FUZZ-IEEE 2011

2011 IEEE International Conference On Fuzzy Systems

Grand Hyatt Taipei, Taipei, Taiwan

June 27-30, 2011

Proceedings

Organized by:

Institute of Electrical and Electronics Engineers (IEEE)

IEEE Computational Intelligence Society (CIS)

National Chiao Tung University, Taiwan, R. O. C.

National University of Tainan, Taiwan, R. O. C.

National Cheng Kung University, Taiwan, R. O. C.

Osaka Prefecture University, Japan

Sponsored by:

National Science Council, Taiwan, R. O. C.

Ministry of Education, Taiwan, R. O. C.

Bureau of Foreign Trade, Taiwan, R. O. C.

© 2011 IEEE. Personal use of this material is permitted. However, permission to reprint/republish this material for advertising or promotional purposes or for creating new collective works for resale or redistribution to servers or lists, or to reuse any copyrighted component of this work in other works must be obtained from the IEEE.

IEEE Catalog Number: CFP11FUZ-USB

ISBN: 978-1-4244-7316-8

ISSN: 1098-7584

Typeset and Printed by DnE Taiwan
www.dneinfo.com
e-mail: nhs@dneinfo.com
Tel: +886-2-22493169

Table of Contents

Welcome Message p.4

Committees p.5

Special Session Organizers p.10

List of Reviewers p.13

Tutorials p.18

Workshops p.19

Plenary Speeches

Plenary Speech I *Jerry M. Mendel* p.20

Plenary Speech II *Piero Bonissone* p.22

Keynote Speeches

Keynote Speech I *Nikhil Pal* p.24

Keynote Speech II *Bernadette Bouchon-Meunier* p.26

Keynote Speech III *Paul Gader* p.28

Invited Talks

Invited Talk I *Kaoru Hirota* p.29

Invited Talk II *James Bezdek* p.31

Invited Talk III *Jim Keller* p.33

Panel Sessions p.35

Competitions p.36

General Information p.40

Conference Venue p.41

Transportation Information p.45

Program-At-A-Glance p.47

Venue Floor Plan p.51

Technical Program Schedule p.52

Contributed Papers p.85

Author Index p.2994

A Message from the Conference Organizers

2011 IEEE International Conference on Fuzzy Systems

It is our great privilege to welcome you to the ***2011 IEEE International Conference on Fuzzy Systems*** (***FUZZ-IEEE 2011***) held in Taipei, Taiwan, June 27-30, 2011. Like the previous conferences in this series, we are confident that FUZZ-IEEE 2011 will provide a forum for fruitful interaction and exchange of ideas between the participants coming from around the world. FUZZ-IEEE 2011 covers all major facets of computational intelligence, but as usual, the primary emphasis will be on fuzzy sets and systems. We are glad to note that 58 different countries from around the world are represented by the authors, thereby making it a truly international event.

The technical program covers four days of presentations including three keynote speeches, two plenary speeches, three invited talks, one Human vs. Computer Go competition, five tutorials, five workshops, two panel sessions, and forty three special sessions given by well-known world class researchers in various fuzzy related subject areas. As for the papers, a total of 358 papers were accepted for oral presentation and 82 for poster presentation out of 618 submissions. So, we expect you to have a great time during these four days. However, we would like to express our sincere gratitude to all the authors and reviewers who have made so many effects for the preparation of their latest researches and all the tutorial and invited speakers who kindly accepted sharing their expertise with the attendees.

No conference can be successful without excellent teamwork and ours is no different. Our special appreciations also go to the sacrifices and perspirations of our colleagues and organizing committee members, for example, Wei-Yen Wang (Local Arrangement Chair), I-Fang Chung (Finance Chair), Shun-Feng Su (Finance Co-Chair), Chia-Feng Juang (Publication Chair), Hani Hagras (Special Sessions Chair), Naoyuki Kubota (Special Sessions Co-Chair), Jyh-Yeong Chang (Registration Chair), Vincenzo Loia (Workshop Chair), Shyi-Ming Chen (Publicity Chair), Mei-Hui Wang (Secretary), Ya-Wen Lin (Secretary), and Hung-Miau Chen (Secretary) in making this conference a smooth process. Most of all, thank you for attending FUZZ-IEEE 2011. We hope this conference will benefit all of us in advancing research activities and building new friendship.

General Chair
Chin-Teng Lin
NCTU, Taiwan

General Co-Chair
Yau-Huang Kuo
NCKU, Taiwan

Program Chair
Chang-Shing Lee
NUTN, Taiwan

Program Co-Chair
Hisao Ishibuchi
OPU, Japan

Program Co-Chair
Wen-June Wang
NCU, Taiwan

Committees

- **Organizing Committee**

Honorary Co-Chairs

Chung-Yu Wu (National Chiao Tung University, Taiwan)
Hsiu-Shuang Huang (National University of Tainan, Taiwan)
Hwung-Hweng Hwung (National Cheng Kung University, Taiwan)
Taketoshi Okuno (Osaka Prefecture University, Japan)

General Chair

Chin-Teng Lin (National Chiao Tung University, Taiwan)

General Co-Chair

Yau-Huang Kuo (National Cheng Kung University, Taiwan)

Program Chair

Chang-Shing Lee (National University of Tainan, Taiwan)

Program Co-Chairs

Hisao Ishibuchi (Osaka Prefecture University, Japan)
Wen-June Wang (National Central University, Taiwan)

Tutorials Chair

Jerry Mendel (University of Southern California, USA)

Keynotes Chair

Jim Keller (University of Missouri-Columbia, USA)

Panels Chair

Nikhil Pal (Indian Statistical Institute, India)

Invited Sessions Chair

Pau-Choo Chung (National Cheng Kung University, Taiwan)

Invited Sessions Co-Chais

Yueh-Min Huang (National Cheng Kung University, Taiwan)
Chih-Min Lin (Yuan Ze University, Taiwan)

Special Sessions Chair

Hani Hagras (University of Essex, UK)

Special Sessions Co-Chair

Naoyuki Kubota (Tokyo Metropolitan University, Japan)

Workshops Chair

Vincenzo Loia (University of Salerno, Italy)

Workshops Co-Chairs

Tzung-Pei Hong (National University of Kaohsiung, Taiwan)
Shi-Jim Yen (National Dong Hwa University, Taiwan)

Fuzzy Competition Chair

Hao Ying (Wayne State University, USA)

Computer Go Competition Chair

Chang-Shing Lee (National University of Tainan, Taiwan)

Computer Go Competition Co-Chairs

Martin Muller (University of Alberta, Canada)
Olivier Teytaud (INRIA-Futurs, TAO, France)
Shun-Chin Hsu (Chang Jung Christian University, Taiwan)

Publicity Chair

Shyi-Ming Chen (National Taiwan University of Science and Technology, Taiwan)

Publicity Co-Chairs

Gary Feng (City University of Hong Kong, Hong Kong)
Francisco Herrera (University of Granada, Spain)
Kok Wai Kevin Wong (Murdoch University, Australia)
Li-Wei Ko (National Chiao Tung University, Taiwan)
Frank Chung-Hoon Rhee (Hanyang University, Korea)
Richard Weber (University of Chile, Chile)
Vladik Kreinovich (University of Texas, USA)
Valentina Balas (Aurel Vlaicu University of Arad, Romania)

Finance Chair

I-Fang Chung (National Yang-Ming University, Taiwan)

Finance Co-Chair

Shun-Feng Su (National Taiwan University of Science and Technology, Taiwan)

Publication Chair

Chia-Feng Juang (National Chung Hsing University, Taiwan)

Publication Co-Chairs

Cheng-Jian Lin (National Chin-Yi University of Technology, Taiwan)
Shin-Mu Tseng (National Cheng Kung University, Taiwan)

Registration Chair

Jyh-Yeong Chang (National Chiao Tung University, Taiwan)

Registration Co-Chairs

Wen-Chieh Lin (National Chiao Tung University, Taiwan)
Sheng-Fu Liang (National Cheng Kung University, Taiwan)

Student Activities Chair

Faa-Jeng Lin (National Central University, Taiwan)

Student Activities Co-Chair

Rong-Ming Chen (National University of Tainan, Taiwan)

Local Arrangement Chair

Wei-Yen Wang (National Taiwan Normal University, Taiwan)

Local Arrangement Co-Chairs

Jin-Tsong Jeng (National Formosa University, Taiwan)
Ching-Hung Lee (Yuan Ze University, Taiwan)
Chun-Fei Hsu (Chung Hua University, Taiwan)
Jiann-Shu Lee (National University of Tainan, Taiwan)
Shing-Tai Pan (National University of Kaohsiung, Taiwan)

Website Chair

Fu-Shine Pai (National University of Tainan, Taiwan)

Website Co-Chair

Ming-Yi Ju (National University of Tainan, Taiwan)

Secretary

Mei-Hui Wang (National University of Tainan, Taiwan)
Yuan-Liang Wang (National University of Tainan, Taiwan)
Ya-Wen Lin (National University of Tainan, Taiwan)
Yi-Ting Fu (Ting) (National Chiao Tung University, Taiwan)
Hung-Miau Chen (NAO) (National Chiao Tung University, Taiwan)

Website maintenance

Hui-Min Wang (National University of Tainan, Taiwan)
Hui-Ju Yang (National University of Tainan, Taiwan)
Yan-Liang Chen (National University of Tainan, Taiwan)

- **Advisory Committee**

James Bezdek (University of West Florida, USA)
Zeungnam Bien (Korea Advanced Institute of Science and Technology, Korea)
Piero Bonissone (GE Global Research, USA)
Bernadette Bouchon-Meunier (University Paris VI, France)
Bor-Sen Chen (National Tsing Hua University, Taiwan)
Jyh-Horng Chou (National Kaohsiung First University of Science and Technology, Taiwan)
Dimitar Filev (Ford Motor Company, USA)
Kaoru Hirota (Tokyo Institute of Technology, Japan)
Laszlo Koczy (Budapest University of Technology and Economics, Hungary)
Enrique H. Ruspini (European Centre for Soft Computing, Spain)
Kay Chen Tan (National University of Singapore, Singapore)
Gwo-Hshiung Tzeng (Kainan University, Taiwan)
Ronald Yager (Iona College, USA)
Gary Yen (Oklahoma State University, USA)
Lotfi A. Zadeh (University of California, USA)

- **Program Committee**

Area Co-Chairs

Intelligent agents and smart environment
Hani Hagras (University of Essex, UK)
Fuzzy control
Jeen-Shing Wang (National Cheng Kung University, Taiwan)
Fuzzy AI - knowledge discovery, reasoning, knowledge representation
Marek Reformat (University of Alberta, Canada)
Basic concepts and mathematics
Qiang Shen (University of Wales Aberystwyth, UK)
Mathematical foundations of fuzzy systems
Baoding Liu (Tsinghua University, China)
Fuzzy robotics
Tzuu-Hseng Li (National Cheng Kung University, Taiwan)
Fuzzy hardware, sensors and architectures
Kaoru Hirota (Tokyo Institute of Technology, Japan)
Fuzzy information processing - information extraction and retrieval, fusion
Witold Pedrycz (University of Alberta, Canada)
Web mining and text mining
Jung-Hsien Chiang (National Cheng Kung University, Taiwan)
Soft computing and hybrid systems - adaptive, hierarchical, evolutionary, neural and nature-inspired systems
Yaochu Jin (University of Surrey, UK)
Software engineering and applications
Jonathan Lee (Chair) (National Central University, Taiwan)
Alan Liu (Co-Chair) (National Chung Cheng University, Taiwan)
Memetic computing
Yew Soon Ong (Nanyang Technological University, Singapore)
Machine learning and cloud computing
Shie-Jue Lee (National Sun Yat-Sen University, Taiwan)
Fuzzy optimization and design, decision support
Hideki Katagiri (Hiroshima University, Japan)
Granular computing
Churn-Jung Liau (Academia Sinica, Taiwan)
Computing with words
Robert John (De Montfort University, UK)
Rough sets, fuzzy human computer interaction
Yo-Ping Huang (National Taipei University of Technology, Taiwan)
Type 2 fuzzy sets and systems
Woei Wan Tan (National University of Singapore, Singapore)
Industrial, financial and medical applications, business intelligence
Fernando Gomide (University of Campinas, Brazil)

Smart interaction and multimedia processing
Hajime Nobuhara (University of Tsukuba, Japan)
Fuzzy reinforcement learning
Hamid Berenji (Intelligent Inference Systems Corp, USA)
Fuzzy systems and Internet - semantic web, ontologies, searching, networks and routing, intrusion detection
Trevor Martin (University of Bristol, UK)
Fuzzy decision making and risk analysis
Didier Dubois (Paul Sabatier University, France)
Genetic fuzzy systems
Rafael Alcalá (University of Granada, Granada, Spain)
Fuzzy image, speech, vision and signal processing
Oscar Cordon (DECSAI, University of Granada, Spain)

Program Committee Members

Rafael Alcalá (University of Granada, Spain)
Plamen Angelov (Lancaster University, UK)
Sansanee Auephanwiriyakul (Chiang Mai University, Thailand)
Robert Babuska (Delft University of Technology, Netherlands)
Gleb Beliakov (Deakin University, Australia)
Oscar Castillo (Tijuana Institute of Technology, Mexico)
Shyi-Ming Chen (National Taiwan University of Science and Technology, Taiwan)
Yung-Yaw Chen (National Taiwan University, Taiwan)
Martine De Cock (Ghent University, Belgium)
Yutaka Hata (University of Hyogo, Japan)
Janusz Kacprzyk (Polish Academy of Science, Poland)
Okyay Kaynak (Bogazici University, Turkey)
Son Kuswadi (Polytechnic Institute of Surabaya, Indonesia)
Yongming Li (Shaanxi Normal University, China)
Kuang-Yow Lian (National Taipei University of Technology, Taiwan)
Radko Mesiar (Slovak University of Technology Bratislava, Slovakia)
Detlef Nauck (Intelligent Systems Research Centre, UK)
Andreas Nürnberger (University of Magdeburg, Germany)
Leszek Rutkowski (Technical University of Czestochowa, Poland)
Mika Sato-Ilic (University of Tsukuba, Japan)
Joao Miguel da Costa Sousa (Technical University of Lisbon, Portugal)
Juhng-Perng Su (National Yunlin University of Science and Technology, Taiwan)
Chin-Wang Tao (National Ilan University, Taiwan)
Nipon Theera-Umpon (Chiang Mai University, Thailand)
Kuo-Yang Tu (National Kaohsiung First University of Science and Technology, Taiwan)
Chi-Hsu Wang (National Chiao Tung University, Taiwan)
Fei-Yue Wang (University of Arizona, USA)
Rahmat Widyanto (University of Indonesia, Indonesia)
Hongwei Wu (Georgia Institute of Technology, USA)

Special Session Organizers

SS01: Fuzzy Ontologies and FML Applications
Organizers: Giovanni Acampora and Chang-Shing Lee

SS02: Evolutionary Fuzzy Systems
Organizers: Yusuke Nojima, Rafael Alcalá, Hisao Ishibuchi, and Francisco Herrera

SS03: Uncertainty and the Semantic Web
Organizers: Fernando Bobillo and Umberto Straccia

SS04: Soft Computing for Operations Research and Optimization
Organizers: Hideki Katagiri, Takashi Hasuike, and M. K. Luhandjula

SS05: Fuzzy Robotics
Organizers: Naoyuki Kubota, Honghai Liu, and Chee Seng Chan

SS06: Intelligent Agents
Organizers: Vincenzo Loia and Hani Hagras

SS07: Metaheuristics and Its Applications
Organizer: Chun-Wei Tsai

SS08: Innovative Fuzzy Approaches to Management Engineering
Organizer: Junzo Watada

SS09: Applications of Fuzzy Logic to Awareness Promotion
Organizers: Kiyota Hashimoto and Shingo Aoki

SS10: Medical and Wellness Engineering
Organizer: Yutaka HATA

SS11: Large-Scale Clustering
Organizer: Timothy Havens

SS12: Recent Advances in Fuzzy-Model-Based Control Systems
Organizers: J. C. Lo and H. K. Lam

SS13: Fuzzy Multiple Criteria Decision Making
Organizer: Gwo-Hshiung Tzeng

SS14: Advances in Fuzzy Theory and their Applications
Organizers: Shyi-Ming Chen and Huey-Ming Lee

SS15: Type-2 Fuzzy Logic Theory
Organizers: Christian Wagner and Robert John

SS16: Fuzzy Interpolation
Organizers: Qiang Shen, László Koczy, and Shyi-Ming Chen

SS17: Practical and Applications Aspects of Type-2 Fuzzy Logic Systems
Organizers: Hani Hagras and Simon Coupland

SS18: Recent Advances in Fuzzy Logic in Image Processing
Organizers: Mike Nachtegael and Gerald Schaefer

SS19: Fuzzy Inference Systems-Theory and Applications
Organizer: Hirosato Seki

SS20: Universal Contents Creation/Distribution and Intelligent System
Organizer: Katsuhiro Honda

SS21: Fuzzy Control in Industrial and Application
Organizer: Shun-Hung Tsai

SS22: Fuzzy Methods in Machine Learning and Data Mining
Organizers: Eyke Huellermeier and Daniel Sanchez

SS23: Industrial Applications of Evolving Fuzzy Systems
Organizers: Kit Yan Chan, Hak Keung Lam, and Steve S. H. Ling

SS24: Hybrid Learning for Fuzzy Systems
Organizer: Jin-Tsong Jeng

SS25: Evolving and Adaptive Fuzzy Systems
Organizers: Plamen Angelov, Dimitar Filev, and Nik Kasabov

SS26: Inter-Relation between Interval and Fuzzy Techniques
Organizers: Eunjin Kim and Vladik Kreinovich

SS27: Communication Robotics and Computational Intelligence Co-creation
Organizers: Yoichi Yamazaki and Fangyan Dong

SS28: Current Development in Pattern Classification-Kernelization, Pairwise Constraints, and Classifiers
Organizer: Yasunori Endo

SS29: Software Engineering with Computational Intelligence
Organizers: Jonathan Lee, Nien-Lin Hsueh, and Chiung-Hon Leon Lee

SS30: Computing With Words
Organizers: Sergio Guadarrama and Jerry Mendel

SS31: Human Symbiotic Systems
Organizers:Yoichiro Maeda and Daisuke Katagami

SS32: Adaptive Fuzzy Logic Control
Organizers:Valentina E. Balas and Tsung-Chih Lin

SS33: Fuzzy and Paraconsistent Intelligent Systems
Organizers: Valentina E. Balas, Jair Minoro Abe, and Kazumi Nakamatsu

SS34: Brain and Learning
Organizers:Isao Hayashi and Toshihiko Watanabe

SS35: Fuzzy Regression Analysis and Its Applications
Organizers: M. Hadi Mashinchi, Mehmet A. Orgun, Witold Pedrycz, Mashaalah Mashinchi, and Chi-Tsuen Yeh

SS36: Fuzzy Systems on Renewable Energy
Organizers: Faa-Jeng Lin and Hong-Tzer Yang

SS37: Fuzzy Logic Based Computer Vision and Its Applications to Guidance and Control
Organizer: Kuo-Hsien Hsia

SS38: Fuzzy Knowledge Discovery and Its Applications
Organizers: Yue-Shi Lee and Rung-Ching Chen

SS39: Fuzzy Based Computation on Biomedical Systems
Organizers: Shing-Tai Pan, Sheng-Fu Liang, and Tzung-Pei Hong

SS40: Fuzzy Approach for Information Security Management
Organizers: Tzung-Nan Chuang, Che-Hung Liu, and Chang-Shing Lee

SS41: Neuro Fuzzy Systems and Their Real World Application
Organizers: Sungshin Kim, Euntai Kim, Kweebo Sim, and Jinwoo Jung

SS42: Fuzzy Cognitive Maps-Theory and Applications
Organizers: Elpiniki I. Papageorgiou and Jose L. Salmeron

SS43: Fuzzy Systems of Unknown Nonlinear Complex Systems
Organizers: Wei-Yen Wang and Hsum Li

List of Reviewers

Hussein A. Abbass
Jair Minoro Abe
Giovanni Acampora
Jose Aguilar
Jesus S Aguilar-Ruiz
Seiki Akama
Rafael Alcala
Jesus Alcala-Fdez
Jose Maria Alonso
Derek Anderson
Plamen Angelov
Cecilio Angulo
Michela Antonelli
Shingo Aoki
Joan Aranda
Nureize Arbaiy
Sansanee Auephanwiriyakul
Mehmet Aydin
Robert Babuska
Afef Bahri
Li Bai
Ying Bai
Rohani Abu Bakar
Valentina E. Balas
Krisztian Balazs
Xiaojun Ban
Ahmad Banakar
Zuhair Bandar
Andrzej Bargiela
Antonio Javier Barragan
Edurne Barrenechea
Senen Barro
Ieroham Baruch
Benjamin Bedregal
Gleb Beliakov
Miguel Bernal
Mohammad Bilgarbegian
Isabelle Bloch
Fernando Bobillo
Andrea Bonarini
Gloria Bordogna
Arsham Borumand Saeid
Patrick Bosc
Janos Botzheim
Rafik Bouaziz
Abdelhamid Bouchachia
Bernadette Bouchon-Meunier
Yiannis Boutalis
Sandra Bringay
Piedad Brox
Humberto Bustince
Vito Calderaro
Silvia Calegari
Raffaele Cannone
Jiangtao Cao
Christer Carlsson
Joao Paulo Carvalho
Jorge Casillas
Ciro Castiello
Oscar Castillo
M. Emre Celebi
Marco Cerami
Quek Hiok Chai
Goutan Chakraborty
Jesus Chamorro-Martinez
Chee Seng Chan
Kit Yan Chan
Sandeep Chandana
Bae-Muu Chang
Cheng-Yuan Chang
Yau-Zen Chang
Yu-Chuan Chang
Brigitte Charnomordic
Bor-Sen Chen
Cheng-Hung Chen
Cheng-Lun Chen
Chin-Sheng Chen
Chun-Hao Chen
Mei-Yung Chen
Ming-Chang Chen
Rung-Ching Chen
Shi-An Chen
Shyi-Ming Chen
Syuan-Yi Chen
Tan Kay Chen
Ta-Tau Chen
Yen-Tzu Chen
Ying-ping Chen
Li-chen Cheng
Chian-Song Chiu
Jyh-Horng Chou
Po-Huan Chou
Chen-Chia Chuang
Tzung-Nan Chuang
I-Fang Chung
Pau-Choo Chung
Marco Cococcioni
Oscar Cordon
Chris Cornelis
Paulo Cortez
Simon Coupland
Pedro Couto
Keeley A Crockett
Darren Dancey
Antonina Dattolo
Martine De Cock
Adolfo R. de Soto
Guy De Tre
Maria Jose del Jesus
Myriam Regattieri Delgado
Danilo Dell'Agnello
Hans DeMeyer
Mustafa Demirci
Bruno DiStefano

Federico Divina
Faiyaz Doctor
Fangyan Dong
Jiuxiang Dong
Antonio Dourado
Xiao-Gang Duan
Didier Dubois
Pietro Ducange
Hakan Duman
Yasunori Endo
Tomoe Entani
Senol Zafer Erdogan
Alexandre G. Evsukoff
Zhun Fan
Paulo Fazendeiro
Gary Feng
Giuseppe Fenza
Javier Fernandez
Dimitar Filev
Gary Fogel
Hichiem Frigui
Wojciech Froelich
Takeshi Furuhashi
Maria Jose Gacto
Paul Gader
Mikel Galar Idoate
Sylvie Galichet
Jose Antonio Gamez
Itziar Garcia-Honrado
Ana Garcia-Serrano
Miguel Garcia-Silvente
Jon Garibaldi
Fathi Gasir
Tom Gedeon
Lluis Godo
Eduardo Gomez
Mario Gongora
Antonio Gonzalez
Pedro Gonzalez
Siegfried Gottwald
Manuel Grana
Bobby Granville
Sarah Greenfield
Jerzy Grzymala-Busse
Dongbing Gu
Sergio Guadarrama
Kevin Guelton
Thierry-Marie Guerra
Serge Guillaume
Alberto Guillen
German Gutierrez
Javier Gutierrez Garcia
Ali Reaza Hadipour
Masafumi Hagiwara
Hani Hagras
Yukihiro Hamasuna
Hussam Hamrawi
Ali Hamzeh
Hugang Han
Hisashi Handa
Ryo Haruna
Kiyota Hashimoto
Tomonori Hashiyama
Takashi Hasuike
Yutaka Hata
Yutaka Hatakeyama
Toshiharu Hatanaka
Timothy Havens
Isao Hayashi
Haibo He
Luis Miramontes Hercog
Francisco Herrera
Sachio Hirokawa
Kaoru Hirota
Katsuhiro Honda
Tzung-Pei Hong
Keiichi Horio
Danilo Horta
Yukinobu Hoshino
Kuo-Hsien Hsia
Chih-Ching Hsiao
Ming-Ying Hsiao
Cheng-Hsiung Hsieh
Chen-Chien (James) Hsu
Chun-Fei Hsu
Nien-Lin Hsueh
Yo-Ping Huang
Eyke Huellermeier
Sajid Hussain
Oscar Ibanez
Hidetomo Ichihashi
Hiroyuki Inoue
Rolly Intan
Masahiro Inuiguchi
Hisao Ishibuchi
Abdelhafidh Jaadari
Dalel Jabri
Jiri Jan
Vladimir Janis
Jin-Tsong Jeng
Jyh-Fu Jeng
Richard Jensen
Yinlai Jiang
Yuncheng Jiang
Jorge Jimenez
Yaochu Jin
Robert John
Chia-Feng Juang
Jin-Woo Jung
Seul Jung
Petr Kadlec
Ilhem Kallel
Achilles Kameas
Akihiko Kanagawa
Masayoshi Kanoh
Yuchi Kanzawa
Cihan Karakuzu
Tomoko Kashima
Daisuke Katagami
Hideki Katagiri

Kosuke Kato
Hiroharu Kawanaka
Ihsan Kaya
Uzay Kaymak
James Keller
Raouf Ketata
Mehdi Khoury
Masayuki Kikuchi
Eunjin Kim
Euntai Kim
Sungshin Kim
Yong-Gi Kim
Erich Peter Klement
Chia-Nan Ko
Syoji Kobashi
Futoshi Kobayashi
Yucel Kocyigit
Laszlo Koczy
Mario Koeppen
Takanori Koga
Stefanos Kollias
Marcin Korytkowski
Dimitrios Koulouriotis
Robert Kozma
Oliver Kramer
Dariusz Krol
Naoyuki Kubota
Daisuke Kurabayashi
Son Kuswadi
Mila Kwiatkowska
Ohbyung Kwon
Chih-Chin Lai
H.K. Lam
Jimmy Lauber
Anne Laurent
Chang-Shing Lee
Ching-Hung Lee
Chiung-Hon Leon Lee
Huey-Ming Lee
Jiann-Shu Lee
Jonathan Lee
Li-Wei Lee
Shie-Jue Lee
Yue-Shi Lee
Zne-Jung Lee
Daniel Leite
Andre Lemos
Zsofia Lendek
Marie-Jeanne Lesot
Yih-Guang Leu
Hongyi Li
I-Hsum Li
Li Li
Yongming Li
Sheng-Fu Liang
Churn-Jung Liau
Chang-Hua Lien
Cheng-Jian Lin
Chih-Min Lin
Faa-Jeng Lin
Hung-Yi Lin
Lee-Chuan Lin
Tsung-Chih Lin
Wen-Chieh Lin
Win-Yang Lin
Yih-Lon Lin
Steve Ling
Alan Liu
Baoding Liu
Che-Hung Liu
FeiLong Liu
Honghai Liu
Xin-Rui Liu
Xinwang Liu
Yonghuai Liu
Ji-Chang Lo
Vincenzo Loia
Daniele Loiacono
Ahmad Lotfi
Hao-Chun Lu
Edwin Lughofer
M. K. Luhandjula
Yiguang Lui
Neil Mac Parthalain
Yoichiro Maeda
Luis Magdalena
Tanja Magoc
Mahdi Mahfouf
Noureddine Manamanni
Francesco Marcelloni
Nicolas Marin
Javier Gomez
Marin-Blazquez
Francisco A. Marquez
Hernandez
Christophe Marsala
Trevor Martin
Maria J. Martin-Bautista
Hadi Mashinchi
Mashaalaah Mashinchi
Mashaalah Mashinchi
Reza Mashinchi
Paris Mastorocostas
Francesco Masulli
Takeshi Matsui
Shimpei Matsumoto
Yoshiyuki Matsumoto
Fuyuko Matsumura
Gilles Mauris
Mauro Mazzieri
Juan Miguel Medina
Miguel Melgarejo
Patricia Melin
Pedro Melo-Pinto
Corrado Mencar
Jerry Mendel
Sumudu Mendis
Olivia Mendoza
Qinggang Meng
Jose M. Merigo Lindahl

Radko Mesiar
Sadaaki Miyamoto
Takatomi Miyata
Tetsuya Miyoshi
Makoto Mizukawa
Masoud Mohammadian
Carlos Molina
Javier Montero
Susana Montes
Oscar Montiel
Eduard Montseny
Ahmed Moussa
Manuel Mucientes
Enrique Munoz
Tadahiko Murata
Toshiaki Murofushi
Zalili Binti Musa
Maybin Muyeba
Mike Nachtegael
Kouki Nagamune
Hirsohi Nakajima
Tsuyoshi Nakamura
Tomoharu Nakashima
Mohammad Narimami
Costas Neocleous
Sing Kiong Nguang
Adam Niewiadomski
Manabu Nii
Hitoshi Nishi
Junji Nishino
Vesa A. Niskanen
Keiichi Niwa
Yusuke Nojima
Akira Notsu
Vilem Novak
Andreas Nuernberger
Alessandro G. Di Nuovo
Hannu Nurmi
Chi-Hyon Oh
Shin-ichi Ohnishi
Hiroshi Ohtake
Manuel Ojeda-Aciego
Hidehiko Okada
Gulay Oke
Jose Angel Olivas
Mehmet Orgun
Mehmet A. Orgun
Albert Orriols-Puig
Juan A. Ortega
James O'Shea
Karen O'Shea
Clemens Otte
Chen-Sen Ouyang
Miguel Pagola
Nikhil Pal
Vasile Palade
Shing-Tai Pan
Endre Pap
Elpiniki Papageorgiou
Daniel Paraschiv
David Parry
Vasile Patrascu
Witold Pedrycz
Wytold Pedrycz
David Pelta
Juan Peralta Donate
Antonio Peregrin
Martin Pereira-Farina
Raul Perez
Irina Perfilieva
Alfredo Petrosino
Fred Petry
Vincenzo Piuri
Hector Pomares
Mihail Popescu
Marjan Popov
Chotipat Pornavalai
Ana Pradera
Belen Prados Suarez
Girijesh Prasad
Cristina Puente Agueda
Dan Ralescu
Marek Reformat
Santiago Romani Also
Bahram Sadeghpour Gildeh
Ryosuke Saga
Yoshitada Sakai
Jose L. Salmeron
Daniel Sanchez
Mika Sato-Ilic
Gerald Schaefer
Hirosato Seki
Kazuhisa Seta
Renping Shao
Ehsan Sharifi
Qiang Shen
Zhiqi Shen
Eri Shimokawara
Pierluigi Siano
Kweebo Sim
Levente Simon
Andrzej Skowron
Isaac Sledge
Dominik Slezak
Stephen Smith
Pilar Sobrevilla
Alejandro Sobrino
Joao Sousa
Dipti Srinivasan
Giorgos Stamou
Umberto Straccia
Maja Stula
Chrysostomos Stylios
Juhng-Perng Su
Ming-Yang Su
Steven Su
Tom Sudkamp
Tsung-Ying Sun
Yeong-Jeu Sun
Kenji Suzuki

Kovacs Szilveszter
Seyed Mahmoud Taheri
Noburu Takagi
Yasutake Takahashi
Takahiro Takeda
Kazuhiro Takeuchi
Woei Wan Tan
Yandong Tang
Tadanari Taniguchi
Chin-Wang Tao
Kai Meng Tay
Maguelonne Teisseire
Andreja Tepavcevic
Settimo Termini
Vladimir Terzija
Ruck Thawonmas
Nipon Theera-Umpon
John B. Theocharis
Chuan-Kang Ting
Vicenc Torra
Enric Trillas
Gracian Trivino
Ching-Chih Tsai
Hung-Hsu Tsai
Kun-Lin Tsai
Men-Shen Tsai
Shun-Hung Tsai
Chung-Shi Tseng
Fan-chuan Tseng
Naoki Tsuchiya
Shusaku Tsumoto
Kuo-Yang Tu
Gwo-Hshiung Tzeng
Silvia Ullo
Takeshi Uno
Alfredo Vaccaro
Gancho Vachkov
Fevrier Valdez
Jose Valente de Oliveira
Marcos Eduardo Valle
Albert Van Der Heide
Patricia A. Vargas
Thanos Vasilakos
Laurentiu Vasiliu
Giovanni Velotto
Enrique Herrera Viedma
Vinicius da F. Vieira
Amparo Vila
Pedro Villar
Karen Villaverde
Autilia Vitiello
Peter Vojtas
Michael Wagenknecht
Christian Wagner
Rong-Jong Wai
Antony Waldock
Igor Walter
Cheng-Yi Wang
Chun-Chieh Wang
Fei-Yue Wang
Feng-Hsu Wang
Jeen-Shing Wang
Jen-Sheng Wang
Ling Wang
Mei-Hui Wang
Shuming Wang
Shyue-Liang Wang
Wei-Yen Wang
Zhenyuan Wang
Junzo Watada
Toshihiko Watanabe
Chih-Chin Wen
Rahmat Widyanto
Anna Wilbik
Andy Wong
Kok Wai Wong
Man Leung Wong
Chih-Hung Wu
Dongrui Wu
Gin-Der Wu
Hongwei Wu
Huai-Ning Wu
Min Wu
Sebastia Xambo
Gang Xiang
Fuding Xie
Zong-Yi Xing
Ning Xiong
Shamshul Bahar Yaakob
Yoshiyuki Yabuuchi
Ronald R. Yager
Naomi Yagi
Yoichi Yamazaki
Hong-Tzer Yang
Longzhi Yang
Hitoshi Yano
Toshiyuki Yasuda
Chi-Tsuen Yeh
I-Cheng Yeh
Shi-Jim Yen
Chenjiu Yin
Tang-Kai Yin
Hao Ying
Jun Yoneyama
Tomohiro Yoshikawa
Ker-Wei Yu
W.S. Yu
Jia Zeng
Xiao-Jun Zeng
Daoyuan Zhai
Baoyong Zhang
Geng Zhang
Hongbin Zhang
Xianxia Zhang
Qiangfu Zhao
Haibo Zhou
Huiyu Zhou
Shang-ming Zhou
William Zhu

Tutorials

T01: Evolutionary Multi-Objective Design of Fuzzy Rule-Based Systems

Instructor: Rafael Alcala

T01-1: Monday, June 27, 2011 (9:00 AM- 10:30 AM) Room: Peacock

T01-2: Monday, June 27, 2011 (11:00 AM- 12:30 PM) Room: Peacock

T02: Interpolative Fuzzy Rule Bases

Instructor: László Koczy

T02-1: Monday, June 27, 2011 (9:00 AM- 10:30 AM) Room: Phoenix

T02-2: Monday, June 27, 2011 (11:00 AM- 12:30 PM) Room: Phoenix

T03: Theoretical and Practical Aspects of Type-2 Fuzzy Systems: Part 1

Instructor: Jerry Mendel

T03-1: Monday, June 27, 2011 (9:00 AM- 10:30 AM) Room: Crane

T03-2 Monday, June 27, 2011 (11:00 AM- 12:30 PM) Room: Crane

T04: Theoretical and Practical Aspects of Type-2 Fuzzy Systems: Part 2

Instructor: Hani Hagras

T04-1: Monday, June 27, 2011 (01:30 PM- 03:00 PM) Room: Peacock

T04-2: Monday, June 27, 2011 (03:30 PM- 05:00 PM) Room: Peacock

T05: Towards a Unified Framework for Intelligent Robotics

Instructors: Honghai Liu and Naoyuki Kubota

T05-1: Monday, June 27, 2011 (01:30 PM- 03:00 PM) Room: Phoenix

T05-2: Monday, June 27, 2011 (03:30 PM- 05:00 PM) Room: Phoenix

Workshops

W01: Fuzzy Approaches to Ambient Intelligent Agents

Organizers:Vincenzo Loiaand Hani Hagras

W01-1: Monday, June 27, 2011 (9:00 AM- 10:30 AM) Room: Egret

W01-2: Monday, June 27, 2011 (11:00 AM- 12:30 PM) Room: Egret

W02: Standards in Computational Intelligence

Organizers:Giovanni Acampora, PlamenAngelov, and Bruno Di Stefano

W02: Monday, June 27, 2011 (9:00 AM- 10:30 AM) Room: Swallow

W03: Computational Intelligence Techniques for Smart Grids

Organizers:Alfredo Vaccaroand Vladimir Terzija

W03-1: Monday, June 27, 2011 (01:30 PM- 03:00 PM) Room: Crane

W03-2: Monday, June 27, 2011 (03:30 PM- 05:00 PM) Room: Crane

W04: Computer Game and Fuzzy-based Game Applications

Organizers:Shun-Chin Hsu, I-Chen Wu, and Shi-Jim Yen

W04-1: Monday, June 27, 2011 (01:30 PM- 03:00 PM) Room: Egret

W04-2: Monday, June 27, 2011 (03:30 PM- 05:00 PM) Room: Egret

W05: Hybrid Computational Intelligence Applications

Organizers:Chuan-Kang Ting and Tzung-Pei Hong

W05-1: Monday, June 27, 2011 (01:30 PM- 03:00 PM) Room: Swallow

W05-2: Monday, June 27, 2011 (03:30 PM- 05:00 PM) Room: Swallow

Plenary Speech I

Date/Time: Tuesday, June 28, 2011 /1:30 PM- 2:30 PM

Room: Grand Ballroom I, Chair: Chang-Shing Lee

Type-2 Fuzzy Sets and Systems: Challenges and Misconceptions.

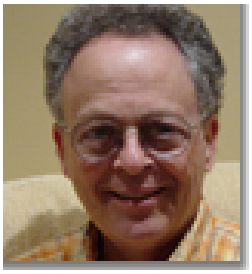

Prof. Jerry M. Mendel

University of Southern California, USA

Abstract

Type-2 fuzzy sets and systems have now moved into the mainstream of world-wide research and should no longer be viewed as an "emerging" research area. During the latter part of 2009 and the first half of 2010 a small group of type-2 researchers created a jointly-authored CI Magazine article, whose title is that of this talk. In addition, in April 2011 there were two panel sessions at the Advances in Type-2 Fuzzy Sets and Systems Symposium, that was a part of the IEEE CIS Symposium Series on CI, held in Paris, France. These panel sessions were also on the topics in the title of this talk. In this talk, I will summarize the main conclusions from the magazine article and the two panels (and ensuing discussions) about the challenges and misconceptions of type-2 fuzzy sets and systems. This should be of great interest to researchers who want to know the directions of the vectors of most promising type-2 research.

Biography

Jerry M. Mendel is Professor of Electrical Engineering and Systems Architecting Engineering at the University of Southern California in Los Angeles, where he has been since 1974. He has published over 480 technical papers and is author, co-author and/or editor of nine books, including Uncertain Rule-based Fuzzy Logic Systems: Introduction and New Directions and Perceptual Computing: Aiding People in Making Subjective Judgments (2010). His present research interests include: type-2 fuzzy logic systems and their applications to a wide range of problems, including smart oil field technology and computing with words. He is a Life Fellow of the IEEE, a Distinguished Member of the IEEE Control Systems Society, and a Fellow of the International Fuzzy Systems Association (2009). He was President of the IEEE Control Systems Society in 1986. He was a member of the Administrative Committee of the IEEE Computational Intelligence Society (2004-2009) and was Chairman of its Fuzzy Systems Technical Committee. He is presently Chair of

the Computing With Words Task Force of the IEEE Computational Intelligence Society. Among his awards are the 1983 Best Transactions Paper Award of the IEEE Geoscience and Remote Sensing Society, the 1992 Signal Processing Society Paper Award, the 2002 Transactions on Fuzzy Systems Outstanding Paper Award, a 1984 IEEE Centennial Medal, an IEEE Third Millenium Medal, and a Fuzzy Systems Pioneer Award (2008) from the IEEE Computational Intelligence Society.

Plenary Speech II

Date/Time: Wednesday, June 29, 2011 /1:30 PM- 2:30 PM

Room: Grand Ballroom I, Chair: Faa-Jeng Lin

Soft Computing in Prognostics and Health Management (PHM) Applications: A Case Study in Anomaly Detection

Dr. Piero Bonissone

GE Global Research, USA

Abstract

Soft Computing (SC) is a term that has evolved, since its inception in 1991, to represent a methodology and a set of techniques covering the aspects of data-driven models design, domain knowledge integration, model generation, and model tuning. We distinguish between offline Meta-heuristics (MH's), used for model design and tuning, and online MH's, used for models selection or aggregation. This view suggests the use of hybrid SC at each MH's level as well as at the object level. We manage model complexity by finding the best model architecture to support problem decomposition, generate local models with high-performance in focused applicability regions, provide smooth interpolations among local models, and increase robustness to imperfect data by aggregating diverse models. We illustrate this concept with a case study in anomaly detection for a fleet of physical assets (such as an aircraft engines or a gas turbines.) Anomaly detection typically uses unsupervised learning techniques to extract the underlying structural information from the data, define normal structures and regions, and identify departures from such regions. We focus on one of the most common causes for anomalies: the inadequate accuracy of the anomaly detection models, which are prone to create false alarms. To address this issue, we propose a hybrid approach based on a fuzzy supervisory system and an ensemble of locally trained auto associative neural networks (AANN's.) The design and tuning of this hierarchical model is performed using evolutionary algorithms. In our approach we interpolate among the outputs of the local models (AANN's) to assure smoothness in operating regime transition and provide continuous condition monitoring to the system. Experiments on simulated data from a high bypass, turbofan aircraft engine model demonstrated promising results.

Biography

Piero Bonissone A Chief Scientist at GE Global Research, Dr. Bonissone has been a pioneer in the field of fuzzy logic, AI, soft computing, and approximate reasoning systems applications

since 1979. He is a Coolidge Fellow at GE Global Research (1993). He is also a Fellow of the Association for the Advancement of Artificial Intelligence (1996), the IEEE (2004), and the International Fuzzy Systems Association (2005). He served as Editor in Chief of the International Journal of Approximate Reasoning for 13 years (1993-2005). He co-edited six books and co-authored 150 publications. He received 54 patents issued from the USPTO (plus 50 pending). He has co-chaired 12 scientific conferences and symposia focused on Multi-Criteria Decision-Making, Fuzzy sets, Diagnostics, Prognostics, and Uncertainty Management in AI. In 2002, he was President of the IEEE Neural Networks Society (now Computational Intelligence Society). He has been an Executive Committee member of NNC/NNS/CIS society since the past 16 years and an IEEE CIS Distinguished Lecturer since 2004. In 2008 he received the II Cajastur International Prize for Soft Computing, from CajAstur and the Foundation for the Advancement of Soft Computing. He is the Chair of the Scientific Committee of the European Centre of Soft Computing.

Keynote Speech I

Date/Time: Tuesday, June 28, 2011 /10:50 AM- 12:00 PM

Room: Grand Ballroom I, Chair: Jyh-Yeong Chang

Inferring Disease Related Gene-Gene Interactions: A Fuzzy Logic Based Approach

Prof. Nikhil Pal

Indian Statistical Institute, India

Abstract

There have been many attempts to infer gene-gene interactions from microarray data based on different approaches such as mutual information, Bayesian networks, and differential equations. The gene-gene interactions identified by such methods reveal important and interesting biological functions, but all of these may not be related to a phenotype, say, a particular cancer. In this talk we shall focus on identification of gene-gene interactions, which are related to a particular disease. Two genes individually may be related to a particular cancer but we are not interested in such pairs. The objective here is to identify pairs of genes whose cooperative behavior make them related to the disease. There have been a few attempts to address this problem based on information theoretic concepts. In this talk first we shall discuss the main philosophy behind such approaches and some associated issues/problems. Then we shall present a very simple fuzzy set theoretic method for inferring gene-gene interactions associated to a particular type of disease/cancer. Our method is based on a set of fuzzy rules. The advantages of this fuzzy approach over the existing ones will be discussed. Finally, we shall demonstrate the effectiveness of our method on a benchmark data set.

Biography

Nikhil R. Pal is a Professor in the Electronics and Communication Sciences Unit of the Indian Statistical Institute. He has also served as a Chair Professor at the National Chiao Tung University, Taiwan and as a visiting professor at other universities. He has coauthored, edited/co-edited several books. His current research interest includes bioinformatics, brain science, fuzzy logic, image and pattern analysis, neural networks, and evolutionary computation. He serves on the editorial /advisory board/ steering committee of several journals including the International Journal of Approximate Reasoning, Applied Soft Computing, Neural Information

Processing—Letters and Reviews, International Journal of Knowledge-Based Intelligent Engineering Systems, International Journal of Neural Systems, Fuzzy Sets and Systems ,International Journal of Intelligent Computing in Medical Sciences and Image Processing, Fuzzy Information and Engineering : An International Journal, and the IEEE Transactions on Systems Man and Cybernetics—B. He has been serving as the Editor-in-Chief of the IEEE Transactions on Fuzzy Systems since 2005. He has given many plenary/keynote speeches in different premier international conferences in the area of computational intelligence. He was the president of the Asia Pacific Neural Net Assembly. He was the Program Chair of the 4th International Conference on Advances in Pattern recognition and Digital Techniques, December 1999, Calcutta, India and was a co-program chair of 2005 IEEE International Conference on Fuzzy Systems and 2006 IEEE International Conference on Fuzzy Systems. He was the General Chair of 2002 AFSS International Conference on Fuzzy Systems, Calcutta, 2002 and the 11th International Conference on Neural Information Processing, ICONIP 2004. He is a Fellow of the National Academy of Sciences, India, a Fellow of the Indian National Academy of Engineering, a Fellow of the International Fuzzy Systems Association (IFSA), and a Fellow of the IEEE, USA.

Keynote Speech II

Date/Time: Wednesday, June 29, 2011 /10:50 AM- 12:00 PM

Room: Grand Ballroom I, Chair: Chia-Feng Juang

Fuzzy Approaches to Information Fusion

Prof. Bernadette Bouchon-Meunier

University Paris VI, France

Abstract

Fusion is a major issue in all steps of the management of information, from data representation to data mining and decision-making, from basic granules of information to consensus of opinions or semantic interpretation of situations. The complexity of data is due to various factors : heterogeneous media, large size available data on the web or provided by all kinds of sensors, incomplete data bases, imprecise or subjective information granules, the reliability of sources, to mention a few of them. Fuzzy approaches provide interesting solutions to cope with such problems. We will address two main levels in information fusion. The first one is technical and concerns basic needs in image processing, prototype construction or classifier fusion. The second one is more abstract and deals with the interpretation of results, the recognition of high level features in images or videos, or the issue of information scoring.

Biography

Bernadette Bouchon-Meunier is a director of research at the National Center for Scientific Research, head of the department of Databases and Machine Learning in the Computer Science Laboratory of the University Paris 6. Graduate from the Ecole Normale Superieure at Cachan, she received the degrees of B.S. in Mathematics and Computer Science, Ph.D. in Applied Mathematics and D. Sc. in Computer Science from the University of Paris. She is the Editor-in-Chief of the International Journal of Uncertainty, Fuzziness and Knowledge-based Systems (World Scientific), She is also a member of the editorial board of the International Journal of Approximate Reasoning, Fuzzy Sets and Systems, International Journal of Fuzzy Systems, International Journal of Information Technology and Intelligent Computing, Journal of Uncertain Systems. She is the (co)-editor of 21 books and the (co)-author of four books in French and one in vietnamese on Fuzzy Logic and Uncertainty Management in Artificial Intelligence. She is a co-founder and co-executive

director of the International Conference on Information Processing and Management of Uncertainty in Knowledge-based Systems (IPMU) held every other year since 1986. She is an IEEE senior member and an International Fuzzy Systems Association fellow. Her present research interests include approximate and similarity-based reasoning, as well as the application of fuzzy logic and machine learning techniques to decision-making, data mining, risk forecasting, information retrieval and user modelling.

Keynote Speech III

Date/Time: Thursday, June 30, 2011 /10:50 AM- 12:00 PM

Room: Grand Ballroom I, Chair: Jung-Hsien Chiang

Soft Computing for Hard Pattern Recognition Problems

Prof. Paul Gader

University of Florida, USA

Abstract

A survey of research and development of fuzzy set related approaches for use in difficult applications involving pattern recognition. Approaches include fuzzy clustering, fuzzy k-nearest neighbors, ordered weighted averaging operators, fuzzy integrals, and random sets. Applications will be drawn from medical image and signal analysis, landmine detection, language processing, and hyperspectral image analysis for remote sensing, face recognition, and trace material detection.

Biography

Paul Gader received his Ph.D. in Mathematics for image processing related research in 1986 from the University of Florida. He has worked as a Senior Research Scientist at Honeywell's Systems and Research Center, as a Research Engineer and Manager at the Environmental Research Institute of Michigan, and as a faculty member at the University of Wisconsin - Oshkosh, the University of Missouri - Columbia, and the University of Florida, where he is currently a Professor of Computer and Information Science and Engineering. His research has spanned a number of areas related to image analysis and pattern recognition including applied mathematics, parallel image processing, mathematical morphology, fuzzy and random sets, handwriting recognition, bio-medical image analysis, automatic target recognition, landmine detection, hyperspectral image analysis, and information fusion. He enjoys trying to devise theoretical approaches and translate them into applications and trying to understand what the important issues are in that process.

Invited Talk I

Date/Time: Wednesday, June 29, 2011 /08:00 AM- 9:00 AM

Room: Grand Ballroom I, Chair: Yau-Hwang Kuo

Casual Communication between Robots and Humans based on Robot Technology Middleware and Multimedia Recognition

Prof. Kaoru Hirota

Tokyo Institute of Technology, Japan

Abstract

The Mascot Robot System has been developed by the author's group as a part of the "Development Project for a Common Basis of Next-Generation Robots" sponsored by NEDO (New Energy and industrial technology Development Organization). The main purpose of the mascot robot system is to perform casual communication between robots and humans mainly based on the speech recognition module mounted on household robots. The system is implemented as a network of multi-robots freely connected by RT middleware (RTM). It consists of 5 robots, i.e., 4 fixed robots (placed on a TV, a darts game machine, an information terminal, and a mini-bar) and 1 mobile robot. Each of them includes an eye robot, a speech recognition module, and a notebook PC that controls the robot and the speech recognition module. These robots connect together with a server through the internet by RTM, thus constituting the Robot System. The Mascot Robot System's functioning is demonstrated in an ordinary living room, where casual communication between 5 robots and 4 human beings (1 host, 2 guests, and 1 walk-in) is conducted based on speech recognition and mentality expression of eye robots. The experimental results are shown by DVD files.

The NEDO project is extended to JSPS (Japan Society for Promotion of Science) project ongoing, where computational intelligence based gesture recognition method is proposed and embedded in the mascot robot system to realize casual communication between robots and humans. It utilized both video image data from web camera, voice information by microphone, and motion data given by a wearable 3D acceleration sensor on human wrists to identify the intentions and emotions, i.e., multi media recognition technology. To demonstrate the validity, the proposed method is now applied to a part of a mascot robot system, where a home party scenario performed

by five eye robots and four human participants. On going results show the possibility that the proposed method may be used to improve the interaction between human and robotic systems.

Biography

Kaoru HIROTA received Dr. E. degrees from Tokyo Institute of Technology in 1979. After his career at Sagami Institute of Technology and Hosei University, he has been with Tokyo Institute of Technology. His research interests include fuzzy systems, intelligent robot, and image understanding. He experienced president-elect and fellow of IFSA (International Fuzzy Systems Association), and president of SOFT (Japan Society for Fuzzy Theory and Systems.) He is a chief editor of J. of Advanced Computational Intelligence and Intelligent Informatics. Banki Donat Medal, Henri Coanda Medal, Grigore MOISIL Award, SOFT best paper award, Acoustical Society of Japan best paper award, honorary professorships from de La Salle University and Changchun Univ. of Science & Technology, and Honoris Causa from Bulacan state university, Budapest Technical University, and Szechenyi Istvan University were awarded to him. He organized more than 10 international conferences/symposiums as a founding/general/program chair. He has been publishing about 250 journal papers, 50 books, and 450 conference papers.

Invited Talk II

Date/Time: Wednesday, June 29, 2011 /05:00 PM- 06:00 PM

Room: Swan, Chair: Li-Wei Ko

Acceleration and Scalability for c-Means Clustering

Prof. James Bezdek

University of West Florida, USA

Abstract

This talk begins with characterization the three canonical problems of clustering: tendency assessment (does the data have cluster substructure?); clustering (how do we find partitions of the data?); and validation (are the partitions we find accurate and/or useful?). I identify the four types of models used in clustering: partition only (single linkage); prototype only (self-organizing maps); partition and prototypes (hard, fuzzy and possibilistic c-means); and (partition, prototype, other parameter) models (EM algorithm for Gaussian mixture decomposition). I will give a brief account of the basic models and algorithms for hard, fuzzy, possibilistic c-means. These algorithms are reliable, but can be slow, and may not scale well for very large data sets. So, the main issues when dealing with huge data sets are acceleration and scaling.

There have been many ideas for acceleration of FCM advanced over the years. I will review eight methods that can be used to speed up clustering with FCM when the entire data set is loadable. Included are AFCM, mrFCM, brFCM and a method for acceleration that depends on mounting the algorithm on a GPU instead of a conventional computer. Reported improvements in speed range from 2:1 to 100:1.

The final part of the talk covers two approaches for (approximate) FCM clustering in VL data. First I will discuss two methods that are based on incremental, distributed clustering (spFCM and oFCM). The second set of three methods considers approaches to approximating FCM clusters for VL data by a much different method – viz., sampling followed by non-iterative extension. This general technique can be used for EM and many other algorithms that are not discussed in this talk. The three algorithms are eFFCM (efficient fast FCM for image data); geFFCM (for feature vector data); and eNERF (for relational data). We will have time to look at only eFFCM here.

Biography

James Bezdek Jim received the PhD in Applied Mathematics from Cornell University in 1973. Jim is past president of NAFIPS (North American Fuzzy Information Processing Society), IFSA (International Fuzzy Systems Association) and the IEEE CIS (Computational Intelligence Society): founding editor the Int'l. Jo. Approximate Reasoning and the IEEE Transactions on Fuzzy Systems: Life fellow of the IEEE and IFSA; and a recipient of the IEEE 3rd Millennium, IEEE CIS Fuzzy Systems Pioneer, and IEEE technical field award Rosenblatt medals. Jim's interests: woodworking, optimization, motorcycles, pattern recognition, cigars, clustering in very large data, fishing, visual methods for clustering, blues music, wireless sensor networks, poker and co-clustering in rectangular relational data. Jim retired in 2007, and will be coming to a university near you soon (especially if there is fishing nearby).

Invited Talk III

Date/Time: Wednesday, June 29, 2011 /06:00 PM- 07:00 PM

Room: Swan, Chair: Li-Wei Ko

Activity Summarization from 3D Video Systems in an Eldercare Environment

Prof. Jim Keller

University of Missouri-Columbia, USA

Abstract

This talk concerns eldercare. Older adults are living longer and more fulfilled lives, and they desire to live as independently as possible in the home of their choice. However, independent lifestyles come with risks that are complicated by chronic illness and impairments in mobility, cognition, and the senses. In response to this trend, the University of Missouri has been investigating new approaches in caring for the elderly. This research focus has resulted in TigerPlace, an apartment complex for seniors that opened in Columbia, Missouri in 2004. A joint venture between MU's Sinclair School of Nursing and Americare Systems Inc., TigerPlace is one of four projects granted state approval to operate under the "aging in place" model of care giving. Under that model, residents who would otherwise be required by state law to live in nursing homes may have health services brought to them in their apartments instead. One focus of our large multidisciplinary research team, including faculty and students from Engineering, Nursing, Health Management and Informatics, Medicine, Social Work, and Physical Therapy, is the creation of intelligent systems that use sensors to uncover patterns of activity helpful to caregivers, especially targeting mobility and cognitive impairment. Details can be found at http://eldertech.missouri.edu.

The larger research program fits perfectly into the concept of Recognition Technology, as defined by L. Zadeh, to be current or future systems that have the potential to provide a "quantum jump in the capabilities of today's recognition systems", and includes systems that incorporate new sensors, novel signal processing and soft computing. In this talk, I will concentrate on generating linguistic activity summarization for large amounts of multiple camera video data, depicting activities that might take place in a single person apartment. Using 2 cameras, a 3-D "voxel person" is constructed (made possible by our high speed GPU construction of silhouettes from image sequences), and sophisticated position and shape features are calculated. A hierarchical fuzzy logic system is built to determine memberships in various states, followed by another set of rules to classify activities (early focus on fall detection). Extensions to a fuzzy voxel person to model the

uncertainty of reconstruction in some areas of the field of view will be discussed. Additionally, we have recently investigated and constructed a real time multiple stereo camera system that produces true depth-based 3-D objects, providing comprehensive models of the environment and the human within it. This representation is completely insensitive to (even abrupt) lighting changes and shadows, incorporates a human detector that provides false alarm reduction for change detection regarding movement of nonhuman objects (e.g. chairs) and objects manipulated by a person, and has a natural way to address tracking and updating, i.e. not adapting stationary humans into the background while still absorbing moved objects even under significant lighting variations.

Biography

Jim Keller James M. Keller received the Ph.D. in Mathematics in 1978. He holds the University of Missouri Curators' Professorship in the Electrical and Computer Engineering and Computer Science Departments on the Columbia campus. He is also the R. L. Tatum Professor in the College of Engineering. His research interests center on computational intelligence: fuzzy set theory and fuzzy logic, neural networks, and evolutionary computation with a focus on problems in computer vision, pattern recognition, and information fusion including bioinformatics, spatial reasoning in robotics, geospatial intelligence, sensor and information analysis in technology for eldercare, and landmine detection. His industrial and government funding sources include the Electronics and Space Corporation, Union Electric, Geo-Centers, National Science Foundation, the Administration on Aging, The National Institutes of Health, NASA/JSC, the Air Force Office of Scientific Research, the Army Research Office, the Office of Naval Research, the National Geospatial Intelligence Agency, the Leonard Wood Institute, and the Army Night Vision and Electronic Sensors Directorate. Professor Keller has coauthored over 350 technical publications.

Jim is a Fellow of the Institute of Electrical and Electronics Engineers (IEEE) for whom he has presented live and video tutorials on fuzzy logic in computer vision, is an International Fuzzy Systems Association (IFSA) Fellow, an IEEE Computational Intelligence Society Distinguished Lecturer, a national lecturer for the Association for Computing Machinery (ACM) from 1993 to 2007, and a past President of the North American Fuzzy Information Processing Society (NAFIPS). He received the 2007 Fuzzy Systems Pioneer Award and the 2010 Meritorious Service Award from the IEEE Computational Intelligence Society. He finished a full six year term as Editor-in-Chief of the IEEE Transactions on Fuzzy Systems, is an Associate Editor of the International Journal of Approximate Reasoning, and is on the editorial board of Pattern Analysis and Applications, Fuzzy Sets and Systems, International Journal of Fuzzy Systems, and the Journal of Intelligent and Fuzzy Systems. Jim was the Vice President for Publications of the IEEE Computational Intelligence Society from 2005-2008, and is currently an elected Adcom member. He was the conference chair of the 1991 NAFIPS Workshop, program co-chair of the 1996 NAFIPS meeting, program co-chair of the 1997 IEEE International Conference on Neural Networks, and the program chair of the 1998 IEEE International Conference on Fuzzy Systems. He was the general chair for the 2003 IEEE International Conference on Fuzzy Systems.

Panel Sessions

PASI: Interpolation and Approximation in Fuzzy Rule Bases

Organizer and Chair: Laszlo Koczy

Panelists: Kaoru Hirota, Qiang Shen, Christophe Marsala, Mathieu Serrurier, Laszlo Koczy

Tuesday, June 28, 2011 (8:00 AM- 10:20 AM) Room: Grand Ballroom I

PASII: Computing With Words

Organizer and Chair: Nikhil Pal

Panelists: Jerry Mendel, Hani Hagras, Jon Garibaldi, Jim Keller, Janusz Kacprzyk, Nikhil Pal

Tuesday, June 28, 2011 (5:00 PM- 7:00 PM) Room: Grand Ballroom I

IPAS: Birth and Evolution of Fuzzy Logic

Honorary Organizer: Lotfi Zadeh

Chair: James Bezdek

Panelists: Piero Bonissone, Jim Keller, James Bezdek, Hisao Ishibuchi,
Wen-June Wang, Bernadette Bouchon-Meunier, Tan Woei Wan

Tuesday, June 28, 2011 (2:50 PM- 4:30 PM) Room: Grand Ballroom I

Human vs. Computer Go Competition

Description

The technique of Monte Carlo Tree Search (MCTS) has revolutionized the field of computer game-playing, and is starting to have an impact in other search and optimization domains as well. In past decades, the dominant paradigm in game algorithms was alpha-beta search. This technique, with many refinements and game-specific engineering, lead to breakthrough performances in classic board games such as chess, checkers and Othello. After Deep Blue's famous victory over Kasparov in 1996, some of the research focus shifted to games where alpha-beta search was not sufficient. Most prominent among these games was the ancient Asian game of Go. During the last few years, the use of MCTS techniques in Computer Go has really taken off, but the groundwork was laid much earlier. In 1990, Abramson [1] proposed to model the expected outcome of a game by averaging the results of many random games. In 1993, Bruegmann [2] proposed Monte-Carlo techniques for Go using almost random games, and developed the refinement he termed all-moves-as-first (AMAF). Ten years later, a group of French researchers working with Bruno Bouzy took up the idea [3]. Bouzy's Indigo program used Monte-Carlo simulation to decide between the top moves proposed by a classical knowledge-based Go engine [4]. RemiCoulom's Crazy Stone [5] was the first to add the crucial second element, a selective game tree search controlled by the results of the simulations. he last piece of the puzzle was the Upper-Confidence Tree (UCT) algorithm of Kocsis and Szepesvari [6], which applied ideas from the theory of multi-armed bandits to the problem of how to selectively grow a game tree. Gelly and Wang developed the first version of MoGo [7], which among other innovations combined Coulom's ideas, the UCT algorithm, and pattern-directed simulations. AMAF was revived and extended in Gelly and Silver's Rapid Action Value Estimate (RAVE), which computes AMAF statistics in all nodes of the UCT tree. Rapid progress in applying knowledge and parallelizing the search followed. Today, programs such as MoGo/MoGoTW, Crazy Stone, Fuego, Many Faces of Go, and Zen have achieved a level of play that seemed unthinkable only a decade ago. These programs are now competitive at a professional level for 9×9 Go and amateur Dan strength on 19×19 [4], [8].

One measure of success is competitions. In Go, Monte-Carlo programs now completely dominate classical programs on all board sizes (though no one has tried boards larger than 19×19). Monte-Carlo programs have achieved considerable success in play against humans. An early sign of things to come was a series of games on a 7×7 board between Crazy Stone and professional 5th Dan Guo Juan. Crazy Stone demonstrated almost perfect play. Since 2008, National University of Tainan (NUTN) in Taiwan and other academic organizations have hosted or organized several human vs. computer Go-related events, including the 2008 Computational Intelligence Forum & World 9×9 Computer Go Championship [8], and 2009 Invited Games for MoGo vs. Taiwan Professional Go Players (Taiwan Open 2009) [9]. Besides, the FUZZ-IEEE 2009: Panel, Invited Sessions, and Human vs. Computer Go Competition [10] was held at the 2009 International Conference on Fuzzy Systems in Aug. 2009. This event was the first human vs. computer Go competition hosted by the IEEE Computational Intelligence Society (CIS) at the IEEE CIS flag conference. In 2010, MoGo and Many Faces of Go achieved wins against strong amateur players on 13×13 with only two handicap stones. On the full 19×19 board, programs have racked up a number of wins (but still a lot more losses) on 6 and 7 handicap stones against top professional Go players [11], [12]. Also, computer Go Programs have won both as White and Black against top players in 9×9 game [13]. Additionally, in April 2011, MoGoTW broke a new world record by winning the first 13×13 game against the 5th Dan professional Go player with handicap 3 and reversed komi of 3.5. It also won 3 out of 4 games of Blind Go in 9×9.

Date
June 27-June 29, 2011

Place
Magpie Room

Website
http://fuzzieee2011.nutn.edu.tw/go/

Human
More than 10 Taiwanese Professional Go Players will join this competition

- Chun-Hsun Chou (9P)
- Ping-Chiang Chou (5P)
- Joanne Missingham (5P)
- Other 10 professional Go players

Computer Go Program

- MoGo/MoGoTW (France / Taiwan)
- Fuego (Canada)
- Many Faces of Go (USA)
- Zen (Japan)

Organizers

- IEEE / IEEE Computational Intelligence Society (CIS)
- National University of Tainan (NUTN), Taiwan
- INRIA, France
- National Science Council (NSC), Taiwan
- Grid 5000 Project, France
- Taiwanese Association for Artificial Intelligence (TAAI), Taiwan
- Taiwan Association of Cloud Computing (TACC), Taiwan

Co-Chairs

- Chang-Shing Lee, National University of Tainan, Taiwan
- Martin Mueller, University of Alberta, Canada
- Olivier Teytaud, TAO-Inria, France
- Shun-Chin Hsu, Chang Jung Christian University, Taiwan

Potential List of Panelists: (tentative)

- Chang-Shing Lee, National University of Tainan, Taiwan
- Martin Mueller, University of Alberta, Canada

- Wen-Yang Lin, National University of Kaohsiung, Taiwan
- Olivier Teytaud, TAO-Inria, France
- Kuo-Ning Chiang, National Center for High-Performance Computing, Taiwan
- Hani Hagras, University of Essex, UK
- Tzung-Pei Hong, National University of Kaohsiung, Taiwan
- Vincenzo Loia, University of Salerno, Italy
- Shi-Jim Yen, National Dong Hwa University, Taiwan
- Gary Yen, Oklahoma State University, USA
- Shun-Chin Hsu, Chang Jung Christian University, Taiwan
- Piero Bonissone, GE Global Research, USA
- Shang-Rong Tsai, Chang Jung Christian University, Taiwan
- Giovanni Acampora, University of Salerno, Italy
- Yeh-Ching Chung, National TsingHua University, Taiwan
- Fabien Teytaud, TAO-Inria, France
- Chun-Nan Hsu, Academia Sinica, Taiwan
- Yau-Hwang Kuo, National Cheng-Kung University, Taiwan

References

[1] B. Abramson, Expected-outcome: a general model of static evaluation, IEEE Transactions on Pattern Analysis and Machine Intelligence, vol. 12, no. 2, pp. 182-193, 1990.

[2] B. Brugmann, Monte Carlo Go, 1993. Online at http://www.ideanest.com/vegos/MonteCarloGo.pdf.

[3] B. Bouzy and T. Cazenave, “Computer Go: an AI-oriented survey,” Artificial Intelligence Journal, vol. 132, no. 1, pp. 39-103, 2001.

[4] C. S. Lee, M. Mueller, and O. Teytaud, “Special Issue on Monte Carlo Techniques and Computer Go”, IEEE Transactions on Computational Intelligence and AI in Games, vol. 2, no. 4, pp. 225-228. Dec. 2010.

[5] R. Coulom, “Efficient selectivity and backup operators in Monte-Carlo tree search,” in Proceeding of 5th International Conference on Computers and Games, Turin, Italy, 2006, pp. 72–83

[6] L. Kocsis and C. Szepesvari, “Bandit based Monte-Carlo planning,” Machine Learning ECML, vol. 4212, pp. 282-293, Springer, 2006.

[7] Y. Wang and S. Gelly, “Modifications of UCT and sequence-like simulations for Monte-Carlo Go,” in Proceedings of the 2007 IEEE Symposium on Computational Intelligence and Games (CIG07), Hawaii, USA, 2007, pp. 175-182.

[8] C. S. Lee, M. H. Wang, C Chaslot, J. B. Hoock, A. Rimmel, O. Teytaud, S. R. Tsai, S. C. Hsu, and T. P. Hong, “The computational intelligence of MoGo revealed in Taiwan's computer Go tournaments,” IEEE Transactions on Computational Intelligence and AI in Games, vol. 1, no. 1, pp. 73-89, Mar. 2009.

[9] C. S. Lee, M. H. Wang, T. P. Hong, G. Chaslot, J. B. Hoock, A. Rimmel, O. Teytaud, and Y. H. Kuo, "A novel ontology for computer Go knowledge management," in Proceeding of the 2009 IEEE International Conference on Fuzzy Systems (FUZZ-IEEE 2009), Jeju Island, Korea, Aug. 19-14, 2009, pp. 1056–1061.

[10] S. J. Yen, C. S. Lee, and O. Teytaud, “Human vs. computer Go competition in FUZZ-IEEE 2009,” International Computer Games Association, vol. 32, no. 3, pp. 178–180, Sept. 2009.

[11] J. B. Hoock, C. S. Lee, A. Rimmel, F. Teytaud, M. H. Wang, and O. Teytaud, “Intelligent agents for the game of Go,” IEEE Computational Intelligence Magazine, vol. 5, no. 4, pp. 28-42, Nov. 2010.

[12] C. S. Lee, M. H. Wang, O. Teytaud, and Y. L. Wang, “The game of Go @ IEEE WCCI 2010,” IEEE Computational Intelligence Magazine, vol. 5, no. 4, pp. 6-7, Nov. 2010.

[13] M. H. Wang, C. S. Lee, Y. L. Wang, M. C. Cheng, O. Teytaud, and S. J. Yen, “The 2010 contest: MoGoTW vs. human Go players,” International Computer Games Association, vol. 33, no. 1, pp. 47-50, Mar. 2010.

Fuzzy Competition

Date

11:00 AM-12:30 PM, June 27, 2011

Place

Swallow Room

Organizers

- IEEE / IEEE Computational Intelligence Society (CIS)
- Task Force on Competitions of the IEEE CIS's Fuzzy Systems Technical Committee

Co-Chairs

- Hao Ying, Wayne State University, USA
- Plamen Angelov, Lancaster University, UK
- Mohammad Biglarbegian, Ryerson University, Canada
- Asli Celikyilmaz, Microsoft Research, USA
- Xinyu Du, Wayne State University, USA
- Dimitar Filev, Ford Motor Company, USA
- Yanqing Ji, Gonzaga University, USA
- Zhao Lu, Tuskegee University, USA
- Edwin Lughofer, Johannes Kepler University of Line, Austria
- Fazal U. Syed, Ford Motor Company, USA
- Tadanari Taniguchi, Tokai University, Japan
- Xiao-Jun Zeng, University of Manchester, UK
- Haibo Zhou, Central South University, China

General Information

Conference Location

The registration, tutorials, workshops, plenary speeches, keynotes, invited talks, competition, and technical sessions are all held at 3F, Grand Hyatt Taipei, Taipei, Taiwan.

Social Programs

- Welcome Reception: 6:00 PM- 9:00 PM, Monday, June 27, 2011
  Venue: Gordon Biersch (GB) Brewery Restaurant, 2F, No.11, Songshou Rd., Xinyi District, Taipei City
- Opening Ceremony: 10:50 AM, Tuesday, June 28, 2011
  Room/Venue: Grand Ballroom I, 3F, Grand Hyatt Taipei Hotel
- Banquet: 7:30 PM-10:00 PM, Wednesday, June 29, 2011
  Room/Venue: Grand Ballroom II, 3F, Grand Hyatt Taipei Hotel

Internet Access

Free internet access is available at 3F, Grand Hyatt Taipei Hotel. There will be tables and chairs for delegates to relax and have discussions.

Conference Venue

- **Introduction to Taiwan**

Taiwan is a medium-sized archipelago in East Asian. It is located off the southeastern coast of China, at the western edge of the Pacific Ocean, between Japan and the Philippines. The Central Mountain Range divides the east and west coasts and stretches from north to south. A wonderful variety of geo-graphical contrasts exist: mountains, hills, plateaus, plains, basins, and coastline, all in which a diversity of unique flora and fauna thrive. Taipei is the capital of Taiwan. Fig. 1 shows basic information of Taiwan. Taiwan was first known to the West as Ilha Formosa or Beautiful Island.

Fig. 1. Taiwan geographical location.

Taiwan has many tourist attractions such as (1) Taipei 101: The world's tallest certified building; (2) Yushan National Park: the highest mountain in Northeast Asia (Yushan means Mt. Jade); (3) National Palace Museum: one of the five top museums in the world; (4) Taroko National Park: the world-class natural landscapes. We also have some of the friendliest people in the world, 24-hour bookstores and convenience shops, and hustling and bustling night markets—all of which imprint indelible memories in the minds of visitors. Taiwan also has the advantage of convenient transportation and an excellent travel environment that you will want to enjoy again and again. For example, Taiwan High Speed Rail (THSR) makes the tourists easier extend their journey from Taipei to Kaohsiung (the biggest city in southern Taiwan) and it only takes 90 minutes by THSR. For more detailed tourist attractions in Taiwan, the FUZZ-IEEE 2011 attendances can connect to Taiwan Tourism Bureau.

- **Introduction to Taipei**

Taipei is located in the valley of the Danshui River in northern Taiwan. It is Taiwan's capital, as well as Taiwan's busy center of commerce, government, and culture. Taipei itself has a population of almost 3 million and it has 12 administrative districts, listed in Fig. 2. In addition, Taipei also provides Taipei Metro with eight lines: Muzha Line, Danshui Line, Zhonghe Line, Xindian Line, Banqiao Line, Nangang Line, Tucheng Line, and Xiaonanmen Line. Fig. 3 shows the Map of Taipei Metro and also indicates some of the Taipei's most popular attraction areas' locations, including Taipei 101, National Palace Museum, Longshan Temple, ShiLin Night Market, Yangmingshan National Park, Beitou Hot Springs, Danshui Fisherman's Wharf, and Bitan Scenic Area.

Fig. 2. District Map of Taipei.

Fig. 3. Map of Taipei Metro.

- **Introduction to Grand Hyatt Taipei**

The conference venue is Grand Hyatt Taipei, which is situated in the foothills of eastern Taipei's XinYi District, an area where the modern face of Taipei shines with glass and steel skyscrapers, one of the tallest buildings in the world (Taipei 101), wide boulevards, and the Taipei World Trade Center complex.The Grand Hyatt Taipei is located in heart of the Taipei, a burgeoning business, shopping and entertainment district, and it is 45 minutes drive from the Taoyuan International Airport. As the political, economic, and cultural center of Taipei, the district houses many landmark buildings, including the Taipei City Hall, Taipei City Council, Sun Yat-Sen Memorial Hall, and Taipei 101. Additionally, the local attractions include National Palace Museum, Shihlin Night Market, Yangmingshan National Park, Lungshan Temple, and Chiang Kai-shek Memorial Hall. Taipei is the capital of Taiwan and is its largest city. Located to the north, its proximity and accessibility to Taiwan's business and production regions is just as appealing as the national parks and eco-reserves that surround and exist within the city itself. Fig. 4 shows the map near Grand Hyatt Taipei.

Fig. 4. Map near Grand Hyatt Taipei.

Transportation Information

Venue: Grand Hyatt Taipei

Address: 2, Songshou Rd., Taipei 11051, Taiwan

Tel: +886-2-2720-1234

Fax: +886-2-2720-1111

Email: taipei.grand@hyatt.com

Website: http://taipei.grand.hyatt.com

From Taiwan Taoyuan International Airport

TPE Airport offers you various direct connections to downtown Taipei. You may select one of the following transportation to arrive at Grand Hyatt Taipei.

Airport Bus

It offers an easy access to the Taiwan Taoyuan International Airport. Fig. 5 shows the Toward You Air Bus (East Line) transportation how to get to the Grand Hyatt Taipei from the Taiwan Taoyuan International Airport and it's about 45-minute ride.

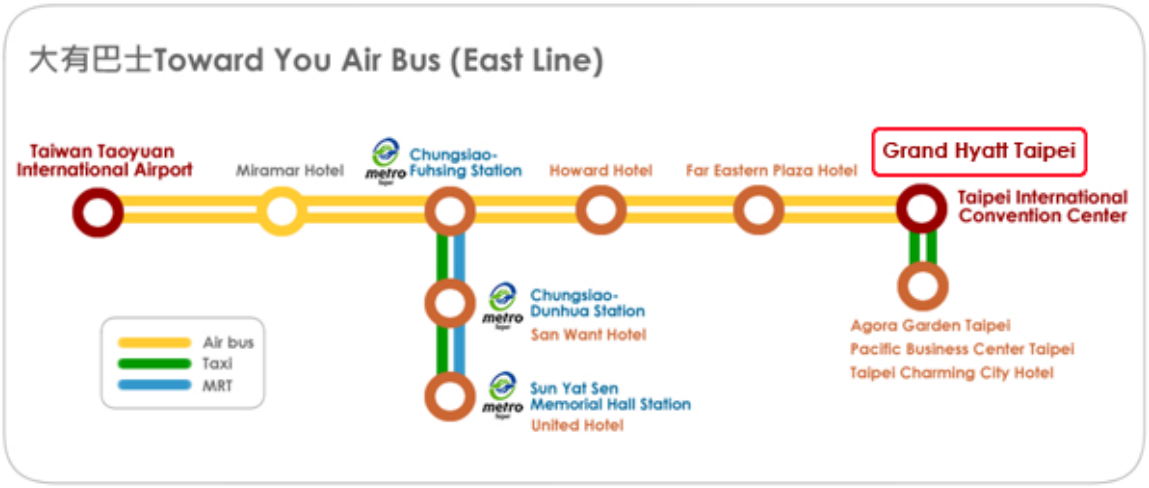

Fig. 5. Toward You Air Bus (East Line) transportation to Grand Hyatt Taipei hotel.

Airport Taxi

Taxi queues are outside the Arrival Halls of both terminals. To ensure the safety of passengers, only the taxis approved by the Aviation Police Bureau are permitted to operate in Taoyuan Airport. The average fare (plus surcharge) to Taipei is about NT$1,200.

Access Grand Hyatt Taipei

By Bus

1. Take bus No. 207, 537, or Blue 5 to TWTC stop, and walk toward Jilong (Keelung) Road.
2. Take bus No. 1, 284, 292, 611, or 650 to TWTC stop, and walk toward Xinyi Road.

By Metro

Take Metro Banqiao Nagang Line (Blue Line) to Taipei City Hall Station, exit at Exit 2 and take Keelung Rd., join onto Songgao Rd., and turn right to Shihfu Rd., then walk toward Xinyi Road. You will see Grand Hyatt Taipei (please refer to Fig. 6 Location Map of Grand Hyatt Taipei).

Fig. 6. Location Map of Grand Hyatt Taipei hotel.

2011 IEEE International Conference on Fuzzy Systems (FUZZ-IEEE 2011)
Timetable

Monday, June 27, 2011						
Time	**Peacock**	**Phoenix**	**Crane**	**Egret**	**Swallow**	**Magpie**
8:00 AM **5:00 PM**	Registration					
9:00 AM **10:30 AM**	**T01-1** Evolutionary Multi-Objective Design of Fuzzy Rule-Based Systems **Rafael Alcala**	**T02-1** Interpolative Fuzzy Rule Bases **László Koczy**	**T03-1** Theoretical and Practical Aspects of Type-2 Fuzzy Systems: Part 1 **Jerry Mendel**	**W01-1** Fuzzy Approaches to Ambient Intelligence **SS06** Intelligent Agents	**W02** Standards in Computational Intelligence	**HCGC-1** Human vs. Computer Go Competition
10:30 AM **11:00 AM**	Coffee Break					
11:00 AM **12:30 PM**	**T01-2** Evolutionary Multi-Objective Design of Fuzzy Rule-Based Systems **Rafael Alcala**	**T02-2** Interpolative Fuzzy Rule Bases **László Koczy**	**T03-2** Theoretical and Practical Aspects of Type-2 Fuzzy Systems: Part 1 **Jerry Mendel**	**W01-2** Fuzzy Approaches to Ambient Intelligence **SS06** Intelligent Agents	**FC** Fuzzy Competition	
12:30 PM **1:30 PM**	Lunch Break					
1:30 PM **3:00 PM**	**T04-1** Theoretical and Practical Aspects of Type-2 Fuzzy Systems: Part 2 **Hani Hagras**	**T05-1** Towards a Unified Framework for Intelligent Robotics **Honghai Liu** **Naoyuki Kubota**	**W03-1** Computational Intelligence Techniques for Smart Grids	**W04-1** Computer Game and Fuzzy-based Game Applications	**W05-1** Hybrid Computational Intelligence Applications	
3:00 PM **3:30 PM**	Coffee Break					
3:30 PM **5:00 PM**	**T04-2** Theoretical and Practical Aspects of Type-2 Fuzzy Systems: Part 2 **Hani Hagras**	**T05-2** Towards a Unified Framework for Intelligent Robotics **Honghai Liu** **Naoyuki Kubota**	**W03-2** Computational Intelligence Techniques for Smart Grids	**W04-2** Computer Game and Fuzzy-based Game Applications	**W05-2** Hybrid Computational Intelligence Applications	
6:00 PM	Welcome Reception					

	Tuesday, June 28, 2011								
Time	**Swan**	**Peacock**	**Phoenix**	**Crane**	**Egret**	**Swallow**	**Grand Ballroom I**	**Grand Ballroom II**	**Magpie**
8:00 AM 5:00 PM	Registration								
8:00 AM 10:20 AM	**SS02-1** Evolutionary Fuzzy Systems	**SS12-1** Recent Advances in Fuzzy-Model-Based Control Systems	**SS14** Advances in Fuzzy Theory and their Applications	**SS28-1** Current Development in Pattern Classification-Kernelization, Pairwise Constraints, and Classifiers	**SS16** Fuzzy Interpolation **SS11** Large-Scale Clustering	**T2FL & FPR** Type-2 Fuzzy Logic and Fuzzy Pattern Recognition	**Panel Session I** Interpolation and Approximation in Fuzzy Rule Bases	**FA-1** Fuzzy Applications	**HCGC-2** Human vs. Computer Go Competition
10:20 AM 10:50 AM	Coffee Break								
10:50 AM 12:00 PM	**Opening Ceremony & Keynote Speech I** Inferring Disease Related Gene-Gene Interactions: A Fuzzy Logic Based Approach **Nikhil Pal** Place: Grand Ballroom I Chair: Jyh-Yeong Chang								
12:00 PM 1:30 PM	Lunch Break IEEE TFS AE Lunch Meeting (TFS AE only) IEEE WCI Lunch Meeting								
1:30 PM 2:30 PM	**Plenary Speech I** Type-2 Fuzzy Sets and Systems: Challenges and Misconceptions **Jerry M. Mendel** Place: Grand Ballroom I Chair: Chang-Shing Lee								
2:30 PM 2:50 PM	Break							**PS01** Poster Session I	
2:50 PM 4:30 PM	**SS05** Fuzzy Robotics	**SS18** Recent Advances in Fuzzy Logic in Image Processing	**SS27** Communication Robotics and Computational Intelligence Co-creation	**SS28-2** Current Development in Pattern Classification-Kernelization, Pairwise Constraints, and Classifiers	**SS42-1** Fuzzy Cognitive Maps-Theory and Applications	**SS21-1** Fuzzy Control in Industrial and Application	**Invited Panel Session** Birth and Evolution of Fuzzy Logic		
4:30 PM 5:00 PM	Coffee Break							**PS02** Poster Session II	
5:00 PM 7:00 PM	**SS10-1** Medical and Wellness Engineering	**SS09** Applications of Fuzzy Logic to Awareness Promotion	**SS08** Innovative Fuzzy Approaches to Management Engineering	**SS37** Fuzzy Logic Based Computer Vision and Its Applications to Guidance and Control	**SS17-1** Practical and Applications Aspects of Type-2 Fuzzy Logic Systems	**SS19** Fuzzy Inference Systems-Theory and Applications	**Panel Session II** Computing With Words		

	Wednesday, June 29, 2011								
Time	**Swan**	**Peacock**	**Phoenix**	**Crane**	**Egret**	**Swallow**	**Grand Ballroom I**	**Grand Ballroom II**	**Magpie**
8:00 AM 5:00 PM	Registration								
8:00 AM 9:00 AM	**SS02-2** Evolutionary Fuzzy Systems	**SS12-2** Recent Advances in Fuzzy-Model-Base d Control Systems	**SS31** Human Symbiotic Systems	**FC&IS** Fuzzy Control and Intelligent Systems	**SS10-2** Medical and Wellness Engineering	**SS13-1** Fuzzy Multiple Criteria Decision Making	**Invited Talk I** Casual Communication between Robots and Humans based on Robot Technology Middleware and Multimedia Recognition **Kaoru Hirota** Chair: Yau-Hwang Kuo	**FA-2** Fuzzy Applications	**HCGC-3** Human vs. Computer Go Competition
9:00 AM 10:20 AM									
10:20 AM 10:50 AM	Coffee Break								
10:50 AM 12:00 PM	**Keynote Speech II** Fuzzy Approaches to Information Fusion **Bernadette Bouchon-Meunier** Place: Grand Ballroom I Chair: Chia-Feng Juang								
12:00 PM 1:30 PM	Lunch Break IEEE FSTC Lunch Meeting								
1:30 PM 2:30 PM	**Plenary Speech II** Soft Computing in Prognostics and Health Management (PHM) Applications: A Case Study in Anomaly Detection **Piero Bonissone** Place: Grand Ballroom I Chair: Faa-Jeng Lin								
2:30 PM 2:50 PM	Break							**PS03** Poster Session III	
2:50 PM 4:30 PM	**SS20** Universal Contents Creation/Distribution and Intelligent System	**SS03** Uncertainty and the Semantic Web	**SS04** Soft Computing for Operations Research and Optimization	**SS01** Fuzzy Ontologies and FML Applications	**SS42-2** Fuzzy Cognitive Maps-Theory and Applications	**SS21-2** Fuzzy Control in Industrial and Application			
4:30 PM 5:00 PM	Coffee Break							**PS04** Poster Session IV	
5:00 PM 6:00 PM	**Invited Talk II** Acceleration and Scalability for c-Means Clustering **James Bezdek** Chair: Li-Wei Ko	**SS40** Fuzzy Approach for Information Security Management	**SS38** Fuzzy Knowledge Discovery and Its Applications	**SS39** Fuzzy Based Computation on Biomedical Systems	**SS17-2** Practical and Applications Aspects of Type-2 Fuzzy Logic Systems	**SS30** Computing With Words **SS43** Fuzzy Systems of Unknown Nonlinear Complex Systems			
6:00 PM 7:00 PM	**Invited Talk III** Activity Summarization from 3D Video Systems in an Eldercare Environment **Jim Keller** Chair: Li-Wei Ko								
7:30 PM		Conference Banquet Place: Grand Ballroom I							

Thursday, June 30, 2011							
Time	**Swan**	**Peacock**	**Phoenix**	**Crane**	**Egret**	**Swallow**	**Magpie**
8:00 AM **5:00 PM**	Registration						
8:00 AM **10:20 AM**	**SS23** Industrial Applications of Evolving Fuzzy Systems	**MFI & RWA** Medical, Financial, Industrial and Other Real World Applications	**FSM & IS** Fuzzy Systems Modeling and Intelligent Systems	**FST & GC** Fuzzy Set Theory and Granular Computing	**SS36-1** Fuzzy Systems on Renewable Energy	**FS & FDM** Fuzzy Clustering and Fuzzy Data Mining	**HA** Hybrids and Other Applications
10:20 AM **10:50 AM**	Coffee Break						
10:50 AM **12:00 PM**	**Keynote Speech III** Soft Computing for Hard Pattern Recognition Problems **Paul Gader** Place: Grand Ballroom I Chair: Jung-Hsien Chiang						
12:00 PM **1:30 PM**	Lunch Break						
1:30 PM **2:30 PM**	**FOD** Fuzzy Optimization and Design	**FO & FEC** Fuzzy Optimization and Fuzzy Emotional Computing	**RS & RDA** Rough Sets and Rough Data Analysis	**T2FL** Type-2 Fuzzy Logic	**SS36-2** Fuzzy Systems on Renewable Energy	**FDM&DSS-1** Fuzzy Decision Making and Decision Support Systems	**HFS** Hybrid Fuzzy Systems
2:30 PM **2:50 PM**	Break						
2:50 PM **4:30 PM**	**SS29** Software Engineering with Computational Intelligence	**SS34** Brain and Learning	**SS35** Fuzzy Regression Analysis and Its Applications	**SS41** Neuro Fuzzy Systems and Their Real World Application	**SS25** Evolving and Adaptive Fuzzy Systems	**SS24** Hybrid Learning for Fuzzy Systems	**SS32** Adaptive Fuzzy Logic Control
4:30 PM **5:00 PM**	Coffee Break						
5:00 PM **6:00 PM**	**SS22** Fuzzy Methods in Machine Learning and Data Mining	**FCW & PT** Fuzzy Computing with Words and Possibility Theory	**SS07** Metaheuristics and Its Applications **SS33** Fuzzy and Paraconsistent Intelligent Systems	**IA** Informatics and Analytics	**SS13-2** Fuzzy Multiple Criteria Decision Making	**FDM&DSS-2** Fuzzy Decision Making and Decision Support Systems	

Venue Floor Plan

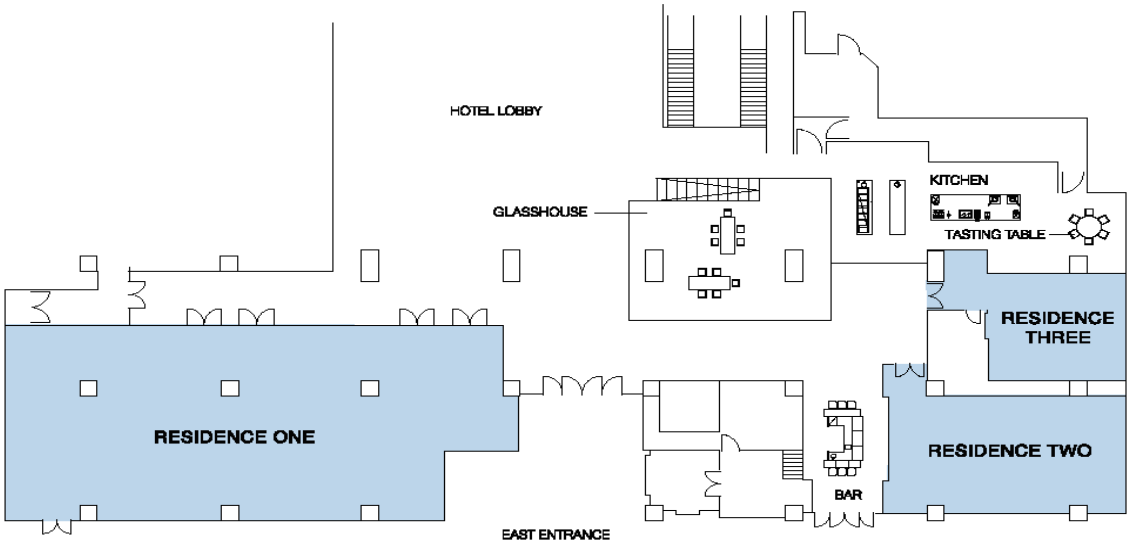

THE GRAND RESIDENCE – LOBBY LEVEL

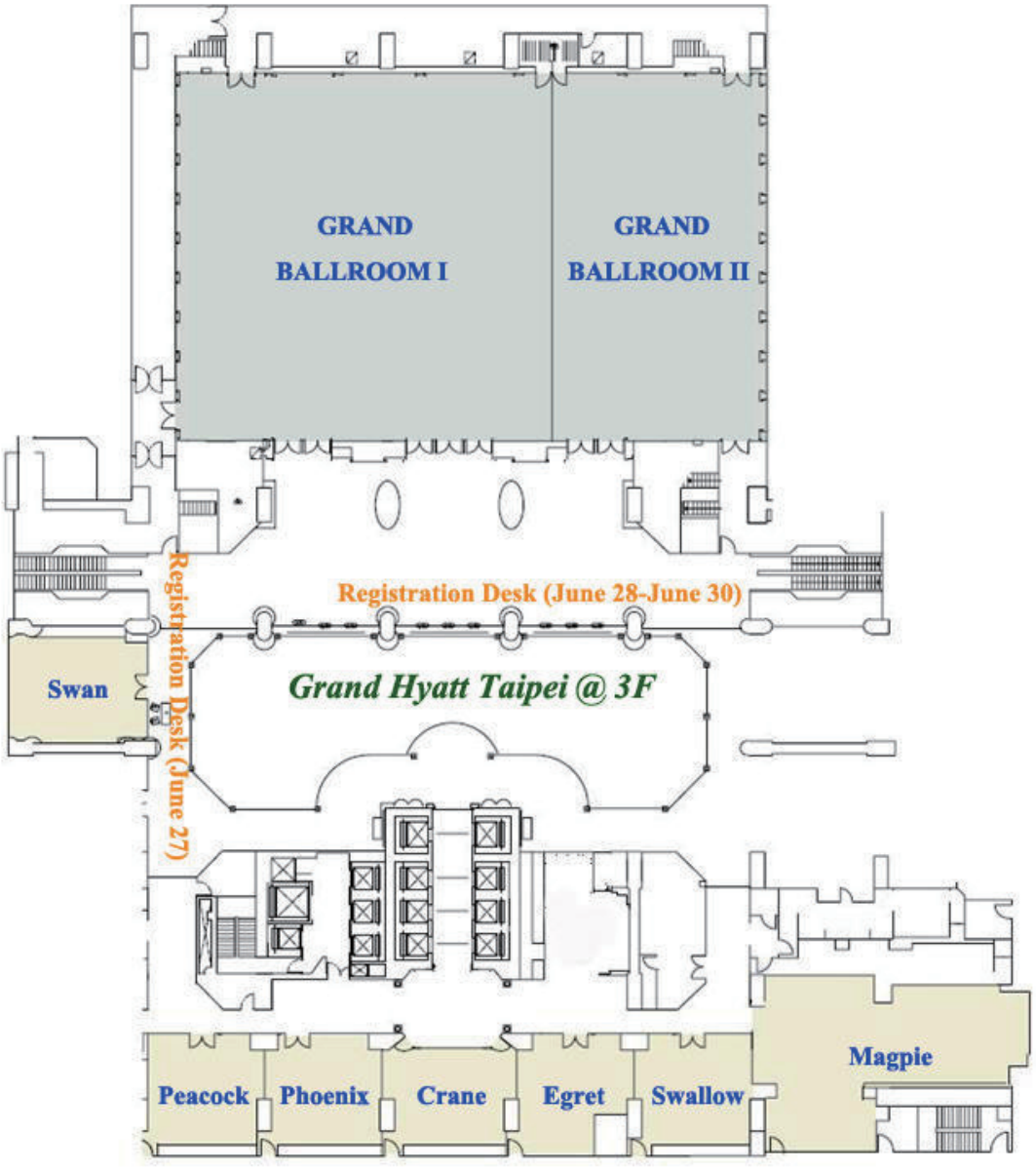

All Session Rooms Are at 3rd Floor, Grand Hyatt Taipei

Technical Program Schedule

DETAILED PROGRAM

Monday, June 27, 9:00AM-10:30AM

(T01-1) Tutorial: Evolutionary Multi-Objective Design of Fuzzy Rule-Based Systems
Monday, June 27, 9:00AM-10:30AM, Room: Peacock, Instructor: Rafael Alcala

(T02-1) Tutorial: Interpolative Fuzzy Rule Bases
Monday, June 27, 9:00AM-10:30AM, Room: Phoenix, Instructor: László Koczy

(T03-1) Tutorial: Theoretical and Practical Aspects of Type-2 Fuzzy Systems: Part 1
Monday, June 27, 9:00AM-10:30AM, Room: Crane, Instructor: Jerry Mendel

(W01-1/SS06) Workshop: Fuzzy Approaches to Ambient Intelligence/Intelligent Agents
Monday, June 27, 9:00AM-10:30AM, Room: Egret, Chair: Vincenzo Loia and Hani Hagras

9:00AM ***Gesture-Based Hybrid Approach for HCI in Ambient Intelligent Environments*** *[#543]*
Stefano Carrino, Elena Mugellini, Omar Abou Khaled and Rolf Ingold

9:20AM ***Understanding the Unknown: Unattested Input Processing in Natural Language*** *[#446]*
Julia M. Taylor and Victor Raskin

9:40AM ***A Fuzzy Agent-based Approach to Trust-based Competency Management*** *[#424]*
Matteo Gaeta, Francesco Orciuoli, Sabrina Senatore and Vincenzo Loia

10:00AM ***Open discussion on current and future trends on Fuzzy Approaches to Ambient Intelligence and Intelligent Agents***

(W02) Workshop: Standards in Computational Intelligence
Monday, June 27, 9:00AM-10:30AM, Room: Swallow, Chair: Plamen Angelov, Giovanni Acampora and Bruno Di Stefano

9:00AM ***New Evolution Algorithm Based On The Standard Particle Swarm Optimization*** *[#166]*
Lipeng Wang, Yangjie Cheng and Liu Dong C

(HCGC-1) Competition: Human vs. Computer Go Competition
Monday, June 27, 9:00AM-10:30AM, Room: Magpie, Chair: Chang-Shing Lee, Martin Muller, Olivier Teytaud, and Shun-Chin Hsu

Monday, June 27, 11:00AM-12:30PM

(T01-2) Tutorial: Evolutionary Multi-Objective Design of Fuzzy Rule-Based Systems
Monday, June 27, 11:00AM-12:30PM, Room: Peacock, Instructor: Rafael Alcala

(T02-2) Tutorial: Interpolative Fuzzy Rule Bases
Monday, June 27, 11:00AM-12:30PM, Room: Phoenix, Instructor: László Koczy

(T03-2) Tutorial: Theoretical and Practical Aspects of Type-2 Fuzzy Systems: Part 1
Monday, June 27, 11:00AM-12:30PM, Room: Crane, Instructor: Jerry Mendel

(W01-2/SS06) Workshop: Fuzzy Approaches to Ambient Intelligence/Intelligent Agents
Monday, June 27, 11:00AM-12:30PM, Room: Egret, Chair: Vincenzo Loia and Hani Hagras

11:00AM ***Intrusion Detection Systems Adapted from Agent-based Artificial Immune Systems*** *[#375]*
Chung-Ming Ou, Yao-Tien Wang and C.R. Ou

11:20AM ***An Adaptive Multi-Agent Memetic System for Personalizing e-Learning Experiences*** *[#309]*
Giovanni Acampora, Matteo Gaeta, Enrique Munoz and Autilia Vitiello

11:40AM ***A hybrid context aware system for tourist guidance based on collaborative filtering*** *[#425]*
Giuseppe Fenza, Enrico Fischetti, Domenico Furno and Vincenzo Loia

12:00AM ***Trainable Estimators for Indirect People Counting: A Comparative Study*** *[#473]*
Giovanni Acampora, Vincenzo Loia, Gennaro Percannella and Mario Vento

(FC) Competition: Fuzzy Competition
Monday, June 27, 11:00AM-12:30PM, Room: Swallow, Chair: Hao Ying

11:00AM ***A TSK Neuro-Fuzzy Approach for Modeling Highly Dynamic Systems*** *[#475]*
Giovanni Acampora

(HCGC-2) Competition: Human vs. Computer Go Competition
Monday, June 27, 11:00AM-12:30PM, Room: Magpie, Chair: Chang-Shing Lee, Martin Muller, Olivier Teytaud, and Shun-Chin Hsu

Monday, June 27, 1:30PM-3:00PM

(T04-1) Tutorial: Theoretical and Practical Aspects of Type-2 Fuzzy Systems: Part 2
Monday, June 27, 1:30PM-3:00PM, Room: Peacock, Instructor: Hani Hagras

(T05-1) Tutorial: Towards a Unified Framework for Intelligent Robotics
Monday, June 27, 1:30PM-3:00PM, Room: Phoenix, Instructor: Honghai Liu and Naoyuki Kubota

(W03-1) Workshop: Computational Intelligence Techniques for Smart Grids
Monday, June 27, 1:30PM-3:00PM, Room: Crane, Chair: Alfredo Vaccaro

1:30PM ***A Bacterial Foraging PSO - DE Algorithm for Solving Reserve Constrained Dynamic Economic Dispatch Problem*** *[#286]*
Praveena Pillala, Vaisakh Kanchapogu and Rama Mohana Rao Sanchana

1:50PM ***A Noisy Data Regression Model Based on General Regression Neural Networks*** *[#384]*
Shih-Chun Shao, Wen-Hui Chen and Jun-Horng Chen

2:10PM ***Estimation of Load Model Parameters from Instantaneous Voltage and Current*** *[#431]*
Pawel Regulski, Francisco Gonzalez-Longatt and Vladimir Terzija

(W04-1) Workshop: Computer Game and Fuzzy-based Game Applications
Monday, June 27, 1:30PM-3:00PM, Room: Egret, Chair: Shun-Chin Hsu, I-Chen Wu, and Shi-Jim Yen

1:30PM ***Apply Different Fuzzy Integrals in Unit Selection Problem of Real Time Strategy Game*** *[#170]*
Y.J. Li, Peter H.F. Ng, H.B. Wang, S.C.K. Shiu and Y. Li

1:50PM ***Unit Formation Planning in RTS game by using Potential Field and Fuzzy Integral*** *[#479]*
Ng Peter, Li Y. J. and Shiu Simon

2:10PM ***Elimination Search for puzzle games : An Application for Hashi Solver*** *[#505]*
Shi-Jim Yen, Shih-Yuan Chiu, Cheng-Wei Chou and Tsan-Cheng Su

2:30PM ***An efficient algorithm for solving Fillomino*** *[#507]*
Shi-Jim Yen, Tsan-Cheng Su and Shun-Chin Hsu

(W05-1) Workshop: Hybrid Computational Intelligence Applications
Monday, June 27, 1:30PM-3:00PM, Room: Swallow, Chair: Chuan-Kang Ting and Tzung-Pei Hong

1:30PM ***Symbiotic Neuron Evolution of a Neural-Network-Aided Grey Model for Time Series Prediction*** *[#302]*
Shih-Hung Yang and Yon-Ping Chen

1:50PM ***A Hybrid Computational Intelligence Approach for Automatic Music Composition*** *[#315]*
Giovanni Acampora, Jose Manuel Cadenas, Roberto De Prisco, Vincenzo Loia, Enrique Munoz and Rocco Zaccagnino

2:10PM ***A Study of a Hybrid Evolutionary Fuzzy Model for Stock Selection*** *[#503]*
Chien-Feng Huang, Chih-Hsiang Chang, Bao Rong Chang and Dun-Wei Cheng

2:30PM ***Upper-Bound Multiple Fuzzy Frequent-Pattern Trees*** *[#526]*
Tzung-Pei Hong, Chun-Wei Lin, Tsung-Ching Lin and Shing-Tai Pan

(HCGC-3) Competition: Human vs. Computer Go Competition
Monday, June 27, 1:30PM-3:00PM, Room: Magpie, Chair: Chang-Shing Lee, Martin Muller, Olivier Teytaud, and Shun-Chin Hsu

Monday, June 27, 3:30PM-5:00PM

(T04-2) Tutorial: Theoretical and Practical Aspects of Type-2 Fuzzy Systems: Part 2
Monday, June 27, 3:30PM-5:00PM, Room: Peacock, Instructor: Hani Hagras

(T05-2) Tutorial: Towards a Unified Framework for Intelligent Robotics
Monday, June 27, 3:30PM-5:00PM, Room: Phoenix, Instructor: Honghai Liu and Naoyuki Kubota

(W03-2) Workshop: Computational Intelligence Techniques for Smart Grids
Monday, June 27, 3:30PM-5:00PM, Room: Crane, Chair: Alfredo Vaccaro

3:30PM ***Exploiting Timed Automata Based Fuzzy Controllers for Voltage regulation in Smart Grids*** *[#441]*
Giovanni Acampora, Vincenzo Loia and Autilia Vitiello

3:50PM ***A Novel Fuzzy System for Wind Turbines Reactive Power Control*** *[#411]*
Geev Mokryani, Pierluigi Siano, Antonio Piccolo, Vito Calderaro and Carlo Cecati

4:10PM ***Terminal Sliding Mode Controlled CVCF Inverters*** *[#282]*
En-Chih Chang, Li-Peng Yin, Rong-Ching Wu and Lung-Sheng Yang,

(W04-2) Workshop: Computer Game and Fuzzy-based Game Applications
Monday, June 27, 3:30PM-5:00PM, Room: Egret, Chair: Shun-Chin Hsu, I-Chen Wu, and Shi-Jim Yen

(W05-2) Workshop: Hybrid Computational Intelligence Applications
Monday, June 27, 3:30PM-5:00PM, Room: Swallow, Chair: Chuan-Kang Ting and Tzung-Pei Hong

3:30PM ***Differential Evolution to Enhance Localization of Mobile Robots*** *[#584]*
Michael Lisowski, Zhun Fan and Ravn Ole

3:50PM ***Fuzzy C-Means Clustering Based Construction And Training For Second Order RBF Network*** *[#571]*
Kanishka Tyagi, Xun Cai and Michael Manry

(HCGC-4) Competition: Human vs. Computer Go Competition
Monday, June 27, 3:30PM-5:00PM, Room: Magpie, Chair: Chang-Shing Lee, Martin Muller, Olivier Teytaud, and Shun-Chin Hsu

Tuesday, June 28, 8:00AM-10:20AM

(SS02-1) Special Session: Evolutionary Fuzzy Systems
Tuesday, June 28, 8:00AM-10:20AM, Room: Swan, Chair: Rafael Alcalá

8:00AM ***Evolutionary Learning of a Laser Pointer Detection Fuzzy System for an Environment Control System*** *[#320]*
Chavez de la O Francisco, Fernandez de Vega Francisco, Alcala Fernandez Rafael, Alcala Fernandez Jesus and Herrera Trigeros Francisco

8:20AM ***A Meta-Fuzzy Classifier for Specifying Appropriate Fuzzy Partitions by Genetic Fuzzy Rule Selection with Data Complexity Measures*** *[#606]*
Yusuke Nojima, Shinya Nishikawa and Hisao Ishibuchi

8:40AM ***Assessing The Effects Of Zero Abundance Data On Habitat Preference Modelling Using A Genetic Takagi-Sugeno Fuzzy Model*** *[#586]*
Shinji Fukuda

9:00AM ***A Multiple-Level Genetic-Fuzzy Mining Algorithm*** *[#512]*
Chun-Hao Chen, Tzung-Pei Hong and Yeong-Chyi Lee

9:20AM ***An Architecture for Constructing Fuzzy Regression Tree Forests Using Opt-aiNet*** *[#314]*
Fathi Gasir, Zuhair Bandar and Keeley Crockett

9:40AM ***Fuzzy C-Means Clustering and Partition Entropy for Species-Best Strategy and Search Mode Selection in Nonlinear Optimization by Differential Evolution*** *[#456]*
Tetsuyuki Takahama and Setsuko Takahama

(SS12-1) Special Session: Recent Advances in Fuzzy-Model-Based Control Systems
Tuesday, June 28, 8:00AM-10:20AM, Room: Peacock, Chair: H. K. Lam

8:00AM ***LMI-Based Stability Conditions for Interval Type-2 Fuzzy-Model-Based Control Systems*** *[#228]*
H.K. Lam, Mohammad Narimani and L.D. Seneviratne

8:20AM ***Robust H-infinite Fuzzy Observer for A Class of Time-Delay Discrete Fuzzy Bilinear Systems with Parameter Uncertainties*** *[#54]*
Shun-Hung Tsai, Ta-Tau Chen, Ming-Ying Hsiao and Chin-Sheng Chen,

8:40AM ***Sum of Squares Solutions Assuring Non-quadratic Discrete Stability*** *[#39]*
Ji-Chang Lo and Jhen-Shun Kao

9:00AM ***Output Feedback Control for Discrete-Time Takagi-Sugeno Fuzzy Systems*** *[#122]*
Nao Ueno, Yuzu Uchida and Jun Yoneyama

9:20AM ***Decentralized control of large scale switched Takagi-Sugeno systems*** *[#156]*
Dalel Jabri, Kevin Guelton and Noureddine Manamanni

9:40AM ***Some Refinements for Non quadratic Stabilization of continuous TS Models*** *[#381]*
Thierry Marie Guerra, Abdelhafidh Jaadari, Juntao Pan and Antonio Sala

10:00AM ***Adaptive fault estimation design for T-S fuzzy systems with interval time varying delay*** *[#496]*
Hamdi Gassara, Ahmed EL Hajjaji and Mohamed Chaabane

(SS14) Special Session: Advances in Fuzzy Theory and their Applications
Tuesday, June 28, 8:00AM-10:20AM, Room: Phoenix, Chair: Shyi-Ming Chen

8:00AM ***Fast Extracting of Change Area from Remote Sensing Image by Fuzzy Theory and Case Base Reasoning*** *[#399]*
Ting-shiuan Wang and Teng-to Yu

8:20AM ***Weights-Learning for Weighted Fuzzy Rule Interpolation in Sparse Fuzzy Rule-Based Systems*** *[#253]*
Shyi-Ming Chen and Yu-Chuan Chang

8:40AM ***On The Type-2 Fuzzy Thresholding Protocol For Event-Driven Wireless Sensor Networks*** *[#458]*
Chung-Ming Own

9:00AM ***A Theoretical Approach to Liu's Generalized Lambda-Fuzzy Measure*** *[#350]*
Hsiang-Chuan Liu and Tung-Sheng Liu

9:20AM ***A Fuzzy Intelligent Decision Support System for Typhoon Disaster Management*** *[#387]*
Wang-Kun Chen, GuangJun Sui and DangLing Tang

9:40AM ***A Robust Fuzzy Trajectory Estimation Design of High Speed Reentry Vehicles*** *[#190]*
Yung-Yue Chen and Chung-Shi Tseng

10:00AM ***Data-driven Based 3-D Fuzzy Logic Controller Design Using Nearest Neighborhood Clustering and Linear Support Vector Regression*** *[#535]*
Zhang Xianxia, Jiang Ye, Zou Tao, Qi Chenkun and Cao Guitao

(SS28-1) Special Session: Current Development in Pattern Classification-Kernelization, Pairwise Constraints, and Classifiers

Tuesday, June 28, 8:00AM-10:20AM, Room: Crane, Chair: Yasunori Endo

8:00AM ***A Method of Explicit Mappings for Kernel Data Analysis and Applications*** *[#276]*
Sadaaki Miyamoto and Keisuke Sawazaki

8:20AM ***Comparison of Scaling Behavior Between Fuzzy c-Means Based Classifier with Many Parameters and LibSVM*** *[#77]*
Hidetomo Ichihashi, Katsuhiro Honda and Akira Notsu

8:40AM ***Ellipse Detection with Hard c-Regression Models and Random Initializations*** *[#106]*
Hidetomo Ichihashi, Li Chieu Lam, Katsuhiro Honda and Akira Notsu

9:00AM ***Trajectory Anonymization From a Time Series Perspective*** *[#141]*
Sergi Martinez-Bea and Vicenc Torra

9:20AM ***On Some Clustering Approaches For Graphs*** *[#205]*
Klara Stokes and Vicenc Torra

9:40AM ***A Study on Regularization Effects of Fuzzified Memberships in FCM Clustering*** *[#57]*
Katsuhiro Honda, Yui Matsumoto, Akira Notsu and Hidetomo Ichihashi

10:00AM ***Constrained Agglomerative Hierarchical Clustering Algorithms with Penalties*** *[#75]*
Sadaaki Miyamoto and Akihisa Teram

(SS16 & SS11) Special Session: Fuzzy Interpolation & Large-Scale Clustering

Tuesday, June 28, 8:00AM-10:20AM, Room: Egret, Chair: Qiang Shen and Timothy Havens

8:00AM ***Adaptive Fuzzy Interpolation with Prioritized Component Candidates*** *[#226]*
Longzhi Yang and Qiang Shen

8:20AM ***Fuzzy Rule Interpolation in Embedded Behaviour-based Control*** *[#558]*
Szilveszter Kovacs

8:40AM ***An Evolutionary-Based Similarity Reasoning Scheme for Monotonic Multi-Input Fuzzy Inference Systems*** *[#119]*
Tay Kai Meng and Lim Chee Peng

9:00AM ***Fuzzy Rule Interpolation Based on Interval Type-2 Gaussian Fuzzy Sets and Genetic Algorithms*** *[#326]*
Shyi-Ming Chen and Yu-Chuan Chang

9:20AM ***Double-Linear Fuzzy Interpolation Method*** *[#546]*
Marcin Detyniecki, Christophe Marsala and Maria Rifqi

9:40AM ***Speedup of Fuzzy and Possibilistic Kernel c-Means for Large-Scale Clustering*** *[#443]*
Timothy Havens, Radha Chitta, Anil Jain and Rong Jin

10:00AM ***Adaptive Fuzzy Interpolation with Uncertain Observations and Rule Base*** *[#397]*
Longzhi Yang and Qiang Shen

(T2FL & FPR) Type-2 Fuzzy Logic and Fuzzy Pattern Recognition

Tuesday, June 28, 8:00AM-10:20AM, Room: Swallow, Chair: Frank Chung-Hoon Rhee

8:00AM ***General Type-2 Fuzzy Membership Function Design and its Application to Neural Networks*** *[#590]*
Eun-A Shim and Frank Chung-Hoon Rhee

8:20AM ***Human Action Recognition via Sum-Rule Fusion of Fuzzy K-Nearest Neighbor Classifiers*** *[#510]*
Teck Wee Chua, Karianto Leman and Nam Trung Pham

8:40AM ***Fuzzy Clustering with Multiple Kernels*** *[#150]*
Naouel Baili and Hichem Frigui

9:00AM ***Kernel-Based Fuzzy Clustering of Interval Data*** *[#52]*
Bruno Pimentel, Anderson Costa and Renata Souza

9:20AM ***Short Term Load Forecasting Using Interval Type-2 Fuzzy Logic Systems*** *[#208]*
Abbas Khosravi, Saeid Nahavandi and Doug Creighton

9:20AM ***An Adaptive Type-2 Input Based Non-SingletonType-2 Fuzzy Logic System for Real World Applications*** *[#528]*
Nazanin Sahab and Hani Hagras

9:40AM ***Hospital Service Quality Evaluation: A Fuzzy Preference Relation Approach*** *[#72]*
Tsung-Han Chang

(HCGC-1) Competition: Human vs. Computer Go Competition
Tuesday, June 28, 8:00AM-10:20AM, Room: Magpie, Chair: Chang-Shing Lee, Martin Muller, Olivier Teytaud, and Shun-Chin Hsu

Panel Session I: Interpolation and Approximation in Fuzzy Rule Bases
Tuesday, June 28, 8:00AM-10:20AM, Room: Grand Ballroom I, Chair: László Koczy

(FA-1) Fuzzy Applications
Tuesday, June 28, 8:00AM-10:20AM, Room: Grand Ballroom II, Chair: Hisao Ishibuchi

8:00AM ***Structural Analysis on Team Internal Soft Factors to Project Success*** *[#49]*
Jyh-Fu (Don) Jeng

8:20AM ***A Robust Portfolio Selection Problem based on a Confidence Interval with Investor's Subjectiviety*** *[#100]*
Takashi Hasuike and Hideki Katagir

8:40AM ***On Some Fuzzy Relations for Color Information*** *[#412]*
Daniel Sanchez, Jose Manuel Soto-Hidalgo, Jesus Chamorro-Martinez and Pedro Martinez-Jimenez

9:00AM ***The Positioning control of an Electro-Hydraulic Variable Rotational Speed Pump-Controlled System Using Adaptive Fuzzy Controller with Self-tuning Fuzzy Sliding Mode Compensation*** *[#463]*
Lian-Wang Lee, I-Hsum Li, Chung-Chieh Chen and Jun-Yi Huang

9:20AM ***Toward Quantitative Definition of Explanation Ability of Fuzzy Rule-based Classifiers*** *[#605]*
Hisao Ishibuchi and Yusuke Nojima

9:40AM ***Multi-level Multi-Objective Decision Problem through Fuzzy Random Regression based Objective Function*** *[#81]*
Nureize Arbaiy and Junzo Watada

Tuesday, June 28, 10:50AM-12:00PM

(HCGC-2) Competition: Human vs. Computer Go Competition
Tuesday, June 28, 10:50AM-12:00PM, Room: Magpie, Chair: Chang-Shing Lee, Martin Muller, Olivier Teytaud, and Shun-Chin Hsu

Keynote Speech I: Inferring Disease Related Gene-Gene Interactions: A Fuzzy Logic Based Approach
Tuesday, June 28, 10:50AM-12:00PM, Room: Grand Ballroom I, Speaker: Nikhil Pal

Tuesday, June 28, 1:30PM-2:30PM

(HCGC-3) Competition: Human vs. Computer Go Competition
Tuesday, June 28, 1:30PM-2:30PM, Room: Magpie, Chair: Chang-Shing Lee, Martin Muller, Olivier Teytaud, and Shun-Chin Hsu

Plenary Speech I: Type-2 Fuzzy Sets and Systems: Challenges and Misconceptions
Tuesday, June 28, 1:30PM-2:30PM, Room: Grand Ballroom I, Speaker: Jerry M. Mendel

Tuesday, June 28, 2:30PM-4:30PM

(PS01) Poster Session I
Tuesday, June 28, 2:30PM-4:30PM, Room: Grand Ballroom II

P101 ***A fuzzy hypothesis test based model for customer satisfaction measurement (Case study in PARS KHODRO CO.)*** *[#22]*
Naimeh Borjalilu, Mahdi Zowghi and Abdolhamid Eshraghniaye Jahromi

P102 ***Permutation Flow Shop Scheduling: Fuzzy Particle Swarm Optimization Approach*** *[#29]*
S. H. Ling, F. Jiang, H. T. Nguyen and K. Y. Chan

P103 ***Patent Valuation with a Fuzzy Binomial Model*** *[#67]*
Xiaolu Wang

P104 ***Natural Topology via Fuzzy Metric*** *[#70]*
Fagner Santana and Regivan Santiago

P105 ***Fault diagnosis of turbine using an improved intuitionistic fuzzy cross entropy approach*** *[#79]*
Hung Kuo-Chen, Lin Kuo-Ping and Weng Chia-Chun

P106 ***Fuzzy delta separation axioms*** *[#91]*
Seok Jong Lee and Sang Min Yun

P107 ***Clustering Data and Imprecise Concepts*** *[#101]*
Zengchang Qin and Weifeng Zhang

P108 ***Fuzzy Variable Structure Control for PWM Inverters*** *[#102]*
En-Chih Chang and Josep M. Guerrero

P109 ***An Adaptive Fuzzy Logic Controller based on Real Coded Quantum-Inspired Evolutionary Algorithm*** *[#103]*
Pintu Shill, Amjad Hossain, Faijul Amin and Kazuyuki Murase

P110 ***An Efficient Hybrid Particle Swarm Optimization for the Job Shop Scheduling Problem*** *[#116]*
Xue-Feng Zhang, Miyuki Koshimura, Hiroshi Fujita and Ryuzo Hasegawa

P111 ***A Framework of Multi-characteristics Fuzzy Dynamic Scheduling for Parallel Video Processing on MPSoC Architecture*** *[#117]*
Da Li, Yibin Hou, Zhangqin Huang and Chunhua Xiao

P112 ***The Drivation of the Analytical Structure of a class of Interval Type-2 fuzzy PD and PI controllers*** *[#127]*
Maowen Nie and Woei Wan Tan

P113 ***Estimation of the Asympototic Stability Region of Uncertain Fuzzy Systems with Bounded Controllers Using Variable Structure System Design Approach*** *[#138]*
Chung-Chun Kung, Ti-Hung Chen, Shuo-Chieh Chang and Chih-Chieh Chen

P114 ***A Study on Atanassov's Intuitionistic Fuzzy Graphs*** *[#157]*
Karunambigai M.G., Parvathi R. and Kalaivani O.K.

P115 ***Fuzzy Controller Based Output Power Leveling Enhancement for a Permanent Mangnet Synchronous Generator*** *[#159]*
Abdul Motin Howlader, Naomitsu Urasaki, Shantanu Chakraborty, Atsushi Yona, Tomonobu Senjyu and Ahmed Y. Saber

P116 ***Important Issues To Be Considered In Developing Fuzzy Cognitive Maps*** *[#548]*
Costas Neocleous, Christos Schizas and Maria Papaioannou

P117 ***A Fall Detection Study on the Sensors Placement Location and a Rule-Based Multi-Thresholds Algorithm Using Both Accelerometer and Gyroscopes*** *[#613]*
Donald Lie, Jerene Jacob and Nguyen Tam

P118 ***A Fuzzy Representation for Non-additive Weights of AHP*** *[#196]*
Shin-ichi Ohnishi, Takahiro Yamanoi and Hideyuki Imai

P119 ***A social cognitive framework of knowledge contribution in the online community*** *[#192]*
Fan-Chuan Tseng and Feng-Yuan Kuo

P120 ***Fuzzy Clustering of Large-Scale Data Sets Using Principal Component Analysis*** *[#188]*
Sassi Minyar and Arfaoui Olfa

P121 ***Soft Subspace Clustering with Competitive Agglomeration*** *[#168]*
Lin Zhu, Longbing Cao and Jie Yang

Tuesday, June 28, 2:50PM-4:30PM

(SS05) Special Session: Fuzzy Robotics
Tuesday, June 28, 2:50PM-4:30PM, Room: Swan, Chair: Honghai Liu

2:50PM ***Hand Motion Recognition via Fuzzy Active Curve Axis Gaussian Mixture Models: A Comparative Study*** *[#96]*
Ju Zhaojie and Liu Honghai

3:10PM ***Trajectory-based Control under ZMP Constraint for the 3D Biped Walking via Fuzzy Control*** *[#294]*
Hsiu-Ming Wu and Chih-Lyang Hwang

3:30PM ***Formation Behavior of Multiple Robots based on Tele-operation*** *[#565]*
Yuki Wagatsuma, Yuichiro Toda and Naoyuki Kubota

3:50PM ***Evaluation of Pointing Navigation Interface for Mobile Robot with Spherical Vision System*** *[#521]*
Kyohei Yoshida, Fuminori Hibino, Yasutake Takahashi and Yoichiro Maeda

4:10PM ***Fuzzy PID Controller Design for Artificial Finger based SMA Actuators*** *[#341]*
Alireza Khodayari, Mohammad Mahdi Kheirikhah and Maryam Talari

(SS18) Special Session: Recent Advances in Fuzzy Logic in Image Processing
Tuesday, June 28, 2:50PM-4:30PM, Room: Peacock, Chair: Mike Nachtegael

2:50PM ***Fuzzy shape Classification exploiting Geometrical and Moments Descriptors*** *[#557]*
Ugo Erra and Sabrina Senatore

3:10PM ***Piece-wise Convex Spatial-Spectral Unmixing of Hyperspectral Imagery using Possibilistic and Fuzzy Clustering*** *[#452]*
Alina Zare and Paul Gader

3:30PM ***Detection of Hyperintense Regions on MR Brain Images using a Mamdani Type Fuzzy Rule-Based System*** *[#603]*
F. Xavier Aymerich, Eduard Montseny, Pilar Sobrevilla and Alex Rovira

3:50PM ***On Fuzzy Partitions for Visual Texture Modelling*** *[#360]*
Jesus Chamorro-Martinez, Pedro Manuel Martinez-Jimenez and Jose Manuel Soto-Hidalgo

(SS27) Special Session: Communication Robotics and Computational Intelligence Co-creation
Tuesday, June 28, 2:50PM-4:30PM, Room: Phoenix, Chair: Yoichi Yamazaki

2:50PM ***Educational System with the Android Robot SAYA and Field Trial*** *[#176]*
Takuya Hashimoto, Naoki Kato and Hiroshi Kobayashi

3:10PM ***Multimodal Gesture Recognition Based on Choquet Integral*** *[#113]*
Kaoru Hirota, Hai An Vu, Phuc Quang Le, Chastine Fatichah and Zhentao Liu

3:30PM ***Emotional States Based 3-D Fuzzy Atmosfield for Casual Communication between Humans and Robots*** *[#172]*
Zhentao Liu, Min Wu, Danyun Li, Fangyan Dong, Yoichi Yamazaki and Kaoru Hirota

3:50PM ***Presence Expression Using Eye Robot for Computer Go System*** *[#455]*
Yoichi Yamazaki, Masaya Hanada, Chang-Shing Lee, Takuya Hashimoto, Fangyan Dong, Makoto Motoki and Kaoru Hirota

4:10PM ***Emotion Recognition based on Human Gesture and Speech Information using RT Middleware*** *[#367]*
An Hai Vu, Yoichi Yamazaki, Fangyan Dong and Kaoru Hirota

(SS28-2) Special Session: Current Development in Pattern Classification-Kernelization, Pairwise Constraints, and Classifiers
Tuesday, June 28, 2:50PM-4:30PM, Room: Crane, Chair: Yasunori Endo

2:50PM ***FCMdd-type Linear Fuzzy Clustering for Incomplete Non-Euclidean Relational Data*** *[#108]*
Takeshi Yamamoto, Katsuhiro Honda, Akira Notsu and Hidetomo Ichihash

3:10PM ***Hybrid Objective Function of Fuzzy c-Varieties and Cross-shape Fuzzy Cluster Extraction*** *[#295]*
Daisuke Yoshida, Katsuhiro Honda, Akira Notsu and Hidetomo Ichihash

3:30PM ***Kernelized Fuzzy c-Means Clustering for Uncertain Data using Quadratic Penalty-Vector Regularization with Explicit Mappings*** *[#114]*
Yasunori Endo, Isao Takayama, Yukihiro Hamasuna and Sadaaki Miyamoto

3:50PM ***On Mahalanobis Distance Based Fuzzy c-Means Clustering for Uncertain Data Using Penalty Vector Regularization*** *[#125]*
Yukihiro Hamasuna, Yasunori Endo and Sadaaki Miyamoto

4:10PM ***On Hard and Fuzzy c-Means Clustering with Conditionally Positive Definite Kernel*** *[#177]*
Yuchi Kanzawa, Yasunori Endo and Sadaaki Miyamoto

(SS42-1) Special Session: Fuzzy Cognitive Maps-Theory and Applications
Tuesday, June 28, 2:50PM-4:30PM, Room: Egret, Chair: Chair: Elpiniki I. Papageorgiou and Sebastian Lozano

2:50PM ***Intuitionistic Fuzzy Reasoning with Cognitive Maps*** *[#477]*
Dimitris Iakovidis and Elpiniki Papageorgiou

3:10PM ***Review study on Fuzzy Cognitive Maps and their applications during the last decade*** *[#516]*
Elpiniki Papageorgiou

3:30PM ***Nonlinear Cause-Effect Relationships In Fuzzy Cognitive Maps*** *[#361]*
Maria Ketipi, Dimitrios Koulouriotis, Evangelos Karakasis, George Papakostas and Vassilios Tourassis

3:50PM ***Case Based Fuzzy Cognitive Maps (CBFCM) : New method for medical reasoning*** *[#567]*
Nassim Douali, Elpiniki Papageorgiou, Jos De Roo and Marie-Christine Jaulent

4:10PM ***Training Fuzzy Cognitive Maps by Using Hebbian Learning Algorithms: A Comparative Study*** *[#343]*
George Papakostas, Athanasios Polydoros, Koulouriotis Dimitrios and Tourassis Vasileios

(SS21-1) Special Session: Fuzzy Control in Industrial and Application
Tuesday, June 28, 2:50PM-4:30PM, Room: Swallow, Chair: Shun-Hung Tsai

2:50PM ***Applications of Fuzzy Classification with Fuzzy C-Means Clustering and Optimization Strategies for Load Identification in NILM Systems*** *[#126]*
Yu-Hsiu Lin, Men-Shen Tsai and Chin-Sheng Chen,

3:10PM ***Knowledge-Based Fuzzy Imbalanced Force Compensator Design for a Single Active Magnetic Bearing Suspended Rotor System*** *[#347]*
Yi Hua Fan and Ying Tsun Lee

3:30PM ***DSP-Based Cross-Coupled Synchronous Control for Dual Linear Motors via Functional Link Radial Basis Function Network*** *[#129]*
Chin-Sheng Chen, Po-Huan Chou and Faa-Jeng Lin,

3:50PM ***An Interactive Fuzzy Satisficing Method for Multiobjective Stochastic Defensive Location Problems*** *[#284]*
Takeshi Uno and Kosuke Kato

(HCGC-4) Competition: Human vs. Computer Go Competition
Tuesday, June 28, 2:50PM-4:30PM, Room: Magpie, Chair: Chang-Shing Lee, Martin Muller, Olivier Teytaud, and Shun-Chin Hsu

Tuesday, June 28, 4:30PM-7:00PM

(PS02) Poster Session II
Tuesday, June 28, 4:30PM-7:00PM, Room: Grand Ballroom II

P301 ***Robust Speed-Controlled Permanent Magnet Synchronous Motor Drive using Fuzzy Logic Controller*** *[#162]*
Gunawan Dewantoro and Yong-Lin Kuo

P302 ***Possibilistic Regression Analysis by Support Vector Machine*** *[#183]*
Pei-Yi Hao

P303 ***Cognitive Simulation-Based on Knowledge Evolution in Fuzzy Discrete Event Systems*** *[#199]*
Paul-Antoine Bisgambiglia, Paul Antoine Bisgambiglia and Jean-Sebastien Gualtieri

P304 ***A Fuzzy Tool for the Validation of Individual Risk Premia in High-Technology Venture Valuation*** *[#202]*
Lars Krueger, Peter Heydebreck and Ralf Salomon

P305 ***Soft-Core Implementation for Centre of Slice Area Average Defuzzifier*** *[#206]*
Antonio Hernandez Zavala, Oscar Camacho Nieto and Cornelio Yanez Marquez

P306 ***Fuzzy Integral-based Composite Facial Expression Generation for a Robotic Head*** *[#234]*
Bum-Soo Yoo, Se-Hyoung Cho and Jong-Hwan Kim

P307 ***Comparing soft clusters and partitions*** *[#243]*
Derek Anderson, James Keller, Ozy Sjahputera, James Bezdek and Mihail Popescu

P308 ***An Adaptive Hybrid Data Fusion Based Identification of Skeletal Muscle Force with ANFIS and Smoothing Spline Curve Fitting*** *[#245]*
Parmod Kumar, Cheng-Hung Chen, Anish Sebastian, Madhavi Anugolu, Chandrasekhar Potluri, Amir Fassih, Yimesker Yihun, Alex Jensen, Yi Tang, Steve Chiu, Ken Bosworth, D. S. Naidu, Marco P. Schoen, Jim Creelman and Alex Urfer

P309 ***A Functional-Link based Interval Type-2 Compensatory Fuzzy Neural Network for Nonlinear System modeling*** *[#249]*
Jyh-Yeong Chang, Yang-Yin Lin, Ming-Feng Han and Chin-Teng Lin

P310 ***Infrared Image Segmentation using Enhanced Fuzzy C-Means clustering for Automatic Detection Systems*** *[#251]*
Sitanshu Gupta and Asim Mukherjee

P311 ***Image-Correlation Data Association with Global Uncertainty Techniques*** *[#274]*
Stephen Stubberud and Kathleen Kramer

P312 ***A Non-Singleton Interval Type-2 Fuzzy Logic System for Universal Image Noise Removal using Quantum-Behaved Particle Swarm Optimization*** *[#291]*
Daoyuan Zhai, Minshen Hao and Jerry Mendel

P313 ***Fuzzy Folksonomy-based Index Creation for e-Learning Content Retrieval on Cloud Computing Environments*** *[#306]*
Wen-Chung Shih, Chao-Tung Yang and Shian-Shyong Tseng

P314 ***Relationship between Intuitionistic Fuzzy Similarity Measures*** *[#308]*
Leila Baccour, Adel M. Alimi and Robert I. John

P315 ***Decomposition of Term-Document Matrix Representation for Clustering Analysis*** *[#316]*
Jianxiong Yang and Junzo Watada

P316 ***Visual-Based Guiding Method for Unmanned Helicopter Approaching to Landmark*** *[#171]*
Kuo-Hsien Hsia, Shao-Fan Lien and Juhng-Perng Su

P317 ***On the Type-1 and Type-2 Fuzziness Measures for Thresholding MRI Brain Images*** *[#200]*
Rajesh R., Senthilkumaran N., Satheesh Kumar J., Shanmuga Priya B., Thilagavathy C. and Priya K

P318 ***A Fast Algorithm for Mining Frequent Closed Itemsets over Stream Sliding Window*** *[#587]*
Show-Jane Yen, Cheng-Wei Wu, Yue-Shi Lee, Vincent S. Tseng and Chaur-Heh Hsieh

P319 ***Neuro-Fuzzy System Design using Differential Evolution with Local Information*** *[#313]*
Lin Chin-Teng, Han Ming-Feng, Lin Yang-Yin, Liao Shih-Hui and Chang Jyh-Yeong

P320 ***Stability Analysis and Synthesis of Markovian Jump Nonlinear Systems with Incomplete Transition Descriptions via Fuzzy Control*** *[#325]*
Min Kook Song, Jin Bae Park and Young Hoon Joo

P321 ***Bio-inspired computing of vision - fuzzy and neurmorphic processing*** *[#426]*
Woo Joon Han and Il Song Han

Tuesday, June 28, 5:00PM-7:00PM

(SS10-1) Special Session: Medical and Wellness Engineering

Tuesday, June 28, 5:00PM-7:00PM, Room: Swan, Chair: Yutaka Hata

5:00PM ***A Testicular Tubule Evaluation Method by Ultrasonic Array Probe*** *[#89]*
Yuya Takashima, Kei Kuramoto, Kobashi Syoji, Hata Yutaka and Ishikawa Tomomoto

5:20PM ***Fuzzy RASP Determination by 1kHz Ultrasonic Probe for Total Hip Arthroplasty*** *[#98]*
Naomi Yagi, Yoshitetsu Oshiro, Osamu Ishikawa, Yutaka Hata and Nao Shibanuma

5:40PM ***A Fuzzy Logic Approach to Predict Human Body Weight Based on AR Model*** *[#88]*
Hideaki Tanii, Hiroshi Nakajima, Tsuchiya Naoki, Kei Kuramoto, Syoji Kobashi and Yutaka Hata

6:00PM ***Consideration of Invasion, Intrusion, and Consciousness in Biomedical Sensing with Uncertainty*** *[#209]*
Hiroshi Nakajima, Naoki Tsuchiya and Yutaka Hata

6:20PM ***Load Forecasting using Fuzzy Wavelet Neural Networks*** *[#273]*
Mahdi Amina and Vassilis Kodogiannis

6:40PM ***Fuzzy Modelling Using a New Compact Fuzzy System: A Special Application to the Prediction of the Mechanical Properties of Alloy Steels*** *[#593]*
Qian Zhang and Mahdi Mahfouf

(SS09) Special Session: Applications of Fuzzy Logic to Awareness Promotion

Tuesday, June 28, 5:00PM-7:00PM, Room: Peacock, Chair: Kiyota Hashimoto

5:00PM ***Agent Simulation for Contents Evaluation with User Models for Hierarchical Knowledge Relations*** *[#356]*
Kiyota Hashimoto and Kazuhiro Takeuchi

5:20PM ***Giving Awareness of Maturity by Capability Assessment*** *[#607]*
Yi-Ling Kuo, Yu Nakamura, Masayuki Sakoda, Hiroshi Tsuji and Chang-Shing Lee

5:40PM ***Medical Care System Evaluation Based on DEA Of Prefectures In Japan*** *[#335]*
Kenji Fukuoka, Shingo Aoki and Yukie Majima

6:00PM ***Structured DEA Model Considering Relation among Input and Output Elements*** *[#331]*
Yamasaki Shingo and Aoki Shingo

6:20PM ***Component-Based Search Engine for Blogs*** *[#490]*
Sachio Hirokawa, Chengjiu Yin and Tetsuya Nakatoh

6:40PM ***Influence of the Space Segmentation and its Adaptive Automation for Reinforcement Learning*** *[#290]*
Akira Notsu, Yuki Komori, Katsuhiro Honda and Hidetomo Ichihashi

(SS08) Special Session: Innovative Fuzzy Approaches to Management Engineering

Tuesday, June 28, 5:00PM-7:00PM, Room: Phoenix, Chair: Junzo Watada

5:00PM ***Learning with Imbalanced Datasets using Fuzzy ARTMAP-based Neural Network Models*** *[#43]*
Shing Chiang Tan, Junzo Watada, Zuwarie Ibrahim, Marzuki Khalid and Wen Jau Lee

5:20PM ***Re-Scheduling the Unit Commitment Problem in Fuzzy Environment*** *[#18]*
Bo Wang, You Li and Junzo Watada

5:40PM ***Building a Fuzzy Multi-objective Portfolio Selection model with Distinct Risk Measurements*** *[#19]*
You Li, Bo Wang and Junzo Watada

6:00PM ***Statistic Test on Fuzzy Portfolio Selection Model*** *[#65]*
Pei-Chun Lin, Junzo Watada and Berlin Wu

6:20PM ***An Approach Based on Takagi-Sugeno Fuzzy Inference System Applied to the Operation Planning of Hydrothermal Systems*** *[#279]*
Ricardo Rabelo, Ricardo Fernandes, Adriano Carneiro and Rosana Braga

6:40PM ***Fuzzy Cognitive Maps in estimating the repercussions of oil/gas exploration on politico-economic issues in Cyprus*** *[#495]*
Costas Neocleous, Maria Papaioannou and Christos Schizas

(SS37) Special Session: Fuzzy Logic Based Computer Vision and Its Applications to Guidance and Control

Tuesday, June 28, 5:00PM-7:00PM, Room: Crane, Chair: Kuo-Hsien Hsia

5:00PM ***The Picked and Placed Control of the Objects for a Pneumatic X-Y Servo Platform by Integrating Image Processing Techniques and a Fuzzy Sliding Mode Controller Design*** *[#390]*
Hong-Ming Chen, Yi-Ping Shyu, Chun-Sheng Shen and Hong-Jia Yang

5:20PM ***The Dynamic Measurement System Design for Stewart Platform by Using Digital Image Processing Method*** *[#161]*
Yu Ker-Wei and Zhou Yu-Quan

5:40PM ***Orientation control of hovercraft systems via an SMFLC and Image-Guided Techniques*** *[#318]*
Chun-Chieh Wang

6:00PM ***PSO-based Estimation for Gaussian Blur in Blind Image Deconvolution Problem*** *[#529]*
Yang-Chih Lai, Chih-Li Huo, Yu-Hsiang Yu and Tsung-Ying Sun

6:20PM ***Fuzzy integrals for the aggregation of confidence measures in speech recognition*** *[#494]*
Julie Mauclair, Laurent Wendling and David Janiszek

6:40PM ***Active Tracking Using Intelligent Fuzzy Controller and Kernel-Based Algorithm*** *[#400]*
Moteaal Asadi Shirzi and M.R. Hairi-Yazdi

(SS17-1) Special Session: Practical and Applications Aspects of Type-2 Fuzzy Logic Systems

Tuesday, June 28, 5:00PM-7:00PM, Room: Egret, Chair: Woei Wan Tan

5:00PM ***An Interval Type 2 Fuzzy Approach to Multilevel Image Segmentation*** *[#591]*
Debanga Raj Neog, Muhammad Amjad Raza and Frank Chung-Hoon Rhee

5:20PM ***Navigation System of Mobile Robot in an Uncertain Environment Using Type-2 Fuzzy Modelling*** *[#585]*
Sittichok Junratanasiri, Sansanee Auephanwiriyakul and Nipon Theera-Umpon

5:40PM ***Multi-attribute Decision Making Models under Interval Type-2 Fuzzy Environment*** *[#95]*
Weize Wang and Xinwang Liu

6:00PM ***A Perceptual Computer Based Method for Supplier Selection Problem*** *[#186]*
Han Shilian and Liu Xinwang

6:20PM ***A Comparison of Non-stationary, Interval Type-2 and Dual-Surface Interval Type-2 Fuzzy Control*** *[#423]*
Naisan Benatar, Uwe Aickelin and Jonathan M. Garibaldi

6:00PM ***A Fuzzy Toolbox for the R Programming Language*** *[#612]*
Christian Wagner, Simon Miller and Jonathan M. Garibaldi

(SS19) Special Session: Fuzzy Inference Systems-Theory and Applications
Tuesday, June 28, 5:00PM-7:00PM, Room: Swallow, Chair: Hirosato Seki

5:00PM ***Type-2 Fuzzy Functional Inference Method*** *[#573]*
Hirosato Seki and Masaharu Mizumoto

5:20PM ***On Extension of Consequent Parts of T-S Inference Model*** *[#553]*
Hirosato Seki and Masaharu Mizumoto

5:40PM ***Optimization of Gaussian Fuzzy Membership Functions and Evaluation of the Monotonicity Property of Fuzzy Inference Systems*** *[#118]*
Tay Kai Meng and Lim Chee Peng,

6:00PM ***Refinement CTIN for General Type-2 Fuzzy Logic Systems*** *[#417]*
Thanh Long Ngo

6:20PM ***On a Strengthening Connective for Flexible Database Querying*** *[#7]*
Patrick Bosc and Olivier Pivert

(HCGC-5) Competition: Human vs. Computer Go Competition
Tuesday, June 28, 5:00PM-7:00PM, Room: Magpie, Chair: Chang-Shing Lee, Martin Muller, Olivier Teytaud, and Shun-Chin Hsu

Panel Session II: Computing With Words
Tuesday, June 28, 5:00PM-6:30PM, Room: Grand Ballroom I, Chair: Nikhil R. Pal

Wednesday, June 29, 8:00AM-10:20AM

(SS02-2) Special Session: Evolutionary Fuzzy Systems
Wednesday, June 29, 8:00AM-10:20AM, Room: Swan, Chair: Rafael Alcalá

8:00AM ***Studying the Behavior of a Multiobjective Genetic Algorithm to design Fuzzy Rule-Based Classification Systems for Imbalanced Data-Sets*** *[#189]*
Pedro Villar, Alberto Fernandez and Francisco Herrera

8:20AM ***On the Cooperation of Interval-Valued Fuzzy Sets and Genetic Tuning to Improve the Performance of Fuzzy Decision Trees*** *[#258]*
Jose Antonio Sanz, Alberto Fernandez, Humberto Bustince and Francisco Herrera

8:40AM ***A Two-Step Approach of Feature Construction for a Genetic Learning Algorithm*** *[#388]*
David Garcia, Antonio Gonzalez and Raul Perez

9:00AM ***Using the Adaboost algorithm for extracting fuzzy rules from low quality data: some preliminary results*** *[#487]*
Ana Palacios, Luciano Sanchez and Ines Couso

9:20AM ***Checking Orthogonal Transformations and Genetic Algorithms for Selection of Fuzzy Rules based on Interpretability-Accuracy Concepts*** *[#324]*
M.Isabel Rey, Marta Galende, Gregorio I. Sainz and MariaJ. Fuente

9:40AM ***A Hierarchical Genetic Fuzzy Rule-Based Classifier for High-Dimensional Classification Problems*** *[#395]*
Dimitris Stavrakoudis, Ioannis Gitas and John Theocharis

10:00AM ***A New Approach to Handle High Dimensional and Large Datasets in Multi-objective Evolutionary Fuzzy Systems*** *[#432]*
Michela Antonelli, Pietro Ducange and Francesco Marcelloni

(SS12-2) Special Session: Recent Advances in Fuzzy-Model-Based Control Systems
Wednesday, June 29, 8:00AM-10:20AM, Room: Peacock, Chair: H. K. Lam

8:00AM ***Generalized Stabilizing Controllers for Fuzzy Systems via Circle Criterion -- LMI and SOS*** *[#40]*
Ji-Chang Lo and Wei-Cheng Liao

8:20AM ***T-S Fuzzy Systems Approach to Approximation and Robust Controller Design for General Nonlinear Systems*** *[#216]*
Qing Gao, Xiao-Jun Zeng, Gang Feng and Yong Wang

8:40AM ***A Polynomial Observer Design for a Wider Class of Polynomial Fuzzy Systems*** *[#62]*
Toshiaki Seo, Hiroshi Ohtake, Kazuo Tanaka, Ying-Jen Chen and Hua O. Wang

9:00AM ***A SVD Approach to $H_$ Decentralized Static Output Feedback Fuzzy Control Design for Nonlinear Interconnected Systems*** *[#45]*
Chung-Shi Tseng and Yung-Yue Chen

9:20AM ***Adaptive Fuzzy Sliding-Mode Control for a Class of Nonlinear Systems with Uncertainties*** *[#111]*
Hugang Han

9:40AM ***Mixed H2/H-Infinity Optimization with Discrete Smith Predictor for Fuzzy Decentralized Control of Nonlinear Interconnected Discrete Dynamic Systems with Large Delay*** *[#44]*
Chih-Lyang Hwang

10:00AM ***A Hybrid Fuzzy Sliding-Mode Control for a Class of Generalized, Under-Actuated and Uncertain Nonlinear Dynamic Systems*** *[#120]*
Chih-Lyang Hwang and Hsiu-Ming Wu

(SS31) Special Session: Human Symbiotic Systems
Wednesday, June 29, 8:00AM-10:20AM, Room: Phoenix, Chair: Daisuke Katagami

8:00AM ***Visualization and Analytical Support of Questionnaire Free-Texts Data based on HK Graph with Concepts of Words*** *[#365]*
Daisuke Kobayashi, Tomohiro Yoshikawa and Takeshi Furuhashi

8:20AM ***Development of Body Mapping from Human Demonstrator to Inverted-Pendulum Mobile Robot for Imitation*** *[#353]*
Takahashi Sataya, Takahashi Yasutake, Maeda Yoichiro and Nakamura Takayauki

8:40AM ***Social Interaction of Cooperative Communication and Group Generation in Multi-Agent Reinforcement Learning Systems*** *[#389]*
Kun Zhang, Yoichiro Maeda and Yasutake Takahashi

9:00AM ***Estimation Of Subjective Stress Via Finger Plethysmogram*** *[#255]*
Yusuke Kobashi, Genma Sano, Tsuyoshi Nakamura and Masayoshi Kanoh

9:20AM ***Human Preference Learning by Robot Partners Based on Multi-objective Behavior Coordination*** *[#560]*
Naoyuki Kubota, Aiko Yaguchi and Utaki Ishikawa

9:40AM ***A Report The Difference Features Of A Multi-agent Using An Overlay Knowledge In The Fire Panic Problem*** *[#554]*
Yukinobu Hoshino

10:00AM ***Group Pressure Generation of Multi-Agents on Cross-cultural Simulation Game*** *[#377]*
Daisuke Katagami and Tam Huynh van

(FC& IS) Fuzzy Control and Intelligent Systems

Wednesday, June 29, 8:00AM-10:20AM, Room: Crane, Chair: Li-Wei Ko

8:00AM ***H2 Guaranteed Cost of Uncertain Continuous T-S Fuzzy Systems by Multiple Lyapunov Function Approach*** *[#87]*
Wen-Ren Horng, Chun-Hsiung Fang, Ching-Hsiang Lee and Jyh-Horng Chou

8:20AM ***Higher Order Sliding Fuzzy Type-2 Interval Control for SISO Uncertain Nonlinear Systems*** *[#508]*
Malik Manceur, Essounbouli Najib and Hamzaoui Abdelaziz

8:40AM ***Output Regulation Using Integral Fuzzy Predictive Control with Piecewise Lyapunov Functions*** *[#248]*
Chien-Hung Liu and Kuang-Yow Lian

9:00AM ***Power Management of a Variable Speed Wind Turbine for Stand-Alone System using Fuzzy Logic*** *[#580]*
Minh Huynh Quang, Frederic Nollet, Najib Essounbouli and Abdelaziz Hamzaoui

9:20AM ***Robust stabilization for continuous fuzzy systems with time varying delay*** *[#550]*
Chedia Latrach, Mourad Kchaou, Ahmed Hajjaji and Ahmed Toumi

9:40AM ***Splitting K-means Generated Neural Fuzzy System with Support Vector Regression*** *[#406]*
Cheng-Da Hsieh and Chia-Feng Juang

10:00AM ***Fuzzy Reinforcement Learning Control for Decentralized Partially Observable Markov Decision Processes*** *[#523]*
Rajneesh Sharma and Matthijs T. J. Spaan

(SS10-2) Special Session: Medical and Wellness Engineering

Wednesday, June 29, 8:00AM-10:20AM, Room: Egret, Chair: Yutaka Hata

8:00AM ***A challenge to biometrics by sole pressure while walking*** *[#338]*
Takahiro Takeda, Kei Kuramoto, Syoji Kobashi and Yutaka Hata

8:20AM ***Six Degree of Freedom Calculation Based on Principal Component Analysis for the Knee Joint in MDCT Image*** *[#433]*
Yosuke Uozumi, Kouki Nagamune, Daisuke Araki, Tomoyuki Matsumoto and Takehiko Matsushita

8:40AM ***Nursing-care Text Classification using Additional Term Information from Web*** *[#336]*
Manabu Nii, Takafumi Yamaguchi, Yusuke Mori, Yutaka Takahashi and Atsuko Uchinuno

9:00AM ***A Development of Navigation System for MOSAIC PLASTY using Electromagnetic Sensor*** *[#413]*
Takayasu Toyoshima, Kouki Nagamune, Daisuke Araki, Tomoyuki Matsumoto and Seiji Kubo

9:20AM ***A Quantitative Measurement System of Endpoint during Lachman tTest with Force Sensor*** *[#379]*
Shogo Kawaguchi, Kouki Nagamune, Daisuke Araki, Tomoyuki Matsumoto and Seiji Kubo

9:40AM ***Human Motion Tracking for Cognitive Rehabilitation in Informationally Structured Space Based on Sensor Networks*** *[#569]*
Yuichiro Toda, Kodai Yuki, Eriko Hiwada and Naoyuki Kubota

10:00AM ***A Pervasive Multi-sensor Data Fusion for Smart Home Healthcare Monitoring*** *[#472]*
Hamid Medjahed, Dan Istrate, Jerome Boudy, Jean-Louis Baldinger and Bernadette Dorizzi

(SS13-1) Special Session: Fuzzy Multiple Criteria Decision Making
Wednesday, June 29, 8:00AM-10:20AM, Room: Swallow, Chair: Gwo-Hshiung Tzeng

8:00AM ***Value Driver Derivations for Embedded Memories by Fuzzy DEMATEL based Hybrid MCDM Methods*** *[#530]*
Chi-Yo Huang and Gwo-Hshiung Tzeng

8:20AM ***Fuzzy Multiple Attribute Decision Making Theory With The Balanced Scorecard Application In Mobile Industry*** *[#369]*
Chiu-Hung Su, Ying-Hsun Hung and Gwo-Hshiung Tzeng

8:40AM ***Fuzzy MCDM Application for Strategy Evaluation*** *[#383]*
Mei-Chen Lo and Gwo-Hshiung Tzeng

9:00AM ***Exploring the SPM System Structure Model by Using Fuzzy DEMATEL for NPD*** *[#342]*
Chang Yu-Yun, Kuan Meng-Jong, Chuang Yen-Ching and Tzeng Gwo-Hshiung

9:20AM ***Interdependent Multiple Objective Programming- A Monte Carlo Method*** *[#398]*
Jih-Jeng Huang and Chin-Yi Chen

9:40AM ***Handling Fuzzy Decision Making Problem based on Linguistic Information and Intersection Concept*** *[#93]*
Chen-Tung Chen, Ping-Feng Pai and Wei-Zhan Hung

10:00AM ***Evaluate and Identify Optimal Weapon Systems Using Fuzzy Multiple Criteria Decision Making*** *[#14]*
Ying Bai and Dali Wang

(HCGC-1) Competition: Human vs. Computer Go Competition
Wednesday, June 29, 8:00AM-10:20AM, Room: Magpie, Chair: Chang-Shing Lee, Martin Muller, Olivier Teytaud, and Shun-Chin Hsu

Wednesday, June 29, 8:00AM-9:00AM

Invited Talk I: Casual Communication between Robots and Humans based on Robot Technology Middleware and Multimedia Recognition
Wednesday, June 29, 8:00AM-9:00AM, Room: Grand Ballroom I, Speaker: Kaoru Hirota

Wednesday, June 29, 8:00AM-10:20AM

(FA-2) Fuzzy Applications
Wednesday, June 29, 8:00AM-10:20AM, Room: Grand Ballroom II, Chair: Qiang Shen

8:00AM ***Fuzzy-rough Classifier Ensemble Selection*** *[#134]*
Ren Diao and Qiang Shen

8:20AM ***Kernel-Based Fuzzy-Rough Nearest Neighbour Classification*** *[#135]*
Yanpeng Qu, Changjing Shang, Qiang Shen, Neil MacParthalain and Wei Wu

8:40AM ***FAPOP: Feature Analysis Enhanced Pseudo Outer-Product Fuzzy Rule Identification System*** *[#240]*
Sau Wai Tung, Chai Quek and Cuntai Guan

9:00AM ***Tracking Control of Surface Vessels via Adaptive Type-2 Fuzzy Logic Control*** *[#256]*
Xue Tao Chen and Woei Wan Tan

9:20AM ***Relaxed Fuzzy Lyapunov Approach for Dynamic Local Model Networks*** *[#263]*
Christian Mayr, Christoph Hametner, Martin Kozek and Stefan Jakubek

9:40AM ***Vehicle Warning System for Land Departure and Collision Avoidance: Using Adaptive Fuzzy Decision Making*** *[#484]*
Chih-Li Huo, Yu-Hsiang Yu, Jhih-Cheng Syu and Tsung-Ying Sun

10:00AM ***Centroid Density of Interval Type-2 Fuzzy Sets: Comparing Stochastic and Deterministic Defuzzification*** *[#444]*
Ondrej Linda and Milos Manic

Wednesday, June 29, 10:50AM-12:00PM

(HCGC-2) Competition: Human vs. Computer Go Competition
Wednesday, June 29, 10:50AM-12:00PM, Room: Magpie, Chair: Chang-Shing Lee, Martin Muller, Olivier Teytaud, and Shun-Chin Hsu

Keynote Speech II: Fuzzy Approaches to Information Fusion
Wednesday, June 29, 10:50AM-12:00PM, Room: Grand Ballroom I, Speaker: Bernadette Bouchon-Meunier

Wednesday, June 29, 1:30PM-2:30PM

(HCGC-3) Competition: Human vs. Computer Go Competition
Wednesday, June 29, 1:30PM-2:30PM, Room: Magpie, Chair: Chang-Shing Lee, Martin Muller, Olivier Teytaud, and Shun-Chin Hsu

Plenary Speech II: Soft Computing in Prognostics and Health Management (PHM) Applications: A Case Study in Anomaly Detection
Wednesday, June 29, 1:30PM-2:30PM, Room: Grand Ballroom I, Speaker: Piero Bonissone

Wednesday, June 29, 2:30PM-4:30PM

(PS03) Poster Session III
Wednesday, June 29, 2:30PM-4:30PM, Room: Grand Ballroom II

P501 ***Statistical Scheme via AIC for Evaluating the Optimal Cut Off Level in Fuzzy Clustering*** *[#370]*
Shuya Kanagawa, Kimiaki Shinkai, Hsunhsun Chung and Kenichi Nagashima

P502 ***Genetic Algorithm Based Fully Automated and Adaptive Fuzzy Logic Controller*** *[#371]*
Pintu Shill, Kishore Pal, Faijul Amin and Kazuyuki Murase

P503 ***A Comparison of Distance-based Semi-Supervised Fuzzy c-Means Clustering Algorithms*** *[#373]*
Daphne Teck Ching Lai and Jonathan M. Garibaldi

P504 ***Applying MDL in PSO for Learning Bayesian Networks*** *[#382]*
Shu-Ching Kuo, Hung-Jen Wang, Hsiao-Yi Wei, Chih-Chuan Chen and Sheng-Tun Li

P505 ***Relational Structure Analysis of Fuzzy Node Fuzzy Graph and its Application*** *[#385]*
Hiroaki Uesu, Kenichi Nagashima, Hsunhsun Chung and Ei Tsuda

P506 ***On another approach to the definition of an L-fuzzy valued integral*** *[#419]*
Vecislavs Ruza and Svetlana Asmuss

P507 ***Evolving Fuzzy Image Segmentation*** *[#422]*
Ahmed Othman and Hamid Tizhoosh

P508 ***On spline methods of approximation under L-fuzzy information*** *[#430]*
Svetlana Asmuss and Alexander Sostak

P509 ***Local Non-Quadratic H-infinity Control For Continuous-Time Takagi-Sugeno Models*** *[#440]*
Miguel Bernal, Adolfo Soto-Cota, Joaquin Cortez, Jose Luis Pitarch and Abdelhafidh Jaadari

P510 ***Fuzzy Active Contour Models*** *[#451]*
Cesar Pereira, Carlos Bastos, Ren Tsang and George Cavalcanti

P511 ***Discretization of fuzzy transitive relations*** *[#470]*
D. Boixader and J. Recasens

P512 ***Tridimensional Fuzzy Pain Assessment*** *[#476]*
Ernesto Araujo and Suzana Miyahira

P513 ***Integrate Variable Precision Rough Sets and Modified PBMF Index Function for Partitioning and Classifying Complex Datasets*** *[#478]*
Kuang Yu Huang and Yu-Hsin Cheng

P514 ***Anti-Swing Control of A New Container Crane With Fuzzy Uncertainties Compensation*** *[#486]*
Weimin Xu, Wei Gu, Aidi Shen, Jianxin Chu and Wangqiang Niu

P515 ***A Robust Method for Image Segmentation of Noisy Digital Images*** *[#492]*
Prabhjot Kaur, I. M. S. Lamba and Anjana Gosain

P516 ***The Fuzzy DEMATEL based Job Accommodation Strategy Definitions for Operators with Hearing Impairments*** *[#534]*
Chi-Yo Huang and Gwo-Hshiung Tzeng

P517 ***A Fuzzy MCDM method to select the best company based on Financial Report Analysis****[#527]*
Jung-Yuan Kung, Tzung-Nan Chuang and Minh Ky Chau

P518 ***Improve Observation-Based Discrete Hidden Markov Model by Fuzzy Vector Quantization -- An example on electroencephalogram (EEG) signal recognition*** *[#572]*
Shing-Tai Pan, Sheng-Fu Liang, Tzung-Pei Hong and Jian-Hong Zeng

P519 ***Design of Interval Type-2 Fuzzy Logic Systems Using Prior Knowledge via Optimization Algorithms*** *[#92]*
Tiechao Wang and Jianqiang Yi

P520 ***Fuzzy Reinforcement Learning for System of Systems (SOS)*** *[#34]*
Hamid Berenji and Mo Jamshidi

Wednesday, June 29, 2:50PM-4:30PM

(SS20) Special Session: Universal Contents Creation/Distribution and Intelligent System
Wednesday, June 29, 2:50PM-4:30PM, Room: Swan, Chair: Katsuhiro Honda

2:50PM ***Partially Exclusive Condition for Sequential Fuzzy Co-cluster Extraction*** *[#48]*
Katsuhiro Honda, Akira Notsu and Hidetomo Ichihashi

3:10PM ***DEA based Hierarchical Structure Evaluation and Vissualization Method*** *[#323]*
Kazushige Inoue, Takeo Ichinotsubo and Shingo Aoki

3:30PM ***Group Decision Focusing on Outliers*** *[#115]*
Tomoe Entani

3:50PM ***PCA-guided k-Means Clustering With Incomplete Data*** *[#15]*
Katsuhiro Honda, Ryoichi Nonoguchi, Akira Notsu and Hidetomo Ichihashi

4:10PM ***Proposed Particle-Filtering Method for Reinforcement Learning*** *[#53]*
Akira Notsu, Katsuhiro Honda and Hidetomo Ichihashi

(SS03) Special Session: Uncertainty and the Semantic Web

Wednesday, June 29, 2:50PM-4:30PM, Room: Peacock, Chair: Fernando Bobillo

2:50PM ***Formalizing Object Membership in Fuzzy Ontology with Property Importance and Property Priority*** *[#298]*
Yi Cai and Ho-fung Leung

3:10PM ***Aggregation Operators and Fuzzy OWL 2*** *[#142]*
Fernando Bobillo and Umberto Straccia

3:30PM ***Are Fuzzy Description Logics with General Concept Inclusion Axioms Decidable?*** *[#310]*
Franz Baader and Rafael Penaloza

3:50PM ***Fuzzy Concept Lattice Construction: A Basis for Building Fuzzy Ontologies*** *[#454]*
Valerie Cross and Meenaskhi Kandasamy

4:10PM ***Fuzziness, OWA and Linguistic Quantifiers for Web Selection Processes*** *[#420]*
Ronald R. Yager, Marek Z. Reformat and Giray Gumrah

(SS04) Special Session: Soft Computing for Operations Research and Optimization

Wednesday, June 29, 2:50PM-4:30PM, Room: Phoenix, Chair: Takashi Hasuike

2:50PM ***Visual Stability Improvement of SOM's Feature Map by Initial Value Assignment*** *[#502]*
Shinji Momoi and Tsutomu Miyoshi

3:10PM ***Study of morphogenesis of a large-span roof that satisfies its form design requirements*** *[#61]*
Yuya Takeda and Kazutoshi Tsutsumi

3:30PM ***Multiobjective Two-Level 0-1 Programming through Distributed Genetic Algorithms*** *[#86]*
Keiichi Niwa, Tomohiro Hayashida and Masatoshi Sakawa

3:50PM ***Optimal Static Output Feedback Control of Fuzzy-Model-Based Control Systems*** *[#12]*
Wen-Hsien Ho, Chen Shinn-Horng, Chou Jyh-Horng and Shu Chun-Chin

4:10PM ***An Interactive Satisficing Method for Multiobjective Random Fuzzy Programming Problems through the Possibility-Based Probability Model*** *[#197]*
Hideki Katagiri, Masatoshi Sakawa and Takeshi Matsui

(SS01) Special Session: Fuzzy Ontologies and FML Applications

Wednesday, June 29, 2:50PM-4:30PM, Room: Crane, Chair: Giovanni Acampora

2:50PM ***Improving Ontology Alignment through Memetic Algorithms*** *[#307]*
Giovanni Acampora, Pasquale Avella, Vincenzo Loia, Salerno Saverio and Autilia Vitiello

3:10PM ***Genetic Fuzzy Markup Language for Diet Application*** *[#468]*
Chang-Shing Lee, Mei-Hui Wang, Zhi-Wei Chen, Chin-Yuan Hsu, Su-E Kuo, Hui-Ching Kuo, Hui-Hua Cheng and Akio Naito

3:30PM ***A Hierarchical Approach to Assess Keyword Dependencies in Fuzzy Keyword Ontologies*** *[#124]*
Christer Carlsson, Robert Fuller and Mario Fedrizzi

3:50PM ***Improving Disease Prediction Using ICD-9 Ontological Features*** *[#148]*
Mihail Popescu and Mohammed Khalilia

(SS42-2) Special Session: Fuzzy Cognitive Maps-Theory and Applications
Wednesday, June 29, 2:50PM-4:30PM, Room: Egret, Chair: Chair: Elpiniki I. Papageorgiou and Sebastian Lozano

2:50PM ***Software Maintenance Scenarios Simulation with Fuzzy Cognitive Maps*** *[#514]*
Cristina Lopez, Jose L. Salmeron and Sebastian Lozano

3:10PM ***Train Fuzzy Cognitive Maps by Gradient Residual Algorithm*** *[#262]*
Huiliang Zhang, Zhiqi Shen and Chunyan Miao

3:30PM ***Causal Modeling Approximations In The Medical Domain*** *[#556]*
Lawrence Mazlack

3:50PM ***Interactive fuzzy programming through possibility measures and probability maximization for two-level linear programming problems involving fuzzy random variable coefficients*** *[#163]*
Masatoshi Sakawa, Hideki Katagiri and Takeshi Matsui

(SS21-2) Special Session: Fuzzy Control in Industrial and Application
Wednesday, June 29, 2:50PM-4:30PM, Room: Swallow, Chair: Shun-Hung Tsai, Chin-Sheng Chen and Ming-Ying Hsiao

2:50PM ***Decentralized Fuzzy Fault Tolerant Control for Multiple Satellites Attitude Synchronization*** *[#265]*
Junquan Li and K. D. Kumar

3:10PM ***T-S Fuzzy Tracking and Synchronous Control in a Gantry Stage*** *[#128]*
Chin-Sheng Chen, Chao-Feng Lee, Po-Huan Chou, Faa-Jeng Lin and Shun-Hung Tsai

3:30PM ***Observer-Based Adaptive FNN Control of Robot Manipulators: PSO-SA Self Adjust Membership Approach*** *[#181]*
Kai-Shiuan Shih, Tzuu-Hseng S. Li and Shun-Hung Tsai

3:50PM ***Design of Digital Battery Charger System Based on PV-Module*** *[#137]*
Ta-Tau Chen, Ming-Ying Hsiao, Shun-Hung Tsai and Che-Nan Lin

4:10PM ***Fuzzy Approaches for Multiobjective Stochastic Linear Programming Problems Considering Both Probability Maximization and Fractile Optimization*** *[#217]*
Hitoshi Yano

(HCGC-4) Competition: Human vs. Computer Go Competition
Wednesday, June 29, 2:50PM-4:30PM, Room: Magpie, Chair: Chang-Shing Lee, Martin Muller, Olivier Teytaud, and Shun-Chin Hsu

Wednesday, June 29, 4:30PM-7:00PM

(PS04) Poster Session IV
Wednesday, June 29, 4:30PM-7:00PM, Room: Grand Ballroom II

P701 ***Performance Enhancement of Hierarchical Document Signature: A Comprehensive Study*** *[#497]*
Sukanya Manna and Tom Gedeon

P702 ***Sliding Adaptive Fuzzy Control for a Class of Time-Delayed Chaotic Systems*** *[#509]*
Negin Farzbod, Hassan Zarabadipour, Mahdi Aliyari Shoorehdeli and Faezeh Farivar

P703 ***Estimating Missing Value in Microarray Gene Expression Data*** *[#515]*
Amit Paul and Jaya Sil

P704 ***Interval Fuzzy Modeling Applied to Model Based Fault Detection of an Active Suspension System*** *[#537]*
Tayebe Sadat Ghiasi, Hassan Zarabadipour and Mahdi Aliyari Shoorehdeli

P705 ***Uncertainty Management in Type-2 Fuzzy Face-Space for Emotion Recognition*** *[#541]*
Rajshree Mandal, Anisha Halder, Pavel Bhowmik, Aruna Chakraborty, Amit Konar and Atulya K. Nagar

P706 ***Generation of Takagi-Sugeno Fuzzy Systems with Minimum Rules in Modeling and Identification*** *[#549]*
Feng Wan and Chenglin Hu

P707 ***Maximum Power Point Tracker for a PV Cell using a Fuzzy Agent adapted by the Fractional Open Circuit Voltage Technique*** *[#551]*
Moustafa Adly, Hisham El-Sherif and Mohamed Ibrahim

P708 ***Improvement of Digital Image Motion Compensation by Fuzzy Inference*** *[#597]*
Sheng-Che Hsu

P709 ***A Semisupervised Feature Extraction Method Based on Fuzzy-type Linear Discriminant Analysis*** *[#598]*
Hui-Shan Chu, Cheng-Hsuan Li, Bor-Chen Kuo and Chin-Teng Lin

P710 ***The Emotion Recognition System with Heart Rate Variability and Facial Image Features*** *[#599]*
Pei-Yang Hsieh and Chiun-Li Chin

P711 ***Fuzzy Control of a Bi-directional Inverter with Nonlinear Inductance for DC Microgrids*** *[#610]*
Gwo-Ruey Yu

P712 ***The Development of the Automatic Lane Following Navigation System for the Intelligent Robotic Wheelchair*** *[#611]*
Wen-Chang Cheng and Chia-Ching Chiang

P713 ***The Prediction of Trust Rating Based on the Quality of Services Using Fuzzy Linear Regression*** *[#614]*
Hadi Mashinchi, Lei Li, Mehmet Orgun and Yan Wang

P714 ***Observer-based Hybrid Fuzzy CMAC Controller for a Class of Uncertain Chaotic Systems*** *[#616]*
Chun-Sheng Chen

P715 ***Automated Boundary Extraction and Visualization System for Coronary Plaque in IVUS Image by Using Fuzzy Inference-based Method*** *[#271]*
Takanori Koga, Eiji Uchino and Noriaki Suetake

P716 ***Multi-source Knowledge Based Unnormalized Interval Type-2 Fuzzy Logic Systems Design*** *[#154]*
Tiechao Wang, Jianqiang Yi and Chengdong Li

P717 ***On the Properties of SIRMs Connected Type-1 and Type-2 Fuzzy Inference Systems*** *[#264]*
Chengdong Li, Guiqing Zhang, Jianqiang Yi and Tiechao Wang

P718 ***Digital controller design for fuzzy systems with packet loss: intelligent digital redesign approach*** *[#333]*
Geun Bum Koo, Jin Bae Park, Young Hoon Joo and Hyoung Seok Jeon

P719 ***Mixed-Time T-S Fuzzy Optimal Estimator for Target Tracking*** *[#517]*
Sun Young Noh, Jin Bae Park and Young Hoon Joo

P720 ***Generalized Projective Synchronization of Time-Delayed Chaotic Systems via Sliding Adaptive Fuzzy Control*** *[#540]*
Negin Farzbod, Hassan Zarabadipour, Mahdi Aliyari Shoorehdeli and Faezeh Farivar

Wednesday, June 29, 5:00PM-6:00PM

Invited Talk II: Acceleration and Scalability for c-Means Clustering
Wednesday, June 29, 5:00PM-6:00PM, Room: Swan, Speaker: James Bezdek

Wednesday, June 29, 5:00PM-7:00PM

(SS40) Special Session: Fuzzy Approach for Information Security Management
Wednesday, June 29, 5:00PM-7:00PM, Room: Peacock, Chair: Che-Hung Liu

5:00PM ***Knowledge Management, Education and Firm's Performance*** *[#416]*
Yen-Tzu Chen, Yun-Chia Yan, Hsiao-Wen Huang and Hua-Wei Huang

5:20PM ***Expert decision making method based on uncertain linguistic variables*** *[#525]*
Tzung-Nan Chuang, Jung-Yuan Kung, Yin-Fang Lin and Hsiang-Chun Ku

5:40PM ***Applying FML and Fuzzy Ontologies to Malware Behavioural Analysis*** *[#575]*
Hsien-De Huang, Giovanni Acampora, Vincenzo Loia, Chang-Shing Lee and Hung-Yu Kao

6:00PM ***Applying Fuzzy AHP to Study the KSFs of Information Security Management*** *[#401]*
Jen-Sheng Wang, Che-Hung Liu, Joseph Z. Shyu and Hsiao-Wen Huang

6:20PM ***An Extension of a Fuzzy Ontology for Flexible Querying*** *[#6]*
Nouredine Tamani, Ludovic Lietard and Daniel Rocacher

6:40PM ***A Computational Linguistic Approach for the Identification of Translator Stylometry using Arabic-English Text*** *[#329]*
Heba El-Fiqi, Eleni Petraki and Hussein A. Abbass

(SS38) Special Session: Fuzzy Knowledge Discovery and Its Applications
Wednesday, June 29, 5:00PM-7:00PM, Room: Phoenix, Chair: Rung-Ching Chen

5:00PM ***Genetic-Fuzzy Association Rules for Network Intrusion Detection Systems*** *[#364]*
Ming-Yang Su, Chun-Yuen Lin, Sheng-Wei Chien and Han-Chung Hsu

5:20PM ***Personalized Recommendation for Web-based Learning Based on Ant Colony Optimization with Segmented-goal and Meta-Control Strategies*** *[#459]*
Feng-Hsu Wang

5:40PM ***A novel fuzzy recommendation system integrated the experts' opinion*** *[#461]*
Li Chen Cheng and Hua An Wang

6:00PM ***Fuzzy Rule-Based Stock Trading System*** *[#464]*
I-Cheng Yeh and Che-hui Lien

6:20PM ***Towards Application of FML in Suspicion of Non-Common Diseases*** *[#582]*
Giovanni Acampora, Tatiana Kiseliova, Karaman Pagava and Autilia Vitiello

6:40PM ***Linguistic summarization of long-term trends for understanding change in human behavior*** *[#296]*
Maria Ros, Derek Anderson, James Keller, Manuel Pegalajar, Miguel Delgado, Amparo Vila and Mihail Popescu

(SS39) Special Session: Fuzzy Based Computation on Biomedical Systems
Wednesday, June 29, 5:00PM-7:00PM, Room: Crane, Chair: Shing-Tai Pan

5:00PM ***Fuzzy Knowledge Approach to Automatic Disease Diagnosis*** *[#281]*
Giuseppe Fenza, Vincenzo Loia, Carmen De Maio, Mariacristina Gallo, Roberto Linciano and Aldo Morrone

5:20PM ***Predicting Laboratory Testing in Intensive Care using Fuzzy and Neural Modeling*** *[#349]*
Federico Cismondi, Andre Fialho, Susana Vieira, Joao Sousa and Shane Reti

5:40PM ***A fuzzy inference system for sleep staging*** *[#109]*
Liang Sheng-Fu, Chen Ying-Huang, Kuo Chih-En, Chen Jyun-Yu and Hsu Sheng-Che

6:00PM ***Fusion of Fuzzy Logic and PD Control for a Five-Fingered Smart Prosthetic Hand*** *[#485]*
Cheng-Hung Chen and D. Subbaram Naidu

6:20PM ***Hierarchical-interpolative Fuzzy System Construction by Genetic and Bacterial Programming Algorithms*** *[#414]*
Krisztian Balazs and Laszlo T. Koczy

6:40PM ***Study on Various Defuzzification Methods for Fuzzy Clustering Algorithms to Improve ROIs Detection in Lung CTs*** *[#140]*
Alberto Rey, Bernardino Arcay and Alfonso Castro

(SS17-2 & SS15) Special Session: Practical and Applications Aspects of Type-2 Fuzzy Logic Systems & Type-2 Fuzzy Logic Theory
Wednesday, June 29, 5:00PM-7:00PM, Room: Egret, Chair: Hani Hagras and Christian Wagner

5:00PM ***Comparison and Practical Implementation of Type-Reduction Algorithms for Type-2 Fuzzy Sets and Systems*** *[#24]*
Dongrui Wu and Maowen Nie

5:20PM ***Interpreting Fuzzy Set Operations and Multi Level Agreement in a Computing with Words Context*** *[#602]*
Christian Wagner and Hani Hagras

5:40PM ***An Adaptive Type-2 Fuzzy Logic Controller for Dynamic Positioning*** *[#211]*
Xue Tao Chen and Woei Wan Tan

6:00PM ***Interval Type-2 Recurrent Fuzzy Neural System Desing via Stable Simultaneous Perturbation Stochastic Approximation Algorithm*** *[#269]*
Feng-Yu Chang and Ching-Hung Lee

6:20PM ***Efficient centroid computation of general type-2 fuzzy sets with linear secondary membership function*** *[#145]*
Liu Xinwang

6:40PM ***Type-2 Fuzzy Airplane Altitude Control: A Comparative Study*** *[#283]*
Sheir Afgen Zaheer and Jong-Hwan Kim

(SS30 & SS43) Special Session: Fuzzy Inference Systems-Theory and Applications &Fuzzy Systems of Unknown Nonlinear Complex Systems
Wednesday, June 29, 5:00PM-7:00PM, Room: Swallow, Chair: Chi-Hsu Wan and Shih-Yu Li

5:00PM ***Solving Zadeh's Magnus Challenge Problem on Linguistic Probabilities via Linguistic Weighted Averages*** *[#436]*
Mohammad Reza Rajati, Jerry Mendel and Dongrui Wu

5:20PM ***Linguistic Weighted Power Means: Comparison with the Linguistic Weighted Average*** *[#68]*
John T. Rickard, Janet Aisbett, Ronald R. Yager and Greg Gibbon

5:40PM ***Finding the Capacity of Fuzzy Neural Networks (FNNs) via Its Equivalent Fully Connected Neural Networks (FFNNs)*** *[#241]*
Jing Wang, Chi-Hsu Wang and C. L. Philip Chen

6:00PM ***On the Classification of Cancer Cell Gene via Expressive Value Distance (EVD) Algorithm and Its Comparison to the Optimally Trained ANN Method*** *[#589]*
Tong Zhang, Sik Chung Tam, Chi-Hsu Wang and C.L. Philip Chen

6:20PM ***Adaptive Neural-Fuzzy Inference System for Classification of Rail Quality Data with Bootstrapping-Based Over-Sampling*** *[#592]*
Yong Yao Yang, Mahdi Mahfouf, George Panoutsos, Steve Thornton and Qian Zhang

6:40PM ***Passive Fuzzy Control for Uncertain Noulinear Stochastic Inverted Pendulum Robot System*** *[#219]*
Wen-Jer Chang, Sin-Sian Jheng and Cheung-Chieh Ku

(HCGC-5) Competition: Human vs. Computer Go Competition
Wednesday, June 29, 5:00PM-7:00PM, Room: Magpie, Chair: Chang-Shing Lee, Martin Muller, Olivier Teytaud, and Shun-Chin Hsu

Wednesday, June 29, 6:00PM-7:00PM

Invited Talk III: Activity Summarization from 3D Video Systems in an Eldercare Environment
Wednesday, June 29, 6:00PM-7:00PM, Room: Swan, Speaker: Jim Keller

Thursday, June 30, 8:00AM-10:20AM

(SS23) Special Session: Industrial Applications of Evolving Fuzzy Systems

Thursday, June 30, 8:00AM-10:20AM, Room: Swan, Chair: Kit Yan Chan

8:00AM ***Economic Load Dispatch using Intelligent Optimization with Fuzzy Control*** *[#105]*
Johnny C.Y. Lai, Frank H. Leung, S. H. Ling and Edwin C. Shi

8:20AM ***Hypoglycemia Detection using Fuzzy Inference System with Genetic Algorithm*** *[#28]*
Sai Ho Ling, Hung Nguyen and F.H.F Leung

8:40AM ***An Approach for Stability Analysis of Polynomial Fuzzy Model-Based Control Systems*** *[#280]*
Mohammad Narimani, Hak-Keung Lam, Kaspar Althoefer, Reza Shams Dilmaghani, Charles Wolfe and Christian Deters

9:00AM ***A Distributed Smart Routing Scheme for Terrestrial Sensor Networks with Hybrid Neural Rough Sets*** *[#588]*
Frank Jiang and Steve Ling

9:20AM ***P2P Traffic Identification and Optimization Using Fuzzy C-means Clustering*** *[#435]*
Duo Liu and Chung-Horng Lung

9:40AM ***Determination Of Process Conditions Of Epoxy Dispensing Processes Using A Genetic Algorithm Based Neural Fuzzy Networks*** *[#30]*
K. Y. Chan, T.S. Dillon, S. H. Ling and C.K. Kwong

10:00AM ***Manufacturing Modeling Using An Evolutionary Fuzzy Regression*** *[#31]*
K.Y. Chan, T.S. Dillon, S.H. Ling and C.K. Kwong

(MFI & RWA) Medical, Financial, Industrial and Other Real World Applications

Thursday, June 30, 8:00AM-10:20AM, Room: Peacock, Chair: James Keller

8:00AM ***A Heuristic Search and its Roughness*** *[#153]*
Chun-Hung Tzeng and Fu-Shing Sun

8:20AM ***Linguistic description of adult skeletal age-at-death estimations from fuzzy integral acquired fuzzy sets*** *[#164]*
Derek Anderson, Melissa Anderson, James Keller and Daniel Wescott

8:40AM ***Moving Pattern-based Approach to Modeling of a Class of Complex Production Processes*** *[#491]*
Zhengguang Xu and Changping Sun

9:00AM ***Multiple Characterisation Modelling of Friction Stir Welding Using a Genetic Multi-objective Data-driven Fuzzy Modelling Approach*** *[#596]*
Qian Zhang, Mahdi Mahfouf, George Panoutsos, Kathryn Beamish and Ian Norris

9:20AM ***Fuzzy Modeling to Predict Administration of Vasopressors in Intensive Care Unit Patients*** *[#429]*
Andre Fialho, Federico Cismondi, Susana Vieira, Joao Sousa, Shane Reti, Leo Celi, Michael Howell and Stan Finkelstein

9:40AM ***Probing Performance Evaluation for NPD Process by Using MCDM Approach*** *[#354]*
Chia-Chun Hsiang, Meng-Jong Kuan and Gwo-Hshiung Tzeng

10:00AM ***Application of Adaptive Self-Organizing CMAC_GBF to Aircraft Landing System*** *[#221]*
Jih-Gau Juang

(FSM & IS) Fuzzy Systems Modeling and Intelligent Systems

Thursday, June 30, 8:00AM-10:20AM, Room: Phoenix, Chair: Honghai Liu

8:00AM ***Optimal Necessary Conditions for General SISO Mamdani Fuzzy Systems as Function Approximators within a Given Accuracy*** *[#522]*
Fuchun Sun, Jin Yang, Minnan Luo and Huaping Liu

8:20AM ***A fuzzy stochastic programming approach to solve the capacitated lot size problem under uncertainty*** *[#493]*
Navid Sahebjamnia and S.Ali Torabi

8:40AM ***Look-ahead intelligent energy management of a parallel hybrid electric vehicle*** *[#278]*
Behnam Ganji, Abbas Z. Kouzani and Hamid Khayyam

9:00AM ***Dynamic Window with Fuzzy Controller in Wireless Sensor Networks for Elliptic Curve Cryptography*** *[#38]*
Xu Huang, Dharmendra Sharma and Pritam Gajkumar Shah

9:20AM ***Regulation for Wind Generation System Using Ant System Based Takagi Sugeno Fuzzy PID*** *[#260]*
Ahmad Besheer and Abdo Tamer

9:40AM ***Actuator Delayed Active Vehicle Suspension Control: A T-S Fuzzy Approach*** *[#396]*
Hongyi Li, Honghai Liu and Huijun Gao

10:00AM ***Hinf Disturbance Attenuation of Fuzzy Large-Scale Systems*** *[#66]*
Mehdi Hosseinzadeh, Nasser Sadati and Iman Zamani

(FST & GC) Fuzzy Set Theory and Granular Computing

Thursday, June 30, 8:00AM-10:20AM, Room: Crane, Chair: Gwo-Hshiung Tzeng

8:00AM ***Dualities between Indistinguishabilities and Related Concepts*** *[#518]*
Gabriel Mattioli and Jordi Recasens

8:20AM ***Graded equipollence and fuzzy c-measures of finite fuzzy sets*** *[#559]*
Michal Holcapek

8:40AM ***On monotonicity of type <1,1> fuzzy quantifiers determined by fuzzy measures*** *[#437]*
Antonin Dvorak and Michal Holcapek

9:00AM ***Generalized Fuzzy Imaginary Ideals of Rings*** *[#104]*
Zuhua Liao, Shu Cao, Qinghe Tian, Miaohan Hu and Yang Zhang

9:20AM ***Cellular Fuzzy Networks*** *[#59]*
Koosha Sadeghi Oskooyee, Mohammad Mansour Riahi Kashani and Mehrdad Jangjou

9:40AM ***Expatriate Manager Selection for an Overseas Manufacturing Site by Using FMCDM Methods*** *[#568]*
Chi-Yo Huang, Chih-Wei Wan and Gwo-Hshiung Tzeng

10:00AM ***On the Geometry of Join and Meet Calculations for General Type-2 Fuzzy Sets*** *[#8]*
Jerry Mendel

(SS36-1) Special Session: Fuzzy Systems on Renewable Energy

Thursday, June 30, 8:00AM-10:20AM, Room: Egret, Chair: Faa-Jeng Lin

8:00AM ***A Fuzzy-Based Output Power Smoothing of WECS using Short-Term Ahead Prediction of Wind Speed*** *[#97]*
Yuya Izumi, Alok Pratap, Yoshihisa Kinjyo, Akie Uehara and Endusa Billy Muhando

8:20AM ***Frequency and Voltage Control by Decentralized Controllable Loads with Fuzzy Control*** *[#332]*
Yoshihisa Kinjyo, Tomonobu Senjyu, Atsushi Yona, Nomitsu Urasaki and Toshihisa Funabashi

8:40AM ***Short-Term Load Forecasting Via Fuzzy Neural Network With Varied Learning Rates*** *[#27]*
Rong-Jong Wai, Yi-Chang Chen and Yung-Ruei Chang

9:00AM ***A Fuzzy Control Maximum Power Point Tracking Photovoltaic System*** *[#133]*
Irwan Purnama, Lo Yu-Kang and Chiu Huang-Jen

9:20AM ***Fuzzy Control of MW-class PV Generation to Reduce Frequency and Tie-line Power Fluctuations in Three Control Area Power System*** *[#391]*
Manoj Datta, Tomonobu Senjyu, Atsushi Yona and Toshihisa Funabashi

9:40AM ***A Fuzzy-Rule Based Power Restoration Approach for a Distribution System with Renewable Energies*** *[#327]*
Hong-Tzer Yang, Jian-Tang Liao and Xiang-He Su

10:00AM ***Neuro-Fuzzy Predictive Model for PV Energy Production based on Weather Forecast*** *[#539]*
Francesco Grimaccia, Marco Mussetta and Riccardo E. Zich

(FS & FDM) Fuzzy Clustering and Fuzzy Data Mining
Thursday, June 30, 8:00AM-10:20AM, Room: Swallow, Chair: Tzung-Pei Hong

8:00AM ***Fuzzy Clustering Approach for Star-Structured Multi-Type Relational Data*** *[#165]*
Jian-Ping Mei and Lihui Chen

8:20AM ***Predicting Septic Shock Outcomes in a Database with Missing Data using Fuzzy Modeling*** *[#427]*
Ruben Pereira, Andre Fialho, Federico Cismondi, Susana Vieira, Joao Sousa, Rui Almeida, Uzay Kaymak, Shane Reti, Michael Howell and Stan Finkelstein

8:40AM ***A normalized soft window-based similarity measure to extend the Rand index*** *[#405]*
Romain Quere and Carl Frelicot

9:00AM ***Fuzzy Clustering With Learnable Cluster Dependent Kernels*** *[#149]*
Ouiem Bchir and Hichem Frigui

9:20AM ***The Interval Autoregressive Time Series Model*** *[#236]*
Xun Wang and Shoumei Li

9:40AM ***Feature Evaluation Based Fuzzy C-Mean Classification*** *[#229]*
Mostafa A. Salama, Aboul Ella Hassanien and Aly A. Fahmy

10:00AM ***A Clustering Method for Geometric Data based on Approximation using Conformal Geometric Algebra*** *[#386]*
Minh Tuan Pham, Kanta Tachibana, Tomohiro Yoshikawa and Takeshi Furuhashi

(HA) Hybrids and Other Applications
Thursday, June 30, 8:00AM-10:20AM, Room: Magpie, Chair: Bor-Sen Chen

8:00AM ***Improving Estimation Accuracy of the COCOMO II Using an Adaptive Fuzzy Logic Model*** *[#237]*
Iman Attarzadeh and Siew Hock Ow

8:20AM ***Fuzzy-Rough Set based Semi-Supervised Learning*** *[#259]*
Neil Mac Parthalain and Richard Jensen

8:40AM ***An Application of Genetic Fuzzy Systems for Wireless Sensor Networks*** *[#418]*
Liliam Leal, Marcus Lemos, Raimir Holanda, Ricardo Rabelo and Fabbio Borges

9:00AM ***On Predicting Learning Styles in Conversational Intelligent Tutoring Systems using Fuzzy Classification Trees*** *[#304]*
Keeley Crockett, Annabel Latham, Zuhair Bandar, James O'Shea and David Mclean

9:20AM ***Signal Transduction Ability Measurement of Signaling Pathways in Intracellular Communication via Fuzzy Method*** *[#501]*
Chia-Chou Wu and Bor-Sen Chen

9:40AM ***Long-term business cycle forecasting using intuitionistic fuzzy least-squares support vector regression*** *[#348]*
Kuo-Ping Lin, Kuo-Chen Hung and Ming-Chang Wu

Thursday, June 30, 10:50AM-12:00PM

Keynote Speech III: Soft Computing for Hard Pattern Recognition Problems
Thursday, June 30, 10:50AM-12:00PM, Room: Grand Ballroom I, Speaker: Paul Gader

Thursday, June 30, 1:30PM-2:30PM

(FOD) Fuzzy Optimization and Design
Thursday, June 30, 1:30PM-2:30PM, Room: Swan, Chair: Chia-Feng Juang

1:30PM ***Production Planning with Uncertain Demands*** *[#35]*
Guillaume Romain, Kobylanski Przemyslaw and Zielinski Pawel

1:50PM ***Min-Max and Two-Stage Possibilistic Combinatorial Optimization Problems*** *[#69]*
Kasperski Adam and Zielinski Pawel

2:10PM ***A Fuzzy Concept for Climate Management in Preventive Conservation*** *[#146]*
Christian Arnold, Steven Lambeck and Christoph Ament

(FO & FEC) Fuzzy Optimization and Fuzzy Emotional Computing
Thursday, June 30, 1:30PM-2:30PM, Room: Peacock, Chair: Chuan-Yu Chang

1:30PM ***Fuzzy Bipolar Conditions of Type "or else"*** *[#33]*
Ludovic Lietard, Nouredine Tamani and Daniel Rocacher

1:50PM ***Fuzzy Optimization Model Based Tolerance Approach to Timetable Rescheduling for High Speed Railway in China*** *[#130]*
Yong Qin, Li Wang, Huan Lian, Xuelei Meng, Xuewen Li, Fugui Shi and Limin Jia

2:10PM ***Online Neuro-Fuzzy CANFIS Hidden-Node Teaching*** *[#402]*
Eiji Mizutani and Jing-Yun Fan

(RS & RDA) Rough Sets and Rough Data Analysis
Thursday, June 30, 1:30PM-2:30PM, Room: Phoenix, Chair: Yo-Ping Huang

1:30PM ***Fuzzy Fusion Fairness Relations for the Evaluation of User Preference*** *[#358]*
Mario Koeppen, Jun Okamoto and Aoi Honda

1:50PM ***Multiple Criteria Group Decision Making with Triangular Interval Type-2 Fuzzy Sets*** *[#409]*
Kuo-Ping Chiao

2:10PM ***Noise Control in Document Classification Based On Fuzzy Formal Concept Analysis*** *[#207]*
Sheng-Tun Li and Fu-Ching Tsai

(T2FL) Type-2 Fuzzy Logic
Thursday, June 30, 1:30PM-2:30PM, Room: Crane, Chair: Hao Ying

1:30PM ***Deriving the Input-Output Mathematical Relationship for a Class of Interval Type-2 Mamdani Fuzzy Controllers*** *[#193]*
Haibo Zhou and Hao Ying

1:50PM ***Design of Interval of Type-2 Fuzzy Logic Controllers for Flocking Algorithm*** *[#231]*
Seung-Mok Lee, Jong-Hwan Kim and Hyun Myung

2:10PM ***Is it rational to partition a data set using Kernel-clustering?*** *[#536]*
Kaushik Sarkar and Nikhil R Pal

(SS36-2) Special Session: Fuzzy Systems on Renewable Energy
Thursday, June 30, 1:30PM-2:30PM, Room: Egret, Chair: Faa-Jeng Lin

1:30PM ***Fuzzy Quantum Computation Based Thermal Unit Commitment Strategy with Solar-battery System Injection*** *[#312]*
Shantanu Chakraborty, Tomonobu Senjyu, Atsushi Yona and Toshihisa Funabashi

1:50PM ***Control of Doubly-Fed Induction Generator System Using PFNN*** *[#46]*
Faa-Jeng Lin, Kuang-Hsiung Tan, Zong-Han Lu and Yung-Ruei Chang

(FDM & DSS-1) Fuzzy Decision Making and Decision Support Systems
Thursday, June 30, 1:30PM-2:30PM, Room: Swallow, Chair: Bao-Rong Chang

1:30PM ***Web User Identification with Fuzzy Fingerprints*** *[#203]*
Nuno Homem and Joao Carvalho

1:50PM ***Fuzzy Multiattribute Evaluation of Airport Performance*** *[#500]*
Chung-Hsing Yeh, Yu-Hern Chang and Yu-Liang Kuo

2:10PM ***An Intelligent Decision Support Tool Based on Belief Rule-Based Inference Methodology*** *[#305]*
Alberto Calzada, Jun Liu, Hui Wang, Luis Martinez and Kashyap Anil

(HFS) Hybrid Fuzzy Systems
Thursday, June 30, 1:30PM-2:30PM, Room: Magpie, Chair: I-Fang Chung

1:30PM ***Fuzzy Controller Design Using Group-Crossover Particle Swarm Optimization for Truck Reversing Control*** *[#225]*
Chia-Feng Juang, Yu-Cheng Chang, Chia-Hung Hsu and I-Fang Chung

1:50PM ***Evolving Ensemble of Fuzzy Models*** *[#85]*
Eng Yeow Cheu, Chai Quek and See Kiong Ng

2:10PM ***Long Term Bank Failure Prediction using Fuzzy Refinement-based Transductive Transfer Learning*** *[#467]*
Vahid Behbood, Jie Lu and Guangquan Zhang

Thursday, June 30, 2:50PM-4:30PM

(SS29) Special Session: Software Engineering with Computational Intelligence
Thursday, June 30, 2:50PM-4:30PM, Room: Swan, Chair: Nien-Lin Hsueh

2:50PM ***Developing a Fuzzy Search Engine Based on Fuzzy Ontology and Semantic Search*** *[#107]*
Lien-Fu Lai, Chao-Chin Wu, Pei-Ying Lin and Liang-Tsung Huang

3:10PM ***Multi-Agent Automatic Negotiation and Argumentation for Courses Scheduling*** *[#213]*
Jong Yih Kuo, Hsuan-KueiI Cheng, Yong-Yi FanJiang and Shang-Pin Ma

3:30PM ***Investment Decision Making by Using Fuzzy Candlestick Pattern and Genetic Algorithm*** *[#563]*
Chiung-Hon Lee, Lindroos Hsu and Yi-Ching Liaw

3:50PM ***Fuzzy Logic as a Basic for Use Case Point Estimation*** *[#577]*
Jonathan Lee, Wen-Tin Lee and Jong-Yih Kuo

4:10PM ***Fuzzy Lymphedema Assessment based on Clinical and Functional Criteria*** *[#524]*
Ernesto Araujo, Patricia Vicentini and Maria C. J. Perez

(SS34) Special Session: Brain and Learning
Thursday, June 30, 2:50PM-4:30PM, Room: Peacock, Chair: Toshihiko Watanabe

2:50PM ***Decision Making Based on Reinforcement Learning and Emotion Learning for Social Behavior*** *[#293]*
Atsushi Matsuda, Hideaki Misawa and Keiichi Horio

3:10PM ***Analysis of Relationship between Characteristics of Driver's Eye Movements and Visual Scene in Driving Events*** *[#561]*
Tetsuya Miyoshi and Hidetoshi Nakayasu

3:30PM ***Directional Control of an Omni-Directional Walker for Walking Support with Forearm Pressures*** *[#233]*
Yinlai Jiang, Shuoyu Wang, Kenji Ishida, Takeshi Ando and Masakatsu G. Fujie

3:50PM ***Construction of Collision Avoidance Behavior Model Induced by Visual Motion*** *[#457]*
Norifumi Watanabe, Hiroaki Mikado and Takashi Omori

4:10PM ***Instruction Knowledge Acquisition for Reinforcement Learning Scheme by PSO Algorithm*** *[#564]*
Toru Sawa and Toshihiko Watanabe

(SS35) Special Session: Fuzzy Regression Analysis and Its Applications
Thursday, June 30, 2:50PM-4:30PM, Room: Phoenix, Chair: M. Hadi Mashinchi

2:50PM ***A Formula for Fuzzy Linear Regression Analysis*** *[#374]*
Chi-Tsuen Yeh

3:10PM ***Real-Time Analysis of Granular Information: Some Initial Thoughts on a Convex Hull-based Fuzzy Regression Approach*** *[#175]*
Azizul Azhar Ramli, Witold Pedrycz, Junzo Watada and Nureize Arbaiy

3:30PM ***An Interval-Based Approach to Fuzzy Regression for Fuzzy Input-Output Data*** *[#215]*
Jalal Chachi, Taheri Seyed Mahmoud and Hojat Rezaei Pazhand

3:50PM ***Study of Dependency between the Input Noise and the Parameter in Fuzzy Linear Regression Model*** *[#372]*
Hongwei Ge, Shitong Wang and Wei Song

(SS41) Special Session: Neuro Fuzzy Systems and Their Real World Application
Thursday, June 30, 2:50PM-4:30PM, Room: Crane, Chair: Sungshin Kim

2:50PM ***Daily Reservoir Inflow Forecasting Using Fuzzy Inference Systems*** *[#542]*
Ivette Raymunda Luna Huamani, Rosangela Ballini, Ieda Geriberto Hidalgo, Paulo Sergio Franco Barbosa and Alberto Luiz Francato

3:10PM ***A Study on Hybrid Model of HMMs and GMMs for Mirror Neuron System Modeling using EEG Signals*** *[#289]*
Seung-Min Park, Junheong Park, Kwang-Eun Ko and Kwee-Bo Sim

3:30PM ***Optimal Input Selection for Neural Fuzzy Modelling With Application to Charpy Energy Prediction*** *[#601]*
Yong Yao Yang, Mahdi Mahfouf and Qian Zhang

3:50PM ***Stereo Vision-Based Self-Localization System for RoboCup*** *[#555]*
Jen-Shiun Chiang, Chih-Hsien Hsia, Hung-Wei Hsu and Chun-I Li

4:10PM ***Training Multilayer Perceptron By Using Optimal Input Normalization*** *[#488]*
Xun Cai, Kanishka Tyagi and Michael Manry

(SS25) Special Session: Evolving and Adaptive Fuzzy Systems
Thursday, June 30, 2:50PM-4:30PM, Room: Egret, Chair: Plamen Angelov

2:50PM ***Automatic Scene Recognition for Low-Resource Devices using Evolving Classifiers*** *[#583]*
Andreu Javier, Dutta Baruah Rashmi and Angelov Plamen

3:10PM ***Real Time Recognition of Human Activities from Wearable Sensors by Evolving Classifiers*** *[#415]*
Javier Andreu, Rashmi Dutta Baruah and Plamen Angelov

3:30PM ***Fuzzy Granular Evolving Modeling for Time Series Prediction*** *[#210]*
Daniel Leite, Fernando Gomide, Rosangela Ballini and Pyramo Costa

3:50PM ***Combustion Engine Modelling using an Evolving Local Model Network*** *[#84]*
Christoph Hametner and Stefan Jakubek

4:10PM ***Rough Set Approach to User Modeling*** *[#71]*
Binghui Helen Wu

(SS24) Special Session: Hybrid Learning for Fuzzy Systems
Thursday, June 30, 2:50PM-4:30PM, Room: Swallow, Chair: Jin-Tsong Jeng

2:50PM ***A Rough-based Robust Support Vector Regression Network for Function Approximation*** *[#212]*
Chih-Ching Hsiao, Shun-Feng Su and Chen-Chia Chuang

3:10PM ***An Immune Symbiotic Evolution Learning for Compensatory Neural Fuzzy Networks and Its Applications*** *[#32]*
Cheng-Hung Chen, Cheng-Jian Lin and Chin-Teng Lin

3:30PM ***Identification of Time-Delay Chaotic System with Outliers: Fuzzy Neural Networks Using Hybrid Learning Algorithm*** *[#214]*
Chia-Nan Ko, Yu-Yi Fu, Guan-Yu Liu and Cheng-Ming Lee

3:50PM ***A New Framework of Fuzzy Clustering Algorithm*** *[#99]*
Horng-Lin Shieh

4:10PM ***Modeling of Fuzzy Integral Based Nonlinear Multi-regressions Systems with QPSO-GS*** *[#270]*
You-Min Jau and Jin-Tsong Jeng

(SS32) Special Session: Adaptive Fuzzy Logic Control
Thursday, June 30, 2:50PM-4:30PM, Room: Magpie, Chair: Tsung-Chih Lin

2:50PM ***Direct Adaptive Fuzzy Control for Nonaffine Nonlinear Systems with Unknown Control direction*** *[#20]*
Salim Labiod and Thierry Marie Guerra

3:10PM ***An Observer Based Adaptive Iterative Learning Control for Robotic Systems*** *[#169]*
Ying-Chung Wang and Chiang-Ju Chien

3:30PM ***Synchronization of uncertain fractional order chaotic systems via adaptive interval type-2 fuzzy sliding mode control*** *[#80]*
Tsung-Chih Lin, Tun-Yuan Lee and Emilia Balas Valentina

3:50PM ***Fractional order chaotic system tracking design based on adaptive hybrid intelligent control*** *[#83]*
Tsung-Chih Lin, Chia-Hao Kuo and Emilia Balas Valentina

Thursday, June 30, 5:00PM-6:00PM

(SS22) Special Session: Fuzzy Methods in Machine Learning and Data Mining
Thursday, June 30, 5:00PM-6:00PM, Room: Swan, Chair: Shi-An Chen and Enrique Munoz

5:00PM ***Towards the Learning from Low Quality Data in a Fuzzy Random Forest ensemble*** *[#299]*
Jose M. Cadenas, M. Carmen Garrido, Raquel Martinez and Piero P. Bonissone

5:20PM ***Non-monotone averaging aggregation*** *[#480]*
Gleb Beliakov, Shui Yu and Daniel Paternain

5:40PM ***Linguistic Local Change Comparison Of Time Series*** *[#147]*
Rita Castillo-Ortega, Nicolas Marin and Daniel Sanchez

(FCW & PT) Fuzzy Computing with Words and Possibility Theory
Thursday, June 30, 5:00PM-6:00PM, Room: Peacock, Chair: Chin-Wang Tao

5:00PM ***Indirect Adaptive Model Predictive Control Supervised by Fuzzy Logic*** *[#434]*
Jerry Mamboundou and Nicolas Langlois

5:20PM ***Maximum likelihood principle for possibility distributions viewed as families of probabilities*** *[#319]*
Mathieu Serrurier and Henri Prade

(SS07 & SS33) Special Session: Metaheuristics and Its Applications & Fuzzy and Paraconsistent Intelligent Systems
Thursday, June 30, 5:00PM-6:00PM, Room: Phoenix, Chair: Chun-Wei Tsai and Shih-Yu Li

5:00PM ***Ant Colony Optimization with Dual Pheromone Tables for Clustering*** *[#378]*
Chun-Wei Tsai, Kai-Cheng Hu, Ming-Chao Chiang and Chu-Sing Yang

5:20PM ***Job Shop Scheduling Based on ACO with a Hybrid Solution Construction Strategy*** *[#376]*
Shih-Pang Tseng, Chun-Wei Tsai, Jui-Le Chen, Ming-Chao Chiang and Chu-Sing Yang

5:40PM ***The Sensing System for the Autonomous Mobile Robot Emmy III*** *[#321]*
Claudio Torres, Jair Abe, Germano Lambert-Torres and Joao da Silva Filho

(IA) Informatics & Analytics
Thursday, June 30, 5:00PM-6:00PM, Room: Crane, Chair: Janusz Kacprzyk and Lawrence Mazlack

5:00PM ***On a benchmark related assessment of the performance of mutual (investment) funds*** *[#297]*
Anna Wilbik and Janusz Kacprzyk

5:20PM ***Discerning Suicide Notes Causality Using Fuzzy Cognitive Maps*** *[#545]*
Ethan White and Lawrence Mazlack

(SS13-2) Special Session: Fuzzy Multiple Criteria Decision Making
Thursday, June 30, 5:00PM-6:00PM, Room: Egret, Chair: Gwo-Hshiung Tzeng

5:00PM ***Constant Penalty Functions to Simplify Optimization of the Choquet Integral under Constraints*** *[#235]*
Tanja Magoc

5:20PM ***Design of a reliable hub-and-spoke network using an interactive fuzzy goal programming*** *[#489]*
Mohammad Hossein Fazel Zarandi, Soheil Davari and Ali Haddad Sisakht

(FDM & DSS-2) Fuzzy Decision Making and Decision Support Systems
Thursday, June 30, 5:00PM-6:00PM, Room: Swallow, Chair: Kuang-Yow Lian

5:00PM ***Connection Manager : A FAHP-based System for Classifier and Decision-Making*** *[#198]*
Chih-Wei Hsu and Sheng-Tzong Cheng

5:20PM ***Approximate Confidence Interval for Generalized Taguchi Process Capability Index*** *[#460]*
Abbas Parchami, Mashaallah Mashinchi and M. Hadi Mashinchi

5:40PM ***Generalized Intuitionistic Fuzzy Soft Set and its Application in Practical Medical Diagnosis Problem*** *[#131]*
Manish Agarwal, Madasu Hanmandlu and Kanad K. Biswas

Contributed Papers

2011 IEEE International Conference on Fuzzy Systems
June 27-30, 2011, Taipei, Taiwan

Gesture-Based Hybrid Approach for HCI in Ambient Intelligent Environmments

Stefano Carrino, Elena Mugellini,
Omar Abou Khaled
Department of Telecommunications
and Computer Science
College of Engineering and Architecture of Fribourg
Fribourg, Switzerland
{Stefano.Carrino, Elena.Mugellini,
Omar.AbouKhaled}@hefr.ch

Rolf Ingold
Department of Informatics
University of Fribourg
Fribourg, Switzerland
Rolf.Ingold@unifr.ch

***Abstract*—In this paper we propose a novel interaction approach, based on gestures, aiming to recognize and enhance interactions between augmented human beings and augmented environments. We explain how this model, we called ARAMIS, allows interaction designers to fill the gap between real and virtual worlds augmenting the human itself. An enhanced interaction is achieved exploiting a hybrid approach. This approach is defined hybrid since it is the combination of several complementary techniques: wearable and pervasive computing paradigms, brute force, fuzzy and ML methods, virtual and real worlds, optical and non-optical sensing technologies. A framework implementing this concept has been developed. Finally, in order to validate our approach, we present a first prototype implemented according to the ARAMIS concept.**

Keywords – HCI, Ambient Intelligence, gesture-based interaction, hybrid-approach

I. INTRODUCTION

People naturally communicate through the voice, gestures, expressions and movements. In HCI area several researches are addressing the design of natural user interfaces allowing the machine to understand the natural language of human beings [1]. In order to allow this kind of communication and bridge the gap between the human and the machine, natural interactions have to be understood by the system. With the same logic the system must provide a feedback as natural as possible. Although these are still opened research fields, at present AmI systems intrinsically have the potential to implement augmented natural-interaction[1]. For instances many of the manipulations used on multi-touch screens, such as the pinch, have no natural counterpart in our interactions with everyday life (it is not possible to pinch a piece of paper to make it smaller, while preserving its aspect ratio). This concept can be highly extended taking into account possibilities provided (at present or in the next years) by novel interaction vectors as smart, mixed reality environments and the approaching internet of things. In these cases the interaction experienced by the users can be extremely richer than the common interaction of every day [2].

The major contribution presented in this paper is the proposition of a hybrid interaction approach, called ARAMIS, aiming to enhance natural gesture-based interaction between humans and smart environments. Our approach is defined hybrid since it is based on four complementary approaches: environmental/wearable paradigms, brute force/fuzzy/machine learning methods, real/virtual worlds, optical/non-optical sensing technologies. ARAMIS uses this heterogeneity in order to exploit the strong points of individual approaches or technologies, and to overcome their weakness (such as light condition sensitivity in vision-based techniques or heavy training for neural network algorithms).

This paper is organized as follow: Section II presents some related work on the interaction between augmented human and smart environments. Section III briefly presents an envisioning scenario highlighting augmented interactions between the user and smart environments. Section IV describes the ARAMIS approach. Section V introduces how the ARAMIS framework handles the information. Section VI illustrates the implementation of the ARAMIS concept and a first prototype. Finally section VII concludes the paper.

II. RELATED WORKS

Studies on human augmentation through the technology have a long history in HCI domain. Since the works of Engelbart [3] the possibility to augment human capacities using the technology was taken into account. If the first studies focused on approaches to improve human abilities to deal with everyday issues, afterwards the problem changed with the years; technology evolved and from human-machine interaction scientific community starts to talk about human-machine cooperation [4], envisioning a kind of communication based on similitudes with the human-human interaction. Moreover, since the environment surrounding the human was progressively changing in something richer and at the same time more complex (in the interfaces, tools and objects), the

[1] Natural interaction is seen in this paper as the computers capability to exploit the perceptive abilities which so far have been a prerogative of human–human communication

978-1-4244-7316-8/11/$26.00 ©2011 IEEE

need of an approach encompassing the wearable and pervasive dimension is becoming a central issue. Under this perspective Greenberg et al. [5] defines a novel interaction approach between users and pervasive devices based on their relative proximity (distance, orientation, identity, movement, and location). Pederson et al. [6] present an egocentric interaction model, in which wearable and pervasive paradigms are combined and interactions are classified based on human perceptual characteristic such as what can be observed and what can be manipulated. This model aimed at bridging the gap between real and mixed reality worlds. We differ from previous approaches by providing a perspective in which also the human has to be augmented in order to extend the interaction toward an augmented natural-interaction and, in addition, we focus on hybrid middleware able to take advantages from different techniques.

III. INTERACTION SCENARIO

This section briefly presents a scenario envisioning the augmented interactions possibilities offered by augmented human in smart environments.

Context: Human-computer interactions (HCI) taken into account in this project have as context a smart environment, with real and virtual interactive devices available inside, and a set of wearable devices woven seamlessly on the user. Alice, the system user, coming back home, is wearing her glasses (actually a head-mounted display). The house is an environment enriched by real and digital elements. Alice through gestures can interact with the surrounding environment in a natural, augmented way.

Interaction with virtual objects (virtual screen): Alice seats in her sofa and with a simple gesture (recognized through sensors woven in her clothes and sensors in the environments) a virtual screen appears in front of her. Passing a hand on the virtual screen, the hand changes shape becoming a mouse pointer and allowing an easier interaction with the screen (without the problem of occlusion, since the virtual objects can be superposed to the real hand). To watch a movie from her sofa she chooses to enlarge the screen and put it on the ceiling: she grabs the virtual screen corners and stretches her arms until the ceiling tuning the screen position, size and orientation (showed in Figure 1). After some time, enjoying the comfort of the sofa, she starts reading a book that is a virtual representation of a real, book that is physically placed in another room.

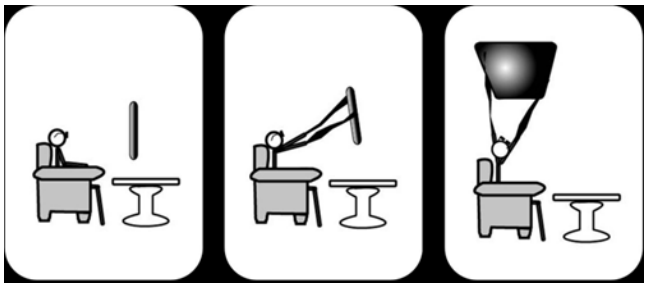

Figure 1. Interaction with a virtual screen

Virtual access to real objects: Alice decides to wear her precious earrings; hence, to open her strongbox, she has to digit the right password in a virtual display that is accessible only in the virtual dimension of the house. In this case the strongbox is a physical object in the real world whereas its command interface is in the digital world.

This scenario highlights the augmented interaction key points and the motivation behind the ARAMIS model. In the next sections it is explained how the presented augmented interactions are modeled in ARAMIS and how ARAMIS handles them.

IV. ARAMIS: BASIC CONCEPT AND BACKGROUND

Gestures are a natural way for a person to interact with the environment, tools and the objects around him [7]. For this reason ARAMIS is focused on gestures as main communication modality. However the ARAMIS approach can be used to model different type of modalities (e.g. voice, touch, etc.) and it can be easily extended toward multimodal approaches.

Since gestures lack in universality (gestures have not the same meaning everywhere) and in order to propose general principles, ARAMIS does not establish a gesture lexicon, but allows detecting different command gestures according to different application and usage contexts.

A. Why a Hybrid Approach

In this section the proposed hybrid approach is presented in its four components highlighting the advantages in the use of these complementary techniques.

Pervasive and Wearable paradigms

Coupling pervasive and wearable paradigms is possible to merge the advantages of both approaches. Table 1 presents the different features form the two approaches as presented in [8] and [9]).

Table 1. Features provided by the pervasive and the wearable approach

FEATURES	*PERVASIVE*	*WEARABLE*
Privacy		**X**
Personalization		**X**
Consistency		**X**
Localized information	**X**	
Localized control	**X**	
Resources	**X**	

Pervasive paradigm provides localized information, controls and resources; whereas wearable paradigm provides privacy, personalization and consistency. Using at the same time pervasive and wearable approaches some features, such as personalization and localized control can be combined to improve user interaction with the system. However the mutual improvement between these paradigms is further increased by our approach. For example information can be fitted and displayed for specified users according to their profiles and interaction context (information from the user and the environment); moreover exploiting virtual elements this

information is still private and personalized. Also the resource management will benefit of our hybrid approach. In ARAMIS data is elaborated in the wearable (mobile) system or/and in the environmental (fixed), according to the type of information to handle, the available devices and the quality of the connection. For instance, data that is troublesome to transfer, such as a high frequency data from the accelerometers, can be elaborated locally on the wearable machine and just the processed information (e.g. extracted features) is sent further. On the other hand information that is heavy to elaborate (e.g. images) can be elaborated at environmental side (more details can be found in [8] and [9]).

As stated above, the merging of these paradigms brings the combination of their related strong points. However to make this possible a lot of issues have to be faced (e.g. heterogeneous devices working asynchronously and with different data rates must be able to rapidly exchange information in order to effectively take advantage one from the other).

Mixed Reality

Gestures are performed in a mixed (real and virtual) world. As presented in the scenario, the presence of digital components is the enabling factor to enhance the interaction. It allows avoid physical constraints (object can be suspended in the air, people can stretch their arms, etc.) and defining new ways of interaction. In ARAMIS two entities are augmented by the technology: the human and the environment. A user avatar is used to represent a human being, and especially the body parts involved in the interaction, in a mixed world (e.g. in a system designed for hands and arms interaction only these parts will be augmented). Since the human representation is digital, the avatar is not tied to physical laws and not necessarily something of visible (e.g. the avatar is not an anthropomorphic digital representation of the user, an avatar can be a simple pointer representing the user hand). Hence, the user avatar can change considerably from an application to another since it depends on the gesture vocabulary, the context and the kind of mixed reality implemented for the interaction and the feedback. Finally the avatar has the goal of facilitating and enhancing the interaction.

Human augmentation becomes valuable in the case the surrounding environment provides rich interfaces of interaction and feedback modalities: we called such ambience augmented (or smart) environment. Our approach defines augmented environments as composed by two kinds of elements: objects and places. 1) Objects can be pure real, pure virtual or enhanced. With the adjective enhanced we classify objects that have the double nature: real and virtual. It means that it is possible to interact with them as normal or virtual objects. For example a book, that can be read directly (physically) or displayed on a screen (virtual representation), belongs to this category. Moreover the simultaneous existence of a real object, its digital counterpart and a suitable feedback interface helps the user in the interaction with tools solving part of the problems tied to the use of a ubiquitous, invisible computer [10]. 2) Places are mixed reality entities integrated in the ARAMIS system that describe interactive objects and their state (id, position, activation state, etc.).

Classification techniques

ARAMIS hybrid approach combines different classification techniques in order to implement decision tasks: brute force, machine learning, fuzzy logic, or neuro-fuzzy [11]. According to the interaction to be implemented and the context of use one or a combination of these techniques can be used.

With a brute force approach is possible to interpret simple data in order to have less computation and, therefore, improve performances [12]. Training is not needed and algorithms are generally simple. This improves speed in recognition but brings limitations in the gestures complexity that can be handled; additional complexity must be introduced in order to make the system user adaptive. With gesture of higher complexity, statistical model and machine learning approaches could be used. Analyzing complex gestures is often not possible or too complicated using brute force algorithms. Machine learning (ML) algorithms can be a solution (especially Hidden Markov Model (HMM) and Artificial Neural Networks (ANN) are used in the gesture recognition field) [13] . However ML solutions require often a large quantity of data to train and to learn the system (for example a neural network can be initialized with random values but it will need training sessions to update these values). Moreover to achieve good results, an algorithm structure may require several calibration sessions and user knowledge of the system can speed up this practice. However tuning such systems can take hours or days of computer time because networks may converge on an inappropriate solution or rule or may fail to converge at all [14]. Neural researchers have proposed hundreds of schemes to alleviate this problem, but none has removed it. Even after a lengthy tuning session, the final rules may not be much better than the first set. Moreover “an impediment to a more widespread acceptance of ANN’s is the absence of a capability to explain to the user, in a human-comprehensible form, how the network arrives at a particular decision. Neither can one say something about the knowledge encoded within the black-box” [11].

Facing these issues and aiming to improve the velocity of the computation is possible using a fuzzy logic (FL). Fuzzy sets are considered to be advantageous in handling higher order processing. Although generally faster than ML often FL systems require experience (of the system developer) in order to configure properly the system. In fact the goal of FL is to simulate the behavior of an expert addressing complex problems, instead of analyzing a problem in detail [15].

Rather than relying on an expert to supply a training set of data and correct a network in the process of learning, unsupervised neural networks learn simply by observing an expert's decisions. In this way, an adaptive fuzzy system can learn to spot rule patterns in the incoming data. In other words adaptive systems can help fuzzy systems learning rules and the merits of both neural and fuzzy systems can be integrated in a neuro–fuzzy approach (NFA). In fact NFA are used to realize a fuzzy system through the connectionist networks, with the advantage that is it possible to extract rules without the need of an expert [16].

The following diagram (in Figure 2) schematizes the strong points and the weakness of these four approaches. The parameters taken into account are: speed of the classification,

need of a large training dataset, capability to recognize complex gestures and need of experience to "tune" the algorithm.

The main idea if ARAMIS concept is to combine these methods flexibly, aiming to take advantage of the more suitable solution according the information to analyze.

Optical and Non-Optical sensing technologies

Combining more acquisition technologies brings several advantages. Different sensors, working with different technologies make possible to have a more robust and accurate dataset. So far, several technologies (vision-based, inertial and acoustic) have been considered. Researches highlighted advantages and drawbacks for any technology. Therefore an approach is usually adapted to specific use cases and contexts [17]. For example optical technologies give very useful information but are expensive in term of processing power if more than one sensor is considered. In addition, sensibility to lighting changes is still an open issue in computer vision domain. Otherwise inertial sensors are more resistant to environmental changes, can be easily embedded in small devices, but suffer for systematic and incremental errors, necessitating a recalibration phase for long measures.

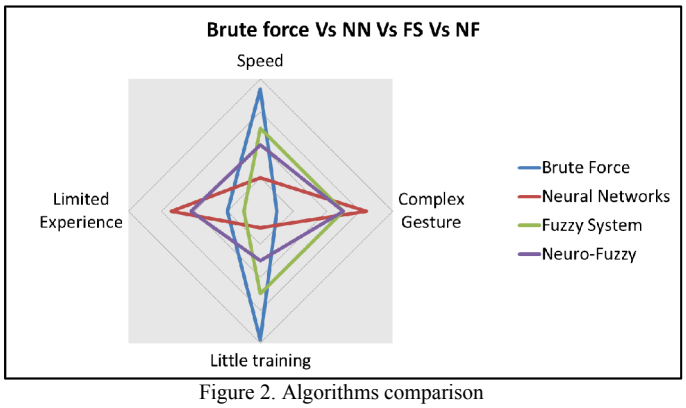

Figure 2. Algorithms comparison

B. *Working Configurations*

Thanks to the proposed hybrid approach ARAMIS is suitable for three working configurations from totally wearable (augmented human) to totally pervasive (augmented environment):

- Augmented human in augmented environment. This is the standard case of use of our system. Our model provides the maximum of augmentation in the interactions. Information provided at the two levels (pervasive and wearable) are merged and exploited to recognize the interaction and provide the feedback.

- Human (without wearable devices) in augmented environment. A reduced interaction lexicon will be recognized at the environment level (e.g. through fixed cameras), and the feedback is presented back to the user in different ways such as acoustic, or visual output.

- Augmented human in normal environment. Also in this case a reduced vocabulary is recognized and the interaction with the environment takes the form of contextual information provided by the wearable devices (e.g. approach used in smart-phones for some augmented reality applications).

The major issue in a combined wearable-environmental approach is the data transmission and fusion between the different entities. Data are heterogeneous and asynchronous. Hence, the elaboration can be complex and, above all, too slow to achieve real-time interaction. Therefore, in order to demonstrate the feasibility of our concept a concrete framework has been realized.

V. ARAMIS: THE FRAMEWORK

Figure 3 shows an overview of the ARAMIS framework and how it handles the information and the decision mechanisms. This framework is service-oriented; it means that each component exposes some method as service that can be flexibly used by other components running on the same machine or exploiting a network.

The framework representation in Figure 3 reflects the hybrid approach presented above separating the environmental and the wearable modules.

A. *Information handling*

Usually, environmental modules have more processing capabilities than wearable modules but the transfer of the information between the different devices can be quite expensive in term of time and bandwidth occupation. In order to optimize the elaboration task the ARAMIS framework allows the information from any sensors to be handled according to three different paths. Raw data that are expensive to be processed (e.g. data from accelerometers needing the extraction of several features) are transmitted to the environmental side and then elaborated (path 1). At the contrary, data that is heavy to transfer (e.g. high quality frames from the camera) has the main features extracted in the module in which is sensed and then sent ahead for further elaboration (such as features fusion according to the path 2). Whereas the information from the worn devices is enough to be analyzed autonomously, gesture can be recognized separately at environmental and wearable side and only the final decision

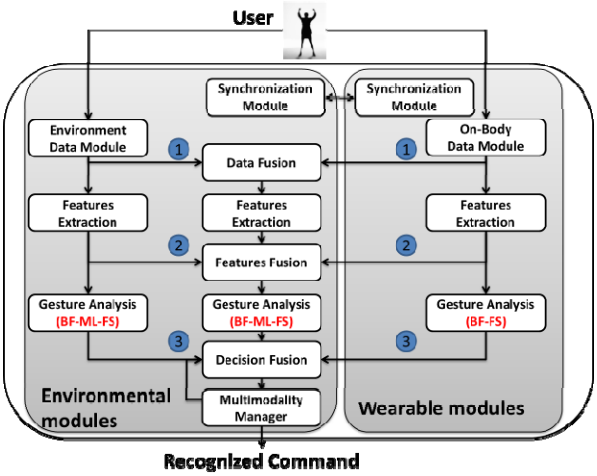

Figure 3. ARAMIS framework – Overview

(path 3) will be pondered and merged (more information about the framework can be bound in the paper [9]).

B. Decision algorithms handling

The gesture analysis modules analyze features in order to classify the input provided by the user. Once again because of the different capabilities between the wearable and pervasive modules it becomes interesting to differentiate and tune the algorithms to be adopted according the type of input and the used devices. At wearable side it will be better to use algorithms fast and requiring small training dataset such as brute force for simple gesture and fuzzy systems to more complex ones. At environmental side all possibilities are opened and also more complex algorithms could be furnished by the framework (Simple Vector Machine, Hidden Markov Model, Neural Networks, Decision Trees, etc.).

VI. ARAMIS: THE IMPLEMENTATION

The previous sections have introduced the ARAMIS approach and how it models the interaction between augmented human beings and the surrounding augmented environments. In this section is presented a first implementation of a system based on the ARAMIS model developed in order to demonstrate its feasibility and benefits. The prototype with the used algorithms, the set-up, and the test of use cases are presented in this section.

A. Gesture lexicon

The gesture lexicon we implemented is composed by several dynamic gestures performed with one arm: goUp, goDown, goLeft, goRight, shake left-right, shake up-down, shake back-forward, rollClockwise, rollCounterclockwise, rollClockwise-&Return. The rolls gestures have to be performed by the arm wearing the gyroscope in order to be recognized. Some more gesture representing numbers drawn in air by one hand are recognized in special context (see section D). In addition a pointing gesture has been introduced in order to indicate and select the device that is the second term of the interaction.
These gestures are been chosen for the sake of simplicity and the minimum effort (cognitive and physic to realize the gesture).

B. Algorithms

Several algorithms have been used in order to face the implementation of a first prototype demonstrating the feasibility of our approach. The complexity of the problem can be resumed in the following main challenges: gesture analysis (features extraction, gesture segmentation, and gestures classification), user recognition and tracking.

Table 2. Algorithms in wearable components

Algorithm	***Goal***
PTAMM	Pointing
PTAMM	World Creation and user tracking
Optical Flow	Dominant arm gesture recognition
Brute Force	Non-dominant arm gesture recognition

Table 3. Algorithms in environmental components

Algorithm	***Goal***
Haar cascade	Face recognition -> hand color extraction
Kalman/ CAMShift	Hand tracking
Speed threshold (or OCR-like)	Gesture Classification
Synchronization	Inspired from [18]

The choice of a simple gesture vocabulary allowed us to use simple classifiers based on brute force to perform recognition at wearable and environmental side. However, as stated before, the system can allow more complex classifiers; for example, at present, is equally possible to use an OCR-like classifier in order to recognize gestures performed facing the camera in the environment and that have reference to alphabet characters. In addition we plan to offer a Hidden Marcov Model (HMM) classifier in order to analyze the data captured by inertial sensors to analyze more complex gestures. However, our simple gesture vocabulary allows us to use simpler and faster brute force classification algorithms without significant changes in the recognition task. A simple vocabulary is possible since a gesture is interpreted differently according to the target of the interaction; this solution allows us to limit to five the number of gestures to be classified in parallel (reducing considerably the possibility of errors). The presence of the user on the in face of the environmental camera is detected by a face detection algorithm (also used to determine in which part of the image is possible to find skin colored elements, as shown in Figure 7).

The pointing gesture requires special effort since the position of the user and the target must be known. A customized version of PTAMM algorithm (presented by Castel et Al. [19] [20]) proved to be suitable for this goal. Moreover it offered the basis to build virtual maps on a real environment realizing the augmented world we need. In fact we use this method to initialize new environments and introducing the interactive objects in the system. A summary of the used algorithms is shown in Table 2 and Table 3 (classified according their use in the wearable or pervasive paradigm).

C. Set-up

Wearable Set-Up

In the implementation of our system we used the wearable devices as illustrated in Figure 4.

The user body is divided in two main parts: the dominant arm and the non-dominant arm. The first is the arm used for most pointing gestures, whereas the second is used for symbolic gestures and as feedback (haptic stimuli) [21]. As segmentation gesture we chose a double rotation of the non-dominant arm (rollClockwise&Return) that has the feature to be easily recognized by gyroscopes and accelerometers (99% of recognition rate with trained users, with negligible false po-

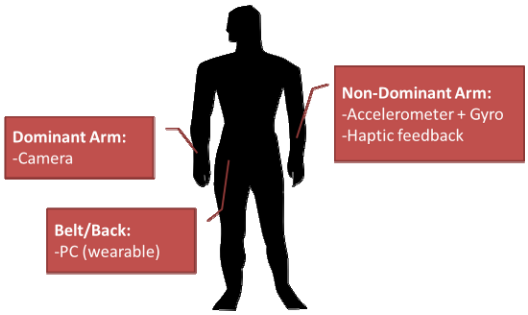

Figure 4. Wearable components set-up

sitives). In the dominant hand (on the upper side of the wrist) is placed a camera. At present the wearable processing part are done on a PC on the user; the use of the only PDA as input, output and processing device is taken into account for the next evolution of the system.

Environmental Set-Up

The augmented environment is realized inside a smart living room. The set-up consists in several pervasive components. A large display (projection on a wall) is used for a visual feedback for the interaction with virtual objects. Using a projection instead of a head mounted display decrease the burden on the user, simplifying the implementation of the scenario. A fixed camera is disposed in front of a couch; this turns the couch into an interactive area in which sensors on the user and in the room can be used at the same time. The enhanced object are a media center PC to play multimedia content, wireless-controlled switches to control some lamps in the room, and processing units hidden in the room performing data elaboration and message routing between elements in the system.

D. *Prototype*

According the working configuration (section IV.B) we developed three interaction scenarios and we present interaction supported by ARAMIS according to the three working configurations.

Case 1 (on Figure 5): augmented human in augmented environment. The user can point and select the media center and start interacting with the menu displayed on a small LCD (such as select the content of a DVD and control the sound).

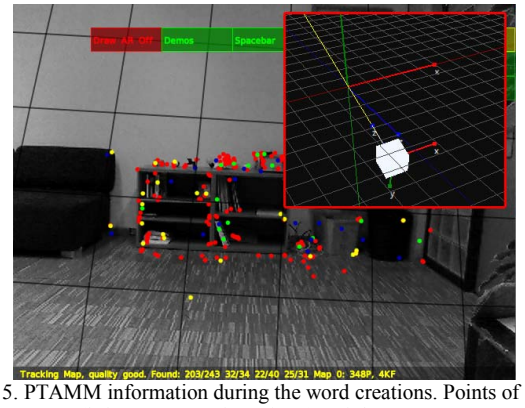

Figure 5. PTAMM information during the word creations. Points of interest (left). Camera orientation (up-right corner).

In addition, complex interactions are allowed, user can grasp a virtual representation of the LCD screen and move it on the wall by pointing at it, now the media center interface will be shown on the wall. With the same gestures the augmented user can point at remote switches and turn on and off the room lighting system. The same gesture is interpreted differently by the system according to the target of the interaction. Whereas the user sits on the couch, a vision-based system for gesture recognition is turned on and the user hands are tracked. Inputs from worn devices and the environment are merged enabling more gesture commands.

Case 2: augmented human in standard environment. The user enters in the environment for a first time. He can include it in the system (creating a new world, as shown in Figure 6) and add virtual objects, which are coupled with the environment only for the position in the space. Due to the lack of feedback (only sound or vibrations), the user should choose conveniently the position of the virtual objects (e.g. a virtual media center on the top of a real media center).

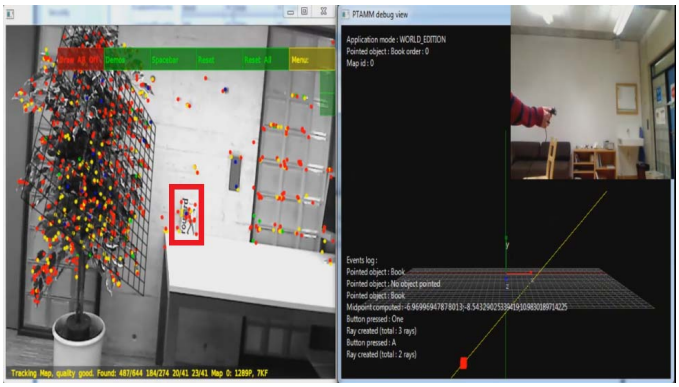

Figure 6. User creating a map. Left: user pointing a book (inside the red rectangle) to add it to the world. Right: ARAMIS perspective, the red cube is the book pointed by the camera.

Case 3 (Figure 7): normal human in augmented environment. In this case the system offers one augmented interaction in a special spot of the room: the couch facing the camera. The interaction is similar to the case 1 with just the gestures from the environment and a simpler gesture vocabulary. Using only a camera an augmented interaction is still possible. Interaction output: only the environment.

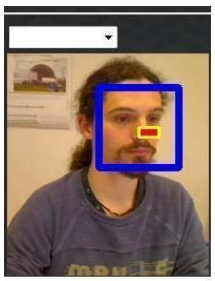

a)

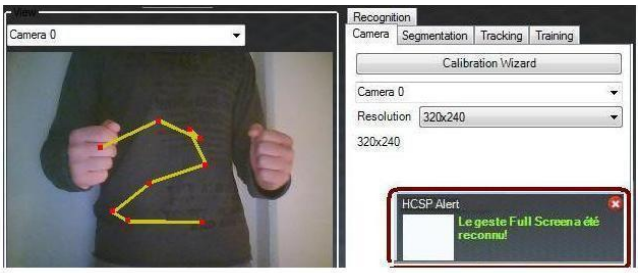

b)

Figure 7. A user facing the camera. a) Haar based face detection and skin color extraction. b) Hand tracking by the environmental camera and with Kalman tracker (working configuration 3)

E. Discussion

The realized scenario implements a part of the hybrid approach described in the section IV. Case 1 (the only having wearable and environmental modules working at the same time), after some speed tests in different configurations, has been implemented according the following principles:

- Wrist worn camera: images are elaborate at wearable side from the features extraction to the gesture analysis (path 3 in Figure 3).
- Worn accelerometers and gyroscopes: raw data is sent at environmental side for features extractions and elaboration (path 1)
- Environmental camera: features are extracted and the gesture analyzed at environmental side.

Data is finally merged at decision level.

It is interesting to highlight that the system is user-location aware: gestures performed in front of the camera are recognized exploiting both the accelerometers and the camera, whereas gestures performed elsewhere (with a reduced lexicon) are recognized only by the worn sensors. For this prototype we have designed a simple gesture vocabulary of ten commands that are interpreted in different ways according to the position of the user in the room and the target of the interaction. The gesture recognition task is made easier by the gesture protocol we used, with five classifiers running in parallel in the worst case (two-three in average).

We have concentrated our efforts to demonstrate the feasibility of the proposed approach. From a technical point of views we evaluate the systems paying attention to real-time issues. We achieved gesture recognition (from features extraction to gesture classification) in less than 250ms. The most of the time is spent by the system sending data (serialization, transfer, and deserialization) between devices on the user and in the environment. It was perceived as acceptable during the tests and it motivates us to proceed with usability tests. However, at this moment, also the proposed gesture language needs more assessments to be deeply evaluated independently of the worn devices (still too cumbersome).

VII. CONCLUSION

In order to achieve novel augmented interactions between human and smart environments, we propose to adopt a hybrid gesture-based approach. Different interaction paradigms and techniques are used at the same time:

- Pervasive and wearable computing paradigms;
- Mixed reality interactive environments;
- Brute force, neuronal, fuzzy or neuro-fuzzy classification approaches;
- Optical and non-optical sensing techniques.

To validate our concept of hybrid approach we realized a framework allowing the system to flexibly handle the information. Data from each sensor can be elaborated in the more suitable way at wearable or environmental side.

We have implemented key elements of the ARAMIS approach demonstrating how to augment the interactions of a user in three different working configurations. The prototype, used to perform feasibility evaluations has demonstrated the system can work in real-time modeling augmented interactions.

In the first prototype we implemented brute force algorithms for simple gesture recognitions, as next step we plan to extend our prototype including a fuzzy approach in order to recognize more complex gestures in real-time. Finally a quantitative evaluation comparing the different solutions (brute force, machine learning and fuzzy approaches) will be done to complete the formalization of the presented interaction.

REFERENCES

[1] OpenNi, http://www.openni.org/.

[2] Dünser, A., Grasset, R., Seichter, H., Billinghurst, M. (2007) "Applying HCI principles to AR systems design" Charlotte, NC, USA: Mixed Reality User Interfaces: Specification, Authoring, Adaptation (MRUI'07: 2nd International Workshop at the IEEE Virtual Reality 2007 Conference), 11 Mar 2007. Mixed Reality User Interfaces: Specification, Authoring, Adaptation (MRUI'07) Workshop Proceedings, 37-42.

[3] D. C. Engelbart, "Augmenting Human Intellect: A conceptual Framework," Summary Report, Contract AF 49(638)-1024, SRI Project 357B, Stanford Research Institute, Menlo Park, California (October 1962), AD 289565.

[4] Hoc, J.-M. "From human–machine interaction to human–machine cooperation". Ergonomics, 43(7), 2000, pp. 833–843.

[5] Greenberg, S., Marquardt, N., Ballendat, T., Diaz-Marino, R., Wang, M. "Proxemic interactions: the new ubicomp?" Interactions 18, 1 (January 2011), 42-50.

[6] Pederson, T. "Towards an activity-aware wearable computing platform based on an egocentric interaction model". UCS□07 Proceedings of the 4th international conference on Ubiquitous computing systems. 211-227 (2007).

[7] Cook, D.J., Das, S.K. "How smart are our environments? An updated look at the state of the art". Pervasive and Mobile Computing. 3, 53–73 (2007).

[8] Rhodes, B.J.; Minar, N.; Weaver, J.; "Wearable computing meets ubiquitous computing: reaping the best of both worlds", Wearable Computers, 1999. Digest of Papers. The Third International Symposium on , vol., no., pp.141-149, 1999

[9] Carrino, S., Mugellini, E., Abou Khaled, O., Ingold, R. "ARAMIS: Toward a Hybrid Approach for Human-Environment Interaction" 14th International Conference on Human-Computer Interaction, HCI International 2011, Orlando, FL, USA, 09-14 July 11.

[10] Rehman, K., Stajano, F., Coulouris, G. “Interfacing with the invisible computer”. Proceedings of the second Nordic conference on Human-computer interaction - NordiCHI ’02. 213 (2002).

[11] Mitra, S., Acharya, T. “Gesture Recognition: A Survey”. IEEE Transactions on Systems, Man and Cybernetics, Part C (Applications and Reviews). 37, 311-324 (2007).

[12] Wobbrock, J.O., Wilson, A.D., Li, Y. “Gestures without libraries, toolkits or training: a $1 recognizer for user interface prototypes”. Proceedings of the 20th annual ACM symposium on User interface software and technology - UIST ’07. 159 (2007).

[13] Elmezain, M., Al-hamadi, A. “A Hidden Markov Model-Based Isolated and Meaningful Hand Gesture Recognition”. Engineering and Technology. 31, 394-401 (2008).

[14] Yuan, X., Wang, Y. “SVM Based Adaptive Inverse Controller for Excitation Control”. Advances in Neural Networks–ISNN 2007. 469–478 (2007).

[15] Nauck, D., Klawonn, F., Kruse, R. “Foundations of neuro-fuzzy systems”. John Wiley & Sons, Inc. New York, NY, USA (1997).

[16] Mitra, S., Hayashi, Y. “Neuro-fuzzy rule generation: survey in soft computing framework”. IEEE transactions on neural networks a publication of the IEEE Neural Networks Council. 11, 748-68 (2000).

[17] Crevoisier, A., Polotti, P. “Tangible acoustic interfaces and their applications for the design of new musical instruments”. Proceedings of the 2005 conference on New interfaces for musical expression. p. 97–100 National University of Singapore (2005).

[18] Castle, R.O., Klein, G., Murray, D.W. “Combining monoSLAM with object recognition for scene augmentation using a wearable camera”. Image and Vision Computing. 28, 1548-1556 (2010).

[19] Castle, R.O., Murray, D.W. “Object recognition and localization while tracking and mapping”. 2009 8th IEEE International Symposium on Mixed and Augmented Reality. 179-180 (2009).

[20] Römer, K. “Time synchronization in ad hoc networks”. In Proceedings of the 2nd ACM international symposium on Mobile ad hoc networking & computing (MobiHoc '01). ACM, New York, NY, USA, 173-182.

[21] Karam, M. “A framework for research and design of gesture-based human computer interactions”. Thesis. Southampton: University of Southampton, (2006)

2011 IEEE International Conference on Fuzzy Systems
June 27-30, 2011, Taipei, Taiwan

Understanding the Unknown:

Unattested Input Processing in Natural Language

Julia M. Taylor
RiverGlass, Inc and Purdue University
USA
jtaylor1@purdue.edu

Victor Raskin
Purdue University and RiverGlass, Inc.
USA
vraskin@purdue.edu

***Abstract*—This paper describes the process of deriving the meaning of an unknown word within the framework of meaning based natural language processing. It uses the clues supplied by the rest of the sentence, taking into account various degrees of possibilities of what the unknown word can mean, according to the previously acquired knowledge resources. The process of finding the meaning is incremental, and thus the derived meaning can evolve as more knowledge is gathered. The paper describes the fuzzy approach to the problem within this framework with regard to the semantic and syntactic acceptability of a sentence.**

Unknown words; computing with words; ontological semantics; natural language understanding; sentence acceptability

I. Introduction

This paper attempts to bring attention to the understanding of previously unseen words based on the meaning of the rest of the sentence. We assume that such trait is necessary for any robust computer system that is capable of communicating intelligently with humans. The necessity is derived from the ongoing changes in natural languages, including constant addition of new terms or senses, i.e. the new meanings of the existing words (think, for instance, of the ever propagated government generated acronyms or of teenage slang terms).

The use of natural language in ambient intelligence seems to be a reasonable bet. This makes it necessary for computer systems to understand natural language at the human proficiency level. If guessing games are to be performed, they have to be built on the platform of solid content and context comprehension to be useful for any reasonable purpose.

We assume, therefore, that an effective computer system that is used to communicate naturally with humans must be equipped with the same ability to learn new terms in a familiar context as the ability that humans possess and utilize under the same circumstances. It is also reasonable to assume that such learning is based on the perception of the situation described in the text, and that, as with most perception-based mechanisms, it is fuzzy.

II. What Kind of Animal Is Unattested Input?

A. First Type: Annetested Input

Annetested input, along with ambiguity, is a major problem for systems attempting to understand natural language: no matter how many words the systems is supposed to be familiar with, there are hundreds of thousands words and senses that it has never encountered and is, therefore, not equipped to handle with the resources it has. However, in order to be robust, such a system must have such a capability.

Annetested input processing can only be meaningful when it happens among the words and in sentences that are well understood other than this one particular unknown occurrence. The task then becomes to guess the meaning of the annestested input on the basis of the fully understood information in the rest of the sentence. In a way, annestested input is being solved just like an inequality system in math is solved, by finding the possible intervals which satisfy it.

Non-meaning based approaches cannot proceed as far because they are not aware of the meaning of the other words or utterances in the sentence. The only reason the famous Jabberwocky poem [1] is understood somewhat by humans is that, besides the felicitous morphological and syntactic guesses, they fully understand quite a few words interspersed with the unknown ones.

The first stanza is, perhaps, the most artful one, because the only known words there are of a grammatical nature: conjunctions, prepositions, determiners and auxiliary verbs. As a result, the understanding is the vaguest and most surprising—in the sense of having any understanding at all:

> Twas brillig, and the slithy toves
> Did gyre and gimble in the wabe:
> All mimsy were the borogoves,
> And the mome raths outgrabe.

By contrast, in the most easily understood stanzas (third and fifth, respectively), the annetested input is limited to very few unknown non-proper-name words each:

> He took his vorpal sword in hand:
> Long time the manxome foe he sought –
> So rested he by the Tumtum tree,
> And stood awhile in thought.

> One, two! One, two! And through and through
> The vorpal blade went snicker-snack
> He left it dead, and with its head
> He went galumphing back.

978-1-4244-7316-8/11/$26.00 ©2011 IEEE

Notice that the first occurrence of *vorpal* is broad: it can be any attribute of a sword. The second occurrence modifies the blade of a sword, thus reducing the set of possible senses of the annetested word. In a similar fashion, the fully familiar and well understood words in this section have compensated, we hope, for our deliberate misspelling of the word *unattested* as *annetested*.

B. *The Vagueness of Vorpal*

One leaves the Jabberwocky poem with a clear understanding that *vorpal* is an attribute of *blade*. This understanding is, however, vague in the sense of the coarsest possible grain size for a blade attribute: it can be such a physical property as sharp (primary function quality), steel (material), masterful (manufacturing execution), heavy (weight), long (dimension); it can also be a non-physical property, such as expensive (price), famous or legendary (extent of what is known about it), heroic (history of performance), merciless (effectiveness), etc. But we cannot yet treat the property as fuzzy because there is no basis for assigning a non-100% degree of membership to any one of the possibilities (cf. [2] on possibilistic theory and the Hartley measure of the uncertainty). So the captured meaning of *vorpal* is uncertain in the sense of vagueness but, perhaps, not yet fuzzy.

III. THE MEANING OF UNKNOWN WORDS

While the meaning of the sentence is not fully compositional in general, many sentence meanings can be put together from individual word meanings, provided that the syntax and semantics make sense. All words in the sentence are connected through some semantic relationships within the syntactic phrases to which they belong. We will assume that some two words in a syntactic phrase are connected through one or more relationships, and each word is connected to at least one other word in the sentence through such relationship. Moreover, there is a finite number of existing relationships. For simplicity, we will describe here binary relations that correspond to such semantic relationships. Such semantic relationships in natural language are fuzzy: we unlock a door with a key, with a code, or with a paper clip[1]. Clearly, $\mu_{\text{INSTRUMENT}}(\text{UNLOCK, KEY}) < \mu_{\text{INSTRUMENT}}(\text{UNLOCK, PAPER-CLIP})$.

Each such relation R(X, Y), where x∈X and y∈Y, has a domain and range, defined respectively as:

$$\mu_{\text{DOM R}}(x) = \max_{y \in Y} \mu_R(x,y), \text{ for each } x \in X.$$

$$\mu_{\text{RAN R}}(y) = \max_{x \in X} \mu_R(x,y), \text{ for each } y \in Y.$$

Furthermore, we assume that each relation has at least some (x, y) such that $\mu_R(x, y)=1$: $\max_{y \in Y} \max_{x \in X} \mu_R(x,y) = 1$.

Semantic relationships typically have well defined and easily calculated inverse relationships, with

$$\mu_{\text{DOM R}^{-1}}(y) = \max_{x \in X} \mu_{R^{-1}}(y,x), \text{ for each } y \in Y.$$

$$\mu_{\text{RAN R}^{-1}}(y) = \max_{y \in Y} \mu_{R^{-1}}(y,x), \text{ for each } x \in X.$$

The relationships are typically verb centered: agent(y, x_1), theme(y, x_2), beneficiary(y, x_3), etc. where y is a verb. Yet, they are rarely all interdependent and, hence, can be dealt with in pairs. When a relationship is object centered, the task is simpler, as the number of such relationships is smaller. As an example, consider the following sentence: *The man opened the door to his house with the key*. The following relationships are of interest: AGENT(OPEN, MAN), THEME(OPEN, DOOR), INSTRUMENT(OPEN, KEY), ENTRY-POINT(DOOR, HOUSE), OWNER(MAN, HOUSE). There are 3 verb centered relationships here, and 2 object centered ones, as shown in Fig. 1.

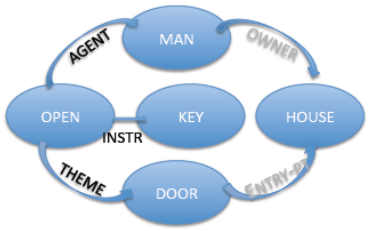

Figure 1. A linked representation of *The man opened the door to his house with the key*.

Whenever a sentence consists of compositional relationships between words, where the words are not interdependent, an unknown word can be calculated based on the domain or range of the relation that corresponds to the semantic relationship between the unknown and the known words. Thus, if in the example above, we don't know the word *man* but somehow know that it is an AGENT of OPEN, we can derive some knowledge of what *man* is from $\mu_{\text{AGENT}}(\text{OPEN, } man)$. Moreover, until more information is found we can approximate *man* as something that maximizes $\mu_{\text{AGENT}}(\text{OPEN, } z)$.

On the other hand, there are situations when an unknown word depends on more than one relationship. This can happen in several situations, some of which are shown in Figure 1. For instance, if the word *house* were unknown, its meaning would be derived from something that can be owned and from something that has a door as an entry. Similarly, if the word *door* was unknown, its meaning would have to be derived from something that is a theme of OPEN and that serves as an entry to HOUSE.

Assuming that there are at least two relations R1(X, Y) and R2(Y, X) such they there is a y∈Y where (x, y) ∈ R1 and (y, z) ∈ R2, a join can be formed between these two relations (R1*R2), such as

$$\mu_{R1*R2}(x,y,z) = \min[\mu_{R1}(x,y), \mu_{R2}(y,z)]$$

for each x∈X, y∈Y, z∈Z ([2], p. 77). Using this formula, the meaning of unknown words—as those in the examples of *door* and *house*—can be calculated.

The formula can be generalized to n relations:

$$\mu_{R1*R2*\ldots*RN}(x_1, x_2, \ldots, x_n, y) = \min[\mu_{R1}(x_1,y), \mu_{R2}(x_2,y), \ldots, \mu_{RN}(x_n,y)]$$

[1] http://www.ehow.com/how_4809693_unlock-locked-door-key.html.

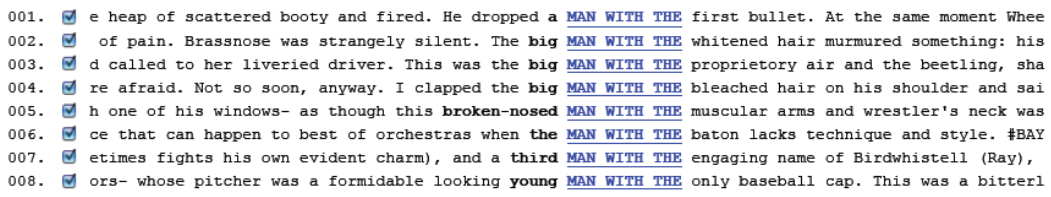

Figure 2. Results for *man with the* __

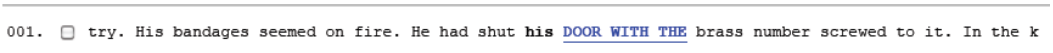

Figure 3. Results for *door with the* __

for each $x_i \in X_i$, $y \in Y$. Using this formula, if word *open* is unknown, its meaning can be derived by considering together its AGENT *man*, its INSTRUMENT *key* and its THEME *door*.

The situation gets more complicated when we consider unknowns that are dependent on other information from the sentence. For example, if we have *A cat opened the door with xyz,* we know that typical instruments of opening the door like keys and code are excluded. On the other hand, if it is a locksmith that opened the door, it is probably not the regular key that was used to open it. Intuitively, in such cases the join should not be done on a single concept but on as many as it takes to derive the correct meaning. Thus, in the case of *cat* or *locksmith*, the agent has to be considered on the join as well or membership functions has to be defined based on individual agents. We will abandon the notion of individual membership function of the INSTRUMENT of OPEN based on the agency for a time being, but note that it is not much different than defining sets for the height of a basketball player: it is easy to define them, but they are not practical from the point of view of natural language usage.

It is easy to see that for the cases of unknown words that are independent arguments of a binary relation, their meaning can be derived from a join of all pertinent relations contained throughout a text: *I lost the xyz that opened the door last time. It fell through the opening in front of the elevator door*. Here, not only do we know that *xyz* is something that opened the door, but it is also slim enough to fall through a centimeter (or so) wide opening. Thus, if somebody disambiguates a sentence, and assigns arguments to each relation, including which relation an unknown word will be in, it is mathematically possible to find the meaning of such word, especially, if it is used in many sentences that describe different functional characteristics. The next section will demonstrate what type of linguistic processes are needed do it automatically.

IV. What Does It Take To Open a Door?

Let us, again, consider the sentence *The man opened the door with the xyz*. In the sentence, *xyz* can be a number of things, including *key, combination code, card, two hanger wires*, or any other instrument with the use of which a lock on the door can be opened. Perhaps somewhat less obviously, *xyz* can be *mirror, picture, hole, ornament*, or any other detail or part of the door. Even less obviously, and somewhat syntactically awkward, *xyz* may stand for *friend, dog*, or any other accompanier for *the man*.

Without the explanation above, the sentence is three-way syntactically ambiguous, depending on the analysis of the prepositional phrase which may pertain to *man*, *open*, or *door*. Thus, similarly to the case of *vorpal*, indicated are the three vague sets of constituents that somehow modify the dominant entities above.

The task of unattested input processing is, then, to determine the semantic features that can satisfy *the man with the xyz*, *open with the xyz*, or *the door with the xyz*. It is here that understanding these phrases and the resulting sentence is necessary. The process of understanding the phrases when all words are known is outlined in Section V.

It is tempting to use the corpus-based approach and look for occurrences of *xyz* given *the man with the, open with the, the door with the xyz.* A brief search[2] of the Brown corpus for the first phrase yielded the results shown in Fig. 2. The results of the second phrase produced nothing, the results of the third phrase yielded one usage, shown in Fig. 3.

The lessons of this example are fast learned: none of the usages received for the first query work for the sentence *The man opened the door with the xyz*. The one usage in the third query is extremely limiting: there are many more possibilities for the detail or part of the door other than having a brass number.

It can be argued that the exact phrase search approach is too narrow and should be expanded to the conceptual search[3], at least of the dominant word. It is possible that it will somewhat enrich the results and give a somewhat higher quantity of the acceptable phrases, such as and beyond *brass number*. It would not, however, correct the situation with the first tried phrase, illustrated in Fig. 2, where none of the results were suitable for the example sentence.

Nirenburg & Raskin [3] sketch an early meaning-based procedure that can be used to find the prevalent crisp set associated with the sense of the one unknown word in a sentence. (See also references there and elsewhere on pre-semantic attempts to account for unattested input: for a representative sample, see [4-19]) Using a much simplified version of early Ontological Semantics, they demonstrate that non-existing word *keegh* can be understood as an instrument of locking/unlocking a door on the basis of the machine-

[2] http://conc.lextutor.ca/concordancers was used

[3] a primitive example of which could be the usage of hypernyms and hyponyms of WordNet.

understood definitions of *lock*, *door*, and the ontological knowledge of the most common artifact that is required to perform the unlocking.

Such an approach, especially on a single sentence, demonstrates that a solution can be found, without validating that it was the optimal solution (see [20] for empirical verification). Consider, for example, a sentence *he unlocked the car door with an xyz*. The range of possibilities here encompasses *key, keyless remote fob, code* (on the door), *wire*, *screwdriver*, *hanger*, *lock pick (Slim Jim)*. In a crisp treatment, *key, keyless remove fob, code*, or maybe *lock pick* and *hanger* will work. The *screwdriver*, on the other hand, will probably draw a blank.

Now suppose, the sentence that follows is *He always had the xyz with him to take the screws off laptops.* The screwdriver, then, an initially unlikely tool, becomes the leading candidate for the unattested input: while it is possible, although hard, to unlock a car door with a screwdriver, none of the other tools are purposefully used to take the screws off laptops.

It appears useful, then, to collect all interpretations, to the lowest possible degree (as unlikely as they may sound), of the tools that could imaginably open a car door. The set of all these interpretations will remain intact until and unless further information is perceived to narrow it down. If decisions have to be made prior to the moment when new, narrowing information is received, then it is natural to accept those tools that have the highest membership in the set as the interpretation of *xyz*. Moreover, it seems natural to select the most probable of them to be used for the interpretation as well. Thus, [3] concluded—or rather, stopped just short of concluding—that the unattested input was an instrument for opening a door, the likeliest of which is, of course, some sort of key.

V. A Meaning-Based Method for Guessing What xyz Is

In this section, we will demonstrate in somewhat simplified non-proprietary technical detail, how the meaning of an unknown word is determined on the basis of the full understanding of everything else in the sentence. The derived meaning will be calculated based on the fuzzy joins of relevant relations. This will be done with the methods and resources of the Ontological Semantic Technology (OST—see [21-23]).

At the core of OST are repositories of world and linguistic knowledge, acquired semi-automatically within the approach and used to disambiguate the different meanings of words and sentences and to represent them. These repositories, also known as the static knowledge resources, consist of the ontology, containing language-independent concepts and relationships between them; one lexicon per supported language (English, Russian, etc), containing word senses anchored in the language-independent ontology which is used to represent their meaning; the Proper Name Dictionary (PND), which contains names of people, countries, organizations, etc., and their description anchoring them in ontological concepts and interlinking them with other PND entries; and a common sense rules resource. A conforming lexicon and ontology, as well as – when needed -- PNDs and common sense rules, are used by the Semantic Text Analyzer (STAn), a software, developed by RiverGlass Inc., that produces Text Meaning Representations (TMRs) from the text that it reads. The format of TMRs conforms to the format and interpretation of the ontology. The processed TMRs are entered into InfoStore, a dynamic knowledge resource of OST, from which information is used for further processing and reasoning.

A. Lexicon

The substantive part of interpreting the sentence *The man opened the door with the xyz* starts with the search for the event of the single clause, and in this case, it is easy: *open* is the only word with any sense anchored in an ontological event concept. For illustrative purposes, we will work with the following senses of *open* as a verb that a semantic analyzer would find in a generic OST lexicon:

1. to allow access [*open the door*]
2. spread out, unfold (open out) [*open the wings*]
3. allow public access, permit access [*open the gallery to the public*]
4. establish [*open a new restaurant*]

…

The formal definition of the above senses is:

```
(open-v1
    (cat(v))
    …
    (syn-struc((subject((root($var1))(cat(np))))
        (root($var0))(cat(v))
        (directobject((root($var2))(cat(np))))
        (pp-adjunct((opt(+))(root(with by))(cat(prep))
            (obj((root($var3))(cat(np))))))
        (pp-adjunct((opt(+))(root(to into of))(cat(prep))
            (obj((root($var4))(cat(np))))))
    ))
    (sem-struc(open
        (agent(value(^$var1)))
        (theme(value(^$var2)))
        (instrument(value(^$var3)))
        (location(value(^$var4)))
    ))
)
(open-v2/v3/v4
    (cat(v))
    …
    (syn-struc((subject((root($var1))(cat(np))))
        (root($var0))(cat(v))
        (phr((opt(+))(root(out up))(cat(prep))))
        (directobject((root($var2))(cat(np))))
        (pp-adjunct((opt(+))(root(for to))(cat(prep))
            (obj((root($var3))(cat(np))))))
    ))
    (sem-struc(unfold/give-access/establish
        (agent(value(^$var1)))
        (theme(value(^$var2)))
        (beneficiary(value(^$var3)))
    ))
)
```

For the simplicity purposes, we will consider only one (physical) sense of *door* (physical movable door), only one sense of *man*, and the following, non phrasal, senses of *with*:

1. accompanier (animate or thing) [*went with a friend*]

2. instrument [*cut with a knife*]
3. beneficiary [*left the parcel with Bob*]
4. object-as-part [*door with a handle*]
5. location-of [*door with a mirror*]
6. containment [*bowl with cherries*]
7. manner [*ate with gusto*]

The first six definitions of *with* can be represented in the following format, where PROP is the property from the list above:

```
(with-prep[1-3]
    …
    (syn-struc((vp((root($var1))(cat(vp))))
        (root($var0))(cat(prep))
        (obj((root($var2))(cat(np))))))
    (sem-struc(^$var1(PROP(value(^$var2)))))
)
(with-prep[4-6]
    …
    (syn-struc((np((root($var1))(cat(np))))
        (root($var0))(cat(prep))
        (obj((root($var2))(cat(np))))))
    (sem-struc(^$var1(PROP(value(^$var2)))))
)
```

The last sense is defined as:

```
(with-prep7
    …
    (syn-struc((vp((root($var1))(cat(vp))))
        (root($var0))(cat(prep))
        (obj((root($var2))(cat(np adv))))))
    (sem-struc(^$var1(manner(value(^$var2)))))
)
```

The same variables in the syntactic and semantic structure (syn-struc and sem-struc) are bound together, with '^' standing for the meaning of the variable that follows the symbol, and '$' standing for the value of the variable. In other words, '$' refers to a word that a variable points to, and '^' to its ontological meaning. Because the lexicon senses only point to the conceptual definitions in the ontology, the bulk of work is carried by the ontology.

B. *Ontology*

The ontology is a lattice that contains the knowledge necessary to accept or reject an interpretation of a sentence. Each concept is defined through properties and their fillers. Each filler is accented by the facet which is interpreted as supplying the degree of membership in a set.

An ontological concept has the following format:

concept-name
    (attribute(facets(literal-value^{+}))$^{+}$)*
    (relation(facet(concept-name^{+}))$^{+}$)*
facet[4]
    sem | value | default | relaxable-to | not

In this paper, we are only interested in relations. The following interpretations for ontological definitions containing fuzzy concepts and relations were defined in [24]:

[4]This list of facets is only applicable to concepts

Given a set of objects $\mathcal{D}$ and given its interpretation function $\mathcal{I}$, for every fuzzy concept B, object x is an element of B with some degree $\mathcal{I}[B](x) \rightarrow [0, 1]$; for every relation Rel, $\mathcal{I}[Rel](x, y) \subseteq \mathcal{D} \times \mathcal{D} \rightarrow [0, 1]$; We will assume that $x \in B$ if $\mathcal{I}[B](x) \rightarrow (0, 1]$.

With this in mind, the following is true for C and D, using [15]:

$\mathcal{I}[C\ D](x) = \max\{\mathcal{I}[C](x), \mathcal{I}[D](x)\}$
$\mathcal{I}[\text{and } C\ D](x) = \min\{\mathcal{I}[C](x), \mathcal{I}[D](x)\}$
$\mathcal{I}[(Rel(D))](x) = \max_{y \in D}\{\mathcal{I}[Rel](y, x)\}$
$\mathcal{I}[(Rel(\text{and } C\ D))](x) = \min\{\mathcal{I}[Rel(C)](x), \mathcal{I}[Rel(D)](x)\}$
$\mathcal{I}[Rel(C\ D)](x) = \max\{\mathcal{I}[Rel(C)](x), \mathcal{I}[Rel(D)](x)\}$
$\mathcal{I}[C(Rel(D))](x) = \min\{\mathcal{I}[C](x), \mathcal{I}[Rel(D)](x)\}$
$\mathcal{I}[C(Rel_1(D))(Rel_2(E))](x)$
$= \min\{\mathcal{I}[C(Rel_1(D))](x), \mathcal{I}[C(Rel_2(E))](x)\}$

For the construction of the ontology, subsumption definition of [25] was followed: C subsumes D iff $\forall x \in \mathcal{D}$: $\mathcal{I}[C](x) \geq \mathcal{I}[D](x)$.

Fuzzy values of facets as the degree of membership is assumed to be set by the ontology engineer, with DEFAULT facet always corresponding to 1, NOT facet corresponding to 0, while the other three facets varying depending on the application and the domain. We will use a slightly different notation in the paper, specifying the exact degree of membership instead of using a facet. Thus, we adopt the following format, where membership-degree is any number between 0 and 1:

concept-name
    (relation(membership-degree(concept-name^{+}))$^{+}$)*

We assume that a parent concept has at most the same membership degree value as a child concept (unless inheritance is blocked). Then, given a concept B that is a descendant of a concept A and an ancestor of a concept C, where $\mu_P(A)$ and $\mu_P(C)$ are known:

$$\mu_P(B) = \mu_P(A) + \frac{\mu_P(C) * \text{dist}(A,B)}{\text{dist}(A,C)},$$

where dist(X, Y) is the logarithmic distance between the lattice nodes X and Y and either ancestor(X, Y) or ancestor(Y, X) holds.

The somewhat simplified ontological concepts OPEN, UNFOLD, GIVE-ACCESS, and ESTABLISH for the 4 lexical senses of *open* above and the concept DOOR for *door* are shown below, without their inherited properties, unless access to them is warranted by the analyzed sentence:

```
(open
   (definition(…("to open a container door window etc")))
   (is-a(1(change-position)))
   (theme(1(container door window))(0.75(artifact))
      (0.1(physical-object)))
   (instrument(1(key))(0.75(artifact)))
   (agent(1(human))(0.5(animal)))
   (accompanier(1(human))(0.75(animal)))
)
(unfold
```

```
    (definition(…("to change configuration of parts of an object")))
    (is-a(1(change-configuration)))
    (theme(0.75(artifact(part-of-object(0.5(physical-object)))
    (instrument(0.9(body-part))(0.5(artifact)))
)
(give-access
    (definition(…("to allow public access")))
    (is-a(1(permit)))
    (theme(1(building))(0.5(organization))
        (0.1(geopolitical-entity)))
    (beneficiary(0.75(human))(0.5(organization))(0.1(animal)))
    (precondition(0.75(communicative-act)))
)
(establish
    (definition(…("to establish an institution")))
    (is-a(1(create-social-object)))
    (theme(0.5(group))(0.65(organization))
        (0.1(geopolitical-entity)))
)
(movable-door
    (definition(…("the slab that is open and closed as opposed to
the hole in the wall")))
    (is-a(1(building-fixture)))
    (inside-of(1(door)))
    (contains(0.05(physical-object)))
    (has-object-as-part(1(handle))(0.8(lock)))
    (locale-of(0.5(mirror hook writing-symbol))(0.3(ornament)))
)
(man
    (definition(…("the slab that is open and closed as opposed to
the hole in the wall")))
    (is-a(1(human)))
    (gender(1(male)))
    (age(1(adult))(0.75(teenager)))
    (has-object-as-part(1(male-body-parts)))
    (locale-of(0.75(garment accessory)))
)
```

In a situation when a word is unknown, humans use the linguistic clues from the sentence as well as their knowledge of the world to come up with some approximate interpretation of the unknown word. The linguistic clues consist of tentative morphological, syntactic and semantic information (such as the lexical senses of the known words), while the knowledge of the world for humans can range from purely encyclopedic to common sense. The ontology tries to capture parts of such knowledge, also relying on InfoStore for facts and common sense rules resources for the rest.

Similarly, a computer calculates the same possibilities, with the membership functions reflecting the semantic preferences. Thus, when the phrase *open the door* is processed, all but the open-v1 sense are excluded due to the membership value of 0 of some phrase interpretations:

μ_{AGENT}(OPEN, MAN)=1; μ_{THEME}(OPEN, DOOR)=1;
μ_{THEME}(UNFOLD, DOOR)=0; μ_{THEME}(GIVE-ACCESS, DOOR)=0;
μ_{THEME}(ESTABLISH, DOOR)=0;

In other words, according to the ontology, it is not possible to unfold a door, allow public access to a door, or to establish a door as an institution.

C. *Back to door with, man with or open with… xyz*

Our sentence is *The man opened the door with the xyz*. The last word before xyz is the article, since there is no other word after it, we can conclude that it is a noun. Thus information is relevant when we create the lexical sense of a word, but not in guessing its meaning in a sentence. We thus continue to the next closest word, which is the preposition *with*. Now we have more clues to work with. According to the lexical senses of with, *xyz* can be one of the following:

1. It can accompany an animate being in any event
2. It can be used as an instrument for a physical event that has a theme.
3. It can be a receiver of something from somebody in an exchange possession or communicative event.
4. It can be a part of a physical object
5. It can be physically located on an (physical) object
6. It can be contained within a physical object
7. It can signify a manner of an event

According to the syntactic structures, we know that the above definition have to conform to the following format in its normalized form:

1. The subject, indirect object and the predicate must be present in the sentence. The subject must precede the verb, while the prepositional phrase containing the indirect object can be in any position.
2. The prepositional phrase containing the instrument must be in the initial or final position, thus preceding or following the predicate with the direct object.
3. The prepositional phrase containing the beneficiary (receiver) must follow the direct object, which in turn follows the predicate.
4. The prepositional phrase must follow a noun (phrase).
5. The prepositional phrase must follow a noun (phrase).
6. The prepositional phrase must follow a noun (phrase).
7. The prepositional phrase must be used adverbially, contain no article, and follow the predicate, not necessarily immediately.

Applying these rules to the sentence, we can rule out *with-prep7* on a purely syntactic ground and *with-prep3* since *open* has no sense that corresponds to the exchange possession event or communicative event on a purely semantic ground.

An interesting case is presented by *with-prep6*: while it is possible in principle to fill the inside of a door (or even an a man's body part) with something, their $\mu_{CONTAINS}$ is very low. Thus, while they are possible and the sense is not discarded, they are unlikely to become serious candidates contributing to the sense of *xyz* unless some other information props them up. In the case of *door* as a container filled with *xyz*,

$\mu_{CONTAINS}$(MOVABLE-DOOR, *xyz*)=0.05,

where *xyz* is any PHYSICAL-OBJECT small enough to fit inside a hollow part of a door, if any.

The cases of *with-prep4,5* remain valid. The difference between *with-prep4* and *with-prep5* is that the former realized only when the following noun is a part of something while the latter is realized when the following noun is located on something. The following interpretations are then valid:

$\mu_{LOCALE\text{-}OF}$(MOVABLE-DOOR, *xyz*)=0.5,

where *xyz* is any descendant of MIRROR, HOOK, WRITING-SYMBOL;

$\mu_{\text{LOCALE-OF}}$(MOVABLE-DOOR, *xyz*)=0.3,

where *xyz* is any descendant of ORNAMENT;

$\mu_{\text{HAS-OBJECT-AS-PART}}$(MOVABLE-DOOR, *xyz*)=1,

where *xyz* is any descendant of HANDLE;

$\mu_{\text{HAS-OBJECT-AS-PART}}$(MOVABLE-DOOR, *xyz*)=0.8,

where *xyz* is any descendant of LOCK.

In theory,

$\mu_{\text{LOCALE-OF}}$(MAN, *xyz*)=0.75,

where *xyz* is any descendant of GARMENT or ACCESSORY;

$\mu_{\text{HAS-OBJECT-AS-PART}}$(MAN, *xyz*)=1,

where *xyz* is any descendant of MALE-BODY-PARTS. However, the strongly prescriptive direct word order in English makes it extremely syntactically unlikely that the prepositional phrase at the end of the sentence would modify *man* (μ_{syntax}(*man*, xyz)=0.05), thus, lowering this possibility to practically non-existent. Unlike the case of *with-prep6*, where additional semantic information could prop the sense up, it is considerably less likely for such propping syntactic information to be found.

Also valid are the cases of *with-prep1,2*. The only event that can be considered with these two senses of *with* is OPEN, as UNFOLD, GIVE-ACCESS and ESTABLISH were excluded above due to their incompatibility with *door* (the corresponding concept, MOVEABLE-DOOR).

We will consider with-prep1 first. According to its syntactic and semantic structures, it needs a subject that is an agent of an event that can be accompanied by an animate object that is part of the prepositional phrase. Thus, *man* is an agent of *open* and *xyz* must then be an accompanier of *man* in this event:

$\mu_{\text{ACCOMPANIER}}$(MAN, *xyz*)=1,

where *xyz* is HUMAN, and

$\mu_{\text{ACCOMPANIER}}$(MAN, *xyz*)=0.75,

where *xyz* is ANIMAL.

In the case of *with-prep2*, *xyz* must be an instrument of opening the door. Thus,

$\mu_{\text{INSTRUMENT}}$(OPEN, *xyz*)=1,

where *xyz* is KEY, and

$\mu_{\text{INSTRUMENT}}$(OPEN, *xyz*)=0.75,

where *xyz* is any other ARTIFACT.

Similarly to the case of *with-prep6*, we now have to consider the word order in the resulting interpretations in relation to the prescriptive and preferred English sentence word order. Thus, we have to use yet another membership function, that corresponding to the perceived syntactic appropriateness or smoothness.

μ_{SYNTAX}(The man opened the door with the dog)<< μ_{SYNTAX}(The man with the dog opened the door)

In more general terms,

μ_{SYNTAX}(AGENT EVENT THEME *with* ACCOMPANIER)=0.2<< μ_{SYNTAX}(AGENT *with* ACCOMPANIER EVENT THEME)=1

Thus, we have the following possible interpretations of xyz, all with different degrees of acceptability of the alternative sentences: mirror, hook, writing-symbol; ornament; handle; lock; garment, accessory; male-body-parts; human; animal; key; artifact. The acceptability depends both on the semantics and syntax of the resulting sentences.

VI. Putting it all together: Calculating degrees of acceptability

We define an interpretation as acceptable if and only if it is acceptable both syntactically and semantically. We treat such acceptability as the intersection of the syntactic and semantic sets.

Syntactic acceptability of a sentence is defined as a minimum acceptability of all of its (binarized) phrases; where the acceptability of each phrase is maximized to the most acceptable syntactic analysis in case of syntactic ambiguity:

$$\mu_{\text{SYNTAX}}(\text{sent}) = \min_{phr \in sent} \max_{x,y \in phr} [\mu_{\text{phr}}(x,y)]$$

Semantic acceptability is similarly defined as a minimum of acceptability of all semantic relations on the maximally acceptable interpretation of each relation:

$$\mu_{\text{SEMANTICS}}(\text{sent}) = \min_{R \in sent} \max_{x,y \in R} [\mu_{\text{R}}(x,y)]$$

The overall syntactic/semantic acceptability of a sentence is, then:

$\mu_{\text{ACCEPTABILITY}}$(sentence) = min[μ_{SYNTAX}, $\mu_{\text{SEMANTICS}}$]

In *The man opened the door with the xyz*, we have eleven possible components that vary with different meanings of *xyz*:

$\mu_{\text{ACCEPTABILITY}}$([very small] PHYS-OBJECT [contained in door]) = min{1, 0.05}=0.05

$\mu_{\text{ACCEPTABILITY}}$(MIRROR, HOOK, WRITING-SYMBOL [on door]) = min{1, 0.5}=0.5

$\mu_{\text{ACCEPTABILITY}}$(ORNAMENT [on door])=min{1, 0.3}=0.3

$\mu_{\text{ACCEPTABILITY}}$(HANDLE [part of door])=min{1, 1} = 1

$\mu_{\text{ACCEPTABILITY}}$(LOCK [part of door])=min{1, 0.8} = 0.8

$\mu_{\text{ACCEPTABILITY}}$(GARMENT, ACCESSORY [of man]) = min{0.05,0.75} = 0.05

$\mu_{\text{ACCEPTABILITY}}$(BODY-PART [of man]) = min{0.05, 1} = 0.05

$\mu_{\text{ACCEPTABILITY}}$(HUMAN [accompanies man]) = min{0.2, 1}= 0.2

$\mu_{\text{ACCEPTABILITY}}$(ANIMAL [with man]) = min{0.2, 0.75} = 0.2

$\mu_{\text{ACCEPTABILITY}}$(KEY [as instrument]) = min{1, 1} = 1

$\mu_{\text{ACCEPTABILITY}}$(ARTIFACT [instrument]) = min{1, 0.75} = 0.75

Thus, the two interpretations of the sentence, where xyz results in the highest syntax-semantic acceptability, are:

- *The man opened the door with the handle.*
- *The man opened the door with the key.*

While it appears to be intuitively correct, in neither interpretation is it really necessary to communicate the prepositional phrase. We propose an interesting observation: things that have the membership value of 1 are there by default, as it were, and are likely to be dropped from the sentence. The exception is when these defaults are modified: it is unlikely that

we would hear *he unlocked the door with a key* – what else can he unlock the door with by default? – but it is ok to say *he unlocked the door with a golden key* or *spare key*, or *his friend's key*.

Thus, if we wish to model human communication, we should be more likely to consider concept candidates for the unknown words that are a little less than 1 than those at exactly 1. On the other hand, the grammaticality of a sentence should not be compromised. Thus, if a verb requires a direct object, and the unknown word is this direct object, then preferring the membership value of less than 1 should not play into the decision process–as the unknown word must be in the sentence for it to be grammatically correct. It is plausible that such transitive verbs develop an intransitive variant, in which case the preferred membership of exactly 1 consideration is no longer valid: it is then so preferred that it becomes trivial and must be dropped.

More generally, acceptability, which is typically barely mentioned in linguistics, cannot be explored scientifically without a serious fuzzy logic influx, and the math, tentatively offered here, may have to be developed further to capture the individual dimensions of this phenomenon as well as combining them together. Besides the syntactic and semantic dimensions that we have touched upon here, there are the:

- appropriateness dimension, which renders the sentence, *This is the best night of my life*, with the membership degree of 1 on both the syntactic and semantic dimensions, totally inappropriate (or humorous, metaphoric, or poetic) when uttered in the middle of the day;
- relevance dimension that demands that each sentence in a text be clearly related to the surrounding sentences or see its membership degree sharply decreased;
- saliency dimension, where, again, a sentence with the degree membership of 1 on the other dimensions may have a much lower value if it does not convey new and important information.

And the list is not exhaustive because, for instance, humorous, metaphoric, and poetic are probably also additional dimensions. While the membership functions will be more difficult to define in the current state of scholarship on those dimensions, the principle of calculating the acceptability of a sentence, which in turn helps with determining meanings of unknown words, will—we believe—remain essentially unchanged.

VII. REFERENCES

[1] L. Carroll, Through the Looking-Glass and What Alice Found There. 1872.

[2] G. J. Klir and T. A. Folger, Fuzzy Sets, Uncertainty, and Information. Englewood Cliffs, NJ: Prentice-Hall, 1988.

[3] S. Nirenburg and V. Raskin, Ontological Semantics. Cambridge, MA: MIT Press, 2004.

[4] J. Smarr and C. D. Manning, "Classifying unknown proper noun phrases without context," in: Technical Report dbpubs/2002-46, NLP Group, Stanford University, 2002.

[5] D, Bikel, R. Schwartz, and R. Weischedel, "An algorithm that learns what's in a name," *Machine Learning* 1999, 34:pp. 211–231.

[6] A. Mikheev, "Automatic rule induction for unknown word guessing," *Computational Linguistics* 1997, 23(3), pp. 405-423.

[7] M. Ciaramita and M. Johnson,. "Supersense tagging of unknown nouns in WordNet," in: Proceedingsof EMNLP-2003, pp. 594-602.

[8] J. Curran, "Supersense tagging of unknown nouns using semantic similarity," in: Proceedings of ACL-2006, pp. 26-33.

[9] Collins, M. and Y. Singer, Unsupervised models for named entity classification. In *Proceedings of EMNLP/VLC'99*, P. Fung and J. Zhou (Eds.),College Park, MD: ACL, 1999.

[10] S. Cucerzan and D. Yarowsky, "Language independent named entity recognition combining morphological and contextual evidence," in: *Proceedings of EMNLP/VLC'99*, P. Fung and J. Zhou Eeds.), College Park, MD: ACL, 1999.

[11] S. Buchholz and A. Van Den Bosch, "Integrating seed names and n-grams for a named entity list and classifier," in: Proceedings of the Second International Conference on Language Resources and Evaluation, Athens, Greece, 2000.

[12] J. R. Curran. "Supersense tagging of unknown nouns using semantic similarity," in: Proc. of ACL, Ann Arbor, MI: University of Michigan, 2005, pp. 26–33.

[13] Murawaki, Yugo and Sadao Kurohashi, "Online acquisition of Japanese unknown morphemes using morphological constraints," in: Proc. of EMNLP, 2008, pp. 429–437.

[14] R. M. Weischedel, M. Meteer, R. M. Schwartz, L. A. Ramshaw, J. Palmucci, "Coping with ambiguity and unknown words through probabilistic models," Computational Linguistics, 1993, 19(2): pp. 359-382.

[15] M. Ciaramita, "Boosting automatic lexical acquisition with morphological information," in: *Proceedings of the Workshop on Unsupervised Lexical Acquisition*, Philadelphia, PA, USA, 2002, pp. 17–25.

[16] D. A. Campbell and S. B. Johnson, "A technique for semantic classification of unknown words using UMLS resources," in: Proc AMIA Symp. 1999: pp. 716–720.

[17] D. Nadeau and S. Sekine, "A survey of named entity recognition and classification." In Named entities: Recognition, classification and use, S. Sekine & E. Ranchhod (Eds.), Amsterdam: John Benjamins, 2009, pp. 3-25.

[18] Y. Wilks, "Making preferences more active," *Artificial Intelligence* 11(3), 1972, pp. 197– 223.

[19] Y. Wilks, and R. Catizone, "Lexical tuning." Proceedings of Computational Linguistics and Intelligent Text Processing, Third International Conference (CICLING 2002), Mexico City, Mexico. 2002, pp, 105-126.

[20] J. M. Taylor, V. Raskin, and C. F. Hempelmann, "Towards computational guessing of unknown word meanings: The ontological semantic approach," submitted to CogSci 2011.

[21] V. Raskin. C. F. Hempelmann, and J. M. Taylor, "Guessing vs. knowing: The two approaches to semantics in natural language processing," A. E. Kibrik (Ed.), *Proceedings of Annual International Conference Dialogue,* Moscow, Russia, AABBY/Yandex, 2010.

[22] J. M. Taylor, V. Raskin, V., and C. F. Hempelmann, "On an automatic acquisition toolbox for ontologies and lexicons in Ontological Semantics," *International Conference on Artificial Intelligence,* Las Vegas, NE. 2010..

[23] C. F. Hempelmann, J. M. Taylor, and V. Raskin, "Application-guided ontological engineering," *Proceedings of International Conference on Artificial Intelligence,* H. A. Arabnia, D. de la Fuente, E. B. Kozerenko, and J. A. Olivas (Eds.), Las Vegas, NE, 2010.

[24] J. M. Taylor and V. Raskin, "Fuzzy Ontology for Natural Language," Proceedings of NAFIPS 2010, Toronto, Canada, 2010

[25] J. Yen, "Generalizing term subsumption languages to fuzzy logic," *Proc. of the 12th Int. Joint Conf. on Artificial Intelligence (IJCAI-91)*, 1991, pp. 472-477.

2011 IEEE International Conference on Fuzzy Systems
June 27-30, 2011, Taipei, Taiwan

A Fuzzy Agent-based Approach to Trust-based Competency Management

Matteo Gaeta, Francesco Orciuoli
Department of Electronic Engineering
and Information Engineering
University of Salerno
via ponte don Melillo
84084 Fisciano (SA), Italy
email: {gaeta, orciuoli}@diima.unisa.it

Vincenzo Loia, Sabrina Senatore
Dipartimento di Informatica
University of Salerno
via ponte don Melillo
84084 Fisciano (SA), Italy
email: {loia, ssenatore}@unisa.it

***Abstract*—In an era in which organizations increasingly consider the competencies of their employees as a crucial resource, human management becomes a key activity for improving staff and business performances. Important is also knowing who knows what inside the organization, so that project teams are assembled as the right mix of skill, knowledge and workforce abilities. At the same time, trust, an essential component, related to understanding interpersonal and group behavior, is an indisputable prerequisite for organizational effectiveness, in terms of social-cognitive capital, global competency as well as economic exchange and social and political stability.**

This paper defines an approach to support competency-based management by providing recommendations about the reliability of a worker in terms of trust information and own competencies. The approach lies on an agent-based architecture which supervises the Human Resources Management (HRM). Task-oriented agents monitor the employees' profiles and capabilities by maintaining update the competencies and the trusts in the organizational social network. Particularly an agent endowed by fuzzy reasoning capabilities provides recommendation about workers' competencies in HRM decision-making processes.

***Index Terms*—Competency-Based Management, fuzzy rules, multi-agent systems, trust/distrust**

I. Introduction

In a climate of global competitiveness, organizations can retain their competitive position by providing innovative products, services, and processes. The innovative potential of an organization depends on features such as skills, abilities, knowledge, experience, perspectives, and social network ties that it can draw on [1]. Organizations succeed in leveraging high levels of trust that represent a necessary condition that must be met for reaching the competitiveness potential. Trust has been defined as the "social glue" [2], that correlates positively with high degrees of personnel involvement, commitment, and organizational success. At the same time, it is " a mental state comprising expectancy (the trustor expects a specific behavior from the trustee) and belief" [3]. Computational trust models have recently been drawing the attention of many scientific communities from various disciplines [6], [7] to analyze interpersonal or inter-organizational trust in different domains such as e-commerce [8] and social web applications [9].

In literature [14], several works provide models for the trust management in virtual communities and social networks. Yet, they do not always consider the relationship existing between trust in competencies and the workers employed on specific jobs. A set of organizational processes identified by Competency-Based Management (CBM) guarantees that there is the right worker with the right competency in the right position at the right time in order to pursue high level of organizational productivity and effectiveness. Typically, CBM processes are top-down organizational processes supported by enterprise software that cannot be exploited to support team building operations in not-formal working activities.

It would be desirable to define an approach to enrich CBM with trust information in order to support the Human Resource Management in finding competencies. On the other hand, because trust is subjective measure of human beings, some works have exploited fuzzy logic as a possible best fit approach for manage uncertainties within organizational data. On the other hand, trust can be naturally expressed by linguistics terms rather than numerical values. In [8], trust has been modeled through Fuzzy Logic by defining a model for identify the information that customers expect to find on a vendors to increase their trust. The work described in [12] instead, exploits the theory of Fuzzy Cognitive Time Maps (FCTMs) into modeling and evaluating trust relationships in the virtual enterprises setting. Similarly to our approach, a fuzzy inference system has been exploited [13] to model trust measurement. The approach has been applied to improve knowledge sharing within a community to lead organizations to high level of productivity: the fuzzy system returns the degree of knowledge sharing. The goal of our approach instead is mainly devoted to suggest recommendations through the agents' supervision in HRM decision-making processes: our fuzzy system, embedded in an agent reasoning, suggests for each selected worker, the personal acquired level of competency.

Many researchers have studied the concept of trust in inter-organizational relationships and investigated trust between organizations [5], evidencing the important benefits produced by exploiting trust both individually and collectively. The

978-1-4244-7316-8/11/$26.00 ©2011 IEEE

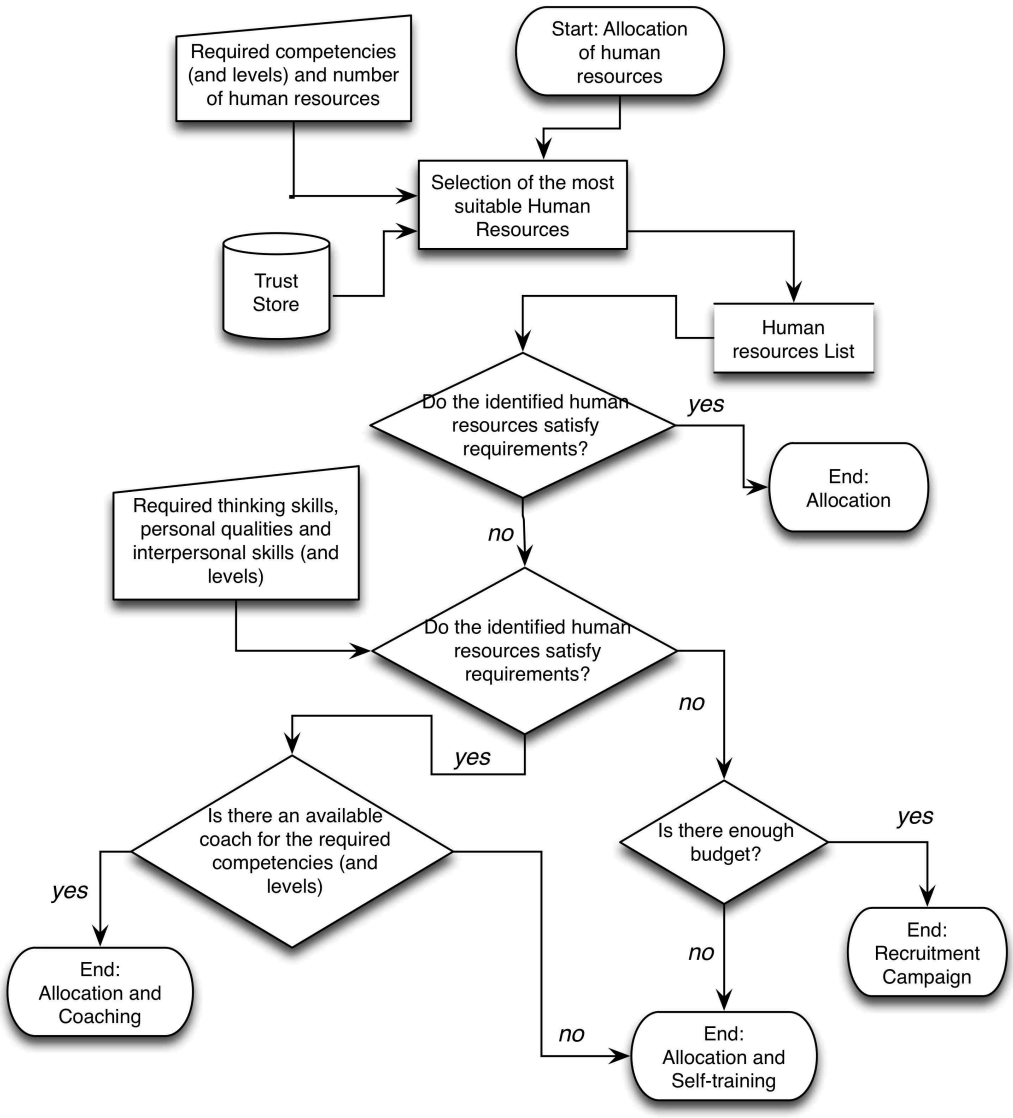

Fig. 1. Activities flow of an organizational strategy

influence of organizational procedures on attributions regarding organization' trustworthiness has been investigated in [5]. These procedures tend to increase trust between worker and supervisor or, in general, the trustworthiness in the organization. Trust might have positive effects on attitudes, perceptions, behaviors, and performance outcomes within organizational settings. In fact, the receipt of positive outcomes constitute evidence that the organization can be counted on to perform behaviors desired by the trustors and is related to employee job satisfaction and overall perceptions of organizational effectiveness.

This work presents an agent-based approach to support competency-based management in an organization. Recommendations address organizational strategies as well as the trustworthiness of a worker in terms of acquired trust degree and own competency levels. Fundamental role to reach this goal is played by the team builder agent which embeds fuzzy reasoning capabilities, in order to provide recommendation about workers' competency in Human Resources Management (HRM) activities.

The remaining of this paper is organized as follows. Section II presents the main step of an enterprise strategy for the human resources management. The role of trust for the human resources allocation is presented in Section III where the concepts of trust and also distrust are formally given. Section IV depicts the logical view of the framework and the role of the agent-based platform. The tasks accomplished by each agent and their interactions are given too. Particularly, Section V provides a closer look on the task accomplished by the team builder agent; it implements a fuzzy inference system to deduce a single overall measure of the worker's competency. Then, Section VI gives an example of applicative scenario. Finally,

conclusion and future works close the paper.

II. Organizational Strategies

In order to refine the human resource allocation process we also need to consider the specific enterprise strategy with respect to human resource management. Figure 1 shows an example of an enterprise strategy aimed at allocating workers whose profiles meet the competency (and level) required by the Decision Support System (briefly, DSS).

In [11], a set of strategic human resource management practices are described. The most relevant, for the purpose of this work, are "Recruitment and Selection" and "Training and Development". During a human resource allocation process, in situations where there is not a perfect match between the required competencies (and levels) and the available competencies (and levels), the awareness of the enterprise strategy could help the decision making. As shown in Figure 1, when there are no workers that match the required competencies and level, the strategy is designed to apply one of two practices. When the company's strategies aim at growing its employees professionally, Training and Development is the favorite practice. It is selected if there are workers in the company that have the required competency, even though with a different (lower) level. In particular, additional skills (e.g. continuous learning, teamwork, etc.) and personal qualities are required for the human resources to be allocated. The strategy foresees a training time (individual or flanked by a coach if available) for them. Otherwise, if the organizational budget allows it, a recruitment campaign (Recruitment and Selection practice) can be activated. The flow of Figure 1 is only one of the plausible practices that an organization could use with respect to the current adopted strategies. A practice can be defined and executed by using a Decision Support System.

In the following sections an approach to refine and improve these practices, by using trust information, will be proposed.

III. Trustor, Trustees and Trust in Competencies

Trust emphasizes how people work together and build effective relationships; it is a critical link to all good relationships, both personal and professional.When workers believe that they are working for trustworthy organization, they are willing to invest their time and talents in making a real contribution in the activities where they are involved. People who trust supervisor will invest more of themselves in their work. Similarly, the trustor evaluates the worker's behavior on the activities, providing a trust degree which be rewarding and incentives him to do better. High trust degrees lead to a great sense of self responsibility, interpersonal insight and collective wishes to reach common goals.

In this work, the trustor is the corporate identified as the community of its employees, the trustees are the employees and we are interested in trust in competencies:

$$trust_c(e, x, k), \tag{1}$$

Category	Sub-category	Examples
Technical Competencies	Knowledge	Java language syntax
		Description logics
		UML notation
	Technical Skills	Java programming
		OWL modeling
		Project management
Behavioural and Cognitive Competencies	Thinking Skills	Problem-solving
		Innovation & creativity
		Continuous learning
	Interpersonal Skills	Teamwork
		Relationship management
		Communication
		Teaching others
	Action Skills	Decision-making
		Results orientations
		Planning & organization
	Personal Qualities	Integrity
		Self-motivation
		Responsibility
		Self-management

Fig. 2. Different types of competencies

The statement 1 indicates that the corporate (trustor) trusts employee e (trustee) regarding the capability of e to apply competency x in context k. Similarly, the distrust is defined as following:

$$distrust_c(e, x, k), \tag{2}$$

The statement 2 indicates that the corporate (trustor) does not trust employee e (trustee) regarding the capability of e to apply competency x in context k.

In the organizations, it seems to be a good choice to divide competencies into behavioral and technical competencies (see Figure 2). *Behavioral competencies* include all those soft skills and attitudes that enable a person to perform well in a specific function, such as *communication*, *problem-solving*, *integrity*, *planning and organization*, etc. *Technical competencies* are specific and depending on the job. These latter could range, for instance, from the knowledge of software development methodologies to skill for Java programming. Authors in [10] propose to calculate trust values in terms of frequencies of positive experiences between the trustor and the trustee. In our proposal, an experience is modeled as a work activity (or task). For each task there are a worker (an employee) and a supervisor. The underlying idea is that the supervisor assigns a rate to the performance of the employee involved in the task. The rate can be interpreted as a value indicating how the required competencies have been applied during the execution of the task. Our goal is to calculate the corporate trust in competencies for each employee. More in details, in the case of **trust in competencies**, formula (3) can be used. In this case the `trustor` is the corporate (intended as the community of

the employees) and the `trustees` are the employees.

$$\alpha = td_c(e, x, k) = n/m, \tag{3}$$

where m is the total number of situations in which e (trustee) has applied competency x in the context k, and n is the number of positive experiences in that set, β (distrust) can be calculated with the same formula (3) of α by replacing n with l and td_c with dtd_c, where l is the number of negative experiences in the same set. Values for n and l can be calculated with the following:

$$n = \sum_{m}^{i=1} e_p(i), l = \sum_{m}^{i=1} e_n(i), \tag{4}$$

where $e_p(i), e_n(i) \in [0, 1]$, representing the degree of the experience i being positive or negative separately, and $e_p(i) + e_n(i) \leq 1$. In the context of this work, a positive (negative) experience is represented by a task, that requires competency x, where any supervisor has provided a positive (negative) review rate $e_p(i)$ ($e_n(i)$) to the worker e for the application of competency x in the context k. Untrust γ can be calculated by using the formula $\alpha + \beta + \gamma = 1$ [10].

IV. Architecture Overview

The proposed approach is based on an agent-based platform aimed at sustaining and exploiting trust-based competency management by improving decision making processes with respect to human resource management activities. The approach also foresees a mechanism to weigh up each decision with organizational strategies and policies. Figure 3 provides a sketched sample enterprise IT environment showing all the components/systems involved in our approach.

- **Human Resource Management (HRM) System** is a typical system used in enterprise context in order to manage employees' profiles, competencies, career plans, payroll, allocations, etc. Typically, HRM systems are not in charge of the trust management.
- **Competency Assessment System** represents a set of tools used to assess employees' competencies and relative competencies levels. These tools can range from questionnaires (electronic form-based, papery, etc.) to Web-based e-Testing System.
- **Collaborative Working Environment (CWE)** is a set of tools used, in the organization, to support employees' tasks. Document Management Systems, Collaborative Workspaces, Wiki, Blog, Instant Messaging and Videoconferencing are examples of these tools.
- **Decision Support System** represents an environment providing human resource managers with suggestions regarding decision making processes. In this work, we focus on decision making about human resource management.
- **Trust Store** is the database in which, for each employee, trust degrees are stored and associated to employees' competencies (and levels). Data used to calculate trust degrees for each employee are also maintained in Trust Store. We assume that for each employee there is a set of tuples <*competency, competency level, context, trust, distrust, untrust*> that states all the competencies owned by the employee. The first three values come from the Human Resource Management System. Trust, distrust and untrust values are calculated by agents exploiting a social approach. Competency is a label representing a specific competency (e.g. Project Management), competency level is a value in the set {*novice*, *advanced beginner*, *competent*, *proficient*, *expert*} (according to Dreyfus model of skill acquisition [4]), context is a label (e.g. R&D Projects) representing the domain in which the competency is applied.

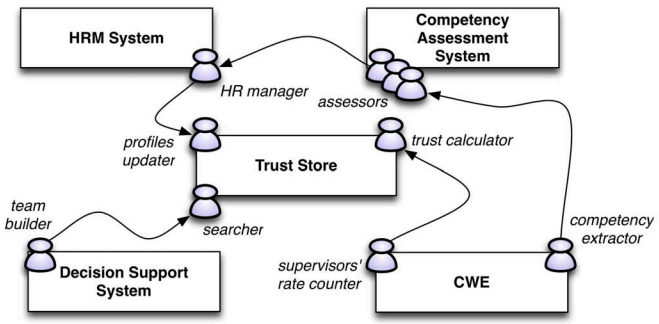

Fig. 3. Logical overview of the architecture

The agent-based paradigm represents the glue to make the several and heterogeneous systems communicating though distributed interactions. In fact, task-oriented agents are designed for each system to guarantee ACL-based communication, monitoring the interaction to each other and support a competency management in human resource processes such as, for instance, effective project team building. Let us introduce the role of each agent, associated to the components of the architecture.

- **HR manager agent**: handles workers' competency profiles inside the HRM system by updating them when new competencies must be added to a specific worker (this information comes from assessors agents) and by communicating last updates to the profiles and network updater agent.
- **Assessors agents**: handle different types (formal and informal) of workers' competency assessment. For instance, this agent is responsible for receive and elaborate the information extracted from collaborative sessions data and content in order to discover unknown competencies from actions and results of workers during their collaborative work activities carried out by using CWE.
- **Competency extractor agent** is responsible for extracting information about employees' competencies from content and data tracked by CWE and for communicating it to the assessor agent.
- **Supervisor's rate counter agent** is responsible for no-

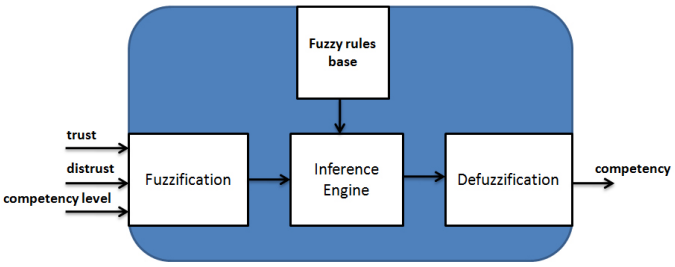

Fig. 4. Fuzzy Inference System

tifying new rates added by a supervisor to judge the performance (applying a specific competency) of a worker (trustee) with respect to a specific task. This agent communicates new posted rates to the trust calculator agent.

- **Trust calculator agent** uses supervisors' rates to produce trust degrees and updates values into the Trust Store.
- **Searcher agent** answers to the queries coming from decision support systems in order, for instance, to find workers owning specific competencies.
- **Team builder agent** provides recommendations about project team composition with respect to a set of needed competencies (and levels). This agent produces recommendations by elaborating information coming from the searcher agent.
- **Profiles updater agent** handles updates into the Trust Store with respect to employees' profiles (modifications to the owned competencies and levels) according to HR manager agent.

V. A CLOSER LOOK AT THE TEAM BUILDER AGENT

The aim of the team builder agent is to support DSS in the competency-based management and suggest recommendations for selecting suitable human resources to recommend to DSS. Precisely, this agent provides a list of workers whose competency matches the DSS request, in terms of competencies and associated levels. The goal of the agent is to provide not only the suitable workers that match the request, but, at the same time, evaluate the "accumulated" trust of the worker (during his previous organizational tasks) on the requested competency. In this way the agent suggests information which represents a kind of trade-off between the two different types of information: on one hand, the trust assigned (and calculated through the above described social approach) by the corporate to the worker on the requested competency, on the other hand, his competency and level in his profile. This balanced evaluation represents an added value that is not directly traceable by the DSS, but it is computed by agent exploiting its embedded reasoning model.

The team builder agent indeed incorporates a fuzzy inference system, which exploits a fuzzy rules base to deduct the overall evaluation of competency of a worker.

Fuzzy inference systems (FIS) are very simple conceptually (see Figure 4). They consist of an input stage, a processing stage, and an output stage. The input maps inputs to the appropriate membership functions and truth values (fuzzification). The processing stage invokes each appropriate fuzzy rule and generates a result for each, then combines the results of the rules (fuzzy reasoning). Finally, the output stage converts the combined result back into a specific control output value (defuzzification). The use of fuzzy inference system makes more intuitive the interpretation of values describing the trust (or the distrust) in a competency of the worker (i.e., trustee). In the real world, when human beings inquire to each other about the competency of an entity, preferably the answers are expressed through a linguistic terms, such as HIGLY COMPETENT, NO COMPETENT, etc., rather than using numerical values. In the light of this consideration, the team builder agent has been designed to simulate the human behavior, then it should provide answers using the same terminology as humans to make it more believable.

The fuzzy inference process exploits Mamdani's fuzzy inference method [15], which takes as input two numerical values representing the number of positive and negative experiences of some trustor for that worker (on a given context) and a competency level (assigned by the organization on the same context). Figure 4 shows information flows from three input variables to a single-output. Let us observe that the organization, by means HRM System, stores competencies (and levels) for each employee. Levels are defined according to the Dreyfus model of skill acquisition [4] which identifies five levels of competencies (detailed in Section IV). The competencies are assigned a priori to each workers through the organizational policy of competency Assessment System, through the assessors agents (see Figure 3), in accordance with their capabilities, certification and past working experiences. Competencies are always associated to a specific context in which they are applied, as said in Section IV.

The output of the fuzzy rules is a "synthetic" value that describes the overall competency of that worker for a specific context. Precisely, the IF-THEN fuzzy rules composing the knowledge based have the following form:

- IF trust is *high* AND distrust is *low* AND comp_level is *expert* THEN competence is *very high*
- IF trust is *high* AND distrust is *low* AND comp_level is *proficient* THEN competence is *high*
- IF trust is *medium* AND distrust is *low* AND comp_level is *proficient* THEN competence is *high*
- ...
- IF trust is *low* AND distrust is *low* AND comp_level is *advanced beginner* THEN competence is *low*
- IF trust is *low* AND distrust is *low* AND comp_level is *novice* THEN competence is *very low*

These rules evaluate a worker regarding to a specific competence by exploiting associated supervisors' trust and

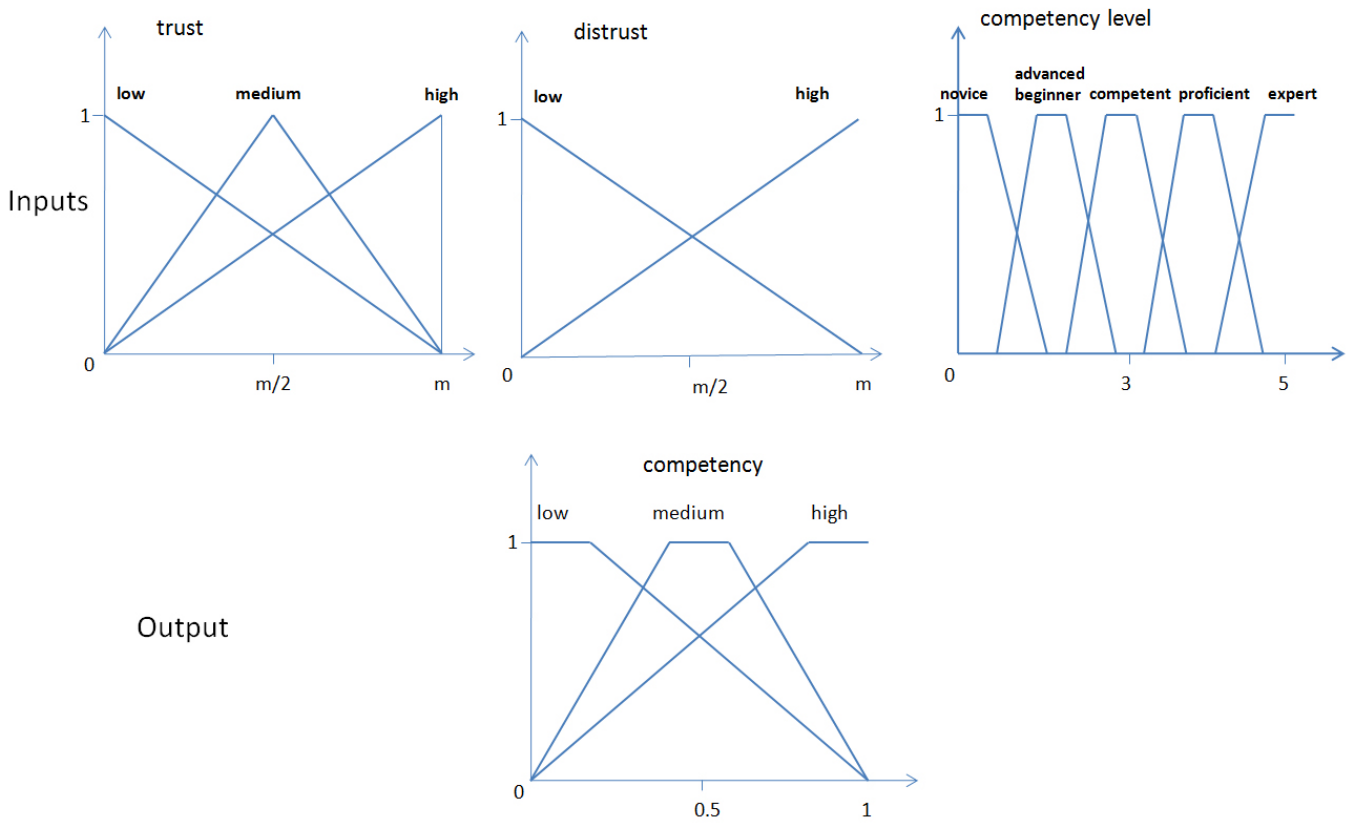

Fig. 5. Inputs and Output fuzzy sets for the reasoning of the team builder agent.

competence level.

Although the specific competency of each worker is related to the trust of the corporate, it is not influential in this stage, because we exploit only the type (positive or negative) of experiences gained during his working activities. Then, the untrust is not considered in this modeling. Figure 5 shows the fuzzy sets associated to the fuzzy reasoning embedded into the team builder agent. The linguistic terms of trust and distrust are modeled as triangular fuzzy sets, while the competence level is described by trapezoidal membership functions; similarly, the output is represented by trapezoidal membership functions. These functions seem good enough to capture the vagueness of those linguistic assessments. Due to many rules associated to knowledge base defined to model our variables, we give just same example of them. Moreover, the output fuzzy variable is defined through its primary terms: *low, medium and high*, the other are derived by applying linguistic modifiers (not shown in Figure 5).

Note the function memberships describing the inputs have the same distribution for all the worker, even though the input fuzzy sets are defined on a domain which depends on a parameter m. The value m represents the total number of situations in which the trustee has exploited his own competency in a certain context, according to the definition of *trust in competencies* (see formula (3)). This value strictly depends on the worker. Specifically, for each worker, the team builder agent loads the relative fuzzy rules based knowledge and applies the inference based on the instanced set of fuzzy rules.

According to the Mamdani-type inference, the output of the fuzzy system is a single value computed by defuzzification of the aggregated output fuzzy sets. Herein, we have exploited the most popular defuzzification method, i.e. the centroid calculation, which returns the center of area under the curve representing the aggregated output. This value represent the "overall" competency of a given worker in a given context.

For each selected worker, the team builder agent returns a synthetic competency value. Then a ranked list of workers is returned. It represents the recommendation to send DSS.

VI. An Example Scenario

Let us suppose a team building request occurs. The DSS requires for some specific competencies with the associated level of assessment about those competencies in some specified context. For instance, one of the desired requirements might be to select a human resource whose competence level is *expert* in Java programming and *proficient* in team working. The searcher agent, which is in charge of complying this request, returns to the team builder agent the set of workers that have both the competencies. For each worker, the agent instantiates the set of fuzzy rules associated to him: his value m of total number of situations (experienced by trustors) and the fuzzy set representing the own competence level as well. In

other words, if the worker *d* has competence level *competent* in Java programming and his number of experiences in this context is 7, the relative fuzzy rules base will be the domain [0, ..., 7] of membership functions for trust and distrust (see Figure 5) and the linguistic term used will be *competent*. Thus, the team builder agent applies the inference model on the knowledge based associated to that worker and deduces how he is "competent" in the specific context. At the end, the ranked list of all the workers is returned.

It is interesting to observe that sometimes an organization prefers to select workers with competencies levels that are slightly lower than the desired ones, for internal policy such as personnel cost, career development, etc. As said in Section II, Figure 1, the organizational strategies/policies could be to apply "Training and Development" practice. In fact, it would be desirable that, when the team builder agent is committed to find human resources with a specific competency level (in a given context), it does not answer with a perfect match, but provides workers whose competency level and trustworthiness together approximate the request.

The agents should select all the workers that have competency in a requested context (for instance, in Java programming), without further filtering on the required competence level. An idea is to use for each worker twice the fuzzy inference system: firstly, compute the overall competency by exploiting his competence level, as described in Section V. We call the final value of inference process the *personal competence* of each worker. Then we would evaluate the expected overall competency of the selected worker, considering instead the required its competence level. The goal is to compare the two output values. Thus, when the team builder agent instantiates the fuzzy inference rules associated to a worker, executes once the inference with is personal rule base. Then it executes a modified version of the worker rules base that substitutes the fuzzy linguistic term describing the competence level of worker with the required one.

After the inference, the agent obtains two values that represent the competency: the *personal* and the *expected* ones. By comparing the two values, it possible to assess how much the personal value of worker's competence approximate the expected one. Thus, the agent will return the worker whose difference between these two values is minimum. Let us note that when the agent selects a worker whose competence level fully matches the the requested one, the two values will be equal. This comparison allows us to get the worker whose competence approximates to desired one. More important, the output values include an evaluation with respect to the trust. In other words, we evaluate the competence of a worker (with respect to the requested one), taking into account also the trustworthiness of the worker. The final ranked list will be a pool of suitable human resources, which could do not fully match the DSS request, but meets the organizational policy.

Modelling the competence level, trust and distrust allows us to get a new measure of competence as a balanced mix of these parameters that could better reflect the organization policy. This result is preferable to a crisp reply for the request "all and just the workers with a given competence level on a context", that can mean an high cost in terms of resources allocation. As said in Section II, the organization can be interested in activity of "Training and Development", to professionally increase the competencies levels of its employees. The fuzzy inference model of the team builder agent can provide this kind of answers.

VII. Conclusion

This paper defines an agent based framework which supports competency-based management. The trustworthiness of a worker is evaluated as combination of his accumulated trust and competency levels for a specific context. A fuzzy inference system, embedded into the team builder agent, accomplishes the combined evaluation which provides an added value to the overall evaluation of a worker, through an adequate balancing of human expertise, competencies and capabilities. The agent returns recommendations to DSS request, providing a ranked list of the workers which matches or just approximates the request competency and level.

In this work, we have exploited Fuzzy Logic to model the trust (and distrust) in competency as well as the competency level. Although the modeling of this framework is still in progress, as future work, we intend to extend the fuzzy modelling to other parameters related to organizational strategies and the human resource management. The approach will be experimented in ARISTOTELE FP7 EU-Project.

References

[1] I. Nonaka, G. F. von Krogh, and S. C. Voelpel, Organizational knowledge creation theory: Evolutionary paths and future advances. Organization Studies 27: 1179-1208, 2006.

[2] S. Atkinson, and D. Butcher, Trust in Managerial Relationships, Journal of Managerial Psychology, Vol. 18 No. 4, pp. 282304, 2003.

[3] R. C. Mayer, J. H. Davis, & F. D. Schoorman, An integrative model of organizational trust. Academy of Management Review, 20:3 pp.709 734, 1995.

[4] S. E. Dreyfus Formal models versus human situational understanding: Inherent limitations on the modelling of business expertise (ORC 81-3). Berkley: Operations Research Center, University of California, 1981

[5] R. M. Kramer, "Trust and Distrust in Organizations: Emerging Perspectives, Enduring Questions, Annual Reviews Psychology, 50, 569-598, 1999.

[6] D. H. McKnight,V. Choudhury, and C. Kacmar, Developing and Validating Trust Measures for E-Commerce:An Integrative Typology," Information Systems Research, 13(3), 334-359, 2002.

[7] X. Li, J. S. Valacich, and T. J. Hess. Predicting User Trust in Information Systems: A Comparison of Competing Trust Models. In Proceedings of the 37th Annual Hawaii International Conference on System Sciences (HICSS'04), Washington, DC, USA, 2004.

[8] S. Nefti, F. Meziane, and K. Kasiran. A Fuzzy Trust Model for E-Commerce. In Proceedings of the Seventh IEEE International Conference on E-Commerce Technology (CEC '05). IEEE Computer Society, Washington, DC, USA, 401-404, 2005.

[9] F. Skopik, D. Schall, and S. Dustdar. Modeling and mining of dynamic trust in complex service-oriented systems. Inf. Syst. 35, 7 (November 2010), 735-757, 2010.

[10] J. Huang and D. Nicol, , A Formal-Semantics-Based Calculus of Trust, IEEE Internet Computing, 14, 5, 38-46, 2010.

[11] Z. Hui, Computer Technology and Development, ICCTD '09. International Conference on Practice of Strategic Human Resource Management In the Enterprise, volume 1, 683 -686, 2009.

[12] Z. Wei, L. Lu, Z. Yanchun, Using fuzzy cognitive time maps for modeling and evaluating trust dynamics in the virtual enterprises, Expert Systems with Applications, Volume 35, Issue 4, 2008, Pages 1583-1592, 2008.

[13] B. ZadJabbari, S. Mohseni, P. Wongthongtham, Fuzzy logic based model to measure knowledge sharing, 3rd IEEE International Conference on Digital Ecosystems and Technologies, 2009. DEST '09, pp.507-510, 1-3 June 2009
[14] D. Artz and Y. Gil, A survey of trust in computer science and the semantic web, J. Web Sem., vol. 5, no. 2, pp. 5871, 2007.
[15] E.H. Mamdani,and S. Assilian, An experiment in linguistic synthesis with a fuzzy logic controller, International Journal of Man-Machine Studies, Vol. 7, No. 1, pp. 1-13, 1975.

2011 IEEE International Conference on Fuzzy Systems
June 27-30, 2011, Taipei, Taiwan

New Evolution Algorithm Based On The Standard Particle Swarm Optimization

Lipeng Wang[1], Yangjie Cheng[2], Dong C. Liu[3]
[1, 2, 3] Computer Science College, Sichuan University, Chengdu, China
Email: wlpscu@126.com

***Abstract*—The particle swarm optimization (PSO) is an alternative for global optimization. A standard for PSO (SPSO) was defined which took into the latest developments, and was used as a baseline for performance testing of improvements. In SPSO, however, particles need to search the optimal solution in the constraint space, and the item velocity in PSO makes particles difficult to adjust themselves to meet those complicated constraints. A new PSO without the item velocity based on SPSO is proposed in this article. The new algorithm inherits the capability of SPSO with fast convergence and high accuracy. This research proves that the convergence process of PSO has nothing to do with the velocity and the proposed method modified simple PSO (msPSO) can converge. The experiments show that msPSO is able to achieve a good result.**

Keywords- particle swarm optimization; constraint space; optimal solution

I. INTRODUCTION

Particle swarm optimization (PSO) was first proposed by Eberhart and Kennedy in 1995[1]. For the sake of simplicity, we call the original PSO algorithm traditional particle swarm optimization (TPSO). This method, inspired by simulation of bird flocking or fish schooling, is a stochastic global optimization. In TPSO, each particle adjusts itself in the search space according to the best position it has found so far and the best position of all the particles in the swarm. The iteration will terminate when the particle converges to the global best point. In TPSO, particles represent potential solutions for the optimized problem. In the search process, each particle has its own position and velocity, represented by X and V respectively.

Compared to other evolutionary algorithms, such as genetic algorithms, artificial neural networks, genetic programming and ant colony optimization, PSO has the advantage of easy implementation and fast convergence. It is amenable to solve complex and diverse issues. PSO has been applied in function optimization, artificial neural network, fuzzy system control, machine learning and so on [2].

TPSO is mainly dependent on the experience of the corresponding particle and the particle's companions. Under some extreme conditions, convergence of TPSO will be very slow with low accuracy during the process of iteration; moreover, the particles will always "spiral" around the local extreme value. An inertia coefficient is added to TPSO to increase the probability of jumping out of local minimum [3]. The inertia coefficient can also balance between global and local search. TPSO is non-linear, and until now there still has not been an effective way to mathematically determine the value of parameters in TPSO to simulate the search process. A fuzzy system was proposed to dynamically adapt the inertia coefficient of TPSO, which could adaptively adjust the coefficients [4]. Another modified PSO (MPSO) was proposed to discard the velocity to get rid of restrictions of the range of velocity and the process was only controlled by the particle's position [5]. PSO has developed a lot with many researchers exploring the concepts and application of the algorithm. Because of different kinds of PSO existing, it is hard for researchers to find a reference to improve. A standard for PSO (SPSO) was defined which took into account current developments. SPSO is regarded as the extension of the TPSO, and can improve performance effectively [6]. The algorithm is intended as a baseline of improvements and provides a valuable point of comparison which can be used for researchers to better test new advances. However, SPSO is still limited to velocity. In some situation, the particle still has the problem with divergence and low accuracy. This research proves that the iteration of SPSO has nothing with the velocity, and proposes a new modified simple PSO (msPSO). The new algorithm removes the constraints of velocity and is proved to converge at a fixed position. The experiment illustrates that msPSO can improve its performance for the five benchmark functions.

The paper is organized as follow: In Section Ⅱ, the related background is presented in details. In Section Ⅲ, a new modified particle swarm optimization is proposed. What is more, the research also proves that the convergence process of PSO has nothing to do with the velocity and the proposed method msPSO can converge. Experiments are done on five benchmark functions and results are analyzed in Section Ⅳ. Finally we conclude the paper in Section Ⅴ.

II. RESEARCH BACKGROUND

TSPO is a global optimization algorithm. The search space for a specific problem is represented by a swarm with a great number of particles. During the process of iteration, the position X and velocity V of the corresponding particle are updated according to the particle's individual best position of its experience, denoted by "iBest", and the swarm's best position, represented by "gBest". The criterion of judging the position for a particle is presented by a "fittness" function. TPSO can be formulated as follows:

$$V_{id}(t+1)=\omega V_{id}(t)+c_1r_1(P_{iBest}(t)-X_{id}(t))+c_2r_2(P_{gBest}(t)-X_{id}(t)) \quad (1)$$

$$X_{id}(t+1)=X_{id}(t)+V_{id}(t+1) \quad (2)$$

where $i=1,2...N$, N is the number of particles in the swarm, $d=1,2...D$,D is the dimension of particles. c_1 and c_2 are nonnegative constants, r_1 and r_2 are random number uniformly distributed in[0,1]. $V_{id}\in[-V_{\max},V_{\max}]$, when V_{id} is more than $V_{\max}$, set $V_{id}=V_{\max}$, and on the other hand, when V_{id} is less than $-V_{\max}$, set $V_{id}=-V_{\max}$, $V_{\max}$ is a pre-set parameter. ω is the inertial weight, which is a constant value distributed in[0,1] . `

Clerc et.al [7] add a constraint factor α to control V as:

$$X_{id}(t+1)=\alpha X_{id}(t)+V_{id}(t+1) \quad (3)$$

[5] shows the evolution of TPSO has nothing to do with the particle velocity, and proposes a modified PSO (MPSO). In MPSO, the velocity V is removed so the discussion of V is avoided, which can simplify the process of iteration. The algorithm is presented by:

$$X_{id}(t+1)=\omega X_{id}(t)+c_1r_1(P_{iBest}-X_{id}(t))+c_2r_2(P_{gBest}-X_{id}(t)) \quad (4)$$

In 2007, Daniel Bratton and James Kennedy designed a standard particle swarm optimization (SPSO), which is the extension of TPSO[6]. SPSO combined the latest developments of PSO, and could improve the performance of iteration effectively. SPSO is denoted by:

$$V_{id}(t+1)=\chi(V_{id}(t)+c_1r_1(P_{iBest}(t)-X_{id}(t))+c_2r_2(P_{gBest}(t)-X_{id}(t))) \quad (5)$$

$$X_{id}(t+1)=X_{id}(t)+V_{id}(t+1) \quad (6)$$

subject to:

$$\varphi=c_1+c_2 \quad (7)$$

$$\chi=\frac{2}{|2-\varphi-\sqrt{\varphi^2-4\varphi}|} \quad (8)$$

The research has found that when $\varphi<4$, particles will spiral around the best found solution in the search space with no guarantee of convergence. While $\varphi>4$, SPSO can converged quickly.

SPSO is different from TPSO . The difference is as follows:

1) *Swarm Communication Topology:*

The global topology is used in TPSO, as shown in Fig.1 (a). In this topology, the global extreme is chosen by the comparison of all the particles in the swarm. While in SPSO, a local topology is used, and the global extreme for a specific particle is obtained by comparison of its neighbors, as shown in Fig.1 (b). To distinguish between the two concepts, in this paper, the global extreme obtained by the global topology is called the global optimal solution, while chosen by the local topology is called the local optimal solution.

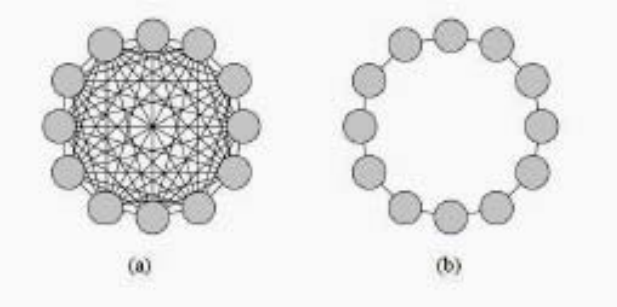

Fig.1. TPSO and SPSO topologies

2) *Inertia weight*

In TPSO, the inertia weight is used to adjust the influence of velocity in the previous step affected on the present step. By adjusting the inertia factor, particles in TPSO can be bound into the region containing the global optimal solution, while not trapped into local optimal solution. A new variable λ is introduced into SPSO which removes the inertia weight. Experiments show that compared with TPSO, SPSO gets better results while maintains the same simplicity with TPSO. Because SPSO is a combination of the latest PSO developments, it can be used as a reference for future work, thus avoid the redundant work of comparison.

III. METHOD

SPSO includes both velocity (V) and position(X). In practice, due to a lot of restrictions with X, the existence of V makes it very difficult to limit X into a designed search space. In this paper, it is found that evolutionary process of SPSO is independent of V.

Theorem A: SPSO has nothing to do with the particle velocity

Proof: let $\omega=c_1r_1\lambda p_0+c_2r_2\lambda p_g$, $\varphi=c_1r_1\lambda+c_2r_2\lambda$. In SPSO, the constraint factor $\alpha=1$. [7] has proved that the constraint of V is equivalent to the constraint factor α , so the scope of V will not be considered. Excluding P_{iBest} and P_{gBest} on the impact of each dimension, each dimension is dependent of each other. In order to simplify the certification process, we can just consider the case of one-dimension, and the subscript d can be omitted. Assuming that the other particles are kept fixed except the i - particle, the subscript i can also be omitted. For SPSO, after one iteration, we can get:

$$V(t+2)=\lambda V(t+1)+\omega-\varphi X(t+1) \quad (9)$$

$$X(t+2)=X(t+1)+V(t+2) \tag{10}$$

From equation (9) and(10), we can get:

$$V(t+1)=\frac{1}{\lambda}(X(t+2)-X(t+1)-\omega+\varphi X(t+1)) \tag{11}$$

Put equation(11) into equation(6):

$$X(t+2)+(\varphi-\lambda-1)X(t+1)+\lambda X(t)-\omega=0 \tag{12}$$

From equation(12), SPSO has no concept of V, which can simplify the process of PSO. Because SPSO is independent of V, so the item V can be removed from SPSO, just as:

$$X_{id}(t+1)=\chi(X_{id}(t)+c_1r_1(P_{iBest}-X_{id}(t))+c_2r_2(P_{gBest}-X_{id}(t))) \tag{13}$$

The research calls this new algorithm modified simple particle swarm optimization (msPSO). In msPSO, the global extreme is obtained through the local topology.

Theorem B: if the average behavior of msPSO is observed through its expected value, msPSO converges

Proof: For ease of exposition, the symbols in theorem A will be used, and the equation(13) can be formatted as:

$$X(t+1)=(\chi-\chi c_1r_1-\chi c_2r_2)X(t)+\chi c_1r_1P_{iBest}+\chi c_2r_2P_{gBest} \tag{14}$$

The equation (14) is a first order differential equation, and we can set:

$$X(t+1)=X(t)+X'(t)(t+1-t) \tag{15}$$

From the equation(15), the equation (14) can be deformed as:

$$X'(t)+(\chi c_1r_1+\chi c_2r_2-\chi-1)X(t)=\chi c_1r_1P_{iBest}+\chi c_2r_2P_{gBest} \tag{16}$$

Solution for the differential equation is:

$$X(t)=\frac{\chi c_1r_1P_{i\mathrm{Best}}+\chi c_2r_2P_{\mathrm{gBest}}}{\chi c_1r_1+\chi c_2r_2-\chi+1}+\mathrm{C}e^{-(\chi c_1r_1+\chi c_2r_2-\chi+1)t} \tag{17}$$

Since the first half items of equation(17) is constant, they can be omitted. If $\lim_{t\to\infty}X(t)$ converges, then:

$$\lim_{t\to\infty}\left|\frac{\mathrm{C}e^{-(\chi c_1r_1+\chi c_2r_2-\chi+1)(t+1)}}{\mathrm{C}e^{-(\chi c_1r_1+\chi c_2r_2-\chi+1)t}}\right|<1 \tag{18}$$

Equation (18) is equivalent to equation(19):

$$\chi c_1r_1+\chi c_2r_2-\chi+1>0 \tag{19}$$

Since r_1 and r_2 are uniformly distributed, the average behavior of msPSO is observed through its expected value.

$$E(r_1)=\int_0^1\frac{x}{1-0}dx=\frac{1}{2} \tag{20}$$

$$E(r_2)=\int_0^1\frac{x}{1-0}dx=\frac{1}{2} \tag{21}$$

From the equation(20) and the equation(21), we can infer that the equation(19) is equivalent to equation(22)

$$\chi(c_1+c_2-2)>-2 \tag{22}$$

Since $\chi>0, c_1+c_2>4$, the equation(22) holds. Equation(13) converges to:

$$\lim_{t\to\infty}X(t)=\frac{\chi c_1r_1P_{iBest}+\chi c_2r_2P_{gBest}}{1-\chi+\chi c_1r_1+\chi c_2r_2}=\frac{2\chi c_1P_{iBest}+2\chi c_2P_{gBest}}{2-2\chi+\chi c_1+\chi c_2} \tag{23}$$

IV. EXPERIMENTS AND RESULTS

To analysis the effect of the proposed algorithm, five benchmark functions are provided for the comparison of particle swarm optimization:

Sphere f1: $f_1(x)=\sum_{i=1}^{n}x_i^2$

Griewank f2: $f_2(x)=\frac{1}{4000}\sum_{i=1}^{n}(x_i)^2-\prod_{i=1}^{n}\cos(\frac{x_i}{\sqrt{i}})+1$

Rastrigin f3: $f_3(x)=\sum_{i=1}^{n}(x_i^2-10\cos(2\pi x_i)+10)$

Duadric f4: $f_4(x)=\sum_{d=1}^{n}\left(\sum_{j=1}^{d}x_j\right)^2$

Shaffer f5: $f5(x)=0.5+\frac{\left(\sin\sqrt{x^2+y^2}\right)-0.5}{\left(1.0+0.001\left(x^2+y^2\right)\right)^2}$

The details about the five benchmake functions described as table 1. In table 1, Dim represents the particle dimension, and Range is the search range of particles. Optimal is the extreme value of the corresponding functions and Goal

represents the accuracy of optimization. Four PSO algorithms (MPSO, msPSO, TPSO, SPSO) will be compared using the five functions. To increase the difficulty of the optimization process, the paper expands the dimension of functions and increases the target precision. With these harsh conditions, it can be more easily for us to compare and highlight performance. In our research, the number of particles is 15, and the maximum number of iterations is 500000. After 500000 iterations, iteration will terminate even the result does not meet the target accuracy. For the other parameters in PSO, the recommended parameters in [5] will be used. In MPSO and msPSO, $c_1 = c_2 = 2.05$, $\omega = 1.0$; in TPSO and SPSO, $c_1 = c_2 = 2.05$, $\omega = 0.8$, $V \in [-2,2]$.

The convergence precision and speed with the fix number of iterations is as shown as fig.2. In Fig.2, X axis represents the iteration number and Y axis represents logarithm of the global optimal solution. When the algorithm reach the required precision after less than 500000 iterations, it will exit and the global optimal.

It can be found in Fig.2 that the five functions can meet the precision requirements with less than 50 iterations. For the function f3, TPSO, SPSO and MSPO always hover around a local minimum, and can not converge; however msPSO can meet the required precision in the number of 50 iterations or less. Compared with other three algorithms, msPSO has a good performance to escape the local minimum. In addition, from the Fig.2, it can be found that for all the objective functions msPSO can achieve the target in less than 500000 iterations, which means that msPSO has good capability of convergence.

Table 2 shows the number of iterations with the accuracy of 0.00005 for PSO to train the five baseline functions. ">500000" represents that the algorithm is not able to achieve the required precision after 500000 iterations. From Table 2, TPSO, which relates to the selection of too many unknown parameters, is not able to convergence in a fixed number of iterations for f1-f4.

TABLE 1 BENCHMARK FUNCTION

Function name	Dim	Range	Optimal	Goal
Sphere f1	30	$[-100,100]^{30}$	0	0.00005
Griewank f2	30	$[-600,600]^{30}$	0	0.00005
Rastrigin f3	30	$[-100,100]^{30}$	0	0.00005
Duadric f4	30	$[-100,100]^{30}$	0	0.00005
Shaffer f5	2	$[-100,100]^{2}$	0	0.00005

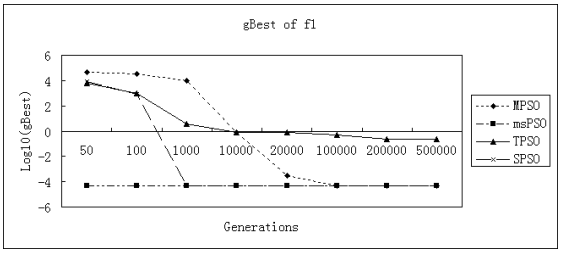

(a)

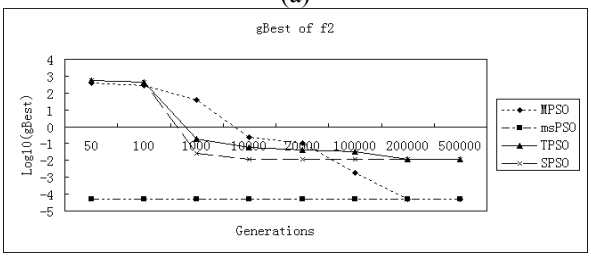

(b)

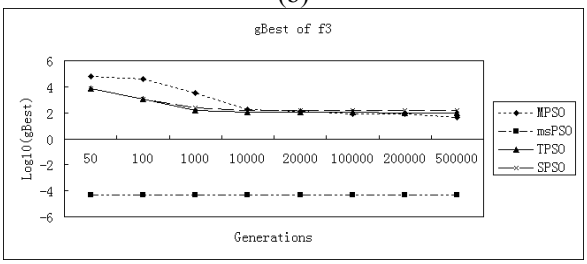

(c)

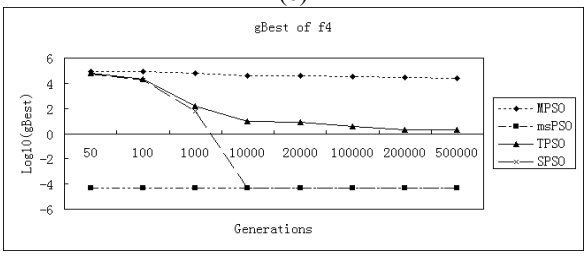

(d)

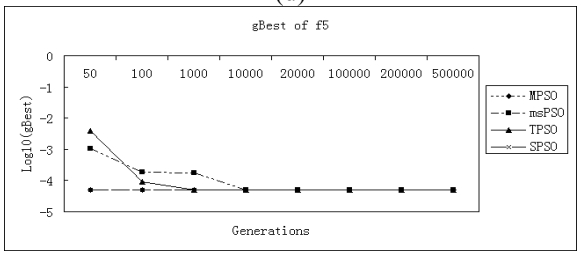

(e)

Fig.2. the evolution curve of the global optimal value for f1-f5

TABLE 2 NUMBERS OF INTERATION UNDER TARGET PRECISION

Function name	Iterations of MSPO	Iterations of msPSO	Iterations of TPSO	Iterations of SPSO
f1	21725	34	>500000	723
f2	123397	35	>500000	>500000
f3	>500000	46	>500000	>500000
f4	>500000	35	>500000	7782
f5	42	3279	105	26

SPSO takes into account the current latest progress of PSO, and its convergence speed has achieved a lot of improvements for f1, f4, f5. Just because of the item V to be considered in SPSO, f2 and f3 still diverge after 500000 iterations. MSPO has been improved a lot to get rid of the constraint of V compared with TPSO, and achieves a good result for f1, f2 and f5. In terms of SPSO msPSO removes the restrictions of V and improve the convergence speed and accuracy.

V. CONCLUSION

In reality, optimization problems face up with many complex and varied constraints. PSO is one of the methods to solve them. However, the velocity V makes X difficult to meet those constraints. The paper proposes msPSO based on SPSO. The new algorithm inherits the capability of SPSO with fast convergence and high accuracy, and gets rid of the item V. This research proves that the convergence process of PSO has nothing to do with V and the proposed method msPSO can converge. The experiments show that msPSO is able to achieve a good result.

REFERENCES

[1] J. Kennedy and R. Eberhart, “Optimization Particle Swarm, ” in Proceedings of the 1995 IEEE International Conference on Evolutionary Computing, Washington DC, 1995, pp. 1942-1948.

[2] Z. You and T. Ying, "GPU-based Parallel Particle Swarm Optimization," in IEEE Congress on Evolutionary Computation 2009, Trondheim, 2009, pp. 1493-1500.

[3] Y. Shi and R. Eberhart, "A modified particle swarm optimizer," in IEEE Conference on Evolutionary Computation, Anchorage, AK , USA, 1998, pp. 69-73.

[4] Y. Shi and R. Eberhart, "Fuzzy adaptive particle swarm optimization," in IEEE Conference on Evolutionary Compution, Seoul , South Korea, 2001, pp. 101 - 106.

[5] H. Wang and L. Zhi-Shu, "A simpler and more effective particle swarm optimization algorithm," Journal of Software, vol. 18, pp. 861-868, 2007.

[6] D. Bratton and J. Kennedy, "Defining a Standard for Particle Swarm Optimization," in Proceedings of the 2007 Swarm Intelligence Symposium, Honolulu, HI, 2007, pp. 120 - 127.

[7] M. Clerc, "Towards a deterministic and adaptive particle swarm optimization," in Proceedings of the 1999 Congress on Evolutionary Computation, Washington, 1999, pp. 1951-1957

2011 IEEE International Conference on Fuzzy Systems
June 27-30, 2011, Taipei, Taiwan

Intrusion Detection Systems Adapted from Agent-based Artificial Immune Systems

Chung-Ming Ou
Department of Information Management
Kainan University
Luchu 33857, Taiwan
Email: cou077@mail.knu.edu.tw

Yao-Tien Wang
Department of Computer Science and Information Engineering
Hungkuang University
Taichung 433, Taiwan
Email: ytwang@sunrise.hk.edu.tw

C.R. Ou
Department of Electrical Engineering
Hsiuping Institute of Technology
Taichung 412, Taiwan
Email: crou@mail.hit.edu.tw

***Abstract*—Agent-based artificial immune system (ABAIS) is applied to intrusion detection systems (IDS). A multiagent-based IDS (ABIDS) inspired by the danger theory of human immune system is proposed. The intelligence behind ABIDS is based on the functionality of dendritic cells in human immune systems and the danger theory, while dentritic cells agents (DC agent) are emulated for innate immune subsystem and artificial T-cell agents (TC agent) are for adaptive immune subsystem. Antigens are profiles of system calls while corresponding behaviors are regarded as signals. This ABIDS is based on the dual detections of DC agent for signals and TC agent for antigen, where each agent coordinates with other to calculate danger value (DV). ABAIS is an intelligent system with learning and memory capabilities. According to DVs, immune response for malicious behaviors is activated by either computer host or Security Operating Center (SOC).**

Multiple agents are "embedded" to ABIDS, where agents coordinate one another to calculate mature context antigen value (MCAV) and update activation threshold for security responses. Accordingly, computer hosts met with malicious intrusions can be effectively detected via input signals and temporary output signals such as PAMP, danger and safe signals.

***Index Terms*—intrusion detection, multiagent, artificial immune systems, dendritic cell algorithm**

I. Introduction

The Internet has become a major environment for propagating malicious codes, in particular, through web applications. Internet worms spread through computer networks by searching, attacking and infecting remote computers automatically. Intrusions, in particular, web-based ones, have become increasing threats for information assets. In order to defend against network attacks, one efficient way is to understand various properties of virus, which include the impact of patching, awareness of other human countermeasures and the impact of network traffic, even the ways how these malicious codes reside in a certain hosts, etc.

Forrest et al. [1] proposed an instance of computer immunology to protect the computer systems using the principles of human immune systems. Gu et al. [2] proposed an architecture of combining multiagent systems and dendritic cells. Most AIS researches focus on the development of specialized AIS algorithms inspired by theories such as the negative selection theory or the danger theory. Applying AIS algorithm to IDS can be traced back to [3].

Greensmith et al. [4] employed dendritic cells (DCs) within AIS which coordinate T-cell immune responses. Kim et al. [5] proposed "CARDINAL" which embedded T-cell process within the danger-theory-based AIS. Greensmith et al. [4], [6] proposed the Dendritic Cell Algorithm (DCA) whose purpose is to correlate data in the form of antigens and signals, then to identify groups of antigens as normal or anomalous. DCA achieves such missions through a generation of an anomaly coefficients, namely, *mature context antigen value (MCAV)*. It is believed that a DC is better performed by agent technology while considering its adoption to network environment. This antigen-plus-context information is passed on to a class of responder cells, termed T-cells. DCs are natural intrusion detection agents, which monitor the host tissue for evidence of cell damage. DC agents in our agent-based intrusion detection system (ABIDS) will evaluate antigens and corresponding signals according to DCA to determine whether antigens are malicious nor not.

For information security, one important aspect learned from immunology is the following: a computer security system should protect a host or network of hosts from unauthorized intruders, which is analogous in functionality to the immune system protecting the body from invasions by foreign pathogens. For example, anti-virus software has recently adopted some features analogous to the innate immune system, which can detect malicious patterns. However, most commercial products do not yet have the adaptive immune system's ability to address novel threats.

The motivation of this research is the following. Can agent-based information security systems learn itself to effectively determine whether the abnormality is "actually" incurred by some malicious attacks? This paradigm is very similar to the danger theory proposed in the immunology [7]. The arrangement of this paper is as follows. In section 2, preliminary knowledge such as AIS, danger theory, intelligent agents system and computer security are introduced. For section 3, IDS based on ABAIS model inspired by DT is discussed Simulations of two agent-based algorithms for ABIDS based on different scenarios will be given in section 4.

978-1-4244-7316-8/11/$26.00 ©2011 IEEE

II. Background

A. Intrusion Detection Systems (IDS)

Intrusion detection systems (IDS) focus on exploiting attacks, or attempted attacks, on networks and systems, in order to take effective measures based on the system security policies, if abnormal patterns or unauthorized access is being suspected. However, there are two potential mistakes by IDS, namely, false positive error (FPE) and false negative error (FNR). For FPE (FNE), a pattern is mistakenly determined as abnormal (normal).

The main goal of IDSs is to detect unauthorized use, misuse and abuse of computer systems by both systems insiders and external intruders. It can be a device or software application that monitors network and/or system activities for malicious activities or policy violations and produces reports to a Management Station. A host-based intrusion detection system (HIDS) consists of an agent on a host that identifies intrusions by analyzing system calls, application logs, file-system modifications (binaries, password files, capability databases, Access control lists, etc.) and other host activities and state. In a HIDS, sensors usually consist of a software agent. Some application-based IDS are also part of this category. It is an crucial issue of establishing principles of designing an IDS. According to [5]. there are three such principles as follows.

1) Types of system response should be determined by attack severity and certainty.
2) For performing adequate magnitudes of responses, both local and peer information needs to be taken into account.
3) Optimize the number of peer hosts polled.

B. Human Immune System (HIS)

The human immune system (HIS) consists of the antibodies and lymphocytes, which include T-cells and B-cells. HIS uses a large number of highly specific B- and T-cells to recognize antigens. Only B-cells secrete antibodies. Clonal selection theory explains the details of antibody secretion specific to an antigen where T-cells help regulating. The binding between antigen and specific lymphocytes trigger proliferation from immature lymphocytes to mature one and the secretion of antibodies.

HIS can be categorized as innate and adaptive immune system. The innate immune system is characterized by three roles, namely, host defense in the early stages of infection, induction of the adaptive immune response and determination of the type of adaptive response through antigen presenting cells (APCs) [8]. On the other hand, the main characteristics of the adaptive immune system are recognitions of pathogens.

1) Dendritic Cells: The dendritic cell (DC) is a vital link between the innate and adaptive immune system and provides the initial detections of pathogenic invaders. DC is an APC which captures antigen protein from the surrounding area and processes it by ingesting and digesting the antigen. DCs are also part of innate immune system; once activated, they migrate to the lymphoid tissues where they interact with T-cells and B-cells to initiate the adaptive immune response. Moreover, adaptive immune response is ”orchestrated” by DCs.

DCs are the first defense line for HISs which will arrive at the locations where antigens intrude and then swallow the latter to the pieces. These pieces will be attached to APCs and presented to the T-cells. DCs can be regarded as the commanders for HISs; they can combine the danger and safe signal information to decide if the tissue environment is in distress or is functioning normally.

2) T-Cell: DCs will influence the differentiation of T-cells by releasing particular cytokines. In other words, DCs drive the T-cell to react to the antigen in an appropriate manner. Naive T-cells are those who have survived the negative and positive selection processes within the thymus, and have migrated to circulation system between the blood and lymphoid organs where they wait antigen presentation by DC's. Naive T-cells reach an activated state when the T-cell receptor (TCR) on their surfaces binds to the antigen-peptide-MHC molecules on the surfaces of DC's, and co-stimulatory molecules are sufficiently upregulated on the surface of the DCs to show the degree of danger signals. The activated T-cells proliferate and their clones will differentiate into other cells such as helper t-cell and cytototoxic T-cells (CTL).

C. Artificial Immune Systems

Artificial Immune Systems (AIS), which is based on HIS, have been applied to anomaly detections [2][3][5][9][10]. AISs have been developed according to negative selection algorithm and clonal selection algorithm which are based on the classical self-nonself theory; nonselfs are entities which are not part of human organisms. This so-called self-nonself classification theory had been challenged while failing to explain several immunological phenomena. Some alternative theories have been proposed, for example, the danger theory (DT). DT postulates that the human immune systems respond to the presence of molecules known as danger signals, which are released as results of unnatural cell deaths.

D. Danger Theory (DT)

Matzinger [7] proposed the Danger Theory, which has become more popular among immunologists in recent years for the development of peripheral tolerance (tolerance to agents outside of the host). DT states that the immune system will only respond when damage is indicated and is actively suppressed otherwise. DT proposes that APCs, (in particular, DCs), have danger signal receptors (DSR) which recognize signals sent out by distressed or damaged cells. These signals inform the immune systems to initiate immune responses. APCs are activated via the danger signals. These activated APCs will be able to provide the necessary signals to the T-cells (more precisely, T-helper cells) which control the adaptive immune response.

Danger signals are generated by ordinary cells of the body that have been injured due to attacks by pathogens. These signals are detected by DCs. There are three modes of operation: immature, semi-mature and mature. In the DC's immature

state, it collects antigens along with safe and danger signals from its local environment. DC is able to integrate these signals to decide whether the environment is safe or dangerous. If it is safe, DC becomes semi-mature. Upon presenting antigens to T-cells, DC will cause T-cells tolerance. If it is dangerous, DC becomes mature and causes the T-cells to become reactive on antigen-presentations.

E. Agent-based Artificial Immune Systems

Agent is an entity that has the ability of consciousness, solving problem, self-learning and adapting to the environment, which is very similar to immune systems in functionalities. Table I summaries such similarities between AIS and multiagent systems (MAS). Accordingly, AIS can be contributed to the learning mechanism of agents: the immune system response attributes of specificity, diversity, memory and self/non-self recognition are needed. It may be used to optimize the agent's responses to intruders. Functionalities of the biological immune system, such as content addressable memory, adaptation, etc., can be utilized in intelligent agents.

TABLE I
COMPARISONS BETWEEN MAS AND AIS

System	MAS	AIS
Diversity Generation	Yes	Yes
Self Tolerance	Yes	No
Learning	Yes	No
SNS Act. Threshold	Yes	Yes
Self Maintenance	Yes	Yes
Short-term Memory	Yes	Yes
Long-term Memory	Yes	No

Adaptiveness is a challenge and also an important feature for MAS to interact with the environment. Three major stages for ABAIS inspired by the clonal selection theory are diversity generation, self-maintenance and memory of nonself. The last two properties define the adaptiveness of the IBMAS. These steps are carried out by agents distributed over the MAS.

- **Diversity Generation**: Continuous diversity generation leads to the "adaptation" of ABAIS. Diverse agents with distinct specificity of the receptor and the effector are generated by way of mutations.
- **Self-Maintenance**: Agents are adjusted to be insensitive to known patterns (self) during the developmental phase. Negative selection theory is a central of this phase.
- **Memory of Nonself**: Agents are adjusted to be more sensitive to unknown patterns (nonself) during the working phase.

III. INTRUSION DETECTION MECHANISM BASED ON ABAIS

According to [10][11][12], we propose improved IDS based on ABAIS, or ABIDS in short. Different from traditional self-nonself paradigm for immune systems, our IDS will first detect danger signals emitted by computer hosts. These danger signals are based on some security threat profile, which defines by system calls generated by running processes. According to [9][11], threat profile may be composed of excessive CPU, memory load at the host, bandwidth saturation, high connection number of the host, etc. In this multi-agent system, several agents are generated which can communicate each other to emulate functionalities extracted from DT-inspired AIS (Fig 1).

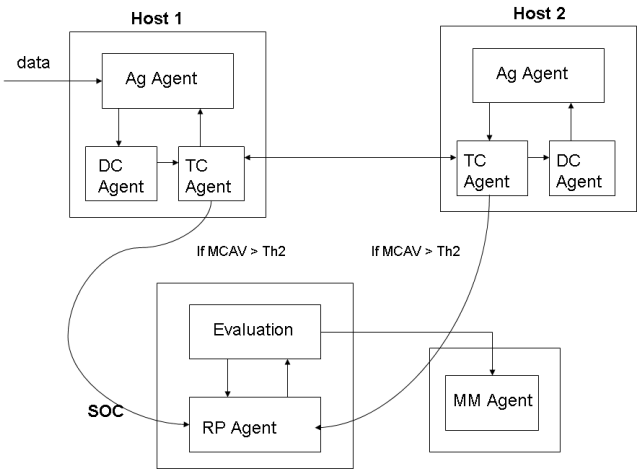

Fig. 1. Architecture of ABIDS.

A. Antigen

For most network detecting systems (for example, those adopting self-nonself paradigm), an antigen is defined as an information vector extracted from network packet. For example, antigens are binary strings extracted from the IP packets, which include IP address, port number, protocol types, etc. However, the antigen defined at Our ABIDS is related to system calls rather than network packets. A system call is the way how a program requests a service from an operating system's kernel. System calls provide the interface between a process and the operating system. Each process invokes some system calls. The more active the process, the more system calls it makes. Each system call is captured and converted into an antigen [13].

B. Intelligent Agents in AIS

We design a MAS with antigen agents, DC agents, T-Cell agents, Responding agents and Memory agents to perform functionalities of ABIDS such as DCAs, antigen memorization, etc.

1) Antigen Agent (Ag Agent): Antigen agents, which are installed at computer hosts, represent data item from the nonself dataset. They extract and record selected attributes from these data items. According to the agent-based DCA (ABDCA) which will be described later, each Ag agent sends corresponding DC agent a picked message when a nonself antigen appears.

2) Dendritic Cell agent (DC agent): In order to determine whether a malicious behavior is taking place, ABIDS needs to analyze antigens. DC agents are the kernel of the ABAIS which are complex compared to other agents; they are installed and distributed at each computer hosts. When an Ag agent issues a picked signal, corresponding DC agent will evaluate the risk

state facing by the host by calculating the danger value (DV). Similar to nature DC, each DC agent has three stages, namely immature, semimature and mature. DC agents are started from immature stages. When a picked signal issued from the Ag agent, DC agent executes data processing function such as the ABDCA. When a DC agent is at either semimature state or nature state, it returns the mature context to corresponding TC agent.

3) T-cell agent (TC Agent): TC agents are also installed at each computer hosts. TC agents are activated by the signals from DC agents when the DVs exceed thresholds. Each TC agent have three numerical values associated with it; these represent the accumulated certainties and severities of attack: *T-cell activation threshold, Th1 activation threshold, Th2 activation threshold*. These TC agents will communicate each other for exchanging these numerical values. There are two perspectives of this agent communications.

- For TC agent issuing malicious act warning for corresponding antigen, it informs TC agents "nearby" by exchanging its numerical values.
- For TC agent not issuing malicious act warning for this antigen, it simply update its numerical values according "nearby" TC agents issuing malicious act warning.

4) Responding Agent (RP agent): Ag agents, DC agents and TC agents are coordinating one another to perform malicious act responses. After DV exceeds threshold value , TC agents will inform RP agent, which is installed at SOC and each computer host. RP agents will activate some control measure to such malicious act. Two measures are considered:

1) Reporting to the SOC or security manager, for example, patches downloaded, activate relevant anti-virus software on this infected host and removes virus.
2) Disruption of intrusion, discards a suspicious packets, kill the related process, cut-off infected sub-network. These can prevent large-scale spreading of computer viruses, in particular internet worms, which have high spreading rate by their natures.

C. Algorithm: Agent-based Dendritic Cell Algorithm (ABDCA)

If an antigen is collected in an environment of danger, the context of this antigen is marked as anomalous and such antigen collected by the DC agent is potentially an intruder. While in the immature state, DC agent performs the following three functions:

1) Antigen Sampling: DC agents collect antigens from some external sources (in this case, from computer hosts) and places these antigens in its own antigen storage.
2) Update input signals: DC agent collect values of all input signals present in the signal storage area.
3) Calculate interim output signals: each DC agent calculates its three temporary output signal values from the received input signals, then derives its final output signal.

We observe that multiple DCs present multiple copies of the same antigen type for invoking an immune response; it leads to an error-tolerance immune system as a single DC is far from stimulating a "false positive" error. The ABDCA is listed as follows.

Algorithm 1 Agent-based DCA (ABDCA)

```
input : Antigens and signals
output: Antigen context (0 for safe/1 for danger)
Initialize DC agents (Immature state);
for each DC_agent_i do
    get antigen (Ag);
    store antigen;
    get input_signal;
    calculate output_signal_i;
    if output_signal_i > Activation_Threshold_i then
        Ag_context is assigned as 0;
        State of DC_agent_i="semi-mature";
    else
        Ag_context is assigned as 1;
        state of DC_agent_i="mature";
    end if
end for
update cumulative output_signals;
```

Three temporary output signals are PAMP signal, danger signal and safe signal. According to Greensmith et al. [13], the system should respond with a very high rate of false positives by switching the PAMP and safe signal. The definitions of PAMP, danger and safe signals, by way of parameters of computer hosts such as CPU usage, memory load, network connection (number) and bandwidth saturation, are as follows.

1) PAMP Signal: Network Connection $>$ th_netconnection AND bandwidth Saturation $>$ th_bandsaturation.
2) Danger Signal: CPU Usage $>$ th_cpuload OR Memory Load $>$ th_memoryload.
3) Safe Signal: All parameters $<$ th_parameter.

Where "th_parameter" represents the threshold value of the parameter. Now the computation of output signals by three temporary output values is the following.

$$output_signal = \frac{W_P \cdot C_P + W_D \cdot C_D + W_S \cdot C_S}{W_P + W_D + W_S} \quad (1)$$

According to empirical experiments [4], the weights for this output signal is $W_P = 2$, $W_D = 1$, $W_S = 1$. C_P, C_D, C_S represent PAMP signal, danger signal and safe signal. The principle for this weights is the following: PAMP signal will decide whether the danger signal will be a "really" harmful one. Whether output signal is harmful or nor is defined by the Table II.

TABLE II
DEFINITIONS OF OUTPUT SIGNAL.

Output Signal	C_P	C_D	C_S
Normality	0	0	1
Harmless Abnormality	0	1	0
Harm Abnormality	1	1	0

D. Algorithm: Agent-based IDS

Now according to ABDCA, we propose an algorithm describing agent-based IDS. This algorithm is also illustrated as Fig. 2. ABDCA can provide information not only a network packet but also a group of network packets is anomalous or not. This is achieved by the generation of an anomaly coefficient value, namely MCAV.

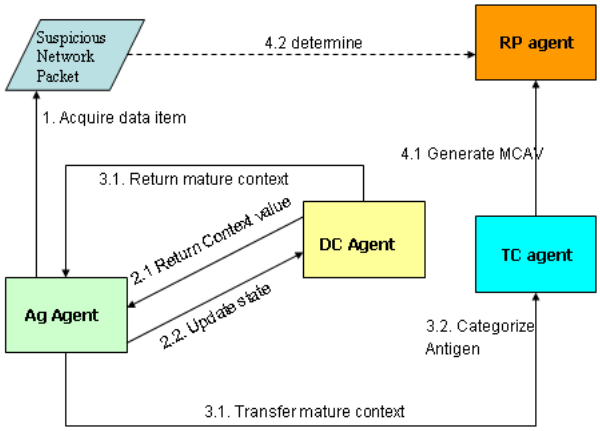

Fig. 2. Diagrammatic Illustration of Agent-based intrusion detection system.

Algorithm 2 Agent-based IDS (ABIDS)

Input: Antigen and Signals
Output: Antigen Types
1. Data Processing:
1.1 Ag agent extracts antigen from network traffic signal according to ag agent attribute.

2. Agent response:
2.1 DC agent returns context value according to threat profile; also according to the policy of the SOC if necessary.
2.2 DC agents will response to such antigen by updating its state according to DCA.

3. Danger Signal processing:
3.1
if this DC agent returns mature values to Ag agent **then**
Ag agent transfers it to the TC agent.
end if
3.2 TC agent categorizes such antigen according to the(updated)threat profile.

4. MCAV generation:
4.1 TC agent generates MCAV, which is sent to the RP agent.
4.2 RP agent determines if the corresponding antigen is malicious or not.
5. Antigen Memory:
5.1 Memory Agent stores necessary MCAV information

For the step 4 of the Algorithm 2, each nonself antigen gets a binary string of mature contexts from every selected DC agent installed at corresponding computer host. MCAV can be calculated through the number of context "1" divided by the number of all contexts. According to [2], it is similar to a voting system, where the antigen is the candidate and the DC agents are the voters. If the context is "1" ("0"), it means the DC agent determines this antigen is malicious (benign). The MCAV is actually the probability of that this antigen is being malicious.

The reactions of RP agents can be multiple according to the SOC's security policies. For example, passive reaction is initiated by sending some alarm signal such as an e-mail to the administrator and a strategy proactive is defined through mobile agents that implement the characteristics of the reaction. According to [11], for example, an applied reaction is defined for each of the following internet protocols such as DNS, FTP, HTTP, POP3 and SMTP. The issue of RP agents is out of the scope of this paper.

E. Agent Communications

One advantage of ABIDS is the communications and coordination between DC agents and TC agents. The basic idea is as follows. TELL and ASK-based communication permit agents share their internal information, enhancing their performances to respond to intruders [10]. On the other hand, useful knowledge obtained by DC agents and TC agents should be stored in some databases. These databases could also be shared by each DC and TC agent to improve their detection efficiencies. Suitable mechanisms of agent communications can contributed to better performance of ABIDS.

On the other hand, if a TC agent determines its host is under malicious attack by analyzing the corresponding MCAV, it will inform other TC agent "nearby". Such communication is direct and does not pass through proxy server or SOC. The activation threshold of this TC will be updated according to the following equation.

$$T(t) = T(t-1)+\alpha E(t-1)(E(t-1)-T(t-1)), t = 1, 2, \ldots, t_b \quad (2)$$

where E_i is the excitation level of TC agent, and t_b is the attacking time by this antigen.

Table III and Table IV illustrate the agent communications [14].

TABLE III
AGENTS AND THEIR COMMUNICATIONS (1).

Communication	Initiator	Receiver
eRaiseWarning	Ag Agent	DC agent
eContextReturned	DC Agent	TC Agent
eMaliciousOrNot	DC agent	TC agent
eEvidenceResponse	TC Agent	RP agent
eMemoryInitiation	RP agent	Memory Agent

TABLE IV
AGENTS AND THEIR COMMUNICATIONS(2).

Communication	Description
eRaiseWarning	Notify of a possible malicious attack
eContextReturned	sending MCAV
eMaliciousOrNot	Identify the malicious antigen
eEvidenceResponse	Implement the system response according to TC agent's information
eMemoryInitiation	Memorize the nonself antigen being encountered; update antigen database of Proxy server

F. Agent Platform

One advantage of this ABIDS is the following: it is feasible to be adapted into large-scale computer networks such as cloud computing environment, as TC agents will collect information from computer hosts to calculate MCAVs, and also update threat profile if necessary. Fig. 3 illustrates the agent interactions between SOC and computer hosts on agent platforms.

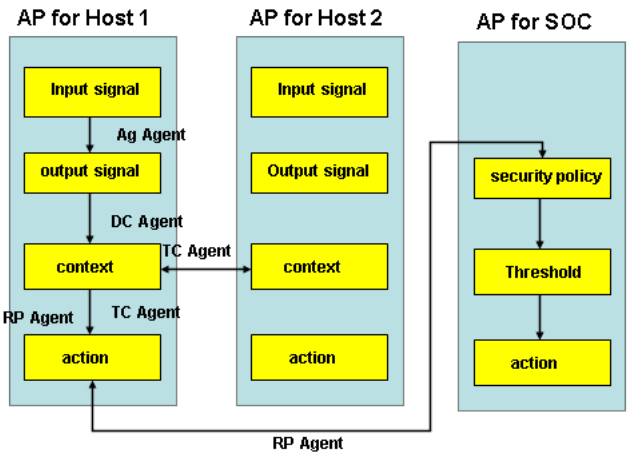

Fig. 3. Agent Interaction for ABIDS.

Table V and Table VI are the comparisons for goals and services fulfilled by these agents.

TABLE V
AGENTS, GOALS AND SERVICES (1).

Agent	Goals
Ag Agent	Data Parsing
DC Agent	Detect malicious codes or network attacks at the input sources
TC Agent	Categorize nonself antigen
RP Agent	Reduce the malicious antigen
Memory Agent	Memorize the nonself antigen

TABLE VI
AGENTS, GOALS AND SERVICES (2).

Agent	Services
Ag Agent	antigen label and signal association
DC Agent	MCAV estimation, update activation threshold
TC Agent	Identify the malicious antigen
RP Agent	Implement the system response
Memory Agent	Update the antigen database of the proxy server

IV. SIMULATION

A. Malicious Behaviors determined by ABDCA

According to essence of the danger theory, the advantage of ABIDS is the following: it can determine some nonself-antigenic behavior which is at the verge of normality and abnormality. For example, for those network behaviors with short attacking time. In this section, we simulate several critical cases for this ABIDS. The threshold of S, C and T are the following $S_{th} = 0.50$, $C_{th} = 0.50$ and $T_{th} = 0.5$. The number of computer hosts within this network is 2000. Each host has its fixed vector of weights. Simulation principle is to determine those critical behaviors, which include one extremely high factor with other low factors, or some factors are closing to the corresponding threshold values.

1) Nonself Antigen with High Severity, Low Certainty and Short Attacking Time: While an antigen intrudes a computer host with behaviors of high severity but low certainty and short attacking time, it is difficult sometimes to determine if this is a malicious attack. In this case, we consider the threat profile TP=$[0.9, 0.01, 0.01]$ for the ABDCA algorithm.

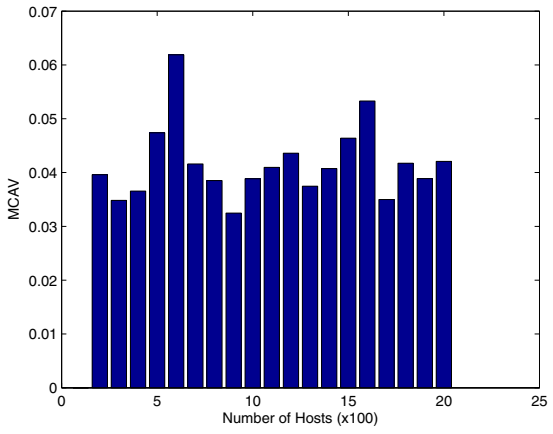

Fig. 4. Average MCAV for an Antigen with High Severity solely.

We expect the simulation should be "stable" for reasonable many hosts as Fig. 4. MCAV is around 0.03 and 0.05, which shows that this nonself antigen is normal.

2) Nonself Antigen with Edge Behavior: While an antigen intrudes a computer host with edge behavior such that severity, certainty and attacking time are all closing to their threshold values, respectively. It is also difficult to determine if this is a malicious attack or not. In this case, we consider TP=$[0.65, 0.65, 0.65]$.

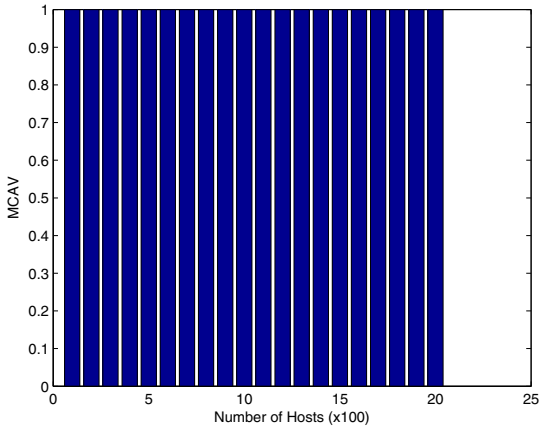

Fig. 5. Average MCAV for an Antigen with Critical Threshold Behavior.

The simulation also show a stable result (see Fig. 5); average MCAV is equal to 1, which indicates that this nonself antigen is harmfully abnormal.

3) Nonself Antigen with Short Time Attack: In this simulation, an antigen causes computer hosts with both high severity and certainty, but relative medium attacking time. It is difficult to determine if this is a malicious attack or not. In this case, we consider TP=$[0.9, 0.9, 0.4]$.

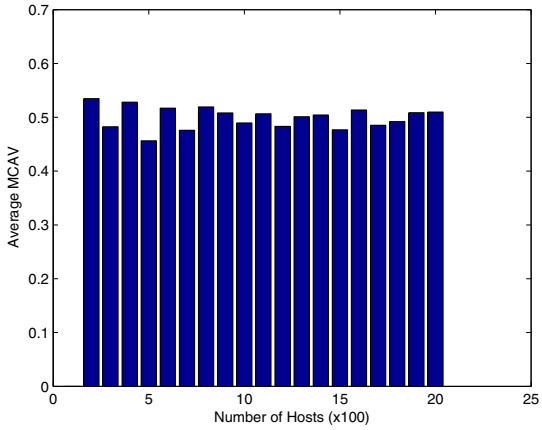

Fig. 6. Average MCAV for an Antigen with High Severity and certainty, but relatively short Attacking Time.

The simulation show a stable result (see Fig. 6); average MCAV is around 0.5, which indicates that this nonself antigen can be harmfully or harmful abnormal depending on the SOC's security profile.

B. Simulation of TC Agents' Coordinations

1) Interactions between Two TC Agents: We consider two computer hosts with TC interactions. TC1 and TC2 are informing each other for confirmed attack from the corresponding antigen.

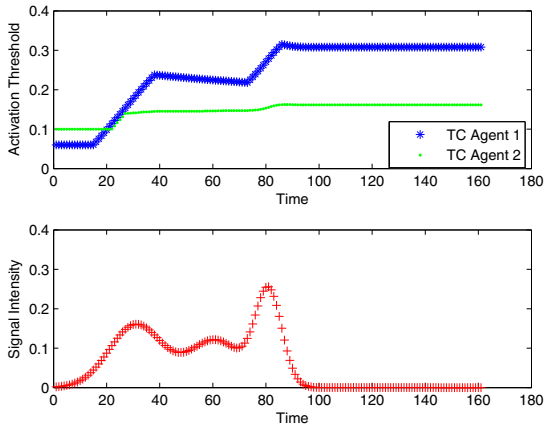

Fig. 7. Activation Thresholds of Two TC agents within the attacking cycle.

According to Fig. 7, even two TC agents will lead to "more" complex threshold behaviors.

2) Interactions among Three TC Agents: We consider three computer hosts with TC agents interactions. TC1, TC2 and TC3 are informing each other for confirmed attack from the corresponding antigen.

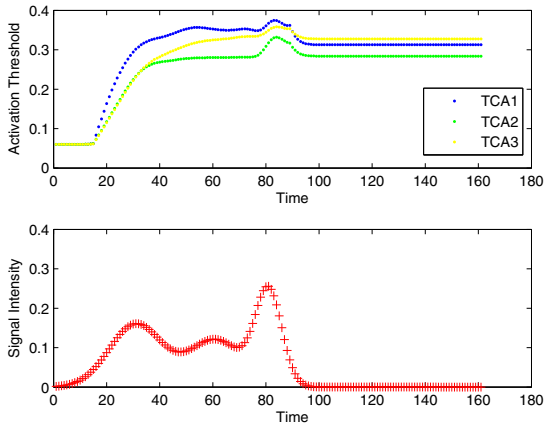

Fig. 8. Activation Thresholds of Three TC agents within the attacking cycle.

V. Conclusion

We propose a multiagent-based intrusion detection system. The intelligence behind such system is based on the danger theory of human immune systems. In particular computations of danger values with dynamic thresholds will reduce the false positive rate of danger signals issued by computer hosts. Three agents, namely, Ag agent, DC agent and TC agents are

coordinated to exchange information of intrusion detections. The evaluations of three factors S, C, and T are pragmatic issues. On the other hand, threshold values have to be defined by SOCs according to security profiles.

REFERENCES

[1] S. Forrest, A. Hofmeyr, T. Somayaji, and Longstaff, "A sense of self for unix processes," in *Proceedinges of the 1996 IEEE Symposium on Research in Security and Privacy*, 1996, p. 120V128.

[2] F. Gu, U. Aickelin, and J. Greensmith, "An agent-based classification model," in *9th European Agent Systems Summer School (EASSS2007)*, 2007.

[3] U. Aickelin, P. Bentley, S. Cayzer, and J. Kim, "Danger theory: The link between ais and ids," *Lecture Notes in Computer Sciences*, vol. 2787, pp. 144–165, 2003.

[4] J. Greensmith, J. Feyereisl, and U. Aickelin, "The dca: Some comparison," *Evolutionary Intelligence*, vol. 1, no. 2, pp. 85–112, 2008.

[5] Kim, *An Artificial Immune System Architecture for Computer Security Applications*. New York: John Wiley and Sons, 1978.

[6] J. GreensmithU, Aickelin, and S. Cayzer, "Detecting danger: The dendritic cell algorithm," *Robust Intelligent Systems*, vol. 12, pp. 89–112, 2008.

[7] P. Matzinger, "Tolarance, danger and the extended family," *Annual Review in Immunology*, vol. 12, pp. 991–1045, 1994.

[8] K.-W. Yeom and J.-H. Park, "An artificial immune system model for multi agents based resource discovery in distributed environments," in *Proceedings of the First International Conference on Innovative Computing, Information and Control*, 2006, pp. 234–239.

[9] J. Zhang and Y. Liang, "Integrating innate and adaptive immunity for worm detection," in *Proceedings of the Second International Workshop on Knowledge Discovery and Data Mining*, 2009, pp. 693–696.

[10] H. Fu, X. Yuan, and N. Wang, "Multi-agents artificial immune system (maais) inspired by danger theory for anomaly detection," in *2007 International Conference on Computational Intelligence and Security Workshops*, 2007, pp. 570–573.

[11] A. Boukerche, R. Machado, K. Juca, J. Sobral, and M. Motare, "An agent based and biological inspired real-time intrusion detection and security model for computer network operations," *Computer Communications*, vol. 20, pp. 2649–2660, 2007.

[12] J. Kim, *Integrating artificial immune algorithms for intrusion detection*. University College London: Ph. D thesis, 2002.

[13] J. Greensmith, U. Aickelin, and G. Tedesco, "Information fusion for anomaly detection with the dendritic cell algorithm." *Information Fusion*, vol. 11, no. 1, pp. 21–34, 2010.

[14] P. Harmer, P. Williams, G. Gunsch, and G. Lamont, "An artificial immune system architecture for computer security applications," *IEEE Transactions on Evolutionary Computations*, vol. 65, no. 3, pp. 252–280, November 2002.

2011 IEEE International Conference on Fuzzy Systems
June 27-30, 2011, Taipei, Taiwan

An Adaptive Multi-Agent Memetic System for Personalizing e-Learning Experiences

Giovanni Acampora*, Matteo Gaeta†, Enrique Muñoz‡ and Autilia Vitiello*
*Dept. of Computer Science, University of Salerno, Fisciano, Italy 84084
Email: {gacampora, loia, avitiello}@unisa.it
†Centro di Ricerca in Matematica Pura ed Applicata, Fisciano, Italy 84084
Email: gaeta@crmpa.unisa.it
‡European Centre for Soft Computing, Mieres, Spain 33600
Email: enriquemuba@um.es

***Abstract*—The rapid changes in modern knowledge, due to exponential growth of information sources, are complicating learners' activity. For this reason, novel approaches are necessary to obtain suitable learning solutions able to generate efficient, personalized and flexible learning experiences. From this point of view, the use of different cooperative intelligent agents can be exploited to analyze learner's preferences and generate high quality learning presentations which provide attractive learning solutions. In particular, to achieve this goal this paper exploits an ontological representation of the learning environment and an adaptive memetic algorithm based on a cooperative multi-agent framework. In this framework different agents analyze the e-learning instance and solve it in a parallel way, cooperating among them. This cooperation is performed by jointly exploiting data mining, via fuzzy decision trees, together with a decision making framework exploiting fuzzy methodologies. As will be shown in the experimental results section, this multi-agent strategy is capable of speeding up the convergence to high-quality personalized e-learning experiences.**

***Index Terms*—Adaptive Memetic Algorithms, Multi-Agent Systems, E-learning.**

I. Introduction

Multi-agent systems have been applied to many different fields obtaining outstanding results. By using intelligent agents we are able to solve complex problems, typically difficult to solve individually, but that can be solved by the interaction of different entities. One of this kind of problems are optimization problems, which are those problems in which the best solution has to be found among a set of feasible solutions. In the context of e-learning, the problem of binding subjects and technologies with learning activities and leaner's preferences can be modeled as an optimization problem, in particular the one called *Learning Presentation Problem* (LPP). For this reason, we believe that a multi-agent framework can help us in its resolution.

Regarding e-learning solutions, for many years most of them have been modeled as learning software platforms which constrain learners to learn following a predefined approach without taking into account their preferences. In addition, they tend to ignore several tools provided by Web 2.0, that could improve learners' experience. In order to face these weaknesses, new e-learning solutions should support the whole learning process, and manage new e-learning 2.0 scenarios [1] by incorporating tools like Blogs, Wikis, Podcast, and so on. Moreover, next generation Learning Management Systems (LMSs) should dynamically and intelligently create personalized e-learning experiences adapted in the Web 2.0 environment.

In this scenario, a representation model to describe both educational domains and learners characteristics is required. Ontologies [2] are a good methodology to model the e-learning contexts and enable a convenient way to bind subjects with learning activities in order to fit specific learning objectives, which we defined as LPP. LPP could be viewed as a modified version of the Uncapacited Facility Location Problem (UFLP) [3] and, consequently, solved through a specific deterministic algorithm. However, this approach is not convenient for Web 2.0 environment characterized by distributed repositories and a wide number of learning activities and learning paths made by numerous subjects.

Starting from this consideration, this work proposes an adaptive multi-agent memetic algorithm which decides, depending on the instance being solved, how to combine and configure different optimization agents in order to derive high-quality learning experiences in the e-learning 2.0 scenarios. In detail, a collection of agents analyzes learner preferences and generates high quality learning presentations by executing, in a parallel way, different cooperating optimization strategies. The metaheuristics cooperation is performed by exchanging solutions among optimization methods in precise moments and under certain conditions that are controlled by a set of fuzzy rules. The fuzzy engine uses knowledge obtained by a preliminary machine learning process that analyzes the performances of different optimization methods applied to well-defined problem's instances.

As will be shown in the experimental results section, where a plug-in for an open-source LMS has been designed and tested, the proposed strategy is capable of speeding up the convergence to high-quality personalized e-learning experiences.

II. The Ontological e-Learning Environment

Our e-Learning system is based on 1) a set of models able to represent the main entities involved in the process of teaching/learning and on 2) a set of methodologies, leveraging on such models, for the generation of individualized learning experiences with respect to learning objectives, pre-existing

978-1-4244-7316-8/11/$26.00 ©2011 IEEE

knowledge and learning preferences. The four models adopted by our solution, based on the *Learning Model* [4], are summarized below:

- the *domain model* represents the knowledge domain that is object of teaching by means of concepts, relations among concepts and teaching preferences connected with concepts;
- the *learner model* represents a learner including concepts that he knows as well as his learning preferences;
- the *learning activity model* represents a single learning object or service that may be used as a building block to generate a learning experience;
- the *unit of learning model* represents a whole learning experience personalized for a single learner and composed by a set of target concepts and a sequence of learning activities needed to learn the target concepts.

By exploiting these models, our system generates a personalised *learning path* (sequence of concepts to be taught) for each learner through a *learning path generation algorithm* and introduces placeholders for testing activities.

Once the learning path is available, the system selects a fragment of the learning path and efficiently generates the best *learning presentation* (sequence of learning activities) for each enrolled learner by applying our proposal of Multi-Agent Memetic Algorithm. The learner then undertakes the learning and testing activities of the learning presentation until its end. When the learner ends a presentation fragment, his learner model is updated on the basis of the results of testing activities and a new learning presentation fragment is generated (possibly including recovery activities for concepts that he did not understand).

A. The Domain Model

The domain model describes, in a machine-understandable way, the piece of the educational domain that is relevant for the e-learning experience we want to define, concretize and broadcast. Our approach is design an ontology composed by a set of concepts representing the topics to be taught and a set of relations between concepts representing connections among topics. Such a structure can be formally represented as a $(n+1)$-tuple $G(C, R_1, \ldots, R_n)$ where C is the set of nodes representing domain concepts and each R_i is a set of arcs corresponding to the i^{th} kind of relation. Several kinds of relations are allowed. As an example we can consider a concept graph $G(C, BT, IRB, SO)$ with three relations BT, IRB and SO whose meaning is explained below (where a and b are two concepts of C):

- $BT(a, b)$ means that the concept *a belongs to b*, i.e., b can be understood if every a so that a belongs to b is already learned. (hierarchical relation);
- $IRB(a, b)$ means that the concept *a is required by b*, i.e., a necessary condition to study b is to have understood a (ordering relation);
- $SO(a, b)$ means that the *suggested order* between a and b is that a precedes b, i.e., to favour learning, it is desirable to study a before b (ordering relation).

TABLE I
EXAMPLE OF DIDACTICAL PROPERTIES AND FEASIBLE VALUES.

Properties	**Feasible Values**
didactic method	deductive, inductive, etc.
activity type	text reading, video clip, simulation discussion with a peer, discussion with the teacher, etc.
interactivity level	high, medium, low

A set of *teaching preferences* may be added to the domain model to define feasible teaching strategies that may be applied for each available concept. Such preferences are represented as a function $TP(C \times Props \times PropVals) \rightarrow [0, 10]$ where $Props$ is the set of didactical properties and $PropVals$ is the set of feasible values for such properties. The Table I provides some (non exhaustive) example of didactical property and associated feasible values. It is worth noting that TP is defined only for couples of $Props$ and $PropVals$ elements belonging to the same row in Table I.

B. The Learner Model

The learner is the main actor of the whole learning process and it is represented with a cognitive state and a set of learning preferences. The *cognitive state* represents the knowledge reached by a learner at a given time and it is represented as a function $CS(C) \rightarrow [0, 10]$ where C is the set of concepts of a given domain model. Given a concept c, $CS(c)$ indicates the degree of knowledge (or grade) reached by a given learner for c; the value 0 indicates *no knowledge*, whereas, the value 10 indicates *full knowledge*. If such grade is greater than a given "passing" threshold θ then c is considered as known, otherwise it is considered as unknown.

The *learning preferences* provide an evaluation of learning strategies that may be adopted for a given learner. They are represented as an application $LP(Props \times PropVals) \rightarrow [0, 10]$ where $Props$ and $PropVals$ are the same sets defined in Table I for teaching preferences, whereas, the value 0 and 10, represent, respectively, the lowest and highest level of learning preference. Differently from teaching preferences, learning preferences are not linked to a domain concept but refer to a specific learner. The cognitive state of any learner is initially void (i.e., $CS(c) = 0$ for any c included in a given domain model) and may be initialized on a teaching domain with a pre-test. Learning preferences may be initialized by the teacher or directly by learners through a questionnaire capable of evaluating learners styles and transform them in suitable values for learning preferences. Both parts of the learner model are automatically updated by the system during learning activities.

C. The Learning Activity Model

A *learning activity* must be performed by a learner to acquire one or more domain concepts. Activities may relate to learning objects (e.g., textual lessons, presentations, videoclips, podcasts, simulations, exercises, etc.) or learning services (e.g.,

virtual labs, wikis, folksonomies, forums, etc.). Our system uses learning activities as bricks to generate learning experiences. In order to be used in this way, a learning activity LO is described through the following elements:

- a set of *concepts* C_{LO} related to a given domain model, that are covered by in the learning activity;
- a set of *didactical properties* expressed as an application $DP_{LO}(property) = value$ representing learning strategies applied by the learning activity;
- a set of *cost properties* expressed as an application $CP_{LO}(property) = value$ that must be taken into account in the optimisation process connected with the *learning presentation generation algorithm.*

Didactical properties components have the same meaning with respect to teaching and learning preferences, i.e., property and value may assume values from a closed vocabulary (see table I). Differently from learning and teaching preferences, they are neither linked to a domain concept nor to a specific student but to a learning activity. Cost properties are couples that may be optionally associated to learning activities, whose properties may assume values from the closed vocabulary {price, duration} and whose values are positive real numbers representing, respectively the price of a single learning resource and its average duration in minutes.

D. The Unit of Learning Model

A unit of learning represents a sequence of learning activities needed for a learner in order to understand a set of target concepts in a given domain with respect to a set of defined cost constraints [6]. It is composed by the following elements:

- a set of *target concepts* TC part of a domain model, that have to be mastered by a given learner in order to successfully accomplish the unit of learning;
- a set of *cost constraints* $CC(property) = value$ that must be taken into account in the optimisation process connected with the learning presentation generation algorithm;
- a *learning path* $LPath(c_1, \ldots, c_n)$, i.e., an ordered sequence of concepts that must be taught to a specific learner in order to let him master target concepts;
- a *learning presentation* $LPres(lo_1, \ldots, lo_m)$, i.e., an ordered sequence of learning activities that must be presented to a specific learner in order to let him/her master the target concepts.

While target concepts are defined by the course teacher, the learning path and the learning presentation are created by the generation algorithms described below. Concerning cost constraints, the property may assume values from the closed vocabulary {price, duration}. Feasible values are positive real numbers representing, respectively the maximum total price and the maximum total duration of the unit of learning.

The generation of the learning path is the starting point to completely generate a unit of learning. Starting from a set of *target concepts* TC and from a *domain model*, a feasible learning path must be generated taking into account the concepts graph $G(C, BT, IRB, SO)$ part of the domain model (with $TC \subseteq C$).

The four steps of the learning path generation algorithm are summarized below:

- The *first step* builds the graph $G'(C, BT, IRB', SO')$ by propagating ordering relations downward the hierarchical relation. IRB' and SO' are initially set to IRB and SO respectively and then modified by applying the following rule: for each arc $ab \in IRB' \cup SO'$ substitute it with arcs ac for all $c \in C$ such that there exist a path from c to b on the arcs from BT.
- The *second step* builds the graph $G''(C', R)$ where C' is the subset of C including all concepts that must be taught according to TC, i.e., C' is composed by all nodes of G' from which there is an ordered path in $BT \cup IRB'$ to concepts in TC (including target concepts themselves). R is initially set to $BT \cup IRB' \cup SO'$ but all arcs referring to concepts external to C' are removed.
- The *third step* finds a linear ordering of nodes of G'' by using a depth-first search that visits the graph nodes along a path as deep as possible. The obtained list L will constitute a first approximation of the learning path.
- The fourth step generates the final learning path $LPath$ by deleting from L all non-atomic concepts with respect to the graph G, i.e., $LPath$ will include any concept of L apart concepts b so that $ab \in BT$ for some a. This ensures that only leaf concepts will be part of $LPath$.

Successively it is necessary to generate the learning presentation suitable for a specific learner based on a *learning path* $LPath$ that has to be covered, on a set of teaching preferences TP belonging to a *domain model*, on a cognitive state CS and a set of learning preferences LP both part of the *learner model* associated to the target learner, on a set of optional *cost constraints* CC and on a set of available *learning activities*. The learning presentation is generated by following the steps below:

- The *first step* is to select the sub-list L of $LPath$ that has to be converted in a presentation. L is the sequence of all the concepts of $LPath$ not already known by the learner (i.e., any concept a so that $CS(a) < \theta$). If L is empty then the algorithm ends because the learner already knows all concepts of the learning path.
- The *second step* is to define the best sequence of learning activities P, selected from available learning activities, covering L on the basis of TP, LP and CC. This sequence definition has been given the name of *Learning Presentation Problem (LPP).*

LPP problem represents the core of this work, in fact, its solution defines the learning experiences personalization. Hereafter, LPP problem will be modeled by means of well known UFLP problem and, successively, it will be efficiently solved through an innovative memetic algorithm.

In order to model LPP by means of UFLP problem, first of all a measure of distance $d_{TP}(lo, c)$ between an activity lo and the set of preferences TP has to be defined with respect

to a concept c. In a similar way a measure of distance $d_{LP}(lo)$ based on LP may be defined. A further measure $d(lo, c)$ shall be defined as a weighted sum of the two measures.
Once the measure of distance is defined the problem of selecting the best set of activities P covering concepts of L becomes a UFLP that may be outlined with the bi-partite graph in Fig. 1, where available activities are displayed on the left and concepts to be covered on the right.

There is an arrow between a learning object LO_i (considering the available activities related to learning objects) and a subject C_j only if the metadata instance of LO_i includes a semantic link to the subject C_j

For each couple (LO_i, C_j) linked in the bipartite graph there is an assigned value $d(i, j)$ representing the distance between LO_i and C_j. Short distances define good coverings. Furthermore, to each learning object LO_i, a value $p(i)$ representing the cost of the introduction of the learning object LO_i into the sequence of LOs delivered to the learner is associated . Assume that distances $d(i, j)$ are calculated applying a specific function that evaluates the matching between the metadata values of LO_i covering C_j and the learning preferences of the learner who requests the personalized e-learning experience. Then, P must be built as the smallest set of activities covering all concepts of L with the minimum sum of distances between activities and covered concepts. Now, consider m as the number of learning objects available and n the number of subjects in the Learning Path to be filled. Set y as a binary vector where each element y_i, $(i = 1, \ldots, m)$, assumes value 1 if you decide to use the learning object LO_i, 0 otherwise, and x as binary vector in which each entry x_{ij}, $(i = 1, \ldots, m$ and $j = 1, \ldots, n)$, assumes value 1 if subject C_j is covered by the learning object LO_i, 0 otherwise. Then, the linear programming model which formalizes the whole problem is described as follows:

$$\min \sum_{i=1}^{m} p(i) y_i + \sum_{i=1}^{m} \sum_{j=1}^{n} d(i, j) x_{ij} \tag{1}$$

subject to constraints

$$\begin{array}{lll} \sum_{j=1}^{n} x_{ij} = 1 & i = 1, \ldots, m & \\ x_{ij} \leq y_i & i = 1, \ldots, m & j = 1, \ldots, n \\ x_{ij} \in \{0, 1\} & i = 1, \ldots, m & j = 1, \ldots, n \\ y_i \in \{0, 1\} & i = 1, \ldots, m & \end{array} \tag{2}$$

The optimal solution of the LPP means the identification of the optimal set of learning objects that better match (minimal distance) the learner preferences.

III. A Novel Memetic Approach to Solve Learning Presentation Problem

As any other optimization problem, LPP can be solved by means of a deterministic algorithm. This approach is valid when we consider a repository with a limited number of learning activities and subjects. However in e-Learning 2.0 scenario, the number of learning activities and subjects tends to be very high, and thus we need to look for more flexible

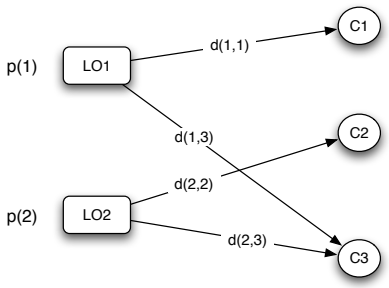

Fig. 1. Formalization of LPP.

approaches. Metaheuristics have been used extensively in the literature obtaining satisfactory results for all kind of problems. Among metaheuristics, Memetic Algorithms (MAs) [8] have become one of the most used approaches due to their ability to combine a high exploration of the search space and a high exploitation of the most promising regions.

Starting from this consideration, our proposal is to design an innovative memetic algorithm capable of efficiently generating learning presentations. In detail, this work introduces a novel parallel cooperative adaptive memetic algorithm aimed to personalize e-learning environment by combining and configuring cooperative evolutionary and local search metaheuristics in order to improve overall performance. The cooperation among the different optimization strategies is performed by intelligently exchanging solutions in precise moments and under certain conditions. The exchange control is supervised by a set of fuzzy rules, which exploits knowledge modeled by a collection of fuzzy decision trees and obtained using a preliminary learning process. With this knowledge the fuzzy engine can predict the behavior of each metaheuristic and adapt it to the presentation being personalized.

Hereafter, this section precisely describes the proposed novel multi-agent memetic algorithm capable of efficiently solving the LPP problem and, consequently, supporting e-learning environments to define high-quality personalized learning experiences.

A. A Novel Multi-agent Based Memetic Algorithm

In this section the proposed Multi-Agent Memetic Algorithm (MAMA) is introduced. MAMA is computed in two steps (see fig. 2), dealing respectively with evolutionary and local methodologies. In the first step, a collection of different evolutionary optimization strategies (Genetic Algorithm, Particle Swarm Optimization, ...) are executed in a *parallel* way in order to locate the best region of problem's search space. Successively a set of local search strategies (Tabu Search, Simulated Annealing, ...) simultaneously exploits this region in order to find a high quality solution. In each step, the optimization strategies, *intelligently choose* their configuration parameters and *cooperate* by exchanging their solutions in *adaptive* way. The adaptability is achieved by means of a fuzzy rule base able to evaluate information extracted by a preliminary machine learning approach [9] that ranks computational

performances related to evolutionary and local metaheuristics applied to a given optimization problem.

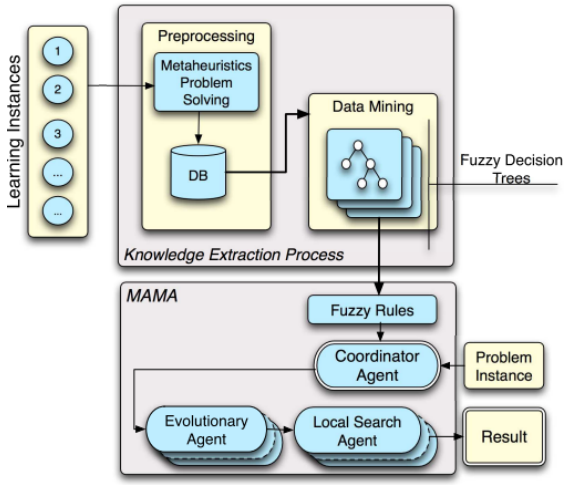

Fig. 2. Adaptive Memetic Architecture.

The parallel and distributed nature of our approach is fully suitable to be modeled using a multi-agent system [7] where a set of so called *optimization agents* computes the cooperating metaheuristics under the supervision of a *coordinator agent* whose intelligence is provided by the aforementioned fuzzy rules and machine learning approach. The coordinator agent is responsible of initiating optimization process by parallel activating optimization agents and, in each phase, it coordinates the cooperation among optimization agents by choosing their configuration parameters and exchanging their solutions in an adaptive way.

The adaptability task of coordinator agent is performed by considering knowledge coming from machine learning (see section III-B) coded by means of a collection of fuzzy decision trees. In particular, trees' analysis supports coordinator agent to 1) choose the best metaheuristic parameters and 2) rank the metaheuristics suitability to solve the instance using numerical weights in the range $[0, 1]$. Through weights analysis, coordinator may realize that a metaheuristic is poorly performing and, consequently, it may update its solutions by adding a set of better solutions computed by other more suitable metaheuristics. This process allows poor metaheuristics to restart their optimization task in a more interesting point of the search space.

The cooperation is performed in the following way, optimization agents evaluate, during a certain period, the objective function then they stop their computation in order to allow the coordinator agent to collect their information and make decisions. After that, each optimization agent continues exploring the search space but executing coordinator agent's orders.

To perform the communication between coordinator and optimization agents, a blackboard architecture [10] will be used. Blackboards are data structures usually used as general communication mechanisms. In our proposal each agent has an assigned space on the blackboard where it periodically *writes* information about the solution it has found. The coordinator *reads* this information and directs the search of each agent.

1) Modeling intelligence of the coordinator agent: A crucial question of proposed memetic architecture is how to model the coordinator agent's intelligence in order to allow it to evaluate metaheuristics performances and control the cooperation among related optimization agents. This goal is achieved by using a set of fuzzy rules able to exploit the knowledge obtained by machine learning. More precisely, the coordinator agent uses fuzzy inference to:

- choose the best metaheuristics' parameters values;
- individuate when poor evolutionary metaheuristics have to receive a collection of individuals from other strategies that are showing a better behavior.
- individuate when local search methods have to reinitiate their search using the solution of another one which is showing a better behavior.

Coordinator agent implements first behavior by using a collection of fuzzy decision trees, as many as metaheuristics, obtained through machine learning. These trees analyze the instance in order to infer the most suitable parameters values for each metaheuristic. Moreover, the coordinator agent realizes the remaining two behaviors by considering two additional trees coming from machine learning. In detail, these trees analyze the instance and respectively rank evolutionary metaheuristics and local search metaheuristics, by returning a weights collection Ω where each $\omega_i \in \Omega$ takes a value in the range $[0, 1]$, the sum of the weights of evolutionary metaheuristics is 1, as the sum of the weights of local search metaheuristics. In short, each weight ω_i is associated with a metaheuristic and represents its suitability to solve the instance under consideration , i.e., the higher the weight of a metaheuristic the more suited it is.

In each phase, the coordinator agent uses a collection of fuzzy rules (one for each metaheuristic) exploiting Ω in order to derive the collection of poor strategies. For the sake of simplicity the rule shown below is related to evolutionary strategies (however rules acting in local phase are equivalent):

> IF [$(\omega_1 \cdot d_1$ OR ... OR $\omega_{|E|} \cdot d_{|E|})$ IS *enough*] THEN change the current solution of m_h.

where:

- m_h is the metaheuristic being evaluated by the rule;
- $d_i = (\xi(m_i) - \xi(m_h))/\max(\xi(m_i), \xi(m_h))$, where ξ is a measure of performance shown by metaheuristics. It is defined by the user;
- $\omega_i \in [0, 1]$ is the weight of m_i;
- $enough$ is a fuzzy set with trapezoidal membership function defined by a quadruplet (a, b, c, d) and whose universe of discourse is the range $[0, 1]$.

The main goal of each rule is to change the position in the search space of a metaheuristic which is showing a bad performance for a position near the solution of another metaheuristic with a better behavior. It should be noted that this rule tries to solve the problem that appears in parallel strategies where the exchange of solutions is unrestricted [11]

and which tend to prematurely converge to local optimums characterized by a low quality.

To perform the firing of the fuzzy rules, $\alpha - cuts$ are used. In other words, only those rules whose activation value exceeds the defined $\alpha - cut$, are fired. In the event that more than one rule is activated then the coordinator applies all of them. In this way, the coordinator agent is capable of simultaneously adapt the behavior of several poor metaheuristics.

The metaheuristics' solution exchange is performed by taking into account two different situations: 1) a single antecedent clause of rule is fired or 2) many clauses are fired during inference process. In detail, let S be the collection of strategies related to fired clauses and let m_h be the poor metaheuristic that have to receive better solutions. If a single clause is fired then $|S| = 1$ otherwise $|S| > 1$.

Then, during the first phase (evolutionary phase), the poor metaheuristics' solutions changing is performed as follows:

1) $|S| = 1$. A proportion of the worst individuals of m_h is substituted by a set of solutions consisting of the best members of the population of strategy $m_k \in S$. The proportion is equals to ω_k.
2) $|S| > 1$. A proportion of the worst individuals of m_h is replaced by a set of solutions where each meta-heuristic chooses its solutions as said before. The proportion is equals to $\sum_{i=1}^{|S|} \omega_i$.

Differently from first phase, during the local optimization phase the changing is performed as follows:

- A solution "near" to the best solution obtained among the meta-heuristics $m_k \in S$ is sent to m_h. Where "near" means that the best solution is changed by applying, $\lceil \frac{1}{(2 \cdot \omega_k)} \rceil$ times, a mutation operator that depends on the problem. This operation is performed in order to introduce some diversification, since the exchange of identical solutions can cause that all metaheuristics perform the search in the same space.

B. MAMA Configuration through Machine Learning

As previously mentioned the adaptability of the proposed MA is provided by the knowledge obtained through an extraction process introduced in this section. The aim of the knowledge extraction process is to evaluate the performances of metaheuristics composing the MA when applied to instances of the problem under consideration. This process returns a set of trees containing: two trees respectively modeling the suitability of the evolutionary and local search strategies by providing the aforementioned weights Ω and, on the other hand, one tree for each metaheuristic which provides the most suitable parameters choice for each metaheuristic.

The Knowledge extraction process is subdivided in two subphases, as can be seen in figure 2, Preprocessing and Data Mining.

1) Preprocessing: In preprocessing phase, metaheuristics that compose the system are applied to a set of training instances in order to build a collection of databases, named *refined databases*, that will be exploited by data mining to compute the trees that guide the coordinator. The obtaining of these databases is carried out in two steps. First, information about the performance of metaheuristics is stored in a set of so called *raw databases*, where each raw database is associated to a different metaheuristic. Successively, data contained in raw databases are processed in order to compute the final refined databases, which contain additional information useful to extract significant knowledge during data mining.

In particular, the obtaining of raw databases is carried out in the following way. For each metaheuristic and each parameter configuring this metaheuristic, a set of parameter values is chosen, after that each metaheuristic is executed k times with each possible combination of parameter values, being k an *iterative factor*, i.e., a predefined value used to obtain more accurate performance estimations. For each one of these executions a row is inserted into the raw database related to the metaheuristic being evaluated. In details, a raw database row contains:

- a description of the specific instance of the problem;
- the values of the parameters used in the execution of each metaheuristic;
- the final solution obtained.

Next step is to analyze raw databases in order to compute the refined databases. Refined databases are smaller than raw databases and contain additional information useful to extract significant knowledge during data mining. In detail, for each metaheuristic a refined database is computed which contains information about its best parameters combinations, i.e., which parameters values obtained a better performance. Besides, two more refined databases are computed which respectively contain information about the weights Ω associated to evolutionary and local search strategies.

In order to build databases concerning parameters for each metaheuristic its raw database is processed as follows:

1) for each instance and for each parameters combination calculate the average fitness value of its k executions.
2) for each instance select the parameter combination computing the best average fitness value;
3) the refined database is updated with a new entry containing the description of instance and the best parameter combination.

The remaining two databases are directly related to evolutionary strategies and local search methods. In detail, the refined database related to evolutionary methods is processed as follows:

1) for each metaheuristic, for each instance and for each parameters combination calculate the average fitness value of its k executions.
2) for each metaheuristic and each instance, select the best average fitness value and compute the *metaheuristic suitability weight* ω_i as:

$$\omega_i = \frac{fit^i_{best}}{\sum_{l=1}^{\#evolutionary_strategies} fit^l_{best}}$$

3) for each metaheuristic and each instance the refined database is updated with a new entry containing the de-

scription of the instance and the metaheuristic suitability weight ω_i.

Database associated to local search methods is analogously built by replacing evolutionary strategies with local search methods. Refined databases represent the output result of Preprocessing phase and they will be used by a data mining technique to complete the Knowledge Extraction Process in computational efficient way.

2) Data Mining: Once gathered performance information and collected it through refined databases, the Data Mining phase extracts the collection of knowledge models through data mining. Our data mining approach exploits a fuzzy decision tree (FDT) technique [12] to extract knowledge from refined databases and build the aforementioned collection of trees. Two main reasons have guided the choice of FDTs. First their interpretability, decision trees stand out on account of their simplicity and readability, which is an important issue in data mining, and enable a full understanding of the knowledge that guides the coordinator. Second, their fuzziness, i.e., the possibility of dealing with fuzzy theory, which can improve inference performance by means of approximate reasoning and provide an easy way to obtain the weights Ω, one of the most important parts of coordinator's knowledge.

Once this phase is finished the collection of fuzzy decision trees that models coordinators's knowledge, is obtained, and it is ready to control the execution of the optimization agents.

IV. Experimental Results

In this section we want to asses the validity of the proposed approach, MAMA. The main purpose of MAMA is to help improving the e-learning process. For this reason we plan to include it as a plug-in of a learning management system. In particular, we plan to include it in Sakai project[1]. Sakai is an open source learning management which enables powerful teaching, learning and research collaboration within a feature-rich, enterprise platform. However, Sakai does not provide the possibility of automatically personalize e-learning experiences in the previously explained way. We consider this an essential feature for modern e-learning solutions, and thus believe that the development of a plug-in that adds this feature can improve learners' experience. In the design of the planned plug-in, a crucial issue has been the choice of the metaheuristics that will made up the system. For the problem being considered we have chosen four strategies, two evolutionary metaheuristics, a Genetic Algorithm (GA) and a Particle Swarm Optimization (PSO), and two local search metaheuristics, a Tabu Search (TS) and a Simulated Annealing (SA). Other metaheuristics could have been chosen or even added, but as a first step we have chosen these four.

Hereafter, the results of some preliminary performance tests and a study with real learners will indicate the positive impact of MAMA in the process of e-learning.

[1]www.sakaiproject.org

TABLE II
Parameters values for each metaheuristic

GA		*PSO*	
parameter	*value*	*parameter*	*value*
Selection op.	Roulette	Topology	Local Best 2N
Cross prob.	0.6	ω	0.729844
Mutation prob.	0.01	r_p	2
Population size	100	r_g	2
		# of particles	100
TS		*SA*	
parameter	*value*	*parameter*	*value*
Tabu list size	10	Cooling schedule	Hyperbolic Tangent
Diversification t.	50	Inner iterations	5000

A. Computational experiments

In this subsection, we perform some tests in order to assess the validity of MAMA, comparing its results with those obtained by the different non-adaptive MAs that can be obtained from the combination of the single metaheuristics that compose MAMA in a sequential way, namely:

- Genetic Algorithm + Tabu Search (GA+TS).
- Genetic Algorithm + Simulated Annealing (GA+SA).
- Particle Swarm Optimization + Tabu Search (PSO+TS).
- Particle Swarm Optimization + Simulated Annealing (PSO+SA).

The parameters used by each metaheuristic are shown in Table II.

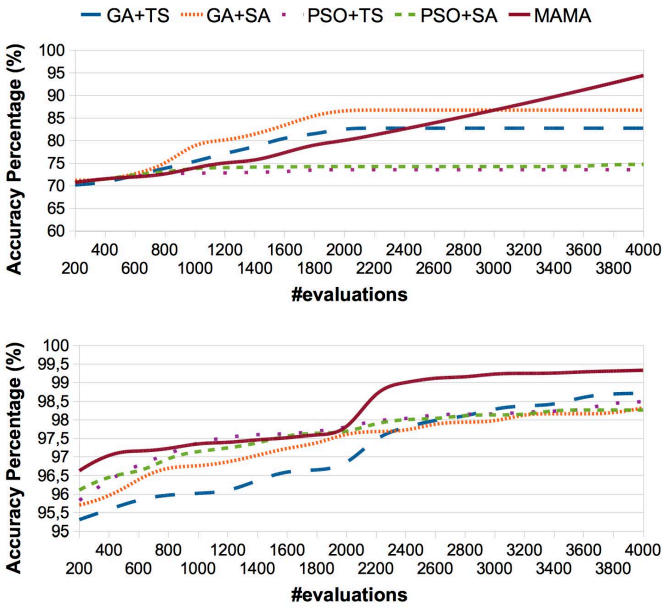

Fig. 3. Evolutions of the different strategies.

1) Performance tests: As a first approach it would be interesting to perform some preliminary tests in order to asses the validity of the proposed strategy. In order to perform these tests we have created an instance generator able to construct artificial instances of the learning presentation problem. We

have identified some instance's features that may influence the behavior and performance of different solving strategies:

- Number of learners.
- Ratio between learning objects and learners.
- Connection percentage between learning objects and learners.

We have carried out two tests with two different instances generated using the aforementioned generator. The purpose of these tests was to graphically interpret the behavior of the different strategies during their search of the optimum. The results are shown in Fig. 3, this figure illustrates the evolution of the 5 strategies. The graphics plot the fitness value obtained by each strategy at each moment of the execution, showing the average of 10 executions of 4000 evaluations. From these graphics we can extract interesting information about the behavior of MAMA. In particular, it can be observed that although MAMA's convergence is not the fastest, it obtains in both instances the best performance. These are promising results which seem to indicate that MAMA solves e-learning LPP problem in a more efficient way than other static memetic approaches and, as will be shown afterwards, it generates very suitable personalized learning experiences.

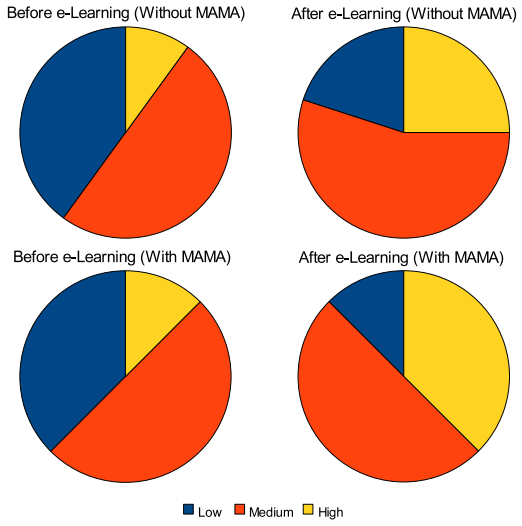

Fig. 4. Experimentation results on a group of 38 learners with and without the proposed memetic Sakai plug-in prototype.

2) Learning Comparative Studies: Once we have demonstrated the effectiveness of MAMA with artificial instances, we perform a real world test, involving real learners that want to train on enterprise management. The control and experimental groups were made up of 20 and 18 learners respectively. Data corresponding to the control group comes from historical data from a previous experiment, and shows the results of learning using Sakai without the help of MAMA. On the other hand, data corresponding to experimental group was obtained from the results achieved by a new group of learners, which were able to use the capabilities of MAMA. All the voluntary learners were tested before and after a training phase on the same topics. In all the tests the learners' skills in the chosen domain were quantified using three ability ranges: low-level (0-3 scores), medium-level (4-7 scores) and high-level (8-10 scores). Figure 4 presents a summary of the results. As can be observed, both e-Learning approaches provide the necessary tools to improve learners' knowledge, in fact the quantifications of the knowledge are statistically better with a significance of the 99.9% after using e-learning. Moreover those learners that have used MAMA have obtained better results than those which not, with an statistical significance of the 95%. These results are very promising and support the creation of a plug-in for Sakai able to include MAMA's capabilities.

V. Conclusions

Recent advances in Web 2.0 have impulsed the development of the so called e-learning 2.0. In this context, Learning Management Systems should promote new e-learning trends by means of suitable models and processes that dynamically and intelligently create personalized e-learning experiences adapted to learner expectations and objectives. Our work proposed an innovative memetic algorithm capable of efficiently generating personalized learning presentations. In detail, we have proposed a parallel cooperative adaptive memetic algorithm aimed to personalize e-learning environment by combining and configuring cooperative evolutionary and local search metaheuristics in order to improve overall performance. The cooperation is supervised by a set of fuzzy rules, which exploits knowledge modeled by a collection of fuzzy decision trees and obtained using a preliminary learning process. As shown by experimental results, our proposal enhances significantly the learning framework in terms of flexibility and efficiency.

References

[1] M. Ebner, "E-Learning 2.0 = e-Learning 1.0 + Web 2.0?," in *Proc. 2nd Int. Conf. Availability, Reliability and Security*, pp. 1235–1239, 2007.

[2] T. Gruber, "Toward Principles for the Design of Ontologies Used for Knowledge Sharing," *Int. J. Human-Computer Studies* vol. 43, pp. 907-928, 1994.

[3] G. Cornuejols, G. L. Nemhauser, and L. A. Wolsey, "The uncapacited facility location problem," *Discrete Location Theory*, P. Mirchandani and R. Francis (Eds.), John Wiley and Sons Inc., New York, pp. 119-171, 1990.

[4] G. Albano, M. Gaeta, and S. Salerno, "E-learning: a model and process proposal," *Int. J. Knowledge and Learning*, vol. 2, pp. 73–88, 2006.

[5] G. Albano, M. Gaeta, and P. Ritrovato, "Testing hypotheses in the functional linear model," *Scandinavian J. Statistics*, vol. 30, pp. 241–251, 2007.

[6] G. Acampora, M. Gaeta, V. Loia, P. Ritrovato, and S.Salerno, "Optimizing Learning Path Selection through Memetic Algorithms," *IEEE Int. Joint Conf. Neural Networks*, pp. 3869–3875, 2008.

[7] M.J. Wooldridge, *Multi-agent Systems : An Introduction*, John Wiley and Sons, 2002.

[8] P. Moscato, "On evolution, search, optimization, GAs and martial arts: toward memetic algorithms," California Inst. Technol., Pasadena, CA, Tech. Rep. Caltech Concurrent Comput. Prog. Rep. 826, 1989.

[9] J.M. Cadenas, M.C. Garrido, and E. Muñoz, "Using machine learning in a cooperative hybrid parallel strategy of metaheuristics," *Information Sciences*, vol.179, pp. 3255–3267. 2009.

[10] Daniel D. Corkill. "Blackboard Systems," *AI Expert*, vol. 6, no. 9, pp. 40-47, September 1991.

[11] T. G. Crainic, M. Gendreau, P. Hansen, and N. Mladenovic, "Cooperative parallel variable neighborhood search for the p-median," J. Heuristics, vol. 10, pp. 293–314, 2004.

[12] C.Z. Janikow, "Fuzzy decision trees: issues and methods," *IEEE Trans. Syst. Man Cybern. B, Cybern.*, vol. 28, no. 1, pp. 1–14, 1998.

2011 IEEE International Conference on Fuzzy Systems
June 27-30, 2011, Taipei, Taiwan

A hybrid context aware system for tourist guidance based on collaborative filtering

G. Fenza, E. Fischetti, D. Furno, V. Loia
Department of Computer Science &
CORISA (Consorzio Ricerca Sistemi ad Agenti)
University of Salerno
E-mail: {gfenza, efischetti, dfurno, loia}@unisa.it

Abstract— **In the area of ambient intelligence there is a need to address user needs according with context features. Recently, the synergy between context aware computing and collaborative filtering is leading to enhance recommender systems with capabilities always nearer to user needs. Specifically, in the domain of tourism it is useful to proactively suggest right sets of attractive locations, events and so on. This work defines a context aware recommender system aimed at suggesting pertinent points of interest (POIs) to tourists. In particular, the approach is strongly based on the synergy between soft computing and data mining techniques. The general framework integrates user profiles, history of social networking and POIs data. Then by defining collaborative filtering approach on the history meaningful POIs are extracted. Indeed, soft computing techniques are mainly applied in order to support activity of unsupervised users and POIs classification. On the other hand, data mining techniques are exploited in order to extract rules able to associate user profile and context features with an eligible set of recommendable POIs. Experimental results show performance in terms of recommendations accuracy.**

Keywords-component; context-awareness; fuzzy data analysis; data mining; recommender system; points of interest

I. INTRODUCTION

The tourism sector is one of the biggest in the global market employing 200 million people and serving 700 million tourists worldwide. Furthermore, this trend is intended to grow in the next years. Additionally, Information Technology with its constant progress has decisively affected the way that tourism services are performed and provided. In effect, tourists thanks to advances in Information and Communication Technologies (ICTs) are enabled to access tourist information as well as to reservations and plans in a more reliable, accurate, inexpensive and efficient way. As a result, services related to tourism are increasingly influenced by the Internet and related technologies, so much so that it is possible to find most of them on line without the necessity of relying on travel agency. On the other hand, ICTs and the Internet have increased the number of choices so dramatically that is very difficult for the users to retrieve what they are looking for. The appropriate discovery of tourism services is one of the main drawbacks when people travel [1]. According to [2] research, the reasons of consumers not purchasing travel products online are the lack of personal service, security issues, lack of experience, and time consuming. Furthermore, different users have different preferences and needs. So a remedy for these problems is to develop systems with an ability to adapt their behavior to the profile, context and other features of individual users and groups of them. An interesting solution for reducing Internet researches complexity and overcoming the aforementioned difficulties is provided by so called recommender systems. Recommender systems have already been applied to several application domains such as finding books, movies, tv-programs, news, music, web-pages, etc. One of the main characteristics of a recommender system is that it can personalize its interaction to each individual user according with context. In that case, personalization involves the design of enabling systems to capture or infer the needs of each person and then to satisfy those needs in a known context [3]. Context-awareness computing and recommender systems can enhance and complement each other; they both help users in finding relevant and interesting objects based on their interests and current context.

In the specific of this paper, our intention is to propose a hybrid context-aware recommender system aimed at adaptively and proactively suggesting points of interest (POIs) to tourists according to their profile, but also to their context. In particular, the work defines an integrated environment applying content based and collaborative filtering on historical data through soft computing and data mining techniques in order to predict and suggest POIs to users. In other words, the main goal of the proposed work is related to define context-aware recommender system whose quality of feedback relies on the acquisition of user context and profile by means of a robust theoretical approach. So, the overall framework is composed of two main workflows: knowledge discovery and recommendation. In particular, Knowledge Discovery Process concerns the fuzzy data analysis of users and POIs. Indeed, fuzzy clustering and classifiers enable us to integrate cluster of users and POIs with historical data. Then association rule mining activity points out a correspondence between user, contexts and cluster of POIs. On the other hand, Recommendation Process foresees activities of user classification and rule matching in order to provide some ranked recommendation about pertinent POIs.

The paper is organized as follows: Section II presents some related works available in literature; Section III proposes a theoretical background for supporting workflows description; Section IV and Section V introduce workflows of the framework by focusing on the Knowledge Discovery Process and Recommendation Process, respectively. Then, Section VI describes the system performance in terms of accuracy. Finally, conclusions and future works close the paper.

978-1-4244-7316-8/11/$26.00 ©2011 IEEE

II. RELATEDWORKS

The aim of this section is to depict the research trend with reference to context aware recommender systems in ambient intelligence for tourist guidance and to point out the benefits of the proposed approach. Among research works regarding personalized and/or location-based recommender systems based on web service, with specific reference to tourist domain, Kakaletris et al. [4] address the design and implementation issues for delivering location-based tourism-related content services. By illustrating an example of generic tourist guide, Scherp and Boll [5] emphasize on supporting the dynamic generation of personalized multimedia content in respect of the tourist's interests and preferences, current location and environment, and mobile device used. Aiming at effectively coordinating and integrating disparate information and service resources anytime and anywhere, Chiu and Leung [6] propose a ubiquitous tourist assistance system that is built upon multi-agent and semantic web technologies for providing personalized assistance and automation to the tourists with different preferences and often changing requirements during their trips. Five agent clusters specified in the system architecture include tourist assistant, ontology maintenance and search, requirement/preference management, package planning, and local tour planning. Ricci and Nguyen [7] present a critique-based mobile recommender system that lets users expressing session-specific preferences in addition to the long-term collected preferences. The objective is to provide on-tour system support to mobile travelers for selecting products or services based on the integration of both types of preferences. The COMPASS system [8] allows easy creation of context-aware personalized applications and the services that are part of such a platform, including a service registry, a context manager and a recommendation engine. Console et al. [9] created a prototype system called MastroCARonte, which provides personalized services that adapt to the user and his context onboard cars. This research focuses on the effects of having such adaptive systems onboard cars.

Among research works regarding more specifically context aware and adaptive recommender systems for tourist guidance, the Intrigue system [10] is an interactive agenda offered by a tourist information server that assists the user in creating a personalized tour along tourist attractions. This research focuses on planning and scheduling a personalized tour taking into account the location of each tourist attraction and the interests of the user. A last example of a tourist guide project is the GUIDE project of the University of Lancaster [11]. This project develops a context sensitive tourist guide for the visitors to the city of Lancaster. Specifically, in this project Users have a portable PC that communicates with a Wireless LAN to retrieve information. The used context information is knowledge of the user and knowledge of the environment (including the physical location of the user). Based on the location and user preferences, visitors can obtain information in two ways. All the required information is broadcasted by cell base-stations to portables either as part of a regular schedule (information relevant for the region the station covers) or in response to user requests. The system determines the location of the user by the cell coverage, or the user can specify in which location he/she is.

The aforementioned works provide the user with tourist recommendations but do not manage uncertainty among user interests. Furthermore, most of them are only content based, omitting collaborative information that is a crucial aspect for user recommendations personalization. In this sense, our approach presents an hybrid system which main aim is related to provide an integrated environment for tourist guidance that combines collaborative and content based filtering. Indeed, the main idea of this work is related to enhanced context awareness by means of data analysis, computational intelligence and rule mining techniques in order to obtain a recommender system able to suggest users in the tourist domain with pertinent POIs. Strictly related approach is described in [12] where a personalization method for tourist Point of Interest (POI) Recommendation is defined by considering both user preferences and collaborative aspects. Indeed, [12] exploits a memory based algorithm to carry out suggestions. In particular, our system define a model based approach that trains itself by performing activities of fuzzy context data analysis in order to support both POIs and user's context identification by means of fuzzy classifiers.

III. THEORETICAL BACKGROUND

The overall system takes into account users data, available POIs and historical data in order to provide proper recommendations (i.e., POIs) according to his/her preferences and context. In particular, algorithms of clustering and classification allow to tackle the huge amount of incoming data (Users and POIs). On the other hand, association rules mining algorithm on historical data allows to extract correspondences with pertinent tourist POI categories.

Since, this work relies on a mathematical model that exploits soft computing and data mining techniques, this section provides some theoretical basis in order to support understanding of the overall framework workflows.

A. Fuzzy clustering

Once data, about users and POIs, are collected and arranged adequately, they are processed by Fuzzy C-Means (briefly FCM) algorithm [15][16]. FCM is an unsupervised clustering algorithm, which considers a prior fixed number of clusters. In order to give more accurate partitions of data, many researchers have studied the cluster validity criteria [17]. In our past studies and experimentations we have achieved good results by the application of Xie and Beni's validity measure [18]; so we have also selected it for the approach proposed in this work. Advanced approaches to (fuzzy) clustering methods could be exploited, according to the nature of the data space and the inherent relationships. As said, we exploit the well-know FCM algorithm, particularly useful for flexible data organizationally. It takes as input a data matrix and it tries to get an "optimal" partitioning of the feature space (composed by the data matrix). FCM aims at maximizing the homogeneity, grouping into the same cluster the patterns which are closer. Herein, each pattern is a row of matrix. FCM recognizes spherical "clouds of points" in a multi dimensional data space (i.e. data matrix) and each cluster is represented by its center point (prototype or centroid). The function minimizes the weighted sum of the

distances between data points *x* and the centroid *v*, according to this formula:

$$V(U)=\sum_{l=1}^{c}\left(\sum_{i=1}^{n}w_{i,l}\sum_{j=1}^{p}(\underline{x}_{i,j}-\underline{v}_{l,j})^2+\gamma\sum_{i=1}^{n}w_{i,l}\sum_{j=p+1}^{m}\partial(\underline{x}_{i,j},\underline{v}_{l,j})\right) \quad (1)$$

where $c \geq 2$ is the number of clusters, $w_{i,l} \in [0,1]$ is the membership degree of $x_{i,j}$ in the l-th cluster and *m* is the features number. In particular, since our feature set is mixed, because of numeric and nominal features, the *m* features are partitioned in two set, namely a numeric feature set composed by the features from *1* to *p* and a nominal feature set composed by the features from *p+1* to *m*. As a result, the first term in (1) is the squared Euclidean distance measure on the numeric attributes and the second term is a semantic distance on the nominal attributes, where ∂ is equal to a linear combination between a semantic distance taxonomy based [13] and Google similarity distance [14]; finally, γ is used to weight features. After the FCM execution, data partitions are returned, in a prior fixed number *c* of clusters. Anyway, with the application of validity measures it is possible to execute clustering without a prior number of clusters specification.

Details about how Fuzzy Clustering has been applied in this framework are given in Section IV and V, where the workflows of the whole proposed system are detailed.

B. Fuzzy Classifier Design

In computational intelligence literature, fuzzy rules have been often exploited in different approaches for decoding the knowledge in a way closer to the human understanding. In neural network [22] approach, if-then fuzzy rules enable the emulation of the decisions or reasoning of a human expert, whereas fuzzy number and compositional rules of inference have been employed for fuzzy decision making in medical diagnosis [23]. The fuzzy if-then rules provide an interpretation of the clusters, closer to the human understanding and easier to evaluate, with respect to the values range of each feature. Outputs of previous phase are prototypes and a partitioning matrix of the data patterns. This matrix contains the memberships of the elements of the given data set in each of the c clusters. Generally, the linear interpolation of memberships is computed; in order to easily assign linguistic label, the membership function is computed by linear interpolation of the projected membership to each axis (according to the n-dimension space), for each cluster. More specifically, exploiting the cylindrical extension technique [15] (a projection-based method of n-dimensional argument vector), the generic i-th fuzzy cluster can be described by a fuzzy rule, where each features is described through a fuzzy set. Each fuzzy cluster K_i with i = 1, . . . , c can be represented through n functions A_{i1} , A_{i2} , . . . , A_{in}, obtained by the projected and interpolated memberships. The generated rules are subject to a proper validation by experts of the specific domain and then exploited for suitable classifications. In our work, the fuzzy rules are exploited to classify new tourist POIs and users. Just to provide an example, a fuzzy rule, supposed to be in the form of Takagi-Sugeno model [19] is described as follows:

R_i : **If** x_1 is A_{i1} AND x_2 is A_{i2} AND … AND x_n is A_{in} **then** $y_i = a_{i1}\, x_1 + a_{i2}\, x_2 + \ldots + a_{in}\, x_n + b_i$,

with weight $[w_i]$ i = 1, … , c

where R_i is the i-th rule, x_1, x_2, . . ., x_n are the input variables, A_{i1},A_{i2}, . . .,A_{in} are the fuzzy sets assigned to corresponding input variables, variable y_i represents the value of the i-th rule output, and $a_i = [a_{i1}, a_{i2}, \ldots, a_{in}]$ and b_i are parameters of the consequent function. As said before, the antecedent fuzzy sets are usually achieved by projecting the membership degrees in the fuzzy partitions matrix U onto the axes of individual antecedent variable x_j to obtain a point-wise defined antecedent fuzzy set A_{ij}. Then we approximate it by a normal bell-shaped membership function [20]; indeed the uniform structure of bell-shaped function is suitable for identification, analysis and optimization. Hence, each fuzzy set A_{ij} is calculated from the sampled input data $x_j = [x_{1j}, \ldots, x_{nj}]^T$ and the fuzzy partition matrix $U = [u_{ij}]$ as follows:

$$A_{ij}(z)=\exp\left\{-\frac{1}{2}\left(\frac{z-\alpha_{iq}}{\beta_{iq}}\right)^2\right\} \quad (2)$$

where

$$\alpha_{iq}=\frac{\sum_{j=1}^{n}u_{ij}x_{qj}}{\sum_{j=1}^{n}u_{ij}} \quad and \quad \beta_{ij}=\sqrt{\frac{\sum_{j=1}^{n}u_{ij}(x_{qj}-\alpha_{iq})^2}{\sum_{j=1}^{n}u_{ij}}} \quad (3)$$

represent the mean and standard deviation of the bell-shaped membership function, respectively.

On the other hand, the computation of parameters $a_i = [a_{i1}, a_{i2}, \ldots, a_{in}]^T$ and b_i in the consequent part requires a deepened study, in order to evaluate the firing strength w_i of the i-th rule and the value of y_i [21].

Goal is to evaluate the final output of the TS fuzzy model y_i for an arbitrary x_j input sample, which is calculated using the following formula [21]:

$$\hat{y}_k=\sum_{i=1}^{c}[\underline{w}_i(\underline{x}_k)(\underline{x}_k\,\underline{a}_i+b_i)] \quad (4)$$

with k = 1, 2, 3, . . .,n and where $\underline{w}_i(\underline{x}_k)$ represent the firing strength of i-th rule for the k-th pattern. Thus, in order to compute the parameters of consequent part of a rule, a regression model of the compact form $\hat{Y} = X'\,[a_i^T, b_i] + \varepsilon$ is evaluated: herein ε is the approximation error, X' assumes the form: $X' = [w_1, x_k^T, 1, w_2\, x_k^T\, 1, \ldots, w_c\, x_k^T, 1]$. Vectors $[a_i^T, b_i]$ are determined using the least-squares method [21].

C. Rule Mining

The proposed approach foresees activities of rule mining on historical data, in order to associate user contexts and tourist POI categories. The problem of mining association rules over was introduced in [24]. An example of an association rule in our case might be that 90% of users arriving in a tourist town in the morning, being scientific researchers and walking, select POI about the nearer science museum. The following is a

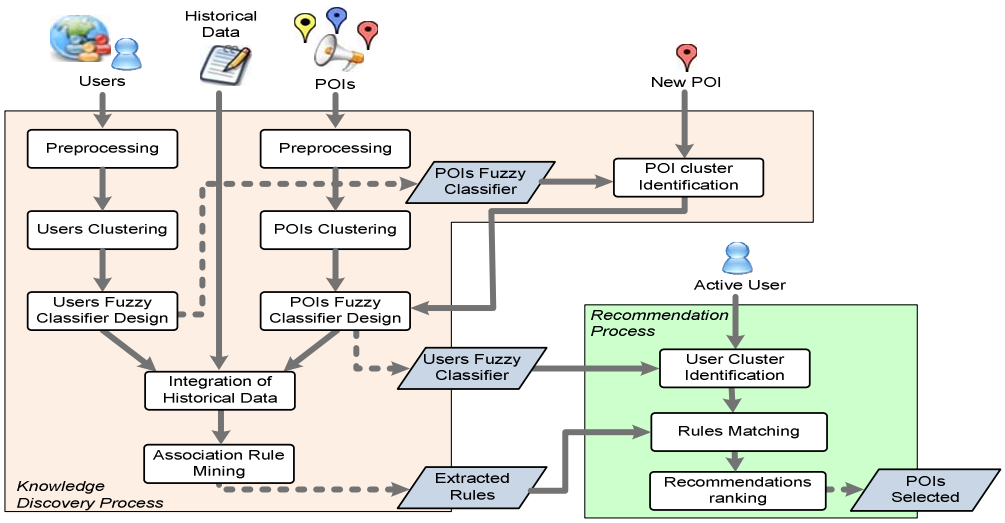

Figure 1. Workflows of the overall framework: Knowledge Discovery Process, Recommendation Process.

formal statement of the problem [24]: given a set of items $I = \{I_1, I_2, \ldots, I_m\}$ and a database of transactions $D = \{t_1, t_2, \ldots, t_n\}$

where $t_i = \{I_{i1}, I_{i2}, \ldots, I_{ik}\}$ and $I_{ij} \in I$, an association rule is an implication of the form $X \Rightarrow Y$ where $X, Y \subset I$ are sets of items called itemsets and $X \cap Y = \emptyset$. X is called the antecedent and Y is called the consequent. We are generally not interested in all implications but only those that are important.

Here, two features called support and confidence are usually used to measure the importance of association rules. The support for an association rule $X \Rightarrow Y$ is the percentage of transactions in the database that contain $X \cup Y$. The confidence for an association rule $X \Rightarrow Y$ is the ratio of the number of transactions that contain $X \cup Y$ to the number of transactions that contain X. Rules that satisfy both the minimum support (MinSup) and confidence (MinConf) thresholds are called strong rules. An algorithm for finding all association rules, henceforth referred to as the AIS algorithm, was presented in [24]. Another algorithm for this task, called the SETM algorithm, has been proposed in [25].

In this work, we use an algorithm, Apriori [26], that differ fundamentally from these algorithms and exhibits better performance. Furthermore, in our future works we would like to experiment a Formal Concept Analysis-based Association Rule Mining Algorithm as proposed in [27].

IV. KNOWLEDGE DISCOVERY PROCESS

As highlighted in Fig.1, the overall framework consists of two main workflows: *Knowledge Discovery Process* and *Recommendation Process*. Following subsections detail the first one.

A. Users and POIs Preprocessing

Preprocessing tasks on Users and POIs data allow to start the process of Knowledge Discovery. In particular, gathering and normalization activities take place in order to prepare data for the next phase, that is, *Users and POIs clustering*. Specifically, preprocessing carries out the user and POIs data sets, as shown in Table I (A) and (B). In the example the user data set includes three features (i.e., age, skill and interest), whereas POIs data set is composed of five features (i.e., type, lat, long, when, period). Furthermore, as highlighted in the Table I features may be numerical or nominal. For instance, in the user data set features space, *age* is a numerical attribute whereas *skill* and *interest* are rather nominal.

B. Users and POIs clustering

Analogously with the previous step, clustering execution takes place on user and POIs data sets. We stress that users and POIs are considered in two off-line separate processes and the subsequent extraction of classification rules enable us to properly add new users and POIs to clusters. So, the execution of these two distinct processes should not be time consuming, because there is no need to execute clustering again whenever a new user or POI must be considered. Specifically, the framework exploits FCM algorithm in order to arrange data according to their similarities. In particular, in order to use mixed features, namely, numeric and nominal, a light variant of FCM is performed.

TABLE I. (A) USER DATA SET AND (B) POIS DATA SETS

(A)

ID User	Features		
	age	*skill*	*interest*
U1	28	researcher	Science
U2	43	truck driver	restaurant reservation
U3	22	student	entertainment
U4	24	student	Science
U5	28	lawyer	restaurant reservation
…			

(B)

ID POI	Features				
	type	*lat*	*long*	*when*	*period*
P1	zoo	41.24	14.06	all day	always
P2	restaurant	42.23	12.34	all day	ever, except monday
P3	disco	44.55	16.80	from midnight	every weekend
P4	restaurant	40.20	14.02	all day	ever, except tuesday
P5	museum	42.20	19.46	from 9 a.m.	always
…					

TABLE II. (A) USER PROFILE PARTITION MATRIX AND (B) POI PARTITION MATRIX

(A)

ID User	*Clusters*		
	UC1	*UC2*	*UC3*
U1	0,68	0,12	0,2
U2	0,2	0,7	0,1
U3	0,05	0,35	0,6
U4	0,7	0,1	0,2
U5	0,15	0,65	0,2
…			

(B)

ID POI	*Clusters*			
	PC1	*PC2*	*PC3*	*PC4*
P1	0,6	0,05	0,3	0,05
P2	0,07	0,7	0,03	0,2
P3	0,06	0,25	0,04	0,65
P4	0,07	0,7	0,03	0,2
P5	0,2	0,07	0,7	0,03
…				

The input of this algorithm are matrices similar to Table I (A) and (B), and the output consists of partition matrices that synthesize users and POIs in different clusters (see Section III for more details).

Anyway, since we use a fuzzy algorithm for clustering, we obtain that each user or POI belongs to several clusters with different membership degrees. Table II shows part of the aforementioned partition matrices.

C. Users and POIs fuzzy classifier design

In this step, the previously obtained user and POI clusters are used to design fuzzy classifiers that are useful to relate new incoming data, such as POI or active user, with the existing clusters.

This design process extracts lists of if-then rules characterizing clusters obtained in the previous step. By designing classifiers the system trains itself in order to avoid clustering execution every time to position new POIs or new users. Theoretical details about this phase can be found in Section III. Table III (A) and (B) shows part of rules concerning users and POI classifiers.

D. Integration of historical data

One of the main aim of the proposed approach is to apply collaborative filtering on historical data, in order to recommend POIs to users that meet their context and preferences. Each record in such historical data asserts interest of a certain user that is identified in a specific context for a proper tourist POI. In this step, an integration between historical data and clusters obtained in the previous steps is achieved by exploiting fuzzy classifiers. Specifically, for each row of the historical data, if the user data in a historical transition are:

- age = 20
- skill = student
- interest = science

then these data can be replace with UC1 (User Cluster 1) according to classifier in Table III (A). Similarly, if the POI attribute values in a transition are the following:

- type = museum
- lat = 42.20
- long = 19.46
- when = from 9 a. m.
- period = always

then, data can be replaced with PC3 (POI Cluster 3) according to classifier in Table III (B). In Fig. 2, are highlighted the substitutions described above, but it is important to point out that a historical transition is also characterized by context data, that is, the context where the user was when he/she selected the specific POI. This further information will be exploit in the next step and it will be of use to provide context aware recommendations to users.

E. Association rules mining

As said before (see Section III) a Apriori algorithm have been selected to carry out association rule on historical data. In particular, in this step, extracted rules synthesize the relation between cluster of users, context and POIs clusters. These rules are useful to recommend eligible POIs to the tourists according with context and user features. Extracted rules are in the following form:

{lat=40/42, long=13/15, time=morning, date=saturday, walk/drive=walk, User Cluster=UC1} ⇒{Poi Cluster=PC3}.

Furthermore, to each rule is associated an importance degree by two features, namely, support and confidence. These features allow to set thresholds (i.e. MinSup, MinConf), in order to trigger only the so called strong rules (see Section III).

V. RECOMMENDATION PROCESS

The results obtained from *Knowledge Discovery Process*, are exploited to recommend POIs to users according to their context and preferences. In particular, the recommendation process, described in this section, consists of three steps detailed below.

TABLE III. (A) USER CLASSIFIER AND (B) POI CLASSIFIER

(A)

ID User Profile Rule	*User Profile Rules*			
	IF			*THEN*
	age	*profession*	*interest*	*Cluster*
UPR1	young	student	science	UC1
UPR2	middle	truck driver	restaurant reservation	UC2
…				

(B)

ID POI Rule	*POI Rules*					
	IF					*THEN*
	type	*lat*	*long*	*when*	*period*	*Cluster*
PR4	restaurant	40/45	13/20	all day	ever, except tuesday	PC2
PR5	museum	40/45	13/20	morning	always	PC3
…						

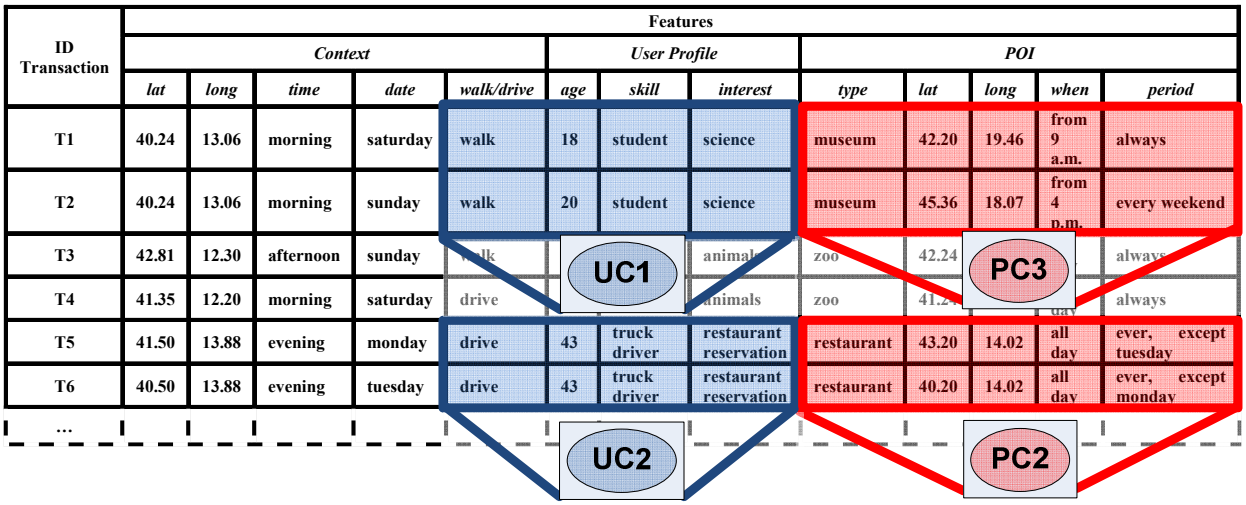

Figure 2. Historical Social Networking and clusters association

TABLE IV. ACTIVE USER CLASSIFICATION

ID User	*Clusters*		
	UC1	*UC2*	*UC3*
U1	0,1	0,2	0,7
U2	0,65	0,2	0,15
U_{Active}	0,1	0,7	0,2
...			

A. User cluster identification

The aim of this step is to identify the cluster of the active user that have "checked-in" to the application system. Thanks to the user classifier, it is not needed to run clustering again in order to determine the belonging of the active user to a specific cluster. When there is a new active user or already registered user changes him preferences the classification take place. In that cases, through the execution of classification rules (see Table III) a new row is added to the user partition matrix as shown in the Table IV. More specifically, Table IV highlights that the considered active user belongs to User Cluster 2 (UC2) with a membership degree higher than the other clusters; therefore, the active user is considered belonging to UC2.

B. Rules matching

In this step, the triggering of a specific rule is achieved according to higher degree of matching between the active user and extracted rules. In particular, a matching degree is calculated by considering a matching matrix M where the rows are represented by the extracted rules ranked according to their support and confidence features, whereas the columns are represented by active user context features and user cluster. Let be *M* the matching matrix, the maximum matching degree M_{max} is given by the following formula:

$$M_{max} = \max_{k} \left(\frac{\sum_{j=1}^{m} \mu_{ij}}{m} \right) \quad i = 1,\ldots, n \quad k = 1,\ldots, n \tag{5}$$

$$\mu_{ij} = S(u_j, a_{ij}) \quad i = 1,\ldots,n \quad j = 1,\ldots,m \tag{6}$$

$$S(u_j, a_{ij}) = 1 - \partial(u_j, a_{ij}) \quad i = 1,\ldots,n \quad j = 1,\ldots,m \tag{7}$$

where u_i represents the context and profile features of the active user, a_{ij} represents the antecedent clause of each extracted rule in the knowledge discovery process and ∂ is defined as described in Section III. So, Table V shows an example of maximum matching degree between the active user and the extracted rules according to (5), (6) and (7).

TABLE V. MAXIMUM MATCHING BETWEEN ACTIVE USER AND RULES

Matching User/Rule	*Context*					*User Cluster*	*POI Cluster*
	lat	*long*	*time*	*date*	*walk/drive*		
$User_{Active}$	41.50	13.88	evening	monday	drive	UC2	???
$Rule_{Active}$	40/42	13/15	evening	monday	drive	UC2	PC2
$S(User_{Active}, Rule_{Active})$	0,75	0,68	1	1	1	0,7	
M_{max}	(0,75 + 0,68 + 1 + 1 + 1 + 0,7)/6 = **0,855**						

C. Recommendations ranking

In the last step of this process, we determine the ranked list of POIs that may be suggested to the user.

In particular, the previous step determines the maximum matching between a new user that starts a transaction and the extracted rules. Rules matching evaluation, defines the highest match of the active user respect with extracted rules. Since, the consequent of a rule is represented by a POI Cluster, this match points out that POIs belonging to a specific cluster can be recommended as relevant for the active user. For instance, user is in a certain context and with a determinate profile if the active rule is the following:

{lat=40/42, long=13/15, time=evening, date=monday, walk/drive=drive, User Cluster=UC2} ⇒ {Poi Cluster=PC2}

then, the ranked list of POIs consists of those belonging to the cluster PC2, as shown in Table V.

TABLE VI. POIs RECOMMENDATION RANKING

ID POI	*Features*					*Cluster*	*Recommendation Ranking*
	type	*lat*	*long*	*when*	*period*	*PC2*	$\rho_i = b_{ic} \times M_{\max}$
P8	restaurant	40.33	14.14	all day	ever, except thuersday	0,8	0,684
P2	restaurant	42.23	12.34	all day	ever, except Tuesday	0,7	0,6
…	…	…	…	…	…	…	…
P5	restaurant	40.20	14.02	all day	ever, except monday	0,55	0,47
P3	hotel	42.90	15.30	all day	always	0,47	0,4
P1	zoo	41.24	14.06	all day	always	0,34	0,3
…							

In order to carry out the ranked list of POIs the framework assigns a ranking value to each POI corresponding to b_{ic} , that is the belonging degree of the i-th POI to the cluster c (i.e., PC2) in the consequent of rule with maximum matching in the antecedent and n is the number of POIs. Table VI shows an example of POIs recommendation ranking.

I. EXPERIMENTAL RESULTS

This section presents the performance results of our proposed recommender system. In particular, Mean Absolute Error (MAE) and Root Mean Square Error (RMSE) are used in order to evaluate the accuracy of the system. Specifically, by considering different set of features the system has been evaluated in the following variants:

- LS - System considering Location
- LUC - System considering Location and User Context
- LUP - System considering Location and User Profile
- HRS - Hybrid Recommender System considering Location, User Context and User Profile

The system has been evaluated with 20 users and 200 POIs. Obviously, little by little the history data grow the system retrieve more meaningful results (the history considered contains about 1000 records). As previously said, MAE and RMSE are used for performance evaluation of the proposed recommender system. MAE is a quantity used to measure how close forecasts or predictions are to the eventual outcomes. On the other hand, RMSE measures the average magnitude of the error, that is, the difference between forecast and corresponding observed values, where each of these differences is squared and then averaged over the sample; so, a relatively high weight is given to large errors. MAE and RMSE can be used together to diagnose the variation in the forecasting errors.

Since the lower the MAE, the more accurately the recommendation engine predicts user ratings [28], the obtained results, shown in Fig. 3, highlight a clear superiority of the overall proposed recommender system among the other variants. Furthermore, since the greater difference between MAE and RMSE, the greater the variance in the individual errors in the sample, Table VII points out that all the errors are of the same magnitude.

II. CONCLUSIONS AND FUTURE WORKS

As a result of demands continuously growing in ambient intelligence for systems able to exploit context for satisfaction of user preferences, a context aware recommender system for tourist guidance is proposed in this paper.

The proposed system presents several improvements. Firstly, user context and profile are considered in order to effectively identify his preferences. Uncertainty among user interests is an important issue which is clearly considered in this approach in order to establish an effective recommendation strategy. Additionally, this approach provides dynamic user clustering for active users and supports them with a personalized and adaptive environment. Moreover, any POIs change can be simply notified to all interested users. Anyway, there are some limitations in this research area that we consider as future research directions. FCM alternative clustering algorithms that work better with mixed data can be experimented as well as alternative rule mining algorithms using fuzziness and based on lattice. However, the proposed framework confirms the useful of considering context factor in recommender systems and provides us with reasonable results in terms of recommendation accuracy as evidenced by the experimental results.

TABLE VII. RECOMMENDER SYSTEMS MAE COMPARISON

Recommender System	LS	LUC	LUP	Hybrid Recommender System
MAE	0,932	0,869	0,851	0,811
RMSE	0,932	0,869	0,851	0,811

REFERENCES

[1] Tak Kee Hui, David Wan, Alvin Ho, Tourists' satisfaction, recommendation and revisiting Singapore, Tourism Management, Volume 28, Issue 4, August 2007, Pages 965-975.

[2] Wolfe, K., Hsu, C. H. C. & Kang, S. K. (2005). Buyer Characteristics Among Users of Various Travel Intermediaries. Journal of Travel & Tourism Marketing, 17(2), 51-62.

[3] Doug Riecken. 2000. Introduction: personalized views of personalization. Commun. ACM 43, 8 (August 2000), 26-28.

[4] G. Kakaletris, D. Varoutas, D. Katsianis, T. Sphicopoulos, and G. Kouvas. 2004. Designing and Implementing an Open Infrastructure for Location-Based, Tourism-Related Content Delivery. Wirel. Pers. Commun. 30, 2-4 (September 2004), 153-165.

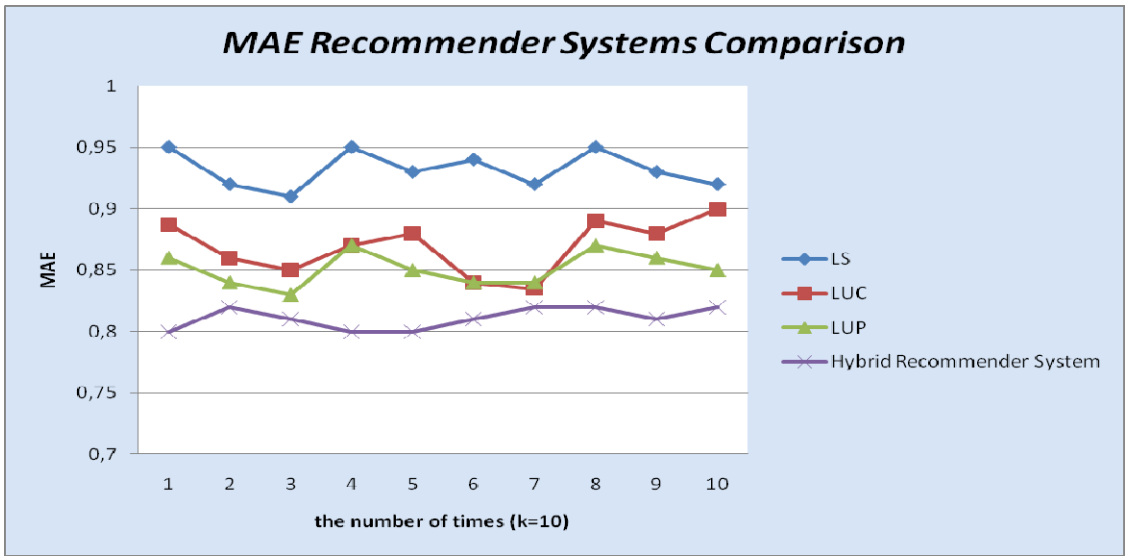

Figure 3. Mean Absolute Error experimental results (k=10)

[5] Ansgar Scherp and Susanne Boll. 2004. Generic support for personalized mobile multimedia tourist applications. In Proceedings of the 12th annual ACM international conference on Multimedia (MULTIMEDIA '04). ACM, New York, NY, USA, 178-179.

[6] Dickson K. W. Chiu and Ho-fung Leung. 2005. Towards ubiquitous tourist service coordination and integration: a multi-agent and semantic web approach. In Proceedings of the 7th international conference on Electronic commerce (ICEC '05). ACM, New York, NY, USA, 574-581.

[7] Francesco Ricci and Quang Nhat Nguyen. 2007. Acquiring and Revising Preferences in a Critique-Based Mobile Recommender System. IEEE Intelligent Systems 22, 3 (May 2007), 22-29.

[8] Mark van Setten, Stanislav Pokraev, and Johan Koolwaaij. Context-Aware Recommendations in the Mobile Tourist Application COMPASS. In Adaptive Hypermedia and Adaptive Web-Based Systems, pages 235–244. 2004.

[9] Console, L., Gioria, S., Lombardi, I., Surano, V., Torre, I.: Adaptation and Personalization on Board Cars: A Framework and Its Application to Tourist Services. In: De Bra, P., Brusilovsky, P., Conejo, R. (eds) Adaptive Hypermedia and Adaptive Web-Based Systems, Proceedings of the second International Conference, AH 2002, Málaga, Spain, May, Springer-Verlag, LNCS 2347 (2002) 112-121.

[10] Ardissono, L., Goy, A., Giovanna, P., Segnan, S., Torasso, P.: Ubiquitous User Assistance in a Tourist Information Server. In: De Bra, P., Brusilovsky, P., Conejo, R. (eds) Adaptive Hypermedia and Adaptive Web-Based Systems, Proceedings of the second International Conference, AH 2002, Málaga, Spain, May, Springer-Verlag, LNCS 2347 (2002) 14-23.

[11] Nigel Davies, Keith Mitchell, Keith Cheverst, Gordon Blair: Developing a Context Sensitive Tourist Guide, Proceedings of the First Workshop on Human Computer Interaction for Mobile Devices, Department of Computing Science, University of Glasgow, UK, May 1998, pp. 64-68.

[12] Eui-young Kang, Hanil Kim, and Jungwon Cho. Personalization method for tourist point of interest (POI) recommendation. In Bogdan Gabrys, Robert Howlett, and Lakhmi Jain, editors, Knowledge-Based Intelligent Information and Engineering Systems, volume 4251 of Lecture Notes in Computer Science, chapter 48, pages 392–400. Springer Berlin / Heidelberg, Berlin, Heidelberg, 2006.

[13] El Sayed, A.; Hacid, H.; Zighed, D.; , "A New Context-Aware Measure for Semantic Distance Using a Taxonomy and a Text Corpus," *Information Reuse and Integration, 2007. IRI 2007. IEEE International Conference on* , vol., no., pp.279-284, 13-15 Aug. 2007.

[14] Rudi L. Cilibrasi and Paul M. B. Vitányi. The Google Similarity Distance. Knowledge and Data Engineering, IEEE Transactions on, 19(3):370–383, 2007.

[15] Hoppner F., Klawonn F., Kruse R., Runkler T. Fuzzy Cluster Analysis - Methods for Image Recognition. J. Wiley, N. York, 1999.

[16] J. C. Bezdek, Pattern Recognition with Fuzzy Objective Function Algorithms. Plenum Press, New York, 1981.

[17] L.Jegatha Deborah, R.Baskaran and A.Kannan, A Survey on Internal Validity Measure for Cluster Validation, Anna University – Chennai.

[18] X. Xie and G. Beni, "A Validity Measure for Fuzzy Clustering," IEEE Trans. Pattern Analysis and Machine Intelligence (PAMI), vol. 13, no. 8, pp.841 - 847, 1991.

[19] Takagi, T., and Sugeno, M.: 'Fuzzy identification of systems and its applications to modeling and control', IEEE Trans. Syst., Man Cybern., 1985, 15, pp. 116–132.

[20] C.C. Kung and J.Y. Su Affine Takagi-Sugeno fuzzy modelling algorithm by fuzzy c-regression models clustering with a novel cluster validity criterion, IET Control Theory Appl., 2007, 1, (5), pp. 1255–1265.

[21] Dragan Kukolj Design of adaptive Takagi–Sugeno–Kang fuzzy models, Applied Soft Computing 2 (2002) 89–103.

[22] S. Mitra,; Y. Hayashi,; Neuro-fuzzy rule generation: survey in soft computing framework IEEE Transactions on Neural Networks, Volume 11, Issue 3, May 2000 Page(s):748 – 768.

[23] J.F.-F. Yao, J.-S.Yao, Fuzzy decision making for medical diagnosis based on fuzzy number and compositional rule of inference, Fuzzy Sets and Systems, 120 (2001), pp 351-366.

[24] R. Agrawal, T. Imielinski, and A. Swami. Mining association rules between sets of items in large databases. In Proc. of the ACM SIGMOD Conference on Management of Data, Washington, D.C., May 1993.

[25] M. Houtsma and A. Swami. Set-oriented mining of association rules. Research Report RJ 9567, IBM Almaden Research Center, San Jose, California, October 1993.

[26] Rakesh Agrawal and Ramakrishnan Srikant. Fast Algorithms for Mining Association Rules, Proceedings of 20th International Conference on Very Large Data Bases, September 12-15, 1994, Santiago de Chile, Chile.

[27] G.Fenza, V.Loia, S.Senatore, "Friendly Web Services Selection exploiting Fuzzy Formal Concept Analysis", Soft Computing, 2008.

[28] Good, N., Schafer, B., Konstan, J., Borchers, A. Sarwar, B., Herlocker, J., Riedle, J.: Combining Collaborative Filtering with Personal Agents for Better Recommendation. In Proc. of the AAAI conference (1999) 439-446.

2011 IEEE International Conference on Fuzzy Systems
June 27-30, 2011, Taipei, Taiwan

Trainable Estimators for Indirect People Counting: A Comparative Study

Giovanni Acampora and Vincenzo Loia
Dept. of Computer Science
University of Salerno
Fisciano, Italy 84084
Email: {gacampora, loia}@unisa.it

Gennaro Percannella and Mario Vento
Dept. of Electronic Engineering and Information Engineering
University of Salerno
Fisciano, Italy 84084
Email: {pergen, mvento}@unisa.it

***Abstract*—Estimating the number of people in a scene is a very relevant issue due to the possibility of using it in a large number of contexts where it is necessary to automatically monitor an area for security/safety reasons, for economic purposes, etc. The large number of people counting approaches available in the literature can be roughly abscribed to two categories: direct approaches and indirect ones. In the first category there are methods that first detect people and then count them; differently, the indirect methods face the counting problem by establishing a relation between some scene features and the estimated number of people. Some recent comparative evaluations carried out in the framework of the PETS initiative have demonstrated that the indirect methods tends to be more robust than direct ones, above all when they are used in very crowded conditions. In this paper, we analyze the behavior of an indirect approach that is based on a trainable estimator that does not require an explicit formulation of a priori knowledge about the perspective and density effects present in the scene at hand. In particular, we investigate on the way the counting accuracy in different crowding conditions is affected by the choice of the trainable estimator.**

***Index Terms*—Indirect People Counting, Trainable Estimators, ANFIS, ϵ-SVR.**

I. Introduction

Knowing the number of people present in an area is a so important issue in the framework of video surveillance applications, that an increasing number of papers on this topic have been proposed in the recent past.

Despite of the fact that recently some pioneering systems have been made available, further improvements are still necessary, especially concerning their generality and flexibility. Many aspects make the problem really challenging: systems are required to work in real time on general purpose computers, possibly in parallel on different video streams coming from megapixel cameras, so as to supply up to date information on crowd density. Of course, the computational charge is a crucial but a less important issue with respect to the expected accuracy: as the output is mainly used for safety issues, the estimation accuracy of the number of people must be sufficiently high, even in presence of dense crowds. To this concern, it is worth pointing out that in these situations only parts of people's body appear in the image; the occluded parts generally cause significant underestimation in the counting process; it means that the partial occlusions must be forecasted and suitably taken into account starting from the information about the crowd density. Another crucial point is the unavoidable presence of perspective distortions: the optical equipment of the cameras, especially those with wide angle views, cause that people far from the camera appear small while the close ones significantly bigger. So, methods must deal with this perspective issue, so as to obtain an estimation independent from the local scale of the image. Moreover, it is convenient that the system works with uncalibrated cameras, as calibration is generally time consuming and demands for suitable technical skills, not owned by the end user. Consequently, the availability of simple training procedures, not requiring knowledge about the internal organization of the computational model, but possibly depending on simple geometric properties derivable from the scene, is an extremely desirable feature.

The literature on people counting presents two conceptually different ways to face this task. In the *direct approach* (also called *detection-based*), each person in the scene is individually detected, using some form of segmentation and object detection; the number of people is then trivially obtainable. In the *indirect approach* (also called *map-based* or *measurement-based*), instead, counting is performed using the measurement of some features that do not require the separate detection of each person in the scene; these features then have to be put somehow in relation to the number of people.

The direct approach has the advantage that people detection is often already performed on a scene for other purposes (e.g. detecting events based on a person's position or trajectory), and as long as people are correctly segmented, the count is not affected by perspective, different people densities and, to some extent, partial occlusions. On the other hand, correct segmentation of people is a complex task by itself, and its output is often unreliable, especially in crowded conditions (which are of primary interest for people counting). Recent examples of the direct approach can be found in [1], [2] and [3].

The indirect approach, instead, is more robust, since it is based on features that are simpler to detect, but it is often not easy to find an accurate correspondence between these features and the number of people, especially if people may appear in the scene at different distances from the camera, and in groups

This research has been partially supported by A.I.Tech s.r.l., a spin-off society of the University of Salerno (www.aitech-solutions.eu).

978-1-4244-7316-8/11/$26.00 ©2011 IEEE

with diverse densities. For the indirect approach, methods such as the use of measurements such as the amount of moving pixels [4], blob size [5], fractal dimension [6] or other texture features [7] have been proposed.

However, one of the most recent indirect approaches has been presented in [8] where the estimation of the count is obtained through a trainable estimator that takes into account perspective effects and the influence of people density on the detection of corner points, and consequently, can be easily adapted to the characteristics of a new scene. This paper is devoted to analyze the behavior of the mentioned approach when it is used with two different estimators: ANFIS and ϵ-SVR.

As will be shown in the experimental results, even though the two approaches yield similar global performance, the neuro-fuzzy based estimator is more efficient when the scenes are characterized by a high density crowd, whereas, the approach based on ϵ-SVR works in a better way when the scenes are characterized by a low density crowd. This comparative analysis opens new scenarios for the development of novel indirect approaches for people counting able to adaptively select the most suitable estimator that reduces the output error measure under particular scene conditions.

II. An Indirect People Counting Approach based on a Trainable Estimator

In this section, a description of an indirect approach based on a trainable estimator is provided in order to evaluate its performance when different regression methods are used to estimate the number of people. The approach uses as its features the moving interest points, where the interest points are first detected using a feature detector from the state of the art, and then the static ones are filtered out on the basis of a motion vector estimation.

An outline of the considered method is described by the following steps: Moving SURF points detection, SURF point Clustering and Feature extraction and regression. More in details, in the first step, SURF algorithm proposed by H. Bay et al. in 2006 [9] is adopted in order to detect interest points; in the second step, the detected points are partitioned into clusters corresponding to separated groups of persons, as to be able to compute for each group its distance from the camera and its density; in the last step, a trainable function estimator is exploited to estimate the number of people in a scene.

This paper focuses on the last step. Precisely, the aim of this work is to compare two different regression methods, ANFIS and ϵ-SVR, when they are used to implement the trainable function estimator of an indirect people counting approach.

However, before presenting the description of the explored methods, in the following subsections, a description of the architecture (see Fig. 1) of the considered approach is given.

A. Moving SURF points detection

In order to detect interest points associated to people, two basic assumptions are made: persons within the scene are not static and there are no other moving elements in the scene. Thus, if we compute the interest points of the image and the associated motion information, the above assumptions guarantee that only the interest points with a non null motion vector must be associated to people. As proposed in [10], the interest points associated to people are extracted in two steps. First, we determine all the interest points within the frame under analyzis. Then, we prune the points not associated to persons by taking into account their motion information. In this approach, interest points are determined by using the SURF algorithm.

In order to remove the static interest points (that are not associated to people), for each point detected by the SURF algorithm we estimate the motion vector with respect to the previous frame by using a block-matching technique. Then the algorithm distinguishes between static and moving interest points on the basis of the following rule:

$$p(x,y) = \begin{cases} \text{moving point} & \text{if } |\vec{v}(x,y)| > \beta \\ \text{static point} & \text{if } |\vec{v}(x,y)| \leq \beta \end{cases} \quad (1)$$

where $p(x,y)$ is the interest point at the x,y coordinates, $|\vec{v}(x,y)|$ is the magnitude of the motion vector calculated in x,y with respect to the previous frame; β is a bias value (in our experiments we set $\beta = 0.0$).

B. SURF point Clustering

In order to compensate for changes in the number of points due to perspective and to partial occlusions, the algorithm needs to partition the detected points into clusters corresponding to separated groups of persons, so as to be able to compute for each group its distance from the camera and its density.

The faced clustering problem is characterized by the fact that there is no priori knowledge about the number and the

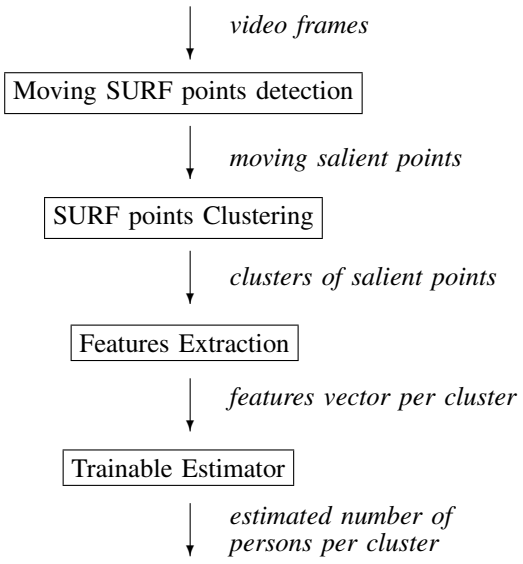

Fig. 1. System architecture.

shape of the clusters to be found. As observed in [11], the clustering algorithms based on graph theory are well suited to face clustering problems where no assumptions can be made about the clusters. In particular, the considered algorithm adopts the technique presented in [12], since (differently from other algorithms in the graph-based clustering family) it requires no parameters to be tuned or adapted to the particular application.

This algorithm represents the set of points as a graph in which each point corresponds to a node and each edge is labeled with the distance between its endpoints. The minimum spanning tree (MST) of the graph is computed; this tree will contain some edges that are between nodes in the same cluster (intra-cluster edges) and other edges between nodes of different clusters (inter-cluster edges). Assuming that the clusters are well separated, it can be expected that the intra-cluster edges are shorter than the inter-cluster edges. So the algorithm uses a thresholding to divide the edges in two sets (the ones below the threshold, say it λ, and the ones above the threshold λ). The edges in the second set are deleted, and the remaining connected components are the clusters output by the algorithm.

The use of a fixed value for the threshold λ would be problematic, since the threshold would need to be adjusted depending on the resolution, the distance from the camera and so on. Instead, this approach used a threshold proportional to the average edge length, computed as:

$$\lambda = \gamma \cdot \frac{1}{N} \sum_{i=1}^{N} x_i \tag{2}$$

where γ is the proportionality factor, N is the number of edges of the spanning tree, while x_i is the weight of the i-th edge of the tree. We have experimentally found that the choice $\gamma = 2.0$ works adequately for all the considered scenes.

C. Feature extraction and regression

In this stage of the algorithm, a feature vector is computed from each cluster detected in the previous step, and is fed into a regressor. The output of the regressor is the estimated number of persons in the group represented by the cluster.

The considered approach reasonably assumes that when the density of people increase,the detected points get closer to each other. So, the density of the points as related to people density is considered, and indirectly it is possible to take into account people density by establishing a relation between the average number of points per person and the point density.

The relation between the number of interest points and the number of people appears more complex than a direct proportionality, because it is possible to take into account also the distance of the people from the camera and the point density. This relation can be formulate as:

$$n_{people} = f(n_{points}, \rho, d) \tag{3}$$

where:

- n_{people} is the estimated number of people;
- n_{points} is the number of interest points within the cluster;
- ρ is the average density of the points in the cluster: the value is obtained as the ratio between the number of points into the cluster and the area of the bounding box. Note that the area of the bounding box is computed with respect to real world coordinates. This allows us to normalize the average density of the points to the value it would have if the cluster were moved to a predefined distance from the camera;
- d is the distance of the cluster from the camera: assuming that the bottom points of the bounding box lie on the ground plane, the calculation is done by applying an Inverse Perspective Mapping and is referred to the center of the bottom edge of the cluster's bounding box.

Since the analytical form of f is not known a priori, the considered approach choices to learn this function from a set of labeled examples by using a regression method.

In particular, this paper aims to compare two different techniques to implement the aforementioned function estimator: the ϵ-SVR regressor and ANFIS. Both explored methods are able to learn a non linear relation and show a good generalization ability. In details, they receive as inputs the number of points of a cluster, the distance from the camera and the point density of the cluster, and are trained (using a set of training frames) to output the estimated number of people in the cluster. However, as will be shown in section IV, ANFIS obtains better results when the people counting is applied to high density crowd, whereas the ϵ-SVR regressor provides more benefits when the indirect people counting method is used to estimate the number people in low density crowd.

III. Trainable Estimators: ANFIS and ϵ-SVR

In this section, a description of the two methods useful to implement the trainable function estimator for indirect people counting is provided. In particular, a brief description about ANFIS and ϵ-SVR is given.

A. Adaptive Neuro Fuzzy Inference System

Adaptive Neuro-Fuzzy Inference Systems (ANFIS) [13] is a class of adaptive networks that are functionally equivalent to conventional fuzzy inference systems. An adaptive network is a multilayer feed forward network in which each node performs a particular function (node function) on incoming signals using a set of parameters specific to this node [14]. The form of node functions may vary from node to node, and the choice of each node function depends on the overall function, which the adaptive network is designed to implement. Adaptive networks are composed by two different classes of nodes: *adaptive nodes* and *fixed nodes*. Adaptive nodes are characterized by a collection of modifiable parameters, named *parameter set*, whereas, the fixed nodes only deal with unmodifiable parameters. Adaptive networks work in order to achieve a desired input-output relationships by updating the parameter sets according to given training data and a gradient-based update procedure. ANFIS exploits this updating feature to learn and adapt the parameters of a given Takagi-Sugeno-Kang (TSK) fuzzy inference system.

As an example, Fig. 2 shows an adaptive network that models a first-order TSK fuzzy inference system composed by two rules:

1) If x is A_1 and y is B_1 Then $f_1 = p_1 \cdot x + q_1 \cdot y + r_1$
2) If x is A_2 and y is B_2 Then $f_2 = p_2 \cdot x + q_2 \cdot y + r_2$

where the symbols $x$and y are the system's inputs, A_1, A_2, B_1 and B_2 are linguistic labels determined by fuzzy sets defined on the universe of discourse related to the variables x and y whereas, the f_1 and f_2 are linear functions computing the output value of the TSK inference system.

To reflect the ANFIS adaptive capabilities, in Fig. 2 the square nodes represent the adaptive nodes, whereas the circle nodes represent the fixed nodes.

Each ANFIS layer implements a particular fuzzy inference subtask. In detail:

Layer 1 Every node i in this layer implements the node function:

$$O_i^1 = \mu_{A_i}(x) \tag{4}$$

where x is the input to node i , and A_i is a linguistic label. From a fuzzy inference point of view, O_i^1 is the membership function related to the fuzzy set A_i, and it specifies the degree to which the input x satisfies A_i. Typically, A_i is a bell-shaped function characterized by a set of three parameters $\{a, b, c\}$ corresponding to the parameter set of the node i.

Layer 2 The nodes labeled with Π multiply their input signals:

$$w_i = \mu_{A_i}(x) \times \mu_{B_i}(y) \text{ with } i = 1, 2; \tag{5}$$

where w_i represents the firing strength of a rule.

Layer 3 The node in this layer calculate the ratio of the i^{th} rules firing strength to the sum of all rules firing strengths:

$$\overline{w_i} = \frac{w_i}{w_1 + w_2} \text{ with } i = 1, 2. \tag{6}$$

The value w_i represents the *normalized firing strenght*.

Layer 4 The adaptive node i in this layer computes the following function:

$$O_i^4 = \overline{w_i} f_i = \overline{w_i}(p_i x + q_i y + r_i) \tag{7}$$

where the collection $\{p_i, q_i, r_i\}$ is the parameter set of the node i and corresponds to the TSK consequent parameters.

Layer 5 The single and fixed node in this layer, labeled Σ, computes the overall network output as the summation of all incoming signals:

$$O_i^5 = \sum_i \overline{w_i} f_i = \frac{\sum_i w_i f_i}{w_i} \tag{8}$$

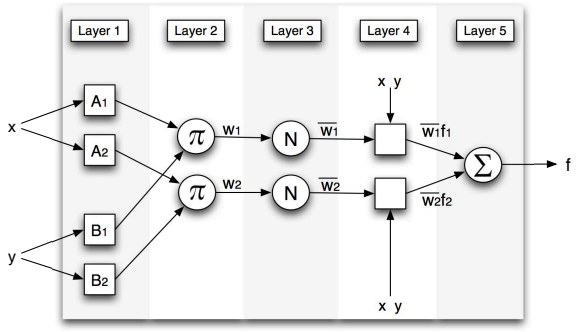

Fig. 2. The Adaptive Neuro Fuzzy Inference System.

B. ϵ-Support Vector Regression

The ϵ-SVR is a variant of the Support Vector Machines(SVM) designed to face the regression estimation task.

SVM is a class of learning algorithms originally developed for classification task, where in order to find a decision rule with good generalization ability one selects some (small) subset of the trained data called *Support Vectors*. Optimal separation of the Support Vectors is equivalent to optimal separation the entire data. In order to deal with the SV Regression, Vapnik [15] devised the so-called ϵ-insensitive loss function which does not penalize errors below some $\epsilon > 0$, chosen a priori [16]. Hereafter, a formal description of ϵ-SVR method is given.

As described in [17], let $G(x)$ be the unknown function where the vector $\mathbf{x} = [x_1, x_2, \ldots, x_d]$ is the *input space* characterized by a dimensionality equal to d. Let $F = (\mathbf{x}, \mathbf{w})$ be a family of functions parameterized by $\mathbf{w}$ and $\hat{\mathbf{w}}$ be the value of $\mathbf{w}$ which minimizes the error between $G(\mathbf{x})$ and $F = (\mathbf{x}, \hat{\mathbf{w}})$. The objective is to estimate $\mathbf{w}$ with $\hat{\mathbf{w}}$ by observing N training instances $\mathbf{v}_j$, $j = 1, \ldots, N$.

In order to achieve this aim, the approximation function F, employed by the SVR method, is defined:

$$F(\mathbf{x}, \hat{\mathbf{w}}) = \sum_{i=1}^{N} (\alpha_i^* - \alpha_i)(\mathbf{v}_i \cdot \mathbf{x} + 1)^p + b)$$

This function represents an expansion which explicitly uses the N training vectors. Indeed, different from other approximation functions, F depends on $2N+1$ coefficients α_i^*, α_i and b that must be determined from the training examples. Now, let $\boldsymbol{\alpha}$ represent the $2N$ values of α_i^* and α_i, the optimum values for the components of $\hat{\mathbf{w}}$ or $\boldsymbol{\alpha}$ depends on the definition of the objective function. Formally, the objective function is defined as:

$$||\mathbf{w}||^2 + C \sum_{j=1}^{N} L[y_j - F(\mathbf{v}_j, \hat{\mathbf{w}})]$$

where L is a general loss function, F is the approximation function, y_j is the observation of $G(\mathbf{x})$ in the presence of noise, and the first term, i.e, the 2-norm of the weight vector $\hat{\mathbf{w}}$, is a regularizer. Finally, the constant C represents a further regularization.

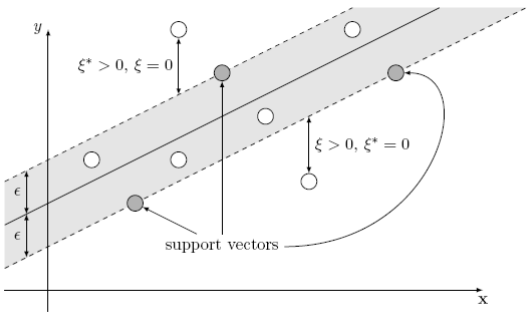

Fig. 3. The ϵ-SVR representation

In particular, the ϵ-SVR exploits as loss function the so-called ϵ-insensitive loss function defined as:

$$L = \begin{cases} 0 & \text{if } |y_j - F(\mathbf{x}_i, \hat{\mathbf{w}})| < \epsilon \\ |y_j - F(\mathbf{x}_i, \hat{\mathbf{w}})| - \epsilon & \text{otherwise} \end{cases} \quad (9)$$

This function defines an ϵ tube [18] (see Figure 3) so that if the predicted value is within the tube the loss is zero, while if the predicted point is outside the tube, the loss is the magnitude of the difference between the predicted value and the radius ϵ of the tube.

In this way, the objective function becomes to minimize this specific function:

$$\frac{1}{2} \cdot \mathbf{w}^2 + C(\sum_{i=1}^{N} \xi_i + \xi_i^*)$$

where ξ_i and ξ_i^* represents the so-called *slack variables* for each input point x_i. Precisely, ξ_i measures positive deviation of more than ϵ, while ξ_i^* indicates negative deviations. So, if a data point is is situated within the tube, both slack variables are 0. However, since no point can be on both sides simultaneously, at least one of the two slack variables is always 0. This is mathematically expressed by means of the ϵ-insensitive loss function defined in the equation 9.

Finally, in order to complete the description of the ϵ-SVR method, the constraints on the objective function are described:

$$\begin{aligned} & y_i - (\mathbf{w} \cdot \mathbf{v}_i) - b \leq \epsilon + \xi_i \\ & (\mathbf{w} \cdot \mathbf{v}_i) + b - y_i \leq \epsilon + \xi_i^* \\ & \xi_i \geq 0 \\ & \xi_i^* \geq 0 \end{aligned} \quad (10)$$

IV. Experimental Results

In this section, the performances of the indirect people counting approach are evaluated on a specific dataset by using two different estimators, ANFIS and ϵ-SVR, in order to compare the results provided by these regression methods.

In particular, the performance of the proposed methods has been assessed using the PETS2009 dataset [1]. The dataset is organized in four sections, but our attention is primarily focused on the section named S1 that was used to benchmark algorithms for the "'Person Count and Density Estimation"' PETS2009 contest. The main characteristics of the subset of video sequences of the PETS 2009 dataset used for assessing the performance of the proposed method are summarized in the Table I in terms of their length, number of people in the scene (minimum, maximum and average number) and other elements as density of the crowd, illumination conditions, etc.

For our experimentations, four videos of the view 2, namely S1.L1.13-57, S1.L2.14-06, S1.L2.14-31 and S3.MF.12-43, are used. For all the sequences the number of people in the whole frame is computed.

(a)

(b)

Fig. 4. Examples of the frames of the video sequences (a) S1.L2.14-06 and (b) S3.MF.12-43 used for the test

In order to exploit the proposed function estimators for people counting, a phase of training is necessary. The training set was built by manually collecting some samples of people groups from a subset of the test frames. For each selected box, the feature vector and the associated ground truth, i.e. the true number of persons that are inside the box, are calculated. Samples were carefully selected in order to guarantee that all the possible combinations in terms of number of persons in

[1] http://www.cvg.rdg.ac.uk/PETS2009/

TABLE I
RELEVANT CHARACTERISTICS OF THE FOUR SEQUENCES OF THE PETS 2009 DATASETS USED FOR ASSESSING THE PERFORMANCE OF THE PROPOSED METHOD.

Video sequence View 2	Length (frames)	Conditions	Number of people		
			Min	AVG	Max
S1.L1.13-57	221	medium density crowd, overcast	8	34.19	46
S1.L2.14-06	201	high density crowd, overcast	3	37.10	46
S1.L2.14-31	131	high density crowd, overcast	10	35.19	43
S3.MF.12-43	108	very low density crowd, overcast	1	4.99	7

TABLE II
PERFORMANCE OF THE ANFIS AND ϵ-SVR. IN EACH CELL THERE ARE REPORTED THE VALUES OF THE MAE AND OF THE MRE (IN PARENTHESIS).

Video view 2	ϵ-SVR	Anfis
S1.L1.13-57	11.76 (30.0%)	11.02 (28.32%)
S1.L2.14-06	18.03 (43.0%)	11.61 (30.02%)
S1.L2.14-31	5.64 (18.8%)	6.99 (20.52%)
S3.MF.12-43	0.63 (18.8%)	1.79 (41.67%)

TABLE III
PERFORMANCE OF THE ANFIS AND ϵ-SVR. IN EACH CELL THERE ARE REPORTED THE VALUES OF THE MAE AND OF THE MRE (IN PARENTHESIS).

Video (view)	ϵ-SVR	Anfis
medium density crowd	11.76 (30.0%)	11.02 (28.32%)
high density crowd	11.84 (30.9%)	9.3 (25.27%)
low density crowd	0.63 (18.8%)	1.79 (41.67%)

the group, points density and distance from the camera were adequately represented in the training set. In our tests, about 30-40 training frames, which correspond to about 5% of the frames within the whole dataset, have been taken into account.

Testing has been carried out by comparing the actual number of people in the video sequences and the number of people calculated by the two considered function estimators, ANFIS and ϵ-SVR. The indices used to report the performance are the Mean Absolute Error (MAE) and the Mean Relative Error (MRE) defined as:

$$MAE = \frac{1}{N} \cdot \sum_{i=1}^{N} |G(i) - T(i)| \tag{11}$$

$$MRE = \frac{1}{N} \cdot \sum_{i=1}^{N} \frac{|G(i) - T(i)|}{T(i)} \tag{12}$$

where N is the number of frames of the test sequence and $G(i)$ and $T(i)$ are the guessed and the true number of persons in the i-th frame, respectively.

This index is very useful to exactly quantify the error in the estimation of the number of person which are in the focus of the camera, but it does not relate this error to number of people; in fact, the same absolute error can be considered negligible if the number of persons in the scene is high while it becomes significant if the number of person is of the same order of magnitude. For this reason, we introduced also the MRE index which takes into account the estimation error related to the true people number.

The performances of the ANFIS and ϵ-SVR algorithms applied on the adopted dataset are reported in Table II.

Starting from the Table II, it is possible to summarize that the two tested function estimators show a different behavior depending on the scene features. In particular, ANFIS method is more suitable to estimate number of people in scenes characterized by a high density crowd, instead, the ϵ-SVR is more adequate for scene with a low density crowd. The results are summarized in the table III.

V. CONCLUSIONS

In this paper, we have analyzed and evaluated the performance of an indirect method for counting moving people in video-surveillance scenes by considering two different trainable estimators, ANFIS and ϵ-SVR. As highlighted in experiments both methods achieve good performances when applied to two different kinds of scenes. Precisely, the neuro-fuzzy based estimator obtains good performance when scenes are characterized by a high density crowd, whereas, the approach based on ϵ-SVR works in a better way when the scenes are characterized by a low density crowd. As a future work, we may use these different estimation behaviors to design an adaptive people counting method capable of identifying the scene features and dynamically selecting the most suitable estimator to deal with these features.

ACKNOWLEDGMENT

The authors would like to thank the PhD student Autilia Vitiello for her precious support to Matlab™ programming.

REFERENCES

[1] J. Rittscher, P. Tu, and N. Krahnstoever, "Simultaneous estimation of segmentation and shape," in *IEEE Conf. on Computer Vision and Pattern Recognition*, 2005, pp. 486–493.

[2] G. J. Brostow and R. Cipolla, "Unsupervised bayesian detection of independent motion in crowds," in *IEEE Conf. on Computer Vision and Pattern Recognition*, 2006, pp. 594–601.

[3] T. Zhao, R. Nevatia, and B. Wu, "Segmentation and tracking of multiple humans in crowded environments," *IEEE Trans. Pattern Anal. Mach. Intell.*, vol. 30, no. 7, pp. 1198–1211, 2008.

[4] S.-Y. Cho, T. W. S. Chow, and C.-T. Leung, "A neural-based crowd estimation by hybrid global learning algorithm," *IEEE Transactions on Systems, Man, and Cybernetics, Part B*, vol. 29, no. 4, pp. 535–541, 1999.

[5] D. Kong, D. Gray, and H. Tao, "A viewpoint invariant approach for crowd counting," in *International Conference on Pattern Recognition*, 2006, pp. 1187–1190.

[6] A. N. Marana, L. da F. Costa, R. A. Lotufo, and S. A. Velastin, "Estimating crowd density with mikowski fractal dimension," in *Int. Conf. on Acoustics, Speech and Signal Processing*, 1999.
[7] H. Rahmalan, M. S. Nixon, and J. N. Carter, "On crowd density estimation for surveillance," in *The Institution of Engineering and Technology Conference on Crime and Security*, 2006.
[8] P. Foggia, G. Percannella, F. Tufano, and M. Vento, "A method for counting people in crowded scenes," in *2010 Seventh International Conference on Advanced Video and Signal Based Surveillance*, 2010.
[9] H. Bay, A. Ess, T. Tuytelaars, and L. V. Gool, "Surf: Speeded up robust features," *Computer Vision and Image Understanding*, vol. 110, no. 3, pp. 346–359, 2008.
[10] A. Albiol, M. J. Silla, A. Albiol, and J. M. Mossi, "Video analysis using corner motion statistics," in *IEEE International Workshop on Performance Evaluation of Tracking and Surveillance*, 2009, pp. 31–38.
[11] S. Theodoridis and K. Koutroumbas, *Pattern Recognition, Third Edition*. Academic Press, February 2006.
[12] P. Foggia, G. Percannella, C. Sansone, and M. Vento, "A graph-based algorithm for cluster detection," *International Journal of Pattern Recognition and Artificial Intelligence*, vol. 22, no. 5, pp. 843–860, 2008.
[13] J.-S. Jang, "Anfis: adaptive-network-based fuzzy inference system," *Systems, Man and Cybernetics, IEEE Transactions on*, vol. 23, no. 3, pp. 665 –685, may/jun 1993.
[14] E. Purwanto, S. Arifin, and B.-S. So, "Application of adaptive neuro fuzzy inference system on the development of the observer for speed sensor less induction motor," in *Electrical and Electronic Technology, 2001. TENCON. Proceedings of IEEE Region 10 International Conference on*, vol. 1, 2001, pp. 409 –414 vol.1.
[15] V. Vapnik, *The Nature of Statistical Learning Theory (Information Science and Statistics)*, 2nd ed. Springer, November 1999. [Online]. Available: http://www.cs.orst.edu/ bulatov/papers/Vapnik, V. (2000) The Nature of Stastical Learning Theory, 167p.pdf
[16] B. Schölkopf, P. Bartlett, A. Smola, and R. Williamson, "Support vector regression with automatic accuracy control," in *Proceedings of ICANN'98*, ser. Perspectives in Neural Computing, L. Niklasson, M. Bodén, and T. Ziemke, Eds. Berlin: Springer Verlag, 1998, pp. 111–116. [Online]. Available: /papers/SchBarSmoWil98.ps.gz
[17] H. Drucker, C. J. Burges, L. Kaufman, C. J. C, B. L. Kaufman, A. Smola, and V. Vapnik, "Support vector regression machines," 1996.
[18] S. Klement, "Incremental Support Vector Regression for Steering Hot Rolling Mills," Diploma Thesis, Universität zu Lübeck, 2006.

2011 IEEE International Conference on Fuzzy Systems
June 27-30, 2011, Taipei, Taiwan

A TSK Neuro-Fuzzy Approach for Modeling Highly Dynamic Systems

Giovanni Acampora
Department of Computer Science
University of Salerno
Fisciano, Salerno 84084
Email: gacampora@unisa.it

***Abstract*—This paper introduces a new type of TSK-based neuro-fuzzy approach and its application to modeling highly dynamic systems. In details, our proposal performs an adaptive supervised learning on a collection of time series in order to create a so-called Timed Automata Based Fuzzy Controller, i.e. an evolvable fuzzy controller whose dynamic features yield high performances in variable structure systems representation. The adaptive learning is accomplished by merging together theories from the area of times series analysis such as the Adaptive Piecewise Constant Approximation method, with a well-known neuro-fuzzy framework, the Adaptive Neuro Fuzzy Inference System. As will be shown in our experiments, where our proposal has been tested on a Fuzz-IEEE 2011 Fuzzy Competition dataset, this approach reduces the output error measure and achieves a better performance than a standard application of the ANFIS algorithm when applied to highly dynamic systems.**

***Index Terms*—Dynamic Systems Modeling, Neuro-Fuzzy Systems, Time Series Approximation, Variable Structure Systems, Timed Automata based Fuzzy Controllers.**

I. Introduction

Traditional systems modeling exploits conventional mathematical methods, such as differential equations, that are not able to deal with complex systems characterized by high levels of imprecision and uncertainty. By contrast, the *fuzzy control theory* [1][2] uses collections of linguistic *if...then* rules in order to model the above mentioned systems by considering qualitative aspects of human knowledge and reasoning processes without employing a precise quantitative analysis[3]. Thanks to their versatility, fuzzy systems have found a great variety of applications ranging from control engineering, qualitative modeling, pattern recognition, signal processing, information processing, machine intelligence, decision making, management, finance, medicine, motor industry, robotics, and so on [4].

However, in spite of their wide applicability, fuzzy systems suffer from some design weaknesses:

1) there are no recognized techniques for capturing human knowledge or experience through a fuzzy rule base;
2) some effective methods for learning and/or tuning the membership functions are necessary to minimize the output error measure or maximize performance index;
3) fuzzy control paradigm does not allow the modeling of systems characterized by a discontinuous nonlinear behavior or, in other words, it cannot directly represent highly dynamic systems and Variable-Structure Systems (VSSs)[5].

In order to solve these drawbacks, this paper introduces an adaptive supervised learning algorithm, based on a neuro-fuzzy approach, able to infer the different behaviors that a system exhibits during its life-cycle, and return a so-called *Timed Automata based Fuzzy Controller (TAFC)*, i.e. a novel kind of evolvable fuzzy inference engine whose dynamic features yield high performances in dynamic systems representation. The main idea underlying the learning algorithm is to identify the time ranges where the system shows a behavior characterized by soft oscillations and, for each range, to compute the most appropriate TSK fuzzy controller [6] modeling the system behavior in that range.

More in detail, the proposed neuro-fuzzy approach learns a suitable TAFC for modeling a given system by performing two sequential subtasks. The first subtask, that is based on the *Adaptive Piecewise Constant Approximation (APCA)* method [7], analyzes a collection of time series representing the temporal evolution of the system variables and identifies a set of disjointed temporal ranges where such variables are simultaneously characterized by soft oscillations or, in other words, by a low variance. This choice will allow the following subtask to work on a more reliable data collection. The second subtask takes as inputs the temporal ranges computed by the first subtask and, for each range, uses the *Adaptive Neuro-Fuzzy Inference Engine (ANFIS)* in order to compute the most suitable TSK controller that models the system behavior in that range. Finally, the computed temporal ranges and TSK controllers will be used to determine the main components of a TAFC modeling the whole system life-cycle.

As will be shown in experiments, where our proposal has been tested on a Fuzz-IEEE 2011 Fuzzy Competition dataset, the TAFC obtained by means of the proposed neuro-fuzzy approach reduces the output error measure error and achieves performances better than a conventional application of the ANFIS algorithm, when applied to highly dynamic systems.

II. Basic Concepts and Background

The following subsections will be devoted to present the main methodologies used by our approach: TAFC, APCA and ANFIS. Successively, the section III will formally introduce the proposed supervised learning algorithm.

978-1-4244-7316-8/11/$26.00 ©2011 IEEE

A. Timed Automata based Fuzzy Controllers

A complete and theoretical discussion about the TAFC definition can be found in [8]. However, in this section a brief description about the most important features characterizing this evolvable inference engine is presented.

TAFCs are evolvable fuzzy systems mainly useful for modeling variable structure systems. In particular, they extend standard fuzzy controllers (Mamdani or TSK) by using three additional concepts: *control eras*, *control configurations* and *control time*. By means of these concepts, the life-cycle of a given system can be considered as composed of a sequence of disjointed time intervals (the control eras) where each era is characterized by a well-defined fuzzy controller (the control configuration) suitable for controlling the system during that era; the control time is the mechanism that allows the system to switch between adjacent control eras; in other words, the control time set the current control configuration of the system and the duration of the control eras.

In order to extend the fuzzy control vision with above said concepts, a modified version of Timed Automata has been used. A timed automaton is a standard finite-state automaton extended with a finite collection of real-valued clocks providing a straightforward way to represent time related events. Conventional automata-based approaches cannot offer this feature. The clocks can be reset to 0 (independently of each other) with the transitions of the automaton, and keep track of the time elapsed since the last reset. The transitions of a timed automaton are labeled with a *guard* (a condition on clocks), an *action* or *symbol* on alphabet Σ, and a *clock reset* (a subset of clocks to be reset). Intuitively, a timed automaton starts execution with all clocks set to zero. Clocks increase uniformly with time while the automaton is within a node. A transition may be taken only if the current values of the clocks satisfy the associated constraints. By taking the transition, all clocks in the clock reset will be set to zero, while the remaining keep their values.

In our vision, TAFCs use the nodes of a timed automaton to implement control era and control configuration, whereas the clocks and transitions realize the control time idea. In particular, when a TAFC transits from a state S_1 to a state S_2 through a transition T_1, an opportune control configuration (or fuzzy controller) C is activated to manage the system until a successive transition T_2 will be taken. The time that elapses between the two transitions is the duration of the control era related to the control configuration C. The control configuration C is obtained by transforming a previous control configuration related to the state S_1 by means of particular transformation operators that are related to the transition T_1. In details, transformation operators change a TAFC's control configuration by means of the following operations: adding ($\oplus$) or deleting ($\ominus$) a variable; adding ($\boxplus^k$), removing ($\boxminus^k$) or changing ($\boxdot^k$) k rules in the rule base; changing implication method of the rule base ($\sim$); adding ($\circledast$), deleting ($\oslash$) or changing ($\circledcirc$) a term to a variable; changing defuzzify method ($\propto$), aggregation method ($\bowtie$) or default value ($\divideontimes$) of an output variable; changing lower bound ($\ltimes$) or upper bound ($\rtimes$) of

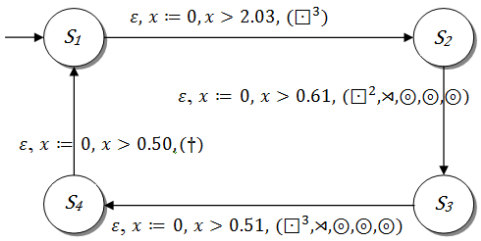

Fig. 1. A Sample of Timed Automata based Fuzzy Controller: an evolution scheme for the Matlab^{TM}Tipper

the universe of discourse of a variable. This process is iterated for each transition taken. A sample of TAFC is shown in Fig. 1. This TAFC evolves the classical tipper controller used as sample of fuzzy system in Mathworks Matlab^{TM}. The Tipper system manages the following issue: what is the right amount to tip your waitperson working in a restaurant placed in a sea village? The system determines the amount of tip by analyzing two data: the quality of service and the quality of served food. Although, it may seem a very simple system, the Tipper can be considered as a dynamic system since it changes its structure and behaviour over the time. Indeed, usually, the tip amount is higher in high season than low season and, as consequence, the fuzzy variable modeling this value should be gradually modified among the four year seasons. In details, it is possible to individuate four periods where the Tipper can show different behavior: from october 10^{th} to april 30^{th}, from may 1^{th} to june 30^{th}, from july 1^{th} to august 20^{th} and from august 21^{th} to october 9^{th}.

As proved in [9], where a comparison between a standard TSK controller and a TAFC has been accomplished, a TAFC results more efficient when it is devoted to control a dynamic system such as the Tipper.

In following sections, an introduction to APCA and ANFIS will be provided in order to define a supervised learning algorithm capable of analyzing a collection of time series related a given system and learning the control eras, the control configurations and the control time of the TAFC most suitable to model a system.

B. Adaptive Piecewise Constant Approximation

The APCA is a method for time series approximation originally designed for solving the problem of similarity search in large time series databases. In particular, APCA is a method for approximating a time series by dividing it into M varying-length segments and recording the mean value of the datapoints that fall within the segment. In our context, this approach is used to identify the collection of temporal ranges where a system shows a soft oscillation behavior. Hereafter, an introduction to APCA is provided starting from the time series definition.

A time series is a sequence of data points, measured at successive times spaced at uniform time intervals. A sample of time series is shown in Fig. 2. A common formal notation

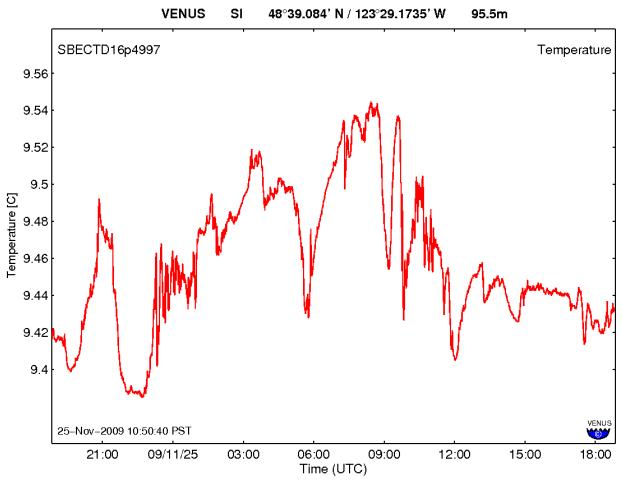

Fig. 2. A Sample of Time Serie for Representing Temperature Variations.

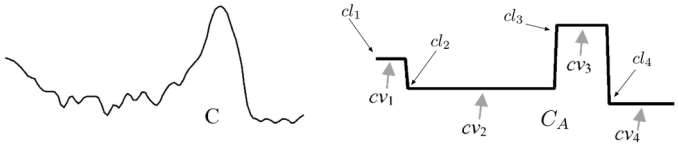

Fig. 3. A time series C and its APCA representation C_A, with $M = 4$.

specifying a time series C is:

$$C = \{c_1, c_2, c_3, \ldots, c_n\} \tag{1}$$

where c_i is the i^{th} datapoint in time series C sampled at the times $\{t_i, i = 1, \ldots, n\}$, with $t_i - t_{i-1} = \delta$ and $\delta \in \mathbb{R}$ (δ is the fixed sampling step).

Given a time series $C = \{c_1, \ldots, c_n\}$, an APCA approximation is represented as:

$$C_A = \{\langle cv_1, cl_1\rangle, \ldots, \langle cv_M, cl_M\rangle\} \tag{2}$$

where cv_i is the mean value of datapoints in the i^{th} segment (i.e., $cv_i = mean(c_{cl_i}, \ldots, c_{cl_{i+1}-1})$) and cl_i the left endpoint of the i^{th} segment. The length of the i^{th} segment can be calculated as $(cl_{i+1} - cl_i)$. Fig. 3 illustrates this notation.

In our neuro-fuzzy context, the APCA is used to analyze the temporal behavior of the variables related to a given system and compute a collection of temporal ranges enabling the proposed learning algorithm to learn the set of desired TAFC control eras.

C. Adaptive Neuro Fuzzy Inference System

Adaptive Neuro-Fuzzy Inference Systems (ANFIS) is a class of adaptive networks that are functionally equivalent to conventional fuzzy inference systems. An adaptive network is a multilayer feed forward network in which each node performs a particular function (node function) on incoming signals using a set of parameters specific to this node [3]. The form of node functions may vary from node to node, and the choice of each node function depends on the overall function, which the adaptive network is designed to implement. Adaptive networks are composed by two different classes of nodes: *adaptive nodes* and *fixed nodes*. Adaptive nodes are characterized by a collection of modifiable parameters, named *parameter set*, whereas, the fixed nodes only deal with an unmodifiable parameters. Adaptive networks work in order to achieve a desired input-output by updating the parameter sets according to given training data and a gradient-based update procedure [10]. ANFIS exploit this updating feature to learn and adapt the parameters of a given TSK fuzzy inference system.

As example, Fig. 4 shows an adaptive network that models a first-order TSK fuzzy inference systems composed by two rules:

1) If x is A_1 and y is B_1 Then $f_1 = p_1 \cdot x + q_1 \cdot y + r_1$
2) If x is A_2 and y is B_2 Then $f_2 = p_2 \cdot x + q_2 \cdot y + r_2$

To reflect the ANFIS adaptive capabilities, in Fig. 4 the square nodes represent the adaptive nodes, whereas the circle nodes represent the fixed nodes.

Each ANFIS layer implements a particular fuzzy inference subtask. In detail:

Layer 1 Every node i in this layer implements the node function:

$$O_i^1 = \mu_{A_i}(x) \tag{3}$$

where x is the input to node i , and A_i is a linguistic label. From a fuzzy inference point of view, O_i^1 is the membership function related to the fuzzy set A_i, and it specifies the degree to which the input x satisfies A_i. Typically, A_i is a bell-shaped function characterized by a set of three parameters $\{a, b, c\}$ corresponding to the parameter set of the node i.

Layer 2 The nodes labeled with Π multiply their input signals:

$$w_i = \mu_{A_i}(x) \times \mu_{B_i}(y) \text{ with } i = 1, 2; \tag{4}$$

where w_i represents the firing strength of a rule.

Layer 3 The node in this layer calculate the ratio of the i^{th} rules firing strength to the sum of all rules firing strengths:

$$\overline{w_i} = \frac{w_i}{w_1 + w_2} \text{ with } i = 1, 2. \tag{5}$$

The value w_i represents the *normalized firing strenght*.

Layer 4 The adaptive node i in this layer computes the following function:

$$O_i^4 = \overline{w_i} f_i = \overline{w_i}(p_i x + q_i y + r_i) \tag{6}$$

where the collection $\{p_i, q_i, r_i\}$ is the parameter set of the node i and corresponds to the TSK consequent parameters.

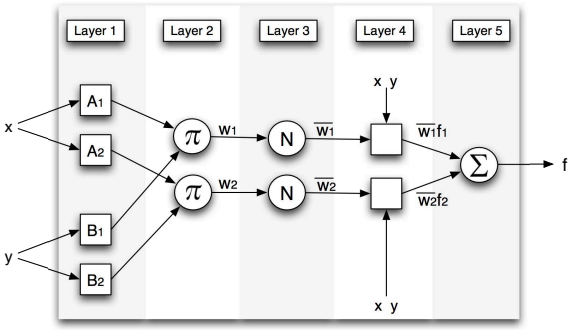

Fig. 4. The Adaptive Neuro Fuzzy Inference System.

Layer 5 The single and fixed node in this layer, labeled Σ, computes the overall network output as the summation of all incoming signals:

$$O_i^5 = \sum_i \overline{w_i} f_i = \frac{\sum_i w_i f_i}{w_i} \tag{7}$$

In our learning context, ANFIS is used to compute a collection of TSK controllers, each one useful to control a given system during a particular control era previously computed by the APCA approach.

III. A Supervised Learning Algorithm for Modeling Highly Dynamic Systems through TAFCs

This section formally introduces our proposal of a neuro-fuzzy approach for learning the TAFC most suitable to modeling the behavior of a given system. The proposed algorithm achieves this goal by taking as input a collection of time series representing the temporal evolution of the different variables of the system. The main idea underlying the learning algorithm is to identify the time ranges where the system shows a behavior characterized by soft oscillations and, for each range, to compute the most appropriate TSK controller modeling the system behavior in that range. Starting from the time ranges and TSK controllers the algorithm returns the control eras, the control configurations and the control time of the TAFC that better models the system under modeling.

The algorithm is essentially based on two steps, the *temporal learning step* and *qualitative learning step* (see Fig. 5). The first step uses the APCA in order examine the time series and computes the sequence of aforementioned time intervals; the second step, taking as input the sequence of time intervals, returns the appropriate (one for each time interval) TSK controller, computed by means of ANFIS.

A. Temporal Learning Step

Let S be a system characterized by n_i input variables and n_o output variables belonging, respectively, to the following sets:

$$\begin{aligned} V_i &= \{v_j, j = 1, \ldots, n_i\} \\ V_o &= \{v_j, j = n_i + 1, \ldots, n_i + n_o\} \end{aligned} \tag{8}$$

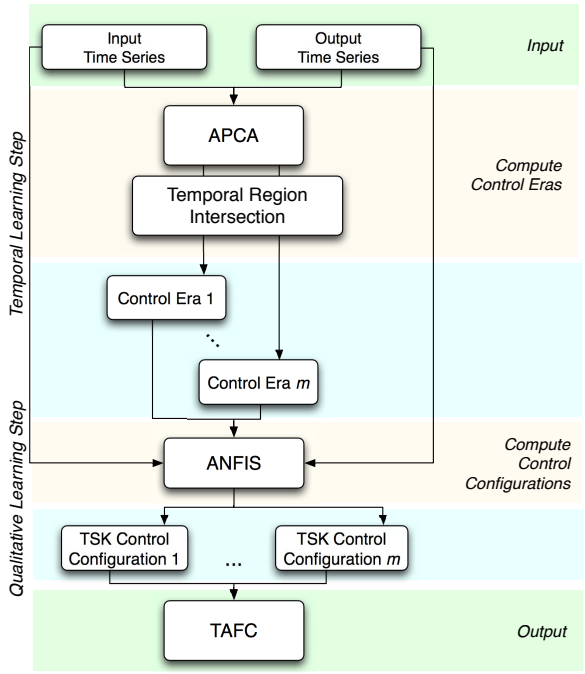

Fig. 5. The Supervised Learning Algorithm for modeling Highly Dynamic Systems: a Flow Chart

For each variable $v_j \in V_i \cup V_o$, let $C^j = \{c_1^j, c_2^j, \ldots, c_n^j\}$ be a time series containing the values of the variable v_j sampled at the time t_i with $i = 1, \ldots, n$ by a fixed sampling step δ.

The main aim of the temporal learning step is to analyze, for each output variable $v' \in V_o$, the time series C^j in order to identify the temporal ranges where the variables $v_j \in V_i \cup \{v'\}$ are simultaneously characterized by soft oscillations. In order to achieve this goal, the APCA method is applied. More in detail, the APCA method is executed on each time series C^j in order to compute the following time series approximation:

$$C_A^j = \{\langle cv_1^j, cl_2^j \rangle, \ldots, \langle cv_{M_j}^j, cl_{M_j}^j \rangle\}$$

where cv_i^j is the mean value of variable v_j in the i^{th} segment and $cl_i^j \in \{t_1, t_2, \ldots, t_n\}$ is the left endpoint of the i^{th} segment. Successively, the algorithm extracts from C_A^j a collection of M_j time instants, $T^j = \{cl_1^j, cl_2^j, \ldots, cl_{M_j}^j\}$, corresponding to the left endpoints of the time ranges where the variable v_j is characterized by soft oscillations. A sample of this process, with $M = 9$, is shown in Fig. 6.

Once APCA has computed the collection T^j for each variable $v_j \in V_i \cup V_o$, it is necessary to identify a further collection of time instants, $\mathbf{T} = \{\tau_1, \tau_2, \ldots, \tau_p\}$, corresponding to the left endpoints of the time ranges where the system variables are 'simultaneously' characterized by soft oscillations. This operation is performed by a *temporal intersection operator*. We give an algorithmic representation of this operator (see Algorithm 1) and an example of temporal intersection applied to two sequences $T^1 = \{0, 27, 289, 437, 595, 759\}$ and $T^2 = \{0, 27, 389, 547\}$ whose temporal intersection returns $\mathbf{T} = \{0, 27, 289, 389, 437, 547, 595, 759\}$ (see Fig. 8).

Starting from $\mathbf{T} = \{\tau_1, \tau_2, \ldots, \tau_p\}$, the algorithm computes the collection of control eras as follows:

$$E = \{\langle \tau_1, \tau_2 - \delta \rangle, \langle \tau_2, \tau_3 - \delta \rangle, \ldots, \}$$

We remind that δ is the fixed sampling step related to time series C^j. In order to compute the TAFC control configurations, the qualitative learning step prepares a collection of datasets, each one of the related to a given control era in E, and successively uses ANFIS to complete the learning process.

Algorithm 1 T-INTERSECTION$(T^1, \ldots, M^1, \ldots)$

Require: The collections $T^1, T^2, \ldots, T^{n_i+n_o}$
Ensure: The collection $\mathbf{T} = \{\tau_1, \tau_2, \ldots, \tau_p\}$.

```
T ← ∅
k ← 1
for i = 1 to |T^1| + |T^2| + ... + |T^{n_i+n_o}| do
    for j = 1 to (n_i + n_o) do
        if |T^j| > 0 then
            m_j ← min(T^j)
        else
            m_j ← +∞
        end if
        {m_j is the minimum value of T^j}
    end for
    τ ← min({m_j, j = 1, ..., n_i + n_o})
    if (τ ∉ T) then
        τ_k ← τ
        T ← T ∪ {τ_k}
        k ← k + 1
    end if
end for
return T
```

B. Qualitative Learning Step

The qualitative learning step applies the ANFIS system to a collection of dataset $D = \{D_i, i = 1, \ldots, |E|\}$ where D_i is the dataset related to the control era $\langle \tau_i, \tau_{i+1} - \delta \rangle$. Precisely, D_i is a matrix with n_i+1 rows and $\frac{(\tau_{i+1}-\delta)-\tau_i}{\delta}$ columns where the j^{th} row corresponds to the values taken by variable v_j at time instants:

$$\tau_i, \tau_i + \delta, \tau_i + 2 \cdot \delta, \ldots, \tau_i + \frac{(\tau_{i+1} - \delta) - \tau_i}{\delta} \cdot \delta$$

These values are extracted from the time series C^j related to the variable v_j.

Once each dataset D_i has filled, the qualitative learning step uses ANFIS in order to learn the best suitable TSK controller modeling the system S in the i^{th} control era: $\phi_i = \text{ANFIS}(D_i)$. The set $\Phi = \{\phi_i, i = 1, \ldots, |E|\}$ is the collection of control configurations related to the TAFC modeling the system S and the time instants $\tau_i + \frac{(\tau_{i+1}-\delta)-\tau_i}{\delta} \cdot \delta$ $(i = 1, \ldots, |E| - 1)$ are used by the control time to move the TAFC from the state corresponding to the controller ϕ_i to the next state corresponding to the controller ϕ_{i+1}.

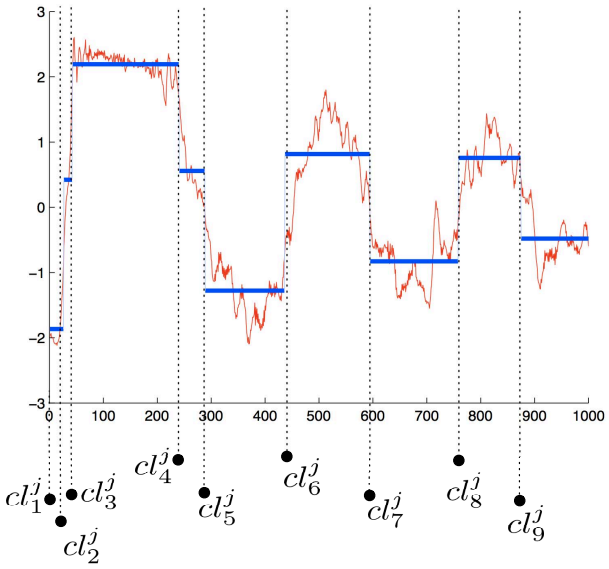

Fig. 6. The time ranges computed by APCA.

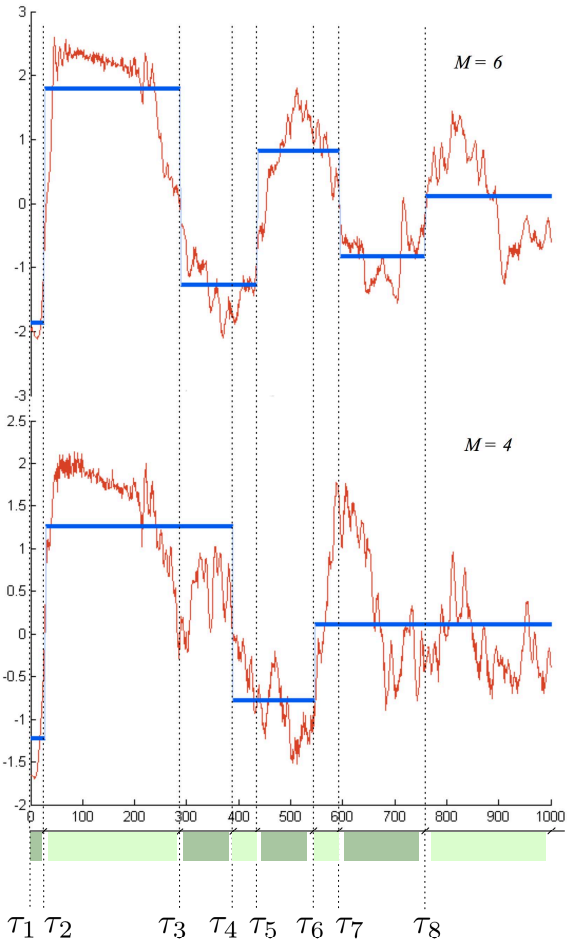

Fig. 7. The time ranges computed by the temporal intersection operator.

IV. Experimental Results

In order to verify and validate the benefits provided by our neuro-fuzzy approach, a dataset from FUZZ-IEEE 2011

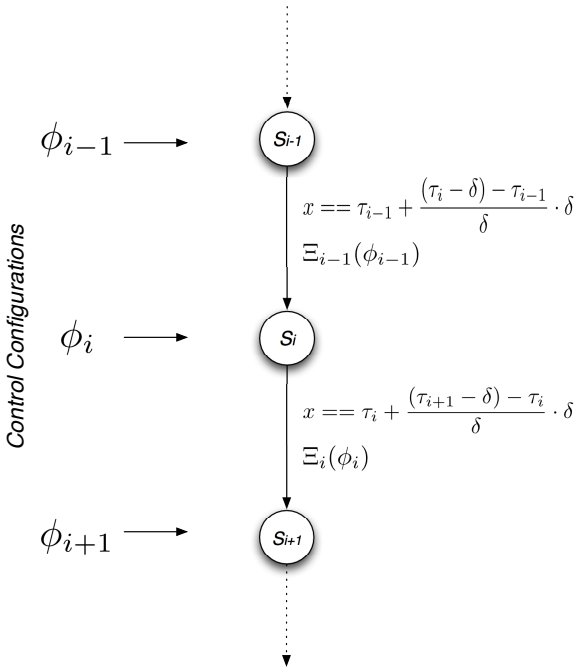

Fig. 8. A portion of TAFC returned by the learning algorithm.

Competition has been used. This dataset is related to a Multi-Input Multi-Output system with output couplings. An important feature of such a system is that each of the system's output variables may depend on all the input variables.

In particular, this competition dataset involves a nonlinear coupling system with four inputs and four outputs. Through data acquisition, 1000 input-output data points (namely, $u_1(n)$, $u_2(n)$, $u_3(n)$, $u_4(n)$, $y_1(n)$, $y_2(n)$, $y_3(n)$, $y_4(n)$, $n = 1, 2, ..., 1000$) were collected from the system with the sampling period $Ts = 0.0005s$. This data acquisition is used to create eight different time series $C_1, C_2, \ldots, C_8$, where the series $C_1, \ldots, C_4$ correspond to the four input variables, whereas the time series C_5 and C_8 correspond to the output variables.

The proposed neuro-fuzzy modeling system approach applies the APCA method to the time series C_i with $i = 1, \ldots, 8$ in order to obtain $M_1 = 4$ temporal segments for the variable u_1, $M_2 = 4$ temporal segments for the variable u_2, $M_3 = 5$ temporal segments for the variable u_3, $M_4 = 4$ temporal segments for the variable u_4, $M_5 = 8$ temporal segments for the variable y_1, $M_6 = 8$ temporal segments for the variable y_2, $M_7 = 6$ temporal segments for the variable u_3 and $M_8 = 6$ temporal segments for the variable y_4. In particular, for each output variable, the approach uses APCA method in order to compute the time instants corresponding to the left endpoints where the variables shows a soft oscillation. For example, considering the output variable y_4, the following collections are obtained:

$$
\begin{aligned}
T^1 &= \{0, 0.126, 0, 0.225, 0.297\} \\
T^2 &= \{0, 0.159, 0.283, 0.379\} \\
T^3 &= \{0, 0.056, 0.192, 0.291, 0.381\} \\
T^4 &= \{0, 0.176, 0.268, 0.334\} \\
T^8 &= \{0, 0.014, 0.17, 0.215, 0.268, 0.335\}
\end{aligned}
$$

The temporal intersection operator 'merges' together the collection T^1, T^2, T^3, T^4, $T^8$and obtains the time instants collection $\mathbf{T}$:

$$
\begin{aligned}
\mathbf{T} = \{&0, 0.0140, 0.056, 0.126, 0.159, 0.170, 0.176, \\
&0.192, 0.215, 0.225, 0.268, 0.283, 0.291, 0.297, \\
&0.335, 0.379, 0.381\}
\end{aligned}
$$

The collection $\mathbf{T}$ is used to learn 17 TAFC control eras:

$$
\begin{aligned}
E = \{&\langle 0, 0.0135\rangle \langle 0.0140, 0.0555\rangle, \langle 0.056, 0.1255\rangle, \\
&\langle 0.126, 0.1585\rangle \langle 0.159, 0.1695\rangle, \\
&\langle 0.170, 0.1755\rangle \langle 0.176, 0.1915\rangle, \\
&\langle 0.192, 0.2145\rangle, \langle 0.115, 0.2245\rangle, \\
&\langle 0.225, 0.2675\rangle \langle 0.268, 0.2825\rangle, \\
&\langle 0.283, 0.2905\rangle \langle 0.291, 0.2965\rangle, \\
&\langle 0.297, 0.3345\rangle \langle 0.335, 0.3785\rangle \\
&\langle 0.379, 0.3805\rangle \langle 0.381, 0.5\rangle\}
\end{aligned}
$$

Starting from E, the collection of ANFIS dataset $D = \{D_i, i = 1, \ldots, 17\}$ is computed in order to learn the control configurations $\Phi = \{\phi_i, i = 1, \ldots, 17\}$ and the control time of the TAFC modeling the behavior of the output variable y_4. The TAFC modeling the behavior of the systems regarding the output variable y_4 is shown in Fig. 9.

By iterating the learning process for each output variables, the performance of our neuro-fuzzy approach can be evaluated. In particular, this performance has been assessed according to the following error measure:

$$
\begin{aligned}
&\hat{e}_{total} = \hat{e_1} + \hat{e_2} + \hat{e_3} + \hat{e_4} = \\
&= \sum_{i=1}^{1000} (y_1(n) - \hat{y_1}(n))^2 + \\
&+ \sum_{i=1}^{1000} (y_2(n) - \hat{y_2}(n))^2 + \\
&+ \sum_{i=1}^{1000} (y_3(n) - \hat{y_3}(n))^2 + \\
&+ \sum_{i=1}^{1000} (y_4(n) - \hat{y_4}(n))^2
\end{aligned}
$$

where $\hat{y}_i$ with $i = 1, \ldots, 4$, are the output value computed by the TAFC model. We used Matlab to the learn the TAFCs related to the FUZZ-IEEE 2011 Competition and we obtained

the following error measures:

$$\begin{aligned}
&\sum_{i=1}^{1000}(y_1(n)-\hat{y_1}(n))^2 = 0.0645\\
&\sum_{i=1}^{1000}(y_2(n)-\hat{y_2}(n))^2 = 0.0474\\
&\sum_{i=1}^{1000}(y_3(n)-\hat{y_3}(n))^2 = 0.5906\\
&\sum_{i=1}^{1000}(y_4(n)-\hat{y_4}(n))^2 = 0.6512
\end{aligned} \tag{9}$$

and, as a consequence:

$$\hat{e}_{total} = 0.0645 + 0.0474 + 0.5906 + 0.6512 = 1.3536 \tag{10}$$

In order to validate the benefit provided by the proposed approach, a comparison between the total error shown in equation 10 and the error $\dot{e}_{total}$ returned by a conventional ANFIS application is given. Indeed, by using the conventional ANFIS approach, the following errors are measured:

$$\begin{aligned}
&\dot{e}_{total} = 455.2466 + 377.2482 + 315.9917 + 300.0843 =\\
&= 1.4486 \times 10^3
\end{aligned} \tag{11}$$

with a percentage improvement:

$$\Delta_E = \frac{(1.4486 \times 10^3 - 1.3536)}{1.4486 \times 10^3} \times 100 = 99.9066\%$$

The values $\hat{e}_{total}$ and Δ_E strongly depend upon the number of control eras returned by the temporal intersection operator. In turn, the number of control eras is related to M_j with $j = 1, \ldots, 8$ i.e, the number of segments used by APCA to approximate the time series C_j related to the variable v_j. In this experiment, we have chosen the M_j values in an empirical way in order to minimize the value of the total error $\hat{e}_{total}$ and try to avoid the overfitting issue. In the future works, a more accurate study about overfitting question will be done by validating the learned TAFCs by means of opportune testing datasets.

V. Conclusion

This paper introduced a novel of TSK-based neuro-fuzzy approach and its application to dynamic system modeling. This approach used the ANFIS system together with a time series approximation method, the APCA, in order to identify the time ranges where the system shows a behavior characterized by soft oscillations and, for each range, to compute the most appropriate TSK controller modeling the system behavior in that range. Successively, the time ranges and TSK controllers have been used in order to define the control eras, the control configurations and the control time of a TAFC, an innovative evolvable fuzzy inference engine. As show in experimental results section, our approach reduces the output error measure and achieves a better performance than a standard application of the ANFIS algorithm when applied to a highly dynamic system. In the future, we will test our neuro-fuzzy system on real-world scenarios in order to further validate the provided benefits.

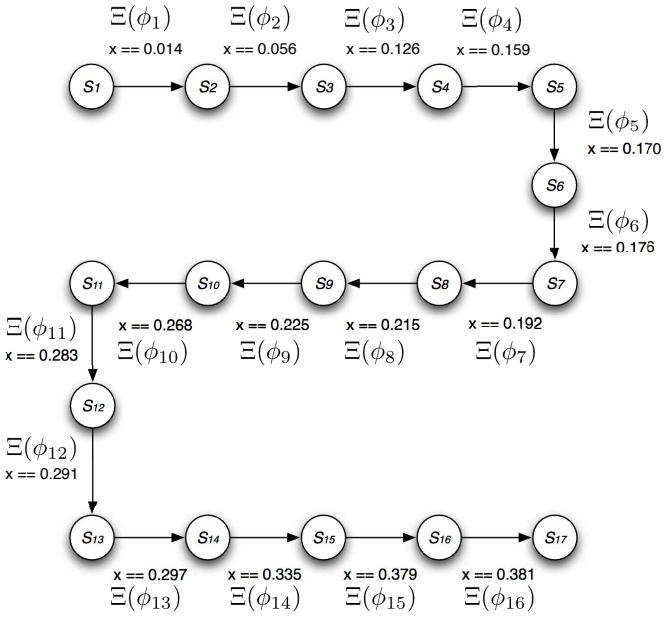

Fig. 9. The TAFC modeling the FUZZ-IEEE 2011 Competition dataset regarding to the output variable y_4.

Acknowledgment

The author would like to thank the PhD student, Autilia Vitiello, for her precious support to Matlab programming.

References

[1] E. H. Mamdani, "Applications of fuzzy algorithms for simple dynamic plants," *Procedings of IEEE,* vol. 121, no. 12, pp. 1585–1588, 1974.

[2] L.A. Zadeh,"Fuzzy sets," *Information and Control*, vol. 8, pp. 338–353,1965.

[3] Jang, J.-S.R., "ANFIS: adaptive-network-based fuzzy inference system," *Systems, Man and Cybernetics, IEEE Transactions on*, vol.23, no.3, pp.665-685, May/Jun 1993, doi: 10.1109/21.256541.

[4] G. Feng, *"Analysis and Synthesis of Fuzzy Control Systems A Model-Based Approach,"* CRC Press, 2010.

[5] S.V. Emelyanov, S.V. Utkin, V.A. Taran, N.E. Kostyleva, A.M. Subladze, V.B. Ezerov, E.N. Dubrovskij, *"Theory of Variable Structure Systems"*, (in Russian), Nauka, Moscow, 1970.

[6] T. Takagi and M. Sugeno, "Fuzzy identification of systems and its applications to modeling and control," *IEEE Transactions Systems, Man & Cybernetics*, vol. 15, no. 1, pp. 116–132, 1985.

[7] J. Scargle, B. Jackson and J. Norris, "Adaptive Piecewise-constant Modeling of Signals in Multidimensional Spaces," in *Proceedings of PHYSTAT2003*, pp. 157-161, 2003.

[8] G. Acampora,"Exploiting Timed Automata-based Fuzzy Controllers and data mining to detect computer network intrusions," *Fuzzy Systems (FUZZ), 2010 IEEE International Conference on,* pp.1-8, July 2010.

[9] G. Acampora, V. Loia, A. Vitiello, "Hybridizing fuzzy control and timed automata for modeling variable structure fuzzy systems," *Fuzzy Systems (FUZZ), 2010 IEEE International Conference on*, pp.1-8, July 2010.

[10] J.S.R. Jang, "Self-learning fuzzy controllers based on temporal back-propagation," *IEEE Trans. Neural Networks*, vol. 3, pp. 714-723, Sept. 1992.

2011 IEEE International Conference on Fuzzy Systems
June 27-30, 2011, Taipei, Taiwan

A Bacterial Foraging PSO – DE Algorithm for Solving Reserve Constrained Dynamic Economic Dispatch Problem

K.Vaisakh
Department of Electrical Engineering
Andhra University
Visakhapatnam, AP, India
vaisakh_k@yahoo.co.in

P.Praveena
Department of Electrical Engineering
Andhra University
Visakhapatnam,AP,India
nambaripraveena@gmail.com

S.Rama Mohana Rao
Department of Electrical Engineering
Andhra University
Visakhapatnam,AP,India
ramu_sanchana@yahoo.com

***Abstract*--This paper introduces a solution to Dynamic Economic Dispatch (DED) problem using a hybrid optimization methodology bacterial foraging and PSO-DE (BPSO-DE) by integrating Bacterial foraging optimization Algorithm (BFOA), Particle Swarm Optimization (PSO) and Differential Evolution (DE). In the proposed method BFOA performs local search and global search for entire search space is accomplished through PSO-DE operators in this way they move to reach the global optimization. The BFOA also takes care of the constraints such as ramp-rate limits, valve-point loading effects, system load demand, prohibited operating zones, power losses and spinning reserve capacity. A ten unit test system is considered to show the effectiveness of the proposed method over other existing methods.**

***Index Terms* -- Bacterial Foraging, Particle Swarm Optimization, Differential Evolution**

I. NOMENCLATURE

D : Dimension of search space.

N_b : The number of bacteria in the population.

N_C : The number of chemo-tactic steps.

N_{re} : The number of reproduction steps.

N_{ed} : The number of elimination-dispersal events.

N_S : Swimming length N_S is the maximum number of steps taken by each bacterium when it moves from low nutrient area to high nutrient area.

P_{ed} : Probability of elimination and dispersal

CS : The size of the step taken in the random direction specified by the tumble.

w : The inertia weight.

$P(t,j,k,l,m)$: Position vector of j^{th} unit in t^{th} hour, k^{th} bacterial population, l^{th} reproduction and m^{th} elimination-dispersal, where $k=1,2,.....,N_b$, $l=1,2,....,N_{re}$ and $m=1,2,....,N_{ed}$.

$V(t,j,k)$: Velocity vector of the j^{th} unit in t^{th} hour and k^{th} bacterial population.

$pbest$: The best previous position of k^{th} particles.

$gbest$: The index of the best particle among all particles in the group.

sf : The scale factor

CR : The Cross over probability

C_1, C_2 : Acceleration constants

rand, Rand : Random value in the range [0,1]

$J(k,l,m)$: Cost value of k^{th} bacterial population, l^{th} reproduction and m^{th} elimination-dispersal

$JF(k,l,m)$: Fitness value of k^{th} bacterial population, l^{th} reproduction and m^{th} elimination-dispersal

r_2, r_3 : Parameter vectors chosen randomly from the current population.

II. INTRODUCTION

DED problem determines the optimal generation schedule of on-line generators, so as to meet the predicted load demand over a time horizon satisfying dynamic constraint such as ramp-rate limits. The goal of DED problem is to minimize operating cost under various system and operational constraints. The ramp-rate limits must be properly modeled in production simulation as the operational decision at an hour t may affect the operational decision at a later hour. So DED is a most difficult dynamic optimization problem.

The literature addresses DED problem with convex cost functions [1]–[4], though in reality, large steam turbines generally have a number of fuel admission valves which are opened sequentially in order to increase the production. When the valve is opened, the throttling losses increases rapidly as a

978-1-4244-7316-8/11/$26.00 ©2011 IEEE

result of which, the incremental heat rate rises suddenly. The valve-point effects and prohibited operating regions contribute non-convexity in the fuel cost function of the generating units [5]-[9]. The generators operating in prohibited operating region experience amplification of vibrations in their shaft bearing [10], [11] due to physical operation limits such as faults in the machines themselves or the associated auxiliaries, such as boiler, feed pumps, etc. Traditional methods like gradient projection method [1], Lagrangian relaxation [12], and dynamic programming when used to solve DED problem often use more approximations to limit the complexity of the problem and take longer solution time. Hence these methods suffer from solution stagnation problem leading them to a less desirable performance. Genetic Algorithm (GA) [5], [13], evolutionary programming (EP) [6], [14]-[16], simulated annealing (SA) [17], [18], particle swarm optimization (PSO) [7] and differential evolution (DE) [19], [20] may prove to be very effective in solving nonlinear ED problems without any restriction on the shape of the cost curves. They often provide fast and reasonable solutions. EP seems to be a good method to solve optimization problems, when applied to problems consisting of more number of local optima the solutions obtained from EP method when combined with sequential quadratic programming (SQP) is just near global optimum[21]-[24]. Recently, a variable scaling hybrid differential evolution (VSHDE) and hybrid differential evolution (HDE) [25] methods are used to solve the DED problem.

The Bacterial Foraging Optimization Algorithm (BFOA) is currently gaining popularity in the community of researchers, for its effectiveness in solving certain difficult real-world optimization problems. BFOA is based on the foraging strategies of Ecoli bacterium cells and was proposed by Prof. K. M. Passino in 2001 [26]. PSO and DE are excellent heuristics like other evolutionary algorithms [29]. Practical experiences suggest that they reach stagnation after certain number of generations as the population is not converged locally, so they will stop proceeding towards global optimal solutions. The stochastic search methods are proven in reaching global solutions for certain difficult real world optimization problems [30]-[36]. Hence this article comes up with a hybrid approach involving PSO-DE and BFOA algorithm for solving non-convex DED problem considering valve-point loading effects, ramp-rate limits, prohibited operating regions and spinning reserve capacity. The new method is shown to be statistically significantly better on a test systems consisting of ten generating units. The results obtained through the proposed method are compared with those reported in the literature.

III. Dynamic Economic Dispatch Problem Formulation

The classic DED problem minimizes the following incremental cost function associated to dispatchable units

$$Min \quad F = \sum_{t=1}^{T}\sum_{i=1}^{N} F_{it}(P_{it}) \qquad (\$) \qquad (1)$$

where F is the total generating cost over the whole dispatch period, T is the number of intervals in the scheduled horizon, N is the number of generating units, and $F_{it}(P_{it})$ is the fuel cost in terms of its real power output P_{it} at time t. Taking into account of the valve-point effects, the fuel cost function of i^{th} thermal generating unit is expressed as the sum of a quadratic and a sinusoidal function in the following form

$$F_{it}(P_{it}) = a_i P_{it}^2 + b_i P_{it} + c_i + \left| e_i \sin(f_i(P_{i\min} - P_{it})) \right| \qquad (2)$$

$$J = F_{it}(P_{it}) \qquad (3)$$

$$JF = 1/J \qquad (4)$$

where a_i, b_i and c_i are cost coefficients, e_i and f_i are constants from the valve point effect of the i^{th} generating unit, and P_i is the power output of the i^{th} unit in megawatts. The minimization of the generation cost is subjected to the following equality and inequality constraints

1) Real power balance constraint

$$\sum_{i=1}^{N} P_{it} - P_{Dt} - P_{Lt} = 0 \qquad (5)$$

where t = 1, 2, …, T. P_{Dt} is the total power demand at time t in megawatts and P_{Lt} is the transmission power loss at time t in megawatts. P_{Lt} is calculated using the B-Matrix loss coefficients and the general form of the loss formula using B-coefficients is

$$P_{Lt} = \sum_{i=1}^{N} B_{ii} P_{it}^2 \qquad (6)$$

2) Real power generation limit

$$P_{i\min} \le P_{it} \le P_{i\max} \qquad (7)$$

where $P_{i\min}$ is the minimum limit, and $P_{i\max}$ is the maximum limit of real power of the i^{th} unit in megawatts.

3) Generating unit ramp rate limits

$$\begin{aligned} P_{it} - P_{i(t-1)} &\le UR_i, \qquad i = 1,2,3,.....,N \\ P_{i(t-1)} - P_{it} &\le DR_i, \qquad i = 1,2,3,.....,N \end{aligned} \qquad (8)$$

where UR_i and DR_i are the ramp-up and ramp-down limits of i^{th} unit in megawatts. Thus the constraint of (8) due to the ramp rate constraints is modified as

$$\max(P_{i\min}, P_{i(t-1)} - DR_i) \le P_{it} \le \min(P_{i\max}, P_{i(t-1)} + UR_i) \qquad (9)$$

such that

$$\begin{aligned} P_{it,\min} &= \max(P_{i\min}, P_{i(t-1)} - DR_i) \\ &\text{and} \\ P_{it,\max} &= \min(P_{i\max}, P_{i(t-1)} + UR_i) \end{aligned} \qquad (10)$$

4) Prohibited operating zones

$$\begin{aligned} P_{it,\min} &\le P_i \le P_{i,1}^L \\ P_{i,q-1}^U &\le P_i \le P_{i,q}^L \\ P_{i,ni}^U &\le P_i \le P_{it,\max}, \; q = 2,3,.....,n_i \end{aligned} \qquad (11)$$

where

i = unit index

n_i = the number of prohibited zones for unit i.

q = the index of prohibited zones for unit i.

$P_{i,q}^{L}$ = the lower boundary of q^{th} prohibited zone for unit i.

$P_{i,q}^{U}$ = the upper boundary of q^{th} prohibited zone for unit i.

5) System spinning reserve constraint

$$\sum_{i=1}^{N} S_{it} \geq S_{Rt}$$
$$S_{it} = \min\{(P_{it\max} - P_{it}), S_{i\max}\} \quad (12)$$

where S_{it} = reserve contribution of the i^{th} unit at t^{th} interval

S_{Rt} = spinning reserve demand at t^{th} interval in megawatts

$S_{i\max}$ = maximum reserve contribution of i^{th} unit

IV. An Overview of Integrated Techniques

The Particle Swarm Optimization was introduced by James Kennedy and Russell C. Eberhart in 1995 [26]. PSO is motivated from the simulation of the behavior of social systems such as fish schooling and birds flocking. It is similar to other evolutionary computation techniques like Genetic Algorithm (GA) and Evolutionary Programming (EP) in that PSO also initializes a population of individuals randomly. These individuals are known as particles and have positions and velocities. Each particle adjusts its velocity dynamically corresponding to its flying experiences and its neighbors. The three main components that affect the changing of the velocity are internal, cognitive and social components. Internal component represents the particles behavior for moving in the previous direction. The cognitive component represents the memory of the particle for attracting to its best position ($pbest$) based on its own thinking. The social component represents the memory of the particle for attracting its previous best position among the group ($gbest$), here the particle changes its velocity based on the social-psychological adaptation of knowledge. So the velocity of the particle is updated to new position according to its modified velocity. The best evaluation function (fitness) is evaluated for the entire run and is stored in $gbest$. The velocity of i^{th} particle is represented as $V_i = (V_{i1}, V_{i2}, ...V_{ij})$. Hence the modified velocity of each particle can be calculated using the information.

a) The current velocity
b) The distance between the current position and $pbest$.
c) The distance between the current position and $gbest$.

$$V_{ij}(it+1) = w * V_{ij}(it) + C_1 * rand_1 * (pbest_{ij} - x_{ij}(it)) + C_2 * rand_2 * (gbest_i - x_{ij}(it)) \quad (13)$$

where

$x_{ij}(it)$ = current position of the i^{th} particle in j^{th} dimension at iteration it.

$V_{ij}(it)$ = velocity of the i^{th} particle in j^{th} dimension at iteration it.

The i^{th} particle position can be represented as $x_i = (x_{i1}, x_{i2}, x_{i3}, ..., x_{iN})$ in the N-dimensional space. The best previous position of the i^{th} particle is stored and represented as $x_{besti} = (x_{best,i1}, x_{best,i2}, ..., x_{best,ij})$. The updated position of each particle is expressed as

$$x_{ij}(it+1) = x_{ij}(it) + V_{ij}(it+1) \quad (14)$$

The new positions are calculated repeatedly till a pre-specified maximum number of iterations are reached.

Differential Evolution is one of the excellent evolutionary algorithms for global optimization developed by Price and Storn in 1995 [27]. It is a simple population based, stochastic parallel search evolutionary algorithm developed for nonlinear and non-differentiable continuous space functions in order to attain global optimization. DE is a robust statistical method for cost function minimization, which does not make use of a single parameter vector but instead uses a population of equally important vectors. To generate a new generation the evolutionary operator's mutation, recombination, and selection are applied to every population member. In each generation to change each population member X_i, a donor vector v_i is created. Three parameter vectors *r*1, *r*2, and *r*3 are chosen in a random fashion from the current population. A scalar number sf scales the difference of any two of the three vectors and the scaled difference is added to the third one. Donor vector for j^{th} component of k^{th} population at G generation is expressed as

$$v_{i,j}(G+1) = X_{r1,j}(G) + sf * (X_{r2,j}(G) - X_{r3,j}(G)) \quad (15)$$
where $j = 1,2,...,D$

The mutation factor sf is a control parameter which scales the difference of any two of the three vectors and the scaled difference is added to the third one. This step is known as differential variation and the result is known as the mutant vector. DE is sensitive to the choice of mutation factor and to avoid search stagnation it is usually taken in the range 0.1 to 1. In recombination a trial vector is generated by replacing certain parameters of the target with the corresponding parameters of a randomly selected donor vector. The crossover constant CR is taken in the range [0, 1].

$$u_{i,j}(G+1) = v_{i,j}(G+1) \ \ if \ \ rand(0,1) < CR$$
$$u_{i,j}(G+1) = X_{i,j}(G) \quad otherwise \quad (16)$$

The evaluated fitness value of population vector and the

trial vector are compared and the best is selected as in equation (16). Hence the fitness of each trial vector $u_{ij}(G+1)$ is compared with that of its parent target vector $X_{ij}(G)$ and the maximum fitness or minimum cost one is allowed to proceed to the next generation.

Bacterial foraging algorithm was proposed by Passino in 2002 [28], the BFO approach was based upon the fact of survival of bacteria especially Escherichia coli, in the natural changing environment. The process depends upon their fitness criteria which depend upon their food searching and motile behavior. The law of evolution supports the bacteria with good foraging strategies and eliminates or reshapes those with poor strategies. The genes of bacteria with good foraging strategies are propagated in evaluation chain since they posses ability to reproduce even better bacteria in future generations. The foraging strategy of Escherichia coli bacteria is explained by three steps chemo-tactic, reproduction and elimination–dispersal with the help of which global searching capability of this algorithm is executed. Chemo-tactic process of bacterial foraging describes the movement of an E.coli cell through swimming and tumbling via flagella. It can move in two different ways, it can swim for a definite period of time or it can tumble and it alternates between these two modes of operation for the entire lifetime. For example if θ_k denotes the k^{th} bacterium and CS_k is the size of the step taken in the random direction specified by the tumble.

$$\theta_k = \theta_k + CS_k * Delta_k$$

$$Delta_k = \frac{\Delta_k}{\sqrt{\Delta_k^T \cdot \Delta_k}} \tag{17}$$

where Δ is a unit length vector in the random direction

In this article we come up with a hybrid optimization technique, which synergistically couples the BFOA with the PSO and DE. The proposed algorithm performs local search through the chemo-tactic movement operation of BFOA whereas the global search over the entire search space is accomplished by a PSO-DE operator. In this way it balances between exploration and exploitation enjoying best of both the worlds.

V. Bacterial Foraging PSO-DE Algorithm for DED Problem

The steps for implementation of the Bacterial Foraging and PSO-DE optimization are given below.

Step1: Initializing parameters

1a) Randomly initialize positions $P(t,j,k,l,m)$ and velocities $V(t,j,k)$ in t^{th} hour for j^{th} unit, k^{th} bacterial population, l^{th} reproduction $(l=1)$ and m^{th} elimination-dispersal $(m=1)$.

1b) Define each particle best as $pbest$ and the best position of all particles as $gbest$.

Step2: Starting of the elimination-dispersal loop $(m=m+1)$.

Step3: Starting of the reproduction loop $(l=l+1)$.

Step4: Starting of the chemo-tactic loop $(iter=iter+1)$.

Step5: For each bacteria $(k=k+1)$.

Step6: Compute fitness function $JF(k,l,m)$ and cost function $J(k,l,m)$, let

$$JFlast = JF(k,l,m) \tag{18}$$

$$JF = \frac{1}{J + penality\ function} \tag{19}$$

$$penality\ function(k) = \begin{cases} k_c \left| (P_k - P_{k,\lim}) \right| & if\ violated \\ 0 & otherwise \end{cases} \tag{20}$$

where k_c is a constant value and $P_{k,\lim}$ is the specified boundary limits

Step7: Move to new position

7a) Compute $CS(k) = rand * k_d$ (21)

7b) $P(t,j,k,l,m) = P(t,j,k,l,m) + CS(k) * Delta(t,j,k)$ (22)

$where\ Delta(t,j,k) = V(t,j,k)$ for k=1, 2, 3……, N_b

7c) Handle constraints

- generation limit
- ramp rate limit
- prohibited operating zones
- system spinning reserve

7d) Compute fit and cost- JF and J

Step8: swimming

8a) $swim-count = 0$

8b) while ($swim-count < N_s$) and $JF(k,l,m) > JFlast$

I. $swim-count = swim-count+1$

II. $JFlast = JF(k,l,m)$

III. $P(t,j,k,l,m) = P(t,j,k,l,m) + CS(k) * Delta(t,j,k)$

IV. Handle constraints

- generation limit
- ramp rate limit
- prohibited operating zones
- system spinning reserve

V. Compute JF and J

Step9: Differential Evolution

9a) $while(rand < CR)$

$$P_{def}(t,j,k,l,m) = P(t,j,k,l,m) + sf * (P(t,j,r_2,l,m) - P(t,j,r_3,l,m) \tag{23}$$

9b) Handle constraints

- generation limit
- ramp rate limit
- prohibited operating zones
- system spinning reserve

9c) Compute cost and fit- J_{def}, JF_{def}

Step10:

$if\,(JF_{def} > JF)\quad then$

$JF = JF_{def}, P = P_{def}, J = J_{def}$

Step11: Update best location $pbest$ and $gbest$ for JF, J and P.

Step12: 12a) Compute new velocity

$$V(t,j,k) = w * V(t,j,k) + C_1 * rand * (pbest(t,j,k) - P(t,j,k,l,m)) + C_2 * rand * (gbest(t,j) - P(t,j,k,l,m)) \quad (24)$$

12b) $Delta = V$

Step13: If $k < S$ then go to step5

Step14: If $iter < N_c$ then go to step4

Step15: Reproduction operations

15a) $JFhealth$ is the measure of particles with good fitness (good fitness means higher fitness and lower cost)

$$JFhealth(k) = pbestJF(k,l,m) \quad (25)$$

where $pbestJF$ is the population of best fitness of the current generation

15b) Sort bacteria in the order of ascending fit. The weaker $N_{br} = N_b / 2$ bacteria die and the rest N_{br} best bacteria each split into two bacteria which are placed at the same location.

15b) If $l < N_{re}$ then go to step3 to start the next generation in the chemo-tactic loop else go to step16.

Step16: Elimination-dispersal operation

16a) For k=1, 2, 3……, N_b a random number is generated and if it is less than or equal to P_{ed} than that bacterium is dispersed to a new random location else it remains at its original location.

16b) If $m < N_{ed}$ then go to step2 otherwise stop.

In the original bacterial foraging algorithm CS_k indicate a basic chemo-tactic step size (chemo-tactic step size is the lengths of steps taken during runs). This value should be greater than zero. It is taken in the tumble and swimming operations so that it moves in a direction specified by them and helps in reduction of cost. The normal choice for this step size is 0.1. The chemo-tactic step size in this paper is proposed to vary in the range (approximately 0.1 to 4.5) by using the relation

$$CS(k) = rand(0,1) * k_d \quad (26)$$

Usually the k_d value is a number between 1 and 5; rand (0, 1) is a uniformly distributed random number within the range [0, 1]. For every chemo-tactic step in the tumble and swimming operation the step size value taken in this paper lead to fine reduction in cost.

VI. Results and Discussions

The feasibility of the method BPSO-DE is demonstrated on a test system (ten-unit) for scheduled time duration one day divided into 24 intervals. The spinning reserve is required to be greater than or equal to 5% of the load demand at every dispatch interval. The proposed method satisfies the constraint load demand in each interval, prohibited operating zones, system spinning reserve and also dynamic constraint ramp-rate constraint. An experimentation is done for different values of control parameters such as C_1, C_2, CR, sf and k_d. It is observed that for C_1=0.1, C_2=0.1, CR=0.8 and sf =0.1 and k_d =5 the convergence leads to better cost.

Example: ten-unit system

Ten-unit system data such as cost coefficients, generation limits, ramp-rate limits, spinning reserve maximum limit for each unit and load demand in each interval is taken from [25]. The parameters chosen for this system are $N_c = 500$, N_{ed} =2, N_{re} =2, N_s =4, N_b =120 and P_{ed} =0.2. The convergence characteristic are plotted for number of evaluation (number of evaluation= $N_c * N_{ed} * N_{re}$) and total generation cost is as in Figure 1, Figure 2 represents the cost for each hour and Figure 3 compares the spinning reserve per hour with 5% load demand.

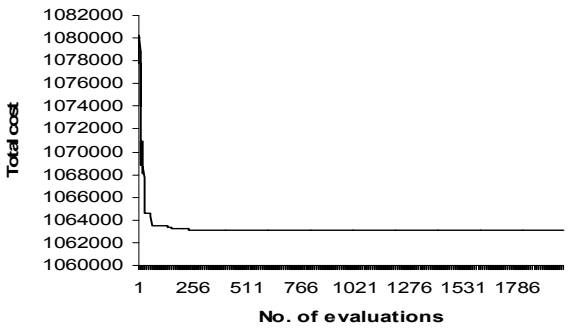

Fig. 1. Cost convergence characteristics for ten-unit system

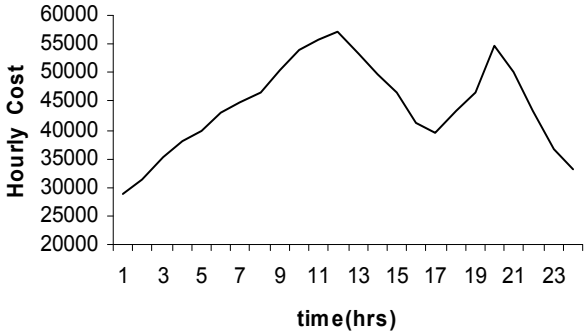

Fig. 2. Hourly cost curve for ten-unit system

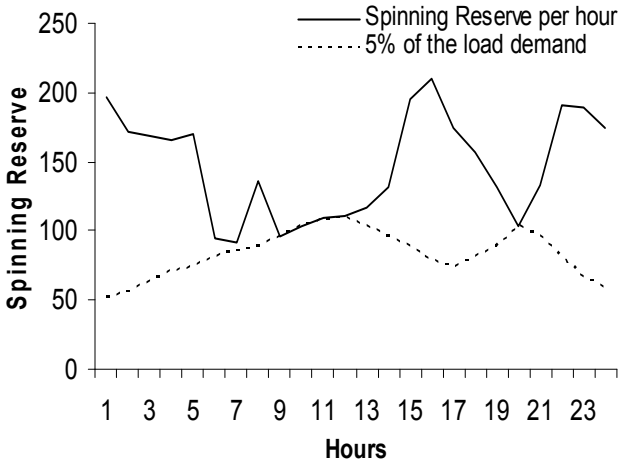

Fig. 3. Comparison of spinning reserve with 5% of the load demand for each hour

From simulation it is observed that the proposed method reduces the total generation cost when compared with other heuristic methods like HDE and VSHDE as shown on Table I. The optimum scheduling of generating units for 24 hours using the proposed method is tabulated in Table II. Computation time of the proposed method per a chemo-tactic step is 7.065seconds.

TABLE I
COMPARISON OF RESULTS FOR TEN-UNIT SYSTEM

Method	HDE [25]	VSHDE [25]	BPSO-DE
Fuel Cost ($)	1343243.2	1100666.4	1063048

VII. CONCLUSION

In this article a new heuristic technique is developed by integrating BFOA, PSO and DE techniques for solving DED problem. PSO-DE operators work effectively when combined with BFOA and leads to reach global solutions. The efficiency of the proposed BPSO-DE method for solving non-convex DED problem considering prohibited operating zones, valve-point loading effect and spinning reserve is observed from its solutions and compared with the results obtained from heuristic methods like HDE and VSHDE. The comparative study reveals the superiority and feasibility of BPSO-DE technique to solve the DED problem. Due to its superiority in reaching good quality solution this method in future work can be extended to solve for security constraints.

VIII. REFERENCES

[1] G.P.Granelli, P.Marannino, M.Montagna, and A.Silvestri, "Fast and efficient gradient projection algorithm for dynamic generation dispatching," *Proc. Inst. Elect. Eng., Gener. Transm. Distrib.,vol.136, no. 5,* pp.295-302, Sep. 1989.

[2] F.Li, R.Morgan, and D.Williams, "Hybrid genetic approaches to ramping rate constrained dynamic economic dispatch," *Elect. Power Syst. Res., vol. 43, no. 2,* pp. 97-103, Nov. 1997.

[3] X.S.Han, H.B.Gooi, and Daniel S.Kirschen, "Dynamic economic dispatch: feasible and optimal solutions," *IEEE Trans. Power Syst., vol. 16, no.1,* pp. 22-28, Feb. 2001.

[4] T.Aruldoss Albert Victoire, and A.Ebenezer Jeyakumar, "Deterministically guided PSO for dynamic dispatch considering valve-point effect," *Elect. Power Syst. Res., vol. 73, no.3,* pp.313-322, 2005

[5] D.C.Walters and G.B.Sheble, "Genetic algorithm solution of economic dispatch with valve point loadings," *IEEE Trans. Power Syst., vol. 8, no.3,* pp.1325-1331, Aug. 1993.

[6] T.Jayabharathi, K.Jayaprakash,N.Jeyakumar, and T.Raghunathan,"Evolutionary programming techniques for different kinds of economic dispatch problems," *Elect. Power Syst. Res., vol. 73, no. 2,* pp.169-176, Feb. 2005.

[7] Zwe-Lee Gaing, "Particle swarm optimization to solving the economic dispatch considering the generator constraints," *IEEE Trans. Power Syst., vol. 18, no.3*, pp. 1187-1195, Aug. 2003.

[8] B.K.Panigrahi, V.Ravikumar Pandi, Sanjoy Das, "Adaptive Particle Swarm Optimization approach for static and dynamic economic load dispatch", *Energy Conversion and Management 49(2008)*, pp. 1407-1415.

[9] Pichet Sriyanyong, "A Hybrid Particle Swarm Optimization Solution to Ramping Rate Constrained Dynamic Economic Dispatch", *World Academy of Science, Engineering and Technology 47, 2008*.

[10] Nima Amjady and Hadi Nasiri-Rad, " Non convex economic dispatch with AC constraints by a new real coded genetic algorithm", *IEEE Trans. Power Syst., vol. 24 no. 3,* pp. 1489-1502, Aug. 2009.

[11] Jong-Bae Park, Yun-Won Jeong, Joong-Rin Shin and Kwang Y. Lee, "An improved Particle Swarm Optimization for non convex economic dispatch problems", *IEEE Trans. Power Syst., vol. 25, no. 1,* pp. 156-166, Feb. 2010.

[12] K.S.Hindi and M.R.Ab Ghani, "Dynamic economic dispatch for large scale power systems: a Lagrangian relaxation approach," *Elect. Power Syst. Res., vol. 13, no. 1*, pp. 51-56, 1991.

[13] D.C.Walters and G.B.Sheble, "Genetic algorithm solution of economic dispatch with valve-point loadings," *IEEE Trans. Power Syst., vol. 8, no.3,* pp.1325-1331, Aug. 1993.

[14] H.T.Yang, P.C.Yang, and C.L.Huang, "Evolutionary programming based economic dispatch for units with non-smooth incremental fuel cost function," *IEEE Trans. Power Syst., vol. 11, no.1,* pp.112-118, Feb. 1996.

[15] N.Sinha, R.Chakrabarti, and P.K.Chattopadhyay, "Evolutionary programming techniques for economic load dispatch," *IEEE Trans. Evol. Comput., vol. 7,* no.1, pp. 83-94, Feb. 2003.

[16] K. Shanti Swarup, Anand Natarajan, "Constrained Optimization using Evolutionary Programming for Dynamic Economic Dispatch", *Proceedings of ICISIP 2005*.

[17] K.P.Wong and Y.W.Wong, "Genetic and genetic/simulated-annealing approaches to economic dispatch," *Proc. Inst. Elect. Eng., Gener. Transm. Distrib., vol. 141, no. 5*, pp.507-513, Sept. 1994.

[18] C.K.Panigrahi, P.K.Chattopadhyay, R.N.Chakrabarti, and M.Basu, "Simulated annealing technique for dynamic economic dispatch," *Electric power components and systems, vol. 34, no.5,* pp.577-586, May 2006.

[19] R.Balamurugan, S.Subramanian, "An Improved Differential Evolution Based Dynamic Economic Dispatch with Nonsmooth Fuel Cost Function", *Journal of Electrical Systems 3-3(2007)*:151-16

[20] Hao, Z. F, Guo, G. H., Huang, H., "A Particle Swarm Optimization Algorithm with Differential Evolution", *in IEEE Int.Conf. Systems, man and Cybernetics, Aug. 2007, Vol. 2,* pp. 1031-1035.

[21] D.Attaviriyanupap, H.Kita, E.Tanaka, and J.Hasegawa, "A hybrid EP and SQP for dynamic economic dispatch with nonsmooth incremental fuel cost function," *IEEE Trans. Power Syst., vol. 17, no.2,* pp.411-416, May 2002. .

[22] T.Aruldoss Albert Victoire, and A.Ebenezer Jeyakumar, "Reserve constrained dynamic dispatch of units with valve-point effects," *IEEE Trans. Power Syst., vol. 20, no.3,* pp.1273-1282, Aug. 2005.

[23] S. Titus and A. Ebenezer Jeyakumar, "A Hybrid EP-PSO-SQP Algorithm for Dynamic Dispatch Considering Prohibited Operating Zones", *Electical Power Components and Systems, vol. 36, no. 5,* pp. 449-467, May 2008.

[24] W. G. Wood, "Spinning reserve constrained static and dynamic economic dispatch", *IEEE Transactions on Power Apparatus and Systems, Vol. PAS-101, No. 2* February 1982.

[25] J.P.Choiu, "A variable scaling hybrid differential evolution for solving large-scale power dispatch problems", *IET Generation, Transmission & Distribution, Vol. 3, Iss. 2,* pp. 154–163, 2009

[26] Kennedy.J, Eberhart.R, "Particle swarm optimization", *In Proceedings of IEEE International Conference on Neural Networks,* (1995) 1942-1948.
[27] R.Storn,and K.Price, "Differential evolution – A simple and efficient heuristic for global optimization over continuous space," *J. Global Optimization, 11,* pp.341-359, 1997.
[28] Passino.K.M, "Biomimicry of Bacterial Foraging for Distributed Optimization and Control", *IEEE Control Systems Magazine, 52-67*, (2002).
[29] Praveena, P, Vaisakh, K, S R M Rao, "A Bacterial Foraging and PSO-DE Algorithm for Solving Dynamic Economic Dispatch Problem with Valve-Point Effects," Integrated Intelligent Computing (ICIIC), 2010 First International Conference on , vol., no., pp.227-232, 5-7 Aug. 2010.
[30] G. Acampora, M. Gaeta, and V. Loia, "Exploring e-learning knowledge through ontological memetic agents," IEEE Comput. Intell. Mag., vol. 5, no. 2, pp. 66-77, 2010.
[31] Ling-Ning Xing, Ying-Wu Chen, Ke-Wei Yang, Feng Hou, Xue-Shi Shen, Huai- Ping Cai, "A hybrid approach combining an improved genetic algorithm and optimization strategies for the asymmetric traveling salesman problem", Engineering Applications of Artificial Intelligence, Volume 21, Issue 8, Pages 1370-1380, December 2008.
[32] G. Acampora, M. Gaeta, and V. Loia, "Hierarchical optimization of personalized experiences for e-learning systems through evolutionary models," Neural Comput. Applicat.,2009.
[33] Huizhi Yang, Jianguo Shi, "A Hybrid Approach Based on Immune Genetic Algorithm and Integer Linear Programming for the Container Loading Problem," Education Technology and Computer Science, International Workshop on, pp. 323-326, 2010 Second International Workshop on Education Technology and Computer Science, 2010.
[34] Haiyan Zhao, Zhili Pei, Jingqing Jiang, Renchu Guan, Chaoyong Wang and Xiaohu Shi, "A Hybrid Swarm Intelligent Method Based on Genetic Algorithm and Artificial Bee Colony ," Lecture Notes in Computer Science, 2010, Volume 6145/2010, pp. 558-565, DOI: 10.1007/978-3-642-13495-1_68.
[35] Xiaohui Yuan, Liang Wang, Yongchuan Zhang, Yanbin Yuan, "A hybrid differential evolution method for dynamic economic dispatch with valve-point effects", Expert Systems with Applications, Volume 36, Issue 2, Part 2, Pages 4042-4048, March 2009.
[36] T.S. Chung, T.W. Lau, "Hybrid PSO and DE approach for dynamic economic dispatch with non-smooth cost functions", International Journal of Modelling, Identification and Control 2009 - Vol. 8, No.4 pp. 317 - 326.

TABLE II
BEST SCHEDULING OF TEN-UNIT SYSTEM (BPSO-DE)

Unit	1	2	3	4	5	6	7	8	9	10	Loss
Hour	(MW)	(MW)	(MW)	(MW)	(MW)	(MW)	(MW)	(MW)	(MW)	(MW)	(MW)
1	303.3107	135.0954	76.1023	120.4930	73.0667	121.9583	93.1576	47.0012	20.0088	55.0000	9.1940
2	303.1047	135.0172	144.0161	118.1940	122.2406	112.6885	63.4516	47.0031	20.0454	55.0000	10.7612
3	303.2802	184.8563	185.0678	159.1366	122.8930	121.9701	43.0133	47.0035	49.8917	55.0000	14.1126
4	326.5068	225.1377	256.8599	181.0907	172.7197	121.9962	20.0175	47.0058	20.0190	55.0000	20.3533
5	303.1970	305.0000	282.5101	180.7022	138.0052	121.6518	20.0278	47.0021	49.9778	55.0000	23.0741
6	379.8711	305.0000	315.5119	223.7387	173.8315	114.4116	20.0192	47.0063	22.7838	55.0000	29.1740
7	456.7183	305.0000	339.8606	244.7551	124.4338	121.9990	20.0141	47.0026	20.0104	55.0000	32.7938
8	453.9357	385.0000	273.5526	231.5744	172.2982	121.6684	20.0609	47.0016	49.3123	55.0000	33.4041
9	420.8934	400.2324	322.5569	241.3323	221.1822	122.0000	49.9804	76.9809	52.0260	55.0000	38.1845
10	428.5658	459.9303	339.9960	242.4761	223.2954	159.9182	69.4463	85.2107	52.0261	55.0000	43.8649
11	456.7193	459.9644	307.7184	257.7640	241.5928	159.9996	93.0807	85.3439	73.5565	55.0000	44.7396
12	423.2593	450.9271	340.0000	295.7597	242.9963	159.9999	93.1312	85.2921	79.6214	55.0000	46.9870
13	443.5317	384.5473	298.1866	299.9900	242.9553	159.4991	93.0246	85.2413	51.6094	55.0000	41.5853
14	428.0703	304.9407	297.3060	299.8588	222.5140	122.0000	93.0787	85.2300	52.0471	55.0000	36.0456
15	379.8416	304.6283	297.2481	250.0262	222.9617	121.9576	82.0084	71.5163	22.5337	55.0000	31.7219
16	379.9198	225.2108	257.4714	241.0372	174.2891	121.9534	56.5162	47.0023	20.0123	55.0000	24.4125
17	379.6118	303.6819	197.7146	198.3923	126.2865	121.8149	52.2891	47.0037	20.0073	55.0000	21.8022
18	379.7567	381.9008	261.5448	237.4783	131.8385	120.6646	22.2964	47.0024	20.0075	55.0000	29.4899
19	380.2061	396.7896	286.3196	234.7688	176.9342	121.9344	50.5152	57.3339	49.0884	55.0000	32.8901
20	420.7247	459.9857	339.9737	248.6047	223.7195	159.1565	55.8475	77.7104	75.0658	55.0000	43.7885
21	379.8003	380.0543	285.7954	297.2375	222.3685	156.7065	84.6191	47.7181	52.0418	55.0000	37.3417
22	379.0003	304.2104	231.2800	247.4262	192.0941	121.9266	54.7050	47.0063	22.1893	55.0000	26.8381
23	316.3778	225.3004	188.8902	203.6083	146.5196	121.9951	24.7158	47.0330	20.0304	55.0000	17.4708
24	303.1660	146.7164	172.0509	157.8998	122.8888	121.9967	20.0078	47.0042	49.9400	55.0000	12.6706

2011 IEEE International Conference on Fuzzy Systems
June 27-30, 2011, Taipei, Taiwan

A Noisy Data Regression Model Based on General Regression Neural Networks

Shih-Chun Shao Wen-Hui Chen
Graduate Institute of Automation Technology
National Taipei University of Technology
Taipei, Taiwan
t8618007@ntut.edu.tw whchen@ntut.edu.tw

Jun-Horng Chen
Department of Communication Engineering
Oriental Institute of Technology
New Taipei, Taiwan
jhchen@mail.oit.edu.tw

***Abstract*—Analysis of noisy data gathered from measurement devices is challenging in the power grid. In this study, an effective noisy data regression approach based on general regression neural networks (GRNN) is employed to deal with the problem for remote terminal units (RTU) in power SCADA systems. Experimental results show the proposed model is able to handle noisy data for practical applications, and has good performance in removing the unintended changes to the original data.**

Keywords- general regression neural networks; genetic algorithms; remote terminal units; power SCADA systems

I. INTRODUCTION

Supervisory control and data acquisition (SCADA) systems are indispensable in the operation of modern power systems. A SCADA system is a centralized control and monitoring system that typically consists of a master station, communication networks, and remote terminal units (RTUs). In power SCADA systems, all the field data are collected by RTUs, and transmit to the host computer in the control center based on some protocol through communication networks. Data acquisition at the RTU includes meter readings and equipment status reports. In the data transmission process, there will be a chance that parts of the collected data are corrupted due to noise interference. Past research indicated the processing of the noisy data at RTU is necessary in SCADA systems [1]-[2].

In the data transmission process, there are different data processing stages between field sites and the control center, including raw data acquisition, transformation, conversion, and transmission in various devices. Spikes or power surges can cause data corruption in the data transmission process, which makes the acquired data become unreliable. For data integrity, it is essential to process the raw data in the substation level before transmitting them to the host computer in the control center. How to handle the corrupted data for improving information accuracy becomes essential as it can have an impact on the system operation and can influence dispatchers during the decision-making process.

To take the data corruption issue into consideration, the converted data in the RTU needs to be processed using data processing techniques before converting back to practical engineering values in the host computer. For improving the data accuracy, in [2], the authors applied fuzzy logic theory to deal with the problem of data uncertainty. In the application of fuzzy logic theory, the selection of membership functions is a key issue, and is time-consuming by try-and-error process. As inappropriate membership functions can cause bad results. The authors in [3] applied genetic algorithms to adjust the required parameters of the membership function to improve the estimation results. However, it is not easy to obtain the optimal membership function using few sample data.

In this study, a computational approach based on general regression neural networks (GRNN) was proposed to construct a systematic fitting model for RTU noisy data processing. The proposed approach is employed to examine the analogue data collected by RTUs as a data preprocessing step to reduce errors existing in the conversion process before running the required data analysis.

The rest of the paper is organized as follows. Section II introduces the proposed GRNN model for dealing with the noisy data. Section III provides an example to verify the effectiveness of the proposed GRNN model. Conclusions are finally drawn in section IV.

II. METHODOLOGY

A. GRNN Architecture

The GRNN is a powerful regression tool proposed in [4] as an alternative neural network based learning paradigm. The network training speed of GRNN is extremely fast as it adopts a one-pass learning algorithm with a highly parallel structure. In addition, the parameter that needs to be determined in GRNN is much fewer than the widely used back-propagation neural networks (BPNN). Due to the simplicity of network structure and ease of implementation, GRNN has been applied to a variety of applications including noisy data removal [5], function approximation [6], active vibration control [7], and fault diagnosis [8].

In GRNN, each training sample is operated as a kernel during the training process. The regression surface is established by using Parzen window estimator. The estimation of GRNN is based on non-parametric regression analysis to make the best fit of the observed data. As such, GRNN does not require prior knowledge of the regression function. These

978-1-4244-7316-8/11/$26.00 ©2011 IEEE

features are useful for obtaining a better estimation of noisy data in the problem of RTU data processing.

Assume that the underlying scalar function to be approximated is denoted as $y=f(\boldsymbol{x})$ where $\boldsymbol{x}\in R^{m}$ is an independent variable and $y\in R^{1}$ is a dependent variable. Regression in the GRNN is carried out by calculating the expected conditional mean of y given $\boldsymbol{x}$ as shown in (1). The Parzen probability density estimator $g(\boldsymbol{x},y)$ with Gaussian function defined in (2) is based on sample values $\boldsymbol{x}_i$ and y_i of the random variable $\boldsymbol{x}$ and y, where n is the number of training samples and m is the dimension of $\boldsymbol{x}$.

$$E[y \mid \boldsymbol{x}] = \frac{\int_{-\infty}^{\infty} y g(\boldsymbol{x}, y)dy}{\int_{-\infty}^{\infty} g(\boldsymbol{x}, y)dy} \tag{1}$$

$$\begin{aligned} g(\boldsymbol{x}, y) = & \frac{1}{(2\pi)^{(m+1)/2}\sigma^{(m+1)}} \\ & \cdot \frac{1}{n}\sum_{i=1}^{n} \exp[-\frac{(\boldsymbol{x}-\boldsymbol{x}_i)^T(\boldsymbol{x}-\boldsymbol{x}_i)}{2\sigma^2}] \\ & \cdot \exp[-\frac{(y-y_i)^2}{2\sigma^2}] \end{aligned} \tag{2}$$

The probability estimator $g(\boldsymbol{x},y)$ assigns the sample probability of width σ for each sample $\boldsymbol{x}_i$ and y_i, and the probability estimate is the sum of those sample probabilities. The non-negative constant σ called smoothing parameter or spread constant is the only parameter that needs to be determined in the GRNN-based approach, and is related to how much the neural network will generalize. Therefore, the performance of the GRNN is affected by the adjustment of spread constants.

When the spread constant is made large, the estimation is forced to be smooth but it does not represent the training samples very precisely. On the other hand, a small value of spread constant allows the estimation that represents the training samples very well but it has many wiggles in the fitting curve. Therefore, a tradeoff between smoothness and minimal error has to be made between precision and smoothness.

Substituting the joint probability estimator in (2) into the conditional mean in (1) yields the desired estimated value as follows,

$$\hat{y}(\boldsymbol{x}) = \frac{\sum_{i=1}^{n} y_i \exp(-\frac{D_i^2}{2\sigma^2})}{\sum_{i=1}^{n} \exp(-\frac{D_i^2}{2\sigma^2})} \tag{3}$$

where D_i is defined as

$$D_i^2 = (\boldsymbol{x}-\boldsymbol{x}_i)^T(\boldsymbol{x}-\boldsymbol{x}_i) \tag{4}$$

The distance, D_i, between the training sample and the point of estimation is used as a measure of how well each training sample can represent the position of estimation. With (3) it is possible to estimate values of the fitting function based on training samples.

B. Noisy Data Regression Using GRNNs

The use of GRNN to build a regression model for noisy data from RTUs is described in this subsection. A feed-forward neural network, as shown in Fig. 1, is used to estimate the regression variable y from a measurement vector $\boldsymbol{x}$.

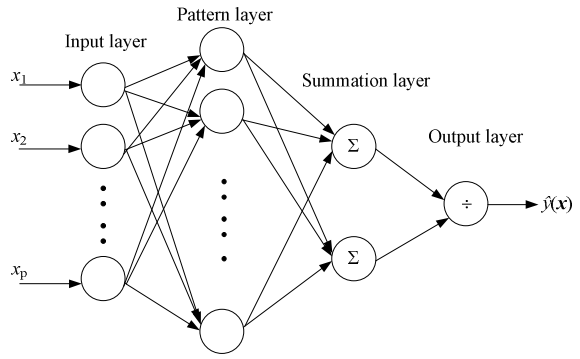

Fig. 1 Schematic diagram of the GRNN architecture.

There are four different types of layers in the structure of the GRNN model: input layer, pattern layer, summation layer, and the output layer. The input neurons in the input layer are merely distribution units, which provide all of the measurement variables to the second layer, the pattern layer. The pattern layer is a latent regression layer. Each neuron in the pattern layer is corresponding to a training sample or one cluster center. The calculations performed in each pattern neuron are the normal distribution centered at each training sample.

The summation layer performs a dot product between a weight vector and a vector composed of the signals from the pattern layer. It includes two units. One is the denominator summation unit, and the other is the numerator summation unit. The first unit adds up the weight values coming from each of the hidden neurons. The numerator summation unit adds up the weight values multiplied by the actual target value for each hidden neuron.

The output layer generates the desired estimation of y, denoted by $\hat{y}$. It divides the value accumulated in the numerator summation unit by the value in the denominator summation unit, and uses the result as the estimated value. This estimated value is an exponentially weighted average of all observed values y_i.

The training of GRNN does not need to determine the connection weights between the neurons in different layers but to adjust the spread constant to make the estimation model best fit the sample data. In other words, the generalization ability of GRNN is controlled by this spread constant. Traditionally, the value of spread constant of GRNN is usually selected by a try-and-error process. In the GRNN-GA model,

the genetic algorithm is used to optimize the spread constant of GRNN.

Genetic algorithms (GA) are population-based search algorithms based on the mechanics of natural selection and genetics. GA is able to globally exploring a solution space searching for potential solutions, and has been applied to solve many optimization problems [9]-[11].

The process of GA begins with a randomly selected population of chromosomes. Each chromosome string contains possible solution to the spread constant of GRNN. GA is used for searching an appropriate spread constant that can minimize the mean square errors between the target values and training samples. The fitness function f is defined as follows,

$$f \equiv \frac{\sum_{i=1}^{n}[y_i - \hat{y}(\boldsymbol{x}_i)]^2}{n} \tag{5}$$

where n is the number of samples.

The optimum solution can be obtained by minimizing the fitness function defined in (5). The fitness function is used to evaluate the quality of each chromosome. The lower fitness value chromosome at each searching step will be chosen to be the parent of the next generation, while the higher fitness one will be discarded. In creating the new offspring, the selected parent chromosomes will get through the reproduction process by performing GA operations, such as crossover and mutation as described in [12]. The process continues updating newer and more suitable chromosome until a predefined stopping condition is satisfied.

III. Experimental Results

The performance of the proposed GRNN model was evaluated by a set of RTU data and is described in this section. The optimal spread constant of the GRNN model is determined according to the mean square error (MSE) criterion using GA searching technique.

The program codes in this experiment are written in MATLAB language for all the simulations. The performance evaluation used in this study is the mean absolute percentage error (MAPE) in accuracy. This value is calculated by first taking the absolute deviation between the actual value y_i and the estimated value $\hat{y}_i$. Then the total ratio of deviation with its actual value is calculated. The percentage of the average of this ratio is the mean absolute percentage error. The process of calculating the MAPE is shown in (6).

$$\text{MAPE} = \frac{\sum_{i=1}^{n}(|y_i - \hat{y}_i|/y_i)}{n} \times 100\% \tag{6}$$

where n is the total number of test data.

To examine the performance of the proposed GRNN model, a comparison with an existing method was given. The test data was adopted from [3]. Suppose that a bus voltage recorded from a substation varies from 180 kV to 260 kV (nominal 220 kV with 18% variations). The voltage values are converted to the value in pulse counts, ranging from 19800 to 28600 (110 counts per kV). Table I lists the test examples and their corresponding calibrated values. In Table I, the measurands in the second column are measurements that contain errors, which are transformed to the pulse output via A/D converters in terms of counts. Actual values in the fourth column are calibrated quantities without errors.

TABLE I
Test Examples and Their Corresponding Calibrated Values

No. of samples	Measurand (kV)	Counts	Actual values (kV)
1	180	19800	180.911
2	190	20900	190.0015
3	200	22000	200.00
4	210	23100	210.0005
5	220	24200	220.00
6	230	25300	230.0005
7	240	26400	240.2563
8	250	27500	250.00
9	260	28600	259.6281

In this experiment, the parameters of GA are initialized with a population of 40 chromosomes, and the crossover probability and mutation probability are taken as 0.85 and 0.01, respectively. Fig. 2 depicts the relation between the number of iterations and the corresponding spread constants. The MSE is plotted versus the number of iterations in Fig. 3. The optimal spread constant was set at 0.6647 to leverage the smooth of fitting function and the mean square error.

The performance evaluation of the Fuzzy-GA (FGA) model proposed in [3] and the proposed GRNN model is listed in Table II. From the results, it can be seen that the performance of the proposed model outperforms that of the FGA model. These results justify the proposed approach is able to approximate the fitting function more accurate than that in [3].

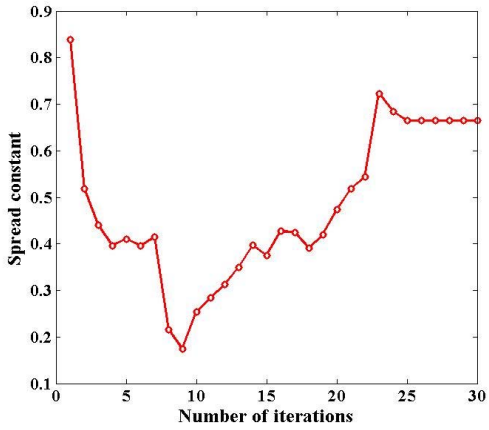

Fig. 2 The iteration-spread constant graph.

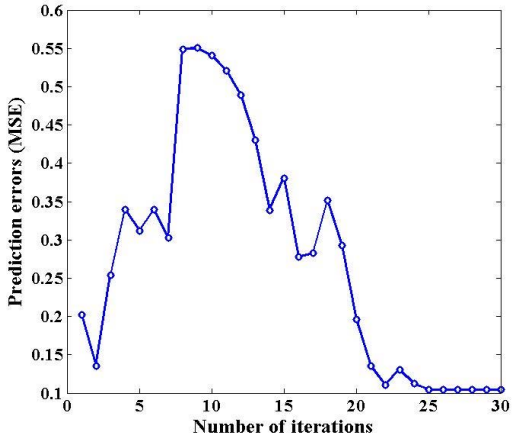

Fig. 3 The MSE-spread constant graph.

TABLE II
PERFORMANCE EVALUATION BETWEEN GRNN AND FGA MODELS

Counts	Actual value (kV)	FGA model (kV)	The proposed GRNN model (kV)
19800	180.911	181.822	182.5051
20900	190.0015	190.003	190.1614
22000	200.00	200.000	200.0015
23100	210.0005	210.001	210.0004
24200	220.00	220.000	220.0005
25300	230.0005	230.001	230.0379
26400	240.2563	240.512	240.1800
27500	250.00	250.00	249.9565
28600	259.6281	249.243	257.9410
	MAPE	0.5124	0.1868

IV. CONCLUSION

This paper has presented an efficient noisy data regression model for the RTU application using GRNN approach. The main merits of the proposed method include its simple computational framework, precision in nonlinear approximation, and fast learning speed. Although we only provide the voltage parameter for demonstration, the proposed approach can also be applied to other analogue quantities in the measurement of remote terminal units.

ACKNOWLEDGMENT

This work was partially supported by the projects sponsored by the National Science Council, Taiwan, under the Grant No. 98-2221-E-027-072 and 99-2218-E-002-005.

REFERENCES

[1] A. G. Bruce, "Reliability analysis of electric utility SCADA systems," *IEEE Trans. Power Systems*, vol. 13, no. 3, pp. 844–849, Aug. 1998.

[2] P. Kumar, V. K. Chandna, and M. S. Thomas, "Intelligent algorithm for preprocessing multiple data at RTU," *IEEE Trans. Power Systems.*, vol. 18, no. 4, pp.1566-1572, Nov. 2003.

[3] P. Kumar, V. K. Chandna, and M. S. Thomas, "Fuzzy-genetic algorithm for preprocessing data at the RTU," *IEEE trans. Power Systems*, vol. 19, no.2, pp.718-723, May 2004.

[4] D. F. Specht, "A general regression neural network," *IEEE Trans. Neural networks*, vol. 2, no. 6, pp. 568-576, Nov. 1991.

[5] W. M. Lee, C. P. Lim, K. K. Yuen, and S. M. Lo, "A hybrid neural network model for noisy data regression," *IEEE Trans. Systems, Man, and Cybernetics-Part B*, vol. 34, no. 2, pp. 951-960, April 2004.

[6] J. Y. Goulermas, P. Liatsis, X. J. Zeng, and P. Cook, "Density-driven generalized regression neural networks (DD-GRNN) for function approximation," *IEEE Trans. Neural networks*, vol. 18, no. 6, pp.1683-1696, Nov. 2007.

[7] A. Madkour, M. A. Hossain, K. P. Dahal, and H. Yu, "Intelligent learning algorithms for active vibration control," *IEEE Trans. Systems, Man, and Cybernetics-Part C*, vol. 37, no. 5, pp.1022-1033, Sept. 2007.

[8] B. G. Hyun and K. Nam, "Faults diagnoses of rotating machines by using neural nets: GRNN and BPN," in *Proc. IEEE 21st Int. IECON Conf. Industrial Electronics, Control, Instrumentation*, vol. 2, 1995, pp.1456-1461.

[9] Sangameswar Venkatraman and Gary Yen, "A genetic framework for constrained optimization using genetic algorithm," *IEEE Trans. Evolutionary Computation*, vol. 9, no.4, pp. 424-435, August 2005.

[10] Zne-Jung Lee, Shun-Feng Su, and Chou-Yuan Lee, "A genetic algorithm with domain knowledge for weapon-target assignment problems," *Journal of the Chinese Institute of Engineers*, vol. 25, no. 3, pp. 287-295, 2002.

[11] Shu-Chien Huang and Chu-Fu Wang, "Genetic algorithms for approximation of digital curves with line segments and circular arcs," *Journal of the Chinese Institute of Engineers*, Vol. 32, no. 4, pp. 437-444, 2009.

[12] D. E. Goldberg, *Genetic algorithms in search, optimization, and machine learning*, Addison-Wesley Inc., 1989.

2011 IEEE International Conference on Fuzzy Systems
June 27-30, 2011, Taipei, Taiwan

Estimation of Load Model Parameters from Instantaneous Voltage and Current

P. Regulski, F. Gonzalez-Longatt, *Senior Member, IEEE,* and V. Terzija*, Senior Member, IEEE*
School of Electrical and Electronic Engineering
University of Manchester
Manchester, UK
pawel.regulski@postgrad.manchester.ac.uk

***Abstract*— Load modeling is a very important aspect of voltage stability analysis as load characteristics governs voltage behavior. In this paper a compact solution to extract parameters of a load model is presented, which includes estimation of power components based on Improved Recursive Newton Type Algorithm and estimation of parameters of a dynamic Load Model using Genetic Algorithms. The paper demonstrates the influence of the preprocessing of the instantaneous values on the final estimation of load parameters. All tests were carried out using 9-buses P.M.Anderson system built in DIgSILENT.**

Keywords—load modeling, parameter estimation, genetic algorithm, power components

I. INTRODUCTION

Power system loads have a significant impact on system stability. It is known that load dynamic response is one of the key elements driving the system to voltage instability or even to voltage collapse [1], so it is crucial to use appropriate load models within Voltage Stability Assessment applications. Additional difficulty related to power system loads is caused by the constantly changing demand, which means that the characteristics of loads vary in time on daily, weekly, monthly and seasonal basis. It is thus essential not only to estimate load parameters once but also to update them when unacceptable difference between model output and power system response is detected. One of two possible approaches to load modelling is the Measurement-based approach [2-5] which enables updating of load parameters whenever it is necessary by taking new measurements at substation. The method consists in comparing measured post disturbance system response versus load model output and based on that, the model's parameters are adjusted. The second method, Component-based approach [6], consists in modelling different types of loads separately, thus requires specific information about contribution of particular devices (e.g. induction motors, heating devices, lighting devices) and classes of loads (e.g. industrial, commercial, residential). Generally, it is difficult to gather all these information precisely enough to create a reliable load model, hence the Measurement-based approach was adopted in this paper.

Currently, the results of estimation of load parameters presented in the literature are mostly based on the assumption of the availability of the measurements of active and reactive power as well as voltage *RMS* value. It is well known that these values are not directly available from the measurements, but they are a product of Digital Signal Processing based on a variety of existing algorithms capable of extracting signal parameters from instantaneous values of voltage and current. It has been proven that sensitivity of different methods may influence the final result, especially when the signal's frequency deviates from its nominal value [7].

In this paper the estimation of active power, reactive power and voltage *RMS* value has been obtained by using a recursive estimation method – Improved Recursive Newton Type Algorithm (IRNTA) [8]. Then the result of this signal processing has been sent to the input of the algorithm estimating the parameters of the load model, which in this case is a widely used Artificial Intelligence (AI) method called Genetic Algorithms (GA) [2], [4] and [5]. The final result will be compared against an estimation performed on the *RMS* values obtained directly from the simulation software (the estimation of *RMS* values is not applied).

The rest of the paper is organized as follows: first the load model and the signal models are described in Section II, then both estimation methods are presented in Section III, after which the simulation results are presented in Section IV, finally conclusions are given in Section V.

II. MODELS

The first part of this Section contains a description of a dynamic load model, parameters of which are being estimated in the experiment. The second part presents an instantaneous power model developed in [7] which is used to obtain active power P and reactive power Q. This part also includes a description of a traditional sine signal model, which has been used to obtain the *RMS* voltage from the instantaneous signal.

A. Exponential Recovery Load Model

Exponential Recovery Load Model (ERLM) is a general load model and it is formulated as a mathematical description of the relationship between voltage and active/reactive power (dynamic, voltage dependent load model). Equations (1)-(4) present the model for both, active and reactive power [1], [9].

$$T_P \dot{z}_P = \left(\frac{V}{V_0}\right)^{\alpha_s} - z_P \left(\frac{V}{V_0}\right)^{\alpha_t} \tag{1}$$

$$P_d = z_P P_0 \left(\frac{V}{V_0} \right)^{\alpha_t} \tag{2}$$

$$T_Q \dot{z}_Q = \left(\frac{V}{V_0} \right)^{\beta_s} - z_Q \left(\frac{V}{V_0} \right)^{\beta_t} \tag{3}$$

$$Q_d = z_Q Q_0 \left(\frac{V}{V_0} \right)^{\beta_t} \tag{4}$$

where z_P and z_Q are the state variables, T_P and T_Q are the recovery time constants, whereas V_0, P_0 and Q_0 are the pre-disturbance voltage, active and reactive power, respectively. P_d and Q_d are the load power demands, α_s and β_s are the static exponents and α_t and β_t are the transient exponents. Vectors of unknown parameters to be estimated are as follows (5-6):

$$\theta_P = [\alpha_s, \alpha_t, T_P] \tag{5}$$

$$\theta_Q = [\beta_s, \beta_t, T_Q] \tag{6}$$

Since the load model for active power is not mathematically related to the reactive power, the unknown parameters can be grouped into two vectors and the estimation process can be performed separately (or in parallel). Maintaining the Integrity of the Specifications

B. Signal Model

Extraction of the *RMS* values (*P*, *Q* and *V*) required by the load model is crucial since its quality will directly influence the final accuracy of the estimated load model. In this paper it is not assumed that the *RMS* values are readily available, instead the instantaneous signals of voltage and current are used (7-8):

$$v(t) = V_{\mathrm{m}} \cos\left(\omega t + \varphi_v\right) \tag{7}$$

$$i(t) = I_{\mathrm{m}} \cos\left(\omega t + \varphi_i\right) \tag{8}$$

where V_m and I_m are the voltage and current magnitudes, respectively, φ_v and φ_i are voltage and current phase angles, respectively and ω is the system angular frequency.

Based on [7] the instantaneous power model is described as follows (9):

$$p(t) = v(t) \cdot i(t) = V_{\mathrm{m}} I_{\mathrm{m}} \cos\left(\omega t + \varphi_v\right) \cos\left(\omega t + \varphi_i\right) \tag{9}$$

which after some mathematical manipulations yields (10):

$$p(t) = \frac{1}{2} V_m I_m \cos\varphi + \frac{1}{2} V_m I_m \cos\left(2\omega t + \varphi\right) = \\ = P + S\cos\left(2\omega t + \varphi\right) \tag{10}$$

where P is the active power, S is the apparent power and φ is the power angle (phase difference between voltage and current).

Now IRNTA can be applied to (10) and both P and S can be directly extracted from the instantaneous power signal. Q can be simply obtained by applying the following formula (11):

$$Q = \sqrt{S^2 - P^2} \tag{11}$$

The vector of unknown parameters for the instantaneous power model consists of (12):

$$\theta_{IP} = [P, S, \omega, \varphi] \tag{12}$$

By treating ω as an unknown parameter, the model becomes insensitive to system frequency deviations, which is increasing the overall quality of the estimation [7].

Similarly, V_{RMS} can be easily obtained by applying IRNTA directly to (7) to extract V_m, which is related to V_{RMS} in the following way (13):

$$V_{RMS} = \frac{V_m}{\sqrt{2}} \tag{13}$$

and the vector of unknown parameters is defined as (14):

$$\theta_V = [V_m, \omega, \varphi_v] \tag{14}$$

Here also ω is estimated together with the amplitude, which makes this signal model insensitive to possible deviations of system frequency.

The next Section presents the estimation methods (IRNTA and GA) and explains in detail how the load model and the signal models are related in this experiment.

III. Parameter Estimation Methods

There are two optimization tasks in this experiment. The first one is related to extraction of the *RMS* values of *P*, *Q* and *V* from the instantaneous signals *v(t)* and *i(t)* and the second one is the estimation of load model parameters based on the previously extracted *RMS* values. An overall picture of this process is shown in fig. 1.

Both stages of the whole procedure can be defined as a curve fitting problem where the task is to minimize the difference between the output of the model and the 'measured' value with respect to the vector of unknown parameters, which in general can be expressed by (15).

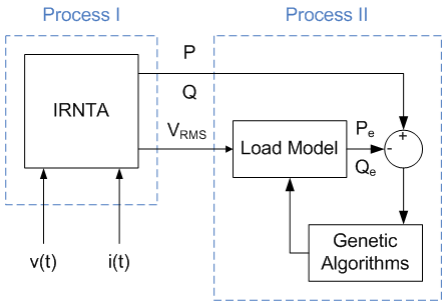

Figure 1. Block diagram of the optimization procedure

$$\min \varepsilon(\theta) = \min \frac{1}{n} \sum_{k=1}^{n} \left(y(k) - M(\theta, k) \right)^2 \tag{15}$$

where *y(k)* is the 'measurement' and $M(\theta, k)$ is the model output, θ is the vector of unknown parameters, and n is the number of samples in the data set.

In this paper IRNTA has been incorporated to extract the *RMS* values of the required signals (find optimal θ_{IP} and θ_V) and GA are used to obtain the parameters of the assumed load model (find optimal θ_P and θ_Q). Both methods are described in the following subsections.

A. *Genetic Algorithms*

GA have become popular in the estimation of load model parameters because of their ability to find a global solution. The method is based on the evolution theory and it is imitating such mechanisms as natural selection, mating of individuals in a population and mutation of genes [4]. The algorithm starts by producing an initial population of individuals, where each individual is vector of unknown parameters θ with randomly selected values. Then, so called fitness is calculated for each individual in the following way (16):

$$f = \frac{1}{\varepsilon(\theta)} \tag{16}$$

which means that fitness is simply a reciprocal of the model error formulated by (15) and this indicates the accuracy of the optimization represented by each individual in the population (the smaller the error the higher the fitness). After identifying the strongest individuals (with the highest fitness) the next generation is bred by applying one of the genetic operators called crossover. In this process the information carried by two selected individuals is exchanged to create two new individuals. The selection of individuals for the crossover is such that the individual with higher fitness have better chance to take part in the process (imitation of mating). The last stage in producing of the next generation is application of the second genetic operator – mutation. This is accomplished by introducing small random changes to randomly selected parameters contained in an individual undergoing a mutation.

The process is repeated until the maximum number of generations is reached or a satisfactory accuracy is achieved. The whole procedure is illustrated in fig. 2.

To improve the overall performance of GA the mutation level is adjusted according to achieved accuracy. At the start of the algorithm, mutations make significant changes to selected parameters contained in an individual, but when the procedure gets closer to the solution, the level of the changes is smaller. This improves the exploration of the searching space at the beginning as well as the fine tuning of the final solution.

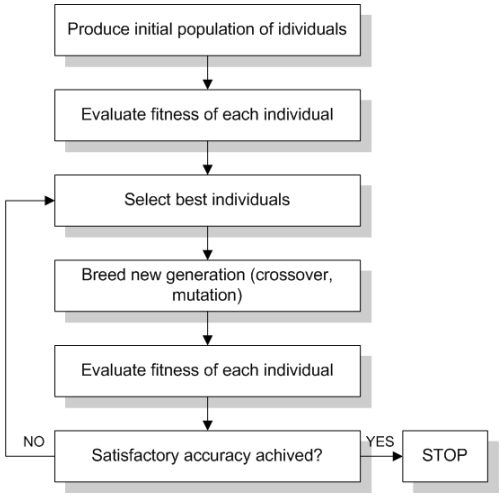

Figure 2. Block diagram of GA procedure

B. *Improved Recursive Newton Type Algorithm*

IRNTA is a recursive variation of the traditional Newton-type algorithm proposed in [8]. The method has several advantages over the classical algorithm because it can be easily applied in real-time applications and it does not require inversion of the Jacobian matrix. The method is formulated in the following way (17-18):

$$\theta_{k+1} = \theta_k + \mathbf{P}_{k+1} \mathbf{j}_{k+1} \left(y(k+1) - M\left(\theta_k, k\right) \right) \tag{17}$$

$$\mathbf{P}_{k+1} = \frac{1}{\lambda_{k+1}} \left(\mathbf{P}_k - \frac{\mathbf{P}_k \mathbf{j}_{k+1} \mathbf{j}_{k+1}^T \mathbf{P}_k}{\lambda_{k+1} + \mathbf{j}_{k+1}^T \mathbf{P}_k \mathbf{j}_{k+1}} \right) \tag{18}$$

where $\mathbf{j}_k = [j_1, j_2, \ldots, j_m]$ is the k-th row of the Jacobian matrix, λ is the forgetting factor and $\mathbf{P}$ is a matrix through which the inversion of the Jacobian matrix is carried out in a recursive way. The forgetting factor λ is a nonlinear function defined as follows (19):

$$\lambda_{k+1} = g\left(\lambda_{\min}, \lambda_{\max}, R_0, R_{k+1}\right) = \lambda_{\min} + \left(\lambda_{\max} - \lambda_{\min}\right) e^{-R_{k+1}/R_0} \tag{20}$$

where $\lambda_{\min}$, $\lambda_{1\max}$, ($\lambda_{\min} \le \lambda_{\max}$) and R_0 are the tuning parameters and R_{k+1} is the sum of absolute values of residual errors (21-22):

$$R_{k+1} = \sum_{p=k+1-L}^{k+1} |r_p| \tag{21}$$

$$r_{k+1} = y(k) - M(\theta_k) \tag{22}$$

where L is the size of the data window.

As it can be seen from (17) that at each discrete time step k the method is giving a new estimation of the unknown parameters defined in vector θ. This means that the algorithm has to start from an initial guess θ_0 provided by the user at the start of the procedure.

IV. Simulation Results

This section is divided into two parts: first the result of the estimation of the RMS values is presented, then in the second part this result is used to obtain parameters of the assumed load model. The simulation data was obtain from DIgSILENT software, where the well known 9-buses P.M.Anderson network [10] was built, and the mathematical analysis of the results were carried out in MATLAB. The simulated event was a loss of a line (causing a sudden voltage drop across the system) and the measurements (v(t) and i(t)) were taken at a bus, where a dynamic load was connected.

A. Signal Processing

Figs. 3 and 4 present the measurements of *v(t)* and *p(t)* (according to (9)), respectively. These signals were used directly to estimate P, Q and V by applying IRNTA. This result is compared against the same signals obtained directly for the simulation software (figs. 5-7).

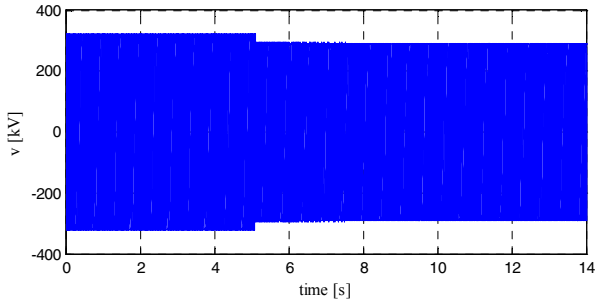

Figure 3. Instantaneous voltage

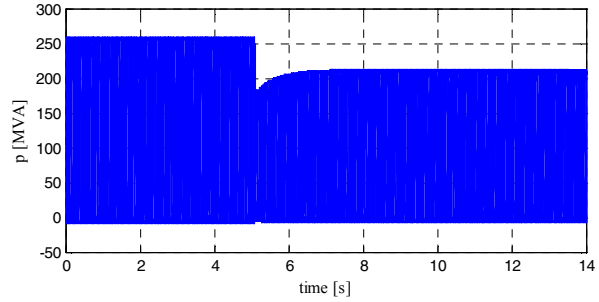

Figure 4. Instantaneous power

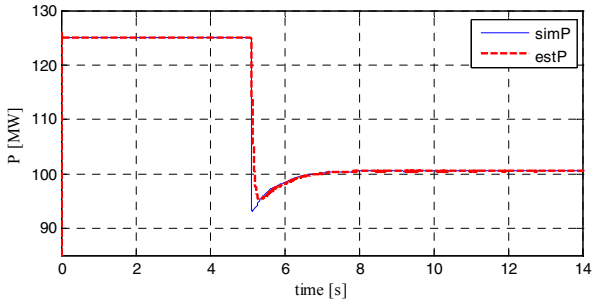

Figure 5. Simulated P versus estimated P

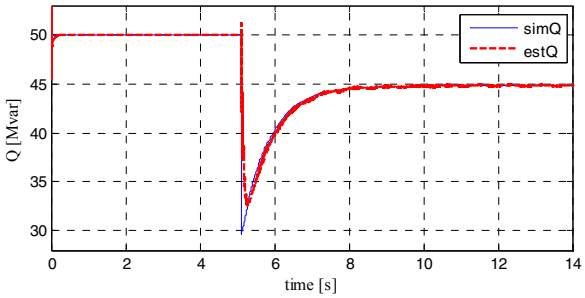

Figure 6. Simulated Q versus estimated Q

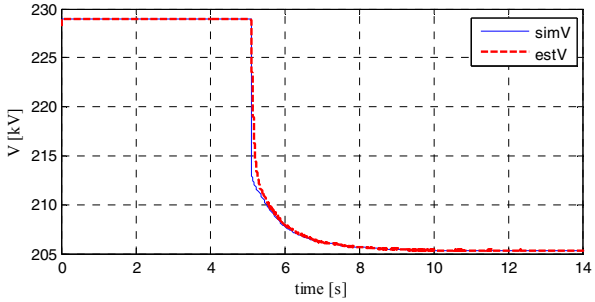

Figure 7. Simulated V versus estimated V

From figs. 5-7 it is clear IRNTA gives a very good estimation of the electrical quantities despite the frequency deviation, which occurs right after the loss of a line at t = 5s. As expected, in the steady state the method gives an error practically equal to zero and during the dynamic state the algorithm produces an error related to the convergence properties of the method, which are considerably good.

In the following subsection these results will be used to obtain parameters of the load model to investigate the influence of the dynamic error introduced during the estimation of the *RMS* values of *P*, *Q* and *V*.

B. Estimation of Load Model Parameters

In this part of the experiment the estimation has been carried out by GA. To ensure that the accuracy of the result is optimal, in each case the algorithm has been apply 10 times to obtain mean value and standard deviation of each estimated parameter.

In the first case original simulated *P*, *Q* and *V* (*simP*, *simQ* and *simV* in fig. 5, 6 and 7, respectively) has been used to

perform the estimation of unknown parameters defined in (5) and (6). The results are presented in tab. I and II and the corresponding plots are shown in fig. 8 and 9.

TABLE I. ESTIMATED PARAMETERS RELATED TO ACTIVE POWER

	α_s	α_t	T_P
mean	1.9991	4.2302	0.3426
std dev	0.0004	0.0282	0.0048

TABLE II. ESTIMATED PARAMETERS RELATED TO REACTIVE POWER

	β_s	β_t	T_Q
mean	0.9848	7.8145	0.2453
std dev	0.0019	0.0226	0.0017

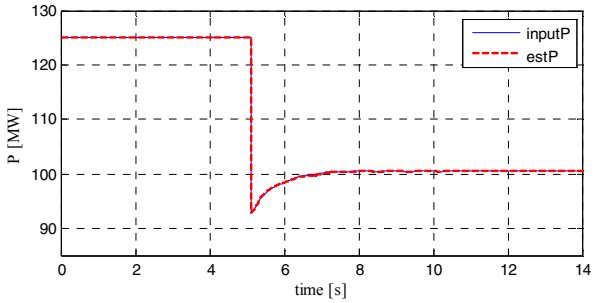

Figure 8. Load model response (active power)

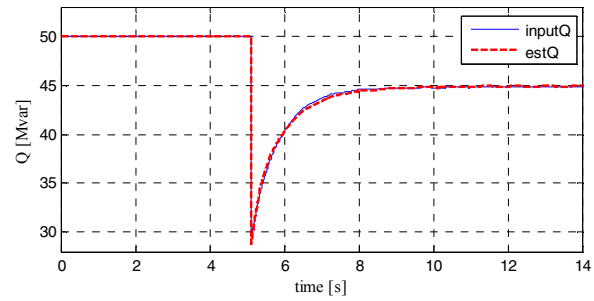

Figure 9. Load model response (reactive power)

From figs. 8 and 9 it can be noted that the quality of estimation is considerably high, which confirms that the algorithm is suitable for this task.

In the second case the parameters of the load model are obtained from the estimated *P*, *Q* and *V* (*estP*, *estQ* and *estV* in fig. 5, 6 and 7, respectively). The results are presented in tab. III and IV and in fig. 10 and 11.

TABLE III. ESTIMATED PARAMETERS RELATED TO ACTIVE POWER

	α_s	α_t	T_P
mean	1.9987	4.1774	0.3518
std dev	0.0031	0.0169	0.0041

TABLE IV. ESTIMATED PARAMETERS RELATED TO REACTIVE POWER

	β_s	β_t	T_Q
mean	0.9845	7.6615	0.2547
std dev	0.0068	0.0909	0.0051

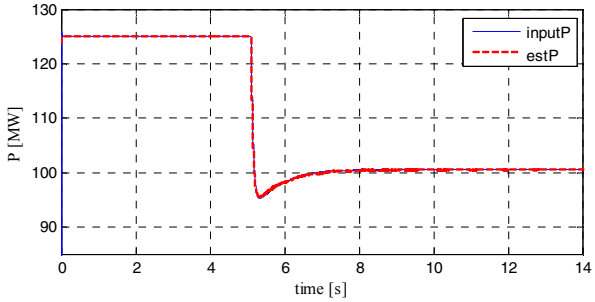

Figure 10. Load model response (active power)

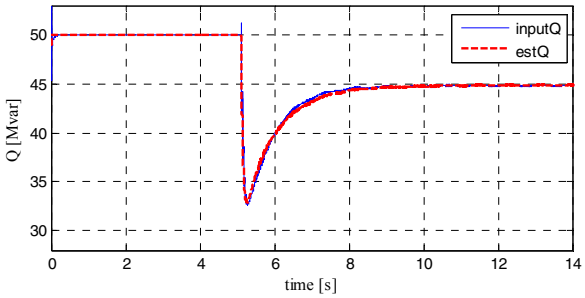

Figure 11. Load model response (reactive power)

In this case GA again confirmed its good performance in this task. By comparing the mean values of the parameters obtained in tab. I and II against the results presented in tab. III and IV, respectively, it is clear that the result is not the same in both cases. Tab. V is summarizing the differences (between mean values) expressed in percents with respect to the original results (mean values in tab. I and II).

TABLE V. DIFFERENCES BETWEEN THE ESTIMATED PARAMETERS

	α_s	α_t	T_P
diff [%]	negligible	1.2482	2.6853
	β_s	β_t	T_Q
diff [%]	negligible	1.9579	3.8320

As expected most affected are parameters governing the dynamic behavior of the model (transient exponents α_t and β_t and recovery time constants T_P and T_Q) whereas the parameters characterizing steady state behavior of the model are practically the same. This result proves that the estimation technique used to obtain the *RMS* values will introduce additional error to the final values of extracted parameters of load model. In this experiment the differences are acceptable, which means that this combination of methods can be efficient and accurate enough to be used in Measurement-based approach to load modeling.

V. CONCLUSIONS

A compact procedure for obtaining parameters of a load model based on instantaneous measurements has been proposed in this paper. The method has been tested in two stages using 9-buses P.M.Anderson test system. Firstly the quality of extracted RMS values has been presented (IRNTA), followed by the estimation of parameters of a dynamic load model performed by GA. The procedure returned considerably good results proving that the combination of both methods is suitable for this task. In the next step the algorithm should undergo extensive testing using more simulated cases and finally its performance should be tested on real data captured by recording equipment in the power system.

REFERENCES

[1] T. Van Cutsem, C. Vournas, *Voltage Stability of Electrical Power System*, Kluwer Academic Publishers, 1998

[2] Jin Ma, Dong Han, Ren-Mu He, Zhao-Yang Dong, D.J. Hill, **"**Reducing Identified Parameters of Measurement-Based Composite Load Model", *Power Systems, IEEE Transactions on*, vol. 23, no. 1, pp. 76 – 83, Feb. 2008

[3] Byoung-Kon Choi, Hsiao-Dong Chiang, Yinhong Li, Hua Li, Yung-Tien Chen, Der-Hua Huang, M.G. Lauby, "Measurement-based dynamic load models: derivation, comparison, and validation", *Power Systems, IEEE Transactions on*, vol. 21, no. 3, pp. 1276 – 1283, Aug. 2006

[4] Jin Ma, Zhao-yang Dong, Ren-mu He, D.J. Hill, **"**Measurement-based Load Modeling using Genetic Algorithms", *Evolutionary Computation, 2007. CEC 2007. IEEE Congress on,* pp. 2909 – 2916, 25-28 Sept. 2007

[5] P.Regulski, G.Valverde, W.Rebizant, V.Terzija, "Estimation of Load Model Parameters for Long-term Voltage Stability Assessment Studies", APAP Conference, 2009

[6] J.Y. Lim, P.S. Ji, A. Ozdemir, C. Singh, "Component-based load modeling including capacitor banks", *Power Engineering Society Summer Meeting, 2001. IEEE,* vol. 2, pp. 1199 – 1204, 15-19 July 2001

[7] V.Terzija et al., "Frequency and Power Components Estimation from Instantaneous Power Signal", IEEE Transaction on Instrumentation and Measurement, 2010, accepted for publication on 22/7/2010

[8] V.Terzija, "Improved Recursive Newton Type Algorithm for Frequency and Spectra Estimation in Power Systems", IEEE Trans. on Instrumentation and Measurement, Volume 52, Issue 5, October 2003, pp.1654-1659

[9] A. Borghetti, R. Caldon, C. A. Nucci, "Generic dynamic load models in long-term voltage stability studies", *International Journal of Electrical Power & Energy System*, vol. 22, no. 4, pp. 231-311, 2000

[10] P. M. Anderson and A. A. Fouad, Power System Control and Stability, Iowa State University Press, Ames, IA, 1977

2011 IEEE International Conference on Fuzzy Systems
June 27-30, 2011, Taipei, Taiwan

Apply Different Fuzzy Integrals in Unit Selection Problem of Real Time Strategy Game

Y.J. Li, Peter H. F. Ng, H. B. Wang, S. C. K. Shiu
Department of Computing
Hong Kong Polytechnic University
Hong Kong, China
(csyjli, cshfng, cshbwang, csckshiu)@comp.polyu.edu.hk

Y. Li
College of Mathematics & Computer Science
Hebei University
Baoding, China
polyuliyan@yahoo.com.cn

***Abstract*—Choquet Integral (CI), which is known as a fuzzy measure-based technique, has been a general aggregation tool for multi-criteria decision making problem. In this paper, we apply Choquet Integral to unit selection problem in Real Time Strategy (RTS) game. In addition, three new fuzzy integrals named Mean-based Fuzzy Integral (Me-based FI), Max-based Fuzzy Integral (Ma-based FI), and Order-based Fuzzy Integral (Or-based FI) are developed, which relax the monotonicity requirement of the traditional fuzzy measures and consider different properties of game play. We compare the performance of Choquet Integral and the new proposed ones on this practical application with highly non-monotonic data. Experiments show that the proposed new fuzzy integrals achieved better learning performance and testing result.**

Keywords-Real time strategy game; feature interacton; fuzzy integral; fuzzy measure; Warcraft III

I. INTRODUCTION

Sugeno [1] (1974) proposed the concepts of fuzzy measure and fuzzy integral which are working by finding the disordered means among cases. Suppose we have a dataset X, and A is a subset of it. As an extension of the probability measure, the fuzzy measure of A, expressed as $\mu(A)$, demonstrates the degree of belief or confidence of its elements. Fuzzy integrals cover a wide range of aggregation criteria and able to represent the interactions among variables. In addition, Choquet Integral is a powerful nonlinear aggregation tool. By considering non-additive set function, it has been widely used in information fusion [2] and data mining [3]. Mostly, the adopted non-additive set function is referred to as the class of fuzzy measures which are constrained by the monotonic property. Although Murofushi [4] has proved that the Choquet Integral is meaningful in the case of non-monotonic situation, there are few literatures in real application.

Real time strategy (RTS) game is a genre of computer war-games which does not process incrementally in turn. Players need to control the use of limited resource, create units and buildings, and lead their armies to attack their opponents. This kind of interactive game provides a rich environment for incremental research on human-level Artificial Intelligence (AI), especially real-time planning [6] and decision making under uncertainty [7]. The core of strategy planning is to build up the army with appropriate unit types which can gain massive destroy power against enemy's army in a short time. On the other hand, the army is taking great risk of being easily defeated by other kinds of units [16]. Thus, understand the effect of unit combination in this complicated game play design is a different problem and it already becomes one of the major challenges to game players. Furthermore, there are feature interactions existing among different unit types ranging from redundancy to synergy [17]. In this situation, the effectiveness of unit combinations cannot be simply computed by weighted average. This leads to a more difficult task of dealing with non-additive properties in game. In this paper, we try to apply fuzzy integrals in unit selection problem of RTS game.

The rest of the paper is organized as follows. In section II, we review the fuzzy measure and Choquet Integral. Section III explains our methodology of fuzzy measure learning with different integrals. Section IV compares the performance of Choquet Integral and our new developed fuzzy integrals on game problem. Finally, conclusions are drawn in Section V.

II. FUZZY MEASURE FND CHOQUET INTEGRAL

To increase the modeling ability, the original non-additive fuzzy measure is preferred. Some experiments are performed by using Sugeno-λ and K-additive fuzzy measure, but unfortunately, both of them achieved poor results with high error. One possible reason is the sense of monotonic assumption. Building a balanced army with many kinds of unit types is improper in game environment.

In this section we review the concepts of fuzzy measure and Choquet Integral. The concept of non-monotonicity and some related properties of the Choquet Integral will also be given.

A. Fuzzy Measure

Additive property is the main characteristic of classical measures. This is an effective and convenient nature, but is often too rigid in many practical applications. Fuzzy Measure extends the application area by replacing the additive property with weaker condition as monotonicity.

Definition 1: A fuzzy measure on a measurable space (X, F) is a real-valued set function $\mu : F \to (-\infty, +\infty)$ satisfying:

(MM1) $\mu(\phi) = 0$,

(MM2) $\mu(A) \geq \mu(B)$ whenever $A \in F$, $B \in F$, $A \subseteq B$.

In case of emphasizing the monotonicity, we can also call it a monotonic fuzzy measure [4].

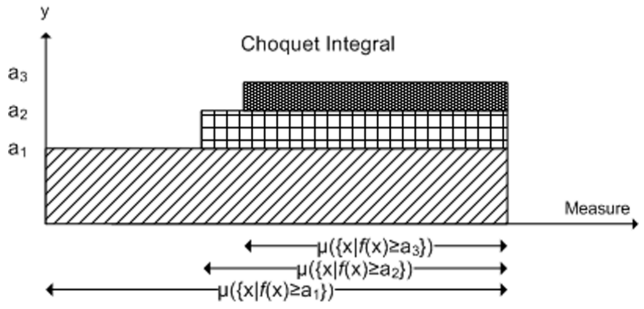

Figure 1. Choquet integral. μ is the fuzzy measure of function *f(x)*

Definition 2: A non-monotonic fuzzy measure on (X, F) is a real-valued set function $\mu : F \to (-\infty, +\infty)$ satisfying $\mu(\phi) = 0$.

B. Choquet Integral

Choquet Integral (Figure 1), as a classical fuzzy measure and an expansion of Lebesgue Integral, is defined by *Definition3*. Over decades, it has gained considerable attention and success in multi-criteria decision making and data mining.

Definition 3: Suppose a fuzzy measure μ on X. The discrete Choquet integral of a function $f : X \to \mathbb{R}^+$ can be written as:

$$(c)\int f(x) \circ \mu(X) = \sum_{i=1}^{n} [f(x_i) - f(x_{i-1})] \cdot \mu\{[x \mid f(x) \geq f(x_i)]\} \qquad (1)$$

Where x_i is permutation on X and $f(x_0) = 0$.

Choquet Integral has the following 3 basic properties:

1) $(c)\int 1_A d\mu = \mu(A)$

2) If $f < g$ then $(c)\int f d\mu \leq (c)\int g d\mu$

3) If a is non-negative real number and b is a real number, then

$$(c)\int (af + b) d\mu = a(c)\int f d\mu + b\mu(X)$$

As Murofushi introduced in [4], non-monotonic measure occurs when resources are limited. The basic properties of the Choquet integral are still useful for a non-monotonic fuzzy measure. RTS game provides a very similar environment with limited time and resource. If player wastes his resource in developing overmuch types of unit, the enemy will get opportunities to destroy his resources.

III. Proposed Methodology

RTS game provides a complicated environment which consists hundreds of buildings and units with different properties [5]. The various characters lead to various combinations. Even the most expensive and powerful units can be easily defeated by cheap units. In this setting, pro-gamer prefers to develop an unbalanced army with only several unit types [15]. Different combination performs different destroy power to certain kinds of unit types and buildings. Furthermore, the combinations are usually affected by a third dependent variable. By tracing the players' historical action, we find that there are substantial feature interactions among units. For example, melee unit often cooperates with magic and rang unit. With this positive interaction, the model is considered as super additive, i.e., $f(x+y) \geq f(x)+f(y)$. When the interaction is negative, the model is considered as sub additive, i.e., $f(x+y) \leq f(x)+f(y)$.

Quantitative interactions among groups of data can be detected by Analysis of Variance (ANOVA) test [8]. If the calculated p-value is smaller than a certain level (usually 5%), we can acquire a strong confidence to confirm that there are interactions among these testing variables. In this section, we describe how to learning fuzzy measure with different integrals for RTS game.

A. Strategy Definition in RTS Games

Strategy is defined as arranging the army with appropriate unit selection which can gain massive destroy power against enemy's unit. The knowledge was extracted from replay file which is provided by game system of Warcraft III. Each replay file consists of sequential records of players' actions which are designed for reviewing the game battle. We develop a C# program to decrypt and extract the features from replay file. Each battle represents a strategy case and has been divided into three parts as goal, situation, and scores.

Strategy Case = {Goal, Situation, Scores}

"Goal" is the creation of a suitable army mixed with certain proportion, e.g., 10% peasants, 50% footman and 40% rifleman.

"Situation" is used to describe what circumstances the player is dealing with. In this paper we define it as enemy's unit combination. Cases will be clustered into different groups with different races and unit combinations.

"Score" is the point obtained from each battle. It can be regarded as the outcome evaluation for each in-game player. Higher performance will represent better unit combination. We use these scores in learning the fuzzy measure.

B. Learning Fuzzy Measure by GA

Genetic Algorithm (GA) is a stochastic search technique with a parallel random search mechanism which aims to achieve a global minimum on error space. We use it to learn the non-additive fuzzy measure in our application problem [9][10]. The flowchart is shown as in Figure 2.

In Warcraft III, each player will get several scores in each battle as the performance evaluation. The higher score denotes the higher chance of winning. We define our score, i.e., *Score* as the differences between player and enemy.

$$Score(x) = Score_{WarcrafIII,\,player} - Score_{WarcrafIII,\,enemy} \qquad (2)$$

Fuzzy integrals are used to calculate the estimated scores which combine unit production statistic (i.e, *f(x)*) and non-monotonic fuzzy measure. Each fuzzy measure *μ(x)* describes

an interaction of the corresponding unit combination. The *Score(x)* wil be normalized between 0 to 1 and compare with the estimated score.

$$Score_{Different}(x) = \left| Score_{Estimate}[f(x)] - Score(x) \right| \qquad (3)$$

Our fitness function is designed to obtain the average differences between real scores and estimated scores in all the training replays. We apply Wang's fitness function as shown in (5).

$$\text{Fitness value} = -\frac{1}{1+e} \text{ where } e = \left(\frac{1}{N}\sum_{i=1}^{N} score_{Different}^{2}(i)\right)^{\frac{1}{2}} \qquad (4)$$

In our GA algorithm, each chromosome consists 2^{n-1} fuzzy measures of $\mu(X)$ including the entire unit combinations i.e.: $\mu(x_1)$, $\mu(x_2)$, ..., $\mu(x_1, x_2)$, ..., $\mu(x_1, x_2, ..., x_n)$. x_1, x_2, ..., x_n represent n kinds of unit types. Each fuzzy measure is first corrected to seven decimal places and then converted into binary form. A number of chromosomes will be initialized randomly at first. The learning process is repeated until the fitness value is stable or exceeds the maximum generation. After that, a reasonable fuzzy measure $\mu(X)$ for training replays is obtained. Population is set as 50, maximum generation is set as 100 and mutation rate is set as 0.01.The detail of the learning process are introduced in [11] [12].

C. Different Fuzzy Integrals

As seen from Figure 2, we define the function $f(x)$ which represents a player unit statistic of one replay:

$$f(x) = f(\text{Unit Statistic}_{\text{Replay i, Player}}).$$

All the unit statistics are normalized and presented by proportion. E.g.: 4 footmen, 6 riflemen and 10 priests will be normalized into $f(x_1)=0.2$, $f(x_2)=0.3$ and $f(x_3)=0.5$ respectively. This definition is useful in all the fuzzy integrals proposed in this paper.

We use Choquet Integral to calculate the estimated score as an example. Suppose there are 7 unit types, i.e.: n=7 and the unit statistic of a replay is $f(X)=\{x_1=0.2, x_2=0.4, x_3=0, x_4=0.3, x_5=0, x_6=0.1, x_7=0\}$. Then, ascending order sorting is performed with respect to the proportion, i.e.: $a_1= x_3=0$, $a_2= x_5=0$, $a_3= x_7=0$, $a_4= x_6=0.1$, $a_5= x_1=0.2$, $a_6= x_4=0.3$, $a_7= x_2=0.4$ where $a_1 \le a_2 \le ... \le a_7$. Given a fuzzy measure as $\mu(X)=\{ ..., \mu(x_6)=0.4, \mu(x_4, x_6)=0.7, \mu(x_1, x_4, x_6)=0.8, \mu(x_1, x_2, x_4, x_6)=0.2, ...\}$, the estimated score is computed by:

$$(c)\int f(x) \circ \mu(X)$$

$$= \sum_{i=1}^{7} (a_i - a_{i-1}) \cdot \mu(\{x \mid f(x) \ge a_i\})$$

$$= ((a_1 - a_0) \cdot \mu(x \mid f(x) \ge a_1)) + ((a_2 - a_1) \cdot \mu(x \mid f(x) \ge a_2)) + ...$$

$$= 0 + ((a_4 - a_3) \cdot \mu(x \mid f(x) \ge a_4)) + ((a_5 - a_4) \cdot \mu(x \mid f(x) \ge a_5)) + ...$$

$$= 0.1 \cdot \mu(x_1, x_2, x_4, x_6) + 0.1 \cdot \mu(x_1, x_4, x_6) + 0.1 \cdot \mu(x_4, x_6) + 0.1 \cdot \mu(x_6)$$

$$= 0.1 \times 0.2 + 0.1 \times 0.8 + 0.1 \times 0.7 + 0.1 \times 0.4$$

$$= 0.21$$

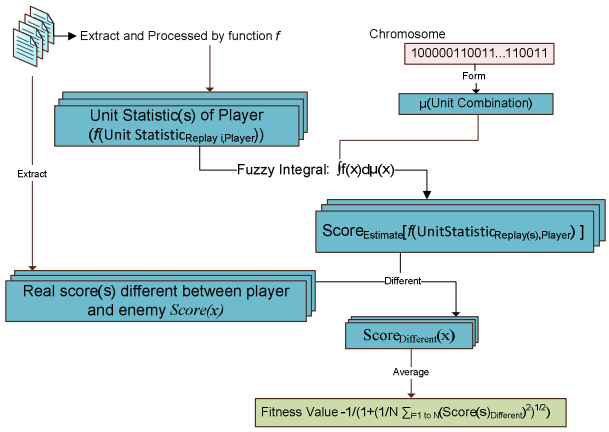

Figure 2. Fitness calculation of one chrommosom

Choquet integral is proved to work in our non-monotonic situation. Unfortunately, according to its fuzzy measure selection, the unit with least production has interaction with all the other units (i.e., basic unit) and the units with most production (i.e., powerful unit) have no interaction with others. This selection cannot well support the Warcraft III game play design. Thus, we develop three new fuzzy integrals based on different considerations. They are named as Max-based Fuzzy Integral (Ma-based FI), Mean-based Fuzzy Integral (Me-based FI) and Order-based Fuzzy Integral (Or-based FI).

1) Max-based Fuzzy Integral

Definition 4: Suppose a fuzzy measure μ on X. The Max-based Fuzzy Integral of a function $f: X \to \mathbb{R}^+$ can be written as:

$$(M)\int f(x) \circ \mu(X) = \sum_{i=1}^{n} x_i \times \max(\mu(S_i)) \qquad (5)$$

Where $x_i \in S_i$ and $\forall x \in S_i, x \neq 0$

Ma-based FI is developed with the thinking of winner takes all. We just consider the most powerful unit combinations which involve the current unit. This setting may lead the fuzzy measure learning process focuses on the important options.

2) Mean-based Fuzzy Integral

Definition 5: Suppose a fuzzy measure μ on X. The Max-based Fuzzy Integral of a function $f: X \to \mathbb{R}^+$ can be written as:

$$(m)\int f(x) \circ \mu(X) = \sum_{i=1}^{n} x_i \times \left(\frac{1}{m_i}\sum_{j=1}^{m_i} \mu(S_{ij})\right) \qquad (6)$$

Where $x_i \in S_{ij}$ and $\forall x \in S_{ij}, x \neq 0$, n is number of unit type, m is the number of set which include x_i

Me-based FI is developed to release the problem of interactions selection. All the fuzzy measures which involve the current unit type will be selected and an average is computed.

3) Order-based Fuzzy Integral

Players may need to develop technology and buildings to unlock advanced unit where the resource weighting in advanced unit is higher and more powerful. According to some data analysis, we found that advanced unit usually dominates the proportion of unit statistic. We infer that most players focus on building their army with advanced units. The advanced units should be considered as having more cooperation with other units. Thus, the largest *f(x)* is combined with the fuzzy measure with most of the units, and the unit type with least production is considered as having no interaction with others.

As Figure.3 shows, players will create labor at the very beginning to exploit resource. Then some basic units will be created for attack or defense. Through some development on building and technology, different kinds of advanced unit are unlocked. Constrained by resource, player will concentrate on certain unit types to build up his army. Proportion of unit combination will also be dominated by the selected unit types in order to maximize the destroy power.

Or-based FI is developed by consider the unit production sequence. Each unit type calculates the interaction with the one who has less production than it. The definition of Or-based FI is shown as follows.

Definition 6: Suppose a fuzzy measure μ on X. The Or-based Fuzzy Integral of a function $f: X \to \mathbb{R}^+$ can be written as

$$(o)\int f(x) \circ \mu(X) = \sum_{i=1}^{n} a_i \cdot \mu(x \mid 0 < f(x) \le a_i) \qquad (7)$$

Where $a_1 \ge \ldots \ge a_{n-1} \ge a_n > 0$

Different from CI, descending order sorting is performed among unit types in Or-based FI. Adopting the same example used in CI, the estimated score is computed as follows.

$$(\mathrm{r})\int f(x) \circ \mu(X)$$

$$= \sum_{i=1}^{4} (a_i) \cdot \mu(\{x \mid 0 < f(x) \le a_i\})$$

$$= a_1(\mu(a_1, a_2, a_3, \ldots, a_7)) + a_2(\mu(a_2, a_3, \ldots, a_7)) + \ldots + a_4(\mu(a_7))$$

$$= x_2(\mu(x_1, x_2, x_4, x_6)) + x_4(\mu(x_1, x_4, x_6)) + x_1(\mu(x_1, x_6)) + x_6(\mu(x_6))$$

$$= 0.4 \times 0.2 + 0.3 \times 0.8 + 0.2 \times 0.7 + 0.1 \times 0.4$$

$$= 0.5$$

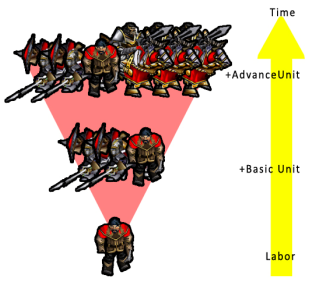

Figure 3. Unit production sequence in Warcraft III

4) Set Selection for Different Fuzzy Integrals

The main difference of these four fuzzy integrals is the set selection. Each *f(x)* will select different fuzzy sets for different fuzzy integrals. According to Wang's [13], the fuzzy measure selection function could be generated by the following equations.

$$K_i = \left\{ k : \frac{i}{2^k} - \left\lfloor \frac{i}{2^k} \right\rfloor \ge 0.5, 1 \le k \le n \right\}$$

$$\overline{K_i} = \{1, 2, \cdots, n\} - K_i$$

where i=1,2,…,2^n-1 and k=1,2,…,n, n is the number of feature $\lfloor a \rfloor$ denotes the integer part for a non-negative number a.

Let δ_i be the set selection operator as defined in (8). Equation (9)-(12) expresses the fuzzy measure selection for different fuzzy integrals: Choquet Integral (10), Or-based- FI (11), Me-based FI (12), and Ma-based FI (13).

$$\delta_i = \max(\min_{k \in K_i} f_k - \max_{k \in \overline{K_i}} f_k, 0) \qquad (8)$$

$$\delta_i = \begin{cases} \min_{k \in K_i} f_k - \max_{k \in \overline{K_i}} f_k, & \min_{k \in K_i} f_k > \max_{k \in \overline{K_i}} f_k \\ 0, & \min_{k \in K_i} f_k \le \max_{k \in \overline{K_i}} f_k \end{cases} \qquad (9)$$

Assume $\min_{k \in \phi} f_k = \max_{k \in \phi} f_k = 0$

$$\delta_i = \begin{cases} \max_{k \in K_i} f_k, & \max_{k \in K_i} f_k < \min_{k \in \overline{K_i}} f_k \\ 0, & \max_{k \in K_i} f_k \ge \min_{k \in \overline{K_i}} f_k \end{cases} \qquad (10)$$

$$\delta_i = \operatorname{avg}_{k \in K_i} f_k \qquad (11)$$

$$\delta_i = \max_{k \in K_i} f_k \qquad (12)$$

The sorting order makes Choquet Integral cannot directly calculate the maximum value. But this mechanism can be applied into Or-based FI. The selected maximum value is then combined with the corresponding unit statistic to calculate the estimated score. The set selection will not involve the assumption of $\min_{k \in \phi} f_k = \max_{k \in \phi} f_k = 0$, while empty set property of $\min_{k \in \phi} f_k = \infty$ is available.

IV. EXPERIMENT

A. Data Collection and Preprocessing

We selected Warcraft III as our research platform. It is a famous RTS game released in 2003 with the award of "Game of the Year" from more than six game publications. It has been sold over 7 million copies and there are concurrently over 200,000 players playing 6,000 battles online.

2,649 replay files of professional one-versus-one competitions from the internet are collected. They consist of two parts of data as shown in TABLE I. The header contains

some demographic data and the other part is composed of different action blocks. Each block is encrypted and stored players' actions in every 250 milliseconds' interval. A detailed example of replay file is shown in TABLE II.

The C# program exacts three kinds of data from these replays: (i) player unit production statistics, (ii) enemy unit type, and (iii) performance scores. Five data sets, as described in TABLE III, with largest amount of cases are prepared for our research. Each data set consist the cases of one race encountering its enemies which have a certain unit combination. Beside two less attended unit types, Figure 4 shows that the unit production follows a normal distribution.

TABLE I. DATA IN WARCRAFT III PEPLAY

	Element
Header	Player Record, Game Name, Map Settings, Map Record, Map & Creator Name, Player Count, Game Type, Language ID, Player List, Game Start Record, Slot Record, Random Seed,
Actions Block	Player ID, Action ID, Action Arguments

TABLE II. SAMPLE OF WARCRAFT III REPLAY

Time	Action
00:00:02:002	Player 1 train 1 Peasant
00:00:02:253	Player 1 select 5 [Peasant]
00:00:02:503	Player 1 Right Click with 0x58a8 at(7296,2432)
00:00:15:241	Player 2 build Altar of Darkness at(-1376,6240)

Player 1 produces 1 Peasants, then select 5 Peasants and move to (X: 7296, Y: 2432). Player 2 builds Altar of Darkness at(X: -1376, Y: 6240)

TABLE III. NATURE OF TESTING DATA SET

Data Set	1	2	3	4	5
Player race Enemy unit	Undead Fm, P	Undead Dr, Fm, P	Orc Pr, So, Sb, P	Orc Fm, P	Elf Fm, P
No. of case	162	65	1004	549	869
No. of Combination	23	16	60	31	31

Fm – Footman, P – Peasant, Dr, Dragon rider, Pr – Priest, So – Sorceress, Sb – Spell breake

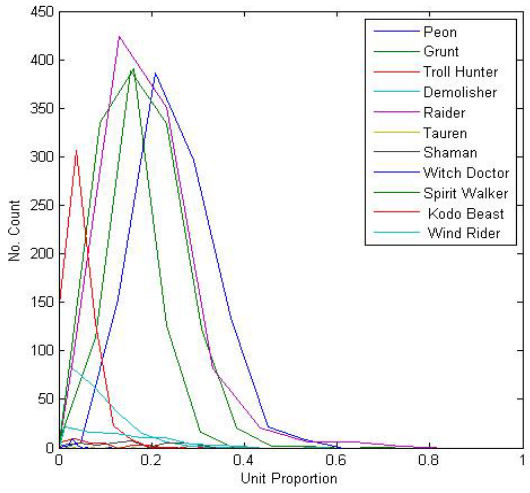

Figure 4. Unit production sequence in Warcraft III

B. *Experimental Comparison of Different Fuzzy Integrals*

In this part, we compare the performance of the four related fuzzy integrals. All the simulations are performed in MATLAB. The machine used is an Intel premium 4 2. 3GHZ with 2GB Ram PC. 70% cases in each dataset are used for training and the rest 30% are for testing.

Classical weight average (WA) method is also considered since we want to survey whether considering interaction can attain better result in our Warcraft III game data. The setting is similar as Yeung's [14] approach. Each unit type is given a weighting w and the unit combination power is calculated as the summation of the corresponding unit type's weighting. The learning process applies genetic algorithm with the same parameters settings as described in section 4.

$$f(X) = \frac{1}{n}\sum_{i=1}^{n} w_i x_i \tag{13}$$

Error is computed as the absolute difference between the estimated score (calculated by fuzzy integrals) and the real

TABLE IV. TRAINING ERROR IN DIFFERENT FUZZY INTEGRAL

Data Cluster	1	2	3	4	5
WA	0.512	0.576	0.799	0.497	0.463
CI	0.194	0.201	0.485	0.195	0.059
Ma-based FI	0.160	0.245	0.048	0.140	0.197
Me-based FI	0.138	0.181	0.078	0.137	0.061
Or-based FI	0.131	0.165	0.100	0.140	0.060

TABLE V. TESTING ERROR IN DIFFERENT FUZZY INTEGRAL

Data Cluster	1	2	3	4	5
WA	0.505	0.683	0.752	0.498	0.490
CI	0.209	0.325	0.483	0.194	0.048
Ma-based FI	0.187	0.234	0.064	0.150	0.212
Me-based FI	0.185	0.236	0.064	0.145	0.054
Or-based FI	0.185	0.247	0.103	0.150	0.056

TABLE VI. TRAINGING TIME IN DIFFERENT FUZZY INTEGRAL

Data Cluster	1	2	3	4	5
WA	6.589s	4.955s	7.752s	6.734s	4.010s
CI	22.906s	10.644s	183.96s	64.723s	96.047s
Ma-based FI	1709s	1567s	34387s	3737s	4017s
Me-based FI	1712s	1572s	34450s	3727s	4014s
Or-based FI	23.809s	10.960s	190.26s	67.722s	99.701s

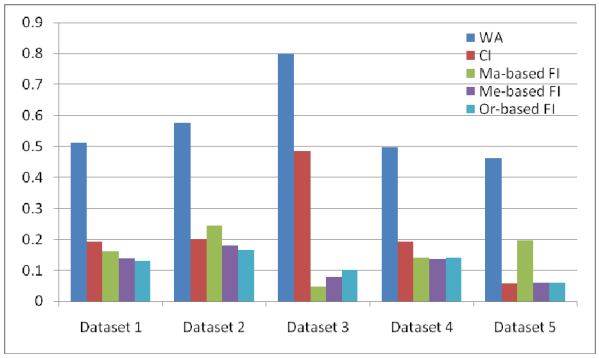

Figure 5. Training error in different Fuzzy Integral

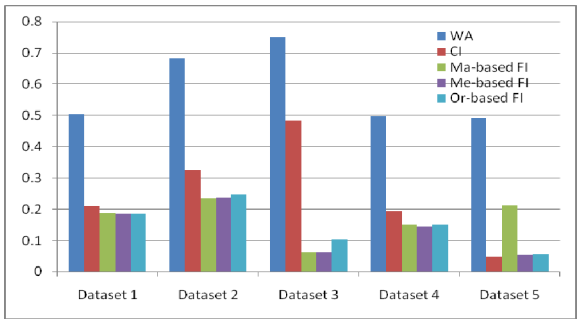

Figure 6. Testing error in different Fuzzy Integral

score from the game system. Training error, testing error and training time of our new fuzzy integrals compared with CI are summarized in TABLE IV-VI, figure 5, and figure 6.

From the experiment result, we provide the following conclusion:

1) Compared with weighted average, fuzzy integrals show an improvement in all the five datasets. Therefore, we believe that non-additive set function has a better representation than weighted average in predicting the power of unit combination.

2) Compared with Choquet Integral, all three new developed fuzzy integrals present better result in both training and testing. Me-based FI has a best performance with the average error of 0.128. Demonstrated by the result of dataset 3, the new fuzzy integrals are more effective if the dataset consists of various combinations. While Choquet Integral has a poor performance in this case.

3) The main weakness of Me-based FI and Ma-based FI is time consuming. Each time for set selection, they need to search for the whole fuzzy set. According table VI, we can observe that both of their training time is about 40 to 180 times more that Choquet Integral.

4) Jointly considering the training time and testing error, Or-based FI shows a best performance among these four methods. It has the similar training time with Choquet Integral with directly addressing the required set. Its training and testing error are similar with Me-based FI, and only 0.005 higher in average. We deem that Or-based FI is more appropriate in interaction detecting on Wacraft III data.

C. *Usage Count of Set in Different Fuzzy Integrals*

We tried to examine the difference of set selection in these four fuzzy integrals. All the selected fuzzy measures in the training process are being recorded and clustered with different amount of elements. As shown in table VIII, the selection of Or-based FI concentrates on the fuzzy measure with two to four elements. The count of selected set with more than five elements is dropped sharply. This phenomenon can be explained as: professional players seldom develop a balance army with many unit types. They usually focus on two to four unit types' cooperation. And this behavior make insufficient or even no data contribute to train up the fuzzy measures with big number of elements.

Or-based FI selects the same amount of fuzzy measures with Choquet Integral, but different selecting result. As show in TABLE II, figure 7 and figure 8, we investigated that Or-based FI concentrates on fewer sets than Choquet Integral. Some fuzzy measures which represent the frequently used unit combination will have a higher chance to be selected by Or-based FI.

We analyze the set selection condition containing different number of elements. According to table VIII， the value of fuzzy sets with less than two elements is concentrating on two unit types which are necessary for each player to create primary. Then the fuzzy measure value concentrates on {1,2,3}, {1,2,4}, {1,2,6} with three elements and {1,2,3,6}, {1,2,6,7} with four elements. Obviously, it shows several different unit production sequences with different advanced units selection. Moreover, because the selection is based on unit production sequence, the battle with longer time which creates more unit types will not be affected by the shorter battle with less unit types. This also avoids the effect of unsuccessful strategy like player being defeated in the early stage and fails to produce the advanced units.

The table also shows that the advanced unit cannot produce alone in a battle. This is because every advanced unit requires additional resource and technology support. In another word, creating the advanced unit requires the contribution of basic unit. The advanced unit should dominate the army and cooperate with other units.

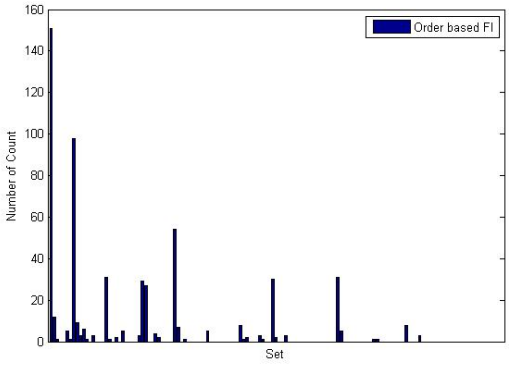

Figure 7. Count of Set selection for Order-based FI in Data cluster 1. X-axis is the set. Statring from the left, they are the set which only contains one element, i.e. , $\{x_2\}$, $\{x_3\}$…etc. Then they are the sets which contain more elements, i.e., $\{x_1, x_2\}$, $\{x_1, x_3\}$,…, $\{x_1, x_2, x_3\}$, etc. The last one on the right is the set which involves the whole set of elements. i.e., $\{x_1, x_{2,\ldots,} x_n\}$

TABLE VII. COUNT OF THE FUZZY MEASURE SELECTION IN DATASET1

No. of variables in Set	Or-based FI	Choquet Integral
1	23.28571	23.85714
2	7.714286	8.000000
3	4.000000	3.942867
4	2.142857	2.085714
5	0.619408	0.666667
6	0	0

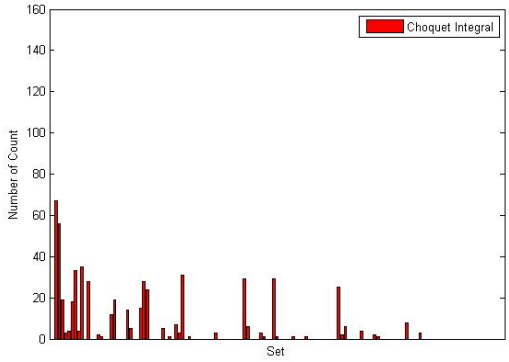

Figure 8. Count of Set selection for Choquet Integral in Data cluster 1

TABLE VIII. FUZZY MEASURE SELECTION IN DATASET1

Fuzzy Measure	Order based FI		Choquet Integral	
	Weighting	Number of count	Weighting	Number of count
{1}	0.460938	151	0.398438	0
{2}	0.617188	12	0.460938	67
{3}	0.734375	1	0.757813	56
{4}	0.859375	0	0.84375	19
{5}	0.789063	0	0.851563	3
{6}	0.296875	5	0.96875	4
{7}	0.578125	1	0.921875	18
{1,2}	0.453125	98	0.515625	33
{1,3}	0.453125	9	0.382813	4
{2,3}	0.601563	3	0.8125	35
{1,4}	0.789063	6	0.140625	0
{2,4}	0.359375	1	0.984375	28
{3,4}	0.429688	0	0.625	0
{1,5}	0.140625	3	0.664063	0
{2,5}	0.523438	0	0.929688	2
{3,5}	0.398438	0	0.046875	1
{4,5}	0.382813	0	0.734375	0
{1,6}	0.875	31	0.679688	0
{2,6}	0.914063	1	0.75	12
{3,6}	0.34375	0	0.976563	19
{4,6}	0.054688	2	0.1875	0
{5,6}	0.203125	0	0.34375	0
{1,7}	0.992188	5	0.242188	0
{2,7}	0.90625	0	0.976563	14
{3,7}	0.179688	0	0.875	5
		…		
{6,7}	0.6875	3	0.96875	15
{1,2,3}	0.367188	29	0.960938	28
{1,2,4}	0.492188	27	0.992188	24
		…		
{1,2,5}	0.835938	4	0.007813	0
{1,3,5}	0.34375	2	0.539063	0
{2,3,5}	0.625	0	0.835938	5
{1,4,5}	0.882813	0	0.359375	0
{2,4,5}	0.6875	0	0.875	1
{3,4,5}	0.6875	0	0.125	0
{1,2,6}	0.585938	54	0.695313	7
{1,3,6}	0.359375	7	0.789063	3
{2,3,6}	0.382813	0	0.992188	31
{1,4,6}	0.140625	1	0.8125	0
{2,4,6}	0.71875	0	0.375	1
		…		
{1,2,7}	0.625	5	0.617188	0
{1,3,7}	0.835938	0	0.828125	0
{2,3,7}	0.632813	0	0.460938	3
		…		
{1,6,7}	0.429688	8	0.90625	0
{2,6,7}	0.882813	1	0.875	29
{3,6,7}	0.554688	2	0.8125	6
		…		
{1,2,3,5}	0.375	3	0.882813	3
{1,2,4,5}	0.421875	1	0.320313	1
		…		
{1,2,3,6}	0.648438	30	0.992188	29
{1,2,4,6}	0.484375	2	0.859375	1
		…		
{1,2,5,6}	0.007813	3	0.1875	0
{1,3,5,6}	0.585938	0	0.664063	0
{2,3,5,6}	0.0625	0	0.28125	1
		…		
{1,2,3,7}	0.773438	0	0.25	1
		…		
{1,2,6,7}	0.476563	31	0.992188	25
{1,3,6,7}	0.71875	5	0.882813	2
{2,3,6,7}	0.164063	0	0.851563	6
		…		
{2,5,6,7}	0.679688	0	0.914063	4
		…		
{1,2,3,4,6}	0.0625	1	0.140625	2
{1,2,3,5,6}	0.101563	1	0.625	1
		…		
{1,2,3,6,7}	0.335938	8	0.945313	8
		…		
{1,2,5,6,7}	0.546875	3	0.421875	3
		…		
{1,2,3,4,5,6,7}	0.90625	0	0.460938	0

1 – Acolyte (Labor), 2 – Ghoul (Basic Melee unit), 3 – Crypt Fiend (Basic ranged unit), 4 – Gargoyle (Basic Air Unit), 5 – Meat Wagon (Advanced Siege Unit), 6 – Obsidian Statue (Advanced Support Unit), 7 – Destroyer (Advanced Air Unit). Number of count of Order based FI and CI = 0 are omitted in this table. Conclusion

V. CONCLUSION

In this paper, we apply different fuzzy integrals in predicting the power of unit combination in Warcraft III data. We found that weighted average cannot achieve an acceptable predicting accuracy. Since feature interaction exists in game data, non-additive method achieves better result. Furthermore, three new fuzzy integrals are developed with different directions to explain the game play. All of them attain a better result than the traditional Choquet Integral. Through the analysis of set selection, we have the evidence of why our methods got a better performance. We deem that for our data, Or-based FI has a better explanation of feature interaction in unit combination by considering the unit production sequence. Our future work regarding this topic includes new fuzzy application in micro-management. We attempt to generate corresponding unit movement to perform the selected strategy and finally lead the AI bots achieve the winning.

ACKNOWLEDGMENT

This research project is supported by the HK Polytechnic University grants 1-ZV5T, A-PJ18 and G-U523, and the NSFC grant no. 60903088.

REFERENCES

[1] M. Sugeno, “Theory of fuzzy integrals and its applications,” Ph.D. thesis, Tokyo Institute of Technology, 1974.

[2] H. Tahani and H J. M. Keller, "Information Fusion in Computer Vision using the Fuzzy Integral," *IEEE Transactions on Systems, Man and Cybernetics*, vol. 15, pp. 733-741, 1990.

[3] K. Hirota and W. Pedrycz, "Fuzzy computing for data mining," *Proceedings of the IEEE*, vol. 87, no. 9, pp. 1575 - 1600,1999.

[4] T. Murofushi, M. Sugeno and M. Machida, "Non-monotonic fuzzy measures and the Choquet integral," *Fuzzy Sets and Systems*, vol. 64, no. 1, pp. 73-86, 1994.

[5] T. Murofushi, M. Sugeno, "The Choquet integral in multiattribute decision making," *Fuzzy measures and integrals: theory and applications*, 333-47, 2000.

[6] D. Aha, M. Molineaux and M. Ponsen, "Learning to Win: Case-Based Plan Selection in a Real-Time Strategy Game," *Case-Based Reasoning Research and Development*, vol. 3620/2005, 2005.

[7] J. L. Hsieh, and C. T. Sun, "Building a player strategy model by analyzing replays of real-time strategy games," Proceedings of IEEE International Joint Conference on Neural Networks, Hongkong, China, June 2008, pp. 3106-3111.

[8] R. Miller, "Beyond ANOVA: basics of applied statistics, Chapman & Hall/CRC," 1997.

[9] Z. Wang, K.S. Leung and J. Wang, "Genetic algorithms used for determining nonadditive set functions in information fusion," *Fuzzy Sets and Systems*, vol. 1, no. 9, pp. 518-521, 1997.

[10] Z. Y. Wang, K. Xu and J. Wang, "Using genetic algorithm to determine non-negative monotone set functions for information fusion in environments with random perturbation," *International Journal of Intelligent System*, pp. 949-962, 1999.

[11] Y.J. Li, Peter H. F. Ng, H. B. Wang, Y. Li and Simon C. K. Shiu, "Applying Fuzzy Integral for Performance Evaluation in Real Time Strategy Game," Proceedings of 2010 2nd International Conference on Information and Multimedia Technology, Hong Kong, December 28-30, 2010,pp. 168-172.

[12] Peter H. F. Ng, Y. J. Li, H. B. Wang, Y. Li and Simon C. K. Shiu, "Bottom-Up Strategy Planning Model by applying Fuzzy Integral in RTS Game," Proceedings of Joint 5th International Conference on Soft Computing and Intelligent Systems and 11th International Symposium on Advanced Intelligent Systems, Okayama, Japan, 8-12 December 2010,pp. 8-12.

[13] J. Wang and Z. Wang, "Using neural networks to determine Sugeno measures by statistics," *Neural Network*, pp.183-195, 1997.

[14] D. Yeung., X. Wang and E. Tsang, "Handling interaction in fuzzy production rule reasoning," *IEEE Transactions on Systems, Man, and Cybernetics, Part B: Cybernetics*, pp. 1979-1987, 2004.

[15] Peter H. F. Ng, Simon C. K. Shiu and H. B. Wang, "Learning Player Behaviors in Real Time Strategy Games from Real Data," Proceedings of Twelve Rough Sets, Fuzzy Sets, Data Mining, and Granular-Soft Computing, pp 321-327, 2009.

[16] Y. Dodge, *The Oxford Dictionary of Statistical Terms,* Oxford University Press. ISBN 0-19-920613-9, 2003.

2011 IEEE International Conference on Fuzzy Systems
June 27-30, 2011, Taipei, Taiwan

Unit Formation Planning In RTS Game By Using Potential Field And Fuzzy Integral

Peter H. F. Ng
Department of Computing
The Hong Kong Polytechnic University
Hong Kong
cshfng@comp.polyu.edu.hk

Y. J. Li and Simon C. K. Shiu
Department of Computing
The Hong Kong Polytechnic University
Hong Kong
{csckshiu, csyjli}@comp.polyu.edu.hk

Abstract— **Unit formation planning and target of attack is the core of micro management in real time strategy (RTS) game. It is more complicated than macro management, such as building and unit production sequence. It consists of a great quantity of possibility. Multiple targets and the non-additive property of unit formation leads the micro-management remains a problem. Traditional tree searching or A* searching is unable to handle these two properties. They are time consuming in runtime and difficult to manage in the AI programming development as there are too many weightings and each of them will interact with the others. In this paper, we applied potential field, fuzzy measure and integral to solve the micro-management. Potential field is suitable for complicated and various environment with multiple targets. However, it does not consider non-additive property. We integrated it with fuzzy measure and integral to extend simple additive property to non-additive property and provide the ability to handle interaction among different targets.**

Keywords-component; Fuzzy Measure, Fuzzy Integral, Potential Field, Real time Strategy Game, unit formation planning, Micro-management, Warcraft III

I. INTRODUCTION

Nowadays, RTS game consists of complicated game rule, hundreds of unit type, various battlefields and decision making under the time pressure. More and more researchers such as Buro [1], Lucas [2], Alexander [3] are interested in it and have recently generated much important outputs in both macro and micro management for the RTS game AI community. RTS game provides a fruitful environment for AI research.

The fundamental game play of a typical RTS game is allocating resources to build an army, design units' combination and defeat the enemy by killing the opponent units. Control of RTS game can be classified into two types. The first type is macro management which is also named game strategy. It involves resource gathering, base building and technology upgrade. The second type is micro management, i.e., tactics, involves planning of the unit movement and control. For the marco-management, many researchers have applied case based reasoning CBR to solve it. CBR is potentially a very useful approach in game AI strategy planning and design. Usually, cases can be collected, learned from real game data or constructed using simulation [4], such as ORTS, MadRTS, Wargus, etc. These cases can be reused according to some similarity and effectiveness measures. However, if cases are continuously accumulated, the time to retrieve solutions will be too long in RTS games. Fast indexing methods is needed such as Peter [5] and Puo [6] approaches. In our previous research [7][8], we also applied CBR concept and combined with fuzzy measure and integral to solve macro management, i.e., the unit production planning problem by considering the non-additive property of different unit combination. In this research, we extended the usage of trained fuzzy measure and applied to the micro management. We combined the potential field and fuzzy integral to solve the unit formation and target of attack planning. The methodology extended the normal additive property of potential field to non-additive property and provided the ability to handle the interaction among different targets. We simulated our experiment in Warcraft III. Details step and experimental result are shown in this paper.

II. LITERATURE REVIEW

A. Fuzzy Measure and Integral

Unit formation planning involves unit combinations selection. The unit combination are enormous in RTS game and the combined power of different units is usually "non-linear", i.e., the sum is not simply the total of the individuals [9] and is not additive. Let $X = \{x_1, x_2 ... x_n\}$ be the unit combination where n is the total number of unit types and f be the combined power. We believe that there exists non-additive property, i.e., $f(X) \neq \sum_{i=1}^{n} f(x_i)$. Formally speaking, when the interaction is positive, $f(X)$ is considered as super additive, i.e., $f(X) \geq \sum_{i=1}^{n} f(x_i)$, for all x in the domain of f. This could be easily found in many RTS game designs, such as the melee unit should be supported by magic or range unit. When the interaction is negative, the model is considered as sub additive, i.e., $f(X) \leq \sum_{i=1}^{n} f(x_i)$. If the interaction is

zero, then it will be considered as normal additive model, i.e., $f(X) = \sum_{i=1}^{n} f(x_i)$.

As the non additive properties in unit combination, weighted average and weighted A* searching cannot give a good result in our experiment, we need to find a solution to indicate the interaction. Therefore, the combined power of units can be evaluated. We applied fuzzy measure and integral and the basic idea is illustrated in Fig. 1. All the units, and their possible combinations are assigned with (i.e., learnt from data) some fuzzy measures, μ , and an overall assessment is computed using fuzzy integral. Then, the case's assessment can be computed by referring to known fuzzy measures, and the fuzzy integral. The final strategy selected can be based on these assessments.

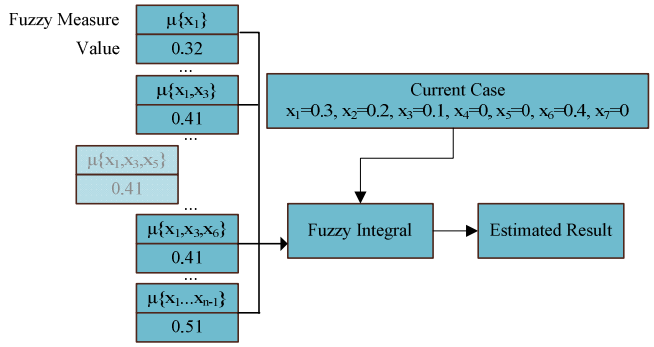

Fig.1. Apply Fuzzy Measure and Integral on Regression

Non additive fuzzy measure is used in our experiment. Non additive fuzzy measure is the original one and can be considered as the basic form of fuzzy measure [10]. It can be regarded as generalization of the classical probability measure. A value is assigned to each combination of variables, i.e., for n variables, there are $2^n - 1$ measures.

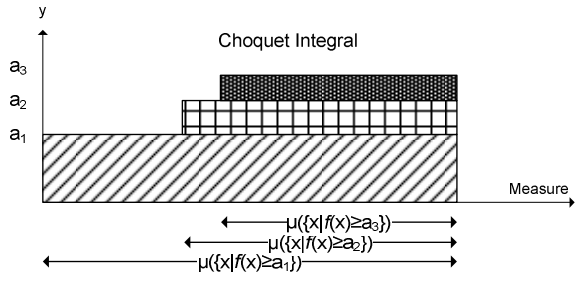

Fig.2. Choquet Integral. μ is the fuzzy measure of a function $f(x)$

$$(c)\int f(x) \circ \mu(X) = \sum_{i=1}^{n} (a_i - a_{i-1}) \cdot \mu(x \mid f(x) \geq a_i) \quad (1)$$

where $a_0 = 0$ and $a_0 \leq a_1 \leq a_2 \leq \ldots a_n$

Choquet Integral (CI) is a kind of fuzzy integral. It has been a general tool for dealing with multiple criteria decision making and is able to model the interactions among different criteria. Sugeno [11] [12] has applied it to the problem of prediction of wooden strength and plant operator. Both of them show a better result than a linear regression. Peter [13] has applied CI in software cost estimation with multiple attribute. Suppose a fuzzy measure $\mu : P(X \rightarrow [0,1])$ and $\mu(\phi) = 0$, definition of CI, see Fig. 2, is shown as follows and a_i is the sorted sequence of x_i

B. *Potential Field*

Potential Field is designed for searching the next movement location in multiple goals and various environments under the time pressure. The classic potential field consists of two virtual forces. One is attractive potential force, $U_{att}(q) = \frac{1}{2}\xi p_g^2$, where ξ is a positive constant scaling factor and $p_g = \|q - q_g\|$ is the Euclidean between the object and the goal. Another force is repulsive potential force, $U_{rep}(q) = \frac{1}{2}\eta(\frac{1}{p(q)} - \frac{1}{p_0})^2$ where η is a positive constant scaling factor, $p(q)$ is the minimum distance from the object to the obstacle and p_0 is a positive constant that presents the influence distance of the obstacles.

Multi-agents Potential Fields of Hagelback [14] [15] and Johan [16] showed the importance to micro management and tactics development. Their experiment result had been proven in events such as Open Real Time Strategy (ORTS) AI competitions which have been held for many years provide a good platform for players to test out their control tactics. They showed a possible solution on micro management in RTS game. Potential field is normal additive. Therefore, it may not have the ability to handle interaction among different goals, especially the sub additive problem, i.e., $f(X) \leq \sum_{i=1}^{n} f(x_i)$.

III. METHODOLOGY

A. *Obtain the Fuzzy Measure from real game data*

Case = {Unit Combination, Situation, Scores}

In our previous research, we try to create a method to evaluate the power of unit combination for macro-management planning, i.e., building sequence and unit production planning [7][8]. A set of fuzzy measure is learnt from real game data. We will briefly explain the flow in this session. A set of game logs which is the replay data of Warcraft III is collected. We converted each replay data, i.e.,

each battle into one case as shown above and divided it into three parts. They are unit combination, situation and scores.

We define the "Unit Combination" of a case as the creation of player and enemy unit production, e.g., player created 10% peasants, 50% footman, 40% rifleman and the enemy created 30% peasants, 70% footman.

"Situation" is used to describe some common circumstances the player is dealing with. For example, if a player faces similar conditions, races, enemy units, etc, we can still think that the player is dealing with similar "situation" or he is under certain typical circumstances. The purpose is to help cluster cases into several similar groups. Depending on the number of training data and game play design, other information, such as map or starting location, could also be selected as the cluster criterion.

Finally, "Score" is the points obtained after the game. It is used for evaluating the outcome of the Warcraft III battle, and is used to guide the training of fuzzy measure, i.e., we can interpret as the higher the scores the more powerful unit combination.

Ontanon [17] [18] and Sharma [19] applied similar approach to index the player action. They used building or architectures as an index to organize the game actions. In our study, we try to use the possible unit that can be produced by player as an index. Game actions are much simplified for the purpose of reducing the complexity of each case description.

After the preprocessing of the game data, we use Genetic Algorithm (GA) to obtain the non additive fuzzy measure [20] [21], i.e., $\mu(X)$ or $\mu(\text{Unit Combination})$, for calculating unit combinations and its' interactions as Fig. 3.

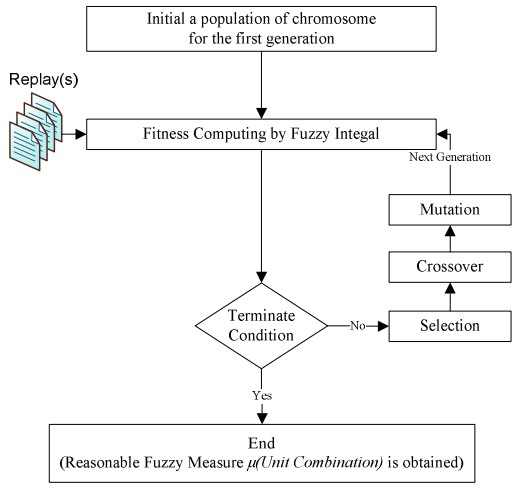

Fig.3. Overview of GA to obtain the Fuzzy Measure

First, a number of chromosomes are generated randomly. Each chromosome represents a fuzzy measure. It is combined by $2^n - 1$ fuzzy measure of $\mu(X)$, where $X = \{x_1, x_2 \ldots x_n\}$ is the unit combination and n is total number of unit type. $\mu(X)$ involves $\mu(x_1)$, $\mu(x_2)$, ..., $\mu(x_1, x_2)$, ..., $\mu(x_1, x_2, ..., x_n)$, each of them represents the fuzzy measure of the unit type sub-set. They are corrected to seven decimal places. Then they are converted into binary form and combined into one chromosome. Population of each generation is set to 50 in our experiment. To simplify the fuzzy measure, the unit types that are not produced in all the replays within the same cluster are not considered.

Each chromosome represents a fuzzy measure. Unit combination in each replay will be extracted and processed by function f. $f(x)$ presents the power of unit combination where x represents a unit combination of a replay, i.e., $f(x) = f(\text{Unit Combination}_{\text{Replay i, Player}})$. Throughout the function f, all the unit productions of player and enemy in the battle (i.e., unit(s) of unit type 1… unit(s) of unit type n) are normalized separately and presented in proportion. We used Choquet Integral (CI) in our experiment to calculate the estimated scores from unit combination, i.e., $f(x)$ and the fuzzy measure chromosome, i.e., $\mu(X)$. The equation is shown in (1).

All the differences between the real scores and the estimation using fuzzy integral in all replays will be summed up and the average is calculated. Then it will become the fitness value of chromosome as shown in (2) where N is the total number of case. We apply Wang's fitness value [22] to calculate the fitness of each chromosome. Finally, after GA operation (100 generations), a reasonable fuzzy measure is learnt.

$$\text{Fitness value} = -\frac{1}{1+e}$$
$$\text{where } e = \frac{1}{N}\sum_{i=1}^{N}\left|(c)\int f(x_i) \circ \mu(X) - score(i)\right| \quad (2)$$

B. *Apply Fuzzy Integral in Unit Formation Planning*

The fuzzy measure has shown improvement on macro-management. We want to extend the usage of trained fuzzy measure to micro-management during the battle, i.e., unit formation planning and target of attack. First, we will discuss about applying fuzzy integral in unit formation planning as shown in Fig.4. When the player decided to fight against the enemy unit in the Warcraft III, the player will divide their army into subgroup and attack the enemy. This is known as formation. We applied fuzzy integral to perform this task.

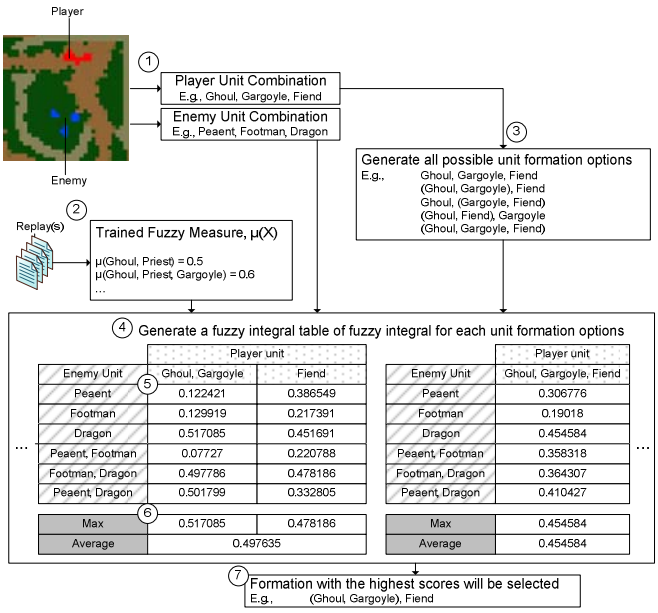

Fig.4. Overview of applying Fuzzy Integral on unit formation planning

1. Fuzzy measure is trained by the replay data.
2. Player and enemy unit proportion is extracted during the battle.
3. When the player decides to fight against the enemy, AI bot will generate all the possible unit formation according player unit type.
4. For each formation, a fuzzy integral table will be generated. Each cell in the table represents the power of the player subgroup to fight against certain the enemy subgroup as shown in Fig. 4
5. The value of each cell is calculated by Choquet integral as shown in (1) by using trained fuzzy measure and unit proportion of the selected player and enemy unit. We can interpret as the higher value the higher chance to win.
6. The maximum fuzzy integral of each player subgroup will be selected and the average will be taken as the score of this unit formation.
7. The unit formation with the highest scores will be selected.

C. *Potential Field with the Fuzzy Integral value*

After AI bot decided unit formation, it needed to decide the target of attack for each subgroup. We applied potential field to perform this task. Player army will be divided into different subgroups according to unit formation planning that described in part B. Then a potential field will be generated for each subgroup of player army as shown in Fig. 5. The centre of the potential field was the middle point of enemy army. The size of potential field was set as 50 x 50 in our experiment. The initial potential field was an empty two dimension array. Each cell of the two dimension array will store the attractive force, , for one coordinate, (x,y) .

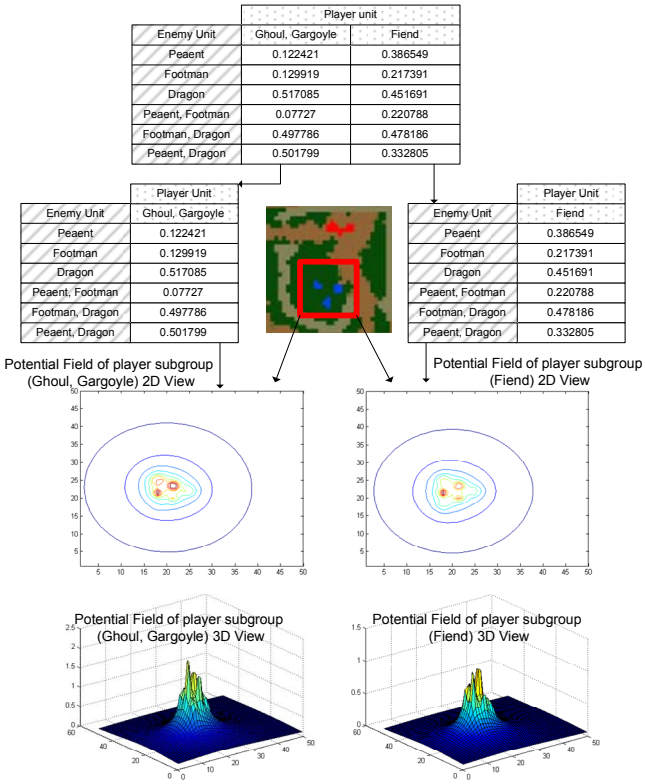

Fig.5. Overview of generating Potential Field by Fuzzy Integral value

$$U(x,y) = \sum_{i=1}^{j} (c)\int f(x) \circ \mu(X) \times d(P_i, P(x,y))^{-1} \qquad (3)$$

We modified the attractive force of potential field, $U(x,y)$ as shown in (3) by applying the idea of opponent force from Johan [14][15]. Each value in the fuzzy integral table will be a point of interest, P_i . Each P_i will generate symmetric surrounding field with the highest attractive force, i.e., fuzzy integral value, $(c)\int f(x) \circ \mu(X)$, in the centre. We used the value that is learnt from real game data instead of expert knowledge. The force will be weakened when it moved away from the center, d where $d(P_i, P(x,y))^{-1} \leq 1$, is used to perform this task.

Fuzzy measure is able to handle the interaction between different units type. To extend this property to potential field, P_i will also consider the outer defense line, i.e., the interaction between different enemy subgroup as shown in the fuzzy integral table. The center of the interaction was set as the middle point of enemy subgroup. Fig. 6 is an example to illustrate our work. The fuzzy integral value of interaction between different enemy subgroup may be negative. Therefore, it changes the simple normal additive property of potential field to non-additive property, especial the sub additive.

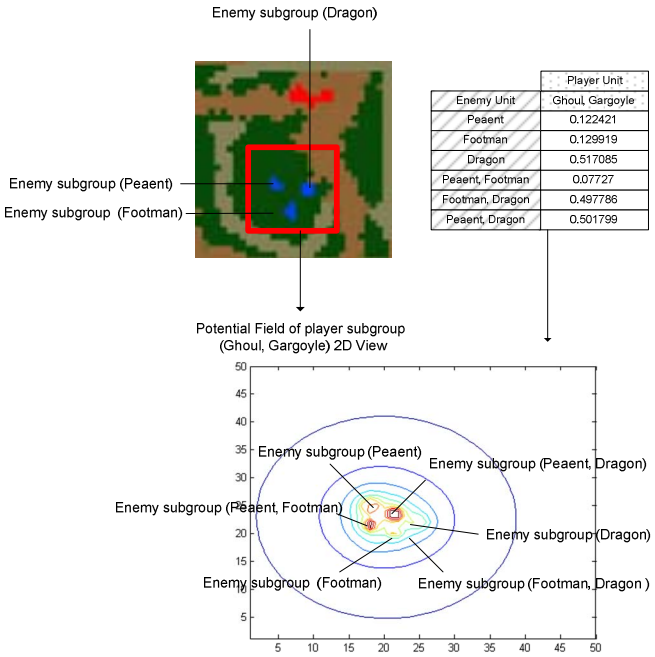

	Player Unit
Enemy Unit	Ghoul, Gargoyle
Peaent	0.122421
Footman	0.129919
Dragon	0.517085
Peaent, Footman	0.07727
Footman, Dragon	0.497786
Peaent, Dragon	0.501799

Fig.6. Example of generating Potential Field by Fuzzy Integral value for one subgroup of player army

D. Apply multi-agent Potential Field in Micro-Management

The advantage of applying potential field in micro management of RTS game is the result can be easily multiplied by complicate RTS terrain properties. In RTS game, some unit type can pass through the blocked area or gain extra attack bonus in some special area. All kind of these information could be stored in another two dimensional array as shown in Fig. 8, e.g., zero is set to the blocked area. Once the potential field has been computed by Part C, it can be multiplied by terrain properties array and the resultant potential field could be computed as shown in Fig. 9. The area with the highest attractive force will be the target of attack for certain player subgroup.

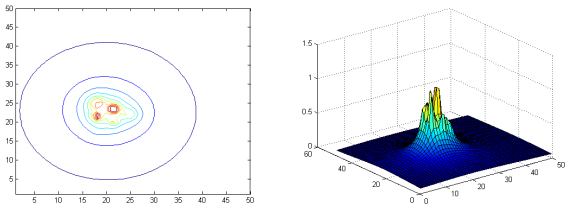

Fig.7. Potential Field by Fuzzy Integral value of one player subgroup

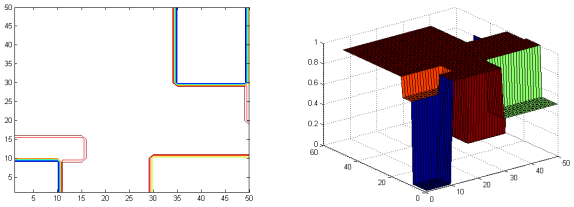

Fig.8. Terrain properties of one player subgroup

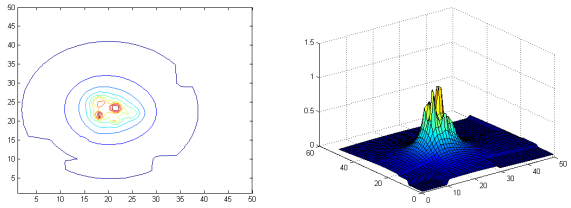

Fig.9. Resultant Potential Field

IV. EXPERIMENTAL RESULT

A. Data Collection

We selected Warcraft III expansion, The Frozen Throne (WIII: TFT) which is a well known and popular RTS game. It is regarded as the best RTS game on the market because of its' interesting, attractive and yet complicated game plays. The purpose of this experiment is to prove our methodology can provide a unit formation and target of attack planning. Hence, the result should be better than Warcraft III AI bot, i.e., the enemy unit scores should be lower.

In this research, 65 replay data are collected to train the fuzzy measure. The player race is Undead and the enemy race is Human. The enemy unit type is peasant, footman and dragon. 5 cases are randomly selected to extract the player and enemy unit combination for simulation.

B. Experimental Setup

For each selected case, player and enemy unit combination is extracted and passed to Matlab for computing the potential field. Then the result will be sent to Warcraft III for simulation.

In Warcraft III, player and enemy units are generated in an official competition field as shown in Fig. 10. Unit formation and the target of attack are set before the battle. After the battle, scores of player and enemy are accorded. For each selected case, 3 additional simulations are performed by using Warcraft III AI bot (Instance) as a comparison of our methodology.

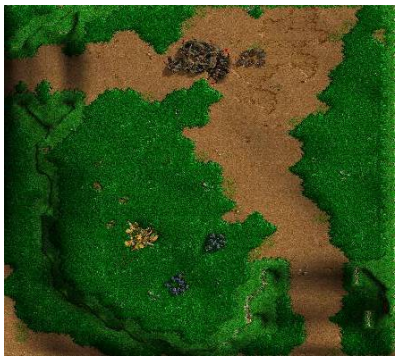

Fig.10. Simulation in Warcraft III

C. Result

As the player won all the selected cases, the scores of players in different simulation are the same. We cannot use it for comparison. We can only compare the scores of enemy. Better micro-management can avoid the enemy to obtain higher scores. Table I shows the enemy scores of using Warcraft III AI bot, while the Table II shows the enemy scores of using potential field and fuzzy integral. Potential field and fuzzy integral obtain a better result in 80% of simulation. The enemy score is lower than the Warcraft III AI bot. Fig. 11 shows the comparison of our methodology and average enemy score that obtained by Warcraft III AI bot. It shows an improvement in 4 selected cases.

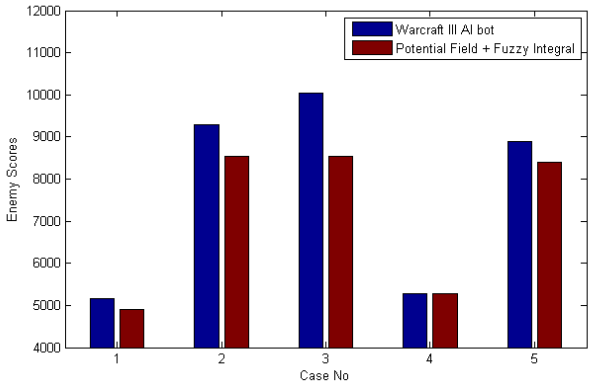

Fig.11. Comparison of our methodology and Warcraft III bot

TABLE I
ENEMY SCORE OF USING WARCRAFT III AI BOT

Case	1	2	3	4	5
Experiment 1	4970	9040	10285	5405	8780
Experiment 2	5350	9295	10160	5165	8950
Experiment 3	5150	9550	9695	5280	8965
Average	**5156**	**9295**	**10046**	**5283**	**8898**

TABLE II
ENEMY SCORE OF USING POTENTIAL FIELD AND FUZZY INTEGRAL

Case	1	2	3	4	5
P.F. + F.I.	**4990**	**8530**	**8540**	**5285**	**8410**

V. CONCLUSION

In this paper, we applied potential field, fuzzy measure and integral to perform a solution on micro management in RTS game. Therefore, the AI bot is able to divide the army into subgroup and perform the unit formation planning. After that the AI bot is also able to consider the interaction among different enemy unit type and decide the target of attack for each player subgroup. Simulation on Warcraft III has been done to test our idea and it shows an improvement.

By integrating the potential field with fuzzy measure and integral, it provides a machine learning approach to obtain the constant scaling factor instead of expert suggestion. It also extends the non-additive property from fuzzy measure and integral to potential field.

Our research is very preliminary. There are still many research problems remain, such as updating and maintaining the fuzzy measure and considering different unit types in player subgroup. We believe that this approach can generate a reasonable solution for AI development in RTS game.

REFERENCES

[1] M. Buro, "Call for AI research in RTS games", Proceedings of the AAAI-04Workshop on Challenges in Game AI, 2004, pp. 139–142

[2] S. M. Lucas , "Computational Intelligence and AI in Games", IEEE TRANSACTIONS ON COMPUTATIONAL INTELLIGENCE AND AI IN GAMES, 2009, VOL. 1, 1-3

[3] N. Alexander, "Game AI is Dead. Long Live Game AI!", Intelligent Systems, 2007, IEEE 22(1): 9-11

[4] S. Bakkes, P. Spronck, "Rapid and Reliable Adaptation of Video Game AI", IEEE Transactions on Computational Intelligence and AI in Games, 2009, 1(2): 93-104

[5] H. Wang, Peter. H. F. Ng, B. Niu, Simon C.K. Shiu, "Case learning and indexing in real time strategy games", Proceedings of the 5th international conference on Natural computation. Tianjin, China, IEEE Press, 2009

[6] P. Huo, Simon C. K. Shiu, H. Wang, "Application and Comparison of Particle Swarm Optimization and Genetic Algorithm in Strategy Defense Game", Proceedings of the 2009 Fifth International Conference on Natural Computation - Volume 05, IEEE Computer Society, 2009

[7] Peter H. F. Ng, Y. J. Li, H. B. Wang, Y. Li and Simon C. K. Shiu. Bottom-Up Strategy Planning Model by applying Fuzzy Integral in RTS Game, Proceeding of Joint 5th International Conference on Soft Computing and Intelligent Systems and 11th International Symposium on Advanced Intelligent Systems (SCIS & ISIS). Okayama, Japan, 2010, pp 8-12

[8] Y. J. Li, Peter H. F. Ng, H. B. Wang, Y. Li and Simon C. K. Shiu, "Applying Fuzzy Integral for Performance Evaluation in Real Time Strategy Game", 2nd International Conference on Information and Multimedia Technology (ICIMT). Hong Kong, RPC China. 2010, pp 28-30.

[9] Y. Dodge, "The Oxford Dictionary of Statistical Terms", Oxford University Press. ISBN 0-19-920613-9, 2003

[10] Gustave Choquet , "Theory of Capacities", Annales de l'Institut Fourier 5, 1953, pp 131–295

[11] K. Ishii, M. Sugeno, "A model of human evaluation process using fuzzy measure", Int. J. Man-Machine Studies, 1985, 22:19-38

[12] T. Murofushi, M. Sugeno, "The Choquet integral in multiattribute decision making", Fuzzy measures and integrals: theory and applications, 2000, pp 333-47

[13] J. Peters, L. Han, S. Ramanna, "The Choquet integral in a rough software cost decision system", Fuzzy Measures and Integrals: Theory and Applications, Studies in fuzziness and soft computing, 1999, pp 392

[14] J. Hagelback and S. Johansson, "Using multi-agent potential fields in real-time strategy games", Proceedings of the 7th international joint conference on Autonomous agents and multiagent systems-Volume 2, pp 631-638, 2008

[15] J. Hagelback, S. Johansson, "Demonstration of multi-agent potential fields in real-time strategy games," International Foundation for Autonomous Agents and Multiagent Systems Richland, SC, 2008

[16] H. Johan. “A Multiagent Potential Field-Based Bot for Real-Time Strategy Games”, International Journal of Computer Games Technology , 2009
[17] S. Ontanon, K. Mishra, N. Sugandh, A. Ram, “Case-Based Planning and Execution for Real-Time Strategy Games”, LECTURE NOTES IN COMPUTER SCIENCE 4626: 164, 2007
[18] S. Ontanon, K. Mishra, A. Ram, “Learning from Demonstration and Case-Based Planning for Real-Time Strategy Games”, Studies in Fuzziness and Soft Computing 226, 2008
[19] M. Sharma, M Holmes, J. Santamaria, A. Irani, C. Isbell, A. Ram, “Transfer learning in real-time strategy games using hybrid CBR/RL”, Proceedings of the Twentieth International Joint Conference on Artificial Intelligence, 2007
[20] Z. Wang, K.S. Leung, J. Wang, “Genetic algorithms used for determining nonadditive set functions in information fusion”, Proc. IFSA'97, vol. 1, pp. 518-521, 1997
[21] Z. Y. Wang, K. Xu, J. Wang, “Using genetic algorithm to determine non-negative monotone set functions for information fusion in environments with random perturbation”, International Journal of Intelligent System, 14: 949-962, 1999
[22] W. Wang, Z. Wang and George J.Klir, “Genetic algorithms for determining fuzzy measures from data”, Journal of Intelligent and Fuzzy Systems 6 171-183, 1998

2011 IEEE International Conference on Fuzzy Systems
June 27-30, 2011, Taipei, Taiwan

Elimination Search for puzzle games : An Application for Hashi Solver

Shi-Jim Yen, Shih-Yuan Chiu, Cheng-Wei Chou and Tsan-Cheng Su

National Dong Hwa University Dept. of CSIE Taiwan, R.O.C

sjyen@mail.ndhu.edu.tw

***Abstract*—This paper proposes an efficient method to solve Hashi, a logical-type puzzle game with N by M grid. By using two methods, intersection method and elimination search, we can solve Hashi quickly and efficiency. The solver is authenticated by solving problems taken from Internet.**

Keywords- Hashi, Elimination search, Puzzle game

I. INTRODUCTION

Recently, many puzzle games become more and more popular. Rules of these puzzle games are usually very simple, but solving them needs excellent logic concept. With contemplation, it is possible to finish these games, such as Sudoku, Nurikabe, Number Link, and so on.

Because of the popularity of puzzle games, many related studies become very popular. There are some directions for these studies. Some put focus on the generation of questions, trying to use the least implied numbers to generate a question with only one answer [1]; some try to demonstrate some puzzle games are NP-Complete problems [2][3]; besides, studying how to use programs to rapidly solve these puzzle games is an important direction. Previous researchers tried to use pattern matching and DFS to solve Nonogram puzzle games [4][5], and had breakthrough in the speed of solving them. However, DFS may step into a wrong track, stuck in it, and cause great deal of resource waste. To avoid this situation, this research tries to use intersection method and elimination search. Elimination search is a useful method for solving puzzle games, we also use it to solve other puzzle games and get good results[6][7][8]. By making use of the feature of elimination search which won't get stuck into a wrong track, Hashi solver in this research is able to solve questions of Hashi.

In this section, we will introduce rules of Hashi in details and the major method used in this research in the second section, including intersection method and elimination search, Experimental results will be presented in the third section, and the fourth section is conclusion.

The initial board of Hashi is shown in Fig. 1(a). In the figure, the circled numbers are "islands;" in addition, the lines connect islands are "bridges." The goal of the game is to connect all the islands with bridges. Correct solutions of the game must follow rules below:

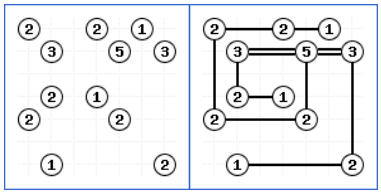

(a) (b)

Figure 1. An example of a Hashi problem (a) and its solution (b)

1. Every bridge can only connect two islands vertically or horizontally, without any other islands between the two islands.
2. The numbers of all the bridges connecting islands must be equal to the numbers on the islands.
3. The number of every island will be between 1~8, and 2 bridges at most are allowed in every direction of an island, up, down, left, and right.
4. A bridge cannot cross another nor has branches.
5. Every island can reach to any other through bridges.

Figure 1 (b) shows the way the game is completed.

II. PROPOSED METHOD

A. Overall Process

The way we use to solve Hashi is intersection method and elimination search. Before using these two methods, we need to do some basic information calculation. The whole process is shown in Fig. 2.

The following three sections will illustrate the methods we use. Section II.B explains basic information calculation. Section II.C explains intersection method, and Section II.D illustrates elimination search method.

B. Basic information calculation

Before using intersection method and elimination search, some preparation has to be done, this is basic information calculation. This step mainly records possible ways for every island to connect. Taking Fig. 3(a) for example, the island with number 2 on the upper left corner has three ways to connect, listed in Fig. 3(b)(c)(d).

978-1-4244-7316-8/11/$26.00 ©2011 IEEE

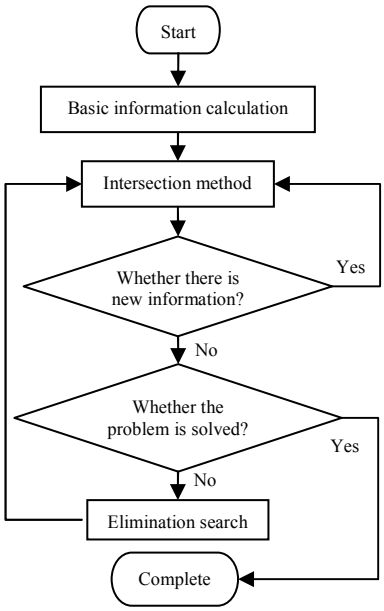

Figure 2. Flow chart of Hashi Solver

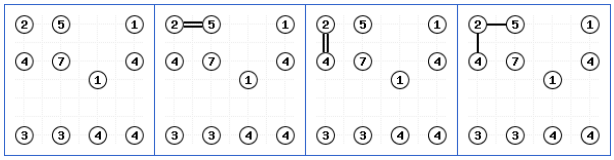

(a) (b) (c) (d)

Figure 3. Possible ways for a island to connect

In addition to the ways of connection, we do some simple judgments to decrease possible ways of connection, increasing the possibility of finding out solutions of intersection method, and decrease the use of elimination search. The way to judge is to delete impossible connection. For example, in Fig. 4(a), if two islands with number 2 connect each other with two bridges, they are impossible to connect other islands, which is against rule 5. Thus, in this step, this possible will be deleted; likewise, in Fig. 4(b), two islands with number 1 connecting together will be against rule 5.

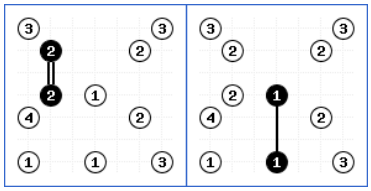

(a) (b)

Figure 4. Connections against rules will be deleted.

Table I lists how the possible connections of two highlighted islands with number 2 will change after the judgment above. Here, we use U(Up), D(Down), L(Left), and R(Right) to represent the connecting directions around a island, and add numbers after directions to show the numbers of bridges. For example, U2 means the island has two bridges connecting the island in the up direction.

TABLE I. HOW THE POSSIBLE CONNECTIONS OF THE TWO HIGHLIGHTED ISLANDS WITH NUMBER 2 IN FIG.4 WILL CHANGE

	Original Possible Connections	Impossible Connections	Actual Possible Connections
Up Islands	R2 D1 R1 D2	R2 D2	D1 R1
Down Islands	U1 R1 U2	U2	U1 R1

C. *Intersection method*

We can use an example to illustrate the main concept of intersection method. Assume an island only has two connecting ways, D1 L1 R2 and D2 L1 R1. Because both of the two possibilities include D1 L1 R1, we can believe that the three bridges, D1, L1, and R1, must exist. In other words, finding possible points in common among lots of possibilities to get information is the concept of intersection method.

Before using intersection method, according to present board, we can use more advanced way of sieving to decrease the possibility of matching so that the intersection method can probably get more information. We use three major ways of sieving here.

Because bridges cannot have branches or cross each other, if island a and island b are separated by bridges not connecting them, there will be no possibility for the two islands to connect. The first kind of sieving is used to exclude these impossible matches. For example, like Fig. 5(a), there are five possible connections for the highlighted island, but through some information calculation, the board situation will change into Fig. 5(b). The highlighted island's connection downward is blocked, so all the connections including down are excluded for its impossibility. Table II shows the specific information.

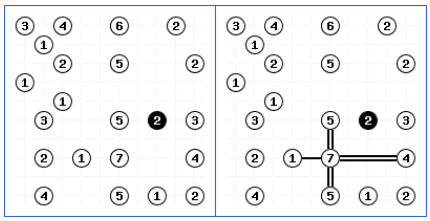

(a) (b)

Figure 5. An example of first kind of sieving

TABLE II. HOW THE POSSIBLE CONNECTIONS OF THE HIGHLIGHTED ISLANDS WITH NUMBER 2 IN FIG.5 WILL CHANGE

Original Possible Connections	Impossible Connections	Actual Possible Connections
R2 L2 R1 L1 D1 L1 D1 R1	 D1 L1 D1 R1	R2 L2 R1 L1

When some islands construct bridges, their ability of containing new bridges will decline; therefore, we can make use of this information to exclude some impossible connections. Like Fig. 6(a), there are five possible connections for the

highlighted island, but, after some basic information calculation, the board changes into Fig. 6(b). The island with number 1 on the right of the highlighted island has one bridge, so its capability of containing new bridges is 0. Thus, all the possibility of connecting islands on its right side will disappear, and all the matches that include connections with islands on the right will be excluded. Specific information is in Table III.

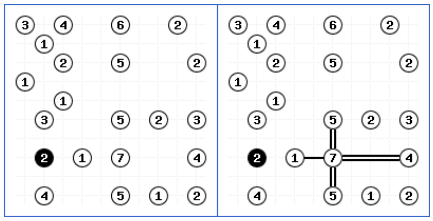

(a) (b)

Figure 6. The second kind of sieving

TABLE III. HOW THE POSSIBLE CONNECTIONS OF THE HIGHLIGHTED ISLANDS WITH NUMBER 2 IN FIG.6 WILL CHANGE

Original Possible Connections	Impossible Connections	Actual Possible Connections
U2		U2
D2		D2
U1 D1		U1 D1
U1 R1	U1 R1	
D1 R1	D1 R1	

At last, considering the original connections of an island itself can effectively exclude some impossibility. Like Fig. 7(b), because the highlighted island already has two bridges downward, all the connections excluding the two can be excluded. Specific information is in Table IV.

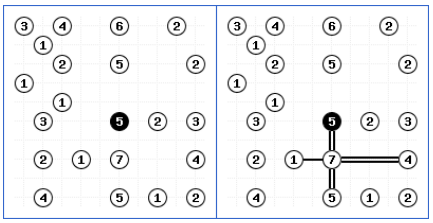

(a) (b)

Figure 7. The third kind of sieving

TABLE IV. HOW THE POSSIBLE CONNECTIONS OF THE HIGHLIGHTED ISLANDS WITH NUMBER 5 IN FIG.7 WILL CHANGE

Original Possible Connections	Impossible Connections	Actual Possible Connections
U1 R2 L2	U1 R2 L2	
U2 D2 L1		U2 D2 L1
U2 R1 L2	U2 R1 L2	
U2 D1 L2	U2 D1 L2	
U2 R2 L1	U2 R2 L1	
U1 D2 L2		U1 D2 L2
D2 R1 L2		D2 R1 L2
U1 D2 R2		U1 D2 R2
D1 R2 L2	D1 R2 L2	
U2 D1 R2	U2 D1 R2	
D2 R2 L1		D2 R2 L1
U2 D2 R1		U2 D2 R1

Before using intersection method to find information, using three kinds of sieving above can greatly decrease possible connections for the benefit of using intersection method. For example, if the present board is like Fig. 8(b), use the three kinds of sieving method to delete impossible connection matches. The result is listed in Table V. The italic marks are impossible connections after using every kind of sieving. Once a connection match is considered to be impossible, it will be deleted as Invalid.

After sieving, there are two possibilities. After intersecting the two possibilities, we can get the conclusion that there is at least one bridge downward, and can condense original 19 possible connections into 2.

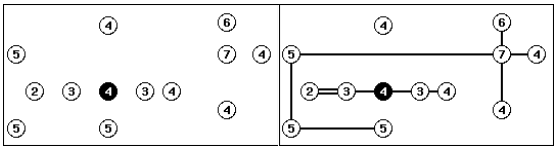

(a) (b)

Figure 8. A board before using intersection method

TABLE V. THE RESULT OF USING THE THREE KINDS OF SIEVING METHOD TO DELETE IMPOSSIBLE CONNECTION MATCHES

Original Possible	Sieving Method 1	Sieving Method 2	Sieving Method 3	Result
U0 D0 L2 R2	Possible	*Impossible*	Possible	~~U0 D0 L2 R2~~
U2 D0 L1 R1	*Impossible*	Possible	Possible	~~U2 D0 L1 R1~~
U0 D2 L0 R2	Possible	Possible	*Impossible*	~~U0 D2 L0 R2~~
U1 D0 L2 R1	*Impossible*	*Impossible*	Possible	~~U1 D0 L2 R1~~
U0 D2 L2 R0	Possible	*Impossible*	*Impossible*	~~U0 D2 L2 R0~~
U1 D0 L1 R2	*Impossible*	Possible	Possible	~~U1 D0 L1 R2~~
U2 D0 L0 R2	*Impossible*	Possible	Possible	~~U2 D0 L0 R2~~
U2 D1 L0 R1	*Impossible*	Possible	Possible	~~U2 D1 L0 R1~~
U2 D0 L2 R0	*Impossible*	*Impossible*	*Impossible*	~~U2 D0 L2 R0~~
U1 D2 L0 R1	*Impossible*	Possible	Possible	~~U1 D2 L0 R1~~
U2 D2 L0 R0	*Impossible*	Possible	*Impossible*	~~U2 D2 L0 R0~~
U1 D1 L0 R2	*Impossible*	Possible	*Impossible*	~~U1 D1 L0 R2~~
U0 D2 L1 R1	Possible	Possible	Possible	**U0 D2 L1 R1**
U2 D1 L1 R0	*Impossible*	Possible	*Impossible*	~~U2 D1 L1 R0~~
U0 D1 L2 R1	Possible	*Impossible*	Possible	~~U0 D1 L2 R1~~
U1 D2 L1 R0	*Impossible*	Possible	*Impossible*	~~U1 D2 L1 R0~~
U0 D1 L1 R2	Possible	Possible	Possible	**U0 D1 L1 R2**
U1 D1 L2 R0	*Impossible*	*Impossible*	*Impossible*	~~U1 D1 L2 R0~~
U1 D1 L1 R1	*Impossible*	Possible	Possible	~~U1 D1 L1 R1~~

D. limination search

Like Fig. 9, when intersection method cannot find any new information anymore, elimination search should be used. By testing every kind of possibility to delete wrong connection match, we can increase the possibility of finding new information.

Elimination search's process is divided into three steps: assumption, extending ratiocination and mistake testing.

STEP1. Assumption: It means to assume some possibility is true for some island, and keep intersecting to change the board situation.

STEP2. Extending ratiocination: Use intersection method to ratiocinate to find more information.

STEP3. Mistake testing: Judge if there is mistake for the situation after extending ratiocination.

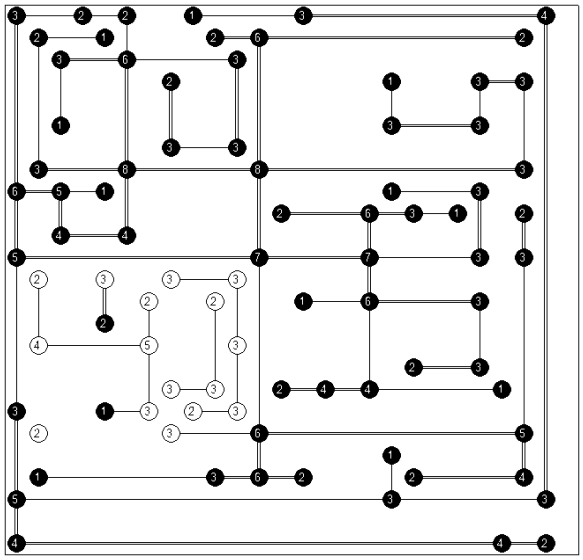

Figure 9. A board that should use elimination search

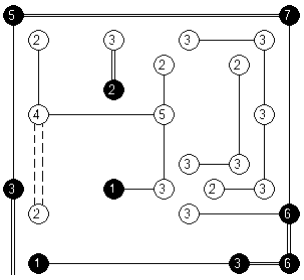

Figure 10. "Assumption" step in a elimination search

We use an example below to illustrate the three steps. Assume the present board is like Fig. 9. Highlighted islands represent those solved, and other islands unsolved. Meanwhile, because intersection method cannot find any information, we will select an unsolved island, and assume some connection is true. For example, possible connections for the unsolved island with number 2 on the left button are R2, U2, and R1U1. Assume the island's connection is U2, and the board will become Fig. 10. The dotted lines are assumed connections.

Next, use extending ratiocination for the new board, and use mistake testing for the board with extending ratiocination to make sure whether it is against rules. Fig. 11 is the board after using extending ratiocination for Fig. 10. The dotted lines are results after using extending assumption. After using mistake testing, we find that because the nine islands in the circle on the left in Fig. 11 cannot connect any direction, they are against rule 5. Besides, the island with number 3 in the center on the up direction can only connect the right direction which is against rule 2 because the capability to contain new bridges of islands on its left, right, and down is 0.

If it is against rules, it is proved that the assumption is not true. In other words, one possibility is excluded, which means we get new information. Because elimination search is slower than intersection method, as long as elimination search has new

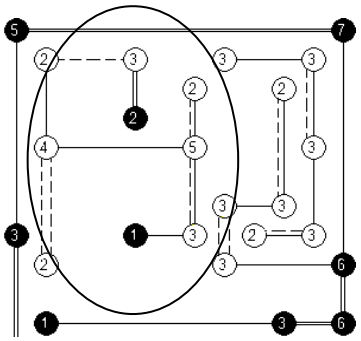

Figure 11. The board after using intersection method

information, we will use intersection method to test if more new information can be found. If it is not against rules after mistake testing, keep using elimination search. In the example above, if the assumption is not true, possible connections for the island with number 2 in the center on the left are U1R1 and R2. After using intersection method, it is found that there must be a bridge connecting the island on the right.

The worst situation is that after using elimination search for all the islands' possibilities, the problem still cannot be solved. However, when we test questions of large size (25X25), we haven't found questions that intersection method and elimination search method cannot solve. Thus, we believe merely using intersection method and elimination search method is enough to deal with the need of solving Hashi.

III. Experiment Results

We use the method in the second section to actually solve questions of Hashi, and list the result here. We use MATLAB 2009 to implement Hashi Solver, and randomly select one thousand questions of 25X25 to the tested objectives from Internet [9]. Our experimental environment is formed by using Intel E8400 CPU, 8G RAM, and the operation system is VISTA64. Testing the one thousand questions, the average time took to solve every question is 0.0342 seconds. Among them, we need only intersection method to solve 76.6% questions without using elimination search, and these questions are those which can be solved without using the rule that "all the islands must connect together." About the comparison between intersection method and elimination search, we list it in Table VI. From the experimental results, intersection method is four times faster than elimination search, which proves that it is a correct way to use intersection method right after finding new information by using elimination search.

TABLE VI. The Comparison Between Intersection Method and Elimination Search

Method	Average Solving Proportion	Average Time Cost	Average Time Cost per 1% Proportion
Intersection	98.9%	0.0327s	3.3064×10^{-4}s
Elimination search	1.1%	0.0015s	13.6364×10^{-4}s

IV. CONCLUSION

This research studies how to quickly solve Hashi. This research tries to use intersection method and elimination search to solve Hashi, and proves that this method can quickly and effectively solve it. According to the experiment results, we can find that over three fourths questions need only intersection method to be completely solved, and the rest of questions can be solved by using elimination search. For every question, 99% information is found by intersection method in average, and only 1% information is provided by elimination search. This proves that the two ways have great performance in solving Hashi. At the same time, because the two methods do not need much domain knowledge basically, we can also try to apply them to other puzzle games and expect there will be great results.

ACKNOWLEDGMENT

This work is supported by the National Science Council of Taiwan under the grant NSC 98-2221-E-259-021-MY3 and NSC 99-2221-E-259-009-MY3.

REFERENCES

[1] G. McGuire, "Sudoku checker and the minimum number of clues problem," In http://www.math.ie/checker.html.

[2] B. McPhail, "Light Up is NP-Complete," Feb. 2005. URL: http://www.cs.umass.edu/~mcphailb/papers/2005lightup.pdf.

[3] G. Kendall, A. Parkes and K. Spoerer, "A Survey Of NP-Complete Puzzles, " *ICGA Journal*, vol. 31, no. 1, pp. 13-34, Mar. 2008.

[4] M. Q. Jing, C. H. Yu, H. L. Lee and L. H. Chen, "Solving Japanese Puzzles with Logical Rules and Depth First Search Algorithm," *Proceedings of the Eighth International Conference on Machine Learning and Cybernetics*, pp. 2962-2967, Jul. 2009.

[5] C. H. Yu, H. L. Lee and L. H. Chen, "An Efficient Algorithm for Solving Nonograms," *Applied Intelligence*, Nov. 2009. http://springer.lib.tsinghua.edu.cn/content/t8288r38q0616g22/fulltext.pdf

[6] S. J. Yen and S. Y. Chiu,"A Simple and Rapid Lights-up Solver," the 14th Game Programming Workshop (GPW-09), pp. 67-70, Nov. 2009.

[7] S. J. Yen, T. C. Su and S. Y. Chiu, "Hitori Solver," the 14th Game Programming Workshop (GPW-09), pp. 87-90, Nov. 2009.

[8] S. J. Yen, S. Y. Chiu and C. W. Chou, "Masyu Solver," the 15th Game Programming Workshop (GPW-010), pp. 82-85, Nov. 2010.

[9] http://www.puzzle-bridges.com/

2011 IEEE International Conference on Fuzzy Systems
June 27-30, 2011, Taipei, Taiwan

An efficient algorithm for solving Fillomino

Shi-Jim Yen
Department of Computer Science & Information Engineering,
National Dong Hwa University,
Hualien, Taiwan, R.O.C.
sjyen@mail.ndhu.edu.tw

Tsan-Cheng Su
Department of Computer Science & Information Engineering,
National Dong Hwa University,
Hualien, Taiwan, R.O.C.
d9821009@ems.ndhu.edu.tw

Shun-Chin Hsu
Department of Information Management,
Chang Jung Christian University,
Tainan, Taiwan, R.O.C.
schsu@mail.cjcu.edu.tw

***Abstract*—Fillomino is a logical puzzle game invented by Nikoli Company in Japan. Fillomino is played on a rectangular cell with no standard size; the internal cell lines are often dotted. Some cells of the cell start containing numbers, referred to as "givens". In this paper, we propose a puzzle solving algorithm to treat these problems. Based on the fact the Fillomino are compact and contiguous, some logical rules are deduced to paint some cells. Experimental results show that our algorithm can solve Fillominos successfully and efficient, and the processing speed is significantly faster than that of depth first search algorithm.**

Keywords- Fillomino, Puzzle Game, CSP.

I. INTRODUCTION

Recently, many puzzle games popular in world. These puzzle games of Rules are usually simple, but solving them needs excellent logic concept. With contemplation, it is possible to finish these games, such as Sudoku, Nurikabe, Number Link, and some puzzle games.

Because of the popularity of puzzle games, many related studies become very popular. There are some directions for these studies. Some put focus on the generation of questions, trying to use the least implied numbers to generate a question with only one answer. Some try to demonstrate some puzzle games are NP-Complete problems [2][8]; besides, studying how to use programs to rapidly solve these puzzle games is an important direction. Previous researchers tried to use pattern match and DFS to solve Nonograms puzzle games [2][5], and had breakthrough in the speed of solving them. However, DFS may step into a wrong track, stuck in it, and cause great deal of resource waste.

In the second section, we will introduce others to the methods to solve puzzle game and introduce rules of fillomino in details in third section. The major method used in this research in the fourth section, including intersection method and logic rules. Experimental results will be presented in the fifth section, and the sixth section is conclusions.

II. PREVIOUS WORKS

Yen[6][7] they used Logical Reasoning and Heuristic to solve Nurikabe and Lights-up, and they can quite efficiency to solve puzzle. Their experimental results show that they can solve successfully and high-speed.

Wiggers [10] proposed a genetic algorithm (GA) and a depth first search (DFS) algorithm to solve Japanese puzzles. In 2004, he compared the performance of these two algorithms. For a small puzzle, the DFS algorithm is faster than the GA; otherwise, GA is faster. However, both methods are slow. In this study, some logical rules will be applied to determine the state filled of as many cells in a Japanese puzzle, then the DFS algorithm with "branch and bound" is used to determine the state of the remaining cells.

Jing and Yu [2][5] proposed a method based on logical rules (LR) and chronological backtracking with an LR filter to solve Japanese puzzles. Their rules exploited with a new concept of "the range of a black run." These rules have three main parts. The first part is used to determine which cells should be colored or left empty; the second part is used to refine the ranges of black runs, and that is used to determine which cells should be colored or left empty and to refine the ranges of black runs. One thing should be mentioned at first, we use row information to build a DFS tree, and the column information is used immediately to verify when a row is used to create a layer. It means that every layer of the DFS tree is composed of row information, and all nodes in each layer are possible solutions (PS) for the corresponding row.

Batenburg [3] described an evolutionary algorithm for Discrete Tomography (DT) then Batenburg and Kosters [4] provided a method to solve Nonogram puzzle. By modifying the fitness function in [3], the evolutionary algorithm can be used to solve Japanese puzzle. Since the evolutionary algorithm in [3] will converge to a local optimum, the obtained solution maybe incorrect.

III. GAME RULES

This Puzzle Game rule below:

A. Clues i said, suggesting that the number of i, the number of cell connected.

The rules need to be shown to satisfy the number of questions on a puzzle, if the clues is "i", that suggest you must have the same number i of connected cell. Like figure 8.

*B. In the game have N * M digits to fill all N * M cells.*

This rule needs to N * M of digits, all cells filled with digits in the N * M of Cells. Like figure 8.

978-1-4244-7316-8/11/$26.00 ©2011 IEEE

C. All of the cells must meet to be number of block.

This rule is necessary to have filled digits all the cells and the number of connection cells must meet the clues number.

D. The same number of blocks can not be connected.

This prompted rule is the same clues number of cells block can not be connected. However, the different clues number of cells block can be connected.

IV. PROPOSED METHOD

The algorithm of our solver contains three phases. The first phase and second phase are logic rule. The third phase is Intersection. The first phase checked point which has only one way to connection with the other cell. If we determine the first one is true, we can link it with the cell which one way to connection. The next phase inspection one cell which only one cell link to other cell, that we must link it. The last phase intersection all the possible answer matches of every cell. If sure one cell belong which one cell, We immediately fill this cell that should belong to the number of cell. Figure 1 that is our algorithm of flow chart.

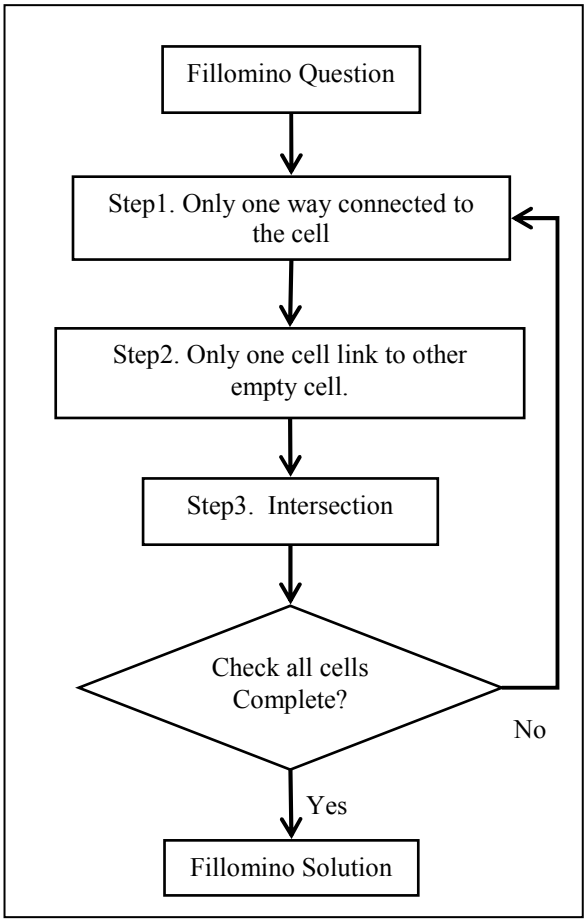

Figure 1. Flow chart of Fillomino.

A. Step1:Only one way connection

One cell that only has one way to connection other cell, that cell must be fill the only other cell numeral. Like figure 2,we marked the cell to fill 「4」.

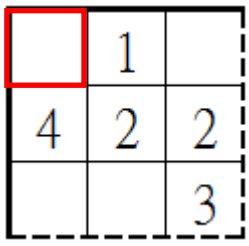

Figure 2. A simple step1.

B. Step2:Only one cell link to other empty cell

We used solid lines mark the cell, which is only one cell link to other cell. If we don't link it we will violation of the rules, and the cell no any numeral to fill it. Like figure 3, we used solid line mark the cell and dotted line mark the cells, these cells must to fill 「6」.

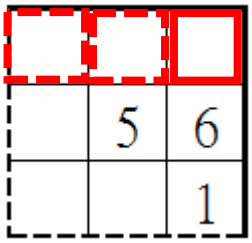

Figure 3. A simple step2.

C. Step3: Intersection

We used Intersection in one cycle of last. Figure 4 is a simple in corner. We do first and second phase, we create all of numeral possibilities pattern for the intersection. Like figure 5.

We intersection again to find intersect of cell. We find Intersect of cell to fill the numeral. Like figure 6. The cell marked that we can fill 「4」.

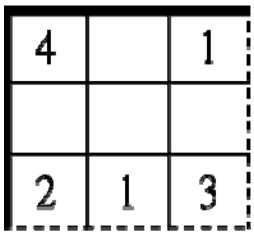

Figure 4. A simple puzzle Part of the corner.

We used three phases repeat continuously until the end of this puzzle. We can efficiently and successfully to solve the puzzle game. Figure 7 and Figure 8 are a simple question and solution.

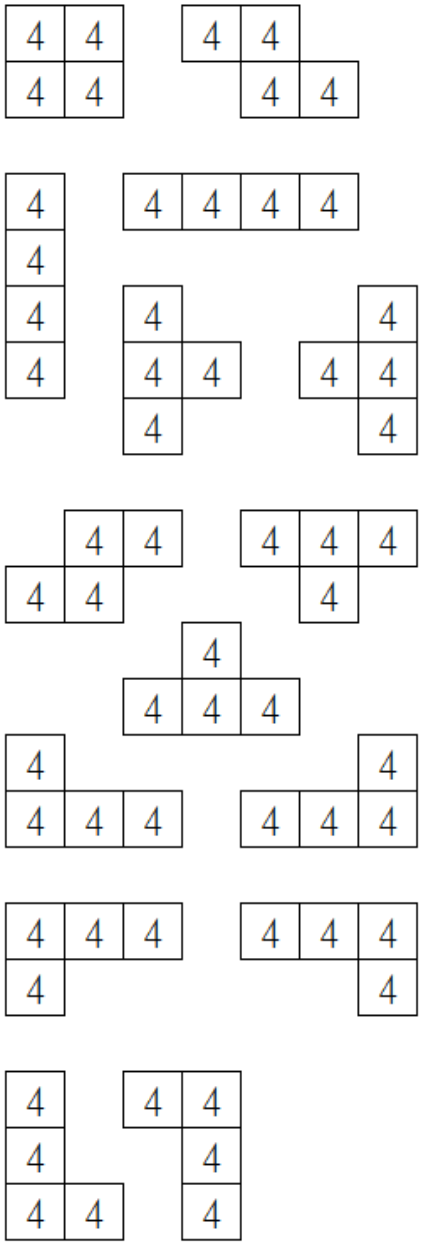

Figure 5. All of numeral possibilities pattern of Fig 4.

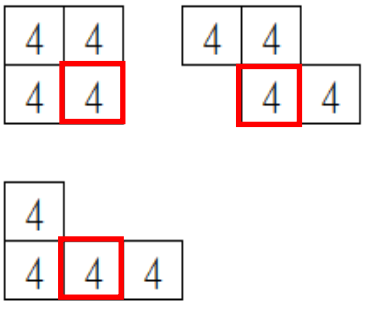

Figure 6. The pattern Intersect of cell.

	1					
4	2	2			5	6
		3				1
6			4			4
4				4		
3	4			5	1	4
					5	

Figure 7. Simple question of Fillomino.

4	1	6	6	6	6	6
4	2	2	3	5	5	6
4	4	3	3	4	5	1
6	6	6	4	4	5	4
4	4	6	6	4	5	4
3	4	4	6	5	1	4
3	3	5	5	5	5	4

Figure 8. Simple solution of Fillomino

Input puzzle of question Q
Do
{
Function1 (Only one way connected to the cell(Q));
{ Output Q_1;}
Function2(Only one cell link to other empty cell(Q_2));
{Output Q_3}
Do Intersection(Q_3);
{Output Q_4;}
Function3(Check All call complete(Q_4));
{
Return True or False;
}
*}while(*all cells Complete*=True)*
If (Function3=True)
{Output the puzzle answer=Q_4; }

Figure 9. our algorithm by pseudo code.

Figure 9: We show our algorithm by pseudo code. Our method is quick to find the answer and our execution time spends very little.

V. EXPERIMENTAL RESULTS

We found 100 of 4 type sizes Fillomino puzzles on [1] to verify the validity of our method. Our Algorithm by Microsoft Visual Studio C# 2008 of program on the computer with CPU of Intel Core 2 Quad Q9550 by 1 thread, 8 GB main memory and Windows Vista 64-bit OS. Table I shows the comparison of our proposed algorithm, Genetic Algorithms (GA) and CSP. Our proposed algorithm takes 2 seconds per question in average. Compared with GA and CSP, our solver is quite efficiency.

	1					
4	2	2			5	6
		3				1
6			4			4
4				4		
3	4			5	1	4
					5	

(a)

4	1	6	6	6	6	6
4	2	2	3	5	5	6
4	4	3	3	4	5	1
6	6	6	4	4	5	4
4	4	6	6	4	5	4
3	4	4	6	5	1	4
3	3	5	5	5	5	4

(b)

				5	5			5	5
4	5		5	3				1	
	3				2	4		4	
	1			2	1				
							6		4
6		2							2
				6	4		1	4	
	3		4	2				1	
					4	3		3	4
6	6			2	3		2		

(c)

4	4	4	1	5	5	5	1	5	5
4	5	5	5	3	2	5	5	1	5
3	3	5	3	3	2	4	2	4	5
3	1	5	6	2	1	4	2	4	5
6	6	6	6	2	4	4	6	4	4
6	3	2	2	6	6	6	6	2	2
4	3	6	1	6	4	4	1	4	4
4	3	6	4	2	2	4	4	1	4
4	4	6	4	4	4	3	2	3	4
6	6	6	2	2	3	3	2	3	3

(d)

			2	7	2				
7	8			7	4		1	4	5
5	8			7	2			4	5
5	8							4	3
			2	8	6			1	
8	8			8	8		1	6	6
4	5			6	2			6	5
									2
4	3			6	5		1	5	5
6	6		2	6	5			2	5
2				5	5				
6	4						1	5	5
6	6	1		3	5			5	3
3	6			6	3			3	3
				4	2		1	2	

(e)

7	7	7	2	7	2	2	5	5	5
7	8	7	2	7	4	4	1	4	5
5	8	7	8	7	2	4	6	4	5
5	8	7	8	7	2	4	6	4	3
5	8	8	8	7	7	7	6	4	3
5	5	2	2	8	6	6	6	1	3
8	8	8	8	8	8	8	1	6	6
4	5	5	5	6	2	6	6	6	5
4	3	6	5	6	2	6	5	5	5
4	3	6	5	6	6	1	5	2	2
4	3	6	2	6	5	5	1	5	5
6	6	6	2	6	5	3	2	2	5
2	2	4	6	5	5	3	3	5	5
6	6	4	6	3	1	5	5	2	2
6	4	4	6	3	5	5	1	5	5
6	6	1	6	3	5	3	5	5	3
3	6	4	6	6	3	3	5	3	3
3	3	4	4	4	2	2	1	2	2

(f)

Figure 10. Testing Puzzle of Question and Answer.

Figure 10: In a comparative experiment many puzzles were solved quickly and completely using this paper of Method. The average execution time was less than about 2 second. Fig. 10 shows the experimental results concerned the testing puzzle of Question and Answer. Fig.10 (a), Fig.10 (c) and Fig.10 (e) are puzzle of Questions. Fig.10 (b), Fig.10 (d) and Fig.10 (f) are solved Fig.10 (a), Fig(c) and Fig.10 (e) by order.

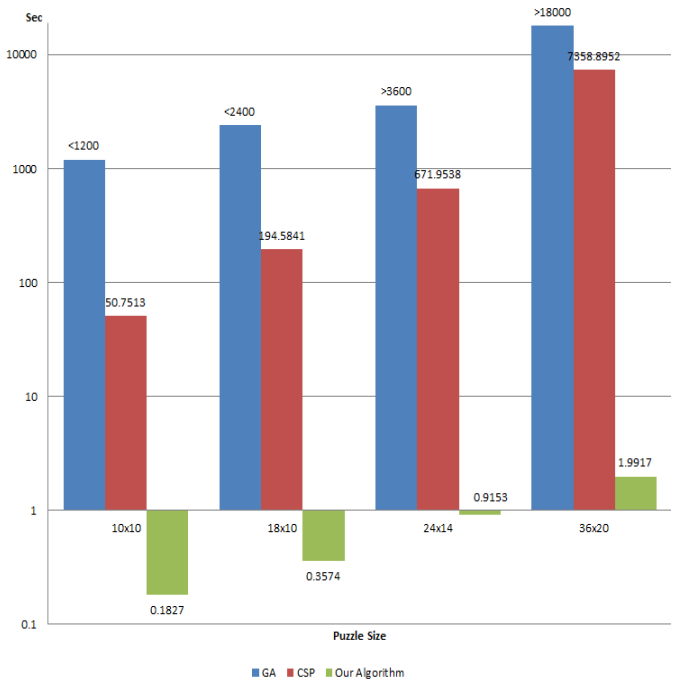

Figure 11. The comparison of the experimental results.

Figure 11: This paper comparison with GA and CSP to solve the Fillomino puzzle. This Figure show this paper method used execution time spend very little.

VI. EXPERIMENTAL

This research studies how to quickly solve Fillomino. This research tries to use intersection method to solve this question, and proves that this method can quickly and effectively solve Fillomino. According to the experiment results, we proved our algorithm than the method using the GA or the CSP more quickly and efficiently. Our algorithm we use is still a drawback to be improved. In Step3 to create all possible patterns, requires a lot of memory resources. This needs to be improved. At the same time, because the three phases do not need much domain knowledge basically, we can also try to apply them to other puzzle games and expect there will be great results.

ACKNOWLEDGMENT

This work is supported by the National Science Council of Taiwan under the grant NSC 98-2221-E-259-021-MY3 and NSC 99-2221-E-259-009-MY3.

TABLE I. TABLE TYPE STYLES

Puzzle Size : Piece	Average Execution time		
	GA	CSP	Our Algorithm
10x10:15	<20 min	50.7513 sec	0.1827 sec
18x10:30	<40 min	194.5841 sec	0.3574 sec
24x14:35	>1 hr	671.9538 sec	0.9153 sec
36x20:20	>5 hr	7358.8952sec	1.9917 sec

REFERENCES

[1] Database of Japanese puzzles : Nicoli.2008. Fillomino 4thed,Japan: Nikoli Co., Ltd..

[2] C. H. Yu, H. L. Lee, and L. H. Chen , "An efficient algorithm for solving nonograms," Applied Intelligence , pp. 1-14, 13 Nov. 2009..

[3] K. J. Batenburg, "An Evolutionary Algorithm for Discrete Tomography," M.Sc. thesis in Computer Science, University of Leiden, The Netherlands, 2003.

[4] K. J. Batenburg and W. A. Kosters, "A Discrete Tomography Approach to Japanese Puzzles,"Proceedings of BNAIC, pp. 243-250, 2004.

[5] M. Q. Jing, C. H. Yu, H. L. Lee and L. H. Chen, "Solving Japanese Puzzles with Logical Rules and Depth First Search Algorithm," Proceedings of the Eighth International Conference on Machine Learning and Cybernetics, pp. 2962-2967, Jul. 2009.

[6] S. J. Yen, T. D. Chuang, S. Y. Chiu and J. C. Chen, "Nurikabe, Heuristic Search, Puzzle," the 14th Game Programming Workshop (GPW-09), pp. 83-86, Nov. 13-15, 2009.

[7] S. J. Yen, S. Y. Chiu ,"A Simple and Rapid Lights-up Solver," the 14th Game Programming Workshop (GPW-09), pp. 67-70, Nov. 13-15, 2009.

[8] B. P. McPhail, "Light Up is NP-Complete," Feb. 2005.URL: http://www.reed.edu/~mcphailb/lightup.pdf.

[9] Ueda N, Nagao T (1996) NP-completeness results for NONOGRAM via parsimonious reductions. Technical report TR96-0008, Department of Computer Science, Tokyo Institute of echnology,May 1996

[10] Gary McGuire, "Sudoku checker and the minimum number of clues problem," In http://www.math.ie/checker.html.

2011 IEEE International Conference on Fuzzy Systems
June 27-30, 2011, Taipei, Taiwan

Symbiotic Neuron Evolution of a Neural-Network-Aided Grey Model for Time Series Prediction

Shih-Hung Yang
Institute of Electrical and Control Engineering
National Chiao Tung University
Hsinchu, Taiwan, R.O.C.
pshong.ece93g@nctu.edu.tw

Yon-Ping Chen
Institute of Electrical and Control Engineering
National Chiao Tung University
Hsinchu, Taiwan, R.O.C.
ypchen@cc.nctu.edu.tw

***Abstract*—This paper introduces a symbiotic neuron evolution algorithm (SNEA) to determine the topology of a neural-network-aided grey model (NNAGM) for time series prediction problem. The SNEA uses an evolutionary approach to evolve partially connected neural networks (NNs) and determine the number of hidden neurons. To achieve symbiotic evolution, SNEA first establishes a neuron population where each neuron is randomly created, and evaluates the neurons by constructing NNs with different numbers of neurons. Each neuron shares fitness from participating NNs. This algorithm then performs evolution on the neuron population by crossover and mutation based on neuron fitness. An NNAGM designed by SNEA is applied to the prediction problems and compared with other methods. The experimental results show that SNEA can produce an NNAGM with appropriate topology and higher prediction performance than other methods.**

Keywords-grey model; symbiotic evolution; neural network; prediction.

I. INTRODUCTION

In time series prediction, a small subset of recent time series information is usually used for prediction. The prediction assumes that the trends of the previous time series will be maintained in the future [1]. This approach is called lagged variables, shift registers, or tapped delay line. This means that accurate predictions can be obtained by using only a finite segment of previous data up to the prediction point [2]-[4]. Many researchers have developed variant systems to address the forecast problem in time series prediction, such as grey theory [5], [6] and neural networks (NNs) [7], [8].

Grey theory, a numerical method, is used to cope with systems with partial information or system dynamic model. The first-order single variable grey model (GM(1,1)) was developed for prediction [9]-[11] based on the gray theory. The GM(1,1) first transforms an amount of historical data into a more exponential-like and smooth signal. The grey differential equation, modified from the first-order ordinary differential equation, is then adopted to calculate the predictive value. Therefore, GM(1,1) can achieve high accuracy in prediction of exponential-type signals, offer the advantages of simplicity, and reduce computation time. However, the precision of this method of prediction is not sufficient for other types of signals.

In addition to GM(1,1), have been developed as a forecasting method based on soft-computing [12], [13]. Cybenko [14] and Hornik et al. [15] suggested that a single hidden layer is sufficient for NNs to approximate any complex nonlinear function and predict time series. Therefore, most researchers use only one hidden layer for prediction purposes. In general, NNs with fewer hidden neurons usually have better generalization ability and present a less severe overfitting problem. However, NNs with too few hidden neurons may not be able to accurately model and learn the data due to limited information processing capability [16], [17]. Thus, determining the number of hidden neurons can be difficult.

Based on the complementary advantages of GM(1,1) and NN, our previous work [18], [19] integrated GM(1,1) and NN into a fusion scheme, neural-network-aided grey model (NNAGM). The NNAGM employed GM(1,1) to predict signals and adopted NN to learn the prediction error of GM(1,1). The NN used in NNAGM has a fully connected topology and the number of hidden neurons is determined by trial-and-error. However, it is possible to have networks that are not fully connected in prediction problems [20]. Thus, automatic design of the topology of NNs is necessary to enable efficient solution of various prediction problems.

Symbiotic evolution is an implicit fitness-sharing algorithm used in an immune system model [21], [22]. In symbiotic evolution, each individual in the population represents a partial solution to a given problem, and complete solutions are constructed from several individuals. The partial solutions can be considered specializations that ensure diversity and prevent a population from converging into suboptimal solutions. The work of [22] proposed symbiotic adaptive neuron evolution to develop NNs according to a population of neurons. The performance of a neuron is determined by how well it cooperates with the other neurons which it combines. This process shows that a neuron that cooperates well with one set of neurons may cooperate poorly with other sets of neurons. However, the number of hidden neurons must be assigned prior to the evolution process. Previous studies have applied symbiotic evolution to design fuzzy controller and neuro-fuzzy systems [23]-[27]. The results of these studies have demonstrated the efficiency and feasibility of symbiotic evolution in reinforcement learning.

978-1-4244-7316-8/11/$26.00 ©2011 IEEE

This paper presents a symbiotic neuron evolution algorithm (SNEA) to design an NNAGM. This algorithm determines the topology of NNAGM, including the number of hidden neurons and connected topology. Section II introduces the concept of NNAGM. Section III indicates that the proposed SNEA does not develop NNs with a fixed number of hidden neurons but rather constructs NNs of different size by selecting the neurons from the neuron population. The neurons are evolved through the crossover and mutation operations, according to the shared fitness from the participating NNs. Section IV demonstrates the ability of the proposed SNEA to create an NNAGM for two prediction problems. Finally, Section V presents the conclusion of this study.

II. Neural-Network-Aided Grey Model

An NNAGM combines a GM(1,1) and an NN where GM(1,1) mainly predicts signals and NN learns the prediction error of GM(1,1) [18]. The structure of an NNAGM is depicted in Fig. 1.

Consider a discrete data sequence of length $n \geq 4$ formed as the following column vector

$$\boldsymbol{x}^{(0)} = \left[x^{(0)}[1] \quad x^{(0)}[2] \quad \cdots \quad x^{(0)}[n] \right]^T \tag{1}$$

where each element has the same numeric sign. In general, the GM(1,1) adopts three fundamental operations, given as

Accumulate Generating Operation (AGO):

$$x^{(1)}[k] = \sum_{l=1}^{k} x^{(0)}[l], \quad k = 1,2,...,n \tag{2}$$

Mean Generating Operation (MGO):

$$z^{(1)}[k] = \alpha x^{(1)}[k] + (1-\alpha) x^{(1)}[k-1], \quad k = 2,3,...,n \tag{3}$$

Inverse Accumulate Generating Operation (IAGO):

$$x^{(0)}[k] = x^{(1)}[k] - x^{(1)}[k-1], \quad k = 2,3,...,n \tag{4}$$

where α is often set as 0.5. According to the GM(1,1) [10], its grey differential equation is presented as

$$x^{(0)}[k] + a z^{(1)}[k] = b, \quad k = 1,2,\cdots,n \tag{5}$$

where a is the development coefficient and b is the grey input. Both a and b are unknown and have to be determined first by rearranging (5) into the following matrix form

$$\boldsymbol{x}^{(0)} = \boldsymbol{X}^{(1)} \begin{bmatrix} a \\ b \end{bmatrix} \tag{6}$$

where

$$\boldsymbol{X}^{(1)} = \begin{bmatrix} -\dfrac{x^{(1)}[1]}{2} & -\dfrac{x^{(1)}[1] - x^{(1)}[1]}{2} \\ 1 & 1 \\ \cdots & -\dfrac{x^{(1)}[n] - x^{(1)}[n-1]}{2} \\ \cdots & 1 \end{bmatrix}^T \tag{7}$$

Then a and b could be solved by the least square method as below

$$\begin{bmatrix} a \\ b \end{bmatrix} = \left(\boldsymbol{X}^{(1)T} \boldsymbol{X}^{(1)} \right)^{-1} \boldsymbol{X}^{(1)T} \boldsymbol{x}^{(0)} \tag{8}$$

Based on the GM(1,1), the solution of the grey first-order differential equation (5) is estimated as [10]

$$\hat{x}^{(1)}[n+j] = \left(x^{(0)}[1] - b/a \right) e^{-a(n+j-1)} + b/a, \quad j \geq 1 \tag{9}$$

Further applying the IAGO in (4) to (9) yields

$$\hat{x}^{(0)}[n+j] = \left(x^{(0)}[1] - b/a \right) e^{-a(n+j-1)} \left(1 - e^{a} \right) \tag{10}$$

which is the so-called predictive data. The one-step-ahead predictive value is then calculated by setting $j = 1$, which is the first predictive value after the original data sequence.

Since the GM(1,1) performs the prediction via the data sequence with the same numeric sign, the preprocess is employed to transform the raw data in (1) into

$$x'^{(0)}[l] = x^{(0)}[l] - \min\left(\boldsymbol{x}^{(0)} \right) + \gamma, \quad l = 1,2,\cdots,n \tag{11}$$

where γ is a constant bias to avoid the output to be zero. Then the transformed value is used to estimate $\hat{x}'^{(0)}[n+j]$ from (2)–(11). As a result, the one-step-ahead predictive value is determined as

$$\hat{x}^{(0)}[n+j] = \hat{x}'^{(0)}[n+j] + \min\left(\boldsymbol{x}^{(0)} \right) - \gamma. \tag{12}$$

Therefore, the GM(1,1) can process the data sequence with different numeric signs.

The NNAGM receives the input data $\boldsymbol{x}^{(0)}[k] = [x^{(0)}[k-n+1]\ x^{(0)}[k-n+2] ... x^{(0)}[k]]^T$ at time step k corresponding to $\boldsymbol{x}^{(0)} = [x^{(0)}[1]\ x^{(0)}[2] ... x^{(0)}[n]]^T$ in (1). Based on (12), the one-step-ahead predictive value is $\hat{x}^{(0)}[k+1]$ whose corresponding prediction error is $e_{\mathrm{GM}}[k]$. To improve the prediction accuracy, NNAGM adopts NN to estimate the prediction error $\hat{e}_{\mathrm{GM}}[k+1]$ by $[e_{\mathrm{GM}}[k-m] \ \cdots \ e_{\mathrm{GM}}[k-1]\ e_{\mathrm{GM}}[k]]$. The weight vector of NN is adjusted by the backpropagation algorithm.

With the fusion scheme, NNAGM integrates the outputs of both GM(1,1) and NN. The NNAGM possesses not only the capacity to predict data using GM(1,1), but also the intelligence to learn to estimate the prediction error using NN. The

remaining problem involves determining the topology of NN, i.e., the number of neurons and connections. The next section introduces the proposed SNEA employed to design the topology of an NN.

III. Symbiotic Neuron Evolution Algorithm

This section presents the proposed SNEA in detail. In its current implementation, SNEA is used to determine the structure of an NNAGM, i.e., the number of neurons and connections. The prior work [18] provided a constraint such that the topology of NN used in an NNAGM should be fully connected. Furthermore, the number of neurons is determined through a trial-and-error method. This paper uses SNEA to design NN in an evolutionary way.

The structure of an NN consists of input neurons, hidden neurons, output neurons, and connections between each layer. The number of neurons in the input and output layer is problem-dependent. For the prediction problem in Section IV, four input neurons and one output neuron are employed. Therefore, SNEA mainly determines the number of hidden neurons and the connected topology between input and hidden neurons.

To evolve the neurons, each neuron is encoded as *bj*, where *b* indicates the connection of bias and *j* indicates the topology related to the input neurons. The value of *j* is a bitwise representation and determines which input neuron is connected to the neuron *bj*. For a four-input-one-output prediction problem, each neuron has 2^4-1 types of topology, i.e., j = 1, 2,…, 9, A,…, F. Note that one input neuron should at least be connected to the hidden neuron. Fig. 2 shows two examples of the coding of two neurons and the topology of an NN constructed from the two neurons.

The main steps of SNEA are summarized in Fig. 3 and further explained as follows.

Step 1) Create a neuron population. The neuron population consists of randomly generated N_{pop} neurons.

Step 2) Randomly select p neurons to construct an NN in the pth group, p = 1,2,…,P. As shown in Fig. 4, each group consists of d NNs where each NN of the pth group includes p neurons.

Step 3) Train each NN using the backpropagation algorithm and then calculate the fitness of each NN where the fitness f_{NN} is the inverse of the root mean square error (RMSE).

Step 4) Share the fitness of NN with each participating neuron. For NN in the pth group, each participating neuron can share fitness as f_{NN}/p.

Step 5) Determine the participating time and fitness of each neuron. The neuron participating T NNs has its fitness f_n as

$$f_n = \frac{1}{T}\sum_{t=1}^{T} f_n^t \tag{13}$$

where f_n^t is the shared fitness in tth NN.

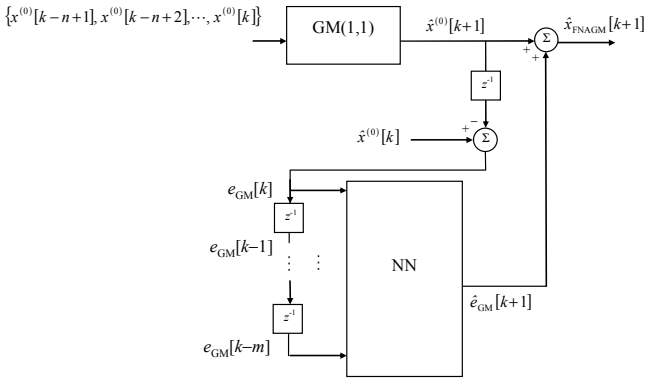

Fig. 1. Neural-network-aided grey model (NNAGM).

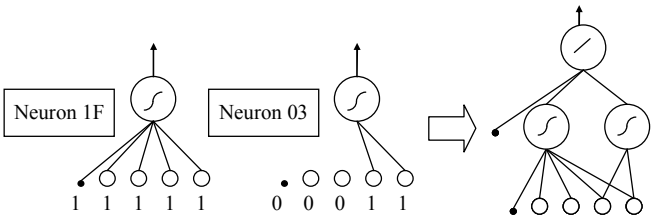

Fig. 2. Coding of two neurons and an NN constructed via two neurons.

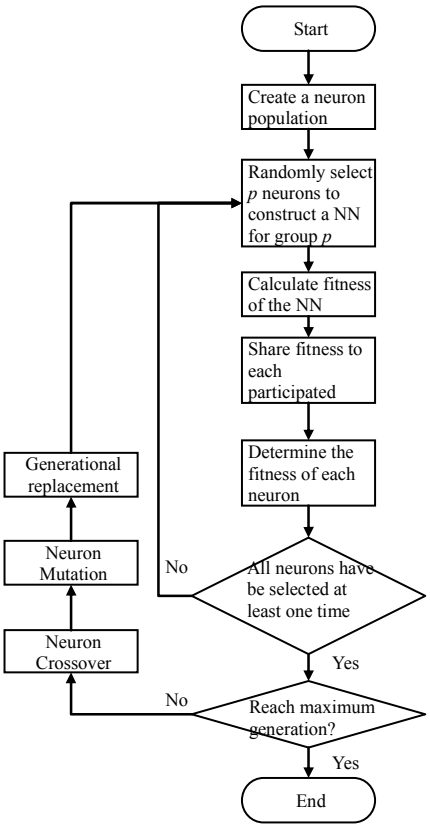

Fig. 3. Flowchart of SNEA.

Step 6) If one of the neurons in the neuron population has not be selected at least one time, then go to Step 2); otherwise, go to Step 7).

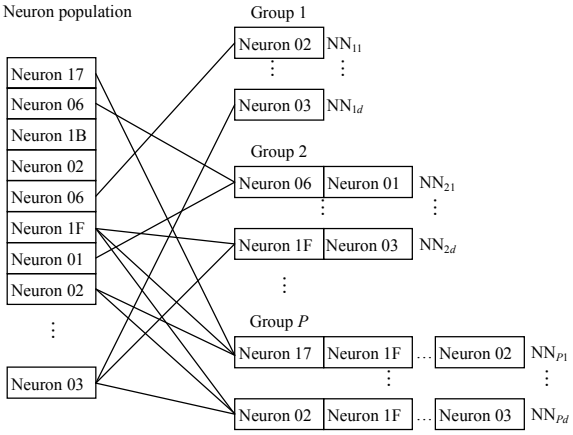

Fig. 4. Construct of NNs of each group from the neuron population.

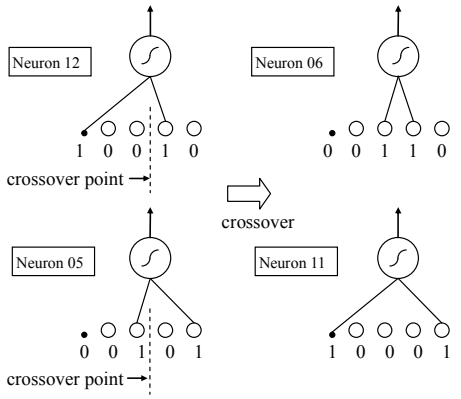

Fig. 5. Neuron crossover.

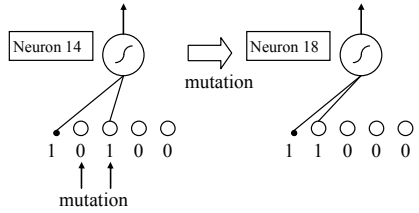

Fig. 6. Neuron mutation.

Step 7) Check the stopping criterion. If the maximum generation is achieved, then stop the algorithm; otherwise, go to Step 8).

Step 8) Perform the neuron crossover to the neuron population. First, the neuron crossover adopts the tournament selection to choose two parents according to their fitness f_n. The crossover point is then randomly assigned, as shown in Fig. 5. Finally, the two parents produce two children by exchanging the connections.

Step 9) Perform neuron mutation on the children. Each connection to either the input or bias might change according to the probability of mutation p_m. For the example shown in Fig. 6, two positions of Neuron 14 are selected to be mutated and then the corresponding connections are disconnected (1→0) or connected (0→1). As a result, Neuron 18 is generated.

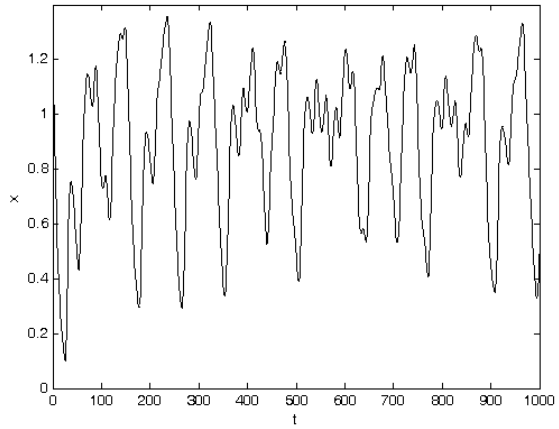

Fig. 7. Mackey-Glass time series.

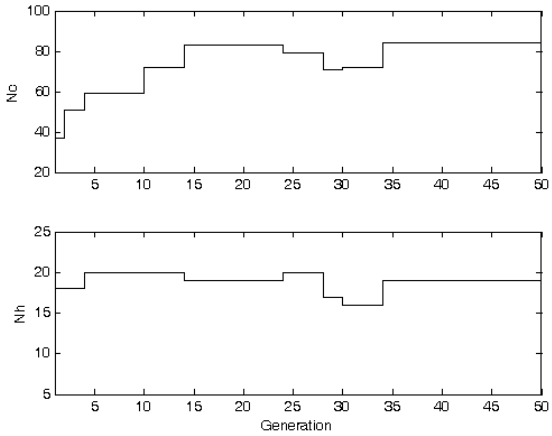

Fig. 8. Evolution progress of neurons and connections for example 1.

Step 10) Perform generational replacement, meaning that all children replace the parents and become parents in the next generation.

IV. Experimental Results

This section provides two examples to verify the performance of the proposed SNEA-NNAGM. The numerical simulations were executed by MATLAB software in an Intel Pentium CPU at 1.5 GHz with 512 MBytes RAM.

Example 1: Chaotic Time Series Prediction

The Mackey-Glass time series shown in Fig. 7 is generated from the following delay differential equation

$$\frac{dx(t)}{dt} = \frac{0.2\,x(t-\tau)}{1+x^{10}(t-\tau)} - 0.1\,x(t) \tag{14}$$

where $\tau = 25$ and $x(0) = 1.2$ in the simulation. The objective involves using $[x(t-3)\ x(t-2)\ x(t-1)\ x(t)]$ to predict $x(t+1)$.

TABLE I. COMPARISON OF PREDICTION RESULTS FOR MACKEY-GLASS TIME SERIES.

	GM(1,1)	Advanced GM(1,1)	NN	NNAGM	SNEA-NNAGM
Training RMSE	---	---	3.27×10^{-4}	2.47×10^{-4}	2.52×10^{-4}
Testing RMSE	1.09×10^{-2}	1.10×10^{-3}	3.58×10^{-4}	2.93×10^{-4}	2.66×10^{-4}
N_h	---	---	34	27	19
N_c	---	---	205	163	84

TABLE II. COMPARISON OF THE PERFORMANCE IN EXAMPLE 2 SUNSPOTS PREDICTION.

	GM(1,1)	Advanced GM(1,1)	NN	NNAGM	SNEA-NNAGM
Training RMSE	---	---	8.24	11.74	12.81
Testing RMSE	30.49	137.52	34.32	65.85	22.01
N_h	---	---	16	14	9
N_c	---	---	97	85	37

Thus, the input of NN of NNAGM is $[e_{GM}(t-3)\ e_{GM}(t-2)\ e_{GM}(t-1)\ e_{GM}(t)]$ and the output is $e_{GM}(t+1)$. The first 500 pairs are used as the training data and the next 500 pairs are the testing data. The parameter of NNAGM is set as $\gamma = 2$ in (12). The parameters of SNEA are set as follows: probability of crossover p_c = 0.8, probability of mutation p_m = 0.5, neuron population size N_{pop} = 40, number of groups N_g = 20, number of group members N_m = 5, and maximum number of generations $G_{\max}$ = 50.

The top side of Fig. 8 shows the number of connections of the evolved NNAGM with the best fitness, N_c, in each generation. The NN has few connections in the first generations and N_c does not always increase. The N_c drops from 83 to 79 in the 24th generation and from 79 to 71 in the 28th generation, implying that more connections do not necessarily result in superior fitness. In other words, appropriate connected topology is the key to improving fitness, not the number of connections. The evolution of NNs almost converges and no further improvement of NN is observed after the 35th generation. The highest quality structure with well-trained weights of NNAGM is then determined.

The bottom side of Fig. 8 shows the number of the hidden neurons, N_h, in the evolved NNAGM. It can be observed that N_h increases to 20 in the 4th generation and decreases to 16 in the 30th generation. As a result, the highest quality structure with well-trained weights of NNAGM has 19 hidden neurons and 84 connections. Clearly, NN of NNAGM is a partially connected network.

Table I shows the prediction results of SNEA-NNAGM compared with other methods including GM(1,1) [9], Advanced GM(1,1) [28], NN [7], and NNAGM [18]. The number of neurons of NNAGM is chosen according to the experimental tests where several NNAGMs with different numbers of neurons, from 1 to 50, were constructed. As a result, a NNAGM with 27 neurons demonstrates the highest performance. The number of neurons of NN is chosen by the same procedure. Consequently, an NN with 34 neurons has the best performance. The neurons of both NN and NNAGM are fully connected. It can be seen that NNAGM has a better RMSE 2.93×10^{-4} than GM(1,1), Advanced GM(1,1), or NN, while SNEA-NNAGM improves the RMSE in advanced 2.66 $\times10^{-4}$ using the evolutionary design of neural networks. It is clear that the evolved NNAGM via SNEA consists of a partially connected NN with 19 neurons and 84 connections. The SNEA-NNAGM obtained a compact structure with fewer neurons and connections, and is superior to NN and NNAGM according to the prediction error.

Example 2: Forecasting the Number of Sunspots

In this example, the sunspots varying nonlinearly from 1709 to 2008 were adopted. The input-output data pair is given as follows:

$$[x[k-3], x[k-2], \cdots, x[k]; x[k+1]] \tag{15}$$

where the four most recent data points are the input data and one step ahead value is the output data. The sunspots of the first 150 years, from 1709 to 1858, were used as the training data and those of the next 150 years, from 1859 to 2008, were the testing data. The input of NN of NNAGM is $[e_{GM}[k-3]\ e_{GM}[k-2]\ e_{GM}[k-1]\ e_{GM}[k]]$ and the output is $e_{GM}[k+1]$. Furthermore, the training data were normalized to the range [0, 1].

Fig. 9 shows the prediction results of the five methods including GM(1,1) [9], Advanced GM(1,1) [28], NNAGM [18], NN [7], and SNEA-NNAGM. The number of neurons of NNAGM is determined by the experimental tests where numerous NNAGMs with different numbers of neurons, from 1 to 50, were constructed. As a result, a NNAGM with 14 neurons has the best performance. The number of neurons of an NN was determined by the same procedure. Consequently, an NN with 16 neurons has the best performance. Note that all neurons in both NNAGM and NN were fully connected. It can be observed that the performance of GM(1,1) was better than the Advanced GM(1,1) in this example, while the performance of NNAGM was better than GM(1,1) due to the use of error prediction via NN. The SNEA-NNAGM further improved the performance by selecting the appropriate structure of NN through SNEA. Table II presents the performance comparison of the five methods. Although SNEA-NNAGM obtained a larger training RMSE than both NN and NNAGM, the testing RMSE is smaller than both of them. Furthermore, the evolved structure of NNAGM via SNEA has 9 neurons and 37 connections. Clearly, the evolved NNAGM is partially connected and is more compact than both NN and NNAGM.

To summarize, through the use of SNEA that designs the structure of NNAGM via symbiotic evolution, SNEA-NNAGM can obtain an appropriate NN structure and outperform NN and NNAGM with a smaller prediction error.

V. CONCLUSION

This paper proposes SNEA to construct automatically NN of an NNAGM. The SNEA determines not only the number of hidden neurons, but also the connected topology between input and hidden layers. The idea behind SNEA is to develop

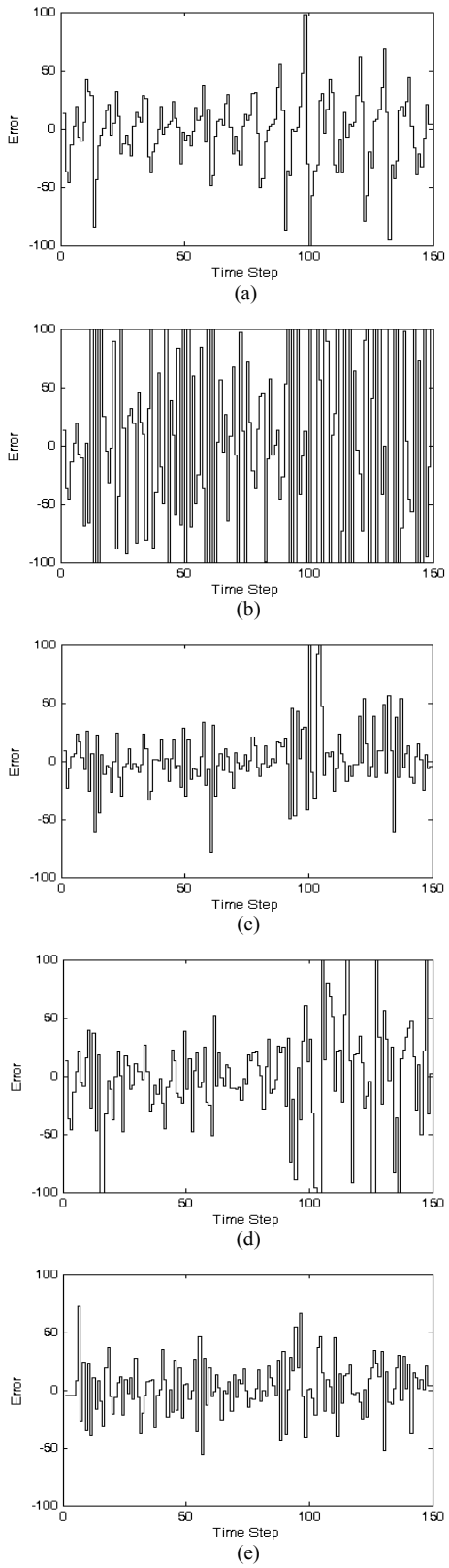

Fig. 9. Prediction errors of (a) GM(1,1) [9], (b) Advanced GM(1,1) [28], (c) NNAGM [18], (d) NN [7], and (e) SNEA-NNAGM.

neurons through symbiotic evolution. This approach facilitates structure learning of NNAGM by evolving neuron population. Each neuron can participate with NNs of different groups and is evaluated through sharing the fitness of the participating NNs. Through symbiotic evolution, NN with appropriate neurons is constructed and the corresponding topology is concurrently established. The experiments in this paper were conducted to evaluate how well SNEA-NNAGM performed in prediction problems. The SNEA can evolve a partially connected NN of an NNAGM with less neurons and connections than a fully connected NN and NNAGM. Furthermore, the prediction performance of SNEA-NNAGM is better than other methods and demonstrates feasibility. Further work should be done to evaluate the performance of this methodology operating in different problems. Thus, future works attempt to analyze the characteristics of this method regarding to the effect of the parameters and apply this method to different numerical experiment and real-world problem.

ACKNOWLEDGMENT

The authors would like to thank anonymous reviewers for their constructive advices and suggestions. This work was supported in part by a grant provided by National Science Council, Taiwan, R.O.C. (NSC 99-2221-E-009 -107) and in part by a grant provided by Industrial Technology Research Institute (Development of Embedded Vision and Intelligent Interactive Behaviors for Home Robots, FY100).

REFERENCES

[1] A. S. Weigend and N. A. Gershenfeld, Time series prediction: Forecasting the future and understanding the past. Addison Wesley, 1994.

[2] J. B. Franch, D. C. Bayarri, “Recurrence plots in nonlinear time series analysis: free software,” Journal of Statistical Software, vol. 7, no. 9, 2002.

[3] F. Takens, “Detecting strange attractors in turbulence,” Dynamical Systems and Turbulence, vol. 898, pp. 366 1981.

[4] D. Ruta and B. Gabrys, “Neural Network Ensembles for Time Series Prediction,” Proc. Int'l Joint Conf. Neural Networks (IJCNN '07), pp. 1204-1209, 2007.

[5] C. C. Hsu and C. Y. Chen, “Applications of improved grey prediction model for power demand forecasting,” Energy Conversion and Management, vol. 44, pp. 2241-2249, 2003.

[6] W. L. Yao, S. C. Chi, and J. H. Chen, “An improved grey-based approach for electricity demand forecasting,” Electric Power Systems Research, vol. 67, no. 3, pp. 217-224, Dec. 2003.

[7] Adya, M., Collopy, F., “How effective are neural networks at forecasting and prediction? A review and evaluation,” Journal of Forecasting, vol. 17, pp. 481–495, 1998.

[8] C. M. Zealand, D. H. Burn, and S. P. Simonovic, “Short term streamflow forecasting using artificial neural networks,” Journal of Hydrology, vol. 214, pp. 32-48, 1999.

[9] J. L. Deng, “Control problems of grey systems,” System & Control Letters, vol. 1, pp. 288-294, 1982.

[10] J. L. Deng, “Introduction of grey system theory,” The J. of Grey System, vol. 1, no. 1, pp. 1-24, 1989.

[11] Kayacan, et. al. Grey system theory-based models in time series prediction. Expert Systems with Applications, vol. 37, pp. 1784-1789, 2010.

[12] V. Viswanathan, V. Krishnan, and L. H. Tsoukalas, “Novel AI approaches in power systems,” Int. Conf. Information Intelligence and Systems, pp. 275-280, 1999.

[13] S. Crone, “Stepwise selection of artificial neural network models for time series prediction,” Journal of Intelligent Systems, vol. 14, no. 2-3, pp 99-122, 2005.

[14] G. Cybenko, “Approximation by superpositions of a sigmoidal function,” Mathematical Control Signals Systems, vol. 2, pp. 303–314, 1989.

[15] K. Hornik, M. Stinchcombe, and H. White, “Multilayer feedforward networks are universal approximators,” Neural Networks, vol. 2, pp. 359–366, 1989.

[16] G. Zhang, B. E. Patuwo, M. Y. Hu, “Forecasting with artificial neural networks: The state of the art,” International Journal of Forecasting, vol. 14, no. 1, pp. 35-62, 1998.

[17] M. M. Islam, M. A. Sattar, M. F. Amin, X. Yao, and K. Murase, “A new adaptive merging and growing algorithm for designing artificial neural networks,” IEEE Trans. Syst., Man, Cybern. B, Cybern., vol. 39, no. 3, pp. 705–722, 2009.

[18] S.-H. Yang and Y.-P. Chen, “Intelligent Forecasting System Based on Grey Model and Neural Network,” IEEE/ASME International Conf. on Advanced Intelligent Mechatronics, pp. 699-704, 2009.

[19] S. H. Yang and Y. P. Chen, “Intelligent Forecasting System Using Grey Model Combined with Neural Network,” *International Journal of Fuzzy Systems*, vol. 13, no. 1, pp. 8-15, 2011.

[20] S.-T. Chen, D. C. Yu, and A. R. Moghaddamjo, “Weather sensitive short-term load forecasting using nonfully connected artificial neural network,” IEEE Trans. Power Systems, vol. 7, no. 3, pp.1098-1105, 1992.

[21] R.E. Smith, S. Forrest and A.S. Perelson, “Searching for diverse, cooperative populations with genetic algorithms,” Evol. Comput., vol. 1, no. 2, pp. 127–149, 1993.

[22] D. E. Moriarty and R. Miikkulainen, “Efficient reinforcement learning through symbiotic evolution,” Mach. Learn., vol. 22, pp. 11–32, 1996.

[23] C. F. Juang, J. Y. Lin, and C. T. Lin, “Genetic reinforcement learning through symbiotic evolution for fuzzy controller design,” IEEE Trans. Syst., Man, Cybern. B, Cybern., vol. 30, no. 2, pp. 290–302, 2000.

[24] C. J. Lin and Y. J. Xu, “A self-adaptive neural fuzzy network with groupbased symbiotic evolution and its prediction applications,” Fuzzy Sets Syst., vol. 157, no. 8, pp. 1036–1056, 2006.

[25] C. J. Lin, C. H. Chen, and C. T. Lin, “Efficient self-evolving evolutionary learning for neurofuzzy inference systems,” IEEE Trans. Fuzzy Syst., vol. 16, no. 6, pp. 1476–1490, 2008.

[26] Y.-C. Hsu and S.-F. Lin, “Reinforcement group cooperation-based symbiotic evolution for recurrent wavelet-based neuro-fuzzy systems,” Neurocomputing, vol. 72, no. 10-12, pp. 2418-2432, 2009.

[27] Y.-C. Hsu, S.-F. Lin, and Y.-C. Cheng, “Multi groups cooperation based symbiotic evolution for TSK-type neuro-fuzzy systems design,” Expert Systems with Applications, vol. 37, no. 7, pp. 5320-5330, 2010.

[28] H. C. Ting, J. L. Chang, C. H. Yeh et al., “Discrete time sliding-mode control design with grey predictor,” International Journal of Fuzzy Systems, vol. 3, pp. 179-185, 2007.

2011 IEEE International Conference on Fuzzy Systems
June 27-30, 2011, Taipei, Taiwan

A Hybrid Computational Intelligence Approach for Automatic Music Composition

Giovanni Acampora*, Jose Manuel Cadenas†, Roberto De Prisco*,
Vincenzo Loia*, Enrique Muñoz‡ and Rocco Zaccagnino*
*Dept. of Computer Science, University of Salerno, Fisciano, Italy 84084
Email: {gacampora, robdep, loia, zaccagnino}@unisa.it
†Dept. of Information and Communications Engineering, University of Murcia, Espinardo, Spain 30003
Email: jcadenas@um.es
‡European Centre for Soft Computing, Mieres, Spain 33600
Email: enriquemuba@um.es

***Abstract*—The use of computers in the production of artifacts has drawn the attention of both artists and computer scientists. Among the different art disciplines, music is one of the arts that most benefited from the use of computers. There are many works which demonstrate the great synergy between these two fields. In this paper we will focus on a specific music composition problem: the figured bass problem, in which we have to automatically generate a 4 voice piece of music, starting from an input the bass line. To solve this problem we use a hybrid strategy, in which different metaheuristics cooperate to find high quality solutions. The cooperation is controlled by means of the combination of fuzzy control and knowledge obtained through Data Mining. As will be shown in the experimental results section, this hybrid strategy is capable of finding musical solutions with an acceptable quality and never discordant which, according to experts, are sound and adhere to scholastic rule.**

***Index Terms*—Computer Music, Evolutionary Computation, Adaptive Memetic Algorithms.**

I. Introduction

The use of computers as means to produce artifacts has been subject of study since the beginning of the computer era. Both artists and computer scientists have been interested in this particular use of the computer. Among the art disciplines, music is one of those that have most benefited from computers. Automatic composition by means of a computer program is almost as old as the computer itself: the ILLIAC suite [1], [2] is a musical piece composed by a computer program and dates back to 1957 just a few years after the introduction of the first computer.

The use of computers in the field of music encompasses many aspects, such as notation programs, sound synthesis, real-time performances, digital instruments, and much more. In this paper we are interested in the aspect of *algorithmic (or automatic) music composition*, that is in the development of computer programs able to automatically generate music, without human intervention.

Algorithmic music composition has fascinated both computer scientists and musicians. We can find works dating back to well before the computer era, which can be considered algorithms for automatic composition (e.g. Mozart's dice game). More recent works include those developed by E.R. Miranda [3] and D. Cope [4], [5], [6].

The tools used to obtain algorithmic composers include many techniques, such as random numbers, formal grammars, cellular automata, fractals, evolutionary algorithms [7][8]. An interesting review of the field can be found in the book by Miranda [9].

Music has a long and interesting history. Music practices have varied during the course of human history developing in various directions also depending on the local culture. This resulted in several formal frameworks for the development of music. The most used one is the so called tempered music system. This system is based on several formal rules that are well suited to be handled by computer programs.

In this paper we are concerned with a very specific tempered music composition problem, known as the *figured bass problem*. A figured bass is a written melody for the bass voice, with indications (numbers or symbols) about the chords to be used. In order to play a figured bass the performer becomes a composer because it is necessary to improvise the other voices in order to obtain a full 4-voice piece of music with the constraints given by the chords indications. The figured bass appeared in the XVI century and was very popular in baroque music. Nowadays it is used (figured or also unfigured) as an exercise for aspiring composers.

So the goal of our automatic composer is that of producing 4-voice piece of music starting from a figured bass line. Formidable examples of 4-voice compositions are Bach's chorales.

Algorithms are frequently used to find optimal or good solutions, where optimal and good are defined according to a precisely defined measure. However, for musical compositions this precise measure does not exist. This is a serious problem, because there is no easy way to decide if a solution is "better" than other. The quality of a musical composition (as the quality of any artistic artifact) is subjective. For the specific problem that we consider in this paper, well known harmony rules can help, although they do not constitute a precise measure. The existence of such a metric would reduce the problem of

978-1-4244-7316-8/11/$26.00 ©2011 IEEE

automatic music composition to an optimization problem with a very large search space. Indeed the figured bass problem, and any other music problem, can be seen as a combinatorial problem where one has to place a finite number of notes on a finite grid (the stave).

In order to "compare" solutions we can exploit harmony rules.

As previously said, there is a broad variety of tools and techniques that can be used to design an algorithmic composer. In this paper we propose the use of a hybrid intelligent tool based on a multi-agent framework and metaheuristics. In this framework different agents analyze a figured bass problem instance and solve it in a parallel way, cooperating between them. This cooperation is performed by jointly exploiting data mining, together with a decision making framework exploiting fuzzy methodologies.

In order to solve the problem each agent implements a metaheuristic. Metaheuristics [10] are intelligent strategies used to design and improve very general heuristic procedures with a high performance. Within metaheuristics, different works [11] have underlined that they can benefit from its combination with fuzzy technologies and data mining improving their results. In this paper we present an adaptive cooperative metaheuristic able to solve figured bass problem. This strategy is able to adapt its behavior depending of the instance being solved. To do that it exploits a set of knowledge models able to code the knowledge obtained from previous executions of the individual metaheuristics. Metaheuristics have already been used for several other problem; to the best of our knowledge, this is the first attempt to use them for a musical problem.

The remainder of the paper is organized as follows. In Section II we introduce some musical concepts necessary to understand the figured bass problem. After that, in Section III the proposed composer is presented. Next, in Section IV we show some results obtained using the composer, and finally in Section V we present some conclusions.

II. Music Background

In this paper we consider the tempered music system, used in western music. This system start from a reference sound (a given frequency, normally 440Hz) and defines *ocatves* as the ranges of frequencies between those sounds obtained by doubling/halving the reference sound. Each octave is divided in 12 equally spaced notes, denoted by the letters A, A♯ or B♭, C, C# or D♭, D, D# or E♭, E, F, F# or G♭, G and G# or A♭. More precisely, if a note has frequency f the "next" note has frequency $f \cdot 2^{\frac{1}{12}}$.

Tempered music is based on the notion of tonality. Roughly speaking, a tonality is a group of notes which form a scale. Using each one of the 12 notes of a scale as starting point we can obtain different tonalities (there are different kinds of tonality for each note, like major, minor, ...). For example, C major scale is C, D, E, F, G, A, B, while D major scale is D, E, F#, G, A, B, C#.

The notes of a scale are often denoted as I, II, III, IV, V, VI, VII, specially when the emphasis is given to the degree of the scale and not to the particular note, which depends on the tonality. Such a notation is possible because all notes are equally spaced.

The interested reader should refer to [12] to get a deeper insight of tempered music.

Usually a tonality is considered the main tonality for a piece, and thus, the notes belonging to the corresponding scale are considered more important than those not belonging to it. Western music, starting from the common practice period, is based on well established harmonic and melodic rules for the tempered music system. We refer the interested reader to any good harmony book as [13] for a discussion about such rules.

In our problem a musical composition is made up of 4 independent voices, called *bass*, *tenor*, *alto*, *soprano*. The bass line is given as input together with numbers, one for each note, that determine the chords to be used.

A musical piece is composed of a sequence of *measures*, each one divided into a given number of *beats*. In each beat the 4 voices play a note (this is a simplification of what really happens, since a composition may also have passing notes, which are not part of the harmony). The vertical set of notes in a beat is a *chord*. The notion of chord is fundamental for this work. There are many types of chords.

In this paper we consider 3- and 4-note chords. Chords are built upon each degree of the scale, that is, I, II, III, IV, V, VI, VII. The note upon which the chord is built, called *root note*, is often given to the bass; however the bass can play any other note which is called chord inversion. Chord inversions usually denoted by a superscript which indicates the inversion (e.g., III^6, V^{46}, I^{357}).

The chords considered on this work are described in Table I (for each one of them we give an example in the tonality of C).

TABLE I
CHORDS CONSIDERED - WITH EXAMPLES IN THE TONALITY OF C

Chord	Root note	Set of notes
Major triad	C	C, E, G
Minor triad	E	E, G, B
Major seventh	C	C, E, G, B
Minor seventh	D	D, F, A, C
Dominant seventh	G	G, B, D, F
Half-diminished seventh	B	B, D, F, A

One of the main rules of tempered music system is that the vertical set of notes has to belong to any of the allowed chords. Other rules may affect sequences of chords. Some sequences are "better" than others, where better is difficult to define, as it is a subjective evaluation. In any case it is largely accepted that particular sequences of chords work better than others. Some chords are "more important" than others because they suggest, prepare, device or enforce tonal centers. The art of tonal music consists precisely in arranging chords in such a way that their interplay is pleasant and significant.

In practice, this is translated into simple rules as the following [13]:

I is followed by IV o V, sometimes VI, less often II o III.
...
...
II is followed by V, sometimes VI, less often I,III o IV.

Besides the rules concerning sequences of chords, we can also find rules about melodic lines. A melodic line is the sequence of notes played by each voice. Rules about melodic lines can refer to the movement of a single voice (for example, a jump bigger than an octave is normally not allowed) or also to the movements of two voices (for example, two voices that proceed by parallel fifth are not allowed). Again, we refer the interested reader to a standard textbook, like [13] for a better and more detailed explanation.

An example of a figured bass problem is provided in Figure 1. Part a of the figure provides the input: only a bass line with indications about the chord; part b provides a solution.

Fig. 1. Chromosome representation

III. An Automatic Music Composer

We propose the use of an adaptive cooperative metaheuristic to solve the figured bass problem. In order to describe the metaheuristic it is necessary to introduce three main aspects: the architecture of the strategy, the cooperation scheme which allows to create a synergy among the different metaheuristics, and the intelligent knowledge extraction process that obtains the data mining models which give adaptability to the strategy.

The development of cooperative metaheuristics lies in the combination of existing metaheuristics to obtain hybrids, in which the different metaheuristics cooperate in a parallel way. Due to their capacity of cooperating in a parallel way, cooperative metaheuristics are closely related to parallel metaheuristics. Many studies have demonstrated [11], [14], [15] that parallel metaheuristics can obtain better results than their sequential components, even when they are allowed to use less time. These studies have shown that the combination of different threads, each one using a different metaheuristic, increments the robustness of the global search independently of the instance being solved.

The proposed strategy combines different metaheuristics which are executed in a parallel way while they exchange information. Information exchange is controlled using previous knowledge about the performance of the individual metaheuristics.

A. Architecture

The strategy is modeled using a multiagent system where we can distinguish two types of agents: *optimization agents* and a *coordinator agent*. Each optimization agent is in charge of executing a metaheuristic, and the coordinator agent is responsible of three tasks: to configure the parameters of the optimization agents depending on the instance being solved, to initiate their parallel execution, and to control their cooperation by deciding how and when they have to exchange information.

Figure 2 shows the architecture of the proposed strategy.

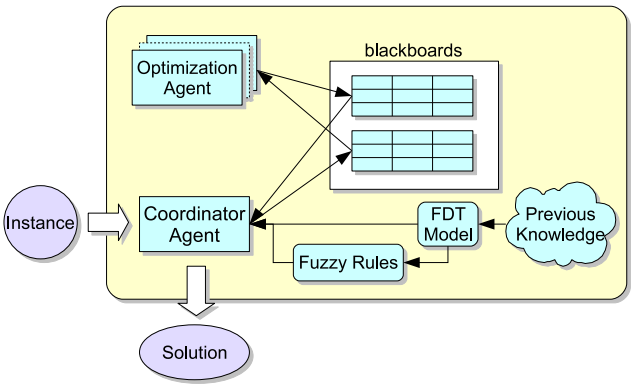

Fig. 2. Architecture of the cooperative metaheuristic strategy

The adaptability of the coordinator is achieved using the knowledge obtained by means of computational learning and coded using a set of trees. In particular, the trees help the coordinator to:

1) choose the best parameters values for each metaheuristic, and
2) sort the suitability of each metaheuristic to solve the instance under consideration, using a set of weights in the range $[0, 1]$.

By analyzing the weights, the coordinator can find out if a metaheuristic is obtaining a poor behavior (according to some measure of performance, e.g. the value of the objective function). As a consequence it can decide to send some solutions to the "bad" metaheuristic from a metaheuristic with a better behavior.

Optimization agents execute in an asynchronous way their associated metaheuristics while send and receive information. The exchange of information is carried out using a blackboard. In detail, two blackboards are used, the first is used by optimization agents to publish the solutions they have found, the second is used by the coordinator in order to indicate the instructions for each agent. Specifically, after a specified period of time, each optimization agent stops and publishes its current solution/population (depending on its type, trajectory or population based). Then the coordinator agent analyzes the behavior of each metaheuristic, using its previous knowledge, and decides if any strategy needs to improve its performance. In this case, the coordinator writes in the second blackboard the new solution/population that the metaheuristic has to use.

B. Cooperation Scheme

The cooperation scheme used by the strategy is mainly defined by the control rules used by the coordinator and the

trees that guide its adaptivity mechanism. These components have to help the coordinator agent to:

- choose the best parameters values for each metaheuristic.
- find out when a metaheuristic is obtaining poor behavior and has to receive new solutions from other metaheuristics with a better behavior.

The first task is carried out using a set of trees obtained through a supervised learning process. Each one of the trees is related to a parameter of a metaheuristic.

The coordinator is able to perform the other task using the information contained in the rest of trees. These trees analyze the instance at hand and sort the different cooperating metaheuristics according to their suitability to solve it. In particular the trees obtain a set of weights $\Omega = \{\omega_i, i = 1, \ldots, n\}$ where n is the number of metaheuristics, $\omega_i \in [0, 1]$ and $\sum_{i=1}^{n} w_i = 1$. Each weight ω_i is associated to a metaheuristic m_i and represents its suitability to solve the instance at hand.

In order to control the exchange of solutions, the coordinator uses the following set of fuzzy rules (this set of rules is replicated once for each metaheuristic):

if $(\omega_1 \cdot \delta_1)$ is *enough* **then**
send solutions from m_1 to m_h

$\ldots$ $\ldots$

if $(\omega_n \cdot \delta_n)$ is *enough* **then**
send solutions from m_n to m_h

where:

- n is the number of metaheuristics.
- m_h is the metaheuristic being evaluated.
- $\delta_i = (\xi_{m_i} - \xi_{m_h})/maximum(\xi_{m_i}, \xi_{m_h})$, where ξ is a measure of performance.
- $\omega_{m_i} \in [0, 1]$ where $\sum_{i=1}^{n} \omega_{m_i} = 1$ and represents the weight of metaheuristic m_i.
- $enough$ is a fuzzy set with trapezodial membership function (with support $\in [0, 1]$) defined by:

$$\mu(x, a, b, c, d) = \begin{cases} 0 & x \leq a \text{ or } x \geq d \\ \frac{x-a}{b-a} & x \in (a, b] \\ \frac{d-x}{d-c} & x \in [c, d) \\ 1 & x \in [b, c] \end{cases}$$

with $(a, b, c, d) = (0, 0.1, 1, 1)$.

Using this set of rules the coordinator is able to know when it has to send new solutions to a given metaheuristic. In detail, it changes the position in the search space of a metaheuristic which is showing a bad performance for a position near the position of another metaheuristic with a better behavior. The firing of the rules is controlled using an α-*cut* defined by the user. In the event that more than a rule is fired, the coordinator applies all of them.

To decide which solutions are sent to a metaheuristic, we consider the following situations:

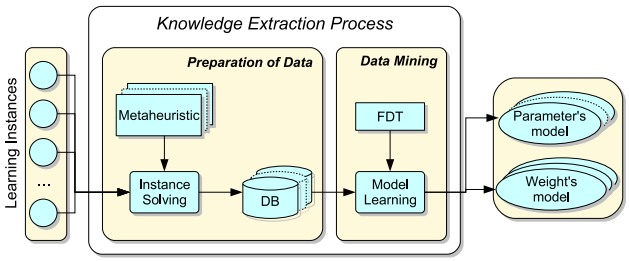

Fig. 3. Obtaining models: Knowledge extraction process

- $m_{receiver}$ is based on trajectories. A solution "near" the best solution obtained by the metaheuristics that have fired the rule is sent. Where "near" means that we apply $\frac{1}{2\omega_{sender}}$ times a mutation operator.
- $m_{receiver}$ is population based:
  - m_{sender} is trajectory based. A proportion of the worst individuals of $m_{receiver}$'s population is substituted by a set of solutions near m_{sender}'s best solution.
  - m_{sender} is population based. A proportion of the worst individuals of $m_{receiver}$'s population is substituted by a set of the best members of m_{sender}.
  - Different metaheuristics have to send solutions. A proportion of the worst individuals of $m_{receiver}$'s population equals to sum of $m'_{sender}s$ ω_i is substituted by a set of solutions where each m_{sender} chooses its solutions as described before.

C. Tree Construction

In order to obtain the models related to weights and parameters we use an intelligent knowledge extraction process, as the one shown in Figure 3.

This process is divided in two different phases, data preparation and data mining. In addition, the process is supervised and previous to strategy's operation.

1) Data Preparation Phase: In this phase the different metaheuristics that compose the strategy are executed several times to solve diverse training instances.

In particular, each metaheuristic is executed using different values for each one of its parameters. Using the information generated in these executions we obtain a dataset which describes the behavior of each metaheuristic.

In detail, we obtain two types of datasets. The first type is related to metaheuristics' parameters and we need one dataset for each parameter of each metaheuristic. The second type is related to metaheuristics' weights and we need one dataset for each metaheuristic.

Focusing on parameters' datasets, each one of them stores for each training instance: a description of the instance and the parameter value that obtained the best performance after solving it. On the other hand, each weights' dataset stores for each training instance: a description of the instance and a weight obtained as

$$\omega_{m_i} = \frac{fit_{best}^{q,i}}{\sum_{l=1}^{n} fit_{best}^{q,l}}$$

where $fit_{best}^{q,i}$ is the best value of the objective function obtained by metaheuristic i for instance q.

2) Data Mining Phase: Once we have obtained the datasets, the data mining phase extracts a collection of fuzzy decision trees which model the information contained in them. Once again we can distinguish two types of models, *parameter models* and *weight models*. The first type is related to the choice of parameters values carried out by the coordinator, and there is one model for each parameter of each metaheuristic. On the other hand, the second type of models is related to the weights Ω, and there is one model for each metaheuristic.

After completing this phase we obtain a set of trees that guide the adaptation of the coordinator. That way it is available to control optimization agents cooperation.

IV. Experimental Analysis

In this section we perform tests in order to asses the validity of the proposed strategy. Each strategy takes as input a figured bass line and produces a complete 4-voice harmonization of the bass line. Some examples of MIDI files generated during the experimental sessions can be listened at http://music.dia.unisa.it/Musimatica/Download.html.

A. Chromosome and gene representation

Figure 4, shows the MIDI-code representation of a chromosome. The time signature $\binom{n_b}{b_\ell}$ is part of the input; we consider as basic time unit the length of the beats. We allow notes of the input to have a length greater than (actually, a multiple of) the beat length. However, if an input note is shorter than the beat length then we consider it only if the note is placed on the beat (otherwise it is only a passage note).

Let n_m denote the number of measures in the input bass line. We can represent a chromosome as an array C of dimension $4 \times n$, where $n \leq n_b \times n_m$. Element $C(i,j)$ contains the j^{th} note for voice i. We place the bass voice in the lower row and the soprano voice in the upper row. Notes are represented using MIDI codes; this allows us to easily play the chromosomes. In the previous example (Figure 4) we have $n_b = 4$, $b_\ell = 1/4$, $n_m = 2$ thus $n = 2 \times 4 = 8$. Notice that this representation doesn't contain information about the notes' length; indeed we do not use such information for the metheuristic. Obviously, we keep the information about the length of the notes in a separate data structure.

For each bass note b_i our goal is to select 3 notes to be played along with the bass note b_i. We will denote such notes with t_i, c_i, s_i. The set of notes $\{b_i, t_i, c_i, s_i\}$ is the chord at position i. We can also think of a (candidate) solution to our problem as an array of $4 \times n$ cells, where each column i contains the four notes b_i, t_i, c_i, s_i. The set of these 4 notes must be one of the allowed chords (see Table I) and must match the indication given in the input.

Since the bass is figured choosing the chord is the easy step, since the input provides already an indication. After choosing the chord we have a huge number of possibilities to place the notes of the chord. Only the bass note is already fixed; notice that the bass not does not necessarily correspond to the root note of the chord.

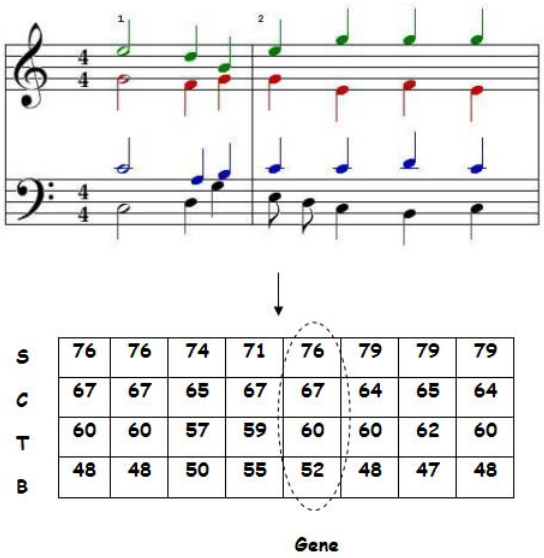

Fig. 4. Chromosome and MIDI representation

B. Fitness function

Our evaluation function takes into account musical composition rules from the common practice period. We consider a simple set of rules, which are detailed in Table II.

To assign a value to a chromosome we start from a reference value which depends on the sequence of chords and thus, depends only on the input, i.e., it is fixed and is based upon harmonic considerations (appropriate sequences of chords);

Given a chromosome x, we assign a reference value by giving a weight for each pair of genes. For each two consecutive bass notes we look at the sequence of the two chords C_1 and C_2 given in x to those two notes and we give the following weights:

- C_1 and C_2 are chords in the same major tonality. The weights are given in Table III.
- C_1 and C_2 are chords in the same minor tonality. The weights are given in Table IV.
- C_1 and C_2 modulate from a major to a major tonality or from a minor to a minor tonality. The weights are given in Table V.
- C_1 and C_2 modulate from a major to a minor tonality or from a minor to a major tonality. The weights are given in Table VI.

The reference value is given by the sum of the weights for pair of genes of x. The weights have been chosen so that good harmonic pattern have heavier weights.

Then to obtain the fitness value of a particular solution we subtract a given cost for each rule violation present in the solution from the reference value. The relations between two consecutive genes (chords) allows us to decide whether the chromosome is good or not. For example, if a voice makes an augmented fourth jump we subtract 40 from the initial value; if two voices make a hidden fifth we subtract 60. If two notes within a chord are at distance greater than an

TABLE II
RULES TABLE

Single voice error	Cost	Type		Two voices error	Cost	Type
sixth	30	normal		hidden unison	40	normal
aug. fourth	40	normal		hidden fifth	60	normal
aug. fifth	40	normal		hidden octave	50	normal
seventh	80	critical		unison	100	critical
$>$ octave	100	critical		parallel fifth	100	critical
				parallel octave	100	critical
Single voice cost	**Cost**	**Type**		**Error within chord**	**Cost**	**Type**
jump	interval	no error		octave leap	30	normal

TABLE V
WEIGHTS FOR MAJOR-TO-MAJOR OR MINOR-TO-MINOR MODULATION.

	C	G	D	A	E	B	G♭	D♭	A♭	E♭	B♭	F
C	2000	0	-500	-1000	-1500	-2000	-2500	-2000	-1500	-1000	-500	0
G	0	2000	0	-500	-1000	-1500	-2000	-2500	-2000	-1500	-1000	-500
D	-500	0	2000	0	-500	-1000	-1500	-2000	-2500	-2000	-1500	-1000
A	-1000	-5000	0	2000	0	-500	-1000	-1500	-2000	-2500	-2000	-1500
E	-1500	-1000	-1000	0	2000	0	-1000	-1000	-1500	-2000	-2500	-2000
B	-2000	-1500	-1500	-5000	0	2000	- 0	-500	-1000	-1500	-2000	-2500
G♭	-2500	-2000	-2000	-1000	-500	0	2000	0	-500	-1000	-1500	-2000
D♭	-2000	-2500	-2500	-1500	-1000	-500	0	2000	0	-500	-1000	-1500
A♭	-1500	-2000	-2000	-2000	-1500	-1000	-500	0	2000	0	-500	-1000
E♭	-1000	-1500	-1500	-2500	-2000	-1500	-1000	-500	0	2000	0	-500
B♭	-500	-1000	-1000	-2000	-2500	-2000	-1500	-1000	-500	0	2000	0
F	0	-500	-1000	-1500	-2000	-2500	-2000	-1500	-1000	-500	0	2000

TABLE VI
WEIGHTS FOR MAJOR-TO-MINOR OR MINOR-TO-MAJOR MODULATION.

	C	G	D	A	E	B	G♭	D♭	A♭	E♭	B♭	F
C	-500	-200	0	500	0	-200	-500	-700	-1000	-1200	-1000	-700
G	-700	-500	-200	0	500	0	-200	-500	-700	-1000	-1200	-1000
D	-1000	-700	-500	-200	0	500	0	-200	-500	-700	-1000	-1200
A	-1200	-1000	-700	-500	-200	0	500	0	-200	-500	-700	-1000
E	-1000	-1200	-1000	-700	-500	-200	0	-500	0	-200	-500	-700
B	-700	-1000	-1200	-1000	-700	-500	-200	0	-500	0	-200	-500
G♭	-500	-700	-1000	-1200	-1000	-700	-500	-200	0	-500	0	-200
D♭	-200	-500	-700	-1000	-1200	-1000	-700	-500	-200	0	-500	0
A♭	0	-200	-500	-700	-1000	-1200	-1000	-700	-500	-200	0	-500
E♭	-500	0	-200	-500	-700	-1000	-1200	-1000	-700	-500	-200	0
B♭	0	-500	0	-200	-500	-700	-1000	-1200	-1000	-700	-500	-200
F	-200	0	-500	0	-200	-500	-700	-1000	-1200	-1000	-700	-500

TABLE III
WEIGHTS FOR STEPPING BETWEEN CHORDS IN THE SAME MAJOR TONALITY.

	I	ii	iii	IV	V	vi	vii^o
I	250	200	50	200	250	50	10
ii	100	100	100	150	2000	150	10
iii	100	100	100	200	100	250	10
IV	250	150	100	200	1500	100	10
V	2000	100	100	100	250	150	10
vi	100	200	150	150	200	200	10
vii	1000	50	150	50	50	100	200

TABLE IV
WEIGHTS FOR STEPPING BETWEEN CHORDS IN THE SAME MINOR TONALITY. THE CHORDS ARE DENOTED $2^*, 3^*$ ETC. BECAUSE IN A MINOR TONALITY ON THESE DEGREES WE CAN HAVE SEVERAL TYPE OF CHORDS (E.G. ON THE SECOND DEGREE WE CAN HAVE ii OR ii°).

	i	2*	3*	4*	5*	6*	7*
i	250	200	50	200	250	50	10
2*	100	100	100	150	2000	150	10
3*	100	100	100	200	100	250	10
4*	250	150	100	200	1500	100	10
5*	2000	100	100	100	250	150	10
6*	100	200	150	150	200	200	10
7*	1000	50	150	50	50	100	200

octave we subtract 30 (except for the couple bass-tenor). For some violations (which we call critical errors) we have bigger penalties. For example for a voice jump bigger than an octave or for two voices that create exposed parallel fifths we have a penalty of 100. Table II provides also the cost that we used for each rule. We construct the possible chords always putting voices in the order bass, tenor, alto and soprano; hence no voice crossing is allowed.

Let's consider an example and again take the one presented in Figure 1. The reference value is the sum of the weights of the chords sequence I - ii - V - I - I - V - I, that is $200 + 2000 + 2000 + 250 + 250 + 2000$, the total is 6700.

To obtain the fitness value of a particular solution, we start from the base value and subtract all the costs listed in Table II.

In this particular case the overall single voices cost is 48, the cost for errors within a chord is 90, the cost of single voices errors 0 and also the cost of two voices errors is 0. Total cost is 138. The fitness value is 6562.

C. Configuration of the Strategy

We will build a strategy using four different individual metaheuristics:

- Genetic Algorithm,
- Tabu Search,
- Simulated Annealing, and
- Particle Swarm Optimization.

After deciding the composition of the metaheuristic, we have to apply the intelligent knowledge extraction process. We will give a brief description of the decisions taken to apply it to a real problem.

- As a first step we have decided to use 36 training instances, in particular this instances have been chosen among J.S. Bach's chorales.
- Each one of them has been solved using each metaheuristic configured with different combination of parameters values. In particular, for each parameter of each metaheuristic we have chosen 4 different values on average. To choose these values we have used previous knowledge about their behavior, however, if there is no previous knowledge we recommend to use, at least, 10 different values.
- After choosing parameters values, we solve each instance 10 times with each possible combination of parameters values, to obtain more precise values.
- Next we obtain parameters and weights datasets.
- Finally we use a fuzzy decision tree construction technique in order to obtain parameters and weights models.

D. Configuration of the Experiments

In order to test the validity of the approach we compare the proposed strategy with the individual metaheuristics that comprise it. To do so, we perform tests with 4 different instances chosen among J.S. Bach's chorales, in particular chorales 26, 112, 266, 606.

Each strategy was executed during 100000 evaluations of the objective function and each instance was solved 10 times. The results show the averages. For the cooperative strategies one can resort to parallel schemes if time is important, or one can simulate the parallelism in a one-processor computer. This is the strategy taken here and the procedure is extremely simple.

We construct an array of solvers and we run them using a round-robin schema. This implementation uses an asynchronous communication mode that is simulated in this way: solvers are executed during a certain number of evaluations of the objective function. This amount of evaluations is a random number in the interval $[5000, 5500]$ and after this period of time, information exchanges are performed. These steps are repeated until the stop condition, given in terms of objective function evaluations, is fulfilled.

The use of the number of objective function evaluations to control the execution of the strategies is broadly extended as a way to perform fairer comparisons with existing techniques. Because in that way we can compare the results independently of the programming language used, the architecture of the computer utilized or the ability of the programmer to optimize his code.

However, we consider that the time can be considered as an important measure of performance, and in that sense we have to point out that the overhead derived from the execution of the coordinator is negligible and that the execution time of the cooperative strategies is always smaller than that of the slower individual metaheuristic for the same number of evaluations of the objective function.

All tests were executed on an Intel Pentium 4 3.20Ghz with 1GB of Memory.

E. Results

The results obtained are shown in Table VII. For each strategy and each instance we present the average percentage of error obtained with respect to the best solution obtained.

From these results we can observe that the proposed strategy (CS) is the one which obtains the lowest error. In order to demonstrate this conclusion we have carried out a statistical analysis [16] of the results. First, we have applied Friedman test to ascertain if there are any differences among the results obtained by all strategies, concluding with a confidence level of 99% that differences do exist. After that we have applied a post-hoc test (Benjamini-Hochberg test together with Wilcoxon test) to study if the error obtained by the proposed strategy is less than that obtained by the rest.

TABLE VII
RESULTS OBTAINED WITH 4 DIFFERENT INSTANCES CHOSEN AMONG J.S. BACH'S CHORALES.

Instance	GA	PSO	SA	TS	CS
Bach's chorale 70	32,03%	26,71%	0,20%	1,41%	0,04%
Bach's chorale 215	39,70%	35,47%	0,88%	5,15%	0,04%
Bach's chorale 266	43,79%	39,38%	12,82%	5,86%	0,02%
Bach's chorale 3604	21,95%	25,66%	4,26%	11,21%	0,02%

The results of these statistical tests indicated with a confidence level of 99% that the results obtained by the cooperative strategy are better.

From these results we can observe the utility of the cooperation between metaheuristics and the adaptive selection of parameters by means of data mining models.

F. Musical analysis

After performing a performance study with respect to the value of the objective function and checking the superiority of the proposed strategy we want to analyze its results from a musical point of view.

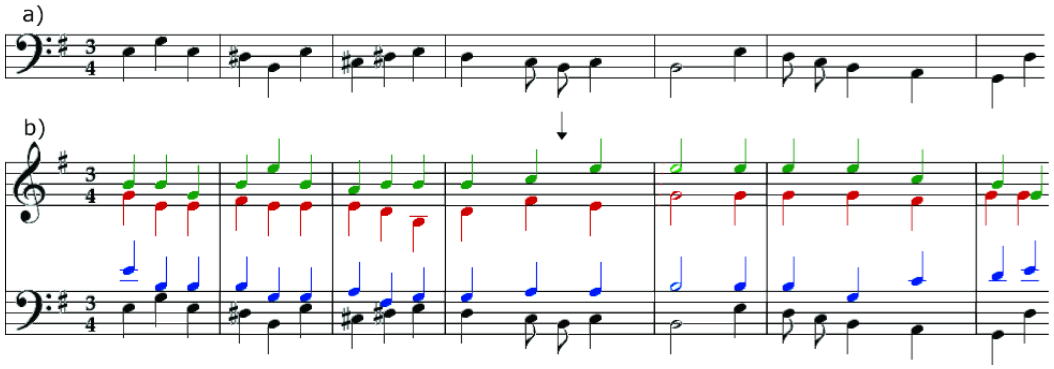

Fig. 5. An example of input - Bach's chorale 266 - (part a) and final solution (part b)

As we have pointed out in the introduction, the quality of a musical composition is a subjective judgment. However the solutions provided do not have any of the errors that guided the search performed by the cooperative metaheuristic.

We have also performed listening tests where we had people, with a music background, listen to the pieces composed by our automatic composer. The avarage response that we had is that the compositions are sound and adhere to scholastic rule. A human composer would probably do better in terms of originality, but most people were surprised that a computer could actually produce such outputs.

V. Conclusions

Figure 5 shows an example of the results obtained by the strategy with Bach's chorale 266. Part a of the figure shows bass line (input) and part b the final solution obtained.

The results obtained fulfill our expectations, returning solutions with an acceptable quality and never discordant. Such results are possible because the cooperative metaheuristic is able to eliminate all critical errors and many of the errors allowed by the used harmonic rules.

In this paper we have presented an automatic composer based on an adaptive cooperative metaheuristic strategy. This composer is able to generate a musical composition without human intervention.

The specific problem under consideration is figured bass problem, in which the objective is the generation of a 4 voice piece starting from bass line. We have tackled the problem using an adaptive cooperative metaheuristic strategy. In this strategy a set of different metaheuristics cooperate under the supervision of a coordinator. This coordinator is modeled using the knowledge extracted by means of a supervised learning process, which is applied to historical data of the execution of individual metaheuristics.

To test the validity of the strategy we have performed different tests obtaining interesting results.

As future work we want to study the similar (but harder) problem called unfigured bass where no indications about the chords is provided in the input. Another interesting direction for future work is the use of an extended set of harmony rules.

Acknowledgements

The authors thank the "Ministerio de Educación y Ciencia" of Spain and the European Fund of Regional Development for the support given to this work under the project TIN2008-06872-C04-03. And the "Fundación Séneca, Agencia de Ciencia y Tecnología de la Región de Murcia (Plan Regional de Ciencia y Tecnología 2007/2010)" which give support under the "Programa de Ayudas a Grupos de Excelencia de la Región de Murcia" of Spain.

References

[1] L. Hiller, Computer music, *Scientific American*, 201(6):109–120, Scientific American Inc., 1959.
[2] L. Hiller, L.M. Isaacson, *Experimental music: Composition with an Electronic Computer*, McGraw-Hill, New York, 1959.
[3] http://neuromusic.soc.plymouth.ac.uk
[4] D. Cope, *Experiments in Musical Intelligence*, Computer Music and Digital Audio Series 12, A-R editions, Madison, WI, 1996.
[5] D. Cope, *The Algorithmic Composer*, Computer Music and Digital Audio Series 16, A-R Editions, Madison, WI, 2000.
[6] D. Cope, *Virtual Music: Computer Synthesis of Musical Style*, MIT Press, Cambridge, 2004.
[7] Y.-p. Chen, "Interactive Music Composition with Evolutionary Computation," *ACM SIGEVOlution*, vol. 2, no. 1, pp. 9-16, 2007.
[8] M. Marques, V. Oliveira, S. Vieira, and A. C. Rosa, "Music composition using genetic evolutionary algorithms," in *Proceedings of the 2000 Congress on Evolutionary Computation (CEC-2000)*, pp. 714-719, 2000.
[9] E.R. Miranda, *Composing Music with Computers* , Music Technology series, Focal Press, 2001.
[10] B. Melián, J.A. Moreno, J.M. Moreno, *Metaheurísticas: una visión global*, Inteligencia Artificial 19:7–28, 2003.
[11] J.M. Cadenas, M.C. Garrido, E. Muñoz, Using machine learning in a cooperative hybrid parallel strategy of metaheuristics, *Information Science*, 179(19):3255–3267, Elsevier, 2009.
[12] G. Loy, *Musimathics vol. 1: The Mathematical Foundations of Music*, The MIT Press, Cambridge, 2006.
[13] W. Piston, M. DeVoto, *Harmony*, Norton, New York, 1987.
[14] T.G. Crainic, M. Toulouse, Parallel Strategies for Metaheuristics, In F. Glover and G.A. Kochenberger, editors, *Handbook of Metaheuristics*, pages 475–513, Kluwer Academic Publisher, 2003.
[15] D. Pelta, C. Cruz, A. Sancho-Royo, J.L. Verdegay, Using memory and fuzzy rules in a cooperative multi-thread strategy for optimization, *Information Sciences*, 176(13): 1849–1868, Elsevier, 2006.
[16] S. García, A. Fernández, J. Luengo, F. Herrera, A study statistical of techniques and performance measures for genetics-based machine learning: accuracy and interpretability, *Soft Computing*, 13(10):959–977, Springer, 2009.

2011 IEEE International Conference on Fuzzy Systems
June 27-30, 2011, Taipei, Taiwan

A Study of a Hybrid Evolutionary Fuzzy Model for Stock Selection

Chien-Feng Huang
Department of Computer Science and Information Engineering
National University of Kaohsiung
Kaohsiung, Taiwan, R.O.C.
cfhuang15@nuk.edu.tw

Chih-Hsiang Chang
Department of Finance
National University of Kaohsiung
Kaohsiung, Taiwan, R.O.C.
cch@nuk.edu.tw

Bao Rong Chang
Department of Computer Science and Information Engineering
National University of Kaohsiung
Kaohsiung, Taiwan, R.O.C.
brchang@nuk.edu.tw

Dun-Wei Cheng
Department of Computer Science and Information Engineering
National University of Kaohsiung
Kaohsiung, Taiwan, R.O.C.
m0985504@mail.nuk.edu.tw

***Abstract*—Stock selection has long been a challenging and important task in finance. Recent advances in machine learning and data mining are leading to significant opportunities to solve these problems more effectively. In this study, we aim at developing a methodology for effective stock selection using fuzzy models as well as genetic algorithms (GA). We first devise a stock scoring mechanism using fundamental variables and apply fuzzy membership functions to re-scale the scores properly. The scores are then used to obtain the relative rankings of stocks. Top-ranked stocks can thus be selected to form a portfolio. Furthermore, we employ GA for optimization of model parameters and feature selection for input variables to the stock scoring model. We will show that the investment returns provided by our proposed methodology significantly outperform the benchmark return. Based upon the promising results obtained, we expect this hybrid fuzzy-GA methodology to advance the research in soft computing for finance and provide an effective solution to stock selection in practice.**

Keywords- Stock selection; fuzzy models; genetic algorithms; model validation

I. INTRODUCTION

Stock selection has long been identified as a challenging and important research area in finance. The success of this task is highly contingent upon reliable selection of stocks that provide above-average return on investment in the future. Recent advances in computational intelligence and data mining are leading to significant opportunities to solve these problems more effectively. Feasible quantitative models include methodologies stemming from soft computing [1] for prediction of financial time series, multi-objective optimization of expected investment return and risk reduction, and portfolio management – selection of investment instruments based on asset ranking using a variety of input variables and historical data, etc. [2-3]. All these research efforts were in an attempt to facilitate the task of decision-making for investment.

In the research area of stock selection and portfolio optimization, several machine learning methodologies have been developed, including artificial neural networks (ANNs), support vector machines (SVMs), evolutionary algorithms (EAs) as well as fuzzy inference models. Quah and Srinivasan [4] studied an ANN stock selection system to choose stocks that are top-ranked performers. They showed their proposed model outperformed the benchmark model in terms of compounded actual returns overtime. Chapados and Bengio [5] also trained neural networks for estimation and prediction of asset behavior in order to facilitate decision-making in asset allocation. Although these models worked in some applications, they often suffer from the overfitting problem and may tend to fall into a local optimum.

For portfolio optimization, Kim and Han [6] proposed a genetic algorithm (GA) approach to feature discretization and the determination of connection weights for ANNs to predict the stock price index. They suggested that their approach was able to reduce the numbers of attributes and the prediction performance was enhanced. In addition, Caplan and Becker [7] employed genetic programming (GP) to develop a stock ranking model for the high technology manufacturing industry in the U.S. More recently, Becker, Fei and Lester [8] explored various single-objective fitness functions for GP to construct stock selection models for particular investment specifics with respect to risk. In a nutshell, these GP-based models rank stocks from high to low according to a pre-defined objective function.

In the area of fuzzy applications in finance, earlier work includes, for instance, Chu *et al.*'s fuzzy multiple attribute decision analysis to select stocks for portfolio construction [9]. Analogously, Zargham and Sayeh [10] employed a fuzzy rule-based system to evaluate a set of stocks for the same purpose. Although these fuzzy approaches denote early efforts in employing computational intelligence for financial applications, they usually lack sufficient learning ability. However, more recently, Chang [11-12] studied a hybrid neuro-fuzzy inference system for the forecast of financial time series. Chang showed that this hybrid model is able to improve the predictive accuracy of irregular non-periodic short-term time series forecast.

Despite the promising performance of the aforementioned approaches in finance, their success is highly contingent upon the input variables (features) to the model. Yang and Honavar [13] indicated that several classification issues are determined by the choice of features that describe given patterns presented

978-1-4244-7316-8/11/$26.00 ©2011 IEEE

to a classifier, such as the classification accuracy of the learned classifier, the computational overhead required for learning a classification function, the number of training examples needed for learning, and the cost associated with the features. Therefore, the goal of feature selection aims to identify useful, non-redundant subsets of features for a given data mining or machine learning task.

In addition, since the variables relevant to the machine learning models usually consist of not only the features but also the models parameters, it is expected that a successful model along this line of research shall take into consideration these two issues simultaneously. Therefore, in this study, we devise a hybrid fuzzy-GA stock selection model for this task, where the GA is used for feature selection and optimization of parameters, simultaneously. Furthermore, in our proposed scheme, feature selection depends on the output of the stock selection model. As a result, our hybrid model can be categorized as a wrapper approach [14-15], as opposed to the filter approach. The wrapper approach for feature selection is employed in this study because of its improved performance over the filter approach [14-18].

In a nutshell, we will conduct the stock scoring mechanism using fuzzy membership functions with the GA-optimized model parameters and subsets of features. Based on the scores calculated, top-ranked stocks are then chosen for portfolio construction. We will report the portfolios constructed by our proposed scheme substantially outperform the benchmark over the long period of time.

This paper is organized into five sections. Section 2 outlines the methods employed in our study. In Section 3 we describe the research data used in this study. In Section 4, we present the experimental design and empirical results are reported and discussed. Section 5 concludes this paper with future research directions.

II. METHODOLOGY

This section first describes our proposed scheme to score stocks using fundamental variables and fuzzy membership functions. Afterwards, model optimization, i.e., parameter optimization and feature selection, by the GA will be discussed.

A. Stock scoring via fundamental variables

In this study, we are concerned with the relative quality of stocks described by the fundamental variables, including firms' share price rationality, growth, profitability, liquidity, efficiency, and leverage attributes. In general, these fundamental variables can be used to determine the value of a stock, defined by the score assigned by our proposed model. Our objective of this scoring model is to imply stocks of higher scores to possess higher potential in future price advancement. Based on these scores one can then rank various stocks and top-ranked stocks are picked to construct the portfolio.

In this study, we first propose a straightforward linear model using these fundamental variables to score stocks. Let $X_{i,j,t}$ denote the score of stock i assigned by variable j at time t, where $X_{i,j,t}$ depends on the value of variable j, $v_{i,j,t}$, for stock i at time t. For instance, in the area of value investing, if the variable is the price-to-book value (P/B ratio), a smaller P/B value tends to imply the stock's higher potential of price increase in the future [19]. On the contrary, if the variable is return-on-asset (ROA), a larger value of ROA usually implies the stock's higher potential of price increase in the future.

Therefore, we propose to sort the stocks according to their values of variable j and the individual score assigned to stock i at time t is:

$$X_{i,j,t} = \rho_{i,j,t},$$

where $\rho_{i,j,t} \in N$ is the ranking of stock i with respect to variable j at time t. Here we denote a stock sorting indicator I_j for variable j and consider two cases for the stock sorting scheme:

$$(1)\ I_j = 0:\ \rho_{i,j,t} \geq \rho_{k,j,t} \ \text{ iff } \ v_{i,j,t} \geq v_{k,j,t} \text{ for } i \neq k.$$

$$(2)\ I_j = 1:\ \rho_{i,j,t} \geq \rho_{k,j,t} \ \text{ iff } \ v_{i,j,t} \leq v_{k,j,t} \text{ for } i \neq k.$$

In addition, let W_j denote the weight of the j-th variable. Then the total score of stock i at time t, $S_{i,t}$, can be defined as

$$S_{i,t} = \sum_j W_j X_{i,j,t}. \tag{1}$$

In this study, to allow more flexibility for our model, we introduce a fuzzy scheme as an extension of the scoring mechanism, which will be discussed next.

B. Fuzzy model for stock scoring

To improve the accuracy of the stock scoring model, the fuzzy membership function is applied. This treatment is to increase the flexibility of the model so that the stock scores calculated by the GA may be adjusted properly to reflect the actual potential of stock price increase in the future. This adjusted score, denoted by $y_{i,t}$, is determined by the score calculated by Eq. (1), $S_{i,t}$, and the fuzzy membership function, $\mu(x)$.

More specifically, in the fuzzy stock scoring model, the score for stock i at time t, $y_{i,t}(\boldsymbol{W}, \boldsymbol{\theta}) \in R$, is defined as

$$y_{i\,t}(\boldsymbol{W}, \boldsymbol{\theta}) = S_{i,t}(\boldsymbol{W}, \boldsymbol{\theta}) * \mu(S_{i,t}(\boldsymbol{W}, \boldsymbol{\theta})),$$

where $\boldsymbol{W}$ denotes the vector of the weights of the input features (i.e., the fundamental variables) used by the stock scoring model and $\boldsymbol{\theta}$ denotes the set of the parameters used by the fuzzy membership function.

In this study, we compare three commonly used fuzzy membership function — the triangle, trapezoid and Gaussian functions. As an illustration, Fig. 1 displays the triangular membership function as shown below, where the shape of the fuzzy model is determined by parameters a, b, and c. In this study, these parameters will be optimized by the GA based on the given fitness function.

$$\mu_A(x) = \begin{cases} 0, & x \le a \\ \dfrac{x-a}{b-a}, & a < x \le b \\ \dfrac{c-x}{c-b}, & b < x \le c \\ 0, & c < x \end{cases}$$

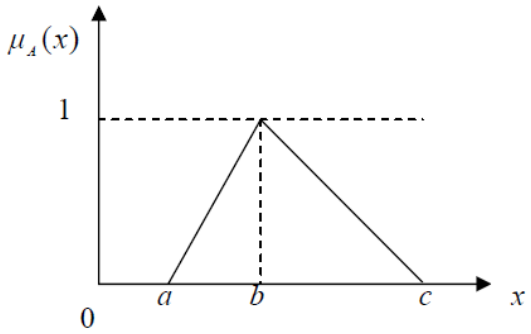

Figure 1. Triangular fuzzy membership function

Our experimental results so far show that the triangle and trapezoid functions exhibited similar, better performance than the Gaussian function. The reason is that the tip and the width of the triangle and trapezoid functions are adjustable, whereas in the Gaussian function, only the width can be adjusted. Therefore, in this paper, we will only demonstrate the experimental results using the triangular membership function.

It is worthwhile to mention that the scores calculated for the stocks may not necessarily represent the precise values of various stocks. Rather, they can serve as surrogates for the actual quality to imply the relative rankings of the stocks. Thus given the scores for all stocks, the ranking of a stock can be defined as:

$$\alpha_{i,t}(\boldsymbol{W}, \boldsymbol{\theta}) = \rho(y_{i,t}(\boldsymbol{W}, \boldsymbol{\theta})), \tag{2}$$

where $\rho(\cdot)$ is a ranking function so that $\alpha_{i,t} \in N$ is the ranking of stock i at time t, and $\alpha_{i,t} \ge \alpha_{j,t}$ iff $y_{i,t} \ge y_{j,t}$.

The task of stock selection can be achieved using these rankings whereby top-ranked m stocks (stocks corresponding to the top m α's) are selected as components of a portfolio. The performance of a portfolio can be evaluated by averaging the actual returns of the stocks in the portfolio, which is defined as:

$$\overline{R_t} = \frac{1}{m}\sum_{i=1}^{m} R_t(s_{i,t}), \tag{3}$$

where $s_{i,t}$ is the i-th ranked stock at time t; $R_t(\cdot)$ is the actual return for a stock at time t and $\overline{R_t}$ is the average return over all the m stocks in the portfolio at time t.

In this study we will use the cumulative total (compounded) return, R_c, to evaluate the performance of a stock selection model, where R_c is defined as the product of the average yearly return, $\overline{R_t}$, of the stocks in a portfolio over n consecutive years as:

$$R_c = \prod_{t=1}^{n} \overline{R_t}. \tag{4}$$

C. Model optimization

The performance of the stock selection model is determined by the set of input features $\boldsymbol{F}$, the set of stock sorting indicators $\boldsymbol{I}$, the weights of the fundamental variables $\boldsymbol{W}$, and the set of parameters $\boldsymbol{\theta}$ to the fuzzy membership function. Therefore, we expect that the selection of optimal subsets of features $\boldsymbol{F}$, and the optimization of $\boldsymbol{I}$, $\boldsymbol{W}$ and $\boldsymbol{\theta}$ will be critical to the effectiveness of the stock selection model. In this study, we propose to use Genetic Algorithms for simultaneous optimization with respect to these tasks. In the next subsections we describe the basics of the GA and the relevant optimization scheme for our stock selection model.

C.1 Genetic algorithms

Genetic algorithms were developed by Holland [20] and have been used as computational models of natural evolutionary systems and as adaptive algorithms for solving optimization problems. GAs operate on an evolving population of artificial organisms, or agents. Each agent is comprised of a genotype (often a binary string) encoding a solution to some problem and a phenotype (the solution itself). GAs regularly start with a population of randomly generated agents within which solution candidates are embedded. In each iteration, a new generation is created by applying variations, such as crossover and mutation, to promising candidates selected according to probabilities biased in favor of the relatively fit agents. As a result, evolution occurs by iterated stochastic variation of genotypes, and selection of the best phenotypes in an environment according to how well the respective solution solves a problem (or problem-specific fitness function). Successive generations are created in the same manner until a well-defined termination criterion is met. The core of this class of algorithms lies in the production of new genetic structures along the course of evolution, thereby providing innovations to solutions for the problem at hand. The steps of a simple GA are shown in the following:

Step 1: Randomly generate an initial population of l agents, each being an n-bit genotype (chromosome).
Step 2: Evaluate each agent's fitness.
Step 3: Repeat until l offspring have been created.
  a) select a pair of parents for mating;
  b) apply variation operators (crossover and mutation);
Step 4: Replace the current population with the new population.
Step 5: Go to Step 2 until terminating condition.

C.2 Chromosome encoding and fitness function

Among many paradigms of search algorithms GAs have been proven to have an advantage over traditional optimization methods in problems with many complex, discontinuous constraints in the search space. This methodology contributes for a global, population-based search in the search space, in contrast with the kind of local, greedy search conducted by most rule-induction and decision-tree algorithms. Lower computation cost is a general advantage of local, greedy search algorithms. However, the solution quality achieved by these algorithms can be greatly degraded if there exists a considerable degree of feature interactions, which is usually the case for real-world problems. Since GAs can be designed to perform a global search for various combinations of sets of features that improve given optimization criteria, this class of algorithms are expected to cope better with feature interaction problems. Therefore, we propose to use the GA method to search for optimal subsets of features for the stock selection model.

Apart from feature selection, three sets of free parameters, $\boldsymbol{I}$, $\boldsymbol{W}$ and $\boldsymbol{\theta}$, are to be provided for the stock selection model. Here we employ the GA for simultaneous optimization of these tasks. In our overall encoding design, the composition of a chromosome is devised to consist of four portions - the candidate set of features $\boldsymbol{F}$, the stock sorting indicators $\boldsymbol{I}$, the weighs $\boldsymbol{W}$ and the fuzzy model parameters $\boldsymbol{\theta}$. In this study, the binary coding scheme is used to represent a chromosome. In Fig. 2, loci b_f^1 through b_f^n represent candidate features 1 through n, respectively. For these features, allele '1' or '0' corresponds to the feature being selected or not. Loci b_i^1 through b_i^n represent the sorting indicators, where 0 represents the variable being used for case (1) of our stock sorting scheme, and 1 represents case (2), respectively. On the right-hand side of Fig. 2 is the encoding of the set of parameters $\boldsymbol{W}$. Fig. 3 shows the detailed binary encoding for the weight of each individual variable, where the value of W_i (the weight for variable i) is encoded by loci b_{Wi}^1 through $b_{Wi}^{n_i}$. For the fuzzy model, the rightmost side of Fig. 2 is the encoding of the set of parameters $\boldsymbol{\theta}$. For example, parameter a is encoded (in binary forms) by loci b_a^1 through $b_a^{n_a}$, as shown in Fig. 4.

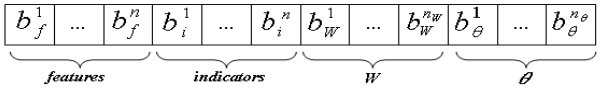

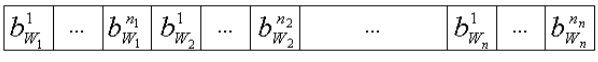

Figure 2. Chromosome encoding

Figure 3. Detail encoding of the weighting terms *Wi's*

Figure 4. Detail encoding of the fuzzy model parameters

In our coding scheme, the portion in the chromosome representing the genotypes of parameter W_i's and $\boldsymbol{\theta}$'s is to be transformed into the phenotype by Eq. (5) for further fitness computation. The precision representing each parameter depends on the number of bits used to encode it in the chromosome, which can be determined as follows:

$$y = \min_y + \frac{d}{2^l - 1} \times (\max_y - \min_y), \tag{5}$$

where y is the corresponding phenotype for the particular parameter; $\min_y$ and $\max_y$ are the minimum and maximum of the parameter; d is the corresponding decimal value, and l is the length of the block used to encode the parameter in the chromosome.

With this encoding scheme, we define the fitness function of a chromosome as the annualized return of the portfolio:

$$fitness = \sqrt[n]{R_c}, \tag{6}$$

where Rc is the cumulative total return computed by Eq. (4).

Our proposed fuzzy-GA model for stock selection is a multi-stage process, including feature selection and parameter optimization by the GA, stock scoring, score fuzzification, stock ranking and selection, as well as performance evaluation. The flowchart of this hybrid algorithm is shown in Fig. 5.

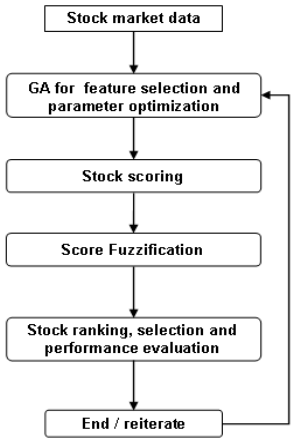

Figure 5. Flow chart of the hybrid fuzzy-GA model

III. DATA AND FUNDAMENTAL VARIABLES

We use the constituent stocks of the 50 largest market capitalizations listed in the Taiwan Stock Exchange as the investment universe. The yearly financial statement data and stock returns used for this research are retrieved from the TEJ

Table I. Attributes used in the stock selection model

Attribute	Ratios	Description	Ref.
Share price rationality	PE ratio	Price-to-earnings ratio = share price / earnings per share	[21, 23-24, 26]
	PB ratio	Price-to-book ratio = share price / book value per share	[21-25]
	PS Ratio	Price-to-sales ratio = share price / sales per share	[21]
Profitability	ROE	Return on equity (after tax) = net income after tax / shareholders' equity	[27-28]
	ROA	Return on asset (after tax) = net income after tax / total assets	[27]
	OPM	Operating profit margin = operating income / net sales	[29]
	NPM	Net profit margin = net income after tax / net sales	[28]
Leverage	DE ratio	Debt-to-equity ratio = total liabilities / shareholders' equity	[27]
Liquidity	CR	Current ratio = current assets / current liabilities	[27]
	QR	Quick ratio = quick assets / current liabilities	[27]
Efficiency	ITR	Inventory turnover rate = cost of goods sold / average inventory	[27]
	RTR	Receivables turnover rate = net credit sales / average accounts receivable	[30]
Growth	OIG	Operating income growth rate = (operating income at the current year – operating income at the previous year) / operating income at the previous year	[31]
	NIG	Net income growth rate = (net income after tax at the current year – net income after tax at the previous year) / net income after tax at the previous year	[32]

(Taiwan Economic Journal Co. Ltd., http://www.tej.com.tw/) database for the period of time from 1995 to 2009. For the choice of fundamental variables, early studies indicated that several financial ratios play key roles in future stock returns. Most of them applied profitability (e.g., ROE, ROA, operating profit margin, and net profit margin), leverage (e.g., DB ratio), liquidity (e.g., current ratio and quick ratio), efficiency (e.g., inventory turnover rate and receivables turnover rate), and growth (e.g., operating rating income growth rate and net income growth rate) related ratios to examine the relationship between fundamentals and stock returns. Mukherji *et al.* [21], Jensen *et al.* [22], Danielson and Dowdell [23], Lewellen [24], Fama and French [25], and Hjalmarsson [26] also showed that the ratios relating to share price rationality, e.g., PE, PB, and PS ratios, are likely to influence future stock returns. According to the previous literature, Table 1 provides the aforementioned six attributes that are to be employed for this study, including fourteen financial ratios. For each year, investable stocks are described by these fourteen financial ratios and their historical returns are provided.

IV. Empirical Results

In this study, standardization was first applied to the research data ─ every original attribute is scaled into the range of [−1, 1] by subtracting the mean, and dividing the result by the standard deviation. This treatment is to ensure that all the attributes lie in the same parameter range, in order to prevent attributes with large ranges from overwhelming others and prediction errors may be reduced.

To examine our proposed model, stock data of all the years is first used for optimization by the GA. Stocks are ranked based on the scores obtained. Top *m* stocks are selected and

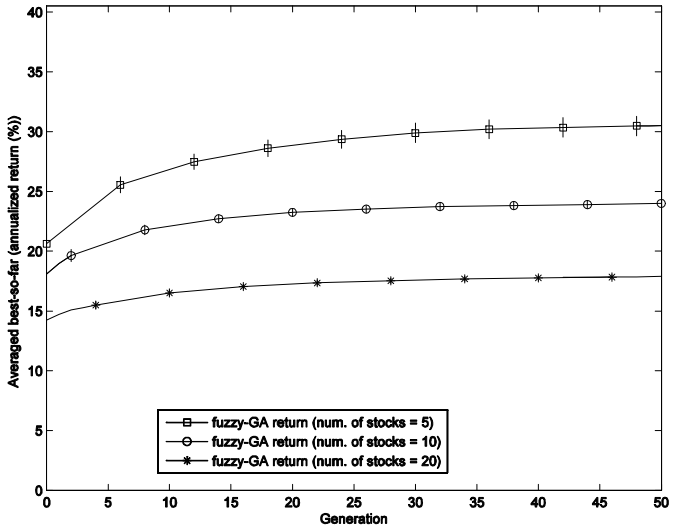

Figure 6. Best-so-far curves by the GA

the average yearly return of these selected stocks are calculated. Fig. 6 displays the averaged best-so-far values for annualized returns over 50 runs attained by the GA over 50 generations.[1] The averaged best-so-far performance curve is calculated by averaging the best-so-fars obtained at each generation for all 50 runs, where the vertical bars overlaying

[1] In order to study the change of the quality of solutions over time, a traditional performance metric for search algorithms is the "best-so-far" curve that plots the fitness of the best individual that has been seen thus far by generation *n* for the GA ─ i.e., a point in the search space that optimizes the objective function thus far. In addition, in this study the GA experiments employ a binary tournament selection [33], one-point crossover and mutation rates of 0.7 and 0.005, respectively.

the curves represent the 95-percent confidence intervals about the means.

Fig. 7 displays an illustration of the cumulative benchmark return (the product of the average yearly returns of the 50 stocks in the investment universe) and the cumulative returns of longing a number of top-ranked stocks recommended by the fuzzy-GA model.[2] This figure shows that the portfolios of maintaining 5, 10 and 20 stocks outperform the benchmark at the end of year 2009. As a result, the optimization on the stock selection model by the GA is advantageous to stock selection.

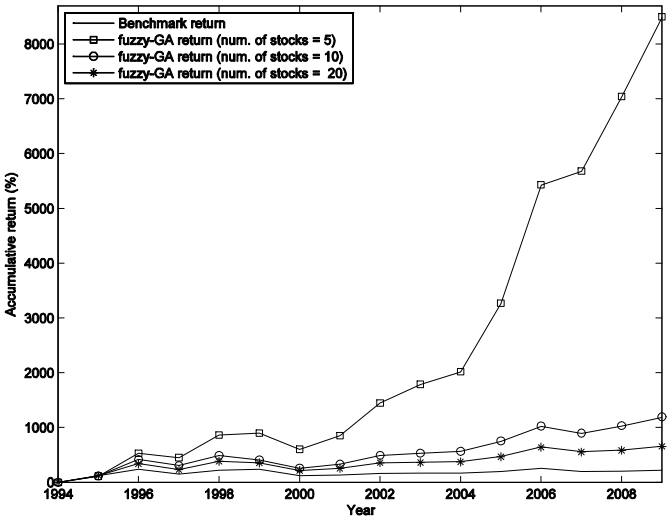

Figure 7. Cumulative returns of benchmark v.s. longing top-ranked stocks by the fuzzy-GA stock selection model

In order to examine the validity of the methodology we proposed, further statistical validation on the model is conducted. In reality, the learned model has to be tested by unseen data. Here, we use the stock data of the first several years to train the fuzzy-GA model, and the remaining years are used for testing the learned model. Thus the average yearly return of the selected stocks for each of the testing year is calculated. The average yearly returns are then compounded to obtain the cumulative total return of the portfolio over the testing years.

Notice that this setup is different from the regular cross-validation procedure where the process of data being split into two independent sets is randomly repeated several times without taking into account the data's temporal order. However, in the stock selection study here, temporal order is critical as practically one would like to use all available data so far to train the model and to apply the models in the future to gain profits.

Here we compare the cumulative benchmark return (the product of the average yearly returns of the 50 stocks in the investment universe) and the cumulative average return of longing a number of top-ranked stocks (5 and 20 stocks) using our stock selection model. Table 2 and 3 show the model validation for selecting 5 and 20 stocks by the fuzzy-GA model for 50 runs. In the 5-stock model, an inspection on the means of annualized model returns shows that 13 out of 14 for the testing cases outperform the annualized benchmark return. For the 20-stock model, in all the 14 testing cases, the means of annualized model returns all outperform the annualized benchmark return.

In the mean time, the standard deviations and standard errors of the annualized model returns decrease as more stocks are being selected into a portfolio. That is, selecting 20 stocks apparently yields more consistent performance on the model

Table II. Statistics of the benchmark and fuzzy-GA stock selection models for 5 stocks

Training period	Annualized benchmark return	Mean of annualized model return	Standard Deviation	Standard error	Testing period	Annualized benchmark return	Mean of annualized model return	Standard Deviation	Standard error
1995	23.1487	61.4170	2.61412	0.36969	1996-2009	4.25672	1.1731	5.34558	0.75598
1995-1996	53.9684	162.6117	10.33728	1.46191	1997-2009	-0.54716	-0.5062	4.02765	0.56959
1995-1997	15.3332	76.9770	3.14302	0.44449	1998-2009	3.07863	5.2559	5.66329	0.80091
1995-1998	22.4658	87.1291	5.02817	0.71109	1999-2009	-0.17093	0.1383	5.11039	0.72271
1995-1999	19.1951	69.1519	5.39052	0.76233	2000-2009	-0.85761	0.9131	5.79058	0.81891
1995-2000	3.7129	43.7078	3.15297	0.44589	2001-2009	6.57475	10.2523	7.24027	1.02393
1995-2001	4.0824	40.2833	2.63405	0.37251	2002-2009	6.60575	13.3479	4.55598	0.64431
1995-2002	6.5905	41.9213	2.32244	0.32844	2003-2009	4.09937	10.1117	5.37307	0.75986
1995-2003	6.1517	39.6470	2.09784	0.29668	2004-2009	4.33343	7.6255	7.19403	1.01739
1995-2004	5.5582	36.0228	1.25193	0.17705	2005-2009	5.14611	11.0043	8.36337	1.18275
1995-2005	6.5087	35.5869	1.82544	0.25815	2006-2009	2.48545	9.02378	7.69611	1.08839
1995-2006	8.124	36.9053	1.67149	0.23638	2007-2009	-4.73667	-1.64134	9.27202	1.31126
1995-2007	5.5105	33.5921	1.64090	0.23205	2008-2009	4.83837	5.25787	9.33182	1.31972
1995-2008	5.3590	31.5289	1.71741	0.24287	2009	6.28742	15.3057	12.88159	1.82173

[2] Beating the benchmark has been a challenging task as discussed in [34-35]; therefore, in this paper, we compare the performance of our stock selection model with the benchmark.

Table III. Statistics of the benchmark and fuzzy-GA stock selection models for 20 stocks

Training period	Annualized benchmark return	Mean of annualized model return	Standard Deviation	Standard error	Testing period	Annualized benchmark return	Mean of annualized model return	Standard Deviation	Standard error
1995	23.1487	39.7684	1.57912	0.2233	1996-2009	4.25672	4.49396	3.07153	0.43438
1995-1996	53.9684	97.5861	2.23359	0.3158	1997-2009	-0.54716	2.12094	2.45705	0.34748
1995-1997	15.3332	39.8031	1.23430	0.1745	1998-2009	3.07863	7.35682	2.40687	0.34038
1995-1998	22.4658	50.1824	1.84520	0.2609	1999-2009	-0.17093	1.37174	2.33844	0.33070
1995-1999	19.1951	40.3479	1.53589	0.2172	2000-2009	-0.85761	0.74860	2.66413	0.37676
1995-2000	3.7129	22.0304	1.36951	0.1936	2001-2009	6.57475	11.0353	1.74344	0.24656
1995-2001	4.0824	21.3027	1.12551	0.1591	2002-2009	6.60575	11.2566	1.96797	0.27831
1995-2002	6.5905	24.0367	1.06560	0.1507	2003-2009	4.09937	8.04446	2.02825	0.28683
1995-2003	6.1517	22.5926	0.96115	0.1359	2004-2009	4.33343	7.75598	2.02601	0.28652
1995-2004	5.5582	20.6871	0.81464	0.1152	2005-2009	5.14611	9.91133	2.24343	0.31727
1995-2005	6.5087	20.3811	0.80881	0.1143	2006-2009	2.48545	8.27924	2.47071	0.34941
1995-2006	8.1249	22.7893	0.79199	0.1120	2007-2009	-4.73667	-1.34713	2.26997	0.32102
1995-2007	5.5105	19.4647	0.53036	0.0750	2008-2009	4.83837	6.23260	2.77440	0.39236
1995-2008	5.3590	18.6817	0.71449	0.1010	2009	6.28742	7.22983	4.71266	0.66647

return from various runs than the 5-stock cases do. As a result, these validations provide a statistical evidence that our proposed stock selection methodology is promising for investment in research and practice.

V. CONCLUSIONS

In this paper we presented a hybrid fuzzy-GA methodology for stock selection. Based on the designed scoring mechanism for a set of stocks, top-ranked stocks can be selected as components in a portfolio. In the mean time, the GA was employed for optimization of model parameters and feature selection for the model. We have evaluated the fuzzy-GA models statistically and validated the effectiveness of this method by comparing the investment return of the models with that of the benchmark. The empirical results showed that the investment return provided by our proposed methodology can significantly outperform the benchmark return. Therefore, we expect this hybrid model to advance the research in computational finance and provide a promising solution to stock selection in practice. In the future, a plausible research direction is to employ more advanced fuzzy and scoring models to investigate how performance of portfolios can be further improved. In addition, in our current model, we consider the first several years as the training set and the next several years as the test set. This may not be sufficient to generate a feasible model; e.g., it might be difficult to infer plausible scores for stocks in the period from 1996 till 2009 if the model uses only the stocks of 1995 for training. Therefore, in the future work, we intend to study a model that would be capable of generating more time-dependent patterns to account for the impact of the more recent past of the stocks. Finally, because investment return and risk management appear to be two distinct objectives, in the future work, we expect that a study for simultaneous optimization on these multi-objectives is also a promising research area.

ACKNOWLEDGMENT

This work is fully supported by the National Science Council, Taiwan, Republic of China, under grant number NSC 99-2221-E-390 -032.

REFERENCES

[1] A. Mochón, D. Quintana, Y. Sáez, “Soft computing techniques applied to finance”, Applied Intelligence, vol.29(2), 2008, pp.111-115.

[2] D. Zhang, L. Zhou, “Discovering golden nuggets: data mining in financial application”, IEEE Transactions on Systems, Man, and Cybernetics—Part C: Applications and Review, vol.34(4), 2004, pp. 513–522.

[3] K. K. Lai, L. Yu, S. Wang, C. Zhou, “A double-stage genetic optimization algorithm for portfolio selection”, the 13th International Conference on Neural Information Processing, 2006, pp. 928–937.

[4] T. S. Quah, B. Srinivasan, “Improving returns on stock investment through neural network selection”, Expert Systems with Applications, vol.17, 1999, pp. 295–301.

[5] N. Chapados, Y. Bengio, “Cost functions and model combination for VaR-based asset allocation using neural networks”, IEEE Transactions on Neural Networks, vol. 12, 2001, pp. 890–906.

[6] K. J. Kim, I. Han, “Genetic algorithms approach to feature discretization in artificial neural networks for the prediction of stock price index”, Expert Systems with Applications, vol.19, 2000, pp. 125–132.

[7] M. Caplan, Y. Becker, “Lessons learned using genetic programming in a stock picking context”, in: U.-M. O'Reilly, T. Yu, R. Riolo, B. Worzel (Eds.), Genetic Programming Theory and Practice II, Springer, Ann Arbor, Michigan, 2004, pp. 87–102, Chapter 6.

[8] Y. Becker, P. Fei, A. Lester, “Stock selection – An innovative application of genetic programming methodology”, in: R. Riolo, T. Soule, B. Worzel (Eds.), Genetic Programming Theory and Practice IV, Genetic and Evolutionary Computation, vol. 5, Springer, Ann Arbor, Michigan, 2006, pp. 315– 334, Chapter 12.

[9] T. C. Chu, C. T. Tsao, Y. R. Shiue, “Application of fuzzy multiple attribute decision making on company analysis for stock selection”, in:

Proceedings of Soft Computing on Intelligent Systems and Information Processing, 1996, pp. 509–514.

[10] M. R. Zargham, M. R. Sayeh, "A web-based information system for stock selection and evaluation", in: Proceedings of the First International Workshop on Advance Issues of E-Commerce and Web-Based Information Systems, 1999, pp. 81-83.

[11] B. R. Chang, "applying nonlinear generalized autoregressive conditional heteroscedasticity to compensate ANFIS outputs tuned by adaptive support vector regression", Fuzzy Sets and Systems, vol.157(13), 2006, pp. 1832-1850.

[12] B. R. Chang, "Resolving the forecasting problems of overshoot and volatility clustering using ANFIS coupling nonlinear heteroscedasticity with quantum tuning", Fuzzy Sets and Systems, vol.159(23), 2008, pp. 3183-3200.

[13] J. Yang, V. Honavar, "Feature subset selection using a genetic algorithm", IEEE Intelligent Systems, vol.13(2), 1998, pp. 44-49.

[14] G. John, R. Kohavi, K. Peger, "Irrelevant features and the subset selection problem," in: Proceedings of the 11th international conference on machine learning, 1994, pp. 121–129.

[15] R. Kohavi, G. John, "Wrappers for feature subset selection," Artificial Intelligence, vol. 97(1–2), 1997, pp. 273–324.

[16] C. L. Huang, C. J. Wang, "A GA-based feature selection and parameters optimization for support vector machines," Expert Systems with Applications, vol. 31, 2006, p. 231–240.

[17] S. Hettich, C. L. Blake, C. J. Merz, "UCI repository of machine learning databases", Department of Information and Computer Science, University of California, Irvine, CA. http://archive.ics.uci.edu/ml/.

[18] I. H. Witten, E. Frank, "Data Mining: Practical Machine Learning Tools and Techniques (2nd Edition)," Morgan Kaufmann, San Francisco, 2005.

[19] J. Piotroski, "Value investing: The use of historical financial statement information to separate winners from losers," Journal of Accounting Research, vol. 38, 2000, pp. 1–41.

[20] J. H. Holland, "Adaptation in natural and artificial systems," University of Michigan Press, Ann Arbor, Michigan, 1975.

[21] S. Mukherji, M. S. Dhatt, Y. H. Kim, "A fundamental analysis of Korean stock returns," Financial Analysts Journal, vol.53(3), 1997, pp. 75-80.

[22] G. R. Jensen, R. R. Johnson, J. M. Mercer, "New evidence on size and price-to-book effects in stock returns," Financial Analysts journal, vol.53(6), 1997, pp.34-42.

[23] M. G. Danielson, T. D. Dowdell, "The return-stages valuation model and the expectations within a firm's P/B and P/E ratios," Financial Management, vol. 30(2), 2001, pp.93-124.

[24] J. Lewellen, "Predicting returns with financial ratio," Journal of Financial Economics, vol. 74(2), 2004, pp. 209-235.

[25] E. F. Fama, K. R. French, "Average returns, B/M, and share issue," Journal of Finance, vol. 63(6), 2008, pp. 2971-2995.

[26] E. Hjalmarsson, "Predicting global stock returns," Journal of Financial and Quantitative Analysis, vol. 45(1), 2010, pp. 49-80.

[27] M. Omran, "Linear versus non-linear relationships between financial ratios and stock returns: empirical evidence from Egyptian firms," Review of Accounting and Finance, vol. 3(2), 2004, 84-102.

[28] R. Bauer, N. Guenster, R. Otten, "Empirical evidence on corporate governance in Europe: the effect on stock returns, firm value and performance," Journal of Asset Management, vol. 5(2), 2004, 91-104.

[29] M. T. Soliman, "The use of DuPont analysis by market Participants," The Accounting Review, vol. 83(3), 2008, 823-853.

[30] T. A. Carnes, "Unexpected Changes in quarterly financial-statement line items and their relationship to stock prices," Academy of Accounting and Financial Studies Journal, vol. 10(3), 2006, 99-116.

[31] D. Ikenberry, J. Lakonishok, "Corporate governance through the proxy contest: evidence and implications," Journal of Business, vol. 66(3), 1993, 405-435.

[32] G. Sadka, R. Sadka, "Predictability and the earnings-returns relation," Journal of Financial Economics, vol. 94(1), 2009, 87-93.

[33] D. E. Goldberg, K. Deb, "A comparative analysis of selection schemes used in genetic algorithms," Foundation of Genetic Algorithms, 1991, pp. 69-93.

[34] B. A. Sensoy, "Performance Evaluation and Self-Designated Benchmark Indexes in the Mutual Fund Industry," Journal of Financial Economics, vol. 92(1), 2009, 25-39.

[35] R. Shukla, S. Singh, "A Performance Evaluation of Global Equity Mutual Funds: Evidence from 1988-95," Global Finance Journal, vol. 8(2), 1997, 279-293.

2011 IEEE International Conference on Fuzzy Systems
June 27-30, 2011, Taipei, Taiwan

Upper-Bound Multiple Fuzzy Frequent-Pattern Trees

Tzung-Pei Hong[1, 2], Chun-Wei Lin[1]
[1]Department of Computer Science and Information Engineering
National University of Kaohsiung
Kaohsiung, Taiwan, R.O.C.
[2]Department of Computer Science and Engineering
National Sun Yat-sen University
Kaohsiung, Taiwan, R.O.C.
tphong@nuk.edu.tw, cwlin@nuk.edu.tw

Tsung-Ching Lin and Shing-Tai Pan
Department of Computer Science and Information Engineering
National University of Kaohsiung
Kaohsiung, Taiwan, R.O.C.
stpan@nuk.edu.tw, m0985507@mail.nuk.edu.tw

***Abstract*—In this paper, a novel two-phase fuzzy mining approach based on the designed upper-bound multiple fuzzy frequent-pattern (UBMFFP) tree is proposed to obtain all fuzzy frequent itemsets from a quantitative database. It prunes unpromising itemsets in the first phase, and then finds the actual fuzzy frequent itemsets in the second phase. Experimental results indicate that the proposed approach has better performance than some previous ones.**

Keywords- fuzzy data mining; fuzzy set; two-phase mining; FP tree; fuzzy frequent itemsets

I. INTRODUCTION

Depending on the classes of knowledge derived, it may be classified as those finding association rules [1], classification rules [12], clustering rules [16], or sequential patterns [2, 20], among others. Especially, finding association rules in large transaction datasets is most commonly seen in data mining research [4, 18]. In these years, fuzzy sets have been used in many fuzzy data mining approaches for managing quantitative data [5, 8-9]. It used membership functions to transform quantitative values in transactions into linguistic terms through fuzzy theory. Papadimitriou *et al.* proposed a tree structure called the fuzzy frequent pattern tree (FFPT) to mine fuzzy association rules [19]. Lin *et al.* then proposed fuzzy data mining approaches to efficiently mine the fuzzy frequent itesmets from the designed tree structures [13-15]. It only considers the term with the maximum cardinality, thus making the number of fuzzy regions processed equal to the number of original items, which reduces the processing time.

In this paper, an upper-bound multiple fuzzy FP tree (UBMFFP tree) algorithm is proposed, which keeps the fuzzy frequent 1-regions whether they are generated from the same item. In the mining process, the fuzzy regions transformed from the same term (item) cannot be joined into fuzzy frequent itemsets using the combination method. Based on the proposed approach, the mining result are more natural and understandable for human beings.

II. REVIEW OF RELATED WORKS

In this section, the fuzzy association rules mining and the FP-growth algorithm are shortly described.

A. Fuzzy Association Rules Mining

The data mining approach is useful to extract knowledge from real-world databases and represented in a comprehensible form. Linguistic representation produces more understandable knowledge for human beings, which is easily implemented by fuzzy sets. Chan *et al.* proposed the F-APACS algorithm to mine fuzzy association rules [3]. Hong *et al.* proposed a fuzzy aprioritid mining algorithm to mine fuzzy rules from quantitative databases [8]. Papadimitriou *et al.* proposed a fuzzy frequent pattern tree (FFPT) to mine fuzzy association rules [19]. Lin *et al.* then proposed the novel fuzzy data mining approaches to efficiently mine the fuzzy frequent itesmets from the designed tree structures [13-15]. The above algorithms, however, were proposed for handling single region with the maximum cardinality among transformed fuzzy regions of an item, thus generating incomplete fuzzy frequent itemsets.

B. FP-growth Algorithm

Han *et al.* proposed the Frequent-Pattern-tree structure (FP-tree) and the FP-growth algorithm for efficiently mining frequent itemsets without generation of candidate itemsets [7]. Three steps were involved in FP-tree construction. The database to be mined was first scanned to find all the items with their counts. The support of an item was then defined as its count divided by the total number of transactions. The items with their supports equal to or larger than a predefined minimum support were then selected as frequent 1-itemsets (items). Next, the frequent items were sorted in a descending order of their frequencies. At last, the database was scanned again to construct the FP tree according to the sorted order of frequent items. The construction process was executed tuple by tuple, from the first transaction to the last one. After all transactions were processed, the FP tree was completely constructed.

After the FP tree was constructed from a database, the FP-growth mining algorithm was then executed to find all frequent itemsets [7]. Several other algorithms based on the FP-tree structure have also been proposed [6, 10].

III. THE PROPOSED UBMFFP CONSTRUCTION ALGORITHM

A special notation is often used to represent fuzzy sets. Assume that x_1 to x_n are the elements in a fuzzy set A, and μ_1 to

μ_2 are, respectively, their membership grades in A. A is usually represented as follows:

$$A = \frac{\mu_1}{x_1} + \frac{\mu_2}{x_2} + \ldots + \frac{\mu_n}{x_n}.$$

A. The UBMFF- tree construction algorithm

The proposed mining approach integrates the fuzzy-set concepts, the FP-tree-like algorithm and the two-phase processing way to efficiently derive fuzzy frequent itemsets from quantitative transactions. The UBMFFP tree construction algorithm is stated as follows.

***UBMFFP tree construction algorithm*:**

INPUT: A quantitative database consisting of n transactions and m items, a set of membership functions, and a predefined minimum support threshold s.

OUTPUT: A constructed UBMFFP tree.

STEP 1: Transform the quantitative value v_{ij} of each item I_j in the *i-th* transaction into a fuzzy set f_{ij} represented as $(f_{ij1}/R_{j1} + f_{ij2}/R_{j2} + \ldots + f_{ijhj}/R_{jhj})$ using the given membership functions, where h_j is the number of fuzzy regions for I_j, R_{jl} is the l-th fuzzy region of I_j, $1 \le l \le h_j$, and f_{ijl} is v_{ij}'s fuzzy membership value in region R_{jl}.

STEP 2: Calculate the scalar cardinality of each fuzzy region R_{jl} in the transaction data as:

$$count_{jl} = \sum_{i=1}^{n} f_{ijl}.$$

STEP 3: Check whether the value $count_{jl}$ of the fuzzy region R_{jl} is greater than or equal to the user-specific minimum count $n*s$. If the count of a fuzzy region R_{jl} is equal to or greater than the minimum count, put the fuzzy region in the set of fuzzy frequent regions (L_1). That is:

$$L_1 = \{R_{jl} \mid count_{jl} \ge n*s,\ 1 \le j \le m\}.$$

STEP 4: While executing the above steps, also find the occurrence number $o(R_{jl})$ of each fuzzy region R_{jl} in the quantitative database. It is later used to decide the item order.

STEP 5: Build the Header_Table by keeping the fuzzy frequent regions in L_1 in the descending order of their occurrence numbers.

STEP 6: Remove the fuzzy regions of the items not in L_1 from the transactions of the transformed database. Sort the remaining fuzzy regions in each transaction according to the order of the fuzzy regions in Header_Table.

STEP 7: Initially set the root node of the UBMFFP tree as ***root***.

STEP 8: Insert the updated transactions in the transformed databases into the UBMFFP tree tuple by tuple. The following two cases may exist to concern.

Substep 8-1: If a fuzzy region R_{jl} in the currently processed i-th transaction appears in the corresponding path of the UBMFFP tree, add the membership value of the region R_{jl} in the transaction to the node with R_{jl};

Substep 8-2: Otherwise, add a new node with R_{jl} to the end of the corresponding path and set the membership value of the region R_{jl} in the currently processed i-th transaction as the value in the node. Insert a link from the node of R_{jl} in the last branch to the current node. If there is no such branch, insert a link from the entry of R_{jl} in Header_Table to the current node.

After STEP 8, the UBMFFP tree finally constructed.

B. An Example

Assume that the predefined minimum support threshold is set at 30%. The quantitative database is shown in Table I.

TABLE I. QUANTITATIVE DATABASE

TID	Items
1	*A*:2, *C*:8, *E*:10
2	*A*:2, *C*:5, *E*:10
3	*B*:4, *C*:8, *D*:5
4	*B*:9, *D*:4
5	*A*:3, *B*:5, *C*:5, *D*:9
6	*A*:2, *B*:7, *C*:11
7	*B*:5, *C*:3, *D*:3, *E*:9
8	*A*:3, *B*:7, *C*:9, *E*:9

Assume that the fuzzy membership functions are the same for all items shown in Figure 1. The UBMFFP tree is constructed as follows.

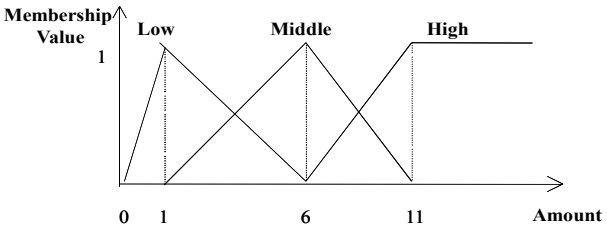

Figure 1. Membership functions used in the example.

The quantitative database in Table I is then transformed into fuzzy sets according to the defined membership function in Figure 1. The results are shown in Table II.

TABLE II. FUZZY SETS TRANSFORMED FROM TABLE I

TID	Items
1	$\frac{0.8}{A.Low}+\frac{0.2}{A.Middle},\frac{0.6}{C.Middle}+\frac{0.4}{C.High},\frac{0.2}{E.Middle}+\frac{0.8}{E.High}$
2	$\frac{0.8}{A.Low}+\frac{0.2}{A.Middle},\frac{0.2}{C.Low}+\frac{0.8}{C.Middle},\frac{0.2}{E.Middle}+\frac{0.8}{E.High}$
3	$\frac{0.4}{B.Low}+\frac{0.6}{B.Middle},\frac{0.6}{C.Middle}+\frac{0.4}{C.High},\frac{0.2}{D.Low}+\frac{0.8}{D.Middle}$
4	$\frac{0.4}{B.Middle}+\frac{0.6}{B.High},\frac{0.4}{D.Low}+\frac{0.6}{D.Middle}$
5	$\frac{0.6}{A.Low}+\frac{0.4}{A.Middle},\frac{0.2}{B.Low}+\frac{0.8}{B.Middle},\frac{0.2}{C.Low}+\frac{0.8}{C.Middle},\frac{0.4}{D.Middle}+\frac{0.6}{D.High}$
6	$\frac{0.8}{A.Low}+\frac{0.2}{A.Middle},\frac{0.8}{B.Middle}+\frac{0.2}{B.High},\frac{1}{C.High}$
7	$\frac{0.2}{B.Low}+\frac{0.8}{B.Middle},\frac{0.6}{C.Low}+\frac{0.4}{C.Middle},\frac{0.6}{D.Low}+\frac{0.4}{D.Middle},\frac{0.4}{E.Middle}+\frac{0.6}{E.High}$
8	$\frac{0.6}{A.Low}+\frac{0.4}{A.Middle},\frac{0.8}{B.Middle}+\frac{0.2}{B.High},\frac{0.4}{C.Middle}+\frac{0.6}{C.High},\frac{0.4}{E.Middle}+\frac{0.6}{E.High}$

The minimum count is then calculated as (8 * 0.3) (= 2.4). The occurrence number of each frequent fuzzy region is calculated and shown in Table III.

TABLE III. COUNTS AND THE OCCURRENCE NUMBERS OF FUZZY REGIONS

Item	Count	Occurrence number
A.Low	3.6	5
B.Middle	4.2	6
C.Middle	3.6	6
C.High	2.4	4
E.High	2.8	4

The fuzzy regions in L_1 are then sorted in descending order of their occurrence numbers and are put in Header_Table. The fuzzy regions not in L_1 are removed from the transactions from Table II. The remaining fuzzy regions in each transaction are then sorted according to the order in the Header_Table. The updated transactions are shown in Table IV.

TABLE IV. THE UPDATED TRANSACTIONS

TID	Fuzzy frequent regions
1	$\frac{0.6}{C.Middle},\frac{0.8}{A.Low},\frac{0.4}{C.High},\frac{0.8}{E.High}$
2	$\frac{0.8}{C.Middle},\frac{0.8}{A.Low},\frac{0.8}{E.High}$
3	$\frac{0.6}{B.Middle},\frac{0.6}{C.Middle},\frac{0.4}{C.High}$
4	$\frac{0.4}{B.Middle}$
5	$\frac{0.8}{B.Middle},\frac{0.8}{C.Middle},\frac{0.6}{A.Low}$
6	$\frac{0.8}{B.Middle},\frac{0.8}{A.Low},\frac{1}{C.High}$
7	$\frac{0.8}{B.Middle},\frac{0.4}{C.Middle},\frac{0.6}{E.High}$
8	$\frac{0.8}{B.Middle},\frac{0.4}{C.Middle},\frac{0.6}{A.Low},\frac{0.6}{C.High},\frac{0.6}{E.High}$

The updated transactions in Table IV are used to construct the UBMFFP tree tuple by tuple from the first transaction to the last one. The results are shown in Figure 2.

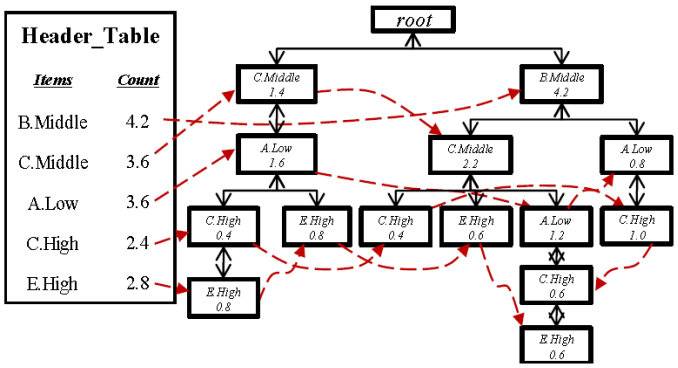

Figure 2. The finally constructed UBMFFP tree.

IV. THE UBMFFP-GROWTH MINING ALGORITHM

After the UBMFFP tree is constructed, the fuzzy frequent itemsets with more than one fuzzy region can then be found by the proposed UBMFFP-growth mining algorithm.

A. Proposed Mining Algorithm

The details of the UBMFFP-growth mining algorithm are as follows.

***UBMFFP-growth mining algorithm*:**

INPUT: The already constructed UBMFFP tree, its corresponding Header_Table, the transferred database, and the predefined minimum support threshold *s*.

OUTPUT: The fuzzy frequent itemsets.

STEP 1: Process the fuzzy regions in Header_Table one by one and bottom-up using the following steps. Let the currently processed fuzzy region be R_{jl}.

STEP 2: Find all the nodes with the fuzzy region R_{jl} in the UBMFFP tree through the links, starting from Header_Table.

STEP 3: Set the variable k = 2, where k is used to keep the number of items in the currently processed itemsets.

STEP 4: Trace the paths with the currently processed fuzzy region R_{jl} to generate the fuzzy k-itemsets except for any of its super-items associated with the same I_j and set their upper-bound fuzzy counts as the minimum of the values in the corresponding nodes, which contain the fuzzy regions in the itemsets.

STEP 5: Sum the upper-bound fuzzy counts of the same fuzzy itemsets from different paths.

STEP 6: If the summed upper-bound fuzzy count of a fuzzy itemset after STEP 5 is larger than or equal to the

predefined minimum count ($n*s$), add it to the candidate set C which will be used to generate fuzzy candidate (k+1)-itemsets.

STEP 7: Set $k = k + 1$ and repeat STEPs 4 to 6 to generate the fuzzy candidate k-itemsets in C based on the downward-closure property recursively. The process is repeated until no more fuzzy itemsets are generated.

STEP 8: Repeat STEPs 2 to 7 for another fuzzy region until all the fuzzy regions in Header_Table are processed.

STEP 9: Rescan the transferred database to get the actual fuzzy counts of the fuzzy candidate itemsets in C and check them against the predefined minimum count.

STEP 10: Output the candidate fuzzy itemsets with their fuzzy counts equal to or larger than the predefined minimum count as the fuzzy frequent itemsets.

B. An Example

For the constructed UBMFFP tree in Figure 2, the proposed UBMFFP-growth mining algorithm finds all the fuzzy frequent itemsets as follows. The variable k is initially set at 2, where k is used to keep the number of items in the currently processed itemsets. The paths with the currently processed fuzzy region are then used to form the candidate fuzzy k-itemsets. The upper-bound fuzzy counts of the same fuzzy itemsets are summed up. The summed upper-bound fuzzy counts of the derived fuzzy itemsets with the currently processed item are checked against the predefined minimum count, which is 2.4. The above steps are repeated for another fuzzy region until all the fuzzy regions in Header_Table are processed. The final candidate fuzzy itemsets with their upper-bound fuzzy counts in C are shown {*A.Low*, *C.Middle*: 2.6}, and {*C.Middle*, *E.High*: 2.8}.

The transferred database is then re-scanned to find the actual fuzzy counts of the derived candidate fuzzy itemsets. The final derived fuzzy frequent itemsets are shown in Table V.

TABLE V. FINAL FUZZY FREQUENT ITEMSETS

1-itemset	*Count*
A.Low	3.6
B.Middle	4.2
C.Middle	3.6
C.High	2.4
E.High	2.8
2-itemset	***Count***
A.Low, *C.Middle*	2.4

V. EXPERIMENTAL RESULTS

A real dataset called FOODMART from an anonymous chain store was used in the experiments [17]. The quantitative database was then transformed into fuzzy 2-regions by the predefined membership functions. Figure 3 shows the comparisons of execution times of the Apriori-based algorithm [1] for mining multiple fuzzy-term frequent itemsets (MF-Apriori), the multiple fuzzy FP tree (MFFP-tree) algorithm [11], and the proposed UBMFFP-tree algorithm. It was obvious to see from Figure 3 that the proposed UBMFFP-tree algorithm ran faster than the other two for the various minimum support thresholds. The experimental results in Figure 4 show the numbers of tree nodes generated from the two algorithms for two fuzzy regions. It reveals that the numbers of nodes in the UBMFFP tree are fewer than the MFFP tree.

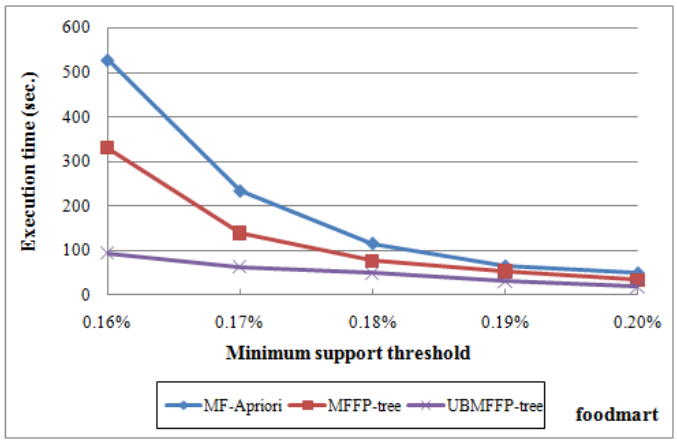

Figure 3. Execution time for three approaches.

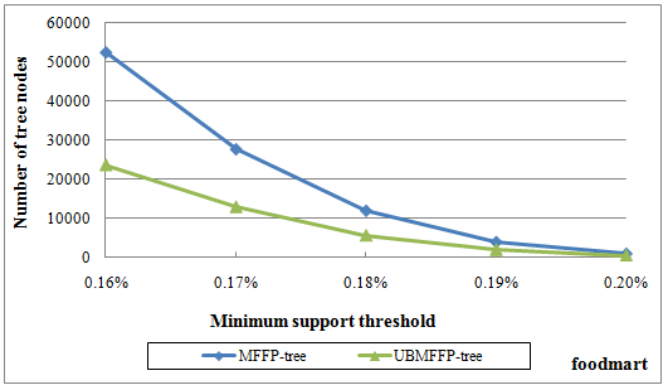

Figure 4. Number of tree nodes generated from the two approaches.

VI. CONCLUSION

In this paper, we proposed a two-phase multiple fuzzy mining algorithm for finding the complete fuzzy frequent itemsets based on the UBMFFP tree. Experimental results show that the proposed approach generates fewer nodes than the fuzzy FP-tree algorithm. In the future, we will further extend the approach to solve other fuzzy mining problems.

REFERENCES

[1] R. Agrawal and R. Srikant, "Fast algorithms for mining association rules in large databases," The 20th International Conference on Very Large Data Bases, pp. 487–499, 1994.

[2] R. Agrawal and R. Srikant, "Mining sequential patterns," The International Conference on Data Engineering, pp. 3–14, 1995.

[3] K. C. C. Chan and W. H. Au, "Mining fuzzy association rules," The 6th International Conference on Information and Knowledge Management, pp. 209–215, 1997.

[4] M. S. Chen, J. Han, and Y. P. S., "Data mining: An overview from a database perspective," IEEE Transactions on Knowledge and Data Engineering, vol. 8, pp. 866–883, 1996.

[5] D. Dubois, E. Hullermeier, and H. Prade, " A systematic approach to the assessment of fuzzy association rules" Data Mining and Knowledge Discovery, vol. 13, pp. 167–192, 2006.

[6] C. I. Ezeife and Y. Su, "Mining incremental association rules with generalized fp-tree," The 15th Conference of the Canadian Society for Computational Studies of Intelligence on Advances in Artificial Intelligence, pp. 147–160, 2002.

[7] J. Han, J. Pei, Y. Yin, and R. Mao, "Mining frequent patterns without candidate generation: A frequent-pattern tree approach," Data Mining and Knowledge Discovery, vol. 8, pp. 53–87, 2004.

[8] T. P. Hong, C. S. Kuo, and S. L. Wang, "A fuzzy aprioritid mining algorithm with reduced computational time," Applied Soft Computing, vol. 5, pp. 1–10, 2004.

[9] T. P. Hong and J. B. Chen, "Finding relevant attributes and membership functions," Fuzzy Sets and Systems, vol. 103, pp. 389–404, 1999.

[10] T. P. Hong, C. W. Lin, and Y. L. Wu, "Incrementally fast updated frequent pattern trees," Expert Systems with Applications, vol. 34, pp. 2424–2435, 2008.

[11] T. P. Hong, C. W. Lin, and T. C. Lin, "Mining complete fuzzy frequent itemsets by tree structures," IEEE International Conference on Systems, Man, and Cybernetics, pp. 563–567, 2010.

[12] K. Hu, Y. Lu, L. Zhou, and C. Shi, "Integrating classification and association rule mining: A concept lattice framework," The 7th International Workshop on New Directions in Rough Sets, Data Mining, and Granular-Soft Computing, pp. 443–447, 1999.

[13] C. W. Lin, T. P. Hong, and W. H. Lu, "Linguistic Data Mining with Fuzzy FP-trees," Expert Systems with Applications, vol. 37, pp. 4560–4567, 2010.

[14] C. W. Lin, T. P. Hong, and W. H. Lu, "An Efficient Tree-based Fuzzy Data Mining Approach," International Journal of Fuzzy Systems, vol. 12, no. 2, pp. 150–157, 2010.

[15] C. W. Lin, T. P. Hong, and W. H. Lu, "A Two-Phase Fuzzy Mining Approach," IEEE International Conference on Fuzzy Systems, pp. 494–498, 2010.

[16] F. Liu, Z. Lu, and S. Lu, "Mining association rules using clustering," Intelligent Data Analysis, vol. 5, pp. 309–326, 2001.

[17] Microsoft. Example database foodmart of microsoft analysis services. Available: http://msdn.microsoft.com/en-us/library/aa217032(SQL.80).aspx

[18] J. S. Park, M. S. Chen, and P. S. Yu, "An effective hash-based algorithm for mining association rules," SIGMOD Record, vol. 24, pp. 175–186, 1995.

[19] S. Papadimitriou and S. Mavroudi, "The fuzzy frequent pattern tree," The 9th WSEAS International Conference on Computers, pp. 1–7, 2005.

[20] R. Srikant and R. Agrawal, "Mining sequential patterns: Generalizations and performance improvements," The 5th International Conference on Extending Database Technology: Advances in Database Technology, pp. 3–17, 1996.

2011 IEEE International Conference on Fuzzy Systems
June 27-30, 2011, Taipei, Taiwan

Exploiting Timed Automata Based Fuzzy Controllers for Voltage regulation in Smart Grids

Giovanni Acampora, Vincenzo Loia, Autilia Vitiello
Department of Computer Science, University of Salerno, Fisciano, Salerno 84084
Email: {gacampora, loia, avitiello}@unisa.it

***Abstract*—The large-scale deployment of the Smart Grid paradigm will support the evolution of conventional electrical power systems toward active, flexible and self-healing web energy networks composed of distributed and cooperative energy resources. In a Smart Grid platform, the optimal coordination of distributed voltage controllers is one of the main issues to address. In this field, the application of traditional control paradigms has some disadvantages that could hinder their application in Smart Grids where the constant growth of grid complexity and the need for massive pervasion of Distribution Generation Systems (DGSs) require more scalable, more flexible control and regulation paradigms. To try and overcome these challenges, this paper proposes the concept of a decentralized non-hierarchical voltage regulation architecture based on intelligent and cooperative smart entities. The distributed voltage controllers employ traditional sensors to acquire local bus variables and mutually coupled oscillators to assess the main variables that characterize the operation of the global Smart Grid. These variables are then amalgamated by a novel fuzzy inference engine, named Timed Automata based Fuzzy Controllers, in order to identify proper control actions aimed at improving the grid voltage profile and reducing power losses.**

***Index Terms*—Distributed Generation Systems, Voltage regulation, Timed Automata based Fuzzy Controllers.**

I. Introduction

The Smart Grid[1] is the convergence of information and operational technologies applied to the electric grid, providing sustainable options to customers and improved security [2][3]. It could play a strategic role in supporting the evolution of conventional electrical grids toward active, flexible and self-healing web energy networks composed of distributed and cooperative energy resources [4][5]. Advances in research on Smart Grids could increase the efficiency of modern electrical power systems by: (i) supporting large-scale penetration of small-scale Distributed Generation Systems (DGSs); (ii) facilitating the integration of Renewable Energy Sources; (iii) reducing system losses and Green House Gas emissions; (iv) increasing the reliability of electricity supply to customers. From this perspective, a crucial issue is how to increase the penetration of DGS into Smart Grids by properly coordinating their operation and by restricting their negative impact on grid operations and control. In this context, effective network voltage regulation is one of the main issues to address [6][7]. Voltage regulation in electrical grids is normally achieved by the optimal coordination of a large set of regulating devices, all used with the aim of supporting the load buses voltages and improving the power quality at the distribution level [8][9]. The presence of DGSs in electrical grids increases the complexity of this regulation process since their power injections, intrinsically random for generators based on renewable sources, could alter the voltage profiles on network buses. This requires the design of a proper methodology aimed at assuring effective grid operation by the optimal coordination of DGS operations with traditional voltage regulating devices. This methodology should require low computational effort in order to assure an effective on-line solution to the voltage regulation problem. In order to address these needs, the application of fuzzy logic theory has been proposed in the literature [10][11]. Fuzzy logic can handle problems with imprecise and incomplete data, and it can model nonlinear functions of arbitrary complexity [12][13][14].

However, the solution to the voltage regulation problem should be prompt, reliable and accurate, but, above all, it should be highly adaptive in order to effectively manage the intrinsic time varying phenomena affecting the smart grid operation. For this reason, in this work, a novel fuzzy inference engine, named Timed Automata based Fuzzy Controllers (TAFCs)[15], is exploited to regulate the reactive power flows injected by the DGSs into the electrical grid. Thanks to its high dynamic features, a TAFC is capable of modelling a system characterized by frequent changes over the time, and, consequently, it results highly suitable for the application in the electrical power systems context.

As shown in the experimental results section, where our proposal has been compared with a conventional fuzzy controller, the proposed strategy results in an effective and suitable method to solve voltage regulation problem.

II. Problem Formulation

The ultimate goal of the voltage regulation process is to identify the optimal asset of voltage regulating devices required to deliver higher service quality, in terms of voltage profile flattening and power losses minimization. Roughly speaking, the solution of the voltage regulation problem requires the identification of the voltage regulation devices asset that minimizes, for each grid state, a set of objectives subject to a number of inequality constraints.

The voltage regulation devices asset is described by the following vector:

$$y = [Q_{dg,1}, \ldots, Q_{dg,N_g}, \ldots, Q_{cap,1}, \ldots, Q_{cap,N_c}, V_{FTS,N_f}, m] \quad (1)$$

where $Q_{dg,i}$ is the reactive power injected by the i^{th} ($i = 1, \ldots, N_g$)DGS connected to the Smart Grid and available for

978-1-4244-7316-8/11/$26.00 ©2011 IEEE

regulation; $Q_{cap,j}$ is the vector of the reactive power injected by the j^{th} ($j = 1, \ldots, N_c$) capacitor bank; $V_{FTS,k}$ is the set point of the kk^{th} ($k = 1, \ldots, N_f$) Flexible AC Transmission System (FACTS) and m is the tap position of the HV/MV line tap changing transformer. Note that the vector $\mathbf{y}$ takes values in the solution space $\mathbf{\Omega}$:

$$\mathbf{y} \in \mathbf{\Omega} \Leftrightarrow \begin{cases} tap_{min} \leq m \leq tap_{max} \\ Q_{dg,min,i} \leq Q_{dg,i} \leq Q_{dg,max,i} & i = 1, \ldots, N_g \\ Q_{cap,min,j} \leq Q_{cap,j} \leq Q_{cap,max,j} & j = 1, \ldots, N_c \\ Q_{FTS,min,k} \leq Q_{FTS,k} \leq Q_{FTS,max,k} & k = 1, \ldots, N_f \end{cases} \tag{2}$$

When solving the voltage regulation problem, several constraints must be satisfied. They include the technical constraints for correct system operation in terms of allowed voltage ranges for the network buses (i.e. $V_{min,i} \leq V_i \leq V_{max,i}$ $i = 1 : n$) and maximum allowable currents for the n_l power lines (i.e. $I_l \leq I_{max,l}$ $l = 1 : n_l$).

The objectives to be minimized in identifying the optimal voltage regulating devices asset takes into account both technical and economic aspects (i.e. power losses, reactive power costs, voltage magnitude). Since the design objectives are in competition, the voltage regulation problem has no unique solution and a suitable trade-off between objectives has to be identified.

III. The proposed Approach

To address the voltage regulation problem in a Smart Grid, an innovative solution approach is proposed here.

The reactive power flows injected by the DGSs into the electrical grid are regulated according to the following control strategy: The proposed algorithm first acquires the global variables characterizing the actual operation of the Smart Grid. These variables are then processed in order to estimate the current grid state. This could be classified on the basis of the mean grid voltage magnitude according to the following set of minimal states:

1) *Grid Voltage Low*: This state is characterized by high load demand. As a result, high power line loading and, consequently, high power losses and a very low value of the mean grid voltage magnitude are expected on the grid.
2) *Grid Voltage High*: This state is characterized by low load demand. As a result, low power line loading and, consequently, low power losses and a very high value of the mean grid voltage magnitude are expected on the grid.
3) *Normal Operation*: This state represents the nominal operating point of the electrical grid. Both the power losses and the value of the mean grid voltage magnitude lie within allowable intervals.

Once the actual Smart Grid state has been assessed, the algorithm identifies proper voltage control strategies for each node. This is implemented according to the following control rules:

- If the Smart Grid state is classified as *Grid Voltage Low* (respectively *Grid Voltage High*), then the control objective is to raise (respectively reduce) the mean grid voltage magnitude V_m by properly increasing (respectively decreasing) the reactive power injected by the DGSs into the grid. In order to obtain a uniform rise in voltage magnitude, the i^{th} controller compares the local bus voltage magnitude (V_i) with the mean grid voltage magnitude (V_M) and:
  1) If $V_i < V_M$, it increases (respectively decreases) the injected reactive power $Q_{dg,i}$ by a quantity directly (respectively inversely) proportional to $|V_M - V_i|$, namely:
  $$\Delta Q_{dg,i} = \alpha_i(V_i) \cdot (V_M - V_i)$$
  respectively
  $$\Delta Q_{dg,i} = \frac{\alpha_i(V_i)}{V_i - V_M}$$
  2) Otherwise, it increases (respectively decreases) the injected reactive power $Q_{dg,i}$ by a quantity inversely (respectively directly) proportional to $|V_M - V_i|$, namely:
  $$\Delta Q_{dg,i} = \frac{\alpha_i(V_i)}{(V_i - V_M)}$$
  respectively
  $$\Delta Q_{dg,i} = \alpha_i(V_i) \cdot (V_M - V_i)$$
- If the Smart Grid state is classified as *Normal operation*, then the control objective is to improve the voltage profile (namely to reduce the voltage magnitude deviation). To address this issue, the i^{th} controller compares the local bus voltage magnitude (V_i) with the mean grid voltage magnitude (V_M) and:
  1) If $V_i < V_M$, it increases the injected reactive power $Q_{dg,i}$ by a quantity directly proportional to $|V_M - V_i|$, namely:
  $$\Delta Q_{dg,i} = \alpha_i(V_i) \cdot (V_M - V_i)$$
  2) Otherwise, it decreases the injected reactive power $Q_{dg,i}$ by a quantity directly proportional to $|V_M - V_i|$, namely:
  $$\Delta Q_{dg,i} = \alpha_i(V_i) \cdot (V_M - V_i)$$
  where $\alpha_i(V_i)$ is a monotonically increasing function of the actual value of the voltage magnitude of the i^{th} bus.

These user-supplied human language rules could be effectively implemented by a Fuzzy Inference System [16]. This system converts these linguistic rules into their mathematical equivalents, thereby simplifying the job of the system designer and resulting in much more accurate representations of the way systems behave in the real world. However, the solution to voltage regulation problem should be characterized by also other characteristics such as reliably and accuracy, but above

all it should be highly adaptive in order to effectively manage the intrinsic time varying phenomena affecting the smart grid operation. In the light of these needs, our proposal is to use a TAFC in order to face the dynamic changes which highly characterize power systems. The exploited fuzzy inference engine is described in detail in the next section.

IV. Timed Automata-based Fuzzy Controllers

This section is devoted to describe the Timed Automata-based Fuzzy Control. This novel fuzzy inference engine improves classic inference methods in terms of dynamism and ability to model variable structure systems that are characterized from a discontinuous nonlinear behaviour. As mentioned, this kind of behaviour strongly characterizes power systems. Consequently, a standard control system could not be sufficient to manage a so complex framework and an alternative scenario is necessary. This scenario is provided by Timed Automata based Fuzzy Controllers.

Before formally defining TAFCs, it is necessary to introduce *timed fuzzy controllers*, i.e, a novel fuzzy inference engine that extends fuzzy control idea with three additional concepts: *control configuration*, *control era* and *control time*. In detail, a timed fuzzy controller uses the control time as a clock moving the controlled systems through several time intervals, known as *control eras*. Each control era is characterized by a specific *control configuration* which is formed by: 1) the number and typology of fuzzy variables and 2) the number and structure of relationships among variables.

Definition 1 (Fuzzy Logic Controller): A fuzzy logic controller c, with n inputs and m outputs, can be considered as a function mapping a vector $\underline{\mathbf{x}} \in \mathbb{R}^n$ with an output vector $\underline{\mathbf{y}} \in \mathbb{R}^m$:

$$c : \mathbb{R}^n \rightarrow \mathbb{R}^m$$

where $\underline{\mathbf{y}} = c(\underline{\mathbf{x}})$ is computed by applying fuzzy inference operators. ■

Definition 2 (Timed Fuzzy Logic Controller): Let $C = \cup_{n\in\mathbb{N}} \cup_{m\in\mathbb{N}} \{c : \mathbb{R}^n \rightarrow \mathbb{R}^m\}$ be the collection of all possible fuzzy controllers and let

$$E = \{e_i = [t'_i, t''_i[\mid i = 1 \dots k, k \in \mathbb{N}, \\ t'_i, t''_i \in \mathbb{R}^+ \text{ with } t'_1 = 0, t''_i = t'_{i+1} \text{ and } t'_i < t'_{i+1}\}$$

be the set of k disjoint control eras. The i^{th} control era, known as e_i, starts at t'_i and ends at t''_i. Once defined C and E, let $f : E \rightarrow C$ be the function that maps each control era to the corresponding control configuration and let $g : \mathbb{R}^+ \rightarrow E$ a function which associates a time instant t_j with the corresponding control era. Then, a *timed fuzzy control* is a function composition $\varphi = f \circ g : \mathbb{R}^+ \rightarrow C$ that maps a time instant $t_j \in \mathbb{R}^+$ belonging to the i^{th} control era to a fuzzy controller $f_i \in C$ representing the associated control configuration. ■

Observation 1: If two instants t_j and t_{j+1}, with $t_j < t_{j+1}$, belong to the same i^{th} control era, the function φ returns the same function f_i:

$$\varphi(t_j) = f(g(t_j)) = f_i = f(g(t_{j+1})) = \varphi(t_{j+1})$$

$$\text{if} \quad t'_i \leq t_j < t_{j+1} < t''_i \quad ■$$

Observation 2: Each fuzzy controller c is a timed fuzzy controller φ_c on 1 control era with following parameters:

$$E = \{[0, t''_1], t''_1 > 0\}$$
$$C = \{c\}$$
$$f([0, t''_1]) = c$$
$$g(t) = [0, t''_1] \quad \forall t \in \mathbb{R}^+$$
$$\varphi_c = f(g(t)) = c \quad \forall t \in \mathbb{R}^+ \quad ■$$

A TAFC is a particular implementation of the function φ based on a theory deriving from formal language: Timed Automata [17].

A. Timed Automata

A timed automaton is a standard finite-state automaton extended with a finite collection of real-valued *clocks* providing a straightforward way to represent time related events, whereas automata-based approaches cannot offer this feature. The clocks can be reset to 0 (independently of each other) with the transitions of the automaton, and keep track of the time elapsed since the last reset. The transitions of a timed automaton are labeled with a *guard* (a condition on clocks), an *action* or *symbol* on alphabet Σ, and a *clock reset* (a subset of clocks to be reset). Intuitively, a timed automaton starts execution with all clocks set to zero. Clocks increase uniformly with time while the automaton is within a node. A transition may be taken only if the current values of the clocks satisfy the associated constraints. The set of behaviours expressed by a system modeled by means of a timed automaton is defined by a *timed language*, i.e., a collection of *timed words*. Both timed concepts are defined in the follows.

Definition 3: A *time sequence* $\tau = \tau_1\tau_2 \dots$ is an infinite sequence of time values $\tau_i \in \mathbb{R}$ with $\tau_i > 0$, satisfying the following constraints:

1) *Monotonicity*: τ increases strictly monotonically; that is, $\tau_i < \tau_{i+1}$ for all $i \geq i + 1$.
2) *Progress*: For every $t \in \mathbb{R}$, there is some $i \geq 1$ such that $\tau_i > t$.

A *timed word* over an alphabet Σ is a pair (σ, τ) where $\sigma = \sigma_1\sigma_2 \dots$ is an infinite word over Σ and τ is a time sequence. A *timed language* over Σ is a set of timed words on Σ. ■

Definition 4: For a set X of clock variables, the set $\Phi(X)$ of *clock constraints* δ is defined inductively by

$$\delta := x \leq c | c \leq x | \neg\delta | \delta_1 \wedge \delta_2$$

where x is a clock in X and c is a constant in $\mathbb{Q}$, the set of nonnegative rationals.

A *clock interpretation* ν for a set X of clocks assigns a real value to each clock; that is, it is a mapping from X to $\mathbb{R}$. We say that a clock interpretation ν for X satisfies a clock constraint δ over X iff δ evaluates to true using the values given by ν. For $t \in \mathbb{R}$, $\nu + t$ denotes the clock interpretation which maps every clock x to the value $\nu(x) + t$, and the clock interpretation $t \cdot \nu$ assigns to each clock x the value $t \cdot \nu(x)$.

For $Y \subseteq X, [Y \mapsto t]\nu$ denotes the clock interpretation for X which assigns t to each $x \in Y$, and agrees with ν over the rest of the clocks. ■

Now, a precise definition of timed transition table, which determines the timed automaton behaviour, is given:

Definition 5: A *timed transition table* $\mathcal{A}$ is a tuple $\langle \Sigma, S, S_0, C, E \rangle$, where

- Σ is a finite alphabet,
- S is a finite set of states,
- $S_0 \subseteq S$ is a set of start states,
- C is finite set of clocks, and
- $E \subseteq S \times S \times \Sigma \times 2^C \times \Phi(C)$ gives the set of transitions. An edge $\langle s, s', a, \lambda, \delta \rangle$ represents a transition from state s to state s' on input symbol a. The set $\lambda \subseteq C$ gives the clocks to be reset with this transition, and δ is a clock constraint over C. ■

If (σ, τ) is a timed word viewed as an input to an automaton, it presents the symbol σ_i at time τ_i. If each symbol σ_i is interpreted to denote an event occurrence then the corresponding component τ_i is interpreted as the time of occurrence of σ_i. Given a timed word (σ, τ), the timed transition table $\mathcal{A}$ starts in one of its start states at time 0 with all clocks initialized to 0. As time advances, the values of all clocks change, reflecting the elapsed time. At time τ_i, $\mathcal{A}$ state from s to s' using some transition of the form $\langle s, s', \sigma_i, \lambda, \delta \rangle$ reading the input σ_i, if the current values of clocks satisfy δ. With this transition the clocks in λ are reset to 0, and thus start continuing time with respect to the time of occurrence of this transition. Formally, this timed behaviour is captured by introducing *runs* of timed transition tables.

Definition 6: A run r, denoted by $(\bar{s}, \bar{\nu})$, of a timed transition table $\langle \Sigma, S, S_0, C, E \rangle$ over a timed word (σ, τ) is an infinite sequence of the form

$$r : \langle s_0, \nu_0 \rangle \xrightarrow[\tau_1]{\sigma_1} \langle s_1, \nu_1 \rangle \xrightarrow[\tau_2]{\sigma_2} \langle s_2, \nu_2 \rangle \xrightarrow[\tau_3]{\sigma_3} \dots$$

with $s_i \in S$ and $\nu_i \in [C \to \mathbb{R}]$, for all $i \geq 0$, satisfying the following requirements:

- *Initiation*: $s_0 \in S_0$ and $\nu_0(x) = 0$ for all $x \in C$.
- *Consecution*: for all $i \geq 1$, there is an edge in E of the form $\langle s_{i-1}, s_i, \sigma_i, \lambda_i, \delta_i \rangle$ such that $(\nu_{i-1} + \tau_i - \tau_{i-1})$ satisfies δ_i and ν_i equals $[\lambda_i \mapsto 0](\nu_{i-1} + \tau_i - \tau_{i-1})$.

■

The timed transition table together with the run concept are the main notions used in our approach to embed dynamism in the standard FLC definition.

B. Merging Timed Automata and Fuzzy Controllers

In an attempt to provide an instrument to model the function φ and consequently to obtain an implementation of a timed fuzzy controller, Timed Automata based Fuzzy Controllers (TAFCs) are proposed. TAFCs represent an integration between two theories: fuzzy control and timed automata.

A TAFC implements a timed fuzzy controller through a timed automaton whose behaviours define all the potential sequences of control eras (and the related control configurations) which the system may cross during its life-cycle. More in detail, TAFCs are able to manage the control configurations by associating each of them with a state in the timed automaton. Timed Automata support control eras progression by using the *run* concept (definition 6) where the i^{th} transition moves the system from the i^{th} control era to the $(i+1)^{th}$ one.

However, in order to change system's configuration among different automaton states, it is necessary to extend timed automata definition by exploiting a collection of so-called *transformation operators*:

$$C_{op} = \{\oplus, \ominus, \boxplus^k, \boxminus^k, \boxdot^k, \sim, \ltimes, \rtimes, \bowtie, \circledast, \oslash, \circledcirc, \divideontimes, \propto\}$$

where $\oplus$ and $\ominus$, respectively, adds and deletes a fuzzy variable from the current configuration; $\boxplus^k$, $\boxminus^k$ and $\boxdot^k$, respectively, adds, removes and modifies k fuzzy rules related to the current configuration; $\sim$ changes the fuzzy implication method of the rule base related to the current configuration; $\circledast$, $\oslash$ and $\circledcirc$, respectively, adds, deletes and modifies a term to a fuzzy variable in the current configuration; $\propto$ modifies the defuzzify method of configuration; $\bowtie$ modifies the fuzzy aggregation method; $\divideontimes$ changes default value of an output variable in the current configuration; $\ltimes$ and $\rtimes$ change, respectively, the lower bound and upper bound of the universe of discourse of a fuzzy variable in the current configuration.

Once that the automaton computation starts over a given timed word, the state transitions will opportunely modify the current control configuration in the successive one. In this vision, a timed word determines how and when to execute the switching among successive control eras. So, a timed word coincides with the control time concept.

The collection C_{op} will be used to extend timed automata and formally define TAFC as a couple of two components: an extended timed automaton that describes the dynamic evolution of a system and a fuzzy logic controller modeling the control behaviour of system during first phase of its existence.

C. Defining an extended timed automaton

Once defined the set of transformation operators C_{op} it is necessary to redefine the Timed Automaton concept in order to introduce a novel kind of transition edges capable of changing the control configuration of the modeled system. In particular, the standard transitions set of timed automata E is replaced with the following:

$$E_C \subseteq S \times S \times \Sigma \times 2^C \times \Phi(C) \times C_{op}^*$$

where C_{op}^* represents the set of all possible sequences of transformation operators, i.e., $C_{op}^* = \cup_{n \geq 1} C_{op}^n$ where C_{op}^n is the set of all possible sequences of n operators with $n \geq 1$. Now, it is possible to provide an extended definition of a timed automaton:

Definition 7: A *timed control transition table* $\mathcal{A}_C$ is a tuple $\langle \Sigma \cup \{\epsilon\}, S, S_0, C, E_C \rangle$, where

- Σ is a finite alphabet;
- ϵ represents the empty event, that is, when it is on a transition, the crossing of this transition depends only by temporal constraints;

- S is a finite set of states;
- $S_0 \subseteq S$ is a set of start states;
- C is finite set of clocks;
- $E_C \subseteq S \times S \times \Sigma \times 2^C \times \Phi(C) \times C_{op}^*$ gives the set of transitions. An edge $\langle s, s', a, \lambda, \delta, o^n \rangle$ represents a transition from state s to state s' on input symbol a which can be also the empty event. The set $\lambda \subseteq C$ gives the clocks to be reset with this transition, δ is a clock constraint over C and $o^n \in C_{op}^*$ is a sequence of n transformation operators, with $n \geq 1$, defined in order to change the current control configuration of modeled system. ■

In each sequence of transformation operators an operator can be repeated in order to execute the same task on different arguments. Besides, it is important to stablish that the operators are executed in the same order of their definition in the sequence (definition 9).

Definition 8: Let F be a fuzzy controller and let $o \in C_{op}$ be a transformation operator then $G = o(F)$ is the fuzzy controller obtained to apply the operator o on fuzzy controller F. ■

Definition 9: Let F be a fuzzy controller and let $o^n \in C_{op}^*$ be a sequence $o^n = (o_1, o_2, ..., o_n)$ where $o_i \in C_{op} \quad \forall i \in \{1, 2, ..., n\}$ then $G = o^n(F) = (o_n(o_{n-1}(...(o_2(o_1(F))))))$ is the fuzzy controller obtained to apply the operators $o_1, o_2, ..., o_{n-1}, o_n$ on fuzzy controller F in the same order of listing in the sequence o^n. ■

D. TAFC formal definition

At this point, it is possible to give a formal definition of a TAFC and the properties characterizing its dynamic behaviour.

Definition 10: A TAFC T is an ordered pair composed by an initial control configuration, represented by a fuzzy controller named F^0, together with a timed control transition table T_C. Formally:

$$T = (F^0, T_C). \quad ■$$

The TAFC properties which define the dynamic behaviour of a system are: *control evolution* and *control run*.

The control evolution is a mapping among the states S contained in T_C and the collection of possible control configurations obtained starting from F^0. More in detail, the control evolution is a mathematical succession, generated in an inductive way, which maps each state in S with a one or more control configurations obtained by sequentially applying over F^0 the transformation operators in $S \times S \times \Sigma \cup \{\epsilon\} \times 2^C \times \Phi(C) \times C_{op}^*$. Then:

Definition 11 (Control evolution): Let $T = (F^0, T_C)$ be a TAFC defined over a timed control transition table $\langle \Sigma \cup \{\epsilon\}, S, S_0, C, E_C \rangle$ with $S = \{s_0, s_1, ..., s_{|S|-1}\}$ the finite set of automaton states; let F^* be the collection of all possible fuzzy controllers; let $\Omega = \{n_1, n_2, ..., n_{|\Omega|}\}$ be a subset of ordered sequences in C_{op}^*, that is, $n_i = (o_1, o_2, ..., o_{|n_i|}) \ \forall i \in \{1, 2, ..., |\Omega|\}$, employed to define the edges in E_C. Then, the control evolution Ψ over a state $s^0 \in S_0$ is:

$$\Psi : \mathbb{N} \to S \times F^*$$

defined inductively, as follows:
The base case ($i = 0$). Let $s^0 \in S_0$ be an initial state of $\langle \Sigma \cup \{\epsilon\}, S, S_0, C, E_C \rangle$, then:

$$\Psi(0) = (s^0, F^0)$$

The inductive step ($i > 0$). Let $\Psi(i-1)$, with $i > 1$, be defined as:

$$\Psi(i-1) = (s^{i-1}, F^{i-1})$$

where $s^{i-1} \in S$ and $F^{i-1} \in F^*$, then:

$$\Psi(i) = (s^i, F^i)$$

with $s^i \in S$, $F^i = n_i(F^{i-1})$, $n_i \in \Omega$ and $\langle s^{i-1}, s^i, a, \lambda, \delta, n_i \rangle \in E_C$. ■

More intuitively, the expression (3) shows the sequence of pairs composing a control evolution over $s^0 \in S_0$ together with the fuzzy transformations obtained by exploiting the n_i sequences of operators.

$$\begin{array}{rcl} \Psi(0) : s^0 \in S_0 & \to & F^0 \\ & & \downarrow n_0 \\ \Psi(1) : s^1 \in S & \to & F^1 \\ & & \downarrow n_1 \\ \Psi(2) : s^2 \in S & \to & F^2 \\ & & \downarrow n_2 \\ \vdots & & \vdots \\ & & \downarrow n_{j-1} \\ \Psi(j) : s^j \in S & \to & F^j \\ & & \downarrow n_j \\ \vdots & & \vdots \end{array} \tag{3}$$

The image of function Ψ, I_Ψ, can be finite or infinite. This depends upon the topology of graph modeling the component T_C of the TAFC. Indeed, if the topology of T_C contains cycles then various FLCs can be associated with a same state $s_h \in S$. In order to explain it, let $\langle s^k, s^{i-1}, a, \lambda, \delta, n_k \rangle \in E_C$ be an edge entering in the state s^{i-1} already crossed, that is, an edge forming a cycle. If it is crossed the current fuzzy controller stored in the state s^{i-1} is replaced by a new one obtained executing the sequence of operators n_k on fuzzy controller stored in the state s^k. Then, crossing again the edge $\langle s^{i-1}, s^i, a, \lambda, \delta, n_i \rangle \in E_C$ also the controller fuzzy stored in s^i is replaced. Indeed, even if the sequence of operators n_i is unchanged from the previous crossing of the edge, a new controller fuzzy is stored in s^i because n_i is executed on the different fuzzy controller which has been stored in s^{i-1} in the previous step. So, states s^{i-1} and s^i are both associated with a new fuzzy controller because of the cycle formed by the edge $\langle s^k, s^{i-1}, a, \lambda, \delta, n_k \rangle$.

Obviously, the control evolution only represents a mapping between the states of timed automaton T_C and the collection of control configurations computable starting from F^0 by applying different sequences of operators in Ω; no dynamic

aspects are considered in the control evolution definition and, therefore, it is necessary to introduce the idea of control run extending the initial idea of the run of standard timed transition table (definition 6).

Definition 12: Let Ψ be a control evolution, then a control run r_c, denoted by $(\bar{s}, \bar{\nu})$, of a timed transition table $\langle \Sigma \cup \{\epsilon\}, S, S_0, C, E_C \rangle$ over a timed word (σ, τ) and a collection of sequences of transformation operators $\Omega = \{n_1, n_2, ..., n_{|\Omega|}\} \subseteq C^*_{op}$, is an infinite sequence of the form

$$r_c : \langle s^0, \nu_0 \rangle \xrightarrow[\tau_1]{\sigma_1, n_1} \langle s^1, \nu_1 \rangle \xrightarrow[\tau_2]{\sigma_2, n_2} \langle s^2, \nu_2 \rangle \xrightarrow[\tau_3]{\sigma_3, n_3} \dots$$

with $s^i \in S$ and $\nu_i \in [C \to \mathbb{R}]$, for all $i \geq 0$, and $n_i \in C^*_{op}$, for all $i \geq 1$, satisfying the following requirements:

- *Initiation*: $s^0 \in S_0$ and $\nu_0(x) = 0$ for all $x \in C$;
- *Consecution*: for all $i \geq 1$, there is an edge in E_C of the form $\langle s^{i-1}, s^i, \sigma_i, \lambda_i, \delta_i, n_i \rangle$ such that $(\nu_{i-1} + \tau_i - \tau_{i-1})$ satisfies δ_i and ν_i equals $[\lambda_i \mapsto 0](\nu_{i-1} + \tau_i - \tau_{i-1})$;
- *Atomicity*: The operators of sequence $n_i \in C^*_{op}$ are atomic operations and their computation time is equals to 0, i.e, they do not modify the duration of permanence in the automaton state $s^i, (\tau_i - \tau_{i-1})$;
- *Evolution*: each state s^i of a pair $\langle s^i, \nu_i \rangle$ in r_c is mapped on a FLC F^i as described by the control evolution Ψ.

■

If $T = (F^0, T_C)$ is a TAFC which models a given system then the set of control run r_c defined over the timed language L, generated by T_C, completely describes the collection dynamic behaviours of the system, whereas, the control run r_c defined over a single word $w_i \in L$ defines a precise dynamic behaviour of the system, so w_i defines the control time.

Definition 13 (Control Time): If $T = (F^0, T_C)$ is a TAFC and T_C is a timed automaton recognizing the timed language $L = w_1, w_2, w_3, ..., w_i, ...$ and w_i is a timed word and r_c is a control run defined over w_i then w_i is a Control Time of the system. ■

Finally, it is possible to give a formal description of control era and control configuration concepts.

Definition 14 (Control era and control configuration): If r_c is a control run defined over the Control Time $w_i = (\sigma, \tau) \in L$:

$$r_c : \langle s^0, \nu_0 \rangle \xrightarrow[\tau_1]{\sigma_1, n_1} \langle s^1, \nu_1 \rangle \xrightarrow[\tau_2]{\sigma_2, n_2} \langle s^2, \nu_2 \rangle \xrightarrow[\tau_3]{\sigma_3, n_3} \dots$$

then time interval between the instant τ_i and τ_{i+1} is the i^{th} control era of system and the FLC F^i which depicts the system during the same interval is defined as the i^{th} control configuration. ■

Therefore, it is important to notice how a TAFC is an implementation of timed fuzzy controller thanks to the concept of the control evolution and control run which perform the task accomplished by previously defined function φ.

Both the control evolution and the control run are potentially based on the infinite concept. In fact, the control evolution can exploit an infinite application of control operators in Ω to compute the mappings between the state s^i and the FLC F^i, whereas, the control run uses a timed word, defined as an infinite sequence of ordered pairs, to describe the dynamic behaviour of the system. Consequently, in order to simulate the behaviour of a TAFC during the first n control eras, the n^{th}-order control evolution and control run are introduced.

Definition 15 (n^{th}-order Control Evolution): If Ψ is a control evolution then the set

$$\Psi^n = \{\Psi(i) = (s^i, F^i) | i = 1, 2, ..., n\}$$

which contains the first n ordered pairs computed by Ψ through definition 11 is the n^{th}-order control evolution. ■

Definition 16 (n^{th}-order Control Run): Let

$$r_c : \langle s^0, \nu_0 \rangle \xrightarrow[\tau_1]{\sigma_1, n_1} \langle s^1, \nu_1 \rangle \xrightarrow[\tau_2]{\sigma_2, n_2} \langle s^2, \nu_2 \rangle \xrightarrow[\tau_3]{\sigma_3, n_3} \dots$$

be a control run defined over a control evolution Ψ, then n^{th}-order control run r^n_c is the sequence of the first n elements of r_c:

$$r^n_c : \langle s^0, \nu_0 \rangle \xrightarrow[\tau_1]{\sigma_1, n_1} \langle s^1, \nu_1 \rangle \xrightarrow[\tau_2]{\sigma_2, n_2} \dots \xrightarrow[\tau_{n-1}]{\sigma_{n-1}, n_{n-1}} \langle s^n, \nu_n \rangle$$

where the mapping between the automaton states s^i and the FLC F^i is computed by the n^{th}-order control evolution related to Ψ. ■

V. Experimental Results

This section discusses the application of the proposed methodology to the task of voltage regulation for the IEEE 30-bus test system depicted in fig. 1.

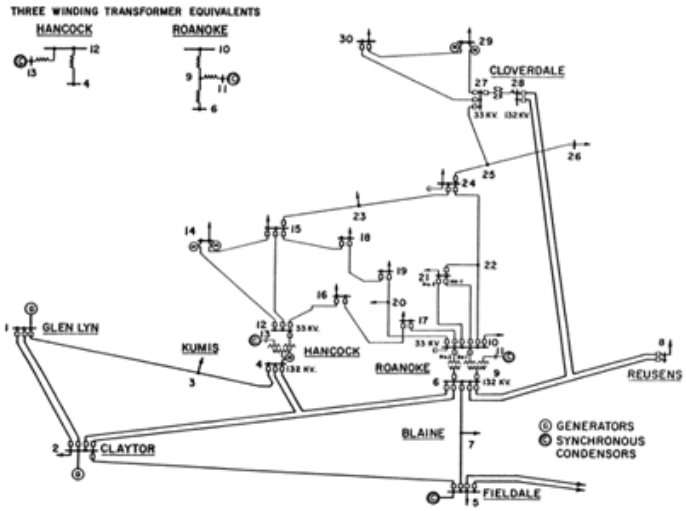

Fig. 1. The IEEE 30-bus test system

Six dispatchable DGSs have been considered in our experiments. The regulating devices asset is, therefore, identified by 6 variables:

$$\mathbf{y} = [Q_{dg,1}, Q_{dg,2}, Q_{dg,3}, Q_{dg,4}, Q_{dg,5}, Q_{dg,6}] \qquad (4)$$

In our experiment, each variable is regulated by an identical voltage TAFC. As far as the regulation performances are

concerned, detailed simulation analyses that consider highly variable load patterns have been developed.

In particular, the TAFC $T = (C, T_A)$ is exploited for regulating the reactive power flows injected by the DGSs where C is a fuzzy logic controller representing the initial configuration of T and modeling the control behaviour of each variable during first phase of its existence, whereas, T_A is the extended timed automaton that describes the dynamic evolution. In particular, in the Fig. 2, the timed automata T_A used to regulate the reactive power flows injected by the DGSs during a simulation run over a time equal to 150 minutes is shown.

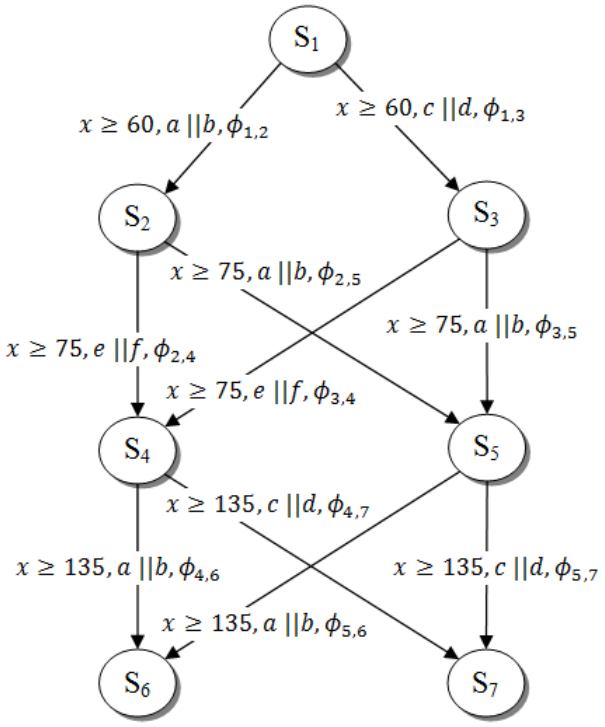

Fig. 2. The timed automata T_A

In details, the timed automaton T_A is composed by seven states $S_1, S_2, \ldots, S_7$. Each state stores a control configuration able to regulate the reactive power flows during the corresponding control era. For sake of simplicity, in the Fig. 2, the description of the transformation operators is replaced by a function $\phi_{i,j}$ capable of calculating the set of operators needed to transform the control configuration related to the state S_i in the control configuration related to the state S_j. The events described through the letters a, b, c, d, e, f on the automaton transitions correspond to the following conditions related to the voltage magnitude M:

- $a \Leftrightarrow M < 0.99$
- $b \Leftrightarrow M > 1.01$
- $c \Leftrightarrow M > 0.99$
- $d \Leftrightarrow M < 1.01$
- $e \Leftrightarrow M < 0.97$
- $f \Leftrightarrow M > 1.03$

In order to show the better performances provided by our strategy, the proposed TAFC T has been compared with a standard fuzzy controller F.

The evaluation of the provided performances has been based on technical and economic aspects, and in particular on the power losses (see fig. 3), reactive power costs (see fig. 4), and voltage magnitude (see fig. 5).

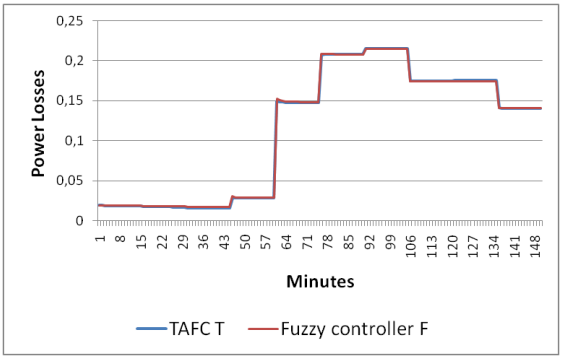

Fig. 3. The power losses values for the TAFC T and the conventional fuzzy controller F

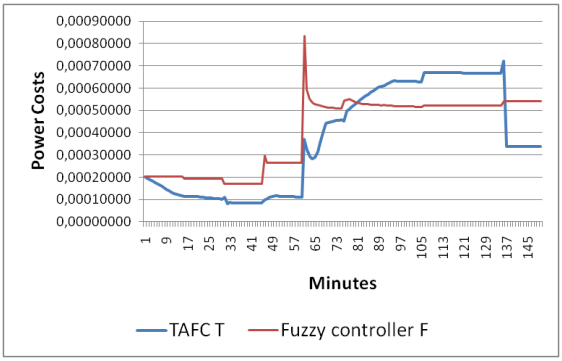

Fig. 4. The reactive power costs values for the TAFC T and the conventional fuzzy controller F

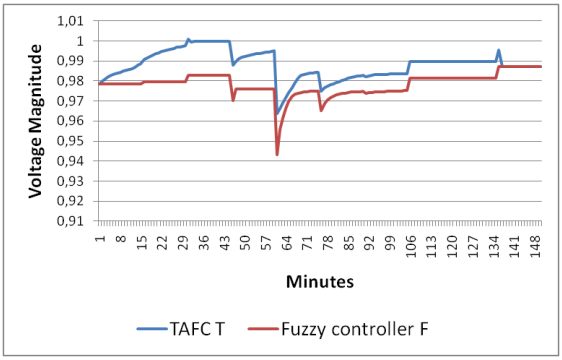

Fig. 5. The voltage magnitude values for the TAFC T and the conventional fuzzy controller F

In order to effectively measure the superiority of the our strategy, the Mean Absolute Errors (MAEs) regarding to the considered performance aspects have been computed for the

compared controllers, T and F. More in detail, the MAE for each aspect has been calculate as:

$$MAE = \frac{1}{N} \cdot \sum_{i=1}^{N} |G(i) - T(i)| \quad (5)$$

where N is the number of iterations of the simulation (equal to the number of minutes of simulation) and $G(i)$ and $T(i)$ are the guessed and the desired value for the performance aspect (power losses, reactive power costs and magnitude voltage) in the i-th iteration, respectively. In particular, the value 0 has been considered as the desired value for the power losses and reactive power costs, whereas, 1 has been considered as the desired value for the magnitude voltage.

The table I shows the computed MAEs concerning the performance aspects for our proposal and the compared conventional fuzzy controller. As highlighted by the perceptual improvement shown in the last column of the table I, the exploited TAFC T provides better performances than a conventional fuzzy controller.

TABLE I
MAEs OF OUR CONTROLLER T AND THE STANDARD F FOR ALL PERFORMANCE ASPECTS. IN THE LAST COLUMN ARE REPORTED THE RELATIVE IMPROVEMENTS.

Performance Aspect	MAE of T_A	MAE of F	Rel. impr.
Power losses	0,1142	0,1146	0,35%
Reactive power costs	3,7245E-4	4,0137E-4	7,2%
Magnitude Voltage	0,0119	0,0216	44,9%

VI. CONCLUSIONS

Modern trends in Smart Grids are oriented toward the employment of advanced regulation architectures that move away from the older centralized paradigm to a system distributed in the field with an increasing pervasion of smart sensors where central controllers play a smaller role. In supporting this complex task, this paper proposes the concept of a decentralized non-hierarchal voltage regulation architecture based on intelligent and cooperative smart entities. The distributed voltage controllers employ traditional sensors to acquire local bus variables and mutually coupled oscillators to assess the main variables that characterize the operation of the global Smart Grid. These variables are then amalgamated by a TAFC in order to identify proper control actions aimed at improving the grid voltage profile and reducing power losses. As far as the regulation performances are concerned, the simulation studies developed confirm the effectiveness of the proposed strategy in solving the voltage regulation problem also in the presence of highly variable load patterns.

REFERENCES

[1] C. Cecati , G. Mokryani, P. Siano, A. Piccolo, "An Overview on the Smart Grid Concept," *36th IEEE Annual Conference of the Industrial Electronics Society (IECON 2010)*, 7-10 November 2010, Phoenix, Arizona, USA, pp. 3316 - 3321, ISBN:978-1-4244-5226-2

[2] V.Madani, R.L.King, "Strategies to meet grid challenges for safety and reliability," *International Journal of Reliability and Safety*, vol. 2, no.1-2, 2008.

[3] S. M. Amin, B.F.Wollenberg, "Toward a Smart Grid," *IEEE Power and Energy Magazine*, vol.3, no 5, pp. 34-38, Sept/Oct. 2005.

[4] A. Schroder, I, Laresgoiti, K.Werlen, B. Schowe-von der brelie ,A. Schnettler, "Intelligent self-describing power grids," *Proc. of the 20th International Conference and Exhibition on Electricity Distribution, 2009. CIRED 2009*, June 2009, Prague, Czech Republic.

[5] R.L. King: "Information services for smart grids," *Proc. of 2008 IEEE Power and Energy Society General Meeting - Conversion and Delivery of Electrical Energy in the 21st Century*, Pittsburgh, PA, July 2008.

[6] G. Joos, B.T. Ooi, D. ;cGillis, F.D. Galiana, R. Marceau, "The potential of distributed generation to provide ancillary services" in *Proc. of IEEE Power Engineering Society Summer Meeting 2000*, vol. 3, pp. 1762 - 1767, July 2000.

[7] G. Bontempi, A.Vaccaro, D.Villacci "An adaptive local learning based methodology for voltage regulation in distribution networks with dispersed generation," *IEEE transactions on Power Systems*, vol.21(3), Aug. 2006, pp.1131-1140.

[8] K. Tomsovich, T. Hiyama, "Intelligent control methods for systems with dispersed generation" in *Proc. of IEEE Power Engineering Society Winter Meeting 2001*, vol.2, pp. 913 - 917, Feb. 2001.

[9] M.I. Marel, E.F. El-Saadany, M.M.A. Salama, "Flexible distributed generation: (FDG)" in *Proc. of IEEE Power Engineering Society Summer Meeting 2002*, vol.1 , pp. 49-53, Jul. 2002.

[10] Spatti, D.H.; da Silva, I.N.; Usida, W.F.; Flauzino, R.A.; "Fuzzy Control System for Voltage Regulation In Power Transformers," *Latin America Transactions, IEEE (Revista IEEE America Latina)*, vol.8, no.1, pp.51-57, March 2010.

[11] Hassan A.R, Sadrul Ula A.H.M, "Design and implementation of a fuzzy controller Based Automatic Voltage Regulator for a Synchronous Generator," *IEEE Trans. on Energy conversion*, vol 9, no 3, September 1994.

[12] M. Pipattanasomporn, H. Feroze, S. Rahman, "Multi-Agent Systems in a Distributed Smart Grid: Design and Implementation," *IEEE PES 2009 Power Systems Conference and Exposition (PSCE'09)*, Mar 2009, Seattle, Washington, USA.

[13] N. Higgins, et al., "Concept of Intelligent Decentralised Power Distribution Automation with IEC 61850, IEC 61499 and Holonic Control," *Proc. IEEE Conference on Systems, Machine and Cybernetics,* 2008.

[14] P. Siano, C. Citro, C. Cecati, A. Piccolo, "Smart Operation of Wind Turbines and Diesel Generators According to Economic Criteria," *IEEE Transactions on Industrial Electronics,* forthcoming, 2011, pp. 1-12.

[15] G. Acampora, V. Loia, A. Vitiello, "Hybridizing fuzzy control and timed automata for modeling variable structure fuzzy systems," *Fuzzy Systems (FUZZ), 2010 IEEE International Conference on*, pp.1-8, July 2010.

[16] Z. Mi, F. Wang, "Substation Reactive Power and Voltage Control Using Fuzzy Control Theory," *Proc. of 2009 International Conference on Industrial and Information Systems*, Haikou, China, Apr. 2009.

[17] R. Alur,"A theory of timed automata," *Theoretical Computer Science*,vol. 126, pp. 183235, 1994.

2011 IEEE International Conference on Fuzzy Systems
June 27-30, 2011, Taipei, Taiwan

A Novel Fuzzy System for Wind Turbines Reactive Power Control

Geev Mokryani, Pierluigi Siano, Antonio Piccolo, Vito Calderaro
Department of Industrial Engineering, University of Salerno, 84084 Fisciano, Salerno, Italy
Emails: gmokryani@ieee.org, psiano@unisa.it, apiccolo@unisa.it, vcalderaro@unisa.it,

Carlo Cecati
Department of Electrical and Information Engineering, University of L'Aquila, 67100 L'Aquila, Italy
Email: carlo.cecati@univaq.it

***Abstract*— The paper proposes a new fuzzy controller for variable speed wind turbines (WTs) in order to compensate the variations at the point of common coupling (PCC) by controlling the reactive power generated by WTs. A protection system is used to disconnect the WTs from the grid when the controller is unable to compensate the voltage variations. Simulations carried out on a real 37-bus Italian weak distribution network demonstrated that the controller allows compensating voltage variations during voltage sags.**

Keywords- Variable speed wind turbines, weak distribution network, voltage sag, fuzzy controller

I. INTRODUCTION

Nowadays, the penetration of the wind turbines (WTs) into electric grids has been increased. With the growing penetration of WTs into electric grids, voltage control, stability and security of the system have been influenced. In many countries, the new established grid codes demand that variable speed WTs should participate in improving voltage control in the distribution networks [1,2]. WTs are usually located in remote and rural areas with a weak network infrastructure. Weak networks are characterized by low X/R ratio and unbalanced voltage conditions. Connection of WTs to a weak distribution system has effects on voltage waveform, voltage variations and steady state voltage level [3]. The main constraints are related to the effect that WTs has on voltage quality.

According to the previous described problems, the Italian standard CEI 11-32, dealing with production systems connected to the grid has been updated with new indications related to WTs such as: disconnection from the grid, power production curtailment during voltage variations and contribution to active and reactive power control.

With regards to the reactive and voltage control, the Italian standard provides that the WTs should be able to control the reactive power at the terminals so that the power factor can be adjustable between 0.95 lagging and 0.95 leading [4].

Recent grid codes prescribed that WTs must withstand voltage variations to a certain percentage of the nominal voltage and for a specified duration. Such requirements are known as Fault Ride- Through (FRT) capability [5,6].

The variable-speed WTs have the ability to control the active and reactive power independently [7,8]. A DFIG based WT can be used as a reactive power source to voltage control with a fewer costs rather than the reactive power compensation devices.

Many previous works has been carried out on the WT reactive power control methods. A control strategy to increase the reactive power output by DFIG based WTs after the fault for improving the voltage variation had been proposed in [9]. Moreover, a mathematical model based on dynamics of DFIG has been defined. In [10], a proportional-integral (PI)-based control algorithm to control the reactive power generated by WTs has been proposed. In [11], the authors have presented a control method for regulating the reactive power generated by DFIGs in a wind farm in order to control voltage variations in the network. The relation between reactive and active power to maintain DFIG operating inside the maximum rotor and stator currents and the steady state stability limit have been described in [12]. In [13], the authors have proposed active network management to exploit maximum wind energy extraction from WTs.

In this paper, a new fuzzy controller for reactive power control of variable speed WTs is presented. The controller is designed in order to compensate the voltage sags at the PCC by controlling reactive power generated by WTs.

This paper is organized as follow: the considered wind turbine model is presented in Section II. The proposed fuzzy controller is described in Section III. Case studies and simulation results are presented and discussed in Section IV, while conclusions are given in Section V.

II. Wind Turbine Generator System

A. WT Modeling

A DFIG is a wound rotor induction generator with the stator connected to the grid directly and with the rotor connected to

978-1-4244-7316-8/11/$26.00 ©2011 IEEE

the network through a back to back converter. The configuration of a DFIG based WT is shown in Fig. 1.

In order to generate active power at constant voltage and frequency, the active power flow between the rotor circuit and the grid must be controlled. Hence, the back to back converter includes two four quadrant IGBT PWM converters (i.e., rotor side converter (RSC) and grid side converter (GSC)) connected back to back by a DC-link capacitor.

The control of the DFIG is obtained by controlling both converters. The aim of the RSC is to control the active and reactive power injected to or absorbed from the grid autonomously, while the GSC has to maintain the DC-link voltage at a set value. A crowbar is also used to short-circuit the RSC in order to protect it from over current in the rotor circuit during disturbances.

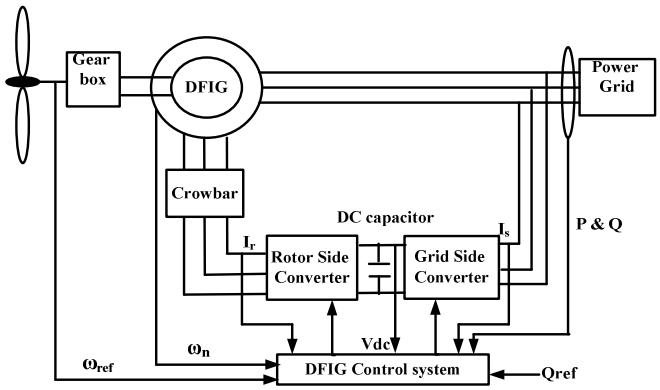

Fig.1. Configuration of DFIG based WT connected to a grid

B. *Grid Side and Rotor Side Converters*

The induction generator converts the power captured by the WT into electrical power and transmits it to the grid. The AC/DC/AC converter consists of the RSC and the GSC. Both RSC and GSC are voltage source converters (VSCs) that use forced commutated power electronic devices to synthesize an AC voltage from a DC voltage source. A capacitor connected on the DC side acts as the DC voltage source and a coupling inductor L is used to connect the GSC to the grid. The three-phase rotor winding is connected to the RSC by slip rings and brushes and the three-phase stator winding is directly connected to the grid.

The pitch angle command and the voltage command signals V_r and V_{gc} for RSC and GSC, respectively, are generated by the control system driving the power of the WT, the DC bus voltage and the voltage at the grid terminals.

The control system for the DFIG, operating under maximum power extraction, is based on a flux oriented control of the induction machine, in which the *d-q* current and voltage values are referred to the reference frame aligned with air-gap flux. The control system is composed by two distinct parts: in the first one, the WT output power and the voltage at the grid terminal are controlled by means of RSC; in the second, the voltage at DC bus capacitor is controlled by means of GSC. The control loop of the RSC, modeled as a voltage source, is shown in Fig. 2(a). The RSC controls both active and reactive power outputs through voltages components V_{qr} and V_{dr}, obtained by two separate Proportional Integral (PI) controllers. The first PI controller, which is the slowest one, controls the sum of the power P_{meas} and the power losses P_{losses} to the reference value P_{ref}, and its output is the reference of the current *d* component I_{dr_ref}. The second PI controller is the rotor current controller tracking the rotor current I_{qr} to the reference value I_{qr_ref} with a faster integration time, typically ten times smaller than the first PI. The aim of the GSC is to keep the DC link voltage constant irrespective of the direction of rotor power flow. Decoupled control of active and reactive powers flowing between rotor and grid is done by using supply voltage vector-oriented control: the scheme of the control is shown in Fig. 2(b). A DC voltage regulator, by comparing the actual voltage and the reference voltage, furnishes the *d*-component of the reference current I_{dgc_ref} for the current regulator. The current regulatory controls the magnitude and phase of the voltage generated by GSC (V_{gc}) from the I_{dgc_ref} produced by the DC voltage regulator and specified by I_{q_ref} reference. A detailed description of the control systems for both the converters and the pitch angle command can be found in [14].

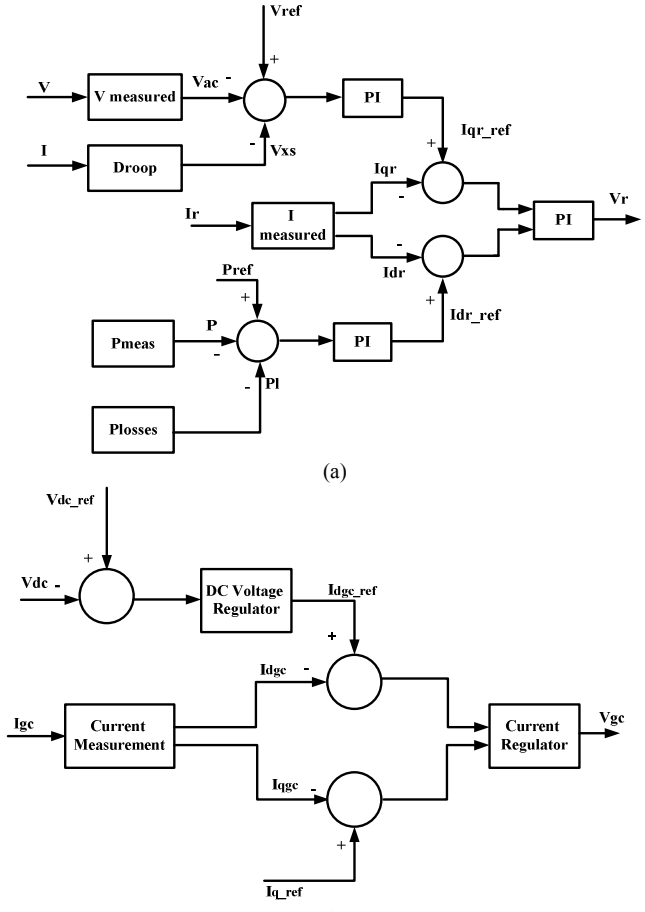

Fig.2. (a) Rotor side converter, (b) Grid side converter

III. Description of the Fuzzy Controller

Due to nonlinearity of power system and linearization problems the control of variable wind speed WTs could be difficult with conventional control methods. For example, Proportional- Integral (PI) controller design requires identifying the WT transfer function, the linear model of the network and defining an accurate tuning process. Because of these reasons, designing a PI controller is not an easy process.

The use of a fuzzy controller can overcome these problems and presents some advantages if compared to a PI controller: it is easy to obtain variable gains depending on the error and to solve problems affected by uncertain models [15-18].

The proposed controller is designed in order to compensate the voltage at the PCC by injecting the reactive power generated by both of the GSC and RSC.

Moreover, it is used in combination with a protection system for disconnecting the WT from the grid when the controller is unable to compensate the voltage variations and respect voltage limits.

The fuzzy controller, as shown in Fig. 3, presents two inputs: the error, the integral of error and one output that is the reference value for the reactive power reference signal (Q_{ref}) sent by the fuzzy controller to the WT local controller.

The error is defined as the difference between the reference voltage (V_{ref}) and the measured voltage at the PCC.

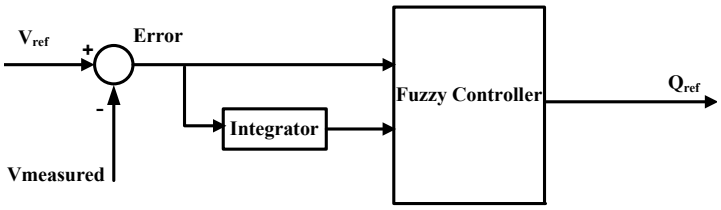

Fig.3. Fuzzy controller

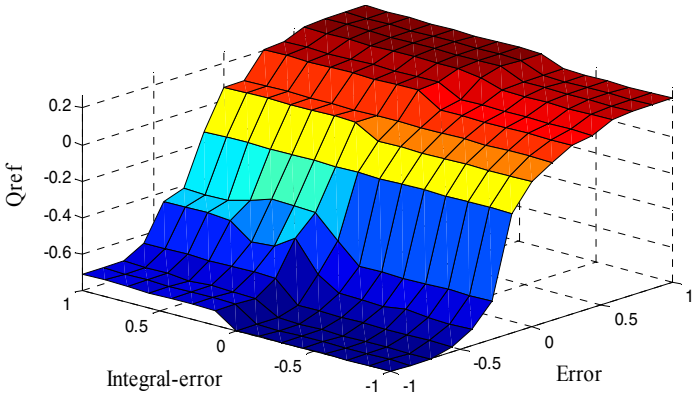

Fig.4. Fuzzy surface of controller

The fuzzy sets of the inputs and outputs assume the following names: "NVB"= Negative-Very-Big, "NB"= Negative-Big, "NM" = Negative-Medium, "NS" = Negative-Small, "ZE" = Zero, and so forth. Nine triangular membership functions have been selected for the inputs and outputs.

A Mamdani-based system architecture is realized; Max-Min and Centroid methods are used in the inference engine and defuzzification process, respectively.

The control surface of the fuzzy controller is provided in Fig.4.

IV. Case Study And Simulation Results

A. Network and WTs data

In order to test the proposed controller, two 1.5-MW WTs connected to a real 20 kV weak distribution system at buses 16, 35 are considered.

The network is characterized by lines with high resistances and low X/R ratios. The WTs and network parameters are provided in the Appendix. The single line diagram of the network is shown in Fig. 5. The base for power and voltage are 1.5/0.9 MVA and 575 V, respectively.

Real wind data sets acquired by the Wind Engineering Research Field Laboratory [19] are considered. The wind speed time history consists of 17500 observations within 50 seconds interval with sampling rate 25 Hz. The wind profile and generated active power profile are shown in Fig.6.

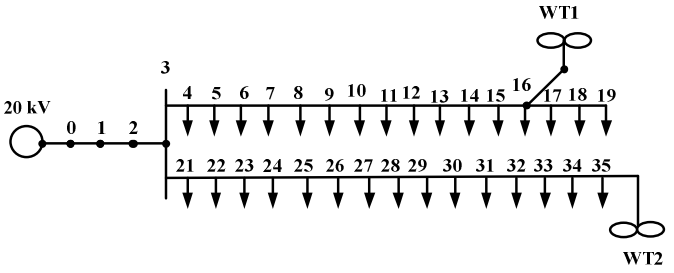

Fig.5. 20kV weak distribution system

The performance of proposed control method is verified considering a 5% voltage sag with a duration of 10 seconds initiated at t=25.

When the voltage at the PCC drops, reactive power is injected by the WTs during the voltage sag in order to help to increase the voltage to about 0.93 and 0.94 p.u., for WT1 and WT2, respectively as shown in Fig. 7.

The injected reactive power varies between about 0.40 MVAR for WT2 to about 0.43 MVAR for WT1, according to the voltages at the connection buses.

It can be also evidenced that the reactive power measured at the PCC follows its reference value as shown in Fig.8.

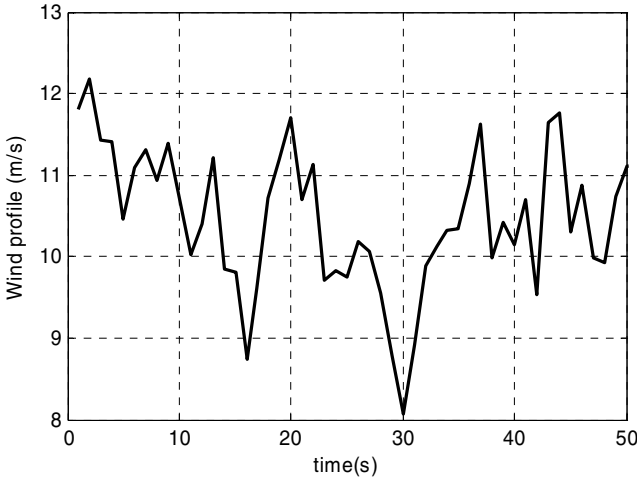

(a)

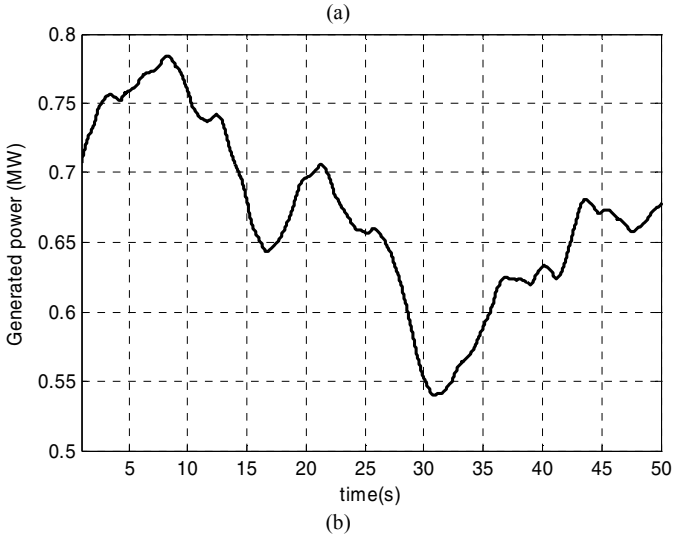

(b)

Fig.6. (a) Wind profile (m/s), (b) Generated active power (MW)

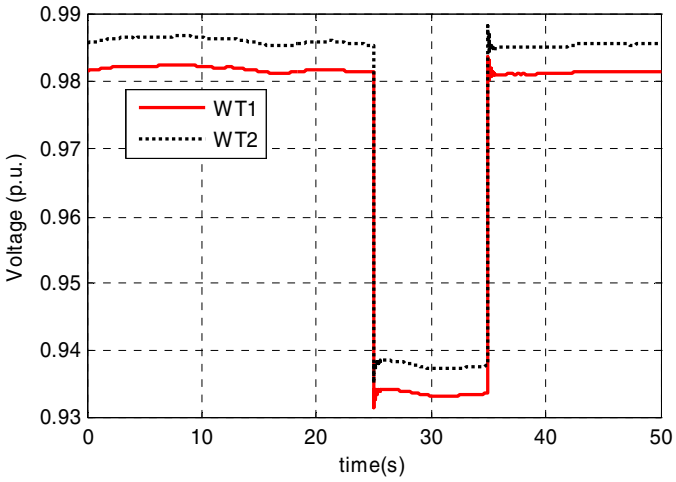

Fig.7. Voltage at the PCC

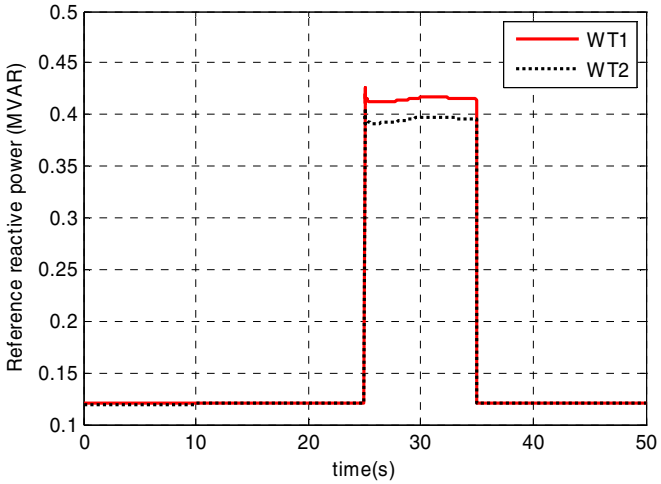

Fig.8. Reference reactive power (MVAR)

In order to evaluate the effectiveness of the proposed controller, its performances are compared with those of a classical PI controller [20] as is shown in Fig. 9.

It can be evidenced that the proposed fuzzy controller exhibits a better voltage compensation compared to the PI controller.

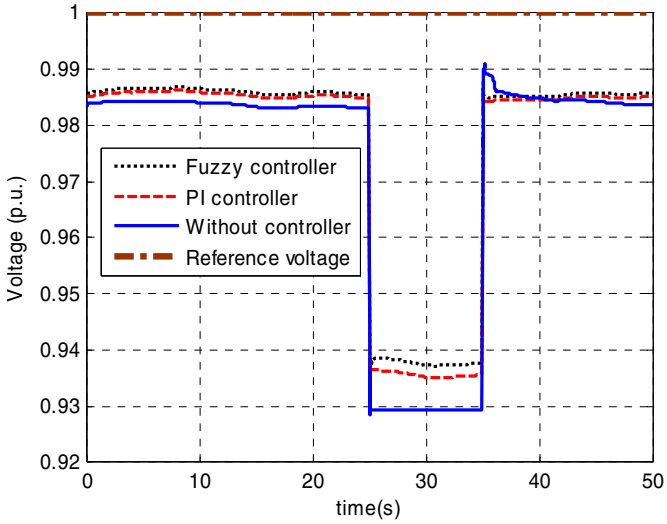

Fig.9. Voltage at bus 35

V. CONCLUSION

This paper proposes a new fuzzy controller for variable speed WTs to compensate voltage variations. at the PCC by controlling the generated reactive power. Simulations carried out on a real 37-bus Italian weak distribution network showed that the proposed controller exhibits good performances and allows compensating voltage variations.

APPENDIX

TABLE I. LOAD DATA

Load No.	P(kW)	Q (kVAR)	Load No.	P(kW)	Q (kVAR)
1	500	200	17	100	50
2	300	100	18	100	50
3	100	50	19	100	50
5	100	50	20	100	100
6	100	50	21	100	100
7	200	100	22	100	100
8	300	100	23	100	100
9	300	100	24	150	100
10	500	200	25	150	100
11	200	100	26	150	200
12	100	50	27	150	200
13	400	200	28	150	200
14	300	100	29	150	200
15	100	100	30	100	50
16	100	150	31	100	50

TABLE II. LINE DATA

Line No.	R (p.u.)	X (p.u.)	X/R	Line No.	R (p.u.)	X (p.u.)	X/R
1	0.0063	0.0031	0.50	19	0.3187	0.15	0.50
2	0.5437	0.3187	0.48	20	0.6375	0.3125	0.51
3	0.8688	0.45	0.49	21	0.0063	0.0031	0.50
5	0.25	0.0938	0.45	22	0.3812	0.15	0.48
6	0.0687	0.0338	0.50	23	0.1125	0.049	0.49
7	0.2375	0.162	0.52	24	0.275	0.1	0.50
8	0.45	0.2287	0.50	25	0.0938	0.045	0.50
9	0.0562	0.0313	0.55	26	0.2437	0.1225	0.50
10	0.1063	0.0625	0.45	27	0.5250	0.25	0.49
11	0.0438	0.0213	0.48	28	0.2575	0.125	0.49
12	0.0750	0.035	0.50	29	0.2575	0.125	0.49
13	0.1375	0.05	0.51	30	0.3125	0.1587	0.50
14	0.3063	0.1563	0.50	31	0.3637	0.1750	0.48
15	0.0125	0.0063	0.50	32	0.1213	0.687	0.49
16	0.3563	0.1437	0.55	33	0.2	0.0813	0.48
17	0.3125	0.1550	0.49	34	0.1375	0.05	0.51
18	0.3562	0.1875	0.50	35	0.2	0.1	0.50

WIND TURBINE PARAMETERS

V_{base} = 575 V S_{base} = 1.5 MVA f_{base} = 60Hz ωs = 1pu
$\omega_b = 2\pi f_b$ = 377 rad/s R_s = 0.00706 p.u. R_r = 0.005 p.u.
L_s = 3.07 p.u. L_r = 3.056 p.u . L_m = 2.9 p.u.

REFERENCES

[1] I. M. de Alegría, J. Andreu, J. L. Martín, P. Ibañez, J. L. Villate, and H. Camblong, "Connection requirements for wind farms: A survey on technical requirements and regulation," Renewable Sustainable Energy Rev., vol. 11, no. 8, Oct. 2007, pp. 1858–1872.

[2] P. Chen, P. Siano, B. Bak-Jensen, Z. Chen, "Stochastic Optimization of Wind Turbine Power Factor Using Stochastic Model of Wind Power", IEEE Transactions on Sustainable Energy, vol. 1(1), 2010, p. 19-29.

[3] John Olav Giúver Tande, "Exploitation of wind-energy resources in proximity to weak electric grids", Vol.65, Issue 1, April 2000, pp. 395-401.

[4] V. Calderaro, V. Galdi, A. Piccolo, P. Siano, "Evaluating the Benefits Deriving from Voltage Control Capabilities of Wind Distributed Generation", IEEE International Conference on Industrial Technology 2009, pp. 1-7.

[5] Jiaqi Liang, Wei Qiao, and Ronald G. Harley, "Feed-Forward Transient Current Control for Low-Voltage Ride-Through Enhancement of DFIG Wind Turbines", IEEE Trans. On Energy Conversion, Vol.25, No.3, Sep. 2010, pp.836- 843.

[6] O. Abdel-Baqi and A. Nasiri, "A dynamic LVRT solution for doubly fed induction generators," IEEE Trans. Power Electron., Vol. 25, No. 1, Jan. 2010, pp. 193–196,

[7] D.J. Atkinson, R.A. Lakin, R. Jones, A vector-controlled doubly-fed induction generator for a variable-speed wind turbine application, Transactions of the Institute of Measurement & Control, Vol.1, Issue 19,1997, pp.2- 12.

[8] R.S. Pena, J.C. Clare, G.M. Asher, Vector control of a variable speed doubly- fed induction machine for wind generation systems, EPE Journal, Vol.3, Issue 6, 1996, pp.60-67.

[9] D. Santos-Martin, S. Arnaltes, J.L.R. Amenedo, Reactive power capability of doubly fed asynchronous generators, Electric Power Systems Research, Vol. 78, No.11, 2008, pp. 1837–1840.

[10] R.G. de Almeida, E.D. Castronuovo, J.A.P. Lopes, Optimum generation control in wind farms when carrying out system operator requests, IEEE Transactions on Power Systems Vol.21, No.2, 2006, pp.718–726.

[11] L. Leclercq, C. Saudemont, B. Robyns, G. Cimuca, M.M. Radulescu, Flywheel energy storage to improve the integration of wind generators into a networks, Proceedings of the 5th International Symposium on Advanced Electromechanical Motion Systems-ELECTROMOTION 2003, vol. 2, Marrakesh, Morocco, November 26–28, 2003, pp.1-7.

[12] C. Abbey, G. Joos, "Integration of energy storage with a doubly fed induction machine for wind power applications", 35th Annual IEE Power Electronics Specialists Conference, 2004, pp. 1-6.

[13] P. Siano, P. Chen, Z., Chen, A. Piccolo, "Evaluating maximum wind energy exploitation in active distribution networks", IET Generation, Transmission & Distribution, vol. 4(5), 2010, pp. 598 608.

[14] Carrasco J.M., Franquelo L.G., Bialasiewicz J.T., Galvan E., Guisado R.C.P., Prats Ma.A.M., Leon J.I., Moreno-Alfonso N., "Power-Electronic Systems for the Grid Integration of Renewable Energy Sources: A Survey", IEEE Trans. on Industrial Electronics, Vol. 53, Issue 4, 2006, pp. 1002- 1016.

[15] V. Galdi, A. Piccolo, P. Siano, "Exploiting maximum energy from variable speed wind power generation systems by using an adaptive Takagi-Sugeno-Kang fuzzy model" Energy Conversion And Management, 2009, vol. 50, pp. 413-421.

[16] V.Calderaro, V. Galdi, A. Piccolo, P. Siano, "A fuzzy controller for maximum energy extraction from variable speed wind power generation systems", Electric Power Systems Research, 2008, vol. 78, p. 1109-1118.

[17] V. Galdi, A. Piccolo, P. Siano, " Designing an adaptive fuzzy controller for maximum wind energy extraction", IEEE Transactions On Energy Conversion, 2008, vol. 23, pp. 559-569.

[18] C. Cecati, F. Ciancetta, P. Siano, (2010) "A Multilevel Inverter for PV Systems with Fuzzy Logic Control", IEEE Transactions on Industrial Electronics, Vol.57, Issue 12, , pp. 4115- 4125.

[19] (http://www.winddata.com/)

[20] SimPower system Toolbox of MATLAB, Mathwork 2009.

2011 IEEE International Conference on Fuzzy Systems
June 27-30, 2011, Taipei, Taiwan

Terminal Sliding Mode Controlled CVCF Inverters

En-Chih Chang* Li-Peng Yin** Rong-Ching Wu*** Lung-Sheng Yang†

*, **, ***Dept. of Electrical Engineering
I-Shou University, Kaohsiung City
84001 Taiwan, R.O.C.

†Dept. of Electrical Engineering
Far East University, Tainan City
74448 Taiwan, R.O.C.

*enchihchang@isu.edu.tw **leepom@isu.edu.tw *** rcwu@isu.edu.tw †yanglungsheng@yahoo.com.tw

***Abstract*—A control technique called Terminal Sliding Mode Control (TSMC) to generate high-quality sinusoidal output voltage for a constant-voltage constant-frequency (CVCF) inverter is presented in this paper. Conventional Sliding Mode Control (SMC) has used extensively due to its robustness and simplicity, but the convergence of the system states to the equilibrium point is usually asymptotic. TSMC not only has the robustness of the SMC but also guarantees the finite reaching time to the equilibrium point. The presented TSMC adjustable parameters are used to decrease the system state error to zero in finite time. With the better robustness of the proposed controller, the output voltage of the CVCF inverter will have the features of low distortion, and insensitively to parameter variations and external disturbances. Simulation results are given to conform that the proposed controller can achieve satisfactory response under linear and nonlinear loads.**

Keywords- Terminal Sliding Mode Control (TSMC), constant-voltage constant-frequency (CVCF) inverter, finite time, distortion, nonlinear loads.

I. INTRODUCTION

Constant-voltage constant-frequency inverters are being broadly adopted in many AC power conditioning systems, such as uninterruptible power supply (UPS) systems, photovoltaic (PV) energy systems, and programmable AC source (PAS) systems [1], [2]. The CVCF inverters are required to maintain the high-quality AC output voltage of low harmonic distortion (THD) and fast dynamic response even feeding distorting loads (especially highly nonlinear loads such as diode rectifiers with electrolytic capacitors) that can be achieved by employing feedback control technique [3], [4]. The variable structure system with sliding mode was initially proposed in the 1950's [5], [6]. The most attractive advantage of a sliding mode is its insensitively to modeling uncertainly, plant parameter variation, and/or external disturbance [7-12]. The sliding mode control system utilizes a switching control laws to drive the system to reach and remain on the intersection of a set of prescribed switching surface. This indicates that in the design procedure of a sliding mode control, the following steps must be satisfied:

1. There exists a sliding cure whenever the trajectory of the state error will be forced toward the sliding cure.
2. When the state error hits the sliding cure, and then the trajectory of the state error must sliding along the cure to the origin.

However, as the above mentioned, the most commonly used switching surfaces are linear hyperplanes [7-12]. The linear hyperplanes guarantee the asymptotic stability of the sliding mode. The system state will converge to the origin in infinite time. Similarly, in more recent literature, the good inverter performance cannot be achieved on account of the infinite system-state convergence time [13-15]. The tracking control scheme based on fixed-frequency SMC technique is applied to the design of Buck-based inverter. In this case, the resulting output voltage also makes a concession between steady state and transient response [13]. A discrete-time SMC method with dual-loop design for UPS inverter is developed by [14]; the system trajectory could not hit the desired sliding surface accurately, and thus a slight distortion exists in the output voltage waveform with a rectified load. In the work [15], a sliding mode controlled PWM inverter is presented, but incurs steady-state error problems.

Thus, in this paper, a terminal sliding mode control through nonlinear hyperplanes is proposed and the system parameter is designed. TSMC not only has the advantages of the conventional SMC but also takes the system to converge the origin point in finite time [16-23]. By using the proposed controller, the high-quality sinusoidal output voltage for a CVCF inverter can be generated and allow for the system state error converge to zero in finite time.

II. MODELING OF THE CVCF INVERTER

The system structure of CVCF inverter is shown in Fig. 1. The inverter output voltage is generally desired to be maintained as the same as possible to a sinusoidal reference waveform. Thus, design of the inverters can be regarded as a typical tracking problem. Let $v_o(t)$ denote the load voltage, $v_o^*(t)$ is the reference waveform, and $v_{in}(t)$ represents the inverter output voltage that takes three values: ($+V_{dc}$, $-V_{dc}$ or 0).

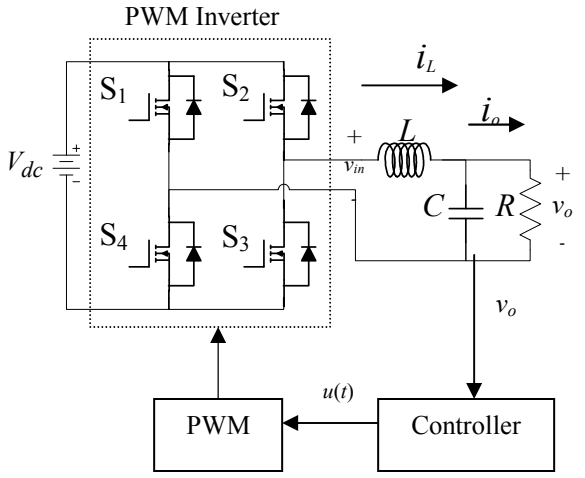

Fig. 1 Block diagram of CVCF inverter

From Fig. 1, we can get two equations:

$$i_L = C\frac{dv_o}{dt} + \frac{v_o}{R} \tag{1}$$

$$L\frac{di_L}{dt} + v_o = v_{in} \tag{2}$$

Substituting (1) into (2) has

$$\frac{d^2v_o}{dt^2} + \frac{1}{RC}\frac{dv_o}{dt} + \frac{1}{LC}v_o = \frac{1}{LC}v_{in} \tag{3}$$

Let

$$\begin{aligned} x_1 &= v_o \\ x_2 &= \dot{x}_1 = \dot{v}_o \\ \dot{x}_2 &= \ddot{x}_1 = \ddot{v}_o \\ u &= v_{in} \end{aligned} \tag{4}$$

$$\therefore \begin{bmatrix} \dot{x}_1 \\ \dot{x}_2 \end{bmatrix} = \begin{bmatrix} 0 & 1 \\ -\frac{1}{LC} & -\frac{1}{RC} \end{bmatrix}\begin{bmatrix} x_1 \\ x_2 \end{bmatrix} + \begin{bmatrix} 0 \\ \frac{1}{LC} \end{bmatrix}u \tag{5}$$

If the desired output voltage is $x_1^* = v_o^*$, and new state variables are defined as:

$$\begin{aligned} e_1 &= x_1 - x_o^* = v_o - v_o^* \\ e_2 &= \dot{e}_1 = \dot{x}_1 - \dot{x}_o^* = \dot{v}_o - \dot{v}_o^* \\ \dot{e}_2 &= \ddot{e}_1 = \ddot{x}_1 - \ddot{x}_o^* = \ddot{v}_o - \ddot{v}_o^* \\ &= -\frac{1}{LC}v_o - \frac{1}{RC}\dot{v}_o + \frac{1}{LC}u - \ddot{v}_o^* \\ &= -\frac{1}{LC}e_1 - \frac{1}{RC}e_2 + \frac{1}{LC}u - \frac{1}{LC}v_o^* - \frac{1}{RC}\dot{v}_o^* - \ddot{v}_o^* \end{aligned} \tag{6}$$

Then, the system dynamics can be represented as follows:

$$\begin{bmatrix} \dot{e}_1 \\ \dot{e}_2 \end{bmatrix} = \begin{bmatrix} 0 & 1 \\ -a_1 & -a_2 \end{bmatrix}\begin{bmatrix} e_1 \\ e_2 \end{bmatrix} + \begin{bmatrix} 0 \\ a_1 \end{bmatrix}u + \begin{bmatrix} 0 \\ -a_1v_o^* - a_2\dot{v}_o^* - \ddot{v}_o^* \end{bmatrix} \tag{7}$$

where a_1 is equal to $1/LC$, a_2 is equal to $1/RC$.

III. CONTROL DESIGN

Define the function as follows:

$$S_0 = e_1 \tag{8}$$

From (8), the terminal sliding surface can be constructed as

$$\sigma = \dot{S}_0 + \beta_1 S_0^{\gamma_1} \tag{9}$$

where $\gamma_1 < 1$. Since γ_1 is less than one, the dynamics will be finite-time convergence; If γ_1 is equal to one, (9) becomes conventional sliding surface, and has an asymptotic convergence time.

Thus, the differentiation of the (9) can be obtained as

$$\begin{aligned} \dot{\sigma} &= \ddot{S}_0 + \beta_1\gamma_1 S_0^{\gamma_1 - 1}\dot{S}_0 \\ &= -\sum_{i=1}^{2} a_i e_i + bu - f(t) + \beta_1\gamma_1 S_0^{\gamma_1 - 1}\dot{S}_0 \\ &= -\sum_{i=1}^{2} a_i e_i + bu - f(t) + \beta_1\frac{d}{dt}S_0^{\gamma_1} \end{aligned} \tag{10}$$

Let

$$\begin{aligned} a_i &= a_{i0} + \Delta a_i \ , \quad i = 1, 2 \\ b &= b_0 + \Delta b \\ f(t) &= a_1 v_o^* + a_2\dot{v}_o^* + \ddot{v}_o^* \end{aligned} \tag{11}$$

where a_{i0} is nominal value of a_i , b_0 is nominal value of b , Δa_i is the variation of a_i , and $f(t)$ is the disturbance.

For system (7), if the control u is designed as

$$u = u_{eq} + u_{tsm} \tag{12}$$

where u_{eq} is the equivalent control input, and is defined as

$$\dot{\sigma}\big|_{u=u_{eq},\, a_1=a_{10},\, a_2=a_{20},\, b=b_0,\, f(t)=0} = 0 \tag{13}$$

$$\therefore u_{eq} = \Big(\sum_{i=1}^{2} a_{i0}e_i - \beta_1\gamma_1 S_0^{\gamma_1 - 1}\dot{S}_0\Big)/b_0 \tag{14}$$

When the system dynamics in sliding motion, $\sigma = 0$, we obtain

$$\dot{S}_0 = -\beta_1 S_0^{\gamma_1} \tag{15}$$

Substitution of equation (15) into (14) yields

$$u_{eq} = \Big(\sum_{i=1}^{2} a_{i0}e_i + \beta_1^2\gamma_1 S_0^{2\gamma_1 - 1}\Big)/b_0 \tag{16}$$

The u_{tsm} is used to eliminate the influence due to the plant parameter variations in Δa_2 to guarantee the existence of a terminal sliding mode as follows:

$$u_{tsm} = \sum_{i=1}^{2}\Omega_i e_i + \sum_{i=1}^{2}\mathrm{H}_i S_0^{2\gamma_1 - 1} + \mathrm{N} \tag{17}$$

The condition for the existence of a sliding motion is $\sigma\dot{\sigma} < 0$, and then

$$\begin{aligned} \sigma\dot{\sigma}\big|_{u=u_{eq}+u_{tsm}} &= \{-\sum_{i=1}^{2} a_i e_i + bu - f(t) + \beta_1^2\gamma_1 S_0^{2\gamma_1 - 1}\}\sigma \\ &= \{-\sum_{i=1}^{2} a_i e_i + [(b_0 + \Delta b)(u_{eq} + u_{tsm})] - f(t) + \beta_1^2\gamma_1 S_0^{2\gamma_1 - 1}\}\sigma \\ &= \{-\sum_{i=1}^{2}\Delta a_i e_i - \Delta a_2 e_2 + [\frac{\Delta b}{b_0}(\sum_{i=1}^{2} a_{i0}e_i)] + [b(\sum_{i=1}^{2}\Omega_i e_i)] \\ &\quad + (b\mathrm{H}_1 + \frac{\Delta b}{b_0}\beta_1^2\gamma_1)S_0^{2\gamma_1 - 1} + (\beta_1^2\gamma_1 S_0^{2\gamma_1 - 1} + bK_2 S_0^{2\gamma_1 - 1}) \\ &\quad + [b\mathrm{N} - f(t)]\}\sigma < 0 \end{aligned} \tag{18}$$

The conditions for satisfying (18) are

$$\Omega_1 = \begin{cases} \rho_1 < (\Delta a_1 - a_{10}\Delta b/b_0)/b & if \quad e_1\sigma > 0 \\ \xi_1 > (\Delta a_1 - a_{10}\Delta b/b_0)/b & if \quad e_1\sigma < 0 \end{cases} \tag{19}$$

$$\Omega_2 = \begin{cases} \rho_2 < (\Delta a_2 - a_{20}\Delta b/b_0)/b & if \quad e_2\sigma > 0 \\ \xi_2 > (\Delta a_2 - a_{20}\Delta b/b_0)/b & if \quad e_2\sigma < 0 \end{cases} \tag{20}$$

$$\mathrm{H}_1 = \begin{cases} h_1 < (-\beta_1^2\gamma_1\Delta b/b_0)/b & if \quad S_0^{2\gamma_1-1}\sigma > 0 \\ \bar{h}_1 > (-\beta_1^2\gamma_1\Delta b/b_0)/b & if \quad S_0^{2\gamma_1-1}\sigma < 0 \end{cases} \tag{21}$$

$$\mathrm{H}_2 = \begin{cases} h_2 < -\beta_1^2\gamma_1/b & if \quad S_0^{2\gamma_1-1}\sigma > 0 \\ \bar{h}_2 > -\beta_1^2\gamma_1/b & if \quad S_0^{2\gamma_1-1}\sigma < 0 \end{cases} \tag{22}$$

$$\mathrm{N} = \begin{cases} \zeta < f(t)/b & if \quad \sigma > 0 \\ \eta > f(t)/b & if \quad \sigma < 0 \end{cases} \tag{23}$$

Remarks:

1. By adjusting the parameters (19) to (23), the system state error can be decrease to zero in finite time.
2. Notice that the control law (12) implies the sign function across the surface σ caused by the derived inequalities form (19) to (23), and thus chattering problem exists. A solution to this problem is to smooth the discontinuous control law in a thin boundary layer. The discontinuous function can be replaced by the following continuous function:

$$\frac{\sigma}{|\sigma| + \varepsilon}, \quad \varepsilon = \begin{cases} \varepsilon_0 & |\sigma| \geq \delta \\ \varepsilon_0 & |\sigma| < \delta \end{cases} \tag{24}$$

where ε_0 and δ are positive constants.

IV. Simulation Results

To demonstrate the feasibility of the single-phase CVCF inverter using the proposed controller, the closed-loop system has been tested by computer simulations. Some key parameters are listed in Table I.

Table I Parameters of the CVCF inverter system

Switching frequency	f_{sw} = 20 kHz
DC source voltage	V_{dc} = 200 V
Rated output voltage	v_O = 110 V
Rated output frequency	f_o = 60 Hz
Rated load	R = 10 Ω
Filter inductor	L = 0.5 mH
Filter capacitor	C = 50 μF

Fig. 2 shows the simulated steady-state output voltage of the inverter with the proposed controller at full resistive load and Fig. 3 shows that with the conventional SMC at the same load condition. Both output voltages show good regulation with low THD sinusoidal waveform. Figure 4 shows the transient response with the load changing from no load to full load at t=0.0208sec. It indicates that the transient response of the proposed control is very fast taking only a few sampling intervals to reach steady-state; On the contrary, the waveforms shown in Fig. 5 with conventional SMC has a significant voltage dip. A final test, as shown in Fig. 6 is done applying a nonlinear load consisting of a diode bridge, a capacitor (200μF) and a resistive load (10 Ω). The %THD computed in the output voltage is 3.11%; The AC voltage is still satisfactory and a good behavior of the inverter is demonstrated also in this critical condition. However, under the same nonlinear loading, Fig. 7 obtained using the conventional SMC exhibits high %THD output voltage (%THD of output voltage is equal to 8.96%). The comparison between TSMC and conventional SMC under linear load and nonlinear load are also given in Table II.

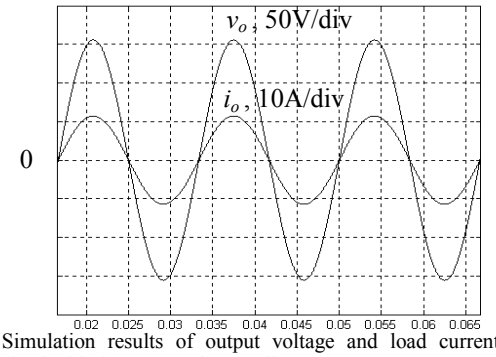

Fig. 2 Simulation results of output voltage and load current under full resistive load with the proposed controller.

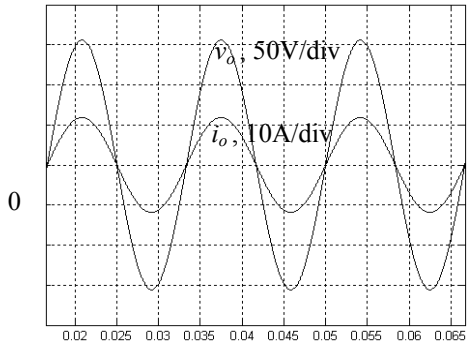

Fig. 3 Simulation results of output voltage and load current under full resistive load with the conventional SMC.

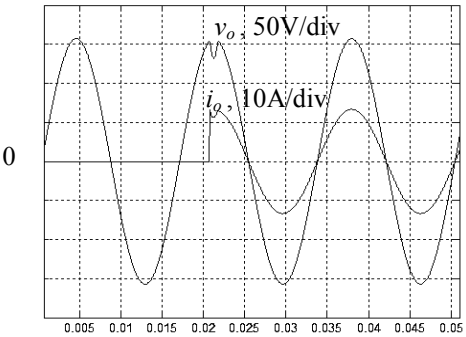

Fig. 4 Simulation results of output voltage and load current under load changing from no load to full load with the proposed controller.

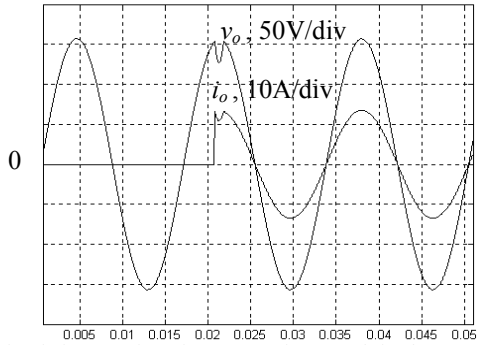

Fig. 5 Simulation results of output voltage and load current under load changing from no load to full load with the conventional SMC.

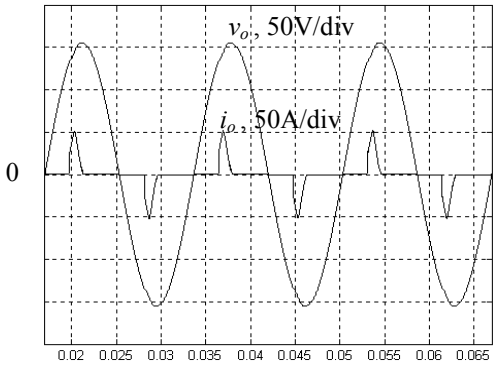

Fig. 6 Simulation results of output voltage and load current under nonlinear load with the proposed controller.

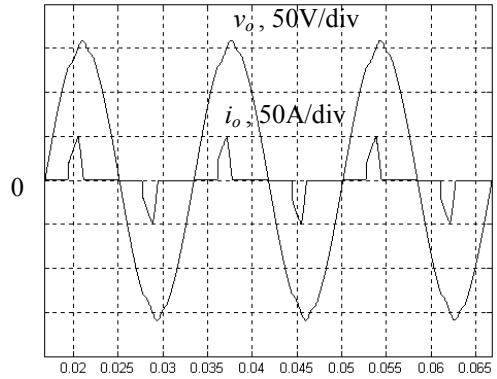

Fig. 7 Simulation results of output voltage and load current under nonlinear load with the conventional SMC.

Table II Comparison of fundamental amplitudes and %THD under linear loads and rectifier loads

		Linear Load	Rectifier Load
		10Ω	
TSMC	Fundamental Amplitude	109.5V	108.1V
	%THD	0.19%	3.11%
SMC	Fundamental Amplitude	109.3V	105.9V
	%THD	0.20%	8.96%

V. CONCLUSIONS

An approach for the control of CVCF inverters is developed on the basis of TSMC with nonlinear switching surface. This method not only possesses the characteristic of SMC but also has the finite time convergence of the system state. Even under nonlinear rectified load, the proposed controller still provides excellent performance. To verify the correct operation of the proposed control method, computer simulation is fulfilled, and good agreement is reported. It is apparent from the simulation results that the proposed CVCF inverter system is robust under different kinds of load conditions

ACKNOWLEDGEMENT

This work was supported by the National Science Council of Taiwan, R.O.C., under contract number NSC99-2218-E-214-002.

REFERENCES

[1] P. Maussion, "Instantaneous feedback control of a single-phase PWM inverter with nonlinear loads by sine wave tracking," in *Proc*. IEEE IECON'89, 1989, pp. 130-135.

[2] T. Kawabata, T. Miyashita, and Y. Yamamoto, "Dead beat Control of three- Phase PWM Inverter," *IEEE Trans. Power Electron*., vol. 5, pp. 21-28, 1990.

[3] K. P. Gokhale, A. Kawamura, and R. G. Hoft, "Dead beat microprocessor control of PWM inverter for sinusoidal output waveform synthesis," in *Proc*. *IEEE PESC*'85, 1985, pp. 28-36.

[4] T. Haneyoshi, A. Kawamura, and R. G. HOFT, "Waveform compensation of PWM inverter cyclic fluctuating loads," *IEEE Trans*. *Ind. Applicat*., vol. 24, no 4, pp. 582-589, 1998.

[5] U. Itkis, Control systems of variable structure. New York: Wiley, 1976.

[6] V. I. Utkin, "Variable Structure System with Sliding Modes," IEEE Transactions on Automatic Control, Vol. 22, pp. 212-222, 1977.

[7] K. Jezernik, and D. Zadravec, "Sliding mode controller for a single phase inverter," in *Proc*. *IEEE APEC'90*, 1990, pp. 185-190.

[8] S. J. Chiang, T. S. Tai, and T. S. Lee, "Variable structure control of UPS inverters," *Proc*. *IEE-Elect*. *Power Applicat*., vol. 145, no. 6, pp. 559-567, 1998.

[9] C. Y. Chan, "Servo-system with discrete-variable structure control," *Syst*. *Contr*. *Lett*., vol. 17, no. 4, pp. 321-325, 1991.

[10] S. L. Jung, Y. Y. Tzou, "Sliding mode control of a closed-loop regulated PWM inverter under large variations," in *Proc*. *IEEE PESC*'93, 1993, pp. 616-622.

[11] S. L. Jung, Y. Y. Tzou, "Discrete feedforward sliding mode control of a PWM inverter for sinusoidal output waveform synthesis," in *Proc*. *IEEE PESC*'94, 1994, pp.552-559.

[12] T. L. Chern, J. Chang, C. H. Chen, and H. T. Su, "Microprocessor-based modified integral discrete variable-structure control for UPS," *IEEE Trans*. *Ind. Electron*., vol. 46, pp. 340-348, 1999.

[13] R. R. Ramos, B. Domingo, E. Fossas, and F. Guinjoan, "A fixed-frequency quasi-sliding control algorithm: application to power inverters design by means of FPGA implementation," *IEEE Trans*. *Power Electron*., vol. 18, no. 1, pp. 344-355, 2003.

[14] T. L. Tai and J. S. Chen, "UPS inverter design using discrete-time sliding-mode control scheme," *IEEE Trans*. *Ind*. *Electron*., vol. 49, n0.1, pp. 67-75 2002.

[15] T. J. Liang, Y. C. Kuo, and J. F. Chen, "Single-stage photovoltaic energy conversion system," *IEE Proc*. *Electr*. *Power Appl*., vol. 148, no.4, pp. 339-344, 2004.

[16] X. H. Yu and M. Zhihong, "On finite time mechanism: terminal sliding modes," in *Proc*. *IEEE VSC'96*, 1996, pp. 164-167.

[17] X. H. Yu and M. Zhihong, "Model reference adaptive control systems with terminal sliding modes," *Int*. *J*. *Contr*., vol. 64, no. 6, pp. 1165-1176, 1996.

[18] X. H. Yu, and M. Zhihong, "Terminal sliding modes with fast transient performance," in *Proc*. *Conf*. *IEEE Decision and Contr*., 1997, vol. 2, pp. 962-963.

[19] D. Yue, S. Xu, and Y. Liu, "Terminal sliding mode control of high-order systems," in Proc. *Conf*. *IEEE Ind*. *Technol*., 1996, pp. 811-815.

[20] R. B. Fernandez and J. K. Hedrick, “Control of multivariable nonlinear systems by the sliding mode method,” *Int*. *J*. *Contr*., vol. 46, no.3, pp. 1019-1040, 1987.
[21] M. Zak, “Terminal Attractors for Addressable Memory in Neural Network,” *Physics Lett*. *A*, vol. 133, no. 1,2, pp. 18-22, 1988.
[22] S. T. Venkataraman and S. Gulati, “Control of nonlinear systems using terminal sliding modes,” in Proc. *Conf*. *American Contr*., 1992, pp. 891-893.
[23] M. Zhihong, A. P. Paplinski, and H. R. Wu, “A robust mimo terminal sliding mode control scheme for rigid robotic manipulators,” *IEEE Trans*. *Autom*. *Contr*., vol. 39, pp. 2464-2469, 1994.

2011 IEEE International Conference on Fuzzy Systems
June 27-30, 2011, Taipei, Taiwan

Differential Evolution to Enhance Localization of Mobile Robots

Michał Lisowski
Department of Management Engineering
Technical University of Denmark
2800 Kgs. Lyngby, Denmark
michlis@gmail.com

Zhun Fan
Department of Management Engineering
Technical University of Denmark
2800 Kgs. Lyngby, Denmark
zhfa@man.dtu.dk

Ole Ravn
Department of Electronic Engineering
Technical University of Denmark
2800 Kgs. Lyngby, Denmark
or@elektro.dtu.dk

***Abstract*—This paper focuses on the mobile robot localization problems: pose tracking, global localization and robot kidnap. Differential Evolution (DE) applied to extend Monte Carlo Localization (MCL) was investigated to better solve localization problem by increasing localization reliability and speed. In addition, a novel mechanism for effective robot kidnap detection was proposed. Experiments were performed using computer simulations based on the odometer data and laser range finder measurements collected in advance by a robot in real-life. Experimental results showed that integrating DE enables MCL to provide more accurate robot pose estimations in shorter time while using fewer particles.**

Keywords-Monte Carlo Localization; Differential Evolution; particle filter; mobile robot

I. INTRODUCTION

With the advances in intelligent sensing and control, in the near future, robots could take over more and more tasks and provide valuable services. Potential applications are diverse, from cleaning and transportation through enhanced communication (e.g. telepresence) and entertainment to security and military use. Unfortunately, nowadays it is still more likely to find mobile robot in structured environment, such as in a research laboratory or in a factory, rather than at home or at the office. Even though a significant progress in mobile robotics field has been made in the last two decades, the levels of autonomy presented by most of mobile robots are still limited, and the interaction and the cooperation between humans and robots are still challenges. To achieve this state, when mobile robots are commonly present in our everyday lives, one of the first remaining problems is localization, which could involve three sub-problems: global localization, pose tracking and kidnap problems.

There is a number of ways to approach the stated problem, which potentially may yield satisfactory solutions. This paper is dedicated to particle filters and evolutionary algorithms, particularly Monte Carlo Localization (MCL) and Differential Evolution (DE). Although both methods are mature and have long history, they were applied together to mobile robot localization problem only once by Moreno et al. [1]. Combining both methods has the potential of yielding a more effective algorithm. To our best knowledge, there was no other evidence in the literature of research in mobile robotics field regarding specifically MCL and DE. Moreno et al. presented an evolutive localization algorithm for mobile robots combining DE and MCL. Algorithm implementation is based on occupancy grid maps and laser range finder sensor.

Thrun et al. [2] presented a comprehensive paper on MCL, which is a family of MCL algorithms including Mixture-MCL. This algorithm combines classic MCL, where poses are predicted based on robots motion, with dual MCL, where information from sensors is used to predict robot poses. One of the interesting observations on classic MCL limitations are that the algorithm performs poorly if not enough particles are placed close to the true robot pose. This requires proposal distribution, from which particles are drawn, to correspond well to the true distribution of robot poses. Recently, Blanco et al. [3] proposed an optimal filtering algorithm, which dynamically generates the minimum number of particles that best represent the true distribution.

An interesting attempt to combine MCL with evolutionary mechanisms is presented by Ronghua and Bingrong [4]. The main focus in this paper is the problem of premature convergence when using MCL in highly symmetric environments. Another solution to mobile robot localization problem based on MCL and evolutionary approach is presented by Gasparri et al. [5]. The key concept of the algorithm presented in this paper is a dynamic clusterization method, which allows applying the evolutionary filter locally in each particle subset. This approach results in parallel exploration of the environment by a number of subsets.

Although not based on MCL, an interesting genetic algorithm for mobile robot localization is presented by Moreno et al. [6]. It also applies evolutionary filter only locally, but uses Extended Kalman Filter (EKF) instead of MCL to provide an estimate of robots pose. The proposed algorithm was tested indoor using a mobile robot equipped with 24 ultrasonic sensors, and demonstrated remarkable improvement in the results and was less computationally expensive than MCL. In this paper, we propose an algorithm combining MCL and DE that can improve the effectiveness of the algorithm, and discusses the performance improvement compared with the standard MCL method.

978-1-4244-7316-8/11/$26.00 ©2011 IEEE

The remaining part of this paper is organized as follows. In Section II, the theory of Monte Carlo Localization and Differential Evolution, and recent solutions to mobile robot localization problem using evolutionary approach and particle filters are introduced. An algorithm combining MCL with DE is presented and discussed. In Section III, an improved algorithm based on MCL and DE is presented and explained. Section IV gives experimental results on comparison of DEMCL with MCL in terms of robot pose tracking, and The proposed modifications to DEMCL algorithm is also evaluated in terms of robot kidnap problem and global localization. Finally, conclusions are presented in Section V.

II. Differential Evolution Monte Carlo Localization (DEMCL)

A. Concepts of Monte Carlo Localization and Differential Evolution

Monte Carlo Localization (MCL) represents a sampling-based class of filters in which theoretical probability distribution on the state space is approximated by a finite set of samples

$$X_t = \{x_t^p; p = 1, 2, ...P\} \tag{1}$$

called particles, for each time-step t. Every particle is a single point in the state space and represents a hypothesis (belief) about the true state.

In robot localization, we are interested in estimating the current state of the robot x_t. Typically, two-dimensional case is considered where $x_t = [x, y, \theta]^T$, i.e. x_t represents robot position in XY-coordinates and orientation. State estimation is based on the input data Y_t. Here, Y_t represents all the data gathered from time-step 0 until t. In mobile robotics, typically two types of data are used: sensor readings $Z_t = \{z_0, ..., z_t\}$ and motion readings (odometry) $U_t = \{u_0, ..., u_t\}$. Often in practice both types of data arrive alternately i.e. $Y_t = \{z_t, u_{t-1}, z_{t-1}, u_{t-2}, ..., z_1, u_0, z_0\}$. Since odometry data u_t represents robots movement (motion command) from state x_t to x_{t+1}, at time-step t the most recent available odometry data is u_{t-1}, as indicated in Figure 1. The MCL algorithm providing recursive state estimation of the robot pose is illustrated in Algorithm 1.

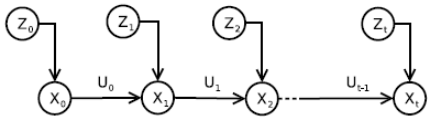

Figure 1. Robot state transformation and input data diagram.

Algorithm 1 MCL(X_{t-1}, u_t, z_t, m)

1: $X'_t = X_t = \phi$
2: **for** $p = 1$ to P **do**
3: x_t^p = **sample_motion_model**(u_t, x_{t-1}^p)
4: w_t^p = **measurement_model**(z_t, x_t^p, m)
5: $X'_t = X'_t + \langle x_t^p, w_t^p \rangle$
6: **end for**
7: **for** $p = 1$ to P **do**
8: draw $p \in [1, \ldots, P]$ with probability $\propto w_t^p$
9: add x_t^p to X_t
10: **end for**
11: **return** X_t

Differential Evolution was proposed by Storn and Price [7] for global optimization problems over continuous spaces. As any other evolutionary algorithm, DE is working with a number of potential solutions, often called a population, rather than a single one. The only requirement for DE is to provide initial population and define an objective function. It allows comparing different solutions in terms of fitness and thus is often referred to as the fitness function. Little requirements result in a wide range of optimization problems which can be addressed with DE. Even the initial requirement for continuous spaces is not valid any more, since in the recent years DE has been extended and successfully applied also to permutation-based combinatorial problems [8].

From the mathematical perspective, DE uses NP parameter vectors

$$x_i^g, i \in [0, NP-1], g \in [0, g_{\max}] \tag{2}$$

forming a population

$$P_g = [x_i^g; i = 1, 2, ..., NP] \tag{3}$$

of potential solutions. Generation index g is an integer equal or greater than zero and limited by g_{max}. P_0 corresponds to initial population, while P_1 represents population after first iteration (step) of the evolutive filter.

Additionally, each parameter vector *i*

$$x_i^g = [x_{i,1}^g, ..., x_{i,D}^g]^T \tag{4}$$

represents a single point in the D-dimensional problem space at generation g.

B. Combination of Monte Carlo Localization and Differential Evolution

Combining MCL with DE is a natural task, because the core concepts of both algorithms are very similar as presented in Table I.

TABLE I. Comparison of core concepts of MCL (particle and set) and DE (individual and population).

MCL	***DE***
$x_t^p = [x, y, \theta]^T$	$x_i^g = [x_{i,1}^g, ..., x_{i,D}^g]^T$
$X_t = \{x_t^p; p = 1, 2, ...P\}$	$P_g = [x_i^g; i = 1, 2, ..., NP]$

If the dimension D of DE parameter vector x_i^g (individual) is set to 3, then it is equivalent to particle x_t i.e. $x_{i,1}^g = x$, $x_{i,2}^g = y$ and $x_{i,3}^g = \theta$. Additionally, particle set X_t becomes equivalent to population P_g, when the number of particles P is equal to the number of parameter vectors NP.

GAs implementation requires a solution space representation and a fitness function. In this case, the most simple and intuitive solution space is $x_t = (x, y, \theta)$, because it can be directly used to represent both particles and individuals. The most obvious choice for fitness function is the measurement model, because it evaluates individual particles in terms of solving the localization problem. Therefore particle weight in MCL can be also considered as a fitness value of individual in DE.

On the algorithm level, DE can successfully replace resampling process in MCL due to crossover and mutation operators [9]. In this way, new algorithm (Algorithm 2) combines DE with MCL and will be referred to as the Differential Evolution Monte Carlo Localization (DEMCL).

As it can be seen in Algorithm 2, each step of DEMCL algorithm starts by updating particles with the most recent robot movement and assigning weights according to the measurement model. This is exactly the same as in MCL, but instead of re-sampling particles are now filtered using DE. In case of Algorithm 2, evolution is performed in a loop for a given number of generations g_{max}. Last generation P_{gmax} becomes the particle set X_t, which estimates robot pose at time t.

Algorithm 2 DEMCL(X_{t-1}, u_t, z_t,m, F,CR, g_{max}))

$X'_t = X_t = \phi$
for $p = 1$ to P do
  $x_t^p = \text{sample_motion_model}(u_t, x_{t-1}^p)$
  $w_t^p = \text{measurement_model}(z_t, x_t^p, m)$
  $X'_t = X'_t + \langle x_t^p, w_t^p \rangle$
end for
$g = 0, P_0 = X'_t$
while $g < g_{max}$ do
  for $p = 1$ to P do
    $v^p = x_t^{r1} + F \cdot (x_t^{r2} - x_t^{r3})$, $r1, r2, r3 \in [1, P]$, $F > 0$
    $u^p = \begin{cases} v_j^p & \text{if } (p_{p,j} \leq CR \text{ or } j = j_{rand}) \\ x_{t,j}^p & \text{otherwise} \end{cases}$ $j = 1, 2, 3$
    $w_u = \text{measurement_model}(z_t, u^p, m)$
    if $w_u > w_t^p$ then
      $P_{g+1} = P_{g+1} + \langle u^p, w_u \rangle$
    else
      $P_{g+1} = P_{g+1} + \langle x_t^p, w_t^p \rangle$
    end if
  end for
  $g = g + 1$
end while
$X_t = P_{g-1}$
return X_t

DE mutation variant used in Algorithm 2 is DE/rand/1/bin with F = 0.5 and CR = 0.7 (which corresponds to ~80% crossover probability).

III. IMPROVED DEMCL

A. Motivation

As demonstrated in the previous chapter, DEMCL is very suitable for solving both global localization and pose tracking problems. However, in the current form it cannot address robot kidnap problem. The main reason is that once population is converged the difference vectors in mutation are small, so evolutionary search is limited only to particles neighborhood. In other words, when all particles are grouped together, new candidate particles are generated by DE only locally. As a result, once the robot is kidnapped to a distant location, the probability of generating a new particle close to its true pose is practically zero and therefore it is almost impossible to recover from the kidnap.

It is evident that in order to solve the kidnap problem it is necessary to modify DEMCL algorithm.

B. Method description

The most straightforward solution to kidnap problem is to extend DE search well beyond the converged population by using high scaling factor F in the mutation operator. Typical F range is (0-1) and in our experiments F=0.5, but theoretically F $\in$ R+. When using high F values, mutated particles are more widely spread in the map and the probability of generating a particle close to the true robot pose after kidnap becomes larger. However, the problem is how to select correct F value. There are two methods for randomizing F via selecting a PDF and deciding how often to draw F, either for each parameter in the vector (jitter) or for every vector (dirther), which require a range of values instead of a single point. However, if the F range is not proper, mutated particles could be often outside the map and this approach would be very inefficient, just as adding random particles to the set.

Taking into account good global localization results of DEMCL, a more efficient solution to kidnap problem would be to reinitialize global localization search once the robot is kidnapped. We propose to modify DEMCL so that the population can be reset by redistributing all particles randomly and uniformly in the map. This approach requires a method to detect the kidnap. We propose following rules to signal when population resetting should be performed:

1. If the average particle weight has decreased recently compared to the long-term average.

2. If the particle set is converged but the long-term average particle weight is low.

3. If the particle set is old and still not converged.

Rule 1 First rule originates from the sensor resetting technique because it also monitors the long term (w_{slow}) and short term (w_{fast}) averages of particles weights using exponential filters. The main purpose of this rule is to signal when the particle set starts to diverge from the true pose distribution. For this rule, the probability of reset is defined as

$$pr_1 = \min(0, 1 - \frac{w_{fast}}{w_{slow}}) \quad (5)$$

where

$$w_{slow} = w'_{slow} + \alpha_{slow}(w_{avg} - w'_{slow}), \alpha_{slow} = 0.2, w_{slow} \in [0,1]$$
$$w_{fast} = w'_{fast} + \alpha_{fast}(w_{avg} - w'_{fast}), \alpha_{fast} = 0.95, w_{fast} \in [0,1]$$

Rule 2 Second rule is designed to assist the first one when the particle set is converged to a wrong pose. In such situations it is reasonable to expect low w_{slow} values, so the probability of reset is defined in this case as

$$pr_2 = \min(0, \alpha_1 - w_{slow}) \quad ()$$

where $1 \in (0, 1)$ is the upper limit of unacceptable w_{slow} values. If w_{slow} 1 than pr2 = 0 and population reset is not triggered by this rule. Parameter1 is introduced in this rule to serve as an adjustable threshold between low and high w_{slow} values. In order to avoid resetting premature populations, for which w_{slow} had not enough time to exceed 1, this rule is applied only to converged populations.

Rule 3 The first two rules cover most of the cases when population reset is needed. However, it is not certain that each population eventually converges and also w_{slow} can be low for an extended period of time, so there is a need for one more rule to trigger population reset in such situations. It would simply reset any population which is old, but not converged. In this case, the probability of reset is defined as

$$pr_3 = \min(\frac{A}{\alpha_2}, 1) \quad ()$$

where A is the population age and $\alpha_2 \in N^+$ is the maximum age, both expressed as the number of simulation steps.

All three rules are defined in probabilistic terms, rather than in deterministic terms, in order to utilize complete range of values of w_{slow} and w_{fast}. We expect such formulation to result in a greater flexibility of our method and ability to work with a wider range of maps. Probabilistic approach is also beneficial from the practical point of view, because the total number of parameters needed to define all rules is reduced to only two α_1 and α_2).

As it can be seen in Algorithm 3, all three rules are independent since the random uniform variable $U(0,1)$ is drawn individually for each rule. Population reset rules are placed at the end of DEMCL algorithm (Algorithm 3).

Algorithm 3 population_reset (X_t, w_{avg}, A, α_1, α_2)

1: $w_{slow} = w'_{slow} + 0.2 \cdot (w_{avg} - w'_{slow})$
2: $w_{fast} = w'_{fast} + 0.95 \cdot (w_{avg} - w'_{fast})$

3: $p_{r1} = \min(0, 1 - \frac{w_{fast}}{w_{slow}})$
4: $p_{r2} = \min(0, \alpha_1 - w_{slow})$
5: $p_{r3} = \min(\frac{A}{\alpha_2}, 1)$

6: **if** $U(0,1) < p_{r1}$ **then**
7: Reset population X_t
8: **end if**
9: **if** X_t is converged AND $U(0,1) < p_{r2}$ **then**
10: Reset population X_t
11: **end if**
12: **if** X_t is not converged AND $U(0,1) < p_{r3}$ **then**
13: Reset population X_t
14: **end if**

Implementation of the resetting rules is relatively simple, since it requires only little additional effort to track population age A and defining convergence criteria (Algorithm 3). In our case, population is being considered as converged if all particles are within 0.25m from the average pose estimated by this population.

IV. EXPERIMANTAL RESULTS

In this section, DEMCL was compared with MCL in terms of robot pose tracking. We are interested in localization speed, pose tracking accuracy and computation time. The proposed modifications to DEMCL algorithm also was evaluated in terms of robot kidnap problem and global localization.

A. *Comparing DEMCL with MCL*

In terms of localization speed, experimental results for MCL and DEMCL are very similar. Figure 2 presents ratio of successful trials which were localized before or exactly at the given step. In other words, all successfully localized trials until given step number are summed up and divided by the total number of successful trials in the experiment.

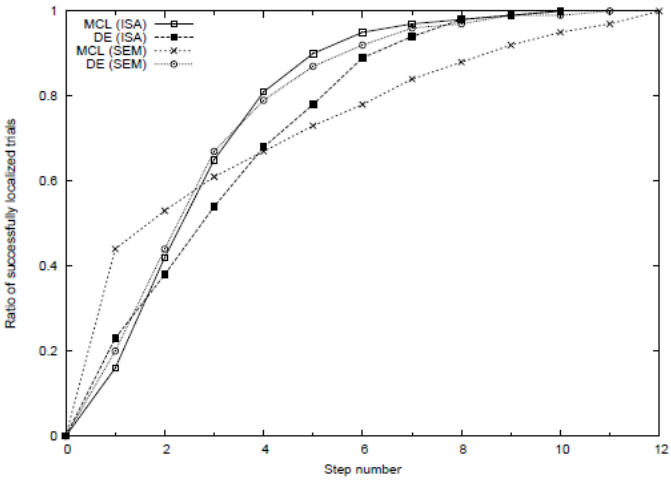

Figure 2. Ratio of successfully localized trials as a function of step number (time).

In terms of localization speed, results obtained show that the number of particles has little influence on pose tracking accuracy, therefore Table II presents only the average results.

On average, DEMCL method is 44% (ISA) and 50% (SEM) more accurate at pose tracking than MCL. Yet, both methods yield results in 0-0.1m range, which should be satisfactory for most real-life applications.

TABLE II. MCL AND DEMCL AVERAGE POSE TRACKING ACCURACY COMPARISON.

MCL	*DEMCL*
ISA 0.072±0.010m	0.050±0.016m
SEM 0.084±0.016m	0.056±0.009m

Increased computation time is the cost of significantly improved DEMCL effectiveness. Table III presents average computation time in ms for 100 particles. In this aspect, DEMCL performance is 53 (ISA map) and 17 (SEM map) times worse than MCL. Such a big difference is surprising, although an increase in computation time could not be avoided due to additional DEMCL calculations in each simulation step. On the other hand, DEMCL was using roughly 10 times less particles than MCL, which reduced the computation effort for DEMCL.

It is important to notice that exact computation time of DEMCL depends highly on the number of generations. Values presented in Table III were calculated using results from experiments with 30 (ISA map) and 10 (SEM map) generations. Any change in the number of generations would influence computation time of DEMCL, so it is not possible to directly compare MCL and DEMCL. Therefore results in Table III should be considered as a general indication of significant computation time increase, rather than as an exact difference.

TABLE III. COMPUTATION TIME IN MS PER 100 PARTICLES.

MCL	*DEMCL (ISA)*	*DEMCL (SEM)*
1.7	89.8	28

The most important observation is DEMCL ability to achieve much better success rates with fewer particles compared to MCL. DEMCL performance is significantly better than MCL in terms of effectiveness and pose tracking accuracy, however it requires much longer computation time.

B. Improved DEMCL

We expect resetting rule 1 to have the most critical influence on the results, therefore two variants of modified DEMCL are tested: with rule 1 only and with all three rules. In addition, global localization results are also presented for DEMCL without modifications. In case of robot kidnap problem, MCL results are included for reference purposes.

Global localization experiment consisted of 100 independent trials with exactly the same setup. At the beginning of each trial particles were initialized randomly and uniformly all over the free space indicated by the map. Next, at each simulation step (single iteration of DEMCL or MCL algorithm) position error was calculated as a distance between the estimated pose and the true robot pose. If this error was less than 0.25m for 5 consecutive steps, global localization was considered to be successful in the particular trial. The maximum length of each trial was set to 50 steps. Starting point in the map was selected randomly for each trial ensuring odometry and sensor data were available at least for 50 steps.

Results presented in Table IV clearly indicate that population resetting with rule 1 gives the best results, except for SEM map. In general, introducing any of the two resetting strategies improves global localization results. The explanation might be the fact that without resetting rules population has only one chance to localize the robot. With resetting there can be numerous attempts to localize the robot as a result of particles being again initialized randomly in the complete map.

TABLE IV. GLOBAL LOCALIZATION RESULTS SUMMARY FOR DEMCL VARIANTS. LGORITHMS ARE ORDERED STARTING FROM THE MOST SUCCESSFUL ONE.

Map	*DEMCL (ISA)*		
ISA	Rule 1	Rule 1-2-3	No resetting
SEM	Rule 1-2-3	Rule 1	No resetting
UWB	Rule 1	No resetting	Rule 1-2-3
COR	Rule 1	Rule 1-2-3	No resetting

Robot kidnap experiment also consisted of 100 independent trials, however the setup was different compared to global localization experiment. First of all, at the beginning of each trial particles were initialized only locally around the random starting position of the robot to avoid the need of global localization. Once the pose tracking was reliable, robot true pose was changed randomly. When pose error decreased to less than 0.25m, within 50 steps from the moment of kidnap, the robot was considered as successfully recovered from kidnap and the trial was counted as successful.

Values of w_{slow} and w_{fast} during a typical trial are presented in Figure 3. In addition, Figure 3 includes the average ratio of new particles created by DE at each generation, which we define as

$$\gamma_{new} = \frac{1}{g_{max}} \sum_{g=1}^{g_{max}} \frac{N_{new}^{g}}{P} \qquad ()$$

where $P = const$ is the total number of particles and N_{new}^{g} is the number of new particles created from population P_g which have higher fitness values than the parents and therefore are added to P_{g+1} (Algorithm 3, lines 13-17). Parameter γ_{new} indicates how effective is the evolutionary search in DE and also how likely it is for a particle to be replaced by a mutated candidate particle.

At the beginning of the trial (Figure 3, steps 1-10), all three parameters are very low. In case of w_{slow} and w_{fast} this is expected because robot is not yet localized, so particle weights are low. Surprisingly, γ_{new} is also very low (~6%), which might

indicate that evolutionary search in DE is not effective, when it is needed the most. However if we take into account the number of generations g_{max}=30, than we can easily calculate that each particle is on average replaced by a better candidate almost twice at each simulation step. This brings us to conclusion that even when γ_{new} is low the particle set is still evolving.

At step 11 w_{fast} rapidly increases which indicates that obtained measurements start to match the expected ones very well. High w_{fast} might signal successful global localization, even though it is not always a sufficient indicator. In general, there might be more than one area in the map resulting in high correlation with obtained measurements. At the same time, also γ_{new} increases from ~6% to ~30%, which suggests that particle set is evolving around five times more often than at the beginning of the trial. This observation might be explained by the fact that it is more likely for a candidate particle to have high fitness value, when particles are converged around the true robot pose, because then mutation acts only locally.

Next, w_{slow} is slowly rising, due to constantly high w_{fast}, and reaches maximum value at step 27. At this point in the simulation, both global localization and pose tracking prove to be successful, so robot kidnap occurs. As a result of sudden change in robot true pose, w_{fast} quickly decreases from 0.97 at step 27 to only 0.07 in the following step, because measurements are not aligned with expectations any more. However, w_{slow} is still quite high (change from 0.94 to 0.76) so the probability of population reset according to rule 1 is high and equal to $p_{rl} = 1 - w_{fast}/w_{slow} = 1 - 0.07/0.76 = 0.91$.

As a consequence of population reset at step 28, both w_{slow} and w_{fast} are set to 0. As seen in Figure 3, at step 35 w_{fast} again suddenly increases and w_{slow} also catches up within steps 35-50, which in this trial indicates successful robot pose recovery after kidnap.

To sum up, in this example trial robot kidnap was quickly detected after one steps (28-29) and after following six steps (29-35) robot pose estimate was successfully recovered.

Overall results from the complete experiment (Table V) prove that DEMCL with resetting rule 1 is clearly the most successful algorithm in solving the kidnap problem. Algorithms are ordered starting from the best.

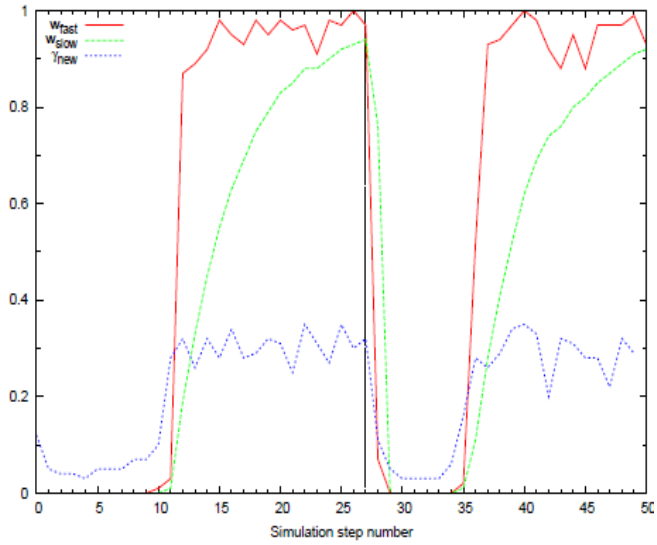

Figure 3. Population parameters in kidnap experiment: long-term (wslow) and short-term (wslow) average particle weights, average ratio of new particles (new) introduced by DE at each generation. Robot kidnap occured at step 27 (indicated by vertical line).

TABLE V. ROBOT KIDNAP OVERALL RESULTS FOR DEMCL AND MCL.

Map	***DEMCL (ISA)***		
ISA	DEMCL (rule 1)	DEMCL (rule 1-2-3)	MCL
SEM	DEMCL (rule 1)	DEMCL (rule 1-2-3)	MCL
UWB	DEMCL (rule 1)	DEMCL (rule 1-2-3)	MCL
COR	DEMCL (rule 1)	DEMCL (rule 1-2-3)	MCL

V. CONCLUSIONS

In this paper, both MCL and DE algorithms have been investigated and demonstrated how they can be easily combined to achieve increased performance. The outcome, modified DEMCL algorithm, is a complete solution for all the localization sub-problems. Experimental evaluation of the proposed algorithm proved significant improvements compared to MCL.

Regarding the challenging robot kidnap problem, the most important advancement was observed, due to the introduced population resetting rule. With sufficient number of particles, modified DEMCL algorithm was able to recover robot pose within 5 to 10 steps after kidnap with effectiveness reaching 100% on 3 out of 4 tested maps (except UWB). Whereas MCL results indicated constantly low effectiveness in recovery from kidnap, with success rates only up to 30% on most favorable map (SEM).

In case of global localization, proposed algorithm demonstrated ability to achieve the same success rates as MCL but with significantly fewer particles. The reduction ratio in particle set size ranges from 14 to 40 times. MCL solution to pose tracking was satisfactory with an average error of 7-8cm.

However modified DEMCL algorithm results in an average error of 5-6cm, which is slightly better.

The future work will focus on the investigation in the following areas: measurement model (fitness function), the improvement in computation cost and efficiency, multiple populations concept applied in DEMCL, and further DE analysis on other mutation and crossover variants or more advanced DE algorithms e.g. based on stochastic ranking. This issue could lead to further improvement of modified DEMCL algorithm and better performance results.

REFERENCES

[1] L. Moreno, S. Garrido, and ML Munoz. Evolutionary filter for robust mobile robot global localization. Robotics and Autonomous Systems, 54(7):590–600, 2006.

[2] S. Thrun, D. Fox, W. Burgard, and F. Dellaert. Robust Monte Carlo localization for mobile robots. Artificial Intelligence, 128(1): 99–141, 2001.

[3] Jose-Luis Blanco, Javier Gonzalez, and Juan-Antonio Fernandez-Madrigal. An optimal filtering algorithm for non-parametric observation models in robot localization. In IEEE International Conference on Robotics and Automation, 2008, pp. 461–466.

[4] L. Ronghua and H. Bingrong. Coevolution Based Adaptive Monte Carlo Localization (CEAMCL). International Journal of Advanced Robotic Systems, 1(3):183–190, 2004.

[5] A. Gasparri, S. Panzieri, F. Pascucci, and G. Ulivi. Monte carlo filter in mobile robotics localization: A clustered evolutionary point of view. Journal of Intelligent and Robotic Systems, 47(2):155–174, 2006.

[6] L. Moreno, J.M. Armingol, S. Garrido, A. De La Escalera, and M.A. Salichs. A genetic algorithm for mobile robot localization using ultrasonic sensors. Journal of Intelligent and Robotic Systems, 34(2):135–154, 2002.

[7] R. Storn and K. Price. Differential evolution-a simple and efficient adaptive scheme for global optimization over continuous spaces. INTERNATIONAL COMPUTER SCIENCE INSTITUTE-PUBLICATIONS-TR, 1995.

[8] G.C. Onwubolu and D. Davendra. Differential Evolution: A Handbook for Global Permutation-based Combinatorial Optimization. Springer Verlag,2009.

[9] T. Higuchi. Monte Carlo filter using the genetic algorithm operators. Journal of Statistical Computation and Simulation, 59(1):1–23, 1997.

2011 IEEE International Conference on Fuzzy Systems
June 27-30, 2011, Taipei, Taiwan

Fuzzy C-Means Clustering Based Construction And Training For Second Order RBF Network

Kanishka Tyagi
Department of Electrical Engineering
The University of Texas at Arlington
Arlington, TX, USA, 76010
kanishka.tyagi@mavs.uta.edu

Xun Cai
School of Computer Science and Technology
Shandong University
Jinan, Shandong, P.R.China, 25010
caixunzh@sdu.edu.cn

Michael T.Manry
Department of Electrical Engineering
The University of Texas at Arlington
Arlington, TX, USA, 76010
manry@uta.edu

***Abstract*—The paper presents a novel two-step approach for constructing and training of optimally weighted Euclidean distance based Radial-Basis Function (RBF) neural network. Unlike other RBF learning algorithms, the proposed paradigms use Fuzzy C-means for initial clustering and optimal learning factors to train the network parameters (i.e. spread parameter and mean vector). We also introduce an optimized weighted Distance Measure (DM) to calculate the activation function. Newton's algorithm is proposed for obtaining multiple optimal learning factor for the network parameters (including weighted DM). Simulation results show that regardless of the input data dimension, the proposed algorithms are a significant improvement in terms of convergence speed, network size and generalization over conventional RBF models which use a single optimal learning factor. The generalization ability of the proposed algorithm is further substantiated by using k-fold validation.**

Keywords- Fuzzy-C means clustering, Hessian Matrix, Newton's Method, Optimal Learning Factor, Orthogonal Least Square.

I. INTRODUCTION

The Radial Basis function (RBF) network is a three layer supervised feed-forward network [1] used in interpolation, probability density function estimation and approximation of smooth multivariate functions [2]-[7]. The RBF was first introduced as a solution to the real multivariate interpolation problem. The RBF model can approximate any multivariate continuous function arbitrarily well on a compact domain if a sufficient number of radial basis functions are given [4].

Fuzzy clustering has been used in RBF networks for many applications. The model presented in [8] uses it for Traffic status evaluation. Though it has been applied only to the simulated data and real traffic condition is still an "open" problem. Conditional Fuzzy Clustering in the design of RBF networks [9]. The idea in [9] is further extended by using supervised Fuzzy clustering to improve RBF performance in regression task [10]. In [11] Fuzzy Clustering is used for designing a RF network used in Modeling of Respiratory system.

A hybrid learning procedure is proposed in [12] which employs unsupervised clustering algorithm like k-means for determining the center for radial basis function and supervised learning for updating output weights connecting the radial basis function unit (hidden unit) to the output unit. In [13] a gradient training algorithm for updating all the network parameters (mean vector, spread parameter and output weights) is presented. A novel space filling curves with genetically evolving parameters is proposed in [14].

In order to train the RBF network mostly first order methods are used. Gradient descent learning described in [15], [16] offers a balance between performance and training speed. These networks can be compared with sigmoid hidden unit based feed forward neural networks in [16]-[18]. The combination of steepest descent and Newton's method would seem to be more promising for unconstrained optimization problems [19]. This method is convergent and has a high convergence rate. Since Newton's method for the RBF often has non-positive definite or even singular Hessian, Levenberg-Marquardt (LM) or other methods are used instead. However second order methods do not scale well and suffer from heavy computational cost. Although first order methods scale better, they are sensitive to input means and gain factor [20].

Using other permissible radial basis function apart from Gaussian function has also been explored by constructing reformulated radial basis function neural networks trained with gradient descent algorithm [20]-[22]. But again the convergence and performance of the gradient descent algorithm is strongly affected by the spread parameter and the radial basis function mean vector.

To solve these problems we introduce an interesting family of RBF networks based on Newton's method. The paper is organized as follows: conventional RBF structure and parameter determining methods are reviewed in section 2; In Section 3, the theoretical and mathematical treatment for the proposed family of RBF models is presented. Section 4 discusses the learning parameters for the proposed model. In Section 5, learning algorithms for the proposed model are elaborated; a detailed algorithm for the proposed RBF models is presented in Section 6; the training performance of various RBF models are compared in Section 7, with single Optimal Learning Factor based RBF model on several bench mark and real life datasets.

II. REVIEW OF RADIAL BASIS FUNCTION NETWORK

Without the loss of generality, we restrict ourselves to a three layer fully connected RBF with non linear activation function

A. Basic RBF topology and notation

The structure of the RBF is shown in Fig. 1. The training dataset consist of N_v training patterns $\{\mathbf{x_p}, \mathbf{t_p}\}$ where the p^{th} input vector $\mathbf{x}_p$, and the p^{th} desired output vector $\mathbf{t}_p$ have dimensions N and M respectively. The input units are directly connected to the single hidden layer with N_h hidden nodes. The scalar weight $m_k(n)$ connects the n^{th} input node and the k^{th} hidden node. For the p^{th} training pattern, the k^{th} hidden unit *net function* is

$$net_p(k) = \sum_{n=1}^{N} (x_p(n) - m_k(n))^2 \quad (1)$$

In order to handle thresholds in the hidden and output layers, the input vectors are augmented by an extra element $x_p(N+1)$ =1, so that $\mathbf{x}_p = [x_p(1), x_p(2) \ldots, x_p(N+1)]^T$. The size of the hidden layer, N_h, is the number of useful clusters. It should be noted here that N_h is the key factor not only for the performance but also the computational complexity of the network.

The k^{th} cluster mean $\mathbf{m}_k$ *(k=1, 2… N_h)* is the center of the k^{th} subclass. In Fig. 1, the dotted line between input- hidden unit signifies that instead of weighted sum/sigmoid activation, each hidden unit output $\mathbf{O_p}$ is obtained by calculating the 'closeness' of the input $\mathbf{x}$ to N_h dimensional parameter $\mathbf{m_k}$ associated with the k^{th} hidden unit. The hidden layer is fully connected to the output weight $w_{oh}(m,k)$ connecting the k^{th} hidden unit's activation $O_p(k)$ to the m^{th} output $y_p(m)$, which has a linear activation. For the p^{th} pattern, the k^{th} hidden unit output $O_p(k)$ is calculated as *a Gaussian basis function*

$$O_p(k) = e^{-\beta(k) net_p(k)} \quad (2)$$

Here $\beta(k)$ is the *spread parameters* defined as the inverse of the width of the receptive field in the input space for hidden unit k. The mean vector $\boldsymbol{m_k}$ and spread parameter $\beta(k)$ constitute the conventional parameters of RBF.

Once the hidden units training are complete, the output weights are optimized. The M dimensional output vector $\mathbf{y_p}$ is given by

$$\mathbf{y_p} = \mathbf{W_{oh}} \mathbf{O_p} \quad (3)$$

Training an RBF typically involves minimizing the mean squared error between the desired and the actual network outputs, defined as

$$E = \frac{1}{N_v} \sum_{p=1}^{N_v} \sum_{m=1}^{M} [t_p(m) - y_p(m)]^2 \quad (4)$$

Here $t_p(m)$ and $y_p(m)$ respectively denote the m^{th} desired and actual outputs for the p^{th} pattern respectively.

B. Classical parameter determining methods and learning algorithms

Broomhead and Lowe [22] proposed a method where the idea is to populate dense regions of the input space with receptive fields. The spread parameter and mean vector need to be found without propagating the output error back through the

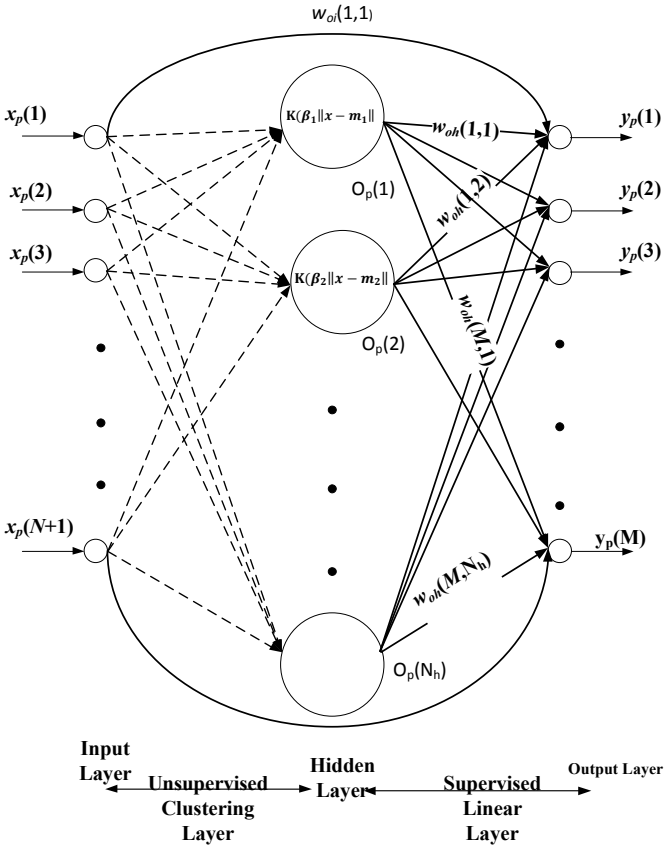

Fig 1: Topology of a fully connected RBF Neural Network

the network. But the disadvantage is for high dimensional space where for 'k' division along each dimension of an N dimensional input space, we require k^{th} basis function to cover the input space. Later Wasserman [23] presented a heuristic that is useful in determining the spread parameters. In [12] a "good" estimate to represent global average over all Euclidean distance between the centers of each unit to its nearest neighbor is suggested.

For mean vector many methods have been suggested, the most popular being choosing the first sample of the training set, some randomly chosen sample from the training set obtained by clustering or classification method.

In [12] unsupervised learning of mean vectors and spread parameters is employed using relatively small number of RBF clusters. Although clustering can be based on statistical model identification, generally competitive learning based clustering methods are used such as self-organizing map (SOM), learning vector quantization (LVQ), neural gas, Adaptive Resonance Theory (ART), C-means, Fuzzy clustering, Fuzzy C-means clustering and mountain/subtractive clustering. Fuzzy based clustering is used in this paper.

To compute the output weight matrix we can use several training algorithms which are classified into three categories: gradient descent methods, conjugate gradient methods, and Newton related method [24]-[26]. The latter is the basis of much of our research in this paper.

III. PROPOSED RBF NETWORK

In this section we illustrate how the second order based Newton's method can be incorporated in the existing RBF network by modifying the conventional RBF Network described in previous section.

Our proposed family of RBF network introduces a new group of network parameters. Referring to the conventional RBF Neural Network shown in Fig. 1; we have bypass weights $w_{oi}(i,n)$ connecting the n^{th} input to the i^{th} output. Including the bypass weights w_{oi}, the linear output response y_p is now given by

$$\mathbf{y_p} = \mathbf{W_{oi}x_p} + \mathbf{W_{oh}O_p} \tag{5}$$

Here the symbols have the usual meaning. The training strategy is a two step procedure, followed in the conventional RBF structure.

A. Phase 1: Initializing the RBF Network

Motivated from the heuristic proposed in [25], we set up the initial parameters for the proposed RBF models as described in following subsection.

1) Setting up initial weighted Distance Measure(DM)

Let elements of vector $\boldsymbol{c}$, of dimension N, denote weights in a weighted Distance Measure (DM). Let elements of $\boldsymbol{\sigma}$ represents the standard deviation of input vector of dimension *N*. Then ***c(n)*** is then defined as :

Then

$$c(n) = \frac{1}{[\sum_{n=1}^{N} 1/\sigma^2(n)]\sigma^2(n)} \tag{6}$$

The input to each hidden unit is now changed to

$$net_p(k) = \sum_{n=1}^{N} c(n)(x_p(n) - m_k(n))^2 \tag{7}$$

where $net_p(k)$ is the weighted DM. Note here that the sum is done over *N,* rather than *N+1*.

2) Setting up initial cluster center using Fuzzy C-means

We use Fuzzy clustering to partition data set into K Fuzzy clusters. The motivation for using Fuzzy clustering is that in several real life applications the data points are on the boundary of two or more classes. Hence they do not belong to any one class. We then assign a membership function which can be seen as a generalization of hard partitions. The Fuzzy C-means clustering algorithm minimizes the cost function J_{fcm} to determine mean vector $'\boldsymbol{m_k}'$ where,

$$J_{fcm} = \sum_{k=1}^{K}\sum_{p=1}^{N_v} (\varepsilon_{kp})^b \left\|x_p - m_k\right\|^2 \tag{8}$$

where $'\varepsilon'$ is the Fuzzy partition and $'b'$ is the free parameter which controls the "bending" of different clusters. If $b > 1$, the cost function allows pattern to belong to multiple cluster. $\boldsymbol{x_p}$ and $\boldsymbol{m_k}$ have their usual meaning.

B. Phase 2: Optimization of network parameters

We now propose a procedure to tune the network parameters via Newton's method which uses first and second order derivatives of the parameters w.r.t the error function.

1) Opimizing weighted DM

A typical error function used in the Training of RBF is described in (4). The hidden unit output is given by

$$O_k(p) = e^{-\beta(k)\overbrace{\sum_{n=1}^{N}(c(n)+d_c(n)).[x_p(n)-(m_k(n)]^2}^{net_p(k)}} \tag{9}$$

where $net_p(k)$ is as defined in (7). $c(n)$ is the weighted DM that will be optimized. The output vector $y_p(i)$ is same as described in (6), i.e

$$y_p(i) = \sum_{k=1}^{N_h} w_o(i,k)\, O_k(p) + \sum_{n=1}^{N} w_{oi}(i,n)\, x_p(n) \tag{10}$$

By calculating the 1st order gradient w.r.t. DM we obtain:

$$g_c(n) = -\frac{\partial E}{\partial d_c(n)} = \frac{2}{N_v}\sum_{p=1}^{N_v}\sum_{i=1}^{M}[t_p(i) - y_p(i)]\frac{\partial y_p(i)}{\partial d_c(n)} \tag{11}$$

where

$$\frac{\partial y_p(i)}{\partial d_c(n)} = -\sum_{k=1}^{N_h} w_o(i,k)O_p(k)(-\beta(k))\big[x_p(n) - m_k(n)\big]^2 \tag{12}$$

calculating the Hessian matrix element we get:

$$h_c(u,v) = -\frac{\partial^2 E}{\partial d_c(u)\partial d_c(v)} = \frac{2}{N_v}\sum_{p=1}^{N_v}\left[\sum_{i=1}^{M}\frac{\partial y_p(i)}{\partial d_c(u)}\frac{\partial y_p(i)}{\partial d_c(v)}\right] \tag{13}$$

One realization that occurs now is that of the following linear equations

$$\boldsymbol{H_c d_c} = \boldsymbol{g_c} \tag{14}$$

This is solved using orthogonal least square (OLS). For n^{th} input unit, $c(n)$ is then changed according to

$$c(n) \leftarrow c(n) + d_c(n) \tag{15}$$

Hence solving (15) we get the optimal d_c via OLS.

2) Optimizing "width" (spread parameter)

Using the same error function as in (4), for p^{th} pattern and k^{th} hidden unit.

$$O_p(k) = e^{(-(\beta(k)+d_\beta(k))\overbrace{\sum_{n=1}^{N} c(n)[x_p(n)-m_k(n)]^2)}^{net_p(k)}} \tag{16}$$

here $d_\beta(k)$ is the learning factor for $\beta(k)$ in each k^{th} hidden unit. For i^{th} output we have,

$$y_p(i) = \sum_{k=1}^{N_h} w_o(i,k) e^{-(\beta(k)+d_\beta(k))\overbrace{\sum_{n=1}^{N} c(n)[x_p(n)-m_k(n)]^2)}^{net_{p(k)}}} \quad (17)$$

We follow the same approach as in the previous sub-section. After calculating $g_\beta(k) = -\frac{\partial E}{\partial d_\beta(k)}$ and Hessian matrix element $h_\beta(u,v) = -\frac{\partial^2 E}{\partial d_\beta(u)\partial d_\beta(v)}$ we obtain

$$\mathbf{H_\beta d_\beta} = \boldsymbol{g_\beta} \quad (18)$$

Solving this again via OLS, $\beta(k)$ is then changed according to

$$\beta(k) \leftarrow \beta(k) + d_\beta(k) \quad (19)$$

3) Optimizing mean vector

In this algorithm we are changing only the mean vectors holding other parameters constant.

$$O_k(p) = e^{-\beta(k)\overbrace{\sum_{n=1}^{N} c(n)[x_p(n)-(m_k(n)+z_k.g_{mean}(k,n)]^2)}^{net_{p(k)}}} \quad (20)$$

For the p^{th} pattern , the i^{th} output unit can be written as

$$y_p(i) = \sum_{k=1}^{N_h} w_o(i,k) e^{-\beta(k)\overbrace{\sum_{n=1}^{N} c(n)[x_p(n)-(m_k(n)+z_k.g_{mean}(k,n)]^2)}^{net_{p(k)}}} \quad (21)$$

Unlike the previous gradients, here we calculate the gradient matrix element $g_{mean}(k,n) = -\frac{\partial E}{\partial m_k(n)}$. In [27] multiple optimal learning factor algorithms (MOLF) is shown to train better than OWO-BP. We therefore update the mean vector $\boldsymbol{m}_k$ based on its own learning factor z_k which is optimal for the k^{th} hidden unit.

The basic idea for MOLF is that while updating the mean vector for every iteration, instead of using a single optimal learning factor 'z' we use a vector $\boldsymbol{z}$ of optimal learning factor called Multiple OLF (MOLF). Each element of $\boldsymbol{z}$ is for each mean vector. We now derive the expression for the MOLF as used in updating mean vector. Using (5), we calculate $g_z(k) = -\frac{\partial E}{\partial z_k}$ and $h_z(u,v) = \frac{\partial^2 E}{\partial z(u)\partial z(v)}$. The Gauss-Newton update guarantees that $\boldsymbol{H_z}$ is non-negative definite. Given the negative gradient vector $\boldsymbol{g}_z = \left[-\frac{\partial E}{\partial z_1}, -\frac{\partial E}{\partial z_2} \ldots, -\frac{\partial E}{\partial z_{N_h}}\right]^T$ and the Hessian $\boldsymbol{H_z}$, we minimize E with respect to the vector $\boldsymbol{z}$ by solving linear equation:

$$\mathbf{H_z z} = \boldsymbol{g_z} \quad (22)$$

Thus we get

$$\boldsymbol{z} = \boldsymbol{H_z^{-1} g_z} \quad (23)$$

During each iteration, the k^{th} mean vector is updated as

$$m_k(n) \leftarrow m_k(n) + z_k.g_{mean}(k,n) \quad (24)$$

Here the MOLF procedure has been used to train the mean vectors. It should also be mentioned here that if MOLF fails then we can combine the optimal learning factors into a single optimal learning factor.

IV. COMBINED LEARNING ALGORITHMS

In this section we describe the construction of advance learning algorithm from the previously described algorithms.

A. Output weight optimization (OWO)

In each iteration of our proposed two stage algorithms we optimize the output weight matrix using a technique called output weight optimization (OWO). Since the outputs have linear activations, finding the weights connected to the outputs is equivalent to solving a system of linear equations. If $\boldsymbol{W_o}$ denotes the output weight matrix, equating $\frac{\partial E}{\partial \boldsymbol{W_o}} = \mathbf{0}$ leads to

$$\boldsymbol{C_a} = \boldsymbol{W_o R_a^T} \quad (25)$$

Where

$$\begin{cases} \boldsymbol{C_a} = \dfrac{1}{N_v}\displaystyle\sum_{p=1}^{N_v} y_p \bar{x}_p^T \\ \boldsymbol{R_a} = \dfrac{1}{N_v}\displaystyle\sum_{p=1}^{N_v} \bar{x}_p \bar{x}_p^T \end{cases} \quad (26)$$

Since the equations in (25) are often ill conditioned [28][29], we solve them using OLS[30] which is equivalent to using the QR decomposition [31].

B. Proposed family of algortihms

In this subsection we combine OWO with the optimization approaches of III (B). In our algorithms we combine a multi-stage training algorithm which can be denote as F[N(*param1*), *param2*] where 'F' represents Fuzzy c-means clustering and 'N' represents Newton's method applied on *param1*, while *param2* are the parameter(s) which have been set during net control and have not been modified or "tuned" during the training process. We also combine all three parameter optimizations where we update weighted DM from (15) and use (19) and (24) to update beta and mean vector. This largest combined algorithms is denotes as F[N(c, β, m.)].

During our investigation we compared our algorithms with RBF models using single OLF (SOLF). Here we discuss the single OLF case for updating spread parameters. Similar equations can be derived for the single OLF for mean vector case. Similar to the proposed algorithms we denote F[SOLF(*param1*), *param2*] where SOLF represents that single OLD has been used for updating the parameters, param1 and param2. We combine both and form a RBF model that will be compared later with the rest of the family of algorithms.

Given the error function as defined in (5) we have,

$$y_p(i) = \sum_{k=1}^{N_h} w_o(i,k) e^{-(\beta(k)+z.g_{\beta(k)})net_p(k)} + \sum_{n=1}^{N} w_{oi}(i,n) x_p(n) \quad (27)$$

Note the similarity in (18) and (23). Instead of using two optimizing parameter, we optimize the performance by using a single parameter $d_\beta(k)$ in (18). By using $g_\beta(u) = -\frac{\partial E}{\partial \beta(k)}$, we calculate $\frac{\partial E}{\partial z}$. The Gauss-Newton approximation of the second partial and 2nd order Taylor series leads to,

$$z = -\frac{\partial E/\partial z}{\partial^2 E/\partial z^2} \quad (28)$$

Instead of using a single optimal learning factor for updating all the parameters, we use Newton's method to estimate a vector of optimal learning factors $\boldsymbol{z}$. One of our investigation aims is to show this novel method to update the parameters to be better than the single optimal learning case

It should be mentioned here that during an iteration, at one time, one parameter is updated followed by OWO and then the next parameter is updated. From a philosophical point of view we modify the two step optimization approach which in turn is similar to EM algorithm where the E denotes expectation as the first step and then in the second step maximization denoted by M.

V. Algorithm for Training the Proposed RBF Network

We follow a two step hybrid learning procedure to train the proposed RBF Network. Contrary to [12] [24], our proposed algorithm efficiently uses Newton Method and Backpropagation algorithm to optimize the network parameters in every epoch. Fig. 2 shows the various stages

VI. Numerical Results

We present the results for the proposed family of algorithms discussed. All algorithm were implemented in MATLAB script. By using different benchmark and real-life dataset we judge the performance of the algorithms by analyzing the effect of applying Newton's method on network parameters. The generalization ability of each algorithm is later shown by using *k-fold* validation procedure all the data set used for the simulation is available from the Image Processing and Neural Networks Lab repository [32] and UCI Machine Learning Repository [33].

For all the figures discussed here, '*B*' denotes the spread parameters $\boldsymbol{\beta}$; $\boldsymbol{m_k}$ as the mean vectors and $\boldsymbol{c}$ is the weighted DM.

For better comparison, initial clusters, initial parameters value and the output synaptic weights of all algorithms are initialized by the same way so that the MSE of the first training iteration is same. The RBF architecture for training each dataset has different number of hidden units, different number of input units and output units. Here, the number of training iterations is fixed as $N_{it} = 50$. In all the data set, the inputs have been normalized to be zero mean and unit variance. The family of networks analyzed, are based on Newton's method with multiple OLF and compared with conventional network based on single OLF for $\boldsymbol{\beta}$ and $\boldsymbol{m_k}$. During our investigation we take two highly correlated ($\rho > 0.8$) and other two as least correlated ($\rho < 0.2$). Here ρ is the correlation coefficient. By doing so, it is found that the performance of the algorithm is severely affected by the data set correlation.

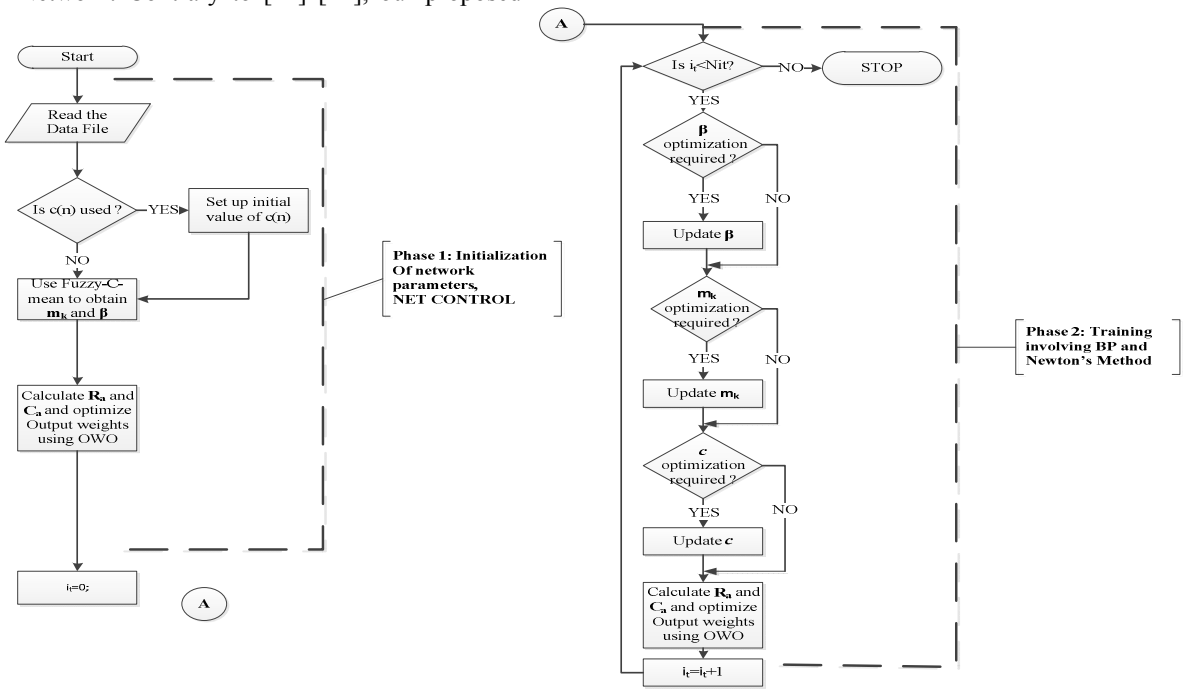

Figure 2: Algorithm for training the proposed family of RBF Network

A. Scattering Parameter Data Set

The training data file contains 1768 patterns. The inputs consist of 8 theoretical values of scattering parameters. The outputs are its 7 corresponding heights, lengths and permittivity. [32] *'twod.tra'* is a highly correlated input data set. We trained all the RBF models with $N_h = 20$. In Fig. 3, the average mean square error (MSE) for training is plotted versus the number of iterations (N_{it}) for each algorithm. From

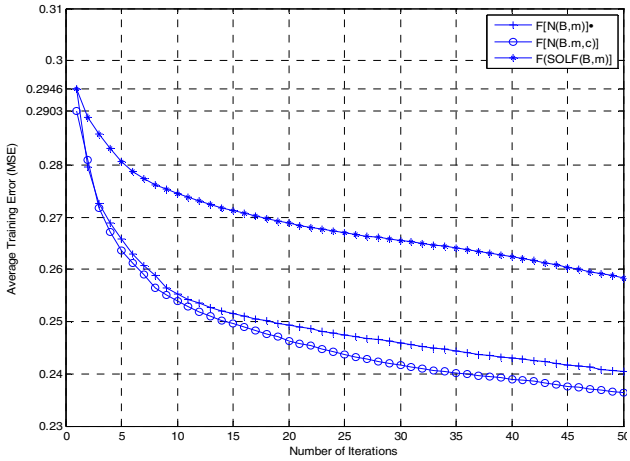

Figure 3 Performance of proposed family of algorithm with single OLF based RBF on twod

The plots we deduce that the network with Newton's method applied on all parameters gives the best performance applied

B. Radar Scattering Data Set

This training set also called '*oh7*', contains polarization at different angles along with the corresponding surface height, surface correlation length, and volumetric soil moisture content [32].

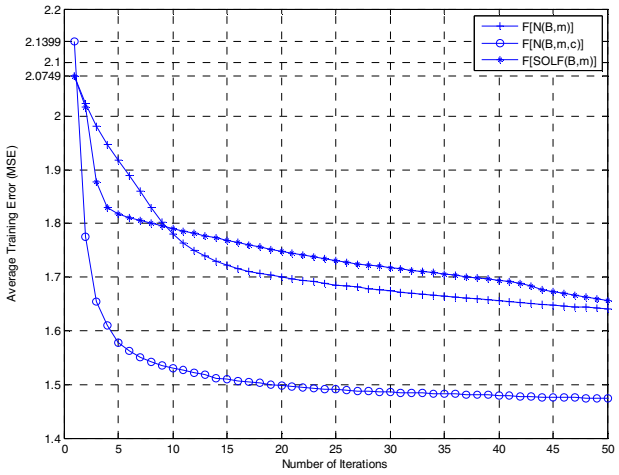

Figure 4 Performance of proposed family of algorithm with single OLF based RBF on oh7

Here not only the input values but also one of the output values is highly correlated with the input values unlike 'twod'. We train all the RBF models with $N_h = 20$. In Fig. 4, the MSE for training is plotted versus N_{it} for each algorithm. The plot shows that the RBF model where we apply Newton's method on all parameters perform best.

C. Inverse Matrix Data Set

Also called '*Mattrn'*, it is an uncorrelated dataset with 2000 training patterns obtained from the inversion of random two-by-two matrices [32]. Each pattern consists of 4 input features and 4 output features. For this data set, all the RBF models are trained with $N_h = 15$. In Fig. 5, MSE for training is plotted versus N_{it} for each algorithm. This data set is uncorrelated and we observe that the model where Newton is applied on $\boldsymbol{\beta}$ and $\boldsymbol{m_k}$*'* performs at par with the model where it is applied on all the parameters.

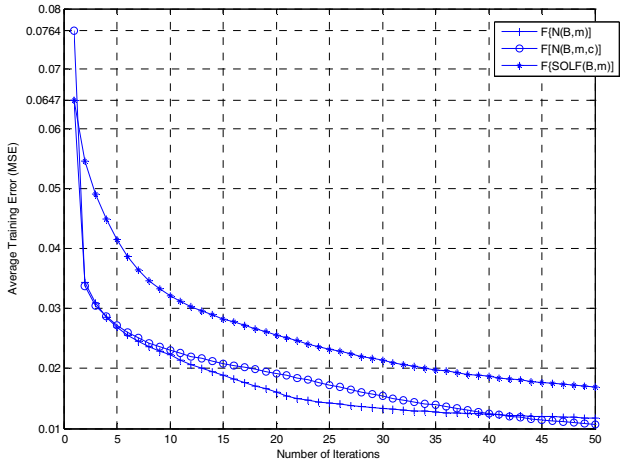

Figure 5 Performance of proposed family of algorithm with single OLF based RBF on mattrn

D. Concrete Compressive Strength Data Set

"Concrete" is an un-correlated dataset used to approximate the nonlinear function of age and ingredients of concrete compressive strength [33]. With a total number of patterns as 1030, this dataset consists of 8 inputs and 1 output and $N_h = 20$.This dataset is also least correlated and we see the same trend as we see in mattrn.tra. The performance of the model with $\boldsymbol{\beta}$ and $\boldsymbol{m_k}$ optimization is close to the model that have weighted DM optimization .

E. K-Fold Crossing Validation

We use the k-fold crossing validation procedure to show the generalization abilities of various RBF models. Choosing *k=10* so for each dataset, we split it randomly into 10 non-overlapping parts of equal size, and use 9 parts of total data for training and leave the remaining one part for testing. This procedure was repeated till we have exhausted all 10 combinations. Then, by training all these combinational datasets, we got the average of training errors. Also, the validation error of each dataset was obtained by averaging all corresponding testing errors on every testing dataset. The training MSEs and test MSEs of k-fold crossing validation on these four datasets are listed as Table 1.

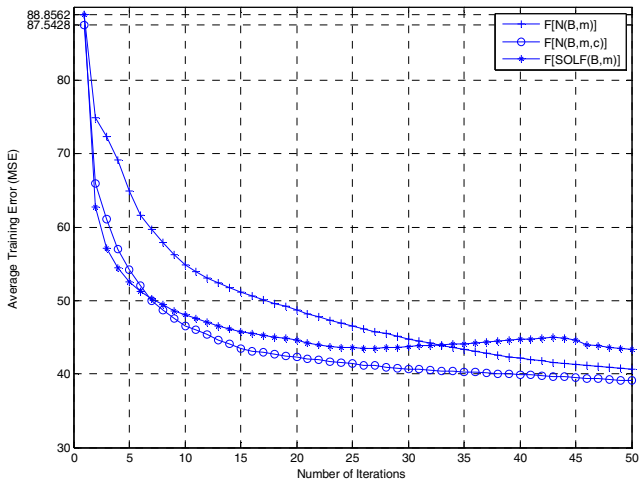

Figure 6 Performance of proposed family of algorithm with single OLF based RBF on concrete

TABLE 1: COMPARISION OF K-FOLD VALIDATION ON DATASET

Data Set	Error	F[N(B,m)]	F[N(B,m,c)]	F[SOLF(B,m)]
Twod	Validation	0.2456	0.2363	0.2587
	Testing	0.2519	0.2433	0.2713
Oh7	Validation	1.6547	1.4738	1.6847
	Testing	1.6843	1.4916	1.7214
mattrn	Validation	0.0118	0.0106	0.0168
	Testing	0.0215	0.0204	0.0181
concrete	Validation	40.5882	39.9854	43.1598
	Testing	41.0689	40.6538	43.2811

VII. CONLCUSION AND FUTURE WORK

The conclusion that we make from our experimental results is that the used of Newton's method on all three parameters helps significantly in improving the performance of RBF networks. Newton's method effect is more pronounced in correlated datasets. Training of the DM weights significantly improves the RBF network. From the experiments we conclude that for un-correlated datasets, optimizing $\boldsymbol{m_k}$ through SOLF has no effects. We have seen that the MOLF training of the $\boldsymbol{m_k}$ is more effective than the training of $\boldsymbol{\beta}$. The experimental results further bolster this conclusion.

REFERENCES

[1] Kumar,S., *Neural Network: a classroom approach,* International ed. McGraw Hill Press, 2005, pp 304-314.

[2] Medgassy,P. 1961. *Decomposition of superposition of distributed functions,* Hungarian academy of Sciences, Budapest.

[3] Micchelli, C.A.1986. *Interpolation of scattered data: Distance and conditionally positive definite functions*, Constructive Approximations, vol.2, pp. 11-22.

[4] Powell, M.J.D 1987. Radial Basis functions for multivariate interpolation: a review, in algorithms for the approximation of Functions and Data. J.C.Mason and M.G.Cox eds., Clarendon Press, Oxford, England.

[5] Duda, R.O., and Hart, P.E.1973. *Pattern Classification and Scene Analysis*, Wiley, New York.

[6] Speecht, D.F. 1990. *Probabilistic neural networks*, Neural Networks, vol 3, pp.109-118.

[7] Poggio, T., and Girosi, F. 1989. *A theory of Networks for Approximation and Learning*. A.I. Memo 1140, MIT, Cambridge.

[8] Liu,X., Sun, D., Chang, Y., and Peng, Z., "Traffic Status Evaluation Based on Fuzzy Clustering and RBF Neural Network," *Intl. Conference on Fuzzy Systems and Knowledge Discovery*, 2010., pp 1405-1409.

[9] Pedrycz, W., "Conditional Fuzzy Clustering in the Design of Radial Basis Function Neural Networks," *IEEE Trans. Neural Network*, vol.9, no.4, pp.601-612, Jul.1998.

[10] Staiano, A., Tagliaferri, R., and Pedrycz, W., "Improving RBF Networks performance in regression tasks by means of a supervised Fuzzy clustering," *Neurocomputing*, pp 1570-1581, 2006.

[11] Madeda, K., Kanae, S., Yang, Z., and Wada, K., " *Design of RBF Network Based on Fuzzy Clustering Method for Modelling of Respiratory System*", Advances in Neural Networks, vol. 3973/2006.

[12] Moddy,J.E., and Darken,C.J., " Fast learning in networks of locally-tuned processing units," *Neural Computation*, vol.1, pp.281-294, 1989.

[13] Cha, I., and Kassam,S.A., " Interference cancellation using radial basis function networks," *Signal Processing*, vol.47, pp.247-268, 1995

[14] Whitehead, B.A., and Chaote,T.D., "Evolving space-filling curves to distribute radial basis functions over an input space," *IEEE Trans. Neural Networks*, vol.5, pp. 15-23, Jan. 1994.

[15] Karayiannis, N.B., "Gradient descent learning of radial basis neural networks," *in Proc.1997 IEEE Int. conf. Neural Networks*, vol.3, Houston, TX, June 9-12, 1997, pp.1815-1820.

[16] Karayiannis, N.B., "Learning algorithms for reformulated radial basis neural networks," in *Proc.1998 Int. Joint Conf. Neural Networks*, Anchorage, AK, 1998, pp.2230-2235.

[17] Karayiannis, N.B., "Reformulated radial basis neural networks trained by gradient descent," *IEEE Trans. Neural Networks*, vol.10, pp.657-671, May 1999.

[18] Karayiannis, N.B., and Behnke,S., 2000 "*New radial basis neural networks and their application in a large-scale handwritten digit recognition problem*," in Recent Advances in Artificial Neural Networks: Design and Applications, L. C. Jain and A. M. Fanelli, Eds. Boca Raton, FL: CRC, pp. 39–94.

[19] Shi, Y., Globally convergent algorithms for unconstrained optimization, *Computational Optimization and Application* vol.16, pp 295-308, 2000.

[20] Malalur,S., Manry,M., " Feed-Forward Network Training Using Optimal Input Gains," *International Conference on Neural Networks*, Atlanata, pp. 1953-1960, Jun 2009.

[21] Cover, T.M., "Geometrical and Statistical Properties of systems of linear inequalities with application in pattern recognition", *IEEE Transaction on Electronic Computers*, Vol. EC-14, pp 326-334, 1965.

[22] Broomhead, D.S. and Lowe, D. (1988), *Multivariate functional interpolation and adaptive networks*, Complex Systems, vol.2, pp. 321-355.

[23] Wasserman, P.D., *Advanced Methods in Neural Computing*, Van Nostrand Reinhold, New York, 1993.

[24] Haykin, S., *Neural Network: A Comprehensive Foundation*, 2nd ed. Englewood Cliffs, NJ: Prentice Hall, 1999.

[25] Flethcer, R., *Practical Methods of Optimization*, 2nd ed. Chichester, NY: John Wiley & Sons, 1987.

[26] Moller, M., *Efficient training of feed forward neural Networks*, Ph.D. dissertation Aarhus University, Denmark, 1997.

[27] Malalur, S., and Manry,M., "Multiple optimal learning factors for feed-forward networks," *Proc. of SPIE: Independent Component Analyses, Wavelets, Neural Networks, Biosystems, and Nanoengineering* VIII, Orlando Florida, vol. 7703 pp. 77030F-1 – 77030F-12, April 7-9, 2010.

[28] Saarein,S., Bramley, R., and Cybenko, G., " Ill-conditioning in neural network training problems." *SIAM Journal on Scientific Computing*, vol.14,pp 693-714, 1993.

[29] Smagt, P., and Hirzinger, G., *Solving the ill-conditioning in neural networks learning, ser. Neural Networks: Tricks of the Trade*. Lecture Notes in Computer Science 1524, G.Orr and K.R.Muller, Eds, Springer Verlag, 1998.

[30] Hadzer et al., "Improved Singular Value Decomposition by Using Neural Network," in *Proc. Of IEEE International Conference on Neural Networks*, 1995, Perth, WA Australia, Nov, 1995, pp.438-442.

[31] Press, W.H.et al., *Numerical Recipes*. NBey York: CAmbirdge University Press, 1986.

[32] http://www-ee.uta.edu/eewb/ip/training_data_files.htm

[33] http://archive.ics.uci.edu/ml/

2011 IEEE International Conference on Fuzzy Systems
June 27-30, 2011, Taipei, Taiwan

Evolutionary Learning of a Laser Pointer Detection Fuzzy System for an Environment Control System

Francisco Chávez and Francisco Fernández
Department of Computer Science
Centro Universitario de Mérida
University of Extremadura
Mérida, Spain 06800
Email: {fchavez,fcofdez}@unex.es

Rafael Alcalá, Jesús Alcalá-Fdez and Francisco Herrera
Department of Computer Science and Artificial Intelligence
Research Center on Information and Communications Technology
University of Granada
Granada, Spain 18071
Email: {alcala, jalcala, herrera}@decsai.ugr.es

***Abstract*—Recent studies in smart homes have proposed methods to use a laser pointer for interacting with home devices, which represents a more user-friendly and less expensive home device control environment. However, detecting the laser spot on the original non-filtered images, using standard and non expensive cameras, and considering real home environments with varying conditions, is currently an open problem.**

In this paper we propose a hybrid technique, combining a classic technique used in image detection processes, such as Template Matching, with an evolutionary learning of a Fuzzy Rule Based Systems for the laser spot detection system in real home environments. This proposal improves the success rate in images without laser spot of the previous classical and non-classical algorithms used for detecting the laser spot in previous works, decreasing the detection of the false offs which could lead to dangerous situations. Experimental results on a real home environment show the effectiveness of the proposed approach.

***Index Terms*—Interaction Systems, Domotic Control Systems, Laser Pointer Detection, Fuzzy rule-based systems, Genetic Learning.**

I. Introduction

Nowadays, a home can be controlled by different devices like special indoors control devices; or by means of mobile phones, personal computer, etc. using Internet if the users are outdoors. Recent research in intelligent homes provide great solutions for controlling home devices [1]–[6].

We can find different kinds of smart homes systems in the specialized literature. Park et al. [2] presented a robotic smart house, by means of which disabled people can be assisted by a robot sending orders with body movements. Other researchers have used non-invasive brain-computer interfaces [3], where a brain computer interface is used to control different devices.

On the other hand, the work presented in [7] makes use of a robot for helping disabled people to pick up different objects. In this work, the authors also proposed an interesting way to point out the desired objects by means of a laser pointer. The robot should then be able to detect the laser spot on an object in order to pick up this object. Since they represent cheap and easy to handle devices, laser pointers have been used as an indicator element for controlling large displays [8]–[11] and now they have been also used in the environment control system.

The main goal in these types of systems is to detect the laser spot effectively. In [7], the authors deal with this problem by using especial physical filters in the video camera while it is taking the environment photos, with the aim of only capturing the laser spot. However, this is still an open problem that can be addressed by using laser spot detection algorithms based on the original non-filtered images avoiding the expenses of using special cameras and filters.

An alternative making use of standard and therefore cheaper cameras can be found in [12] where a set of algorithms, were proposed to detect the laser spot effectively on the image obtained by a standard video camera. Nevertheless, this algorithms present some false offs, when a laser spot is detected by the algorithm but the image does not have any laser spot. In this event, a wrong order is sent to the domotic system which could provoke undesirable, dangerous or at least unexpected, situations. For this reason, in [13] we presented a new approach hybridizing a classic technique with the use of a Fuzzy Rule Based System (FRBS) designed from expert's knowledge [14], [15] for trying to improve the success rate in images without laser spot. Further, this initial FRBS was tuned in [16] by means of a Genetic Algorithm (GA), in order to improve the success rate in images without laser spot.

In this paper, we present a new approach to detect the laser spot in the environment device control system presented in [13], [16] by means of an evolutionary learning of the FRBS for the laser spot detection system. It consists on an embedded evolutionary learning of the Data Base (DB) as the way to effectively obtain a complete Knowledge Base (KB) and it is based on using the linguistic 2-tuples representation [17], which allows the lateral displacement of the labels considering an unique parameter per label, decreasing the complex search space that learning together the Rule Base (RB) and the Data Base (DB) represents. Using this particular representation, the search space is reduced with respect to the classic triangular Membership Functions (MFs) representation in order to easily obtain optimal models. The embedded learning scheme consists of an evolutionary process that learns the DB and wraps a simple method to derive a set of rules for each DB definition. This allows learning the most adequate context for each fuzzy partition (i.e., granularities and MFs displacements) together with the associated RB which will help to significantly improve the performance of the obtained FRBS for the laser spot

978-1-4244-7316-8/11/$26.00 ©2011 IEEE

detection problem. The results obtained by using the proposed approach on a big set of image samples (990 images in total) and following a cross-fold validation model show a better general success rate with respect to the previous techniques, and the most important advantage, the not desired false offs are virtually avoided.

This contribution is arranged as follows. In section II, the environment device system for environment control by using a laser pointer is described together with the previous approaches applied to solve this problem. Section III presents the evolutionary learning of a FRBS for the laser spot detection system used in this work. The results obtained using the classic technique, and the hybrid approaches based on the derivation of a FRBS from expert's knowledge, automatic tuning or automatic learning (respectively) are shown and analyzed by comparing them in section IV. Finally, section V points out some conclusions.

II. System Description and Previous Work

As we mentioned, the laser pointer systems allows to control different home devices. These systems analyze different environment images sent by a video camera, detect the laser spot on these images and automatically recognizes the device which the user has selected with the laser pointer, sending the necessary orders to control the home device by means of a domotic system.

In our case, this system consists of three sections (see figure 1):

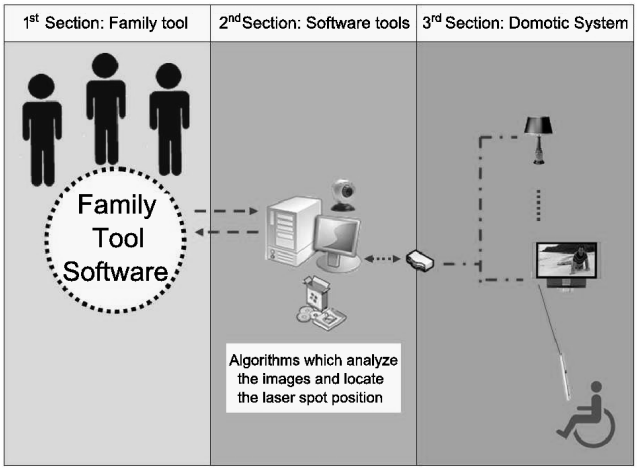

Fig. 1. Environment control system

- 1^{st} *Section*: The configuration tool allows to the users select the home devices that will be controlled by the system. In this tool, they will able to mark the active zone for each home device using the images sent by the video camera.
- 2^{nd} *Section*: In this section the system uses different techniques in order to analyze the image sent by the video camera and to locate the position of the laser spot.
- 3^{rd} *Section*: KNX/EIB architecture [18] let the system to control the different home devices. Once the laser spot is found and it is in an active zone, the system sends to the domotic system the necessary orders to turn on/off the device selected.

This contribution is focused on the 2^{nd} *Section*, in order to improve the laser spot detection ability, which becomes one of the most important tasks in these kinds of systems. In Figure 2, an example of images with and without laser spot is presented.

Fig. 2. Image with laser spot (top), Image without laser spot (bottom)

The algorithms previously used to detect the laser spot on an image have been the following:

1) Dynamic Umbralization (DU)
2) Template Matching (TM)
3) Template Matching + Dynamic Umbralization (TM + DU)
4) Template Matching + FRBS design from Expert's Experience and automatic evolutionary tuning (TM + FRBS).

The home environment control system based on laser pointer presented in [12] used three different classic algorithms, DU, TM and TM + DU. In [13] an initial hybrid model is proposed combining TM with a FRBS obtained from expert's experience, which is after improved by applying a genetic tuning of the FRBS membership functions in [16]. In the following subsections, we will briefly introduce the methods that we have presented in this previous work to detect the laser spot on an image (more information on the 1^{st} and the 3^{rd} *Sections*, and a deeper description of these algorithms can be found in [12], [13], [16]).

A. Dynamic Umbralization

Dynamic Umbralization was the first algorithm used in this system. This algorithm calculates a threshold value, by

means of which, the pixels under this value are eliminated. The threshold value is calculated by means of the following expression:

$$V_{umb} = ((Sv_I_{min}) - (Sv_I_{max})) * \frac{X}{20} + (Sv_I_{min}), \quad (1)$$

where Sv_I_{min} and Sv_I_{max} are the minimum and maximum sub intervals balance, and X is the sum of the balance parameters obtained from the pixel numerical information (see [12], [13] for more information on how this values are calculated). As a consequence of this umbralization, the resultant image has the candidate pixels of the laser spot searched.

B. Template Matching

In order to improve the system performance, we have also used a second technique, namely Template Matching. The algorithm that uses TM is based on convolution techniques. By means of this algorithm, an image named template is searched on the image sent by the video camera. A template is a laser spot image previously stored. Figure 3 shows a template image example.

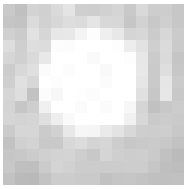

Fig. 3. Laser spot template

Each image sent by the video camera may have a section similar to the used template. The TM algorithm searches for such template on the obtained environment image. This algorithm obtains the probability of coincidence between the analyzed image sections and the template image. This probability ranges between -1 and 1, by using the following expression:

$$\Phi(I_r, I_l) = \frac{\sum_{i,j\in[-w,w]} AB}{\sqrt{\sum_{i,j\in[-w,w]} A^2 \sum_{i,j\in[-w,w]} B^2}},$$

$$A = I_r(x+i, y+j) - \overline{I_r(x,y)},$$

$$B = I_l(x'+i, y'+j) - \overline{I_l(x',y')}, \quad (2)$$

where A contains the set of pixels which are in the principal image section, and B contains the set of laser template pixels (see [12], [13] for more information on how this formula can be applied). The TM algorithm proposes the image section with the highest correlation since, the laser spot should be found in the position of the obtained image section with the highest correlation.

C. Template Matching + Dynamic Umbralization

The algorithm described above has the same problem that the DU algorithm, the false offs. Trying to improve the algorithms and to eliminate the false offs, we proposed a new approach in [12], [13] by joining both techniques in a new algorithm. The first step is to calculate the image section with highest correlation, by using the TM algorithm. The second step is to check if the section calculated is a laser spot image by using the DU algorithm. In this step, if the image calculated has pixels with high energy, these pixels will not be eliminated, and it is possible to say that the image calculated is a laser spot image.

D. Template Matching + Fuzzy Rule Based Systems

In order to improve the results presented in [12], an hybrid approach between TM and FRBSs has been proposed for determining whether an image section provided by TM is detected as a laser spot or not. This way working allows to have a system based on labels [14], [15], with a near human language, making easy the derivation of rules [19] that can provide a positive or negative response for each analyzed image section.

A set of interesting system variables where proposed in [13] by analyzing some example images, with and without laser spots. These variables determined by the expert (five inputs and one output) represent the following information:

- X1: Long standard deviation.
- X2: Cross standard deviation.
- X3: Similarity to perfect circle value.
- X4: Laser spot number of pixels.
- X5: Percentile 80 value.
- Y: Laser spot probability (laser spot is detected if this value is over a threshold).

Once the input variables and their domains were defined, the expert defined useful rules and manually adjusted the membership function definitions for the detection task. The process to determine these variables as well as the finally proposed FRBS from the expert's experience can be found in [13].

The complete recognition task is therefore comprised of two main parts (algorithms). The first algorithm, TM, analyzes the image sent by the video camera together with a template image. This obtains the image section with the highest correlation. The obtained image section is then analyzed by using the FRBS proposed. This new combination of algorithms [13], namely $TM + FRBS_{expert}$, directly presented a better performance than the algorithms described in sections II-A and II-B as we can see in [13].

On the other hand, though that the new approach, $TM + FRBS_{expert}$, presented better results than the previous techniques, it can be further refined by performing a genetic tuning of the MFs [20], i.e., by means of a Genetic Algorithm (GA) [21], [22], the MFs of the FRBS are adjusted. This kind of hybridization between fuzzy logic [14], [15] and GAs is well-known as Genetic Fuzzy Systems (GFSs) [23]–[25].

In this way a new approach, namely $TM + FRBS_{tuned-GA}$, was proposed in [16] to perform an automatic evolutionary tuning of the initial FRBS based on the existence of 105 image samples that were used for training the model. To perform the genetic tuning it was considered a GA that presents a real coding scheme and uses the stochastic universal sampling as selection procedure together with an elitist scheme. The operators employed for performing the individual recombination and mutation were uniform mutation and the max-min-arithmetical crossover.

Once the GA optimizes the MF parameters of the initial FRBS ($FRBS_{expert}$), the new FRBS obtained ($FRBS_{tuned-GA}$) presented better results than the previous techniques used to detect the laser spot, as we can see in [16].

III. Template Matching and Evolutionary Learning of a FRBS for the Laser Spot Detection

In this section, we present a new approach considering the problem to detect the laser spot on an image. This is based on the use of a more advanced technique for a complete learning of the FRBS used to detect the laser spot in the image sections obtained by TM. Therefore, in this work we propose the TM technique in combination with the learning of the complete KB. Learning together the rules and the parameters of the MFs let us consider the interaction between both parts and therefore obtaining more accurate models. Nevertheless, this proposal represents a more complicated search space for the use of a initial RB obtained by an expert and further tuning technique [16].

In order to effectively apply this new approach to our concrete problem, we consider eight input variables: the variables used in the FRBSs presented in subsection II-D, plus 3 input variables which represent the laser spot color (Red, Green and Blue) and one output variable. Using this new approach we obtain a new FRBS named $FRBS_{learning-GA}$ which in combination with the TM technique gives way to a new hybrid approach, namely $TM + FRBS_{learning-GA}$.

In this way, this section presents a learning algorithm of the KB which can efficiently manage the search space. To do that, the learning scheme is presented in the next. Then, a model of representation of the BD is introduced, which decreases the search space with respect to the classical MFs triangular representations. Finally, a specific evolutionary algorithm is proposed, which is applied for machine learning of FRBSs from data.

A. FRBS learning scheme

In addition to the classical approaches, some new directions to apply genetic (evolutionary) techniques to FRBSs can be found in [25]: selection of fuzzy rules, feature selection, learning of KBs via genetic derivation of the DB, interpretability maintenance via multi-objective genetic processes, learning approaches considering different model structures, etc. These kinds of techniques try to find a better trade off between the efficiency of the learning/post-processing process and the dimensionality of the search space.

This is the case of the *learning of KBs via genetic derivation of DBs*, a recent approach involving a simpler search space than the classical learning of KBs. It consists of obtaining the DB and the RB separately, based on the embedded learning of the DB [26]–[29] (see Figure 4). This way to work allows us to learn the most adequate context for each fuzzy partition, which is necessary in different application contexts and different fuzzy rule extraction models.

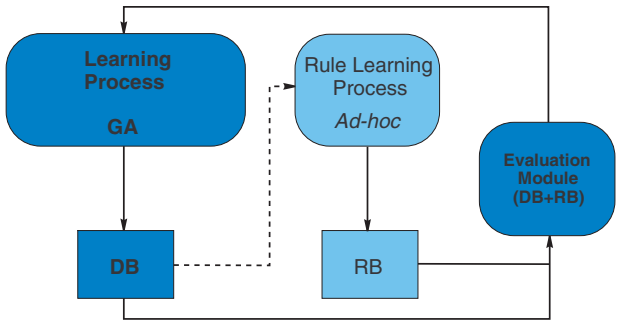

Fig. 4. Learning scheme of the KB

The learning scheme considered in this work belongs to this last group and is comprised of two main components:

- A process to learn the DB, which allows to define:
  - The number of labels for each linguistic variable.
  - The lateral displacements of such labels.

  Triangular membership functions are considered for their simplicity.
- A quick *Ad-hoc data-driven method* to derive the RB [30] considering the DB previously obtained. This method is run from each DB definition generated by a Genetic Algorithm (GA), thus, allowing the proposed hybrid learning process to finally obtain the whole definition of the KB (DB and RB) by means of the cooperative action of both methods.

B. The Linguistic 2-Tuples Representation

In [31], a new model of tuning of FRBSs was proposed considering the linguistic 2-tuples representation scheme introduced in [17], which allows the lateral displacement of the support of a label and maintains the interpretability associated to the obtained linguistic FRBSs. This proposal also introduces a new model for rule representation based on the symbolic translation concept that is a number within the interval [-0.5, 0.5) expressing the domain of a label when it is moving between its two lateral labels. Formally, we have the pair,

$$(s_i, \alpha_i), \;\; s_i \in S, \;\; \alpha_i \in [0.5, -0.5).$$

Figure 5 shows the lateral displacement of the label M. The new label "y_2" is located between B and M, being enough smaller than M but closer to M.

C. Evolutionary Algorithm

In this work, we will consider the use of CHC [32] to design the proposed learning algorithm. CHC is a GA that presents

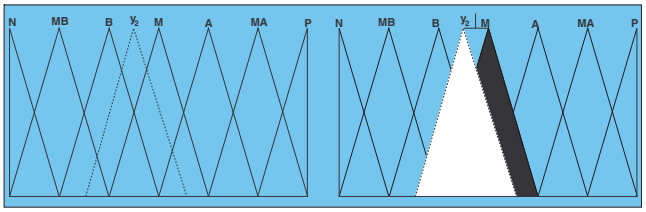

Fig. 5. Lateral Displacement of the Linguistic Label M

a good trade-off between exploration and exploitation, being a good choice in problems with complex search spaces. This genetic model makes use of a mechanism of "Selection of Populations". N parents and their corresponding offspring are combined to select the best N individual to take part of the next population.

Considering this approach, the learning process of the DB have to define both, the granularity of the linguistic partitions and the lateral displacements of the involved labels. For this reason, a double coding scheme is considered (granularity + displacements).

In the following, the components needed to design our FRBS are explained. They are: DB codification, chromosome evaluation, initial gene pool, crossover operator and restarting approach.

1) DB Codification: A double coding scheme ($C = C_1 + C_2$) to represent both parts, *granularity* and *translation parameters*, is considered:

- Number of labels (C_1): This part is a vector of integer numbers with size N (being N the number of system variables). The possible numbers of labels considered are the set $\{3, \ldots, 9\}$:

$$C_1 = (L^1, \ldots, L^N) \ .$$

- Lateral displacements (C_2): This part is a vector of real numbers with size $N*9$ (N variables with a maximum of 9 linguistic labels per variable) in which the displacements of the different labels are coded for each variable. Of course, if a chromosome does not have the maximum number of labels in one of the variables, the space reserved for the values of these labels is ignored in the evaluation process. In this way, the C_2 part has the following structure (where each gene is associated to the tuning value of the corresponding label):

$$C_2 = (\alpha_1^1, \ldots, \alpha_{L^1}^1, \ldots, \alpha_1^N, \ldots, \alpha_{L^N}^N)$$

2) Chromosome Evaluation: To evaluate a determined chromosome we will apply the well-known rule generation method of Wang and Mendel [30] on the DB coded by such chromosome. Once the whole KB is obtained, the following function is minimized:

$$F_C = w_1 \cdot FF + w_2 \cdot NR,$$

where:

- NR is the number of rules of the obtained KB (in order to penalize an excessive number of rules).
- $w_1 = 1$.
- w_2 is computed from the Mean Square Error (MSE) and the number of rules of the KB generated from a DB considering the maximum number of labels (9 labels) and without considering the displacement parameters,

$$w_2 = \alpha \cdot \frac{MSE_{max-lab}}{NR_{max-lab}} \ ,$$

  with α being a weighting percentage given by the system expert that determines the trade-off between accuracy and complexity. Values higher than 1.0 search for linguistic models with few rules, and values lower than 1.0 search for linguistic models with high accuracy. A good neutral choice is for example 1.0 (good accuracy and not too many rules), but in this particular problem we use $\alpha = 1.15$.
- FF is the Fitness Function used to analyze the number of False Negative (FN) and False Positive (FP) obtained with the KB generated,

$$FF = \frac{|FN|}{|D|} + 10 \cdot \frac{|FP|}{|D|}$$

  where $|FN|$ is the number of False Negatives obtained, $|FP|$ is the number of False Positives obtained and $|D|$ is the dataset size. Notice that the number of FPs is penalized in order to avoid the wrong orders to be sent to the domotic system.
  For each input example, the FRBS must generate an output value into interval [0, 1]. If this value is higher than 0.5, the example will be classificated as a laser spot image, in otherwise, it will be classificated as image without a laser spot. Thus, an input example can be considered as:
  - FN: If the example is classified as an image without laser spot and it is a laser spot image.
  - FP: If the example is classified as a laser spot image and it is an image without laser spot.
  - Hit: If the example is correctly classified.

For the fuzzy inference, we have selected the *minimum t-norm* playing the role of the implication and conjunctive operators, and the *center of gravity weighted by the matching* strategy acting as defuzzification operator.

3) Initial Gene Pool: The initial population will be comprised of two different parts (with the same number of chromosomes):

- In the first part, each chromosome has the same number of labels for all the problem variables and considers strong fuzzy partitions with translation parameters initialized to zero.
- In the second part, the only change is that each variable could have a different number of labels.

Since CHC has no mutation operator, the translation parameters remain unchanged and the most promising number of labels is obtained for each linguistic variable. The algorithm operates in this way until the first restarting is reached.

4) Crossover Operator: Two different crossover operators are considered depending on the two parent's scope to obtain two offspring:

- *When the parents encode different granularity levels in any variable*, a crossover point is randomly generated in C_1 and the classical crossover operator is applied on this point in both parts, C_1 and C_2 (exploration).
- *When both parents have the same granularity level per variable*, an operator based on the concept of environments (the offspring are generated around one parent) is applied only on the C_2 part (exploitation). These kinds of operators present a good cooperation when they are introduced within evolutionary models forcing the convergence by pressure on the offspring (as the case of CHC). Particularly, we consider the Parent Centric BLX (PCBLX) operator [33], which is based on the BLX-α.
  The PCBLX is described as follows. Let us assume that $X = (x_1 \cdots x_n)$ and $Y = (y_1 \cdots y_n)$, $(x_i, y_i \in [a_i, b_i] \subset \Re, i = 1 \cdots n)$, are two real-coded chromosomes that are going to be crossed. PCBLX generates the offspring $Z = (z_1 \cdots z_n)$, where z_i is a randomly (uniformly) chosen number from the interval $[l_i, u_i]$, with $l_i = max\{a_i, x_i - I\}$, $u_i = min\{b_i, x_i + I\}$, and $I = \mid x_i - y_i \mid$. The parents X and Y will be named differently: X will be called *female parent*, and Y will be called *male parent*. In this way, by taking X as female parent (Y as male), and then by taking Y as female parent (X as male) our algorithm generates two offspring.
  On the other hand, CHC makes use of an incest prevention mechanism, i.e., two parents are only crossed if their hamming distance divided by 2 is over a predetermined threshold, L. It will be only considered in order to apply the PCBLX operator. Since, we consider a real coding scheme (the C_2 part is going to be crossed), we have to transform each gene considering a Gray Code with a fixed number of bits per gene ($BITSGENE$) determined by the system expert. In this way, the threshold value is initialized as:

$$L = (\#GenesC_2 * BITSGENE)/4.0.$$

Following the original CHC scheme, L is decremented by one when no cross is performed in one generation. In order to avoid very slow convergence, in our case, L will be also decremented by one when no improvement is achieved respect to best chromosome of the previous generation.

5) Restarting approach: To get away from local optima, a restarting mechanism is considered [32] when the threshold value L is lower than cero. In this case, all the chromosomes set up their C_1 parts to that of the best global solution, being the parameters of their C_2 parts generated at random within the interval $[-0.5, 0.5)$. Moreover, if the best global solution had any change from the last restarting point, this is included in the population (the exploitation continues while there is convergence). This operation mode was initially proposed by the CHC authors as a possibility to improve the algorithm performance when it is applied to solve some kinds of problems [32].

IV. Experimental Results

To evaluate the usefulness of the approaches proposed in the previous sections, we have considered the previous environment control system presented in [12]. In order to have a performance measure and to perform the automatic tuning [16] and learning, we extend the 105 example images used in [16] with a big set of data containing 990 images. This set of images has been randomly divided in 5 subsets with the 20 % of the images for each. Applying 5-fold cross-validation method we obtained 5 different sets of images with 792 images for training and 198 images for test.

Table I presents a brief description of the studied methods.

The parameters for the methods $TM + FRBS_{expert}$ and $TM + FRBS_{tuned-GA}$ were selected according to the recommendation of the authors in [13] and [16]. Notice that in the $TM + FRBS_{tuned-GA}$ algorithm, the number of evaluation used by the GA in the tuning process was 50000. The values of the input parameters considered by our proposal are shown in the next:

- Evaluations = 50000
- Population size = 50
- Bits per gene = 30.
- α factor = 1.15

Table II presents the results of $TM + UD$ algorithm using the new set of 990 images divided in 5 subsets and with similar configuration that the algorithm presented in [12].

Tables III and IV show the $TM + FRBS_{expert}$ and $TM + FRBS_{tuned-GA}$ results using the new set of 990 images, with similar input parameters which were presented in [13] and [16] respectively. We can see that classic techniques $TM + UD$ are better than $TM + FRBS_{expert}$ and $TM + FRBS_{tuned-GA}$ using a big set of images. This is due to that the classic technique works with heterogeneous data like brightness and luminosity, otherwise, the FRBS developed by the expert and tuned by GA works with data of the appearance of the image like similarity of circle, etc. This kind of data is useful when we work with learning algorithms, where they are used in corporate form. For this reason, we have combined the classic technique TM with the learning algorithm, obtaining the new hybrid algorithm named $TM + FRBS_{learning-GA}$, the results are the best (see Table V).

We can see that the percentage of success rate in images with laser spot is 70.50 % and in images without laser spot is 98.76 %, very close to 100 %, the optimal success rate.

V. Conclusion

In this paper a new hybrid technique combining Template Matching and an evolutionary learning of the FRBS to detect a laser spot in a home environment is presented. Thanks to the system developed in conjunction with a standard domotic system, we provide a more user-friendly and less expensive home device control environment.

TABLE I
TECHNIQUES USED IN THE EXPERIMENTS

Ref	Method	Year	Description
[12]	$TM + DU$	2008	Template Matching plus Dinamic Umbralization (described in Section II-C)
[13]	$TM + FRBS_{expert}$	2010	Template Matching plus FRBS design from Expert's Experience (described in Section II-D)
[16]	$TM + FRBS_{tuned-GA}$	2010	Template Matching plus FRBS design from Expert's Experience and tuned by GA (described in II-D)
Our proposal	$TM + FRBS_{learning-GA}$		Template Matching plus learning FRBS as explained in Section III.

TABLE II
RESULTS OF $TM + UD$

	Training		Test	
	Average	Standard Deviation	Average	Standard Deviation
General Success Rate	83.48 %	0.01206	83.54 %	0.04705
Success Rate with Laser Sopt	67.86 %	0.01575	68.13 %	0.05705
Success Rate without Laser Spot	98.32 %	0.00481	98.36 %	0.01647

TABLE III
RESULTS OF $TM + FRBS_{expert}$

	Training		Test	
	Average	Standard Deviation	Average	Standard Deviation
General Success Rate	78.59 %	0.01229	78.59 %	0.04917
Success Rate with Laser Sopt	66.21 %	0.01845	66.52 %	0.06770
Success Rate without Laser Spot	90.35 %	0.00821	90.30 %	0.03226

TABLE IV
RESULTS OF $TM + FRBS_{tuned-GA}$

	Training		Test	
	Average	Standard Deviation	Average	Standard Deviation
General Success Rate	75.80 %	1.81965	74.97 %	5.03560
Success Rate with Laser Sopt	51.44 %	3.59527	50.51 %	6.84627
Success Rate without Laser Spot	98.91 %	0.33398	98.35 %	1.34530

An experimental study on a big set of image samples (990 images in total) of the previous algorithms used to detect a laser spot on an image versus the new approach using the evolutionary learning of the FRBS is presented in this paper. We can see how the proposal method has better results than other approaches. However, the most important result is that the new approach has a 98.76 % of success rate in images without laser spot, very close to 100 %, where the false offs will be completely eliminated.

The new approach presented in this paper is particularly useful for remote acting on home devices, the user can reach any device in sight. Moreover, we think the results show the usefulness for any environment where devices are not easily reachable by the user, industrial operation, for instance.

ACKNOWLEDGMENT

This work has been supported by the Spanish Ministry of Education and Science under project TIN2008-06681-C06-01 and National Nohnes project TIN2007-68083-C02-01, and by the University of Extremadura, regional government Junta de Extremadura, Consejería de Economía-Comercio e Innovación and FEDER, under project GRU09105.

REFERENCES

[1] M. Chan, D. Estève, C. Escriba, and E. Campo, *A review of smart homes-present state and future challenges*, Computer Methods and Programs in Biomedicine, vol. 91, no. 1, pp. 55–81, 2008.

[2] K.-H. Park, Z. Bien, J.-J. Lee, B. K. Kim, J.-T. Lim, J.-O. Kim, H. Lee, D. H. Stefanov, D.-J. Kim, J.-W. Jung, J.-H. Do, K.-H. Seo, C. H. Kim, W.-G. Song, and W.-J. Lee, *Robotic smart house to assist people with movement disabilities*, Autonomous Robots, vol. 22, no. 2, pp. 183–198, 2007.

[3] F. Cincotti, D. Mattia, F. Aloise, S. Bufalari, G. Schalk, G. Oriolo, A. Cherubini, M. G. Marciani, and F. Babiloni, *Non-invasive brain-computer interface system: Towards its application as assistive technology*, Brain Research Bulletin, vol. 75, no. 6, pp. 796 – 803, 2008.

[4] N. Noury, G. Virone, P. Barralon, J. Ye, V. Rialle, and J. Demongeot, *New trends in health smart homes*, Healthcom 2003. Proceedings of 5th International Workshop on Enterprise Networking and Computing in Healthcare Industry., pp. 118 – 127, 2003.

[5] M. Nikolova, F. Meijs, and P. Voorwinden, *Remote mobile control of home appliances*, Consumer Electronics, IEEE Transactions on, vol. 49, no. 1, pp. 123 – 127, 2003.

[6] J.-H. Do, H. Jang, S. H. Jung, J. Jung, and Z. Bien, *Soft remote control system in the intelligent sweet home*, IEEE/RSJ International Conference on Intelligent Robots and Systems (IROS 2005)., pp. 3984 – 3989, 2005.

[7] C. Kemp, C. Anderson, H. Nguyen, A. Trevor, and Z. Xu, *A point-and-click interface for the real world: laser designation of objects for mobile manipulation*, Proceedings of the 3rd ACM/IEEE international conference on Human robot interaction (HRI'08). Amsterdam, The Netherlands: ACM, pp. 241–248, 2008.

TABLE V
RESULTS OF $TM + FRBS_{learning-GA}$

	Training		Test	
	Average	Standard Deviation	Average	Standard Deviation
General Success Rate	87.27 %	0.78990	84.92 %	2.90425
Success Rate with Laser Sopt	73.87 %	1.28823	70.50 %	4.48146
Success Rate without Laser Spot	100 %	0.00000	98.76 %	1.14364

[8] J. Olsen, R. Dan, and T. Nielsen, *Laser pointer interaction*, Proceedings of the SIGCHI conference on Human factors in computing systems (CHI'01). Seattle, Washington, USA: ACM, pp. 17–22, 2001.

[9] J.-Y. Oh and W. Stürzlinger, *Laser pointers as collaborative pointing devices*, Proceedings of Graphics Interface, Calgary, Alberta, pp. 141–150, 2002.

[10] L. Zhang, Y. Shi, and J. Chen, *Drag and drop by laser pointer: Seamless interaction with multiple large displays*, Ubiquitous Intelligence and Computing, Lecture Notes in Computer Science, Springer, vol. 4159, pp. 12–20, 2006.

[11] N. W. Kim, S. J. Lee, B.-G. Lee, and J.-J. Lee, *Vision based laser pointer interaction for flexible screens*, Human-Computer Interaction. Interaction Platforms and Techniques, Lecture Notes in Computer Science Springer, vol. 4551, pp. 845–853, 2007.

[12] F. Chávez, F. Fernández, G. Olague, and J. Llano, *An independent and non-intrusive laser pointer environment control device system*, Proceedings of the 5th international conference on Pervasive services (ICPS'08). Sorrento, Italy: ACM, pp. 37–46, 2008.

[13] F. Chávez, F. Fernández, R. Alcalá, J. Alcalá-Fdez, G. Olague, and F. Herrera, *Hybrid laser pointer detection algorithm based on template matching and fuzzy rule-based systems for domotic control inrealhome environments*, Applied Intelligence, pp. 1–17, 10.1007/s10489-010-0268-6, 2010.

[14] L. Zadeh, *Fuzzy sets*, Information and Control, vol. 8, pp. 338–353, 1965.

[15] L. Zadeh, *Outline of a new approach to the analysis of complex systems and decision processes*, IEEE Transactions on Systems, Man, and Cybernetics, vol. SMC-3, pp. 28–44, 1973.

[16] F. Chávez, F. Fernández, J. Alcalá-Fdez, R. Alcalá, F. Herrera, and G. Olague, *Genetic tuning of a laser pointer environment control device system for handicapped people with fuzzy systems*, IEEE International Conference on Fuzzy Systems (FUZZ-IEEE 2010), pp. 1 –8, 2010.

[17] F. Herrera, L. Martínez, and F. Herrera, *A 2-tuple fuzzy linguistic representation model for computing with words*, IEEE Transactions on Fuzzy Systems, vol. 8, pp. 746–752, 1999.

[18] KNX/EIB, *http://www.knx.org*.

[19] R. Alcalá, J. Alcalá-Fdez, M. J. Gacto, and F. Herrera, *Improving fuzzy logic controllers obtained by experts: A case study in HVAC systems*, Applied Intelligence, vol. 31, no. 1, pp. 15–30, 2009.

[20] F. Herrera, M. Lozano, and J. L. Verdegay, *Tuning fuzzy logic controllers by genetic algorithms*, International Journal of Approximate Reasoning, vol. 12, no. 3-4, pp. 299–315, 1995.

[21] D. Goldberg, *Genetic algorithms in search, optimization, and machine learning*. Upper Saddle River, NJ, USA: Addison-Wesley Professional, 1989.

[22] J. Holland, *Adaptation in Natural and Artificial Systems*. Ann Arbor, MI, USA: University of Michigan Press, 1975.

[23] O. Cordón, F. Herrera, F. Hoffmann, and L. Magdalena, *GENETIC FUZZY SYSTEMS. Evolutionary Tuning and Learning of Fuzzy Knowledge Bases*. New York, USA: World Scientific, 2001.

[24] F. Herrera, *Genetic fuzzy systems: taxonomy, current research trends and prospects*, Evolutionary Intelligence, vol. 1, no. 1, pp. 27–46, 2008.

[25] O. Cordón, F. A. C. Gomide, F. Herrera, F. Hoffmann, and L. Magdalena, *Ten years of genetic fuzzy systems: current framework and new trends*, Fuzzy Sets and Systems, vol. 141, no. 1, pp. 5–31, 2004.

[26] J. Casillas, O. Cordón, F. Herrera, and P. Villar, *A hybrid learning process for the knowledge base of a fuzzy rule-based system*, International Conference on Information Processing and Management of Uncertainty in Knowledge-Based Systems, vol. 3, pp. 2189–2196, 2001.

[27] O. Cordón, F. Herrera, L. Magdalena, and P. Villar, *A genetic learning process for the scaling factors, granularity and contexts of the fuzzy rule-based system data base*, Information Sciences, vol. 136, pp. 85–107, 2001.

[28] W. Pedrycz, *Associations and rules in data mining: A link analysis*, International Journal of Intelligent Systems, vol. 19, no. 7, pp. 653–670, 2004.

[29] Y. W. Teng and W. J. Wang, *Constructing a user-friendly ga-based fuzzy system directly from numerical data*, IEEE Transactions on Systems, Man, and Cybernetics, vol. 34, no. 5, pp. 2060–2070, 2004.

[30] L. X. Wang and J. M. Mendel, *Generating fuzzy rules by learning from examples*, IEEE Transactions on Systems, Man, and Cybernetics, vol. 22, no. 6, pp. 1414–1427, 1992.

[31] R. Alcalá and F. Herrera, *Genetic tuning on fuzzy systems based on the linguistic 2-tuples representation*, IEEE International Conference on Fuzzy Systems, vol. 1, pp. 233–238, 2004.

[32] L. Eshelman, *The chc adaptive search algorithm: How to have safe search when engaging in nontraditional genetic recombination*, Foundations of genetic Algorithms, Morgan Kaufman, vol. 1, pp. 265–283, 1991.

[33] F. Herrera, M. Lozano, and A. M. Sánchez, *A taxonomy for the crossover operator for real-coded genetic algorithms: An experimental study*, International Journal of Intelligent Systems, vol. 18, pp. 309–338, 2003.

2011 IEEE International Conference on Fuzzy Systems
June 27-30, 2011, Taipei, Taiwan

A Meta-Fuzzy Classifier for Specifying Appropriate Fuzzy Partitions by Genetic Fuzzy Rule Selection with Data Complexity Measures

Yusuke Nojima, Shinya Nishikawa, Hisao Ishibuchi
Dept. of Computer Science and Intelligent Systems, Osaka Prefecture University
1-1 Gakuen-cho, Naka-ku, Sakai, Osaka, 599-8531, Japan
{nojima@, nishikawa@ci., hisaoi@}cs.osakafu-u.ac.jp

Abstract— **Tens of thousands of classifiers have been proposed so far. There is no best classifier among them for all the existing data sets. The performance of each classifier often depends on the data sets used for comparison. Even for a single classifier, suitable parameters of the classifier also depend on the data sets. That is, there is a possibility that a suited classifier and its parameter specification can be chosen beforehand if the target data sets or their characteristics were known. In recent years, a number of data complexity measures have been proposed to characterize data sets. The aim of this study is to develop a meta-classifier for selecting an appropriate classifier and/or its appropriate parameter specification by means of data complexity measures. In this paper, we focus on the parameter specification of fuzzy classifiers using data complexity measures as a preliminary study. To construct a meta-classifier, we generate a large number of artificial data sets from Keel benchmark data sets. Then we generate meta-patterns which are composed of the values of data complexity measures as inputs and an appropriate fuzzy partition as an output. Using meta-patterns, a meta-classifier is designed by multiobjective genetic fuzzy rule selection. We evaluate the proposed method through leave one-group out cross-validation.**

Keywords-fuzzy classifier design; data complexity measures; meta-learning; pattern classification; knowledge acquisition

I. INTRODUCTION

A lot of comparative studies on pattern classification problems have shown that there is no single best classifier for all the existing data sets. In the practical use of classifiers, we do not know the best classifier for given data sets beforehand. We also do not know an appropriate parameter setting of the classifier used for the data sets. Thus, we usually select a classifier and specify its parameter values in a trial and error manner. This is a very time-consuming task. If we know a best-suited classifier and its appropriate parameter setting, we can reduce the redundant time.

In general, the performance of classifiers strongly depends on the data sets used in the experiments. For example, it would be enough to use a simple classifier for a simple data set. On the other hand, for a complicated data set, it must be necessary to use a complicated classifier which can finely approximate the complicated decision boundaries. It is, however, difficult for us to know whether the data set is simple or complicated. To characterize the data sets, a number of data complexity measures for classification problems have been proposed by Ho and Basu [1,2]. Some researchers analyzed the relationship between the search performance of classifiers and data complexity measures [3-5]. Other researchers utilized data complexity measures to reduce training patterns [6-8].

In this paper, we focus on parameter specification of fuzzy classifiers by means of data complexity measures. We use a Chi-RW classifier which is a Chi's fuzzy classifier [9] with rule weights [10, 11]. The Chi-RW classifier is very famous and useful as a baseline of fuzzy classifiers. The main parameter of the Chi-RW classifiers is the number of fuzzy membership functions (i.e., membership granularity). Thus, we specify the membership granularity by utilizing data complexity measures before constructing fuzzy classifiers in this paper.

In our former study [12], we proposed a meta-classifier that predicts an appropriate granularity by the values of data complexity measures for each data set. While two-dimensional two-class problems were used in [12], we use a large number of data sets derived from Keel data repository in this paper. We propose *Leave one-group out* cross-validation for examining the prediction performance of meta-classifiers. A meta-classifier is obtained by multiobjective genetic fuzzy rule selection with genetic lateral tuning [13-16].

This paper is organized as follows. In Section II, we explain the overall procedure of the proposed framework. From Section III to Section VI, we explain the details on data preparation, data complexity measures, meta-data generation, and multi-objective genetic fuzzy rule selection. Section VII presents computational experiments. Finally, we conclude this paper in Section VIII.

II. OVERALL PROCEDURE OF THE PROPOSED FRAMEWORK

In this section, we briefly explain the overall procedure of the proposed framework by dividing it into two phases: training phase and predicting phase. The basic part of the proposed framework is the same as [12].

A. Training Phase

The procedure of the training phase is as follows:

This study is partially supported by the Japanese Grant-in-Aid for Young Scientists (B) (22700239).

Step 1: A large number of artificial data sets are generated from the real world problems.

Step 2: The values of data complexity measures are calculated for each data set.

Step 3: The performance of a Chi-RW classifier with each candidate parameter setting is examined for each data set.

Step 4: Meta-patterns are generated from the values of data complexity measures and the results on candidate parameter settings.

Step 5: A meta-classifier is obtained by multiobjective genetic fuzzy rule selection using the meta-patterns.

Since existing data sets are limited and too few to cover the wide range of data complexity measures, we generate a large number of artificial data sets by eliminating some patterns from the original data sets, adding small noise into patterns, or generating new patterns nearby the original patterns in Step 1.

As a target classifier, we use a Chi-RW method [9-11] in this paper. It is very famous and well-used as a baseline. We focus on the granularity of fuzzy membership functions (i.e., the number of fuzzy membership functions). A single meta-pattern is corresponding to a single data set. The input vector of a meta-pattern is composed of the values of data complexity measures. The output class of the meta-pattern is the best-suited parameter setting in this paper.

A meta-data set with a large number of meta-patterns is used for designing a meta-classifier. In this paper, we employ multiobjective fuzzy rule selection with genetic lateral tuning [13-16].

B. *Predicting Phase*

The obtained meta-classifier in the training phase is used to predict an appropriate parameter setting of a classifier for unseen data sets. The procedure of the predicting phase is as follows:

Step 1: The values of data complexity measures for an unseen data set are calculated.

Step 2: The meta-classifier predicts class (i.e., an appropriate setting) according to the values of data complexity measures.

It should be noted that it would be possible to select a classifier among alternatives (e.g., RBFN, C4.5, SVM) instead of parameter settings for a Chi-RW classifier. It would be also possible to use other machine learning techniques for designing a meta-classifier.

The details are explained at the subsequent sections.

III. Data Preparation

While we generated two-dimensional artificial data sets in [12], we generate multiple-dimensional artificial data sets from Keel data repository in this paper. Since each artificial data set is derived from one of the real-world data sets, each data structure is not completely meaningless.

To generate artificial data sets, we propose three simple operations. Figure 1 demonstrates a simple example. Each attribute value is normalized within [0.0, 1.0].

1) Random reduction

Randomly remove a number of patterns as in Fig. 1 (b). A prespecified number of data sets are generated by changing the reduction rate.

2) Noise addition

Randomly add noise (e.g., uniform random value [-0.05, 0.05] per variable) to each pattern as in Fig. 1 (c). Each new pattern is replaced with the original patterns. A prespecified number of data sets are generated by changing a random seed.

3) Random generation

Randomly generate new patterns in the neighbor of each pattern as in Fig. 1 (d). A prespecified number of data sets are generated by changing the number of newly-generated patterns.

If the new attribute value is less than 0.0 or more than 1.0, its value is replaced with 0.0 or 1.0, respectively.

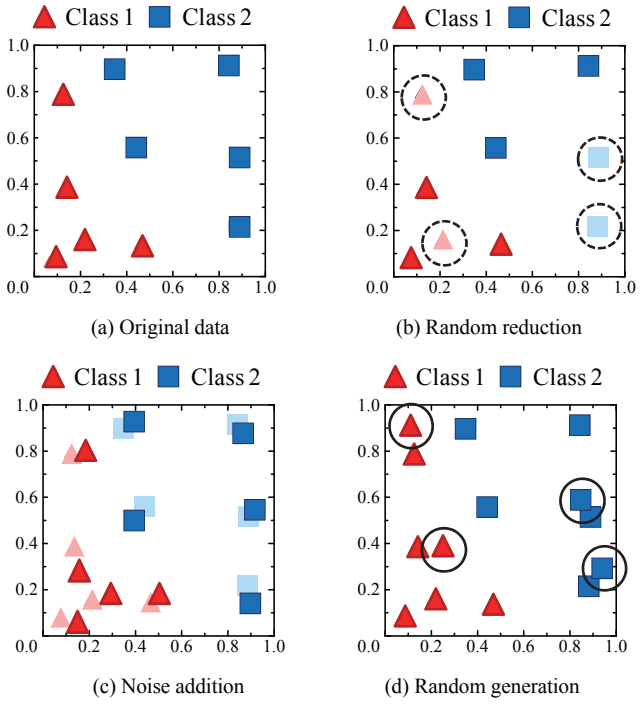

Figure 1. An example of artificial data set generation.

IV. Data Complexity Measures

To describe the characteristics of data sets, this paper uses data complexity measures. In the literature [3-8], some researchers showed the effectiveness of data complexity measures. In this section, we briefly describe representative data complexity measures. Most of them have been originally defined for two-class data sets. The original explanations on the data complexity measures can be found in the literature (Ho and Basu [1, 2] and Orriols-Puig [17]).

A. F1: Maximum Fisher's discriminant ratio

This measure is calculated by the distance and variance between classes. It analyzes the effectiveness of a single attribute. The value is calculated as follows:

$$\mathrm{F1} = \max_{h=1,2,\ldots,d} \frac{(\mu_{h1} - \mu_{h2})^2}{\sigma_{h1}^2 + \sigma_{h2}^2}, \quad (1)$$

where μ_{h1}, μ_{h2}, σ_{h1} and σ_{h2} are the means and the variances of two classes for the h-th attribute, respectively. The d is the number of attributes of the data set.

B. F2: Volume of overlap region

This measure describes how much two classes are overlapping each other, calculating the volume of the overlap region as hypercube of each dimension. This measure is strongly dependent on the number of attributes, because the value of an attribute's overlap region is multiplied as:

$$\mathrm{F2} = \prod_{h=1}^{d} \frac{\mathrm{minmax}_h - \mathrm{maxmin}_h}{\mathrm{maxmax}_h - \mathrm{minmin}_h}, \quad (2)$$

where

$$\mathrm{minmax}_h = \min\{\max(f_h, c_1), \max(f_h, c_2)\},$$
$$\mathrm{maxmin}_h = \max\{\min(f_h, c_1), \min(f_h, c_2)\},$$
$$\mathrm{maxmax}_h = \max\{\max(f_h, c_1), \max(f_h, c_2)\},$$
$$\mathrm{minmin}_h = \min\{\min(f_h, c_1), \min(f_h, c_2)\},$$

where $\max(f_h, c_i)$ and $\min(f_h, c_i)$ are the maximum and minimum values of the h-th attribute in the class c_i (i = 1, 2), respectively (see Fig. 2).

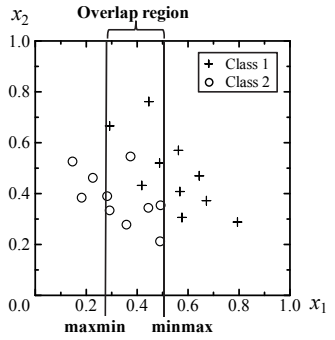

Figure 2. Overlap region of an attribute.

C. F3: Maximum (individual) feature efficiency

This measure describes the level of overlap like F2 measure. Different from F2, it counts the patterns which are falling outside of the overlap region for each attribute and considers the single attribute which has the maximum points. This value is calculated as follows:

$$\mathrm{F3} = \max_{h=1,2,\ldots,d} \frac{|P_h|}{N_e}, \quad (3)$$

$$P_h = \{\mathbf{x}_i \mid x_{ih} \le \mathrm{maxmin}_h \text{ or } x_{ih} \ge \mathrm{minmax}_h\}, \quad (4)$$

where N_e is the number of examples in the data set. x_{ih} is the h-th attribute value of the i-th pattern $\mathbf{x}_i$.

D. F4: Collective feature efficiency

The idea of this measure is derived from F3. In F3, only a single attribute is considered. However, F4 is calculated as follows. First, a single attribute is selected by (3). Then the overlap region on the attribute is calculated. The patterns out of the region are temporally removed. Next, another attribute is selected by (3). This process is repeated until all patterns are removed or all attributes are selected. This measure returns the fraction of all patterns by total removed patterns.

E. L1: The minimized sum of the error distance of a linear classifier.

This measure evaluates how much the training data are linearly separable. Therefore, its value is the sum of the difference between the exception of a linear classifier and the actual class value. Different from Ho and Basu [2], this paper uses a support vector machine (SVM) [18] trained with the sequential minimal optimization (SMO) algorithm [19] to construct the linear classifier. This measure can be used only for two-class problems. For a linearly separable problem, this measure becomes zero.

F. L2: Error rate of linear classifier

This measure is the error rate of the linear classifier designed for L1, measured with the training data set.

G. N1: Fraction of points on class boundary

This measure builds a class-blind minimum spanning tree (see Fig. 3) over the entire data set, and counts the number of points on an edge going across the different classes. This measure returns the fraction of these points over all points in the data set.

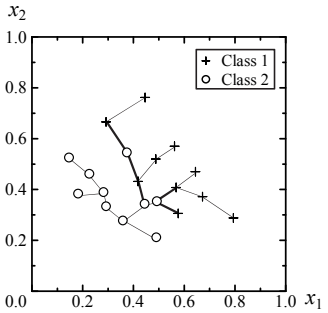

Figure 3. Minimum spanning tree. The bold lines are edges going across the different classes.

H. N2: The ratio of average intra/inter class nearest neighbor distance

This measure compares the spread with distance of within-class to that of the nearest neighbor of other classes. To compute this metric, we first compute the Euclidean distance to the nearest neighbor within the class and to the nearest

neighbor of other classes for all points ($\mathbf{x}_i$) in the data set. Then we compute the average of all the distance to intra class (*intraDist*($\mathbf{x}_i$)) and the average of all the distance to inter class (*interDist*($\mathbf{x}_i$)). This measure returns the ratio of these two averages. This measure is defined as follows:

$$\mathrm{N2} = \frac{\sum_{i=0}^{N_e} intraDist(\mathbf{x}_i)}{\sum_{i=0}^{N_e} interDist(\mathbf{x}_i)}. \quad (5)$$

I. N3: The leave-one-out error rate of 1-NN classifier

This metric simply returns the leave-one-out error rate by the 1-NN classifier.

J. L3: The nonlinearity of a linear classifier

This measure is characterized by a measure of non-linearity proposed by Hoekstra and Duin [20]. When a data set is given, a test set is created by linear interpolation with random coefficients between randomly selected pairs of points which are the same class. A linear classifier used for calculating L1 is also employed. After the classifier trained with the original data set, the error rate is measured by the created test set. This measure returns the error rate.

K. N4: The nonlinearity of 1-NN classifier

This measure creates a test set as proposed by L3, and evaluates the error rate of 1-NN. The value is the error rate.

L. T1: The fraction of maximum covering spheres

Simply speaking, this measure counts the number of balls needed to cover each class. At first, the ball is centered each instances and then grown as much as possible before touching the ball of other classes. The balls included any other ball are removed. This measure returns the fraction of all points by those balls.

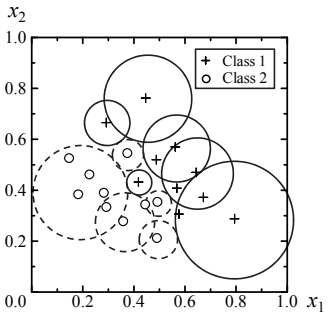

Figure 4. An example of the concept of T1 in the decision space.

Figure 4 shows the concept of T1, where the dashed circle means the balls of Class 2, the other circle means the balls of Class 1. In this example, the number of balls is 11.

M. T2: Average number of points per dimension

This measure represents the density of patterns.

$$\mathrm{T2} = \frac{N_e}{d}. \quad (6)$$

Since the calculation of all the data complexity measure is not computationally costly, we employ these values as inputs. We utilized DCoL (Data Complexity Library in C++) developed by Orriols-Puig et al [16] in order to calculate each data complexity measures.

V. A TARGET CLASSIFIER AND META-DATA GENERATION

In this section, we explain a target classifier (i.e., Chi-RW) and how to generate a meta-data set.

A. Target Classifier

In this paper, as the benchmark classifier, we use a Chi-RW classifier [9-11]. The main parameter of Chi-RW classifiers is the number of fuzzy membership functions (i.e., membership granularity). Thus, we focus on the granularity of fuzzy sets used in the antecedent of Chi-RW classifiers. We examine three different granularity specifications in Fig. 5: (a) coarse granularity (three fuzzy sets), (b) moderate granularity (five fuzzy sets), and (c) fine granularity (seven fuzzy sets). We call the Chi-RW classifiers with those granularities Chi-RW-3, Chi-RW-5, and Chi-RW-7, respectively.

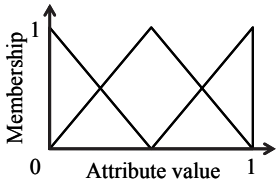

(a) Coarse granularity.

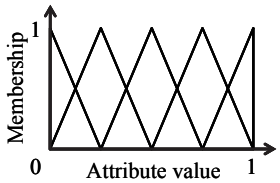

(b) Moderate granularity.

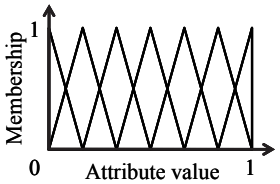

(c) Fine granularity.

Figure 5. Fuzzy membership funcitons used in Chi-RW classifiers.

As explained in introduction, the objective of this paper is to estimate an appropriate granularity of fuzzy membership functions in Chi-RW classifiers for each data set. It can be simply expected that a coarse granularity must be suited for data sets with noisy patterns. On the other hand, a fine granularity must be suited for data sets with complex decision boundaries. For some other data sets, a moderate granularity might be useful.

B. Meta-data generation

We generate a meta-data set composed of a large number of meta-patterns from many data sets. We assume that an appropriate granularity is strongly dependent on each data set. So that, we define each meta-pattern corresponding to one data

set. The input values of each meta-pattern are the values of data complexity measures of a data set explained in Section IV. Let $\mathbf{z}_i = (z_{i1}, z_{i2}, \ldots, z_{ij}, \ldots, z_{in})$, $i = 1, 2, \ldots, D$ be the attribute values (i.e., the values of the data complexity measures) of i-th data set, where D is the number of data sets. We use 13 data complexity measures: F1, F2, F3, F4, N1, N2, N3, N4, L1, L2, L3, T1 and T2 for two-class data sets in this paper (i.e., $n = 13$). For two or more-class data sets, we use nine data complexity measures: F2, F3, F4, N1, N2, N3, N4, T1 and T2. It should be noted that all input values (i.e., the values of data complexity measures) are normalized. This normalization is just to use the same membership functions for each attribute. Since we do not know the actual minimum and maximum values of each data complexity measure, we should examine the effect of this normalization. This is one of our future research issues.

The output class of each meta-pattern is an appropriate granularity of fuzzy membership functions in a Chi-RW classifier for the data set. Let $y_i \in$ {Chi-RW-3, Chi-RW-5, Chi-RW-7} be the consequent class of i-th meta-pattern. For each meta-pattern, three Chi-RW classifiers are performed by a ten-fold cross-validation (10CV). The classifier with the best test data accuracy is chosen as the consequent class of the meta-pattern. We performed 10CV by means of the KEEL data-mining software tool [21].

VI. Meta-Classifier Design by Multiobjective Genetic Fuzzy Rule Selection

From the generated meta-data set, we obtain a meta-classifier that predicts an appropriate fuzzy membership functions. We apply multiobjective genetic fuzzy rule selection (MoGFRS) to the design of a meta-classifier [13-16]. Genetic fuzzy rule selection [22] is one of the well-known methods in the field of genetic fuzzy systems [23,24]. It is a very simple two-stage method [22]. At the first stage, a number of fuzzy if-then rules are generated from numerical data as candidate rules. At the second stage, a subset of candidate rules is chosen by a genetic algorithm with binary strings in which "0" and "1" mean "not selected" and "selected" as a classifier, respectively. By maximizing the classification performance of the classifier and minimizing the complexity of the classifier (e.g., the number of fuzzy rules), an accurate and simple rule set is obtained as the final classifier. Its multiobjective formulation versions have been also studied in [13]. We use the modified version [15] of MoGFRS. There are two modifications: One is the use of a single granularity specification for each attribute [14]. The other is the use of genetic lateral tuning for adjusting fuzzy membership functions [16].

The procedure of our rule selection method is as follows:

Step 1: Rule extraction with multiple granularities.

Step 2: Specification of a single granularity for each attribute based on the extracted rules.

Step 3: Rule extraction with selected single granularities.

Step 4: Multiobjective genetic fuzzy rule selection.

In Step 1, a prespecified number of fuzzy rules of the following type are extracted from the meta-patterns.

$$R_j: \text{If } z_1 \text{ is } A_{j1} \text{ and } \ldots \text{ and } z_n \text{ is } A_{jn} \text{ then Class } y_j \text{ with } CF_j, \quad (7)$$

where R_j is the label of the j-th fuzzy rule, $\mathbf{z} = (z_1, \ldots, z_n)$ is an n-dimensional meta-pattern vector, A_{ji} is an antecedent fuzzy set such as *"Simple"* and *"Complicated"*, y_j is a consequent class, and CF_j is a rule weight. We use 14 fuzzy membership functions shown in Fig. 6 and a *don't care* condition as the antecedent fuzzy set. To obtain interpretable knowledge, we restricted the number of conditions to three or less fuzzy sets.

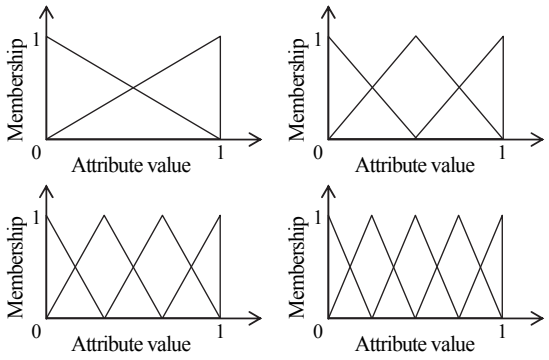

Figure 6. Membership functions for a meta-classifier design.

After extracting the rules, the frequently-used promising granularity is selected for each attribute in Step 2. In Step 3, a prespecified number of fuzzy rules are extracted by using the selected single granularity for each attribute. In Step 4, the combination of extracted rules and the positions of fuzzy membership functions are optimized by NSGA-II of Deb et al. [25].

We use a double coding scheme [15] in our multiobjective genetic fuzzy rule selection with genetic lateral tuning (Fig. 7). Each string includes binary bits and real numbers. Binary bits represent whether each extracted rule is selected for a meta-classifier, or not. Real numbers represent the position of each fuzzy membership function as shown in Fig. 8. The movable range is limited to maintain the interpretability of the fuzzy membership functions.

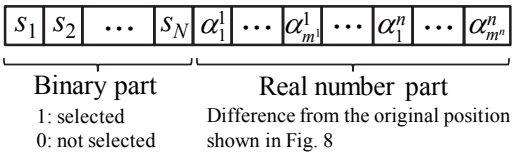

Figure 7. String representation by the double coding scheme. m^n is the total number of linguistic variables (fuzzy membership functions) for n-th input.

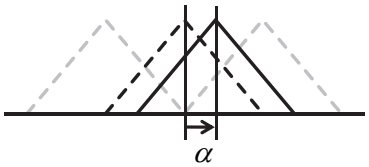

Figure 8. Genetic lateral tuning of fuzzy membership functions.

Each meta-classifier S is evaluated by the following three objective functions.

$f_1(S)$: the number of correctly classified training meta-patterns,

$f_2(S)$: the number of selected fuzzy rules,

$f_3(S)$: the total number of antecedent conditions.

That is, our multiobjective genetic fuzzy rule selection problem is formulated as:

$$\text{Maximize } f_1(S) \text{ and minimize } f_2(S) \text{ and } f_3(S). \quad (8)$$

Uniform crossover and bit-flip mutation are used as genetic operations for the rule selection part.

BLX-α crossover [26] and uniform mutation are used as genetic operations for tuning part.

By our multiobjective genetic fuzzy rule selection, we obtain a number of non-dominated decision systems with respect to the three objective functions. We select the most accurate classifier with respect to the first objective $f_1(S)$ for the training meta-data set, as the final meta-classifier.

VII. Computational Experiments

We examined two cases: One case is the application of the proposed framework to two-class problems. The other case is the application to multiple class problems with two or more classes. We explain the experimental setting and show the experimental results in this section.

A. Experimental Setting

We generated 100 artificial data sets from each data set by each simple operation explained in Section III. Thus, 300 new artificial data sets were generated in total. However, if more than one Chi-RW classifiers with different granularity have the same classification performance, we eliminate such data sets from this experiment.

The parameter settings of data set generation are as follows:

Reduction rate (random reduction): 5%, 10%, ..., 50%,

Generation rate (random generation): 10%, 20%, ..., 100%.

The parameter settings of MoGFRS are as follows:

The number of candidate rules per class: 300,

The number of strings: 200,

The number of generations: 5000,

Crossover probability: 0.9,

Mutation probability: 0.1 (1 to 0), 1/N (0 to 1),

(N is the number of total candidate rules).

Different mutation probabilities are used to select a small number of rules from the candidate ones.

To examine the generalization ability of the obtained meta-classifier, we propose *Leave one-group out* cross-validation shown in Fig. 9. Unlike 10-fold cross-validation (10CV), data sets are not randomly subdivided. All the data sets derived from an original data set are regarded as a group. When some group is used as test data sets, the other groups are used as training data sets. This is because each data set in the same group has somewhat similar data structure to each other. We avoided this affect in our experiments in order to assume the practical use of our proposed framework. As one of future issues, we have to examine whether the generated artificial data sets can cover the input space for unseen data sets or not.

We used the following experimental procedures.

Step 1: Divide artificial data sets into training data sets (T_r) and test data sets (T_s) by leave one-group out cross-validation.

Step 2: Calculate the values of data complexity measures of each artificial data set of T_r.

Step 3: Classify each artificial data set of T_r using each one of three granularities by 10CV.

Step 4: Generate a meta-data set from Step 2 and Step 3.

Step 5: Obtain a meta-classifier by MoGFRS.

Step 6: Calculate the values of data complexity measures of each artificial data set of T_s.

Step 7: Predict an appropriate granularity for each data set.

Step 8: Classify each data set of T_s using the granularity predicted in Step 7.

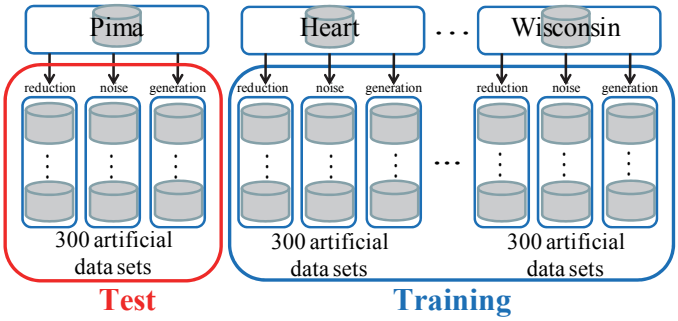

Figure 9. Leave one-group out validation.

B. Experimental Results for Two-class Problems

As two-class problems, we used 13 data sets listed in Table I. They are available from Keel data repository (http://keel.es). By simple operations, we generated 3,900 data sets in total.

The classification rates for test patterns in 10CV are shown in Table II. Chi-RW-3, Chi-RW-5, and Chi-RW-7 represent the results obtained by Chi-RW classifiers with coarse, moderate, and fine granularity, respectively. In those cases, the fixed granularity of fuzzy membership functions was used for all the data sets. "Meta-classifier" represents the result obtained by Chi-RW classifiers in which a granularity was selected by the meta-classifier for each data set. "Best" represents the result obtained by Chi-RW classifiers in which the best granularity was always used for each data set. This is an ideal case and just for a reference. From Table II, we can see that better test data

accuracy was obtained by our proposed method than the classifiers with fixed granularity. Table II also indicates that the result by our proposed method was close to the ideal case.

TABLE I. USED DATA SETS WITH TWO CLASSES

Data sets	Patterns	Attributes	Classes
Appendicitis	106	7	2
Australian	690	14	2
Banana	5300	2	2
Bupa	345	6	2
Haberman	306	3	2
Heart	270	13	2
Mammographic	830	5	2
Monk-2	432	6	2
Pima	768	8	2
Sonar	208	60	2
Titanic	2201	3	2
Wdbc	569	30	2
Wisconsin	683	9	2

TABLE II. CLASSIFICATION RATE OF TWO-CLASS PROBLEMS

	Chi-RW-3	Chi-RW-5	Chi-RW-7	Meta-Classifier	Best
Classification Rate (%)	75.11	65.89	59.77	**77.18**	77.84

The classification rate for test group data sets in *Leave one-group out* cross-validation was 77.00%.

We also analyzed if-then rules of the obtained meta-classifier. Since there were large differences among the meta-classifiers by leave one-group out, we generated a meta-classifier using all the artificial data sets (i.e., there is no test group). Figure 10 shows the best classifier with respect to the first objective $f_1(S)$. It was composed of four fuzzy rules. The black triangles mean the selected fuzzy membership functions. The left end of the x-axis means "simple", while the right end of the x-axis means "complicated".

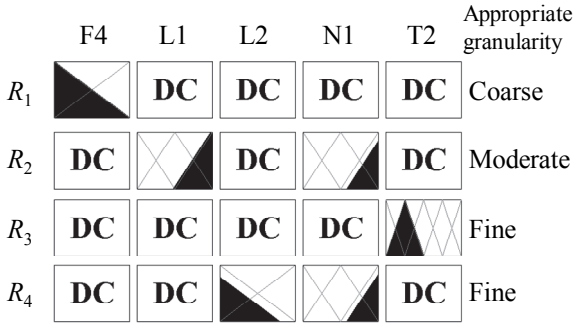

Figure 10. The obtained meta-classifier for two-class problems by MoGFRS.

Figure 10 can be interpreted as follows:

R_1: If the data set is **simple** w.r.t. **F4** then **coarse** fuzzy set is the best.

R_2: If the data set is **complicated** w.r.t. **L1** and **N1** then **moderate** fuzzy set is the best.

R_3: If the data set is **simple** w.r.t. **T2** then **fine** fuzzy set is the best.

R_4: If the data set is **simple** w.r.t **L2** and it is **complicated** w.r.t. **N1** then **fine** fuzzy set is the best.

These rules are counterintuitive except for R_1.

C. Experimental Results for mupliple class Problems

As multiple class problems with two or more classes, we used 24 data sets listed in Table III. They are also available from Keel data repository (http://keel.es). By simple operations, we generated 7,200 data sets in total.

Table IV shows the classification rates for test patterns in 10CV. From Table IV, we can see that better test data accuracy was obtained by our proposed method than the classifiers with fixed granularity. But the difference between our proposed method and Chi-RW-3 seems to be very small.

TABLE III. USED DATA SETS WITH TWO AND MORE CLASSES

Data sets	Patterns	Attributes	Classes
Appendicitis	106	7	2
Australian	690	14	2
Bands	365	19	2
Bupa	345	6	2
Cleveland	297	13	5
Dermatology	358	34	6
Glass	214	9	6
Haberman	306	3	2
Hayes-roth	132	4	3
Heart	270	13	2
Hepatitis	80	19	2
Ionosphere	351	34	2
Iris	150	4	3
Mammographic	830	5	2
Newthyroid	215	5	3
Pasture	36	22	3
Pima	768	8	2
Saheart	462	9	2
Sonar	208	60	2
Tae	151	5	3
Vehicle	846	18	4
Wdbc	569	30	2
Wine	178	13	3
Wisconsin	683	9	2

TABLE IV. CLASSIFICATION RATE OF MULTI-CLASS PROBLEMS

	Chi-RW-3	Chi-RW-5	Chi-RW-7	Meta-Classifier	Best
Classification Rate (%)	75.63	64.25	55.47	**75.72**	77.02

It should be noted that the ratio of data sets for which Chi-RW-3 was the best among three Chi-RW classifiers was 70.37%. Since the classification rate for test group data sets in *Leave one-group out* cross-validation was 70.83%, we can say

that the meta-classifier successfully selected different granularity to some extent.

Figure 11 shows the best classifier with respect to the first objective $f_1(S)$. No rule with moderate class was included in the meta-classifier. N4 measure seems to be a key data complexity measure for this case.

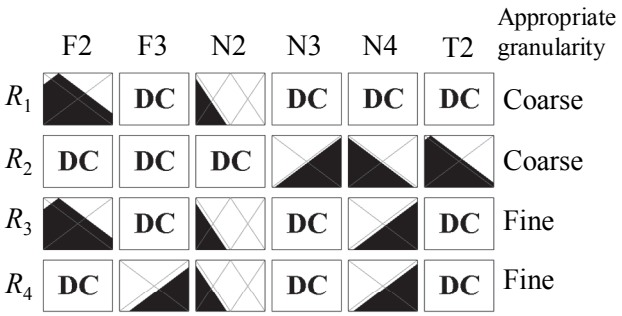

Figure 11. The obtained meta-classifier for multi-class problems by MoGFRS.

VIII. CONCLUSIONS

We proposed a framework for specifying an appropriate parameter setting in the design of Chi-RW classifiers for unseen data sets. The experimental results showed that our proposed framework can correctly predict an appropriate granularity by data complexity measures. The results by our proposed method were better than those by using the same (fixed) granularity for all data sets.

As a future research topic, we will apply this framework to classifier selection in which an appropriate classifier is selected from popular machine learning techniques (e.g., RBFN, SVM, C4.5) by data complexity measures for each data set. It would be necessary to reconsider the artificial data generation in order to generate data sets with various values of data complexity measures. A recent proposal [27] could be an alternative method.

REFERENCES

[1] T. K. Ho and M. Basu, "Complexity measures of supervised classification problems," *IEEE Trans. on Pattern Analysis and Machine Intelligence*, vol. 24, no. 3, March 2002, pp. 289-300.

[2] T. K. Ho, M. Basu, and M. H. Law, "Measures of geometrical complexity in classification problems," M. Basu and T. K. Ho (eds.) *Data Complexity in Pattern Recognition*, Springer-Verlag, 2006, pp. 3-23.

[3] S. Singh, "Multiresolution estimates of classification complexity," *IEEE Trans. on Pattern Analysis and Machine Intelligence*, vol. 25, no. 12, December 2003, pp. 1534-1539.

[4] J. Luengo and F. Herrera, "Domains of competence of fuzzy rule based classification systems with data complexity measures: A case of study using a fuzzy hybrid genetic based machine learning method," *Fuzzy Sets and Systems*, vol. 161, no. 1, 2010, pp. 3-19.

[5] A. Orriols-Puig and J. Casillas, "Fuzzy knowledge representation study for incremental learning in data streams and classification problems," *Soft Computing*, (in press).

[6] J. S. Sanchez, R. A. Mollineda, and J. M. Sotoca, "An analysis of how training data complexity affects the nearest neighbor classifiers," *Pattern Analysis and Application*, vol. 10, no. 3, 2007, pp. 189-201.

[7] R. A. Mollineda, J. S. Sanchez, and J. M. Sotoca, "Data characterization for effective prototype selection," *Proc. of the 2nd Iberian Conf. on Pattern Recognition and Image Analysis*, 2005, pp. 27-34.

[8] S. Garcia, J. R. Cano, E. Bernado-Mansilla, and F. Herrera, "Diagnose effective evolutionary prototype selection using an overlapping measure," *International Journal of Pattern Recognition and Artificial Intelligence*, vol. 23, no. 8, 2009, pp. 1527-1548.

[9] Z. Chi, H. Yan, and T. Pham, *Fuzzy Algorithms: with Applications to Image Processing and Pattern Recognition*, World Scientific, 1996.

[10] O. Cordon, M. J. del Jesus, and F. Herrera, "A proposal on resoning methods in fuzzy rule-based classification systems," *International Journal of Approximate Reasoning*, vol. 20, no. 1, 1999, pp. 21-45.

[11] H. Ishibuchi and T. Yamamoto, "Rule weight specification in fuzzy rule-based classification systems," *IEEE Trans. on Fuzzy Systems*, vol. 13, no. 4, 2005, pp. 428-435.

[12] S. Nishikawa, Y. Nojima, and H. Ishibuchi, "Appropriate granularity specification for fuzzy classifier design by data complexity measures," *Proceedings of the World Congress on Nature and Biologically Inspired Computing*, Kitakyusyu, Japan, December 15-17, 2010, pp. 698-703.

[13] H. Ishibuchi and T. Yamamoto, "Fuzzy rule selection by multi-objective genetic local search algorithms and rule evaluation measures in data mining," *Fuzzy Sets and Systems* vol. 141, 2004, pp. 59-88.

[14] R. Alcala, Y. Nojima, F. Herrera, and H. Ishibuchi, "Generating single granularity-based fuzzy classification rules for multiobjective genetic fuzzy rule selection," *Proc. of the 2009 IEEE International Conference on Fuzzy Systems*, Jeju, Korea, pp 1718-1723.

[15] R. Alcala, Y. Nojima, F. Herrera, and H. Ishibuchi, "Multiobjective genetic fuzzy rule selection of single granularity-based fuzzy classification rules and its interaction with the lateral tuning of membership functions," *Soft Computing* (in press).

[16] R. Alcala, J. Alcalá-Fdez, and F. Herrera, "A Proposal for the genetic lateral tuning of linguistic fuzzy systems and its interaction with rule selection," *IEEE Transactions on Fuzzy Systems,* vol. 15, no. 4, 2007, pp. 616-635.

[17] A. Orriols-Puig, N. Macia, and T. K. Ho, "Documentation for the data complexity library in C++," La Salle - Universitat Ramon Llull, Quatre Camins 2, Barcelona, Spain, 2010001, 2010. http://dcol.sourceforge.net

[18] V. Vapnik, *The Nature of Statistical Learning Theory*, Springer Verlag, New York, 1995.

[19] C. Platt, "Fast training of support vector machines using sequential minimal optimization," *Advances in Kernel Methods: Spport Vector Learning,* MIT Press, Cambridge, MA, USA, 1998, pp. 185-208.

[20] A. Hoekstra and R. P. W. Duin, "On the nonlinearity of pattern classifiers," *Proc. of the 13th International Conference on Pattern Recognition*, Vienna, August, 1996, pp. 271-275.

[21] KEEL A Software Tool to Assess Evolutionally Algorithms for Data Mining Problems. http://keel.es/

[22] H. Ishibuchi, K. Nozaki, N. Yamamoto, and H. Tanaka, "Selecting fuzzy if-then rules for classification problems using genetic algorithms," *IEEE Trans. on Fuzzy Systems*, vol. 3, no. 3, 1995, pp. 260-270.

[23] O. Cordon, F. Herrera, F. Hoffman, and L. Magdalena, *Genetic Fuzzy Systems*, World Scientific, 2001.

[24] F. Herrera, "Genetic fuzzy systems: Taxonomy, current research trends and prospects," *Evolutionary Intelligence*, vol. 1, 2008, pp. 27-46, 2008.

[25] Deb, A. Pratap, S. Agarwal, and T. Meyarivan, "A fast and elitist multiobjective genetic algorithm: NSGA-II," *IEEE Trans. on Evolutionary Computation* , vol. 6, no. 2, April 2002, pp. 182-197.

[26] L. J. Eshelman, K. E. Mathias, and J. D. Schaffer, "Crossover operator biases: Exploiting the population distribution," *Proc of 7th International Conference on Genetic Algorithms*, 1997, pp. 354-361.

[27] N. Macia, A. Orriols-Puig, and E. Bernado-Mansilla, "In search of targeted-complexity problems," *Proc. of Genetic and Evolutionary Computation Conference*, 2010, pp. 1055-1062.

2011 IEEE International Conference on Fuzzy Systems
June 27-30, 2011, Taipei, Taiwan

Assessing The Effects Of Zero Abundance Data On Habitat Preference Modelling Using A Genetic Takagi-Sugeno Fuzzy Model

Shinji Fukuda
Institute of Tropical Agriculture
Kyushu University
Fukuoka, Japan
shinji-fkd@agr.kyushu-u.ac.jp

***Abstract*—In this paper, the effects of zero abundance data on fish habitat modelling using a genetic Takagi-Sugeno fuzzy system were assessed with specific focus on habitat preference curves (HPCs) and model performance. Three independent data sets were prepared from a series of fish habitat surveys conducted in an agricultural canal in Japan. To quantify the effects of zero abundance data, two kinds of data (full abundance data and presence-only abundance data) were used, from which a fuzzy habitat preference model (FHPM) were developed. As a result, the HPCs obtained using presence-only abundance data resulted in similar HPCs across the different data sets used, while those obtained using full abundance data differed by the data sets. Because the model performance with regard to generalization ability was higher, the present study concluded that the use of presence-only abundance data can better capture the habitat preference of the target species.**

Keywords-genetic fuzzy systems; species distribution; habitat model; model error; uncertainty

I. INTRODUCTION

Genetic fuzzy systems (GFSs) have been widely applied to various research fields because of their ability to solve different types of problems [1], [2]. The GFSs have been applied to many disciplines using such approach as linguistic fuzzy models [3] and precise fuzzy models [4], [5] (for a review, see [6]). In ecological modelling, GFSs have also been used for tuning the membership functions of Mamdani–Assilian models [7] and the consequent part of Takagi–Sugeno models [8]–[16]. They are data-driven models, which have been reported to outperform knowledge-based models in the case of habitat modelling [17]. These application studies support the strengths of GFSs, i.e., the flexibility of the model structures and their ability to tune knowledge-based systems according to the new data sets for a given problem. Because the applicability of GFSs depends on the target systems and available data, it is necessary to accumulate both theoretical and application studies to better understand the ability and limitations of GFSs and the related modelling approaches.

In practical implementation of species distribution models (SDMs), presence-only data are often used because of the availability compared to presence-absence or abundance data [18]–[21]. On the one hand, presence data indicate clear evidence that target fish were observed at a surveyed point. On the other hand, zero abundance data (also referred to as absence data in presence-absence analysis) contain essential uncertainty. For instance, there could be a case where target species were absent due to the presence of enemy species or simply because the habitat was not yet occupied by the species. This uncertainty has been used as an explanation for the errors in SDM-related studies [17], [22], [23]. Despite the previous researches [24], [25] on the effects of absence data or prevalence of the data on the predictive performance of the models used, no study evaluated the effects of zero abundance data on habitat preference evaluation. Therefore, it is important to understand the behaviour of a target model in response to different qualities of data, from which existing models can be improved and also new models can be further developed.

The aim of this study is to assess the effects of zero abundance data on model performance and habitat preference evaluation using a genetic algorithm (GA) [26]-optimized fuzzy habitat preference model (FHPM). A series of fish habitat surveys focusing on Japanese medaka (*Oryzias latipes*) were conducted, from which three independent data sets were derived for the analyses. The effects of zero abundance data were assessed on the basis of habitat preference curves (HPCs) and predictive accuracy of spatial distribution of the fish.

II. METHODS

A. Study site and target fish

A series of field surveys was carried out in an agricultural canal located in Kurume City, Fukuoka, Japan (33˚20’ N, 130˚42’ E). The spring-fed canal runs through paddy fields and is used for both irrigation and drainage purposes. The Japanese medaka is one of the most common fish in paddy environments in Japan. This fish is considered to be one of the symbols for the conservation and restoration of rural environments, because the fish is vulnerable to changes in physical habitat conditions such as current velocity. This is partly ascribed to the body length of the Japanese medaka (2–4 cm in length for an adult).

B. Fish Habitat Surveys

The field surveys were conducted on 14 October, 5 and 9 November 2004. The surveys were conducted during a non-

This work was supported in part by the Grant-in-aid for Young Scientists B (21780225) of the Ministry of Education, Culture, Sports, Science and Technology (MEXT), Japan.

irrigation period, and thus the discharge in both reaches remained stable. The habitat use of the Japanese medaka and four physical habitat characteristics of water depth (cm, henceforth referred as depth), current velocity (cm s^{-1}, velocity), lateral cover ratio (%, cover) and percent vegetation coverage (%, vegetation) in the study reach were surveyed on sunny days. After mapping the reach, the habitat use of the fish was observed, and then the physical habitat characteristics within the reach were surveyed.

The habitat use of Japanese medaka was observed visually from the bank; the observer moved slowly and carefully to avoid disturbing the fish. The number of the fish was counted in units of five to consider the habit of school formation; fish in a small school (less than five) were not counted. The fish observations were repeated eight times and the results were averaged in order to reduce observational errors.

Immediately after completing the fish observation, the four physical habitat variables of depth, velocity, cover and vegetation were surveyed to establish a relationship between the habitat variables and the habitat preferences of Japanese medaka. First, depth and velocity were measured, in which depth was measured with a stainless steel ruler and velocity was measured with a portable propeller current meter (KENEK, V-303) at three lateral points comprising a midpoint and two near-shore points at longitudinal intervals of 1 m. Next, the study reach were divided into small water units having a similar condition with regard to depth and velocity. The other two factors of cover and vegetation were then calculated at each water unit. The lateral cover ratio is defined as a function of the presence of a lateral cover, which comprises the water's edge, a dike, or anything that emerges from the water surface and surrounds the water body. The cover thus consists of four components (four lateral sides). The maximum cover ratio is 100%, and each of the cover components is assigned a score of 25%. In the definition of the cover, objects attached to more than 90% of the boundary between water units were regarded as cover components. That is, only instream and undersurface cover structures that may have the same effects as the margin of the stream were considered as cover components. Percent vegetation coverage is defined as the percentage of the area covered with aquatic vegetation in each water unit. Both submerged and emergent vegetation were pooled because of their same roles in providing foods and shelters from predators and fast-flowing currents.

The fish distribution data used in the following analyses were the log-transformed fish population density observed at the i^{th} water unit $FPD_{o,i}$ (individuals per square metre), where i (= 1, 2, …, N) denotes the index of the water units and N is the total number of water units (Fig. 1).

C. *Fuzzy Habitat Preference Model*

In the present study, a fuzzy habitat preference model (FHPM; [8]) was employed. The FHPM is a 0-order Takagi-Sugeno model [27] which relates habitat variables to habitat preference by considering uncertainties such as fish behaviour and measurement errors of the physical habitat variables. FHPMs have been applied to modelling the habitat use of Japanese medaka in a laboratory experiment [7] and at a microhabitat scale [9–15]. The FHPMs has also been applied to habitat evaluations at a larger spatial scale [16]. A FHPM can be viewed as a fuzzified version of a GA-optimized piecewise constant model [12], in which simultaneous optimization of all model parameters enables an FHPM to evaluate habitat preference, even under the nonlinear, complex interactions between habitat variables and habitat preference [11]. The brief description of an FHPM follows.

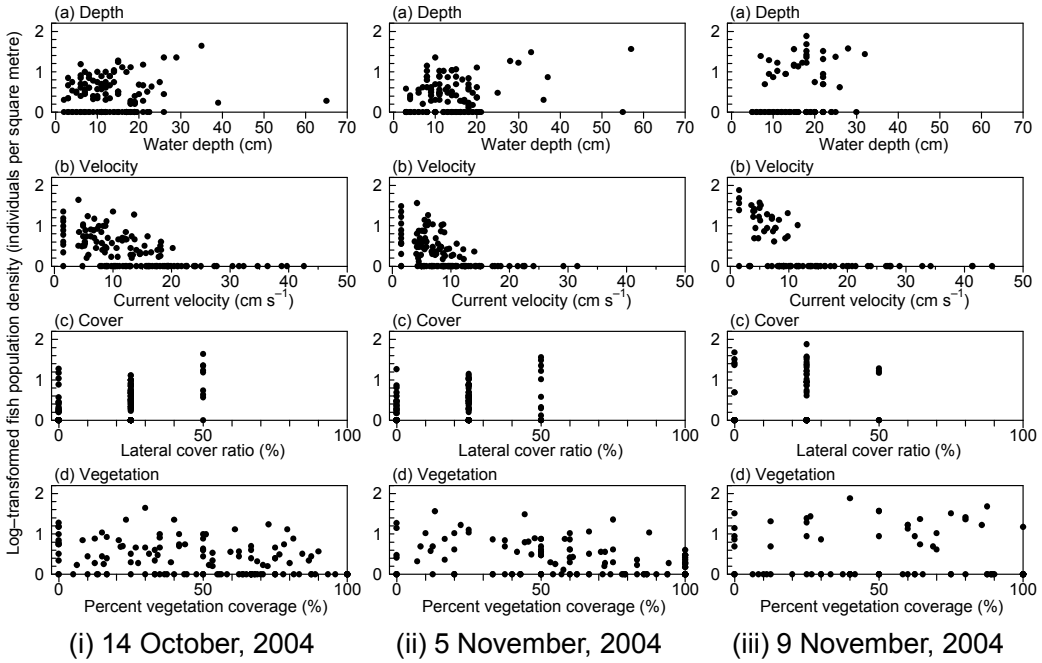

Figure 1. Results of fish habitat surveys.

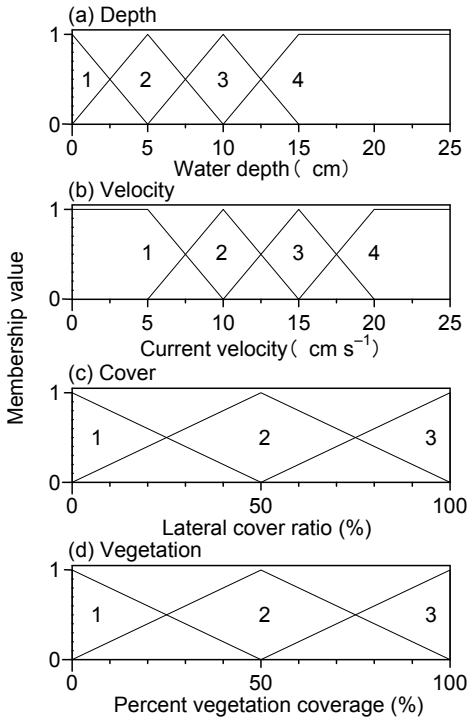

Figure 2. Membership functions.

The present FHPM is a single-input single-output fuzzy system and has 4 sets of if-then rules, comprised of 4 rules for depth and velocity, and 3 rules for cover and vegetation (14 rules in total). The input values (four habitat variables) were expressed by symmetric triangular fuzzy numbers with centre α_m and spread σ_m, where m denotes the habitat conditions of depth, velocity, cover and vegetation, to consider the measurement errors and the spatial variances of the habitat variables. The centre α_m is the observed value and the spread σ_m is determined from the allowable variances when dividing the reach into water units: 1 cm was given for the spread of depth σ_{d}, 1 cm s^{-1} for velocity σ_{v} and 10% each for cover σ_{c} and vegetation σ_{veg}. The abbreviations d, v, c and veg denote depth, velocity, cover and vegetation, respectively. The antecedent parts of the FHPM (the membership functions) were defined to extract habitat requirements of the target fish (Fig. 2). Each membership function has a corresponding singleton value in the consequent part. The habitat preference was calculated by taking a weighted mean of the singleton values in the consequent parts, with the membership degrees as weights. The singleton values in the consequent part are in the range [0, 1] and were determined by a GA so as to minimize the mean squared error (MSE) between the modelled and observed fish population density. That is, the fitness function of the GA is a reciprocal of the MSE. The present GA consisted of a population of 100 individuals, each of which has a 56-bit string (4 bits × 14 singletons). The shape of the habitat preference curves (HPCs), i.e., a set of singletons for a habitat variable, was constrained to have a unimodal or monotone form with maximum preference of one. Specifically, the model was penalized by giving large MSE values when the above regulation was violated. In the estimation of the fish population density, a composite habitat preference according to the four habitat variables was calculated as

$$HP_i = P_{\mathrm{d},i} \times P_{\mathrm{v},i} \times P_{\mathrm{c},i} \times P_{\mathrm{veg},i} \tag{2}$$

where HP_i denotes the habitat preference in the i^{th} water unit, and $P_{\mathrm{d},i}$, $P_{\mathrm{v},i}$, $P_{\mathrm{c},i}$, and $P_{\mathrm{veg},i}$ are the habitat preference to individual habitat variables of depth, velocity, cover and vegetation, respectively. The product operation is reported to produce a FHPM with higher performance with consistent habitat preference curves [16]. The habitat use of Japanese medaka was then estimated using the equation:

$$FPD_{\mathrm{c},i} = \left(HP_i \Big/ \sum_{i=1}^{N} HP_i \right) \cdot \sum_{i=1}^{N} FPD_{\mathrm{o},i} \tag{3}$$

where $\mathrm{FPD}_{\mathrm{c},i}$ is the calculated fish population density in the i^{th} water unit, and $\mathrm{FPD}_{\mathrm{o},i}$ is the observed fish population density. The MSE was calculated accordingly and the GA repeatedly modified the model structure (the singletons in the consequent part) using three genetic operations: roulette wheel selection with an elitist strategy, uniform crossover and mutation at a probability of 5%. After 2,000 iterations, the optimal model was obtained. The GA optimization was repeated using 20 different sets of initial conditions.

D. Model Development and Analysis

To assess the effects of zero abundance data (i.e., data at which no fish was present) on the habitat evaluation of Japanese medaka, two kinds of data were used: full abundance data (henceforth referred to as full data) and the data without zero abundance (henceforth referred to as presence-only abundance data). The full data consist of both abundance data and zero abundance data, whereas presence-only abundance data consist of only abundance data (i.e., full data without zero abundance data). FHPMs were developed using three independent data sets with two kinds (full and presence-only abundance data), in which a data set was used for model calibration and each of the remaining two data sets were used for model validation. HPC for a habitat variable was obtained by providing consecutive values, which were in the range of the corresponding membership functions (in steps of 0.1), to the FHPM of which the output values were plotted against the habitat variable. HPCs were evaluated according to the shapes and variances of all HPCs from 20 different initial conditions. Consistent HPCs indicate that consistent ecological knowledge was extracted by FHPMs. A variance in HPCs reflects the variance in model structures optimized using 20 different initial conditions in the GA optimization, and quantifies the convergence of model parameters. Consistency or a smaller variance in HPCs would thus demonstrate the appropriateness of the model developed.

The accuracy of the model was evaluated based on the MSE between predicted and observed fish population density. The MSE was calculated for the three cases of species distribution modelling of the fish: prediction using full data by FHPMs developed from full data, prediction using full data by FHPMs developed from presence-only abundance data, and prediction using presence-only abundance data by FHPMs

developed from presence-only abundance data. Mean and standard deviation of the MSE values across 20 different initial conditions were used as performance measures. The smaller MSE values in validation data sets indicate the higher generalization ability of the models.

III. RESULTS

The full data and presence-only abundance data result in slightly different HPCs (Figs. 3–4), in which differences are also found across data sets used. The difference can be seen from the shape or trend of HPCs and the degree of preference. For instance, it is observed from the HPCs for depth derived using the full data (Figs. 3a(i)–3a(iii)) that Japanese medaka

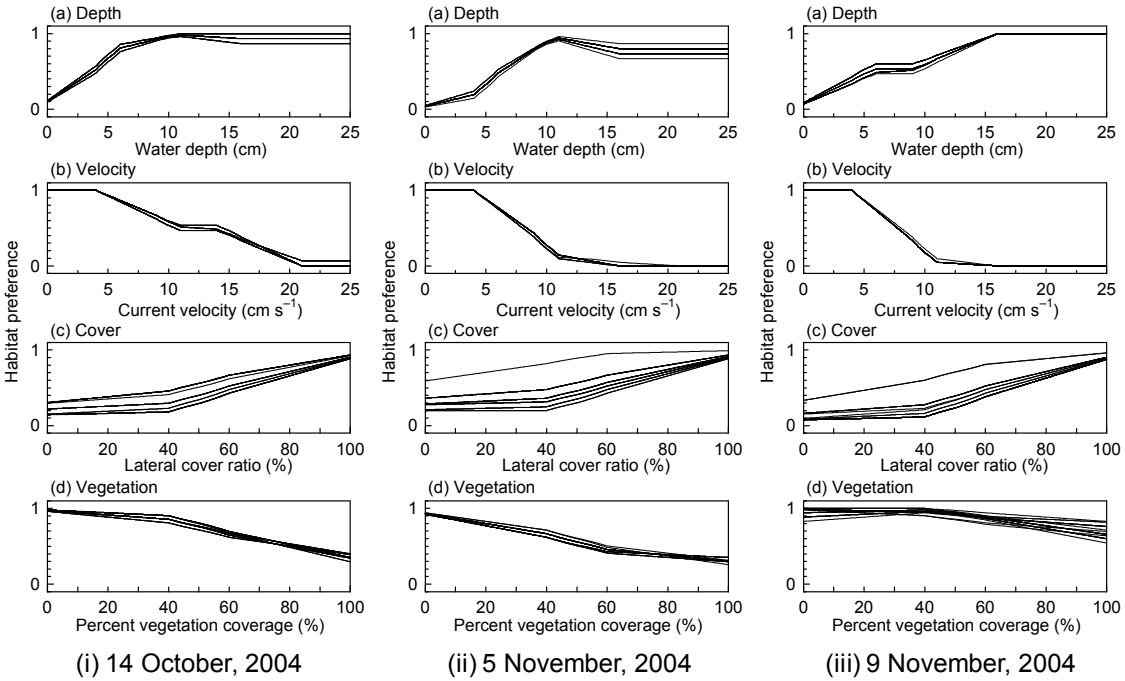

Figure 3. Habitat preference curves of fuzzy habitat preference models developed using full abundance data

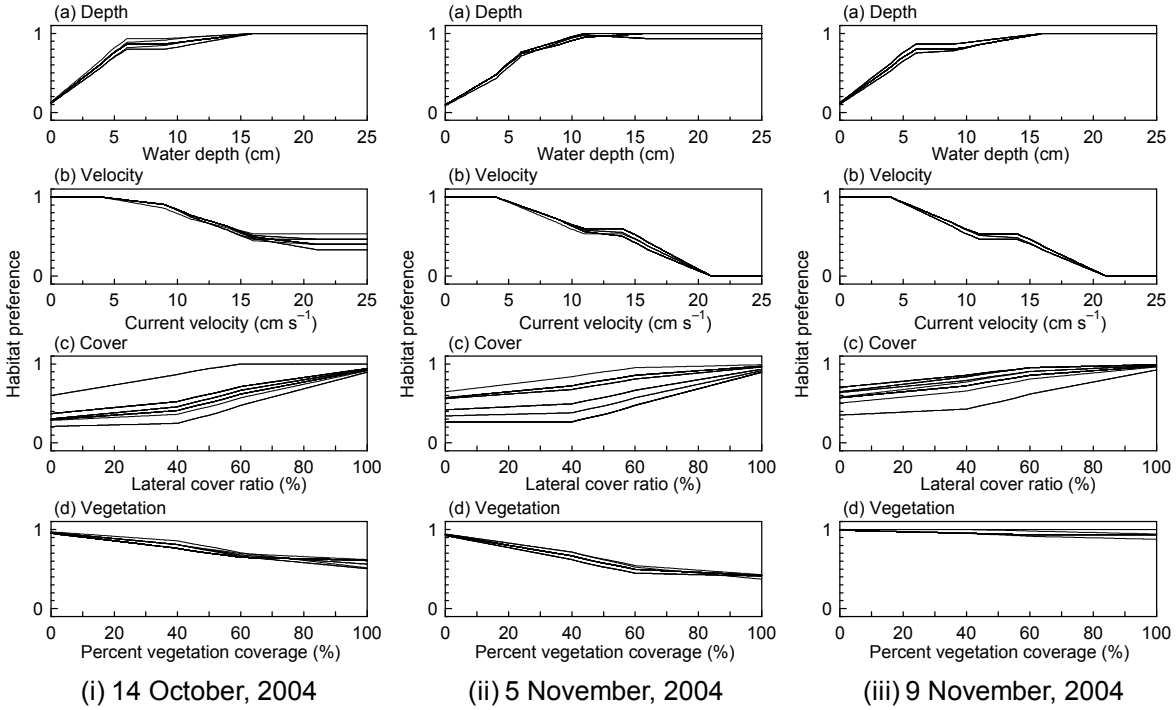

Figure 4. Habitat preference curves of fuzzy habitat preference models developed using presence-only abundance data.

TABLE I. MEAN SQUARED ERRORS BETWEEN PREDICTED AND OBSERVED FISH POPULATION DENSITY, IN WHICH RESULTS FROM DIFFERENT SETTING ARE SHOWN: (A) FUZZY HABITAT PREFERENCE MODELS (FHPMS) CALIBRATED AND EVALUATED USING FULL ABUNDANCE DATA, (B) FHPMS CALIBRATED USING PRESENCE-ONLY ABUNDANCE DATA AND EVALUATED USING FULL ABUNDANCE DATA, AND (C) FHPMS CALIBRATED AND EVALUATED USING PRESENCE-ONLY ABUNDANCE DATA. EACH OF THREE DATA SETS WAS USED FOR MODEL CALIBRATION AND EVALUATION.

	Data Used For Model Evaluation		
(a) FHPM	***14 Oct.***	***5 Nov.***	***9 Nov.***
Model 1	0.0691 ±0.0005	0.0842 ±0.0017	0.2163 ±0.0057
Model 2	0.1457 ±0.0071	0.0665 ±0.0004	0.2056 ±0.0088
Model 3	0.2399 ±0.0418	0.1148 ±0.0162	0.1431 ±0.0013
(b) $FHPM_0$-1			
Model 1	0.0933 ±0.0017	0.1091 ±0.0012	0.2613 ±0.0036
Model 2	0.0768 ±0.0011	0.0927 ±0.0015	0.2361 ±0.0051
Model 3	0.0846 ±0.0018	0.1064 ±0.0025	0.2127 ±0.0049
(c) $FHPM_0$-2			
Model 1	0.0535 ±0.0004	0.0648 ±0.0011	0.1368 ±0.0072
Model 2	0.0698 ±0.0025	0.0566 ±0.0005	0.1862 ±0.0128
Model 3	0.0754 ±0.0028	0.0820 ±0.0020	0.0697 ±0.0005

Mean ±standard deviation are shown.
Model 1 was developed using the data set on 14 October.
Model 2 was developed using the data set on 5 November.
Model 3 was developed using the data set on 9 November.

prefers a larger water depth as a trend, while different degrees of preference around the depth over 10 cm are observed between the three data sets. For velocity, the degrees of preference at the velocity of 10 to 15 cm s^{-1} are found to be different between the data sets of 14 October and the other data sets (Figs. 3b(i)–3b(iii)). The difference of HPCs are not clear for cover (Figs. 3c(i)–3c(iii)), of which the convergence are slightly better in the data sets on 14 October. For vegetation, the degree of preference to the larger vegetation is higher in the data sets on 9 November (Figs. 3d(i)–3d(iii)). These differences between data sets can be the source of errors in validation data sets (Table Ia). Large errors are observed at model 2 for the data set of 14 October and model 3 for the data sets of 14 October and 5 November, which is partly ascribed to the overestimations of fish population density.

In the case where presence-only abundance data were used, the differences in HPCs between data sets are found to be small (Fig. 4). While the degrees of preference are slightly different between the HPCs from different data sets, the trends of HPCs are the same across the data sets. The slight differences in the degree of preference are observed at the HPCs for velocity over 20 cm s^{-1} and those for vegetation (Figs. 4b and 4d). The HPCs for vegetation developed using the presence-only abundance data show weak trend over the variable range (Fig. 4d(iii)), which would indicate a small contribution of the variable in modelling spatial distributions of the fish using the data set. The HPCs obtained from presence-only abundance data result in worse accuracy when testing the FHPMs by the full data (Table Ib) but better accuracy when testing the FHPMs by the presence-only abundance data (Table Ic). Despite the different accuracy between the FHPMs developed using the presence-only abundance data (Table Ib–Ic), the accuracies are better than that of FHPMs developed using the full data (Table Ia).

IV. DISCUSSION

The present results illustrated that the zero abundance data affect model performance of the FHPMs (Figs. 3–4, Table I), which was observed through the HPCs and resulting MSE values. The reduced standard deviation values of MSEs indicate that the zero abundance data can be a source of uncertainties in species distribution modelling (Table I). This is clear, to some extent, because zero abundance contains two possible cases of true and chance absences. The former means that the fish was absent because the fish avoided it, while the latter means that the fish was absent because the habitat was not yet occupied or because of presence of predator or competitive species, even the habitat was preferable for the fish. As a result, model predictions in the former case are evaluated to be perfect fits, while model predictions in the latter case are to be errors. This type of errors is the same as the errors that are reported as false positives in presence-absence modelling [17], [22], [23]. It is also reported that the proportion of presence data to total data, often termed as prevalence, affects the performance of SDMs (see [24], [25] for reviews). Accordingly, it could be concluded that the model performance is affected by not only the prevalence of data but also the proportion of true and chance absences in absence data or zero abundance data. However, it is impossible to distinguish true and chance absences at the moment. Novel methods are, therefore, needed to be developed for better understanding the model behaviour to uncertainties associated with the data used.

The present results demonstrated the higher generalization ability of FHPMs developed using presence-only abundance data, which can be mainly because of the consistent HPCs obtained (Figs 3–4). For instance, the present HPCs show a consistent trend of habitat preference that the fish prefer a larger depth, a slower velocity, a larger cover and a smaller vegetation with a small difference of the degree of preference. This supports the appropriateness of presence-only abundance data in species distribution modelling, especially where HPCs are necessary or important. The differences in HPCs have been reported as a 'transferability' of a habitat model [10], [14], [28]–[31]. References [32], [33] suggested the necessity of a response curve of a model, i.e., a HPC in the present study, for a better understanding towards an improvement of the existing models or development of a new model. Since the response curve of a model illustrate how target species response to a given habitat condition, SDMs should be compared on the basis of both accuracy measures and response curves derived from the models.

V. CONCLUSION

This case study of Japanese medaka demonstrated the effect of zero abundance data in modelling fish habitat preference using a 0-order Takagi-Sugeno fuzzy system. The dual nature of zero abundance (i.e., true and chance absences) would be one of the sources of performance deterioration of the model.

Further studies are needed to develop an approach to distinguish true and chance absences, which contributes to the better understandings of target species and the improvement of SDMs

ACKNOWLEDGMENT

The author thanks Prof. K. Hiramatsu at Faculty of Agriculture, Kyushu University for his sincere assistance in the early phase of this study.

REFERENCES

[1] O. Cordon, F. Herrera, F. Hoffmann, and L. Magdalena, "Genetic fuzzy systems. Evolutionary tuning and learning of fuzzy knowledge bases," World Scientific, Singapore, 2001.

[2] F. Herrera, "Genetic fuzzy systems: taxonomy, current research trends and prospects," Evol. Intel., vol. 1, pp. 27–46, 2008.

[3] H. Ishibuchi, T. Nakashima and M. Nii, "Classification and modeling with linguistic information granules: Advanced approaches to linguistic data mining," Springer Verlag, 2004.

[4] N. Xiong, "Evolutionary learning of rule premises for fuzzy modelling," Int. J. Syst. Sci., vol. 32, pp. 1109–1118, 2001.

[5] O. Cordon and F. Herrera, "A two-stage evolutionary process for designing TSK fuzzy rule-based systems," IEEE Trans. Systems Man Cybernet. B, vol. 29, pp. 703–715, 1999.

[6] M.J. Gacto, R. Alcalá and F. Herrera, "Interpretability of linguistic fuzzy rule-based systems: An overview of interpretability measures," Inform. Sci., in press.

[7] E. Van Broekhoven, V. Adriaenssens, and B. De Baets, "Interpretabilitypreserving genetic optimization of linguistic terms in fuzzy models for fuzzy ordered classification: An ecological case study," Int. J. Approx. Reasoning., vol. 44, pp. 65–90, 2007.

[8] K. Hiramatsu, S. Fukuda, and S. Shikasho, "Mathematical modelling of habitat preference of Japanese medaka for instream water environment using fuzzy inference," Trans. JSIDRE, vol. 228, pp. 65–72,2003 (in Japanese with English abstract).

[9] S. Fukuda, K. Hiramatsu, M. Mori, and S. Shikasho, "Mathematical Characterization of fuzziness in fish habitat preference of Japanese medaka (*Oryzias latipes*) in agricultural canal," Trans. JSIDRE, vol. 239, pp. 43–49, 2005 (in Japanese with English abstract).

[10] S. Fukuda and K. Hiramatsu, "Prediction ability and sensitivity of artificial intelligence-based habitat preference models for predicting spatial distribution of Japanese medaka (*Oryzias latipes*)," Ecol. Model., vol. 215, pp. 301–313, 2008.

[11] S. Fukuda and S. Okushima, "Assessing nonlinearity in fish habitat preference of Japanese medaka (*Oryzias latipes*) using genetic algorithm-optimized habitat prediction models," JARQ-Jpn. Agric. Res. Quart., vol. 42 (2), pp. 97–107, 2008.

[12] S. Fukuda, "Consideration of fuzziness: Is it necessary in modelling fish habitat preference of Japanese medaka (*Oryzias latipes*)?" Ecol. Model., vol. 220, pp. 2877–2884, 2009.

[13] S. Fukuda, "A preliminary analysis for improving model structure of fuzzy habitat preference model for Japanese medaka (*Oryzias latipes*)," Proc. of 13th IFSA World Congress and 6th Conference of EUSFLAT, pp. 1258–1263, 2009.

[14] S. Fukuda, "Assessing transferability of genetic algorithm-optimized fuzzy habitat preference models for Japanese medaka (*Oryzias latipes*)," Proc. of GEFS2010, pp. 57–62, 2010.

[15] S. Fukuda, "Effect of data quality on habitat preference evaluation for Japanese medaka (*Oryzias latipes*) using a simple genetic fuzzy system," Proc. of FUZZ-IEEE2010, pp. 1231–1237, 2010.

[16] S. Fukuda, B. De Baets, A.M. Mouton, W. Waegeman, J. Nakajima, T. Mukai, K. Hiramatsu, and N. Onikura, "Effect of model formulation on the optimization of a genetic Takagi-Sugeno fuzzy system for fish habitat suitability evaluation," Ecol. Model., vol. 222, pp. 1401–1413, 2011.

[17] A.M. Mouton, B. De Baets, and P.L.M. Goethals, "Knowledge-based versus data-driven fuzzy habitat suitability models for river management," Environ. Modell. Softw., vol. 24, pp. 982–993, 2009.

[18] A. Guisan, and N.E. Zimmermann, "Predictive habitat distribution models in ecology," Ecol. Model., vol. 135, pp.147–186, 2000.

[19] A. Guisan, and W. Thuiller, "Predicting species distribution: offering more than simple habitat models," Ecol. Lett., vol. 8, pp.993–1009, 2005.

[20] J. Elith, C.H. Graham, R.P. Anderson, M. Dudík, S. Ferrier, A. Guisan, R.J. Hijmans, F. Huettmann, J.R. Leathwick, A. Lehmann, J. Li, L.G. Lohmann, B.A. Loiselle, G. Manion, C. Moritz, M. Nakamura, Y. Nakazawa, J. M. Overton, A.T. Peterson, S.J. Phillips, K. Richardson, R. Scachetti-Pereira, R.E. Schapire, J. Soberón, S. Williams, M.S. Wisz, and N.E. Zimmermann, "Novel methods improve prediction of species' distributions from occurrence data," Ecography, vol. 29, pp.129–151, 2006.

[21] R. Pino-Mejías, M.D. Cubiles-de-la-Vega, M. Anaya-Romero, A. Pascual-Acosta, A. Jordán-López, and N. Bellinfante-Crocci, "Predicting the potential habitat of oaks with data mining models and the R system," Envion. Modell. Softw., vol. 25, pp.826–836, 2010.

[22] A.M. Mouton, B. De Baets, E. Van Broekhoven, and P.L.M. Goethals, "Prevalence-adjusted optimisation of fuzzy models for species distribution," Ecol. Model., vol. 220, pp. 1776–1786, 2009.

[23] A.M. Mouton, A.P. Dedecker, S. Lek, P.L.M. Goethals, "Selecting Variables for Habitat Suitability of Asellus (Crustacea, Isopoda) by Applying Input Variable Contribution Methods to Artificial Neural Network Models," Environ. Model. Assess., vol. 15, pp. 65–79, 2009.

[24] A.H. Fielding, and J.F. Bell, "A review of methods for the assessment of prediction errors in conservation presence/absence models," Environ. Conserv., vol. 24(1), pp.38–39, 1997.

[25] A.M. Mouton, B. De Baets, P.L.M. Goethals, "Ecological relevance of performance criteria for species distribution models," Ecol. Model., vol. 221, pp.1995–2002, 2010.

[26] D. Goldberg, "Genetic algorithms in search, optimization, and machine learning," Addison-Wesley, 1989.

[27] T. Takagi and M. Sugeno, "Fuzzy identification of systems and its applications to modellingand control," IEEE Trans. Systems Man Cybernet. B, vol. 15, pp. 116–132, 1985.

[28] A. Mäki-Petäy, A. Huusko, J. Erkinaro and T. Muotka, "Transferability of habitat suitability criteria of juvenile Atlantic salmon (*Salmo salar*)," Can. J. Fish. Aquat. Sci. vol. 59, pp. 218–228, 2002.

[29] J.C. Guay, D. Boisclair, M. Leclerc and M. Lapointe, "Assessment of the transferability of biological habitat models for Atlantic salmon parr (*Salmo salar*)," Can. J. Fish. Aquat. Sci. vol. 60, pp. 1398–1408, 2003.

[30] M. Nykänen and A. Huusko, "Transferability of habitat preference criteria for larval European grayling (*Thymallus thymallus*)," Can. J. Fish. Aquat. Sci. vol. 61, pp. 185–192, 2004.

[31] W. Vanreusel, D. Maes and H. Van Dyck, "Transferability of species distribution models: a functional habitat approach for two regionally threatened butterflies," Conserv. Biol. vol. 21(1), pp. 201–212, 2007.

[32] J. Elith, S. Ferrier, F. Huettmann, and J. Leathwick, "The evaluation strip: A new and robust method for plotting predicted responses from species distribution models," Ecol. Model., vol. 186, pp. 280–289, 2005.

[33] J. Elith and C.H. Graham, "Do they? How do they? Wh do they differ? On finding reasons for differing performances of species distribution models," Ecography, vol. 32, pp. 66–77, 2009.

2011 IEEE International Conference on Fuzzy Systems
June 27-30, 2011, Taipei, Taiwan

A Multiple-Level Genetic-Fuzzy Mining Algorithm

Chun-Hao Chen
Department of Computer Science and Information Engineering
Tamkang University
Taipei, Taiwan, R.O.C.
chchen@mail.tku.edu.tw

Tzung-Pei Hong
Department of Computer Science and Information Engineering
National University of Kaohsiung
Kaohsiung, Taiwan, R.O.C.
tphong@nuk.edu.tw

Yeong-Chyi Lee
Department of Information Management
Cheng Shiu University
Kaohsiung, Taiwan, R. O. C.
yeongchyi@csu.edu.tw

***Abstract*—In this paper, we propose a multiple-level genetic-fuzzy mining algorithm for mining membership functions and fuzzy association rule on multiple-concept levels. It first encodes the membership functions of each item class (category) into a chromosome according to the given taxonomy. The fitness value of each individual is then evaluated by the summation of large 1-itemsets of each item in different concept levels and the suitability of membership functions in the chromosome. After the GA process terminates, a better set of multiple-level fuzzy association rules can then be expected with a more suitable set of membership functions. Experimental results on a simulation dataset also show the effectiveness of the algorithm.**

Keywords- data mining, genetic algorithm, multiple-concept levels, membership function, fuzzy association rule.

I. INTRODUCTION

Data mining is most commonly used in attempts to induce association rules from transaction data [2]. An association rule is an expression $X \rightarrow Y$, where X and Y are a set of items. It means in the set of transactions, if all the items in X exist in a transaction, then Y is also in the transaction with a high probability. A variety of mining approaches based on the Apriori algorithm [2] have also been proposed [4, 21]. However, most of them are focus on finding association rules on a single-concept level. Thus, many approaches have also been proposed for mining multiple-concept-level association rules to discovery more specific and important knowledge from data [8, 22].

Most of the mentioned approaches above focused on binary valued transaction data. Transaction data in real-world applications usually consist of quantitative values. Thus, fuzzy data mining algorithms have been proposed for handling quantitative transactions and mining fuzzy association rules [5, 11, 17, 24]. As to multiple-concept levels fuzzy mining, according to the given fuzzy generalization hierarchies, Lee first proposed a generalized fuzzy quantitative association rules mining algorithm [16]. In 2003, Hong et al. then proposed a multiple-level fuzzy association rule mining approach [12]. It first transforms quantitative transactions into fuzzy values by using the predefined membership functions and taxonomy. Then, a top-down progressively deepening approach is used to finding large itemsets and rules. Additionally, in order to reduce the time complexity, only the linguistic term with the maximum cardinality of each item is used in later mining processes. In [14], Kaya et al. proposed a weight fuzzy rule mining approach based on Hong's approach. In 2008, Lee et al. proposed a fuzzy mining algorithm for discovering generalized fuzzy association rules with multiple supports of items for extracting implicit knowledge from quantitative transaction data [18, 19].

Those mentioned approaches assumed the membership functions to be known in advance. The given membership functions may, however, have a critical influence on the final mining results. In recent years, the Genetic-Fuzzy Mining (GFM) approaches have then proposed for deriving appropriate membership functions and mining fuzzy association rules [3, 6, 10, 13, 15]. Kaya *et al.* proposed a GA-based approach to derive a predefined number of membership functions for getting a maximum profit within a user specified interval of minimum supports [13]. Hong *et al.* also proposed a genetic-fuzzy data-mining algorithm for extracting both association rules and membership functions from quantitative transactions [10]. Alcalá-Fdez *et al.* then modified Hong's approach to propose an enhanced approach based on the 2-tuples linguistic representation model [3]. Besides, multi-objective genetic-fuzzy mining approaches have also been proposed [6, 15].

However, those mentioned GFM algorithms are focus on one single-concept level. To the best of our knowledge, there is no GFM algorithm for multiple-concept levels until now. In this paper, we thus propose a multiple-level GFM algorithm for mining membership functions and fuzzy association rule on multiple-concept levels. According to the given taxonomy, it first encodes membership functions of each item class (category) into chromosome. The fitness value of each individual is then evaluated by the summation of large 1-itemsets of each item in different concept levels and the suitability of membership functions in the chromosome. After the GA process terminates, a better set of multiple-level fuzzy association rules can then be expected with a more suitable set of membership functions.

II. A MULTIPLE-LEVEL GENETIC-FUZZY MINING FRAMEWORK

In this section, the fuzzy and GA concepts are used to discover both useful association rules and suitable membership functions from quantitative values. We propose a Multiple-level Genetic-Fuzzy Mining (Multiple-level GFM) framework for searching membership functions suitable for multiple-level mining problems and then use the final best set of membership functions to mine multiple-level fuzzy association rules. The proposed framework is shown in Figure 1.

978-1-4244-7316-8/11/$26.00 ©2011 IEEE

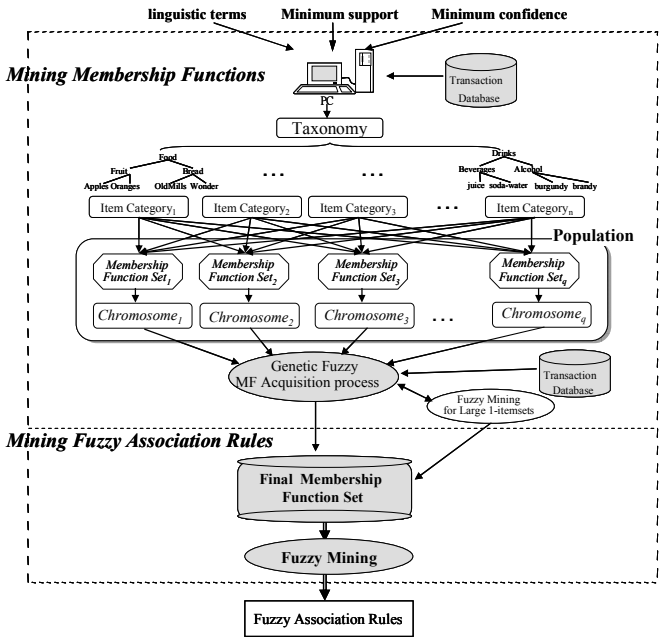

Figure 1. The Multiple-level GFM framework

The proposed framework consists of two phases, namely mining membership functions and mining fuzzy association rules phases. It maintains a population of sets of membership functions, and uses the genetic algorithm to automatically derive the resulting one. In the first phase, according to the given taxonomy, it first transforms each set of membership functions of each item category into a fixed-length string. It then chooses appropriate strings for mating, gradually creating good offspring membership function sets. The offspring membership function sets then undergo recursive evolution until a good set of membership functions has been obtained. In second phase, the derived membership functions are then used to mine multiple-level fuzzy association rules by using rule mining approach [12].

III. COMPONENTS OF THE PROPOSED APPROACHES

In this section, the components of the proposed approach for deriving membership functions and fuzzy association rule on multiple-concept levels are stated. The details of them are described below.

A. Chromosome Representation

It is important to encode membership functions as string representation for GAs to be applied. Several possible encoding approaches have been described in [1, 3, 7, 20, 23]. In this paper, each set of membership functions is encoded as a chromosome and handled as an individual with real-number schema. In order to effectively encode the associated membership functions, we use two parameters to represent each membership function as Parodi and Bonelli did [20]. Thus, in multiple-level fuzzy rule mining, membership functions applied to an item class (category) are then assumed to be isosceles-triangle functions as shown in Figure 2.

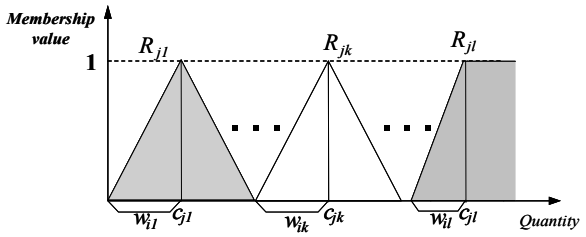

Figure 2. Membership Functions of item class IC_j

where R_{jk} denotes the membership function of the k-th linguistic term of *item class* IC_j, c_{jk} indicates the center abscissa of fuzzy region R_{jk}, and w_{jk} represents half the spread of fuzzy region R_{jk}. As Parodi and Bonelli did, we then represent each membership function as a pair (c, w). Thus, all pairs of (c, w)'s for a certain item class are concatenated to represent its membership functions. Thus the set of membership functions MF_1 for the first item class IC_1 is then represented as a substring of $c_{11}w_{11}\ldots c_{1|IC1|}w_{1|IC1|}$, where $|IC_1|$ is the number of linguistic terms of IC_1.

The entire set of membership functions is then encoded by concatenating substrings of MF_1, MF_2, ..., MF_j. Since c and w are both numeric values, a chromosome is thus encoded as a fixed-length real-number string rather than a bit string.

B. Fitness and Selection

In order to develop a good set of membership functions from an initial population, the genetic algorithm selects *parent* membership function sets with high fitness values for mating. An evaluation function is then used to qualify the derived membership function sets. The performance of membership function sets is then fed back to the genetic algorithm to control how the solution space is searched to promote the quality of the membership functions. In this paper, we thus propose an evaluation function according to the one used in our previous approach [10] as shown below.

$$f(C_q) = \frac{\sum_{k=1}^{levels} | L_{1q}^k |}{suitabilit\,y(C_q)},$$

where the $| L_{1q}^k |$ is the number of large 1-itemsets in level k of chromosome C_q, $1 \le k \le levels$, and the $suitability(C_q)$ is used in the fitness function can reduce the occurrence of the two bad kinds of membership functions, where the first one is too redundant, and the second one is too separate. The suitability of the membership functions in a chromosome C_q is thus defined as:

$$suitability(C_q)$$
$$= \sum_{j=1}^{m} [\, overlap_factor(C_{qj}) + coverage_factor(C_{qj})],$$

where the overlap factor of the membership functions for an item class IC_j in the chromosome C_q is defined as:

$$overlap_factor(C_{qj}) = \sum_{k \ne i} [\max((\frac{overlap(R_{jk}, R_{ji})}{\min(w_{jk}, w_{ji})}), 1) - 1],$$

where the overlap ratio $overlap(R_{jk}, R_{ji})$ of two membership functions R_{jk} and R_{ji} is defined as the overlap length divided by half the minimum span of the two functions. If the overlap length is larger than half the span, then these two membership functions are thought of as a little redundant. Appropriate punishment must then be considered in this case.

The coverage ratio of a set of membership functions for an item class IC_j is defined as the coverage range of the functions divided by the average value of maximum quantity in each level of that item class in the transactions. The larger the coverage ratio is, the better the derived membership functions are. Thus, the coverage factor of the membership functions for an item class IC_j in the chromosome C_q is defined as:

$$coverage_factor(C_{qj}) = \frac{1}{\frac{range(R_{j1}, ..., R_{jl})}{avgmax(IC_j)}},$$

where $range(R_{j1}, R_{j2}, \ldots, R_{jl})$ is the coverage range of the membership functions, l is the number of membership functions for IC_j, and $avgMax(IC_j)$ is the average value of maximum quantity in each level of that item class in the transactions. Note that the overlap factor is designed for avoiding the first bad case "too redundant", and the coverage factor is for the second one "too separate".

C. Genetic Operators

Genetic operators are very important to the success of specific GA applications. Two genetic operators, the *max-min-arithmetical (MMA) crossover* proposed in [9] and the *one-point mutation*, are used in the genetic fuzzy mining framework. In the *max-min-arithmetical (MMA)* crossover operator, it will generate the following four candidate chromosomes from the given two chromosomes. Then, the best two chromosomes of the four candidates are then chosen as the offspring.

The one-point mutation operator will create a new fuzzy membership function by adding a random value ε, for example $\pm w_{jk}$, to the center or to the spread of an existing linguistic term, say R_{jk}. Assume that c and w represent the center and the spread of R_{jk}. The center or the spread of the newly derived membership function will be changed to $c + \varepsilon$ or $w + \varepsilon$ by the mutation operation. Mutation at the center of a fuzzy membership function may however disrupt the order of the resulting fuzzy membership functions. These fuzzy membership functions then need rearrangement according to their center values.

IV. The Proposed Multiple-Level Genetic-Fuzzy Mining Algorithm

According to the above description, the proposed multi-level genetic-fuzzy data mining algorithm for mining both membership functions and fuzzy association rules is described below.

The proposed multiple-level GFM algorithm:

INPUT: A body of n quantitative transaction data, a set of m items, each with a number of linguistic terms, codes of item names, a predefined taxonomy, a support threshold α, and a confidence threshold λ.

OUTPUT: A set of multiple-level fuzzy association rules with its associated set of membership functions.

STEP 1: Encode the predefined taxonomy using a sequence of numbers and the symbol "*", with the t-th number represents the branch number of a certain item on level t.

STEP 2: Translate the item names in the transaction data according to the encoding scheme.

STEP 3: Find level-k representation of the transaction data using following substeps:

SUBSTEP 3.1: Set $k = 1$, where k is used to store the level number being processed.

SUBSTEP 3.2: Group the items with the same first k digits in each transaction datum D_i, where $1 \le i \le$ n. Denote the j-th group on level k in transaction D_i as v^k_{ij}.

SUBSTEP 3.3: If level-k representation is not null, set $k = k + 1$ and go to SUBSTEP 3.2; otherwise, go to next step.

STEP 4: Randomly generate a population of P individuals; each individual is a set of membership functions for items in level-1 classes of the taxonomy.

STEP 5: Encode each set of membership functions into a string representation.

STEP 6: Calculate the fitness value of each chromosome by the following substeps:

SUBSTEP 6.1: Set $k = 1$, where k is used to store the level number being processed.

SUBSTEP 6.2: Transform the quantitative value v^k_{ij} of each transaction datum D_i (i =1 to n) for each encoded group name I^k_j into a fuzzy set f^k_{ij} represented as:

$$\left(\frac{f^{(k)}_{ij1}}{R^k_{j1}} + \frac{f^{(k)}_{ij2}}{R^k_{j2}} + ... + \frac{f^{(k)}_{ijh}}{R^k_{jh}} \right),$$

using the corresponding membership functions represented by the chromosome, where R^k_{jl} is the l-th fuzzy region of item I^k_j, $1 \le l \le$ h, f^k_{ij} is v^k_{ij}'s fuzzy membership value in region R^k_{jl}, and l (= $|I^k_j|$) is the number of linguistic terms for I^k_j.

SUBSTEP 6.3: Calculate the scalar cardinality of each fuzzy region R^k_{jl} in the transactions as follows:

$$count^k_{jl} = \sum_{i=1}^{n} f^k_{ijl} .$$

SUBSTEP 6.4: Check whether the value of each fuzzy region R^k_{jl} is larger than or equal to the predefined minimum support value α. If the value of a fuzzy region R^k_{jl} is equal to or greater than the minimum support value, put it in the large 1-itemsets ($L_1{}^k$) at level k. That is:

$$L_1{}^k = \{ R_{jl}{}^k \mid count_{jl}{}^k \ge \alpha, 1 \le j \le m^k, 1 \le l \le \text{h} \}.$$

SUBSTEP 6.5: If level-k representation is not null, set $k = k + 1$ and go to SUBSTEP 6.1; otherwise, go to next step.

STEP 7: Set the fitness value of the chromosome as the summation of the number of large 1-itemsets in L_1^k for all levels divides by its suitability *suitability*(C_q) as follows:

$$f(C_q) = \frac{\sum_{k=1}^{levels} |L_1^k|}{suitability(C_q)}.$$

STEP 8: Execute crossover operations on the population.
STEP 9: Execute mutation operations on the population.
STEP 10: Using the *selection* criteria to choose individuals for the next generation.
STEP 11: If the termination criterion is not satisfied, go to Step 6; otherwise, do the next step.
STEP 12: Output the set of membership functions with the highest fitness value.

The set of membership functions are then used to mine multiple-level fuzzy association rules from the given transactions. The multiple-level fuzzy mining algorithm proposed in [12] is then adopted to achieve this purpose.

V. Experimental Results

In this section, experiments made to show the performance of the proposed approach are described. They were implemented in Java on a personal computer with Intel Core i5 CUP 661 @ 3.33GHz and 1.8GB RAM. And, 10000 transactions were used in the experiments. The initial population size P was set at 50, the crossover rate p_c was set at 0.8, and the mutation rate p_m was set at 0.001. The parameter d of the crossover operator was set at 0.35 according to [9] and the minimum support α was set at 0.04 (4%).

There were 64 purchased items (terminal nodes) on level 3, 16 generalized items on level 2, and 4 generalized items on level 1. Each non-terminal node had four branches. Only the terminal nodes could appear in transactions. Data sets with different numbers of transactions were run by the proposed algorithm. In the data set, numbers of purchased items in transactions were first randomly generated. The purchased items and their quantities in each transaction were then generated. An item could not be generated twice in a transaction.

After 500 generations, the final membership functions are apparently much better than the original ones. For example, the initial membership functions of four item classes are shown in Figure 3.

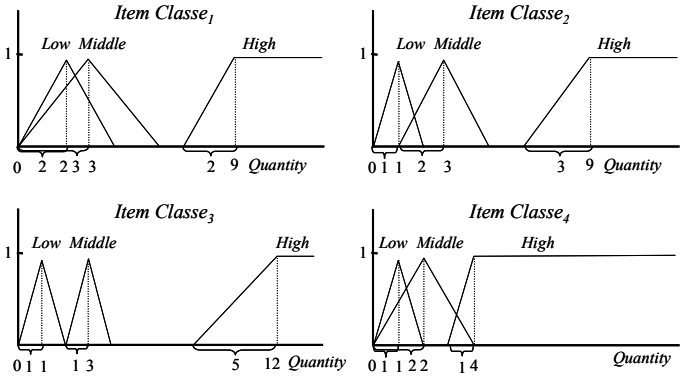

Figure 3. The initial membership functions of four item classes

In Figure 3, the membership functions have the two bad types of shapes according to the definition in the previous section. The membership functions of *Item Class*$_1$, *Item Class*$_2$ and *Item Class*$_3$ are "too separate". The membership functions of *Item Class*$_1$ and *Item Class*$_4$ are "too redundant". After 500 generations, the final membership functions for the four item classes are shown in Figure 4.

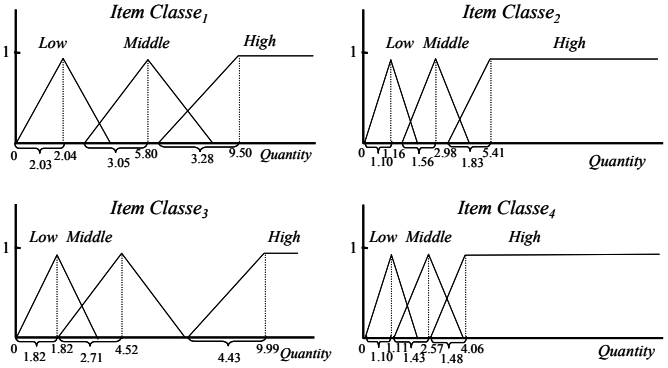

Figure 4. The final membership functions of four item classes after 500 generations

It is easily seen that the membership functions in Figure 4 is better than those in Figure 3. The two bad kinds of membership functions didn't appear in the final results. Then, the five runs average value of average fitness values of the chromosomes along with different numbers of generations are shown in Figure 5.

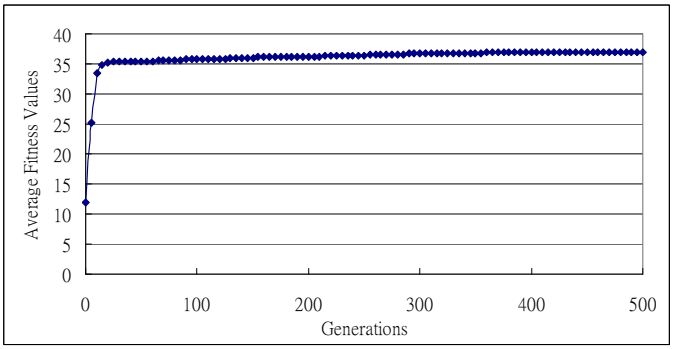

Figure 5. The five runs average values of average fitness values along with different numbers of generations

From Figure 5, we can observe that the curve gradually goes upward, finally converging to a certain value.

VI. Conclusion And Future Works

In this paper, we first propose a Multiple-level Genetic-Fuzzy Mining (Multiple-level GFM) framework for searching membership functions suitable for multiple-level mining problems and then use the final best set of membership functions to mine multiple-level fuzzy association rules. Then, a Multiple-level GFM algorithm is proposed. Experiments on a simulation dataset were also made to show the effectiveness and stableness of the proposed approach. The main contribution of this work is that the proposed algorithm is the first work for mining both membership functions and fuzzy association rules on multiple-concept levels. However, the

proposed approach is just a beginning. In the future, we will continuously to enhance the Multiple-level GFM framework for more complex problems.

ACKNOWLEDGMENT

This research was supported by the National Science Council of the Republic of China under contract NSC 99-2218-E-032 -005.

REFERENCES

[1] R.Alcala, J.Alcala-Fdez, F.Herrera, "Aproposal for the genetic lateral tuning of linguistic fuzzy systems and its interaction with rule selection," *IEEE Transaction on Fuzzy Systems,* Vol. 15, No. 4, pp. 616-635, 2007.

[2] R. Agrawal and R. Srikant, "Fast algorithm for mining association rules," *The International Conference on Very Large Databases*, pp. 487-499, 1994.

[3] J. Alcala-Fdez, R. Alcala, M. J. Gacto, F. Herrera, "Learning the membership function contexts for mining fuzzy association rules by using genetic algorithms," *Fuzzy Sets and Systems*, Vol. 160, No. 7, pp. 905-921, 2009.

[4] S. Brin, R. Motwani, J. D. Ullman and S. Tsur, "Dynamic itemset counting and implication rules for market-basket data," ACM-SIGMOD International Conference in Management of Data, pp. 207-216, 1997.

[5] C. H. Cai, W. C. Fu, C. H. Cheng and W. W. Kwong, "Mining association rules with weighted items," *The International Database Engineering and Applications Symposium*, pp. 68-77, 1998.

[6] C. H. Chen, T. P. Hong, Vincent S. Tseng, "A SPEA2-based genetic-fuzzy mining algorithm," *The IEEE International Conference on Fuzzy Systems*, 2010.

[7] O. Cordón, F. Herrera, and P. Villar, "Generating the knowledge base of a fuzzy rule-based system by the genetic learning of the data base," *IEEE Transactions on Fuzzy Systems*, Vol. 9, No. 4, 2001.

[8] J. Han and Y. Fu, "Discovery of multiple-level association rules from large databases," The International Conference on Very Large Data Bases, pp. 420-431, 1995.

[9] F. Herrera, M. Lozano and J. L. Verdegay, "Fuzzy connectives based crossover operators to model genetic algorithms population diversity," *Fuzzy Sets and Systems,* Vol. 92, No. 1, pp. 21–30, 1997.

[10] T. P. Hong, C. H. Chen, Y. L. Wu and Y. C. Lee, "A GA-based fuzzy mining approach to achieve a trade-off between number of rules and suitability of membership functions", *Soft Computing*, Vol. 10, No. 11, pp. 1091-1101. 2006.

[11] T. P. Hong, C. S. Kuo and S. C. Chi, "Mining association rules from quantitative data", *Intelligent Data Analysis*, Vol. 3, No. 5, pp. 363-376, 1999.

[12] T. P. Hong, K. Y. Lin, B. C. Chien, "Mining Fuzzy Multiple-Level Association Rules from Quantitative Data," *Applied Intelligence*, Vol. 18, No. 1, pp. 79-90, 2003.

[13] M. Kaya, R. Alhajj, "Genetic algorithm based framework for mining fuzzy association rules," *Fuzzy Sets and Systems*, Vol. 152, No. 3, pp. 587-601, 2005.

[14] M. Kaya, R. Alhajj, "Effective Mining of Fuzzy Multi-Cross-Level Weighted Association Rules," *Lecture Notes in Computer Science*, Vol. 4203, pp. 399-408, 2006.

[15] M. Kaya, R. Alhajj, "Utilizing Genetic Algorithms to Optimize Membership Functions for Fuzzy Weighted Association Rules Mining," *Applied Intelligence*, Vol. 24, No. 1, pp. 7-15, 2006.

[16] K. M. Lee, "Mining generalized fuzzy quantitative association rules with fuzzy generalization hierarchies," *IFSA World Congress and 20th NAFIPS International Conference*, Vol. 5, pp. 2977-2982, 2001.

[17] Y. C. Lee, T. P. Hong and W. Y. Lin, "Mining fuzzy association rules with multiple minimum supports using maximum constraints", *Lecture Notes in Computer Science*, Vol. 3214, pp. 1283-1290, 2004.

[18] Y. C. Lee, T. P. Hong, T. C. Wang, "Mining Multiple-Level Association Rules Under the Maximum Constraint of Multiple Minimum Supports," *IEA/AIE*, pp. 1329-1338, 2006.

[19] Y. C. Lee, T. P. Hong, T. C. Wang, "Multi-level fuzzy mining with multiple minimum supports," *Expert Systems with Applications*, Vol. 34, No. 1, pp. 459-468, 2008.

[20] A. Parodi and P. Bonelli, "A new approach of fuzzy classifier systems," *Proceedings of Fifth International Conference on Genetic Algorithms*, Morgan Kaufmann, Los Altos, CA, pp. 223-230, 1993.

[21] A. Savasere, E. Omiecinski and S. Navathe, "An efficient algorithm for mining association rules in large databases," The International Conference in Very Large Data Bases, pp. 432-443, 1995.

[22] R. Srikant and R. Agrawal, "Mining generalized association rules," The International Conference on Very Large Data Bases, pp. 407-419, 1995.

[23] C. H. Wang, T. P. Hong and S. S. Tseng, "Integrating membership functions and fuzzy rule sets from multiple knowledge sources," *Fuzzy Sets and Systems,* Vol. 112, pp. 141-154, 2000.

[24] S. Yue, E. Tsang, D. Yeung and D. Shi, "Mining fuzzy association rules with weighted items," *The IEEE International Conference on Systems, Man and Cybernetics*, pp. 1906-1911, 2000.

[25] J. S. Park, M. S. Chen and P. S. Yu, "An Effective hash-based algorithm for mining association rules," The ACM-SIGMOD International Conference in Management of Data, pp. 175-186, 1995.

2011 IEEE International Conference on Fuzzy Systems
June 27-30, 2011, Taipei, Taiwan

An Architecture for Constructing Fuzzy Regression Tree Forests Using Opt-aiNet

Fathi Gasir
Intelligent Systems Group
School of CMDT
MMU
Manchester, UK
f.gasir@mmu.ac.uk

Zuhair Bandar
Intelligent Systems Group
School of CMDT
MMU
Manchester, UK
z.bandar@mmu.ac.uk

Keeley Crockett
Intelligent Systems Group
School of CMDT
MMU
Manchester, UK
k.crockett@mmu.ac.uk

Abstract— **This paper presents a new approach to combining multiple fuzzy regression trees, which are induced by applying the modified Elgasir fuzzy regression tree algorithm. This method utilises Trapezoidal membership functions for fuzzification and the Takagi-Sugeno fuzzy inference to obtain the final predicted values. A modified version of Artificial Immune Network model (opt-aiNet) is used for the simultaneous optimization of the membership functions across all trees within the forest. Boston housing and Abalone are two real-world datasets from the UCI repository used to evaluate the proposed approach. The empirical results have showed that fuzzy regression tree forests reduce the error rate compared with single fuzzy regression tree.**

Keywords: *fuzzy regression tree forests***,** *Fuzzy inference system, Fuzzy Regression tree, Data mining, Machine learning, Evolutionary algorithms, Artificial Immune system.*

I. INTRODUCTION

Decision trees are a transparent method of representing a set of IF-THEN rules in a graphical way and are generated by learning and reasoning from feature-based examples. There are two well known and distinctive methods for generating decision trees: Regression trees [1,2,3,4,5,6] which are designed to predict continuous outcomes and Classification trees [7,8,9,10,11] which predict discrete outcome classes. AID [12], CHAID [13] and CART (classification and regression tree) [14,15] are crisp regression trees algorithms that describe the approach of building regression trees based on information theory. A well documented weakness of these algorithms is that they induce trees with sharp decision boundaries when the decision space of continuous attributes is partitioned. Moreover the output of crisp regression trees are generated using a discrete function which clearly decreases the prediction accuracy and affect the robustness of the generation crisp regression trees [1,2,3,4].

The application of fuzzy logic to the crisp regression trees has shown improvement in the performance of the traditional regression trees [1...6,16]. This has been achieved using fuzzy membership functions at each crisp regression tree node to soften the sharp node boundaries. The Fuzzy CHAID Induction Algorithm was first proposed by Fowdar et al [5,6] to generate regression trees by using the CHAID algorithm and optimising the amount of Fuzzification using a Genetic Algorithm (GA). The main weakness of Fowdars' approach was in the defuzzification strategy as it could lead to less accurate prediction as a result of using one of varied defuzzification methods to calculate the final output.

The Elgasir algorithm [2] is a method for creating fuzzy regression trees [1] by formulating trapezoidal membership functions for each node in the pre-generated crisp regression trees. This algorithm has shown the capability of overcoming the weakness of crisp decision trees by applying appropriate membership functions for all branch split points, and using Takagi-Sugeno fuzzy inference technique [17] to generate a final continuous output value. Elgasir has successfully alleviated Fowdar's defuzzification problem as a result of having a single numeric value as the output of fuzzy inference [17]. Fuzzification has been successfully used with multiple decision trees models [16,23…26] to induce fuzzy decision tree forests in order to improve the predictive power of a single fuzzy decision tree. Although the use of multiple regression trees has been used to improve the performance of a single fuzzy regression tree [16], little work has been done in this field.

Immune algorithms have been used to solve optimization problems [18] such as: design optimization task for electromagnetic devices [19], optimizing the dynamic function [20] and optimization of a weapon-target assignment problem [21]. An adapted version of Artificial Immune Network model (opt-aiNet) [22] was proposed in [2] to enable the algorithm to be applied to the optimization of fuzzy regression trees and the algorithm was successfully applied to the Elgasir [2]. The adapted version of an artificial immune network model (opt-aiNet) [2] is used in this work for optimizing the proposed framework.

This paper proposes a new approach which applies a modified version of the Elgasir algorithm to the task of creating fuzzy regression tree forests. The modification of the Elgasir algorithm has been done based on an approach by Crockett et al for growing a fuzzy classification based decision tree forest. In the modified Elgasir algorithm, a number of fuzzy regression trees are generated from one training sample, where each tree represents a different view

978-1-4244-7316-8/11/$26.00 ©2011 IEEE

of the problem domain and will represent different associations of independent variables for the same dataset.

The organisation of this paper as follows: Section II provides some background information on Fuzzy Forests. Section III provides a brief outline of the Elgasir algorithm. Section IV describes the methodology used for constructing fuzzy regression tree forests Section V describes the conducted experiments and section VI presents the results and discussion. Finally the paper is concluded in section VII.

II. Fuzzy Forests

Fuzzy multiple decision trees forests models [16, 23… 26] have been used to combine more than one fuzzy decision tree in order to improve the predictive power of a single fuzzy decision tree. Different approaches have been proposed for classification problems [23…26]. These approaches can be described as tree-based ensemble classifiers [23], but they differ by the way that used to induce multiple trees. Bonissone et al [23] have applied fuzzy logic and fuzzy sets to random forest to produce multiple fuzzy classifier system. In Bonissone's method a fuzzy random forest is created by combining several individual classifiers based on Breiman's methodology [27]. This method used a random subset of the total set of available attributes to construct each node. Marsala and Bouchon-Meunier presented a method for generating forests of fuzzy decision trees [24], where each fuzzy decision tree of the forest is induced from a random subset of the whole training dataset. With theses two methods there is no guarantee that the information space has been explored exhaustively. Cezary and Janikow [25] induced fuzzy decision forests by allowing the usage of more than one test attribute at a non‐leaf node. Although this approach can overcome noisy or missing values problems, but it has been unstable [28]. Crockett et al [26] introduced an approach for growing a fuzzy decision forest. In this approach, multiple classification trees are created from same training sample and the strategy for adding classification tree is by restriction the attribute which has highest-ranking to be the root of the tree. This method was shown to be successful but if the number of trees in the forest has a limit in terms of improving performance and once a certain threshold is reached, overfitting of the training set will start to occur. However it was shown that if the number of trees was kept small, then the results justify the computational expense and provide a practical way of improving the classification accuracy. For regression problems, Haskell [16] proposed a method to induce a fuzzy regression trees forest, which used a new splitting criteria based on a generalized Kolmogorov-Smirnov distance to construct fuzzy regression trees associated with a fuzzy cumulative distribution function. The main problem with this method is that a human expert is needed to provide pre-fuzzified data, despite the number and size of the membership functions being automatically determined in Haskell's method.

III. Elgasir Algorithm

The Elgasir algorithm, originally proposed in [1], combined principles of fuzzy theory and Takagi-Sugeno fuzzy inference [17] to generate fuzzy regression trees. This algorithm does not require pre-fuzzified data and therefore can overcome the problems of unnecessary complexity and poor transparency problems often resulting from algorithms which generate fuzzy trees directly from data which has been pre-fuzzified by experts in the domain. Another advantage of the Elgasir algorithm is that the output of fuzzy inference is a single numeric value as a result of using Takagi-Sugeno fuzzy inference technique. In other words, there is no need for a defuzzification operation to calculate the output of the fuzzy regression tree. This has shown to lead to more accurate results by avoiding doing more calculations to transform the output fuzzy sets into a non-fuzzy output [1,2].

The fuzzy rule base generated by Elgasir is produced by applying Trapezoidal membership function to crisp CHAID regression trees. The algorithm is not restricted to just Trapezoidal membership functions and any other membership function can be applied. In addition, the Elgasir methodology can be applied to any other crisp regression tree algorithm. For the purpose of this work the CHAID regression tree algorithm has been used [13]. Full details of the original Elgasir algorithm can be found in [1].

IV. Modified Elgasir Algorithm for Constructing Fuzzy Regression Tree Forests

The modified Elgasir algorithm is the new version of Elgasir algorithm [1], which is used to induce a fuzzy regression tree forest by combing two or more singular fuzzy regression trees, where each one represents a different view of the same domain. The algorithm is optimized using the adapted version of an artificial immune network model (opt-aiNet) [2] in order to establish the optimum fuzzification throughout the tree.

The modified Elgasir algorithm consists of the following stages:

The first stage: multiple crisp regression trees induction

1.1 Creating a series of crisp regression trees:
The CHAID algorithm [13] is used to construct an optimal singular crisp regression tree by applying various values of CHAID algorithm parameters in order to produce a highly optimised regression tree. The attribute selection, branching strategy and terminate growth criteria for growing a crisp tree are based on the information measure entropy. To induce the second crisp regression tree form the same dataset, the attribute which has the smallest adjusted p-value (the highest ranking) is restricted from formulating the root of the second crisp regression tree. This process is repeated in each creating of crisp regression tree. The result is a combination of crisp regression trees, where each tree is

different in representing the association of independent variables for the same dataset.

1.2 Generating IF-THEN rules:

The combination of crisp regression trees are converted into a set of IF-THEN production rules in-order to create a knowledge base using a one-to-one mapping. Each rule represents a path from the root to the leaf node in each crisp CHAID regression tree. The form of the typical rule as following:

$$R_i : \text{IF } x_1 \text{ is } b_{i1} \text{ and....and } x_k \text{ is } b_{ik} \text{ THEN } y_i = b_{i0} \quad (1)$$

where $R_i (i = 1,2,..., n)$ denotes the ith rule, $x_j (j = 1,2,.....,k)$ are the input (antecedent) variables, y_i are the rule output variables, $b_{i0} (i = 1,2,..., n)$ are real numbers.

Due to method used to create each tree there will be no duplication of rules and hence no redundancy.

The Second Stage: applying membership functions and fuzzy inference technique

Appropriate membership functions are applied for all branch split points i within the antecedent rules and the consequent part of rules (1) are parameterized. Then a typical fuzzy rule can be defined as:

$$R_i : \text{IF } x_1 \text{ is } A_{i1} \text{ and } .... \text{ and } x_k \text{ is } A_{ik} \text{ THEN } y_i = \rho_i b_{i0} + a_{i1}.x_1 + ... + a_{ik}.x_k$$

Let $\rho_i b_{i0}, = a_{i0}$ then

$$R_i : \text{IF } x_1 \text{ is } A_{i1} \text{ and } .... \text{ and } x_k \text{ is } A_{ik} \text{ THEN } y_i = a_{i0} + a_{i1}.x_1 + ... + a_{ik}.x_k \quad (2)$$

where $R_i (i = 1,2,..., n)$ denotes the ith fuzzy rule, $x_j (j = 1,2,.....,k)$ are the input (antecedent) variables, y_i are the rule output variables, $A_{i1}, ..., A_{ik}$ are fuzzy sets defined in the antecedent space, and $a_{i0}, a_{i1}, ..., a_{ik}$ are the consequent parameters.

The inferred global output of the proposed framework is computed by taking the weighted average of the individual rules' contributions defined as:

$$y = \frac{\sum_{i=1}^{n} \tau_i(x).(a_{i0} + a_{i1}.x_1 + ... + a_{ik}.x_k)}{\sum_{i=1}^{n} \tau_i(x)} \quad (3)$$

where $\tau_i(x)$ is the degree of fulfilment of the ith fuzzy rule, defined by

$$\tau_i(x) = \min\{\mu_{A_{i1}}(x_1)....\mu_{A_{ik}}(x_k)\}$$

In order to Identify the consequent parameters

Let β_i be

$$\beta_i = \frac{\tau_i(x)}{\sum_{i=1}^{n} \tau_i(x)} \quad (4)$$

then

$$y = \sum_{i=1}^{n} \beta_i.(a_{i0} + a_{i1}.x_1 + ... + a_{ik}.x_k)$$

$$y = \sum_{i=1}^{n} (\beta_i.a_{i0} + \beta_i.a_{i1}.x_1 + ... + \beta_i.a_{ik}.x_k)$$

When we apply a set dataset $x_{j1}, .x_{j2}, ..., x_{jk}$ then the value of the outputs y_j

where $(j = 1,2,..., m)$ as

$$y_1 = (\beta_{11}.a_{10} + \beta_{11}.a_{11}.x_{11} + ... + \beta_{11}.a_{1k}.x_{1k}) + ... + (\beta_{1n}.a_{n0} + \beta_{1n}.a_{n1}.x_{11} + ... + \beta_{1n}.a_{nk}.x_{1k})$$

.

.

.

$$y_m = (\beta_{m1}.a_{10} + \beta_{m1}.a_{11}.x_{m1} + ... + \beta_{m1}.a_{1k}.x_{mk}) + ... + (\beta_{mn}.a_{n0} + \beta_{mn}.a_{n1}.x_{m1} + ... + \beta_{mn}.a_{nk}.x_{mk})$$

The consequent parameters $a_{i0}, a_{i1}, ..., a_{ik}$ $(i = 1,2,..., n)$ can be obtained using the least square method by combining previous equations

Using matrixes and vectors;

Least square equation can be expressed as:

$$Y = \begin{bmatrix} y_j \\ . \\ . \\ . \\ y_m \end{bmatrix}, X = \begin{bmatrix} \beta_{11}, \beta_{11}.x_{11}, ..., \beta_{11}.x_{1k}, ..., \beta_{1n}, \beta_{1n}.x_{11}, ..., \beta_{1n}.x_{1k} \\ . \\ . \\ . \\ \beta_{m1}, \beta_{m1}.x_{m1}, ..., \beta_{m1}.x_{mk}, ..., \beta_{mn}, \beta_{mn}.x_{m1}, ..., \beta_{mn}.x_{mk} \end{bmatrix}, A = \begin{bmatrix} a_{10} \\ a_{11} \\ \vdots \\ a_{1k} \\ \vdots \\ a_{n0} \\ a_{n1} \\ \vdots \\ a_{nk} \end{bmatrix}$$

Where

$$Y = XA$$

X(m×n(k+1) matrix), Y (m vector) and A (n(k+1) vector).

Then the parameter vector A is given by

$$A = (X^T X)^{-1} X^T Y$$

The Third Stage: Optimization

The modified Elgasir algorithm is optimized using the adapted version of an artificial immune network model (opt-aiNet) [2] which is described in Figure 2

```
Initialization: randomly initialize a population
while (stopping criterion is not met)
 {
     for each network cell
     {
     Determine the fitness
      }
      -Normalize the vector of fitness's in the interval [0,1],
        where 0 is assigned to the highest fitness, while 1 is
        assigned to the lowest fitness.
      for each network cell
      {
          Generate a number of clones Nc
       for each clone
          {
               -Mutate each clone proportionally to the fitness
                of its parent cell.
               -Determine the fitness
               -Select the cell with lowest fitness
               -if fitness of best clone less than its parent
                {
                The clone replaces the parent in the network
                }
           }
          }
         if the average error of the population is not
         significantly different from the previous iteration
       {
                    for each network cell
                    {
                      -calculate the affinity between this
                        network  cell and the other network cells
                      -if two cells have an affinity below a
                        pre-defined threshold
                     {
                          the cell with the highest fitness is
                          deleted from the network
                     }
                    }
                    if maximum iteration reached, or there
                    has been no change in the number of cells
                    in the network since the last iteration
                    {
                       Terminate the loop
               }
                    else
                    {
                      Introduce a percentage d% of randomly
                      generated cells
                    }
          }
 }
```

Fig. 2 The modified algorithm opt-aiNet for Elgasir optimization

In order to determine the optimal domain delimiters for the membership function of each node in the regression tree. The membership function $f(x,a,b,c,d)$ is defined as:

$$f(x,a,b,c,d) = \begin{cases} 0 & \text{for } x < a \\ \dfrac{x-a}{b-a} & \text{for } a \le x < b \\ 1 & \text{for } b \le x < c \\ \dfrac{d-x}{d-c} & \text{for } c \le x \le d \\ 0 & \text{for d} < x \end{cases}$$

where

$a = \mathrm{i} - n\sigma$
$b = \mathrm{i} - \alpha$
$c = \mathrm{i} + \alpha$
$d = \mathrm{i} + n\sigma$

where σ is the standard deviation, x is value of attribute A.
$\alpha = m\sigma$ where m = 0.0001, 0.001, 0.01 0.1, n is a real number $n \to [0,\infty]$

The initial membership functions are selected to give fuzzy rules set that are equivalent to crisp rules set where $\sigma = 0$.

Figure.3 shows a generalised example of the tuning of membership function domain delimiters which shows Trapezoidal membership function f of domain $a \ldots d$ that creates a fuzzy region around threshold i.

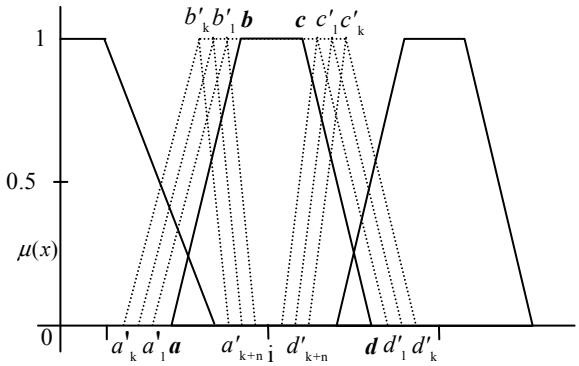

Fig .3 Optimization of Trapezoidal membership function

This optimization system is used to tune the position of the domain delimiters of each membership function, so the points (***a***,***b***,***c***,***d***) can be directed with the constraint $a \le b \le i \le c \le d$ to produce (a'_k, b'_k, c'_k, d'_k). where k and n are natural numbers.

Four domain delimiters (a,b,c,d) are used to represent the membership function within The proposed Elgasir optimization framework as following:
Let Z is a complete set of domain delimiters for a fuzzy regression tree consisting of z branches.

$$Z = \{(a_1,b_1,c_1,d_1), (a_2,b_2,c_2,d_2), \ldots\ldots, (a_z,b_z,c_z,d_z)\}$$

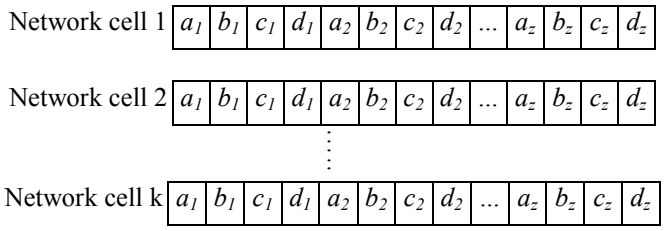

Fig. 4 Network cell representation for fuzzy regression tree.

Figure 4 shows the Network cell representation for membership functions domain delimiters of fuzzy regression tree where *a,b,c,d* real numbers.

The performance of the tree is evaluated by using the MSE (mean square error) which is defined in equation (5).

$$\text{Performance of fuzzy system} = \frac{\sum_{y=1}^{n} (\text{PredictedValue} - \text{ActualValue})^2}{n} \quad (5)$$

Where n = Number of records in the dataset.

V. Experiments

A. Datasets

Experiments were undertaken on two real-valued datasets which known as Boston housing and Abalone datasets. These datasets have numeric outcomes and were retrieved form the well known UCI machine learning repository [29]. The Boston housing dataset consists of 506 records with thirteen continuous attributes and one binary-valued attribute and it has 229 unique outcome values. This dataset is used to predict the Median value of owner occupied homes. The Abalone dataset comprises 4177 instances featuring eight continuous attributes and it has 28 unique outcome values. This data set is concerned with predicting the age of abalone from physical measurements. The main characteristics of these datasets are presented in Table I.

TABLE I
THE MAIN CHARACTERISTICS OF DATASETS

Name	Number of instances	Unique values
boston housing dataset	506	229
abalone dataset	4177	28

B. Methodology

The cross validation approach was used for each experiment. The dataset is divided to n equal-sized disjoint blocks. Each block in turn is used to evaluate both the crisp and the fuzzy trees, which are generated by the remaining $n-1$ blocks. In this work 10-fold cross validation were applied to both datasets. A singular crisp regression tree was first created using the training dataset with various values of the CHAID regression parameters. These parameters include: merge threshold, split threshold, tree depth, node size and child node size. Each parameter was examined in turn to obtain the optimal crisp regression tree. The attribute which has the smallest adjusted p-value (the highest ranking) was restricted from formulating the root of the second crisp regression tree. Hence, this tree will be different in representing the association of independent variables for the same dataset. This process was repeated until 5 crisp regression trees were created. The number of trees was empirically defined by a series of initial experiments which obtained the tree growth saturation threshold of 5. Emperically these experiments showed that no further improvement could be achieved from creating further regression trees of the domain. A set of IF-THEN rules were extracted from the combination of crisp CHAID regression trees. Then the fizzification was applied to these set of IF-THEN rules.

TABLE II- THE OPT-AINET PARAMETERS VALUES

NAME	VALUE
Iterations number	500
Population size	100
Clones number	15
Suppression threshold	0.175
Average error threshold	0.001
Percentage of newcomers	50%
Affinity proportional	75

The adapted version of an artificial immune network model (opt-aiNet) [2] was used to determine the most appropriate domain delimiters of Trapezoidal membership function. Table II presents a summary of the adapted opt-aiNet parameters values which were empirically defined by a series of initial experiments [2].

VI. Results and Discussion

Tables III-VI show the results achieved by the proposed framework for both Abalone and Boston housing datasets. The results show a comparison of results between singular crisp regression trees and fuzzy regression tree forest.

TABLE III
SINGULAR CRISP REGRESSION TREES RESULTS
(ABALONE DATASET)

Tree number	Training dataset (error value)	Test dataset (error value)
1	4.5091	4.5138
2	4.4082	4.4162
3	4.4066	4.4151
4	4.5184	4.5431
5	4.5742	4.6029

TABLE IV
FUZZY REGRESSION TREE FORESTS RESULTS
(ABALONE DATASET)

No of trees	Training dataset (error value)	Test dataset (error value)
1	2.5169	2.8624
2	2.3061	2.4711
3	2.3041	2.4708
4	2.3537	2.4885
5	2.6150	2.9797

TABLE V
SINGULAR CRISP REGRESSION TREES RESULTS
(BOSTON HOUSING DATASET)

Tree number	Training dataset (error value)	Test dataset (error value)
1	21.1749	21.5082
2	20.6497	21.0358
3	20.6562	21.0436
4	20.9841	21.4084
5	21.8231	22.0471

TABLE VI
FUZZY REGRESSION TREE FORESTS RESULTS
(BOSTON HOUSING DATASET)

No of trees	Training dataset (error value)	Test dataset (error value)
1	13.3983	15.9891
2	13.2702	15.6417
3	13.2926	15.6801
4	13.3892	15.7990
5	13.9587	16.3765

For both Abalone and Boston housing datasets the tables III and V show the results of five singular crisp regression trees while the tables IV and VI present the results of combining up to 5 fuzzy regression trees. The tables present the mean square error which was obtained by Equation (5).

The results in Tables III-VI confirmed that the proposed method for creating multiple fuzzy regression trees improves the performance of prediction. The Abalone dataset results show that the combination of three fuzzy regression trees obtained the best rest which reduced the error rate by 14% compared to singular fuzzy regression tree. The biggest improvement in performance for the proposed method with the Boston housing dataset was obtained by the combination of two fuzzy regression trees which reduced the error rate by 2% compared to singular fuzzy regression tree. The proposed framework is most effective on continuous attributes, which is reflected in the improvement of the Abalone dataset. As the number of fuzzy regression tree in the forest increases up to a certain threshold, the prediction accuracy also improves to degree, and once this threshold is reached, overfitting of the training dataset starts to occur, which is dependent on the type, value, distribution and nature of dataset.

VII. CONCLUSION

This study introduced a new framework to creating a fuzzy regression trees forests using the modified Elgasir algorithm. The CHAID algorithm was selected for this work used to induce crisp regression trees. The modified Elgasir algorithm was applied to generate fuzzy regression trees forests using Trapezoidal membership functions to represent tree nodes and the Takagi-Sugeno fuzzy inference technique to combine values down each path. The adapted version of an artificial immune network model (opt-aiNet) was used to optimize the membership functions of the proposed method. The results from two real-valued datasets show that combine fuzzy regression trees can improve the performance by incorporating information from different perspectives of the same dataset. This framework offer promising results in using this kind of technique to reduce the error rate of single fuzzy regression trees. Further studies involve investigating the effects of more complex dataset characteristics in the performance of the proposed method, and comparing the results of the new approach with other approaches to inducing multiple fuzzy regression trees.

REFERENCES

[1] Gasir, F. Bandar, Z. Crockett, K., Elgasir: An algorithm for creating Fuzzy Regression Trees. FUZZ-IEEE International Conference on Fuzzy Systems, Jeju Island, Korea, pp 332-337, 2009.

[2] Gasir, F. Bandar, Z. Crockett, K. Crispin, A., Immune Engineering for Elgasir algorithm optimization. IEEE World Congress on Computational Intelligence, Barcelona, Spain, pp 1918-1924, 2010.

[3] Gasir, F. Bandar, Z. Crockett, K., On Application of Artificial Immune System to Optimize Fuzzy Regression Trees. IEEE International Conference on Systems, Man, and Cybernetics, Istanbul, Turkey, pp 2442-2447, 2010.

[4] Gasir, F. Bandar, Z. Crockett, K., The Effect of Datasets Characteristic in The Induction of Fuzzy Regression Trees Using Elgasir. The International Arab Conference on Information Technology, Benghazi, Libya, 2010

[5] Fowdar, J. Crockett, K. Bandar, Z., On the Use of Fuzzy Trees for Solving Classification Problems with Numeric Outcomes. 2005 IEEE Conference on Fuzzy Systems, Nevada, USA , 2005.

[6] Crockett, K , Bandar, Z. Fowdar, J, O'Shea, J., "Genetic Tuning of Fuzzy Inference within Fuzzy Classifier Systems," The International Journal of Expert Systems, Vol 23, No2, pp 63-82, 2006.

[7] Quinlan, J.R., Induction of Decision Trees, Machine Learning, 1, pp. 81-106, 1986.

[8] Quinlan, J.R., C4.5 program for machine learning, Morgan Kaufmann Publishrs, 1993.

[9] Quinlan, J.R.,, (2002) Is C5.0 better than C4.5; available at ttp://www.rulequest.com/see5-comparison html.

[10] Leland Wilkinson, Tree Structured Data Analysis: AID, CHAID and CART. Sun Valley, ID, Sawtooth/SYSTAT Joint Software Conference, 1992.

[11] Servane Gey and Elodie Nedelec, Model Selection for CART Regression Trees, IEEE Transactions on Information Theory, 51, pp.658-670, 2005.

[12] Morgan, J. N. Sonquist, J. A., Problems in the Analysis of Survey Data and a Proposal, American Statistical Association Journal 58, pp 415-434, 1963.

[13] Kass, G. V., An Exploratory Technique For Investigating Large Quantities Of Categorical Data, Applied Statistics, 29(2) pp 119-127, 1979.

[14] Wilkinson, L., Tree Structured Data Analysis: AID, CHAID and CART. Sun Valley, ID, Sawtooth/SYSTAT Joint Software Conference, 1992..

[15] Gey, S. Nedelec, E., Model Selection for CART Regression Trees, IEEE Transactions on Information Theory, 51, pp.658-670, 2005.

[16] Haskell, R. E., Regression Tree Fuzzy Systems, Proc. ICSC Symposium on Soft Computing, Fuzzy Logic, Artificial Neural Networks and Genetic Algorithms, University of Reading, Whiteknights, Reading, England, pp. B.1–B.6, 1996.

[17] Takagi, T. Sugeno, M., Fuzzy identification of a system and its application to modeling and control, IEEE Trans. Syst. Man and Cybern., vol.15, pp.116-132, 1985.

[18] Cutello, V. Nicosia, G. Oliveto, P. S. Romeo, M., On the Convergence of Immune Algorithms, FOCI 2007, The First IEEE Symposium on Foundations of Computational Intelligence, 2007.

[19] Campelo, F., Guimares, F.G., Igarashi, H., Ramirez, J.A., Noguchi, S., A modified immune network algorithm for multi-modal electromagnetic problems, IEEE Trans. Magn. 42 (April (4)) (2006) 1111–1114, 2006.

[20] Walker, J.H. Garrett, S.M., Dynamic Function Optimization: Comparing the Performance of Clonal Selection and Evolution Strategies, Proceeding of Second International Conference on Artificial Immune Systems (ICARIS2003), Napier University, Edinburgh, UK, September 1-3 2003

[21] Lee, Z-J. Lee, C-Y. Su, S-F., An immunity based ant colony optimization algorithm for solving weapon-target assignment problem, Appl. Soft Comput. 2 (August (1)) (2002) 39–47, 2002.
[22] De Castro, L.N. Timmis, J., An Artificial Immune Network for Multimodal Function Optimisation. Proc. Of IEEE World Congress on Evolutionary Computation. Pp. 669-674, 2002.
[23] Piero P. Bonissone, José Manuel Cadenas, M. Carmen Garrido, R. Andrés Díaz-Valladares: A fuzzy random forest. Int. J. Approx. Reasoning 51(7): 729-747, 2010.
[24] C. Marsala and B. Bouchon-Meunier. Forest of fuzzy decision trees. In M. Mare˘s, R. Mesiar, V. Nov´ak, J. Ramik, and A. Stup˘nanov´a, editors, Proceedings of the Seventh International Fuzzy Systems Association World Congress, volume 1, pages 369–374, Prague, Czech Republic, June 1997.
[25] C. Z. Janikow and M. Faifer. Fuzzy decision forest. In Proceedings of the 19th International Conference of the North American Fuzzy Information Processing Society (NAFIPS'00), p 218–221, July 2000.
[26] Crockett, K, Bandar, Z. Mclean D. Growing a Fuzzy Decision Forest. The 10th IEEE International Conference on Fuzzy Systems - FUZZ-IEEE 2001 Melbourne Australia, ISBN 0-7803-7294-X, December 2001.
[27] L. Breiman, Random forests, Machine Learning 45 (1) (2001) 5–32.
[28] Abu-halaweh, Nael Mohammed, "Integrating Information Theory Measures and a Novel Rule-Set-Reduction Tech-nique to Improve Fuzzy Decision Tree Induction Algorithms" (2009). *Computer Science Dissertations.* Paper 48. http://digitalarchive.gsu.edu/cs_diss/48
[29] Blake, C. L. and C. J. Merz, UCI Repository of machine learning databases. Irvine, CA: Universit of California, Department of Information and Computer Science, 1998.

2011 IEEE International Conference on Fuzzy Systems
June 27-30, 2011, Taipei, Taiwan

Fuzzy C-Means Clustering and Partition Entropy for Species-Best Strategy and Search Mode Selection in Nonlinear Optimization by Differential Evolution

Tetsuyuki Takahama
Department of Intelligent Systems
Hiroshima City University
Asaminami-ku, Hiroshima, 731-3194 Japan
Email: takahama@info.hiroshima-cu.ac.jp

Setsuko Sakai
Faculty of Commercial Sciences
Hiroshima Shudo University
Asaminami-ku, Hiroshima, 731-3195 Japan
Email: setuko@shudo-u.ac.jp

***Abstract*— Differential Evolution (DE) is a newly proposed evolutionary algorithm. DE is a stochastic direct search method using a population or multiple search points. DE has been successfully applied to optimization problems including non-linear, non-differentiable, non-convex and multimodal functions. However, the performance of DE degrades in problems having strong dependence among variables, where variables are related strongly to each other. In this study, we propose to utilize partition entropy given by fuzzy clustering for solving the degradation. It is thought that a directional search is desirable when search points are distributed with bias. Thus, when the entropy is low, algorithm parameters can be controlled to make the directional search. Also, we propose to use a species-best strategy for improving the efficiency and the robustness of DE. The effect of the proposed method is shown by solving some benchmark problems.**

***Index Terms*—differential evolution; rotation-invariant; intensive search; extensive search**

I. Introduction

Optimization problems, especially nonlinear optimization problems, are very important and frequently appear in the real world. There exist many studies on solving optimization problems using evolutionary algorithms (EAs). Differential evolution (DE) is a newly proposed EA by Storn and Price [1]. DE is a stochastic direct search method using a population or multiple search points. DE has been successfully applied to optimization problems including non-linear, non-differentiable, non-convex and multimodal functions [2], [3]. It has been shown that DE is a very fast and robust algorithm.

However, the performance of DE degrades in problems having strong dependence among variables, where variables are related strongly to each other. It is very important to know the distribution of search points to solve the degradation. For example, when search points are uniformly distributed as in the left part of Fig. 1, a nondirectional search is the better choice than a directional search. On the contrary, when variables are strongly related as in the right part of the figure, a directional search is the better choice.

In this study, in order to know the distribution, we propose to utilize partition entropy given by fuzzy clustering. If the entropy is very high, search points are often uniformly distributed. If the entropy is low, search points are distributed with a bias. Thus, when the entropy is low, algorithm parameters can be controlled to make the directional search. It is thought that this idea can be applicable to other EAs than DE.

Also, we propose to use a species-best strategy [4] for improving the efficiency and the robustness of DE. In DE, a mutant vector is generated for each parent by using a base vector and one or more difference vectors which are the difference between two individuals. The parent and the mutant vector are recombined by a crossover operation to generate a child, or a trial vector. There are some strategies for selecting the base vector: The best individual is used as the base vector in the best strategy and a randomly selected individual is used in the rand strategy. In the species-best strategy, a population is divided into several species by speciation, and the seed of the species to which the parent belongs is selected as the base vector. It is thought that the efficiency of the species-best strategy is better than the rand strategy and the robustness of the species-best strategy is better than the best strategy. Thus, it is expected that the strategy improves the efficiency and the robustness of the search.

The effect of the proposed method is shown by solving 13 benchmark problems including multimodal problems and problems with strong dependence.

In Section II, some studies on DE using fuzzy set theory or speciation are briefly reviewed. Fuzzy clustering and par-

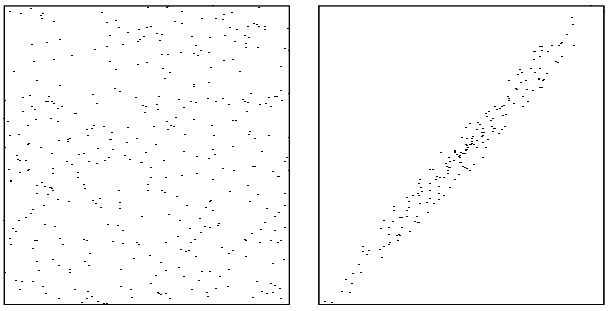

Fig. 1. Uniform Search (left) and Directional Search (right)

978-1-4244-7316-8/11/$26.00 ©2011 IEEE

tition entropy are explained in Section III. DE and DE with speciation using fuzzy clustering are described in Section IV and V, respectively. In Section VI, experimental results on some problems are shown. Finally, conclusions are described in Section VII.

II. Previous Works

In this section, the optimization problem in this study is defined and some studies on DE using fuzzy set theory or speciation are described.

A. Optimization Problems

In this study, the following optimization problem with lower bound and upper bound constraints will be discussed.

$$\begin{array}{ll} \text{minimize} & f(\boldsymbol{x}) \\ \text{subject to} & l_i \leq x_i \leq u_i,\ i = 1, \ldots, D, \end{array} \tag{1}$$

where $\boldsymbol{x} = (x_1, x_2, \cdots, x_D)$ is a D dimensional vector and $f(\boldsymbol{x})$ is an objective function. The function f is a nonlinear real-valued function. Values l_i and u_i are the lower bound and the upper bound of x_i, respectively. Let the search space in which every point satisfies the lower and upper bound constraints be denoted by $\mathcal{S}$.

B. Fuzzy Set Theory

There exist some studies on optimization by DE using fuzzy set theory.

- Fuzzy logic: Fuzzy logic is used to control the parameters of DE. The fuzzy adaptive differential evolution (FADE) [5] is proposed to control parameters for a mutation operation and a crossover operation. In each generation, the movement of individuals (vectors) and the change of function values over the whole population between the last two generations were nonlinearly depressed and used as the inputs for fuzzy logic controllers.
- Fuzzy clustering: The hybrid DE based on fuzzy c-means clustering (FCDE) [6] is proposed, which uses the one-step fuzzy c-means clustering. The clustering acts as a multi-parent crossover operation to utilize the information of a population efficiently. In [7], fuzzy clustering is used to divide a population into several clusters or niches, which are a kind of species described below, for multimodal optimization.

C. Speciation

Speciation is mainly used for multimodal optimization where multiple optimal or suboptimal solutions are obtained simultaneously in one run. Each species evolves to find an optimal or suboptimal solution. There exist some types of research using speciation in DE [8].

- Radius-based speciation: In this category, a population is sorted in increasing objective value order, first. Then, the best individual in the sorted population becomes a new species seed. The population members that exist within the specified radius from the seed are assigned to the species, and the members are deleted from the population. This process is repeated until the population becomes empty [4], [9], [10].
- Clustering-based speciation
  A population is divided into several clusters using a clustering algorithm such as k-means clustering [11] or fuzzy c-means clustering [7]. Each cluster corresponds to a species. If the seed of a species is necessary, an individual that has the best objective value in the species is selected as the seed.

In this study, the clustering-based speciation using fuzzy c-means clustering is used not to multimodal optimization but to usual optimization for finding one optimal solution and improving the efficiency of DE using the species-best strategy. Also, as a quite new approach, the partition entropy obtained by the clustering is used to control the parameter for crossover operation of DE.

III. Fuzzy C-Means Clustering and Entropy

In this section, fuzzy c-means clustering and partition entropy are briefly explained [7], [12].

A. Fuzzy Partition and Partition Entropy

Fuzzy partition allows a data point to belong to two or more clusters. Let $X = \{\boldsymbol{x}_1, \boldsymbol{x}_2, \cdots, \boldsymbol{x}_N\}$ be a set of N data points. A fuzzy partition of X into C clusters can be defined with a matrix $U = \{\mu_{ij}\}, 1 \leq i \leq N, 1 \leq j \leq C$, which satisfies the following conditions:

$$\mu_{ij} \in [0, 1] \tag{2}$$

$$\sum_{j=1}^{C} \mu_{ij} = 1,\ 1 \leq i \leq N \tag{3}$$

$$0 < \sum_{i=1}^{N} \mu_{ij} < N,\ 1 \leq j \leq C \tag{4}$$

where μ_{ij} is the degree of membership of the i-th data $\boldsymbol{x}_i$ in the j-th cluster. The higher μ_{ij} indicates that the i-th data belongs to the j-th cluster more strongly.

Some evaluation criteria for the fuzzy partition are proposed such as partition entropy and so on. The normalized partition entropy is defined as follows:

$$PE(C) = -\frac{1}{N \log_2 C} \sum_{i=1}^{N} \sum_{j=1}^{C} \mu_{ij} \log_2 \mu_{ij} \tag{5}$$

where $0 \leq PE(C) \leq 1$. The minimum value 0 corresponds to a hard partition, where each data point $\boldsymbol{x}_i$ belongs to only a cluster c_i:

$$\mu_{ij} = \begin{cases} 1 & j = c_i \\ 0 & j \neq c_i \end{cases}, 1 \leq i \leq N \tag{6}$$

The maximum value 1 corresponds to the fuzziest partition, where each data point belongs to all clusters equivalently:

$$\mu_{ij} = \frac{1}{C},\ 1 \leq i \leq N, 1 \leq j \leq C \tag{7}$$

In this study, the entropy is used to detect the distribution of search points and alter the mode of the search by DE.

B. Fuzzy C-Means Clustering

Fuzzy C-Means (FCM) is a clustering method which realizes the fuzzy partition. This method is frequently used in pattern recognition. The FCM algorithm minimizes the following function:

$$J_m(U,V) = \sum_{i=1}^{N}\sum_{j=1}^{C}(\mu_{ij})^m ||\boldsymbol{x}_i - \boldsymbol{v}_j||^2,\ 1 \le m < \infty \quad (8)$$

where m is a real number parameter specifying degree of fuzziness, $\boldsymbol{v}_j$ is the center of the j-th cluster, $V = \{\boldsymbol{v}_1, \boldsymbol{v}_2, \cdots, \boldsymbol{v}_C\}$ is a set of the cluster centers, and $||\cdot||$ represents any norm expressing the distance between a data point and the cluster center.

The FCM algorithm is as follows:

1) Assign membership values μ_{ij} of all data in all clusters randomly.
2) Update cluster centers.

$$\boldsymbol{v}_j = \frac{\sum_{i=1}^{N}(\mu_{ij})^m x_i}{\sum_{i=1}^{N}(\mu_{ij})^m} \quad (9)$$

3) Update membership degrees.

$$\mu_{ij} = \frac{1}{\sum_{k=1}^{C}\left(\frac{||\boldsymbol{x}_i - \boldsymbol{v}_j||^2}{||\boldsymbol{x}_i - \boldsymbol{v}_k||^2}\right)^{\frac{1}{m-1}}} \quad (10)$$

4) The algorithm is terminated, when the following condition is satisfied, or the change of membership degrees between two iterations is no more than ε, the given sensitivity threshold.

$$\sum_{i=1}^{N}\sum_{j=1}^{C}(\mu_{ij}^m(t) - \mu_{ij}^m(t-1))^2 \le \varepsilon \quad (11)$$

where $\mu_{ij}^m(t)$ and $\mu_{ij}^m(t-1)$ are the value at the current iteration and that at the previous iteration, respectively.
5) Go back to 2).

This algorithm minimizes intra-cluster variance, but the minimum is a local minimum and the results depend on the initial choice of membership degrees.

IV. Differential Evolution

In this section, the outline of DE is described.

A. Outline of Differential Evolution

In DE, initial individuals are randomly generated within the given search space and form an initial population. Each individual contains D genes as decision variables. At each generation or iteration, all individuals are selected as parents. Each parent is processed as follows: The mutation operation begins by choosing several individuals from the population except for the parent in the processing. The first individual is a base vector. All subsequent individuals are paired to create difference vectors. The difference vectors are scaled by a scaling factor F and added to the base vector. The resulting vector, or a mutant vector, is then recombined with the parent. The probability of recombination at an element is controlled by a crossover rate CR. This crossover operation produces a trial vector. Finally, for survivor selection, the trial vector is accepted for the next generation if the trial vector is better than the parent.

There are some variants of DE that have been proposed. The variants are classified using the notation DE/$base$/num/$cross$ such as DE/rand/1/bin and DE/rand/1/exp.

"$base$" specifies a way of selecting an individual that will form the base vector. For example, DE/rand selects an individual for the base vector at random from the population. DE/best selects the best individual in the population.

"num" specifies the number of difference vectors used to perturb the base vector. In case of DE/rand/1, for example, for each parent $\boldsymbol{x}^i$, three individuals $\boldsymbol{x}^{p1}$, $\boldsymbol{x}^{p2}$ and $\boldsymbol{x}^{p3}$ are chosen randomly from the population without overlapping $\boldsymbol{x}^i$ and each other. A new vector, or a mutant vector $\boldsymbol{x}'$ is generated by the base vector $\boldsymbol{x}^{p1}$ and the difference vector $\boldsymbol{x}^{p2} - \boldsymbol{x}^{p3}$, where F is the scaling factor.

$$\boldsymbol{x}' = \boldsymbol{x}^{p1} + F(\boldsymbol{x}^{p2} - \boldsymbol{x}^{p3}) \quad (12)$$

"$cross$" specifies the type of crossover that is used to create a child. For example, 'bin' indicates that the crossover is controlled by the binomial crossover using a constant crossover rate, and 'exp' indicates that the crossover is controlled by a kind of two-point crossover using exponentially decreasing the crossover rate. Fig. 2 shows the binomial and exponential crossover. A new child $\boldsymbol{x}^{\text{child}}$ is generated from the parent $\boldsymbol{x}^i$ and the mutant vector $\boldsymbol{x}'$, where CR is a crossover rate.

```
binomial crossover DE/·/·/bin
  j_rand=randint(1,D);
  for(k=1; k≤D; k++) {
    if(k == j_rand || u(0,1) < CR) x_k^child=x'_k;
    else x_k^child=x_k^i;
  }
exponential crossover DE/·/·/exp
  k=1; j=randint(1,D);
  do {
      x_j^child=x'_j;
      k=k+1; j=(j+1)%D;
  } while(k ≤ D && u(0,1) < CR);
  while(k ≤ D) {
      x_j^child=x_j^i;
      k=k+1; j=(j+1)%D;
  }
```

Fig. 2. Binomial and exponential crossover operation, where randint(1,D) generates an integer randomly from $[1, D]$ and $u(l, r)$ is a uniform random number generator in $[l, r]$.

B. The Algorithm of Differential Evolution

The algorithm of DE is as follows:

Step1 Initialization of a population. Initial N individuals $P = \{\boldsymbol{x}^i, i = 1, 2, \cdots, N\}$ are generated randomly in the search space and form an initial population.

Step2 Termination condition. If the number of function evaluations exceeds the maximum number of evaluation $FE_{\max}$, the algorithm is terminated.

Step3 DE operations. Each individual $\boldsymbol{x}^i$ is selected as a parent. If all individuals are selected, go to Step4. A mutant vector $\boldsymbol{x}'$ is generated according to Eq. (12). A trial vector (child) is generated from the parent $\boldsymbol{x}^i$ and the mutant vector $\boldsymbol{x}'$ using a crossover operation shown in Fig. 2. If the child is better than or equal to the parent, or the DE operation is succeeded, the child survives. Otherwise the parent survives. Go back to Step3 and the next individual is selected as a parent.

Step4 Survivor selection (generation change). The population is organized by the survivors. Go back to Step2.

Fig. 3 shows a pseudo-code of DE/rand/1.

```
DE/rand/1()
{
// Initialize a population
 P=N individuals generated randomly in S;
 for(t=1; FE ≤ FE_max; t++) {
  for(i=1; i ≤ N; i++) {
// DE operations
     x^p1=Randomly selected from P(p1 ≠ i);
     x^p2=Randomly selected from P(p2 ∉ {i,p1});
     x^p3=Randomly selected from P(p3 ∉ {i,p1,p2});
     x'=x^p1+F(x^p2 − x^p3);
     x^child=trial vector is generated from
           x^i and x' by the crossover operation;
// Survivor selection
     if(f(x^child) ≤ f(x^i))  z^i=x^child;
     else                     z^i=x^i;
     FE=FE+1;
  }
  P={z^i,  i = 1,2,···,N};
 }
}
```

Fig. 3. The pseudo-code of DE, FE is the number of function evaluations.

V. DE with Speciation using Fuzzy Clustering

In this section, DE with speciation using fuzzy clustering (DESFC) is proposed.

A. Species-Best Strategy

The following steps are executed in each generation to realize the species-best strategy.

1) FCM is applied to a population $P = \{\boldsymbol{x}^1, \boldsymbol{x}^2, \cdots, \boldsymbol{x}^N\}$ where N is the population size. The membership grade of the i-th individual $\boldsymbol{x}^i$ in the j-th cluster, μ_{ij}, $1 \leq i \leq N$, $1 \leq j \leq C$ is obtained where C is the number of clusters.
2) Each cluster j corresponds to one species. The i-th individual is assigned to the cluster or the species S_i where μ_{ij} has the maximum value.

$$S_i = \arg \max_{1 \leq j \leq C} \mu_{ij},\ 1 \leq i \leq N \tag{13}$$

3) The seed of j-th species, $seed_j$ is the best individual in the species.

$$seed_j = \arg \min_{\{i | S_i = j\}} f(\boldsymbol{x}^i),\ 1 \leq j \leq C \tag{14}$$

Thus, the seed for the i-th individual can be obtained as $seed_{S_i}$.

The species-best strategy to $\boldsymbol{x}^i$ can be described as follows:

$$\boldsymbol{x}' = \boldsymbol{x}^{seed_{S_i}} + F(\boldsymbol{x}^{p2} - \boldsymbol{x}^{p3}) \tag{15}$$

where $p2$ and $p3$ are random integers in $[1, N]$ and i, $p2$ and $p3$ are different with each other.

B. Algorithm of DESFC

Fig. 4 shows the pseudo-code of DESFC. Some modifications to standard DE are applied for proposed method as follows:

1) The partition entropy $PE(C)$ for $\{\mu_{ij}\}$ is calculated in each generation. If the entropy is low, or $PE(C) < 0.99$, a directional search is desirable. In this study, the crossover rate is set to 0.95 or 0.1 with equal probability using the binomial crossover to search for an area near the parent or the mutant vector. In order to improve the robustness, the species-best strategy and the rand strategy are adopted probabilistically.
2) Continuous generation model [13], [14] is adopted. Usually discrete generation model is adopted in DE and when the child is better than the parent, the child survives in the next generation. In this study, when the child is better than the parent, the parent is immediately replaced by the child. It is thought that the continuous generation model improves efficiency because the model can use newer information than the discrete model.
3) Reflecting back out-of-bound solutions [15] is adopted. In order to keep bound constraints, an operation to move a point outside of the search space $\mathcal{S}$ into the inside of $\mathcal{S}$ is required. There are some ways to realize the movement: generating solutions again, cutting off the solutions on the boundary, and reflecting points back to the inside of the boundary [16]. In this study, reflecting back is used:

$$x_{ij} = \begin{cases} l_i + (l_i - x_{ij}) - \left\lfloor \frac{l_i - x_{ij}}{u_i - l_i} \right\rfloor (u_i - l_i) & (x_{ij} < l_i) \\ u_i - (x_{ij} - u_i) + \left\lfloor \frac{x_{ij} - u_i}{u_i - l_i} \right\rfloor (u_i - l_i) & (x_{ij} > u_i) \\ x_{ij} & (\text{otherwise}) \end{cases} \tag{16}$$

where $\lfloor z \rfloor$ is the maximum integer smaller than or equal to z. This operation is applied when a new point is generated by DE operations.

VI. Solving Optimization Problems

In this paper, well-known thirteen benchmark problems are solved.

A. Test Problems and Experimental Conditions

The 13 scalable benchmark functions are shown in Table I [17]. All functions have an optimal value 0. Some characteristics are briefly summarized as follows: Functions f_1 to f_4 are continuous unimodal functions. The function f_5 is Rosenbrock function which is unimodal for 2- and 3-dimensions but may have multiple minima in high dimension cases [18]. The

```
DESFC()
{
// Initialize a population
 P=N individuals generated randomly in S;
 for(t=1; FE ≤ FE_max; t++) {
// Speciation using FCM
   {μ_ij}=Fuzzy c-means clustering of P;
   for(i=1; i ≤ N; i++)
     S_i=arg max_{1≤j≤C} μ_ij;
   for(j=1; i ≤ C; j++)
     seed_j=arg min_{i|S_i=j} f(x^i);
// Judge distribution of search points
   PE=partition entropy of {μ_ij};
   if(PE ≥ 0.99) isUniform=TRUE;
   else          isUniform=FALSE;

   for(i=1; i ≤ N; i++) {
     CR=CR_0; Select exponential crossover;
     if(i! = seed_{s_i} && u(0,1) < 0.6) {
       if(isUniform==FALSE) {
         if(u(0,1) < 0.5) CR=0.95;
         else             CR=0.1;
         Select binomial crossover;
       }
// DE/species-best/1/{bin,exp}
       p_1=seed_{S_i};
     }
     else
// DE/rand/1/exp
     x^{p_1}=Randomly selected from P(p_1 ≠ i);
     x^{p_2}=Randomly selected from P(p_2 ∉ {i,p_1});
     x^{p_3}=Randomly selected from P(p_3 ∉ {i,p_1,p_2});
     x'=x^{p_1}+F(x^{p_2} − x^{p_3});
     x^c=trial vector is generated from
               x^i and x' by the selected crossover;
     FE=FE+1;
// Survivor selection
     if(f(x^c) ≤ f(x^i))
       x^i=x^c;
   }
 }
}
```

Fig. 4. The pseudo-code of DESFC where CR_0 is an initial crossover rate.

function f_6 is a discontinuous step function, and f_7 is a noisy quartic function. Functions f_8 to f_{13} are multimodal functions and the number of their local minima increases exponentially with the problem dimension [19].

Independent 30 runs are performed for the 13 problems. The dimension of problems is 40 (D=40). Each run stops when a near optimal solution, which has equivalent objective value to the optimal solution, is found. In this study, when the difference between the best objective value and the optimal value becomes less than 10^{-7}, the run stops. In f_7, it is difficult to find the good objective value, because a random noise is added. It is assumed that the optimal value of f_7 is 10^{-2} in this experiment.

The efficiency of two algorithms DE/rand (continuous generation model) and DESFC are compared where the number of clusters C is changed from 2 to 5 in DESFC. The degree of fuzziness m is fixed to 2. The parameters are: $F = 0.7$, $CR = 0.9$ and the exponential crossover is adopted as usual crossover, because these settings showed very good and stable performance [21]. The population size is twice of the dimension size, $N = 2D = 80$. The number of function evaluations (FEs) until finding a near optimal solution is compared. If the number of FEs exceeds 2,000,000, the run is terminated and regarded as a failure run.

TABLE I
TEST FUNCTIONS OF DIMENSION D. THESE ARE SPHERE, SCHWEFEL 2.22, SCHWEFEL 1.2, SCHWEFEL 2.21, ROSENBROCK, STEP, NOISY QUARTIC, SCHWEFEL 2.26, RASTRIGIN, ACKLEY, GRIEWANK, AND TWO PENALIZED FUNCTIONS, RESPECTIVELY [20]

Test functions	Bound constraints
$f_1(\boldsymbol{x}) = \sum_{i=1}^{D} x_i^2$	$[-100, 100]^D$
$f_2(\boldsymbol{x}) = \sum_{i=1}^{D} \lvert x_i \rvert + \prod_{i=1}^{D} \lvert x_i \rvert$	$[-10, 10]^D$
$f_3(\boldsymbol{x}) = \sum_{i=1}^{D} \left(\sum_{j=1}^{i} x_j \right)^2$	$[-100, 100]^D$
$f_4(\boldsymbol{x}) = \max_i \{ \lvert x_i \rvert \}$	$[-100, 100]^D$
$f_5(\boldsymbol{x}) = \sum_{i=1}^{D-1} \left[100(x_{i+1} - x_i^2)^2 + (x_i - 1)^2 \right]$	$[-30, 30]^D$
$f_6(\boldsymbol{x}) = \sum_{i=1}^{D} \lfloor x_i + 0.5 \rfloor^2$	$[-100, 100]^D$
$f_7(\boldsymbol{x}) = \sum_{i=1}^{D} i x_i^4 + rand[0, 1)$	$[-1.28, 1.28]^D$
$f_8(\boldsymbol{x}) = \sum_{i=1}^{D} -x_i \sin \sqrt{\lvert x_i \rvert}$ $+ D \cdot 418.98288727243369$	$[-500, 500]^D$
$f_9(\boldsymbol{x}) = \sum_{i=1}^{D} \left[x_i^2 - 10 \cos(2\pi x_i) + 10 \right]$	$[-5.12, 5.12]^D$
$f_{10}(\boldsymbol{x}) = -20 \exp \left(-0.2 \sqrt{\frac{1}{D} \sum_{i=1}^{D} x_i^2} \right)$ $- \exp \left(\frac{1}{D} \sum_{i=1}^{D} \cos(2\pi x_i) \right) + 20 + e$	$[-32, 32]^D$
$f_{11}(x) = \frac{1}{4000} \sum_{i=1}^{D} x_i^2 - \prod_{i=1}^{D} \cos \left(\frac{x_i}{\sqrt{i}} \right) + 1$	$[-600, 600]^D$
$f_{12}(x) = \frac{\pi}{D} [10 \sin^2(\pi y_1) + \sum_{i=1}^{D-1} (y_i - 1)^2$ $\{1 + 10 \sin^2(\pi y_{i+1})\} + (y_D - 1)^2]$ $+ \sum_{i=1}^{D} u(x_i, 10, 100, 4)$ where $y_i = 1 + \frac{1}{4}(x_i + 1)$ and $u(x_i, a, k, m) =$ $\begin{cases} k(x_i - a)^m & x_i > a \\ 0 & -a \le x_i \le a \\ k(-x_i - a)^m & x_i < -a \end{cases}$	$[-50, 50]^D$
$f_{13}(x) = 0.1[\sin^2(3\pi x_1) + \sum_{i=1}^{D-1} (x_i - 1)^2$ $\{1 + \sin^2(3\pi x_{i+1})\} + (x_D - 1)^2$ $\{1 + \sin^2(2\pi x_D)\}] + \sum_{i=1}^{D} u(x_i, 5, 100, 4)$	$[-50, 50]^D$

B. Experimental Results

Table II shows the experimental results. The mean number of FEs until finding a near optimal value and their standard deviation are shown in the top row for each function. Also, the ratio of the mean number of FEs relative to that of the standard DE is shown in the bottom row using parentheses. The best result is highlighted using bold face fonts.

TABLE II
EXPERIMENTAL RESULTS. MEAN VALUE ± STANDARD DEVIATION AND RATIO OF THE MEAN VALUE RELATIVE TO THAT OF THE STANDARD DE IN 30 RUNS ARE SHOWN

	DE	DESFC ($C = 2$)	DESFC ($C = 3$)	DESFC ($C = 4$)	DESFC ($C = 5$)
f_1	160492.4 ± 1435.2 (1.000)	**117206.1 ± 1564.7** (0.730)	120674.8 ± 1831.4 (0.752)	122346.5 ± 1755.9 (0.762)	124235.9 ± 1194.0 (0.774)
f_2	226925.5 ± 1780.4 (1.000)	**170303.5 ± 2038.4** (0.750)	174018.3 ± 2069.4 (0.767)	177648.0 ± 1673.2 (0.783)	179780.8 ± 1981.5 (0.792)
f_3	1383166.8 ± 17090.3 (1.000)	**810832.5 ± 13592.4** (0.586)	838104.6 ± 16195.6 (0.606)	847113.2 ± 13832.2 (0.612)	861445.0 ± 17661.7 (0.623)
f_4	1435549.4 ± 12435.7 (1.000)	**845085.4 ± 12057.4** (0.589)	884353.9 ± 14714.8 (0.616)	907182.5 ± 14305.0 (0.632)	921243.2 ± 13765.9 (0.642)
f_5	505521.2 ± 6922.3 (1.000)	**375997.1 ± 11190.8** (0.744)	417049.6 ± 10243.3 (0.825)	446234.7 ± 9937.2 (0.883)	464278.1 ± 7319.0 (0.918)
f_6	64055.6 ± 1613.6 (1.000)	**47752.3 ± 1296.9** (0.745)	49372.5 ± 1214.7 (0.771)	49977.7 ± 1297.2 (0.780)	50268.7 ± 1612.4 (0.785)
f_7	798441.2 ± 139293.5 (1.000)	**563133.9 ± 107809.7** (0.705)	572408.3 ± 115549.5 (0.717)	553073.6 ± 95603.7 (0.693)	598517.6 ± 92705.4 (0.750)
f_8	192272.8 ± 2857.9 (1.000)	**144776.4 ± 3354.0** (0.753)	148036.9 ± 3334.3 (0.770)	150478.6 ± 2474.9 (0.783)	151358.5 ± 3162.7 (0.787)
f_9	349435.7 ± 8654.0 (1.000)	**282471.5 ± 10327.1** (0.808)	286350.3 ± 6992.8 (0.819)	293521.2 ± 10027.9 (0.840)	292191.9 ± 7366.3 (0.836)
f_{10}	239050.7 ± 1933.8 (1.000)	**174369.5 ± 2165.9** (0.729)	179843.3 ± 1916.2 (0.752)	183511.6 ± 2097.5 (0.768)	185127.6 ± 1934.2 (0.774)
f_{11}	171085.8 ± 5818.7 (1.000)	**121418.5 ± 3495.4** (0.710)	127356.7 ± 5213.6 (0.744)	128429.4 ± 5079.4 (0.751)	131122.6 ± 5681.8 (0.766)
f_{12}	142630.8 ± 1479.8 (1.000)	**106608.6 ± 2220.4** (0.747)	109387.1 ± 2468.9 (0.767)	110834.6 ± 1590.7 (0.777)	112822.2 ± 2121.4 (0.791)
f_{13}	153476.0 ± 1643.0 (1.000)	**113441.0 ± 1508.6** (0.739)	116932.2 ± 2255.1 (0.762)	118936.9 ± 1966.8 (0.775)	119801.5 ± 1684.0 (0.781)

DESFC can solve all problems in all runs successfully. DESFC outperformed the standard DE in all problems and in all settings of C. The value $C = 2$ showed the best results. DESFC with $C = 2$ can solve the problems f_3 and f_4 within 60% FEs compared with the standard DE, solve the problems f_7 and f_{11} in about 70% FEs, and solve the other problems in about 75% FEs except for f_9 in about 80% FEs.

It is shown that the proposed method can solve 4 problems very fast and 9 problems fast. Thus, it is thought that the method is effective to various problems.

To determine the significance of the proposed method, statistical analysis was performed using one-sided Welch's t-test for the mean FEs of the standard DE and that of DESFC with C being 1, 2, 3, 4 and 5. It is thought that the proposed method is significantly better than the standard DE because p-values in all parameter settings and all functions are less than 0.001.

Figures 5 to 17 show the change of best objective value found over the number of FEs within 200,000 evaluations. Apparently, the proposed method can find better objective values faster than the standard DE in all problems.

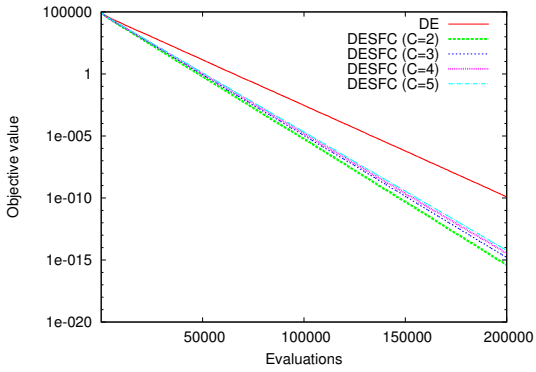

Fig. 5. The graph of f_1

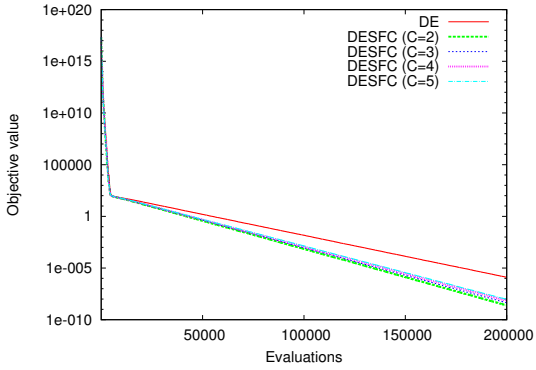

Fig. 6. The graph of f_2

VII. CONCLUSION

Differential evolution is known as a simple, efficient and robust search algorithm that can solve nonlinear optimization problems. In this study, we proposed the DE with speciation using fuzzy clustering and partition entropy to improve the efficiency and also robustness of DE. Especially, it is a quite new approach to detect the distribution of search points using FCM and to control an algorithm parameter. It was shown that DESFC can reduce the number of function evaluations for

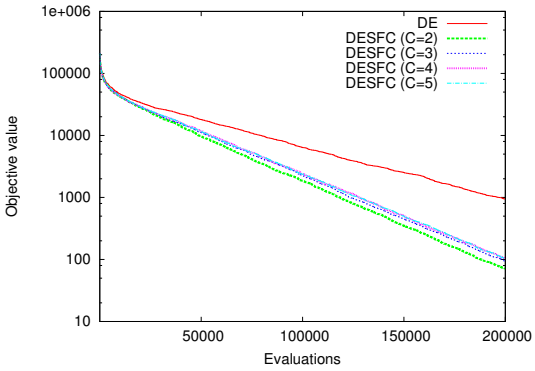

Fig. 7. The graph of f_3

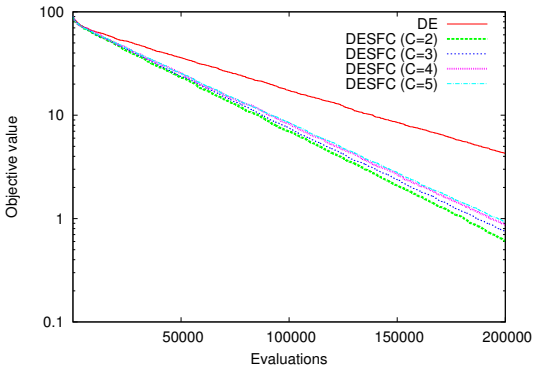

Fig. 8. The graph of f_4

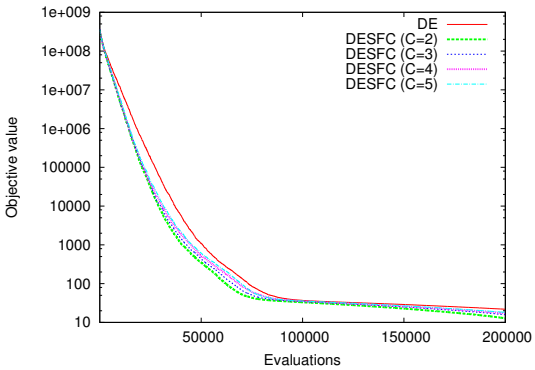

Fig. 9. The graph of f_5

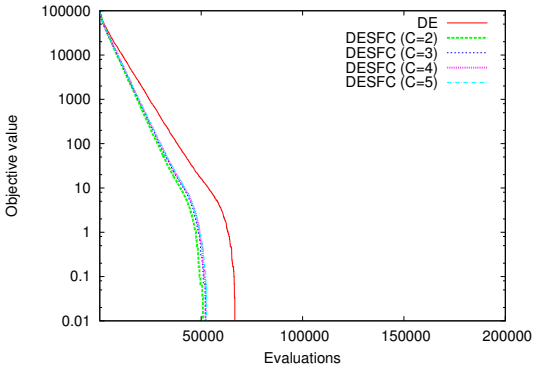

Fig. 10. The graph of f_6

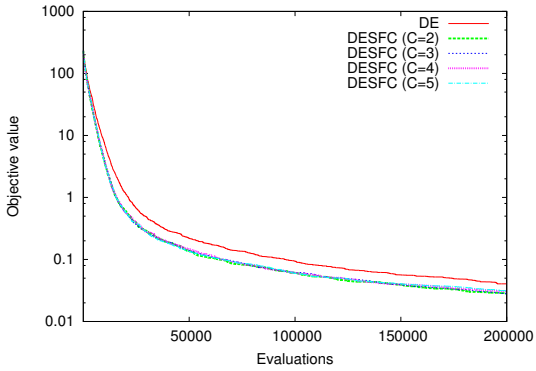

Fig. 11. The graph of f_7

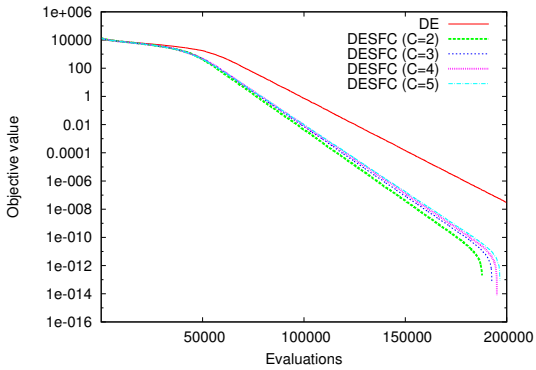

Fig. 12. The graph of f_8

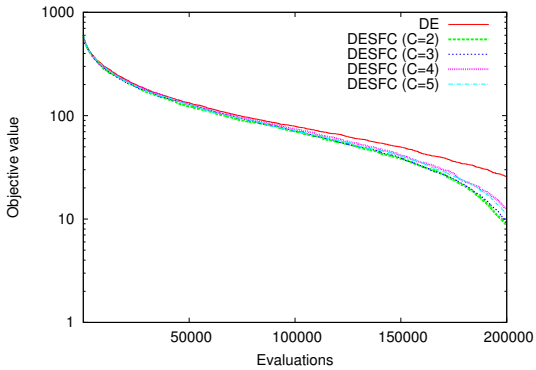

Fig. 13. The graph of f_9

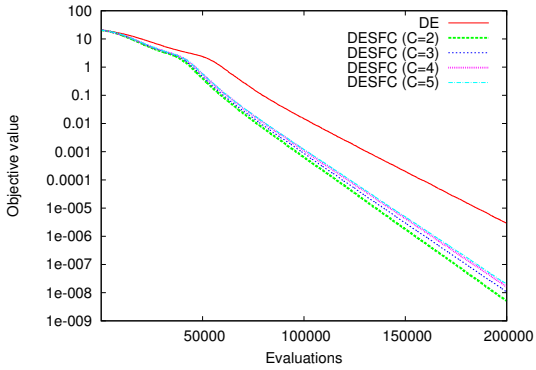

Fig. 14. The graph of f_{10}

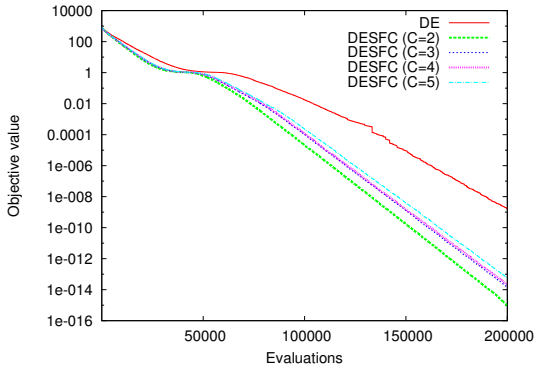

Fig. 15. The graph of f_{11}

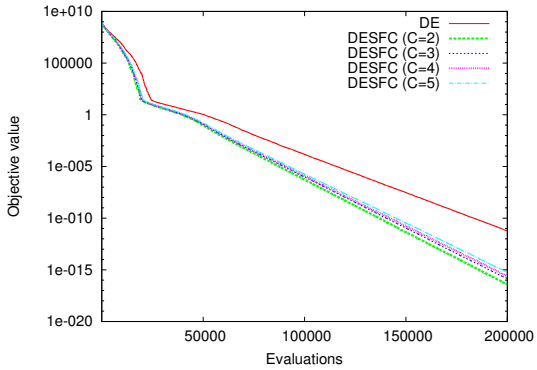

Fig. 16. The graph of f_{12}

finding near optimal solutions more than 25% in 11 problems out of the 13 problems. Thus, it is thought that DESFC is a very efficient optimization algorithm compared with standard DEs.

The effect of the degree of fuzziness m is not studied in this paper. It is thought that a proper value of the degree enhances the ability to discriminate a biased distribution from the uniform distribution. We plan to analyze the effect of the degree.

ACKNOWLEDGMENT

This research is supported in part by Grant-in-Aid for Scientific Research (C) (No. 20500138,22510166) of Japan society for the promotion of science.

REFERENCES

[1] R. Storn and K. Price, "Differential evolution – A simple and efficient heuristic for global optimization over continuous spaces," *Journal of Global Optimization*, vol. 11, pp. 341–359, 1997.

[2] K. V. Price, R. M. Storn, and J. A. Lampinen, *Differential Evolution: A Practical Approach to Global Optimization*. Springer, 2005.

[3] U. K. Chakraborty, Ed., *Advances in Differential Evolution*. Springer, 2008.

[4] M. Shibasaka, A. Hara, T. Ichimura, and T. Takahama, "Species-based differential evolution with switching search strategies for multimodal function optimization," in *Proc. of the 2007 IEEE Congress on Evolutionary Computation*, Sep. 2007, pp. 1183 –1190.

[5] J. Liu and J. Lampinen, "A fuzzy adaptive differential evolution algorithm," *Soft Comput.*, vol. 9, no. 6, pp. 448–462, 2005.

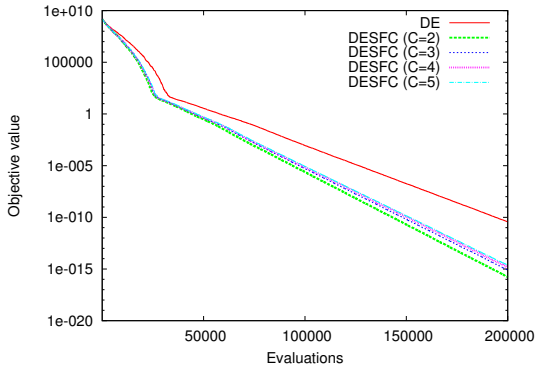

Fig. 17. The graph of f_{13}

[6] W. Gong, Z. Cai, C. X. Ling, and J. Du, "Hybrid differential evolution based on fuzzy c-means clustering," in *Proc. of Genetic and Evolutionary Computation Conference 2009*, 2009, pp. 523–530.

[7] A. E. Imrani, A. Bouroumi, H. Z. E. Abidine, M. Limouri, and A. Essaïd, "A fuzzy clustering-based niching approach to multimodal function optimization," *Journal of Cognitive Systems Research*, vol. 1, no. 2, pp. 119–133, 2000.

[8] J.-P. Li, X.-D. Li, and A. Wood, "Species based evolutionary algorithms for multimodal optimization: A brief review," in *Proc. of the 2010 IEEE Congress on Evolutionary Computation*, Jul. 2010, pp. 1–8.

[9] X. Li, "Efficient differential evolution using speciation for multimodal function optimization," in *Proc. of the 2005 conference on Genetic and evolutionary computation*, 2005, pp. 873–880.

[10] B. Qu and P. Suganthan, "Modified species-based differential evolution with self-adaptive radius for multi-modal optimization," in *Proc. of the 2010 International Conference on Computational Problem-Solving*, Dec. 2010, pp. 326 –331.

[11] A. Passaro and A. Starita, "Particle swarm optimization for multimodal functions: a clustering approach," *Journal of Artificial Evolution and Applications*, vol. 2008, pp. 1–15, January 2008.

[12] J. C. Bezdek, *Pattern Recognition with Fuzzy Objective Function Algorithms*. Norwell, MA, USA: Kluwer Academic Publishers, 1981.

[13] T. Takahama, S. Sakai, and N. Iwane, "Solving nonlinear constrained optimization problems by the ε constrained differential evolution," in *Proc. of the 2006 IEEE Conference on Systems, Man, and Cybernetics*, Oct. 2006, pp. 2322–2327.

[14] T. Takahama and S. Sakai, "Reducing function evaluations in differential evolution using rough approximation-based comparison," in *Proc. of the 2008 IEEE Congress on Evolutionary Computation*, Jun. 2008, pp. 2307–2314.

[15] S. Kukkonen and J. Lampinen, "Constrained real-parameter optimization with generalized differential evolution," in *Proc. of the 2006 IEEE Congress on Evolutionary Computation*. Vancouver, BC, Canada: IEEE Press, 16-21 July 2006, pp. 207–214.

[16] T. Takahama and S. Sakai, "Solving difficult constrained optimization problems by the ε constrained differential evolution with gradient-based mutation," in *Constraint-Handling in Evolutionary Optimization*, E. Mezura-Montes, Ed. Springer-Verlag, 2009, pp. 51–72.

[17] Z. Jingqiao and A. C. Sanderson, "JADE: Adaptive differential evolution with optional external archive," *IEEE Transactions on Evolutionary Computation*, vol. 13, no. 5, pp. 945–958, Oct. 2009.

[18] Y.-W. Shang and Y.-H. Qiu, "A note on the extended rosenbrock function," *Evolutionary Computation*, vol. 14, no. 1, pp. 119–126, 2006.

[19] X. Yao, Y. Liu, , and G. Lin, "Evolutionary programming made faster," *IEEE Transactions on Evolutionary Computation*, vol. 3, pp. 82–102, 1999.

[20] X. Yao, Y. Liu, K.-H. Liang, and G. Lin, "Fast evolutionary algorithms," in *Advances in evolutionary computing: theory and applications*, A. Ghosh and S. Tsutsui, Eds. New York, NY, USA: Springer-Verlag New York, Inc., 2003, pp. 45–94.

[21] T. Takahama and S. Sakai, "Fast and stable constrained optimization by the ε constrained differential evolution," *Pacific Journal of Optimization*, vol. 5, no. 2, pp. 261–282, May 2009.

2011 IEEE International Conference on Fuzzy Systems
June 27-30, 2011, Taipei, Taiwan

LMI-Based Stability Conditions for Interval Type-2 Fuzzy-Model-Based Control Systems

H.K. Lam[1], Mohammad Narimani[2] and L.D. Seneviratne[3]
Division of Engineering,
King's College London,
Strand, London,
WC2R 2LS, United Kingdom
E-mails: [1]hak-keung.lam@kcl.ac.uk, [2]mohammad.narimani@kcl.ac.uk, [3]lakmal.seneviratne@kcl.ac.uk

***Abstract*—This paper investigates the stability of the interval type-2 (IT2) fuzzy-model-based (FMB) control systems. An IT2 T-S fuzzy model is developed to represent the nonlinear plant subject to parameter uncertainties, which are captured by the lower and upper membership functions. An IT2 fuzzy model is then be proposed to close the feedback loop. It is not required that the IT2 fuzzy controller shares the same premise membership functions or the same number of fuzzy rules as those of the IT2 T-S fuzzy model. Consequently, it offers a greater design flexibility to the IT2 fuzzy controllers. However, the mismatched premise membership functions are not favourable to the development of stability conditions and thus leads to a conservative stability analysis result. In this paper, with the consideration of the lower and upper membership functions, which carry the information of the nonlinearities and parameter uncertainties of the nonlinear plant, the stability of the IT2 FMB control systems is investigated based on the Lyapunov stability theory. Stability conditions in terms of linear matrix inequalities are developed to guarantee the stability of the IT2 FMB control systems and synthesize the IT2 fuzzy controller. A simulation example is given to demonstrates the effectiveness of the proposed approach.**

***Index Terms*—Fuzzy Controller, Fuzzy-Model-Based Control, Interval Type-2, Linear Matrix Inequalities (LMIs), Stability Analysis.**

I. Introduction

Type-1 fuzzy-model-based (FMB) control [1] is a promising control approach for complex and ill-defined nonlinear plants, represented by the type-1 Takagi-Sugeno (T-S) fuzzy model [2], [3]. Based on the Lyapunov stability theory, a set of stability conditions in the form of linear matrix inequalities (LMIs) [4], [5] was obtained to guarantee the system stability. The work in [4], [5] provides the basic stability analysis procedure for the type-1 FMB control systems. More relaxed LMI-based stability conditions were obtained in [7]–[12]. Further relaxed stability conditions were obtained in [13]–[20] by considering the information of the type-1 membership functions.

In general, for the type-1 T-S FMB control system under the parallel distributed compensation (PDC) design [4], [5], the fuzzy controller needs to share the same premise membership function as those of the T-S fuzzy model. When the nonlinear plant is subject to parameter uncertainties, the membership functions of the T-S fuzzy model will contain the uncertain parameters and lead to the grades of membership uncertain in value. Consequently, the advantage of the PDC design given to the stability analysis will be vanished.

Type-2 fuzzy sets [21]–[24] have been shown that it is superior to the type-1 ones on dealing with uncertainties. With the lower and upper membership functions, the uncertainties can be captured and the information of the uncertainties is embedded in the footprint of uncertainty (FOU) [21]. In recent years, some properties and theories of type-2 fuzzy sets have been developed to theoretically support the design and implementation of type-2 fuzzy logic systems. However, it is mainly for general type-2 fuzzy logic systems but not mainly for the purposes of fuzzy control. In type-1 FMB control approach, the type-1 T-S fuzzy model [2], [3] plays an important role representing the dynamics of the nonlinear plant to facilitate the stability analysis and control synthesis. A basic interval type-2 (IT2) T-S fuzzy model was proposed in [25] for a limited class of nonlinear plants. We extended the idea and proposed a more general IT2 T-S fuzzy model [26] for a wider class of nonlinear plants to support the analysis and development of IT2 FMB control systems. A preliminary stability analysis result was reported in [26] for an IT2 FMB control systems under perfect premise matching that the IT2 T-S fuzzy model and IT2 fuzzy controller share the same lower and upper membership functions (which implies the same number of fuzzy rules). A set of LMI-based stability conditions was obtained to guarantee the system stability.

In this paper, we investigate the stability of IT2 FMB control systems under imperfect premises matching. As it is not requited that the IT2 T-S fuzzy model and IT2 fuzzy controller share the same lower and upper membership functions, and the same number of fuzzy rules, it enhances the design flexibility of the IT2 fuzzy controller and is able to lower the controller complexity by using a smaller number of fuzzy rules and simple membership functions. However, it makes the stability analysis more difficulty and leads to more conservative stability conditions. To facilitate the stability analysis of IT2 FMB control system, an IT2 T-S fuzzy model [26] is employed to represent the nonlinear plant subject to parameter uncertainties, captured by the lower and upper membership functions. An IT2 fuzzy controller with different lower and upper membership functions is employed to close the feedback loop. We propose a favourable form to represent the lower and upper membership functions for the stability analysis and LMI-based stability conditions are obtained to guarantee the system stability and

978-1-4244-7316-8/11/$26.00 ©2011 IEEE

synthesize the IT2 fuzzy controller.

The organization of this paper is as follows. In Section II, the IT2 fuzzy model representing the nonlinear plant subject to parameter uncertainties, IT2 fuzzy controller and IT2 FMB control systems are presented. In Section III, LMI-based stability conditions are derived based on the Lyapunov stability theory for the IT2 FMB control systems. In Section IV, a simulation example is given to illustrate the merits of the proposed IT2 FMB control scheme. In Section V, a conclusion is drawn.

II. IT2 TS Fuzzy Model, IT2 Fuzzy Controller and IT2 FMB Control System

An IT2 FMB control system is referred to a closed-loop system consisting of the IT2 T-S fuzzy model [25], [26] and the IT2 fuzzy controller connected in a closed loop.

A. IT2 T-S Fuzzy Model

Consider an IT2 T-S fuzzy model [25], [26] with p rules of the following format of which the antecedent of each rule contains some IT2 fuzzy sets and the consequent is a linear dynamical system.

$$\begin{aligned}\text{Rule } i\text{: IF } f_1(\mathbf{x}(t)) \text{ is } \tilde{M}_1^i \text{ AND } \cdots \text{ AND } f_\Psi(\mathbf{x}(t)) \text{ is } \tilde{M}_\Psi^i \\ \text{THEN } \dot{\mathbf{x}}(t) = \mathbf{A}_i\mathbf{x}(t) + \mathbf{B}_i\mathbf{u}(t)\end{aligned} \tag{1}$$

where $\tilde{M}_\alpha^i$ is an IT2 fuzzy set of rule i corresponding to the function $f_\alpha(\mathbf{x}(t))$, α = 1, 2, $\cdots$, Ψ; i = 1, 2, $\cdots$, p; Ψ is a positive integer; $\mathbf{x}(t) \in \Re^n$ is the system state vector; $\mathbf{A}_i \in \Re^{n\times n}$ and $\mathbf{B}_i \in \Re^{n\times m}$ are the known system and input matrices, respectively; $\mathbf{u}(t) \in \Re^m$ is the input vector. The firing strength of the i-th rule is the following interval sets.

$$W_i(\mathbf{x}(t)) = \left[\ \underline{w}_i(\mathbf{x}(t)),\quad \overline{w}_i(\mathbf{x}(t))\ \right], i = 1, 2, \cdots, p \tag{2}$$

where

$$\underline{w}_i(\mathbf{x}(t)) = \prod_{\alpha=1}^{\Psi} \underline{\mu}_{\tilde{M}_\alpha^i}(f_\alpha(\mathbf{x}(t))) \geq 0, \tag{3}$$

$$\overline{w}_i(\mathbf{x}(t)) = \prod_{\alpha=1}^{\Psi} \overline{\mu}_{\tilde{M}_\alpha^i}(f_\alpha(\mathbf{x}(t))) \geq 0, \tag{4}$$

in which $\underline{w}_i(\mathbf{x}(t))$ and $\overline{w}_i(\mathbf{x}(t))$ denote the lower and upper grades of membership, respectively; $\underline{\mu}_{\tilde{M}_\alpha^i}(f_\alpha(\mathbf{x}(t))) \geq 0$ and $\overline{\mu}_{\tilde{M}_\alpha^i}(f_\alpha(\mathbf{x}(t))) \geq 0$ denote the lower and upper membership functions, respectively. It exhibits the property that $\overline{\mu}_{\tilde{M}_\alpha^i}(f_\alpha(\mathbf{x}(t))) \geq \underline{\mu}_{\tilde{M}_\alpha^i}(f_\alpha(\mathbf{x}(t)))$ leading to $\overline{w}_i(\mathbf{x}(t)) \geq \underline{w}_i(\mathbf{x}(t))$ for all i. The inferred IT2 T-S fuzzy model [26] is defined as follows.

$$\dot{\mathbf{x}}(t) = \sum_{i=1}^{p} \tilde{w}_i(\mathbf{x}(t))(\mathbf{A}_i\mathbf{x}(t) + \mathbf{B}_i\mathbf{u}(t)) \tag{5}$$

where

$$\tilde{w}_i(\mathbf{x}(t)) = \underline{\alpha}_i(\mathbf{x}(t))\underline{w}_i(\mathbf{x}(t)) + \overline{\alpha}_i(\mathbf{x}(t))\overline{w}_i(\mathbf{x}(t)) \geq 0\ \forall\ i, \tag{6}$$

$$\sum_{i=1}^{p} \tilde{w}_i(\mathbf{x}(t)) = 1, \tag{7}$$

in which $0 \leq \underline{\alpha}_i(\mathbf{x}(t)) \leq 1$ and $0 \leq \overline{\alpha}_i(\mathbf{x}(t)) \leq 1$ are nonlinear functions and exhibit the property of $\underline{\alpha}_i(\mathbf{x}(t)) + \overline{\alpha}_i(\mathbf{x}(t)) = 1$ for all i.

B. IT2 Fuzzy Controller

An IT2 fuzzy controller with c rules of the following format is proposed to stabilize the nonlinear plant represented by the IT2 T-S fuzzy model (5).

$$\begin{aligned}\text{Rule } j\text{: IF } g_1(\mathbf{x}(t)) \text{ is } \tilde{N}_1^j \text{ AND } \cdots \text{ AND } g_\Omega(\mathbf{x}(t)) \text{ is } \tilde{N}_\Omega^j \\ \text{THEN } \mathbf{u}(t) = \mathbf{G}_j\mathbf{x}(t)\end{aligned} \tag{8}$$

where $\tilde{N}_\beta^j$ is an IT2 fuzzy set of rule j corresponding to the function $g_\beta(\mathbf{x}(t))$, β = 1, 2, $\cdots$, Ω; j = 1, 2, $\cdots$, c; Ω is a positive integer; $\mathbf{G}_j \in \Re^{m\times n}$, j = 1, 2, $\cdots$, c, are the constant feedback gains to be determined. The firing strength of the j-th rule is the following interval sets.

$$M_j(\mathbf{x}(t)) = \left[\ \underline{m}_j(\mathbf{x}(t)),\quad \overline{m}_j(\mathbf{x}(t))\ \right], j = 1, 2, \cdots, c \tag{9}$$

where

$$\underline{m}_j(\mathbf{x}(t)) = \prod_{\beta=1}^{\Omega} \underline{\mu}_{\tilde{N}_\beta^j}(g_\beta(\mathbf{x}(t))) \geq 0, \tag{10}$$

$$\overline{m}_j(\mathbf{x}(t)) = \prod_{\beta=1}^{\Omega} \overline{\mu}_{\tilde{N}_\beta^j}(g_\beta(\mathbf{x}(t))) \geq 0, \tag{11}$$

in which $\underline{m}_j(\mathbf{x}(t))$ and $\overline{m}_j(\mathbf{x}(t))$ denote the lower and upper grades of membership, respectively; $\underline{\mu}_{\tilde{N}_\beta^j}(g_\beta(\mathbf{x}(t))) \geq 0$ and $\overline{\mu}_{\tilde{N}_\beta^j}(g_\beta(\mathbf{x}(t))) \geq 0$ denote the lower and upper membership functions, respectively. It exhibits the property that $\underline{\mu}_{\tilde{N}_\beta^j}(g_\beta(\mathbf{x}(t))) \geq \overline{\mu}_{\tilde{N}_\beta^j}(g_\beta(\mathbf{x}(t)))$ leading to $\overline{m}_j(\mathbf{x}(t)) \geq \underline{m}_j(\mathbf{x}(t))$ for all j. The inferred IT2 fuzzy controller is defined as follows.

$$\mathbf{u}(t) = \sum_{j=1}^{c} \tilde{m}_j(\mathbf{x}(t))\mathbf{G}_j\mathbf{x}(t) \tag{12}$$

where

$$\begin{aligned}&\tilde{m}_j(\mathbf{x}(t)) \\ &= \frac{\underline{\beta}_j(\mathbf{x}(t))\underline{m}_j(\mathbf{x}(t)) + \overline{\beta}_j(\mathbf{x}(t))\overline{m}_j(\mathbf{x}(t))}{\sum_{k=1}^{c}\left(\underline{\beta}_k(\mathbf{x}(t))\underline{m}_k(\mathbf{x}(t)) + \overline{\beta}_k(\mathbf{x}(t))\overline{m}_k(\mathbf{x}(t))\right)} \geq 0\ \forall\ j,\end{aligned} \tag{13}$$

$$\sum_{j=1}^{c} \tilde{m}_i(\mathbf{x}(t)) = 1, \tag{14}$$

in which $0 \leq \underline{\beta}_j(\mathbf{x}(t)) \leq 1$ and $0 \leq \overline{\beta}_j(\mathbf{x}(t)) \leq 1$ are predefined functions and exhibit the property of $\underline{\beta}_j(\mathbf{x}(t)) + \overline{\beta}_j(\mathbf{x}(t)) = 1$ for all j.

C. IT2 FMB Control Systems

An IT2 FMB control system is formed by connecting the IT2 T-S fuzzy model (5) and the IT2 fuzzy controller (12) in a closed loop. From (5) and (12), considering the property of $\sum_{i=1}^{p}\tilde{w}_i(\mathbf{x}(t)) = \sum_{j=1}^{c}\tilde{m}_j(\mathbf{x}(t)) = \sum_{i=1}^{p}\sum_{j=1}^{c}\tilde{w}_i(\mathbf{x}(t))\tilde{m}_j(\mathbf{x}(t)) = 1$, we have,

$$\begin{aligned}\dot{\mathbf{x}}(t) &= \sum_{i=1}^{p}\tilde{w}_i(\mathbf{x}(t))(\mathbf{A}_i\mathbf{x}(t) + \mathbf{B}_i\sum_{j=1}^{c}\tilde{m}_j(\mathbf{x}(t))\mathbf{G}_j\mathbf{x}(t)) \\ &= \sum_{i=1}^{p}\sum_{j=1}^{c}\tilde{w}_i(\mathbf{x}(t))\tilde{m}_j(\mathbf{x}(t))(\mathbf{A}_i + \mathbf{B}_i\mathbf{G}_j)\mathbf{x}(t). \quad (15)\end{aligned}$$

The control objective is to determine the feedback gains, $\mathbf{G}_j$, such that the IT2 fuzzy controller (12) is able to drive the system states towards the origin, i.e., $\mathbf{x}(t) \to \mathbf{0}$ as time $t \to \infty$.

The stability of the FMB based control system in the form of (15) was investigated in [4] and guaranteed to be asymptotically stable if the LMI-based stability conditions in the following theorem are satisfied.

Theorem 1: [4] The FMB control system in the form of (15) is guaranteed to be asymptotically stable if there exist matrices $\mathbf{N}_j \in \Re^{m\times n}$, $j = 1, 2, \cdots, c$, $\mathbf{X} = \mathbf{X}^T \in \Re^{n\times n}$ such that the following LMIs are satisfied.

$$\mathbf{X} > 0;$$
$$\mathbf{Q}_{ij} = \mathbf{A}_i\mathbf{X} + \mathbf{X}\mathbf{A}_i^T + \mathbf{B}_i\mathbf{N}_j + \mathbf{N}_j^T\mathbf{B}_i^T < 0 \;\forall\, i, j,$$

where the feedback gains are defined as $\mathbf{G}_j = \mathbf{N}_j\mathbf{X}^{-1}$ for all j.

However, without considering the information of the membership functions in the development of the stability conditions in Theorem 1 are very conservative. It can be seen from Theorem 1 that employing different feedback gains does not relax the stability conditions (or make the stability conditions to be satisfied easier). The stability conditions can be reduced to $\mathbf{Q}_{ij} = \mathbf{A}_i\mathbf{X}_j + \mathbf{X}_j\mathbf{A}_i^T + \mathbf{B}_i\mathbf{N} + \mathbf{N}^T\mathbf{B}_i^T < 0$ for all i by choosing a common feedback gain, i.e., $\mathbf{N} = \mathbf{N}_j$ for all j. Consequently, the fuzzy controller becomes a linear controller.

In this paper, the IT2 fuzzy control concept is employed to investigate the stability of the IT2 FMB control system (15). In order to facilitate the stability analysis, the state space of interest denoted as Φ is divided into q connected sub-state spaces denoted as Φ_k, $k = 1, 2, \cdots, q$ such that $\Phi = \bigcup_{k=1}^{q}\Phi_k$. We express the IT2 FMB control system (15) in the following favourable form.

$$\dot{\mathbf{x}}(t) = \sum_{i=1}^{p}\sum_{j=1}^{c}\tilde{h}_{ij}(\mathbf{x}(t))(\mathbf{A}_i + \mathbf{B}_i\mathbf{G}_j)\mathbf{x}(t) \quad (16)$$

where

$$\begin{aligned}&\tilde{h}_{ij}(\mathbf{x}(t)) \equiv \tilde{w}_i(\mathbf{x}(t))\tilde{m}_j(\mathbf{x}(t)) \\ &= \underline{\gamma}_{ij}(\mathbf{x}(t))\underline{h}_{ij}(\mathbf{x}(t)) + \overline{\gamma}_{ij}(\mathbf{x}(t))\overline{h}_{ij}(\mathbf{x}(t)) \geq 0 \;\forall\, i, j; \quad (17)\end{aligned}$$

$$\sum_{i=1}^{p}\sum_{j=1}^{c}\tilde{h}_{ij}(\mathbf{x}(t)) = 1, \quad (18)$$

where $0 \leq \underline{\gamma}_{ij}(\mathbf{x}(t)) \leq 1$ and $0 \leq \overline{\gamma}_{ij}(\mathbf{x}(t)) \leq 1$ are two functions, which are not necessary to be known, exhibiting the property that $\underline{\gamma}_{ij}(\mathbf{x}(t)) + \overline{\gamma}_{ij}(\mathbf{x}(t))$ for all i and j. The main purpose of these two nonlinear functions is to reconstruct $\tilde{h}_{ij}(\mathbf{x}(t)) \equiv \tilde{w}_i(\mathbf{x}(t))\tilde{m}_j(\mathbf{x}(t))$ by representing it as a linear combination of $\underline{h}_{ij}(\mathbf{x}(t))$ and $\overline{h}_{ij}(\mathbf{x}(t))$ as shown in (17). The nonlinear functions $\underline{h}_{ij}(\mathbf{x}(t))$ and $\overline{h}_{ij}(\mathbf{x}(t))$ exhibiting the property of $\underline{h}_{ij}(\mathbf{x}(t)) \leq \tilde{w}_i(\mathbf{x}(t))\tilde{m}_j(\mathbf{x}(t)) \leq \overline{h}_{ij}(\mathbf{x}(t))$ for all i, j and $\mathbf{x}(t)$ (or a predefined state space of interest) denote the lower and upper bounds of $\tilde{w}_i(\mathbf{x}(t))\tilde{m}_j(\mathbf{x}(t))$ (which are characterized by the lower and upper membership functions of the IT2 fuzzy model and the IT2 fuzzy controller, i.e., $\underline{w}_i(\mathbf{x}(t))$, $\overline{w}_i(\mathbf{x}(t))$, $\underline{m}_j(\mathbf{x}(t))$ and $\overline{m}_j(\mathbf{x}(t))$), and are defined as follows.

$$\begin{aligned}\underline{h}_{ij}(\mathbf{x}(t)) = &\sum_{k=1}^{q}\sum_{i_1=1}^{2}\sum_{i_2=1}^{2}\cdots\sum_{i_n=1}^{2} \\ &\times\prod_{r=1}^{n}v_{ri_rk}(x_r(t))\underline{\delta}_{iji_1i_2\cdots i_nk} \;\forall\, i, j, k, \quad (19)\end{aligned}$$

$$\begin{aligned}\overline{h}_{ij}(\mathbf{x}(t)) = &\sum_{k=1}^{q}\sum_{i_1=1}^{2}\sum_{i_2=1}^{2}\cdots\sum_{i_n=1}^{2} \\ &\times\prod_{r=1}^{n}v_{ri_rk}(x_r(t))\overline{\delta}_{iji_1i_2\cdots i_nk} \;\forall\, i, j, k, \quad (20)\end{aligned}$$

where $0 \leq \underline{\delta}_{iji_1i_2\cdots i_nk} \leq 1$ and $0 \leq \overline{\delta}_{iji_1i_2\cdots i_nk} \leq 1$ are constant scalars to be determined. The functions $v_{ri_sk}(x_r(t))$ are defined such that $0 \leq v_{ri_sk}(x_r(t)) \leq 1$ and $v_{r1k}(x_r(t)) + v_{r2k}(x_r(t)) = 1$ for $r, s = 1, 2, \cdots, n$; $i_r = 1, 2$; $\mathbf{x} \in \Phi_k$; otherwise, $v_{ri_sk}(x_r(t)) = 0$. As a result, we have the property that $\sum_{k=1}^{q}\sum_{i_1=1}^{2}\sum_{i_2=1}^{2}\cdots\sum_{i_n=1}^{2}\prod_{r=1}^{n}v_{ri_rk}(x_r(t)) = 1$, which is used in the stability analysis.

III. Stability Analysis

In this section, we will investigate the stability of the IT2 FMB control system (15) through the Lyapunov stability theory. A set of LMI-based stability conditions will be derived to guarantee the system stability and facilitate the control synthesis. For brevity, in the following analysis, the time t associated with the variables is dropped for situation without ambiguity, e.g., $\mathbf{x}(t)$ is denoted as $\mathbf{x}$. The variables $\underline{w}_i(\mathbf{x}(t))$, $\overline{w}_i(\mathbf{x}(t))$, $\tilde{w}_i(\mathbf{x}(t))$, $\underline{m}_j(\mathbf{x}(t))$, $\overline{m}_j(\mathbf{x}(t))$, $\tilde{m}_j(\mathbf{x}(t))$, $\tilde{h}_{ij}(\mathbf{x}(t))$, $v_{1i_1k}(x_1(t))$, $v_{2i_2k}(x_2(t))$, $\cdots$, $v_{ni_nk}(x_n(t))$ are denoted by $\underline{w}_i$, $\overline{w}_i$, $\tilde{w}_i$, $\underline{m}_j$, $\overline{m}_j$, $\tilde{m}_j$, $\tilde{h}_{ij}$, v_{1i_1k}, v_{2i_2k}, $\cdots$, v_{ni_nk}, respectively. Furthermore, the property of $\sum_{i=1}^{p}\tilde{w}_i = \sum_{j=1}^{c}\tilde{m}_j = \sum_{i=1}^{p}\sum_{j=1}^{c}\tilde{w}_i\tilde{m}_j = \sum_{i=1}^{p}\sum_{j=1}^{c}\tilde{h}_{ij} = 1$ is utilized.

We consider the following quadratic Lyapunov function candidate to investigate the stability of the IT2 FMB control systems (15) expressed in the form of (16).

$$V = \mathbf{x}^T\mathbf{P}\mathbf{x}, \quad (21)$$

where $0 < \mathbf{P} = \mathbf{P}^T \in \Re^{n\times n}$.

Denote $\mathbf{z} = \mathbf{P}^{-1}\mathbf{x}$ and $\mathbf{X} = \mathbf{P}^{-1}$. Define the feedback gains $\mathbf{G}_j = \mathbf{N}_j\mathbf{X}^{-1}$ where $\mathbf{N}_j \in \Re^{m\times n}$, $j = 1, 2, \cdots, c$, are matrices to be determined. From (16) and (21), we have,

$$\begin{aligned}\dot{V} &= \dot{\mathbf{x}}^T\mathbf{P}\mathbf{x} + \mathbf{x}^T\mathbf{P}\dot{\mathbf{x}} \\ &= \sum_{i=1}^{p}\sum_{j=1}^{c}\tilde{h}_{ij}\mathbf{x}^T\big((\mathbf{A}_i + \mathbf{B}_i\mathbf{G}_j)^T\mathbf{P} + \mathbf{P}(\mathbf{A}_i + \mathbf{B}_i\mathbf{G}_j)\big)\mathbf{x} \\ &= \sum_{i=1}^{p}\sum_{j=1}^{c}(\underline{\gamma}_{ij}\underline{h}_{ij} + \overline{\gamma}_{ij}\overline{h}_{ij})\mathbf{z}^T\mathbf{Q}_{ij}\mathbf{z}, \end{aligned} \tag{22}$$

where $\mathbf{Q}_{ij} = \mathbf{A}_i\mathbf{X} + \mathbf{X}\mathbf{A}_i^T + \mathbf{B}_i\mathbf{N}_j + \mathbf{N}_j^T\mathbf{B}_i^T$.

Recalling the property that $\overline{h}_{ij} \geq \underline{h}_{ij} \geq 0$, $0 \leq \underline{\gamma}_{ij} \leq 1$, $0 \leq \overline{\gamma}_{ij} \leq 1$ and $\underline{\gamma}_{ij} + \overline{\gamma}_{ij} = 1$ for all i and j, we introduce some slack matrices to the stability analysis through the following inequalities using the S-procedure [6].

$$\big(\sum_{i=1}^{p}\sum_{j=1}^{c}(\underline{\gamma}_{ij}\underline{h}_{ij} + \overline{\gamma}_{ij}\overline{h}_{ij}) - 1\big)\mathbf{M} = \mathbf{0}, \tag{23}$$

$$-\sum_{i=1}^{p}\sum_{j=1}^{c}(1 - \underline{\gamma}_{ij})(\underline{h}_{ij} - \overline{h}_{ij})\mathbf{W}_{ij} \geq 0, \tag{24}$$

where $\mathbf{M} = \mathbf{M}_{ij}^T \in \Re^{n\times n}$ are arbitrary matrices and $0 \leq \mathbf{W}_{ij} = \mathbf{W}_{ij}^T \in \Re^{n\times n}$.

From (22), (23) and (24), we have

$$\begin{aligned}\dot{V} \leq& \sum_{i=1}^{p}\sum_{j=1}^{c}(\underline{\gamma}_{ij}\underline{h}_{ij} + (1 - \underline{\gamma}_{ij})\overline{h}_{ij})\mathbf{z}^T\mathbf{Q}_{ij}\mathbf{z} \\ &- \sum_{i=1}^{p}\sum_{j=1}^{c}(1 - \underline{\gamma}_{ij})(\underline{h}_{ij} - \overline{h}_{ij})\mathbf{z}^T\mathbf{W}_{ij}\mathbf{z} \\ &+ \big(\sum_{i=1}^{p}\sum_{j=1}^{c}(\underline{\gamma}_{ij}\underline{h}_{ij} + (1 - \underline{\gamma}_{ij})\overline{h}_{ij}) - 1\big)\mathbf{z}^T\mathbf{M}\mathbf{z} \\ =& \mathbf{z}^T\big(\sum_{i=1}^{p}\sum_{j=1}^{c}(\overline{h}_{ij}\mathbf{Q}_{ij} - (\underline{h}_{ij} - \overline{h}_{ij})\mathbf{W}_{ij} + \overline{h}_{ij}\mathbf{M}) - \mathbf{M}\big)\mathbf{z} \\ &+ \sum_{i=1}^{p}\sum_{j=1}^{c}\underline{\gamma}_{ij}(\underline{h}_{ij} - \overline{h}_{ij})\mathbf{z}^T(\mathbf{Q}_{ij} + \mathbf{W}_{ij} + \mathbf{M})\mathbf{z}. \end{aligned} \tag{25}$$

It can be seen from (21) that $V > 0$ for all $\mathbf{x} \neq \mathbf{0}$. From (25), if the inequalities, $\sum_{i=1}^{p}\sum_{j=1}^{c}(\overline{h}_{ij}\mathbf{Q}_{ij} - (\underline{h}_{ij} - \overline{h}_{ij})\mathbf{W}_{ij} + \overline{h}_{ij}\mathbf{M}) - \mathbf{M} < 0$ and $\mathbf{Q}_{ij} + \mathbf{W}_{ij} + \mathbf{M} > 0$ (as $\underline{\gamma}_{ij}(\underline{h}_{ij} - \overline{h}_{ij}) \leq 0$) for all i and j are satisfied, we have $\dot{V} < 0$ for all $\mathbf{x} \neq \mathbf{0}$. As a result, the IT2 FMB control system is guaranteed to be asymptotically stable in the sense of Lyapunov. The second set of inequalities is in the form of LMI, however, the first one is not due to the existence of the lower and upper membership functions $\underline{h}_{ij}$ and $\overline{h}_{ij}$. With the expression of (19) and (20), recalling that $\sum_{k=1}^{q}\sum_{i_1=1}^{2}\sum_{i_2=1}^{2}\cdots\sum_{i_n=1}^{2}\prod_{r=1}^{n}v_{ri_rk} = 1$, the second first inequality can be written as follows.

$$\begin{aligned}&\sum_{k=1}^{q}\sum_{i_1=1}^{2}\sum_{i_2=1}^{2}\cdots\sum_{i_n=1}^{2}\prod_{r=1}^{n}v_{ri_rk}\big(\sum_{i=1}^{p}\sum_{j=1}^{c}(\overline{\delta}_{iji_1i_2\cdots i_nk}\mathbf{Q}_{ij} \\ &- (\underline{\delta}_{iji_1i_2\cdots i_nk} - \overline{\delta}_{iji_1i_2\cdots i_nk})\mathbf{W}_{ij} + \overline{\delta}_{iji_1i_2\cdots i_nk}\mathbf{M}) \\ &- \mathbf{M}\big) < 0 \end{aligned} \tag{26}$$

It can be seen that the inequality $\sum_{i=1}^{p}\sum_{j=1}^{c}(\overline{h}_{ij}\mathbf{Q}_{ij} - (\underline{h}_{ij} - \overline{h}_{ij})\mathbf{W}_{ij} + \overline{h}_{ij}\mathbf{M}) - \mathbf{M} < 0$ can be achieved if $\sum_{i=1}^{p}\sum_{j=1}^{c}(\overline{\delta}_{iji_1i_2\cdots i_nk}\mathbf{Q}_{ij} - (\underline{\delta}_{iji_1i_2\cdots i_nk} - \overline{\delta}_{iji_1i_2\cdots i_nk})\mathbf{W}_{ij} + \overline{\delta}_{iji_1i_2\cdots i_nk}\mathbf{M}) - \mathbf{M} < 0$ for all i_1, i_2, $\cdots$, i_n and k.

Referring to (26), the advantages of representing the IT2 FMB control system (15) in the form of (16) can be seen. The membership functions $\tilde{h}_{ij}$ are reconstructed by a linear combination of the lower and upper membership functions $\underline{h}_{ij}$ and $\overline{h}_{ij}$. Consequently, as seen from (25), the stability of the IT2 FMB control system is determined by the lower and upper membership functions $\underline{h}_{ij}$ and $\overline{h}_{ij}$. By expressing $\underline{h}_{ij}$ and $\overline{h}_{ij}$ in the form of (19) and (20), respectively, they are characterized by the constant scalars $\underline{\delta}_{iji_1i_2\cdots i_nk}$ and $\overline{\delta}_{iji_1i_2\cdots i_nk}$. Furthermore, as the cross terms $\prod_{r=1}^{n}v_{ri_rk}(x_r(t))$ are independent of i and j, they can be extracted as shown in (26) to facilitate the stability analysis. With these favourable properties, we only need to check $\sum_{i=1}^{p}\sum_{j=1}^{c}(\overline{\delta}_{iji_1i_2\cdots i_nk}\mathbf{Q}_{ij} - (\underline{\delta}_{iji_1i_2\cdots i_nk} - \overline{\delta}_{iji_1i_2\cdots i_nk})\mathbf{W}_{ij} + \overline{\delta}_{iji_1i_2\cdots i_nk}\mathbf{M}) - \mathbf{M} < 0$ at some discrete points ($\underline{\delta}_{iji_1i_2\cdots i_nk}$ and $\overline{\delta}_{iji_1i_2\cdots i_nk}$) instead of every single point of the lower and upper membership functions $\underline{h}_{ij}$ and $\overline{h}_{ij}$ to guarantee the holding of the inequality (26).

Based on the Lyapunov stability theory, the IT2 FMB control system (15) is guaranteed to be asymptotically stable if the LMI-based stability conditions summarized in the following theorem are satisfied.

Theorem 2: The IT2 FMB control system (15) under imperfect premise matching, formed by a nonlinear plant (represented by the IT2 T-S fuzzy model (5)) and an IT2 fuzzy controller (12) connected in a closed loop, is guaranteed to be asymptotically stable if there exist matrices $\mathbf{M} = \mathbf{M} \in \Re^{n\times n}$, $\mathbf{N}_j \in \Re^{m\times n}$, $\mathbf{X} = \mathbf{X}^T \in \Re^{n\times n}$, $\mathbf{W}_{ij} = \mathbf{W}_{ij}^T \in \Re^{n\times n}$, $i = 1, 2, \ldots, p$; $j = 1, 2, \ldots, c$, such that the following LMIs are satisfied.

$$\mathbf{X} > 0; \tag{27}$$

$$\mathbf{W}_{ij} \geq 0,\ \forall\, i, j; \tag{28}$$

$$\mathbf{Q}_{ij} + \mathbf{W}_{ij} + \mathbf{M} > 0,\ \forall\, i, j; \tag{29}$$

$$\begin{aligned}&\sum_{i=1}^{p}\sum_{j=1}^{c}(\overline{\delta}_{iji_1i_2\cdots i_nk}\mathbf{Q}_{ij} - (\underline{\delta}_{iji_1i_2\cdots i_nk} - \overline{\delta}_{iji_1i_2\cdots i_nk})\mathbf{W}_{ij} \\ &+ \overline{\delta}_{iji_1i_2\cdots i_nk}\mathbf{M}) - \mathbf{M} < 0,\ \forall\, i_1, i_2, \cdots, i_n, k; \end{aligned} \tag{30}$$

where $\underline{\delta}_{iji_1i_2\cdots i_nk}$ and $\overline{\delta}_{iji_1i_2\cdots i_nk}$, $i = 1, 2, \ldots, p$; $j = 1, 2, \ldots, c$; $i_1, i_2, \cdots, i_n = 1, 2$; $k = 1, 2, \cdots, q$ are pre-defined constant scalars satisfying (19) and (20);

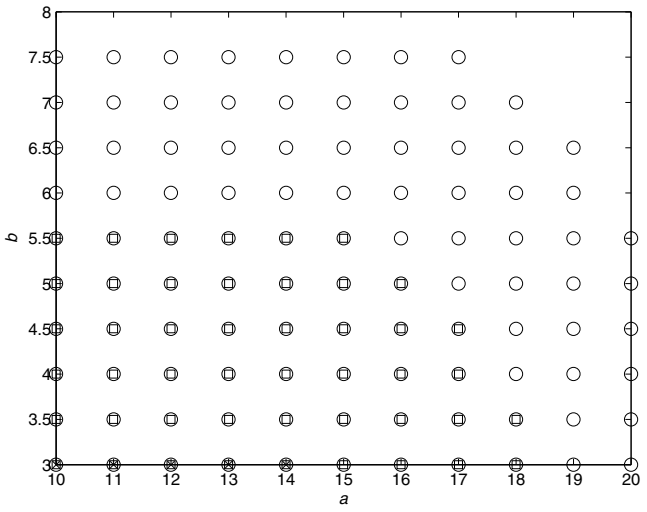

Fig. 1. Stability regions given by the stability conditions in Theorem 2 for Case 1 ('×'); Case 2 ('□'); and Case 3 ('○').

$\mathbf{Q}_{ij} = \mathbf{A}_i\mathbf{X} + \mathbf{X}\mathbf{A}_i^T + \mathbf{B}_i\mathbf{N}_j + \mathbf{N}_j^T\mathbf{B}_i^T$ for all i and j; and the feedback gains are defined as $\mathbf{G}_j = \mathbf{N}_j\mathbf{X}^{-1}$ for all j.

Remark 1: It should be noted that the LMI-based stability conditions in Theorem 2 are for the IT2 FMB control systems under imperfect premise matching that the IT2 fuzzy controller does not require sharing the same lower and upper premise membership functions and the same number of fuzzy rules as those of the IT2 T-S fuzzy model. As a result, compared with the stability conditions for the IT2 FMB control systems under perfect premise matching [26], it offers a higher design flexibility to the IT2 fuzzy controller.

Remark 2: It can be shown that the stability conditions in Theorem 1 is a particular case of Theorem 2 (the solution of the stability conditions in Theorem 1 is that of Theorem 2). Referring to Theorem 1, if there exists a solution, we have $\mathbf{X} > 0$ and $\mathbf{Q}_{ij} < 0$ for all i and j. Referring to Theorem 2, choosing $\mathbf{M} = \varepsilon_1\mathbf{I} > 0$ where $\varepsilon_1 > 0$. The LMIs (28) and (29) must be satisfied by choosing $\mathbf{W}_{ij} = -\mathbf{Q}_{ij} + (-\varepsilon_1 + \varepsilon_2)\mathbf{I} > 0$ for all i and j with sufficiently small non-zero positive value of ε_1 and ε_2. As a result, recalling that $\overline{\delta}_{iji_1i_2\cdots i_nk} \geq \underline{\delta}_{iji_1i_2\cdots i_nk} \geq 0$, the LMIs in (30) become $\sum_{i=1}^{p}\sum_{j=1}^{c}(\overline{\delta}_{iji_1i_2\cdots i_nk}\varepsilon_2\mathbf{I} - \underline{\delta}_{iji_1i_2\cdots i_nk}\mathbf{W}_{ij}) - \varepsilon_1\mathbf{I} < 0$ for all $i_1, i_2, \cdots, i_n$ and k, which will be satisfied by a sufficiently small value of ε_2.

IV. Simulation Example

We consider a nonlinear plant represented by a 3-rule IT2 T-S fuzzy model in the form of (5), with $\mathbf{A}_1 = \begin{bmatrix} 1.59 & -7.29 \\ 0.01 & 0 \end{bmatrix}$, $\mathbf{A}_2 = \begin{bmatrix} 0.02 & -4.64 \\ 0.35 & 0.21 \end{bmatrix}$, $\mathbf{A}_3 = \begin{bmatrix} -a & -4.33 \\ 0 & 0.05 \end{bmatrix}$, $\mathbf{B}_1 = \begin{bmatrix} 1 \\ 0 \end{bmatrix}$, $\mathbf{B}_2 = \begin{bmatrix} 8 \\ 0 \end{bmatrix}$, $\mathbf{B}_3 = \begin{bmatrix} -b+6 \\ -1 \end{bmatrix}$, $\mathbf{x} = [x_1 \quad x_2]^T$, a and b are constant system parameters. For demonstration purposes, the actual membership functions are chosen as $\tilde{w}_1(x_1) = \mu_{M_1^1}(x_1) = 1 - \frac{1}{1+e^{-(x_1+4+\sigma(t))}}$, $\tilde{w}_2(x_1) = \mu_{M_1^2}(x_1) = 1 - \tilde{w}_1(x_1) - \tilde{w}_3(x_1)$ and $\tilde{w}_3(x_1) = \mu_{M_1^3}(x_1) = \frac{1}{1+e^{-(x_1-4+\sigma(t))}}$ where $\sigma(t) \in [-0.1, 0.1]$ represents the parameter uncertainty. The lower and upper membership functions for the IT2 T-S fuzzy model are chosen to be $\underline{w}_1(x_1) = \underline{\mu}_{\tilde{M}_1^1}(x_1) = 1 - \frac{1}{1+e^{-(x_1+4+d_1)}}$, $\underline{w}_3(x_1) = \underline{\mu}_{\tilde{M}_1^3}(x_1) = \frac{1}{1+e^{-(x_1-4-d_1)}}$, $\overline{w}_1(x_1) = \overline{\mu}_{\tilde{M}_1^1}(x_1) = 1 - \frac{1}{1+e^{-(x_1+4-d_1)}}$, $\overline{w}_3(x_1) = \overline{\mu}_{\tilde{M}_1^3}(x_1) = \frac{1}{1+e^{-(x_1-4+d_1)}}$, $\underline{w}_2(x_1) = \underline{\mu}_{\tilde{M}_1^2}(x_1) = 1 - \overline{\mu}_{\tilde{M}_1^1}(x_1) - \overline{\mu}_{\tilde{M}_1^3}(x_1)$ and $\overline{w}_2(x_1) = \overline{\mu}_{\tilde{M}_1^2}(x_1) = 1 - \underline{\mu}_{\tilde{M}_1^1}(x_1) - \underline{\mu}_{\tilde{M}_1^3}(x_1)$ where d_1 is a constant to be determined.

A 2-rule fuzzy controller in the form of (12) is employed to stabilize the nonlinear plant. The lower and upper membership functions are chosen as $\underline{m}_1(x_1) = \underline{\mu}_{\tilde{N}_1^1}(x_1) = 1 - \frac{1}{e^{\frac{-x_1+d_2}{2}}}$, $\overline{m}_1(x_1) = \overline{\mu}_{\tilde{N}_1^1}(x_1) = 1 - \frac{1}{e^{\frac{-x_1-d_2}{2}}}$, $\underline{m}_2(x_1) = \underline{\mu}_{\tilde{N}_1^2}(x_1) = 1 - \overline{\mu}_{\tilde{N}_1^1}(x_1)$ and $\overline{m}_2(x_1) = \overline{\mu}_{\tilde{N}_1^2}(x_1) = 1 - \underline{\mu}_{\tilde{N}_1^1}(x_1)$. From (13), we have $\tilde{m}_j(x_1) = \frac{\underline{\beta}_j\underline{m}_j(x_1) + \overline{\beta}_j\overline{m}_j(x_1)}{\sum_{k=1}^{c}(\underline{\beta}_k\underline{m}_k(x_1) + \overline{\beta}_k\overline{m}_k(x_1))}$ for $j = 1, 2$, where $\underline{\beta}_j$ and $\overline{\beta}_j$ are chosen to be a constant; d_2 is a constant to be determined, in this example.

To determine the lower and upper membership functions $\underline{h}_{ij}(x_1)$ and $\overline{h}_{ij}(x_1)$, we consider $x_1 \in [-10, 10]$ and divide the state space of x_1 into 20 regions, i.e., $\phi_k : \underline{x}_{1,k} \leq x_1 < \overline{x}_{1,k}$, $k = 1, 2, \cdots, 19$ and $\phi_{20} : \underline{x}_{1,20} \leq x_1 \leq \overline{x}_{1,20}$, where $\underline{x}_{1,k} = (k - 11)$ and $\overline{x}_{1,k} = (k - 10)$. The lower and upper membership functions $\underline{h}_{ij}(x_1)$ and $\overline{h}_{ij}(x_1)$ can be defined by choosing $v_{11k}(x_1) = 1 - \frac{x_1 - \underline{x}_{1,k}}{\overline{x}_{1,k} - \underline{x}_{1,k}}$ and $v_{12k}(x_1) = 1 - v_{11k}(x_1)$; and the constant scalars as $\underline{\delta}_{ij1k} = \underline{w}_i(\underline{x}_{1,k})\underline{m}_j(\underline{x}_{1,k})$, $\underline{\delta}_{ij2k} = \underline{w}_i(\overline{x}_{1,k})\underline{m}_j(\overline{x}_{1,k})$, $\overline{\delta}_{ij1k} = \overline{w}_i(\underline{x}_{1,k})\overline{m}_j(\underline{x}_{1,k})$, $\overline{\delta}_{ij2k} = \overline{w}_i(\overline{x}_{1,k})\overline{m}_j(\overline{x}_{1,k})$ for all k.

TABLE I
Parameter values for $\underline{\beta}_j$, $\underline{\beta}_j$, d_1 and d_2.

	Case 1	Case 2	Case 3
$\underline{\beta}_j$	1	0.5	0
$\underline{\beta}_j$	0	0.5	1
d_1	0.3	0.3	0.25
d_2	0.25	0.15	0.15

The stability conditions in Theorem 2 are employed to check the stability of the IT2 FMB control system with the Matlab LMI toolbox. We consider three cases with different values of $\underline{\beta}_j$, $\underline{\beta}_j$, d_1 and d_2, as shown in Table I, to test the stability conditions in Theorem 2. The values of d_1 and d_2 are chosen such that $\tilde{h}_{ij}(x_1)$ in the form of (17) are withing the lower and upper membership functions defined in (19) and (20), respectively. Considering $10 \leq a \leq 20$ at the interval of 1 and $3 \leq b \leq 8$ at the interval of 0.5, with the $\underline{\beta}_j = \overline{\beta}_j = 0.5$, the stability regions are shown in Fig. 1 indicated by '×',

'□' and '○' corresponding to Case 1 to Case 3, respectively. It can be seen that different values of $\underline{\beta}_j$ and $\overline{\beta}_j$, leading to different values of d_1 and d_2, will produce different size of stability regions. It demonstrates a trend that Case 3 produces a larger stability region than Case 2 while Case 3 produces a larger stability region than Case 1 due to different values of d_1 and d_2. For comparison purposes, Theorem 1 is employed to check the stability of the IT2 FMB control system. However, no feasible solution can be obtained. It should be noted that the IT2 FMB control system is under imperfect premise matching, the stability conditions in [26] for perfect premise matching cannot be applied in this example.

V. Conclusion

The stability of IT2 FMB control systems subject to parameter uncertainties under imperfect matching has been investigated. It is not required that both the IT2 T-S fuzzy model and the IT2 fuzzy controller share the same number of rules and/or the same set of premise membership functions. Thus, it offers a greater design flexibility for the IT2 fuzzy controller and is possible to lower the controller complexity by employing a smaller number of rules and simple membership functions. Through the lower and upper membership functions, the information of the nonlinearity and parameter uncertainties embedded in the footprint of uncertainty are brought to the stability analysis. Based on the Lyapunov stability theory, LMI-based stability conditions are obtained to guarantee the stability of the IT2 FMB control system and synthesize the IT2 fuzzy controller. Simulation examples have been given to demonstrate the merits of the proposed approach.

Acknowledgment

The work described in this paper was supported by King's College London.

References

[1] G. Feng, "A survey on analysis and design of model-based fuzzy control systems," *IEEE Trans. Fuzzy Systems*, vol. 14, no. 5, pp. 676–697, Oct. 2006.

[2] T. Takagi and M. Sugeno, "Fuzzy identification of systems and its applications to modelling and control," *IEEE Trans. Sys., Man., Cybern.*, vol. smc-15, no. 1, pp. 116–132, Jan. 1985.

[3] M. Sugeno and G. T. Kang, "Structure identification of fuzzy model," *Fuzzy sets and systems*, vol. 28, no. 1, pp. 15–33, Oct. 1988.

[4] H. O. Wang, K. Tanaka, and M. F. Griffin, "An approach to fuzzy control of nonlinear systems: Stability and design issues," *IEEE Trans. Fuzzy Systems*, vol. 4, no. 1, pp. 14–23, Feb. 1996.

[5] K. Tanaka, T. Ikeda, and H. O. Wang, "Fuzzy regulators and fuzzy observers: Relaxed stability conditions and LMI-based designs," *IEEE Trans. Fuzzy Systems*, vol. 6, no. 2, pp. 250–265, May 1998.

[6] S. P. Boyd, *Linear matrix inequalities in system and control theory*. Society for Industrial and Applied Mathematics (SIAM), 1994.

[7] E. Kim and H. Lee, "New approaches to relaxed quadratic stability condition of fuzzy control systems," *IEEE Trans. Fuzzy Systems*, vol. 8, no. 5, pp. 523–534, Oct. 2000.

[8] M. C. M. Teixeira, E. Assuncao, and R. G. Avellar, "On relaxed LMI-based designs for fuzzy regulators and fuzzy observers," *IEEE Trans. Fuzzy Systems*, vol. 11, no. 5, pp. 613–623, Oct. 2003.

[9] X. Liu and Q. Zhang, "New approaches to H_∞ controller designs based on fuzzy observers for Takagi-Sugeno fuzzy systems via LMI," *Automatica*, vol. 39, no. 9, pp. 1571–1582, Sep. 2003.

[10] ——, "Approaches to quadratic stability conditions and H_∞ control designs for Takagi-Sugeno fuzzy systems," *IEEE Trans. Fuzzy Systems*, vol. 11, no. 6, pp. 830–839, Dec. 2003.

[11] C. H. Fang, Y. S. Liu, S. W. Kau, L. Hong, and C. H. Lee, "A new LMI-based approach to relaxed quadratic stabilization of Takagi-Sugeno fuzzy control systems," *IEEE Trans. Fuzzy Systems*, vol. 14, no. 3, pp. 386–397, Jun. 2006.

[12] A. Sala and C. Ariño, "Asymptotically necessary and sufficient conditions for stability and performance in fuzzy control: Applications of Polya's theorem," *Fuzzy Sets Syst.*, vol. 158, no. 24, pp. 2671–2686, Jul. 2007.

[13] ——, "Relaxed stability and performance conditions for Takagi-Sugeno fuzzy systems with knowledge on membership function overlap," *IEEE Trans. Syst., Man and Cybern., Part B: Cybernetics*, vol. 37, no. 3, pp. 727–732, Jun. 2007.

[14] ——, "Relaxed stability and performance LMI conditions for Takagi-Sugeno fuzzy systems with polynomial constraints on membership function shapes," *IEEE Trans. Fuzzy Systems*, vol. 16, no. 5, pp. 1328–1336, Oct. 2008.

[15] A. Kruszewski, A. Sala, T. Guerra, and C. Arino, "A triangulation approach to asymptotically exact conditions for fuzzy summations," *IEEE Trans. on Fuzzy Systems*, vol. 17, no. 5, pp. 985 –994, Oct. 2009.

[16] H. K. Lam and F. H. F. Leung, "Stability analysis of fuzzy control systems subject to uncertain grades of membership," *IEEE Trans. Syst., Man and Cybern., Part B: Cybernetics*, vol. 35, no. 6, pp. 1322–1325, Dec. 2005.

[17] C. Ariño and A. Sala, "Extensions to "stability analysis of fuzzy control systems subject to uncertain grades of membership"," *IEEE Trans. Syst., Man and Cybern., Part B: Cybernetics*, vol. 38, no. 2, pp. 558 –563, Apr. 2008.

[18] H. K. Lam and M. Narimani, "Stability analysis and performance design for fuzzy-model-based control system under imperfect premise matching," *IEEE Trans. Fuzzy Systems*, vol. 17, no. 4, pp. 949–961, Aug 2009.

[19] M. Narimani and H. K. Lam, "Relaxed LMI-based stability conditions for Takagi-Sugeno fuzzy control systems using regional-membership-function-shape-dependent analysis approach," *IEEE Trans. Fuzzy Systems*, vol. 17, no. 5, pp. 1221–1228, Oct. 2009.

[20] H. K. Lam and M. H. Narimani, "Quadratic stability analysis of fuzzy-model-based control systems using staircase membership functions," *IEEE Trans. Fuzzy Systems*, vol. 18, no. 1, pp. 125–137, Feb. 2010.

[21] J. M. Mendel, R. I. John, and F. Liu, "Interval type-2 fuzzy logic systems made simple," *IEEE Trans. Fuzzy Systems*, vol. 14, no. 6, pp. 808–821, Dec. 2006.

[22] J. M. Mendel and F. Liu, "Super-exponential convergence of the Karnik–Mendel algorithms for computing the centroid of an interval type-2 fuzzy set," *IEEE Trans. Fuzzy Systems*, vol. 15, no. 2, pp. 309–320, Apr. 2007.

[23] S. Coupland and R. John, "Geometric type-1 and type-2 fuzzy logic systems," *IEEE Trans. Fuzzy Systems*, vol. 15, no. 1, pp. 3–15, Feb. 2007.

[24] E. A. Jammeh, M. Fleury, C. Wagner, H. Hagras, and M. Ghanbari, "Interval type-2 fuzzy logic congestion control for video streaming across IP networks," *IEEE Trans. on Fuzzy Systems*, vol. 17, no. 5, pp. 1123–1142, Oct. 2009.

[25] Q. Liang and J. M. Mendel, "Equalization of nonlinear time-varying channels using type-2 fuzzy adaptive filters," *IEEE Trans. Fuzzy Systems*, vol. 8, no. 5, pp. 551–563, Oct. 2000.

[26] H. K. Lam and L. D. Seneviratne, "Stability analysis of interval type-2 fuzzy-model-based control systems," *IEEE Trans. Syst., Man and Cybern., Part B: Cybernetics*, vol. 38, no. 3, pp. 617–628, Jun. 2008.

2011 IEEE International Conference on Fuzzy Systems
June 27-30, 2011, Taipei, Taiwan

Robust H_∞ Fuzzy Observer for A Class of Time-Delay Discrete Fuzzy Bilinear Systems with Parameter Uncertainties

Shun-Hung Tsai*
Graduate Institute of Automation Technology
National Taipei University of Technology
Taipei, Taiwan
shtsai@ntut.edu.tw

Ta-Tau Chen
Department of Electrical Engineering
Kun Shan University
Tainan, Taiwan
chen0221@mail.ksu.edu.tw

Ming-Ying Hsiao
Department of Electrical Engineering
Fortune Institute of Technology
Kaohsiung, Taiwan
myhsiao@center.fotech.edu.tw

Chin-Sheng Chen
Graduate Institute of Automation Technology
National Taipei University of Technology
Taipei, Taiwan
saint@ntut.edu.tw

***Abstract*—In this paper, a robust H_∞ fuzzy observer is proposed for a class of time-delay discrete fuzzy bilinear systems with parameter uncertainties. Utilizing the Lipschitz conditions, a linear matrix inequality approach is developed and a sufficient condition is obtained to design the robust H_∞ fuzzy observer. Besides, the robust H_∞ fuzzy observer for time-delay discrete fuzzy bilinear systems with parameter uncertainties can be obtained through the LMIs without any pre-assigned gain matrices. Finally, a numerical example is illustrated the feasibility and effectively of proposed observer design method.**

Keywords- Time-delay, fuzzy observer, linear matrix inequalities; fuzzy bilinear system.

I. INTRODUCTION

During the last decade, fuzzy technique has attracted great attention from both the academic and industrial applications. Among various fuzzy controls, a so-called Takagi–Sugeno (T–S) fuzzy model [1-3] becomes a popular and convenient tool in analyzing the nonlinear system. Through fuzzy modeling procedure, the T-S fuzzy model can be obtained from a nonlinear system. In addition, the obtained T-S fuzzy model is composed of many linear models; therefore, there are many linear system theories which can be utilized to analyze the T-S fuzzy model. By examining controller design, the parallel distributed compensation (PDC) scheme is adopted for each rule to stabilize the overall T-S fuzzy model. For the problems of stability and stabilization of T-S fuzzy models, the Lyapunov direct method [4-7] is mainly investigated to yield the stability/stabilization conditions. Furthermore, the solutions can be found via linear matrix inequalities (LMIs) techniques [8-11] for the T-S fuzzy control system under consideration. Due to the systematic design procedure, different methodologies have been also proposed for the stabilization problem of T-S fuzzy model [4], [12-13].

Even though T-S fuzzy model is composed of linear models blended together with nonlinear scalar positive functions sharing the convex sum property, and can be utilized the linear system theory to analyze the T-S fuzzy model. But unfortunately, there are many real-world nonlinear systems cannot be adequately approximated by linear models [14], [15]. Due to this reason, [16] first proposed a novel fuzzy modeling method to modelize the nonlinear system into a T-S fuzzy bilinear system (FBS). Besides, [17] studied the H_∞ control problem for a class of discrete fuzzy bilinear systems (DFBSs). Furthermore, [18-20] explored the stabilization problem of T-S FBS with time-delay. In addition to the stabilization problem, [21] investigated the observer design for T-S FBS. [22] explored the output feedback control and proposed an observer for T-S time-delay FBS, but in this paper, some matrices still needs to be pre-assigned for obtaining the observer gains. Moreover, there is no any study proposed a LMI method to obtain the observer gains without any pre-assigned matrices for time-delay FBS/DFBS. Furthermore, there is no any literature to investigate the robust H_∞ fuzzy observer for time-delay DFBS with parameter uncertainties and additive disturbance. Hence, we will explore the robust fuzzy H_∞ observer problem in this paper. The main contributions of this paper include i) Proposing a robust fuzzy H_∞ observer for time-delay DFBSs with parameter uncertainties; ii) The stability conditions for time-delay DFBSs with parameter uncertainties can be formulated as LMIs, and iii) The robust fuzzy H_∞ observer gain for time-delay DFBSs with parameter uncertainties can be obtained from LMIs without any pre-assigned parameter/matrix.

Following the introduction, the paper is organized as follows. In Section II the observer design problem for the time-delay DFBS with parameter uncertainties is introduced. Applying the Lipschitz conditions and some variable transformations, the sufficient conditions for time-delay DFBSs with parameter uncertainties can be transformed into the forms of LMI in Section III. In Section IV, a simulation example is provided to illustrate the effectiveness of the proposed design approach. Finally, in Section V, conclusions are drawn.

II. PROBLEM DESCRIPTION

The T-S fuzzy dynamic model is described by fuzzy IF-THEN rules, which locally represent input-output relations of

The authors would like to thank the National Science Council for financially supporting this research under contract NSC-99-2221-E-027-101 and NSC-98-2622-E-168-013-CC3.

nonlinear systems. Similar to [2], [4], the i th rule of the uncertain DFBS with disturbance can be represented by the following form:

Plant Rule i : IF $s_1(k)$ is F_{i1} and $\cdots$ and $s_g(k)$ is F_{ig}

THEN

$$x(k+1) = (A_i + \Delta A_i)x(k) + (A_{di} + \Delta A_{di})x(k-\tau) + N_i x(k)u(k) + N_{di}x(k-\tau)u(k) + D_{1i}w(k) \quad (1a)$$

$$y(k) = (C_i + \Delta C_i)x(k) + (C_{di} + \Delta C_{di})x(k-\tau) + D_{2i}w(k) \quad (1b)$$

$$z(k) = R_i e(k) + R_{di}e(k-\tau) \quad (1c)$$

$$x(k) = \phi(k) \quad \forall k \in [-\tau, 0],\ i = 1, \cdots r$$

where F_{ij} is the fuzzy set, and r is the number of IF-THEN rules; $s_1(t), s_2(t), \cdots s_g(t)$, are the premise variables. $x(k) \in R^{n\times 1}$ is the system state; $u(k) \in R^{1\times 1}$ is the input and satisfies $|u(k)| \le 1$ for all $k \in \mathbf{Z}$, $w(k) \in R^{q\times 1}$ is the exogenous disturbance which belongs to $l_2[0,\infty)$; $\tau > 0$ is an integer representing the time delay of the fuzzy system; $y(k) \in R^{p\times 1}$ is the measured output; $z(k) \in R^{m\times 1}$ is the controlled output of the error state, A_i , A_{di} , N_i , N_{di} , C_i , C_{di} , D_{1i} , D_{2i} , R_i , and R_{di} are known real matrices with appropriate dimensions. ΔA_i , ΔA_{di} , ΔC_i , and ΔC_{di} are unknown matrices representing time-varying parameter uncertainties, and are assumed to be of the following matched form:

Assumption 1: [8,] [10]

$$[\Delta A_i \quad \Delta A_{di}] = G_{1i}F_{1i}[E_{1i} \quad E_{2i}] \quad (2a)$$

$$[\Delta C_i \quad \Delta C_{di}] = G_{2i}F_{2i}[E_{3i} \quad E_{4i}] \quad (2b)$$

where G_{1i} , G_{2i} , E_{1i} , E_{2i} , E_{3i} , and E_{4i} are known real constant matrices of appropriate dimensions, and $F_{1i}(k)$, and $F_{2i}(k)$ are unknown matrix function with Lebesgue-measurable elements and satisfy $F_{1i}^T(k)F_{1i}(k) \le I$ and $F_{2i}^T(k)F_{2i}(k) \le I$. The parameter uncertainties ΔA_i , ΔA_i , ΔC_i , and ΔC_{di} are said to be admissible if Assumption 1 hold. Similar to [4] and [10], using a center average defuzzifier, product inference, and singleton fuzzifier, the discrete fuzzy bilinear system with time-delay can be expressed as (3a)-(3c).

Where $\mu_i(s(k)) = \prod_{j=1}^{g} F_{ij}(s(k))$, $h_i(s(k)) = \dfrac{\mu_i(s(k))}{\sum_{j=1}^{r}\mu_j(s(k))}$, $F_{ij}(s_j(k))$ is the grade of membership of $s_j(k)$ in F_{ij} , and $s(k) = [s_1(k) \quad s_2(k) \quad \cdots \quad s_n(k)]^T$. Some basic properties of $\mu_i(s(k))$ are $\mu_i(s(k)) \ge 0$ and $\sum_{i=1}^{r}\mu_i(s(k)) > 0$. It is clear that $h_i(s(k)) \ge 0$ and $\sum_{j=1}^{r} h_j(s(k)) = 1$. According to the conception of observer for linear system, we consider the H_∞ fuzzy observer as follows:

$$\hat{x}(k+1) = \sum_{i=1}^{r} h_i(s(k))\big(A_i\hat{x}(k) + A_{di}\hat{x}(k-\tau) + N_i\hat{x}(k)u(k) + N_{di}\hat{x}(k-\tau)u(k) + L_i[y(k) - C_i\hat{x}(k) - C_{di}\hat{x}(k-\tau)]\big) \quad (4)$$

where $\hat{x}(k)$ is the estimated state vector of $x(k)$, and $L_i \in R^{n\times 1}$ are observer parameters to be determined. Besides, $N_i^*(u(k), x(k), x(k-\tau), k) = (N_i x(k)u(k) + N_{di}x(k-\tau)u(k))$ is assumed to satisfy the following global Lipschitz conditions: $N_i^*(u(k), 0, 0, k) = 0$, and

$$\left\| N_i^*(u(k), x, \underset{\sim}{x}, k) - N_i^*(u(k), \hat{x}, \underset{\sim}{\hat{x}}, k) \right\| \quad (5)$$

For all $k \in \mathbf{Z}$, $u(k) \in R^{1\times 1}$ and x , $\underset{\sim}{x}$, $\hat{x}$, $\underset{\sim}{\hat{x}} \in R^{n\times 1}$, where $\bar{N}_i$, $\bar{N}_{di}$ are known matrices with appropriate dimensions.

$$x(k+1) = \sum_{i=1}^{r}\mu_i(s(k))\big((A_i + \Delta A_i)x(k) + (A_{di} + \Delta A_{di})x(k-\tau) + N_i x(k)u(k) + N_{di}x(k-\tau)u(k) + D_{1i}w(k)\big) / \sum_{i=1}^{r}\mu_i(s(k))$$
$$= \sum_{i=1}^{r} h_i(s(k))\big((A_i + \Delta A_i)x(k) + (A_{di} + \Delta A_{di})x(k-\tau) + N_i x(k)u(k) + N_{di}x(k-\tau)u(k) + D_{1i}w(k)\big) \quad (3a)$$

$$y(k) = \sum_{i=1}^{r}\mu_i(s(k))\big((C_i + \Delta C_i)x(k) + (C_{di} + \Delta C_{di})x(k-\tau) + D_{2i}w(k)\big) / \sum_{i=1}^{r}\mu_i(s(k))$$
$$= \sum_{i=1}^{r} h_i(s(k))\big((C_i + \Delta C_i)x(k) + (C_{di} + \Delta C_{di})x(k-\tau) + D_{2i}w(k)\big) \quad (3b)$$

$$z(k) = \sum_{i=1}^{r}\mu_i(s(k))\big(R_i e(k) + R_{di}e(k-\tau)\big) / \sum_{i=1}^{r}\mu_i(s(k))$$
$$= \sum_{i=1}^{r} h_i(s(k))\big(R_i e(k) + R_{di}e(k-\tau)\big) \quad (3c)$$

Let $e(k)=x(k)-\hat{x}(k)$; from (1) and (4) so that we have the fuzzy observer error dynamics as follows:

$$\begin{aligned} e(k+1)=\sum_{i=1}^{r}\sum_{j=1}^{r}h_i(s(k))h_j(s(k))\big((A_i-L_iC_j)e(k) \\ +(A_{di}-L_iC_{dj})e(k-\tau)+\delta_{fi}(k)+G_{1i}\delta_{ai}(k) \\ +L_iG_{2j}\delta_{cj}(k)+(D_{1i}+L_iD_{2j})w(k)\big) \end{aligned} \tag{6}$$

where

$$\delta_{ai}=F_{1i}\left(E_{1i}x(k)+E_{2i}x(k-\tau)\right) \tag{7a}$$

$$\delta_{ci}=F_{2i}\left(E_{3i}x(k)+E_{4i}x(k-\tau)\right) \tag{7b}$$

$$\begin{aligned} \delta_{fi}&=\left(N_ix(k)u(k)+N_{di}x(k-\tau)u(k)\right) \\ &\quad-\left(N_i\hat{x}(k)u(k)+N_{di}\hat{x}(k-\tau)u(k)\right) \\ &=\left(N_ie(k)+N_{di}e(k-\tau)\right)u(k) \end{aligned} \tag{7c}$$

According to (2), (5) and (7a)-(7c), we have the following results

$$\delta_{ai}^T(k)\delta_{ai}(k)\le\begin{bmatrix}x(k)\\x(k-\tau)\end{bmatrix}^T\Lambda_{ai}\begin{bmatrix}x(k)\\x(k-\tau)\end{bmatrix} \tag{8a}$$

$$\delta_{ci}^T(k)\delta_{ci}(k)\le\begin{bmatrix}x(k)\\x(k-\tau)\end{bmatrix}^T\Lambda_{ci}\begin{bmatrix}x(k)\\x(k-\tau)\end{bmatrix} \tag{8b}$$

$$\delta_{fi}^T(k)\delta_{fi}(k)\le\begin{bmatrix}e(k)\\e(k-\tau)\end{bmatrix}^T\Lambda_{fi}\begin{bmatrix}e(k)\\e(k-\tau)\end{bmatrix} \tag{8c}$$

where

$$\Lambda_{ai}=\begin{bmatrix}E_{1i}^TE_{1i} & E_{1i}^TE_{2i}\\ E_{2i}^TE_{1i} & E_{2i}^TE_{2i}\end{bmatrix} \tag{9a}$$

$$\Lambda_{ci}=\begin{bmatrix}E_{3i}^TE_{3i} & E_{3i}^TE_{4i}\\ E_{4i}^TE_{3i} & E_{4i}^TE_{4i}\end{bmatrix} \tag{9b}$$

$$\Lambda_{fi}=\begin{bmatrix}\bar{N}_i^T\bar{N}_i & \bar{N}_i^T\bar{N}_{di}\\ \bar{N}_{di}^T\bar{N}_i & \bar{N}_{di}^T\bar{N}_{di}\end{bmatrix}. \tag{9c}$$

The purpose of this paper is to design the robust fuzzy observer parameters L_i such that the fuzzy observer error dynamics (6) are globally stable independent of the time delay τ and the following conditions $H_\infty-$norm upper-bound constraint is simultaneously guaranteed:

$$\|z(k)\|_{[0,\infty)}\le\gamma\|w(k)\|_{[0,+\infty)} \tag{10}$$

for all nonzero $w(k)\in l_2[0,+\infty)$ and all admissible uncertainties.

III. Main Results

In this section, an LMI approach will be developed to solve the problem of robust H_∞ fuzzy observer for T-S time-delay DFBS with parameter uncertainties formulated in the previous section. Before discussing the theorem, we first give the following results which will be used in our main results.

Lemma 1: [6], [7], [23]: Given any matrices X, Y and ε with appropriate dimensions such that $\varepsilon>0$ we have

$$X^TY+XY^T\le\varepsilon X^TX+\varepsilon^{-1}Y^TY.$$

Theorem 1: Consider the uncertain DFBS with disturbance (1). Given a prescribed H_∞ performance index $\gamma>0$, if there exist positive scalars ε_{1ij}, ε_{2ij} λ, and ρ_{ij} and matrices $P_1>0$; $P_2>0$; $Q_1>0$; $Q_2>0$ and X_i, satisfying the LMIs (11) and (12), shown at the next page, then the fuzzy observer error dynamics (6) with the fuzzy observer (4) with $L_i=P_1^{-1}X_i$ is globally asymptotically stable and with an H_∞ performance bound $\gamma>0$.

Proof: Based on the Lyapunov direct method, Lipschitz conditions, and Lemma 1, one can obtain the LMIs (11) and (12). (Due to the limitation of space, we omit the proof.)

IV. Numerical Example

Consider the time-delay DFBS with parameter uncertainty as follows:

Rule 1:

IF x_1 is about -1

THEN

$$\begin{aligned} x(k+1)&=(A_1+\Delta A_1)x(k)+(A_{d1}+\Delta A_{d1})x(k-\tau) \\ &\quad+(N_1+\Delta N_1)x(k)u(k) \\ &\quad+(N_{d1}+\Delta N_{d1})x(k-\tau)u(k)+D_{11}w(k) \end{aligned} \tag{13a}$$

$$y(k)=(C_1+\Delta C_1)x(k)+(C_{d1}+\Delta C_{d1})x(k-\tau)+D_{21}w(k)$$

$$z(k)=R_1e(k)+R_{d1}e(k-\tau)$$

Rule 2:

IF x_1 is about 1

THEN

$$\begin{aligned} x(k+1)&=(A_2+\Delta A_2)x(t)+(N_2+\Delta N_2)x(t)u(t) \\ &\quad+(A_{d2}+\Delta A_{d2})x(k-\tau) \\ &\quad+(N_{d2}+\Delta N_{d2})x(k-\tau)u(k)+D_{12}w(k) \end{aligned} \tag{13b}$$

$$y(k)=(C_2+\Delta C_2)x(k)+(C_{d2}+\Delta C_{d2})x(k-\tau)+D_{22}w(k)$$

$$z(k)=R_2e(k)+R_{d2}e(k-\tau).$$

$$\begin{bmatrix} -\begin{bmatrix} \Pi_{1ii} & 0 & 0 \\ 0 & \Pi_{2ii} & 0 \\ 0 & 0 & \Pi_{3ii} \end{bmatrix} + \zeta_1 I & \Xi_{ii}^T(k) & \mathbf{0} \\ \Xi_{ii}(k) & -P & PS_{ii} \\ \mathbf{0} & S_{ii}^T P & -\begin{bmatrix} \varepsilon_{1ii} I & 0 \\ 0 & \varepsilon_{2ii} I \end{bmatrix} \end{bmatrix} < 0 \quad (1 \le i \le r) \tag{11}$$

$$\begin{bmatrix} -\begin{bmatrix} \Psi_{1ij} & 0 & 0 \\ 0 & \Psi_{2ij} & 0 \\ 0 & 0 & \Psi_{3ij} \end{bmatrix} + \varsigma_2 I & \Xi_{ij}^T(k) & \mathbf{0} \\ \Xi_{ij}(k) & -\begin{bmatrix} P & 0 \\ 0 & P \end{bmatrix} & \begin{bmatrix} P & 0 \\ 0 & P \end{bmatrix} S_{ij} \\ \mathbf{0} & S_{ij}^T \begin{bmatrix} P & 0 \\ 0 & P \end{bmatrix} & -\begin{bmatrix} \varepsilon_{1ij} I & 0 & 0 & 0 \\ 0 & \varepsilon_{2ij} I & 0 & 0 \\ 0 & 0 & \varepsilon_{1ji} I & 0 \\ 0 & 0 & 0 & \varepsilon_{2ji} I \end{bmatrix} \end{bmatrix} < 0 \quad (1 \le i < j \le r) \tag{12}$$

where $P = \begin{bmatrix} P_1 & 0 \\ 0 & P_2 \end{bmatrix}$, $Q = \begin{bmatrix} Q_1 & 0 \\ 0 & Q_2 \end{bmatrix}$, $\Pi_{1ii} = \begin{bmatrix} P_1 - Q_1 & 0 \\ 0 & Q_1 \end{bmatrix} - \left[\varepsilon_{1ii} \left(\Lambda_{ai} + \Lambda_{fi} \right) + \varepsilon_{2ii} \Lambda_{ai} + \lambda \Lambda_{ci} \right]$, $S_{ii} = \begin{bmatrix} S_i & 0 \\ 0 & S_i \end{bmatrix}$,

$S_{ij} = \begin{bmatrix} S_i & 0 & 0 & 0 \\ 0 & S_j & 0 & 0 \\ 0 & 0 & S_i & 0 \\ 0 & 0 & 0 & S_j \end{bmatrix}$, $S_i = \begin{bmatrix} G_{1i} & I \end{bmatrix}$, $\Lambda_{ci} = \begin{bmatrix} E_{3i}^T E_{3i} & E_{3i}^T E_{4i} \\ E_{4i}^T E_{3i} & E_{4i}^T E_{4i} \end{bmatrix}$, $\Pi_{2ii} = \begin{bmatrix} P_2 - Q_2 & 0 \\ 0 & Q_2 \end{bmatrix} - (\varepsilon_{2ii} \Lambda_{fi} + \Lambda_{ri})$, $\Pi_{3ii} = \begin{bmatrix} \lambda I & 0 \\ 0 & \gamma^2 I \end{bmatrix}$,

$$\Psi_{1ij} = 2\begin{bmatrix} P_1 - Q_1 & 0 \\ 0 & Q_1 \end{bmatrix} - \left[\varepsilon_{1ij} \left(\Lambda_{ai} + \Lambda_{fi} \right) + \varepsilon_{1ji} \left(\Lambda_{aj} + \Lambda_{fj} \right) + \varepsilon_{2ij} \Lambda_{ai} + \varepsilon_{2ji} \Lambda_{aj} + \lambda (\Lambda_{ci} + \Lambda_{cj}) \right],$$

$$\Psi_{2ij} = 2\begin{bmatrix} P_2 - Q_2 & 0 \\ 0 & Q_2 \end{bmatrix} - \left(\varepsilon_{2ij} \Lambda_{fi} + \varepsilon_{2ji} \Lambda_{fj} + \Lambda_{rij} \right), \ \Psi_{3ij} = \begin{bmatrix} \lambda I & 0 & 0 \\ 0 & \lambda I & 0 \\ 0 & 0 & 2\gamma^2 I \end{bmatrix},$$

$$\Xi_{ii}(k) = \Xi_{ii} = \begin{bmatrix} P_1 A_i & P_1 A_{di} & 0 & 0 & 0 & P_1 D_{1i} \\ 0 & 0 & P_2 A_i - X_i C_i & P_2 A_{di} - X_i C_{di} & X_i G_i & P_2 D_{1i} + X_i D_{2i} \end{bmatrix},$$

$$\Xi_{ij}(k) = \Xi_{ij} = \begin{bmatrix} P_1 A_i & P_1 A_{di} & 0 & 0 & 0 & 0 & P_1 D_{1i} \\ 0 & 0 & P_2 A_i - X_i C_j & P_2 A_{di} - X_i C_{dj} & 0 & X_i G_{2j} & P_2 D_{1i} + X_i D_{2j} \\ P_1 A_j & P_1 A_{dj} & 0 & 0 & 0 & 0 & P_1 D_{1j} \\ 0 & 0 & P_2 A_j - X_j C_i & P_2 A_{dj} - X_j C_{di} & X_j G_{2i} & 0 & P_2 D_{1j} + X_j D_{2i} \end{bmatrix},$$

$$\Lambda_{ri} = \begin{bmatrix} R_i^T R_i & R_i^T R_{di} \\ R_{di}^T R_i & R_{di}^T R_{di} \end{bmatrix}, \ \Lambda_{rij} = \frac{1}{2} \begin{bmatrix} (R_i + R_j)^T (R_i + R_j) & (R_i + R_j)^T (R_{di} + R_{dj}) \\ (R_{di} + R_{dj})^T (R_i + R_j) & (R_{di} + R_{dj})^T (R_{di} + R_{dj}) \end{bmatrix}.$$

where $A_1 = \begin{bmatrix} 0.4 & 0.01 \\ 0.02 & -0.55 \end{bmatrix}$, $A_2 = \begin{bmatrix} 0.35 & 0.02 \\ -0.2 & -0.5 \end{bmatrix}$,
$N_1 = \begin{bmatrix} -0.5 & 0 \\ 0 & -0.1 \end{bmatrix}$, $N_2 = \begin{bmatrix} 0.1 & 0 \\ 0 & 0.1 \end{bmatrix}$, $A_{d1} = \begin{bmatrix} 0.1 & 0 \\ 0 & 0.1 \end{bmatrix}$,
$A_{d2} = \begin{bmatrix} -0.1 & 0.1 \\ 0 & 0.1 \end{bmatrix}$, $N_{d1} = \begin{bmatrix} 0.1 & 0 \\ 0 & 0.05 \end{bmatrix}$, $N_{d2} = \begin{bmatrix} 1 & 0 \\ 0 & 0.03 \end{bmatrix}$,
$D_{11} = \begin{bmatrix} 0.3 & 0 \\ 0 & 0.2 \end{bmatrix}$, $D_{12} = \begin{bmatrix} 0.1 & 0 \\ 0 & 0.1 \end{bmatrix}$, $C_1 = \begin{bmatrix} 0.1 & 0 \end{bmatrix}$,
$C_2 = \begin{bmatrix} 0.1 & 0 \end{bmatrix}$, $C_{d1} = \begin{bmatrix} -0.2 & -0.3 \end{bmatrix}$, $C_{d2} = \begin{bmatrix} 0.1 & -0.1 \end{bmatrix}$,
$D_{21} = \begin{bmatrix} 0.2 & 0.7 \end{bmatrix}$, $D_{22} = \begin{bmatrix} 0.3 & 0.5 \end{bmatrix}$, $R_1 = \begin{bmatrix} 0 & 0.2 \end{bmatrix}$,
$R_2 = \begin{bmatrix} 0.3 & 0 \end{bmatrix}$, $R_{d1} = \begin{bmatrix} -0.2 & -0.1 \end{bmatrix}$, $R_{d2} = \begin{bmatrix} 0.1 & -0.2 \end{bmatrix}$ and $\tau = 1$. The membership functions of the state x_1 are defined as $\mu_1(k) = (1 - x_1)/2$ and $\mu_2(k) = (1 + x_1)/2$.

Based on Assumption 1, we can define the matrices G_{ij}, $F_i(t)$, E_{1i}, E_{2i}, E_{3i}, and E_{4i}, where $i, j = 1, 2$, as follows.

$G_{11} = \begin{bmatrix} 0.01 & -0.1 \\ 0.1 & 0.1 \end{bmatrix}$, $G_{12} = \begin{bmatrix} 0.02 & 0.1 \\ 0.1 & 0.1 \end{bmatrix}$, $G_{21} = \begin{bmatrix} 0.02 & 0.1 \end{bmatrix}$,
$G_{21} = \begin{bmatrix} 0.01 & 0.1 \end{bmatrix}$

$$F_1(t) = F_2(t) = 0.1 \times \begin{bmatrix} rand & 0 \\ 0 & rand \end{bmatrix}$$

where *rand* is a random number taken from a normal distribution over $[-1, 1]$.

$$E_{11} = E_{12} = E_{31} = E_{32} = \begin{bmatrix} 0.1 & 0 \\ 0 & 0.1 \end{bmatrix}$$

$$E_{21} = E_{22} = E_{41} = E_{42} = \begin{bmatrix} 0.01 & 0 \\ 0 & 0.01 \end{bmatrix}.$$

By solving the solution to the stability conditions in Theorem 1 using MATLAB LMI toolbox, with $\gamma = 1$, $\lambda = 1$ and $\zeta_1 = \zeta_2 = 0.0001$, where $i, j = 1, 2$, we have

$P_1 = \begin{bmatrix} 0.4332 & 0.0061 \\ 0.0061 & 0.4188 \end{bmatrix}$, $P_2 = \begin{bmatrix} 0.5421 & -0.0191 \\ -0.0191 & 0.4226 \end{bmatrix}$,
$Q_1 = \begin{bmatrix} 0.1333 & -0.0008 \\ -0.0008 & 0.0894 \end{bmatrix}$, $Q_2 = \begin{bmatrix} 0.1458 & -0.0245 \\ -0.0245 & 0.1054 \end{bmatrix}$,
$X_1 = \begin{bmatrix} -0.1373 \\ -0.1201 \end{bmatrix}$, $X_2 = \begin{bmatrix} -0.0312 \\ -0.1830 \end{bmatrix}$ and the robust H_∞ fuzzy observers is (4) with

$$L_1 = P_1^{-1} X_1 = \begin{bmatrix} -0.2991 \\ -0.2824 \end{bmatrix}$$

$$L_2 = P_1^{-1} X_2 = \begin{bmatrix} -0.0629 \\ -0.4361 \end{bmatrix}.$$

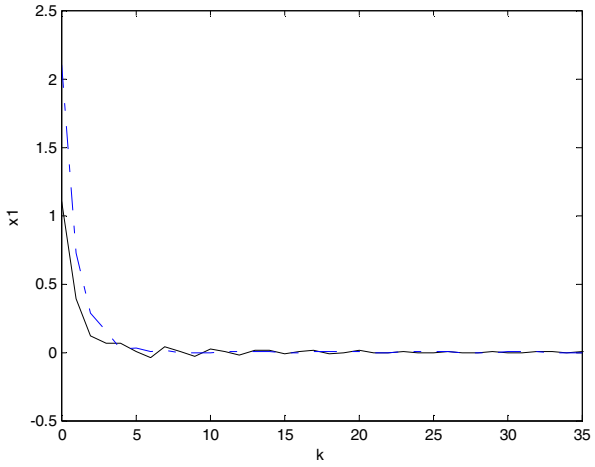

Fig. 1. Responses of $x_1(k)$ and $\hat{x}_1(k)$ for time-delay DFBS with parameter uncertainties.

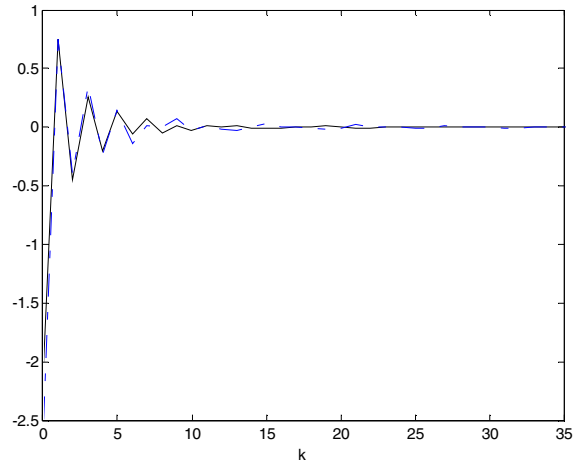

Fig. 2. Responses of $x_2(k)$ and $\hat{x}_2(k)$ for time-delay DFBS with parameter uncertainties.

Applying the controller proposed in [20] with $\rho = 0.3$ and control gain $K_1 = [-0.275 \quad -0.35]$ and $K_2 = [-0.35 \quad -0.25]$ to time-delay DFBS with parameter uncertainties (13). The time-delay DFBS with parameter uncertainties was simulated by choosing a system's initial conditions $x(0) = [1.1 \quad -2.0]^T$ and observer's initial condition $\hat{x}(0) = [2.1 \quad -2.5]^T$ and the exogenous disturbance input $w(k) = \left[0.5e^{-0.1k}\sin(2k) \quad 0.3e^{-0.08k}\cos(k)\right]^T$ are illustrated in Fig. 1 and Fig. 2. From the simulation results, one can find that the state variables of time-delay DFBSs with parameter uncertainties (13) and their estimated by time-delay DFBS observer are almost the same after a short transient instant. Fig. 3 shows the control input. Fig. 4 shows that the designed fuzzy observer ensures the robust asymptotic stability of fuzzy observer error dynamics (6) and guarantees a prescribed H_∞ performance level.

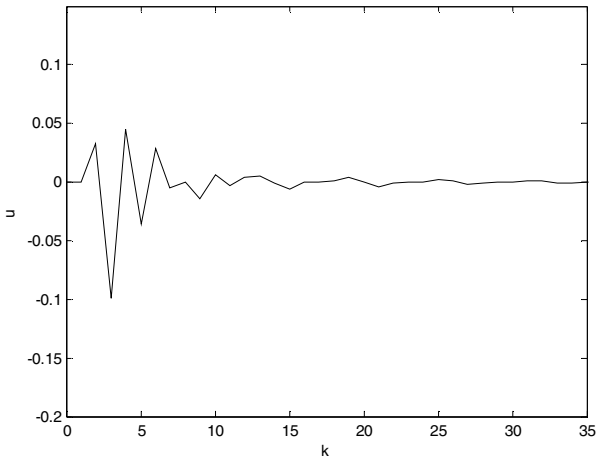

Fig. 3. Control input $u(k)$ for time-delay DFBS with parameter uncertainties.

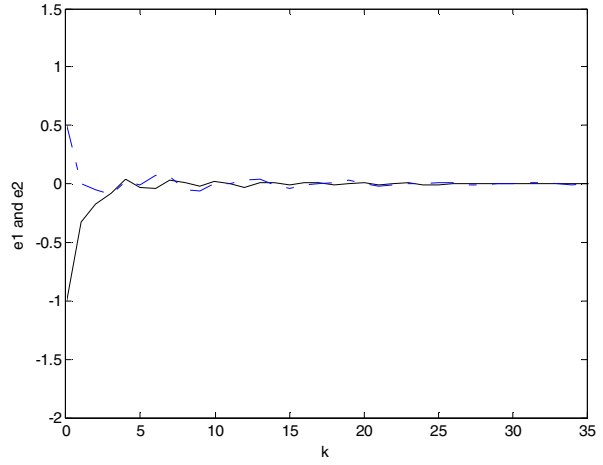

Fig. 4. Responses of e_1 and e_2 for initial conditions $x(0)=[1.1 \quad -2.0]^T$ and $\hat{x}(0)=[2.1 \quad -2.5]^T$.

V. CONSLUSION

In this paper, a robust H_∞ fuzzy observer has been presented for a class of time-delay DFBSs with parameter uncertainties. Based on the Lipschitz condition, the design problem of the H_∞ fuzzy observer can be reformulated as an LMI problem. Besides, the robust H_∞ fuzzy observer for time-delay DFBSs with parameter uncertainties can be obtained from the proposed LMIs without any pre-assigned matrices. The simulation has shown the effectiveness and feasibility of the proposed method to the reconstruction of the state.

ACKNOWLEDGMENT

The work is supported by the National Science Council, Taiwan, under grants NSC-99-2221-E-027-101 and NSC-98-2622-E-168-013-CC3.

REFERENCES

[1] B. Chen, X. P. Lin, S. C. Tong, and C. Lin, "Observer-based stabilization of T-S fuzzy systems with input delay," IEEE Transactions on Fuzzy System, vol. 16, no. 3, pp. 652–663. June 2008.

[2] H. O. Wang, K. Tanaka, and M. F. Griffin, "An approach to fuzzy control of nonlinear systems: stability and design issues," IEEE Trans. Fuzzy Syst., vol. 4, pp. 14–23, Feb. 1996.

[3] T. Takagi and M. Sugeno, "Fuzzy identification of systems and its applications to modeling and control," IEEE Trans. Syst., Man, Cybern., vol. SMC-15, pp. 116–132, Jan. 1985.

[4] K. Tanaka, and H. O. Wang, "A Linear Matrix Inequality Approach. Fuzzy Control Systems Design and Analysis," NY: Wiley. 2001.

[5] X. Liu, and Q. Zhang, "New approaches to H_∞ controller designs based on fuzzy observers for T–S fuzzy systems via LMI," Automatica, vol. 39, no. 9, pp. 1571–1582, June 2003.

[6] M. Teixeira, E. Assunc¸ao, and R. Avellar, "On relaxed LMI-based design for fuzzy regulators and fuzzy observers," IEEE Trans. Fuzzy Syst., vol. 11, no. 5, pp. 613–623. Oct. 2003.

[7] S. Xu, and J. Lam, "Robust H_∞ control for uncertain discrete-time-delay fuzzy systems via output feedback controllers," IEEE Transactions on Fuzzy System, vol. 13, no. 1, pp. 82–93. Feb. 2005.

[8] H. J. Lee, J. B. Park, and G. Chen, "Robust fuzzy control of nonlinear systems with parametric uncertainties," IEEE Transactions on Fuzzy System, vol. 9, pp. 369–379. Apr. 2001.

[9] B. Chen, and X. P. Liu, "Delay-dependent robust H_∞ control for T-S fuzzy systems with time delay," IEEE Transactions on Fuzzy Systems, vol. 13, no. 2, pp. 238–249. Apr. 2005.

[10] J. C. Lo, and M. L. Lin, "Robust H_∞ control for fuzzy systems with Frobenius norm-bounded uncertainties," IEEE Transactions on Fuzzy System, vol. 14, no. 1, pp. 1–15. Feb. 2006.

[11] S. K. Nguang, and P. Shi, "Robust H_∞ output feedback control design for fuzzy dynamic systems with quadratic D-stability constraints: an LMI approach," Information Sciences, vol. 176, pp. 2161–2191. Feb. 2006.

[12] S. Xu, and J. Lam, "Robust H_∞ control for uncertain discrete-time-delay fuzzy systems via output feedback controllers," IEEE Transactions on Fuzzy System, vol. 13, no. 1, pp. 82–93. Feb. 2005.

[13] Z. R. Tsai, Y. Z. Chang, J. D. Hwang, and J. Lee, "Robust fuzzy stabilization of dithered chaotic systems using island-based random optimization algorithm," Information Sciences, vol. 178, pp. 1171–1188. Oct. 2008.

[14] R. R. Mohler, "Nonlinear systems: Vol. 2, *Application to bilinear control*," Prentice-Hall, Englewood Cliffs, NJ, 1991.

[15] D. L. Elliott, Bilinear Systems in Encyclopedia of Electrical Engineering. New York: Wiley, 1999.

[16] T.-H. S. Li and S.-H. Tsai, "T-S fuzzy bilinear model and fuzzy controller design for a class of nonlinear systems," IEEE Trans. Fuzzy Syst., vol. 15, no. 3, pp. 494–506, Jun. 2007.

[17] T.-H. S. Li, S.-H. Tsai, J.-Z. Lee, M.-Y. Hsiao, and C.-H. Chao, " Robust H_∞ fuzzy control for a class of uncertain discrete fuzzy bilinear systems," IEEE Trans. Syst., Man, Cybern. Part B. Vol. 38, No. 2, pp. 510–527, Apr. 2008.

[18] S.-H. Tsai, and T.-H. S. Li, "Robust fuzzy control of a class of fuzzy bilinear systems with time-delay," Chaos, Solitons and Fractals, vol. 39, No. 15, pp. 2028–2040, Mar. 2009.

[19] J. Yoneyama, "Stabilization of Takagi-Sugeno fuzzy bilinear time-delay systems," IEEE Multi-Conference Systems and Control, Yokohama, Japan, 2010, pp. 111–116.

[20] S.-H. Tsai, M.-Y. Hsiao, and K.-L. Tsai, "LMI-based fuzzy control for a class of time-delay discrete fuzzy bilinear system," IEEE Conference on Fuzzy System, Jeju, Korea, 2009, pp. 796–801.

[21] D. SAOUDI, C. MECHMECHE and N. BENHADJ BRAIEK, "T-S fuzzy bilinear observer for a class of nonlinear system," 18th Mediterranean Conference on Control & Automation Congress, Marrakech, Morocco, 2010, PP. 1395–1400.

[22] J. Yoneyama, “Output feedback control design for Takagi-Sugeno Fuzzy bilinear time-delay systems,” IEEE Conference on Systems, Man and Cybernetics, Istanbul, Turkey, 2010, pp. 1671–1677.

[23] K. Zhou and P. Khargonedkar, "Robust Stabilization of linear systems with norm-bounded time-varying uncertainty," System Control Letters, vol. 10, no. 1, pp. 17–20, Jan. 1988.

2011 IEEE International Conference on Fuzzy Systems
June 27-30, 2011, Taipei, Taiwan

Sum of Squares Solutions Assuring Non-quadratic Discrete Stability

Ji-Chang Lo
Mechanical Engineering
National Central University
Jhong-Li, Taiwan
Email: jclo@cc.ncu.edu.tw

Jhen-Shun Kao
Mechanical Engineering
National Central University
Jhong-Li, Taiwan

***Abstract*—A new stability condition in terms of SOS is studied in this paper for discrete-time fuzzy systems. Based on a parameter-dependent Lyapunov function, we study asymptotically SOS relaxation families, reducing the conservatism that commonly exists in the quadratic stability approaches.**

***Index Terms*—TS fuzzy model; Copositive relaxations; Premise-dependent Lyapunov function; Linear matrix inequality; Sum of Squares.**

I. Introduction

For decades a large number of literature on fuzzy control are TS model-based control where, mostly, the common P approach searching for a single Lyapunov function remains active [1], [2], [3]. Another category emphasizes parameter-dependent functions with multiple P_j matrices as a candidate of Lyapunov function [4], [5], [6]. To remove the time-derivative dependence, progress has been made in obtaining less conservative results using non-quadratic approach (multiple Lyapunov functions) [7], [8], [9], [10], [11] where a fuzzy Lyapunov candidate is used for continuous-time T-S fuzzy models and the resulting stability condition is shown to be more relaxed than the condition derived from the common P approach. Although LMI approaches remain the most favorite tool of choice when a Lyapunov-based stability analysis is used, we, in this paper, propose a copositive relaxation combined with premise-dependent Lyapunov functions to derive necessary and sufficient conditions for the TS fuzzy model stability tests. Inspired by recent advances [10]-[20], [21], [22], we investigate copositive relaxation associated to fuzzy stability and control design from sum of squares viewpoints. The main contribution is that the proposed method takes the firing strength into account and

The paper is organized as follows. Section II rehearses some useful results which forms the foundation for later developments. Sum of squares is also introduced. Section III derives the stability conditions for discrete-time fuzzy systems via a parameter-dependent Lyapunov function. SOS relaxation addressed in Section IV. An example is illustrated in Section V and conclusion is drawn in Section VI.

This work was supported in part by the National Science Council of the ROC under grant NSC-98-2221-E-008-110.

Notations: The symbol $\star$ denotes transposed elements in a symmetric matrix. The notation Y_μ stands for $\sum_{i=1}^{r}\mu_i Y_i$ where $\mu_i \geq 0$ and $\sum_{i=1}^{r}\mu_i = 1$. ! denotes factorial for combinatoric expression. Let $\mathcal{K}(h)$, where h is the degree of a polynomial in μ, be the set of r-tuples defined below:

$$\mathcal{K}(h) = \{(k_1, k_2, \cdots, k_r) : k_1 + k_2 + \cdots + k_r = h \quad (1)$$

$$\forall k_i \in I^+(non-negative\ integers), i = 1, 2, \cdots, r\}.$$

Since the number of rules in the fuzzy base is r, the number of elements in $\mathcal{K}(h)$ is given by $J(h) = (r+h-1)!/(h!(r-1)!)$. To ease the presentation, we adopt the short hand notations displayed below:

$$\begin{aligned}
k &= (k_1, k_2, \cdots, k_r)\\
\mu^k &= \mu_1^{k_1}\mu_2^{k_2}\cdots\mu_r^{k_r}\\
e_i &= 0\cdots\underbrace{1}_{i^{th}}\cdots 0\\
k - e_i &= k_1 k_2 \cdots (k_i - 1)\cdots k_r\\
\pi(k) &= (k_1!)(k_2!)\cdots(k_r!)\\
\mathcal{C}_{ii}^k(h) &= \frac{(h!)k_i(k_i-1)}{\pi(k)},\ \mathcal{C}_{ij}^k(h) = \frac{(h!)k_i k_j}{\pi(k)}.
\end{aligned}$$

and

$$\mathcal{C}_{iii}^k(h) = \frac{(h!)k_i(k_i-1)(k_i-2)}{\pi(k)}$$

$$\mathcal{C}_{iij}^k(h) = \frac{(h!)k_i(k_i-1)k_j}{\pi(k)},\ \mathcal{C}_{ijl}^k(h) = \frac{(h!)k_i k_j k_l}{\pi(k)}.$$

II. Preliminaries

To begin with, we introduce the following definitions and terminologies which serve as the entry point to this paper.

Definition 1 (SOS functions): [23] A multivariate polynomial $f(x), x \in R^r$, is a sum of squares if there exist polynomials $g_1(x), g_2(x), \cdots, g_t(x)$ such that

$$f(x) = \sum_{i=1}^{t} g_i^2(x).$$

Definition 2 (Monomials): [23] A monomial in x is a function of the form $x_1^{\alpha_1}x_2^{\alpha_2}\cdots x_r^{\alpha_r}$ where $\alpha_1, \alpha_2, \cdots \alpha_r$ are nonnegative integers and the degree of the monomial is given

by α which is the sum of all α_i. In short, $\alpha = \alpha_1 + \alpha_2 + \cdots + \alpha_r$.

Given the aforementioned definition, it is shown in the articles [23], [24] that $f(x)$ is an SOS if and only if there exists a positive semidefinite matrix $Q \geq 0$ such that

$$f(x) = \tilde{x}' Q \tilde{x} \tag{2}$$

where $\tilde{x}$ is a column vector whose entries are all monomials in x. Terminologically, (2) is referred to the Gram matrix method. It is interesting to know that when $\tilde{x} = x$, $f(x)$ in (2) is a quadratic function.

One can search for such a Q by solving a semidefinite program which is done using SOSTOOLS [25], [26] that uses SeDuMi [27] as the semidefinite programming solver. Note that a function that is SOS always implies the underlying function is nonnegative, the converse is not true. However, numerical experiments seem to indicate that the gap between SOS and nonnegativity is small [24]. We note in passing that an extension of scalar polynomial optimization by SOS decomposition to optimization with scalar polynomial objective and nonlinear matrix constraints is stated in [12], [28].

III. Stability Analysis

In this section, we derive stability conditions for discrete-time open loop fuzzy systems that are displayed below:

$$z(t+1) = \sum_{i=1}^{r} \mu_i A_i z = A_\mu z(t) \tag{3}$$

where A_i is a system matrix of each rule i and $\mu_i \geq 0$ is the firing strength of rule i. z is the state vector.

Considering a premise-dependent non-quadratic Lyapunov function

$$V(z(\cdot)) = z^T(\cdot) X_\mu^{-1} z(\cdot) \tag{4}$$

where $X_\mu = \sum_{j=1}^{r} \mu_j X_j$ and $X_j > 0$ are symmetric, positive definite matrices for all discrete-time index t, we have the following Lemmas.

Lemma 1 (Discrete-time Stability, LMI): The open loop system (3) is stable if there exist matrices $X_j = X_j' > 0, j = 1, \cdots, r$ satisfying the following HPPD:

$$f(\mu) := \sum_{i=1}^{r} \sum_{j=1}^{r} \sum_{l=1}^{r} \mu_i \mu_j \mu_l^+ M_{ijl} < 0 \tag{5}$$

where

$$M_{ijl} = \begin{bmatrix} -X_j & X_j A_i' \\ A_i X_j & -X_l \end{bmatrix}$$

Proof: Given the non-quadratic Lyapunov function (4), it is straightforward to verify

$$\begin{aligned} \Delta V(t) &= V(t+1) - V(t) \\ &= z'(t+1) X_{\mu^+}^{-1} z(t+1) - z'(t) X_\mu^{-1} z(t) \\ &< 0 \end{aligned}$$

where μ^+ means $\mu(t+1)$. Recalling Schur complement and congruence transformation with $diag[X_\mu \ I]$, we have an equivalent form

$$\begin{bmatrix} -X_\mu & X_\mu A_\mu' \\ A_\mu X_\mu & -X_{\mu^+} \end{bmatrix} < 0$$

For Lyapunov stability, a sufficient condition is (5). ■

Notice that the matrices M_{ijl} are real symmetric, matrix-valued and linear functions of decision variables (multiple Lyapunov matrices) X_j.

Up to now, we have the following stability condition expressed by matrix-valued homogeneous polynomial function in μ for discrete-time systems.

$$f(\mu) < 0 \tag{6}$$

By applying matrix-valued Pólya's Theorem [29], [30], [31], (6) leads to an equivalent form

$$\begin{aligned} 0 &> (\sum_{i=1}^{r} \mu_i)^d f(\mu) \\ &= \sum_{k \in \mathcal{K}(d+3)} H^k \mu^k \end{aligned} \tag{7}$$

where $\mathcal{K}(d+3)$ is defined in 1 and

$$\begin{aligned} H^k &= \sum_{i=1}^{r} C_{iii}^k(d) M_{iii} \\ &+ \sum_{i=1}^{r-1} \sum_{j=i+1}^{r} C_{iij}^k(d)(M_{iij} + M_{iji} + M_{jii}) \\ &+ \sum_{i=1}^{r-2} \sum_{j=i+1}^{r-1} \sum_{l=j+1}^{r} C_{ijl}^k(d)(M_{ijl} + M_{jil} \\ &+ M_{ilj} + M_{jli} + M_{lij} + M_{lji}) \end{aligned}$$

For Lemmas 1, the challenge lies on how the above conditions (5) can be verified. We observe that the matrices involved are copositive. The brief review in the preliminaries motivates the following research. Unlike existing LMI-based relaxations, we require Lemma 1 to be sum of squares, asking when (7) has an SOS decomposition.

IV. SOS Relaxations

The sum of squares circumvents the NP-hard problem proving positivity of a polynomial function and provides a computationally tractable technique for the existence of an SOS decomposition [23], [12], [13], [32].

Based on Pólya and Lyapunov theorem, we have established that sufficient conditions for the existence of Parameter-dependent Lyapunov function assuring stability is to verify (5), which is a non-convex problem and NP-hard. Most existing LMI-based relaxations in the literature ignore μ and solve the underlying stability problem as an SDP problem. Unlike those approaches, we take μ into consideration. Particularly *instead of asking*

$$-\sum_{k \in \mathcal{K}(d+3)} H^k \mu^k > 0, \quad \mu \in R_+^r$$

we require them to be sums of squares (SOS) [26]. Having established the rationale, the idea is to find a homogeneous polynomially parameter-dependent (HPPD) function such that

$$-\sum_{k\in\mathcal{K}(d+3)} H^k x^{2k} \text{ is SOS} \tag{8}$$

where $\mu = x^2, x \in R^r$ and v_1 is vector independent of x. We emphasize that the HPPD (8) takes the membership μ into accounts, collects the interactions among the subsystems and yields less conservative results.

Therefore by deliberately working on polynomials consisting of basis monomials, the positive definiteness of the negated condition in Lemma 1 can be relaxed to the existence of SOS decomposition. Under this relaxation, the search for a bounded degree d can be efficiently solved by checking the maximum eigenvalues of Q in 2 [33]. The SOS program is therefore formally stated below.

Theorem 1 (SOS Relaxation): There exist a matrix $X_j = X_j' > 0$ solving (6) if for each $k \in \mathcal{K}(d+3)$ and a sufficiently large $d > 0$ there exist matrices $X_j = X_j' > 0$ such that

$$-\sum_{k\in\mathcal{K}(d+3)} H^k x^{2k} > 0 \tag{9}$$

which is verifiable by SOS displayed below

$$-v_1'\left(\sum_{k\in\mathcal{K}(d+3)} (H^k - \phi_1)x^{2k}\right) v_1 \text{ is SOS}$$
$$v_2'\left(X_i - \phi_2\right) v_2, i = 1, \cdots r \text{ is SOS}$$

where ϕ_1, ϕ_2 are sufficiently small positive constants NEEDED to guarantee positive definiteness of HPPD function. v_1, v_2 are vectors independent of x.

Proof: The sufficiency is readily seen from HPPD (7) and lemma 1. ■

More details are documented in [22] whilst the corresponding LMI details are documented in [21].

V. An Example

In order to appreciate the efficiency of the proposed method, we consider an example where the T-S fuzzy models are borrowed from existing papers.

A. Discrete fuzzy systems

Consider a discrete-time fuzzy system borrowed from [10] in which the system matrices are given as

$$A_1 = \begin{bmatrix} b & -0.5 \\ a & -0.9 \end{bmatrix}, A_2 = \begin{bmatrix} 0.9 & -a \\ -0.6 & 0.8 \end{bmatrix}$$

where the (a, b) parameters are varied during numerical experiments for feasibility test. Also, compared with the relaxation method proposed in [10], the proposed SOS relaxation generates more feasible regions than that of the cited paper.

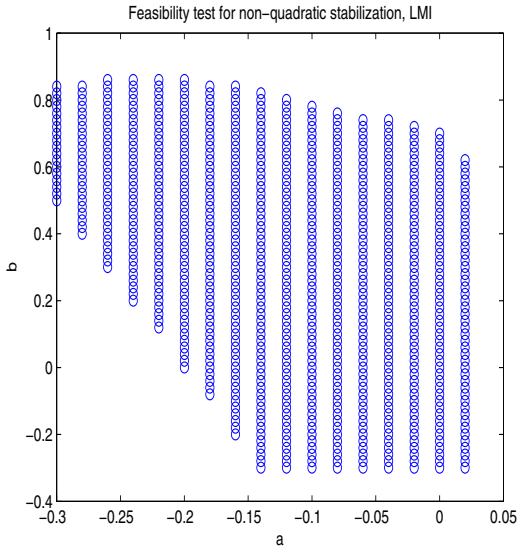

Fig. 1. Feasible regions found by LMI

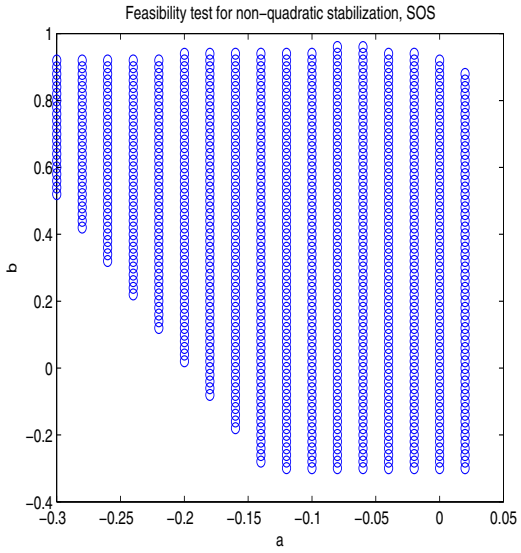

Fig. 2. SOS explores more feasible regions.

VI. Conclusion

In this paper, a stability condition based on sum of squares are developed for discrete-time T-S fuzzy systems. The proposed approach utilizes a premise-dependent Lyapunov function to prove the non-quadratic Lyapunov stability of the underlying fuzzy systems, leading to a family of SOS relaxations that assures existence of non-quadratic Lyapunov function. It is shown and demonstrated via an example that the stability can be cast and solved by SOS .

References

[1] K. Tanaka and H. Wang, *Fuzzy Control Systems Design: A Linear Matrix Inequality Approach*. New York, NY: John Wiley & Sons, Inc., 2001.

[2] J. Lo and M. Lin, "Robust H_∞ control for fuzzy systems with Frobenius norm-bounded uncertainties," *IEEE Trans. Fuzzy Systems*, vol. 14, no. 1, pp. 1–15, Feb. 2006.

[3] ——, "Existence of similarity transformation converting BMI to LMI," *IEEE Trans. Fuzzy Systems*, vol. 15, no. 5, pp. 840–851, Oct. 2007.

[4] M. Johansson, A. Rantzer, and K.-E. Arzen, "Piecewise quadratic stability of fuzzy systems," *IEEE Trans. Fuzzy Systems*, vol. 7, no. 6, pp. 713–722, Dec. 1999.

[5] K. Tanaka, T. Hori, and H. Wang, "A fuzzy Lyapunov approach to fuzzy control system design," in *American Control Conference*, vol. 6, Arlington, VA, 2001, pp. 4790 –4795.

[6] G. Feng, "Stability analysis of discrete-time fuzzy dynamic systems based on piecewise Lyapunov functions," *IEEE Trans. Fuzzy Systems*, vol. 12, no. 1, pp. 22–28, Feb. 2004.

[7] T. Guerra and W. Perruquetti, "Non quadratic stabilization of discrete Takagi Sugeno fuzzy models," in *FUZZ-IEEE2001 Conference*, vol. 1, Melbourne, AU, 2001, pp. 1271–1274.

[8] T. Guerra and L. Vermeiren, "Conditions for non quadratic stabilization of discrete fuzzy models," in *2001 IFAC Conference*, 2001.

[9] K. Tanaka, T. Hori, and H. Wang, "A multiple Lyapunov Function Approach to Stabilization of Fuzzy Control Systems," *IEEE Trans. Fuzzy Systems*, vol. 11, no. 4, pp. 582–589, Aug. 2003.

[10] A. Kruszewski, R. Wang, and T. M. Guerra, "Nonquadratic stabilization conditions for a class of uncertain nonlinear discrete time TS fuzzy models: A New Approach," *IEEE Trans. Automatic Control*, vol. 53, no. 25, pp. 606–611, Mar. 2008.

[11] M. Bernal and T. Guerra, "Generalized non-quadratic stability of continuous-time Takagi-Sugeno models," *IEEE Trans. Fuzzy Systems*, vol. 18, no. 4, pp. 815–822, 2010.

[12] C. Hol and C. Scherer, "Sum of squares relaxations for polynomial semidefinite programming," in *Proc.of MTNS*, 2004, pp. 1–10.

[13] C. Scherer and C. Hol, "Asymptotically exact relaxations for robust LMI problems based on matrix-valued sum-of-squares," in *Proc. 16th Int'l Symposium on Mathematical Theory of Network and Systems*, 2004, pp. 1–11.

[14] V. Montagner, R. Oliveira, and P. Peres, "Necessary and sufficient LMI conditions to compute quadratically stabilizing state feedback controller for Takagi-sugeno systems," in *Proc. of the 2007 American Control Conference*, July 2007, pp. 4059–4064.

[15] ——, "Convergent LMI relaxations for quadratic stabilization and H_∞ control of Takagi-sugeno fuzzy systems," *IEEE Trans. Fuzzy Systems*, no. 4, pp. 863–873, Aug. 2009.

[16] A. Sala and C. Ariño, "Asymptotically necessary and sufficient conditions for stability and performance in fuzzy control: Applications of Polya's theorem," *Fuzzy Set and Systems*, vol. 158, pp. 2671–2686, 2007.

[17] ——, "Design of multiple-parameterization PDC controllers via relaxed condition for multi-dimensional fuzzy summations," in *Proc. of Fuzz-IEEE'07.*, London, UK, 2007, doi:10.1109/FUZZY.2007.4295495.

[18] A. Kruszewski, A. Sala, T. M. Guerra, and C. Ariño, "A triangulation approach to asymptotically exact conditions for fuzzy summations," *IEEE Trans. Fuzzy Systems*, vol. 17, no. 5, pp. 985–994, Oct. 2009.

[19] J. Wan and J. Lo, "LMI relaxations for nonlinear fuzzy control systems via homogeneous polynomials," in *The 2008 IEEE World Congress on Computational Intelligence, FUZZ2008*, Hong Kong, CN, June 2008, pp. 134–140.

[20] J. Lo and C. Tsai, "LMI relaxations for non-quadratic discrete stabilization via Polya theorem," in *Proc. of the* 48^{th} *IEEE Conference on Decision and Control*, Shanghai,CH, Dec. 2009, pp. 7430–7435.

[21] J. Lo and J. Wan, "Studies on LMI relaxations for fuzzy control systems via homogeneous polynomials," *IET Control Theory & Appl.*, vol. 4, no. 11, pp. 2293–2302, Nov. 2010.

[22] J. Lo and M. Liu, "Exact solutions to fuzzy PD-LMIs via SOS," in *The 2010 World Congress on Computational Intelligence; FUZZ-IEEE International Conference on Fuzzy Systems*, Barcelona, SP, July 2010, pp. 1352–1357.

[23] P. Parrilo, *Structured Semidefinite Programs and Semialgebraic Geometry Methods in Robustness and Optimization*. Caltech, Pasadena, CA.: PhD thesis, 2000.

[24] S. Prajna, A. Papachristodoulou, and F. Wu, "Nonlinear control synthesis by sum of squares optimization: A Lyapunov-based Approach," in *Proc. 5th Asian Control Conference*, 2004, pp. 157–165.

[25] S. Prajna, A. Papachristodoulou, and P. Parrilo, "Introducing SOSTOOLS: a general purpose sum of squares programming solver," in *Proc of IEEE CDC*, Montreal, Ca, July 2002, pp. 741–746.

[26] A. Papachristodoulou and S. Prajna, "On the construction of Lyapunov functions using the sum of squares decomposition," in *Proc of IEEE CDC*, Montreal, Ca, July 2002, pp. 3482–3487.

[27] J. Sturm, "Using SeDuMi 1.02, a MATLAB toolbox for optimization over symmetric cones," *Optimization Methods and Software*, vol. 11-12, pp. 625–653, 1999.

[28] H. Ichihara and E. Nobuyama, "A computational approach to state feedback synthesis for nonlinear systems based on matrix sum of squares relaxations," in *Proc. 17th Int'l Symposium on Mathematical Theory of Network and Systems*, Kyoto, Japan, 2006, pp. 932–937.

[29] C. Scherer, "High-order relaxations for robust LMI problems with verifications for exactness," in *Proc. of the 42th IEEE CDC*, Maui, Hawaii, Dec. 2003, pp. 4652–4657.

[30] ——, "Relaxations for robust linear matrix inequality problems with verification for exactness," *SIAM J. Matrix Anal.Appl.*, vol. 27, no. 2, pp. 365–395, 2005.

[31] R. Oliveira and P. Peres, "Stability of polytopes of matrices via affine parameter-dependent Lyapunov functions: Asymptotically exact LMI conditions," *Linear Algebra and its Applications*, vol. 405, pp. 209–228, 2005.

[32] P. Parrilo, "Semidefinite programming relaxations for semialgebraic problems," *Mathematical Programming*, vol. 96, no. 2, pp. 293–320, 2003.

[33] J. Lo and C. Tsai, "Existence of Parameter-dependent Lyapunov Functions Assuring Robust Stability via SOS," in *The 2011 Asia Control Conference*, Kaoshung, TW, May 2011, p. accepted.

2011 IEEE International Conference on Fuzzy Systems
June 27-30, 2011, Taipei, Taiwan

Output Feedback Control for Discrete-Time Takagi-Sugeno Fuzzy Systems

Nao Ueno, Yuzu Uchida, and Jun Yoneyama
Department of Electrical Engineering and Electronics, Aoyama Gakuin University
5-10-1 Fuchinobe, Sagamihara, Kanagawa, Japan
Telephone: +81-42-759-6527
Email: yoneyama@ee.aoyama.ac.jp

***Abstract*—This paper is concerned with output feedback control design for a discrete-time fuzzy system with immeasurable premise variables. It is well known that Takagi-Sugeno fuzzy model describes a wide class of nonlinear systems especially when its premise variables include immeasurable functions. However, when it comes to control design of such a fuzzy system with immeasurable premise variables, a conventional parallel distributed compensator(PDC) is not feasible because it shares the same premise variables as those of a fuzzy system. In this paper, we introduce an output feedback controller with the estimate of the premise variables of an original fuzzy system. We then formulate the stabilization problem for a discrete-time fuzzy system with immeasurable premise variables. Our control design method is based on a set of strict LMI conditions. No tuning parameter is necessary a priori to solve LMI conditions. Our method includes tuning matrices for control gains in a controller and hence they can be chosen to optimize the control performance of the system. Furthermore, we extend our results to a class of discrete-time fuzzy systems with uncertain parameters. A design method of robust controller for such uncertain systems is also given. Numerical examples are finally given to illustrate our control design method.**

keywords-Takagi-Sugeno fuzzy systems, Stabilization, Output feedback control

I. Introduction

It is well-known that the Takagi-Sugeno fuzzy model is one of the efficient mathematical models that describe a wide class of nonlinear systems([6], [10]). Hence, its analysis and control synthesis are important. In the past years, sufficient stability conditions were given, and control design methods were proposed([7], [11], [12], [13]). A conventional approach to control design for a fuzzy system is to employ a parallel distributed compensator(PDC). It is shown that a PDC works well for a fuzzy system because it shares the same premise variables as those of the original fuzzy system. The papers [7] and [13] gave stability conditions and proposed a control design method by a PDC. Furthermore, relaxed stability conditions have been investigated in [11] and [12]. These results were only concerned with the state feedback control design, and the premise variables were assumed to be available. However, this is not always the case in many situations. Especially, in practical situations, the state of the system is not measurable and we need an output feedback control design. In this case, the above mentioned results are infeasible. In fact, if the premise variable is the state, a conventional PDC, which feeds back the state variables, is infeasible. Furthermore, when the premise variable is the state, the Takagi-Sugeno model describes the widest class of nonlinear systems. In other words, a conventional PDC can work only for a limited class of nonlinear systems([16]).

In this paper, we propose a design method of a stabilizing output feedback controller for a discrete-time fuzzy system with immeasurable premise variables. Such a fuzzy system describes a large class of nonlinear systems. The results in [3], [8], [9], [16] do not take care of such a class of fuzzy systems. Yoneyama et al. [16] gave an approximate stabilizing output feedback controller. Assawinchaichote et al. [1] and Yoneyama [15] proposed an uncertain fuzzy system approach. Guerra et al. [2] gave a design method based on non-strict LMI conditions. These results are conservative and are not easy to solve controller design conditions. The paper by Yoneyama [17] proposed a design method based on strict LMI conditions. It gives a two-step procedure to solve the design problem. The paper [17] considers only a class of continuous-time fuzzy systems with immeasurable premise variables. This paper is concerned with a discrete-time counterpart. A control design procedure is also based on strict LMI conditions. No tuning parameter is required in the control design, which is much easier than others in the literature. In addition, we have free scaling matrices that can tune control gain matrices.

We also consider the robust stabilization for fuzzy systems with uncertain parameters. Our method can easily be extended to such a robust stabilization problem. For this robust stabilization problem, we also give a similar two-step procedure with strict LMI conditions, which can easily be calculated via numerical software. Finally, some numerical examples are given to illustrate our design procedure and the effectiveness of our design method.

II. Fuzzy Systems

In this section, we introduce discrete-time Takagi-Sugeno fuzzy systems. Consider the discrete-time Takagi-Sugeno fuzzy model, described by the following IF-THEN rules:

$$\begin{array}{ll} \textbf{IF} & \xi_1 \ is \ M_{i1} \ and \ \cdots \ and \ \xi_p \ is \ M_{ip}, \\ \textbf{THEN} & x(k+1) = A_i x(k) + B_i u(k), \\ & y(k) = C_i x(k), \quad i = 1, \cdots, r \end{array}$$

where $x(k) \in \Re^n$ is the state, $u(k) \in \Re^m$ is the control input and $y(k) \in \Re^q$ is the measurement output. The matrices A_i, B_i

978-1-4244-7316-8/11/$26.00 ©2011 IEEE

and C_i are constant matrices of appropriate dimensions. r is the number of IF-THEN rules. M_{ij} are fuzzy sets and $\xi_1, \cdots, \xi_p$ are premise variables. We set $\xi = [\xi_1 \quad \cdots \quad \xi_p]^T$. The premise variable $\xi(k)$ is assumed to be a function of the state, which is immeasurable.

For simplicity, we define the following notations:

$$X_\xi = \sum_{i=1}^{r} \lambda_i(\xi(k)) X_i,$$
$$X_{\hat{\xi}} = \sum_{i=1}^{r} \lambda_i(\hat{\xi}(k)) X_i,$$
$$X_{\xi\hat{\xi}} = \sum_{i=1}^{r}\sum_{j=1}^{r} \lambda_i(\xi(k))\lambda_j(\hat{\xi}(k)) X_{ij}.$$

and so on.

Then, the state equation and the output equation are described, respectively, by

$$\begin{aligned} x(k+1) &= \sum_{i=1}^{r} \lambda_i(\xi(k))\{A_i x(k) + B_i u(k)\} \\ &\triangleq A_\xi x(k) + B_\xi u(k), \\ y(k) &= \sum_{i=1}^{r} \lambda_i(\xi(k)) C_i x(k) \\ &\triangleq C_\xi x(k), \end{aligned} \tag{1}$$

where $\lambda_i(\xi(k))$

$$\lambda_i(\xi(k)) = \frac{\beta_i(\xi(k))}{\sum_{i=1}^{r} \beta_i(\xi(k))}, \quad \beta_i(\xi(k)) = \prod_{j=1}^{p} M_{ij}(\xi_j(k))$$

and $M_{ij}(\cdot)$ is the grade of the membership function of M_{ij}. We assume

$$\beta_i(\xi(k)) \geq 0, \ i = 1, \cdots, r, \ \sum_{i=1}^{r} \beta_i(\xi(k)) > 0$$

for any $\xi(k)$. Hence $\lambda_i(\xi(k))$ satisfy

$$\lambda_i(\xi(k)) \geq 0, \ i = 1, \cdots, r, \ \sum_{i=1}^{r} \lambda_i(\xi(k)) = 1$$

for any $\xi(k)$.

As stated in [15], [16], a fuzzy system covers a wider class of nonlinear systems when its premise variables are the state variables than the measurement output. In order to design a stabilizing controller for a fuzzy system, a PDC is traditionally used for stabilization because it shares the same premise variables as those of a fuzzy system([7], [13]). However, a PDC is feasible only if the premise variables are measurable or available functions. Thus, most existing results have assumed that the premise variables are measurable([3], [8], [9], [16]). In this paper, we consider an output feedback stabilization where the state is not directly measurable. A fuzzy system is supposed to have the premise variables that are functions of the states, which are immeasurable. In this case, actual values of the premise variables are not available. Hence, we employ the following rules for an output feedback controller with the premise variables being their estimates:

IF $\hat{\xi}_1$ *is* M_{i1} *and* $\cdots$ *and* $\hat{\xi}_p$ *is* M_{ip},
THEN $\hat{x}(k+1) = \hat{A}_i \hat{x}(k) + \hat{B}_i y(k)$
$u(k) = \hat{C}_i \hat{x}(k), \quad i, j = 1, \cdots, r.$

where $\hat{A}_i = \sum_{j=1}^{r} \lambda_j(\hat{\xi}(k)) \hat{A}_{ij}$, and $\hat{A}_{ij}$, $\hat{B}_i$ and $\hat{C}_i$ are constant matrices to be determined. Then the natural choice of a controller is given by

$$\begin{aligned} \hat{x}(k+1) &= \sum_{i=1}^{r}\sum_{j=1}^{r} \lambda_i(\hat{\xi})\lambda_j(\hat{\xi})\{\hat{A}_{ij}\hat{x}(k) + \hat{B}_j y(k)\} \\ &\triangleq \hat{A}_{\hat{\xi}\hat{\xi}}\hat{x}(k) + \hat{B}_{\hat{\xi}} y(k), \\ u(k) &= \sum_{i=1}^{r} \lambda_i(\hat{\xi})\hat{C}_i \hat{x}(k) \triangleq \hat{C}_{\hat{\xi}}\hat{x}(k). \end{aligned} \tag{2}$$

Remark 2.1: One might consider the following controller:

$$\begin{aligned} \hat{x}(k+1) &= \sum_{i=1}^{r} \lambda_i(\hat{\xi})\{\hat{A}_i\hat{x}(k) + \hat{B}_j y(k)\}, \\ u(k) &= \sum_{i=1}^{r} \lambda_i(\hat{\xi})\hat{C}_i\hat{x}(k). \end{aligned}$$

However, this class of controllers is limited, and a general class of controller is given as in (2)(see [10] for more detail.).

The closed-loop system (1) with (2) becomes

$$x_e(k+1) = \bar{A}_{\xi\hat{\xi}\hat{\xi}} x_e(k), \tag{3}$$

where $x_e(k)$ and $\bar{A}_{\xi\hat{\xi}\hat{\xi}}$ are given by

$$x_e(k) = \begin{bmatrix} x(k) \\ \hat{x}(k) \end{bmatrix}, \ \bar{A}_{\xi\hat{\xi}\hat{\xi}} = \begin{bmatrix} A_\xi & B_\xi \hat{C}_{\hat{\xi}} \\ \hat{B}_{\hat{\xi}} C_\xi & \hat{A}_{\hat{\xi}\hat{\xi}}. \end{bmatrix}$$

Our problem is to find an output feedback controller (2) such that the closed-loop system (3) is asymptotically stable.

The following lemma is useful to prove our main results.

Lemma 2.1: ([12])

$$\sum_{i=1}^{r}\sum_{j=1}^{r} \lambda_i(\xi(k))\lambda_j(\xi(k))\Phi_{ij} < 0$$

holds if the followings are satisfied:

$$\begin{aligned} \Phi_{ii} &< 0, \qquad i = 1, \cdots, r, \\ \frac{2}{r-1}\Phi_{ii} + \Phi_{ij} + \Phi_{ji} &< 0, \quad i, j = 1, \cdots, r, \ i \neq j \end{aligned}$$

III. Stability and Stabilization

Here, we consider an output feedback control of a discrete-time fuzzy system. We first give sufficient conditions for the closed-loop system (3) to be asymptotically stable. Then, we propose a design method of an output feedback controller for a discrete-time fuzzy system.

A. Stabilization Analysis

We make the stability analysis of the closed-loop system (3).

Theorem 3.1: An output feedback controller of the form (2) stabilizes the fuzzy system (1) if there exist matrices $X > 0,\ Y > 0,\ L_{\hat{\xi}\hat{\xi}},\ W_{\hat{\xi}},\ Z_{\hat{\xi}}$ such that

$$\left[\begin{array}{cc} X & I \\ I & Y \end{array} \right] > 0, \tag{4}$$

$$\Psi_{\xi\hat{\xi}\hat{\xi}} = \left[\begin{array}{cccc} -X & -I & \Psi_{13\xi\hat{\xi}} & A_{\xi} \\ -I & -Y & \Psi_{23\xi\hat{\xi}\hat{\xi}} & \Psi_{24\xi\hat{\xi}} \\ \Psi_{13\xi\hat{\xi}}^T & \Psi_{23\xi\hat{\xi}\hat{\xi}}^T & -X & -I \\ A_{\xi}^T & \Psi_{24\xi\hat{\xi}}^T & -I & -Y \end{array} \right] < 0. \tag{5}$$

where

$$\begin{array}{rcl} \Psi_{13\xi\hat{\xi}} & = & A_{\xi}X + B_{\xi}Z_{\hat{\xi}}, \\ \Psi_{23\xi\hat{\xi}\hat{\xi}} & = & YA_{\xi}X + YB_{\xi}Z_{\hat{\xi}} + W_{\hat{\xi}}C_{\xi}X + L_{\hat{\xi}\hat{\xi}}, \\ \Psi_{24\xi\hat{\xi}} & = & YA_{\xi} + W_{\hat{\xi}}C_{\xi}. \end{array}$$

Proof: We investigate the stability of the closed-loop system (3). A condition for the system (3) to be asymptotically stable is that there exists a matrix $P > 0$ such that

$$\bar{A}_{\xi\hat{\xi}\hat{\xi}}^T P \bar{A}_{\xi\hat{\xi}\hat{\xi}} - P < 0$$

or equivalently

$$\Lambda = \left[\begin{array}{cc} -P^{-1} & \bar{A}_{\xi\hat{\xi}\hat{\xi}} \\ \bar{A}_{\xi\hat{\xi}\hat{\xi}}^T & -P \end{array} \right] < 0. \tag{6}$$

To solve the matrix inequality (6), we follow the idea of [5] and partition P and P^{-1} as

$$P = \left[\begin{array}{cc} Y & N \\ N^T & V \end{array} \right], \quad P^{-1} = \left[\begin{array}{cc} X & M \\ M^T & U \end{array} \right]. \tag{7}$$

Define a transformation matrix Π as

$$\Pi = \left[\begin{array}{cc} X & I \\ M^T & 0 \end{array} \right]. \tag{8}$$

Then, it can be inferred from $PP^{-1} = I$ that

$$YX + NM^T = I. \tag{9}$$

We take a congruence transformation with Π for P to obtain

$$\Pi^T P \Pi = \left[\begin{array}{cc} X & I \\ I & Y \end{array} \right] > 0,$$

which is exactly the same as (4).

Pre- and post-multiplying Λ by $S = diag[P\Pi\ \Pi]$, we obtain

$$\Psi_{\xi\hat{\xi}\hat{\xi}} = S^T \Lambda S = \left[\begin{array}{cc} -\Pi^T P \Pi & \Pi^T P \bar{A}_{\xi\hat{\xi}\hat{\xi}} \Pi \\ \Pi^T \bar{A}_{\xi\hat{\xi}\hat{\xi}}^T P \Pi & -\Pi^T P \Pi \end{array} \right] < 0,$$

or more exactly we get (5) where we define

$$L_{\hat{\xi}\hat{\xi}} = N\hat{A}_{\hat{\xi}\hat{\xi}}M^T,\ W_{\hat{\xi}} = N\hat{B}_{\hat{\xi}},\ \text{and}\ Z_{\hat{\xi}} = \hat{C}_{\hat{\xi}}M^T. \tag{10}$$

B. Stabilization

This section gives sufficient conditions for the closed-loop system (3) to be asymptotically stable, and a method of controller design base on such stability conditions.

Theorem 3.2: An output feedback controller of the form (2) stabilizes the fuzzy system (1) if there exist matrices $X > 0,\ Y > 0,\ L_{jk},\ W_j,\ Z_j,\ j,k = 1,\cdots,r$ such that (4) holds and

$$\begin{array}{ll} \Psi_{ijj} < 0, & i,j = 1,\cdots,r, \\ \dfrac{2}{r-1}\Psi_{ijj} + \Psi_{ijk} + \Psi_{ikj} < 0, & i,j,k = 1,\cdots,r, \\ & j \neq k. \end{array} \tag{11}$$

where

$$\Psi_{ijk} = \left[\begin{array}{cccc} -X & \Psi_{13ij}^T & \Psi_{23ijk}^T & -I \\ \Psi_{13ij} & -X & -I & A_i \\ \Psi_{23ijk} & -I & -Y & \Psi_{24ij} \\ -I & A_i^T & \Psi_{24ij}^T & -Y \end{array} \right],$$

$$\begin{array}{rcl} \Psi_{13ij} & = & A_iX + B_iZ_j, \\ \Psi_{23ijk} & = & YA_iX + YB_iZ_j + W_jC_iX + L_{jk}, \\ \Psi_{24ij} & = & YA_i + W_jC_i. \end{array}$$

In this case, control gain matrices in (2) are given by

$$\begin{array}{l} \hat{A}_{jk} = N^{-1}L_{jk}M^{-T}, \\ \hat{B}_j = N^{-1}W_j, \\ \hat{C}_j = Z_jM^{-T}, j,k = 1,\cdots,r \end{array} \tag{12}$$

where M and N can be found from the equation $NM^T = I - YX$.

Proof: If conditions (11) are satisfied, it follows from Lemma 2.1 that

$$\sum_{i=1}^{r}\sum_{j=1}^{r}\sum_{k=1}^{r} \lambda_i(\xi(k))\lambda_j(\hat{\xi}(k))\lambda_k(\hat{\xi}(k))\Psi_{ijk} = \Psi_{\xi\hat{\xi}\hat{\xi}} < 0.$$

Taking a congruence transformation with the following T:

$$T = \left[\begin{array}{cccc} 0 & 0 & I & 0 \\ I & 0 & 0 & 0 \\ 0 & I & 0 & 0 \\ 0 & 0 & 0 & I \end{array} \right]$$

and calculating $T^T\Psi_{\xi\hat{\xi}\hat{\xi}}T < 0$, we obtain (5).

By Theorem 3.1, the stability is established. Control gain matrices (12) follow from the relations (10).

Theorem 3.2 does not give LMI conditions. However, the following algorithm provides an efficient LMI-based approach to solve for (4) and (11).

Algorithm 3.1: **Step 1**: Solve $Y > 0,\ W_j,\ j = 1,\cdots,r$ for the following LMI conditions

$$\left[\begin{array}{cc} -Y & \Psi_{24ij} \\ \Psi_{24ij}^T & -Y \end{array} \right] < 0, \quad i,j = 1,\cdots,r.$$

Step 2: Insert matrices $Y,\ W_j,\ j = 1,\cdots,r$, which are obtained in **Step 1**, into Ψ_{ijk}. Solve $X > 0,\ Z_j,\ L_{jk},\ j,k = 1,\cdots,r$ for (4) and (11).

Step 3: If there exists a solution, obtain gain matrices as in (12).

Remark 3.1: It follows from (4) that $Y - X^{-1} > 0$ and hence $NM^T = I - YX$ is nonsingular. M and N can tune control gain matrices in (2), which reflect trajectories of the states of the controlled system. One way to find M is to choose $M = X$. In this case, $\hat{x}$ in (2) becomes an estimate of the state x(see [4] for more detail.), and $N = X^{-1} - Y$.

Remark 3.2: Assawinchaichote et al. [1] and Yoneyama [15] considered the grade $\lambda_i(\xi)$ as uncertainty, and then gave stability conditions. Since their results depend on the maximum upper bound of $\lambda(\xi)$, they are rather conservative. The result of Guerra et al. [2] is based on non-LMI conditions with four scaling parameters, which must be chosen a priori. Algorithm 3.1 is involved with only strict LMI conditions, which are much easier to be solved than other methods.

C. Robust Stabilization

Now, we extend the results in the previous sections to a class of uncertain discrete-time fuzzy systems. Consider the uncertain discrete-time Takagi-Sugeno fuzzy model, described by the following IF-THEN rules:

$$\begin{array}{ll}\textbf{IF} & \xi_1 \ is \ M_{i1} \ and \ \cdots \ and \ \xi_p \ is \ M_{ip}, \\ \textbf{THEN} & x(k+1) = (A_i + \Delta A_i)x(k) \\ & \qquad +(B_i + \Delta B_i)u(k), \\ & y(k) = (C_i + \Delta C_i)x(k), \quad i = 1, \cdots, r\end{array}$$

where ΔA_i, ΔB_i and ΔC_i, $i = 1, \cdots, r$ are uncertain matrices that have the following structures:

$$\left[\begin{array}{cc} \Delta A_i & \Delta B_i \\ \Delta C_i & * \end{array}\right] = \left[\begin{array}{c} H_{1i} \\ H_{2i} \end{array}\right] F_i(k) \left[\begin{array}{cc} E_{1i} & E_{2i} \end{array}\right], \quad i = 1, \cdots, r. \tag{13}$$

and $F_i(k)$ is an uncertain matrix satisfying

$$F_i^T(k)F_i(k) \le I, \ i = 1, \cdots, r,$$

and H_{1i}, H_{2i}, E_{1i} and E_{2i} are constant matrices of appropriate dimensions.

The state and output equations are described by

$$\begin{aligned} x(k+1) = & \sum_{i=1}^{r} \lambda_i(\xi)\{(A_i + H_{1i}F_i(k)E_{1i})x(k) \\ & +(B_i + H_{1i}F_i(k)E_{2i})u(k)\}, \\ \triangleq & A_{\Delta\xi}x(k) + B_{\Delta\xi}u(k), \\ y(k) = & \sum_{i=1}^{r} \lambda_i(\xi)\{(C_i + H_{2i}F_i(k)E_{1i})x(k)\} \\ \triangleq & C_{\Delta\xi}x(k). \end{aligned} \tag{14}$$

If there exists a controller of the form (2) that stabilizes the system (14) for all admissible uncertain matrices ΔA_i, ΔB_i and ΔC_i satisfying (13), then it is called a robust stabilizing controller.

For the system (14), we will find a robust stabilizing controller. To this end, we use the following lemma.

Lemma 3.1: ([14]) Given matrices $Q = Q^T$, H, E and $R = R^T > 0$ of appropriate dimensions

$$Q + HF(k)E + E^TF^T(k)H^T < 0$$

for all $F(k)$ satisfying $F^T(k)F(k) \le R$ if and only if there exists a scalar $\varepsilon > 0$ such that

$$Q + \frac{1}{\varepsilon}HH^T + \varepsilon E^TRE < 0.$$

The closed-loop system (14) with (2) is given by

$$x_e(k+1) = \bar{A}_{\xi\hat{\xi}\hat{\xi}}x_e(k) \tag{15}$$

where $x_e(k)$ and $\bar{A}_{\xi\hat{\xi}\hat{\xi}}$ is given by

$$x_e(k) = \left[\begin{array}{c} x(k) \\ \hat{x}(k) \end{array}\right], \quad \bar{A}_{\xi\hat{\xi}\hat{\xi}} = \left[\begin{array}{cc} A_{\Delta\xi} & B_{\Delta\xi}\hat{C}_{\hat{\xi}} \\ \hat{B}_{\hat{\xi}}C_{\Delta\xi} & \hat{A}_{\hat{\xi}\hat{\xi}} \end{array}\right].$$

Theorem 3.3: An output feedback controller of the form (2) robustly stabilizes the uncertain fuzzy system (14) if there exist matrices $X > 0$, $Y > 0$, L_{jk}, W_j, Z_j, $j, k = 1, \cdots, r$ and scalars $\varepsilon_i > 0$ such that (4) holds and

$$\left[\begin{array}{ccccc} -\frac{1}{\varepsilon_{ij}}I & 0 & \bar{E}_{1ij} & 0 & 0 \\ 0 & -\frac{1}{\varepsilon_{ij}}I & \bar{E}_{2i} & 0 & 0 \\ \bar{E}_{1ij}^T & \bar{E}_{2i}^T & \Xi_{ijj} & \bar{H}_{1i} & \bar{H}_{2ij} \\ 0 & 0 & \bar{H}_{1i}^T & -\varepsilon_{ij}I & 0 \\ 0 & 0 & \bar{H}_{2ij}^T & 0 & -\varepsilon_{ij}I \end{array}\right] < 0, \quad i, j = 1, \cdots, r, \tag{16}$$

$$\left[\begin{array}{ccccc} -\frac{1}{\varepsilon_{ij}}I & 0 & \hat{E}_{1ijk} & 0 & 0 \\ 0 & -\frac{1}{\varepsilon_{ij}}I & \bar{E}_{2i} & 0 & 0 \\ \hat{E}_{1ijk}^T & \bar{E}_{2i}^T & \hat{\Xi}_{ijk} & \bar{H}_{1i} & \hat{H}_{2ijk} \\ 0 & 0 & \bar{H}_{1i}^T & -\varepsilon_{ij}I & 0 \\ 0 & 0 & \hat{H}_{2ijk}^T & 0 & -\varepsilon_{ij}I \end{array}\right] < 0, \quad i, j, k = 1, \cdots, r, \ j \ne k, \tag{17}$$

where

$$\begin{aligned} \Xi_{ijk} &= \left[\begin{array}{cccc} -X & \Xi_{13ij}^T & \Xi_{23ijk}^T & -I \\ \Xi_{13ij} & -X & -I & A_i \\ \Xi_{23ijk} & -I & -Y & \Xi_{24ij} \\ -I & A_i^T & \Xi_{24ij}^T & -Y \end{array}\right], \\ \Xi_{14ij} &= A_iX + B_iZ_j, \\ \Xi_{24ijk} &= YA_iX + YB_iZ_j + W_jC_iX + L_{jk}, \\ \Xi_{25ij} &= YA_i + W_jC_i, \\ \hat{\Xi}_{ijk} &= \tfrac{2}{r-1}\Xi_{ijj} + \Xi_{ijk} + \Xi_{ikj}, \\ \bar{H}_{1i} &= \left[\begin{array}{cccc} 0 & H_{1i}^T & H_{1i}^TY & 0 \end{array}\right]^T, \\ \bar{H}_{2ij} &= \left[\begin{array}{cccc} 0 & 0 & H_{2i}^TW_j^T & 0 \end{array}\right]^T, \\ \hat{H}_{2ijk} &= \tfrac{r+1}{r-1}\bar{H}_{2ij} + \bar{H}_{2ik}, \\ \bar{E}_{1ij} &= \left[\begin{array}{cccc} E_{1i}X + E_{2i}Z_j & 0 & 0 & E_{1i} \end{array}\right]^T, \\ \bar{E}_{2i} &= \left[\begin{array}{cccc} E_{1i}X & 0 & 0 & E_{1i} \end{array}\right]^T, \\ \hat{E}_{1ijk} &= \tfrac{r+1}{r-1}\bar{E}_{1ij} + \bar{E}_{1ik}. \end{aligned}$$

In this case, control gain matrices in (2) are given by (12).

Proof: Replacing A_i, B_i and C_i by $A_i + H_{1i}F_iE_{1i}$, $B_i + H_{1i}F_iE_{2i}$ and $C_i + H_{2i}F_iE_{1i}$, respectively in the first LMI (11), we get

$$\begin{aligned} &\Psi_{ijj} + \bar{H}_{1i}F_i\bar{E}_{1ij} + \bar{E}_{1ij}^TF_i^T\bar{H}_{1i}^T \\ &\quad +\bar{H}_{2ij}F_i\bar{E}_{2i} + \bar{E}_{2i}^TF_i^T\bar{H}_{2ij}^T < 0, \ i, j = 1, \cdots, r. \end{aligned}$$

We apply Lemma 3.1, and obtain an equivalent condition that there exists $\varepsilon_i > 0$ such that

$$\Psi_{ijj} + \varepsilon_i \bar{E}_{1ij}^T \bar{E}_{1ij} + \varepsilon_i \bar{E}_{2i}^T \bar{E}_{2i} + \frac{1}{\varepsilon_i} \bar{H}_{1i} \bar{H}_{1i}^T + \frac{1}{\varepsilon_i} \bar{H}_{2ij} \bar{H}_{2ij}^T < 0, \ i,j = 1, \cdots, r.$$

By Schur complement formula, we finally obtain the LMI in (16).

The LMI in (17) can be obtained in a similar manner. In fact, it follows from (17) that

$$\begin{aligned} &\frac{2}{r-1}\Psi_{ijj} + \Psi_{ijk} + \Psi_{ikj} + \frac{\varepsilon_i(r+1)}{r-1}\bar{E}_{1ij}^T \bar{E}_{1ij} \\ &+\varepsilon_i \bar{E}_{1ik}^T \bar{E}_{1ik} + \frac{2r\varepsilon_i}{r-1}\bar{E}_{2i}^T \bar{E}_{2i} + \frac{2r}{\varepsilon_i(r-1)}\bar{H}_{1i}\bar{H}_{1i}^T \\ &+\frac{r+1}{\varepsilon_i(r-1)}\bar{H}_{2ij}\bar{H}_{2ij}^T + \frac{1}{\varepsilon_i}\bar{H}_{2ik}\bar{H}_{2ik}^T < 0, \\ &\qquad i = 1, \cdots, r, \quad j \neq k = 1, \cdots, r. \end{aligned}$$

Then, the results follow.

The following algorithm is used for the control design.

Algorithm 3.2: **Step 1**: Solve $Y > 0, \ W_j, \ j = 1, \cdots, r$ and $\varepsilon_i > 0, \ i = 1, \cdots, r$ for the following LMI conditions

$$\begin{bmatrix} -Y & \Xi_{24ij} & YH_{1i} & W_j H_{2i} \\ \Xi_{24ij}^T & -Y & 0 & 0 \\ H_{1i}^T Y & 0 & -\varepsilon_{ij} I & 0 \\ H_{2i}^T W_j^T & 0 & 0 & -\varepsilon_{ij} I \end{bmatrix} < 0, \quad i,j = 1, \cdots, r,$$

$$\begin{bmatrix} -\frac{2r}{r-1}Y & \hat{\Xi}_{24ijk} & YH_{1i} & \tilde{H}_{ijk} \\ \hat{\Xi}_{24ijk}^T & -\frac{2r}{r-1}Y & 0 & 0 \\ H_{1i}^T Y & 0 & -\varepsilon_{ij} I & 0 \\ \tilde{H}_{ijk}^T & 0 & 0 & -\varepsilon_{ij} I \end{bmatrix} < 0, \quad i,j,k = 1, \cdots, r, \ \ j \neq k$$

where

$$\begin{aligned} \hat{\Xi}_{24ijk} &= \frac{r+1}{r-1}\Xi_{24ij} + \Xi_{24ik}, \\ \tilde{H}_{ijk} &= \frac{r+1}{r-1} W_j H_{2i} + W_k H_{2i}, \end{aligned}$$

Step 2: Insert matrices $Y, \ W_j, \ j = 1, \cdots, r$ and $\varepsilon_i > 0, \ i = 1, \cdots, r$, which are obtained in **Step 1**, into Ψ_{ijk}. Then, solve $X > 0, \ L_{jk}, \ Z_j, \ j,k = 1, \cdots, r$ for (4), (16) and (17).

Step 3: If there exists a solution, obtain gain matrices as in (12).

Remark 3.3: Algorithm 3.2 also gives LMI approach to solving an output feedback control problem.

IV. Examples

We give two examples. The first one illustrates stabilization for a nominal fuzzy system. The second example is concerned with an uncertain fuzzy system. We note that the results in [3], [8], [9], [16] cannot be applied to these problems because these papers assume the measurable premise variables.

Example 4.1 Consider the fuzzy system (1) with following matrices:

$$\begin{aligned} A_1 &= \begin{bmatrix} 1.2 & -0.2 \\ 0.1 & -0.4 \end{bmatrix}, \\ A_2 &= \begin{bmatrix} 1.2 & -0.2 \\ 0.2 & 0 \end{bmatrix}, \\ B_1 &= \begin{bmatrix} 1.3 \\ 0.7 \end{bmatrix}, \\ B_2 &= \begin{bmatrix} 1.5 \\ 1.0 \end{bmatrix}, \\ C_1 = C_2 &= \begin{bmatrix} 10 & -2 \end{bmatrix}, \\ \lambda_1(x_1) &= \frac{1}{1+e^{-x_1}}, \\ \lambda_2(x_1) &= 1 - \lambda_1(x_1). \end{aligned}$$

The system is descretized with sampling time $t_s = 0.01$. We attempt to obtain a stabilizing output feedback controller of the form (2). In this problem, the output y is the only measurable and premise variable x_1 is immeasurable. Algorithm 3.1 guarantees the existence of a stabilizing output feedback controller. According to the result in [4], we choose $M = X$. In this case, then a stabilizing controller (2) is given with

$$\begin{aligned} \hat{A}_{11} &= \begin{bmatrix} -0.7815 & 0.0775 \\ -0.4765 & -0.1442 \end{bmatrix}, \\ \hat{A}_{12} &= \begin{bmatrix} -1.4191 & 0.7697 \\ 0.4761 & -3.4518 \end{bmatrix}, \\ \hat{A}_{21} &= \begin{bmatrix} -0.4473 & -0.5188 \\ -1.3826 & 3.2341 \end{bmatrix}, \\ \hat{A}_{22} &= \begin{bmatrix} -0.9619 & 0.0924 \\ -0.5902 & -0.1377 \end{bmatrix}, \\ \hat{B}_1 &= \begin{bmatrix} 0.1251 \\ 0.0130 \end{bmatrix}, \\ \hat{B}_2 &= \begin{bmatrix} 0.1471 \\ 0.0274 \end{bmatrix}, \\ \hat{C}_1 &= \begin{bmatrix} -0.5381 & 0.0250 \end{bmatrix}, \\ \hat{C}_2 &= \begin{bmatrix} -0.5253 & 0.0088 \end{bmatrix}. \end{aligned}$$

Simulation results of x_1 and $\hat{x}_1$ with the initial conditions

$$x(0) = \begin{bmatrix} 10 \\ 5 \end{bmatrix}, \ \hat{x}(0) = \begin{bmatrix} 0 \\ 0 \end{bmatrix}.$$

are depicted in Fig. 1. The solid lines show the state x and the dotted lines the estimate $\hat{x}$. The controller stabilizes the system. No tuning parameter is necessary for solving LMI conditions in Algorithm 3.1, while several tuning parameters are required to be given to solve design conditions in [2].

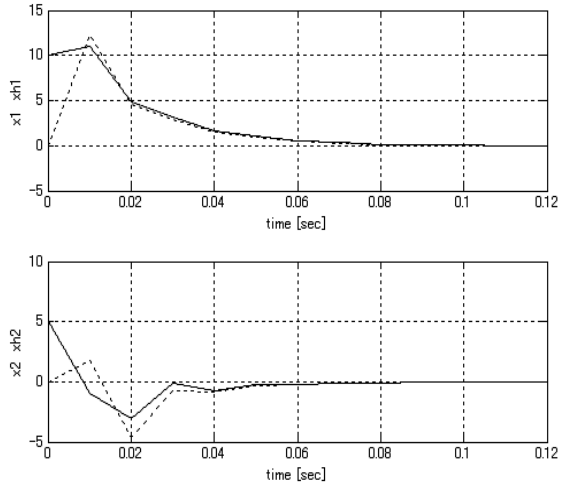

Fig. 1. States of the system

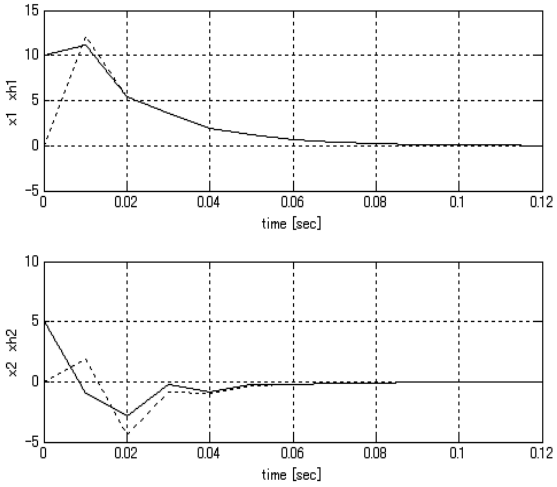

Fig. 2. States of the system

Example 4.2 We consider the system (14) with the following matrices:

$$A_1 = \begin{bmatrix} 1.2 & -0.2 \\ 0.1 & -0.4 \end{bmatrix},$$
$$A_2 = \begin{bmatrix} 1.2 & -0.2 \\ 0.2 & 0 \end{bmatrix},$$
$$B_1 = \begin{bmatrix} 1.3 \\ 0.7 \end{bmatrix},$$
$$B_2 = \begin{bmatrix} 1.5 \\ 1.0 \end{bmatrix},$$
$$C_1 = C_2 = \begin{bmatrix} 10 & -2 \end{bmatrix},$$
$$\lambda_1(x_1) = \frac{1}{1+e^{-x_1}},$$
$$\lambda_2(x_1) = 1 - \lambda_1(x_1),$$
$$H_{11} = H_{12} = 0.1I,$$
$$H_{21} = H_{22} = \begin{bmatrix} 0.1 & 0.1 \end{bmatrix},$$
$$E_{11} = E_{12} = 0.1I,$$
$$E_{21} = E_{22} = \begin{bmatrix} 0.1 \\ 0 \end{bmatrix}.$$

The system is descretized with sampling time $t_s = 0.01$.

Algorithm 3.2 gives a stabilizing output feedback controller (2) with $\hat{\xi} = \hat{x}_1$. Choosing $M = X$, we obtain control gains:

$$\hat{A}_{11} = \begin{bmatrix} -0.7862 & 0.0180 \\ -0.5132 & -0.1761 \end{bmatrix},$$
$$\hat{A}_{12} = \begin{bmatrix} -1.0024 & -0.6752 \\ -1.1031 & -2.2682 \end{bmatrix},$$
$$\hat{A}_{21} = \begin{bmatrix} -0.8287 & 0.8416 \\ 0.2020 & 2.0217 \end{bmatrix},$$
$$\hat{A}_{22} = \begin{bmatrix} -0.8223 & 0.0216 \\ -0.5389 & -0.1751 \end{bmatrix},$$
$$\hat{B}_1 = \begin{bmatrix} 0.1328 \\ 0.0195 \end{bmatrix},$$
$$\hat{B}_2 = \begin{bmatrix} 0.1371 \\ 0.0227 \end{bmatrix},$$
$$\hat{C}_1 = \begin{bmatrix} -0.5091 & -0.0145 \end{bmatrix},$$
$$\hat{C}_2 = \begin{bmatrix} -0.5104 & -0.0184 \end{bmatrix}.$$

Simulation results with the initial conditions and uncertain parameter:

$$x(0) = \begin{bmatrix} 10 \\ 5 \end{bmatrix},\ \hat{x}(0) = \begin{bmatrix} 0 \\ 0 \end{bmatrix},\ F(k) = cos(10k).$$

are shown in Fig. 2. The solid lines show the state x and the dotted lines the estimate $\hat{x}$. The controller robustly stabilizes the system.

V. Conclusions

We have proposed a stabilizing output feedback controller for discrete-time fuzzy systems with immeasurable premise variables. Our design method was based on LMI approach. No tuning parameter is necessary to solve the output feedback controller design problem. Furthermore, we extended the results to the case of robust output feedback controller for a class of uncertain fuzzy systems. Finally, some numerical examples are given to illustrate our design methods.

References

[1] W. Assawinchaichote, S.K. Nguang, and P. Shi, Fuzzy Control and Filter Design for Uncertain Fuzzy Systems, Springer, 2006.

[2] T.M. Guerra, A. Kruszewski, L. Vermeiren, and H. Tirmant, Conditions of output stabilization for nonlinear models in the Takagi-Sugeno's form, Fuzzy Sets and Systems, Vol.157, pp.1248-1259, 2006.

[3] X.J. Ma, Z.Q. Sun, and Y.Y. He, Analysis and design of fuzzy controller and fuzzy observer, IEEE Transactions on Fuzzy Systems, Vol. 6, No. 1, pp.41-50, 1998.

[4] Shusaku Nishikawa and Jun Yoneyama, Guaranteed cost output feedback control of fuzzy systems via LMI approach, Journal of Advanced Computational Intelligence and Intelligent Informatics, Vol.14, No.6, pp.567-573, 2010.

[5] C. Scherer, P. Gahinet, and M. Chilali, Multiobjective output-feedback control via LMI optimization, IEEE Transactions on Automatic Control, Vol. 42, No. 7, pp. 896-911, 1997.

[6] T. Takagi and M. Sugeno, Fuzzy identification of systems and its applications to modeling and control, IEEE Transaction on Systems, Man, Cybernetics, Vol.15, pp.116-132, 1985.
[7] K. Tanaka and M. Sugeno, Stability analysis and design of fuzzy control systems, Fuzzy Sets and Systems, Vol.45, pp.135-156, 1992.
[8] K. Tanaka and M. Sano, On the concepts of regulator and observer of fuzzy control systems, 3rd IEEE International Conference on Fuzzy Systems, pp.767-772, 1994.
[9] K. Tanaka, T. Ikeda, and H.O. Wang, Fuzzy regulators and fuzzy observers: relaxed stability conditions and LMI-based designs, IEEE Transactions on Fuzzy Systems, Vol. 6, No. 2, pp. 1-16, 1998.
[10] K. Tanaka and H.O. Wang, Fuzzy Control Systems Design and Analysis: A Linear Matrix Inequality Approach, Wiley Inter-Science, 2000.
[11] M.C.M. Teixeira, E. Assuncao and R.G. Avellar, On relaxed LMI-based designs for fuzzy regulators and fuzzy observers, Vol.11, pp,613-623, 2003.
[12] H.D. Tuan, P. Apkarian, T. Narikiyo and Y. Yamamoto, Parameterized linear matrix inequality techniques in fuzzy control system design, IEEE Transactions on Fuzzy Systems, Vol.9, pp.324-332, 2001.
[13] H.O. Wang, K. Tanaka, and M. Griffin, An approach to fuzzy control of nonlinear system stability and design issues, IEEE Transactions on Fuzzy Systems, Vol. 4, No. 1, pp. 14-21, 1996.
[14] L. Xie, Output feedback H_∞ control of systems with parameter uncertainty, International Journal of Control, 63 (1996), 741-59.
[15] J. Yoneyama, H_∞ output feedback control for fuzzy systems with immeasurable premise variables: discrete-time case, Applied Soft Computing, Vol. 8, No, 2, pp.949-958, 2008.
[16] J. Yoneyama, M. Nishikawa, H. Katayama and A. Ichikawa, Design of output feedback controllers for Takagi-Sugeno fuzzy systems, Fuzzy Sets and Systems, Vol.121, No.1, pp.127-148, 2001.
[17] Jun Yoneyama, LMI Approach to output feedback control for fuzzy systems, IEEE International Conference on Fuzzy Systems, pp.2174-2179, Barcelona, 2010.

2011 IEEE International Conference on Fuzzy Systems
June 27-30, 2011, Taipei, Taiwan

Decentralized Control of Large Scale Switched Takagi-Sugeno Systems

Dalel Jabri, Kevin Guelton, Noureddine Manamanni
University of Reims Champagne-Ardenne
CReSTIC EA3804, Moulin de la Housse
BP 1039, 51687 Reims Cedex 2, France
kevin.guelton@univ-reims.fr

Abstract— **This paper deals with decentralized stabilization of large scale switched nonlinear systems under arbitrary switching laws. A global large scale switched system can be split into a set of smaller interconnected switched Takagi Sugeno fuzzy subsystems. Then, in order to stabilize the overall closed-loop system, a set of switched non-PDC controllers is employed. The latter is designed based on Linear Matrix Inequalities (LMI) conditions obtained from a multiple switched non quadratic like-Lyapunov candidate function. A numerical example is proposed to illustrate the effectiveness of the suggested decentralized switched controller design approach.**

Keywords- switched fuzzy system, decentralized control, stabilizing non-PDC control law, arbitrary switching laws, multiple switched non quadratic like-Lyapunov functional.

I. INTRODUCTION

Among control theory, switched linear systems has grown interest since they provide a convenient modeling approach for many physical systems such as computer networks, embedded control systems, traffic control systems, automatic highway systems, chemical process [1-4]. This special class of hybrid system is represented by a family of time-invariant systems switching together in accordance to a stabilizing or an arbitrary law.

In the past decades, many studies focused on the stability analysis and stabilization issue for both linear and nonlinear switched systems [5-10]. The main challenge in treating such problems is to guaranty the stability of the whole system at the switching time. Indeed, the well-know example in [11] show that the stability of each subsystem may not involve the stability of the whole switched system. Hence, switching between subsystems may introduce instable behavior.

Attempting to solve this problem, several primary results dealing with switched linear systems propose to find a common quadratic Lyapunov function satisfying some linear matrix inequality (LMI) conditions [11]. Despite the simplicity of the obtained LMI formulation, finding a common Lyapunov function leads to conservatism. Thus, in order to reduce the conservatism, some relaxed approaches has been proposed by using piecewise quadratic Lyapunov functions [12] or multiple Lyapunov functions [13-16]. In [14], besides to the conditions ensuring the decreasing behaviors for each local Lyapunov function, an additional condition at the switching time to ensure the stability of the whole switched system. Some other works suggest verifying the decreasing behaviour of like-Lyapunov function's switching sequences, see e.g. [8] for more details.

In this study, the problem of designing decentralized switched controllers ensuring the stability of continuous time large scale switched nonlinear systems is addressed. Based on the well-known universal approximator property of Takagi-Sugeno (TS) fuzzy models for nonlinear problems [17,18], there is a growing attention on studying switched nonlinear systems based on TS fuzzy modeling, see e.g. [19]. This kind of systems, known as switched fuzzy systems, involves TS models to represent nonlinear continuous modes. This class of hybrid dynamical systems may be useful to describe precisely both continuous and discrete dynamics as well as their interactions in real-world systems [19,20]. Despite switched linear systems, few studies have been done in the switched nonlinear case. A common Lyapunov candidate function has been firstly employed to ensure the stabilization of switched fuzzy systems [11]. In [21], authors propose to employ a switched PDC controller as well as a switched fuzzy Lyapunov candidate function. However, the authors don't mention any condition to guarantee the stability of the whole system at the switching times.

According to the above described studies and since complex physical configuration and high dimension of many real systems, several works have dealt with stability and stabilization issues of large scale dynamical systems; see e.g. [22-26]. Nevertheless, few investigations can be found in the literature dealing with stability and stabilization problems of large scale switched systems [24,27,28]. In our previous works, one has proposed LMI based stabilization for large scale switched linear systems [24]. Moreover, to the best of the authors' knowledge, the stabilization issue of interconnected switched nonlinear systems hasn't yet been investigated.

Note also that, regarding to TS based approaches, the fuzzy Lyapunov function remains one of the least conservative in terms of LMI. However, the appearance of the membership function derivatives is often considered as a drawback. For more details on some recent results in TS based nonquadratic state feedback controller design, one can refer to [29-31]. Nevertheless, the meaning of this paper is not to cope with this problem. Hence, the goal is to propose a LMI based

This work has been supported by the GIS 3SGS within the framework of the project COSMOS II and by the Région Champagne-Ardenne and the FEDER within the CPER MOSYP.

methodology, in the nonquadratic framework, for the design of decentralized switched non-PDC controllers for a class of large scale switched nonlinear systems under arbitrary switching laws.

This paper is organized as follows: First, the studied class of continuous-time interconnected switched fuzzy systems will be described. Then, a set of decentralized switched non-PDC controller is proposed. Hence, LMI stability conditions are provided based on a switched fuzzy like-Lyapunov function candidate. Finally, a simulation example is proposed to illustrate the efficiency of the designed approach.

II. PROBLEM STATEMENT

Let us consider the class of nonlinear hybrid systems S composed of n continuous time switched nonlinear subsystem S_i based on TS modelling. The n state equations of the whole interconnected switched fuzzy system S are given as follows:

$$\text{For } i=1,...,n:$$
$$\dot{x}_i(t)=\sum_{j_i=1}^{m_i}\sum_{s_{j_i}=1}^{r_{j_i}}\xi_{j_i}(t)h_{s_{j_i}}\left(z_{j_i}(t)\right)\left[A_{s_{j_i}}x_i(t)+B_{s_{j_i}}u_i(t)+\sum_{\substack{\alpha=1\\ \alpha\neq i}}^{n}F_{i,\alpha,s_{j_i}}x_\alpha(t)\right] \tag{1}$$

where $x_i(t)\in\mathbb{R}^{\eta_i}$, $u_i(t)\in\mathbb{R}^{\upsilon_i}$ represent respectively the state and the input vectors associated to the i^{th} subsystem; m_i is the number of switching modes of the i^{th} subsystem; r_{j_i} is the number of fuzzy rules associated to the i^{th} subsystem in the j_i^{th} mode; for $i=1,...,n$, $j_i=1,...,m_i$ and $s_{j_i}=1,...,r_{j_i}$, $A_{s_{j_i}}\in\mathbb{R}^{\eta_i\times\eta_i}$, $B_{s_{j_i}}\in\mathbb{R}^{\eta_i\times\upsilon_i}$ and $F_{i,\alpha,s_{j_i}}\in\mathbb{R}^{\eta_i\times\eta_\alpha}$ are constant matrices describing the local dynamics of each polytops; $F_{i,\alpha,s_{j_i}}$ express the interconnections between subsystems, i.e. the influence of the α^{th} subsystem on the i^{th} one; $z_{j_i}(t)$ are the premises variables and $h_{s_{j_i}}\left(z_{j_i}(t)\right)$ are positive membership functions satisfying the convex sum proprieties $\sum_{s_{j_i}=1}^{r_{j_i}}h_{s_{j_i}}\left(z_{j_i}(t)\right)=1$; $\xi_{j_i}(t)$ is the switching rules of the i^{th} subsystem, considered arbitrary but assumed to be real time available, these are defined such that the active system in the l_i^{th} mode lead to:

$$\begin{cases}\xi_{j_i}(t)=1 & \text{if } j_i=l_i\\ \xi_{j_i}(t)=0 & \text{if } j_i\neq l_i\end{cases} \tag{2}$$

In order to ensure the stabilization of the overall closed-loop fuzzy switched S, a set of decentralized state feedback switched non-PDC control laws is proposed as:

$$\text{For } i=1,...,n:$$
$$u_i(t)=\sum_{j_i=1}^{m_i}\sum_{k_{j_i}=1}^{r_{j_i}}\xi_{j_i}(t)h_{s_{j_i}}\left(z_{j_i}(t)\right)K_{k_{j_i}}\left(\sum_{s_{j_i}=1}^{r_{j_i}}h_{s_{j_i}}\left(z_{j_i}(t)\right)X_{s_{j_i}}\right)^{-1}x_i(t) \tag{3}$$

where $K_{k_{j_i}}$ and $X_{s_{j_i}}=X_{s_{j_i}}^T>0$ are the gain matrices to be synthesized.

Notations : The time t will be omitted when there is no ambiguity. However, one denotes $t_{j_i\to j_i^+}$ the switching instants of the i^{th} subsystem between the current mode j_i (at time t) and the upcoming mode j_i^+ (at time t^+), therefore:

$$\begin{cases}\xi_{j_i}(t)=1\\ \xi_{j_i^+}(t)=0\end{cases}\text{ and }\begin{cases}\xi_{j_i}(t^+)=0\\ \xi_{j_i^+}(t^+)=1\end{cases} \tag{4}$$

In order to lighten the mathematical expression, the premises entries z_{j_i} will be omitted and the following notations will be employed in the sequel:

$$G_{h_{j_i}}=\sum_{s_{j_i}=1}^{r_{j_i}}h_{s_{j_i}}G_{s_{j_i}}\text{ and }Y_{h_{j_i},h_{i_i}}=\sum_{s_{j_i}=1}^{r_{j_i}}\sum_{k_{j_i}=1}^{r_{j_i}}h_{s_{j_i}}h_{k_{j_i}}Y_{s_{j_i},k_{j_i}}\ .$$

We will also distinguish, for a regular quantity $\Gamma_{s_{j_i}}$ of appropriate dimension:

$$\left(\Gamma_{h_{j_i}}\right)^{-1}=\left(\sum_{s_{j_i}=1}^{r_{j_i}}h_{s_{j_i}}\Gamma_{s_{j_i}}\right)^{-1}.$$

For matrices of appropriate dimensions we will denote :

$$\dot{X}_{h_{j_i}}=\frac{dX_{h_{j_i}}}{dt}\text{ and }\left(\dot{X}_{h_{j_i}}\right)^{-1}=\frac{d\left(X_{h_{j_i}}\right)^{-1}}{dt}.$$

As usual, a star (*) indicates a transpose quantity in a symmetric matrix.

The basic idea is to synthesize a global decentralized (3) controller composed of n local switched non-PDC controllers ensuring the stability of each subsystem S_i regarding to the influence of the others subsystems' dynamics. Hence, substituting (3) into (1), one expresses the overall closed-loop dynamics S_{cl} described by:

$$\text{For } i=1,...,n:$$
$$\dot{x}_i=\sum_{j_i=1}^{m_i}\xi_{j_i}\left\{\left[A_{h_{j_i}}+B_{h_{j_i}}K_{h_{j_i}}\left(X_{h_{j_i}}\right)^{-1}\right]x_i+\sum_{\substack{\alpha=1\\ \alpha\neq i}}^{n}F_{i,\alpha,h_{j_i}}x_\alpha\right\} \tag{5}$$

The following lemma will be useful in the sequel.

Lemma [32]: Let us consider two matrices A and B with appropriate dimension, the following inequality is satisfied with the scalar $\tau > 0$:

$$A^T B + B^T A \le \tau A^T A + \tau^{-1} B^T B \tag{6}$$

III. LMI Based Decentralized Controller Design

In this section, the goal is to propose a methodology for the design of decentralized switched non-PDC controller (3) ensuring the closed-loop stability of (5). The main result is given in the following theorem.

Theorem : Assume that for each subsystem i of (1), the active mode is denoted by j_i and, for $j_i = 1,...,m_i$ and $s_{j_i} = 1,...,r_{j_i}$, $\dot{h}_{s_{j_i}}\left(z(t)\right) \ge \lambda_{s_{j_i}}$. The overall interconnected switched Takagi-Sugeno system (1) is stabilized by a set of n decentralized switched non-PDC control laws (3), if there exists, for all combinations of $i = 1,...,n$, $j_i = 1,...,m_i$ $j_i^+ = 1,...,m_i$, $s_{j_i} = 1,...,r_{j_i}$, $k_{j_i} = 1,...,r_{j_i}$ and $l_{j_i} = 1,...,r_{j_i}$, the matrices $X_{k_{j_i}} = \left(X_{k_{j_i}}\right)^T > 0$, $W_{s_{j_i},k_{j_i}}$, $K_{k_{j_i}}$ and the positive scalars, $\tau_{1,i}$, … $\tau_{i-1,i}$, $\tau_{i+1,i}$,…, $\tau_{n,i}$ (excepted $\tau_{i,i}$ which don't exist since there is no interaction between a subsystem and himself), such that the LMIs described by (7), (8) and (9)are satisfied.

$$X_{k_{j_i}} - \mu_{j_i \to j_i^+} X_{k_{j_i}} \le 0 \tag{7}$$

$$X_{l_{j_i}} + W_{s_{j_i},k_{j_i}} > 0 \tag{8}$$

$$\left(\begin{array}{c|ccccc|ccccc} \Gamma_{s_{j_i},k_{j_i}} & X_{k_{j_i}} & \cdots & \cdots & X_{k_{j_i}} & X_{k_{j_i}} & \cdots & \cdots & X_{k_{j_i}} \\ \hline X_{k_{j_i}} & -\tau_{1,i} I & 0 & \cdots & 0 & 0 & \cdots & \cdots & 0 \\ \vdots & 0 & \ddots & \ddots & \vdots & \vdots & \ddots & 0 & \vdots \\ \vdots & \vdots & \ddots & \ddots & 0 & \vdots & 0 & \ddots & \vdots \\ X_{k_{j_i}} & 0 & \cdots & 0 & -\tau_{i-1,i} I & 0 & \cdots & \cdots & 0 \\ \hline X_{k_{j_i}} & 0 & \cdots & \cdots & 0 & -\tau_{i+1,i} I & 0 & \cdots & 0 \\ \vdots & \vdots & \ddots & 0 & \vdots & 0 & \ddots & \ddots & \vdots \\ \vdots & \vdots & 0 & \ddots & \vdots & \vdots & \ddots & \ddots & 0 \\ X_{k_{j_i}} & 0 & \cdots & \cdots & 0 & 0 & \cdots & 0 & -\tau_{n,i} I \end{array}\right) < 0 \tag{9}$$

with

$$\Gamma_{s_{j_i},k_{j_i}} = X_{k_{j_i}} \left(A_{s_{j_i}}\right)^T + A_{s_{j_i}} X_{k_{j_i}} - \Phi_{s_{j_i},k_{j_i}} + \left(K_{k_{j_i}}\right)^T \left(B_{s_{j_i}}\right)^T + B_{s_{j_i}} K_{k_{j_i}} + \sum_{\substack{\alpha=1 \\ \alpha \ne i}}^{n} \tau_{i,\alpha} F_{i,\alpha,s_{j_i}} \left(F_{i,\alpha,s_{j_i}}\right)^T$$

and

$$\Phi_{s_{j_i},k_{j_i}} = \sum_{l_{j_i}=1}^{r_{j_i}} \lambda_{l_{j_i}} \left(X_{l_{j_i}} + W_{s_{j_i},k_{j_i}}\right).$$

Proof: Let us define the following multiple like-Lyapunov functional candidate:

$$V\left(x_1, x_2, ..., x_n\right) = \sum_{i=1}^{n} \sum_{j_i=1}^{m_i} \xi_{j_i} v_{j_i}\left(x_i\right) > 0 \tag{10}$$

where $v_{j_i} = x_i^T \left(X_{h_{j_i}}\right)^{-1} x_i = x_i^T \left(\sum_{s_{j_i}=1}^{r_{j_i}} h_{s_{j_i}} X_{s_{j_i}} \right)^{-1} x_i$

with $X_{h_{j_i}} = \left(X_{h_{j_i}}\right)^T > 0$.

According to the overview [15], the closed-loop interconnected switched system (5) is asymptotically stable if:

$$\forall t \ne t_{j_i \to j_i^+}, \ \dot{V}\left(x_1, x_2, ..., x_n\right) < 0 \tag{11}$$

and

$$v_{j_i^+}\left(t_{j_i \to j_i^+}\right) \le \mu_{j_i \to j_i^+} v_{j_i}\left(t_{j_i \to j_i^+}\right) \tag{12}$$

where $\mu_{j_i \to j_i^+}$ are positive scalars.

First, let us focus on the inequalities (12). Their aim is to ensure the global behaviour of the like-Lyapunov function (10) at the switching time $t_{j_i \to j_i^+}$. These inequalities are verified if :

For $i = 1,...,n$:

$$\left(X_{h_{j_i^+}}\right)^{-1} \le \mu_{j_i \to j_i^+} \left(X_{h_{j_i}}\right)^{-1} \tag{13}$$

which can be rewritten in its extended form as:

For $i = 1,...,n$:

$$\sum_{s_{j_i}=1}^{r_{j_i}} \sum_{s_{j_i^+}=1}^{r_{j_i^+}} h_{s_{j_i}} h_{s_{j_i^+}} \left(X_{s_{j_i}} - \mu_{j_i \to j_i^+} X_{s_{j_i^+}}\right) \le 0 \tag{14}$$

Inequality (14) is verified if (7) hold for all $i = 1,...,n$, $j_i = 1,...,m_i$, $j_i^+ = 1,...,m_i$, $s_{j_i} = 1,...,r_{j_i}$ and $s_{j_i^+} = 1,...,r_{j_i^+}$.

Now, let us deal with (11), with the above defined notations, it can be rewritten as, $\forall t \ne t_{j_i \to j_i^+}$:

$$\sum_{i=1}^{n} \left[\dot{x}_i^T \left(X_{h_{j_i}}\right)^{-1} x_i + x_i^T \left(X_{h_{j_i}}\right)^{-1} \dot{x}_i + x_i^T \left(\dot{X}_{h_{j_i}}\right)^{-1} x_i \right] < 0 \tag{15}$$

Substituting (5) into (15), one can write, $\forall t \ne t_{j_i \to j_i^+}$:

$$\sum_{i=1}^{n}\Bigg\{x_i^T\Bigg[\left(A_{h_{ji}}\right)^T\left(X_{h_{ji}}\right)^{-1}+\left(X_{h_{ji}}\right)^{-1}A_{h_{ji}}+\left(\dot{X}_{h_{ji}}\right)^{-1}$$
$$+\left(X_{h_{ji}}\right)^{-1}\left(K_{h_{ji}}\right)^T\left(B_{h_{ji}}\right)^T\left(X_{h_{ji}}\right)^{-1}+\left(X_{h_{ji}}\right)^{-1}B_{h_{ji}}K_{h_{ji}}\left(X_{h_{ji}}\right)^{-1}\Bigg]x_i$$
$$+\sum_{\substack{\alpha=1\\ \alpha\neq i}}^{n}\Bigg[\left(x_\alpha\right)^T\left(F_{i,\alpha,h_{ji}}\right)^T\left(X_{h_{ji}}\right)^{-1}x_i+x_i^T\left(X_{h_{ji}}\right)^{-1}F_{i,\alpha,h_{ji}}x_\alpha\Bigg]\Bigg\}<0 \tag{16}$$

From (6), the inequality (16) can be bounded by, $\forall t\neq t_{j_i\to j_i^+}$:

$$\sum_{i=1}^{n}x_i^T\Bigg\{\left(A_{h_{ji}}\right)^T\left(X_{h_{ji}}\right)^{-1}+\left(X_{h_{ji}}\right)^{-1}A_{h_{ji}}+\left(\dot{X}_{h_{ji}}\right)^{-1}$$
$$+\left(X_{h_{ji}}\right)^{-1}\left(K_{h_{ji}}\right)^T\left(B_{h_{ji}}\right)^T\left(X_{h_{ji}}\right)^{-1}+\left(X_{h_{ji}}\right)^{-1}B_{h_{ji}}K_{h_{ji}}\left(X_{h_{ji}}\right)^{-1}$$
$$+\sum_{\substack{\alpha=1\\ \alpha\neq i}}^{n}\tau_{i,\alpha}\left(X_{h_{ji}}\right)^{-1}F_{i,\alpha,h_{ji}}\left(F_{i,\alpha,h_{ji}}\right)^T\left(X_{h_{ji}}\right)^{-1}\Bigg\}x_i+\sum_{i=1}^{n}\sum_{\substack{\alpha=1\\ \alpha\neq i}}^{n}\tau_{i,\alpha}^{-1}x_\alpha^Tx_\alpha<0 \tag{17}$$

where, for $i=1,...,n$, $\alpha=1,...,n$ and $\alpha\neq i$, $\tau_{i,\alpha}$ are positive scalars (note that, $\tau_{i,i}$ don't exist).

Since $\sum_{i=1}^{n}\sum_{\substack{\alpha=1\\ \alpha\neq i}}^{n}\tau_{i,\alpha}^{-1}x_\alpha^Tx_\alpha=\sum_{i=1}^{n}\sum_{\substack{\alpha=1\\ \alpha\neq 1}}^{n}\tau_{\alpha,i}^{-1}x_i^Tx_i$, $\forall x_i$, (17) is satisfied if, for $i=1,...,n$ and $\forall t\neq t_{j_i\to j_i^+}$:

$$\left(A_{h_{ji}}\right)^T\left(X_{h_{ji}}\right)^{-1}+\left(X_{h_{ji}}\right)^{-1}A_{h_{ji}}+\left(\dot{X}_{h_{ji}}\right)^{-1}$$
$$+\left(X_{h_{ji}}\right)^{-1}\left(K_{h_{ji}}\right)^T\left(B_{h_{ji}}\right)^T\left(X_{h_{ji}}\right)^{-1}+\left(X_{h_{ji}}\right)^{-1}B_{h_{ji}}K_{h_{ji}}\left(X_{h_{ji}}\right)^{-1} \tag{18}$$
$$+\sum_{\substack{\alpha=1\\ \alpha\neq i}}^{n}\Bigg[\tau_{i,\alpha}\left(X_{h_{ji}}\right)^{-1}F_{i,\alpha,h_{ji}}\left(F_{i,\alpha,h_{ji}}\right)^T\left(X_{h_{ji}}\right)^{-1}+\tau_{\alpha,i}^{-1}I\Bigg]<0$$

Left and right multiplying the inequalities (18) respectively by $X_{h_{ji}}$ and since $-\left(\dot{X}_{h_{ji}}\right)^{-1}=\left(X_{h_{ji}}\right)^{-1}\dot{X}_{h_{ji}}\left(X_{h_{ji}}\right)^{-1}$, it yields, for $i=1,...,n$ and $\forall t\neq t_{j_i\to j_i^+}$:

$$X_{h_{ji}}\left(A_{h_{ji}}\right)^T+A_{h_{ji}}X_{h_{ji}}-\dot{X}_{h_{ji}}+\left(K_{h_{ji}}\right)^T\left(B_{h_{ji}}\right)^T+B_{h_{ji}}K_{h_{ji}}$$
$$+\sum_{\substack{\alpha=1\\ \alpha\neq i}}^{n}\Bigg[\tau_{i,\alpha}F_{i,\alpha,h_{ji}}\left(F_{i,\alpha,h_{ji}}\right)^T+\tau_{\alpha,i}^{-1}X_{h_{ji}}X_{h_{ji}}\Bigg]<0 \tag{19}$$

Let us now focus on the term $\dot{X}_{h_{ji}}$. Since the inequality (19) is a double sum ($h_{j_i}h_{j_i}$) and, by extension to the relaxation scheme proposed in [20], additional slack decision matrices can be introduced. Indeed, since the membership functions holds the convex sum property, one has $\sum_{s_{ji}=1}^{r_{ji}}\dot{h}_{j_i}=0$ and so $\sum_{l_{ji}=1}^{r_{ji}}\dot{h}_{l_{ji}}W_{h_{ji},h_{ji}}=0$. Therefore, one can write:

$$\dot{X}_{h_{ji}}=\sum_{l_{ji}=1}^{r_{ji}}\dot{h}_{l_{ji}}\left(X_{l_{ji}}+W_{h_{ji},h_{ji}}\right) \tag{20}$$

Then, let us assume that, for $i=1,...,n$, $j_i=1,...,m_i$, $s_{j_i}=1,...,r_{j_i}$, $\lambda_{s_{ji}}$ are the lower bound of $\dot{h}_{l_{ji}}$, one can write :

$$-\dot{X}_{h_{ji}}\leq-\Phi_{h_{ji},h_{ji}} \tag{21}$$

with $\Phi_{h_{ji},h_{ji}}=\sum_{s_{ji}=1}^{r_{ji}}\sum_{k_{ji}=1}^{r_{ji}}h_{s_{ji}}h_{k_{ji}}\sum_{l_{ji}=1}^{r_{ji}}\lambda_{l_{ji}}\left(X_{l_{ji}}+W_{s_{ji},k_{ji}}\right)$ and :

$$X_{l_{ji}}+W_{s_{ji},k_{ji}}>0 \tag{22}$$

Thus, from (21) and applying the Schur complement, (19) is satisfied if, for $i=1,...,n$ and $\forall t\neq t_{j_i\to j_i^+}$:

$$\left(\begin{array}{c|ccccc|ccccc}
\Gamma_{h_{ji},h_{ji}} & X_{h_{ji}} & \cdots & \cdots & X_{h_{ji}} & X_{h_{ji}} & \cdots & \cdots & X_{h_{ji}} \\
\hline
X_{h_{ji}} & -\tau_{1,i}I & 0 & \cdots & 0 & 0 & \cdots & \cdots & 0 \\
\vdots & 0 & \ddots & \ddots & \vdots & \vdots & \ddots & 0 & \vdots \\
\vdots & \vdots & \ddots & \ddots & 0 & \vdots & 0 & \ddots & \vdots \\
X_{h_{ji}} & 0 & \cdots & 0 & -\tau_{i-1,i}I & 0 & \cdots & \cdots & 0 \\
\hline
X_{h_{ji}} & 0 & \cdots & \cdots & 0 & -\tau_{i+1,i}I & 0 & \cdots & 0 \\
\vdots & \vdots & \ddots & 0 & \vdots & 0 & \ddots & \ddots & \vdots \\
\vdots & \vdots & 0 & \ddots & \vdots & \vdots & \ddots & \ddots & 0 \\
X_{h_{ji}} & 0 & \cdots & \cdots & 0 & 0 & \cdots & 0 & -\tau_{n,i}I
\end{array}\right)<0 \tag{23}$$

with

$$\Gamma_{h_{ji},h_{ji}}=X_{h_{ji}}\left(A_{h_{ji}}\right)^T+A_{h_{ji}}X_{h_{ji}}-\Phi_{h_{ji},h_{ji}}$$
$$+\left(K_{h_{ji}}\right)^T\left(B_{h_{ji}}\right)^T+B_{h_{ji}}K_{h_{ji}}+\sum_{\substack{\alpha=1\\ \alpha\neq i}}^{n}\tau_{i,\alpha}F_{i,\alpha,h_{ji}}\left(F_{i,\alpha,h_{ji}}\right)^T.$$

Then, (22) and (23) are satisfied if respectively (8) and (9) hold. That ends the proof. ■

Remark: When $\mu_{j_i\to j_i^+}$ are unknown, conditions of theorem above are not LMI. In order to obtain LMI conditions, one may choose the positive decreasing rates $\mu_{j_i\to j_i^+}$ according to :

$$\prod_{\substack{j_i=1 \\ j_i^+ \neq j_i}}^{m_i} \mu_{j_i \to j_i^+} \leq 1 \qquad (24)$$

IV. NUMERICAL EXAMPLE

This section is dedicated to illustrate the efficiency of the proposed approaches. We consider the following system composed of two interconnected switched takagi-sugeno subsystems given by:

Subsystem 1:

$$\dot{x}_1 = \sum_{j_1=1}^{2} \sum_{s_{j_1}=1}^{2} \xi_{j_1} h_{s_{j_1}} \left[A_{s_{j_1}} x_1 + B_{s_{j_1}} u_1 + F_{1,2,s_{j_1}} x_2 \right] \qquad (25)$$

with

$$x_1 = \begin{bmatrix} x_{11} \\ x_{12} \end{bmatrix} A_{1_{1_1}} = \begin{bmatrix} -2 & 1 \\ 0.1 & -2.1 \end{bmatrix}, A_{2_{1_1}} = \begin{bmatrix} -2 & 1 \\ 0.1 & -1.1 \end{bmatrix},$$

$$A_{1_{2_1}} = \begin{bmatrix} -1 & 1 \\ 0.1 & -2 \end{bmatrix}, A_{2_{2_1}} = \begin{bmatrix} -1 & 1 \\ 0.1 & -3 \end{bmatrix}, B_{1_{1_1}} = \begin{bmatrix} -1.2 \\ 0.2 \end{bmatrix},$$

$$B_{2_{1_1}} = \begin{bmatrix} -1.2 \\ 1.2 \end{bmatrix}, B_{1_{2_1}} = \begin{bmatrix} -1.5 \\ -0.5 \end{bmatrix}, B_{2_{2_1}} = \begin{bmatrix} -1.5 \\ -1.5 \end{bmatrix},$$

$$F_{1,2,1_{1_1}} = \begin{bmatrix} 0.01 & 0.001 & 0.1 \\ 0.01 & 0.01 & 0.1 \end{bmatrix}, F_{1,2,2_{1_1}} = \begin{bmatrix} 0.01 & 0.01 & 0.1 \\ 0.01 & 0.01 & 0.1 \end{bmatrix},$$

$$F_{1,2,1_{2_1}} = \begin{bmatrix} 0.01 & 0.01 & 0.01 \\ 0.07 & 0.2 & 0.2 \end{bmatrix}, F_{1,2,2_{2_1}} = \begin{bmatrix} 0.01 & 0.001 & 0.01 \\ 0.08 & 0.02 & 0.2 \end{bmatrix}$$

and the membership functions:

$$h_{1_{1_1}}\left(x_1(t)\right) = \sin^2\left(x_{11}(t)\right),\ h_{2_{1_1}}\left(x_1(t)\right) = \sin^2\left(x_{12}(t)\right),$$

$$h_{1_{2_1}}\left(x_1(t)\right) = 1 - h_{1_{1_1}}\left(x_1(t)\right), \text{ and } h_{2_{2_1}}\left(x_1(t)\right) = 1 - h_{2_{1_1}}\left(x_1(t)\right).$$

Subsystem 2:

$$\dot{x}_2 = \sum_{j_2=1}^{2} \sum_{s_{j_2}=1}^{2} \xi_{j_2} h_{s_{j_2}} \left[A_{s_{j_2}} x_2(t) + B_{s_{j_2}} u_2(t) + F_{2,1,s_{j_2}} x_1(t) \right] \qquad (26)$$

with

$$x_2 = \begin{bmatrix} x_{21} \\ x_{22} \\ x_{23} \end{bmatrix} A_{1_{1_2}} = \begin{bmatrix} -2 & 2 & 0 \\ 0 & -1 & 0 \\ 1 & 0.1 & -1.1 \end{bmatrix}, A_{2_{1_2}} = \begin{bmatrix} -2 & 2 & 0 \\ 0 & -1 & 0 \\ 0 & 0.1 & -2.1 \end{bmatrix},$$

$$A_{1_{2_2}} = \begin{bmatrix} -2 & 1 & 0 \\ 1 & -2 & 0 \\ 0 & 1.1 & -1 \end{bmatrix}, A_{2_{2_2}} = \begin{bmatrix} -2 & 1 & 0 \\ 1 & -3 & 0 \\ 0 & 0.1 & -1 \end{bmatrix}, B_{1_{2_2}} = \begin{bmatrix} -0.1 \\ 0.5 \\ 0.1 \end{bmatrix},$$

$$B_{2_{1_2}} = \begin{bmatrix} -0.1 \\ 0.5 \\ 1.1 \end{bmatrix}, B_{1_{2_2}} = \begin{bmatrix} 0.1 \\ 0.5 \\ 0.2 \end{bmatrix}, B_{2_{2_2}} = \begin{bmatrix} 0.1 \\ 0.5 \\ 1.2 \end{bmatrix}, F_{2,1,1_{1_2}} = \begin{bmatrix} 0.01 & 0.6 \\ 0.3 & 0.2 \\ 0.2 & 0.1 \end{bmatrix},$$

$$F_{2,1,2_{1_2}} = \begin{bmatrix} 0.01 & 0.6 \\ 0.3 & 0.2 \\ 0.02 & 0.1 \end{bmatrix}, F_{2,1,1_{2_2}} = \begin{bmatrix} 0.01 & 0.5 \\ 0.1 & 0.4 \\ 0.2 & 0.2 \end{bmatrix},$$

$$F_{2,1,2_{2_2}} = \begin{bmatrix} 0.01 & 0.5 \\ 0.1 & 0.04 \\ 0.2 & 0.2 \end{bmatrix}$$

and the membership functions

$$h_{1_{1_2}}\left(x_2(t)\right) = \sin^2\left(x_{21}(t)\right),\ h_{2_{1_2}}\left(x_2(t)\right) = \sin^2\left(x_{22}(t)\right),$$

$$h_{1_{2_2}}\left(x_2(t)\right) = 1 - h_{1_{1_2}}\left(x_2(t)\right),\ h_{2_{2_2}}\left(x_2(t)\right) = 1 - h_{2_{1_2}}\left(x_2(t)\right).$$

Let us assume that each subsystem switches under within the frontier defined by: $\mathrm{H}_{11} = 0.9x_{11} + x_{12}$, $\mathrm{H}_{12} = -0.2x_{11} + 9x_{12}$, $\mathrm{H}_{21} = -x_{21} + x_{22}$ and $\mathrm{H}_{22} = x_{21} - 2x_{22}$.

A set of decentralized switched controllers (3) is synthesized based on theorem 1 via the Matlab LMI toolbox. To do so, the decreasing rates are chosen as $\mu_{1_1 \to 2_1} = 0.4$, $\mu_{2_1 \to 1_1} = 2$, $\mu_{1_2 \to 2_2} = 0.4$, $\mu_{2_1 \to 1_1} = 2$ according to (24) and the lower bounds of membership functions as $\lambda_{1_{1_1}} = -4$, $\lambda_{1_{2_1}} = -1$, $\lambda_{1_{1_2}} = -6.5$ and $\lambda_{1_{2_2}} = -1.5$.

The close-loop subsystem dynamics are shown in Figure 1 for the initial states $x_1(0) = \begin{bmatrix} 2 & 2 \end{bmatrix}^T$ and $x_2(0) = \begin{bmatrix} -1 & 1.5 & -1 \end{bmatrix}^T$.

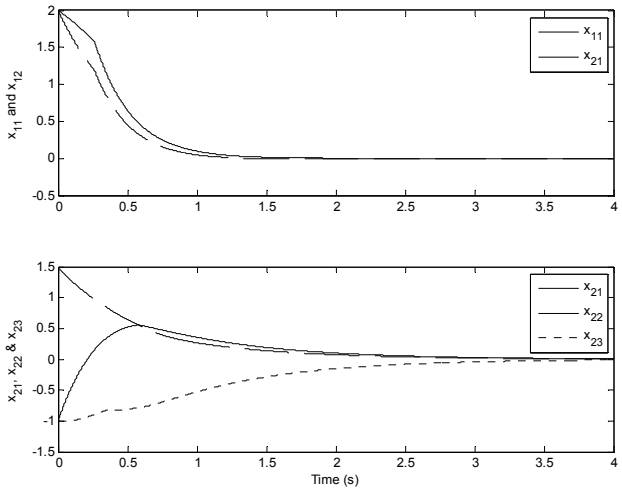

Figure 1. States dynamics of the overall closed-loop interconnected switched Takagi-Sugeno system.

Figure 2 shows the control signals as well as the switching modes' evolution. As expected, the synthesized decentralized switched controller stabilizes the overall large scale switched system composed of (25) and (26).

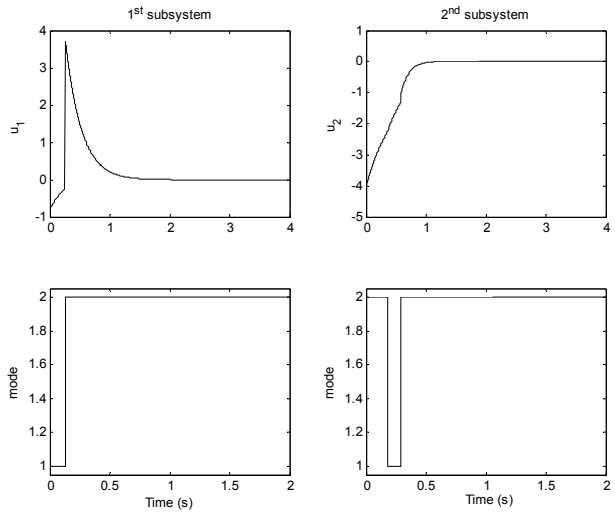

Figure 2. Control signals and switched laws' evolutions.

Figure 3 shows that like-Lyapunov functions $v_1(x_1)$ and $v(x_2)$ of both the subsystems, as well as the global like-Lyapunov function $V(x_1, x_2, ..., x_n)$, have a global decreasing behavior along the systems' trajectories.

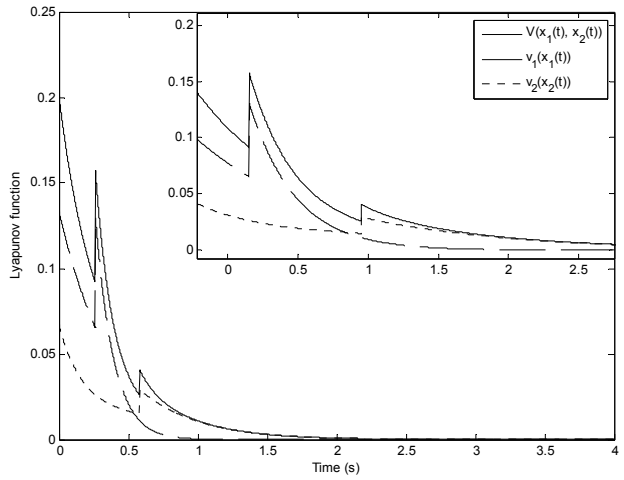

Figure 3. Behaviour of the like-Lyapunov functions.

Figure 4 provides the time evolution of the membership functions derivatives $\dot{h}_{1_{1_1}}(x_1(t))$, $\dot{h}_{2_{1_1}}(x_1(t))$, $\dot{h}_{1_{1_2}}(x_2(t))$ and $\dot{h}_{2_{1_2}}(x_2(t))$. This shows that the assumed lower bounds are verified in simulation for the considered initial conditions.

V. CONCLUSION

This study has focused on large scale switched nonlinear systems where, due to their well-known universal approximator properties, each nonlinear mode has been represented by a fuzzy Takagi-Sugeno system. Hence, the considered class of hybrid dynamical systems is composed by a set of interconnected switched Takagi-Sugeno subsystems. To ensure the stability of the whole system in closed-loop, a set of decentralized switched non-PDC controllers has been proposed. Therefore, LMI based conditions for the decentralized controller design has been obtained through the consideration of a candidate multiple switched non quadratic like-Lyapunov functional. Finally, a numerical example has been proposed to show the effectiveness of the proposed approach.

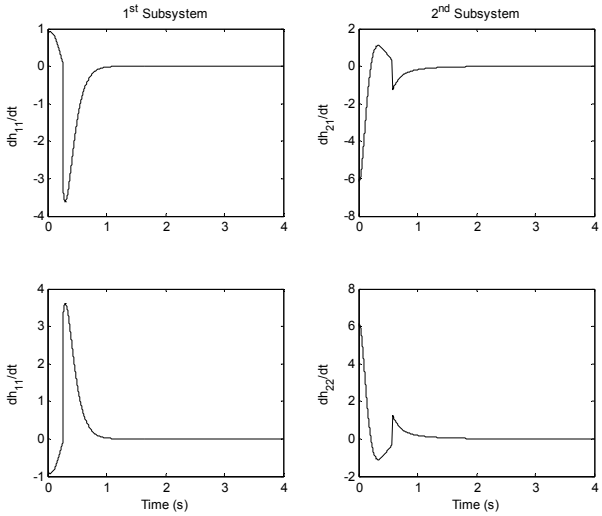

Figure 4. Evolution of membership functions derivatives.

ACKNOWLEDGMENT

The authors would like to thank Mr Sherpa Maal for his valuable comments.

REFERENCES

[1] D. Corona, J. Buisson, B. De Schutter and A. Giua, "Stabilization of switched affine systems: An application to the buck-boost converter," American Control Conference, New York, pp. 6037–6042, 2007.

[2] S. Mourik, H. Zwart and K.J. Keesman. "Switching input controller for a food storage room", Control Engineering Practice, vol. 18, 5, pp 507-514, 2010.

[3] Y. Song, Z. Xiang, Q. Chen and W. Hu, "Control of switched systems with actuator saturation", Journal of Control Theory and Applications, vol 1, pp. 38–43, 2006.

[4] H. Sun, and J. Zhao, "Control Lyapunov functions for switched control systems", American Control Conference, Arlington, USA, vol. 3, pp. 1890-1891, 2001.

[5] M-S. Branicky, "Stability of hybrid systems: state of the art", 36th Conf. Decision and Control, San Diego, USA, pp. 120–125, 1997.

[6] G.P. Chesi, J. C. Colaneri, R. Geromel, Middleton and R. Shorten, "Computing upper-bounds of the minimum dwell time of linear switched systems via homogeneous polynomial lyapunov functions", American Control Conference, Marryland, USA, 2010.

[7] J.P. Hespanha and A.S. Morse, "Stability of switched systems with average dwell-time". 38th IEEE Conf. Decision and Control, Phoenix, Arizona, USA, 3, pp 2655-2660, 1999.

[8] H. Lin and P. Antsaklis, “Stability and stabilizability of switched linear systems: A survey of recent results”, IEEE Transactions on Automatic Control, vol. 54, 2, pp. 308-322, 2009.

[9] Z. Wang, L. Xie, G. Xie and F. Hao, “Linear matrix inequality approach to quadratic stabilisation of switched systems”, IEE Proceedings Control Theory Application, vol. 151, 3, pp. 289–294, 2004.

[10] B. Mansouri, N. Manamanni, K. Guelton and M. Djemai, “Robust pole placement controller design in LMI region for uncertain and disturbed switched systems”, Nonlinear Analysis: Hybrid Systems, vol. 2, 4, pp 1136-1143, 2008.

[11] D. Liberzon and A.S. Morse, “Basic problems in stability and design of switched systems”, IEEE Control Systems Magazine, vol. 19, 5, pp. 59-70, 1999.

[12] M. Johansson, “Piecewise linear control systems - A computational approach”, Lecture Notes in Control and Information Science, 284, Springer, Heidelberg, Germany, 2003.

[13] J. Daafouz, P. Riedinger and C. Iung, “Stability analysis and control synthesis for switched systems: a switched Lyapunov function approach”, IEEE Transactions on Automatic Control, vol. 47, 11, pp 1883–1887, 2002.

[14] R.A. Decarlo, M.S. Branicky, S. Pettersson and B. Lennartson, “Perspectives and results on the stability and stabilizability of hybrid systems”, Proceedings of the IEEE, vol. 88, 7, pp. 1069-1082, 2000.

[15] M.S. Mahmoud, P. Shi·and A.W.A. Saif, “Stabilization of linear switched delay systems: H2 and H∞ methods”, Journal of Optimization Theory and Application, vol. 142, 3, pp. 583–601.

[16] G. Zhai, I. Matsune, J. Imae and T. Kobayashi, “A note on multiple Lyapunov functions and stability condition for switched and hybrid systems”, 16th IEEE International Conference on Control Applications, Singapore, vol. 5, 5, pp. 1189-1199, 2009.

[17] T. Takagi and M. Sugeno, “Fuzzy identification of systems and its application to modelling and control”, IEEE Trans. Syst., Man and Cyber, vol. 1115, pp. 116-132, 1985.

[18] K. Tanaka, T. Hori and H.O. Wang, “A multiple Lyapunov function approach to stabilization of fuzzy control systems,” Transactions on Fuzzy Systems, vol. 11, pp. 582–589, 2003.

[19] V. Ojleska and G. Stojanovski, “Switched fuzzy systems: overview and perspectives”, 9th International PhD Workshop on Systems and Control: Young Generation Viewpoint, Slovenia, 2008.

[20] A. Núñez, D. Sáez, S. Oblak and I. krjanc, “Fuzzy-model-based hybrid predictive control”, ISA Transactions, vol. 48, pp. 24-31, 2009.

[21] B. Jia, G. Ren and Z. Xiu, “Fuzzy switching controller for multiple model”, Lecture Notes in Computer Science, vol. 3613, pp 1011-1014, 2005.

[22] D. Jabri, K. Guelton, N. Manamanni and M.N. Abdelkrim, “Fuzzy Lyapunov decentralized control of Takagi-Sugeno interconnected descriptors”, IEEE Symposium Series on Computational Intelligence - IEEE Symposium on Computational Intelligence in Control and Automation, Nashville, USA, 2009.

[23] D. Jabri, K. Guelton and N., Manamanni, “Decentralized static output feedback control of interconnected fuzzy descriptors”, IEEE Multi-conference on Systems and Control, Yokohama, Japan, 2010.

[24] D. Jabri, N. Manamanni, K. Guelton and M.N. Abdelkrim, “Decentralized stabilization of discrete-time large scale switched systems”, 18th Mediterranean Conference on Control and Automation, IEEE, Marrakech, Morocco, 2010.

[25] H. Mukaidani, “A numerical analysis of the nash strategy for weakly coupled large-scale systems”, IEEE Transactions on Automatic Control, vol 51, 8, pp. 1371 – 1377, 2006.

[26] N. Sandell, P. Varaiya, M. Athans and M. Safonov, “Survey of decentralized control methods for large scale systems”, IEEE Transactions on Automatic Control, vol 23, 2, pp. 108-128, 1987.

[27] J-S. Chio, “Stability analysis for a class of switched large-scale time-delay systems via time-switched method”, IEE Control theory and applications, vol. 6, pp. 684–688, 2006.

[28] M.S. Mahmoud and F.M. AL-Sunni, “Interconnected continuous-time switched systems: Robust stability and Stabilization”, Nonlinear Analysis: Hybrid Systems, vol. 4, 3, pp 531-542, 2010.

[29] L.A. Mozelli, R.M. Palhares, F.O. Souza and E.M.A.M. Mendes, “Reducing conservativeness in recent stability conditions of TS fuzzy systems”, Automatica, vol. 45, 6, pp. 1580-1583, 2009.

[30] B.J. Rhee and S. Won, “A new Lyapunov function approach for a Takagi-Sugeno fuzzy control system design”, Fuzzy Sets and Systems, vol. 157, 9, pp. 1211-1228, 2006.

[31] T.M. Guerra, M. Bernal, A. Jaadari and K. Guelton, “Stabilisation non quadratique locale pour des modèles continus de type Takagi-Sugeno”, 6ème Conférence Internationale Francophone d'Automatique (CIFA 2010), Nancy, 2010.

[32] K. Zhou and P. Khargonedkar, “Robust stabilization of linear systems with norm-bounded time-varying uncertainty”, System Control Letters, vol. 10, pp. 17-20, 1988.

2011 IEEE International Conference on Fuzzy Systems
June 27-30, 2011, Taipei, Taiwan

Some Refinements for Non quadratic Stabilization of continuous TS Models

T.M. Guerra[1], A. Jaadari[1,2], J. Pan[1,3], A. Sala[2]

[1] LAMIH FRE CNRS 3304, University of Valenciennes Hainaut-Cambrésis, France
{guerra Abdelhafidh.Jaadari}@univ-valenciennes.fr,

[2] Dept. of Systems Engineering & Control, polytechnic University of Valencia, Spain
asala@isa.upv.es

[3] School of Automation, Southeast University, Nanjing, China
jtpan@yahoo.cn,

Abstract – Quadratic stability / stabilization / estimation for Takagi-Sugeno models have now reached maturity. Lots of results concerning performances (H_2, H_∞, D-stability) for TS models with uncertainties, noise, time-delays … exist in the literature. Nevertheless, it is illusive thinking to solve every nonlinear problem of stability using a simple quadratic Lyapunov function. Moreover, most of the nonlinear systems only have properties of local stability. This work follows the idea of using non quadratic Lyapunov functions for continuous Takagi-Sugeno models restricting the global asymptotic stability to a local one. Therefore, it tries to estimate the best stabilization domain possible. A rather "simple" LMI constraints problem is derived to answer to this question.

Index Terms — Takagi-Sugeno (TS) models, Linear Matrix Inequality (LMI), Fuzzy Lyapunov Function (FLF), Local Stabilization.

I. INTRODUCTION

The so-called Takagi-Sugeno models [1] have reached a very big attention in the control community. The results for stability, stabilization, estimation [2, 3, 4] are now converging towards quasi-LPV models results [5]. A global view of the last works can give the conclusion that more or less, lots of new results just represent outperforming previous ones, using the same techniques. Of course, some of these improvements are particularly important and allows dealing with problems that were unfeasible before. Among these nice improvements, we can cite the Polya's approach that gives sufficient and necessary conditions for the copositivity problem [6], piecewise Lyapunov functions when restricted to specific TS models [7, 8], non quadratic Lyapunov functions for discrete TS models with important results [9, 10, 11, 12].

The paper focuses on non quadratic stabilization for continuous TS models where the results are not satisfactory, especially when compared with the discrete case. Two families of results have to be described. As the derivative of the Lyapunov function will involve the derivative of the membership function of the TS model, several results propose just to bound them a priori [13, 14, 15]. This way of doing is not satisfactory because the verification of these bounds can only be done a posteriori on a case by case approach. On another side, independent path Lyapunov functions were used in [16] that present a fine result but restricted to specific TS models. Notice also that for stabilization, the problem remains BMI. All these approaches consider the problem of global stability which is far to be the general rule for nonlinear systems. Therefore, some works proposed to reduce this goal to local stability and estimate a domain of convergence [17, 18]. A tentative for stabilization has been presented in [19] which introduced bounds on the control law and complicated treatments of the problem. The work presented therein allows solving the stabilization problem in a local stabilization framework without this drawback.

The work is organized as follows. Part 1 recalls some properties; part 2 presents the problem of NQ stabilization and part 3 introduces the main result of the paper. An example illustrates the interest of the results and a conclusion ends the paper.

II. PRELIMINARIES

First, we will present some notations and properties helpful to derive the main result of the work.

As usual, a star $(*)$ in a symmetric matrix denotes the transpose element. When suitable, the next notations are used. Consider nonlinear functions $h_i(z) \geq 0$ sharing the convex sum property, i.e. $\sum_{i=1}^{r} h_i(z) = 1$, then:

$$\Upsilon_z = \sum_{i=1}^{r} h_i(z(t))\Upsilon_i, \qquad \Upsilon_z^{-1} = \left(\sum_{i=1}^{r} h_i(z(t))\Upsilon_i\right)^{-1}$$

and for multiple sums: $\Upsilon_{zz} = \sum_{i=1}^{r}\sum_{j=1}^{r} h_i(z(t))h_j(z(t))\Upsilon_{ij}$.

Property 1: for $y \in \mathbb{R}^n$ and $\beta > 0$ the following equivalence holds:

$$y^T y - \beta < 0 \Leftrightarrow yy^T - \beta I < 0 \qquad (1)$$

Proof: it follows directly using the Schur complement:

$$y^T y < \beta \Leftrightarrow \begin{bmatrix} \beta & y^T \\ y & I \end{bmatrix} > 0 \Leftrightarrow \beta^{-1} yy^T - I < 0 \Leftrightarrow yy^T < \beta I .$$

Property 2: with $P = P^T > 0$ and $\delta \in \mathbb{R}$, $\delta > 0$ the following property holds:

$$P_z \geq \delta I \Rightarrow P_z^2 \geq \delta P_z . \quad (2)$$

Proof: consider $x^T P_z x \geq \delta x^T x$ and the change of variable: $x = P_z^{1/2} y$, it follows directly: $y^T P_z^2 y \geq \delta y^T P_z y$.

Property 3 [18]: with X, Y two matrices of appropriate dimension $\delta, \lambda \in \mathbb{R}$, $\lambda > 0$ and $|\delta| \leq \lambda$ the following implication holds:

$$S = S^T > 0, \quad Y + \frac{1}{2}\left(\lambda^2 S + X S^{-1} X\right) \leq 0 \quad \Rightarrow \quad Y + \delta X \leq 0 . \quad (3)$$

Proof: use the completion of squares, i.e. with $S = S^T > 0$, $U^T V + V^T U \leq U^T S U + V^T S^{-1} V^T$. Thus, with $U = \delta I$ and $V = X$ it is direct.

Property 4 [20]: (relaxation lemma).
Let Υ_{ij}, $i, j \in \{1, \cdots, r\}$ be matrices of appropriate dimensions.

$\Upsilon_{zz} = \sum_{i=1}^{r} \sum_{j=1}^{r} h_i(z(t)) h_j(z(t)) \Upsilon_{ij} \geq 0$ holds if

$$\frac{2}{r-1} \Upsilon_{ii} + \Upsilon_{ij} + \Upsilon_{ji} > 0, \; i, j \in \{1, \cdots, r\}. \quad (4)$$

Remark: conditions (4) represent one of the numerous possible relaxations, see [6] for example. Notice that once the quantities Υ_{ij} defined and being LMI constraints, any relaxation can be used.

Recall that the open loop TS model [1] writes:

$$\dot{x}(t) = A_z x(t) + B_z u(t), \quad (5)$$

with $x(t) \in \mathbb{R}^n$ the state vector, $u(t) \in \mathbb{R}^m$ the input vector, $z(t) \in \mathbb{R}^p$ the premise vector. This latter is linked to the state vector $x(t)$ via a linear or a nonlinear mapping.

Consider also the validity domain of the TS model [21] which is a compact set of the state space:

$$C = \left\{ x \in \mathbb{R}^n, \underline{x}_i \leq x \leq \overline{x}_i, i = 1, \ldots, n \right\}; \quad (6)$$

and $0 \in C$, as the equilibrium point is 0 without lack of generality. It is supposed that the functions $h_i(z) \geq 0$ are obtained via the sector nonlinearity approach [2]. Therefore, we can write [18]:

$$h_i = h_{1+i_1+i_2 \times 2 + \cdots + i_p \times 2^{p-1}} = \prod_{j=1}^{p} w_{i_j}^j (z_j), \quad (7)$$

with $i \in \{1, \ldots, 2^p\}$, $i_j \in \{0, 1\}$ and $w_1^j(\cdot) = 1 - w_0^j(\cdot)$.

Remark: other possible compact sets are possible, such as for example: $C = \left\{ x \in \mathbb{R}^n, \|x\| \leq \lambda_x \right\}$, the form (6) is classically used because of the sector nonlinearity approach [2].

Hypothesis 1: In this work the functions $h_i(z)$ and the mapping between the premise vector $z(t)$ and the state vector $x(t)$ are of class C^1 on the defined compact set C; i.e. the partial derivatives are well-defined.

III. NON QUADRATIC STABILIZATION

This section recalls some basics on NQ stabilization for continuous TS models. First of all, a non-PDC control law is used:

$$u(t) = F_z P_z^{-1} x(t). \quad (8)$$

Therefore, the closed loop writes:

$$\dot{x}(t) = \left(A_z + B_z F_z P_z^{-1}\right) x(t), \quad (9)$$

whose stability properties will be investigated through the following non-quadratic fuzzy Lyapunov function candidate:

$$V(x(t)) = x^T(t) P_z^{-1} x(t), \quad (10)$$

where $P_z > 0$. Its derivative along the trajectories of the closed-loop TS model (9) is:

$$\dot{V}(x) = x^T \left(P_z^{-1} \left(A_z + B_z F_z P_z^{-1} \right) + \left(A_z + B_z F_z P_z^{-1} \right)^T P_z^{-1} + \dot{P}_z^{-1} \right) x$$

Since elementary matrix manipulations show that is verified if

$$A_z P_z + B_z F_z + \left(A_z P_z + B_z F_z \right)^T - \dot{P}_z < 0 . \quad (11)$$

Recall now that $\dot{P}_z$ writes:

$$\dot{P}_z = \sum_{i=1}^{r} \dot{h}_i P_i = \sum_{i=1}^{r} \left(\frac{\partial h_i(z)}{\partial z} \right)^T \dot{z} P_i . \quad (12)$$

Using the definition of the functions $h_i(z)$ and w_0^j equation (7) and after some manipulations see [17, 18], (12) can be written as:

$$\begin{aligned} \dot{P}_z &= \sum_{i=1}^{r} \sum_{k=1}^{p} h_i \frac{\partial w_0^k}{\partial z_k} \dot{z}_k \left(P_{g_1(i,k)} - P_{g_2(i,k)} \right) \\ &= \sum_{k=1}^{p} \frac{\partial w_0^k}{\partial z_k} \dot{z}_k \left(P_{g_1(z,k)} - P_{g_2(z,k)} \right) \end{aligned} \quad (13)$$

with $g_1(i,k) = \left\lfloor (i-1)/2^{p+1-k} \right\rfloor \times 2^{p+1-k} + 1 + (i-1) \bmod 2^{p-k}$ and $g_2(i,k) = g_1(i,k) + 2^{p-k}$, $\lfloor . \rfloor$ being the floor function.

Remark: it is ***very important*** to notice that the expression (13) shows that if a quadratic Lyapunov function exists than $\dot{P}_z = 0$ is guaranteed via $P_{g_1(\alpha,k)} = P_{g_2(\alpha,k)}$ for each $i \in \{1, \cdots, r\}$ and $k \in \{1, \cdots, p\}$. This remark will hold also for the LMI constraints thereinafter. Therefore, every conditions derived in this work are ***always*** including the quadratic case.

Theorem 1 (Local stabilizability): If there exist matrices of the proper size $P_i = P_i^T > 0$, F_i, $i \in \{1, \ldots, r\}$ such that $A_z P_z + B_z F_z + P_z A_z^T + F_z^T B_z^T < 0$, then there exists a domain D, $0 \in D$, such that TS model (5) is locally asymptotically stabilizable under control law (8).

Proof: The NQLF candidate (10) satisfies $V(0)=0$ and $V(x)\geq 0$ in $\mathbb{R}^n$. Its time-derivative (11) holds $\dot{V}(0)=0$. Provided that $A_zP_z+B_zF_z+P_zA_z^T+F_z^TB_z^T<0$ it is implied that there exists a sufficiently small $\lambda>0$ such that $A_zP_z+B_zF_z+P_zA_z^T+F_z^TB_z^T+\lambda I<0$ which can be used to define $D=\{x: x\in B, \|\dot{P}_z\|<\lambda\}$. The origin belongs to domain D since

$$\begin{aligned}\dot{P}_z &= \sum_{i=1}^{r}\dot{h}_iP_i=\sum_{i=1}^{r}\left(\frac{\partial h_i}{\partial z}\right)^T\frac{\partial z}{\partial x}^T\dot{x}P_i \\ &= \sum_{i=1}^{r}\left[\left(\frac{\partial h_i}{\partial z}\right)^T\frac{\partial z}{\partial x}^T\left(A_z+B_zF_zP_z^{-1}\right)x(t)\right]P_i\end{aligned} \tag{14}$$

depends on the state vector $x(t)$. Since $V(x)>0$ and $\dot{V}(x)<0$ in $D-\{0\}$, the equilibrium point $x=0$ is locally asymptotically stable, thus concluding the proof.

Remark: conditions for theorem 1 can be ensured for example with property 4, i.e. define $\Upsilon_{ij}=A_iP_j+B_iF_j+P_jA_i^T+F_j^TB_i^T$, find $P_i=P_i^T>0$, F_i, $i\in\{1,\ldots,r\}$ such that:

$$\frac{2}{r-1}\Upsilon_{ii}+\Upsilon_{ij}+\Upsilon_{ji}>0,\ i,j\in\{1,\cdots,r\}. \tag{15}$$

IV. MAIN RESULT

A precedent work [19] used a bound on the control law to derive conditions of stabilization. Therein a more interesting way to cope with the stabilization problem is used in order to remove this drawback. Let us focus on the real $\dot{z}_k\in\mathbb{R}$. In a general framework, the premise vector $z(t)$ depends linearly or not on the state vector $x(t)$. Thus:

$$\dot{z}_k=\left(\frac{\partial z_k}{\partial x}\right)^T\dot{x}=\left(\frac{\partial z_k}{\partial x}\right)^T\left(A_z+B_zF_zP_z^{-1}\right)x. \tag{16}$$

Therefore the goal is to find a "nice" bound $\beta_k>0$ for:

$$\left|\frac{\partial w_0^k}{\partial z_k}\dot{z}_k\right|\leq\beta_k, \tag{17}$$

which is equivalent to:

$$\left|\frac{\partial w_0^k}{\partial z_k}\left(\frac{\partial z_k}{\partial x}\right)^T\left(A_zP_z+B_zF_z\right)P_z^{-1}x\right|\leq\beta_k. \tag{18}$$

Remark: it is also important to note that this is ***not equivalent*** to other approaches found in the literature [13, 14, 15] where the required condition is in the form of: $\left|\dot{h}_i(z(t))\right|\leq\phi_i$. In this later case, ϕ_i is given a priori and can only be checked a posteriori. In the presented case, the bounds β_k are ***included*** in the problem to solve.

In order for (18) to hold, we will introduce (19):

$$\left(\frac{\partial w_0^k}{\partial z_k}\left(\frac{\partial z_k}{\partial x}\right)^T\left(A_zP_z+B_zF_z\right)P_z^{-1}x\right)^2\leq\beta_k^2. \tag{19}$$

Or equivalently:

$$\left(\frac{\partial w_0^k}{\partial z_k}\right)^2\left(\frac{\partial z_k}{\partial x}\right)^T\left(A_zP_z+B_zF_z\right)P_z^{-1}xx^TP_z^{-1}\left(A_zP_z+B_zF_z\right)^T\frac{\partial z_k}{\partial x}-\beta_k^2\leq 0 \tag{20}$$

Knowing that $\|x\|^2\leq\lambda_x^2 \Leftrightarrow xx^T\leq\lambda_x^2I$ (property 1 (1)), (20) holds if:

$$\lambda_x^2\left(\frac{\partial w_0^k}{\partial z_k}\right)^2\left(\frac{\partial z_k}{\partial x}\right)^T\left(A_zP_z+B_zF_z\right)P_z^{-1}P_z^{-1}\left(A_zP_z+B_zF_z\right)^T\frac{\partial z_k}{\partial x}-\beta_k^2\leq 0 \tag{21}$$

Applying again property 1 to (21) gives:

$$\lambda_x^2\left(\frac{\partial w_0^k}{\partial z_k}\right)^2P_z^{-1}\left(A_zP_z+B_zF_z\right)^T\frac{\partial z_k}{\partial x}\left(\frac{\partial z_k}{\partial x}\right)^T\left(A_zP_z+B_zF_z\right)P_z^{-1}-\beta_k^2I\leq 0 \tag{22}$$

At last, as the functions w_0^k are known explicitly, thus bounding $\frac{\partial w_0^k}{\partial z_k}$ is direct. On the other side, $\frac{\partial z_k}{\partial x}$ represents the linear or nonlinear mapping between $z(t)$ and $x(t)$, and it is also known. Therefore we can compute easily the bounds: $\left(\frac{\partial w_0^k}{\partial z_k}\right)^2\left\|\frac{\partial z_k}{\partial x}\right\|^2\leq\lambda_k^2 \Leftrightarrow \left(\frac{\partial w_0^k}{\partial z_k}\right)^2\frac{\partial z_k}{\partial x}\left(\frac{\partial z_k}{\partial x}\right)^T\leq\lambda_k^2I$.

These bounds define regions in the state space:

$$R_k=\left\{x\in\mathbb{R}^n,\left(\frac{\partial w_0^k}{\partial z_k}\right)^2\left\|\frac{\partial z_k}{\partial x}\right\|^2\leq\lambda_k^2\right\}, \tag{23}$$

and it follows that:

$$\lambda_x^2\lambda_k^2P_z^{-1}\left(A_zP_z+B_zF_z\right)^T\left(A_zP_z+B_zF_z\right)P_z^{-1}-\beta_k^2I\leq 0 \tag{24}$$

Then, multiplying left and right with P_z gives:

$$\lambda_x^2\lambda_k^2\left(A_zP_z+B_zF_z\right)^T\left(A_zP_z+B_zF_z\right)-\beta_k^2P_z^2\leq 0. \tag{25}$$

Considering now that $P_z\geq\delta I$ and using property 2 (2), (17) is satisfied if:

$$\lambda_x^2\lambda_k^2\left(A_zP_z+B_zF_z\right)^T\left(A_zP_z+B_zF_z\right)-\beta_k^2\delta P_z\leq 0.$$

Thus with the help of the Schur complement:

$$\begin{aligned}&\lambda_x^2\lambda_k^2\left(A_zP_z+B_zF_z\right)^T\beta_k^{-2}\delta^{-1}\left(A_zP_z+B_zF_z\right)-P_z\leq 0\\ &\Leftrightarrow\begin{bmatrix}P_z & (*)\\ \lambda_x\lambda_k\left(A_zP_z+B_zF_z\right) & \beta_k^2\delta I\end{bmatrix}>0\end{aligned} \tag{26}$$

Now, coming back to (11) we can use

$$A_z P_z + B_z F_z + \left(A_z P_z + B_z F_z\right)^T - \sum_{k=1}^{p} \frac{\partial w_0^k}{\partial z_k} \dot{z}_k \left(P_{g_1(z,k)} - P_{g_2(z,k)}\right) < 0 \tag{27}$$

And we have the bound: $\left|\frac{\partial w_0^k}{\partial z_k} \dot{z}_k\right| \le \beta_k$.

Thus using property 3 second part (3) we can derive the theorem 2. Note that introducing matrices $S_{zz}^k > 0$ we can write:

$$\begin{aligned} &\frac{\partial w_0^k}{\partial z_k} \dot{z}_k \left(P_{g_1(z,k)} - P_{g_2(z,k)}\right) \\ &\le \frac{1}{2}\left(\beta_k^2 S_{zz}^k + \left(P_{g_1(z,k)} - P_{g_2(z,k)}\right)\left(S_{zz}^k\right)^{-1}\left(P_{g_1(z,k)} - P_{g_2(z,k)}\right)\right) \end{aligned} \tag{28}$$

Therefore, let us consider the following quantities:

$$\Gamma_{ij} = \begin{bmatrix} A_i P_j + B_i F_j + P_j A_i^T + F_j^T B_i^T + \frac{1}{2}\sum_{k=1}^{p} \beta_k^2 S_{ij}^k & (*) & \cdots & & (*) \\ P_{g_1(i,1)} - P_{g_2(i,1)} & -2S_{ij}^1 & 0 & \cdots & 0 \\ \vdots & 0 & \ddots & \ddots & \vdots \\ & \vdots & \ddots & \ddots & 0 \\ P_{g_1(i,p)} - P_{g_2(i,p)} & 0 & \cdots & 0 & -2S_{ij}^p \end{bmatrix} \tag{29}$$

$$\Upsilon_{ij} = \begin{bmatrix} P_i & (*) \\ \lambda_x \lambda_k \left(A_i P_j + B_i F_j\right) & \beta_k^2 \delta I \end{bmatrix} \tag{30}$$

Theorem 2: consider the TS closed loop model (9) and expressions defined in (30) and (29). If there exist matrices P_i, F_i, $S_{ij}^k > 0$, $i, j \in \{1, \cdots, r\}$, $k \in \{1, \cdots, p\}$ such that the following LMI are satisfied:

$$P_i \ge \delta I \,,\ i \in \{1, \cdots, r\} \tag{31}$$

$$\frac{2}{r-1}\Upsilon_{ii} + \Upsilon_{ij} + \Upsilon_{ji} > 0 \,,\ i, j \in \{1, \cdots, r\} \tag{32}$$

$$\frac{2}{r-1}\Gamma_{ii} + \Gamma_{ij} + \Gamma_{ji} < 0 \,,\ i, j \in \{1, \cdots, r\} \tag{33}$$

Then, the control law (8) stabilizes the TS open loop model (5) in a local domain. An estimation of this domain is given by the outermost Lyapunov level contained in $R = C \cap \left\{\bigcap_{k=1}^{p} R_k\right\}$ with C defined in (6) and R_k in (23).

Proof: from (27), repeating (28) for each term of the sum, gives and applying the Shur complement gives directly $\Gamma_{zz} < 0$.

(26) represents $\Upsilon_{zz} > 0$. Thus, conditions (32) and (33) just expresses the sum relaxation (4) to $\Upsilon_{zz} > 0$ and $\Gamma_{zz} < 0$.

Remark: notice that (31)~(33) are LMI constraints only if the scalars β_k^2 and δ are known.

A procedure to determine these values is possible, inspired from [22] for static output feedback. Recall that if the conditions of theorem 1 are satisfied it ensures the existence of a local stability domain for theorem 2. Therefore, the procedure is based on this remark.

A first step consists in obtaining a solution to theorem 1 conditions (15). The obtained gains give a control law that can be seen as stabilizing the "frozen" time-invariant continuous TS model. Thus bounds β_k^2 and δ can be directly obtained from this first step.

The second step is the solution to the theorem 2 conditions (31)~(33).

V. Example

Example 1: Consider the following TS model [23]:

$$\dot{x}(t) = A_z x(t) = \sum_{i=1}^{2} h_i\left(z(t)\right)\left(A_i x(t) + B_i u(t)\right) \tag{34}$$

with $A_1 = \begin{bmatrix} 3.6 & -1.6 \\ 6.2 & -4.3 \end{bmatrix}$, $A_2 = \begin{bmatrix} -0.35 & -1.6 \\ 6.2 & -4.3 \end{bmatrix}$, $B_1 = \begin{bmatrix} -0.45 \\ -3 \end{bmatrix}$, $B_2 = \begin{bmatrix} -0.5 \\ -3 \end{bmatrix}$, $z_1(t) = x_1(t)$, $h_1 = w_0^1 = \frac{1 - \sin x_1}{2}$ and $h_2 = w_1^1 = \frac{1 + \sin x_1}{2}$ defined in the compact set $C = \left\{x : |x_i| \le \pi/2\right\}$, $i = 1, 2$.

Fig. 1 shows the stabilization region (region $R_0 = \left\{x : x^T P_z^{-1} x \le r\right\}$ enclosed by a solid line).

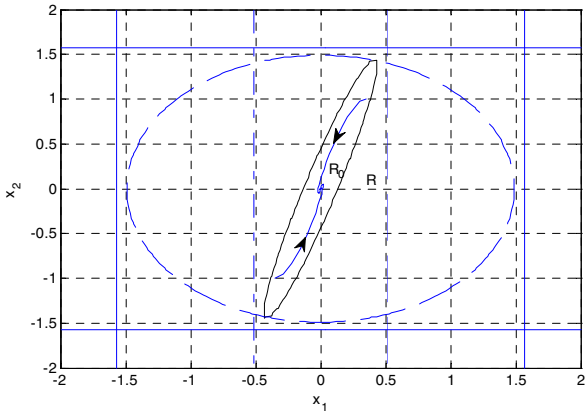

Figure 1: Stabilization region for TS model

The gains and the matrices involved in the control law are :

$$F_1 = \begin{bmatrix} -30.9367 & -64.6603 \end{bmatrix},\ F_2 = \begin{bmatrix} -7.9679 & 0.8826 \end{bmatrix}$$

$$P_1 = \begin{bmatrix} 14.1439 & 44.8202 \\ 44.8202 & 156.7774 \end{bmatrix}, P_2 = \begin{bmatrix} 14.0601 & 44.4733 \\ 44.4733 & 155.5855 \end{bmatrix}$$

$$\lambda_k = 0.19\ ,\ \gamma = 1\ ,\ \beta_k = 370 \text{ and } \lambda_x = 2.2214\ .$$

The control law evolution for initial states $x_0 = \begin{bmatrix} 0.35 & 1 \end{bmatrix}$ can be seen in Fig. 2.

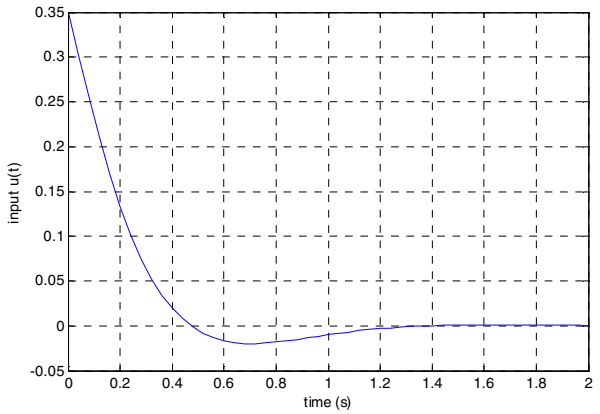

Fig. 2: Control law evolution.

Acknowledgments

The present paper has been supported by the International Campus on Safety and Intermodality in Transportation, the Nord-Pas-de-Calais Region, the European Community, the Regional Delegation for Research and Technology, the Ministry of Higher Education and Research, and the National Center for Scientific Research. The authors gratefully acknowledge the support of these institutions.

This work has been done during the one year PhD stay of Juntao Pan at LAMIH, University of Valenciennes Hainaut-Cambresis (France) under the China Scholarship Council Postgraduate scholarship program.

References

[1]. T. Takagi and M. Sugeno, "Fuzzy identification of systems and its application to modeling and control", IEEE Trans. on System Man and Cybernetics, Vol.15(1), pp116-132. 1985.

[2]. K. Tanaka and H.O. Wang, "Fuzzy control systems design and analysis. A linear matrix inequality approach". John Wiley and Sons, New York, USA. 2001.

[3]. Zs. Lendek, T.M. Guerra, R. Babuska, B. De Schutter, "Stability analysis and nonlinear observer design using Takagi-Sugeno fuzzy models" – Studies in Computational Intelligence, Springer-Verlag. 2010

[4]. G. Feng, "A Survey on Analysis and Design of Model-Based Fuzzy Control Systems", IEEE T. Fuzzy Systems, 14 (5), 676-697. 2006

[5]. C. Scherer, S. Weiland, "Linear Matrix Inequalities in Control" (lecture notes). 2004

[6]. A. Sala, C. Ariño, "Asymptotically necessary and sufficient conditions for stability and performance in fuzzy control: Applications of Polya's theorem" Fuzzy Sets and Systems, Vol. 158, (24), pp 2671-2686, 2007.

[7]. M. Johansson, A. Rantzer, K. Arzen, "Piecewise quadratic stability of fuzzy systems". IEEE Trans. on Fuzzy Systems, Vol.7, pp713-722,1999.

[8]. G. Feng, C.L. Chen, D. Sun, Y. Zhu, "H∞ controller synthesis of fuzzy dynamic systems based on piecewise Lyapunov functions and bilinear matrix inequalities". IEEE Trans. On Fuzzy Systems, Vol. 13 (1), pp 94-103, 2005.

[9]. T.M. Guerra and L. Vermeiren, "LMI-based relaxed non-quadratic stabilization conditions for nonlinear systems in Takagi-Sugeno's form", Automatica, Vol. 40(5), pp823-829. 2004.

[10]. B.C. Ding, H.X. Sun, P. Yang, "Further studies on LMI-based relaxed stabilization conditions for nonlinear systems in Takagi-Sugeno's form". Automatica Vol. 42, pp503-508, 2006.

[11]. A. Kruszewski, R. Wang, T.M. Guerra, "Non-quadratic stabilization conditions for a class of uncertain non linear discrete-time T-S fuzzy models: a new approach". IEEE Trans. on Automatic Control, 53 (2), pp. 606-611, 2008.

[12]. T.M. Guerra, A. Kruszewski, M. Bernal, "Control Law Proposition for the Stabilization of Discrete Takagi-Sugeno Models". *IEEE Trans. on Fuzzy Systems,* 17 (3), 724-731, 2009.

[13]. K. Tanaka, T. Hori, H.O. Wang, "A multiple Lyapunov function approach to stabilization of fuzzy control systems", IEEE Trans. on Fuzzy Systems, Vol. 11 (4), pp 582-589, 2003.

[14]. M. Bernal, P. Hušek, V. Kučera, "Non quadratic stabilization of continuous-time systems in the Takagi-Sugeno form", Kybernetika, vol. 42 (6), pp. 665-672, 2006.

[15]. L. Mozelli, R. Palhares, G.S.C. Avellar, "A systematic approach to improve multiple Lyapunov function stability and stabilization conditions for fuzzy systems", Information Sciences, Vol. 179(8), pp 1149-1162.

[16]. B.J. Rhee, S. Won, "A new fuzzy Lyapunov function approach for a Takagi–Sugeno fuzzy control system design", Fuzzy Sets & Systems, Vol. 157(9), pp1211-1228, 2006.

[17]. T.M. Guerra and M. Bernal, "A way to escape from the quadratic framework", in Proc. FUZZ-IEEE Conference, Jeju, Korea, 2009

[18]. M. Bernal, T.M. Guerra, "Generalized non-quadratic stability of nonlinear models in the Takagi-Sugeno form", IEEE T. on Fuzzy Systems18 (4), 815-822. 2010

[19]. M. Bernal, T.M. Guerra, A. Jaadari, "Non-quadratic stabilization of Takagi-Sugeno models: a local point of view", Fuzz'IEEE Barcelona, Spain. 2010

[20]. H.D. Tuan, P. Apkarian, T. Narikiyo, and Y. Yamamoto. "Parameterized linear matrix inequality techniques in fuzzy control system design". IEEE Trans. on Fuzzy Systems, 9(2), 324–332. 2001

[21]. T. Taniguchi, K. Tanaka, H.O. Wang, "Model construction, rule reduction and robust compensation for generalized form of Takagi-Sugeno fuzzy systems", IEEE T. Fuzzy Systems, 9 (4), 525-537. 2001

[22]. D. Mehdi, E. K. Boukas, O. Bachelier, "Static output feedback design for uncertain linear discrete time systems," IMA J. Mathematical Control Information, 21 (1), 1–13, 2004.

[23]. L. Mozelli, R. Palhares, G.S.C. Avellar, "A systematic approach to improve multiple Lyapunov function stability and stabilization conditions for fuzzy systems", Information Sciences, Vol. 179(8), pp 1149-1162.

2011 IEEE International Conference on Fuzzy Systems
June 27-30, 2011, Taipei, Taiwan

Adaptive Fault Estimation Design For T-S Fuzzy Systems With Interval Time Varying Delay

Hamdi Gassara and Ahmed El Hajjaji
Modeling, Information and Systems Laboratory,
University of Picardie Jules Verne,
MIS, 7 Rue du Moulin Neuf 80000 Amiens France
{hamdi.gassara, ahmed.hajjaji}@u-picardie.fr)

Mohamed Chaabane
Department of Electrical Engineering,
Research Unit of Automatic Control,
National School of Engineering of Sfax, University of Sfax,
Route Soukra Km 3.5, B.P. 1173, 3038 Sfax, Tunisia

***Abstract*—This paper is concerned with fault estimation design for continuous-time Takagi-Sugeno (T-S) fuzzy systems with time delay by using adaptive fault diagnostic observer. Through constructing an appropriate type of Lyapunov function, criteria is established to reduce the conservatism of the design procedure. Based on appropriate type of Lyapunov function, new sufficient delay-dependent conditions are given to guarantee the stability of error dynamics in terms of Linear Matrix Inequalities (LMI). Finally, the effectiveness of the proposed approach is illustrated through a simulation example.**

Keyword: Linear Matrix Inequalities, Takagi-Sugeno fuzzy systems, fault tolerant control.

I. Introduction

In many applications the problem of fault detection and isolation FDI is a crucial issue that has been theoretically and experimentally investigated with different types of approaches. Adaptive Fault Diagnostic Observer (AFDO) approach has the advantage to estimate the state vector and actuator faults simultaneously. As consequence, the use of this approach has attracted an increasing interest in the last decade ([2], [3], [4]). Recent years have witnessed rapidly growing in the study of T-S fuzzy model since it is well known that this model is a powerful tool in approximating a wide class of nonlinear systems ([6], [7], [8], [9]). Still, time delay is one of the instability sources of dynamical processes. For this reason, T-S fuzzy model has been extended to deal with nonlinear systems with time delay. Different delay-independent methodologies have been proposed for analysis and synthesis for T-S fuzzy systems with time delay ([10], [11], [12]). It is generally recognized that delay-dependent results are usually less conservative than delay-independent ones. That's why, delay-dependent techniques have been reported in ([13], [14], [15]).

Considering the AFDO design, the problem of fault estimation for linear system are treated in [3]. This idea is extended to deal with T-S fuzzy models with constant time delay in [4]. The obtained result is delay-independent. By adopting the free weighting matrix technique, delay-dependent results are obtained for linear systems with bounded time delay [5]. However, the price under additional variables is the growth of computational burden in the meantime. In this paper, we investigate the delay-dependent AFDO design for T-S fuzzy systems with interval time varying delay without using any free weighting matrices. The advantages of the developed criteria are: (1) the reduction of conservatism; (2) the reduction of computational complexity and (3) the removing of condition $\dot{\tau}(t) < 1$ which makes it applicable to both slow and fast time varying delay.

Notations $W + W^T$ is denoted as $W + (*)$ for simplicity.

II. Problem formulation and preliminaries

Consider a nonlinear system with time delay which could be approximated by a time delay T-S fuzzy model.

The i^{th} rule of the system is expressed in the following IF-THEN rules.

Plant Rule $i(i = 1, 2, \cdots, r)$: If θ_1 is μ_{i1} and $\cdots$ and θ_p is μ_{ip} THEN

$$\begin{aligned} \dot{x}(t) &= A_i x(t) + A_{\tau i} x(t - \tau(t)) + B_i u(t) \\ &\quad + E_i f(t) \\ y(t) &= Cx(t) \\ x(t) &= \psi(t), \quad t \in [-\tau,\ 0] \end{aligned} \tag{1}$$

where $\theta_j(x(t))$ and $\mu_{ij}(i = 1, \cdots, r, j = 1, \cdots, p)$ are respectively the premise variable and the fuzzy sets; $\psi(t)$ is the initial condition; $x(t) \in \Re^{n_x}$ is the state; $u(t) \in \Re^{n_u}$ is the control input; $f(t) \in \Re^{n_f}$ represents the actuator fault vector. It is assumed that the derivative of $f(t)$ with respect to time is norm bounded, i.e. $\|\dot{f}(t)\| \leq f_1$ and $0 \leq f_1 < \infty$. r is the number of IF-THEN rules.

The AFDO is constructed as

Observer Rule $i(i = 1, 2, \cdots, r)$: If θ_1 is μ_{i1} and $\cdots$ and θ_p is μ_{ip} THEN

$$\begin{aligned} \dot{\hat{x}}(t) &= A_i \hat{x}(t) + A_{\tau i} \hat{x}(t - \tau(t)) + B_i u(t) \\ &\quad + E_i \hat{f}(t) - L_i(\hat{y}(t) - y(t)) \\ \hat{y}(t) &= C\hat{x}(t) \end{aligned} \tag{2}$$

Denote $e_x(t) = \hat{x}(t) - x(t)$, $e_y(t) = \hat{y}(t) - y(t)$, $e_f(t) = \hat{f}(t) - f(t)$

then the error dynamic is given by

$$\begin{aligned} \dot{e}_x(t) &= (A(t) - L(t)C)e_x(t) \\ &\quad + A_\tau(t)e_x(t - \tau(t)) + E(t)e_f(t) \\ e_y(t) &= Ce_x(t) \end{aligned}$$

where

$$A(t)=\sum_{i=1}^{r}h_iA_i;A_\tau(t)=\sum_{i=1}^{r}h_iA_{\tau i};E(t)=\sum_{i=1}^{r}h_iE_i$$

The following result has been given in [4] which treats the case of constant delay ($\tau(t)=\tau$).

Theorem 1: [4] If there exist symmetric positive definite matrices $P>0$, $Q>0$, $M>0$, Y_i and F_i such that the following LMI hold:

$$\Psi_{ij}+\Psi_{ji}<0,\qquad i,j=1,2,\cdots,r,i\leq j \tag{3}$$

$$E_i^TP=F_iC,\qquad i=1,2,\cdots,r \tag{4}$$

then the fuzzy Fast Adaptive Fault Estimation (FAFE) algorithm

$$\dot{\hat{f}}(t)=-\Gamma\sum_{i=1}^{r}h_iF_i(\dot{e}_y(t)+e_y(t)) \tag{5}$$

can realize $e_x(t)$ and $e_f(t)$ uniformly ultimately bounded, where

$$\Psi_{ij}=\begin{bmatrix}\Psi_{ij}^{11} & PA_{\tau i} & -A_i^TPE_j+C^TY_i^TE_j\\ * & -Q & -A_{\tau i}^TPE_j\\ * & * & -E_i^TPE_j-E_j^TPE_i+M\end{bmatrix}$$

in which

$$\Psi_{ij}^{11}=PA_i+A_i^TP-Y_iC-C^TY_i^T+Q$$

In this case, the gains L_i are given by

$$L_i \;=\; Y_iP^{-1} \tag{6}$$

the symmetric positive definite matrix Γ is the learning rate.

In this paper, we will develop another design method which improves that in theorem (1).

III. Improved result

In this section, we first present useful lemma and then present the main result.

Lemma 1: Given matrices x and y.
For a symmetric positive definite matrix P, the following inequality holds

$$2x^Ty\leq x^TPx+y^TP^{-1}y$$

Lemma 2 Consider a negative definite matrix $\Pi<0$.
Given a symmetric matrix X of appropriate dimension such that $X^T\Pi X<0$, then, $\exists\lambda\in\Re^+$ such that

$$X^T\Pi X\leq-2\lambda X-\lambda^2\Pi^{-1}$$

Lemma 3 Given matrices $M,E,F(t)$ with compatible dimensions and $F(t)$ satisfying $F(t)^TF(t)\leq I$.
Then, the following inequalities hold for any $\epsilon>0$
$MF(t)E+E^TF(t)^TM^T\leq\epsilon MM^T+\epsilon^{-1}E^TE$

The following theorem gives the new LMI-based conditions in order to reduce the conservatism in theorem (1). Furthermore, we consider interval time-varying delay rather than constant delay.

the interval time varying delay satisfies

$$0<\tau_m\leq\tau(t)\leq\tau_M,\dot{\tau}(t)\leq\beta \tag{7}$$

Denote

$$\tau_1=\frac{\tau_m+\tau_M}{2};\tau_2=\frac{\tau_M-\tau_m}{2}$$

Theorem 2: For given positif scalar λ, if there exist matrices $P>0$, $Q_l>0(l=1,2,3,4,5)$, $R_m>0(m=1,2,3,4)$ such that (4) and the following LMI hold

$$\Xi_{ij}+\Xi_{ji}<0,\qquad i,j=1,2,\cdots,r,i\leq j \tag{8}$$

where

$$\Xi_{ij}=\begin{bmatrix}\xi_{ij}^{11} & R_4 & PA_{\tau i} & 0\\ * & \xi_{22} & R_3 & Q_2+R_1\\ * & * & \xi_{33} & 0\\ * & * & * & \xi_{44}\\ * & * & * & *\\ * & * & * & *\\ * & * & * & *\end{bmatrix}\begin{bmatrix}0 & \xi_{ij}^{16} & \xi_{ij}^{17}\\ 0 & 0 & 0\\ R_3 & -A_{\tau i}^TPE_j & A_{\tau i}^TP\\ -Q_2+R_2 & 0 & 0\\ \xi_{55} & 0 & 0\\ * & \xi_{ij}^{66} & E_i^TP\\ * & * & \xi_{ij}^{77}\end{bmatrix}$$

in which

$$\begin{aligned}
\xi_{ij}^{11} &= PA_i-Y_iC+A_i^TP-C^TY_i^T+Q_4+Q_5-R_4;\\
\xi_{ij}^{16} &= -A_i^TPE_j+C^TY_i^TE_j;\\
\xi_{ij}^{17} &= A_i^TP-C^TY_i^T\\
\xi^{22} &= Q_1-Q_5-R_1-R_3-R_4;\\
\xi^{33} &= -(1-\beta)Q_4-2R_3;\\
\xi^{44} &= Q_3-Q_1-R_1-R_2;\\
\xi^{55} &= -Q_3-R_2-R_3;\\
\xi_{ij}^{66} &= -E_i^TPE_j-E_j^TPE_i+M;\\
\xi_{ij}^{77} &= -2\lambda P\\
&\quad+\lambda^2((\tau_2)^2R_1+(\tau_2)^2R_2+(2\tau_2)^2R_3+(\tau_m)^2R_4)
\end{aligned}$$

then the fuzzy Fast Adaptive Fault Estimation (FAFE) algorithm (5) can realize $e_x(t)$ and $e_f(t)$ uniformly ultimately bounded,

In this case, the L_i are given by (6).

Proof:
Consider the following Lyapunov function

$$V(t)=\sum_{i=1}^{6}V_i(t) \tag{9}$$

where

$$\begin{aligned} V_1(t) &= e_x(t)^T P e_x(t) + \int_{t-\tau_1}^{t-\tau_m} \{e_x(s)^T Q_1 e_x(s) \\ &\quad +2e_x(s)^T Q_2 e_x(s-\tau_2) \\ &\quad +e_x(s-\tau_2)^T Q_3 e_x(s-\tau_2)\} ds \\ &\quad + \int_{t-\tau(t)}^{t} e_x(s)^T Q_4 e_x(s) ds \\ &\quad + \int_{t-\tau_m}^{t} e_x(s)^T Q_5 e_x(s) ds \end{aligned}$$

$$\begin{aligned} V_2(t) &= \tau_2 \int_{-\tau_1}^{-\tau_m} \int_{t+\sigma}^{t} \dot{e}_x(s)^T R_1 \dot{e}_x(s) ds d\sigma \\ V_3(t) &= \tau_2 \int_{-\tau_M}^{-\tau_1} \int_{t+\sigma}^{t} \dot{e}_x(s)^T R_2 \dot{e}_x(s) ds d\sigma \\ V_4(t) &= 2\tau_2 \int_{-\tau_M}^{-\tau_m} \int_{t+\sigma}^{t} \dot{e}_x(s)^T R_3 \dot{e}_x(s) ds d\sigma \\ V_5(t) &= \tau_m \int_{-\tau_m}^{0} \int_{t+\sigma}^{t} \dot{e}_x(s)^T R_4 \dot{e}_x(s) ds d\sigma \\ V_6(t) &= e_f(t)^T \Gamma^{-1} e_f(t) \end{aligned}$$

Taking the derivation of $V(t)$, we have

$$\dot{V}_1(t) = 2e_x(t)^T P \dot{e}_x(t) + \Delta$$

where

$$\begin{aligned} &\Delta = e_x(t-\tau_m)^T Q_1 e_x(t-\tau_m) + 2e_x(t-\tau_m) Q_2 e_x(t-\tau_1) \\ &+e_x(t-\tau_1) Q_3 e_x(t-\tau_1) - e_x(t-\tau_1)^T Q_1 e_x(t-\tau_1) \\ &-2e_x(t-\tau_1)^T Q_2 e_x(t-\tau_M) - e_x(t-\tau_M)^T Q_3 x(t-\tau_M) \\ &+e_x(t)^T Q_4 e_x(t) - (1-\dot{\tau}(t)) e_x(t-\tau(t)) Q_4 e_x(t-\tau(t)) \\ &+e_x(t)^T Q_5 e_x(t) - e_x(t-\tau_m)^T Q_5 e_x(t-\tau_m) \end{aligned}$$

$$\begin{aligned} \dot{V}_2(t) &= \tau_2 \{\dot{e}_x(t)^T R_1 \dot{e}_x(t) \\ &\quad - \int_{t-\tau_1}^{t-\tau_m} \dot{e}_x(s)^T R_1 \dot{e}_(s) ds\} \end{aligned} \quad (10)$$

Similarly, we obtain

$$\begin{aligned} \dot{V}_3(t) &= \tau_2 \{\tau_2 \dot{e}_x(t)^T R_2 \dot{e}_x(t) \\ &\quad - \int_{t-\tau_M}^{t-\tau_1} \dot{e}_x(s)^T R_2 \dot{e}_x(s) ds\} \\ \dot{V}_4(t) &= 2\tau_2 \{2\tau_2 \dot{e}_x(t)^T R_3 \dot{e}_x(t) \\ &\quad - \int_{t-\tau_M}^{t-\tau_m} \dot{e}_x(s)^T R_3 \dot{e}_x(s) ds\} \\ \dot{V}_5(t) &= \tau_m \{\tau_m \dot{e}_x(t)^T R_4 \dot{e}_x(t) \\ &\quad - \int_{t-\tau_m}^{t} \dot{e}_x(s)^T R_4 \dot{e}_x(s) ds\} \end{aligned}$$

By using the FAFE algorithm given in (5), we obtain

$$\begin{aligned} \dot{V}_6(t) &= -2e_f(t)^T F(t) C(\dot{e}_x(t) + e_x(t)) \\ &\quad -2e_f(t)^T \Gamma^{-1} \dot{f}(t) \end{aligned}$$

By considering equality (4), we obtain:

$$\begin{aligned} &\dot{V}_1(x(t)) + \dot{V}_6(x(t)) \\ &= 2e_x(t)^T P[(A(t) - L(t)C)e_x(t) + A_\tau(t) e_x(t-\tau(t)) \\ &+E(t) e_f(t)] \\ &+\Delta - 2e_f(t)^T F(t) C(\dot{e}_x(t) + e_x(t)) - 2e_f(t)^T \Gamma^{-1} \dot{f}(t) \\ &= 2e_x(t)^T P[(A(t) - L(t)C)e_x(t) + A_\tau(t) e_x(t-\tau(t))] \\ &+\Delta - 2e_f(t)^T F(t) C \dot{e}_x(t) - 2e_f(t)^T \Gamma^{-1} \dot{f}(t) \\ &+ \underbrace{2e_x(t)^T P E(t) e_f(t) - 2e_f(t)^T F(t) C e_x(t)}_{0} \end{aligned}$$

From lemma (1), we can obtain that

$$\begin{aligned} &-2e_f(t)^T \Gamma^{-1} \dot{f}(t) \leq \\ &e_f(t)^T M e_f(t) + \dot{f}(t)^T \Gamma^{-1} M^{-1} \Gamma^{-1} \dot{f}(t) \leq \\ &e_f(t)^T M e_f(t) + \delta \end{aligned} \quad (11)$$

where

$$\delta = f_1^2 \lambda_{max}(\Gamma^{-1} M^{-1} \Gamma^{-1})$$

Applying Jensen's integral inequality [1] to deal with the cross product items, we have

$$\begin{aligned} &-\tau_2 \int_{t-\tau_1}^{t-\tau_m} \dot{e}_x(s)^T R_1 \dot{e}_x(s) ds \\ &\leq \begin{bmatrix} e_x(t-\tau_m) \\ e_x(t-\tau_1) \end{bmatrix}^T \begin{bmatrix} -R_1 & R_1 \\ * & -R_1 \end{bmatrix} \begin{bmatrix} e_x(t-\tau_m) \\ e_x(t-\tau_1) \end{bmatrix} \end{aligned}$$

$$\begin{aligned} &-\tau_2 \int_{t-\tau_M}^{t-\tau_1} \dot{e}_x(s)^T R_2 \dot{e}_x(s) ds \\ &\leq \begin{bmatrix} e_x(t-\tau_1) \\ e_x(t-\tau_M) \end{bmatrix}^T \begin{bmatrix} -R_2 & R_2 \\ * & -R_2 \end{bmatrix} \begin{bmatrix} e_x(t-\tau_1) \\ e_x(t-\tau_M) \end{bmatrix} \end{aligned}$$

$$\begin{aligned} &-2\tau_2 \int_{t-\tau_M}^{t-\tau_m} \dot{e}_x(s)^T R_3 \dot{e}_x(s) ds \\ &\leq -(\tau(t) - \tau_m) \int_{t-\tau(t)}^{t-\tau_m} \dot{e}_x(s)^T R_3 \dot{e}_x(s) ds \\ &-(\tau_M - \tau(t)) \int_{t-\tau_M}^{t-\tau(t)} \dot{e}_x(s)^T R_3 \dot{e}_x(s) ds \\ &\leq \begin{bmatrix} e_x(t-\tau_m) \\ e_x(t-\tau(t)) \\ e_x(t-\tau_M) \end{bmatrix}^T \begin{bmatrix} -R_3 & R_3 & 0 \\ * & -2R_3 & R_3 \\ * & * & -R_3 \end{bmatrix} \\ &\begin{bmatrix} e_x(t-\tau_m) \\ e_x(t-\tau(t)) \\ e_x(t-\tau_M) \end{bmatrix} \end{aligned}$$

$$-\tau_m \int_{t-\tau_m}^{t} \dot{e}_x(s)^T R_4 \dot{e}_x(s) ds$$
$$\leq \begin{bmatrix} e_x(t) \\ e_x(t-\tau_m) \end{bmatrix}^T \begin{bmatrix} -R_4 & R_4 \\ * & -R_4 \end{bmatrix} \begin{bmatrix} e_x(t) \\ e_x(t-\tau_m) \end{bmatrix}$$

Let $\eta(t) = [e_x(t)^T, e_x(t-\tau_m)^T, e_x(t-\tau(t))^T, e_x(t-\tau_1)^T, e_x(t-\tau_M)^T, e_f(t)^T]^T$.

$$\dot{V}(t) \leq \eta(t)^T \Omega(t) \eta(t) \quad (12)$$
$$+\dot{e}_x(t)^T((\tau_2)^2 R_1 + (\tau_2)^2 R_2 + (2\tau_2)^2 R_3 + (\tau_m)^2 R_4)\dot{e}_x(t) + \delta$$

where

$$\Omega(t) = \begin{bmatrix} \omega_{11}(t) & R_4 & PA_\tau(t) & 0 & 0 & \omega_{16}(t) \\ * & \xi_{22} & R_3 & Q_2+R_1 & 0 & 0 \\ * & * & \xi_{33} & 0 & R_3 & A_\tau(t)^T PE(t) \\ * & * & * & \xi_{44} & -Q_2+R_2 & 0 \\ * & * & * & * & \xi_{55} & 0 \\ * & * & * & * & * & \omega_{66}(t) \end{bmatrix}$$

in which

$$\begin{aligned} \omega_{11}(t) &= P(A(t)-L(t)C) + (A(t)-L(t)C)^T P \\ &\quad +Q_4 + Q_5 - R_4; \\ \omega_{16}(t) &= -(A(t)-L(t)C)^T PE(t); \\ \omega_{66}(t) &= -2E(t)^T PE(t) + M \end{aligned}$$

By the Schur complement, we obtain

$$\Phi(t) = \begin{bmatrix} \Omega(t) & \phi_{12}(t) \\ * & -P((\tau_2)^2 R_1 + (\tau_2)^2 R_2 \\ & +(2\tau_2)^2 R_3 + (\tau_m)^2 R_4)^{-1} P \end{bmatrix}$$

where

$$\phi_{12}(t)^T = \begin{bmatrix} P(A(t)-L(t)C) & 0 & PA_\tau(t) \\ 0 & 0 & PE(t) \end{bmatrix}^T \quad (13)$$

Applying lemma 2, if $\Xi_{ij}+\Xi_{ji} < 0, i,j = 1,2,\cdots,r, i \leq j$, then there exist a scalar $\epsilon > 0$ such that $\dot{V}(t) < -\epsilon\|\eta(t)\|^2 + \delta$. It follows that $\dot{V}(t) < 0$ for $\epsilon\|\eta(t)\|^2 > \delta$, which means that $\eta(t)$ converges to a small set $S = \{\eta(t) | \|\eta(t)\|^2 \leq \frac{\delta}{\epsilon}\}$ according to Lyapunov stability theory. Therefore, estimation errors of both the state and the fault are uniformly ultimately bounded.

We can extend the result in theorem 2 to the uncertain case: A_i and $A_{\tau i}$ are replaced by $A_i + \Delta A_i$ and $A_{\tau i} + \Delta A_{\tau i}$, respectively.

$$\Delta A_i = M_{Ai} F_i(t) E_{Ai}, ; \quad \Delta A_{\tau i} = M_{A\tau i} F_i(t) E_{A\tau i}$$

We obtain the following theorem

Theorem 3 For given positif scalar λ, if there exist matrices $P, Q_l (l = 1,2,3,4,5), R_m (m = 1,2,3,4)$ and scalars ϵ_{Ai} and $\epsilon_{A\tau i}$ such that (4) and the following LMI hold

$$\Upsilon_{ij} + \Upsilon_{ji} < 0, \qquad i,j = 1,2,\cdots,r, i \leq j \quad (14)$$

where

$$\begin{aligned} \Upsilon_{ij} &= \begin{bmatrix} \Xi_{ij} & U_i & V_i \\ * & -\epsilon_{Ai} I & 0 \\ * & * & -\epsilon_{A\tau i} I \end{bmatrix} \\ &\quad +diag(\epsilon_{Ai} E_{Ai}^T E_{Ai}, 0, \epsilon_{A\tau i} E_{A\tau i}^T E_{A\tau i}, 0_{1\times 6}) \end{aligned}$$

in which

$$U_i = \begin{bmatrix} PM_{Ai} \\ 0_{4\times 1} \\ -E_j^T PM_{Ai} \\ PM_{Ai} \end{bmatrix}$$

$$V_i = \begin{bmatrix} PM_{A\tau i} \\ 0_{4\times 1} \\ -E_j^T PM_{A\tau i} \\ PM_{A\tau i} \end{bmatrix}$$

then the fuzzy Fast Adaptive Fault Estimation (FAFE) algorithm (5) can realize $e_x(t)$ and $e_f(t)$ uniformly ultimately bounded,

In this case, the L_i are given by (6).

Proof:

In the case with uncertainty, we obtain theorem (2) in which Ξij is replaced by $\bar{\Xi} ij$ such that

$$\bar{\Xi}_{ij} = \Xi_{ij} + \Delta\Xi_{ij}$$

The uncertain part is given by

$$\Delta\Xi_{ij} = \begin{bmatrix} \Delta\Xi_{ij}^{11} & 0 & P\Delta A_{\tau i} & 0_{1\times 2} & -\Delta A_i^T PE_j & \Delta A_i^T P \\ & 0 & 0 & 0_{1\times 2} & 0 & 0 \\ & * & 0 & 0_{1\times 2} & -\Delta A_{\tau i}^T PE_j & \Delta A_{\tau i}^T P \\ & * & * & 0_{1\times 2} & 0 & 0 \\ & * & * & 0_{1\times 2} & 0 & 0 \\ & * & * & 0_{1\times 2} & 0 & 0 \\ & * & * & 0_{1\times 2} & 0 & 0 \end{bmatrix}$$

in which

$$\Delta\Xi_{ij}^{11} = P\Delta A_i + \Delta A_i^T P$$

$$\begin{aligned} \Delta\Xi_{ij} &= U_i F(t) \begin{bmatrix} E_{Ai} & 0_{1\times 6} \end{bmatrix} + (*) \\ &\quad +V_i F(t) \begin{bmatrix} 0_{1\times 2} & E_{A\tau i} & 0_{1\times 4} \end{bmatrix} + (*) \quad (15) \end{aligned}$$

By applying lemma 3 and schur complement, we obtain theorem 3.

Remark 1 It is easy to solve inequality (3) and (14) by using LMI Toolbox. For equations (4), we can make a transform into the following optimization problem:

Minimize $\rho > 0$ subject to

$$\begin{bmatrix} \rho I & E_i^T P - F_i C \\ * & \rho I \end{bmatrix} > 0, i = 1, \cdots, r \qquad (16)$$

Remark 2 Compared with theorem (1), theorem 2 contains some new improvements as follows:

(i) The result of theorem (2) is less conservative than that of theorem (1). This is because the conditions (3) is recovered by setting $Q_1 = Q_2 = Q_3 = Q_5 = R_1 = R_2 = R_3 = R_4 = 0$, $\tau(t) = \tau$, $\beta = 0$ in conditions (14).

(ii) Theorem 1 consider an interval time varying delay which is more general than constant time delay.

Furthermore, the uncertain case has been considered in theorem (3).

Remark 3 Based on the on-line fault estimate, an observer-based fast active fault tolerant controller can be designed to compensate for the effects of faults. This design is presented in ([4]) by using the basic concept of generalized inverse.

IV. Simulation Result

Consider the following T-S fuzzy model

$$\dot{x}(t) = \sum_{i=1}^{2} h_i[A_i x(t) + A_{\tau i} x(t - \tau(t)) + B_i u(t)] \qquad (17)$$

The membership functions for rules 1 and 2 are:

$$\begin{aligned} h_1(x_2(t)) &= 1 - \frac{x_2(t)^2}{2.25} \\ h_2(x_2(t)) &= 1 - h_1(x_2(t)) \end{aligned} \qquad (18)$$

where

$$A_1 = \begin{bmatrix} -0.1125 & -0.0200 \\ 1 & 0 \end{bmatrix}, A_2 = \begin{bmatrix} -0.1125 & -1.5270 \\ 1 & \end{bmatrix}$$

$$A_{\tau 1} = \begin{bmatrix} -0.0125 & -0.0050 \\ 0 & 0 \end{bmatrix}, A_{\tau 2} = \begin{bmatrix} -0.0125 & -0.2300 \\ 0 & 0 \end{bmatrix}$$

$$B_1 = B_2 = \begin{bmatrix} 1 \\ 1 \end{bmatrix}, C = \begin{bmatrix} 0 & 1 \end{bmatrix}$$

Assume that time varying fault $f(t)$ is created as

$$\begin{aligned} f(t) &= 0, \qquad 0 \le t < 3 \\ &= 0.7 + 0.15\sin(t), 3 \le t \le 10 \end{aligned} \qquad (19)$$

By using theorem 2 for $\tau(t) = 0.2 + 0.1\sin(t)(\tau_m = 0.1; \tau_M = 0.3, \beta = 0.1)$ with the choice of $\lambda = 5$, we can obtain the following feasible solution:

$$P = 10^3 \times \begin{bmatrix} 1.5409 & -1.5409 \\ -1.5409 & 3.3868 \end{bmatrix}$$

$$F = 10^3 \times 1.8459$$

$$L_1 = \begin{bmatrix} 1.7056 \\ 2.1581 \end{bmatrix}, L_2 = \begin{bmatrix} 0.1081 \\ 2.1555 \end{bmatrix}$$

The simulation result is shown in figure 1.

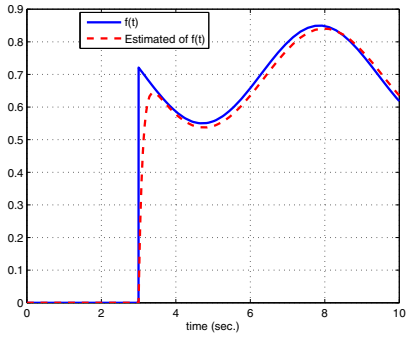

Fig. 1. Fault $f(t)$ and its estimated

V. Conclusion

The problem of delay dependent AFDO design to a class of T-S fuzzy systems with interval time varying delay has been investigated. Based on improved Lyapunov function, a delay dependent conditions for the existence of the fault estimator are given in terms of linear matrix inequalities. This result overcomes the drawbacks of delay independent results. An illustrative example has been presented to demonstrate the potential of the method.

References

[1] K. Gu, V. L. Kharitonov and J. Chen *Stability of time delay systems*. Birhauser, 2003.

[2] B. Jiang, M. Staroswiecki, V. Cocquempot *Fault accommodation for nonlinear dynamic systems*. IEEE Trans. Automat. Contr. 51(9), 1578-1583 (2006)

[3] K. Zhang, B. Jiang, V. Cocquempot, *Adaptive observer-based fast fault estimation*. Int. J. Control Autom. Syst. 6(3), 320-326 (2008)

[4] K. Zhang, B. Jiang, P. Shi *A New Approach to Observer-Based Fault-Tolerant Controller Design for Takagi-Sugeno Fuzzy Systems with State Delay*. Circuits Syst Signal Process, 28, 679-697 (2009)

[5] B. Jiang, K. Zhang, P. Shi *Less conservative criteria for fault accommodation of time-varying delay systems using adaptative fault diagnosis observer*. I. Journal Of Adaptative Control and Signal Processing, (2009)

[6] Zhang Y, Heng P A., *Stability of fuzzy control systems with bounded uncertain delays*, IEEE Transactions on Fuzzy Systems, 2002.

[7] M. Chadli and A. El Hajjaji, *A Observer-based robust fuzzy control of nonlinear systems with parametric uncertaintie*. Fuzzy Sets and Systems, 2006.

[8] E. Kim and H. Lee, *New approaches to relaxed quadratic stability condition of fuzzy control systems*. IEEE Trans. Fuzzy Syst., vol. 8, no. 5, pp. 523-534, 2000.

[9] E. Boukas and A. El Hajjaji, *On Stabilizability of Stochastic Fuzzy Systems*. Proceedings of the 2006 American Control Conference Minneapolis, Minnesota, USA ,p. 4362-4366, 2006.

[10] B. Chen and X. Liu, *Fuzzy guaranteed cost control for nonlinear systems with time-varying delay*. IEEE Trans., vol. 13, no. 2, pp. 238-249, 2005.

[11] K. R. Lee, J. H. Kim, E. T. Jeung, and H. B. Park, *Output feedback robust H_∞ control of uncertain fuzzy dynamic systems with time-varying delay*. IEEE Trans. Fuzzy Syst., vol. 8, no. 6, pp. 657-664, 2000.

[12] S. Xu and J. Lam, *Robust H_∞ control for uncertain discrete-time-delay fuzzy systems via output feedback controllers*. IEEE Trans. Fuzzy Syst., vol. 13, no. 1, pp. 82-93, 2005.

[13] C. Li, H. Wang, and X. Liao, *Delay-dependent robust stability of uncertain fuzzy systems with time-varying delays*. Proc. Inst. Elect. Eng. Control Theory Appl., vol. 151, no. 4, pp. 417-421, 2004.

[14] X.-P. Guan and C.-L. Chen, *Delay-dependent guaranteed cost control for T-S fuzzy systems with time delays*. IEEE Trans. Fuzzy Syst., vol. 12, no. 2, pp. 236-249, 2004.

[15] B. Chen and X. Liu, *Delay-dependent robust H_∞ control for T-S fuzzy systems with time delay*. IEEE Trans. Fuzzy Syst., vol. 13, no. 2, pp. 238-249, 2005.

2011 IEEE International Conference on Fuzzy Systems
June 27-30, 2011, Taipei, Taiwan

Fast Extracting of Change Area from Remote Sensing Image by Fuzzy Theory and Case Base Reasoning

Ting-shiuan Wang
Department of Resource Engineering, Ph.D. students
National Cheng-Kung University
Tainan, Taiwan
n4896111@mail.ncku.edu.tw

Teng-to Yu
Department of Resource Engineering, Assistant Professor
National Cheng-Kung University
Tainan, Taiwan
yutt@mail.ncku.edu.tw

Abstract—**This study presents the technology to combine the remote sensing image of SPOT and FORMOSAT-2 satellite image by Fuzzy theory and case base reasoning. This method adopt three experience identify factors of NDVI, shape, and color to establish the membership function. The Fuzzy theory was applied to estimate the process of thinking as the human brain; while the Case Base Reasoning method was used to increase the capability of self-loop learning and support its consistency with the real nature. The results show that the successful rate of identification was between 90 percent. The Case Base Reasoning results show that the two data similarity was between 46 percent. The Fuzzy and Case Base Reasoning difference factor was (satellite sensors, inclination, date, shadowing, etc.). The rate can be increase if there is enough experienced data. It reveal that fuzzy theory with case base reasoning indeed can rapid screen the change area from remote sensing image in before and after the disaster event.**

Keywords: fuzzy theory, case base reasoning, image extraction, image variation

I. INTRODUCTION

The objective of monitoring the change of catchment area is to avoid the damage from the nature disaster or excessive development. Previous method uses the software to identify the build the land category, and followed by the human experience to check it one by one. However, it has to spend a lot of time to identify the image from the remote sensing images. If it is possible to automatically study and train the capability of selection system, then the time of distinguish can be effectively reduced.

Using image segmentation software to produce the image segmentation vector and extract the variation region is a common practice for remote sensing technique in the past. The process is: select image to segment, output the segmentation vector file, use the software to extract the vector layer, and screen for variation area. The work was done by the accumulation of human experience. The memory capability of human can accumulate the previous experience, and it can compile the things touched to the rules of information.

Human brain can trigger the corresponding rules to the next move. If there were no corresponding rules, it can also trigger the fuzzy space for self-learning and reasoning. This capability can be simulated by the case base reasoning with fuzzy theory. Therefore, we use the fuzzy theory and case base reasoning to construct a quantitative fuzzy space structure to learn the human brain logic and estimate the variation region in the remote sensing image.

II. METHODOLOGY

Jose et al.[3]using Case Base Reasoning design remote sensing search system. Every image have severl classify index in database. The user can use these index combination search any image conform their demand. All user need not understand any programming language or Structured Query Language (SQL) in search process. Hsu and Hong[2]research typhoon remote sensing image classified according Wavelet Transform and Fuzzy Neural Network. They used Case Base Reasoning and Fuzzy damage estimated agricultural products and inhabitants damage. The experiment shows that their method can fast estimate typhoon damage area.

A. Set the membership function and numerical value of prediction indexes

Three indexes were adopted in this study as the experience rules for quick discrimination, which were: NDVI value difference, shape ratio, and color difference ratio (TABLE 1).

1) NDVI.

The meaning of NDVI value difference is to compare the ratio of red light absorption and near-infrared light reflection by green plant in the remote sensing image. The numerical value of NDVI difference is the difference of the early image and late image. Its value was ranged between -2～2.

- Define the NDVI value of previous image is a, and the value of post-image is b. The range of a single NDVI value is between -1 to 1.
- Let f(a) = {1,-1} f(b)= {-1,1} ,then f(b)-f(a) = -2 and 2 , so the maximum threshold value is between -2~2.

- The different value of NDVI is in the range between -2 to 2. According to the induction of manual experience, if the difference values of NDVI lower than 0.3, it could be regarded as no change.
- Let f(a)= {0.2,0.5} f(b)= {0.5,0.2} , we set the range as.
- If the value is between -0.3 to 0.3, then there is no change. If the value is between 02 to -0.3, then there is change exists.

The function of NDVI is to rapidly analyze the plant growth rate in the variation region. Otsu have proposed a rule for plant in the remote sensing image in 1979.[4]The color value of image was divided into two area as vegetation and non-vegetation.

2) Shape ratio

The definition of shape ratio is the ratio of post stage area to the previous stage area. It has to be assigned with the value accordant to the error factors of location, shape, and twist, etc. If the values lower than 1, then it is the reduction change. If the value is 1 to 1.5, then there is no change. If the value is greater than 1.5, then it is the diffusion change.

The shape ratio is not applicable to the land use type as: from never to have, from having to no, and the simplest change of type. The shape ratio is applicable to the condition when the land use types have no change, and only the area shape changes. The shape ratio is also applicable to the area which has been labeled as the variable region.

3) Color difference value

The color difference value is the total post RGB value minus the previous value of previous RGB in the same area. The total RGB value in the remote sensing image should nor over 255+255+255=765. So the category range for the index is:

- Set the total RGB for the previous image is a, and for the post image is b. Then b-a = 765 or-765.
- Therefore, the range of the maximum threshold value is between -765 to 765.

According to the induction of manual experience, the value of RGB difference lower than 30 is an acceptable value. Therefore, the membership function value of the fuzzy interval is defined as the following. If the value is lower than 30, than it is similar. If the value is between 30 to 765 or 765 to 30, then it is not similar.

B. Construct fuzzy and case base reasoning

The MATLAB fuzzy toolbox was used to construct a structure of rapid extraction. Three groups of indicators were identified. The functional forms and membership function value were shown as Figure1. to Figure 4..

Since, every index has three attribute of fuzzy interval. So,every index has four critical range. Kaufmann,Gupta[1] induced several kinds type of membership function. Most suitable for all index are trapezoidal fuzzy number. As in（1）:

$$f(x,a,b,c,d)=\begin{cases} 0 & x \le a \\ \dfrac{x-a}{b-a} & a \le x \le b \\ 1 & b \le x \le c \\ \dfrac{d-x}{d-c} & c \le x \le d \\ 0 & x \ge d \end{cases} \quad (1)$$

$a \le b, c \le d$

The trapezoidal function was chosen in this study because the interval of threshold value for the three indexes in this study is relatively fixed. Twenty seven rules of < IF…THEN > were formulating as the following:

1. If (NDVI is nochange) and (shape is nochange) and (color is Similar) then (expectedvalue is nochange)
2. If (NDVI is nochange) and (shape is nochange) and (color is Dissimilar) then (expectedvalue is yeschange)
3. If (NDVI is nochange) and (shape is nochange) and (color is Dissimilar) then (expectedvalue is yeschange)
4. If (NDVI is nochange) and (shape is Reduction) and (color is Similar) then (expectedvalue is yeschange)
5. If (NDVI is nochange) and (shape is Reduction) and (color is Dissimilar) then (expectedvalue is yeschange)
6. If (NDVI is nochange) and (shape is Reduction) and (color is Dissimilar) then (expectedvalue is yeschange)
7. If (NDVI is nochange) and (shape is Diffusion) and (color is Similar) then (expectedvalue is yeschange)
8. If (NDVI is nochange) and (shape is Diffusion) and (color is Dissimilar) then (expectedvalue is yeschange)
9. If (NDVI is nochange) and (shape is Diffusion) and (color is Dissimilar) then (expectedvalue is yeschange)
10. If (NDVI is negative) and (shape is nochange) and (color is Similar) then (expectedvalue is yeschange)
11. If (NDVI is negative) and (shape is nochange) and (color is Dissimilar) then (expectedvalue is yeschange)
12. If (NDVI is negative) and (shape is nochange) and (color is Dissimilar) then (expectedvalue is yeschange)
13. If (NDVI is negative) and (shape is Reduction) and (color is Similar) then (expectedvalue is yeschange)
14. If (NDVI is negative) and (shape is Reduction) and (color is Dissimilar) then (expectedvalue is yeschange)
15. If (NDVI is negative) and (shape is Reduction) and (color is Dissimilar) then (expectedvalue is yeschange)
16. If (NDVI is negative) and (shape is Diffusion) and (color is Similar) then (expectedvalue is yeschange)
17. If (NDVI is negative) and (shape is Diffusion) and (color is Dissimilar) then (expectedvalue is yeschange)
18. If (NDVI is negative) and (shape is Diffusion) and (color is Dissimilar) then (expectedvalue is yeschange)
19. If (NDVI is positive) and (shape is nochange) and (color is Similar) then (expectedvalue is yeschange)
20. If (NDVI is positive) and (shape is nochange) and (color is Dissimilar) then (expectedvalue is yeschange)
21. If (NDVI is positive) and (shape is nochange) and (color is Dissimilar) then (expectedvalue is yeschange)
22. If (NDVI is positive) and (shape is Reduction) and (color is Similar) then (expectedvalue is yeschange)
23. If (NDVI is positive) and (shape is Reduction) and

(color is Dissimilar) then (expectedvalue is yeschange)
24. If (NDVI is positive) and (shape is Reduction) and (color is Dissimilar) then (expectedvalue is yeschange)
25. If (NDVI is positive) and (shape is Diffusion) and (color is Similar) then (expectedvalue is yeschange)
26. If (NDVI is positive) and (shape is Diffusion) and (color is Dissimilar) then (expectedvalue is yeschange)
27. If (NDVI is positive) and (shape is Diffusion) and (color is Dissimilar) then (expectedvalue is yeschange) .

TABLE 1. MEMBERSHIP FUNCTION AND NUMERICAL VALUE OF THE THREE EVALUATION INDEXES

evaluation index of Variation regional	Type of membership function	Attribute of fuzzy interval	Membership function value
Differences in NDVI values	Trapezoidal	*NDVI ddifferences values is positive*	0.3 ~ 2
		NDVI no change	-0.3 ~ 0.3
		NDVI differences values is negative	-2 ~ -0.3
Shape ratio	Trapezoidal	*No change*	1 to 1.5 times
		Diffusion change	1.5 times to 10 times
		Reduction change	0 ~ 1 time
Color difference value	Trapezoidal	*Similar*	-30 ~ 30
		Dissimilar, positive value	30 ~ 765
		Dissimilar, negative value	-765 ~ -30

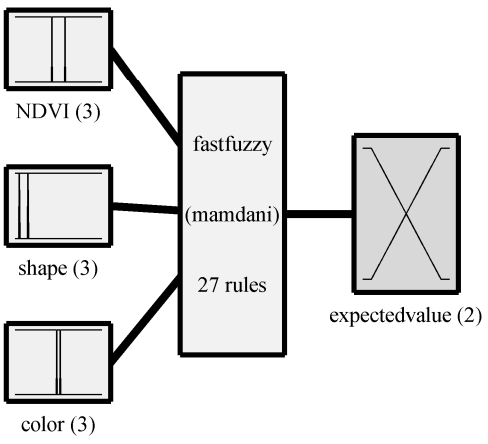

System fastfuzzy: 3 inputs, 1 outputs, 27 rules

Figure 1. Module chart (there are 3 indexes, 1 simulator, 27 rules)

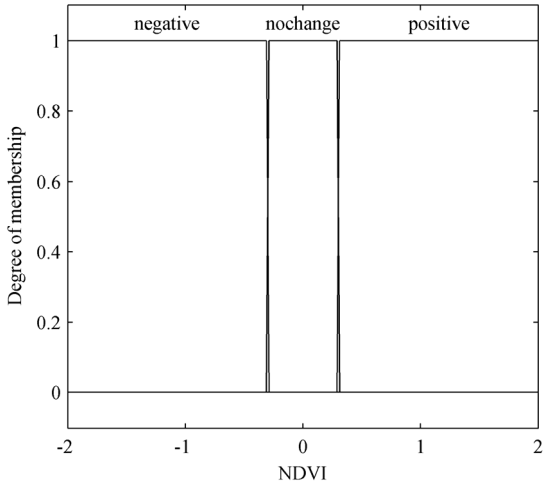

Figure 2. Differences in NDVI values

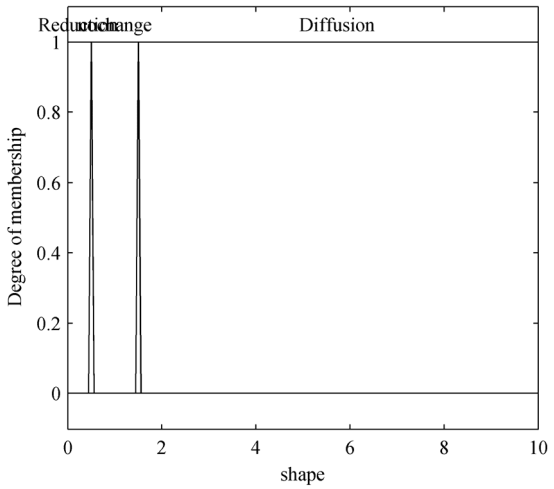

Figure 3. Shape ratio

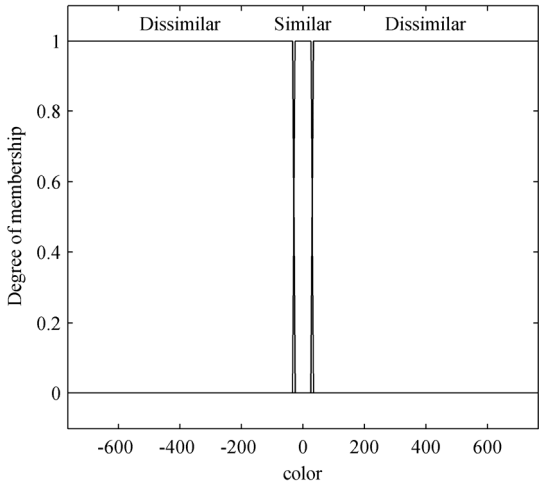

Figure 4. Color difference value

III. RESULTS AND DISCUSSION

The study area was Shihmen Reservoir in Taoyuan County, Taiwan (Figure 6). The area of orchard planting showed rapid growth in the catchment area, according to the third stage governance planning of Shihmen Dam by Water Resource Agency, Ministry of Economic Affairs, Taiwan. These area were distributed in the slope place above 800 meters. It is more suitable for the planting of temperate fruit trees such as honey peach. And the low attitude area is more suitable for the planting of citrus trees. It shows that the land use was influenced by the demand of tourism and economic effect. There is a substantial degree of change comparing to the types of agriculture crop planting in earlier stage.

The forth stage investigation data from the project of SWCB-97-157 in 2008 were taken as the experience cases. Using four FORMOSAT-2 and SPOT panchromatic (pan) and multispectral (MS) images. The results were further verified by the three indexes. The expected value of variations was calculated by the module and obtains the value of 0.67, as shown in Figure 5. It means that if there is a possibility of change, its value will be greater than 0.67. Otherwise, the value of change will be lower than 0.67. The results of experience cases were shown in TABLE 2.

From the above TABLE 2 results, there are three cases with the expected value of variance lower than 0.67 among the thirty two cases. So the success rate of distinguish is 33-3/33=0.90. The recognition rate is about 90%.

From the above TABLE 3 ~TABLE 6 results, using fourth contrast third case data and count total mean similarity. The total mean similarity is about 46 %(Figure 7).

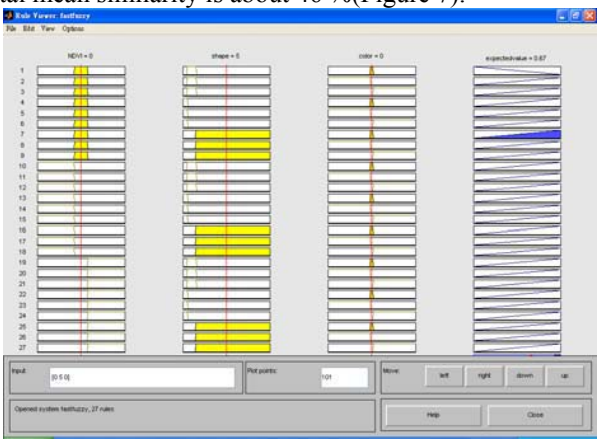

Figure 5 Interface of operation module

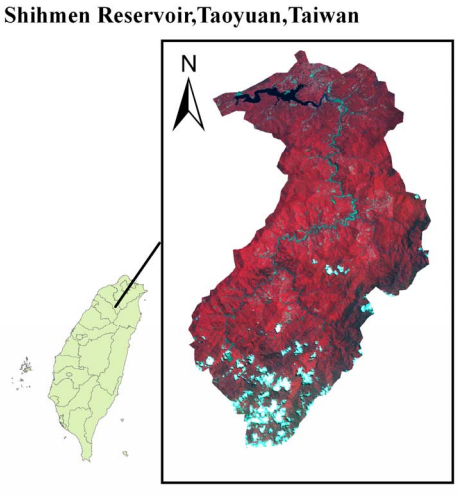

Figure 6 Shihmen reservoir

TABLE 2. THE FOURTH EXPERIENCE CASE IN 2008

No	Differences in NDVI values	Shape ratio	Color difference value	expected value of Variations
D1	-0.25	1.00	-128.00	0.67
D2	-0.63	1.00	-3.00	0.67
D3	-0.62	1.00	-13.00	0.67
D4	-0.47	1.00	-22.00	0.67
D5	-0.22	1.00	-93.00	0.67
D6	-0.34	1.00	-53.00	0.67
D7	-0.50	1.00	-1.00	0.67
D8	-0.38	2.56	-26.00	0.67
D9	-0.14	1.00	-90.00	0.67
D10	-0.42	1.00	-35.00	0.67
D11	-0.10	1.00	-47.00	0.67
D12	-0.40	1.00	29.00	0.67
D13	-0.35	1.00	66.00	0.67
D14	-0.51	1.00	10.00	0.67
D15	-0.54	1.00	-16.00	0.67
D16	-0.42	1.00	-14.00	0.67
D17	-0.58	1.00	-38.00	0.67
D18	-0.44	1.00	-23.00	0.67
D19	-0.30	1.00	-12.00	0.498
D20	-0.44	1.00	20.00	0.67
D21	-0.41	1.00	-100.00	0.67
D22	-0.35	1.00	15.00	0.67
D23	-0.27	1.00	-92.00	0.67
D24	-0.22	1.00	-62.00	0.67
D25	-0.42	1.00	41.00	0.67
D26	-0.56	1.00	-75.00	0.67
D27	-0.56	1.00	-40.00	0.67
D28	-0.43	1.00	-20.00	0.67
D29	-0.45	1.00	-47.00	0.67

D30	-0.28	1.00	-19.00	0.324
D31	-0.30	1.00	26.00	0.498
D32	-0.57	1.00	-3.00	0.67
D33	-0.05	1.00	-104.00	0.67

TABLE 3. FOURTH CONTRAST THIRD EVERY CASE SIMILARITY(D1~D9)

	D1	D2	D3	D4	D5	D6	D7	D8	D9
C1	0.67	*0.33*	*0.33*	0.67	0.67	0.67	0.67	0.67	0.67
C2	0.67	*0.33*	*0.33*	0.67	0.67	0.67	0.67	0.67	0.67
C3	0.67	*0.33*	*0.33*	*0.33*	0.67	1.00	*0.33*	0.67	1.00
C4	*0.33*	*0.33*	*0.33*	*0.33*	0.67	0.67	*0.33*	*0.33*	0.67
C5	0.67	0.67	0.67	0.67	0.67	0.67	0.67	0.67	0.67
C6	*0.33*	*0.33*	*0.33*	*0.33*	0.67	*0.33*	*0.33*	*0.33*	0.67
C7	0.67	0.67	0.67	0.67	0.67	0.67	0.67	0.67	0.67
C8	0.67	*0.33*	*0.33*	*0.33*	0.67	0.67	*0.33*	0.67	0.67
C9	*0.33*	*0.33*	*0.33*	*0.33*	*0.33*	0.67	*0.33*	*0.33*	*0.33*
C10	*0.33*	*0.33*	*0.33*	*0.33*	*0.33*	*0.00*	*0.33*	*0.33*	*0.33*
C11	*0.33*	0.67	0.67	0.67	0.67	*0.33*	0.67	0.67	0.67
C12	*0.33*	*0.33*	*0.33*	*0.33*	0.67	*0.33*	*0.33*	*0.33*	0.67
C13	0.67	*0.33*	*0.33*	*0.33*	0.67	*0.33*	*0.33*	*0.33*	0.67
C14	*0.33*	*0.33*	*0.33*	*0.33*	0.67	*0.33*	*0.33*	*0.33*	0.67
C15	*0.33*	*0.33*	*0.33*	*0.33*	*0.33*	*0.33*	0.67	*0.33*	*0.33*
C16	*0.33*	*0.33*	*0.33*	*0.33*	*0.33*	*0.33*	*0.33*	*0.33*	*0.33*
C17	*0.33*	*0.33*	*0.33*	*0.33*	*0.33*	*0.33*	*0.33*	*0.33*	0.67
C18	*0.33*	*0.33*	0.67	*0.33*	*0.33*	*0.33*	0.67	*0.33*	*0.33*
C19	*0.00*	*0.00*	*0.00*	*0.00*	*0.33*	*0.00*	*0.00*	*0.00*	*0.33*
C20	*0.33*	*0.33*	*0.33*	*0.33*	*0.33*	0.67	*0.33*	0.67	*0.33*
C21	*0.33*	*0.33*	*0.33*	*0.33*	0.67	0.67	*0.33*	*0.33*	1.00
C22	0.67	*0.33*	*0.33*	0.67	0.67	0.67	*0.33*	0.67	0.67
Similarity	0.44	0.36	0.38	0.41	0.55	0.48	0.42	0.45	0.59

TABLE 4. FOURTH CONTRAST THIRD EVERY CASE SIMILARITY(D10~D18)

	D10	D11	D12	D13	D14	D15	D16	D17	D18
C1	0.67	0.67	0.67	1.00	0.67	0.67	0.67	0.67	0.67
C2	0.67	0.67	0.67	0.67	0.67	0.67	0.67	0.67	0.67
C3	1.00	1.00	0.67	0.67	*0.33*	*0.33*	0.67	0.67	0.67
C4	*0.33*	*0.33*	*0.33*	*0.33*	*0.33*	*0.33*	*0.33*	*0.33*	*0.33*
C5	0.67	*0.33*	0.67	0.67	0.67	0.67	0.67	0.67	0.67
C6	*0.33*	0.67	*0.33*	0.67	*0.33*	*0.33*	*0.33*	*0.33*	*0.33*
C7	*0.33*	0.67	0.67	0.67	0.67	0.67	0.67	*0.33*	0.67
C8	*0.33*	0.67	*0.33*	0.67	*0.33*	*0.33*	*0.33*	*0.33*	*0.33*
C9	*0.33*	0.67	*0.00*	*0.33*	*0.00*	*0.33*	*0.33*	*0.33*	*0.33*
C10	*0.33*	*0.33*	*0.00*	*0.00*	*0.33*	*0.33*	*0.33*	*0.00*	*0.33*
C11	0.67	1.00	*0.33*	*0.33*	*0.33*	0.67	0.67	0.67	0.67
C12	*0.33*	0.67	*0.33*	*0.33*	*0.33*	*0.33*	*0.33*	*0.33*	*0.33*
C13	*0.33*	*0.33*	*0.33*	*0.33*	*0.33*	*0.33*	*0.33*	*0.33*	*0.33*
C14	*0.33*	0.67	*0.33*	*0.33*	*0.33*	*0.33*	*0.33*	*0.33*	*0.33*
C15	*0.33*	*0.33*	0.67	*0.33*	0.67	*0.33*	*0.33*	*0.33*	*0.33*
C16	*0.33*	*0.33*	*0.33*	0.67	*0.33*	*0.33*	*0.33*	*0.33*	*0.33*
C17	*0.33*	0.67	0.67	0.67	*0.33*	*0.33*	*0.33*	*0.33*	*0.33*
C18	*0.33*	0.67	0.67	*0.33*	0.67	0.67	0.67	*0.33*	*0.33*
C19	*0.00*	*0.33*	*0.00*	*0.33*	*0.00*	*0.00*	*0.00*	*0.00*	*0.00*
C20	0.67	0.67	*0.33*	*0.33*	*0.33*	*0.33*	*0.33*	0.67	0.67
C21	*0.33*	1.00	*0.33*	*0.33*	*0.33*	*0.33*	*0.33*	*0.33*	*0.33*
C22	0.67	0.67	0.67	0.67	*0.33*	*0.33*	0.67	*0.33*	0.67
similarity	0.44	0.61	0.42	0.48	0.39	0.41	0.44	0.39	0.44

TABLE 5. FOURTH CONTRAST THIRD EVERY CASE SIMILARITY(D19~D27)

	D19	D20	D21	D22	D23	D24	D25	D26	D27
C1	0.67	0.67	0.67	0.67	0.67	0.67	0.67	0.67	0.67
C2	0.67	0.67	0.67	0.67	0.67	0.67	0.67	0.67	0.67
C3	0.67	0.67	0.67	0.67	1.00	1.00	0.67	0.67	0.67
C4	*0.33*	*0.33*	0.67	*0.33*	0.67	0.67	*0.33*	0.67	*0.33*
C5	0.67	0.67	0.67	0.67	0.67	0.67	0.67	0.67	0.67
C6	*0.33*	*0.33*	*0.33*	*0.33*	0.67	0.67	0.67	*0.33*	*0.33*
C7	1.00	0.67	*0.33*	1.00	0.67	0.67	0.67	*0.33*	*0.33*
C8	0.67	*0.33*	*0.33*	0.67	0.67	0.67	*0.33*	*0.33*	*0.33*
C9	0.67	*0.00*	*0.00*	*0.33*	*0.33*	*0.33*	*0.00*	*0.00*	*0.33*
C10	*0.33*	*0.33*	*0.00*	*0.33*	*0.00*	*0.33*	*0.00*	*0.00*	*0.00*
C11	0.67	*0.33*	*0.33*	*0.33*	*0.33*	0.67	*0.33*	*0.33*	0.67
C12	*0.33*	*0.33*	0.67	*0.33*	0.67	*0.33*	*0.33*	0.67	*0.33*
C13	*0.33*	*0.33*	0.67	*0.33*	0.67	*0.33*	*0.33*	*0.33*	*0.33*
C14	*0.33*	*0.33*	0.67	*0.33*	0.67	1.00	*0.33*	0.67	*0.33*
C15	*0.33*	0.67	*0.33*	0.67	*0.33*	*0.33*	0.67	*0.33*	*0.33*
C16	*0.33*	*0.33*	*0.33*	*0.33*	*0.33*	*0.33*	*0.33*	*0.33*	*0.33*
C17	*0.33*	0.67	*0.33*	0.67	*0.33*	*0.33*	0.67	*0.33*	*0.33*
C18	0.67	0.67	*0.33*	0.67	*0.33*	*0.33*	0.67	*0.33*	*0.33*
C19	*0.00*	*0.00*	*0.00*	*0.00*	*0.00*	*0.33*	*0.33*	*0.00*	*0.00*
C20	*0.33*	*0.33*	*0.33*	*0.33*	*0.33*	0.67	*0.33*	0.67	0.67
C21	*0.33*	*0.33*	0.67	*0.33*	0.67	0.67	*0.33*	0.67	*0.33*
C22	0.67	0.67	0.67	0.67	0.67	0.67	0.67	*0.33*	*0.33*
Similarity	0.48	0.44	0.44	0.48	0.52	0.56	0.45	0.42	0.39

TABLE 6. FOURTH CONTRAST THIRD EVERY CASE SIMILARITY(D28~D32)

	D28	D29	D30	D31	D32	D33
C1	0.67	0.67	0.67	0.67	0.67	0.67
C2	0.67	0.67	0.67	0.67	0.67	0.67
C3	0.67	1.00	0.67	0.67	*0.33*	0.67
C4	*0.33*	*0.33*	*0.33*	*0.33*	*0.33*	0.67
C5	0.67	0.67	0.67	0.67	0.67	*0.33*
C6	*0.33*	*0.33*	0.67	*0.33*	*0.33*	0.67

C7	0.67	*0.33*	1.00	1.00	0.67	0.67
C8	*0.33*	*0.33*	0.67	0.67	*0.33*	0.67
C9	*0.33*	*0.33*	0.67	*0.33*	*0.33*	*0.33*
C10	*0.33*	*0.00*	*0.33*	*0.00*	*0.33*	*0.33*
C11	0.67	0.67	0.67	*0.33*	0.67	0.67
C12	*0.33*	*0.33*	*0.33*	*0.33*	*0.33*	1.00
C13	*0.33*	*0.33*	*0.33*	*0.33*	*0.33*	0.67
C14	*0.33*	*0.33*	*0.33*	*0.33*	*0.33*	1.00
C15	*0.33*	*0.33*	0.67	0.67	*0.33*	*0.33*
C16	*0.33*	*0.33*	*0.33*	*0.33*	*0.33*	0.67
C17	*0.33*	*0.33*	*0.33*	0.67	*0.33*	0.67
C18	*0.33*	*0.33*	*0.33*	0.67	0.67	0.67
C19	*0.00*	*0.00*	*0.00*	*0.00*	*0.00*	*0.33*
C20	*0.33*	0.67	*0.33*	*0.33*	*0.33*	0.67
C21	*0.33*	0.67	*0.33*	*0.33*	*0.33*	0.67
C22	0.67	0.67	0.67	0.67	*0.33*	0.67
Similarity	0.42	0.44	0.50	0.47	0.41	0.62

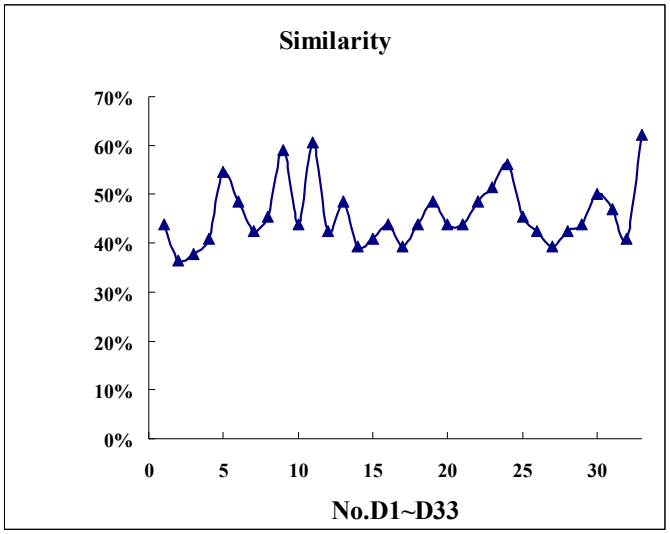

Figure 7 Fourth contrast third case total mean similarity

IV. CONCLUSION

It is necessary to appropriately monitor the environment according to the characteristic of land use in the watershed. If it was done by human observation to understand the hillside use condition, then it will take more time and more cost consuming. Remote sensing technology helps to provide the real time data, and can quickly glimpse the land picture status of watershed. This technology enforce the capability of variation region monitoring, and could save the time and cost. How to use this technology in the conservation of hillside deserves our attention.

ACKNOWLEDGMENT

This research was supported by Soil and Water Conservation Bureau of Council of Agriculture, under the project【Interpretation and investigation of the satellite image variation point of Shihmen Dam catchment area】(Project No.：970102860)

REFERENCES

[1] A. Kaufmann, M.M., "Gupta, Introduction to Fuzzy Arithmetic Theory and Applications," *Van Nostrand Reinhold*, New York, 1991.

[2] Chien-Chang Hsu, Zhi-Yu Hong,"An Intelligent Typhoon Damage Prediction System from Aerial Photographs," *KES(1)*, pp. 747-756, 2007.

[3] Jose, B., Singh, B. P., Venkataraman, S., and Krishnan, R. "Vector based image matching for indexing in case-based reasoning systems," *In Proceedings of the 4th German Workshop on Case-based Reasoning*; System Development and Education, Berlin, pp. 20-22,1996.

[4] Otsu, N. "A threshold selection method from gray-level histograms," *IEEE Transactions on System Man Cybernet*, Vol. 9, No. 1, pp. 62-69, 1979.

2011 IEEE International Conference on Fuzzy Systems
June 27-30, 2011, Taipei, Taiwan

Weights-Learning for Weighted Fuzzy Rule Interpolation in Sparse Fuzzy Rule-Based Systems

Shyi-Ming Chen and Yu-Chuan Chang
Department of Computer Science and Information Engineering, National Taiwan University of Science and Technology, Taipei, Taiwan, R. O. C.
e-mail: smchen@mail.ntust.edu.tw, D9315003@mail.ntust.edu.tw

***Abstract*—In this paper, we present a weights-learning algorithm based on the CHC algorithm, which is a specialization of traditional genetic algorithms, to automatically learn the optimal weights of the antecedent variables of the fuzzy rules for the proposed weighted fuzzy interpolative reasoning method based on bell-shaped membership functions. We also apply the proposed method to deal with the truck backer-upper control problem. The experimental results show that the proposed method using the optimally learned weights gets better accuracy rates than the existing methods for dealing with the truck backer-upper control problem.**

Keywords-Fuzzy interpolative reasoning; sparse fuzzy rule-based systems; weighted antecedent variables; genetic algorithms

I. INTRODUCTION

Sparse fuzzy rule bases contain blank areas uncovered by fuzzy rules in the universe of discourse with respect to the input variables. When the observation occurs in these blank areas, traditional fuzzy rule-based systems may get improper fuzzy reasoning results. Because fuzzy interpolation techniques can make inferences with sparse fuzzy rule bases effectively, fuzzy interpolation is an essential solution for inference in sparse fuzzy rule-based systems. Some fuzzy interpolative reasoning methods have been presented for sparse fuzzy rule-based systems [1]-[7], [10], [11], [13], [14], [17], [18].

In this paper, we present a weights-learning algorithm based on the CHC algorithm [8], which is a specialization of traditional genetic algorithms (GAs) [12], to automatically learn the optimal weights of the antecedent variables of the fuzzy rules for the proposed weighted fuzzy interpolative reasoning method, based on bell-shaped membership functions. We also apply the proposed method to deal with the truck backer-upper control problem. The experimental results show that the proposed method using the optimally learned weights gets smaller error rates than the existing methods [1], [6], [7], [11], [15].

II. PRELIMINARIES

A bell-shaped fuzzy set A in the universe of discourse U can be represented by $e^{-\left(\frac{x-c}{a}\right)^{2b}}$, where the parameters a and b alter the width of the membership function curve of A, the parameter c denotes the mean (i.e., the center) of the membership function of A and $b \geq 0$. For simplicity, a bell-shaped fuzzy set A can be represented by (a, b, c). For example, Figure 2 shows a bell-shaped fuzzy set A, where $A = (2, 2, 5)$. The representative value "$Rep(A)$" of a bell-shaped fuzzy set A is defined as follows:

$$Rep(A) = c. \tag{1}$$

Let c_A and c_B be the representative values of two bell-shaped fuzzy sets A and B, respectively. If $c_A \leq c_B$, then A is at the left-hand side of B and the total ordering relationship between A and B is denoted by "$A \prec B$". Otherwise, A is at the right-hand side of B and the total ordering relationship between A and B is denoted by "$B \prec A$".

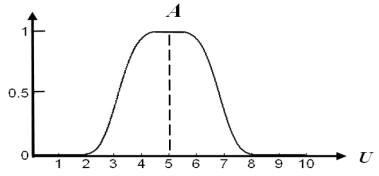

Figure 1. Bell-shaped fuzzy set $A = (2, 2, 5)$.

Generally speaking, the larger the values of the parameters a_A and b_A of the bell-shaped fuzzy set A, the larger the fuzziness of the fuzzy set A. Let A and B be two bell-shaped fuzzy sets, where $A = (a_A, b_A, c_A)$ and $B = (a_B, b_B, c_B)$. The ratios of the fuzziness $RF_a(A, B)$ and $RF_b(A, B)$ of the bell-shaped fuzzy set A to the fuzziness of the bell-shaped fuzzy set B with respect to the parameters a and b, respectively, are defined as follow:

$$RF_a(A, B) = \frac{a_A}{a_B}, \tag{2}$$

$$RF_b(A, B) = \frac{b_A}{b_B}. \tag{3}$$

III. A WEIGHTED FUZZY INTERPOLATIVE REASONING METHOD FOR SPARSE FUZZY RULE-BASED SYSTEMS USING BELL-SHAPED MEMBERSHIP FUNCTIONS

In this section, we present a weighted fuzzy interpolative reasoning method for sparse fuzzy rule-based systems using bell-shaped membership functions. Consider the following weighted multiple fuzzy rules interpolation scheme using bell-shaped membership functions:

***Rule* 1: If** X_1 is A_{11} (w_1) **and** X_2 is A_{12} (w_2) **and** ...**and** X_m is A_{1m} (w_m) **Then** Y is B_1
***Rule* 2: If** X_1 is A_{21} (w_1) **and** X_2 is A_{22} (w_2) **and** ...**and** X_m is A_{2m} (w_m) **Then** Y is B_2
⋮
***Rule n*: If** X_1 is A_{n1} (w_1) **and** X_2 is A_{n2} (w_2) **and** ...**and** X_m is A_{nm} (w_m) **Then** Y is B_n
***Observation*:** X_1 is A_1^* **and** X_2 is A_2^* **and** ...**and** X_m is A_m^*

***Conclusion*:** Y is B^*

where X_j denotes the jth antecedent variable, Y denotes the consequence variable, the antecedent fuzzy set A_{ij} of *Rule i* is represented by $(a_{A_{ij}}, b_{A_{ij}}, c_{A_{ij}})$, the consequence fuzzy set B_i of *Rule i* is represented by $(a_{B_i}, b_{B_i}, c_{B_i})$, the jth observation fuzzy set A_j^* is represented by $(a_{A_j^*}, b_{A_j^*}, c_{A_j^*})$, the interpolated consequence fuzzy set B^* is represented by $(a_{B^*}, b_{B^*}, c_{B^*})$, w_j denotes the weight of the antecedent variable X_j, $0 \le w_j \le 1$, $1 \le j \le m$, m denotes the number of antecedent variables appearing in the fuzzy rules and n denotes the number of fuzzy rules. Based on the weighted multiple fuzzy rules interpolation scheme, the proposed method for fuzzy rule interpolation using bell-shaped membership functions is now presented as follows:

Step 1: Choose p neighboring fuzzy rules *Rule* 1, *Rule* 2, …, and *Rule p* with respect to the observation as the closest fuzzy rules [5] with respect to the observation, where each antecedent fuzzy set A_{ij} of the closest fuzzy rule *Rule i* is either the left nearest fuzzy set or the right nearest fuzzy set of the observation fuzzy set A_j^*, $1 \le j \le m$ and $1 \le p \le n$.

Step 2: Based on [5], calculate the weight W_i of *Rule i*, where $1 \le i \le p$. Assume that $A_{l_j j}$ and $A_{r_j j}$ are the left nearest antecedent fuzzy set and the right nearest antecedent fuzzy set with respect to the observation fuzzy set A_j^*, respectively, where $1 \le l_j \le p$ and $1 \le r_j \le p$. Let

$$\lambda_{l_j j} = \begin{cases} \left(1 - \dfrac{\left|c_{A_j^*} - c_{A_{l_j j}}\right|}{\left|c_{A_{r_j j}} - c_{A_{l_j j}}\right|}\right), & \text{if } A_{l_j j} \prec A_j^* \prec A_{r_j j}, \\ 1, & \text{if } A_{ij} \prec A_j^*, \text{ where } 1 \le i \le p, \end{cases} \tag{4}$$

$$\lambda_{r_j j} = \begin{cases} \left(1 - \dfrac{\left|c_{A_{r_j j}} - c_{A_j^*}\right|}{\left|c_{A_{r_j j}} - c_{A_{l_j j}}\right|}\right), & \text{if } A_{l_j j} \prec A_j^* \prec A_{r_j j}, \\ 1, & \text{if } A_j^* \prec A_{ij}, \text{ where } 1 \le i \le p, \end{cases} \tag{5}$$

where $1 \le j \le m$. Let

$$W_i = \frac{\underset{1 \le j \le m}{\text{Min}}\, w_j \lambda_{ij}}{\sum_{q=1}^{p} \underset{1 \le j \le m}{\text{Min}}\, w_j \lambda_{qj}}, \tag{6}$$

where W_i denotes the weight of the fuzzy rule *Rule i*, $0 \le W_i \le 1$, $\sum_{i=1}^{p} W_i = 1$ and $1 \le i \le p$.

Step 3: Calculate the mean c_{B^*} of the interpolated consequence fuzzy set B^*, shown as follows:

$$c_{B^*} = \sum_{i=1}^{p} W_i \times c_{B_i}, \tag{7}$$

where $0 \le W_i \le 1$, $\sum_{i=1}^{p} W_i = 1$ and $1 \le i \le p$.

Step 4: Calculate the ratio RF_b of the composite fuzziness of the observation fuzzy sets to the composite fuzziness of the antecedent fuzzy sets with respect to the parameter b, shown as follows:

$$CF_b^* = \sum_{j=1}^{m} w_j \times b_{A_j^*}, \tag{8}$$

$$CF_{b,i} = \sum_{j=1}^{m} w_j \times b_{A_{ij}}, \quad \text{where } 1 \le i \le p \tag{9}$$

$$RF_b = \frac{RF_b^*}{\sum_{i=1}^{p} W_i \times RF_{b,i}}, \tag{10}$$

where CF_b^* denotes the composite fuzziness of the observation fuzzy sets A_1^*, A_2^*, …, and A_m^* with respect to the parameter b, $CF_{b,i}$ denotes the composite fuzziness of the antecedent fuzzy sets A_{i1}, A_{i2}, …, and A_{im} of the fuzzy rule *Rule i* with respect to the parameter b, RF_b denotes the ratio of the composite fuzziness of the observation fuzzy sets to the composite fuzziness of the antecedent fuzzy sets A_{ij} with respect to the parameter b, $RF_b \ge 0$, $0 \le W_i \le 1$, $\sum_{i=1}^{p} W_i = 1$, $1 \le j \le m$ and $1 \le i \le p$. Calculate the value of b_{B^*} of the interpolated consequence fuzzy set $B^* = (a_{B^*}, b_{B^*}, c_{B^*})$, shown as follows:

$$b_{B^*} = RF_b \times \left(\sum_{i=1}^{p} W_i \times b_{B_i}\right), \tag{11}$$

where $0 \le W_i \le 1$, $\sum_{i=1}^{p} W_i = 1$ and $1 \le i \le p$.

Step 5: Calculate the ratio RF_a of the composite fuzziness of the observation fuzzy sets to the composite fuzziness of the antecedent fuzzy sets with respect to the parameter a, shown as follows:

$$CF_a^* = \sum_{j=1}^{m} w_j \times a_{A_j^*}, \tag{12}$$

$$CF_{a,i} = \sum_{j=1}^{m} w_j \times a_{A_{ij}}, \tag{13}$$

$$RF_a = \frac{CF_a^*}{\sum_{i=1}^{p} W_i \times CF_{a,i}}, \tag{14}$$

where CF_a^* denotes the composite fuzziness of the observation fuzzy sets A_1^*, A_2^*, … and A_m^* with respect to the parameter a, $CF_{a,i}$ denotes the composite fuzziness of the antecedent fuzzy sets A_{i1}, A_{i2}, …, and A_{im} of the fuzzy rule *Rule i* with respect to the parameter a, RF_a denotes the ratio of the composite fuzziness of the observation fuzzy sets A_j^* to the composite fuzziness of the antecedent fuzzy sets A_{ij} with respect to the parameter a, $RF_a \ge 0$, $0 \le W_i \le 1$, $\sum_{i=1}^{p} W_i = 1$, $1 \le j \le m$ and $1 \le i \le p$. Calculate the value of a_{B^*} of the interpolated consequence fuzzy set $B^* = (a_{B^*}, b_{B^*}, c_{B^*})$, where

$$a_{B^*} = RF_a \times \left(\sum_{i=1}^{p} W_i \times a_{B_i} \right), \quad (15)$$

$0 \le W_i \le 1$, $\sum_{i=1}^{p} W_i = 1$ and $1 \le i \le p$. Therefore, we can get the interpolated consequence fuzzy set B^*, where $B^* = (a_{B^*}, b_{B^*}, c_{B^*})$.

IV. A Weights-Learning Algorithm to Automatically Learn the Optimal Weights of the Antecedent Variables of the Fuzzy Rules

In this section, we present a weights-learning algorithm based on the CHC algorithm [8], which is a specialization of traditional genetic algorithms (GAs) [12], to automatically learn the optimal weights of the antecedent variables of the fuzzy rules for the weighted fuzzy interpolative reasoning method. The CHC algorithm [8] uses the crossover generation, elitist selection, heterogeneous recombination and cataclysmic mutation for evolution. Assume that a fuzzy rule-based system has a knowledge base consisting of n fuzzy rules, where X_1, X_2, …, and X_m denote the antecedent variables of the fuzzy rules with respect to the inputs x_1, x_2, …, and x_m, respectively, and Y denotes the consequence variable of the fuzzy rules with respect to the output. Let W_{X_j} denote the weight of the antecedent variable X_j, where $1 \le j \le m$. Given a set S of training samples, where $S = \{S_1, S_2, \ldots, S_P\}$, the input values of each training sample S_i are represented by $(x_{i1}, x_{i2}, \ldots, x_{im})$, the target output of training sample S_i is represented by y_i, $1 \le i \le P$ and P denotes the number of training samples. In the proposed weights-learning algorithm, a population consists of l chromosomes and each chromosome consists of m genes, where the value g_j of the jth gene denotes the weight W_{Xj} of the antecedent variable X_j of the fuzzy rules, $0 \le g_j \le 1$ and $1 \le j \le m$, as shown in Figure 2. Assume that h denotes the heterogeneous recombination threshold for incest prevention.

Chromosome	g_1	g_2	g_3	…	g_{m-1}	g_m

Figure 2. Encoding the weights of the antecedent variables into a chromosome.

The proposed weights-learning algorithm is now presented as follows:

Step 1: Initialize two chromosomes, where one chromosome has the weights 0, 1, 0, 1, …, 0, 1 and the other chromosome has the weights 1, 0, 1, 0, …, 1, 0. Then, the system randomly generates the remaining l - 2 chromosomes to form the initial population. Let $h = \left\lceil \frac{m}{4} \right\rceil$.

Step 2: For each chromosome in the current population, decode the chromosome into the weight W_{X_j} of each antecedent variable X_j of the fuzzy rules, where $1 \le j \le m$. Based on the weighted fuzzy rules interpolation scheme, let the input values $x_{i1}, x_{i2}, \ldots$, and x_{im} of each training sample S_i $(x_{i1}, x_{i2}, \ldots, x_{im}, y_i)$ be the input observation "$X_1 = x_{i1}$, $X_2 = x_{i2}$, …, and $X_m = x_{im}$", where $1 \le i \le P$ and y_i denotes the target output of S_i. For each training sample $S_i = (x_{i1}, x_{i2}, \ldots, x_{im}, y_i)$, apply the proposed weighted fuzzy interpolative reasoning method to generate the fuzzy interpolated result B_i^* with respect to the input observation "$X_1 = x_{i1}$, $X_2 = x_{i2}$, …, $X_m = x_{im}$", where $1 \le i \le P$. For each B_i^*, if B_i^* is a fuzzy set, then use the center of gravity defuzzification method [16] to defuzzify B_i^* into a crisp-valued inferred output y_i^*, where $1 \le i \le P$. Based on a predefined fitness function, calculate the fitness value of each chromosome between the inferred outputs and the target outputs of the training samples.

Step 3: Select chromosomes from the current population based on the binary tournament selection method [9] to form a mating pool. The system repeatedly randomly selects two chromosomes from the current population and puts the chromosome having the larger fitness value into the mating pool and then puts the two selected chromosomes back into the current population. Repeatedly perform the above process until the number of chromosomes in the mating pool is equal to l, where l denotes the number of chromosomes of a population.

Step 4: Perform the blend crossover (BLX-α) method [8] with the chromosomes in the mating pool, where $0 \le \alpha < 1$ (Note: In this paper, we let $\alpha = 0.5$). For each chromosome C_i in the mating pool, the system randomly generates a real value between 0 and 1. If the randomly generated real value is smaller than a predefined crossover rate γ, where $\gamma \in [0, 1]$, then the system randomly chooses another chromosome C_j from the mating pool in which the number of distinct genes between C_i and C_j is larger than the value of h, and randomly chooses $\left\lceil \frac{m}{4} \right\rceil$ crossover points to perform the BLX-α crossover [8] with the selected chromosomes C_i and C_j. Figure 3 shows an example how the system updates the genes between the two selected chromosomes C_i and C_j, where the values of the genes g_2 and g_7 of C_i and C_j shown in Figure 3 are updated by the system, respectively.

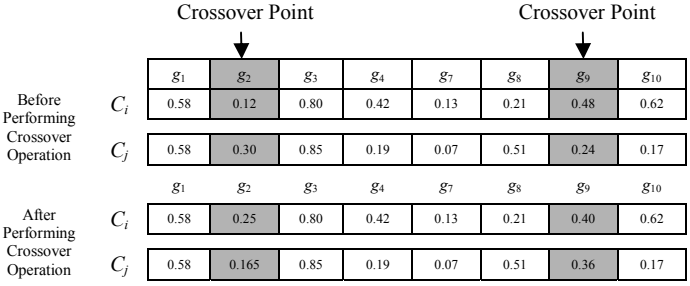

Figure 3. The system updates the genes between the two selected chromosomes.

Step 5: For each chromosome in the mating pool, decode the chromosome into the weight W_{X_j} of each antecedent variable X_j of the fuzzy rules, where $1 \le j \le m$. Based on the weighted fuzzy rules interpolation scheme, let the input values $x_{i1}, x_{i2}, \ldots$, and x_{im} of each training sample $S_i = (x_{i1}, x_{i2}, \ldots, x_{im}, y_i)$ be the input observation "$X_1 = x_{i1}$, $X_2 = x_{i2}$, …, and $X_m = x_{im}$", where $1 \le i \le P$ and y_i denotes the target output of S_i. For each training sample $S_i = (x_{i1}, x_{i2}, \ldots, x_{im}, y_i)$, apply the proposed weighted

fuzzy interpolative reasoning method to generate the fuzzy interpolated result B_i^* with respect to the input observation "$X_1 = x_{i1}, X_2 = x_{i2}, \ldots, X_m = x_{im}$", where $1 \le i \le P$. For each B_i^*, if B_i^* is a fuzzy set, then use the center of gravity defuzzification method [16] to defuzzify B_i^* into a crisp-valued inferred output y_i^*, where $1 \le i \le P$. Based on a predefined fitness function, calculate the fitness value of each chromosome between the inferred outputs and the target outputs of the training samples. Perform the elitist replacement to form the population of the next generation. The system selects chromosomes having the top l largest fitness values from the l chromosomes in the current population together with the l chromosomes in the mating pool to form the population of the next generation. If the number of selected chromosomes from the mating pool is equal to zero, then let $h = h - 1$. Otherwise, go to Step 6. If $h = 0$, then go to Step 7. Otherwise, go to Step 6.

Step 6: If the number of evolutions meets a predefined maximum number of evolutions, then let the chromosome, which has the largest fitness value be the optimal chromosome and go to Step 8. Otherwise, go to Step 2.

Step 7: Reinitialize the population using the cataclysmic mutation method [8]. The system puts the best chromosome having the largest fitness value in the current population into the population of the next generation and mutates the remaining l - 1 chromosomes of the current population to form the l - 1 chromosomes in the population of the next generation. For each gene of a mutated chromosome, the system randomly generates a real value between 0 and 1. If the generated real value is smaller than 0.5, then the system replaces the value of the gene with a randomly generated real value between 0 and 1. Let $h = \left\lceil \frac{m}{4} \right\rceil$, where m denotes the number of genes in a chromosome, and go to Step 2.

Step 8: Decode the chromosome having the largest fitness value into the weights W_{X_1}, W_{X_2}, …, and W_{X_m} to be used in the proposed weighted fuzzy interpolative reasoning method.

V. Experimental Results

In this section, we apply the proposed weights-learning algorithm to automatically learn the optimal weights of the antecedent variables of the fuzzy rules for the weighted fuzzy interpolative reasoning method to deal with the truck backer-upper control problem [15].

The goal of the truck backer-upper control problem [15] is to back up a truck to a loading dock as precisely as possible, where the behavior of the truck can be described by three state variables $x \in [0, 100]$, $y \in [0, 200]$ and $\phi \in [-90, 270]$, x denotes the horizontal axis, y denotes the vertical axis and ϕ denotes the azimuth angle. The truck starts from an initial state and should back up to the loading dock with the target state (50, 200, 90), i.e., $x = 50$, $y = 200$, and $\phi = 90$. In order to control the truck, the steering angle $\theta \in [-30, 30]$ is provided for each move of the truck. In general, it is assumed that the distance between the truck and the loading dock is quite large, and the state variable y can be ignored, so that the truck backer-upper control problem can be simplified into $\theta = f(x, \phi)$ [11]. In [11], Huang and Shen used a more compact fuzzy rule base of the six fuzzy rules shown in Figure 4 for truck backer-upper control. In this paper, we adopt the fuzzy rule base of the six fuzzy rules shown in Figure 4 for truck backer-upper control, where each row shown in Figure 4 denotes a fuzzy rule, shown as follows:

If x is A and ϕ is B **Then** θ is C,

where x and ϕ are the antecedent variables denoting the horizontal axis and the azimuth angle, respectively, θ is the consequence variable denoting the steering angle, and A, B and C are the possible fuzzy sets of x, ϕ and θ, respectively.

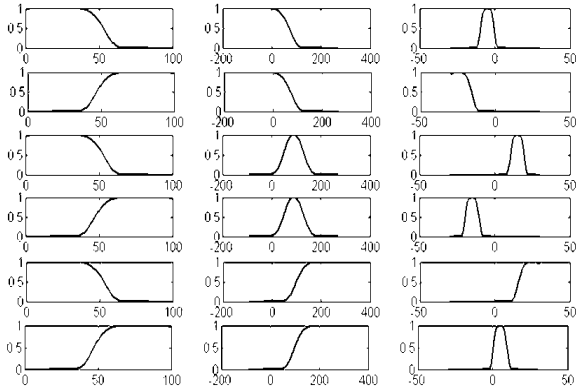

Figure 4. Membership functions of the six fuzzy rules [11].

Based on the weighted multiple fuzzy rules interpolation scheme, assume that each fuzzy rule of the six fuzzy rules for truck backer-upper control is represented as follows:

If x is A (w_x) and ϕ is B (w_ϕ) **Then** θ is C,

where x and ϕ are the antecedent variables denoting the horizontal axis and the azimuth angle, respectively, θ is the consequence variable denoting the steering angle, A, B and C are the possible fuzzy sets of x, ϕ and θ, respectively, and w_x and w_ϕ denote the weights of the antecedent variables x and ϕ, respectively. Let each chromosome have two genes g_1 and g_2 which denote the weights w_x and w_ϕ of the antecedent variables x and ϕ, respectively, where $0 \le g_1 \le 1$ and $0 \le g_2 \le 1$. Based on the fuzzy rule base shown in Figure 4 and the 64 initial states shown in Table I, we apply the proposed weights-learning algorithm for truck backer-upper control shown in Figure 5 to learn the optimal weights of w_x and w_ϕ for the proposed weighted fuzzy interpolative reasoning method, where the population size is 30, the crossover rate is 0.95 and the number of evolutions is 100. In this paper, we use the following fitness function to calculate the fitness value *Fitness* of each chromosome for truck backer-upper control:

$$Fitness = \left(\frac{1}{64} \sum_{i=1}^{64} \frac{|x_i^f - 50| + |\phi_i^f - 90|}{2} \right)^{-1}, \tag{16}$$

where $1 \le i \le 64$.

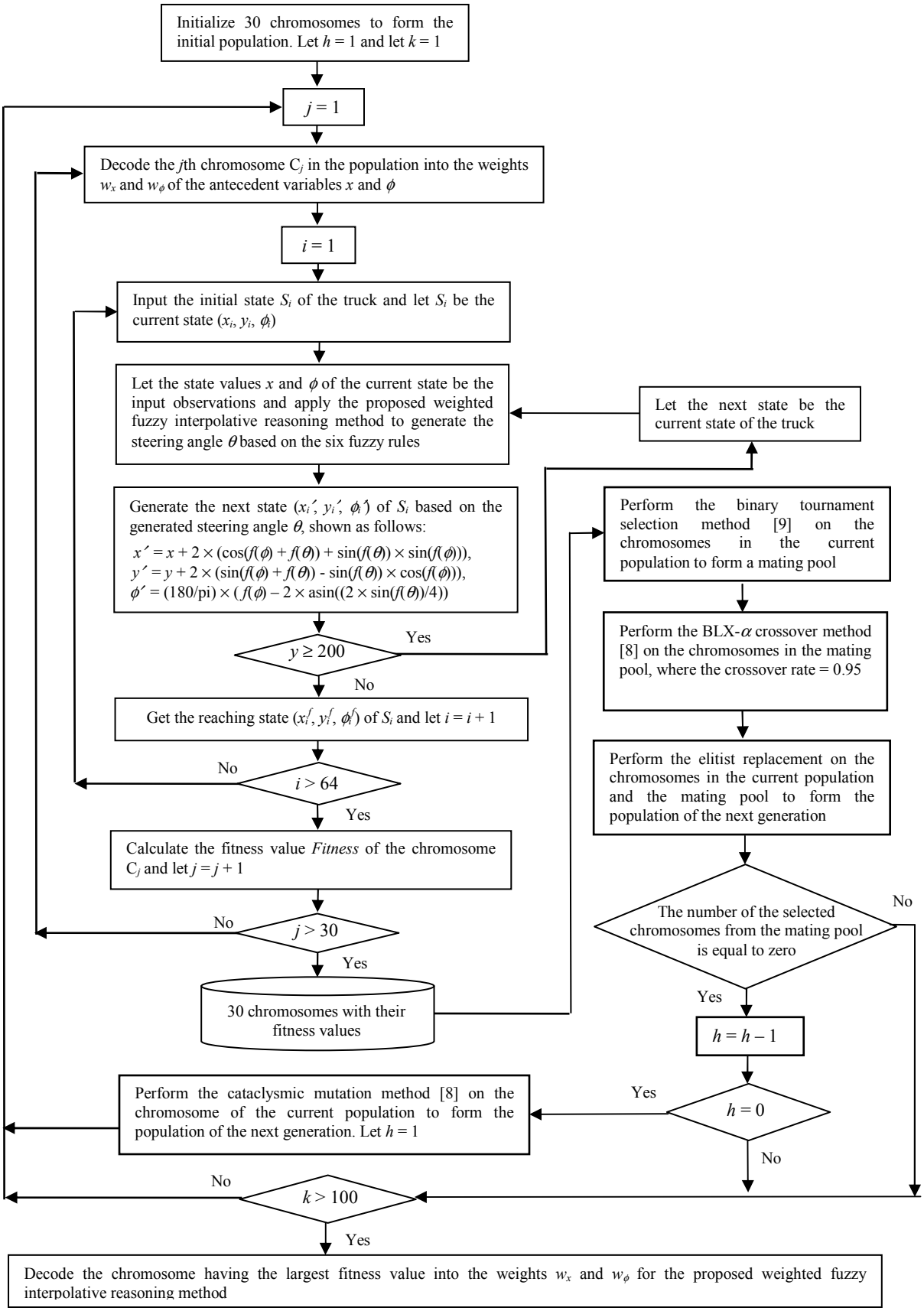

Figure 5. The flowchart of the proposed weights-learning algorithm for truck backer-upper control.

TABLE I
64 INITIAL STATES WITH RESPECT TO THE TARGET STATE (50, 200, 90)

Initial States S_i	(x_i^s, y_i^s, ϕ_i^s)	Initial States S_i	(x_i^s, y_i^s, ϕ_i^s)	Initial States S_i	(x_i^s, y_i^s, ϕ_i^s)
S_1	(10, 10, 270)	S_{23}	(30, 70, 0)	S_{45}	(60, 50, 90)
S_2	(10, 20, 225)	S_{24}	(30, 80, -45)	S_{46}	(60, 60, 45)
S_3	(10, 30, 180)	S_{25}	(40, 10, 270)	S_{47}	(60, 70, 0)
S_4	(10, 40, 135)	S_{26}	(40, 20, 225)	S_{48}	(60, 80, -45)
S_5	(10, 50, 90)	S_{27}	(40, 30, 180)	S_{49}	(70, 10, 270)
S_6	(10, 60, 45)	S_{28}	(40, 40, 135)	S_{50}	(70, 20, 225)
S_7	(10, 70, 0)	S_{29}	(40, 50, 90)	S_{51}	(70, 30, 180)
S_8	(10, 80, -45)	S_{30}	(40, 60, 45)	S_{52}	(70, 40, 135)
S_9	(20, 10, 270)	S_{31}	(40, 70, 0)	S_{53}	(70, 50, 90)
S_{10}	(20, 20, 225)	S_{32}	(40, 80, -45)	S_{54}	(70, 60, 45)
S_{11}	(20, 30, 180)	S_{33}	(50, 10, 270)	S_{55}	(70, 70, 0)
S_{12}	(20, 40, 135)	S_{34}	(50, 20, 225)	S_{56}	(70, 80, -45)
S_{13}	(20, 50, 90)	S_{35}	(50, 30, 180)	S_{57}	(80, 10, 270)
S_{14}	(20, 60, 45)	S_{36}	(50, 40, 135)	S_{58}	(80, 20, 225)
S_{15}	(20, 70, 0)	S_{37}	(50, 50, 90)	S_{59}	(80, 30, 180)
S_{16}	(20, 80, -45)	S_{38}	(50, 60, 45)	S_{60}	(80, 40, 135)
S_{17}	(30, 10, 270)	S_{39}	(50, 70, 0)	S_{61}	(80, 50, 90)
S_{18}	(30, 20, 225)	S_{40}	(50, 80, -45)	S_{62}	(80, 60, 45)
S_{19}	(30, 30, 180)	S_{41}	(60, 10, 270)	S_{63}	(80, 70, 0)
S_{20}	(30, 40, 135)	S_{42}	(60, 20, 225)	S_{64}	(80, 80, -45)
S_{21}	(30, 50, 90)	S_{43}	(60, 30, 180)		
S_{22}	(30, 60, 45)	S_{44}	(60, 40, 135)		

Based on the proposed weights-learning algorithm for truck backer-upper control shown in Figure 5, we can get the optimally learned weights $w_x = 0.55$ and $w_\phi = 0.70$ with respect to the antecedent variables x and ϕ, respectively. Table II shows a comparison of the reaching states of the four trajectories for different methods with respect to the target state (50, 200, 90). From Table II, we can see that the proposed method using the optimally learned weights $w_x = 0.55$ and $w_\phi = 0.70$ gets better truck backer-upper control results than the ones using the traditional fuzzy inference system [15], the CCL method [1], the CK method [6], the CKCP method [7] and the HS method [11].

TABLE II
A COMPARISON OF REACHING STATES OF THE FOUR TRAJECTORIES FOR DIFFERENT METHODS WITH RESPECT TO THE TARGET STATE (50, 200, 90)

Initial States	(20, 20, 90)	(80, 30, 120)	(60, 40, -90)	(10, 30, 220)
9 Rules without Interpolation [15]	(53.35, 200, 89.69)	(53.45, 200, 90.52)	(53.37, 200, 90.35)	(53.57, 200, 90.58)
6 Rules without Interpolation [15]	(53.44, 200, 89.51)	(53.40, 200, 90.45)	(53.43, 200, 90.84)	(53.48, 200, 90.84)
6 Rules with the HS Method [11]	(49.68, 200, 84.65)	(49.49, 200, 84.83)	(49.84, 200, 97.97)	(49.71, 200, 97.98)
6 Rules with the CCL Method [1]	(41.42, 200, 84.61)	(56.50, 200, 89.94)	(63.44, 200, 94.34)	(44.5, 2001, 86.94)
6 rules with the CK Method [6]	(50.39, 200, 88.36)	(50.57, 200, 89.34)	(50.58, 200, 89.94)	(50.54, 200, 90.00)
6 rules with the CKCP Method [7]	(49.99, 200, 89.96)	(50.01, 200, 90.05)	(50.03, 200, 90.05)	(50.00, 200, 89.99)
6 Rules with the Proposed Method Using the Optimally Learned Weights $w_x = 0.55$ and $w_\phi = 0.70$	(49.9997, 200, 89.9997)	(50.0026, 200, 90.0081)	(50.0028, 200, 90.0064)	(49.9988, 200, 89.9974)

VI. CONCLUSION

In this paper, we have presented a weights-learning algorithm based on the CHC algorithm to automatically learn the optimal weights of the antecedent variables of the fuzzy rules for the weighted fuzzy interpolative reasoning method. We also apply the proposed method to deal with the truck backer-upper control problem. The experimental results show that the proposed method using the optimally learned weights gets better accuracy than the existing methods [1], [6], [7], [11], [15] for dealing with the truck backer-upper control problem.

ACKNOWLEDGMENT

This work was supported in part by the National Science Council, Republic of China, under Grant NSC 97-2221-E-011-107-MY3.

REFERENCES

[1] Y. C. Chang, S. M. Chen, and C. J. Liau, "Fuzzy interpolative reasoning for sparse fuzzy rule-based systems based on the areas of fuzzy sets," *IEEE Trans. Fuzzy Syst.*, vol. 16, no. 5, pp. 1285-1301, 2008.

[2] Y. C. Chang and S. M. Chen, "A new method for multiple fuzzy rules interpolation with weighted antecedent variables," in *Proc. 2008 IEEE Int. Conf. Systems, Man and Cybernetics*, Singapore, 2008, pp. 76-81.

[3] Y. C. Chang and S. M. Chen, "A new fuzzy interpolative reasoning method based on interval type-2 fuzzy sets," in *Proc. 2008 IEEE Int. Conf. Systems, Man and Cybernetics*, Singapore, 2008, pp. 82-87.

[4] S. M. Chen and Y. C. Chang, "A new weighted fuzzy rule interpolation method based on GA-based weights-learning techniques," in *Proc. 2010 International Conference on Machine Learning and Cybernetics*, Qingdao, Shandong, China, 2010, pp. 2705-2711.

[5] S. M. Chen and Y. C. Chang, "A new method for weighted fuzzy interpolative reasoning based on weights-learning techniques," in *Proc. 2010 IEEE International Conference on Fuzzy Systems*, Barcelona, Spain, 2010, pp. 339-344.

[6] S. M. Chen and Y. K. Ko, "Fuzzy interpolative reasoning for sparse fuzzy rule-based systems based on α-cuts and transformation techniques," *IEEE Trans. Fuzzy Syst.*, vol. 16, no. 6, pp. 1626-1648, 2008.

[7] S. M. Chen, Y. K. Ko, Y. C. Chang, and J. S. Pan, "Weighted fuzzy interpolative reasoning based on weighted incremental transformation and weighted ratio transformation techniques," *IEEE Trans. Fuzzy Syst.*, vol. 17, no. 6, pp. 1412-1427, 2009.

[8] L. Eshelman, "The CHC adaptive search algorithm: How to have safe search when engaging in nontraditional genetic recombination," *Foundations of Genetic Algorithms*, pp. 265–283, San Mateo, Morgan Kaufmann, 1991.

[9] D. E. Goldberg and K. Deb, "A comparison analysis of selection schemes used in genetic algorithms," *Foundations of Genetic Algorithms*, pp. 69-93, San Mateo, Morgan Kaufmann, 1991.

[10] Z. H. Huang and Q. Shen, "Fuzzy interpolative reasoning via scale and move transformations," *IEEE Trans. Fuzzy Syst.*, vol. 14, no. 2, pp. 340-359, 2006.

[11] Z. H. Huang and Q. Shen, "Fuzzy interpolation and extrapolation : A practical approach," *IEEE Trans. Fuzzy Syst.*, vol. 16, no. 1, pp. 13-28, 2008.

[12] J. H. Holland, *Adaptation in Natural and Artificial Systems*, Cambridge. MA: MIT Press, 1975.

[13] L. T. Koczy and K. Hirota, "Approximate reasoning by linear rule interpolation and approximation," *Int. J. Approx. Reasoning*, vol. 9, no. 3, pp. 197-225, 1993.

[14] Y. M. Li, D. M. Huang, E. C. C. Tsang, and L. N. Zhang, "Weighted fuzzy interpolative reasoning method," in *Proc. 2005 IEEE Int. Conf. Machine Learning and Cybern.*, Guangzhou, China, 2005, pp. 18-21.

[15] A. Lotfi, "Fuzzy inference system toolbox for matlab (FISMAT)," 2000 [Online]. Available: http://www.lotfi.net/research/fismat/index.html.

[16] S. G. Nash and A. Sofer, *Linear and Nonlinear Programming*. NY: McGraw Hill, 1996.

[17] Y. Yam, M. L. Wong, and P. Baranyi, "Interpolation with function space representation of membership functions," *IEEE Trans. Fuzzy Syst.*, vol. 14, no. 3, pp. 398-411, 2006.

[18] L. Yang and Q. Shen, "Towards adaptive interpolative reasoning," in *Proc. 2009 IEEE International Conference on Fuzzy Systems*, Korea, 2009, pp. 542-549.

2011 IEEE International Conference on Fuzzy Systems
June 27-30, 2011, Taipei, Taiwan

On the Type-2 Fuzzy Thresholding Protocol For Event-Driven Wireless Sensor Networks

Chung-Ming Own
Department of Computer and Communication Engineering
St. John's University
Tamsui Taipei, Taiwan 62107, R.O.C
Email:cmown@mail.sju.edu.tw

***Abstract*—Network lifetime is one of the most vital issues in wireless sensor network and is fundamental to any design and development effort. Extending the life time requires energy efficiency in every aspect. Besides, fuzziness, a feature of imperfect information was used to measure the distances between the sensed values. Involved with type-2 fuzzy sets, an effectively thresholding method is proposed and discussed in this study. Given an adaptive threshold value, the membership function of a sensed value is implemented, and the potential improvement gained by using our method is demonstrated by the simulated results presented.**

Keywords-type-2 fuzzy sets, entropy, measufes of fuzziness, wireless sensor network

I. INTRODUCTION

Over the last half a century, computers are becoming small and cheap, the single-purpose computers with embedded sensors are practical from both economical and theoretical points; the revolution has been taking place. Wireless sensor networks (WSNs), which combine wireless network and context aware computations as the next logical step, make the technology easy enough to be implemented by non-specialists [1]. Thought a range of impending applications are envisaged in the area of WSNs, which are categorized as event driven monitoring, continuous monitoring and hybrid methods.

In event driven monitoring application, sensors derived the data packet when events are triggered. On the other hand, in continuous monitoring approach, data was generated continuously with a predefined reporting frequency. The representativeness is to aggregate data in a cluster-based architecture with low energy adaptive clustering hierarchy (LEACH) [2]. The former approach reports time critical data reactively, however, the later reports the periodic data proactively. Thus, continuous monitoring approach would send data to the sink even if there is no significant importance of the sensed values; the result causes the wastage of resources. To resolve these problems, a hybrid protocol has been proposed by adapting the periodic threshold-sensitive time.

The main goals of this study are to reduce the power consumption of sensor nodes and to improve data quality received by the sink node in event driven monitoring application. However, the author assumes that different nodes detect different signal strength of the event, that is, the fault tolerances are distinct. Some sensor nodes may send packets to sink node when no event occurs due to the noise in the environment, and some sensor nodes may not send packets when an event occurs. A new thresholding technique will be introduced in this study.

Fuzziness, a feature of imperfect information, results from the lack of crisp distinction between the elements belonging and not belonging to a set. In 1969, Zadeh introduced the fuzziness/fuzzy-entropy for the first time [3], and in 1972 DE Luca and Termini introduced the axiom construction of entropy of fuzzy sets and referred to Shannon's probability entropy [4]. Due to intrinsic similarity to the equations in the Shannon entropy, fuzziness and entropy are significance of equality. It's very different from the classical entropy measure which measures probabilistic information. The index of fuzziness represents the average amount of fuzziness by measuring the distance between the sensed values. Accordingly, in this paper, based on the concept of type-2 fuzzy set, an effectively thresholding method is proposed. Given an adaptive threshold value, the membership function of a sensed value is defined by the absolute difference between the sensed value and average value. The larger the absolute difference is, the smaller the membership value becomes. In addition, the optimal threshold can then be effectively determined by minimizing the measure of fuzziness of nodes.

II. RELATED WORK

A. Event-Driven WSNs

Because the power consumption and data quality are usually the most important issues in WSNs, many research efforts have been proposed to find the best tradeoff between these two issues. Besides, in the event-driven WSNs, no event occurs at most of the time. Therefore, how to reduce the power consumption in the idle time is the another important aspect of energy saving. The authors in [5] proposed an energy efficient S-MAC protocol to arrange sensor nodes falling into sleep periodically. In [6], the authors propose an efficient sleep scheduling to exploit the timing semantics of WSNs. The proposed algorithm is light-weight because of no TDMA schedules or communication backbones needed, and the simulation results show the robust in the dynamic WSNs. In [7],

978-1-4244-7316-8/11/$26.00 ©2011 IEEE

a distributed, cross layer scheduling scheme was proposed to communicate with its parent for transmission. The authors design an efficient schedule for the query processing with the following processing cycle, sampling, computing, communicating, and falling sleep. The experimental results show that the algorithm achieves the great power saving goal on the sensor nodes. In [8], the authors proposed an energy efficient protocol, multiple thresholds, and dynamic sampling/hop frequency to save energy when there is no event and wakes up the corresponding sensor nodes quickly when an event occurs.

B. Entropy and Measures of Fuzziness

The fuzziness of a fuzzy set, or entropy, tries to answer the following question: how fuzzy is a fuzzy set? Thus, De Luca and Termini first axiomatically proposed non-probabilistic entropy, they assume that E is a set-to-point mapping $E: F(2^x) \rightarrow [0,1]$, thus E is a fuzzy set defined on fuzzy universal sets [4]. Besides, if E is also satisfies the four DE Luca and Termini axioms, it is an entropy measure,

1. $E(A) = 0$ if $A \in 2^x$ $(A\ non-fuzzy)$,
2. $E(A) = 1$ if $\mu_A(x_i) = 0.5$ $for\ all\ i$,
3. $E(A) \leq E(B)$ if A is $less\ fuzzy\ than\ B, i.e.,$ if
   $\mu_A(x) \leq \mu_B(x)$ $when\ \mu_B(x) \leq 0.5$ and
   $\mu_A(x) \geq \mu_B(x)$ $when\ \mu_B(x) \geq 0.5$,
4. $E(A) = E(A^C)$.

Accordingly, there are several approaches of measuring fuzziness have been proposed, the most famous approaches are modified by Shannon's function and Yager's measuring functions [9][10]. According to the Shannon's function, De Luca and Termini defined the entropy of a fuzzy set X as

$$E(A) = \frac{1}{n\ln 2}\sum_i S\big(\mu_A(x_i)\big), \quad i = 1,2,\dots,n$$

With the Shannon's function

$$S(\mu_A(x_i)) = -\mu_A(x_i)\ln[\mu_A(x_i)] - [1-\mu_A(x_i)]\ln[1-\mu_A(x_i)].$$

Using the histogram information, the above equation can be revised as [11]

$$E(A) = \frac{1}{MN\ln 2}\sum_g S\big(\mu_A(g)\big)h(g), \quad g = 1,2,\dots,L,$$

where $h(g)$ denotes the number of occurrences at the data input level of g. On the other hand, Yager defines the major distinction between the fuzzy set and the traditional crisp set is on the discontent of the law of the excluded middle [9]. He argued that the measure of fuzziness should be dependent on the relationship between the fuzzy set A and its complement $\bar{A}$. Thus, he defined the distance between them as

$$D(A,\bar{A}) = [\sum_i |\mu_A(x_i) - \mu_{\bar{A}}(x_i)|^p]^{\frac{1}{p}}, \quad p = 1,2,\dots,$$

where $\mu_{\bar{A}}(x_i) = 1 - \mu_A(x_i)$. The measure of fuzziness of X is denoted as

$$\eta_p(A) = 1 - \frac{D(A,\bar{A})}{|A|^{1/p}}.$$

Accordingly, to compute $D(X,\bar{X})$ can be simplified by adding the histogram information as

$$D(A,\bar{A}) = [\sum_g |\mu_A(g) - \mu_{\bar{A}}(g)|^p]^{\frac{1}{p}} h(g)$$
$$g = 1,2,\dots,L.$$

Note that, for p=1, D(.) is called the Hamming metric, and for p=2, D(.) is called the Euclidean metric.

C. Type-2 Fuzzy Sets

Type-2 fuzzy sets are designed by making membership function in three dimensions where each element in type-2 fuzzy sets has membership value in range [0, 1]. The third dimension is an extension and adds degrees of freedom to get more information in represented fuzzy sets. Type-2 fuzzy sets are very useful when there is a difficulty in deciding appropriate membership function with ambiguity. Membership value in type-2 fuzzy sets can be any value in range [0, 1]. The based membership is called by primary membership, besides, related to the primary membership, there is a secondary membership by assigning possibility in range [0, 1] to the primary membership. To clarify statement, the fuzzy set 'tall' is represented as

$$tall = \frac{0.95}{\text{Michael}} + \frac{0.4}{\text{Danny}} + \frac{0.6}{\text{Robert}}.$$

Conversely, the interpretation by type-2 fuzzy set could be

$$tall = \frac{High}{\text{Michael}} + \frac{Low}{\text{Danny}} + \frac{Medium}{\text{Robert}},$$

where *High*, *Low* and *Medium* are themselves fuzzy sets. The previous set is measured by one condition for one element, on the contrary, the latter defined set is measured by several conditions for one element. Type-2 fuzzy sets are useful when the exact membership for a usual fuzzy set cannot be easily determined, and hence are advantageous for incorporating uncertainties.

D. Measure of Ultrafuzziness

Accordingly to [11], to measure the threshold value as type-2 fuzzy sets is what we called "how ultrafuzzy is a fuzzy set". If membership value degree in a fuzzy set can be decided clearly and without ambiguity, then ultrafuzzy value is zero. Whenever the membership value can only state as value interval, then its ultrafuzziness total value will be increased.

Measure of ultrafuzziness $\tilde{\gamma}$ with L level $g \in [0, L-1]$, the histogram $h(g)$ and the membership function $\mu(g)$ can be written as follows [11],

$$\tilde{\gamma} = \frac{1}{N}\sum_{g=0}^{L-1} h(g)\, x[\mu_U(g) - \mu_L(g)]$$

where

$\mu_U(g) = [\mu(g)]^{1/\alpha}$,

$\mu_L(g) = [\mu(g)]^{\alpha}, \alpha \in [1,2]$.

Note that $\mu_U(g)$ and $\mu_L(g)$ are the upper/lower bound of fuzzy set respectively.

III. Proposed Algorithm

In this study, the author employs the network environment as the static event-driven WSN, and the approach is based on the following observations;

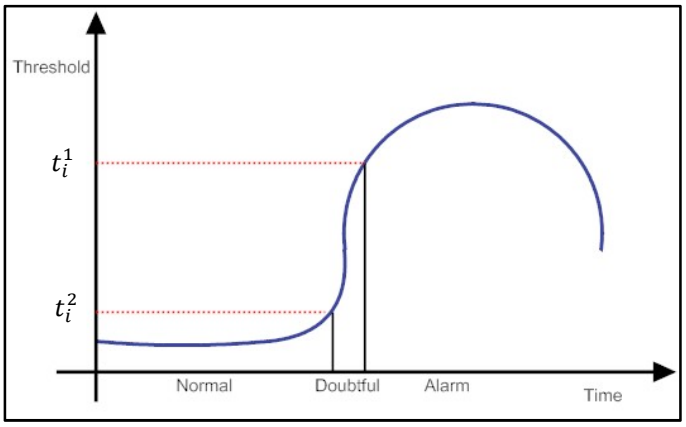

Figure 1. Multi-level thresholding

1. The sensor nodes have different quality with different signal-to-noise ratio and different memory capability, and all have limited processing and basic decision ability.
2. In some case, when an event occurs, several sensor nodes would be activated and deliver packets for response simultaneously. Thus, the network will leads to data implosion and redundancy. For the severely limited bandwidth, these nodes may have contention on the packet transmissions and ACKs overload.
3. Because of distinct signal-to-noise ratios, a sensor node with low signal-to-noise ratio may generate more irregularly data than those with high ratio when there is no event occurred.
4. With the same detected signal strength, the more sensor nodes can receive packets from sensor nodes with higher priority than ones with lower priority. In the meantime, most of retransmitted packets are redundant and useless.
5. The sink node has more resources, computation ability and memory capability.
6. For the purpose to reduce packet transmissions, each sensor node i have multiple threshold t_i^j to determine the packet need to be transmitted or not. That means that if there is no event occurred or only with noise interference, the packet don't need to be transmitted or are only transmitted to its neighbors within a small number of hops.
7. Based on the "positive feed-back" algorithm, when an event occurs, several nodes sense the varying of the environment, the transmission hops and frequency of these nodes are also increase. Then the frequency of received packets for nodes near these sensor nodes increases, and these neighbor nodes also increase the sensing frequency too.

In this study, because of the distinct noise tolerance for each node, the author attempts to develop multi-level thresholds in the histogram of a sensor node based on the fuzziness measure, please review Figure 1. Our proposed method performs an iterative operation for each node, and we assume the target histogram contains K different non-empty data levels. The method is listed as follows;

1. Choose type of membership function to determine membership value $\mu(g)$ and initialize value of α. In this paper, three membership functions derived as the normal, doubtful and alarm states respectively.
2. Compute the history data histogram.
3. Determine initial position location of membership functions.
4. Shift membership function along data range to calculate fuzziness total in each position as shown in Figure 2.
5. Compute upper membership value $\mu_U(g)$ and lower membership value $\mu_L(g)$ in each position.
6. Calculate ultrafuzziness value for each state.
7. Compute ultrafuzziness total value with the following equation:

$$\tilde{\Upsilon}_{total} = \tilde{\Upsilon}_{normal} \times \tilde{\Upsilon}_{doubtful} \times \tilde{\Upsilon}_{alarm}.$$

8. Find the optimum threshold positions with maximum ultrafuzziness total value.
9. Threshold data using this optimum value.

Using the above method, significant differences among different states are achieved. Therefore, optimal thresholding among them can be derived.

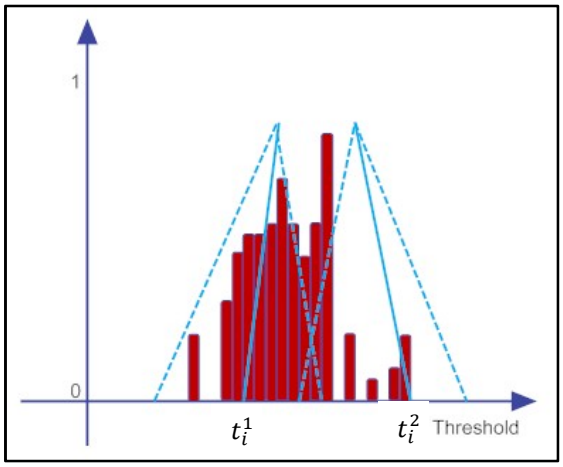

Figure 2. Shifting two membership functions

IV. RESUTL AND DISCUSSION

To evaluate the performance of our method, the author simulates the transmission by TinyOS simulator TOSSIM [12]. Here real data is used for the evaluation of the techniques (Intel lab data for both sensed and network connectivity data [13]). The comparison method is the general transmission protocol to flood sensing data when nodes sense the even occurred. Figure 3 shows the average energy consumptions of our proposed protocol and general protocol over the time (1200-4000 seconds) with 20 nodes deployments. The result shows our proposed method gains the better performance than the general case. Intuitively in this case the energy efficiency is achieved on the expense of loosing data accuracy.

V. CONCLUSIONS

Network lifetime is one of the most vital issues in WSNs and is fundamental to any design and development effort. Extending the lifetime of WSNs requires energy efficiency in every aspect of the utilized techniques such as energy efficient medium access control, energy efficient routing, aggregation and son on. This study presents a simple transmission technique that maintains the data accuracy while utilizing spatiotemporal correlation of data. The presented technique is to reduce the power consumption of sensor nodes and to improve data quality based on the type-2 fuzzy thresholding protocol. The potential improvement gained by using our method is demonstrated by the simulated results presented.

ACKNOWLEDGMENT

The author would like to thank the National Science Council of the Republic of China, Taiwan for partially supporting this research under Contract No. NSC *99-2218-E-129 -001*, and NSC 99-2221-E-129 -014.

REFERENCES

[1] K. Lorincz and M. Welsh, "Motetrack: a robust, decentralized approach to RF-based location tracking," International Workshop on Location-and Context-Awareness, 2005.

[2] R. Vidhyapriya and P. T. Vanathi, "Eneryg aware routing for wireless snsor networks," Proceedings of International Confernece on Signal Processing, Communications and Networking, pp. 545-550, 2007.

[3] L.A. Zadeh, Fuzzy Sets and Systems, in Proc. Symp. On Systems Theory, New Yourk, 1965.

[4] A. De Luca, S. Termini, "A definition of a non-probabilistic entropy in the setting of fuzzy sets theory," Inform. And Control 20, pp. 301-312, 1972.

[5] W. Ye, J. Heidemann, and D. Estrin, "An energy-efficient mac protocol for wireless sensor networks," Proceedings of IEEE INFOCOM, 2002.

[6] O. Chipara, C. Lu, and G.-C. Roman, "Efficient power management based on application timing semantics for wireless sensors," Proceedings of the 25th IEEE International Conference on Distributed Computing Systems, pp. 361-370, 2005.

[7] H. Wu, Q. Luo, and W. Xue, "Distributed cross-layer scheduling for in-network sensor query processing," Proceedings of the Fourth Annual IEEE International Conferecne on Pervasive Computing and Communications, pp. 180-189, 2006.

[8] Y. Sun, H. Liu, M.S. Kim, "Energy-efficient routing protocol in event-driven wireless sensor networks," International Conference on Communications Workshops of IEEE, pp. 1-5, 2010.

[9] L.A. Zadeh, "Fuzzy sets and their applications to cognitive and decision processes," Academic Press, London, pp. 1-39, 1975.

[10] R. R. Yager, "On the measure of fuzziness and negation," Part I: Membership in the unit interval, Int. J. gen. Syst. 5, pp. 221-229, 1979.

[11] H.R. Tizhoosh, "Image thresholding using type II fuzzy sets," Pattern Recognition, pp. 2363-2371, 2005.

[12] P. Levis, N. Lee, M. Welsh, and D. Culler, "TOSSIM: accurate and scalable simulation of entire tinyos application," 1st ACM Conference on Embedded Networked Sensor Systems, 2003.

[13] http://db.csail.mit.edu./labdata/labdata.html.

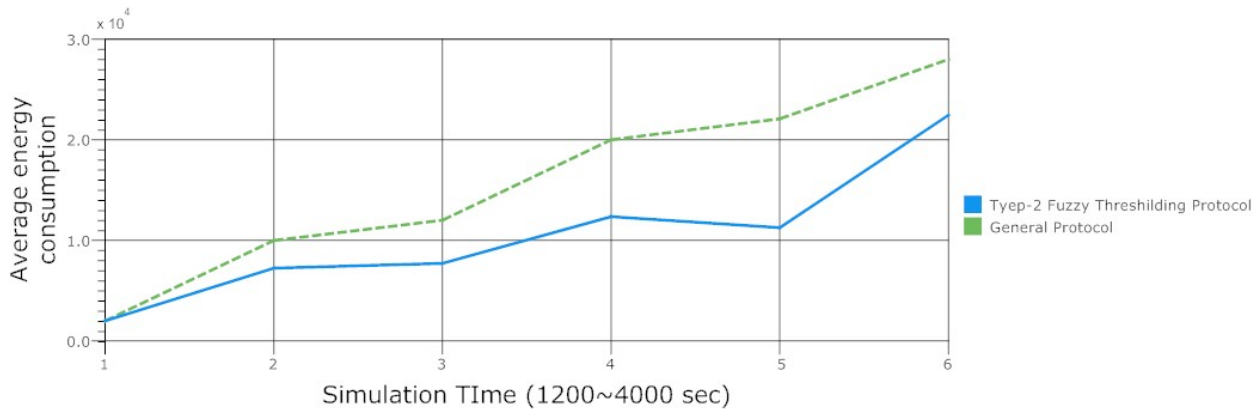

Figure 3. Performance comparison

2011 IEEE International Conference on Fuzzy Systems
June 27-30, 2011, Taipei, Taiwan

A Theoretical Approach to Liu's Generalized Lambda-Fuzzy Measure

Hsiang-Chuan Liu
Department of Bioinformatics and Medical Informatics
Asia University,
Graduate Institute of Acupuncture Science
China Medical University
Taichung, Taiwan, ROC
lhc@asia.edu.tw

Tung-Sheng Liu
Graduate School of Criminology
National Taipei University
Department of criminal justice
Military Police School
Taipei, Taiwan, ROC
tommy0366@yahoo.com.tw

***Abstract*—λ-measure, P-measure, additive measure and B-measure are four well known fuzzy measure, all of them are univalent fuzzy measure with only one formulaic fuzzy measure solution. In this paper, first of all, it is proved that both λ-measure and additive measure are larger than P-measure and less than B-measure, in other words, both λ-measure and additive measure are never equal to the smallest fuzzy measure, P-measure and the largest fuzzy measure, B-measure. Furthermore, a novel multivalent fuzzy measure with infinitely many fuzzy measure solutions based on λ-measure, called a generalized λ-measure, is proposed. It is proved that the measure function of this new measure is continuous and increasing on λ, each different λ value corresponding different fuzzy measure, from the smallest fuzzy measure, P-measure to the largest fuzzy measure, B-measure, and containing λ-measure itself, in other words, all of above four univalent fuzzy measures are special cases of this new fuzzy measure. Moreover, this new generalized λ-measure is also satisfying the monotone condition rather than the old generalized λ-measure proposed by L.-Z. Yang, M.-H. Ha, X.-J. Wang and Z.-R. Zhang. However, the old one is just the λ-measure without the monotone condition. It is a generalized measure but no more a fuzzy measure. Hence, this new and true generalized fuzzy measure is called Liu's generalized λ-measure. Some properties about this new measure are also discussed.**

Keywords- λ-measure; P-measure; B-measure; L-measure; Liu's generalized λ-measure

I. INTRODUCTION

When interactions among independent variables exist in forecasting problems, the performances of the multiple linear regression models and ridge regression models [1] are not good enough. For improving this situation, G. Choquet proposed his fuzzy integral, called Choquet integral, in 1953 [2], M. Sugeno rediscovered the concepts of fuzzy integral and fuzzy measure and also proposed his λ-measure in 1974 [3], L. A. Zadeh's simple sub-additive fuzzy measure with closed form, P-measure, was proposed in 1978 [4], the author, H.-C. Liu, proved that the P-measure is the smallest fuzzy measure and proposed the largest fuzzy measure, B-measure in 2009 [6], all of above measures and traditional additive measure [5] are univalent fuzzy measure with only one formulaic fuzzy measure solution, the author, H.-C. Liu, proposed some multivalent fuzzy measures with infinitely many fuzzy measure solutions, called L-measure, completed L-measure, maximized L-measure, etc, [6-9]. It is showed that the interactions problem can be improved by using Choquet integral regression models with λ-measure and above multivalent fuzzy measures [6-9].

However, although all of L-measure, completed L-measure and maximized L-measure are multivalent fuzzy measures with infinitely many fuzzy measure solutions, but they do not contain λ-measure, in other words, λ-measure is not a special case of above multivalent fuzzy measures and all of the above multivalent fuzzy measures are not a generalized λ-measure.

L.-Z. Yang, M.-H. Ha, X.-J. Wang, and Z.-R. Zhang proposed a generalized λ-measure by deleting the monotone condition of λ-measure in 2008 [10], and then λ-measure is a a special case of their generalized λ-measure, but if the monotone condition is not satisfied, then this generalized λ-measure is not a fuzzy measure, in other words, this generalized λ-measure is a generalized measure of λ-measure, but not a generalized fuzzy measure of λ-measure, since a fuzzy measure must be a monotone measure.

In this paper, a novel multivalent fuzzy measure satisfying the monotone condition with infinitely many fuzzy measure solutions based on λ-measure also containing λ-measure itself and rather than the generalized λ-measure proposed by L.-Z. Yang, M.-H. Ha, X.-J. Wang, and Z.-R. Zhang, is considered. t. Some relative properties about this new generalized λ-measure are also considered.

II. FUZZY MEASURES

A. Fuzzy measures

Definition 1. [3,5] A measure μ on a finite set X is a fuzzy measure, if its measure function $g_\mu : 2^X \to [0,\infty)$ satisfying

(i) $g_\mu(\phi) = 0$ (vanishing at the empty set) (1)

(ii) $A \subseteq B \Rightarrow g_\mu(A) \le g_\mu(B)$ (monotonicity) (2)

B. Fuzzy support function, support

Definition 2. [6] A fuzzy support function of a fuzzy measure μ on a finite set X is a function $s : X \to [0,\infty)$ satisfying:

$$s(x)=\mu(\{x\}),\ x\in X \tag{3}$$

$s(x)$ is called the support value of singleton x.

C. Additive measure

Definition 3. [5] For a given fuzzy support function, $s(x)$ on a finite set X, a measure σ on X is an additive measure, if its measure function $g_\sigma : 2^X \to [0,\infty)$ satisfying :

(i) $g_\sigma(\phi)=0$ (vanishing at the empty set) (4)

(ii) $$\forall A\in 2^X \Rightarrow g_\sigma(A)=\sum_{x\in A}s(x)=\sum_{x\in A}g_\sigma(\{x\}) \tag{5}$$

Theorem 1. [5] An additive measure on a finite set X is a fuzzy measure on X satisfying

(i) $$A,B\in 2^X,\ A\cap B=\phi \Rightarrow g_\sigma(A\cup B)=g_\sigma(A)+g_\sigma(B) \tag{6}$$

(ii) $$A,B\in 2^X,\ A\subseteq B \Rightarrow g_\sigma(A)\le g_\sigma(B) \tag{7}$$

Proof:

(i) $A,B\in 2^X,\ A\cap B=\phi$

$$\Rightarrow g_\sigma(A\cup B)=\sum_{x\in A\cup B}g_\sigma(\{x\})=\sum_{x\in A}g_\sigma(\{x\})+\sum_{x\in B}g_\sigma(\{x\}) =g_\sigma(A)+g_\sigma(B) \tag{8}$$

(ii) $$A,B\in 2^X,\ A\subseteq B \Rightarrow g_\sigma(A)=\sum_{x\in A}g_\sigma(\{x\})\le\sum_{x\in B}g_\sigma(\{x\})=g_\sigma(B) \tag{9}$$

D. λ-measure [3]

Definition 4. [3] For a given fuzzy support function, $s(x)$, on a finite set X, a measure on X is a λ-measure, if its measure function $g_\lambda : 2^X \to [0,\infty)$ satisfying

(i) $g_\lambda(\phi)=0$ (Vanishing at the empty set) (10)

(ii) $$\lambda\in\left[-\frac{1}{\max_{A\subset X}\{g_\lambda(A)\}},\infty\right) \tag{11}$$

(iii) $A,B\in 2^X,\ A\cap B=\phi,\ A\cup B\ne X$

$$\Rightarrow g_\lambda(A\cup B)=g_\lambda(A)+g_\lambda(B)+\lambda g_\lambda(A)g_\lambda(B) \tag{12}$$

(iv) $$\forall A\subset X\Rightarrow g_\lambda(A)=\begin{cases}\frac{1}{\lambda}\left(-1+\prod_{x\in A}[1+\lambda s(x)]\right) & \lambda\ne 0\\ \sum_{x\in A}s(x) & \lambda=0\end{cases} \tag{13}$$

Note that

(i) Eq. (12) and Eq. (13) are called $\sigma-\lambda-$ rule of λ-measure.

(ii) Eq. (11) is the monotone condition of λ-measure.

E. P-measure

Definition 5. [4] For a given fuzzy support function, $s(x)$, on a finite set X, a measure is called P-measure, g_P, if its measure function $g_P : 2^X \to [0,\infty)$ satisfying

(i) $g_P(\phi)=0$ (vanishing at the empty set)

(ii) $$\forall A\in 2^X \Rightarrow g_P(A)=\max_{x\in A}\{s(x)\}=\max_{x\in A}g_P(\{x\}) \tag{14}$$

III. NORMALIZED FUZZY MEASURES

A. Normalized fuzzy measures [2,3]

Definition 6. [5,6] A fuzzy measure μ on a finite set X is a normalized fuzzy measure, if its measure function $g_\mu : 2^X \to [0,1]$ satisfying the following axioms:

(i) $g_\mu(\phi)=0,\ g_\mu(X)=1$ (normalized conditions) (15)

(ii) $A\subseteq B\Rightarrow g_\mu(A)\le g_\mu(B)$ (monotonicity) (16)

B. Fuzzy density function

Definition 7. A fuzzy density function of a normalized fuzzy measure μ on a finite set X is a function $d : X\to[0,1]$ satisfying:

$$s(x)=g_\mu(\{x\}),\ x\in X \tag{17}$$

$s(x)$ is called the density of singleton x.

C. Normalized additive measure

Definition 8. [5] For a given fuzzy density function, $d(x)$ on a finite set X, a measure σ on X is an normalized additive measure, if its measure function $g_\sigma : 2^X \to [0,1]$ satisfying :

(i) $g_\sigma(\phi)=0,\ g_\sigma(X)=1$ (Normalized conditions) (18)

(ii) $$\forall A\in 2^X \Rightarrow g_\sigma(A)=\sum_{x\in X}s(x)=\sum_{x\in X}g_\sigma(\{x\}) \tag{19}$$

Theorem 2. [5] An normalized additive measure on a finite set X is a fuzzy measure on X satisfying

(i) $$A,B\in 2^X,\ A\cap B=\phi \Rightarrow g_\sigma(A\cup B)=g_\sigma(A)+g_\sigma(B) \tag{20}$$

(ii) $$A,B\in 2^X,\ A\subseteq B \Rightarrow g_\sigma(A)\le g_\sigma(B) \tag{21}$$

(iii) $$\sum_{x\in X}g_\sigma(\{x\})=1 \tag{22}$$

D. Normalized λ-measure

Definition 9. [3] For a given fuzzy density function, $d(x)$, on a finite set x, a normalized fuzzy measure is called a normalized **λ**-measure, if its measure function $g_\lambda : 2^X \to [0,1]$ satisfying the following axioms:

(i) $g_\lambda(\phi)=0,\ g_\lambda(X)=1$ (normalized conditions) (23)

(ii) $$\lambda\in[-1,\infty) \tag{24}$$

(iii) $A,B\in 2^X,\ A\cap B=\phi,\ A\cup B\ne X$

$$\Rightarrow g_\lambda(A\cup B)=g_\lambda(A)+g_\lambda(B)+\lambda g_\lambda(A)g_\lambda(B) \tag{25}$$

(iv) $$\forall A\subset X\Rightarrow g_\lambda(A)=\begin{cases}\frac{1}{\lambda}\left(-1+\prod_{x\in A}[1+\lambda d(x)]\right) & \lambda\ne 0\\ \sum_{x\in A}d(x) & \lambda=0\end{cases} \tag{26}$$

(v) $$\prod_{x\in X}[1+\lambda d(x)]=1+\lambda>0,\ d(x)=g_\lambda(\{x\}) \tag{27}$$

Note that Eq. (27) is the upper bounded condition of Definition 9.

Theorem 3. [3] If $d(x)$ is the fuzzy density function of a normalized λ-measure on a finite set X, then normalized λ-measure is a normalized fuzzy measure on X with exact one solution of the value of λ satisfying

(i) $$\sum_{x\in X} d(x) > 1 \Rightarrow -1 \le \lambda < 0, \quad (28)$$

(ii) $$\sum_{x\in X} d(x) = 1 \Rightarrow \lambda = 0 \quad (29)$$

(iii) $$\sum_{x\in X} d(x) < 1 \Rightarrow \lambda > 0, \quad (30)$$

Definition 10. [3] Let μ be a normalized fuzzy measure, $g_\mu : 2^X \to [0,1]$ be its measure function

(i) If the formula (31) is satisfied, then μ is called a normalized sub-additive measure,

$$\forall A, B \in 2^X,\ A \cap B = \phi \Rightarrow g_\mu(A \cup B) < g_\mu(A) + g_\mu(B) \quad (31)$$

(ii) If the formula (32) is satisfied, then μ is called a normalized additive measure,

$$\forall A, B \in 2^X,\ A \cap B = \phi \Rightarrow g_\mu(A \cup B) = g_\mu(A) + g_\mu(B) \quad (32)$$

(iii) If the formula (33) is satisfied, then μ is called a normalized supper-additive measure,

$$\forall A, B \in 2^X,\ A \cap B = \phi \Rightarrow g_\mu(A \cup B) > g_\mu(A) + g_\mu(B) \quad (33)$$

Theorem 4. [3] Let $d(x)$ be the fuzzy density function of a normalized λ-measure on a finite set X,

(i) If $\sum_{x\in X} s(x) > 1$, then normalized λ-measure is a normalized sub-additive measure

(ii) If $\sum_{x\in X} s(x) = 1$, then normalized λ-measure is a normalized additive measure

(iii) If $\sum_{x\in X} s(x) < 1$, then normalized λ-measure is a normalized supper-additive measure

E. Normalized P-measure

Definition 11. [4] For a given fuzzy density function $d(x)$ on a finite set X, a normalized fuzzy measure is called a normalized P-measure, if its measure function $g_P : 2^X \to [0,1]$ satisfying

(i) $g_P(\phi) = 0$, $g_P(X) = 1$ (normalized conditions) (34)

(ii) $$\forall A \in 2^X \Rightarrow g_P(A) = \max_{x\in X}\{s(x)\} = \max_{x\in X}\{g_P(\{x\})\} \quad (35)$$

IV. Regular Fuzzy Measures

Definition 12. A fuzzy density function $d(x)$ of a normalized fuzzy measure μ on a finite set X is called a regular fuzzy density function, if it satisfies

$$\forall x \in X \Rightarrow d(x) = g_\mu(\{x\}) > 0 \quad (36)$$

Definition 13. Any normalized fuzzy measure is called a regular fuzzy measure, if its fuzzy density function is a regular fuzzy density function

Definition 14.

(i) A normalized additive measure is called a regular additive measure, if its fuzzy density function is a regular fuzzy density function

(ii) A normalized sub-additive measure is called a regular sub-additive measure, if its fuzzy density function is a regular fuzzy density function.

(iii) A normalized supper-additive measure is called a regular supper-additive measure, if its fuzzy density function is a regular fuzzy density function

(iv) A normalized λ-measure is called a regularλ-measure, if its fuzzy density function is a regular fuzzy density function

(v) A normalized P-measure is called a regular P-measure, if its fuzzy density function is a regular fuzzy density function.

V. Comparison between two measures

A. B-measure

Definition 15. [6] For any given fuzzy density function, $d(x)$, on a finite set, X, a normalized fuzzy measure is called a B-measure, if its measure function, $g_B : 2^X \to [0,1]$, satisfies

$$g_B(A) = \begin{cases} 0 & A = \phi \\ d(x) & A = \{x\}, x \in X \\ 1 & |A| > 1, A \subset X \end{cases} \quad (37)$$

Definition 16. A B-measure is called a regular B-measure, if its fuzzy density function is a regular fuzzy density function.

B. Definition of Comparisons of fuzzy measures

Definition 17. [6] Comparison of two fuzzy measure

For any given fuzzy density function, $d(x)$, on a finite set, X, let μ_1 and μ_2 be two normalized fuzzy measures on X,

(i) If $g_{\mu_1}(A) = g_{\mu_2}(A), \forall A \subset X,$, then we say that μ_1-measure is equal to μ_2-measure, denoted as

$$\mu_1 - measure = \mu_2 - masure. \quad (38)$$

(ii) If $g_{\mu_1}(A) < g_{\mu_2}(A), \forall A \subset X, 1 < |A| < |X|$ then we say that μ_1-measure is less than μ_2-measure, or μ_2-measure is larger than μ_1-measure, denoted as

$$\mu_1 - measure < \mu_2 - masure. \quad (39)$$

(iii) If $g_{\mu_1}(A) \le g_{\mu_2}(A), \forall A \subset X, 1 < |A| < |X|$, then we say that μ_1-measure is not larger than μ_2-measure, or μ_2-measure is not smaller than μ_1-measure, denoted as

$$\mu_1 - measure \le \mu_2 - masure . \quad (40)$$

C. Important properties for comparisons of fuzzy measures

Theorem 5. For any given fuzzy density function $d(x)$ on a finite set X, P-measure is not larger than any other fuzzy measure μ, that is

$$P - measure \le \mu - measure \quad (41)$$

Proof.

Let $\forall A \subset X$ and $1 < |A| < |X|$,

From the definition of monotonicity, we have

$$g_\mu(A) \ge g_\mu(\{x\}), \forall x \in A \quad (42)$$

And then

$$g_\mu(A) \ge \max_{x \in A}\{g_\mu(\{x\})\} \quad (43)$$

Since $g_\mu(\{x\}) = g_p(\{x\}) = d(x), \forall x \in A$ (44)

We can obtain

$$g_\mu(A) \ge \max_{x \in A}\{g_\mu(\{x\})\} = \max_{x \in A}\{g_p(\{x\})\} = g_P(A) \quad (45)$$

That is $g_P(A) \le g_\mu(A), \forall A \subset X$, the proof is completed.

Theorem 6. For any given fuzzy density function $d(x)$ on a finite set X, B-measure is not less than any other fuzzy measure μ, that is

$$\mu - measure \le B - measure \quad (46)$$

Proof.

Let $\forall A \subset X$ and $1 < |A| < |X|$,

From the definition of B-measure, we have

$$g_\mu(A) \le g_B(A) = 1, \forall x \in A \quad (47)$$

That is $g_\mu(A) \le g_B(A), \forall A \subset X$, the proof is completed

Theorem 7.

$$regular\ P - measure < regular\ \lambda - measure$$

Proof:

i) Let $\forall A \subset X$ and $1 < |A| < |X|$ (48)

Satisfy $A = B \cup C, B \ne \phi \ne C, B \cap C = \phi$ (49)

From the definition of regular fuzzy measure, we know that $d(x) > 0, \forall x \in X$ (50)

Since $B \ne \phi \ne C$, then $g_\lambda(B), g_\lambda(C), g_p(B), g_p(C) > 0$ (51)

ii) From the definition of regular λ- measure, we know that

$$\lambda > -1 \quad (52)$$

We can get $g_\lambda(C)[1 - \lambda g_\lambda(B)] > 0$ (53)

Then

$$\begin{aligned} g_\lambda(A) &= g_\lambda(B \cup C) = g_\lambda(B) + g_\lambda(C) - \lambda g_\lambda(B) g_\lambda(C) \\ &= g_\lambda(B) + g_\lambda(C)[1 - \lambda g_\lambda(B)] > g_\lambda(B), \end{aligned} \quad (54)$$

That is $g_\lambda(A) = g_\lambda(B \cup C) > g_\lambda(B)$, (55)

Similarly we have $g_\lambda(A) = g_\lambda(B \cup C) > g_\lambda(C)$, (56)

Then $g_\lambda(A) = g_\lambda(B \cup C) > \max[g_\lambda(B), g_\lambda(C)]$ (57)

In general, we can obtain

$$\begin{aligned} &g_\lambda(A) > \max_{x \in A}\{g_\lambda(\{x\})\} = \max_{x \in A}\{g_P(\{x\})\} = g_P(A) \\ &\Rightarrow g_\lambda(A) > g_P(A), \forall A \subset X, 1 < |A| < |X| \end{aligned} \quad (58)$$

Then $regular\ P - measure < regular\ \lambda - measure$.

Theorem 8.

$$regular\ \lambda - measure < B - measure$$

Proof:

(i) Suppose that $regular\ \lambda - measure < B - measure$ is not true, then there exist $A \subset X$ such that $1 < |A| < |X|$ satisfies

$$g_\lambda(A) = 1 \quad (59)$$

(ii) Since $1 < |A| < |X|$, then $A' = X - A \ne \phi$ (60)

and $A \ne \phi \ne A'$ (61)

From the definition of regular λ-measure, we know that $\lambda > -1$ and $g_\lambda(A') > 0$

then $g_\lambda(A')[1 + \lambda] > 0$ (62)

(iii) Since

$$\begin{aligned} g_\lambda(X) &= g_\lambda(A \cup A') \\ &= g_\lambda(A) + g_\lambda(A') + \lambda g_\lambda(A) g_\lambda(A') \\ &= g_\lambda(A) + g_\lambda(A')[1 + \lambda g_\lambda(A)] \\ &= 1 + g_\lambda(A')[1 + \lambda] > 1 \end{aligned} \quad (63)$$

But $g_\lambda(X) = 1$, it leads a contradiction,

hence $\lambda - measure < B - measure$.

Theorem 9.

$$regular\ P - measure < regular\ \lambda - measure < B - measure \quad (64)$$

Proof: It is trivial!

Theorem 10.

$$regular\ P - measure < regular\ additive\ measure$$

Proof:

(i) Let $\forall A \subset X$ and $1 < |A| < |X|$ (65)

Satisfy $A = B \cup C, B \ne \phi \ne C, B \cap C = \phi$ (66)

From the definition of regular fuzzy measure, we know that $d(x) > 0, \forall x \in X$ (67)

Since $B \ne \phi \ne C$, then $g_\sigma(B), g_\sigma(C) > 0$ (68)

ii) From the definition of regular additive measure, we know that

$$g_\sigma(A) = g_\sigma(B \cup C) = g_\sigma(B) + g_\sigma(C) \quad (69)$$

That is $g_\lambda(A) = g_\lambda(B \cup C) > g_\lambda(B)$, (70)

and $g_\lambda(A) = g_\lambda(B \cup C) > g_\lambda(C)$, (71)

Then $g_\lambda(A) = g_\lambda(B \cup C) > \max[g_\lambda(B), g_\lambda(C)]$ (72)

In general, we can obtain

$$g_\sigma(A) > \max_{x\in A}\{g_\sigma(\{x\})\} = \max_{x\in A}\{g_P(\{x\})\} = g_P(A)$$
$$\Rightarrow g_\sigma(A) > g_P(A), \forall A \subset X, 1 < |A| < |X| \quad (73)$$

Then *regular* $P-$*measure* < *regular additive measure* .

Theorem 11.

regular additive measure < $B-$*measure*

Proof:

(i) Suppose that *regular additive measure* < $B-$*measure* is not true,

then there exist $A \subset X$ such that $1 < |A| < |X|$ satisfies

$$g_\sigma(A) = 1 \quad (74)$$

(ii) Since $1 < |A| < |X|$, then $A' = X - A \neq \phi$ (75)

and $A \neq \phi \neq A'$ (76)

From the definition of regular additive measure, we know that $g_\sigma(A') > 0$ (77)

(iii) Since

$$g_\sigma(X) = g_\sigma(A \cup A') = g_\sigma(A) + g_\sigma(A') > g_\sigma(A) = 1 \Rightarrow g_\sigma(X) > 1 \quad (78)$$

But $g_\lambda(X) = 1$, it leads a contradiction,

Hence *regular additive measure* < $B-$*measure* .

Theorem 12.

regular $P-$*measure* < *regular additive measure* < $B-$*measure* (79)

Proof: It is trivial!.

Note that

(i) If there is no confusion, for brief, the regular fuzzy measure is also called fuzzy measure.

(ii) Both λ-measure and additive measure are larger than the smallest fuzzy measure, P-measure and less than the largest fuzzy measure, B-measure.

VI. YANG'S GENERALIZED LAMBDA MEASURE

Yang's generalized λ-measure was proposed by L.-Z. Yang, M.-H. Ha, X.-J. Wang and Z.-R. Zhang in 2008 [10], its formal definition is list as below'

Definition 18. [10] For a given fuzzy support function, $s(x)$, on a finite set X, a measure on X is a Yang's generalized λ-measure, if its measure function $g_\lambda : 2^X \to [0,\infty)$ satisfying

(i) $g_\lambda(\phi) = 0$ (Vanishing at the empty set) (80)

(ii) $$A, B \in 2^X, A \cap B = \phi, A \cup B \neq X$$
$$\Rightarrow g_\lambda(A \cup B) = g_\lambda(A) + g_\lambda(B) + \lambda g_\lambda(A) g_\lambda(B) \quad (81)$$

(iii) $$\forall A \subset X \Rightarrow g_\lambda(A) = \begin{cases} \frac{1}{\lambda}\left(-1 + \prod_{x\in A}\left[1+\lambda s(x)\right]\right) & \lambda \neq 0 \\ \sum_{x\in A} s(x) & \lambda = 0 \end{cases} \quad (82)$$

Note that

(i) Eq. (84) and Eq. (85) are called $\sigma - \lambda -$ rule of λ - measure.

(ii) To compare the definition of Yang's generalized λ-measure with the definition of λ -measure, we know that Yang's generalized λ-measure is just the λ -measure without the monotone condition $\lambda \in \left[-\frac{1}{\max_{A\subset X}\{g_\lambda(A)\}}, \infty\right)$, in other words, Yang's generalized λ-measure is a generalization of λ-measure not necessarily monotone,

(iii) Since a fuzzy measure must be a monotone measure. If a Yang's generalized λ-measure does not satisfy the monotone, condition, then it is not a fuzzy measure, hence Yang's generalized λ-measure is only a generalized measure of λ-measure, but not a generalized fuzzy measure of λ-measure

VII. LIU'S GENERALIZED LAMBDA FUZZY MEASURE

A. Definition of multivalent fuzzy measures

Definition 19. [6] Multivalent fuzzy measures

(i) A fuzzy measure is called a univalent fuzzy measure, if it has only one fuzzy measure solution.

(ii) A fuzzy measure is called a multivalent fuzzy measure, if its fuzzy measure solutions are more than one

(iii) A normalized fuzzy measure is called a univalent normalized fuzzy measure, if it has only one normalized fuzzy measure solution.

(iv) A normalized fuzzy measure is called a multivalent normalized fuzzy measure, if its normalized fuzzy measure solutions are more than one

(v) A regular fuzzy measure is called a univalent regular fuzzy measure, if it has only one regular fuzzy measure solution.

(vi) A regular fuzzy measure is called a multivalent regular fuzzy measure, if its regular fuzzy measure solutions are more than one

B. Definition of multivalentλ- measures

Definition 20. Multivalent λ- measures

For any $$\lambda \in \left[-\frac{1}{\max_{A\subset X}\{g_\lambda(A)\}}, \infty\right) \quad (83)$$

and a given fuzzy support function, $s(x)$ on a finite set X, a measure on X is a multivalent λ - measure, if its measure function $g_\lambda : 2^X \to [0,\infty)$ satisfying

(i) $g_\lambda(\phi) = 0$ (Vanishing at the empty set) (84)

(ii) $$\forall A, B \in 2^X, A \cap B = \phi$$
$$\Rightarrow g_\lambda(A \cup B) = g_\lambda(A) + g_\lambda(B) + \lambda g_\lambda(A) g_\lambda(B) \quad (85)$$

(iii) $$\forall A \subset X \Rightarrow g_\lambda(A) = \begin{cases} \frac{1}{\lambda}\left(-1 + \prod_{x\in A}\left[1+\lambda s(x)\right]\right) & \lambda \neq 0 \\ \sum_{x\in A} s(x) & \lambda = 0 \end{cases} \quad (86)$$

Note that multivalent λ - measure do not need the condition;

$$\prod_{x\in X}\left[1+\lambda s(x)\right]=1+\lambda>0,\ s(x)=g_\lambda(\{x\})$$

Theorem 13. Multivalent λ - measure is a multivalent fuzzy measure

Proof;

(I) For any $\lambda\in\left[-\frac{1}{\max\limits_{E\subset X}\{g_\lambda(E)\}},\infty\right)$, let $\forall A,B\in 2^X$, $A\subseteq B$,

to prove that $g_\lambda(A)\le g_\lambda(B)$ (87)

Since $\lambda\in\left[-\frac{1}{\max\limits_{E\subset X}\{g_\lambda(E)\}},\infty\right)$,

then $\lambda>-\frac{1}{\max\limits_{E\subset X}\{g_\lambda(E)\}}\Rightarrow 1+\lambda\max\limits_{E\subset X}\{g_\lambda(E)\}>0$ (88)

(i) if $-\frac{1}{\max\limits_{E\subset X}\{g_\lambda(E)\}}<\lambda<0$ (89)

Then $1+\lambda g_\lambda(A)\ge 1+\lambda\max\limits_{E\subset X}\{g_\lambda(E)\}>0$ (90)

$$\begin{aligned}g_\lambda(B)&=g_\lambda\left(A\cup(B-A)\right)\\&=g_\lambda(A)+g_\lambda(B-A)+\lambda g_\lambda(A)g_\lambda(B-A)\\&=g_\lambda(A)+g_\lambda(B-A)\left[1+\lambda g_\lambda(A)\right]\\&\ge g_\lambda(A)+g_\lambda(B-A)\left[1-\frac{g_\lambda(A)}{\max\limits_{E\subset X}\{g_\lambda(E)\}}\right]\\&\ge g_\lambda(A)\end{aligned}\quad(91)$$

(ii) if $\lambda\ge 0$ (92)

$$\begin{aligned}g_\lambda(B)&=g_\lambda\left(A\cup(B-A)\right)\\&=g_\lambda(A)+g_\lambda(B-A)+\lambda g_\lambda(A)g_\lambda(B-A)\\&\ge g_\lambda(A)\end{aligned}\quad(93)$$

(II) For any $\forall A\subset X$ to prove $g_\lambda(\phi)=0$

$$\begin{aligned}&g_\lambda(\phi)=g_\lambda(\phi\cup\phi)=g_\lambda(\phi)+g_\lambda(\phi)+\lambda g_\lambda(\phi)g_\lambda(\phi)\\&=2g_\lambda(\phi)+\lambda\left[g_\lambda(\phi)\right]^2\\&\Rightarrow g_\lambda(\phi)+\lambda\left[g_\lambda(\phi)\right]^2=g_\lambda(\phi)\left[1+\lambda g_\lambda(\phi)\right]=0\\&Since\quad\left[1+\lambda g_\lambda(\phi)\right]>0\\&\Rightarrow g_\lambda(\phi)=0\end{aligned}\quad(94)$$

The proof is completed.

Definition 21. Multivalent normalizedλ- measures

For any $\lambda\in[-1,\infty)$ (95)

and a given fuzzy density function $d(x)$ on a finite set X, a measure on X is a multivalent normalized λ - measure, if its measure function $g_\lambda:2^X\to[0,1]$ satisfying

(i) $g_\lambda(\phi)=0,\ g_\lambda(X)=1$ (normalized conditions) (96)

(ii) $\forall A,B\in 2^X,\ A\cap B=\phi$

$$\Rightarrow g_\lambda(A\cup B)=\left[g_\lambda(A)+g_\lambda(B)+\lambda g_\lambda(A)g_\lambda(B)\right]\wedge 1 \quad(97)$$

(iii) $\forall A\subset X\Rightarrow g_\lambda(A)=\begin{cases}\left[\frac{1}{\lambda}\left(-1+\prod\limits_{x\in A}\left[1+\lambda d(x)\right]\right)\right]\wedge 1 & \lambda\ne 0\\ \sum\limits_{x\in A}d(x) & \lambda=0\end{cases}$ (98)

Note that multivalent normalized λ - measure also do not need the condition; $\prod_{x\in X}\left[1+\lambda d(x)\right]=1+\lambda>0,\ d(x)=g_\lambda(\{x\})$.

Theorem 14. Multivalent normalized λ - measure is a multivalent normalized fuzzy measure

Proof;

(I) For any $\lambda\in[-1,\infty)$, let $\forall A,B\in 2^X$, $A\subseteq B$,

to prove that $g_\lambda(A)\le g_\lambda(B)$

(i) if $-1\le\lambda\le 0$ then $1+\lambda g_\lambda(A)\ge 1-g_\lambda(A)\ge 0$ (99)

$$\begin{aligned}g_\lambda(B)&=g_\lambda\left(A\cup(B-A)\right)\\&=g_\lambda(A)+g_\lambda(B-A)+\lambda g_\lambda(A)g_\lambda(B-A)\\&=g_\lambda(A)+g_\lambda(B-A)\left[1+\lambda g_\lambda(A)\right]\ge g_\lambda(A)\end{aligned}\quad(100)$$

(ii) if $\lambda>0$ then

$$\begin{aligned}g_\lambda(B)&=g_\lambda\left(A\cup(B-A)\right)\\&=g_\lambda(A)+g_\lambda(B-A)+\lambda g_\lambda(A)g_\lambda(B-A)\\&=g_\lambda(A)+g_\lambda(B-A)\left[1+\lambda g_\lambda(A)\right]\ge g_\lambda(A)\end{aligned}\quad(101)$$

(II) For any $\lambda\in[-1,\infty)$, and any $A\subset X$ to prove

$$0\le g_\lambda(A)\le 1 \quad(102)$$

From (I), we know that $0=g_\lambda(\phi)\le g_\lambda(A)\le g_\lambda(X)=1$

The proof is completed.

Definition 22. Multivalent regularλ- measures

For any $\lambda\in[-1,\infty)$ (103)

and a given fuzzy regular density function $d(x)$ on a finite set X, a measure on X is a multivalent regular λ - measure, if its measure function $g_\lambda:2^X\to[0,1]$ satisfying

(i) $g_\lambda(\phi)=0,\ g_\lambda(X)=1$ (Normalized conditions) (104)

(ii) $\forall A,B\in 2^X,\ A\cap B=\phi$

$$\Rightarrow g_\lambda(A\cup B)=\left[g_\lambda(A)+g_\lambda(B)+\lambda g_\lambda(A)g_\lambda(B)\right]\wedge 1 \quad(105)$$

(iii) $\forall A\subset X\Rightarrow g_\lambda(A)=\begin{cases}\left[\frac{1}{\lambda}\left(-1+\prod\limits_{x\in A}\left[1+\lambda d(x)\right]\right)\right]\wedge 1 & \lambda\ne 0\\ \sum\limits_{x\in A}d(x) & \lambda=0\end{cases}$ (106)

Theorem 15. Multivalent regular λ - measure is a multivalent regular fuzzy measure

Proof: it is trivial.

C. Completed measure

Definition 23 [6] **C**ompleted measure

For any given fuzzy density function, $d(x)$, on a finite set, X, a multivalent fuzzy measure,μ-measure, with determined coefficient, $\mu \in R$ it is called a completed fuzzy measure, if it satisfies

(i) $\forall \mu \in [a,b]$ ∋ μ-measure is a fuzzy measure

(ii) $\mu = a \Rightarrow g_\mu(A) = g_p(A), \forall A \subset X$ (107)

(iii) $\mu = b \Rightarrow g_\mu(A) = g_B(A), \forall A \subset X$ (108)

Note that all of regular λ-measure, multivalent λ - measure and multivalent normalized λ - measure are not completed fuzzy measure.

Definition 23 Liu's generalizedλ-measure

For any given fuzzy density function $d(x)$ on a finite set X,

$$\text{And} \quad \forall \lambda \in [a,b] = \left[\frac{-2}{\min\limits_{0 \neq x \in X} \{d(x)\}}, \frac{1}{\left[\min\limits_{0 \neq x \in X} \{d(x)\}\right]^2} \right] \tag{109}$$

a measure on X is called a Liu's generalized λ - measure, if its measure function $g_\lambda : 2^X \to [0,1]$ satisfying

(i) $g_\lambda(\phi) = 0, g_\lambda(X) = 1$ (Normalized conditions) (110)

(ii) $\forall A, B \in 2^X, A \cap B = \phi$

$$\Rightarrow g_\lambda(A \cup B) = \begin{cases} \frac{\lambda+1}{a+1} \max\limits_{x \in A \cup B} \{d(x)\} + \frac{a-\lambda}{a+1}\left[g_\lambda(A) + g_\lambda(B) - g_\lambda(A) g_\lambda(B)\right] & a \le \lambda < -1 \\ \left[g_\lambda(A) + g_\lambda(B) + \lambda g_\lambda(A) g_\lambda(B)\right] & -1 \le \lambda \le 0 \\ \left[g_\lambda(A) + g_\lambda(B) + \lambda g_\lambda(A) g_\lambda(B)\right] \wedge 1 & 0 < \lambda \le b \end{cases} \tag{111}$$

$$a = \frac{-2}{\min\limits_{0 \neq x \in X} \{d(x)\}} < -1, \quad b = \frac{1}{\left[\min\limits_{0 \neq x \in X} \{d(x)\}\right]^2} > 1 \tag{112}$$

(iii) $$\forall A \subset X \Rightarrow g_\lambda(A) = \begin{cases} \frac{\lambda+1}{a+1} \max\limits_{x \in A} \{d(x)\} + \frac{a-\lambda}{a+1} f_{-1}(A) & a \le \lambda < -1 \\ f_\lambda(A) & -1 \le \lambda < 0 \\ \sum\limits_{x \in A} s(x) & \lambda = 0 \\ \left[f_\lambda(A)\right] \wedge 1 & 0 < \lambda \le b \end{cases} \tag{113}$$

where $$f_\lambda(A) = \left[\frac{1}{\lambda} \left(-1 + \prod_{x \in A} \left[1 + \lambda d(x)\right] \right) \right] \tag{114}$$

Theorem 16. Liu's generalizedλ-measure is a **C**ompleted, continuous and increasing normalized fuzzy measure

Proof:

(I) Let $\forall A \in 2^X$ to prove that $0 \le g_\lambda(A) \le 1$,

From (113) and the definition of fuzzy density function we know that

If $A = \phi, or\ A = X, or\ |A| = 1 \Rightarrow 0 \le g_\lambda(A) \le 1$ (115)

If $|A| > 1,\ A = B \cup C, B \cap C = \phi, B \neq \phi \neq C$ (116)

From (113), we know that

$$0 \le \max_{x \in A}\{d(x)\} = \max_{x \in B \cup C}\{d(x)\} \le g_\lambda(B \cup C) = g_\lambda(A) \le 1 \tag{117}$$

(II) Let $\forall A, B \in 2^X, A \subseteq B$ to prove that $g_\lambda(A) \le g_\lambda(B)$

From (102) and (106), we can obtain that

$$\forall A \in 2^X \Rightarrow g_\lambda(A) \ge \max_{x \in A}\{d(x)\} = g_P(A) \tag{118}$$

Since $B = A \cup (B - A)$, then we have

$$g_\lambda(B) = g_\lambda(A \cup (B - A)) = \begin{cases} \frac{\lambda+1}{a+1} \max\limits_{x \in B}\{d(x)\} + \frac{a-\lambda}{a+1}\left[g_\lambda(A) + g_\lambda(B-A) - g_\lambda(A) g_\lambda(B-A)\right] & a \le \lambda < -1 \\ \left[g_\lambda(A) + g_\lambda(B-A) + \lambda g_\lambda(A) g_\lambda(B-A)\right] & -1 \le \lambda \le 0 \\ \left[g_\lambda(A) + g_\lambda(B-A) + \lambda g_\lambda(A) g_\lambda(B-A)\right] \wedge 1 & 0 < \lambda \le b \end{cases} \tag{119}$$

(i) if $0 < \lambda \le b$, then $g_\lambda(A) \le g_\lambda(B)$ is trivial.

(ii) if $-1 \le \lambda \le 0$, since $0 \le g_\lambda(A) \le 1$ then

$\lambda g_\lambda(A) \ge \lambda \ge -1$ and $\left[1 + \lambda g_\lambda(A)\right] \ge 0$ we can obtain

$$\begin{aligned} g_\lambda(B) &= g_\lambda(A) + g_\lambda(B - A) + \lambda g_\lambda(A) g_\lambda(B - A) \\ &= g_\lambda(A) + g_\lambda(B - A)\left[1 + \lambda g_\lambda(A)\right] \ge g_\lambda(A) \end{aligned} \tag{120}$$

That is $g_\lambda(A) \le g_\lambda(B)$

(iii) if $a \le \lambda < -1$ then $g_\lambda(B) = \frac{\lambda+1}{a+1} g_P(B) + \frac{a-\lambda}{a+1} f_{-1}(B)$ (121)

Where $g_P(A) \le g_P(B), f_{-1}(A) \le f_{-1}(B)$

We can obtain

$$g_\lambda(A) = \frac{\lambda+1}{a+1} g_P(A) + \frac{a-\lambda}{a+1} f_{-1}(A) \le \frac{\lambda+1}{a+1} g_P(B) + \frac{a-\lambda}{a+1} f_{-1}(B) = g_\lambda(B) \tag{122}$$

And we know that Liu's generalizedλ-measure is a fuzzy measure.

(II) Let $\lambda = a = \frac{-2}{\min\limits_{0 \neq x \in X}\{d(x)\}}$ to prove

$$g_\lambda(A) = g_a(A) = \max_{x \in A}\{d(x)\} = g_P(A) \tag{123}$$

Let $\forall A, B \subset X, A \cap B = \phi$, and $\lambda = a = \frac{-2}{\min\limits_{0 \neq x \in X}\{d(x)\}}$

then

$$\begin{aligned} & a \le -\left(\frac{1}{\min\limits_{0 \neq x \in A}\{d(x)\}} + \frac{1}{\min\limits_{0 \neq x \in B}\{d(x)\}} \right) \le -\left(\frac{1}{g_a(A)} + \frac{1}{g_a(B)} \right) \\ & \le \frac{-g_a(A) - g_a(B)}{g_a(A) g_a(B)} \le \frac{\max\limits_{x \in A \cup B}\{d(x)\} - g_a(A) - g_a(B)}{g_a(A) g_a(B)} \\ & \Rightarrow a g_a(A) g_a(B) \le \max_{x \in A \cup B}\{d(x)\} - g_a(A) - g_a(B), \forall A, B \subset X \\ & \Rightarrow \left[g_a(A) + g_a(B) + a g_a(A) g_a(B)\right] \le \max_{x \in A \cup B}\{d(x)\} \end{aligned} \tag{124}$$

Then we can obtain

$$g_a(A\cup B)$$
$$=\left[g_a(A)+g_a(B)+\alpha g_a(A)g_a(B)\right]\vee\max_{x\in A\cup B}\left\{d(x)\right\}=\max_{x\in A\cup B}\left\{d(x)\right\} \quad (125)$$
$$\Rightarrow g_a(A\cup B)=\max_{x\in A\cup B}\left\{d(x)\right\}$$

That is

$$g_\lambda(A)=g_a(A)=\max_{x\in A}\left\{d(x)\right\}=g_P(A),\forall A\subseteq X$$

(III) Let $$\lambda=b=\frac{1}{\left[\min_{0\neq x\in X}\left\{d(x)\right\}\right]^2} \quad (126)$$

to prove $$g_\lambda(A)=g_b(A)=g_B(A),\forall A\subseteq X,|A|>1 \quad (127)$$

let

$$\forall A,B\subset X, A\cap B=\phi, g_\lambda(A)g_\lambda(B)>0,,$$

$$|A\cup B|>1,\ \lambda=b=\frac{1}{\left[\min_{0\neq x\in X}\left\{d(x)\right\}\right]^2} \quad (128)$$

then $$\lambda=b=\frac{1}{\left[\min_{0\neq x\in X}\left\{d(x)\right\}\right]^2}\geq\frac{1}{\left[g_b(A)\wedge g_b(B)\right]^2} \quad (129)$$
$$\geq\frac{1}{g_b(A)g_b(B)}\geq\frac{1-g_b(A)-g_b(B)}{g_b(A)g_b(B)}$$

$$\Rightarrow g_b(A)+g_b(B)+bg_b(A)g_b(B)\geq 1,\forall A,B\subset X$$
$$\Rightarrow g_b(A\cup B)=\left[g_b(A)+g_b(B)+bg_b(A)g_b(B)\right]\wedge 1=1 \quad (130)$$

In other words, $$\forall A\subseteq X,|A|>1\Rightarrow g_b(A)=1$$

Then $$g_\lambda(A)=g_b(A)=g_B(A),\forall A\subseteq X,|A|>1$$

(IV) From above we know that Liu's generalizedλ-measure is a **C**ompleted normalized fuzzy measure

(V) It is trivial that the measure function of Liu's generalizedλ-measure is a continuous and increasing function on λvalue.

VIII. CONCLUSIONS AND FUTURE WORKS

In this paper, first of all, it is proved that both λ-measure and additive measure are never equal to the smallest fuzzy measure, P-measure and the largest fuzzy measure, B-measure.

Second, this paper pointed out that the generalized λ-measure proposed by L.-Z. Yang, M.-H. Ha, X.-J. Wang, and Z.-R. Zhang, is a generalized measure of λ-measure, but not a generalized fuzzy measure of λ-measure, since a fuzzy measure must be a monotone measure.

Furthermore, a novel multivalent fuzzy measure with infinitely many fuzzy measure solutions based on λ-measure, called Liu's generalized λ-measure, is proposed. It is proved that the measure function of this new measure is continuous and increasing on λ, each different λ value corresponding different fuzzy measure, from the smallest fuzzy measure, P-measure to the largest fuzzy measure, B-measure, and containing additive measure and λ-measure itself, Moreover, it is a generalize fuzzy measure of λ-measure satisfying the monotone condition, and rather than the old generalized λ-measure proposed by L.-Z. Yang, M.-H. Ha, X.-J. Wang, and Z.-R. Zhang. Some properties about this new measure are also discussed.

In the future, we can use Choquet integral with respect to this new fuzzy measure to analysis forecasting problem and multiple criterion decision making problem.

ACKNOWLEDGMENT

This paper is partially supported by the National Science Council grant (NSC 99-2511-S-468-001).

REFERENCES

[1] A. E. Hoerl, R. W. Kenard, and K. F. Baldwin, "Ridge regression: Some simulation," Communications in Statistics, 1975, vol. 4, No. 2, pp. 105-123.

[2] G. Choquet, "Theory of capacities," Annales de l'Institut Fourier, 1953, Vol. 5, pp. 131-295

[3] M. Sugeno, "Theory of fuzzy integrals and its applications," unpublished doctoral dissertation , Tokyo Institute of Technology, Tokyo, Japan, 1974.

[4] L. A. Zadeh, "Fuzzy sets as a basis for a theory of possibility, " Fuzzy Sets and Systems., 1978, vol. 1, pp.3-28..

[5] Z. Wang, and G. J. Klir, 'Generalized Measure Theory", Springer Press, New York, 2009

[6] H.-C. Liu, "A theoretical approach to the completed L-fuzzy measure", 2009 International Institute of Applied Statistics Studies (IIASS), 2nd Conference, Qindao, China, July 24-29, 2009

[7] H.-C. Liu, Maximized L-measure and its Choquet integral regression model, Proceedings of the 10th International Symposium on Pervative Systems, Algorithms, and Networks (I-SPAN2009). December 14-16, 2009.

[8] H.-C. Liu , W.-S. Chen , C.-C. Chen, Y.-D. Jheng , D.-B. Wu,. Choquet Integral with Respect to High Order Extensional L- Measure. Applied Mechanics and Materials, 2010, Vol. 44-47. pp.3579-3583..

[9] H.-C. Liu. Choquet integral on Liu's generalized intuitionistic fuzzy numbers, Proceedings of the 2010 International Conference on Machine Learning and Cybernetics (ICMLC 2010) Qingdao, 11-14 July 2010. Volume: 6, pp.2390-2395.

[10] L.-Z. Yang, M.-H. Ha, X.-J. Wang and Z.-R. Zhang, A generalized λ −fuzzy measure and its application in image enhancement, Proceedings of the 2008 International Conference on Wavelet Analysis and Pattern Recognition, Hong Kong, 30-31 Aug. 2008, pp. 35-40.

2011 IEEE International Conference on Fuzzy Systems
June 27-30, 2011, Taipei, Taiwan

A Fuzzy Intelligent Decision Support System for Typhoon Disaster Management

Wang-Kun. Chen[1]
1 Department of Environment and Property Management, Jinwen University of Science & Technology, Taipei, Taiwan E-mail: wangkun@just.edu.tw

GuangJun. Sui[2]
2 Guangdong University of Foreign Studies, Guangzhou, China

DangLing Tang[3]
3 Research Center for Remote sensing of Marine Ecology/Environment, LED, South China Sea Institute of, Oceanology, Chinese Academy of Sciences,Guangzhou, China

***Abstract*—This paper presents the conceptual framework of fuzzy intelligent decision support system for typhoon disaster management. The typhoon risk management pattern was mentioned in the first section. Several types of database should be established in the decision support system. There are three steps to predict the typhoon risk. The first one is the feature extraction of typhoon pattern. The second one is the damage estimation by case base reasoning method. And the third one is the linguistic estimation of typhoon risk. An example of risk evaluation from the experiment data shows that the decision supporting system can be further improved if there is a complete and accurate dataset in this system.**

Keywords-component; fuzzy theory, decision support system, disaster management, risk analysis

I. INTRODUCTION TO TYPHOON DISASTER MANAGEMENT

Typhoon is one of the most worrisome natural disasters in Taiwan. Its management is related to the location because typhoon is a variable vector in the space. The concept of geospatial information system helps us to construct the geographic database. However, the prediction of typhoon must have large amount of observational data. The choice of these data is a process worthy of careful condition.

Typhoon disaster is a decision analysis process under uncertain condition. We need to concern about the combination of information on human identification and instrumental observation to make consolidated conclusion.

The aim of this study was to build a decision support system for typhoon mitigation. The system can provide the disaster prevention and rescue unit to temporary reduce risk and disaster preparedness. Besides, it can support the operations as decision making or disaster recovery. The system has to integrate with the function of geographical information system to incorporate the typhoon forecasting and analysis model. A model bank with the spatial decision support system was included in this system to obtain the necessary knowledge of typhoon risk management.

How to obtain the wisdom related to typhoon disaster management is an important issue in constructing the intelligent system. The theory of ontology can systematically organize the human knowledge.(Hadzic et al., 2009) Knowledge ontology allows us to share the wisdom and knowledge more easily. It can also quickly help us to find the required information and data. The knowledge ontology in this study also accumulates the technical results of typhoon risk prevention and assists the researchers to identify the topic worthy of further research. (Chang and Wang, 1996)

II. MATHEMATICAL MODEL

A. Feature extraction

Feature extraction of typhoon risk includes the image decomposition, pattern recognition and noise filtering. Many researchers have applied the Artificial Neural Network (ANN) model in feature extraction. ANN has capacity to simulate the brain's thinking process objectively and avoid the influence of the forecasters' subjective judgment.

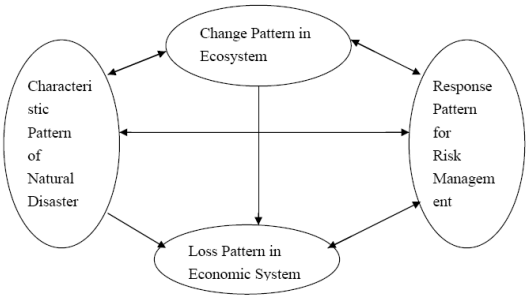

Fug 1 the four types of pattern in the typhoon risk management system

Chen et al have used the multivariable method to clarify the relationship of typhoon pattern. (Chen et al, 2010) We may consider the feature of typhoon has the following four categories: (1) typhoon natural itself; (2) change in ecosystem; (3) loss in economic system; (4) response for risk management. (Chen, 2010) (Schuermann, 1996) (Richard et al, 2001)

B. Damage prediction

The typhoon damage can be estimated by the basic principle of case-based reasoning (CBR). CBR is one of the new reasoning methods of artificial intelligence, and it is the simplest way to perform fuzzy risk assessment and calculate the fuzzy expected value. Case base reasoning method can also convert the fuzzy risk into the non-fuzzy risk by converting it to a clear number. Decision support system of typhoon uses various risk factors of typhoon to analyze the damage by the case base reasoning method.

C. Risk analysis

Prediction of typhoon risk is difficult because the term "risk" is a very subjective work. Some people think that is very dangerous, but others believe that not dangerous. For example, if the damage of typhoon can be represented as: very safe, safe, medium, serious, very serious, then we can use fuzzy logic operation to convert it into an objective amount. The Triangle Fuzzy Number (TFN)r is often used in the representation of a vague amount. For example, the i^{th} damage of the j^{th} area, X_{ij}, the fuzzy equation can be written as $F_{ij} = (LF_{ij}, MF_{ij}, RFi_j)$, where F_{ij} is the characteristic value of X_{ij}, LF_{ij} is the lowest value of F_{ij}, RF_{ij} is the maximum value of F_{ij}, MF_{ij} is the most probable value of F_{ij}, and ${}^{L}F_{ij} < {}^{M}F_{ij} < {}^{R}F_{ij}$.(Figure 2a)

We can use the membership function $\mu_A(x)$ represented by (a_1, a_2, a_3) to express the triangular fuzzy number (TFN). Thus the characteristic number of the i^{th} damage of the j^{th} area is $a_1 = {}^{L}F_{ij}$, $a_2 = {}^{M}F_{ij}$, $a_3 = {}^{R}F_{ij}$. The membership function by TFN then becomes

$$\mu_A(x) = \begin{cases} 0 & , \quad x < a_1 \\ \dfrac{x - a_1}{a_2 - a_1} & , \quad a_1 \le x \le a_2 \\ \dfrac{a_3 - x}{a_3 - a_2} & , \quad a_2 \le x \le a_3 \\ 0 & , \quad x > a_3 \end{cases} \qquad (1)$$

Since the range of fuzzy interval for everyone is different, so the value of TFN is not the same. Figure 2b describe that there are various TFN value from different observer.

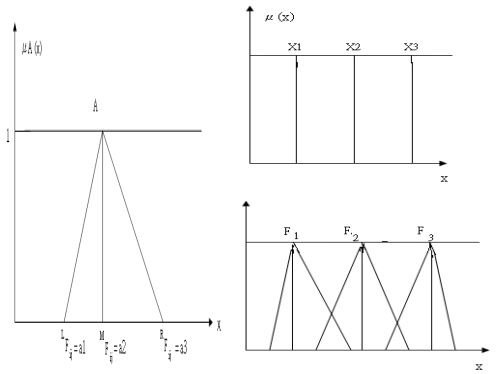

(a) (b)

Fig 2 (a) Membership function of the triangular fuzzy numbers (TFN) (b) Converting the original results into a normalized fuzzy number

III. System Description

The knowledge bank of typhoon disaster management is shown as figure 3.

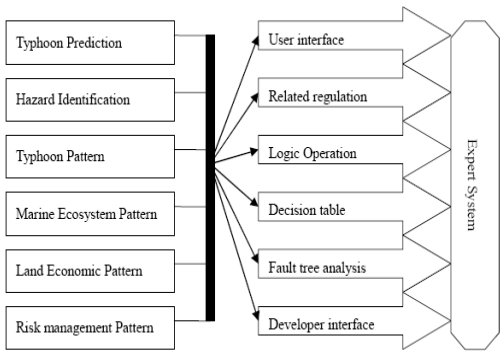

Fig 3 Intelligent knowledge-based expert system

A. Knowledge bank and data base design

The input data of typhoon disaster decision support system includes the following: real- time meteorological data, forecast typhoon data, historical typhoon data, and other basic typhoon information. There are two types of real time data, the real-time meteorological data and the forecast typhoon data. Therefore the system must have the real-time data loading capability in order to meet the "real time" feature.

The real-time meteorological data can be obtained from the government. The typhoon forecast data is also real-time information; however, it may not so complete as the general meteorological data. Most of this information is image base, such as satellite image, typhoon forecasting, or typhoon path map, etc.

B. Real-time and historical information query

The real-time information of typhoon includes the real-tine trend of typhoon. These includes typhoon the previous typhoon path and forecast typhoon path, satellite images, and related descriptive statistics information.

The historical information of typhoon provides the function of query. The query is through the configuration condition by name, landing time, landing location, and generating location, etc. the information available in this system are: landing data, landing time, generating location, generating time, typhoon grade, cumulative rainfall, total rainfall, satellite image, and disaster description.

C. Typhoon damage prediction

Typhoon damage prediction can be performed by the case base reasoning method as described in section 2.3. The major disaster of typhoon is flooding and landslides which were caused by the precipitation due to typhoon. The major function of typhoon damage prediction is to provide the real time rainfall data as for the risk analysis. It includes the spatial and temporal distribution of real time rainfall and accumulates rainfall.

D. Typhoon risk analysis

The results of risk analysis provide the decision maker the information about the loss of life and property. Typhoon risk prediction can be performed by the linguistic risk analysis as described in section 2.3. In this study, we selected five

grades of typhoons in this system: 1.very strong; 2. strong; 3. medium; 4. weak; 5.very weak.

There are many variable for describing the degree of risk. These include: extent of flooding, number of death, number of disappear, number of injury, housing collapse(all), housing collapse(half), housing loss, and agriculture loss.

E. Scenario simulation and information display

The scenario simulation and information display of typhoon should consider the space and time characteristic of typhoon. Since the typhoon disaster is a space-time event, we define the event by the same equation. The scenario simulation was based on the historical typhoon information. The case base reasoning can help us to simulate the possible damage in order to prevent the disaster.

Typhoon can be represented by a mathematical vector. The space geographical information can be represented by the following equation:

$$I = \sum_{i=1}^{m} \left[\sum_{j=1}^{n} \begin{bmatrix} S_{ij}(T_{ij}) \\ A_{ij}(T_{ij}) \\ T_{ij} \end{bmatrix} \right] \quad T_{ij}(t_b, t_e)_{ij} \qquad (2)$$

Where I is the collection of space geographical information; i is the individual vector for the i^{th} item, j is the state of this item; $S_{ij}(T_{ij})$ and $A_{ij}(T_{ij})$ represent the characteristics of this item in time t_b to t_e.

Because the decision support system is based on the core concept of geographical information system, therefore the information should fully demonstrate the characteristic of spatial information. It has to show the relationship between the space and spatial distribution. In addition, it has to integrate the traditional text, statistics, reports, and display mode.

F. Intelligent decision support system

Spatial Decision Support Systems is one of the major development item of Geographic Information Science. (Goodchild, 2005;Sengupta and Bennett , 2003;) The development of intelligent decision support system should include the intelligence and knowledge for this kind of decision making.

In this system, the database includes the real-time meteorological data, with this information and other data; it can provide the related table and figure for the decision maker.

To solve the decision making problem of typhoon disaster management, we need to utilize our information technology. Intelligent spatial decision support system (ISDSS), which is now the major research direction in geographic information science and decision makers, can help us integrate the data base in various types of information and knowledge.

IV. EXAMPLE AND DISCUSSION

An example of risk analysis was presented in this section to explain the importance of database. The prediction of typhoon risk has to use the available data. There are three different types of data for the prediction of typhoon risk. The first one is the value with definite quantity; the second one is the value with fuzzy interval, and the third one is the linguistic expression.

In order to compare the different types of data, we have to adjust these data into the same type. **W**e use three types of fuzzy degree to calculate the fuzzified number, 20%, 10%, and 5%. The fuzzified results were shown in figure 4. Then, the normalized risk was calculated and the aggregate results of total risk were shown in figure 5.

In figure 5, there are different fuzzy degree ranges with different type of typhoon, from very strong to very weak. If it is twenty percent fuzzy degree as figure 5(a), then there is a very wide range of risk interval; however, if the fuzzy degree is low, such as figure 5(c), then the range of risk interval will be decreased.

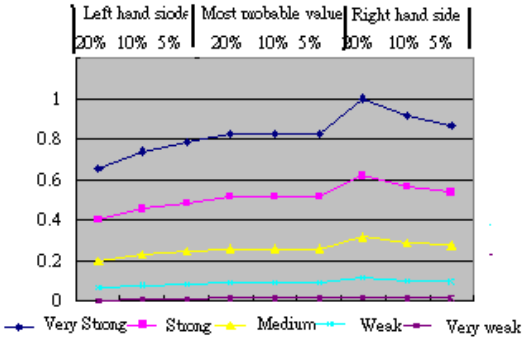

Figure 4 the evaluation results of the typhoon risk

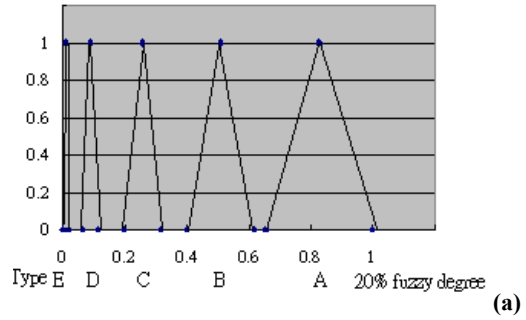

(a)

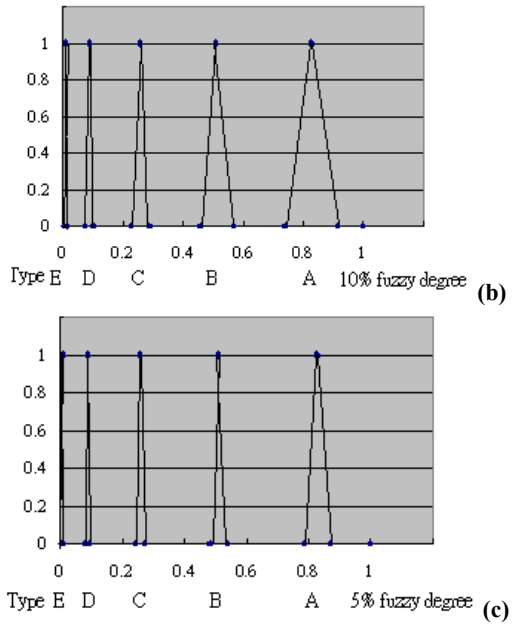

Figure 5 Different fuzzy degree range with different type of typhoon, A: very strong B: strong C: medium D: weak E: very weak

The reasons for the discrepancy of these results were due to the reliable extent of information. The damage prediction need adequate data to support the decision making process. However, the determination of the availability of information is very cumbersome. The decision maker does not have enough time to determine. Therefore, more unreliable information cause more credible decision-making. The best way to improve the efficiency of this decision support system is to increase the reliability completeness of the database.

The feature extraction and damage prediction help us to confirm the extent of harm by typhoon. In this article, there is not enough space to elaborate. Hope there will have more research appeared in this area.

V. CONCLUSION

This paper describes the framework of a fuzzy intelligent decision support system for typhoon disaster management. The development of spatial decision support system was introduced in this article. The mathematical model of the intelligent system includes the feature extraction by artificial neural network, damage estimation by case base reasoning, and risk prediction by fuzzy linguistic transformation. An example of the typhoon risk analysis show that the improvement of this system is depends upon the accuracy and completeness of its knowledge. And the development of feature extraction and damage estimation will be of great benefit of these results.

Acknowledgement

The present research was supported by: (1) Guangdong National Science Foundation, China (8351030101000002), (2) Natural National Science Foundation of China (40976091), (3) The CAS/SAFEA International Partnership Program for Creative Research Teams (KZCX2-YW-T001).

REFERENCES

[1] Kaufmann A., Gupta M.M., Introduction to Fuzzy Arithmetic Theory and Applications, Van Nostrand Reinhold, New York, 1991.

[2] Chang, N.B. and Wang, S. F., "The Development of an Environmental Decision Support System for Municipal Solid Waste Management," *Computers, Environment and Urban System*, 20(3), 201-212, 1996.

[3] Goodchild, F. M., Kryiakidids, P., Rice, M., and Schneider, P. (2005) Spatial Web. In Report of the NCGIA Specialist Meeting on Spatial Webs, 73-78.

[4] Hadzic, M., Wongthongtham, P., Dillon, T., and Chang, E. (2009). Ontology-Based Multi-Agent Systems. Springer-Verlag Berlin

[5] Heidelberg Kolas, D., Hebeler, J., and Dean, M. (2005) . Geospatial Semantic Web: Architecture of Ontologies. Paper read at First International Conference, GeoS 2005, at Mexico City, Mexico.

[6] Sengupta, R. R. and Bennett, D. A. (2003). Agent-based modeling environment for spatial decision support, International *Journal of Geographical Information Science* 17, no.2, p. 157-180.

[7] Zadeh L. A. (1965) "Fuzzy sets". *Information and Control* 8 (3) 338–353.

[8] Schuermann, J. (1996): *Pattern Recognition,* Wiley&Sons, 1996, ISBN 0-471-13534-8

[9] Richard O. Duda, Peter E. Hart, David G.Stork (2001) *Pattern Recognition* (2nd), Wiley, New York, ISBN

2011 IEEE International Conference on Fuzzy Systems
June 27-30, 2011, Taipei, Taiwan

A Robust Fuzzy Trajectory Estimation Design of High Speed Reentry Vehicles

Yung-Yue Chen[1], *IEEE Member*
Department of Electrical Engineering
National Yunlin University of Science and Technology
Douliou 64002, Taiwan
Email: chenyuyu@yuntech.edu.tw

Chung-Shi Tseng[2], *Senior Member, IEEE*
Department of Electrical Engineering
Ming Hsin University of Science and Technology
Hsin-Feng 30401, Taiwan
Email: cstseng@must.edu.tw

Abstract—**An H_∞ fuzzy trajectory estimation is proposed for robust tracking guidance and early warning in antitactical ballistic missile systems with model uncertainties and external disturbances. In order to avoid solving the nonlinear Hamilton-Jacobi-Isaac(H-J-I) partial differential equation for H_∞ trajectory estimation of the nonlinear reentry vehicle (RV) dynamic equation, the Takagi and Sugeno fuzzy linear model is employed to interpolate piecewise to approximate the RV nonlinear dynamic equation. Then, from the fuzzy linear model, a fuzzy H_∞ state estimator is developed for robust trajectory estimation of RV with optimal attenuation of the worst-case effect of system uncertainties such as approximation error, external disturbance, maneuver and unpredictable external forces in flight and other sources. The proposed method parameterizes the H_∞ trajectory estimation problem in terms of an eigenvalue problem (EVP), so that the worst-case effect of system uncertainties on the trajectory estimation error is minimized in the robust trajectory estimation design subject to certain linear matrix inequality (LMI) constraints. Convex optimization techniques are employed to solve the EVP of the H_∞ fuzzy trajectory estimation in antitactical ballistic missile systems. Simulation results indicate that the proposed method possesses a satisfactory performance.**

Keywords-Tactical ballistic missile; H_∞ Trajectory estimation

I. INTRODUCTION

In antitactical ballistic missile (ATBM) systems, trajectory estimation of a reentry vehicle from a single radar plays an important role in radar tracking, missile guidance, and early-warning systems. Trajectory estimation of the reentry vehicle in the terminal phase is typically investigated in postflight analysis to identify state variables and key parameters from available flight data measured by radar, satellite, and on-board sensor [1]-[4]. Since the ATBM system is uncertain and nonlinear, one of the major topics behind trajectory estimation problems is related to model uncertainties, which are normally induced by simplification of assumptions, parameter uncertainty, maneuver and unpredictable external forces in flight, and other sources.

In general, an on-line optimal trajectory estimation in ATBM warfare is more difficult because one needs to solve a nonlinear partial differential Hamilton Jacobi (H-J) equation and all mathematical model quantities to be identified must be measurable by radar [1]. Therefore, a simplified model is desired, but this may induce a more serious model uncertainty problem. Klein et al. have introduced an important stepwise regression method in the determination of air plane model structure with both model orders and control derivatives [5]. However, it is too complex to be implemented in on-line trajectory estimations. Furthermore, the on-line trajectory estimation only operates well with a simplified model and needs to maintain a low sensitivity in order to avoid uncertainties.

In recent years, trajectory estimation of a RV in antitactical missile systems has received more attention. A filtering algorithm for state and parameter estimation has been developed by Chang et al. for a maneuvering RV subject to a simplified dynamic model with maneuver forces in terms of related coefficients like drag force [7]. They proposed an augmented state vector which contains position, velocity, and corresponding parameters to drag and maneuver forces in their filter. In order to avoid solving the nonlinear estimation problem by H-J equation, the extended Kalman filter was employed to perform the trajectory estimation work. The trajectory estimation performance, however, is degraded if the maneuvering forces are absent. Furthermore, the simplified dynamic model also confines the applications to maneuvering cases and is rarely applied to real flight. Manohar and Krishnan have proposed a trajectory reconstruction algorithm for a rocket system by using a differential correction method [8]. The dynamic equations for trajectory construction contain an unmodeled acceleration term to take care of all the forces acting on the vehicle other than those from aerodynamic, propulsive, and gravitational sources. In their trajectory algorithm, trajectory states and unmodeled acceleration values are estimated simultaneously. However, the required data are beyond what a simple radar can provide.

In the past two decades, input estimation methods have been successfully applied to tracking problems and initial leveling of strapdown inertial navigation system. A trajectory estimation algorithm using input estimation technique has recently been proposed for a RV via an extended Kalman filter to provide accuracy and fast trajectory estimation with low sensitivities. Since the estimation algorithm is developed from the linearized dynamic model on the present estimated state vector, the estimation errors may propagate with increasing

978-1-4244-7316-8/11/$26.00 ©2011 IEEE

estimation steps. Furthermore, input estimation needs a large amount of computations and precise statistic knowledge of external noises, which may confine its practical applications. H_∞ filter has been employed for state estimation of nonlinear systems with uncertain external noises by minimizing the worst-case effect of external noises. However, a nonlinear partial H-J-I equation needs to be solved. At present, an effective method for treating the H-J-I equation has not been found.

Recently, fuzzy techniques have been effectively used to approximate nonlinear dynamics and successfully applied to control system design. In this study, a fuzzy nonlinear H_∞ filter based on Takagi-Sugeno fuzzy is proposed. At first, the three-dimensional (3D) RV dynamic system is approximated by a fuzzy system motivated by a Takagi-Sugeno fuzzy model, which is obtained by interpolating several linearized systems at different operation points through the smoothing of fuzzy basis functions. Then, the nonlinear H_∞ estimation problem of RV systems is solved by fuzzy interpolation filtering method via an eigenvalue technique. For the convenience of design, the nonlinear H_∞ trajectory estimation problem via the fuzzy filtering approach is characterized in terms of an EVP, i.e., the worst-case effect of external disturbances on the estimation error is minimized subject to certain LMI constraints. The EVP or LMIP is to be solved via convex optimization techniques with the help of LMI optimization toolbox of Matlab. Finally, a simulation example is given to illustrate the design procedure and to confirm the estimation performance of our proposed method.

II. System Description and Problem Formulation

Consider the RV along a ballistic trajectory. For trajectory estimation and analysis, a mathematical model of ballistic missile system must be constructed first with some simplified assumptions to describe its motion. Fig. 1 shows a vehicle in the reentry phase over a flat, nonrotating earth with constant gravity. Since the RV has flown over several hundred kilometers along a ballistic trajectory above the rotating earth, the distance that the RV travels in this phase is shorter than the distance traveled before reentry. The RV can be considered as a point mass with constant weight following a ballistic trajectory in which two types of significant forces, i.e., drag and gravity, act on the RV. Extra forces induced by model uncertainties or disturbances must be considered when assumptions on the system are violated or the RV undertakes a maneuver. These effects can be grouped as uncertain accelerations in each axis. Suppose the RV system model in radar coordinates *(O, X, Y, Z) centered at radar site can be expressed as,*

$$\begin{aligned}
\dot{v}_x(t) &= -\frac{\rho v^2(t)}{2\beta} g\cos\gamma_1(t)\sin\gamma_2(t) + a_x(t) \\
\dot{v}_y(t) &= -\frac{\rho v^2(t)}{2\beta} g\cos\gamma_1(t)\cos\gamma_2(t) + a_y(t) \\
\dot{v}_z(t) &= -\frac{\rho v^2(t)}{2\beta} g\sin\gamma_1(t) - g + a_z(t)
\end{aligned} \tag{1}$$

Where v_x, v_y, and v_z denote the velocity components along *X*, *Y*, and *Z*, respectively, $a_x(t)$, $a_y(t)$ and $a_z(t)$ are uncertain accelerations due to model uncertainties and RV's maneuvering along *X*, *Y*, and *Z*, respectively, ρ stands for the air density. γ_1, γ_2 and the ballistic coefficient β are defined as,

$$\begin{aligned}
\gamma_1(t) &= \tan^{-1}\left(-\frac{v_z(t)}{\sqrt{v_x^2(t)+v_y^2(t)+v_z^2(t)}}\right) \\
\gamma_2(t) &= \tan^{-1}\left(\frac{v_x(t)}{v_y(t)}\right) \\
\beta &= \frac{W}{sC_{D0}}
\end{aligned} \tag{2}$$

where *s*, *W*, and C_{D0} represent the reference area, weight, and zero-lift drag coefficient, respectively. (1) can be translated into the following equations,

$$\begin{aligned}
\dot{v}_x(t) &= -\frac{\rho}{2\beta} g\left(\sqrt{v_x^2(t)+v_y^2(t)+v_z^2(t)}\cdot v_x(t)\right) + a_x(t) \\
\dot{v}_y(t) &= -\frac{\rho}{2\beta} g\left(\sqrt{v_x^2(t)+v_y^2(t)+v_z^2(t)}\cdot v_y(t)\right) + a_y(t) \\
\dot{v}_z(t) &= -\frac{\rho}{2\beta} g\left(\sqrt{v_x^2(t)+v_y^2(t)+v_z^2(t)}\cdot v_z(t)\right) - g + a_z(t)
\end{aligned} \tag{3}$$

Let us denote the state vector as,

$$\begin{aligned}
x(t) &= \left[x_1(t)\,x_2(t)\,x_3(t)\,x_4(t)\,x_5(t)\,x_6(t)\right]^T \\
&= \left[x_m(t) \quad y_m(t) \quad z_m(t) \quad v_x(t) \quad v_y(t) \quad v_z(t)\right]^T
\end{aligned} \tag{4}$$

where $x_m(t)$, $y_m(t)$, and $z_m(t)$ are the RV positions in *X*, *Y*, and *Z*, respectively; $v_x(t)$, $v_y(t)$ and $v_z(t)$ are the RV velocities along *X*, *Y*, and *Z*, respectively. Then, we get the nonlinear state equation for RV trajectories as follows:

$$\dot{x}(t) = F\left(x(t)\right) + Dw(t) \tag{5}$$

where,

$$F\left(x(t)\right) = \begin{bmatrix}
x_4(t) \\
x_5(t) \\
x_6(t) \\
-\left(\frac{\rho}{2\beta}\right)\left(\sqrt{x_4^2(t)+x_5^2(t)+x_6^2(t)}\cdot x_4\right)\cdot g \\
-\left(\frac{\rho}{2\beta}\right)\left(\sqrt{x_4^2(t)+x_5^2(t)+x_6^2(t)}\cdot x_5\right)\cdot g \\
-\left(\frac{\rho}{2\beta}\right)\left(\sqrt{x_4^2(t)+x_5^2(t)+x_6^2(t)}\cdot x_6\right)\cdot g - g
\end{bmatrix}$$

$$D = \begin{bmatrix} 0_{3\times3} & 0_{3\times3} \\ 0_{3\times3} & I_{3\times3} \end{bmatrix}$$

$$w(t) = \begin{bmatrix} 0\ 0\ 0\ a_x(t)\ a_y(t)\ a_z(t) \end{bmatrix}$$

(6)

The air density ρ in (3) is a function of altitude and the altitude dramatically changes as RV flies over 44 km. An

approximate model of air density ρ in g/cm3 is given as follows:

$$\rho = 0.12492((1-0.0000225577\cdot z_m(t))^{4.2561} \quad (7)$$

for $z_m(t) < 44332m$

For conventional air defense missile systems, the ground radar is the major instrument for detecting the RV. The measurement equation is then,

$$y(t) = Cx(t) + n(t) \quad (8)$$

where $n(t)$ denotes the measurement noise vector, and $C = I_{6\times 6}$ denotes the response distribution matrix.

Suppose the following fuzzy system is employed to approximate the nonlinear RV system in (5) and (8), the *ith* rule of this fuzzy model for the nonlinear RV system (5) is of the following form;

System Rule i:

If $a_1(t)$ is G_{i1} and …and $a_g(t)$ is G_{ig},

Then $\dot{x}(t) = A_i x(t) + Dw(t)$

$y(t) = Cx(t) + n(t)$, for $i = 1, 2, ..., l$ (9)

where, G_{ij} is the fuzzy set, $A_i \in R^{6\times 6}$, $D \in R^{6\times 6}$, l is the number of If-Then rules, and $a_1(t)$, ..., $a_g(t)$ are the premise variables.

The overall fuzzy RV system is inferred as follows :

$$\dot{x}(t) = \frac{\sum_{i=1}^{l}\mu_i(a(t))(A_i x(t))}{\sum_{i=1}^{l}\mu_i(a(t))} + Dw(t)$$
$$y(t) = Cx(t) + n(t) \quad (10)$$

or,

$$\dot{x}(t) = \sum_{i=1}^{l} h_i(a(t))(A_i x(t)) + Dw(t)$$
$$y(t) = Cx(t) + n(t) \quad (11)$$

where,

$$\mu_i(a(t)) = \prod_{j=1}^{g} G_{ij}(a_j(t))$$

$$h_i(a(t)) = \frac{\mu_i(a(t))}{\sum_{i=1}^{l}\mu_i(a(t))}$$

$$a(t) = [a_1(t),\ a_2(t),\ ...,\ a_g(t),]$$

and $G_{ij}(a_j(t))$ is the grade of membership of $a_j(t)$ in G_{ij}.

In this study, we assume

$\mu_i(a(t)) \geq 0$,for $i = 1, 2, \ldots, l$

and

$$\sum_{i=1}^{l}\mu_i(a(t)) > 0$$

for all *t*. Therefore, we get the certainty functions,

$h_i(a(t)) \geq 0$

(12)

for $i = 1, 2, \ldots, l$ and

$$\sum_{i=1}^{l} h_i(a(t)) > 1$$

(13)

The physical meaning of the fuzzy system in (11) is that the local linearized systems $\dot{x}(t) = A_i x(t) + Dw(t)$ at different operation regions (different fuzzy set G_{ij}) are interpolated via the fuzzy basis functions $h_i(a(t))$ to approximate the nonlinear RV system in (6).

Therefore, form (9), we get,

$$\begin{aligned}\dot{x}(t) &= F(x(t)) + Dw(t)\\ &= \sum_{i=1}^{l} h_i(a(t))(A_i x(t)) + Dw(t)\\ &+ \left\{F(x(t)) - \sum_{i=1}^{l} h_i(a(t))(A_i x(t))\right\}\end{aligned} \quad (14)$$

where $\left\{F(x(t)) - \sum_{i=1}^{l} h_i(a(t))(A_i x(t))\right\}$ and $h_i(a(t)) \geq 0$ denotes the approximation error and interpolation function between the nonlinear RV system (6) and the fuzzy RV model (9). Let us denote the sum of approximation error and external disturbance as the following uncertain disturbance,

$$\xi(t) = \left[F(x(t)) - \sum_{i=1}^{l} h_i(a(t))(A_i x(t))\right] + Dw(t)$$

Then, we get the fuzzy RV system in the following equivalent form,

$$\dot{x}(t) = \sum_{i=1}^{l} h_i(a(t))(A_i x(t)) + \xi(t)$$
$$y(t) = Cx(t) + n(t) \quad (15)$$

This study proposes using the following fuzzy trajectory estimator to deal with the state estimation of nonlinear RV system in (6) and (8) or the fuzzy equivalent system in (11), on Rule i:

If $a_1(t)$ is G_{i1} and …and $a_g(t)$ is G_{ig}

Then $\hat{x}(t) = A_i\hat{x}(t) + L_i\left(y(t) - \hat{y}(t)\right)$ (16)

where L_i is the estimator parameter to be designed for $i = 1, ..., l$. The overall fuzzy trajectory estimator in (16) is equivalent to,

$$\dot{\hat{x}}(t) = \sum_{i=1}^{l} h_i\left(a(t)\right)\left\{A_i\hat{x}(t) + L_i\left(y(t) - C\hat{x}(t)\right)\right\} \quad (17)$$

Now let us denote the estimation error as

$$\tilde{x}(t) = x(t) - \hat{x}(t) \quad (18)$$

By differentiating (18), and from (11) and (17), it is seen,

$$\dot{\tilde{x}}(t) = \sum_{i=1}^{l} h_i\left(a(t)\right)\left\{\left(A_i - L_iC\right)\tilde{x}(t) - L_in(t)\right\} + \xi(t) \quad (19)$$

After some manipulations, (19) can be expressed in a compact form:

$$\dot{\tilde{x}}(t) = \sum_{i=1}^{l} h_i\left(a(t)\right)\left\{\tilde{A}_i\tilde{x}(t) + \tilde{E}_i\tilde{w}(t)\right\} \quad (20)$$

Where

$$\tilde{A}_i = \left[A_i - L_iC\right],\ \tilde{E}_i = \left[-L_i \quad I\right],\ \tilde{w}(t) = \begin{bmatrix} n(t) \\ \xi(t) \end{bmatrix} \quad (21)$$

In order to attenuate the effect of uncertain disturbance $\tilde{w}(t)$ resulting form the uncertain target accelerations, approximation error and measurement noise $n(t)$ on the performance of the above estimation error dynamics, the H_∞ estimation performance is proposed to attenuate the worst-case effect of $\tilde{w}(t)$ on $\tilde{x}(t)$ as follows;

$$\frac{\int_0^{t_f} \tilde{x}^T(t)Q\tilde{x}(t)}{\int_0^{t_f} \tilde{w}^T(t)\tilde{w}(t)\,dt} \le \gamma^2,\ \forall\tilde{w}(t) \in L_2\left[0, t_f\right] \quad (22)$$

where Q is a weighting matrix with $Q^T = Q \ge 0$ and γ^2 denotes a prescribed attenuation level which is always chosen to be less than 1. The above equation is equivalent to

$$\int_0^{t_f} \tilde{x}^T(t)Q\tilde{x}(t)\,dt \le \gamma^2 \int_0^{t_f} \tilde{w}^T(t)\tilde{w}(t)\,dt,\ \forall\tilde{w}(t) \in L_2\left[0, t_f\right]$$

Theorem 1: *Suppose the fuzzy estimator in (17) is employed in the nonlinear trajectory estimation of RV dynamic system in (6) and (8), and P=P^T > 0 is the common solution of the following Riccati-like inequalities,*

$$\tilde{A}_i^T P + PA_i + P\left(\frac{1}{\gamma^2}\tilde{E}_i\tilde{E}_i^T\right)P + Q < 0, \text{ for, } i = 1, 2, ..., l \quad (23)$$

the H_∞ estimation performance in (22) is guaranteed for the fuzzy trajectory estimator in (17) with a prescribed γ^2 in presence of external uncertain disturbance $\tilde{w}(t)$.

III. Simulation Results

To demonstrate the performance robustness of the proposed estimation method, the following case of initial condition is considered in the simulation example.

*Case*1 : the reentry target is with $\beta = 2400$ (kg/m^2) and maneuvering accelerations of $4g$ and $-4g$ in X and Y, respectively, during $14(\text{sec}) \le t \le 18(\text{sec})$ and $7(\text{sec}) \le t \le 9(\text{sec})$ as figure 2, respectively as Fig. 2. The following is the initial condition of the high speed reentry target:

$$x_m(0) = 4km,\quad y_m(0) = 4km,\quad z_m(0) = 55km,$$
$$v_x(0) = -550m/s,\quad v_y(0) = -650m/s,\quad v_z(0) = -1800m/s.$$

and the initial condition for the estimation system is set up as follows:

$$\hat{x}_m(0) = 6km,\quad \hat{y}_m(0) = 6km,\quad \hat{z}_m(0) = 70km,$$
$$\hat{v}_x(0) = -900m/s,\quad \hat{v}_y(0) = -800m/s,\quad \hat{v}_z(0) = -1900m/s.$$

As seen in Figs 3-6, the proposed nonlinear H_∞ fuzzy tilter yields satisfactory estimation results under ballistic coefficient $\beta = 2400$ (kg/m^2) and the strong effect of a maneuvering acceleration: step maneuver as shown in Fig. 2. Figs. 3 show the 3D profiles of the true trajectory of RV systems and their estimation result by the proposed trajectory estimation method corresponding to the above high differentiation in initial conditions between high speed reentry target and the estimator. These results imply that the proposed method is robust in overriding the effect of modeling uncertainties: modeling uncertainties of reentry targets in our design procedures include 1. model approximation errors, 2. unpredictable accelerations of targets and 3. measurement noise. Since, the proposed method has minimized the worst-case effect of modeling uncertainties in advance; the superior performance of proposed fuzzy H_∞ filter is predictable. This is reasonable because several linearized models around different operation points of the nonlinear system were first obtained by the ANFIS algorithm, hence, the interpolation model of the local linear models by the fuzzy basis function are very similar to that of the nonlinear RV system, i.e., the nonlinear RV systems are approximated piecewise by the fuzzy-interpolated local linear models with small approximation errors, and then the worst-case effect of the proposed method has been eliminated with a systematic analysis. From simulation results, it is obvious that the state trajectories of the RV system can be efficiently estimated by the proposed fuzzy H_∞ filter.

IV. Conclusions

In this study, a nonlinear fuzzy H_∞ filter is successfully developed for the state estimation of high speed reentry vehicles. In general, it needs to solve the Hamilton-Jacobi-Isaac equation for obtaining a robust filter with noise reduction and modeling uncertainty elimination ability. To

avoid solving the complicated Hamilton-Jacobi-Isaac equation in the conventional H_∞ filter design, the robust fuzzy H_∞ filter design problem is first transformed to an eigenvalue problem with the fuzzy approximation technology and then formulates it as a solvable LMI so that the trajectory estimation problem of reentry vehicles could be efficiently solved with the available computer software. The simulation results reveal that the proposed method yield accurate and satisfactory estimation ability. Simulation results also show that the proposed H_∞ filter offers the potential application in the precise trajectory estimation of RV systems.

REFERENCES

[1] A. S., Abutableb, "Improved trajectory estimation of maneuvering reentry vechicles using a nonlinear filter based on the pontryagin minimum principle," *Proc. Of IEEE Iner. Radar Conf.,* New York, pp.424-429,1985.

[2] A. G., Lindgren, A. J., Irz, and S. C., Nardone, "Trajectory estimation with uncertain and nonassociated data," *IEEE Trans. on Aerosp. And Electron. Syst.,* vol. AES-22,no. 1, pp.71-78,1986.

[3] N. J., Denis, "Space-based tactical ballistic missile launch parameter estimation," IEEE Trans. on Aerosp. And Electron, Syst., vol. 29, no 2, pp.412424,1993.

[4] Q. P., Chu, J. A., Mulder, and P. T. L. M., van Woerkom, "Modified recursive maximum likehood adaptive filter for nonlinear aircraft flight path reconstruction," *J. Guidance, Contr., and Dyn.*, vol 19, no 6, pp.1285-1295,1996.

[5] Klein, V., Batterson, J. G., and Murphy, P/ C., "Determination of Airpplane Model Structure from Flight Data by Using modified Stepwise Regression," NASA TP-1916,1981.

[6] J. S. R., Jang, "ANFIS: Adaptive-network-based fuzzy inference systems", *IEEE Trans.Syst., Man, and Cybern.,* vol. 23, no. 3, pp.665-685,1993.

[7] C. B., Chang, R. H., Whiting, and M., Athans, "On the state and parameter estimation for maneuvering reentry vehicles", *IEEE Trans. Automat. Contr.,* vol. AC-22, no. 1, pp.99-105,1977.

[8] D. R., Manohar, and S., Krishnan, "Trajectory reconstruction during thrusting phase of rockets using differential corrections," *J. Guidance, Contr., and Dyn.*, vol 8, no 3, pp.406-408,1985.

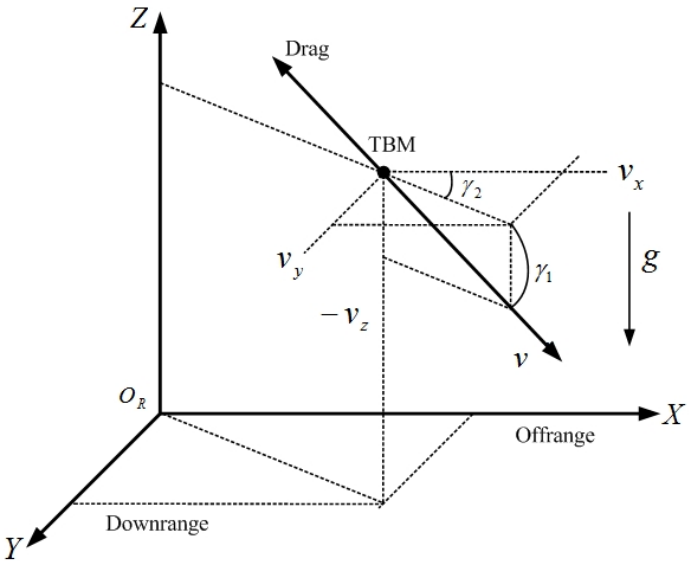

Fig.1 Tactical ballistic missile geometry

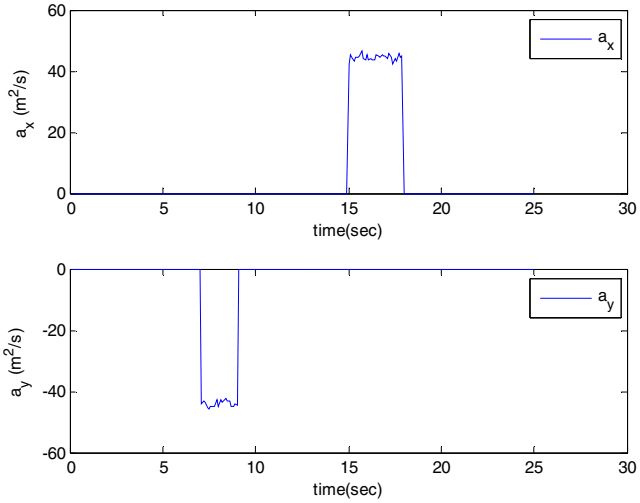

Fig.2 TBM's random maneuver in X and Y axis

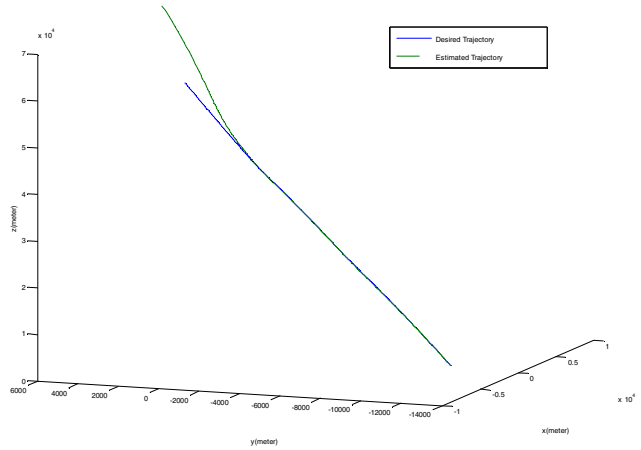

Fig.3 Three dimensional profiles of the trajectory estimations corresponding to the initial conditions of Case 1

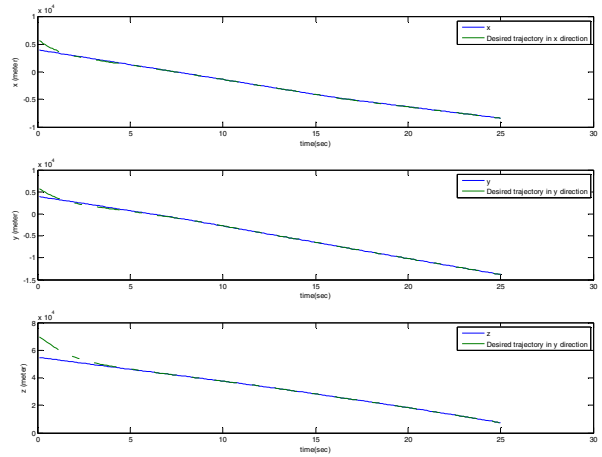

Fig.4 Estimation results of altitude x_m, downrange y_m and offrange z_m

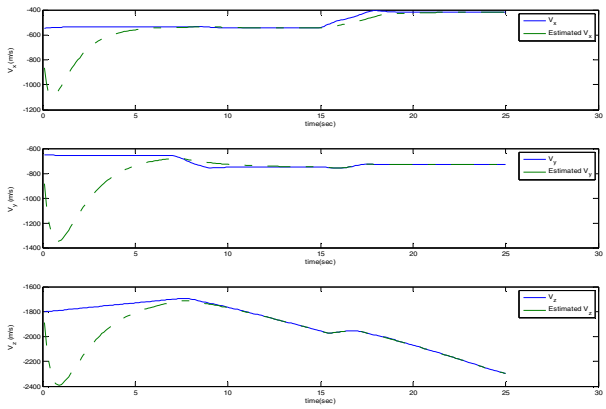

Fig.5 Estimation results of altitude v_x , downrange v_y and offrange v_z

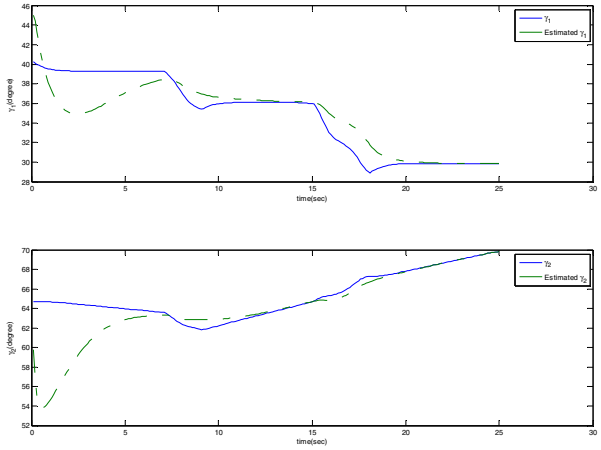

Fig.6 Estimation results of Azimuth γ_1 and elevation angle γ_2

2011 IEEE International Conference on Fuzzy Systems
June 27-30, 2011, Taipei, Taiwan

Data-driven Based 3-D Fuzzy Logic Controller Design Using Nearest Neighborhood Clustering and Linear Support Vector Regression

Xianxia Zhang, Ye Jiang
Shanghai Key Laboratory of Power Station Automation Technology
School of Mechatronics and Automation
Shanghai University
Shanghai 200072, China
e-mail:ye924@shu.edu.cn

Tao Zou
College of Information Engineering
Zhejiang University of Technology
Hangzhou 310014, China

Chenkun Qi
School of Mechanical Engineering
State Key Laboratory of Mechanical System and Vibration
Shanghai Jiao Tong University
Shanghai 200240, China

Guitao Cao
Software Engineering Institute
East China Normal University
Shanghai 200062, China

***Abstract*—Three-dimensional fuzzy logic controller (3-D FLC) is a novel FLC developed for spatially distributed parameter systems. In this study, we are concerned with data-based 3-D FLC design. A nearest neighborhood clustering algorithm is employed to extract fuzzy rules from input-output data pairs, and then an optimization algorithm based on geometric similarity measure is used to reduce the obtained rule base. The consequent parameters are estimated using linear support vector regression. Finally, a catalytic packed-bed reactor is taken as an application to demonstrate the effectiveness of the 3-D FLC.**

Keywords-3-D fuzzy set; three-dimensional fuzzy logic controller; nearest neighborhood clustering; linear support vector regression

I. INTRODUCTION

In the real world, many physical processes and systems have the characteristics of spatial distribution, and are usually called spatially distributed systems. Recently, A novel three-dimensional fuzzy logic controller (3-D FLC) [1] has been developed for the control of such systems. 3-D FLC employs 3-D fuzzy sets [1], which is composed of the traditional fuzzy set plus a third dimension for the spatial information, and carries out 3-D rule inference engine. It has an inherent capability to express and process spatial information. The design of 3-D FLC is usually divided into two different approaches: expert experience based approach and data-driven based approach. When much domain knowledge from human experts or operators is obtained, a satisfied 3-D FLC can be designed by expert experience such as in [1]. On the other hands, if the domain knowledge is not available, or the domain knowledge is very hard to be extracted or described by human's words, but effective input-output data is available, the 3-D FLC can also be designed using the data information such as in [2].

In [2], a table look-up scheme that took into account the tempo-spatial nature sufficiently was applied to the 3-D FLC design. Each input-output data pair generates one rule; as a result, the number of rules is very large. To reduce the number of rules, a degree is assigned to a rule, and then only the rule with maximum degree from a conflict group is accepted. However, it is equal to the number of boxes of the base when the fuzzy rule base is complete, and then, it increases exponentially as the dimension of the input space increases. Instead of the most direct way to partition the input space, fuzzy clustering algorithms provide a more flexible partition, such as the nearest neighborhood clustering in [3]. In this study, we adopt the Frobenius norm as a distance measurement, instead of the Euclidean norm in the traditional counterpart. Via comparing the inverse of sum of unit and distance with a given threshold, a new fuzzy rule is determined whether to be generated. To simplify the redundancy fuzzy sets in the input space partition, similarity measures techniques are usually used, such as in [4]- [6], which can be divided into two categories [6]: geometric similarity measures and set-theoretic similarity measures. For the 3-D fuzzy set, a distance-based similarity measure [4], as a special geometric similarity measures method, is employed to combine similar fuzzy sets. After constructing the antecedent parts, the linear support vector regression (SVR, i.e. ε-linear support vector regression) will be used to determine the parameters in consequent parts.

The paper is divided into five sections. In Section II, preliminaries on 3-D FLC and SVR are described. In Section III, the proposed data-based 3-D FLC design is presented in detail. Application to the catalytic packed-bed reactor and experimental results are given in Section IV. Finally, conclusions and future works are given in Section V.

978-1-4244-7316-8/11/$26.00 ©2011 IEEE

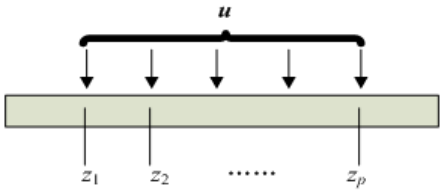

Figure 1. Sketch of a DPS with a distributed actuator u and p point measurement sensors.

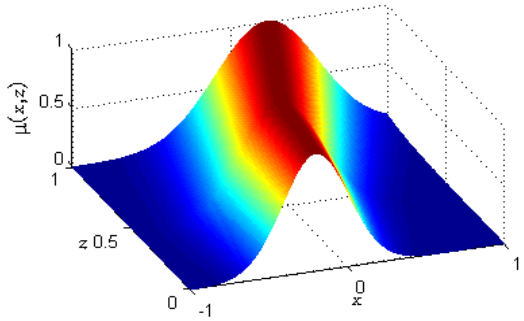

Figure 2. 3-D fuzzy set.

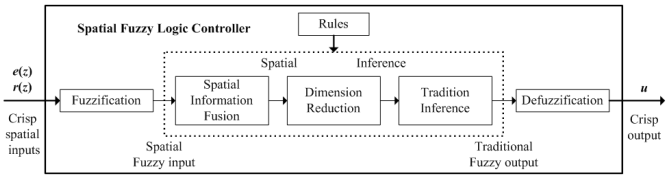

Figure 3. Basic structure of 3-D FLC.

II. PRELIMINARIES

A. *Three-dimensional fuzzy logic controller*

The 3-D FLC is designed to have the inherent capability to deal with spatial information and its basic structure is shown in Fig. 3. It has a similar functional structure similar to the traditional FLC, which consists of three basic blocks: fuzzification, rule inference, and defuzzification. However, it will differ in the detailed operations because of the spatial processing requirement [1]. Generally, the 3-D FLC will be involved with the following basic designs: 3-D membership function (MF), 3-D fuzzification, 3-D rule base, 3-D rule inference, and defuzzification. One can refer to [1] for detailed description. In this study, we consider the multi-input single-output (MISO) cases where the finite sensors are employed; extensions to general multi-input multi-output (MIMO) cases are straightforward. Given N fuzzy rules with the following form

$$\bar{R}^l\text{: IF } x_1(z) \text{ is } \bar{C}_1^l \text{ and..and } x_s(z) \text{ is } \bar{C}_s^l, \text{THEN } u \text{ is } B^l \quad (1)$$

where $x_i(z)\,(i=1,...,s)$ denotes the ith spatial input variable; $z \in Z$ is a point in one-dimensional space Z; In discrete space, Z can be represented by $Z=\{z_1,z_2,...,z_p\}$, $z_1,z_2,...,z_p$ denote the discrete space positions; $\bar{C}_i^l$ denotes a 3-D fuzzy set; u denotes output variable (the control action). B^l denotes a traditional fuzzy set; $l=1,...,N$.

To design a 3-D fuzzy set, for instance $\bar{C}_i^l$ $(i=1,...,s,$ $l=1,...,N)$ in (1), one simple method is to decompose the 3-D fuzzy set into the multiple 2-D fuzzy sets. As a result, the design method from the traditional 2-D fuzzy sets can be used. Similarly, the 3-D fuzzification can be regarded as the assembly of the traditional 2-D fuzzification at each sensing location. When the Gaussian type fuzzy set is chosen for 3-D fuzzy set, it means that MF of the ith spatial input variable $x_i(z)$ at the sensing location $z=z_j$ is Gaussian MF, which can be written as

$$\mu_{Gij}(x_i(z_j))=\exp\left(-(x_i(z_j)-v_{ij}^l)^2/(\sigma_{ij}^l)^2\right) \quad (i=1,...,s,\ j=1,...,p,\ l=1,...,N) \quad (2)$$

where v_{ij}^l and σ_{ij}^l are center and width of the Gaussian MF, respectively.

If we choose singleton fuzzification, product for the spatial information fusion operation, the centroid approach for the dimension reduction, product inference, center-of-sets defuzzification, and Gaussian MF in (2), then the input-output mapping of the 3-D FLC, $u: R^{p\times s} \to R$, is given by

$$u(x_z)=\frac{\sum_{l=1}^N u^l \sum_{j=1}^p a_j^l \prod_{i=1}^s \mu_{Gij}(x_i(z_j))}{\sum_{l=1}^N \sum_{j=1}^p a_j^l \prod_{i=1}^s \mu_{Gij}(x_i(z_j))} \quad (3)$$

where u^l is the centroid of the consequent set, i.e. the center of Gaussian MF, such that $\mu(u^l)=1$; a_j^l denotes the time-variant weight with the following form

$$\begin{cases} a_1^l=\Delta\theta_1^l/\left(2\sum_{k=1}^{p-1}\Delta\theta_k^l\right) \\ a_j^l=\left(\Delta\theta_{j-1}^l+\Delta\theta_j^l\right)/\left(2\sum_{k=1}^{p-1}\Delta\theta_k^l\right) \quad j=2,...,p-1 \\ a_p^l=\Delta\theta_{p-1}^l/\left(2\sum_{k=1}^{p-1}\Delta\theta_k^l\right) \\ \Delta\theta_k^l=\sqrt{\left(\mu_{W^l}(z_{k+1})-\mu_{W^l}(z_k)\right)^2+\left(z_{k+1}-z_k\right)^2} \\ \mu_{W^l}(z_k)=\prod_{i=1}^s \mu_{Gik}(x_i(z_k)) \end{cases} \quad (4)$$

Let

$$\phi^l(x_z)=\frac{\sum_{j=1}^p a_j^l \prod_{i=1}^s \mu_{Gij}(x_i(z_j))}{\sum_{l=1}^N \sum_{j=1}^p a_j^l \prod_{i=1}^s \mu_{Gij}(x_i(z_j))} \quad l=1,...,N \quad (5)$$

be the fuzzy basis functions (FBF) of 3-D FLC and u^l be constants, then (3) can be viewed as a linear combination of fuzzy basis functions.

$$u(x_z)=\sum_{l=1}^N \phi^l(x_z)\theta^l \quad (6)$$

where $\theta^l \in R$ are constants, i.e. $\theta^l=u^l$.

From (1) and (5), we can see that each FBF corresponds to a fuzzy IF-THEN rule.

B. *Linear support vector regression*

In this subsection, we will briefly introduce the basic theory of linear SVR (i.e. ε-linear support vector regression) [7].

Suppose there is a set T composed of n input-output training data pairs

$$T=\{(x_i,y_i)\big|x_i\in R^s, y_i\in R, i=1,...,n\} \tag{7}$$

In ε-linear SVR, the aim is to find a decision function $f(x)$ that has at most ε deviation from the actually obtained targets y_i for all the training data pairs, and at the same time is as flat as possible. $f(x)$ has the following form

$$f(x)=\langle w,x\rangle+b \text{ with } w\in R^s, b\in R \tag{8}$$

where $\langle\cdot,\cdot\rangle$ denotes the dot product in R^s; w is a high-dimensional weight vector, and b is a bias term. Flatness in the case of (8) means that one seeks a small w. One way to ensure this is to minimize $\|w\|^2=\langle w,w\rangle$.

If the considered problem is infeasible or some errors are allowed, then the task is to minimize the following convex optimization problem by introducing slack variables ξ_i,ξ_i^*.

$$\begin{aligned}&\min_{w,b,\xi^{(*)}} \quad \frac{1}{2}\|w\|^2+C\sum_{i=1}^{n}(\xi_i+\xi_i^*)\\ &s.t. \quad \begin{cases} y_i-(w\cdot x_i+b)\le\varepsilon+\xi_i\\ (w\cdot x_i+b)-y_i\le\varepsilon+\xi_i^*\\ \xi_i,\xi_i^*\ge 0,\ i=1,...,n\end{cases}\end{aligned} \tag{9}$$

where constant C determines the trade-off between the flatness of f and the amount up to which deviations larger than ε are tolerated. This corresponds to dealing with a so called ε-insensitive loss function $|\xi|_\varepsilon$ described by

$$|\xi|_\varepsilon:=\begin{cases}0 & \text{if } |\xi|\le\varepsilon\\ |\xi|-\varepsilon & \text{otherwise.}\end{cases}$$

The corresponding dual optimization problem of convex optimization problem in (9) is given by

$$\begin{aligned}&\max_{\alpha^{(*)}\in R^{2l}} \quad \begin{cases}-\frac{1}{2}\sum_{i,j=1}^{n}(\alpha_i-\alpha_i^*)(\alpha_j-\alpha_j^*)\langle x_i,x_j\rangle\\ -\varepsilon\sum_{i=1}^{n}(\alpha_i+\alpha_i^*)+\sum_{i=1}^{n}y_i(\alpha_i-\alpha_i^*)\end{cases}\\ &s.t. \quad \sum_{i=1}^{n}(\alpha_i-\alpha_i^*)=0 \text{ and } \alpha_i,\alpha_i^*\in[0,C]\end{aligned} \tag{10}$$

The vector w has the form: $w=\sum_{i=1}^{n}(\alpha_i-\alpha_i^*)x_i$ and therefore

$$f(x)=\sum_{i=1}^{n}(\alpha_i-\alpha_i^*)\langle x_i,x\rangle+b \tag{11}$$

The points with $(\alpha_i-\alpha_i^*)\neq 0$ are defined as support vectors.

III. Data-Based 3-D FLC Design

The design of 3-D FLC includes two steps: structure learning and parameter learning. In structure learning, the nearest neighborhood clustering is employed to mine the underlying knowledge of the data set S such that fuzzy rules and Gaussian 3-D MFs in the antecedent part are constructed, and then an optimization algorithm based on similarity measure is utilized to combine similar MFs and then simplify the rule base. In parameter learning, the linear SVR algorithm is used to estimate the parameters of the traditional Gaussian-type fuzzy sets in the consequent part.

Firstly, the concerned 3-D FLC can be defined as follows.

Definition 1: The set of 3-D FLC with fuzzy rule base in (1), singleton fuzzification, product inference, center-of-sets defuzzification, and Gaussian MF can be described mathematically in (12)

$$u(x_z)=\frac{\sum_{l=1}^{N}u^l\sum_{j=1}^{p}a_j^l\prod_{i=1}^{s}\mu_{Gij}(x_i(z_j))}{\sum_{l=1}^{N}\sum_{j=1}^{p}a_j^l\prod_{i=1}^{s}\mu_{Gij}(x_i(z_j))}+b \tag{12}$$

From (12), we can see that each 3-D FLC in the set combines a 3-D FLC in (3) and a constant b. b is included for the bias term in the linear SVR. The motivation of this study is to determine a mapping u in (12) using the fuzzy rules generated from a set S represented by (13), which consists of input-output data pairs from a spatially distributed system.

$$S=\{(x_z^k,u^k)\big|x_z^k\in R^{p\times s}, u^k\in R, k=1,...,n\} \tag{13}$$

where $x_z^k=(x_1^k(z),...,x_s^k(z))$ denotes the value of all s spatial input variables at the kth sampling time, $x_i^k(z)=(x_i^k(z_1),...,x_i^k(z_p))^T$ $(i=1,...,s)$, u^k denotes the output value at the kth sampling time, n denotes the number of sampling time, and p denotes sensor number.

A. Structure Learning

Define abbreviations and acronyms the first time they are used in the text, even after they have been defined in the abstract. Abbreviations such as IEEE, SI, MKS, CGS, sc, dc, and rms do not have to be defined. Do not use abbreviations in the title or heads unless they are unavoidable.

1) Nearest neighborhood clustering: Different from the traditional vector input-output data pairs, the input-output data pairs S in (13) are of matrix form. Therefore, the Frobenius norm will be used for defining the distance in a nearest neighborhood clustering algorithm [3]. By comparing the inverse of sum of unit and distance with a given threshold, we can determine whether to add a new fuzzy rule. The nearest neighborhood clustering algorithm is summarized as follows:

Step 1: Begin from the first input-output data pair x_z^1. Let the first cluster center c_z^1 be x_z^1, the number of data pairs m_1 be 1 in this cluster, and the threshold be ρ_0 for generating new fuzzy rules.

Step 2: Suppose that the kth input-output data pair $x_z^k(k=2,...,n)$ is considered, when N clusters have been generated and their centers are $c_z^1,...,$and c_z^N, respectively. Firstly, the distance between x_z^k and each center of N clusters is computed using $\|x_z^k-c_z^l\|_F$ $(l=1,...,N)$, where $\|\cdot\|_F$ denotes the Frobenius norm, $\|X\|_F=\sqrt{tr(X^TX)}$ $(X\in R^{p\times s})$. Then, threshold ρ is given by (14)

$$\rho=\max_{l=1,...,N}\left(1\Big/\left(1+\|x_z^k-c_z^l\|_F\right)\right) \tag{14}$$

Hence, the corresponding cluster center $c_z^{l_k}$ is taken as the nearest neighborhood cluster of x_z^k.

Step 3: If $\rho < \rho_0$, then x_z^k is taken as the new cluster center. Let $N = N+1$, $m_N = 1$, and $c_z^N = x_z^k$. Otherwise, x_z^k belongs to the cluster $c_z^{l_k}$, by introducing a learning rate $\eta = \eta_0/(m_{l_k}+1)$ ($\eta_0 \in [0,1]$) [1] described by (15) for tuning the center of l_kth cluster;

$$c_z^{l_k} = c_z^{l_k} + \eta(x_z^k - c_z^{l_k});\ m_{l_k} = m_{l_k} + 1 \tag{15}$$

Step 4: Let $k = k+1$. If $k \geq n+1$, then quit; otherwise, back to Step 2.

2) Rule extraction and 3-D MF construction: After clustering learning, we can obtain a input space partition with N cluster centers $c_z^1, c_z^2, ..., c_z^N$. Then, we will produce antecedent part of rule base and construct 3-D MF in terms of the partition. Each cluster corresponds to a fuzzy rule, and the cluster center corresponds to the center of Gaussian 3-D MFs in the antecedent part. Thus, the number of fuzzy rules is equal to the number of clusters N. Finally, let the width of 3-D Gaussian MFs have the same value as in (16) [1] at each sensing location.

$$\sigma(z_j) \approx \max_{1 \leq i \leq s} \left((x_i^{\max}(z_j) - x_i^{\min}(z_j))/10 \right) \tag{16}$$

where $x_i^{\max}(z_j)$ and $x_i^{\min}(z_j)$ are the maximum and the minimum bound value of the ith spatial input in S, respectively. Similarly, the width of traditional Gaussian MF in the consequent part is given as

$$\sigma_B \approx (\max(u) - \min(u))/10 \tag{17}$$

where $\max(u)$ and $\min(u)$ are the maximum and the minimum bound value of the output in S, respectively.

3) Optimization algorithm: The obtained input space partition may have redundancy in terms of highly overlapping membership functions. It is necessary to optimize the above obtained fuzzy partition. The optimization task includes: removing 3-D fuzzy sets similar to the universal set or the singleton set, and merging some similar 3-D fuzzy sets and some rules with similar antecedent part.

Firstly, the definition of the similarity of two 3-D fuzzy sets is given as follows.

Definition 2: Define the similarity of two 3-D fuzzy sets $\overline{A}$ and $\overline{B}$ as

$$\overline{S}(\overline{A}, \overline{B}) = \frac{1}{1 + d(\overline{A}, \overline{B})} \quad \overline{S}(\cdot) \in (0,1] \tag{18}$$

where $d(\overline{A}, \overline{B})$ is the distance between $\overline{A}$ and $\overline{B}$. Since Gaussian type membership functions are chosen, the following simple expression can be used to approximate the distance.

$$d(\overline{A}, \overline{B}) = \left\| \begin{bmatrix} c_{\overline{A}(z_1)} & \sigma_{\overline{A}(z_1)} \\ \vdots & \vdots \\ c_{\overline{A}(z_p)} & \sigma_{\overline{A}(z_p)} \end{bmatrix} - \begin{bmatrix} c_{\overline{B}(z_1)} & \sigma_{\overline{B}(z_1)} \\ \vdots & \vdots \\ c_{\overline{B}(z_p)} & \sigma_{\overline{B}(z_p)} \end{bmatrix} \right\|_F \tag{19}$$

where $c_{\overline{A}(z_j)}(c_{\overline{B}(z_j)})$ and $\sigma_{\overline{A}(z_j)}(\sigma_{\overline{B}(z_j)})$ are center and width of Gaussian MF at sensing location $z = z_j$ $(j = 1, ..., p)$ respectively.

If 3-D fuzzy sets $\overline{A}$ and $\overline{B}$ are similar, then they will be merged into a new spatial fuzzy set $\overline{C}$, the center and width of which are viewed as the average value of the two original 3-D fuzzy sets, i.e. $c_{\overline{C}(z_j)} = (c_{\overline{A}(z_j)} + c_{\overline{B}(z_j)})/2, \sigma_{\overline{C}(z_j)} = (\sigma_{\overline{A}(z_j)} + \sigma_{\overline{B}(z_j)})/2$.

The similarity of fuzzy rules only measures their similarity in antecedent part. Therefore, the similarity between two fuzzy rules $\overline{R}^{l_1}$ and $\overline{R}^{l_2}$ can be computed by (20).

$$\overline{S}_{rule}(\overline{R}^{l_1}, \overline{R}^{l_2}) = \min_{1 \leq i \leq s} \left\{ \overline{S}(\overline{C}_i^{l_1}, \overline{C}_i^{l_2}) \right\} \tag{20}$$

The rule base simplification algorithm in [1] can be extended to this study only for antecedent part, where the similarity measure is replaced by (18) and two thresholds γ (for removing fuzzy sets similar to the universal set) and λ (for merging two similar fuzzy sets) are required. In this study, we choose $\gamma \in (\lambda, 1]$ and $\lambda \in [0.6, 0.9]$.

B. Parameter Learning

For a complete rule base, the rest task is to determine the consequent part parameters. In this subsection, a linear SVR algorithm is applied to estimate the consequent part parameter b^l $(l = 1, ..., N)$ in the 3-D FLC. Each input x_z^k $(k = 1, ..., n)$ in S is transformed into a corresponding FBF $\phi(x_z^k) = (\phi^1(x_z^k), \phi^2(x_z^k), ..., \phi^N(x_z^k))$. Hence, the original data set S in (13) can be represented by (21)

$$S = \{(\phi(x_z^k), u^k) \,|\, \phi(x_z^k) \in R^N, u^k \in R, k = 1, ..., n\} \tag{21}$$

From (13), the final decision function $f(\phi(x_z^k))$ can be described in the following form

$$f(\phi(x_z^k)) = \sum_{k=1}^n (\alpha_k - \alpha_k^*) \langle \phi(x_z^k), \phi(x_z) \rangle + b \tag{22}$$

where α_k^* and α_k are obtained by solving the dual optimization problem in (10). Then (22) can further be expressed as follows

$$\begin{aligned} u(x_z) &= \sum_{k=1}^n (\alpha_k - \alpha_k^*) \sum_{l=1}^N \phi^l(x_z^k) \phi^l(x_z) + b \\ &= \sum_{l=1}^N \left(\sum_{k=1}^n (\alpha_k - \alpha_k^*) \phi^l(x_z^k) \right) \phi^l(x_z) + b \\ &= \sum_{l=1}^N u^l \phi^l(x_z) + b \end{aligned} \tag{23}$$

We can see that (23) is equal to (12), namely, $u^l = \sum_{k=1}^n (\alpha_k - \alpha_k^*) \phi^l(x_z^k)$. Thus, the parameters u^l $(l = 1, ..., N)$ in consequent parts are obtained, which can be modified as follows.

$$u^l = \sum_{k \in SV} (\alpha_k - \alpha_k^*) \phi^l(x_z^k) \tag{24}$$

where SV denotes the support vectors of linear SVR. It is noted that C in (9) is an adjustable parameter. In this study, we choose a better one through several turns of simulation."

IV. Application To Catalytic Packed-bed Reactor

We take a catalytic packed-bed reactor [1] [10] as an example. A reaction of the form $C \rightarrow D$ takes place on the catalyst. The reaction is endothermic and a jacket is used to

heat the reactor. A dimensionless model that describes this nonlinear tubular chemical reactor is provided as follows:

$$\varepsilon_p \frac{\partial T_g}{\partial t} = -\frac{\partial T_g}{\partial z} + \alpha_c (T_s - T_g) - \alpha_g (T_g - u)$$
$$\frac{\partial T_s}{\partial t} = \frac{\partial^2 T_s}{\partial z^2} + B_0 \exp\left(\frac{\gamma T_s}{1+T_s}\right) - \beta_c (T_s - T_g) - \beta_p (T_s - b(z)u) \quad (25)$$

Subject to the boundary conditions

$$z = 0, T_g = 0, \frac{\partial T_s}{\partial z} = 0; z = 1, \frac{\partial T_s}{\partial z} = 0 \quad (26)$$

where T_g, T_s, and u denote the dimensionless temperature of the gas, the catalyst, and jacket, respectively. The values of the process parameters are given as follows:

$\varepsilon_p = 0.01, \gamma = 21.14, \beta_c = 1.0, \beta_p = 15.62, B_0 = -0.003, \alpha_c = 0.5, \alpha_g = 0.5$

A sin distribution heat source is used with $b(z) = 1 - \cos(\pi z)$, $0 \le z \le 1$. The spatial reference profile is given as $T_{sd}(z) = 0.42 - 0.2\cos(\pi z)$.

Five point sensors are uniformly located along the length of the reactor with $z = (0, 0.25, 0.5, 0.75, 1)^T$ for collecting the spatial distribution of the temperature T_s. Two spatial inputs are error $e^*(z) = [e_1^*, ..., e_5^*]^T$ and error in change $r^*(z) = [r_1^*, ..., r_5^*]^T$, where $e_i^* = T_s(z_i, q) - T_{sd}(z_i)$ $r_i^* = e_i^*(q) - e_i^*(q-1)$; q and $q-1$ denotes the qth and q-1th sampling time, respectively. Δu^* denotes the incremental output at the qth sampling time.

It should be noted that the model represented by (25)-(26) is just used to unveil the system dynamics and is employed as the simulated model by the method of lines [11] to evaluate the control scheme. The only information we can utilize is the measured input-output data pairs.

Two groups data set are obtained from [1] by adding Pseudo-Random Quinary Sequence (PRQS) signal [12] with different amplitude (i.e. 0.447 and 0.1) to the control input. The scaling factors of 3-D FLC in [1] are set as 2.0, 0.001 and 0.8716 respectively. Each group has 150 data pairs composed of $e^*(z), r^*(z)$ and Δu^* with the sampling time 0.2s. The group generated from the control input with amplitude 0.447 is taken as the training data set, while the other group is taken as the test data set. The design process of data-based 3-D FLC is given as follows:

- Apply the nearest neighborhood clustering algorithm to partition the input space. Let $\rho_0 = 0.7$ and $\eta_0 = 0$. Then 16 fuzzy rules were generated, where the width of 3-D MF was $\sigma_z \approx [0.0620, 0.0902, 0.1518, 0.2008, 0.2175]^T$ as in (16).
- Optimization algorithm with $\gamma = 0.95$ and $\lambda = 0.9$ was used to simplify the obtained fuzzy rules and 3-D fuzzy sets.
- The linear SVR algorithm was used to obtain optimal consequent part parameters, where the width of Gaussian MF is set as $\sigma_B \approx 0.1247$ by (17). Let ε be 0.01, and C be a real number in [10, 10^7]. Root Mean-Squared Error (RMSE) defined in (27) was chosen as the quantitative performance to select the best approximated 3-D FLC, and then the *RMSEs* of the training data set and the test data set under different parameter C were listed in the Table I. From Table I, we can find that when $C = 10^7$, *RMSE* has a minimal value. Therefore, we choose $C = 10^7$ in this study. The extracted 3-D rule base and the related MFs were depicted in Fig. 4.

The proposed data-based 3-D FLC is applied to the control of catalytic packed-bed reactor, where simulation time is 10s. We select the same quantitative performance criteria as in [1]: steady-state error (SSE), integral of the absolute error (IAE), and integral of time multiplied by absolute error (ITAE). The control performance is given in Table II, and the control profile is given in Fig. 5. We can find that the data-based 3-D FLC has comparable control performance with the expert experience based 3-D FLC in [1] both in ideal condition and in disturbed condition.

TABLE I. *RMSE*S OF THE TRAINING AND TEST DATA SETS FOR DIFFERENT C

C	***RMSE*(training)**	***RMSE*(test)**
10	0.0452	0.0324
10^2	0.0452	0.0325
10^3	0.0452	0.0324
10^4	0.0451	0.0322
10^5	0.0441	0.0317
10^6	0.0401	0.0253
10^7	**0.0401**	**0.0249**

TABLE II. PERFORMANCE COMPARISONS

Performance index	Data-based 3-D FLC	Expert-based 3-D FLC [1]
Number of rules	16	49
No disturbance		
ISS ($\times 10^{-2}$)	1.74	1.69
IAE ($\times 10^{-1}$)	2.603	2.557
ITAE($\times 10^{-1}$)	8.896	8.646
With 50% increase disturbance in velocity of gas		
ISS ($\times 10^{-2}$)	1.82	1.78
IAE ($\times 10^{-1}$)	2.721	2.680
ITAE($\times 10^{-1}$)	9.297	9.062

V. CONCLUSION

In this paper, a new data-based 3-D FLC is designed by using a nearest neighborhood clustering algorithm, fuzzy similarity measurement techniques, and a linear SVR algorithm. Firstly, the nearest neighborhood clustering algorithm is used to partition the input space and construct 3-D rule base and 3-D MFs. Then, geometric similarity measure is employed to reduce the rule base. Finally, a linear SVR algorithm is used to estimate the optimal consequent part parameters. The proposed 3-D FLC was applied to the control of catalytic packed-bed reactor. The simulation results show that the designed 3-D FLC had a satisfied control performance compared with the expert experience based 3-D FLC.

ACKNOWLEDGMENT

This work was supported in part by the National Nature Science Foundation of China under Grant 60804033, Grant 61074059, and Grant 61004047, in part by the Shanghai Municipal Natural Science Foundation (Grant: 09ZR1409600), in part by Specialized Research Fund for the Doctoral Program of Higher Education of China (20100073120045), and in part by National Hi-Tech Research and Development Program of China (863 Program, Grant No. SQ2011AA0403839001).

REFERENCES

[1] H. X. Li, X. X. Zhang, S. Y. Li, "A three-dimensional fuzzy control methodology for a class of distributed parameter systems", IEEE Trans. Syst., Vol. 15, No. 3, pp. 470–481, Jun. 2007.

[2] Y. Jiang, X. X. Zhang, T. Zou, G. T. Cao, A novel 3-D fuzzy logic controller design using table look-up scheme, 2010 International Conference on Computer Application and System Modeling (ICCASM), pp.V4388-V4393, Oct. 2010.

[3] L. X. Wang, Y. J. Wang, A course in fuzzy systems and control, Beijing: Tsinghua University Press, 2003. (in Chinese)

[4] Yaochu Jin, Fuzzy modeling of high-dimensional systems: Complexity reduction and interpretability improvement, IEEE Trans. On Fuzzy System 8 (2) pp.212-221, 1994.

[5] Min-You Chen, D.A. Linkens, Rule-base self-generation and simplification for data-driven fuzzy models, Fuzzy Sets and Systems 142 pp.243-265, 2004.

[6] M. Setnes, R. Babuška, U. Kaymak, and H. R. van Nauta Lemke, Similarity measures in fuzzy rule base simplification, IEEE Trans. Systems, Man, and Cybernetics – Part B: Cybernetics, 28(3) pp.379-386, Jun. 1998.

[7] A. J. Smola, B. Schölkopf, A tutorial on support vector regression, Statistics and Computing, 14(3) pp.199-222, Sep. 2003.

[8] Jia Li, J. P. Shi, M. S. Qiu, Fuzzy neural model with global convergence for batch process, Information and Control, 38(6) pp.685-691, Dec. 2009.(in Chinese)

[9] Yinghua Lin, A fuzzy approach to input variable identification, Proceedings of the Third IEEE Conference on Fuzzy Systems, Orlando, 3: pp.2031-2036, 1994.

[10] W. H. Ray, Advanced process control, New York: McGraw-Hill, 1981.

[11] W.E. Schiesser, The Numerical Methods Of Lines Integration Of Partial Differential Equations, Academic Press, San Diego, 1991.

[12] X. F. Wang, G. Z. Lu, System modelling and identification, Beijing: Publishing House of Electronics Industry, 2004. (in Chinese)

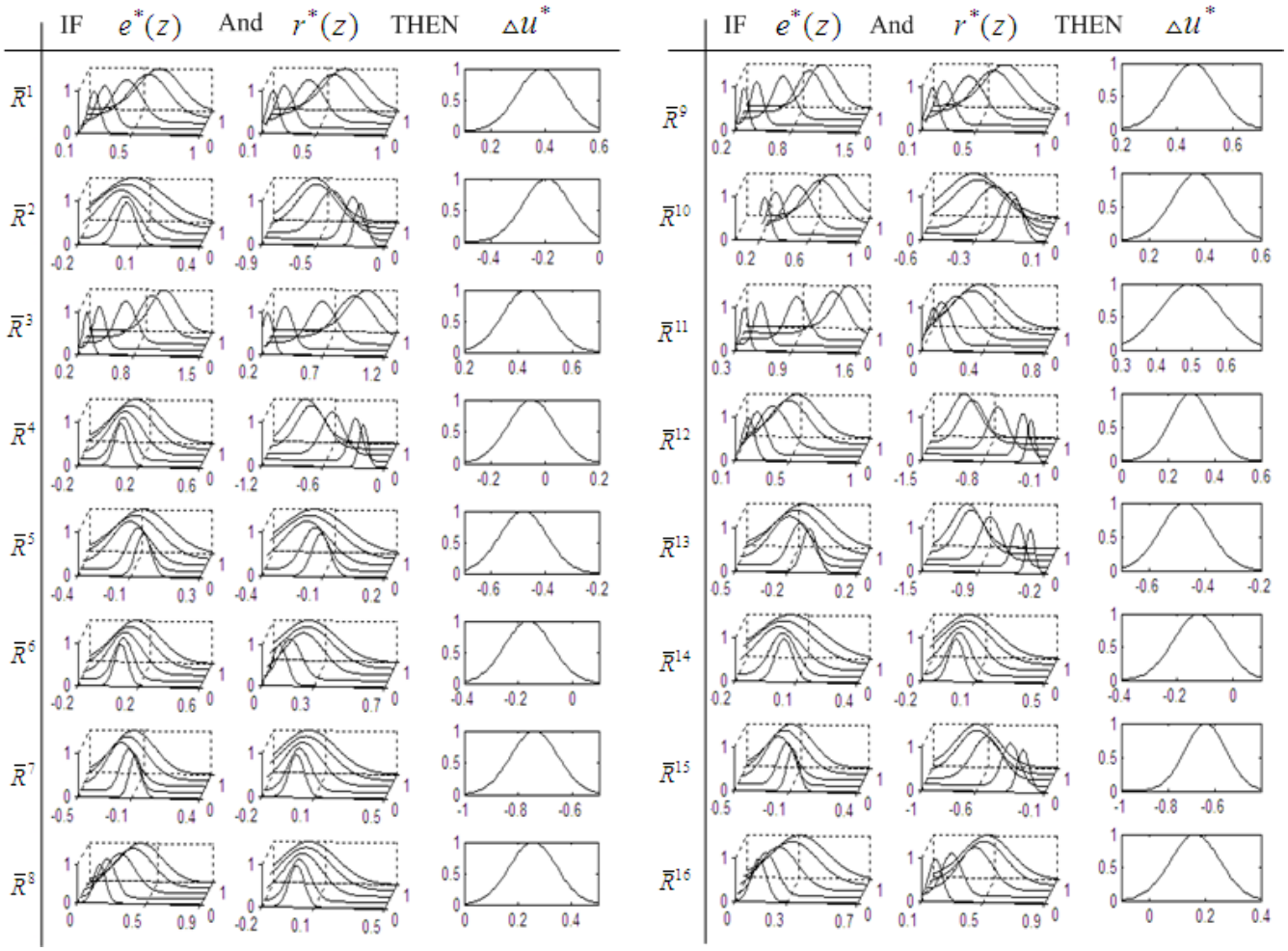

Figure 4. 3-D rule base extracted from input-output data pairs.

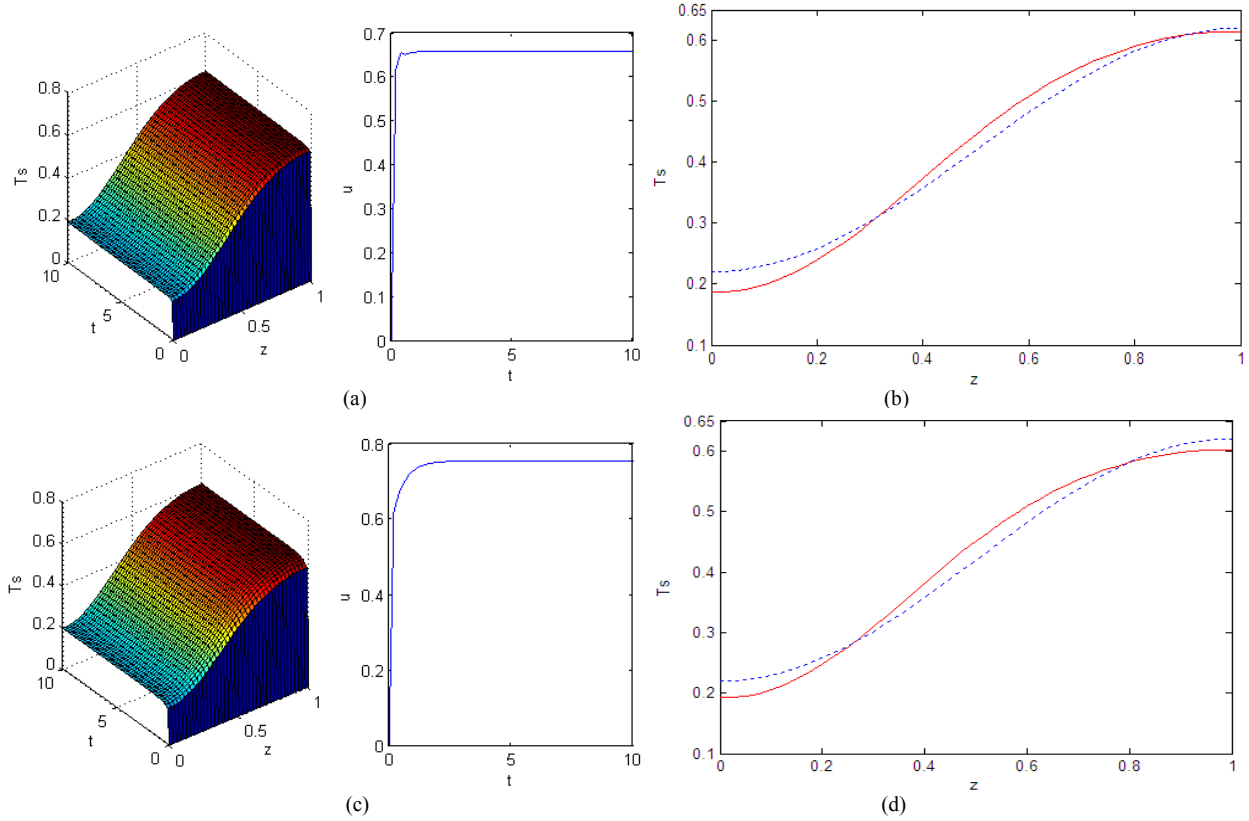

Figure 5. Data-based 3-D FLC controlled catalyst temperature evolution profile and manipulated input under ideal situations, respectively. (b) Catalyst temperature profiles in steady state under ideal condition. (c) Data-based 3-D FLC controlled catalyst temperature evolution profile and manipulated input under disturbance situations, (d) Catalyst temperature profiles in steady state under disturbed condition. (Dotted line: Reference profile. Solid line: Actual temperature profile.)

2011 IEEE International Conference on Fuzzy Systems
June 27-30, 2011, Taipei, Taiwan

A Method of Explicit Mappings for Kernel Data Analysis and Applications

Sadaaki Miyamoto
Department of Risk Engineering
University of Tsukuba
Ibaraki 305-8573, Japan
Email: miyamoto@risk.tsukuba.ac.jp

Keisuke Sawazaki
Master's Program in Risk Engineering
University of Tsukuba
Ibaraki 305-8573, Japan
Email: sawazaki@soft.risk.tsukuba.ac.jp

***Abstract*—The method of kernel data analysis is now a standard tool in modern data mining. An implicit mapping into a high-dimensional feature space is assumed in this method, in other words, an explicit form of the mapping is unknown but their inner product should be known instead. Contrary to this common assumption, we propose a method of explicit mappings. The reason why we use explicit mappings is as follows. (1) The use of these mappings does not lose any fundamental information in kernel data analysis. (2) We have the same formulas in kernel methods with and without the explicit mappings. (2) Usually the derivation becomes simpler by using these mappings. (3) New applications of the kernel methods become possible using these mappings. Two types of the mappings are proposed, one of which uses $\Phi(x_k) = \boldsymbol{e}_k$ $(k = 1, \ldots, N)$ while the second type uses $\Phi(x_k) = K^{\frac{1}{2}}\boldsymbol{e}_k$, where $K = (K(x_i, x_j))$ is $N \times N$ matrix. As an application we consider L_1 space fuzzy c-means clustering and lower dimensional approximation of kernel K. The effectiveness of the proposed method is shown by numerical examples.**

Keywords-data mining; kernel function; explicit mapping; clustering.

I. Introduction

Kernel functions [7] have been used in support vector machines [8] and are now becoming a standard tool in many applications of data mining. The *kernel trick* is commonly used in this method which means that we consider a mapping, e.g. $\Phi(x)$, from a data space into a high-dimensional feature space of which an explicit form is unknown, but we know the explicit functional form of their inner product $K(x, y) = \langle \Phi(x), \Phi(y) \rangle$ in the feature space. The function $K(x, y)$ is called a kernel function. Hence formulas in data analysis should be described in terms of the inner product of $\Phi(x)$, since the functional form of $\Phi(x)$ is unknown.

Kernel functions are known to be useful in many applications, but the derivations are generally complicated, since original formulas should be rewritten by the inner product forms. A typical example is kernel fuzzy c-means clustering [4] and kernel VQ clustering [5].

Contrary to this common understanding, we propose a method of kernel functions using explicit mappings. The idea is simple: the original idea is to assume a mapping $\Phi\colon \boldsymbol{R}^p \to H$, where $\boldsymbol{R}^p$ is the data space and H is the feature space. Instead, we assume $\Phi\colon \{x_1, \ldots, x_N\} \to \boldsymbol{R}^p$, where $\{x_1, \ldots, x_N\}$ is the set of objects to be analyzed. As a result we do not need to have the full functional form of $K(x, y)$; it is sufficient to know $K(x_i, x_j)$ $(1 \le i, j \le N)$. However, we do not know the actual form of $\Phi(x_k)$ but we know only $K = (K(x_i, x_j))$. How to handle $\Phi(x_k)$? The answer is simple: we consider two mappings:

1) $\Phi(x_k) = \boldsymbol{e}_k$;
2) $\Phi(x_k) = K^{\frac{1}{2}}\boldsymbol{e}_k$.

By these mappings the derivation of a kernel method becomes simpler, and some new techniques can be developed, as we will see later.

To illustrate the effectiveness of the present method, a typical result of kernel fuzzy c-means clustering with L_2 and L_1 norms will be shown. Further, a low dimensional approximation of a kernel is shown.

II. Explicit Mappings for Kernel Functions

A. Preliminary consideration

A set of objects $X = \{x_1, \ldots, x_N\} \subset \boldsymbol{R}^p$ is assumed to be given. They are points in the p-dimensional real space: $x_k = (x_k^1, \ldots, x_k^p)^\top \in \boldsymbol{R}^p$. We consider a mapping into a high-dimensional feature space $\Phi\colon \boldsymbol{R}^p \to H$ and associated kernel function as usual:

$$K(x, y) = \langle \Phi(x), \Phi(y) \rangle$$

where $\langle \cdot, \cdot \rangle$ is the inner product of H. We also assume $\| \cdot \|_H$ is the norm of H.

In this section we first suppose, as usual, we do not know an explicit form of function $\Phi(\cdot)$ but we know $K(x, y)$. Specifically, the Gaussian kernel is frequently used:

$$K(x, y) = \exp(-\lambda \|x - y\|^2),$$

where $\lambda > 0$ and $\|x\|$ is the norm of $\boldsymbol{R}^p$.

1) Kernel-based fuzzy c-means clustering: Let us review the method of kernel-based fuzzy c-means clustering [4], [5]. In this section we do not use an explicit mapping.

An objective function of fuzzy c-means using the feature space H is the following.

$$J_H(U, W) = \sum_{i=1}^{c} \sum_{k=1}^{N} (u_{ki})^m \|\Phi(x_k) - W_i\|_H^2, \quad (m > 1)$$

where $U = (u_{ki})$ is $n \times c$ membership matrix of x_k to cluster i. U has the next constraint when it is optimized.

$$M = \{U = (u_{ki}) : \sum_{i=1}^{c} u_{ki} = 1,\ u_{\ell j} \geq 0, \forall \ell, j\},$$

while $W = (W_1, \ldots, W_c)$ is a collection of cluster centers in H.

The iterative algorithm of fuzzy c-means clustering [1] is basically an alternative minimization of $J_H(U, W)$ with respect to U and W until convergence. We have the next solutions [5]:

$$u_{ki} = \left[\sum_{j=1}^{c} \left(\frac{D(x_k, W_i)}{D(x_k, W_j)} \right)^{\frac{1}{m-1}} \right]^{-1}, \tag{1}$$

$$W_i = \frac{\sum_{k=1}^{N} (u_{ki})^m \Phi(x_k)}{\sum_{k=1}^{N} (u_{ki})^m}, \tag{2}$$

where we put

$$D(x_k, W_i) = \|\Phi(x_k) - W_i\|_H^2. \tag{3}$$

Equations (1) and (2) should be repeated until convergence, but since $\Phi(x_k)$ is unknown, we use another formula for kernel fuzzy c-means clustering.

The formula is derived by eliminating (2) from iteration, i.e., we substitute (2) into (3) to have an updating formula for $D(x_k, W_i)$ [4]:

$$D(x_k, W_i) = K(x_k, x_k) - \frac{2}{\sum_{k=1}^{N} (u_{ki})^m} \sum_{j=1}^{N} (u_{ji})^m K(x_j, x_k) + \frac{1}{\{\sum_{k=1}^{N} (u_{ki})^m\}^2} \sum_{j=1}^{N} \sum_{\ell=1}^{N} (u_{ji} u_{\ell i})^m K(x_j, x_\ell). \tag{4}$$

We thus repeat (1) and (4) until convergence in kernel-based fuzzy c-means clustering.

B. Two explicit mappings

The above derivation needs transformation of an original algorithm into another one, due to the fact that no explicit mapping is available.

In contrast, if we have an explicit mapping, then no additional derivation is needed and we can use an existing algorithm.

We show two explicit mappings. First mapping is very simple:

$$\Phi_1(x_k) = \boldsymbol{e}_k \quad (k = 1, 2, \ldots, N) \tag{5}$$

where $H = \boldsymbol{R}^N$ and $\boldsymbol{e}_k$ is the k-th unit vector that has unity as ith component and all other components are zero. Note that $\Phi_1 \colon X \to \boldsymbol{R}^N$, i.e., $\Phi(\cdot)$ is not defined on $\boldsymbol{R}^p$ but is limited to the finite set X. We also assume that the inner product of $\boldsymbol{R}^N$ is

$$\langle \boldsymbol{e}_k, \boldsymbol{e}_\ell \rangle = K(x_k, x_\ell) \tag{6}$$

instead of the standard inner product $\langle \boldsymbol{e}_k, \boldsymbol{e}_\ell \rangle = \delta_{k\ell}$ ($\delta_{k\ell}$ is the Kronecker delta).

We have the next proposition.

Proposition 1: If kernel function $K(x, y)$ is positive-definite, $\langle \boldsymbol{e}_k, \boldsymbol{e}_\ell \rangle$ defined by (6) satisfy the axioms of the inner product of $\boldsymbol{R}^N$, that is, $\boldsymbol{R}^N$ with (6) is an inner product space.

(*Proof*) The detailed proof is given in standard textbooks [7]. As a rough sketch of the proof, note that the Mercer condition [8]

$$\int \int K(x, y) \eta(x) \eta(y) dx dy \geq 0$$

for all $\eta(x)$ guarantees

$$\sum_{i,j} K(x_i, x_j) \zeta_i \zeta_j \geq 0$$

$\forall \zeta_i \in \boldsymbol{R}$, by putting $\eta(x) = \sum_i \zeta_i \delta(x - x_i)$. Thus the matrix $K = (K(x_i, x_j))$ is positive semi-definite. (*QED*)

We introduce second explicit mapping that may be more time consuming in calculation but useful in applications. Note that a positive definite matrix K can be divided into $K = K^{\frac{1}{2}} K^{\frac{1}{2}}$. We thus define the second mapping:

$$\Phi_2(x_k) = K^{\frac{1}{2}} \boldsymbol{e}_k \quad (k = 1, 2, \ldots, N) \tag{7}$$

In this case, $\Phi_2 \colon X \to \boldsymbol{R}^N$, i.e., the domain and the codomain are the same as Φ_1, but now the inner product of $\boldsymbol{R}^N$ is standard:

$$\langle \boldsymbol{e}_k, \boldsymbol{e}_\ell \rangle = \delta_{k\ell}. \tag{8}$$

We now apply mappings Φ_i ($i = 1, 2$) to fuzzy c-means clustering. It is sufficient to show the optimal solution of W_i.

Proposition 2: For all positive semi-definite kernel $K(x, y)$ and mapping Φ_1 by (5), the cluster centers are given by

$$W_i = \left(\frac{(u_{1i})^m}{\sum_{k=1}^{N} (u_{ki})^m}, \ldots, \frac{(u_{ni})^m}{\sum_{k=1}^{N} (u_{ki})^m} \right)^T, \quad i = 1, \ldots, c \tag{9}$$

When Φ_2 by (7) is used, the cluster centers are given by

$$W_i = K^{\frac{1}{2}} \left(\frac{(u_{1i})^m}{\sum_{k=1}^{N} (u_{ki})^m}, \ldots, \frac{(u_{ni})^m}{\sum_{k=1}^{N} (u_{ki})^m} \right)^T, \quad i = 1, \ldots, c \tag{10}$$

(*Proof*) The proof of this proposition is not difficult by observing closely (2). Note that W_i given by (2) is the solution of

$$\min_{W_i} \sum_{k} (u_{ki})^m \|x_k - W_i\|^2$$

where the space can be an arbitrary inner product space, since the derivation of (2) uses a general variational principle valid for any Hilbert space. Note moreover that we substitute (9) into (1) to have the optimal solution of U. It should be noted that although optimal W_i is the same for all positive definite

kernel, optimal U differs because (6) give different values for different kernels. (*QED*)

The proof of the next proposition is almost trivial and is omitted.

Proposition 3: Substituting (9) or (10) into (3), we have (4).

That is, (9) (or (10)) derived from mapping (5) (or (7)) has all necessary and sufficient information for kernel fuzzy c-means clustering.

The mappings (5) and (7) are moreover useful for application to SOM [3] and VQ clustering [5], where vectors for updating quantization vectors should be based on learning. The explicit mappings enable vector representations in $\boldsymbol{R}^N$, and hence we can use every formulas in VQ and SOM.

C. L_1 space fuzzy c-means

Let us consider a method specific to an explicit mapping. Although kernel-based methods assume Euclidean spaces, we use an L_1 space clustering [5], which may be useful in applications. The L_1 space fuzzy c-means clustering uses

$$J_H(U,W) = \sum_{i=1}^{c}\sum_{k=1}^{N}(u_{ki})^m \|\Phi(x_k) - W_i\|_{L_1}, \quad (m>1),$$

where we assume the second mapping: $\Phi(x_k) = K^{\frac{1}{2}}\boldsymbol{e}_k$. Hence

$$\|\Phi(x_k) - W_i\|_{L_1} = \sum_{j=1}^{N} |(K^{\frac{1}{2}}\boldsymbol{e}_k)^j - W_i^j|$$

where $\boldsymbol{z}^j$ is j-th component of $\boldsymbol{z}$.

Accordingly the solution is

$$u_{ki} = \left[\sum_{j=1}^{c}\left(\frac{\|\Phi(x_k) - W_i\|_{L_1}}{\|\Phi(x_k) - W_j\|_{L_1}}\right)^{\frac{1}{m-1}}\right]^{-1},$$

while calculation of W_i needs an algorithm of an weighted median [5] of which the details are omitted for simplicity. We note, however, that calculation of an weighted median is frequently faster than the weighted centroid in the ordinary L_2-space based method.

Note also that this algorithm is valid only for the explicit mapping, since it does not assume an Euclidean feature space.

D. Low dimensional approximation of kernels

Another method specific to the explicit mapping is a low dimensional approximation of kernels. As we will see in the next section of numerical examples, the effectiveness of a kernel data analysis frequently depends on a small dimension of those subspaces of a few top eigenvalues of the kernel matrix. This means that a low dimensional approximation of the kernel simplifies the analysis and yet preserves its effectiveness. Such approximation is also suitable when an original kernel matrix is not known to be positive-definite. Then we can take a subspace of a number of top positive eigenvalues.

Let us assume that the original $N \times N$ kernel matrix K is decomposed into

$$K = T^\top \Lambda T,$$

where T is an orthogonal matrix which is composed of eigenvectors, and

$$\Lambda = diag(\lambda_1, \lambda_2, \ldots, \lambda_N)$$

is the diagonal matrix of eigenvalues with $\lambda_1 \geq \lambda_2 \geq \cdots \geq \lambda_N$. Let us consider D-dimensional approximation by taking

$$\hat{\Lambda} = diag(\lambda_1, \lambda_2, \ldots, \lambda_D, 0, \ldots, 0),$$

where $D < N$ and $\lambda_D > 0$. Accordingly we put

$$\hat{K} = T^\top \hat{\Lambda} T,$$

and use $\hat{K}$ instead of K. We thus assume $\Phi_2(x_k) = \hat{K}^{\frac{1}{2}}\boldsymbol{e}_k$, where

$$\begin{aligned}\hat{K} &= T^\top \hat{\Lambda}^{\frac{1}{2}} T \\ &= T^\top diag(\sqrt{\lambda_1}, \sqrt{\lambda_2}, \ldots, \sqrt{\lambda_D}, 0, \ldots, 0)T.\end{aligned}$$

It is easily seen that the feature space is now D-dimensional and when $D << N$, we have a low-dimensional approximation of the kernel space.

Note 1: This approximation appears similar to the kernel principal component analysis, but the concepts and the derivations are different. The method herein is an approximation of kernel K, while the kernel principal component analysis is approximation of a covariance matrix. Note also that, when D is two or three, we can visualize the 'principal part' of a kernel feature space. Thus the low dimensional approximation is useful as a visualization method for the feature space.

III. Numerical Examples

A set of data shown in Fig. 1 was used to show the effectiveness of the proposed method. This example is well-known in the sense that a usual fuzzy c-means (abbreviated as FCM) algorithm cannot separate the outer circle and the inner ball, while a kernel-based c-means algorithm can. Figure 2 depicts the result of an ordinary FCM, while Fig. 3 with the kernel-based FCM with the explicit mappings of the Gaussian kernel successfully separated the two groups.

Moreover Fig. 4 shows two major principal components with mapping Φ_2, where the method of the ordinary principal component analysis has been applied. In contrast, Figure 5 shows the two-dimensional approximation ($D = 2$) of the Gaussian kernel, which shows a similar, yet different configuration of the points.

The same result of perfect separation in Fig. 2 was obtained by the L_1-based method with an L_1 exponential kernel:

$$K(x,y) = \exp(-const\|x - y\|_{L_1})$$

which has been proved to be a kernel function [8], [2]. The two-dimensional approximation with this kernel is shown in Fig. 6.

Note that both Φ_1 and Φ_2 give the successful separation in Fig. 2 because they are equivalent to (4), while Φ_1 cannot

be used for the principal component analysis, since the coordinates for Φ_1 does not satisfy $\langle \boldsymbol{e}_k, \boldsymbol{e}_\ell \rangle = \delta_{k\ell}$ which is necessary in the principal component analysis.

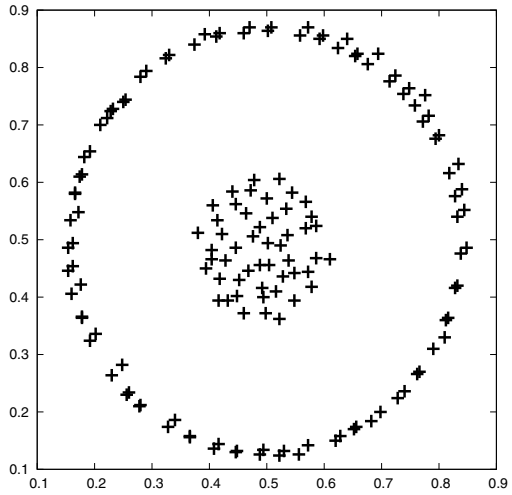

Fig. 1. A ball in a circle with 150 data points.

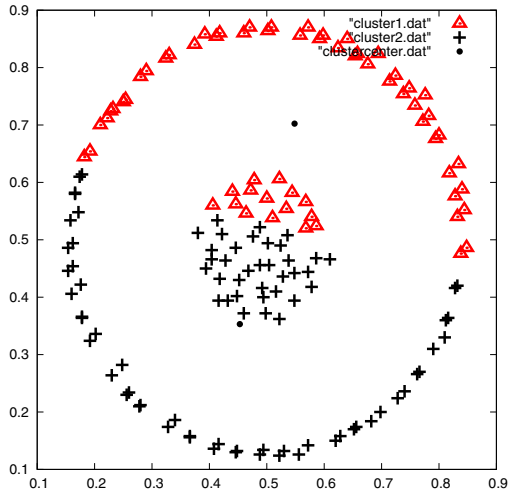

Fig. 2. The result of ordinary FCM applied to data in Fig. 1.

IV. Conclusions

We have proposed the method of explicit mappings for kernel based data analysis. Either one of Φ_1 and Φ_2 can be used, as there is no fundamental difference between the two, but the second mapping seems to be more useful in applications. Indeed, the L_1-based method and the low dimensional approximation of kernels has been developed for the second mapping. The low dimensional approximation is also useful when we do not know whether a kernel function is positive-definite or not, since it may be difficult to prove positive-definiteness in real applications.

In summary, we note the following advantages of the present method.

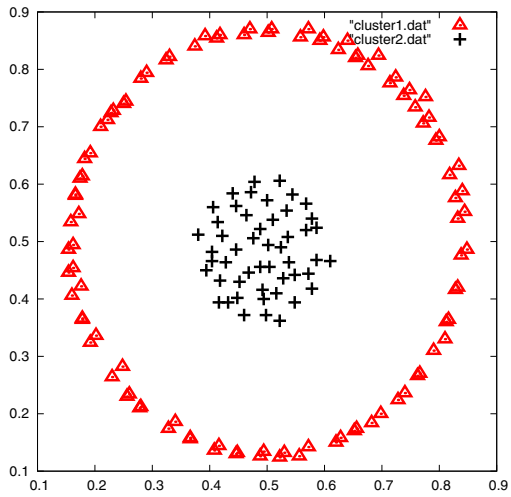

Fig. 3. The result of kernel-based FCM applied to data in Fig. 1.

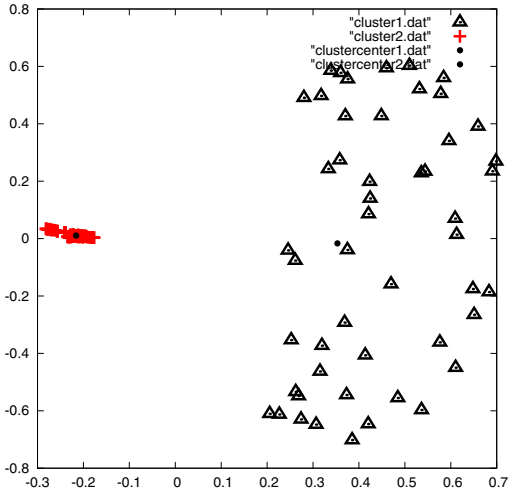

Fig. 4. The display of two major principal components to data in Fig. 1 with mapping $\Phi_2(x_k)$.

1) Using this mapping, we do not lose any fundamental information in kernel data analysis.
2) Generally the derivation becomes simpler using this mapping.
3) New applications of the kernel methods become possible using this mapping.

The last statement should be further studied. In relation to fuzzy clustering, the method of fuzzy c-varieties [1] should be considered. We also have many research possibilities related to SOM and LVQ [3].

Moreover we have other possibility to use nonlinear methods of data analysis such as LLE [6] to the transformed data, where the above explicit mapping is essential. Without such a mapping, we cannot apply a nonlinear tool of data analysis.

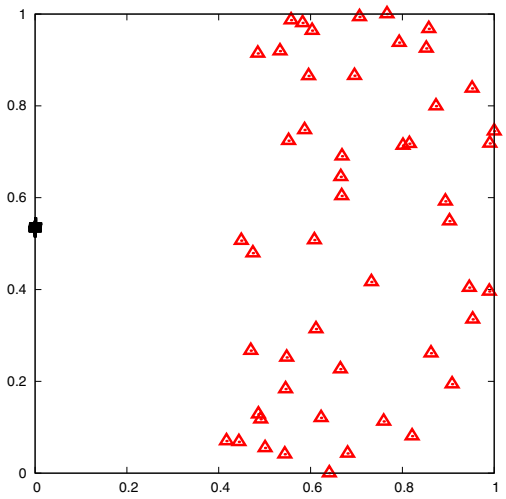

Fig. 5. The display of the low dimensional approximation to data in Fig. 1 with mapping $\Phi_2(x_k)$.

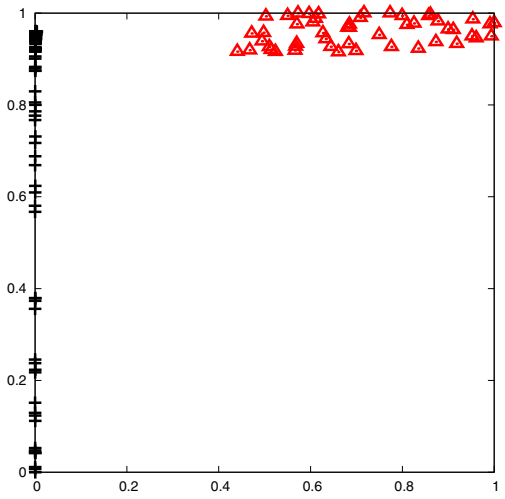

Fig. 6. The display of the low dimensional approximation to data in Fig. 1 with mapping $\Phi_2(x_k)$. L_1-based FCM with L_1-exponential kernel was applied.

ACKNOWLEDGMENT

This research has partly been supported by the Grant-in-Aid for Scientific Research, JSPS, Japan, No.19300074.

REFERENCES

[1] J.C. Bezdek, Pattern Recognition with Fuzzy Objective Functions, Plenum Press, New York, 1981.
[2] N. Cristianini, J. Shawe-Talor, *An Introduction to Support Vector Machines*, Cambridge Univ. Press, 2000.
[3] T. Kohonen, Self-Organizing Maps, 2nd Ed., Springer, Berlin, 1995.
[4] S. Miyamoto, D. Suizu, Fuzzy *c*-means clustering using transformations into high dimensional spaces, Proc. of FSKD'02: 1st International Conference on Fuzzy Systems and Knowledge Discovery, Nov. 18-22, 2002, Singapore, Vol.2, pp. 656–660.
[5] S. Miyamoto, H. Ichihashi, K. Honda, Algorithms for Fuzzy Clustering, Springer, Berlin, 2008.
[6] S.T. Roweis, L.K. Saul, Nonlinear Dimensionality Reduction by Locally Linear Embedding, *Science*, Vol.290, No.22, pp.2323-2326, 2000.
[7] B. Schölkopf, A.J. Smola, Learning with Kernels, the MIT Press, Cambridge, 2002.
[8] V.N. Vapnik, *Statistical Learning Theory*, Wiley, 1998.

2011 IEEE International Conference on Fuzzy Systems
June 27-30, 2011, Taipei, Taiwan

Comparison of Scaling Behavior Between Fuzzy c-Means Based Classifier with Many Parameters and LibSVM

Hidetomo Ichihashi, Katsuhiro Honda, Akira Notsu
Department of Computer Science and Intelligent Systems
Osaka Prefecture University
1-1 Gakuen-cho, Nakaku, Sakai, Osaka 599-8531, Japan
Email: {ichi, honda, notsu}@cs.osakafu-u.ac.jp

***Abstract*—This paper reports the scaling behavior of the fuzzy c-means based classifier (FCMC) with many parameters. FCMC is a classifier based on clustering approaches. The classification accuracy on test sets (i.e., the generalization capability) is not necessarily improved by increasing the number of clusters. Especially when the number of training samples is relatively small, not only the classification boundary over-fits the data, but also covariance matrices and cluster centers are computed incorrectly, since the number of samples in each cluster becomes smaller. Hence, the test set accuracy deteriorates.**

The performance of FCMC with two clusters in each class and the number of training samples less than 1000, was reported in the literature. This paper reports the scaling behavior of FCMC by testing with variously-sized training samples. The number of clusters of FCMC is increased up to eight. The number of clusters used in this paper is not very large but the number of parameters is relatively large. So, the parameters are optimized to training sets.

LibSVM is one of the widely known state of the art tools for support vector machines (SVM). The test set accuracy, training time and testing time (i.e., the detection time) of FCMC are compared with LibSVM by varying the size of training sets. FCMC shows a good generalization capability, though the parameters are optimized to training sets. When the number of training samples is increased by 10 times, the training time of FCMC increases by 10 times, but that of LibSVM increases by a factor of 100. The testing time is also much shorter than LibSVM when the size of the training set is large.

***Index Terms*—classifier, clustering, large data set, scaling behavior.**

I. Introduction

Fuzzy c-means based classifier (FCMC) [1], [2], [3], [4] is a classifier based on clustering approaches. We put FCMC in practical use for the vehicle detection system at several parking lots in Japan [4].

In this paper, for testing scaling behaviors of FCMC, the number of clusters is increased up to 8 for each class. Large-sized training sets with samples from 100,000 to 1,000,000 are used and the size of the training set is variously varied. Mixing proportions of clusters are parameterized. So, FCMC has many parameters, though the number of clusters is not very large. The parameters are optimized to training sets and the test set accuracy is evaluated on the test set.

When the number of training samples is relatively small, the classifier tends to over-fits the data. The obtained covariance matrices and cluster centers become incorrect, because the number of samples in each cluster is small.

For parameter optimization, PSO [5], [6], [7] is implemented just because PSO is as simple as the random search method. The selection of the optimization method is not essential because small improvement in training time on average is not significant in practice.

Support vector machines (SVMs) deliver superb performance in many real-world applications. SVMs are the standard tools for machine learning and data mining. We also give results with LibSVM: a library for support vector machines by Chang and Lin [8] for the sake of comparison. LibSVM incorporates SMO [9], which is a standard in SVM resolution for large size data sets and LibSVM is a state-of-the-art approach to SVM.

We need to compare the performance of FCMC from the following two points of view.

1) Comparison of scaling behaviors by varying the number of training samples. The number of clusters in each class is increased up to 8, and the mixing proportions of clusters are parameterized for FCMC. The parameters are optimized to training sets and are not regarded as free parameters.

2) Comparison of classification performances on very large datasets, when the number of clusters in each class is increased as many as possible for FCMC. The number of free parameters is set to less than or equal to 3 and the rage for parameter search is limited for both FCMC and LibSVM.

This paper reports the results of 1). Free parameters (hyper-parameters) of LibSVM and FCMC, which are optimized to test sets or validation sets, are assumed to be known from the knowledge about the given set of data. Our results indicate that FCMC surpasses LibSVM with properly chosen parameters in classification accuracy when the size of training set is reduced by sampling. So, we can reduce the training time by a simple sampling of training data. For FCMC, the training time and the testing time are proportional to the size of training set and the size of testing set respectively.

The choice of the free parameters of SVM does not only

978-1-4244-7316-8/11/$26.00 ©2011 IEEE

influence greatly the accuracy but also the training and testing time. These computation times are usually difficult to estimate in advance because the time largely depends on the number of support vectors, which is not known in advance. Our experiments on LibSVM show similar behaviors as those reported in the literature concerning training size and performance.

The advantages of FCMC with many parameters are the high generalization capability and the fast testing time.

II. Fuzzy c-Means Based Classifier

The first phase of FCMC is clustering or partitioning, which is modified from [10], [11]. See [3] for details of the derivation of the algorithm. The objective function of FCM with regularization by Kullback-Leibler divergence (KLFCM) [12], [10] is linearized and the update rules are derived by using Lagrangian multiplier method. Let $x_k \in \mathcal{R}^p$ be a feature vector and

$$D(x_k, v_i; S_i) = (x_k - v_i)^\top S_i^{-1}(x_k - v_i) \tag{1}$$

be squared Mahalanobis distance from x_k to $v_i \in \mathcal{R}^p$. S_i is a covariance matrix of data samples of the i-th cluster written as:

$$S_i = \frac{\sum_{k=1}^N u_{ki}(x_k - v_i)(x_k - v_i)^\top}{\sum_{k=1}^N u_{ki}}. \tag{2}$$

$$v_i = \frac{\sum_{k=1}^N u_{ki} x_k}{\sum_{k=1}^N u_{ki}} \tag{3}$$

is a cluster center and the mixing proportion of i-th cluster is

$$\alpha_i = \frac{\sum_{k=1}^N u_{ki}}{\sum_{j=1}^c \sum_{k=1}^N u_{kj}} = \frac{1}{N}\sum_{k=1}^N u_{ki}. \tag{4}$$

c denotes the number of clusters and N denotes the number of samples. The above updating rule is repeated and called as the generalized hard c-means [12], [11].

Initial locations of cluster centers or membership values are usually given randomly in the clustering approach. Since the classification performance is sensitive to the initialization, our approach does not use random initializations and use the principal component analysis (PCA) instead. Let $f_k, k = 1, ..., N$ be PCA scores of the data set $X = (x_1, ..., x_N)^\top$ of a class. f_k are associated with the largest singular value of mean corrected X. First, initial membership values of the two clusters of a class are given by

$$\begin{aligned} u_{k1} &= \begin{cases} 1 & (f_k \le 0) \\ 0 & (\text{otherwise}) \end{cases} \\ u_{k2} &= \begin{cases} 0 & (f_k \le 0) \\ 1 & (\text{otherwise}). \end{cases} \end{aligned} \tag{5}$$

This bisection method is repeated on each cluster, and the number of clusters (c) is increased. The resultant leaf nodes of the binary tree are the clusters. In this paper, the number of clusters is less than or equal to 8 for each class. The number of parameters to be optimized by PSO increases with the number of clusters (c). Moreover, when c is large, the number of training samples in each cluster becomes small, and covariance matrices and cluster centers become inaccurate. This leads to the deterioration of classification accuracy. We can not use many more clusters for testing scaling behaviors.

One of the impediments for FCMC is the singularity of covariance matrices, which frequently occurs when feature dimension is relatively high and the number of samples in each cluster is small. So, the low-rank approximation of covariance matrices in the mixture of probabilistic principal component analysis (MPCA) [13] and the character recognition [14] is applied. By reducing the number r of basis vectors in the approximation of S_i, the algorithm becomes stably convergent. When r=0, S_i is a diagonal matrix, hence is non-singular, and $D(x_k, v_j; S_j)$ is reduced to Euclidean distance. The clustering is done on a per class bases.

The classification (i.e., the second phase) is performed by computing fuzzy memberships. Let π_q denote the mixing proportion of class q, i.e., the $a\ priori$ probability of class q. Let α_{qj} be α_i in (4) for cluster j of class q. The class membership of k-th data x_k to class q is computed as:

$$u^*_{qjk} = \alpha_{qj}|S_{qj}|^{-\frac{1}{\gamma}}(D(x_k, v_{qj}; S_{qj}) + \nu)^{-\frac{1}{m}}, \tag{6}$$

$$\tilde{u}_{qk} = \frac{\pi_q \sum_{j=1}^c u^*_{qjk}}{\sum_{s=1}^Q \pi_s \sum_{j=1}^c u^*_{sjk}}, \tag{7}$$

where c denotes the number of clusters of each class and Q denotes the number of classes. We selected the functional form of u^* based on the membership functions derived from the generalized FCM objective function [12] and that of FCM with regularization by Kullback-Leibler divergence [12], [10].

At the completion of clustering for all classes in the first phase of FCMC, we then compute Mahalanobis distances by (1) for all the samples in the training sets. The second phase of FCMC is the supervised classification and the parameters, i.e., $m \in [0, 2], \gamma \in [0, 20], \nu \in [0, 200]$ and the change rates of $\alpha_{qj} \in [-0.5, 0.5]$ (see [3]), are selected to minimize error rate on the training sets. Since we have Q classes and c clusters for each class, the number of α_{qj} is $Q \times c$. The distances by (1) for all the samples in the training set are fixed and the best setting of the parameters are searched by PSO [5], [6], [7]. The free parameters (C, γ) of LibSVM in Section III are chosen to fit the given test set. But, the parameters $(m, \gamma, \nu, \alpha_{qj})$ of FCMC are optimized to training set since the number of parameters is much larger than LibSVM. After the optimization, the test set accuracy on the test set is evaluated.

III. Experiments

In this Section, we implement FCMC and LibSVM, and illustrate the scaling behavior of FCMC on several benchmark data sets. Table I summarizes the characteristics of the data sets used. The parking lot image data were used for the vehicle detection system in [4]. Checkerboard data are artificial data. Other data sets are downloaded from http://www.cse.ust.hk/~ivor/cvm.html (Ivor W. Tsang, Andras Kocsor, James T. Kwok [15]). FCMC is implemented in

Matlab. FCMC has several to dozens of parameters, which are optimized by PSO. But FCMC has other parameters that are not automatically optimized. They are the number c of clusters and the number r of basis vectors for the low-rank approximation of covariance matrices. c is chosen from $\{2, 4, 8\}$ and $r \in \{0, 2, 5, 20, 40, 30\}$ and they also need to be selected. But in this paper, we assume that these two parameters are the free parameters and their optimum values are known from the knowledge about the given data sets. The free parameters (C, γ) of LibSVM are also assumed to be known. We use the Gaussian kernel $k(x, y) = \exp(-\gamma|x-y|^2)$ for nonlinear classification. The kernel parameter γ and the regularization parameter C are the free parameters of LibSVM.

For medium-sized problems, cross validation might be the most reliable way for parameter selection. But, for large-sized problems as in Table I, it is hard to implement cross validation procedure since it takes very long computation time. Therefore, in this paper PSO in FCMC is used for optimizing training accuracy on training set. Then, we evaluate the accuracy on the given test set. The free parameters of LibSVM are also chosen manually. We tested various parameter values including those reported in the literatures of SVM, and we report the best results.

Experiments are performed on DELL T5400 3.16GHz, 4GB. Each experiment reports the error rate on test set, the training time on training set, and the testing time (i.e., the detection time).

TABLE I
DATA SETS USED FOR PERFORMANCE COMPARISON

data	features	training	testing
Parking lot image	50 (1,024)	135,000	135,000
USPS zero-one	50 (676)	266,079	75,383
Checkerboard	2 (2)	1,000,000	2000
KDD-CUP 1999	5 (127)	2,449,216 (4,989,431)	311,029
MNIST	50 (576)	60,000	10,000

Parking Lot Image Data

First, we use the set of image data with 50 feature dimensions. The image data are used for the vehicle detection system in [4]. The camera images of a parking lot are first stored in JPEG format of 704 × 576. Vehicle/parking space sub-windows are cropped from each picture. Each RGB image of the sub-windows is thinned as 32×32×3 and transformed into HSV and then into gray scale image of 32×32 (=1,024). 50 PCA (principal component analysis) basis vectors were computed using a subset of sample images. PCA for image compression is also know as the Hotelling, or Karhunen and Leove (KL), transform. All the collected gray scale image data were compressed by multiplying PCA basis vectors (i.e., inner product). The obtained 270,000 vectors with 50 feature dimensions were used. The first half (135,000 image data) is used for training and the latter half (135,000) is used for testing. The best accuracy by LibSVM is obtained with $C = 1.0$ and $\gamma = 5.0$. We found this parameter values by testing many times. We make the training size varies. Fig. 1 shows the results for experiments where the training size is growing. The error rate of FCMC on the test set is smaller than LibSVM as shown in Fig. 1, though the training time (dashed line) is slightly longer than LibSVM with the proper values of C and γ. The straight line with circles show the result of FCMC with the best settings of the parameters, while the dashed line shows the result by PSO for each reduced set of training samples. It should be noted that to increase the numbers of iterations and particles of PSO does not necessarily improve the testing accuracy, since PSO optimize the parameters to training sets. The straight line with circles shows the results when the parameters are fixed to the best setting, i.e., the change rate of α_{qj}= (0.2035, 0.7642, 0.3540, 0.1885, 0.7342, 0.7632, 0.4914, -0.1085, 0.6106, 0.1501, 0.7356, 0.5202, 0.4685, 0.9049, 0.2748, 1.1440), m=0.1143, γ=8.2049, and ν=173.8178. The testing time of LibSVM is much longer than that of FCMC when the size of training set is large as shown in Fig. 3. For FCMC, we set as c=8, and r=30. The number of particles in PSO is 50 and the number of iterations is 10 (denoted as 50×10).

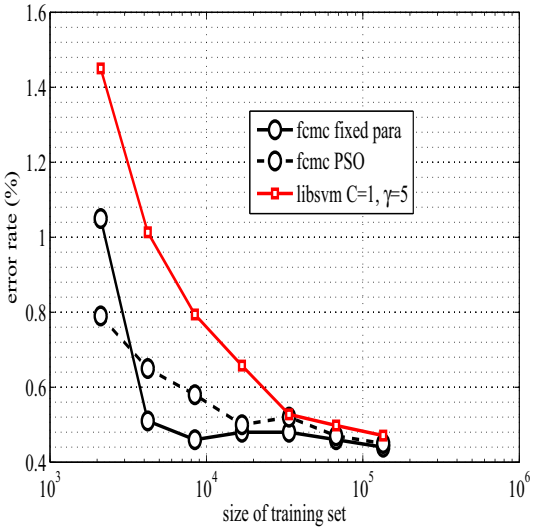

Fig. 1. Error rates (%) on the test sets of the parking lot image data (FCMC: PSO 50×10, c=8, r=30). Note that the size of the training set is in log scale.

Extended USPS Zero-one Data

In this experiment, our task is to classify digits zero from one in an extended version of the USPS data set. The original training set has 1,005 zeros and 1,194 ones, while the test set has 359 zeros and 264 ones. To better study the scaling behavior, Tsang, Kwok and Cheung [15] extend this data set by first converting the resolution from 16×16 to 26×26, and then generate new images by shifting the original ones in all directions for up to

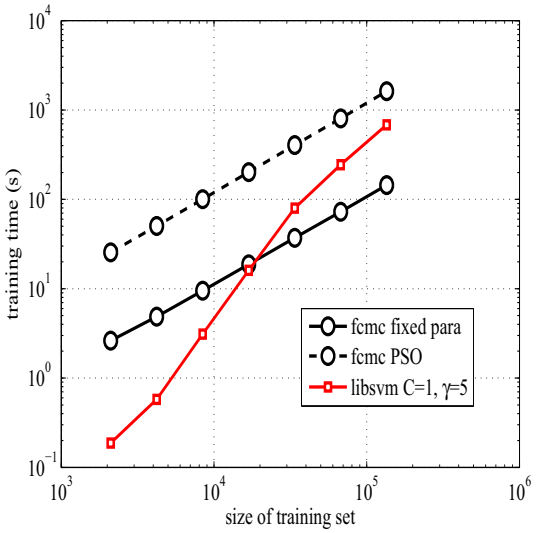

Fig. 2. Training time (s) on the parking lot image data (FCMC: PSO 50×10, c=8, r=30). Note that the training time is also in log scale.

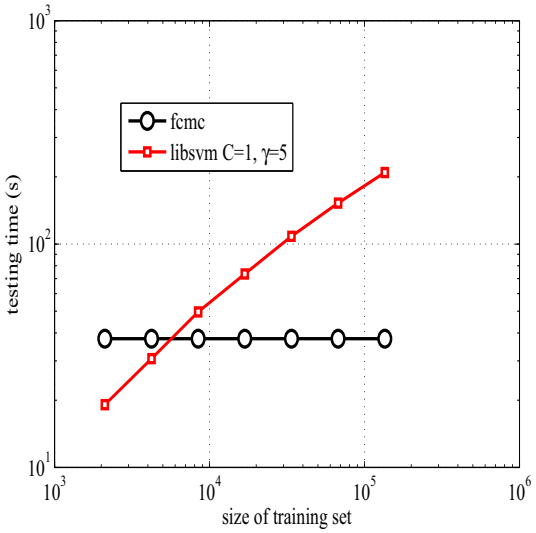

Fig. 3. Testing time (s) on the test sets of the parking lot image data (FCMC: PSO 50×10, c=8, r=30)

five pixels. Thus, the resultant training set has a total of (1005+1194)×112 =266,079 samples while the extended test set has (359+264)×112 = 75,383 samples (http://www.kernel-machines.org/data/usps.mat.gz). 50 PCA basis vectors were computed using a subset of image data. All the image data were compressed by multiplying PCA basis vectors. The obtained training and testing samples with 50 feature dimensions were used. As shown in Fig. 4, the accuracy of LibSVM deteriorates with the decreasing number of training samples. The straight line with circles show the result of FCMC with the best settings of the parameters, while the dashed line shows the result by a single trial of PSO (20×10) for each reduced set of training samples. Therefore, the training time can not be reduced for LibSVM by a simple sampling of the training data, though FCMC's accuracy is high for a wide range of training set sizes. When the size of training set is larger than 30,000, the best set of the parameters in terms of testing accuracy is $C = 1, \gamma = 0.03$ for LibSVM, and the training time is nearly equal to FCMC with $c = 8$, and $r = 5$. This, however, is true only when we know the best parameter values. If we test LibSVM with $C = 1, \gamma = 0.1$, it takes 10 times longer than FCMC as shown in Fig. 5. So, the total training time including parameter search may become extremely long for LibSVM. And, the testing time is longer than that of FCMC by more than an order of magnitude as shown in Fig. 6.

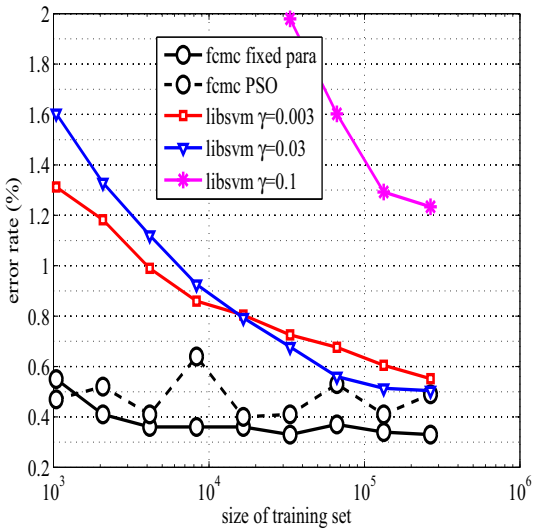

Fig. 4. Error rates (%) on the test sets of the extended USPS digits data (LibSVM: C=1, FCMC: PSO 20×10, c=8, r=5).

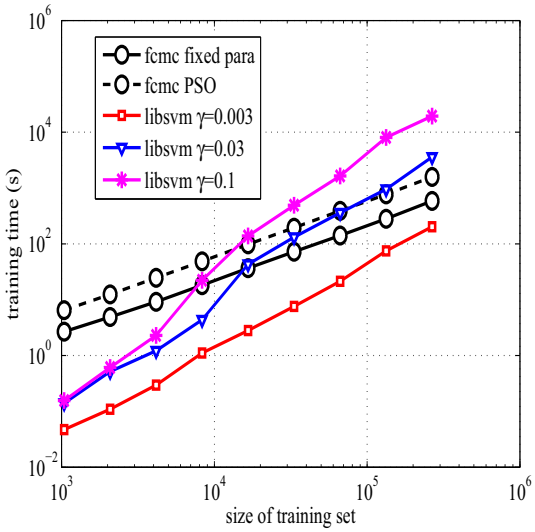

Fig. 5. Training time (s) on the extended USPS digits data (LibSVM: C=1, FCMC: PSO 20×10, c=8, r=5)

Checkerboard Data

We experiment on the 4×4 checkerboard data commonly

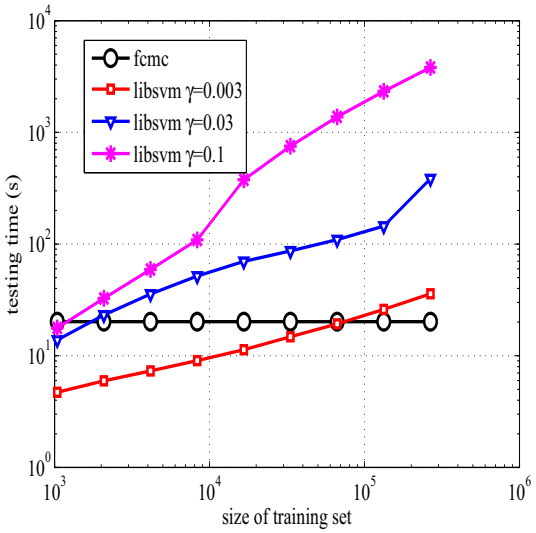

Fig. 6. Testing time (s) on the test sets of the extended USPS digits data (LibSVM: C=1, FCMC: PSO 20×10, c=8, r=5)

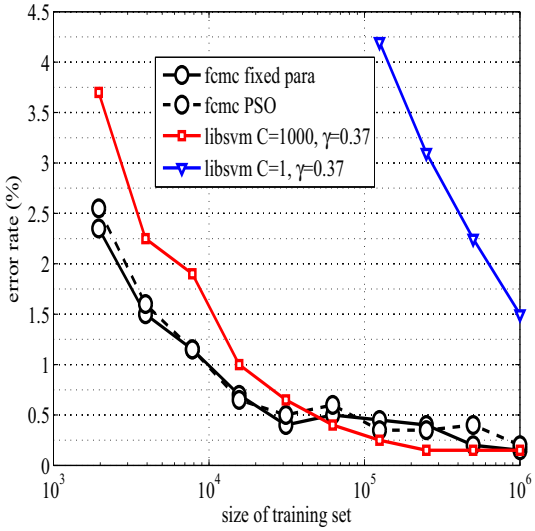

Fig. 7. Error rates (%) on the test sets of the checkerboard data (FCMC: PSO 50×10, c=8, r=0)

used for evaluating large-scale non-linear SVM implementations [15], [16]. We use training sets with a maximum of 1 million points and 2,000 independent points for testing.

Fig. 7 shows that the accuracy of both approaches deteriorates as the training samples are reduced by sampling. For relatively small training sets, with less than 100,000 samples, the error rate of LibSVM is twice larger than FCMC. But, LibSVM is faster as shown in Fig. 8. When the number of training samples is 1,000,000, the training time is nearly the same. This, however, is true when we know the best parameter values of LibSVM. If we test LibSVM with $C = 10, \gamma = 0.001$, it takes 10 times longer than FCMC. So, the total training time of LibSVM for parameter search may become extremely long. The testing time for LibSVM with the best parameter setting is 10 times longer than FCMC as shown in Fig. 9. As we know the clusters are all squares of the same size on the checker board and the number of clusters is 8 for each class. we set as $c = 8, r = 0$

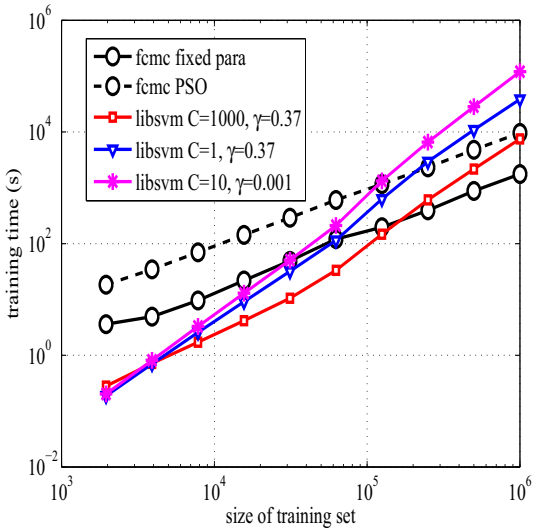

Fig. 8. Training time (s) on the checkerboard data (FCMC: PSO 50×10, c=8, r=0)

KDDCUP-99 Intrusion Detection Data

This intrusion detection data set has been used for the Third International Knowledge Discovery and Data Mining Tools Competition, which was held in conjunction with KDD-99. Each original sample has 34 continuous features and 7 symbolic features (http://kdd.ics.uci.edu/databases/kddcup99/kddcup99.html). The original training set contains 4,898,431 connection records, which are processed from about four gigabytes of compressed binary TCP dump data from seven weeks of network traffic. Another two weeks of data produced the test data with 311,029 samples. The data set includes a wide variety of intrusions simulated in a military network environment. There are a total of 24 training attack types, and an additional 14 types that appear in the test data only. The task is to separate normal connections from attacks. We used 2 million samples for training. Each sample is compressed with PCA and has only 5 feature (PCA score) dimensions because of not enough memory. As the test results show, the accuracy does not deteriorate by the significant reduction of the feature dimensionality. This is the case only for the KDD data. We computed 5 PCA basis vectors by using first 300,000 training samples and then multiply them with all training and testing samples. We used the compressed data for both FCMC and LibSVM.

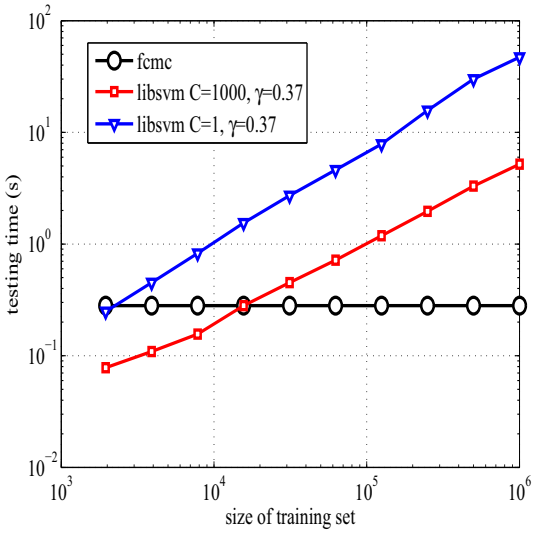

Fig. 9. Testing time (s) on the test sets of the checkerboard (FCMC: PSO 50×10, c=8, r=0)

When $C = 1,000,000$ and $\gamma = 0.1$, LibSVM attains the best accuracy, but the differences between LibSVM with some other parameter settings and FCMC are slight for a wide range of sizes of training samples as shown in 10. The training time for FCMC is shorter than LibSVM when the size is larger than 1,000,000 as shown in Fig. 11. The testing time is shorter than LibSVM with $C = 1, \gamma = 0.0001$ by two orders of magnitude as shown in Fig. 12.

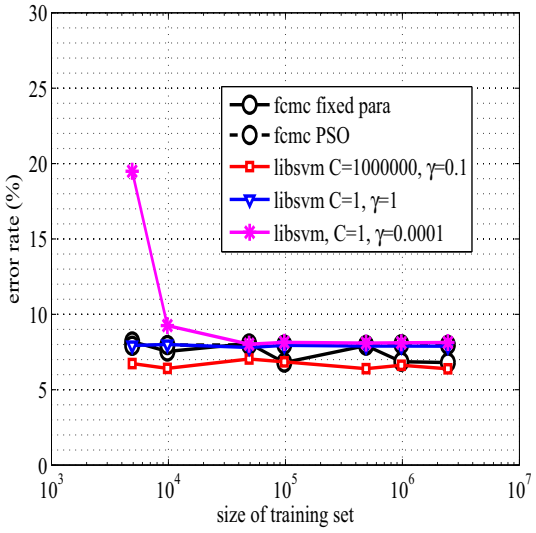

Fig. 10. Error rates (%) on the test sets of the KDD data (FCMC: PSO 20×10, c=2, r=2)

MNIST Data

The MNIST database of handwritten digits (10-class problem), has a training set of 60,000 samples, and a test set of 10,000 samples. It is a subset of a larger set available from NIST by LeCun research group at AT&T lab [17]. A 576-dimensional directional feature based

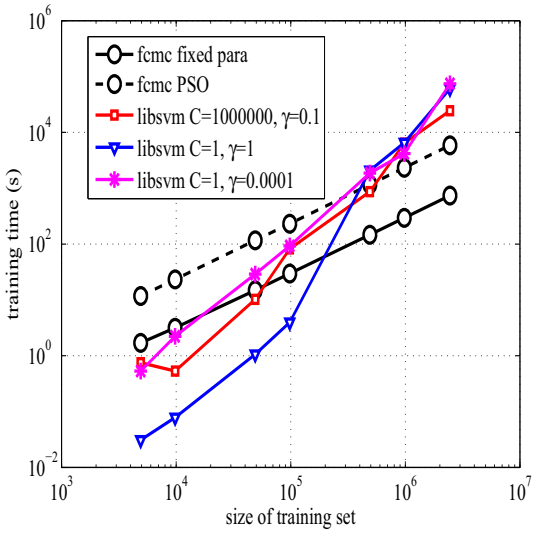

Fig. 11. Training time (s) on the KDD data with (FCMC: PSO 20×10, c=2, r=2)

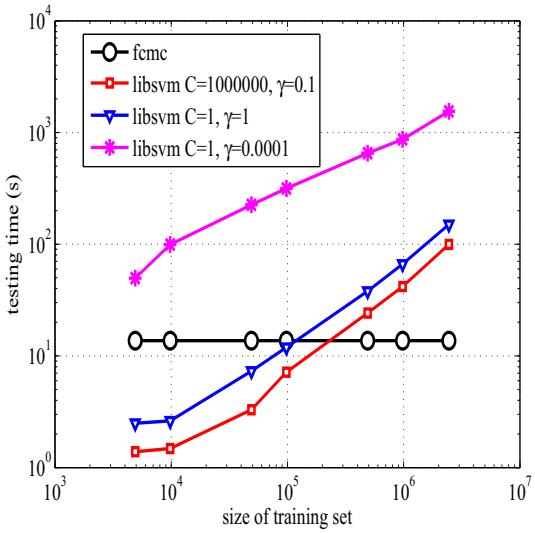

Fig. 12. Testing time (s) on the test sets of the KDD data (FCMC: PSO 20×10, c=2, r=2)

on gradient of gray-level image was extracted by using Robert edge operator. The data set is available from http://www.cenparmi.concordia.ca/~jdong/HeroSvm.html.

Results are shown in Figs. 13-15. When the number of training samples is smaller, the accuracy of FCMC is better for $c = 2$, but when the number is larger than 20,000, $c = 8$ is better. LibSVM use the "one-against-one" approach in which $Q(Q-1)/2$ classifiers are constructed and each one trains data from two different classes. In classification a voting strategy is used: each binary classification is considered to be a voting where votes can be cast for all data points x - in the end point is designated to be in a class with maximum number of votes. LibSVM's training time and testing time is short, since the number of training samples handled by each classifier is small. We used the same data set of 50 dimensional feature vectors for

both LibSVM and FCMC. It should be noted that the training time does not include the time for parameter search, hence in practice a long computation time is indispensable for LibSVM.

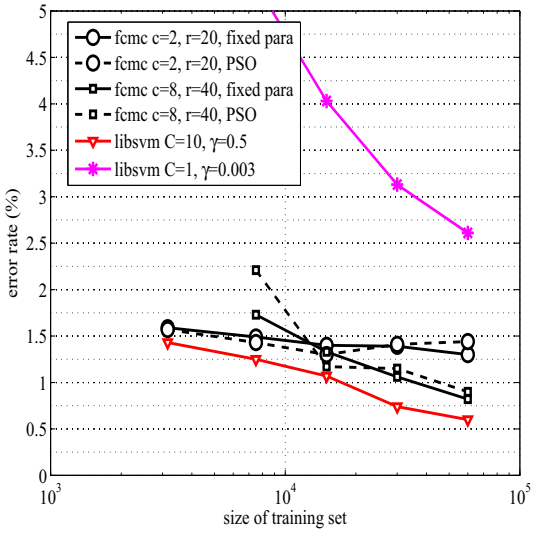

Fig. 13. Error rates (%) on the test sets of the MNIST 10-class data (FCMC: PSO 20×10)

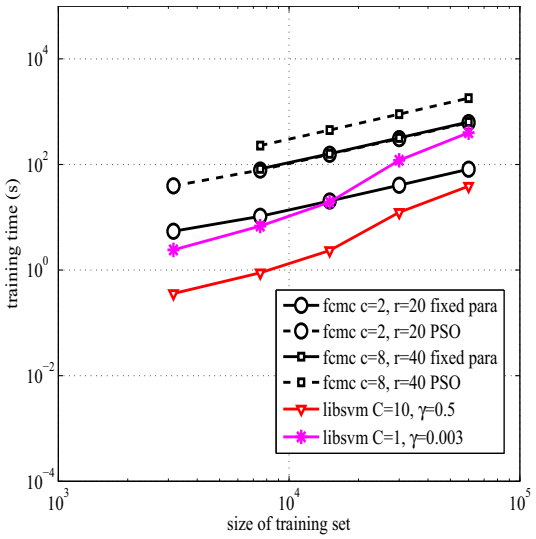

Fig. 14. Training time (s) on the MNIST 10-class data with (FCMC: PSO 20×10)

IV. Conclusion

We have demonstrated the performance of FCMC by comparing with LibSVM. We used five large sized data sets whose feature values are mainly continuous real numbers.

When the number of clusters of FCMC is increased, in order for cluster covariance matrices and cluster centers to be correctly estimated, a very large-sized training set is necessary. Therefore, we tested the performance with the number of clusters less than or equal to 8, and the number of parameters $c \times Q + 3$. The results are summarized as follows:

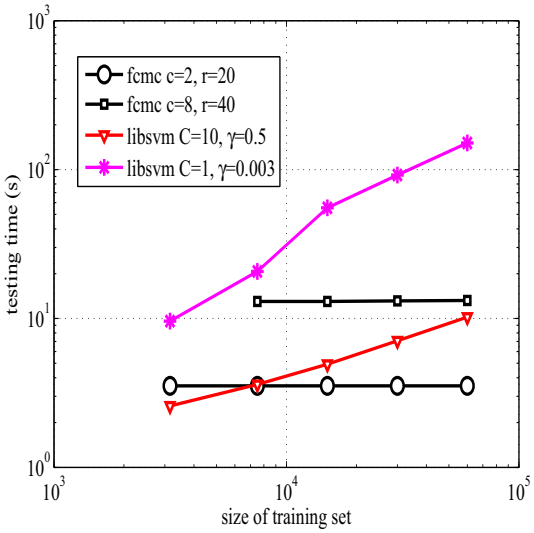

Fig. 15. Testing time (s) on the test sets of the MNIST 10-class data (FCMC: PSO 20×10)

1) When the number of training samples is large, the difference in the test set accuracy (i.e., the generalization capability) between FCMC and LibSVM is slight.

2) When the size of training set is reduced, the test set accuracy of FCMC surpasses LibSVM in many data sets.

3) Training time of FCMC proportionally increases with the size of training set (i.e., $O(N)$). But, the time needed for LibSVM increases more rapidly than FCMC (i.e., $O(N^2)$ for LibSVM). Thus, the training is faster than LibSVM, when the size of training set is large.

4) The testing time (detection time) is faster than LibSVM by an order of magnitude, when the size of training set is large.

There may be other types of benchmark data such as those with many categorical features. To confirm the discriminative power on various benchmark data is left for our future work.

References

[1] H. Ichihashi, K. Honda, A. Notsu and K. Ohta, "Fuzzy *c*-means classifier with particle swarm optimization," *Proc. of the IEEE International Conference on Fuzzy System, World Congress on Computational Intelligence*, Hong Kong, China, pp. 207-215, 2008.

[2] H. Ichihashi, A. Notsu and K. Honda, "Triplet of FCM classifiers," *Proc. of 2009 IEEE International Conference on Fuzzy System*, Jeju, Korea, Aug. 20-24, 2009.

[3] H. Ichihashi, A. Notsu and K. Honda, "Semi-hard *c*-means clustering with application to classifier design," *Proc. of the IEEE International Conference on Fuzzy System, World Congress on Computational Intelligence*, Barcelona, Spain, pp. 2788-2795, 2010.

[4] H. Ichihashi, A. Notsu, K. Honda, T. Katada and M. Fujiyoshi, "Improvement in the performance of camera based vehicle detector for parking lot," *Proc. of 2010 IEEE International Conference on Fuzzy System*, Barcelona, Spain, Juli. 18-23, 2010.

[5] R. C. Eberhart and J. Kennedy, "A new optimizer using particle swarm theory," *Proc. of the 6th International Symposium on Micro Machine and Human Science*, Nagoya, Japan, pp. 39-43, 1995.

[6] J. Kennedy and R. C. Eberhart, "Particle swarm optimization ," *Proc. of the IEEE International Conference on Neural Networks*, Piscataway, NJ, vol. 4, pp. 1942-1948, 1995.

[7] M. Clerc, *Particle Swarm Optimization*, Wiley, 2006.

[8] Chih-Chung Chang and Chih-Jen Lin, LIBSVM : a library for support vector machines, 2001. Software available at http://www.csie.ntu.edu.tw/˜cjlin/libsvm.

[9] J. C. Platt, “Fast training of support vector machines using sequential minimal optimization. ,” *Advances in Kernel Methods - Support Vector Learning, Eds. B. Scholkopf, C. J. C. Burges, and A. J. Smola*, Cambridge, MA, 1998. MIT Press, pp. 185-208, 1999.

[10] H. Ichihashi, K. Miyagishi and K. Honda, “Fuzzy *c*-means clustering with regularization by K-L information,” *Proc. of 10th IEEE International Conference on Fuzzy Systems*, Melbourne, Australia, vol.3, pp.924-927, 2001.

[11] S. Miyamoto, T. Yasukochi, R. Inokuchi, “A family of fuzzy and defuzzified *c*-means algorithms, ” *Proc. of the International Conference on Computational Intelligence for Modelling, Control and Automation*, Vienna, Austria, pp.170-176, 2005.

[12] S. Miyamoto, H. Ichihashi, and K. Honda, *Algorithms for Fuzzy Clustering, Methods in c-Means Clustering with Applications*, Springer-Verlag, Berlin, 2008.

[13] M.E. Tipping and C.M. Bishop, “Mixtures of probabilistic principal component analyzers,” *Neural Computation*, vol.11, pp.443-482, 1999.

[14] F. Sun, S. Omachi, and H. Aso, “Precise selection of candidates for hand written character recognition,” *IEICE Trans. Information and Systems*, vol.E79-D, no.3, pp.510-515, 1996.

[15] I. W. Tsang, J. T. Kwok, and P.-M. Cheung, “Core vector machines - Fast SVM training on very large data sets,” *Journal of Machine Learning Research*, vol.6, pp. 363-392, 2005.

[16] G. Loosli and S. Canu, “Comments on the ‘Core vector machines: Fast SVM training on very large datasets’, ” *Journal of Machine Learning Research*, vol.8 , pp. 291-301, 2007.

[17] Y. LeCun, L. Bottou, Y. Bengio, and P. Haffner, “Gradient-based learning applied to document recognition,” *Proc. of the IEEE*, vol. 86, no. 11, pp. 2278-2324, 1998.

2011 IEEE International Conference on Fuzzy Systems
June 27-30, 2011, Taipei, Taiwan

Ellipse Detection with Hard c-Regression Models and Random Initializations

Hidetomo Ichihashi, Li Chieu Lam, Katsuhiro Honda, Akira Notsu
Department of Computer Science and Intelligent Systems
Osaka Prefecture University
Sakai, Osaka
Email: ichi@cs.osakafu-u.ac.jp

***Abstract*—Shell clustering methods partition data sets into several shell-shape clusters by extracting local circles or ellipses as prototypes of clusters. This paper proposes hard c-regression models (HCRMs) for shell clustering. The procedure is a defuzzified switching regression models. HCRMs successfully detect ellipses by using random initializations. We report the performance using 20 data sets each of which consists of two ellipses. The detection time on average is 14 milliseconds on DELL PRECISION T5400 3.16GHz.**

***Index Terms*—ellipse detection, clustering, switching regression, random initializations.**

I. Introduction

Figs. 1-2 illustrates an application of ellipse detection, where a robot grasps a saucer placed upside-down. First, Sobel edge detection method is applied on the gray scale image. Then the coordinate of pixels on the edges are picked by thresholding the gray scale values and thinned by sampling every 10 points. The data set consisted of the coordinate of points on edge is used for ellipse detection. The robot can know the relative position of the saucer precisely and can grasp it correctly, since the mathematical formula of the ellipses are obtained.

A standard method of detecting ellipses is the Hough transform (HT). The Hough transform extracts geometrical parameters of an image and maps them into the Hough domain. Standard HT, however, is not really used for fast ellipse detection since it requires a lot of computational processing. An ellipse has five parameters and requires intensive memory.

The 5-dimensional parameter space is decomposed into several subspaces of fewer dimensions via parallel edge points in [3]. A multistage HT approach using the polar and pole definition of ellipses has been proposed in [4]. Ellipses were extracted by relating local geometric features of a parametric representation to the local features in an image in [5]. In [6] a global geometric symmetry method was utilized to locate the centers of ellipses and circles and then used the accumulative concept of the Hough transform to extract all ellipses and circles in an image. Another HT variant is the Randomized Hough Transform (RHT) [7] which is well-suited to ellipse detection due to its lessened usage of memory and fast processing characteristic as proposed in [8].

Some non-Hough transform methods were also proposed for detecting ellipses. Dave [9] used the fuzzy c-shells to detect circles and ellipses. Shell clustering methods divide data into clusters, each one representing a circle or an ellipse. Fuzzy c-Shells (FCS) [9] and Adaptive Fuzzy c-Shells (AFCS) [10] are represented by a prototype of nonlinear function; FCS is effective for dividing data into circle clusters and into ellipse clusters. However for each iteration, it is necessary to solve a set of nonlinear equations, so there is a problem in terms of complexity. R. Krishnapuram's Fuzzy c-Spherical

A saucer placed upside-down

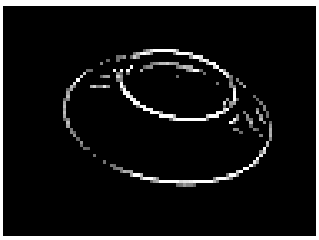

Sobel edge detection

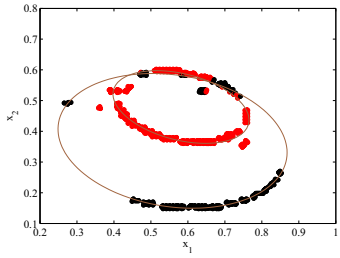

Ellipse detection after thresholding intensity and thinning the edges by sampling

Fig. 1. Detecting saucer placed upside-down

978-1-4244-7316-8/11/$26.00 ©2011 IEEE

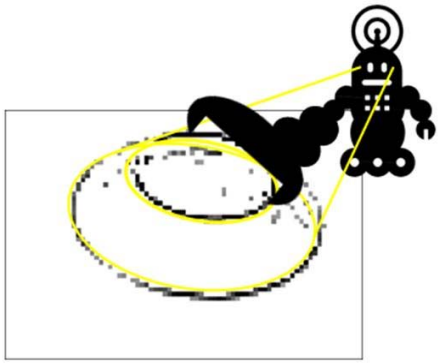

Fig. 2. Robot grasps the saucer

Shells (FCSS) [11] improves the computational efficiency by calculating prototypes analytically with "algebraical" distance. Fuzzy c-Quadratic Shells (FCQS) adopts quadratic polynomial as a distance function, and extracts clusters in the shape of ellipsoid, hyperbola, and parabola. Probabilistic approach for FCQS and robust FCQS which are less affected by noise also have been studied [12], [13], [14]. FCV-based robust shell clustering is proposed but there are problems in terms of computational time [15].

For improving computational time and detection accuracy, we defuzzify fuzzy c-regression models (FCRM) [16] and formulate hard c-regression models (HCRMs). Hence, the first half of our approach can be regarded as one of the switching regression models [1], [2] on an extended high dimensional space. The approach is based on an objective function. The procedure is repetitive and the termination condition by using another error evaluation function is adopted.

HCRMs quickly extract circles or ellipses by repeating random initializations. We test the performance using 20 data sets and report that the detection time on average is 14 milliseconds.

II. Shell clustering with hard c-regression models

Fuzzy c-regression models (FCRM) regards c-regression equations as clustering prototypes. In this section, we formulate the methods which capture nonlinear structures of data sets efficiently by applying hard clustering to FCRM.

Two dimensional data (i.e., points on a plane), each of which is written as $\mathbf{x}_k = (x_{k1}, x_{k2})^\top$, are extended as:

$$\mathbf{x}_k^* = (x_{k1}, x_{k2}, {x_{k1}}^2, {x_{k2}}^2, x_{k1}x_{k2})^\top \quad k = 1, \cdots, n, \tag{1}$$

where $\mathbf{x}_k^*$ denotes the vector of dependent variables. We minimize the squared errors of the following regression equation so that z_{ki} is as close to 1 as possible.

$$\begin{aligned} z_{ki} &= a_{i1}x_{k1} + a_{i2}x_{k2} + a_{i3}{x_{k1}}^2 \\ &+ a_{i4}{x_{k2}}^2 + a_{i5}x_{k1}x_{k2} \\ &= \mathbf{x}_k^{*\top}\mathbf{a}_i \\ \mathbf{a}_i &= (a_{i1}, a_{i2}, a_{i3}, a_{i4}, a_{i5})^\top, \end{aligned} \tag{2}$$

where i denotes the cluster number ($i = 1, \cdots, c$). (2) represents an ellipse when z_{ki} is a positive constant. We choose $\mathbf{a}_i$ such that z_{ki} are all close to a constant value. The constant value can be 1, and the squared error between 1 and z_{ki} is defined as:

$$\begin{aligned} d_{ki}^2 &= (a_{i1}x_{k1} + a_{i2}x_{k2} + a_{i3}{x_{k1}}^2 \\ &+ a_{i4}{x_{k2}}^2 + a_{i5}x_{k1}x_{k2} - 1)^2 \\ &= (\mathbf{x}_k^*\mathbf{a}_i - 1)^2 \end{aligned} \tag{3}$$

and the objective function is defined as:

$$L = \sum_{i=1}^{c}\sum_{k=1}^{n} u_{ki}d_{ki}^2. \tag{4}$$

$u_{ki} \in [0,\ 1]$ is the membership and 1 or 0 is assigned to u_{ki}, since L is linear with respect to u_{ki}. For updating u_{ki}, following rule is adopted.

$$u_{ki} = \begin{cases} 1 & (i = \arg\min_{1\le j\le c} d_{kj}^2), \\ 0 & (\text{otherwise}). \end{cases} \tag{5}$$

Regression coefficient $\mathbf{a}_i$ is the least squares estimator of the following simultaneous equations.

$$\begin{bmatrix} u_{1i}\mathbf{x}_1^{*\top}\mathbf{a}_i \\ u_{2i}\mathbf{x}_2^{*\top}\mathbf{a}_i \\ \vdots \\ u_{ni}\mathbf{x}_n^{*\top}\mathbf{a}_i \end{bmatrix} = \begin{bmatrix} u_{1i} \\ u_{2i} \\ \vdots \\ u_{ni} \end{bmatrix}. \tag{6}$$

Let us rewrite (6) as:

$$X\mathbf{a}_i = \mathbf{u}_i. \tag{7}$$

Then, $\mathbf{a}_i$ is computed with singular value decomposition

$$X = Z\Lambda P^\top, \tag{8}$$

where Z is an n $\times$ 5 matrix, Λ is the diagonal matrix of singular values $\lambda_j, j = 1, ..., 5$, and $P^\top$ denotes the transpose of P, an 5 $\times$ 5 matrix. Column vectors of Z and P are all length 1.

By using the pseudoinverse, the solution becomes:

$$\mathbf{a}_i = P\Lambda^+ Z^\top \mathbf{u}_i, \tag{9}$$

where Λ^+ is a inverse of Λ and $1/\lambda_j$ is replaced by zero when $\lambda_j = 0$. This solution procedure is embedded by certain programming languages, such as Matlab.

As $\mathbf{a}_i$ and u_{ki} are updated repeatedly, the above mentioned regression method can be seen as one of the switching regression models [1], [2]. In our proposed method, initial values of $\mathbf{a}_i$ are given randomly and then the initial membership values are calculated. We choose $\mathbf{a}_i$ which minimize the objective

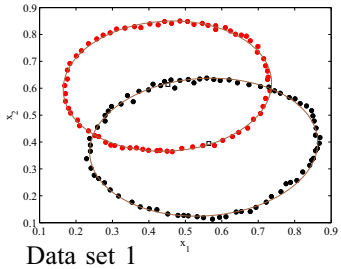

Data set 1

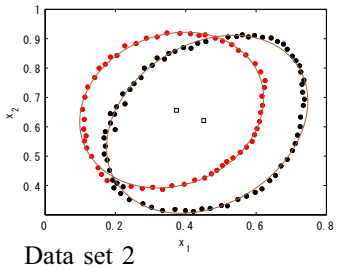

Data set 2

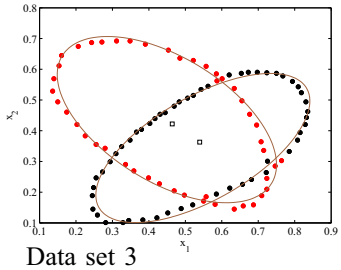

Data set 3

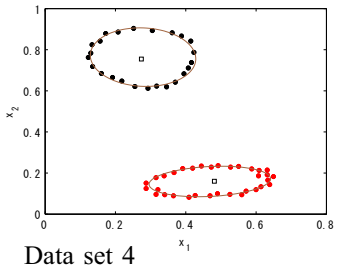

Data set 4

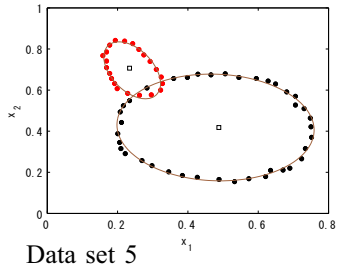

Data set 5

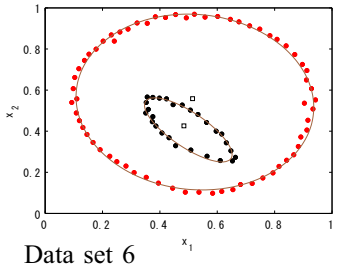

Data set 6

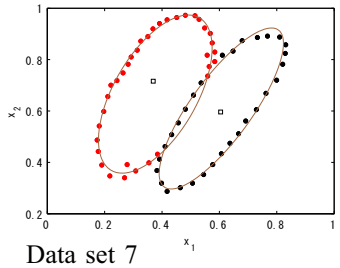

Data set 7

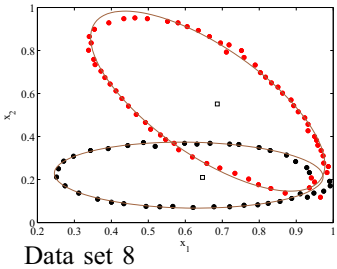

Data set 8

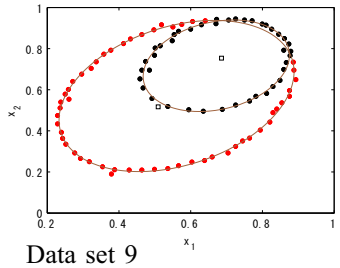

Data set 9

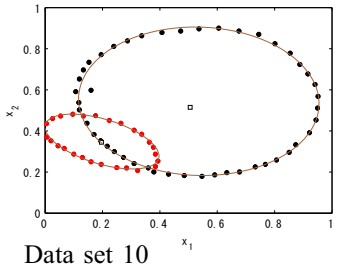

Data set 10

Fig. 3. Data sets 1 - 10

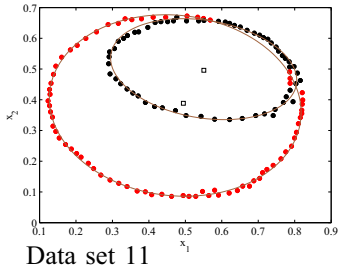

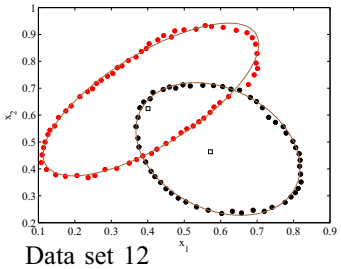

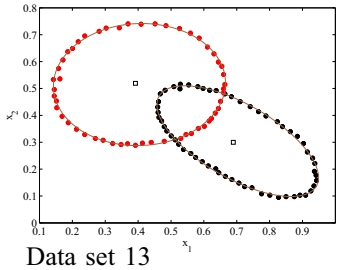

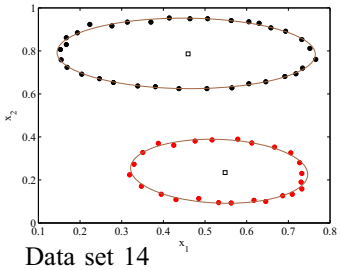

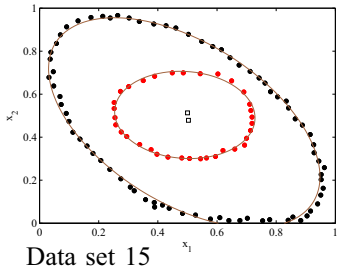

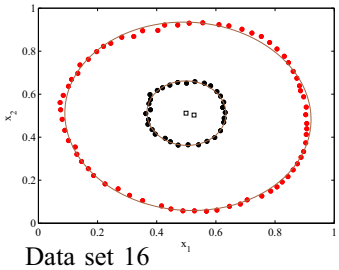

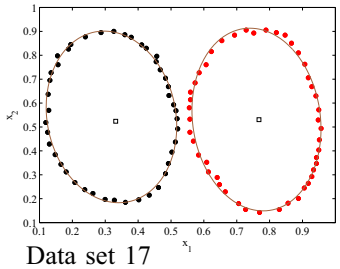

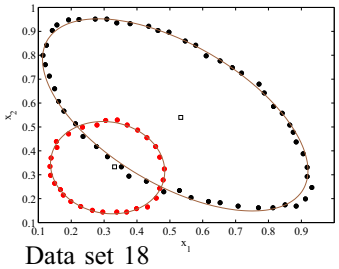

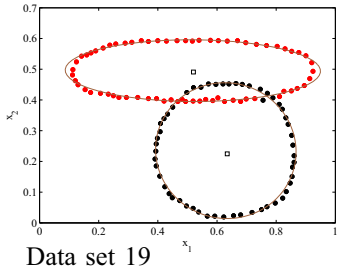

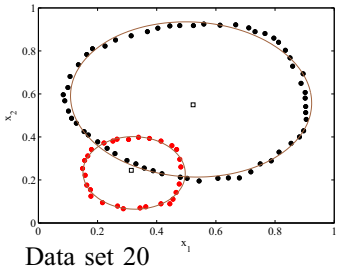

Fig. 4. Data sets 11 - 20

function L. But, for example, for data set 4 in Fig. 3, L often becomes smaller when the detection is false than when the detection is correct. So, we repeatedly change initial values until the following evaluation function E becomes less than a given threshold e.

$$E = \sum_{i=1}^{c} \left(\sum_{k=1}^{n} u_{ki}\beta_{ki} \mid \mathbf{x}_k - \mathbf{v}_i \mid / \sum_{k=1}^{n} u_{ki} \right) \tag{10}$$

$\mathbf{v}_i$ is a center and $\mid \cdot \mid$ denotes the Euclidean distance. β_{ki} is calculated such that $\mathbf{y}_k$ is the projection of $\mathbf{x}_k$ on the oval.

$$\begin{gathered} \mathbf{y}_k = \mathbf{x}_k + \beta_{ki}(\mathbf{x}_k - \mathbf{v}_i) \\ \mathbf{y}_k^{*\top} \mathbf{a}_i = 1, \end{gathered} \tag{11}$$

where $\mathbf{y}_k^*$ are extended 5 dimensional data of $\mathbf{y}_k$. The smallest absolute value of β_{ki} is chosen.

The procedure is repeated to a maximum of r-times if the condition $E < e$ is not met, then $\mathbf{a}_i$ which minimizes E is chosen.

The detection algorithm using the above mentioned update rules is as follows.

1. Extend $\mathbf{x}_k$ to $\mathbf{x}_k^*$.
2. Initialize regression coefficients $\mathbf{a}_i$ randomly.
3. Compute the errors by (3).
4. Update the membership value u_{ki} by (5).
5. Update $\mathbf{a}_i$ by (6).
6. If the change in the objective function values (4) becomes small enough ($|L^{old} - L^{new}| < 10^{-7}$), then go to 7, else go to 3.
7. Compute evaluation function (10) for detecting ellipses.
8. If repetition time is less than r and $E > e$, then go to 2, else go to 9.
9. Select $\mathbf{a}_i$ which minimizes the evaluation function (10).

In the next section we set as $r = 200$ and $e = 0.02$.

III. Detection Performance

To evaluate the effectiveness of the proposed method, experiments were conducted using the 20 different data sets shown in Figs. 3-4. Table II-I shows the results. Initial values of $\mathbf{a}_i$ are given as:

$$\begin{aligned} \mathbf{a}_1 &= (2.10561.3352 - 1.6725 - 1.6585 - 0.1724) \times 1.1 \\ &+ (rand - 0.5) \times 2 \\ \mathbf{a}_2 &= (2.10561.3352 - 1.6725 - 1.6585 - 0.1724) \times 1.8 \\ &+ (rand - 0.5) \times 2 \end{aligned}$$

where $rand$ denotes a vector of uniform random numbers $rand \in [0, 1]$. The program stops when E in (10) is less than 0.02.

Each data set is tested 10 times and values of E, detection times and the number of repetitions (i.e., the numbers of initializations of $\mathbf{a}_i$ until $E < 0.02$ is satisfied) are given in Tables II-III. In all cases, the algorithm terminated before reaching the final termination condition ($r = 200$). For Data set 1, E=0.0107 is attained in 18 milliseconds on average. The detected ellipses are shown in Fig. 3 upper left. For example, the maximum detection time for Data set 10 is 6 milliseconds, the mean time is 4 milliseconds and the minimum time is 3 milliseconds. Table I shows the results on all data sets. The mean detection time on all the data sets is 14 milliseconds. Experiments are performed on DELL PRECISION T5400 3.16GHz 4GB.

TABLE I
DETECTION TIME ON ALL DATA SET

	E	time (s)	repetitions (initializations)
Max	0.0197	0.155	155
Mean	0.0139	**0.014**	11.2
Min	0.0075	0.002	1

The methods based on Hough transform are most popular for ellipse detection. By comparison, the time for detecting two ellipses by Hough-based ellipse detection algorithm is about 1500 seconds and that of Randomized Hough Transform is about 15 seconds [8]. 10% detection error at minimum is reported in [8].

IV. Conclusion

The shell clustering method in this paper is based on the hard c-regression models with random initializations. An additional evaluation function is used for terminating the repetitive algorithm. With this enhancement, HCRM accurately detects circles or ellipses very quickly.

Our possible future work includes setting more effective initial random values, coping with a large number of clusters, and robustizing the method by using the noise clustering approach [17].

References

[1] S. M. Goldfeld and R. E. Quandt, "Techniques for estimating switching regressions," *Studies in Nonlinear Estimation (eds. by S. M. Goldfeld and R. E. Quandt)*, pp. 3-35, Ballinger, Cambridge, Massachusetts, 1976.

[2] R. E. Quandt, "A new approach to estimating switching regressions," *Journal of American Statistical Association*, vol. 67, pp. 306-310, 1972.

[3] K. K. R. Yip, K. S. P. Tam and N. K. D. Leung, "Modification of Hough transform for circles and ellipses detection using a 2-dimensional array," *Pattern Recognition*, vol. 25, pp. 1007-1022, 1992.

[4] J. H. Yoo and I. K. Sethi, "An ellipse detection method from the polar and pole definition of conics," *Pattern Recognition*, vol. 26, pp. 307-315, 1993.

[5] A. S. Aguado, M. E. Montiel and M. S. Nixon, , "Ellipse detection via gradient direction in the Hough transform," *Proceedings of 5th IEEE International Conference on Image Processing and its Applications,* Edinburgh, UK, pp. 375-378, 1995.

[6] C. T. Ho, and L. H. Chen, "A fast ellipse/circle detector using geometry symmetry," *Pattern Recognition*, vol. 28, no. 1, pp. 117-124, 1995.

[7] P. Kultanen, L. Xu, and E. Oja, "Randomized hough transform (rht)," *In Proc., 10th Int'l Conf. Pattern Recognition*, vol. 1, pp. 631-635, 1990.

[8] R. A. McLaughlin, "Randomized hough tranform: Improved ellipse detection with comparison," *Pattern Recognition Letters*, vol. 19, no. 3-4, pp.299-305, 1998.

[9] R. N. Dave, "Fuzzy shell-clustering and application to circle detection in digital images," *Int. J.Gen. syst.*, vol.16, pp.343-355, 1990.

TABLE II
DETECTION TIME ON DATA SETS 1 - 10

data set 1			
	E	time (s)	repetitions (initializations)
Max	0.0107	0.043	16
Mean	0.0107	**0.018**	6.4
Min	0.0107	0.003	1
data set 2			
	E	time (s)	repetitions (initializations)
Max	0.0168	0.155	110
Mean	0.0142	**0.041**	26.8
Min	0.0118	0.006	2
data set 3			
	E	time (s)	repetitions (initializations)
Max	0.0197	0.070	70
Mean	0.0197	**0.022**	20.8
Min	0.0197	0.002	1
data set 4			
	E	time (s)	repetitions (initializations)
Max	0.0138	0.015	16
Mean	0.0138	**0.005**	5.3
Min	0.0138	0.002	1
data set 5			
	E	time (s)	repetitions (initializations)
Max	0.0122	0.018	21
Mean	0.0121	**0.004**	4.0
Min	0.0121	0.002	1
data set 6			
	E	time (s)	repetitions (initializations)
Max	0.0158	0.154	155
Mean	0.0158	**0.074**	74.0
Min	0.0158	0.007	5
data set 7			
	E	time (s)	repetitions (initializations)
Max	0.0188	0.045	51
Mean	0.0188	**0.017**	18.4
Min	0.0186	0.004	2
data set 8			
	E	time (s)	repetitions (initializations)
Max	0.0192	0.032	17
Mean	0.0188	**0.011**	5.9
Min	0.0185	0.003	1
data set 9			
	E	time (s)	repetitions (initializations)
Max	0.0196	0.035	31
Mean	0.0148	**0.014**	11.8
Min	0.0095	0.003	1
data set 10			
	E	time (s)	repetitions (initializations)
Max	0.0116	0.006	5
Mean	0.0115	**0.004**	2.5
Min	0.0110	0.003	1

TABLE III
DETECTION TIME ON DATA SETS 11 - 20

data set 11			
	E	time (s)	repetitions (initializations)
Max	0.0100	0.028	2
Mean	0.0098	**0.006**	1.2
Min	0.0095	0.003	1
data set 12			
	E	time (s)	repetitions (initializations)
Max	0.0125	0.042	31
Mean	0.0125	**0.012**	7.0
Min	0.0125	0.003	1
data set 13			
	E	time (s)	repetitions (initializations)
Max	0.0075	0.025	15.0
Mean	0.0075	**0.008**	3.7
Min	0.0075	0.003	1
data set 14			
	E	time (s)	repetitions (initializations)
Max	0.0115	0.004	4.0
Mean	0.0115	**0.002**	1.5
Min	0.0115	0.002	1
data set 15			
	E	time (s)	repetitions (initializations)
Max	0.0166	0.030	25
Mean	0.0166	**0.010**	7.1
Min	0.0166	0.003	1
data set 16			
	E	time (s)	repetitions (initializations)
Max	0.0126	0.075	38
Mean	0.0126	**0.016**	10.4
Min	0.0126	0.002	1
data set 17			
	E	time (s)	repetitions (initializations)
Max	0.0125	0.007	5
Mean	0.0125	**0.004**	2.7
Min	0.0125	0.003	1
data set 18			
	E	time (s)	repetitions (initializations)
Max	0.0135	0.007	5
Mean	0.0135	**0.004**	2.5
Min	0.0135	0.002	1
data set 19			
	E	time (s)	repetitions (initializations)
Max	0.0122	0.048	5
Mean	0.0122	**0.008**	1.9
Min	0.0122	0.002	1
data set 20			
	E	time (s)	repetitions (initializations)
Max	0.0187	0.023	24
Mean	0.0187	**0.010**	10.1
Min	0.0187	0.005	3

[10] R. N. Dave and K. Bhaswan, "Adaptive fuzzy *C*-shells clustering and detection of ellipses," *IEEE Trans. on Neural Networks*, vol.3, No.5, pp.643-662, 1992.
[11] R. Krishnapuram, O. Nasraoui and H. Frigui, "The fuzzy C spherical shells algorithms: A new approach," *IEEE Trans. on Neural Networks*, vol.3, no.5, pp.663-671, 1992.
[12] R. Krishnapuram, H. Frigui and O. Nasraoui, "Quadric shell clustering algorithms and the detection of second degree curves," *Pattern RecognitionLett*, vol.14, no.7, pp.545-552, 1993.
[13] R. Krishnapuram, H. Frigui and O. Nasraoui, "Fuzzy and possiblistic shell clustering algorithms and their application to boundary detection and surface approximation - partI," *IEEE Trans. on Fuzzy systems*, vol.3, no.1, pp.29-43, 1995.
[14] R. Krishnapuram, H. Frigui and O. Nasraoui, "Fuzzy and possiblistic shell clustering algorithms and their application to boundary detection and surface approximation - partII," *IEEE Trans. on Fuzzy systems*, vol.3, no.1, pp.44-60, 1995.
[15] K. Honda, N. Togo, H. Ichihashi, "Generalization of FCV and robust shell clustering based on least absolute deviations," *Journal of Japan Society for Fuzzy Theory and Intelligent informatics*, Vol.15, No.6, pp.693-701, 2003.
[16] R. Hathaway and J. Bezdek, "Switching regression model and fuzzy clustering," *IEEE Trans. on Fuzzy systems*, vol. 1, pp. 195-204, 1993.
[17] R. N. Dave, "Characterization and detection of noise in clustering," *Pattern Recognition Letters*, vol.12, pp. 657-664, 1991.

2011 IEEE International Conference on Fuzzy Systems
June 27-30, 2011, Taipei, Taiwan

Trajectory Anonymization from a Time Series Perspective

Sergi Martínez-Bea
IIIA - Institut d'Investigació en Intel·ligència Artificial
CSIC - Consejo Superior de Investigaciones Científicas
Campus de la UAB, 08193 Bellaterra, Catalonia, Spain
Email: smartinez@iiia.csic.es

Vicenç Torra
IIIA - Institut d'Investigació en Intel·ligència Artificial
CSIC - Consejo Superior de Investigaciones Científicas
Campus de la UAB, 08193 Bellaterra, Catalonia, Spain
Email: vtorra@iiia.csic.es

***Abstract*—In a world of constant technological evolution, the expansion of location tracking technologies is a fact. Most of us may have a device which can tell us our location with more or less accuracy. Most of those devices collect our location information and, usually, the trajectories we make. Publishing this information is essential for companies to improve their marketing strategies, for the traffic department in order to have some control about the traffic, and for many other entities. With the publishment of this information an important problem arises, the privacy. On the literature, many approaches to trajectory protection are provided. We contribute to the scene providing a framework with a protection method and measures for both the computation of the perturbation added to the data, and the risk of linking a protected trajectory to its original.**

***Index Terms*—Trajectory anonymization, location privacy, information loss, disclosure risk.**

I. Introduction

Nowadays, it is very common to have devices equiped with technologies that can localize you, such as smartphones, GPS navigators, etc. Those devices can store data about the trajectories you made. Those trajectories might be very useful for companies, e.g. they can know which are the most common places that people visit, the most transited roads, etc. The problem here is that this data can easily compromise your privacy. If this data falls in the hands of the wrong person, he could identify an individual and have the information about all their moves, which can be highly dangerous. The rationale, in order to avoid this, is to protect the data. There are many approaches in the literature for this purpose such as [1], [2], [3], and [4] between others. Some of them, for example [1], [2], and [3], only focus on protecting the data. Others, like [4], prevent the disclosure and try to preserve the data utility as high as possible. There is literature that focus on using generalization as a protection method, like in [1]. Generalization receives n trajectories and it returns n undistinguishable trajectories. Therefore, the re-identification of an individual becomes more difficult. In this paper, we focus on using microaggregation as a protection method, like in [4], and we provide a framework to evaluate the information loss (i.e. the amount of perturbation added to the data) and the disclosure risk. In contrast to [4], our work aims to be as generic as possible for the information loss calculation. This is specially important as there is a wide range of uses that this data can be given. This paper is organized as follows. In Section 2 we present some preliminar information that will be used across all the text. In Section 3 we talk about protection methods and we present our approach. In Section 4, the information loss measures are presented. In Section 5, we explain the disclosure risk measure we use. In Section 6, we present the experiments made in order to validate our framework and we present the results. Finally, Section 7 concludes and give some directions for future research.

II. Preliminaries

In this section we review several definitions on trajectories that are needed in the rest of the paper.

A. Trajectories

A trajectory can be defined as a sequence of places or spots that a given object or person has gone through. We will define each place or spot with their coordinates x and y and a timestamp t that determines the time when the object or person was there. Therefore, we can define formally a trajectory as:

$$\{(x_1, y_1, t_1), (x_2, y_2, t_2), \ldots, (x_n, y_n, t_n)\} \text{ where } n \in \mathbb{N}$$

In this way, we can observe a trajectory as numerical data that varies over time, and thus we can find similarities with the definition of time series. Recall that they are defined as:

$$\{(x_1, t_1), (x_2, t_2), \ldots, (x_n, t_n)\} \text{ where } n \in \mathbb{N}$$

Given this, we can easily adapt distances and statistics from time series to trajectories. The first part of this section includes a section for distances and another for the autocorrelation function. The original distances were taken from [5].

B. Distances between trajectories

As we have already pointed out, there is a similarity between trajectories and time series. Due to this, we take two distance functions from time series and adapt them to trajectories. Trajectories can be totally overlapped over time, partially overlapped over time, or non overlapped at all. The distances adapted should take into account all those cases. It is important, though, that when we apply a distance to a pair of trajectories, the two trajectories have the same number of points.

978-1-4244-7316-8/11/$26.00 ©2011 IEEE

1) Adapted Euclidean Distance: The common Euclidean distance does not take into account the time. As the distance between two trajectories partially overlapped over time should be less than the distance between two trajectories non overlapped, we need to include the time factor in the distance calculation.

Given two time series r and s as follows

$$r = \{p_1, p_2, \ldots, p_n\}$$
$$s = \{q_1, q_2, \ldots, q_n\}$$

with their elements p_i and q_i represented as

$$p = (p_x, p_y, p_t)$$
$$q = (q_x, q_y, q_t)$$

we can define the Adapted Euclidean Distance between r and s as:

$$d_{EU}(r, s) = \sqrt{\sum_{i=1}^{n} d_e(r_i, s_i)}$$

where

$$d_e(p, q) = (1 + (p_t - q_t)^2) \cdot ((p_x - q_x)^2 + (p_y - q_y)^2)$$

2) Adapted Short Time Series Distance: Adapting the Short Time Series distance to trajectories is quite straightforward. It is enough to add the y coordinate to the distance formula. Therefore, we can define the Adapted Short Time Series Distance as:

$$d_{STS_A}(r, s) = \sqrt{\sum_{i=1}^{n} d_s(r_i, s_i)}$$

where

$$d_s(p, q) = \left[\left(\frac{q_{x_{i+1}} - q_{x_i}}{q_{t_{i+1}} - q_{t_i}} - \frac{p_{x_{i+1}} - p_{x_i}}{q_{t_{i+1}} - q_{t_i}}\right)^2\right] + \left[\left(\frac{q_{y_{i+1}} - q_{y_i}}{p_{t_{i+1}} - p_{t_i}} - \frac{p_{y_{i+1}} - p_{y_i}}{p_{t_{i+1}} - p_{t_i}}\right)^2\right]$$

C. Adapted Autocorrelation Function

The Autocorrelation function applied to time series is used in [5] as part of the computation of data utility. In the same way as the distances, we adapt this function to work with trajectories. Again, it is quite straightforward. It is enough to add the y coordinate to the formula.

Given the time series r represented by

$$r = \{p_1, p_2, \ldots, p_n\}$$

with the elements p_i with the following components

$$p = (p_x, p_y, p_t)$$

we can define the Adapted Autocorrelation Function as:

$$\rho(h) = \frac{\gamma'_A(h)}{\gamma'_A(0)}$$

where

$$\gamma'_A(h) = n^{-1} \cdot \sum_{i=1}^{n-|h|} \left(p_{x_{t+|h|}} - \mu_x\right) \cdot \left(p_{x_t} - \mu_x\right) + \left(p_{y_{t+|h|}} - \mu_y\right) \cdot \left(p_{y_t} - \mu_y\right)$$

and

$$\mu_x = \frac{1}{n} \sum_{i=1}^{n} p_x$$
$$\mu_y = \frac{1}{n} \sum_{i=1}^{n} p_y$$

III. Protection Methods

As stated before, the objective of trajectory anonymization is to preserve the privacy of the individuals whose trajectory data has been collected. In order to achieve this, we need a protection method.

Given a data set X a protection method transforms X into a protected data set X'. In general, X can be seen as a matrix with n rows (records) and m columns (attributes). We can classify the attributes in two types: identifiers and quasi-identifiers. A given attribute is considered an identifier when it unambiguously identifies an individual (e.g the social security number), in contrast an attribute is considered a quasi-identifier when it can not identify an individual by itself but a set of them can. Note that a concrete group of quasi-identifier attributes can identify an individual depending on the scenario. E.g. age and sex can be quasi-identifiers in a small company but not in a class. Quasi-identifier attributes can be divided in two classes: confidential and non-confidential depending on whether they contain private information. For instance, let us imagine that an attacker A has some quasi-identifier attributes of an individual, as e.g age, birth place, sex and medical history. The first three attributes are non-confidential while the last one is confidential. In a very large database those attributes would not give the attacker the necessary information to identify an individual as lots of people of the same sex may have been born in the very same place at the same year. But if we have a different scenario, e.g. a database with the employees of a company, where those quasi-identifier attributes are unique in the whole data set, the attacker could clearly identify the individual.

Our scenario is the same as the scenario presented in [5]. In the standard scenario (see eg. [6] [7] [8] [9] [10] [11]) before releasing a data set X with confidential attributes, a protection method ρ is applied, leading to a protected data set X'. Indeed, we will assume the following: (i) identifier attributes in X are either removed or encrypted, therefore we will write $X = X_{nc}||X_c$; (ii) confidential quasi-identifier attributes X_c are not modified, so we have $X'_c = X_c$; (iii) the protection method itself is applied to non-confidential quasi-identifier

attributes in order to preserve the privacy of the individuals whose confidential data is being released. Therefore, we have $X'_{nc} = \rho(X_{nc})$.

In the remaining part of this section we discuss microaggregation, one of the most effective data protection methods. We describe our approach for applying microaggregation to trajectories.

A. Microaggregation

Microaggregation is a protection method that ensures k-anonymity by building small clusters of at least k elements and replacing the original values with the centroid of the cluster to which the record belongs to.

In order to solve the information loss problem of the basic microaggregation method, multivariate microaggregation is used at the cost of increasing the disclosure risk. Specifically, after dividing attributes into different blocks and applying the basic microaggregation technique to each block separately. This means that the k records which fall in the same cluster for the first block of attributes, may fall in a different cluster for any of the other block of attributes. So, the resulting protected records will not be equal and no k-anonymity is ensured.

In order to preserve information loss as low as possible, microaggregation methods try to minimize the total sum of distances between all the elements to be protected and the centroid of the cluster where an element belongs to, i.e. to minimize the total Sum of Square Errors (SSE):

$$SSE = \sum_{i=1}^{C} \sum_{x_{ij} \in C_i} (X_{ij} - \bar{X}_i)^T (X_{ij} - \bar{X}_i),$$

where c is the total number of clusters, C_i is the ith cluster and $\bar{x}_i$ is the centroid of C_i. The restriction is $|C_i| \geq k$, for all $i = 1, \ldots, c$. In general, the larger the value of k the lower the disclosure risk. Therefore, in order to parametrize microaggregation methods, k has to be large enough to ensure confidentiality but not too large to compromise the statistical utility of the protected information.

The rationale of this process is to make the protected data as similar as possible to the original one. In any case, methods should provide clusters with at least k elements. Finding the optimal multivariate microaggregation has been proven to be an NP-Hard problem. For this reason, heuristic methods have been proposed in the literature.

In our work, we will adapt for trajectories one of the most used methods for heuristic multivariate microaggregation: the MDAV (Maximum Distance to Average Vector) algorithm.

B. MDAV microaggregation

The *MDAV (Maximum Distance to Average Vector)* algorithm is an heuristic algorithm for clustering records in a data set X so that each cluster is constrained to contain at least k records. You can see the *MDAV* algorithm description in Algorithm 1.

The generic *MDAV* algorithm can be used for different data types, but then it requires the appropiate definitions for distance and average. When we want to apply the *MDAV* algorithm to a particular type of data, we need to define what the most distant record means, which the closest records of a given record are, and the average record of a set of records. The average vector will be used in step (3) and to mask the original data in steps (4) and (8).

Algorithm 1: MDAV

Input: X: original microdata, k: integer
Output: X': protected microdata
1: **while** $|X| > k$ **do**
2: Compute the average record $\bar{x}$ of all records X
3: Consider the most distant record x_r to the average record $\bar{x}$
4: Form a cluster around x_r. The cluster contains x_r together with the $k-1$ closest records to x_r
5: Remove these records from microdata file X
6: **if** $|X| > k$ **then**
7: Find the most distant record x_s from record x_r
8: Form a cluster around x_s. The cluster contains x_s together with the $k-1$ closest records to x_s
9: Remove these records from microdata file X
10: **end if**
11: **end while**
12: Form a cluster with the remaining records

C. Trajectory microaggregation

In order to apply the *MDAV* algorithm to trajectories we need to determine which distance and which average functions we are going to use in order to implement the general *MDAV* algorithm described in Algorithm 1.

- **Distance functions.** We use our *Adapted Euclidean Distance* and our *Adapted Short Time Series Distance*, which were already explained in section 2.
- **Average.** As we are working with trajectories, using an average function would not give realistic results. Given a cluster, when doing the aggregation process, that is, the step when you replace the original values with the centroid of the cluster, if the centroid is computed with an average function, the microaggregated trajectories could have points that fall inside a building, which would be correct if the individual is a pedestrian, but not if it is an automobile. In the latter case, the trajectory would not have any utility. We assume that there can not be points inside a building. In order to avoid that, we propose two approaches based on the median function.
  - The first approach, which we call *(X median, Y median)*, is to calculate the median for the X coordinate of points of different trajectories that have the same timestamp t and fall into the same cluser. Then, do the same with the Y coordinate, so you end up having a trajectory that represents all the trajectories in that cluster.
    E.g. Given the trajectories r, s and u defined as

$$r = (r_1, r_2, r_3)$$
$$s = (s_1, s_2, s_3)$$
$$u = (u_1, u_2, u_3)$$

    where

$$r_1 = (3, 6, 1), r_2 = (1, 7, 2), r_3 = (8, 5, 3)$$
$$s_1 = (2, 9, 1), s_2 = (7, 8, 2), s_3 = (2, 4, 3)$$
$$u_1 = (0, 3, 1), u_2, = (6, 2, 2), u_3 = (9, 2, 3)$$

we calculate the median for the X and Y coordinate of the points with the same timestamp t, resulting in a single trajectory v. That is,

$$v = (v_1, v_2, v_3)$$

where

$$v_1 = (2, 6, 1), v_2 = (6, 7, 2), v_3 = (8, 4, 3)$$

– The second approach, which we call *(X median, Y)* is not very different. Again, calculate the median for the X coordinate of the same points of the different trajectories that fall into the same cluster. Then instead of doing the same with the Y coordinate, search through all the trajectories in the same cluster for that X value, and get the corresponding Y value. This gives a trajectory with real points (i.e. points that will not fall inside a building), that represents all the trajectories in that cluster.
E.g. Given the trajectories r, s and u that fall into the same cluster, defined as

$$r = (r_1, r_2, r_3)$$
$$s = (s_1, s_2, s_3)$$
$$u = (u_1, u_2, u_3)$$

where

$$r_1 = (3, 6, 1), r_2 = (1, 7, 2), r_3 = (8, 5, 3)$$
$$s_1 = (2, 9, 1), s_2 = (7, 8, 2), s_3 = (2, 4, 3)$$
$$u_1 = (0, 3, 1), u_2, = (6, 2, 2), u_3 = (9, 2, 3)$$

we calculate the median for the X coordinate of the points with the same timestamp t and get the Y coordinate corresponding to that X value, resulting in a single trajectory v. That is,

$$v = (v_1, v_2, v_3)$$

where

$$v_1 = (2, 9, 1), v_2 = (6, 2, 2), v_3 = (8, 5, 3)$$

In section 6 we show how one approach or the other, affect the results.

IV. Information Loss measures

Trajectories information can have a wide range of uses. It can be used by companies to improve their advertisement strategy, for marketing purposes, for traffic control, etc. In our scenario, we assume no concrete use can be specified before its protection.

When applying any perturbative methods to protect a data set, there is always some kind of information loss. I.e, the perturbation inflicted to the data decreases their utility. As we would like to minimize this loss, we need a measure to compare different perturbations due to different parameters within a method or even different methods.

Information loss clearly depends on the uses that will be given to the protected data. Nervertheless, as stated above we focus on generic uses. In this case, it is desirable to have a generic way to measure this information loss. It should reflect the amount of perturbation that is being added with a given protection method and the decay of data utility for a range of data uses.

In order to achieve this goal, we define information loss in terms of three components: IL_1, IL_2, IL_3. They are partial information loss measures described below.

- IL_1. It is defined as the average value of the measures $IL_{1.1}$ and $IL_{1.2}$ which are defined below. That is,

  $$IL_1 = \frac{IL_{1.1} + IL_{1.2}}{2}$$

  $IL_{1.1}$ is the average of the difference between the means of both original and protected trajectories, and $IL_{1.2}$ is the average of the difference between the autocorrelation functions of both original and protected trajectories. They are defined by:

  $$IL_{1.1} = \frac{1}{2s}\left(\sum_{i=1}^{s} \frac{|\mu_{x_i} - \mu'_{x_i}|}{Max(|\mu_{x_i}|, |\mu'_{x_i}|)} + \frac{|\mu_{y_i} - \mu'_{y_i}|}{Max(|\mu_{y_i}|, |\mu'_{y_i}|)}\right)$$

  $$IL_{1.2} = \frac{1}{4}\sum_{h=0,n/4,n/2,3n/4}\left(\frac{1}{s}\sum_{i=1}^{s} \frac{|\rho_i(h) - \rho_i(h)'|}{Max(|\rho_i(h)|, |\rho_i(h)'|)}\right)$$

  where s is the number of trajectories in the given data set, μ_x the average of the X coordinate, μ_y the average of the Y coordinate, and the $\rho_i(h)$ is the *Adapted Autocorrelation Function* explained on the preliminaries.
- IL_2. It is defined as the absolute differences between original and protected data. That is,

  $$IL_2 = \frac{1}{2 \times s \times n}\sum_{i=1}^{s \times n}\left(\frac{||x_i| - |x'_i||}{Max(|x_i|, |x'_i|)} + \frac{||y_i| - |y'_i||}{Max(|y_i|, |y'_i|)}\right)$$

  where s is the number of trajectories in the given data set, n the number of points of a trajectory (i.e. its length), x and y the coordinates of a point that belongs to a non protected trajectory and x' and y' the coordinates of a point that belongs to a protected trajectory. Each pair of x, y - x', y' has the same timestamp t.

- IL_3. This measure was taken from [4] and is called *Space Distortion*. The aim of this measure is to capture the distortion of the shape of an anonymized trajectory. The definition on [4], takes into account that the distances used for the protection process are not defined for all kind of trajectories (i.e. totally overlapped over time, partially overlapped over time or non overlapped over time). As our distances can be applied to all of those trajectories we can simplify the Space Distortion measure presented in [4]. The *Simplified Space Distortion measure (SSD)* is defined as

$$SSD = \sum_{i=1}^{s} \sqrt{(x_i - x'_i)^2 + (y_i - y'_i)^2}$$

where s is the number of trajectories of a given data set, x and y the coordinates of a point that belongs to a non protected trajectory and x' and y' the coordinates of a point that belongs to a protected trajectory. Each pair of x, y - x', y' has the same timestamp t.
After the SSD calculation, a min-max range normalization is applied as it is desirable to have this value in the range $[0, 1]$.

V. Disclosure risk measure

When protecting trajectories or any data in general, the main goal is to maintain the privacy of the individuals. As it is desirable to keep the data useful, the protection method has to try to achieve a minimum information loss. The problem is that while the information loss decreases, it resembles more the original data and, therefore, the disclosure risk increases. Then a way to measure this disclosure risk is needed.

A. Record Linkage method

One direct approach to measure the disclosure risk is to get both the original and protected data and try to establish some links between the individuals in both data sets. That is what an attacker would do in case he gets the original and protected data sets. This method is based on the standard *Distance Based Record Linkage (DB-RL)* which can only be applied when a distance measure exists between a pair of records. This method links every protected record to the closest original one. Here, we use two different distances. Those distances are the same that were used in the microaggregation process, i.e. *Adapted Euclidean Distance* and *Adapted Short Time Series Distance*. Consider *AEULD (Adapted Euclidean distance Linkage Disclosure)* and *ASTSLD (Adapted Short Time Series distance Linkage Disclosure)*, then, we compute the disclosure risk (DR) as

$$DR = Max(AEULD, ASTSLD)$$

The DB-RL process for trajectories is detailed below, in Algorithm 2.

Algorithm 2: Trajectory Record Linkage

Input: X: original data set, k: protected data set
Output: X': LP: linked pairs
1: **foreach** $a \in X$ **do**
2: $b' = arg_min_{b \in X'} d_{tr}(a, b)$
3: $LP = LP \cup (a, b')$
4: **end foreach**

VI. Experiments

In this section we present the experiments we made, in order to empirically analyze our framework. The experiments consist in applying our protection method to some data sets (those data sets are explained in detail later in this section). Once the data sets are protected, the information loss and the disclosure risk is computed. As stated before, as information loss decreases, disclosure risk increases, and viceversa. Due to this, a trade-off between the two measures is needed to evaluate the method. There are several approaches in the literature, some of them use a graphical representation, for instance R-U maps [12], others are analytical. For example, in [13] , the authors use a combination of both information loss and disclosure risk, which they call *Score*, using the arithmetic mean between these two values. In this way, we can have a numerical value to determine the effectiveness of the method in different scenarios. The score is defined as

$$score = \frac{IL + DR}{2}$$

where IL is the information loss measure and DR the disclosure risk measure. Note that the lower the score, the best is the protection method.

A detailed explanation of the data sets we used as well as the process applied for the experiments and the commented results are found below.

A. Data sets

When doing experiments it is desirable that the data sets are real data from the real world instead of random generated data. In our case, in order to get data sets as real as possible, we used Brinkhoff's generator [14] to obtain trajectories of moving entities. The trajectories generated this way, have the same behaviour that would have real trajectories. That is because moving objects in a city usually follow a network (e.g. the street map) made of interconnected nodes (e.g. cross-streets), and also because of the large ammount of trajectories generated as well as their variable length. The synthetic trajectories are precisely generated this way. This generator has also been used for evaluation of approaches like [15] and [16]. We generated 1049 trajectories separated in 10 different data sets. The generated trajectories are over the map of Oldenburg in Germany, with 5 moving entities (object classes). As the object classes can represent different moving entities such pedestrians or automobiles, the microaggregation process is applied to each object class separately.

B. Process

In the clustering part of the microaggregation process, there is a parameter k that constraints each cluster to have at least k trajectories. Due to this, varying this parameter affects the final results as the microaggregated trajectories will not be the same for different values of k. Therefore, in our experiments, we considered applying the protection process for different values of k to each data set. That is, $k \in \{2, 3, 6, 9, 12, 14\}$. As we stated before, in the microaggregation we have two ways of doing the aggregation process. Recall that *(X median, Y median)* is the process where the median for the X coordinate and the median for the Y coordinate is calculated, and *(X median, Y)* the process where the median for the X coordinate is calculated and its corresponding Y coordinate is taken. We also stated before that we use two different distances, the *AEUD (Adapted Euclidean Distance)* and the *ASTSD (Adapted Short Time Series Distance)*. This gives us two more ways of applying the microaggregation. The experiments take into account those two distances as well as the *(X median, Y median)* and *(X median, Y)* methods for doing the aggregation process.

C. Results

This section presents the results on our experiments. In order to present them as clearly as possible, we only present the common behaviours detected from the analyzed results.

Figures 1(a) - 1(b) and 2(a) - 2(b) present four graphics as a representation of all the results. The graphics for the other data sets have a similar behaviour so we omit them.

In these figures, in the X axis we have the different values for the k parameter, on the Y axis we have the *Score* value (the lower, the better). Each graphic represents the *Score* for each k value, for the different object classes.

In general all the graphics have a similar shape. The *Score* value starts decreasing until it reaches a minimum value and then, they increase or they keep equal. The common behaviour of the *Score* value is precisely this. We stated that information loss and disclosure risk are contrary measures (i.e. when one increases the other decreases) and they both have the same relevance when computing the *Score*. This means that the best result for a given k value will be the one that has the lower *Score*. Thinking in this way, we observe that, among the different object classes, the lowest values for the *Score* are at $k = 9$, Except for the case of Figure 1(b) where the best k value is $k = 12$.

In all the results there are two object classes (4 and 5) that stand out of the others, not for they high *Score* values but for they shape: The *Score* is monotonically stable. This is because the information loss and the disclosure risk measures have the same relevance on the *Score* computation so, when they equilibrate each other, the *Score* does not change.

We stated before that we use two different distances for the microaggregation process as well as two different ways of doing the aggregation process, so it is interesting to compare the obtained results. Focusing at the k value that gives, in general, the best result (i.e. $k = 9$) and comparing the

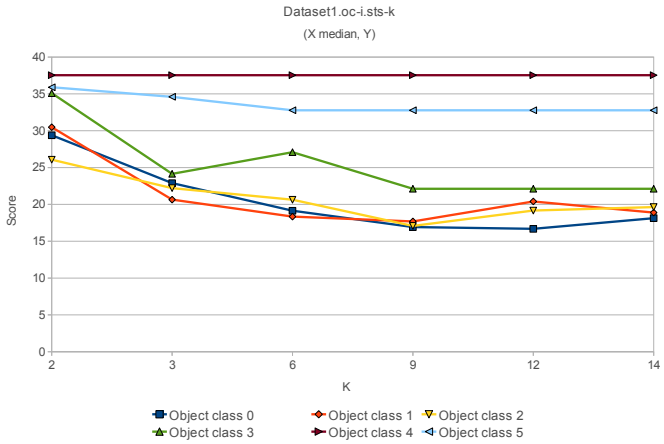

(a) *AdaptedEuclidean distance, X median - Y*

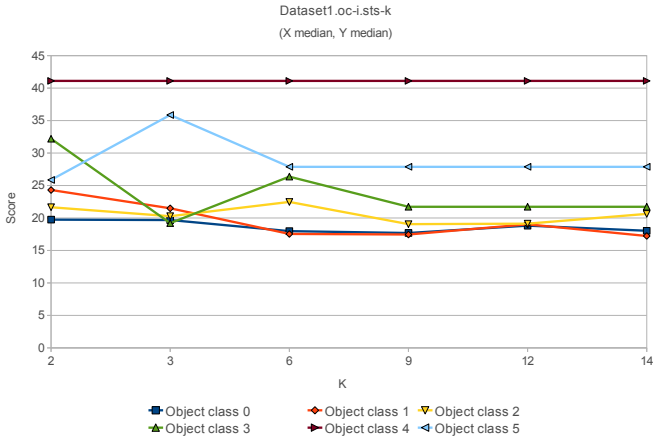

(b) *Adapted Euclidean distance, X median - Y median*

Fig. 1. *Adapted Euclidean distance results*

AEUD microaggregation with the *ASTSD* microaggregation in combination of the two different aggregation methods the *(X median, Y median)* and the *(X median, Y)*, the differences between them are not remarkable but the combination of the *ASTSD* microaggregation with the *(X median, Y)* aggregation process seems to be the best. That is because the value of the *Score* is the lowest at each object class, except for the object class 5. This behaviour is due to a high value of the information loss measure for the *ASTSD* microaggregation with the *(X median, Y)* aggregation process, which come from the microaggregation process, where, in this case, the anonymity achieved is not high enough to equilibrate the information loss. Therefore, the *Score* value is higher for this object class. This can be appreciated on Figure 3.

Figure 4 represents the *Disclosure Risk* and *Information Loss* measures for each pair consisting of the microaggregation of an object class using a particular aggregation process. In the figure, the nearer a pair to $(0, 0)$, the better. Note that $(0, 0)$ stands for data with no information loss and no disclosure risk. Also, the exceptional cases commented above can be appreciated.

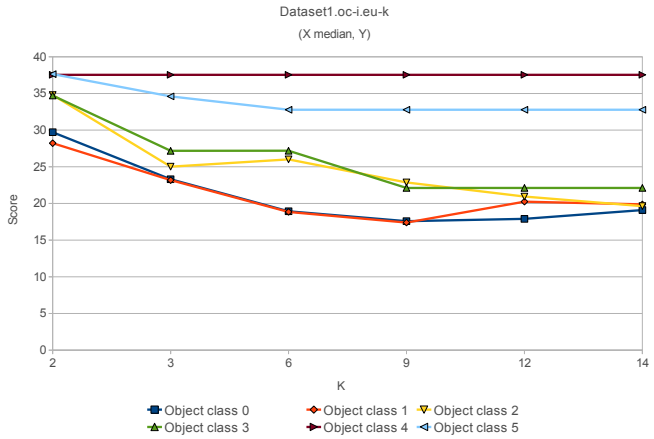

(a) *Adapted Short Time Series distance, X median - Y*

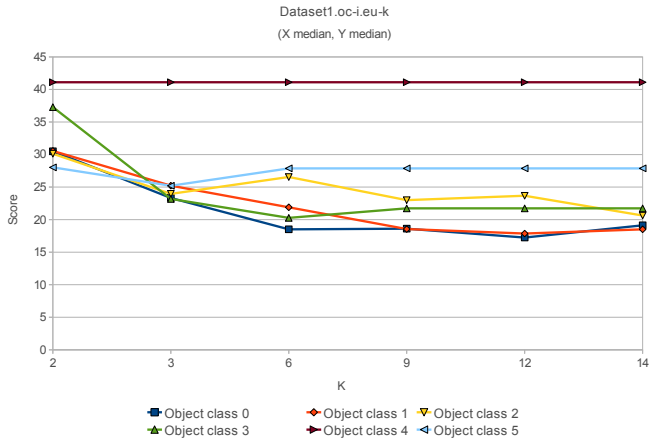

(b) *Adapted Short Time Series distance, X median - Y median*

Fig. 2. *Adapted Short Time Series Results*

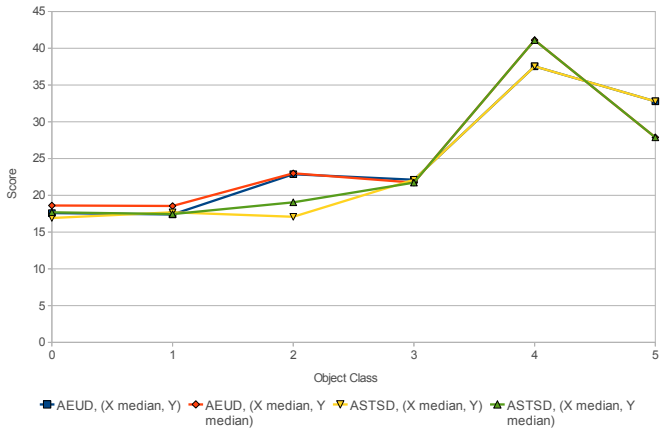

Fig. 3. *Score comparison for $k = 9$*

VII. Conclusions and Further Work

In this paper, we have presented a new framework for trajectory anonymization. We adapted the microaggregation protection method in order to apply it to trajectory anonymization. We have introduced a set of information loss measures which try to cover the general uses of trajectories. We adapted the distance based record linkage for trajectories. We adapted

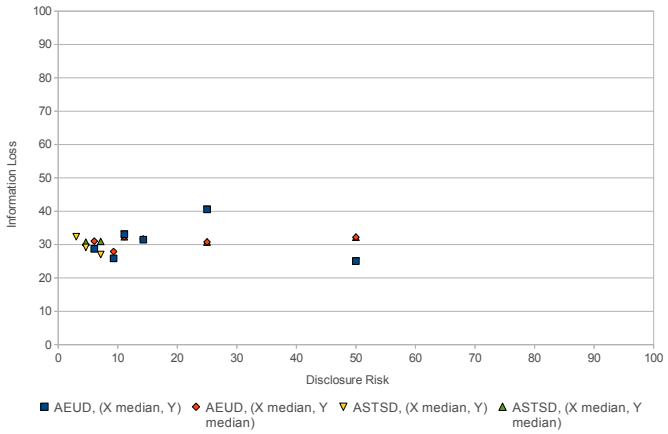

Fig. 4. *R-U Map for $k = 9$*

a couple of existing distances so that they can be applied to trajectories, no matter what their overlapping degree is. Finally, we have presented some results from applying the microaggregation method to different data sets in order to get the best parameter combination for this method when working with trajectories.

As future work, new protection methods can be found or adapted as well as new information loss and disclosure risk measures.

Acknowledgements

Partial support by the Spanish MICINN (projects eAEGIS TSI2007-65406-C03-02 and ARES - CONSOLIDER INGENIO 2010 CSD2007-00004) is acknowledged.

References

[1] G. Andrienko, N. Andrienko, F. Giannotti, A. Monreale, and D. Pedreschi, "Movement data anonymity through generalization," in *Proceedings of the 2nd SIGSPATIAL ACM GIS 2009 International Workshop on Security and Privacy in GIS and LBS*, ser. SPRINGL '09. New York, NY, USA: ACM, 2009, pp. 27–31. [Online]. Available: http://doi.acm.org/10.1145/1667502.1667510

[2] G. Ghinita, "Private queries and trajectory anonymization: a dual perspective on location privacy," *Trans. Data Privacy*, vol. 2, pp. 3–19, April 2009. [Online]. Available: http://www.tdp.cat/issues/tdp.a018a09.pdf

[3] D. Lin, E. Bertino, R. Cheng, and S. Prabhakar, "Location privacy in moving-object environments," *Trans. Data Privacy*, vol. 2, pp. 21–46, April 2009. [Online]. Available: http://www.tdp.cat/issues/tdp.a019a09.pdf

[4] J. Domingo-Ferrer, M. Sramka, and R. Trujillo-Rasúa, "Privacy-preserving publication of trajectories using microaggregation," in *Proceedings of the 3rd ACM SIGSPATIAL International Workshop on Security and Privacy in GIS and LBS*, ser. SPRINGL '10. New York, NY, USA: ACM, 2010, pp. 26–33. [Online]. Available: http://doi.acm.org/10.1145/1868470.1868478

[5] J. Nin and V. Torra, "Towards the evaluation of time series protection methods," *Inf. Sci.*, vol. 179, no. 11, pp. 1663–1677, 2009.

[6] J. Domingo-Ferrer and V. Torra, "A quantitative comparison of disclosure control methods for microdata," in *Confidentiality, disclosure, and data access : Theory and practical applications for statistical agencies*. Elsevier, 2001, pp. 111–113.

[7] J. Nin, J. Herranz, and V. Torra, "Rethinking rank swapping to decrease disclosure risk," *Data Knowl. Eng.*, vol. 64, pp. 346–364, January 2008. [Online]. Available: http://dx.doi.org/10.1016/j.datak.2007.07.006

[8] J. Nin, J. Herranz, and V. Torra, "How to group attributes in multivariate microaggregation," *International Journal of Uncertainty, Fuzziness and Knowledge-Based Systems*, vol. 16, no. Supplement-1, pp. 121–138, 2008.

[9] V. Torra, J. M. Abowd, and J. DomingoFerrer, "Using mahalanobis distance-based record linkage for disclosure risk assessment," in *Lecture Notes in Computer Science*, 2006, p. 233242.

[10] W. E. Winkler, "Re-identification methods for masked microdata," in *In Proc. Privacy in Statistical Databases 2004, Springer LNCS 3050*. Springer, 2004, pp. 216–230.

[11] W. E. Yancey, W. E. Winkler, and R. H. Creecy, "Disclosure risk assessment in perturbative microdata protection," in *Inference Control in Statistical Databases, From Theory to Practice*. London, UK, UK: Springer-Verlag, 2002, pp. 135–152. [Online]. Available: http://portal.acm.org/citation.cfm?id=645539.657842

[12] G. T. Duncan, S. A. Keller-mcnulty, and S. L. Stokes, "Disclosure risk vs. data utility: The r-u confidentiality map," Chance, Tech. Rep., 2001.

[13] V. Torra and J. Domingo-Ferrer, "Disclosure control methods and information loss for microdata," in *Confidentiality, disclosure, and data access : Theory and practical applications for statistical agencies*. Elsevier, 2001, pp. 91–110.

[14] T. Brinkhoff, "Generating traffic data," *Bulletin of the Technical Committee on Data Engineering, IEEE Computer Society*, no. 26, p. 2003.

[15] O. Abul, F. Bonchi, and M. Nanni, "Never walk alone: Uncertainty for anonymity in moving objects databases," in *InProceedings ICDE*, 2008, pp. 376–385.

[16] M. E. Nergiz, M. Atzori, and Y. Saygin, "Towards trajectory anonymization: a generalization-based approach," in *Proceedings of the SIGSPATIAL ACM GIS 2008 International Workshop on Security and Privacy in GIS and LBS*, ser. SPRINGL '08. New York, NY, USA: ACM, 2008, pp. 52–61. [Online]. Available: http://doi.acm.org/10.1145/1503402.1503413

2011 IEEE International Conference on Fuzzy Systems
June 27-30, 2011, Taipei, Taiwan

On Some Clustering Approaches For Graphs

Klara Stokes
Universitat Rovira i Virgili
Dept. of Computer Engineering and Maths,
UNESCO Chair in Data Privacy
Av. Països Catalans 26,
43007 Tarragona, Catalonia, Spain
Email: klara.stokes@urv.cat

Vicenç Torra
IIIA, Institut d'Investigació en Intel·ligència Artificial
CSIC, Consejo Superior de Investigaciones Científicas
Campus Universitat Autònoma de Barcelona,
08193 Bellaterra,
Catalonia, Spain
Email: vtorra@iiia.csic.es

***Abstract*—In this paper we discuss some tools for graph perturbation with applications to data privacy. We present and analyse two different approaches. One is based on matrix decomposition and the other on graph partitioning. We discuss these methods and show that they belong to two traditions in data protection: noise addition/microaggregation and k-anonymity.**

***Index Terms*—Data privacy, clustering, k-anonymity, microaggregation, graph**

I. Introduction

Graphs are useful mathematical structures for representing a large variety of data. In particular, they can be used to represent social networks and other kind of data where elements establish relationships with other elements.

In this paper we discuss methods for protection of data represented in terms of a graph. More specifically, we focus on problems in which the graph can be represented in an explicit way in terms of an adjacency matrix of manageable size.

The interest of this work is twofold. First, it is useful for protection of social networks with a limited number of nodes, as e.g. the data from a company or a university department. Naturally, this approach can be adapted to subsets of larger networks. Second, as these methods can be applied to a network that can be expressed in its entirety in a compact way, they permit us to analyse with some detail their effect as well as the effect of their parameterizations. In particular, we can study their effectiveness with respect to disclosure risk and information loss.

A. Our scenario in data privacy

We discuss in this section the scenario of data privacy we are considering in this paper. The scenario is basically the same as in previous research in the area of data privacy (see e.g. [1], [2]), although those papers focus on standard databases and not on relational data representable as graphs.

Scenario 1.1: A company or a national office wants to release data to a third party for doing some kind of analysis. Nevertheless, confidentiality should be ensured and so, no confidential information should be inferred by this third party from the data received.

In the framework of this scenario, existing tools for data privacy can be roughly classified in two broad classes:

- Cryptographic or computation oriented methods. They are methods based on cryptographic tools which try to avoid any disclosure at all. These methods are developed ad hoc for a particular analysis. That is, given a particular computation – a function of the data, a particular protocol is built which computes the function without giving to the data suppliers more information than the result of the function. As such, these methods are computation oriented, as they need to know and are based on the function to be computed.
- Perturbative or data oriented methods. These methods try to avoid disclosure manipulating the original data set and introducing some noise into the set. Then the perturbated data is released to the third party who can apply any analysis to the data. In this way, there is no need of knowing the function to be computed. That is why these methods are data oriented. Disclosure is (partially) avoided because of the perturbation inflicted to the data. Nevertheless, some disclosure risk is inherent in the data and, therefore, needs to be quantified. At the same time, the perturbation modifies the data and some information loss occurs. So, information loss also needs to be quantified.

Following [1], [3], we focus on the data oriented approach. That is, we focus on perturbative methods that add some kind of noise to the data. As stated above, the evaluation of these methods requires the quantification of information loss and disclosure risk. Then, we consider that a method has a good performance (i.e., it is a good data protection method) if for a particular type of data it achieves a good compromise between disclosure risk (i.e., the risk of disclosing sensitive information) and information loss (i.e., the amount of *data utility* that is lost when data is perturbated).

Among all possible data types, this paper focus on data protection tools for data representable in terms of graphs. The literature already presents some tools for data protection of graph structures. See e.g. the survey in [4]. There are tools [5] for graph perturbation based on random addition and deletion of nodes, and others [6] based on k-anonymity.

In this paper we focus on tools for small graphs. More specifically, in tools for graphs that can be representable in their entirety by a adjacency matrix or an equivalent structure and small enough to be stored and operated in memory. That is, we focus on tools for graph perturbation to be applied to

978-1-4244-7316-8/11/$26.00 ©2011 IEEE

graphs of limited size. Then, we develop methods based on the decomposition of the matrix and on similarities between the nodes of the graph. This diverges from previous works.

The goal of this paper is to present a set of tools for data privacy that will be further studied in detail for analysing its effectiveness. We discuss the appropriateness of our approach and illustrate it with some examples. Then, in a further research, we can develop approximate solutions for larger datasets, or apply them to subsets of larger sets.

The structure of the paper is as follows. In Section II we review some basic concepts that are needed in the rest of the paper. Then, in Section III we present some approaches for graph perturbation. The paper finishes with some conclusions.

II. Preliminaries

In this section we review some concepts that are needed later on in this paper. We focus on some tools we use later for operating with graphs. In particular, in methods of matrix decomposition.

A. Matrix decomposition

We will denote by U^H the conjugate transpose of U. That is, U^H is the transpose of the conjugate matrix. Recall that the conjugate of the complex number $a + bi$ is $a - bi$. When U only contains real numbers, U^H is the standard transpose of U.

A matrix M is said to be unitary when $MM^T = I_n$. Here I_n stands for the diagonal matrix of dimension n.

The singular value decomposition of a matrix M consists of a factorization of M in three matrices U, D and V as follows:

$$M = UDV^H$$

where U and V are unitary matrices and where D is a nonnegative diagonal matrix.

Here, if M is an $m \times n$ matrix, then U is an $m \times m$ matrix, D is an $m \times n$ matrix, and V is an $n \times n$ matrix.

The eigendecomposition or spectral decomposition of a square matrix M of dimension n consists of the factorization of M in terms of two matrices V and D as follows:

$$M = VDV^{-1}$$

where V is an $n \times n$ matrix with the eigenvalues of M, and D is an $n \times n$ diagonal matrix with the eigenvalues of M on the diagonal.

Both decompositions are related for some particular matrices. In particular, if M is symmetric and positive definite, then the spectral decomposition corresponds to a singular value decomposition.

III. Graph perturbation

In this section we discuss two different approaches for graph perturbation. One is based on matrix decomposition, and the other on graph partitioning. Both follow the tradition of perturbation methods. Nevertheless, they can be seen as belonging to two different *traditions*. We will discuss this later in Section III-C.

A. Methods based on matrix decomposition

In statistics a dimension reduction is a reduction of the number of random variables under consideration. The dimension reduction can be performed using the spectral decomposition or the singular value decomposition (SVD) of the matrix representing the data. If we apply the same methods to the adjacency matrix of a graph, then we accomplish a perturbation of the matrix. Appropriate selection of the eigenvalues in the spectral method and of the singular values in the SVD method will reduce the *complexity* of the matrix so that the most significant features of the structure is kept. In this way it is possible to perturbate the graph while keeping its most significative edges.

The rationale of the approach is to perform a transformation similar to random addition and deletion of edges (as in e.g. [5]) but in a more learned way. We define the approach below. We start with the method based on the spectral decomposition.

Definition 3.1: Let $G = (V, E)$ be a graph and let M be its adjacency matrix, let p be a parameter such that $0 \leq p \leq |V|$. Then, the SD-graph protection method consists in (i) computing the spectral decomposition of M: let $M = UDU^{-1}$ be the spectral decomposition of M; (ii) returning $M' = UD'U^{-1}$ where D' includes only the first p eigenvalues of D.

Here, as usual in spectral decomposition, we assume that the eigenvalues of D are arranged in descending order with respect to the size of their absolute value.

We now define the method based on singular value decomposition.

Definition 3.2: Let $G = (V, E)$ be a graph and let M be its adjacency matrix, let p be a parameter such that $0 \leq p \leq |V|$. Then, the SVD-graph protection method consists in (i) computing the singular value decomposition of M: let $M = U\Sigma W^H$ be the singular value decomposition of M; (ii) returning $M' = U\Sigma' W^H$ where Σ' includes only the first p values of the diagonal of Σ, where these are arranged in descending order.

As we saw in the introduction, the SVD and the spectral decomposition are related. For undirected graphs we get the following proposition.

Proposition 3.3: For undirected graphs the methods defined in Definition 3.1 and Definition 3.2 are equivalent.

Proof: The adjacency matrix of an undirected graph is symmetric and real, but in general not positive definite. The singular values of the matrix are the absolute values of its eigenvalues. This implies that for undirected graphs the two methods are equivalent. ■

For both methods, the smaller the number p, the larger the distortion inflicted to the graph. Naturally, when p equals the dimension of the matrix (i.e., $p = |V|$), data protection methods cause no distortion to the graph; in contrast, when $p = 0$, the distortion is maximal as the graph is completely distorted. Note that for $p = 0$, all edges are lost.

Therefore, the parameter p controls the degree of noise. This is in line of most perturbative data protection methods for databases. Note that e.g. the parameter k in microaggregation [7] permits the user a rank of results from maximal

distortion (all records are replaced by the same value) to no distortion at all (all records are published as they are). Similar situation occurs with the different variants of rank swapping [8].

Although both methods are a natural way to implement a perturbation that introduces noise to the original data, they have two drawbacks.

The first one is that while the original matrix M contains only binary values to represent presence or absence of an edge, the matrix obtained as output from the method has coefficients with values in the real numbers. They are not restricted to [0,1] and can even be negative. This requires to develop a post processing in which the resulting matrix is transformed into a proper graph. For example, this binarization process could consist in transforming M' into a set of probabilities, and then using these probabilities for building a new matrix $\tilde{M}'$. Another approach for binarization consists in assigning zero or one according to a threshold. This latter approach has been applied in Example 3.4.

The second one is that, once the binarization process is applied, the *graph* represented by M' is quite similar to M for several of the parameterizations of the methods. That is, although M' is no longer a binary matrix, zero values in M result into values near zero in M', and unitary values in M result into values near one in M'. For example, for the matrix in Example 3.4, using a binarization with a threshold of 0.5, we have that we have to perform a dimension reduction of at least 6 ($p = 4$) in order to obtain a graph which is different from the original one. With $p = 4$ we remove two edges, with $p = 3$ we remove 8 edges and with $p = 2$ we remove 16 edges. With $p = 1$, 23 edges are changed (7 added and 16 removed) and, of course, all 28 edges are removed taking $p = 0$.

Example 3.4: This is a graph on 10 vertices with 14 edges:

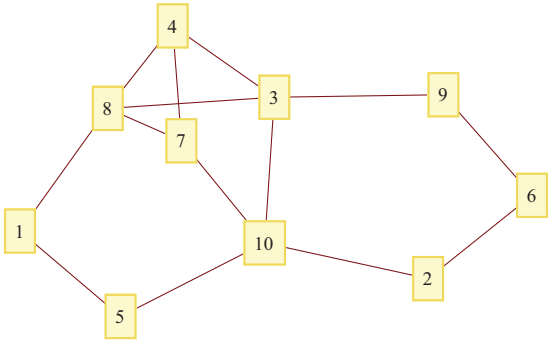

This is the adjacency matrix of the graph:

$$\begin{pmatrix} 0 & 0 & 0 & 0 & 1 & 0 & 0 & 1 & 0 & 0 \\ 0 & 0 & 0 & 0 & 0 & 1 & 0 & 0 & 0 & 1 \\ 0 & 0 & 0 & 1 & 0 & 0 & 0 & 1 & 1 & 1 \\ 0 & 0 & 1 & 0 & 0 & 0 & 1 & 1 & 0 & 0 \\ 1 & 0 & 0 & 0 & 0 & 0 & 0 & 0 & 0 & 1 \\ 0 & 1 & 0 & 0 & 0 & 0 & 0 & 0 & 1 & 0 \\ 0 & 0 & 0 & 1 & 0 & 0 & 0 & 1 & 0 & 1 \\ 1 & 0 & 1 & 1 & 0 & 0 & 1 & 0 & 0 & 0 \\ 0 & 0 & 1 & 0 & 0 & 1 & 0 & 0 & 0 & 0 \\ 0 & 1 & 1 & 0 & 1 & 0 & 1 & 0 & 0 & 0 \end{pmatrix}$$

The singular values of this matrix are approximately

$$\{3.16, 2.52, 1.83, 1.63, 1.56, 1.28, 0.83, 0.77, 0.41, 0.31\}.$$

We applied first dimension reduction using SVD on the adjacency matrix of the graph. All values of p between 0 and 10 were considered. Below we list the correlations between the original matrix and the result as a function of p, using the function implemented in R [9].

dimensionality reduction$(1-p)$	*correlation*
0	1
1	0.4283313
2	0.475191
3	0.3822435
4	0.4283313
5	0.3360108
6	0.3822435
7	0.28843
8	0.2375955

Then we applied a binarization process to the result with a threshold of 0.5. Below we list the correlations between the original matrix and the binarized matrix as a function of p. For $p = 10$ no correlation can be computed because the perturbated graph has no edge.

dimensionality reduction$(1-p)$	*correlation*
0	1
1	1
2	1
3	1
4	1
5	1
6	0.948448
7	0.7953949
8	0.4516129
9	0.5663766
10	$--$

The selection of the threshold was done heuristically, defined as the mid point between 0 and 1 with respect to the perturbation of the matrix. This selection results into a rather conservative selection. For $p = 2$, except a threshold of 0.4 that leads to 13 changes in the matrix, all other thresholds lead to the same or more changes (with maximums of 49 and 20 changes for thresholds of 0.1 and 0.9).

When constructing a method for data perturbation with the ambition to obtain data privacy it is important to verify that the perturbation is hard to reverse, since otherwise the method implies no privacy, or at most limited privacy. The following arguments are made under the assumption that the graphs are undirected and simple (i.e. without multiedges and loops). Research on spectral graph theory has shown that 'almost all' graphs are uniquely determined by their spectra [10], so that in many cases given a sequence of eigenvalues, there is only one graph which has an adjacency matrix with these

eigenvalues. This is so due to the difficulties to find a set of eigenvectors which brings the diagonal matrix to a space where the matrix is symmetric, with entries either 0 or 1 and with the diagonal all 0. Suppose that we apply to a graph one of the methods for graph perturbation defined above. Before applying the binarization process, the result is a matrix M with p of the eigenvalues equal to the largest p eigenvalues of the original adjacency matrix A, ordered by their absolute value. The rest of the eigenvalues of M are all 0. The eigenvectors of M are the same as the eigenvectors of A. Counting the number of the eigenvectors of M which are 0, we can bound the number of removed eigenvectors. The absolute value of a removed eigenvalue (i.e. any eigenvalues of A which is not an eigenvalue of M) is smaller than the smallest absolute value of all the eigenvalues of M. Given M this significantly restrict the possible choices of A. If we also remember that since the diagonal of an adjacency matrix of a simple undirected graph is always 0, so is its trace, then it is clear that in some cases it is very easy to given M deduce A. For example when only one eigenvalue is removed, the missing eigenvalue is minus the sum of the other eigenvalues.

This observation highlights the importance of binarization process. Indeed, through the binarization process perturbations are introduced into the *eigenvectors* of the graph. This destroys the possibility to easily reverse the perturbation process. Important aspects of the privacy therefore relies on the binarization process, implying that the choice of binarization process could be most significant for the degree of privacy supplied by the method. Since the information loss of course also depends on the binarization process, the choice of the binarization process should be further investigated in the future.

B. Methods based on graph partitioning

The literature for database protection includes a large number of methods for achieving k-anonymity [2], [11], [12]. A file is said to be compliant with k-anonymity if for each record there are other $k-1$ indistinguishable records.

k-anonymity is used for data protection based on the following rationale:

> No disclosure takes place when any individual is indistinguishable of $k-1$ other different individuals.

Then, methods transform the original data file so that only sets of k-indistinguishable records are found in the data. Naturally, all such methods use k as one of the parameters. These methods act by means of clustering, generalizations and suppressions.

In the framework of k-anonymity, disclosure risk is usually not analysed but taken for granted once k is settled. This is so because the parameter k is assumed to be a threshold of the satisfactory disclosure risk. So, only information loss is evaluated here.

Methods for graph partitioning can be used for achieving protection following the idea of k-anonymity. In its simplest form, graph partitioning divides the vertices in two sets of equal size such that the number of edges between these two parts is minimized. In a more general formulation, the vertices are divided in p disjoint subsets of equal size.

Therefore, we can conceive a kind of k-anonymity from the results of graph partitioning. Let $G = (V, E)$ represent a graph, and let $\Pi_V = \{V_1, \ldots, V_p\}$ represent a partition of the edges of this graph into p clusters. Then, we consider the vertices of each cluster V_i as indistinguishable. So, given p, this results in $k = |V|/p$-anonymity. At this point, two alternatives can be foreseen.

1) Direct partitioning: In this case, we apply a partitioning algorithm to the original graph (i.e., to the original matrix). This causes clusters to be built on the basis of good connectivity. That is, the method detects sets of vertices that are well connected among themselves but with a low connectivity with the other ones.

This approach has an inconvenience. The partitioning algorithm does not distinguish between the different roles that vertices might have in well connected regions. To illustrate this point, let us consider the following example.

Let $G = (V, E)$ be a graph representing the relationships among members of a university. Let the vertices V represent the staff of the university and edges E represent mails and other types of communication among staff members. In this case, for an appropriate value of p, a graph partitioning algorithm will form p clusters. Such clusters shall roughly correspond to departments. Note that communication links between department members is likely to be more intense than communication links between members belonging to different departments.

So, in general, this approach is unable to detect and distinguish that within the department, some of the members might be administrative staff, other senior research staff, and other students. The approach proposed in the next section focuses on the detection of such roles.

2) Indirect partitioning: In this case, the partitioning algorithm is applied to a similarity matrix computed from the graph. Therefore, this is a two step process.

- First, we define a matrix $S : V \times V \to [0, 1]$ representing the edge similarity between the pairs of vertices in the graph with $|V| = n$.

  $$S(v_i, v_j) = \text{similarity}(v_i, v_j)$$

  where the similarity function should be selected in order to give a satisfactory clusterization.
- Second, we apply a graph partitioning algorithm to the matrix S.

While in the direct approach the algorithm clusters together well connected vertices, in the indirect approach we cluster vertices with a similar role in the graph. In some sense, this is similar to the approach in [6] which discusses the isomorphism between edges in the graph.

We have considered two distinct definitions of similarity between vertices: one based on the l_1 or Manhattan distance and the other based on which neighbors the vertices have in common. We define these two similarities below and discuss their properties. We represent the edges of a vertex v_i by the

row vector $A(i)$ of the adjacency matrix A (or equivalently, the column vector $A(j)$) corresponding to the vector.

Definition 3.5: Using the Manhattan or the l_1 distance, the similarity between two vertices v_i and v_j with edges $A(i)$ and $A(j)$ in a graph on n vertices is defined as

$$\text{similarity}_{l_1}(v_i, v_j) = n - \sum_{k=1}^{n} |A(i,k) - A(j,k)|$$

$$= \sum_{k=1}^{n} (1 - |A(i,k) - A(j,k)|) .$$

Definition 3.6: The 2-path similarity between two vertices v_i and v_j with edges $A(i)$ and $A(j)$ in a graph on n vertices is defined as

$$\text{similarity}_{2-path}(v_i, v_j) = \sum_{k=1}^{n} A(i,k)A(j,k).$$

Observe that since an adjacency matrix of an undirected graph is symmetric, the ith row is the ith column transposed.

The 2-path similarity is augmented with one for every neighbor the two vertices have in common. The similarity based on the Manhattan distance is also augmented with one for every neighbor the two vertices have in common, but it is augmented with one for every non-neighbor they have in common as well.

The 2-path similarity highlights the fact that similarity between vertices is based on the existing edges, and not on the missing edges. The following example illustrates this point.

Example 3.7: This is a graph with 7 vertices and 10 edges:

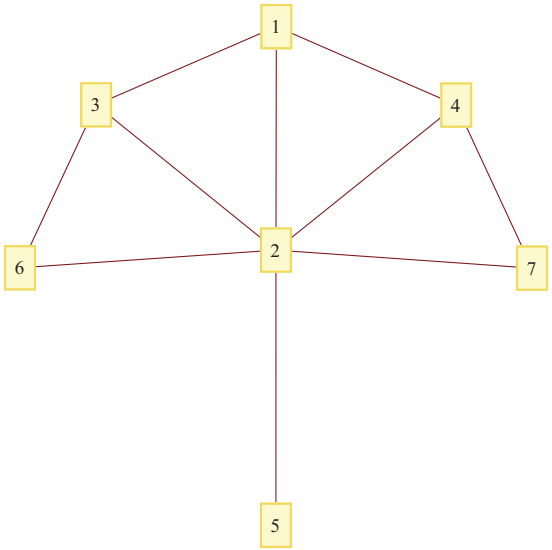

This is the adjacency matrix of the graph:

$$\begin{pmatrix} 0 & 1 & 1 & 1 & 0 & 0 & 0 \\ 1 & 0 & 1 & 1 & 1 & 1 & 1 \\ 1 & 1 & 0 & 0 & 0 & 1 & 0 \\ 1 & 1 & 0 & 0 & 0 & 0 & 1 \\ 0 & 1 & 0 & 0 & 0 & 0 & 0 \\ 0 & 1 & 1 & 0 & 0 & 0 & 0 \\ 0 & 1 & 0 & 1 & 0 & 0 & 0 \end{pmatrix}$$

The distance from vertex 1 to the other vertices is listed below.

vertex	similarity$_{l_1}$	similarity$_{2-path}$
2	2	2
3	3	1
4	3	1
5	5	1
6	6	2
7	6	2

The example illustrates the differences between the two similarities. It can be seen that while the similarity between vertex 1 and vertex 5 is much larger for the Manhattan distance than the similarity between vertex 1 and 2, in the 2-step similarity we have the reversal.

This is due to the fact that vertices 1 and 5 share four non-neighbours, while 1 and 2 do not share any of them. In contrast, vertices 1 and 2 share two neighbors and vertices 1 and 5 share only one. The 2-step similarity focuses on the common neighbors.

In relation to the interest of the approach of indirect partitioning with respect to the one of direct partitioning, let us consider the following scenario.

Example 3.8: Let us consider a social network where vertices can either represent individuals or mass media. While in the direct approach, individuals and media might be clustered together according to communities of news producers and consumers, in the indirect approach, producers and consumers can be kept disaggregated. That is, consumers with similar interests (reading newspaper n_1, n_2 and listening radios r_1, r_2) will be aggregated together in the same cluster. At the same time, media with a similar audience will also be clustered together (n_1, n_2, r_1 and r_2 will form a cluster).

We include below an example that illustrates this situation with a graph, and showing the results of the approach for indirect partitioning.

Example 3.9: This is a graph on 25 vertices with 33 edges:

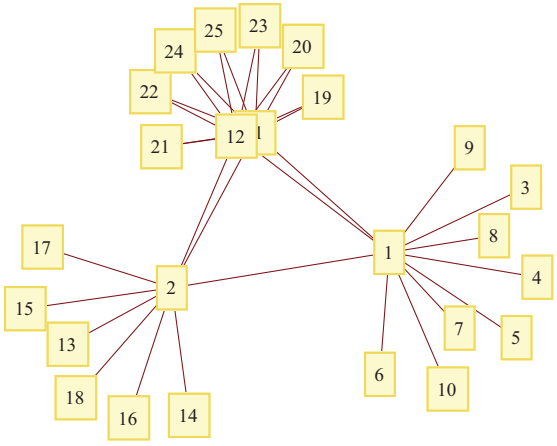

In this example vertices 1, 2, 11, and 12 represent the mass media and the rest of the vertices represent individuals. Edges from individuals to mass media represent that the individuals access/use the mass media while edges between pairs of mass media represent interactions among them. Graph partitioning

using the similarity based on the Manhattan distance results in the following partition:

$$\{1, 2, 3, 4, 5, 6, 11, 12\}$$

$$\{8, 9, 10, 13, 14, 15, 16, 17, 18\}$$

$$\{7, 19, 20, 21, 22, 23, 24, 25\}$$

and graph partitioning using the 2-path similarity results in the following partition:

$$\{1, 2, 19, 20, 21, 22, 23, 24, 25\}$$

$$\{11, 12, 13, 14, 15, 16, 17, 18\}$$

$$\{3, 4, 5, 6, 7, 8, 9, 10\}$$

It can be seen that this partition includes in the partition elements the consumers of a (group) of media while the media themselves are disaggregated from the individuals. In contrast, graph partitioning using Manhattan distance does not show this behaviour as the media are clustered with their individuals. For example, the partition of the Manhattan distance contains 1, 2, 3, 4, 5, 6, 11, 12 but the 2-path distance contains 3, 4, 5, 6, 7, 8, 9, 10. Note that this latter cluster contains all vertices related to 2, but not the vertice 2. In contrast, the former contains a mix of nodes connected to 2, with node 2.

Example 3.10: In the graph below there are two leafs, the vertices 8 and 9. We want the vertices of the graph to be clusterized so that vertices with a similar role in the graph end up in the same cluster. What we mean with this depends on what we mean when we say that two vertices play a similar role. In this case, if the role is to be a leaf, then we probably want 8 and 9 to go together. However, if the role is to be connected to more or less the same vertices, then vertices 8 and 9 should be in different clusters.

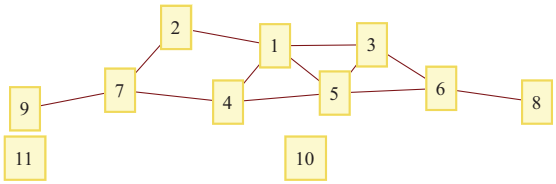

Clustering the graph with respect to the Manhattan distance using the partition algorithm in METIS we obtain the partition

$$\{1, 5, 7\} \quad \{2, 8, 9, 10, 11\} \quad \{3, 4, 6\}$$

and if the clusterization is performed with respect to the 2-path distance, then the same partition algorithm gives us

$$\{8, 10, 11\} \quad \{2, 3, 4, 9\} \quad \{1, 5, 6, 7\}.$$

If we use the partition algorithm from Mathematica instead, in the last case we obtain

$$\{1, 7, 5, 6, 3, 8\} \quad \{2, 4, 9\} \quad \{10\} \quad \{11\}.$$

This illustrates that if the partition algorithm is calibrated in an adequate way (in this case it means that the number of partitions should be adequate), then the 2-path similarity creates clusters which collect vertices which more or less are connected to the same vertices, while the similarity based on the Manhattan distance rather tends to cluster vertexes together which are similar also in their non-existing edges, like for example two leafs or two isolated vertices like vertices 10 and 11. Indeed it is clear that the similarity based on the Manhattan distance considers similarity with respect to non-existing edges equally important as similarity with respect to existing edges.

Graph partitioning does not fully define a method compliant with k-anonymity. The correct application of this approach to a graph requires that the resulting partition satisfies two requirements: (i) that the number of vertices in a cluster is large enough; (ii) that the edges between vertices are reconstructed.

For solving the first issue, we propose the use of graph partitioning algorithms that lead to solutions with a similar number of vertices in all partitions. Then, if we require at least k vertices in each partition element, we should select a number of clusters less than $|V|/k$. The algorithm for graph partitioning implemented in METIS [13], [14] proceeds in this way.

As forcing solutions of this form might result into unnatural clusters for large graphs, an alternative approach is to proceed in a two step process. First, partitioning the vertices without any constraint (or a loose constraint) on the number of vertices in each cluster (the clustering algorithm in Mathematica proceeds in this way), and, then, refine the largest clusters applying a more constrained clustering algorithm.

The second element to be considered is about edge reconstruction. Once clusters are defined, the original edges have to be updated. First, vertices within the cluster are connected among themselves according to a pre-specified algorithm. Then, vertices should be connected to the other clusters, and all vertices from one cluster should be connected in the same way to vertices in another cluster. The decision of a connection can be done according to the majority of presence or absence of edges between the corresponding vertices.

The following proposition is crucial for how to choose the connections for the reconstruction between vertices in the same cluster.

Proposition 3.11: We call a cycle of length 3 a triangle. If the original graph is triangle-free, then the 2-path distance will cluster the graph so that the vertices in the same cluster are not connected.

Proof: We may suppose that two vertices a and b in the same cluster have at least one neighbor c in common, making a and b similar. Suppose that there is an edge between a and b. Then, since we have the path bca, there is the cycle $abca$ of length 3, that is, a triangle. This implies that in triangle-free graphs there are no edges between the vertices in the same cluster if the cluster was made using 2-path similarity. ■

The proposition implies that whenever the graph is triangle-free, assuming that it is desirable to preserve this property, the reconstruction of the graph from the clusters should be such that vertices in the same cluster are not connected.

Observe that if we cluster with respect to the similarity based on the Manhattan distance, Proposition 3.11 does not

apply, since two vertices in the same cluster not necessarily have any neighbors in common. Indeed, the similarity based on the Manhattan distance groups all isolated vertices together.

C. Discussion on graph perturbation

We have introduced two different families of methods for graph perturbation. One family consists on methods based on matrix decomposition, and the second one consists on methods based on graph partitioning.

While both methods perturbate the original graph resulting into a new graph with changes on the edges, they can be seen as belonging to two different traditions of perturbative approaches.

Methods based on matrix decomposition, with the parameter p, result into methods which try to find a good trade-off between information loss and disclosure risk. That is, on the tradition of noise addition and microaggregation. In contrast, methods based on graph partitioning follow the tradition of k-anonymity.

IV. Concluding remarks

In this paper we have presented some perturbation methods for graphs of limited size. We have discussed briefly some of the properties of the approaches, and we have given some examples of their behaviour. Further research should concentrate on analysing the properties of these methods further, and it is necessary to perform additional experiments for graphs of larger sizes. Future research should also include a comparative study of the results obtained by applying the different methods.

Acknowledgments

The first author was partially supported by the Spanish Government through projects TIN2009-11689 "RIPUP", CONSOLIDER INGENIO 2010 CSD2007-00004 "ARES", and FPU grant (BOEs 17/11/2009 and 11/10/2010) and by the Government of Catalonia under grant 2009 SGR 1135.

The second author was partially supported by the Spanish MEC (projects ARES – CONSOLIDER INGENIO 2010 CSD2007-00004 – and eAEGIS – TSI2007-65406-C03-02). The authors are with the UNESCO Chair in Data Privacy, but their views do not necessarily reflect those of UNESCO nor commit that organization.

References

[1] J. Domingo-Ferrer and V. Torra, "A quantitative comparison of disclosure control methods for microdata," in Confi dentiality, Disclosure and Data Access: Theory and Practical Applications for Statistical Agencies, P. Doyle, J. I. Lane, J. J. M. Theeuwes and L. Zayatz, Eds. North-Holland, 2001, pp. 111-134.

[2] L. Sweeney, "k-anonymity: a model for protecting privacy," Int. J. of Unc., Fuzz. and Knowledge Based Systems, vol. 10:5, pp. 557-570, 2002.

[3] W.E. Yancey, W.E. Winkler and R.H. Creecy, "Disclosure risk assessment in perturbative microdata protection," in Inference Control in Statistical Databases, J. Domingo-Ferrer, Eds. Lecture Notes in Computer Science 2316, 2002, pp. 135-152.

[4] D. Nettleton, V. Torra, "Data privacy for simply anonymized social network logs represented as graphs," unpublished.

[5] M. Hay, G. Miklau, D. Jensen, P. Weis, S. Srivastava, "Anonymizing social networks," Technical Report 07-19, University of Massachusetts Amherst, 2007. Published at VLDB 2008.

[6] K. Liu, E. Terzi, "Towards Identity Anonymization of Graphs," In proceedings of SIGMOD, 2008.

[7] J. Domingo-Ferrer, J.M. Mateo-Sanz, "Practical data-oriented microaggregation for statistical disclosure control," IEEE Trans. on Knowledge and Data Engineering, vol. 14:1, pp. 189-201, 2002.

[8] J. Nin, J. Herranz, V. Torra, "Rethinking Rank Swapping to Decrease Disclosure Risk," Data and Knowledge Engineering, vol. 64:1 pp. 346-364, 2008.

[9] T. Butts, Package 'sna', Project R, 2011.

[10] E.R. van Dam, W.H. Haemers, "Spectral characterizations of some distance-regular graphs," Journal of Algebraic Combinatorics, vol. 15:2 pp. 189–202, 2002.

[11] P. Samarati, "Protecting Respondents' Identities in Microdata Release," IEEE Trans. on Knowledge and Data Engineering, vol. 13:6, pp. 1010-1027, 2001.

[12] P. Samarati, L. Sweeney, "Protecting privacy when disclosing information: k-anonymity and its enforcement through generalization and suppression," SRI Intl. Tech. Rep, 1998.

[13] http://glaros.dtc.umn.edu/gkhome/metis/metis/overview

[14] G. Karypis, V. Kumar, "Multilevel k-way Partitioning Scheme for Irregular Graphs," J. Parallel Distrib. Comput. vol. 48:1,pp. 96-129, 1998.

2011 IEEE International Conference on Fuzzy Systems
June 27-30, 2011, Taipei, Taiwan

A Study on Regularization Effects of Fuzzified Memberships in FCM Clustering

Katsuhiro Honda, Yui Matsumoto, Akira Notsu, Hidetomo Ichihashi
Department of Computer Science and Intelligent Systems
Osaka Prefecture University
1-1 Gakuen-cho, Nakaku, Sakai, Osaka 599-8531, Japan
Email: {honda, notsu, ichi}@cs.osakafu-u.ac.jp

***Abstract*—FCM clustering is a fundamental technique for capturing intrinsic cluster structures of multivariate data sets. This paper presents a comparative study on the regularization effects of Fuzzy c-Means memberships estimated by two different fuzzification approaches: standard approach and entropy regularization approach. In this paper, the characteristics of the two fuzzification approaches are also discussed in noise fuzzy clustering (NFC) and it is revealed that the noise rejection mechanism of NFC can contribute to weakening the influence of initialization problems in entropy regularization approach although the approach is generally more sensitive to initial partition than the standard approach.**

***Keywords*—fuzzy clustering, regularization, noise clustering.**

I. Introduction

Fuzzy c-Means (FCM) [1] is a basic method for estimating fuzzy c-partitions and is a fuzzy variant of k-Means clustering model [2], in which bivariate cluster indicators of k-Means are fuzzified so that they represent the relative typicalities of degree of belongingness to clusters. In order to estimate "fuzzy memberships" drawn from the interval $[0, 1]$, the linear programming problem of k-Means is transformed into a non-linear one by introducing an additional weighting exponent.

Entropy regularization [3] is another approach to fuzzification of k-Means cluster memberships, in which a non-linear penalty term (regularization term) is added to the k-Means objective function so that the full objective function is non-linear with respect to memberships. Using an entropy-like penalty term, the FCM model has close relation to Gaussian mixture models (GMMs) with Expectation-Maximization (EM) algorithm [4], in which the weight for the penalty term corresponds to the variance parameter in GMMs [5]. Besides the entropy term, other non-linear penalty terms such as a quadratic term [6] and a K-L information term [7] were also proved to be useful in fuzzification of memberships [8].

Although the FCM models with various fuzzification approaches derive similar clustering results in many cases, an important difference between the standard fuzzification approach and the regularization approach is seen in their classification functions [9]. The classification function of the standard approach has the maximum value of "1" on cluster centers and has the "fuzziest" value in the area far distant from all cluster centers. On the other hand, the classification function of the entropy regularization approach does not have the maximum value on cluster centers and the value becomes large as a point goes away from all cluster centers.

This work was funded in part by the Ministry of Education, Culture, Sports, Science and Technology, Japan, under Grant-in-Aid for Scientific Research (20700214).

In this paper, the regularization effects of the standard fuzzification and entropy regularization are compared. It has been known that regularization of objective functions contributes to avoiding singular solutions. In the FCM clustering, we can expect that the fuzzified objective functions improve the possibility of avoiding local minima. Additionally, in this paper, the regularization effects are also compared in a robust clustering context. Noise fuzzy clustering [10], [11] is a robust clustering model, in which noise samples that are far distant from all cluster centers are dumped into an additional "noise cluster" in order to robustly estimate cluster centers. If we consider the noise rejection situation, the entropy regularization approach may have a similar classification function to the standard approach.

The remainder of this paper is organized as follows: Section II briefly reviews fuzzification approaches in the FCM clustering and noise fuzzy clustering. Section III considers the regularization effects of fuzzified objective function through a toy example. Section IV presents several experimental results to compare the characteristic features of the fuzzification approaches. Section V summarizes the conclusions of this paper.

II. Membership Fuzzification in FCM and Noise Rejection

A. Standard FCM

Let $\boldsymbol{x}_i = (x_{i1}, \cdots, x_{im})^\top$, $i = 1, \cdots, n$ denote m dimensional observations of n samples and the goal be to partition the sample into C clusters, in which samples belonging to same clusters are mutually similar. k-Means clustering [2] uses mean vector $\boldsymbol{b}_c$ as the prototype of cluster c and estimates cluster indicators (membership of each sample) by minimizing the following within-group-sum-of-errors.

$$L_{km} = \sum_{c=1}^{C}\sum_{i=1}^{n} u_{ci} d_{ci} = \sum_{c=1}^{C}\sum_{i=1}^{n} u_{ci}(\boldsymbol{x}_i - \boldsymbol{b}_c)^\top(\boldsymbol{x}_i - \boldsymbol{b}_c), \quad (1)$$

978-1-4244-7316-8/11/$26.00 ©2011 IEEE

where u_{ci} represents the membership of data point $\boldsymbol{x}_i$ to cluster c and is given based on the nearest prototype principle as

$$u_{ci} = \begin{cases} 1; & \boldsymbol{x}_i \text{ belongs to cluster } c \\ 0; & \text{otherwise} \end{cases}$$

and

$$\sum_{c=1}^{C} u_{ci} = 1, \qquad i = 1, \cdots, n. \tag{2}$$

The clustering algorithm is a 2-step iterative procedure of calculation of memberships u_{ci} and mean vectors $\boldsymbol{b}_c$ [2].

In fuzzy clustering, memberships are generalized to $u_{ci} \in [0, 1]$ so that membership matrix $U = (u_{ci})$ represents a fuzzy partition composed of relative typicalities of belongingness to clusters. Equation (1) is, however, a linear function with respect to memberships and the optimal memberships are given in the extremal points ($u_{ci} \in \{0, 1\}$). Then, Standard Fuzzy c-Means (FCM^s) algorithm [1] introduced an additional weighting exponent into the linear objective function so that it becomes non-linear with respect to u_{ci}.

$$L^s_{fcm} = \sum_{c=1}^{C} \sum_{i=1}^{n} u_{ci}^{\theta} d_{ci}, \tag{3}$$

where $\theta (\theta > 1)$ is the additional weighting exponent of "fuzzifier". If $\theta = 1$, the clustering model is reduced to the (hard) k-Means model. The larger the θ, the fuzzier the memberships. θ is often set as $\theta = 2$ or sometime $\theta = 1.5$ in real applications. The clustering algorithm has similar formula to that of k-Means. New prototypes are derived as the weighted centers of clusters (mean vectors). Memberships are calculated under the constraint of Eq.(2) called "probabilistic constraint" [12]. The constraint forces memberships to have similar meaning to posterior probabilities in the EM algorithm [4] with probabilistic mixture models so that they represent the relative typicalities in clusters.

The FCM algorithm with standard fuzzification approach is summarized as follows:

Algorithm: Standard Fuzzy c-Means (FCM^s)

Step 1 Initialize memberships $u_{ci}, c = 1, \cdots, C, i = 1, \cdots, n$ randomly, and normalize the memberships so that they satisfy the probabilistic constraint. Choose termination threshold ε.

Step 2 Update $\boldsymbol{b}_c, c = 1, \cdots, C$ as

$$\boldsymbol{b}_c = \frac{\sum_{i=1}^{n} u_{ci}^{\theta} \boldsymbol{x}_i}{\sum_{i=1}^{n} u_{ci}^{\theta}}. \tag{4}$$

Step 3 Update $u_{ci}, c = 1, \cdots, C, i = 1, \cdots, n$ as

$$u_{ci} = \begin{cases} \left[\sum_{l=1}^{C} \left(\frac{d_{ci}}{d_{li}} \right)^{\frac{1}{\theta - 1}} \right]^{-1} & ; I_i = \emptyset \\ 1/|I_i| & ; I_i \neq \emptyset, c \in I_i \\ 0 & ; I_i \neq \emptyset, c \notin I_i \end{cases} \tag{5}$$

where I_i is the set of indices such that d_{ci} is zero, i.e., $I_i = \{c : d_{ci} = 0\}$.

Step 4 If

$$\max_{c,i} \mid u_{ci}^{NEW} - u_{ci}^{OLD} \mid < \varepsilon,$$

then stop. Otherwise, return to Step 2.

This standard FCM algorithm has the following characteristics [9]: If we use the membership calculation rules of Eq.(5) as fuzzy classification rules u_c, the maximum value $(u_c = 1)$ is given on the cluster center, and u_c moves toward $1/C$ as $||\boldsymbol{x}|| \to \infty$.

B. Fuzzy Clustering with Regularized Objective Function

If the goal is to fuzzify memberships in k-Means clustering, we can add a non-linear penalty term in order to make the objective function non-linear with respect to memberships. Miyamoto and Mukaidono [3] introduced a regularization term with a positive parameter λ into the objective function based on the regularization concept. Adding an entropy term, the objective function of FCM with regularization by entropy (FCM^e) is defined as

$$L^e_{fcm} = \sum_{c=1}^{C} \sum_{i=1}^{n} u_{ci} d_{ci} + \lambda \sum_{c=1}^{C} \sum_{i=1}^{n} u_{ci} \log u_{ci}, \tag{6}$$

where the entropy term works like the weighting exponent in the standard FCM algorithm and the parameter λ plays a role for tuning the degree of fuzziness of membership values. The larger the λ, the fuzzier the memberships.

This objective function has similar formulation to the negative log-likelihood in the EM algorithm with GMMs, in which λ correspond to the variance parameter of Gaussian distributions [5].

The clustering algorithm is also composed of the 2-step procedure, in which the updating rules for memberships and cluster centers are derived as follows:

$$u_{ci} = \frac{\exp(-\frac{1}{\lambda} d_{ci})}{\sum_{l=1}^{c} \exp(-\frac{1}{\lambda} d_{li})}, \tag{7}$$

$$\boldsymbol{b}_c = \frac{\sum_{i=1}^{n} u_{ci} \boldsymbol{x}_i}{\sum_{i=1}^{n} u_{ci}}. \tag{8}$$

From the classification viewpoint, the fuzzy classification function have different features from that of FCM^s [9]. u_c does NOT have the maximum value $(u_c = 1)$ on the cluster center and u_c moves toward 1 as $||\boldsymbol{x}|| \to \infty$. So, a data point that is far distant from all clusters may have a very large membership value.

The regularization approach can also be performed by using other regularization terms [6], [7], [13].

C. Noise Fuzzy Clustering

Noise fuzzy clustering [10], [11] introduced an additional noise cluster in order to damp noise samples into the noise cluster with the goal being to estimate robust cluster centers. In the noise clustering model, it is assumed that all samples have a constant (same) distance to the noise cluster, and that all samples, whose distance to all real cluster centers are greater

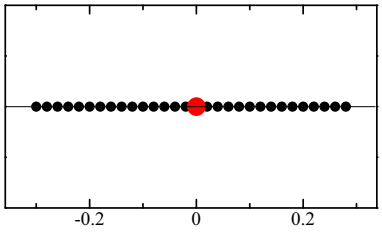

Fig. 1. an 1-D artificial data

than the constant distance, should be assigned to the noise cluster. In the FCM^s formulation, the objective function is given as

$$L^s_{nfc} = \sum_{c=1}^{C}\sum_{i=1}^{n} u_{ci}^{\theta} d_{ci} + \sum_{i=1}^{n} \delta \left(1 - \sum_{c=1}^{C} u_{ci}\right)^{\theta}, \quad (9)$$

where $1 - \sum_{c=1}^{C} u_{ci}$ represent the membership degree to the noise cluster and δ is the weight parameter that is identified with the distance to noise cluster. So, the conventional probabilistic constraint is redefined as

$$\sum_{c=1}^{C} u_{ci} \leq 1. \quad (10)$$

The membership updating rule of Eq.(5) (case of $I_i = \emptyset$) is modified as

$$u_{ci} = \left[\sum_{l=1}^{C} \left(\frac{d_{ci}}{d_{li}}\right)^{\frac{1}{\theta-1}} + \left(\frac{d_{ci}}{\delta}\right)^{\frac{1}{\theta-1}}\right]^{-1}. \quad (11)$$

In the same way, for the FCM^e formulation, Eq.(7) is modified as

$$u_{ci} = \frac{\exp(-\frac{1}{\lambda} d_{ci})}{\sum_{l=1}^{c} \exp(-\frac{1}{\lambda} d_{li}) + \exp(-\frac{1}{\lambda}\delta)}, \quad (12)$$

III. Consideration on Regularization Effects of Fuzzified Objective Functions

In this section, a toy example is shown in order to demonstrate the regularization effects of fuzzified objective functions. Figure 1 shows an 1-D artificial data composed of 30 samples uniformly distributed in a 1-D space.

Assume that we partition the samples into 3 clusters and the third cluster center ($\boldsymbol{b}_3$) is fixed on the center (red circle). Figure 2 shows the 3D contour surface of the k-Means objective function Eq.(1) calculated by changing $\boldsymbol{b}_1$ and $\boldsymbol{b}_2$ in the interval $[-0.35, 0.35]$. Local minima are shown by red marks. The figure indicates that we have the optimal (global) solution of $(\boldsymbol{b}_1, \boldsymbol{b}_2) = (0.21, -0.21)$ or $(\boldsymbol{b}_1, \boldsymbol{b}_2) = (-0.21, 0.21)$ and that we also have several other local minima. So, k-Means is severely influenced by initial partitions and is often trapped in local minima.

Figure 3 shows the 3D contour surfaces of the FCM objective functions Eqs.(3) and (6). The fuzzification coefficients were set as $\theta = 2$ and $\lambda = 0.05$, respectively. In the fuzzified objective functions, the contour surfaces were smoothened

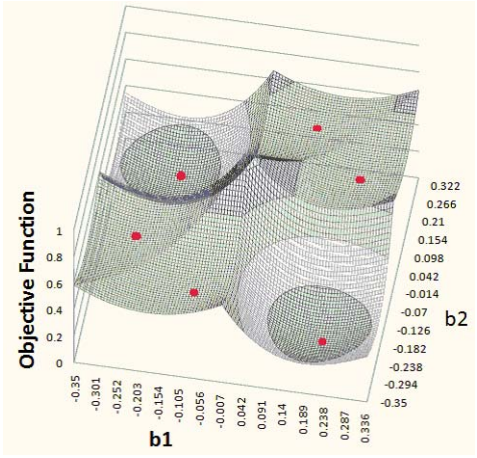

Fig. 2. Objective function of k-Means in toy example

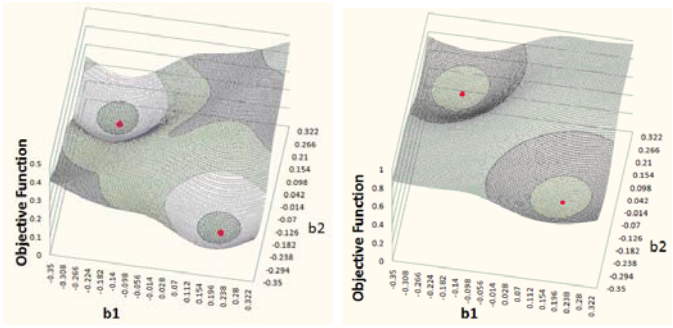

(a) standard fuzzification (b) entropy regularization

Fig. 3. Objective function of FCM in toy example

and the possibility of being trapped into local minima was weakened. In this way, both fuzzification approaches have the regularization effects in k-Means clustering.

IV. Numerical Experiments

In this section, several experimental results are shown in order to compare the regularization effects of fuzzification approaches.

A. Artificial data Set

The first experiment was performed with a 2-D ($m = 2$) artificially generated data set shown in Fig. 4, in which 200 samples ($n = 200$) were drawn from one of 4 Gaussian distributions (50 samples each) with unit variances whose mean vectors were (-1,-1), (-1,1), (1,-1) and (1,1), respectively. In order to compare the possibilities of being trapped into local minima, the samples were partitioned into 4 clusters with various initial partitions.

Applying the k-Means algorithm, 2 different partitions shown in Fig. 5 were derived. Figure 5-(a) is the optimal k-Means partition having the smallest objective function value and was given in 62% trials. On the other hand, another local optimal solution shown in Fig. 5-(b) was also derive in the remaining trials. The result implies that the (hard) k-Means

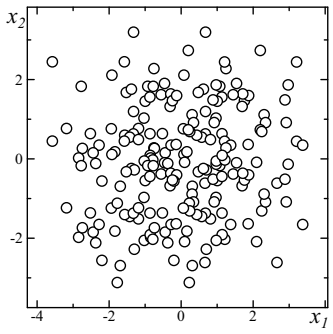

Fig. 4. 2-D artificial data set

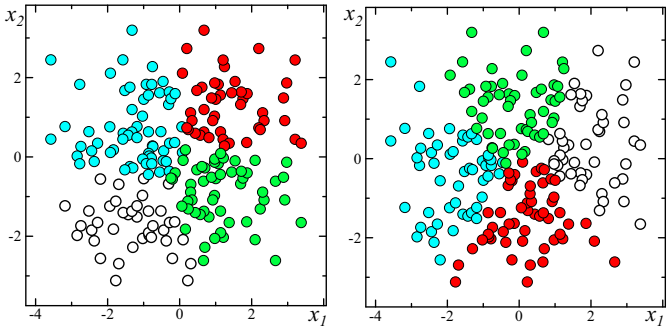

(a) partition a (b) partition b

Fig. 5. Derived partitions with 2-D artificial data set

algorithm is very sensitive to initial partitions and is often trapped into local minima.

Next, fuzzy c-partitions were estimated by the standard fuzzification approach and the entropy regularization approach comparing the regularization effects. Tables I and tab: Comparison of local solution FCM-e compare the frequencies of the local solutions (LS(%)) in 1820 trials, in which the initial cluster centers were located on $b_{cj} = \{x_{ij}^{\min}, \frac{1}{3}x_{ij}^{\min} + \frac{2}{3}x_{ij}^{\max}, \frac{2}{3}x_{ij}^{\max} + \frac{1}{3}x_{ij}^{\min}, x_{ij}^{\max}\}$ for each coordinate without duplication. The local solutions mean the case where the clustering algorithm failed to capture the c-partition of Fig. 5-(a). The tables imply that both fuzzification approach have regularization effects and contribute to avoiding being trapped into local minima as the weight parameters were increased.

Here, the fuzzy c-partitions derived by the two fuzzification approaches are compared using several clustering criteria. Partition coefficient (PC) and partition entropy (average entropy: AE) [1] are the average values of squared membership values u_{ci} and entropy of fuzzy memberships $-u_{ki}\log u_{ki}$. The criteria are used for evaluating the degree of fuzziness of fuzzy c-partition. A small PC and a large AE values imply a fuzzier partition with overlapping clusters. Xie-Beni index (XB) [14] is a cluster criterion considering the geometric features of FCM partitions:

$$XB = \frac{\sum_{c=1}^{C}\sum_{i=1}^{n} u_{ci}||\boldsymbol{x}_i - \boldsymbol{b}_c||^2}{n(\underbrace{\min}_{c\neq j}||\boldsymbol{b}_c - \boldsymbol{b}_j||^2)}. \quad (13)$$

TABLE I
COMPARISON OF FREQUENCIES OF LOCAL SOLUTIONS AND CLUSTER CRITERIA WITH 2-D ARTIFICIAL DATA SET (FCM^s)

θ	LS(%)	PC	AE	XB
1.01	62.4	1.000	0.000	0.274
1.05	21.5	0.987	0.006	0.269
1.1	12.1	0.968	0.014	0.257
1.15	12.1	0.948	0.023	0.245
1.17	11.8	0.940	0.026	0.241
1.18	11.8	0.936	0.028	0.239
1.19	0.0	0.932	0.030	0.237

TABLE II
COMPARISON OF FREQUENCIES OF LOCAL SOLUTIONS AND CLUSTER CRITERIA WITH 2-D ARTIFICIAL DATA SET (FCM^e)

λ	LS(%)	PC	AE	XB
0.05	23.6	0.997	0.000	0.273
0.1	22.5	0.988	0.005	0.272
0.2	11.9	0.971	0.012	0.263
0.4	11.7	0.934	0.028	0.250
0.45	11.3	0.925	0.032	0.248
0.49	10.9	0.917	0.036	0.247
0.5	0.0	0.915	0.037	0.246

A small XB value implies compact-separated clusters.

Comparing the cluster criteria in the situation where the local solutions were disappeared, the entropy regularization approach needs a "fuzzier" memberships than the standard approach in order to avoid local solutions and the derived fuzzy c-partition is more compact and separated.

It may be because FCM^e can assign larger memberships to samples that are far distant from all cluster centers as mentioned in Section II-2. If we gave a bad initial partition, some "noisy" samples having large memberships may illegally pull cluster centers.

B. Iris Data Set

A similar experiment was performed with Iris data set that is downloadable from UCI Machine Learning Repository [15]. In this experiment, 150 instances ($n = 150$) with 4 dimensional observation ($m = 4$) drawn from 3 classes were partitioned into 3 clusters without using the class label.

Tables III and IV compare the clustering performance with various fuzzification parameters. In this experiment, the cluster partition corresponding to the 3 Iris classes were regarded as the optimal solution. The frequencies and the average values were calculated after 85320 trials with a similar initialization strategy to the previous experiment in 4-D data space. In the same way with the previous experiment, FCM^s successfully derived a stable solution by using a suitable fuzzification weight. On the other hand, FCM^e was still trapped into local minima using larger fuzzification weights. Especially, when $\lambda \geq 1.0$, Xie-Beni index significantly increased, i.e. some clusters might be severely overlapping.

In this sense, FCM^s seems to work better than FCM^e from the viewpoint of regularization of k-Means objective function.

TABLE III
COMPARISON OF FREQUENCIES OF LOCAL SOLUTIONS AND CLUSTER CRITERIA WITH IRIS DATA SET (FCM^s)

θ	LS(%)	PC	AE	XB
1.1	8.5	0.991	0.005	0.160
1.5	1.8	0.919	0.049	0.142
1.7	0.6	0.867	0.081	0.136
1.8	0.3	0.840	0.098	0.135
1.9	0.1	0.812	0.115	0.135
2.0	0.0	0.783	0.132	0.137

TABLE IV
COMPARISON OF FREQUENCIES OF LOCAL SOLUTIONS AND CLUSTER CRITERIA WITH IRIS DATA SET (FCM^e)

λ	LS(%)	PC	AE	XB
0.08	12.1	0.995	0.003	0.162
0.09	12.1	0.994	0.003	0.161
0.1	12.1	0.994	0.004	0.161
0.5	13.5	0.929	0.039	0.166
1.0	14.6	0.854	0.077	0.204
1.5	15.1	0.777	0.114	0.323

C. Combination With Noise Fuzzy Clustering

Finally, the regularization effects of membership fuzzification are also compared in a robust clustering context using the 2-D data set shown in Fig. 4. Additional noise cluster adopted in noise fuzzy clustering [10] contributes to decreasing the membership degree of samples that are far distant from all cluster centers. We can expect that the robust feature may improve the effect of bad initial partitions in the entropy regularization approach by assigning smaller memberships to noisy samples. In noise fuzzy clustering, initial partitions are often given by FCM without noise rejection mechanism. In this experiment, however, the initial partition was given in the same initialization strategy with Section IV-A.

Table V compares the partition performance, in which the number of samples assigned to noise cluster "noise" was also shown with various noise weights δ. The fuzzification weights were set as $\theta = 1.19$ in order to consider the situation where the local solutions were first disappeared in Section IV-A. In this experiment, when $\delta \leq 1.5$, more than 30 out of 200 samples were regarded as noise and the plausible cluster centers could not be estimated. The table implies that the noise rejection mechanism increases the possibility of being trapped into local minima in FCM^s. In this sense, the FCM-guided initialization in noise fuzzy clustering seems to be plausible.

Next, Table VI shows the results given by FCM^e. The fuzzification paramter was set as $\lambda = 0.49$ where local solutions were still remained in Section IV-A. The table indicates that the noise rejection mechanism with large δ did not increase local solutions. Especially, when $\delta = 3.0$, the clustering performances were almost equivalent to those of $\lambda = 0.5$ in Table II, i.e., the noise rejection mechanism contributed to avoiding being trapped into local minima. It may be bacause the noise cluster plays a role for decreasing the membership values of samples far distant from all clusters, which would illegally draw in some cluster centers.

TABLE V
COMPARISON OF FREQUENCIES OF LOCAL SOLUTIONS AND CLUSTER CRITERIA WITH NOISE REJECTION (FCM^s)

δ	LS(%)	PC	XB	noise
1.0	–	0.451	0.078	97
1.25	–	0.570	0.132	72
1.5	–	0.727	0.124	33
1.75	28.8	0.788	0.160	25
2.0	16.3	0.852	0.172	12
2.25	20.5	0.887	0.193	4
2.5	16.6	0.908	0.209	2
2.75	15.8	0.919	0.219	1
3.0	14.9	0.925	0.227	0

TABLE VI
COMPARISON OF FREQUENCIES OF LOCAL SOLUTIONS AND CLUSTER CRITERIA WITH NOISE REJECTION (FCM^e)

δ	LS(%)	PC	XB	noise
1.0	–	0.311	0.042	90
1.25	–	0.472	0.070	66
1.5	–	0.637	0.107	37
1.75	25.1	0.748	0.139	27
2.0	17.6	0.828	0.172	13
2.25	19.0	0.878	0.204	5
2.5	0.0	0.905	0.223	2
2.75	0.0	0.913	0.234	1
3.0	0.0	0.915	0.242	0

The result implies that the noise rejection mechanism may have another role for tackling initialization problems in the regularized objective functions of FCM.

V. CONCLUSION

This paper discussed the effects of fuzzified memberships of k-Means clustering from the view point of the regularization of objective functions. Several experimental results revealed that the standard fuzzification approach is more useful for decreasing the effects of bad initial partitions than the entropy regularization approach, which can be identified with a sort of GMMs. In this paper, the regularization effects were also compared in the robust clustering context. An experimental result implied that the noise fuzzy clustering mechanism can also contribute to decreasing the effects of noisy samples in bad initial partitions by assigning smaller memberships in the entropy regularization approach.

Comparative study with other fuzzification approaches is remained in future work.

REFERENCES

[1] J. C. Bezdek, *Pattern Recognition with Fuzzy Objective Function Algorithms*, Plenum Press, 1981.

[2] J. B. MacQueen, "Some methods of classification and analysis of multivariate observations," *Proc. of 5th Berkeley Symposium on Math. Stat. and Prob.*, pp. 281-297, 1967.

[3] S. Miyamoto, and M. Mukaidono, "Fuzzy c-Means as a regularization and maximum entropy approach," *Proc. of the 7th International Fuzzy Systems Association World Congress*, vol. 2, pp 86-92, 1997.

[4] A. P. Dempster, N.M. Laird, and D.B. Rubin, "Maximum likelihood from incomplete data via the EM algorithm," *J. of the Royal Statistical Society*, Series B, vol. 39, pp. 1–38, 1977.

[5] K. Honda and H. Ichihashi, "Regularized linear fuzzy clustering and probabilistic PCA mixture models," *IEEE Trans. on Fuzzy Systems*, vol. 13, no. 4, pp. 508-516, 2005.
[6] S. Miyamoto, S. Umayahara, "Fuzzy clustering by quadratic regularization," Proc. 1998 IEEE Int. Conf. Fuzzy Syst., pp.1394-1399, 1998.
[7] H. Ichihashi, K. Miyagishi, K. Honda, "Fuzzy *c*-means clustering with regularization by K-L information," Proc. 2001 IEEE Int. Conf. Fuzzy Syst., pp.924-927, 2001.
[8] S. Miyamoto, H. Ichihashi and K. Honda, *Algorithms for Fuzzy Clustering*, Springer, 2008.
[9] Z.-Q. Liu, S. Miyamoto (eds.), *Soft Computing and Human-Centered Machines*, Springer-Verlag, 2000.
[10] R. N. Davé, "Characterization and detection of noise in clustering," *Pattern Recognition Letters*, vol. 12, no. 11, pp. 657-664, 1991.
[11] R. N. Davé and R. Krishnapuram, "Robust clustering methods: a unified view," *IEEE Trans. on Fuzzy Systems*, vol.5, pp.270-293, 1997.
[12] F. Höppner, F. Klawonn, R. Kruse, and T. Runkler, *Fuzzy Cluster Analysis*, Jhon Wiley & Sons, 1999.
[13] K. Honda and H. Ichihashi, "A new approach to fuzzification of memberships in cluster analysis," *Modeling Decisions for Artificial Intelligence (MDAI) 2005*, Lecture Notes in Artificial Intelligence 3558, Springer, pp.172-182, 2005.
[14] X. L. Xie and G. Beni, "A validity measure for fuzzy clustering," *IEEE Trans. on Pattern Anal. Machine Intell.*, vol. 13, no. 8, pp. 841-847, 1987.
[15] A. Asuncion and D.J. Newman, UCI Machine Learning Repository [http://www.ics.uci.edu/ mlearn/MLRepository.html], Irvine, CA: University of California, School of Information and Computer Science, (2007).

2011 IEEE International Conference on Fuzzy Systems
June 27-30, 2011, Taipei, Taiwan

Constrained Agglomerative Hierarchical Clustering Algorithms with Penalties

Sadaaki Miyamoto
Department of Risk Engineering
University of Tsukuba
Ibaraki 305-8573, Japan
Email: miyamoto@risk.tsukuba.ac.jp

Akihisa Terami
Master's Program in Risk Engineering
University of Tsukuba
Ibaraki 305-8573, Japan
Email: e0611387@edu.esys.tsukuba.ac.jp

***Abstract*—Semi-supervised clustering with constraints has widely been studied, but there are few studies on constrained agglomerative hierarchical algorithms. We have shown modified kernel algorithms of agglomerative hierarchical clustering, but there is a drawback that the modified kernels are not positive-definite in general. In this paper we consider another idea of agglomerative hierarchical algorithms with pairwise constraints. That is, merging of clusters is with penalties. The centroid method and the Ward method with and without a kernel are considered. Typical numerical examples show effectiveness of the proposed algorithms in generating clusters with nonlinear cluster boundaries. We also compare the results with those by COP K-means, showing that the proposed algorithms outperform the COP K-means.**

Keywords-semi-supervised clustering; pairwise constraints; agglomerative hierarchical clustering.

I. Introduction

As cluster analysis is becoming a standard tool for data mining, various techniques have been developed and at the same time fundamental problems to be solved are addressed; three of them are as follows:

1) how traditional methods of agglomerative hierarchical clustering [6], [9], [10] should be used;
2) how clusters with nonlinear boundaries [11] should be generated;
3) how to semi-supervised clustering should be handled.

These three problems have sound reasons why they are important. First, agglomerative hierarchical clustering is frequently used for application to many contemporary problems including bioinformatics. Second, the theory of positive-definite kernels [1], [13] has been found to be useful to have nonlinearity in classification and clustering. Third, there are many studies in semi-supervised clustering using different ideas [4]. As to the last problem, various researches have been revealed that clustering with pairwise constraint is useful as a technique to handle semi-supervised classification [15], [2], [3], [8].

This paper concerns all these three problems and intends to give partial solutions to them. First, it proposes a constrained centroid method and a constrained Ward method of agglomerative hierarchical clustering. In contrast to our former paper [12] which uses a modified kernel function, the method herein does not use any kernel function and yet generates clusters with nonlinear boundaries, using a simple method of penalties in merging clusters. This paper also shows that the standard method of COP K-means [15] with pairwise constraint cannot generate clusters with nonlinear boundaries without a kernel function, while the present method can do this.

There are well-known typical examples with nonlinear boundaries that we can handle by the present method. We show the effectiveness of the proposed method and moreover compare performances of the proposed method and the COP K-means which shows the usefulness of the proposed method.

II. Agglomerative Clustering with Penalties

Let the set of objects for clustering be $X = \{x_1, \ldots, x_N\}$. We assume that object x_k $(k = 1, \ldots, N)$ is a point of a Euclidean space $\boldsymbol{R}^p$ with the Euclidean norm $\|\cdot\|$.

Generally a hard cluster denoted by G_i is a subset of X. The family of clusters is denoted by $\mathcal{G} = \{G_1, G_2, \ldots, G_K\}$, where the clusters form a crisp partition of X:

$$\bigcup_{i=1}^{K} G_i = X, \qquad G_i \cap G_j = \emptyset \quad (i \neq j).$$

Agglomerative hierarchical clustering uses a dissimilarity measure, frequently called a distance, between two clusters $d(G, G')$ $(G, G' \in \mathcal{G})$ which also is called an inter-cluster dissimilarity. In the following we sometimes write $d_{cn}(G, G')$ which means that the centroid method is used. Moreover, $d_{wm}(G, G')$ means that the Ward method is used. The two methods use the following definitions of the inter-cluster dissimilarity:

Centroid method:

Let the centroid of a cluster G be

$$M(G) = \frac{1}{|G|} \sum_{x_k \in G} x_k, \tag{1}$$

and let

$$d_{cn}(G, G') = \|M(G) - M(G')\|^2. \tag{2}$$

Ward method:

Assume $M(G)$ is the centroid as above, and let

$$E(G) = \sum_{x_i \in G} \|x_i - M(G)\|^2. \tag{3}$$

978-1-4244-7316-8/11/$26.00 ©2011 IEEE

Define

$$d_{wm}(G, G') = E(G \cup G') - E(G) - E(G'). \quad (4)$$

Although there are other three methods of the single linkage, complete linkage, and average linkage are often used, they are not studied in this paper.

Let us first describe a general procedure of agglomerative hierarchical clustering [9], [10] with a variation that a term $\mathcal{P}(G, G')$ is attached in the merging step, which is called **AHCP** (Agglomerative Hierarchical Clustering with Penalties) here. The definition of this term is described after the procedure.

AHCP Algorithm:

AHCP1: Assume that initial clusters are given by
$\mathcal{G} = \{\hat{G}_1, \hat{G}_2, \ldots, \hat{G}_{N_0}\}$.
Set $K = N_0$.
(K is the number of clusters and N_0 is the initial number of clusters)
$G_i = \hat{G}_i$ $(i = 1, \ldots, K)$.
Calculate $d(G, G')$ for all pairs $G, G' \in \mathcal{G}$.

AHCP2: Search the pair of minimum dissimilarity:

$$(G_p, G_q) = \arg \min_{G, G' \in \mathcal{G}} \{d(G, G') + \mathcal{P}(G, G')\}. \quad (5)$$

Merge: $G_r = G_p \cup G_q$.
Add G_r to $\mathcal{G}$ and delete G_p, G_q from $\mathcal{G}$.
$K = K - 1$.
if $K = 1$ then stop and output the dendrogram.

AHCP3: Update dissimilarity $d(G_r, G'')$ for all $G'' \in \mathcal{G}$.
Go to **AHCP2**.

End AHCP.

Assume that K_0 is given and it is necessary to have K_0 clusters, then we stop **AHCP** algorithm when K_0 clusters are obtained in **AHCP2**.

A. Pairwise constraints and penalties

A set $ML = \{(x_i, x_j)\} \subset X \times X$ consists of *must-link* pairs so that x_i and x_j should be in a same cluster, while another set $CL = \{(x_k, x_l)\} \subset X \times X$ consists of *cannot-link* pairs so that x_i and x_j should be in different clusters. ML and CL are assumed to be symmetric in the sense that if $(x_i, x_j) \in ML$ then $(x_j, x_i) \in ML$, and if $(x_k, x_l) \in CL$ then $(x_l, x_k) \in CL$.

Note that ML is regarded as an undirected graph in which nodes are objects appeared in ML, and an undirected edge is $(x_i, x_j) \in ML$. Accordingly, $V(ML)$ is the set of objects in graph ML. The connected components of graph ML is denoted by $ML_1, \ldots, ML_\ell$. Moreover the constraints are assumed to be consistent in the sense that if $(x_k, x_l) \in CL$, x_k and x_l are in different components of graph ML.

The must-link constraints are realized in **AHCP** algorithm by putting the initial clusters $\mathcal{G} = \{\hat{G}_1, \hat{G}_2, \ldots, \hat{G}_{N_0}\}$ to be the connected components $ML_1, \ldots, ML_\ell$.

In contrast, the following penalty term realizes the cannot-link constraints in **AHCP**:

$$\mathcal{P}(G, G') = W_{CL} \sum_{x \in G, x' \in G', (x, x') \in CL} \quad (6)$$

where W_{CL} is a positive constant. If W_{CL} is sufficiently large, the cannot-link constraints will never be broken.

Note: We handle ML to be hard constraints, while CL is treated to be *soft* constraints in (6). It is, however, straightforward to treat ML as soft constraints as well. For this purpose we modify (6) as follows:

$$\mathcal{P}(G, G') = W_{CL} \sum_{x \in G, x' \in G', (x, x') \in CL} - W_{ML} \sum_{x \in G, x' \in G', (x, x') \in ML} \quad (7)$$

Note also that the CL constraints become hard when W_{CL} is sufficiently large, which we assume later for the examples herein.

B. Positive-definite kernels in agglomerative clustering

It has been known that a high-dimensional mapping with a kernel function which is used in support vector machines [14], [13], [1] is also useful in agglomerative hierarchical clustering [5]. That is, regardless whether a high-dimensional mapping is used or not, the updating formulas for merging clusters remain the same in the centroid method and the Ward method [5]:

$$\begin{aligned} d_{cm}(G_r, G'') = & \frac{|G_p|}{|G_p| + |G_q|} d_{cm}(G_p, G'') \\ & + \frac{|G_q|}{|G_p| + |G_q|} d_{cm}(G_q, G'') \\ & - \frac{|G_p||G_q|}{(|G_p| + |G_q|)^2} d_{cm}(G_p, G_q), \end{aligned} \quad (8)$$

$$\begin{aligned} d_{wm}(G_r, G'') = & \frac{1}{|G_p| + |G_q| + |G''|} \Big[\\ & (|G_p| + |G''|) d_{wm}(G_p, G'') \\ & + (|G_q| + |G|) d_{wm}(G_q, G'') \\ & - |G''| d_{wm}(G_p, G_q) \Big]. \end{aligned} \quad (9)$$

except that the initial dissimilarities are different:

$$d_{cm}(x, y) = \|x - y\|^2 = K(x, x) + K(y, y) - 2K(x, y),$$
$$d_{wm}(x, y) = \frac{1}{2}\|x - y\|^2 = \frac{1}{2}\{K(x, x) + K(y, y) - 2K(x, y)\}.$$

for two objects $x, y \in X$ from which $d_{cm}(\hat{G}, \hat{G}')$ and $d_{wm}(\hat{G}, \hat{G}')$ are easily calculated.

We compare the results from the centroid method and the Ward method with and without the Gaussian kernel:

$$K(x, y) = \exp(-const. \|x - y\|^2).$$

III. Numerical Examples

Three illustrative examples are shown, in which cluster boundaries are nonlinear. First set of data is shown in Fig. 1 which has two obvious clusters of "double circles"; the outer circle has 100 objects while the inner has 50. Second data set in Fig. 2 has a ball inside a shape like a crescent, which is called " a moon and a ball." Third set of data in Fig. 3 is called "two moons" which also cannot be separated by a line. Each "moon" has 150 objects.

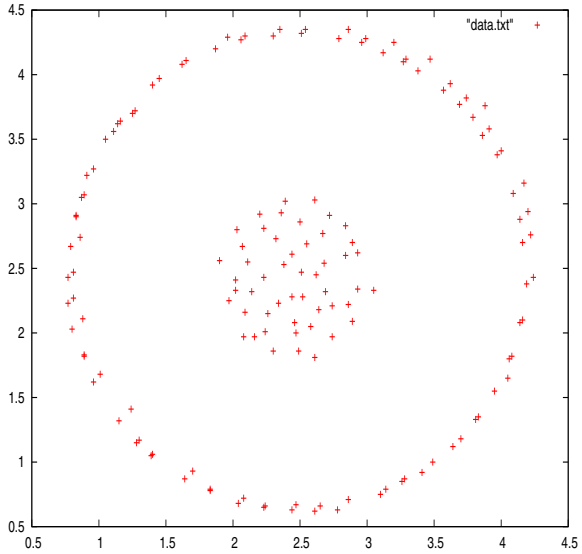

Fig. 1. First data set: double circles

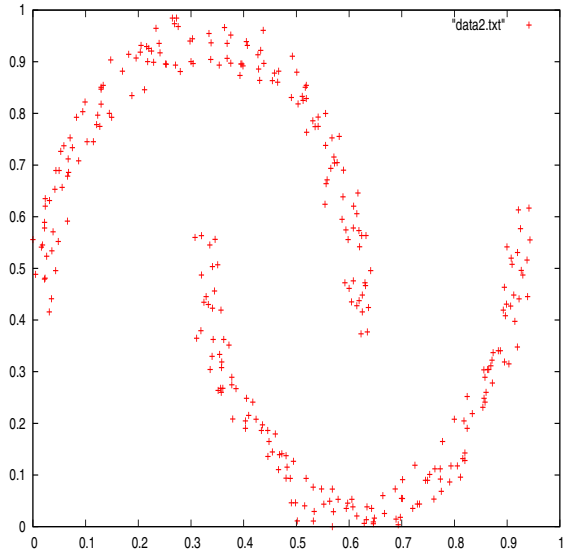

Fig. 3. Third data set: two moons

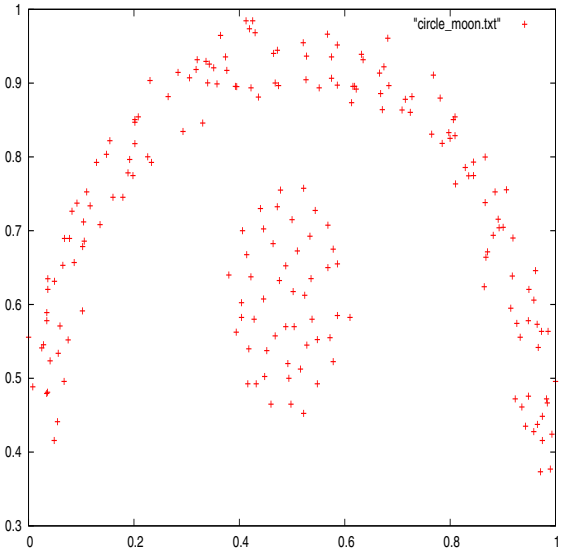

Fig. 2. Second data set: A moon and a ball

We generated ML and CL randomly, with the obvious restriction that ML are in the same (correct) cluster and CL connects two objects in different clusters. The penalty W_{CL} was sufficiently large so that CL pair did not be in a same cluster. Thus CL was handled as a hard constraint.

The numbers of constraints in ML and CL were changed in the numerical experiment and the ratios of correct results were evaluated as follows.

The Rand index which is one of the standard evaluation criteria was used:

$$Rand(a,b) = \frac{a+b}{N(N-1)/2}, \tag{10}$$

where a is the number of pairs that has to be in the same cluster and actually in the same cluster in the result, and b is the number of pairs that has to be in different clusters and actually in different clusters in the results. In short, $Rand(a,b)$ is the ratio of correct pairs in the whole number of pairs. Hence if the result is perfect, $Rand(a,b) = 1$.

The proposed method was compared with the COP K-means [15] with $K = 2$ in both examples.

We fixed the number of constraints and then generated the constraints randomly 1000 times, then generated clusters by the proposed method and the COP K-means. Then the averages of the rand index were calculated.

The number of constraints were then changed from 0 to 50 shown on the horizontal axis in Figs. 4–9.

In the following six kinds of results are compared; we did not mix ML and CL but included ML or CL alone:

1) results of the centroid method with ML (and no CL), shown by red line with $+$ in Figs. 4–9;
2) results of the centroid method with CL (and no ML) shown by green line with $\times$;
3) results of the Ward method with ML (and no CL) shown by blue line with $*$;
4) results of the Ward method with CL (and no ML) shown by pink line with $\square$;
5) results of the COP K-means with ML (and no CL) shown by light blue line with $\blacksquare$;
6) results of the COP K-means with CL (and no ML) shown by black line with $\bullet$.

Figures 4 and 5 respectively show the results without a kernel and those with the Gaussian kernel applied to the data set of the double circles. The all results from the COP K-means was without a kernel. Note that it has been known that K-means with the Gaussian kernel can separate the two clusters of the two circles.

It is observed that the centroid and the Ward methods with

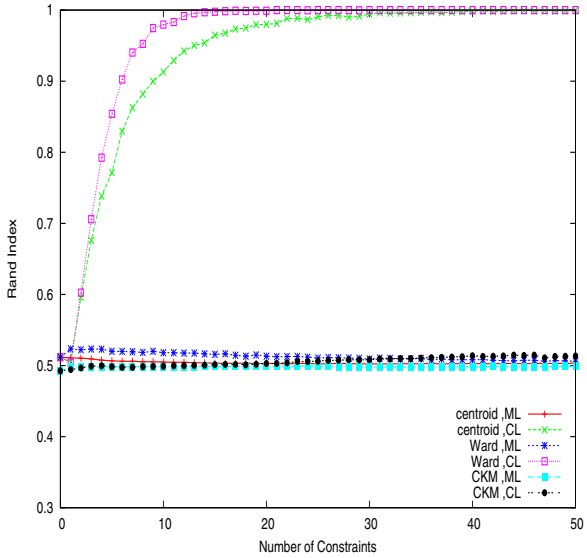

Fig. 4. The ratios of $Rand(a, b)$ by the proposed method without a kernel and the COP K-means applied to the double circle data set

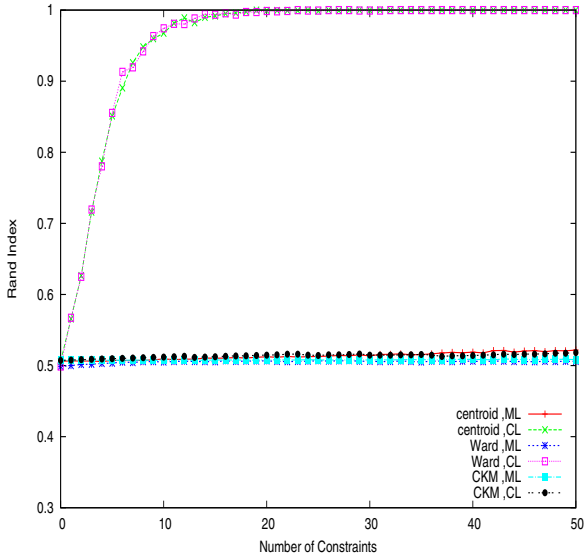

Fig. 6. The ratios of $Rand(a, b)$ by the proposed method without a kernel and the COP K-means applied to the moon and ball data set

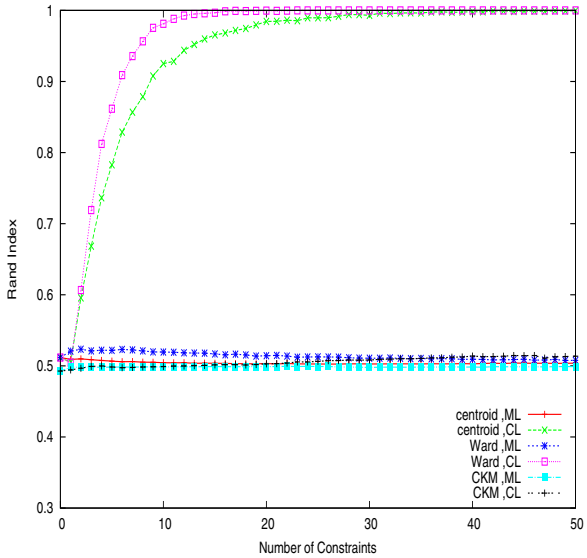

Fig. 5. The ratios of $Rand(a, b)$ by the proposed method with the Gaussian kernel ($const. = 0.01$) and the COP K-means applied to the double circle data set

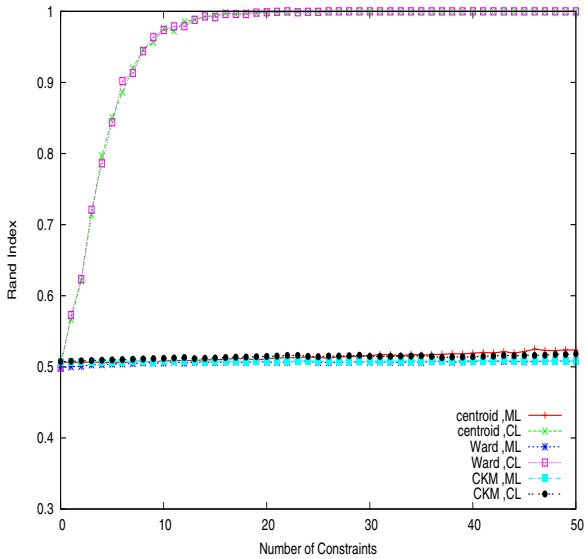

Fig. 7. The ratios of $Rand(a, b)$ by the proposed method with the Gaussian kernel ($const. = 0.01$) and the COP K-means applied to the moon and ball data set

CL better separated the two clusters as the number of the cannot-link constraints increase, while the other methods could not separate these two.

Figures 6 and 7 respectively show the results without a kernel and those with the Gaussian kernel applied to the data set of the "moon and ball." The same tendency as the first example is observed: the centroid and the Ward methods with CL better separated the two clusters as the number of the cannot-link constraints increase, whereas the other methods could not separate the moon and the ball.

Figures 8 and 9 respectively show the results without a kernel and those with the Gaussian kernel applied to the data set of the two moons. The COP K-means was used again without a kernel function. Note that in this case it is generally difficult to separate the two clusters using K-means, even with the Gaussian kernel.

It is observed again that the centroid and Ward methods with CL separated the two moons as the number of the cannot-link constraints increase, while the other methods could not separate the two clusters. It is moreover seen that the Gaussian kernel improved the performance in the second example when compared with the centroid and the Ward methods without a

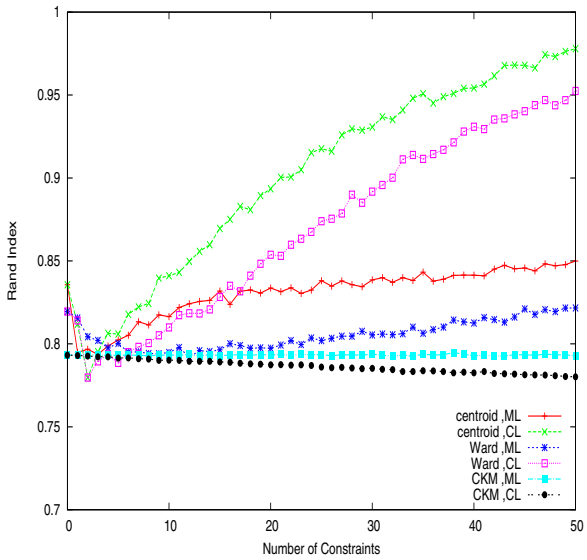

Fig. 8. The ratios of $Rand(a, b)$ by the proposed method without a kernel and the COP K-means applied to the two moons data set

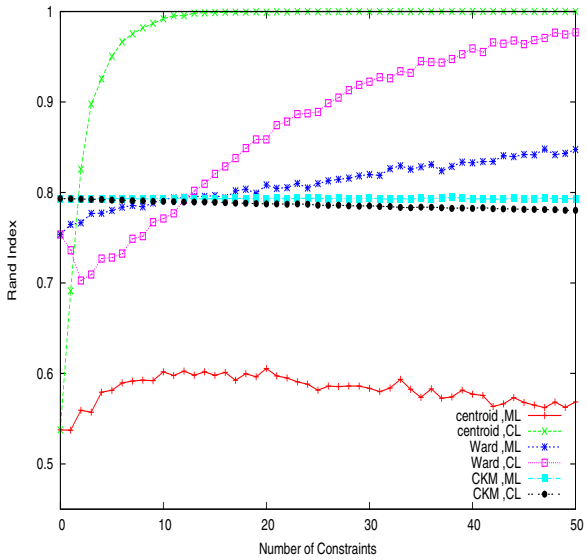

Fig. 9. The ratios of $Rand(a, b)$ by the proposed method with the Gaussian kernel ($const. = 10$) and the COP K-means applied to the two moons data set

kernel.

A. Discussion

The three illustrative examples show that the proposed method with CL outperforms other methods. It is also observed that the two clusters in the first and the second examples were separated without the use of a kernel function. This contrasts the general understanding that K-means type methods including fuzzy c-means without a kernel cannot separate clusters with nonlinear boundaries. Even if we use the COP K-means, the cluster boundaries remained the same with the exception of the pairwise constraints, and hence no perfect separation of the two clusters was observed for the COP K-means.

In contrast, the third data set of two moons could perfectly be separated with the use of the Gaussian kernel, which shows the effectiveness of a kernel function, as it generally is more difficult to separate the two moons than the two circles.

The three examples moreover show the generalization ability of the CL constraints especially in the first two examples, since the two clusters were almost perfectly classified when the number of CL constraints is 10, where the complete cannot links should have 50 constraints.

In contrast, we observed ML was not so effective as CL. Why ML was not so effective in agglomerative algorithms should be further investigated. We also observed that the increase in the number in ML did not result in the improvement of the rand index. The reason is unknown but similar tendency has also been observed in other studies (e.g. [7]).

IV. Conclusion

We have proposed the centroid method and the Ward method of agglomerative hierarchical clustering with penalties of the pairwise constraints. The three illustrative examples showed their effectiveness in extracting clusters with nonlinear boundaries. The idea herein is simple and can be implemented without difficulty. Note that agglomerative hierarchical clustering is frequently used in a variety of applications. We thus showed that the proposed method enhances the usefulness of the agglomerative algorithms.

When compared with our former proposal which uses modification of a kernel function [12], the present method is better in the sense that a kernel function is unnecessary and it does not have a drawback of indeterminate kernel which the former method of us has.

Future studies include testing its effectiveness in real examples and dendrogram output showing pairwise penalties. Comparison with fuzzy c-means with semi-supervision [16] which is not yet an established technique should also be considered.

References

[1] S. Akaho, *Kernel Multivariate Analysis*, Iwanami-Shoten, Tokyo, 2008 (in Japanese).
[2] S. Basu, M. Bilenko, R.J. Mooney, A Probabilistic Framework for Semi-Supervised Clustering, *Proc. of the Tenth ACM SIGKDD (KDD-2004)*, pp.59-68, 2004.
[3] S. Basu, A. Banerjee, R.J. Mooney, Active Semi-Supervision for Pairwise Constrained Clustering, *Proc. of the SIAM International Conference on Data Mining*, (SDM-2004), pp. 333-344, 2004.
[4] O. Chapelle, B. Schölkopf, A. Zien, eds., *Semi-Supervised Learning*, MIT Press, 2006.
[5] Y. Endo, H. Haruyama, T. Okubo, On some hierarchical clustering algorithms using kernel functions, *Proc. of FUZZ-IEEE 2004*, Budapest, Hungary, July 25-29, 2004, CD-ROM Proc. pp. 1–6.
[6] B.S. Everitt, *Cluster Analysis, 3rd Ed.*, Arnold, London, 1993.
[7] D. Klein, S.D. Kamvar, C. Manning, From Instance-level Constraints to Space-level Constraints: Making the Most of Prior Knowledge in Data Clustering, *Proc. of the Intern. Conf. on Machine Learning*, pp.307-314, Sydney, Australia, 2002.
[8] B. Kulis, S. Basu, I. Dhillon, R. Mooney, Semi-supervised graph clustering: a kernel approach, *Mach. Learn.*, Vol.74, pp.1-22, 2009.

[9] S. Miyamoto, *Fuzzy Sets in Information Retrieval and Cluster Analysis*, Kluwer, Dordrecht, 1990.
[10] S. Miyamoto, *Introduction to Cluster Analysis: Theory and Applications of Fuzzy Clustering*, Morikita-Shuppan, Tokyo, 1990 (in Japanese).
[11] S. Miyamoto, H. Ichihashi, K. Honda, *Algorithms for Fuzzy Clustering*, Springer, 2008.
[12] S. Miyamoto, A. Terami, Semi-Supervised Agglomerative Hierarchical Clustering Algorithms with Pairwise Constraints, *Proc. of WCCI 2010 IEEE World Congress on Computational Intelligence*, July, 18-23, 2010 - CCIB, Barcelona, Spain, pp.2796-2801 (2010).
[13] B. Schölkopf, A. Smola, *Learning with Kernels*, MIT Press, 2002.
[14] V.N. Vapnik, *Statistical Learning Theory*, Wiley, New York, 1998.
[15] K. Wagstaff, C. Cardie, S. Rogers, S. Schroedl, Constrained K-means Clustering with Background Knowledge, *Proc. of the 9th ICML*, pp. 577-584, 2001
[16] N. Wang, X. Li, X. Luo, Semi-supervised Kernel-based Fuzzy *c*-Means with Pairwise Constraints, *Proc. of WCCI 2008*, pp.1099-1103, 2008.

2011 IEEE International Conference on Fuzzy Systems
June 27-30, 2011, Taipei, Taiwan

Adaptive Fuzzy Interpolation with Prioritized Component Candidates

Longzhi Yang and Qiang Shen
Department of Computer Science
Aberystwyth University
Aberystwyth, SY23 3DB, UK
Email: {lly07,qqs}@aber.ac.uk

***Abstract*—Adaptive fuzzy interpolation strengthens the potential of fuzzy interpolative reasoning. It first identifies all possible sets of faulty fuzzy reasoning components, termed the candidates, each of which may have led to all the contradictory interpolations. It then tries to modify one selected candidate in an effort to remove all the contradictions and thus restore interpolative consistency. This approach assumes that all the candidates are equally likely to be the real culprit. However, this may not be the case in real situations as certain identified reasoning components may be more liable to resulting in inconsistencies than others. This paper extends the adaptive approach by prioritizing all the generated candidates. This is achieved by exploiting the certainty degrees of fuzzy reasoning components and hence of derived propositions. From this, the candidate with the highest priority is modified first. This extension helps to quickly spot the real culprit and thus considerably improves the approach in terms of efficiency.**

***Index Terms*—Adaptive fuzzy interpolation, assumption-based truth maintenance systems, reliability-based general diagnostic engine.**

I. Introduction

Fuzzy rule interpolation enhances the robustness of fuzzy reasoning. When given observations have no overlap with any antecedent values, no rule can be fired in classical inference. However, interpolative reasoning through a sparse rule base may still obtain certain conclusions and thus improve the applicability of fuzzy models. Also, with the help of fuzzy interpolation, the complexity of a rule base can be reduced by omitting those fuzzy rules which may be approximated from their neighboring ones. A number of important interpolation approaches have been presented in the literature, including [1], [2], [3], [4], [7], [8], [9], [10], [11], [12], [13], [14]. In particular, the scale and move transformation-based approach can handle both interpolation and extrapolation, which involve multiple fuzzy rules, with each rule consisting of multiple antecedents. This approach also guarantees the uniqueness as well as normality and convexity of the resulting interpolated fuzzy sets. Yet, it is possible that more than one object value of a single variable may be derived in fuzzy interpolation. This implies that certain inconsistencies may have resulted.

To address this problem, *adaptive fuzzy interpolation* has recently been proposed [15]. This approach is capable of efficiently detecting inconsistencies, locating possible fault candidates and modifying the candidates in an effort to remove all the inconsistencies. It works by viewing the interpolative inference procedures as artificial system components, and then utilizing an assumption-based truth maintenance system (ATMS) [5] to record the dependencies between an interpolated value and its proceeding interpolation components. From this, the classical algorithm of general diagnostic engine (GDE) [6] is employed to manipulate the sets of dependent components of contradictions to hypothesize all possible candidates of defective rules.

The adaptive approach of [15] assumes that all the component candidates are equally reliable, but this may not be true in reality. This is because: i) two derived object values for a common variable which have led to a contradiction may not be equally reliable (moreover, one may be correct and the other wrong); and ii) all the interpolation components that jointly entail one of the two contradictory object values may not be equally reliable. Given information on such differences, all the generated component candidates may be prioritized. This is achieved by firstly extending the traditional ATMS not only to record dependencies, but also to record how reliable these dependencies are. Then GDE is modified in an effort to prioritize all the component candidates. The prioritization of candidates will inevitably help the modification procedure to quickly arrive at a consistent solution and thus save computational effort.

The rest of this paper is structured as follows. Sec. II reviews the adaptive fuzzy interpolation approach. Sec. III presents the extension that shows how component candidates can be efficiently prioritized. Sec. IV reconsiders the example given in [15] to illustrate how this extension can improve the original approach. Sec. V concludes the paper and points out important future research directions.

II. Adaptive Fuzzy Interpolation

Adaptive interpolative reasoning [15] provides a way to ensure that inference results remain consistent throughout the fuzzy interpolative process. The degree of consistency is typically expressed as the degree of matching. In particular, the matching degree between two fuzzy sets A_{ij} and A_{ik}, denoted as $M(A_{ij}, A_{ik})$, in the domain D_{x_i} of variable x_i is defined as follows, which is used to evaluate consistency efficiently (though distance-based measure may also be used for this):

$$M(A_{ij}, A_{ik}) = \sup_{x \in D_{x_i}} [\min(\mu_{A_{ij}}(x), \mu_{A_{ik}}(x))]. \quad (1)$$

978-1-4244-7316-8/11/$26.00 ©2011 IEEE

Then, the degree β of a contradiction with respect to two propositions P (x_i is A_{ij}) and P'(x_i is A_{ik}) is defined by:

$$\beta = 1 - M(A_{ij}, A_{ik}). \tag{2}$$

A predefined threshold β_0 ($0 \leq \beta_0 \leq 1$) is adopted in order to determine those values assigned to a common variable with an unacceptable contradictory degree. A contradiction is called a β_0-*contradiction* if the corresponding degree of contradiction $\beta > \beta_0$.

In implementing fuzzy interpolation, each pair of neighboring rules is defined as a *fuzzy reasoning component*. Such a component takes an input, an observation or a previously interpolated result, including that obtained by extrapolation (which are all hereafter referred to as an observation for simplicity), and produces another (the consequent of the interpolated rule) as output. The process of adaptive interpolation is summarized in Fig. 1. Firstly, the interpolator carries out interpolation and passes the interpolated results to the ATMS for dependency-recording. Then, the ATMS relays any β_0-*contradictions* as well as their dependent fuzzy reasoning components to the GDE which diagnoses the problem and generates all possible component candidates. After that, a modification process takes place to correct a certain candidate to restore consistency. A brief description of each of these key methods is given below.

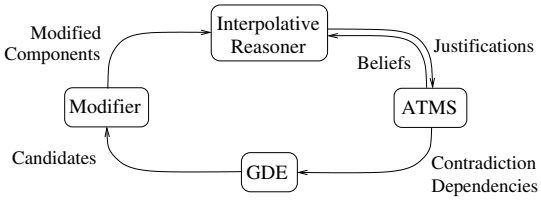

Fig. 1. Adaptive interpolative reasoning

A. Truth maintenance

ATMS is utilized to record the dependency of the interpolated results and that of contradictions, upon the fuzzy reasoning components from which they are inferred. Thus, propositions, contradictions and fuzzy interpolative reasoning components are all represented as ATMS nodes. In addition to the so-called datum field, which trivially denotes the actual meaning of the node, an ATMS node has two other fields: justification and label.

1) Justification: Briefly, a justification describes how a node is derivable from other nodes. Any ATMS node with an inferred proposition is represented by an ATMS justification as:

$$O, R_i R_j \Rightarrow C, \tag{3}$$

where $R_i R_j$ stands for the fuzzy reasoning component containing the two neighboring rules R_i and R_j ($i \neq j$) that have been used to infer the outcome C from the observation O.

According to the definition of contradiction above, any two propositions P (x_i is A_{ij}) and P'(x_i is A_{ik}) concerning the same variable x_i are contradictory to a certain degree β. When β is not higher than β_0, the contradictory degree is acceptable and the two considered propositions are treated as being consistent in ATMS. Otherwise, a β_0-$contradiction$ is deduced, which can be represented as:

$$P, P' \Rightarrow_{\beta_0} \perp. \tag{4}$$

2) Label and label-updating: A label is a set of environments, each of which supports the associated node. In particular, an environment is a minimal set of fuzzy reasoning components that jointly entail the supported node, thereby describing how the node ultimately depends on those fuzzy reasoning components. An environment is said to be β_0-*inconsistent* if β_0-contradiction is derivable propositionally by the environment and a given justification. An environment is said to be $(1-\beta_0)$-*consistent* if it is not β_0-inconsistent.

The label of each node is guaranteed to be $(1-\beta_0)$-consistent, sound, minimal and complete by the label updating algorithm, except that the label of the special "false" node is guaranteed to be β_0-inconsistent rather than $(1-\beta_0)$-consistent. In particular, the label of the special "false" node gathers all minimal β_0-inconsistent environments. Its corresponding label-updating process is given as follows. Whenever a β_0-contradiction is detected, each environment in its label is added into the label of "false" node and all such environments and their supersets are removed from the label of every other node. Also, any such environment which is a superset of another is removed from the label of the node "false".

B. Candidate generation

GDE [6] generates minimal candidates by manipulating the label of the specific "false" node. A candidate is a particular set of nodes or fuzzy reasoning components which may be responsible for the whole set of current contradictions. Because a β_0-inconsistent environment indicates that at least one of its elements is faulty, a candidate must have a non-empty intersection with each β_0-inconsistent environment. Thus, each candidate is constructed by taking one fuzzy reasoning component from each environment in the label of "false" node. Supersets removal then ensures such generated candidates to be minimal. In light of this, a successful correction of any single candidate will remove all the contradictions.

C. Candidate modification

Consistency can be restored by successfully correcting any single candidate because each single candidate explains the entire set of current contradictions. Given a set of candidates, the modification procedure is shown in Fig. 2.

For convenience, in the rest of this paper, A^*_{ij} is used to denote the modified consequence of a culprit interpolated rule whose consequent value is A_{ij}, and $A^*_{ij}{}'$ and λ^*_{ij} are used to denote the corresponding modified intermediate rule consequence and the *relative placement factor* [15] of A^*_{ij}, respectively. Also, for simplicity, only rules with a single antecedent are considered here, through extension to multi-antecedent rules is straightforward. Suppose that the neighboring rules $A_{11} \Rightarrow A_{21}$ and $A_{1n} \Rightarrow A_{2n}$ are the two rules used

CONSISTENCYRESTORING($\mathbb{Q}$)
$\mathbb{Q}$, the candidate set sorted in descending cardinality, each element of which is a set of fuzzy reasoning components (f); MODIFY(f), the modification procedure for single fuzzy reasoning component (f). Return **true** when modification succeeds and **false** otherwise.

(1) $success \leftarrow$ **false**
(2) **do**
(3) $C \leftarrow Dequeue(\mathbb{Q})$
(4) **foreach** $f \in C$
(5) $success \leftarrow$ MODIFY(f)
(6) **if** ($success ==$**false**)
(7) **break**
(8) **until** (($success ==$**true**) or ($\mathbb{Q} == \varnothing$))
(9) **return** $success$

Fig. 2. The CONSISTENCYRESTORING procedure

for interpolation by a defective fuzzy reasoning component, that $A_{12}, A_{13}, ..., A_{1(n-1)}$ are observations or previously interpolated results located in between A_{11} and A_{1n}, and that A_{1j} $(2 \leq j \leq n-1)$ is the middle most observation. The modification procedure for single fuzzy reasoning component can then be summarized as follows:

1. Find the rule $(A_{1j} \Rightarrow A_{2j})$ whose antecedent is located in the middle most of the neighborhood of the antecedents of any two rules that may be used for interpolation, with respect to their representative values. Assume that the *relative placement factor* of its consequence λ_{2j} is modified to λ^*_{2j}.

2. Calculate the *correction rate pair* according to the *relative placement factor* modification of rule $A_{1j} \Rightarrow A_{2j}$:

$$\begin{cases} c^- = \frac{\lambda^*_{2j}}{\lambda_{2j}} \\ c^+ = \frac{1-\lambda^*_{2j}}{1-\lambda_{2j}}. \end{cases} \tag{5}$$

3. Calculate the modified *relative placement factors* of consequences of all other interpolated rules which are generated from the same defective fuzzy reasoning component as per the *correction rate pair* computed above, where $i \in \{2, 3, ..., j-1\}$ and $k \in \{j+1, j+2, ..., n-1\}$:

$$\begin{cases} \lambda^*_{2i} = \lambda_{2i} \cdot c^- \\ 1 - \lambda^*_{2k} = (1 - \lambda_{2k}) \cdot c^+. \end{cases} \tag{6}$$

4. Calculate the modified consequences of all interpolated rules which are generated from the same defective fuzzy reasoning component in accordance with their modified *relative placement factors*:

$$\begin{cases} {A^*_{2x}}' = (1 - \lambda^*_{2x})A_{21} + \lambda^*_{2x}A_{2n} \\ T(A_{1x}', A_{1x}) = T(A^*_{2x}', A^*_{2x}), \end{cases} \tag{7}$$

where $x \in \{2, 3, ..., n-1\}$, and $T(A', A)$ represents the scale and move transformations [7], [8] from fuzzy set A' to A.

5. Restrict the modified consequence so that it is consistent with the context. Suppose that m object values $A_{i1}, A_{i2}, ..., A_{im}$ are obtained for variable x_i. If they are $(1-\beta_0)$-consistent, they must satisfy:

$$\bigcap_{j=1}^{m} (A_{ij})_{\beta_0} \neq \varnothing, \tag{8}$$

where $(A_{ij})_{\beta_0}$ denotes the β_0-*cut* of fuzzy set A_{ij}.

6. Restrict the propagations of all modified consequences so that they are consistent with the context. For simplicity, let function $I(A_{ij}, R_l R_r) = A_{kj}$ denote the standard interpolation from the antecedent fuzzy set A_{ij} to the consequent value A_{kj}, through fuzzy reasoning component $R_l R_r$. Suppose that m object values $A_{i1}, A_{i2}, ..., A_{im}$ of variable x_i, located between the antecedent values of rules R_l and R_r, are modified, that the corresponding modified object values of variable x_k are A^*_{kj}, $j \in \{1, 2, ..., m\}$, and that n object values A_{kl}, $l \in \{1, 2, ..., n\}$, of variable x_k are already derived previously. If the modified consequences A^*_{kj} are all $(1-\beta_0)$-consistent, then they must satisfy:

$$\begin{cases} A^*_{kl} = I(A^*_{ij}, R_l R_r) \\ \left(\bigcap_{j=1}^{m} (A^*_{kj})_{\beta_0} \right) \bigcap \left(\bigcap_{l=1}^{n} (A_{kl})_{\beta_0} \right) \neq \varnothing. \end{cases} \tag{9}$$

7. Solve all these simultaneous equations. The result is the modified solution which ensures inconsistency-free.

III. THE EXTENSION

The approach described above assumes that each candidate is equally likely to be the real culprit and naturally the candidate with the smallest cardinality is always tentatively modified first. However, this may not be true in real-world problems and, as argued earlier, differences exist amongst such candidates. In order to prioritize all the generated candidates, fuzzy reasoning components and derived propositions need to be ranked first in accordance with their certainty or reliability degrees.

A. Certainty degrees of fuzzy reasoning components

In this work, a fuzzy reasoning component composed by a pair of neighboring rules is used to represent the fuzzy interpolation mechanism which uses these two rules. In particular, the approach is based on the use of the scale and move transformation-based fuzzy interpolation techniques. Essentially, it is a fuzzy extension of classical linear interpolation. Thus, it is expected that such an artificial component will be more appropriate to represent those pairs of neighboring rules where relative distance between the two antecedents is closer to the corresponding relative distance between the two consequences than otherwise. In other words, the fuzzy reasoning components which are defined on such pairs of neighboring rules are more certain to derive correct interpolated results than the others, under the linearity assumption.

Suppose that fuzzy reasoning component $R_i R_j$ is composed by the following two rules:

$$\begin{array}{l} R_i: \text{ If } x_1 \text{ is } A_{1i}, \text{ then } x_2 \text{ is } A_{2i}; \\ R_j: \text{ If } x_1 \text{ is } A_{1j}, \text{ then } x_2 \text{ is } A_{2j}. \end{array} \tag{10}$$

Inspired by the above observation, the certainty degree $c_{R_iR_j}$ of fuzzy reasoning component R_iR_j can therefore be defined by:

$$c_{R_iR_j} = 1 - \left| \frac{d(A_{1i}, A_{1j})}{max_1 - min_1} - \frac{d(A_{2i}, A_{2j})}{max_2 - min_2} \right|, \quad (11)$$

where $d(A_{ki}, A_{kj})$, $k \in \{1, 2\}$, is the distance between fuzzy sets A_{ki} and A_{kj} (given a certain distance metric); max_k and min_k are the maximum and minimum of the domain values of variable x_k, respectively. Obviously, $c_{R_iR_j} \in [0, 1]$.

B. Certainty degree of an interpolated result

Given an observation or previously inferred result O and a fuzzy reasoning component R_iR_j which is composed by two rules R_i and R_j that flank the given observation O, a logical consequence C can be generated by the scale and move transformation-based fuzzy interpolation approach. The certainty degree c_C of the conclusion C is then calculated by:

$$c_C = c_O \otimes c_{R_iR_j}, \quad (12)$$

where the composition operator $\otimes$ can be minimum, algebraic product or any other T-norm operator. If O is an observation, it is regarded fully certain in this research and hence, c_O is assumed to be 1. Otherwise, c_O is calculated from a previous interpolation.

In general, the certainty degree of an interpolated result should also depend on the certainty degree (reliability) of the two rules used for interpolation. However, in this research, as with its preceding work, all given rules are presumed to be fixed and true. That is, the certainty degree of any rule in the rule base is 1. Therefore, the contribution of any rule's certainty degree can be ignored in the calculation of the certainty degree of an interpolated result.

Note that two different applications of interpolation procedures may result in the same interpolated result C, but with two different certainty degrees associated, say c_C and $c_{C'}$. Then the overall certainty degree of C, denoted as c is updated such that

$$c = c_C \oplus c_{C'}, \quad (13)$$

where $\oplus$ is the maximum operator, or any other S-norm operator.

C. Reliability-based ATMS

Having introduced the certainty degrees of fuzzy reasoning components and those of the interpolated results, ATMS needs to be extended accordingly in order to represent such information within the ATMS network. For this purpose, an extra filed, termed certainty degree, is introduced to each ATMS node, which measures to what extent the corresponding node can be (logically disjunctively) derived from all the label environments according to the entire set of current justifications. Each extended ATMS node is therefore of the following form:

$$\langle N, c, \{E_1, E_2, ..., E_n\}, \{J_1, J_2, ..., J_m\} \rangle, \quad (14)$$

where N is the underlying meaning of the node, c is the certainty degree of N, $\{E_1, E_2, ..., E_n\}$ is the ATMS label and $J_1, J_2, ..., J_m$ are the justifications. In addition, each label environment E_i $(1 \leq i \leq n)$ is of the form:

$$E_i = \{N_{11}, N_{12}, ..., N_{1k_i}\}, \quad (15)$$

where N_{ij}, $j \in \{1, 2, ..., k_i\}$, are those ATMS nodes which jointly support N.

1) Justification: A justification within this extended ATMS conveys two types of information: i) how the present node is derived from other nodes; and ii) to what extent the node is derivable from the other nodes. The first type of information is the same as that conveyed by the classical ATMS. For all nodes but the special "false" node, any justification is of the form of Eq. 3. Thus, the second type of information can be calculated with respect to Eq. 12.

Note that, for the special "false" node, the justifications are of the form of Eq. 4. However, in this research, no direct use of such justifications is required. Hence, any calculation involving the second type of information for this node is omitted.

2) Label and label-updating: In the extended ATMS, the set of fuzzy reasoning components that compose a label environment not only jointly entails their supported node, but also determines how certain the supported node can be logically derived from that environment. From this, the overall certainty degree of the supported node can be determined by the entire set of label environments. Without losing generality, suppose that node N can be derived by n different environments and that the kth $(1 \leq k \leq n)$ environment consists of m_k fuzzy reasoning components $F_{k1}, F_{k2}, ..., F_{km_k}$. Then the node N can be derived through the kth environment to the degree:

$$c_{N_k} = c_{F_{k1}} \otimes c_{F_{k2}} \otimes ... \otimes c_{F_{Km_k}}. \quad (16)$$

This is simply the generalized case of Eq. 12 by multiple applications of Eq. 12. By applying Eq. 13, the overall certainty degree c_N of the node N can be calculated such that

$$\begin{aligned} c_N &= c_{F_1} \oplus c_{F_2} \oplus ... \oplus c_{F_n} \\ &= (c_{F_{11}} \otimes c_{F_{12}} \otimes ... \otimes c_{F_{1m_1}}) \\ &\quad \oplus (c_{F_{21}} \otimes c_{F_{22}} \otimes ... \otimes c_{F_{2m_2}}) \\ &\quad \oplus ... \\ &\quad \oplus (c_{F_{n1}} \otimes c_{F_{n2}} \otimes ... \otimes c_{F_{nm_n}}). \end{aligned} \quad (17)$$

In general, to update the overall certainty degree of a given node, the label-updating algorithm needs to be applied. Hence, when a new justification is present, the extended label-updating algorithm not only updates the label of the node in question in exactly the same way as that of the classical ATMS, but also updates the overall certainty degree of this node according to Eq. 17.

D. Reliability-based GDE

In this work, a β_0-contradiction appears when two object values are derived for a common variable and the contradictory degree of the two object values is greater than a given threshold β_0. A contradiction indicates that at least one of the two derived object values is faulty. In earlier work such as [15], due to lack of information, both derived object values are supposed to be equally faulty. With additional information on certainty

degrees, and with the assistance of reliability-based ATMS, any two object values for a common variable can be distinguished. In effect, given a β_0-contradiction, the real defective fuzzy reasoning components which have caused this contradiction are more likely within the label environments of the less certain object value. Note that there may be more than one defective fuzzy reasoning component for a certain contradiction because there may be multiple environments each supporting the same contradiction. Amongst each label environment of one of the two object values which has caused the contradiction, the fuzzy reasoning component with the smallest certainty degree is intuitively regarded as the most likely to be the real culprit.

In the same way, all the components in each label environment of the special "false" node can be ranked. For this, a ranking value r is attached to every component of each of such label environments. The ranking value of each of those components which are in a label environment of the less certain object value, is set to its certainty degree. The ranking value of any other component in the label environments of the special "false" node is then set to its original certainty degree plus 1. Note that the range of a certainty degree is $[0, 1]$. Thus, the integer part of a ranking value indicates whether the environment that contains the given component entails a more certain object value, whilst the decimal part of the ranking value simply denotes the certainty degree of that component.

Example 3.1: Assume that a contradiction is derived from propositions P_1 and P_2, that the label of P_1 is $\{\{F_1, F_2\}, \{F_3\}\}$, and that the label of P_2 is $\{\{F_4\}\}$. Then the label of the contradiction is $\{\{F_1, F_2, F_4\}, \{F_3, F_4\}\}$ as illustrated in Fig. 3.

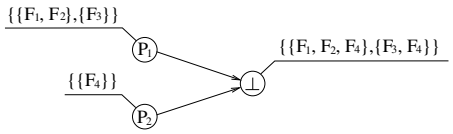

Fig. 3. The contradiction and its dependencies

Suppose that the certainty degrees of F_i, $i \in \{1, 2, 3, 4\}$, are: $c_{F_1} = 0.80$, $c_{F_2} = 0.40$, $c_{F_3} = 0.70$, $c_{F_4} = 0.50$. The certainty degrees of propositions P_1 and P_2 can be calculated with respect to Eq. 17. If the maximum and algebraic product operators are used to implement $\oplus$ and $\otimes$, respectively, then:

$$\begin{aligned} c_{P_1} &= \max\{c_{F_1} \times c_{F_2}, c_{F_3}\} \\ &= \max\{0.80 \times 0.40, 0.70\} \\ &= 0.70. \end{aligned}$$

Similarly, c_{P_2} can be calculated and the result is: $c_{P_2} = 0.50$. For label environment $\{F_1, F_2, F_4\}$ of the "false" node, because $c_{P_1} > c_{P_2}$ and F_4 is an element of the label environment of node P_2, the ranking value of F_4 is set to itself, i.e. $r_{F_4} = 0.50$, and the ranking values of F_1 and F_2 are set to their original certainty degrees plus 1, i.e. $r_{F_1} = 1.80$ and $r_{F_2} = 1.40$. In the same way, the ranking values of components in the label environment $\{F_3, F_4\}$ are set as: $r_{F_3} = 1.70$ and $r_{F_4} = 0.50$.

Without losing generality, suppose that $E_\perp$ is one of the label environments of the "false" node and it is deduced by two contradictory propositions P and P', represented by ATMS nodes N_P and $N_{P'}$ respectively. Then there must exist environments $E = \{F_1, F_2, ..., F_m\}$ and $E' = \{F'_1, F'_2, ..., F'_n\}$ which entail nodes N_P and $N_{P'}$ respectively such that $E \cup E' = E_\perp$. Suppose that the certainty degrees of propositions P and P' are c and c', respectively. Note that c is not necessarily equal to the certainty degree of which the environment E entails node N_P. The same holds for c' and $N_{p'}$. This is because: (1) an object value may be supported by more than one environment (or derived by more than one inference path), and (2) the certainty degree of the object value indicates the overall extent to which this object value may be supported by all its environments (or derived by all possible inference paths). Of course, certain elements in E may be identical to some in E'. In this case, the ranking value of each of those elements will take the less value (i.e. the one with higher priority). The procedure of attaching a ranking value to each element of $E_\perp$ is outlined in Fig. 4.

COMPONENTRANKING(E,E',c,c')

```
(1)  E⊥ = E ∪ E'
(2)  foreach F ∈ E⊥
(3)      if (c ≤ c' && F ∈ E)
(4)          r_F = c_F
(5)      else
(6)          if (c ≥ c' && F ∈ E')
(7)              r_F = c_F
(8)          else
(9)              r_F = c_F + 1
```

Fig. 4. The COMPONENTRANKING procedure

Each label environment of the special "false" node entails a contradiction and each candidate is formed by taking one element from each environment of the special "false" node. Therefore, if all the duplications are deliberately kept, all the candidates have the same cardinality which is equal to the number of label environments in the special "false" node. From this, all candidates can be prioritized according to the ranking values of their components. This is achieved by two steps of sorting as outlined in Fig. 5. In this figure, $\mathbb{S}$ is the generated candidate set and each candidate C is itself a set of fuzzy reasoning components. SORT(C) can be any standard sorting procedure, which sorts the fuzzy reasoning components in a given candidate C in an ascending order with respect to their ranking values. STABLESORT($\mathbb{S}, i$) is any stable sorting algorithm which ranks all the candidates in the candidate set $\mathbb{S}$ in an ascending order by the ranking value of the ith reasoning component. Since each candidate is a set of components, any duplication needs to be removed. Also, in order to generate only a minimal candidate set, all those candidates which are a superset of one other candidate are removed. Of course, such removals do not affect the overall ranking of the remaining candidates.

Example 3.2: Continue Ex. 3.1. Suppose that the contradiction in question is the only one in the system. Therefore,

TABLE I
THE CANDIDATES SORTING PROGRESS

Candidates with duplications	Every candidate sorted	Stable-sorted (2nd elements)	Stable-sorted (1st elements)
$C_1 = [(F_1, 1.80), (F_3, 1.70)]$	$C_1 = [(F_3, 1.70), (F_1, 1.80)]$	$C_6 = [(F_4, 0.50), (F_4, 0.50)]$	$C_6 = [(F_4, 0.50), (F_4, 0.50)]$
$C_2 = [(F_1, 1.80), (F_4, 0.50)]$	$C_2 = [(F_4, 0.50), (F_1, 1.80)]$	$C_4 = [(F_4, 0.50), (F_2, 1.40)]$	$C_4 = [(F_4, 0.50), (F_2, 1.40)]$
$C_3 = [(F_2, 1.40), (F_3, 1.70)]$	$C_3 = [(F_2, 1.40), (F_3, 1.70)]$	$C_3 = [(F_2, 1.40), (F_3, 1.70)]$	$C_5 = [(F_4, 0.50), (F_3, 1.70)]$
$C_4 = [(F_2, 1.40), (F_4, 0.50)]$	$C_4 = [(F_4, 0.50), (F_2, 1.40)]$	$C_5 = [(F_4, 0.50), (F_3, 1.70)]$	$C_2 = [(F_4, 0.50), (F_1, 1.80)]$
$C_5 = [(F_4, 0.50), (F_3, 1.70)]$	$C_5 = [(F_4, 0.50), (F_3, 1.70)]$	$C_1 = [(F_3, 1.70), (F_1, 1.80)]$	$C_3 = [(F_2, 1.40), (F_3, 1.70)]$
$C_6 = [(F_4, 0.50), (F_4, 0.50)]$	$C_6 = [(F_4, 0.50), (F_4, 0.50)]$	$C_2 = [(F_4, 0.50), (F_1, 1.80)]$	$C_1 = [(F_3, 1.70), (F_1, 1.80)]$

CANDIDATESORTING($\mathbb{S}$)

(1) **foreach** $C \in \mathbb{S}$
(2) SORT (C)
(3) **foreach** $i = |C| : 1$
(4) STABLESORT$(\mathbb{S}, i)$

Fig. 5. The CANDIDATESORTING procedure

the label of this contradiction is the same as that of the special "false" node. By deliberately keeping all the duplications, six candidates are generated as illustrated in the first column of Tab. I. The second column of this table is the result of sorting all the components of each candidate. Because the cardinality of these candidates are 2, the stable sorting subroutine will be invoked twice. The third column is the result of the first calling which is carried out by comparing the second elements of these candidates. The last column is the result of the second calling (and also the final result) achieved by comparing the first elements of all the candidates based on the previous sorting result. After removing all element duplications in each candidate and all the candidate duplications, there are three candidates remaining, which (in ascending order of priority) are: $C_6 = [(F_4, 0.50)]$, $C_3 = [(F_2, 1.40), (F_3, 1.70)]$, $C_1 = [(F_3, 1.70), (F_1, 1.80)]$.

Having generated the set of prioritized candidates, the next step is to correct a single candidate in order to remove all the contradictions and thus restore system consistency. By the ranking procedure, the higher priority a candidate has, the more likely the candidate is to be the real culprit. Therefore, the tentative modification always starts from the candidate with the highest priority. If the tentative modification succeeds, the algorithm terminates. Otherwise, the candidate will be removed from the candidate set and the candidate with the next highest priority in the current set will be tried, and so on.

IV. AN ILLUSTRATIVE EXAMPLE

To illustrate the potential of this extended adaptive approach, the problem given in [15] is reconsidered. The rule base is given as follows:
R_1: If x_1 is A_{11}, then x_2 is A_{21};
R_2: If x_1 is A_{12}, then x_2 is A_{22};
R_3: If x_2 is A_{23}, then x_3 is A_{31};
R_4: If x_2 is A_{24}, then x_3 is A_{32};
R_5: If x_2 is A_{25}, then x_4 is A_{41};
R_6: If x_2 is A_{26}, then x_4 is A_{42};
R_7: If x_3 is A_{33}, then x_5 is A_{51};
R_8: If x_3 is A_{34}, then x_5 is A_{52};
R_9: If x_4 is A_{43}, then x_5 is A_{53};
R_{10}: If x_4 is A_{44}, then x_5 isA_{54}.

Given $\beta_0 = 0.5$ and three observations, $x_1 = A_{13} = (7.0, 8.0, 9.0)$, $x_1 = A_{14} = (7.6, 8.6, 9.6)$ and $x_4 = A_{45} = (12.0, 13.0, 14.0)$, the interpolation procedures are illustrated in Fig. 6 and the original observations as well as interpolated results by scale and move transformation-based interpolation are presented in Fig. 7. Note that in this example, to keep the illustration simple, it has been assumed that the variable x, takes two different object values A_{13} and A_{14}. In practice, this may be caused by the fact that the observations are taken by different agents or that one is a real observation and the other may be produced by other inference mechanism.

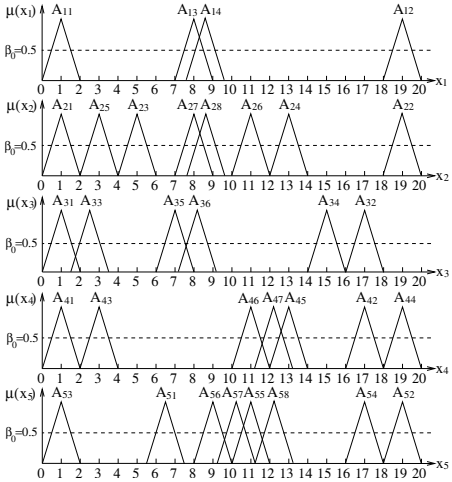

Fig. 7. Fuzzy sets used in the example

A. Certainty degree calculation for reasoning components

The certainty degree of each fuzzy reasoning component can be calculated by applying the approach obtained in Eq. 11. In particular, the distance between two fuzzy sets in this example is defined as the distance between their representative values. For instance, the certainty degree of fuzzy reasoning component R_1R_2 is calculated as follows:

$$\begin{aligned} c_{R_1R_2} &= 1 - \left| \frac{d(A_{11}, A_{12})}{max_1 - min_1} - \frac{d(A_{21}, A_{22})}{max_2 - min_2} \right| \\ &= 1 - \left| \frac{\mathrm{Rep}(A_{12}) - \mathrm{Rep}(A_{11})}{max_1 - min_1} - \frac{\mathrm{Rep}(A_{22}) - \mathrm{Rep}(A_{21})}{max_2 - min_2} \right| \\ &= 1 - \left| \frac{19-1}{20-0} - \frac{19-1}{20-0} \right| \\ &= 1.00, \end{aligned}$$

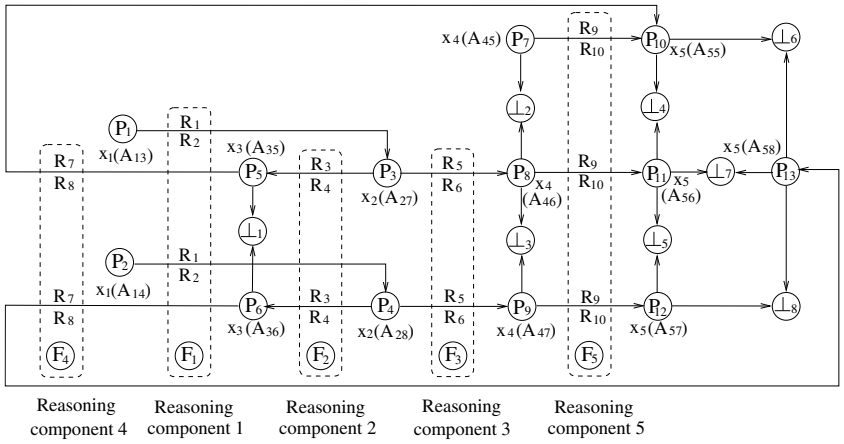

Fig. 6. Discrepancy records in ATMS

where $\mathrm{Rep}(A_{ij})$ denotes the representative value of fuzzy set A_{ij}, $i, j = 1, 2$. Similarly, the certainty degrees of all other fuzzy reasoning components can be calculated. The detailed calculation process is omitted here, but the results are: $c_{R_3R_4} = 0.60$, $c_{R_5R_6} = 0.60$, $c_{R_7R_8} = 1.00$, $c_{R_9R_{10}} = 1.00$.

B. Dependency recording by ATMS

In Fig. 6, an arrowed line which is flanked by two rules R_i and R_{i+1} represents a fuzzy reasoning component, which is denoted as R_iR_{i+1}, $i \in \{1, 3, 5, 7, 9\}$, where R_i and R_{i+1} are the neighboring rules used for interpolation. ATMS nodes and contradictions are represented by circles. Particularly, each F_j, $j \in \{1, 2, ..., 5\}$, is a node denoting a fuzzy reasoning component; each of P_k, $k \in \{1, 2, ..., 13\}$, is a node denoting a proposition; and each $\perp_l$, $l \in \{1, 2, ..., 8\}$, denotes a β_0-contradiction. These ATMS nodes and contradictions are listed as follows, with all justifications omitted:

$F_1 : \langle R_1R_2, 1.00, \{\{R_1R_2\}\}\rangle$;
$F_2 : \langle R_3R_4, 0.60, \{\{R_3R_4\}\}\rangle$;
$F_3 : \langle R_5R_6, 0.60, \{\{R_5R_6\}\}\rangle$;
$F_4 : \langle R_7R_8, 1.00, \{\{R_7R_8\}\}\rangle$;
$F_5 : \langle R_9R_{10}, 1.00, \{\{R_9R_{10}\}\}\rangle$;
$P_1 : \langle x_1 = A_{13}, 1.00, \{\{\}\}\rangle$;
$P_2 : \langle x_1 = A_{14}, 1.00, \{\{\}\}\rangle$;
$P_3 : \langle x_2 = A_{27}, 1.00, \{\{R_1R_2\}\}\rangle$;
$P_4 : \langle x_2 = A_{28}, 1.00, \{\{R_1R_2\}\}\rangle$;
$P_5 : \langle x_3 = A_{35}, 0.60, \{\{R_1R_2, R_3R_4\}\}\rangle$;
$P_6 : \langle x_3 = A_{36}, 0.60, \{\{R_1R_2, R_3R_4\}\}\rangle$;
$P_7 : \langle x_4 = A_{45}, 1.00, \{\{\}\}\rangle$;
$P_8 : \langle x_4 = A_{46}, 0.60, \{\{R_1R_2, R_5R_6\}\}\rangle$;
$P_9 : \langle x_4 = A_{47}, 0.60, \{\{R_1R_2, R_5R_6\}\}\rangle$;
$P_{10} : \langle x_5 = A_{55}, 1.00, \{\{R_1R_2, R_3R_4, R_7R_8\}, \{R_9R_{10}\}\}\rangle$;
$P_{11} : \langle x_5 = A_{56}, 0.60, \{\{R_1R_2, R_5R_6, R_9R_{10}\}\}\rangle$;
$P_{12} : \langle x_5 = A_{57}, 0.60, \{\{R_1R_2, R_5R_6, R_9R_{10}\}\}\rangle$;
$P_{13} : \langle x_5 = A_{58}, 0.60, \{\{R_1R_2, R_3R_4, R_7R_8\}\}\rangle$;
$\perp_1 : \langle \perp, \{\{R_1R_2, R_3R_4\}\}\rangle$;
$\perp_2 : \langle \perp, \{\{R_1R_2, R_5R_6\}\}\rangle$;
$\perp_3 : \langle \perp, \{\{R_1R_2, R_5R_6\}\}\rangle$;
$\perp_4 : \langle \perp, \{\{R_1R_2, R_5R_6, R_9R_{10}\}\}\rangle$;
$\perp_5 : \langle \perp, \{\{R_1R_2, R_5R_6, R_9R_{10}\}\}\rangle$;
$\perp_6 : \langle \perp, \{\{R_1R_2, R_3R_4, R_7R_8\}\}\rangle$;
$\perp_7 : \langle \perp, \{\{R_1R_2, R_3R_4, R_5R_6, R_7R_8, R_9R_{10}\}\}\rangle$;
$\perp_8 : \langle \perp, \{\{R_1R_2, R_3R_4, R_5R_6, R_7R_8, R_9R_{10}\}\}\rangle$.

Note that a certainty degree is attached to each fuzzy reasoning component and proposition, which is calculated and then recorded within the ATMS network, except the certainty degrees of any contradictions which are irrelevant to the present work and hence omitted. Also, as stated previously, the certainty degree of each observation is assumed to be 1 in this research. The certainty degree of any derived node can be calculated by Eq. 17. Within this illustrative example, maximum and algebraic product are used to implement $\oplus$ and $\otimes$ of Eq. 17, respectively. For example, the certainty degree of proposition P_{10} is computed by:

$$\begin{aligned} c_{P_{10}} &= \max\{c_{R_1R_2} \times c_{R_3R_4} \times c_{R_7R_8}, c_{R_9R_{10}}\} \\ &= \max\{1.00 \times 0.60 \times 1.00, 1.00\} \\ &= 1.00. \end{aligned}$$

A specific ATMS node "false", denoted by $P_\perp$, which collectively represents all the contradictions listed above from $\perp_1$ to $\perp_8$, is given as follows:

$P_\perp : \langle \perp, \{\{R_1R_2, R_3R_4\}, \{R_1R_2, R_5R_6\}\}\rangle$.

C. Candidate generation and prioritization

It is recorded in the ATMS that the label environment $\{R_1R_2, R_3R_4\}$ entails contradiction $\perp_1$, which is derived from propositions P_5 and P_6, while P_5 and P_6 are inferred through the same path. A ranking value is computed and attached to each component of this label using the procedure of Fig. 4. Similarly, each component in label environment $\{R_1R_2, R_5R_6\}$ is also attached by a ranking value by the same approach. The result is given as follows:

$\{(R_1R_2, 1.00), (R_3R_4, 0.60)\}$;
$\{(R_1R_2, 1.00), (R_5R_6, 0.60)\}$.

From this, by deliberately keeping all the duplications, four component candidates are generated as follows:

$$C_1 = [(R_1R_2, 1.00), (R_1R_2, 1.00)];$$
$$C_2 = [(R_1R_2, 1.00), (R_5R_6, 0.60)];$$
$$C_3 = [(R_1R_2, 1.00), (R_3R_4, 0.60)];$$
$$C_4 = [(R_3R_4, 0.60), (R_5R_6, 0.60)].$$

Because these four candidates have the same cardinality size, they can be prioritized following the algorithm of Fig. 4. The prioritized result is: C_4, C_2, C_3, C_1, in a descending order. After removing the duplicate candidate component R_1R_2 in component C_1, and then removing supersets C_2 and C_3 (of C_1), the final minimal candidate set consists of two candidates C_1' and C_4':

$$C_1' = [(R_1R_2, 1.00)];$$
$$C_4' = [(R_3R_4, 0.60), (R_5R_6, 0.60)],$$

where C_4' is of a higher priority.

D. Candidate modification

The candidate with the highest priority, i.e. candidate C_4' in this example, needs to be modified first according to the consistency restoring algorithm given in Fig. 2. Following the modification procedure for single candidates as outlined in Sec. II, a set of simultaneous equations and inequations can be calculated. One of the solutions resulting from solving these equations and inequations simultaneously is illustrated in Fig. 8. It is clear from this figure that there is no β_0-contradiction any more and thus consistency has been restored. This means that the original inconsistent interpolation process has been corrected with consistent interpolated results throughout. Note that the other candidate, C_1' cannot lead to any consistent solution although it has a smaller cardinality size, which shows the potential of the proposed work.

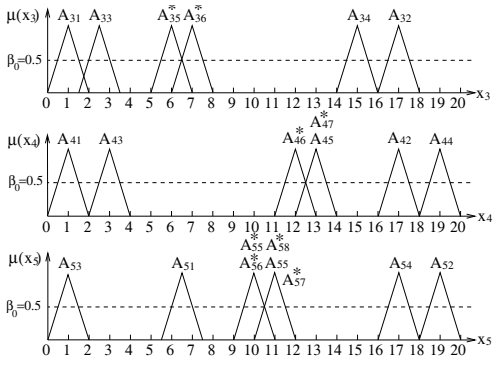

Fig. 8. The solution of the example

V. Conclusions

This paper has extended the recent work on adaptive fuzzy interpolation. It has introduced the concept of the certainty degree of a fuzzy reasoning component and that of the certainty degree of a derived proposition. From this, the classical ATMS has been extended not only to record the dependencies of a node but also to record to what degree the node can be derived from their supporting environments. This is followed by a modified GDE, which is able to prioritize all the generated minimal candidates by exploiting certainty degrees. The actual modification procedure, the same as the one described in [15], takes place, carrying out tentative modification to each minimal candidate of the highest priority until a solution is found. Whilst the working of this method has been illustrated with a practically significant example, real-world applications remain as further work.

Other improvements may enhance the potential of the proposed approach. Currently, the extended approach is only applicable to fuzzy interpolation with two single antecedent rules. It is worthwhile to generalize the approach for fuzzy interpolation with multiple antecedent rules and fuzzy extrapolation. Also, all the rules given in the initial rule base are assumed to be true and fixed. However, this may not be the case in certain real-world situations, despite that it is a common assumption made in the literature of interpolative reasoning. Thus, it is interesting to consider extending the proposed work to allow rules in the given rule base to become themselves diagnosable and modifiable. The initial investigation into such issue has been reported in [16].

References

[1] P. Baranyi, L. T. Kóczy, and T. D. Gedeon, "A generalized concept for fuzzy rule interpolation," *IEEE T. Fuzzy Syst.*, vol. 12, no. 6, pp. 820–837, 2004.

[2] Y.-C. Chang, S.-M. Chen, and C.-J. Liau, "Fuzzy interpolative reasoning for sparse fuzzy-rule-based systems based on the areas of fuzzy sets," *IEEE T. Fuzzy Syst.*, vol. 16, no. 5, pp. 1285–1301, Oct. 2008.

[3] S.-M. Chen, Y.-K. Ko, Y.-C. Chang, and J.-S. Pan, "Weighted fuzzy interpolative reasoning based on weighted increment transformation and weighted ratio transformation techniques," *IEEE T. Fuzzy Syst.*, vol. 17, no. 6, pp. 1412 –1427, 2009.

[4] S.-M. Chen and Y.-K. Ko, "Fuzzy interpolative reasoning for sparse fuzzy rule-based systems based on α-cuts and transformations techniques," *IEEE T. Fuzzy Syst.*, vol. 16, no. 6, pp. 1626–1648, Dec. 2008.

[5] J. de Kleer, "An assumption-based TMS," *Artif. Intell.*, vol. 28, no. 2, pp. 127–162, 1986.

[6] J. de Kleer and B. C. Williams, "Diagnosing multiple faults," *Artif. Intell.*, vol. 32, no. 1, pp. 97–130, 1987.

[7] Z. Huang and Q. Shen, "Fuzzy interpolative reasoning via scale and move transformations," *IEEE T. Fuzzy Syst.*, vol. 14, no. 2, pp. 340–359, 2006.

[8] ——, "Fuzzy interpolation and extrapolation: a practical approach," *IEEE T. Fuzzy Syst.*, vol. 16, no. 1, pp. 13–28, 2008.

[9] L. T. Kóczy and K. Hirota, "Approximate reasoning by linear rule interpolation and general approximation," *Int. J. Approx. Reason.*, vol. 9, no. 3, pp. 197–225, 1993.

[10] ——, "Size reduction by interpolation in fuzzy rule bases," *IEEE T. Syst., Man Cybern.*, vol. 27, no. 1, pp. 14–25, 1997.

[11] D. Tikk and P. Baranyi, "Comprehensive analysis of a new fuzzy rule interpolation method," *IEEE T. Fuzzy Syst.*, vol. 8, no. 3, pp. 281–296, Jun 2000.

[12] K. W. Wong, D. Tikk, T. Gedeon, and L. Kóczy, "Fuzzy rule interpolation for multidimensional input spaces with applications: a case study," *IEEE T. Fuzzy Syst.*, vol. 13, no. 6, pp. 809–819, Dec. 2005.

[13] Y. Yam and L. Kóczy, "Representing membership functions as points in high-dimensional spaces for fuzzy interpolation and extrapolation," *IEEE T. Fuzzy Syst.*, vol. 8, no. 6, pp. 761–772, Dec 2000.

[14] Y. Yam, M. L. Wong, and P. Baranyi, "Interpolation with function space representation of membership functions," *IEEE T. Fuzzy Syst.*, vol. 14, no. 3, pp. 398–411, June 2006.

[15] L. Yang and Q. Shen, "Towards adaptive interpolative reasoning," in *Proc. IEEE Int. Conf. Fuzzy Syst.*, 2009, pp. 542–549.

[16] ——, "Adaptive fuzzy interpolaion with uncertain observations and rule base," in *Proc. IEEE Int. Conf. Fuzzy Syst.*, 2011.

2011 IEEE International Conference on Fuzzy Systems
June 27-30, 2011, Taipei, Taiwan

Fuzzy Rule Interpolation in Embedded Behaviour-based Control

Szilveszter Kovács
Department of Information Technology
University of Miskolc
Miskolc, Hungary
szkovacs@iit.uni-miskolc.hu

Abstract— **Fuzzy Rule Interpolation (FRI) methods are efficient structures for knowledge representation with relatively few rules. In spite of the good knowledge representation efficiency, the usually high computational demand turns the FRI methods hardly suitable for embedded real-time applications, where the short reasoning time has a high importance. On the other hand the fact of increasing computational power of nowadays available devices gives an opportunity to the FRI methods for appearance in real-time embedded applications. The goal of this paper is to introduce the benefit of adapting low computational and resource demanded FRI methods in embedded behavior-based control applications.**

Keywords - fuzzy rule interpolation (FRI); low computational demand FRI; fuzzy automata; behavior-based control.

I. INTRODUCTION

The idea of behavior-based control is in a great extent originated from the existence of descriptive verbal models based on numerous observations of living creature's reactions in different situations. Many of them are built around a predefined sequence of environmental situations and events, where the reactions are in details noted and evaluated. The knowledge representation this case is a series of observations of various facts and action-reaction rules. For mathematical modeling of such a system, the rule-based knowledge representation is straightforward. Moreover the need of following observed sequences requires a model structure of a state machine or an automaton. Adding the fact, that the observable or hidden states are continuous measures, the situation is quite complicated. Summarizing the above requirements, the model has to have a rule-based knowledge representation, and the ability of describing event sequences of continuous values and continuous states. The suggested modeling method is the adaptation of the fuzzy automaton, where the state is a vector of membership values, the state-transitions are controlled by a fuzzy rule-base and the observations and conclusions are continuous values. The main problem in case of practical implementation of such a fuzzy automaton based model is the size of the state-transition rule base. In classical fuzzy reasoning the rule base size is exponential with the number of observations, in this case with the length of the state vector. In case of a behavior-based control model of moderate complexity it could be 10-20 state variables i.e. thousands of rules required for the complete classical rule base (e.g. the Zadeh-Mamdani-Larsen Compositional Rule of Inference (CRI) (Zadeh [1]) (Mamdani [2]) (Larsen [3]) or the Takagi-Sugeno fuzzy inference (Sugeno [4], Takagi-Sugeno [5]).

Moreover, having a verbal model, the existing knowledge is usually a few dozen verbal rules, which means, that most of the rules are undefined. In case of classical fuzzy reasoning this contradiction is hardly solvable.

The solution suggested in this paper for the exponential complexity problem of the required fuzzy automation state-transition rule base is the application of the Fuzzy Rule Interpolation (FRI) methods (one of the first methods was introduced in [6]). By the application of FRI methods the number of the rules required for the FRI state-transition fuzzy model can be reduced to the existing (known from the verbal model) rules. Moreover in case of automatic model generation or fine tuning based on given input-output sample data, the application of the FRI model can also lead to fewer rules and hence less parameters, which means better convergence of the optimization algorithm.

The behavior-based model implementation introduced in this paper is built upon the framework of fuzzy automaton and low computational demand Fuzzy Rule Interpolation (FRI) [7], [8], [9], and [10]. The knowledge representation style of FRI method fits well the conceptually "spare rule-based" structure of the descriptive verbal models, where the "completeness" of the rule-base is essentially not required. FRI methods can provide reasonable (interpolated) conclusions even if none of the existing rules fires under the current observation. From the beginning of 1990s numerous FRI methods have been proposed [11].

II. FUZZY RULE INTERPOLATION (FRI)

Traditional fuzzy rule based systems (e.g. the Zadeh-Mamdani-Larsen CRI ([1], [2], [3]) or the Takagi-Sugeno fuzzy inference ([4], [5]) requires a complete rule base with all of the possible rules set, even though lots of these rules are unimportant from the viewpoint of the actual application. A fuzzy rule base is called sparse or incomplete if an observation may exists, which does not hit any of the rules in the rule base. Accordingly there can be observations, where no conclusion can be gained with traditional fuzzy reasoning techniques. On

978-1-4244-7316-8/11/$26.00 ©2011 IEEE

the other hand, in many embedded control application areas having no conclusion is an avoidable situation. One real solution for the sparse rule base is the application of fuzzy rule interpolation (FRI) methods. This case the derivable rules are intentionally missing from the rule base, as FRI methods are capable of providing reasonable (interpolated) conclusions even if none of the existing rules fire under the current observation. The FRI rule base could contain the most significant fuzzy rules alone without risking the chance of having no conclusion for some of the observations. In this case having an efficient knowledge representation, a considerable amount of unnecessary work can be avoided during the rule base creation. On the other hand most of the FRI methods are sharing the burden of high computational demand, e.g. the task of searching for the two closest surrounding rules to the observation, and calculating the conclusion at least in some characteristic α-cuts. Moreover in some methods the interpretability of the fuzzy conclusion gained is also not straightforward [12]. There have been a lot of efforts to rectify the interpretability of the interpolated fuzzy conclusion [13]. In [14] Baranyi *et al.* give a comprehensive overview of the recent existing FRI methods. Beyond these problems, some of the FRI methods are originally defined for one dimensional input space, and need special extension for the multidimensional case (e.g. [15], [16]). In [11] Wong *et al.* gave a comparative overview of the multidimensional input space capable FRI methods. In [15] Jenei introduced a way for axiomatic treatment of the FRI methods. In [17] Johanyák introduces an automatic way for sparse fuzzy model identification from sample data. The high computational demand, mainly the search for the two closest surrounding rules to an arbitrary observation in the multidimensional antecedent space makes many of these methods hardly suitable for real-time applications. Some FRI methods, (e.g. the method introduced by Jenei *et al.* in [16], or FRIPOC [18]), eliminate the search for the two closest surrounding rules by taking all the rules into consideration, hence speeding up the reasoning process. On the other hand, keeping the goal of constructing fuzzy conclusion, and not simply speeding up the reasoning process, they still require some additional (or repeated) computational steps for the elements of the level set (or at least some relevant α levels). An application oriented aspect of the FRI, the low computational and resource demand is emerging in the concept of 'FIVE' (Fuzzy Interpolation based on Vague Environment). In the followings some details of this method will be briefly introduced.

III. FRI BASED ON VAGUE ENVIRONMENT: FIVE

In the concept of 'FIVE' an application oriented aspect, the need for low computational and resource demand has a high importance. The method was originally introduced in [7], [8], [9], and extended in [10] for satisfying the speed requirements of direct fuzzy control, where the conclusions of the fuzzy controller are applied directly as control actions in a real-time system.

The main idea of FIVE is based on the fact that most of the control applications serves crisp observations and requires crisp conclusions from the controller. Adopting the concept of the Vague Environment (VE) [19], FIVE can handle the antecedent and consequent fuzzy partitions of the fuzzy rule base by scaling functions [19] and therefore turn the fuzzy interpolation to crisp interpolation. The idea of a VE is based on the indistinguishability of elements. In VE the fuzzy membership function $\mu_A(x)$ is indicating level of similarity of x to a specific element a which is a representative or prototypical element of the fuzzy set $\mu_A(x)$, or, equivalently, as the degree to which x is indistinguishable from a (see e.g. on Figure 1) [19]. Two values in a VE are ε-indistinguishable if their distance is less or equal than ε. The distances in a VE are weighted distances (1). The weighting factor or function is called scaling function (factor) [19]:

$$\delta_s(a,b)=\left|\int_a^b s(x)dx\right|\le\varepsilon\ , \tag{1}$$

where $\delta_s(a,b)$ is the scaled distance of the values a, b and $s(x)$ is the scaling function on X.

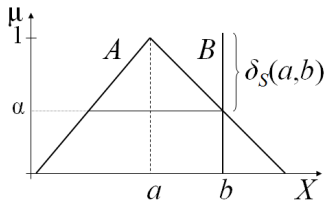

Figure 1. The α-cuts of $\mu_A(x)$ contain the elements that are (1−α)-indistinguishable from a.

If the VE of a fuzzy partition (the scaling function or at least the approximate scaling function [7], [8], [9]) exists, the member sets of the fuzzy partition can be characterized by points in that VE (see e.g. exact scaling function s on Figure 2 and an approximate scaling function on Figure 3).

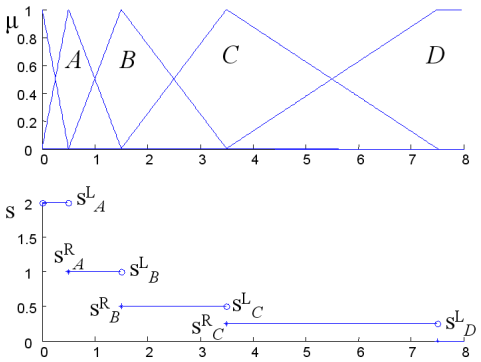

Figure 2. A Ruspini fuzzy (A, B, C, D) partition and its scaling function s.

Having the VE concept and the scaling function based similarity calculation, any crisp interpolation, extrapolation, or regression method can be adapted very simply for FRI [7], [8], [9]. Because of its simple multidimensional applicability, in FIVE the Shepard operator based interpolation (first introduced in [20]) is adapted (see e.g. Figure 4).

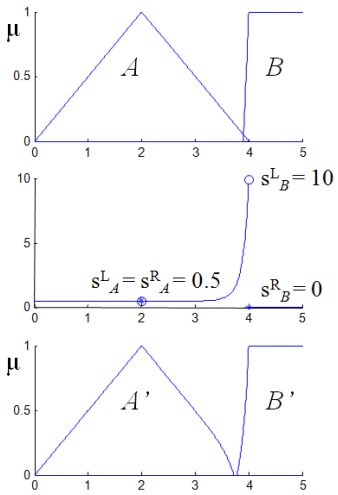

Figure 3. A fuzzy partition (A, B), its approximate scaling function s [7], [8] and the corresponding approximated partition (A', B').

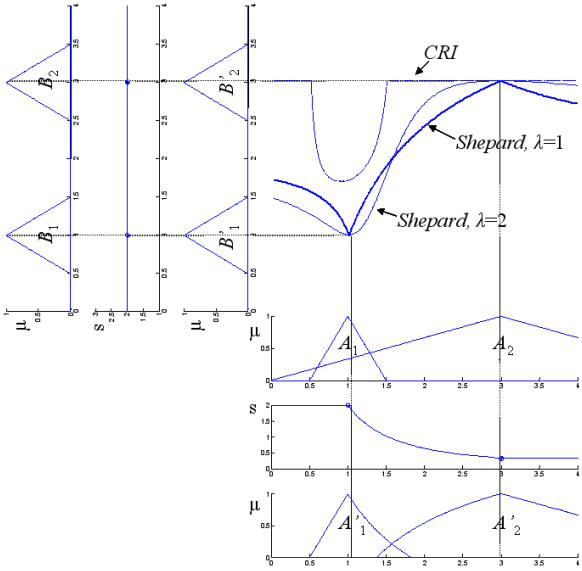

Figure 4. Interpolation of two fuzzy rules (R_i: $A_i \rightarrow B_i$), by the Shepard operator based FIVE (3), and for comparison the min-max CRI with centre of gravity defuzzification.

In case of singleton rule consequents (c_k) the fuzzy rules R_k has the following form:

$$\textbf{If } x_1 = A_{k,1} \textbf{ And } x_2 = A_{k,2} \textbf{ And } \ldots \textbf{ And } x_m = A_{k,m} \textbf{ Then } y = c_k \qquad (2)$$

Adapting the VE concept and the scaling function based similarity calculation to the Shepard operator based interpolation, the conclusion of the interpolative fuzzy reasoning can be obtained as:

$$y(\mathbf{x}) = \begin{cases} c_k & \text{if } \mathbf{x} = \mathbf{a}_k \text{ for some } k, \\ \left(\sum_{k=1}^{r} c_k / \delta_{s,k}^{\lambda}\right) \Big/ \left(\sum_{k=1}^{r} 1/\delta_{s,k}^{\lambda}\right) & \text{otherwise.} \end{cases} \qquad (3)$$

where $\delta_{s,k}$ are scaled distances:

$$\delta_{s,k} = \delta_s(\mathbf{a}_k, \mathbf{x}) = \left[\sum_{i=1}^{m}\left(\int_{a_{k,i}}^{x_i} s_{X_i}(x_i)dx_i\right)^2\right]^{1/2}, \qquad (4)$$

and s_{X_i} is the i^{th} scaling function of the m dimensional antecedent universe, $\mathbf{x}$ is the m dimensional crisp observation and $\mathbf{a}_k$ are the cores of the m dimensional fuzzy rule antecedents $\boldsymbol{A}_k$.

The code of the FIVE FRI together with other FRI methods is freely available as a MATLAB FRI Toolbox [21], and it can be downloaded from [22] and [23].

IV. FRI BASED FUZZY AUTOMATON

There are numerous versions and understanding of the fuzzy automaton can be found in the literature (a good overview van be found in [24]). In our case we start from the most common definition of Fuzzy Finite-state Automaton (FFA, summarized in [24]), where the FFA is defined by a tuple (according to [24], [25] and [26]):

$$\widetilde{F} = (Q, \Sigma, \delta, R, Z, \omega), \qquad (5)$$

where

Q is a finite set of states, $Q=\{q_1,q_2,...,q_n\}$.

Σ is a finite set of input symbols, $\Sigma=\{a_1,a_2,...,a_m\}$.

$R \in Q$ is the (possibly fuzzy) start state of $\widetilde{F}$.

Z is a finite set of output symbols, $Z=\{b_1,b_2,...,b_n\}$.

$\delta : Q \times \Sigma \times Q \rightarrow [0,1]$ is the fuzzy transition function which is used to map a state (current state) into another state (next state) upon an input symbol, attributing a value in the fuzzy interval [0,1] to the next state.

$\omega : Q \rightarrow Z$ is the output function which is used to map a (fuzzy) state to the output.

Extending the concept of FFA from finite set of input symbols to finite dimensional input values turns to the following:

$$\widetilde{F} = (S, X, \delta, P, Y, \omega), \qquad (6)$$

where

S is a finite set of fuzzy states, $S = \{\mu_{s1}, \mu_{s2}, ..., \mu_{sn}\}$.

X is a finite dimensional input vector, $X = \{x_1, x_2, ..., x_m\}$.

$P \in S$ is the fuzzy start state of $\widetilde{F}$.

Y is a finite dimensional output vector, $Y = \{y_1, y_2, ..., y_l\}$.

$\delta : S \times X \to S$ is the fuzzy state-transition function which is used to map the current fuzzy state into the next fuzzy state upon an input value.

$\omega : S \times X \to Y$ is the output function which is used to map the fuzzy state and input to the output value. See e.g. on Figure 5.

In case of fuzzy rule based representation of the state-transition function $\delta : S \times X \to S$, the rules have $n+m$ dimensional antecedent space, and n dimensional consequent space. Applying classical fuzzy reasoning methods, the complete state-transition rule base size can be approximated by the following formula:

$$|R| = n \cdot i^n \cdot j^m, \tag{7}$$

where n is the length of the fuzzy state vector S, m is the input dimension, i is the number of the term sets in each dimensions of the state vector, and j is the number of the term sets in each dimensions of the input vector.

According to (7) the state-transition rule-base size is exponential with the length of the fuzzy state vector and the number of the input dimensions.

Applying FRI methods for the state-transition function fuzzy model can dramatically reduce the rule base size. See e.g. [27], where the originally exponential sized state-transition rule base of a simple heuristic model turned to be polynomial thanks to the FRI.

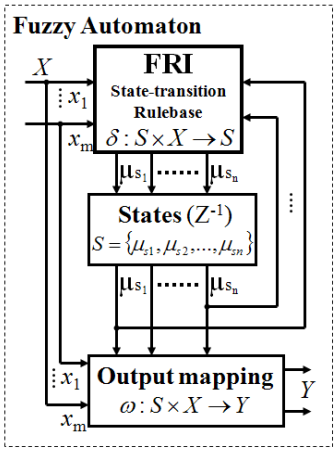

Figure 5. FRI based Fuzzy Automaton.

V. Behaviour-based Control

In behaviour-based control systems (a good overview can be found in [28]), the actual behaviour of the system is formed as one of the existing component behaviours (which fits best the actual situation), or a kind of fusion of the component behaviours appeared to be the most appropriate to handle the actual situation. Beyond the construction of the component behaviors, this structure has two main tasks. The first is the behavior coordination, the decision, which component behavior is needed, or in cases of behavior fusion the determination of the weights for each component behaviors in solving the actual situation. The second is the way of the behavior fusion.

In case of direct application of the suggested FRI based Fuzzy Automaton for behaviour-based control structures, the output function $\omega : S \times X \to Y$ can be decomposed to parallel component behaviors and independent behavior fusion. This case we can get a very similar structure as it is expected in behaviour-based control (see Figure 6).

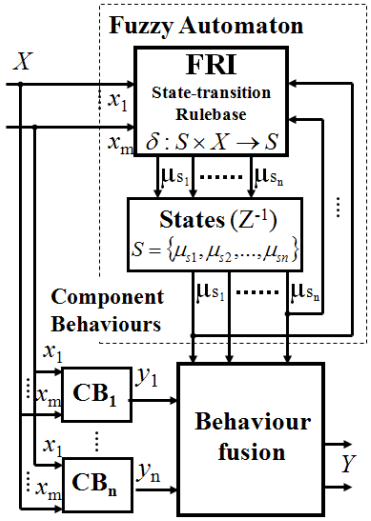

Figure 6. The suggested FRI behaviour-based structure.

VI. Navigation Example

The application example of the proposed structure is a simulated steering control of an automated guided vehicle (AGV) already introduce more detailed in [29], [30].

The reason of the application example in this paper is a demonstration for the simple state-transition FRI rule base creation concept, not for competing in collision avoidance performance with other solutions.

In the example application the steering control has two main goals, the path tracking (to follow a guide path) and the collision avoidance. The simulated AGV is first trying to follow a guide path with minimal path tracking error, and in the case if it is impossible (because of the obstacles) leave it, and as the collision situation is avoided try to find the guide path and follow it again (see Figure 8).

In the collision avoidance strategies, two different collision situations, the frontal and the side collision are distinguished. Having the preconditions of motionless obstacles, it is sufficient to have three ultrasonic distance sensors (on the front of the AGV, one in the middle (U_M) and one-one on both sides (U_L, U_R) (see Figure 7)) to approximate both the collision conditions [30].

In the example, there are four different component behaviours:

Path tracking and restricted collision avoidance strategy: The main goal of this strategy is following the guide path and

as a sub goal, avoiding obstacles if it is possible without risking the chance of losing the guide path [30].

The collision avoidance strategy: A simple collision avoidance steering strategy. Its only goal is to avoid collisions.

The collision avoidance with left/right tendency strategy: The same as the collision avoidance steering strategy, except the left or right turning tendencies in case of no left or right turning difficulties. These strategies are needed to aid finding the path after leaving it.

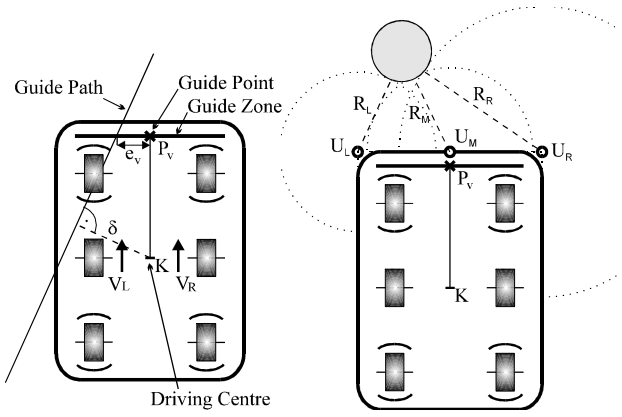

Figure 7. Differential steered AGV with guide zone, e_v is the distance of the guide path and the guide point, P_v is the guide point, K is the driving centre, R_L, R_R, R_M are the distances measured by the left, right and middle ultrasonic sensors (U_L, U_R, U_M).

Having four known component behaviours, the automaton has four state variables (see Figure 6). These are the weight for the path tracking and restricted collision avoidance strategy (S_P), the weight for the collision avoidance strategy (S_C), the weights for the collision avoidance strategy with right tendency (S_{CR}), and for the left tendency (S_{CL}). Having four conclusions, four state-transition rule bases are needed. The $\mathbf{R_{SP}}$ state-transition rule base is determining the next value of the S_P state variable, $\mathbf{R_{SC}}$ is for determining S_C, $\mathbf{R_{SCR}}$ for S_{CR}, and $\mathbf{R_{SCL}}$ for S_{CL}.

The observations of the state-transition rule bases are the distance between the guide path and the driving centre (e_v), the distance measured by the middle ultrasonic sensor ($R_{M)}$ (see Figure 7), the approximated maximal left and right turning angle without side collision (α_{ML}, α_{MR}), the previous state variables (S_P, S_{CR}, S_{CL}), and the availability of path sensing (P_V).

The rules of the state-transition rule bases have the following common form ($R_{Sx,i}$):

If $S_P=A_{1,i}$ **And** $S_{CR}=A_{2,i}$ **And** $S_{CL}=A_{3,i}$ **And** $e_v=A_{4,i}$ **And** $P_V=A_{5,i}$ **And** $R_M=A_{6,i}$ **And** $\alpha_{ML}=A_{7,i}$ **And** $\alpha_{MR}=A_{8,i}$ **Then** $S_x=B_i$.

The state-transition rule bases for the FRI fuzzy automaton are summarized in Tab. 1.

Figure 8 and Figure 9 introduces some results of the simulated application (see more detailed in [30]). The results on Figure 9 shows, that in the tested situation the suggested FRI based Fuzzy Automaton behavior coordination was able to follow the state changes in acceptable level.

TABLE I. STATE-TRANSITION RULE BASES

$\mathbf{R_{SP}}$:

S_P	S_{CR}	S_{CL}	e_v	PV	R_M	α_{ML}	α_{MR}	S_P
			Z	*V*	*L*			*L*
			PL	*V*			*S*	*Z*
			NL	*V*		*S*		*Z*
				NV				*Z*

$\mathbf{R_{SC}}$:

S_P	S_{CR}	S_{CL}	e_v	PV	R_M	α_{ML}	α_{MR}	S_P
				V	*S*			*L*
				V	*L*			*Z*
				NV				*Z*

$\mathbf{R_{SCR}}$:

S_P	S_{CR}	S_{CL}	e_v	PV	R_M	α_{ML}	α_{MR}	S_P
L			*NL*	*V*				*L*
	L			*NV*				*L*
			Z	*V*	*L*			*Z*
		L						*Z*

$\mathbf{R_{SCL}}$:

S_P	S_{CR}	S_{CL}	e_v	PV	R_M	α_{ML}	α_{MR}	S_P
L			*PL*	*V*				*L*
		L		*NV*				*L*
			Z	*V*	*L*			*Z*
	L							*Z*

where the linguistic labels of the antecedent and consequent fuzzy sets are stand for *N*: negative, *P*: positive, *VL*: very large, *L*: large, *S*: small, *Z*: zero, *V*: path valid, *NV*: path not valid.

VII. CONCLUSION

The application of the suggested FRI based Fuzzy Automaton in embedded behavior-based control applications can dramatically simplify the state-transition rule base creation. In case of the simple example of the paper, the $\mathbf{R_{SP}}$ rule base has only 4 rules, while the complete rule base should have at least $5 \cdot 2 \cdot 2 \cdot 2^2 = 80$, $\mathbf{R_{SCR}}$ and $\mathbf{R_{SCL}}$ has 4 rules, while their complete counterpart has at least $2^3 \cdot 5 \cdot 2 \cdot 2 = 160$.

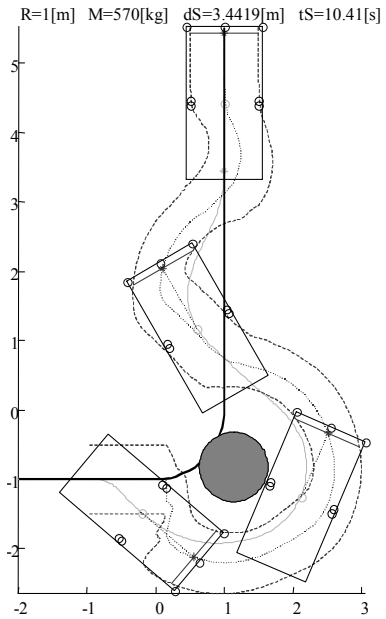

Figure 8. Track of a single run in case of one obstacle.

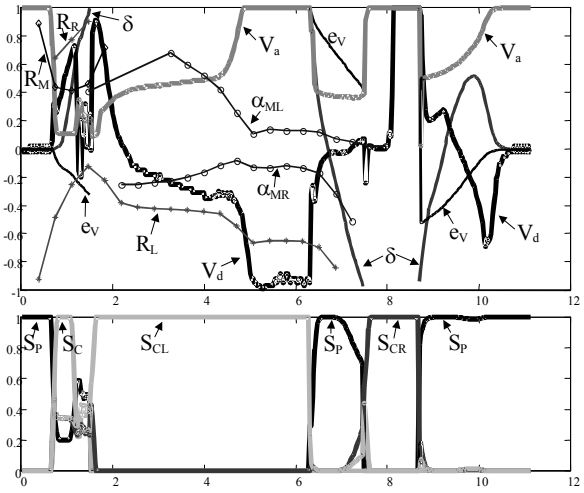

Figure 9. Time function of observations, conclusions and system state values (S_P, S_C, S_{CL}, S_{CR}) related to the track of Figure 8.

ACKNOWLEDGMENT

This research was supported by the Hungarian National Scientific Research Fund grant no: OTKA K77809.

REFERENCES

[1] L. A. Zadeh, "Outline of a new approach to the analysis of complex systems and decision processes", IEEE Trans. on SMC, (3), 1973, pp.28-44.

[2] E. H. Mamdani and S. Assilian, "An experiment in linguistic synthesis with a fuzzy logic controller", Int. J. of Man Machine Studies, (7), 1975, pp.1-13.

[3] P. M. Larsen, "Industrial application of fuzzy logic control", Int. J. of Man Machine Studies, (12) 4, 1980, pp.3-10.

[4] M. Sugeno, "An introductory survey of fuzzy control", Information Science, (36), 1985, pp.59-83.

[5] T. Takagi and M. Sugeno, "Fuzzy identification of systems and its applications to modeling and control", IEEE Trans. on SMC, (15), 1985, pp.116-132.

[6] L. T. Kóczy and K. Hirota, "Rule interpolation by α-level sets in fuzzy approximate reasoning", In J. BUSEFAL, Automne, URA-CNRS. Vol. 46. Toulouse, France, 1991, pp. 115-123.

[7] Sz. Kovács, "New Aspects of Interpolative Reasoning", Proceedings of the 6th. International Conference on Information Processing and Management of Uncertainty in Knowledge-Based Systems, Granada, Spain, 1996, pp. 477-482.

[8] Sz. Kovács, and L.T. Kóczy, "Approximate Fuzzy Reasoning Based on Interpolation in the Vague Environment of the Fuzzy Rule base as a Practical Alternative of the Classical CRI", Proceedings of the 7th International Fuzzy Systems Association World Congress, Prague, Czech Republic, 1997, 144-149.

[9] Sz. Kovács, and L.T. Kóczy, "The use of the concept of vague environment in approximate fuzzy reasoning", Fuzzy Set Theory and Applications, Tatra Mountains Mathematical Publications, Mathematical Institute Slovak Academy of Sciences, Bratislava, Slovak Republic, vol.12, 1997, pp. 169-181.

[10] Sz. Kovács, "Extending the Fuzzy Rule Interpolation "FIVE" by Fuzzy Observation", Advances in Soft Computing, Computational Intelligence, Theory and Applications, Bernd Reusch (Ed.), Springer Germany, ISBN 3-540-34780-1, 2006, pp. 485-497.

[11] K. W. Wong, D. Tikk, T. D. Gedeon, and L. T. Kóczy, "Fuzzy Rule Interpolation for Multidimensional Input Spaces With Applications", IEEE Transactions on Fuzzy Systems, ISSN 1063-6706, Vol. 13, No. 6, December, 2005, pp. 809-819.

[12] L. T. Kóczy and Sz. Kovács, "On the preservation of the convexity and piecewise linearity in linear fuzzy rule interpolation", Tokyo Inst. Technol., Yokohama, Japan, Tech. Rep. TR 93-94/402, LIFE Chair Fuzzy Theory, 1993.

[13] D. Tikk and P. Baranyi, "Comprehensive analysis of a new fuzzy rule interpolation method", In IEEE Trans. Fuzzy Syst., vol. 8, No. 3, June, 2000, pp. 281-296.

[14] P. Baranyi, L. T. Kóczy, and Gedeon, T. D., "A Generalized Concept for Fuzzy Rule Interpolation", IEEE Trans. on Fuzzy Systems, vol. 12, No. 6, 2004, pp. 820-837.

[15] S. Jenei, "Interpolating and extrapolating fuzzy quantities revisited – an axiomatic approach", Soft Comput., vol. 5., 2001, pp. 179-193.

[16] S. Jenei, E. P. Klement and R. Konzel, "Interpolation and extrapolation of fuzzy quantities – The multiple-dimensional case", Soft Comput., vol. 6., 2002, 258-270.

[17] Zs. Cs. Johanyák, "Sparse fuzzy model identification Matlab toolbox - RuleMaker toolbox", Proceedings of IEEE 6th International Conference on Computational Cybernetics ICCC, Stara Lesná, Slovakia, 2008, pp. 69-74.

[18] Zs. Cs. Johanyák, Sz. Kovács, "Fuzzy Rule Interpolation Based on Polar Cuts", Computational Intelligence, Theory and Applications, Springer Berlin Heidelberg, 2006, pp. 499-511.

[19] F. Klawonn, "Fuzzy Sets and Vague Environments", Fuzzy Sets and Systems, 66, 1994, pp. 207-221.

[20] D. Shepard, "A two dimensional interpolation function for irregularly spaced data", Proc. 23rd ACM Internat. Conf., 1968, pp. 517-524.

[21] Zs. Cs. Johanyák, D. Tikk, Sz. Kovács, K. W. Wong "Fuzzy Rule Interpolation Matlab Toolbox – FRI Toolbox", Proc. of the IEEE World Congress on Computational Intelligence (WCCI'06), 15th Int. Conf. on Fuzzy Systems (FUZZ-IEEE'06), July 16-21, Vancouver, BC, Canada, Omnipress. ISBN 0-7803-9489-5, 2006, pp. 1427-1433.

[22] The FRI Toolbox is available at: http://fri.gamf.hu/

[23] Some FRI applications are available at: http://www.iit.uni-miskolc.hu/~szkovacs/

[24] M. Doostfatemeh, S. C. Kremer, "New directions in fuzzy automata", International Journal of Approximate Reasoning, 38, 2005, pp. 175-214.

[25] W. Omlin, C.L. Giles, K.K. Thornber, "Equivalence in knowledge representation: automata, rnns, and dynamical fuzzy systems", Proc. IEEE 87 (9), 1999, pp. 1623–1640.

[26] R. Belohlavek, "Determinism and fuzzy automata", Inf. Sci. 143, 2002, pp. 205–209.

[27] Sz. Kovács, "Interpolative Fuzzy Reasoning in Behaviour-based Control", Advances in Soft Computing, Vol. 2, Computational Intelligence, Theory and Applications, Bernd Reusch (Ed.), Springer, Germany, ISBN 3-540-22807-1, 2005, pp.159-170.

[28] P. Pirjanian, "Behavior Coordination Mechanisms - State-of-the-art", Tech-report IRIS-99-375, Institute for Robotics and Intelligent Systems, School of Engineering, University of Southern California, October, 1999.

[29] Sz. Kovács, and L.T. Kóczy, "Application of the Approximate Fuzzy Reasoning Based on Interpolation in the Vague Environment of the Fuzzy Rulebase in the Fuzzy Logic Controlled Path Tracking Strategy of Differential Steered AGVs", Computational Intelligence - Theory and Applications, Lecture Notes in Computer Science, 1226, Springer, Germany, 1997, pp.456-467.

[30] Sz. Kovács, "Fuzzy Behaviour-based Control Techniques in Adaptive System Applications", Proceedings of the ICCC 2003, IEEE International Conference on Computational Cybernetics, August 29-31, Siófok, Hungary, ISBN 963 7154 18 3, 2003, p. 6.

2011 IEEE International Conference on Fuzzy Systems
June 27-30, 2011, Taipei, Taiwan

An Evolutionary-Based Similarity Reasoning Scheme for Monotonic Multi-Input Fuzzy Inference Systems

Kai Meng Tay
Faculty of Engineering
Universiti Malaysia Sarawak, Sarawak
Malaysia
kmtay@feng.unimas.my

Chee Peng Lim
School of Computer Sciences
University of Science Malaysia
Malaysia

***Abstract*—In this paper, an Evolutionary-based Similarity Reasoning (ESR) scheme for preserving the monotonicity property of the multi-input Fuzzy Inference System (FIS) is proposed. Similarity reasoning (SR) is a useful solution for undertaking the incomplete rule base problem in FIS modeling. However, SR may not be a direct solution to designing monotonic multi-input FIS models, owing to the difficulty in getting a set of monotonically-ordered conclusions. The proposed ESR scheme, which is a synthesis of evolutionary computing, *sufficient conditions*, and SR, provides a useful solution to modeling and preserving the monotonicity property of multi-input FIS models. A case study on Failure Mode and Effect Analysis (FMEA) is used to demonstrate the effectiveness of the proposed ESR scheme in undertaking real world problems that require the monotonicity property of FIS models.**

Keywords- Multi-input fuzzy inference system, monotonicity propery, similarity reasoning, fuzzy rule interpolation

I. INTRODUCTION

Recent advances in fuzzy modeling focus on evolutionary fuzzy systems and similarity reasoning (SR)-based techniques. The former attempts to use Evolutionary Computation (EC) techniques to search, learn, or optimize a fuzzy model. Indeed, many problems in fuzzy modeling can be expressed as an optimization problem (either single objective or multi-objectives), and EC have shown to be a promising solution to these problems. Jang *et al*, [1] examined the use of a data-driven fuzzy modeling as a system identification problem which could be expressed as an optimization problem. Ishibuchi *et al.* [2] proposed a Genetic Algorithm (GA)-based technique for selecting a small number of significant fuzzy if-then rules to construct a compact fuzzy classification system with high accuracy. Besides, multi-objective GAs have been used to search for a pareto set of fuzzy models with interpretability and accuracy trade-off [3]. The latter has been proposed as a solution to undertake the incomplete rule base problems. Similarity Reasoning (SR) techniques, e.g. Analogical Reasoning (AR) [4] and Fuzzy Rule Interpolation (FRI) [5], have been exemplified as a type of qualitative reasoning by Zadeh [6]. A conventional Fuzzy Inference System (FIS) assumes that an observation of a rule is mapped to zero, if its conclusion is not defined [7]. However, this may not always be true, and is the so-called "tomato classification problem" [7]. SR is able to deduce a conclusion for an observation, based on a set of incomplete rule base, whereby each rule assumes in the form of antecedent and consequent. In short, a similarity measure (either based on overlapping of membership functions or distance) is obtained between the observation and antecedents of the available rules from the incomplete rule base. A mathematical function is adopted so that the property (or properties) of the conclusion is obtained from the consequent parts of the available rules [8], usually with a weighted addition or average. Similarity measure is then used to indicate the relative weightage of each consequent of the available rules contributing to the conclusion. In this paper, FRI is viewed as a type of SR technique. FRI considers the distance between the observation and the antecedent as a similarity measure, which is further used as an indication to what extend the property (or properties) of the consequent part contributes to the conclusion.

Another recent trend in FIS modeling is the fulfillment of the monotonicity property. Consider an FIS model, $y = f(x_1, x_2, \dots, x_i, \dots, x_n)$, that satisfies the monotonicity condition between its output, y, with respect to its i^{th} input, x_i. Output y monotonically increases or decreases as x_i increases, i.e. $f(x_1, x_2, \dots, x_i^1, \dots, x_n) \leq f(x_1, x_2, \dots, x_i^2, \dots, x_n)$ or $f(x_1, x_2, \dots, x_i^1, \dots, x_n) \geq f(x_1, x_2, \dots, x_i^2, \dots, x_n)$, respectively, for $x_i^1 < x_i^2$. The importance of this line of study has been highlighted in a number of recent publications [9-15]. Among the important aspects include: (1) many real-world systems and control problems obey the monotonicity property [10-11, 14-16]; (ii) the validity of the FIS output needs to be ensured for undertaking comparison, selection, and decision making problems [10, 12-13]; (iii) in the case when the number of data samples is small or the fuzzy rule set is incomplete, it is important to fully exploit the available qualitative information/ knowledge [9]; (iv) taking the additional qualitative information/knowledge of the system into consideration makes the model identification process less vulnerable to noise and inconsistencies in data samples, as well as mitigates the over-fitting phenomenon [9]. However, there are only a few articles that address the issues on how to design monotonicity-preserving FIS models [10].

From the literatures, several investigations on the mathematical conditions for a monotonic FIS model have been reported. Generally, theoretical proof of exact monotonicity in FIS is difficult [11]. But, there are some mathematical conditions that are useful for preserving monotonicity in FIS models. In [14], a set of mathematical conditions (i.e., the *sufficient conditions*) have been derived with the assumption that the first derivative of a Sugeno FIS is always *greater than or equal to* zero, or *less than or equal to* zero, for a

monotonically increasing or decreasing function, respectively. The *sufficient conditions* suggest that two mathematical conditions (at the antecedent and consequent parts) are essential to obtain a monotonicity-preserving FIS model. For a fuzzy partition (at rule antecedent), maintaining a monotonically-ordered rule base can preserve the monotonicity property. This condition has been used and extended in [10, 12-13, 15]. In [9], it has been verified that for three basic T-norms (minimum, product, and Lukasiewicz), a monotonic input-output behavior is obtained for any monotonic rule bases. Some useful guidelines have also been proposed [9]. The relationships among the monotonicity property, monotonic rule base, and comparable fuzzy sets for single-input-rule-modules-connected FIS model are discussed in [11]. The findings in [9-15] indicate that it is important to maintain a monotonic rule base for FIS models.

The aim of this paper is to investigate on the use of SR for preserving the monotonicity property of multi-input FIS models. The focus is on the zero-order Sugeno FIS model coupled with the *sufficient conditions*. In our previous work [17-18], it has been shown that conventional SR that attempts to deduce each FIS rule consequent separately, with a simple weighted average or addition, is useful; but, it may not be a direct solution to preserving the monotonicity property in multi-input FIS models. This is because SR suffers from the difficulty in getting a set of monotonically-ordered conclusions, with respect to a set of observations which are comparable among themselves as well as comparable with the existing incomplete rule base. Thus, in [18], we have investigated the use of optimization techniques for SR with simulated data.

In this study, an Evolutionary-based SR (ESR) scheme is investigated. Instead of a simple weighted average or weighted addition, SR for monotonicity-preserving multi-input FIS models is formulated as a constrained optimization problem. The proposed ESR scheme adopts the *sufficient conditions* [14] as the hard constraints, and employs certain features of SR as the objective function. An evolutionary computing technique is used to search for a set of conclusions for the associated observations. This is a practical SR model, as the constraints in monotonicity-preserving multi-input FIS models are included. We further demonstrate the use of the ESR scheme with a real case study, i.e., an FIS-based Risk Priority Number (RPN) model in Failure Mode and Effect Analysis (FMEA) methodology.

This paper is organized as follows. In section II, the background of FIS models, the *sufficient conditions*, and SR is presented. A summary of our previous analysis [17-18] is also described. In section III, the proposed ESR scheme is explained in detail. A case study and the results are reported in section IV. Concluding remarks are presented in section V.

II. BACKGROUND

A. Fuzzy Inference Systems

The fuzzy production rules for an n-input FIS model, where $n > 1$ can be represented as follows.

$R^{j_1,j_2,\ldots,j_n}$:

$If\ (x_1 is\ A_1^{j_1})AND\ (x_2 is\ A_2^{j_2})\ldots AND(x_n is\ A_n^{j_n})$,

$THEN(y\ is\ B^{j_1,j_2,\ldots,j_n})$

The AND operator in the rule antecedent part is the product function. For the x_i domain, its membership functions are $\mu_i^1(x_i), \mu_i^2(x_i)$, …, and $\mu_i^{n_i}(x_i)$. The output is obtained by using the weighted average of a representative value, $b^{j_1,j_2,\ldots,j_n}$, with respect to its compatibility grade, as in (1).

$$y = \frac{\sum_{j_{n=1}}^{j_{n=M_n}} \ldots \sum_{j_{2=1}}^{j_{2=M_2}} \sum_{j_{1=1}}^{j_{1=M_1}} \left(\mu_1^{j_1}(x_1) \times \mu_2^{j_2}(x_2) \times .. \times \mu_n^{j_n}(x_n) \times b^{j_1,j_2,\ldots,j_n}\right)}{\sum_{j_{n=1}}^{j_{n=M_n}} \ldots \sum_{j_{2=1}}^{j_{2=M_2}} \sum_{j_{1=1}}^{j_{1=M_1}} \left(\mu_1^{j_1}(x_1) \times \mu_2^{j_2}(x_2) \times .. \times \mu_n^{j_n}(x_n)\right)} \quad (1)$$

where $b^{j_1,j_2,\ldots,j_n}$ is a representative value of $B^{j_1,j_2,\ldots,j_n}$, i.e., $b^{j_1,j_2,\ldots,j_n} = Rep\,(B^{j_1,j_2,\mathrm{e}\,j_n})$. The representative value represents the overall location of the membership function (MF). It can be obtained with defuzzification, or with the point that the membership value is 1.

B. Sufficient Conditions

The first derivative of an FIS model, as in (1), returns a weighted addition series. The *sufficient conditions* assume that all the components in the weighted addition series are always *greater than or equal to* zero, or *less than* or *equal to* zero. In general, two conditions can be derived [10, 12-14]:

Condition 1. At the rule antecedent part, $(d\mu_i^p(x)/dx)/\mu_i^p(x) \geq (d\mu_i^q(x)/dx)/\mu_i^q(x)$, where $p > q$. Note that $(d\mu(x)/dx)/\mu(x)$ is the ratio between the rate of change in the membership degree and the membership degree itself. The derivative of a Gaussian MF with respect to x is $G'(x) = -((x-c)/\sigma^2)G(x)$. Note that $(d\mu(x)/dx)/\mu(x)$ for a Gaussian MF , i.e., $(G'(x)/G(x))$, returns a linear function, i.e. $E(x) = G'(x)/G(x) = -(1/\sigma^2)x + (c/\sigma^2)$.

Condition 2. At the rule consequent part, $b^{j_1,j_2,\ldots,j_i=p,..,j_n} - b^{j_1,j_2,\ldots,j_i=q,..,j_n} \geq 0$ or $b^{j_1,j_2,\ldots,j_i=p,..,j_n} - b^{j_1,j_2,\ldots,j_i=q,..,j_n} \leq 0$ for $dy/dx_i \geq 0$ or $dy/dx_i \leq 0$, respectively. This condition suggests that a monotonically-ordered rule base is required.

C. Similarity Reasoning

In this paper, SR is viewed as a computing paradigm, as in Fig. 1. An example of SR [6] is as follows.

If pressure is *high* Then volume is *small*

If pressure is *low* Then volume is *large*

Thus: If pressure is *medium* Then volume is $(w_1 \wedge small + w_2 \wedge large)$, where $w_1 = sup(high \wedge medium)$, and $w_2 = sup(low \wedge medium)$.

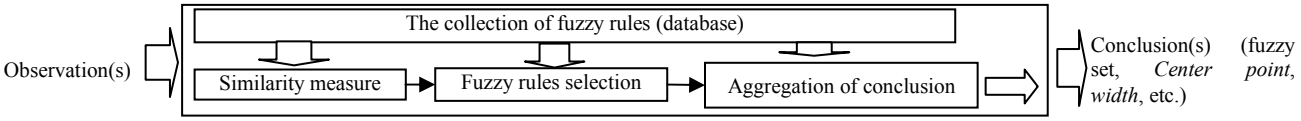

Figure 1 The Similarity reasoning paradigm

The above notion was further extended, and a number of SR schemes have been proposed to allow an unknown conclusion of an observation (in the form of a fuzzy set) to be deduced or predicted, based on a collection of fuzzy rules (database). Note that the "If" part of a fuzzy rule is called the antecedent while the "Then" part is called the consequent. The "If" part of an unknown rule is called the observation, while the "Then" part is called the conclusion.

An observation (in the form of a fuzzy set) acts as an input to the computing paradigm. The observation is compared with the antecedent of each fuzzy rule in the database, and a similarity measure is produced for each fuzzy rule. The similarity measure represents how similar a fuzzy rule is with respect to the observation. There are many ways how this similarity measure can be derived. For example, similarity measure models have been reviewed, compared, and analyzed in [4,8]. In [5, 7, 19], another class of similarity measure that is based on distance has been proposed.

Fuzzy rules from the database are selected for aggregation and for arriving at the conclusions. As an example, in [4], a threshold has been introduced to select fuzzy rules with similarity measure above the threshold. In [19], the n closest fuzzy rules from the observation are selected for use with the Fuzzy Rule Interpolation (FRI) scheme. The importance of the ordering criteria in the selection of fuzzy rules is pointed out in [5,17].

The conclusion is formed by aggregating the selected fuzzy rules. In this stage, a mathematical function is adopted so that the property (or properties) of the conclusion is obtained. The similarity measure is used as an indication of the degree to which the property (or properties) of the consequent of each selected fuzzy rule contributes to the conclusion. In [5], the *center point* and *width* of the conclusion are aggregated using a distance-based similarity measure via a weighted average function. In [6], the conclusion is aggregated using a similarity measure via a weighted addition function. Usually, each conclusion is predicted separately.

D. An Example

In the following section, a summary of our previous work [17-18] is presented. In order to have a better understanding of the work, a numerical example is provided, as follows. A monotonic two-input FIS model, $z = f(x, y)$, is considered. It is known that the relationship between $f(x, y)$ and its inputs, x and y, increases monotonically. Each x and y consists of five Gaussian MFs, i.e., , mf_{x1}, mf_{x2}, mf_{x3}, mf_{x4} and mf_{x5}, and mf_{y1}, mf_{y2} , mf_{y3} , mf_{y4} and mf_{y5} , respectively. These MFs fulfil ***Condition 1***, and can be projected using the ratio as suggested in ***Condition 1*** $(d\mu_i(x)/dx)/\mu_i(x)$, for x and y, respectively.

A complete rule base is expected to have 25 rules. The output domain, z , consists of five MFs , namely mf_{z1} , mf_{z2}, mf_{z3}, mf_{z4} and mf_{z5}, with the representative values of 1, 2, 3, 4, and 5, respectively. In this example, assume that there are eight available rules, as summarized in Fig. 2. Note that the available rules satisfy ***Condition 2***. This problem can also be presented as a rule matrix, as in Fig. 3. As an example, R_1 from Fig. 2 is represented as R_1: mf_{z1}, and located in the cell with coordinate (mf_{x1}, mf_{y1}). Observation $\boldsymbol{A_1^*}$, with coordinate (mf_{x1}, mf_{y2}) is mapped to an unknown conclusion, $\boldsymbol{B_1^*}$, which needs to be predicted by using SR.

R_1: If x is mf_{x1} and y is mf_{y1}, Then z is mf_{z1}
R_2: If x is mf_{x1} and y is mf_{y3}, Then z is mf_{z3}
R_3: If x is mf_{x2} and y is mf_{y4}, Then z is mf_{z5}
R_4: If x is mf_{x3} and y is mf_{y1}, Then z is mf_{z2}
R_5: If x is mf_{x3} and y is mf_{y2}, Then z is mf_{z2}
R_6: If x is mf_{x5} and y is mf_{y1}, Then z is mf_{z3}
R_7: If x is mf_{x5} and y is mf_{y3}, Then z is mf_{z4}
R_8: If x is mf_{x5} and y is mf_{y5}, Then z is mf_{z5}

Figure 2. The fuzzy rules in data base

mf_{x5}	R_6: mf_{z3}	$\boldsymbol{A_{16}^*}$->$\boldsymbol{B_{16}^*}$	R_7: mf_{z4}	$\boldsymbol{A_{17}^*}$->$\boldsymbol{B_{17}^*}$	R_8: mf_{z5}
mf_{x4}	$\boldsymbol{A_{11}^*}$->$\boldsymbol{B_{11}^*}$	$\boldsymbol{A_{12}^*}$->$\boldsymbol{B_{12}^*}$	$\boldsymbol{A_{13}^*}$->$\boldsymbol{B_{13}^*}$	$\boldsymbol{A_{14}^*}$->$\boldsymbol{B_{14}^*}$	$\boldsymbol{A_{15}^*}$->$\boldsymbol{B_{15}^*}$
mf_{x3}	R_4: mf_{z2}	R_5: mf_{z2}	$\boldsymbol{A_8^*}$->$\boldsymbol{B_8^*}$	$\boldsymbol{A_9^*}$->$\boldsymbol{B_9^*}$	$\boldsymbol{A_{10}^*}$->$\boldsymbol{B_{10}^*}$
mf_{x2}	$\boldsymbol{A_4^*}$->$\boldsymbol{B_4^*}$	$\boldsymbol{A_5^*}$->$\boldsymbol{B_5^*}$	$\boldsymbol{A_6^*}$->$\boldsymbol{B_6^*}$	R_3: mf_{z5}	$\boldsymbol{A_7^*}$->$\boldsymbol{B_7^*}$
mf_{x1}	R_1: mf_{z1}	$\boldsymbol{A_1^*}$->$\boldsymbol{B_1^*}$	R_2: mf_{z3}	$\boldsymbol{A_2^*}$->$\boldsymbol{B_2^*}$	$\boldsymbol{A_3^*}$->$\boldsymbol{B_3^*}$
	mf_{y1}	mf_{y2}	mf_{y3}	mf_{y4}	mf_{y5}

Figure 3 Rule matrix for a numerical example

Fig. 4 depicts a surface plot of z versus x and y, using FRI based on a weighted average function. A simple distance, i.e., the Euclidian distance, between the representative values of fuzzy sets, is used. Note that the use of the representative values has been suggested in [19]. In short, a non-monotonic surface is obtained.

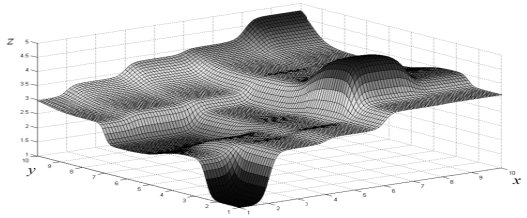

Figure 4 Surface plot of z versus x and y, using an FRI

This phenomenon occurs because a set of non-monotonically-ordered conclusions is deduced by FRI. Two situations as highlighted in [17-18] are:

Situation 1*:* A deduced conclusion of an observation may not be comparable with the collection of fuzzy rules.

Situation 2: It is difficult to deduce a set of conclusions (for a set of observations) that are comparable among one another.

Situation 1 can be solved by adding an ordering criterion [17]. But, ***Situation 2*** suggests that it is necessary to consider the relationship among the conclusions in an SR model. Based on the example, how do we ensure that $B_6^* \geq B_5^*$? Optimization techniques provide a solution to this problem.

III. THE EVOLUTIONARY-BASED SIMILARITY REASONING SCHEME

A. A General Formulation

Consider a multi-input FIS model with $n_{available}$ ($n_{available} > 1$) fuzzy rules $(R_1, R_2, \dots, R_{n_{available}})$, $R_n: A_n \rightarrow B_n$,. There are n_{empty} observations ($A_1^*, A_2^*, \dots, A_{n_{empty}}^*$), where $n_{empty} > 1$. The conclusions for the n_{empty} observations are $B_1^*, B_2^*, \dots, B_{n_{empty}}^*$, respectively. We suggest a SR scheme for monotonicity-preserving multi-input FIS models as a constrained optimization problem. Here, we predict the representative value, instead of the actual membership function, i.e.,

Minimizing

$f\left(b_1^*, b, \dots, b_{n_{empty}}^*\right)$, where $b = rep(B)$

Subject to

Constraint #1: Each conclusion is comparable with the rule collection, i.e, $\overline{b_i} \geq b_i \geq \underline{b_i}$. $\overline{b_i}$ and $\underline{b_i}$ are the highest and lowest possible representative values for the consequent of the observation, respectively. As an example, in Fig. 3, the conclusion of observation $\boldsymbol{A_6^*}$ is $\boldsymbol{B_6^*}$, $\overline{b_6^*} \geq b_6^* \geq \underline{b_6^*}$. The fuzzy rules that are expected to have higher and lower consequents are highlighted in dark-grey and light-grey, respectively. Hence, $\overline{b_6^*}$= **min** (*rep* (mf_{z5}), *rep* (mf_{z4}), *rep* (mf_{z5})), $\underline{b_6^*}$= **max** (*rep* (mf_{z1}), *rep* (mf_{z3})).

Constraint #2: Conclusions are comparable among themselves. In other words, a monotonic ordering of conclusions exist, i.e., $b_i \geq b_j \geq b_k$. As an example, in Fig. 3, $rep(\boldsymbol{B_4^*}) \leq rep(\boldsymbol{B_5^*}) \leq rep(\boldsymbol{B_6^*}) \leq rep(\boldsymbol{B_7^*})$.

In this paper, we investigate the use of a *proximity measure* function that is to be minimized in SR. Each conclusion is further predicted with an SR scheme (as explained in section II(C)), and a set of *reference consequents* is obtained. A *reference conclusion* of a conclusion, $Rep\,(B^*)$, is denoted by $Rep\,(B^*)_R$. For a set of candidates denoted by $(Rep\,(B_1^*)_C, Rep\,(B_2^*)_C, \dots, Rep\,(B_{n_{empty}}^*)_C)$, the *proximity measure* is expressed with a root mean square function, as in (2). It is a measure of "closeness" between the candidates and the *reference conclusions*. The lower the *proximity measure*, the closer the candidate is.

$$Proximity\ measure = \sqrt[2]{\sum_{n=1}^{n_{empty}} (b_{n\,R}^* - b_{n\,C}^*)^2}, \quad (2)$$

where $b = rep(B)$

B. Genetic Algorithem Search

The problem formulated in Section III (A) can be solved using an evolutionary computation technique, e.g. the Genetic Algorithm (GA) [20]. GA is a population-based stochastic optimization technique. Each potential solution set, in a form of $\left(b_1^*, b, \dots, b_{n_{empty}}^*\right)$, is represented by a chromosome. The GA search procedure is used to find the solution set with the best fitness value. Fig. 5 shows the GA procedure.

```
%Note: Initialize variable
Determine the lowest possible representative value and highest
possible representative value of each conclusion.
Determine an reference Conclusion for each conclusion with an SR
scheme
Initial conclusion_candidate_set(s)
While stopping criteria is not triggered
{
Evaluate conclusion_candidate_set(s) with (3)
Record the best conclusion_candidate_set(s)
Crossover
Mutation
Evaluate the stopping criteria
}
```

Figure 5. Pseudo-code of the proposed GA based SR scheme

The hard constraints, i.e., **constraints #1** and **#2**, are considered as penalties of the objective function to be minimized, as in (3).

$$\begin{aligned} &Objective\ function \\ &= w \times \left(\begin{cases} 0\ if\ constraints\ \#1 \text{ and } \#2\ fulfilled \\ 1\ if\ constraints\ \#1 \text{ and } \#2\ not\ fulfilled \end{cases}\right) \\ &+ proximity\ measure \end{aligned} \quad (3)$$

IV. EXPERIMENTAL RESULTS AND DISCUSSION

A. Failure Mode and Effect Analysis

Failure Mode and Effective Analysis (FMEA) is a popular problem prevention methodology that can be interfaced with many engineering and reliability models [13, 21]. FMEA uses an RPN model to evaluate the risk associated with each failure mode. The RPN model considers three risk factors, i.e., severity (S), occurrence (O), and detect (D), and produces a RPN score ($RPN = g_{RPN}(S, O, D)$). The three input factors are estimated by domain experts in accordance with the scale from "1" to "10" based on a set of commonly agreed evaluation criteria, which are presented in the scale tables.

In this paper, the focus is on designing a monotonicity-preserving FIS-based RPN model. FIS-based RPN models are popular, and they have been widely used [13, 21]. They act as a solution for decision making and selection problems for FMEA methodology. An FIS-based RPN model considers S, O, and D as the inputs and the RPN as the output. MFs of S, O, and D are generated from the designated scale tables. The relationships between S, O, and D and the RPN are expressed by a set of fuzzy If-Then rules. In our previous work [13, 21], it has been shown that an effective FIS-based RPN model should satisfy the monotonicity property. This is because the inputs (i.e., S, O, and D ratings) are defined in such a way that the higher the rating, the more critical the situation is. The output (i.e., the RPN score) is a measure of the failure risk. The monotonicity property is important to allow a valid comparison among all failure modes to be made [12-13]. A prediction is deemed illogical if the RPN model yields a contradictory result [12-13].

To validate the proposed procedure, a series of experiments with data and information collected from a semiconductor manufacturing process is conducted. Specifically, the test handler process of the Flip Chip Ball

Grid Array (FCBGA) product is considered. MFs of S, O, and D of the FIS-based RPN model are constructed using the scale tables in [21]. A fuzzy rules base is formed by collecting information from the domain experts, i.e., engineers in charge of the test handler process. Experiments are conducted according to the following conditions : (1) the fuzzy rule base is incomplete (50% of the fuzzy rules are randomly selected) and without SR; (2) the fuzzy rule base is incomplete (50% of the fuzzy rules are randomly selected) and FRI is used to deduce the missing fuzzy rules; (3) the fuzzy rule base is incomplete (50% of the fuzzy rules are randomly selected) and the ESR scheme (as in section III) is used to deduce the missing fuzzy rules. Note that when SR is not used, the conclusions are mapped to zero.

B. Experimental Results

Fig. 6 depicts the objective function versus the number of generations of the GA simulation, with, $w = 20$, for 150 iterations. The objective function of the best individual is subject to GA operations, i.e., crossover and mutation.

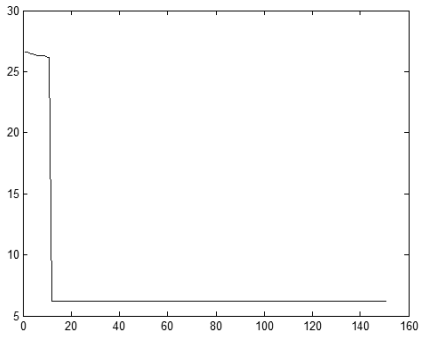

Figure 6 Objective function versus the number of generations of the GA-based procedure for 150 iterations.

The monotonicity property of an FIS model can be observed by using the surface plot. Figures 7, 8, and 9 depict the surface plots of the RPN scores versus O and D when S is fixed at 8, for 50% fuzzy rules.

Without FRI, the surface plot, as shown in Fig. 7, is not monotonic. There are areas where the RPN scores are close to zero because some of the conclusions are undefined, and they are mapped to zero. This is the co-called "tomato classification problem".

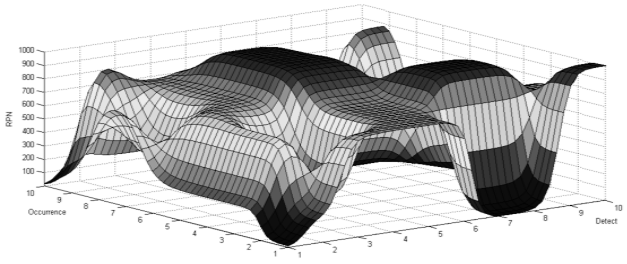

Figure 7 Surface plot for 50% fuzzy rules and without FRI

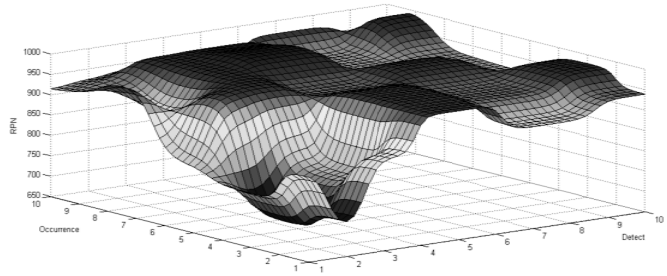

Figure 8 Surface plot for 50% fuzzy rules and with FRI

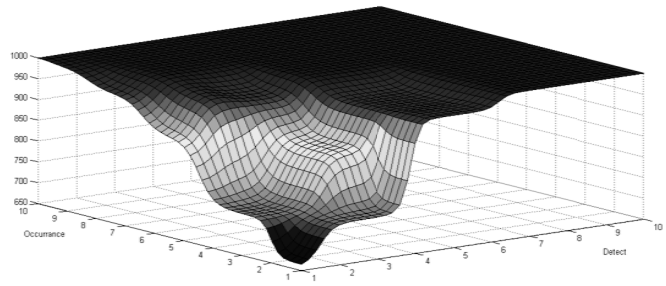

Figure 9 Surface plot for 50% fuzzy rules and with ESR

The use of FRI improves the situation partially. Fig. 8 depicts a "smoother" surface than that of Fig. 7. The effect of the "tomato classification problem" is reduced, as the RPN scores are not mapped to zero. However, the monotonicity property is not satisfied. This is because the rule base obtained is not monotonically-ordered. With the ESR scheme, a monotonic surface plot is obtained, as shown in Fig. 9. In short, the monotonicity property is fulfilled by using the proposed ESR scheme.

C. Evaluation

Fulfillment of the monotonicity property of FIS models can also be evaluated by a test for monotonicity [22]. In this paper, the test for monotonicity of the FIS-based RPN model is conducted by comparing the outputs in pairs. The aim of the test is to examine the relationships between the output (the RPN score) and the inputs (S, O, or D). The test allows the monotonic relationship to be represented by a numerical value, from 0 to 1. We attempt to generate all possible comparable pairs between the output and each of the inputs. The number of monotonic pairs is counted, and the degree of monotonicity is obtained as in (4).

$$Degree\ of\ monotonicity = \frac{\#\ Monotone\ pairs(D)}{\#Comparable\ pairs\ (D)} \qquad (4)$$

The $Degree\ of\ monotonicity$ is 1 for an ideal monotonic FIS model. The $Degree\ of\ monotonicity$ is 0 if the FIS model violates totally the condition of monotonicity. A higher $Degree\ of\ monotonicity$ implies a better fulfillment of the monotonicity property by the FIS model under test.

As an example, comparable pairs in the form of [S,O,D] are generated, i.e., [1,1,1] and [2,1,1], [2,1,1] and [3,1,1],…, [9,1,1] and [10, 1,1], …, and finally [9, 10, 10] and [10, 10, 10]. The RPN scores for [1,1,1] and [2,1,1] are compared, and its fulfillment towards monotonicity is checked. The same goes to other comparable pairs. In this case, 900 comparable pairs are generated between the RPN and S. The same applies to the RPN and O as well as the RPN and D. Thus, a total of 2700 comparable pairs are available. Table 1 shows the results.

Table1 The measure of monotonicity

Experiment	#Comparable pairs	#Monotonic pairs	Degree of monotonicity
Without SR	2700	1376	0.51
With FRI	2700	1981	0.73
With ESR	2700	2700	1.00

As can be seen in Table 1, without SR, there are 1376 monotonic pairs, and the *degree of monotonicity* is 0.51. An improvement is achieved with FRI, i.e., 1981 monotonic pairs, with the *degree of monotonicity* of 0.73. The ESR scheme is able to generate 2700 monotonic pairs, with the *Degree of monotonicity* of 1. This indicates that a full fulfilment of monotonicy among the RPN and S, O, and D ratings. In other words, the monotonicity property is fully perserved with the use of the ESR scheme.

V. SUMMARY

In this paper, it is argued that SR that predicts each rule consequent separately, using a simple weighted average function, may not be a direct solution for designing a monotonic multi-input FIS model. An alternative SR scheme, i.e., ESR, is thus proposed. It is formulated as a constrained optimization problem. An optimization procedure, i.e., GA, is adopted to search for a set of conclusions that obey the *sufficient conditions*, with the minimum proximity measure. An experiment has been conducted with real data collected from industry, i.e., an FIS-based RPN model for FMEA. The results show that without SR, the output does not fulfill the monotonicity property, and some regions are mapped to zero, hence leading to the "tomato classification problem". With SR, the situation is improved, but the output is still not able to satisfy the monotonicity property. With the proposed ESR scheme, the monotonicity property can be preserved. As a result, ESR provides a solution to designing multi-input FIS models that preserve the monotonicity property.

For further work, investigations into other evolutionary models, e.g. particle swarm optimization, harmonic search etc., can be conducted. Alternative methods of handling constraints will be studied. In addition to FMEA, experiments in different domains are needed to fully evaluate the proposed ESR scheme in designing useful monotonic multi-input FIS models for various applications.

ACKNOWLEDGMENT

The financial support provided by the Fundamental Research grant (No. FRGS/02(10)/752/2010(38)) and USM RU Grant (No. 814089) for this work is highly appreciated.

REFERENCES

[1] J.S.R. Jang, C.T. Sun, and E. Mizutani, Neural-Fuzzy and Soft Computing. Prentice-Hall,1997.

[2] H. Ishibuchi, K. Nozaki, N. Yamamoto, and H. Tanaka, "Selecting Fuzzy If-Then Rules for Classification Problems Using Genetic Algorithms," *IEEE Trans. Fuzzy Syst*., vol.3, no.3, pp.260-270, 1995.

[3] H. Ishibuchi and Y. Nojima, "Analysis of interpretability-accuracy tradeoff of fuzzy systems by multiobjective fuzzy genetics-based machine learning," *Int. J. Approx. Reason.*, vol.44, no.1, pp. 4-31, 2007.

[4] I.B. Turksen, and Z. Zhao, "An approximate analogical reasoning approach based on similarity measures," *IEEE Trans. Syst. Man Cyb*., vol.18, no.6, pp.1049-1056,1988.

[5] L.T. Kóczy and K. Hirota, "Size reduction by interpolation in fuzzy rule bases," *IEEE Trans. Syst. Man Cy. B*, vol.27, no.1, pp.14-25, 1997.

[6] L.A. Zadeh, "Knowledege representation in fuzzy logic," *IEEE Trans. Knowl. Data En.*, vol.1, no.1, pp.89-100, 1989.

[7] W-H Hsiao, S-M Chen and C-H Lee, "A new interpolative reasoning method in sparse rule based system," *Fuzzy Sets Syst*., vol.93, no.1, pp. 17-22, 1998.

[8] S. Raha, N.R. Pal, and K.S. Ray, "Similarity-Based Approximate Reasoning Methodology and Application," *IEEE Trans. Syst. Man Cy. A*, vol.32, no.4, pp.541-547, 2002.

[9] E.V. Broekhoven and B.D. Baets, "Only Smooth Rule Bases Can Generate Monotone Mamdani–Assilian Models Under Center-of-Gravity Defuzzification," *IEEE Trans. Fuzzy Syst*., vol.17, no.5, pp.1157-1174, 2009.

[10] V.S. Kouikoglou and Y.A. Phillis, "On the monotonicity of hierarchical sum-product fuzzy systems," *Fuzzy Sets Syst*., vol.160, no.24, pp.3530-3538, 2009.

[11] H. Seki, H. Ishii, and M. Mizumoto, "On the Monotonicity of Fuzzy-Inference Methods Related to T–S Inference Method," *IEEE Trans. Fuzzy Syst.*, vol.18, no.3, pp.629 – 634, 2010.

[12] K.M. Tay and C.P. Lim, "On the Use of Fuzzy Inference Techniques in Assessment Models: Part I: Theoretical Properties," *Fuzzy Optim Decis Making*, vol.7, no.3, pp.269-281, 2008.

[13] K.M. Tay and C.P. Lim, "On the Use of Fuzzy Inference Techniques in Assessment Models: Part II: Industrial Applications," *Fuzzy Optim Decis Making*, vol.7, no.3, pp.283-302, 2008.

[14] J.M. Won, S.Y. Park, and J.S. Lee, "Parameter conditions for monotonic Takagi-Sugeno-Kang fuzzy system," *Fuzzy Sets Syst.*, vol.132, no.2, pp.135-146, 2002.

[15] K.M. Tay and C.P. Lim. "A Fuzzy Inference System-Based Criterion-Referenced Assessment Model," *Expert Syst. Appl*., vol.38, no.9, pp. 11129-11136, 2011.

[16] P. Lindskog and L. Ljung, "Ensuring monotonic gain characteristics in estimated models by fuzzy model structures," *Automatica*, vol.36, no.2, pp.311-317, 2000.

[17] K.M. Tay and C.P. Lim, "On the Use of Fuzzy Rule Interpolation Techniques for Monotonic Multi-Input Fuzzy Rule Base Models," in *Proc. 2009 IEEE Int. Conf. Fuzzy Syst*., pp.1736-1740, 2009.

[18] K.M. Tay and C.P. Lim, "A Similarity Reasoning Scheme for Modelling of Monotonic Multi-Input Fuzzy Inference Systems," in *Proc. 2010 Fourth International Conference on Genetic and Evolutionary Computing*, pp.214-218, 2010.

[19] Z.H. Huang and Q. Shen, "Fuzzy interpolation and extrapolation: a practical approach", *IEEE Trans. Fuzzy Syst.*, vol.16, no.1, pp.13–28, 2008.

[20] DE Goldberg, Genetic algorithms in search, optimization, and machine learning. Addison-Wesley Professional, 1989.

[21] K.M. Tay and C.P. Lim, "Enhancing the Failure Mode and Effect Analysis methodology with Fuzzy Inference Techniques," *J. Intell. Fuzzy Syst.*, vol.21, no.1-2, pp.135-146, 2010.

[22] H. Daniels and M. Velikova, "Monotone and partially monotone neural network," *IEEE Trans. Neural Netw.*, vol.21, no.6, pp.906-917, 2010.

2011 IEEE International Conference on Fuzzy Systems
June 27-30, 2011, Taipei, Taiwan

Fuzzy Rule Interpolation Based on Interval Type-2 Gaussian Fuzzy Sets and Genetic Algorithms

Shyi-Ming Chen and Yu-Chuan Chang
Department of Computer Science and Information Engineering, National Taiwan University of Science and Technology, Taipei, Taiwan, R. O. C.
e-mail: smchen@mail.ntust.edu.tw, D9315003@mail.ntust.edu.tw

***Abstract*—In this paper, we present a new method for fuzzy rule interpolation with interval type-2 Gaussian fuzzy sets for sparse fuzzy rule-based systems based on genetic algorithms. The proposed fuzzy rule interpolation method deals with the interpolation of fuzzy rules based on the multiple fuzzy rules interpolation scheme. We also present a new learning method to learn optimal interval type-2 Gaussian fuzzy sets for sparse fuzzy rule-based systems based on genetic algorithms. We apply the proposed fuzzy rule interpolation method and the proposed learning method to deal with the Mackey-Glass chaotic time series prediction problem. The experimental result shows that the proposed fuzzy rule interpolation method using the optimally learned interval type-2 Gaussian fuzzy sets obtained by the proposed learning method gets higher average accuracy rates than the existing methods to deal with the Mackey-Glass chaotic time series prediction problem.**

Keywords-Fuzzy rule interpolation; sparse fuzzy rule-based systems; interval type-2 Gaussian fuzzy sets; type-1 Gaussian fuzzy sets; genetic algorithms

I. INTRODUCTION

In recent years, some methods [4], [6], [7], [17] have been presented to deal with fuzzy rule interpolation in sparse fuzzy rule-based systems based on interval type-2 fuzzy sets [18]. In [4], Chang and Chen presented a method for fuzzy rule interpolation based on the principle membership functions and the uncertainty grade functions of interval type-2 fuzzy sets. In [6], Chen and Chang presented a method for fuzzy rule interpolation based on the ratios of fuzziness of interval type-2 fuzzy sets. In [7], Chen and Chang presented a method for fuzzy rule interpolation based on the uncertainty ratios of interval type-2 fuzzy sets. In [17], Lee and Chen presented a method for fuzzy rule interpolation based on the ranking values of interval type-2 fuzzy sets.

In this paper, we present a new method for fuzzy rule interpolation with the learned interval type-2 Gaussian fuzzy sets for sparse fuzzy rule-based systems based on genetic algorithms. The proposed fuzzy rule interpolation method deals with the interpolation of fuzzy rules based on the multiple fuzzy rules interpolation scheme. We also present a new learning method to learn optimal interval type-2 Gaussian fuzzy sets for sparse fuzzy rule-based systems based on genetic algorithms. We apply the proposed learning method and the proposed fuzzy rule interpolation method to deal with the Mackey-Glass chaotic time series prediction problem. The experimental result shows that the proposed fuzzy rule interpolation method using the optimally learned interval type-2 Gaussian fuzzy sets obtained by the proposed learning method gets higher average accuracy rates than the existing methods [2], [8], [13] to deal with the Mackey-Grass chaotic time series prediction problem.

II. PRELIMINARIES

In this section, we briefly introduce the concepts of interval type-2 Gaussian fuzzy sets [16], [18]. A type-1 Gaussian fuzzy set $\widetilde{A}$ represented by the membership function $e^{-\frac{(x-m)^2}{2\sigma^2}}$ can be denoted by $\widetilde{A} = <m, \sigma>$, as shown in Fig. 1, where m and σ denote the mean and the standard deviation of the type-1 Gaussian fuzzy set $\widetilde{A}$, respectively.

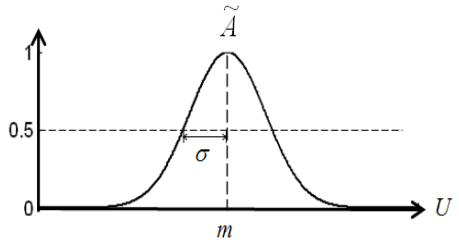

Fig. 1. A type-1 Gaussian fuzzy set $\widetilde{A}$.

Definition 2.1 **[18]:** An interval type-2 Gaussian fuzzy set $\widetilde{\widetilde{A}}$ can be represented by $< \widetilde{\widetilde{A}}^{U}, \widetilde{\widetilde{A}}^{L} >$, where $\widetilde{\widetilde{A}}^{U}$ and $\widetilde{\widetilde{A}}^{L}$ denote the upper membership function and the lower membership function of $\widetilde{\widetilde{A}}$, respectively, and both $\widetilde{A}^{U}$ and $\widetilde{A}^{L}$ are type-1 Gaussian fuzzy sets.

Let us consider the adjacent type-1 Gaussian fuzzy sets $\widetilde{A}_1 = <m_1, \sigma_1>$ and $\widetilde{A}_2 = <m_2, \sigma_2>$ shown in Fig. 2. Based on [16], we can get an interval type-2 Gaussian fuzzy set $\widetilde{\widetilde{A}} = < \widetilde{\widetilde{A}}^{U}, \widetilde{\widetilde{A}}^{L} >$ obtained from $\widetilde{A}_1$ and $\widetilde{A}_2$, as shown in Fig. 3, where

$$\widetilde{\widetilde{A}} = <[m_1, m_2], \sigma_1; \sigma_2>, \quad (1)$$

$[m_1, m_2]$ denotes the interval-valued mean of the interval type-2 Gaussian fuzzy set $\widetilde{\widetilde{A}}$, σ_1 and σ_2 are called the left standard deviation and the right standard deviation of the interval type-2 Gaussian fuzzy set $\widetilde{\widetilde{A}}$, respectively, $m_1 \le m_2$, $\sigma_1 > 0$ and $\sigma_2 > 0$.

978-1-4244-7316-8/11/$26.00 ©2011 IEEE

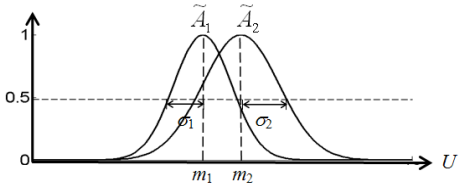

Fig. 2. Two adjacent type-1 Gaussian fuzzy sets $\tilde{A}_1 = <m_1, \sigma_1>$ and $\tilde{A}_2 = <m_2, \sigma_2>$.

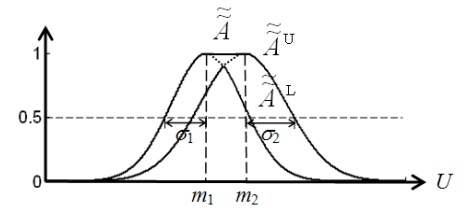

Fig. 3. An interval type-2 Gaussian fuzzy set $\tilde{\tilde{A}} = <[m_1, m_2], \sigma_1; \sigma_2>$.

Let us consider an interval type-2 Gaussian fuzzy set $\tilde{\tilde{A}}$ having an interval-valued mean $[m_1, m_2]$, a left standard deviation σ_1 and a right standard deviation σ_2, as shown in Fig. 3, where $\tilde{\tilde{A}} = <[m_1, m_2], \sigma_1; \sigma_2>$, $m_1 < m_2$, $\sigma_1 > 0$ and $\sigma_2 > 0$. If $m_1 = m_2$ and $\sigma_1 = \sigma_2$, then the interval type-2 Gaussian fuzzy set $\tilde{\tilde{A}}$ becomes the type-1 Gaussian fuzzy set $\tilde{A}$, as shown in Fig. 1.

Definition 2.2: The representative value $Rep(\tilde{\tilde{A}})$ of the Gaussian interval type-2 fuzzy set $\tilde{\tilde{A}} = <[m_1, m_2], \sigma_1; \sigma_2>$ is calculated as follows:

$$Rep(\tilde{A}) = \frac{m_1 \times \sigma_1 + m_2 \times \sigma_2}{\sigma_1 + \sigma_2}, \tag{2}$$

where $m_1 \le Rep(\tilde{A}) \le m_2$, $\sigma_1 > 0$ and $\sigma_2 > 0$

From Eq. (2), we can see that the larger the value of the standard deviation σ_i, the closer the representative value $Rep(\tilde{\tilde{A}})$ to m_i, where $1 \le i \le 2$.

III. A New Method For Fuzzy Rule Interpolation Based on Interval Type-2 Gaussian Fuzzy Sets

In this section, we present a new method for fuzzy rule interpolation based on interval type-2 Gaussian fuzzy sets. Let us consider the following multiple fuzzy rules interpolation scheme using interval type-2 Gaussian fuzzy sets:

Rule 1: If X_1 is $\tilde{\tilde{A}}_{1,1}$ and X_2 is $\tilde{\tilde{A}}_{1,2}$ and ... and X_m is $\tilde{\tilde{A}}_{1,m}$ **Then** Y is $\tilde{\tilde{B}}_1$

Rule 2: If X_1 is $\tilde{\tilde{A}}_{2,1}$ and X_2 is $\tilde{\tilde{A}}_{2,2}$ and ... and X_m is $\tilde{\tilde{A}}_{2,m}$ **Then** Y is $\tilde{\tilde{B}}_2$

$\vdots$

Rule p: If X_1 is $\tilde{\tilde{A}}_{p,1}$ and X_2 is $\tilde{\tilde{A}}_{p,2}$ and ... and X_m is $\tilde{\tilde{A}}_{p,m}$ **Then** Y is $\tilde{\tilde{B}}_p$

Observation: X_1 is $\tilde{\tilde{A}}_1^*$ and X_2 is $\tilde{\tilde{A}}_2^*$ and ... and X_m is $\tilde{\tilde{A}}_m^*$

Conclusion: Y is $\tilde{\tilde{B}}^*$

the jth antecedent variable X_j, $\tilde{\tilde{B}}^* = <[m_{\tilde{\tilde{B}}^*,1}, m_{\tilde{\tilde{B}}^*,2}], \sigma_{\tilde{\tilde{B}}^*,1}; \sigma_{\tilde{\tilde{B}}^*,2}>$ is the interval type-2 Gaussian fuzzy set of the fuzzy interpolated result, m denotes the number of antecedent variables in the fuzzy rules, p denotes the number of fuzzy rules, $1 \le j \le m$ and $1 \le k \le p$. In this paper, we use the neighboring fuzzy rules [5] with respect to the observation as the closest fuzzy rules with respect to the observation for fuzzy rule interpolation, where each antecedent fuzzy set $\tilde{\tilde{A}}_{k,j}$ of the closest fuzzy rule *Rule k* is either the left nearest fuzzy set or the right nearest fuzzy set with respect to the observation fuzzy set $\tilde{\tilde{A}}_j^*$, where $1 \le j \le m$ and $1 \le k \le p$.

The proposed method for fuzzy rule interpolation using interval type-2 Gaussian fuzzy sets is now presented as follows:

Step 1: Based on Eq. (2), calculate the representative values $Rep(\tilde{\tilde{A}}_{k,j})$ of each antecedent interval type-2 fuzzy set $\tilde{\tilde{A}}_{k,j}$ appearing in fuzzy rule *Rule k* and calculate the representative values $Rep(\tilde{\tilde{A}}_j^*)$ of each observation interval type-2 fuzzy set $\tilde{\tilde{A}}_j^*$, respectively, where

$$Rep(\tilde{\tilde{A}}_{k,j}) = \frac{m_{\tilde{\tilde{A}}_{k,j},1} \times \sigma_{\tilde{\tilde{A}}_{k,j},1} + m_{\tilde{\tilde{A}}_{k,j},2} \times \sigma_{\tilde{\tilde{A}}_{k,j},2}}{\sigma_{\tilde{\tilde{A}}_{k,j},1} + \sigma_{\tilde{\tilde{A}}_{k,j},2}}, \tag{3}$$

$$Rep(\tilde{\tilde{A}}_j^*) = \frac{m_{\tilde{\tilde{A}}_j^*,1} \times \sigma_{\tilde{\tilde{A}}_j^*,1} + m_{\tilde{\tilde{A}}_j^*,2} \times \sigma_{\tilde{\tilde{A}}_j^*,2}}{\sigma_{\tilde{\tilde{A}}_j^*,1} + \sigma_{\tilde{\tilde{A}}_j^*,2}}, \tag{4}$$

$1 \le k \le p$ and $1 \le j \le m$.

Step 2: Calculate the weight W_k of the closest fuzzy rule *Rule k* with respect to the observation fuzzy sets [3], where

$$w_k = \min_{1 \le j \le m} \left(1 - \left| \frac{Rep(\tilde{\tilde{A}}_j^*) - Rep(\tilde{\tilde{A}}_{k,j})}{Rep(\tilde{\tilde{A}}_{r_j,j}) - Rep(\tilde{\tilde{A}}_{l_j,j})} \right| \right), \tag{5}$$

$$W_k = \frac{w_k}{\sum_{q=1}^{p} w_q}, \tag{6}$$

$Rep(\tilde{\tilde{A}}_{l_j,j})$ and $Rep(\tilde{\tilde{A}}_{r_j,j})$ are the representative values of the left nearest antecedent fuzzy sets $\tilde{\tilde{A}}_{l_j,j}$ and the right nearest antecedent fuzzy set $\tilde{\tilde{A}}_{r_j,j}$ with respect to the observation fuzzy set $\tilde{\tilde{A}}_j^*$, respectively, $0 \le W_k \le 1$, $\sum_{k=1}^{p} W_k = 1$ and $1 \le k \le p$.

Step 3: Construct an intermediate interpolated fuzzy rule, shown as follows:

If X_1 is $\tilde{\tilde{A}}_1'$ and X_2 is $\tilde{\tilde{A}}_2'$ and ... and X_m is $\tilde{\tilde{A}}_m'$ Then Y is $\tilde{\tilde{B}}'$.

where $\tilde{\tilde{A}}'_j = <[\, m_{\tilde{\tilde{A}}'_j,1}, \, m_{\tilde{\tilde{A}}'_j,2}\,], \, \sigma_{\tilde{\tilde{A}}'_j,1}; \, \sigma_{\tilde{\tilde{A}}'_j,2}>$ is an interval type-2 Gaussian fuzzy set appearing in the *j*th antecedent of the constructed intermediate interpolated fuzzy rule, $\tilde{\tilde{B}}' = <[\, m_{\tilde{\tilde{B}}',1}, \, m_{\tilde{\tilde{B}}',2}\,], \, \sigma_{\tilde{\tilde{B}}',1}; \, \sigma_{\tilde{\tilde{B}}',2}>$ is an interval type-2 Gaussian fuzzy set appearing in the consequence of the constructed intermediate interpolated fuzzy rule and $1 \le j \le m$. The interval-valued mean $[\, m_{\tilde{\tilde{A}}'_j,1}, \, m_{\tilde{\tilde{A}}'_j,2}\,]$, the left standard deviation $\sigma_{\tilde{\tilde{A}}'_j,1}$ and the right standard deviation $\sigma_{\tilde{\tilde{A}}'_j,2}$ of the interval type-2 Gaussian fuzzy set $\tilde{\tilde{A}}'_j = <[\, m_{\tilde{\tilde{A}}'_j,1}, \, m_{\tilde{\tilde{A}}'_j,2}\,], \, \sigma_{\tilde{\tilde{A}}'_j,1}; \, \sigma_{\tilde{\tilde{A}}'_j,2}>$ are calculated as follows:

$$m_{\tilde{\tilde{A}}'_j,1} = \sum_{k=1}^{p} (W_k \times m_{\tilde{\tilde{A}}_{k,j},1}), \tag{7}$$

$$m_{\tilde{\tilde{A}}'_j,2} = \sum_{k=1}^{p} (W_k \times m_{\tilde{\tilde{A}}_{k,j},2}), \tag{8}$$

$$\sigma_{\tilde{\tilde{A}}'_j,1} = \sum_{k=1}^{p} (W_k \times \sigma_{\tilde{\tilde{A}}_{k,j},1}), \tag{9}$$

$$\sigma_{\tilde{\tilde{A}}'_j,2} = \sum_{k=1}^{p} (W_k \times \sigma_{\tilde{\tilde{A}}_{k,j},2}), \tag{10}$$

where $0 \le W_k \le 1$, $\sum_{k=1}^{p} W_k = 1$, $1 \le k \le p$ and $1 \le j \le m$. The interval-valued mean $[\, m_{\tilde{\tilde{B}}',1}, \, m_{\tilde{\tilde{B}}',2}\,]$, the left standard deviation $\sigma_{\tilde{\tilde{B}}',1}$ and the right standard deviation $\sigma_{\tilde{\tilde{B}}',2}$ of the interval type-2 Gaussian fuzzy set $\tilde{\tilde{B}}' = <[\, m_{\tilde{\tilde{B}}',1}, \, m_{\tilde{\tilde{B}}',2}\,], \, \sigma_{\tilde{\tilde{B}}',1}; \, \sigma_{\tilde{\tilde{B}}',2}>$ are calculated as follows:

$$m_{\tilde{\tilde{B}}',1} = \sum_{k=1}^{p} (W_k \times m_{\tilde{\tilde{B}}_k,1}), \tag{11}$$

$$m_{\tilde{\tilde{B}}',1} = \sum_{k=1}^{p} (W_k \times m_{\tilde{\tilde{B}}_k,2}), \tag{12}$$

$$\sigma_{\tilde{\tilde{B}}',1} = \sum_{k=1}^{p} (W_k \times \sigma_{\tilde{\tilde{B}}_k,1}), \tag{13}$$

$$\sigma_{\tilde{\tilde{B}}',2} = \sum_{k=1}^{p} (W_k \times \sigma_{\tilde{\tilde{B}}_k,2}), \tag{14}$$

where $0 \le W_k \le 1$, $\sum_{k=1}^{p} W_k = 1$ and $1 \le k \le p$.

Step 4: Get the interval-valued mean $[\, m_{\tilde{\tilde{B}}^*,1}, \, m_{\tilde{\tilde{B}}^*,2}\,]$, the left standard deviation $\sigma_{\tilde{\tilde{B}}^*,1}$ and the right standard deviation $\sigma_{\tilde{\tilde{B}}^*,2}$ of the fuzzy interpolated result $\tilde{\tilde{B}}^* = <[\, m_{\tilde{\tilde{B}}^*,1}, \, m_{\tilde{\tilde{B}}^*,2}\,], \, \sigma_{\tilde{\tilde{B}}^*,1}; \, \sigma_{\tilde{\tilde{B}}^*,2}>$, respectively, where

$$m_{\tilde{\tilde{B}}^*,1} = m_{\tilde{\tilde{B}}',1}, \tag{15}$$

$$m_{\tilde{\tilde{B}}^*,2} = m_{\tilde{\tilde{B}}',2}, \tag{16}$$

$$\sigma_{\tilde{\tilde{B}}^*,1} = \sigma_{\tilde{\tilde{B}}',1} \times \frac{\sum_{j=1}^{m} \sigma_{\tilde{\tilde{A}}^*_j,1}}{\sum_{j=1}^{m} \sigma_{\tilde{\tilde{A}}'_j,1}}, \tag{17}$$

$$\sigma_{\tilde{\tilde{B}}^*,2} = \sigma_{\tilde{\tilde{B}}',2} \times \frac{\sum_{j=1}^{m} \sigma_{\tilde{\tilde{A}}^*_j,2}}{\sum_{j=1}^{m} \sigma_{\tilde{\tilde{A}}'_j,2}}. \tag{18}$$

Then, we can get the fuzzy interpolated result $\tilde{\tilde{B}}^*$, where $\tilde{\tilde{B}}^* = <[\, m_{\tilde{\tilde{B}}^*,1}, \, m_{\tilde{\tilde{B}}^*,2}\,], \, \sigma_{\tilde{\tilde{B}}^*,1}; \, \sigma_{\tilde{\tilde{B}}^*,2}>$.

IV. A New Method To Learn the Optimal Interval Type-2 Gaussian Fuzzy Sets for Sparse Fuzzy Rule-Based Systems Based on Genetic Algorithms

In this section, we present a new learning method to learn optimal interval type-2 Gaussian fuzzy sets for sparse fuzzy rule-based systems based on genetic algorithms [11], [12], [15]. Given a sparse fuzzy rule base with type-1 Gaussian fuzzy sets constructed by the existing fuzzy rule base generation method [20], we can construct a new sparse fuzzy rule base with interval type-2 Gaussian fuzzy sets, where each interval type-2 Gaussian fuzzy set corresponds to a type-1 Gaussian fuzzy set in the original sparse fuzzy rule base. Assume that the new sparse fuzzy rule base has *m* antecedent variables $X_1, X_2, \ldots, X_m$ and has a consequence variable *Y*, where each antecedent variable and the consequence variable has *n* possible interval type-2 Gaussian fuzzy sets in the universe of discourse, the *k*th possible interval type-2 Gaussian fuzzy set $\tilde{\tilde{A}}_{k,j}$ of the *j*th antecedent variable X_j is denoted by $\tilde{\tilde{A}}_{k,j} = <[\, m_{\tilde{\tilde{A}}_{k,j},1}, \, m_{\tilde{\tilde{A}}_{k,j},2}\,], \, \sigma_{\tilde{\tilde{A}}_{k,j},1}; \, \sigma_{\tilde{\tilde{A}}_{k,j},2}>$, the *k*th possible interval type-2 Gaussian fuzzy set $\tilde{\tilde{B}}_k$ of the consequence variable *Y* is denoted by $\tilde{\tilde{B}}_k = <[\, m_{\tilde{\tilde{B}}_k,1}, \, m_{\tilde{\tilde{B}}_k,2}\,], \, \sigma_{\tilde{\tilde{B}}_k,1}; \, \sigma_{\tilde{\tilde{B}}_k,2}>$, $1 \le k \le n$ and $1 \le j \le m$. Given a set of *P* training samples, where the input observations of each training sample S_i are represented by $(x_{i1}, x_{i2}, \ldots, x_{im})$, the target output of the training sample S_i is represented by y_i, $1 \le i \le P$ and *P* denotes the number of training samples. Because

the shape of an interval type-2 Gaussian fuzzy set $\tilde{\tilde{A}} = <[m_1, m_2], \sigma_1; \sigma_2>$ varies with its left standard deviation σ_1 and its right standard deviation σ_2, the proposed method encodes the left standard deviations and the right standard deviations of interval type-2 Gaussian fuzzy sets appearing in the rules into the genes of a chromosome, where each chromosome in a population has $2n\times(m + 1)$ genes $g_{1,1,1}$, $g_{1,1,2}$, $g_{2,1,1}$, $g_{2,1,2}$, …, $g_{k,j,1}$, $g_{k,j,2}$, …, $g_{n,m,1}$, $g_{n,m,2}$, $g_{1,m+1,1}$, $g_{1,m+1,2}$, $g_{2,m+1,1}$, $g_{2,m+1,2}$, …, $g_{k,m+1,1}$, $g_{k,m+1,2}$, …, $g_{n,m+1,1}$ and $g_{n,m+1,2}$, where the two successive genes $g_{k,j,1}$ and $g_{k,j,2}$ represent the values $\sigma_{\tilde{\tilde{A}}_{k,j},1}$ and $\sigma_{\tilde{\tilde{A}}_{k,j},2}$ of the kth possible interval type-2 Gaussian fuzzy set $\tilde{\tilde{A}}_{k,j} = <[m_{\tilde{\tilde{A}}_{k,j},1}, m_{\tilde{\tilde{A}}_{k,j},2}], \sigma_{\tilde{\tilde{A}}_{k,j},1}; \sigma_{\tilde{\tilde{A}}_{k,j},2}>$ of the antecedent variable X_j, respectively, $0 \le g_{k,j,1} \le \frac{\left| m_{\tilde{\tilde{A}}_{k,j},2} - m_{\tilde{\tilde{A}}_{k,j},1} \right|}{2}$, $0 \le g_{k,j,2} \le \frac{\left| m_{\tilde{\tilde{A}}_{k,j},2} - m_{\tilde{\tilde{A}}_{k,j},1} \right|}{2}$, the two successive genes $g_{k,m+1,1}$ and $g_{k,m+1,2}$ represents the values of $\sigma_{\tilde{\tilde{B}}_k,1}$ and $\sigma_{\tilde{\tilde{B}}_k,2}$ of the kth possible interval type-2 Gaussian fuzzy set $\tilde{\tilde{B}}_k = <[m_{\tilde{\tilde{B}}_k,1}, m_{\tilde{\tilde{B}}_k,2}], \sigma_{\tilde{\tilde{B}}_k,1}; \sigma_{\tilde{\tilde{B}}_k,2}>$ of the consequence variable Y, respectively, $0 \le g_{k,m+1,1} \le \frac{\left| m_{\tilde{\tilde{B}}_k,2} - m_{\tilde{\tilde{B}}_k,1} \right|}{2}$, $0 \le g_{k,m+1,2} \le \frac{\left| m_{\tilde{\tilde{B}}_k,2} - m_{\tilde{\tilde{B}}_k,1} \right|}{2}$, $1 \le k \le n$ and $1 \le j \le m$. Fig. 4 shows the genes of a chromosome encoding the left standard deviations and the right standard deviations of the interval type-2 Gaussian fuzzy sets appearing in the fuzzy rules.

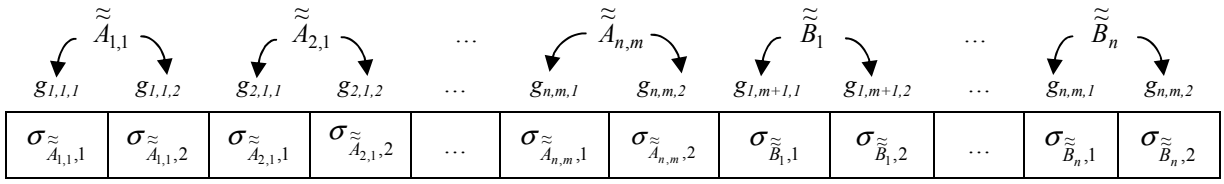

Fig. 4. A chromosome.

The proposed learning method to learn the optimal left standard deviations and the optimal right standard deviations of interval type-2 Gaussian fuzzy sets for sparse fuzzy rule-based systems is now presented as follows:

Step 1: Construct a new sparse fuzzy rule base with the interval type-2 Gaussian fuzzy sets, where each interval type-2 Gaussian fuzzy set $\tilde{\tilde{A}} = <[m_1, m_2], \sigma_1; \sigma_2>$ appearing in the new fuzzy rules is constructed from the corresponding type-1 Gaussian fuzzy set $\tilde{A} = <m, \sigma>$ in the original fuzzy rule, $m_1 = m - \frac{\sigma}{t}$, $m_2 = m + \frac{\sigma}{t}$, t is a parameter determining the values m_1 and m_2 of $\tilde{\tilde{A}}$, $2 \le t \le \infty$, $\sigma_1 = \sigma$ and $\sigma_2 = \sigma$.

Step 2: Encode the left standard deviations and the optimal right standard deviations of the interval type-2 Gaussian fuzzy sets appearing in the fuzzy rules into the genes of the chromosomes. Randomly generate N chromosomes to form the initial population.

Step 3: Decode each chromosome of the population into the left standard deviations and the optimal right standard deviations of the interval type-2 Gaussian fuzzy sets appearing in the fuzzy rules. Apply the proposed fuzzy rule interpolation method to generate the interpolated consequence fuzzy set with respect to the input observations (x_{i1}, x_{i2}, …, x_{im}) of each training sample S_i and then calculate the representative value of the fuzzy interpolated result as the inferred output with respect to the input observations of the training sample S_i, where $1 \le i \le P$ and P denotes the number of training samples. Based on the target output and the inferred output of each training sample, calculate the fitness value *Fitness* of each chromosome using the following fitness function:

$$RMSE = \sqrt{\frac{\sum_{i=1}^{P} \left(y_i - y_i^* \right)^2}{P}}, \tag{19}$$

$$Fitness = \frac{1}{RMSE}, \tag{20}$$

where *RMSE* denotes the root mean square error between the inferred outputs $y_1^*, y_2^*, \ldots, y_P^*$ and the target outputs $y_1, y_2, \ldots, y_P$ of the training samples $S_1, S_2, \ldots$ and S_P, and P denotes the number of training samples. The larger the fitness value *Fitness* of a chromosome, the better the chromosome.

Step 4: Select chromosomes from the current population using the binary tournament selection method [12] to form a mating pool. The system repeatedly randomly selects two chromosomes from the current population and puts the chromosome having the larger fitness value into the mating pool and then puts the two selected chromosomes back into the current population. Repeatedly perform the above process until the number of chromosomes in the mating pool is equal to N, where N is the number of chromosomes in a population.

Step 5: Apply the multi-points crossover method [15] to the chromosomes in the mating pool. For each chromosome C_i in the mating pool, the system randomly generates a real value between 0 and 1. If the randomly generated real value is smaller than a predefined crossover rate γ, where $\gamma \in [0, 1]$, then the system randomly chooses another chromosome C_j

from the mating pool. Then, the system randomly chooses $\left\lfloor \frac{m \times n}{4} \right\rfloor$ crossover points to replace the values of the genes of the crossover points between the selected chromosomes C_i and C_j.

Step 6: Decode each chromosome of the mating pool into the left standard deviations and the optimal right standard deviations of the interval type-2 Gaussian fuzzy sets appearing in the fuzzy rules. Apply the proposed fuzzy rule interpolation method to generate the interpolated consequence fuzzy set with respect to the input observations (x_{i1}, x_{i2}, …, x_{im}) of each training sample S_i and then calculate the representative value of the fuzzy interpolated result as the inferred output with respect to the input observations of the training sample S_i, where $1 \le i \le P$ and P denotes the number of training samples. Based on the target outputs and the inferred outputs of training samples, calculate the fitness value *Fitness* of each chromosome based on the fitness function shown in Eq. (20).

Step 7: Perform the elitist replacement method [11] to form the population of the next generation. The system selects the chromosomes having the top N largest fitness values in the current population and the mating pool to form the population of the next generation. If the number of selected chromosomes from the mating pool is equal to zero, go to **Step 8**. Otherwise, go to **Step 9**.

Step 8: Reinitialize the population using the cataclysmic mutation method [11]. The system puts the best chromosome having the largest fitness value in the current population into the population of the next generation. Mutates the remaining $N - 1$ chromosomes of the current population to generate the $N - 1$ chromosomes in the population of the next generation.

Step 9: If the number of generations is larger than a predefined number of generations, then go to **Step 10**, else go to **Step 3**.

Step 10: Decode the best chromosome having the largest fitness value in the current population into the left standard deviations and the right standard deviations of the interval type-2 Gaussian fuzzy sets appearing in the fuzzy rules. Output the fuzzy rules represented by the optimally learned interval type-2 Gaussian fuzzy sets for the sparse fuzzy rule-based system.

V. Experimental Results

In this section, we apply the proposed fuzzy rule interpolation method and the proposed learning method to deal with the Mackey-Glass chaotic time series prediction problem [10]. We also compare the experimental results of the proposed method with the results obtained by the existing methods [2], [8], [13]. The goal of the Mackey-Glass chaotic time series prediction problem [10] is to achieve a high prediction accuracy for forecasting the time series based on the following equation:

$$\frac{dx(t)}{dt} = \frac{0.2x(t-\tau)}{1+x^{10}(t-\tau)} - 0.1x(t). \tag{21}$$

In [10], Cowder extracted 1000 input-output data pairs using four past values for predicting the Mackey-Glass chaotic time series, shown as follows:

$$[x(t-18), x(t-12), x(t-6), x(t); x(t+6)], \tag{22}$$

where $x(t-18)$, $x(t-12)$, $x(t-6)$ and $x(t)$ are the four input attributes of the data pair at time $t-18$, $t-12$, $t-6$ and t, respectively, $x(t+6)$ is the output attribute of the data pair at time $t+6$, $\tau = 17$, $x(0) = 1.2$ and $0.42 \le x(t) \le 1.31$. In this paper, we also use the 1000 input-output data pairs (i.e., from $x(1)$ to $x(1000)$) as the data set of the Mackey-Glass chaotic time series prediction problem, where the first 500 input-output data pairs (i.e., from $x(1)$ to $x(500)$) are used as the training data set and the remaining 500 input-output data pairs (i.e., from $x(501)$ to $x(1000)$) are used as the testing data set. We apply the fuzzy rules generation method presented in [20] to construct a sparse fuzzy rule base consisting of 116 fuzzy rules using type-1 Gaussian fuzzy sets for the Mackey-Glass chaotic time series prediction problem based on the 500 training input-output data pairs, where each linguistic variable has seven possible type-1 Gaussian fuzzy sets $\tilde{A}_1$, $\tilde{A}_2$, $\tilde{A}_3$, $\tilde{A}_4$, $\tilde{A}_5$, $\tilde{A}_6$ and $\tilde{A}_7$, as shown in Fig. 5, which are evenly distributed over the universe of discourse, where $\tilde{A}_1$ = <0.42, 0.07>, $\tilde{A}_2$ = <0.57, 0.07>, $\tilde{A}_3$ = <0.72, 0.07>, $\tilde{A}_4$ = <0.87, 0.07>, $\tilde{A}_5$ = <1.02, 0.07>, $\tilde{A}_6$ = <1.17, 0.07> and $\tilde{A}_7$ = <1.31, 0.07>. Then, we apply the rule-cutting threshold 0.3 to reduce the constructed sparse fuzzy rule base of 116 fuzzy rules into a more compact sparse fuzzy rule base of 51 fuzzy rules by removing the fuzzy rules whose degrees of brief are smaller than 0.3.

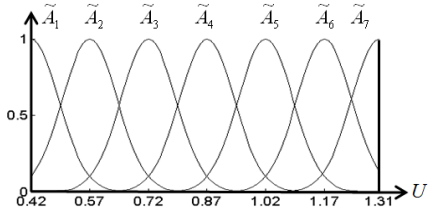

Fig. 5. Seven type-1 Gaussian fuzzy sets used in each variable for the Mackey-Glass chaotic time series prediction problem.

Based on Step 1 of the proposed learning method shown in Section IV, we can construct a new sparse fuzzy rule base using interval Gaussian type-2 fuzzy sets, where each interval type-2 Gaussian fuzzy set $\tilde{\tilde{A}}_i$ = < $[m_{i,1}, m_{i,2}]$, $\sigma_{i,1}$; $\sigma_{i,2}$> appearing in the fuzzy rules corresponds to the original type-1 Gaussian fuzzy set $\tilde{A}_i$ = <m_i, σ_i> appearing in the fuzzy rules of the original sparse fuzzy rule base, $m_{i,1} = m_i - \frac{\sigma_i}{4}$, $m_{i,2} = m_i + \frac{\sigma_i}{4}$, $\sigma_{i,1} = \sigma_i$, $\sigma_{i,2} = \sigma_i$ and $1 \le i \le 7$. Fig. 6 shows the seven possible interval type-2 Gaussian fuzzy sets used for each variable for the Mackey-Glass chaotic time series prediction problem.

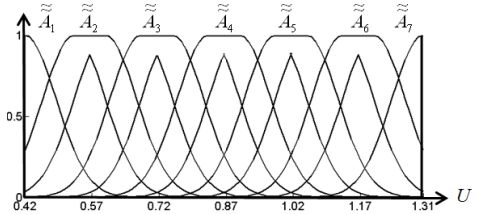

Fig. 6. Seven interval type-2 Gaussian fuzzy sets used in each variable for the Mackey-Glass chaotic time series problem.

After applying Step 1 of the proposed learning method, the above 51 fuzzy rules using type-1 Gaussian fuzzy sets are transformed into the 51 fuzzy rules using interval type-2 Gaussian fuzzy sets, where $\tilde{\tilde{A}}_1$ = <[0.42, 0.42], [0.07, 0.07]>, $\tilde{\tilde{A}}_2$ = <[0.53, 0.6], [0.07, 0.07]>, $\tilde{\tilde{A}}_3$ = <[0.68, 0.75], [0.07, 0.07]>, $\tilde{\tilde{A}}_4$ = <[0.83, 0.9], [0.07, 0.07]>, $\tilde{\tilde{A}}_5$ = <[0.98, 1.05], [0.07, 0.07]>, $\tilde{\tilde{A}}_6$ = <[1.13, 1.2], [0.07, 0.07]> and $\tilde{\tilde{A}}_7$ = <[1.31, 1.31], [0.07, 0.07]>, as shown in Fig. 6. Because there are four antecedent variables and one consequence variable appearing in the fuzzy rules and because each antecedent variable and the consequence variable have seven possible interval type-2 Gaussian fuzzy sets shown in Fig. 5, there are a total of 35 (i.e., (4 + 1) × 7 = 35) individual interval type-2 Gaussian fuzzy sets appearing in the 51 fuzzy rules. Therefore, we encode the left standard deviations and the right standard deviations of the 35 individual interval type-2 Gaussian fuzzy sets into chromosomes, and each chromosome has 70 genes representing the left standard deviations and the right standard deviations of the 35 interval type-2 Gaussian fuzzy sets. Each two successive genes represents the left standard deviation $\sigma_{i,1}$ and the right standard deviation $\sigma_{i,2}$ of the corresponding Gaussian interval type-2 fuzzy set $\tilde{\tilde{A}}_i$ = < [$m_{i,1}$, $m_{i,2}$], $\sigma_{i,1}$; $\sigma_{i,2}$>, where $1 \le i \le 7$. Based on the new sparse fuzzy rule base with the interval type-2 Gaussian fuzzy sets and the training data set of the 500 training data pairs of the Mackey-Glass chaotic time series prediction problem, we apply the proposed learning method to learn the optimal left standard deviations and the optimal right standard deviations of the interval type-2 Gaussian fuzzy sets appearing in the fuzzy rules, where the population size is 60, the number of evolutions is 300 and the crossover rate is 0.9. Fig. 7 shows an example of the learned optimal interval type-2 Gaussian fuzzy sets obtained by the proposed learning method.

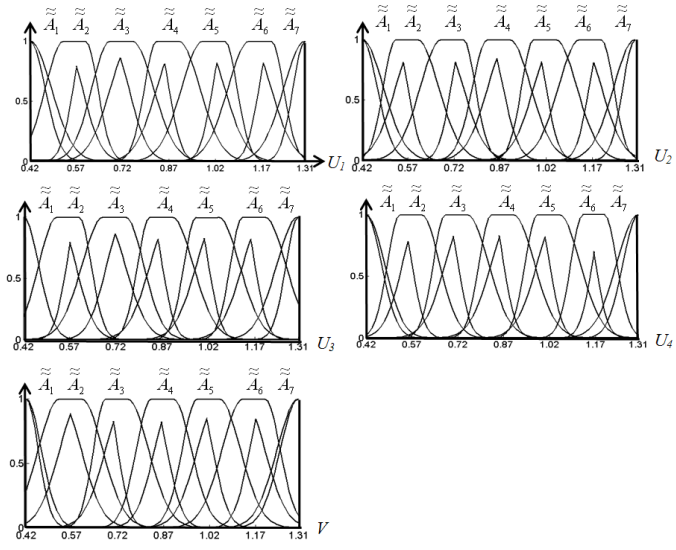

Fig. 7. Optimally learned interval type-2 Gaussian fuzzy sets for the Mackey-Glass chaotic time series problem based on the proposed learning method.

Based on the 51 fuzzy rules with the optimally learned interval type-2 Gaussian fuzzy sets obtained by the proposed learning method, we apply the proposed fuzzy rule interpolation method to produce the interpolated outputs with respect to the testing samples in the 500 testing data pairs. For example, based on the 51 fuzzy rules with the optimally learned interval type-2 Gaussian fuzzy sets shown in Fig. 7, the proposed fuzzy rule interpolation method has the root mean square error 0.0486 with respect to the testing data set.

We have implemented a program based on the proposed learning method and the proposed fuzzy rule interpolation method using Eclipse Version 3.4.2 in a Core 2 duo x86 PC. The system executes the program ten times and the mean of the RMSEs of these ten runs is used as the average RMSE of the proposed method. We then compare the experimental results of the proposed method with the HS method [13], the CCL method [2] and the CK method [8]. Table I shows a comparison of the average root mean square errors for different methods for dealing with the Mackey-Glass chaotic time series prediction problem [10]. From Table I, we can see that the proposed fuzzy rule interpolation method using the optimally learned interval type-2 Gaussian fuzzy sets gets a smaller average root mean square error than the HS method [13], the CCL method [2] and the CK method [8].

TABLE I
A COMPARISON OF THE AVERAGE ROOT MEAN SQUARE ERRORS FOR DIFFERENT METHODS FOR THE MACKEY-GLASS CHAOTIC TIME SERIES PREDICTION PROBLEM

Methods	HS Method [13] (Using Type-1 Gaussian Fuzzy Sets)	CCL Method [2] (Using Type-1 Gaussian Fuzzy Sets)	CK Method [8] (Using Type-1 Gaussian Fuzzy Sets)	The Proposed Method (Using Type-1 Gaussian Fuzzy Sets)	The Proposed Method (Using the Optimally Learned Interval Type-2 Gaussian Fuzzy Sets)
Average RMSE	0.0546	0.1547	0.0630	0.0515	0.0485

Note: The system executes the proposed fuzzy rule interpolation method and the proposed learning method to deal with the Mackey-Glass chaotic time series prediction problem ten times, where the population size of the genetic algorithm is 60, the number of evolutions is 300 and the crossover rate is 0.9.

VI. CONCLUSION

In this paper, we have presented a new method for fuzzy rule interpolation with the learned interval type-2 Gaussian fuzzy sets for sparse fuzzy rule-based systems based on genetic algorithms. The proposed fuzzy rule interpolation method deals with the interpolation of fuzzy rules based on the multiple fuzzy rules interpolation scheme. We also have presented a new learning method to learn optimal Gaussian interval type-2 fuzzy sets for sparse fuzzy rule-based systems based on genetic algorithms. We also have applied the proposed learning method and the proposed fuzzy rule interpolation method to deal with the Mackey-Glass chaotic time series prediction problem. From Table I, we can see that the proposed fuzzy rule interpolation method using the optimally learned interval type-2 Gaussian fuzzy sets obtained by the proposed learning method gets a higher average accuracy rate than the existing methods [2], [8], [13].

ACKNOWLEDGMENT

This work was supported in part by the National Science Council, Republic of China, under Grant NSC 97-2221-E-011-107-MY3.

REFERENCES

[1] K. Balazs, J. Botzheim, and L. T. Koczy, "Comparative analysis of interpolative and noninterpolative fuzzy rule based machine learning systems applying various numerical optimization methods," in *Proc. 2010 IEEE International Conference on Fuzzy Systems*, Barcelona, Spain, 2010, pp. 975-982.

[2] Y. C. Chang, S. M. Chen, and C. J. Liau, "Fuzzy interpolative reasoning for sparse fuzzy rule-based systems based on the areas of fuzzy sets," *IEEE Trans. Fuzzy Syst.*, vol. 16, no. 5, pp. 1285-1301, 2008.

[3] Y. C. Chang and S. M. Chen, "A new method for multiple fuzzy rules interpolation with weighted antecedent variables," in *Proc. 2008 IEEE Int. Conf. Systems, Man and Cybernetics*, Singapore, 2008, pp. 76-81.

[4] Y. C. Chang and S. M. Chen, "A new fuzzy interpolative reasoning method based on interval type-2 fuzzy sets," in *Proc. 2008 IEEE Int. Conf. Systems, Man and Cybernetics*, Singapore, 2008, pp. 82-87.

[5] S. M. Chen and Y. C. Chang, "A new method for weighted fuzzy interpolative reasoning based on weights-learning techniques," in *Proc. 2010 IEEE International Conference on Fuzzy Systems*, Barcelona, 2010, pp. 339-344.

[6] S. M. Chen and Y. C. Chang, "A new method for fuzzy rule interpolation based on the ratio of fuzziness of interval type-2 fuzzy sets" in *Proc. 2010 IEEE International Conference on Fuzzy Systems*, Barcelona, 2010, pp. 333-338.

[7] S. M. Chen and Y. C. Chang, "Fuzzy interpolative reasoning based on the footprints of uncertainty of interval type-2 fuzzy sets," in *Proc. 2010 International Conference on Computational Aspects of Social Networks*, Taiyuan, China, 2010, pp. 569-572.

[8] S. M. Chen and Y. K. Ko, "Fuzzy interpolative reasoning for sparse fuzzy-rule-based systems based on cutting and transformation techniques," *IEEE Trans. Fuzzy Syst.*, vol. 16, no. 6, pp. 1626-1648, 2008.

[9] S. M. Chen, Y. K. Ko, Y. C. Chang, and J. S. Pan, "Weighted fuzzy interpolative reasoning y interpolative reasoning based on weighted incremental transformation and weighted ratio transformation techniques," *IEEE Trans. Fuzzy Syst.*, vol. 17, no. 6, pp. 1412-1427, 2009.

[10] R. S. Cowder, "Predicting the Mackey-Glass time series with cascade-correlation learning," in *Proc. 1990 Connectionist Models Summer School*, pp. 117-123, 1990.

[11] L. Eshelman, "The CHC adaptive search algorithm: How to have safe search when engaging in nontraditional genetic recombination," *Foundations of Genetic Algorithms*, pp. 265–283, San Mateo, Morgan Kaufmann, 1991.

[12] D. E. Goldberg and K. Deb, "A comparison analysis of selection schemes used in genetic algorithms," *Foundations of Genetic Algorithms*, pp. 69-93, San Mateo, Morgan Kaufmann, 1991.

[13] Z. H. Huang and Q. Shen, "Fuzzy interpolative reasoning via scale and move transformations," *IEEE Trans. Fuzzy Syst.*, vol. 14, no. 2, pp. 340-359, 2006.

[14] Z. H. Huang and Q. Shen, "Fuzzy interpolation and extrapolation: A practical approach," *IEEE Trans. Fuzzy Syst.*, vol. 16, no. 1, pp. 13-28, 2008.

[15] J. H. Holland, *Adaptation in Natural and Artificial Systems*, Cambridge. MA: MIT Press, 1975.

[16] C. F. Juang and Y. W. Tsao, "A self-evolving interval type-2 fuzzy neural network with online structure and parameter learning," *IEEE Trans. Fuzzy Syst.*, vol.16, no. 6, pp. 1411-1424, 2008.

[17] L. W. Lee and S. M. Chen, "Fuzzy interpolative reasoning using interval type-2 fuzzy sets," *in Proceedings of the Twenty First International Conference on Industrial, Engineering & Other Applications of Applied Intelligent Systems*, Wroclaw, Poland, 2008, pp. 92-101.

[18] J. M. Mendel and R. I. John, "Type-2 fuzzy sets made simple," *IEEE Trans. Fuzzy Syst.*, vol. 10, no. 2, pp. 117-127, 2002.

[19] J. M. Mendel, R. I. John, and F. L. Liu, "Interval type-2 fuzzy logic systems made simple," *IEEE Trans. Fuzzy Syst.*, vol. 14, no. 6, pp. 808-821, 2006.

[20] L. X. Wang and J. M. Mendel, "Generating fuzzy rules by learning from examples," *IEEE Trans. Syst., Man, Cybern.*, vol. 22, no. 6, pp. 1414-1426, 1992.

[21] L. Yang and Q. Shen, "Towards adaptive interpolative reasoning," in *Proc. 2009 IEEE International Conference on Fuzzy Systems*, Korea, 2009, pp. 542-549.

[22] L. Yang and Q. Shen, "Adaptive fuzzy interpolation and extrapolation with multiple antecedent rules," in *Proc. 2010 IEEE International Conference on Fuzzy Systems*, Barcelona, Spain, 2010, pp. 565-572.

[23] L. A. Zadeh, "Fuzzy sets," *Information and Control*, vol. 8, pp. 338-353, 1965.

2011 IEEE International Conference on Fuzzy Systems
June 27-30, 2011, Taipei, Taiwan

Double-Linear Fuzzy Interpolation Method

Marcin Detyniecki, Christophe Marsala, and Maria Rifqi
UPMC Univ. Paris 06, CNRS, UMR 7606, LIP6
4 place Jussieu, F-75005 Paris, France
Email: *firstname.lastname*@lip6.fr

***Abstract*—In this paper, we present an original fuzzy interpolation method. In contrast to existing approaches, our method is able to always construct an interpolated fuzzy interval without a need of a special step dedicated to the "standardization" of non-viable solutions, which fractures the sense of the interpolation. In fact, these "standardization" steps imply that, for instance, a point obtained from the interpolation of the upper limit (right side) of the fuzzy sets, is used to build the lower limit (left side) of the interpolated conclusion, breaking the underlying hypothesis of (linear) graduality. To achieve the direct interpolation, our method is based on the deviation of the observation from the expected linearly interpolated solution and constrains of the constructed solution between extreme cases. We illustrate and discuss the behavior of our method by comparison to other well-known fuzzy interpolation methods.**

Keywords: **Fuzzy Interpolation, approximate reasoning, sparse rule base.**

I. Introduction

Interpolation of fuzzy rules has been intensively studied since 1991 with a first paper proposing a method [1] (or more accessible [2]). Since then, many different points of views were adopted: α-cuts approaches (recent ones proposed in [3], [4], [5] or [6]), analogy or similarity based approaches ([7], [8], [9]), logical approaches, among others. The interested reader can find a quasi exhaustive list of references in [10] and [11].

Some methods suppose that fuzzy data are represented only by trapezoidal fuzzy intervals, some others are more general and propose methods applicable to all membership function. Frameworks were proposed to compare different existing methods [10], [12], [13], or to unify them [11], [14]. The latter framework is an interesting theoretical approach enabling to write many methods in a unique way thanks to an analytic approach, but, unfortunately, it is not easy to instantiate the different behaviors in concrete situations.

Most methods agree on the *position* of the interpolated conclusion. Thus differences arise when dealing with the challenge of constructing an adequate shape, with the risk of obtaining a non viable fuzzy set. The reason of the latter, as shown in this paper, is that the shape of the fuzzy sets can *not* be linearly interpolated. Thus, very often a standardization step dedicated to ensure that the obtained membership is actually a viable normalized function is proposed. Unfortunately, as we point out in this paper, these steps break several fundamental underlying hypotheses, as for instance the graduality one. In fact, state of the art "standardization" steps always imply that, for instance, a point obtained from the interpolation of the upper limit (right side) of the fuzzy sets, is used to build the lower limit (left side) of the interpolated conclusion, breaking the underlying hypothesis of (linear) graduality. Moreover, the fact of "swaping" points in a "standardization" steps also implies that the associated uncertainty (which was actually used to identify the concerned points for the interpolation) is ignored. As consequence, for instance, almost uncertain values may be used (via the "standardization" step) to build the totally certain kernel of the interpolated solution.

To achieve a direct estimation of the solution, we perform a double linear interpolation by, first, linearly interpolating the expected shape value based on the known rules and secondly, by linearly interpolating the deviation from that value.

Another major difference of the method described in this paper compared to the state of the art is that it constrain the solutions between two know natural boundaries. In the one extreme, we know that the shape of the solution cannot be more precise than a certain single value and in the other limit we assume that the solution has to fall between the *know* rules. In other words, our solution takes into account, indirectly, the spread between the rules to constrain the solution: a novelty.

Our paper is organized as follows. In the next section we present the notations, before describing our method which is divided in two phases: the interpolation of the position as described in Section III and the interpolation of the shape as described in Section IV. In SectionV, we present some empirical comparisons with known methods putting in contrast the differences and common behaviors. Finally, we conclude and provide some hints about future works.

II. Interpolative Reasoning and Notations

A. Interpolative reasoning general principles

Let us consider two numerical variables X and Y defined on the universe $\mathbf{R}$ of real numbers. Let $\mathbf{F}$ denote the set of fuzzy sets of $\mathbf{R}$. We suppose that we are given fuzzy sets A_i in $\mathbf{F}$, $1 \leq i \leq n$, such that: $A_1 \preceq A_2 ... \preceq A_i \preceq A_{i+1} ... \preceq A_n$, for a given order $\preceq$ on $\mathbf{F}$. We also suppose that we are given fuzzy sets B_i in $\mathbf{F}$, $1 \leq i \leq n$, which are also ordered according to $\preceq$.

The context of study concerns sparse fuzzy rule-based systems where fuzzy rules are of the type : (R_i): "if X is A_i then Y is B_i". The sparsity of the system means that the premises of the rules do not cover the input space $\mathbf{F}$ and there exist inputs A_* such that $\exists i / A_i \preceq A_* \preceq A_{i+1}$.

The aim of a fuzzy interpolation method is to provide the conclusion corresponding to the observation A_* by considering only the two rules R_i and R_{i+1} when $A_i \preceq A_* \preceq A_{i+1}$.

978-1-4244-7316-8/11/$26.00 ©2011 IEEE

B. Notations and hypotheses

Our approach is based on three fundamental hypothesis. The first hypothesis lies in the fact that Y has a *gradual behavior* with regard to X. The second hypothesis is that there is a *gradual behavior* for the space of forms. This hypothesis translates the intuition that if an observation is smaller (i.e more precise) than the premisses, then the conclusion should be smaller than the known conclusions. The third hypothesis is that the interpolated conclusion has to be *between* the conclusions of the adjacent rules. Intuitively, we know that on the extremes, rules 1 and 2 apply, and thus, if something is observed in the middle, the conclusion should also be in the middle.

Moreover, we require that for $A_i \preceq A_{i+1}$ the order $\preceq$ verifies no value of the support (respectively kernel) of A_{i+1} is smaller than any value of the support ((respectively kernel) of A_i and no value of the support (respectively kernel) of A_i is greater than any value of the support (respectively kernel) of A_{i+1}.

In this paper we focus on trapezoidal fuzzy sets. We choose to describe such a fuzzy set $A_i = [a_{i1}, a_{i2}, a_{i3}, a_{i4}]$, with the following four parameters. For a visual illustration see Fig. 1:

- its position defined as the center of its kernel:

$$A_i^P = \frac{a_{i2} + a_{i3}}{2} \tag{1}$$

- its certain values range characterized by the kernel's amplitude left and right from its center, as computed by:

$$\overline{A}_i^L = \overline{A}_i^R = \frac{a_{i3} - a_{i2}}{2} \tag{2}$$

- the extend of the uncertainty on the left and on the right, defined by:

$$\underline{A}_i^L = a_{i2} - a_{i1} \tag{3}$$

$$\underline{A}_i^R = a_{i4} - a_{i3} \tag{4}$$

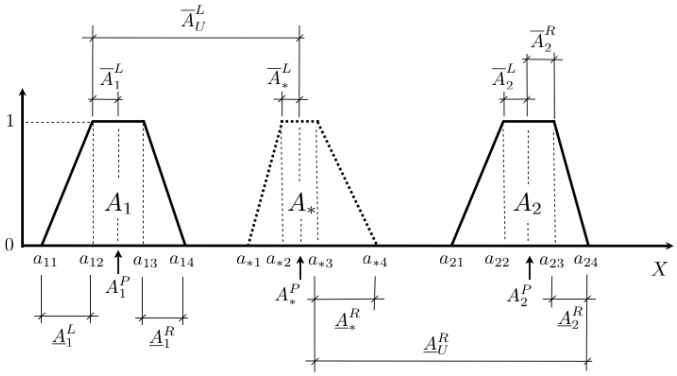

Fig. 1. A trapezoidal fuzzy set $A_i = [a_{i1}, a_{i2}, a_{i3}, a_{i4}]$ has a position A_i^P. Its kernel's form is described by its left and right length: $\overline{A}_i^L = \overline{A}_i^R$. $\underline{A}_i^L$ (and $\underline{A}_i^R$) describe its left (and right) uncertainties. We claim that in an interpolative reasoning problem it is necessary to know the range of values between the known rules to constraint the solutio. Thus, we define the global uncertainty for the kernel on the left $\overline{A}_U^L$ and on the right $\overline{A}_U^R$. Analogously $\underline{A}_U^R$ defines the global uncertainty right, ranging from the largest possible value of the left premise A_2 to the largest certain value of the observation A_*.

III. Interpolating the position

The linear hypothesis for the position states that the position of the observation A_* and the premises A_1 and A_2 are in a linear relationship with coefficient α and that the interpolated conclusion B_* and the conclusions B_1 and B_2 are also in a linear relationship with the *same* coefficient α. Formally, we have:

$$A_*^P = \alpha \cdot A_1^P + (1 - \alpha) \cdot A_2^P \tag{5}$$

$$B_*^P = \alpha \cdot B_1^P + (1 - \alpha) \cdot B_2^P \tag{6}$$

Now, using these two equations we can easily compute the position of the interpolated conclusion B_*. First, based on equation 5, we obtain α:

$$\alpha = \frac{A_2^P - A_*^P}{A_2^P - A_1^P} \tag{7}$$

Second, using that value in equation 5, we obtain the position B_*^P.

IV. Interpolating the shape

On Fig. 2 we observe that the shape of observation A_* is not necessarily in a linear relationship with the shapes of the premises A_1 and A_2, when considered in the universe of description X (which coincides with position). One could argue that this lack of linearity depends upon the way the shapes are measured, but in fact for any non trivial measure it is easy to imagine a case breaking the linearity.

In fact, a simple way to achieve this is by, first computing the expected shape value (linearly) and then building a fuzzy set observation A_* (the counterexample), which has a different shape value. This counterexample exists because the measure is assumed not trivial.

Moreover, this non linearity applies not only to any general description of the shape but also to any shape measure based on a length descriptor. Thus, any α-cut based method will suffer from this non-linearity. This fundamental limitation has also been been observed in [15].

One of the direct consequences is that any method attempting to linearly interpolate the shape (based on the position) will produce degenerated shapes, as pointed out in [7]. The more recent methods avoid ill solutions, by using heuristics that wisely choose among a set of points the ones providing a viable solution. Unfortunately these heuristics are solely designed to avoid degenerative solutions, ignoring any interpolative argumentation.

To overcome the above fundamental reality, we propose to compute the value of the interpolated conclusion in a two step interpolation: first linearly interpolate the *expected shape values* (between the premises and between the conclusions) and then linearly interpolate the *shape deviation* between the expected shape and a limit case, which follows our fundamental assumptions. De facto, our two limit cases correspond, in the one extreme, to zero (assuming that any shape measure is positive), and in the other extreme, to the shape measure of the global uncertainty. The latter corresponds to the assumption,

mentioned in Section II-B, that the interpolated conclusion must be between the known conclusions.

As a result, the solutions are constrained to a reasonable range, corresponding to the limit cases, in which they linearly evolve. The shapes of the premises and conclusions influence *only indirectly* the solution via the double linear interpolation: first the linear interpolation of the expected value and second the linear interpolation of the deviation.

A. Describing the shape of a trapezoidal fuzzy set

The shape of a fuzzy set, and in particular of a trapezoidal one, can be described in numerous ways. For instance it could be described by a single value, as the surface (or integral of the membership function), which summarizes the global spread of uncertainty. But more refined ways, with several parameters, can also be imagined. In this paper we choose to describe the shape of a trapezoidal fuzzy set with the four parameters $\overline{A}_i^L$, $\overline{A}_i^R$, $\underline{A}_i^L$ and $\underline{A}_i^R$, defined in Section II-B. This description focuses on the amplitudes, and symmetry, of the kernel and the support sets.

Since these are all length-descriptors, the double linear interpolation required by the nature of the problem, as described above, has to be applied. In the following we describe how this is performed, analogously in the four cases.

B. Interpolating the kernel's length

In order to interpolate the kernel's shape, we compute two double linear interpolations: one for the left lengths $\overline{A}_i^L$ and one for the right ones $\overline{A}_i^R$. Since the calculations are identical, in the following we only describe the left case.

For the first linear interpolation, we estimate the linearly expected shapes $\overline{A}_E^L$ and $\overline{B}_E^L$ using the kernels' left lengths of the premises $\overline{A}_1^L$ and $\overline{A}_2^L$, and of the conclusions' $\overline{B}_1^L$ and $\overline{B}_2^L$. As illustrated on Fig. 2 and 3, using simple mathematics we obtain :

$$\overline{A}_E^L = \left(\overline{A}_1^L - \overline{A}_2^L\right) \cdot \left(\frac{A_2^P - A_*^P}{A_2^P - A_1^P}\right) + \overline{A}_2^L \tag{8}$$

$$\overline{B}_E^L = \left(\overline{B}_1^L - \overline{B}_2^L\right) \cdot \left(\frac{B_2^P - B_*^P}{B_2^P - B_1^P}\right) + \overline{B}_2^L \tag{9}$$

Then, for the second interpolation, we linearly calculate the deviation of the observed kernel $\overline{A}_*^L$ from the expected kernel $\overline{A}_E^L$. As we will see below two scenarios appear depending on the relative magnitude of $\overline{A}_*^L$ with respect to $\overline{A}_E^L$. It is noteworthy to observe that both scenarios can not be integrated in a single linear transformation.

1) Smaller-shape deviation: Let us assume that $\overline{A}_*^L < \overline{A}_E^L$. In this case the observation is more precise than the expected interpolation. Knowing that any shape measure, and in particular one based on the length, is always positive (or equals to 0), using the linear hypothesis for the deviation we have:

$$\overline{A}_*^L = \beta_L \cdot \overline{A}_E^L + (1 - \beta_L) \cdot 0 = \beta_L \cdot \overline{A}_E^L \tag{10}$$

$$\overline{B}_*^L = \beta_L \cdot \overline{B}_E^L + (1 - \beta_L) \cdot 0 = \beta_L \cdot \overline{B}_E^L \tag{11}$$

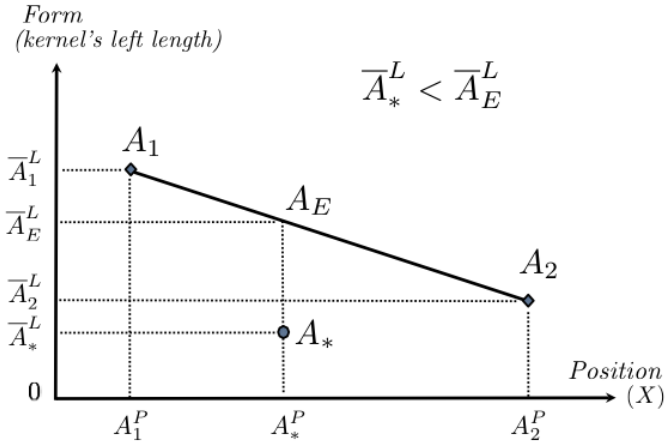

Fig. 2. The shape description of observation A_* is not necessarily in a linear relationship with the shape descritions of the premises A_1 and A_2.

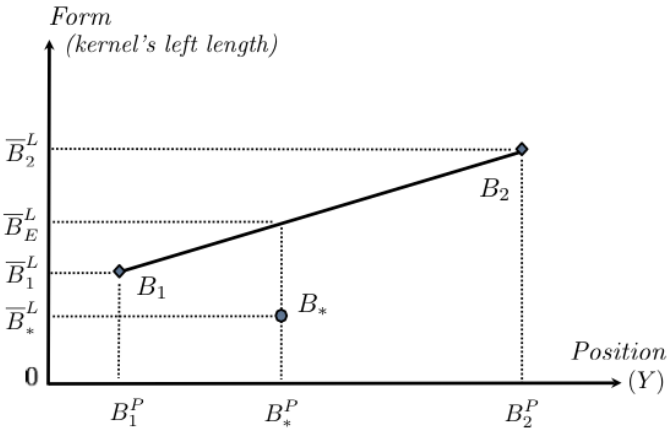

Fig. 3. The shape description of the interpolated conclusion B_* should be in the same linear deviation from the expected shape value, as is the case for the premises.

Thus, in order to obtain the interpolated conclusion's kernel left length, we use Equation 10 to obtain:

$$\beta_L = \frac{\overline{A}_*^L}{\overline{A}_E^L} \tag{12}$$

Which is then used in Equation 11 to obtain the length $\overline{B}_*^L$. The same exact equations, replacing L by R, can be used for the right description of the kernels and, thus, obtain $\overline{B}_*^R$.

2) Larger-shape deviation: It may happen that the observation is less precise than the linearly expected value: $\overline{A}_*^L \geq \overline{A}_E^L$. In that case Equation 10 do not apply, since we have a deviation that implies an increase of the shape and therefore can not be constrained, by a lower boundary, as in a reduction scenario. In other words, since the length of the observation is larger than expected, we would like the length of the conclusion to be *also* larger than the expected linearly interpolated conclusion $\overline{B}_E^L$. In addition, the third of hypothesis mentioned in Section II-B implies that its range can not be larger that the gap between the rules. In the case of the kernel's

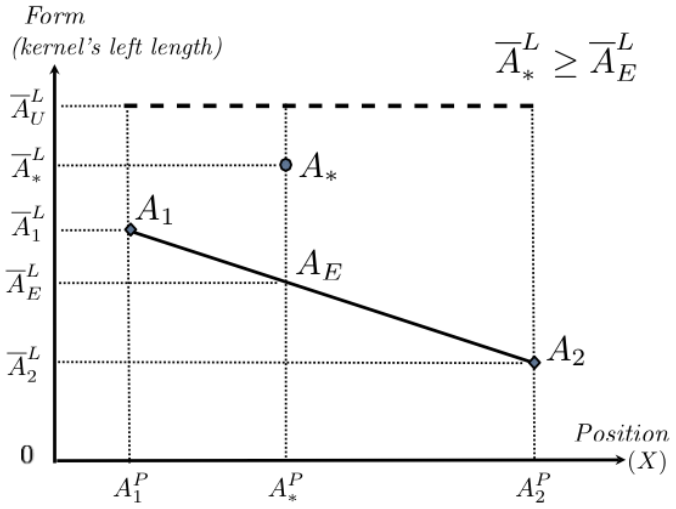

Fig. 4. The shape description of observation A_*, as for instance here the left kernel length $\overline{A}_*^L$, may be larger than the linearly expected value $\overline{A}_E^L$. We propose to constrain the solution by linearly interpolating between the linearly expected shape and the left kernel uncertainty $\overline{A}_U^L$.

left length calculations the uncertainty left between the kernel's premises estimated by:

$$\overline{A}_U^L = A_*^P - a_{12} \tag{13}$$

as shown on Fig. 1.

Consequently, assuming a linear hypothesis for the deviation, we obtain:

$$\overline{A}_*^L = \beta_L \cdot \overline{A}_E^L + (1 - \beta_L) \cdot \overline{A}_U^L \tag{14}$$

$$\overline{B}_*^L = \beta_L \cdot \overline{B}_E^L + (1 - \beta_L) \cdot \overline{B}_U^L \tag{15}$$

The same way as with the smaller shape reduction, in order to obtain the conclusion's kernel-left-length, we use Equation 14 to obtain:

$$\beta_L = \left(\frac{\overline{A}_U^L - \overline{A}_*^L}{\overline{A}_U^L - \overline{A}_E^L} \right) \tag{16}$$

which is then used in Equation 15 to obtain the length $\overline{B}_*^L$. Again, by replacing in the equations L by R we know how to obtain $\overline{B}_*^R$.

C. Interpolating the left and right uncertainties

At this point we know the interpolated conclusion's fuzzy set position (Section III) and its kernel's shape (Section IV-B). Now we interpolate, analogously as for the kernel's lengths, the left and right uncertainties. We first interpolate the expected forms, here only for the right uncertainties:

$$\underline{A}_E^R = \left(\underline{A}_1^R - \underline{A}_2^R\right) \cdot \left(\frac{a_{23} - a_{*3}}{a_{23} - a_{13}} \right) + \underline{A}_2^R \tag{17}$$

$$\underline{B}_E^R = \left(\underline{B}_1^R - \underline{B}_2^R\right) \cdot \left(\frac{b_{23} - b_{*3}}{b_{23} - b_{13}} \right) + \underline{B}_2^R \tag{18}$$

where $b_{*3} = B_*^P + \overline{B}_*^R$. Notice that we anchor, as for the kernels, the length description to the point where the interval starts.

Now, in the same way as for the kernels, we have two scenarios depending of the the relative value of the expected length and the observed length.

If $\underline{A}_*^R < \underline{B}_E^R$, then the double interpolated right uncertainty is obtained by:

$$\underline{B}_*^R = \gamma_R \cdot \underline{B}_E^R = \left(\frac{\underline{A}_*^R}{\underline{A}_E^R} \right) \cdot \underline{B}_E^R \tag{19}$$

But, if $\overline{A}_*^L \geq \overline{A}_E^L$, , then the double interpolated right uncertainty is obtained by:

$$\underline{B}_*^R = \gamma_R \cdot \underline{B}_E^R + (1 - \gamma_R) \cdot \underline{B}_U^R \tag{20}$$

where

$$\gamma_R = \left(\frac{\underline{A}_U^R - \underline{A}_*^R}{\underline{A}_U^R - \underline{A}_E^R} \right) \tag{21}$$

V. Empirical comparisons

In this section, we compare the double-linear fuzzy interpolation method (DoLFIn for short) with some well-known methods: [16] (DP), [10] (BTKY), and [7] (BMR). We consider several scenarios:

- all the shapes are similar
- specific observation
- specific premises or specific conclusions
- extremely unspecific observation

Moreover, to extend our comparison to other state of the art approaches, we use some examples shared by the following papers [3] (HS), [4] (CK), [17] (CCL).

Figures Fig. 5 to Fig. 12 should be read as follows. The first row shows the two premises A_1 and A_2 and the observation A_*. The other four rows present the conclusions by each of the four studied approaches. For the comparison the two known conclusions B_1 and B_2 are always the same, and only the obtained result B_* changes between the rows.

A. All the shapes are similar

A first interesting scenario arises when the observation is similar to the premise. In this case, the observation can be considered as a translation of one of the premises. It is a typical case of interpolative reasoning.

In Fig. 5 and Fig. 6, it can be seen that the three approaches BTKY, BMR, and DolFIn propose the exact same conclusion. The unique method which offers a different solution is the DP, which is very unspecific and uncertain.

B. Precise observation

A second interesting case arises when the observation is precise. It is often the case in real-world applications for decision-making process when no fuzzification of the input data is processed.

In Fig. 7 and Fig. 8, it can be seen that the results are different for the four methods. As previously seen, again DP

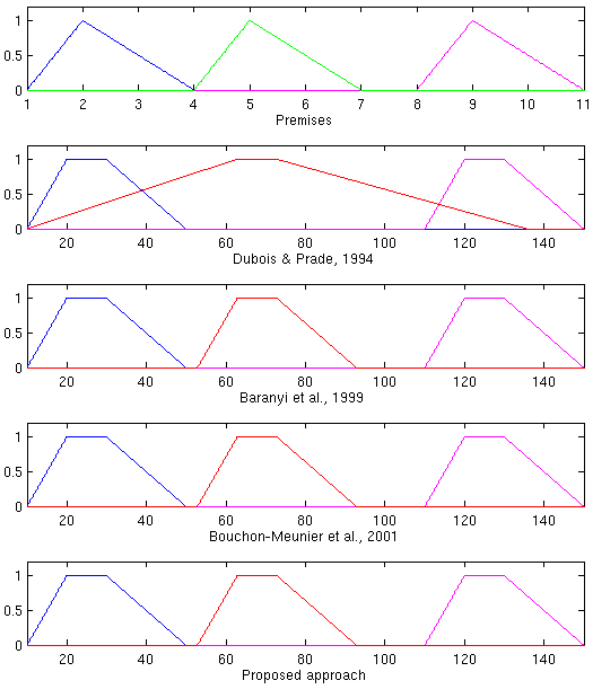

Fig. 5. All the shapes are similar (1)

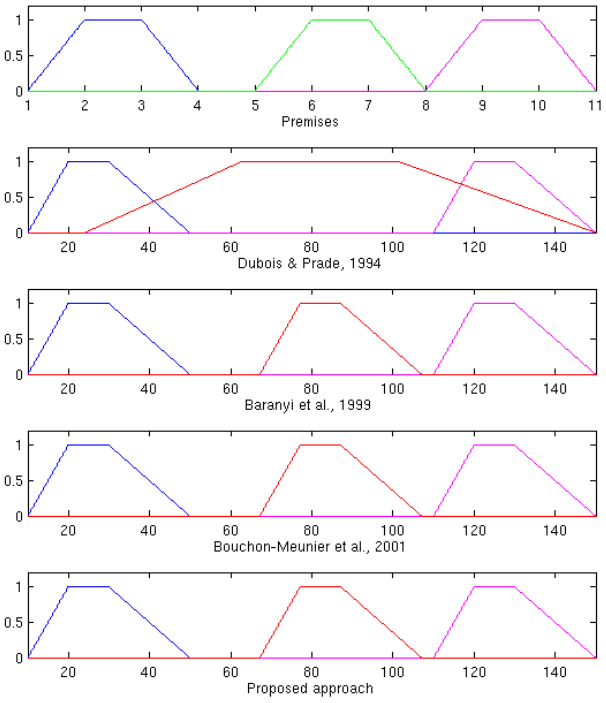

Fig. 6. All the shapes are similar (2)

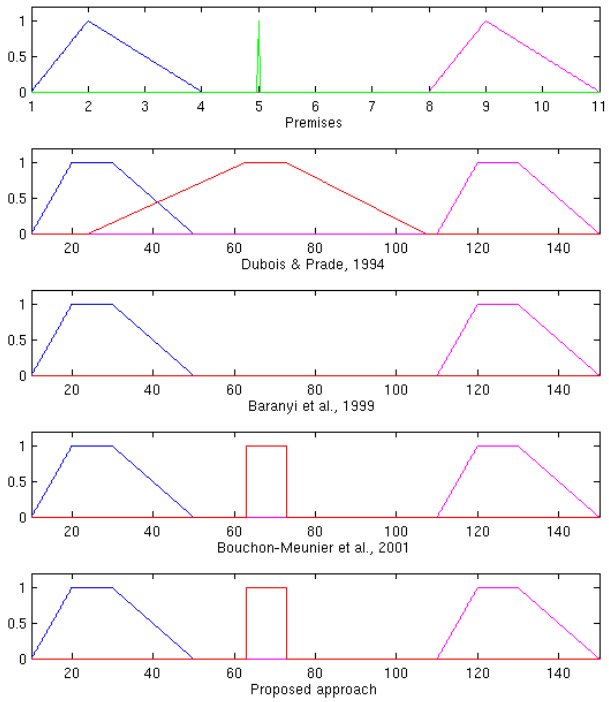

Fig. 7. Precise observation (1)

offers a very specific solution that can hardly be linked to the preciseness of the observation. BTKY proposes a non viable solution. Concerning BMR and DoLFIn, the results are different depending on the form of the premises and the conclusions. In a case, Fig. 7, BMR and DoLFIn methods propose a similar result. On the other case, Fig. 8, the results are very different: BMR proposes a fuzzy solution where DoLFIn constructs a precise solution.

The difference between the situations of Fig. 7 and Fig. 8 is that the forms of the premises are smaller than the forms of the conclusions on the first one, and greater on the second one. In this case, BMR method does not always provide a specific conclusion in presence of a specific observation.

In general, for a precise observation we obtain either a vague solution or no solution at all. While DoLFIn guarantees a specific conclusion in this case.

C. Precise premises

When premises are precise and the observation is imprecise and uncertain (see Fig. 9) all the methods except DoLFIn provide a solutions very imprecise and uncertain, sometimes going beyond the scope of the conclusions.

DoLFIn method proposes an interesting solution with a reasonable support size. Moreover, as for the observation and the premises, the solution respects the requirements imposed by the order $\preceq$ defined in Section II-B.

D. Extremely unspecific observations

When the observation is in the limit case of an extremely unspecific but precise interval that covers the whole space between the premises, see Fig. 10, DoLFIn is the only approach

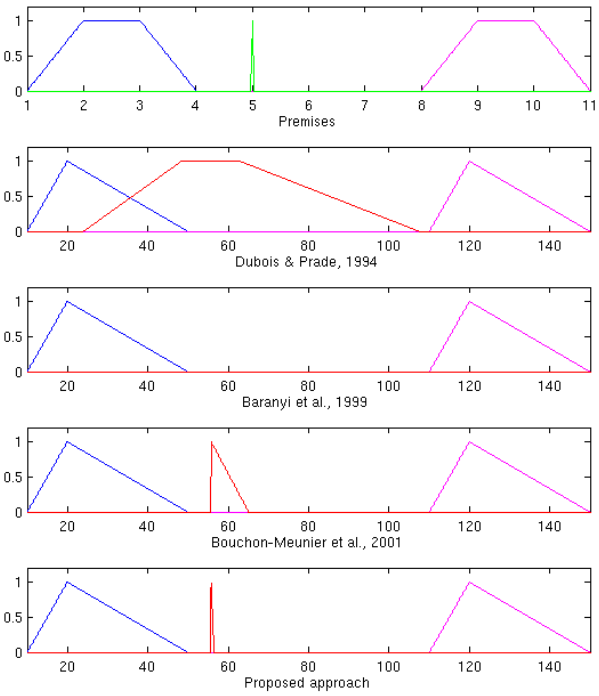

Fig. 8. Precise observation (2)

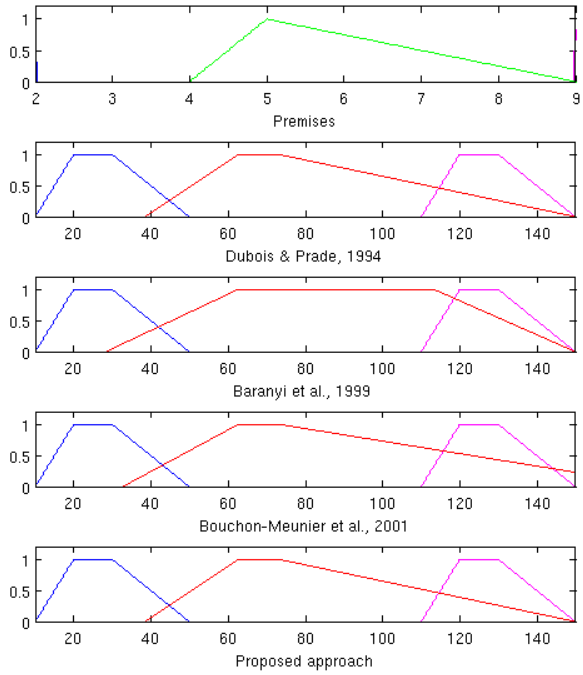

Fig. 9. Precise premises

that leads to an unspecific and precise conclusion. In this case, BTKY does not propose a viable solution, and BMR and DP construct imprecise solutions.

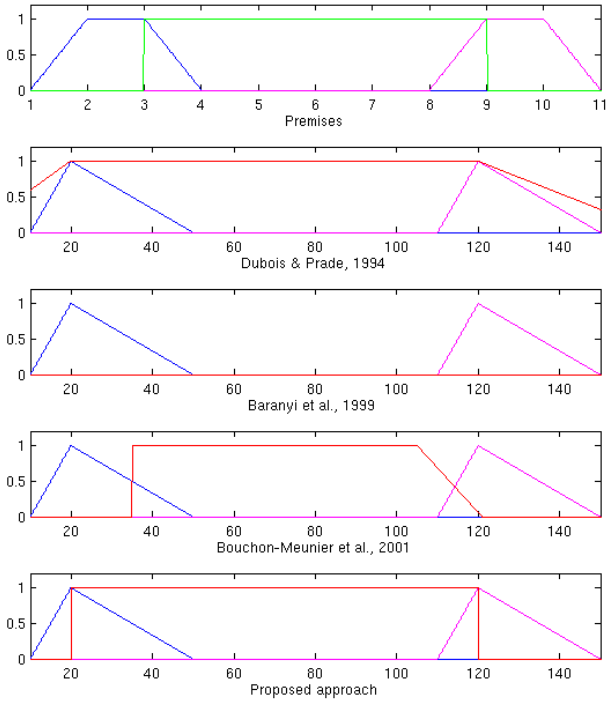

Fig. 10. Extremely unspecific observations

E. Remarkable examples

In figures Fig. 11 to Fig. 12, we extend our comparison by using some remarkable examples pointed out and shared by the following papers [3] (HS), [4] (CK), [17] (CCL). We invite the reader to refer to those papers for further details.

In Fig. 11, it can been seen that DP produces a very unspecific solution and BTKY constructs a non viable solution. The remaining approaches provide similar results with slight differences. BMR proposes a solution with a very steep right slope due to the fact that there is a strong transformation from the right slope of the premises to the observation. The result by DoLFIn is more fuzzy and with a different location than the solution by HS and CK. DoLFIn and CCL produce an almost identical conclusion.

A second remarkable example is presented in Fig. 12. Here again, it can been seen that DP produces a very unspecific conclusion. BTKY constructs a non viable solution. This time all the remaining approaches[1] (BMR, DoLFIn, CCL, and CK) produce a very similar result.

In general DoLFIn is able to provide a reasonable solution to all the remarquable examples identified by the above mentioned authors.

[1]The comparison with HS is not available because this example is not treated in [3].

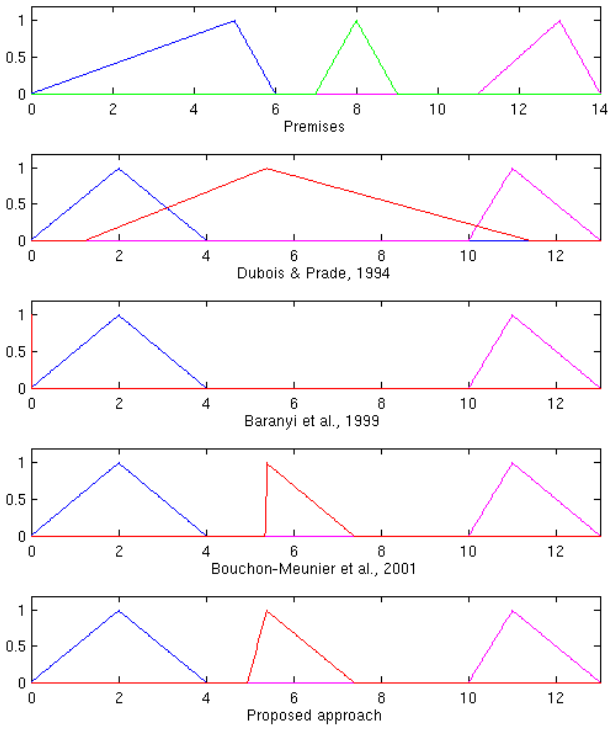

Fig. 11. Remarkable example (1)

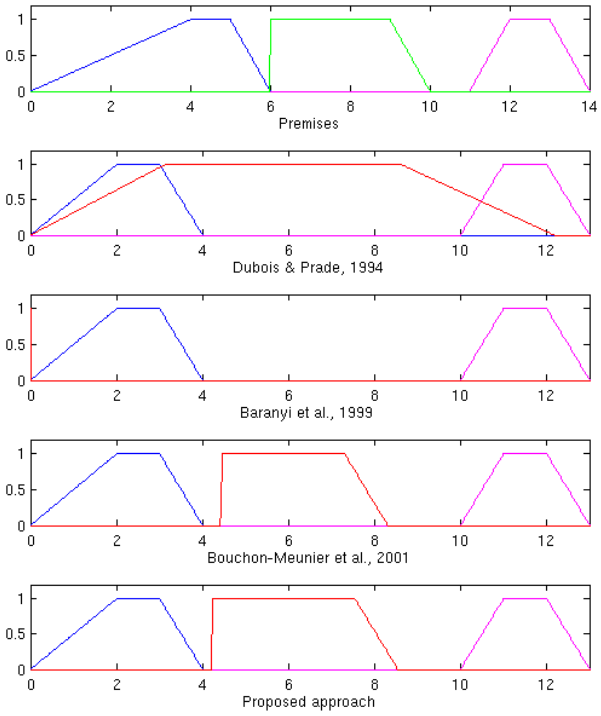

Fig. 12. Remarkable example (2)

F. Discussion

It can be seen in the presented comparison that for each of the scenarios, a group of methods (not always the same ones) provides adequate solutions.

DP proposes always a solution which is very unspecific and imprecise. BTKY generates conclusions often very pertinent but suffers of a problem of viability. BMR is very robust and can handle a large set of particular cases without having a problem of viability thanks to its standardization step [7]. However, the constructed solution can have a fuzzy conclusion with a precise observation, or a conclusion which is out of the scope of the known conclusions.

The proposed DoLFIn method has none of the mentioned drawbacks and proposes a pertinent and viable solution in all the studied cases without the use of a standardization step.

VI. Conclusion

Our method is based on the deviation to the expected linearly interpolated solution and constrains the constructed solution between extreme cases. We discovered that from the fundamental assumptions, mathematically, two scenarios appear: one where the form is expected to diminish but constrained to be positive and a second where the form is expected to grow but is constrained by the two known rules.

The presented study suggests that DoLFIn produces always a pertinent solution for a large set of diverse situations. Its pertinence is reinforced by the fact that each time the solution coincides with at least the result of another method.

An extensive and detailed comparison with a larger set of examples and methods coded in the FRI toolbox [18], is under development. We believe that its conclusion will not reveal any major differences with the conclusions of the presented paper. Future works will focus on the extension of the presented method to general shaped fuzzy sets and to the more complex multi-premise rules interpolation problem.

References

[1] L. T. Kóczy and K. Hirota, "Rule interpolation in approximate reasoning based fuzzy control," in *IFSA World Congress*, Brussels, 1991.

[2] ——, "Interpolative reasoning with insufficient evidence in sparse fuzzy rule bases," *Information Sciences*, vol. 71, no. 1–2, pp. 169–201, 1993.

[3] Z. Huang and Q. Shen, "Fuzzy interpolative reasoning via scale and move transformations," *Fuzzy Systems, IEEE Transactions on*, vol. 14, no. 2, pp. 340–359, april 2006.

[4] S.-M. Chen and Y.-K. Ko, "Fuzzy interpolative reasoning for sparse fuzzy rule-based systems based on α-cuts and transformations techniques," *IEEE Transactions on Fuzzy Systems*, vol. 16, no. 6, pp. 1626–1648, 2008.

[5] L.-W. Lee and S.-M. Chen, "Fuzzy interpolative reasoning for sparse fuzzy rule-based systems based on the ranking values of fuzzy sets," *Expert Systems with Applications*, vol. 35, pp. 850–864, 2008.

[6] S.-M. Chen and Y.-C. Chang, "Weighted fuzzy interpolative reasoning forsparse fuzzy rule-based systems," *Expert Systems with Applications*, Article in Press.

[7] B. Bouchon-Meunier, C. Marsala, and M. Rifqi, "Interpolative reasoning based on graduality," in *FUZZIEEE'00*, vol. 1, San Antonio, 2000, pp. 483–487.

[8] F. Esteva, M. Rifqi, B. Bouchon-Meunier, and M. Detyniecki, "Similarity-based fuzzy interpolation method," in *International conference on Information Processing and Management of Uncertainty in knowledge-based systems, IPMU 2004*, Perugia, July 2004.

[9] B. Bouchon-Meunier, F. Esteva, L. Godo, M. Rifqi, and S. Sandri, "A principled approach to fuzzy rule base interpolation using similarity relations," in *EUSFLAT–LFA 2005*, Barcelona, 2005, pp. 757–763.

[10] P. Baranyi, D. Tikk, L. T. Kóczy, and Y. Yam, "Investigation of a new alpha-cut based fuzzy interpolation method," The Chinese University of Hong Kong, Tech. Rep. CUHK-MAE-99-06, 1999.

[11] I. Perfilieva, D. Dubois, H. Prade, F. Esteva, L. Godo, and P. Hodakova, "Interpolation of fuzzy data: Analytical approach and overview," *Fuzzy Sets and Systems*, vol. 17, no. 1, pp. 134–160, Article in Press.

[12] P. Baranyi, D. Tikk, Y. Yam, L. Kczy, and L. Nadai, "A new method for avoiding abnormal conclusion for alpha;-cut based rule interpolation," in *FUZZ-IEEE'99*, vol. 1, Seoul, 1999, pp. 383–388.

[13] B. Bouchon-Meunier, D. Dubois, C. Marsala, H. Prade, and L. Ughetto, "A comparative view of interpolation methods between sparse fuzzy rules," in *IFSA'01 World Congress*, Vancouver, July 2001, pp. 2499–2504.

[14] I. Perfilieva, "Towards a theory of a fuzzy rule base interpolation," in *30^{th} Linz Seminars on Fuzzy Set Theory*, 2009.

[15] L. T. Koczy and S. Kovacs, "Shape of the fuzzy conclusion generated by linear interpolation in trapezoidal fuzzy rule bases," in *European Congress on Intelligent Techniques and Soft Computing*, Aachen, 1994, pp. 1666–1670.

[16] D. Dubois and H. Prade, "On fuzzy interpolation," in *Proceedings of the 3rd International Conference on Fuzzy Logic & Neural Networks*, Iizuka, Japan, August 1994, pp. 353–354.

[17] Y.-C. Chang, S.-M. Chen, and C.-J. Liau, "Fuzzy interpolative reasoning for sparse fuzzy-rule-based systems based on the areas of fuzzy sets," *Fuzzy Systems, IEEE Transactions on*, vol. 16, no. 5, pp. 1285 –1301, oct. 2008.

[18] Z. C. Johanyak, D. Tikk, S. Kovacs, and K. K. Wong, "Fuzzy rule interpolation matlab toolbox - fri toolbox," in *IEEE World Congress on Computational Intelligence (WCCI'06)*, Vancouver, BC, Canada, July 2006, pp. 1427–1433.

2011 IEEE International Conference on Fuzzy Systems
June 27-30, 2011, Taipei, Taiwan

Speedup of Fuzzy and Possibilistic Kernel c-Means for Large-Scale Clustering

Timothy C. Havens, Radha Chitta, Anil K. Jain, and Rong Jin
Department of Computer Science and Engineering
Michigan State University, East Lansing, MI 48824
E-mail: havenst@gmail.com, {chittara, jain, rongjin}@msu.edu

***Abstract*—The ubiquity of personal computing technology has produced an abundance of staggeringly large data sets—the Library of Congress has stored over 160 terabytes of web data and it is estimated that Facebook alone logs over 25 terabytes of data per day. There is a great need for systems by which one can elucidate the similarity and dissimilarity among and between groups in these data sets. Clustering is one way to find these groups. In this paper, we propose an approximation method for the fuzzy and possibilistic kernel c-means clustering algorithms. Our approximation constrains the cluster centers to be linear combinations of a size m randomly selected subset of the n input objects, where $m << n$. The proposed algorithm only requires an $m \times n$ rectangular portion of the full $n \times n$ kernel matrix and the n diagonal values, resulting in significant memory savings. Furthermore, the computational complexity of the c-means algorithm is substantially reduced. We demonstrate that up to 3 orders of magnitude of speedup are possible while achieving almost the same performance as the original kernel c-means algorithm.**

***Index Terms*—clustering, large-scale data, kernel methods, fuzzy partitions, possibilistic partitions**

I. Introduction

Clustering algorithms are an integral part of both computational intelligence and pattern recognition. Often researchers are mired in data sets that are large and unlabeled. There are many methods, under the heading exploratory data analysis, by which researchers can elucidate these data. Clustering is one such exploratory tool for deducing the nature of the data by providing labels to individual objects that describe how the data separate into groups. Clustering has also been shown to improve the performance of other algorithms or systems by separating the problem-domain into manageable sub-groups—a different algorithm or system is tuned to each cluster [1, 2]. Also, clustering has been used to infer the properties of unlabeled objects by clustering these objects together with a set of labeled objects (of which the properties are well understood) [3, 4].

The problem domains and applications of clustering are innumerable. Virtually every field, including biology, engineering, medicine, finance, mathematics, and the arts, have used clustering. Its function—grouping objects according to a measure of similarity—is a basic part of intelligence and is ubiquitous to the scientific endeavor.

Consider a set of n objects, denoted $O = \{o_1, \ldots, o_n\}$, e.g., sets of vintage bass guitars, freshwater fish, or genes in a microarray experiment. Each object is typically represented by an associated set of vectors $X = \{\mathbf{x}_1, \ldots, \mathbf{x}_n\} \in \mathbb{R}^d$, where each $\mathbf{x}$ is a numerical feature vector that describes the objects' attributes — examples include height, weight, length, or expression value.

Clustering in unlabeled data X is defined as the assignment of *labels* to groups of similar (unlabeled) objects O. In other words, objects are *partitioned* into groups such that each group is composed of objects with similar attributes. There are two important factors that all clustering algorithms must consider: 1) the number (and, perhaps, type) of clusters to seek and, 2) a mathematical way to determine the similarity between various objects (or groups of objects). Let c denote the integer number of clusters. The number of clusters can take the values $c = 1, 2, \ldots, n$, where $c = 1$ results in the universal cluster—every object is in one cluster—and $c = n$ results in single-object clusters—each object is a cluster. A wide array of algorithms exists for clustering unlabeled object data O. Descriptions of many of these algorithms, both relational and not, can be found in the following general references on clustering: [5–12].

A *partition* of the objects is defined as the set of cn values, where each value $\{u_{ik}\}$ represents the degree to which an object o_k is in the ith cluster. The c-partition is often represented as a $c \times n$ matrix $U = [u_{ik}]$, where each row represents a cluster and each column represents an object. There are three main types of partitions, crisp, fuzzy (or probabilistic), and possibilistic [7, 13]. *Crisp* partitions of the unlabeled objects are non-empty mutually-disjoint subsets of O such that the union of the subsets covers O. The set of all non-degenerate (no zero rows) crisp c-partition matrices for the object set O is described in (1), where u_{ik} is the *membership* of object o_k in cluster i; the partition element $u_{ik} = 1$ if o_k is labeled i and is 0 otherwise.

Fuzzy (or probabilistic) partitions are more flexible than crisp partitions in that each object can have membership in more than one cluster. Note, if U is probabilistic, the partition values are interpreted as a probability $p(i|o_k)$ that o_k is in the i-th class. We assume, in this paper, that fuzzy and probabilistic partitions are essentially equivalent from the point of view of clustering algorithm development. The set of all fuzzy c-partitions is described in (2). Each column of the fuzzy partition U must sum to 1, thus ensuring that every object is involved in a partition ($\sum_i u_{ik} = 1$).

Possibilistic partitions relax this condition, allowing partition columns that do not necessarily sum to 1. Possibilistic

978-1-4244-7316-8/11/$26.00 ©2011 IEEE

$$M_{hcn} = \left\{ U \in \mathbb{R}_{0,+}^{c\times n} | u_{ij} \in 0,1, \forall j,i; 0 < \sum_{i=1}^{n} u_{ij} < n, \forall j; \sum_{j=1}^{c} u_{ij} = 1, \forall i \right\} \quad (1)$$

$$M_{fcn} = \left\{ U \in \mathbb{R}_{0,+}^{c\times n} | u_{ij} \in [0,1], \forall j,i; 0 < \sum_{i=1}^{n} u_{ij} < n, \forall j; \sum_{j=1}^{c} u_{ij} = 1, \forall i \right\} \quad (2)$$

$$M_{pcn} = \left\{ U \in \mathbb{R}_{0,+}^{c\times n} | u_{ij} \in [0,1], \forall j,i; 0 < \sum_{i=1}^{n} u_{ij} < n, \forall j; \max_{1\le j\le c} u_{ij} > 0, \forall i \right\} \quad (3)$$

$$\min_{U} \left\{ J_m(U;H,K) = \sum_{j=1}^{c} \left(\sum_{i=1}^{n}\sum_{k=1}^{n} \left(u_{ij}^m u_{kj}^m d_\kappa(\mathbf{x}_i,\mathbf{x}_k) \right) / 2 \sum_{l=1}^{n} u_{lj}^m \right) + \sum_{j=1}^{c} \nu_j \sum_{i=1}^{n} (1-u_{ij})^m \right\} \quad (4)$$

clustering has been shown to be especially effective in partitioning data that has outliers and intersecting clusters [13]. The set of all possibilistic c-partitions is described in (3), where u_{ik} is the possibility that o_k is in cluster i (this was also described in [13] as the *typicality* of o_k to cluster i). Notice that the possibilistic partition ensures that there is at least one object that has a non-zero possibility of being in each cluster (the empty cluster cannot exist). An interesting property of these three types of partitions is that all crisp partitions are fuzzy partitions and all fuzzy partitions are possibilistic partitions. Equations (1), (2), and (3), show that $M_{hcn} \subset M_{fcn} \subset M_{pcn}$.

All cluster analyses address the same questions, independent of the type of partition. The three main questions are: i) *Cluster tendency*—are there clusters, and how many clusters are there? ii) *Partitioning*—which objects belong to which cluster and to what degree? And iii) *cluster validity*—are the partitions "good"? There are many algorithms that attempt to answer these questions. This paper focuses on a specific form of question ii), namely soft c-means partitioning of large datasets in kernel-induced spaces.

A. Kernel c-Means

Consider some non-linear mapping function $\phi : \mathbf{x} \rightarrow \phi(\mathbf{x}) \in \mathbb{R}^{D_K}$, where D_K is the dimensionality of the transformed feature vector $\mathbf{x}$. With kernel clustering, we do not need to explicitly transform $\mathbf{x}$, we simply need to represent the dot product $\phi(\mathbf{x}) \cdot \phi(\mathbf{x}) = \kappa(\mathbf{x},\mathbf{x})$. The kernel function κ can take many forms, with the polynomial $\kappa(\mathbf{x},\mathbf{y}) = (\mathbf{x}^T\mathbf{y}+1)^p$ and radial-basis-function (RBF) $\kappa(\mathbf{x},\mathbf{y}) = \exp(||\mathbf{x}-\mathbf{y}||^2/\sigma)$ being two of the most well known. Given a set of n objects X, we can thus construct an $n \times n$ kernel matrix $K = [K_{ij} = \kappa(\mathbf{x}_i,\mathbf{x}_j)]^{n\times n}$. This kernel matrix K represents all pairwise dot products of the feature vectors associated with n objects in the transformed high-dimensional space—called the Reproducing Kernel Hilbert Space (RKHS).

Given a kernel matrix K, the kernel c-means can be generally defined as the constrained optimization in (4), where $U \in M_{pcn}$, $H = \{\nu_1,\ldots,\nu_c\} \in \mathbb{R}_{0,+}$ is the cluster radii set (which only applies to possibilistic clustering), $m \geq 1$ is the fuzzification parameter, and $d_\kappa(\mathbf{x}_i,\mathbf{x}_k)$ is the kernel-based distance between the ith and kth objects. All three of the major c-means algorithms—hard, fuzzy, and possibilistic—can be instantiated by adjusting the parameters appropriately in the objective function in (4). Table I shows how the parameters of (4) are set for each algorithm. For simplicity, we denote the cluster center to object distance $d_\kappa(\mathbf{v}_j,\mathbf{x}_i)$ as $d_\kappa(j,i)$.

TABLE I: Hard, Fuzzy, and Possibilistic Variations of Solving the c-Means Optimization in Eq. (4) [14]

Algorithm	m	H	U
Hard (Crisp)	$m=1$	$\nu_j = 0,\ \forall j$	Use Eq. (5)
Fuzzy	$m>1$	$\nu_j = 0,\ \forall j$	Use Eq. (6)
Possibilistic	$m>1$	$\nu_j > 0,\ \forall j$	Use Eq. (7)

Hard c-means membership update [15]:

$$u_{ij} = \begin{cases} 1, & d_\kappa(j,i) = \min_{1\le k\le c} d_\kappa(k,i) \\ 0, & \text{else} \end{cases}, \ \forall j,i \quad (5)$$

Fuzzy c-means membership update [15]:

$$u_{ij} = \left(\sum_{k=1}^{c} \left(\frac{d_\kappa(j,i)}{d_\kappa(k,i)} \right)^{\frac{2}{m-1}} \right)^{-1}, \ \forall i,j \quad (6)$$

Possibilistic c-means membership update [15]:

$$u_{ij} = \left(1 + \left(\frac{d_\kappa(j,i)}{\nu_j} \right)^{\frac{2}{m-1}} \right)^{-1}, \ \forall i,j \quad (7)$$

The partition update equations in Table I are all based on a kernel distance between an object and a cluster center, which is computed as

$$d_\kappa(j,i) = ||\phi(\mathbf{v}_j) - \phi(\mathbf{x}_i)||^2, \quad (8)$$

where

$$\phi(\mathbf{v}_j) = \frac{\sum_{l=1}^{n} u_{lj}^m \phi(\mathbf{x}_l)}{\sum_{l=1}^{n} u_{lj}^m}. \quad (9)$$

We can simplify (8) by using the identity $K_{ij} = \phi(\mathbf{x}_i) \cdot \phi(\mathbf{x}_j)$ and denoting $\tilde{\mathbf{u}}_j = \mathbf{u}_j^m / ||\mathbf{u}_j^m||_1$ ($\mathbf{u}_j$ is the jth column of U),

which gives

$$\begin{aligned} d_\kappa(j,i) &= \frac{\sum_{l=1}^n \sum_{s=1}^n u_{lj}^m u_{sj}^m \phi(\mathbf{x}_l)\cdot\phi(\mathbf{x}_s)}{\sum_{l=1}^n u_{lj}^{2m}} \\ &\quad +\phi(\mathbf{x}_i)\cdot\phi(\mathbf{x}_i) - 2\frac{\sum_{l=1}^n u_{lj}^m \phi(\mathbf{x}_l)\cdot\phi(\mathbf{x}_i)}{\sum_{l=1}^n u_{lj}^m} \\ &= \tilde{\mathbf{u}}_j^T K \tilde{\mathbf{u}}_j + \mathbf{e}_i^T K \mathbf{e}_i - 2\tilde{\mathbf{u}}_j^T K \mathbf{e}_i \\ &= \tilde{\mathbf{u}}_j^T K \tilde{\mathbf{u}}_j + K_{ii} - 2(\tilde{\mathbf{u}}_j^T K)_i, \end{aligned} \tag{10}$$

where $\mathbf{e}_i$ is a length n unit vector with the ith element equal to 1.

In *possibilistic c-means* (PCM), the parameters ν determine the influence of each cluster on the value of the objective function in (4), where the second term in (4) penalizes the trivial solution of $u_{ij} = 0,\ \forall i, j$.

Algorithms 1, 2, and 3 outline the kernel-based variants of *hard c-means* (HCM), *fuzzy c-means* (FCM), and PCM, respectively. This variant of the PCM algorithm first initializes the memberships by using FCM, then the ν parameter is estimated by

$$\nu_j = \Theta \frac{\sum_{i=1}^n u_{ij}^m d_\kappa(j,i)}{\sum_{i=1}^n u_{ij}^m},\ \forall j, \tag{11}$$

where $\Theta > 0$ and is usually set to $\Theta = 1$ [8, 13].

Algorithm 1: Hard c-Means (HCM) Kernel Clustering Algorithm

Input: K - $n \times n$ kernel matrix
Data: $m = 1$, $U \in \{0,1\}^{c\times n}$ cluster membership matrix
Initialize U
while $\max\{|U - U'|\} > 0$ **do**
  $U' = U$
  Compute $d_\kappa(j,i)$, $\forall i, j$, using Eq.(10)
  Update U using Eq. (5)

Algorithm 2: Fuzzy c-Means (FCM) Kernel Clustering Algorithm

Input: K - $n \times n$ kernel matrix; m - fuzzifier
Data: $U \in [0,1]^{c\times n}$ cluster membership matrix
Initialize U
while $\max\{|U - U'|\} > \epsilon$ **do**
  $U' = U$
  Compute $d_\kappa(j,i)$, $\forall i, j$, using Eq.(10)
  Update U using Eq. (6)

In all these c-means variants, Eq.(10) is computationally expensive for large number of objects n as it requires $O(n^2)$ operations. Furthermore, the entire kernel matrix K is required and producing and storing this matrix for the entire data set is often very computationally expensive; e.g., $n = 100,000$ requires 40 gigabytes of memory, which is not a small amount by today's standards. We approximate $d_\kappa(j,i)$ by constraining the space in which the cluster centers exist.

Algorithm 3: Possibilistic c-Means (PCM) Kernel Clustering Algorithm [13, 16]

Input: K - $n \times n$ kernel matrix; m - fuzzifier
Data: $U \in [0,1]^{c\times n}$ cluster membership matrix
Run FCM to initialize U
Estimate ν_j by Eq. (11)
while $\max\{|U - U'|\} > \epsilon$ **do**
  $U' = U$
  Compute $d_\kappa(j,i)$, $\forall i, j$, using Eq. (10)
  Update U using Eq.(7)

II. Large Scale c-Means Approximation Algorithms

The cluster centers in kernel c-means algorithms are represented by a linear sum of the high-dimensional transformed features $\phi(\mathbf{x}_i)$,

$$\phi(\mathbf{v}_j) = \sum_{i=1}^n \tilde{u}_{ij}\phi(\mathbf{x}_i), \tag{12}$$

where this equation is equivalent to (9) with $\tilde{u}_{ij}$ substituted. In data where the number of objects n is large, we hypothesize that the cluster centers $\phi(\mathbf{v}_j)$ can be accurately represented by a subset of the feature vectors $\phi(\mathbf{x})$. Let $\xi = (\xi_1, \ldots, \xi_n)$ be binary variables indicating the instances that are selected for constructing the cluster centers, with $\xi_i = 1$ if $\mathbf{x}_i$ is selected and 0 otherwise. Let s denote the number of selected objects, where $s = \sum_i \xi_i$. The following derivation follows, very closely, that of our previous work [17] on approximating HCM for large-scale data.

In our approximation, the cluster centers are approximated by a linear sum of the selected feature vectors

$$\hat{\phi}(\mathbf{v}) = \sum_{i=1}^n a_i \xi_i \phi(\mathbf{x}_i), \tag{13}$$

where a_i is the weight of the ith feature vector. We are only interested in the values of a_i when $\xi_i = 1$; hence, we denote the weights for the jth cluster center as $\alpha_j = (\alpha_{1j} = a_{(1)}, \ldots, \alpha_{sj} = a_{(s)})$, where $a_{(1)}, \ldots, a_{(s)}$ are the set of associated weights where $\xi = 1$. Although this notation seems cumbersome, it dramatically simplifies the description of our derivation. With this notation, we can rewrite (13) for the jth cluster center as

$$\hat{\phi}(\mathbf{v}_j) = \sum_{i=1}^s \alpha_{ij}\phi(\mathbf{x}_{(i)}), \tag{14}$$

where it is clear now that we are representing the cluster center $\phi(\mathbf{v}_j)$ as a linear sum of s selected objects.

Now we want to solve for the weights α_j such that the distance between the true cluster center and the approximated cluster center, $||\phi(\mathbf{v}_j) - \hat{\phi}(\mathbf{v}_j)||^2$, is minimized. This distance

can be written as

$$||\phi(\mathbf{v}_j) - \hat{\phi}(\mathbf{v}_j)||^2 = \left|\left|\sum_{i=1}^{n} \tilde{u}_{ij}\phi(\mathbf{x}_i) - \sum_{i=1}^{n} a_i\xi_i\phi(\mathbf{x}_i)\right|\right|^2$$
$$= \tilde{\mathbf{u}}_j^T K \tilde{\mathbf{u}}_j + (\mathbf{a}\circ\xi)_j^T K (\mathbf{a}\circ\xi)_j - 2\tilde{\mathbf{u}}_j^T K(\mathbf{a}\circ\xi)_j, \quad (15)$$

where $\circ$ indicates the Hadamard product or element-by-element multiplication (.* in MATLAB) and $(\mathbf{a}\circ\xi)_j$ is an n-length vector that represents the weights of the approximated cluster center $\hat{\phi}(\mathbf{v}_j)$. We can substitute α_j into (15) by defining two sub-matrices of the kernel matrix K,

$$K_{\xi\xi} = [K_{ij}]^{s\times s},\ \xi_i = 1, \xi_j = 1, \quad (16)$$
$$K_{\xi} = [K_i]^{n\times s},\ \xi_i = 1, \quad (17)$$

where K_i is the ith column of K. Notice that $K_{\xi\xi}$ is the $s\times s$ square matrix corresponding to the pairwise elements of K for the ξ-selected objects. K_ξ is the $n\times s$ rectangular matrix corresponding to the columns of K for the ξ-selected objects; also, $K_{\xi\xi}$ is a sub-matrix of K_ξ. Hence, we can now rewrite (15) as

$$||\phi(\mathbf{v}_j) - \hat{\phi}(\mathbf{v}_j)||^2 = \tilde{\mathbf{u}}_j^T K \tilde{\mathbf{u}}_j + \alpha_j^T K_{\xi\xi}\alpha_j - 2\tilde{\mathbf{u}}_j^T K_\xi \alpha_j. \quad (18)$$

We determine α_j by minimizing (18) with respect to α, which is solved by setting the derivative of (18) with respect to α_j to zero,

$$\frac{d||\phi(\mathbf{v}_j) - \hat{\phi}(\mathbf{v}_j)||^2}{d\alpha_j} = 2K_{\xi\xi}\alpha_j - 2\tilde{\mathbf{u}}_j^T K_\xi = 0,$$

leading to the solution

$$\alpha_j = -\left(K_{\xi\xi}^{-1} K_\xi^T \tilde{\mathbf{u}}_j\right)^T. \quad (19)$$

In practice, $K_{\xi\xi}$ could be rank-deficient (have a number of relatively small eigenvalues); hence, it is advisable to use a pseudo-inverse when computing $K_{\xi\xi}^{-1}$, which we denote as $K_{\xi\xi}^\dagger$. Also, the calculation of $K_{\xi\xi}^{-1}K_\xi^T$ only needs to be performed once, at the beginning of the algorithm, with the result stored.

The key element of our approximation algorithms is the redefinition of Eq. (10) using the solution of α_j, i.e.,

$$\hat{d}_\kappa(j,i) = \alpha_j^t K_{\xi\xi}\alpha_j + K_{ii} - 2(K_\xi\alpha_j)_i. \quad (20)$$

Notice that we no longer require the full kernel matrix to compute the distance $\hat{d}_\kappa(j,i)$; the only required kernel matrix elements are the diagonal elements (which for the RBF are all equal to one) and the s columns of K corresponding to the selected objects.

We are now ready to define our large-scale approximations of the kernel FCM and PCM algorithms. Algorithms 4 and 5 outline the approximations of the kernel FCM and PCM algorithms, respectively, which we call akFCM and akPCM.

The computational complexity of the distance calculation in (20) is $O(sn)$, which for $s << n$ is a significant improvement on the $O(n^2)$ complexity of the full-kernel distance calculation in (10). Furthermore, only $sn + n - s$ elements of K need to be calculated—the sn elements of K_ξ and the $n - s$ additional diagonal elements—which both reduces the computation time to produce the kernel elements and the storage requirements. However, for very large n both the computational and memory requirements can still be significant—e.g. a $10,000\times 1,000,000$ array of floats (4 bytes) requires 40 gigabytes of working memory. While this memory requirement is large (at the time this paper was written), it is manageable compared to the 4 terabyte memory requirement for the full $1,000,000\times 1,000,000$ kernel matrix.

The computational complexity of the pseudo-inverse of $K_{\xi\xi}$ is $O(m^3)$, which could lead to problems for large m. However, in practice, one could employ gradient descent to solve for α.

Next, we move on to some experiments.

Algorithm 4: Approximate Fuzzy c-Means (akFCM) Kernel Clustering Algorithm

Input: K_ξ - $n\times s$ kernel sub-matrix; diag(K) - Kernel matrix diagonal; m - fuzzifier; ξ - selection vector
Data: $U\in[0,1]^{c\times n}$ cluster membership matrix
Initialize U
$\hat{K} = -K_{\xi\xi}^\dagger K_\xi^T$
while $\max\{|U - U'|\} > \epsilon$ **do**
  $U' = U$
  $\alpha_j = \left(\hat{K}\tilde{\mathbf{u}}_j\right)^T,\ \forall j$
  $\hat{d}_\kappa(j,i) = \alpha_j^t K_{\xi\xi}\alpha_j + K_{ii} - 2(K_\xi\alpha_j)_i,\ \forall i,j$
  Update U using Eq. (6)

Algorithm 5: Approximate Possibilistic c-Means (akPCM) Kernel Clustering Algorithm

Input: K_ξ - $n\times s$ kernel sub-matrix; diag(K) - Kernel matrix diagonal; m - fuzzifier; ξ - selection vector
Data: $U\in[0,1]^{c\times n}$ cluster membership matrix
$\hat{K} = -K_{\xi\xi}^\dagger K_\xi^T$
Run akFCM to initialize U
Estimate ν_j by Eq. (11)
while $\max\{|U - U'|\} > \epsilon$ **do**
  $U' = U$
  $\alpha_j = \left(\hat{K}\tilde{\mathbf{u}}_j\right)^T,\ \forall j$
  $\hat{d}_\kappa(j,i) = \alpha_j^t K_{\xi\xi}\alpha_j + K_{ii} - 2(K_\xi\alpha_j)_i,\ \forall i,j$
  Update U using Eq. (7)

III. Experiments

We performed two sets of experiments. The first compared the performance of the proposed algorithms with the full kernel solution. The second set of experiments applies the proposed algorithms to data sets for which computing the full kernel solution was impossible because of memory limitations.

The experiments described in this paper were performed on a single core of an AMD Opteron in a Sun Fire X4600 M2 server with 256 gigabytes of memory. All code was written in the MATLAB [18] computing environment.

A. Evaluation Criteria

We judge the performance of our proposed algorithms with three criteria. Each criteria is computed for 20 independent runs. For each run, we initialize the full kernel c-means and the sampled kernel c-means algorithms with the same initialization. Thus, both the approximation algorithm and the full kernel algorithm begin with the same initial partition, with a different initialization for each run. We initialize U by choosing c objects as the initial cluster centers. The value of $\epsilon = 1 \times 10^{-3}$ and the fuzzifier $m = 2$.

1) Speedup Factor: This criteria represents an actual run-time comparison. Speedup is defined as t_{full}/t_{samp}, where these values are times in seconds for computing the membership matrix U. Note that we de not include the time savings from having to only compute a portion of the kernel matrix in our calculation. Thus, the speedup we present is a conservative measure. In practice, one would see further improvement by only calculating the necessary portions of the kernel matrix—the $m \times n$ rectangular matrix K_ξ and the diagonal of K.

2) Cluster Purity: This measure is defined as

$$P = \frac{1}{n} \sum_{j=1}^{c} \max_{\omega \in \Omega} |\omega \cap C_j|, \tag{21}$$

where Ω is the set of all class labels and C_j is the set of labels of the objects in the jth cluster. This measure cannot be directly applied to soft partitions; hence, we first *harden* the partitions before applying (21). Hardening is the process of setting the maximum cluster membership in each column of U to 1 and all else to 0.

The figures in this paper show *relative purity*, which is calculated as $P_{samp} - P_{full}$ for each run.

3) Squared Error Distortion: This criteria is the c-means objective and is defined as

$$E = \sum_{j=1}^{c} \sum_{i=1}^{n} u_{ji}^m ||\phi(\mathbf{v}_j) - \phi(\mathbf{x}_i)||^2 = \sum_{j=1}^{c} \sum_{i=1}^{n} u_{ji}^m d_\kappa(j,i). \tag{22}$$

We present the % error in E, which is calculated as

$$\%\ \text{Error} = \frac{E_{samp} - E_{full}}{E_{full}} * 100.$$

As with relative purity, % Error is only calculated between the approximation result and the full kernel result that start with the same initialization. By doing this, we are negating the effect that the initialization has on the result.

B. Comparison with Full Kernel c-Means

We compared the proposed approximation to the full kernel method on two different data sets.

1) **A3**: These data are composed of 7,500 2-dimensional vectors, with a visually-preferred grouping into 50 clusters.[1] Figure 1 shows a plot of these data. We used the RBF kernel with $\sigma = 0.5$.

[1]The A3 data was designed by Ilja Sidoroff and can be downloaded at http://cs.joensuu.fi/~isido/clustering/.

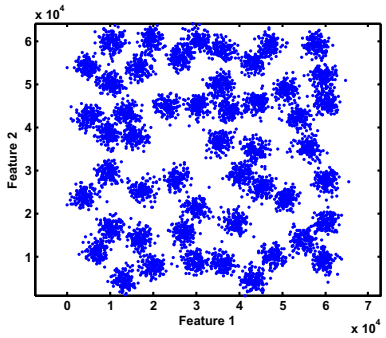

Fig. 1: Plot of A3 data set.

2) **MNIST**: This data set is a subset of the collection of handwritten digits available from the *National Institute of Standards and Technology* (NIST)[2]. There are 70,000 28×28 pixel images of the digits 0 to 9. Each pixel has an integer value between 0 and 255. We normalize the the pixel values to the interval $[0, 1]$ by dividing by 255 and concatenate each image into a 784-dimensional column vector. The kernel used for this example was a degree-5 polynomial kernel $\kappa(\mathbf{x}, \mathbf{y}) = (\mathbf{x}^T\mathbf{y} + 1)^5$, which was shown to be effective in [19].

Figure 2 illustrates the evaluation criteria for the sFCM clustering algorithm on the A3 data set. The error-bars indicate the maximum and minimum values of each criteria over 20 independent runs. View (a) shows that an order of magnitude speedup is attained with sample sizes $m \leq 250$, or at a 3% sampling rate. Views (b) and (c) show that even at very low sample rates, the quality of the approximated clustering solution is equal to that of the full kernel solution and in one instance, at sample size $m = 1500$, the cluster purity was 2% greater than that of the full kernel solution.

The results of the akPCM algorithm on the A3 data set are illustrated in Fig. 3. View (a) shows that akPCM provides similar speedup results as akFCM and views (b) and (c) demonstrate that the quality of the solution is better than that of the full kernel algorithm. We conjecture that this is because the influence of objects in regions where classes overlap is perhaps lessened by the sampling process.

Figures 4 and 5 show the results of the experiments performed on the MNIST data set. The results of the akFCM algorithm show significant speedup at low sampling rates (the two lowest sampling rates are 0.1% and 0.2%, respectively) with negligible difference in the quality of the clustering, relative to the full kernel c-means. Figure 3(a) shows that 1-2 orders of magnitude in speedup is achieved; however, in the akPCM experiments, a degradation in the cluster purity of about 3% was observed. Again, the lower sampling rates perform better than the higher sampling rates. We aim to investigate this phenomenon in subsequent studies and conjecture that this behavior is either due to the psuedo-inverse calculation in the approximation algorithm or because of the influence of outlier

[2]The MNIST data can be downloaded at http://yann.lecun.com/exdb/mnist/.

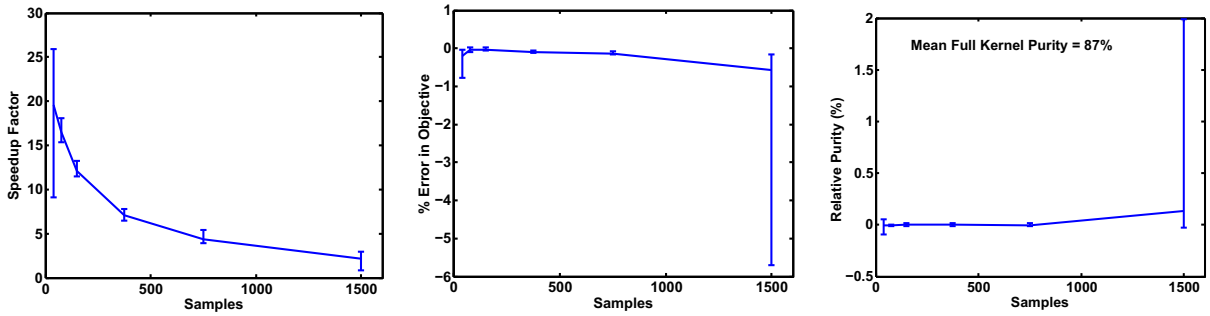

(a) Speedup — t_{full}/t_{samp} (b) % Error in squared distortion — $(E_{samp} - E_{full})/E_{full}$ (c) Relative cluster purity — $P_{samp} - P_{full}$

Fig. 2: Performance of akFCM on *A3* data set using RBF kernel with $\sigma = 0.5$, $n = 7500$, $c = 50$. Lines denotes mean values over 21 runs; error-bars represent maximum and minimum values. Membership matrix was hardened to compute cluster purity.

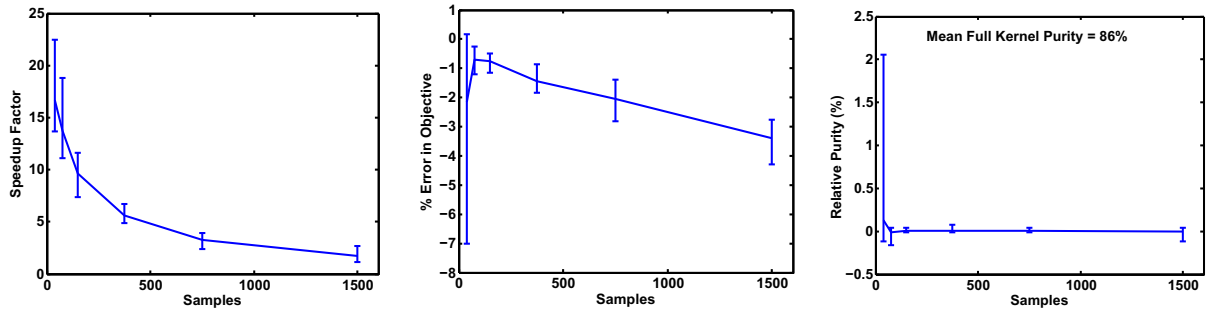

(a) Speedup — t_{full}/t_{samp} (b) % Error in squared distortion — $(J_{samp} - J_{full})/J_{full}$ (c) Relative cluster purity — $P_{samp} - P_{full}$

Fig. 3: Performance of akPCM on *A3* data set using RBF kernel with $\sigma = 0.5$, $n = 7500$, $c = 50$. Lines denote mean values over 21 runs; error-bars represent maximum and minimum values. Membership matrix was hardened to compute cluster purity.

and overlapping classes.

C. Performance on Very Large Data Sets

Now we present the results of our proposed approximation algorithms on two data sets which are considerably larger than than the those in the previous experiments.

To store the full kernel matrix for either of the data sets in this section in single-precision format would require 1+ terabytes (1,000 gigabytes) of memory. At the time of this study, 1 terabyte of memory was an exceptionally large amount. Without considering distributed memory architectures, this is out of reach for most researchers and consumers.

1) **Forest Cover Type** [20][3]: These data are composed of cartographic variables obtained from *United States Geological Survey* (USGS) and *United State Forest Service* (USFS) data. There are 10 quantitative variables, such as elevation and horizontal distance to hydrology, 4 binary wilderness area designation variables, and 40 binary soil type variables. These features were collected from a total of 581,012 30×30 meter cells, which were then determined to be one of 7 forest cover types by the USFS. We normalize the features to the interval $[0, 1]$.

[3]The *Forest Cover Type* and *Quadreped Mammals* data sets can be downloaded at http://uisacad2.uis.edu/dstar/data/clusteringdata.html.

2) **Quadruped Mammals** [20]: These data are generated by the program animals.c, which can be downloaded from the UCI Machine Learning depository. The program generates instances of 72-dimensional feature vectors which belong to one of 4 classes of animals: dogs, cats, horses, and giraffes. We use 500,000 examples from this data set, with an approximately equal number of each class.

These problems become manageable by applying our approximation algorithms. We collected results for these two data sets at sample rates, $m = 0.01\%n$, $0.05\%n$, and $0.1\%n$. We produced 5 random draws of the selection variable ξ and for each random draw computed the akFCM and akPCM solutions for 5 different initializations; thus, a total of 25 experiments were done at each sample rate. Two different kernels were used, a degree-2 polynomial and an RBF with $\sigma = 2$.

Table II contains the run-time and cluster purity values for the two very large data sets. These results show that the akFCM algorithm can be used to cluster the Mammals data set in 8 seconds, with a cluster purity of 85%, and the Cover Type data set in 58 seconds, with a cluster purity of 52%.

For comparison, it was reported in [21] that the CLUTO [22] hard clustering algorithm achieved a purity score of 0.49 in on the Cover Type data and 0.82 purity on the Mammals data set. Our approximation algorithm produces results slightly

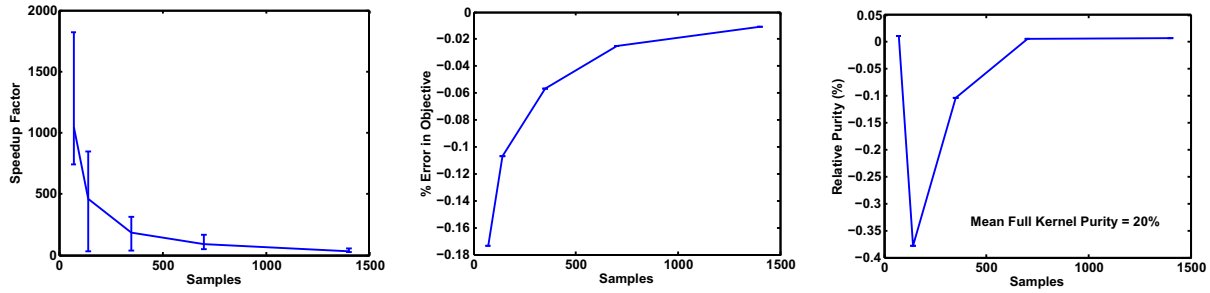

(a) Speedup — t_{full}/t_{samp} (b) % Error in squared distortion — $(J_{samp} - J_{full})/J_{full}$ (c) Relative cluster purity — $P_{samp} - P_{full}$

Fig. 4: Performance of akFCM on *MNIST* data set using degree-5 polynomial kernel, $n = 70000$, $c = 10$. Lines denote mean values over independent 21 runs; error-bars represent maximum and minimum values. Membership matrix was hardened to compute cluster purity.

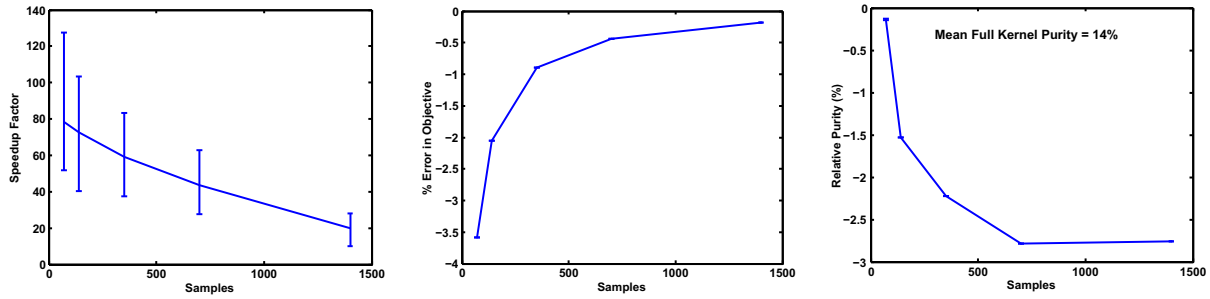

(a) Speedup — t_{full}/t_{samp} (b) % Error in squared distortion — $(J_{samp} - J_{full})/J_{full}$ (c) Relative cluster purity — $P_{samp} - P_{full}$

Fig. 5: Performance of akPCM on *MNIST* data set using degree-5 polynomial kernel, $n = 70000$, $c = 10$. Lines denote mean values over independent 21 runs; error-bars represent maximum and minimum values. Membership matrix was hardened to compute cluster purity.

TABLE II: Clustering Results of akFCM and akPCM Algorithms on Very-Large Data

Data Set	Quadruped Mammals						Forest Cover Type					
Kernel	Degree-2 Polynomial			RBF ($\sigma = 1$)			Degree-2 Polynomial			RBF ($\sigma = 1$)		
Sample size m	50	250	500	50	250	500	59	291	582	59	291	582
akFCM	$c = 4$						$c = 7$					
Run-time (secs)	8	34	91	8	60	88	75	229	416	58	154	384
Purity	0.85	0.86	0.86	0.85	0.86	0.86	0.53	0.53	0.53	0.52	0.52	0.52
akPCM	$c = 4$						$c = 7$					
Run-time (secs)	30	129	199	35	151	224	125	352	600	87	215	570
Purity	0.68	0.69	0.71	0.68	0.69	0.69	0.50	0.50	0.50	0.49	0.49	0.49

better to those of CLUTO on these data. The GARDEN$_{HD}$ hard clustering algorithm [21] achieved a purity score of 0.65 on the Cover Type data; although, this algorithm is based on recursive division of the vector data and determined that the Cover Type data has 84 clusters. Cluster purity, by definition, tends to increase as the number of clusters increases; e.g., when the number of clusters $c = n$, purity $= 1$. Thus, comparing our results directly against GARDEN$_{HD}$ is not advised. The GARDEN$_{HD}$ algorithm achieved a purity of 0.76 with 1250 clusters and a purity of 1 with 6314 clusters on the Mammals data set. In comparison, akFCM achieved a purity of 0.86 with 4 clusters on this data and many of the individual runs in our experiment did produce a perfect cluster purity of 1. We believe that these results show that our algorithm is producing results that are as good as or better than existing algorithms that work on large scale data.

IV. Conclusion

We proposed an approximation of the fuzzy and possibilistic kernel c-means that has a reduced computational complexity and memory requirement. Our experimental results show that run-time can be decreased by 1-2 orders of magnitude, while achieving equal clustering performance to the classical kernel c-means. Furthermore, the memory requirements of our approximation is $O(mn)$, compared to $O(n^2)$ for the full kernel solution, where $m << n$.

In the future we are going to do a theoretical analysis on the loss imposed on the fuzzy and possibilistic c-means objective functions by the error in our approximation of the kernel-based

distance between the cluster-center and objects. We have done analysis on a related approximation of the hard c-means, which can be found in [17]. In short, we discovered that with some modest assumptions the error imposed by our approximation on the hard c-means objective decreases at the rate of $O(1/m)$, which is intuitively pleasing. We expect similar results with the soft partitioning algorithms.

Also, we plan to investigate other sampling methods. There have been many sampling methods, both random and deterministic, proposed and analyzed for the Nyström method of approximating a kernel matrix [23, 24]. We aim to further investigate and build upon these methods to optimize the trade-off between the computational complexity and memory requirements and the imposed error.

ACKNOWLEDGEMENTS

Timothy Havens is supported by the National Science Foundation under Grant #1019343 to the Computing Research Association for the CI Fellows Project.

REFERENCES

[1] H. Frigui, *Advances in Fuzzy Clustering and Feature Discrimination with Applications*. John Wiley and Sons, 2007, ch. Simultaneous Clustering and Feature Discrimination with Applications, pp. 285–312.

[2] W. Bo and R. Nevatia, "Cluster boosted tree classifier for multi-view, multi-pose object detection," in *Proc. ICCV*, October 2007.

[3] S. Khan, G. Situ, K. Decker, and C. Schmidt, "GoFigure: Automated Gene Ontology annotation," *Bioinf.*, vol. 19, no. 18, pp. 2484–2485, 2003.

[4] The UniProt Consotium, "The universal protein resource (UniProt)," *Nucleic Acids Res.*, vol. 35, pp. D193–D197, 2007.

[5] R. Duda, P. Hart, and D. Stork, *Pattern Classification*, 2nd ed. Wiley-Interscience, October 2000.

[6] S. Theodoridis and K. Koutroumbas, *Pattern Recognition*, 4th ed. San Diego, CA: Academic Press, 2009.

[7] J. Bezdek, *Pattern Recognition With Fuzzy Objective Function Algorithms*. New York: Plenum, 1981.

[8] J. Bezdek, J. Keller, R. Krishnapuram, and N. Pal, *Fuzzy Models and Algorithms for Pattern Recognition and Image Processing*. Norwell: Kluwer, 1999.

[9] J. Hartigan, *Clustering Algorithms*. New York: Wiley, 1975.

[10] R. Xu and D. Wunsch II, *Clustering*. Psicataway, NJ: IEEE Press, 2009.

[11] A. Jain, M. Murty, and P. Flynn, "Data clustering: A review," *ACM Computing Surveys*, vol. 31, no. 3, pp. 264–323, September 1999.

[12] A. Jain and R. Dubes, *Algorithms for Clustering Data*. Englewood Cliffs, NJ: Prentice-Hall, 1988.

[13] R. Krishnapuram and J. Keller, "A possibilistic approach to clustering," *IEEE Trans. on Fuzzy Sys.*, vol. 1, no. 2, May 1993.

[14] I. Sledge, T. Havens, J. Bezdek, and J. Keller, "Relational duals of cluster validity functions for the c-means family," *IEEE Trans. Fuzzy Systems*, vol. 18, no. 6, pp. 1160–1170, Dec. 2010.

[15] R. Hathaway and J. Bezdek, "Optimization of clustering criteria by reformulation," *IEEE Trans. Fuzzy Systems*, vol. 3, pp. 241–245, 1995.

[16] R. Krishnapuram and J. Keller, "The possibilistic c-means: insights and recommendations," *IEEE Trans. Fuzzy Systems*, vol. 4, pp. 385–393, 1996.

[17] R. Chitta, T. Havens, A. Jain, and R. Jin, "Large scale clustering using approximate kernel k-means," in *To be submitted, Proc. ACM SIGKDD*, 2011.

[18] *Using MATLAB*, The Mathworks, Natick, MA, November 2000.

[19] R. Zhang and A. Rudnicky, "A large scale clustering scheme for kernel k-means," in *Proc. Int. Conf. Pattern Recognition*, 2002, pp. 289–292.

[20] A. Asuncion and D. Newman, "UCI machine learning repository," http://www.ics.uci.edu/~mlearn/MLRepository.html, 2007.

[21] R. Orlandia, Y. Lai, and W. Lee, "Clustering high-dimensional data using an efficient and effective data space reduction," in *Proc. ACM Conf. Information and Knowledge Management*, 2005, pp. 201–208.

[22] G. Karypis, "CLUTO: A clustering toolkit," University of Minnesota, Computer Science, Tech. Rep. 02-017, 2003.

[23] P. Drineas and M. Mahoney, "On the Nyström method for approximating a gram matrix for improved kernel-based learning," *J. Machine Learning Research*, vol. 6, pp. 2153–2175, 2005.

[24] S. Kumar, M. Mohri, and A. Talwalkar, "Sampling techniques for the Nyström method," in *Proc. Int. Conf. Artificial Intelligence and Statistics*, 2009.

2011 IEEE International Conference on Fuzzy Systems
June 27-30, 2011, Taipei, Taiwan

Adaptive Fuzzy Interpolation with Uncertain Observations and Rule Base

Longzhi Yang and Qiang Shen
Department of Computer Science
Aberystwyth University
Aberystwyth, SY23 3DB, UK
Email: {lly07,qqs}@aber.ac.uk

***Abstract*—Adaptive fuzzy interpolation strengthens the potential of fuzzy interpolative reasoning. It views interpolation procedures as artificially created system components, and identifies all possible sets of faulty components that may each have led to all detected contradictory results. From this, a modification procedure takes place, which tries to modify each of such components, termed candidates, in an effort to remove all the contradictions and thus restore consistency. This approach assumes that the employed interpolation mechanism is the only cause of contradictions, that is all given observations and rules are believed to be true and fixed. However, this may not be the case in certain real situations. It is common in fuzzy systems that each observation or rule is associated with a certainty degree. This paper extends the adaptive approach by taking into consideration both observations and rules also, treating them as diagnosable and modifiable components in addition to interpolation procedures. Accordingly, the modification procedure is extended to cover the cases of modifying observations or rules in a given rule base along with the modification of fuzzy reasoning components. This extension significantly improves the robustness of the existing adaptive approach.**

***Index Terms*—Fuzzy interpolation, uncertain observations, uncertain rules.**

I. Introduction

Fuzzy rule interpolation enables inference in systems with sparse rule bases and helps reduce the complexity of fuzzy models. When given observations have no overlap with any antecedent values, no rule can be fired in classical inference. However, interpolative reasoning through a sparse rule base may still obtain certain conclusions and thus improve the applicability of fuzzy models. Also, with the help of fuzzy interpolation, the complexity of a large rule base can be reduced by omitting those fuzzy rules which may be approximated from their neighboring ones. A number of important interpolation approaches have been presented in the literature, including [1], [2], [3], [7], [8], [9], [12], [13]. In particular, the scale and move transformation-based approach can handle both interpolation and extrapolation, which involve multiple fuzzy rules with each rule consisting of multiple antecedents. This approach also guarantees the uniqueness as well as the normality and convexity of the resulting interpolated fuzzy sets. Yet, it is possible that more than one object value of a single variable may be derived in fuzzy interpolation. This implies that certain inconsistencies may result.

To address this problem, *adaptive fuzzy interpolation* has recently been proposed [14], [15]. This approach is capable of efficiently detecting inconsistencies, locating possible fault candidates and effectively modifying the candidates in an effort to remove all the inconsistencies. It works by viewing the interpolative inference procedures as artificial system components, and then utilizing an assumption-based truth maintenance system (ATMS) [4] to record the dependencies between an interpolated value and its proceeding interpolative procedures. From this, the classical algorithm of general diagnostic engine (GDE) [5] is employed to hypothesize all possible candidates of defective rules, by manipulating the sets of the artificial (fuzzy reasoning) components that led to the detected contradictions.

The adaptive approach of [14], [15] presumes that the underlying interpolation procedures have caused all the contradictory interpolated results. This limits its application to the reasoning components only. However, in general, observations and rules in a given rule base may also be faulty and be so to a certainty degree. Fortunately this is not fundamentally restricted by the underlying approach. This work extends that of [14], in order to allow that observations and rules are also diagnosable and modifiable. Due to the ability of using more information, this extension will considerably improve the approach in two aspects. First, one interpolative solution may still be derived when the existing approach fails. Second, the solution generated may be more reasonable than that by the existing approach.

The reminder of this paper is structured as follows. Sec. II reviews the adaptive fuzzy interpolation approach. Sec. III extends the candidate generation procedure by taking observations, rules, and fuzzy interpolative procedures as diagnosable components. Sec. IV generalizes the candidate modification procedure in order that all kinds of candidate component are modifiable. Sec. V reconsiders the example given in [14] to illustrate how this extension can improve the original approach. Sec. VI concludes the paper and points out important future research directions.

II. Adaptive Fuzzy Interpolation

Adaptive interpolative reasoning [14] provides a way to ensure that inference results remain consistent throughout the fuzzy interpolative process. In this work, the fuzzy interpolation procedure based on each pair of neighboring rules R_i and R_j $(i \neq j)$ is defined as a *fuzzy reasoning component*, denoted

978-1-4244-7316-8/11/$26.00 ©2011 IEEE

as R_iR_j. Such a component takes an input, an observation or a previously interpolated result, including that obtained by extrapolation (which are all hereafter referred to as an observation for simplicity), and produces another (the consequent of the interpolated rule) as output. The process of adaptive interpolation is summarized in Fig. 1. Firstly, the interpolator carries out interpolation and passes the interpolated results to the ATMS for dependency-recording. Then, the ATMS relays to the GDE any β_0-*contradiction* (i.e. inconsistency between two values for a common variable that at least differ to the degree of a given threshold β_0, $0 \leq \beta_0 \leq 1$) as well as their dependent fuzzy reasoning components. Next, GDE diagnoses the problem and generates all possible component candidates which may have led to the detected inconsistencies. After that, a modification process takes place to correct a certain candidate in order to restore consistency. A brief description of each of these key methods is given below.

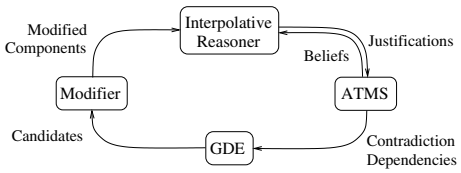

Fig. 1. Adaptive interpolative reasoning

A. Truth maintenance

ATMS is utilized to record the dependency of the interpolated results and that of contradictions, upon the fuzzy reasoning components from which they are inferred. Thus, propositions, contradictions and fuzzy interpolative reasoning components are all represented as ATMS nodes. In addition to the so-called datum field, which trivially denotes the actual meaning of the node, an ATMS node has two other fields: justification and label.

1) Justification: Briefly, a justification describes how a node is derivable from other nodes. Any ATMS node with an inferred proposition can be verified by an ATMS justification:

$$O, R_iR_j \Rightarrow C, \tag{1}$$

which means that the outcome C is inferred form observations O through the interpolation procedure R_iR_j $(i \neq j)$ by firing rules R_i and R_j.

By definition, any two propositions P (x_i is A_{ij}) and P'(x_i is A_{ik}) concerning the same variable x_i are contradictory if the values differ at least by a given degree β_0, which can be represented as:

$$P, P' \Rightarrow_{\beta_0} \perp. \tag{2}$$

2) Label and label-updating: A label is a set of environments, each of which supports their associated node. In particular, an environment is a minimal set of fuzzy reasoning components that jointly entail the supported node, thereby describing how the node ultimately depends on those fuzzy reasoning components. An environment is said to be β_0-*inconsistent* if β_0-contradiction is derivable propositionally by the environment and a given justification. An environment is said to be $(1-\beta_0)$-*consistent* if it is not β_0-inconsistent.

The label of each node is guaranteed to be $(1-\beta_0)$-consistent, sound, minimal and complete by the label updating algorithm, except that the label of the special "false" node is guaranteed to be β_0-inconsistent rather than $(1-\beta_0)$-consistent. In particular, the label of the special "false" node gathers all minimal β_0-inconsistent environments. The corresponding label-updating process for this special node is given as follows. Whenever a β_0-contradiction is detected, each environment in its label is added into the label of "false" node and all such environments and their supersets are removed from the label of every other node. Also, any such environment which is a superset of another is removed from the label of the node "false".

B. Candidate generation

GDE [5] generates minimal candidates by manipulating the label of the specific "false" node. A candidate is a particular set of nodes or fuzzy reasoning components which may be responsible for the whole set of current contradictions. Because a β_0-inconsistent environment indicates that at least one of its elements is faulty (contradictory to the extent of β_0), a candidate must have a non-empty intersection with each β_0-inconsistent environment. Thus, each candidate is constructed by taking one fuzzy reasoning component from each environment in the label of "false" node. Supersets removal then ensures such generated candidates to be minimal. In light of this, a successful correction of any single candidate will remove all the contradictions.

C. Candidate modification

Consistency can be restored by successfully correcting any single candidate because each single candidate explains the entire set of current contradictions. Given a set of candidates, the modification procedure is shown in Fig. 2.

CONSISTENCYRESTORING($\mathbb{Q}$)
$\mathbb{Q}$, the candidate set sorted in descending cardinality, each element of which is a set of fuzzy reasoning components (f);
MODIFY(f), the modification procedure for a single fuzzy reasoning component (f), which returns **true** when modification succeeds and **false** otherwise.

```
(1)  success ← false
(2)  do
(3)      C ← Dequeue(ℚ)
(4)      foreach f ∈ C
(5)          success ← MODIFY(f)
(6)          if (success ==false)
(7)              break
(8)  until ((success ==true) or (ℚ == ∅))
(9)  return success
```

Fig. 2. The CONSISTENCYRESTORING procedure

For convenience, in the rest of this paper, A^*_{ij} is used to denote the modified consequence of a culprit interpolated

rule whose consequent value is A_{ij}, and $A_{ij}^{*\prime}$ and λ_{ij}^{*} are used to denote the corresponding modified intermediate rule consequence and the *relative placement factor* [14] of A_{ij}^{*}, respectively. Also, for simplicity, only rules with a single antecedent are considered here, though extension to multi-antecedent rules is straightforward. Suppose that the neighboring rules $A_{11} \Rightarrow A_{21}$ and $A_{1n} \Rightarrow A_{2n}$ are the two rules used for interpolation by a defective fuzzy reasoning component, that $A_{12}, A_{13}, ..., A_{1(n-1)}$ are observations or previously interpolated results located in between A_{11} and A_{1n}, and that A_{1j} $(2 \leq j \leq n-1)$ is the middle most observation (which informally, is the one that is closest to both antecedent values of the neighboring rules). The modification procedure for a single fuzzy reasoning component is summarized as follows:

1. Find the rule $(A_{1j} \Rightarrow A_{2j})$ whose antecedent is located in the middle most of the neighborhood of the antecedents of any two rules that may be used for interpolation, with respect to their representative values [7]. Assume that the *relative placement factor* of its consequence λ_{2j} is modified to λ_{2j}^{*}.

2. Calculate the *correction rate pair* according to the *relative placement factor* modification of rule $A_{1j} \Rightarrow A_{2j}$:

$$\begin{cases} c^{-} = \frac{\lambda_{2j}^{*}}{\lambda_{2j}} \\ c^{+} = \frac{1-\lambda_{2j}^{*}}{1-\lambda_{2j}}. \end{cases} \tag{3}$$

3. Calculate the modified *relative placement factors* of the consequences of all other interpolated rules which are generated from the same defective fuzzy reasoning component as per the *correction rate pair* computed above, where $i \in \{2, 3, ..., j-1\}$ and $k \in \{j+1, j+2, ..., n-1\}$:

$$\begin{cases} \lambda_{2i}^{*} = \lambda_{2i} \cdot c^{-} \\ 1 - \lambda_{2k}^{*} = (1 - \lambda_{2k}) \cdot c^{+}. \end{cases} \tag{4}$$

4. Calculate the modified consequences of all interpolated rules which are generated from the same defective fuzzy reasoning component in accordance with their modified *relative placement factors*:

$$\begin{cases} A_{2x}^{*\prime} = (1 - \lambda_{2x}^{*}) A_{21} + \lambda_{2x}^{*} A_{2n} \\ T(A_{1x}^{\prime}, A_{1x}) = T(A_{2x}^{*\prime}, A_{2x}^{*}), \end{cases} \tag{5}$$

where $x \in \{2, 3, ..., n-1\}$, and $T(A', A)$ represents the scale and move transformations [7], [8] from fuzzy set A' to A.

5. Restrict the modified consequence such that if m object values $A_{i1}, A_{i2}, ..., A_{im}$ are obtained for variable x_i then they must satisfy:

$$\bigcap_{j=1}^{m} (A_{ij})_{\beta_0} \neq \varnothing, \tag{6}$$

where $(A_{ij})_{\beta_0}$ denotes the β_0-*cut* of fuzzy set A_{ij} That is, all derived values for a given variable are at least $(1 - \beta_0)$-consistent.

6. Restrict the propagations of all modified consequences so that they are mutually consistent to the extent of at least $(1 - \beta_0)$. For simplicity, let function $I(A_{ij}, R_l R_r) = A_{kj}$ denote the standard interpolation from the antecedent fuzzy set A_{ij} to the consequent value A_{kj}, through fuzzy reasoning component $R_l R_r$. Suppose that m object values $A_{i1}, A_{i2}, ..., A_{im}$ of variable x_i, located between the antecedent values of rules R_l and R_r, are modified, that the corresponding modified object values of variable x_k are A_{kj}^{*}, $j \in \{1, 2, ..., m\}$, and that n object values A_{kl}, $l \in \{1, 2, ..., n\}$, of variable x_k are already derived previously. If the modified consequences A_{kj}^{*} are all $(1 - \beta_0)$-consistent, then they must satisfy:

$$\begin{cases} A_{kl}^{*} = I(A_{ij}^{*}, R_l R_r) \\ \left(\bigcap_{j=1}^{m} (A_{kj}^{*})_{\beta_0} \right) \bigcap \left(\bigcap_{l=1}^{n} (A_{kl})_{\beta_0} \right) \neq \varnothing. \end{cases} \tag{7}$$

7. Solve all these simultaneous equations. The result is the modified solution which ensures β_0-inconsistency-free.

III. Generalizing Candidate Generation

The approach described above assumes that observations and rules in a given rule base are true and fixed and thus, inference procedures are the only possible cause of any inconsistencies. Consequently, only inference procedures (i.e. fuzzy reasoning components) are treated as diagnosable and modifiable components. However, this may not be true in real-world problems as observations and rules in a given rule base may also be faulty to a certain degree. Therefore, observations and rules in a rule base may also need to be diagnosed and modified. A generalization of the existing approach is described below.

A. Certainty degrees of observations and rules

Conceptually, inexact information may be classified into the following four general categories [6]: i) vagueness, which arises due to lack of sharp distinctions or boundaries between pieces of information and is usually modeled by a fuzzy set that identifies a soft constraint on a set of elements; ii) uncertainty, which depicts the reliability or confidential weight of a given piece of information stated in a proposition and can be captured by a numerical value or a fuzzy set; iii) both vagueness and uncertainty, which means that information of type i) and type ii) coexists but the uncertainties are expressed by numerical values; iv) Both vagueness and uncertainty with the latter also expressed in vague terms (i.e. fuzzy sets). The previous work [14] involves in type i information only. This work extends that by introducing type ii information into the system, but using numerical uncertainty representation only. This results in the use of type iii information. How to further extend this work to deal with type iv information remains active research.

In particular, an observation in this work is of the form:

$$O\text{: } x_i \text{ is } A_{ij} \ (c), \tag{8}$$

where c, a crisp number between 0 and 1, represents the certainty degree of observation O. According to the aforementioned categories of inexactness, an object value is modeled as a fuzzy set because no clear boundary between pieces of information is available; the certainty degree of the observation is expressed as a crisp number because the current description

of the object value (i.e. the fuzzy set) may not be of full confidence or fully reliable.

Since c represents the certainty degree, $1-c$ then naturally describes the uncertainty degree of the same piece of information. Thus, an uncertainty degree value as given in Eq. 8 may be interpreted being the extent to which the factual object value of O is located on the left side or right side of its current position. From this, intuitively, the modifiable range of object value O is bounded to the proportion of $1-c$ in reference to the entire variable domain. That is, it can shift leftwards or rightwards to a maximal distance of $\frac{1-c}{2}(max_i - min_i)$, where max_i and min_i are the maximum and minimum of the domain values of variable x_i. Note that the shifting of a fuzzy set does not affect the vague term (i.e. the shape and area of the fuzzy set). It is equivalent to add a crisp number to the representative value of the original fuzzy set [10]. In summary, the modified value A^*_{ij} of observation O as given in Eq. 8 must satisfy:

$$\begin{cases} A^*_{ij} \geq A_{ij} - \frac{1-c}{2}(max_i - min_i) \\ A^*_{ij} \leq A_{ij} + \frac{1-c}{2}(max_i - min_i). \end{cases} \tag{9}$$

It is possible that the shifting may be out of the variable domain. In order to keep the shifting result within the underlying domain, the shifting also needs to satisfy:

$$\begin{cases} min(supp(A^*_{ij})) \geq mix_i \\ max(supp(A^*_{ij})) \leq max_i, \end{cases} \tag{10}$$

where $supp(A^*_{ij})$ is the support of fuzzy set A^*_{ij}.

A uncertain rule is of the form as follows:

$$R: \text{ If } x_k \text{ is } A_{kj}, \text{ then } x_i \text{ is } A_{ij} \ (c), \tag{11}$$

which indicates that rule R is certain to the degree of c. Similar to the meaning of the certainty degree of an observation, this is interpreted as that the factual consequence object value A_{ij} may be located in the left or right side of the current position. Again, the shifting must satisfy Eqs. 9 and 10.

B. Dependency recording

In adaptive fuzzy interpolation, ATMS is used to record the dependencies of the interpolated results and contradictions upon the artificial (fuzzy reasoning) components. In this extended work, such dependencies can also be upon observations and rules in a given rule base. That is, propositions (including observations), contradictions, fuzzy reasoning components, and rules in a rule base are all represented as ATMS nodes.

Recall that a justification describes how a node is derivable from other nodes. Observations, rules in a given rule base and fuzzy reasoning components are assumed to be initially true and may be established to be false subsequently. For each of such nodes (i.e. assumptions in classical ATMS terms [4]), its justification simply assumes itself to be true. Any ATMS node with an inferred proposition (i.e. a derived node in [4]), which is obtained through the scale and move transformation-based interpolation, may now be verified by an ATMS justification:

$$O, R_i, R_j, R_iR_j \Rightarrow C. \tag{12}$$

Note that when rules R_i and R_j $(i \neq j)$ are fixed and true, there is no point to keep these dependencies and then Eq. 12 degenerates to Eq. 1. The justification of a β_0-contradiction in this extended work is the same as that in the existing work.

Note that if a consequence that is justified by a new interpolation does not already exist in the ATMS network, a new node will be created. Then, the label of every node will be updated, which is achieved by the so called label-updating algorithm. In order to avoid duplications, the label-updating algorithm is omitted here because it is basically the same as that used in the existing approach to adaptive fuzzy interpolation [14].

C. Candidate generation

From recorded dependencies of all contradictions within the ATMS network, GDE is employed to generate the candidate set. In particular, each candidate is formed by taking one element from each label environment of each contradiction. Of course, duplication and superset removal takes place for each candidate to ensure that the generated candidate set is minimal. Although candidate generation procedure in this work is similar to that in [14], the constituent components of the generated candidates hence may be different from those in the existing approach. This is obvious because an element of a certain candidate may now be an observation, a rule in a given rule base or a fuzzy reasoning component rather than just a fuzzy reasoning component.

To facilitate the modification of a candidate, it is necessary to determine whether multiple related components with respect to a single step of interpolation can appear within one candidate. If any candidate contains at most one element with respect to a single interpolation step, the modification of the candidate can be decomposed to the modification of its individual elements. Otherwise, the modification of related components needs to be implemented jointly.

Suppose that a step of interpolation $O, R_i, R_j, R_iR_j \Rightarrow C$ is given. Let N_O, N_{R_i}, N_{R_j}, $N_{R_iR_j}$ and N_C be the identity nodes, regarding O, R_i, R_j, R_iR_j and C, respectively. As stated previously, each observation, rule or fuzzy reasoning component has an environment containing only one node which represents itself. According to the label updating algorithm, each label environment of node N_O and those of nodes $\{N_{R_i}, N_{R_j}, N_{R_iR_j}\}$ jointly form a label environment of node N_C. Without losing generality, assume that N_C contributes to a certain contradiction directly or indirectly. Then, if any of its label environments contains $N_{R_iR_j}$, it must also contain N_{R_i} and N_{R_j}, and vice versa. Therefore, it is impossible that $\{N_{R_i}, N_{R_iR_j}\}$ or $\{N_{R_j}, N_{R_iR_j}\}$ is contained within one candidate in the minimal candidate set. This is because a candidate is generated by taking one element from each label environment of each contradiction and any candidate which is a superset of any other candidate is removed.

Similarly, if O is an observation, $\{N_O, N_{R_i}\}$, $\{N_O, N_{R_j}\}$, or $\{N_O, N_{R_iR_j}\}$ cannot be contained in any one candidate in the minimal candidate set. However, it is possible that N_{R_i} and N_{R_j} are contained within the same candidate. This is because

N_{R_i} may also be used in conjunction with another rule to carry out interpolation rather than N_{R_j}, and vice versa. Thus, one label environment of the special "false" node may only contains N_{R_i} but not N_{R_j} while another may only contains N_{R_j} but not N_{R_i}. Therefore, it is possible to generate a candidate in the minimal candidate set such that it contains both N_{R_i} and N_{R_j}.

IV. Generalizing Candidate Modification

Having generated the minimal candidate set, a certain candidate needs to be selected for modification in an effort to remove all the contradictions and thus to restore consistency. The principle underlying the consistency-restoring algorithm as outlined in Fig. 2 can be extended for use here. However, the extension is not straightforward due to the involvement of vague and uncertain information. This is because the constituent components of a fault candidate can now also be observations or rules given in a rule base apart from fuzzy reasoning components. However, as indicated in Sec. III-C, for the particular application of GDE in the present problem, elements contained within any minimal candidate returned by the GDE are independent amongst themselves except that a pair of rules that were used for interpolation may be contained within one certain candidate. Thus, their modification can be carried out independently except that the modification of a pair of neighboring rules should be carried out jointly. The modification of fuzzy reasoning components has been outlined in Sec. II-C. The modifications of observations and rules in a given rule base are described in the rest of this section.

A. Observation modification

For a given defective observation associated with certainty degree c, what the modification needs to do is to shift the fuzzy set along the variable axis while fixing its shape and area. This follows a naturally appealing interpretation of certainty degrees in the present context. In particular, the shifting must satisfy the three constraints below:

1) The shifting must be bounded by Eqs. 9 and 10, with respect to the given c.
2) The shifted observation needs to be consistent with the rest observations (or interpolated results), which corresponds to point 5 of the modification procedure for fuzzy reasoning components as outlined in Sec. II-C.
3) The propagation of the shifted observation needs to be mutually consistent with other consequences, which corresponds to point 6 of the modification procedure for fuzzy reasoning components outlined in Sec. II-C.

All three constraints can be satisfied by posing and then solving a set of simultaneous equations and inequations. The solution guarantees that the interpolated results using the modified observation are at least $(1-\beta_0)$-consistent throughout.

B. Rule modification

The situation that only one of two neighboring rules is defective is considered first. Similar to the modification of an observation, given a defective rule with certainty degree c, what the modification needs to do is to shift the consequence of the rule along with the consequent axis by satisfying Eqs. 9 and 10. However, because the defective rule has been used for interpolation, all the interpolated results which have been generated by employing this defective rule also need to be modified accordingly. There are two cases to consider in order to modify the defective rule, depending on whether the antecedent of the other rule that was used together with it to carry out interpolation is on which side of its own antecedent.

Without losing generality, suppose that $x_1 = A_{1i} \Rightarrow x_2 = A_{2i}$ and $x_1 = A_{1d} \Rightarrow x_2 = A_{2d}$ are the two neighboring rules which flank a given observation A_{1j} and that the second rule is defective, where $1 \leq i, d \leq N$ with N being the cardinality of the rule base, and $1 \leq j \leq M$ with M being the number of all given observations (including derived values) for x_1. Assume that A_{1i} is on the left hand side of A_{1d}, the antecedent of the defective rule.

Note that in implementing the scale and move transformation-based fuzzy interpolation, given an observation and two neighboring rules which flank the observation, the logical consequence of the observation is derived from the consequent fuzzy set of an artificially created intermediate rule via the scale and move transformations. This is achieved by minimizing the area and shape differences between the observation and the antecedent of the intermediate rule. Therefore, the area and shape of the logical consequence ultimately depend on the value of the relative placement factor λ (see [14] for details), the areas and shapes of the observation, and all the fuzzy sets defined in the rules used for interpolation. Thus, to maintain the interpretability of the fuzzy models and reasoning, it is desirable to modify a defective rule without changing the shape and area of its consequence. The only aspect that is modifiable is its location.

The overall location of a fuzzy set may be approximately captured by a crisp number, termed representative value [7]. In carrying out interpolation, the location relation between A_{1j} and its corresponding interpolated consequence A_{2j} can be mapped by a line which is determined by the locations of the the antecedents and consequences of two neighboring rules used for interpolation. This corresponds to the line P_1P_3 shown in Fig. 3. Suppose that the consequence of the defective rule

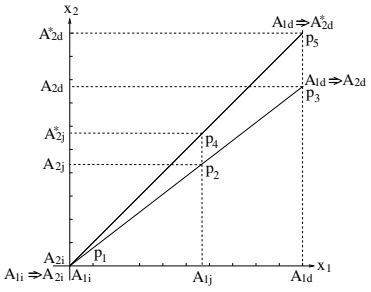

Fig. 3. Rule modification propagation

is modified to A^*_{2d}, then the location relation line P_1P_3 is accordingly shifted to line P_1P_5. In order to measure the extent

of such shifting, the following *correction rate* c^- is introduced:

$$c^- = \frac{d(A_{2i}, A^*_{2d})}{d(A_{2i}, A_{2d})}, \tag{13}$$

where $d(A, A')$ stands for the distance between the locations of the two fuzzy sets A and A' (shorted as the distance between fuzzy sets A and A' hereafter for simplicity). Denote the modified result of A_{2j} as A^*_{2j}, then the distance between A_{2i} and A^*_{2j} can be calculated by applying the correction rate c^- to the distance between A_{2i} and A_{2j}. Having known the locations of A_{2i} and A_{2j}, the location of A^*_{2j} can be calculated. Given only location is modified, A^*_{2j} is then obtained. For any other given interpolated results, if their corresponding observations are flanked by the same pair of original neighboring rules, their locations are corrected in a similar manner.

Of course, such modified results need to be consistent with the rest, so do their propagations. The procedure required is the same as points 5 and 6 of the modification procedure of a fuzzy reasoning component as outlined in Sec. II-C. Putting the above together, a set of constraints in terms of equations and inequations is constructed. The solution of these equations and inequations in conjunction with those imposed by all other elements of the same candidate in question guarantees the modified result of the candidate to be β_0-contradiction-free.

The case discussed so far covers the situation where all the observations which have invoked the use of the defective rule for interpolation are located on the left side of its antecedent. For the case where observations are located on the right side of its antecedent, the modification follows a mirrored procedure, with a different *correction rate* c^+. Suppose that a given observation A_{1k}, $1 \leq k \leq M$ is flanked by the defective rule and its right neighboring rule, $x_1 = A_{1l} \Rightarrow x_2 = A_{2l}$, $1 \leq l \leq N$, then c^+ is calculated by:

$$c^+ = \frac{d(A^*_{2d}, A_{2l})}{d(A_{2d}, A_{2l})}. \tag{14}$$

Similar to the left hand side case, the modified result of observation A_{1k} can then be computed by utilizing this correction rate. From this, the rest of the modification procedure is the same as the previous case.

The above has addressed the situations where only one of the two neighboring rules is defective. For the situation where both neighboring rules are defective, the modification can be done by modifying the two individual defective rules separately in a sequence. This is because the modified result is independent of the order of modifications.

The independence of the order of modifications carried out is proven below. Without losing generality, following the above description, suppose that rule $x_1 = A_{1l} \Rightarrow x_2 = A_{2l}$ is also defective, that the modified consequence of the left neighboring rule is A^*_{2d}, and that the modified consequence of the right neighboring rule is A^*_{2l}. Then, the final modification corresponds to the replacement of the location mapping line P_1P_3 by line P_6P_5 as illustrated in Fig. 4(b). This is because if the left defective rule is modified first as shown in Fig. 4(a), the modification of the right defective rule will be performed using the result of the modification of the left rule as illustrated in the final result of Fig. 4(b). If, however, the modification starts from the right defective rule, then the modification process is illustrated in Fig. 5, which also leads to the final result that is the same as the one given in the line P_6P_5 of Fig. 4(b). Thus, the modification in this case is simply a combination of the two procedures previously introduced.

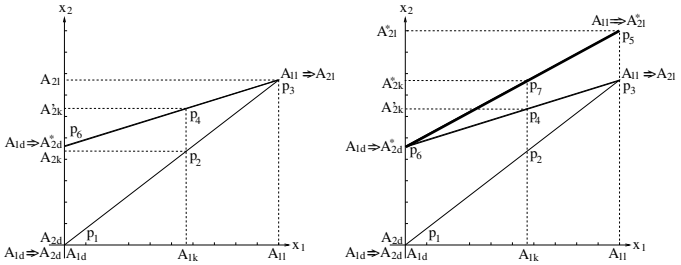

(a) Left rule modification (b) Right rule modification

Fig. 4. The left defective rule is modified first

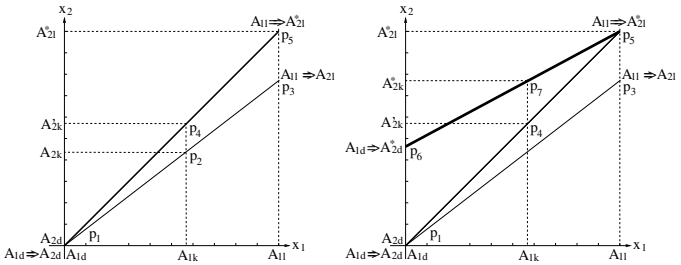

(a) Right rule modification (b) Left rule modification

Fig. 5. The right defective rule is modified first

V. An illustrative Example

To illustrate the potential of this extended adaptive approach, the problem given in [14] is reconsidered, with information on certainty degrees added. The rule base is given as follows:

R_1: If x_1 is A_{11}, then x_2 is A_{21} (0.82);
R_2: If x_1 is A_{12}, then x_2 is A_{22} (0.79);
R_3: If x_2 is A_{23}, then x_3 is A_{31} (0.93);
R_4: If x_2 is A_{24}, then x_3 is A_{32} (0.64);
R_5: If x_2 is A_{25}, then x_4 is A_{41} (0.75);
R_6: If x_2 is A_{26}, then x_4 is A_{42} (0.88);
R_7: If x_3 is A_{33}, then x_5 is A_{51} (0.82);
R_8: If x_3 is A_{34}, then x_5 is A_{52} (0.86);
R_9: If x_4 is A_{43}, then x_5 is A_{53} (0.90);
R_{10}: If x_4 is A_{44}, then x_5 isA_{54} (0.62).

Given $\beta_0 = 0.5$ and three observations, $x_1 = A_{13} = (7.0, 8.0, 9.0)$ (0.95), $x_1 = A_{14} = (7.6, 8.6, 9.6)$ (0.83) and $x_4 = A_{45} = (12.0, 13.0, 14.0)$ (0.92), the interpolation procedures are illustrated in Fig. 6 and the original observations as well as the results obtained by scale and move transformation-based interpolation are presented in Fig. 7. Note that in this example, to keep the illustration simple, it has been assumed that the variable x_1 takes two different object values A_{13} and A_{14} with different certainty degrees. In practice, this may be caused by the fact that the observations are taken by different

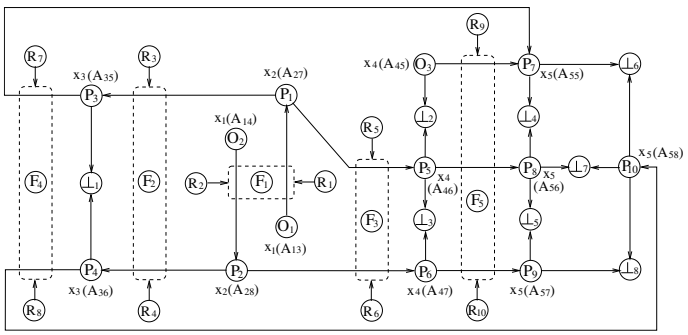

Fig. 6. Discrepancy records in ATMS

agents or that one is a real observation and the other may be produced by another inference mechanism.

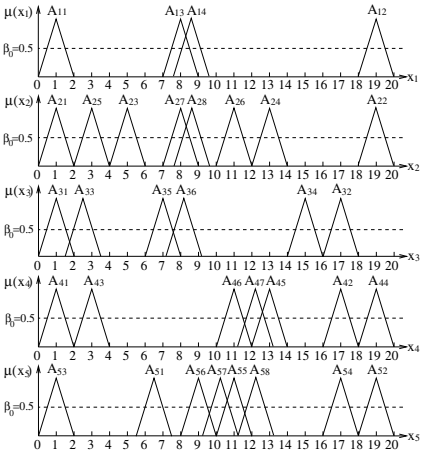

Fig. 7. Fuzzy sets used in the example

A. Dependency recording

In Fig. 6, ATMS nodes and contradictions are represented by circles. Particularly, each of $O_g,\ g \in \{1,2,3\}$, is a node denoting an observation; each of $R_h,\ h \in \{1,2,...,10\}$, is a node denoting a rule in the rule base; each of $F_i,\ i \in \{1,2,...,5\}$, is a node denoting a fuzzy reasoning component; each of $P_j,\ j \in \{1,2,...,10\}$, is a node denoting a proposition; and each of $\perp_k,\ k \in \{1,2,...,8\}$, denotes a β_0-contradiction. These ATMS nodes and contradictions are listed as follows, with all justifications omitted:

$R_1 : \langle x_1 = A_{11} \Rightarrow x_2 = A_{21}, \{\{R_1\}\}\rangle$;
$R_2 : \langle x_1 = A_{12} \Rightarrow x_2 = A_{22}, \{\{R_2\}\}\rangle$;
$R_3 : \langle x_2 = A_{23} \Rightarrow x_3 = A_{31}, \{\{R_3\}\}\rangle$;
$R_4 : \langle x_2 = A_{24} \Rightarrow x_3 = A_{32}, \{\{R_4\}\}\rangle$;
$R_5 : \langle x_2 = A_{25} \Rightarrow x_4 = A_{41}, \{\{R_5\}\}\rangle$;
$R_6 : \langle x_2 = A_{26} \Rightarrow x_4 = A_{42}, \{\{R_6\}\}\rangle$;
$R_7 : \langle x_3 = A_{33} \Rightarrow x_5 = A_{51}, \{\{R_7\}\}\rangle$;
$R_8 : \langle x_3 = A_{34} \Rightarrow x_5 = A_{52}, \{\{R_8\}\}\rangle$;
$R_9 : \langle x_4 = A_{43} \Rightarrow x_5 = A_{53}, \{\{R_9\}\}\rangle$;
$R_{10} : \langle x_4 = A_{44} \Rightarrow x_5 = A_{54}, \{\{R_{10}\}\}\rangle$;
$O_1 : \langle x_1 = A_{13}, \{\{O_1\}\}\rangle$;
$O_2 : \langle x_1 = A_{14}, \{\{O_2\}\}\rangle$;
$O_3 : \langle x_4 = A_{45}, \{\{O_3\}\}\rangle$;
$F_1 : \langle R_1 R_2, \{\{F_1\}\}\rangle$;
$F_2 : \langle R_3 R_4, \{\{F_2\}\}\rangle$;
$F_3 : \langle R_5 R_6, \{\{F_3\}\}\rangle$;
$F_4 : \langle R_7 R_8, \{\{F_4\}\}\rangle$;
$F_5 : \langle R_9 R_{10}, \{\{F_5\}\}\rangle$;
$P_1 : \langle x_2 = A_{27}, \{\{O_1, R_1, R_2, F_1\}\}\rangle$;
$P_2 : \langle x_2 = A_{28}, \{\{O_2, R_1, R_2, F_1\}\}\rangle$;
$P_3 : \langle x_3 = A_{35}, \{\{O_1, R_1, R_2, F_1, R_3, R_4, F_2\}\}\rangle$;
$P_4 : \langle x_3 = A_{36}, \{\{O_2, R_1, R_2, F_1, R_3, R_4, F_2\}\}\rangle$;
$P_5 : \langle x_4 = A_{46}, \{\{O_1, R_1, R_2, F_1, R_5, R_6, F_3\}\}\rangle$;
$P_6 : \langle x_4 = A_{47}, \{\{O_2, R_1, R_2, F_1, R_5, R_6, F_3\}\}\rangle$;
$P_7 : \langle x_5 = A_{55}, \{\{O_1, R_1, R_2, F_1, R_3, R_4, F_2, R_7, R_8, F_4\},$
$\{O_3, R_9, R_{10}, F_5\}\}\rangle$;
$P_8 : \langle x_5 = A_{56}, \{\{O_1, R_1, R_2, F_1, R_5, R_6, F_3, R_9, R_{10}, F_5\}\}\rangle$;
$P_9 : \langle x_5 = A_{57}, \{\{O_2, R_1, R_2, F_1, R_5, R_6, F_3, R_9, R_{10}, F_5\}\}\rangle$;
$P_{10} : \langle x_5 = A_{58}, \{\{O_2, R_1, R_2, F_1, R_3, R_4, F_2, R_7, R_8, F_4\}\}\rangle$;
$\perp_1 : \langle \perp, \{\{O_1, O_2, R_1, R_2, F_1, R_3, R_4, F_2\}\}\rangle$;
$\perp_2 : \langle \perp, \{\{O_1, O_3, R_1, R_2, F_1, R_5, R_6, F_3\}\}\rangle$;
$\perp_3 : \langle \perp, \{\{O_1, O_2, R_1, R_2, F_1, R_5, R_6, F_3\}\}\rangle$;
$\perp_4 : \langle \perp, \{\{O_1, O_3, R_1, R_2, F_1, R_5, R_6, F_3, R_9, R_{10}, F_5\}\}\rangle$;
$\perp_5 : \langle \perp, \{\{O_1, O_2, R_1, R_2, F_1, R_5, R_6, F_3, R_9, R_{10}, F_5\}\}\rangle$;
$\perp_6 : \langle \perp, \{\{O_2, O_3, R_1, R_2, F_1, R_3, R_4, F_2, R_7, R_8, F_4\}\}\rangle$;
$\perp_7 : \langle \perp, \{\{O_1, O_2, R_1, R_2, F_1, R_3, R_4, F_2, R_5, R_6, F_3, R_7, R_8, F_4, R_9,$
$R_{10}, F_5\}\}\rangle$;
$\perp_8 : \langle \perp, \{\{O_2, R_1, R_2, F_1, R_3, R_4, F_2, R_5, R_6, F_3, R_7, R_8, F_4, R_9, R_{10},$
$F_5\}\}\rangle$.

In particular, a specific ATMS node "false", denoted by $P_\perp$, which collectively represents all the contradictions listed above from $\perp_1$ to $\perp_8$, is given as follows:

$P_\perp : \langle \perp, \{\{O_1, O_2, R_1, R_2, F_1, R_3, R_4, F_2\},$
$\{O_1, O_3, R_1, R_2, F_1, R_5, R_6, F_3\},\ \{O_1, O_2, R_1, R_2, F_1, R_5, R_6, F_3\},$
$\{O_2, O_3, R_1, R_2, F_1, R_3, R_4, F_2, R_7, R_8, F_4\}\}\rangle$.

B. Candidate generation

After removing all duplications in each candidate and all candidates which are supersets of any other candidate, twenty four minimal candidates are generated, each of which is formed by taking one element from each environment in the label of the "false" node:

$C_1 = [R_1];\ C_2 = [R_2];\ C_3 = [F_1];\ C_4 = [O_1, O_2];\ C_5 = [O_1, O_3];$
$C_6 = [O_1, R_3];\ C_7 = [O_1, R_4];\ C_8 = [O_1, F_2];\ C_9 = [O_1, R_7];$
$C_{10} = [O_1, R_8];\ C_{11} = [O_1, F_4];\ C_{12} = [O_2, R_5];\ C_{13} = [O_2, O_3];$
$C_{14} = [O_2, R_6];\ C_{15} = [O_2, F_3];\ C_{16} = [R_3, R_5];\ C_{17} = [R_3, R_6];$
$C_{18} = [R_3, F_3];\ C_{19} = [R_4, R_5];\ C_{20} = [F_2, R_5];\ C_{21} = [R_4, F_3];$
$C_{22} = [R_4, R_6];\ C_{23} = [F_2, R_6];\ C_{24} = [F_2, F_3].$

C. Candidate modification

As with the existing approach, candidates of the smallest cardinality are examined first. Those candidates which only contain one element, i.e. candidates C_1, C_2 and C_3 in this example, are therefore chosen to be modified first. Particularly, C_1 is randomly chosen as the first to be modified in this case. According to Eqs. 9 and 10, the modified consequence of rule R_1 must satisfy:

$$\begin{cases} A^*_{21} \geq A_{21} - \frac{1-0.82}{2}(20-0) \\ A^*_{21} \leq A_{21} + \frac{1-0.82}{2}(20-0) \\ min(supp(A^*_{21})) \geq 0 \\ max(supp(A^*_{21})) \leq 20. \end{cases}$$

Note that each of the following two rules has been used to form the neighboring rules in conjunction with the defective rule R_1 to carry out interpolation:

IR_1 : If x_1 is A_{13}, then x_2 is A_{27};
IR_2 : If x_1 is A_{14}, then x_2 is A_{28}.

Since both the antecedent of IR_1 and that of IR_2 are on the right hand side of their counterpart of the defective rule, the following correction rate is used:

$$c^+ = \frac{d(A^*_{21}, A_{22})}{d(A_{21}, A_{22})}$$

Then, the locations of the modified interpolated results must satisfy:

$$\begin{cases} d(A^*_{27}, A_{22}) = d(A_{27}, A_{22}) \cdot c^+, \\ d(A^*_{28}, A_{22}) = d(A_{28}, A_{22}) \cdot c^+. \end{cases}$$

These are in turn, used to calculate the modified interpolated results as follows:

$$\begin{cases} A^*_{27} = A_{27} + (d(A^*_{27}, A_{22}) - d(A_{27}, A_{22})) \\ A^*_{28} = A_{28} + (d(A^*_{28}, A_{22}) - d(A_{28}, A_{22})). \end{cases}$$

From this, the rest of the modification is to pose a set of equations and inequations to ensure that the modified results and their propagations are consistent with the rest, which is the same as that of the modification of a fuzzy reasoning component and thus omitted here. Unfortunately, solving all these simultaneous equations and inequations does not lead to any solution. This is also the case when the single candidates C_2 and C_3 are examined.

According to the general candidate modification procedure given in Fig. 2, a candidate of a cardinality of 2 is then randomly taken for modification. In this particular case, suppose that candidate C_4 is taken first, which is comprised of two observations O_1 and O_2. By satisfying the first constraint of a modified observation as given in Sec. IV-A, the modified result of O_1 must satisfy:

$$\begin{cases} A^*_{13} \geq A_{13} - \frac{1-0.95}{2}(20-0) \\ A^*_{13} \leq A_{13} + \frac{1-0.95}{2}(20-0) \\ min(supp(A^*_{13})) \geq 0 \\ max(supp(A^*_{13})) \leq 20. \end{cases}$$

Similarly, a set of constraining inequations can be posed on the modified observation O_2. From this, the rest of the modification, which correspond to the second and third constraints outlined in Sec. IV-A, is the same as that of the modification of a fuzzy reasoning component and thus omitted. Again, this leads to no solution.

The tentative modification continues until one modification succeeds. In this case, candidate C_{12} leads to one solution as illustrated in Fig. 8. It is clear from this figure that there is no β_0-contradiction any more and thus consistency has been successfully restored. This means that the original inconsistent interpolation process has been corrected with consistent interpolated results throughout.

VI. Conclusions

This paper has extended the recent work on adaptive fuzzy interpolation by allowing observations and rules in a given rule base to be diagnosable and modifiable. In particular, it first represents the concepts of generalized adaptive fuzzy interpolation in ATMS terms. Then, GDE is employed to generate the minimal candidates by making use of the label of the specific "false" node within the ATMS. The consequence of this is that a candidate may consist of observations, rules and/or fuzzy reasoning components. While the modification method for individual fuzzy reasoning components has been given previously, this work proposes an extended approach to modifying individual observations and individual rules. The working of this method is illustrated with an example, though scale-up applications remain as active research. Theoretical analysis of the general properties of the work however, requires future investigation.

Further improvements may enhance the potential of the proposed research. Firstly, the extended approach can only be applied to fuzzy interpolation with two single-antecedent rules. It is worthwhile to generalize the approach to cope with fuzzy interpolation with multi-antecedent rules and fuzzy extrapolation. Also, due to more complex and uncertain information has been introduced into the underlying knowledge representative scheme used, the number of candidates grows dramatically. Thus, how to reduce the candidate set size and prioritize these candidates require further research. Use of an uncertainty-based ATMS such as that of [11] may help addressing this issue.

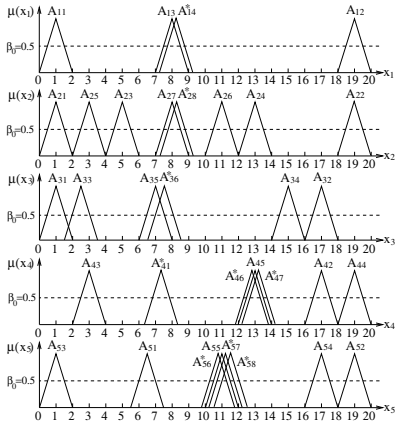

Fig. 8. Solution for the running example

References

[1] P. Baranyi, L. T. Kóczy, and T. D. Gedeon, "A generalized concept for fuzzy rule interpolation," *IEEE T. Fuzzy Syst.*, vol. 12, no. 6, pp. 820–837, 2004.

[2] Y.-C. Chang, S.-M. Chen, and C.-J. Liau, "Fuzzy interpolative reasoning for sparse fuzzy-rule-based systems based on the areas of fuzzy sets," *IEEE T. Fuzzy Syst.*, vol. 16, no. 5, pp. 1285–1301, Oct. 2008.

[3] S. Chen, Y. Ko, Y. Chang, and J. Pan, "Weighted fuzzy interpolative reasoning based on weighted increment transformation and weighted ratio transformation techniques," *IEEE T. Fuzzy Syst.*, vol. 17, no. 6, pp. 1412–1427, 2009.

[4] J. de Kleer, "An assumption-based TMS," *Artif. Intell.*, vol. 28, no. 2, pp. 127–162, 1986.

[5] J. de Kleer and B. C. Williams, "Diagnosing multiple faults," *Artif. Intell.*, vol. 32, no. 1, pp. 97–130, 1987.

[6] X. Fu and Q. Shen, "Fuzzy compositional modeling," *IEEE T. Fuzzy Syst.*, vol. 18, no. 4, pp. 823 –840, 2010.

[7] Z. Huang and Q. Shen, "Fuzzy interpolative reasoning via scale and move transformations," *IEEE T. Fuzzy Syst.*, vol. 14, no. 2, pp. 340–359, 2006.

[8] ——, "Fuzzy interpolation and extrapolation: a practical approach," *IEEE T. Fuzzy Syst.*, vol. 16, no. 1, pp. 13–28, 2008.

[9] L. T. Kóczy and K. Hirota, "Size reduction by interpolation in fuzzy rule bases," *IEEE T. Syst., Man Cybern.*, vol. 27, no. 1, pp. 14–25, 1997.

[10] Q. Shen and R. Leitch, "Fuzzy qualitative simulation," *IEEE T. Syst., Man Cybern.*, vol. 23, no. 4, pp. 1038–1061, Jul/Aug 1993.

[11] Q. Shen and R. Zhao, "A credibilistic approach to assumption-based truth maintenance," *IEEE T. Syst., Man and Cybern. A*, vol. 41, no. 1, pp. 85–96, 2011.

[12] D. Tikk and P. Baranyi, "Comprehensive analysis of a new fuzzy rule interpolation method," *IEEE T. Fuzzy Syst.*, vol. 8, no. 3, pp. 281–296, Jun 2000.

[13] Y. Yam, M. L. Wong, and P. Baranyi, "Interpolation with function space representation of membership functions," *IEEE T. Fuzzy Syst.*, vol. 14, no. 3, pp. 398–411, June 2006.

[14] L. Yang and Q. Shen, "Towards adaptive interpolative reasoning," in *Proc. IEEE Int. Conf. Fuzzy Syst.*, 2009, pp. 542–549.

[15] ——, "Adaptive fuzzy interpolation," *under minor revision for publication in IEEE T. Fuzzy Syst.*, 2011.

2011 IEEE International Conference on Fuzzy Systems
June 27-30, 2011, Taipei, Taiwan

General Type-2 Fuzzy Membership Function Design and its Application to Neural Networks

Eun-A Shim
School of Electrical Engineering and Computer Science
Hanyang University
Korea
sea0209@fuzzy.hanyang.ac.kr

Frank Chung-Hoon Rhee
School of Electrical Engineering and Computer Science
Hanyang University
Korea
frhee@fuzzy.hanyang.ac.kr

***Abstract*— Several type-1 fuzzy membership function (T1 FMF) generation methods have been proposed to model the uncertainty of pattern data. However, if we cannot obtain satisfactory results using type-1 fuzzy sets, employment of type-2 fuzzy sets (T2 FSs) for managing uncertainty may allow us to obtain desirable results. In this paper, a general T2 FMF design method and its application to back propagation (BP) neural networks is proposed. The general T2 FMF is designed using data histograms and then type-1 fuzzy membership values which are extracted from the centroid of the T2 FMF are used as inputs to the BP neural network. Applying our proposed membership assignment to the BP neural networks shows improvement of the classification performance since the uncertainty of pattern data are desirably controlled by the T2 fuzzy memberships. Experimental results for several data sets are given.**

Keywords - type-2 fuzzy membership function generation; neural network; fuzzy input

I. INTRODUCTION

The generation of appropriate fuzzy membership functions has been an important issue in fuzzy data analysis. Several T1 FMF generation methods have been proposed [1]-[4]. However, in the real world, there are several problems where T1 FMF may not properly represent the uncertainty of the pattern data [5]-[12]. To overcome this issue, many applications of T2 FSs using interval type-2 fuzzy membership functions (IT2 FMF) have been proposed [7]-[13]. However, the generation methods of IT2 FMF have been very rarely discussed. Recently, B. Choi and F. Rhee [7] proposed several IT2 FMF generation methods to effectively represent a pattern set.

Although IT2 FMF has been used primarily due to the computational complexity of general T2 FSs, our interest in using general T2 FMF cannot be overlooked since it may manage the uncertainties of the data more effectively due to the flexibility in its secondary membership. Moreover, the computational complexity can be reduced by employing the α-plane representation to compute the centroid of T2 FSs using α-plane computations that are very simple. This is possible since computations can be performed using Karnik-Mendel algorithms that are applied to each α-plane [14]-[15].

In this paper, we propose a general T2 FMF generation method, where the upper and lower membership functions for each class and feature are obtained by fitting appropriate parameterized functions to the histograms of the pattern data and the secondary membership functions are estimated by again fitting appropriate parameterized functions to the histograms of the upper and lower membership values for each vertical slice. In Section II, we briefly review histogram based IT2 FMF generation method [7]-[8]. In Section III, we propose our general T2 FMF generation method. In Section IV, we apply our proposed general T2 FMF generation method to back propagation (BP) neural networks. Experimental results are given in Section V. Finally, in Section VI, we present some conclusions.

II. INTERVAL TYPE-2 FUZZY MEMBERSHIP FUNCTION GENERATION METHODS

In this section, we briefly introduce histogram based IT2 FMF generation method [7]-[8]. The histogram of the feature values describes the distribution of input patterns for each feature. Therefore, the membership function generated from the histogram of the input data can suitably represent the data. To generate the histogram based IT2 FMF, the histogram of the pattern data is obtained for each labeled class and feature by smoothing the domain of each feature using a symmetric window (e.g., a triangular window). In doing so, the vertex of the triangular function is positioned at the first bin of the histogram and the weighted moving average is calculated, then the vertex is moved to the next bin. This procedure is repeated for all of the bins. For simplicity, we use a one class data set. Fig. 1(a) and (b) shows a scatter plot of pattern data and the histogram of the data for feature 1, respectively.

Next, appropriate parameterized functions are fitted to the histogram. To do so, a polynomial function is first fitted to the histogram to determine the number and approximate parameter values for the parameterized function(s). The parameter values for each function are then optimized to fit the histogram using the gradient descent method. In this example, we selected a Gaussian function as our parameterized function. Fig. 1(c) shows a Gaussian function fitted to the histogram of the data.

Then, to estimate an IT2 FMF, Gaussian function fitting to the upper and lower histogram values is needed. Gaussian function fitted to the upper (lower) histogram is used as the

978-1-4244-7316-8/11/$26.00 ©2011 IEEE

upper (lower) membership function. Fig. 1(d) shows the upper and lower membership function obtained that represent the IT2 FMF. The region between upper and lower membership function represents the FOU of the IT2 FMF and hence represents the IT2 FMF, since its secondary membership values are all 1.

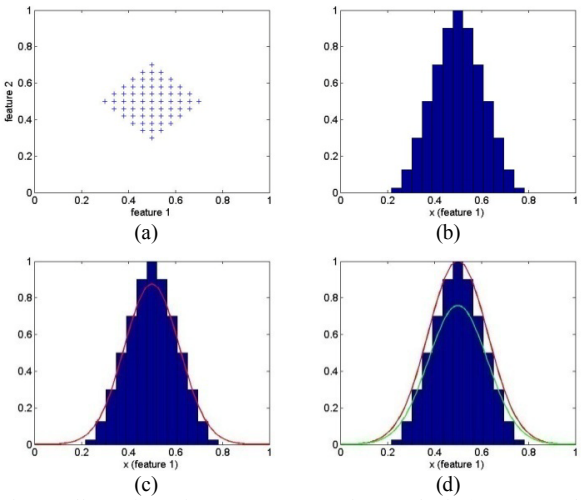

Fig. 1. Illustration of IT2 FMF generation method: (a) scatter plot, (b) histogram for feature 1, (c) Gaussian function fitting for histogram of data, and (d) upper and lower membership function.

III. General Type-2 Fuzzy Membership Function Design Method

In this section, we propose a general T2 FMF design method. For explanation purposes, we use the same data as in Fig. 1. First, to estimate the FOU of a general T2 FMF, we perform Gaussian function fitting to the histogram of data set as in the IT2 FMF generation method. The difference between the general T2 FMF and IT2 FMF generation method is to use window functions of different size for smoothing to obtain the histogram. For example, if we choose to use 6 triangular window functions of size 3, 5, 6, 7, 9, and 13 (i.e., base length), we can obtain 6 smoothed histograms each having a upper and lower membership function. Among all upper and lower membership functions, the smallest value is considered to be the lower membership value and the largest value is considered to be upper membership value for each vertical slice. For illustration purposes, Fig. 2(a) and (b) shows the smoothed histogram and upper/lower membership function for only window size 3 and 7, respectively. Fig. 2(c) represents upper and lower membership functions obtained by fitting Gaussian functions to all 6 smoothed histograms and Fig. 2(d) shows FOU of the general T2 FMF.

Next, the histogram for the upper and lower membership values is obtained at each vertical slice x domain values. For example, if six windows of different size are used we can get six upper and lower membership values at each vertical slice x domain value. Then we can obtain the histogram for the membership value domain at each vertical slice. Here, a smoothing window is again used to smooth the histogram. To estimate the secondary membership function, Gaussian function fitting to this histogram is performed. Fig. 2(e) illustrates the secondary membership function estimated by fitting the histogram of upper and lower membership values at $x = 0.35$, which denotes the vertical slice at $x = 0.35$. With this procedure, we can estimate the secondary membership function for all x domain values. Fig. 2(f) shows the 3D version of the general T2 FMF.

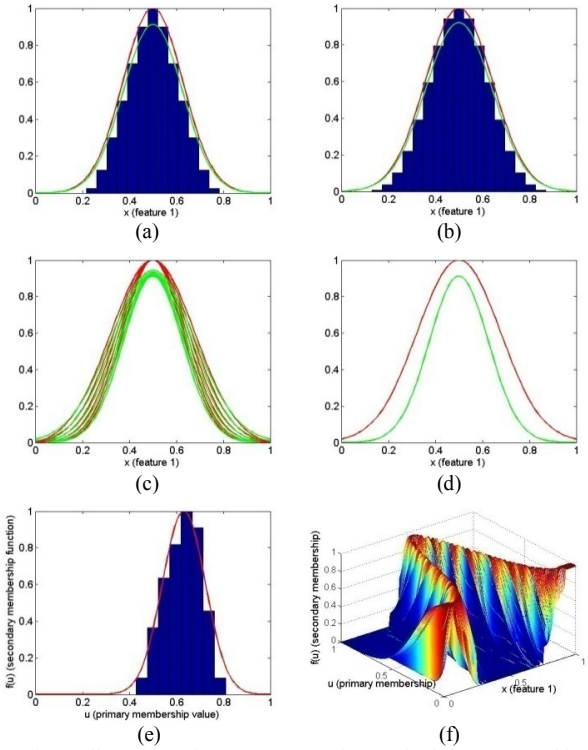

Fig. 2. Illustration of T2 FMF generation method: (a) upper and lower membership functions using 3-window size, (b) upper and lower membership functions using 7-window size, (c) all upper and lower membership functions, (d) FOU, (e) vertical slice at $x = 0.35$, and (f) 3D plot

IV. Application to Backpropagation Neural Network

To apply T2 FSs to the BP neural network, we extract type-1 fuzzy membership values using the centroid of each T2 FMF which is calculated by performing type reduction and defuzzification. The centroid of a T2 FS, which is $C_{\tilde{A}}(x)$, can be represented by the union of the centroids of all the embedded T2 FSs of $\tilde{A}$, i.e., [12]

$$C_{\tilde{A}}(x) = \int_{\forall\theta_1 \in J_{x_1}} \cdots \int_{\forall\theta_N \in J_{x_N}} \min\left(f_{x_1}(\theta_1),\ldots,f_{x_N}(\theta_N)\right) / \frac{\sum_{i=1}^{N} x_i\theta_i}{\sum_{i=1}^{N}\theta_i}, \quad (1)$$

where x_i is input feature pattern and θ_i is the primary membership for x_i. This centroid can be computed using α-plane representations [14]-[15].

The α-plane representation is as follows,

$$C_{\tilde{A}}(x) = \bigcup_{\alpha\in[0,1]} \alpha / C_{\tilde{A}_\alpha}(x), \quad (2)$$

where $C_{\tilde{A}_\alpha}(x)$ is the centroid of the α-plane, $\tilde{A}_\alpha$. Since each $\tilde{A}_\alpha$ is an IT2 FS, its centroid is an interval set, i.e.,

$$C_{\tilde{A}_\alpha}(x) = \left[l_{\tilde{A}_\alpha}, r_{\tilde{A}_\alpha} \right]. \quad (3)$$

This centroid can be obtained using the enhanced Karnik-Mendel algorithms [13] that are applied to each α-plane and the defuzzification value of each α-plane can be calculated as follows,

$$C_\alpha = \frac{l_{\tilde{A}_\alpha} + r_{\tilde{A}_\alpha}}{2}. \quad (4)$$

Then, the centroid of $\tilde{A}$, C, is obtained by calculating the mean value of defuzzification values of each α-plane, i.e.,

$$C = \frac{\sum_{\text{All } \alpha} \alpha C_\alpha}{\sum_{\text{All } \alpha} \alpha}. \quad (5)$$

Now, we can extract the type-1 fuzzy membership value of input pattern **x** for class *j* according to the distance between the centroid and input pattern, i.e., [7]-[8]

$$f_j(\mathbf{x}) = 1 - \left| \mathbf{x} - C_j \right|, \quad (6)$$

where C_j is the centroid of class *j*. It is to be noted that the input patterns are normalized in the interval [0,1].

The type-1 fuzzy membership values of input patterns for each class are used as inputs to the BP neural network. Therefore, the dimension of the input to the BP neural network is the same as the number of classes. Fig. 3 illustrates the structure of our proposed general T2 FMF generation method applied to a BP neural network.

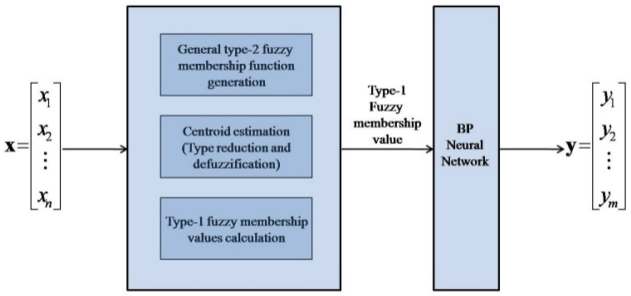

Fig. 3. Structure of the proposed general T2 FMF generation method applied in a BP neural network.

V. EXPERIMENTAL RESULTS

To show the performance of our proposed general T2 FMF design, BP neural network classification results are given for "T-shape" data sets and segmentation results for real images.

A. "T-shape" data

For our first example, we use the "T-shape" data set that consists of 447 patterns (228 and 219 patterns for each class) with 2 features and 2 classes. All pattern features are normalized between 0 and 1. We select 10% patterns for testing and the remaining patterns for training. This procedure is repeated for all the patterns, hence, every pattern will be tested only one time. Fig. 4 shows the scatter plot of the data.

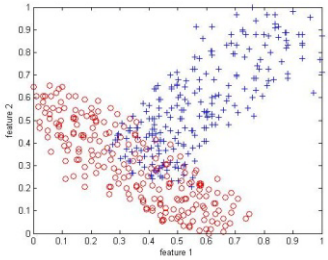

Fig. 4. Scatter plot for "T-shape" data.

As described above, we obtain general T2 FMFs by fitting Gaussian functions to the histograms of the lower and upper membership values at each vertical slice *x* domain values for each class and feature, which are obtained from the histograms of the training data. Fig. 5(a) and (b) ((c) and (d)) shows the FOU and 3D plot of the general T2 FMF for class 1 of feature 1(2), respectively. Fig. 5(e) and (f) ((g) and (h)) shows the FOU and 3D plot of the general T2 FMF for class 2 of feature 1(2), respectively.

We next estimate the centroid of the general T2 FSs by performing type reduction and defuzzification procedure using the α-plane representation and Karnik-Mendel algorithms. We extract type-1 fuzzy membership values for training data using the distance between the centroid and training data.

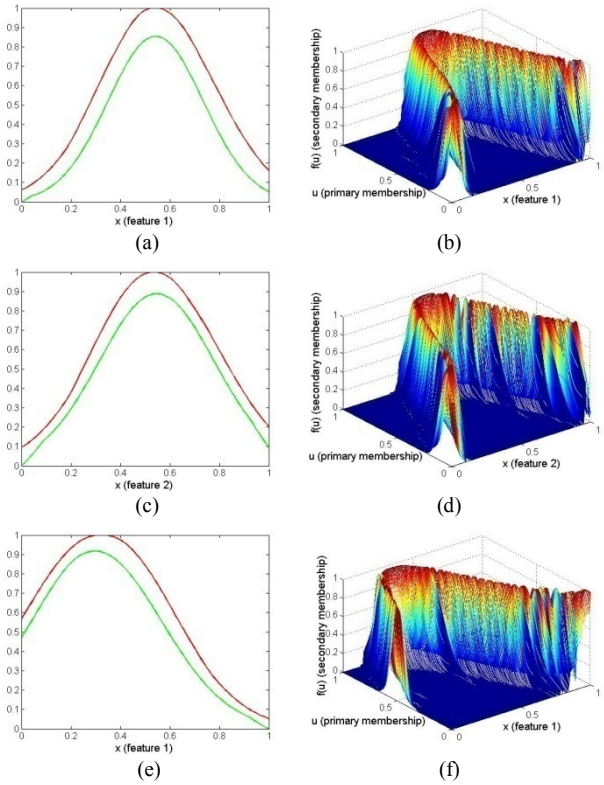

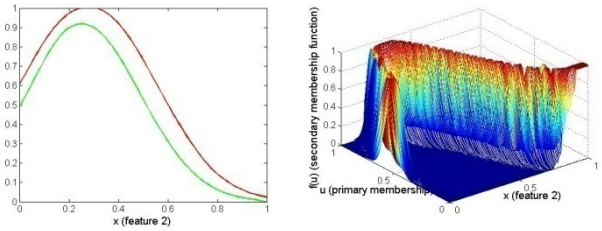

(g) (h)

Fig. 5. FOUs and 3D graph of general T2 FMF for: (a) and (b) class1 of feature1, (c) and (d) class 1 of feature2, (e) and (f) class2 of feature1, and (g) and (h) class2 of feature2.

Next, we train a BP neural network using the type-1 fuzzy membership values for training data as inputs. The test patterns are then classified using the trained BP neural network. Fig. 6 shows the classification results for the type-1 fuzzy membership values using IT2 FMF and general T2 FMF method, and for crisp input patterns as inputs to the BP neural network according to the number of hidden neurons. As shown in figure, BP neural networks trained with fuzzy inputs outperform the case with crisp inputs.

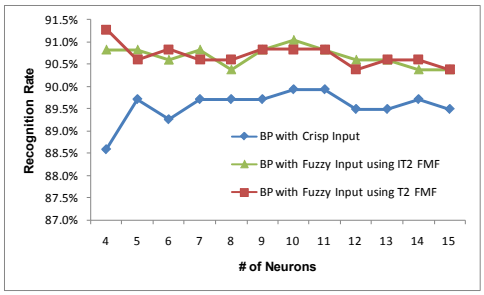

Fig. 6. Classification results for "T-shape" data.

B. *Real image data segmentation*

In this example, we show segmentation results for a 200×200 real scene image that consists of three regions, namely road, forest, and sky. The gray levels of median and excess green filtered images were used as feature values. We then randomly select 100 samples in each region and the feature values are used for training data. Fig. 7(a) and (b) shows the original image and the scatter plot of randomly selected sample data, respectively.

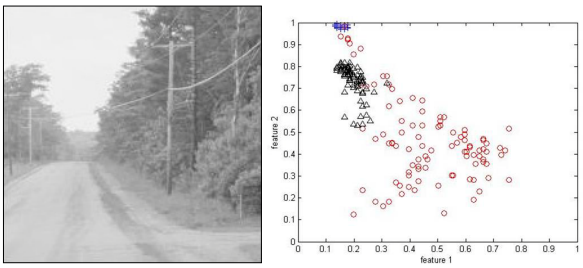

(a) (b)

Fig. 7. Real image example: (a) original image and (b) scatter plot of sample data.

As in the previous example, we generate general T2 FMFs and extract type-1 fuzzy membership values for training data. Next, we train BP neural networks using the type-1 fuzzy membership values for training data. Finally, fuzzy membership values for all feature data of the original image were classified into three classes using the trained BP neural network. Fig. 8(a), (b) and (c) shows the segmentation results for crisp inputs, fuzzy inputs using the IT2 FMF, and fuzzy inputs using the general T2 FMF, respectively, when 10 hidden neurons were used. Fig. 9 shows the recognition rate according to the number of hidden neurons. The recognition rate was improved by 3.2% compared to IT2 FMF method. Table I shows the confusion matrix for the results in Fig. 8. Although the recognition showed little improvement, the segmentation result showed a more significant visual improvement.

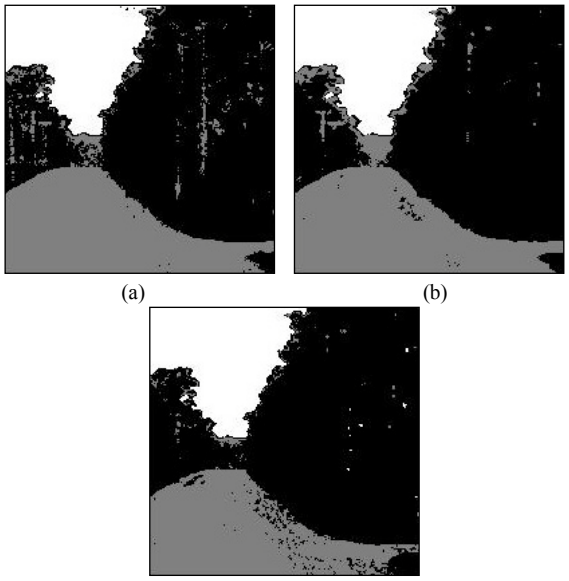

(a) (b)

(c)

Fig. 8. Segmentation results for BP neural network with 10 hidden neurons: (a) crisp input, (b) fuzzy input using IT2 FMF, and (c) fuzzy input using T2 FMF.

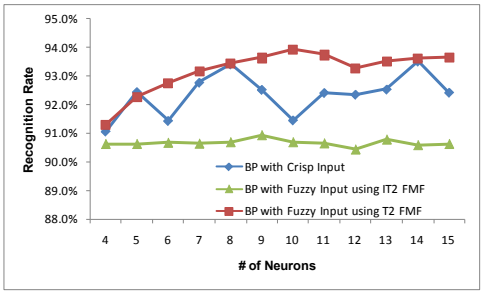

Fig. 9. Recognition rate of real image for various number of neurons.

TABLE I
CONFUSION MATRIX FOR SEGMENTATION RESULTS IN FIG. 8(B) AND (C)

Real Image	BP neural network using fuzzy inputs using IT2 FMF Recognition rate = 90.7%			BP neural network using fuzzy inputs using T2 FMF Recognition rate = 93.9%		
	Road	Forest	Sky	Road	Forest	Sky
Road	8150	70	0	7876	344	0
Forest	3162	21785	499	1536	23381	529
Sky	3	16	6315	3	16	6315

C. Noisy image data segmentation

For our final experiment, we apply 5% Gaussian noise to Fig. 7(a). The training and testing procedure are the same as previous example. Fig. 10(a) and (b) shows the noisy image and the scatter plot of sample data, respectively. Fig. 11(a), (b), and (c) illustrates the segmentation results for crisp inputs, fuzzy inputs using IT2 FMF, and fuzzy inputs using general T2 FMF, respectively, when 8 hidden neurons were used in BP neural network training. As shown in Fig. 12, the recognition rate was improved about 4% at most compared to crisp input and the variation of results for various neurons is more stable than the IT2 FMF method.

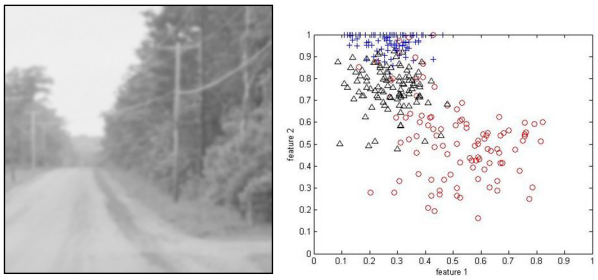

(a) (b)

Fig. 10. Real noisy image example: (a) noisy image and (b) scatter plot of sample data.

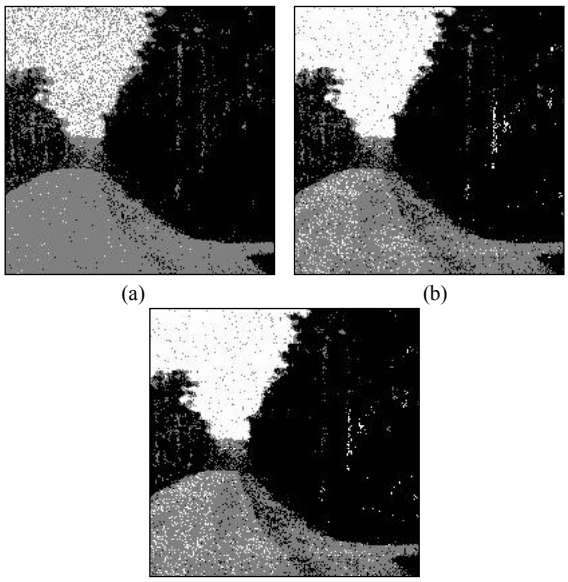

(a) (b)

(c)

Fig. 11. Segmentation results for BP neural network with 8 hidden neurons: (a) crisp input, (b) fuzzy input using IT2 FMF, and (c) fuzzy input using T2 FMF.

VI. CONCLUSION

In this paper, we proposed a general T2 FMF design method and applied the type-1 fuzzy membership values, which are estimated from the centroid of the T2 FMF, as inputs to train BP neural networks. The experimental results showed an improvement in classification performance over the case when crisp inputs were trained and IT2 FMF was used.

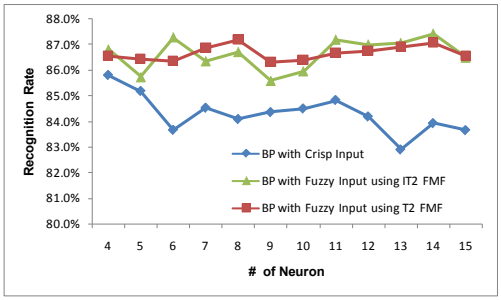

Fig. 12. Recognition rate of noisy image for various number of neurons.

This indicates that our proposed general T2 FMF design method can effectively manage the uncertainty of pattern data. Other general T2 FMF generation methods are currently under investigation.

REFERENCES

[1] M. Makrehchi, O. Basir, and M. Karnel, "Generation of fuzzy membership function using information theory measures and genetic algorithm," *Lecture notes in computer science,* no. 275, pp. 603-610, 2003.

[2] S. Medasani, J. Kim, and R. Krishnapuram, "An overview of membership function generation techniques for pattern recognition," *Int. J. Approximate Reasoning*, vol. 19, no.3/4, pp. 391-417, 1998.

[3] S. Wang, "Generating fuzzy membership functions: a monotonic neural network," *Fuzzy Sets and Systems*, vol. 61, no. 1, pp. 71-81, 1993.

[4] C. Yang and N. Bose, "Generating fuzzy membership function with self-organizing feature map," *Pattern recognition letters*, vol. 27, no. 5, pp. 356-365, 2006.

[5] H. Hagras, "A hierarchical type-2 fuzzy logic control architecture for autonomous mobile robots," *IEEE Trans. Fuzzy Syst*., vol. 12, no. 4, pp. 524-539, Aug. 2004.

[6] D. Wu and W. Tan, "A type-2 fuzzy logic controller for the liquid-level process,", in *Proc. IEEE Int. Conf. Fuzzy Syst*., Budapest, Hungary, Jul. 2004, pp. 953-958.

[7] F. Rhee and B. Choi, "Interval type-2 fuzzy membership function design and its application to radial basis function neural networks," in *Proc. FUZZ-IEEE,* London, U.K., Jul. 2007, pp. 2047-2052.

[8] B. Choi and F. Rhee, "Interval type-2 fuzzy membership function generation methods for pattern recognition," *Information Sciences*, vol. 179, no. 13, pp. 2102-2122, June 2009.

[9] C. Hwang and F. Rhee, "Uncertain fuzzy clustering : interval type-2 fuzzy approach to C-means," *IEEE Trans. Fuzzy Syst.*, vol. 15, no. 1, pp. 107-120, Feb. 2007.

[10] F. Rhee, "Uncertain fuzzy clustering: insights and recommendations," *IEEE Computational Intelligence Magazine,* vol. 2, no. 1, Feb. 2007.

[11] J. Min, E. Shim, and F. Rhee, "An interval type-2 fuzzy PCM algorithm for pattern recognition,", in *Proc. FUZZ-IEEE*, Jeju Island, Korea, Aug. 2009, pp. 480-483.

[12] J. Mendel, *Uncertain Rule-Based Fuzzy Logic Systems*: *Introduction and New Directions,* Prentice Hall, 2001.

[13] D. Wu and J. Mendel, "Enhanced Karnik-Mendel algorithms," *IEEE Trans. Fuzzy Syst.*, vol. 17, no. 4, pp. 923-934, Aug. 2009.

[14] J. Mendel, F. Liu, and D. Zhai, "α-plane representation for type-2 fuzzy sets: theory and application," *IEEE Trans. Fuzzy Sys.*, vol. 17, no. 5, pp. 1189-1207, Oct. 2009.

[15] J. Mendel, "Comments on 'α-plane representation for type-2 fuzzy sets: theory and application'," *IEEE Trans. Fuzzy Sys.*, vol. 18, no. 1, pp. 229-230, Feb. 2010.

[16] S. Kumar, *Neural Networks: A Class Approach*, McGraw-Hill, 2005.

2011 IEEE International Conference on Fuzzy Systems
June 27-30, 2011, Taipei, Taiwan

Human Action Recognition via Sum-Rule Fusion of Fuzzy K-Nearest Neighbor Classifiers

Teck Wee Chua Karianto Leman Nam Trung Pham

Institute for Infocomm Research
A*STAR (Agency for Science, Technology and Research), 1 Fusionopolis Way, Singapore
{tewchua, karianto, ntpham}@i2r.a-star.edu.sg

***Abstract*—Shape and motion are two most distinct cues observed from human actions. Traditionally, K-Nearest Neighbor (K-NN) classifier is used to compute crisp votes from multiple cues separately. The votes are then combined using linear weighting scheme. Usually, the weights are determined in a brute-force or trial-and-error manner. In this study, we propose a new classification framework based on sum-rule fusion of fuzzy K-NN classifiers. Fuzzy K-NN classifier is capable of producing soft votes, also known as fuzzy membership values. Based on Bayes theorem, we show that the fuzzy membership values produced by the classifiers can be combined using sum-rule. In our experiment, the proposed framework consistently outperforms the conventional counterpart (K-NN with majority voting) for both Weizmann and KTH datasets. The improvement may attribute to the ability of the proposed framework to handle data ambiguity due to similar poses present in different action classes. We also show that the performance of our method compares favorably with the state-of-the-arts.**

***Index Terms*—Action recognition, Sum-Rule Fusion, Fuzzy K-NN**

I. Introduction

Human can recognize an action in a seemingly effortless fashion. In contrast, the solutions using computer vision have, in many cases, proved to be immensely difficult. The challenges include: huge collection of possible actions, poor recording settings, temporal variations, inter/intra-personal differences etc. In addition, the choice of optimal representation for an action is still an open problem. Recent approaches can be categorized into global and local representations. For global representation, the region-of-interest (obtained by tracking or background subtraction) is encoded as a whole. In other words, the entire human figure is considered. Silhouette, optical flow, edge and space-time volume fall into this category. Efros *et al.* [1] used blurred optical flows to recognize the actions of small human figures. Blank *et al.* [2] stacked silhouettes over a sequence to form space-time volumes. Poisson equation was used to compute local space-time saliency and orientation features. Ikizler *et al.* [3] extended the motion descriptor of Efros by using spatial and directional binning and then combined it with line shape descriptor. Following that, they proposed to use histogram of oriented rectangles as the shape descriptor [4]. Likewise, Lin *et al.* [5] used silhouettes as the shape descriptor by counting the number of foreground pixels and motion-compensated optical flow as motion descriptor. On the contrary, local representation encodes the image or video frames as a collection of local patches. Common local representation includes spatio-temporal interest points such as 3D Harris, cuboid, Hessian, Dense etc. Usually the interest points are extracted at different spatial and temporal scales. Laptev and Lindeberg [6] proposed to extend Harris corner detector to the third dimension. Dollár *et al.* [7] cuboid detector is based on temporal Gabor filter. Willems *et al.* [8] measured the saliency with the determinant of the 3D Hessian matrix.

According to Ikizler *et al.* [4], an action is defined by three key elements: (a) pose of the body, (b) speed of body motion, and (c) relative ordering of the poses. Actions such as jogging, walking and running can be easily confused if only pose information is used due to similar postures in the action sequences. It has been suggested that combinations of multiple cues may overcome the limitations of a single representation [9]. This is because different inputs may offer complimentary information about the patterns to be classified. In view of this, previous studies which used multiple cues were mainly based on linear weighting of classifiers' votes [3], feature vectors concatenation [5], [10], and hierarchical system [4], [3], [11]. While linear weighting scheme may seem straightforward, the weights are usually obtained in a brute-force or trial-and-error manner.

Apart from the uncertainty in determining the correct weight, most of the previous studies relied on conventional K-nearest neighbor classifier [12]. However, the algorithm has a major drawback: each prototype is considered equally important in the assignment of input patterns. Atypical data are weighted as much as the data from the true class. This can cause ambiguity in those places where the data overlap.

In this work, we address the aforementioned problems in two ways. First, we propose to use fuzzy K-NN classifiers to classify shape and motion feature respectively. The outputs of the classifiers can be regarded as the confidence levels of the input belonging to different classes. Next, we show that based on Bayes theorem the outputs of the classifiers can be fused using sum-rule.

The paper is organized as follows. In Section II we give an overview of the proposed action recognition framework. Next, we describe the details of shape and motion feature extraction in Section III. Subsequently, we outline the fuzzy K-NN algorithm and propose the sum-rule as the fusion strategy of the fuzzy outputs in Section IV. Section V sets the backdrop

978-1-4244-7316-8/11/$26.00 ©2011 IEEE

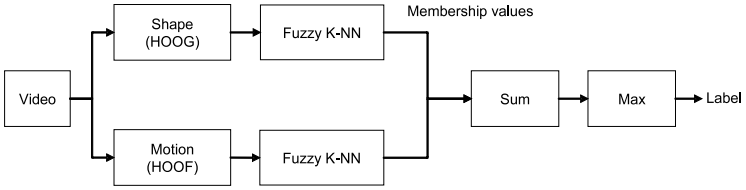

Fig. 1. The proposed shape-motion path combination strategy using Fuzzy K-NN with sum-rule.

for the experimental evaluation while Section VI shows the results with some comparisons to the state-of-the-art methods. Finally, Section VII gives the conclusion remarks of the paper.

II. System Overview

The proposed system is illustrated in Fig. 1. From the shape path, fuzzy K-NN classifier produces membership value $\boldsymbol{\mu}_i = \{\mu_{i1}, \mu_{i2}, \ldots, \mu_{iC}\}$ for each snippet where C denotes the number of classes. Given a video sequence with M snippets, we then compute the average of the membership values from all snippets, i.e., $\boldsymbol{U_s} = (\sum_i \boldsymbol{\mu}_i)/M = \{U_1, U_2, \ldots, U_C\}$ and normalize it to $\widetilde{\boldsymbol{U_s}} \in [0, 1]$. Likewise, we compute the normalized membership values $\widetilde{\boldsymbol{U_m}}$ from the motion path. Next, we combined the membership values from both shape and motion inputs using sum-rule

$$\boldsymbol{U} = \widetilde{\boldsymbol{U}}_{\boldsymbol{s}} + \widetilde{\boldsymbol{U}}_{\boldsymbol{m}} \tag{1}$$

Finally, we apply winner-takes-all principle to determine the class label.

Since the proposed system will be compared with the conventional system (K-NN with majority voting), we briefly discuss the architecture of the latter (see Fig. 2). Consider the shape path first, for each test snippet we find the K-nearest snippets from the training set and assign its label to the class most common among its neighbors. We can obtain crisp votes $\boldsymbol{v}_i = \{v_{i1}, v_{i2}, \ldots, v_{iC}\}$ from the i-th snippet. The votes from the individual snippets (from the same video) are then summed up, i.e., $\boldsymbol{V_s} = \sum_i \boldsymbol{v}_i = \{V_1, V_2, \ldots, V_C\}$. The step is repeated for the motion path to obtain the votes $\boldsymbol{V_m}$. The crisp votes from the shape and motion paths are combined using linear weighting scheme

$$\boldsymbol{V} = \alpha \boldsymbol{V_s} + (1 - \alpha)\boldsymbol{V_m} \tag{2}$$

where $\alpha \in [0, 1]$ is a design parameter that adjust the relative importance of shape and motion votes. Finally, the video is assigned to the class that has the highest votes, $\boldsymbol{V}$.

III. Motion and Shape Feature Extraction

As delineated in the introduction part, observing shape and motion is a very natural way to recognize an action. Motivated by the robustness of the histogram of feature, we use histogram-of-oriented gradient (HOOG) and histogram-of-oriented optical flow (HOOF) as the shape and motion descriptors respectively. We adopt the histogram formation method which was originally introduced by Chaudhry *et al.* [13]. The method is more robust against scale variation and the change of motion direction. The method is illustrated in Fig. 3(a) with example of creating a 4-bin histogram. The main idea is to bin the vectors according to their primary angles from the horizontal axis. Therefore, the vectors are symmetry about the vertical axis. As a result, the histogram of a person moving from left to right will be same as the one with a person moving in the opposite direction. The contribution of each vector is proportional to its magnitude. The histogram is normalized to sum up to unity to make it scale-invariant. Therefore, we do not normalize the size of the bounding box. We further enhance Chaudhry *et al.* algorithm by including spatial information. This is done by dividing the bounding box of the subject into 4×4 regions as shown in Fig. 3(b).

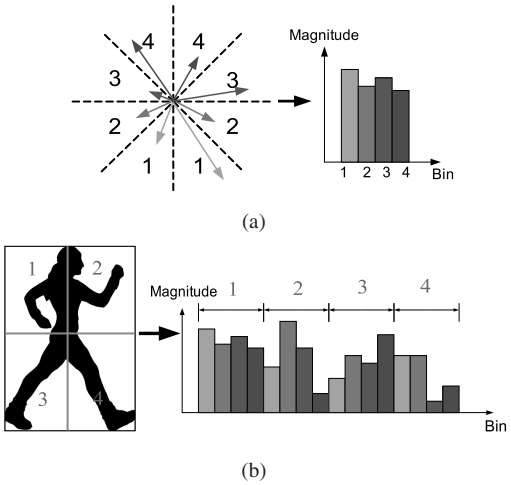

Fig. 3. (a) Histogram binning, (b) the bounding box is divided into 4×4 grid and the resultant histograms from each region are concatenated.

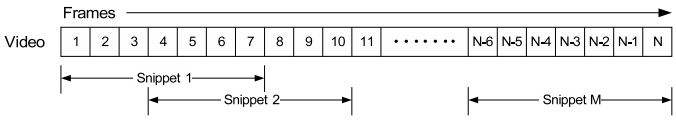

Fig. 4. An example of video sequence that is divided into overlapping snippets.

The pose ordering and time-warping effect can be handled by using overlapping snippets instead of a single frame. Fig. 4 shows an example of 7-frame snippet with four overlapped frames, which is the setting that we used for all experiments in this study.

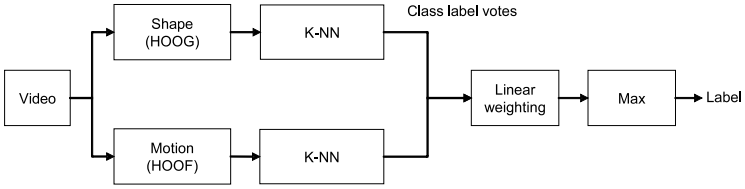

Fig. 2. The conventional shape-motion path combination strategy using K-NN with linear weighting.

IV. Sum-Rule Fusion of Fuzzy K-Nearest Neighbor Classifiers

Unlike the conventional crisp K-NN, fuzzy K-NN algorithm [14] assigns class membership value to an input data rather than class label. The membership assignment is based on the distance between the input data and its K-nearest neighbors and those neighbors' memberships (pre-computed during initialization process) in the possible classes. Let $S = \{\mathbf{x}_1, \mathbf{x}_2, \cdots, \mathbf{x}_n\}$ be a set of n labeled samples. Also, let $\mu_j(\mathbf{x})$ be the membership assigned to the input data $\mathbf{x}$, and $\mu_{ij}(\mathbf{x})$ be the membership in the jth class of the ith labeled prototype.

$$\mu_j(\mathbf{x}) = \frac{\sum_{i=1}^{K} \mu_{ij}\left(1/\hbar(\mathbf{x}, \mathbf{x}_i)^{2/(m-1)}\right)}{\sum_{i=1}^{K}\left(1/\hbar(\mathbf{x}, \mathbf{x}_i)^{2/(m-1)}\right)} \tag{3}$$

Note that in this work $\hbar(\mathbf{x}, \mathbf{x}_i)$ denotes Hellinger distance instead of Euclidean distance [14] because the former provides a more accurate histogram-type feature similarity measure. The parameter m ($m > 1$) is used to scale the effect of the distance measure. The algorithm requires the prototype membership value to be initialized:

$$\mu_{ij}(x) = \begin{cases} 0.51 + (n_j/K) * 0.49 & \text{if } j = i \\ (n_j/K) * 0.49 & \text{if } j \neq i \end{cases} \tag{4}$$

where n_j is the number of the neighbors which belong to the jth class. This initialization procedure ensures the prototype is more informative. The more accurate the initial membership value is, the more accurate the classification result will be.

Suppose there are R classifiers and each rth classifier will classify a distinct input vector $\mathbf{x}_r$, $(r = 1, \ldots, R)$. Bayes rule can be applied to find the class label, c_{j^*}:

$$j^* = \arg\max_j \left(P(c_j|\mathbf{x}_1, \ldots, \mathbf{x}_R)\right) \tag{5}$$

where

$$P(c_j|\mathbf{x}_1, \ldots, \mathbf{x}_R) = \frac{p(\mathbf{x}_1, \ldots, \mathbf{x}_R|c_j)P(c_j)}{p(\mathbf{x}_1, \ldots, \mathbf{x}_R)} \tag{6}$$

In order to evaluate (5), the joint probability density function $p(\mathbf{x}_1, \ldots, \mathbf{x}_R|c_j)$, which is difficult to infer, must be computed. Based on two assumptions, sum-rule can be used to combine the outputs of multiple classifiers [9]. The assumptions are: (a) the inputs $\mathbf{x}_r$ are conditionally statistically independent, and (b) a posteriori probabilities of individual classifier $P(c_j|\mathbf{x}_r)$ will not deviate from the prior probabilities $P(c_j)$ by a large margin. The first assumption is readily satisfied because we are using two types of representations: shape and motion. Moreover, the second assumption can be satisfied when the discriminatory information is highly ambiguous due to the high level of noise. For example, KTH dataset has very strong intra-subject variations due to different recording scenarios. The sum-rule is given as:

$$j^* = \arg\max_j \left[(1-R)P(c_j) + \sum_{r=1}^{R} P(c_j|\mathbf{x}_r)\right] \tag{7}$$

When priors are equal, (7) can be reduced to:

$$j^* = \arg\max_j \left(\sum_{r=1}^{R} P(c_j|\mathbf{x}_r)\right) \tag{8}$$

For fuzzy K-NN, we can approximate $P(c_j|\mathbf{x})$ as:

$$P(c_j|\mathbf{x}) \approx \mu_j(\mathbf{x}) \tag{9}$$

Notice that unlike the estimation of posterior probability from Neural Network where normalization of output is required [9], there is no need to normalize the output of fuzzy K-NN classifier because $\mu_j(\mathbf{x}) \in [0, 1]$.

There are some other forms of classifiers combination strategies such as product-rule, min-rule, max-rule, and majority voting proposed by Kittler *et al.* [9]. We will compare the performance of sum-rule to these variants in Section VI.

V. Experiments

We performed various experiments to evaluate the proposed action recognition framework on two publicly available datasets (see Fig. 5):

- **Weizmann** The dataset was originally introduced in [2]. The dataset contains 90 low-resolution (180×144 pixels) video sequences with 9 subjects performing 10 actions: bend (*bend*), jumping-jack (*jack*), jump-forward (*jump*), jump-in-place (*pjump*), run (*run*), gallop-sideways (*side*), jump-forward-one-leg (*skip*), walk (*walk*), wave-one-hand (*wave1*), and wave-two-hands (*wave2*)[1]. We used the silhouettes provided to compute the bounding boxes for the subjects. HOOG and HOOF features are extracted from the silhouettes.

- **KTH** The dataset was introduced in [15]. There are 25 subjects performing 6 actions: boxing, handclapping, handwaving, jogging, running, and walking. The low resolution (160×120) videos were recorded under four

[1]Note that there are two versions of Weizmann dataset, the original one has 9 actions while the augmented version has 10 which includes *skip* action.

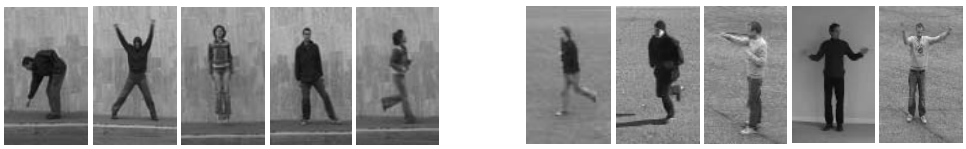

Fig. 5. Examples of different actions from databases Weizmann (left) and KTH (right).

scenarios (s1- outdoors, s2- outdoors with scale variation, s3- outdoor with different clothes, s4- indoors with lighting variation) and each video was split into 4 sub-clips. Originally, the dataset has (4 settings) $\times$ (25 subjects) $\times$ (6 actions) $\times$ (4 sub-clips) = 2400 clips. However, only 2391 clips are available because 8 clips were missing. We used the bounding box provided by Lin *et al.* [5] to locate the subject. Nevertheless, we did not compute the silhouette because object segmentation is not our focus in this work. Therefore, HOOG and HOOF features are extracted directly from the raw grayscale video frames.

In the literature, KTH dataset has been regarded either as one large set with strong intra-subject variations (*all-in-one*) or as four independent scenarios. In the latter case, each scenario is trained and tested separately. In this work, we only focus on the *all-in-one* case. Since KTH dataset size is much larger than Weizmann dataset, we use K-means algorithm to cluster the training data. Each class is quantized into 500 clusters. This can reduce the intra-class variation and computational time. Leave-one-out cross validation (LOOCV) protocol is used in all evaluations.

For Fuzzy K-NN, we set parameter $m = 2$ such that the influence of of each neighbor is weighted by the square of reciprocal of its distance from the query point. The parameter K is varied from 3, then 5 to 7 to evaluate the effect of the neighborhood size.

VI. Results and Discussions

From the experiment on Weizmann dataset using the proposed framework and the conventional framework, it is evident that neighborhood size of 3 consistently gives better performance than other sizes. Table I shows the LOOCV recognition rate for Weizmann dataset when using neighborhood of K = 3. By comparing the results using single representation (either shape or motion feature only), it is noticed that fuzzy K-NN always performed better than K-NN counterparts with improvement of 3.33% and 2.22% when using the shape and motion features respectively. When the outputs from fuzzy K-NN classifiers were combined using sum-rule, the proposed system yielded 100% accuracy. In contrast, the conventional K-NN with linear weighting scheme only achieved 97.78%. Note that for this conventional scheme, the weight, α was set to 0.5 so that the shape and motion features were equally important to facilitate a common comparison setting for both systems.

The result for KTH dataset is tabulated in Table II. It is worth noting that fuzzy K-NN consistently outperforms K-NN counterpart when using single representation only. The advantage of the proposed framework is even more prominent when both shape and motion inputs are combined. The classification accuracy is improved by as much as 5% when $K = 3$. We also investigate the effect of neighborhood size K. The results show that $K = 3$ gives the best results for both frameworks. Considering all three neighborhood sizes, the proposed framework outperforms the conventional counterpart by 3.59% in classification accuracy on average.

TABLE I
Weizmann Average Accuracy (K=3, LOOCV).

Framework	Shape	Motion	Combined
KNN + Linear weighting	92.22%	92.22%	97.78%
Fuzzy K-NN + Sum Rule	95.55%	94.44%	**100**%

TABLE II
KTH Average Accuracy (*all-in-one*, LOOCV).

Framework	K	Shape	Motion	Combined
KNN + Linear weighting	3	74.22%	82.44%	85.80%
	5	72.73%	82.14%	85.46%
	7	72.57%	82.14%	85.12%
Fuzzy K-NN + Sum Rule	3	77.97%	83.13%	**90.80**%
	5	76.91%	82.25%	88.43%
	7	74.76%	83.59%	87.93%

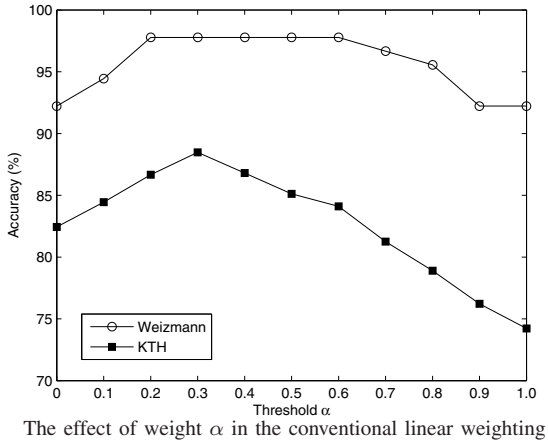

Fig. 6. The effect of weight α in the conventional linear weighting scheme on the average classification rate for Weizmann and KTH datasets. The weight is used to control the relative importance of the votes from shape and motion cues. $\alpha = 0$ corresponds to motion only while $\alpha = 1$ corresponds to shape only. The neighbor size, K is set to 3.

The results from Table I and II suggest that the contribution of each feature is dataset dependant. For instance, the shape feature is slightly better than the motion feature for

Fig. 7. Similar poses observed from *jogging* (left) and *running* (right) action sequences.

Weizmann dataset. On the other hand, we observe that for KTH dataset motion feature is much more discriminative than the shape feature. This implies that in the conventional linear weighting approach the contribution of each feature must be pre-determined by finding a suitable weight, α. Therefore, we evaluated the effect of α as shown in Fig. 6. The best results are only 97.78% for Weizmann and 88.48% for KTH. This provides clear evidence that regardless of the weight values, the conventional framework is still inferior to our implicitly weight-free framework. Another interesting observation from Table II is that the performance improvement brought by fuzzy K-NN classifier is more significant on the classification based on shape rather than motion features. The reason could be that fuzzy K-NN is able to handle the uncertainty in the poses better compared to conventional K-NN classifier. The uncertainty can arise from similar postures in action sequences such as jogging and running as shown in Fig. 7. Recall that fuzzy K-NN has an initialization procedure to weight the training sample which potentially resolves the data overlap problem. On the contrary, conventional K-NN suffers from the drawback that each training sample is considered equally important which causes atypical sample is weighted as much as the sample from the true class.

Finally, we investigate the performance of sum-rule compared to other combining schemes. The result from Table III clearly show that sum-rule delivers the best classification rate, closely followed by product-rule, max-rule, min-rule, and majority voting schemes. The result is consistent with Kittler *et al.* [9] findings that sum-rule produces the most reliable decisions due to its robustness against estimation error.

TABLE III
CLASSIFICATION RATE FOR KTH DATASET USING DIFFERENT COMBINING SCHEMES

Combining Schemes	Accuracy (%)
Sum-rule	**90.80**
Product-rule	89.61
Max-rule	87.94
Min-rule	86.09
Majority vote	81.94

The confusion matrix for KTH is given in Fig. 8. Most of the errors occur when *running* action is misclassified as *jogging* action. This is followed by *boxing* and *clapping* actions. This observation is consistent with the results reported in [10], [8], [16]. Although the main goal of this work is to compare our framework to the conventional K-NN with linear weighting method, we also compare the results against state-of-the-art action recognition approaches. Table IV shows that our method achieved the same perfect accuracy as [17] for Weizmann dataset. As for KTH dataset, it may be argued that the results are not directly comparable as different authors employed different evaluation protocol (splits vs. LOOCV). While not definitive, Table V still provides some indicative comparison. The result shows that our system remains competitive compared to the other methods. In fact, our method achieved the second best result (only slightly inferior to Lin *et al.* [5]). One possible reason is that Lin *et al.* used silhouette for feature extraction. It is well known that silhouette requires good background modelling which is more restrictive than the bounding box-based approach. In contrast, our KTH experiment only used the original grayscale image containing inside the bounding box. From the result, it can be deduced that our method can perform very well even without using silhouette. In addition, it should be noted that in Lin *et al.* work the prototype tree is only used for quantization when matching the frame to prototype. The algorithm still relies on dynamic time warping which are computationally expensive when the video is long. Our framework has the advantage of efficient computation.

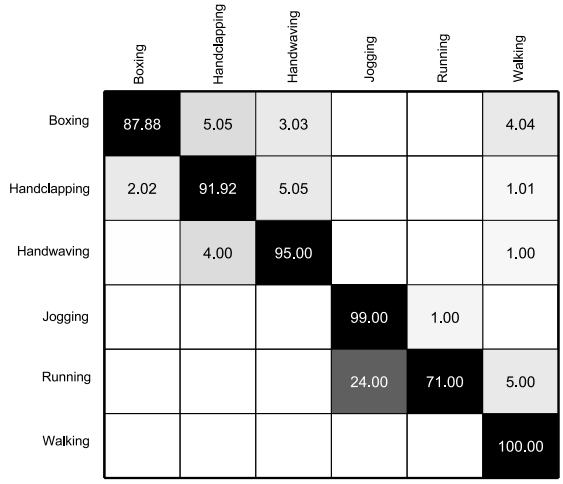

Fig. 8. Confusion matrix for KTH (K = 3).

TABLE IV
COMPARISON OF RECOGNITION RATES FOR WEIZMANN.

Method	Accuracy (%)
Our method	**100.00**
Fathi [17]	100.00
Blank [2]	99.64
Jhuang [11]	98.80
Wang [18]	97.78
Saad [19]	95.75
Chaudhry [13]	94.44
Niebles [20]	90.00

TABLE V
COMPARISON OF RECOGNITION RATES FOR KTH.

Method	Protocol	Accuracy (%)
Our method	LOOCV	**90.80**
Lin [5]	LOOCV	93.43
Fathi [17]	Splits	90.50
Ahmad [21]	Splits	88.83
Willems [8]	Splits	84.26
Niebles [20]	LOOCV	83.33
Dollár [7]	LOOCV	81.17
Ke [16]	LOOCV	80.90
Schüldt [15]	Splits	71.72

VII. CONCLUSION

This paper presents a new fuzzy-KNN with sum-rule fusion framework to perform action recognition from shape-motion features. The novelty is in the new approach to fuse the decisions from shape-motion cues which is very efficient in implementation. We demonstrated that fuzzy K-NN classifier can deliver better performance than the conventional K-NN classifier especially when dealing with data uncertainty. This is evident when classifying actions with similar poses. The introduction of sum-rule to combine fuzzy K-NN classifiers outputs has shown promising results compared to other combining schemes such as product-rule, max-rule etc. One major advantage of using sum-rule is that the process of choosing the suitable weight through trial-and-error is no longer required. The method described in this paper facilitates a generic framework that can also be used to combine the classification results from heterogenous inputs other than shape and motion.

REFERENCES

[1] A. A. Efros, A. C. Berg, G. Mori, and J. Malik, "Recognizing action at a distance," in *Proc. of International Conference on Computer Vision (ICCV)*, Nice, France, 2003.

[2] M. Blank, L. Gorelick, E. Shechtman, M. Irani, and R. Basri, "Actions as space-time shapes," in *Proc. of International Conference on Computer Vision (ICCV)*, Beijing, China, 2005.

[3] N. Ikizler, R. G. Cinbis, and P. Duygulu, "Human action recognition with line and flow histograms," in *Proc. of International Conference on Pattern Recognition (ICPR)*, Tampa, Florida, USA, 2008.

[4] N. Ikizler and P. Duygulu, "Histogram of oriented rectangles: A new pose descriptor for human action recognition," *Image and Vision Computing*, vol. 27, no. 10, pp. 1515–1526, 2009.

[5] Z. Lin, Z. Jiang, and L. S. Davis, "Recognizing actions by shape-motion prototype trees," in *Proc. of International Conference on Computer Vision (ICCV)*, Kyoto, Japan, 2009.

[6] I. Laptev and T. Lindeberg, "Space-time interest points," in *Proc. of International Conference on Computer Vision (ICCV)*, Nice, France, 2003.

[7] P. Dollár, V. Rabaud, G. Cottrell, and S. Belongie, "Behavior recognition via sparse spatio-temporal features," in *Proc. of IEEE International Workshop on Visual Surveillance and Performance Evaluation of Tracking and Surveillance (VS-PETS)*, Beijing, China, 2005.

[8] G. Willems, T. Tuytelaars, and L. Van Gool, "An efficient dense and scale-invariant spatio-temporal interest point detector," in *Proc. of European Conference on Computer Vision (ECCV)*, Marseille, France, 2008.

[9] J. Kittler, M. Hatef, R. P. Duin, and J. Matas, "On combining classifiers," *IEEE Trans. Pattern Anal. Mach. Intell.*, vol. 20, no. 3, pp. 226–239, 1998.

[10] K. Schindler and L. Van Gool, "Action snippets: How many frames does human action recognition require?" in *Proc. of IEEE Conference on Computer Vision and Pattern Recognition (CVPR)*, Anchorage, Alaska, 2008.

[11] H. Jhuang, T. Serre, L. Wolf, and T. Poggio, "A biologically inspired system for action recognition," in *Proc. of International Conference on Computer Vision (ICCV)*, Rio de Janeiro, Brazil, 2007.

[12] R. Poppe, "A survey on vision-based human action recognition," *Image and Vision Computing*, vol. 28, no. 6, pp. 976–990, June 2010.

[13] R. Chaudhry, A. Ravichandran, G. Hager, and R. Vidal, "Histograms of oriented optical flow and binet-cauchy kernels on nonlinear dynamical systems for the recognition of human actions," in *Proc. of IEEE Conference on Computer Vision and Pattern Recognition (CVPR)*, Miami, Florida, 2009.

[14] J. M. Keller, M. R. Gray, and J. A. Givens, "A fuzzy K-NN neighbor algorithm," *IEEE Trans. Syst., Man, Cybern.*, vol. 15, no. 4, pp. 580–585, 1985.

[15] C. Schüldt, I. Laptev, and B. Caputo, "Recognizing human actions: A local SVM approach," in *Proc. of International Conference on Pattern Recognition (ICPR)*, Cambridge, UK, 2004.

[16] Y. Ke, R. Sukthankar, and M. Hebert, "Spatio-temporal shape and flow correlation for action recognition," in *Proc. of IEEE Conference on Computer Vision and Pattern Recognition (CVPR)*, Minnesota, USA, 2007.

[17] A. Fathi and G. Mori, "Action recognition by learning mid-level motion features," in *Proc. of IEEE Conference on Computer Vision and Pattern Recognition (CVPR)*, Anchorage, Alaska, 2008.

[18] L. Wang and D. Suter, "Recognizing human activities from silhouettes: Motion subspace and factorial discriminative graphical model," in *Proc. of IEEE Conference on Computer Vision and Pattern Recognition (CVPR)*, Minnesota, USA, 2007.

[19] S. Ali and M. Shah, "Human action recognition in videos using kinematic features and multiple instance learning," *IEEE Trans. Pattern Anal. Mach. Intell.*, vol. 32, no. 2, pp. 288–303, 2010.

[20] J. C. Niebles, H. Wang, and L. Fei-fei, "Unsupervised learning of human action categories using spatial-temporal words," *Int'l J. Computer Vision*, vol. 79, no. 3, pp. 299–318, 2008.

[21] M. Ahmad and S. Lee, "Human action recognition using shape and CLG-motion flow from multi-view image sequences," *Pattern Recognition*, vol. 41, no. 7, pp. 2237–2252, July 2008.

2011 IEEE International Conference on Fuzzy Systems
June 27-30, 2011, Taipei, Taiwan

Fuzzy Clustering with Multiple Kernels

Naouel Baili
Multimedia Research Lab
CECS Department
University of Louisville, USA
Email: n0bail02@louisville.edu

Hichem Frigui
Multimedia Research Lab
CECS Department
University of Louisville, USA
Email: h.frigui@louisville.edu

***Abstract*—In this paper, the kernel fuzzy c-means clustering algorithm is extended to an adaptive cluster model which maps data points to a high dimensional feature space through an optimal convex combination of homogenous kernels with respect to each cluster. This generalized model, called Fuzzy C-Means with Multiple Kernels (FCM-MK), strives to find a good partitioning of the data into meaningful clusters and the optimal kernel-induced feature map in a completely unsupervised way. It constructs the kernel from a number of Gaussian kernels and learns a resolution specific weight for each kernel function in each cluster. This allows better characterization and adaptability to each individual cluster. The effectiveness of the proposed algorithm is demonstrated for several toy and real data sets.**

***Index Terms*—Fuzzy Clustering, Multiple Kernels, Resolution Weights.**

I. Introduction

Clustering methods have been used extensively in computer vision and pattern recognition. Fuzzy clustering, where an object can belong to multiple clusters with a certain degree of membership, has been shown to be more effective than crisp clustering where a point can be assigned to only one cluster. This is particularly useful when the boundaries among the clusters are not well separated and ambiguous. Moreover, the memberships may help in discovering more hidden relations between a given object and the disclosed clusters. The Fuzzy C-Means (FCM) is one of the most popular fuzzy clustering algorithms [1]. The basic FCM uses the squared-norm to measure similarity between prototypes and data points, and is suitable for identifying spherical clusters. Many extensions of the FCM have been proposed to cluster more general data set. Most of those algorithms are realized by replacing the squared-norm in the object function of FCM with other similarity measures [1][2]. Others, such as the Kernel-based fuzzy c-means (KFCM) [3] adopts a kernel-induced metric in the data space to replace the original Euclidean norm. By replacing the inner product with an appropriate kernel function, one can implicitly perform a nonlinear mapping to a high dimensional feature space without increasing the number of parameters. This kernel approach has been successfully applied to many learning systems [4], such as Support Vector Machines (SVMs), kernel principal component analysis and kernel fisher discriminant analysis [5].

Kernel-based clustering relies on a kernel function to project data samples into a high-dimensional kernel-induced feature space. A good choice of the kernel function is therefore imperative to the success of the clustering. However, one of the central problems with kernel methods in general is that it is often unclear which kernel is the most suitable for a particular task [6][7][8]. Thus, instead of using a single fixed kernel, recent developments in SVM and other supervised kernel methods have shown encouraging results in constructing the kernel from a number of homogeneous or even heterogeneous kernels [7][9] [10][11]. This provides extra flexibility and also allows domain knowledge from possibly different information sources to be incorporated to the base kernels. However, previous work in this so-called multiple kernel learning approach have all been focused on the supervised and semi-supervised learning settings. Therefore, how to efficiently learn and adopt multiple kernels in unsupervised learning, or fuzzy clustering in particular, is still an interesting yet unexplored research topic.

In this paper, we propose a new fuzzy clustering with multiple kernels algorithm (FCM-MK). FCM-MK strives to find a good partitioning of the data into meaningful clusters and the optimal kernel-induced feature map in a completely unsupervised way. FCM-MK is a generalization of the KFCM algorithm and uses a new optimization criterion to learn the optimal convex combination of homogenous kernels with respect to each cluster. It constructs the kernel from a number of Gaussian kernels and learns a resolution-specific weight for each kernel function in each cluster. This allows better characterization and adaptability to each individual cluster.

The organization of this paper is as follows. In section II, we give a brief overview of the Kernel-based learning algorithms. In section III, we describe the proposed fuzzy c-means with multiple kernels algorithm. Experiments are discussed in section IV and conclusions are provided in section V.

II. Related work

Kernel-based learning algorithms [12][13], are based on Cover's theorem. By nonlinearly transforming a set of complex and nonlinearly separable patterns into a higher-dimensional feature space, it is possible to separate these patterns linearly [14]. The difficulty of the curse of dimensionality can be overcome by the kernel trick, arising from Mercer's theorem [14]. By designing and calculating an inner-product kernel, we can avoid the time-consuming, sometimes even infeasible process to explicitly describe the nonlinear mapping $\Phi : X \mapsto \mathcal{F}$ from the input space X to a high dimensional feature space $\mathcal{F}$ and

978-1-4244-7316-8/11/$26.00 ©2011 IEEE

compute the corresponding points in the transformed space. Computing the Euclidean distances in $\mathcal{F}$ without explicit knowledge of Φ is possible using the so called distance kernel trick:

$$\begin{aligned}\|\Phi(x_i) - \Phi(x_j)\|^2 &= (\Phi(x_i) - \Phi(x_j)).(\Phi(x_i) - \Phi(x_j)) \\ &= \Phi(x_i).\Phi(x_i) + \Phi(x_j).\Phi(x_j) - 2\Phi(x_i).\Phi(x_j) \\ &= K(x_i, x_i) + K(x_j, x_j) - 2K(x_i, x_j) \end{aligned} \quad (1)$$

Thus, the computation of the distances in the feature space is just a function of the input vectors. In fact, every algorithm in which input vectors appear only in dot products with other input vectors can be kernelized [15].
In (1), $K(x_i, x_j) = \Phi(x_i).\Phi(x_j)$ is the Mercer Kernel. It is a symmetric function $K : X \times X \to \mathbb{R}$ and satisfies

$$\sum_{i=1}^{N}\sum_{j=1}^{N} c_i c_j K(x_i, x_j) \geq 0 \qquad \forall n \geq 2, \quad (2)$$

where $c_r \in \mathbb{R}$, and $r = 1, \ldots, N$. Examples of Mercer kernels include [16]

- Linear

$$K^{(l)}(x_i, x_j) = x_i.x_j \quad (3)$$

- Polynomial of degree p

$$K^{(p)}(x_i, x_j) = (1 + x_i.x_j)^p, \qquad p \in \mathbb{N} \quad (4)$$

- Gaussian

$$K^{(g)}(x_i, x_j) = \exp\left(-\frac{\|x_i - x_j\|}{2\sigma^2}\right), \qquad \sigma \in \mathbb{R} \quad (5)$$

Kernel-based clustering algorithms have the following main advantages.

1) They are more likely to obtain a linearly separable hyperplane in the high-dimensional, or even in an infinite feature space;
2) They can identify clusters with arbitrary shapes;
3) Kernel-based clustering algorithms, like support vector clustering (SVC), have the capability of dealing with noise and outliers;
4) For SVC, there is no requirement for prior knowledge to determine the system topological structure. In [17], the kernel matrix can provide the means to estimate the number of clusters.

The kernelized metric Fuzzy C-Means [18] is one of the most common kernel-based clustering algorithm. It minimizes the following objective function.

$$J^{\phi} = \sum_{i=1}^{K}\sum_{j=1}^{N} u_{ij}^m \|\phi(x_j - \phi(v_i)\|^2, \quad (6)$$

subject to

$$u_{ij} \in [0, 1] \quad and \quad \sum_{i=1}^{K} u_{ij} = 1 \; \forall j \quad (7)$$

In (6), u_{ij} denotes the membership of x_j in cluster i, v_i is the center of cluster i in the input space, and ϕ is the mapping from the input space $\mathcal{X}$ to the feature space $\mathcal{F}$. Minimization of the function in (6) has been proposed only in the case of a Gaussian kernel. The reason is that the derivative with respect to the v_i in this case allows to use the kernel trick:

$$\frac{\partial K(x_j, v_i)}{\partial v_i} = \frac{(x_j, v_i)}{\sigma^2} K(x_j, v_i) \quad (8)$$

It can be shown [18] that the update equation for the membership is

$$u_{ij}^{-1} = \sum_{h=1}^{K} \left(\frac{1 - K(x_j, v_i)}{1 - K(x_j, v_h)}\right)^{1/(m-1)}, \quad (9)$$

and for the codevectors

$$v_i = \frac{\sum_{j=1}^{N} u_{ij}^m K(x_j, v_i) x_j}{\sum_{j=1}^{N} u_{ij}^m K(x_j, v_i)}. \quad (10)$$

A critical issue related to kernel-based clustering is the selection of an "optimal" kernel for the problem at hand. In fact, the performance of a kernel-based clustering depends critically on the selection of the kernel function, and on the setting of the involved parameters. The kernel function in use must conform with the learning objectives in order to obtain meaningful results. While solutions to estimate the optimal kernel function and its parameters have been proposed in a supervised setting [19][20][21][22], the problem presents open challenges when no labeled data are provided.

III. Fuzzy C-Means with Multiple Kernels

Given N data points, $x_j \in \mathbb{R}^d$, for $j = 1, \ldots, N$. Then, x_j is transformed via S mappings $\Phi_l(x_j) \mapsto \mathbb{R}^{d_l'}$ for $l = 1, \ldots, S$ from the input space into S feature spaces $(\Phi_1(x_j), \ldots, \Phi_S(x_j))$ where d_l' denotes the dimensionality of the l^{th} feature space. By using the closure properties of kernel functions [23], we construct a new cluster dependent similarity based on kernel K^i, between object j and cluster i. In particular, we define K^i as a linear combination of S Gaussian kernels $K_1, \ldots, K_S$, with spread parameters $\sigma_1, \ldots, \sigma_S$, respectively. That is,

$$\begin{aligned} K^{(i)}(x_j, v_i) &= \sum_{l=1}^{S} w_{il} K_l(x_j, v_i) \\ &= \sum_{l=1}^{S} \frac{w_{il}}{\sigma_l} \exp\left(-\frac{\|x_j - v_i\|^2}{2\sigma_l^2}\right) \end{aligned} \quad (11)$$

In (11), $W = [w_{il}]$, where $w_{il} \in [0, 1]$ is a resolution-specific weight for the kernel matrix K_l with respect to cluster i. A low value of w_{il} indicates that the bandwidth of kernel K_l is not relevant for the density estimation of cluster i, and that this matrix should not have a significant impact on the creation of this cluster. Similarly, a high value of w_{il} indicates that the bandwidth of kernel K_l is highly relevant for the density estimation of cluster i, and that this matrix should be the main factor in the creation of this cluster.
We normalize the kernel $K^{(i)}$ to construct a new kernel $\widetilde{K}^i$,

where $\widetilde{K}^i(x_j, x_j) = 1$, for $j = 1, \ldots, N$. This normalized kernel is defined as

$$\widetilde{K}^{(i)}(x_j, v_i) = \frac{K^{(i)}(x_j, v_i)}{\sqrt{K^{(i)}(x_j, x_j).K^{(i)}(v_i, v_i)}} = \sum_{l=1}^{S} \frac{w_{il}}{\sigma_l} \exp(-\frac{\|x_j - v_i\|^2}{2\sigma_l^2}) \times \frac{1}{\sum_{l=1}^{S} \frac{w_{il}}{\sigma_l}} \quad (12)$$

After kernel normalization, the distance in (1) becomes

$$\|\widetilde{\Phi}^{(i)}(x_j) - \widetilde{\Phi}^{(i)}(v_i)\|^2 = 2 - 2\widetilde{K}^{(i)}(x_j, v_i) \quad (13)$$

Substituting the distance in (13) into the kernelized metric Fuzzy C-Means objective function (6), we define the objective function of the proposed FCM-MK algorithm as

$$J(U, V, W) = 2 \sum_{i=1}^{C} \sum_{j=1}^{N} u_{ij}^m \left(1 - \sum_{l=1}^{S} \frac{w_{il}}{\sigma_l} \exp(-\frac{\|x_j - v_i\|^2}{2\sigma_l^2}) \times \frac{1}{\sum_{l=1}^{S} \frac{w_{il}}{\sigma_l}}\right) \quad (14)$$

subject to

$$u_{ij} \in [0, 1], \; and \sum_{i=1}^{C} u_{ij} = 1, \; for \, j = 1, \ldots, N; \quad (15)$$

and

$$w_{il} \in [0, 1], \; and \sum_{l=1}^{S} w_{il} = 1, \; for \, i = 1, \ldots, C. \quad (16)$$

In (14), C and N represent the number of clusters and the number of data points respectively, u_{ij} is the fuzzy membership of point x_j in cluster i, v_i are the centers or prototypes of the clusters, and $m \in (1, \infty)$ denotes the fuzzifier.

The goal of the FCM-MK is to identify the resolution-specific weight w_{il}, the membership values u_{ij} and the cluster prototypes v_i by optimizing (14). In order to compute the optimal values of w_{il}, u_{ij} and v_i, we use an alternating optimization method, where we will alternate the optimization of w_{il}, u_{ij} and of v_i.

To optimize (14) with respect to the memberships, we first rewrite (14) as

$$J(U, V, W) = \sum_{i=1}^{C} \sum_{j=1}^{N} u_{ij}^m dist_{ij}^2 \quad (17)$$

where

$$dist_{ij}^2 = \left(2 - 2 \sum_{l=1}^{S} \frac{w_{il}}{\sigma_l} \frac{\exp(-\frac{\|x_j - v_i\|^2}{2\sigma_l^2})}{\sum_{l=1}^{S} \frac{w_{il}}{\sigma_l}}\right) \quad (18)$$

Note that in (18), $dist_{ij}^2$ is not a function of the fuzzy memberships u_{ij}.

Then, to optimize (17) with respect to u_{ij} subject to (15), we use the Lagrange multiplier technique and obtain

$$J = \sum_{i=1}^{C} \sum_{j=1}^{N} u_{ij}^m dist_{ij}^2 - \sum_{j=1}^{N} \lambda_j \left(\sum_{i=1}^{C} u_{ij} - 1\right). \quad (19)$$

By setting the gradient of J to zero, we obtain the following update equation for the membership

$$u_{ij} = \frac{1}{\sum_{t=1}^{C} (dist_{ij}^2 / dist_{tj}^2)^{\frac{1}{m-1}}} \quad (20)$$

where $dist_{ij}^2$ is as defined in (18).

To optimize (14) with respect to te cluster prototypes v_i, we take the first derivative of J with respect to v_i and set it to zero. This yields the following update equation for the prototypes

$$v_i = \frac{\sum_{j=1}^{N} u_{ij}^m \overline{K}^{(i)}(x_j, v_i) x_j}{\sum_{j=1}^{N} u_{ij}^m \overline{K}^{(i)}(x_j, v_i)} \quad (21)$$

where

$$\overline{K}^{(i)}(x_j, v_i) = \left(\sum_{l=1}^{S} \frac{w_{il}}{\sigma_l^3} \exp(-\frac{\|x_j - v_i\|^2}{2\sigma_l^2}) \times \frac{1}{\sum_{l=1}^{S} \frac{w_{il}}{\sigma_l}}\right) \quad (22)$$

The optimization of (14) with respect to the resolution-specific weights has no closed form solution. Thus, we use the gradient descent method and update w_{il} iteratively using

$$w_{il}^{(new)} = w_{il}^{(old)} - \rho \frac{\partial J}{\partial w_{il}} \quad (23)$$

where ρ is a scalar parameter that determines the learning rate. In our approach, ρ is optimized via a line-search method.
It can be shown that the gradient of J with respect to w_{il} is given by

$$\frac{\partial J}{\partial w_{il}} = -2 \sum_{j=1}^{N} \frac{u_{ij}^m}{\sigma_l} \left(\frac{\exp(-\frac{\|x_j - v_i\|^2}{2\sigma_l^2})}{\sum_{t=1}^{S} \frac{w_{it}}{\sigma_t}} - \frac{\sum_{t=1}^{S} \frac{w_{it}}{\sigma_t} \exp(-\frac{\|x_j - v_i\|^2}{2\sigma_t^2})}{\left(\sum_{t=1}^{S} \frac{w_{it}}{\sigma_t}\right)^2}\right) = -2 \sum_{j=1}^{N} \frac{u_{ij}^m}{\sigma_l \sum_{t=1}^{S} \frac{w_{it}}{\sigma_t}} \left(K_l(x_j, v_i) - \widetilde{K}^{(i)}(x_j, v_i)\right) \quad (24)$$

The resulting FCM-MK algorithm is summarized in Algorithm 1.

The time complexity of the first step of the algorithm is $\mathcal{O}(NCdS)$ where N is the number of samples or data points, C is the number of clusters, d is the number of features or dimensions and S is the number of Gaussian kernels. In the second step of FCM-MK to update the prototypes, the time complexity is also $\mathcal{O}(NCdS)$. The time spend in the membership update is $\mathcal{O}(NC^2)$. We use the gradient descent technique to update the resolution-specific weight. If we note by τ_{gd} the number of iterations for the gradient descent

Algorithm 1 Fuzzy C-Means with Multiple Kernels

Fix the number of clusters C, fuzzification parameter $m > 1$, stopping criterion ϵ, maximum number of iterations $qmax$ and iteration counter $q = 1$;
Initialize the fuzzy partition matrix **U**;
Initialize cluster prototypes **V**;
Pick the Gaussian parameters $\sigma_1, \ldots, \sigma_S$ and initialize $w_{il}^{(0)} = 1/S$
repeat
1. Compute total similarities $\widetilde{K}^{(i)}$ using (12);
2. Update cluster prototypes using (21);
3. Update fuzzy membership using (20);
repeat
4.1 Update $w_{il}^{(q-1)} = w_{il}^{(q)}$
4.2 Compute the gradients $\frac{\partial J}{\partial w_{il}}$ using (24)
4.3 Update resolution-specific weights using (23);
until $\|w_{il}^{(q)} - w_{il}^{(q-1)}\| < \epsilon$ or $q = qmax$
until (fuzzy memberships do not change);

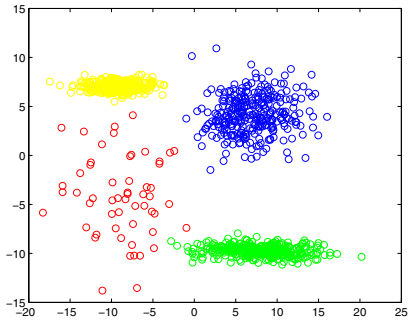

Fig. 1. Data set with 4 clusters of different shapes and densities

to converge, the time complexity of step 6 is $\mathcal{O}(\tau_{gd} NdS)$. Therefore, the total computational complexity of FCM-MK is

$$\mathcal{O}\left(\tau(NCdS + NC^2) + \tau\tau_{gd} NdS\right) \tag{25}$$

where τ is the number of iterations.

IV. Experimental results

To illustrate the ability of FCM-MK to learn appropriate local density fitting functions and cluster the data simultaneously, we use it to categorize a synthetic data set (refer to figure 1), that includes categories with unbalanced sizes and densities, and two real-world data sets selected from the UCI repository (digits and ionosphere). For the digits data, we focus on the pair 3 vs 8 that is difficult to differentiate [24]. We summarize all of these in Table I.

For each data set, we show the effectiveness of the proposed algorithm by evaluating the resolution specific weights assigned to each kernel induced-similarity. A low value of w_{il} indicates that the bandwidth σ_l of kernel K_l is not relevant for the density fitting of cluster i, and that the distance matrix computed with this kernel should not have significant impact on the creation of this cluster. Similarly, a high value of w_{il} indicates that the bandwidth σ_l of kernel K_l is highly relevant for fitting the points in cluster i, and that this matrix should be the main factor in the creation of this cluster. We demonstrate the effectiveness of FCM-MK by comparing the clustering results to the following algorithms:

1) FCM with the Euclidean norm;
2) Kernel metric FCM (KFCM) where K is a gaussian kernel with S different values of σ, $\sigma_1, \ldots, \sigma_S$;
3) KFCM with a kernel K constructed as the sum of the S Gaussian kernels, $K(x_j, v_i) = \sum_{l=1}^{S} \exp(-\frac{\|x_j - v_i\|^2}{2\sigma_l^2})$

For all algorithms, we use the same initialization, the same number of clusters, and the same fuzzifier. In all experiments, we choose the number of kernels $S = 4$ and $\sigma = 0.1 * D, 0.2 * D, 0.3 * D, 0.4 * D$ where $D = \left[\sum_{k=1}^{d} \left(\max(X^k) - \min(X^k)\right)^2\right]^{\frac{1}{2}}$ and X^k is the k^{th} attribute of the data set.

To assess the performance of the different clustering algorithms and compare them, we assume that the ground truth is known and we use some relative cluster evaluation measures [25]: the accuracy rate (Q_{RR}), the *Jaccard coefficient* (Q_{JC}), the *Folkes-Mallows index* (Q_{FMI}) and the *Hubert index* (Q_{HI}).

TABLE I
Description of the data sets

Data	Size	Dimension	Class
Synthetic data set	1078	2	4
ionosphere	351	34	2
digits3v8	345	64	2
digits0689	692	64	4

TABLE II
Resolution weights learned by FCM-MK for the data in figure 1

	$\sigma_1 = 0.5$	$\sigma_2 = 1$	$\sigma_3 = 3$	$\sigma_4 = 5$	True (σ_x, σ_y)
Cluster1	0.203	0.294	0.387	0.115	(3.20, 1.99)
Cluster2	0.106	0.298	0.395	0.201	(3.80, 4.09)
Cluster3	0.212	0.284	0.358	0.145	(3.77, 0.54)
Cluster4	0.296	0.390	0.202	0.114	(2.10, 0.42)

The FCM algorithm cannot categorize the data in figure 1 as it can be seen in figure 2a. This is due to the fact that FCM is designed to seek compact spherical clusters. However, the geometry of this data is more complex. The clusters are close to each others and have different densities. Similarly, the KFCM algorithm, using a single bandwidth, was not able to categorize this data correctly as it can be seen from figures 2b-2e. The KFCM algorithm, using a kernel constructed as the average of the 4 Gaussian kernels K_l with bandwidth σ_l, also cannot categorize the data. This is because one global bandwidth cannot take into account the variations of the different clusters.

On the other hand, the resolution weights learned by our approach (see table II) make it possible to identify the four clusters correctly. In table II, cluster4 has an ellipsoidal shape with a true standard deviation of 2.10 in the horizontal

TABLE III
RESOLUTION WEIGHTS LEARNED BY FCM-MK FOR DIGITS3V8

	$\sigma_1 = 5$	$\sigma_2 = 10$	$\sigma_3 = 15$	$\sigma_4 = 20$	True σ
digit3	0.198	0.356	0.256	0.190	7.89
digit8	0.202	0.395	0.236	0.167	7.25

TABLE IV
RESOLUTION WEIGHTS LEARNED BY FCM-MK FOR IONOSPHERE

	$\sigma_1 = 0.5$	$\sigma_2 = 1$	$\sigma_3 = 1.5$	$\sigma_4 = 2$	True σ
Cluster1	0.174	0.266	0.361	0.199	1.41
Cluster2	0.172	0.202	0.258	0.368	1.59

direction and 0.42 in the vertical direction. The geometry of cluster4 is captured by our algorithm. In fact, higher weights were assigned to $\sigma_l = 0.5$ and $\sigma_l = 1$ which reflects the existence of some points with small variance along the horizontal direction and some points with larger variance along the vertical direction. Similarly, the other three clusters were assigned different weights. The clustering performances of the different algorithms on this data are reflected on the cluster evaluation measures in table VI. As it can be seen, the statistics provided by FCM-MK are higher than the statistics provided by the other algorithms.

For the digits0689 data set, the FCM-MK assigned high weight to $\sigma_l = 10$ for all clusters (refer to table V). This is an indication that the clusters within this data have similar distributions and one global σ is sufficient for this data. This explains the comparable behavior of FCM-MK with KFCM with kernel K_2 as reported in table IX.

On the other hand, for the ionosphere data set, FCM-MK assigned different weights to the different clusters as reported in table IV. This indicates that the clusters within this data have different distributions. Thus, the statistics provided by FCM-MK are higher than the statistics of the other competing algorithms.

V. CONCLUSIONS

In this paper, we proposed a new fuzzy clustering algorithm with multiple kernels. The proposed FCM-MK algorithm uses a fixed set of kernels with different resolutions that cover the spectrum of the entire data. Data points are mapped to a high dimensional feature space through a convex combination of these kernels. The kernel weights are adapted to the different clusters to reflect their distributions. The FCM-MK algorithm optimizes one objective function to identify the optimal clusters' prototypes, their fuzzy membership degrees, and the optimal convex combination of the homogeneous kernels in an unsupervised way.

The effectiveness of the proposed algorithm is demonstrated and compared to similar algorithms using synthetic and real data sets. We showed that when the data has clusters with similar densities, the FCM-MK performance is comparable to the kernel FCM with one kernel. However, for data sets that have clusters with different densities, the proposed FCM-MK learns different kernel weights and outperforms the kernel FCM.

TABLE V
RESOLUTION WEIGHTS LEARNED BY FCM-MK FOR DIGITS0689

	$\sigma_1 = 5$	$\sigma_2 = 10$	$\sigma_3 = 15$	$\sigma_4 = 20$	True σ
digit0	0.281	0.384	0.261	0.074	6.45
digit6	0.174	0.377	0.343	0.106	7.55
digit8	0.203	0.414	0.335	0.048	7.25
digit9	0.144	0.412	0.352	0.102	9.25

In the current implementation, the FCM-MK algorithm uses fuzzy memberships that are constrained to sum to one. This makes the algorithm sensitive to noise and outliers. In fact, noise points can lead the algorithm to learn kernel weights that do not reflect the overall distribution of the clusters. One way to address this limitation is to adapt the FCM-MK to use possibilistic membership functions. We are currently investigating this alternative.

ACKNOWLEDGMENT

This work was supported in part by U.S. Army Research Office Grants Number W911NF-08-0255 and by a grant from the Kentucky Science and Engineering Foundation as per Grant Agreement No. KSEF-2079-RDE-013 with the Kentucky Science and Technology Corporation.

REFERENCES

[1] J. Bezdek, *Pattern recognition with fuzzy objective function algorithms*. New York: Plenum, 1981.
[2] K. Wu and M. Yang, "Alternative c-means clustering algorithms," P*attern* R*ecognition*, vol. 35, pp. 2267–2278, 2002.
[3] W. X. Z. Wu and J. Yu, "Fuzzy c-means clustering algorithm based on kernel method," C*omputational* I*ntelligence and* M*ultimedia* A*pplications*, 2003.
[4] D. Graves and W. Pedrycz, "Kernel-based fuzzy clustering and fuzzy clustering: A comparative experimental study," *Fuzzy Sets and Systems*, vol. 161, no. 4, pp. 522 – 543, 2010.
[5] N. Cristianini and J. Taylor, "An introduction to SVMs and other kernel-based learning methods," *Cambridge* U*niv.* P*ress*, 2000.
[6] O. Bousquet and D. Herrmann, "On the complexity of learning the kernel matrix," *NIPS*, 2003.
[7] L. G. P. B. G. Lanckriet, N. Cristianini and M. Jordan, "Learning the kernel matrix with semidefinite programming," *JMLR*, vol. 5, pp. pp. 27–72, 2006.
[8] A. S. C. Ong and R. Williamson, "Learning the kernel with hyperkernels," *JMLR*, vol. 6, pp. pp. 1043–1071, 2005.
[9] G. L. F. Bach and M. Jordan, "Multiple kernel learning, conic duality, and the smo algorithm," *ICML*, 2004.
[10] S. C. A. Rakotomamonjy, F. Bach and Y. Grandvalet, "More efficiency in multiple kernel learning," *ICML*, 2007.
[11] S. J. J. Ye and J. Chen, "Learning the kernel matrix in discriminant analysis via quadratically constrained quadratic programming," *SIGKDD*, 2007.
[12] G. R. K. T. K. Muller, S. Mika and B. Scholkopf, "An introduction to kernel-based learning algorithms," *IEEE Trans. Neural Network*, vol. 12, no. 2, pp. pp. 181–201, 2001.
[13] B. Scholkopf and A. Smola, *Learning with kernels: Support vector machines, regulization, optimization and beyond*. Cambridge, MA: MIT Press, 2002.
[14] S. Haykin, *Neural networks: S comprehensive foundation*, 2nd ed. Englewood Cliffs, NJ: Prentice-Hall, 1999.
[15] B. Scholkopf and A. J. Smola, *Learning with Kernels: Support Vector Machines, Regularization, Optimization, and Beyond*. MIT Press, Cambridge, MA, USA, 2001.
[16] V. Vapnik, *The Nature of Statistical Learning Theory*. Inc., New York, NY, USA, 1995.
[17] M. Girolami, "Mercer kernel based clustering in feature space," *IEEE Trans. Neural Netw.*, vol. 13, no. 3, pp. pp. 780–784, 2002.

[18] W. X. Z.D. Wu and J. Yu., "Fuzzy c-means clustering algorithm based on kernel method," *Computational Intelligence and Multimedia Applications*, 2003.
[19] J. S.-T. N. Cristianini and A. Elisseeff, "On kernel-target alignment," *Neural Information Processing Systems (NIPS)*, 2001.
[20] O. Chapelle and V. Vapnik, "Choosing mutiple parameters for support vector machines," *Machine Learning*, vol. 46, no. 1, pp. pp. 131–159, 2002.
[21] W. L. W. Wang, Z. Xu and X. Zhang, "Determination of the spread parameter in the gaussian kernel for classification and regression," *Neurocomputing*, vol. 55, no. 3, p. pp. 645, 2002.
[22] W. C. J. Huang, P.C. Yuen and J. Lai, "Kernel subspace lda with optimized kernel parameters on face rcognition," *The sixth IEEE International Conference on Automatic Face and Gesture Recognition*, 2004.
[23] J. Taylor and N. Cristianini, *Kernel methods for pattern analysis*. Cambrige University, 2004.
[24] A. Asuncion and D. Newman, "Uci machine learning repository," 2007.
[25] C. H. H. Frigui and F. C.-H. Rhee, "Clustering and aggregation of relational data with applications to image database categorization," *Pattern Recognition*, vol. 40, no. 11, pp. 3053–3068, 2007.

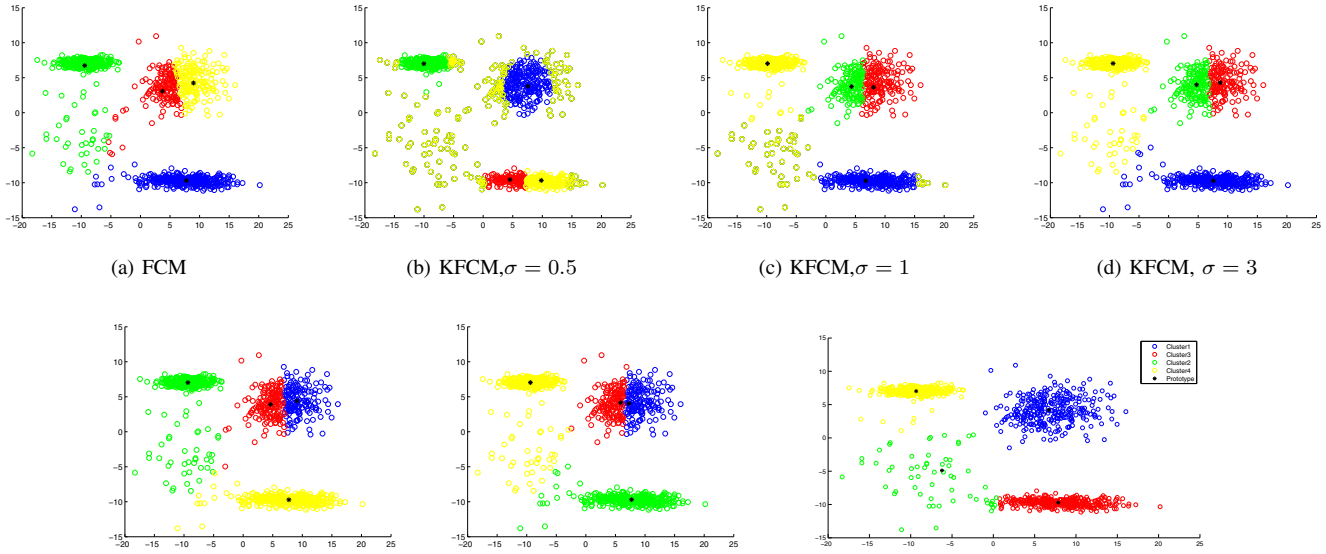

(a) FCM (b) KFCM,$\sigma = 0.5$ (c) KFCM,$\sigma = 1$ (d) KFCM, $\sigma = 3$

(e) KFCM,$\sigma = 5$ (f) KFCM,$\frac{1}{S}\sum_{l=1}^{S} K_l$ (g) FCM-MK

Fig. 2. Comparison of the partitions of the data set in figure 1 generated by the different algorithms

TABLE VI
COMPARISON OF THREE DIFFERENT ALGORITHMS ON THE DATA SET IN FIGURE 1

	FCM	KFCM					FCM-MK
		K_1	K_2	K_3	K_4	$\frac{1}{S}\sum_{l=1}^{S} K_l$	
Q_{RR}	84.9%	73.9%	86.7%	83.6%	82.7%	81.2%	98.9%
Q_{JC}	0.535	0.163	0.178	0.295	0.416	0.193	0.640
Q_{FMI}	0.687	0.281	0.303	0.456	0.588	0.325	0.781
Q_{HI}	0.569	0.007	0.035	0.241	0.423	0.065	0.691

TABLE VII
COMPARISON OF THREE DIFFERENT ALGORITHMS ON DIGITS3V8

	FCM	KFCM					FCM-MK
		K_1	K_2	K_3	K_4	$\frac{1}{S}\sum_{l=1}^{S} K_l$	
Q_{RR}	94.6%	90%	94.6%	94.4%	91.7%	88.7%	97.9%
Q_{JC}	0.189	0.189	0.189	0.189	0.19	0.189	0.396
Q_{FMI}	0.342	0.341	0.342	0.342	0.343	0.341	0.608
Q_{HI}	0	0	0	0	0.003	0	0.431

TABLE VIII
COMPARISON OF THREE DIFFERENT ALGORITHMS ON IONOSPHERE

	FCM	KFCM					FCM-MK
		K_1	K_2	K_3	K_4	$\frac{1}{S}\sum_{l=1}^{S} K_l$	
Q_{RR}	68%	86%	77%	72%	67%	62%	91%
Q_{JC}	0.297	0.326	0.322	0.317	0.298	0.294	0.396
Q_{FMI}	0.461	0.495	0.489	0.485	0.462	0.457	0.56
Q_{HI}	0.012	0.066	0.014	0.05	0.014	0.006	0.102

TABLE IX
COMPARISON OF THREE DIFFERENT ALGORITHMS ON DIGITS0689

	FCM	KFCM					FCM-MK
		K_1	K_2	K_3	K_4	$\frac{1}{S}\sum_{l=1}^{S} K_l$	
Q_{RR}	42.3%	93.1%	96.6%	94.1%	84.5%	82%	97.7%
Q_{JC}	0.119	0.255	0.257	0.255	0.207	0.160	0.399
Q_{FMI}	0.215	0.317	0.379	0.318	0.234	0.227	0.577
Q_{HI}	0	0.004	0.011	0.006	0.008	0.001	0.462

2011 IEEE International Conference on Fuzzy Systems
June 27-30, 2011, Taipei, Taiwan

Kernel-Based Fuzzy Clustering of Interval Data

Bruno A. Pimentel
Centro de Informatica/UFPE
Recife, Brazil
Email: bap@cin.ufpe.br

Anderson F. B. F. da Costa
Centro de Informatica/UFPE
Recife, Brazil
Email: afbfc@cin.ufpe.br

Renata M. C. R. de Souza
Centro de Informatica/UFPE
Recife, Brazil
Email: rmcrs@cin.ufpe.br

***Abstract*—Kernel clustering methods have been very important in application of non-supervised machine learning to real problems. Kernel methods possess many advantages other than non-linearity such as modularity, ability to work with heterogeneous descriptions of data, incorporation of prior knowledge etc. In this paper, we present a clustering method based on kernel functions for partitioning a set of interval-valued data. In addition, this method is compared to a fuzzy partitioning approach for interval data introduced previously. Experiments with real and syntectic symbolic interval-valued data sets are presented. The evaluation of the clustering results furnished by the methods is performed regarding the computation of an external cluster validity index and the global error rate of classification.**

***Index Terms*—Kernel, clustering, interval-valued data, fuzzy.**

I. Introduction

With the growing interest in automatically to understand, process and summarize data, several application domains like pattern recognition, machine learning, data mining, computer vision, computational biology and classification of statistical findings in social studies have used clustering algorithms [1] [2]. The objective of the cluster analysis is to group a set of elements into clusters such that elements within a cluster have a high degree of similarity, while elements belonging to different clusters have a high degree of dissimilarity. Clustering techniques may be divided into hierarchical clustering and partitioning clustering: hierarchical clustering groups data objects with a sequence of partitions dividing one group with all individuals in singleton clusters or vice versa, while partitioning clustering directly divides data objects into some fixed number of clusters with no hierarchical structure [3] and makes this division based on the optimization of a suitable objective function.

The partitioning methods may be classified in hard partitioning and fuzzy partitioning. The hard partitioning associates each element of the data to a single class, while in the fuzzy partitioning each element of the data is associated with all classes of the partition, the elements not belong a single cluster only and so that the memberships are calculated. When the memberships have values between 0 and 1, the sum of the all possibilities of an element belong to some classes is equal to 1 and the method is the type probabilistic [4]. But when the memberships have values 0 or 1, the method is the type crisp and the fuzzy method becomes equivalent to a hard method [5].

Kernel clustering methods have been very important in the application of non-supervised machine learning to real problems. These methods are able to produce nonlinear separating hyper surfaces among clusters [6]. The use of kernels allows to map implicitly data into a high dimensional space, called feature space; computing a linear partitioning in this feature space results in a nonlinear separation between clusters in the input space. Several clustering methods has been modified including the use of the kernel functions such as SOM [7], k-means [8], fuzzy c-means (FCM)[9] and so on. The kernel k-means was proposed [10] as an extension of the standard hard partitioning method k-means and the kernel fuzzy c-means was proposed [11] aiming to replace a kernel-induced distance metric for the original Euclidean distance of the fuzzy partitioning method.

In classical cluster analysis, data are often represented as arrays of quantitative or qualitative values, where each column represents a variable. In particular, each individual takes a single value for each variable. However, research study has shown that this presentation is not as rich in information to represent the complexity of data such as intervals or distributions found in real problems [12]. The main goal of *Symbolic Data Analysis* (SDA) concerns to model more complex information through a set-valued (interval or multi-valued) or modal (weight or probability distribution) variables also termed symbolic and extend classical data analysis techniques, such as, clustering, factorial techniques, decision trees and other to symbolic data. These data allow to take account variability and/or uncertainty, making the symbolic data analysis more comprehensive than the classical data analysis.

In this paper, we present a new clustering method based in kernel functions for partitioning a set of interval-valued data. This method is an extension of the fuzzy c-means cluster algorithm based on kernelization of metric [11] to interval-valued data. In addition, this method is compared with a fuzzy c-means method for interval data introduced in [13]. The paper is organized as follows. In Section 2, we describe the fuzzy c-means clustering method for symbolic interval data. In Section 3, we introduce the new kernel-based fuzzy clustering method for symbolic interval data. In order to validate this new method, Section 4 presents experiments with real and syntectic symbolic interval data sets. The evaluation of the clustering results furnished by the methods is based on the computation of an external cluster validity index and the global error rate of classification. In Section 5, the concluding remarks are given.

978-1-4244-7316-8/11/$26.00 ©2011 IEEE

II. Introduction to a fuzzy c-means method for interval data

This section initially shows an brief description of the fuzzy c-means method for symbolic interval data [13] (here called FCM-IV). This method is a suitable extension of the standard fuzzy c-means clustering algorithm that furnishes a fuzzy partition and a prototype for each cluster by optimizing an adequacy criterion based on a suitable squared Euclidean distance between vectors of intervals.

Consider Ω a set of n objects indexed by i and formed by p symbolic interval-valued variables indexed by j. Each object i is represented by a vector of intervals $\mathbf{x}_i = ([a_i^1, b_i^1], \ldots, [a_i^p, b_i^p])^T$. Similar to the object, the prototype of a cluster C_k $(k = 1, \ldots, K)$ is also represented as a vector of intervals $\mathbf{y}_k = ([\alpha_i^1, \beta_i^1], \ldots, [\alpha_i^p, \beta_i^p])^T$. Thus the partition $P = (C_1, \ldots, C_K)$ from Ω in K clusters where each cluster has a prototype L_k described by the vector $\mathbf{y}_k$.

The problem of clustering concerns to find a partition of Ω into K disjoint clusters $C_1, \ldots, C_K$ such that minimizes locally a clustering criterion defined as

$$J(P, L) = \sum_{k=1}^{K} \sum_{i \in C_k} (u_{ik})^m d^2(x_i, y_k). \quad (1)$$

where the squared Euclidian distance d^2 measuring the dissimilarity between a pair of vectors of intervals is given as

$$d^2(x_i, y_k) = \sum_{j=1}^{p} \left[\left(a_i^j - \alpha_k^j \right)^2 + \left(b_i^j - \beta_k^j \right)^2 \right]. \quad (2)$$

The term u_{ik} is the membership degree of pattern i in cluster C_k and $m \in]1, +\infty[$ is a parameter that controls the fuzziness of membership for each pattern i. The membership degree $u_{ik} (i = 1, \ldots, n)$ of each pattern i in each cluster C_k, minimizing the clustering criterion J under $u_{ik} \geq 0$ and $\sum_{k=1}^{K} u_{ik} = 1$, is updated according to the following expression:

$$u_{ik} = \left[\sum_{h=1}^{K} \left(\frac{\sum_{j=1}^{p} \left[\left(a_i^j - \alpha_k^j \right)^2 + \left(b_i^j - \beta_k^j \right)^2 \right]}{\sum_{j=1}^{p} \left[\left(a_i^j - \alpha_h^j \right)^2 + \left(b_i^j - \beta_h^j \right)^2 \right]} \right)^{\frac{1}{m-1}} \right]^{-1}. \quad (3)$$

The prototype $\mathbf{y}_k = ([\alpha_i^1, \beta_i^1], \ldots, [\alpha_i^p, \beta_i^p])^T$ of C_k which minimizes the clustering criterion J has the bounds of each interval $[\alpha_i^j, \beta_i^j]$ $(j = 1, \ldots, p)$ updated according to the following expressions:

$$\alpha_k^j = \frac{\sum_{i=1}^{n} (u_{ik})^m a_k^j}{\sum_{i=1}^{n} (u_{ik})^m} \quad (4)$$

$$\beta_k^j = \frac{\sum_{i=1}^{n} (u_{ik})^m b_k^j}{\sum_{i=1}^{n} (u_{ik})^m} \quad (5)$$

The algorithm schema of the FCM-IV algorithm for interval data is as follows:

Schema of the FCM-IV algorithm

1) **Initialization step**
   The parameters c $(2 \leq c \leq n)$, m $(1 < m < \infty)$ and $\varepsilon > 0$ are fixed.
   1.1 Initialize u_{ik} $(i = 1, \ldots, n)$ and $(k = 1, \ldots, K)$ such that $u_{ik} \geq 0$ and $\sum_{k=1}^{K} u_{ik} = 1$.
   1.2 Compute J^0 using Eq. 1 and do $t = 1$.
2) **Representation step**
   Compute the prototype $\mathbf{y}_k$ of the cluster $C_k (k = 1, \ldots, K)$ using the Eqs. 4 and 5.
3) **Fuzzy membership step**
   Update the fuzzy membership degree u_{ik} of the pattern i belonging to cluster $C_k (k = 1, \ldots, K)$ using the Eq. 3.
4) **Stopping criterion**
   If $|J_t - J_{t-1}| \leq \varepsilon$, STOP; else update $t = t + 1$ and go step 2.

III. A Kernel Fuzzy c-Means Method for Interval Data

The kernel fuzzy c-means (KFCM) method is an extension of the fuzzy c-means (FCM) cluster algorithm proposed in [11]. KFCM adopts a new kernel-induced metric in the data space to replace the original Euclidean norm metric in FCM, thus KFCM can implicitly perform a nonlinear mapping to a high dimensional feature space.

This section presents an extension of the kernel fuzzy c-means method to interval-valued data. The main idea of this method (here called KFCM-IV) consist in manipulating a kernel function for interval data and to use the approach fuzzy for generate a fuzzy partitions based on the idea of partial membership expressed by the degree of membership of each pattern in a given cluster.

Regarding interval data, each object i $(i = 1, \ldots, n)$ of Ω is represented as a vector of intervals $\mathbf{x}_i = ([a_i^1, b_i^1], \ldots, [a_i^p, b_i^p])^T$ and a nonlinear function $\xi : \mathbf{x}_i \to \xi(\mathbf{x}_i)$ performs the mapping from the input space to a high dimensional feature space H. Consider k centers $\mathbf{g}_1^\xi, \ldots, \mathbf{g}_k^\xi$ as prototypes of the clusters where $\mathbf{g}_k^\xi \subset H$ $(k = 1, \ldots, K)$.

Using the classic kernel fuzzy c-means methodology, the problem of clustering concerns to find a partition of Ω into K disjoint clusters $C_1, \ldots, C_K$ such that minimizes a clustering error defined as:

$$E = \sum_{k=1}^{K} \sum_{i \in C_k} u_{ik}^m \|\xi(\mathbf{x}_i) - \xi(\mathbf{v}_k)\|^2 \quad (6)$$

The squared Euclidian distance between $\xi(\mathbf{x}_i)$ and $\xi(\mathbf{v}_k)$ is given by:

$$\|\xi(\mathbf{x}_i) - \xi(\mathbf{g}_k)\|^2 = K(\mathbf{x}_i, \mathbf{x}_i) - 2K(\mathbf{x}_i, \mathbf{v}_k) + K(\mathbf{v}_k, \mathbf{v}_k) \quad (7)$$

The Gaussian kernel function $K_{il} = K(\mathbf{x}_i, \mathbf{x}_l)$ for interval data is defined as:

$$K(\mathbf{x}_i, \mathbf{x}_l) = exp(-\|\mathbf{x}_i - \mathbf{x}_l\|^2 / 2\delta^2) \quad (8)$$

with

$$\|\mathbf{x}_i - \mathbf{x}_l\|^2 = \sum_{j=1}^{p} \left[(a_i^j - a_l^j)^2 + (b_i^j - b_l^j)^2 \right]$$

The membership u_{ik} of the object x_i in class C_k assuming values in the interval $[0, 1]$ and satisfying $\sum_{k=1}^{K} u_{ik} = 1$ is defined as:

$$u_{ik} = \frac{(1/(1 - K(x_i, v_k)))^{1/(m-1)}}{\sum_{l=1}^{K} (1/(1 - K(x_i, v_l)))^{1/(m-1)}} \quad (9)$$

The prototypes are given by:

$$v_k = \frac{\sum_{i=1}^{n} u_{ik}^m K(x_i, v_k) x_i}{\sum_{i=1}^{n} u_{ik}^m K(x_i, v_k)} \quad (10)$$

The weighting exponent m is called the fuzzifier and it can have an influence on the clustering performance of the method. The algorithm schema of the KFCM-IV algorithm for interval data is as follows:

SCHEMA OF THE KFCM-IV ALGORITHM

1) **Pre-processing step: compute a kernel matrix**
   Compute the matrix $\boldsymbol{K}$ using the Eq. 8 for $i = 1, \ldots, n$ and $l = 1, \ldots, n$.
2) **Initialization step**
   The parameters c $(2 \leq c \leq n)$, m $(1 < m < \infty)$ and $\varepsilon > 0$ are fixed.
   1.1 Initialize u_{ik} $(i = 1, \ldots, n)$ and $(k = 1, \ldots, K)$ such that $u_{ik} \geq 0$ and $\sum_{k=1}^{K} u_{ik} = 1$.
   1.2 Compute the criterion error E^0 using Eq. 6 and do $t = 1$.
3) **Representation step**
   Update the prototypes v_k $(k = 1, \ldots, K)$ with Eq. 7.
4) **Membership step**
   Update the memberships u_{ik} $(k = 1, \ldots, K)$ and $(i = 1, \ldots, n)$ with Eq. 6.
5) **Stopping criterion**
   If $|E_{t+1} - E_t| \leq \varepsilon$ then STOP calculate error criterion E using the Eq. 5, otherwise do $t = t + 1$ and go to step 3.

IV. EXPERIMENTAL RESULTS

In order to validate the proposed method for interval data, this section presents the experimental results regarding synthetic and real symbolic data sets. Our aim is to achieve a comparison between this method and the fuzzy c-means method introduced in the Section II. The evaluation was performed in the framework of a Monte Carlo experience with 100 replications for each synthetic interval data set. Concerning real symbolic data, an application with two data sets is also considered.

To assess the clustering results provided by FCM-IV and KFCM-IV methods, we used the corrected Rand index (CR) and the overall error rate of classification (OERC). The index CR [14] takes its values in the interval $[-1, 1]$ where the value 1 indicates a perfect agreement between the partitions, values close to 0 correspond to more or less random cluster agreement, and negative values to insufficient recovery properties. The OERC takes its values in the interval $[0, 1]$ where the value 0 indicates a perfect agreement between the partitions, unlike the value 1.

In all experiments for KFCM-IV method, it was used the Gaussian kernel defined in Eq. 8 with parameter $\sigma = 1$. For FCM-IV and KFCM-IV methods, it used the parameter m equal to 2.

A. The Monte Carlo experiment results and comparison

First, we simulated two classical quantitative data sets in $\Re^2$ with nonlinear clusters. Thus, interval data sets is built from these quantitative data sets, each point (y_1, y_2) of these data sets is considered as the 'seed' of a rectangle. Each rectangle is therefore a vector of two intervals defined by:

$$([y_1 - \gamma_1/2, y_1 + \gamma_1/2], [y_2 - \gamma_2/2, y_2 + \gamma_2/2])$$

The parameters γ_1 and γ_2 are the width and the height of the rectangle. They are drawn randomly within a given range of values.

Data set 1 is formed by two rings, each representing a class. The first ring has radius equals to 12 and 100 individuals. The second ring has radius equals to 5 and 50 individuals. From this data, we can observe that the classes are nonlinearly separable and similar points sets can be found in [10]. Figure 1 represents an interval data set with two rings using width and the height of all the rectangles drawn randomly within the interval $[1, 2]$.

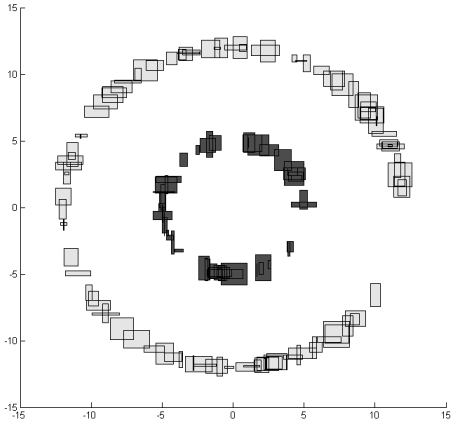

Fig. 1. Symbolic interval data set 1: two rings

Data set 2 is formed by data follow a similar training to Archimedean spiral, where each arm of the spiral is defined in polar coordinates (r, θ) by the equation:

$$r = a + b\theta \quad (11)$$

where a and b are real numbers and θ in angular measurements. The parameter a controls the initial radius of the each arm of the spiral, while b is related with distance between successive turns. This data set has 90 individuals distributed among the classes contained 15, 20, 25 and 30. The total angle $\theta = 120$ degrees with $a = 10$ and $b = 5$. Figure 2 represents the interval data set 2 width and the height of all the rectangles drawn randomly within the interval $[1, 5]$.

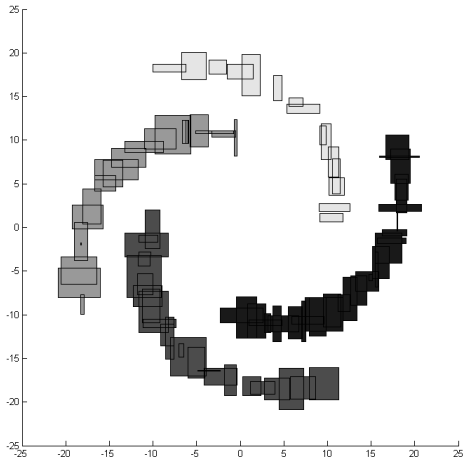

Fig. 2. Symbolic interval data set 2: spiral of four classes

In the framework of a Monte Carlo experiment, 100 replications of the previous process were carried out for parameters γ_1 γ_2 drawn randomly 100 times from each of the following intervals: $[1, 2], [1, 5], [1, 10]$, $[1, 15]$ and $[1, 20]$. This process has also been repeated for interval data sets 1 and 2. The KFCM-IV and FCM-IV methods have been performed on these data sets. The cluster partition obtained with these clustering methods were compared with the class partition known a priori based on CR index and the OERC metric. For each 100 replications, the average CR index and the average OERC are calculated.

Tables I and II give the values of the average and standard-deviation (in parenthesis) of the CR index and OERC for the FCM-IV and KFCM-IV methods and the data sets 1 and 2, respectively. As expected, the KFCM-IV method outperforms the FCM-IV one considering CR index and OERC metric.

TABLE I
COMPARISON OF THE CLUSTERING METHODS FOR DATA SET 1

Predefined Interval	FCM-IV		KFCM-IV	
	CR index	OERC	CR index	OERC
[1,2]	0.0000 (0.0114)	0.4771 (0.0345)	0.4391 (0.0665)	0.1352 (0.0155)
[1,5]	-0.0001 (0.0099)	0.4767 (0.0354)	0.4401 (0.0756)	0.1359 (0.0177)
[1,10]	0.0001 (0.0113)	0.4776 (0.0354)	0.3725 (0.0573)	0.1516 (0.0132)
[1,15]	0.0012 (0.0134)	0.4769 (0.0389)	0.2695 (0.0615)	0.1742 (0.0140)
[1,20]	-0.0005 (0.0091)	0.4782 (0.0328)	0.1609 (0.0787)	0.1996 (0.0176)

B. Results and comparison with a city-temperature interval data set

This interval data set [15] concerns 37 cities, each city is described by 12 interval variables which are minimum and the maximum temperatures of 12 months in degree centigrade. Table III shows part of this data set.

The 4-cluster partitions obtained with these clustering methods were compared with the 4-cluster partition known a priori.

TABLE II
COMPARISON OF THE CLUSTERING METHODS FOR DATA SET 2

Predefined Interval	FCM-IV		KFCM-IV	
	CR index	OERC	CR index	OERC
[1,2]	0.3207 (0.0030)	0.5482 (0.0285)	0.3814 (0.0412)	0.2809 (0.0274)
[1,5]	0.3204 (0.0028)	0.5481 (0.0318)	0.3826 (0.0425)	0.2837 (0.0295)
[1,10]	0.3204 (0.0026)	0.5471 (0.0306)	0.3843 (0.0423)	0.2799 (0.0264)
[1,15]	0.3204 (0.0023)	0.5523 (0.0267)	0.3815 (0.0382)	0.2827 (0.0292)
[1,20]	0.3213 (0.0028)	0.5492 (0.0291)	0.3752 (0.0381)	0.2871 (0.0303)

TABLE III
MINIMUM AND THE MAXIMUM TEMPERATURES OF CITIES IN DEGREE CENTIGRADE

Cities	**January**	**February**	...	**November**	**December**
Amsterdan	$[-4, 4]$	$[-5, 3]$	...	$[1, 10]$	$[-1, 4]$
Athens	$[6, 12]$	$[6, 12]$	...	$[11, 18]$	$[8, 14]$
Bahrain	$13, 19]$	$[14, 19]$	...	$[20, 26]$	$[15, 21]$
Bombay	$[19, 28]$	$[19, 28]$	...	$[14, 26]$	$[10, 20]$
Calcutta	$[13, 27]$	$[16, 29]$	...	$[18, 29]$	$[13, 26]$
Colombo	$[22, 30]$	$[22, 30]$	...	$[23, 29]$	$[22, 30]$
⋮	⋮	⋮	⋮	⋮	⋮
Toronto	$[-8, -1]$	$[-8, -1]$	...	$[-1, 17]$	$[-5, 1]$
Vienna	$[-2, 1]$	$[-1, 3]$	...	$[2, 7]$	$[1, 3]$
Zurich	$[-11, 9]$	$[-8, 15]$	...	$[0, 19]$	$[-11, 8]$

The a priori classification, indicated by the suffix attached to the city temperature, is as follows:

a) Class 1: Bahraim: 3, Bombay: 4, Cairo: 5, Calcutta: 6, Colombo: 7, Dubal: 9, Hong Kong: 12, Kula Lampur: 13, Madras: 16, Manila: 18, Mexico: 20, Nairobi: 23, New Delhi: 24, Sydney: 30 and Singapore: 32
b) Class 2: Amsterdam: 1, Athens: 2, Copenhagen: 8, Frankfurt: 10, Geneva: 11, Lisbon: 14, London: 15, Madrid: 17, Moscow: 21, Munich: 22, New York: 25, Paris: 26, Rome: 27, San Francisco: 28, Seoul: 29, Stockholm: 31, Tokyo: 34, Toronto: 35, Vienna: 36 and Zurich: 37
c) Class 3: Mauritius: 19
d) Class 4: Tehran: 33

Table IV shows the clusters (individual labels) given by the a priori partition according to the categorical variable, as well as the clusters obtained by the kernel fuzzy c-means and fuzzy c-means methods concerning the temperature interval data set.

The CR index obtained from the comparison between the a priori partition and the partitions given by the FCM-IV and KFCM-IV methods are, respectively, 0.466 and 0.714. The OERC for FCM-IV and KFCM-IV methods are, respectively, 0.405 and 0.216. Therefore, the KFCM-IV method is very superior to FCM-IV for this data set.

C. Results and comparison with the agaricus interval data set

This data set was extracted from [16] and contains information on species of fungi. Agaricus is a genus of mostly medium to large gilled mushrooms. Well known members of the genus

TABLE IV
CLUSTERING RESULTS FOR TEMPERATURE OF CITIES DATA SET

	Cluster 1	Cluster 2	Cluster 3	Cluster 4
A priori Partition	3 4 5 6 7 9 12 13 16 18 20 23 24 30 32	1 2 8 10 11 14 15 17 21 22 25 26 27 28 29 31 34 35 36 37	19	33
FCM-IV	3 5 9 12 20 23 24 32	1 8 10 11 15 21 22 26 31 35 36 37	2 14 17 25 27 28 29 33 34	4 6 7 13 14 18 19 30
KFCM-IV	3 4 6 7 9 13 16 18 24 30	1 8 10 11 14 15 17 21 22 25 26 27 28 29 31 34 35 36 37	2 5 12 20 33	19 23 32

Agaricus are the bisporus, the "button mushroom" common in supermarkets and the campestris, the "meadow mushroom", a popular edible mushroom which is common in pastures and grasslands in many temperate areas of the world. This data set consists of 24 mushrooms, each mushroom described by 5 interval variables: width of the pileus, width of the stipe, thickness of the stipe, height and width of spores. Table V shows part of this data set. It is composed of two classes: edible (E) and inedible (I).

TABLE V
INFORMATION ABOUT AGARICUS SPECIES KNOWN TO OCCUR IN CALIFORNIA

Species	pileus's width	stipe's width	stipe's thickness	spores's height	spores's width
Albolutescens	$[6, 12]$	$[2, 7]$	$[1.5, 3]$	$[6, 7.5]$	$[4, 5]$
Arvensis	$[6, 21]$	$[4, 14]$	$[1, 3.5]$	$[6.5, 9]$	$[4.5, 6]$
Benesii	$[4, 8]$	$[5, 11]$	$[1, 2]$	$[5, 6]$	$[3, 4]$
Bernardii	$[7, 16]$	$[4, 7]$	$[3, 4.5]$	$[5.5, 7]$	$[5.5, 6.5]$
Bisporus	$[5, 12]$	$[2, 5]$	$[1.5, 2.5]$	$[6, 8.5]$	$[4.5, 6]$
⋮	⋮	⋮	⋮	⋮	⋮
Subrutilescens	$[6, 14]$	$[6, 12]$	$[1, 2]$	$[4, 6]$	$[3.5, 4.5]$
Subrufescens	$[6, 13]$	$[6, 12]$	$[1.5, 2.5]$	$[5.5, 6.5]$	$[4, 4.5]$
Xanthodermus	$[5, 17]$	$[4, 14]$	$[1, 3.5]$	$[5, 6]$	$[4, 5.5]$

Table VI shows the elements grouped by clusters given by the a priori partition according to the categorical variable edible or inedible, as well as the clusters obtained by the kernel fuzzy c-means and fuzzy c-means methods concerning the agaricus interval data set.

TABLE VI
CLUSTERING RESULTS FOR AGARICUS DATA SET

	Cluster 1	Cluster 2
A priori Partition	1 2 3 4 5 6 8 9 10 11 12 14 15 16 17 19 20 21 22 23	7 13 18 24
FCM-IV	2 4 6 11 13 14 16 17 18 20 21 22 23 24	1 3 5 7 8 9 10 12 15 19
KFCM-IV	1 2 3 4 5 6 7 8 9 10 11 12 15 16 17 19 20 21 22 23	13 14 18 24

The CR index calculated from the comparison between the a priori partition and the partitions given by the FCM-IV and KFCM-IV methods are, respectively, -0.037 and 0.613. The OERC for the FCM-IV and KFCM-IV methods are, respectively, 0.500 and 0.082. Again, the KFCM-IV is very superior to the FCM-IV for the agaricus data set.

V. CONCLUSIONS

In this paper, we have presented a new clustering method for symbolic interval data based on kernel. This method is an extension of the kernel fuzzy c-means to symbolic interval data. The evaluation of this method in comparison with a fuzzy c-means clustering method for interval data was carried out. The accuracy of the results provided by these clustering methods regarding synthetic interval data sets were assessed by the corrected Rand index and overall error rate in the framework of a Monte Carlo experience. An application with two real interval data sets was also performed. Concerning the CR index and overall error rate, the proposed method in this paper surpassed the fuzzy c-means method in all interval data sets.

ACKNOWLEDGMENT

The authors would like to thank CNPq and FACEPE (Brazilian Agencies) for their financial support.

REFERENCES

[1] A. K. Jain, M. N. Murty and P. J. Flynn Data clustering: a review. ACM Computing Surveys, 31(3):264-323, 1999.
[2] R. O. Duda, P. E. Hart, and D. G. Stork Pattern Classification, John Wiely and Sons, 2001.
[3] Xu, R.; Wunsch, D. I. I. Survey of clustering algorithms. IEEE Transactions on Neural Networks, p. 645-678, 2005.
[4] Nikhil, R. Pal; Pal, K.; Keller, James M.; Bezdek, James C. A Possibilistic Fuzzy c-Means Clustering Algorithm. IEEE Transactions on fuzzy Sysyems, 2005.
[5] Yang, M.-S., Wu, K.-L. Unsupervised possibilistic clustering. Pattern Recog. p. 521, 2006.
[6] M. Filippone, F. Camastra, F.Masulli, and S. Rovetta. A survey of kernel and spectral methods for clustering. Pattern recognition, p. 176-190, 2008.
[7] R. Inokuchi and S. Miyamoto. LVQ clustering and som using a kernel function. volume 3, p. 1497-1500, 2004.
[8] M. Girolami. Mercer kernel based clustering in feature space. I.E.E.E. Transactions on Neural Networks, p. 780-784, 2002.
[9] Dao Q. Zhang and Song C. Chen. Kernel based fuzzy and possibilistic cmeans clustering. In Proceedings of the International Conference Artificial Neural Network, p. 122-125. Turkey, 2003.
[10] I. S. Dhillon, Y. Guan, and B. Kulis. Kernel k-means, spectral clustering and normalized cuts. in Proc. ACMSIGKDD Intl Conf Knowledge Discovery and Data Mining, Seattle, WA, 2004.
[11] D.-Q. Zhang and S.-C. Chen. Kernel based fuzzy and possibilistic c-means clustering. in Proc. ICANN, Istanbul, Turkey, p. 122125, 2003.
[12] E. Diday and M. Noirhomme-Fraiture. Symbolic Data Analysis And The Sodas Software. Wiley-Interscience Publishers, 2008.
[13] de Carvalho, F.d.A.T., Fuzzy c-means clustering methods for symbolic interval data, Pattern Recog. Lett. doi:10.1016/j.patrec.2006.08.014, 2006.
[14] Hubert, L. and Arabie. P. Comparing Partitions. Journal of Classification. p. 193-218, 1985.
[15] D.S. Guru, B.B. Kiranagi,and P. Nagabhushan. Multivalued type dissimilarity measure and concept of mutual dissimilarity value for clustering symbolic patterns. Pattern Recognition, p. 1203-1213, 2004.
[16] Wood, M.; Stevens, F. Agaricus. http://www.mykoweb.com/CAF/genera/Agaricus.html. Accessed July, 2010.

2011 IEEE International Conference on Fuzzy Systems
June 27-30, 2011, Taipei, Taiwan

Short Term Load Forecasting Using Interval Type-2 Fuzzy Logic Systems

Abbas Khosravi, Saeid Nahavandi, Doug Creighton
Centre for Intelligent Systems Research
Deakin University, Geelong, VIC, 3217, Australia
Email: {abbas.khosravi,saeid.nahavandi,douglas.creighton@deakin.edu.au}

***Abstract*—Accurate Short Term Load Forecasting (STLF) is essential for a variety of decision making processes. However, forecasting accuracy may drop due to presence of uncertainty in the operation of energy systems or unexpected behavior of exogenous variables. This paper proposes the application of Interval Type-2 Fuzzy Logic Systems (IT2 FLSs) for the problem of STLF. IT2 FLSs, with extra degrees of freedom, are an excellent tool for handling prevailing uncertainties and improving the prediction accuracy. Experiments conducted with real datasets show that IT2 FLS models appropriately approximate future load demands with an acceptable accuracy. Furthermore, they demonstrate an encouraging degree of accuracy superior to feedforward neural networks used in this study.**

***Index Terms*—Load forecasting, type-2 fuzzy logic.**

I. Introduction

By definition, forecasting is a phenomenon of calculating or estimating a measure in the next coming time periods. Tools and models for accurate forecasting of electric power load are essential to the operation and planning of utility companies. Load forecasts are used by participants in electric energy generation, transmission, distribution, and markets for a variety of decision-making processes, such as economy dispatch, unit commitment, hydro-thermal coordination, transaction evaluation, and expansion planning.

There has always been a need for accurate forecasting of future load demands. However, the need has intensified in the last decade due to deregulation of the energy industries in developed countries. As the energy prices may be boosted by a factor of ten or more during periods of peak demands, precise short and medium term load forecasting becomes vitally important to the utilities. Taking into account this as well as rapid fluctuations of demands and abrupt changes in weather condition, access to reliable models for accurate prediction of load demand is essential.

Studies conducted by scholars and industry practioners for load forecasting can be divided into two broad categories: (i) traditional methods, such as Box-Jenkins models, regression models, Autoregressive Integrated Moving Average (ARIMA) (in general time series), Kalman filtering models, and splines [1] [2], [3] [4]; and (ii) Artificial Intelligence (AI) methods, such as Neural Networks (NNs), Fuzzy Logic Systems (FLSs), and expert systems. Models in the former category are typically linear and cannot cope with the level of nonlinearity and seasonality present in the behavior of electric loads. There exists no best method that always outperforms others in the field of load forecasting. However, recent reviewing studies in the field of prediction and forecasting show that AI-based models, and in particular NNs, often outperform the traditional modeling techniques in terms of prediction accuracy and generalization power [5].

Both NN and FLSs are universal approximators with the capability of identification and approximation of nonlinear relationships between independent (inputs) and dependent (targets) variables to any arbitrary degree of accuracy [6] [7]. While black-box NN models have their excellent learning capabilities, transparent FLS models can simultaneously handle quantitative and qualitative information, and as so uncertainties. Both model types are of the best alternatives for modeling, prediction, and forecasting purposes. A good review of NN-based Short Term Load Forecasting (STLF) can be found in [6] and [7] (and references within) [1]. Recently Khosravi et al. [9] [10] investigated the application of NN–based prediction intervals for quantifying uncertainties associated with forecasted loads. They showed that prediction intervals provide more information about uncertainties present in the process of load forecasting. However, construction of prediction intervals using the proposed methods is computationally expensive.

Studies on application of FLSs and neuro-fuzzy systems for STLF can be found in [11] [12] [13]. The Achilles heel of traditional FLSs is their precise Type-1 Fuzzy Sets (T1 FSs). Once the type-1 Membership Functions (MFs) are selected and adjusted, all uncertainties disappear. Type-2 FLS (T2 FLS) is a new emerging paradigm that uses Type-2 Fuzzy Sets (T2 FS). T2 FSs are characterized by a three dimensional fuzzy MF including a footprint of uncertainty. The footprint of uncertainty and the third dimension of MFs provide additional degrees of freedom that make it possible to directly model and handle uncertainties. Therefore, a T2 FLS has the potential to outperform a Type-1 FLS (T1 FLS) [14].

Zadeh [15] originally introduced the concept of type-2 fuzzy sets as an extension of the concept of an ordinary type-1 fuzzy set in 1975. Mendel [16] and Karnik et al. [17] [18] further developed the theory of T2 FLSs. The structure of rules in the T2 FLS and its inference engine are similar to those in T1 FLS. A T2 FLS includes a fuzzifier, a rule base, fuzzy inference engine, and an output processing unit composed of a type reducer and a defuzzifier (Fig. 1).

[1] Similar studies for the case of electricity price forecasting can be found in [8].

978-1-4244-7316-8/11/$26.00 ©2011 IEEE

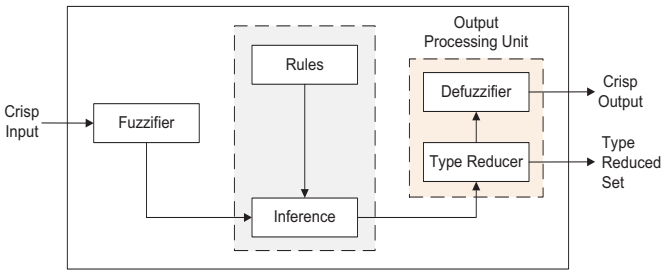

Fig. 1. Structure of a T2 FLS.

The computational complexity of general T2 FLSs has until recently hindered their widespread use in practical applications. As a restricted class of T2 FLSs, Interval T2 FLSs (IT2 FLSs) [19] were introduced to avoid massive computational requirement (mainly due to type reduction stage). IT2 FLSs are characterized by secondary MFs that only take the value of 1 over their domain. Such a restriction greatly reduces the computational burden of performing inference compared with general T2 FLSs. In the last few years, T2 FLSs, and in particular, to IT2 FLSs have drawn a great deal of attention from both academia and industry. IEEE Computational Intelligence Magazine, February 2007 contains several papers reviewing theory and application of T2 FLSs and IT2 FLSs [20] [21] [22]. Also more recent work on application of IT2 FLSs and their combination with neural networks can be found in [23] [24].

Motivated by these recent trends in academia, this paper investigates the use of IT2 FLSs for STLF problem. Takagi-Sugeno-Kang (TSK) fuzzy inference systems are used for developing IT2 TSK FLSs for load forecasting. It is expected that load forecasting accuracy will be improved due to excellent capabilities of IT2 FLSs in handling uncertainties in data. Feedforward NN models are also used for STLF problem and their forecasting performance and accuracy is compared with performance of IT2 TSK FLS models.

The rest of this article is organized as follows: Section II introduces IT2 TSK FLSs. Section III describes how IT2 TSK FLSs are developed and trained in this study. Experimental procedure and used datasets are discussed in Section IV. Simulation results are demonstrated in Section V. Finally, we draw conclusions and discuss future work in section VI.

II. Interval Type-2 TSK Fuzzy Logic Systems

IT2 TSK FLSs are TSK fuzzy models, where (at least) antecedent MFs are IT2 FSs. As per this definition, three classes of models can be formed:

- A2-C1: Antecedents are IT2 FSs, and consequents are interval T1 FSs.
- A2-C0: Antecedents are similar to the case of A2-C1 model, however, consequent parameters are crisp (similar to the case of traditional type-1 TSK fuzzy models).
- A1-C1: Antecedents and consequents are both type-1 fuzzy sets.

We use class A2-C1 in this study, as it is the most general form of IT2 TSK FLS models with the largest degrees of freedom. The extra flexibility of these models allows for efficient handling of uncertainties and minimizing their effects on the quality of forecasts.

In an IT2 TSK FLS (A2-C1) with a rule base of M rules in which each rule has p antecedents, let the lth rule be denoted by R^l,

$$R^l: \; If \; x_1 \; is \; \tilde{F}_1^l, \; x_2 \; is \; \tilde{F}_2^l, \cdots, \; and \; x_p \; is \; \tilde{F}_p^l, \; then$$
$$y^l \; = \; C_0^l + \sum_{i=1}^{p} C_i^l \; x_i \tag{1}$$

where $l = 1, ..., M$. $\tilde{F}_i^l$ is the ith IT2 FS ($i = 1, ..., p$) composed of a lower and upper bound MFs,

$$\mu_{\tilde{F}_i^l}(x_i) = [\underline{\mu}_{\tilde{F}_i^l}(x_i), \; \bar{\mu}_{\tilde{F}_i^l}(x_i)] \tag{2}$$

C_i^l is also an interval T1 FS, where its center and spread are c_i^l and s_i^l respectively,

$$C_i^l = [c_i^l - s_i^l, \; c_i^l + s_i^l] \tag{3}$$

Given an input $x = (x_1, x_2, ..., x_p)$, the result of the input and antecedent operations (firing strength) is an interval type-1 set, $F^l = [\underline{f}^l, \bar{f}^l]$, where,

$$\underline{f}^l(x) = \underline{\mu}_{\tilde{F}_1^l}(x_1) * \underline{\mu}_{\tilde{F}_2^l}(x_2) * \cdots * \underline{\mu}_{\tilde{F}_p^l}(x_p) \tag{4}$$

$$\bar{f}^l(x) = \bar{\mu}_{\tilde{F}_1^l}(x_1) * \bar{\mu}_{\tilde{F}_2^l}(x_2) * \cdots * \bar{\mu}_{\tilde{F}_p^l}(x_p) \tag{5}$$

where * represents a t-norm. It is assumed that singleton fuzzyfier is used in obtaining (4) and (5).

y^l in (1) is the output from the lth If-Then rule, which is a T1 FS, $Y^l = [y_L^l, y_R^l]$. y_L^l and y_R^l are evaluated as,

$$y_L^l = \sum_{i=1}^{p} c_i^l \; x_i + c_0^l \; - \; \sum_{i=1}^{p} s_i^l \; |x_i| - s_0^l \tag{6}$$

$$y_R^l = \sum_{i=1}^{p} c_i^l \; x_i + c_0^l \; + \; \sum_{i=1}^{p} s_i^l \; |x_i| - s_0^l \tag{7}$$

The final output of the IT2 TSK FLS model is obtained through combining the outcomes of M rules, as shown in (8).

$$Y = [y_L, y_R] = \int_{y^1 \in [y_L^1, y_R^1]} \cdots \int_{y^M \in [y_L^M, y_R^M]} \int_{f^l \in [f_L^l, f_R^l]} \cdots \int_{f^M \in [f_L^M, f_R^M]} \frac{1}{\frac{\sum_{l=1}^{M} f^l y^l}{\sum_{l=1}^{M} f^l}} \tag{8}$$

Before generating a crisp output, the outputs of the inference engine should be type-reduced and then defuzzified.

Unfortunately, there is no direct theoretical solution (closed-form formula) for calculation of y_L and y_R in (8). However, they can be calculated using the iterative Karnik-Mendel (KM) procedure [18] for type reduction (transferring a T2 FS into a T1 FS using the concept of center of sets). In the KM algorithm, y_L^l are reordered in ascending order. A switch point, L, is iteratively found that minimizes the value of y_L. The same procedure can be applied for calculation of y_R, where a switch point, R, is determined for maximizing y_R. y_L and y_R are given below,

$$y_L = \frac{\sum_{l=1}^{L} \bar{f}_i^l y_L^l + \sum_{l=L+1}^{M} \underline{f}_i^l y_L^l}{\sum_{l=1}^{L} \bar{f}_i^l + \sum_{l=L+1}^{M} \underline{f}_i^l} \tag{9}$$

$$y_R = \frac{\sum_{l=1}^{R} \underline{f}_i^l y_R^l + \sum_{l=K_R+1}^{M} \bar{f}_i^l y_R^l}{\sum_{l=1}^{R} \underline{f}_i^l + \sum_{l=K_R+1}^{M} \bar{f}_i^l} \tag{10}$$

Details of the KM type reduction algorithm can be found in [18] [25]. Finally, the defuzzified crisp output from the IT2 TSK FLS is the mean of y_L and y_R,

$$y = \frac{y_L + y_R}{2} \tag{11}$$

III. Structure and Training of IT2 TSK FLS Models

A. Membership Functions of IT2 TSK FLS

The performance of an IT2 TSK FLS depends on several factors, such as type and quantity of MFs, training algorithm, number of inputs, and the amount of available data for training. The antecedent MFs used in this study are assumed to be Gaussian with a fixed mean and uncertain standard deviations,

$$\mu_{\tilde{F}_i^l}(x_{i,k}) = exp\left[-\frac{1}{2}\left(\frac{x_{i,k} - m_i^l}{\sigma_i^l}\right)^2\right] = \mathcal{N}(m_i^l, [\sigma_{i,1}^l, \sigma_{i,2}^l]) \tag{12}$$

where $i = 1, ..., p$, $l = 1, ..., M$, and k indicates the sample index. The upper and lower MFs are,

$$\underline{\mu}_{\tilde{F}_i^l}(x_{i,k}) = \mathcal{N}(m_i^l, \sigma_{i,1}^l) \tag{13}$$

$$\bar{\mu}_{\tilde{F}_i^l}(x_{i,k}) = \mathcal{N}(m_i^l, \sigma_{i,2}^l) \tag{14}$$

Fig. 2 shows the graphical representation of these two MFs for arbitrary chosen values for m_i^l, $\sigma_{i,1}^l$, and $\sigma_{i,2}^l$. The uniformly shaded region is the footprint of uncertainty for the IT2 Gaussian MF.

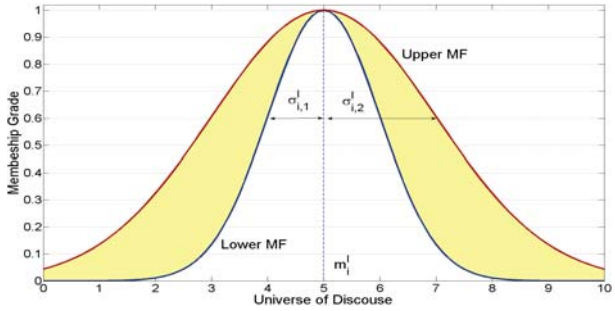

Fig. 2. The IT2 Gaussian MFs with fixed mean and uncertain standard deviation.

B. Genetic Algorithm for Training

The Genetic Algorithm (GA) is used for adjusting parameters of the IT2 TSK FLS models. By simultaneously exploring different parts of the parameter space, GAs increase the probability of finding the global solution to the minimization problem. The GA includes three main operators, namely reproduction (elitism), crossover, and mutation. Offsprings (new populations) are generated through crossover and mutation. Reproduction is a process in which individual chromosomes are copied according to their scaled fitness function values. Mutation introduces random changes to the chromosomes by altering the value to a gene with a probability called the mutation rate. Crossover operator determines how the GA combines two parents to form an offspring (crossover child) for the next generation.

Once a decision on the number of inputs and MFs per input is made, we can code the IT2 TSK FLS parameters into a chromosome. In each rule, premise parameters (mean and two standard deviations of each input membership function) and consequent parameters, as shown in (3), are coded as real variables and allowed to take real values. The Root Mean Squared Error (RMSE) is considered as the fitness function,

$$RMSE = \sqrt{\frac{1}{n}\sum_{i=1}^{n}(Act_i - Pre_i)^2} \tag{15}$$

where Act_i and Pre_i are the ith actual load and the ith forecasted load. n is also the number of load samples.

Parameters of premise and consequent parts of IT2 TSK FLS (A2-C1) are randomly initialized. Exploration of solution space continues until termination conditions are met. The maximum number of iterations, a minimum convergence speed, and a satisfactory small value of RMSE are the stopping criteria used in our experiments. After termination of the GA optimization, test samples are used for examining performance of the trained model.

Table I lists parameters used in the optimization algorithm. The cross over method is single point. This randomly selects a crossover point within a chromosome, and then interchanges the two parent chromosomes at this point to produce two new offspring. Parameters summarized in Table I are obtained through trial and error. The preliminary experiments were

TABLE I
PARAMETERS USED IN EXPERIMENTS AND GA-BASED TRAINING METHOD

Parameter	Numerical value
Population size	100
Parent selection	Stochastic uniform
Reproduction (elite count)	2
Cross over fraction (single point)	0.8
Number of MFs	3
Type of MFs	Gaussian (Fig. 2)
D_{train}	80% of all samples
D_{test}	20% of all samples

carried out with the aim to ensure optimization convergence within a short time (minimum number of generations), but to avoid premature convergence.

IV. DATA AND EXPERIMENT PROCEDURE

A. Data

The dataset in this study is the same that used previously in [9] and [10]. The purpose is to forecast the two-day-ahead loads based on past observations. The inputs to the IT2 TSK FLS models have been listed in Table II. These inputs are the mean of loads in the last three hours, the current temperature, and the day of week (coded as a number between 1 and 7). Other combinations of inputs and inclusion of lagged loads (up to even one year ago) can improve the quality of load forecasting results, however, determination of such a subset is beyond the scope of this paper. Furthermore, inclusion of more inputs will substantially increase the complexity of developed models.

The profile of loads for three years is shown in Fig 3. There is seasonal behavior with rapid fluctuations in the amount of consumed loads. Load peaks occur in summer, where load demand is minimum in winter. Additionally, there is an upward trend in the curve, which indicates an annual growth load demand.

IT2 TSK FLSs are data-driven techniques, and their forecasting performance intimately hinges on data used for their training. With the purpose of an objective assessment, the available dataset is split into training samples (80%, D_{train}) and test samples (20%, D_{test}). The IT2 TSK FLS is first trained using training samples, where the fitness function (RMSE) is minimized using the GA.

All available data are pre-processed to have zero mean and unit variance. This is done in particular for inputs (those listed in Table II) to give them an equal chance for contribution to models and load forecasting.

For the purpose of comparison, we benchmark performance of IT2 TSK FLS models by feedforward Neural Network (NNs). A two layer NN with 10 neurons in each hidden layer is trained using the Levenberg-Marquardt training algorithm. Simulations and forecasting procedure are repeated twenty times and averaged results are reported. This is done to avoid misleading results and subjective judgment due to random initialization of NN parameters.

TABLE II
INPUTS OF IT2 TSK FLS FOR STLF

Input	Quantity
Load demand in the last three hours	3
Current temperature	1
Day of the week	1

B. Performance Evaluation

Prediction performance of the developed models for STLF can be measured using three statistical measures. Coefficient of determination, designated by R^2, is one of the best choices, as it provides a measure of target variation captured by the model. R^2 is calculated as follows,

$$R^2 = 1 - \frac{\sum_{i=1}^{n} \left(Act_i - Pre_i\right)^2}{\sum_{i=1}^{n} \left(Act_i - \overline{Act}\right)^2} \tag{16}$$

where Act_i, Pre_i, and $\overline{Act}$ are the ith actual load, the ith forecasted load, and the mean of loads, respectively. A coefficient of determination close to unity (or 100%)) is an indication that forecasted values are close to actual data, and performance of the developed model is acceptable.

The two other performance measures used are RMSE (which also used as the fitness function) and correlation coefficient.

V. RESULTS AND ANALYSIS

The convergence behavior of the optimization algorithm and minimization of the fitness function (RMSE) is illustrated in Fig. 4. The fitness function is reduced several orders of magnitude from its initial value. The fitness function continuously decreases at a high rate up to generation 60. The optimization process then slows and converges to the optimal solution at iteration 109. During optimization, the fitness function drops from 0.5019 to 0.1283. This indicates that randomly selected initial values for IT2 TSK FLS (A2-C1) models are not optimal, leading to a large forecasting error.

Fig. 5 shows the plot of forecasted load demands versus their actual values. It is evident that there is a good agreement between the observed and forecasted load demands. The correlation coefficient between these values is 89.92%, which is sufficiently large. Also, forecasting errors are shown in Fig. 6. In some cases, the gap between actual and forecasted values is large. The maximum forecasting error (underestimation) is 3185 MWs. Such a large error can be due to unknown patterns in data or lack of informative variables.

Table III summarizes quantitative values of three performance measures for results obtained from IT2 TSK FLS (A2-C1) and NN models. These results are for test samples, which were not used for model training. The performance measures for NNs are averaged values obtained from 20 replicates of experiments. The main conclusions from the results listed in Table III are as follows:

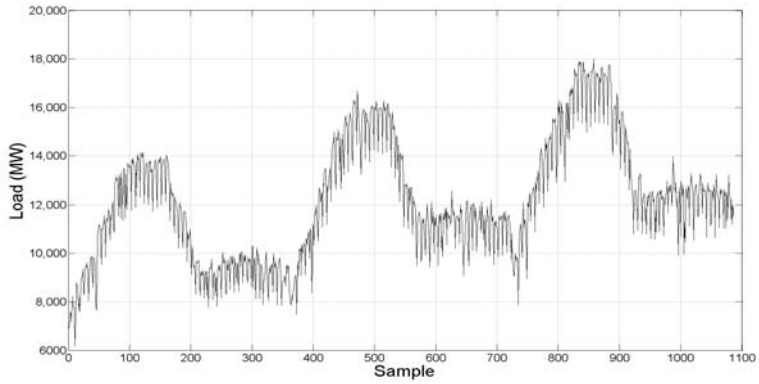

Fig. 3. The profile of loads used in this study.

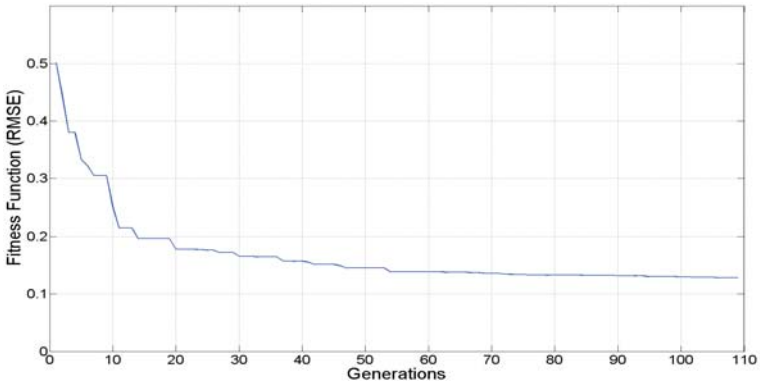

Fig. 4. Illustration of the convergence history of optimization algorithm for minimization of fitness function (RMSE) and adjusting parameters of IT2 TSK FLS (A2-C1).

- IT2 TSK FLS (A2-C1) models accurately forecast two day ahead load demands for test samples. A large R^2 and a small RMSE are indications of satisfactory results.
- The performance of IT2 TSK FLS (A2-C1) model is superior to multilayer NN models for STLF. This superiority is due to use of IT2 MFs in our forecasting models. This supports the claim that T2 FLSs have an excellent capability in handling uncertainties and minimizing their effects.
- NN models cannot appropriately cope with uncertainties in data. These uncertainties significantly degrade performance of NN models and cause a large forecasting error. This is due to fact that NNs are deterministic models and show a poor performance in case of multivalued targets [9] [26] [10] [27].

TABLE III
PERFORMANCE MEASURES FOR IT2 TSK FLS AND NN MODELS

Performance Measure	Neural Network	IT2 TSK FLS (A2-C1)
Correlation coefficient	86.48%	89.92%
RMSE	0.1685	0.1394
R^2	62.52%	77.02%

STLF performance of IT2 TSK FLS (A2-C1) models can be further improved through the use of other types of IT2 MFs with more degrees of freedom. An example is the Gaussian MF with uncertain mean and standard deviation. The number of MFs per inputs is 3 in experiments conducted (totally 81 rules). Increasing resolution of models by considering more MFs will improve the forecasting performance of models. The forecasting error for more complicate models (with more MFs) will also be further decreased in case of applying more generations in GAs for training of models. Inclusion of more inputs and using a validation set will also improve the accuracy of forecasting results obtained from both IT2 TSK FLS (A2-C1) and NN models.

VI. CONCLUSION

In this paper, interval type-2 TSK fuzzy logic systems are used for the problem of short term load forecasting. Lagged load demands and weather and calendar information are used as inputs to the forecasting model. Created models are trained using the genetic algorithm, where mean squared error is the cost function. The conclusion of this research is that short term power demand can be accurately forecasted using interval type-2 TSK fuzzy logic systems. The extra degrees of freedom of these models provide the analyzers with sufficient capacity for modeling nonlinear relationships and handling of uncertainties. The coefficient of determination between actual and forecasted loads is 77%, which is approximately 15%

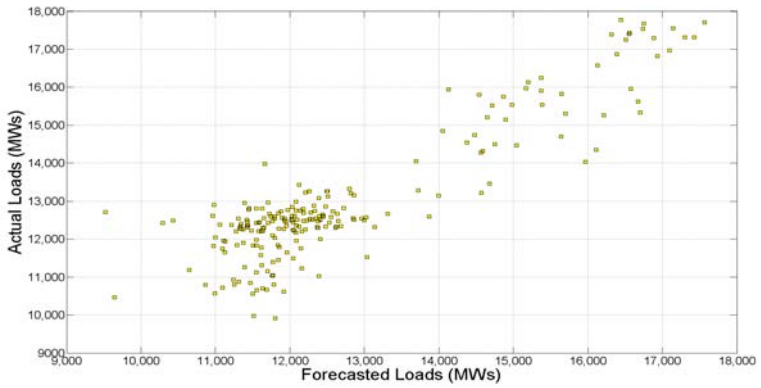

Fig. 5. Forecast vs. actual power demand with a correlation coefficient equal to 89.92%.

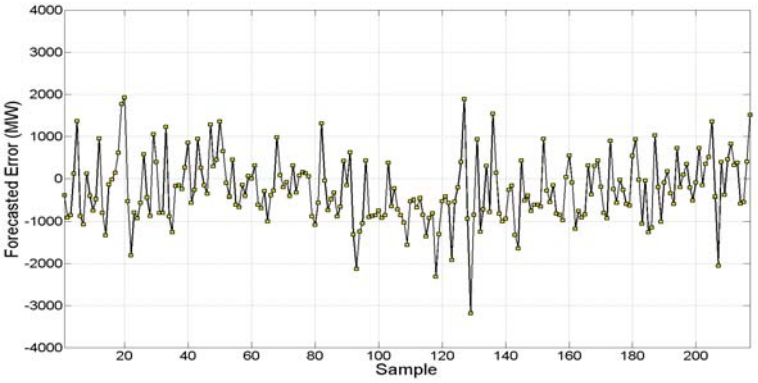

Fig. 6. Forecasting error for test samples (D_{test}).

greater than coefficient of determination for results obtained using neural networks.

IT2 TSK FLS (A2-C1) models used in this study can also be applied to the problem of medium and long term load forecasting. It is expected that these models will efficiently handle uncertainties and minimize their effects on forecasted long and short term load demands. Electricity price estimation is another research field, where these models could be used to handle prevailing uncertainties. Further research in these fields is continuing.

The work presented in this paper is a pioneer study on application of IT2 TSK FLS (A2-C1) for STLF problem. It will have a significant impact on the way artificial intelligence methods are used to forecast power load demands. It is expected that results of this paper will encourage other research groups to devote further effort into the application of IT2 FLS models for addressing problems in the power engineering field.

ACKNOWLEDGMENT

This research was fully supported by the Centre for Intelligent Systems Research (CISR) at Deakin University.

REFERENCES

[1] A. Papalexopoulos and T. Hesterberg, "A regression-based approach to short-term system load forecasting," *IEEE Transactions on Power Systems*, vol. 5, no. 4, pp. 1535–1547, 1990.

[2] H. M. Al-Hamadi and S. A. Soliman, "Short-term electric load forecasting based on kalman filtering algorithm with moving window weather and load model," *Electric Power Systems Research*, vol. 68, no. 1, pp. 47–59, Jan. 2004.

[3] S.-J. Huang and K.-R. Shih, "Short-term load forecasting via arma model identification including non-gaussian process considerations," *IEEE Transactions on Power Systems*, vol. 18, no. 2, pp. 673–679, 2003.

[4] J. D. Cryer, *Time Series Analysis*. Duxbury Press, 1986.

[5] M. Paliwal and U. A. Kumar, "Neural networks and statistical techniques: A review of applications," *Expert Systems with Applications*, vol. 36, no. 1, pp. 2–17, Jan. 2009.

[6] H. Hippert, C. Pedreira, and R. Souza, "Neural networks for short-term load forecasting: a review and evaluation," *IEEE Transactions on Power Systems*, vol. 16, no. 1, pp. 44–55, 2001.

[7] K. Metaxiotis, A. Kagiannas, D. Askounis, and J. Psarras, "Artificial intelligence in short term electric load forecasting: a state-of-the-art survey for the researcher," *Energy Conversion and Management*, vol. 44, no. 9, pp. 1525–1534, Jun. 2003.

[8] S. K. Aggarwal, L. M. Saini, and A. Kumar, "Electricity price forecasting in deregulated markets: A review and evaluation," *International Journal of Electrical Power & Energy Systems*, vol. 31, no. 1, pp. 13–22, Jan. 2009.

[9] A. Khosravi, S. Nahavandi, and D. Creighton, "Construction of optimal prediction intervals for load forecasting problem," *IEEE Transactions on Power Systems*, vol. 25, pp. 1496–1503, 2010.

[10] ——, "Load forecasting and neural networks: A prediction interval-based perspective," *B.K. Panigrahi et al. (Eds.): Computational Intelligence in Power Engineering, SCI 302*, pp. 131–150, 2010.

[11] D. Srinivasan, S. S. Tan, C. Cheng, and E. K. Chan, "Parallel neural network-fuzzy expert system strategy for short-term load forecasting: system implementation and performance evaluation," *IEEE Transactions on Power Systems*, vol. 14, no. 3, pp. 1100–1106, 1999.

[12] L.-C. Ying and M.-C. Pan, "Using adaptive network based fuzzy infer-

ence system to forecast regional electricity loads," *Energy Conversion and Management*, vol. 49, no. 2, pp. 205–211, Feb. 2008.
[13] Z. Yun, Z. Quan, S. Caixin, L. Shaolan, L. Yuming, and S. Yang, "Rbf neural network and anfis-based short-term load forecasting approach in real-time price environment," *IEEE Transactions on Power Systems*, vol. 23, no. 3, pp. 853–858, 2008.
[14] H. Hagras, "A hierarchical type-2 fuzzy logic control architecture for autonomous mobile robots," *IEEE Transactions on Fuzzy Systems*, vol. 12, no. 4, pp. 524–539, 2004.
[15] L. A. Zadeh, "The concept of a linguistic variable and its application to approximate reasoning–i," *Information Sciences*, vol. 8, no. 3, pp. 199–249, 1975.
[16] J. Mendel and R. John, "Type-2 fuzzy sets made simple," *IEEE Transactions on Fuzzy Systems*, vol. 10, no. 2, pp. 117–127, 2002.
[17] N. Karnik, J. Mendel, and Q. Liang, "Type-2 fuzzy logic systems," *IEEE Transactions on Fuzzy Systems*, vol. 7, no. 6, pp. 643–658, 1999.
[18] N. N. Karnik and J. M. Mendel, "Centroid of a type-2 fuzzy set," *Information Sciences*, vol. 132, no. 1-4, pp. 195–220, Feb. 2001.
[19] Q. Liang and J. Mendel, "Interval type-2 fuzzy logic systems: theory and design," *IEEE Transactions on Fuzzy Systems*, vol. 8, no. 5, pp. 535–550, 2000.
[20] J. Mendel, "Type-2 fuzzy sets and systems: an overview," *IEEE Computational Intelligence Magazine*, vol. 2, no. 1, pp. 20–29, 2007.
[21] H. Hagras, "Type-2 flcs: A new generation of fuzzy controllers," *IEEE Computational Intelligence Magazine*, vol. 2, no. 1, pp. 30–43, 2007.
[22] R. John and S. Coupland, "Type-2 fuzzy logic: A historical view," *IEEE Computational Intelligence Magazine*, vol. 2, no. 1, pp. 57–62, 2007.
[23] J. R. Castro, O. Castillo, P. Melin, and A. Rodrguez-Daz, "A hybrid learning algorithm for a class of interval type-2 fuzzy neural networks," *Information Sciences*, vol. 179, no. 13, pp. 2175–2193, Jun. 2009.
[24] T. Dereli, A. Baykasoglu, K. Altun, A. Durmusoglu, and I. B. Trksen, "Industrial applications of type-2 fuzzy sets and systems: A concise review," *Computers in Industry*, vol. 62, no. 2, pp. 125–137, Feb. 2011.
[25] J. M. Mendel, *Uncertain Rule-Based Fuzzy Logic Systems: Introduction and New Directions*. Prentice Hall, Englewood Cliffs, NJ, 2001.
[26] R. A. Kilmer, A. E. Smith, and L. J. Shuman, "Computing confidence intervals for stochastic simulation using neural network metamodels," *Computers & Industrial Engineering*, vol. 36, no. 2, pp. 391–407, Apr. 1999.
[27] A. Khosravi, S. Nahavandi, D. Creighton, and A. F. Atiya, "A lower upper bound estimation method for construction of neural network-based prediction intervals," *IEEE Transactions on Neural Networks*, vol. 22, no. 3, pp. 337 – 346, 2011.

2011 IEEE International Conference on Fuzzy Systems
June 27-30, 2011, Taipei, Taiwan

An Adaptive Type-2 Input Based Nonsingleton Type-2 Fuzzy Logic System for Real World Applications

Nazanin Sahab
The Computational Intelligence Centre, School of Computer Science and Electronic Engineering
University of Essex
United Kingdom
E-mail: nsahab@essex.ac.uk

Hani Hagras
The Computational Intelligence Centre, School of Computer Science and Electronic Engineering
University of Essex
United Kingdom
E-mail: hani@essex.ac.uk

***Abstract*—A Fuzzy Logic System (FLS) is generally credited with being an adequate methodology for real world applications which are subject to high uncertainty levels. Recent works have shown that interval type-2 FLSs can outperform type-1 FLSs in the applications which encompass high uncertainty levels. However, the majority of interval type-2 FLSs handle the linguistic and input numerical uncertainties using singleton interval type-2 FLSs that mix the numerical and linguistic uncertainties to be handled only by the linguistic labels type-2 fuzzy sets. This ignores the fact that if input numerical uncertainties were present, they should affect the incoming inputs to the FLS. Even in the papers that employed nonsingleton type-2 FLSs, the input signals were assumed to have a predefined shape (mostly Gaussian or triangular) which might not reflect the real uncertainty distribution which can vary with the associated measurement. In our previous work, we have presented some of the theoretical basis for generating an adaptive type-2 fuzzy input which is better able to represent the encountered uncertainty at a given measurement. The nonsingleton type-2 fuzzy inputs are dynamic and they are automatically generated from data and they do not assume a specific shape about the uncertainty distribution associated with the given sensor. In this paper, we will present an overview on how the adaptive type-2 input based nonsingleton interval type-2 FLS can operate in real time. We will present real world experiments using a mobile robot which will show how under high input uncertainty levels, the nonsingleton type-2 FLS can give a good performance and outperform its singleton type-2 and type-1 FLSs counterparts.**

Keywords- type-2 nonsingleton, interval type-2 fuzzy logic systems, uncertainty, measurement data, mobile robots

I. INTRODUCTION

The Fuzzy Logic System (FLS) is credited with being an adequate methodology for dealing with the uncertainties and imprecision present in real world applications. While traditionally type-1 FLSs have been widely employed in real world applications, recent years have shown a rapidly growing interest in the research and application of type-2 FLSs. This is because, it has become apparent that type-1 FLSs cannot fully handle the large amounts of uncertainties encountered in real world environments and applications. Interval type-2 FLSs have shown to provide better performance when compared to type-1 FLSs in applications with high levels of uncertainty. The difference in performance has been attributed to the nature of interval type-2 fuzzy sets which can better account for the uncertainties as they incorporate a Footprint of Uncertainty (FOU) and they can be assumed to embed a large number of type-1 fuzzy sets. However, the majority of the type-2 FLSs handle the linguistic and input numerical uncertainties using singleton interval type-2 FLSs that mix the numerical and linguistic uncertainties to be handled only by the linguistic labels type-2 fuzzy sets. Input numerical uncertainties are associated with the noise, imprecision and uncertainty associated with sensors and input devices. However, the linguistic uncertainties are associated with human words and perceptions. Hence, it seems paradoxical to use singleton type-2 FLSs to handle the input numerical uncertainties, as this ignores the fact that if input numerical uncertainties were present, they should affect the incoming inputs to the FLS. Thus we cannot treat the incoming FLS inputs as perfect signals as in the case of singleton FLSs. Hence, there is a need to employ nonsingleton FLSs to handle the input numerical uncertainties by modelling the inputs as fuzzy inputs rather than crisp values.

Although, there are many papers on type-1 FLSs, limited number of papers considered the usage of type-1 nonsingleton FLSs such as [1-6] and even fewer number considered type-2 nonsingleton FLS [7-11]. The work done so far in (type-1 and type-2) nonsingleton FLSs use predefined shapes for the uncertainty distribution affecting the FLSs inputs (mainly Gaussian and triangular) which might not reflect the real uncertainty distribution associated with the given sensor [12-14]. For example in the case of a sonar sensor, the numerical input uncertainties depend on many factors such as the shape and type of objects reflecting the sonar signal as well as wind speed, humidity and temperature. Moreover, the uncertainty distribution also varies with the measured values where for the case of a sonar sensor, the amount of uncertainty affecting measurement readings at 20cm distance could be much less than the uncertainties affecting the measurement at large distances such as 3m. Hence, it is not fair to consider that there

978-1-4244-7316-8/11/$26.00 ©2011 IEEE

is specific shape for the uncertainty distribution (triangular, Gaussian, etc.) with fixed parameters (average, standard deviation, etc.) for all the measured values.

In our previous work [15], we have presented some of the theoretical basis for generating an adaptive type-2 fuzzy input which is better able to represent the encountered uncertainty at a given measurement. The nonsingleton type-2 fuzzy inputs are dynamic and they are automatically generated from data and they are piece-wise linear type-2 fuzzy sets which are changing for different measurements to model the encountered uncertainty. Piece-wise linear fuzzy sets were used in [16] for the representation of membership functions. However, we use piece-wise linear fuzzy sets to represent the type-2 fuzzy input variables. In this paper, we will present an overview on how the adaptive type-2 input based nonsingleton interval type-2 FLS can operate in real time. We will present real world experiments using a mobile robot which will show how under high input uncertainty levels, the nonsingleton type-2 FLS can give a good performance and outperform its singleton type-2 and type-1 FLSs counterparts.

Section II will give a summary of the structure of the real – time type-2 nonsingleton type-2 FLS. Section III will present the experiments and results. Finally Section IV provides conclusions and future work.

II. THE TYPE-2 NONSINGLETON TYPE-2 FLS

A. The Structure of Type-2 Nonsingleton Type-2 FLS

The structure of the type-2 nonsingleton type-2 FLS [15] is illustrated in Fig.1. The type-2 nonsingleton type-2 FLS employs interval type-2 fuzzy sets to handle the encountered linguistic uncertainty associated with the linguistic labels while the nonsingleton type-2 fuzzy input variables handle the encountered numerical input uncertainties.

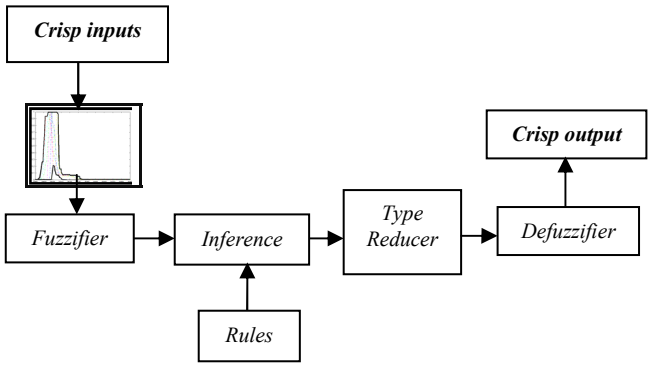

Figure 1. The structure of type-2 nonsingleton type-2 FLS.

B. Modeling Type-2 Fuzzy Input Variables

Fig.2 shows a high level overview on the steps taken to model the type-2 fuzzy input variables at given measurement values. The first step involves sampling the given input at different measurements by logging many readings at the same measurement value (for example for a sonar sensor, collecting 10,000 readings at 20cm, 40cm, etc.) which will create a data distribution (or a histogram). The data distributions are then converted into piece-wise linear type-1 fuzzy sets that are convex and normal as explained in [15] and [17]. We then repeat the same process under various uncertainty conditions (for the sonar sensors, subjecting it to humidity, heat, wind, different surfaces, etc.) which will create different type-1 fuzzy sets for the different uncertainty conditions [15], [17]. We then combine the various type-1 fuzzy sets at the given measurement value to form a type-2 fuzzy set that models the uncertainty at the given measurement value.

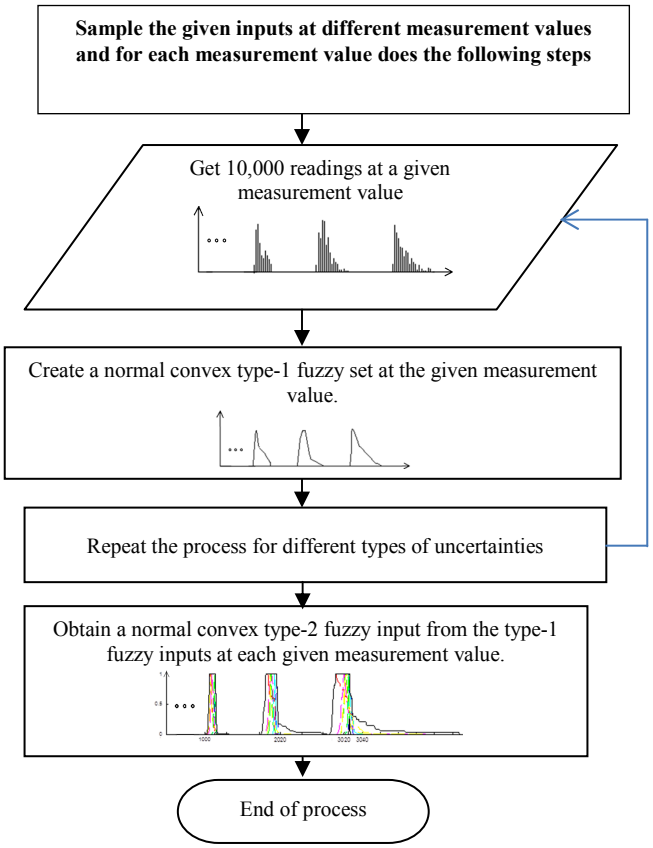

Figure 2. The off-line process of obtainig the type-2 fuzzy input at certain measusrement values.

As we cannot generate the type-2 fuzzy sets for all the measurements values, hence, we need to interpolate the type-2 fuzzy set for an incoming measurement value by interpolating the type-2 fuzzy sets representing the measurements to the left and right of the incoming measurement value. For each control cycle (as shown in Fig.3), we have a measurement window which takes 5 consecutive crisp measurements from the sensor at the given instance and takes the average to form an incoming measurement value which interpolates type-2 fuzzy sets at the right and left of the incoming measurement to generate an interpolated type-2 fuzzy input as explained in [17]. The type-2 fuzzy input is then fuzzified and then it triggers the inference engine and the rule base to generate a type-2 fuzzy output which is then type-reduced and defuzzified to generate the final crisp output of the FLS.

Fig.4-6 present the real-world shapes of the nonsingleton type-2 fuzzy inputs generated at given measurements of a given sonar sensor at 1m, 2m, and 3m respectively. The top figures of each pair set of figures (Fig.4-Fig.6) are the type-2 fuzzy input variable for the front sonar sensor and the figures below are

related to back sonar sensor of the mobile robot shown in Fig.11. For each given measurement, we log 10,000 readings from the sensor. In the case of a sonar sensor for the robot shown in Fig.11, we keep the distance fixed and read 10,000 readings at the same fixed distance which will result in a data distribution or a histogram. Following the steps in Fig. 2, we then create a normal convex type-1 fuzzy set from the given data distribution, which will model the uncertainties at the given measurement conditions. We then apply various environmental conditions, which could affect the input measurements. As for the case of a sonar sensor, we can consider changing shapes and materials of the objects as well as changing temperature, sound noise and wind. Each condition will then have an associated type-1 fuzzy set which models the uncertainty at the given measurement (fixed distance). We then combine the various type-1 fuzzy sets to create a convex type-2 fuzzy set (as explained in [15] and [17]) which models the various uncertainties encountered at each measurement value.

The upper and lower membership functions of type-2 fuzzy input for the considered sonar sensors are shown by black lines in Fig.4-Fig.6, while the related type-1 fuzzy input for each case of uncertainty is shown by dashed lines. Fig.4-Fig.6 illustrate that not only the shape of type-2 fuzzy sets change for different range of distances, but also the sonar sensors may not be effected in a same way.

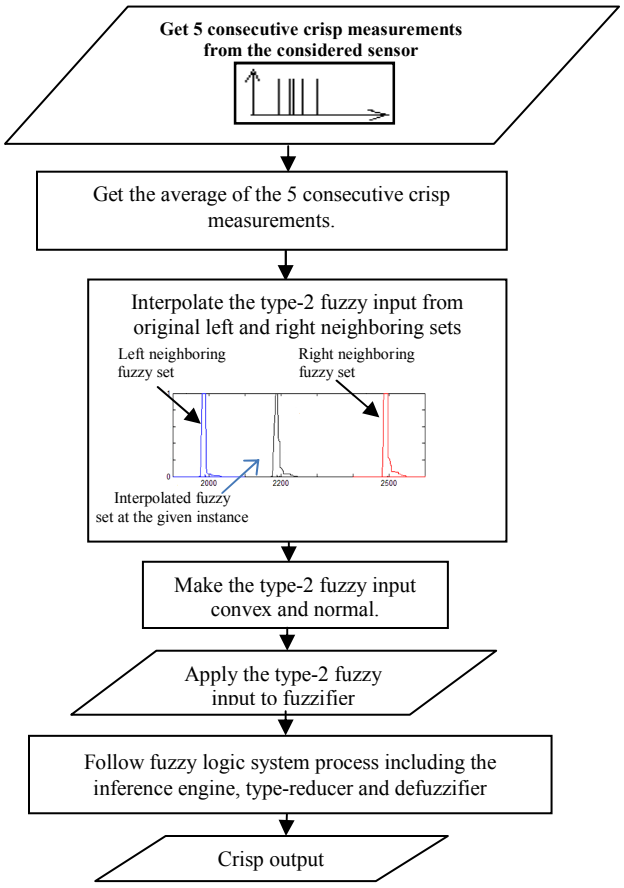

Figure 3. The process of the on-line nonsingleton type-2 FLS

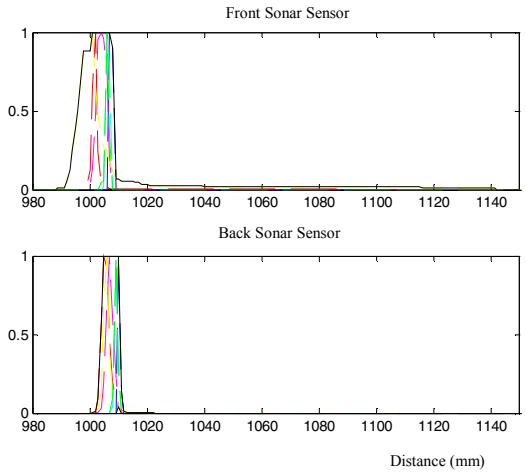

Figure 4. The generated input type-2 fuzzy sets for the front sonar sensor (top figure) and the back sonar sensor (bottom figure) of the robot in Fig.11 when the edge is set around 1 m from the robot.

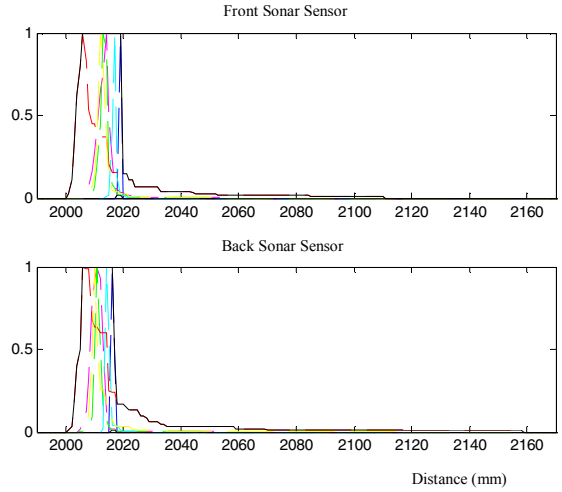

Figure 5. The generated input type-2 fuzzy sets for the front sonar sensor (top figure) and the back sonar sensor (bottom figure) of the robot in Fig.11 when the edge is set around 2m from the robot.

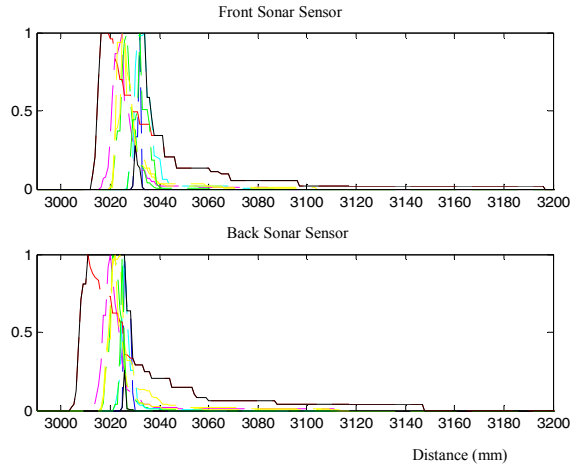

Figure 6. The generated input type-2 fuzzy sets for the front sonar sensor (top figure) and the back sonar sensor (bottom figure) of the robot in Fig.11 when the edge is set around 3m from the robot.

C. The Type-2 Nonsingleton Type-2 Fuzzification

The fuzzifier converts the fuzzy inputs into linguistic labels with given membership values to activate the rule base and inference engine. The fuzzification operation between the type-2 fuzzy input variables and the type-2 fuzzy sets assigned for linguistic labels (the antecedent type-2 fuzzy set specified by F_k^l) to obtain lower and upper membership values of input k within rule l are shown in Equations (1) and (2) respectively:

$$\overline{\mu}_k^l(x_k) = \sup_{x_k \in X_k} (\overline{\mu}_{x_k}(x_k) * \overline{\mu}_{F_k^l}(x_k)) \quad (1)$$

$$\underline{\mu}_k^l(x_k) = \sup_{x_k \in X_k} (\underline{\mu}_{x_k}(x_k) * \underline{\mu}_{F_k^l}(x_k)) \quad (2)$$

The $\overline{\mu}_{x_k}(x_k)$ and $\underline{\mu}_{x_k}(x_k)$ are the upper and lower membership functions of the type-2 fuzzy input variable and $\overline{\mu}_{F_k^l}(x_k)$ and $\underline{\mu}_{F_k^l}(x_k)$ are the upper and lower membership functions of the antecedent type-2 fuzzy sets (representing the linguistic labels) respectively. The sup operation has been considered as maximum t-conorm, and the * operation is minimum t-norm. In [17], we described the theory of type-2 nonsingleton type-2 FLS, and how the fuzzification output is calculated for the upper membership functions. The process of finding the output of the fuzzifier follows Equations (1) and (2) to find the upper and lower membership values to the given respective linguistic label. Due to the limited space, in this subsection, we will concentrate on presenting the process followed to find the lower membership value to the given respective linguistic label. The process is quite complicated as the input type-2 fuzzy variable is a piece-wise linear function (as shown in Fig.7).

According to Equation (2), to get lower bound of the membership to the given respective linguistic label, we need to apply the t-norm (minimum operation) between the type-1 membership functions $\underline{\mu}_{x_k}(x_k)$ and $\underline{\mu}_{F_k^l}(x_k)$. This will result in a type-1 fuzzy set (shown by thick line in Fig.8 - Fig.10), where we need to find its sup (maximum) to find $\underline{\mu}_k^l(x_k)$.

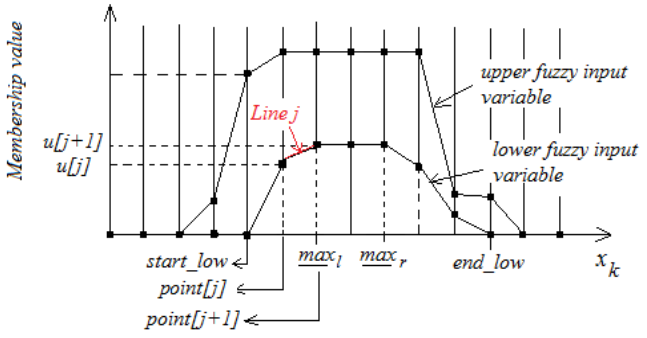

Figure 7. The piece-wise linear type-2 fuzzy input variable.

Due to the limited space in this paper, we will present a sample for the operation between the antecedent type-2 fuzzy set and the type-2 fuzzy input variable for the lower bound when the starting point *start_low* (shown in Fig.8 - Fig.10) (of the lower membership function for type-2 fuzzy input variable) is smaller than d_{m2} (of the lower membership function antecedent type-2 fuzzy set) and the ending point *end_low* (of the lower membership function for type-2 fuzzy input variable) is greater than a_{m2} (of the lower membership function of antecedent type-2 fuzzy set).

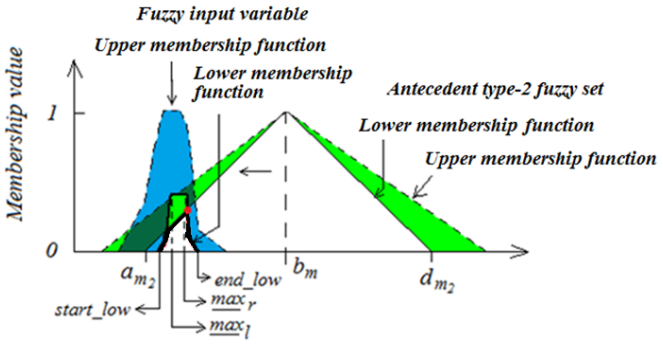

Figure 8. Finding $\underline{\mu}_k^l(x_k)$ for Case 1 .

The case 1 in Fig.8 happens when the intersection between the lower membership function of the type-2 fuzzy input and the lower membership function of the antecedent is located on the antecedent line from b_m to a_{m2} , but the intersection does not happen on the maximum of the lower membership function of the type-2 fuzzy input. In that case, we need to obtain the first intersection point from right to left starting from the pieces of line j ending at *end_low*. As the slope of the antecedent line from b_m to a_{m2} is positive, the first intersection from right side has the highest membership value, which will be the result of max-min operation between the two fuzzy sets to lead to $\underline{\mu}_k^l(x_k)$.

The given line *j* (of fuzzy input) ranges from *point[j]* to *point [j+1]* in the x-axis line where *j+1* is the line connecting to the line *j* and located at its right in the piece-wise linear function. The *u[j]* and *u[j+1]* are also membership value at *point[j]* and *point[j+1]* respectively. The membership value for any point x_k located on line *j* is obtained from Equation (3) as follows:

$$\frac{\mu_{x_k}(x_k) - u[j]}{x_k - point[j]} = \frac{u[j+1] - u[j]}{point[j+1] - point[j]}$$

$$\mu_{x_k}(x_k) = \frac{u[j+1] - u[j]}{point[j+1] - point[j]} x_k + \frac{point[j+1]u[j] - point[j]u[j+1]}{point[j+1] - point[j]} \quad (3)$$

The membership value $\mu_{F_k^l}(x_k)$ of any point x_k on a line of the antecedent fuzzy set (starting from an extreme left point "*left*" (a_{m2} in our case) and ending at an extreme right point "*right*" (b_m in our case)) is obtained as follows:

$$\frac{\mu_{F_k^l}(x_k) - \mu_{F_k^l}(left)}{x_k - left} = \frac{\mu_{F_k^l}(right) - \mu_{F_k^l}(left)}{right - left}$$

$$\mu_{F_k^l}(x_k) = \frac{\mu_{F_k^l}(right) - \mu_{F_k^l}(left)}{right - left} x_k + \frac{right\mu_{F_k^l}(left) - left\mu_{F_k^l}(right)}{right - left} \quad (4)$$

At the intersection point $x_{k,c}$ between an antecedent line and a line j of the fuzzy input variable, $\mu_{x_k}(x_k)$ in Equation (3) is equal to $\mu_{F_k^l}(x_k)$ in Equation (4). Hence $x_{k,c}$ could be found as follows:

$$x_{k,c} = \frac{\left[\begin{array}{l}(right\mu_{F_k^l}(left) - left\mu_{F_k^l}(right))(po\,\mathrm{int}[j+1] - po\,\mathrm{int}[j]) + \\ (right - left)(po\,\mathrm{int}[j]u[j+1] - po\,\mathrm{int}[j+1]u[j])\end{array}\right]}{\left[\begin{array}{l}(right - left)(u[j+1] - u[j]) + \\ (\mu_{F_k^l}(left) - \mu_{F_k^l}(right))(po\,\mathrm{int}[j+1] - po\,\mathrm{int}[j])\end{array}\right]} \quad (5)$$

Subsistuting with the value of $x_k = x_{k,c}$ in Equation (3) or (4), we can find $\underline{\mu}_k^l(x_k) = \mu_k^l(x_k)$.

The case 2 in Fig.9 happens when at least one intersection between lower membership function of the type-2 fuzzy input and the lower membership function of the antecedent happens on the maximum of the lower membership function of the type-2 fuzzy input (or it can happens when the fuzzy input variable is within a_{m2} to d_{m2} domain but no intersection occurres). In that case, $\underline{\mu}_k^l(x_k)$ is equal to the maximum membership value of the lower membership function of type-2 fuzzy input.

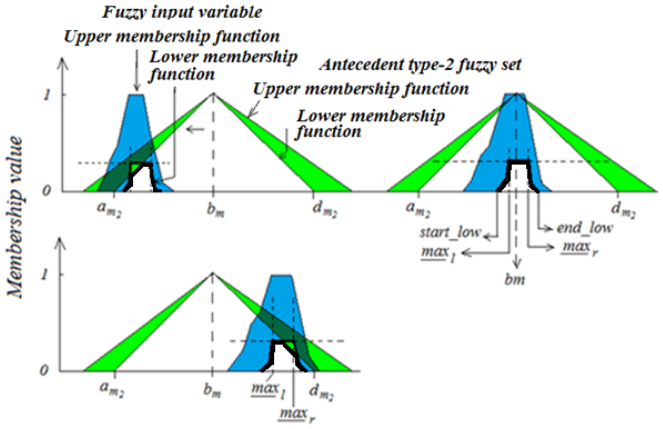

Figure 9. Finding $\underline{\mu}_k^l(x_k)$ for Case 2 .

The case 3 in Fig.10 happens when the intersection between lower membership function of the type-2 fuzzy input and the lower membership function of the antecedent is located on the antecedent line from b_m to d_{m2}, but the intersection does not happen on the maximum of the lower membership function of the type-2 fuzzy input. In that case, we need to obtain the first intersection point from left to right side strating from the pieces of line j starting at *start_low*. As the slope of the antecedent line from b_m to d_{m2} is negative, the first intersection from left has the highest membership value. Hence $\underline{\mu}_k^l(x_k)$, could be found using the same approach followed in Equations (3 –5).

Following the same procedure the upper and lower membership values ($\underline{\mu}_k^l(x_k)$ and $\overline{\mu}_k^l(x_k)$) could be found for the various cases as explained in [17].

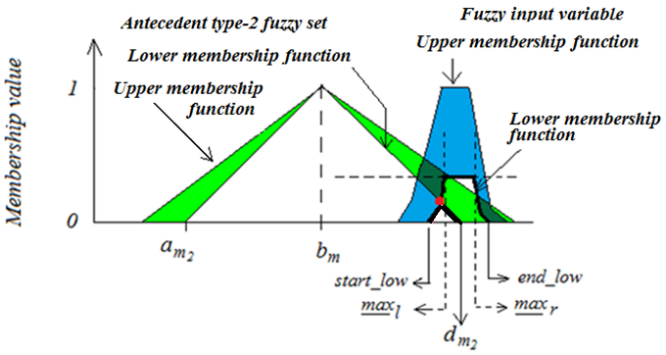

Figure 10. Finding $\underline{\mu}_k^l(x_k)$ for Case 3 .

D. Rule Base

The rule base of singleton and nonsingleton FLS are similar. Considering a FLS having inputs $x_1 \in X_1, \ldots, x_p \in X_p$ and one output y∈ Y, the rule *l* is defined as [12]:

$$\text{If } x_1 \text{ is } \tilde{F}_1^l \ldots \text{and } x_p \text{ is } \tilde{F}_p^l, \text{ then y is } \tilde{G}^l \quad (6)$$

Where *l=1, ..., M* and *M* is the total number of rules in the rule base. The $\tilde{F}_k^l$ is the antecedent membership function for input *k* and rule *l*, and $\tilde{G}^l$ is consequent membership function for rule *l*.

E. Inference Engine

We have shown in the fuzzifier subsection, how to find the upper and lower membership values of a given type-2 fuzzy input variable to a given linguistic label. The process needs to be done for all inputs *(k=1,..., p)*. At the end, the firing strength of each rule $F^l = [\underline{f}^l, \overline{f}^l]$ could be found where $\underline{f}^l$ and $\overline{f}^l$ will be obtained as follows:

$$\underline{f}^l = T_{k=1}^p \{\underline{\mu}_k^l(x_k)\} \quad (7)$$

$$\overline{f}^l = T_{k=1}^p \{\overline{\mu}_k^l(x_k)\} \quad (8)$$

F. Type-Reduction and Defuzzification

After obtaining the lower and upper firing strengths for each rule from the inference engine and obtaining the centroid of consequent membership function, the center of sets type-reducer [12] is used to produce the type-reduced sets. We then take the average of the type-reduced set to provide the final defuzzified crisp output.

III. Experiments and Results

A. The Robots and the Experimental Setup

In our experiments, we have employed a four-wheel mobile robot (shown in Fig. 11) with two sonar sensors to follow an edge made of cylindrical objects. In order to test the robot under unseen input uncertainties, we have applied various sources of uncertainties to the input sonar sensors as shown in Fig.11a where we have used a hair dryer stuck on robot to blow hot air through the path of front sonar sensor. We have also employed a fan fixed at a certain position on ground to create cold wind at the starting robot position. These employed

uncertainties are introduced during the online operation of the robot and they have not been seen by the robot during the FLS design. We chose changing the wind speed (through the fan and dryer) and temperature (through the hair dryer) to introduce input uncertainties to the sonar sensors. This is because the wind, temperature variations and atmospheric turbulences are all meteorological conditions [18] that have an effect on sound propagation (as we used sonar sensors). The speed of sound in air is proportional to the square root of absolute temperature as follows:

$$c = 20.05\sqrt{T + e/p} \tag{9}$$

Where T is absolute temperature in Kelvin, and e is partial pressure of water vapor, and p is barometric pressure. Wind is also another factor affecting the sound travel. The wind in the same direction of sound will cause the wave propagation to be bent downward, and in the upwind direction, sound waves move upward which cause no direct sound penetration [18].

To obtain the position of the robot in a precise way, the VICON system is used in which six cameras are employed. To be able to recognize the robot, four markers are used (as shown in Fig.11). The top of the cylinders are also marked to be able to check if the edges of the cylinders are in a same line where the starting and ending cylinders are modeled in VICON to be able to distinguish the certain position of wall (one of them is shown in Fig.11b).

B. The FLSs Design

We have designed a type-1 FLS which is able to give a good performance under the normal lab conditions. The performance of the type-1 FLS is considered to be acceptable when it produces small overshoots/undershoots and small steady state error in a usual room temperature without applying external uncertainty. The antecedent membership functions for the type-1 FLS are shown in Fig.12 (drawn with thin line). We have then blurred the type-1 fuzzy sets by a given uncertainty value to generate the FOU of the type-2 fuzzy sets (shown in Fig.12 by thick line) for the interval (singleton and nonsingleton) type-2 FLS. The consequent membership functions (for all FLSs) are type-1 fuzzy sets as there are no major uncertainties associated with robot outputs. The rule-base (employed for all FLSs) is shown in Table I.

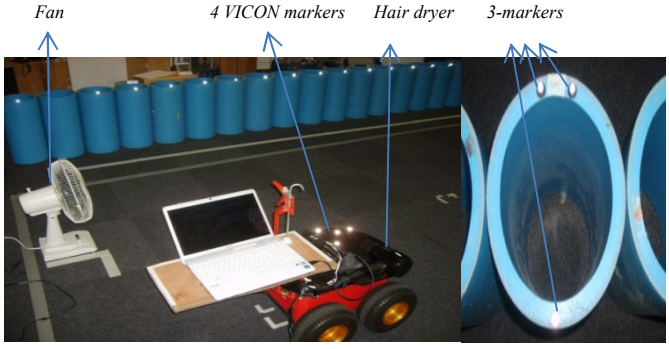

(a) (b)

Figure 11. (a) The Experimenal setup where the robot is marked to be tracked by VICON camera system in robot arena. (b) One of the cylindars modeled in VICON system using three markers to know the exact position of wall.

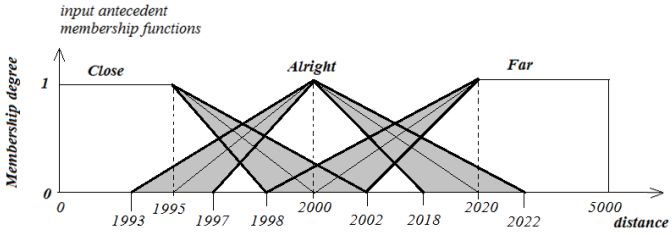

Figure 12. Antecedent membership functions for both the front and back senors. The type-1 fuzzy sets are shown in thin line while the interval type-2 fuzzy sets are shown in thick lines.

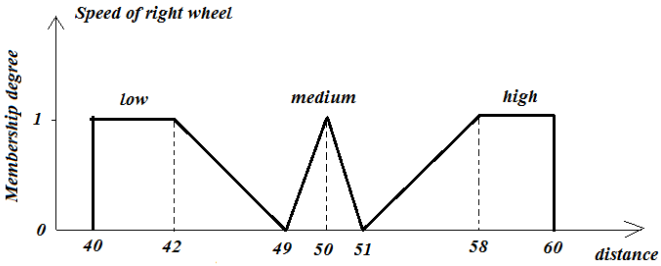

Figure 13. The consequent type-1 fuzzy sets for the used FLSs

TABLE I. THE RULE BASE FOR ALL THE FLSS. THE RULE BASE OUTPUT IS THE SPEED OF RIGHT WHEEL.

Front sonar	Back sonar		
	Close	Alright	Far
Close	*low*	*low*	*low*
Alright	*low*	*medium*	*low*
Far	*high*	*high*	*high*

C. Control Surface Analysis

The control surface graphically represents the unknown function articulated by the FLS. Fig. 14 shows the control surfaces for the singleton type-1 and type-2 FLSs and the type-2 nonsingleton type-2 FLS. The control surfaces show the front and back sensors plotted against the speed of right wheel. Note that a smooth shape of a control surface translates to a smooth control response that can deal with uncertainty and imprecision.

As seen from Fig.14a, the control surface of the type-1 FLS is rather steep which means it can be affected by high levels of uncertainties in the inputs where small change in the inputs can result in large output changes which might cause high overshoots/undershoots and steady state errors in addition to moving towards an unstable situation. On the other hand the control surface of the singleton type-2 FLS (shown in Fig.14b) is smoother than the type-1 FLS, which means it can handle higher level of uncertainties. However, the control surface of the type-2 nonsingleton type-2 FLS (shown in Fig.14c) is much smoother where there are smooth transition at all parts of the control surface where any small change in inputs will

result in a small change in the outputs. Thus using the type-2 input based nonsingleton type-2 FLS result in a control surface which is smoother than the singleton type-1 and type-2 FLSs. This smooth response will consequently give a very good control performance that can handle the high levels of uncertainties and disturbances where small variations in inputs will not cause significant changes to outputs. Thus, it is expected that the type-2 nonsingleton type-2 FLS will be able to handle higher levels of uncertainties than its singleton type-1 and type-2 FLSs counterparts. This will be evidenced in the real world experiments reported in the following subsection.

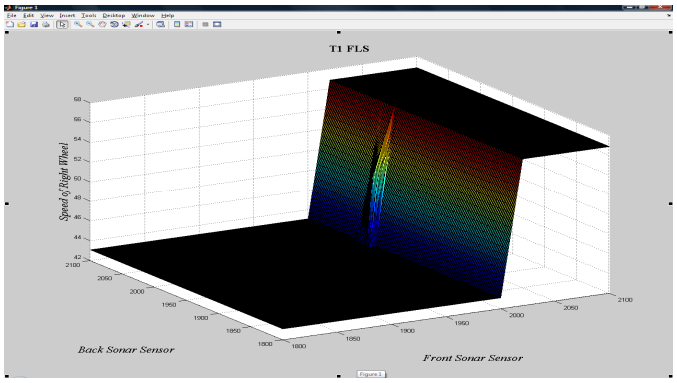

(a)

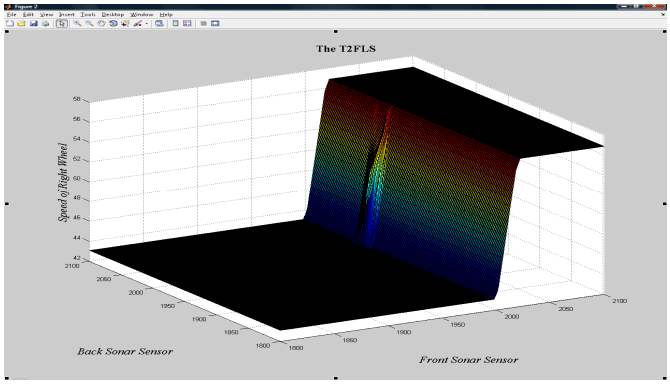

(b)

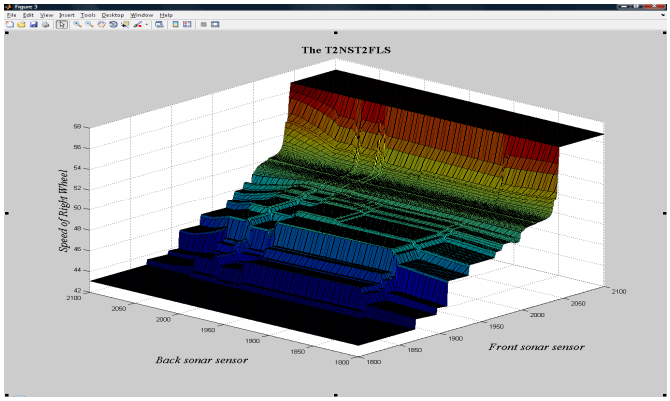

(c)

Figure 14. The control surface of (a) The singleton type-1 FLS. (b) The singleton interval type-2 FLS. (c) The type-2 nonsingleton intreval type-2 FLS.

D. Real World Experiments

Fig.15 and Fig.16 show the results of some robotic experiments, which compare the performance of singleton type-1, singleton type-2 and type-2 input based nonsingleton type-2 FLS to realize an edge following behavior at a desired distance of 2m. The robot starts from the distance of 1.8m from the nearest edge. Fig. 15 shows the robots paths of singleton type-1, type-2 and nonsingleton type-2 FLS under no induced uncertainty. As shown in Fig.15 and Table II (as expected under no uncertainty), the performance of all the FLSs will be quite similar where the type-1 FLS will be slightly better. However, as high levels of uncertainties are introduced (by blowing hot wind through the way of one sonar) as shown in Fig.16 and Table II, the type-2 nonsingleton type-2 FLS gives the best performance in terms of the Root Mean Squared Error (RMSE) (which could represent the average error) and the Standard Deviation (STD) (which could represent the size of the overshoots/undershoots from the average). In terms of control performance, the type-2 nonsingleton type-2 FLS provides the best performance followed (by a large margin) by the singleton type-2 FLS and then the singleton type-1 FLS which performs poorly.

Fig.16 evidences the control surface analysis in Fig.14 where the type-2 nonsingleton type-2 FLS recovers quickly from the uncertainties with relatively smaller overshoot/undershoot.

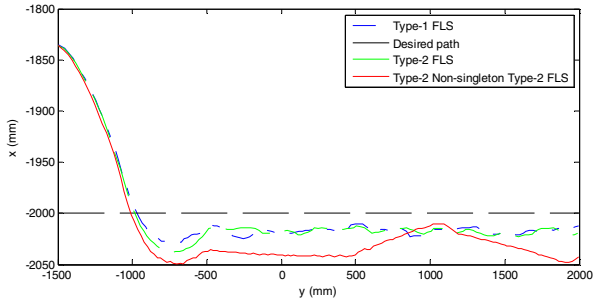

Figure 15. The robot's paths when employing singleton type-1, type-2 and nonsingleton type-2 FLS under no uncerantity.

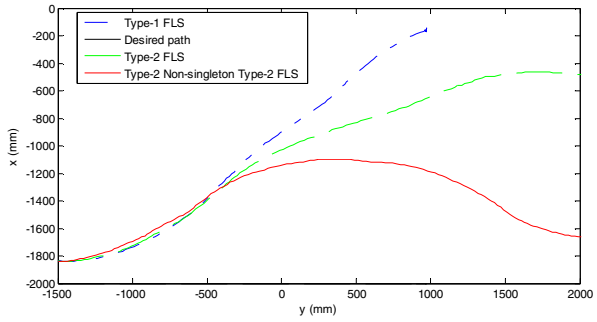

Figure 16. The robot's paths when employing singleton type-1, type-2 and nonsingleton type-2 FLS under high uncerantity levels.

TABLE II. SUMMARY RESULTS OF WALL FOLLOWING FOR THE THREE TYPES OF FLSS.

Different Conditions	Different Types of FLS		
	Type-1 FLS	***Type-2 FLS***	***Type-2 nonsingleton Type-2***
No uncertainty	STD =45.7 RMSE =45.6	STD =46.7 RMSE=46.6	STD =48.1 RMSE=51.2
Large uncertainty	STD =626.7 RMSE=1268.2	STD=478.7 RMSE=1037.8	STD =245.0 RMSE=634.4

IV. CONCLUSION

In this paper, we have presented an adaptive type-2 fuzzy input based nonsingleton type-2 FLS which is better able to handle the encountered input uncertainties. The nonsingleton type-2 fuzzy inputs are dynamic and they are automatically generated from data and they do not assume a specific shape about the uncertainty distribution associated with the given sensor. We have presented an overview on how the adaptive type-2 input based nonsingleton interval type-2 FLS can operate in real time. We have shown through control surface analysis, how the nonsingleton type-2 FLS can produce much smoother control surface than the singleton type-1 and type-2 FLSs. This should result in a better control response that handles high uncertainty levels. This was evidenced through the real world experiments using mobile robots where under high uncertainty levels, the nonsingleton type-2 FLS can outperform its singleton type-2 and type-1 FLSs counterparts. This work has shown the benefits achieved when using type-2 nonsingleton type-2 FLSs in applications characterized by high input uncertainty levels. In our future work, we aim to allow the various parameters of the type-2 nonsingleton type-2 FLSs to be learnt directly from data online.

ACKNOWLEDGMENT

The authors would like to thank Mr. Robin Dowling who supported the project by providing facilities and Mr. John Oyekan who helped to obtain data from VICON system.

REFERENCES

[1] A. Perez-Neira, J. Sueiro, and J. Roca and M. Lagunas, "A dynamic non-singleton fuzzy logic system for DS/CDMA communications," IEEE International Conference on Fuzzy Systems, vol. 2, 1998, pp. 1494-1499.

[2] M. Benedetti, A. Casagranda, and M. Donelli, and A. Massa, "An adaptive multiscaling imaging technique based on a fuzzy-logic strategy for dealing with the uncertainty of noisy scattering data," IEEE Transactions on Antennas and Propagation, vol. 55, no. 11, November 2007, pp. 3265-3278.

[3] C. Makropoulos and D. Butler, "Spatial decisions under uncertainty: fuzzy inference in urban water management," Journal of Hydroinformatics, IWA publishing, pp. 3-18, 2004.

[4] C. Quek and R. Zhou, "Structure and learning algorithms of a nonsingleton input fuzzy neural network based on the approximate analogical reasoning schema," International Journal on Information Science and Engineering Science (Fuzzy Sets and Systems), Elsevier, vol.157, no. 13, pp. 1814-1831, July 2006.

[5] E. Cavallaro, S. Micera, and P. Dario, and W. Jensen, and T. Sinkjaer," IEEE Transactions on Biomedical Engineering, vol.50, no. 9, pp. 1063-1073, September 2003.

[6] T. Chua and W. Tan, "Non-singleton genetic fuzzy logic system for arrhythmias classification," Engineering Applications of Artificial Intelligence, Elsevier, vol. 24, no. 2, March 2011, Pages 251-259.

[7] G. Mendez, L. Leduc-Lezama and R. Colas and G. Murilo-Perez and J. Ramirez-Cuellar and J. Lopez, "Application of interval type-2 fuzzy logic systems for control of the coiling entry temperature in a hot strip mill," Book chapter, Hybrid Artificial intelligent systems, Springer Berlin 2009, vol. 5572 , 2009, pp. 352-359.

[8] H. Wu and J. Mendel, "Classification of battlefield ground vehicles using acoustic features and fuzzy logic rule-based classifiers," IEEE transactions on Fuzzy Systems, vol.15, no. 1, pp. 56-72, February 2007.

[9] G. Mendez, I. Lopez-Juarez, and L. Leduc, and R. Soto, and A. Cavazos, "Temperature prediction in hot strip mill bars using a hybrid type-2 fuzzy algorithm," International Journal of simulation systems, Science and Technology, vol. 6, no. 9, pp. 33-43, 2005.

[10] G. Mendez and A. Hernandez, " Hybrid learning of interval type-2 fuzzy systems based on orthogonal least squares and back propagation for manufacturing applications," Journal of Automation, mobile robotics & Intelligent systems, vol. 2, no. 1, pp. 23-32, 2008.

[11] G. Mendez and M. Hernandez," Hybrid learning for interval type-2 fuzzy logic systems based on orthogonal least-squares and back-propagation methods," International Journal on Information Sciences, Elsevier, vol.179, no. 13, pp. 2146-2157, June 2009.

[12] J. M. Mendel, "Uncertain rule-based fuzzy logic systems, introduction and new direction," Prentice Hall PTR Upper Saddle River, NJ, 2001.

[13] G. C. Mouzouris and J. M. Mendel, "Dynamic nonsingleton fuzzy logic systems for non-linear modelling," IEEE Transactions on Fuzzy Systems, vol.5, no. 2, pp.199-208, May 1997.

[14] G. C. Mouzouri and J. M. Mendel, "Nonsingleton fuzzy logic systems: theory and application," IEEE Transactions on Fuzzy Systems, vol.5, no. 1, pp. 56-71, February 1997.

[15] N. Sahab and H. Hagras, "A hybrid approach to modeling input variables in non-singleton type-2 fuzzy logic systems," UK workshop on computational intelligence (UKCI), September 2010, pp.1-6.

[16] S. Coupland and R. John, " Geometric interval type-2 fuzzy systems," Proceedings of the joint 4th Conference of the European Society for Fuzzy Logic and Technology (EUSFLAT 2005) and the 11th Rencontres Francophones sur la Logique Floue et ses Applications (LFA 2005 joint EUSFLAT-LFA 2005, pp.449-454.

[17] N. Sahab and H. Hagras, "A type-2 nonsingleton type-2 fuzzy logic system to handle linguistic and numerical uncertainties in real world environments," 2011 IEEE International Symposium on Advances in Type-2 Fuzzy Logic Systems April 2011, Paris, in press.

[18] J. Lamancusa (2000), "Outdoor sound propagation," noise control, ME 458:Engineering noise control. Penn state university 2009, pp.10-19.

2011 IEEE International Conference on Fuzzy Systems
June 27-30, 2011, Taipei, Taiwan

Hospital Service Quality Evaluation: A Fuzzy Preference Relation Approach

Tsung-Han Chang
Department of Information Management, Kao Yuan University
1821, Jhongshan Road, Lujhu District
Kaohsiung City 821, Taiwan
t90082@cc.kyu.edu.tw

***Abstract*—This paper proposes a fuzzy preference relation approach to evaluate the hospital service quality in Taiwan. Pairwise comparisons based on consistent reciprocal additive transitivity are utilized to derive the importance weights of evaluation criteria and to obtain the performance rating of feasible hospitals with respect to each criterion. By multiplying the importance weights of evaluation criteria, and the performance ratings of feasible hospitals, the service qualities of hospital are determined. An illustrative example elicited from 5 public hospitals in southern Taiwan is used to demonstrate the evaluation procedures of this proposed approach.**

Keywords-hospital service quality; fuzzy preferece relations; performance evaluation; consistent reciprocal additive transitivity

I. INTRODUCTION

In 1995, Taiwanese National Health Insurance program was put into practice, the residents enjoyed high quality but relatively cheaper medical care compared with the developed countries. Hospital care is an industry with the characteristics of highly specialized medical capability and close contact with many persons. The importance of medical service and quality leaves no room for doubt, since good or bad quality of medical treatments directly affect the survival possibility. Recently the request for hospital service quality is gaining momentum in the world [1]. To manage a hospital successfully, the primary goals are providing good medical service quality and meeting various kinds of demands for the patients then retaining as many customers as possible [2]. Hospital, like other commercial or non-profit organizations, uses resources to provide many types of services, which is a measure of output for health-care organizations [3]. At the end of 2010, there are 19,329 public and private medical care institutions in Taiwan, so it is very difficult and complicated for the government to manage them. In order to manage so many medical care institutions efficiently, comparative performance evaluation, usually evaluated with itself over time or by comparison with others in the same industry, is used as an essential resolution of the managerial control function [3]. There are papers discussing the hospital or medical care service quality evaluation problems. Andaleeb [4] compared the quality of services provided by private and public hospitals in urban Bangladesh. Li [5] explored the relationship between hospital quality management and service quality performance for a sample of US community hospitals using a path analytic model. Raju [6] examined the impact of service quality and marketing on financial performance in the hospital industry. Andaleeb [7] surveyed the service quality perceptions and patient satisfaction of hospitals in a developing country. Li [8] identified strategic operations management decisions in the US community hospitals, showed their causal relationships, and identified their effects on hospital performance. Goldman [9] compared the quality of rural hospitals participating in a public reporting initiative to that of their urban counterparts using Hospital Compare, a new national database containing process measures. Tsai [10] used fuzzy hierarchy sensitive with Delphi method to evaluate hospital organization performance. Many critical factors are considered in the hospital service quality evaluation; so this issue is regarded as a multicriteria decision making problem. This study therefore proposes an analytic hierarchy framework based on the consistent fuzzy preference relations to evaluate the service quality of these medical care institutions. The next section will briefly discuss the consistent fuzzy preference relations. An analytic hierarchy framework based on the consistent reciprocal additive transitivity for evaluate hospital service quality is derived in Section III. In Section IV, an illustrative example is presented. Finally, discussion and conclusion are given in Section V.

II. CONSISTENT FUZZY PREFERENCE RELATIONS

The decision information is frequently represented with the system of preference relations in many decision-making approaches. Herrera-Viedma et al. [11] proposed the consistent fuzzy preference relations, with the ability which not only enables decision makers to express preferences over a set of alternatives with the least judgments, but also avoids checking the inconsistency in decision-making process. Wang and Parkan [12] investigated the aggregation of fuzzy preference relations with an application to broadband internet service selection. Wang and Chen [13] applied fuzzy linguistic preference relations to improve the inconsistency of fuzzy AHP. Chao and Chen [14] evaluated the criteria and effectiveness of distance e-learning with consistent fuzzy preference relations. Chang and Wang [15] measured the success possibility of implementing advanced manufacturing technology by utilizing the consistent fuzzy preference relations. Wang and Chang [16] applied the consistent fuzzy preference relations in predicting the success of knowledge management implementation. Wang and Chang [17] forecasted the probability of successful knowledge management by consistent fuzzy preference

978-1-4244-7316-8/11/$26.00 ©2011 IEEE

relations. Wang and Chen [18] applied the consistent fuzzy preference relations to partnership selection. Wang and Lin [19] applied consistent fuzzy preference relations to select merger strategy for commercial banks in new financial environments. The following briefly describes some definitions and propositions discussed in [20-28].

Given $X=\{x_1,x_2,...,x_n,\ n\geq 2\}$ be a finite set of alternatives to be pairwise assessed by a finite set of experts ($E=\{e_1,e_2,...,e_m,\ m\geq 2\}$). We can assume that the experts' preferences toward the set of alternatives X may be expressed in the following ways [29]:

(1) ***Multiplicative preference relation***. A multiplicative preference relation A on a set of alternatives X is indicated by a matrix $A\subset X\times X$, $\mathrm{A}=(a_{ij})$, a_{ij} is the ratio of the preference degree of alternative x_i over alternative x_j, A is assumed multiplicative reciprocal, that is

$$a_{ij}\otimes a_{ji}=1\ \ \forall i,j\in\{1,...,n\} \tag{1}$$

(2) ***Additive fuzzy preference relation***. An expert's preferences on a set of alternatives X is denoted by a positive preference relation matrix $P\subset \mathrm{X}\times\mathrm{X}$, with membership function: $\mu_p:\mathrm{X}\times\mathrm{X}\to[0,\ 1]$, where $\mu_p(x_i,x_j)=p_{ij}$ indicates the ratio of the preference intensity of alternative x_i over alternative x_j. If $p_{ij}=\frac{1}{2}$ implies indifference between x_i and x_j ($x_i\sim x_j$), $p_{ij}=1$ indicates x_i is absolutely preferred to x_j, $p_{ij}=0$ indicates x_j is absolutely preferred to x_i. P is assumed additive reciprocal, given by

$$p_{ij}+p_{ji}=1\ \ \forall i,j\in\{1,...,n\} \tag{2}$$

Suppose there is a set of alternatives being associated with a multiplicative preference relation $\mathrm{A}=(a_{ij})$ with $a_{ij}\in[\frac{1}{9},\ 9]$. Then the corresponding fuzzy preference relation $P=(p_{ij})$ with $p_{ij}\in[0,\ 1]$ to $\mathrm{A}=(a_{ij})$ is defined as:

$$p_{ij}=g(a_{ij})=\tfrac{1}{2}(1+\log_9 a_{ij}) \tag{3}$$

A consistent fuzzy preference relation P' on $X=\{x_1,x_2,...,x_n,\ n\geq 2\}$ from $n-1$ preference values $\{p_{12},p_{23},...,p_{n-1n}\}$ can be constructed as follow.

$$B=\{p_{ij},i<j\wedge p_{ij}\notin\{p_{12},p_{23},...,p_{n-1n}\}\} \tag{4}$$

$$p_{ji}=\frac{j-i+1}{2}-p_{ii+1}-p_{i+1i+2}\cdots-p_{j-1j} \tag{5}$$

$$a=\left|\min\{B\cup\{p_{12},p_{23},...,p_{n-1n}\}\}\right| \tag{6}$$

$$P=\{p_{12},...,p_{n-1n}\}\cup B\cup\{1-p_{12},...,1-p_{n-1n}\}\cup\neg B \tag{7}$$

$$f:[-a,\ 1+a]\to[0,\ 1],\quad f(x)=\frac{x+a}{1+2a} \tag{8}$$

III. Framework to Evaluate Hospital Service Quality by Using Fuzzy Preference Relations

This section proposes an analytic hierarchy model based on fuzzy preference relations to evaluate the hospital service quality. The procedures consist of: determining the importance weights of evaluation criteria, evaluating the performance rating of feasible hospitals with respect to each criterion, and ranking the alternative hospitals.

A. Identify the evaluation criteria for hospital service quality

The evaluation criteria are derived through literature review [2], widespread investigation and consultation with several experts. They are: ***hospital environment*** (C_1:well-equipped medical equipment, warm and comfortable environment in the hospital, clear marked signs in the hospital); ***service attitude*** (C_2: tidy appearance of service personnel, service personnel with good communication skills, caring attitude of medical staff, cordial attitude of service personnel); ***pharmacy treatment*** (C_3: pharmacist's advices on taking medicine, medicine preservation advices by pharmacists, feeling a sense of security when medical services are provided); ***professional capability*** (C_4: medical staff with professional abilities, trusted medical staff with professional competence of health care, detailed description of the patient's condition by the medical doctor, service personnel with immediate problem-solving abilities) and ***administrative policy*** (C_5: ease of use of hospital reservation system, operating procedures of the emergency room, exact outpatient locations guided by service personnel, patient meals services, outpatient drug-picking services, outpatient waiting time for medical treatment, processes of hospitalized services).

B. Determining the importance weight of evaluation criterion

This study provides the evaluators linguistic variables quantified in a scale of $[\frac{1}{9},\ 9]$ to express their preferences toward the importance weights of evaluation criteria (see Table I) and the performance rating of feasible alternatives (see Table II) with respect to each criterion [30]. Fuzzy preference relations proposed by Herrera -Viedma et al. [11] are employed in this study since it constructs a complete preference relation matrix that has n elements with the least ($n-1$) pairwise comparisons.

TABLE I
LINGUISTIC VARIABLES FOR THE IMPORTANCE WEIGHT OF CRITERIA

Definition	Intensity of importance
Equally important (EQ)	1
Weakly more important (WK)	3
Strongly more important (ST)	5
Very strongly more important (VS)	7
Absolutely more important (AB)	9
Intermediate values presenting compromise	2,4,6,8

TABLE II
LINGUISTIC VARIABLES FOR THE PERFORMANCE RATING OF ALTERNATIVES

Definition	Intensity of importance
Medium good (M)	1
Fairly good (FG)	3
Good (G)	5
Very good (VG)	7
Absolutely good (AG)	9
Intermediate values presenting compromise	2,4,6,8

(1) The evaluators (E_k, $k=1,2,...,m$) are asked which is the more important of each two adjoining evaluation criteria (C_i, $i=1,2,...,n$) for a set of $n-1$ preference values $\{a_{12}, a_{23}, ..., a_{n-1n}\}$, for example

$$A^k = \begin{array}{c} \\ C_1 \\ C_2 \\ C_3 \\ \vdots \\ C_n \end{array} \begin{array}{c} \begin{array}{ccccc} C_1 & C_2 & C_3 & \cdots & C_n \end{array} \\ \begin{bmatrix} 1 & a_{12}^k & \times & \times & \times \\ \times & 1 & a_{23}^k & \times & \times \\ \times & \times & 1 & a_{34}^k & \times \\ \vdots & \vdots & \vdots & \ddots & a_{n-1n}^k \\ \times & \times & \times & \times & 1 \end{bmatrix} \end{array} \tag{9}$$

where a_{ij}^k denotes the preference intensity toward criterion i and criterion j assessed by k^{th} evaluator. The sign "×" indicates the remaining a_{ij}^k which can be obtained by inverse comparison methods.

(2) Use Eq. (3) to transform the preference value $a_{ij}^k \in [\frac{1}{9}, 9]$ into $p_{ij}^k \in [0, 1]$. The remaining p_{ij}^k can be calculated using Eqs. (2) and (5). If this preference matrix contains any values that are not included in the interval $[0, 1]$, then a transformation function is required to preserve the reciprocity and additive transitivity, given by

$$f(p_{ij}^k) = \frac{p_{ij}^k + a}{1+2a}, \tag{10}$$

where $a = \left|\min\{p_{12}, p_{23}, ..., p_{n-1n}\}\right|$

(3) Utilize the method of average value to integrate the judgments of m evaluators, namely

$$p_{ij} = \frac{1}{m}(p_{ij}^1 + p_{ij}^2 + ... + p_{ij}^m) \tag{11}$$

(4) Use r_{ij} to indicate the normalized fuzzy preference value of each criterion, such as

$$r_{ij} = \frac{p_{ij}}{\sum_{i=1}^{n} p_{ij}}, \quad i,j = 1,2,\ldots,n \tag{12}$$

(5) Given the ϖ_i denoting the importance weight of evaluation criterion i, the importance weight of which is obtained by

$$\varpi_i = \frac{\sum_{j=1}^{n} r_{ij}}{\sum_{i=1}^{n}\sum_{j=1}^{n} r_{ij}} \tag{13}$$

C. Evaluating the performance rating of feasible alternatives with respect to each criterion

The evaluators are invited to express their subjective judgments regarding the performance ratings of feasible alternatives (A_u, $u=1,2,...,t$) with respect to each criterion by using linguistic variables, as listed in Table II.

(1) Under each criterion, the evaluators are asked to compare the performance rating of adjoining alternatives for a set of $t-1$ preference data $\{b_{12}, b_{23}, ..., b_{t-1t}\}$, for example

$${}_iB = \begin{array}{c} \\ A_1 \\ A_2 \\ A_3 \\ \vdots \\ A_t \end{array} \begin{array}{c} \begin{array}{ccccc} A_1 & A_2 & A_3 & \cdots & A_t \end{array} \\ \begin{bmatrix} 1 & {}_ib_{12}^k & \times & \times & \times \\ \times & 1 & {}_ib_{23}^k & \times & \times \\ \times & \times & 1 & {}_ib_{34}^k & \times \\ \vdots & \vdots & \vdots & \ddots & {}_ib_{t-1t}^k \\ \times & \times & \times & \times & 1 \end{bmatrix} \end{array} \tag{14}$$

where ${}_ib_{uv}^k$ represents the performance rating assessed by k^{th} evaluator for alternative A_u and alternative A_v with respect to evaluation criterion i.

(2) Using Eq. (3), the performance rating ${}_ib_{uv}^k$ is transformed into ${}_iq_{uv}^k$ in a scale $[0, 1]$. If this preference matrix contains any values that are not included in the interval $[0, 1]$, then a transformation function is required, given by

$$f({}_iq_{uv}^k) = \frac{{}_iq_{uv}^k + a}{1+2a}, \tag{15}$$

where $a = \left|\min\{q_{12}, q_{23}, ..., q_{t-1t}\}\right|$

(3) Synthesize the different judgments of m evaluators, namely

$${}_iq_{uv} = \frac{1}{m}({}_iq_{uv}^1 + {}_iq_{uv}^2 + ... + {}_iq_{uv}^m) \tag{16}$$

(4) Take ${}_i\lambda_u$ to indicate the normalized performance rating of alternative A_u with respect to evaluation criterion i.

$${}_i\lambda_u = \frac{{}_iq_{uv}}{\sum_{u=1}^{t}\sum_{v=1}^{t} {}_iq_{uv}}, \quad u,v = 1,2,\ldots,t \tag{17}$$

D. Ranking the alternatives

Ranking the alternatives by the performance value Q which is defined as

$$Q_u = \sum_{i=1}^{n} {}_i\lambda_u \varpi_i \tag{18}$$

where ϖ_i is the importance weight of evaluation criterion i, and the best alternative is the one which has the largest performance value Q.

IV. EMPERICAL ANALYSIS

This study chooses 4 public hospitals located in southern Taiwan to be evaluated by 5 evaluators according to 5 major evaluation criteria (including 21 sub-criteria). Analytic hierarchy selections based on the fuzzy preference relations are adopted to solve this multiple criteria performance evaluation problem. The computations of this proposed framework are described as follows.

A. Weighting calculation for evaluation criteria

Pairwise comparisons for these 5 major evaluation criteria are obtained via a series of interviews with 5 evaluators. The following examples clarify the computational process involved in obtaining the importance weights of evaluation criteria using the consistent fuzzy preference relations.

(1) The pairwise comparison matrices derived from 5 evaluators for a set of 4 adjoining evaluation criteria $\{a_{12}, a_{23}, a_{34}, a_{45}\}$ are listed in Table III.

TABLE III
LINGUISTIC TERMS ASSIGNED FOR 5 CRITERIA BY 5 EVALUATORS

	E_1	E_2	E_3	E_4	E_5	
C_1	VT	LVS	LVS	LST	LAB	C_2
C_2	ST	AB	LST	VS	SW	C_3
C_3	LAB	LVLA	LAB	LVS	LVS	C_4
C_4	AB	VS	AB	AV	VS	C_5

(2) Using Eq. (3) to transform the linguistic variables quantified in $[\frac{1}{9}, 9]$ listed in Table III into an interval $[0, 1]$, taking E_1 as an example and yielding the following values:

$a_{12} = VT = 6$, $p_{12} = (1+\log_9 6)/2 = 0.908$
$a_{23} = LST = \frac{1}{5}$, $p_{23} = (1+\log_9 \frac{1}{5})/2 = 0.134$
$a_{34} = \mathrm{LVS} = \frac{1}{7}$, $p_{34} = (1+\log_9 \frac{1}{7})/2 = 0.057$
$a_{45} = VS = 7$, $p_{45} = (1+\log_9 7)/2 = 0.943$

(3) Using Eq. (11), the aggregated pairwise comparison matrix is obtained. The result is shown in Table IV.

TABLE IV
AGGREGATIVE MATRIX OF IMPORTANCE WEIGHT OF CRITERIA

	C_1	C_2	C_3	C_4	C_5
C_1	2.500	1.405	2.674	0.913	2.672
C_2	3.595	2.500	3.768	2.008	3.767
C_3	2.326	1.232	2.500	0.740	2.498
C_4	4.087	2.992	4.260	2.500	4.259
C_5	2.328	1.233	2.502	0.741	2.500
Total	14.836	9.362	15.704	6.902	15.696

(4) The importance weight and rank of each evaluation criterion is then obtained by Eqs. (12) & (13), and the results are listed in Table V. Taking ϖ_1 as an example,

$$r_{11} = \frac{2.5}{2.5 + 3.595 + 2.326 + 4.087 + 2.328} = 0.169$$

$$\varpi_1 = \frac{0.169 + 0.150 + 0.286 + 0.132 + 0.170}{0.907 + 1.443 + 0.822 + 1.684 + 0.822} = 0.160$$

TABLE V
NORMALIZED MATRIX OF IMPORTANCE WEIGHT AND RANK OF EVALUATION CRITERIA

	C_1	C_2	C_3	C_4	C_5	Weight (ϖ_i)	Rank
C_1	0.169	0.150	0.286	0.132	0.170	0.160	**3**
C_2	0.242	0.267	0.403	0.291	0.240	0.254	**2**
C_3	0.157	0.132	0.267	0.107	0.159	0.145	**5**
C_4	0.275	0.320	0.455	0.362	0.271	0.297	**1**
C_5	0.157	0.132	0.267	0.107	0.159	0.145	**4**

The results show that the importance order of 5 evaluation criteria is: professional capability (0.297) > service attitude (0.254) > hospital environment (0.160) > administrative policy (0.145) > pharmacy treatment (0.145).

B. Calculation the performance rating of feasible hospitals with respect to criteria

The performance rating of 4 feasible hospitals is calculated as follows.

(1) These 5 evaluators are interviewed to assess which hospital is better than another according to each evaluation criterion. The linguistic variables derived from Evaluator 1 are used as examples and listed in Table VI. The linguistic terms are translated into corresponding numbers, then into the interval $[\frac{1}{9}, 9]$ and finally in $[0, 1]$.

(2) Since there are values in Table VII are not in the range of $[0, 1]$, this study uses Eq. (15) to transform the values. The transformed results are shown in Table VIII. We find that the absolute vale of minimum in Table VII is 0.158, so the $f({}_1q_{12}^1) = \frac{0.057 + 0.158}{1 + 2 * 0.158} = 0.163$.

(3) Use Eq. (16) to aggregate the different evaluators' preference, the aggregated decision matrix is shown in Table IX.

(4) Using Eq. (17) to normalize the performance rating of 4 feasible hospitals with respect to evaluation criteria. The results are listed in Table IX.

TABLE VI
EVALUATOR 1 PAIWISE COMPARES THE ALTERNATIVE IN CRITERION 1 WITH LINGUISTIC VARIABLES

	E_1	A1	A2	A3	A4
C_1	A1	X	LVG		
	A2		X	MF	
	A3			X	AG
	A4				X

TABLE VII
LINGUISTIC TERMS TRANSLATED INTO NUMBER

	E_1	A1	A2	A3	A4
C_1	A1	0.500	0.057	0.215	0.715
	A2	0.943	0.500	0.658	**1.158**
	A3	0.785	0.342	0.500	1.000
	A4	0.285	**-0.158**	0.000	0.500

TABLE IX
AGGREGATED AND NORMALIZED DECISION MATRIX

		A1	A2	A3	A4	NORM
C_1	A1	2.500	1.499	0.740	1.431	0.154
	A2	3.501	2.500	1.741	2.431	0.254
	A3	4.260	3.259	2.500	3.190	0.330
	A4	3.569	2.569	1.810	2.500	0.261
		A1	A2	A3	A4	NORM
C_2	A1	2.500	3.393	1.921	2.653	0.262
	A2	1.607	2.500	1.029	1.760	0.172
	A3	3.079	3.971	2.500	3.231	0.320
	A4	2.347	3.240	1.769	2.500	0.246
		A1	A2	A3	A4	NORM
C_3	A1	2.500	3.225	2.445	4.300	0.312
	A2	1.775	2.500	1.720	3.575	0.239
	A3	2.555	3.280	2.500	4.355	0.317
	A4	0.700	1.425	0.645	2.500	0.132
		A1	A2	A3	A4	NORM
C_4	A1	2.500	2.804	2.450	2.807	0.264
	A2	2.196	2.500	2.146	2.502	0.234
	A3	2.550	2.854	2.500	2.856	0.269
	A4	2.193	2.498	2.144	2.500	0.233
		A1	A2	A3	A4	NORM
C_5	A1	2.500	3.290	1.799	2.583	0.254
	A2	1.710	2.500	1.009	1.793	0.175
	A3	3.201	3.991	2.500	3.284	0.324
	A4	2.417	3.207	1.716	2.500	0.246

**NORM: Normalization value*

TABLE VIII
TRANSFORMED NUMBERS

	E_1	A1	A2	A3	A4
C_1	A1	0.500	0.163	0.283	0.663
	A2	0.837	0.500	0.620	**1.000**
	A3	0.717	0.380	0.500	0.880
	A4	0.337	**0.000**	0.120	0.500

C. *Ranking the performance degree of hospitals*

Using Eq. (18) to multiply the importance weights of evaluation criteria by the performance ratings of feasible hospitals, an aggregative performance value Q_u for hospital A_u is obtained. Generally speaking, the performance value is the-larger-the-better. Taking Q_3 as an example,

$$Q_3 = (0.160\times0.330\ ) + (0.254\times0.320\ ) + (0.145\times0.317\ ) + (0.297\times0.269\ ) + (0.145\times0.324\ ) = 0.307$$

The performance values of 4 feasible hospitals are listed in Table X. The ranking of 4 hospitals is Q3>Q1>Q4>Q2. The best hospital is A3.

TABLE X
PERFORMANCE VALUE AND RANK OF 4 HOSPITALS

	A1	A2	A3	A4
Q	0.251	0.214	0.307	0.228
Rank	**2**	**4**	**1**	**3**

V. CONCLUSION

Good service quality is a significant factor leads to the success of a hospital operation and management. The proposed approach is based on the reciprocal additive consistent fuzzy preference relations, rather than using conventional multiplicative preference relation. Namely, this method considers only $n-1$ pairwise comparisons, whereas the traditional AHP takes $\frac{n(n-1)}{2}$ judgments in a preference matrix with n elements, it is clear that the proposed approach is faster to execute and more efficient than the conventional pairwise comparison methods. According to the importance weights of evaluation criteria, the professional capability and service attitude are more important than other criteria. Furthermore, this proposed method is proved to be applicable in solving the multiple criteria decision making problems.

ACKNOWLEDGMENT

The author would like to thank the National Science Council of the Republic of China, Taiwan for financially supporting this research under Contract No. NSC 98-2410-H-244-002-MY2.

REFERENCES

[1] S. J. Welch and T. L. Allen, "Data-driven quality improvement in the Emergency Department at a level one trauma and tertiary care hospital," Journal of Emergency Medicine, vol. 30, pp. 269-276, 2006.

[2] J.-I. Shieh, H.-H. Wu, and K.-K. Huang, "A DEMATEL method in identifying key success factors of hospital service quality," Knowledge-Based Systems, vol. 23, pp. 277-282, 2010.

[3] H.-h. Chang, "Determinants of Hospital Efficiency: the Case of Central Government-owned Hospitals in Taiwan," Omega, vol. 26, pp. 307-317, 1998.

[4] S. S. Andaleeb, "Service quality in public and private hospitals in urban Bangladesh: a comparative study," Health Policy, vol. 53, pp. 25-37, 2000.

[5] L. X. Li, "Relationships between determinants of hospital quality management and service quality performance--a path analytic model," Omega, vol. 25, pp. 535-545, 1997.

[6] P. S. Raju and S. C. Lonial, "The impact of service quality and marketing on financial performance in the hospital industry: an empirical

examination," Journal of Retailing and Consumer Services, vol. 9, pp. 335-348, 2002.
[7] S. S. Andaleeb, "Service quality perceptions and patient satisfaction: a study of hospitals in a developing country," Social Science & Medicine, vol. 52, pp. 1359-1370, 2001.
[8] L. X. Li, W. C. Benton, and G. K. Leong, "The impact of strategic operations management decisions on community hospital performance," Journal of Operations Management, vol. 20, pp. 389-408, 2002.
[9] L. E. Goldman and R. A. Dudley, "United States rural hospital quality in the Hospital Compare database--Accounting for hospital characteristics," Health Policy, vol. 87, pp. 112-127, 2008.
[10] H.-Y. Tsai, C.-W. Chang, and H.-L. Lin, "Fuzzy hierarchy sensitive with Delphi method to evaluate hospital organization performance," Expert Systems with Applications, vol. 37, pp. 5533-5541, 2010.
[11] E. Herrera-Viedma, F. Herrera, F. Chiclana, and M. Luque, "Some issues on consistency of fuzzy preference relations," European Journal of Operational Research, vol. 154, pp. 98-109, 2004.
[12] Y.-M. Wang and C. Parkan, "Optimal aggregation of fuzzy preference relations with an application to broadband internet service selection," European Journal of Operational Research, vol. 187, pp. 1476-1486, 2008.
[13] T.-C. Wang and Y.-H. Chen, "Applying fuzzy linguistic preference relations to the improvement of consistency of fuzzy AHP," Information Sciences, vol. 178, pp. 3755-3765, 2008.
[14] R.-J. Chao and Y.-H. Chen, "Evaluation of the criteria and effectiveness of distance e-learning with consistent fuzzy preference relations," Expert Systems with Applications, vol. 36, pp. 10657-10662, 2009.
[15] T.-H. Chang and T.-C. Wang, "Measuring the success possibility of implementing advanced manufacturing technology by utilizing the consistent fuzzy preference relations," Expert Systems with Applications, vol. 36, pp. 4313-4320, 2009.
[16] T.-C. Wang and T.-H. Chang, "Application of consistent fuzzy preference relations in predicting the success of knowledge management implementation," European Journal of Operational Research, vol. 182, pp. 1313-1329, 2007.
[17] T.-C. Wang and T.-H. Chang, "Forecasting the probability of successful knowledge management by consistent fuzzy preference relations," Expert Systems with Applications, vol. 32, pp. 801-813, 2007.
[18] T.-C. Wang and Y.-H. Chen, "Applying consistent fuzzy preference relations to partnership selection," Omega, vol. 35, pp. 384-388, 2007.
[19] T.-C. Wang and Y.-L. Lin, "Applying the consistent fuzzy preference relations to select merger strategy for commercial banks in new financial environments," Expert Systems with Applications, vol. 36, pp. 7019-7026, 2009.
[20] F. Chiclana, F. Herrera, and E. Herrera-Viedma, "Integrating three representation models in fuzzy multipurpose decision making based on fuzzy preference relations," Fuzzy Sets and Systems, vol. 97, pp. 33-48, 1998.
[21] F. Chiclana, F. Herrera, and E. Herrera-Viedma, "Integrating multiplicative preference relations in a multipurpose decision-making model based on fuzzy preference relations," Fuzzy Sets and Systems, vol. 122, pp. 277-291, 2001.
[22] F. Herrera and E. Herrera-Viedma, "Choice functions and mechanisms for linguistic preference relations," European Journal of Operational Research, vol. 120, pp. 144-161, 2000.
[23] F. Herrera, E. Herrera-Viedma, and F. Chiclana, "Multiperson decision-making based on multiplicative preference relations," European Journal of Operational Research, vol. 129, pp. 372-385, 2001.
[24] F. Herrera, E. Herrera-Viedma, and J. L. Verdegay, "A sequential selection process in group decision making with a linguistic assessment approach," Information Sciences, vol. 85, pp. 223-239, 1995.
[25] F. Herrera, E. Herrera-Viedma, and J. L. verdegay, "A model of consensus in group decision making under linguistic assessments," Fuzzy Sets and Systems, vol. 78, pp. 73-87, 1996.
[26] F. Herrera, E. Herrera-Viedma, and J. L. Verdegay, "A rational consensus model in group decision making using linguistic assessments," Fuzzy Sets and Systems, vol. 88, pp. 31-49, 1997.
[27] T. Tanino, "Fuzzy preference orderings in group decision making," Fuzzy Sets and Systems, vol. 12, pp. 117-131, 1984.
[28] Z. Switalski, "General transitivity conditions for fuzzy reciprocal preference matrices," Fuzzy Sets and Systems, vol. 137, pp. 85-100, 2003.
[29] F. Chiclana, F. Herrera, E. Herrera-Viedma, and L. Martínez, "A note on the reciprocity in the aggregation of fuzzy preference relations using OWA operators," Fuzzy Sets and Systems, vol. 137, pp. 71-83, 2003.
[30] T. L. Saaty, "Exploring the interface between hierarchies, multiple objectives and fuzzy sets," Fuzzy Sets and Systems, vol. 1, pp. 57-68, 1978.

2011 IEEE International Conference on Fuzzy Systems
June 27-30, 2011, Taipei, Taiwan

Structural Analysis on Team Internal Soft Factors to Project Success

Don Jyh-Fu Jeng
Institute of International Management
National Cheng Kung University
Tainan, Taiwan
jeng@mail.ncku.edu.tw

***Abstract*—Project has witnessed a high rate of failure. The project management is concerned with disciplines that better manage the project inherent strengths and weaknesses. In contrast to the hard factors, soft factors are very often ignored during project management. Such factors, involved with the internal services within the team, are concerned with working with people, ensuring customer satisfaction and creating a conducive environment for the project team to deliver high quality products which meeting stakeholder expectations. This research aims to investigate the intertwined effects of project team internal soft factors. Combining the exploratory factor analysis and fuzzy decision making trial and evaluation laboratory (DEMATEL) technique, an empirical case is demonstrated to show the effectiveness of the proposed method. The exploratory factor analysis is applied for extracting the dimension and criteria structure. The fuzzy DEMATEL technique is then used to analyze the intertwined effect. The proposed method has proven to be an effective one for analyzing the complex interrelation of human psychological concerns.**

Keywords-exploratory factor analysis, decision making trial and evaluation laboratory (DEMATEL), fuzzy logic, project management, internal service.

I. INTRODUCTION

Project management is important in order to control projects throughout the entire project life cycle and to eventually lead to project success and better project performance. It can also have "strategic value when a clear connection is made between how efficiently and effectively a project is done and how the project's products and services provide business value" [23] (p.19). In order to properly manage a project, it is necessary to understand the controllable factors and its intertwined effects that impact the project team's performance.

There has been a significant amount of research done on project success factors within the Western cultural settings (e.g. [1],[6],[37],[38]). However, most of these researches focused on the team hard factors and rarely discuss how soft factors internally in the project team may influence the overall project success. Hard factors relate to technical abilities in implementing the project, while soft factors relate to teamwork and interpersonal skills. Soft factors are often neglected in previous studies; however, it plays significant in project success.

As culture impacts the values and norms [15][20], the culture setting must be taken into consideration when investigating impact factors in non-Western settings. No research has been found that investigate the impact of soft factors have within a Chinese cultural setting on project performance. In addition, the research of soft skills on project management has rarely seen in the literatures. Understand the intertwined effects of soft factors on project success is critical to managers who conduct projects. These criteria that affecting that project success are numerous and influence one another.

The purpose of this paper is to first indentify the hierarchy structure of soft skills that influence on project success and then analyze the intertwined effects between the criteria. Exploratory factor analysis is applied to generate the independent factors/criteria. Then, the DEMATEL (Decision Making Trial and Evaluation Laboratory) technique [10][11] is adopted. In recent years, a number of scholars have proposed Multiple Criteria Decision-Making (MCDM) theories to strengthen the comprehensiveness and reasonableness of the decision-making process [28][46][50], and DEMATEL technique is commonly used to illustrate the interrelations among criteria.

The remainder of this paper is organized as follows. The research background and literature reviews on factors that impact project performance are presented in Section 2. In Section 3, a brief introduction of exploratory factor analysis and the fuzzy DEMATEL technique is given. An empirical study in the case of soft factors on project success is presented in Section 4, while a hierarchy structure with dimension and criteria is proposed and its intertwined effects is analyzed by fuzzy DEMATEL. In Section 5, the analysis result is discussed and the implication is drawn. Finally, the concluding remarks are presented in Section 6.

II. FACTORS IMPACT PROJECT PERFORMANCE

Project performance metrics can be viewed as the key attributes and objectives which must be met or reached to consider a project successful [27]. Most researchers agree that time, cost, and quality should be used as performance metrics and the key determinants of project success [1][6] [7][27][37][47]. However, many agree that success criteria should not be limited to the iron triangle of time, cost, and quality [1][27][29][47].

978-1-4244-7316-8/11/$26.00 ©2011 IEEE

A team's project performance is influenced by factors both external and internal to the team, while culture and soft factors are highly impacted.

A. Cultural Context

Culture, both national and corporate [16], can be defined as "the collective programming of the mind which distinguishes the members of one group or society from those of another" (p. 82). Within each nation, there can be dominant groups and non-dominant groups. All the groups will have their own and sometimes similar group-ideologies, beliefs, and values, but the national culture will resemble the largest or more influential dominant group's. Therefore, it is vital to understand the dominant group's underlying views if one is to gain a general understanding of the views of the people within that culture [44]. As previous studies have taken place in Western cultural settings, their findings are not adequate when applying in the Chinese cultural context, which is highly influenced by the teachings of Confucius. "Confucian social theory is concerned with the question of how to establish a harmonious secular order in the man-centered world" [25](p.65). The term guanxi (role-relationship) is deeply embedded in Confucian social theory and uses the term architect to refer to Confucian individuals who build their guanxi throughout their life, creating their own social networks outside their family structure [19][25].

In Taiwan, Hofstede's [15] study has found that in supporting the Confucianism regarding unequal relationships, it was found to rank on the higher end of power distance, meaning hierarchal structures are common. For the Confucianism regarding the importance of upholding 'he', or harmony, Hofstede [15] showed that the Taiwanese culture leans toward collectivism rather than individualism, meaning that individuals are focused on the group's interest rather than their individual self. This is further supported by the findings of Gao [12], who conducted a study on understanding Chinese speaking practices, and found that in the Chinese culture the self involves and is made up of multiple relationships. For Hofstede's [15] last two dimensions (*i.e.* uncertainty avoidance and masculinity), Taiwanese would prefer to avoid uncertainty and show characteristics of both masculinity and femininity as the masculinity score is modest. Further studies have confirmed that both the Confucian values and cultural dimensions are reflected in the work values that Taiwanese employees hold [16][17].

B. Soft Factors

A team's project performance will depend heavily on how well the team works together. The factors that impact these dynamics are the relationships between the team members, and the perceived quality of the 'internal services' between the team members as work flows between them. The scope of the internal-team factors for this study is limited to interactions and relationships between project group members.

In terms of work-flow, McGrath's [32] paper on the theory of group's assumes groups to be "complex, intact social systems…that engage in purposeful activity at three partially nested levels: projects, tasks, and steps" (p. 151). It is thus clear that work may flow from one team member to the next at the level of steps and tasks. This work-flow is an internal service between the team members, and the interaction related to the work being passed on to the next step is the service encounter. The service encounter can be viewed as the "dyadic interaction between an internal customer and an internal service provider" [13](p.35).

The perceived quality of the service encounter is evaluated by an internal customer after the service encounter takes place, whereby an internal customer evaluates the individual internal service quality attributes to gain an overall perception of the quality of the service encounter [13]. Improving and managing this perceived quality is important for organizations since researchers have found linkages between high levels of internal service quality (ISQ) and higher productivity, improved relationships between departments and groups, lower employee turnover, increased external customer satisfaction, and increased profits [13][35] [36][39][41].

While previous studies have mostly applied western internal service quality attributes to the Taiwanese setting (e.g. [8][9][28][30]), as an organization's culture – which is based largely on national culture – has a direct impact on the internal service providers and internal customers' values, norms, behavior, or even way of thinking [4][20][42], using Western attributes in an Eastern cultural setting could produce inadequate results as cultural differences create unique work places with different views, values, practices, etc. [16]. To overcome this limitation, Stanworth et al. [43] developed the internal service quality attribute that is Taiwanese context based, which 29 service quality attributes were derived.

As stated, Confucianism is shown to have an undisputable impact on the national and organizational culture of Taiwan, where it is important to maintain harmony within relationships [16]. Furthermore, studies related to group project performance within the Chinese context have shown that focusing on creating friendly relationships within organizations and groups can positively impact project performance by increasing their odds of success [22][24], while Bromiley and Cummings [2] found that a harmonious relationship based on trust can lead to lower costs and shorter durations when conducting business. Thus, as relationships play a major role within Taiwan due to the Confucian influence. Furthermore, Katz [24] found that high levels of internal communication between all project members will lead to higher project performance.

Based on the above literature reviews, this research adopts Stanworth et al.'s [43] internal service quality structure and slightly modified as follows: two items are removed when changing the negative attributes to a positive (Incomplete Professional Knowledge and Quarrel), as they are in fact a polar opposites of positives already present (Detailed Professional Knowledge and Consensus), and one item is expanded into two separate items (Work Loading to Work Loading and Accessible) to better capture the complexity of the attribute. This leaves a total of 26 attributes. In addition, Pinto and Prescott's [37] two trouble-shooting attributes (trouble-shooting and handle deviations), and Jin and Ling's [22] seven relationship attributes were added to our list. Thus, the final scale to be investigated in this study is made up of 35 team internal soft factors includes friendly (chin-chieh), polite (ke-

chi), patience, positive/proactive (jiji), responsible, trouble-shooting, handle deviations, please supervisor, competent, effective, detailed and professional knowledge, consensus, shows empathy, shared objective, considerate, reliable, internal efficiency, external efficiency, harmony, personnel connection, emotionally stable, internal communication, litigation, risk exposure, change orders and claims, mutual understanding, client satisfaction, learning culture, help each other, cooperation, coordination, work loading, accessible, bureaucracy, exchange thoughts.

III. Building a Structural Model

In reality, it is difficult to quantify a precise value in human psychological feeling. However, the complex phenomenon can be divided into many criteria to more easily judge differences or measure scores of the divided criteria. The exploratory factor analysis method is commonly used to gather criteria into groups. These criteria may have interdependent relationships; therefore, the DEMATEL technique is used to construct the interrelations between criteria.

A. Finding Independent Factors for Building a Hierarchical System

Based on the suitable measuring method, the criteria can be categorized into distinct aspects. When the evaluated criteria are too large to determine the dependent or independent relation with others, using factor analysis can verify independent factors.

Exploratory factor analysis is a dimension reduction method of multivariate statistics, which explores the latent variables from manifest variables. It is used to uncover the underlying structure of a relatively large set of variables. The main procedure of exploratory factor analysis can be described in the following steps:

Step 1: Find the correlation matrix (***R***) or variance-covariance matrix for the objects to be assessed.

Step 2: Find the eigenvalues $(\lambda_k, k = 1, 2, \ldots, m)$ and eigenvectors $(\beta_k = [\beta_{1k}, \ldots, \beta_{ik}, \ldots, \beta_{pk}])$ for assessing the factor loading $(a_{ik} = \sqrt{\lambda_k}\beta_{ik})$ and the number of factors (m).

Step 3: Consider the eigenvalue ordering $(\lambda_1 > \cdots > \lambda_k > \cdots > \lambda_m; \lambda_m > 1)$ to decide the number of common factors, and pick the number of common factors to be extracted by a predetermined criterion.

Step 4: To facilitate the interpretation of factors, choose a rotation methods. In this study, the promax rotation method is applied which allows the factors to be correlated.

Step 5: Name the factor referring to the combination of manifest variables.

When a large set of variables are factored, the method first extracts the combinations of variables, explaining the greatest amount of variance, and then proceeds to combinations that account for progressively smaller amounts of variance. Two kinds of criteria are used for selecting the number of factors: latent root criterion and percentage of variance criterion. The former criterion is that any individual factor should account for the variance $(\mathrm{Var}(Y_k) = \lambda_k)$ of at least a single variable if it is to be retained for interpretation. In this criterion only the factors having eigenvalues greater than 1 (*i.e.* $\lambda_k \geq 1, k = 1, 2, \ldots, m$) are considered significant. The latter criterion is based on achieving a specified cumulative percentage of total variance extracted by successive factors. Its purpose is to ensure the extracted factors can explain at least a specified amount of variance. Practically, to be satisfactory the total amount of variance explained by factors should be at least 95% in the natural sciences, and 60% in the social sciences. However, no absolute threshold has been adopted for all applications [14].

B. Fuzzy DEMATEL Technique for Building Structural Model

DEMATEL [10][11] is a comprehensive method for building and analyzing a structural model involved of causal relationships between complex factors. It was developed in the belief that the proper use of scientific research methods could facilitate comprehension of the specific problematique, the cluster of intertwined problems, and contribute to recognition of practical solutions by a hierarchical structure. The methodology, according to the characteristics of objective affairs, can verify the interdependence among the variables/attributes/criteria and confine the relation that reflects the characteristics with an essential system and evolution trend [5][18]. The method is a practical and useful tool, especially for visualizing the structure of complex causal relationships with matrices or digraphs. The matrices or digraphs show a contextual relation between the elements of the system, in which a numeral represents the strength of influence of each element. Thus, the DEMATEL technique is able to convert the relationship between the causes and effects of criteria into an intelligible structural model of systems [48].

Fuzzy set theory can be efficiently dealt with the vagueness of human thought and expression in making decisions. To tackle the ambiguities involved in the process of decision-making, the linguistic terms can be more effective in estimation.

A fuzzy set $\widetilde{A}$ is a subset of a universe of discourse X, which is a set of ordered pairs and is characterized by a membership function $\mu_{\widetilde{A}}(x)$ representing a mapping $\mu_{\widetilde{A}}(x): X \to [0,1]$. The function value of $\mu_{\widetilde{A}}(x)$ for the fuzzy set $\widetilde{A}$ is called the membership value of x in $\widetilde{A}$, which represents the degree of truth that x is an element of the fuzzy set $\widetilde{A}$. It is assumed that $\mu_{\widetilde{A}}(x): X \in [0,1]$, where $\mu_{\widetilde{A}}(x) = 1$ reveals that x completely belongs to $\widetilde{A}$, while $\mu_{\widetilde{A}}(x) = 0$ indicates that x does not belong to the fuzzy set $\widetilde{A}$.

$$\widetilde{A} = \left\{\left(x, \mu_{\widetilde{A}}(x)\right)\right\}, \quad x \in X \tag{1}$$

where $\mu_{\widetilde{A}}(x)$ is the membership function and $X = \{x\}$ represents a collection of elements x.

A triangular fuzzy number $\widetilde{N}$ can be defined as a triplet (l, m, u), and the membership function $\mu_{\widetilde{N}}(x)$ is defined as:

$$\mu_{\widetilde{N}}(x)=\begin{cases}0, & x<l\\ (x-l)/(m-l), & l\le x\le m\\ (r-x)/(u-m), & m\le x\le u\\ 0, & x>u\end{cases} \tag{2}$$

where l, m, and r are real numbers and $l < m < u$.

To deal with the problems of group decision-making in a fuzzy environment, an effective fuzzy aggregation method is required. The human judgments with fuzzy linguistic variables are fuzzy numbers, which a defuzzification method is required to transform the crisp elements into scores. Proposed by Opricovic & Tzeng [33], the CFCS (Converting Fuzzy data into Crisp Scores) defuzzification method is based on the procedure of determining the low and up scores by fuzzy min and fuzzy max, and the total score is determined as a weighted average according to the membership functions. This would provide a more appropriate crisp value comparing with other methods.

Let $\widetilde{z}_{ij}^{k}=\left(l_{ij}^{k},m_{ij}^{k},u_{ij}^{k}\right)$ indicates the fuzzy assessment of evaluator k (k=1,2,…,p) about the degree to which the criterion i affects the criterion j, the CFCS algorithm can be described in following five steps:

(1) Normalization:

$$xl_{ij}^{k}=\left(l_{ij}^{k}-\min l_{ij}^{k}\right)\Big/\Delta_{\min}^{\max} \tag{3}$$

$$xm_{ij}^{k}=\left(m_{ij}^{k}-\min l_{ij}^{k}\right)\Big/\Delta_{\min}^{\max} \tag{4}$$

$$xr_{ij}^{k}=\left(r_{ij}^{k}-\min l_{ij}^{k}\right)\Big/\Delta_{\min}^{\max} \tag{5}$$

where $\Delta_{\min}^{\max}=\max r_{ij}^{k}-\min l_{ij}^{k}$.

(2) Compute left (ls) and right (rs) normalized value:

$$x\,\mathrm{ls}_{ij}^{k}=xm_{ij}^{k}\Big/\left(1+xm_{ij}^{k}-xl_{ij}^{k}\right) \tag{6}$$

$$x\,\mathrm{rs}_{ij}^{k}=xr_{ij}^{k}\Big/\left(1+xr_{ij}^{k}-xm_{ij}^{k}\right) \tag{7}$$

(3) Compute total normalized crisp value:

$$x_{ij}^{k}=\left[x\,\mathrm{ls}_{ij}^{k}\left(1-x\,\mathrm{ls}_{ij}^{k}\right)+x\,\mathrm{rs}_{ij}^{k}\,x\,\mathrm{rs}_{ij}^{k}\right]\Big/\left[1-x\,\mathrm{ls}_{ij}^{k}+x\,\mathrm{rs}_{ij}^{k}\right] \tag{8}$$

(4) Compute crisp values:

$$z_{ij}^{k}=\min l_{ij}^{k}+x_{ij}^{k}\Delta_{\min}^{\max} \tag{9}$$

To further the practicality of the conventional DEMATEL technique for group decision-making in a fuzzy environment, the process is illustrated as follows:

Step 1: Design the fuzzy linguistic scale. To deal with the ambiguities of human assessments, the linguistic variable ''influence'' is used with five linguistic terms as {No, Very low, Low, High, Very high} that are expressed in positive triangular fuzzy numbers $\left(l_{ij},m_{ij},u_{ij}\right)$.

Step 2: Calculate the fuzzy direct-influence matrix by scores (depending on the views of the experts by linguistic scales of natural language) and evaluate the relationship among elements based on Table 2, we can obtain the fuzzy direct-influence matrix $\widetilde{\boldsymbol{D}}$ by Eq. (15).

$$\widetilde{\boldsymbol{D}}=[\widetilde{d}_{ij}]_{n\times n},\ \text{where}\ \widetilde{d}_{ij}=(d_{ij}^{l},d_{ij}^{m},d_{ij}^{u}) \tag{10}$$

Step 3: Normalize the fuzzy direct-influence matrix: Based on the fuzzy direct-influence matrix $\widetilde{\boldsymbol{D}}$, the normalized fuzzy direct-relation matrix $\widetilde{\boldsymbol{N}}$ is acquired by using Eq. (16).

$$\widetilde{\boldsymbol{N}}=\widetilde{\boldsymbol{D}}/u \tag{11}$$

where

$u=\max\limits_{i,j}\left\{\max_i\sum_{j=1}^{n}d_{ij},\max_j\sum_{i=1}^{n}d_{ij}\right\},\ i,j\in\{1,2,\ldots,n\}$,

$\widetilde{\boldsymbol{N}}=[\widetilde{e}_{ij}]_{n\times n}$, $\widetilde{e}_{ij}=(e_{ij}^{l},e_{ij}^{m},e_{ij}^{u})$.

Step 4: Attain the fuzzy total-influence matrix: once the normalized fuzzy direct-influence matrix $\widetilde{\boldsymbol{N}}=(\boldsymbol{N}^{l},\boldsymbol{N}^{m},\boldsymbol{N}^{u})$ obtained, where $\boldsymbol{N}^{l}=[e_{ij}^{l}]_{n\times n}$, $\boldsymbol{N}^{m}=[e_{ij}^{m}]_{n\times n}$, and $\boldsymbol{N}^{u}=[e_{ij}^{u}]_{n\times n}$; the fuzzy total-influence matrix $\widetilde{\boldsymbol{T}}$ is arrived at through Eq. (12), in which the $\boldsymbol{I}$ is denoted as the identity matrix.

$$\widetilde{\boldsymbol{T}}=[\widetilde{t}_{ij}]_{n\times n},\ \text{where}\ \widetilde{t}_{ij}=(t_{ij}^{l},t_{ij}^{m},t_{ij}^{u}) \tag{12}$$

where, $\boldsymbol{T}^{l}=[t_{ij}^{l}]_{n\times n}=\boldsymbol{N}^{l}(\boldsymbol{I}-\boldsymbol{N}^{l})^{-1}$,

$\boldsymbol{T}^{m}=[t_{ij}^{m}]_{n\times n}=\boldsymbol{N}^{m}(\boldsymbol{I}-\boldsymbol{N}^{m})^{-1}$ and

$\boldsymbol{T}^{u}=[t_{ij}^{u}]_{n\times n}=\boldsymbol{N}^{u}(\boldsymbol{I}-\boldsymbol{N}^{u})^{-1}$ respectively; the elements of triangular fuzzy numbers in fuzzy total-influence matrix $\widetilde{\boldsymbol{T}}$ are divided into $\boldsymbol{T}^{l}$, $\boldsymbol{T}^{m}$ and $\boldsymbol{T}^{u}$, and $\boldsymbol{T}^{l}=[t_{ij}^{l}]_{n\times n}\prec\boldsymbol{T}^{m}=[t_{ij}^{m}]_{n\times n}\prec\boldsymbol{T}^{u}=[t_{ij}^{u}]_{n\times n}$, when $e_{ij}^{l}<e_{ij}^{m}<e_{ij}^{u}$ for any $i,j\in\{1,2,\ldots,n\}$.

Step 5: Defuzzy into the crisp values. Using the CFCS method showing in Eqs. (3)-(9), the total fuzzy influence matrix $\widetilde{\boldsymbol{T}}=[\widetilde{t}_{ij}]_{n\times n}$ are defuzzified as crisp values into the total-influence matrix $\boldsymbol{T}=[t_{ij}]_{n\times n}$.

Step 6: Analyze the results: in the stage, the sum of rows (given influence) and the sum of columns (received influence) are separately expressed as influential vector $\boldsymbol{d}=\left(d_1,\ldots,d_i,\ldots,d_n\right)'$ by factor j (j = 1,2,...,n) and influential vector $\boldsymbol{r}=\left(r_1,\ldots,r_j,\ldots,r_n\right)'$ by factor i (i = 1,2,...,n) using Eqs. (13)-(15). Then, when $i,j\in\{1,2,\ldots,n\}$ and $i=j$ the horizontal axis vector ($\boldsymbol{d}$+$\boldsymbol{r}$) is made by adding vector $\boldsymbol{d}$ to vector $\boldsymbol{r}$, which exhibits total important influence of each criterion. Similarly,

the vertical axis vector ($\boldsymbol{d}-\boldsymbol{r}$) is made by deducting vector $\boldsymbol{d}$ from vector $\boldsymbol{r}$, which may separate criteria into a cause group and an affected group. In general, when the value of d_i-r_i is higher, the criterion is belonging to the cause group. On the contrary, if the value of d_i-r_i is lower, the criterion is belonging to the affected group. Therefore, the causal-and-effect graph can be achieved by plotting the data set of $\{(d_i+r_i,\ d_i-r_i) \mid i = 1,2,\ldots,n\}$, providing valuable approaching for making decisions.

$$\boldsymbol{T} = \left[t_{ij}\right]_{n\times n}, \quad i, j \in \{1,2,\ldots,n\}, \tag{13}$$

$$d = \left[\sum_{j=1}^{n} t_{ij}\right]_{n\times 1} = \left[t_i\right]_{n\times 1} = \left[d_i\right]_{n\times 1}, \tag{14}$$

$$r = \left[\sum_{i=1}^{n} t_{ij}\right]_{n\times 1}' = \left[t_j\right]_{n\times 1} = \left[r_j\right]_{n\times 1}, \tag{15}$$

where vector $d = (d_1,\ldots, d_i, \ldots, d_n)$ and vector $r = (r_1,\ldots, r_j,\ldots, r_n)$ express the sum of rows and the sum of columns based on total-influence matrix $\boldsymbol{T} = [t_{ij}]_{n\times n}$, separately.

IV. Empirical Study: Case of Project Success

The empirical experiment was focused on Taiwanese firms that consist of project group. The study includes two parts, the exploratory factor analysis and fuzzy DEMATEL analysis, as detail described below.

A. The Exploratory Factor Analysis to Obtain Independent Criteria Groups

The questionnaire was sent to several Taiwanese companies that have project groups consisting of Taiwanese working professionals, and was explained that through the study, they can receive a clearer understanding of which factors are perceived to lead to greater project performance, which ultimately leads to increasing the probability of project success. A total of 224 questionnaires were collected for this study, while 16 questionnaires were not fully completed, this makes 208 useable feedbacks.

For the soft factor items, a clear structure emerged on the third iteration using a kappa rotation of 7. The Kaiser-Meyer-Olkin (KMO) test and the Bartlett's test are both acceptable on each iteration, with the lowest KMO being 0.949 and highest Bartlett's being 0.000. The Cronbach's Alpha and Pearson's Correlation were also both acceptable on each iteration with the lowest alpha being 0.851 and the lowest correlation being 0.618. After iterations one and two, the original 35 item list was reduced to a final 26 items that categorized into eight dimensions. Eigenvalues are all greater than 1 and all items' item-to-total correlations are above the cutoff value 0.5. The exploratory factor analysis final iteration result is shown in Table I.

B. The Fuzzy DEMATEL Method to Find the Interrelation between Criteria

According to the factor analysis results, 50 project managers and senior team members were invited to score the influence level of criteria based on the fuzzy DEMATEL method.

TABLE I. Dimension and Criteria Extracted

Extracted Dimensions	Items / Criteria	Factor Loading	Eigenvalues (Rotated)	Item-to-Total Correlation
Synergy (D_1)	Work Loading (C_{11})	1.22	14.27	0.79
	Accessible (C_{12})	0.95		0.84
	Reliable (C_{13})	0.90		0.79
	Considerate (C_{14})	0.87		0.83
	Coordination (C_{15})	0.83		0.87
	Help each other (C_{16})	0.81		0.84
	Cooperation (C_{17})	0.74		0.86
	Consensus (C_{18})	0.68		0.83
	Shared objective (C_{19})	0.63		0.75
Competence (D_2)	Trouble-shooting (C_{21})	0.95	12.08	0.80
	Handle deviations (C_{22})	0.93		0.86
	Positive/proactive (jiji) (C_{23})	0.86		0.85
	Responsible (C_{24})	0.80		0.81
Attitude (D_3)	Polite (ke-chi) (C_{31})	1.08	9.93	0.77
	Friendly (chin-chieh) (C_{32})	0.86		0.79
	Patience (C_{33})	0.69		0.70
Relationship (D_4)	Learning culture (C_{41})	1.04	11.62	0.69
	Client satisfaction (C_{42})	0.81		0.79
	Bureaucracy (C_{43})	0.59		0.68
Consideration (D_5)	Shows empathy (C_{51})	0.85	10.43	0.75
	Competent (C_{52})	0.84		0.73
	Effective (C_{53})	0.53		0.69
Risk Exposure (D_6)	Risk exposure (C_{61})	0.86	4.92	N/A
	Change orders and claims (C_{62})	0.80		N/A
Litigation (D_7)	Litigation (C_{71})	0.91	3.71	N/A
Personnel Connection (D_8)	Personnel connection (C_{81})	0.84	2.49	N/A

TABLE II. THE DEFUZZIED TOTAL-INFLUENCE MATRIX $\boldsymbol{T}$ ($\times 10^{-4}$)

	C_{11}	C_{12}	C_{13}	C_{14}	C_{15}	C_{16}	C_{17}	C_{18}	C_{19}	C_{21}	C_{22}	C_{23}	C_{24}	C_{31}	C_{32}	C_{33}	C_{41}	C_{42}	C_{43}	C_{51}	C_{52}	C_{53}	C_{61}	C_{62}	C_{71}	C_{81}
C_{11}	367	875	360	755	800	930	856	671	459	635	790	314	464	608	605	802	488	838	539	647	468	880	702	587	628	530
C_{12}	344	211	324	453	467	680	495	623	444	242	258	211	215	201	225	198	686	885	53	205	188	282	92	73	89	863
C_{13}	517	346	80	182	256	250	235	206	208	230	285	247	673	377	421	343	273	882	45	248	517	290	65	57	69	723
C_{14}	259	754	204	187	383	818	696	635	344	209	318	163	165	300	445	330	312	817	39	691	178	263	75	48	55	846
C_{15}	582	370	181	352	265	801	693	728	700	685	729	290	247	341	280	618	400	982	58	370	556	737	78	78	97	570
C_{16}	608	766	304	716	374	275	811	404	320	290	282	256	229	258	392	266	485	602	56	273	213	347	109	79	96	845
C_{17}	275	264	129	182	276	677	183	717	734	222	209	114	212	159	146	125	588	564	44	107	155	650	76	64	185	626
C_{18}	198	163	101	177	240	224	258	120	620	173	208	59	103	98	71	76	478	609	37	86	103	588	51	45	42	228
C_{19}	163	326	130	117	282	340	358	500	134	197	247	71	165	71	66	80	282	671	35	60	99	626	39	42	37	193
C_{21}	469	170	125	142	530	290	244	193	181	128	339	147	167	142	132	644	206	714	53	145	652	397	76	264	106	237
C_{22}	228	207	104	240	554	228	278	255	360	478	133	207	140	224	181	310	240	708	32	130	606	312	54	60	196	256
C_{23}	534	224	125	150	192	313	257	202	179	127	179	63	355	152	148	125	497	661	51	105	496	448	102	67	186	450
C_{24}	398	145	110	111	138	158	147	133	123	93	108	191	45	93	91	76	253	383	38	73	139	135	54	47	72	200
C_{31}	302	691	151	224	662	324	267	272	241	147	249	144	125	109	446	225	549	837	39	137	127	227	64	54	54	800
C_{32}	300	757	221	242	287	319	310	273	262	164	193	159	174	321	108	195	347	815	35	258	173	258	59	49	47	838
C_{33}	260	302	141	145	354	183	162	153	142	103	397	87	120	124	115	73	363	579	38	130	140	306	46	40	45	553
C_{41}	192	193	94	104	262	368	415	395	451	134	198	61	83	81	76	70	125	516	195	63	90	348	278	289	212	206
C_{42}	464	184	79	118	441	278	433	239	554	194	223	122	114	147	163	149	481	232	44	118	174	276	63	56	60	579
C_{43}	645	69	28	57	120	79	138	138	81	113	119	26	43	45	43	64	178	84	64	47	43	84	404	714	734	49
C_{51}	246	582	148	715	251	706	369	289	237	144	197	155	140	296	336	216	414	633	34	112	138	237	63	48	50	761
C_{52}	418	128	66	86	153	257	225	136	157	447	411	113	138	74	74	103	340	648	38	74	93	402	55	54	58	204
C_{53}	198	131	199	96	187	125	178	184	163	117	302	259	113	66	64	119	356	542	27	70	247	96	47	36	44	139
C_{61}	443	62	31	55	76	64	79	68	56	88	78	25	37	39	35	53	182	63	435	44	38	63	128	680	698	38
C_{62}	702	105	48	114	385	157	351	338	305	458	458	49	71	71	67	160	287	188	129	87	108	184	701	137	688	102
C_{71}	95	12	6	12	30	16	28	27	23	44	34	5	8	8	8	15	31	18	182	10	11	17	698	624	95	10
C_{81}	380	735	322	368	803	529	484	701	443	347	434	234	216	544	469	214	480	891	45	306	233	371	73	64	68	315

Followed by the above mentioned steps, the initial fuzzy direct-influence matrix $\widetilde{\boldsymbol{D}}$ was produced. The normalized fuzzy direct-influence matrix $\widetilde{\boldsymbol{N}}$ is then retrieved based on Eq. (11). Subsequently, the fuzzy total-influence matrix $\widetilde{\boldsymbol{T}}$ was calculated. Next, the CFCS method listed on Eq. (3)-(9) was used to aggregate the fuzzy data. Table II shows the defuzzied total-influence matrix $\boldsymbol{T}$. The degree of influence in dimension level and criteria level are presented in Table III and IV, respectively. Based on the above analysis, the dimension and criteria impact relation maps can be generated in Fig. 1 and Fig. 2, respectively.

TABLE III. THE INFLUENCE OF CONCERN FACTORS IN DIMENSION LEVEL

	d_i	r_i	d_i+r_i	d_i-r_i
D_1	0.2676	0.2185	0.4861	0.0492
D_2	0.1748	0.1462	0.3210	0.0287
D_3	0.2083	0.1409	0.3493	0.0674
D_4	0.1723	0.2468	0.4191	-0.0746
D_5	0.1576	0.1567	0.3143	0.0009
D_6	0.1895	0.1765	0.3660	0.0131
D_7	0.0917	0.1575	0.2492	-0.0659
D_8	0.2473	0.2660	0.5133	-0.0187

V. DISCUSSION AND IMPLICATION

The proposed hybrid method has proven to be an effective model for evaluating the complex psychological intertwined effects. Based on our empirical experiments, factor analysis was used to classify each element/criteria into eight different independent factors/dimensions. Those criteria under the same dimension had some interrelations with each other. The direct/indirect influential relationship of criteria was figured using the fuzzy DEMATEL method.

A clear structure of the Team-Internal impact factors for project performance within the Taiwanese cultural context was created through exploratory factor analysis (see Table I). By combining Stanworth et al.'s [43] 26 attributes from ISQ, Pinto and Prescott's [37] two trouble-shooting attributes, Jin and Ling's [22] seven relationship attributes, thus the final scaleinvestigated in this study was made up of 35 attributes. The exploratory factor analysis was then conducted and extracted a final structure of eight dimensions and 26 criteria: Synergy (9 criteria), Competence (4 criteria), Attitude (3 criteria), Relationship (3 criteria), Consideration (3 criteria), Risk Exposure (2 criteria), Litigation (1 criterion), and Personnel Connection (1 criterion).

According to the fuzzy DEMATEL analysis, the factors which show greater values of (d_i-r_i) are intensely affecting others, the factors show lesser values of (d_i-r_i) are intensely

TABLE IV. THE INFLUENCE OF CONCERN FACTORS IN CRITERIA LEVEL

	d_i	r_i	d_i+r_i	d_i-r_i
C_{11}	1.6598	0.9587	2.6185	0.7011
C_{12}	0.9005	0.8771	1.7776	0.0234
C_{13}	0.8021	0.3812	1.1833	0.4210
C_{14}	0.9532	0.6098	1.5630	0.3434
C_{15}	1.1789	0.8766	2.0555	0.3024
C_{16}	0.9657	0.9388	1.9045	0.0269
C_{17}	0.7684	0.8949	1.6633	-0.1266
C_{18}	0.5156	0.8601	1.3757	-0.3446
C_{19}	0.5330	0.7920	1.3250	-0.2589
C_{21}	0.6893	0.6211	1.3105	0.0682
C_{22}	0.6722	0.7378	1.4100	-0.0656
C_{23}	0.6389	0.3773	1.0162	0.2616
C_{24}	0.3556	0.4563	0.8118	-0.1007
C_{31}	0.7468	0.4947	1.2415	0.2521
C_{32}	0.7163	0.5205	1.2368	0.1957
C_{33}	0.5101	0.5650	1.0751	-0.0548
C_{41}	0.5497	0.9320	1.4817	-0.3824
C_{42}	0.5986	1.5364	2.1350	-0.9378
C_{43}	0.4211	0.2386	0.6597	0.1824
C_{51}	0.7515	0.4594	1.2109	0.2921
C_{52}	0.4952	0.5986	1.0938	-0.1034
C_{53}	0.4106	0.8824	1.2930	-0.4718
C_{61}	0.3657	0.4253	0.7910	-0.0596
C_{62}	0.6449	0.4351	1.0801	0.2098
C_{71}	0.2067	0.4713	0.6781	-0.2646
C_{81}	1.0068	1.1162	2.1230	-0.1093

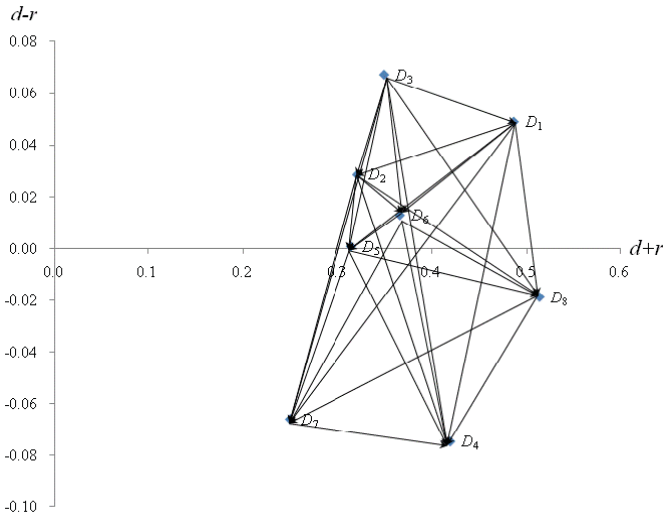

Figure 1. Dimensional impact relation map

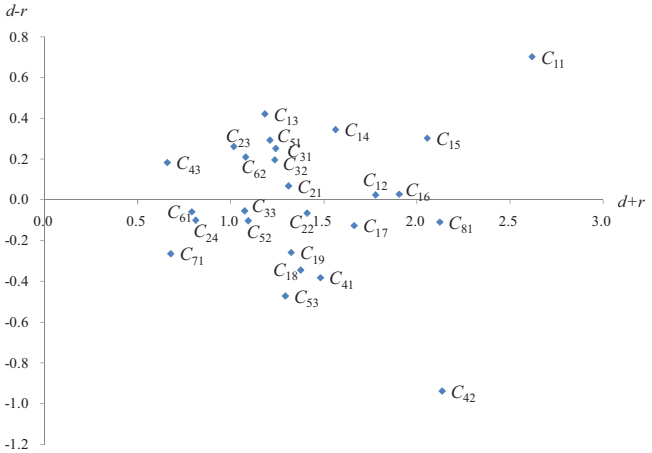

Figure 2. Criteria impact relation map

affected by the others. Figure 1 and 2 show a clear picture of intertwined effect in between dimensions and criteria.

Based on Figure 1, the attitude (D_3) plays a significant role that highly influences other soft factors towards the project success. On the other hand, the relationship (D_4) is impacted by all dimensions. The personal connection (D_8) presents a high relationship with other dimensions. From Figure 2 cross-dimensionally, the work loading (C_{11}) is a key factor that greatly impacts all other criteria, while ultimately meets the customer satisfaction (C_{42}). Bureaucracy (C_{43}) and litigation (C_{71}) show less relationship with other factors.

Project leadership requires more than just technical competence and encompasses the ability to manage a team. Stated by Kloppenborg and Petrick [26], skills in managing relationships are critical to achieve stakeholder satisfaction through all stages of the project. Creating the right relationships between team members is one of the biggest challenges that face project managers [3][45][34]. Whitty [49] mentioned that "projects are simply a synthesis of human sensations and expectations about how multiple resources are to be used" (p.577). Ropponen and Lyytinen [40] stated that personnel management is one of the major risk components in software development project. Above evidences highlight the importance of understanding the interrelation of project team soft factors.

The result of this study gives a clear picture to the project manager on the intertwined effects of team internal soft factors. As work loading plays as a key influencer, when more resources such as people are needed than are available, the tasks need to be rescheduled concurrently or even sequentially to manage the constraint. The project manager should apply resource leveling to resolve the conflicts of schedule instead of overloading the work to a single resource. Attitude is the one that project team should emphasize in order to create a harmony working environment, which can further build the team synergy. From internal service point of view, Jeng [21] stated that rewards and recognition can be the best strategy to enhance the team internal service operation.

VI. Concluding Remarks

This research proposed a hybrid method combines the factor analysis and fuzzy DEMATAL technique to understand the factors intertwined effect in complex system. Supported by previous qualitative studies, exploratory factor analysis is applied to extract a clear factor structure consist of dimension and criteria. Then, the fuzzy DEMATEL technique is utilized to analyze the intertwined effect between the extracted dimension and criteria. Based on the impact relation map, project manager can gain a clear picture on the impact of soft factors on project performance. A project manager may set the strategies to better manage the working environment and team atmosphere. The result provides directions to enhance the team synergy, increase relationship, and ultimately achieving the project success. This study may also provides the information for a company to further adopt effective training agenda and employee assistance programs (EAPs) that improve the working atmosphere of the project team.

References

[1] R. Atkinson, "Project management: Cost, time and quality, two best guesses and a phenomenon, its time to accept other success criteria," International Journal of Project Management, vol. 17, no. 6, pp.337-342, 1999.

[2] P. Bromiley, and L.L. Cummings, "Transactions costs in organizations with trust," Research on Negotiation in Organizations, vol. 5, pp.219-250, 1995.

[3] A. Bucero, "Smart emotions," PM Network, vol. 18, no. 11, p.22, 2004.

[4] D.M. Cable, and T.A. Judge, "Person-organization fit, job choice decisions, and organizational entry," Organizational Behavior and Human Decision Processes, vol. 67, no. 3, pp.294-311, 1996.

[5] Y.J. Chiu, H.C. Chen, G.H. Tzeng, and J.Z. Shyu, "Marketing strategy based on customer behaviour for the LCD-TV," International Journal of Management and Decision Making, vol. 7, no. 2/3, pp.143-165, 2006.

[6] T. Cooke-Davies, "The "real" success factors on projects," International Journal of Project Management, vol. 20, no. 3, pp.185-190, 2002.

[7] A. De Wit, "Measurement of project success," International Journal of Project Management, vol. 6, no. 3, pp.164-170, 1988.

[8] W. Deng, S. Chiang, C. Tsai, and S. Tsai, “The relationship of internal service quality, external service quality and overall customer satisfaction,” Quality Monthly, vol. 43, no. 10, pp.52-58, 2007.

[9] W. Deng, M. Lin, M., and C. Tsai, “Employee satisfaction as the foundation for assessing internal service quality: An international hotel example,” Quality Monthly, vol. 41, no. 11, pp.79-83, 2005.

[10] E. Fontela, and A. Gabus, The DEMATEL Observer, DEMATEL 1976 Report, Battelle Geneva Research Center, Geneva, Switzerland, 1976.

[11] A. Gabus, and E Fontela, Perceptions of The World Problematique: Communication Procedure, Communicating with Those Bearing Collective Responsibility, DEMATEL Report No. 1, Battelle Geneva Research Center, Geneva, Switzerland, 1973.

[12] G. Gao, “"Don't take my word for it."--understanding Chinese speaking practices,” International Journal of Intercultural Relations, vol. 22, no. 2, pp.163-186, 1998.

[13] D.D. Gremler, M.J. Bitner, and K.R. Evans, “The internal service encounter,” International Journal of Service Industry Management, vol. 5, no. 2, pp.43-56, 1994.

[14] J.S. Hair, R.E. Anderson, R.L. Tetham, and W.C. Black, Multivariate Data Analysis (5 ed.), New Jersey: Prentice Hall, 1998.

[15] G. Hofstede, “Cultural dimensions in management and planning,” Asia Pacific Journal of Management, vol. 1, no. 2, pp.81-99, 1984.

[16] G. Hofstede, and M.H. Bond, “The Confucius connection: From cultural roots to economic growth,” Organizational Dynamics, vol. 16, no. 4, pp.4-21, 1988.

[17] G. Hofstede, B. Neuijen, D.D. Ohayv, and G. Sanders, “Measuring organizational cultures: A qualitative and quantitative study across twenty cases,” Administrative Science Quarterly, vol. 35, no. 2, pp.286-316, 1990.

[18] C.Y. Huang, and G.H. Tzeng, “Reconfiguring the innovation policy portfolios for Taiwan’s SIP mall industry,” Technovation, vol. 27, no. 12, pp.744-765, 2007.

[19] K.-K. Hwang, “The deep structure of Confucianism: A social psychological approach,” Asian Philosophy: An International Journal of the Philosophical Traditions of the East, vol. 11, no. 3, pp.179-204, 2001.

[20] B.-S. Jaw, Y.-H. Ling, C.Y.-P. Wang, and W.-C. Chang, “The impact of culture on Chinese employees' work values,” Personnel Review, vol. 36, no. 5, pp.763-780, 2007.

[21] D.J.F. Jeng, “Multiple criteria decision making approach for internal service operation strategy by nonadditive fuzzy integral,” International Journal of Innovative Computing, Information and Control, in press.

[22] X.-H. Jin, and F.Y.Y. Ling, “Key relationship-based determinants of project performance in China,” Building and Environment, vol. 41, no. 7, pp.915-925, 2006.

[23] K. Jugdev, and R. Muller, “A restropective look at our evolving understanding of project success,” Project Management Journal, vol. 36, no.4, pp.19-31, 2005.

[24] R. Katz, “The effects of group longevity on project communication and performance,” Administrative Science Quarterly, vol. 27, no. 1, pp.81-104, 1982.

[25] A. Y.-c. King, “Kuan-hsi and network building: A sociological interpretation,” Daedalus, vol. 120, no. 2, pp.63-84, 1991.

[26] T. Kloppenborg, and J. Petrick, “Leadership in project life cycle and team character development,” Project Management Journal, vol. 30, no. 2, pp.8-13, 1999.

[27] A. Lester, Project Management, Planning and Control (Fifth Edition). Oxford: Butterworth-Heinemann, 2007.

[28] J.F. Liao, C.H.J. Wu, Y.H. Jou, and Y.Y. Huang, “A study of the relationship between of internal marketing, job satisfaction and customer-oriented behaviors,” Sun Yat-Sen Management Review, vol. 12, no. 5, pp.181-201, 2004.

[29] C.S. Lim, and M.Z. Mohamed, “Criteria of project success: an exploratory re-examination,” International Journal of Project Management, vol. 17, no. 4, pp.243-248, 1999.

[30] I.Y. Lu, and Y.H. Cheng, “The study on the relationships among the factors of internal service quality, service ability, job satisfaction and external service quality: The case of nurse,” Journal of Quality, vol. 14, no. 2, pp.161-179, 2007 (in Chinese).

[31] J.J.H. Liou, and G.H. Tzeng, “A dominance-based rough set approach to customer behavior in the airline market,” Information Sciences, vol. 180, no. 11, pp.2230-2238, 2010.

[32] J.E. McGrath, “Time, interaction, and performance (TIP): A theory of groups,” Small Group Research, vol. 22, no. 2, pp.147-174, 1991.

[33] S. Opricovic, and G.H. Tzeng, “Defuzzification within a multicriteria decision model,” International Journal of Uncertainty, Fuzziness and Knowledge-Based Systems, vol. 11, no. 5, pp.635-652, 2003.

[34] I. Pant, and B. Baroudi, “Project management education: The human skills imperative,” International Journal of Project Management, vol. 26, no. 2, pp.124-128, 2008.

[35] A. Paraskevas, “Internal service encounters in hotels: An empirical study,” International Journal of Contemporary Hospitality Management, vol. 13, no. 6, pp.285-292, 2001.

[36] A. Parasuraman, L.L. Berry, and V.A. Zeithaml, “Perceived service quality as a customer-based performance measure: An empirical examination of organizational barriers using an extended service quality model,” Human Resource Management, vol. 30, no. 3, pp.335-364, 1991.

[37] J.K. Pinto, and J.E. Prescott, “Variations in critical success factors over the stages in the project life cycle,” Journal of Management, vol. 14, no. 1, pp.5-18, 1988.

[38] J.K. Pinto, and D.P. Slevin, “Critical factors in successful project implementation,” IEEE Transactions on Engineering Management, vol. 34, no. 1, pp.22-27, 1987.

[39] J. Reynoso, and B. Moores, “Towards the measurement of internal service quality,” International Journal of Service Industry Management, vol. 6, no. 3, pp.64-83, 1995.

[40] J. Ropponen, and K. Lyytinen, “Components of software development risk: How to address them? A project manager survey,” IEEE Transactions on Software Engineering, vol. 26, no. 2, pp.98-112, 2000.

[41] L.L. Stanley, and J.D. Wisner, “Internal service quality in purchasing: An empirical study,” The Journal of Supply Chain Management, vol. 34, no. 3, pp.50-60, 1998.

[42] S.H. Schwartz, and L. Sagiv, “Identifying culture-specifics in the content and structure of values,” Journal of Cross-Cultural Psychology, vol. 26, no. 1, pp.92-116, 1995.

[43] J. Stanworth, S. Chen, and R. Hsu, “Understanding Chinese employees’ (dis)satisfaction in the internal service encounter,” National Changhua University of Education, Unpublished Research Article, 2009.

[44] E.F. Stone-Romero, and D.L. Stone, “Cognitive, affective, and cultural influences on stigmatization: Impact on human resource management processes and practices,” Research in Personnel and Human Resources Management, vol. 26, pp.111-161, 2007.

[45] H.J. Thamhain, “Linkages of project environment to performance: lessons for team leadership,” International Journal of Project Management, vol. 22, no. 7, pp.533-544, 2004.

[46] G.H. Tzeng, Y.P. Ou Yang, C.T. Lin, and C.B. Chen, “Hierarchical MADM with fuzzy integral for evaluating enterprise intranet web sites,” Information Sciences, vol. 169, no. 3-4, pp.409-426, 2005.

[47] X. Wang, and J. Huang, “The relationships between key stakeholders' project performance and project success: Perceptions of Chinese construction supervising engineers,” International Journal of Project Management, vol. 24, no. 3, pp.253-260, 2006).

[48] P.L. Wei, J.H. Huang, G.H. Tzeng, and S.I. Wu, “Causal modeling of web-advertising effects by improving SEM based on DEMATEL technique,” International Journal of Information Technology & Decision Making, vol. 9, no. 5, pp.799-829, 2010.

[49] S.J. Whitty “A memetic paradigm of project management,” International Journal of Project Management, vol. 23, no. 8, pp.575-583, 2005.

[50] J.L. Yang, H.N. Chiu, G.H. Tzeng, and R.H. Yeh, “Vendor selection by integrated fuzzy MCDM techniques with independent and interdependent relationships,” Information Sciences, vol. 178, no. 21, pp.4166-4183, 2008.

2011 IEEE International Conference on Fuzzy Systems
June 27-30, 2011, Taipei, Taiwan

A Robust Portfolio Selection Problem based on a Confidence Interval with Investor's Subjectiviety

Takashi Hasuike
Graduate School of Information Science and Technology
Osaka University, Japan
2-1 Yamadaoka, Suita, Osaka 565-0871, Japan
thasuike@ist.osaka-u.ac.jp

Hideki Katagiri
Graduate School of Engineering
Hiroshima University, Japan
1-4-1 Kagamiyama, Higashi-Hiroshima City, Hiroshima
739-8527, Japan
katagiri-h@hiroshima-u.ac.jp

***Abstract*—This paper considers a robust portfolio selection problem considering a confidence interval with subjectivity to the weight for the standard deviation. Since the proposed model is formulated as an ill-defined problem due to fuzziness and bi-object derived from maximizing both robustness and investor's satisfaction level to the total profit, it is hard to solve it directly. Therefore, introducing fuzzy goals for the bi-objective functions, the proposed model is transformed into the deterministic equivalent problem. Furthermore, in order to obtain the exact optimal portfolio analytically, the solution method is developed introducing a parameter and doing the equivalent transformations.**

Keywords-component; portfolio selection problem; robust programming; confidential interval; fuzzy goal;

I. INTRODUCTION

In recent years, not only big companies and institutional investors but also many individual investors take part in investment. Therefore, the role of investment theory, which is generally called portfolio theory, becomes increasingly important. Of course, investors confront several uncertainties derived from changes in social conditions such as price escalation and burst of the economic bubble which have a great influence on the future return, and from insufficiency of available information. Under such conditions, investors must find ways to reduce risks as well as maximizing the total profit.

Until now, various studies concerning portfolio selection problems have been performed. Regarding the research history on the mathematical approach, Markowitz [21] proposed the mean-variance model. Since then, it has been the centre of research activities in the real financial field, and numerous researchers have contributed to the development of modern portfolio theory. Then, many researchers have proposed models of portfolio selection problems that have extended the Markowitz model; mean-absolute-deviation model (Konno et al. [18, 19]), semi-variance model (Bawa and Lindenberg [1]), safety-first model (Elton and Gruber [7]), Value-at-Risk (VaR) and conditional Value-at-Risk model (CVaR) (Rockafellar and Uryasev [22]) etc..

On the other hand, investors may receive a lot of data or information in the current market, but it is almost impossible to determine strict random distributions of future returns. These distributions may be statistically determined as a confidence interval to the total profit involving the mean value and variance. Therefore, using these statistical distributions, it is more important to considering that decision makers optimize the problem in the worst case; i.e. robust optimization problem.

Recently, the robust optimization problem becomes a more active area of research, and there exists various studies (For example, Ben-Tal and Nemirovski [2, 3], Ghaoui and Lebret [8]). Particularly, there are some studies of robust portfolio selection problems determining optimal investment strategy using the robust approach (For example, Goldfarb and Iyengar [9], Lobo [20]). The expected return and variance of each asset are mainly estimated from historical data based on the statistical analysis. However, in the case that we consider the value of received information, the investor's subjectivity to the trend of current market, and the satisfaction function to the achievement of objects such as maximizing the total profit, we need to consider that statistical distribution or confidential interval considering these conditions includes some ambiguity and is involved some flexibility. In this paper, we propose an extended model of robust portfolio selection problems including fuzziness.

Until now, there are some basic researches under various uncertainty conditions with respect to portfolio selection problems (Bilbao-Terol et al. [4], Carlsson et al. [5], Guo and Tanaka [10], Hasuike et al. [11], Huang [12, 13], Inuiguchi et al. [14, 15], Katagiri et al. [17, 18], Tanaka et al. [23, 24], Watada [25]). However, there are few models considering the confidential interval with investor's subjectivity. Furthermore, there are no researches which are analytically extended and explicitly solved these types of portfolio selection problems. Therefore, we develop the exact solution algorithm for the proposed robust portfolio selection problem. Since our model is a multi-objective programming problem with investor's subjectivity, in this paper, we transform main problems into the deterministic equivalent problems, and obtain the exact optimal portfolio.

This paper is organized as follows. In Section II, we introduce a robust portfolio selection problem maximizing the region of confidential interval to the total profit. Furthermore, we propose the bi-objective programming problem maximizing

This work was supported by The Ministry of Education, Culture, Sports, Science and Technology (MEXT), Grant-in-Aid for Young Scientists (B) (22700233).

978-1-4244-7316-8/11/$26.00 ©2011 IEEE

the total profit as well as the region of confidential interval. In Section III, introducing fuzzy goals to both objective functions, we propose the maximin robust portfolio selection problem and develop the strict solution algorithm. In the solution algorithm, we need to solve a convex programming problem, repeatedly. Therefore, in order to solve the problem analytically and explicitly, in Section IV, we perform the deterministic equivalent transformations, and obtain the exact optimal portfolio. Finally, in Section V, we conclude this paper and discuss future researches.

II. Formulation of a Robust Portfolio Selection Problem with Confidential Interval

In this section, we consider a robust portfolio selection problem with a confidential interval. First of all, we set parameters in portfolio optimization. The expected return of total future profit $E(\boldsymbol{r})$ and the total variance $\mathbf{Var}(\boldsymbol{r})$ is defined as follows:

$$E(\boldsymbol{r}) = \bar{\boldsymbol{r}}^t \phi, \quad \mathbf{Var}(\boldsymbol{r}) = \phi^t \mathbf{V} \phi \tag{1}$$

where the notation means as follows:
$\boldsymbol{r}$: Future return vector assumed to be a random variable
$\bar{\boldsymbol{r}}$: Mean value vector of random variable $\boldsymbol{r}$
$\mathbf{V}$: Variance-covariance matrix of random variable $\boldsymbol{r}$
ϕ : Portfolio with respect to each asset j, $(j = 1, 2, ..., n)$

In general, a confidential interval is represented by mean value and standard deviation of each random variable such as normal distribution, student's t-distribution, etc.. Therefore, in this paper, we define d -confidential interval using $E(\boldsymbol{r})$ and $\mathbf{Var}(\boldsymbol{r})$ based on the study (Watada et al. [26]):

$$\left[E(\boldsymbol{r}) - d\sqrt{\mathbf{Var}(\boldsymbol{r})}, E(\boldsymbol{r}) + d\sqrt{\mathbf{Var}(\boldsymbol{r})}\right] \tag{2}$$

With respect to this confidential interval, in this case that constant value of parameter d is larger, the considerable region is also wide, and it urges the investor to deal with more robust case than the small value of d . In this paper, in terms of considering such robust case by maximizing parameter d , the following robust portfolio selection problem is formulated:

$$\begin{aligned} &\text{Maximize } d \\ &\text{subject to } E(\boldsymbol{r}) - d\sqrt{\mathbf{Var}(\boldsymbol{r})} \geq f, \\ &\qquad E(\boldsymbol{r}) \geq f', \\ &\qquad \mathbf{1}^t \phi = 1 \end{aligned} \tag{3}$$

where f and f' are the worst and standard target values of total future return, respectively. In this paper, we assume $f \leq f'$ and these parameters are initially determined by the investor. Since the first constraint of problem (3) is equivalently transformed into the following form;

$$E(\boldsymbol{r}) - d\sqrt{\mathbf{Var}(\boldsymbol{r})} \geq f \;\Leftrightarrow\; \frac{E(\boldsymbol{r}) - f}{\sqrt{\mathbf{Var}(\boldsymbol{r})}} \geq d,$$

problem (3) is equivalently transformed into the following problem:

$$\begin{aligned} &\text{Maximize } \frac{E(\boldsymbol{r}) - f}{\sqrt{\mathbf{Var}(\boldsymbol{r})}} \\ &\text{subject to } E(\boldsymbol{r}) \geq f', \\ &\qquad \mathbf{1}^t \phi = 1 \end{aligned} \tag{4}$$

This problem is a convex programming problem similar to the probability maximization model, and so we obtain the optimal solution using the convex programming approach.

However, in practical investment situations, it is natural for the investor to consider maximizing the target total profit as well as minimizing the total risk, i.e., maximizing the region of confidential interval in terms of robustness. Therefore, the proposed model is reformulated as the following problem:

$$\begin{aligned} &\text{Maximize } d \\ &\text{Maximize } f \\ &\text{subject to } E(\boldsymbol{r}) - d\sqrt{\mathbf{Var}(\boldsymbol{r})} \geq f, \\ &\qquad E(\boldsymbol{r}) \geq f', \\ &\qquad \mathbf{1}^t \phi = 1 \end{aligned} \tag{5}$$

III. Fuzzy Programming Approach to the Proposed Robust Portfolio Selection Problem

In addition to bi-criteria in Section 2, taking account of subjectivity of investment decision and flexibility for the execution of portfolio management, the investor often has satisfaction functions for target parameters d and f called fuzzy goals. In this paper, we defined each fuzzy goal as the fuzzy set characterized by a linear membership function:

$$\begin{aligned} \mu_{\tilde{d}}(\omega) &= \begin{cases} 1 & (d_U \leq \omega) \\ \dfrac{\omega - d_L}{d_U - d_L} & (d_L < \omega < d_U) \\ 0 & (\omega \leq d_L) \end{cases} \\ \mu_{\tilde{G}}(f) &= \begin{cases} 1 & (f_U \leq f) \\ \dfrac{f - f_L}{f_U - f_L} & (f_L < f < f_U) \\ 0 & (f \leq f_L) \end{cases} \end{aligned} \tag{6}$$

where d_L, d_U and f_L, f_U are constant values determined by the investor. Then, substituting $z_d(\boldsymbol{x}) = \dfrac{E(\boldsymbol{r}) - f}{\sqrt{\mathbf{Var}(\boldsymbol{r})}}$ into fuzzy goal $\mu_{\tilde{d}}(\omega)$, the following formula is obtained:

$$\mu_{\tilde{g}(d)}(z_d(\boldsymbol{x})) = \begin{cases} 1 & (\omega \leq g_U(d)) \\ \dfrac{g_L(d) - \omega}{\left((d_U - d_L)\sqrt{\mathbf{Var}(\boldsymbol{r})}\right)} & (g_U(d) < \omega < g_L(d)) \\ 0 & (g_L(d) \leq \omega) \end{cases} \tag{7}$$

$$g_L(d) = E(\boldsymbol{r}) - d_L\sqrt{\mathbf{Var}(\boldsymbol{r})},\ g_U(d) = E(\boldsymbol{r}) - d_U\sqrt{\mathbf{Var}(\boldsymbol{r})}$$

With respect to problem (5), this problem is a bi-objective programming problem, and so without introducing some criterion of optimality for the bi-objective functions, it is hard to solve this problem directly. Therefore, considering fuzzy goals (6) and (7) for the bi-object and $f' = f_U$ for the standard target profit, we transform problem (5) into the following maximin programming problem:

$$\begin{aligned} &\text{Maximize} \ \min\left\{\mu_{\tilde{g}(d)}\left(z_d(\boldsymbol{x})\right), \mu_{\tilde{G}}(f)\right\} \\ &\text{subject to} \ E(\boldsymbol{r}) \geq f_U, \\ &\qquad \mathbf{1}^t\boldsymbol{\phi} = 1 \end{aligned} \tag{8}$$

This problem is also equivalently transformed into the following single-objective programming problem introducing parameter h which means the common target satisfaction level:

$$\begin{aligned} &\text{Maximize} \ h \\ &\text{subject to} \ \min\left\{\mu_{\tilde{g}(d)}\left(z_d(\boldsymbol{x})\right), \mu_{\tilde{G}}(f)\right\} \geq h, \\ &\qquad E(\boldsymbol{r}) \geq f_U, \\ &\qquad \mathbf{1}^t\boldsymbol{\phi} = 1 \end{aligned} \tag{9}$$

With respect to the first constraint of problem (9), we obtain the following deterministic equivalent transformations:

$$\begin{aligned} &\min\left\{\mu_{\tilde{g}(d)}\left(z_d(\boldsymbol{x})\right), \mu_{\tilde{G}}(f)\right\} \geq h, \\ &\Leftrightarrow \ \mu_{\tilde{g}(d)}\left(z_d(\boldsymbol{x})\right) \geq h, \ \mu_{\tilde{G}}(f) \geq h \\ &\Leftrightarrow \ \exists f : \frac{g_L(d) - f}{\left((d_U - d_L)\sqrt{\mathbf{Var}(\boldsymbol{r})}\right)} \geq h, \ \frac{f - f_L}{f_U - f_L} \geq h \\ &\Leftrightarrow \ \exists f : g_L(d) + h(d_L - d_U)\sqrt{\mathbf{Var}(\boldsymbol{r})} \geq f, f \geq (1-h)f_L + hf_U \\ &\Leftrightarrow \ E(\boldsymbol{r}) - d_L\sqrt{\mathbf{Var}(\boldsymbol{r})} + h(d_L - d_U)\sqrt{\mathbf{Var}(\boldsymbol{r})} \geq (1-h)f_L + hf_U \\ &\Leftrightarrow \ E(\boldsymbol{r}) - d_L\sqrt{\mathbf{Var}(\boldsymbol{r})} - f_L \geq h\left((d_U - d_L)\sqrt{\mathbf{Var}(\boldsymbol{r})} + (f_U - f_L)\right) \\ &\Leftrightarrow \ \frac{E(\boldsymbol{r}) - d_L\sqrt{\mathbf{Var}(\boldsymbol{r})} - f_L}{(d_U - d_L)\sqrt{\mathbf{Var}(\boldsymbol{r})} + (f_U - f_L)} \geq h \end{aligned} \tag{10}$$

Consequently, the proposed model is transformed into the following problem:

$$\begin{aligned} &\text{Maximize} \ h \\ &\text{subject to} \ \frac{E(\boldsymbol{r}) - d_L\sqrt{\mathbf{Var}(\boldsymbol{r})} - f_L}{(d_U - d_L)\sqrt{\mathbf{Var}(\boldsymbol{r})} + (f_U - f_L)} \geq h, \\ &\qquad E(\boldsymbol{r}) \geq f_U, \\ &\qquad \mathbf{1}^t\boldsymbol{\phi} = 1 \end{aligned} \tag{11}$$

i.e.,

$$\begin{aligned} &\text{Maximize} \ \frac{E(\boldsymbol{r}) - d_L\sqrt{\mathbf{Var}(\boldsymbol{r})} - f_L}{(d_U - d_L)\sqrt{\mathbf{Var}(\boldsymbol{r})} + (f_U - f_L)} \\ &\text{subject to} \ E(\boldsymbol{r}) \geq f_U, \\ &\qquad \mathbf{1}^t\boldsymbol{\phi} = 1 \end{aligned} \tag{12}$$

This objective function is fractional, but the numerator $E(\boldsymbol{r}) - d_L\sqrt{\mathbf{Var}(\boldsymbol{r})} - f_L$ is a concave function and the denominator $(d_U - d_L)\sqrt{\mathbf{Var}(\boldsymbol{r})} + (f_U - f_L)$ is a convex function, and so the objective function is convex. Then, all constraints are linear functions, and so problem (12) is a convex programming problem. Furthermore, this problem is similar to the model proposed by Dinkelbach [6].

In Dinkelbach [6], the following parametric programming problem $\mathbf{P}(q)$ introducing parameter q has been considered:

$$\begin{aligned} &\text{Maximize} \ E(\boldsymbol{r}) - d_L\sqrt{\mathbf{Var}(\boldsymbol{r})} - f_L \\ &\qquad - q\left((d_U - d_L)\sqrt{\mathbf{Var}(\boldsymbol{r})} + (f_U - f_L)\right) \\ &\text{subject to} \ E(\boldsymbol{r}) \geq f_U, \\ &\qquad \mathbf{1}^t\boldsymbol{\phi} = 1 \\ &\Leftrightarrow \ \text{Maximize} \ E(\boldsymbol{r}) - (1-q)f_L - qf_U \\ &\qquad - \left((1-q)d_L + qd_U\right)\sqrt{\mathbf{Var}(\boldsymbol{r})} \\ &\quad \text{subject to} \ E(\boldsymbol{r}) \geq f_U, \\ &\qquad \mathbf{1}^t\boldsymbol{\phi} = 1 \end{aligned} \tag{13}$$

With respect to this problem $\mathbf{P}(q)$, the following theorem holds.

Theorem 1 (Dinkelbach [6]): Let the objective function of $\mathbf{P}(q)$ be $F(q, \boldsymbol{\phi})$, and optimal solution of problem (12) be $\boldsymbol{\phi}^*$. Then,

$$q^* = \frac{\overline{\boldsymbol{r}}^t\boldsymbol{\phi}^* - d_L\sqrt{\boldsymbol{\phi}^{*t}\mathbf{V}\boldsymbol{\phi}^*} - f_L}{(d_U - d_L)\sqrt{\boldsymbol{\phi}^{*t}\mathbf{V}\boldsymbol{\phi}^*} + (f_U - f_L)}$$

if, and only if, $F(q^*, \boldsymbol{\phi}^*) = 0$.

Consequently, we develop the following exact solution algorithm for the proposed robust portfolio selection problem based on Dinkelbach [6].

Solution algorithm.

STEP1: Set $q_0 = 0$, and solve $\mathbf{P}(q_0)$. If there is no feasible solution, then terminate this algorithm. In this case, there is no feasible solution of main problem and it is necessary to reset fuzzy goals. Else if there is an optimal portfolio, let the optimal portfolio of $\mathbf{P}(q_0)$ be $\boldsymbol{\phi}_1$, and set $k = 1$. Go to STEP2.

STEP2: Evaluate

$$q_k = \frac{\overline{\boldsymbol{r}}^t\boldsymbol{\phi}_k - d_L\sqrt{\boldsymbol{\phi}_k^t\mathbf{V}\boldsymbol{\phi}_k} - f_L}{(d_U - d_L)\sqrt{\boldsymbol{\phi}_k^t\mathbf{V}\boldsymbol{\phi}_k} + (f_U - f_L)},$$

and go to STEP3.

STEP3: Solve $\mathbf{P}(q_k)$, and denote the optimal solution by $\boldsymbol{\phi}_{k+1}$. Go to STEP4.

STEP4: With respect to sufficiently small number ε, if $F(q_k, \boldsymbol{\phi}_{k+1}) < \varepsilon$, then terminate this algorithm. In

this case, ϕ_{k+1} is the optimal portfolio. Else if $F(q_k, \phi_{k+1}) \geq \varepsilon$, $k \leftarrow k+1$ and return to STEP2.

IV. Exact Optimal Portfolio of $\mathbf{P}(q)$

In the solution algorithm in Section 3, we need to solve problem $\mathbf{P}(q_k)$ on each q_k, repeatedly. Therefore, it is also important to consider the solution algorithm for $\mathbf{P}(q)$. In this section, we develop the strict solution algorithm to obtain the exact optimal portfolio of $\mathbf{P}(q)$.

We consider the following problem which is equivalent to be $\mathbf{P}(q)$:

$$\begin{aligned} &\text{Minimize} \quad -\bar{\boldsymbol{r}}^t\phi + f_q + d_q\sqrt{\phi^t\mathbf{V}\phi} \\ &\text{subject to} \quad \bar{\boldsymbol{r}}^t\phi \geq f_U, \\ &\qquad\qquad \mathbf{1}^t\phi = 1 \end{aligned} \tag{14}$$

where $f_q = (1-q)f_L + qf_U$ and $d_q = (1-q)d_L + qd_U$. Then, f_q and d_q are positive values. With respect to this problem, since $\mathbf{V}$ is a variance-covariance matrix which is positive definite, we perform the following equivalent transformations of variables:

$$\begin{aligned} &\phi^t\mathbf{V}\phi = \boldsymbol{x}^t\boldsymbol{x} \\ &\mathbf{V} = \mathbf{Q}^t\mathbf{\Lambda}\mathbf{Q}, \ \begin{pmatrix}\mathbf{Q}: \textit{unitary matrix} \\ \textit{consisting of eigen vectors of } \mathbf{V}\end{pmatrix} \\ &\mathbf{\Lambda} = \begin{pmatrix}\lambda_1 & & \mathbf{0} \\ & \ddots & \\ \mathbf{0} & & \lambda_n\end{pmatrix}, \ (\lambda_i : \textit{eigen value of } \mathbf{V}) \\ &\mathbf{\Lambda} = \left(\mathbf{\Lambda}^{1/2}\right)^t\mathbf{\Lambda}^{1/2}, \ \mathbf{\Lambda}^{1/2} = \left(\mathbf{\Lambda}^{1/2}\right)^t = \begin{pmatrix}\sqrt{\lambda_1} & & \mathbf{0} \\ & \ddots & \\ \mathbf{0} & & \sqrt{\lambda_n}\end{pmatrix} \\ &\boldsymbol{x} = \mathbf{\Lambda}^{1/2}\mathbf{Q}\phi, \ \bar{\boldsymbol{r}}' = \left(\mathbf{\Lambda}^{1/2}\right)^{-1}\mathbf{Q}\bar{\boldsymbol{r}}, \ \boldsymbol{a} = \left(\mathbf{\Lambda}^{1/2}\right)^{-1}\mathbf{Q}\mathbf{1} \end{aligned} \tag{15}$$

Using these transformations of variables, problem (15) is equivalently transformed into the following problem:

$$\begin{aligned} &\text{Minimize} \quad -\bar{\boldsymbol{r}}'^t\boldsymbol{x} + f_q + d_q\sqrt{\boldsymbol{x}^t\boldsymbol{x}} \\ &\text{subject to} \quad \bar{\boldsymbol{r}}'^t\boldsymbol{x} \geq f_U, \\ &\qquad\qquad \boldsymbol{a}^t\boldsymbol{x} = 1 \end{aligned} \tag{16}$$

This problem still includes a square root term as well as problem (14). Therefore, in order to obtain the exact optimal portfolio to problem (16), we introduce the following auxiliary problem using a parameter R not including the square root term:

$$\begin{aligned} &\text{Minimize} \quad R\left(-\bar{\boldsymbol{r}}'^t\boldsymbol{x} + f_q\right) + \frac{d_q}{2}\left(\boldsymbol{x}^t\boldsymbol{x}\right) \\ &\text{subject to} \quad \bar{\boldsymbol{r}}'^t\boldsymbol{x} \geq f_U, \\ &\qquad\qquad \boldsymbol{a}^t\boldsymbol{x} = 1 \end{aligned} \tag{17}$$

Since this problem is a quadratic convex programming problem, we solve problem (17) more easily than problem (16). Furthermore, with respect to the relation between problem (16) and its auxiliary problem (17), the following theorem holds.

Theorem 2: Let the optimal solution of auxiliary problem (17) be $\boldsymbol{x}(R)$. If $R = \sqrt{\sum_{j=1}^{n} x_j(R)^2}$ is satisfied, $\boldsymbol{x}(R)$ is also the optimal solution of problem (16).

Proof: We compare Karush-Kuhn-Tucker (KKT) conditions of problem (16) with that of problem (17). the KKT condition of problem (16) is as follows:

$$\begin{aligned} L &= -\sum_{j=1}^{n}\bar{r}'_j x_j + f_q + d_q\sqrt{\sum_{j=1}^{n}x_j^2} \\ &\quad + u\left(f_U - \sum_{j=1}^{n}\bar{r}'_j x_j\right) + v\left(1 - \sum_{j=1}^{n}a_j x_j\right) \\ \frac{\partial L}{\partial x_j} &= -\bar{r}'_j + d_q\frac{x_j}{\sqrt{\sum_{j=1}^{n}x_j^2}} - u\bar{r}'_j - va_j = 0 \end{aligned} \tag{18}$$

the KKT condition of auxiliary problem (17) is also obtained as follows:

$$\begin{aligned} L' &= -R\sum_{j=1}^{n}\bar{r}'_j x_j + Rf_q + \frac{d_q}{2}\left(\sum_{j=1}^{n}x_j^2\right) \\ &\quad + u'\left(f_U - \sum_{j=1}^{n}\bar{r}'_j x_j\right) + v'\left(1 - \sum_{j=1}^{n}a_j x_j\right) \\ \frac{\partial L'}{\partial x_j} &= -R\bar{r}'_j + d_q x_j - u'\bar{r}'_j - v'a_j = 0 \end{aligned} \tag{19}$$

With respect to these KKT conditions, we set $u = u'/R$, $v = v'/R$. Then, satisfying $R = \sqrt{\sum_{j=1}^{n} x_j(R)^2}$, the KKT condition of problem (17) is equal to that of problem (16). Therefore, this theorem holds. □

This theorem means that we can obtain the optimal solution of problem (14) by solving the auxiliary quadratic programming problem (17) setting the appropriate parameter R.

With respect to problem (17) and the KKT condition (19), we consider the following two cases. We reconsider the following KKT condition of problem (17) including complementary conditions:

$$\begin{cases} \dfrac{\partial L}{\partial \boldsymbol{x}} = -R\overline{\boldsymbol{r}}' + d_q \boldsymbol{x} - u\overline{\boldsymbol{r}}' - v\boldsymbol{a} = 0 \\ u\left(f_U - \overline{\boldsymbol{r}}'^t \boldsymbol{x}\right) = 0 \\ \boldsymbol{a}^t \boldsymbol{x} = 1 \end{cases} \tag{20}$$

First, in the case of $f_U - \overline{\boldsymbol{r}}'^t \boldsymbol{x} = 0$, KKT condition (20) is degenerated as follows:

$$\begin{cases} -R\overline{\boldsymbol{r}}' + d_q \boldsymbol{x} - u\overline{\boldsymbol{r}}' - v\boldsymbol{a} = 0 \\ f_U - \overline{\boldsymbol{r}}'^t \boldsymbol{x} = 0 \\ \boldsymbol{a}^t \boldsymbol{x} = 1 \end{cases} \tag{21}$$

Since we obtain $\boldsymbol{x} = \dfrac{(R+u)\overline{\boldsymbol{r}}' + v\boldsymbol{a}}{d_q}$ from the first equation of (21), we calculate the following solution for each parameter:

$$\begin{cases} v = \dfrac{d_q\left(\left\|\overline{\boldsymbol{r}}'\right\|^2 - f_U\left(\overline{\boldsymbol{r}}'^t \boldsymbol{a}\right)\right)}{\left\|\overline{\boldsymbol{r}}'\right\|^2 \left\|\boldsymbol{a}\right\|^2 - \left(\overline{\boldsymbol{r}}'^t \boldsymbol{a}\right)^2} \\ (R+u) = \dfrac{d_q\left(f_U \left\|\boldsymbol{a}\right\|^2 - \left(\overline{\boldsymbol{r}}'^t \boldsymbol{a}\right)\right)}{\left\|\overline{\boldsymbol{r}}'\right\|^2 \left\|\boldsymbol{a}\right\|^2 - \left(\overline{\boldsymbol{r}}'^t \boldsymbol{a}\right)^2} \end{cases} \tag{22}$$

Consequently, we obtain the optimal portfolio of problem (14) as follows:

$$\begin{aligned} \boldsymbol{x}^* &= \frac{\overline{\boldsymbol{r}}'}{d_q}\left(\frac{d_q\left(f_U \left\|\boldsymbol{a}\right\|^2 - \left(\overline{\boldsymbol{r}}'^t \boldsymbol{a}\right)\right)}{\left\|\overline{\boldsymbol{r}}'\right\|^2 \left\|\boldsymbol{a}\right\|^2 - \left(\overline{\boldsymbol{r}}'^t \boldsymbol{a}\right)^2}\right) + \frac{\boldsymbol{a}}{d_q}\left(\frac{d_q\left(\left\|\overline{\boldsymbol{r}}'\right\|^2 - f_U\left(\overline{\boldsymbol{r}}'^t \boldsymbol{a}\right)\right)}{\left\|\overline{\boldsymbol{r}}'\right\|^2 \left\|\boldsymbol{a}\right\|^2 - \left(\overline{\boldsymbol{r}}'^t \boldsymbol{a}\right)^2}\right) \\ \Leftrightarrow \quad \boldsymbol{x}^* &= \frac{\left(f_U \left\|\boldsymbol{a}\right\|^2 - \left(\overline{\boldsymbol{r}}'^t \boldsymbol{a}\right)\right)}{\left\|\overline{\boldsymbol{r}}'\right\|^2 \left\|\boldsymbol{a}\right\|^2 - \left(\overline{\boldsymbol{r}}'^t \boldsymbol{a}\right)^2}\overline{\boldsymbol{r}}' + \frac{\left(\left\|\overline{\boldsymbol{r}}'\right\|^2 - f_U\left(\overline{\boldsymbol{r}}'^t \boldsymbol{a}\right)\right)}{\left\|\overline{\boldsymbol{r}}'\right\|^2 \left\|\boldsymbol{a}\right\|^2 - \left(\overline{\boldsymbol{r}}'^t \boldsymbol{a}\right)^2}\boldsymbol{a} \\ \Leftrightarrow \quad \boldsymbol{\Lambda}^{1/2}\mathbf{Q}\boldsymbol{\phi}^* &= \frac{\left(f_U \left\|\left(\boldsymbol{\Lambda}^{1/2}\right)^{-1}\mathbf{Q}\mathbf{1}\right\|^2 - \left(\overline{\boldsymbol{r}}'^t \mathbf{Q}^t \boldsymbol{\Lambda}^{-1}\mathbf{Q}\mathbf{1}\right)\right)}{\left\|\left(\boldsymbol{\Lambda}^{1/2}\right)^{-1}\mathbf{Q}\overline{\boldsymbol{r}}\right\|^2 \left\|\left(\boldsymbol{\Lambda}^{1/2}\right)^{-1}\mathbf{Q}\mathbf{1}\right\|^2 - \left(\overline{\boldsymbol{r}}'^t \mathbf{Q}^t \boldsymbol{\Lambda}^{-1}\mathbf{Q}\mathbf{1}\right)^2}\overline{\boldsymbol{r}}' \\ &\quad + \frac{\left(\left\|\left(\boldsymbol{\Lambda}^{1/2}\right)^{-1}\mathbf{Q}\overline{\boldsymbol{r}}\right\|^2 - f_U\left(\overline{\boldsymbol{r}}'^t \mathbf{Q}^t \boldsymbol{\Lambda}^{-1}\mathbf{Q}\mathbf{1}\right)\right)}{\left\|\left(\boldsymbol{\Lambda}^{1/2}\right)^{-1}\mathbf{Q}\overline{\boldsymbol{r}}\right\|^2 \left\|\left(\boldsymbol{\Lambda}^{1/2}\right)^{-1}\mathbf{Q}\mathbf{1}\right\|^2 - \left(\overline{\boldsymbol{r}}'^t \mathbf{Q}^t \boldsymbol{\Lambda}^{-1}\mathbf{Q}\mathbf{1}\right)^2}\boldsymbol{a} \\ \Leftrightarrow \quad \boldsymbol{\phi}^* &= \frac{\left(f_U\left(\mathbf{1}^t\mathbf{V}^{-1}\mathbf{1}\right) - \left(\overline{\boldsymbol{r}}'^t\mathbf{V}^{-1}\mathbf{1}\right)\right)\overline{\boldsymbol{r}}' + \left(\left(\overline{\boldsymbol{r}}'^t\mathbf{V}^{-1}\overline{\boldsymbol{r}}\right) - f_U\left(\overline{\boldsymbol{r}}'^t\mathbf{V}^{-1}\mathbf{1}\right)\right)\boldsymbol{a}}{\left(\overline{\boldsymbol{r}}'^t\mathbf{V}^{-1}\mathbf{1}\right)\left(\mathbf{1}^t\mathbf{V}^{-1}\mathbf{1}\right) - \left(\overline{\boldsymbol{r}}'^t\mathbf{V}^{-1}\mathbf{1}\right)^2} \end{aligned} \tag{23}$$

From solution (23), by calculating only inverse matrix $\mathbf{V}^{-1}$ of variance-covariance matrix $\mathbf{V}$, we obtain optimal portfolio $\boldsymbol{\phi}^*$. Furthermore, we find that the optimal portfolio of problem $\mathbf{P}(q)$ in the case $f_U - \overline{\boldsymbol{r}}'^t \boldsymbol{x} = 0$ does not depend on parameter d_q to represent robustness.

Second, in the case of $f_U - \overline{\boldsymbol{r}}'^t \boldsymbol{x} > 0$, i.e., $u = 0$, KKT condition (20) is degenerated as follows:

$$\begin{cases} \dfrac{\partial L}{\partial \boldsymbol{x}} = -R\overline{\boldsymbol{r}}' + d_q \boldsymbol{x} - v\boldsymbol{a} = 0 \\ \boldsymbol{a}^t \boldsymbol{x} = 1 \end{cases} \tag{24}$$

Since we obtain $\boldsymbol{x} = \dfrac{R\overline{\boldsymbol{r}}' + v\boldsymbol{a}}{d_q}$ from the first equation of (24), we calculate the following solution for v:

$$\begin{aligned} & \boldsymbol{a}^t \boldsymbol{x} = 1 \\ \Leftrightarrow \ & \boldsymbol{a}^t\left(\frac{R\overline{\boldsymbol{r}}' + v\boldsymbol{a}}{d_q}\right) = 1 \\ \Leftrightarrow \ & v = \frac{d_q - R\left(\overline{\boldsymbol{r}}'^t \boldsymbol{a}\right)}{\left\|\boldsymbol{a}\right\|^2} \end{aligned} \tag{25}$$

Therefore, we also calculate solution $\boldsymbol{x}$ including parameter R as follows:

$$\begin{aligned} & \boldsymbol{x} = \frac{R}{d_q}\overline{\boldsymbol{r}}' + \frac{v}{d_q}\boldsymbol{a} = \frac{R}{d_q}\overline{\boldsymbol{r}}' + \frac{d_q - R\left(\overline{\boldsymbol{r}}'^t \boldsymbol{a}\right)}{d_q\left\|\boldsymbol{a}\right\|^2}\boldsymbol{a} \\ \Leftrightarrow \ & \boldsymbol{x}(R) = \frac{R}{d_q}\left(\overline{\boldsymbol{r}}' - \frac{\left(\overline{\boldsymbol{r}}'^t \boldsymbol{a}\right)}{\left\|\boldsymbol{a}\right\|^2}\boldsymbol{a}\right) + \frac{\boldsymbol{a}}{\left\|\boldsymbol{a}\right\|^2} \end{aligned} \tag{26}$$

By substituting $\boldsymbol{x}(R)$ of (26) into optimal condition for parameter R : $R = \sqrt{\sum_{j=1}^{n} x_j(R)^2}$, we solve the following equation:

$$\begin{aligned} R^2 &= \left(\frac{R}{d_q}\left(\overline{\boldsymbol{r}}' - \frac{\left(\overline{\boldsymbol{r}}'^t \boldsymbol{a}\right)}{\left\|\boldsymbol{a}\right\|^2}\boldsymbol{a}\right) + \frac{\boldsymbol{a}}{\left\|\boldsymbol{a}\right\|^2}\right)^t \left(\frac{R}{d_q}\left(\overline{\boldsymbol{r}}' - \frac{\left(\overline{\boldsymbol{r}}'^t \boldsymbol{a}\right)}{\left\|\boldsymbol{a}\right\|^2}\boldsymbol{a}\right) + \frac{\boldsymbol{a}}{\left\|\boldsymbol{a}\right\|^2}\right) \\ R^2 &= \frac{R^2}{d_q^2}\left(\overline{\boldsymbol{r}}' - \frac{\left(\overline{\boldsymbol{r}}'^t \boldsymbol{a}\right)}{\left\|\boldsymbol{a}\right\|^2}\boldsymbol{a}\right)^t \left(\overline{\boldsymbol{r}}' - \frac{\left(\overline{\boldsymbol{r}}'^t \boldsymbol{a}\right)}{\left\|\boldsymbol{a}\right\|^2}\boldsymbol{a}\right) \\ &\quad + \frac{2R}{d_q}\left(\overline{\boldsymbol{r}}' - \frac{\left(\overline{\boldsymbol{r}}'^t \boldsymbol{a}\right)}{\left\|\boldsymbol{a}\right\|^2}\boldsymbol{a}\right)\frac{\boldsymbol{a}}{\left\|\boldsymbol{a}\right\|^2} + \frac{1}{\left\|\boldsymbol{a}\right\|^2} \\ R^2 &= \frac{R^2}{d_q^2}\left(\left\|\overline{\boldsymbol{r}}'\right\|^2 - \frac{\left(\overline{\boldsymbol{r}}'^t \boldsymbol{a}\right)^2}{\left\|\boldsymbol{a}\right\|^2}\right) + \frac{1}{\left\|\boldsymbol{a}\right\|^2} \\ d_q^2\left\|\boldsymbol{a}\right\|^2 R^2 &= R^2\left(\left\|\overline{\boldsymbol{r}}'\right\|^2 \left\|\boldsymbol{a}\right\|^2 - \left(\overline{\boldsymbol{r}}'^t \boldsymbol{a}\right)^2\right) + 1 \\ \left(d_q^2\left\|\boldsymbol{a}\right\|^2 + \left(\overline{\boldsymbol{r}}'^t \boldsymbol{a}\right)^2 - \left\|\overline{\boldsymbol{r}}'\right\|^2 \left\|\boldsymbol{a}\right\|^2\right) R^2 &= 1 \\ R^* &= \sqrt{\frac{1}{d_q^2\left\|\boldsymbol{a}\right\|^2 + \left(\overline{\boldsymbol{r}}'^t \boldsymbol{a}\right)^2 - \left\|\overline{\boldsymbol{r}}'\right\|^2 \left\|\boldsymbol{a}\right\|^2}} \ \left(\because R \geq 0\right) \end{aligned} \tag{27}$$

Consequently, we obtain the exact optimal solution of $\boldsymbol{x}$ as

$$\boldsymbol{x}^* = \frac{R^*}{d_q}\left(\overline{\boldsymbol{r}}' - \frac{\left(\overline{\boldsymbol{r}}'^t \boldsymbol{a}\right)}{\left\|\boldsymbol{a}\right\|^2}\boldsymbol{a}\right) + \frac{\boldsymbol{a}}{\left\|\boldsymbol{a}\right\|^2},$$

and so the exact optimal solution of problem (14) is represented as the following form:

$$\phi^* = \mathbf{V}^{-1}\left(\frac{R^*}{d_q}\left(\bar{\boldsymbol{r}} - \frac{\left(\bar{\boldsymbol{r}}^t\mathbf{V}^{-1}\mathbf{1}\right)}{\mathbf{1}^t\mathbf{V}^{-1}\mathbf{1}}\mathbf{1}\right) + \frac{1}{\mathbf{1}^t\mathbf{V}^{-1}\mathbf{1}}\mathbf{1}\right)$$
$$R^* = \sqrt{\frac{1}{\left(d_q^2 - \left(\bar{\boldsymbol{r}}^t\mathbf{V}^{-1}\bar{\boldsymbol{r}}\right)\right)\left(\mathbf{1}^t\mathbf{V}^{-1}\mathbf{1}\right) + \left(\bar{\boldsymbol{r}}^t\mathbf{V}^{-1}\mathbf{1}\right)}} \qquad (28)$$

From solution (28), by calculating only inverse matrix $\mathbf{V}^{-1}$ of variance-covariance matrix $\mathbf{V}$, we obtain optimal parameter R^* and portfolio ϕ^*. Furthermore, we find that the optimal portfolio of problem $\mathbf{P}(q)$ in the case $f_U - \bar{\boldsymbol{r}}'^t\boldsymbol{x} > 0$ does not depend on parameter f_U to represent the standard target profit.

V. CONCLUSION

In this paper, we have proposed a robust portfolio selection problem considering the confidential interval to the total profit with investor's subjectivity. Since the proposed model is a bi-objective programming problem with fuzziness, we have introduced fuzzy goals for both objective functions, and transformed it into the deterministic equivalent problems. Furthermore, in order to obtain the explicit optimal portfolio, we have developed the exact solution algorithm based on the Dinkelbach's algorithm and auxiliary quadratic programming problem without loss of optimality. Our proposed model includes some existing robust portfolio selection problems, and specific random distributions are not assumed in the model. Therefore, we may apply our models to the more flexible and complex portfolio selection problems in real investment markets than the previous models.

As future studies, we need to consider the application of our proposed model and solution algorithm to large-scale or multi-period portfolio selection problems. Then, we are now attacking the sensitivity analysis for parameters of the proposed robust portfolio model.

REFERENCES

[1] V.S. Bawa and E.B. Lindenberg, "Capital market equilibrium in a mean-lower partial moment framework", *Journal of Financial Economics*, 5, pp. 189-200, 1977.

[2] A. Ben-Tal and A. Nemirovski, "Robust solutions of uncertain linear programs", *Operations Research Letters*, 25(1), pp. 1-13, 1999.

[3] A. Ben-Tal and A. Nemirovski, "Lectures on modern convex optimization", SIAM, Philadelphia, PA, 2001.

[4] A. Bilbao-Terol, B. Perez-Gladish, M. Arenas-Parra and M.V. Rodriguez-Uria, "Fuzzy compromise programming for portfolio selection", *Applied Mathematics and Computation*, 173, pp. 251-264, 2006.

[5] C. Carlsson, R. Fuller, and P. Majlender, "A possibilistic approach to selecting portfolios with highest utility score", *Fuzzy Sets and Systems*, 131, pp.12-21, 2002.

[6] W. Dinkelbach, "On nonlinear fractional programming", *Management Science*, 13(7), pp. 492-498, 1967.

[7] E.J. Elton and M.J. Gruber, *Modern Portfolio Theory and Investment Analysis*, Wiley, New York, 1995.

[8] L.E. Ghaoui and H. Lebret, "Robust solutions to least squares problems with uncertain data", *Journal of Matrix Analysis and Applications*, 18, pp.1035-1064, 1997.

[9] D. Goldfarb and G. Iyengar, "Robust portfolio selection problems", *Mathematics of Operations Research*, 28, pp. 1-38, 2003

[10] P. Guo and H. Tanaka, "Possibility data analysis and its application to portfolio sekection problems", *Fuzzy Economic Rev*., 3, pp. 3-23, 1998.

[11] T. Hasuike, H. Katagiri, and H. Ishii, "Portfolio selection problems with random fuzzy variable returns", *Fuzzy Sets and Systems*, 160, pp. 2579-2596, 2009.

[12] X. Huang, "Fuzzy chance-constrained portfolio selection", *Applied Mathematics and Computation*, 177, pp. 500-5007, 2006.

[13] X. Hung, "Two new models for portfolio selection with stochastic returns taking fuzzy information", *European Journal of Operational Research*, 180, pp. 396-405, 2007.

[14] M. Inuiguchi and J. Ramik, "Possibilisitc linear programming: A brief review of fuzzy mathematical programming and a comparison with stochastic programming in portfolio selection problem", *Fuzzy Sets and Systems*, 111, pp. 3-28, 2000.

[15] M.Inuiguchi and T. Tanino, "Portfolio selection under independent possibilistic information", *Fuzzy Sets and Systems*, 115, pp. 83-92, 2000.

[16] H. Katagiri, H. Ishii, and M. Sakawa, "On fuzzy random linear knapsack problems", *Central European Journal of Operations Research*, Vol.12 No.1, pp. 59-70, 2004.

[17] H. Katagiri, M. Sakawa, and H. Ishii, "A study on fuzzy random portfolio selection problems using possibility and necessity measures", *Scientiae Mathematicae Japonicae,* Vol.65 No.2, pp.361-369, 2005.

[18] H. Konno and H. Yamazaki, "Mean-Absolute Deviation Portfolio Optimization Model and Its Applications to Tokyo Stock Market", *Management Science*, 37, pp. 519-531, 1991.

[19] H. Konno, H. Shirakawa, and H. Yamazaki, "A mean-absolute deviation-skewness portfolio optimization model", *Annals of Operations Research*, 45, pp. 205-220, 1993.

[20] M.S. Lobo, *Robust and convex optimization with applications in finance*, Doctor thesis of the Department of Electrical Engineering and the Committee on Graduate Studies, Stanford University, 2000

[21] H.M. Markowitz, "Portfolio Selection", *The Journal of Finance*, 7(1), pp. 77–91, 1952.

[22] R.T. Rockafellar and S. Uryasev, "Optimization of conditional value-at-risk", *Journal of Risk*, 2(3), pp. 1-21, 2000.

[23] H. Tanaka and P. Guo, "Portfolio selection based on upper and lower exponential possibility distributions", *European Journal of Operational Researches*, 114, pp. 115-126, 1999.

[24] H. Tanaka, P. Guo, and I.B. Turksen, "Portfolio selection based on fuzzy probabilities and possibility distributions", *Fuzzy Sets and Systems*, 111, pp. 387-397, 2000.

[25] J. Watada, "Fuzzy portfolio selection and its applications to decision making", *Tatra Mountains Math. Pub.*, 13, pp. 219-248, 1997.

[26] J. Watada, S. Wang, and W. Pedrycz, "Building confidence-interval-based fuzzy random regression models", *IEEE Transaction on Fuzzy Systems*, 17(6), pp. 1273-1283, 2009.

2011 IEEE International Conference on Fuzzy Systems
June 27-30, 2011, Taipei, Taiwan

On Some Fuzzy Relations for Color Information

D. Sánchez
European Centre for Soft Computing
Mieres, Asturias, Spain
daniel.sanchezf@softcomputing.es

J. M. Soto-Hidalgo
Dept. Computer Architecture,
Electronics, and Electronic Technology
University of Córdoba, Spain
jmsoto@uco.es

J. Chamorro-Martínez, P. Martínez-Jiménez
Dept. Computer Science and A.I.
University of Granada, Spain
{jesus,pedromartinez}@decsai.ugr.es

***Abstract*—In this paper we introduce several fuzzy resemblance relations between different combinations of crisp and fuzzy colors. As a starting point, we discuss about fuzzy colors and fuzzy color spaces as a way to represent color information, providing examples of conjunctive and disjunctive use of fuzzy colors for this purpose. Then we determine different types of relations measuring the degree of matching between color information of different kinds, using well known results from fuzzy sets and possibility theories. We study the particular case in which the user considers there is no resemblance between the fuzzy colors comprising the fuzzy color space under consideration. The proposal is based on definitions of fuzzy color and fuzzy color space provided by the authors in previous works.**

***Index Terms*—Fuzzy Color Information, Fuzzy Relations.**

I. Introduction

Humans and computers describe colors in a completely different way, a problem that is known as the *semantic gap*. Whilst computers represent colors as points in some three-dimensional (color) space, humans employ a comparatively much smaller collection of linguistic terms like *red*, *light blue*, and *strong green*.

This fact poses very interesting problems when developing applications for managing color information in which the source or destination of part of the information is a human user, whilst the rest has been obtained by means of sensors or has been generated synthetically [1]. This is the case in applications like generating descriptions of pictures for visually impaired people, determining the suitability of a certain soil for a specific cultivation, or detecting potentially cancerogenous areas in the skin, just to mention a few among a huge number.

In this paper, we are interested in problems about uncertainty in both the representation and the relationships between pieces of color information. Several authors have pointed out the suitability of the theory of fuzzy sets for this purpose, leading to the introduction of notions like *fuzzy color* for representing the compatibility between triplets of real values (crisp colors) and linguistic terms [2]–[12].

However, to the best of our knowledge, no deep study of how to use these concepts for representing uncertain color information, or relating pieces of color information for flexible query answering, have been made available in the literature. Our objective in this work is to go a step forward in this direction.

This work has been partially supported by the Spanish Government under project TIN2009-08296.

The rest of the paper is organized as follows. In section II we describe the approach to fuzzy colors and fuzzy color spaces introduced in [12]. Possible uses of fuzzy colors for representing color information are described in section III. In section IV we introduce different fuzzy relations for evaluating different types of matching queries involving color information. These relations are particularized to the case of a specific resemblance relation between fuzzy colors in section V. Finally, section VI contains our conclusions and future research plans in this area.

II. Fuzzy Modelling of Colors

All along the paper, we will consider the notions of fuzzy color (section II-A) and fuzzy color space (section II-B) introduced in [12]. We introduce these notions in the following sections.

A. Fuzzy color

In order to represent the semantic compatibility between crisp colors and linguistic color terms, in [12] we introduce the following definition of fuzzy color:

Definition 2.1: [12] A fuzzy color $\widetilde{C}$ is a normalized fuzzy subset of crisp colors.

As previously explained, crisp colors can be represented as a triplet of real numbers corresponding to coordinates in a color space. Hence, a fuzzy color can be defined as a normalized fuzzy subset of points of a color space. From now on, we shall assume that a generic color space with components X, Y and Z whose domains are D_X, D_Y and D_Z respectively, is employed. We shall call this color space XYZ (not to be confused with the CIE XYZ color space, which is just one particular case). This leads to the following more specific definition [12]:

Definition 2.2: [12] A fuzzy color $\widetilde{C}$ is a linguistic label whose semantics is represented in a color space XYZ by a normalized fuzzy subset of $D_X \times D_Y \times D_Z$.

Def. 2.2 implies that for each fuzzy color $\widetilde{C}$ there is at least one crisp color $\mathbf{r}_{\widetilde{C}}$ such that $\widetilde{C}(\mathbf{r}_{\widetilde{C}}) = 1$. Also, the membership function is not required to be convex. This leaves open the possibility to define color terms like for example *chocolat*, that may be represented by the union of the fuzzy sets for color

978-1-4244-7316-8/11/$26.00 ©2011 IEEE

terms like *white*, *dark brown*, and *black*. Following this idea, we shall consider two kind of fuzzy colors:

- *Atomic colors*, those colors that are not defined on the basis of other colors, like *white*, *dark brown*, and *black* in the previous example. We shall consider that atomic colors are represented by means of convex fuzzy sets; in particular this implies ${}^{\alpha}\widetilde{C}$ is a convex volume $\forall \alpha \in (0,1]$, where ${}^{\alpha}\widetilde{C}$ is the α-cut of degree α of the fuzzy color $\widetilde{C}$.
- *Derived colors*, those defined on the basis of other colors by means of logical operations, like the color *chocolat* of the previous example.

Since the representation of fuzzy colors is a matter of semantics, we have that not every convex fuzzy subset of colors corresponds necessarily to an atomic fuzzy set. Another important problem related to the semantics arises because it is possible to represent the same fuzzy color by means of different fuzzy subsets on different color spaces, provided they have the same expressive power. For example, a fuzzy color *red* may be represented as a fuzzy subset with semantics "approximately [255,0,0]" if we employ the RGB color space or as a fuzzy subset with semantics "approximately [0,1,128]" if we use the HSV space. However, if we apply a transformation of the crisp colors in "approximately [255,0,0]" to HSV and we maintain the membership degrees, the result may not be "approximately [0,1,128]"; even worst, when performing such transformations from one color space to another, we can obtain a non-convex fuzzy set! Hence, a fuzzy subset of colors that semantically is an atomic fuzzy color has a non-convex representation in other spaces.

A particular case of this problem comes from the fact that the expressive power (the *gamut*) is not the same for every color space, so it could be the case that some crisp colors with degree 0 appear inside the convex volume when changing the representation, corresponding to colors that the original color space is not able to represent. However, non-convexity on the support of the fuzzy set could in principle arise as well because of the transformation from one color space to another because of a spatial redistribution of crisp colors in the color space, even if both color spaces have the same gamut. As a consequence, the notion of atomic fuzzy color may be dependent on the color space employed in the definition of the membership function. Hence, we introduce the following definitions: let XYZ be a (crisp) color space.

Definition 2.3: [12] A XYZ fuzzy color is a fuzzy color whose membership function is defined on XYZ.

Definition 2.4: [12] An atomic XYZ fuzzy color is a fuzzy color whose membership function is convex on XYZ.

From now on we will say that a fuzzy color is simply *atomic* when it is atomic in some color space XYZ.

B. Fuzzy color space

For extending the concept of color space to the case of fuzzy colors, and assuming a fixed color space XYZ, with D_X, D_Y and D_Z being the domains of the corresponding color components, the following definition is introduced in [12]:

Definition 2.5: [12] A fuzzy color space $\widetilde{XYZ}$ is a set of atomic XYZ fuzzy colors that define a partition of $D_X \times D_Y \times D_Z$.

We consider that a fuzzy partition of the color space XYZ is a crisp set of m fuzzy colors $\widetilde{C}_1, \ldots, \widetilde{C}_m$ verifying the following properties [12]:

1) $\bigcup_{\{1,\ldots,m\}} sup(\widetilde{C}_i) = XYZ$, i.e., the union of the support of the $\widetilde{C}_i$ covers the whole space.
2) $ker(\widetilde{C}_i) \cap ker(\widetilde{C}_j) = \emptyset \ \forall i \neq j$, i.e., the kernels of the $\widetilde{C}_i$ and $\widetilde{C}_j$ are pairwise disjoint.
3) $\forall i \in \{1,\ldots,m\} \ \exists \mathbf{c} \in XYZ$ such that $\widetilde{C}_i(\mathbf{c}) = 1$, i.e., there is at least one object fully representative of the fuzzy color $\widetilde{C}_i$.

Condition 3 is always verified by definition of fuzzy color. Condition 1 implies $\forall \mathbf{c} \in XYZ \ \exists i \in \{1,\ldots,m\}$ such that $\widetilde{C}_i(\mathbf{c}) > 0$. Conditions 2 and 3 imply $\widetilde{C}_i \not\subseteq \widetilde{C}_j \ \forall i \neq j$.

III. Color Information

Fuzzy colors allow us to represent color information in a computer, filling the semantic gap with human's perception of color. However, it is important to remark that the same fuzzy color may represent information with different semantics depending on its use.

Fuzzy colors can be used both in a conjunctive and disjunctive way as pieces of information [13]–[16]. An example of a conjunctive use is to answer with a fuzzy color $\widetilde{C}$ to the question "which are the red colors?". In this case, each crisp color c is part of the answer with a degree given by $\widetilde{C}(c)$. An example of disjunctive use is to provide a fuzzy color for answering the question "what's the color of that car?". In this second case, the true answer is a single crisp color, but we do not know exactly what one, so we answer by giving a restriction on the set of crisp colors given by the fuzzy color $\widetilde{C}$, i.e., the possibility that a certain crisp color c is the color of the car is $\widetilde{C}(c)$. Hence, a disjunctively-used fuzzy color is a possibility distribution on the set of crisp colors. From now on we shall denote the conjunctive (resp. disjunctive) use of fuzzy colors as Cu (resp. Du), i.e., we shall say that a fuzzy color is conjunctively used (Cu) or disjunctively used (Du).

Hence, in this paper we shall consider that color information may be expressed by means of:

1) A crisp color $c \in XYZ$, e.g., *this pixel has color* **[0,0,0]** *in RGB*.
2) A conjunctively-used fuzzy color, e.g., *I like* **red** *cars*; *the grass is* **green**. It defines the compatibility degree between a linguistic term and the crisp colors in a crisp color space.
3) A disjunctively-used fuzzy color (possibility distribution on the set of crisp colors), corresponding to a description by means of a flexible restriction of our knowledge about the actual value of a variable whose possible values are crisp colors. For example, *my car is* **red**;

Table I indicates the actual information represented by each of the previous cases, as well as the presence of imprecision and/or uncertainty.

TABLE I
COLOR INFORMATION, TYPE OF VALUE REPRESENTED, AND PRESENCE OF IMPRECISION AND/OR UNCERTAINTY IN THE REPRESENTATION.

Representation	Value	Imprec.	Uncert.
Crisp	Crisp color	No	No
Cu	Cu Fuzzy Color	Yes	No
Du	Crisp color	No	Yes

IV. MATCHING COLOR INFORMATION

Matching color information is crucial for practical applications involving fuzzy color spaces. In particular, when we are given statements involving color information coming from different sources, the assessment of these statements depends usually in the degree of matching between them. In this section we propose how to calculate the degree of matching associated to certain expressions involving two pieces of color information, depending on the semantics of the color information employed (any of those explained in the previous section).

The basic information to be employed in color information matching is intimately linked to the own definition of a fuzzy color space, since the representation of each fuzzy color is the fuzzy set of crisp colors that are compatible with the fuzzy color. This representation induces a resemblance relation for crisp colors based on the idea that crisp colors appearing to a certain degree in the representation of a fuzzy color are supposed to be resemblant at least to the minimum of those degrees. This notion of *resemblance induced by a fuzzy color* can be extended to *resemblance induced by a fuzzy color space* just taking the maximum degree among all the fuzzy colors of the fuzzy color space, as we shall see. We shall denote by $r_{\widetilde{C}}$ and $R_{\widetilde{XYZ}}$ the resemblance relations induced by $\widetilde{C}$ and $\widetilde{XYZ}$, respectively. For the sake of simplicity, when there is a single clear fuzzy color space $\widetilde{XYZ}$, we shall denote the relations as r and R, respectively.

In addition to defining each fuzzy color, we shall consider that users can provide their perception of *resemblance between fuzzy colors* by means of a fuzzy resemblance relation (reflexive and symmetric), that we will denote by $S_{\widetilde{XYZ}}$ (or, again, simply S when the fuzzy color space is known). Notice that S is not expected to be transitive in general, and this is consistent with our view of fuzzy color resemblance. For example, one might say that *red* and *orange* are resemblant to some degree, and *orange* and *yellow* are resemblant to the same degree, but *red* and *yellow* are resemblant to a lesser degree than the former. Let us point out that this resemblance is to be taken into account only when the fuzzy color is used in a conjunctive way (as a whole).

Let us remark that compatibility and resemblance of fuzzy colors are different relations, in particular we assume S to be independent of the representation of fuzzy colors. Hence, there is no problem in considering that two fuzzy colors are compatible to a certain degree $\alpha > 0$ (i.e., there is at least one crisp color whose membership degree to both fuzzy colors is at least α) and, at the same time, their resemblance is 0, meaning that both colors are semantically distinguishable and different. This is also consistent with the fact that the user considered both colors in his/her definition of the fuzzy color space since, conceptually, the fuzzy color space is a (fuzzy) partition of the crisp color space.

TABLE II
MOST USUAL CASES WHEN MATCHING PIECES OF COLOR INFORMATION, AND THE CORRESPONDING EQUATION NUMBER.

	c'	Cu $\widetilde{C}'$	Du $\widetilde{C}'$
c	R (2)	K (3)	Pos (4) Nec (5)
Cu $\widetilde{C}$		K (6) R (7)	Pos (8) Nec (9)
Du $\widetilde{C}$			Pos (10) Nec (11) Inc (15) R (17)

Hence, we separate the relationship between a crisp and a fuzzy color from the relationship between fuzzy colors. In other words, S is not necessarily obtained by performing operations on the representations of the fuzzy colors. As a particular case, in this work we devote some effort to the study of the relation S^0 given by $S^0(\widetilde{C}, \widetilde{C'}) = 1$ iff $\widetilde{C} = \widetilde{C'}$, and 0 otherwise. This is the simplest relation one may consider, and it is fully consistent with the view of $\widetilde{XYZ}$ as a partition of the set of crisp colors (though a fuzzy one in which colors may be compatible to some degree). The fact that under S^0 colors are all different but compatible illustrates very clearly the independence between fuzzy color definition and similarity. Other relations and how to obtain them for representing specific semantics will be studied in forthcoming papers.

The possible situations we may encounter when matching pieces of color information correspond to the cells in Table II, where **c**, **c'** $\in XYZ$ are crisp colors, and $\widetilde{C}$, $\widetilde{C}' \in \widetilde{XYZ}$ are fuzzy colors. We shall denote R=resemblance relation, K=compatibility relation, Inc=inclusion. Pos and Nec mean possibility and necessity, respectively.

A first notion of resemblance between crisp colors is that of resemblance induced by a single fuzzy color, defined as follows:

Definition 4.1: The resemblance between crisp colors induced by a single fuzzy color $\widetilde{C}$ is

$$r_{\widetilde{C}}(c, c') = \min(\widetilde{C}(c), \widetilde{C}(c')) \quad (1)$$

It is easy to show that $r_{\widetilde{C}}$ is symmetric and max-min transitive, but not reflexive unless $\widetilde{C}$ is crisp. Reflexivity may be imposed by forcing $r_{\widetilde{C}}(c, c) = 1$ in the previous definition, allowing us to interpret directly a fuzzy color as a group of similar crisp colors, defined by a fuzzy equivalence relation. However, this introduces a discontinuity in the fuzzy set "being similar to c following $\widetilde{C}$", whose membership function is given for every c' by $r_{\widetilde{C}}(c, c')$, even when $\widetilde{C}$ is continuous. This condition may be eliminated if continuity is desired and

reflexivity is not mandatory. Anyway, this discussion is not very important from a practical point of view, since what is important in practical applications is the generalization of this notion to that of resemblance induced by a whole fuzzy color space, considering a user-defined resemblance relation S between fuzzy colors, as follows:

Definition 4.2: The resemblance between crisp colors c and c' induced by a fuzzy color space $\widetilde{XYZ}$ is

$$R_{\widetilde{XYZ}}(c,c') = \max_{(\widetilde{C},\widetilde{C}')\in\widetilde{XYZ}\times\widetilde{XYZ}} \min\{\widetilde{C}(c),\widetilde{C}'(c'),S(\widetilde{C},\widetilde{C}')\} \tag{2}$$

Definition 4.2 is useful in practice when answering questions like *What RGB colors are resemblant to color c?*, or *Give me images containing colors that resemble that of pixel p*, etc. Notice that in this case, the relation is reflexive iff the kernels of the fuzzy colors form a crisp partition of the crisp color space; otherwise, we have to impose $R_{\widetilde{XYZ}}(c,c)=1$ and we have again a discontinuity in the similarity to a fixed crisp color c. Notice however that, taking into account the notion of fuzzy partition that we consider in Section II-B, we are allowed to consider a fuzzy color space consisting of non-crisp fuzzy subsets of colors whose kernels form a crisp partition of the color space, since we allow $\sum_{\widetilde{C}\in\widetilde{XYZ}}\widetilde{C}(c)>1$. Hence, we may obtain a reflexive fuzzy relation $R_{\widetilde{XYZ}}$ in which $R_{\widetilde{XYZ}}(c,c')$ is continuous for every fixed c (provided every $\widetilde{C}\in\widetilde{XYZ}$ is continuous) from a suitable fuzzy color space $R_{\widetilde{XYZ}}$ having non-crisp fuzzy colors.

The following definitions correspond to the rest of cases as shown in Table II. We shall assume from now on that we work with a fuzzy color space $\widetilde{XYZ}$, avoiding it explicitly in the notations. Notice that we shall always employ the same notation (letters R and K to denote resemblance and compatibility, respectively, etc.), although the definitions correspond to different resemblance and compatibility relations. Finally, we shall assume that only a subset of crisp colors in the color space XYZ are considered (this is always the case when working with computers).

Definition 4.3: The compatibility between a crisp color c and a Cu fuzzy color $\widetilde{C}\in\widetilde{XYZ}$ is

$$K(c,\widetilde{C}) = \max_{\widetilde{C}'\in\widetilde{XYZ}} \min\{\widetilde{C}(c),\widetilde{C}'(c),S(\widetilde{C},\widetilde{C}')\} \tag{3}$$

Definition 4.3 is useful when answering questions like *To what degree pixel p is* **red***?*, or *Give me images containing* **red** *pixels*, etc.

Definition 4.4: The possibility and the necessity that a certain color variable V takes value c knowing that its value is in a Du fuzzy color $\widetilde{C}\in\widetilde{XYZ}$ are, respectively

$$pos(V=c|V \text{ is } \widetilde{C}) = \widetilde{C}(c) \tag{4}$$

and

$$nec(V=c|V \text{ is } \widetilde{C}) = 1 - \max_{c'\in\widetilde{XYZ} \mid c'\neq c} \{\widetilde{C}(c')\} \tag{5}$$

Definition 4.4 is useful when answering questions like *Knowing that my car is* **red***, what is the possibility/necessity that my car is painted in the RGB color c?*. Notice that for any fuzzy color $\widetilde{C}\in\widetilde{XYZ}$ such that its kernel is not a singleton, $Nec(V=c|V \text{ is } \widetilde{C})=0$. On the other hand, if $\widetilde{C}$ is a singleton, it is easy to show that

$$pos(V=c|V \text{ is } \{c'\}) = Nec(V=c|V \text{ is } \{c'\}) = \\ = \begin{cases} 1 & c=c' \\ 0 & \text{otherwise} \end{cases}$$

Definition 4.5: The compatibility between two Cu fuzzy colors is

$$K(\widetilde{C},\widetilde{C'}) = \max_{(\widetilde{C''},\widetilde{C'''})\in\widetilde{XYZ}\times\widetilde{XYZ}} \max_{c\in XYZ}\{ \\ \min\{S(\widetilde{C},\widetilde{C''}),\widetilde{C''}(c),S(\widetilde{C'},\widetilde{C'''}),\widetilde{C'''}(c)\}\} \tag{6}$$

Definition 4.5 is useful when answering questions like *To what extent it is possible to find a crisp color that is* **red** *and* **orange***?*.

Definition 4.6: The resemblance between two Cu fuzzy colors is

$$R(\widetilde{C},\widetilde{C'}) = S(\widetilde{C},\widetilde{C'}) \tag{7}$$

where S is a resemblance relation defined by the user.

Definition 4.6 is useful when answering questions like *To what extent* **red** *is similar to* **orange***?*.

Definition 4.7: The possibility and the necessity that a certain color variable V takes a value compatible with a Cu fuzzy color $\widetilde{C}$ knowing that the value of V is in a Du fuzzy color $\widetilde{C'}$ are, respectively

$$pos(K(V,\widetilde{C})|V \text{ is } \widetilde{C'}) = \\ = \max_{\widetilde{C''}\in\widetilde{XYZ}} \max_{c\in XYZ} \min\{\widetilde{C'}(c),\widetilde{C''}(c),S(\widetilde{C},\widetilde{C''})\} \tag{8}$$

and

$$nec(K(V,\widetilde{C})|V \text{ is } \widetilde{C'}) = 1 - pos(\neg K(V,\widetilde{C})|V \text{ is } \widetilde{C'}) = \\ = 1 - \max_{\widetilde{C''}\in\widetilde{XYZ}} \max_{c\in XYZ} \min\{\widetilde{C'}(c),1-\widetilde{C''}(c),S(\widetilde{C},\widetilde{C''})\} \tag{9}$$

where $pos(\neg K(V,\widetilde{C})|V \text{ is } \widetilde{C'})$ is the possibility that V *does not* take a value compatible with $\widetilde{C}$ given that the value of V is in $\widetilde{C'}$.

Definition 4.7 is useful when answering questions like *She told me the car was* **red***, what is the possibility/necessity that the car was* **orange***?*

Definition 4.8: The possibility and the necessity that a certain color variable V takes a value compatible with a Du fuzzy color $\widetilde{C}$ knowing that the value of V is in a Du fuzzy color $\widetilde{C'}$ are, respectively

$$pos(K(V,\widetilde{C})|V \text{ is } \widetilde{C'}) = \max_{c\in XYZ} \min\{\widetilde{C'}(c),\widetilde{C}(c)\} \tag{10}$$

$$nec(K(V,\widetilde{C})|V \text{ is } \widetilde{C'}) = 1 - \max_{c\in XYZ} \min\{\widetilde{C'}(c),1-\widetilde{C}(c)\} \tag{11}$$

Definition 4.8 is useful when answering questions like *Jim saw a* ***red*** *car, and Tim saw an* ***orange*** *car, what's the*

possibility/necessity that both cars were painted in the same color?.

In order to define degrees of inclusion, we will employ the following definition from [17]:

Definition 4.9 ([17]): Let I a contrapositive fuzzy implication[1] satisfying:

1) $(\forall x, y \in [0,1])(x \leq y \Leftrightarrow I(x,y) = 1)$
2) $(\forall x, y \in [0,1])(x = 1 \wedge y = 0 \Leftrightarrow I(x,y) = 0)$

and let A, B be two fuzzy sets defined on a crisp set X. Then, the family of functions given by

$$Sub(A,B) = \min_{x \in X} I(A(x), B(x)) \tag{12}$$

is a family of *inclusion indicators* that satisfy all the Sinha-Dougherty axioms [17].

An example of contrapositive fuzzy implication I satisfying the conditions above is the Lukasiewicz's implicator [17], given by

$$I_a(x,y) = \min(1, 1 - x + y) \tag{13}$$

On this basis, a family of similarity indicators between fuzzy sets can be defined as follows [18]: let A, B be two fuzzy sets defined on a crisp set X. Then, the family of functions given by

$$Sim(A,B) = \min\{Sub(A,B), Sub(B,A)\} \tag{14}$$

is a family of similarity indicators.

The inclusion indicator (resp. similarity indicator) between pieces of color information is useful when answering questions like *To what extent Jim's knowledge about my car's color is more specific than (resp. similar to) Tim's?*.

Definition 4.10: The degree of inclusion of a Du fuzzy color $\widetilde{C}$ in another Du fuzzy color $\widetilde{C'}$ is calculated by means of a suitable, application-depending inclusion indicator in the family given by Eq. 12, i.e.,

$$Inc(\widetilde{C}, \widetilde{C'}) = Sub(\widetilde{C}, \widetilde{C'}) = \min_{c \in \widetilde{XYZ}} I(\widetilde{C}(c), \widetilde{C'}(c)) \tag{15}$$

In particular, the degree of inclusion of a Du fuzzy color $\widetilde{C}$ in another Du fuzzy color $\widetilde{C'}$ based on Lukasiewicz's implicator is

$$Inc(\widetilde{C}, \widetilde{C'}) = \min_{c \in \widetilde{XYZ}} \min(1, 1 - \widetilde{C}(c) + \widetilde{C'}(c)) \tag{16}$$

Definition 4.11: The degree of resemblance between two Du fuzzy colors $\widetilde{C}$ and $\widetilde{C'}$ is calculated by means of one function of the family Sim given by Eq. 14, i.e.,

$$R(\widetilde{C}, \widetilde{C'}) = Sim(\widetilde{C}, \widetilde{C'}) \tag{17}$$

[1]A fuzzy implication I is contrapositive if $I(x,y) = I(N_I(y), N_I(x))$ $\forall x, y \in [0,1]$, with N_I being the induced negator of I defined as $N_I(x) = I(x,0)$ $\forall x \in [0,1]$.

TABLE III
MATCHING PIECES OF COLOR INFORMATION USING S^0, AND THE CORRESPONDING EQUATION NUMBER.

	c'	Cu $\widetilde{C'}$	Du $\widetilde{C'}$
c	R (18)	K (19)	Pos (4) Nec (5)
Cu $\widetilde{C}$		K (20) R (21)	Pos (22) Nec (23)
Du $\widetilde{C}$			Pos (10) Nec (11) Inc (15) R (17)

V. THE CASE OF THE RESEMBLANCE RELATION S^0

In this section we consider the particular case of the relation S^0 given by $S^0(\widetilde{C}, \widetilde{C'}) = 1$ iff $\widetilde{C} = \widetilde{C'}$, and 0 otherwise. As explained in the previous section, the resemblance relation S between fuzzy colors is not necessarily obtained from the membership functions of the fuzzy colors. In principle, we assume there is independence between both these aspects, i.e., they are two different types of information to be provided by humans. Whilst membership functions define the compatibility between crisp and fuzzy colors, the resemblance relation S define the semantic resemblance between fuzzy colors, that depend on how a particular use perceive and use them.

Since a fuzzy color space is defined as a partition of a crisp color space using fuzzy colors, it is reasonable to consider that these fuzzy colors are the different groups that may be distinguished and separated. The fact that the partition is fuzzy allows fuzzy colors to be compatible, i.e., to share crisp colors in their support, but this is not incompatible with the view that colors in $\widetilde{XYZ}$ are totally different.

This consideration is useful for building a fuzzy color space by asking users to enumerate the collection of different colors they can clearly distinguish as different. Hence, S^0 is the simplest relation between fuzzy colors and, at the same time, the less computationally complex. In [12] we proposed an approach for defining a fuzzy color space from a collection of color names and a corresponding set of representative crisp colors, one for each name, both sets provided by the user. If the user is asked to provide these sets by assuming S^0 as the resemblance between fuzzy colors, we have in a very simple way all the necessary information for defining a fuzzy color space and for using this space for representing and matching color information for different purposes.

Using S^0, the relations studied in section IV reduce to those referred in Table III. Some expressions (those not involving the similarity between fuzzy colors S) are the same. New formulae are given in equations (18) - (23).

$$R_{\widetilde{XYZ}}(c,c') = \max_{\widetilde{C} \in \widetilde{XYZ}} \min\{\widetilde{C}(c), \widetilde{C}(c')\} \tag{18}$$

$$K(c, \widetilde{C}) = \widetilde{C}(c) \tag{19}$$

$$K(\widetilde{C}, \widetilde{C'}) = \max_{c \in \widetilde{XYZ}} \min\{\widetilde{C}(c), \widetilde{C'}(c)\} \tag{20}$$

$$R(\widetilde{C}, \widetilde{C'}) = 1 \text{ if } C = C',\ 0 \text{ otherwise.} \tag{21}$$

$$pos(K(V,\widetilde{C})|V \text{ is } \widetilde{C'}) = \max_{c\in XYZ} \min\{\widetilde{C}(c), \widetilde{C'}(c)\} \quad (22)$$

$$nec(K(V,\widetilde{C})|V \text{ is } \widetilde{C'}) = 1 - pos(\neg K(V,\widetilde{C})|V \text{ is } \widetilde{C'}) =$$

$$= 1 - \max_{c\in XYZ} \min\{\widetilde{C'}(c), 1-\widetilde{C}(c)\} \quad (23)$$

VI. Conclusions and future work

Our work lies in the framework of Zadeh's Computational Theory of Perceptions [19]. Fuzzy color spaces are intended to represent the collection of terms employed by a particular user, either in general or in a certain application, for describing his/her perception about colors. By representation we understand the (fuzzy) compatibility between crisp colors and these terms, expressed as membership functions defined on a crisp color space. In addition, we consider separately the user's perception of resemblance between colors, the latter seen as abstract notions, by means of a fuzzy relation S. These models allow us to fill the semantic gap between the representation of colors in computers and the perception of colors by humans, and to represent different types of color information. As a consequence, we are able to provide computational procedures for matching color information of different types, something very useful in determining the compatibility between linguistic terms and images for color image description, for image and visual information retrieval, flexible query answering in image databases, etc.

As future work, we shall use the relations introduced here in many applications, in particular for developing image retrieval systems working with linguistic queries and flexible queries to image databases, as well as for identifying visual concepts and the automatic generation of linguistic descriptions of images on the basis of color information [20]. We will also employ these techniques for color image segmentation [21], [22]. Another important future work concerns the study of the computational complexity of calculating the measures proposed in this work, when it is possible to precalculate this information, and how to develop efficient algorithms for using them in practice. Finally, we shall study the semantics of different similarity relations between fuzzy colors, in particular on the basis of hierarchical fuzzy color spaces, a notion that we are currently developing.

References

[1] A. Plouznikoff, N. Plouznikoff, J. Robert, and M. Desmarais, "Enhancing human-machine interactions: virtual interface alteration through wearable computers," in *CHI '06: Proceedings of the SIGCHI conference on Human Factors in computing systems*. New York, NY, USA: ACM, 2006, pp. 373–376.

[2] P. Kay and C. McDaniel, "The linguistic significance of the meanings of soft basic color terms," *Language*, vol. 3, no. 54, pp. 610–646, 1978.

[3] J. Lammens, "A computational model of color perception and color naming," State University of New York, Tech. Rep. 94-26, 24, 1994.

[4] N. Sugano, "Color-naming system using fuzzy set theorical approach," in *IEEE Int. Conference on Fuzzy Systems*, 2001, pp. 81–84.

[5] ——, "Fuzzy set theoretical approach to the RGB color triangle," in *Knowledge-Based Intelligent Information and Engineering Systems. LNCS 4253*. Springer-Verlag, 2006, pp. 948–955.

[6] H. Zhu, H. Zhang, and Y. Yu, "Deep into color names: Matching color descriptions by their fuzzy semantics," *LNAI 4183*, pp. 138–149, 2006.

[7] A. Mojsilovic, "A computational model for color naming and describing color composition of images," *IEEE Transactions on Image Processing*, vol. 14, no. 5, pp. 690 – 699, 2005.

[8] A. Younes, I. Truck, and H. Akdag, "Color image profiling using fuzzy sets," *Turkish Journal of Electrical Engineering and Computer Sciences*, vol. 13, no. 3, p. 343359, 2005.

[9] J. Chamorro-Martínez, J. Medina, C. Barranco, E. Galán-Perales, and J. Soto-Hidalgo, "Retrieving images in fuzzy object-relational databases using dominant color descriptors," *Fuzzy Sets and Systems*, vol. 158, no. 3, pp. 312 – 324, 2007.

[10] H. Aboulmagd, N. El-Gayar, and H. Onsi, "A new approach in content-based image retrieval using fuzzy," *Telecommunication Systems*, vol. 40, no. 2, pp. 55–66, 2009.

[11] R. Benavente, M. Vanrell, and R. Baldrich, "Parametric fuzzy sets for automatic color naming," *Journal of the Optical Society of America A*, vol. 25, no. 10, pp. 2582–2593, Oct 2008. [Online]. Available: http://cat.uab.cat/Publications/2008/BVB08

[12] J. Soto-Hidalgo, J. Chamorro-Martínez, and D. Sánchez, "A new approach for defining a fuzzy color space," in *Proceedings WCCI 2010*, 2010, pp. 292–297.

[13] L. Zadeh, "PRUF - a meaning representation language for natural languages," *International Journal of Man-Machine Studies*, vol. 10, pp. 395–460, 1978.

[14] R. Yager, "Set-based representations of conjunctive and disjunctive knowledge," *Information Sciences*, vol. 41, no. 1, pp. 1–22, 1987.

[15] D. Dubois and H. Prade, "Incomplete conjunctive information," *Computers & mathematics with applications*, vol. 15, pp. 797–810, 1988.

[16] ——, "Gradualness, uncertainty and bipolarity: Making sense of fuzzy sets," *Fuzzy Sets and Systems*, vol. In Press, Corrected Proof, 2010.

[17] C. Cornelis, C. Van der Donck, and E. Kerre, "Sinha-Dougherty approach to the fuzzification of set inclusion revisited," *Fuzzy Sets and Systems*, vol. 134, pp. 283–295, 2003.

[18] I. Beg and S. Ashraf, "Similarity measures for fuzzy sets," *Appl. and Comput. math.*, vol. 8, no. 2, pp. 192–202, 2009.

[19] L. Zadeh, "A new direction in AI. Toward a computational theory of perceptions," *AI Magazine*, vol. 22, no. 1, pp. 73–84, 2001.

[20] R. Castillo-Ortega, J. Chamorro-Martínez, N. Marín, D. Sánchez, and J. Soto-Hidalgo, "Describing images via linguistic features and hierarchical segmentation," in *Proceedings WCCI 2010*, 2010, pp. 1104–1111.

[21] J. Chamorro-Martínez, D. Sánchez, B. Prados-Suarez, and E. Galán-Perales, "Fuzzy connectivity measures for path-based image segmentation," in *IEEE International Conference on Fuzzy Systems*. Reno, Nevada (USA), May 2005, pp. 218–223.

[22] B. Prados-Suárez, J. Chamorro-Martínez, D. Sánchez, and J. Abad, "Region-based fit of color homogeneity measures for fuzzy image segmentation," *Fuzzy Sets and Systems*, vol. 158, no. 3, pp. 215–229, 2007.

2011 IEEE International Conference on Fuzzy Systems
June 27-30, 2011, Taipei, Taiwan

The Positioning control of an Electro-Hydraulic Variable Rotational Speed Pump-Controlled System Using Adaptive Fuzzy Controller with Self-tuning Fuzzy Sliding Mode Compensation

Lian-Wang Lee
Department of Graduate School of Engineering Technology, Lunghwa University of Science and Technology, Taiwan
Email: leelw@mail.lhu.edu.tw

I-Hsum Li
Department of Computer Science and Information Engineering, Lee-Ming Institute of Technology, Taiwan.
Email: i-hsum@orion.ee.ntust.edu.tw

Chung-Chieh Chen
Department of Mechanical Engineering, De Lin Institute of Technology, Taiwan.
Email: eversafe@seed.net.tw

Jun-Yi Huang
Department of Graduate School of Engineering Technology, Lunghwa University of Science and Technology, Taiwan
Email: dickymails@yahoo.com.tw

***Abstract*—The electro-hydraulic variable rotational speed pump-controlled system (EHVRSPCS) performs specific characteristics on non-linearity and time-varying. An exact model-based controller is difficult to be realized. In this study, the design method and experimental implementation of an adaptive fuzzy controller with on-line self-tuning fuzzy sliding-mode compensation (AFC-STFSMC) are proposed to deal with the system time-varying and non-linear uncertain behaviours by adjusting the control rule parameters. This control strategy employs the adaptive fuzzy approximation technique to design the equivalent controller of the conventional sliding-mode control (SMC). Furthermore, the fuzzy sliding-mode control scheme with self-tuning ability is introduced to compensate the approximation error of the equivalent controller for improving the control performance. The tuning algorithms are derived in the sense of the Lyapunov stability theorem; thus, the stability of the system can be guaranteed. The experimental results show that the AFC-STFSMC can perform excellent positioning control for the EHVRSPCS.**

Keywords: electro-hydraulic pump-controlled system, AC servo motor, fuzzy sliding mode control, adaptive fuzzy, sliding-mode control

I. INTRODUCTION

Hydraulic servo systems are widely used in the industry due to the advantages of high power-weight ratio, large driving forces, high response and good conduction of heat out of components by pressure fluid. However, oil viscosity, friction force, and leakage cause highly nonlinear time-variant dynamics, load sensitivity and parameter uncertainty in the hydraulic servo control systems result in the control complexity and difficulty [1-2]. In view of the hydraulic circuits, two different hydraulic systems are classified as the high-response but low-energy efficiency hydraulic valve-controlled system and the high-energy efficiency but lower response hydraulic pump-controlled system. The hydraulic valve-controlled systems have been applied widely in the industrial servo control. And, recently, the investigations on high response pump-controlled systems driven by AC servo motors or switch reluctance motor are introduced [3]. Helduser [3] first presented the concept of hydraulic pump-controlled system, driven by gear pumps and AC servo motors with variable rotational speed for injection moulding machines in 1995. Ruhlicke [4] studied the position control of asymmetrical cylinder with double pump-controlled system driven by AC servo motor with variable rotational speed, which the position accuracy, about 50μm, is still unsatisfactory. Kazmeier and Feldmann [5] used Fuzzy control to study the pump-controlled system with variable rotational speed for positioning control with small power, max. 330W, and small stroke 0,5mm. Helduser [6] developed an electric-hydrostatic drive using AC servo motor and constant displacement internal gear pump for energy-saving power and motion control system. In recent years, AC servo motors combined with internal gear pumps were used mostly, and they can reach 50μm accuracy in position control. New applications of the high response in different hydraulic servo machines are still being developed. Therefore, this paper aims to investigate the position control performance of the high response pump-controlled system driven by an AC servo motor with variable rotational speed. Instead of internal gear pumps, a constant displacement axial piston pump is used in this paper for positioning control of hydraulic servo machines.

The classical SMC [7-9] have been proposed for solving the hydraulic servo control problems during the past decades. However, the drawbacks of classical SMC, such as chattering, large control effort and difficulty for deciding the equivalent control, limit its practical applicability. Moreover, the boundary of the uncertainty has to be estimated in order to guarantee the stability of the SMC systems. Thus, the SMC systems are still difficulty in real-world applications.

The fuzzy control, which doesn't require mathematical models of the system, has been used in several industrial applications. Zhao and Vivalo [10-11] developed a fuzzy state controller for a hydraulic position servo system with unknown load. Deticek [12] proposed an intelligent position control of electro-hydraulic drive using hybrid FC structure. The design of a traditional fuzzy controller mostly depends on expert experience for establishing the fuzzy rule base However, for complex systems there are no guide rules for designing the fuzzy rule base and parameters. Thus, self-tuning algorithms were introduced in FC for adjusting fuzzy parameters and improving the control performance based upon a specified performance index [13-14]. However, a complicated learning mechanism or a specific performance decision table designed by trial-and-error is required. Thus, its application still presents certain difficulty, and the large amount of the fuzzy rules also makes the analysis complex.

For reducing the fuzzy rules in FC, FC design methods based on SMC scheme, namely fuzzy sliding-mode control (FSMC), have proposed [15-16]. Since only one variable is defined as the fuzzy input variable, the main advantage of FSMC lies in less fuzzy rules than FC. Although FC and FSMC are both effective design methods, their major drawback is that the fuzzy rules should be previously tuned by time-consuming trial-and-error procedures. In order to tackle this problem, adaptive fuzzy control (AFC) based on the Lyapunov synthesis approach has been extensively studied [17-18]. With this approach, the fuzzy rules can be automatically adjusted to achieve system response by an adaptive law.

The objective of this paper is forcing on experimental implementation of the adaptive fuzzy controller with self-tuning fuzzy sliding-mode compensation (AFC-STFSMC) for the positioning control with high response in the EHVRSPCS. The AFC-STFSMC combines the adaptive fuzzy control and the self-tuning fuzzy sliding-mode control scheme. The adaptive fuzzy approximation method is to establish the unknown equivalent controller for releasing the model-based requirement. Furthermore, the fuzzy sliding-mode control scheme with self-tuning ability is introduced to compensate the function approximation error of the equivalent controller for improving the control performance and reducing the implementation difficulty. The AFC-STFSMC approach comprises the advantages of which the fuzzy rules can be automatically adjusted, similar to AFC, and can reduce the fuzzy rules, like FSMC. All controller parameters of this scheme are tuned in the Lyapunov sense, thus the stability of the system can be guaranteed.

II. FORMULATION OF ELECTRO-HYDRAULIC VARIABLE ROTATIONAL SPEED PUMP-CONTROLLED SYSTEM

The EHVRSPCS is designed and set up for investigating the dynamic performance and control effect. The test rig layout of the EHVRSPCS is shown in Fig.1. The hydraulic servo cylinder system of EHVRSPCS contains a double-rod symmetrical hydraulic cylinder fitted with a linear encoder with the resolution of 0.1 μm. The hydraulic power supply system, which consists of a swash plate axial piston pump with constant displacement of 12 ml/rev and is driven by an AC servo motor of 7.0 kW, adjusts the supply volume flow by the rotational speed controlled by the AC servo motor. The mathematics models of the main elements in this system are discussed as below:

(a) Servo motor control unit

The servo motor control unit proportionally transfers the input voltage into the rotational speed of the servo motor, and can be described as

$$\omega = K_a \cdot u \tag{1}$$

where w indicates the rotational speed of the servo motor, K_a is the gain of servo control unit and u is the input voltage.

(b) Swash plate axial piston pump with constant displacement

The pump volumetric displacement of the swash plate axial piston pump D_l is supposed to be constant. The load volume flow Q_l from the pump to the controlled hydraulic cylinder can be described as

$$Q_l = D_l \cdot w - C_l \cdot P_l \tag{2}$$

where w indicates the pump rotational speed, C_l is the leakage coefficient of the pump, P_l is the load pressure.

(c) The controlled cylinder

The continuity equation of the controlled cylinder chamber is given by

$$Q_l = A_p \dot{x}_p + C_t P_l + \left(\frac{V_t}{4\beta_e} \right) \dot{P}_l \tag{3}$$

where A_p is the effective area of piston, x_p is the position of piston rod, C_t is the leakage coefficient of cylinder, V_t is the total compressed volume and β_e is the effective bulk modulus of hydraulic oil. Substituting Eq. (1) and Eq. (2) into Eq. (3), we have

$$D_l \cdot k_a \cdot u = A_p \dot{x}_p + \left(C_l + C_t \right) P_l + \left(\frac{V_t}{4\beta_e} \right) \dot{P}_l \tag{4}$$

According to the Newton's 2nd law, the motion equation of controlled cylinder on position control can be derived as

$$A_P P_l - f_l = M \ \ddot{x}_P + B\dot{x}_P + Kx_P \tag{5}$$

where M indicates the total mass of piston, rod and load, B is the viscous damping coefficient, K is the spring constant and f_l is the arbitrary load force on piston. By combining Eqs. (1)-(5), the state equations of the EHVRSPCS model can be achieved as follows

$$\begin{aligned} \dot{x}_1 &= x_2(t) \\ \dot{x}_2 &= x_3(t) \\ \dot{x}_3 &= -\sum_1^3 a_i x_i(t) + g(\underline{x})u + d(\underline{x}) = f(\underline{x}) + g(\underline{x})u + d(\underline{x}) \end{aligned} \tag{6}$$

where

$$\underline{x}(t) = \left[x_1(t) \quad x_2(t) \quad x_3(t) \right]^T = \left[x_p(t) \quad \dot{x}_p(t) \quad \ddot{x}_p(t) \right]^T$$

$$a_1(t)=\frac{4\beta_e(C_l+C_t)K}{MV_t} \quad a_2(t)=\frac{K}{M}+\frac{4\beta_e A_p^2}{MV_t}+\frac{4\beta_e(C_l+C_t)B}{MV_t}$$

$$a_3(t)=\frac{B}{M}+\frac{4\beta_e(C_l+C_t)}{V_t},\ g(\underline{x})=\frac{4A_p\beta_e D_l K_a}{MV_t}$$

$$d(\underline{x})=-(\frac{4\beta_e(C_l+C_t)}{V_t M}f_l+\frac{1}{M}\dot{f}_l)$$

in which $g(\underline{x})$ is a constant with positive value.

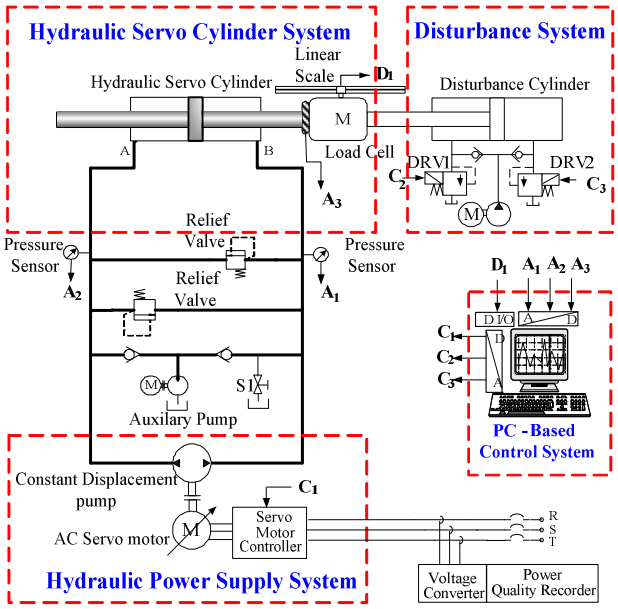

Fig. 1: Layout of the electro-hydraulic variable rotational speed pump-controlled system

III. CONTROLLER DESIGN AND STABILITY ANALYSIS

The design of a sliding mode controller requires the system models and has to find the inverse form of the inertia term in system dynamics. However, the accurate mathematical models are sometimes difficult to be formulated or even not available. To solve these problems, an AFC-STFSMC is proposed in this paper for realizing the positioning control in EHVRSPCS. The block diagram of the AFC-STFSMC control system for EHVRSPCS is shown in Fig.2 in the last page.

A. Fuzzy control

According to the definitions [12], the basic configuration of fuzzy logic systems consists of four components: a fuzzifier, a fuzzy rule base, a fuzzy inference engine and a defuzzifier. In this paper single-input single-output rules will be used in formulation of the control law. Assume that there are *n* rules in a fuzzy base and each of them has the following form:

$$R^i: \text{IF } S \text{ is } F^i \text{ THEN } u \text{ is } \alpha_i \qquad (7)$$

where S is the input variable of the fuzzy system; u is the output variable of the fuzzy system; F^i are the triangular-type membership functions; and α_i are the singleton control actions for $i=1,2,...,n$. The defuzzification of the FC output is accomplished by the method of center-of-gravity [12]

$$u=\frac{\sum_{i=1}^{n}\alpha_i\times w_i}{\sum_{i=1}^{n}w_i}=\underline{\alpha}^T\underline{\xi} \qquad (8)$$

where w_i is the firing weight of the *i*th rule, $\underline{\alpha}=[\alpha_1,\alpha_2,...,\alpha_n]^T$ is the parameter vector and $\underline{\xi}=[\xi_1,\xi_2,...,\xi_n]^T$ is the vector of fuzzy basis functions

$$\xi_i=\frac{w_i}{\sum_{i=1}^{n}w_i} \qquad (9)$$

In conventional FC, the control actions α_i should be previously assigned through a lot of trails for achieving satisfactory control performance. In this paper, an adaptive algorithm will be proposed to tune these control actions on-line.

B. Fuzzy Sliding-Mode Control

Hwang *et al.* [13] proposed the methods to design the fuzzy sliding-mode controller for a non-linear system with 2nd order where the error and the error change rate were used to synthesize fuzzy reasoning rules. However, the rule number was larger and did not give the mathematical expression. Thus, it is difficult to analyze the properties of the control system. To overcome this problem, this paper adopts the sliding surface $S=0$ of SMC and extends it to the fuzzy sliding surface $\tilde{S}=\tilde{0}$, and make S be a linguistic description of $\tilde{S}$. In this study the two triangular-typed functions are used to define the membership functions of IF-part and THEN-part, which are depicted in Figs.3 (a) and 3(b) respectively. The fuzzy rules are given in the following form

$$R^l: \text{IF } S \text{ is } \tilde{F}_s^l \text{ THEN } u_{fs} \text{ is } \tilde{F}_u^{8-l},\ l=1,...,7. \qquad (10)$$

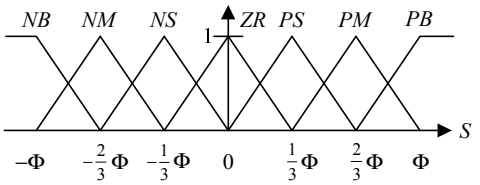

(a)

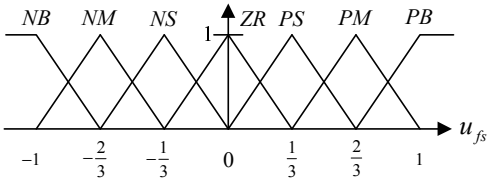

(b)

Figs.3 Fuzzy partitions and membership functions of S and u_{fs} in the respective universe of discourse

According to the sup-min compositional rule of inference and the defuzzification of the control output accomplished by the method of center-of-area, the mathematical expression can be derived as

$$u_{fs}=\begin{cases} 1 & ,if \quad z<-1 \\ \dfrac{7.5z^2+13.5z+5}{9z^2+15z+5} & ,if \quad -1\le z<-\dfrac{2}{3} \\ \dfrac{9z^2+11z+2}{18z^2+18z+2} & ,if \quad -\dfrac{2}{3}\le z<-\dfrac{1}{3} \\ \dfrac{1.5z^2+1.5z}{9z^2+3z-1} & ,if \quad -\dfrac{1}{3}\le z<0 \\ \dfrac{-1.5z^2+1.5z}{9z^2-3z-1} & ,if \quad 0\le z<\dfrac{1}{3} \\ \dfrac{-9z^2+11z-2}{18z^2-18z+2} & ,if \quad \dfrac{1}{3}\le z<\dfrac{2}{3} \\ \dfrac{-7.5z^2+13.5z-5}{9z^2-15z+5} & ,if \quad \dfrac{2}{3}\le z<1 \\ -1 & ,if \quad z\ge 1 \end{cases} \tag{11}$$

where $z=\dfrac{S}{\Phi}$, and as $|S|\ge\Phi$, it is easy to check $u_{fs}=-\mathrm{sgn}(S)$.

C. Adaptive Fuzzy Controller with Self-Tuning Fuzzy Sliding-Mode Compensation

The control objective is to find a control law that can make the hydraulic actuator of EHVRSPCS tracking the desired target $x_d(t)$. Define the tracking error $e(t)$ as

$$e(t)=x_d(t)-x(t) \tag{12}$$

where $x(t)$ indicates the control output and $x_d(t)$ is the desired target. Define a sliding surface as

$$S(t)=\ddot{e}(t)+k_1\dot{e}(t)+k_2e(t) \tag{13}$$

where k_1 and k_2 are non-zero positive constants. Assume that parameters of the system in Eq. (6) are well known and the external load disturbance is measurable, then the control law can be defined as

$$u^*=g^{-1}(\underline{x})[\eta S_\Delta(t)-f(\underline{x})-d(\underline{x})+\ddot{x}_d+k_1\ddot{e}(t)+k_2\dot{e}(t)] \tag{14}$$

where $S_\Delta(t)=S(t)-\Phi sat(S(t)/\Phi)$ and Φ is the boundary layer width of the sliding surface S. The properties of the function S_Δ that are useful in the design of adaptive law [14] are described as below.

Property1: As $|S|>\Phi,\ \Rightarrow |S_\Delta|=|S|-\Phi$ and $\dot{S}_\Delta=\dot{S}$.

Property2: When $|S|\le\Phi,\ \Rightarrow S_\Delta=\dot{S}_\Delta=0$.

The above properties of the boundary layer concept are exploited in the design of controller to cease adaptation as soon as the boundary layer is reached and to avoid the possibility of unbounded growth. Differentiating Eq. (13), we have

$$\dot{S}(t)=-f(\underline{x})-g(\underline{x})u-d(\underline{x})+\dddot{x}_d+k_1\ddot{e}(t)+k_2\dot{e}(t) \tag{15}$$

Substituting Eq. (16) into Eq.(17) gives

$$\dot{S}(t)+\eta S_\Delta(t)=0,\qquad \eta>0. \tag{16}$$

Equation (16) shows that $\underline{e}(t)=[e(t),\dot{e}(t),\ddot{e}(t)]$ will converge to the neighborhood of zero as $t\to\infty$, and the value of the neighborhood depends on the value of Φ [19]. However, the system parameters may be unknown or perturbed; the controller u^* cannot be precisely implemented. Therefore, in accordance with the universal approximation theorem [11], for any $\rho^*>0$, an optimal fuzzy control $\hat{u}_{fz}(S,\underline{\alpha}^*)$ exists in the form of Eq. (10) that satisfies

$$\left|u^*-\hat{u}_{fz}(S,\underline{\hat{\alpha}}^*)\right|=\rho^* \tag{17}$$

where ρ^* is assumed to be bounded by $|\rho^*|\le M$. Utilize a fuzzy controller $\hat{u}_{fz}(S,\underline{\hat{\alpha}})$ to approximate u^* as

$$\hat{u}_{fz}(S,\underline{\hat{\alpha}})=\underline{\hat{\alpha}}^T\underline{\xi} \tag{18}$$

where $\underline{\hat{\alpha}}$ is the estimated values of $\underline{\alpha}^*$. The control law for the developed AFC-STFSMC is defined as the following form:

$$u=\hat{u}_{fz}(S,\underline{\hat{\alpha}})+u_{comp}(S) \tag{19}$$

where the fuzzy controller $\hat{u}_{fz}$ is designed to approximate the control u^* and the fuzzy sliding-mode compensation u_{comp} is proposed to compensate the difference between the controller u^* and fuzzy controller $\hat{u}_{fz}(S,\underline{\hat{\alpha}})$. Through Eqs. (14), (15) and (19), the dynamical equation can be derived as:

$$\dot{S}(t)+\eta S_\Delta(t)=g[u^*-\hat{u}_{fz}(\mathrm{S},\underline{\hat{\alpha}})-u_{rb}(S)] \tag{20}$$

In order to derive the adaptive laws for ensuring convergence to the boundary layer, a candidate Lyapunov function is defined as:

$$V(S_\Delta,\underline{\tilde{\alpha}},\tilde{\rho})=\frac{1}{2}\frac{S_\Delta^2}{g}+\frac{1}{2\eta_1}\underline{\tilde{\alpha}}^T\underline{\tilde{\alpha}}+\frac{1}{2\eta_2}\tilde{\rho}^2 \tag{21}$$

where $\underline{\tilde{\alpha}}^{\mathrm{T}}=\underline{\hat{\alpha}}^{*\mathrm{T}}-\underline{\hat{\alpha}}^{\mathrm{T}}$ and $\tilde{\rho}=\rho^*-\hat{\rho}$ are the approximation error of the parameter vectors $\underline{\hat{\alpha}}^{*\mathrm{T}}$ and ρ^* respectively. In addition, η_1 and η_2 are positive constants. Differentiate Eq. (21) with respect to time as

$$\dot{V}(S_\Delta,\underline{\tilde{\alpha}},\tilde{\rho})=\frac{S_\Delta\dot{S}_\Delta}{g}+\frac{1}{\eta_1}\underline{\tilde{\alpha}}^T\underline{\dot{\tilde{\alpha}}}+\frac{1}{\eta_2}\tilde{\rho}\dot{\tilde{\rho}}. \tag{22}$$

Thus, if $|S|\le\Phi$, then $S_\Delta=0$, it follows $\dot{V}(S_\Delta,\underline{\tilde{\alpha}},\tilde{\rho})=0$. If $|S|>\Phi$, then $\dot{S}_\Delta=\dot{S}$. By substituting Eq. (20) into Eq. (22), Eq. (23) can be obtained

$$\dot{V}(S_\Delta,\underline{\tilde{\alpha}},\tilde{\rho})=-\eta\frac{S_\Delta^2}{g}+S_\Delta[u^*-\hat{u}_{fz}(S,\underline{\hat{\alpha}})]-S_\Delta u_{rb}(S)+\frac{1}{\eta_1}\underline{\tilde{\alpha}}^T\dot{\underline{\tilde{\alpha}}}+\frac{1}{\eta_2}\tilde{\rho}\dot{\tilde{\rho}}$$
$$=-\eta\frac{S_\Delta^2}{g}+S_\Delta[u^*-\hat{u}_{fz}(S,\underline{\hat{\alpha}}^*)+\hat{u}_{fz}(S,\underline{\hat{\alpha}}^*)-u_{fz}(S,\underline{\hat{\alpha}})]-S_\Delta u_{rb}(S)+\frac{1}{\eta_1}\underline{\tilde{\alpha}}^T\dot{\underline{\tilde{\alpha}}}+\frac{1}{\eta_2}\tilde{\rho}\dot{\tilde{\rho}}$$
$$\le-\eta\frac{S_\Delta^2}{g}+|S_\Delta|\left|u^*-\hat{u}_{fz}(S,\underline{\hat{\alpha}}^*)\right|+S_\Delta[\hat{u}_{fz}(S,\underline{\hat{\alpha}}^*)-\hat{u}_{fz}(S,\underline{\hat{\alpha}})]-S_\Delta u_{rb}(S)+\frac{1}{\eta_1}\underline{\tilde{\alpha}}^T\dot{\underline{\tilde{\alpha}}}+\frac{1}{\eta_2}\tilde{\rho}\dot{\tilde{\rho}}$$
$$=-\eta\frac{S_\Delta^2}{g}+[|S_\Delta|\rho^*-S_\Delta u_{rb}(S)-\frac{1}{\eta_2}\tilde{\rho}\dot{\hat{\rho}}]+\underline{\tilde{\alpha}}^T(S_\Delta\xi(S)-\frac{1}{\eta_1}\dot{\underline{\hat{\alpha}}}) \tag{23}$$

For achieving $\dot{V}(S_\Delta,\underline{\tilde{\alpha}},\tilde{\rho})\le 0$, the adaptive laws of AFC-STFSMC are chosen as

$$\dot{\underline{\hat{\alpha}}}=\eta_1\cdot S_\Delta\cdot\xi(S) \tag{24}$$

$$u_{comp}(S)=-\hat{\rho}\cdot u_{fs} \tag{25}$$

$$\dot{\hat{\rho}}=\eta_2\cdot|S_\Delta| \tag{26}$$

Thus Eq. (23) can be rewritten as

$$\dot{V}(S_\Delta,\underline{\tilde{\alpha}},\tilde{\rho})\le-\eta\cdot\frac{S_\Delta^2}{g}\le 0 \tag{27}$$

Equations (24)-(27) guarantee only $S_\Delta\in L_\infty$ but don't guarantee convergence. Integrating both sides of (27) and using some derivation, we have

$$\int_0^\infty S_\Delta^2 dt\le\frac{V(S_\Delta(\infty),\underline{\tilde{\alpha}},\tilde{\rho})-\dot{V}(S_\Delta(0),\underline{\tilde{\alpha}},\tilde{\rho})}{\frac{\eta}{g}}. \tag{28}$$

Since the right side of Eq. (28) is bounded, $S_\Delta\in L_2$. Using Barbalat's lemma [19], $\lim_{t\to\infty}S_\Delta=0$ can be shown. That means that the inequality $|S|\le\Phi$ is obtained asymptotically, so the tracking error $e(t)$ converges to neighborhood of zero. In summary, AFC-STFSMC is derived in Eq. (19), where $\hat{u}_{fz}$ is given in Eq. (18) with the parameters $\underline{\hat{\alpha}}$ adjusted by Eq. (24) and u_{comp} is given in Eq. (25) with the parameter $\hat{\rho}$ adjusted by Eq. (26). By applying these adaptive laws, the controller of Eq. (19) can be guaranteed the EHVRSPCS to be stable.

IV. EXPERIMENTS

For verifying the control performance of the proposed AFC-STFSMC controller, the positioning control experiments in EHVRSPCS are implemented under different strokes and different external loadings.

(a) Positioning control at different strokes with external loading force

The experiment is respectively achieved for different stroke set points such as 100, 200 and 300 mm with external loading force 30kN. Fig.4 shows the response for different strokes. The experimental results show that the piston of cylinder can, at different strokes with loading force 30kN, reach the set point within a little overshoot 18μm and remain the steady state error within 10μm.

(b) Positioning control under different loading conditions

For confirming the control performance under different external loading conditions, the experiments of position control under three constant external loading conditions, such as 10kN, 30kN and 50kN, are investigated. Fig.5 indicates the step responses of the position control of 300 mm stroke with different loadings. The experimental results show that the piston of cylinder can, under 10kN and 30kN loading conditions, reach the set point within a little overshoot 14μm and remain the steady state error within 3.6μm. Even under 50kN loading condition, the piston can reach the set point within 38μm overshoot and remain the steady state error within 17μm.

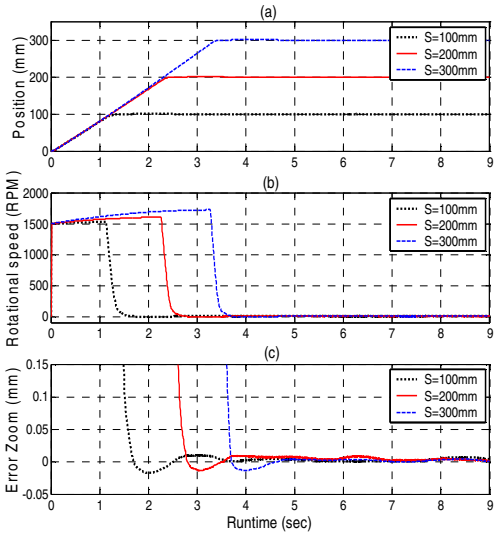

Fig.4: Experimental results of positioning control for different strokes with loading force 30kN in variable rotational speed pump-controlled system: (a) position control response (b) controller input (c) control error

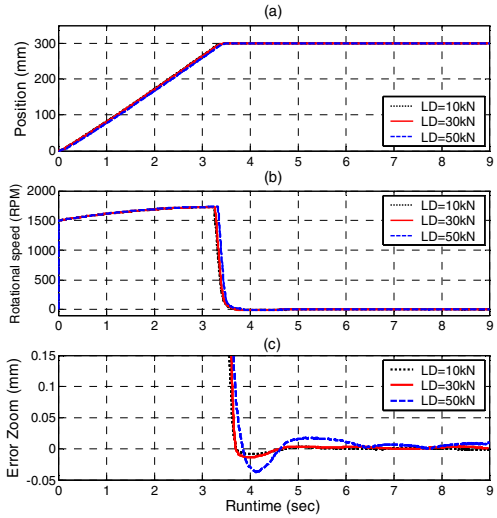

Fig.5: Experimental results of positioning control of 300mm stroke with different loadings in variable rotational speed pump-controlled system: (a) position control response (b) controller input (c) control error

V. CONCLUSIONS

This paper develops a new EHVRSPCS driven by an AC servo motor for realizing motion control of hydraulic servo machines with high response. The swash plate axial piston pump with constant displacement combines with the AC servo motor due to the better response, instead of the internal gear pump used in [3-6]. The positioning control in different loading conditions are implemented and verified experimentally for EHVRSPCS in this paper. For achieving better control performance, an AFC-STFSMC is proposed for positioning control of the EHVRSPCS. The AFC-STFSMC strategy combining with the adaptive fuzzy control and the self-tuning fuzzy sliding-mode control scheme is comprised of the adaptive fuzzy approximation technique to establish the equivalent controller of the traditional SMC and the FSMC scheme with self-tuning ability for compensating the approximation error of equivalent controller and external disturbance. Excellent self-adaptability with regard to various strokes and uncertain external disturbance force are verified experimentally.

ACKNOWLEDGMENT

This work was supported by the National Science Council, Taiwan under grant NSC 99-2221-E-234-001.

REFERENCES

[1] H. Murrenhoff, Servohydraulik, Lecture Notes, RWTH Aachen University, 2003.
[2] H. E. Merrit, Hydraulic control systems, John Wiley, New York, 1976.
[3] Helduser S, "Moderne hydraulische Antriebe und Steuerungen am Beispiel von Kunststoff-Spritgiessmaschinen" (in German), O+P Ölhydraulik und Pneumatik 39, No.10, 1995.
[4] Ruhlicke I, "Elektro-hydraulische Antriebssysteme mit drehzahlveränderbarer Doppelpumpe", *(in German), O+P Ölhydraulik und Pneumatik 41*, No.10, 1997.
[5] Kazmeier B and Feldmann D-G, "Ein neues Konzept füreinen kompakten elektrohydraulischen Linearantrieb" (in German), *Proc. of 1. International Fluid Power Conference (1.IFK)*, Aachen, Germany, Band 1, pp.345-358, 1998.
[6] Helduser S, "Electric-hydrostatic drive – an innovative energy-saving power and motion control system", *Proc. of Institution of Mechanical Engineers*, Vol. 213, Part I, pp.427-439, 1999.
[7] A. Bonchis, P. I. Corke, D. C. Rye, Q. P. Ha, "Variable Structure Methods in Hydraulic Servo Systems," *Automatica*, vol. 37, pp.589–595, 2001.
[8] J. P. Su, "Robust Control of a Class of Nonlinear Cascade Systems: A Novel Sliding Mode Approach," *Proc. IEE Control Theory Appl.*, vol. 149, No. 2, pp.131-136, 2001.
[9] H. M. Chen, J. P. Su, J. C. Renn, "A Novel Sliding Mode Control of an Electro-hydraulic Position Servo System," *IEEE Trans. Fundam Electron.*, Vol. 85, No. 8, pp.1928-1936, 2002.
[10] T, Zhao. ,T, Virvalo., "Fuzzy control of a hydraulic position servo with unknown load," *IEEE Trans. Fuzzy Syst.*, pp. 785-788, 1993.
[11] T, Zhao., T, Virvalo., "Development of fuzzy state controller for a hydraulic position servo," *IEEE Trans. Fuzzy Syst.*, pp. 1075-1080, 1994.
[12] E, Decticek, "An Intelligent Position Control of Electrohydraulic Drive Using Hybrid Fuzzy Control Structure," *Proceedings of the IEEE International Symposium on Industrial Electronics*, vol. 3:3, pp. 1008-1013, 1999.
[13] M. Maeda, S. Murakami, "A self-tuning fuzzy controller," *Fuzzy Sets Syst.*, vol. 47, pp. 13–21, 1992.
[14] W. Z. Qiao, W. P. Zhung, T. H. Heng, "AS rule self-regulating fuzzy controller," *Fuzzy Sets Syst.*, vol. 47, pp.13–21, 1992.
[15] S. W, Kim., J. J. Lee, "Design of fuzzy controller with fuzzy sliding surface," *Fuzzy Sets Syst.*, vol. 71, pp.359–369, 1995.
[16] B. J. Choi, S. W. Kwak, B. K. Kim, "Design of a single-input fuzzy logic controller and its properties," *Fuzzy Sets Syst.*, vol. 106, pp.299–308, 1999.
[17] L. X. Wang, Adaptive Fuzzy Systems and Control: Design and Stability Analysis, Englewood Cliffs, NJ: Prentice-Hall, 1994.
[18] H. Lee. M. Tomizuka, "Robust adaptive control using a universal approximator for SISO nonlinear systems," *IEEE Trans. Fuzzy Syst.*, vol. 8, pp. 95-106, Feb. 2001.
[19] J. E. Slotin, W. Li, Applied Nonlinear Control, Prentice-Hall Inc, New Jersey, 1991.

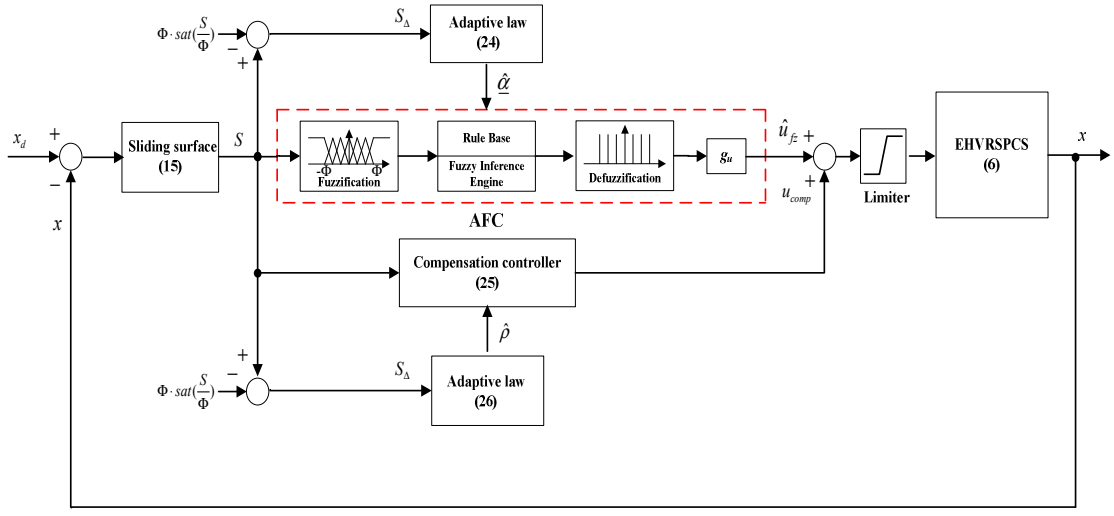

Fig.2. Adaptive Fuzzy Controller with Self-Tuning Fuzzy Sliding-Mode Compensation for Electro-Hydraulic Variable Rotational Speed Pump-Controlled System

2011 IEEE International Conference on Fuzzy Systems
June 27-30, 2011, Taipei, Taiwan

Toward Quantitative Definition of Explanation Ability of Fuzzy Rule-based Classifiers

Hisao Ishibuchi
Department of Computer Science and Intelligent Systems
Osaka Prefecture University
1-1 Gakuen-cho, Naka-ku, Sakai, Osaka 599-8531, Japan
hisaoi@cs.osakafu-u.ac.jp

Yusuke Nojima
Department of Computer Science and Intelligent Systems
Osaka Prefecture University
1-1 Gakuen-cho, Naka-ku, Sakai, Osaka 599-8531, Japan
nojima@cs.osakafu-u.ac.jp

***Abstract*—Explanation ability of a fuzzy rule-based classifier is its ability to explain why an input pattern is classified as a particular class in a convincing way. This ability is important especially when fuzzy rule-based classifiers are used as support systems for human users. This is because human users often want to know why the current input pattern is classified as a particular class. The explanation ability looks similar to the interpretability. They are, however, clearly different concepts. Whereas the explanation ability is directly related to the classification of each pattern, the interpretability is usually independent of classification results. The interpretability has been taken into account in multiobjective design of fuzzy rule-based classifiers. However, the explanation ability has not been used for fuzzy rule-based classifier design. This is because its quantitative definition is very difficult. In this paper, we discuss various factors that are related to quantitative definition of the explanation ability of fuzzy rule-based classifiers. Using simple numerical examples, we explain that the complexity minimization of fuzzy rule-based classifiers does not always lead to the explanation ability maximization. We also explain that the accuracy of fuzzy rules is related to the explanation ability.**

Keywords—pattern classification; fuzzy systems; fuzzy rule-based classifiers; explanation ability; interpretability; complexity.

I. INTRODUCTION

Fuzzy rule-based classifier design has been often handled as the search for accurate and interpretable fuzzy rule-based classifiers. That is, accuracy and interpretability have been used as design criteria in fuzzy rule-based classifier design. These two criteria are combined into a single overall criterion in single-objective approaches [1]-[4] whereas they are handled as different objectives in multiobjective approaches [5]-[9]. Since there exists a tradeoff relation between these two criteria [10], multiobjective approaches usually find a large number of non-dominated fuzzy rule-based classifiers with different tradeoffs (i.e., from simple classifiers with high interpretability and low accuracy to complicated classifiers with high accuracy and low interpretability). It is implicitly assumed that a single fuzzy rule-based classifier is chosen from a large number of obtained non-dominated ones by human users based on their preference in multiobjective approaches. In single-objective approaches, parameter values in a single overall design criterion are often assumed to be specified by human users' preference.

In some early studies on multiobjective fuzzy rule-based classifier design [5], [6], interpretability maximization was formulated as complexity minimization using complexity measures such as the number of fuzzy rules and the total number of antecedent conditions (i.e., total rule length). Recently more sophisticated interpretability measures have been used in multiobjective approaches to fuzzy rule-based classifier design [7]-[9]. Definition of interpretability itself is currently a hot research issue in fuzzy systems [11]-[19].

Whereas the interpretability of fuzzy rule-based classifiers has been frequently discussed in the literature [11]-[19], the explanation ability has not been discussed in many studies [20]-[24]. In this paper, we use the term "*explanation ability*" to mean the ability of a fuzzy rule-based classifier to explain why an input pattern is classified as a particular class in a convincing way. It should be noted that the interpretability and the explanation ability are different concepts. On the one hand, the interpretability of a fuzzy rule-based classifier is often defined by its structural features (e.g., the shape of membership functions, the overlap of adjacent membership functions, the number of fuzzy rules, and the number of antecedent conditions) independent of the classification of each pattern. On the other hand, the explanation ability is directly related to classification results from its definition: the ability of a fuzzy rule-based classifier to explain why an input pattern is classified as a particular class in a convincing way.

In this paper, we discuss various factors that are related to quantitative definition of the explanation ability of a fuzzy rule-based classifier. We assume the use of a single winner-based fuzzy reasoning method for pattern classification. This means that each input pattern is classified by a single winner rule. Thus the explanation of the classification result of an input pattern is performed by showing the corresponding single winner rule. In this situation, the following factors seem to be related to the explanation ability:

(1) Compatibility of the input pattern with its winner rule: If the winner rule has high compatibility with the input pattern, it may have high explanation ability since its antecedent conditions can be viewed as describing the input pattern very well (i.e., without large inconsistency).
(2) Interpretability of the winner rule: If the winner rule has high interpretability, it may have high explanation ability since the explanation is easy for human users to understand.
(3) Accuracy of the winner rule: If the winner rule has high accuracy, it may have high explanation ability since the

978-1-4244-7316-8/11/$26.00 ©2011 IEEE

classification result is highly reliable.

(4) Coverage of the winner rule: If the winner rule classifies many patterns, it may have high explanation ability since the same explanation is applicable to many patterns.

For discussing these factors, this paper is organized as follows. First we explain our fuzzy rule-based classifier with the single winner-based fuzzy reasoning method in Section II. Then we discuss mathematical formulations of the above-mentioned four factors in details in Section III using simple numerical examples. Finally we conclude this paper in Section IV where we also suggest some future research directions.

II. Fuzzy Rule-Based Classifiers

We assume that we have an M-class pattern classification problem in an n-dimensional normalized hyper-cube $[0, 1]^n$. For this problem, we use fuzzy rules of the following type:

$$\text{Rule } R_q: \text{If } x_1 \text{ is } A_{q1} \text{ and } \ldots \text{ and } x_n \text{ is } A_{qn} \text{ then Class } C_q \text{ with } CF_q, \quad (1)$$

where R_q is the label of the qth fuzzy rule, $\mathbf{x}=(x_1, \ldots, x_n)$ is an n-dimensional pattern vector, A_{qi} is an antecedent fuzzy set $(i=1,2,\ldots,n)$, C_q is a class label, and CF_q is a real number in the unit interval [0, 1] which represents a rule weight. The rule weight can be specified by a heuristic manner [25]. It can be also adjusted by a learning algorithm [26]. We use the n-dimensional fuzzy vector $\mathbf{A}_q=(A_{q1}, \ldots, A_{qn})$ for representing the antecedent part of the fuzzy rule R_q in (1) in a concise manner.

Let S be a set of fuzzy rules of the type in (1). That is, S is a fuzzy rule-based classifier. When an n-dimensional input pattern $\mathbf{x}_p=(x_{p1}, \ldots, x_{pn})$ is presented to S, first the compatibility grade of $\mathbf{x}_p$ with the antecedent part $\mathbf{A}_q$ of each fuzzy rule R_q in S is calculated by the product operator as

$$\mu_{\mathbf{A}_q}(\mathbf{x}_p) = \mu_{A_{q1}}(x_{p1}) \times \cdots \times \mu_{A_{qn}}(x_{pn}) \quad \text{for } R_q \in S, \quad (2)$$

where $\mu_{Aqi}(.)$ shows the membership function of A_{qi}. Then a single winner rule $R_{w(\mathbf{x}_p)}$ is identified for $\mathbf{x}_p$ as follows:

$$CF_{w(\mathbf{x}_p)} \times \mu_{\mathbf{A}_{w(\mathbf{x}_p)}}(\mathbf{x}_p) = \max\{CF_q \times \mu_{\mathbf{A}_q}(\mathbf{x}_p) \mid R_q \in S\}, \quad (3)$$

where $w(\mathbf{x}_p)$ denotes the rule index of the winner rule for $\mathbf{x}_p$.

The pattern $\mathbf{x}_p$ is classified by the single winner rule $R_{w(\mathbf{x}_p)}$ as its consequent class. If there is no fuzzy rule with a positive compatibility grade with $\mathbf{x}_p$ (i.e., if $\mathbf{x}_p$ is not covered by any fuzzy rules in S), the classification of $\mathbf{x}_p$ is rejected. The classification of $\mathbf{x}_p$ is also rejected if multiple fuzzy rules with different consequent classes have the same maximum value in the right-hand side of (3). In this case, $\mathbf{x}_p$ is exactly on the classification boundary between the different classes.

We use the single winner-based fuzzy reasoning method in (3) for pattern classification. This is because a responsible fuzzy rule can be always identified for the classification result of each input pattern when we use the single winner-based fuzzy reasoning method. For other fuzzy reasoning methods (e.g., a voting-based method), see [27]-[29] where other types of fuzzy rules (e.g., fuzzy rules with no rule weights, fuzzy rules with multiple consequent classes) were also explained.

III. Explanation Ability

In this section, we discuss each of the four factors related to the explanation ability of a fuzzy rule-based classifier in detail: compatibility, interpretability, accuracy and coverage.

A. A Simple Test Problem and Fuzzy Rule-Based Classifiers

For visual explanation, let us consider a simple three-class two-dimensional pattern classification problem with 20 patterns from each class in Fig. 1. Using three linguistic values (*small*, *medium* and *large*) in Fig. 1 as antecedent fuzzy sets for each of the two attributes, we can generate 3×3 fuzzy rules. Let S_1 be the fuzzy rule-based classifier with those nine fuzzy rules (for simplicity, the rule weight is specified as 1.0 in S_1):

S_1: Fuzzy rule-based classifier with nine fuzzy rules

R_1: If x_1 is *small* and x_2 is *small* then Class 2 with 1.0,
R_2: If x_1 is *small* and x_2 is *medium* then Class 2 with 1.0,
R_3: If x_1 is *small* and x_2 is *large* then Class 1 with 1.0,
R_4: If x_1 is *medium* and x_2 is *small* then Class 2 with 1.0,
R_5: If x_1 is *medium* and x_2 is *medium* then Class 2 with 1.0,
R_6: If x_1 is *medium* and x_2 is *large* then Class 1 with 1.0,
R_7: If x_1 is *large* and x_2 is *small* then Class 3 with 1.0,
R_8: If x_1 is *large* and x_2 is *medium* then Class 3 with 1.0,
R_9: If x_1 is *large* and x_2 is *large* then Class 3 with 1.0.

The location of each rule is shown in Fig. 2 (a). All the 60 patterns in Fig. 1 are correctly classified by S_1 with these nine rules in S_1 as shown in Fig. 3 (a).

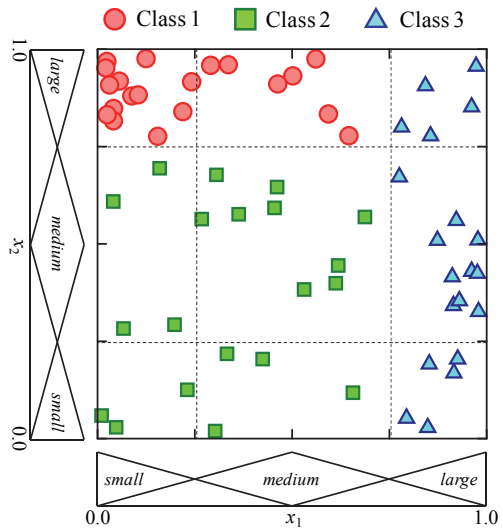

Fig. 1. A simple three-class two-dimensional test problem.

Let us try to simplify the fuzzy rule-based classifier S_1. We can see from Fig. 1 that all training patters with large values of x_1 are from Class 3. Accordingly, the last three fuzzy rules R_7, R_8 and R_9 in S_1 with the same antecedent condition "x_1 is *large*" have the same consequent class (i.e., Class 3). This

observation suggests us to combine the last three rules R_7, R_8, and R_9 of S_1 into a single fuzzy rule:

R_{789}: If x_1 is *large* then Class 3 with 1.0.

Using this fuzzy rule, S_1 can be simplified as follows:

S_2: Fuzzy rule-based classifier with seven fuzzy rules

R_1: If x_1 is *small* and x_2 is *small* then Class 2 with 1.0,
R_2: If x_1 is *small* and x_2 is *medium* then Class 2 with 1.0,
R_3: If x_1 is *small* and x_2 is *large* then Class 1 with 1.0,
R_4: If x_1 is *medium* and x_2 is *small* then Class 2 with 1.0,
R_5: If x_1 is *medium* and x_2 is *medium* then Class 2 with 1.0,
R_6: If x_1 is *medium* and x_2 is *large* then Class 1 with 1.0,
R_{789}: If x_1 is *large* then Class 3 with 1.0.

This fuzzy rule-based classifier S_2 is illustrated in Fig. 2 (b). All the 60 patterns in Fig. 1 are correctly classified by S_2 as shown in Fig. 3 (b). From Fig. 3 (a) and Fig. 3 (b), we can see that S_1 and S_2 have slightly different classification boundaries.

If we use the negation of *large* (i.e., "*not large*") in the antecedent part, the number of fuzzy rules in S_2 can be further decreased as follows:

S_3: Fuzzy rule-based classifier with three fuzzy rules

R_{1245}: If x_1 is *not large* and x_2 is *not large*
then Class 2 with 1.0,
R_{36}: If x_1 is *not large* and x_2 is *large* then Class 1 with 1.0,
R_{789}: If x_1 is *large* then Class 3 with 1.0.

The membership function of "*not large*" is defined as

$$\mu_{not\ large}(x) = 1 - \mu_{large}(x) \quad for\ 0 \le x \le 1, \tag{4}$$

where $\mu_{large}(x)$ is the membership function of the antecedent fuzzy set *large*.

The fuzzy rule-based classifier S_3 with the three fuzzy rules is illustrated in Fig. 2 (c). All the 60 patterns are correctly classified by S_3 as shown in Fig. 3 (c). From Fig. 3 (a)-(c), we can see that the three fuzzy rule-based classifiers S_1, S_2 and S_3 have slightly different classification boundaries.

The fuzzy rule-based classifier S_3 can be viewed as having the following tree-structure:

If x_1 is *large* then Class 3 with 1.0,
else if x_2 is *large* then Class 1 with 1.0,
else Class 2 with 1.0. (5)

A simple fuzzy rule-based classifier can be also obtained by selecting fuzzy rules from S_1 rather than combining fuzzy rules. For example, the following fuzzy rule-based classifier with four fuzzy rules has the same classification boundaries as S_1 with the nine fuzzy rules (see Fig. 2 (d) and Fig. 3 (d)):

S_4: Fuzzy rule-based classifier with four fuzzy rules

R_5: If x_1 is *medium* and x_2 is *medium* then Class 2 with 1.0,
R_6: If x_1 is *medium* and x_2 is *large* then Class 1 with 1.0,
R_8: If x_1 is *large* and x_2 is *medium* then Class 3 with 1.0,
R_9: If x_1 is *large* and x_2 is *large* then Class 3 with 1.0.

Strictly speaking, patterns with $x_1 = 0.0$ or $x_2 = 0.0$ cannot be classified by S_4 whereas those patterns can be classified by S_1. Thus the classification results by S_1 and S_4 are not exactly the same. However, except for those special cases, S_1 and S_4 have the same classification results as shown in Fig. 3.

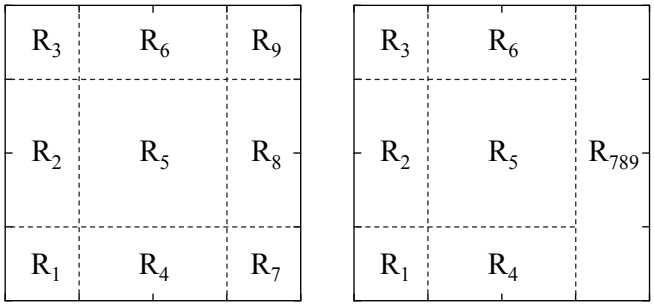

(a) Fuzzy rule-based classifier S_1. (b) Fuzzy rule-based classifier S_2.

(c) Fuzzy rule-based classifier S_3. (d) Fuzzy rule-based classifier S_4.

Fig. 2. Fuzzy rules in S_1, S_2, S_3 and S_4.

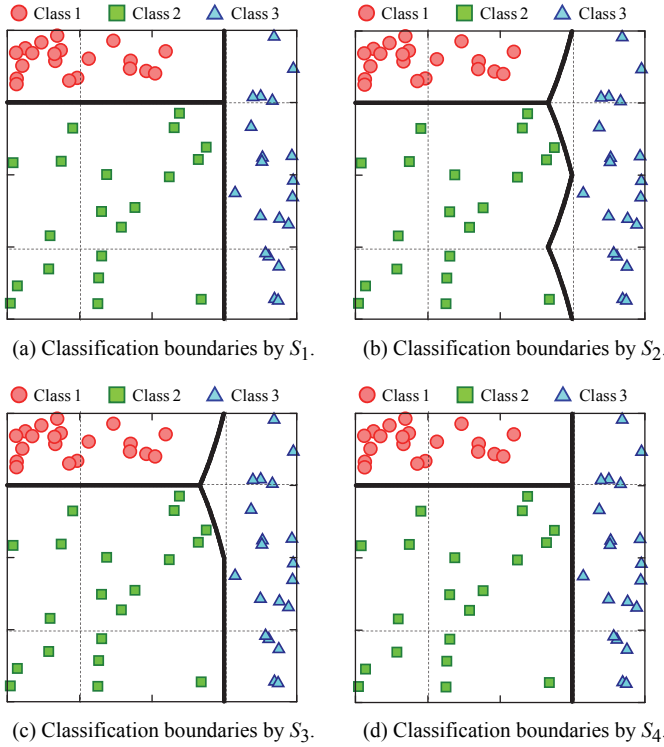

(a) Classification boundaries by S_1. (b) Classification boundaries by S_2.

(c) Classification boundaries by S_3. (d) Classification boundaries by S_4.

Fig. 3. Classification boundaries by S_1, S_2, S_3 and S_4.

Since S_4 is a subset of S_1, it is clear that S_4 is simpler (i.e., less complicated) than S_1 (see Fig. 2 (a) and Fig. 2 (d)). It is also clear that S_2 is simpler than S_1 since the three fuzzy rules R_7, R_8 and R_9 in S_1 are merged into the single fuzzy rule R_{789} in S_2. However, the comparison of S_3 with the other fuzzy rule-based classifiers is not easy since S_3 has the special antecedent fuzzy set "*not large*". If we use the number of fuzzy rules as a complexity measure, we have the following order of the four fuzzy rule-based classifiers with respect to their complexity:

$$Complex(S_1) > Complex(S_2) > Complex(S_4) > Complex(S_3), \quad (6)$$

where $Complex(S)$ is a complexity measure.

If we think that fuzzy rules with "*not large*" are more complicated than other fuzzy rules with no negations, we may have the following order

$$Complex(S_1) > Complex(S_2) > Complex(S_3) > Complex(S_4). \quad (7)$$

B. Compatibility of Each Input Pattern with Its Winner Rule

Let us consider the classification of a new pattern $\mathbf{x}_1 = (0.05, 0.05)$ by the four fuzzy rule-based classifiers S_1, S_2, S_3 and S_4. This pattern is classified as Class 2 by the following winner rule in each classifier:

R_1 in S_1: If x_1 is *small* and x_2 is *small* then Class 2 with 1.0,

R_1 in S_2: If x_1 is *small* and x_2 is *small* then Class 2 with 1.0,

R_{1245} in S_3: If x_1 is *not large* and x_2 is *not large* then Class 2 with 1.0,

R_5 in S_4: If x_1 is *medium* and x_2 is *medium* then Class 2 with 1.0.

It seems that the fuzzy rule R_1 is a convincing explanation about the classification of $\mathbf{x}_1$ as Class 2. This is because $\mathbf{x}_1$ is linguistically described as "x_1 is *small* and x_2 is *small*", which means that $\mathbf{x}_1$ has high compatibility with the antecedent part of the fuzzy rule R_1. The compatibility is calculated as

$$\mu_{\mathbf{A}_1}(\mathbf{x}_1) = \mu_{small}(0.05) \times \mu_{small}(0.05) = 0.9 \times 0.9 = 0.81. \quad (8)$$

On the contrary, it seems that the fuzzy rule R_5 in S_4 is not a convincing explanation about the classification of $\mathbf{x}_1$ as Class 2. This is because $\mathbf{x}_1$ does not have high compatibility with the antecedent part of R_5. Human users do not think that the input pattern $\mathbf{x}_1 = (0.05, 0.05)$ is well-described by the antecedent conditions "x_1 is *medium* and x_2 is *medium*". The compatibility of $\mathbf{x}_1$ with the antecedent part of R_5 is calculated as

$$\mu_{\mathbf{A}_5}(\mathbf{x}_1) = \mu_{medium}(0.05) \times \mu_{medium}(0.05) = 0.1 \times 0.1 = 0.01. \quad (9)$$

From these discussions, we can see that the compatibility of the input pattern $\mathbf{x}_p$ with the antecedent part $\mathbf{A}_{w(\mathbf{x}_p)}$ of its winner rule $R_{w(\mathbf{x}_p)}$ is related to the explanation ability of the fuzzy rule-based classifier. Let D_{Test} be the set of input patterns to be classified. This pattern set can be viewed as testing data that are not used for the design of the fuzzy rule-based classifier. The average compatibility of each input pattern with the antecedent part of its winner rule is calculated over the pattern set D_{Test} as follows:

$$Compatibility(S, D_{\text{Test}}) = \frac{\sum_{\mathbf{x}_p \in D_{\text{Test}}} \mu_{\mathbf{A}_{w(\mathbf{x}_p)}}(\mathbf{x}_p)}{|D_{\text{Test}}|}, \quad (10)$$

where S is a fuzzy rule-based classifier, $|D_{\text{Test}}|$ is the cardinality of D_{Test} (i.e., the number of patterns in D_{Test}), and $\mathbf{A}_{w(\mathbf{x}_p)}$ is the antecedent part of the winner rule $R_{w(\mathbf{x}_p)}$ for the input pattern $\mathbf{x}_p$ in D_{Test}. Since the winner rule $R_{w(\mathbf{x}_p)}$ is selected from the fuzzy rule-based classifier S, S is included in the left hand side whereas S is not explicitly shown in the right hand side.

The input pattern $\mathbf{x}_1 = (0.05, 0.05)$ is fully compatible with the antecedent part of th fuzzy rule R_{1245} in S_3:

$$\mu_{\mathbf{A}1245}(\mathbf{x}_1) = \mu_{not\ large}(0.05) \times \mu_{not\ large}(0.05) = 1.0 \times 1.0 = 1.0. \quad (11)$$

Thus the fuzzy rule R_{1245} in S_3 has high explanation ability in terms of the compatibility with the input pattern. One may think that R_1 in S_1 seems to have higher explanation ability than R_{1245} in S_3 whereas R_{1245} has higher compatibility than R_1. This intuition is related to the interpretability of each rule, which will be discussed later in the next section.

Let us consider another input pattern $\mathbf{x}_2 = (0.95, 0.05)$. This pattern is classified as Class 3 by the following winner rules:

R_7 in S_1: If x_1 is *large* and x_2 is *small* then Class 3 with 1.0,

R_{789} in S_2: If x_1 is *large* then Class 3 with 1.0,

R_{789} in S_3: If x_1 is *large* then Class 3 with 1.0,

R_8 in S_4: If x_1 is *large* and x_2 is *medium* then Class 3 with 1.0.

The fuzzy rule R_7 seems to be a convincing explanation about the classification of $\mathbf{x}_2$ because $\mathbf{x}_2$ is linguistically described as "x_1 is *large* and x_2 is *small*". The compatibility of $\mathbf{x}_2$ with the antecedent part of R_7 is calculated as

$$\mu_{\mathbf{A}_7}(\mathbf{x}_2) = \mu_{large}(0.95) \times \mu_{small}(0.05) = 0.9 \times 0.9 = 0.81. \quad (12)$$

Whereas S_4 is simpler than S_1, S_4 does not have higher explanation ability than S_1. For example, the fuzzy rule R_8 in S_4 seems to be less convincing than R_7 in S_1 because "x_1 is *large* and x_2 is *medium*" is not highly compatible with $\mathbf{x}_2 = (0.95, 0.05)$. The compatibility of $\mathbf{x}_2$ with the antecedent part of R_8 is calculated as

$$\mu_{\mathbf{A}_8}(\mathbf{x}_2) = \mu_{large}(0.95) \times \mu_{medium}(0.05) = 0.9 \times 0.1 = 0.09. \quad (13)$$

On the contrary, the fuzzy rule R_{789} in S_2 and S_3 seems to be a good linguistic explanation. This is because its antecedent condition "x_1 is *large*" describes $\mathbf{x}_2 = (0.95, 0.05)$ very well. The compatibility of $\mathbf{x}_2$ with the antecedent part of R_{789} is

$$\mu_{\mathbf{A}_{789}}(\mathbf{x}_2) = \mu_{large}(0.95) = 0.90. \quad (14)$$

These discussions on the classification of $\mathbf{x}_2 = (0.95, 0.05)$ also suggest that the compatibility of the input pattern $\mathbf{x}_p$ with

the antecedent part $\mathbf{A}_{w(\mathbf{x}_p)}$ of its winner rule $R_{w(\mathbf{x}_p)}$ is related to the explanation ability of the fuzzy rule-based classifier.

C. Interpretability of the Winner Rule for Each Input Pattern

In a fuzzy rule-based classifier with the single winner-based fuzzy reasoning method, the winner rule for an input pattern is used as the explanation for its classification result. Thus the interpretability of the winner rule is directly related to the explanation ability of the fuzzy rule-based classifier.

Let us consider the classification of the input pattern $\mathbf{x}_1 = (0.05, 0.05)$ again. This pattern is classified by R_1 in S_1:

R_1 in S_1: If x_1 is *small* and x_2 is *small* then Class 2 with 1.0.

The fuzzy rule R_1 seems to have higher interpretability than the winner rule R_{1245} in S_3:

R_{1245} in S_3: If x_1 is *not large* and x_2 is *not large* then Class 2 with 1.0.

This is because R_{1245} looks more complicated than R_1.

When the same pattern $\mathbf{x}_1$ is presented to the fuzzy rule-based classifier S_4, it is classified as Class 2 by R_5:

R_5 in S_4: If x_1 is *medium* and x_2 is *medium* then Class 2 with 1.0.

This winner rule R_5 in S_4 can be viewed as having the same interpretability as R_1 in S_1. This is because these two fuzzy rules have the same structure. As explained in the previous subsection, R_1 seems to have higher explanation ability for $\mathbf{x}_1$ than R_5 because R_1 has higher compatibility. However, with respect to their interpretability, we cannot differentiate these two fuzzy rules.

Let us consider the other input pattern $\mathbf{x}_2 = (0.95, 0.05)$. This pattern is classified as Class 3 by R_7 in S_1 and R_{789} in S_2:

R_7 in S_1: If x_1 is *large* and x_2 is *small* then Class 3 with 1.0,

R_{789} in S_2: If x_1 is *large* then Class 3 with 1.0.

The interpretability of R_{789} seems to be higher than that of R_7. This is because R_{789} has a simpler antecedent condition than R_7. As in the case of the comparison between the two fuzzy rules R_1 and R_5, the winner rule R_7 in S_1 can be viewed as having the same interpretability as the winner rule R_8 in S_4:

R_8 in S_4: If x_1 is *large* and x_2 is *medium* then Class 3 with 1.0.

Let $R_{w(\mathbf{x}_p)}$ be the winner rule of the input pattern $\mathbf{x}_p$. As in the previous subsection, let D_{Test} be the set of input patterns to be classified. In this case, the average interpretability of the winner rules over the pattern set D_{Test} is calculated as follows:

$$Interpretability(S, D_{\text{Test}}) = \frac{\sum_{\mathbf{x}_p \in D_{\text{Test}}} Interpretability(R_{w(\mathbf{x}_p)})}{|D_{\text{Test}}|}. \quad (15)$$

In (15), the problem is how to define the interpretability of each fuzzy rule. In the above discussions, we intuitively use the complexity of the antecedent part of each fuzzy rule. A simple measure to evaluate the complexity of the antecedent part is the number of antecedent conditions. This measure seems to be too simple because it cannot differentiate between R_{1245} with the antecedent condition "If x_1 is *not large* and x_2 is *not large*" and R_1 with the antecedent condition "If x_1 is *small* and x_2 is *small*".

We may be able to refer to a lot of existing studies on the interpretability of fuzzy rule-based systems [11]-[19]. It should be noted, however, that the interpretability in those studies was usually discussed for fuzzy rule-based classifiers rather than each individual fuzzy rule. In (15), the interpretability of each winner rule is used. The interpretability in (15) can be viewed as the understandability of the winner rule for human users.

D. Accuracy of the Winner Rule for Each Input Pattern

In multiobjective fuzzy rule-based classifier design, the accuracy of classifiers is not viewed as a factor related to the interpretability. This is because the accuracy is handled as a separate objective from the interpretability in multiobjective fuzzy rule-based classifier design. However, the accuracy of the winner rule seems to be an important factor related to the explanation ability of fuzzy rule-based classifiers.

Let us consider the following fuzzy rule-based classifier with three rules for our three-class test problem:

S_5: Fuzzy rule-based classifier with three fuzzy rules

R_{123}: If x_1 is *small* then Class 1 with 1.0,
R_{456}: If x_1 is *medium* then Class 2 with 1.0,
R_{789}: If x_1 is *large* then Class 3 with 1.0.

The classification boundaries by S_5 are shown in Fig. 4. Several training patterns from Class 1 and Class 2 are misclassified while all the 20 patterns from Class 3 are correctly classified in Fig. 4.

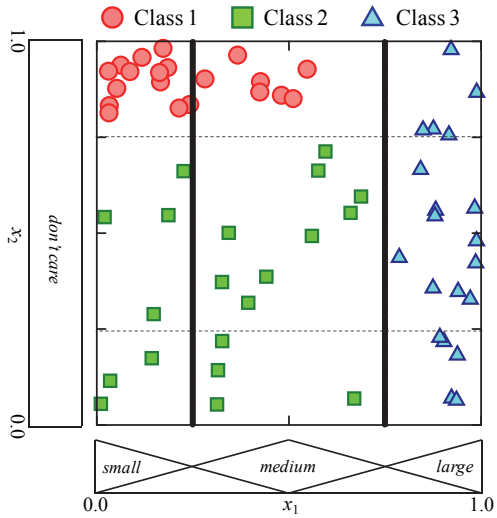

Fig. 4. Classification boundaries by S_5.

As in the previous two subsections, let us consider the classification of the input pattern $\mathbf{x}_1 = (0.05, 0.05)$. This pattern is classified as Class 1 by the winner rule R_{123} in S_5:

R_{123} in S_5: If x_1 is *small* then Class 1 with 1.0.

This winner rule R_{123} has high compatibility with $\mathbf{x}_1 = (0.05, 0.05)$. This winner rule has also has high interpretability thanks to its simple antecedent condition. As a result, this winner rule is viewed as having high explanation ability with respect to the compatibility and the interpretability. However, we do not think that the winner rule R_{123} explains the classification result of $\mathbf{x}_1$ in a convincing manner. The winner rule R_{123} classifies $\mathbf{x}_1 = (0.05, 0.05)$ as Class 1. However, this classification result is not likely to be correct in Fig. 4 because many training patterns close to $\mathbf{x}_1$ in Fig. 4 are from Class 2. That is, we may think that the explanation ability of R_{123} is low since the accuracy of R_{123} is low.

From these discussions, we can see that the accuracy of the winner rule is related to the explanation ability of a fuzzy rule-based classifier. The average accuracy of the winner rule $R_{w(\mathbf{x}p)}$ can be defined over the pattern set D_{Test} as follows:

$$Accuracy(S, D_{\text{Test}}) = \frac{\sum_{\mathbf{x}_p \in D_{\text{Test}}} Accuracy(R_{w(\mathbf{x}_p)})}{|D_{\text{Test}}|} . \quad (16)$$

In (16), the problem is the definition of the accuracy of each fuzzy rule. One candidate definition is as follows:

$$Accuracy(R_q) = \frac{\text{Number of patterns correctly classified by } R_q}{\text{Number of patterns classified by } R_q} . \quad (17)$$

Let us assume that a single fuzzy rule correctly classifies 18 out of 20 patterns for which it is selected as the winner rule. The accuracy of this rule is calculated as 18/20 (i.e., 0.9) in (17). This accuracy is summed up 20 times in the numerator of (16), which is calculated as 18 (i.e., the same as the number of correctly classified patterns by this fuzzy rule). From this discussion, we can see that (16) is the same as the classification rate when we use (17) as the accuracy of each fuzzy rule:

$$Accuracy(S, D_{\text{Test}}) = \frac{\text{Number of patterns correctly classified by } S}{|D_{\text{Test}}|} . \quad (18)$$

In this definition based on (16) and (17), the accuracy of the fuzzy rule-based classifier S is directly used as a factor related to its explanation ability.

The accuracy of the fuzzy rule R_q can be also defined as

$$Accuracy(R_q) = \frac{\sum_{\mathbf{x}_p \in D_{\text{Test}}(C_q)} \mu_{\mathbf{A}_q}(\mathbf{x}_p)}{\sum_{\mathbf{x}_p \in D_{\text{Test}}} \mu_{\mathbf{A}_q}(\mathbf{x}_p)} , \quad (19)$$

where $D_{\text{Test}}(C_q)$ is the set of patterns in D_{Test} from Class C_q (i.e., the same class as the consequent class of the fuzzy rule R_q). In the field of fuzzy data mining [29]-[32], the accuracy in (19) is referred to as the confidence of the fuzzy rule R_q.

In (19), it is possible to use the training data rather than the test data. In data mining, the confidence is usually defined using the training data. If we use the 60 patterns in Fig. 4 as the data set D_{Test} in (19), the accuracy (i.e., confidence) of each rule in S_5 is calculated from (19) as follows:

$Accuracy(R_{123}) = Confidence(R_{123}) = 0.591,$
$Accuracy(R_{456}) = Confidence(R_{456}) = 0.469,$
$Accuracy(R_{789}) = Confidence(R_{789}) = 0.911.$

If we also use the 60 patterns in Fig. 4 as the data set D_{Test} in (16), the accuracy measure of the fuzzy rule-based classifier S_5 is calculated as follows:

$Accuracy(S_5, D_{\text{Test}}) = 0.657.$

For comparison, we calculate the accuracy measure for each of the other fuzzy rule-based classifiers S_1, S_2, S_3 and S_4 in the same manner as follows:

$Accuracy(S_1, D_{\text{Test}}) = 0.846,$
$Accuracy(S_2, D_{\text{Test}}) = 0.848,$
$Accuracy(S_3, D_{\text{Test}}) = 0.837,$
$Accuracy(S_4, D_{\text{Test}}) = 0.784.$

We can see that S_1, S_2, S_3 and S_4 with no misclassified pattern have larger values of the accuracy measure than S_5 with many misclassified patterns.

E. Coverage of the Winner Rule for Each Input Pattern

Roughly speaking, fuzzy rules with small covering regions in the pattern space tend to have high accuracy. Let us consider an extreme case where each fuzzy rule covers only a single pattern. In this extreme case, the accuracy of each fuzzy rule is always 1.0. However, such a fuzzy rule with a very small covering region may have small explanation ability.

Let us consider the following two cases:

Case 1: Most patterns are classified by a few winner rules. That is, many patterns share the same winner rule.

Case 2: Each pattern is classified by a different winner rule. That is, each winner rule classifies only a single pattern.

We think that Case 1 has higher explanation ability than Case 2. This is because human users do not have to examine many winner rules in Case 1.

In fuzzy data mining, coverage is defined as follows:

$$Coverage(R_q) = \frac{\sum_{\mathbf{x}_p \in D_{\text{Test}}(C_q)} \mu_{\mathbf{A}_q}(\mathbf{x}_p)}{|D_{\text{Test}}(C_q)|} , \quad (20)$$

where $|D_{\text{Test}}(C_q)|$ is the number of D_{Test} from Class C_q.

We can also define the coverage of R_q using the number of correctly classified patterns as

$$Coverage(R_q) = \frac{\text{Number of correctly classified patterns by } R_q}{|D_{\text{Test}}(C_q)|} . \quad (21)$$

We can see that the coverage of a fuzzy rule in (21) is large when it correctly classifies many patterns (i.e., when it is selected as the winner rule for many patterns from its consequent class). The coverage in (20) has a similar meaning: The coverage of a fuzzy rule in (20) has a large value when it covers many patterns from its consequent class.

The average value of coverage of the winner rule is calculated over the pattern set D_{Test} as follows:

$$Coverage(S, D_{\text{Test}}) = \frac{\sum_{\mathbf{x}_p \in D_{\text{Test}}} Coverage(R_{w(\mathbf{x}_p)})}{|D_{\text{Test}}|} . \quad (22)$$

If we use the 60 patterns in Fig. 4 as the pattern set D_{Test}, the average value of coverage in (22) is calculated for each fuzzy rule-based classifier for the definition in (21) as follows:

$Coverage(S_1, D_{\text{Test}}) = 0.408$,
$Coverage(S_2, D_{\text{Test}}) = 0.617$,
$Coverage(S_3, D_{\text{Test}}) = 1.000$,
$Coverage(S_4, D_{\text{Test}}) = 0.875$,
$Coverage(S_5, D_{\text{Test}}) = 0.767$.

We can see that high coverage is obtained from fuzzy rule-based classifiers with a small number of fuzzy rules (e.g., S_3 and S_5 with three fuzzy rules, and S_4 with four fuzzy rules). Since many patterns are misclassified by S_5, its coverage by (21) is much smaller than S_3 whereas they have the same number of fuzzy rules.

If we use the definition of (20), the average value of coverage in (22) is calculated for each fuzzy rule-based classifier as follows:

$Coverage(S_1, D_{\text{Test}}) = 0.326$,
$Coverage(S_2, D_{\text{Test}}) = 0.494$,
$Coverage(S_3, D_{\text{Test}}) = 0.875$,
$Coverage(S_4, D_{\text{Test}}) = 0.364$,
$Coverage(S_5, D_{\text{Test}}) = 0.641$.

We can also see that high coverage is obtained from fuzzy rule-based classifiers with a small number of fuzzy rules (e.g., S_3 and S_5 with three fuzzy rules). Since many patterns are misclassified by S_5, its coverage by (20) is much smaller than S_3 whereas they have the same number of fuzzy rules.

IV. CONCLUSIONS

In this paper, first we defined the explanation ability as "the ability of a fuzzy rule-based classifier to explain why an input pattern is classified as a particular class in a convincing way." Then we pointed out the following four factors related to the quantitative definition (i.e., mathematical formulation) of the explanation ability:

(1) Compatibility of an input pattern with its winner rule
(2) Interpretability of the winner rule
(3) Accuracy of the winner rule
(4) Coverage of the winner rule

We discussed the formulation of each factor. It was clearly shown through the discussions on these four factors that the explanation ability of a fuzzy rule-based classifier is related to both its accuracy and its interpretability. Since we formulated each factor, we may be able to formulate the explanation ability by combining those formulations into a single overall measure. A discussion on how to combine them into a single overall measure is a future research issue. This issue does not exclude the possibility of combining the four factors into two measures with different characteristic features.

We may need further discussions on each factor as well as the above-mentioned discussions on their integration. It may be interesting to examine relations among the four factors. We also need further discussions on the possibility of other factors that are related to the explanation ability. Moreover, it may be a promising research issue to use the explanation ability instead of or together with the interpretability in multiobjective fuzzy rule-based classifier design. In this case, both of the classifier-level accuracy and the rule-level accuracy will be used to measure different aspects of fuzzy rule-based classifiers.

REFERENCES

[1] H. Ishibuchi, K. Nozaki, N. Yamamoto, and H. Tanaka, "Selecting fuzzy if-then rules for classification problems using genetic algorithms," *IEEE Trans. on Fuzzy Systems* 3 (3) 260-270, 1995.

[2] M. Setnes and H. Roubos, "GA-fuzzy modeling and classification: Complexity and performance," *IEEE Trans. on Fuzzy Systems* 8 (5) 509-522, 2000.

[3] L. Castillo, A. González, and R. Pérez, "Including a simplicity criterion in the selection of the best rule in a genetic fuzzy learning algorithm," *Fuzzy Sets and Systems* 120 (2) 309-321, 2001.

[4] J. Abonyi, J. A. Roubos, and F. Szeifert, "Data-driven generation of compact, accurate, and linguistically sound fuzzy classifiers based on a decision-tree initialization," *International Journal of Approximate Reasoning* 32 (1) 1-21, 2003.

[5] H. Ishibuchi, T. Murata, and I. B. Türksen, "Single-objective and two-objective genetic algorithms for selecting linguistic rules for pattern classification problems," *Fuzzy Sets and Systems* 89 (2) 135-150, 1997.

[6] H. Ishibuchi, T. Nakashima, and T. Murata, "Three-objective genetics-based machine learning for linguistic rule extraction," *Information Sciences* 136 (1-4) 109-133, 2001.

[7] P. Pulkkinen and H. Koivisto, "Fuzzy classifier identification using decision tree and multiobjective evolutionary algorithms," *International Journal of Approximate Reasoning* 48 (2) 526-543, 2008.

[8] P. Ducange, B. Lazzerini, and F. Marcelloni, "Multi-objective genetic fuzzy classifiers for imbalanced and cost-sensitive datasets," *Soft Computing* 14 (7) 713-728, May 2010.

[9] Y. Zhang, X. B. Wu, Z. Y. Xing, and W. L. Hu, "On generating interpretable and precise fuzzy systems based on Pareto multi-objective cooperative co-evolutionary algorithm," *Applied Soft Computing* 11 (1) 1284-1294, 2011.

[10] H. Ishibuchi and Y. Nojima, "Analysis of interpretability-accuracy tradeoff of fuzzy systems by multiobjective fuzzy genetics-based machine learning," *International Journal of Approximate Reasoning* 44 (1) 4-31, 2007.

[11] J. Casillas, O. Cordón, F. Herrera, and L. Magdalena (eds.), *Interpretability Issues in Fuzzy Modeling*, Springer, 2003.

[12] J. Casillas, O. Cordón, F. Herrera, and L. Magdalena (eds.), *Accuracy Improvements in Linguistic Fuzzy Modeling*, Springer, 2003.

[13] S. Guillaume, "Designing fuzzy inference systems from data: An interpretability-oriented review," *IEEE Trans. on Fuzzy Systems* 9 (3) 426-443, 2001.

[14] R. Mikut, J. Jäkel, and L. Gröll, "Interpretability issues in data-based learning of fuzzy systems," *Fuzzy Sets and Systems* 150 (2) 179-197, 2005.

[15] C. Mencar and A. M. Fanelli, "Interpretability constraints for fuzzy information granulation," *Information Sciences* 178 (24) 4585-4618, 2008.

[16] S. M. Zhou and J. Q. Gan, "Low-level interpretability and high-level interpretability: a unified view of data-driven interpretable fuzzy system modelling," *Fuzzy Sets and Systems* 159 (23) 3091-3131, 2008.

[17] A. Botta, B. Lazzerini, F. Marcelloni, and D. C. Stefanescu, "Context adaptation of fuzzy systems through a multi-objective evolutionary approach based on a novel interpretability index," *Soft Computing* 13 (5) 437-449, 2009.

[18] J. M. Alonso, L. Magdalena, and G. González-Rodríguez, "Looking for a good fuzzy system interpretability index: An experimental approach." *International Journal of Approximate Reasoning*, 51 (1) 115-134, 2009.

[19] C. Mencar, C. Castiello, R. Cannone, and A. M. Fanelli, "Interpretability assessment of fuzzy knowledge bases: A cointension based approach," *International Journal of Approximate Reasoning* 52 (4) 501-518, June 2011.

[20] H. Ishibuchi, Y. Kaisho, and Y. Nojima, "Designing fuzzy rule-based classifiers that can visually explain their classification results to human users," *Proc. of 3rd International Workshop on Genetic and Evolving Fuzzy Systems*, 5-10, 2008.

[21] H. Ishibuchi, Y. Kaisho, and Y. Nojima, "A visual explanation system for explaining fuzzy reasoning results by fuzzy rule-based classifiers," *Proc. of 2008 North American Fuzzy Information Processing Society Conference*, CD-ROM Proceeding (6 pages), 2008.

[22] H. Ishibuchi and Y. Nojima, "Discussions on Interpretability of Fuzzy Systems using Simple Examples," *Proc. of 13th IFSA World Congress and 6th Conference of EUSFLAT*, 1649-1654, 2009.

[23] H. Ishibuchi, Y. Kaisho, and Y. Nojima, "Complexity, interpretability and explanation capability of fuzzy rule-based classifiers," *Proc. of 2009 IEEE International Conference on Fuzzy Systems*, 1730-1735, Jeju Island, Korea, August 20-24, 2009.

[24] H. Ishibuchi, Y. Kaisho, and Y. Nojima, "Design of linguistically interpretable fuzzy rule-based classifiers: A short review and open questions," *Journal of Multiple-Valued Logic and Soft Computing* 17 (2-3) 101-134, 2011.

[25] H. Ishibuchi and T. Yamamoto, "Rule weight specification in fuzzy rule-based classification systems," *IEEE Trans. on Fuzzy Systems* 13 (4) 428-435, 2005.

[26] K. Nozaki, H. Ishibuchi, and H. Tanaka, "Adaptive fuzzy rule-based classification systems," *IEEE Trans. on Fuzzy Systems* 4 (3) 238-250, 1996.

[27] O. Cordón, M. J. del Jesus, and F. Herrera, "A proposal on reasoning methods in fuzzy rule-based classification systems," *International Journal of Approximate Reasoning* 20 (1) 21-45, 1999.

[28] H. Ishibuchi, T. Nakashima, and T. Morisawa, "Voting in fuzzy rule-based systems for pattern classification problems," *Fuzzy Sets and Systems* 103 (2) 223-238,1999.

[29] H. Ishibuchi, T. Nakashima, and M. Nii: *Classification and Modeling with Linguistic Information Granules: Advanced Approaches to Linguistic Data Mining*, Springer, Berlin, 2004.

[30] H. Ishibuchi, T. Yamamoto, and T. Nakashima, "Fuzzy data mining: Effect of fuzzy discretization," *Proc. of 2001 IEEE International Conference on Data Mining*, 241-248, 2001.

[31] T. P. Hong, C. S. Kuo, and S. C. Chi, "Trade-off between computation time and number of rules for fuzzy mining from quantitative data," *International Journal of Uncertainty Fuzziness and Knowledge-Based Systems* 9 (5) 587-604, 2001.

[32] T. P. Hong, K. Y. Lin, and S. L. Wang, "Fuzzy data mining for interesting generalized association rules," *Fuzzy Sets and Systems* 138 (2) 255-269, 2003.

2011 IEEE International Conference on Fuzzy Systems
June 27-30, 2011, Taipei, Taiwan

Multi-level Multi-Objective Decision Problem through Fuzzy Random Regression based Objective Function

[1,2]Nureize Arbaiy
[1]Graduate School of Information, Production and System, Waseda University, 2-7 Hibikino, Wakamatsu, Kitakyushu, 808-0135 Japan.
[2]Faculty of Comp. Science and Information Technology, Univ. Tun Hussein Onn Malaysia, 86400 Johor, Malaysia.
[1]nureize@uthm.edu.my

Junzo Watada
Graduate School of Information, Production and System, Waseda University, 2-7 Hibikino, Wakamatsu, Kitakyushu, 808-0135 Japan.
[2]junzow@osb.att.ne.jp

***Abstract*—A multi-level decision making problem confronts several issues especially in coordinating decision in hierarchic processes and in compromising conflicting objectives for each decision level. Therefore, its mathematical model plays a pivotal role in solving such problem, and is influencing to the final result. However, it is sometimes difficult to estimate the coefficients of objective functions of the model in real situations specifically when the statistical data contain random and fuzzy information. Thus, decision making scheme should provide an appropriate method to handle the presence of such uncertainties. Hence, this paper proposes a fuzzy random regression method to estimate the coefficients value for the objective functions of multi-level multi-objective model. The algorithm is constructed to obtain a satisfaction solution, which fulfills at least weak Pareto optimality. A numerical example illustrates the proposed solution procedure.**

Keywords- fuzzy random regression model, multi-level problem; multi-objective; additive fuzzy goal programming.

I. INTRODUCTION

Organizational decision making is usually based on the multi-level structure that consists of the top-level decision maker and subsequent levels of decision making power. At least, one decision maker (DM) is located at each level and controls a decision for optimizing their level or unit's objectives. Decision making process in multi-level organization should pay an attention to the central administrations issues and the coordination among lower-level activities. Although the execution of decision moves from an upper level to a lower level, the reaction of a lower-level decision maker affects the optimization of the decision at an upper level decision maker ([1]; [2]; [3]). In such cases, a proper distribution of decision powers with respect to problem belongs to the DM in the respective level must be addressed in most multi-level decision situations.

The structure of multi-objective problem in each level of organization increases the complexities of decision making and planning. DM has to resolve several conflicting objectives at different levels and preference which cause dissatisfaction among decision makers. Although the standard mathematical programming problems are able to solve the multi-objective problem, it is usually considering only one DM in a single-level structure. Thus, multi-objective optimizations in the multi-level structure are required to address this problem. Mathematical programming that takes a multi-level structure, with each level controlling several conflicting objectives is known as multi-level multi-objective programming ([4]; [5]).

In a multi-level decision-making context, each DM which represents decision-making unit should have a motivation to cooperate with others. The satisfactions of a DM at other levels are important and must be considered to accomplish overall organization's goal. Therefore, a satisfaction approach is needed to support the decision-making in multi-level structure that confronts a multiple objective problem at each level. Even though the standard mathematical programming was used to solve the multi-objective problem, these kinds of model are basically unable to accommodate multi-objective problem in multi-level structure due to the presence of decision makers in each level of decision structure.

Moreover, one often needs to make a decision under uncertainty in the real-situation decision making problems. In this study, uncertainties are characterized by fuzzy and random information. The uncertainties were observed during the model settings where the statistical data used to estimate the coefficients may include either random or fuzzy information. We explain the situation as follows. Assume that a profit of crop is reliant on weathers, which this scenarios occur in random. The profit itself may be estimated as a fuzzy number as well. That is, the profit is expressed by a fuzzy random variable. Furthermore, if multiple decision makers are involved in evaluating the same subject, for instance in the multi-attribute evaluation problem, the difference of decision maker's evaluation also should be considered ([6]; [7]). Hence, such situation may take place in real situation and should be handled sufficiently.

Additionally, estimating the model coefficients is essential under the coexistence of fuzzy and random information in the decision evaluation. Though, the coefficients usually are not exactly known, as relevant data are sometimes not given or are

978-1-4244-7316-8/11/$26.00 ©2011 IEEE

sometimes difficult to obtain. However, it makes these decisions crucial and influential to the model's result and the occurrence of errors in the determination of the coefficients might ruin the model formulation [8]. Consequently, the model coefficients are then important in the model settings and should be determined.

Motivated by the above situations, in this paper the satisfaction-based optimization method of additive FGP is introduced to solve multi-level multi-objective (MLMO) problem where the objective functions are developed from Fuzzy Random Regression (FRR) model in the initial phase of model setting. The methodology presented in this paper embraces two objectives. First, the FRR model is used to estimate the coefficients and develop the fuzzy random based objective functions for multi-objective model settings. Second, the additive FGP method is then used to solve the multi-objective linear problem in the multi-level decision making structures.

The remainder of this paper is divided into six sections. Section II describes the construction of fuzzy random objective function. Section III explains important components of FGP based on additive model. Section IV describes the algorithm for solving MLMO decision making with fuzzy random objective function built in prior. An illustrative example of production planning is presented in Section V. Discussions and conclusions are given in Sections VI and VII.

II. BUILDING FUZZY RANDOM OBJECTIVE FUNCTION

Building appropriate objective function in the multi-objective model problem is important and influence the overall model result. Thus this section is spent to explain the solution to estimate the model coefficient and further develop a fuzzy random objective function by using FRR model [6].

The FRR model is constructed based on fuzzy random variables and its confidence intervals. To describe the fuzzy random variables, let Pos be a possibility measure defined on the power set $P(\Gamma)$ in a universe Γ. Let $\Re$ be the set of real numbers. A function $Y : \Gamma \to \Re$ is a fuzzy variable defined on Γ [9]. The possibility distribution μ_Y of Y is defined by $\mu_Y(t) = Pos\{Y = t\}, t \in \Re$ which is the possibility of the event $\{Y = t\}$. The possibility and necessity of the event $\{Y \le r\}$ for fuzzy variable Y with possibility distribution μ_Y, are given respectively in the following forms:

$$\begin{aligned} Pos\{Y \le r\} &= \sup_{t \le r} \mu_Y(t), \\ Nec\{Y \le r\} &= 1 - \sup_{t > r} \mu_Y(t). \end{aligned} \tag{1}$$

The expected value of a fuzzy variable is defined as follows:

Definition 1: Let Y be a fuzzy variable. The expected value of Y where the two integrals are finite is defined as

$$\begin{aligned} E[Y] = &\int_0^\infty \left(\frac{1}{2}\left[1 + \sup_{t \ge r} \mu_Y(t) - \sup_{t < r} \mu_Y(t) \right] \right) dr \\ &- \int_{-\infty}^0 \left(\frac{1}{2}\left[1 + \sup_{t \le r} \mu_Y(t) - \sup_{t > r} \mu_Y(t) \right] \right) dr, \end{aligned} \tag{2}$$

From (1), the expected value of Y is $E[Y] = \frac{1}{4}\left(a^l + 2c + a^r\right)$ when Y is a triangular fuzzy number (c, a^l, a^r). Fuzzy random variables and their expected value operators are defined as follows.

Definition 2: Let (Ω, Σ, Pr) be a probability space and F_v, a collection of fuzzy variables defined on possibility space $(\Gamma, P(\Gamma), \mathrm{Pos})$. A fuzzy random variable is a map $X : \Omega \to F_v$ such that for any Borel subset B of $\Re$, $Pos\{X(\omega) \in B\}$ is a measureable function of ω.

Let X be a fuzzy random variable on Ω. For any fuzzy random variable X on Ω, the expected value of the fuzzy variable $X(\omega)$ is denoted by $E[X(\omega)]$ [10].

The expected value of the fuzzy random variable X is then defined as the mathematical expectation of the random variable $E[X(\omega)]$.

Definition 3: Let X be a fuzzy random variable defined on a probability space $(\Omega, \Sigma, \mathrm{Pr})$. The expected value of X is defined as

$$E[X] = \int_\Omega \left[\int_0^\infty \left(\frac{1}{2}[a] \right) dr - \int_{-\infty}^0 \left(\frac{1}{2}[b] \right) dr \right] Pr(d\omega) \tag{3}$$

where $a = 1 + \sup_{t \ge r} \mu_{X(\omega)^{(t)}} - \sup_{t < r} \mu_{X(\omega)^{(t)}}$ and $b = 1 + \sup_{t \le r} \mu_{X(\omega)^{(t)}} - \sup_{t > r} \mu_{X(\omega)^{(t)}}$.

Definition 4: Let X be a fuzzy random variable defined on a probability space $(\Omega, \Sigma, \mathrm{Pr})$ with expected value e. The variance of X is defined based on $e = E[X]$ from Definition 3, as follows:

$$var[X] = E[(X-e)^2]. \tag{4}$$

The fuzzy random data Y_i and X_{ik} for all $i = 1, \cdots, N$ and $k = 1, \cdots, K$ are defined as $Y_i = \bigcup_{t=1}^{M_{Y_i}} \{(Y_i^t, Y_i^{t,l}, Y_i^{t,r})_\Delta, p_i^t\}$, and $X_{ik} = \bigcup_{t=1}^{M_{X_{ik}}} \{(X_{ik}^t, X_{ik}^{t,l}, X_{ik}^{t,r})_\Delta, q_{ik}^t\}$, with probability p_i^t and q_{ik}^t for $i = 1, \cdots, N$, $k = 1, \cdots, K$ and $t = 1, \cdots, M$ or $t = 1, \cdots, M_{X_{ik}}$, respectively.

Let us denote a fuzzy linear model with fuzzy coefficients $\tilde{C}_i, \cdots, \tilde{C}_K$ as $\overline{Y}_i = \tilde{C}_i X_{i1} + \cdots + \tilde{C}_K X_{iK}$. Each $\overline{Y}_i$ denotes an estimate of the output and

$\widetilde{C}_k = \left(\frac{1}{2}\left[\widetilde{c}_k^{\,l} + \widetilde{c}_k^{\,r}\right], \widetilde{c}_k^{\,l}, \widetilde{c}_k^{\,r} \right)_{\Delta}$ are symmetric triangular fuzzy coefficients for given triangular fuzzy random data X_{ik} for $i = 1, \cdots, N$ and $k = 1, \cdots, K$.

The input data $X_{ik} = (x_{ik}, x_{ik}^{l}, x_{ik}^{r})_{\Delta}$ and output data $\overline{Y}_i = (y_k, y_i^{l}, y_i^{r})_{\Delta}$ for all $i = 1, \cdots, N$ and $k = 1, \cdots, K$, are fuzzy random variables. Therefore, the following relation should hold:

$$\overline{Y}_i = \widetilde{C}_i X_{i1} + \ldots + \widetilde{C}_K X_{iK} \underset{FR}{\supseteq} Y_i, \quad i = 1, \cdots, N , \tag{5}$$

where $\underset{FR}{\supseteq}$ is a fuzzy random inclusion relation. The inclusion relation is based on the expectation-based inclusion and the fuzzy random regression was converted to the expected value regression model with fuzzy inclusion relation at level h [11].

By using the one-sigma $(1 \times \sigma)$ confidence interval, the interval is obtained by the expectation and variance of a fuzzy random variable as follows:

$$I[e_X, \sigma_X] \underline{\Delta} \left[E(X) - \sqrt{var\,(X)}, \quad E(X) + \sqrt{var\,(X)}\right] \tag{6}$$

Hence, the FRR model with $1 \times \sigma$ – confidence intervals is expressed as follows:

$$\begin{aligned} &\underset{A}{min} \;\; J(C) = \sum_{k=1}^{K} \left(\widetilde{C}_k^{r} - \widetilde{C}_k^{l}\right) \\ &\widetilde{C}_k^{r} \geq \widetilde{C}_k^{l}, \\ &Y_i = \widetilde{C}_i\, I\left[e_{X_{i1}}, \sigma_{X_{i1}}\right] + \cdots + \widetilde{C}_K I\left[e_{X_{i1}}, \sigma_{X_{i1}}\right] \underset{\widetilde{h}}{\supseteq} I\left[e_{Y_i}, \sigma_{Y_i}\right] \\ &\text{for } \; i=1,\cdots,N \quad k=1,\cdots,K. \end{aligned} \tag{7}$$

The FRR model with the confidence interval is given in the following form:

$$\overline{Y}_i^{*} = \widetilde{C}_K\, I[e_{X_{iK}} + \sigma_{X_{iK}}], \quad i = 1,...,N \tag{8}$$

Using the fuzzy random variables-based regression model, we estimate the coefficient ξ_{ij} for decision parameters. The coefficients of FRR model results in a close interval $\left[c_j^{l}, c_j^{r}\right]$. Considering the center value of $\hat{\xi}_{ij} = \frac{\left(c^{l} + c^{r}\right)}{2}$, the fuzzy random based objective function is built as

$$F_j(x) = \left\{\overline{Y}_i = \xi_{ij}(X_i)\right\}. \tag{9}$$

Hence, the coefficients c_{ij} of objective function are identified through regression model that is based on a hybrid uncertainty including the fuzziness and the randomness that co-exist in formal decision problem, and these objective functions are further used in the setting of multi-objective model.

III. MLMO Decision Making based on Fuzzy Goal Programming: An Additive Model.

Let us consider an organization that has a multi-level programming problem with multi-objective function $f_i(x)$ for $i = 1, \cdots, p,$. Assume that the decisions are made sequentially beginning with top level DM_1, which controls a vector $x_1 \in X_1$, down through DM_p , which controls a vector $x_p \in X_p$, where x_i is nonempty subset of $\Re^{n_i}$, $i = 1, \cdots, p$, $n_i = n_1 + \cdots + n_p$ and $x_i = x_1, \cdots, x_p$.

The decision maker DM_i at the i^{th} level has authority over the decision variable x_i . Mathematically, the multi-level multi-objective linear programming problem is a nested optimization problem ([1]; [12]) and has the following structures:

$$\begin{aligned} &\text{Find } x \text{ so as to satisfy} \\ &\min_{x_1 \in X_1} F_1(x) = \min_{x_1}\left\{f_{11}(x), \cdots, f_{1m_1}(x)\right\}, \\ &\text{where } x_1 \text{ solves} \\ &\min_{x_2 \in X_2} F_2(x) = \min_{x_2}\left\{f_{21}(x), \cdots, f_{2m_1}(x)\right\}, \\ &\vdots \\ &\text{where } x_2, \ldots, x_p \text{ solves} \\ &\min_{x_p \in X_p} F_p(x) = \min_{x_p}\left\{f_{p1}(x), \cdots, f_{pm_p}(x)\right\} \\ &\text{subject to :} \\ &x \in X \\ &X = \left\{x \in \Re^{n} : Ax(\leq, \geq, =) b, x \geq 0\right\} \end{aligned} \quad \begin{matrix} \left.\vphantom{\begin{matrix}a\\b\\c\\d\end{matrix}}\right\}\text{level p} \\ \left.\vphantom{\begin{matrix}a\\b\\c\\d\end{matrix}}\right\}\text{level 2} \\ \left.\vphantom{\begin{matrix}a\\b\\c\\d\end{matrix}}\right\}\text{level 1} \end{matrix} \tag{10}$$

where $f_{ij}(x) = c_1^{ij} x_1 + \cdots + c_p^{ij} x_p$, $i = 1, \cdots, p,$ $j = 1, \cdots, m_i,$ is the objective function. c_k^{ij} are the constants, and A_i are coefficients matrices of size $m \times n_i$. n_i is the number of decision makers involved.

The FGP [13] based optimization solution is utilized to solve problem model (10). The goal value g_{ij} and tolerance value μ_{ij} are determined by computing the individual best and least solution to obtain the satisfaction degree [14].

The linear membership functions for the fuzzy objective $\mu_{f_{ij}}(x)$ for maximization case of $F_i(x) \gtrsim g_i$ can be formulated as follows:

$$\mu_{F_i}(x) = \begin{cases} 1 & \text{if } f_{ij}(x) \geq \mu_{ij} \\ \dfrac{f_{ij}(x) - \mu_{ij}}{g_{ij} - \mu_{ij}} & \text{if } \mu_{ij} \leq f_{ij}(x) \leq g_{ij} \\ 0 & \text{if } f_{ij}(x) \leq \mu_{ij} \end{cases} \tag{11}$$

In a multi-level decision-making situation in which the decisions made at each level are influenced by the upper level's decision, there exist decision variables that are controlled by upper-level decision makers. Let $t_k^{i_L}$ and $t_k^{i_R}$ be the lower bound and upper bound of tolerance values for the decision vectors considered by the i^{th} level decision maker, respectively.

The triangular fuzzy numbers of decision vectors x_{ik} are $\left(x_{ik}^{*}-t_k^{i_L}, x_{ik}^{*}, x_{ik}^{*}+t_k^{i_R}\right)$. Thus, the linear membership functions for each of the K_i components of the decision vector $x^{i*}=\left(x_1^{i*},\ldots,x_p^{i*}\right)$ controlled by the decision makers of the upper $p-1$ levels can be formulated as follows:

$$\mu_{x_{ik}}(\mathbf{x})=\begin{cases}\dfrac{x_{ik}-\left(x_{ik}^{*}-t_k^{i_L}\right)}{t_k^{i_L}} & \text{if } x_{ik}^{*}-t_k^{i_L}\le x_{ik}\le x_{ik}^{*}\\ \dfrac{\left(x_{ik}^{*}+t_k^{i_R}\right)-x_{ik}}{t_k^{i_R}} & \text{if } x_{ik}^{*}\le x_{ik}\le x_{ik}^{*}+t_k^{i_R}\\ 0 & \text{otherwise}\end{cases} \quad (12)$$

Let V represent the fuzzy achievement function consisting of membership functions for fuzzy objectives μ_i. Recall the fuzzy random objective function of Equation (9), the additive FGP model for multi-level decision-making with fuzzy random objective function is written as follows:

$$\begin{aligned}&\max\ V(\mu_p)=\sum_{j=1}^{m_1}\mu_{1j}+\cdots+\sum_{j=1}^{m_p}\mu_{pj}+\sum_{k=1}^{n_{p-1}}\left[\mu(x)_{p-1k}^{L}+\mu(x)_{p-1k}^{R}\right],\\ &\text{subject to}\\ &\mu_{\mathrm{F}_i(\mathbf{x})}=\frac{\mu_{ij}-\left(\xi_1^{ij}x_1+\cdots+\xi_p^{ij}x_p\right)}{g_{ij}-\mu_{ij}},\ i=1,\ldots,p,\ j=1,\ldots,m_i,\\ &\mu_{x_{ik}(\mathbf{x})}^{L}=\frac{x_{ik}-\left(x_{ik}^{*}-t_k^{i_L}\right)}{t_k^{i_L}},\ i=1,\ldots,p-1,k=1,\ldots,m_{K_i},\\ &\mu_{x_{ik}(\mathbf{x})}^{R}=\frac{\left(x_{ik}^{*}-t_k^{i_R}\right)-x_{ik}}{t_k^{i_R}},\ i=1,\ldots,p-1,k=1,\ldots,m_{K_i},\\ &A_1x_1+\cdots+A_px_p(\le,\ge,=)b,\ \mathbf{x}\ge 0,\\ &\mu_i\in[0,1],\ i=1,\ldots,m.\end{aligned} \quad (13)$$

Because the objectives are fuzzy unlike the conventional goal programming that minimizes deviation, the fuzzy decision function consisting of μ_i must be maximized.

IV. The Additive Fuzzy Goal Programming for MLMO Problem Based on Fuzzy Random Objective Function

The process flow of decision-making under multi-level additive FGP model is illustrated in the following algorithm. The additive FGP is separately solved for the i^{th} level multi-objective program where $i=1,\ldots,p-1$.

Phase I: Building fuzzy random objective functions

1) Determine all the objectives for MLMO problem.
2) Solve each objective described in the model to find the estimate's coefficients. For each of the goal constraints $f_{ij}(x)$,
   - prepare the fuzzy random input-output data.
   - calculate the one sigma confidence interval in terms of Equation (6).
   - perform FRR model by means of Equation (7).
3) Build fuzzy random based objective function as Equation (9) including the confidence interval value.
4) Formulate the MLMO linear program model (10) to illustrate the model for the respective problem. Substitute the fuzzy random-based objective function as Equation (9) that is derived from Step 3) in the MLMO model.

Phase II: Solving MLMO problems

For each objective established at each level in the MLMO Model (10), compute the individual solutions to determine the target goal g_{ij} and tolerance μ_{ij}, respectively.

A: First-Level Additive-FGP

1) Assume $p=l$. Set $l=1$.
2) Create the fuzzy achievement function V_{μ_1} consisting of μ_{ij} for $i=1,\ldots,p \quad j=1,\ldots,m_i$ in level 1.
3) Create the fuzzy objective membership function $\mu_{F_i(x)}$ with the aspiration value g_{ij} and μ_{ij} for the fuzzy goals of the first level controlled by DM_1.
4) Formulates the additive FGP model based on Model (10) for the first-level problem to obtain a satisfactory solution.
5) Send the obtained solutions of the objective function $\mathrm{x}^{1*}=\left(\mathrm{x}_1^{1*},\ldots,\mathrm{x}_p^{1*}\right)$ decisions to the next lower level.

B: Second-Level towards p^{th} -Level Additive-FGP.

1) Set $l=l+1$. Determine the obtained solutions $\mathrm{x}^{l-1*}=\left(\mathrm{x}_1^{l-1*},\ldots,\mathrm{x}_p^{l-1*}\right)$ decisions from the higher level l–1.
2) Let the decision maker decide the lower bound and upper bound of the tolerance values $t_k^{i_L}$ and $t_k^{i_R}$ on the decision vector $\mathrm{x}^{l-1*}=\left(\mathrm{x}_1^{1*},\ldots,\mathrm{x}_p^{1*}\right)$.
3) Develop the fuzzy achievement function V_{μ_p} consisting of $\mu_{f_{ij}}$ for $i=1,\ldots,l,\ j=1,\ldots,m_l$ and $\mu_{x_{ik}}$ for $i=1,\ldots,l-1;$ $k=1,\ldots,n_{l-1}$.
4) Create the fuzzy objectives membership function $\mu_{f_i(x)}$ with the aspiration values g_{ij} and μ_{ij} for the fuzzy goals of the first level controlled by the DM_1.
5) Develop the decision vector membership function $\mu_{x_{ik}(x)}, i=1,\ldots,p-1, k=1,\ldots,K_i$ based on Equation (12).
6) Formulate the additive-FGP Model (10) of the p -level problem to obtain a satisfactory solution to the first-level FGP problem.
7) Solve the model to obtain $\mathrm{x}^{l*}=\left(\mathrm{x}_1^{l*},\ldots,\mathrm{x}_p^{l*}\right)$.
8) Repeat step 1 until $l<p$, to generate a satisfactory solution $\mathrm{x}^{l*}=\left(\mathrm{x}_1^{l*},\ldots,\mathrm{x}_p^{l*}\right)$ for the MLMO linear programming problem.

TABLE I. THE OBJECTIVES

Decision Maker	*The Objectives*	
Government level, DM_1 (upper-level)	f_{11}	Maximize the export revenue
	f_{12}	Maximize the national level profit
	f_{13}	Minimize the capital,
State level, DM_2 (middle-level)	f_{21}	Maximize the production volume
	f_{22}	Maximize the profit for state level
	f_{23}	Minimize the cost of production
City level, DM_3 (lower-level)	f_{31}	Maximize the production volume
	f_{32}	Minimize the cost of production

V. NUMERICAL EVALUATIONS AND DISCUSSIONS

The following multi-objective linear programming problem is illustrated to demonstrate the proposed procedure. The problem situation is described as follows. One export-oriented country is concentrating on producing three important products x_1 , x_2 and x_3 which are manufactured by company C_m, $m = 1, \cdots, M$. This company has distributed branch B_m, $m = 1, \cdots, M$, in city level for producing the products.

There are 3 levels of decision making related to this case and each level are responsible to accomplish the objectives that are decided in prior. Table 1 summarizes the objectives decided in each level.

Let us assume f_{ij} represent the DM_i objective in each level. The multi-level multi-objective problem can be summarized as follows:

Find x so as to satisfy:

$$\begin{aligned}
&[\text{Level1}]\\
&\min_{x_1} F_1(x) = \{f_{11}(x), f_{12}(x), f_{13}(x)\},\\
&\text{where } x_2 \text{ and } x_3 \text{ solve}\\
&[\text{Level2}]\\
&\min_{x_2} F_2(x) = \{f_{21}(x), f_{22}(x), f_{23}(x)\},\\
&\text{where } x_3 \text{ solves}\\
&[\text{Level3}]\\
&\min_{x_3} F_3(x) = \{f_{31}(x), f_{32}(x)\},
\end{aligned} \tag{14}$$

Subject to constraints:

$$\begin{aligned}
&\text{raw} && 3.815x_1 + 0.910x_2 + 0.220x_3 <= 87.75;\\
&\text{labor} && 0.650x_1 + 0.900x_2 + 0.125x_3 <= 4.425;\\
&\text{mills} && 17.50x_1 + 2.160x_2 + 4.775x_3 <= 95.20;\\
&\text{capital} && 1.350x_1 + 0.980x_2 + 0.890x_3 <= 20.15;
\end{aligned} \tag{15}$$

Phase I: Building fuzzy random objective functions

The initial step in this phase is the data preparation to estimate the decision coefficients through a fuzzy random-based regression and further develop the objective function. The previously collected data set is then pre-processed ([7]; [15]). In this example, three types of product are produced from three different production plants. The probabilities are assigned as the proportion of product being produced in i^{th} plant to the total production numbers.

An FRR model (7) is used to estimate the weights of the decision parameters x_1, x_2 and x_3 and to develop the objective function for each objective that was defined in Table 1. Using the fuzzy random data format of input-output data, we solve the linear program (7) and obtain the estimated coefficients c_i^l and c_i^r for all objectives. For the other objective functions we run the same procedure. The interval $\left[c_i^l, c_i^r\right]$ shows the estimated coefficients for the decision parameters.

The objective functions are developed based on the central value of the interval coefficients as follows:

$$F_1 = \begin{cases} f_{11} = (2.078)_T I[e_{X_1}, \sigma_{X_1}] + (0.260)_T I[e_{X_2}, \sigma_{X_2}] + (0.170)_T I[e_{X_3}, \sigma_{X_3}] \\ f_{12} = (1.010)_T I[e_{X_1}, \sigma_{X_1}] + (1.700)_T I[e_{X_2}, \sigma_{X_2}] + (0.476)_T I[e_{X_3}, \sigma_{X_3}] \\ f_{13} = (0.438)_T I[e_{X_1}, \sigma_{X_1}] + (0.796)_T I[e_{X_2}, \sigma_{X_2}] + (0.512)_T I[e_{X_3}, \sigma_{X_3}] \end{cases} \tag{16}$$

$$F_2 = \begin{cases} f_{21} = (1.126)_T I[e_{X_1}, \sigma_{X_1}] + (0.100)_T I[e_{X_2}, \sigma_{X_2}] + (0.097)_T I[e_{X_3}, \sigma_{X_3}] \\ f_{22} = (0.856)_T I[e_{X_1}, \sigma_{X_1}] + (1.473)_T I[e_{X_2}, \sigma_{X_2}] + (0.443)_T I[e_{X_3}, \sigma_{X_3}] \\ f_{23} = (0.380)_T I[e_{X_1}, \sigma_{X_1}] + (0.737)_T I[e_{X_2}, \sigma_{X_2}] + (0.277)_T I[e_{X_3}, \sigma_{X_3}] \end{cases} \tag{17}$$

$$F_3 = \begin{cases} f_{31} = (0.921)_T I[e_{X_{31}}, \sigma_{X_{31}}] + (0.050)_T I[e_{X_{32}}, \sigma_{X_{32}}] + (0.526)_T I[e_{X_{33}}, \sigma_{X_{33}}] \\ f_{32} = (0.380)_T I[e_{X_{31}}, \sigma_{X_{31}}] + (0.737)_T I[e_{X_{32}}, \sigma_{X_{32}}] + (0.216)_T I[e_{X_{33}}, \sigma_{X_{33}}] \end{cases} \tag{18}$$

The three sets of objective functions (16), (17) and (18) represent the objective functions on each decision making level. At this step, we end the Phase I on the development of objective functions. Next, we move to the second phase to solve the MLMO problem through an additive-FGP approach.

Phase II: Solving MLMO problem

The MLMO problem (10) can be rewritten by considering the result from Phase I as follows:

$$\min_{x_1} = \begin{pmatrix} f_{11} = 2.078\,x_1 + 0.260\,x_2 + 0.170\,x_3, \\ f_{12} = 1.010\,x_1 + 1.700\,x_2 + 0.476\,x_3, \\ f_{13} = 0.438\,x_1 + 0.796\,x_2 + 0.512\,x_3. \end{pmatrix}$$

where x_2 and x_3 solves,

$$\min_{x_2} = \begin{pmatrix} f_{21} = 1.126\,x_1 + 0.100\,x_2 + 0.097\,x_3, \\ f_{22} = 0.856\,x_1 + 1.473\,x_2 + 0.443\,x_3, \\ f_{23} = 0.380\,x_1 + 0.737\,x_2 + 0.277\,x_3. \end{pmatrix} \tag{19}$$

whe re x_3 solves,

$$\min_{x_3} = \begin{pmatrix} f_{31} = 0.921\,x_1 + 0.050\,x_2 + 0.526\,x_3, \\ f_{32} = 0.380\,x_1 + 0.737\,x_2 + 0.216\,x_3. \end{pmatrix}$$

subject to : system constraint s (15);

$x_i \geq 0$;

The first step for solving MLMO problem starts with computation of the individual solutions to determine the goal g_{ij} and its tolerance u_{ij} of each objective function. Table 2

tabulates the individual solutions of all objectives functions for the three levels of the MLMO problem.

Based on the procedure stated in Phase II, the equivalent linear program (19) for the first-level decision making as follows:

$$\begin{aligned}
&\max = u_1 + u_2 + u_3; \\
&u_1 = 0.183x_1 + 0.023x_2 + 0.015x_3; \\
&u_2 = 0.078x_1 + 0.131x_2 + 0.036x_3; \\
&u_3 = 1\text{-}(0.038x_1 + 0.069x_2 + 0.044x_3); \\
&\text{system constraint s (15);} \\
&x_i \geq 0.
\end{aligned} \tag{20}$$

LINGO© computer software is used to run the equivalent ordinary linear programming model. The solution of the first level is $x^{1*} = (x_1^{1*}, x_2^{1*}, x_3^{1*}) = (5.30, 1.08, 0.00)$. Let DM_1 decide $x_1^1 = 5.30$ from the first level solution and the negative and positive tolerance are decided to be $t_1^{1L} = 0.5$ and $t_1^{1R} = 0.5$ respectively. The second level solution proceeds as follows:

$$\begin{aligned}
&\max = u_1 + u_2 + u_3 + u_4 + u_5 + u_6 + ux_1^L + ux_1^R; \\
&u_1 = 0.183x_1 + 0.023x_2 + 0.015x_3; \\
&u_2 = 0.078x_1 + 0.131x_2 + 0.036x_3; \\
&u_3 = 1\text{-}(0.038x_1 + 0.069x_2 + 0.044x_3); \\
&u_4 = 0.183x_1 + 0.016x_2 + 0.015x_3; \\
&u_5 = 0.072x_1 + 0.125x_2 + 0.037x_3; \\
&u_6 = 1\text{-}(0.054x_1 + 0.106x_2 + 0.040x_3); \\
&ux_1^L = 2x_1\text{-}9.6; \\
&ux_1^R = 9.6\text{-}2x_1; \\
&\text{system constraint s (15);} \\
&x_i \geq 0.
\end{aligned} \tag{21}$$

The solution of the second level is observed as $x^{2*} = (x_1^{2*}, x_2^{2*}, x_3^{2*}) = (4.80, 1.19, 1.80)$. Let DM_2 decide $x_2^2 = 1.19$, $t_1^{2L} = 0.75$ and $t_1^{2R} = 0.25$. The solution for the third level is shown in the following equivalent linear programming problem.

$$\begin{aligned}
&\max = u_1 + u_2 + u_3 + u_4 + u_5 + u_6 + u_7 \\
&+ u_8 + ux_1^L + ux_1^R + ux_2^L + ux_2^R; \\
&u_1 = 0.183x_1 + 0.023x_2 + 0.015x_3; \\
&u_2 = 0.078x_1 + 0.131x_2 + 0.036x_3; \\
&u_3 = 1\text{-}(0.038x_1 + 0.069x_2 + 0.044x_3); \\
&u_4 = 0.183x_1 + 0.016x_2 + 0.015x_3; \\
&u_5 = (0.072x_1 + 0.125x_2 + 0.037x_3); \\
&u_6 = 1\text{-}(0.054x_1 + 0.106x_2 + 0.040x_3); \\
&u_7 = 0.087x_1 + 0.004x_2 + 0.009x_3; \\
&u_8 = 1\text{-}(0.065x_1 + 0.127x_2 + 0.037x_3); \\
&ux_2^R = 2x_1\text{-}9.6; \\
&ux_2^R = 9.6\text{-}2x_1; \\
&ux_2^R = 1.333x_2\text{-}0.586; \\
&ux_2^R = 3.76\text{-}4x_2; \\
&\text{system constraint s (15);} \\
&x_i \geq 0.
\end{aligned} \tag{22}$$

The satisfactory solution of the MLMO problem is $x^{3*} = (x_1^{3*}, x_2^{3*}, x_3^{3*}) = (4.80, 0.69, 0.00)$. The procedure brings to an end as $l = p = 3$, and the satisfactory solution is obtained.

TABLE II. INDIVIDUAL SOLUTIONS

f_{ij}	f_i^-	f_i^+
f_{11}	0.00	11.30
f_{12}	0.00	12.89
f_{13}	0.00	11.50
f_{21}	0.00	6.12
f_{22}	0.00	11.74
f_{23}	0.00	6.92
f_{31}	0.00	10.48
f_{32}	0.00	5.77

TABLE III. FUZZY RANDOM BASED COEFFICIENTS

Decision Making Level	***Goal***	***Fuzzy Random-Based Coefficient***		
		Product 1	***Product 2***	***Product 3***
1	Export revenue	[2.031, 2.215]	[0.200, 0.320]	[0.120, 0.220]
	Profit	[0.935, 1.086]	[1.206, 2.194]	[0.420, 0.532]
	Capital	[0.365, 0.512]	[0.735, 0.857]	[0.412, 0.613]
	Production	[1.098, 1.154]	[0.000, 0.200]	[0.092, 0.103]
2	Profit	[0.856, 0.856]	[1.006, 1.940]	[0.354, 0.352]
	Cost	[0.305, 0.455]	[0.680, 0.794]	[0.203, 0.532]
3	Production	[0.872, 0.971]	[0.000, 0.100]	[0.082, 0.970]
	Cost	[0.305, 0.455]	[0.680, 0.794]	[0.200, 0.232]

TABLE IV. MLMO ADDITIVE-FGP RESULTS

FGP solution		***The Solution***
Objective	***Achievement***	
$f_{11} = 10.154$	$\mu_{11} = 0.89$	11.30
$f_{12} = 6.021$	$\mu_{12} = 0.46$	12.89
$f_{13} = 2.652$	$\mu_{13} = 0.77$	11.50
$f_{21} = 5.474$	$\mu_{21} = 0.89$	6.12
$f_{22} = 5.125$	$\mu_{22} = 0.43$	11.74
$f_{23} = 2.333$	$\mu_{23} = 0.67$	6.92
$f_{31} = 4.458$	$\mu_{31} = 0.42$	10.48
$f_{32} = 2.84$	$\mu_{32} = 0.60$	5.77

VI. Results and Discussions

In this section, the results of the industrial problem case are explained. The FRR Model (7) was applied to the datasets of the manufacturing production. The coefficients are obtained as shown in Table III, where each coefficient is represented in interval-valued form. This result illustrates the coefficients for each attribute and shows the range of their evaluations. The coefficients ξ_i are the fuzzy random coefficients for the decision variables x_i.

The coefficients values derived by the FRR approach are represented by the interval valued form which shows the fuzzy judgments and supports the range of values around expected value that is likely to contain the estimation target. Table IV summarizes the objective function value and the achievement of each objective function. Objective f_{11} and f_{21} in the first and second level achieve about 90% which maximized the export revenues. However, the objective of maximizing the profit only achieved about 46% and 43% in the government and state level. 77% goal achievement is gained for the objective to maximize the capital in the government level. From the results, decision makers can perform decision analysis to consider the solution derived by the mathematical approach. The decision maker can reevaluate the solution and change the decision and repeat the process. Since the proposed method is based on satisfaction approach, the decision makers may involve in evaluating the results to achieve better satisfying solution.

VII. Conclusions

In this study, an additive FGP approach is used to solve multi-level multi-objective decision problem. The initial model setting specifically the objective functions were developed by FRR model to treat the fuzziness and randomness in the evaluation. In the solution, each multi-objective problem at each level was solved separately, starting with the highest level. The main advantage of this algorithm is to allow a decision maker to select the desired satisfactory value from the higher level that is then used in the following level. The procedure also enables the decision maker of the respective decision making unit to decide the decision value by means of the mathematical solution based on their satisfaction. Additionally, the proposed method uses one-sigma confidence intervals when developing the objective functions which include the mean interval values of all samples in the model. Using the confidence intervals, we could provide a more complete description of the information in the data about the estimation target. Our model also supports the range of values around expected value that is likely to contain the estimation target.

Acknowledgment

A. Nureize would like to thank to University Tun Hussein Onn Malaysia (UTHM) and Ministry of Higher Education (MOHE) for a study leave.

References

[1] I. A. Baky, (2010). "Solving multi-level multi-objective linear programming problems through fuzzy goal programming approach," *Applied Mathematical Modeling*, 34 (9), 2377-2387.

[2] G. Anandalingam, (1988). "A mathematical programming model of decentralized multilevel systems," *Journal of Operational Research Society*, 39 (11), 1021-1033.

[3] M. Mesarovic, D. Macko and Y. Takahara, (1970). *Theory of Hierarchical Multi-level Systems*. Academic Press, New York.

[4] SB. Sinha, and S. Sinha, (2004). "A linear programming approach for linear multi-level programming problems," *Journal of the Operational Research Society*, 55 (3), 312-316.

[5] H-S. Shih, Y-J. Lai, and E. S. Lee, (1996). "Fuzzy Approach for Multi-level Programming Problems," *Computers Operations Research*, 23 (1), 73-911.

[6] J. Watada, S. Wang, and W. Pedrycz, (2009). "Building confidence interval-based fuzzy random regression model," *IEEE Transactions on Fuzzy Systems*, 11 (6), 1273 - 1283.

[7] A. Nureize, and J. Watada, (2010). "Constructing fuzzy random goal constraints for stochastic fuzzy goal programming," V.-N. Huynh et al. (Eds.): Integrated Uncertainty Management and Applications, 293-304, Springer-Verlag Berlin Heidelberg.

[8] M. J. Schniederjans, "Goal programming," Methodology and Applications. Kluwer, Boston, 1995.

[9] S. Nahmias, (1978), "Fuzzy variables," *Fuzzy Sets and Systems*, 1 (2), 97 – 111.

[10] Y-K. Liu and B. Liu, (2003). "Fuzzy random variable: A scalar expected value operator," *Fuzzy Optimization and Decision Making*, 2 (2), 143–160.

[11] J. Watada and S. Wang, "Regression model based on fuzzy random variables," Seising Rodulf (Ed.), Chapter 26, *Views on Fuzzy Sets and Systems from Different Perspectives,* Spring-Verlag, Berlin, 2009.

[12] M. Sakawa, *Fuzzy sets and interactive multi-objective optimization*, Applied Information Technology, Plenum Press. New York (1993).

[13] R.N. Tiwari, S. Dharmar, and J.R. Rao, (1987), "Fuzzy goal programming – an additive model," *Fuzzy Sets and Systems*, 24 (1), 27–34.

[14] H.J. Zimmermann, (1978), "Fuzzy programming and linear programming with several objective functions*," Fuzzy Sets and Systems*, 1 (1), 45-55.

[15] A. Nureize and J. Watada (2010), "Approximation of Goal Constraint Coefficients in Fuzzy Goal Programming," *2010 Second International Conference on Computer Engineering and Applications*, 1, 161-165.

2011 IEEE International Conference on Fuzzy Systems
June 27-30, 2011, Taipei, Taiwan

A Fuzzy Hypothesis Test Based Model For Customer Satisfaction Measurement

(Case Study in PARS KHODRO CO.)

Naimeh Borjalilu
Corresponding author: MSc of Industrial Engineering (System Management and Productivity), Quality Assurance Engineering in IRANAIR Co.
Tehran, IRAN
n.borjalilu@yahoo.com
Mahdi Zowghi
MSc of Industrial Engineering (System Management and Productivity)
Tehran, IRAN
Mahdizowghi@yahoo.com

Abdolhamid Eshraghniaye Jahromi
Associate professor of Industrial Engineering, Department of Industrial engineering, Sharif University of Technology
Tehran, IRAN
eshragh@sharif.edu

Abstract- **The article proposes a model for customer satisfaction measuring, which is adapted to use in automobile industries. The proposed methodology evaluates the satisfaction level of a set of customers in different aspect of customer focus based on hypothesis values. It permits to evaluate the validity of a service/manufacturing operation from the point of view of consumers. The main advantages of this method are fully considered the qualitative form of customers' judgments through fuzzy theory and evaluate customers' satisfaction in different aspect of customer focus. This model also allows fully evaluates by analysis of all possible hypothesis cases. In the end, we implement our model in KHODRO CO. in IRAN and show the results. This research does asking the opinions of the experts through a number of questionnaires related to the L90 auto customers of PARS KHODRO CO. in 5 fields. Customer's satisfaction of L90 auto in above fields attains among 81 hypotheses and concludes the following result:**

"Product quality is good, financial problems is good, Total quality of services is good and Guarantee is medium then customer satisfaction is good''. Finally, future research directions are provided.

Keywords- fuzzy hypothesis test; customer satisfaction analysis; subjective judgments

I. Introduction

Paper's introduction is in two parts as customer satisfaction models and fuzzy hypothesis testing. According to our knowledge and researches, there is not a method for customer satisfaction measuring based on fuzzy hypothesis testing approach.

A. Customer satisfaction models

Globalization and free trade carry on remodeling the business environment and expanding global competition. Customer satisfaction is a resume notion and show the actual state of satisfaction which can vary from person to person and product/service to product/service. Therefore, customer satisfaction should be determined and rendered into a number of quantifiable parameters [1]. Also Since, customer satisfaction index (CSI) have been widely developed in both theory and applications [2, 3, 4, 5], especially in the fields of marketing, education, medical treatment, guesthouse management ,therefore customer satisfaction has been one of the most frequently surveyed topics in literature. The work done by Berry et al. [6] between 1985 and 1988 delivered SERVQUAL (it is a service-quality scheme that has been incorporated into customer-satisfaction surveys [7]), supports the basis for the measurement of customer satisfaction with a service by using the gap between the customer's expectation of achievement and their perceived experience of achievement. In 1989, the first model of CSI was built by Swedish researchers [8]. The American customer satisfaction index (ASCI) was set up in 1994 [9]. Another well-known CSI was built by 11 countries of European Union in 1999 [10, 11]. Some researchers introduce modified CSI for using in the different fields. Hsu (2008) proposes an index for online customer satisfaction, which was adapted from an American Customer Satisfaction Index (ACSI). It predicts customer loyalty and overall customer satisfaction via a way that was similar to the average for the online retail industry in ACSI and the partial least squares (PLS) method [12]. Web-based customer satisfaction don´t terminate in the above paper. Customer satisfaction measurement index system via mail service is designed by LIU et al. (2006) [13]. Some of researches also focused on the relationship between customer satisfaction and financial performance [14, 15,16]. According to Grigoroudis et al. (2000), customer satisfaction information is analyzed based

on a preference disaggregation model. Their tool (Software) is termed as TELOS that follows the principles of Multicriteria analysis and uses subjective customers' judgments [17]. Therefore, they propose a model that called MUSA (Multicriteria Satisfaction Analysis). It is a preference disaggregation model following the principles of ordinal regression analysis. Same as their mentioned paper, MUSA model uses subjective customers' judgments, too [18]. The Research of Mihelis et al are concerned with a model that is based on the principles of Multicriteria analysis and preference disaggregation modeling and it is implemented in private bank sector. It determines critical service dimensions and the investigation to customer classes with distinctive preferences and expectations [19]. Jaime and Fonseca (2009) consider the latent segment models (LSM) approach for evaluation of customer's service satisfaction that quantified through multiple indicators. They selected a three latent segment model that represents "The Very Satisfied", "The Well Satisfied" and "Satisfaction Demanders" [20]. Since Zadeh introduces fuzzy set theory in 1965 [21], researchers intend to use it in their quests. For example, Xiaohong (2008) introduce new method for calculating the e-commerce customer satisfaction index (ECSI), using fuzzy techniques [22], so that ECSI obtains by fusion of comparison customers' cognition in e-commerce and their acclaims and complaints.

The purpose of our study is to utilize the fuzzy hypothesis testing for customer satisfaction measuring, such that, satisfaction level is caused by six fields as product quality , financial problems , total quality of services , guarantee , complaints and loyalty. The fuzzy hypothesis test is developed crisp hypothesis testing but it challenge the all possible hypotheses. In other hand, it utilizes ambiguity and vagueness of subjective judgments by fuzzy logic.

B. Fuzzy hypothesis testing

As discussed in previous section, main structure of our method is based on fuzzy hypothesis testing. In the real world, sometimes data cannot be recorded or collected precisely. Therefore, the fuzzy sets theory is naturally used as an appropriate tool in modeling the statistical models when the fuzzy data have been observed [23]. The concept of fuzzy sets used here was originally introduced in [21] and described in more detail e.g. in [24, 25]. It should be noted that in this paper only the hypotheses are allowed to be fuzzy and the data are assumed to remain crisp. Furthermore, the 'classical' way of statistical inference is generalized to fuzzy hypothesis. Note that there is a fundamental difference between a membership function of a linguistic term and a prior probability distribution. The membership function just gives a description of the linguistic term, whereas a prior probability distribution gives prior information about the truth of the hypotheses under consideration. Arnold [26, 27] proposed the fuzzification of usual statistical hypotheses and considered the hypotheses testing under fuzzy constraints on the type I and II errors. Casals and Gil [28] and Son et al. [29] considered the Neyman–Pearson type testing hypotheses. Saade [30, 31] considered the binary hypotheses testing and discussed the fuzzy likelihood functions in the decision making process by applying a fuzzified version of the Bayes criterion. Gil et al. [32] also discussed the likelihood ratio test for goodness of fit with fuzzy observations by means of the minimum inaccuracy principle of point estimation. Casals and Gil [33], Casals and Gil [34], and Gil et al. [35] considered the Bayesian sequential tests and χ^2 tests for goodness of fit with fuzzy observations by means of the notion of fuzzy information. Grzegorzewski [36], Watanabe and Imaizumi [37] proposed the fuzzy test for hypotheses testing with vague data, and the fuzzy test gave the acceptability of the null and alternative hypotheses. Niskanen [38] discussed the applications of soft statistical hypotheses in the human sciences. The fuzzy hypothesis testing is developed of classic statistical hypothesis testing which zero and one are using for acceptance or rejection of any hypothesis. However, fuzzy hypothesis testing has two strength points versus classic statistical hypothesis testing. They are: (1) it considers all the possible hypotheses and (2) accepts them relatively by numbers in [0,1]. The fuzzy hypothesis testing – like the classic statistical hypothesis testing - has four steps: hypothesis formulation, sampling, hypothesis testing and decision-making. In hypothesis formulation step, all the possible hypotheses are formulated. Classical hypotheses define two type hypotheses as null hypothesis and alternative. However, fuzzy hypotheses formulated by a block consist of hard-core and associated auxiliary hypotheses. In the sampling step, subsets of all data are selected. The sample should has enough data to be a good indication of the all data. In hypothesis testing step, fuzzy conclusion for any hypothesis is done and then, results are aggregated by aggregation function. In final step, total result has to be analyzed and associated decisions made.

The paper organization is according to the follows:

Section II, describes information collection tools, its validity and reliability, and some information about case location. Section III, is describes our methodology which is consist of fuzzy hypothesis concept, structure of our approach, model implementing and its finding. Finally the last section, conclude the models efficiency and results.

II. Information Collection

A. Case Location and Sampling

Pars Khodro Company (P.K.C.) is an automobile manufacturer company that is established in 1956 and since then is operational. In P.K.C. the environment of the competitive markets changes intensely and it is necessary to improve the manufacturing quality continuously. Hence, we introduce a way to evaluate the P.K.C's manufacturing quality, which is based on the degree of user satisfaction. The statistical universe of this

paper is considered from total customers of L90 (one of the Pars Khodro products started in 2009) .In this paper, random systematic method for sampling is used [39] and due to list of total customers of L90 in 2009, Morgan table is utilized for numbers of samples [40] in which the best sample numbers corresponded to any universe cardinality. Accordingly, a sample of 380 from 20000 customers is considered as good representative of total data.

B. Tools

In this paper, main information collecting tool is questionnaires and interviews. Interview is used to analyze customers' viewpoints before questionnaire designing. Questionnaire also is used to measure the satisfaction samples in framework of hypothesis. Initial questionnaire has six essential fields and each field has several sub-fields as follows:

1. Product quality
1.1. Apparent form
1.2. Safety
1.3. Car body specifications
1.4. Motor power and fuelling
1.5. Good ventilation and power means
1.6. Technical documents quality

2. Financial problems
2.1. Cost of product
2.2. Fair relation between cost and quality
2.3. Purchase styles
2.4. Financial operation rapidity
2.5. Attention and clarity in financial affairs

3. Total quality of services
3.1. Managers and experts communication manner
3.2. Inform manner quality
3.3. Delivery quality
3.4. Guarantee conditions

4. Guarantee
4.1. Provide the spare parts
4.2. Parts ampleness and quality
4.3. Guarantee access
4.4. Repairs quality
4.5. Guarantee cost and wage

5. Complaints
5.1. Complaints receiving ways
5.2. Complaints investigation quickness
5.3. Complaints consideration

6. Loyalty
6.1. Continuing cooperation
6.2. Looking forward to the fresh products
6.3. Suggest to other peoples

After the initial collection of 30 questionnaires and evaluation of feedbacks, we integrate them with experts' opinions. Accordingly, due to overlapping and concluded by another, loyalty eliminated from questionnaires and then, final questionnaire is formed. The Response of any question was set according to Likert scale [41], which scaled as: poor satisfaction ، Medium poor satisfaction ، Fair ، medium good satisfaction and good satisfaction.

C. Validity and Reliability

The method of explority factor analysis has been used to analyze the questionnaire validity [39]. The KMO* value of questionnaire is 0.895 in 0.01 significant level which imply to sampling sufficiency for method of explority factor analysis. Varimax rotation was used for explority factor analysis, and result implies that: first factor (product quality) explains the 75% changes, second factor (financial problems) explains the 81% changes, third factor (Total quality of services) explains the 73% changes, Guarantee factor explains 74% changes and finally, complaints factor explains the 79% changes. Generally, the questionnaire forecast the 73% changes that indicate the validity. Of course, load factor of fields was greater than 0.5. The Cronbach's alpha method has been used to analyze the questionnaire reliability [42] which was calculated Cronbach's alpha for product quality , 75% ; financial problem , 79% ; Total quality of services , 72% ; Guarantee , 80% and complaints, 79%. This result indicates the reliability of customer satisfaction measurement scale. It is necessary to mention that the investigations have been done by MINITAB 15.0 software.

III. Mathematical Framework of Fuzzy Hypothesis Testing

Fuzzy hypothesis test is extension of classical statistics hypothesis test. It leads to importance degree of each hypothesis compare with auxiliary rules. Let, X be universes of discourse, $D = \{x_1 , x_2 , \dots , x_n\}$ be sample set and $H = \{H_1 , H_2 , \dots , H_n\}$ be if-then rule statements. In this view, we can demonstrate a fuzzy if-then rule as follows:

H_i: IF $\{\text{Condition } 1, \text{Condition } 2, \dots , \text{Condition } k\}$ to be considered true, THEN x is a member of F by membership degree $\mu(x)$ .Nevertheless, general structure of fuzzy hypothesis test is as Table 1:

*Kaiser - Meyer- Olkin

TABLE1. Fuzzy hypothesis test matrix

If-then statements	Samples				$M_j(D)$
	x_1	x_2	…	x_n	
H_1					
H_2					
⋮					
H_r					
					Summation=1

It should be noted that, auxiliary rules are in $\{\text{Condition } 1, \text{Condition } 2, \ldots, \text{Condition k}\}$ and main hypothesis is included in F notation. The if-part of the rule is called the antecedent, while the then-part is called the consequent or conclusion. Each sample x_i satisfies condition 1 ، condition 2 through condition k within $\mu_1(x_i)$ ، $\mu_2(x_i)$ through $\mu_k(x_i)$, respectively. In other hand, x_i satisfies the consequent within $\mu(x)$ that is defined as:

$$\mu : (H, x) \rightarrow [0,1] \quad (1)$$

Due to multiple parts related to the antecedent and consequent, apply fuzzy logic operators and resolve them to a single number between 0 and 1,therefore we apply multiplication operator (P.M. Larson relation) for combining the antecedent and consequent such as fuzzy logic operators. So, satisfaction degree of each hypothesis by x_i sample calculates by equation (2). Hence, attain associated array of j^{th} row and i^{th} column for Table (1).

$$\text{Sat}_{x_i}(H_j) = \mu_1(x_i) \times \mu_2(x_i) \times \ldots \times \mu_k(x_i) \times \mu(x_i) \quad (2)$$

To determine the verification degree of each hypothesis (claim), so it is necessary to calculate all possible $\text{Sat}_{x_i}(H_j)$ $\forall i, j$ and then, find arithmetic mean as follows:

$$M_j(D) = \frac{\sum_{i=1}^{n} \text{Sat}_{x_i}(H_j)}{n} \quad j = 1,2, \ldots, r \quad (3)$$

A. Fuzzy hypothesis testing in customer satisfaction measuring

In this section, we intend to introduce the set of hypothesis in our model. Claims $H = \{H_1, H_2, \ldots, H_n\}$ have been introduced and are calculated verification degree of each ($\mu_k(x_i)$). As discussed in section II., five fields are used in this model ; product quality, financial problems, Total quality of services, Guarantee are antecedents and then complaints is rule's consequent that implies to customer satisfaction level. We classify each of them in to the three scales as, good ، medium and bad. As an example, Total qualities of services investigate in the three classes; good Total quality، medium Total quality and bad Total quality. So, to analyze the total classifications of fields, we will have $3 \times 3 \times 3 \times 3 = 81$ hypothezies. All hypothezies have been analyzed in our paper. As an example, one of the hypothesis could be "product quality is good, financial problem is good, Total quality of services is bad, Guarantee is medium and then customer satisfaction level (complaints) is medium". The fuzzy classifications are as shown in Fig. 1.

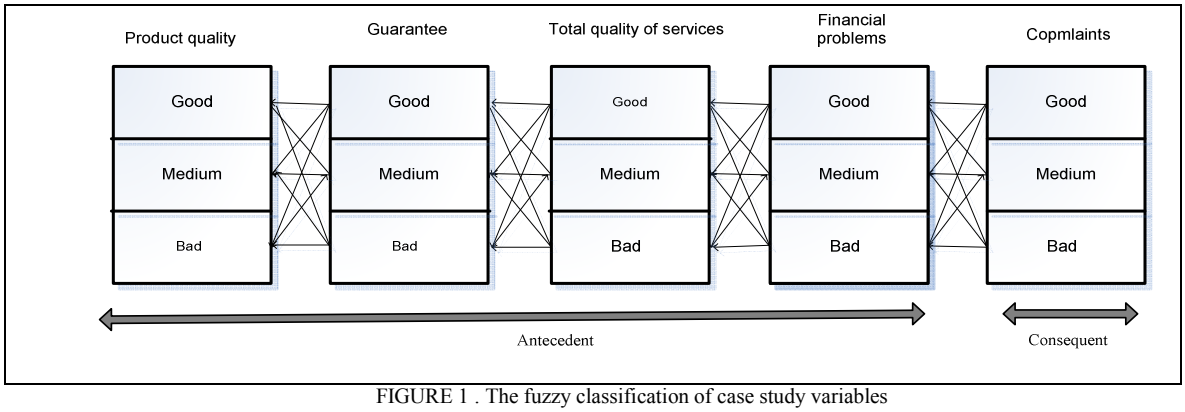

FIGURE 1 . The fuzzy classification of case study variables

As discussed in above, linguistic terms have been used in any classifications. Good ، medium and bad are our linguistic terms. So, accordingly we need to design theirs fuzzy distributions. Fig. 2 demonstrates the linguistic values of any linguistic variable in which ranges have been got from interview with company experts. Note that, concept of

The parameters have been allotted as Fig. 2.So, the membership functions of good, medium and bad linguistic terms are indicated as follows:

"complaint" is negative, so, the more values imply to worse condition. Fig. 3 demonstrates the linguistic terms that are based on the parameters which are different in each field.

$$\mu_{good}(x) = \begin{cases} \frac{1}{e-d}(x-d) & x \in [d,e] \\ 1 & x \in [e,f] \end{cases} \quad (4)$$

$$\mu_{medium}(x) = \begin{cases} \frac{1}{c-b}(x-b) & x \in [b,c] \\ 1 & x \in (c,d] \\ \frac{-1}{e-d}(x-d)+1 & x \in (d,e] \end{cases} \quad (5)$$

$$\mu_{bad}(x) = \begin{cases} \frac{1}{a}x & x \in [0,a] \\ 1 & x \in (a,b] \\ \frac{-1}{c-b}(x-c) & x \in (b,c] \end{cases} \quad (6)$$

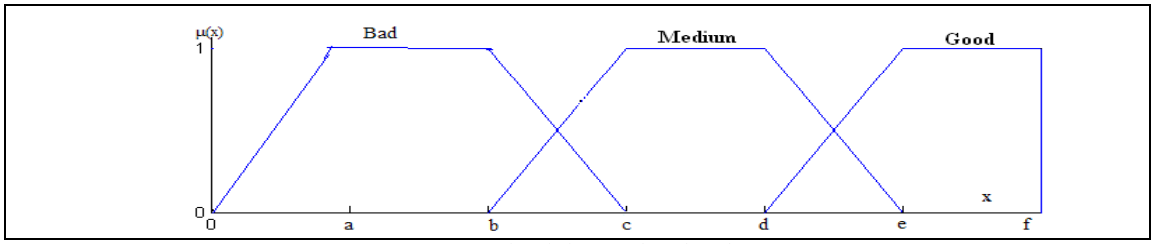

FIGURE 3 . Linguistic terms based on the parameters

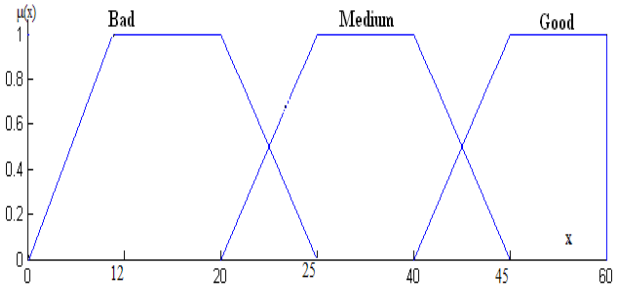	Bad = (0,12,20,25) Medium=(20,25,40,45) Good=(40,45,60,60)	Product Quality
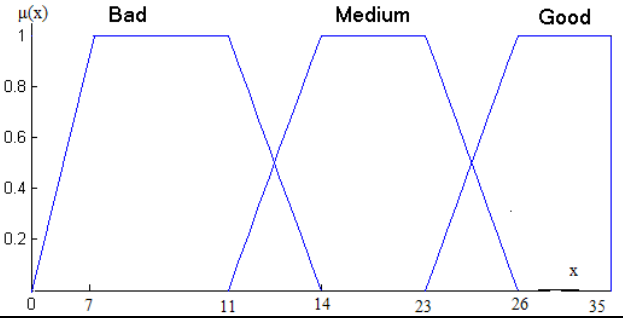	Bad = (0,7,11,14) Medium=(11,14,23,26) Good=(23,26,35,35)	Financial problems
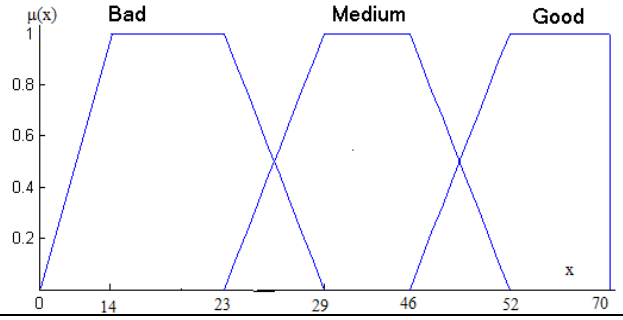	Bad = (0,14,23,29) Medium=(23,29,46,52) Good=(46,52,70,70)	Total quality of service
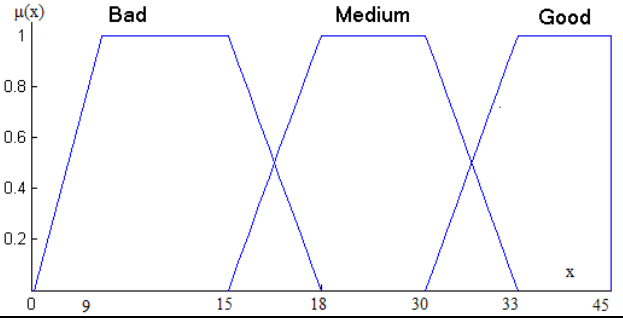	Bad = (0,9,15,18) Medium=(15,18,30,33) Good=(30,33,45,45)	Guarantee
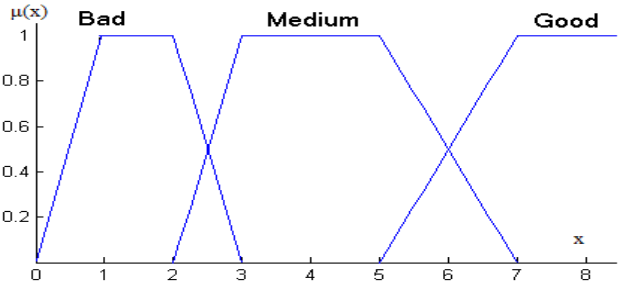	Good = (0,1,2,3) Medium=(2,3,5,7) Bad =(5,7,inf,inf)	Complaints

FIGURE 2 . Distribution of good, medium and bad linguistic values

In this stage, the verification degree of each claim has been calculated according to the customers´ data. As an example, let "product quality is medium, financial problems is good, total quality of services is medium, Guarantee is medium and customer satisfaction level is medium" for one of the customer (Due to Table 2). So, the verification degree for this customer is $0.8 \times 0.25 \times 0.14 \times 0.87 \times 1 = 0.02$. In a similar way, via each customer, the verification degree for other hypotheses has been calculated. This procedure repeats for other customers and the verification degree of each 81 hypothesis are calculated as described in section III. Note that, customer i play role of x_i that is explained in sectionIII. Table 2 depicts satisfaction degree of each linguistic variable by one of the customer .

TABLE 2 . Satisfaction degree of each linguistic variable by one of the customer

Ling. variables	**Product quality**				**Financial problem**				**Total quality of services**				**Guarantee**				**Customer satisfaction level (Complaint)**			
Ling. values	G[1]	M[2]	B[3]	Score	G	M	B	Score	G	M	B	Score	G	M	B	Score	G	M	B	Score
Sat. degree	0.2	0.8	-	42	0.25	0.75	-	36	0.86	0.14	-	32	0.13	0.87	-	35	-	1	-	4

1. G : Good 2. M : Medium 3. B : Bad

B. Findings

The results of hypotheses testing have been introduced as $M_{H_1}, M_{H_2}, \ldots, M_{H_{81}}$ which are verification degrees of $H_1, H_2, \ldots, H_{81}$ hypotheses. If verification degrees of H_i be greater than other hypotheses, then, we can conclude that H_i accurance possibility is greater than others. As shown in Table 3, the top five highest verification degrees are shown and the hypothesis "product quality is good, financial problem is good, Total quality of services is good and Guarantee is medium and as a result, customer satisfaction is good'' has the highest verification degree among the others. So, we can say, this claim has the more conformances in company case. This findings lead to get safeguarding strategy in product quality, financial problem, Total quality of services fields and improvement strategy in Guarantee approach.

TABLE 3.The top five highest verification degrees of hypotheses for L90

Priority	**Hypothesis**
1	product quality is good , financial problems is good, Total quality of services is good , Guarantee is medium and as a result, customer satisfaction is good
2	product quality is good , financial problems is good, Total quality of services is good , Guarantee is good and as a result, customer satisfaction is good
3	product quality is medium, financial problems is good, Total quality of services is medium , Guarantee is medium and as a result, customer satisfaction is medium
4	product quality is good , financial problems is medium, Total quality of services is medium , Guarantee is medium and as a result, customer satisfaction is medium
5	product quality is medium, financial problems is medium, Total quality of services is medium , Guarantee is bad and as a result, customer satisfaction is medium

IV. Conclusion

Due to increase global competition, customer satisfaction should be determined and rendered into a number of quantifiable parameters. Accordingly, different methods have been introduced to customer satisfaction measurement. Nevertheless, none of them did not use vagueness of customers' judgments and did not probe comprehensively the varied satisfaction fields. The proposed Method used the fuzzy hypothesis testing for utilizing the intuitive judgments and decision-making vagueness and Diagnoses the satisfaction customers associated fields. It Leads to the real satisfaction level and specifies the foible, strength and improvement opportunity, which they are essential information in the strategic management and latest planning in a company. This paper was implemented in Pars Khodro Co. and study L90 satisfaction customers in 2009. Finally, the result of this research emphasize on "product quality is good, financial problem is good, Total quality of services is good and Guarantee is medium then customer satisfaction is good'' hypothesis. Compare to the other researches, this approach presents more realistic results.

REFERENCES

[1] R. F. Gerson," Measuring customer satisfaction: A guide to managing quality service". Menlo Park: Crisp Publications, 1993.

[2] C. Albert,"Service Loyalty: the effects of service quality and the mediating role of customer satisfaction", European Journal of Marketing,vol.36 ,pp.810–823, . 2002.

[3] E.,Grigoroudis,Y.,Siskos,"Preference disaggregation for measuring and analysing customer satisfaction: The MUSA method,European", Journal of Operational Research, vol.143(1), pp.148–170, 2002.

[4]W. Band,"Create a customer satisfaction index (CSI) to improve your performance", Sales Market. Management. Can, vol. 31 (7) ,pp.58–59,1990.

[5]P.Hackl,A.H.Westlund,"On structural equation modeling for customer satisfaction measurement", J. Total Quality Meas., vol.11 ,pp.820–825,2000.

[6]L.,Berry,A.Parasuraman, Marketing Services: Competing Through Quality,New York: Free Press,1991 .

[7] J.,Michael, A.,Gustafssonb,T.,Andreassenc,L.,Lervikc, J., Cha," The evolution and future of national customer satisfaction index models",Journal of Economic Psychology,vol.22(2),pp. 217–245,2001.

[8]C. Fornell,"A national customer satisfaction barometer: the Swedish experience", Journal of Marketing, vol. 56 ,pp.6–21,1992.

[9] ACSI-American Customer Satisfaction Index Methodology report. The National Quality Research Center (1995).

[10] A., Martensen, K., Kristensen, L., Gronholdt,"Customer satisfaction measurement at post Denmark: results of application of the European Customer Satisfaction Index methodology", Total Quality Management, vol.11 ,pp.1007–1015,2000.

[11] A.H. Westlund, J. Eklof,"The Pan-European Customer Satisfaction Index Program current work and the way ahead", J. Total Quality Measure, vol.13,pp. 1099–1106,2002.

[12] S.H. Hsu," Developing an index for online customer satisfaction: Adaptation of American Customer Satisfaction Index", Expert Systems with Applications, vol.34(4), pp.3033-304,2008.

[13] H.,LIU, J.,LI, Y.,GE,"Design of Customer Satisfaction Measurement Index System of EMS Service", The Journal of China Universities of Posts and Telecommunications, vol.13(1), pp.109-113,2006.

[14] K.L., Bernhardt, N., Donthu, P.A., Kennett," A longitudinal analysis of satisfaction and profitability", Journal of Business Research, vol. 47, pp.161–171,2000.

[15] E.C., Nelson, R.T., Rust, A., Zahorik, R.L., Rose, P., Batalden, B.A., Siemanski," Do patient perceptions of quality relate to hospital financial performance?",Journal of Health Care Marketing, pp. 6–13,1992.

[16] D., Gursoy, N., Swanger," Performance-enhancing internal strategic factors: impacts on financial success", International Journal of Hospitality Management, vol.26 (1),pp. 213–227,2007.

[17] E., Grigoroudis, Y., Siskos, O., Saurais," TELOS: A customer satisfaction evaluation software", Computers and Operations Research , vol.27, pp.799-817,2000.

[18] E.W. Anderson, C. Fornell," Foundations of the American Customer Satisfaction Index",Total Quality Management, vol.11 ,pp.869–882,2000.

[19] G. Mihelis, E. Grigoroudis, Y. Siskos, Y. Politis, Y. Malandrakis,"Customer satisfaction measurement in the private bank sector", European Journal of Operational Research, vol.130,pp.347-360,2001.

[20] R., Jaime ,S. Fonseca," Customer satisfaction study via a latent segment model", Journal of Retailing and Consumer Services, vol. 16(5),pp. 352-359,2009.

[21] L.A. Zadeh,"Fuzzy sets", Inform. Control , vol.8 ,pp.338–353,1965.

[22] L., Xiaohong , Z., Xianyi , X., Yang , K.,Ludovic," A fuzzy model of customer satisfaction index in e-commerce", Mathematics and Computers in Simulation, vol.77(5), pp.512-521,2008.

[23] D. Dubois, H. Prade,"Fuzzy Sets and Systems—Theory and Applications", New York :Academic Press,1980.

[24] H. ,Bandemer, S. ,Gottwald,"Einfuhrun 9 in Fuzzy- Methoden"(4th ed) , Berlin :Akademie Verlag,1993.

[25] H.-J. Zimmermann ,"Fuzzy set theory - and its applications"(2nd edition) , Dordrecht :Kluwer Academic Publishers,1991.

[26] B.F. Arnold," Statistical tests optimally meeting certain fuzzy requirements on the power function and on the sample size" ,Fuzzy Sets and Systems, vol.75 ,pp.365–372,1995.

[27] B.F. Arnold,"Testing fuzzy hypotheses with crisp data", Fuzzy Sets and Systems, vol.94 ,pp.323–333,1998.

[28] M.R. Casals, M.A. Gil," A note on the operativeness of Neyman–Pearson tests with fuzzy information", Fuzzy Sets and Systems , vol.30 ,pp.215–220,1992.

[29] J.Ch. Son, I. Song, H.Y. Kim,"A fuzzy decision problem based on the generalized Neymen–Pearson criterion", Fuzzy Sets and Systems , vol.47 ,pp.65–75,1992.

[30] J.J. Saade, H. Schwarzlander,"Fuzzy hypothesis testing with hybrid data", Fuzzy Sets and Systems , vol.35 ,pp.197–212,1990.

[31] J.J. Saade,"Extension of fuzzy hypothesis testing with hybrid data", Fuzzy Sets and Systems , vol.63 ,pp.57–71,1994.

[32] M.A. Gil, N. Corral, M.R. Casals,"The likelihood ratio test for goodness of fit with fuzzy experimental observations", IEEE Transactions on Systems, Man, and Cybernetics, vol.19 ,pp.771–779,1989.

[33] M.R. Casals, P. Gil," .Bayesian sequential test for fuzzy parametric hypotheses from fuzzy information", Information Sciences , vol.80 ,pp.283–298,1994.

[34] M.R. Casals, M.A. Gil, P. Gil. (1986) .The Fuzzy decision problem: an approach to the problem of testing statistical hypotheses with fuzzy information, European Journal of Operational Research, 27 ,pp.371–382.

[35]M.A. Gil, N. Corral, P. Gil,"The minimum inaccuracy estimates in X^2 tests for goodness of fit with fuzzy observations", Journal of Statistical Planning and Inference , vol.19 ,pp.95–115,1988.

[36] P. Grzegorzewski,"Testing statistical hypotheses with vague data", Fuzzy Sets and Systems , vol.112 ,pp.501–510,2000.

[37] N. Watanabe, T. Imaizumi," A fuzzy statistical test of fuzzy hypotheses", Fuzzy Sets and Systems , vol.53 ,pp.167–178,1993.

[38] V.A. Niskanen,"Prospects for soft statistical computing: describing data and inferring from data with words in the human sciences", Information Sciences, vol.132 ,pp.83–131,2001.

[39] D., Nachmias, C., Nachmias, research methods in sicial sciences new york, st. Martin's Press,1987.

[40] R.V., Krejcie, D.W., Morgan," determine sample size for research actives ", journal of education & psychological measure, vol.3, pp.607-670,1970.

[41] N. Hill. (2006).handbook of customer satisfaction measurement(3 edition), publisher: G,ower technical press.

[42] J. ,Reynaldo, A. Santos,"Cronbach's Alpha: A tool for Assessing the reliability of scales", Journal of extension, vol.37 (2),1999.

2011 IEEE International Conference on Fuzzy Systems
June 27-30, 2011, Taipei, Taiwan

Permutation Flow Shop Scheduling: Fuzzy Particle Swarm Optimization Approach

Sai Ho Ling
Faculty of Engineering
and Information Technology,
University of Technology, Sydney,
NSW 2007, Australia
Email: Steve.Ling@uts.edu.au
Telephone: (61)2-95142390
Fax: (61)2-95142435

Frank Jiang and Hung T. Nguyen
Faculty of Engineering
and Information Technology,
University of Technology, Sydney,
NSW 2007, Australia
Email: frankj@eng.uts.edu.au,
Hung.Nguyen@uts.edu.au

Kit Yan Chan
Digital Ecosystems and
Business Intelligence Institute,
Curtin University of Technology,
Perth, Australia
Email: Kit.Chan@curtin.edu.au

***Abstract*—A fuzzy particle swarm optimization (PSO) for the minimization of makespan in permutation flow shop scheduling problem is presented in this paper. In the proposed fuzzy PSO, the inertia weight of PSO and the control parameter of the cross-mutated operation are determined by a set of fuzzy rules. To escape the local optimum, cross-mutated operation is introduced. In order to make PSO suitable for solving permutation flow shop scheduling problem, a roulette wheel mechanism is proposed to convert the continuous position values of particles to job permutations. Meanwhile, a swap-based local search for scheduling problem is designed for the local exploration on a discrete job permutation space. Flow shop benchmark functions are employed to evaluate the performance of the fuzzy PSO for flow shop scheduling problems and the results indicate that the algorithm performs better compared with existing hybrid PSO algorithms.**

***Index Terms*—Flow shop Scheduling, Fuzzy logic, Particle swarm optimization.**

I. Introduction

Permutation flow shop scheduling problem is a NP hard problem, existing mathematical methods, i.e., integer programming, branch-and-prune method, dynamic programming, etc, are only applicable to small-scale problem and they are difficult to find the global solution of the problem. Thus, various global algorithms such as genetic algorithm (GA) [1] ,differential evolution (DE) [2] and ant colony optimization (ACO) [3] [4] are proposed. Recently, a new global searching algorithm namely particle swarm optimization (PSO) is widely used to different industrial areas [5]–[8]. Especially, it is effectively to tackle the flow shop scheduling problems [9]–[14]. Comparing with other population based stochastic optimization methods, such as evolutionary algorithms, PSO has comparable or even superior search performance for many hard optimization problems with faster and more stable convergence rates [15], [16]. However, observations reveal that PSO converges sharply in the early stage of the searching process, but saturates or even terminates in the later stage. It behaves like the traditional local searching methods that trap in local optima.

Recently, different hybrid PSO methods have been proposed to overcome the drawback of trapping in local optima. The hybrid PSO has been first proposed in 1998 [17], in which a standard selection mechanism is integrated with PSO. A new hybrid gradient descent PSO (HGPSO), which is integrated with gradient information to achieve faster convergence without getting trapped in local minima is proposed [18]. However, the computational demand of HGPSO is increased by the process of the gradient descent. In addition, it is poor to handle the multimodel problem that contain many local minima. In [19], a hybrid PSO algorithm named HGAPSO is proposed, which incorporates GA's evolutionary operations of crossover, mutation and reproduction. In the paper [5], a hybrid PSO named HPSOM is proposed, in which a constant mutating space is used in mutation. In both HGAPSO and HPSOM, the solution space can be explored by performing mutation operations on particles along the search, and premature convergence is more likely to be avoided. However, the mutating space is kept unchanged all the time throughout the search, and the space for the permutation of particles in PSO is also fixed. It can be improved by varying the mutating space along the search. A hybrid PSO with wavelet mutation operation (HPSOWM) is proposed [8], which the mutating space is varying by applying wavelet theory. The solution quality and solution reliability (standard deviation upon many trials) are improved.

In order to make PSO be suitable to solve the combinational (scheduling) problem, a converting process from the continuous position values of particles to job permutations is used. Conventionally, the Smallest Position Value (SPV) rule [11]–[13] is actually a mapping from an N-dimensional continuous space to a sequence with N numbers. The corresponding sequence is represented by the order of the vector. As we know, the positions of the particles in PSO are updated that causes velocity and evolution. In some case, the positions of the particles are updated, the corresponding sequence is still unchange by using SPV rule [14]. This kind of inefficiency of the continuous space will result in the decrease in convergence rate. To overcome this drawback, a sequence-order system based on the roulette wheel mechanism is proposed in this paper. In this mechanism, the probability representation is instead of the position value which is represented by SPV rule.

978-1-4244-7316-8/11/$26.00 ©2011 IEEE

In [20], an improved version of PSO with an inertia weight factor is introduced. The aim of the inertia weight provides a balance between the global exploration and local exploitation and it is governed by a linear characteristic function. However, not all the optimization problems are linear. Thus, in this paper, a hybrid fuzzy logic-based PSO with cross-mutated operation is proposed. This proposed approach can be divided into two main parts. First, an adaptive inertia weight is proposed, which incorporates with the fuzzy inference system. Fuzzy logic is good in representing some expert knowledge and experience in some linguistic rule which can be easily understood by the human being. Using fuzzy inference to determine the inertia weight of PSO, such that, the characteristic of function of inertia weight becomes nonlinear. It will be shown that the nonlinear characteristic of the inertia weight performs more better solution quality in this paper. Second, a new operation namely cross-mutated (CM) operation is introduced. The CM operation effectively solves the drawback of PSO, which makes PSO easier to trap in the local optima. In CM operation, the control parameter is determined by fuzzy rules and the operation becomes adaptive. Additionally, a swap-based local search method is designed for the local exploration on a discrete job permutation space. This method is used to fine tune the sequence of the flow shop scheduling problem. In this paper, a suite of benchmark problems for permutation flow shop scheduling problem are used to illustrate the performance of the proposed approach. The resulting adaptive inertia weight and CM operation aid the proposed fuzzy logic-based PSO with cross-mutated operation to perform better solution quality compared with improved PSO (IPSO) [20] and other hybrid PSO methods [5], [8], [18], [19].

This paper is organized as follows. Section 2 presents the formulation of flow shop scheduling problem. The implementation of the flow shop scheduling problem with hybrid PSO will be discussed in Section 3. In this section, the solution representation, hybrid fuzzy-based PSO with cross-mutated operation, and the swap local search method are discussed. In Section 4, benchmark problems will be given to evaluate the performance of the proposed method. Finally, a conclusion will be drawn in Section 5.

II. Permutation Flow shop scheduling problem formulation

The formulation of the permutation flow shop scheduling problem is described in this section. Suppose there is a set of n jobs to be processed in a set of m machines in the same order. The processing time $p_{j,k}$ for job j $(j = 1, 2, ..., n)$ on machine k $(k = 1, 2, ..., m)$ is given. The objective is to find a sequence for the processing of jobs in the machines to minimize the total completion time or makespan (C_{max}). There are several assumptions on this scheduling problem [21]: 1) Each job j can be processed at most on one machine k at the same time; 2) Each machine m can process only one job j at a time; 3)The processing of a job j on a machine k cannot be interrupted; 4) All jobs are independent and are available for processing at time 0; 5) The setup times of the jobs on machines are negligible; 6) The machines are continuously available; and 7) If the next machine on the sequence needed by a job is not available, the job can wait and join the queue at that machine.

Let $\pi = J_1, J_2, ..., J_n$ denote a permutation of all jobs, and $C(J_j, k)$ denotes the completion time of job J_j on the machine, then the completion time $C(J_j, k)$ can be calculated as follows:

$$C\left(J_1, 1\right) = p_{J_1,1} \tag{1}$$

$$C\left(J_j, 1\right) = C\left(J_{j-1}, 1\right) + p_{J_j,1}, j = 2, ..., n \tag{2}$$

$$C\left(J_1, k\right) = C\left(J_1, k-1\right) + p_{J_1,k}, k = 2, ..., m \tag{3}$$

$$C\left(J_j, k\right) = \max\left\{C\left(J_{j-1}, k\right), C\left(J_j, k-1\right)\right\} + p_{J_j,k}, \quad j = 2, ..., n, k = 2, ..., m \tag{4}$$

$$C_{\max}\left(\pi\right) = C\left(J_n, m\right). \tag{5}$$

So, the flow shop problem with the makespan criterion is to find a permutation π^* in the set of all permutations Π such that,

$$C_{\max}\left(\pi^*\right) \leq C\left(J_n, m\right), \forall \pi \in \Pi \tag{6}$$

III. The hybrid fuzzy-based PSO for flow shop scheduling

A. Solution representation: roulette wheel mechanism

As mentioned in the introduction section, the existing solution representation method, smallest position value (SPV) rule has a drawback which is to decrease the convergence rate and performance. In this section, a sequence-order system based on the *roulette wheel mechanism* is proposed. In this method, the value of the continuous position of particles represents the probability of the higher ranking. In other words, the position of the higher value of the element of particles will have a higher chance to be select to job sequence list firstly. In this section, the process of the methodology is discussed.

The process of the solution representation with roulette wheel mechanism is described as follows. The roulette wheel mechanism is shown in Fig. 1.

(1) Given a continuous position (element) of the particle x_j, j = 1, 2,... , n.
(2) Assign a probability q_j to the x_j such that: $q_j = \frac{x_j}{\sum_{j=1}^{n} x_j}$. Note that $\sum q_j$ should equal to 1.
(3) Evaluate a cumulative probability $\hat{q}_j$ for each x_j such as: $\hat{q}_j = \sum_{l=1}^{j} q_l$.
(4) Generate a set of floating-point numbers $d_h \in \left[\begin{array}{cc} 0 & 1 \end{array}\right]$ randomly, $h = 1, 2, ..., \eta$; η is the number of generated floating-point number. These floating point numbers should be sorted with ascending order. Normally, the

number of generated floating-point number η equals to $20 \times n$.

(5) Count the total number of the floating-point numbers for each j are in the range of $\left[\ \hat{q}_{j-1} \quad \hat{q}_j\ \right]$ such as: $S_j = count\left(\hat{q}_{j-1} \le d_h \le \hat{q}_j\right)$, where $count()$ is a function to count how many statement is met the condition. Note that $\hat{q}_0 = 0$.

(6) Convert the continuous position of S_j to the sequence of job by using largest position value rule. For a given continuous position like [23, 12, 41, 6], the corresponding sequence is represented by the order of the value. For example, in decent order, 41 is the largest value, so the first of the sequence should be 3; the second largest value is 2, so the second job of sequence should be 1. Thus, we can obtain the corresponding job sequence π is [3, 1, 2, 4].

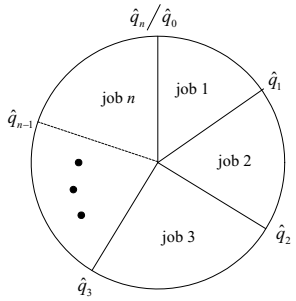

Fig. 1. The roulette wheel mechanism

B. Fuzzy logic-based PSO with cross-mutated operation

Particle swarm optimization (PSO) is a stochastic optimization method which developed in 1995 [15]. It models the processes of the sociological behavior associated with bird flocking and fish schooling. It uses a number of particle that constitute a swarm. Each particle traverses the search space looking for the global optimum. In recently, an improved PSO (IPSO) is proposed [20] where constriction and inertia weight factors are introduced and the searching ability is improved compared with standard PSO [15]. Based on the IPSO, an improved fuzzy logic-based particle swarm optimization with cross-mutated operation namely FPSOCM is proposed to tackle the permutation flow shop scheduling problem and shown in Fig. 2.

From Fig.2, $X\left(t\right)$ is denoted as a swarm at the t-th iteration. Each particle $\mathbf{x}^i\left(t\right) \in X\left(t\right)$ contains n elements $x_j^i\left(t\right) \in \mathbf{x}^i\left(t\right)$ at the t-th iteration, where i = 1, 2,... , γ and j = 1, 2,... , n; γ denotes the number of particles in the swarm and n is the dimension of a particle. First, the particles of the swarm are initialized and then evaluated by a defined cost (objective) function. The evaluation cost value is represented by $f\left(\mathbf{x}^i\left(t\right)\right)$. In the same time, current generation number t is initially set at 0. The objective of PSO is to minimize the cost values of particles iteratively. The swarm evolves from iteration $t+1$ by repeating the processes as shown in Fig.2.

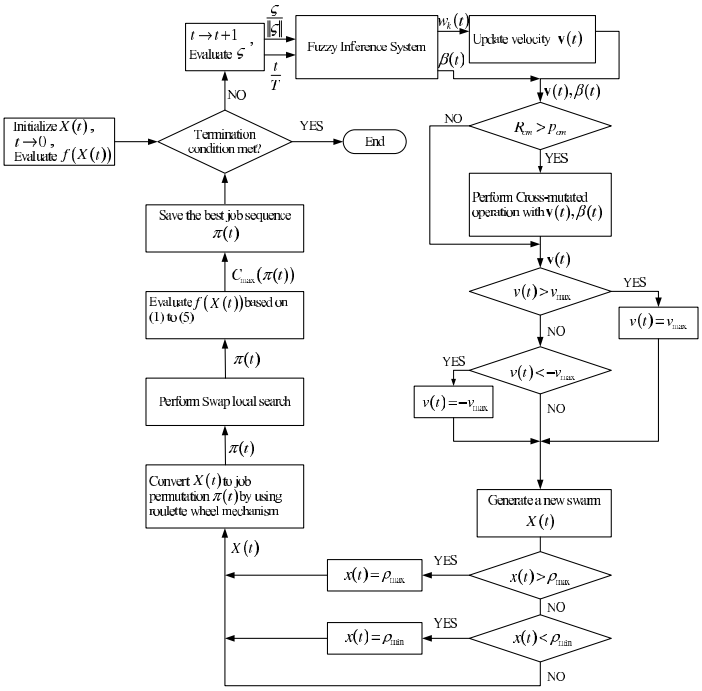

Fig. 2. The process diagram of FPSOCM for flow shop scheduling

In PSO, there has one important term and called velocity. The velocity is corresponding to the flight speed in the search space. The velocity $v_j^i\left(t\right)$ and the position $x_j^i\left(t\right)$ of the j-th element of the p-th particle at the t-th generation can be calculated using the following formulae:

$$v_j^i\left(t\right) = k \cdot \left\{\omega_k\left(t\right) \cdot v_j^i\left(t-1\right) + \varphi_1 \cdot r_1 \cdot \left(p_j^i - x_j^i\left(t-1\right)\right) + \varphi_2 \cdot r_2 \cdot \left(g_j - x_j^i\left(t-1\right)\right)\right\} \tag{7}$$

$$x_j^i\left(t\right) = x_j^i\left(t-1\right) + v_j^i\left(t\right) \tag{8}$$

where $p^i = \left[\ p_1^i \quad p_2^i \quad ,\ldots \quad p_n^i\ \right]$ and $g = \left[\ g_1 \quad g_2 \quad ,\ldots \quad g_n\ \right]$; the best position of a particle i is represented as p^i; the position of the best particle among all the particles is represented as g; r_1 and r_2 return a uniform random number in the range of [0,1], where ω_k is an inertia weight factor to provide a balance between the global and local explorations; φ_1 and φ_2 are acceleration constants; k is a constriction factor derived from the stability analysis of equation (7) to ensure the system to be converged but not prematurely [20]. Mathematically, k is a function of φ_1 and φ_2 as reflected in the following equation:

$$k = \frac{2}{\left|2 - \varphi - \sqrt{\varphi^2 - 4\varphi}\right|} \tag{9}$$

where $\varphi = \varphi_1 + \varphi_2$ and $\varphi > 4$.

In this proposed fuzzy PSO, there are two main contributions that will enhance the performance of searching compared to other PSO methods. Firstly, an adaptive inertia weight $\omega_k(t)$ is proposed to improve the solution quality of searching. Secondly, cross-mutated (CM) operation is given to solve the drawback of IPSO that it is easier to trap into local minima. From Fig.2, we can see that the adaptive inertia weight $\omega_k(t)$ and the control parameter $\beta(t)$ of CM operation are determined by a fuzzy inference system.

1) Adaptive inertia weight: In IPSO [20], the inertia weight is used to provide a balance between the global exploration and local exploitation. A linear inertia weight is adopted in IPSO. In IPSO, when the value of t/T is smaller which implies that it is doing global exploration. Similarly, higher value of t/T implies that it is doing fine-tuning (local exploitation). We can see that the characteristic of this function is linear. However, some of the optimization problems are nonlinear. Thus, an adaptive (nonlinear) inertia weight is proposed to enhance the performance of the searching. In this paper, an adaptive inertia weight $\omega_k(t)$ is proposed, which is incorporated with a fuzzy inference system. In a fuzzy inference system, there are two inputs and two outputs. One of the output is adaptive inertia weight $\omega_k(t)$, the other one is control parameter $\beta(t)$ of CM (It will discussed in later). The inputs of the fuzzy system are $\varsigma(t)/\|\varsigma(t)\|$ and t/T. $\varsigma(t)/\|\varsigma(t)\|$ is a normalized standard deviation of cost value among all the particles. A larger value of $\varsigma(t)/\|\varsigma(t)\|$ implies that the variance between each cost value of particle $f(X^p(t))$ is larger. Conversely, when the value of $\varsigma(t)/\|\varsigma(t)\|$ is smaller, that means the variance between each cost value of particle $f(X^i(t))$ is smaller. In other words, the location of each particles are closer. The formulation of $\varsigma(t)/\|\varsigma(t)\|$ is defined as follows:

$$\varsigma(t) = \sqrt{\frac{1}{\gamma}\sum_{i}^{\gamma}\left(f\left(\mathrm{x}^i(t)\right) - \bar{f}\left(\mathrm{x}^i(t)\right)\right)^2} \tag{10}$$

where

$$\bar{f}\left(\mathrm{x}^i(t)\right) = \frac{1}{\gamma}\sum_{i=1}^{\gamma} f\left(\mathrm{x}^i(t)\right) \tag{11}$$

$\|\cdot\|$ denotes the l_2 vector norm.

The adaptive inertia weight $\omega_k(t)$ is governed by the following fuzzy rules:

$$\text{Rule } j: \text{IF } \varsigma(t)/\|\varsigma(t)\| \text{ is } \mathrm{N}_1^j, \text{ AND } t/T \text{ is } \mathrm{N}_2^j, \text{ THEN } \omega_k(t) = \sigma_j,$$

$$j = \quad 1, \quad 2, \quad \ldots, \quad \varepsilon \tag{12}$$

where N_1^j and N_2^j are fuzzy terms of rule j, ε denotes the number of rules, $\sigma_j \in \left[\begin{array}{cc} \omega_{min} & \omega_{min} \end{array}\right]$ is the singleton to be determined. In this paper, ω_{min} and ω_{min} are set at 0.1 and 1.1 respectively [8]. The final value of $\omega_k(t)$ is given by:

$$\omega_k(t) = \sum_{j=1}^{\varepsilon} m_j(t)\sigma_j \tag{13}$$

where

$$m_j(t) = \frac{\mu_{\mathrm{N}_1^j}\left(\varsigma(t)/\|\varsigma(t)\|\right) \times \mu_{\mathrm{N}_2^j}(t/T)}{\sum_{j=1}^{r_m}\left(\mu_{\mathrm{N}_1^j}\left(\varsigma(t)/\|\varsigma(t)\|\right) \times \mu_{\mathrm{N}_2^j}(t/T)\right)} \tag{14}$$

$\mu_{\mathrm{N}_1^j}\left(\varsigma(t)/\|\varsigma(t)\|\right)$ and $\mu_{\mathrm{N}_2^j}(t/T)$ are the membership function corresponding to N_1^j and N_2^j respectively.

In the proposed algorithm, there are 3 membership functions for each input and shown in Fig. 3. The 3 fuzzy terms are namely L (Low), M (Middle), and H (High). Based on the characteristic of $\varsigma(t)/\|\varsigma(t)\|$ and t/T, there are 9 linguistic IF-THEN fuzzy rules and the fuzzy rule table for determine $\omega_k(t)$ is shown in Fig. 4 (a). The rationale of the selected fuzzy rules for determine $\omega_k(t)$ is described as follows: the value of $\omega_k(t)$ is determined by fuzzy inputs $\varsigma(t)/\|\varsigma(t)\|$ and t/T. The value of t/T represents the iteration stage (smaller value of t/T represents the searching process in the early stage, a larger value of t/T represents the searching process in the later stage). The value of $\omega_k(t)$ should be higher as the value of t/T is smaller (in early stage) implies that a larger value of velocity of particle element is given for global searching. Similarly, a larger value of t/T implies that a higher value of velocity of particle element for local searching. Because of it, the values of $\omega_k(t)$ at t/T is "L", are larger than t/T is set at"M". For the same reason, the values of $\omega_k(t)$ at t/T is "M" are larger than that as t/T is "H". The value of $\omega_k(t)$ should be smaller as t/T increase in order to reduce the value of velocity of particle element for fine-tuning.

As mentioned before, $\varsigma(t)/\|\varsigma(t)\|$ is a normalized standard deviation of cost value among all the particles. A larger value of $\varsigma(t)/\|\varsigma(t)\|$ implies that the variance between each cost value of particle $f(X^i(t))$ is larger. In other words, the location of each particle is far away. At t/T is "L", which the searching process is in early stage and when $\varsigma(t)/\|\varsigma(t)\|$ is "H", that implied the location of each particle is far away in early stage. Thus, a larger value of $\omega_k(t)$ should be given for global exploration. In a special case, when $\varsigma(t)/\|\varsigma(t)\|$ is "L", that implies the location of each particle is closed in early stage.

We also set $\omega_k(t)$ to a larger value, because there has a high chance that the solutions are trap into local optima (it is affected from the smaller value of $\varsigma(t)/\|\varsigma(t)\|$). Therefore, a larger value of $\omega_k(t)$ is given to force the particle escape the local optima. As the value of $\varsigma(t)/\|\varsigma(t)\|$ is "M", we set the value of $\omega_k(t)$ is slight smaller than that $\varsigma(t)/\|\varsigma(t)\|$ is "L" and $\varsigma(t)/\|\varsigma(t)\|$ is "H" in early stage (t/T is "L"). When t/T is "M", which the searching process is in middle stage. The rationale of the suggested value of $\omega_k(t)$ is similar to rules that when When t/T is "L". However, there is one difference that when $\varsigma(t)/\|\varsigma(t)\|$ is "L", the value of $\omega_k(t)$ is smaller than $\varsigma(t)/\|\varsigma(t)\|$ is "H". It is because the optimal solution may be found in middle stage where a smaller value of $\omega_k(t)$ is given. At t/T is "H", which the searching process is in later stage . In this stage, the searching process is undergo fine-tuning process (local exploitation) to find the optimal solution. Because of it, when the value of $\varsigma(t)/\|\varsigma(t)\|$ is "L" that implied the position

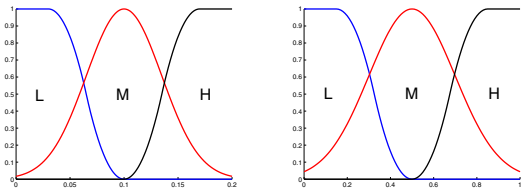

(a) fuzzy input 1: $\varsigma/\|\varsigma\|$ (b) fuzzy input 2: t/T

Fig. 3. Membership functions a) (x-axis: $\varsigma(t)/\|\varsigma(t)\|$,y-axis: $\mu_{N_1}(\varsigma(t)/\|\varsigma(t)\|)$) and b) (x-axis: t/T ,y-axis: $\mu_{N_2}(t/T)$)

of most particles are closed and near the best solution. Thus, a smallest value of $\omega_k(t)$ is given.

$\frac{t}{T}$ \ $\frac{\varsigma(t)}{\|\varsigma(t)\|}$	L	M	H
L	1.1	0.9	1.1
M	0.6	0.5	0.7
H	0.1	0.2	0.3

(a)

$\frac{t}{T}$ \ $\frac{\varsigma(t)}{\|\varsigma(t)\|}$	L	M	H
L	0.5	0.4	0.6
M	0.4	0.3	0.5
H	0.1	0.2	0.2

(b)

Fig. 4. The fuzzy rule table for determining (a) $w_k(t)$, and (b) $\beta(t)$

2) Cross-mutated operation: In this section, a cross-mutated (CM) operation is introduced. This new CM operation is merged the idea of crossover and mutation operation of genetic algorithm. The aim of the CM operation is force the particle escape the local optima. Furthermore, a control parameter $\beta(t)$ is introduced into the CM operation, and the operation becomes more adaptive. This control parameter is governed by some fuzzy rules with human knowledge. By introducing the CM operation, the performance of the proposed PSO method is improved.

The details of the CM operation is as follows. Every velocity of particle element of the swarm will have a chance to undergo CM operation governed by a probability of cross-mutated operation, $p_{cm} \in \left[\begin{array}{cc} 0 & 1 \end{array}\right]$, which is defined by user. For each velocity of particle element, a random number R_{cm} between 0 and 1 will be generated such that if it is less than or equal to p_{cm}, the CM operation will take place on that element. The sensitivity of the p_{cm} with experimental results and the analysis will be discussed in later. The choice of the p_{cm} will affect the quality of solution.

The resulting velocity of particle element under the CM operation is given by:

$$\bar{v}_j^i(t) = (1-\beta(t))\, v_j^i(t) + \beta(t)\tilde{v}_j^i(t) \qquad (15)$$

where

$$\tilde{v}_j^i(t) = \frac{1}{4}\left\{r_3 \cdot \left(\rho_{\max_j} - \rho_{\min_j}\right) - \rho_{\max_j}\right\} \qquad (16)$$

$v_j^i(t)$ is determined by (7), $\tilde{v}_j^i(t)$ is a random velocity of particle element and the value of this velocity is randomly generated and bounded with 0.25 of the dynamic range of the particle element. $r_3 \in \left[\begin{array}{cc} -1 & 1 \end{array}\right]$ is an uniform random number. In (15), the resulting velocity of particle element $\bar{v}_j^i(t)$ is combined with the information of $v_j^i(t)$ and $\tilde{v}_j^i(t)$. This information exchanging process is like as crossover operation. However, in CM operation, $\bar{v}_j^i(t)$ is changed (mutated) one-by-one which is like as mutation operation. Therefore, we called it is cross-mutated (CM) operation.

In (15), the control parameter $\beta(t)$ provides a balance to control the resulting velocity $\bar{v}_j^i(t)$ converge toward $v_j^i(t)$ or $\tilde{v}_j^i(t)$. If $\beta(t)$ is approaching 0, the $\bar{v}_j^i(t)$ will tends to the $v_j^i(t)$. Conversely, when $\beta(t)$ is approaching 1,the $\bar{v}_j^i(t)$ will tends to the $\tilde{v}_j^i(t)$. The proposed random velocity $\tilde{v}_j^i(t)$ in (16) has ability to force the particle element to escape the local optima with a random movement. In this operation, the value of the $\beta(t)$ is governed by nine fuzzy-rules. The fuzzy inference system is same as before we mentioned. The inputs of the fuzzy system are same. They are $\varsigma(t)/\|\varsigma(t)\|$ and t/T. Now, there are 9 linguistic fuzzy rules and the fuzzy rule table for determine $\beta(t)$ is shown in Fig. 4 (b).

The rationale of the selected fuzzy rules is similar to the rules of adaptive inertia weight in last sub-section. The brief description of the choosing fuzzy rules for CM operation is given as follows: the value of $\beta(t)$ is determined by $\varsigma(t)/\|\varsigma(t)\|$ and t/T, and some fuzzy rules. As mention before, the value of the t/T represents the iteration stage. We can see as t/T is "L", where the searching process is in early stage and as t/T is "H", where the searching process is in later stage, the values of $\beta(t)$ in early stage are larger than the values of $\beta(t)$ in later stage. It is because a significant random velocity (higher value of $\beta(t)$ in (15)) provides a global exploration in early stage. Conversely, the effect of the random velocity should be reduced in later stage for fine-tuning (local exploitation) with smaller value of $\beta(t)$.

Till now, we have discussed about the effect of the $\varsigma(t)/\|\varsigma(t)\|$, the concept is same as the rules of adaptive inertia weight. In the early stage, when $\varsigma(t)/\|\varsigma(t)\|$ is "L", that implies the location of each particle is closed. Thus, we need to set the value of $\beta(t)$ to be larger than that when $\varsigma(t)/\|\varsigma(t)\|$ is "M". The reason lies in the fact that a higher chance that the solution being trapped into a local optimum. Conversely, in the later stage, the searching process undergoes fine-tuning process (local exploitation) to find the optimal solution. Because of this, when the value of $\varsigma(t)/\|\varsigma(t)\|$ is "L" that implies the position of most particles are closed (similar) and near the best solution. Thus, a smallest value of $\beta(t)$ is given.

In (7), the particle velocity is limited by a maximum value $v_{\max}$. The parameter $v_{\max}$ determines the resolution with which regions are to be searched between the present

position and the target position. This limit enhances the local exploitation of the problem space and it realistically simulates the incremental changes of human learning. If $v_{\max}$ is too high, particles might fly past good solutions. If $v_{\max}$ is too small, particles may not explore sufficiently beyond local solutions. Empirically, $v_{\max}$ is often set at 10% to 20% of the dynamic range of the element on each dimension.

A new swarm $X(t)$ is updated after the velocity of all particles are updated. To ensure all particle elements x_j^i in $X(t)$ fall within the range $\left[\ \rho_{\mathbf{min}},\ \ \rho_{\mathbf{max}}\ \right]$, the following conditions are considered as follows: If $x_j^i(t)\ > \rho_{\max_j}$, then the updated $x_j^i(t)$ should equal to $\rho_{\max_j}$. Similarly, If $x_j^i(t)\ < \rho_{\min_j}$, then the updated $x_j^i(t)$ should equal to $\rho_{\min_j}$. Here, $\rho_{\mathbf{min}} = \left[\ \rho_{\min_1}\ \ \rho_{\min_2}\ \ \cdots\ \ \rho_{\min_n}\ \right]$ and $\rho_{\mathbf{max}} = \left[\ \rho_{\max_1}\ \ \rho_{\max_2}\ \ \cdots\ \ \rho_{\max_n}\ \right]$; $\rho_{\min_j}$ and $\rho_{\max_j}$ are minimum and maximum values of $x_j^i(t)$ respectively and $j = 1, 2, ..., n$.

After an updated swarm is generated. Next, convert all the particles in the swarm to job permutation $\pi(t)$ by using the sequence-order system based on the roulette wheel mechanism. After going through the process of the sequence-order system, a set of job sequence will be formed and then undergo swap based local search operation for local exploration on a job permutation space.

3) Swap based-Local search: Local searches are very important for the exploitation. In this paper, a swap-based local search method is designed for fine-tuning on the flow shop scheduling problem. The operation of this local search is simply to swap the selected two job order number. The operation of swap based local searching method is described as follows.

(1) Given a sequence of jobs π, where $\pi = J_1, J_2, ..., J_{i-1}, J_i, J_{i+1}, ...J_n$.
(2) Randomly picks 2 jobs, i.e., J_i and J_{i+1} .
(3) Swap the selected 2 jobs.

After the process, the new sequence of jobs should be J_1, J_2, ..., J_{i-1}, J_{i+1}, J_i, ...J_n. An example of swap based-local search method is given in Fig.5. In this figure, the job 7 and the job 1 are selected to undergo the swap process. After going through the swap operation, a new job sequence is generated. By using (1)-(5), a updated makespan C_{max} will be evaluated. The optimization process will repeat until a termination condition is met. The iterative process will be terminated when a defined number of iteration is met.

IV. Computational results

To test the performance of the proposed FPSOCM to flow shop scheduling problem, computational simulation is carried out with a suite of flow shop benchmark problems [22].

A. Experimental setup

The performance of HPSOWM [8], HPSOM [5], HGAPSO [19], HGPSO [18], IPSO [20], and the proposed FPSOCM on solving the flow-shop benchmarking problems are evaluated.

The following simulation conditions are in use:

For All PSOs:

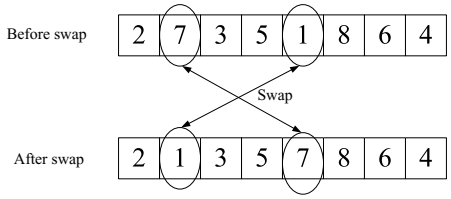

Fig. 5. The example of the swap-based local search method.

- Swarm size (γ): 100
- Number of runs: 20
- Acceleration constant φ_1: 2.05
- Acceleration constant φ_2: 2.05
- Maximum velocity v_{max}: 0.2
- Initial population: it is generated uniformly at random

For FPSOCM:

- Probability of cross-mutated operation (p_{cm}):
  p_{cm} = 0.05 for Car3, Car8;
  p_{cm} = 0.01 for Car1, Car2, Car4, Car5, Car6, Car7;

For HPSOWM, HPSOM, and HGAPSO:

- Probability of mutation operation (p_m): it is chosen by trial and error through experiments for good performance for all functions. (p_m= 0.2 for Car1 - Car8)

For HPSOWM:

- Shape parameter of the wavelet mutation: it is chosen by trial and error through experiments for good performance for all functions
- Parameter g of the wavelet mutation: 10000

For HGPSO:

- Learning rate: it is chosen by trial and error through experiments for good performance for all functions

For HGAPSO:

- Probability of crossover operation: 0.8

B. Results

In this section, the results for the 8 flow shop problem are given to validate the FPSOCM, which is proven to perform well on flow shop scheduling problem. The experimental results in terms of the average relative error (ARE), best relative error (BRE), and worst relative error (WRE) are summarized in Table I. The number of iterations 100 is adopted in all approaches. From the table, we can see that FPSOCM algorithm obtains a smaller ARE, BRE and WRE in all problems. In problem Car6 which is a 8 jobs 9 machines flow shop scheduling problem, the ARE of the FPSOCM is 0. Comparing with other algorithms, only FPSOCM can reach the optimal value. In Problem Car3, the ARE of FPSOCM is 0.06 which imply around 2.5 - 6 times improvement compared

(A)

Method		Problem			
		Car1 $n,m=11,5;\ C^*=7038$	Car2 $n,m=13,4;\ C^*=7166$	Car3 $n,m=12,5;\ C^*=7312$	Car4 $n,m=14,4;\ C^*=8003$
FPSOCM	ARE	0	0	0.06	0
	BRE	0	0	0	0
	WRE	0	0	0.602	0
HPSOWM	ARE	0	0	0.157	0
	BRE	0	0	0	0
	WRE	0	0	1.203	0
HPSOM	ARE	0	0	0.260	0
	BRE	0	0	0	0
	WRE	0	0	1.504	0
HGAPSO	ARE	0	0	0.356	0
	BRE	0	0	0	0
	WRE	0	0	1.504	0
HGPSO	ARE	0	1.036	0.345	0.012
	BRE	0	0	0	0
	WRE	0	2.930	1.504	0.062
IPSO	ARE	0	0	0.343	0
	BRE	0	0	0	0
	WRE	0	0	1.792	0

(B)

Method		Problem			
		Car5 $n,m=10,6;\ C^*=7720$	Car6 $n,m=8,9;\ C^*=8505$	Car7 $n,m=7,7;\ C^*=6590$	Car8 $n,m=8,8;\ C^*=8366$
FPSOCM	ARE	0.019	0	0	0
	BRE	0	0	0	0
	WRE	0.389	0	0	0
HPSOWM	ARE	0.161	0.153	0	0124
	BRE	0	0	0	0
	WRE	0.622	0.764	0	1.960
HPSOM	ARE	0.282	0.115	0	0
	BRE	0	0	0	0
	WRE	1.308	0.764	0	0
HGAPSO	ARE	0.549	0.076	0	0.152
	BRE	0	0	0	0
	WRE	1.308	0.764	0	1.960
HGPSO	ARE	0.194	0.223	0	0.294
	BRE	0	0	0	0
	WRE	0.609	0.764	0	1.960
IPSO	ARE	0.343	0.483	0	0.144
	BRE	0	0	0	0
	WRE	1.308	2.787	0	1.960

n: Number of jobs

m: Number of machines

C^*: The optimal value known so far

TABLE I
COMPARISON RESULTS OF FPSOCM, HPSOWM, HPSOM, HGAPSO, HGPOS, AND IPSO. ALL RESULTS ARE AVERAGED ONES OVER 20 RUNS (A: CAR1-4, B: CAR5-8).

with other algorithm. Similarly, in Problem Car5, the ARE of FPSOCM is 0.019 which imply around 8 - 18 times improvement. So FPSOCM algorithm for flow shop scheduling problem to minimize makespan is more effective.

V. CONCLUSION

In this paper, we have proposed a hybrid particle swarm optimization which incorporates a fuzzy system and a new cross-mutated operation to tackle job shop scheduling problem. An adaptive inertia weight of PSO is presented. It is determined by a fuzzy system. Moreover, in order to solve the local optimum problem of PSO, a new operation namely cross-mutated operation is proposed. With these proposed operations, the solution quality is improved. The performance of the proposed hybrid PSO is compared with other hybrid PSOs with respect to the same set of flow scheduling problems. The results demontrate the effectiveness of the proposed algorithm for the flow shop scheduling problem.

REFERENCES

[1] C. R. Reeves, "A genetic algorithm for flowshop sequencing",*Comput. Oper. Res.,* vol. 22, no. 4, pp. 5-13, 1995.

[2] G. Onwubolo and D. Davendra, "Scheduling flow shops using differential evolution algorithm",*Eur. J. Oper. Res.*, vol. 171, pp. 674-692, 2006.

[3] C. Rajendran and H. Ziegler, "Two ant-colony algorithms for minimizing total flowtime in permutation flowshops",*Comput. & Ind. Engg.*, vol. 48, pp. 789-797, 2005.

[4] K.C. Ying and C. J. Liao, "An ant colony system for premutation flowshop sequencing", *Comput. Oper. Res.*, vol. 31, pp. 791-801, 2004.

[5] A. A. E. Ahmed, L. T. Germano and Z. C.Antonio, "A hybrid particle swarm optimization applied to loss power minimization", *IEEE Trans. Power Syst.*, vol. 20, no. 2, pp. 859-866, 2005.

[6] J. Hazra and A. K. Sinha, "Congestion Management Using Multiobjective Particle Swarm Optimization", *IEEE Trans. Power Syst.* vol. 22 no. 4, pp. 1726-1734, 2007.

[7] S. L. Ho, S. Y. Yang, G. Z. Ni and K. F. Wong, "An improved PSO method with application to multimodal functions of inverse problems", *IEEE Trans. Magnetics*, vol. 4, pp. 1597-1600, 2007.

[8] S. H. Ling, H. H. C. Iu, K. Y. Chan, H. K. Lam, C. W. Yeung and F. H. F. Leung, "Hybrid particle swarm optimization with wavelet mutation and its industrial applications", *IEEE Trans. Syst. Man and Cybern. B*, vol. 38, no. 3, pp. 743-763, 2008.

[9] Z. Lian, X. Gu and B. Jiao, "A novel particel swarm optimization algorithm for permutation flow-shop scheduling to minimize makespan", *Chaos, Solitons and Fractals* vol. 35, pp. 851-861, 2008.

[10] B. Liu, L. Wang and Y. H. Jin, "An effective hybrid PSO-based algorithm for flow shop scheduling with limited buffers", *Comput. Oper. Res.*, vol. 35, pp. 2791-2806, 2008.

[11] B. Liu, L. Wang and Y. H. Jin, "An effective PSO-based memetic algorithm for flow shop scheduling", *IEEE Trans. Syst. Man and Cybern. B*, vol. 37, pp. 18-27, 2007.

[12] K. Sun and G. Yang, "An effective hybrid optimization algorithm for the flow shop scheduling problem", *Proc. 30th IEEE Conf. Decision and Control*, New Orleans, USA, 1995, pp. 1942–1948.

[13] M. F. Tasgetiren and Y. C. Liang and M. Sevkli and G. Gencyilmaz, "A particle swarm optimization algorithm for makespan and total flowtime minimization in the permutation flowshop sequencing problem", *Eur. J. Oper. Res.*, vol. 177, pp. 1930-1947, 2007.

[14] L. Yuan and Z. D. Zhao, "A modified binary particle swarm optimization algorithm for permutation flowshop problem", *Proc. 6th Int. Conf. on Machine Learing and Cybernetics*, Hong Kong, 2007, pp. 902–907.

[15] J. Kennedy and R. Eberhart, "Particle swarm optimization", *Proceedings of IEEE International Conference on Neural Networks*, Piscataway, NJ, 1995, pp. 1942–1948.

[16] J. Kennedy, R. Eberhart and Y. Shi, *Swarm Intelligence* ,Morgan Kaufmann Publishers, San Fransisco, USA, 2001.

[17] P. Angeline, "Using selection to improve particle swarm optimization", *Proc. IEEE Congress on Evolutionary Computing*, Anchorage, 1998, pp. 84–89.

[18] M. M. Noel and T. C. Jannett, "Simulation of a new hybrid particle swarm optimization algorithm", *Proc. 36th Southeastern Symposium on System Theory*, Atlanta, USA, 1994, pp. 150–153.

[19] C. F. Juang, "A hybrid genetic algorithm and particle swarm optimization for recurrent network design", *IEEE Trans. Syst. Man and Cybern. B*, vol. 34, no.2, pp. 997-1006, 2004.

[20] R. C. Eberhart and Y. Shi, "Comparing inertia weights and constriction factors in particle swarm optimization", *Proc. IEEE Congress on Evolutionary Computing*, 2000, pp. 84–88.

[21] K. R. Baker, *Introduction to Sequencing and Scheduling*, John Wiley and Sons, New York, 1974.

[22] J. Carlier, "Ordonnancements a contraintes disjonctives", *R.A.I.R.O. Oper. Res.*, vol. 12, no. 4, pp. 333-351, 1978.

2011 IEEE International Conference on Fuzzy Systems
June 27-30, 2011, Taipei, Taiwan

Patent Valuation with a Fuzzy Binomial Model

Xiaolu Wang
Institute for Advanced Management Systems Research
Åbo Akademi University
Turku, Finland
Email: xiaolu.wang@abo.fi

***Abstract*—Patent valuation has always been a difficult task due to the considerable uncertainty involved in both the patent application procedure and the patent exploitation. This paper proposes, under the fuzzy framework, a multiperiod binomial approach for patent valuation of the latter case. We depart from the model introduced in S. Muzzioli et al. [1] by utilizing binomial tree to simulate the movement of patent monopoly benefits through time and representing the volatility of the patent monopoly benefits with fuzzy numbers, which is triggered by the fact that, in most cases, the Intellectual Property Rights (IPR) managers may not have good information on the parameters, and that the conventional probability theory is incapable of capturing this type of imprecision. Our model also reveals the values of the managerial flexibilities embedded in the patent exploitation.**

***Keywords*—Patent valuation; fuzzy sets; American call option**

I. Introduction

Patented inventions have played a very important role in human life and, in fact, pervaded every aspect of it, from telephone (patent held by Alexander Graham Bell) and first computer (patent held by Herman Hollerith), to insulin (patent held by the University of Toronto) and holography (patent held by Gábor Dénes). Having been granted the right to negate the use of the underlying inventions by others, which is also known as the underlying intellectual asset, the patent holders are obliged to disclose information on their inventions publicly for exploitation and further improvement by other researchers and inventors, which "enriches the total body of technical knowledge in the world, and therefore promotes further creativity and innovation in others" [2]. In addition to the monopolistic status, another principal incentive to file for patents is the interdependency between patent protection and research and development (R&D). On the one hand, powerful patent protection stimulates and facilitates economically efficient R&D, and the investments in R&D, on the other hand, require legal protection for its outputs. E. Eicher et al. [3] describes this interdependency between expenditures in IPR protection and research investments as follows "a lower degree of protection reduces the returns from research and hence the incentives to do R&D; similarly, a low level of R&D will reduce the return to investment in IPR protection". Therefore, it is of great interest to not only the patent applicants, but also those who manage granted patents and are to make crucial decisions about their management to know the values of both the underlying inventions and their patents (if granted) accurately and adequately. It is worth emphasizing that projects of commercializing the underlying inventions and patents protecting those inventions are two distinct entities [4], and in our study, we focus on the latter alone. Additionally, the patent valuation model to be presented is considered from the microeconomic perspective, that is to say, it is designed to evaluate individual patents, patent families and patent portfolios instead of the benefits they bring to the economy as a whole.

Patent valuation, however, is often a difficult task, primarily because both patent application process and patent exploitation are subject to various choices and decisions at a number of successive stages and thus involve a particularly high degree of flexibility. For example, patents can be licensed, sold, abandoned at any time in the post-grant phase or simply kept in force for own use by paying the annual renewal fee. Even the patent applicants may confront the decisions as to whether to file a foreign application and whether to continue with the on-going patent application at several decision points. It therefore makes perfect sense to employ real option valuation methods in hope of capturing the embedded flexibilities and thus acquiring a more accurate estimate of the value of the underlying patents. There has been much research on patent valuation that is based on real options-thinking and can be categorized into different subsets according to the methodologies that have been used. A. Pakes [5] considers the post-grant phase of a patent as *a series of call options* on the monopoly benefits of the coming year with the strike price of each option being the next renewal fee. He also claims that the IPR manager will renew the patent only if the monopoly benefits over the coming year plus the value of the option to renew the patent at the end of the year exceeds the renewal fee. H. Weeds [6] takes into consideration the possibilities of sleeping patents and studies a two-stage investment project, with research carried out and then a patent filed for the new invention in the first stage and irreversible market entry in the second, and models the two-stage problem as *real sequential compound options*. In more specific terms, exercising the option to conduct research and file a patent for any resultant invention buys the inventor a second option to commercialize the innovation. In addition, extensive literature on the management of patenting decisions has combined game theory and real option theory to study the effect of *strategic interactions* between different firms, as in R. Meng [7]. This is promoted by the fact that, in many real-world asset markets, the firms under consideration are not necessarily "monopolists or entities in a perfectly competitive market" [7], and therefore "exercise strategies cannot be determined separately, but must be formed as part of a strategic equilibrium" [8].

978-1-4244-7316-8/11/$26.00 ©2011 IEEE

Another problem which could arise when we deal with patent valuation is that the volatility of the underlying asset, which is assumed to be constant in the Discounted Cash Flow (DCF) analysis and Black-Scholes formula, is likely to vary drastically throughout both the patent application process and the life of the patent since "the fact that the patent has survived thus far makes it increasingly likely that it will be successful and profitable" [4]. This therefore provides the incentives for using fuzzy set theory to better formalize these uncertainties as "fuzzy sets are sets that allow gradation of belonging and serve as a representation of uncertain or imprecise knowledge" [9]. M. Collan et al. [10] introduced patent valuation with the fuzzy pay-off method [9], which is based on real option-thinking and specifically suitable for asset valuation involving uncertainty on the future cash-flow and estimation inaccuracy. E. Agliardi [11] also combined a real option to litigate with fuzzy valuation due to the unpredictable outcomes of trials.

Our study is an extension of the ideas of applying the conventional multiperiod binomial model to patent valuation, which is also juiced up with the work of S. Muzzioli et al. [1]. The original idea was triggered by the observation that the managerial flexibilities embedded in patents resemble the possibilities financial options grant their holders, and more specifically, that a patent asset is like an American call option with the underlying asset being the cash flow generated from the patent, which can be priced under the risk-neutral valuation paradigm by adopting numerical methods of finance such as the binomial model. In Section (II), we briefly introduce the multiperiod binomial pricing model for American (call) options and continue shortly on fuzzy sets and fuzzy numbers. Section (III) is devoted to the proposed patent valuation method. The last section concludes and suggests the possible future work.

II. Preliminaries

A. The Binomial Model for the Pricing of an American Option

An American option is a financial instrument which gives its holder the right, but not the obligation, to trade in a certain amount of underlying assets at a predetermined price at or before a specified date. A call (resp. put) option gives the right to buy (resp. sell) the underlying assets. The Cox-Ross-Rubinstein (or CRR) model presented in Cox et al. [12] is a simple discrete-time binomial model for option pricing, which allows preference-free or arbitrage pricing of every contingent claim[1], and only requires the following inputs: the strike price K, the present value of the underlying asset S_0, the number of time steps to maturity n, the risk-free interest rate r and the upward and downward jumping factors of the underlying asset price u and d, respectively. Cox et al. [12] also makes the following fundamental assumptions:

1) The asset price satisfies a multiplicative binomial process over discrete periods.
2) There are no transaction costs, margin requirements or taxes.
3) The risk-free interest rate r is constant.
4) In order to rule out arbitrage opportunities, it is assumed that $d < 1 + r < u$.
5) The model is complete.

In addition, we assume for simplicity that no dividends will be paid during the entire life cycle of the option.

First we look at the single-period binomial model, which is $n = 1$. In a complete market, the fair price of every contingent claim H is equal to the initial value of the unique replicating portfolio V_0, which can be calculated explicitly as the expected value of the discounted claim $\overline{H}$ under the risk-neutral probability measure Q defined by $(q, 1-q)$ such that $Q(S_1 = uS_0) = q$ and $Q(S_1 = dS) = 1 - q$. Therefore, for a single-period binomial model, we have

$$V_0 = \mathbb{E}_Q[\overline{H}].$$

The discounted asset price also has constant expectation under the risk-neutral probability measure Q so as to fulfill the no-arbitrage assumption, which implies[2]

$$S_0 = \mathbb{E}_Q[\overline{S}_1]$$

that is

$$1 = q\frac{u}{1+r} + (1-q)\frac{d}{1+r}$$

leading to

$$q = \frac{(1+r)-d}{u-d}, \tag{1}$$

$$1-q = \frac{u-(1+r)}{u-d}. \tag{2}$$

The upward and downward jumping factors of the underlying asset price are approximated by (see Cox et al. [12])

$$u = e^{\sigma\sqrt{\Delta t}}, \tag{3}$$

$$d = e^{-\sigma\sqrt{\Delta t}}, \tag{4}$$

where σ is the volatility of the underlying asset.

For the multiperiod binomial model, the replicating portfolio at each stage is formed exactly in the same way as in the single-period model. Therefore, without loss of generality, the values of the American (call) option at the terminal and intermediate stages can be determined as follows:

$$\begin{aligned}
V_n^i &= \left(S_n^i - K\right)^+, \\
S_n^i &= S_0 u^i d^{n-i},\ i = 0, \ldots, n, \\
V_m^j &= \max\left(S_m^j - K, \frac{1}{1+r}\left(qV_{m+1}^{j+1} + (1-q)V_{m+1}^j\right)\right), \\
S_m^j &= S_0 u^j d^{m-j},\ m = 0, \ldots, n-1,\ j = 0, \ldots, m.
\end{aligned}$$

[1] "A contingent claim represents the potential liability inherent in a derivative security". (Elliott and Kopp [13])

[2] We compute the risk-neutral probabilities based on the risk neutrality assumption which gives the same result as the replicating portfolio approach (or the arbitrage pricing theory approach), which is presented in Elliott and Kopp [13] and Shreve [14].

B. Fuzzy Sets and Fuzzy Numbers

Fuzzy sets serve as a approach of representing vague concepts expressed in natural language [15]. It provides us with a tool of describing the ambiguous notions, such as "the weather today is sunny" and "someone is tall". Mathematically, a fuzzy set A in a given universal set X can be defined as a set of ordered pairs, with the first element of each pair from X and the second element being its grade of membership standing for the degree to which the individual in the universe corresponds to the concept represented by the fuzzy set A, and with exactly one ordered pair assigned to each element of X. This implies the following membership function of A

$$\mu_A = X \to [0,1]\,,$$

where 0 and 1 represent non-membership and complete membership respectively, while the values in between represent the intermediate degrees of membership.

The γ-cut is an important concept associated with fuzzy sets, which is defined as follows:

Definition 1. *A γ-cut (or γ-level set) of a fuzzy set A of X is a non-fuzzy set denoted by $[A]^\gamma$ and defined by*

$$[A]^\gamma = \begin{cases} \{x \in X \mid A(x) \geq \gamma\}\,, & \text{if } \gamma > 0 \\ cl(suppA), & \text{if } \gamma = 0 \end{cases}$$

where $cl(suppA)$ denotes the closure of the support of A, which has the following form

$$supp(A) = \{x \in X \mid A(x) > 0\}\,.$$

Before we can bring up the definition of fuzzy numbers, the following concepts are needed first,

Definition 2. *[16] A fuzzy set A of X is called convex if $[A]^\gamma$ is a convex subset of X for all $\gamma \in [0,1]$.*

Definition 3. *[16] A fuzzy set A of a classical set X is called normal if there exists an $x \in X$ such that $A(x) = 1$. Otherwise A is subnormal.*

Essentially fuzzy numbers are nothing more than a special type of fuzzy sets which are defined on the real line $\mathbb{R}$, and their membership functions have the form

$$\mu_A = \mathbb{R} \to [0,1]\,.$$

Therefore they are generally used to "capture our intuitive conceptions of approximate numbers or intervals" [15]. For example a triangular fuzzy number (with center a) and a trapezoidal fuzzy number (with core $[a,b]$) can be seen as fuzzy quantities "x is approximately equal to a given real number a" and "x is approximately in a given interval $[a,b]$ of real numbers", respectively.

Definition 4. *[16] A fuzzy number A is a fuzzy set of the real line with a normal, (fuzzy) convex and continuous membership function of bounded support.*

Remark 1. *The terms membership function and fuzzy set and their notations can be interchangeably used since each fuzzy set is uniquely defined by its membership function [15].*

Definition 5. *A fuzzy set A is called a triangular fuzzy number with center (or peak) a, left width $\alpha > 0$ and right width $\beta > 0$ if its membership function has the following form*

$$A(x) = \begin{cases} 0, & \text{for } x < a-\alpha \text{ and } x > a+\beta \\ 1 - \frac{a-x}{\alpha}, & \text{for } a-\alpha \leq x \leq a \\ 1 - \frac{x-a}{\beta}, & \text{for } a < x \leq a+\beta \end{cases}$$

and can be denoted by $A = (\alpha, a, \beta)$. It is easy to show that

$$\begin{aligned} [A]^\gamma &= [a-(1-\gamma)\alpha, a+(1-\gamma)\beta] \\ &= [a-\alpha+\gamma\alpha, a+\beta-\gamma\beta] \end{aligned}$$

for all $\gamma \in [0,1]$, and therefore the support of A is $(a-\alpha, a+\beta)$.

Definition 6. *A fuzzy set A is called a trapezoidal fuzzy number with core (or tolerance interval) $[a,b]$, left width $\alpha > 0$ and right width $\beta > 0$ if its membership function has the following form*

$$A(x) = \begin{cases} 0, & \text{for } x < a-\alpha \text{ and } x > a+\beta \\ 1 - \frac{a-x}{\alpha}, & \text{for } a-\alpha \leq x < a \\ 1, & \text{for } a \leq x \leq b \\ 1 - \frac{x-b}{\beta}, & \text{for } b < x \leq b+\beta \end{cases}$$

and can be denoted by $A = (a, b, \alpha, \beta)$. It is easy to verify that

$$\begin{aligned} [A]^\gamma &= [a-(1-\gamma)\alpha, b+(1-\gamma)\beta] \\ &= [a-\alpha+\gamma\alpha, b+\beta-\gamma\beta] \end{aligned}$$

for all $\gamma \in [0,1]$, and therefore the support of A is $(a-\alpha, b+\beta)$.

III. The Fuzzy Binomial Model for Patent Valuation

Before proceeding to the discussion of the proposed model, it is worth emphasizing the concept of patents first. A patent can be defined as a set of exclusive rights, usually granted by national governments, to make exclusive use of a new, non-obvious invention for a predetermined (limited) period of time in return for publication of the underlying invention. Generally speaking, most patent applicants and patentees face the following four basic decision types at different stages [4]

1) Whether to file a patent application.
2) Whether to continue with the ongoing patent application at a few decision points.
3) Whether to maintain any patent granted in effect or abandon it.
4) Whether and how to exploit the patent after it is granted.

Here we only consider decision type 4, that is to say, we want to maintain the patent granted by paying renewal fees annually and look to make extra profits by licensing, besides monopoly benefits due to holding the patent.

In this study, a fuzzy binomial model is adopted to simulate the movement of patent monopoly benefits through time. As mentioned above, the opportunity of licensing for extra revenues is also taken into consideration on a regular basis,

which is usually once a year. That is, the patent would be evaluated annually and licensed to other investors if the monopoly benefits are high enough. This, however, would have an effect upon the existing competitive edge to some extent and would bring down the monopoly profits accordingly. Therefore, this flexibility takes the form of enabling the patent to be licensed in exchange for licensing fees and royalties on incurring a reduction in the monopoly profits, which is very similar to an embedded American option.

To capture the side effect on the monopoly benefits due to patent licensing, we introduce a triangular fuzzy discount factor[3] $\delta = (\alpha_\delta, a_\delta, \beta_\delta)$, which, by the conception of fuzzy numbers presented in Section (II-B), represents "the set of real numbers close to a_δ" [15]. This is to be determined according to experts' estimation and has the following form

$$\begin{aligned} \delta &= [\delta_{\min}, \delta_{\max}] \\ &= [a_\delta - \alpha_\delta, a_\delta - \beta_\delta], \end{aligned}$$

where $0 < a_\delta - \alpha_\delta < a_\delta - \beta_\delta < 1$.

A triangular fuzzy number $\sigma = (\alpha_\sigma, a_\sigma, \beta_\sigma)$ is also utilized to represent the volatility of the monopoly benefits, which, for simplicity of the notations, is defined in terms of its γ-cut by

$$\begin{aligned} \sigma &= [a_\sigma - (1-\gamma)\alpha_\sigma, a_\sigma + (1-\gamma)\beta_\sigma] \\ &= [a_\sigma - \alpha_\sigma + \gamma\alpha_\sigma, a_\sigma + \beta_\sigma - \gamma\beta_\sigma], \end{aligned} \tag{5}$$

where $\gamma \in [0,1]$. According to (3) and (4), the fuzzy[4] upward and downward jumping factors can be determined as follows:

$$\begin{aligned} u &= [u_{\min}, u_{\max}] \\ &= \left[e^{a_\sigma - \alpha_\sigma + \gamma\alpha_\sigma}, e^{a_\sigma + \beta_\sigma - \gamma\beta_\sigma}\right] \\ d &= [d_{\min}, d_{\max}] \\ &= \left[e^{-(a_\sigma + \beta_\sigma - \gamma\beta_\sigma)}, e^{-(a_\sigma - \alpha_\sigma + \gamma\alpha_\sigma)}\right] \end{aligned}$$

where $\triangle t = 1$ in our case since the evaluation is performed annually. Assumption 4. in Section (II-A) implies that

$$d_{\max} < 1 + r < u_{\min}$$

which is

$$-(a_\sigma - \alpha_\sigma) < \ln(1+r) < a_\sigma - \alpha_\sigma$$

when γ is set to be 0.

Next we adopt the approach presented in S. Muzzioli et al. [1] to determine the fuzzy risk-neutral probabilities. By using (1) and (2), we have

$$\frac{\partial q}{\partial u} = \frac{\partial\left(\frac{(1+r)-d}{u-d}\right)}{\partial u} = \frac{d-(1+r)}{(u-d)^2} < 0$$

and

$$\frac{\partial q}{\partial d} = \frac{\partial\left(\frac{(1+r)-d}{u-d}\right)}{\partial d} = \frac{(1+r)-u}{(u-d)^2} < 0,$$

which implies that the maximum (resp. minimum) of q is obtained at $u_{\min}$ and $d_{\min}$ (resp. $u_{\max}$ and $d_{\max}$). Analogously, it is easy to verify

$$\frac{\partial(1-q)}{\partial u} = \frac{\partial\left(\frac{u-(1+r)}{u-d}\right)}{\partial u} = \frac{(1+r)-d}{(u-d)^2} > 0$$

and

$$\frac{\partial(1-q)}{\partial d} = \frac{\partial\left(\frac{u-(1+r)}{u-d}\right)}{\partial d} = \frac{u-(1+r)}{(u-d)^2} > 0,$$

that is, the maximum (resp. minimum) of $1-q$ is obtained at $u_{\max}$ and $d_{\max}$ (resp. $u_{\min}$ and $d_{\min}$). Therefore, the fuzzy risk-neutral probabilities are as follows:

$$\begin{aligned} q &= [q_{\min}, q_{\max}] \\ &= \left[\frac{(1+r)-d_{\max}}{u_{\max}-d_{\max}}, \frac{(1+r)-d_{\min}}{u_{\min}-d_{\min}}\right], \\ 1-q &= [(1-q)_{\min}, (1-q)_{\max}] \\ &= \left[\frac{u_{\min}-(1+r)}{u_{\min}-d_{\min}}, \frac{u_{\max}-(1+r)}{u_{\max}-d_{\max}}\right], \end{aligned}$$

and they satisfy the following equalities

$$q_{\min} + (1-q)_{\max} = 1 \text{ and } q_{\max} + (1-q)_{\min} = 1.$$

By applying the fuzzy risk-neutral probabilities and the fuzzy upward and downward jumping factors, our model becomes[5]

$$\begin{aligned} V_n^i &= \max\left(S_n^i - R, \delta S_n^i - R + L\right), \\ S_n^i &= S_0\left[u_{\min}^i, u_{\max}^i\right] \otimes \left[d_{\min}^{n-i}, d_{\max}^{n-i}\right],\ i = 0, \ldots, n, \\ V_m^j &= \max\Bigg(\delta S_m^j - R + L, \frac{1}{1+r}\Big([q_{\min}, q_{\max}] V_{m+1}^{j+1} \oplus \\ &\qquad [(1-q)_{\min}, (1-q)_{\max}] V_{m+1}^j\Big)\Bigg), \\ S_m^j &= S_0\left[u_{\min}^j, u_{\max}^j\right] \otimes \left[d_{\min}^{m-j}, d_{\max}^{m-j}\right], \\ &\qquad m = 0, \ldots, n-1, j = 0, \ldots, m, \end{aligned}$$

[3]Triangular fuzzy numbers are adopted for simplicity.

[4]See G. J. Klir et al. [15] for the characteristics of arithmetic operations on fuzzy numbers. From this point forward, all fuzzy numbers are represented by the bounded intervals, which should not be confused with the γ-cut.

[5]We define the arithmetic operations on fuzzy number and the ordering of fuzzy numbers as follows: let $A = [a_1, a_2]$ and $B = [b_1, b_2]$ be two fuzzy numbers, we define

$$\begin{aligned} A \oplus B &= [a_1 + b_1, a_2 + b_2], \\ A \ominus B &= [a_1 - b_2, a_2 - b_1], \\ A \otimes B &= [a_1 b_1, a_2 b_2], \end{aligned}$$

and, provided that $0 \notin [b_1, b_2]$,

$$A \oslash B = [a_1/b_1, a_2/b_2];$$

let $c \in \mathbb{R}$, then we define

$$\begin{aligned} \max(A, B) &= [\max(a_1, b_1), \max(a_2, b_2)], \\ \max(A, c) &= [\max(a_1, c), \max(a_2, c)]. \end{aligned}$$

where

V = the fuzzy patent values
S_0 = the present value of the monopoly benefits from the underlying patent
R = annual patent renewal fees
L = patent licensing fees and royalties[6]
δ = the fuzzy discount rate of the monopoly profits due to patent licensing
n = time periods to patent maturity.

Note that, by adjusting γ in (5), this valuation model is capable of providing the patentees varying weighted intervals of the fair price of the patent. If $\gamma = 1$, the bounded interval collapses to one crisp number which is the "most likely" [17] patent value.

IV. Discussion and conclusions

In this paper, we extend the ideas of applying the conventional multiperiod binomial model to patent valuation by taking into consideration the uncertainty on the volatility of the patent monopoly benefits, which is formalized in our study through fuzzy set-based methodology. We started from determining the fuzzy upward and downward jumping factors according to Cox et al. [12], which leads to the fuzzy risk-neutral probabilities calculated by following the method presented in S. Muzzioli et al. [1]. Additionally, we take into consideration the side effect of patent licensing through introducing a fuzzy discount factor on the monopoly benefits. Together with the derived fuzzy risk-neutral probabilities, the patent value is determined in the similar way as in the American option pricing method.

Our model allows direct input of estimates of the volatility parameter, instead of assuming an interval of possible values for the upward and downward jumping factors respectively as in S. Muzzioli et al. [1] and [17]. However, the single option to license the underlying patent is a limitation of this model, since the option of direct commercialization, a combination of commercialization and licensing, outright sale or abandonment [4] may also exist in practical cases. For example, S.-H. Liao et al. [18] have proposed an approach to evaluate investment project under uncertainty, which has taken into account the managerial flexibility to expand or contract its scale of operation at a specific time.

In our model, we only consider the case when the underlying patent has been granted and we want to exploit it while keeping the patent in force. However, the decision type 1 and 2 mentioned in Section (III) are also of great interest to IPR managers as the patent application procedure is not just "a simple investment project with initial costs and near certain future returns" [4] but a very complex process, each stage of which involves cost, actual profits or potential future profits with great uncertainties and decision-making points of whether to continue the application or not. Therefore, patent application valuation is intuitively the natural candidate for our future work.

[6]Both patent licensing fees and royalties are assumed to be constant for simplicity.

References

[1] S. Muzzioli and H. Reynaerts, "American option pricing with imprecise risk-neutral probabilities," International Journal of Approximate Reasoning, vol. 49, 2008, pp. 140-147.

[2] (2011, Jan.) Frequently Asked Questions: What Role do Patents Play in Everyday Life? [Online]. Available: http://www.wipo.int/patentscope/en/patents_faq.html#protection

[3] T. Eicher and C. Garca-Pealosa, "Endogenous strength of intellectual property rights: Implications for economic development and growth," European Economic Review, vol. 52, 2008, pp. 237–258.

[4] R. Pitkethly, "The valuation of patents: a review of patent valuation methods with consideration of option based methods and the potential for further research," Judge Institute Working Paper WP 21/97, The Judge Institute of Management Studies, Trumpington Street, Cambridge CB2 1AG.

[5] A. Pakes, "Patents as options: some estimates of the value of holding European patent stocks," Econometrica, vol. 54, no. 4, 1986, pp. 755-784.

[6] H. Weeds, "Sleeping patents and compulsory licensing: an options analysis," Warwick economic research papers, no. 577, 1999, 34 pages.

[7] R. Meng, "A patent race in a real options setting: investment strategy, valuation, CAPM beta, and return volatility," Journal of Economic Dynamics & Control, vol. 32, 2008, pp. 3192–3217.

[8] S. R. Grenadier, "Option exercise game: an application to the equilibrium investment strategies of firms," Rev. Financ. Stud, vol. 15, 2002, pp. 691-721.

[9] M. Collan, R. Fullér and J. Mezei, "A fuzzy pay-off method for real option valuation," Journal of Applied Mathematics and Decision Sciences, 2009, Article ID 238196, 14 pages.

[10] M. Collan and M. Heikkilä, "Valuation of patents with the pay-off method," 5th International Forum on Knowledge Asset Dynamics, July 2010, Matera, Italy.

[11] E. Agliardi, "The fuzzy value of patent litigation under imprecise information," 12th International Conference on Real Options: Theory and Applications, July 2008, Rio de Janeiro, Brazil.

[12] J. Cox, S. Ross and M. Rubinstein, "Option pricing: a simplified approach," Journal of Financial Economics, vol. 7, 1979, pp. 229-263.

[13] R. Elliott and P. Kopp, Mathematics of Financial Markets, Springer Verlag, 1999.

[14] S. E. Shreve, Stochastic Calculus for Finance I: The Binomial Asset Pricing Model, Springer Verlag, 2004.

[15] G. J. Klir and B. Yuan, Fuzzy Sets and Fuzzy Logic: Theory and Applications, Prentice Hall PTR, 1995.

[16] R. Fullér, Fuzzy Reasoning and Fuzzy Optimization, Turku Centre for Computer Science, TUCS General Publication No 9, September 1998.

[17] S. Muzzioli and C. Torricelli, "A multiperiod binomial model for pricing options in a vague world," Journal of Economic Dynamics & Control, vol. 28, 2004, pp. 861 – 887.

[18] S.-H. Liao and S.-H. Ho, "Investment project valuation based on a fuzzy binomial approach," Information Sciences, vol. 180, 2010, pp. 2124–2133.

2011 IEEE International Conference on Fuzzy Systems
June 27-30, 2011, Taipei, Taiwan

Natural Topology via Fuzzy Metric

Fagner Santana
Department of Mathematics
UFRN
RN, Brazil, postal code 59072-970
Email: fagner@ccet.ufrn.br

Regivan Santiago
Department of Informatics and Applied Mathematics
UFRN
RN, Brazil, postal code 59072-970
Email: regivan@dimap.ufrn.br

***Abstract*—In this paper, we propose a natural way to define topologies by using fuzzy metrics; here the value of the distance between two points is a non-negative fuzzy number. With such topology, we also define notions like continuity, convergent sequence, Cauchy sequences and complete spaces. As an application, we provide a fixed point theorem quite similar to the classical Banach's theorem.**

Keywords: *Fuzzy metric, fixed point, fuzzy numbers, α-cuts, intervals, topology, continuity.*

I. Introduction

The first concept of *fuzzy metrics* was introduced by Kramosil and Michalek [1], which adaptated the notion of statistical metric spaces — or Menger spaces (see [2]) — to the fuzzy viewpoint. There, the distance between two points, a and b, is seen as a probabilistic distribution, and the expression $d(a,b)(t)$ denotes the assertion: "the probability of the distance from a to b is less than t". In [3], Kaleva and Seikkala introduced another concept of fuzzy metric; in this case, the distance between two points is a non-negative fuzzy number and the same expression $d(a,b)(t)$ now means: "the possibility (see [4]) of the distance between a and b is t".

There are several investigations concerning such approaches of fuzzy metric spaces, with results such as: fixed-point theorems, completions, separability, etc. (see [5], [6], [7]). In both cases, such generalizations are based on changing the usual valuation space $\langle \mathbb{R}^+, \leq \rangle$ to a suitable one. With the usual valuation, a metric on a set M is a function, satisfying some properties, which returns a quantitative information about the distance between two points. With such formalization it is possible to define a topology on M by using the concept of open ball; which is an entity with a strong geometric appeal. With this kind of topology, it is possible to abstract important concepts which reside in the world of real numbers; namely: continuity, completeness, compactness, etc.

The basic metric properties are stated in terms of the natural order, "$\leq$", and the sum on $\mathbb{R}$. This establishes a connection between the axiomatics and the structure of the valuation. Thus, in principle, to modify the valuation space in order to preserve basic properties, the new valuation space should retain both: a notion of sum and a notion of order. However, in [8], we introduced a new kind of generalization by modifying the usual valuation; $\mathbb{R}$ was replaced by an ordered (preordered) set $(G, \leq)$ with smallest element, also endowed with a new kind of relation; called: *semi-auxiliary relation* for $\leq$. The resulting valuation space was named *Informative Metric Valuation* or just **IMV** and a function $d : M \times M \rightarrow G$ satisfying suitable axioms was designated by *Informative Metrics*. Such generalization produced topologies very similar to the usual case; since the basic building blocks (open balls) where easily recovered.

Kaleva and Seikkala showed in [3] that, in a particular case, their proposed fuzzy metrics is very similar to the usual metric when an addition and an order relation are defined on the set of non-negative fuzzy numbers. In that case, the resulting fuzzy metric space becomes a *generalized metric* in the sense of [9], which is a bridge to the IMV approach. Following such bridge, we apply the ideas of [8] to define a natural topology on a fuzzy metric space. With such topology, concepts like: continuity, completeness, convergent and Cauchy sequences arise naturally. They are investigated here and an application of them: a fixed-point theorem is provided. A very important aspect of such applicaton is that its proof follows steps similar to those in the proof of classical Banach theorem (see [10]) which depend only on the topological concepts listed above. This does not happen with the most of the proofs of fixed-points theorems for fuzzy metric spaces, revealing that our approach does not only have an advantage, but that it also gives a way to obtain similar classical results and notions that are built on usual topological concepts.

mds
January 13, 2011

II. Preliminaries

In this section, we introduce the basic concepts that will be used in the whole paper, such as: fuzzy numbers, fuzzy arithmetic, partial order on the fuzzy numbers and some required properties.

A. Fuzzy Numbers: arithmetic and order

A fuzzy number is a fuzzy set $A : \mathbb{R} \longrightarrow [0,1]$ satisfying:

1) A is normal (exists $t \in \mathbb{R}$ such that $A(t) = 1$);
2) The support of A — i.e. the set $suppA = \{t \in \mathbb{R};\ A(t) > 0\}$ — is a bounded set;
3) For every $\alpha \in (0,1]$, the α-cut $A_\alpha = \{t \in \mathbb{R};\ A(t) \geq \alpha\}$ is a closed interval.

Every real number r can be seen as a fuzzy number, by the following membership function:

$$\mu_r(t) = \begin{cases} 1, \text{ if } t = r \\ 0, \text{ if } t \neq r \end{cases}.$$

978-1-4244-7316-8/11/$26.00 ©2011 IEEE

This fuzzy numbers will be denoted by $\tilde{r}$. For other examples of fuzzy numbers, like triangular and trapezoidal fuzzy numbers, see [11].

The following theorem gives the characterization of fuzzy numbers.

Theorem II.1. *Let $A : \mathbb{R} \longrightarrow [0,1]$ be a fuzzy set. Then, A is a fuzzy number iff there exists a closed interval $[a,b]$ and functions $l : (-\infty, a) \longrightarrow [0,1]$ and $r : (b, \infty) \longrightarrow [0,1]$, where l is non-decreasing, continuous from the right and there exists ω_1 such that $l(t) = 0$, for all $t < \omega_1$ and r is non-increasing, continuous from the left and there exists $\omega_2 \in \mathbb{R}$ such that $r(t) = 0$ for all $t > \omega_2$ such that:*

$$A(t) = \begin{cases} 1, \text{ if } t \in [a,b] \\ l(t), \text{ if } t < a \\ r(t), \text{ if } t > b \end{cases}.$$

Proof: See [11]. ■

A non-negative fuzzy number A is a fuzzy number such that $A(t) = 0$ for all $t < 0$. If $r > 0$, then $\tilde{r}$ is a non-negative fuzzy number. The set of all non-negative fuzzy numbers will be denoted by G.

If $A \in G$ and $\alpha \in (0,1]$, then we use the notation $A_\alpha = [\underline{a_\alpha}, \overline{a_\alpha}]$.

Since the fuzzy sets are uniquely defined by your α-cuts, we can define an arithmetic and a partial order in G from an arithmetic and a partial order on the set of closed real intervals $\mathbb{IR}$.

Let $\mathbb{IR}^+$ be the set of all intervals $[a,b]$ such that $0 \leq a \leq b$. We consider the following operations on $\mathbb{IR}^+$:

i) $[a,b] + [c,d] = [a+b, c+d]$;
ii) $[a,b] \cdot [c,d] = [ac, bd]$.

This operations are the same operations defined by Moore (see [12]) for the set $\mathbb{IR}$ of all closed intervals. We define the partial order $\leq_{km}$ (Kulisch-Miranker order, see [13]) by: $[a,b] \leq_{km} [c,d] \Leftrightarrow a \leq c$ *and* $b \leq d$. The next proposition gives some properties of $\mathbb{IR}^+$.

Proposition II.1. *Let $A, B, C, D \in \mathbb{IR}^+$, where $A = [\underline{a}, \overline{a}]$, $B = [\underline{b}, \overline{b}]$, $C = [\underline{c}, \overline{c}]$ and $D = [\underline{d}, \overline{d}]$. The following properties are hold:*

1) $[0,0] \leq_{km} A$, *for all* $A \in \mathbb{IR}^+$;
2) $A + (B + C) = (A + B) + C$ *and* $A \cdot (B \cdot C) = (A \cdot B) \cdot C$;
3) $A^n = [\underline{a}^n, \overline{a}^n]$;
4) *If* $A \leq_{km} B$ *and* $C \leq_{km} D$, *then* $A + C \leq_{km} B + D$ *and* $A \cdot C \leq_{km} B \cdot D$;
5) *If* $\overline{b} < 1$, *then* $A \cdot B <_{km} A$, *ie,* $A \cdot B \leq_{km} A$ *and* $A \cdot B \neq A$.

Proof: For items 2) and 3) see [12]. The proof of items 1), 4) and 5) are immediate. ■

From the above interval operations, we can define similar operations on G.

Definition II.1. *Let $A, B \in G$. We define:*

1) *The sum between A and B is the fuzzy number $A \oplus B \in G$ such that $(A \oplus B)_\alpha = A_\alpha + B_\alpha$, for all $\alpha \in (0,1]$;*
2) *The product between A and B is the fuzzy number $A \odot B \in G$ such that $(A \odot B)_\alpha = A_\alpha \cdot B_\alpha$, for all $\alpha \in (0,1]$;*
3) *The partial order $\preceq$ is defined by $A \preceq B \Leftrightarrow A_\alpha \leq_{km} B_\alpha$, for all $\alpha \in (0,1]$.*

Proposition II.2. *Let $A, B, C, D \in G$. The following properties are hold:*

1) $\tilde{0} \preceq A$, *for all* $A \in G$;
2) $A \oplus (B \oplus C) = (A \oplus B) \oplus C$ *and* $A \odot (B \odot C) = (A \odot B) \odot C$;
3) $(A^n)_\alpha = (A \odot ... \odot A)_\alpha = [\underline{a_\alpha}^n, \overline{a_\alpha}^n]$, *for all* $\alpha \in (0,1]$;
4) *If* $A \preceq B$ *and* $C \preceq D$, *then* $A \oplus C \preceq B \oplus D$ *and* $A \odot C \preceq B \odot D$;
5) *If* $\overline{b_\alpha} < 1$, *for all* $\alpha \in (0,1]$, *then* $A \odot B \prec A$, *ie,* $A \odot B \leq_{km} A$ *and* $A \odot B \neq A$.

Proof: It's straightforward from the proposition II.1. ■

In an usual metric space, we define the open balls $B(a,r)$ using the strict relation $<$. The strict relation $\prec$ on G — namely $A \preceq B$ iff $A \preceq B$ and $A \neq B$ — has proved inadequate for this purpose, so we need to define a relation that will make the role of the strict relation.

Definition II.2. *Let $A, B \in G$. The relation $\prec\prec$ is defined by: $A \prec\prec B$ iff there exists $r_1, r_2 > 0$ such that $\underline{b_\alpha} - \underline{a_\alpha} > r_1$ and $\overline{b_\alpha} - \overline{a_\alpha} > r_2$, for all $\alpha \in (0,1]$.*

Example II.1. *If $a, b \in \mathbb{R}^+$, with $a < b$, then $\tilde{a} \prec\prec \tilde{b}$.*

Example II.2. *A triangular fuzzy numbers is a fuzzy set with a "triangle shape". Its membership function A is defined by: $A(x) = 0$, if $x \leq a_1$, $A(x) = l(x)$, if $a_1 \leq x \leq a_2$, where $l(x)$ is the straight line connecting the points $(a_1, 0)$ and $(a_2, 1)$, $A(x) = r(x)$, if $a_2 \leq x \leq a_3$, where $r(x)$ is the straight line connecting the points $(a_2, 1)$ and $(a_3, 0)$ and $A(x) = 0$, if $x \geq a_3$. The numbers a_1, a_2 and a_3 completely determine A, so we use the notation $A = (a_1, a_2, a_3)$. If $A = (a_1, a_2, a_3)$ and $B = (b_1, b_2, b_3)$ are two triangular fuzzy numbers, then $A \prec\prec B$ if, and only if, $a_1 < b_1$, $a_2 < b_2$ and $a_3 < b_3$.*

Proposition II.3. *Let $A, B, C, D \in G$. The following properties are valid:*

1) *If* $A \prec\prec B$, *then* $A \prec B$;
2) *If* $A \preceq B \prec\prec C \preceq D$, *then* $A \prec\prec D$;
3) *If* $A \preceq C$ *and* $B \prec\prec D$, *then* $A \oplus B \prec\prec C \oplus D$.

Proof:

1) It's straighforward.
2) There exists $r_1, r_2 > 0$, such that $\underline{c_\alpha} - \underline{b_\alpha} > r_1$ and $\overline{c_\alpha} - \overline{b_\alpha} > r_2$, for all $\alpha \in (0,1]$. Since $\underline{b_\alpha} \geq \underline{a_\alpha}$, $\overline{b_\alpha} \geq \overline{a_\alpha}$, $\underline{d_\alpha} \geq \underline{c_\alpha}$ and $\overline{d_\alpha} \geq \overline{c_\alpha}$, for all $\alpha \in (0,1]$, we can conclude that $\underline{d_\alpha} - \underline{a_\alpha} > r_1$ and $\overline{d_\alpha} - \overline{a_\alpha} > r_2$, for all $\alpha \in (0,1]$, so $A \oplus B \prec\prec C \oplus D$
3) There exists $r_1, r_2 > 0$ such that $\underline{d_\alpha} - \underline{b_\alpha} > r_1$ and $\overline{d_\alpha} - \overline{b_\alpha} > r_2$. We have $\underline{c_\alpha} - \underline{a_\alpha} \geq 0$ and $\underline{c_\alpha} - \underline{a_\alpha} \geq 0$, so $\underline{d_\alpha} - \underline{b_\alpha} + \underline{c_\alpha} - \underline{a_\alpha} > r_1$ and $\overline{d_\alpha} - \overline{b_\alpha} + \overline{c_\alpha} - \overline{a_\alpha} > r_2 \Rightarrow A \oplus B \prec\prec C \oplus D$.

■

Corollary II.2. *Let $A, B, C \in G$. Then:*

1) *If $A \preceq B \prec\prec C$, then $A \prec\prec C$;*
2) *If $A \prec\prec B \preceq C$, then $A \prec\prec C$.*

Proof: It's straightforward. ∎

It also follows from the above results that the relation $\prec\prec$ is transitive.

The next results are very important to ensure that the class of open sets in the following is Hausdorff.

Theorem II.3. *If $A, B \in G$, with $\tilde{0} \prec\prec A$ and $\tilde{0} \prec\prec B$ then exists $C \in G$, with $\tilde{0} \prec\prec C$, such that $C \preceq A$ and $C \preceq B$.*

Proof: Since $\tilde{0} \prec\prec A$ and $\tilde{0} \prec\prec B$, then exists $r_1, r_2 > 0$ such that $\overline{a_\alpha} \geq \underline{a_\alpha} > r_1$ and $\overline{b_\alpha} \geq \underline{b_\alpha} > r_2$. So take $C \in G$ defined by $C = \tilde{r}$, where $r = \min\{r_1, r_2\} > 0$. So, trivially we have $\tilde{0} \prec\prec C$, $C \preceq A$ and $C \preceq B$. ∎

Theorem II.4. *If $A, B \in G$ with $A \prec\prec B$, then there exists $C \in G$, with $\tilde{0} \prec\prec C$ such that $A \oplus C \prec\prec B$.*

Proof: There exists $r_1, r_2 > 0$ such that $\underline{b_\alpha} - \underline{a_\alpha} > r_1$ and $\overline{b_\alpha} - \overline{a_\alpha} > r_2$. It sufficient to take $C \in G$ defined by $C(t) = \begin{cases} 1, \text{ if } t = r/2 \\ 0, \text{ if } t \neq r/2 \end{cases}$, where $r = \min\{r_1, r_2\}$. ∎

Theorem II.5. *If $A \in G$, with $\tilde{0} \prec\prec A$, then exists $B, C \in G$, with $\tilde{0} \prec\prec B$ and $\tilde{0} \prec\prec C$ such that $B \oplus C \prec\prec A$.*

Proof: Since $\tilde{0} \prec\prec$, there exists $r > 0$ such that $\overline{a_\alpha} \geq \underline{a_\alpha} > r$. It sufficient to take $B, C \in G$ defined by $B(t) = C(t) = \begin{cases} 1, \text{ if } t \in [r/8, r/4] \\ 0, \text{ if } t \notin [r/8, r/4] \end{cases}$. ∎

III. Fuzzy Metric

In their paper, Kaleva and Seikkala gave the following definition of fuzzy metric:

Definition III.1. *Let be M a non-empty set, a mapping $d : M \times M \longrightarrow G$ and $L, R : [0,1] \times [0,1] \longrightarrow [0,1]$ two mappings symmetric, non-decreasing on both arguments and satisfying $L(0,0) = 0$ and $R(1,1) = 1$. The quadruple (X, d, L, R) is called a fuzzy metric space and d a fuzzy metric, when:*

i) $d(x,y) = \tilde{0}$ if and only if $x = y$;
ii) $d(x,y) = d(y,x)$, for all $x, y \in M$;
iii) Given $x, y \in M$, use notation $[d(x,y)]_\alpha = [\lambda_\alpha(x,y), \rho_\alpha(x,y)]$. Thus, for all $x, y, z \in M$,

1) *$d(x,y)(s+t) \geq L(d(x,z)(s), d(y,z)(t))$, whenever $s \leq \lambda_1(x,z)$, $t \leq \lambda_1(z,y)$ and $s + t \leq \lambda_1(x,y)$;*
2) *$d(x,y)(s+t) \leq R(d(x,z)(s), d(y,z)(t))$, whenever $s \geq \lambda_1(x,z)$, $t \geq \lambda_1(z,y)$ and $s + t \geq \lambda_1(x,y)$;*

Example III.1 (Kaleva and Seikkala)**.** *Let E be the set of all fuzzy numbers. The function $d : E \times E \longrightarrow G$ defined by*

$$d(x,y) = \begin{cases} |x - y| & , \text{ if } x \neq y \\ \tilde{0} & , \text{ if } x = y \end{cases} \quad (1)$$

is a fuzzy metric where $L \equiv 0$ and $R = \max$

There are several functions L and R satisfying the conditions in Definition III.1. For example, for $L = \min$ and $R = \max$ the following result is hold:

Theorem III.1. *In a fuzzy metric space $(X, d, \min, \max)$, the condition $iii)$ of the definition III.1 is equivalent to:*

$$d(x,z) \preceq d(x,y) \oplus d(y,z).$$

Proof: See [3]. ∎

In this case, a function $d : M \times M \longrightarrow G$ is a fuzzy metric if and only if it satisfies:

i) $d(x,y) = \tilde{0}$ if and only if $x = y$;
ii) $d(x,y) = d(y,x)$, for all $x, y \in M$;
iii') $d(x,z) \preceq d(x,y) \oplus d(y,z)$.

Thus, a fuzzy metric is a generalized metric in the sense given in [9]. The condition iii'), or triangle inequality, takes a closer way than usual. In this paper, we consider only fuzzy metric in this sense and we will call them gf-metrics.

Example III.2. *If $d : M \times M \longrightarrow \mathbb{R}$ is an usual metric, then $d_f : M \times M \longrightarrow G$ defined by $d_f(x,y) = \tilde{d(x,y)}$ is a **gf-metric**.*

Example III.3. *Let $d_1, d_2, d_3, d_4 : M \times M \longrightarrow \mathbb{R}$ be usual metrics such that $d_1 \leq d_2 \leq d_3 \leq d_4$. The function $d_f : M \times M \longrightarrow G$ defined by:*

$$d_f(x,y)(t) = \begin{cases} 1/2, \text{ if } d_1(x,y) \leq t < d_2(x,y) \\ 1, \text{ if } d_2(x,y) \leq t \leq d_3(x,y) \\ 1/2, \text{ if } d_3(x,y) < t \leq d_4(x,y) \\ 0, \text{ in other cases} \end{cases}$$

is a gf-metric.

Theorem III.2. *Let $d : M \times M \longrightarrow G$ be a gf-metric. If $d(a,b) \prec\prec R$, where $\tilde{0} \prec\prec R$, then exists $\tilde{0} \prec\prec D$ such that $d(b,c) \prec\prec D \Rightarrow d(a,c) \prec\prec R$.*

Proof: Since $d(a,b) \prec\prec R$, it follows from theorem II.4 that there exists $\tilde{0} \prec\prec D$ such that $d(a,b) \oplus D \prec\prec R$. Suppose that $d(b,c) \prec\prec D$. So, follows from the proposition II.3 that $d(a,b) \oplus d(b,c) \prec\prec d(a,b) \oplus D \prec\prec R \Rightarrow d(a,b) \oplus d(b,c) \prec\prec R$. From the triangle inequality, it follows that $d(a,c) \preceq d(a,b) \oplus d(b,c) \prec\prec R \Rightarrow d(a,c) \prec\prec R$. ∎

The above theorem guarantees that all fuzzy metric is an informative metric, where the IMV is $(G, \preceq, \prec\prec, \tilde{0})$ (see [8]).

A. Topology via Fuzzy Metric

We begin this section with a definition of open ball that has the same geometric sense of open balls in usual metric spaces.

Definition III.2. *Let (M, d) be an gf-metric space. Given $a \in M$ and $R \in G$, with $\tilde{0} \prec\prec R$, the open ball of center a and radius R is the set $B(a,R) = \{b \in M; d(a,b) \prec\prec R\}$. A subset $O \subseteq M$ is an **open set**, if for every $a \in O$ exists an open ball $B(a,R)$, such that $B(a,R) \subseteq O$.*

Observation III.1. *The empty set is an open set by convention.*

Theorem III.3. *Let (M, d) be an gf-metric space. The class $\Im(M)$ of the open sets of M is a topology on M.*

Proof: It must be proved that: $\emptyset, M \in \Im(M)$, if $\{A_\lambda\}_{\lambda\in L} \subseteq \Im(M)$, then $\bigcup_{\lambda\in L} A_\lambda \in \Im(M)$, and if $A, B \in \Im(M)$, then $A \cap B \in \Im(M)$. The first two conditions are immediate. Let $A, B \in \Im(M)$. Take $a \in A \cap B$. Since A and B are open sets, there are two open balls $B(a, R_1)$ and $B(a, R_2)$ such that $B(a, R_1) \subseteq A$ and $B(a, R_2) \subseteq B$. By the definition of open ball, we have $\tilde{0} \prec\prec R_1$ and $\tilde{0} \prec\prec R_2$, so, from the theorem II.3, there is $D \in G$, with $\tilde{0} \prec\prec D$ such that $D \preceq R_1$ and $D \preceq R_2$. Thus, consider the open ball $B(a, D)$. Take $b \in B(a, D)$, which implies that $d(a, b) \prec\prec D$. Thus, follows from the proposition II.3 that $d(a, b) \prec\prec R_1 \Rightarrow b \in B(a, R_1)$ which implies that $B(a, D) \subseteq B(a, R_1)$. Similarly it is proved that $B(a, D) \subseteq B(a, R_2)$. Thus, $B(a, D) \subseteq A \cap B$, and so $A \cap B \in \Im(M)$. ∎

Proposition III.1. *Let (M, d) be an gf-metric space. Every open ball are open sets.*

Proof: Follows directly from theorem III.2. ∎

The class of all open balls in a gf-metric space (M, d) is a basis for the topology $\Im(M)$.

In [3], the authors defined a topology generated by a fuzzy metric space (M, d, L, R), it is based on the following definition of open ball:

$$B(a, \varepsilon, \alpha) = \{y \in M; \rho_\alpha(x, y) < \varepsilon\} \tag{2}$$

Note that, the definition in 2 depends only on the upperbound of α-cuts $d(x, y)_\alpha$. Thus, the topology generated does not fully incorporate the vagueness expressed by the fuzzy number $d(x, y)$. However, the definition proposed here incorporates all the information contained in $d(x, y)$, since the relation used to define the open balls depends both: on upper and lowerbounds of each α-cut.

Remark III.1. *In usual metric spaces the strong order "$<$" is used to define open balls. Those spaces has the property: "$0 < d(x, y)$, whenever $x \neq y$". In the last section we defined the notion of open balls in terms of "$\prec\prec$" relation and in what follows we define gf-spaces which share the corresponding property.*

Definition III.3 (Hausdorff gf-metric spaces)**.** *A gf-metric space which satisfies: "$\tilde{0} \prec\prec d(x, y)$, whenever $x \neq y$" is called a **Hausdorff gf-metric space**.*

Theorem III.4. *Let (M, d) be a Hausdorff gf-metric space. The resulting topology, $\Im(M)$, is a Hausdorff topology.*

Proof: Let (M, d) be a gf-metric space. Take $a, b \in M$, where $a \neq b$. Thus, we have $\tilde{0} \prec\prec d(a, b)$. From the theorem II.5 follows that there exists $B, C \in G$, with $\tilde{0} \prec\prec B$ and $\tilde{0} \prec\prec C$ such that $B \oplus C \prec\prec d(a, b)$. Define the open balls $B(a, B)$ and $B(b, C)$. Suppose there exists $c \in B(a, B) \cap B(b, C)$, which implies $d(a, c) \prec\prec B$ and $d(c, b) \prec\prec C$, so $d(a, b) \preceq d(a, c) \oplus d(b, c) \prec\prec B \oplus C \prec\prec d(a, b) \Rightarrow d(a, b) \prec\prec d(a, b)$, so $d(a, b) \prec d(a, b)$, which is a contradiction. ∎

From now on we consider just Hausdorff gf-metric spaces.

Definition III.4. *Let x_n be a sequence in a gf-metric space (M, d). We shall say that x_n **converges to** $L \in M$ if for every $\tilde{0} \prec\prec R$, there exists $n_0 \in \mathbb{N}$, such that if $n \geq n_0$, then $d(x_n, L) \prec\prec R$. In this case, we say x_n is **gf-convergent** and L is the **gf-limit of** x_n; we use the notation: "$x_n \longrightarrow L$". A sequence x_n is said to be a **gf-cauchy sequence**, if for every $\tilde{0} \prec\prec R$, there exists $n_0 \in \mathbb{N}$, such that if $m, n \geq n_0$, then $d(x_m, x_n) \prec\prec R$.*

Observation III.2. *The theorem III.4 guarantees the unicity of the limit of a convergent sequence.*

Definition III.5. *A gf-metric space is said to be complete if every gf-cauchy sequence is convergent.*

Example III.4. *In a gf-metric space, every convergent sequence is a gf-cauchy sequence.*

In fact, if $x_n \longrightarrow L$, then for every $\tilde{0} \prec\prec R$, there exists $n_1 \in \mathbb{N}$ such that $n > n_1 \Rightarrow d(x_n, L) \prec\prec R_1$, and there exists $n_2 \in \mathbb{N}$, such that $m > n_2 \Rightarrow d(x_m, L) \prec\prec R_2$, where $\tilde{0} \prec\prec R_1$, $\tilde{0} \prec\prec R_2$ and $R_1 \oplus R_2 \prec\prec R$. Define $n_0 = \max\{n_1, n_2\}$. Thus, if $n > n_0$, then $d(x_n, x_m) \preceq d(x_n, L) \oplus d(L, x_m) \prec\prec R_1 \oplus R_2 \preceq R \Rightarrow d(x_n, x_m) \prec\prec R$.

B. gf-Continuity

In this section, we present the concept of gf-continuity, which represents the idea of contunuity in the fuzzy context.

Definition III.6. *A function $f : M \longrightarrow N$ between the two gf-metric spaces (M, d_1) and (N, d_2) is called **gf-continuous at** $a \in M$, if for every $\tilde{0} \prec\prec R$ there exist $\tilde{0} \prec\prec D$ such that, if $d_1(a, b) \prec\prec D$, then $d_2(f(a), f(b)) \prec\prec R$. If f is gf-continuous for all $a \in M$, then we will simply say that f is gf-continuous.*

The next theorem shows how the gf-continuity is linked with the usual topological concept of continuity.

Theorem III.5. *A function $f : M \longrightarrow N$ is continuous with respect to the topologies $\Im(M)$ and $\Im(N)$ iff f is gf-continuous.*

Proof: The proof follows the same steps of the usual case (see [10]). ∎

If $(\mathbb{R}^n, d)$ is a gf-metric space then constant functions, the identity function, sums and products(for $n = 1$) of gf-continuous functions are all gf-continuous functions.

Theorem III.6. *Let (M, d_1) and (N, d_2) be two gf-metric spaces and consider the mapping $f : M \longrightarrow N$. If f is gf-continuous at $a \in M$ and x_n is a sequence in M such that $x_n \longrightarrow a$, then $f(x_n) \longrightarrow f(a)$.*

Proof: Given $\tilde{0} \prec\prec R$, there exists $\tilde{0} \prec\prec D$ such that $d(a, x) \prec\prec D \Rightarrow d(f(a), f(x)) \prec\prec R$. Since $x_n \longrightarrow a$, there exists $n_0 \in \mathbb{N}$ such that $n > n_0 \Rightarrow d(x_n, a) \prec\prec D$, so $d(f(x_n)f(a)) \prec\prec R$, ie, $f(x_n) \longrightarrow f(a)$. ∎

IV. Application: Fixed Point Theorem

The fixed point theorems play an important role in applications. All these theorems involves convenient definitions of

contractions. Below, we present the definition of contractions in gf-metric spaces.

Definition IV.1. *Let (M,d) be a gf-metric space and $T : M \longrightarrow M$ a mapping. We say that T is a **gf-contraction** if exists $K \in G$, with $K \prec\prec \tilde{1}$, such that $d(T(x),T(y)) \preceq K \odot d(x,y)$.*

Observation IV.1. *Note that if $K \prec\prec \tilde{1}$, then there exists $0 < r < 1$ such that $\overline{k_\alpha} < r$, for all $\alpha \in (0,1]$.*

Proposition IV.1. *Let (M,d) be a gf-metric space and $T : M \longrightarrow M$ a mapping. If T is a gf-contraction, then T is gf-continuous*

Proof: Let $a \in M$. Since T is a gf-contraction, we have $d(T(x),T(y)) \preceq d(x,y)$, for all $x,y \in M$. Thus, given $\tilde{0} \prec\prec R$, take $D = R$ and suppose that $d(a,x) \prec\prec D = R$. So, $d(T(a),T(x)) \preceq d(a,x) \prec\prec D = R \Rightarrow d(T(a),Y(x)) \prec\prec R$. Thus, T is gf-continuous at any $a \in M$ and so, T is gf-continuous. ∎

Below, we proof a fixed point theorem in gf-metric spaces which is very similar to the classical Banach's theorem.

Theorem IV.1 (Fixed Point Theorem)**.** *Let (M,d) be a complete gf-metric space and $T : M \longrightarrow M$ a contraction. Thus, T has a unique fixed point.*

Proof: Take $x_0 \in M$ and define the sequence x_n by $x_1 = T(x_0)$ and $x_{n+1} = T(x_n)$. Thus, $d(x_2,x_1) = d(T(x_1),T(x_0)) \preceq K \odot d(x_1,x_0)$, $d(x_3,x_2) = d(T(x_2),T(x_1)) \preceq K \odot d(x_2,x_1) \preceq K \odot (K \odot d(x_1,x_0)) = K^2 \odot d(x_1,x_0)$, etc.. In general, we have

$$d(x_{n+1},x_n) \preceq K^n \odot d(x_0,x_1). \tag{3}$$

Given $m,n \in \mathbb{N}$, with $m > n$, using the triangle inequality and (3) we have:

$$\begin{aligned} d(x_m,x_n) &\preceq d(x_n,x_{n+1}) \oplus d(x_{n+1},x_{n+2}) \\ &\oplus \ldots \oplus d(x_{m-1},x_m) \\ &\preceq (K^n \odot d(x_1,x_0)) \oplus (K^{n+1} \odot d(x_1,x_0)) \\ &\oplus \ldots \oplus (K^{m-1} \odot d(x_1,x_0)) \\ &= \left(K^n \oplus \ldots \oplus K^{m-1}\right) \odot d(x_1,x_0), \text{ so} \\ d(x_m,x_n) &\preceq \left(K^n \oplus \ldots \oplus K^{m-1}\right) \odot d(x_1,x_0) \end{aligned} \tag{4}$$

Consider $r > 0$ as in the observation IV.1.

If $K_\alpha = [\underline{k_\alpha}, \overline{k_\alpha}]$, for all $\alpha \in (0,1]$, then $K_\alpha^n = [\underline{k_\alpha}^n, \overline{k_\alpha}^n]$, so

$$\begin{aligned} \left(K^n \oplus \ldots \oplus K^{m-1}\right)_\alpha &= \left[\sum_{i=n}^{m-1} \underline{k_\alpha}^i, \sum_{i=n}^{m-1} \overline{k_\alpha}^i\right] \\ &\leq_{km} \left[\sum_{i=n}^{m-1} r^i, \sum_{n=1}^{m-1} r^i\right]. \end{aligned} \tag{5}$$

Since the serie $\sum r^n$ is convergent, given $\varepsilon > 0$, there exists $n_0 \in \mathbb{N}$ such that $m > n > n_0 \Rightarrow \sum_{i=n}^{m-1} \underline{k_\alpha}^i \leq \sum_{i=n}^{m-1} \overline{k_\alpha}^i \leq \sum_{i=n}^{m-1} r^i < \varepsilon$, for all $\alpha \in (0,1]$, so

$$\left[\sum_{i=n}^{m-1} \underline{k_\alpha}^i, \sum_{i=n}^{m-1} \overline{k_\alpha}^i\right] \leq_{km} [\varepsilon,\varepsilon], \text{ for all } \alpha \in (0,1]. \tag{6}$$

Since *supp* $d(x_1,x_0)$ is bounded, there exists $l > 0$ such that $0 < \lambda_\alpha(x_1,x_0) \leq \rho_\alpha(x_1,x_0) < l$, for all $\alpha \in (0,1]$, where $(d(x_1,x_0))_\alpha = [\lambda_\alpha(x_1,x_0), \rho_\alpha(x_1,x_0)]$.

Given $\tilde{0} \prec\prec R$, we know there is $d > 0$ such that $d < \underline{r_\alpha} \leq \overline{r_\alpha}$, for all $\alpha \in (0,1]$. Take $0 < \varepsilon < \frac{d}{2l}$. Thus, there exists $n_0 \in \mathbb{N}$ such that:

$$\begin{aligned} m > n > n_0 \quad &\Rightarrow \quad \left(K^n \oplus K^{n+1} \oplus \ldots \oplus K^{m-1}\right)_\alpha \\ &\leq_{km} \quad [\varepsilon,\varepsilon] \\ &\Rightarrow \quad \left(K^n \oplus K^{n+1} \oplus \ldots \oplus K^{m-1}\right)_\alpha \\ &\cdot \quad [\lambda_\alpha(x_1,x_0), \rho_\alpha(x_1,x_0)] \\ &\leq_{km} \quad [\varepsilon,\varepsilon] \cdot [\lambda_\alpha(x_1,x_0), \rho_\alpha(x_1,x_0)] \end{aligned} \tag{7}$$

Thus, we have $\left[\left(K^n \oplus \ldots \oplus K^{m-1}\right) \odot d(x_1,x_0)\right]_\alpha \leq_{km} [\varepsilon\lambda_\alpha(x_1,x_0), \varepsilon\rho_\alpha(x_1,x_0)]$, for all $\alpha \in (0,1]$, ie,

$$\left(K^n \oplus \ldots \oplus K^{m-1}\right) \odot d(x_1,x_0) \preceq [\varepsilon,\varepsilon] \odot d(x_1,x_0). \tag{8}$$

Note that $\lambda_\alpha(x_1,x_0) < l \Rightarrow \varepsilon\lambda_\alpha(x_1,x_0) < \varepsilon l < \frac{d}{2l} l = \frac{d}{2}$, so, from $\underline{r_\alpha} > d$, follows that $\underline{r_\alpha} - \frac{d}{2} > \frac{d}{2} \Rightarrow \underline{r_\alpha} - \varepsilon\lambda_\alpha(x_1,x_0) > \frac{d}{2}$. Analogously, we proof that $\overline{r_\alpha} - \varepsilon\rho_\alpha(x_1,x_0) > \frac{d}{2}$. Thus, we can conclude that $[\varepsilon\lambda_\alpha(x_1,x_0), \varepsilon\rho_\alpha(x_1,x_0)] \prec\prec R$, so, for all $m > n > n_0$, we have

$$\begin{aligned} d(x_m,x_n) &\preceq \left(K^n \oplus K^{n+1} \oplus \ldots \oplus K^{m-1}\right) \odot d(x_1,x_0) \\ &\preceq [\varepsilon,\varepsilon] \odot d(x_1,x_0) \\ &\prec\prec R. \end{aligned}$$

Thus, we conclude that x_n is a gf-Cauchy sequence. Since the gf-metric space (M,d) is complete, we have that x_n is convergent. Let $a \in M$ such that $x_n \longrightarrow a$. Since T is continuous, we have $T(x_n) \longrightarrow T(a)$, but, $T(x_n) = x_{n+1}$, so $T(x_n) \longrightarrow a$. Thus, as the limit of x_n is unique, we have $T(a) = a$, ie, a is a fixed point of T.

Now, suppose that $x,y \in M$ and $T(x) = x$, $T(y) = y$, with $x \neq y$. Follows that:

$$\begin{aligned} d(x,y) &= d(T(x),T(y)) \preceq K \odot d(x,y) \prec d(x,y) \\ &\Rightarrow d(x,y) \prec d(x,y), \text{ which is a contradiction.} \end{aligned}$$

So, the fixed point must to be unique. ∎

V. Conclusion

The fuzzy metric proposed by Kaleva and Seikkala with $L = \min$ and $R = \max$ satisfies a very natural triangle inequality. In this case we showed how to define a Hausdorff topology, which carries more information than the original one defined in [3], since it depends on $d(x,y)$, and not just on a piece of $d(x,y)$, as in the original definition. With this definition it was possible to create natural notions of fuzzy continuity and fuzzy convergent sequence, from which we proved a fixed point theorem very similar to the classical Banach's theorem. In future works, we attempted to verify other classical results

on metric spaces in the fuzzy context and, mainly, to investigate ways to reduce the triangle inequality iii) for a more natural form, where L and R are arbitrary functions satisfying the conditions of the Kaleva and Seikkala's definition. We also intend to propose a concept of fuzzy quasi-metric, following the same ideas developed in this paper. Achieving that, we have in hands a topology that can not be Hausdorff, but will have other properties of separability, like the T_1 spaces (see [10]).

REFERENCES

[1] I. Kramosil and J. Michalek, *Fuzzy Metric and Statistical Metric Spaces*, Kybernetika, vol. 11, pp. 336-344, 1975.

[2] K. Menger, *Statistical Metric*, Proc. Nat. Acad. Sci., USA, vol. 28, pp. 535-537, 1942.

[3] O. Kaleva and S. Seikala, *On Fuzzy Metric Spaces*, Fuzzy sets and Systems, 12, pp. 215-229, 1984.

[4] L. Zadeh, *Fuzzy Sets as a Basis for a Theory of Possibility*, Fuzzy Sets and Systems, vol. 100 (suplement), pp. 9-34, 1999.

[5] L. Ciri, *Solving the Banach Fixed Point Principle for Nonlinear Contractions in Probabilistic Metric Spaces*, Nonlinear Analysis: Theory, Methods & Applications, vol. 72, pp 2009-2018, 2010.

[6] B. Singh and S. Jain, *Semicompatibility and Fixed Point Theorems in Fuzzy Metric Space Using Implicit Relation*, International Journal of Mathematics and Mathematical Sciences, vol. 16, pp 2617-2629, 2005.

[7] B. Lee, S. Lee and K. Park, *The Completions of Fuzzy Metric Spaces and Fuzzy Normed Linear Spaces*, Fuzzy Sets and Systems, vol. 106, pp 469-473, 1999.

[8] F. Santana and R. Santiago, *Informative Metrics. Introducing Interval Metrics*, Interval Mathematics and Connections in Teachingand Scientific Development, edited by R. Reiser and M. Pilla, Federal University of Pelotas, University Publisher, pp 131-144, 2010.

[9] M. Khamsi, V. Kreinovich and D. Misane, *A New Method of Proving the Existence of Answer Sets for Disjunctive Logic Programs: a Metric Fixed-point Theorem for Multivalued Mappings*, Vancouver: Proc. Workshop on logic programming with Incomplete Information, pp. 58-73, 1993.

[10] J. Dugundji, *Topology*, Allyn and Bacon Inc, Boston, 1966.

[11] G. Klir and B. Yuan, *Fuzzy Sets and Fuzzy Logic: Theory and Applications*, New Jersey, Prentica Hall, 1995.

[12] R. Moore, *Interval Analysis*, Englewood Cliffs, Prentice Hall, 1966.

[13] U. Kulisch and W. Miranker, *Computer Arithmetic in Theory and Practice*, New York: Academic press, 1981.

2011 IEEE International Conference on Fuzzy Systems
June 27-30, 2011, Taipei, Taiwan

Fault Diagnosis of Turbine Using an Improved Intuitionistic Fuzzy Cross Entropy Approach

Kuo-Chen Hung
Department of Logistics Management
National Defense University
Taipei, Taiwan
Kuochen.hung@msa.hinet.net

Kuo-Ping Lin
Department of Information Management
Lunghwa University of Science and Technology, Taoyuan, Taiwan
kplin@mail.lhu.edu.tw

Chia-Chun Weng
Department of Logistics Management
National Defense University
Taipei, Taiwan
daurlgr@gmail.com

***Abstract*—The fuzzy cross entropy of intuitionistic fuzzy sets, so-called intuitionistic cross entropy, is introduced by analogy with the cross entropy of probability distributions. This paper introduces the concepts of discrimination information and cross-entropy in the intuitionistic fuzzy sets. Based on this improved entropy measure, we add information of an intuitionistic fuzzy index and reveal an intuitive and mathematical connection between the notions of entropy for intuitionistic fuzzy sets in terms of fuzziness and intuitionism. Finally, a fault diagnosis example of the turbine has been illustrated. The example demonstrates that the proposed method cannot only diagnose the main fault types of the turbine, it can also detect useful information for future trends and multi-fault analysis.**

Keywords-Intuitionistic fuzzy sets; cross-entropy; similarity measure; fault diagnosis

I. INTRODUCTION

The technique of fault diagnosis has produced the huge economic benefits by scheduling preventive maintenance and preventing extensive downtime periods caused by extensive failure. Therefore, it has become a research hotspot. However, fault occurred in a very complex mechanism, the same set of signs of failure which were observed, may be caused by the other failure reasons, in addition, the Characteristics of state failure which were extracted from the failure detection often have a characteristics of fuzziness, coupled with the uncertainty of the signs and the very failures, such as the fuzziness of the sign, the uncertainty of the knowledge of empirical diagnosis and so on, making the problems of diagnosis even more difficult. Fuzzy relative theory can be a good description and characterization of this complex concept, and use the method of computing and transform the vague sets for fault diagnosis and reasoning.

The steam turbine generator unit is a kind of important equipments in power plant with complexity in equipment structure and particularity in operating environment. Failures of steam turbine generator units can usually be specified according to the different amplitude ratio of vibration signal in several different frequency ranges [16]. Since the failure and its vibration symptom are not one-to-one corresponding, many studies have been performed on the intelligent diagnosis methods for turbine generator based on expert system (such as [22], [23], [13], [7], [24]), artificial neural network (such as [17], [6], [9], [28], [11]) fuzzy theory or their combination in recent years (such as [10], [8], [25], [26]).

In the problem at hand, little research has been devoted to the situation where the value of the amplitude ratio of vibration signal is vague and linguistic ambiguity. Actually the value of the amplitude ratio of vibration signal in real circumstance is usually inaccuracy and vague valued. The estimation of precise value of possibility becomes very difficult in many cases. So the methods mentioned above would thus obtain wrong results under the intuitionistic fuzzy circumstance for they could not get the precise value of amplitude ratio of vibration signal.

The aim of this paper is to develop a fault diagnosis method of turbine based on an improved cross entropy measures under the intuitionistic fuzzy circumstance. In order to handle the uncertain situation and insufficient vague information, a concept of intuitionistic fuzzy sets (IFSs) developed by Atanassov [1] is introduced in this paper. The fundamental characteristics of IFSs are that the values of its membership function and non-membership vague values rather than exact numbers. Therefore, it could be used to simulate any activities and process requiring human expertise and knowledge, which are inevitably imprecise values. The distance between two IFSs is also defined taking into account the intuitionistic fuzzy values. And the similarity measure is conducted based on the Euclidean distance. Then, a new method of the fault diagnosis of turbine is presented in the basis of the cross entropy measures among IFSs. The similarity degree between the detecting sample and the knowledge of system fault is evaluated in the fault diagnosis of turbine vibration by the proposed measured method among IFSs. The smaller the value of distance measure, the more the similarity between the detecting sample and a type of fault knowledge. Then, the type of vibration fault is determined according to the value of similarity measure. Examples explain the validity and reasonability in the fault diagnosis problems based on the distance measures among IFSs.

The remainder of this study is organized as follows: In Section II, the relative basic concepts including IFSs, fuzzy cross-entropy (FCE) and intuitionistic fuzzy cross-entropy (IFCE) method are described. Section III presents an improved

978-1-4244-7316-8/11/$26.00 ©2011 IEEE

IFCE approach, and illustrates an example for fault diagnosis in Section IV. Finally, a conclusion is drawn in section V.

II. Related works

A. IFSs Theroy

Fuzzy sets theory has proposed by Zadeh in 1965 [27], has shown successful applications in various fields. A fuzzy set is defined as: $\tilde{A} = \{(x, \mu_{\tilde{A}}(x)) | x \in U, \mu_{\tilde{A}}(x) \in [0, 1]\}$, where U э x is the universe of discourse and $\mu_{\tilde{A}}(x) \in [0, 1]$ is the membership function of A. For further details, the reader may refer to [27].

In this theory, the membership of an element to a fuzzy set is a single value between zero and one. But in reality, it may not always be certain that the degree of non-membership of an element to a fuzzy set is just equal to 1 minus the degree of membership, i.e. there may be some intuitionistic fuzzy index. Thus, as a generalization of fuzzy sets, the concept of IFSs was introduced by Atanassov in 1986. Bustince and Burillo [5] showed that this notion coincides with the notion of vague sets (VSs).

The IFSs is as an extension of fuzzy sets. An IFSs A in a fixed set E is an objective with the expression

$$A = \{\langle x, \mu_A(x), \nu_A(x)\rangle | x \in E\}, \tag{1}$$

where the functions $\mu_A : E \to [0,1]$ and $\nu_A : E \to [0,1]$ denote the degree of membership and the degree of non-membership of the element $x \in E$, respectively. For every $x \in E$,

$$0 \le \mu_A(x) + \nu_A(x) \le 1. \tag{2}$$

When $\mu_A(x) + \nu_A(x) = 1$, for every $x \in E$, then the IFSs will degenerate to a fuzzy set. Hence, we can consider a fuzzy set with its membership function $u_A(x)$, having the IFSs expression as

$$A = \{\langle x, \mu_A(x), 1 - \mu_A(x)\rangle | x \in E\}. \tag{3}$$

Under the condition of $v_A(x) = 1 - u_A(x)$, for every $x \in E$.

For each IFSs A in E, "intuitionistic fuzzy index" has consideration. We call the intuitionistic fuzzy index of an element $x \in E$ in A by the following expression:

$$\pi_A(x) = 1 - \mu_A(x) - \nu_A(x), \tag{4}$$

we can consider $\pi_A(x)$ as an intuitionistic fuzzy index of x to A. From Eq.(4) it is evident that

$$0 \le \pi_A(x) \le 1 \text{ for all } x \in E. \tag{5}$$

Therefore, to describe an intuitionistic fuzzy set completely; we need at least two functions from the triplet ([2][3]): (1) membership function; (2) non-membership function; (3) intuitionistic fuzzy index.

B. FCE Method

Let us recall the definition of the cross entropy by Shannon in 1948 [19]. Let $P = \{p(x_i), i = 1,2,...,n\}$ is a probability distribution on X. where $p(x_i) \in [0,1]$ and $\sum_{i=1}^{n} p(x_i) = 1$. Then the entropy of probability distribution P has been defined as follows,

$$H(P) = -\sum_{x_i \in X} p(x_i) \ln p(x_i). \tag{6}$$

Kullback [12] advance lets $Q = \{q(x_i), i = 1,2,...,n\}$ as the other probability distributions of the discrete random variable X, where $q(x_i) \in [0,1]$ and $\sum_{i=1}^{n} q(x_i) = 1$. Then the cross-entropy measure of P from Q can be obtained as

$$H(P,Q) = \sum_{x_i \in X} p(x_i) \ln \frac{p(x_i)}{q(x_i)}, \tag{7}$$

which measures the amount of discrimination of P from Q. However, Lin [15] pointed out that Eq. (7) is undefined if $q(x_i) = 0$ and $p(x_i) = 0$ for any $x_i \in X$. In order to overcome this drawback, a modified cross-entropy measure has be provided as

$$H(P,Q) = \sum_{x_i \in X} p(x_i) \ln \frac{p(x_i)}{\frac{1}{2}p(x_i) + \frac{1}{2}q(x_i)}. \tag{8}$$

Based on Eq. (8), Shang and Jiang [18] defined the FCE approach between two fuzzy numbers as the following,

$$M_{FS}(\tilde{A},\tilde{B}) = \sum (\mu_{\tilde{A}}(x_i) \ln \frac{\mu_{\tilde{A}}(x_i)}{\frac{1}{2}(\mu_{\tilde{A}}(x_i) + \mu_{\tilde{B}}(x_i))} + (1 - \mu_{\tilde{A}}(x_i)) \ln \frac{1 - \mu_{\tilde{A}}(x_i)}{1 - \frac{1}{2}(\mu_{\tilde{A}}(x_i) + \mu_{\tilde{B}}(x_i))}). \tag{9}$$

Due $M_{FS}(\tilde{A},\tilde{B})$ is not symmetric with respect to its arguments. Thus, Shang and Jiang [18] have also defined a symmetric discrimination information measure as the following,

$$D_{FS}(\tilde{A},\tilde{B}) = M_{FS}(\tilde{A},\tilde{B}) + M_{FS}(\tilde{B},\tilde{A}). \tag{10}$$

In addition, Shang and Jiang [18] have proofed that $D_{FS}(\tilde{A},\tilde{B}) \ge 0$ and $D_{FS}(\tilde{A},\tilde{B}) = 0$ if and only if $\tilde{A} = \tilde{B}$.

Based on above mentions theoretical background, an intuitionistic fuzzy cross entropy method has been described as the next subsection.

C. IFCE Method

Let us consider two sets $A, B \in U(X)$. In order to derive a cross-entropy measure for IFSs, we have to exploit the information carried by both the membership and the non-membership function. In an analogous manner to Bhandari and Pal [4], we consider the following quantity:

$$H^{\mu}(A,B;x_i) = \ln \frac{\mu_A(x_i)}{\mu_B(x_i)}, \tag{11}$$

as the amount of information for discrimination of $u_A(x_i)$ from $u_B(x_i)$. Therefore, the expected information for discrimination of A against B, based solely on the membership function, is given by

$$H^{\mu}(A,B) = \sum_{i=1}^{n} \mu_A(x_i) \ln \frac{\mu_A(x_i)}{\mu_B(x_i)}. \tag{12}$$

Similarly, considering the non-membership function we have

$$H^{v}(A,B)=\sum_{i=1}^{n}\nu_A(x_i)\ln\frac{\nu_A(x_i)}{\nu_B(x_i)}. \quad (13)$$

Hence, the information for discrimination in favor of A against B is obtained as the sum of the quantities $H^{u}(A,B)$ and $H^{v}(A,B)$, i.e.,

$$H''_{IFS}(A,B)=\sum_{i=1}^{n}\left[\mu_A(x_i)\ln\frac{\mu_A(x_i)}{\mu_B(x_i)}+\nu_A(x_i)\ln\frac{\nu_A(x_i)}{\nu_B(x_i)}\right]. \quad (14)$$

In order to overcome the drawback of Eq. (14) being undefined if $u_B(x_i)=0$ or $v_B(x_i)=0$ for any $x_i\in X$, a modified version of Eq. (14) is introduced based on Eq. (8) and is given by

$$H_{IFS}(A,B)=\sum_{i=1}^{n}\left[\mu_A(x_i)\ln\frac{\mu_A(x_i)}{\frac{1}{2}(\mu_A(x_i)+\mu_B(x_i))}+\nu_A(x_i)\ln\frac{\nu_A(x_i)}{\frac{1}{2}(\nu_A(x_i)+\nu_B(x_i))}\right] \quad (15)$$

According to Shannon's inequality, Lin [15] pointed out that one can easily prove that $H_{IFS}(A,B)\geq 0$ and $H_{IFS}(A,B)=0$ if and only if $A = B$. A similar measure for FSs, denoted by $H_{FS}(\tilde{A},\tilde{B})$, was defined by Bhandari and Pal [4]. For FSs in general $H_{FS}(\tilde{A},\tilde{B})\neq H_{FS}(\tilde{A}^c,\tilde{B}^c)$. However, for IFSs the following equality holds:

$$H_{IFS}(A,B)=H_{IFS}(A^c,B^c), \quad (16)$$

where A^c and B^c are the complementary sets of A and B, respectively. Therefore, in analogy with Eq. (9), we proceed to the following definition of the intuitionistic fuzzy cross-entropy.

Definition 1. For two sets $A,B\in U(X)$, $H_{IFS}(A,B)$ is the intuitionistic fuzzy cross-entropy between A and B. $H_{IFS}(A,B)$ can also be called discrimination information for IFSs. However, one can observe that $H_{IFS}(A,B)$ is not symmetric with respect to its arguments. Therefore, a symmetric measure is defined as follows:

Definition 2. For two sets $A,B\in U(X)$,

$$D_{IFS}(A,B)=H_{IFS}(A,B)+H_{IFS}(B,A) \quad (17)$$

is called a symmetric discrimination information measure for IFSs. It can easily be verified that $H_{IFS}(A,B)$ and $D_{IFS}(A,B)$ degenerate to their fuzzy counterparts when A and B are FSs.

III. An Improved IFCE Approach

It is easy to see that cross-entropy proposed by Vlachos and Sergiadis [21] only involve the first two parameters. That is, the membership degree and non-membership degree of IFSs. Furthermore, it dose not take the third parameter (intuitionistic fuzzy index) into account in the above derivation and discrimination measure of IFSs.

Furthermore, Szmidt and Kacprzyk [20] have showed that omitting one of the three parameters may lead to incorrect results, and thus all the three parameters should be taken into account when calculating association or distance between two IFSs.

Motivated by the idea of Szmidt and Kacprzyk [20], we improve the feasibility of original IFCE by add the third parameter (intuitionistic fuzzy index) consideration. Therefore, a modified formulation is improved to reach better discrimination measure of IFCE approach.

Following the Eqs. (12) and (13), we may keep considering the function of an intuitionistic fuzzy index for discrimination measure similarly. Thus, we can obtained

$$H^{\pi}(A,B)=\sum_{i=1}^{n}\pi_A(x_i)\ln\frac{\pi_A(x_i)}{\pi_B(x_i)}. \quad (18)$$

Next, the information for discrimination in favor of A against B can be calculated as the sum of the quantities $H^{u}(A,B)$, $H^{v}(A,B)$, and $H^{\pi}(A,B)$. The Eq. (14) can be revised as

$$H'_{IFS}(A,B)=\sum_{i=1}^{n}\left[\mu_A(x_i)\ln\frac{\mu_A(x_i)}{\mu_B(x_i)}+\nu_A(x_i)\ln\frac{\nu_A(x_i)}{\nu_B(x_i)}+\pi_A(x_i)\ln\frac{\pi_A(x_i)}{\pi_B(x_i)}\right]. \quad (19)$$

To avoid the drawback of Eq. (19) being undefined if $u_B(x_i)=0$, $v_B(x_i)=0$ or $\pi_B(x_i)=0$ for any $x_i\in X$, an improved version of Eq. (19) is introduced based on Eq. (15) and is given as

$$H_{IFS}(A,B)=\sum_{i=1}^{n}\left[\mu_A(x_i)\ln\frac{\mu_A(x_i)}{\frac{1}{2}(\mu_A(x_i)+\mu_B(x_i))}+\nu_A(x_i)\ln\frac{\nu_A(x_i)}{\frac{1}{2}(\nu_A(x_i)+\nu_B(x_i))}+\pi_A(x_i)\ln\frac{\pi_A(x_i)}{\frac{1}{2}(\pi_A(x_i)+\pi_B(x_i))}\right] \quad (20)$$

One can also prove that $H_{IFS}(A,B)\geq 0$ and $H_{IFS}(A,B)=0$ if and only if $A = B$, according to Shannon's inequality. A similar measure for IFSs, the following equality also holds:

$$H_{IFS}(A,B)=H_{IFS}(A^c,B^c), \quad (21)$$

where A^c and B^c are the complementary sets of A and B, respectively. Therefore, in analogy with Eq. (20), we can also proceed to the symmetric discrimination definition of the proposed intuitionistic fuzzy cross-entropy.

$$D_{IFS}(A,B)=H_{IFS}(A,B)+H_{IFS}(B,A) \quad (22)$$

IV. Illustrative Example for Fault Diagnosis of Turbine

In this section, the proposed measured method is applied to fault diagnosis of steam turbine generator unit under intuitionistic fuzzy circumstance. The knowledge of system fault and detecting sample adopted from Li and Wan [14] are listed. We select the amplitude ratio of vibration signal in six different frequency ranges, such as less than 0.4*f*, 0.5*f*, *f*, 2*f*, 3*f* and more than 3*f*, as the characteristic value. Therein, *f* is the fundamental frequency of the rotor. Three typical failures are selected as failures pattern. Here, P_1 is oil whip, P_2 is unbalance, P_3 is misalignment. And B_1, B_2 are the two samples to be evaluated.

Table I presents the six different frequency ranges for the failures pattern. Another, the six different frequency ranges for two samples are be evaluated in Table II. Each element of the tables, is given in the form of a pair of numbers corresponding to the membership, non-membership values, respectively, e.g., the pattern (P_1) vs. frequency (< 0.4f) is described by (μ, ν) = (0.06, 0.84).

TABLE I. THE KNOWLEDGE OF SYSTEM FAULT PATTERN

	< 0.4f	0.5f	f	2f	3f	>3f
P_1	(0.06, 0.84)	(0.84, 0.02)	(0.20, 0.75)	(0.02, 0.89)	(0.20, 0.75)	(0.01, 0.92)
P_2	(0.01, 0.93)	(0.02,0. 90)	(0.90, 0.01)	(0.08, 0.85)	(0.01, 0.89)	(0.02, 0.93)
P_3	(0.01, 0.94)	(0.01, 0.94)	(0.40, 0.42)	(0.40, 0.44)	(0.28, 0.56)	(0.10, 0.61)

TABLE II. THE CHARACTERISTIC FOR THE SAMPLES CONSIDERED

	< 0.4f	0.5f	f	2f	3f	>3f
B_1	(0.01, 0.96)	(0.00, 0.97)	(0.37, 0.60)	(0.46, 0.51)	(0.31, 0.66)	(0.21, 0.75)
B_2	(0.00, 0.98)	(0.05, 0.92)	(0.69, 0.27)	(0.04, 0.93)	(0.03, 0.94)	(0.00, 0.97)

In order to find a proper diagnosis, we calculate for each sample, B_i, where $i \in \{1,2\}$, the symmetric discrimination information measure for IFSs $D_{IFS}(P_j, B_i)$ between sample characteristics and the set of knowledge for system fault pattern that are characteristics for each fault diagnosis P_j, with $j \in \{1,2,3\}$. Based on Eq. (22), we assign the lowest symmetric discrimination information measure to the ith sample the diagnosis. Therefore, we assign to the ith sample the diagnosis whose characteristics have the lowest symmetric discrimination information measure from sample's characteristics. The fault diagnosed results for the considered samples are given in Table III.

According to Table III, we know that the degree of distance between failure pattern P_j , j = 1, 2, 3, and sample B_1 has been ranked and we have $D_{IFS}(P_3, B_1) \succ D_{IFS}(P_2, B_1) \succ D_{IFS}(P_1, B_1)$. It is clear that the degree of distance between P_3 and B_1 is the smallest one, the sample B_1 belongs to fault P_3 and the most possible type of vibration fault is misalignment. Also we have $D_{IFS}(P_2, B_2) \succ D_{IFS}(P_3, B_2) \succ D_{IFS}(P_1, B_2)$. from Table III and the degree of distance between P_2 and B_2 is the smallest one, the sample B_2 belongs to fault P_2 and the most possible type of vibration fault is unbalance.

TABLE III. THE DIAGNOSED RESULTS BY THE IMPROVED IFCE APPROACH

	Information measure		
	$D_{IFS}(P_1, B_1)$	$D_{IFS}(P_2, B_1)$	$D_{IFS}(P_3, B_1)$
Sample 1	2.5233	1.5131	0.4754
Rank	**3**	**2**	**1**
	$D_{IFS}(P_1, B_2)$	$D_{IFS}(P_2, B_2)$	$D_{IFS}(P_3, B_2)$
Sample 2	2.1259	0.3906	1.2854
Rank	**3**	**1**	**2**

V. CONCLUSIONS

In this paper, taking into account the intuitionistic fuzzy sets, an improved cross entropy measure of IFSs on the basis of the Euclidean distance was defined. And the proposed method has been applied to the fault diagnosis of turbine among IFSs in this paper. This method can overcome the situation that the value of the amplitude ratio of vibration signal is uncertain and thus has promising future in the engineering application. Furthermore, ranking of the similarity degree can not only reveal the most possible type of fault occurred but also point out the sequence of fault diagnosis. Finally, an illustrative example has been provided to illustrate the validity and reasonability of the developed approach.

ACKNOWLEDGMENTS

This research is partially supported by the National Science Council of the Republic of China, Taiwan with Grant no. NSC 99-2410-H-606-005.

REFERENCES

[1] K. T. Atanassov, "Intuitionistic fuzzy sets," *Fuzzy Sets and Systems*, vol. 20, pp. 87–96, 1986.

[2] K. T. Atanassov, "More on intuitionistic fuzzy sets," *Fuzzy Sets and Systems*, vol. 33, pp. 37–46, 1989.

[3] K. T. Atanassov, *Intuitionistic Fuzzy Sets: Theory and Applications*, Physica-Verlag, Heidelberg, 1999.

[4] D. Bhandari and N. R. Pal, "Some new information measures for fuzzy sets," *Information Sciences*, vol. 67, pp. 209–228, 1993.

[5] P. Burillo and H. Bustince, "Entropy on intuitionistic fuzzy sets and on interval-valued fuzzy sets," *Fuzzy Sets and Systems*, vol. 78, pp. 305–316, 1996.

[6] Y. B. Chen, X. Li, and E. Orady, "Integrated diagnosis using information-gainweighted radial basis function neural networks," *Computers Industrial Engineering*, vol. 30, no. 2, pp. 243–255, 1996.

[7] M. Demetgul, I. N. Tansel, and S. Taskin, "Fault diagnosis of pneumatic systems with artificial neural network algorithms," *Expert Systems with Applications*, vol. 36, no. 7, pp. 10512–10519, 2009.

[8] Z. Ge, Y. Niu, and R. Li, "Study on selflearning vibration fault diagnosis system of turbo generator unit", *Proceedings of the CSEE*, vol. 20, no. 5, pp. 76–79, 2000.

[9] S. Hayashi, T. Asakura, and S. Zhang, "Study of machine fault diagnosis using neural networks," *Proceedings Neural Networks (IJCNN'02)*, vol. 1, pp. 956–961, 2002.

[10] M. Jia and G. Wang, "Multi-fault diagnosis with an improve neural networks with ellipsoidal activation functions," *Proceedings of the CSEE*, vol. 30, no. 2, pp. 243–255, 1999.

[11] S. Khomfoi and L. M. Tolbert, "Fault diagnostic system for a multilevel inverter using a neural network," *IEEE Transactions on Power Electronics*, vol. 22, no. 3, pp. 1062–1069, 2007.

[12] S. Kullback, *Information Theory and Statistics*, Dover Publications, New York, 1968.

[13] D. Leung and J. Romagnoli, "Dynamic probabilistic modelbased expert system for fault diagnosis," *Computers and Chemical Engineering*, vol. 24, no. 11, pp. 2473–2492, 2000.

[14] H. Li and S. Wan, "Improved BP algorithm in vibration failure diagnosis of steam turbine generator set," *Journal of Chongqing University(Natural Science Edition)*, vol. 22, no. 5, pp. 47–52, 1999.

[15] J. Lin, "Divergence measures based on the Shannon entropy," *IEEE Transactions on Information Theory*, vol. 37, pp. 145–151, 1991.

[16] J. S. Mitcheel, *Machinery Analysis and Monitoring*, Pennwell Publishing Company, United States, 1981.

[17] R. Rengaswamy and V. Venkatasubramanian, "A syntactic pattern-recognition approach for process monitoring and fault diagnosis,"

Engineering Applications of Artificial Intelligence, vol. 8, no. 1, pp. 35–51, 1995.

[18] X. G. Shang and W. S. Jiang, "A note on fuzzy information measures," *Pattern Recognition Letters*, vol. 18, pp. 425–432, 1997.

[19] C. E. Shannon, "A mathematical theory of communication," *Bell System Technical Journal*, vol. 27, pp. 379–423, 1948.

[20] E. Szmidt and J. Kacprzyk, "On distances between intuitionistic fuzzy sets," *Fuzzy Sets and Systems*, vol. 114, pp. 505–518, 2000.

[21] I. K. Vlachos and G. D. Sergiadis, "Intuitionistic fuzzy information-applications to pattern recognition," *Pattern Recognition Letters*, vol. 28, pp. 197–206, 2007.

[22] X. Wang and S. Yang, "A parallel distributed knowledge-based system for turbine generator fault diagnosis," *Artificial Intelligence in Engineering*, vol. 4, no. 4, pp. 335–341, 1996.

[23] M. Wo, W. Gui, D. Shen, and Y. Wang, "Export fault diagnosis using role models with certainty factors for the leaching process," *In Proceedings of the Third World Congress on Intelligent Control and Automation*, vol. 1, pp. 238–241, 2000.

[24] J. D. Wu and C. H. Liu, "An expert system for fault diagnosis in internal combustion engines using wavelet packet transform and neural network," *Expert Systems with Applications*, vol. 36, no. 3, pp. 4278–4286, 2009.

[25] J. Ye, "Research on fault diagnosis of turbine based on similarity measures between vague sets," *Proceedings of the CSEE*, vol. 26, no. 1, pp. 16–20, 2006.

[26] J. Ye, "Cosine similarity measures for intuitionistic fuzzy sets and their applications," *Mathematical and Computer Modelling*, vol. 53, no. 1-2, pp. 91–97, 2011.

[27] L. A. Zadeh, "Fuzzy sets," *Information and Control*, vol. 8, pp. 338–353, 1965.

[28] S. Zhang, T. Asakura, X. Xu, and B. Xu, "Fault diagnosis system for rotary machines based on fuzzy neural networks," *IEEE/ASME International Conference on Advanced Intelligent Mechatronics (AIM)*, pp. 199–204, 2003.

2011 IEEE International Conference on Fuzzy Systems
June 27-30, 2011, Taipei, Taiwan

Fuzzy Delta Separation Axioms

Seok Jong Lee
Department of Mathematics
Chungbuk National University
Cheongju 361-763 Korea
Email: sjl@cbnu.ac.kr

Sang Min Yun
Department of Mathematics
Chungbuk National University
Cheongju 361-763 Korea
Email: javesm@freechal.com

***Abstract*—We introduce a new type of separation axioms, which is called fuzzy δ-separation axioms by using the concept of fuzzy δ-open sets. Also we investigate the relation between the separation property and the subspaces. We show that fuzzy δ-separation axioms are hereditary in fuzzy regular open subspaces.**

***Index Terms*—fuzzy logic, fuzzy topology, separation axiom**

I. Introduction and Preliminaries

The usual notion of a set was generalized with the introduction of fuzzy sets by Zadeh in the classical paper [1]. The concept of fuzzy topology was first defined by Chang[2] and later redefined in a somewhat different way by Lowen[3] and Hutton and Reilly[4] and others. Several authors have expansively developed the theory of fuzzy sets and its applications. Closure and interior are alternative approaches to open sets in topology. So, many researchers have studied for these notions. The notions of fuzzy δ-closure and fuzzy θ-closure of a fuzzy set in a fuzzy topological space were introduced by Ganguly and Saha[5] and Mukherjee and Sinha[6], respectively. Furthermore, the notion of strong δ-continuity was investigated in [7] and the concept of δ-continuity on function spaces was studied in [8]. The notion of θ-closure and θ-interior also expanded in more generalized spaces, intuitionistic fuzzy topological spaces [9]. In [10] we also have introduced fuzzy δ-topology and fuzzy δ-compactness, and studied their properties.

In order to prove many important theorems of topology we need the Hausdorff condition, because Hausdorff condition implies the uniqueness of limit. Moreover most of the important spaces in mathematics are Hausdorff spaces. For this reason, many different definitions are introduced and studied as in [11], [12], [13], [14], [15], [16], [17], [18]. The aim of this paper is to introduce separation axioms in a fuzzy δ-topological space, which is both harmonious in itself and compatible with fuzzy δ-compactness. In this manner, we will define a new type of separation axioms, which is called fuzzy δ-separation axioms by using the concept of fuzzy δ-open sets introduced in [10]. We will investigate the relation between the separation property and the subspaces. We will show that fuzzy δ-separation axioms are hereditary in fuzzy regular open subspaces. It is interesting that there are some deviations in the behavior of these axioms as compared to those in the general topology.

Throughout this paper by $(X, \mathcal{T})$ or simply by X, we mean a fuzzy topological space (briefly fts) due to Chang [2]. A fuzzy point in X with support $x \in X$ and value $\alpha (0 < \alpha \leq 1)$ is denoted by x_α. When no confusion will arise, we omit the value α and write the fuzzy point x_α simply as x. For a fuzzy set A in X, a fuzzy point $x_\alpha \in A$ iff $\alpha \leq A(x)$. A fuzzy point x_α is said to be quasi-coincident (q-coincident, for short) with A, denoted by $x_\alpha \; q \; A$, iff $\alpha > A^c(x)$, or $\alpha + A(x) > 1$, where A^c denotes the complement of A, defined by $A^c = 1 - A$. A fuzzy set A in a fts X is said to be a q-neighbourhood (q-nbd, for short) of a fuzzy point x_α iff there exists a fuzzy open set B such that $x_\alpha \; q \; B$ and $B \leq A$. For two fuzzy sets A and B, $A \leq B$ iff $A \tilde{q} B^c$. A fuzzy point $x_\alpha \in \mathrm{cl}(A)$ iff each q-nbd of x_α is q-coincident with A (See [19]). A fuzzy set A in a fts X is called a fuzzy regular open set iff A = int(cl(A)), and the complement of a fuzzy regular open set is called a fuzzy regular closed set (See [20]).

Definition 1.1: ([5]) A fuzzy point x_α is said to be a fuzzy δ-cluster point of a fuzzy set A iff every fuzzy regular open q-nbd U of x_α is q-coincident with A. The set of all fuzzy δ-cluster points of A is called the fuzzy δ-closure of A, and denoted by $\mathrm{cl}_\delta(A)$.

Remark 1.2: ([10]) For any fuzzy set A in a fts $(X, \mathcal{T})$, the δ-closure of A is represented as follows;

$$\mathrm{cl}_\delta(A) = \bigwedge \{\mathrm{cl}(U) \mid A \leq \mathrm{cl}(U), U \in \mathcal{T}\}.$$

Definition 1.3: ([6]) A fuzzy set A is said to be a fuzzy δ-nbd of a fuzzy point x_α iff there exists a fuzzy regular open q-nbd V of x_α such that $V \leq A$.

Definition 1.4: ([5]) A fuzzy set A is said to be fuzzy δ-closed iff $A = \mathrm{cl}_\delta(A)$, and the complement of a fuzzy δ-closed set is called a fuzzy δ-open set.

Since δ-open set is the complement of an δ-closed set, G is δ-open iff $G = \mathrm{int}_\delta(G)$. And we know that $1 - \mathrm{int}_\delta(1 - A) = \mathrm{cl}_\delta(A)$. A fuzzy set A is fuzzy δ-open in a fts X if and only if for each fuzzy point x_α with $x_\alpha q A$, A is a fuzzy δ-nbd of x_α ([21]).

It is easy to show that $\mathrm{cl}(A) \leq \mathrm{cl}_\delta(A) \leq \mathrm{cl}_\theta(A)$ for any fuzzy set A in a fts X. However, for a fuzzy open set A in a fts $(X, \mathcal{T})$, we have $\mathrm{cl}(A) = \mathrm{cl}_\delta(A)$ (See [6]). Moreover, it is clear that any regular open set is δ-open, and any δ-open set is open.

978-1-4244-7316-8/11/$26.00 ©2011 IEEE

For any fuzzy set A in a fts $(X, \mathcal{T})$, $\mathrm{cl}_\delta(A)$ is a fuzzy δ-closed set. That is, $\mathrm{cl}_\delta(\mathrm{cl}_\delta(A)) = \mathrm{cl}_\delta(A)$ (See [10]).

Definition 1.5: ([5]) A function $f : X \to Y$ is said to be *fuzzy δ-continuous (f.δ.c., for short)* if and only if for each fuzzy point x_α in X and for any regular open q-nbd V of $f(x_\alpha)$ in Y, there exists a regular open q-nbd U of x_α such that $f(U) \leq V$.

Remark 1.6: ([10]) $f : X \to Y$ is fuzzy δ-continuous if and only if for each fuzzy δ-open set U of Y, $f^{-1}(U)$ is fuzzy δ-open in X. Therefore the composition of two fuzzy δ-continuous mappings is also fuzzy δ-continuous.

Definition 1.7: Let $f : (X, \mathcal{T}) \to (Y, \mathcal{H})$ be a fuzzy mapping.
(1) f is *fuzzy δ-open* if for each fuzzy δ-open set A in X, $f(A)$ is a fuzzy δ-open in Y.
(2) f is *fuzzy δ-closed* if for each fuzzy δ-closed set B in X, $f(B)$ is fuzzy δ-closed in Y.

Theorem 1.8: ([10]) If $f : X \to Y$ is fuzzy δ-continuous, then the following are equivalent.
(a) $f(\mathrm{cl}_\delta(A)) \leq \mathrm{cl}_\delta(f(A))$.
(b) $\mathrm{cl}_\delta(f^{-1}(A)) \leq f^{-1}(\mathrm{cl}_\delta(A))$.
(c) For each fuzzy δ-closed set A in Y, $f^{-1}(A)$ is fuzzy δ-closed in X.
(d) For each fuzzy δ-open set A in Y, $f^{-1}(A)$ is fuzzy δ-open in X.

In 1993, M. Macho Stadler and M.Á. De Prada Vicente[22] have introduced a new concept of subspaces in fuzzy topological spaces. In Section 4 we will define the concept of fuzzy δ-separation axioms in this subspace.

Definition 1.9: ([22]) Let $(X, \mathcal{T})$ be a fts and $\mu \in I^X$. Let $X^\mu = \{V \wedge \mu \mid V \in I^X\}$. The family $\mathcal{T}^\mu = \{V \wedge \mu \mid V \in \mathcal{T}\}$ is called the fuzzy μ-topology induced by $\mathcal{T}$ over μ. The ordered pair $(\mu, \mathcal{T}^\mu)$ is called the subspace. The elements of $\mathcal{T}^\mu$ are called fuzzy open sets in the subspace μ. $V \in X^\mu$ is called fuzzy closed in μ if $\mu - V \in \mathcal{T}^\mu$.

Definition 1.10: Let x_r be a fuzzy point in μ, i.e. $x_r \in \mu$. We say that $N \in X^\mu$ is a fuzzy neighborhood of x_r in the subspace μ if there is a $U \in \mathcal{T}^\mu$ such that $x_r \in U \leq N$.

Remark 1.11: In [22] "$x_r \in U$" means that $r < U(x)$. But in this paper it means that $r \leq U(x)$. And if $\mu = \chi_A$ for any crisp fuzzy subset $A \subseteq X$, then $\mathcal{T}^\mu$ is a subspace in the sense of general topology.

Theorem 1.12: ([22]) Let $U \in X^\mu$. Then $U \in \mathcal{T}^\mu$ iff for each $x_r \in U$, U is a fuzzy neighborhood of x_r in μ.

Definition 1.13: ([22]) Let $V \in X^\mu$. We define the interior of V in the subspace μ as the largest fuzzy open set in μ contained in V, that is

$$\mathrm{int}^\mu(V) = \sup_{U \in \mathcal{T}^\mu} \{U \mid U \leq V\}.$$

Similarly we define the closure of V in μ as the smallest closed set in μ contains V, that is

$$\mathrm{cl}^\mu(V) = \inf_{U \in \mathcal{T}^\mu} \{\mu - U \mid V \leq \mu - U\}.$$

Definition 1.14: ([23]) Let $A \in X^\mu$ and $x_r \in X$. x_r is said to be q-coincident with A in the subspace μ if $r + A(x) > \mu(x)$. And $x_r q A[\mu]$ represents it.

Definition 1.15: ([23]) Let $x_r \in \mu$. We say that $N \in X^\mu$ is a fuzzy q-nbd of x_r in μ if there is a $U \in \mathcal{T}^\mu$ such that $x_r q U[\mu]$ and $U \leq N$.

Theorem 1.16: ([23]) Let $U \in X^\mu$. Then $U \in \mathcal{T}^\mu$ iff for each $x_r q U[\mu]$, U is a q-neighborhood of x_r in μ.

Lemma 1.17: ([22]) Let $(X, \mathcal{T})$ be a fuzzy topological space and $(\mu, \mathcal{T}^\mu)$ a fuzzy subspace.
(1) If $A \in X^\mu$, then $\mathrm{int}(A) \leq \mathrm{int}^\mu(A)$.
(2) $\mathrm{int}(A) = \mathrm{int}^\mu(A) \wedge \mathrm{int}(\mu)$ for any fuzzy subset $A \in X^\mu$.
(3) If $\mu \in \mathcal{T}$ and $A \in X^\mu$, $\mathrm{int}(A) = \mathrm{int}^\mu(A)$.

II. FUZZY δ-SEPARATION AXIOMS

In this section, we construct new separation axioms, by using the concept of fuzzy δ-open sets. As for the fuzzy disjointness, we know that only the implication $\mu_1 \wedge \mu_2 = 0 \Rightarrow \mu_1 \leq \mu_2^c$ holds, but the reverse implication does not hold. With this principle, we now define a new fuzzy δ-separation axioms.

Definition 2.1: A fts X is called fuzzy δ-T_0 if for any pair of fuzzy points p and q with different supports in X, there is a fuzzy δ-open set U with $p \leq U \leq q^c$ or $q \leq U \leq p^c$.

This separation axiom is different from the fuzzy T_0 axiom as in the following example.

Example 2.2: Let $X = [0, 1]$ and for any $\alpha \in (0, 1)$

$$U_\alpha(x) = \begin{cases} 1 & \text{if } 0 \leq x \leq \alpha \\ 0 & \text{if } \alpha < x \leq 1. \end{cases}$$

Let $\mathcal{T} = \{\bar{0}, \bar{1}\} \cup \{U_\alpha \mid \alpha \in (0, 1)\}$. Then clearly $\mathcal{T}$ is a fuzzy topology on X and the set of all fuzzy δ-open sets in $(X, \mathcal{T})$ is $\{\bar{0}, \bar{1}\}$. Therefore for any two distinct fuzzy points of $(X, \mathcal{T})$ there is a fuzzy open subset of X which contains one but not the other. Hence $(X, \mathcal{T})$ is fuzzy T_0 but not fuzzy δ-T_0.

Theorem 2.3: Let $f : X \to Y$ be injective and fuzzy δ-continuous. If Y is fuzzy δ-T_0, then so is X.

Proof: Take any two points p and q with different supports in X. Since f is injective, $f(p)$ and $f(q)$ are two fuzzy points with different supports in Y. Since Y is fuzzy δ-T_0, there is a fuzzy δ-open set U with $f(p) \leq U \leq f(q)^c$ or $f(q) \leq U \leq f(p)^c$. Therefore $p \leq f^{-1}(U) \leq q^c$ or $q \leq f^{-1}(U) \leq p^c$. And since f is fuzzy δ-continuous, $f^{-1}(U)$ is fuzzy δ-open. Hence X is fuzzy δ-T_0. □

Definition 2.4: A fts X is called fuzzy δ-T_1 if for any pair of fuzzy points p and q with different supports in X, there are two fuzzy δ-open sets U_1, U_2 with $p \leq U_1 \leq q^c$ and $q \leq U_2 \leq p^c$.

Clearly every fuzzy δ-T_1 space is fuzzy δ-T_0.

Example 2.5: Let $X = \{a, b\}$ and $\mathcal{T} = \{b_s \mid s \in [0, 1]\} \cup \{\bar{1}, \bar{0}\}$, where b_s is the fuzzy point with value s at the support b. Then clearly $\mathcal{T}$ is a fuzzy topology and all elements in $\mathcal{T}$ are fuzzy regular open, so they are fuzzy δ-open. Take any two fuzzy points a_r and b_s where r and s are nonzero. Then there is a fuzzy δ-open set b_s such that $b_s \leq b_s \leq a_r^c$, and $\bar{1}$ is an only fuzzy δ-open set with $a_r \leq \bar{1}$. Clearly, for any s, $\bar{1} \not\leq b_s^c$. Hence $(X, \mathcal{T})$ is fuzzy δ-T_0, but it is not fuzzy δ-T_1.

Theorem 2.6: A fts X be fuzzy δ-T_1 iff any crisp fuzzy point in X is fuzzy δ-closed.

Proof: Let X be fuzzy δ-T_1. Take any crisp fuzzy point p in X. We will show that p^c is fuzzy δ-open. We can take a fuzzy point $q \in p^c$ with different support from p. Since X is fuzzy δ-T_1, there is a fuzzy δ-open set U with $q \leq U \leq p^c$. Thus $p^c = \bigcup_{q \in p^c} \{U \mid q \leq U \leq p^c, U \text{ is fuzzy } \delta\text{-open in } X\}$. Since $\bigcup_{q \in p^c} \{U \mid q \leq U \leq p^c, U \text{ is fuzzy } \delta\text{-open in } X\}$ is fuzzy δ-open, p^c is fuzzy δ-open. Hence p is fuzzy δ-closed. □

Corollary 2.7: Let X be a fuzzy topological space. X is fuzzy δ-T_1 if and only if $x_\alpha = \bigcap\{\text{cl}_\delta(U) \mid x_\alpha \leq \text{cl}_\delta(U)\}$.

Theorem 2.8: Let $f : X \to Y$ be injective and fuzzy δ-continuous. If Y is fuzzy δ-T_1, then so is X.

Proof: Take any two fuzzy points p and q with different supports in X. Since f is injective, $f(p)$ and $f(q)$ are two fuzzy points with different supports in Y. Since Y is fuzzy δ-T_1, there are two fuzzy δ-open sets U_1, U_2 with $f(p) \leq U_1 \leq f(q)^c$ and $f(q) \leq U_2 \leq f(p)^c$. Therefore $f^{-1}(U_1)$ and $f^{-1}(U_2)$ are fuzzy δ-open sets in X with $p \leq f^{-1}(U_1) \leq q^c$ and $q \leq f^{-1}(U_2) \leq p^c$. Hence X is fuzzy δ-T_1. □

Definition 2.9: A fts X is called fuzzy δ-Hausdorff, or fuzzy δ-T_2, if for any pair of fuzzy points p and q with different supports in X, there are fuzzy δ-open sets U_1 and U_2 with $p \leq U_1 \leq q^c$, $q \leq U_2 \leq p^c$ and $U_1 \leq U_2^c$.

Obviously every fuzzy δ-T_2 space is fuzzy δ-T_1.

Theorem 2.10: Let $(X, \mathcal{T})$ be a fuzzy δ-T_1 space. If the complement of each fuzzy δ-open set is also fuzzy δ-open, then $(X, \mathcal{T})$ is fuzzy δ-T_2.

Proof: Take any two fuzzy points p and q in X with different supports. Since X is fuzzy δ-T_1, there is a fuzzy δ-open set U such that $p \leq U \leq q^c$ or $q \leq U \leq p^c$. We may assume that $p \leq U \leq q^c$. Then we have that $q \leq U^c \leq p^c$. By the assumption, U^c is fuzzy δ-open. Hence $(X, \mathcal{T})$ is fuzzy δ-T_2. □

Theorem 2.11: If for any $x \in X$ the crisp fuzzy point x_1 is fuzzy δ-open in $(X, \mathcal{T})$, then $(X, \mathcal{T})$ is fuzzy δ-T_2.

Proof: Take any two fuzzy points p and q with different supports. Then $p \leq p_1 \leq q^c$ and $q \leq q_1 \leq p^c$. Clearly $p_1 \leq q_1^c$, and by the assumption p_1 and q_1 are fuzzy δ-open. Hence $(X, \mathcal{T})$ is fuzzy δ-T_2. □

Theorem 2.12: Let $f : X \to Y$ be injective and fuzzy δ-continuous. If Y is fuzzy δ-T_2, then so is X.

Proof: Take any two points p and q with different supports in X. Since f is injective, $f(p)$ and $f(q)$ are two fuzzy points with different supports in Y. Since Y is fuzzy δ-T_2, there are two fuzzy δ-open sets U_1, U_2 with $f(p) \leq U_1 \leq f(q)^c$, $f(q) \leq U_2 \leq f(p)^c$ and $U_1 \leq U_2^c$. Therefore $f^{-1}(U_1)$ and $f^{-1}(U_2)$ are fuzzy δ-open sets in X with $p \leq f^{-1}(U_1) \leq q^c$ and $q \leq f^{-1}(U_2) \leq p^c$. Furthermore $f^{-1}(U_1) \leq (f^{-1}(U_2))^c$. Hence X is fuzzy δ-T_2. □

Definition 2.13: A fts X is called fuzzy δ-regular if for any fuzzy point p in X and any fuzzy δ-closed set K with $p \leq K^c$, there are fuzzy δ-open sets U_1 and U_2 with $p \leq U_1$, $K \leq U_2$ and $U_1 \leq U_2^c$. A fts X is called fuzzy δ-T_3 if it is fuzzy δ-regular and fuzzy δ-T_1.

We can easily prove that every fuzzy δ-T_3 space is fuzzy δ-T_2.

We have known that for any fuzzy closed set K, $\text{int}(K)$ is fuzzy regular open. Thus it is also fuzzy δ-open. Therefore the following theorem is hold.

Theorem 2.14: For a fts $(X, \mathcal{T})$, the following are equivalent:
(1) X is fuzzy δ-regular.
(2) For any fuzzy point p and any fuzzy δ-open set V containing p, there is a fuzzy δ-open set U such that $p \leq U \leq \text{cl}_\delta(U) \leq V$.
(3) For any fuzzy δ-closed set K and any fuzzy point p such that $p \leq K^c$, there are fuzzy δ-open sets U_1 and U_2 such that $p \leq U_1, K \leq U_2$ and $\text{cl}(U_1) \leq (\text{cl}(U_2))^c$.
(4) For any fuzzy δ-closed set K and any fuzzy point p such that $p \leq K^c$, there are fuzzy open sets U_1 and U_2 such that $p \leq U_1, K \leq U_2$ and $\text{cl}(U_1) \leq (\text{cl}(U_2))^c$.

Proof: (1) $\Rightarrow$ (2) Let p be a fuzzy point set and V a fuzzy δ-open set containing p. Then there exist fuzzy δ-open sets U_1 and U_2 such that $p \leq U_1, 1 - V \leq U_2$ and $U_1 \leq 1 - U_2$. So $p \leq U_1 \leq 1 - U_2 \leq V$. Thus $p \leq U_1 \leq \text{cl}_\delta(U_1) \leq \text{cl}_\delta(1 - U_2) = 1 - U_2 \leq V$.
(2) $\Rightarrow$ (3) Let K be a fuzzy δ-closed subset of X and p a fuzzy point set such that $p \leq K^c$. Then $1 - K$ is a fuzzy δ-open set with $p \leq K^c$. By (2) there is a fuzzy δ-open set U such that $p \leq U \leq \text{cl}_\delta(U) \leq 1 - K$. Since U is a fuzzy δ-open set containing p, there is a fuzzy δ-open set V such that $p \leq V \leq \text{cl}_\delta(V) \leq U \leq \text{cl}_\delta(U) \leq 1 - K$. Put $U_1 = V$ and $U_2 = (\text{cl}_\delta(U))^c$. Then U_1 and U_2 are fuzzy δ-open sets with $p \leq U_1, K \leq U_2$. Furthermore $\text{cl}(U_2) \leq \text{cl}((\text{cl}_\delta(U))^c) \leq \text{cl}(U^c) = U^c$. Hence $\text{cl}(U_1) = \text{cl}(V) \leq U \leq (\text{cl}(U_2))^c$.
(3) $\Rightarrow$ (4) it is obvious.
(4) $\Rightarrow$ (1) Let K be a fuzzy δ-closed subset of X and p a fuzzy point set such that $p \leq K^c$. By (4), there are fuzzy open sets U and V such that $p \leq U, K \leq V$ and $\text{cl}(U) \leq (\text{cl}(V))^c$. Since $p \leq U \leq \text{cl}(U)$, $p \leq \text{int}(U) = U \leq \text{int}(\text{cl}(U))$. Put $U_1 = \text{int}(\text{cl}(U))$, then U_1 is fuzzy δ-open and $p \leq U_1$. Since $K \leq V \leq \text{cl}(V)$, $K \leq \text{int}(V) = V \leq \text{int}(\text{cl}(V))$. Put $U_2 = \text{int}(\text{cl}(V))$, then U_2 is fuzzy δ-open and $K \leq U_2$. Furthermore, since $\text{int}(\text{cl}(U)) \leq \text{cl}(U) \leq (\text{cl}(V))^c \leq (\text{int}(\text{cl}(V)))^c$, we have $U_1 \leq U_2^c$. □

Definition 2.15: A fts X is called fuzzy δ-normal if for any pair of fuzzy δ-closed subsets K, L with $K \leq L^c$ in X,

there are fuzzy δ-open sets U_1 and U_2 in X with $K \leq U_1$, $L \leq U_2$ and $U_1 \leq U_2^c$. A fts X is called fuzzy δ-T_4 if it is fuzzy δ-T_1 and fuzzy δ-normal.

Clearly every fuzzy δ-T_4 space is a fuzzy δ-T_3 space.

Theorem 2.16: For a fts $(X, \mathcal{T})$, the following are equivalent:

(1) X is fuzzy δ-normal.

(2) For any fuzzy δ-closed set K and any fuzzy δ-open set U containing K, there exists a fuzzy δ-open set V such that $K \leq V \leq \text{cl}(V) \leq U$.

(3) For any fuzzy δ-closed set K and any fuzzy δ-open set U containing K, there exists a fuzzy open set V such that $K \leq V \leq \text{cl}(V) \leq U$.

(4) For any pair of fuzzy δ-closed subsets K, L with $K \leq L^c$ in X, there are fuzzy open sets U_1 and U_2 with $K \leq U_1$, $L \leq U_2$ and $\text{cl}(U_1) \leq (\text{cl}(U_2))^c$.

Proof: (1)⇒(2) Let K be a fuzzy δ-closed set and U a fuzzy δ-open set containing K. Then U^c is a fuzzy δ-closed set with $U^c \leq K^c$. Thus there are fuzzy δ-open sets V_1 and V_2 such that $K \leq V_1, U^c \leq V_2$ and $V_1 \leq V_2^c$. So $K \leq V_1 \leq V_2^c \leq U$ and $V_1 \leq \text{cl}_\delta(V_1) \leq \text{cl}_\delta(V_2^c) = V_2^c$. Hence $K \leq V_1 \leq \text{cl}(V_1) \leq \text{cl}_\delta(V_1) \leq U$.

(2)⇒(3) It is obvious.

(3)⇒(4) Let K and L be fuzzy δ-closed subsets of X with $K \leq L^c$. Then L^c is a fuzzy δ-open set containing K. By (3) there is a fuzzy open set V such that $K \leq V \leq \text{cl}(V) \leq L^c$. Since $\text{cl}(V)$ is fuzzy δ-closed and L^c is a fuzzy δ-open set containing $\text{cl}(V)$, there is a fuzzy open set U such that $K \leq V \leq \text{cl}(V) \leq U \leq \text{cl}(U) \leq L^c$. Let $U_1 = V$ and $U_2 = (\text{cl}(U)^c$, then U_1 and U_2 are fuzzy open sets with $K \leq U_1, L \leq U_2$. And $\text{cl}(U_2) = \text{cl}((\text{cl}(U))^c) \leq \text{cl}(U^c) = U^c$. So $\text{cl}(U_1) = \text{cl}(V) \leq U \leq (\text{cl}(U_2))^c$.

(4)⇒(1) Let K and L be fuzzy δ-closed subsets of X with $K \leq L^c$. Then, by (4), there are fuzzy open sets U and V such that $K \leq U, L \leq V$ and $\text{cl}(U) \leq (\text{cl}(V))^c$. Furthermore since $K \leq U \leq \text{cl}(U)$, $K \leq U = \text{int}(U) \leq \text{int}(\text{cl}(U)$. Put $U_1 = \text{int}(\text{cl}(U)$, then U_1 is fuzzy δ-open and $K \leq U_1$. Similarly put $U_2 = \text{int}(\text{cl}(V))$, then U_2 is fuzzy δ-open and $L \leq U_2$. And since $\text{int}(\text{cl}(U)) \leq \text{cl}(U) \leq (\text{cl}(V))^c \leq (\text{int}(\text{cl}(V)))^c$, $U_1 \leq U_2^c$. □

Example 2.17: Let $X = [0, 1]$ and for each $\alpha \in X$, $U_\alpha(x) = \alpha$ for all $x \in X$. And let $\mathcal{T} = \{U_\alpha \mid \alpha \in X\}$. Then $\mathcal{T}$ is a fuzzy topology and each U_α is fuzzy δ-open. Therefore $\mathcal{T}$ is fuzzy δ-normal and fuzzy δ-regular. But it is not fuzzy δ-T_1. So it is neither fuzzy δ-T_3 nor fuzzy δ-T_4.

Example 2.18: Let $X = [0, 1]$ and for each $\alpha \in X$

$$U_\alpha(x) = \begin{cases} 1 & \text{if } 0 \leq x \leq \alpha \\ 0 & \text{if } \alpha < x \leq 1, \end{cases}$$

$$V_\alpha(x) = \begin{cases} 0 & \text{if } 0 \leq x \leq \alpha \\ 1 & \text{if } \alpha < x \leq 1. \end{cases}$$

Let $\mathcal{T}$ be a fuzzy topology on X generated by the subbase $\{U_\alpha \mid \alpha \in X\} \cup \{V_\alpha \mid \alpha \in X\}$. Then $\mathcal{T}$ is a fuzzy topology and $\text{int}(\text{cl}(U_\alpha)) = U_\alpha$ for all $\alpha \in X$. So every U_α is fuzzy δ-open. Similarly every V_α is also fuzzy δ-open. Therefore $(X, \mathcal{T})$ is fuzzy δ-T_4 and also fuzzy δ-T_3.

III. Fuzzy δ-closure and δ-interior in the fuzzy subspace μ

Let $(X, \mathcal{T})$ be a fuzzy topological space and μ a fuzzy subset of X. We denote by $(\mu, \mathcal{T}^\mu)$ the fuzzy subspace on μ. If μ is fuzzy regular open(regular closed) in X, then $(\mu, \mathcal{T}^\mu)$ is said to be a fuzzy regular open(resp. regular closed) subspace.

Definition 3.1: Let $A \in X^\mu$. We say that A is fuzzy regular open(regular closed) in the subspace μ if $A = \text{int}^\mu(\text{cl}^\mu(A))$ (resp. $\text{cl}^\mu(\text{int}^\mu(A))$).

Definition 3.2: Let $A \in X^\mu$. A fuzzy point $x_r \in \mu$ is said to be a fuzzy δ-cluster point of A in μ iff every fuzzy regular open q-nbd U of x_r in μ is q-coincident with A in μ. The set of all fuzzy δ-cluster point of A in μ is called the fuzzy δ-closure of A in μ and is denoted by $\text{cl}_\delta^\mu(A)$.

Theorem 3.3: Let $A \in X^\mu$ and $x_r \in \mu$. $x_r \in \bigwedge\{F \in X^\mu \mid A \leq F, F = \text{cl}^\mu(\text{int}^\mu(F))\}$ if and only if every fuzzy regular open q-nbd U of x_r in μ is q-coincident with A in μ.

Proof: Suppose that N is a fuzzy regular open q-nbd of x_r with $N\tilde{q}A$. Then N is also a fuzzy open set in μ such that $x_r q N \leq N$ and $A\tilde{q}N$. Since N^c is fuzzy regular closed and $A \leq N^c$, $\bigwedge\{F \in X^\mu \mid A \leq F, F = \text{cl}^\mu(\text{int}^\mu(F))\} \leq N^c$. And since $x_r \notin N^c$, we have $x_r \notin \bigwedge\{F \in X^\mu \mid A \leq F, F = \text{cl}^\mu(\text{int}^\mu(F))\}$. Conversely suppose that $x_r \notin \bigwedge\{F \in X^\mu \mid A \leq F, F = \text{cl}^\mu(\text{int}^\mu(F))\}$. Then there is a fuzzy regular closed set F such that $x_r \notin F$ and $A \leq F$. Thus F^c is a fuzzy regular open set with $x_r q F^c$ and $A\tilde{q}F^c$. Hence x_r is not a fuzzy δ-cluster point of A in μ. □

By the above theorem, in a fuzzy subspace $(\mu, \mathcal{T}^\mu)$, we have

$$\text{cl}_\delta^\mu(A) = \bigwedge\{F \in X^\mu \mid A \leq F, F = \text{cl}^\mu(\text{int}^\mu(F))\}$$

for any set $A \in X^\mu$. Now we define the δ-interior in a subspace.

Definition 3.4: Let $A \in X^\mu$. The δ-interior of A in μ is defined as follows;

$$\text{int}_\delta^\mu(A) = \mu - \text{cl}_\delta^\mu(\mu - A).$$

We have known that $\text{cl}^\mu(A) = \mu - \text{int}^\mu(\mu - A)$ for any fuzzy subset A of X^μ. So we have the following remark.

Remark 3.5:

$$\begin{aligned} \text{int}_\delta^\mu(A) &= \mu - \text{cl}_\delta^\mu(\mu - A) \\ &= \mu - \bigwedge\{F \in X^\mu \mid \mu - A \leq F, \\ &\quad F = \text{cl}^\mu(\text{int}^\mu(F))\} \\ &= \bigvee\{\mu - F \in X^\mu \mid \mu - F \leq A, \\ &\quad \mu - F = \mu - \text{cl}^\mu(\text{int}^\mu(F))\} \\ &= \bigvee\{U \in X^\mu \mid U \leq A, U = \text{int}^\mu(\text{cl}^\mu(U))\}. \end{aligned}$$

We will show that for any fuzzy set A in a fuzzy subspace $(\mu, \mathcal{T}^\mu)$,

$$\mathrm{cl}^\mu_\delta(A) = \bigwedge\{\mathrm{cl}^\mu(U) \mid A \le \mathrm{cl}^\mu(U), U \in \mathcal{T}^\mu\}.$$

For the sake, we will prove two lemmas.

Lemma 3.6: Let $(\mu, \mathcal{T}^\mu)$ be a fuzzy subspace. If $V \in \mathcal{T}^\mu$, then $\mathrm{cl}^\mu(V)$ is fuzzy regular closed in μ.

Proof: Since $V \le \mathrm{cl}^\mu(V)$, $V = \mathrm{int}^\mu(V) \le \mathrm{int}^\mu(\mathrm{cl}^\mu(V))$ and hence $\mathrm{cl}^\mu(V) \le \mathrm{cl}^\mu(\mathrm{int}^\mu(\mathrm{cl}^\mu(V)))$. Conversely since $\mathrm{int}^\mu(\mathrm{cl}^\mu(V)) \le \mathrm{cl}^\mu(V)$, $\mathrm{cl}^\mu(\mathrm{int}^\mu(\mathrm{cl}^\mu(V))) \le \mathrm{cl}^\mu(\mathrm{cl}^\mu(V)) = \mathrm{cl}^\mu(V)$. Hence $\mathrm{cl}^\mu(V) = \mathrm{cl}^\mu(\mathrm{int}^\mu(\mathrm{cl}^\mu(V)))$. □

Lemma 3.7: Let $(\mu, \mathcal{T}^\mu)$ is a fuzzy subspace. Then $\{\mathrm{cl}^\mu(U) \mid U \in \mathcal{T}^\mu\} = \{F \in X^\mu \mid F$ is fuzzy regular closed in $\mu\}$.

Proof: We know that for any fuzzy open set U in μ, $\mathrm{cl}^\mu(U)$ is fuzzy regular closed in μ. Conversely, take any fuzzy regular closed set F in μ. Then $F = \mathrm{cl}^\mu(\mathrm{int}^\mu(F)) = \mathrm{cl}^\mu(\bigvee\{U \mid U \le F, U \in \mathcal{T}^\mu\}) \in \{\mathrm{cl}^\mu(U) \mid U \in \mathcal{T}^\mu\}$. □

We may have a problem in finding the fuzzy δ-closure of any fuzzy set. But from the above lemmas we have the clue to find it.

Theorem 3.8: For any fuzzy set A in a fuzzy subspace $(\mu, \mathcal{T}^\mu)$,

$$\mathrm{cl}^\mu_\delta(A) = \bigwedge\{\mathrm{cl}^\mu(U) \mid A \le \mathrm{cl}^\mu(U), U \in \mathcal{T}^\mu\}.$$

Proof: The proof is straightforward. □

In general, $\mathrm{cl}^\mu(A) \ne \mathrm{cl}(A) \wedge \mu$ and $\mathrm{int}(A) = \mathrm{int}^\mu(A) \wedge \mathrm{int}(\mu)$ for any fuzzy subset $A \in X^\mu$. But for any crisp fuzzy subset Y of X, if $\mu = \chi_Y$, then $\mathrm{cl}^\mu(A) = \mathrm{cl}(A) \wedge \mu$ for any fuzzy subset $A \in X^\mu$ (See [19]).

Furthermore, if μ is fuzzy open in X and $\mu = \chi_Y$, $\mathrm{cl}^\mu_\delta(A) = \mathrm{cl}_\delta(A) \wedge \mu$ for any fuzzy subset A of μ. Now we will prove it.

Lemma 3.9: Let X be a fuzzy topological space and $\mu = \chi_Y$ a fuzzy open subset of X. Suppose that $A \in X^\mu$. If A is fuzzy regular open in X, then A is fuzzy regular open in μ.

Proof: For any fuzzy subset $A \in X^\mu$, the following holds.

$$\begin{aligned}
\mathrm{int}^\mu(\mathrm{cl}^\mu(A)) &= \mathrm{int}^\mu(\mathrm{cl}(A) \wedge \mu) \\
&= \mathrm{int}(\mathrm{cl}(A) \wedge \mu) \\
&= \mathrm{int}(\mathrm{cl}(A)) \wedge \mathrm{int}(\mu) \\
&= \mathrm{int}(\mathrm{cl}(A)) \wedge \mu.
\end{aligned}$$

Hence if $A = \mathrm{int}(\mathrm{cl}(A))$, then $\mathrm{int}^\mu(\mathrm{cl}^\mu(A)) = \mathrm{int}(\mathrm{cl}(A)) \wedge \mu = A \wedge \mu = A$. □

Theorem 3.10: Let $(X, \mathcal{T})$ is a fuzzy topological space and Y a crisp fuzzy subset of X. If $\mu = \chi_Y$ and μ is fuzzy regular open in X, then

$$\mathrm{cl}^\mu_\delta(A) = \mathrm{cl}_\delta(A) \wedge \mu$$

for any fuzzy subset $A \in X^\mu$.

Proof: Suppose that $x_r \notin \mathrm{cl}^\mu_\delta(A)$. Then there is a fuzzy regular open q-nbd N of x_r in μ with $N\tilde{q}A[\mu]$. i.e. $\mathrm{int}^\mu(\mathrm{cl}^\mu(N)) \le A^c$. Since $x_r q N[\mu]$, $x_r q N$ and N is fuzzy open in X, $N = \mathrm{int}(N) \le \mathrm{int}(\mathrm{cl}(N))$. Note that $\mathrm{int}(\mathrm{cl}(N))$ is a fuzzy regular open q-nbd of x_r in X. Since $\mathrm{int}(\mathrm{cl}(N)) = \mathrm{int}(\mathrm{cl}(N \wedge \mu)) = \mathrm{int}(\mathrm{cl}^\mu(N)) \le \mathrm{int}^\mu(\mathrm{cl}^\mu(N))\tilde{q}A[\mu]$, we have $\mathrm{int}(\mathrm{cl}(N))\tilde{q}A$. Thus $x_r \notin \mathrm{cl}_\delta(A) \wedge \mu$. Conversely take $x_r \in \mathrm{cl}^\mu_\delta(A)$ and a fuzzy regular open q-nbd N of x_r in X. Then $N(x) + r > 1$ and so $(N \wedge \mu)(x) + r > 1$. Thus $N \wedge \mu$ is a fuzzy regular open q-nbd of x_r in X. By the above lemma, $N \wedge \mu$ is also a fuzzy regular open q-nbd of x_r in μ. Since $x_r \in \mathrm{cl}^\mu_\delta(A)$, $(N \wedge \mu) q A$. Hence NqA. Therefore x_r is a fuzzy δ-cluster point of A in X. □

In general every fuzzy regular open subset in μ is not fuzzy regular open in X. On the other hand, if $\mu = \chi_Y$ is a fuzzy regular open set in X, then a fuzzy δ-open set in X which is contained in X^μ is also fuzzy δ-open in μ. The following theorem shows it.

Theorem 3.11: Let $(X, \mathcal{T})$ be a fuzzy topological space and Y a crisp fuzzy subset of X. Let $\mu = \chi_Y$ be fuzzy regular open in X and $A \in X^\mu$. Then

$$\mathrm{int}^\mu_\delta(A) = \mathrm{int}_\delta(A).$$

Proof:

$$\begin{aligned}
\mathrm{int}^\mu_\delta(A) &= \mu - \mathrm{cl}^\mu_\delta(\mu - A) \\
&= \mu - (\mathrm{cl}_\delta(\mu - A) \wedge \mu) \\
&= \mu \wedge (\mathrm{cl}_\delta(\mu - A) \wedge \mu)^c \\
&= \mu \wedge ((\mathrm{cl}_\delta(\mu - A))^c \vee \mu^c) \\
&= \mu \wedge (\mathrm{cl}_\delta(\mu - A))^c \\
&= \mu \wedge (1 - \mathrm{cl}_\delta(\mu - A)) \\
&= \mu \wedge \mathrm{int}_\delta(1 - (\mu - A)) \\
&= \mathrm{int}_\delta(\mu \wedge (1 - (\mu - A))) \\
&= \mathrm{int}_\delta(A).
\end{aligned}$$

□

IV. Fuzzy δ-separation axioms in the fuzzy subspace μ

Now we define the fuzzy δ-separation axioms on the fuzzy subspaces. Note that $A^c = \mu - A$ in the fuzzy subspace μ, for any set $A \in X^\mu$.

Definition 4.1: A fuzzy subspace $(\mu, \mathcal{T}^\mu)$ is called fuzzy δ-T_0 if for any pair of fuzzy points p and q with different supports in μ, there is a fuzzy δ-open set U in μ with $p \le U \le q^c$ or $q \le U \le p^c$.

Theorem 4.2: Let $(X, \mathcal{T})$ be a fuzzy δ-T_0 space. Suppose that Y is a crisp fuzzy subset of X and a fuzzy regular open set of X. Then $(\mu = \chi_Y, \mathcal{T}^\mu)$ is fuzzy δ-T_0.

Proof: Let X be a fuzzy δ-T_0 space and $\mu = \chi_Y$ a fuzzy regular open subset of X. Take any fuzzy points p and q with different supports in a subspace $(\mu, \mathcal{T}^\mu)$. Then p and q

are also fuzzy points with different supports in the space X. Since X is fuzzy δ-T_0, there is a fuzzy δ-open set U in X with $p \leq U \leq q^c$ or $q \leq U \leq p^c$. And since $U \wedge \mu$ is fuzzy δ-open in X with $U \wedge \mu \leq \mu$, $U \wedge \mu$ is also fuzzy δ-open in μ. Furthermore $p \leq U \wedge \mu \leq (\mu - q)$ or $q \leq U \wedge \mu \leq (\mu - p)$. Hence $(\mu, \mathcal{T}^\mu)$ is fuzzy δ-T_0. □

Definition 4.3: A fuzzy subspace $(\mu, \mathcal{T}^\mu)$ is called fuzzy δ-T_1 if for any pair of fuzzy points p and q with different supports in μ, there are two fuzzy δ-open sets U_1, U_2 in μ with $p \leq U_1 \leq q^c$ and $q \leq U_2 \leq p^c$.

Theorem 4.4: A fuzzy subspace $(\mu, \mathcal{T}^\mu)$ is fuzzy δ-T_1 iff every crisp fuzzy point in μ is fuzzy δ-closed in μ.

Proof: Take any crisp fuzzy point p in μ. We will show that $\mu - p$ is fuzzy δ-open in μ. We can take a fuzzy point $q \in \mu - p$ with different support from p. Since $(\mu, \mathcal{T}^\mu)$ is fuzzy δ-T_1, there is a fuzzy δ-open set U in μ with $q \leq U \leq \mu - p$. Thus $\mu - p = \bigcup_{q \in \mu - p} \{U \mid q \leq U \leq \mu - p, U \text{ is fuzzy } \delta\text{-open in } \mu\}$. Since $\bigcup_{q \in \mu - p} \{U \mid q \leq U \leq \mu - p, U \text{ is fuzzy } \delta\text{-open in } \mu\}$ is fuzzy δ-open in μ, $\mu - p$ is fuzzy δ-open in μ. Hence p is fuzzy δ-closed in μ. □

Corollary 4.5: Let $(\mu, \mathcal{T}^\mu)$ be a fuzzy subspace. μ is fuzzy δ-T_1 if and only if $x_\alpha = \bigcap \{\mathrm{cl}_\delta(U) \mid x_\alpha \leq \mathrm{cl}_\delta(U)\}$ for any $x_\alpha \in \mu$.

Theorem 4.6: Let $(X, \mathcal{T})$ be a fuzzy δ-T_1 space. Suppose that Y is a crisp fuzzy subset of X and fuzzy regular open in X. Then $(\mu = \chi_Y, \mathcal{T}^\mu)$ is fuzzy δ-T_1.

Proof: It is obvious. □

Definition 4.7: A fuzzy subspace $(\mu, \mathcal{T}^\mu)$ is called fuzzy δ-Hausdorff, or fuzzy δ-T_2, if for any pair of fuzzy point p and q with different supports in μ, there are fuzzy δ-open sets U_1 and U_2 in μ with $p \leq U_1 \leq q^c$, $q \leq U_2 \leq p^c$ and $U_1 \leq U_2^c$.

Obviously every fuzzy δ-T_2 subspace is fuzzy δ-T_1.

Theorem 4.8: Let $(X, \mathcal{T})$ be a fuzzy δ-T_2 space. Suppose that Y is a crisp fuzzy subset of X and fuzzy regular open in X. Then $(\mu = \chi_Y, \mathcal{T}^\mu)$ is fuzzy δ-T_2.

Proof: Take any fuzzy points p and q with different supports in a subspace $(\mu, \mathcal{T}^\mu)$. Then p and q are also fuzzy points with different supports in the space X. Since X is fuzzy δ-T_2, there are fuzzy δ-open sets U_1 and U_2 in X such that $p \leq U_1 \leq 1 - q$, $q \leq U_2 \leq 1 - p$ and $U_1 \leq 1 - U_2$. Thus there are fuzzy δ-open sets $U_1 \wedge \mu$ and $U_2 \wedge \mu$ in μ such that $p \leq (U_1 \wedge \mu) \leq (1 - q) \wedge \mu = \mu - q$, $q \leq (U_2 \wedge \mu) \leq (1 - p) \wedge \mu = \mu - p$ and $(U_1 \wedge \mu) \leq (1 - U_2) \wedge \mu = \mu - (U_2 \wedge \mu)$. So μ is fuzzy δ-T_2. □

Definition 4.9: A fuzzy subspace $(\mu, \mathcal{T}^\mu)$ is called fuzzy δ-regular if for every pair consisting of a fuzzy point p in μ and a fuzzy δ-closed set K in μ with $p \leq K^c$, there are fuzzy δ-open sets U_1, U_2 in μ with $p \leq U_1$, $K \leq U_2$ and $U_1 \leq U_2^c$. A fuzzy subspace $(\mu, \mathcal{T}^\mu)$ is called fuzzy δ-T_3 if it is fuzzy δ-regular and fuzzy δ-T_1.

We can easily prove that every fuzzy δ-T_3 subspace is fuzzy δ-T_2.

We have known that for any fuzzy closed set K in μ, $\mathrm{int}^\mu(K)$ is fuzzy regular open in μ. Thus it is also fuzzy δ-open. Therefore the following theorem holds.

Theorem 4.10: For a fuzzy subspace $(\mu, \mathcal{T}^\mu)$, the following are equivalent:
(1) $(\mu, \mathcal{T}^\mu)$ is fuzzy δ-regular.
(2) For any fuzzy point p and any fuzzy δ-open set V containing p in $(\mu, \mathcal{T}^\mu)$, there is a fuzzy δ-open set U in μ such that $p \leq U \leq \mathrm{cl}^\mu_\delta(U) \leq V$.
(3) For any fuzzy δ-closed set K and any fuzzy point p in $(\mu, \mathcal{T}^\mu)$ such that $p \leq (\mu - K)$, there are fuzzy δ-open sets U_1 and U_2 in μ such that $p \leq U_1, K \leq U_2$ and $\mathrm{cl}^\mu(U_1) \leq (\mu - \mathrm{cl}^\mu(U_2))$.
(4) For any fuzzy δ-closed set K and each fuzzy point p in $(\mu, \mathcal{T}^\mu)$ such that $p \leq (\mu - K)$, there are fuzzy open sets U_1 and U_2 in $(\mu, \mathcal{T}^\mu)$ such that $p \leq U_1, K \leq U_2$ and $\mathrm{cl}^\mu(U_1) \leq (\mu - \mathrm{cl}^\mu(U_2))$.

Proof: (1) ⇒ (2) Let p be a fuzzy point set in μ and V a fuzzy δ-open set in μ containing p. Then there exist fuzzy δ-open sets U_1 and U_2 in μ such that $p \leq U_1, \mu - V \leq U_2$ and $U_1 \leq \mu - U_2$. So $p \leq U_1 \leq \mu - U_2 \leq V$. Thus $p \leq U_1 \leq \mathrm{cl}^\mu_\delta(U_1) \leq \mathrm{cl}^\mu_\delta(\mu - U_2) = \mu - U_2 \leq V$.
(2) ⇒ (3) Let K be a fuzzy δ-closed subset in μ and p a fuzzy point in μ such that $p \leq \mu - K$. Then $\mu - K$ is a fuzzy δ-open set in μ with $p \leq \mu - K$. By (2) there is a fuzzy δ-open set U in μ such that $p \leq U \leq \mathrm{cl}^\mu_\delta(U) \leq \mu - K$. Since U is a fuzzy δ-open set in μ containing p, there is a fuzzy δ-open set V in μ such that $p \leq V \leq \mathrm{cl}^\mu_\delta(V) \leq U \leq \mathrm{cl}^\mu_\delta(U) \leq \mu - K$. Put $U_1 = V$ and $U_2 = \mu - \mathrm{cl}^\mu_\delta(U)$. Then U_1 and U_2 are fuzzy δ-open sets in μ with $p \leq U_1, K \leq U_2$. Furthermore $\mathrm{cl}^\mu(U_2) \leq \mathrm{cl}^\mu(\mu - \mathrm{cl}^\mu_\delta(U)) \leq \mathrm{cl}^\mu(\mu - U) = \mu - U$. Since $\mathrm{cl}^\mu(V) \leq \mathrm{cl}^\mu_\delta(V)$, $\mathrm{cl}^\mu(U_1) = \mathrm{cl}^\mu(V) \leq U \leq \mu - \mathrm{cl}^\mu(U_2)$.
(3) ⇒ (4) it is obvious.
(4) ⇒ (1) Let K be a fuzzy δ-closed subset in μ and p a fuzzy point in μ such that $p \leq \mu - K$. By (4), there are fuzzy open sets U and V in μ such that $p \leq U, K \leq V$ and $\mathrm{cl}^\mu(U) \leq \mu - \mathrm{cl}^\mu(V)$. Since $p \leq U \leq \mathrm{cl}^\mu(U)$, $p \leq \mathrm{int}^\mu(U) = U \leq \mathrm{int}^\mu(\mathrm{cl}^\mu(U))$. Put $U_1 = \mathrm{int}^\mu(\mathrm{cl}^\mu(U))$, then U_1 is fuzzy δ-open in μ and $p \leq U_1$. Since $K \leq V \leq \mathrm{cl}^\mu(V)$, $K \leq \mathrm{int}^\mu(V) = V \leq \mathrm{int}^\mu(\mathrm{cl}^\mu(V))$. Put $U_2 = \mathrm{int}^\mu(\mathrm{cl}^\mu(V))$, then U_2 is fuzzy δ-open in μ and $K \leq U_2$. Furthermore, since $\mathrm{int}^\mu(\mathrm{cl}^\mu(U)) \leq \mathrm{cl}^\mu(U) \leq \mu - \mathrm{cl}^\mu(V) \leq \mu - \mathrm{int}^\mu(\mathrm{cl}^\mu(V))$, $U_1 \leq \mu - U_2$. □

Definition 4.11: A fuzzy subspace $(\mu, \mathcal{T}^\mu)$ is called fuzzy δ-normal if for any pair of fuzzy δ-closed subsets K, L in μ with $K \leq L^c$, there are fuzzy δ-open sets U_1, U_2 in μ with $K \leq U_1$, $L \leq U_2$ and $U_1 \leq U_2^c$. A fuzzy subspace $(\mu, \mathcal{T}^\mu)$ is called fuzzy δ-T_4 if it is fuzzy δ-T_1 and fuzzy δ-normal.

Clearly every fuzzy δ-T_4 subspace is fuzzy δ-T_3.

Theorem 4.12: For a fuzzy subspace $(\mu, \mathcal{T}^\mu)$, the following are equivalent:
(1) $(\mu, \mathcal{T}^\mu)$ is fuzzy δ-normal.
(2) For any fuzzy δ-closed set K and any fuzzy δ-open set U containing K in $(\mu, \mathcal{T}^\mu)$, there exists a fuzzy δ-open set V in

μ such that $K \leq V \leq \mathrm{cl}^{\mu}_{\delta}(V) \leq U$.
(3) For any fuzzy δ-closed set K and any fuzzy δ-open set U containing K in $(\mu, \mathcal{T}^{\mu})$, there exists a fuzzy δ-open set V in μ such that $K \leq V \leq \mathrm{cl}^{\mu}(V) \leq U$.
(4) For any fuzzy δ-closed set K and any fuzzy δ-open set U containing K in $(\mu, \mathcal{T}^{\mu})$, there exists a fuzzy open set V in μ such that $K \leq V \leq \mathrm{cl}^{\mu}(V) \leq U$.
(5) For any pair of fuzzy δ-closed subsets K and L with $K \leq \mu - L$ in $(\mu, \mathcal{T}^{\mu})$, there are fuzzy open sets U_1 and U_2 in μ with $K \leq U_1$, $L \leq U_2$ and $\mathrm{cl}^{\mu}(U_1) \leq (\mu - \mathrm{cl}^{\mu}(U_2))$.

Proof: (1)⇒(2) Let K be a fuzzy δ-closed set in μ and U a fuzzy δ-open set in μ containing K. Then $\mu - U$ is a fuzzy δ-closed set in μ with $\mu - U \leq \mu - K$. Thus there are fuzzy δ-open sets V_1 and V_2 in μ such that $K \leq V_1, \mu - U \leq V_2$ and $V_1 \leq \mu - V_2$. So $K \leq V_1 \leq \mu - V_2 \leq U$ and $V_1 \leq \mathrm{cl}^{\mu}_{\delta}(V_1) \leq \mathrm{cl}^{\mu}_{\delta}(\mu - V_2) = \mu - V_2$. Hence $K \leq V_1 \leq \mathrm{cl}^{\mu}_{\delta}(V_1) \leq U$.
(2)⇒(3), (3)⇒(4) It is obvious.
(4)⇒(5) Let K and L be fuzzy δ-closed subsets in μ with $K \leq \mu - L$. Then $\mu - L$ is a fuzzy δ-open set in μ containing K. By (3) there is a fuzzy open set V in μ such that $K \leq V \leq \mathrm{cl}^{\mu}(V) \leq \mu - L$. Since $\mathrm{cl}^{\mu}(V)$ is fuzzy δ-closed in μ and $\mu - L$ is a fuzzy δ-open set in μ containing $\mathrm{cl}^{\mu}(V)$, there is a fuzzy open set U in μ such that $K \leq V \leq \mathrm{cl}^{\mu}(V) \leq U \leq \mathrm{cl}^{\mu}(U) \leq \mu - L$. Let $U_1 = V$ and $U_2 = \mu - \mathrm{cl}^{\mu}(U)$, then U_1 and U_2 are fuzzy open sets in μ with $K \leq U_1$ and $L \leq U_2$. Also $\mathrm{cl}^{\mu}(U_2) = \mathrm{cl}^{\mu}(\mu - \mathrm{cl}^{\mu}(U)) \leq \mathrm{cl}^{\mu}(\mu - U) = \mu - U$. So $\mathrm{cl}^{\mu}(U_1) = \mathrm{cl}^{\mu}(V) \leq U \leq \mu - \mathrm{cl}^{\mu}(U_2)$.
(5)⇒(1) Let K and L be fuzzy δ-closed subsets in μ with $K \leq \mu - L$. Then, by (4), there are fuzzy open sets U and V in μ such that $K \leq U, L \leq V$ and $\mathrm{cl}^{\mu}(U) \leq \mu - \mathrm{cl}^{\mu}(V))$. Since $K \leq U \leq \mathrm{cl}^{\mu}(U)$, we have $K \leq U = \mathrm{int}^{\mu}(U) \leq \mathrm{int}^{\mu}(\mathrm{cl}^{\mu}(U)$. Put $U_1 = \mathrm{int}^{\mu}(\mathrm{cl}^{\mu}(U)$, then U_1 is fuzzy δ-open in μ and $K \leq U_1$. Similarly put $U_2 = \mathrm{int}^{\mu}(\mathrm{cl}^{\mu}(V))$, then U_2 is fuzzy δ-open in μ and $L \leq U_2$. And since $\mathrm{int}^{\mu}(\mathrm{cl}^{\mu}(U)) \leq \mathrm{cl}^{\mu}(U) \leq \mu - \mathrm{cl}^{\mu}(V) \leq \mu - \mathrm{int}^{\mu}(\mathrm{cl}^{\mu}(V))$, we have $U_1 \leq \mu - U_2$. □

Theorem 4.13: Let $(X, \mathcal{T})$ be a fuzzy δ-regular space. Suppose that Y is a crisp fuzzy subset of X and fuzzy regular open in X. Then $(\mu = \chi_Y, \mathcal{T}^{\mu})$ is fuzzy δ-regular.

Proof: Let U be a fuzzy δ-open set in μ and p a fuzzy point in μ with $p \leq U$. Since μ is fuzzy regular open in X, U is also fuzzy δ-open in X. Since X is fuzzy δ-regular, there is a fuzzy δ-open set W of X such that $p \leq W \leq \mathrm{cl}_{\delta}(W) \leq U$. Thus there is a fuzzy δ-open set $W_{\mu} = W \wedge \mu$ in μ such that $p \leq W_{\mu} \leq \mathrm{cl}_{\delta}(W) \wedge \mu = \mathrm{cl}^{\mu}_{\delta}(W_{\mu}) \leq U \wedge \mu = U$. Hence μ is fuzzy δ-regular. □

Lemma 4.14: Let $(X, \mathcal{T})$ be a fuzzy δ-normal space. Suppose that μ is a crisp fuzzy subset of X and fuzzy regular closed in X. If $K \in X^{\mu}$ is fuzzy regular closed in μ, then K is also fuzzy regular closed in X.

Proof: $K = \mathrm{cl}^{\mu}_{\delta}(K) = \mathrm{cl}_{\delta}(K) \wedge \mu = \mathrm{cl}_{\delta}(K) \wedge \mathrm{cl}_{\delta}(\mu) \geq \mathrm{cl}_{\delta}(K \wedge \mu) = \mathrm{cl}_{\delta}(K) \geq K$. □

Theorem 4.15: Let $(X, \mathcal{T})$ be a fuzzy δ-normal space. Suppose that Y is a crisp fuzzy subset of X and fuzzy regular clopen in X. Then $(\mu = \chi_Y, \mathcal{T}^{\mu})$ is fuzzy δ-normal.

Proof: Let X be a fuzzy δ-normal space and μ a fuzzy δ-clopen subspace of X. Let K, L be fuzzy δ-closed subsets in μ with $K \leq (\mu - L)$. Since μ is fuzzy δ-closed in X, K and L are also fuzzy δ-closed in X with $K \leq (1 - L)$. Since X is fuzzy δ-normal, there exist fuzzy δ-open sets U_1 and U_2 in X with $K \leq U_1$, $L \leq U_2$ and $U_1 \leq U_2^c$. So there exist fuzzy δ-open sets $(\mu \wedge U_1)$ and $(\mu \wedge U_2)$ in μ with $K \leq (\mu \wedge U_1)$, $L \leq (\mu \wedge U_2)$ and $(\mu \wedge U_1) \leq \mu - (\mu \wedge U_2)$ in the subspace μ. □

V. Conclusion

In this paper, we introduced fuzzy δ-separation axioms in fuzzy topological spaces, and proved that

$$\delta\text{-}T_4 \Rightarrow \delta\text{-}T_3 \Rightarrow \delta\text{-}T_2 \Rightarrow \delta\text{-}T_1 \Rightarrow \delta\text{-}T_0.$$

Also we defined fuzzy δ-separation axioms in the fuzzy subspace in the sense of [22]. We have shown the hereditariness of fuzzy δ-separation in the fuzzy regular subspaces. However we cannot find counterexamples for the reverse directions of the above implications except $\delta\text{-}T_0 \not\Rightarrow \delta\text{-}T_1$. In the subsequential research, we will find these examples and investigate other properties of fuzzy separation axioms.

Acknowledgment

This work was supported by the research grant of the Chungbuk National University in 2010.

References

[1] L. A. Zadeh, "Fuzzy sets," *Information and Control*, vol. 8, pp. 338–353, 1965.
[2] C. L. Chang, "Fuzzy topological spaces," *J. Math. Anal. Appl.*, vol. 24, pp. 182–190, 1968.
[3] R. Lowen, "Fuzzy topological spaces and fuzzy compactness," *J. Math. Anal. Appl.*, vol. 56, no. 3, pp. 621–633, 1976.
[4] B. Hutton and I. Reilly, "Separation axioms in fuzzy topological spaces," *Fuzzy Sets and Systems*, vol. 3, no. 1, pp. 93–104, 1980.
[5] S. Ganguly and S. Saha, "A note on δ-continuity and δ-connected sets in fuzzy set theory," *Simon Stevin*, vol. 62, no. 2, pp. 127–141, 1988.
[6] M. N. Mukherjee and S. P. Sinha, "On some near-fuzzy continuous functions between fuzzy topological spaces," *Fuzzy Sets and Systems*, vol. 34, no. 2, pp. 245–254, 1990.
[7] K. Dutta and S. Ganguly, "On strongly δ-continuous functions," *Carpathian J. Math.*, vol. 19, no. 1, pp. 51–66, 2003.
[8] S. Ganguly and K. Dutta, "δ-continuous functions and topologies on function spaces," *Soochow J. Math.*, vol. 30, no. 4, pp. 419–430, 2004.
[9] S. J. Lee and Y. S. Eoum, "Intuitionistic fuzzy θ-closure and θ-interior," *Commun. Korean Math. Soc.*, vol. 25, no. 2, pp. 273–282, 2010.
[10] S. J. Lee and S. M. Yun, "Fuzzy δ-topology and compactness," *submitted*.
[11] M. H. Ghanim, E. E. Kerre, and A. S. Mashhour, "Separation axioms, subspaces and sums in fuzzy topology," *J. Math. Anal. Appl.*, vol. 102, no. 1, pp. 189–202, 1984.
[12] S. Ganguly and S. Saha, "On separation axioms and separations of connected sets in fuzzy topological spaces," *Bull. Calcutta Math. Soc.*, vol. 79, no. 4, pp. 215–225, 1987.
[13] A. A. Fora, "Separation axioms for fuzzy spaces," *Fuzzy Sets and Systems*, vol. 33, no. 1, pp. 59–75, 1989.
[14] T. Kubiak, "On L-Tychonoff spaces," *Fuzzy Sets and Systems*, vol. 73, no. 1, pp. 25–53, 1995. Fuzzy topology.
[15] S.-G. Li, "Separation axioms in L-fuzzy topological spaces. I. T_0 and T_1," *Fuzzy Sets and Systems*, vol. 116, no. 3, pp. 377–383, 2000.
[16] C. De Mitri, C. Guido, and R. E. Toma, "Fuzzy topological properties and hereditariness," *Fuzzy Sets and Systems*, vol. 138, no. 1, pp. 127–147, 2003.

[17] M. Alimohammady and M. Roohi, "Separation of fuzzy sets in fuzzy minimal spaces," *Chaos Solitons Fractals*, vol. 31, no. 1, pp. 155–161, 2007.
[18] U. Höhle and T. Kubiak, "A note on Hausdorff separation in L-TOP," *Fuzzy Sets and Systems*, vol. 159, no. 19, pp. 2606–2610, 2008.
[19] P. M. Pu and Y. M. Liu, "Fuzzy topology. I. Neighborhood structure of a fuzzy point and Moore-Smith convergence," *J. Math. Anal. Appl.*, vol. 76, no. 2, pp. 571–599, 1980.
[20] K. K. Azad, "On fuzzy semicontinuity, fuzzy almost continuity and fuzzy weakly continuity," *J. Math. Anal. Appl.*, vol. 82, no. 1, pp. 14–32, 1981.
[21] J. R. Choi, B. Y. Lee, and J. H. Park, "On fuzzy θ-continuous mappings," *Fuzzy Sets and Systems*, vol. 54, no. 1, pp. 107–113, 1993.
[22] M. Macho Stadler and M. Á. De Prada Vicente, "On fuzzy subspaces," *Fuzzy Sets and Systems*, vol. 58, no. 3, pp. 365–373, 1993.
[23] A. M. Zahran, "On fuzzy subspaces," *Kyungpook Math. J.*, vol. 41, no. 2, pp. 361–369, 2001.

2011 IEEE International Conference on Fuzzy Systems
June 27-30, 2011, Taipei, Taiwan

Clustering Data and Imprecise Concepts

Weifeng Zhang
Intelligent Computing and Machine Learning Lab
School of Automation Science and Electrical Engineering
Beihang University, China
Email: zwf.zhang@gmail.com

Zengchang Qin
[1] Intelligent Computing and Machine Learning Lab
School of ASEE, Beihang University
[2] Robotics Institute, CMU, USA
Email: zcqin@andrew.cmu.edu

***Abstract*—Cluster analysis is the assignment of grouping a set of observations into clusters so that observations in the same cluster are similar in some sense. One of the key features for clustering is how to define a sensible similarity measure. However, classical clustering algorithms have no ability to cluster data instances and imprecise concepts using traditional distance measures. In this paper, we proposed a (dis)similarity measure based on a new knowledge representation framework called label semantics. Based on this new measure, we can automatically cluster data instance and descriptive concepts represented by logical expressions of linguistic labels. Experimental results on a toy problem in image classification demonstrate the effectiveness of the new proposed clustering algorithm. Since the new proposed measure can be extended to measuring distance between any two granularities, the new clustering algorithms can also be extended to clustering data instance and imprecise concepts represented by other granularities.**

***Index Terms*—Clustering; Label Semantics; Linguistic Expressions; K-means; Imprecise Concept Modeling**

I. Introduction

Cluster analysis is considered as the most important forms of unsupervised learning [17]. It deals with finding similar patterns in a collection of unlabeled data. A cluster is therefore a collection of objects which are "similar" and are "dissimilar" to the objects belonging to other clusters. Another kind of clustering is conceptual clustering. Two or more objects belong to the same cluster if this one defines a concept common to all objects. In other words, objects are grouped according to their fit to descriptive concepts, not according to simple similarity measures.

Clustering algorithms can be applied in many fields, such as marketing, bio-informatics, video analysis [13] and so on. Hence, in past decades, many classical clustering algorithms, for example K-means, Fuzzy K-means, Hierarchical clustering algorithms, have been proposed and some of them have been successfully applied in resolving practical problems. They group the "similar" objects into one cluster. In this sense, the clustering results depend heavily on the distance measure between objects. Euclidean distance and Mahalanobis distance are two of the most used distance measure. Other (dis)similarity measures may be used for some particular data type. For example, Kullback-Leibler (KL) distance is good for measuring the divergence between two probability distributions. But its unsymmetrical properties make it unsuitable as to be a good universal measure of data distance. In literatures, the objects handled by these classical clustering algorithms are restricted to numerical data, though they could be high-dimensional complex data. However, what we hope to cluster are not limited to numerical data, it could be some high-level knowledge of imprecise concepts or linguistic descriptions [11]. For example, if we are given a set of human age $Age = \{16, 17, 19, 22, 40, 67, 68, 70, 82\}$ and three descriptive concepts $\{young, middle\text{-}aged, old\}$ which are defined by fuzzy membership functions. How can we cluster these two type of data if given the cluster number $K = 3$? Ideally, if the imprecise concept of human age are sensibly defined, we should obtain the following 3 clusters: $\{young, 16, 17, 19, 22\}$, $\{middle\text{-}aged, 40\}$ and $\{old, 67, 68, 70, 82\}$.

Unfortunately, these objects can not be well handled by the existed clustering algorithms. The main reason is there is no good metric for measuring dissimilarity between numerical data and linguistic descriptions [3][6]. In this paper we proposed a novel distance measure which can measure the distance between numeral data and logical expressions of linguistic labels based on *label semantics* [5]. Label semantics uses a set of linguistic labels to represents imprecise concepts in terms of a probability distribution on appropriate label sets. This new proposed measure make it possible to cluster a set of objects including numerical data, concepts, and linguistic descriptions, by modifying the distance measure based on the classical K-means clustering algorithm.

II. Label Semantics

In order to understand the use of natural language for information and knowledge processing in computer systems, Zadeh proposed the concept of Computing with Words paradigm [14]. He suggested a form of precisiated natural language (PNL) based on the theory of generalized constraints and linguistic variables: $\mathbf{x}$ *isr* θ, where $\mathbf{x}$ is the constrained variable, r is the constraining relation, and r is a discrete valued modal variable. The "is" in *isr* is simply its natural meaning- the conjugated verb "to be" and other defined modalities include: possibilistic ($r = blank$); probabilistic ($r = p$); veristic ($r = v$); random set ($r = rs$); fuzzy graph($r = fg$); bimodal ($r = bm$); and Pawlakset ($r = ps$) [15]. However, since the invention of PNL, there is no applicable calculus developed to solve problems in natural language understanding, though some thoughts had been used in designing a search engines by combining it with other computational linguistics technologies [1][10]. Label semantics, proposed by Lawry [4] [5], provides an alternative

978-1-4244-7316-8/11/$26.00 ©2011 IEEE

representation for modeling with words. In contrast to Zadeh's methodology this approach is based on measures of an agent's subjective belief that a logical expression is appropriate to describe a particular object or value. It provides a set of applicable calculus that has been successfully used in many supervised learning applications [4] [9] [11].

Label semantics is a random set framework for modeling with words. The fundamental notion underlying label semantics is that when individuals make assertion of the form ' $\mathbf{x}$ is θ ', different from Zadeh's approach discussed above [15], they are essentially providing information about what labels are appropriate for the value of the underlying variable $\mathbf{x}$ [5]. For $x \in \Omega$ the label description of x is a random set from V into the power set of $\mathbb{L}$, denoted by D_x, with associated distribution m_x, which is referred to as mass assignment:

$$\forall S \subseteq \mathbb{L}, m_x(S) = P(I \in V : D_x^I = S). \tag{1}$$

To evaluate how appropriate a label is for describing a particular value of variable x, *appropriateness degrees* are defined.

$$\forall x \in \Omega, \forall L \in \mathbb{L}, \mu_L(x) = \sum_{S \subseteq \mathbb{L}: L \in S} m_x(S) \tag{2}$$

Example 1: Given a set of labels defined on the height of an adult: $\mathbb{L}_{Height} = \{short, medium, tall\}$ and a voting space with size of 10. Suppose 4 of 10 people agree that *medium* is the only appropriate label for the height of $173cm$ and 6 support that both *short* and *medium* are appropriate labels, according to Eq. 1, the mass assignment for $173cm$ is: $m_{173} = \{medium\} : 0.4, \{short, medium\} : 0.6$. Based on the appropriateness measure given in Eq. 2, the appropriateness degree of *medium* as a description of $173cm$ is

$$\mu_{medium}(173) = 0.4 + 0.6 = 1 \tag{3}$$

and that of *short* is $\mu_{short}(173) = 0.6$.

The mass assignment is extendable to multi-dimensional case. For example, multi-dimensional color labels $\{red, orange, yellow, \ldots\}$ can be used to describe a pixel of color image $\mathbf{p}$ in the HSV space. The mass assignment can be represented in the form of

$$m_{\mathbf{p}} = \{red, orage\} : 0.3, \{red\} : 0.7$$

Such representations will be used in our experiments.

Given a universe of discourse Ω containing a set of objects or instances to be described, it is assumed that all relevant expression can be generated recursively from a finite set of basic labels $\mathbb{L} = \{L_1, L_2, ..., L_n\}$ Operators for combing expressions are restricted to the standard logical connectives of negation '$\neg$', conjunction '$\wedge$', disjunction '$\vee$' and implication '$\rightarrow$'. Hence, the set of logical expressions of labels can be formally defined as follows:

Definition 1 (Logical expressions of labels): The set of logical expressions, *LE*, is defined recursively as follows:

(i) $L_i \in LE \quad for \quad i = 1, 2, ..., n$. (ii) If θ, $\varphi \in LE$ then $\neg\theta, \theta \wedge \varphi, \theta \vee \varphi, \theta \rightarrow \varphi \in LE$.

Basically, we interpret the main logical connectives as follows:

- $\neg L$ means that L is not an appropriate label.
- $L_1 \wedge L_2$ means both L_1 and L_2 are appropriate labels.
- $L_1 \vee L_2$ means that either L_1 or L_2 are appropriate labels.
- $L_1 \rightarrow L_2$ means that L_2 is an appropriate label whenever L_1 is.

As well as labels for a single variable, we may want to evaluate the appropriateness degree of a complex logical expression $\theta \in LE$. Consider the set of logical expressions LE obtained by recursive application of the standard logical connectives. In order to evaluate the appropriateness degrees of such expressions we must identify what information they provide regarding the appropriateness of labels. In general, for any logical expression θ we should be able to identify a maximal set of label sets, $\lambda(\theta)$, that are consistent with θ so that the meaning of θ can be interpreted as the constraint $D_x \in \lambda(\theta)$.

Definition 2 (λ-Function): Let θ and φ be expressions generated by recursive application of the connectives $\neg, \wedge, \vee$ and $\rightarrow$ to the elements of $\mathbb{L}$ (i.e. $\theta \in LE$). Then the set of possible label sets defined by a linguistic expression can be determined recursively as follows:

(i) $\lambda(L_i(x)) = \{S \subseteq \mathbb{F} | \{L_i\} \subseteq S\}$.
(ii) $\lambda(\neg\theta) = \overline{\lambda(\theta)}$.
(iii) $\lambda(\theta \vee \varphi) = \lambda(\theta) \bigcap \lambda(\varphi)$.
(iv) $\lambda(\theta \wedge \varphi) = \lambda(\theta) \bigcup \lambda(\varphi)$.
(v) $\lambda(\theta \rightarrow \varphi) = \overline{\lambda(\theta)} \bigcap \lambda(\varphi)$.

where $\mathbb{F}$, which is refereed to as *focal set*, represents the subsets of labels with possible non-zero masses into the power set of $\mathbb{L}$. The formal definition of focal set is as follows:

Definition 3 (Focal set): Given a universe Ω for variable x, the focal set of $\mathbb{L}$ is a set of focal elements defined as:

$$\mathbb{F} = \{S \subseteq \mathbb{L} | \exists x \in \Omega, m_x(S) > 0\} \tag{4}$$

In label semantics theory, λ-function is a useful tool to represent logical expressions into a set of linguistic labels [11], i.e.: $\lambda(\mathbb{L}) \rightarrow \mathbb{F}$. More details on the label semantics theory are available in [4]. Label semantics has been well applied in data mining and machine learning, a brief review on label semantics based data mining algorithms are given in [12].

III. Distance of Logical Expressions

Based on theory of fuzzy sets many similarity/dissimilarity measures [3] [6] have been proposed for measuring the degree of similarity between fuzzy sets. But those measures are not proper to deal with the similarity/dissimilarity measures between logical expressions which are concepts based on given linguistic variables. Label semantics focus on the decision making process, an intelligent agent must go through in order to identify which labels or logical expressions can actually be used to describe an object or value. For this reason, the appropriateness degree is proposed for measuring the appropriateness of using a particular subset of labels to describe

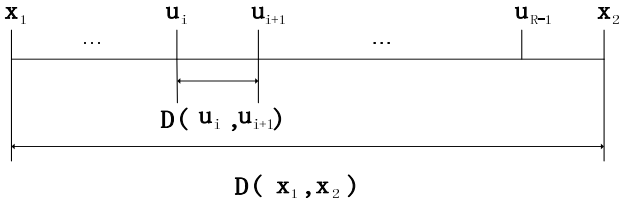

Fig. 1. Illustration of calculating the distance between two data points. The overall dissimilarity between $\mathbf{x}_1$ and $\mathbf{x}_2$ is the aggregated dissimilarity of all the neighboring points $\mathbf{u}_i$ and $\mathbf{u}_{i+1}$ for $i \in R$.

an object or value. One step further, we present a measure to evaluate the dissimilarity of logical expressions based on the mass assignments which can quantize the divergences between logical expressions. This measure is also extendable to measure distance between any two granular sets.

Definition 4 (Distance between data points): Given two data points $\mathbf{x}_1$ and $\mathbf{x}_2$ from an multi-dimensional universe Ω who is fully covered by n labels $\mathbb{L} = \{L_1, ..., L_n\}$, then the distance between $\mathbf{x}_1$ and $\mathbf{x}_2$ in this linguistic label space is defined by:

$$D(\mathbf{x}_1, \mathbf{x}_2) = \sum_{i=0}^{R-1} D(\mathbf{u}_i, \mathbf{u}_{i+1}) \tag{5}$$

where

$$D(\mathbf{u}_i, \mathbf{u}_{i+1}) = \sum_{S \in \lambda(\mathbb{L})} (m_{\mathbf{u_i}}(S) - m_{\mathbf{u_{i+1}}}(S))^2 \tag{6}$$

$$\mathbf{u}_i = \mathbf{x}_1 + \frac{i}{R}(\mathbf{x}_2 - \mathbf{x}_1) \tag{7}$$

Fig. 1 intuitively explains the above definition. To calculate the distance between two data points, we divide the distance between them into R ($R > 0$) pieces and calculate the the dissimilarity $D(\mathbf{u}_i, \mathbf{u}_{i+1})$ between two neighboring points $(\mathbf{u}_i, \mathbf{u}_{i+1})$ in the space of linguistic labels. The overall dissimilarity $D(\mathbf{x}_1, \mathbf{x}_2)$ is the sum of the above R pieces of dissimilarity. Thus the accuracy of the distance measure will be improved with increasing the value of R. As we can easily seen that this measure can be generalized to calculate the dissimilarity between any granular sets or a data point to a granular set. In addition, this distance measure has two important properties:

Theorem 1: The distance defined by Equation 5 is symmetric.

$$D(\mathbf{x}_i, \mathbf{x}_j) = D(\mathbf{x}_j, \mathbf{x}_i) \tag{8}$$

Theorem 2: If given $\mathbf{x}_1 < \mathbf{x}_2 < \mathbf{x}_3$[1], then

$$D(\mathbf{x}_1, \mathbf{x}_3) \geq D(\mathbf{x}_1, \mathbf{x}_2) \tag{9}$$

Theorem 2 demonstrates that this measure has non-negative correlation with the distance of $\mathbf{x}$. Both theorems have been proved in [16].

Above definition tells us the way of calculating distance between two data elements. Now we consider the question of how can we design a measure to calculate the distance between a data element point and an imprecise concept represented by logical expressions of linguistic labels. Given a data point $\mathbf{x}_0$ and a linguistic label set $S \in \mathbb{F}$ that covers a continuous area $\delta(S)$ on the universe Ω, the distance between $\mathbf{x_0}$ and S is defined as follows:

$$D(\mathbf{x}_0, S) = \frac{\int_{\delta(S)} D(\mathbf{x}_0, \mathbf{x}) d\mathbf{x}}{\delta(S)} \tag{10}$$

Furthermore, distance of sets of labels which is used to measure the divergence between them can be defined as follows:

Definition 5 (Distance between sets of labels): Given two sets of labels S_i, $S_j \in \mathbb{F}$ and S_i covering a continuous area $\delta(S_i)$ and S_j covering a continuous area $\delta(S_j)$. Then distance between these two sets is defined as:

$$D(S_i, S_j) = \frac{\int_{\delta(S_i)} \int_{\delta(S_j)} D(\mathbf{x}_i, \mathbf{x}_j) d\mathbf{x}_i d\mathbf{x}_j}{\delta(S_i)\delta(S_j)} \tag{11}$$

where $\mathbf{x}_i \in \delta(S_i), \mathbf{x}_j \in \delta(S_j)$, and when $i = j$:

$$D(S_i, S_j) = D(S_i, S_i) = 0 \tag{12}$$

For the symmetry of the distance between two variables, it is obviously that the distance of sets of labels is also symmetric. As we have discussed in Section II, λ-function provides a way of mapping from logical expressions of labels to random set descriptions of labels. So we also can define the distance between two logical expressions as the following.

Definition 6 (Distance between logical expressions): Given two logical expressions $\theta, \varphi \in LE$, then the distance between θ and φ is

$$D(\theta, \varphi) = \frac{1}{pr} \sum_{i=1}^{r} \sum_{j=1}^{p} D(S_i^{\theta \wedge \neg\varphi}, S_j^{\varphi}) - \frac{1}{qt} \sum_{k=1}^{t} \sum_{l=1}^{q} D(S_k^{\varphi \wedge \neg\theta}, S_l^{\theta}) \tag{13}$$

where p, q, r, t, respectively, represent the cardinality of label set $\mathbb{S}^{\varphi}$, $\mathbb{S}^{\theta}$, $\mathbb{S}^{\theta \wedge \neg\varphi}$, $\mathbb{S}^{\varphi \wedge \neg\theta}$, respectively, where:

$$S_i^{\theta} \in \mathbb{S}^{\theta} = \{S | S \in \lambda(\theta)\}, i = 1, 2, ..., q.$$

$$S_j^{\varphi} \in \mathbb{S}^{\varphi} = \{S | S \in \lambda(\varphi)\}, j = 1, 2, ..., p.$$

$$S_k^{\theta \wedge \neg\varphi} \in \mathbb{S}^{\theta \wedge \neg\varphi} = \{S | S \in \lambda(\theta) \bigcap \overline{\lambda(\varphi)}\}, k = 1, 2, ..., r.$$

$$S_l^{\varphi \wedge \neg\theta} \in \mathbb{S}^{\varphi \wedge \neg\theta} = \{S | S \in \lambda(\varphi) \bigcup \overline{\lambda(\theta)}\}, l = 1, 2, ..., t.$$

When $\mathbb{S}^{\varphi \wedge \neg\theta} = \emptyset$,

$$D(\theta, \varphi) = \frac{1}{pr} \sum_{i=1}^{r} \sum_{j=1}^{p} D(S_i^{\theta \wedge \neg\varphi}, S_j^{\varphi}) \tag{14}$$

[1]if $dim(\mathbf{x}) > 2$, we define: $\mathbf{x}_1 \geq \mathbf{x}_2$ if $d(\mathbf{x}_1, 0) \geq d(\mathbf{x}_2, 0)$, where $d(\cdot)$ is the Euclidean distance.

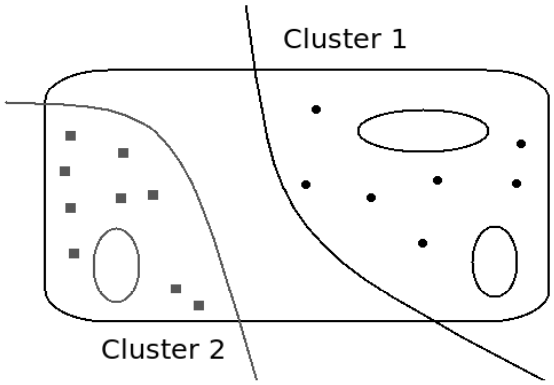

Fig. 2. A schematic illustration of mixed objects clustering. The imprecise concepts are represented by ellipses and data instances are by dots.

When $\mathbb{S}^{\theta\wedge\neg\varphi} = \emptyset$,

$$D(\theta,\varphi) = \frac{1}{qt}\sum_{k=1}^{t}\sum_{l=1}^{q} D(S_k^{\varphi\wedge\neg\theta}, S_l^{\theta}) \tag{15}$$

The above logical expression is one dimensional, which can be used by agents to describe one of the features of the object. If we have a multi-dimensional objects, linguistic rule can be used to described the object such as "x is *big* AND y is *medium* $\wedge$ *large*".

Based on Definition 1, a linguistic rule is a rule that can be represented as a multi-dimensional logical expressions of linguistic labels.

Definition 7: (Multi-dimensional logical expressions of labels) $MLE^{(n)}$ is the set of all multi-dimensional label expressions that can be generated from the logical label expression $LE_j : j = 1, ..., n$ and is defined recursively by

(i) If $\theta \in LE_j$ for $j = 1, ..., n$ then $\theta \in MLE^{(n)}$.

(ii) If $\theta, \varphi \in MLE^{(n)}$ then $\neg\theta, \theta \wedge \varphi, \theta \vee \varphi, \theta \rightarrow \varphi \in MLE^{(n)}$

Similarly we could give the definition of distance between two $MLE^{(n)}$.

Definition 8: (Distance between multi-dimensional logical expressions) Given two n-dimensional logical expressions: Φ, Ψ with

$$\Phi = \theta_{D_1} \wedge \theta_{D_2} \wedge ... \wedge \theta_{D_n}$$

$$\Psi = \varphi_{D_1} \wedge \varphi_{D_2} \wedge ... \wedge \varphi_{D_n}$$

where θ_{D_i}, φ_{D_i} respectively means the logical expressions in dimension D_i. hence, the distance between Φ and Ψ is defined as follows:

$$D(\Phi,\Psi) = \sqrt{\sum_{i=1}^{n} |D(\theta_{D_i}, \varphi_{D_i})|^2} \tag{16}$$

TABLE I
THE DESCRIPTION OF LOGICAL DISTANCE BASED K-MEANS ALGORITHM

Given unlabeled data set DB=$\{\mathbf{obj}_i : i = 1, ..., N\}$ in $\mathbb{R}^d$ and cluster number $K > 0$, counter $p = 0$, $\varepsilon > 0$
Randomly initialize the K centers $\mathbf{c}_1$,..., $\mathbf{c}_K$

While(TRUE): $p++$

Step 1: For each $i \in \{1, ..., N\}$, determine the cluster for all objects in DB: $\mathbf{obj}_i \leftarrow c_j$, if:
$D(\mathbf{obj}_i, \mathbf{c}_j^{(p-1)})$=min$\{D(\mathbf{obj}_i, \mathbf{c}_k^{(p-1)}) : k = 1, ..., K\}$

Step 2: Compute the cluster centers $\mathbf{c}_i^{(p)}$ which satisfy:
$\sum_{\mathbf{obj}_j \in \mathbb{C}_i} D(\mathbf{c}_i^{(p)}, \mathbf{obj}_j)$=min$\{\sum_{\mathbf{obj}_j \in \mathbb{C}_i} D(\mathbf{x}, \mathbf{obj}_j)\}$

Until $|\mathbf{c}^{(p)}$-$\mathbf{c}^{(p-1)}| < \varepsilon$.

IV. CLUSTERING OF MIXED OBJECTS

Based on the above dissimilarity measure, the distance between objects including numerical data, concepts, and linguistic description can be easily measured. Further more, a set of these objects can be grouped into clusters using clustering algorithms.

K-means [8] is one of the simplest unsupervised learning algorithms that solve clustering problem. The procedure follows a simple way to group a given data set to a certain number of clusters. Suppose that we have N sample feature vectors $\langle \mathbf{x}_1, \mathbf{x}_2, ..., \mathbf{x}_N \rangle$ that are all from the same class, and we know that they fall into K ($K < N$) compact clusters, . Let $\mathbf{m}_j$ be the mean of the vectors in cluster j. We can use a minimum-distance to separate them. That is, we can say $\mathbf{x}$ belongs to cluster j if $||\mathbf{x} - \mathbf{m}_j||$ is the minimum of all the K distances. Hence, this algorithm aims at minimizing an objective function J:

$$J = \sum_{j=1}^{K}\sum_{i=1}^{N} ||\mathbf{x}_i^{(j)} - \mathbf{m}_j||^2 \tag{17}$$

Fig. 2 gives a schematic illustration of mixed objects clustering where the ellipses represent some imprecise concepts can could be interpreted into linguistic labels or other granularity. Such mixed objects can be clustered by combining the classical clustering algorithms with our proposed distance measure. Formally, suppose we are given an unlabeled data set $\mathbf{obj}_1, ..., \mathbf{obj}_n$ in which there are numerical data, labels (concepts), and logical expressions (linguistic description). Now we focus on clustering them using K-means algorithm. The algorithm is as same as the classical K-means clustering and the pseudo-code are shown in Table I.

There are two points which are worthy of highlighting. First and the most important, we adopted the new proposed distance metric in last section as the distance measure of these mixed objects. The novel distance definition makes it possible to cluster data and imprecise concepts represented by linguistic labels. Second, in the algorithm implementation, the center of each cluster should be numerical data but not logical expressions.

TABLE II
DISTANCES BETWEEN SETS OF LABELS DEFINED ON H VALUES.

	$\{r\}$	$\{r,o\}$	$\{o\}$	$\{o,y\}$	$\{y\}$
$\{r\}$	0	0.0288	0.0626	0.0950	0.1246
$\{r,o\}$	0.0288	0	0.0354	0.0673	0.0968
$\{o\}$	0.0626	0.0354	0	0.0336	0.0626
$\{o,y\}$	0.0950	0.0673	0.0336	0	0.0304
$\{y\}$	0.1246	0.0968	0.0626	0.0304	0

TABLE III
DISTANCES BETWEEN EACH TWO LOGICAL EXPRESSIONS θ, φ AND γ DEFINED ON H VALUES.

	$\theta = \neg orange$	$\varphi = red \vee orange$	$\gamma = red$
$\theta = \neg orange$	0	0.1413	0.1735
$\varphi = red \vee orange$	0.1413	0	0.0650
$\gamma = red$	0.1735	0.0650	0

V. EXPERIMENTAL STUDIES

In this section we did two experiments to verify the new proposed measure and the clustering problem. The first experiment is to illustrate the properties of the proposed logical distance measure. The second experiments shows image scene clustering based on a benchmark problem.

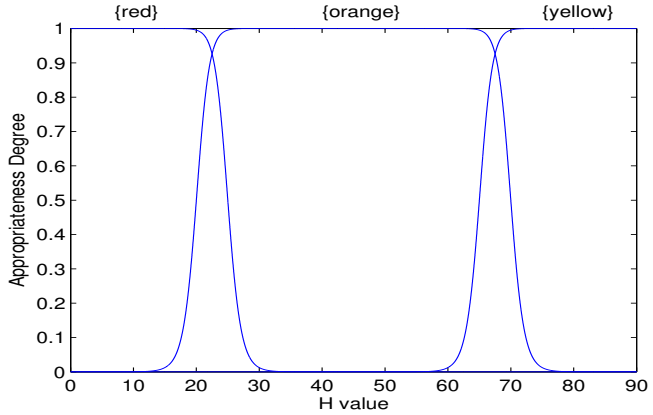

Fig. 3. Three linguistic labels: red (r), orange (o) and yellow (y). They are defined by bell-shape fuzzy sets on the Hue (H) values.

A. Logical Distance

Color of an object is a vague concept and largely depends on the observer's subjective belief. Human eye can distinguish about 10 million different colors but we only use very limited number of words to describe them. There is no general principle for human beings to decide using the most appropriate word such as yellow or red to describe the color of an object. However, people know the difference among these colors, which is difficult to be defined with some specific numerical value. We often make classifications based on these vague and subjective differences among objects. We can use the method proposed in this research to quantize these differences in order to let the agents have the ability to distinguish different objects.

HSV color space can be well visualized by the conical representation model accords with human beings' visual features. Fig. 3 shows three linguistic labels defined on the Hue (H)

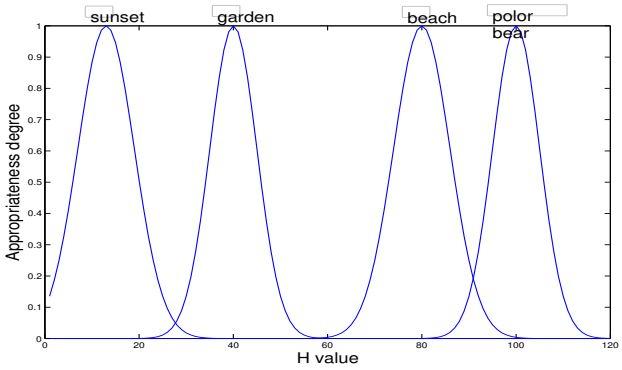

Fig. 4. Four image labels are predefined on the HSV space. This is the mapping of the labels on Hue (H) axis.

value. Based on Definition 3, we can infer that the focal set is:

$$\mathbb{F} = \{\{r\}, \{r,o\}, \{o\}, \{o,y\}, \{y\}\}$$

The distances between these label sets based on Definition 5 is calculated and shown into Table II, from which we can clearly see the symmetric property of this distance measure.

Given the same example above, if there is imprecise concept of the color is not orange, or formally denoted by θ: $\theta = \neg orange$. There are also two other descriptions about the colors φ and γ:

$$\varphi = red \vee orange, \ \gamma = red$$

According to Definition 2, the possible label sets of the given logical expressions θ, γ and φ are calculated as follows:

$$\lambda(\neg o) = \{\{r\}, \{y\}\}, \ \lambda(r) = \{\{r\}, \{r,o\}\}$$
$$\lambda(o) = \{\{r,o\}, \{o\}\, \{o,y\}\}$$

so that

$$\lambda(\theta) = \{\{r\}, \{y\}\}, \ \lambda(\gamma) = \{\{r\}, \{r,o\}\}$$
$$\lambda(\varphi) = \{\{r\}, \{r,o\}, \{o\}\, \{o,y\}\}$$

Then according to Definition 6 and Table II, we could calculate all the distances and fill in Table III. It is illustrated that distances between LEs are symmetric and could reasonably reflect the logical divergences between LEs.

B. Images and Labels Clustering

To show how to use our proposed approach to cluster data and imprecise concept, we built a toy application which can cluster images and image labels which are defined based on image global color feature. One hundred images are evenly picked up from four categories of the Corel image data set [2][7]. And each category has 25 images. We first resize these images into 192×128. We then artificially designed four linguistic labels on color: "$sunset$", "$beach$", "$garden$", and "$polar\ bear$" based on the image content. These labels can be considered as the linguistic descriptors of images which convey the semantic of images. Since the main goal of this

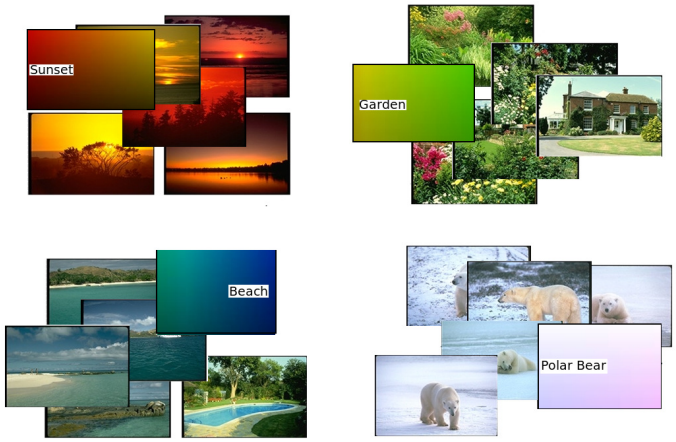

Fig. 5. Sample results of images and linguistic labels clustering. Linguistic labels on color: *sunset, garden, beach* and *polar bear* are areas of color in HSV space. For each cluster, four images and one label (the colored shape on the top of stack of images) are shown.

TABLE IV
PERFORMANCE OF THE IMAGE CLUSTERING.

	sunset	*beach*	*garden*	*polar bear*
Performance	72%	60%	64%	96%

work is to present a new approach to cluster data and vague concepts, we did not use complicated image features like SIFT and LBP.

The only feature we used in this experiment is the global average of HSV color. Fig. 4 shows the mappings of these predefined labels on the Hue (H) axis. The original labels are 3-dimensional granularity in the HSV space. Thus after artificially designing the image labels and extracting image color feature, the data set need to be clustered is with one hundred images and the above four image labels which are represented by granularity on HSV space. The experimental results are shown in Table IV and the code and image set are also open to public at the web address of [18] and [19], respectively. In the future work, such linguistic labels can be used as constraints guide clustering process by using high-level knowledge. It allows us to develop a new human-machine interface by using linguistic labels.

In addition although low-level image features, such as color and texture, are useful information to describe images in this experiment. In practice the features extraction are very important and the clustering algorithms are always only one step of the procedure. High-level image features can convey much more accurate information of the content of the images. In real-world application of image clustering, SIFT, LBP or other complex image features are better choice.

VI. CONCLUSION

In this paper we proposed a novel clustering algorithm by employing a new distance measure based on label semantics. The new algorithm can be used to cluster data and imprecise concepts. The distance defined in linguistic label space differs from the other measures by focusing on the difference of logical meanings the objects convey. It has the ability to measure the linguistic divergence between numerical data and concepts which are presented in the form of linguistic labels. Experimental studies on a toy image clustering problem showed that our approach is an effective to group data and linguistic labels reasonably.

Because the new proposed measure is calculated by considering the accumulated dissimilarities alone the trials connecting to imprecise concepts. It is extendable to measuring distance between any granularities. In the future work, we hope to apply this clustering algorithms to other application areas beside image classification. We will also investigate the advantages and disadvantages of this measure studying other concepts represented by other granularity.

ACKNOWLEDGEMENTS

This work is partially funded by the NCET Program of MOE, China and the SRF for ROCS. The second author also thanks the China Scholar Council for visiting fellowship (No. 2010307502).

REFERENCES

[1] M.M.S. Beg, M. Thint and Z. Qin, PNL-enhanced restricted domain question answering system, *the Proceedings of IEEE-FUZZ*, (2007) pp. 1277-1283.
[2] G. Carneiro, A.B. Chan, P.J. Moreno, and N. Vasconcelos, Supervised learning of semantic classes for image annotation and retrieval, *IEEE Transactions on Pattern Analysis and Machine Intelligence*, Vol. 29 (3) (2006), pp. 394-410.
[3] L.K. Hyung, Y.S. Song, K.M. Lee, Similarity measure between fuzzy sets and between elements, *Fuzzy Sets and System* Vol. 62 (1994), pp. 291-293.
[4] J. Lawry, *Modelling and Reasoning with Vague Concepts* (2006), Springer.
[5] J. Lawry, A Framework for Linguistic Modelling, *Artificial Intelligence*, Vol. 155 (2004), pp. 1-39
[6] D.-F. Li, Some measures of dissimilarity in intuitionistic fuzzy structures, *Journal of Computer and System Sciences* Vol. 8 (2004), pp. 115-122.
[7] V. Lavrenko, R. Manmatha, and J. Jeon, A model for learning the semantics of pictures, *Proceedings of NIPS*, (2004).
[8] J.B. MacQueen, Some methods for classification and analysis of multivariate observations, *Proceedings of 5th Berkeley Symposium on Mathematical Statistics and Probability*, University of California Press (1967), pp. 281-297.
[9] Z. Qin, J. Lawry, Decision tree learning with fuzzy labels, *Inform. Sci.* 172(1-2) (2005), pp. 91-129.
[10] Z. Qin, M. Thint and M.M.S. Beg Deduction engine designs for PNL-based question answering systems, *Foundations of Fuzzy Logic and Soft Computing*, LNAI 4529 (2007) pp. 253-262.
[11] Z. Qin, J. Lawry, LFOIL:Linguistic rule induction in the label semantics framework, *Fuzzy sets and systems* Vol. 159 (2008), pp. 435-448.
[12] Z. Qin, J. Lawry, Knowledge discovery in a framework for modelling with words. *Soft Computing for Knowledge Discovery and Data Mining* (2008): pp. 241-276.
[13] T. Wan and Z. Qin, A new technique for summarizing video sequences through histogram evolution, *Proceedings of Int. Conf. on Signal Processing and Communications (SPCOM)* (2010), pp. 1-5.
[14] L.A. Zadeh, Fuzzy Logic=Computing with Words, *IEEE Transaction on Fuzzy Systems* Vol. 4(1996), pp. 103-111.
[15] L.A. Zadeh, The Concept of Linguistic Variable and its Application to Approximate Reasoning Part 2, *Information Science* Vol. 8 (1975), pp. 301-357.
[16] W. Zhang, and Z. Qin, Dissimilarity measure of logical expressions, *Proceedings of Int. Conf. of Machine Learning and Cybernetics (ICMLC)* (2010), pp. 199-203.
[17] http://en.wikipedia.org/wiki/Unsupervised_learning
[18] icmll.buaa.edu.cn/projects/FUZZ-IEEE2011/code.rar
[19] icmll.buaa.edu.cn/projects/FUZZ-IEEE2011/image.rar

2011 IEEE International Conference on Fuzzy Systems
June 27-30, 2011, Taipei, Taiwan

Fuzzy Variable Structure Control for PWM Inverters

En-Chih Chang
Power Electronics Lab
Dept. of Electrical Engineering
I-Shou University, Kaohsiung City
84001 Taiwan, R.O.C.
enchihchang@isu.edu.tw

Josep M. Guerrero
Distributed Generation and Microgrids Lab
Dept. of Automatic Control Systems
Universitat Politècnica de Catalunya
08036 Barcelona, Spain
josep.m.guerrero@upc.edu

***Abstract*—This paper proposes the practical realization of a fuzzy variable structure control applied to a PWM inverter. Variable structure Control (VSC) is a robust control method for handling nonlinear systems where occur parameter variations and external disturbances. However, control input chattering round sliding surface exists, and may deteriorate the system performance. To reduce the chattering, a fuzzy logic for VSC is applied to overcome the problem. By composing the advantages of both VSC and fuzzy logic (FL), the PWM Inverter system can be designed and produces low total harmonic distortion (THD) output voltage and fast dynamic response under different types of load. Experimental results on a single-phase PWM inverter laboratory prototype controlled by a dSPACE-based DSP controller are presented to illustrate the improved performance, particularly under severe rectifier load. Moreover, for comparison purposes, a conventional variable structure controlled single-phase PWM inverter is also tested on the same experimental system.**

Keywords-Variable structure Control (VSC), chattering, fuzzy logic (FL),total harmonic distortion (THD), PWM Inverter

I. INTRODUCTION

With the increasing demands for high-quality power sources, a pulse-width modulated PWM inverter has been used as a key element for a high-performance power conversion system for critical loads, like data processing systems, telephone switching systems, and life support equipment in hospitals. In that kind of applications it is necessary that the inverter generates by itself the voltage waveform. That kind of inverters, named voltage source inverters, are becoming more and more popular in standalone applications like Microgrids, being able to operate in parallel by using droop method or virtual inertias.

The critical point of these inverters is its performance that generally lies on the following criteria: (1) output voltage waveform with low harmonic distortion (THD) for linear and nonlinear loads; (2) fast transient response for load step changes; and (3) the steady-state error as small as possible. In order to achieve above criteria, proportional-integral (PI) controllers perform reasonably well under constant load conditions. However, the consistent regulation performance is not achieved when the process is subject to fluctuating load disturbances [1], [2], [3]. Also, various control schemes can be found in literature, such as the multi-loop control [4], the deadbeat control [5], the fourier transform (DFT)-based harmonic elimination technique [6], and so on. However, these methods require complex mathematical models or large computation time.

Variable structure control has been recognized as a powerful device capable of exhibiting good robustness, even invariant under certain condition, with respect to system parameter variations and external disturbances [7], [8]. Many VSC applications to PWM inverter systems have been reported. In [9], a control strategy for DC/AC inverter is proposed in which an inverter is controlled by a double-loop regulation scheme. However, the control design uses a typical VSC and cumbersome analog implementation, and thus incurs distorted output voltage during steady-state operation when supplying a nonlinear load. Reference [10] utilizes two sliding control laws to achieve DC/AC converter tracking control. This method has a complicated hardware design and an undesirable chattering phenomenon. In the earlier works of [11] and [12], they adopt conventional VSC for PWM inverters, resulting in problems of chattering and steady-state errors. However, as mentioned above [9-12], owing to the sampling action of digital implementation and delay of switch device, the chattering exists in a VSC system is fearful to control system; In case of these inverter applications, chattering has caused serious voltage harmonics.

FL was developed in 1970s [13], and further developed in inverter applications, since its operation principle does not require precise knowledge of the load parameters, FL controllers have the potential of operating successfully under a wide range of load variation [14], [15]. Thus, in this paper, we will use a simple FL to reduce the chattering effect. By incorporating a VSC with FL, not only the sliding surface is fuzzified by FL, thus reducing the chattering, but also VSC accomplishes the rejection of system uncertainties. This proposed algorithm is then applied to the control of a PWM inverter system in which the control law is realized on a dSPACE DSP and will show the effectiveness of low output voltage distortion, fast dynamic response, and insensitive to load variation even under rectifier loads. Experimental results are finally shown to validate the performance of this proposed controller.

978-1-4244-7316-8/11/$26.00 ©2011 IEEE

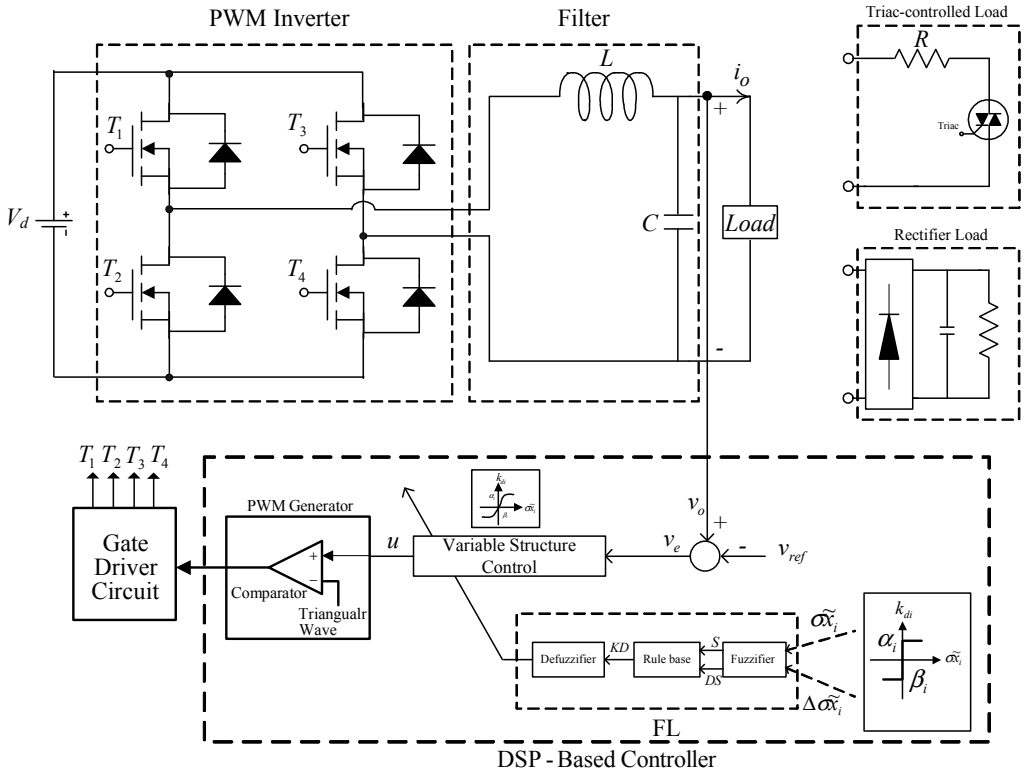

Fig. 1 Block diagram of PWM inverter system.

II. MATHEMATICAL MODELING

The system block diagram of PWM Inverter is shown in Fig. 1 [16]. Let v_o be the load voltage, v_{ref} be the desired sinusoidal waveform, and $v_e = v_o - v_{ref}$ be the voltage error. Assuming that the switching frequency is high enough, PWM inverter can be regarded as a constant gain, K_{pwm}. Choosing $\tilde{x}_1 = v_e$ and $\dot{\tilde{x}}_1 = \tilde{x}_2$, the resulting error dynamic state equation can be derived as

$$\begin{bmatrix} \dot{\tilde{x}}_1 \\ \dot{\tilde{x}}_2 \end{bmatrix} = \underbrace{\begin{bmatrix} 0 & 1 \\ -\frac{1}{LC} & -\frac{1}{RC} \end{bmatrix}}_{A} \begin{bmatrix} \tilde{x}_1 \\ \tilde{x}_2 \end{bmatrix} + \underbrace{\begin{bmatrix} 0 \\ \frac{K_{pwm}}{LC} \end{bmatrix}}_{B} u + \underbrace{\begin{bmatrix} 0 \\ -\frac{1}{LC} v_{ref} - \frac{1}{RC} \dot{v}_{ref} - \ddot{v}_{ref} \end{bmatrix}}_{f} \quad (1)$$

The control objective is to make the output voltage be equal to a reference input. The above system takes the following form

$$\dot{\tilde{x}} = A\tilde{x} + Bu + f \quad (2)$$

where $\tilde{x}$ is the error state vector, u is the control input, A is the system matrix, B is the control matrix, and f is the disturbance.

Then the sliding function is given by

$$\sigma = c_1\tilde{x}_1 + \tilde{x}_2 = c^T\tilde{x} \quad (3)$$

where c is the sliding surface coefficient vector.

The control input u is chosen as

$$u = -K^T\tilde{x} \quad (4)$$

where K is the feedback gain vector.

The dynamics in sliding motion can be written as

$$\dot{\sigma} = 0 \quad (5)$$

Then, for $det(cB) \neq 0$, the equivalent control u_{eq} is derived as follows

$$\dot{\sigma}\big|_{u=u_{eq},\, f=0} = c^T\dot{\tilde{x}} = c^T(A\tilde{x} + Bu_{eq}) = 0 \quad (6)$$

Therefore, the equivalent control can be expressed as

$$u_{eq} = -K_{eq}^T\tilde{x} \quad (7)$$

where K_{eq}^T is the equivalent feedback gain vector.

From (6) and (7), it yields obtains

$$K_{eq}^T = (c^TB)^{-1}c^TA \quad (8)$$

The hitting control law guarantees a system trajectory that moves toward the sliding surface from any initial condition if the following condition occurs:

$$\lim_{\sigma \to 0} \sigma\dot{\sigma} < 0 \quad (9)$$

Let system control u be composed by K_{eq}^T and $K_s^T sign(\sigma\tilde{x})$, that is,

$$u = -K_{eq}^T - K_s^T sign(\sigma\tilde{x}) \quad (10)$$

For two-order system case, K_s^T can be written as

$$K_s^T = \begin{bmatrix} k_{s1} \\ k_{s2} \end{bmatrix} \tag{11}$$

and k_{si}, $i = 1$ to 2 is given by

$$k_{si} = \begin{cases} \alpha_i & if \quad \sigma\tilde{x}_i > 0 \\ 0 & if \quad \sigma\tilde{x}_i = 0 \\ \beta_i & if \quad \sigma\tilde{x}_i < 0 \end{cases} \tag{12}$$

Thus, the condition in (12) is represented to satisfy the inequality (9) and the system state (2) will be transferred on the sliding surface (5). Obviously, (12) uses a sign function and often causes chattering problem in practice. To solve such a problem, fuzzy logic is introduced, and the design is described in detail in Section III.

III. Design of Fuzzy Variable Structure Control

FL is a direct method for controlling a system without the need of a mathematical model. FL gets crisp data from various sensors. These data are changed to linguistic or fuzzy membership functions via the fuzzification process. After that, they go through a set of fuzzy "IF-THEN" rules in an inference engine and result in fuzzy outputs. These fuzzy outputs are then changed back to crisp values by the defuzzification.

If the VSC is implemented by means of a digital signal processor (DSP), the switching actions with chattering will occur in (12), which is a crisp version. In other words, the sliding surface is a particular fuzzy case, and its membership function is defined as

$$\mu_{\sigma=0} = \begin{cases} 1 & , \quad \sigma = 0 \\ 0 & , \quad \text{otherwise} \end{cases} \tag{13}$$

To alleviate the chattering, fuzziness of the sign function and sliding surface are shown as Fig. 2 and Fig. 3, respectively.

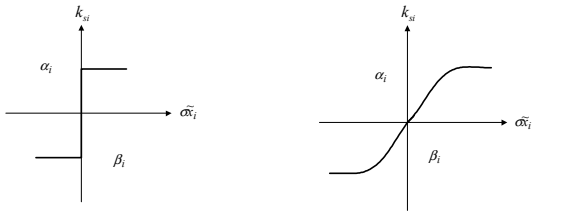

(a) (b)

Fig. 2 (a) Switching criteria with the sign function, and (b) fuzziness of the *sign* function.

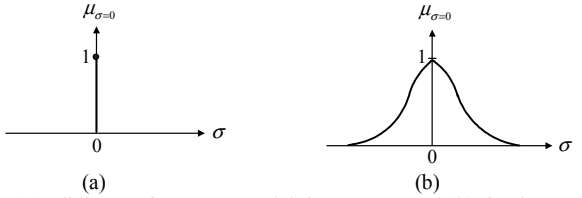

(a) (b)

Fig. 3 (a) Sliding surface as a special fuzzy case, and (b) fuzziness of the sliding surface.

Then the human experience is fixed as linguistic rules with the help of in the following statements:

IF farther from the sliding surface
THEN larger feedback gain (14)

The design steps are described as follows:

Step 1: To govern system dynamic, define two inputs, $\sigma\tilde{x}_i$ and $\Delta\sigma\tilde{x}_i$ (the change of $\sigma\tilde{x}_i$).

Step2: To determine the system dynamic behavior, we define a crisp sliding surface, $\sigma = c^T\tilde{x}$.

Step3: The fuzzy linguistics and the membership functions of the fuzzy input and output variables S, DS, KD are nominated as shown in Fig. 4.

Step 4: The output of each rule is determined by inference method as follows:

IF S.P and DS.P THEN KD.PB
IF S.P and DS.ZO THEN KD.PM
IF S.P and DS.N THEN KD.PS
IF S.ZO and DS.P THEN KD.PS
IF S.ZO and DS.ZO THEN KD.ZO
IF S.ZO and DS.N THEN KD.NS
IF S.N and DS.P THEN KD.NS
IF S.N and DS.ZO THEN KD.NM
IF S.N and DS.N THEN KD.NB

where

S.P: S is positive
S.ZO: S is zero
S.N: S is negative
DS.P: DS is positive
DS.ZO: DS is zero
DS.N: DS is negative
KD.PB: KD is positive big
KD.PM: KD is positive medium
KD.PS: KD is positive small
KD.NS: KD is negative small
KD.NM: KD is negative medium
KD.NB: KD is negative big

Step 5: Quantification of the crisp input variables $\sigma\tilde{x}_i$ and $\Delta\sigma\tilde{x}_i$ is carried out by multiplying the scaling factors GS and GDS, respectively, i.e., $\sigma\tilde{x}_i \times GS$, and $\Delta\sigma\tilde{x}_i \times GDS$.

$$k_{si} = T(\bullet) \times GKS \tag{15}$$

where $T(\bullet)$ indicates the fuzzy rules, and GKS is the scaling factor of k_{si}.

Step 6: The control input u is written as

$$u = -\sum_{i=1}^{2} (k_{eqi} + k_{di})\tilde{x}_i \tag{16}$$

where k_{eqi} are the elements of equivalent feedback gain, K_{eq}^T.

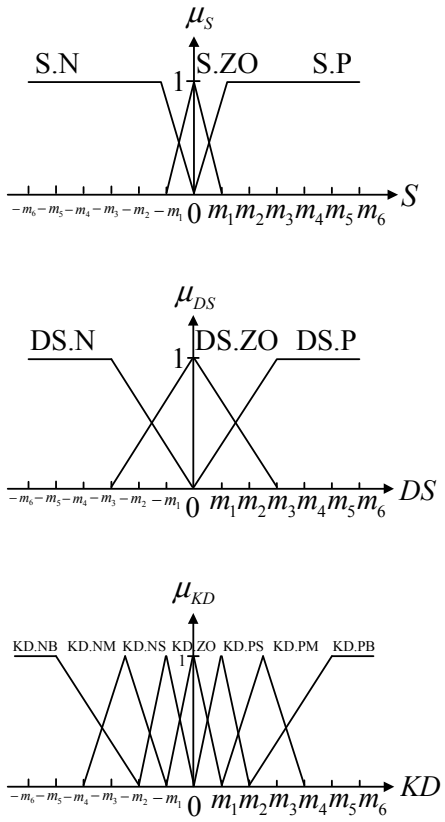

Fig. 4 Fuzzy membership functions of *S*, *DS* and *KD*.

IV. EXPERIMENTAL RESULTS

In order to confirm the effective performance of the PWM inverter, key experiment under rectifier load were done. The controller is validated with a hardware setup. The control algorithms are designed and implemented using MATLAB/Simulink and the codes are then compiled and loaded to a dSPACE DS1102 controller board implement the controller. The system parameters are summarized in Table I.

Table I System parameters

DC-bus Voltage V_d	250V
Output Voltage V_o	$110V_{rms}$
Output Frequency f	60 Hz
Filter Inductor L	2 mH
Filter Capacitor C	30 μF
Switching Frequency f_s	18 kHz
Rated Load R	20 Ω

In order to test the transient performance, the load-step change response is shown in Fig. 5 when the rated load is suddenly connected. We found that the proposed controller exhibits small voltage sag and fast recover time under load-step changes. On the contrary, the waveform shown in Fig. 6 with conventional VSC exhibits worst voltage compensation at the firing angle. The rectifier load consists of a full wave rectified with a parallel resistor, a 55Ω resistance and 100μF filter capacitor. A comparison of the performance by using the proposed controller and the conventional VSC are shown in Fig. 7 and Fig. 8, respectively. Fig. 7 depicts the output voltage waveform which is nearly sinusoidal and has low distortion (%THD of 2.89%), which is under the industrial standard of 5%. Fig. 8 exhibits a noticeable distortion (%THD of 8.15%). Indeed, the chattering is alleviated by the proposed controller, and thus the inverter output voltage can obtain a significant improvement reducing the voltage THD under rectifier-type load condition.

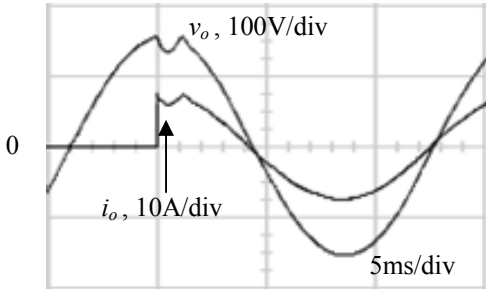

Fig. 5 Load step changes (from full load to no load at 90^0) with fuzzy VSC.

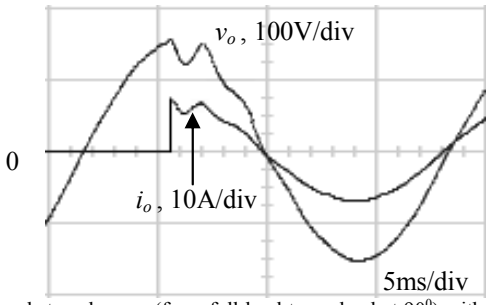

Fig. 6 Load step changes (from full load to no load at 90^0) with conventional VSC.

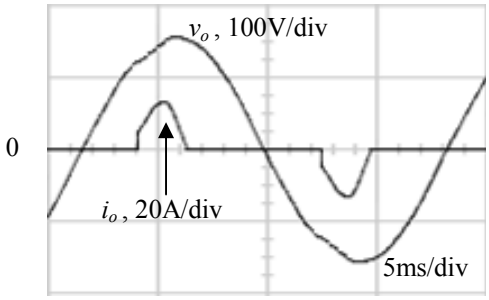

Fig. 7 Voltage and current waveforms when supplying a rectifier load, using fuzzy VSC

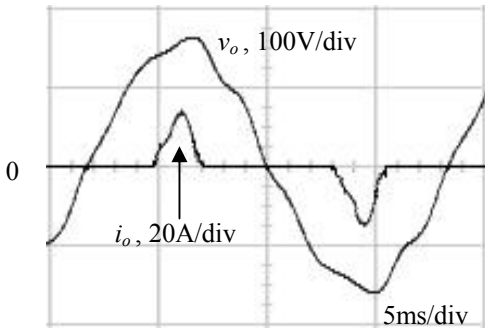

Fig. 8 Voltage and current waveforms when supplying a rectifier load, using conventional VSC

V. CONCLUSIONS

This paper proposes a fuzzy VSC applied to PWM inverter in order to achieve the following features: fast dynamic response, chattering reduction, and low THD output voltage. The proposed controller not only has the merits of the conventional VSC but also reduces the chattering problem by using fuzzy logic. The system's performance has been verified by means of experimental tests on a laboratory inverter prototype, confirming the proposed methodology. Compared to the conventional VSC under the same operating conditions, the proposed controller exhibits better inverter performance.

ACKNOWLEDGEMENT

This work was supported by the National Science Council of Taiwan, R.O.C., under contract number NSC99-2218-E-214-002.

REFERENCES

[1] H. I. Cha, S. S. Kim, M. G. Kang, and, Y. H. Chung, "Real-time digital control of PWM inverter with PI compensator UPS," in Proc. IEEE Industry Applications Society Annual Meeting Conf., pp. 1124-1128, 1990.

[2] R. Caceres, R. Rojas, and O. Camacho, "Robust PID control of a buck-boost UPS converter," in Proc. IEEE INTELEC, pp. 180-185, 2000.

[3] W. K. Ho, K. W. Lim, and W. Xu "Optimal gain and phase margin tuning for PID controllers," *Automatica*, vol. 34, pp. 1009-1014, 1998.

[4] S. L. Jung, H. S. Hung, M. Y. Chang, and Y. Y. Tzou "DSP-based multiple-loop control strategy for single-phase inverters used in ac power sources," in Proc. IEEE Power Electronics Specialists Conf., vol. 1, pp. 706-712, 1997.

[5] A. Kawamura, T. Haneyoshi, and R. G. Hoft, "Dead beat controlled PWM inverter with parameter estimation using only voltage sensor," in Proc. IEEE Power Electronics Specialists Conf., pp. 576-583, 1986.

[6] A. V. Jouanne, P. N. Enjeti, and D. J. Lucas, "DSP control of high-power UPS system feeding nonlinear loads," *IEEE Trans. Ind. Electron.*, vol. 43, pp.121-125, 1996.

[7] U. Itkis, Control Systems of Variable Structure. New York: Wiley, 1976.

[8] K. D. Young, V. I. Utkin, and U. Ozguner, "A control engineer's guide to sliding mode control," *IEEE Transactions Control System Technology*, vol. 7, pp. 328-342, 1999.

[9] P. Sanchis, A. Ursaea, E. Gubia, and L. Marroyo, "Boost DC-AC inverter: A new control strategy," *IEEE Trans. Power Electron.*, vol. 20, no. 2, pp. 343-353, 2005.

[10] D. Biel, F. Guinjoan, E. Fossas, and J. Chavarria, "Sliding-mode control design of a boost-buck switching converter for AC signal generation," *IEEE Tran. Circuits Syst. I*, vol. 51, no. 8, pp. 1539-1551, 2004.

[11] T. J. Liang, Y. C. Kuo, and J. F. Chen, "Single-stage photovoltaic energy conversion system," *Proc. IEE-Elect. Power Applicat.*, vol. 148, no. 4, pp. 339-344, 2004.

[12] J. F. Chen, Y. C. Kuo, and T. J. Liang, "Voltage and current hybrid controlled PWM inverters using variable structure control," in Proc. IEEE Power Electronics and Drive Systems Conf., pp. 1010-1014, 1999.

[13] L. A. Zadeh, "Fuzzy sets," Inform Control, vol. 8, pp. 338-353, 1965.

[14] B. R. Lin and R. G. Hoft, "Real-time digital control of PWM inverter with fuzzy logic compensator for nonlinear loads," in Proc. IEEE Industry Applications Society Annual Meeting Conf., vol. 2, pp. 862-869, 1993.

[15] Y. T. Tzou, L. H. Ho, and R. S. Ou, "Fuzzy control of a closed-loop regulated PWM inverter under large load variations," in Proc. IEEE Industrial Electronics, Control, and Instrumentation Conf., vol. 1, pp. 267-272, 1993.

[16] F. J. Chang, T. J. Liang, and E. C. Chang, "Integral terminal sliding-mode control of PWM inverters," in Proc. Systemic, Cybernetics, and Informatics Conf., pp. 33-36, 2004.

2011 IEEE International Conference on Fuzzy Systems
June 27-30, 2011, Taipei, Taiwan

An Adaptive Fuzzy Logic Controller based on Real Coded Quantum-Inspired Evolutionary Algorithm

Pintu Chandra Shill†, Md. Amjad Hossain‡, Md. Faijul Amin†, Kazuyuki Murase†
† Department of System Design Engineering, University of Fukui, 3-9-1 Bunkyo, Fukui-910-8507, Japan
‡ Khulna University of Engineering and Technology, Khulna, Bangladesh
{pintu,amin,murase}@ synapse.his.u-fukui.ac.jp, amjad_kuet@yahoo.com

Abstract—**In this paper, fuzzy logic control systems and real coded quantum inspired evolutionary algorithm (RCQIEA) are integrated for intelligent control. Here, RCQIEAs is utilized as an adaptive method for selection and definition of fuzzy control rules and for tuning the parameters of membership function for each fuzzy control rule in two different ways. The majority of fuzzy logic controllers (FLCs) to date are working based on the expert knowledge base derived from heuristic knowledge of experienced operators. These approaches are difficult and time consuming for experts. Moreover, because manual coded FLCs use expert knowledge, there is no guarantee that the FLCs obtained will have sufficiently good performance, especially for a complex system problem with a large number of input variables. On the contrary, our proposed approach is an automatic knowledge acquisition learning method for generating or adapting FLCs using RCQIEA. In order to check the effectiveness of our proposed approach, it has been applied to solve the truck-and-trailer controller, which is well known test-bed for fuzzy control systems. The fuzzy controller obtained by the proposed approach performs better and effectively realizes the trajectory control of the truck with trailer.**

Keywords-Fuzzy Logic Controller; Fuzzy Rule Base; Real Coded Quantum-Inspired Evolutionary Algorithm; Optimization; Truck-and-Trailer controller

I. INTRODUCTION

Fuzzy rule-based model is used to solve a wide range of problems providing flexible solutions. A fuzzy rule-based model is a set of fuzzy rules and the associated membership functions (MFs) that maps inputs to outputs. Fuzzy rules are either provided by human experts or learned from sample data. Many decision-making and problem-solving tasks are too complex to be understood quantitatively. People however succeed by using knowledge that is imprecise rather than precise. The construction of fuzzy logic controllers (FLCs) based on the appropriate expert knowledge base (KB) can be quick and effective. On the other hand, without such an expert KB the design of FLCs can be slow as it relies on trial and error rather than a guided approach.

To surmount this shortcoming, real coded quantum inspired evolutionary algorithm (RCQIEA) can be considered as a powerful tool to find out efficient fuzzy rule sets [1], and tuning of MFs parameters. These algorithms mimics the natural evolution and provide an effective way for searching a large and complex solution space to give close to optimal solutions in much faster times than random trial-and-error.

For most fuzzy logic control problems, the most important issue is to determine the parameters that define the MFs. Because of this, the MFs optimization problems can be regarded as parameter optimization problems. These parameters are generally based on the expert KB that is derived from heuristic knowledge of experienced control engineers and/or generated automatically. A variety of methods such as genetic algorithms (GAs), neural networks (NNs), self-organizing feature map (SOFM), tabu search (TS), particle swarm optimization (PSO) have been used to improve the behavior of parameter optimization problem as well as selection and definition of fuzzy rules.

GA was used by Belarbi [2] in fuzzy rule base (RB) minimization. Belarbi applied GA to design FLC for the control of the pole and cart system and the control of the concentration in continuously stirred tank reactor. Kim [1] presented a method to find out efficient fuzzy rule sets using quantum inspired evolutionary. They design a fuzzy logic control system for path planning of mobile robot. Meredith [3] also applies GA to the fine tuning of MFs in a FLC for a helicopter. Bagis [4] have presented an approach for the determination of the structure and parameters of fuzzy RB. He applied this approach in the modeling of the nonlinear or complex systems. Bai and Chen [5] proposed an automatic method for a students' evaluation task. The purpose was to automatically construct the grade MFs of lenient-type grades, strick-type grades, and normal-type grades of fuzzy rules. Yang and Bose [6] has presented a method for generating fuzzy MFs with an unsupervised learning using SOFM. The SOFM approach is a two-step procedure; firstly, generate the proper clusters and secondly generate the fuzzy MF according to the clusters in the first step. They applied this method to pattern recognition. Huang [7] has presented a fuzzy knowledge integration technique based on the PSO. Their proposed approach consists of two phases: Firstly, it encodes the fuzzy rule sets and fuzzy sets with its corresponding MFs. Secondly, the particle swarm algorithm is used to explore the fuzzy rule sets, fuzzy sets and MFs to its optimal or the approximately optimal extent. Koga, et. al. [8] has presented a method, the self-organizing relationship (SOR) network with fuzzy inference based evaluation for backing up a truck-and-trailer controller. They use SOR network to establish desired I/O (Rule base) relationship of a target system.

In a classical evolutionary algorithm like GA, information is stored as classical binary (0 or 1) format. So information stored in a classical register represents a single state. But in quantum inspired evolutionary algorithm, smallest unit of information is called Q-bit which may be in '0'state or '1'

978-1-4244-7316-8/11/$26.00 ©2011 IEEE

state or any superposition state of them. Superposition of logical state can be expressed as "$\alpha|0\rangle+\beta|1\rangle$". Another way of writing "superposition" is as a vector:

$$\alpha|0\rangle+\beta|1\rangle \leftrightarrow \begin{pmatrix}\alpha\\ \beta\end{pmatrix}$$

The complex number α and β are called the "amplitudes" of the superposition. $|\alpha_i|^2$ gives the probability that the Q-bit will be found in "0" state and $|\beta_i|^2$ gives the probability that the Q-bit will be found in "1" and they satisfy the normalization condition $|\alpha_i|^2+|\beta_i|^2=1$. A Q-bit individual as a string of m Q-bits is defined as:

$$q=\begin{bmatrix}\alpha_1 & \alpha_2 & \dots & \alpha_m\\ \beta_1 & \beta_2 & \dots & \beta_m\end{bmatrix}$$

where $|\alpha_i|^2+|\beta_i|^2=1$, $i=1, 2, 3\ldots..m$. So a Q-bit individual of m bits can represent 2^m states at a time.

Quantum inspired evolutionary algorithms has a better characteristic of population diversity than others, since it can represent linear superposition of states probabilistically. But higher value of m needs higher computing time of the algorithm. For an optimization problem with fitness function $f(x_1, x_2, \cdots, x_n)$, if we represent each real variable x_i by k bits then the total number of Q-bits in an Q-bit individual $m=k\times n$. So if we apply the evolutionary operators on huge number of bits then they will definitely take a significant amount of time to execute.

In this paper, FLCs and RCQIEA are integrated for the intelligent control of a truck-and-trailer controller problem. RCQIEA is employed as an adaptive method for selection and definition of fuzzy control rules of the FLC as well as shape of MFs. It is found that our proposed integrated architecture is able to generate comprehensible and reliable fuzzy rules with appropriate shape of MFs by a self-learning adaptive method.

The organization of this paper is as follows: In Section II, we review the literature relevant to the FLC. In the third section we explain the problem truck-and-trailler controller in a greater detail. In section IV, we provide the integrated FLCs and RCQIEA architecture and also show how it can be used to solve highly nonlinear complex problems. We also introduce the basic principle of RCQIEAs and discuss how they can be used to generate a satisfactory fuzzy rule base and select appropriate shape of MFs simultaneously for FLCs. Section V presents our simulation results. Finally, section VI provides some concluding remarks and future directions.

II. FUZZY LOGIC CONTROLLER

The idea of fuzzy logic was first introduced in 1960s by Professor Lofti Zadeh [9]. The general configuration of FLC, can be divided into four main parts; fuzzification interface, a rule base, an inference mechanism and defuzzification interface (Fig.1).

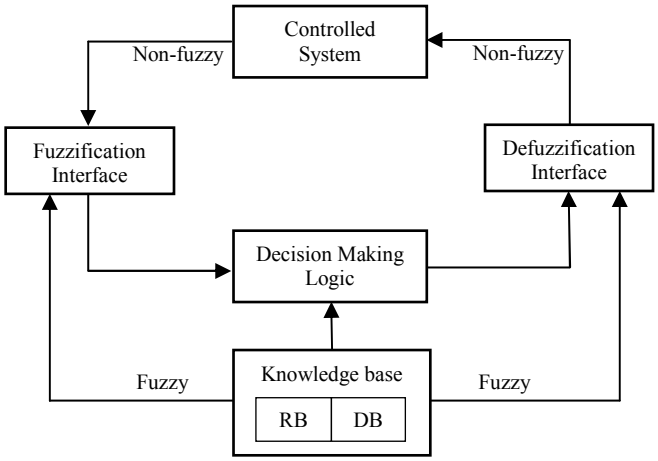

Figure 1. Fuzzy Logic Controller (FLC)

A. Fuzzifier

Fuzzy sets can be defined as μ_A, membership function that associates with each element $x\in X$ where X is the universe of discourse, a number called membership grade $\mu_A(x)\in[0,1]$. The *function* of the *fuzzifier* is to map a crisp input value $x\in X$ into a fuzzified value in $A\in U(universe)$.

B. Fuzzy rule base

The general form of a fuzzy rule used in most FLCs is as follows:

R^k : IF x_1 is F_1^k,....., and x_n is F_n^k, THEN y is G^k.

$l=1, 2, 3,....., M$, M = number of rules in the RB

where $x_1, x_2,....., x_n$, and y are the input and output linguistic variables respectively. F_i^k and G^k are type-1 fuzzy sets in input sets $X\in X_1\times X_2\times X_n$ and output sets *Y*.

B. Fuzzy Inference Engine

A fuzzy relation R^l can be defined as:

$$R^l : X\times Y=\{(\vec{x}, y) : x\in X, y\in Y\}$$

where $\vec{x}$ is a vector of the form $(x_1, x_2, ...x_n)^T$. This relation R^l is the actual process of mapping from fuzzy sets in X to fuzzy sets in Y, $F_1^l\times F_2^l\times....F_n^l\rightarrow G^l$, can be called fuzzy inference process.

C. Modified Height Defuzzifier

The modified height defuzzifer was used to handle the consequent uncertainty [10, 11], The expression generally used for a fuzzy set is as follows:

$$y_{mh}=\frac{\sum_{i=1}^{M} y^k \mu_{B^k}(\bar{y^k})/\delta^{k^2}}{\sum_{i=1}^{M} y^k \mu_{B^k}(\bar{y^k})/\delta^{k^2}}$$

where δ^k is the spread measure of the *kth* consequent set. For gaussian membership function δ^k is the standard deviation whereas triangular membership function δ^k is the length of its base.

III. PROBLEM STATEMENT

A. Model of Backing up a Truck-and-Trailer

The task is to back up a simulated truck-and-trailer to a loading dock in planner parking lot, depicted in Fig. 2. The four state variables ϕ_t, ϕ_c, x and y exactly determine the truck-and-trailer position. The angle ϕ_t specifies the angle of the trailer with the horizontal and ϕ_c is the relative angle of the cab with the trailer. The coordinate pair (x, y) specifies the position of the rear center of the trailer in the plane. The goal is to make the trailer arrive at the loading dock at a right angle $(\phi_t = 90^0)$ and to align the position (x, y) of the trailer with the desired loading dock (x_f, y_f) and the truck is allowed to move backward by some fixed distance *b* at every stage. The loading zone corresponded to the plane $[0,0]\times[100,100]$ and (x_f, y_f) equaled (50, 100). At every stage our proposed approach should produce the output angle β to update the θ and angle ϕ_t of the trailer with horizontal that backs up the trailer to the loading dock from any initial position. The truck-and- trailer only moves backward with fixed distance. The variable ranges were as follows:

$$-100 \le x \le 100$$
$$-90^0 \le \phi_t \le 270^0$$
$$-90^0 \le \phi_c \le 90^0$$
$$-30^0 \le \beta \le 30^0$$

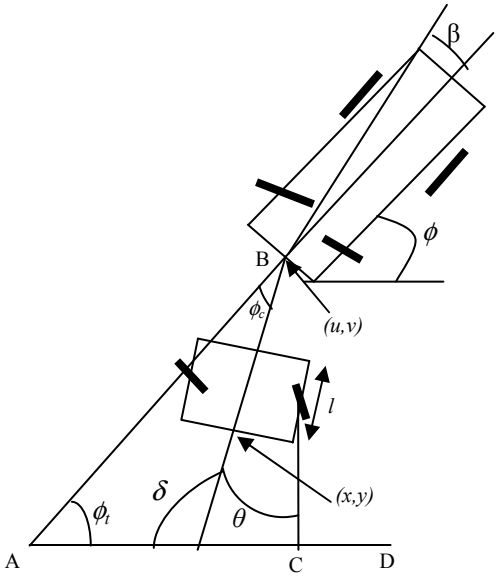

Figure 2. Diagram of truck-and-trailer

The state space of the system is four dimensional. The variable *x* gives the horizontal position of the midpoint of the rear of the trailer and the variable *y* gives the vertical position of the midpoint. Fuzzy variable ϕ_t specified the angle of the trailer with the horizontal. The fuzzy variable ϕ_c specified the relative cab angle with respect to the center line along the trailer. The extreme cab angle 90^0 and -90^0 corresponds to two "jack knife" positions of the cab with respect to the trailer. Positive ϕ_c value indicated that the cab resided on the left-hand side of the trailer. Negative value indicated that is resides on the right hand side and Fig.2 shows a positive angle value of ϕ_c.

The following inputs and outputs are chosen to represent the system and illustrated in Fig.2.

Three Inputs:

- *x,* Cartesian *x*-coordinate of truck rear end.
- ϕ_t, Angle of the trailer with horizontal.
- ϕ_c, Relative angle of the cab with the trailer.

One Output

- β, Angle of the trailer updated at each step.

Fuzzy variable ϕ_t, ϕ_c and x defined the input variables. Fuzzy variable β defined the output variable. The angle that is needed to update the trailer is β. With the output β value computed, the updated angle of the trailer with the horizontal is $\phi_t^/$:

$$\phi_t^/ = \phi_t + \beta \tag{1}$$

The trailer position is (x, y) moved to the new position $(x^/, y^/)$:

$$x^/ = x + r\cos(\phi_t^/)$$
$$y^/ = y + r\sin(\phi_t^/) \tag{2}$$

where *r* denotes a fixed backing distance. Then the joint of the truck and trailer (u, v) moved to the new position $(u^/, v^/)$:

$$u^/ = x^/ - l\cos(\phi_t^/)$$
$$y^/ = y^/ - l\sin(\phi_t^/) \tag{3}$$

Where *l* denotes the trailer length.

Again, the steering angle

$$\theta = \phi_{c,h}^/ - \phi_{c,h}$$
$$\phi_{c,h}^/ = \phi_{c,h} + \theta \tag{4}$$

Where $\phi_{c,h}^/$ denotes the updated cab angle with horizontal and $\phi_{c,h}$ denotes the cab angle with horizontal.

From ΔABC,

$$180^0 = \phi_c + \phi_t + \delta$$
$$\delta = 180^0 - (\phi_c + \phi_t) \quad (5)$$

And from $\angle BCA$ and $\angle$BCD,

$$\angle BCA + \angle \text{BCD} = 180^0$$
$$\delta + \phi_{c,h} = 180^0$$
$$180^0 - (\phi_c + \phi_t) + \phi_{c,h} = 180^0$$
$$\phi_{c,h} = \phi_c + \phi_t \quad (6)$$

Let, $\theta = \frac{\beta}{2}$

From equation (4) and equation (6) the updated relative angle of the cab with the trailer:

$$\phi'_{c,h} = \phi'_c + \phi'_t$$
$$\theta + \phi_{c,h} = \phi'_c + \phi'_t$$
$$\phi'_c = \theta + \phi_{c,h} - \phi'_t$$
$$\phi'_c = -\frac{\beta}{2} + \phi_c + \phi_t - \beta - \phi_t$$
$$\therefore \phi'_c = \phi_c - \frac{3}{2}\beta \quad (7)$$

Then the steering angle value $\theta = \phi'_{c,h} - \phi_{c,h}$ where $\phi_{c,h}$ denotes the cab angle with the horizontal.

IV. Integration Of FLCs And RCQIEA

The first step in designing an integrated FLC and RCQIEA, as shown in Fig.3, is to decide which parts of the KB are subject to be optimized by the RCQIEA. The KB of fuzzy system is made of two components: the parameters of the fuzzy RB, constituted of the collection of fuzzy rules as well as the shape of MFs and MFs type associated with the linguistic labels of each fuzzy control rule. In this case, selection and definition of fuzzy control rules as well as the shape of MFs are adapted using RCQIEA.

In RCQIEA, each Q-bit contains directly a real variable x_i along with two probability amplitudes (α_i, β_i) consisting an allele of real coded triploid chromosome. So each real coded triploid chromosome requires only n Q-bits (alleles) and thus reduces the execution time of the evolutionary operators, hence whole algorithm.

In this paper, *Ri*, a fuzzy rule is similar to the x_i described above. Each *Ri* consists of several real variables and those will need so many Q-bits if we use quantum inspired evolutionary algorithm. To reduce the execution time we use RCQIEA instead of quantum inspired evolutionary algorithm. Moreover, RCQIEA uses discrete crossover operator which expand the search space providing better exploration and exploitation characteristic of the algorithm.

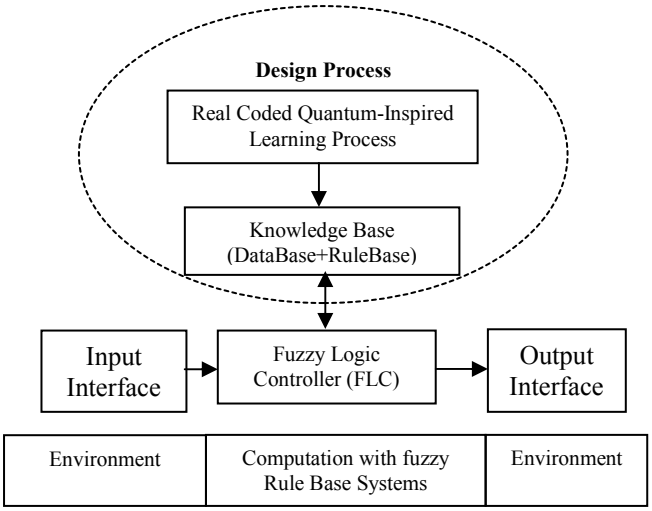

Figure 3. Learning schema of Real Coded Quantum Inspired Evolutionary Algorithm based FLCs

A. Divide the input output variables range

At first identify the variables (inputs, states and outputs) of the problem. Then partition the input and output universe of discourse or the interval spanned by each variable into a number of fuzzy regions (fuzzy sets) and assign a fuzzy MF, i.e., linguistic term of each region. For truck-and-trailer controller divide the state space input x, ϕ_t, and ϕ_c variable space and output β variable space into fuzzy regions and assign a fuzzy MFs of each region. In our running example, we divide the domain for x, ϕ_t, ϕ_c and θ into 5, 7, 3and 7 regions respectively. The linguistic levels for these regions are defined as of Table 1.

TABLE I. DEFINITION OF LINQUISTIC VARIABLE

x	ϕ_t	ϕ_c	β
LE – Left End LC – Left Center CE – Center RC – Right Center RE – Right End	LB – Left Below LU – Left Upper LV – Left Vertical VE – Vertical RV – Right Vertical RB – Right Below RU – Right Upper	NE-Negative ZR -Zero PO -Positive	NL – Negative Large NM – Negative Medium NS – Negative Small ZE – Zero PS – Positive Small PM – Positive Medium PL – Positive Large

B. Encoding Technique

After defining the regions, encode the input and output spaces fuzzy regions into strings (real value) and the fuzzy rule is written a string (real valued) as depicted in Fig.4.

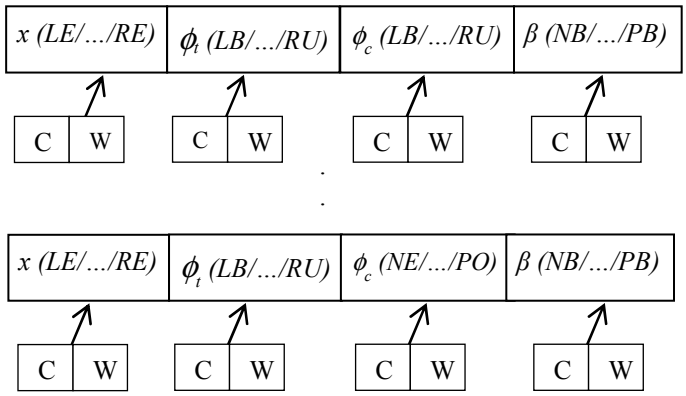

Figure 4. Chromosome structure

C. Real Coded Quantum-Inspired Evolutionary Procedure

The choice of input-output (IO) control signal to be set for each fuzzy rule is made by the RCQIEA. It initializes randomly a population of complete real valued strings. Each of these real values strings is then decoded into fuzzy rules and evaluated by a FLC. Each real valued string's fitness is defined as the error between the state of the system and the target set. RCQIEA procedures, such as selection, crossover and mutation then proceed according to the fitness values produced by the FLC for each real valued-string. The RCQIEA then performs a self-directed search, learning to look for better and better fuzzy rules and optimal MFs parameters. A mechanism for acceptance of a set of fuzzy control rules generated by the RCQIEA is needed. We only accept a set of fuzzy rules with generation ρ , where ρ is a specified number. The overall real coded quantum inspired evolutionary procedure to adapt the FLCs is shown in Fig.5.

D. Representation of RB and MFs in RCQIEA

In this paper, we consider RCQIEA where population consists of real coded triploid chromosomes [12]. Each chromosome of RCQIEA population is defined based on the fuzzy rules. So, the chromosome for this control system can be defined as follows:

$$\begin{pmatrix} R_1 \cdots R_i \cdots R_n \\ \alpha_1 \cdots \alpha_i \cdots \alpha_n \\ \omega_1 \cdots \omega_i \cdots \omega_n \end{pmatrix} \quad (8)$$

where $(R_i\ \alpha_i\ \omega_i)^T$, i =1, 2…. n is the *i-th* allele of real-coded triploid chromosome, R_i is the *i-th* rule in the fuzzy rule base and it is represented using center (c) and width (w) of input and output variables as follows:

C_1W_1	C_2W_2	C_3W_3	C_4W_4
Input x	Input φ_t	Input φ_c	Output β

A pair of probability amplitudes of one Q-bit is $(\alpha_i,\ \omega_i)^T$ which must satisfy the normalization condition $|\alpha_i|^2+|\omega_i|^2=1$. Here, n is the length of real-coded triploid chromosome which is 105 for this fuzzy controller. At each generation t RCQEA maintains a population of real- coded triploid chromosome $P^t=\{p_1^t,\cdots,p_j^t,\cdots,p_N^t\}$, where$p_j^t$ is an individual defined in (8). A rule $R_{j,i}^t$ in p_j^tcontains eight values, center (c) and width (w) for each of four variables ($x, \varphi_c, \varphi_t$and β).

E. Fitness function

An evaluation function is used for evaluating the status of each chromosome or string and consider as an important link between the RCQIEA and the system. The FLCs generates a fitness value for each RB and MFs parameters according to the following evaluation function defined based on the trajectory error:

Trajectory error/fitness =

$$\frac{Length\ of\ truck\ trajectory}{Distance(\ initial\ position,\ \ desired\ final\ position)} \quad (9)$$

F. Mutation

In RCQIEA, evolutionary operators (mutation and crossover) are applied to make change in the population having fuzzy rules which helps to adjust the FLCs to back up the truck-and-trailer more perfectly. Mutation operator is applied to i^{th} allele selected randomly from p_j^t. The fuzzy rule of that allele is updated by using gaussian mutation where centers for the input and output variables are changed as follows:

$$C^{t+1} = C^t + (\ Max - Min)\ N\ (0,\ (\sigma_{j,i}^t)^2) \quad (10)$$

Where Max and Min are respectively upper and lower bound of the regions in which the center C^t lies. The value of

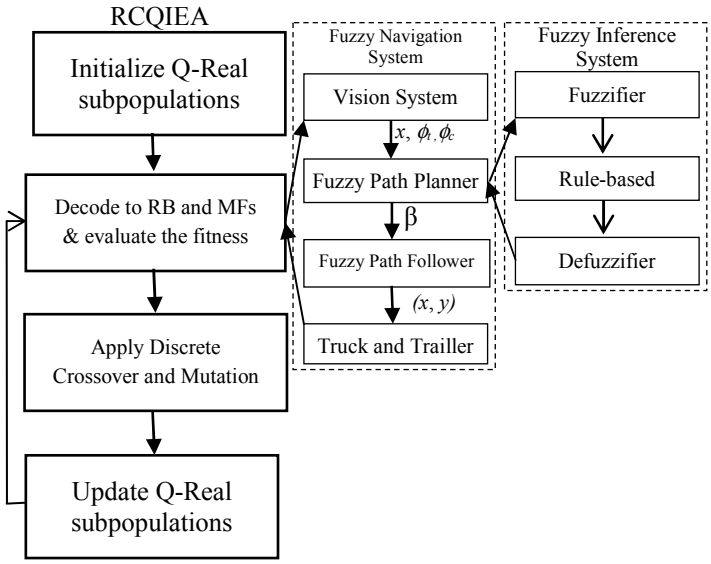

Figure 5. Data flow of proposed RCQIEA with fuzzy navigation system and fuzzy inference system

C^{t+1} may not remain in the region of C^t so it is clipped into that region. The center of β is not kept in a particular region rather its range is considered always the whole range of β. The value of variance $(\sigma_{j,i}^t)^2$ is either $|\alpha_{j,i}^t|^2$ or $|\omega_{j,i}^t|^2/5$ subject to "Fine Search" or "Coarse Search" to be implemented [12]. Now the width (W^{t+1}) of each center is calculated from the new centers of the variables as follows:

$$W^{t+1} = \begin{cases} r * (Max - C^{t+1}) & if C^{t+1} > (Max + Min)/2 \\ r * (C^{t+1} - Min) & Otherwise \end{cases} \quad (11)$$

Where r is the uniformly distributed random number in the range [0, 1]. The pair probability amplitudes of the i^{th} allele is updated by the rotation gate as follows:

$$\begin{pmatrix} \alpha_{j,i}^{t+1} \\ \omega_{j,i}^{t+1} \end{pmatrix} = \begin{pmatrix} \cos(\Delta\Theta_{j,i}^t) & -\sin(\Delta\Theta_{j,i}^t) \\ \sin(\Delta\Theta_{j,i}^t) & \cos(\Delta\Theta_{j,i}^t) \end{pmatrix} \begin{pmatrix} \alpha_{j,i}^t \\ \omega_{j,i}^t \end{pmatrix} \quad (12)$$

where rotation angle $\Delta\Theta_{j,i}^t$ of qubit is calculated as follows,

$$\Delta\Theta_{j,i}^t = sgn(\alpha_{j,i}^t \omega_{j,i}^t)\Theta_0 \exp\left(\frac{|\omega_{j,i}^t|}{|\alpha_{j,i}^t| + \gamma}\right) \quad (13)$$

where Θ_0 is the initial rotation angle, γ is the scale parameter, Θ_0 and γcontrol the value of the rotation angle together and

have an effect on the speed of convergence, the sign *sgn*(.) determines the direction of the rotation angle.

G. Discrete Crossover and Elitism

To backing up the truck-and-trailer with minimized trajectory error (fitness value) the FLCs have to search for the suitable angle of the trailer β with respect to input variables. Discrete Crossover (DC) is used here to expand the search space for the FLC. DC is performed after a fixed number of generations that is after a defined interval τ. Here DC is performed m times for each individual of the population. The process of DC can be explained as follows: First, for individual p_u^t, $u = 1,\cdots,n$, select randomly another individual p_v^t, $v = 1,\cdots,n$, where $u \neq v$. Let p_u^t and p_v^t be considered as parents. Then, every corresponding allele of them is exchanged with a 0.5 probability, and two new individuals (off springs) p_k^t, $k = 1, 2$, are formed. Figure 6 describes DC.

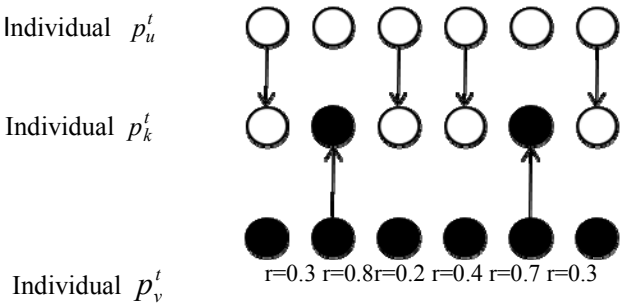

Figure 6. Discrete Crossover

The elitism technique is used to select the individuals with minimized fitness value which also ensure that the rule bases with best fitness value will not be lost.

V. EXPERIMENTAL RESULTS

This section presents the simulation results obtained from the proposed FLC simulating the truck and trailer controller problem. The RCQEA runs for 5 times with generation = 200, population size =10, scale parameter $\gamma = 5$ and initial rotation angle $\Theta_0 = 0.1\pi$. Table 2 shows the simulation parameters of RCQIEA for FLC. Figure 7(a) shows the shape of the membership functions by RCQIEA and 7 (b) shows an example of MF form of fuzzy rule.

An important characteristic of fuzzy models, FM, is the partitioning of the input and output space of system variables (input, output) into fuzzy regions using fuzzy sets [8]. The range of x is divided into five non-uniform intervals [0, 32.5], [32.5, 47.5], [47.5, 52.5], [52.5, 67.5], and [67.5, 100]. The range of ϕ_t is divided into seven non-uniform regions [-90, 0], [0, 66.5], [66.5. 86], [86.5, 94.5], [94.5, 113.5], [113.5, 182.5], [182.5, 270]. For another input ϕ_c, the linguistic variables are NE (Negative), ZR (Zero) and PO (Positive) and the space $-90 \le \phi_c \le 90$ has been divided into three intervals [-90,-12.5], [-12.5, 12.5], [12.5, 90]. Similarly seven divided regions of the range of β [-30, -20], [-20, -7.5], [-7.5, -2.5], [-2.5, 2.5], [2.5, 7.5], [7.5, 20], [20, 30] are represented by variables NL, NM, NS, ZE, PS, PM and PL.

TABLE II. MFS AND RULE SET PARAMETERS (OPTIMAL SOLUTION)

Rule No.	RCQIEA(Optimal Solution)							
	Input						*Output*	
	x		ϕ_t		ϕ_c		β	
	Center	Width	Center	Width	Center	Width	Center	Width
1	16.981	17.1579	-77.340	79.0289	-19.8562	54.732	4.41199	17.4324
2	13.9245	29.9475	-67.792	107.416	-1.15573	121.796	5.94693	18.7478
.	.	.	.	.	.	.	.	.
.	.	.	.	.	.	.	.	.
104	80.3251	16.3588	195.069	148.051	2.2023	39.6526	-3.4602	17.0375
105	96.1698	49.7159	252.462	186.979	77.97409	51.664	-1.7170	20.9209

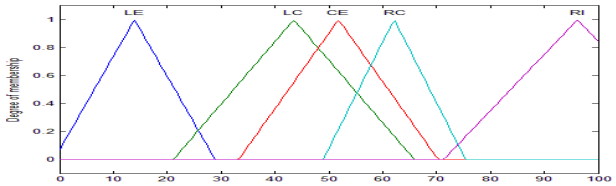

(a)

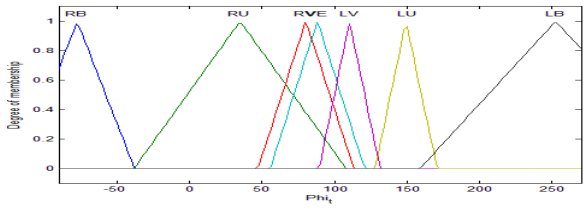

(b)

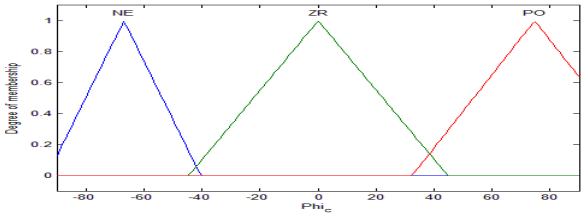

(c)

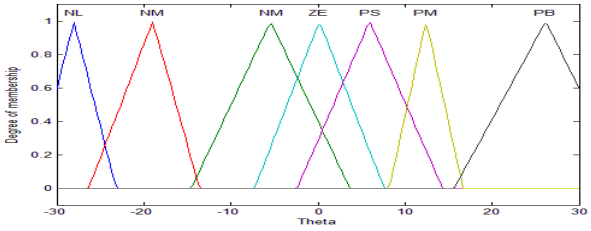

(d)

Figure 7(a).Tuned MFs using RCQIEA (a) Input x (b) ϕ_t (c) Input ϕ_c (d) Output β

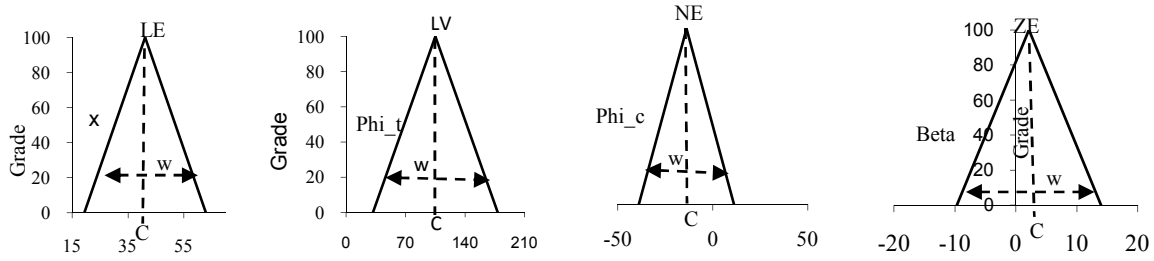

Rule 7: If x=LE and ϕ_t=LV and ϕ_c=NE Then β=ZE

Figure 7(b). MF (triangular) form of fuzzy rule

ϕ_C \ ϕ_t

β	LB	LU	LV	VE	RV	RU	RB
NE	[1]PS	[4]PB	[7]ZE	PS	NS	PS	PS
ZR	[2]PS	NM	NM	NM	PS	NS	PS
PO	[3]ZE	PM	NB	NS	NM	NM	PB

x=LE

ϕ_C \ ϕ_t

β	LB	LU	LV	VE	RV	RU	RB
NE	NM	ZE	NS	PS	PS	PS	NM
ZR	NM	NM	NM	NS	PS	ZE	PM
PO	PS	NM	NM	NS	PB	ZE	NS

x=LC

ϕ_C \ ϕ_t

β	LB	LU	LV	VE	RV	RU	RB
NE	PS	PB	PS	ZE	PS	PB	PM
ZR	NM	NS	ZE	ZE	PS	ZE	PM
PO	NM	NS	ZE	NS	NS	NS	NS

x=CE

ϕ_C \ ϕ_t

β	LB	LU	LV	VE	RV	RU	RB
NE	NM	PB	PS	PM	PB	PB	NS
ZR	NM	ZE	PS	NS	PM	NS	PB
PO	PS	NS	NS	ZE	PM	NS	ZE

x=RC

ϕ_C \ ϕ_t

β	LB	LU	LV	VE	RV	RU	RB
NE	NS	PS	PM	PM	PB	PS	PM
ZR	NS	PS	PS	NS	PM	PM	NS
PO	ZE	NM	NS	PS	NS	NB	ZE

x=RE

Figure 8. FAM bank of the truck–and-trailler control System

At the beginning of the simulation, the antecedent and consequent part of each rule, i.e., fuzzy associative memories (FAM) cells are empty. To get the antecedent and consequent part of each rule in terms of linguistic language form and shape of MFs from the developed RCQIEA generator block, we start the simulation from twenty initial positions (x_o, y_o, ϕ_{t0} , ϕ_{c0}): (25, 30, 60^0, 30^0), (80, 30, 150^0, and 60^0)..etc. The initial positions are randomly selected and cover the simulated truck-and-trailer loading zone.

For all the given initial positions the RCQIEA converges to some sets of fuzzy IF-THEN rules. During the simulation, we generate twenty sets of values associated to fuzzy rules from twenty different initial positions. After translating the parameter values into sets of rules, these RB are combined together to form the final FAM as shown in Fig.8 using Fuzzy Amalgamation (FA) methodology [13]. The FA method starts with an empty new FAM. Then it compares and combines two FAMs as follows. If the corresponding cells of two FAMs are same then add the cell entries into the corresponding cell of the new FAM. On the other hand, if corresponding cells of two FAMs are different, then an average of the two different entries is computed using the following formula:

$$Numeric - Value(NV) = \frac{1}{n}\sum_{i=1}^{n} N_i$$

where n is the number of combining tables (Here n = 2), N_i is the numeric values (center) of fuzzy rule. Find the linguistic term (fuzzy set) for NV where it has the highest membership value, and return that linguistic term as a result of two different entries into the corresponding cell of the new FAM. There are 105 fuzzy rules (fuzzy RB or FAM can be formed as a 5×(3×7) tables with rows to hold the corresponding actions (outputs) as shown in fig.8.

With the above FAM rules (shown in Fig.8), the fuzzy truck- and-trailler controller produced successful truck–and-trailler trajectories starting form any given initial condition. Figure 9 shows the typical example of fuzzy truck-and-trailler trajectories.

In each generation, all chromosomes are evaluated by the FLC to generate the fitness error. Chromosomes are sorted according to the fitness error and the best one among all chromosomes is selected in each generation. Figure 10 shows a graph of fitness generation by generation.

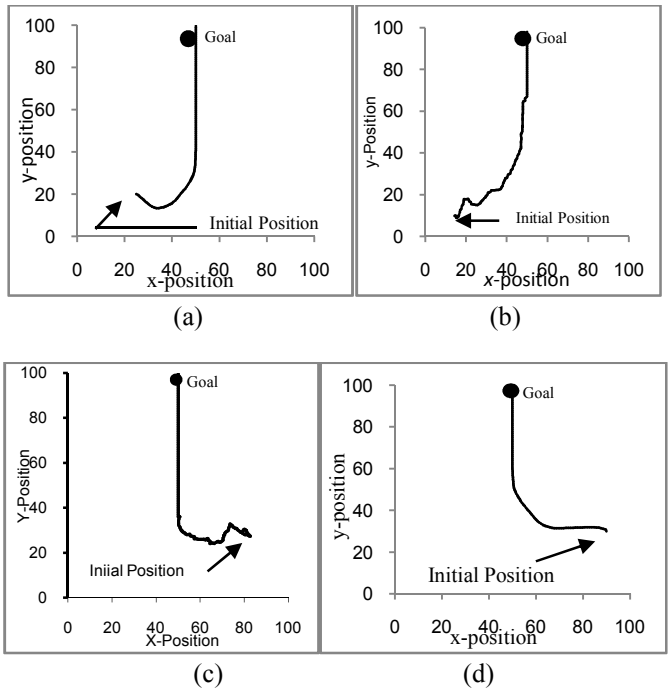

Figure 9. Sample truck-and-trailler trajectories of the fuzzy controller for the initial conditions (X, Y, ϕ, ϕ_c): (a) (25,20,-45°,60) (b) (80, 30, 10 and 20) (c) (15,10,-20°,45°) (d)(90,30,145°,30°)

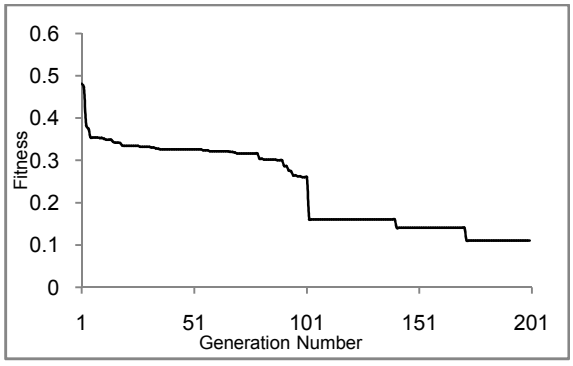

Figure 10. Fitness function value of the solution populations

VI. CONCLUSIONS

In this paper, a new RCQIEA is applied to search for optimal settings of the MFs shapes and gains of the inputs and outputs of FLC for a truck-and-trailer controller problem. The proposed RCQIEA represents a new way of self-learning adaptive FLCs. The simulation results show that it can generate the fuzzy control rules and the MFs in a consequent way automatically without any priori expert knowledge. Moreover the designed adapted fuzzy logic controller effectively realizes the trajectory control of the truck with trailer. The proposed approach may be seen as a step in the development of a better accepting of how to incorporate a fuzzy logic controller with a quantum inspired evolutionary algorithm to achieve asignificant adaptive learning capability.

Suggestions for follow-up works that may come after this paper are as follows: This research work is to be extended for intelligent control of a mobile robot, control of a robotic arm in the presence of moving or fixed obstacle, the path planning problem for multiple mobile robots with more than one obstacle either moving or fixed in the workspace. Moreover, this work also to be extended in the analysis of the behavior of the cooperative real coded quantum inspired evolutionary learning proposal with high dimensional problems, where it might be necessary to include a variable feature selection component into the learning approach.

REFERENCES

[1] Y. H. Kim and J.H. Kim, "Multiobjective quantum-inspired evolutionary algorithm for fuzzy path planning of mobile robot," *in Proc. IEEE Congress Evol. Comput.*, May 2009.

[2] K. Belarbi, F. Titel, W. Bourebia, and K. Benmahammed, "Design of mamdani fuzzy logic controllers with rule base minimisation using genetic algorithm," *J. Engg. Appl. Artificial Intell.,* vol. 18 pp. 875–880, Oct. 2005.

[3] D. L. Meredith, C. L. Karr, and K. K. Kumar, "The use of genetic algorithms in the design of fuzzy logic controllers," *in Proc. third workshop on neural netw.,* vol. 1721, 1992, pp. 549-555.

[4] A. Bagis, "Fuzzy rule base design using tabu search algorithm for nonlinear system modeling," *ISA Trans.,* vol. 47, no. 1, pp. 32–44, Jan. 2008.

[5] S. Bai and S. Chen, "Automatically constructing grade membership functions of fuzzy rules for students' evaluation," *Expert Syst. Appl.,* vol. 35, pp.1408–1414, Oct. 2008.

[6] C. C. Yang and N. K. Bose, "Generating fuzzy membership function with self-organizing feature map," *Pattern Recog. Letters*, vol.27, no.4, pp. 356–365, Apr. 2006.

[7] A. F. M. Huang, S .J .H. Yang, M. Wang, and J. J.P. Tsai, "Improving fuzzy knowledge integration with particle swarm optimization," *Expert Syst. Appl.*, vol. 37, iss. 12, pp. 8770–8783, Dec. 2010.

[8] T. Koga, K. Horio, and T. Yamakawa, "Self-organizing relationship (SOR) retwork with ruzzy inference based evaluation and its application to trailer-truck back-up control," *in Proc. 11th int. conf. neural inform. Processing*, 2006, pp. 368-374.

[9] L.A. Zadeh, "Fuzzy sets," Information and Control 8 (3), pp. 338–353, 1965.

[10] L. X. Wang, *Adaptive Fuzzy systems and control: Design and Stability Analysis*. Englewood cliffs, NJ: Prentice-Hall PTR, 1994.

[11] G. C. Mouzouris and J. M. Mendel, "Nonsingleton fuzzy logic systems and application," *IEEE Trans. Fuzzy Syst*., vol.5, no.1, Feb. 1997.

[12] R. Zhang and H. Gao, "Real -coded quantum evolutionary algorithm for complex function with high dimension," *in Proc. IEEE Int. Conf. Mechatronics and Automation*, Aug. 2007, pp. 2974-2979.

[13] M. Mohammadian and R. J. Stonier, "Generating fuzzy rules by genetic algorithms," *in Proc. IEEE Int. Works. Robot and Human Comm.,* 1994, pp.362-367.

[14] Do-Hyeon Kim, Kwang-Baek Kim and Eui-Young Cha, "Fuzzy truck control scheme for obstacle avoidance," *J. Neural Comput. Appl.,* vol. 18, no. 7, pp. 801-811, Oct. 2009.

[15] T. Yamakawa and T. Koga,"Bio-inspired self-organizing relationship network as knowledge acquisition tool and fuzzy inference engine," *in Proc. IEEE world conf. Comput. Intell.,* 2008, pp. 159-180.

[16] Y. Li and Y. Li, "Neural-fuzzy control of truck backer-upper system using a clustering method," *Neurocomputing*, vol. 70, pp-680-688, Jan. 2007.

[17] K. H. Han and J. H. Kim, "Quantum-inspired evolutionary algorithm for a class of combinatorial optimization," IEEE Trans. Evolutionary Comput., vol. 6, no. 6, pp.580–593, Dec. 2002.

[18] K. H. Han and J. H. Kim , "Quantum-Inspired evolutionary algorithms with a new termination criterion, he gate, and two-phase scheme," *IEEE Trans. Evolutionary Comput.,* vol. 8, no.2, pp.156-169, Apr. 2004.

2011 IEEE International Conference on Fuzzy Systems
June 27-30, 2011, Taipei, Taiwan

An Efficient Hybrid Particle Swarm Optimization for the Job Shop Scheduling Problem

Xue-Feng Zhang
Graduate School of Information
Science and Electrical Engineering
Kyushu University
Fukuoka, Japan 819–0382
Email: xuefeng@ar.is.kyushu-u.ac.jp

Miyuki Koshimura
Graduate School of Information
Science and Electrical Engineering
Kyushu University
Fukuoka, Japan 819–0382
Email: koshi@inf.kyushu-u.ac.jp

Hiroshi Fujita
Graduate School of Information
Science and Electrical Engineering
Kyushu University
Fukuoka, Japan 819–0382
Email: fujita@inf.kyushu-u.ac.jp

Ryuzo Hasegawa
Graduate School of Information
Science and Electrical Engineering
Kyushu University
Fukuoka, Japan 819–0382
Email: ryuzo@inf.kyushu-u.ac.jp

***Abstract*—This paper proposes a hybrid particle swarm optimization algorithm for solving Job Shop Scheduling Problems (JSSP) to minimize the maximum makespan. A new hybrid heuristic, based on Particle Swarm Optimization (PSO), Tabu Search (TS) and Simulated Annealing (SA), is presented. PSO combines local search (by self-experience) with global search (by neighboring experience), achieving a high search efficiency. TS uses a memory function to avoid being trapped at a local minimum, and has emerged as an effective algorithmic approach for the JSSP. This method can also be referred to as calculation of the horizontal direction. SA employs certain probability to avoid becoming trapped in a local optimum and the search process can be controlled by the cooling schedule (also known as calculation of vertical direction). By reasonably combining these three different search algorithms, we develop a robust, fast and simply implemented hybrid optimization algorithm HPTS (Hybrid of Particle swarm optimization, Tabu search and Simulated annealing). This hybrid algorithm is applied to the standard benchmark sets and compared with other approaches. The experimental results show that the proposed algorithm could obtain the high-quality solutions within relatively short computation time. For 6 of 43 instances, new upper bounds among the unsolved problems are found in a short time in HPTS.**

***Index Terms*—Job Shop Scheduling Problem, Particle Swarm Optimization, Tabu Search.**

I. Introduction

The Job Shop Scheduling Problem (JSSP) is one of the existing combinatorial optimization problems and it has been demonstrated to be an NP-hard problem [1]. In JSSP, each one of n jobs ($n \geq 1$) must be processed passing through m machines ($m \geq 1$) in a given sequence. The sequence of m machines is different for each different job and cannot be changed during the processing. When one job was processed on a machine, it can be considered as one operations, each job j needs a combination of m operations to complete the work. One operation is processed on one of m machines, and just only one operation can be processed at a time. Any job cannot interrupt the machine that is processing one operation of another job. Each machine can process at most one operation at the same time. The main objective of the JSSP is to find a schedule of operations that can minimize the maximum completion (called makespan) that is the completed time of carrying out total operations in the schedule for n jobs and m machines [2].

JSSP can be applied to the manufacture processing and actually effects the production time and the cost of production for a plant. During the past few decades, JSSP has attracted many researchers to develop algorithms. Because JSSP is an NP-hard problem, it is difficult to develop a perfect algorithm to find a solution with a reasonable time especially for higher dimensions. Recently, many researchers made use of evolution algorithm to solve the problem. such as shifting bottleneck approach (SB) [3], tabu search algorithm(TS) [4], genetic algorithm(GA) [5], simulated annealing(SA) [6], particle swarm optimization(PSO) [7], and ant colony(ACO) [8]. Most studies indicate that a single technique can not solve this stubborn problem. Much work has been done on hybrid methods involving GA,SA,TS,and SB techniques as hybrid methods can provide high-quality solution within reasonable computing time, such as Goncalves' HGA [5], Tsung-Lieh Lin's MPSO [2], Wei-Jun Xia's HPSO [9], Fevrier Valdez's PSO+GA [10] [11]. A comprehensive survey of scheduling techniques can be seen from Blazevicz et al. and Jain and Meeran. In addition, many research results of the JSSP show that it is very difficult to obtain a good-enough solution only by single search scheme. Motivated by these perspectives, we propose an efficient hybrid intelligent algorithm for the JSSP based on PSO, TS and SA. PSO, TS and SA are evolution computation techniques. They exhibit implicit parallelism and contain certain redundancy and

978-1-4244-7316-8/11/$26.00 ©2011 IEEE

historical information of past solutions. Moreover, TS and SA also have better local search features. Therefore, the proposed hybrid particle swarm optimization algorithm also effectively exploits the capabilities of distributed and parallel computing of swarm intelligence approaches to achieve the better solution for JSSP.

In this paper, we present an efficient hybrid particle swarm optimization for the Job Shop Scheduling Problem. The remainder of the paper is organized as follows. In Section II, we present the different classes of schedules. In section III, we discusses and analyzes our approach to solve the JSSP. Section IV gives experimental results of the HPTS algorithm and other competitive approaches. Finally, the main conclusions are drawn.

II. Problem Formulation

A. Job Shop Scheduling Problem

The JSSP consists of n jobs and m machines. Each job must go through m machines to complete its work. We consider one job consists of m operations. Each operation uses one of m machines to complete one job's work for a fixed time interval. Once one operation is processed on a given machine, it cannot be interrupted before it finishes the job's work. The sequence of operations of one job should be predefined and maybe different for any job. In general, one job being processed on one machine is considered as one operation as noted above, then every job has a sequence of m operations. Each machine can process only one operation during the time interval. The objective of JSSP is to find an appropriate operation permutation for all jobs that can minimize the makespan C_{max}, i.e., the maximum completion time of the final operation in the schedule of $n \times m$ operations.

Let $J = 0, 1, ..., n, n+1$ denote the set of operations to be scheduled and $M = 0, 1, ..., m, m+1$ the set of machines. The operations 0 and $n+1$ are dummy, have no duration and represent the initial and final operations. The operations are interrelated by two kinds of constraints. Firstly, the precedence constraints, which force each operation j to b scheduled after all predecessor operations, P_i, are completed. Secondly, operation j can only be scheduled if the machine it requires is idle. Further, let dj denote the fixed duration (processing time) of operation j.

Let F_j represent the finish time of operation j. A schedule can be represented by a vector of finish times $(F_1, ...F_m, F_{m+1})$. Let $A(t)$ be the set of operations being processed at time t, and let r_{jm} = 1 if operation j requires machine m to be processed and r_{jm} = 0 otherwise.

The conceptual model of the JSSP can be described in the following way [5]:

$$Minimize F_{n+1}(C_{max}) \tag{1}$$

$$F_k \leq F_j - d_j, j = 1, ...n+1, k \in P_j \tag{2}$$

$$\sum_{j \in A(t)} r_{jm} \leq 1, m \in M, t \geq 0 \tag{3}$$

$$F_j \geq 0, j = 1, ...n+1 \tag{4}$$

The objective of Eq.1 minimizes the finish time of operation $n+1$ (the last operation), and therefore minimizes the makespan. Constraints in Eq.2 impose the precedence relations between operations and constraints in Eq.3 state that one machine can only process one operation at a time. Finally Eq.4 forces the finish times to be nonnegative.

B. Particle Swarm Optimization

Particle Swarm Optimization (PSO) algorithm is introduced by Kennedy and Eberhart [12] [13] based on the social behavior metaphor. In PSO, a group of particles, without quality and volume, fly through a D-dimensional space, adjusting their positions in search space according to their own experience and their neighbors. Although approximation methods do not guarantee achieving optimal solutions, they are able to attain near-optimal solutions. Therefore, approximation methods are more suitable for larger problems. The particle swarm concept was based on the premise of social behavior. The original intent was to graphically simulate the graceful but unpredictable choreography of a bird flock. A PSO algorithm mimics the behavior of flying birds and their means of information exchange to solve optimization problems. PSO has been introduced as an optimization technique in real-number spaces. But many optimization problems are set in a space featuring discrete components. Typical examples include problems that require ordering and route planning, such as in scheduling and routing problems [14]. They are described as follows [15]:

$$\begin{aligned} V_{id} &= \omega \times V_{id} + C_1 \times \mathrm{Rand}() \times \left(\mathrm{P}_{\mathrm{id}}^{\mathrm{best}} - \mathrm{P}_{\mathrm{id}}\right) \\ &+ C_2 \times \mathrm{Rand}() \times \left(\mathrm{P}_{\mathrm{gid}}^{\mathrm{best}} - \mathrm{P}_{\mathrm{id}}\right) \end{aligned} \tag{5}$$

$$P_{id} = P_{id} + V_{id} \tag{6}$$

where V_{id} represents the velocity of particle i. It also can be regarded as the distance to be traveled by particle i from its current position. P_{id} represents the particle position, P_{id}^{best} called "pbest", the local best solution, represents particle i's best previous position, and P_{gid}^{best} called "gbest", the global best solution, represents the best position among all particles in the swarm. ω is an inertia weight. It regulates the trade-off between the global exploration and local exploitation abilities of the swarm. The acceleration constants C_1 and C_2 represent the weights of the stochastic acceleration terms that pull each particle toward "pbest" and "gbest" positions. $\mathrm{Rand}()$ is a random function with range $[0, 1]$.

For Eq.5, the first part represents the inertia of previous velocity; the second part is the "cognition" part, which represents individuals thinking independently; and the third part is the "social" part, which represents cooperation among the particles [16].

III. The Proposed algorithm for JSSP

A. Implementation of Hybrid Particle Swarm Optimization

Some issues are in applying PSO algorithm to solve scheduling problems. The original PSO design is developed

to solve continuous function. The PSO algorithm is problem-independent, which means little specific knowledge relevent to a given problem is required. All we have to know is the fitness evaluation of each solution. This advantage makes PSO more robust than many other search algorithms. However, since PSO is a stochastic search algorithm, it is prone to inadequate global search at the end of a run. PSO may fail to find the required optimum in cases when the problem to be solved is too complicated and complex. SA employs certain probability to avoid becoming trapped in a local optimum, and the search process can be controlled by the cooling schedule. by designing the neighborhood structure and cooling schedule of TS and SA, we can control the search process and avoid individuals being trapped in local optimum more efficiently. Therefore, a hybrid algorithm of PSO, TS and SA, named HPTS, is presented in Figure 1.

1) Encoding scheme and initial solution: Suppose that the searching space is D-dimensional and m particles form the swarm. The ith particle represents a D-dimensional vector X_i (i = 1, 2,..., m). It means that the ith particle locates at X_i = (x_{i1}, x_{i2},..., x_{iD}) (i = 1, 2,..., m). The position of each particle is a potential result. We could calculate the particle's fitness by putting its position into a designated objective function. The ith particle "flying" velocity is also a D-dimensional vector, denoted as V_i = (v_{i1}, v_{i2},..., v_{iD}) (i = 1, 2,..., m). Denote the best position of the ith particle as P_i = (p_{i1}, p_{i2},..., p_{iD}), and the best position of the swarm as G_i = (g_{i1}, g_{i2},..., g_{iD}), respectively.

2) The neighborhood search: The neighborhood search strategy is directly effective on the efficiency of the local search for the JSSP, and unnecessary and infeasible moves must be eliminated if it is possible. Currently, the most well-known neighborhood structures are all based on the concept of blocks. In the HTPS algorithm, taking into account a balance of the effectiveness and efficiency, we ultimately adopt $N6$[1] neighborhood structure, which is introduced by Balas and Vazacopoulos [17].

3) Tabu list: The main task is to avoid the search process turning back to the solutions visited in the previous steps. The elements stored in the tabu list are the attributes of moves, rather than the attributes of solutions for the considered problem. The main purpose of using this attributive representation is to reduce the computational cost. In HPTS, the size of the list is set the same as the swarm size. During the algorithm running, the tabu list will be updated dynamically.

4) Fitness function: Fitness function is usually used as the performance evaluation of particles in the swarm, which is represented to map an original objective function value to a fitness function that represents relative superiority of particles. In HPTS, each particle's fitness function is expressed by the makespan of the corresponding schedule.

5) Cooling schedule: The SA process can be controlled by the cooling schedule. In general, the cooling schedule is specified by several parameters and/or methods, namely the initial temperature T_0, the rule designated how to lower the temperature, and the termination condition. In proposed algorithm, the initial temperature T_0 is set by $T_0 = \Delta\ f_{max}$, where $\Delta\ f_{max}$ is the maximal difference in fitness values between any two neighboring solutions. We specify the temperature with T_k = $B \times T_{k-1}$ during the kth epoch (k = 1,2,3,...), where B is a parameter called decreasing rate and has a value less than 1.

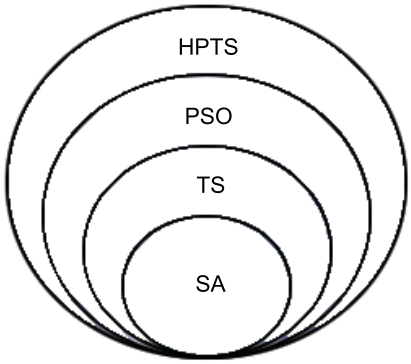

Fig. 1. The structure of HPTS.

6) Termination criterion: If one of the following conditions is satisfied: whether the algorithm stops when the algorithm has performed a given total number of iterations, or the elite solution stack has been exhausted, or the solution is proved to be optimal.

B. The Process of Proposed Algorithm

In the HPTS, three different operations are defined: PSO operation, TS operation and SA operation. PSO combines local search (by self-experience) with global search (by neighboring experience), achieving a high search efficiency. TS uses a memory function to avoid being trapped at a local minimum. It has emerged as an effective algorithmic approach for the JSSP. This method can also be referred to as calculation of the horizontal direction. SA employs certain probability to avoid being trapped in a local optimum and the search process can be controlled by the cooling schedule (also known as calculation of vertical direction). The groups use a random initialization, which generates initial particle's initial position and velocity in the search space. Each particle's best position is set to the current location. The current position of the corresponding fitness value is calculated for each particle, according to the evolutionary structure. The hybrid HPTS framework can be converted to the traditional PSO that provides initial solution for TS and SA during the hybrid search process. Such hybrid HPTS strategy retains the advantages of TS and SA, which provides a promising methodology to solve JSSP. In addition, HPTS can be applied to many combinatorial optimization problems by simple modification. The description of HPTS is shown in algorithm 1 and algorithm 2. The process of implementing the framework is as follows:

$Step$ 1: Initialize a swarm of particles with random position and velocities in the D-dimensional problem space.

$Step$ 2: For each particle, evaluate the desired optimization fitness function.

Step 3: Individual particle's fitness value are with D-dimensional problem space. If the current value is better than , then set the position equal to the current value, and the position equal to the current position in the D-dimensional problem space.

Step 4: Compare the fitness evaluation value with the swarm's best fitness value obtained so far. If current value is better than , then reset to the current particle's fitness value.

Step 5: Change the velocity and position of the particle according to Eq.5 and Eq.6, respectively.

Step 6: Loop to step (2) until a termination criterion is met, usually a sufficiently good fitness or a specified number of generations.

Algorithm 1 PSO

1: **while** the maximum of generation is not met **do**
2: Generation++;
3: Generate next swarm;
4: Find a new local optimum ($gbest$) and a global optimum ($pbest$);
5: Update $gbest$ and $pbest$;
6: **end while**

Algorithm 2 TS (SA)

1: Set iteration $iter$ = $iter$ + 1, generate neighbors of the current solution $s*$ by a neighborhood structure. If the $s*$ is optimal, then stop;
2: Select the best neighbor which is not tabu or satisfies the aspiration criterion, and store it as the new current solution $s*$, update the tabu list;
3: **for** $gbest$ particle s of swarm **do**
4: Tempreture T_k = T_0;
5: **while** $T_k \geq T_{end}$ **do**
6: Generate a neiborhood solution $s*$ from s by pair-exchange method;
7: Compute the fitness of $s*$;
8: Evaluate $s*$, Δ = f(s*)-f(s);
9: **if** min[1,exp(-Δ/T_k)] $<$ random[0,1] **then**
10: Accept $s*$;
11: Update the best solution found so far if possible;
12: **end if**
13: **end while**
14: T_k= B * T_{k-1} (weight value parameters are included in B);
15: **end for**
16: If $iter \leq improveiter$ then go to loop;
17: If a termination criterion is satisfied then stop. Otherwise 'pop' a solution on top of the solution stack L, shift the solution to active schedule and install the active solution as the current solution s*, set $iter$ = 0, and empty tabu list. Go to step 2;

TABLE I
THE SETTINGS OF THE CONTROL PARAMETERS.

Iterations	**The number of particles**	**Inertia weight**
K = 300	N = 400	w_{max} = 0.4, w_{min} = 0.2
Acceleration	**Initial temperature**	**Cooling parameters**
c_1 = c_1= 0.2	T_0 =10	$Alpha$ =0.97

TABLE II
THE EXPERIMENTAL RESULTS.

Problem	**Size**	**BKS**	**HGA**	**MPSO**	**HPSO**	**HPTS**
FT06	6 × 6	55	55	55	55	55
FT10	10 × 10	930	930	930	930	930
FT20	20 × 5	1165	1165	1165	1178	1165
LA01	10 × 5	666	666	666	666	666
LA02	10 × 5	655	655	655	655	655
LA03	10 × 5	597	597	597	597	597
LA04	10 × 5	590	590	590	590	590
LA05	10 × 5	593	593	593	593	593
LA06	15 × 5	926	926	926	926	926
LA07	15 × 5	890	890	890	890	890
LA08	15 × 5	863	863	863	863	863
LA09	15 × 5	951	951	951	951	951
LA10	15 × 5	958	958	958	958	958
LA11	20 × 5	1222	1222	1222	1222	1222
LA12	20 × 5	1039	1039	1039	1039	1039
LA13	20 × 5	1150	1150	1150	1150	1150
LA14	20 × 5	1292	1292	1292	1292	1292
LA15	20 × 5	1207	1207	1207	1207	1207
LA16	10 × 10	945	945	945	945	945
LA17	10 × 10	784	784	784	784	784
LA18	10 × 10	848	848	848	848	848
LA19	10 × 10	842	842	842	842	842
LA20	10 × 10	902	902	902	907	902
LA21	15 × 10	1046	1046	1046	1046	1046
LA22	15 × 10	927	927	927	927	927
LA23	15 × 10	1032	1032	1032	1032	1032
LA24	15 × 10	935	953	941	938	**935**
LA25	15 × 10	977	986	977	977	977
LA26	20 × 10	1218	1218	1218	1218	1218
LA27	20 × 5	1235	1256	1239	1236	**1236**
LA28	20 × 5	1216	1232	1216	1216	1216
LA29	20 × 5	1152	1196	1173	1164	**1166**
LA30	20 × 5	1355	1355	1355	1355	1355
LA31	30 × 10	1784	1784	1784	1784	1784
LA32	30 × 10	1850	1850	1850	1850	1850
LA33	30 × 10	1719	1719	1719	1719	1719
LA34	30 × 10	1721	1721	1721	1721	1721
LA35	30 × 10	1888	1888	1888	1888	1888
LA36	15 × 15	1268	1279	1278	1269	**1268**
LA37	15 × 15	1397	1408	1411	1401	**1399**
LA38	15 × 15	1196	1219	1208	1208	**1201**
LA39	15 × 15	1233	1246	1233	1240	**1233**
LA40	15 × 15	1222	1241	1225	1226	**1222**

IV. EXPERIMENTAL RESULTS

To illustrate the effectiveness of the HPTS algorithm for JSSP to minimize the makespan, 43 instances taken from OR-Library [18] as test benchmarks to test our new proposed algorithm. In the 43 instances, FT06, FT10, and FT20 were designed by Fisher and Thompson [19]. Instances LA01-LA40 that were designed by Lawerence [20].

The proposed approach was coded in MATLAB programming language and run on a 2.27 GHz Intel(R) Core(TM)2 Duo CPU, RAM 4GB personal computer. Each instance is executed for 10 runs. The algorithm ran with the settings of the control parameters which can be shown in Tabel I. The proper

values of these parameters were experimentally determined in a pre-processing phase. Specifically, the performance of the proposed HPTS was compared against that of Goncalves' HGA [5], Tsung-Lieh Lin's MPSO [2], Wei-Jun Xia's HPSO [9].

Due to the stochastic behavior of these algorithms, and the fact that none of them has a natural termination point, it was decided to run the algorithms for the same fix time duration and report the best solution obtained after this time has elapsed. The benchmarks range from small size instances with 6 jobs and 6 machines to large size instances with 30 jobs and 10 machines.

In Tabel II, $Problem$ denotes the JSSP problems, $Size$ represents the Problem size n jobs on m machines. BKS represents the well-known optimal solutions in the benchmark. Among 43 instaces, HPTS can find the well-known optimal solutions with 40 instances that is much better than HGA (33), MPSO (36), and HPSO (35). Moreover, in about 93 % of the instances, and the deviation of the minimum found makespan from the well-known optimal solutions is only on average 0.4 %. The proposed algorithm yields a significant improvement in solution quality with respect to almost all the other algorithms, except for the HGA, MPSO and HPSO approaches that has a better performance in the LA29, LA36, LA37, LA38, LA40 instances mainly. For instances LA24, LA25, LA27, LA28, LA29, LA36, LA37, LA38, LA39, LA40, the deviation between the best minimum founded solution and the best known solution are all less than the deviation results of HGA. HPTS can obtain better solution for instances LA24, LA27, LA29, LA36, LA37, LA38, LA40 than MPSO. Except for LA29, HPTS also can obtain better solution (LA24, LA36, LA37, LA38, LA39, LA46) than HPSO.

Obviously, the experimental results show that HPTS is more efficient than other existing discrete particle swarm optimization and genetic algorithms, respectively. The superior results also indicate the successful incorporation of the improved PSO, TS and SA, which facilitates the escape from local minimum points and increases the possibility of finding a better solution. Therefore, the computational results show that the proposed algorithm could obtain the high-quality solutions within relatively short computation time. So, it is a robust, fast and simply hybrid optimization algorithm.

V. Conclusion

Although there are many literatures on classical PSO, the PSO for JSSP does not have rich literatures. In this paper, a new hybrid heuristic HPTS, based on Particle Swarm Optimization (PSO), Tabu Search (TS) and Simulated Annealing (SA), is presented. We have applied the HPTS algorithm to JSSP in minimizing makespan. The experimental results show the effectiveness of the proposed approach. Moreover, our HPTS algorithm outperforms HGA, MPSO, and HPSO algorithms in some solution quality thoroughly. For 6 of 43 instances, new upper bounds among the unsolved problems are found in a short time in HPTS. It can achieve the optimal value in the search space quickly with smaller population size, making use of its better local searching ability to get the final optimal solution at the end of evolution.

In addition, we have proposed a new algorithm structure: three-tier structure of hybrid algorithm, which brings the new research direction and inspiration for the hybrid algorithm. To improve the algorithm performance, we plan to apply parallel and distributed computing to the HPTS algorithm.

Acknowledgment

This paper is supported by the research fund JSPS KAKENHI (20240003, 21300054). Xue-Feng Zhang is sponsored by the China Scholarship Council (CSC).

References

[1] M. Garey,D. Johnson, R. Sethi, "The complexity of flow shop and job shop scheduling," Mathematics of Operations Research, 1, 1976, pp. 117-129.

[2] L. Tsung-Lieh, H. Shi-Jinn, "An effiecient job-shop scheduling algorithm based on particle swarm optimization," Expert Systems with Applications, 37(2010), pp.2629-2636.

[3] J. Adams, E. Balas, D. Zawack, "The shifting bottleneck procedure for job shop scheduling," Management Science, 34(1988), pp.391-401.

[4] E. Nowicki, C. Smutnicki, "An advanced tabu search algorithm for the job shop problem," Journal of Scheduling, 8(2005), pp.145-159.

[5] J.F. Goncalves, J.J.D.M Mendes, M.G.C. Resende, "A hybrid genetic algorithm for job shop scheduling," European Joural of Operational Research, 167(2005), pp.77-95.

[6] R.K. Sursh, A. Albrecht, K.C. Wong, "Pareto archived simulated annealing for job shop scheduling with multiple objectives," The International Journal of Advanced Manufacture Technology, 29(2005), pp.184-196.

[7] H.W. Ge, L. Sun, Y.C. Liang, "An effective PSO and AIS-based hybrid intelligent algorithm for job-shop scheduling," IEEE Transactions on Systems, Man and Cybernetics, Part A, 38(2008), pp.358-368.

[8] A. Udomsakdigool, V. Kachitvichyanukul, "Multiple colony ant algorithm for job-shop scheduling," International Journal of Production Research, 46(2008), pp.4155-4175.

[9] X. Weijun, W. Zhiming, "A Hybrid particle swarm optimization approach for the job-shop scheduling problem," Int J Manuf Technol, 29(2006), pp. 360-366

[10] V. Fevrier, M. Patricia, C. Oscar, M. Oscar, "A New Evolutionary Method with a Hybrid Approach Combining Particle Swarm Optimization and Genetic Algorithms using Fuzzy Logic for Decision Making," IEEE Congress on Evolutionary Computation, 2008, pp. 1333-1339

[11] V. Fevrier, M. Patricia, C. Oscar, "An improved evolutionary method with fuzzy logic for combining Particle Swarm Optimization and Genetic Algorithms," Appl. Soft Comput, 2011, 11(2): 2625-2632

[12] J. Kennedy, R. Eberhart, "Particle swarm optimization," In Proceedings of IEEE international conference on neural network , 1995, pp.1942-1948.

[13] R. Eberhart, J. Kennedy, "A new optimizer using particle swarm theory," In: Proceedings of Sixth International Symposium on Micro Machine and Human Science, Japan, 1995, pp. 39-43.

[14] D.Y. Sha, L. Hsinghung, "A particle swarm optimization for multi-objective flowshop scheduling," Original Article Int J Adv Manuf Technol, (45) 2009, pp. 749-758.

[15] Y. Shi, R. Eberhart, "Empirical study of particle swarm optimization," In: Proceedings of Congress on Evolutionary Computation, 1999, pp.1945-1950.

[16] J. Kennedy, "The particle swarm: social adaptation of knowledge," In: Proceedings of IEEE International Conference on Evolutionary Computation, 1997, pp.303-308.

[17] E. Balas, A. Vazacopoulos, "Guided local search with shifting bottleneck for job shop scheduling," Management Science, (44)1988, pp. 62-75.

[18] J.E. Beasley, "Or-library: Distributing test problems by electronic mail," Journal of the Operational Research Society, (14)1990, pp. 1069-1072.

[19] H. Fisher, G.L. Thompson, "Probabilistic learning combinations of local job shop scheduling rules," Prentice-Hall, NJ: Englewood Cliffs, 1963, pp. 225-251.

[20] S. Lawrence, "An experimental investigation of heuristic scheduling techniques," In supplement to resource constrained project scheduling, GSIA, Pittsburgh, PA: Carnegie Mellon University, 1984.

2011 IEEE International Conference on Fuzzy Systems
June 27-30, 2011, Taipei, Taiwan

A Framework of Multi-characteristics Fuzzy Dynamic Scheduling for Parallel Video Processing on MPSoC Architecture

Da Li, Yibin Hou, Zhangqin Huang, Chunhua Xiao
School of Electronics and Information Engineering, Xi'an Jiaotong University, Xi'an, P.R. China
Embedded Software and Systems Instiute, Beijing University of Technology (BJUT), Beijing, P.R. China
lida1204@gmail.com

***Abstract*—This paper addresses the inherent unreliability and instability of the multiple uncertain characteristics of complex embedded multiprocessor systems, such as MPSoC (multi-processor system on chip) systems. In this work, we propose a fuzzy sets description for the multiple uncertain characteristics of system, and using fuzzy set membership calculation to determine the scheduling priorities of tasks and resources, in order to improve the capability of concurrent executions of tasks. And also we present a method estimation of comprehensive analysis on the multiple performances in order to increase utilization factor and balancing loads on processors. Through simulation, we demonstrate that the fuzzy dynamic scheduling algorithm can handle wide variety requirements of multiple performances, and we also show an improved approach to solve its demerit of partial adjustment. We implemented a prototype MPSoC system, which utilizes the proposed fuzzy dynamic scheduling algorithm to allocating tasks onto the multiprocessors. And in our case studies, we design a parallel architecture h.264 encoder, running on a multicore MPSoC system on FPGA. The speedup ratio of this prototype application system is up to 12.69.**

Keywords-MPSoC System; Dynamic Scheduling; Multi-characteristics; Priority Level; Fuzzy Set; Video Processing; Parallel Processing

I. INTRODUCTION

With the rapid improvement of microprocessor technology, MPSoC system, featured as high in performance, extensible, small in size and low in power consumption, is able to meet requirements of complex embedded systems for computing performance, power consumption and cost, thus having become one of the mainstream development trends of embedded systems [1], [2]. Currently, MPSoC is widely used in computer communication, digital media, auto electronics, medical electronics, aviation and aerospace, industrial control and many other fields, and the relevance of research topics on MPSoC has engaged many enterprises and institutes in research on MPSoC, such as programming model, task scheduling, system development, debugging environment and system safety; among these, real-time dynamic scheduling has become an important topic [3], [4].

While scheduling of multicore processor is NP-Hard [5], there is no optimal polynomial-time algorithm. Meanwhile, realization of a scheduler applicable to systems of different structures and application fields becomes a new challenge. Researchers apply heuristic search to find a partial optimal scheduling solution for this system [16], [17], [18], [19]. Priority scheduling algorithms are most commonly used. Scheduling algorithms based on task priority mainly include RM, EDF, LSF [6], [7], [8], [9], and some complex fix-priority policies such as the policy of integrated priority [10], [11]. And the myopic [12], [13], thrift [14], group-proper [15] algorithms analyzed in this paper are integrated priority.

However, the above algorithms are dependent on prior characteristic values of the system and loads, and can only provide performance guarantee in a predictable environment when all constraints of system and tasks are known accurately. In actual applications however, characteristics of many tasks are always uncertain and fuzzy. Furthermore, execution performance of computing and control algorithms, real-time operating system, scheduling and network delay may cause delays and errors, and system overload or failures may also lead to uncertain changes in the system. And also some characteristics of tasks are time-varying, such as the laxity time of tasks, the executed ratio of tasks and the remaining ratio of tasks. These characteristics can't be calculated completely accurately, so they can be considered as fuzzy and uncertain random variables. Further, the key features of tasks are relative, and it is not suitable to use a certain value describing the criticality of tasks distinguishingly.

Hence some researchers have proposed to utilize the fuzzy theory for dynamic scheduling, fuzzy sets for description of uncertainties and priority levels of different tasks, and the rules of fuzzy sets for determination of priority levels. Some fuzzy dynamic scheduling algorithms [16], [17] and some fuzzy model [18], [19] for representation of fuzzy constraint rules, but most description functions in these papers are certain, it is inflexible to use certain functions for description of time-varying uncertain characteristics; in addition, all the above methods give no consideration to other characteristics such as key features of tasks, resource factor or limited priority levels, and more system performances. They just only focus on a certain feature or a certain performance of system scheduling, that is unable to meet diversified requirements of a system, such as success ratio of scheduling, schedule time length etc.

This work was supported by the China National Natural Science Foundation under Grant 60773186, and the High-level Personnel Training Project of Beijing University of Technology.

978-1-4244-7316-8/11/$26.00 ©2011 IEEE

The main goal of this paper is to establish fuzzy model of complex MPSoC system, and apply proper scheduling policy to meet composite requirements for multiple performances. In order to do that, we propose a new real-time fuzzy scheduling algorithm for MPSoC, multi-characteristics fuzzy dynamic scheduling (Multi-Fuzzy algorithm), It uses language fuzzy sets for modeling various characteristics of tasks and system, and calculates the target priority functions of tasks and resources based on the membership rules of these fuzzy sets, and this paper further proposes the solution for partial adjustment.

The rest of this paper is organized as follows: section II Introduces our models, definitions and computation methods of algorithm, section III discusses the multi-characteristics fuzzy dynamic scheduling algorithm. In section IV a case study and simulation results are presented and discussed. Finally, section V summarizes the work.

II. CONCEPTS, DEFINITIONS, METHODS

A. System and Task Model

Provided a real-time MPSoC system S has m processors (m>1), r resources (r>1) and n tasks in a task set (n>>1), this system can be described as below:

$$S = \{P_m, R_r\} \mid T_n \mid H$$

Definitions of the key parameters are summarized in Table I.

TABLE I. SYMBOLS AND DEFINITIONS IN ALGORITHM

symbol	definition
$t_{a\tau}$	Task arriving time
$t_{d\tau}$	Task deadline
$t_{e\tau}$	Task executing time
$ret(\tau)$	The remaining executing time of task τ
$ts(\tau)$	The laxity time of task τ , $ts(\tau) = td\tau - t - ret(\tau)$;
wt_1, wt_2	The weights in time factor for tasks
EAT	The earliest available time
ft	Factor time, $ft = [t_{d\tau} + wt_1 \times EAT(\tau) + wt_2 * ts(\tau)] / t_{e\tau}$
fp	Factor parallel level $fp = \min(tk_{R1}(\tau), ..., tk_{Rn}(\tau))$
fc	Factor parallel level $fc = fc_0 + t_{e\tau} - ret(\tau)$
wp	The weights in processors priority
$U_P(p)$	The utilization ratio of processors
$EAT_P(p)$	The earliest available time of processors

In system resource R_k has r_k access tokens tk (maximum number of shared access), tokens are independent and each enables a shared access. The available resource state can be signed as

$$\{tk_1^{Rk}(EAT_1^{Rk}), \ldots, tk_{r_k}^{Rk}(EAT_{r_k}^{Rk})\}$$

Each of the r_k access tokens has a time label EAT^{Rk}..it means this token's earliest available time. And setting EAT_{Rk_s} , EAT_{Rk_e} denote the EAT of resource R_k in shared mode and exclusive mode, then

$$\begin{aligned} EAT_{Rk_s} &= \min(EAT_j^{Rk}), \\ EAT_{Rk_e} &= \max(EAT_j^{Rk}), \\ 0 &< j \le r_k \end{aligned} \quad (1)$$

So, the EAT f source for task τ s denoted as:

$$EAT_R = \max(\max(EAT_{Rj_e}), \max(EAT_{Rj_s})) \quad (2)$$

The EAT of system processors is

$$EAT_P = \min(EAT_{Pj}), 0 < j \le m \quad (3)$$

EAT_{Pj} is the EAT of processor *Pj*.

Then, the earliest available time of task τ should be

$$EAT(\tau) = \max(t_{a\tau}, EAT_p, EAT_R(\tau)) \quad (4)$$

B. Fuzzy Set Model

Fuzzy sets are described based on uncertain multi-characteristics of tasks, and target priority function $H_T(\tau)$ is worked out after computation and quantitative evaluation based on the rules of fuzzy sets.

- Relative time ft

ft is an evaluation value of the time factor of all tasks. It changes with increase of scheduling time. As described in Table 1, ft is a weighted comprehensive estimation of $t_{d\tau}$, $EAT(\tau)$ and $ts(\tau)$. Therefore, the relative time of tasks is uncertain and can be described with fuzzy sets, such as "most urgent (shortest)", "urgent (short)", "moderate (medium)", "slack (long)", "slackest (longest)" and etc., and expressed as $A(sa_1), \ldots, A(sa_n)$ fuzzy sets. It is denoted as

$$Sa(ft) = \frac{u_{A(sa1)}(ft)}{A(sa1)} + \ldots + \frac{u_{A(san)}(ft)}{A(san)}, \quad (5)$$

Here $u_{A(sai)}(ft)$ is the membership of relative time to fuzzy set $A(sa_i)$, and $\sum_{i=1}^{n} u_{A(sai)}(ft) = 1$.

- Parallel level fp

Similarly, the capability of parallel execution of tasks is decided by the resources available tokens at that time. fp is equal to the minimum of number of available resources tokens($fp \geq 0$), and task of lower fp value will be given higher priority. The system resources access tokens are time-varying by the system scheduling process. So fp is also uncertain and can be described with fuzzy sets, classified as "higher", "medium", "lower", and denoted as

$$Sb(fp) = \frac{u_{b1}(fp)}{B(s_{b1})} + \ldots + \frac{u_{bn}(fp)}{B(s_{bn})}, \tag{6}$$

- Key feature fc

Key feature is the importance mark of a task in the task set, which is describing the criticality of tasks. And as shown in Table 1, it is related to the executed time of task, which is time-varying. So we use fuzzy sets express it as "important", "ordinary" and "unimportant", and denoted as

$$Sc(fc) = \frac{u_{C1}(fc)}{C(sc_1)} + \ldots + \frac{u_{Cn}(fc)}{C(sc_n)}, \tag{7}$$

C. Calculation Methods

- Composite target function of task priority

Let g indicating uncertain characteristics be represented by $\{A, \ldots, G\}$, and the jth fuzzy set of uncertain characteristic xi as $A(aj)(xi)$; fuzzy membership $u_{A(aj)(xi)}$ is the possibility of task τ belonging to $A(aj)(xi)$; then matrix $Q_f(\tau)$ represents the possible membership of a task in various fuzzy sets:

$$Q_f(\tau) = \begin{bmatrix} u_{A(sa1)(x1)} & \ldots & u_{A(san)(x1)} \\ \ldots & \ldots & \ldots \\ u_{G(sg1)(xg)} & \ldots & u_{G(sgn)(xg)} \end{bmatrix} \tag{8}$$

To decide the importance of fuzzy sets and multi-characteristics in priority levels, we set up resultant weight vector W_f and evaluation level vector Δ_f of different fuzzy characteristics, shown as:

$$H_T(\tau) = W_f \circ Q_f(\tau) \cdot \Delta_f \tag{9}$$

Here,

$$\Delta_f = [\Delta_{f1}, \ldots, \Delta_{f\eta}]^T, W_f = [w_1, \ldots, w_g]$$

We get the membership of task priority level, through the computation on max-min rules of fuzzy set, as $Pb = W_f \circ Q_f(\tau) = [p_{b1}, \ldots, p_{b\eta}]$ and then Pb is multiplied by Δ_f to get the corresponding value of $H_T(\tau)$. Scheduling of tasks should be decided according to the $H_T(\tau)$ value of current tasks. And generally, the smaller the $H_T(\tau)$ value is, the higher the priority level is.

- Target function of processor priority

In the policy of processor selection, we should consider the relationships between the feasible time of tasks, available time of resources and available time of processors, and select the appropriate processor in available processor subsets to reduce the schedule time length of task sets and improve processor utilization.

$$\begin{aligned} &H_P(p) = EAT_P(p) + W_P * U_P(p), \\ &Pchoose() \\ &= \{p_{\min} \mid H_P(p_{\min}) = \min(H_P(p_j)), p_j \in P\} \end{aligned} \tag{10}$$

- Auto-adjustment

```
Algorithm 3.1 : multi-fuzzy algorithm
Input:  {T}^n, {P}^m, {R}^r;
Output: construct a complete schedule Schedule(T)
        if T is feasible; otherwise reject.
1   f ← 1, b ← N ;//system initalization
2   Schedule(T) ← NULL
3   while (t_ar ≤ t) do UpdateTask(t,T) od;//
    update T_ready when new task is ready
4   case  // scheduling
5   for i=1 to n do
6   f ← feasible(ws) ;// feasibility analysis
7     if (f = 1)
8       then // get a local scheduling for ws
9       Schedule(Ti) ← localScheduling(ws,l) ;
10      stPi,stRi,utPi,utRi ← stPi+1,stRi+1,utPi+1,utRi+1 ;//
      update system state tables and usage tables
11      else   // backward to the former schedule
12      Schedule(Ti) ← Schedule(Ti-1) ;
13      stPi,stRi,utPi,utRi ← stPi-1,stRi-1,utPi-1,utRi-1 ;//
      backward system state tables and usage tables
14      b ← N-1, f ← fP(r) ;
15    fi;
16    if (b ≤ 0) then abort fi;
17    if (SR < SR0 or URP < URP0) //
      auto-adjustment of the weight W
18    then w ← w + Δw ;
19    fi;
20  od
21  return ;
```

Figure 1. Multi-Fuzzy Algorithm

The method of auto-adjustment is for purposes of better comprehensive performances in scheduling success, schedule time length and resource utilization, and modification of the weights of various fuzzy characteristics of priority levels , if the schedule performance of a partial task subset is lower than the initial threshold value during scheduling of task sets, namely $W_f' = W_f + \Delta W_f$; and then adjusting step by step until the

schedule performance reaches the initial threshold, so as to improve scheduling performance of task sets.

III. MULTI-FUZZY SCHEDULING ALGORITHM

A. Description of Multi-Fuzzy Algorithm

As described in Fig.1, multi-fuzzy algorithm is divided into several parts: Lines1 to 2 are designed for initial setting of the system, and line 3 for updating tasks ready for the task ready queue T_ready, in the order of increasing deadlines; Lines 4 to 19for heuristic scheduling; specifically, lines 6 for feasibility analysis of tasks in the search window ws; lines 8 to 10 for further extension of partial schedule only when feasible, selecting proper tasks and processors for execution, updating the status table after execution, while system scheduling goes to line 5 for the next scheduling; lines 12 to 14 forces search tree to backtrack to the upper level schedule and for resetting the processor choose l when unfeasible, while lines 17 to 19 for auto-adjustment of the algorithm's weight parameter W, so as to properly adjust weight ratios between various characteristics.

B. Metrics for Performance Evaluation

For task scheduling of MPSoC, success ratio is an important metric for evaluation; meanwhile, other metrics such as schedule time length, average scheduling cost and processor utilization, affect scheduling performance directly and reflect the scheduling efficiency per unit of time, the power consumption of the system and effective utilization of resources. Hence this paper studies the metrics of these performances.

- Success Ratio $SR(T)$:

$$SR(T) = N_{success} / N_{sum} \times 100\% \quad (11)$$

$N_{success}$, number of task sets that can be successfully scheduled; N_{sum} , total number of task sets.

- Scheduling Time Length $\overline{TL}$:

$$\overline{TL} = \sum_{i=1}^{N_{success}} t_{finish}(i) / N_{success} \quad (12)$$

$t_{finish}(i)$, scheduling time for each task set; $\overline{TL}$, the average value of schedule time of all the task set available for scheduling;

- Average scheduling cost $\overline{N}_H$

$\overline{N}_H$ refers to the number of times that local scheduling function is called during scheduling of task sets, namely the average length of total schedule number of calculation of task priority and evaluation value of processors.

- Processor Utilization UR_P :

$$UR_{Pj} = \sum_{Pj} t_{e\tau} / t_{finish} \times 100\% \quad (13)$$

$\sum_{Pj} t_{e\tau}$ refers to the total execution time of tasks allocated to processor P_j .

IV. CASE STUDIES

A. Simulation Experiments

The primary MPSoC system is built on the XUPV5-LX110T Development Board from Xilinx, this board has a Virtex-5 XC5VLX110T FPGA, and a video VGA input and DVI output hardware. Our experiments are simulated on the FPGA, setting the MPSoC system on FPGA processing the video data, and output the video multi-display onto a PC screen.

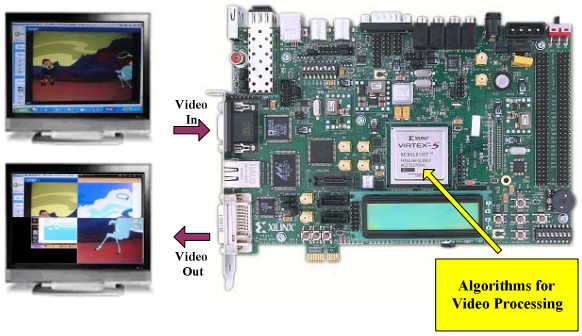

Figure 2. Experiment Platform Overview.

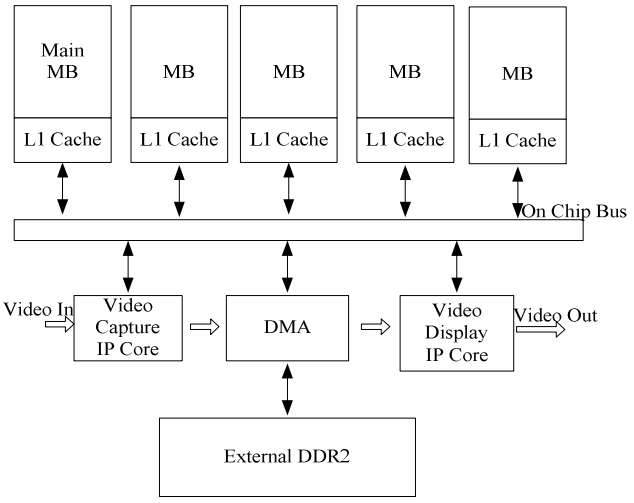

Figure 3. Architecture of MPSoC System for Video Processing.

The video processing is divided into some tasks to be executed on multiprocessors, and each processor has a local BRAM resource and share an external DDR2 SDRAM. The overview of the experiment platform is given in Fig. 2. And the

architecture of MPSoC System for Video Processing is shown in Fig. 3.

B. Results Analysis

Fig. 4 shows effects of laxity r on success ratio SR of algorithms. SR of the four algorithms becomes higher when r increases; specifically, when r falls in the interval (0, 0.1), SR of multi-fuzzy algorithms are relatively low; but it increases rapidly when r is over 0.3, exceeds other algorithms when r is around 0.5 and remains the highest when r is above 0.5. For multi-fuzzy algorithm with different weights, the success ratio varies significantly when r value is small, and the rate of change is different as r increases, but after r exceeds 0.5, the

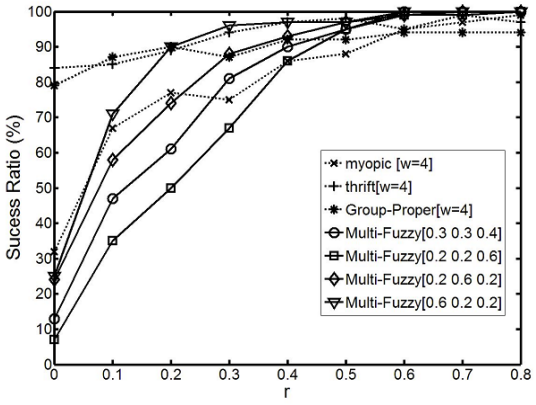

Figure 4. Success Ratio of Scheduling.

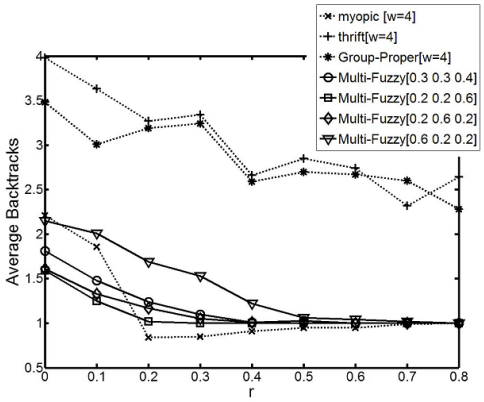

Figure 5. Average Number of Backtracking.

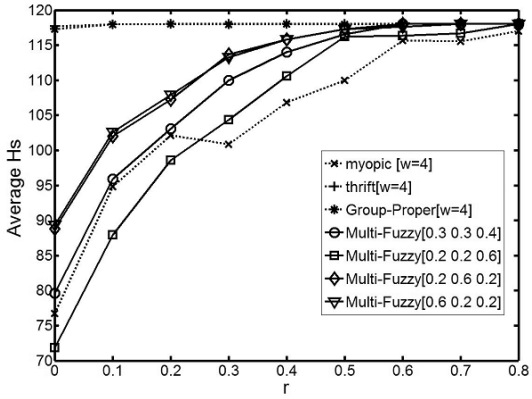

Figure 6. Average Scheduling Cost

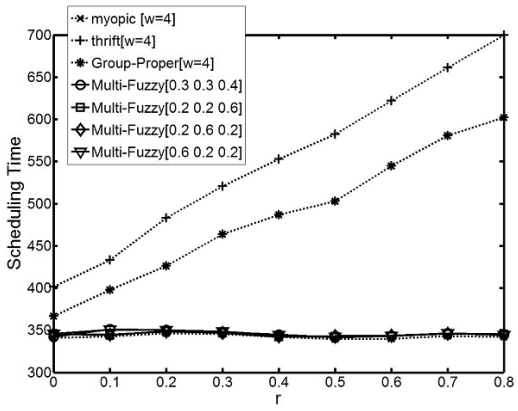

Figure 7. Average Scheduling Time Length.

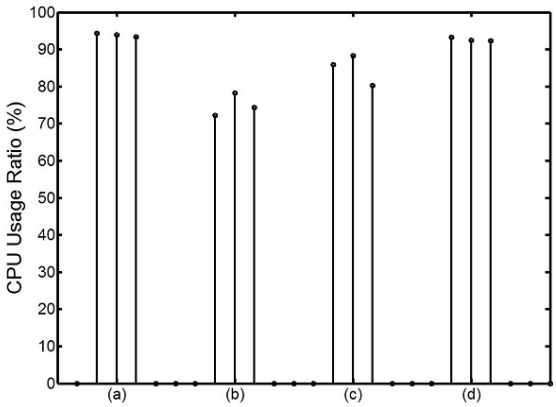

Figure 8. Processor Utilization: (a) Myopic. (b) Thrift. (c) Group-Proper. (d) Multi-Fuzzy

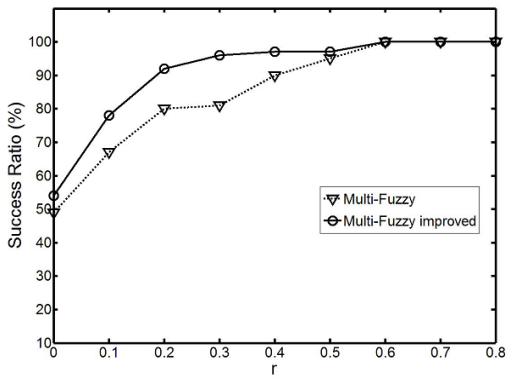

Figure 9. Improvement of Multi-Fuzzy Algorithm

difference becomes insignificant, falling within 10%. The performance test of Average number of backtracking sets maximum backtracking number N as 10. As show in Fig. 5, all algorithms decreases slowly with r; thrift algorithm is the highest, 3-4 times per task set; that of group-proper algorithm is the second highest with a level of 2.5-3.5 times per task set; and larger number of backtracking means a lower probability of successful search for a feasible solution, and the corresponding scheduling cost and time of the scheduler are added. In Fig. 6, scheduling costs of thrift and group-proper algorithms are obviously higher when r value is small; as r the scheduling costs of algorithms increases, and when laxity r is over 0.6, SR of all algorithms is close to each other, multi-fuzzy algorithm is just only higher than myopic algorithm. $\overline{N}_H$ (shown in Fig. 7) of thrift and group-proper is longer and increases linearly with laxity r, while that of myopic and multi-fuzzy algorithms tend to be stable around 340-350 time units, close to the basic time length of task set generator SC(330 on average); this resulted from effects of the policy of processor allocation of algorithms. And for UR_P in Fig. 8, single processor utilization of the thrift algorithm is the highest, up to 94%; that of myopic and group-proper algorithms are 74% and 85% respectively, and that of the multi-fuzzy algorithm is 92%. In terms of equalizing in processor utilization, performance of the multi-fuzzy algorithm is the best, for loads on various processors are the most even.

C. *Improvement Policy of Multi-Fuzzy Algorithm*

In the test in section IV-A, SR of multi-fuzzy algorithm is not so high when laxity *r* is low, thus we adjust part of the scheduling policy. Standards for processor selection can be properly loosened so as to select feasible processors with a suboptimal evaluation function value or a value closer to the average, providing more opportunities for those infeasible tasks. For example, the processor with a $H_P(P)$ value close to $\overline{H}_P$ can be selected, as

$$f_P(r)=\begin{cases}1, & r>0.3\\ Lt(\overline{H}_P), & r\le 0.3\end{cases} \tag{14}$$

with set $f_P(r)$ as a selection parameter of the algorithm. When r is no higher than 0.3, $Lt(\overline{H}_P)$ is the sequence number of processor whose $H_P(P)$ is closest to and less than $\overline{H}_P$; A simulation test is performed in reference to the adjustment policy. It can be seen from simulation results in Fig. 9 that the algorithm is significantly improved when time constraints are tight (r≤0.3), in that SR is increased from 20%-30% to 50%.

D. *Implement h.264 Encoder on FPGA*

A high performance FPGA was used to implement an MPSoC of h.264 encoder, as shown in Fig. 10, and the heterogeneous multi-core processor architecture has been designed for the special use of mass data computation. The MPSoC has five MBs (MicroBlaze), which is a software IP core of 32bit general CPU. These MBs are connected by the on chip high speed interconnection network directly. The Main Processor is in charge of the system initialization and system controlling, and other Synergistic Processors execute parallel video data computation separately. Each processor has a local L1 cache to load and store data used by executing unit. So there is potential competition to the occupation of data transmission. The Multi-Fuzzy Scheduling is running on the Main MB to be evaluated for scheduling and communication of system.

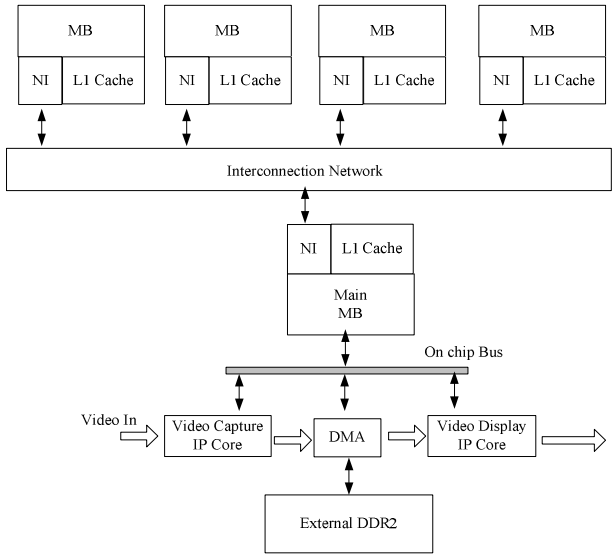

Figure 10. Architecture of Heterogeneous Multiprocessor System for Video Processing

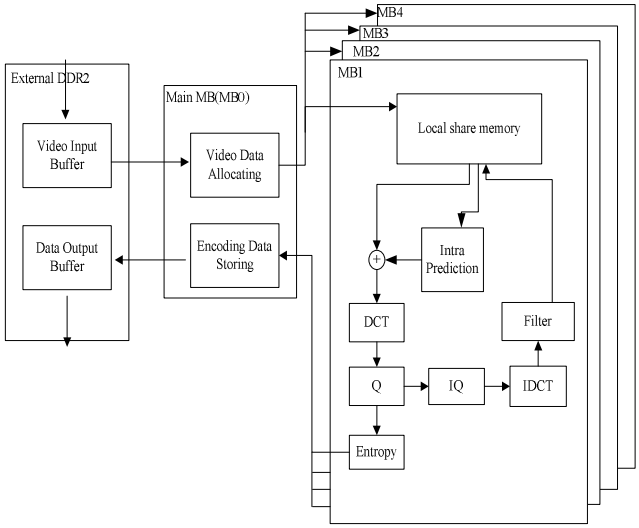

Figure 11. The Data Flow and Task Allocation of h.264 Encoder

In the h.264 video encoding application, the prototype system will capture the video stream as input, encode these video data and stored the encoded data to the output buffer. Fig. 11 outlines the data flow and task mapping of this application. In this application, the main MB is charge for allocating video stream data to the other Synergistic Processors, and gathering the encoded data from the video processing

processors to output into the external memory. Each MB will execute a complete h.264 encoding process. This process is divided up into several tasks: Intra Prediction, Forward and Inverse Transforms, Forward and Inverse Quantization, Reconstruction and Entropy Coder. We map these tasks onto different cores in each MB subsystem.

In the h.264 encoding processing, a frame is divided into many macroblocks. Hence it becomes the basic processing object for each core. The shared local memory (L1 cache) and some buffers between cores (such as FIFOs) are using for cache data, by which the one-way data stream can be divided into Multi-stage pipeline to greatly improve the system parallel performances.

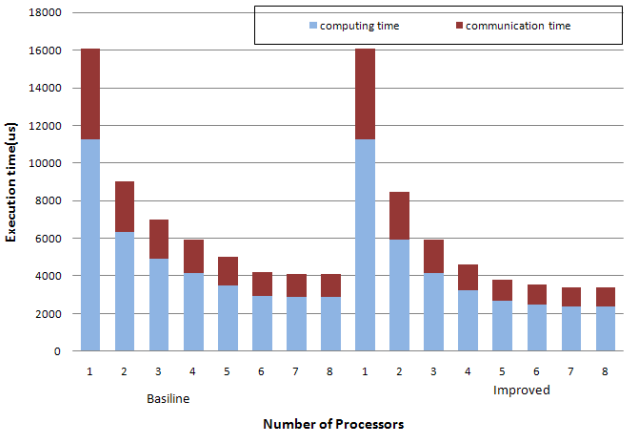

Figure 12. Execution Time of h.264 Encoder

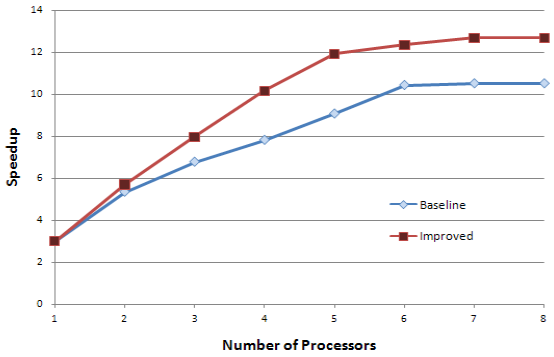

Figure 13. Speedup Ratio of h.264 Encoder

The Fig. 12 shows the execution time of the h.264 encoding for different number of processors. We have run the encoder under 100MHz system clock. In this example the baseline case allocates the tasks with the invariable macroblocks onto these processors, and the improved case use the fuzzy dynamic scheduling to allocate the macroblocks onto the appropriate processor. And the Fig. 13 shows the parallel speedup ratio performance, with the increase of number of processors, the speedup ratio of this application is improved. The highest speedup ratio is up to 10.53 and 12.69 in baseline case and improved case. The improved case can achieve better speedup ratio performance, because it minimize the difference of each processor's executing time so that there are less communications and high utilization.

V. CONCLUSION

The multiple performances are keys for scheduling algorithms and scheduler. By referring to these scheduling performance parameters, we can study the corresponding performances in detail, such as cost efficiency, scheduling efficiency. The multi-fuzzy algorithm is better suited to task scheduling in a complex system with multiple characteristics, and it works well in various scheduling performances, thus able to meet the requirements for dynamic task scheduling more effectively.

In different target systems actually designed, performance parameter standards and weights may vary significantly due to difference in design key points. Therefore, algorithms should be applied according to actual conditions during design of scheduler.

And we implement a prototype design with the fuzzy dynamic scheduling method for the hierarchical MPSoC architecture, which adopts a MPSoC h.264 encoder. The speedup ratio of this prototype application system is up to 12.69.

REFERENCES

[1] Tilak Agerwala, Siddhartha Chatterijee, "Computer architecture: Challenges and opportunities for the next decade," IEEE Micro, vol. 25, no. 3, pp. 58-69, 2005

[2] Wayne Wolf, "The future of multiprocessor systems-on-chips," Proc. 41st Annual Conference on Design Automation, pp. 681-684, 2004

[3] Baruah S, Nathan F, "The feasibility analysis of multiprocessor real-time systems," Proc. EuroMicro Conference on Real-Time Systems, pp. 85-94, 2006

[4] Liu Sha, Tarek Abdelzaher, Karlerik Arzen, "Real time scheduling theory: A historical perspective," J. Real-Time Systems, vol. 28, no. 2, pp. 101-155, 2004

[5] Mok,A.K. "Fundamental Design Problems of Distributed Systems for the Hard Real-Time Environment," PhD dissertation, Dept. of Electrical Eng, MIT, Cambridge, 1983.

[6] Liu C L, Layland J W, "Scheduling algorithms for multiprogrammingin a hard real-time environment," J. ACM, vol. 20, no. 1, pp. 46-61, 1973

[7] Tarek A. AlEnawy, Hakan Aydin, "Energy-Aware Task Allocation for Rate Monotonic Scheduling," Proc. 11th IEEE Real-Time and Embedded Technology and Applications Symp, pp. 213-223, 2005

[8] Theodore P. Baker, "An Analysis of EDF Schedulability on a Multiprocessor," IEEE Trans. on Parallel and Distributed Systems, vo1. 16, no. 8, pp. 760-768, August 2005

[9] Myunggwon Hwang, Pankoo Kim, Dongjin Choi, "Least Slack Time Rate First: New Scheduling Algorithm for Multi-Processor Environment," Proc. 4th IEEE Int'l Conf. Complex, Intelligent and Software Intensive Systems, pp. 806 – 811, 2010

[10] Jin Hong; Wang Hong An; Wang Qiang; Dai Guo Zhong, "An Integrated Design Method of Task Priority," J. Software, vol. 14, no. 3, pp. 376-382, 2003

[11] Xianbo He, Li Yang, Feng Yin ,Chunlin He,Gangyuan Zhang, "A fuzzy scheduling model based on multi-characteristics of tasks in embedded soft real-time Systems oriented to communication field," Proc. 2nd IEEE Int'l Conf. on Computer Science and Information Technology,pp. 270-274,2009

[12] Ramamritham,K.J.,Stankovic,A.,Shiah,P.-F, "Efficient scheduling algorithms for real-time multiprocessor systems," IEEE Trans. on Parallel and Distributed Systems, vol. 1, no. 2, pp. 184~194, 1990

[13] Manimaran,G.,Murthy,C.S.R.,"An efficient dynamic scheduling algorithm for multiprocessor real-time systems," IEEE Trans. on Parallel and Distributed Systems, vol. 9, no. 3, pp. 312-319, 1998

[14] WangKun, QiaoYing, WangHong An, FangTing, Zou Bing, DaiGuo-Zhong, "Study of a dynamic scheduling algorithm for realtime heterogeneous systems," J. Computer Research and Development, vol. 39, no. 6, pp. 725-731, 2002

[15] Bin Xuelian, Yang Yuhai, Jin Shiyao., "A new dynamic scheduling algorithm for real-time multiprocessor systems based on grouping and properly choosing policies," J. Computers, vol. 29, no. 1, pp. 81-91, 2006

[16] Terrier F.,Chen Z., "Fuzzy calculus applied to real time scheduling," Proc. 3rd IEEE Int'l Conf. on Fuzzy Systems, vol. 3, pp. 1905-1910, 1994

[17] Salmani, V.,Ensafi, R.,Khatib-Astaneh, N., Naghibzadeh, M, "A Fuzzy-Based Multi-criteria Scheduler for Uniform Multiprocessor Real-Time Systems," Proc. IEEE 10th Int'l Conf. on Integration Technology, pp. 179 – 184,2007

[18] Litoiu M., Tadei R., "Real-time task scheduling with fuzzy deadlines and processing times," J. Fuzzy Set and Systems, vol. 117, no. 1, pp. 35-45, 2001

[19] Dai Hongjun, Xu XinShun, Jia Zhiping, "A Fuzzy algorithm for parallelizability evaluation and load balance on the multi-core processor," Proc. 4th IEEE Int'l Conf.on Granular Computing, pp. 168 – 171, 2008

2011 IEEE International Conference on Fuzzy Systems
June 27-30, 2011, Taipei, Taiwan

The Derivation of the Analytical Structure of a class of Interval Type-2 Fuzzy PD and PI Controllers

Maowen Nie
Department of Electrical and Computer Engineering
National University of Singapore
Email: g0700223@nus.edu.sg

Woei Wan Tan
Department of Electrical and Computer Engineering
National University of Singapore
Email: wwtan@nus.edu.sg

***Abstract*— Analytical structure of a fuzzy logic system (FLS) is to establish its mathematical input-output relationship. In this paper, the analytical structure of a class of Interval type-2 (IT2) fuzzy PD and PI controllers are derived by dividing the input space and identifying the input-output relationship for each region. Unlike the symmetric fuzzy PD and PI controller [12] which have three different consequent sets $H_4 < H_3 = H_2 < H_1$, the IT2 fuzzy PD and PI controllers considered in this paper have four different consequent sets $H_4 < H_3 < H_2 < H_1$. Compared with the symmetric IT2 fuzzy controllers investigated in [12], the relatively large number of divisions of the input space indicates the potential of this class of IT2 fuzzy controllers in achieving better performance. The equations describing the input-output relationship for each region provide mathematical tools for further investigations of these IT2 fuzzy PD controllers.**

***Index Terms*— Interval type-2 fuzzy logic system, analytical structure, fuzzy PD and PI controller, Karnik-Mendel type-reduction method.**

I. Introduction

Numerical studies have shown that the IT2 fuzzy logic controller (FLC) may outperform the type-1 (T1) FLC in complex control systems, particularly in faces of complicated imprecision and uncertainty. One possible reason is that the 3-dimensional structure of an IT2 FS allows additional design parameters to be introduced. These additional design freedom may enable the IT2 FLC to produce satisfactory performance. But most of the efforts to demonstrate the advantages of the IT2 FLC over the T1 FLC have been made through case studies, and their conclusions may not be general enough to provide guidelines for the design of IT2 FLCs for other complex plants. As a result, the IT2 FLCs are generally treated as black-box systems whose parameters are optimized through genetic algorithms or other optimization algorithms only. Such FLCs may not be amenable for analysis and interpretation by engineers.

As an efficient theoretical tool, the analytical structure of a T1 fuzzy controller may be described by mathematical equations relating the output of the fuzzy controller and its inputs [3]-[10]. This analytical tool can overcome the limitation of fuzzy logic system—lack of explicit model, and reveal how the design parameters affect the input-output relationship. More importantly, this analytical tool can provide guidelines for the design of T1 FLCs in choosing a t-norm operation, the shapes of antecedent sets and tuning the design parameters. An early effort to derive the analytical structure of IT2 fuzzy controllers has been made in [11]. In this work, the authors approximated the output of the controller by averaging 16 embedded T1 FLSs, instead of the widely used Karnik-Mendel (KM) type-reduction method.

The KM type-reduction method is established on wavy-slice representation theorem: an IT2 fuzzy set (FS) contains an infinite number of embedded T1 FSs whose centroids will form an interval, the type-reduced set. In an IT2 FLS, the type-reduced set is formed by the centroid of all possible embedded T1 FLSs. The smallest and largest centroid which are the left and right endpoints of the interval respectively, can be searched using the Karnik-Mendel iterative algorithm [2]. There lacks closed-form expressions relating the output and inputs of an IT2 FLS. The left and right endpoints have been proven to be generated by the centroids of the output sets weighted by the upper or lower bound of the corresponding firing sets. Therefore, the challenge that impedes the derivation of analytical structure for IT2 fuzzy controllers is to figure out the situations when the upper or lower bound of firing sets should be applied. An effort has been made to derive the analytical structure for a class of symmetrical IT2 fuzzy PD or PI controllers [12]. Although this work has shed some lights on how to derive the analytical structure for IT2 fuzzy controllers, it is limited to symmetrical IT2 FLSs whose consequent sets H_1, H_2, H_3, H_4 satisfy $H_1 > H_2 = H_3 > H_4$. In this paper, another class of IT2 fuzzy controllers whose consequent sets satisfy $H_1 > H_2 > H_3 > H_4$ is considered. The main contribution of this paper is to propose an algorithm for deriving the analytical structure of the considered IT2 FLCs and to derive the analytical structure by following the proposed algorithm. The following parts of this paper are organized as: Section II describes the configurations of IT2 fuzzy PD and PI controllers; Section III presents the algorithm to derive their analytical structure, followed by the detailed derivation of the analytical structure of IT2 fuzzy controllers In Section IV. A conclusion is given in Section V.

II. Configuration Of Interval T2 Fuzzy PD and PI Controller

Fig. 1 contains the schematic diagram of an IT2 FLS. A two-inputs single-output fuzzy system commonly used for feedback control may be defined as

$$\triangle U(n) = f(E(n), R(n)) \tag{1}$$

978-1-4244-7316-8/11/$26.00 ©2011 IEEE

where $E(n) = K_e e(n) = K_e(SP(n) - y(n))$, $R(n) = K_r r(n) = K_r(e(n) - e(n-1))$, $y(n)$ is the output of the closed-loop system, $SP(n)$ is the reference signal, K_e and K_r are the scaling constants. The output $\triangle U(n)$ may be interpreted directly as the control signal or as the rate of change in the actuation signal. Depending how the output of the fuzzy controller is defined, it may be interpreted as a fuzzy PD or a fuzzy PI controller.

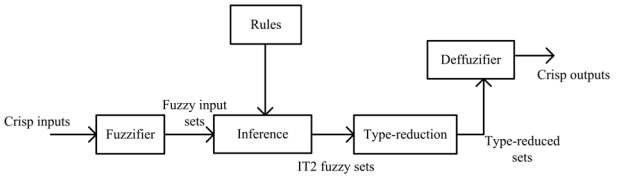

Fig. 1. The structure of IT2 FLS

For this study, two IT2 FSs are used to partition the space of each input: EN and EP for $E(n)$, **RN** and **RP** for $R(n)$. By shifting the membership of two symmetrical T1 FSs vertically by the amount of θ_1, the upper and lower membership of EN and EP, $\overline{\mathbf{EN}}$, $\underline{\mathbf{EN}}$, $\overline{\mathbf{EP}}$ and $\underline{\mathbf{EP}}$ in Fig. 2, can be obtained. In the same way, θ_2 represents the amount by which the upper and lower membership of RN and RP are shifted to obtain $\overline{\mathbf{RN}}$, $\underline{\mathbf{RN}}$, $\overline{\mathbf{RP}}$ and $\underline{\mathbf{RP}}$ in Fig. 3. Based on whether its value depends on the inputs, the lower bound or upper bound of any antecedent set can be decomposed into dependent part or independent segment (0 or 1). For example,

$$\overline{\mathbf{EN}} = \begin{cases} \overline{EN} = \frac{1}{2L_1}E(n) + 0.5 + \theta_1 \\ \qquad \text{for } -L_1 + P_1 \le E(n) \le L_1 + P_1 \\ 0 \qquad \text{for } E(n) \ge L_1 + P_1 \\ 1 \qquad \text{for } E(n) \le -L_1 + P_1 \end{cases} \tag{2}$$

where $\overline{EN}$ is the segment of the membership function of $\overline{\mathbf{EN}}$ that is dependent on the input, while the other part are independent of the input. (2) reveals the relationship between the membership grade and the input.

For fuzzy systems that partition the input space using IT2 fuzzy sets shown in Fig. 2 and 3, a commonly used rule base comprises of the following IF-THEN statements:

- Rule 1: IF $E(n)$ is Positive AND $R(n)$ is Positive THEN $\triangle U(n)$ is H_1
- Rule 2: IF $E(n)$ is Positive AND $R(n)$ is Negative THEN $\triangle U(n)$ is H_2
- Rule 3: IF $E(n)$ is Negative AND $R(n)$ is Positive THEN $\triangle U(n)$ is H_3
- Rule 4: IF $E(n)$ is Negative AND $R(n)$ is Negative THEN $\triangle U(n)$ is H_4

where H_1, H_2, H_3 and H_4 are the four singleton consequent fuzzy sets.

The result of the input and antecedent operations is an IT1 set called the firing set. Using Zadeh fuzzy AND operator as the t-norm operator, the firing set for each rule are as follows:

$$R_1 = [\underline{R}_1, \overline{R}_1] = [\min(\underline{\mathbf{EP}}, \underline{\mathbf{RP}}), \min(\overline{\mathbf{EP}}, \overline{\mathbf{RP}})] \quad \text{for } \triangle U(n) = H_1 \tag{3}$$

$$R_2 = [\underline{R}_2, \overline{R}_2] = [\min(\underline{\mathbf{EP}}, \underline{\mathbf{RN}}), \min(\overline{\mathbf{EP}}, \overline{\mathbf{RN}})] \quad \text{for } \triangle U(n) = H_2 \tag{4}$$

$$R_3 = [\underline{R}_3, \overline{R}_3] = [\min(\underline{\mathbf{EN}}, \underline{\mathbf{RP}}), \min(\overline{\mathbf{EN}}, \overline{\mathbf{RP}})] \quad \text{for } \triangle U(n) = H_3 \tag{5}$$

$$R_4 = [\underline{R}_4, \overline{R}_4] = [\min(\underline{\mathbf{EN}}, \underline{\mathbf{RN}}), \min(\overline{\mathbf{EN}}, \overline{\mathbf{RN}})] \quad \text{for } \triangle U(n) = H_4 \tag{6}$$

The output of the fuzzy inference engine, an interval type-2 fuzzy set, is obtained by combining the fired output consequent sets, where each fired output consequent set is the union of the firing set and the output consequent sets. Using the Mendel-John Representation theorem [1] (Theorem 1), the IT2 FS formed by the fuzzy inference engine may be viewed as the collection of all of its embedded IT1 FSs. Hence, the output of the inference engine may be type-reduced into an IT1 set comprising of the centroids of all embedded T1 FSs.

$$\triangle U_j = \frac{R_1^* * H_1 + R_2^* * H_2 + R_3^* * H_3 + R_4^* * H_4}{R_1^* + R_2^* + R_3^* + R_4^*} \tag{7}$$

where R_i^* is a value within the lower and upper bound of the firing set for the ith rule, R_i. In summary, the type-reduced set $\triangle U_{TR}(n)$ may be expressed mathematically as $[\triangle U_j^{min}, \triangle U_j^{max}]$, $\triangle U_j^{min}$ and $\triangle U_j^{max}$ are respectively the smallest and largest centroid of all the possible embedded T1 FS. Lastly, using the height defuzzification, the crisp output of the IT2 FLC is

$$\triangle U(n) = \frac{\triangle U_j^{min} + \triangle U_j^{max}}{2} \tag{8}$$

The four singleton consequent sets H_4, H_3, H_2, H_1 are equally spaced. Further, it is assumed that $H_4 < H_3 < H_2 < H_1$, which is shown in Fig. 4.

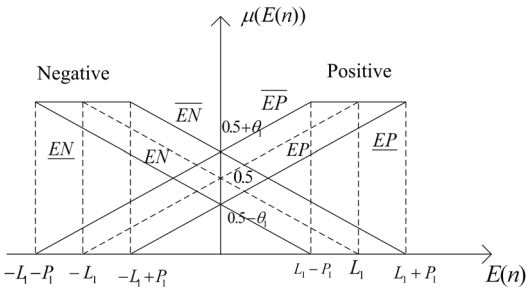

Fig. 2. IT2 FSs EN and EP as antecedent sets for the input $E(n)$ ($P_1 = 2L_1\theta_1$)

III. Algorithms to Derive the Analytical Structure of IT2 Fuzzy PD Controllers

This section will first establish the mathematical model of the left and right endpoints $\triangle U_j^{min}$ and $\triangle U_j^{max}$, and then present the algorithm to identify the mathematical expression for each firing strength in the IT2 fuzzy PD controller.

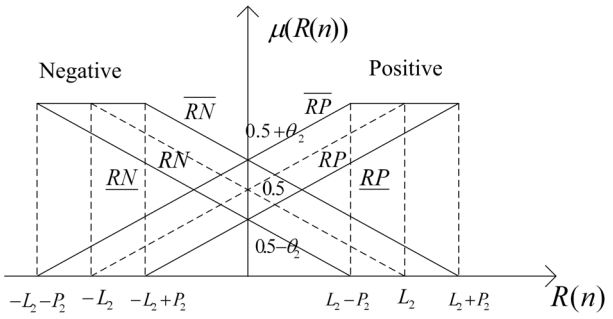

Fig. 3. IT2 FSs RN and RP as antecedent sets for the input $R(n)$ ($P_2 = 2L_2\theta_2$)

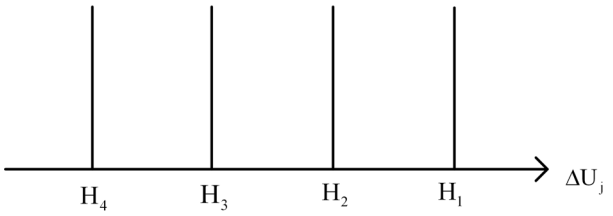

Fig. 4. Singleton consequent fuzzy sets of IT2 fuzzy PD controller

A. Mathematical model for the left endpoint $\triangle U_j^{min}$

From the Karnik-Mendel type-reduction method [2], the left and right endpoint $\triangle U_j^{min}$ and $\triangle U_j^{min}$ can be re-expressed as

$$\triangle U_j^{min} = \frac{\sum_{i=1}^{L-1} \underline{R}_i H_i + \sum_{i=L}^{4} \overline{R}_i H_i}{\sum_{i=1}^{L-1} \underline{R}_i + \sum_{i=L}^{4} \overline{R}_i} \tag{9}$$

$$\triangle U_j^{max} = \frac{\sum_{i=1}^{R-1} \overline{R}_i H_i + \sum_{i=R}^{4} \underline{R}_i H_i}{\sum_{i=1}^{R-1} \overline{R}_i + \sum_{i=R}^{4} \underline{R}_i} \tag{10}$$

where the switch point L and R coincide with the location of one of the 3 singleton consequent sets (H_1, H_2, H_3, H_4). From the derivation of the Karnik-Mendel type-reduction method [2], the following can be observed:

$$H_L \leq \triangle U_j^{min} < H_{L-1} \tag{11}$$

$$H_R \leq \triangle U_j^{max} < H_{R-1} \tag{12}$$

Due to the constraint that the switch point L and R must be positioned at one of the three singleton consequent sets and the inequalities in (11) and (12), it may be concluded that L and R can assume one of the three values i.e. $L = \{4, 3, 2\}$ and $R = \{4, 3, 2\}$. Hence, the only three possible expressions for $\triangle U_j^{min}$ may be written as

$$\begin{aligned}
&\text{Mode 1}: \quad \text{When } H_4 \leq \triangle U_j^{min} \leq H_3 \Leftrightarrow L = 4, \\
&\triangle U_j^{min} = \triangle U_{j1}^{min} \\
&= \frac{\overline{R}_4 * H_4 + \underline{R}_3 * H_3 + \underline{R}_2 * H_2 + \underline{R}_1 * H_1}{\overline{R}_4 + \underline{R}_3 + \underline{R}_2 + \underline{R}_1}
\end{aligned} \tag{13}$$

$$\begin{aligned}
&\text{Mode 2}: \quad \text{When } H_3 \leq \triangle U_j^{min} \leq H_2 \Leftrightarrow L = 3 \\
&\triangle U_j^{min} = \triangle U_{j2}^{min} \\
&= \frac{\overline{R}_4 * H_4 + \overline{R}_3 * H_3 + \underline{R}_2 * H_2 + \underline{R}_1 * H_1}{\overline{R}_4 + \overline{R}_3 + \underline{R}_2 + \underline{R}_1}
\end{aligned} \tag{14}$$

$$\begin{aligned}
&\text{Mode 3}: \quad \text{When } H_2 \leq \triangle U_j^{min} \leq H_1 \Leftrightarrow L = 2 \\
&\triangle U_j^{min} = \triangle U_{j3}^{min} \\
&= \frac{\overline{R}_4 * H_4 + \overline{R}_3 * H_3 + \overline{R}_2 * H_2 + \underline{R}_1 * H_1}{\overline{R}_4 + \overline{R}_3 + \overline{R}_2 + \underline{R}_1}
\end{aligned} \tag{15}$$

Based on the output conditions for Mode 1 ($H_4 \leq \triangle U_j^{min} \leq H_3$), Mode 2 ($H_3 \leq \triangle U_j^{min} \leq H_2$) and Mode 3 ($H_2 \leq \triangle U_j^{min} \leq H_1$), the input conditions when the three embedded T1 FLSs in (13)-(15) are respectively used as the left endpoint $\triangle U_j^{min}$ may be established as follows:

1) The condition when the switch point changes from the position of $L = 4$ to $L = 3$ and vice versa can be established as

$$\triangle U_j^{min} = \triangle U_{j1}^{min} = \triangle U_{j2}^{min} = H_3 \tag{16}$$

By replacing $\triangle U_{j1}^{min}$ and $\triangle U_{j2}^{min}$ with the expressions (13) and (14), the above equation may be written as

$$\overline{R}_4(H_4 - H_3) = \underline{R}_2(H_3 - H_2) + 2\underline{R}_1(H_3 - H_1)$$

Because of the assumption that the four consequent sets are equally spaced and $H_4 < H_2 < H_3 < H_1$, the condition established above may be reduced to

$$\overline{R}_4 = \underline{R}_2 + 2\underline{R}_1 \tag{17}$$

Further, the input subregions where (13) is used to calculate the left endpoint of the type-reduced set (Mode 1) can be found using its corresponding output condition:

$$\triangle U_j^{min} = \triangle U_{j1}^{min} \leq H_3 \Leftrightarrow \overline{R}_4 \geq \underline{R}_2 + 2\underline{R}_1 \tag{18}$$

and the areas where the IT2 fuzzy PD controller operate in Mode 2, i.e. the output is defined by (14), should satisfy the condition:

$$\triangle U_j^{min} = \triangle U_{j2}^{min} \geq H_3 \Leftrightarrow \overline{R}_4 \leq \underline{R}_2 + 2\underline{R}_1 \tag{19}$$

2) The condition when the switch point changes from the position of $L = 3$ to $L = 2$ and vice versa can be established as

$$\triangle U_j^{min} = \triangle U_{j2}^{min} = \triangle U_{j3}^{min} = H_2 \tag{20}$$

By replacing $\triangle U_{j2}^{min}$ and $\triangle U_{j3}^{min}$ with the corresponding expression in (14)-(15), the above equation may be written as

$$2\overline{R}_4 + \overline{R}_3 = \underline{R}_1 \tag{21}$$

Further, the subregions where (14) is used to calculate the left endpoint of the type-reduced set (Mode 2) can be found using the following equality

$$\triangle U_j^{min} = \triangle U_{j1}^{min} \leq H_2 \Leftrightarrow 2\overline{R}_4 + \overline{R}_3 \geq \underline{R}_1 \quad (22)$$

and the areas where the IT2 fuzzy PD controller operates in Mode 3, i.e. the output is defined by (15), should satisfy the condition:

$$\triangle U_j^{min} = \triangle U_{j3}^{min} \geq H_2 \Leftrightarrow 2\overline{R}_4 + \overline{R}_3 \leq \underline{R}_1 \quad (23)$$

B. Methodology for deriving analytical structure of IT2 fuzzy PD controller

An investigation of the conditions (18)-(19) and (22)-(23) reveals that

1) As stated above, the regions in the input space where the left endpoint $\triangle U_j^{min}$ is operating at Mode 1 and Mode 2 satisfy the condition (18) and (19) respectively. For the embedded T1 FLS of Mode 3, its corresponding region in the input space also satisfies (19) because its output condition $\triangle U_j^{min} \geq H_2$ and the assumption $H_2 > H_3$ may lead to $\triangle U_j^{min} > H_3$. Due to the complementarities between (18) and (19), the inequality (18) can be used to identify the corresponding region for the embedded T1 FLS of Mode 1.
2) Similarly, the regions in the input space which correspond to Mode 2 and Mode 3 satisfy (22) and (23) respectively. The corresponding region of Mode 1 in the input space also satisfies the inequality (22) because its output condition $\triangle U_j^{min} \leq H_3$ and the assumption $H_3 < H_2$ may result in $\triangle U_j^{min} < H_2$. Consequently, the region for the embedded T1 FLS of Mode 3 can be identified using the inequality (23).

On the other hand, by comparing the expressions of the three embedded T1 FLSs in (13)-(15), their properties can be generalized as

1) The weight associated with H_1 is always the lower bound of the firing set for Rule 1. Similarly, H_4 is weighted by the upper bound of the firing set for Rule 4. Consequently, the weight on H_1 and H_4 is independent of the switch points L and R.
2) In Mode 1, H_3 is weighted by the lower bound $\underline{R}_3$, while the corresponding upper bounds $\overline{R}_3$ is used to weight H_3 in Mode 2 and 3. On the other hand, the lower bound $\underline{R}_2$ weights H_2 in Mode 1 and 2, while in Mode 3 H_2 is weighted by the corresponding upper bound $\overline{R}_2$.

The first property shows that the firing strength of Rule 1 and Rule 4 used to calculate $\triangle U_j^{min}$ is independent of the switch point L, and the firing strength of Rule 1 and Rule 4 is always governed by the lower and upper bound of the firing set i.e. $\underline{R}_1$ and $\overline{R}_4$. Based on this observation, the first step in partitioning the input space in order to derive closed form firing level is performed by considering the outcomes of Zadeh AND operations (minimum operator) for Rule 1 and Rule 4. As stated in the second property, the firing strength for Rule 2 and Rule 3 can be the lower or upper bound of their corresponding firing set, depending on which embedded T1 FLS in (13)-(15) dominates the sub-region. Hence, the specification of the firing strength for Rule 2 and Rule 3 can be done only after the regions for the three embedded T1 FLSs in (13)-(15) are identified.

Because the conditions (18) and (23) contains three of R_1, R_2, R_3 and R_4, the challenge is how to identify the sub-regions in the input space for the three embedded T1 FLSs when only the expressions of R_1 and R_4 are known. To achieve the goal of identifying the regions for Mode 1 and Mode 3, the following technique will be used in the second step:

- Assuming that $\underline{R}_2$ weights H_2 in the whole input space, the firing strength of Rule 2 can be specified by considering the following Zadeh AND operation:

$$\underline{R}_2 = \min(\underline{\mathbf{EP}}, \underline{\mathbf{RN}}) \quad (24)$$

  Then the relative value of $\underline{R}_1$, $\underline{R}_2$ and $\overline{R}_4$ can be examined via (18) to identify the region for Mode 1.
  This assumption does not enlarge the area of the region for Mode 1 because in the region where H_2 is weighted by its upper bound $\overline{R}_2$, the property $2\overline{R}_4 + \underline{R}_3 \leq \underline{R}_1$ holds which leads to $\overline{R}_4 < \underline{R}_2 + 2\underline{R}_1$ and thus contradicts the inequality (18).
- Under the assumption that H_3 is weighted by its corresponding upper bound $\overline{R}_3$, the firing strength of Rule 3 can be mathematically expressed by considering the following Zadeh operation:

$$\overline{R}_3 = \min(\overline{\mathbf{EN}}, \overline{\mathbf{RP}}) \quad (25)$$

  According to (23), the relative value of $\underline{R}_1$, $\overline{R}_3$ and $\overline{R}_4$ may be examined to determine the sub-regions for Mode 3.
  The assumption made above does not affect the size of the region for Mode 3. This is because the regions where the lower bound $\underline{R}_3$ weights H_3 satisfies $\overline{R}_4 \geq \underline{R}_2 + 2\underline{R}_1$ which contradicts the inequality (23).

Once the regions for Mode 1 and Mode 3 are respectively identified, the firing strength for Rule 2 and Rule 3 may also be mathematically expressed by considering the corresponding Zadeh AND operations in the subregions. In summary, the proposed algorithm to derive the mathematical expression of the firing strength in $\triangle U_j^{min}$ may be presented as:

Step 1 : The firing strength of Rule 1 ($\underline{R}_1$) and Rule 4 ($\overline{R}_4$) can be specified by dividing the input space via the outcomes of Zadeh AND operations (minimum operator) for Rule 1 and Rule 4 i.e.

$$\underline{R}_1 = \min\{\underline{\mathbf{EP}}, \underline{\mathbf{RP}}\} \quad (26)$$

$$\overline{R}_4 = \min\{\overline{\mathbf{EN}}, \overline{\mathbf{RN}}\} \quad (27)$$

Step 2 : This step is to identify the regions in the input space that correspond to Mode 1 and Mode 3 respectively. Then the other region must correspond to Mode 2.

1) *Step 2.1* : Assuming that H_2 is weighted by its corresponding lower bound $\underline{R}_2$ in the whole input space, $\underline{R}_2$

can be specified as

$$\underline{R}_2 = \min(\underline{\mathbf{EP}}, \underline{\mathbf{RN}}) \tag{28}$$

The partitions obtained using $\underline{R}_1$, $\overline{R}_4$ in Step 1 and $\underline{R}_2$ are further examined to find out the group for Mode 1 (M_{L1}) satisfying the following inequality (18):

$$\text{Mode 1}: \quad \overline{R}_4 \geq \underline{R}_2 + 2\underline{R}_1$$

2) *Step 2.2* : Assume that in the input space H_3 is always weighted by its upper bound $\overline{R}_3$ and thus specify $\overline{R}_3$ as

$$\overline{R}_3 = \min(\overline{\mathbf{EN}}, \overline{\mathbf{RP}}) \tag{29}$$

The relative values of $\overline{R}_4$, $\underline{R}_1$ obtained in Step 1 and $\overline{R}_3$ are examined to find out the group for Mode 3 (M_{L3}) which satisfies the inequality (23):

$$\text{Mode 3}: \quad 2\overline{R}_4 + \overline{R}_3 \leq \underline{R}_1$$

Step 3 : In Step 3, the firing strength associated with Rule 2 and 3 can be specified via the Zadeh AND operation.

1) *Step 3.1* : Since Step 2.1 divides the whole input space into two parts: the group M_{L1} for Mode 1 and the other region for Mode 2 and 3, the firing strength associated with Rule 3 can be respectively specified as follows:
In the group M_{L1}, H_3 is weighted by its lower bound $\underline{R}_3$. By considering the Zadeh AND operation the firing strength for Rule 3 may be specified as

$$\underline{R}_3 = \min\{\underline{\mathbf{EN}}, \underline{\mathbf{RP}}\} \tag{30}$$

In the other regions for Mode 2 and Mode 3, the corresponding upper bound $\overline{R}_3$ weights H_3 and thus the firing strength for Rule 3 can be specified as

$$\overline{R}_3 = \min\{\overline{\mathbf{EN}}, \overline{\mathbf{RP}}\} \tag{31}$$

2) *Step 3.2* : The whole input space is divided into two parts in Step 2.2: the group M_{L3} for Mode 3 and the other region for Mode 1 and Mode 2. Therefore, the firing strength for Rule 2 can be specified by using Zadeh AND operation to divide the input space as follows:
The upper bound $\overline{R}_2$ weights H_2 in the region M_{L3}. The regions M_{L3} is divided by the Zadeh AND operation as

$$\overline{R}_2 = \min\{\overline{\mathbf{EP}}, \overline{\mathbf{RN}}\} \tag{32}$$

In the other regions, H_2 is weighted by the corresponding lower bound $\underline{R}_2$. The Zadeh AND operation divides the regions as

$$\underline{R}_2 = \min\{\underline{\mathbf{EP}}, \underline{\mathbf{RN}}\} \tag{33}$$

Step 4 : Superimpose all the partitions obtained by considering the mode switch and Zadeh AND operations.

Similarly, the firing strength for the right endpoint $\triangle U_j^{max}$ can be specified.

IV. Derivation of the analytical structure of IT2 Fuzzy PD controller

By following the proposed algorithm presented in the last section, the analytical structure of the fuzzy PD controller will be derived in this section.

A. The specification of the firing strength

By following the proposed algorithm, the specification of the firing strength for the left endpoint $\triangle U_j^{min}$ will be derived as an example to show the procedures:

Step 1 is to mathematically express the firing strength for Rule 1 ($\underline{R}_1$) and Rule 4 ($\overline{R}_4$) by dividing the input space into regions.

Step 2 is to sperate the input space into the three groups where the three embedded T1 FLSs in (13)-(15) are respectively used as the left endpoint $\triangle U_j^{min}$.

1) By superimposing the partitions of $\overline{R}_1$, $\underline{R}_3$ and $\underline{R}_4$, nine regions in Fig. 5(a) are generated: S_{L1}^1-S_{L9}^1. Whether the IT2 fuzzy PD controller operates in Mode 1 (M_{L1}) depends on the relative values of $\overline{R}_4$, $\underline{R}_1$ and $\underline{R}_2$.
   - Region S_{L1}^1: $\underline{R}_2 = \underline{R}_1 = 0$ and $\overline{R}_4 > 0$. Hence, $\overline{R}_4 > \underline{R}_2 + 2\underline{R}_1$ and thus for any input pair in Region S_{L1}^1, the IT2 fuzzy PD controller is operating in Mode 1. ($S_{L1} \in M_{L1}$)
   - Region S_{L2}^1: $\overline{R}_4 = \overline{RN}, \underline{R}_2 = 0, \underline{R}_1 = \underline{EP}$. The inequality (18) can be simplified into $\overline{RN} \geq 2\underline{EP}$. As shown in Fig. 5(b), the condition $\overline{RN} = 2\underline{EP}$ is denoted by the red line EG.
   - Region S_{L3}^1: $\overline{R}_4 = \overline{EN}, \underline{R}_2 = 0, \underline{R}_1 = \underline{RP}$. The fact $\overline{EN} < \overline{RN}$ and $\overline{RN} < \underline{RP}$ in Region S_{L3}^1 lead to $\overline{EN} < \underline{RP}$. Hence, in Region S_{L3}^1, the property $\overline{R}_4 < \underline{R}_2 + 2\underline{R}_1$ holds and the IT2 fuzzy PD controller operates in Mode 2 or 3.
   - Region S_{L4}^1: $\overline{R}_4 = \overline{RN}, \underline{R}_2 = \underline{RN}, \underline{R}_1 = \underline{EP}$. The inequality (18) leads to $\overline{RN} \geq \underline{RN} + 2\underline{EP}$ which is the left side of the red line IJ in Fig.5(b).
   - Region S_{L5}^1: $\overline{R}_4 = \overline{RN}, \underline{R}_2 = \underline{EP}, \underline{R}_1 = \underline{EP}$ and then the condition (18) can be simplified into $\overline{RN} > 3\underline{EP}$. The line EF includes all input pairs where $\overline{RN} = 3\underline{EP}$ holds in Region S_{L5}.
   - Region S_{L6}^1: $\overline{R}_4 = \overline{EN}, \underline{R}_2 = \underline{EP}, \underline{R}_1 = \underline{RP}$. The condition in (18) leads to $\overline{EN} \geq \underline{EP} + 2\underline{RP}$. The boundary $\overline{EN} = \underline{EP} + 2\underline{RP}$ is denoted by the red line MG in Fig.5(b).
   - Region S_{L7}^1: $\overline{R}_4 = \overline{EN}, \underline{R}_2 = \underline{RN}, \underline{R}_1 = \underline{RP}$. Due to the fact $\overline{R}_4 < \underline{R}_2 + 2\underline{R}_1$ in Region S_{L7}, the IT2 fuzzy PD controller is operating at Mode 2 or 3.
   - Region S_{L8}^1: $\overline{R}_4 = \overline{EN}, \underline{R}_2 = \underline{EP}, \underline{R}_1 = 0$. The condition (18) can be reduced to $EN_U \geq EP_L$, which is the left side of the red line GN in Fig.5(b).
   - Region S_{L9}^1: $\overline{R}_4 = \overline{EN}, \underline{R}_2 = \underline{RN}, \underline{R}_1 = 0$. In Region S_{L9}, there exists $\overline{R}_4 < \underline{R}_2 + 2\underline{R}_1$ and thus Region S_{L9}^1 does not belong to M_{L1}.
2) Step 2.2 seeks to identify the region M_{L3} where the IT2 fuzzy PD controller is operating at Mode 3. As stated in the proposed algorithm, the superimposition of the partitions of $\underline{R}_1$, $\overline{R}_3$ and $\overline{R}_4$ creates 5 regions in Fig. 6(a): S_{L1}^2-S_{L5}^2. As shown in Fig. 6(b), in the regions above the line QSV, the IT2 fuzzy controller is operating at Mode 3 while in the other regions, the fuzzy controller works at Mode 1 or Mode 2.

In this manner, the whole input space is divided into the three parts: M_{L1}, M_{L2} and M_{L3}, where the fuzzy controller is operating at Mode 1, Mode 2 or Mode 3, respectively.

Step 3 This step is to specify the firing strength for Rule 2 and Rule 3 by considering the corresponding Zadeh AND operation in the subregions for Mode 1-3.

1) In the region M_{L1} for Mode 1, the firing strength for Rule 3 can be specified by considering the following Zadeh AND operation: $\underline{R}_3 = \min\{\underline{\mathbf{EN}}, \underline{\mathbf{RP}}\}$ while in the other regions M_{L2} and M_{L3}, the following Zadeh AND operation is considered to specify the firing strength for Rule 3:$\overline{R}_3 = \min\{\overline{\mathbf{EN}}, \overline{\mathbf{RP}}\}$ The red and blue lines in Fig. 7 show the divisions of the input space for Rule 3.
2) As shown in Fig. 7, the red lines and yellow lines show the partition for Rule 2. In the subregion M_{L1} and M_{L2}, H_2 is weighted by the lower bound $\underline{R}_2$. Hence, the firing strength for Rule 2 in these regions can be specified by considering $\underline{R}_2 = \min\{\underline{\mathbf{EP}}, \underline{\mathbf{RN}}\}$ In the subregion M_{L3}, the firing strength for Rule 2 can be specified using $\overline{R}_2 = \min\{\overline{\mathbf{EP}}, \overline{\mathbf{RN}}\}$.

Step 4 Similarly, the partitions by the right endpoint $\triangle U_j^{max}$ can be derived in Fig. 8. At last, the partition of the input space for the IT2 fuzzy controllers in Fig. 9 can be obtained by superimposing all the results derived in Step 1-3.

B. The expressions of IT2 fuzzy PD controller

Fig. 10 shows the partitions of the input space when $\theta_1 = \theta_2$. The mathematical expressions of the firing strengths for 34 regions in Fig. 10 has been listed in Table I. By replacing the firing strength in (9) and (10) with their mathematical expressions, the mathematical equations relating the output of the fuzzy controller and its inputs can be derived. The region IC 1 is taken as an example to show the procedure. Table I shows that in IC1, $R_4 = R_2 = \overline{RN} = -\frac{1}{2L_2}R(n) + 0.5 + \theta_2$, $R_3 = \overline{EN} = -\frac{1}{2L_1}E(n) + 0.5 + \theta_1$, $R_1 = \underline{EP} = \frac{1}{2L_1}E(n) + 0.5 - \theta_1$. After simple manipulation, $\triangle U_j^{min}$ for IC 1 can be expressed into functions of $E(n)$ and $R(n)$ in (34).

C. Discussion

Comparing with the IT2 FLSs in [12], the introduction of the additional consequent set results in three possible embedded T1 FLSs for each endpoint $\triangle U_j^{min}$ or $\triangle U_j^{max}$, instead of the two in [12]. An observation of Fig. 7 and 8 indicates that the input space is divided into three parts that corresponds to the embedded T1 FLSs which produce the left or right endpoint $\triangle U_j^{min}$ or $\triangle U_j^{max}$. A comparative study of the partitions in Fig. 9 and that in [12] shows the introduced parameters produces 14 more regions, which indicates the potential of the considered IT2 fuzzy controllers to produce better performance.

V. Conclusion

In this paper, the analytical structure of the IT2 fuzzy controller has been derived by following the proposed algorithm. The relative large number of divisions provides the potential to produce better performance. The unique divisions may assistant the research community to understand the configurations of the considered IT2 fuzzy controllers. The equations relating the output and the input of the IT2 fuzzy controller provide tools for further investigations of their characteristics.

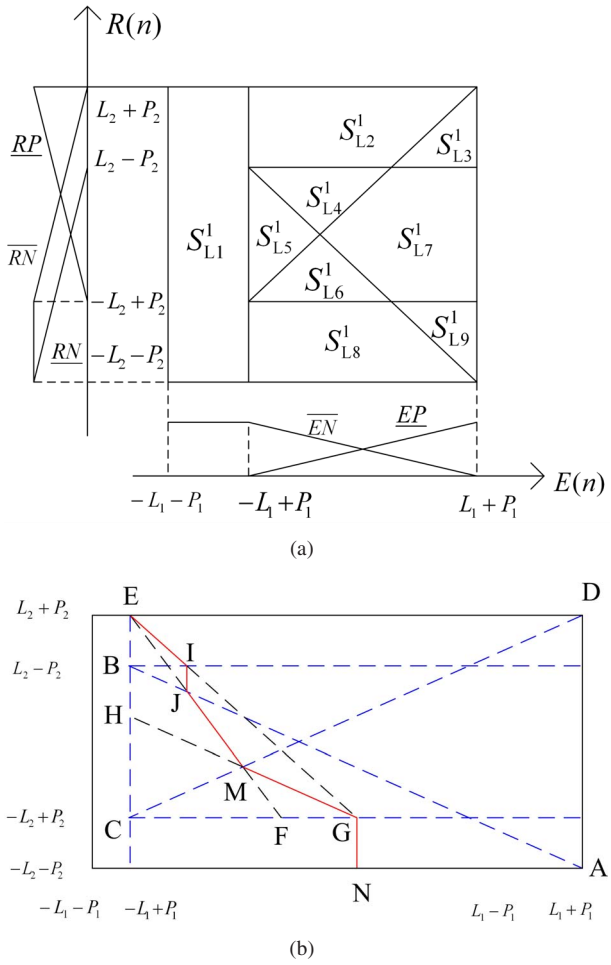

Fig. 5. Partition of the input space by $\triangle U_j^{min}$ (a) The superimposition of $\overline{R}_4$, $\underline{R}_1$ and $\underline{R}_2$. (b) The boundary between subregions for Mode 1 and the other modes: $\overline{R}_4 = \underline{R}_2 + 2\underline{R}_1$

References

[1] J. M. Mendel and R. I. B. John, "Type-2 fuzzy sets made simple", *IEEE Trans. Fuzzy Syst.*, vol. 10, no.2, pp. 117-127, 2002.

[2] J. M. Mendel, *Uncertain Rule-Based Fuzzy Logic Systems: Introduction and New Directions*, Upper Saddle River, NJ: Prentice-Hall, 2001.

[3] H. Ying, "The simplest fuzzy contollers using different inference methods are different nonlinear proportinal-integral controller with variable gains", *Automatica*, vol. 26, no. 6, pp. 1579-1589, 1993

[4] H. Ying, ""Practical Design of Nonlinear Fuzzy Controllers with Stability Analysis for Regulating Processes with Unknown Mathematical Models", *Automatica*, vol. 30, no. 7, pp. 1185-1195, 1994.

[5] H. Ying, "Fuzzy Control and Modeling: Analytical Foundations and Applications", Piscataway, NJ: IEEE Press, 2000.

[6] H. Ying, W. Siler and J. Buckley, "Fuzzy Control Theory: a Nonlinear Case", *Automatica*, vol.26, no.3, pp. 513-520, 1990

[7] J. Buckley and H. Ying, "Linear Fuzzy Controller: It Is a Linear Non-fuzzy Controller", *Inf. Sci.*, vol.51, no.2, pp.183-192, 1990.

$$\triangle U_{jIC1}^{min} = \frac{R_4^* * H_4 + R_3^* * H_3 + R_2^* * H_2 + R_1^* * H_1}{R_4^* + R_3^* + R_2^* + R_1^*}$$
$$= \frac{\overline{RN} * H_4 + \overline{EN} * H_3 + \overline{RN} * H_2 + \underline{EP} * H_1}{\overline{RN} + \overline{EN} + \overline{RN} + \underline{EP}}$$
$$= \frac{[-\frac{1}{2L_2}R(n) + 0.5 + \theta_1](H_2 + H_4) + [-\frac{1}{2L_1}E(n) + 0.5 + \theta_1]H_3 + [\frac{1}{2L_1}E(n) + 0.5 - \theta_1]H_1}{2[-\frac{1}{2L_2}R(n) + 0.5 + \theta_2] + [-\frac{1}{2L_1}E(n) + 0.5 + \theta_1] + [\frac{1}{2L_1}E(n) + 0.5 - \theta_1]}$$
$$= \frac{-L_1(H_2 + H_4)R(n) + L_2(H_1 - H_3)E(n)}{4L_1L_2(1 + \theta_2) - 2L_1R(n)}$$
$$- \frac{2L_1L_2[(0.5 + \theta_1)(H_2 + H_4) + (0.5 - \theta_1)H_1 + (0.5 + \theta_1)H_3]}{4L_1L_2(1 + \theta_2) - 2L_1R(n)}$$
$$= K_p^1 E(n) + K_d^1 R(n) + \delta^1 \quad (34)$$

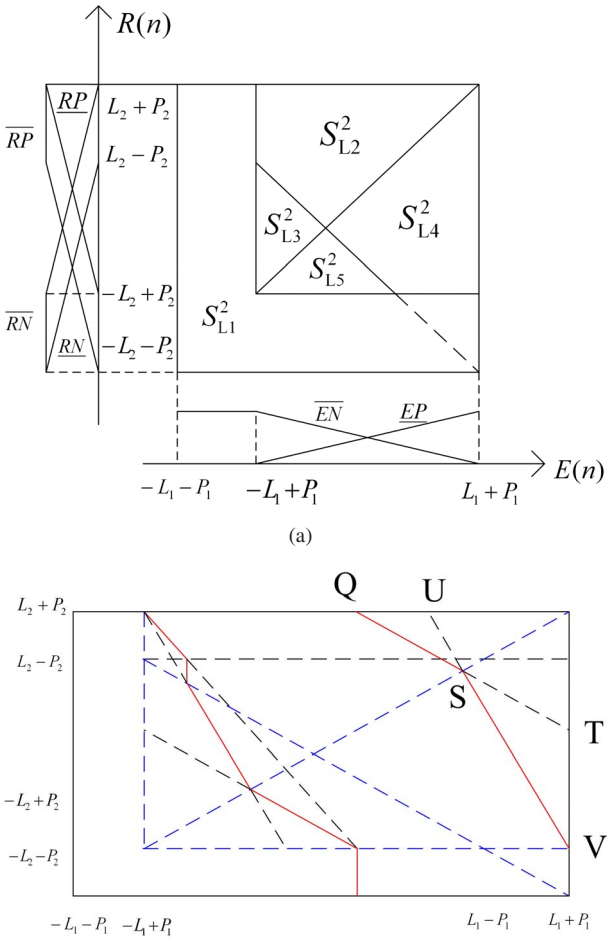

Fig. 6. Partition of the input space by $\triangle U_j^{min}$: (a) The superimposition of $\overline{R}_4$, $\underline{R}_1$ and $\overline{R}_3$. (b) The boundary between subregions for Mode 3 and the other modes: $2\overline{R}_4 + \overline{R}_3 = \underline{R}_1$

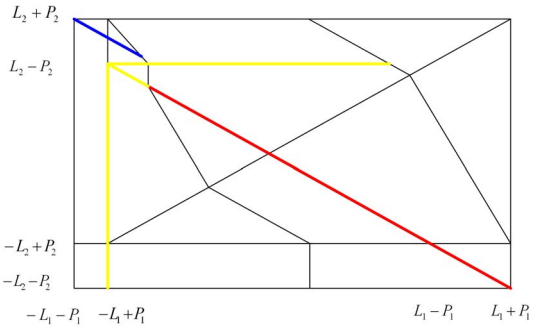

Fig. 7. The partition of the input space for the left endpoint $\triangle U_j^{min}$

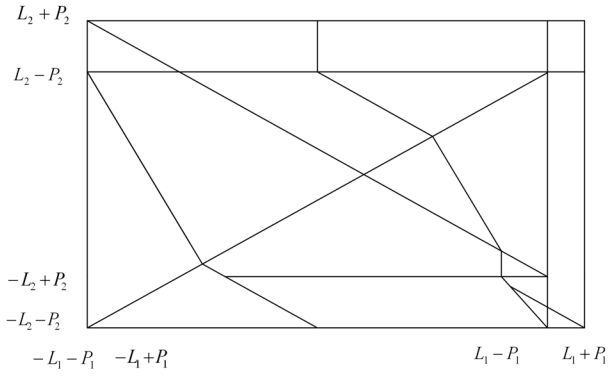

Fig. 8. The partition of the input space for the right endpoint $\triangle U_j^{max}$

[8] H. Amin, and H. Ying, "Structural and Stability Analysis of Fuzzy Controllers with Nonlinear Input Fuzzy Sets with Relation to Nonlinear PID Control with Variable Gains", *Automatica*, vol.40, no. 9, pp. 1551-1559, 2004.

[9] H. Ying, "Deriving Analytical Input-Output Relationship for Fuzzy Controllers Using Arbitrary Input Fuzzy Sets and Zadeh Fuzzy AND Operator", *IEEE Trans. Fuzzy Syst.*, vol. 14, no. 5, pp. 654-662, 2006.

[10] H. Ying, "A General Technique for Deriving Analytical Structure of Fuzzy Controllers That Use Arbitrary Trapezoidal/Triangular Input Fuzzy Sets and Zadeh Fuzzy Logic AND Operator", *Automatica*, vol.39, no. 7, pp. 1171-1184, 2003

[11] X. Du and H. Ying, "Deriving Analytical Structure of a Type-2 Fuzzy PD/PI Controller", in *Proc. North Amer. Fuzzy Inf. Process. Soc. Conf.*, New York, May 2008, pp. 1-6.

TABLE I

THE FIRING STRENGTHS OF FOUR RULES IN $\triangle U_j^{min}$

IC No.	$\triangle U_j^{min}$			
	Rule 4	Rule 3	Rule 2	Rule 1
1	$\overline{RN}$	$\overline{EN}$	$\overline{RN}$	$\underline{EP}$
2	$\overline{RN}$	$\overline{EN}$	$\underline{RN}$	$\underline{EP}$
3	$\overline{RN}$	$\overline{EN}$	$\underline{RN}$	$\underline{EP}$
4	$\overline{RN}$	$\overline{RP}$	$\underline{EP}$	$\underline{EP}$
5	$\overline{RN}$	$\underline{EN}$	$\underline{RN}$	$\underline{EP}$
6	$\overline{RN}$	$\underline{RP}$	$\underline{EP}$	$\underline{EP}$
7	$\overline{RN}$	$\underline{RP}$	$\underline{EP}$	$\underline{EP}$
8	$\overline{EN}$	$\underline{RP}$	$\underline{EP}$	$\underline{RP}$
9	$\overline{EN}$	$\underline{RP}$	$\underline{EP}$	$\underline{RP}$
10	$\overline{EN}$	$\overline{RP}$	$\underline{EP}$	$\underline{RP}$
11	$\overline{EN}$	$\overline{EN}$	$\underline{RN}$	$\underline{RP}$
12	$\overline{EN}$	$\overline{EN}$	$\underline{RN}$	$\underline{RP}$
13	$\overline{EN}$	$\overline{EN}$	$\overline{RN}$	$\underline{RP}$
14	$\overline{EN}$	$\overline{RP}$	$\underline{EP}$	$\underline{RP}$
15	$\overline{EN}$	$\overline{EN}$	$\overline{RN}$	$\underline{RP}$
16	$\overline{RN}$	$\overline{EN}$	$\overline{RN}$	$\underline{EP}$
17	$\overline{RN}$	$\overline{EN}$	$\overline{RN}$	$\underline{EP}$
18	$\overline{RN}$	$\overline{EN}$	0	$\underline{EP}$
19	$\overline{RN}$	$\overline{EN}$	0	$\underline{EP}$
20	$\overline{RN}$	$\underline{EN}$	0	$\underline{EP}$
21	$\overline{RN}$	$\underline{EN}$	0	0
22	$\overline{RN}$	$\underline{RP}$	0	0
23	$\overline{RN}$	$\underline{RP}$	0	0
24	$\overline{RN}$	$\underline{RP}$	0	0
25	1	0	0	0
26	1	0	0	0
27	$\overline{EN}$	0	$\underline{EP}$	0
28	$\overline{EN}$	0	$\underline{EP}$	0
29	$\overline{EN}$	$\overline{RP}$	$\underline{EP}$	0
30	$\overline{EN}$	$\overline{RP}$	$\underline{EP}$	0
31	$\overline{EN}$	$\overline{RP}$	$\underline{EP}$	0
32	$\overline{EN}$	$\overline{EN}$	$\underline{RN}$	0
33	$\overline{EN}$	$\overline{EN}$	$\underline{RN}$	$\underline{RP}$
34	$\overline{EN}$	$\overline{EN}$	$\overline{RN}$	$\underline{RP}$

[12] M. Nie and W. W. Tan, "Derivation Of The Analytical Structure Of Symmetrical IT2 Fuzzy PD And PI Controllers", in *Proc. IEEE Intl Conf. on Fuzzy Systems* , Barcelona, July 2010, pp. 1-8.

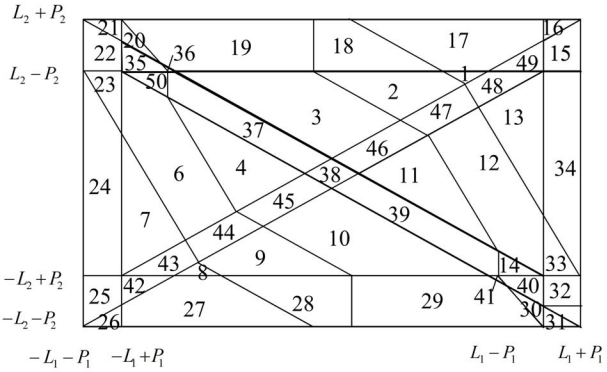

Fig. 9. The partition of the input space for the IT2 FLC

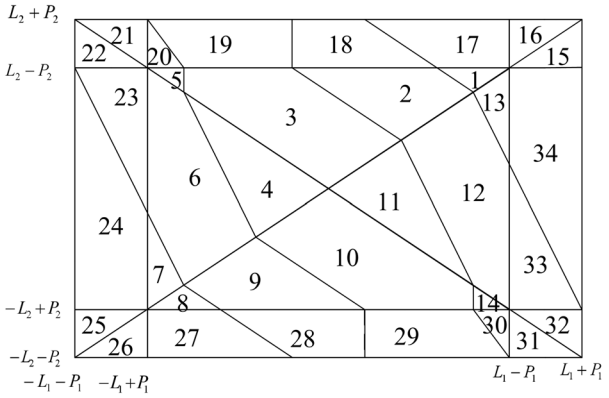

Fig. 10. The partition of the input space for the IT2 FLC when $\theta_1 = \theta_2$

2011 IEEE International Conference on Fuzzy Systems
June 27-30, 2011, Taipei, Taiwan

Estimation of the Asympototic Stability Region of Uncertain Fuzzy Systems with Bounded Controllers Using Variable Structure System Design Approach

Chung-Chun Kung*, Ti-Hung Chen**, Shuo-Chieh Chang, and Chih-Chieh Chen
Department of Electrical Engineering, Tatung University*
Department of Computer Information and Network Engineering, Lunghwa University of Science and Technology**
Taipei, Taiwan, R.O.C.
e-mail: cckung@ttu.edu.tw*, cth@mail.lhu.edu.tw**

***Abstract*—In this paper, the problem of estimating the asymptotic stability region (ASR) of uncertain nonlinear systems is considered. Our approach is based on Takagi-Sugeno (T-S) fuzzy model and variable structure control (VSC) technique. To simplify the problem, we use a state transformation to reduce the system order of the T-S fuzzy systems. Then we design the sliding surface for the transformed system. By the Lyaponov stability theorem, the ASR can be estimated. A simulation example is presented to verify the effectiveness of the proposed scheme.**

Keywords-component; asymptotic stability region; Takagi-Sugeno fuzzy model; variable structure control; sliding mode controller

I. INTRODUCTION

As we know that, design a sliding mode control system[1-5], only need to use a rough mathematical model to describe the physical system. Design of the controller and analysis of the complex nonlinear systems is very difficult task. Thus, the fuzzy technique has been widely adopted to model complex nonlinear plants [6]. Among the many types of fuzzy modules, the Takagi-Sugeno (T-S) fuzzy model [7] is a popular and convenient tool for nonlinear system. T-S type fuzzy models which are the local dynamics in different state-space regions are represented by linear models and the nonlinear system is approximated by the overall fuzzy linear models. In recent years, the problem of fuzzy control systems based on T-S model for complex nonlinear system has become more and more popular [8-17].

Although the complex nonlinear system can be represented by T-S model, there are many uncertainties in actual situations for the nonlinear system. The uncertainty may include parameter variations, modeling errors, extraneous disturbances, and fuzzy approximation errors, etc. To solve this problem, some authors [5, 18-21], use the variable structure control (VSC) theory to deal with the problem of an uncertainty, it can more effectively achieve the control objective.

The VSC technique has been used to control complex nonlinear systems with their T-S fuzzy models [19-23]. The robust variable structure controller is designed to ensure the existence of a sliding mode and to overcome the effect of the uncertainty. If the VSC theory and T-S fuzzy model are combined to apply to the nonlinear systems, the dynamic performance of nonlinear systems can be improved by taking advantage of their respective merit [24-27].

In VSS, due to physical constraints, the control input magnitude must be bounded. The problem of estimating the asymptotic stability region (ASR) for uncertain systems with bounded sliding mode controllers is proposed in [28]. In [28], the conception of combining different Lyapunov function along with a state transformation is used to estimate ASR. By using an example and under the same conditions, the method of estimating the ASR in [29] is better than in [28]. These methods [28 , 29] of using state transformation matrices are indirect and complex. So, they do not seem to be useful in designing a sliding surface. Thus, the method of using linear matrix inequalities (LMIs) to deal with the problem is presented [30], and its method of estimating the ASR is better than the methods presented in [28 , 29]. But, these cases are limited to the explicit linear system [28 – 30], their examples are only the numerical example, it does not seem to be useful in estimating the ASR of the real model. In this paper, the method of estimating the ASR via T–S fuzzy modeling method and VSC technique is presented. Our approach is to use the T-S fuzzy model to approximately a class of the complex nonlinear systems, and design the sliding mode controllers for the T-S fuzzy model.

II. SYSTEM DESCRIPTION

The fuzzy model is described by fuzzy If-Then rules and will be employed here to deal with the control design problem for nonlinear systems. In this section, we consider the following uncertain T-S fuzzy control systems with r plant rules that can be represented as:

Plant Rule *i*:

If ϕ_1 is F_1^i and $\cdots$ and ϕ_n is F_n^i

Then (1)

$$\dot{\mathbf{x}}(t) = (\mathbf{A}_i + \Delta\mathbf{A}_i(t))\,\mathbf{x}(t) + (\mathbf{B}_i + \Delta\mathbf{B}_i(t))\,\mathbf{u}(t) + \mathbf{g}_i(t,\mathbf{x})$$

where $\mathbf{x}(t) = [x_1(t),\ldots, x_n(t)]^T \in \Re^n$ is the state vector, $\mathbf{u}(t) \in \Re^m$ is the input vector, $\phi_j\,(j = 1,2,\ldots,n)$ are the state variables, $F_1^i,\ldots, F_n^i$ are the fuzzy sets $(i = 1,2,\ldots,r)$,

This work was supported in part by the National Science Council of Taiwan under Grant NSC 99-2221-E-036-021 and NSC 99-2221-E-262 -021.

$\mathbf{A}_i \in \Re^{n\times n}$ and $\mathbf{B}_i \in \Re^{n\times m}$ are system matrices, $\Delta\mathbf{A}_i(t)$ and $\Delta\mathbf{B}_i(t)$ stand for the uncertainties in $\mathbf{A}_i$ and $\mathbf{B}_i$, respectively, $\mathbf{g}_i(t,\mathbf{x})$ is the external disturbances.

Given the a pair $(\mathbf{x},\mathbf{u})$, using the singleton fuzzifier, product inference, and center average defuzzifier [7], the final state of the uncertain T-S fuzzy control systems is obtained as follows:

$$\dot{\mathbf{x}}(t)=\sum_{i=1}^{r} h_i(\phi_j)[(\mathbf{A}_i+\Delta\mathbf{A}_i(t))\mathbf{x}(t)+(\mathbf{B}_i+\Delta\mathbf{B}_i(t))\mathbf{u}(t) + \mathbf{g}_i(t,\mathbf{x})] \tag{2}$$

where $h_i(\phi_j)$ is the fuzzy basis functions given as

$$h_i(\phi_j)=\frac{\prod_{j=1}^{n}\mu_{ij}(\phi_j)}{\sum_{i=1}^{r}\prod_{j=1}^{n}\mu_{ij}(\phi_j)},\ i=1,2,\ldots,r \tag{3}$$

in which $\mu_{ij}(x_j(t))$ is the grade of membership function of $x_j(t)$ in F_j^i, $h_i(\phi_j)$ can be regarded as the normalized weight of each If-Then rule and satisfies

$$h_i(\phi_j)\ge 0,\ \ i=1,\ldots,r \tag{4}$$

and

$$\sum_{i=1}^{r} h_i(\phi_j)=1 \tag{5}$$

To simplify the formula (2), we make the following assumptions:

Assumption 1 [21]: There exist $\boldsymbol{\beta}_A(t)\in\Re^{m\times n}$, $\boldsymbol{\beta}_B(t)\in\Re^{m\times n}$ and $\mathbf{f}(t,\mathbf{x})\in\Re^{m\times 1}$ such that $\Delta\mathbf{A}_i(t)=\mathbf{B}_i\boldsymbol{\beta}_A(t)$, $\Delta\mathbf{B}_i(t)=\mathbf{B}_i\boldsymbol{\beta}_B(t)$ and $\mathbf{g}_i(t)=\mathbf{B}_i\mathbf{f}(t,\mathbf{x})$.

Assumption 2 [21]: There exist known continuous positive scalar-valued functions $\rho_A(t,\mathbf{x})$, $\rho_f(t,\mathbf{x})$ and known constant $0\le\varphi<1$ such that $\|\boldsymbol{\beta}_A(t)\mathbf{x}(t)\|\le\rho_A(t,\mathbf{x})$, $\|\mathbf{f}(t,\mathbf{x})\|\le\rho_f(t)$, and $\|\boldsymbol{\beta}_B(t)\|\le\varphi$.

Assumption 3 [21]: The $n\times m$ matrix $\mathbf{B}$ has full rank m defined by

$$\mathbf{B}=\frac{1}{r}\sum_{i=1}^{r}\mathbf{B}_i \tag{6}$$

According to assumption 1, assumption 2 and assumption 3, the uncertain T-S fuzzy control systems (2) can be rewritten as follows:

$$\dot{\mathbf{x}}(t)=\sum_{i=1}^{r} h_i(\phi_j)\mathbf{A}_i\mathbf{x}(t)+\overline{\mathbf{B}}[\mathbf{u}(t)+\mathbf{h}(t,\mathbf{u},\mathbf{x})] \tag{7}$$

where $\overline{\mathbf{B}}=\mathbf{B}+\mathbf{KFR}$, $\mathbf{K}=\frac{1}{2}[(\mathbf{B}-\mathbf{B}_1),\cdots,(\mathbf{B}-\mathbf{B}_r)]\in\Re^{n\times rm}$, $\mathbf{F}=Diag[(1-2h_1)\mathbf{I},\cdots,(1-2h_r)\mathbf{I}]\in\Re^{n\times rm}$, $\mathbf{R}=[\mathbf{I},\cdots,\mathbf{I}]^T\in\Re^{rm\times m}$, and $\mathbf{h}(t,\mathbf{u},\mathbf{x})$ is the lumped uncertainty given as $\mathbf{h}(t,\mathbf{u},\mathbf{x})=\boldsymbol{\beta}_A(t)\mathbf{x}(t)+\boldsymbol{\beta}_B(t)\mathbf{u}(t)+\mathbf{f}(t,\mathbf{x})$.

III. Estimation of Asymptotic Stability Region of System State

A variable structure system (VSS) is a control system implementing different control laws in different regions of the state space. The regions of the VSS are divided by a set of boundary manifolds which represent the checking conditions of the VSS. Thus, we consider the uncertain T-S fuzzy control systems (7) and define the following linear switching surface [2].

$$\Omega=\{\mathbf{x}:\boldsymbol{\sigma}(\mathbf{x})=\mathbf{S}\mathbf{x}(t)=0\} \tag{8}$$

where $\mathbf{S}\in\Re^{m\times n}$ with full rank *m*. We assume that the switching surface parameter matrix $\mathbf{S}$ satisfies the following properties [21, 30].

Property 1: $\mathbf{S}\overline{\mathbf{B}}>0$ for any $h_i(\phi_j)$ satisfying $h_i(\phi_j)\ge 0$ and $\sum_{i=1}^{r}h_i(\phi_j)=1$.

Property 2: By using an appropriately chosen stabilizing feedback control law, the system trajectory is already stably restricted to the linear switching surface $\mathbf{S}\mathbf{x}(t)=0$, the reduced (*n-m*)th order sliding mode dynamics is asymptotically stable.

Our problem can be formulated as follows: 1) Design a sliding mode control for the complex nonlinear systems with matched uncertainties so that the systems are asymptotically stable. 2) Estimate the ASR of (7) for a given $\mathbf{S}$ satisfying *Property 1* and *Property 2*.

Referring to [30], we define nonsingular transformation matrix $\mathbf{M}$ as follows:

$$\mathbf{M}=\begin{bmatrix}\boldsymbol{\Phi}^T\\ (\overline{\mathbf{B}}^T\overline{\mathbf{B}})^{-1}\overline{\mathbf{B}}^T\end{bmatrix}\ \text{and}\ \mathbf{M}^{-1}=[\boldsymbol{\Phi}\quad\overline{\mathbf{B}}]. \tag{9}$$

And we have the associated state $\mathbf{v}(t)$ by (9) as follows:

$$\mathbf{v}(t)=\begin{bmatrix}\mathbf{v}_1(t)\\ \mathbf{v}_2(t)\end{bmatrix}=\mathbf{M}\mathbf{x}(t)=\begin{bmatrix}\boldsymbol{\Phi}^T\mathbf{x}(t)\\ (\overline{\mathbf{B}}^T\overline{\mathbf{B}})^{-1}\overline{\mathbf{B}}^T\mathbf{x}(t)\end{bmatrix} \tag{10}$$

where $\mathbf{v}_1(t)\in\Re^{(n-m)\times 1}$ and $\mathbf{v}_2(t)\in\Re^{m\times 1}$. From (8), (9) and (10), we obtain

$$\mathbf{S}\mathbf{x}(t)=\mathbf{S}\mathbf{M}^{-1}\mathbf{v}(t)=\mathbf{S}\boldsymbol{\Phi}\,\mathbf{v}_1(t)+\mathbf{S}\overline{\mathbf{B}}\,\mathbf{v}_2(t)=\mathbf{0}. \tag{11}$$

Under a sliding condition, the trajectory asymptotically goes to the zero of the phase plant. The dynamics can be formulated as (11). Thus, from the equivalent control method [1], we can design the equivalent controllers as follows:

$$\mathbf{u}_{eq}(t)=-\sum_{i=1}^{r}h_i(\phi_j)(\mathbf{S}\overline{\mathbf{B}})^{-1}\mathbf{S}\mathbf{A}_i\mathbf{x}(t)-\mathbf{h}(t,\mathbf{u},\mathbf{x}). \tag{12}$$

Proposition 1: If there exists positive scalar $\varepsilon\in\Re$ and positive-define matrix $\mathbf{P}$ satisfy the following conditions

$$\mathbf{P}>0,\boldsymbol{\Phi}^T(\mathbf{A}_i\mathbf{P}+\mathbf{P}\mathbf{A}_i^T)\boldsymbol{\Phi}<0,\ i=1,2,\ldots,r \tag{13}$$

$$\varepsilon>0,\quad \mathbf{S}\mathbf{P}=\varepsilon\overline{\mathbf{B}}^T \tag{14}$$

then the switching surface parameter matrix $\mathbf{S}$ satisfying *Property 1* and *Property 2* for the uncertain T-S fuzzy control systems (2.5) where $\boldsymbol{\Phi}\in\Re^{n\times(n-m)}$ is any full rank matrix such that $\overline{\mathbf{B}}^T\boldsymbol{\Phi}=\mathbf{0}$ and $\boldsymbol{\Phi}^T\boldsymbol{\Phi}=\mathbf{I}$.

Proof:

Our aim is to choose an appropriate $\mathbf{P}$ such that the systems motion on the sliding surface is asymptotically stable. In order to obtain the dynamics on the sliding surface, we must do a transformation for the state $\mathbf{x}(t)$.

From the above transformation and the time derivative of (10), the dynamics as follows:

$$\begin{aligned}\dot{\mathbf{v}}(t) &= \mathbf{M}\left(\sum_{i=1}^{r} h_i(\phi_j)\,\mathbf{A}_i\mathbf{x}(t) + \overline{\mathbf{B}}[\mathbf{u}(t)+\mathbf{h}(t,\mathbf{u},\mathbf{x})]\right)\\ &= \sum_{i=1}^{r} h_i(\phi_j)\,\mathbf{M}\mathbf{A}_i\mathbf{M}^{-1}\mathbf{v}(t) + \mathbf{M}\overline{\mathbf{B}}[\mathbf{u}(t)+\mathbf{h}(t,\mathbf{u},\mathbf{x})]\\ &= \sum_{i=1}^{r} h_i(\phi_j)[\boldsymbol{\Phi} \quad \overline{\mathbf{B}}(\overline{\mathbf{B}}^T\overline{\mathbf{B}})^{-1}]^T\mathbf{A}_i[\boldsymbol{\Phi} \quad \overline{\mathbf{B}}(\overline{\mathbf{B}}^T\overline{\mathbf{B}})^{-1}]^{-T}\mathbf{v}(t)\\ &\quad + [\boldsymbol{\Phi} \quad \overline{\mathbf{B}}(\overline{\mathbf{B}}^T\overline{\mathbf{B}})^{-1}]^T\overline{\mathbf{B}}[\mathbf{u}(t)+\mathbf{h}(t,\mathbf{u},\mathbf{x})]\\ &= \sum_{i=1}^{r} h_i(\phi_j)\begin{bmatrix}\boldsymbol{\Phi}^T\mathbf{A}_i\boldsymbol{\Phi} & \boldsymbol{\Phi}^T\mathbf{A}_i\overline{\mathbf{B}}\\ (\overline{\mathbf{B}}^T\overline{\mathbf{B}})^{-1}\overline{\mathbf{B}}^T\mathbf{A}_i\boldsymbol{\Phi} & (\overline{\mathbf{B}}^T\overline{\mathbf{B}})^{-1}\overline{\mathbf{B}}^T\mathbf{A}_i\overline{\mathbf{B}}\end{bmatrix}\mathbf{v}(t)\\ &\quad + \begin{bmatrix}\mathbf{0}\\ \mathbf{I}\end{bmatrix}(\mathbf{u}(t)+\mathbf{h}(t,\mathbf{u},\mathbf{x})).. \end{aligned} \tag{15}$$

Substituting (12) into (15) and consider (11), we obtain the dynamics $\mathbf{v}_1(t)$ and $\mathbf{v}_2(t)$ as follows:

$$\begin{bmatrix}\dot{\mathbf{v}}_1(t)\\ \dot{\mathbf{v}}_2(t)\end{bmatrix} = \sum_{i=1}^{r} h_i(\phi_j)\begin{bmatrix}\boldsymbol{\Phi}^T\mathbf{A}_i\boldsymbol{\Phi}\mathbf{v}_1(t) - \boldsymbol{\Phi}^T\mathbf{A}_i\overline{\mathbf{B}}(\mathbf{S}\overline{\mathbf{B}})^{-1}\mathbf{S}\boldsymbol{\Phi}\boldsymbol{\Phi}_1(t)\\ ((\overline{\mathbf{B}}^T\overline{\mathbf{B}})^{-1}\overline{\mathbf{B}}^T\mathbf{A}_i - \mathbf{B}(\mathbf{S}\overline{\mathbf{B}})^{-1}\mathbf{S}\mathbf{A}_i)\mathbf{M}^{-1}\mathbf{v}(t)\end{bmatrix} \tag{16}$$

From (16), we have the reduced $(n-m)$ order sliding mode dynamics restricted to the switching surface $\boldsymbol{\sigma}(\mathbf{x}) = \mathbf{S}\mathbf{x}(t) = 0$, i.e., the reduced $(n-m)$ order equivalent system dynamics is given by

$$\dot{\mathbf{v}}_1(t) = \sum_{i=1}^{r} h_i(\phi_j)[\boldsymbol{\Phi}^T\mathbf{A}_i\boldsymbol{\Theta}\boldsymbol{\Phi}\mathbf{v}_1(t)]\,. \tag{17}$$

where $\boldsymbol{\Theta} = \mathbf{I} - \overline{\mathbf{B}}(\mathbf{S}\overline{\mathbf{B}})^{-1}\mathbf{S}$.

Now, we consider the Lyapunov function candidate $\overline{V} = \mathbf{v}_1^T(t)\mathbf{P}_0^{-1}\mathbf{v}_1(t)$, then, the equivalent system dynamics (17) is asymptotically stable if there exists a positive definite matrix $\mathbf{P}_0^{-1} \in \Re^{(n-m)\times(n-m)}$ such that

$$\dot{\overline{V}}(t) = \mathbf{v}_1^T(t)\mathbf{P}_0^{-1}\dot{\mathbf{v}}_1^T + \dot{\mathbf{v}}_1^T(t)\mathbf{P}_0^{-1}\mathbf{v}_1^T < 0\,. \tag{18}$$

Substituting (17) into (18), we have

$$\begin{aligned}\dot{\overline{V}}(t) &= \sum_{i=1}^{r} h_i(\phi_j)\{\mathbf{v}_1(t)\mathbf{P}_0^{-1}\boldsymbol{\Phi}^T\mathbf{A}_i\boldsymbol{\Theta}\mathbf{P}_0\mathbf{P}_0^{-1}\mathbf{v}_1(t)\\ &\qquad + \mathbf{v}_1(t)\mathbf{P}_0^{-1}\mathbf{P}_0\boldsymbol{\Phi}^T\boldsymbol{\Theta}^T\mathbf{A}_i^T\boldsymbol{\Phi}\mathbf{P}_0^{-1}\mathbf{v}_1(t)\}\\ &= \sum_{i=1}^{r} h_i(\phi_j)\{\mathbf{v}_1(t)\mathbf{P}_0^{-1}[\boldsymbol{\Phi}^T\mathbf{A}_i\boldsymbol{\Theta}\mathbf{P}_0\\ &\qquad + \mathbf{P}_0\boldsymbol{\Phi}^T\boldsymbol{\Theta}^T\mathbf{A}_i^T\boldsymbol{\Phi}]\,\mathbf{P}_0^{-1}\mathbf{v}_1(t)\}\\ &= \sum_{i=1}^{r} h_i(\phi_j)\{\mathbf{v}_1(t)\mathbf{P}_0^{-1}\boldsymbol{\Phi}^T[\boldsymbol{\Phi}^T\mathbf{A}_i\boldsymbol{\Theta}\mathbf{P}_0\boldsymbol{\Phi}^T\\ &\qquad + \boldsymbol{\Phi}\mathbf{P}_0\boldsymbol{\Phi}^T\boldsymbol{\Theta}^T\mathbf{A}_i^T\boldsymbol{\Phi}]\,\boldsymbol{\Phi}\mathbf{P}_0^{-1}\mathbf{v}_1(t)\}\\ &= \sum_{i=1}^{r} h_i(\phi_j)\{\mathbf{v}_1(t)\mathbf{P}_0^{-1}\boldsymbol{\Phi}^T[\mathbf{A}_i\mathbf{P}^T + \mathbf{P}\mathbf{A}_i^T]\,\boldsymbol{\Phi}\mathbf{P}_0^{-1}\mathbf{v}_1(t)\} \end{aligned} \tag{19}$$

where

$$\mathbf{P} = \boldsymbol{\Phi}\mathbf{P}_0\boldsymbol{\Phi}^T\boldsymbol{\Theta}^T = \boldsymbol{\Phi}\mathbf{P}_0\boldsymbol{\Phi}^T(\mathbf{I} - \overline{\mathbf{B}}(\mathbf{S}\overline{\mathbf{B}})^{-1}\mathbf{S})^T\,. \tag{20}$$

From (19) and (20), we get the dynamics (17) is asymptotically stable if $\boldsymbol{\Phi}^T(\mathbf{A}_i\mathbf{P}^T + \mathbf{P}\mathbf{A}_i^T)\boldsymbol{\Phi} < 0$ and $\mathbf{P} > 0$ where the matrix $\mathbf{P}$ satisfy the condition (14). The dynamics (17) is asymptotically stable imply that the $\mathbf{v}_2(t) = 0$ by (11).

Lemma: $\mathbf{P} = \boldsymbol{\Phi}\mathbf{P}_0\boldsymbol{\Phi}^T(\mathbf{I} - \overline{\mathbf{B}}(\mathbf{S}\overline{\mathbf{B}})^{-1}\mathbf{S})^T$ is a positive definite matrix in (20).

Proof:

Form $\mathbf{P} = \boldsymbol{\Phi}\mathbf{P}_0\boldsymbol{\Phi}^T(\mathbf{I} - \overline{\mathbf{B}}(\mathbf{S}\overline{\mathbf{B}})^{-1}\mathbf{S})^T$ we obtain

$$(\mathbf{I} - \overline{\mathbf{B}}(\mathbf{S}\overline{\mathbf{B}})^{-1}\mathbf{S})\mathbf{P} = (\mathbf{I} - \overline{\mathbf{B}}(\mathbf{S}\overline{\mathbf{B}})^{-1}\mathbf{S})\boldsymbol{\Phi}\mathbf{P}_0\boldsymbol{\Phi}^T(\mathbf{I} - \overline{\mathbf{B}}(\mathbf{S}\overline{\mathbf{B}})^{-1}\mathbf{S})^T \tag{21}$$

By (21) and must be satisfy (14), we have

$$\mathbf{P} = (\mathbf{I} - \overline{\mathbf{B}}(\mathbf{S}\overline{\mathbf{B}})^{-1}\mathbf{S})\boldsymbol{\Phi}\mathbf{P}_0\boldsymbol{\Phi}^T(\mathbf{I} - \overline{\mathbf{B}}(\mathbf{S}\overline{\mathbf{B}})^{-1}\mathbf{S})^T + \varepsilon\overline{\mathbf{B}}(\mathbf{S}\overline{\mathbf{B}})^{-1}\overline{\mathbf{B}}^T \tag{22}$$

where if there exists $\mathbf{P}_0$, ε in proposition 1 and $\mathbf{S}$ satisfying property 1, we have $\mathbf{P} > 0$.

Suppose that the proposition 1 has a solution for $\mathbf{P}$ and ε, then there exists a linear switching surface parameter matrix $\mathbf{S}$ satisfying property 1 and property 2, it can be parameterized as follows [2]:

$$\boldsymbol{\sigma}(\mathbf{x}) = \mathbf{S}\mathbf{x}(t) = \overline{\mathbf{B}}^T\mathbf{P}^{-1}\mathbf{x}(t) \tag{23}$$

By the *Projection lemma* and *Finsler's lemma* [32], (13) is equivalent to the following linear matrix inequalities (LMIs) [31]:

$$\mathbf{P} > 0,\ \mathbf{A}_i\mathbf{P} + \mathbf{P}\mathbf{A}_i^T - \mathbf{E}\overline{\mathbf{B}}^T - \overline{\mathbf{B}}\mathbf{E}^T < 0, i = 1,2,\cdots,r. \tag{24}$$

$$\begin{bmatrix}\mathbf{P} & \mathbf{E}\\ \mathbf{E}^T & \mathbf{I}\end{bmatrix} > 0 \tag{25}$$

$$\begin{bmatrix}\mathbf{P} & \mathbf{I}\\ \mathbf{I} & \alpha\mathbf{I}\end{bmatrix} > 0 \tag{26}$$

where $\alpha > 0$. Therefore we have the following theorem.

Theorem 1: If there exists symmetric matrix $\mathbf{P}_0 \in \Re^{(n-m)\times(n-m)}$, matrix $\mathbf{E} \in \Re^{n\times m}$ and positive scalars $\varepsilon \in \Re$, $\alpha \in \Re$ satisfy the following LMIs

$$\boldsymbol{\Theta}\boldsymbol{\Phi}\mathbf{P}_0\boldsymbol{\Phi}^T\boldsymbol{\Theta}^T + \varepsilon\overline{\mathbf{B}}(\mathbf{S}\overline{\mathbf{B}})^{-1}\overline{\mathbf{B}}^T > 0 \tag{27}$$

$$\begin{aligned}&\mathbf{A}_i\boldsymbol{\Theta}\boldsymbol{\Phi}\mathbf{P}_0\boldsymbol{\Phi}^T\boldsymbol{\Theta}^T + \varepsilon\mathbf{A}_i\overline{\mathbf{B}}(\mathbf{S}\overline{\mathbf{B}})^{-1}\overline{\mathbf{B}}^T - \mathbf{E}\overline{\mathbf{B}}^T\\ &+ (\mathbf{A}_i\boldsymbol{\Theta}\boldsymbol{\Phi}\mathbf{P}_0\boldsymbol{\Phi}^T\boldsymbol{\Theta}^T + \varepsilon\mathbf{A}_i\overline{\mathbf{B}}(\mathbf{S}\overline{\mathbf{B}})^{-1}\overline{\mathbf{B}}^T - \overline{\mathbf{B}}\mathbf{E}^T)^T < 0\end{aligned} \tag{28}$$

$$\begin{bmatrix}\boldsymbol{\Theta}\boldsymbol{\Phi}\mathbf{P}_0\boldsymbol{\Phi}^T\boldsymbol{\Theta}^T + \varepsilon\overline{\mathbf{B}}(\mathbf{S}\overline{\mathbf{B}})^{-1}\overline{\mathbf{B}}^T & \mathbf{E}\\ \mathbf{E}^T & \mathbf{I}\end{bmatrix} > 0 \tag{29}$$

$$\begin{bmatrix}\boldsymbol{\Theta}\boldsymbol{\Phi}\mathbf{P}_0\boldsymbol{\Phi}^T\boldsymbol{\Theta}^T + \varepsilon\overline{\mathbf{B}}(\mathbf{S}\overline{\mathbf{B}})^{-1}\overline{\mathbf{B}}^T & \mathbf{I}\\ \mathbf{I} & \alpha\mathbf{I}\end{bmatrix} > 0 \tag{30}$$

then the switching surface parameter matrix **S** satisfies *Property 1* and *Property 2*.

Proof:

By *Projection lemma* and *Finsler's lemma* we can show that any **S** satisfying *Property 1* and *Property 2* if exists a solution $\mathbf{P}_0$, **E** and ε , α satisfy (27)-(30) in which **P** can be obtained by (22). From *Lemma*, we know that **P** is a positive definite matrix and satisfy the condition (14) if there exists symmetric matrix $\mathbf{P}_0$ and positive scalar $\varepsilon \in \Re$, and from (13) we see that the sliding mode dynamics (17) is asymptotically stable.

Referring to [2] and [30], we consider the following switching feedback control law.

Control Rule i :

If ϕ_1 is F_1^i and $\cdots$ and ϕ_n is F_n^i

$$\text{Then } \mathbf{u}(t) = -\eta_i \frac{\boldsymbol{\sigma}(\mathbf{x})}{\|\boldsymbol{\sigma}(\mathbf{x})\|} \tag{31}$$

where $\phi_j (j = 1,2,\ldots,n)$ are the state variables and $\eta_i (i = 1,2,\ldots,r) \in \Re$ are the controller parameters for each subsystems and $\eta_{\max} = \max\{\eta_1, \eta_2, \ldots, \eta_r\}$ is assumed.

The overall controller inferred as the weighted average of the each local controller as follows:

$$\mathbf{u}(t) = -\sum_{i=1}^{r} h_i(\phi_j)\eta_i \frac{\boldsymbol{\sigma}(\mathbf{x})}{\|\boldsymbol{\sigma}(\mathbf{x})\|} \tag{32}$$

To support the following theorem, we make the assumptions as follows:

Assumption 4: There exist a known nonnegative constant $\rho = \dfrac{\rho_A + \rho_B}{1-\varphi}$ such that $\mathbf{h}(t,\mathbf{u},\mathbf{x}) \le \rho$ for all *t*.

Assumption 5: The difference $\eta_{\max} - \rho = \zeta$ is positive.

Theorem 2: Suppose that assumption 4 and assumption 5 hold and a switching surface $\boldsymbol{\sigma}(\mathbf{x}) = 0$ guaranteeing *Property 1* and *Property 2* are satisfied. Consider the uncertain T-S fuzzy system of (7) with the controller (32). The following region is an estimate of the ASR:

$$B_S = \left\{ \mathbf{x}(t) : \| \mathbf{x}(t) \| \le \frac{\zeta}{\sqrt{\alpha}} \right\} \tag{33}$$

proof:

We define the Lyapunov function as

$$V = \mathbf{x}(t)\mathbf{P}^{-1}\mathbf{x}(t) \tag{34}$$

The time of derivative of the Lyapunov function V is as follows:

$$\begin{aligned}
\dot{V} &= 2\sum_{i=1}^{r} h_i(\phi_j)\mathbf{x}^T(t)\mathbf{P}^{-1}\mathbf{A}_i\mathbf{x}(t) + 2\mathbf{x}^T(t)\mathbf{P}^{-1}\overline{\mathbf{B}}(\mathbf{u}(t) + \mathbf{h}(t,\mathbf{u},\mathbf{x})) \\
&= \sum_{i=1}^{r} h_i(\phi_j)\mathbf{x}^T(t)\mathbf{P}^{-1}[\mathbf{A}_i\mathbf{P} + \mathbf{P}\mathbf{A}_i^T - \mathbf{E}\overline{\mathbf{B}}^T - \overline{\mathbf{B}}\mathbf{E}^T]\mathbf{P}^{-1}\mathbf{x}(t) \\
&\quad + 2\mathbf{x}^T(t)\mathbf{P}^{-1}\overline{\mathbf{B}}(\mathbf{u}(t) + \mathbf{E}^T\mathbf{P}^{-1}\mathbf{x}(t) + \mathbf{h}(t,\mathbf{u},\mathbf{x}))
\end{aligned} \tag{35}$$

Substituting (32) into (35), we have

$$\begin{aligned}
\dot{V} &= \sum_{i=1}^{r} h_i(\phi_j)\mathbf{x}^T(t)(-\mathbf{Q}_i)\mathbf{x}(t) \\
&\quad + 2\mathbf{x}^T(t)\mathbf{P}^{-1}\overline{\mathbf{B}}(-\sum_{i=1}^{r} h_i(\phi_j)\eta_i \frac{\boldsymbol{\sigma}(\mathbf{x})}{\|\boldsymbol{\sigma}(\mathbf{x})\|} + \mathbf{E}^T\mathbf{P}^{-1}\mathbf{x}(t) \\
&\quad + \mathbf{h}(t,\mathbf{u},\mathbf{x})) \\
&\le \sum_{i=1}^{r} h_i(\phi_j)\mathbf{x}^T(t)(-\mathbf{Q}_i)\mathbf{x}(t) \\
&\quad + \left\| 2\mathbf{x}^T(t)\mathbf{P}^{-1}\overline{\mathbf{B}}(-\sum_{i=1}^{r} h_i(\phi_j)\eta_i \frac{\boldsymbol{\sigma}(\mathbf{x})}{\|\boldsymbol{\sigma}(\mathbf{x})\|} + \mathbf{E}^T\mathbf{P}^{-1}\mathbf{x}(t) \right. \\
&\quad \left. + \mathbf{h}(t,\mathbf{u},\mathbf{x})) \right\|
\end{aligned} \tag{36}$$

where $\mathbf{P}^{-1}[\mathbf{A}_i\mathbf{P} + \mathbf{P}\mathbf{A}_i^T - \mathbf{E}\overline{\mathbf{B}}^T - \overline{\mathbf{B}}\mathbf{E}^T]\mathbf{P}^{-1} = -\mathbf{Q}_i$ and $\mathbf{Q}_i > 0, \forall i = 1,2,\ldots,r.$

From assumption 4 and assumption 5, (36) implies that

$$\begin{aligned}
\dot{V} &\le -\sum_{i=1}^{r} h_i(\phi_j)\lambda_{\min}(\mathbf{Q}_i)\| \mathbf{x}(t) \|^2 + 2\| \mathbf{x}^T(t)\mathbf{P}^{-1}\overline{\mathbf{B}} \| \\
&\quad \cdot (\| \mathbf{E}^T\mathbf{P}^{-1}\mathbf{x}(t) \| - \zeta)
\end{aligned} \tag{37}$$

Therefore, in the region

$$\Omega_0 = \{\mathbf{x}(t) : \mathbf{x}^T(t)\mathbf{P}^{-1}\mathbf{E}\mathbf{E}^T\mathbf{P}^{-1}\mathbf{x}(t) \le \zeta^2\} \tag{38}$$

the following inequality holds:

$$\dot{V} \le -\sum_{i=1}^{r} h_i(\phi_j)\lambda_{\min}(\mathbf{Q}_i)\| \mathbf{x}(t) \|^2 \le 0 \tag{39}$$

and implies that the $\Omega_1 = \{\mathbf{x}(t) : \mathbf{x}^T(t)\mathbf{P}^{-1}\mathbf{x}(t) \le \zeta^2\}$.

The constraint $\Omega_1 \subset \Omega_0$ is satisfied if $\mathbf{P}^{-1} > \mathbf{P}^{-1}\mathbf{E}\mathbf{E}^T\mathbf{P}^{-1}$ which can be rewritten as the LMI (25) by using the Schur complement formula [31]. From (26), we can find the inequality $\alpha\mathbf{I} > \mathbf{P}^{-1}$ satisfying the constraint $\Omega_{ASR} \subset \Omega_1$ where the region Ω_{ASR} is an estimate of the ASR as follows:

$$\Omega_{ASR} = \{\mathbf{x}(t) : \mathbf{x}^T(t)\alpha\mathbf{I}\,\mathbf{x}(t) \le \zeta^2\} \tag{40}$$

From (40), we can obtain (33).

Remark: If the uncertain systems (1) satisfy assumption 1-assumption 5, then there exist a positive definite matrix **P** satisfy (24)-(26). The switching surface can be designed and some LMI problems of the (27)-(30) can be solved. The ASR can be estimated.

IV. Simulation Example

We consider the inverted pendulum via gear train [27], described by the following sates equation:

$$\begin{bmatrix} \dot{x}_1(t) \\ \dot{x}_2(t) \\ \dot{x}_3(t) \end{bmatrix} = \begin{bmatrix} x_2(t) \\ (g/l)\sin(x_1) + (NK_m/ml^2)x_3 \\ -(V_b/L_a)x_2 - (R_a/L_a)x_3 \end{bmatrix} + \begin{bmatrix} 0 \\ 0 \\ 1/L_a \end{bmatrix} u(t) \tag{41}$$

where $x_1(t)$ is the angle of the pendulum, $x_2(t)$ is the angle velocity, $x_3(t)$ is the current of the motor. K_m is the motor torque constant, V_b is the back emf constant, R_a is the resistance, L_a is the inductance of armature circuit, N is the gear ratio.

In this simulation, $g = 9.8m/s^2$, $l = 1m$, $m = 1kg$, $N = 10$, $K_m = 0.1Nm/A$, $K_b = 0.1Vs/rad$, $R_a = 1\Omega$, and $L_a = 100mH$. Using the values of the system parameter in (41), we have

$$\begin{bmatrix} \dot{x}_1(t) \\ \dot{x}_2(t) \\ \dot{x}_3(t) \end{bmatrix} = \begin{bmatrix} x_2(t) \\ 9.8\sin(x_1) + x_3 \\ -10x_2 - 10x_3 \end{bmatrix} + \begin{bmatrix} 0 \\ 0 \\ 10 \end{bmatrix} u(t) \tag{42}$$

The following dynamic fuzzy model is used to represent the nonlinear system (42):

Plant Rule 1 :

If x_1 is G_1

$$\text{Then } \dot{\mathbf{x}}(t) = \begin{bmatrix} 0 & 1 & 0 \\ 9.8 & 0 & 1 \\ 0 & -10 & -10 \end{bmatrix} \mathbf{x}(t) + \begin{bmatrix} 0 \\ 0 \\ 10 \end{bmatrix} u(t) \tag{43}$$

Plant Rule 2:

If x_1 is G_2

$$\text{Then } \dot{\mathbf{x}}(t) = \begin{bmatrix} 0 & 1 & 0 \\ 0 & 0 & 1 \\ 0 & -10 & -10 \end{bmatrix} \mathbf{x}(t) + \begin{bmatrix} 0 \\ 0 \\ 10 \end{bmatrix} u(t) \tag{44}$$

and we consider $\rho_A = 0.25$, $\varphi = 0.1$, $\rho_f = 0$, and $\eta_{\max} = 7$. The membership functions as follows [27]:

$$G_1 = \frac{1 - 1/[1 + \exp(-5(x_1 - 1))]}{1 + \exp(-5(x_1 - 1))} \text{ and } G_2 = 1 - G_1 \tag{45}$$

Now, we checking the $\overline{\mathbf{B}}^T\mathbf{\Phi} = \mathbf{0}$ and $\mathbf{\Phi}^T\mathbf{\Phi} = \mathbf{I}$, the $\mathbf{\Phi}^T = \begin{bmatrix} 0 & 1 & 0 \\ -1 & 0 & 0 \end{bmatrix}$ can be obtained from MATLAB code [33]. By solving the LMI problem we can obtain the following arguments:

$$\mathbf{P} = \begin{bmatrix} 2.6795 & -8.8122 & 16.3451 \\ -8.8122 & 32.6026 & -97.2679 \\ 16.3451 & -97.2679 & 632.8051 \end{bmatrix}, \ \mathbf{E} = \begin{bmatrix} -0.6149 \\ 2.1290 \\ -2.6274 \end{bmatrix}$$

$$\mathbf{P}_0 = \begin{bmatrix} 32.6026 & 8.8122 \\ 8.8122 & 2.6795 \end{bmatrix}, \ \alpha = 120.1430, \text{ and } \varepsilon = 1.8074.$$

And we can be obtained the estimate of ASR as follows:

$$ASR = \{\mathbf{x}(t) : \| \mathbf{x}(t) \| \le 0.61\} \tag{46}$$

Fig. 1 gives the simulation results of $x_1(t)$. Fig. 2 gives the simulation results of $x_2(t)$. Fig. 3 gives the simulation results of $x_3(t)$. From Fig. 4, it can be clearly seen here that the system enters into a sliding mode and is confined to the vicinity of the switching surface.

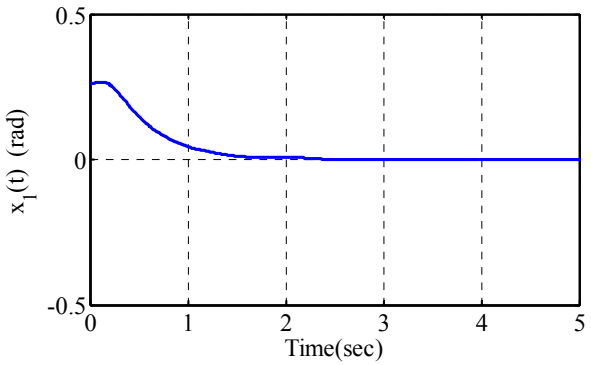

Fig. 1. The locus of $x_1(t)$ for initial conditions $\mathbf{x}(0) = [\pi/12 \quad 0 \quad 0]^T$.

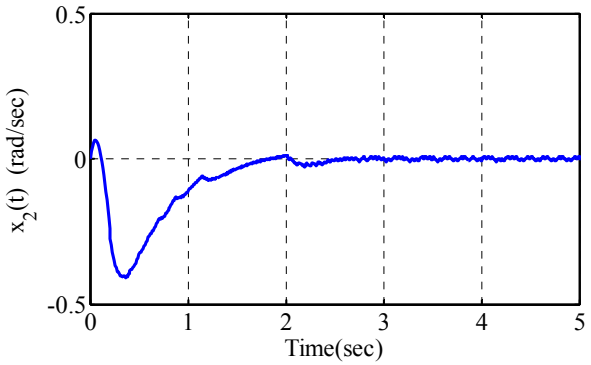

Fig. 2. The locus of $x_2(t)$ for initial conditions $\mathbf{x}(0) = [\pi/12 \quad 0 \quad 0]^T$.

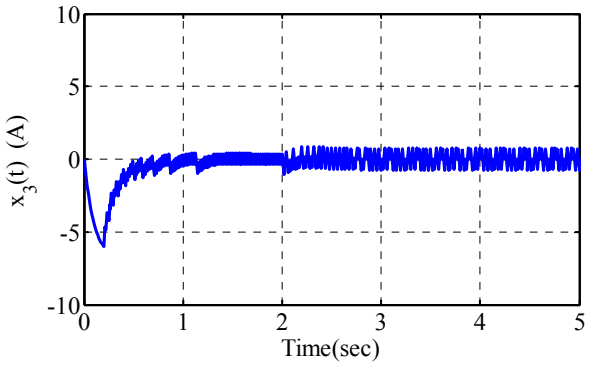

Fig. 3. The locus of $x_3(t)$ for initial conditions $\mathbf{x}(0) = [\pi/12 \quad 0 \quad 0]^T$.

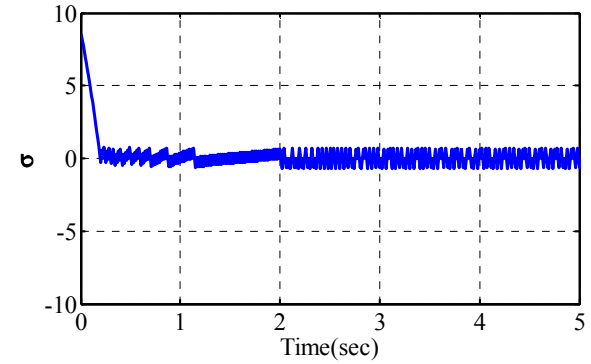

Fig. 4. The switching surface for initial conditions $\mathbf{x}(0) = [\pi/12 \quad 0 \quad 0]^T$.

V. CONCLUSIONS

The T-S fuzzy model is presented to approximate the uncertain nonlinear systems. By the Lyapunov stability theorem, the variable structure controllers can be designed with the linear matrix inequalities (LMIs). And the asymptotic stability region (ASR) can be obtained. The simulation example showed the effectiveness of the proposed scheme.

ACKNOWLEDGMENT

Financial support of this research by National Science Council of Taiwan, Republic of China, under Grant NSC 99-2221-E-036-021 is gratefully acknowledged.

REFERENCES

[1] V. I. Utkin, "Variable structure systems with sliding modes," *IEEE Transactions on Automatic Control*, vol. 22, no. 2, pp. 212–222, Feb. 1977.

[2] H. H. Choi, "An explicit formula of linear sliding surfaces for a class of uncertain dynamic systems with mismatched uncertainties," *Automatica,* vol. 34, no 8, pp. 1015–1020, Aug. 1998.

[3] M. Zohdy, M. S. Fadali, and J. Liu, "Variable structure control using system decomposition," *IEEE Transactions on Automatic Control.*, vol. 37, no. 10, pp. 1514–1517, Oct. 1992.

[4] W. J. Wang, G. H. Wu, and D. C. Yang, "Variable structure control design for uncertain discrete-time systems," *IEEE Transactions on Automatic Control.*, vol. 39, no. 1, pp. 99-102, Jan. 1994.

[5] C. Lin, Q. G. Wang, and T. H. Lee, "Stabilization of uncertain fuzzy time-delay systems via variable structure control approach," *IEEE Transactions on Fuzzy Systems.*, vol. 13, no. 6, pp. 787–798, Dec. 2005.

[6] L. X. Wang, "Adaptive fuzzy systems and control: design and stability analysis," Upper Saddle River, NJ: Prentice-Hall, 1994.

[7] T. Tagaki and M. Sugeno, "Fuzzy identification of systems and its applications to modeling and control," *IEEE Transactions on Systems, Man and Cybernetics*, vol. 15, no. 1, pp. 116–132, Jan. 1985.

[8] H. O. Wang, K. Tanaka, and M. F. Griffin, "An approach to fuzzy control of nonlinear systems: Stability and design issues," *IEEE Transactions on Fuzzy System*, vol. 4, no. 1, pp. 14–23, Feb. 1996.

[9] M. C. M. Teixeira and S. H. Zak, "Stabilizing controller design for uncertain nonlinear systems using fuzzy models," *IEEE Transactions on Fuzzy Systems*, vol. 7, no. 2, pp. 133–142, Apr. 1999.

[10] S. H. Zak, "Stabilizing fuzzy system models using linear controllers," *IEEE Transactions on Fuzzy Systems*, vol. 7, no. 2, pp. 236–240, Apr. 1999.

[11] K. Tanaka, T. Ikeda, and H. O. Wang, "Robust stabilization of a class of uncertain nonlinear systems via fuzzy control: Quadratic stabilization H_∞ control theory and linear matrix inequalities," *IEEE Transactions on Fuzzy Systems*, vol. 4, no. 1, pp. 1–13, Jan. 1996.

[12] H. D. Tuan, P. Apkarian, T. Narikiyo, and Y. Yamamoto, "Parameterized linear matrix inequality techniques in fuzzy control system design," *IEEE Transactions on Fuzzy Systems*, vol. 9, no. 2, pp. 324–332, Apr. 2001.

[13] H. J. Uang and G. S. Huang, "A robust fuzzy model following observer-based control design for nonlinear system," *IEEE International Conference on Control Applications Taipei, Taiwan*, Sep. 2004.

[14] K. Tanaka and M. Sano, "Stability analysis and design of fuzzy control system," *Fuzzy Sets and System*, vol. 45, pp. 135-156, 1992.

[15] K. Tanaka and M. Sano, "Fuzzy stability criterion of a class of linear," *Information Sciences*, vol. 71, no. 1, pp. 3-26, June 1993.

[16] K. Tanaka, T. Ikeda, and H. O. Wang, "Fuzzy regulators and fuzzy observers: Relaxed stability conditions and LMI-based designs," *IEEE Transactions on Fuzzy Systems*, vol. 6, no. 2, pp. 250-265, May 1998.

[17] S. G. Cao, N. W. Rees, and G. Feng, "Analysis and design for a class of complex control systems part II: Fuzzy controller design," *Automatica*, vol. 33, no. 6, pp. 1029-1039, June 1997.

[18] F. Zheng, Q. G. Wang, and T. H. Lee, "Output tracking control of MIMO fuzzy nonlinear systems using variable structure control approach," *IEEE Transactions on Fuzzy Systems*, vol. 10, no. 6, pp. 686–697, Dec. 2002.

[19] X. Yu, Z. Man, and B. Wu, "Design of fuzzy sliding-mode control systems," *Fuzzy Sets and Systems*, vol. 95, no. 3, pp. 295-306, May 1998.

[20] C. L. Hwang, "A novel Takagi-Sugeno-based robust adaptive fuzzy sliding-mode controller," *IEEE Transactions on Fuzzy Systems*, vol. 12, no. 5, pp. 676-687, Oct. 2004.

[21] H. H. Choi, "Robust stabilization of uncertain fuzzy systems using variable structure system approach," *IEEE Transactions on Fuzzy Systems*, vol. 16, no. 3, pp. 715–724, June 2008.

[22] R. Palm and P. Bergsten "Sliding mode observer for a Takagi Sugeno fuzzy system," *IEEE International Conference on Fuzzy Systems*, vol. 2, pp. 665–670, May 2000.

[23] C. C. Kung, S. C. Chang, and P. S. Huang, "Design of adaptive fuzzy integral sliding mode control for uncertain nonlinear systems with state and input delays," *IEEE International Conference on Systems, Man and Cybernetics*. pp. 944–949, Oct. 2008.

[24] W. S. Yu, "T-S fuzzy controller design for nonlinear large-scale systems with time-varying uncertainties," *IEEE International Conference on Fuzzy Systems*, pp. 879–886, June 2008.

[25] J. C. Wu and T. S. Liu, "A sliding mode approach to fuzzy control design," *IEEE Transactions Fuzzy Systems*, vol. 4, no. 2, pp. 141–151, Mar. 1996.

[26] N. Sadati and A. Talasaz, "A robust fuzzy sliding mode control for uncertain dynamic systems," *IEEE International Conference on Systems, Man and Cybernetics*, vol. 3, pp. 2225–2230, Oct. 2004.

[27] K. Suiyang, M. Zhihong, and Z. Shengkui, "Sliding mode control of Fuzzy dynamic Systems," *International Conference on Control, Automation, Robotics and Vision*, pp. 1–6, Dec. 2006.

[28] S. M. M. Esfahani, M. Hached, and S. H. Zak, "Estimation of sliding mode domains of uncertain variable structure systems with bounded controllers," *IEEE Transactions on Automatic Control*, vol. 35, no. 4, pp. 446–449, Mar. 1990.

[29] H. H. Choi and M. J. Chung, "Estimation of asymptotic stability region of uncertain systems with bounded sliding mode controllers," *IEEE Transactions on Automatic Control*, vol. 39, no. 11, pp. 2275–2278, Dec. 1994.

[30] H. H. Choi, "An analysis and design method for uncertain variable structure systems with bounded controllers," *IEEE Transactions on Automatic Control,* vol. 49, no. 4, pp. 602–607, Apr. 2004.

[31] S. Boyd, L. E. Ghaoui, E. Feron, and V. Balakrishnan, "Linear matrix inequalities in system and control theory," Philadelphia, PA: SIAM, 1994.

[32] P. Gahinet and P. Apkarian, "A linear matrix inequality approach to H_∞ control," *International Journal, Robust, Nonlinear Control*, vol. 4, pp. 421–448, 1994.

[33] P. Gahinet, A. Nemirovski, and A. J. Laub, "LMI Control toolbox user's guide." Natick, MA: The Math Works, Inc., 1995.

2011 IEEE International Conference on Fuzzy Systems
June 27-30, 2011, Taipei, Taiwan

A Study on Atanassov's Intuitionistic Fuzzy Graphs

M.G.Karunambigai
Department of Mathematics
Sri Vasavi College
Erode, Tamilnadu
India
Email: gkaruns@yahoo.co.in

R. Parvathi
Department of Mathematics
Vellalar College for Women
Erode, Tamilnadu
India
Email: paarvathis@rediffmail.com

O.K.Kalaivani
Department of Mathematics
T.John Institute of Technology
Bangalore,Karnataka
India
Email: kalaivani83@gmail.com

***Abstract*—Atanassov [1][9][10] defined Intuitionistic Fuzzy Graphs(IFGs) using five types of Cartesian products. In this paper IFGs so defined are named. Homomorphism, weak isomorphism and co-weak isomorphism of minmax IFGs are defined with suitable illustrations. Some of the properties of isomorphism on IFG and isomorphism on strong IFG are also analyzed.**

***Index Terms*—$\mu-$product IFG, $\nu-$product IFG, minmax IFG, maxmin IFG, homomorphism, weak isomorphism and co-weak isomorphism.**

I. Introduction

The motivation for introducing IFGs is due to [1][9][10]. The first definition and concept of Intuitionistic Fuzzy Graph(IFG) was introduced by Krassimir T. Atanassov 1994[1]. R.Parvathi and M.G.Karunambigai analyzed the properties of minmax IFGs in [3][8]. Shannon and Atanassov[1][9][10] defined intuitionistic fuzzy graphs using five types of Cartesian products. In this paper IFGs so defined are named. Some isomorphic properties on IFGs are discussed. Nagoor Gani, et al., discussed the properties of isomorphism on fuzzy graphs and properties of isomorphism on strong fuzzy graphs in [4][5][6] which motivated us to develop the same on IFGs and on strong IFGs.

The main aim of this study is to build basic definitions of an IFG which will be useful for the researchers for their future study in IFGs. Since Atanassov[1][9][10] is the pioneer of our study, the title of the paper is given so. For graph theoretical definitions see[2] and throughout this paper all the properties are analyzed for simple minmax IFG.

II. Atanassov's IFG

Definition 2.1: [1] Let E_1 and E_2 be two universes and let
A = $\{\langle x, \mu_A(x), \nu_A(x)\rangle / x \in E_1\}$
B = $\{\langle x, \mu_B(x), \nu_B(x)\rangle / x \in E_2\}$
be two IFSs; A $-$over E_1 and B $-$over E_2. Then define
$A \otimes_1 B = \{\langle\langle x, y\rangle, \mu_A(x) \bullet \mu_B(y), \nu_A(x) \bullet \nu_B(y)\rangle | \langle x, y\rangle \in E_1 \times E_2\}$,
$A \otimes_2 B = \{\langle\langle x, y\rangle, \mu_A(x) + \mu_B(y) - \mu_A(x) \bullet \mu_B(y), \nu_A(x) \bullet \nu_B(y)\rangle | \langle x, y\rangle \in E_1 \times E_2\}$,
$A \otimes_3 B = \{\langle\langle x, y\rangle, \mu_A(x) \bullet \mu_B(y), \nu_A(x) + \nu_B(y) - \nu_A(x) \bullet \nu_B(y)\rangle | \langle x, y\rangle \in E_1 \times E_2\}$,
$A \otimes_4 B = \{\langle\langle x, y\rangle, min(\mu_A(x), \mu_B(y)), max(\nu_A(x), \nu_B(y))\rangle | \langle x, y\rangle \in E_1 \times E_2\}$,
$A \otimes_5 B = \{\langle\langle x, y\rangle, max(\mu_A(x), \mu_B(y)), min(\nu_A(x), \nu_B(y))\rangle | \langle x, y\rangle \in E_1 \times E_2\}$.

We must note that $A \times_i B$ is an IFS, but it is an IFS over the universe $E_1 \times E_2$, where $\otimes_i$ is one of the five Cartesian products above, $\times$ is the classical Cartesian product on ordinary sets and $\bullet$ is a crisp product. An Intuitionistic Fuzzy Graph (IFG) is of the form $G = (V, E)$ where

(i) $V = \{v_1, v_2, ..., v_n\}$ such that $\mu_1 : V \to [0, 1]$ and $\nu_1 : V \to [0, 1]$, denotes the degree of membership and non-membership of the element $v_i \in V$ respectively and $0 \leq \mu_1(v_i) + \nu_1(v_i) \leq 1$, for every $v_i \in V, (i = 1, 2, ..., n)$,

(ii) $E \subseteq V \times V$ where $\mu_2 : V \times V \to [0, 1]$ and $\nu_2 : V \times V \to [0, 1]$, are such that
$\mu_2(v_i, v_j) \leq (\mu_1(v_i) \circ \mu_1(v_j))$
$\nu_2(v_i, v_j) \leq (\nu_1(v_i) \circ \nu_1(v_j))$,
denotes the degree of membership and non-membership of an edge $(v_i, v_j) \in E$ respectively, where, $\circ \in \{\otimes_1, \otimes_2, \otimes_3, \otimes_4, \otimes_5\}$ and $0 \leq \mu_2(v_i, v_j) + \nu_2(v_i, v_j) \leq 1$, for every $(v_i, v_j) \in E$.

Notations 2.1: The triple $(v_i, \mu_{1i}, \nu_{1i})$ denotes the degree of membership and non-membership of the vertex v_i. The triple $(e_{ij}, \mu_{2ij}, \nu_{2ij})$ denotes the degree of membership and non- membership of the edge relation $e_{ij} = (v_i, v_j)$ on V.

Note 2.1: (1) When $\mu_{2ij} = 0, \nu_{2ij} = 0$ for some i and j, then there is no edge between v_i and v_j.

(2) When either one of the following is true, then there is an edge between v_i and v_j
- $\mu_{2ij} = 0$ or $\nu_{2ij} > 0$
- $\mu_{2ij} > 0$ or $\nu_{2ij} = 0$

The IFGs defined by Atanassov[1] by using five Cartesian products and those IFGs are defined and named here as follows:

A. Product IFG

An Intuitionistic Fuzzy Graph (IFG) $G = (V, E)$ is said to be a product IFG if

(i) $V = \{v_1, v_2, ..., v_n\}$ such that $\mu_1 : V \to [0, 1]$ and $\nu_1 : V \to [0, 1]$, denotes the degree of membership and non-membership of the element $v_i \in V$ respectively and $0 \leq \mu_1(v_i) + \nu_1(v_i) \leq 1$, for every $v_i \in V, (i = 1, 2, ..., n)$,

(ii) $E \subseteq V \times V$ where $\mu_2 : V \times V \to [0, 1]$ and $\nu_2 : V \times V \to [0, 1]$, are such that
$\mu_2(v_i, v_j) \leq (\mu_1(v_i) \bullet \mu_1(v_j))$
$\nu_2(v_i, v_j) \leq (\nu_1(v_i) \bullet \nu_1(v_j))$,
denotes the degree of membership and non-membership

of an edge $(v_i, v_j) \in E$ respectively, where, $0 \leq \mu_2(v_i, v_j) + \nu_2(v_i, v_j) \leq 1$, for every $(v_i, v_j) \in E$.

B. $\mu-$Product IFG

An Intuitionistic Fuzzy Graph (IFG) $G = (V, E)$ is said to be a $\mu-$ product IFG if

(i) $V = \{v_1, v_2, ..., v_n\}$ such that $\mu_1 : V \to [0, 1]$ and $\nu_1 : V \to [0, 1]$, denotes the degree of membership and non-membership of the element $v_i \in V$ respectively and $0 \leq \mu_1(v_i) + \nu_1(v_i) \leq 1$, for every $v_i \in V$, $(i = 1, 2, ..., n)$,

(ii) $E \subseteq V \times V$ where $\mu_2 : V \times V \to [0, 1]$ and $\nu_2 : V \times V \to [0, 1]$, are such that
$\mu_2(v_i, v_j) \leq (\mu_1(v_i) \bullet \mu_1(v_j))$
$\nu_2(v_i, v_j) \leq (\nu_1(v_i) + \nu_1(v_j) - \nu_1(v_i) \bullet \nu_1(v_j))$,
denotes the degree of membership and non-membership of an edge $(v_i, v_j) \in E$ respectively, where, $0 \leq \mu_2(v_i, v_j) + \nu_2(v_i, v_j) \leq 1$, for every $(v_i, v_j) \in E$.

C. $\nu-$Product IFG

An Intuitionistic Fuzzy Graph (IFG) $G = (V, E)$ is said to be a $\nu-$ product IFG if

(i) $V = \{v_1, v_2, ..., v_n\}$ such that $\mu_1 : V \to [0, 1]$ and $\nu_1 : V \to [0, 1]$, denotes the degree of membership and non-membership of the element $v_i \in V$ respectively and $0 \leq \mu_1(v_i) + \nu_1(v_i) \leq 1$, for every $v_i \in V, (i = 1, 2, ..., n)$,

(ii) $E \subseteq V \times V$ where $\mu_2 : V \times V \to [0, 1]$ and $\nu_2 : V \times V \to [0, 1]$, are such that
$\mu_2(v_i, v_j) \leq (\mu_1(v_i) + \mu_1(v_j) - \mu_1(v_i) \bullet \mu_1(v_j))$
$\nu_2(v_i, v_j) \leq (\nu_1(v_i) \bullet \nu_1(v_j))$,
denotes the degree of membership and non-membership of an edge $(v_i, v_j) \in E$ respectively, where, $0 \leq \mu_2(v_i, v_j) + \nu_2(v_i, v_j) \leq 1$, for every $(v_i, v_j) \in E$.

D. Minmax IFG

An Intuitionistic Fuzzy Graph (IFG) $G = (V, E)$ is said to be a minmax IFG if

(i) $V = \{v_1, v_2, ..., v_n\}$ such that $\mu_1 : V \to [0, 1]$ and $\nu_1 : V \to [0, 1]$, denotes the degree of membership and non-membership of the element $v_i \in V$ respectively and $0 \leq \mu_1(v_i) + \nu_1(v_i) \leq 1$, for every $v_i \in V$, $(i = 1, 2, ..., n)$,

(ii) $E \subseteq V \times V$ where $\mu_2 : V \times V \to [0, 1]$ and $\nu_2 : V \times V \to [0, 1]$, are such that
$\mu_2(v_i, v_j) \leq min(\mu_1(v_i), \mu_1(v_j))$
$\nu_2(v_i, v_j) \leq max(\nu_1(v_i), \nu_1(v_j))$,
denotes the degree of membership and non-membership of an edge $(v_i, v_j) \in E$ respectively, where, $0 \leq \mu_2(v_i, v_j) + \nu_2(v_i, v_j) \leq 1$, for every $(v_i, v_j) \in E$.

E. Maxmin IFG

An Intuitionistic Fuzzy Graph (IFG) $G = (V, E)$ is said to be a maxmin IFG if

(i) $V = \{v_1, v_2, ..., v_n\}$ such that $\mu_1 : V \to [0, 1]$ and $\nu_1 : V \to [0, 1]$, denotes the degree of membership and non-membership of the element $v_i \in V$ respectively and $0 \leq \mu_1(v_i) + \nu_1(v_i) \leq 1$, for every $v_i \in V, (i = 1, 2, ..., n)$,

(ii) $E \subseteq V \times V$ where $\mu_2 : V \times V \to [0, 1]$ and $\nu_2 : V \times V \to [0, 1]$, are such that
$\mu_2(v_i, v_j) \leq max(\mu_1(v_i), \mu_1(v_j))$
$\nu_2(v_i, v_j) \leq min(\nu_1(v_i), \nu_1(v_j))$,
denotes the degree of membership and non-membership of an edge $(v_i, v_j) \in E$ respectively, where, $0 \leq \mu_2(v_i, v_j) + \nu_2(v_i, v_j) \leq 1$, for every $(v_i, v_j) \in E$.

F. Type n IFG

An Intuitionistic Fuzzy Graph (IFG) $G = (V, E)$ is said to be a type n IFG if

(i) $V = \{v_1, v_2, ..., v_n\}$ such that $\mu_1 : V \to [0, 1]$ and $\nu_1 : V \to [0, 1]$, denotes the degree of membership and non-membership of the element $v_i \in V$ respectively and $0 \leq \mu_1(v_i) + \nu_1(v_i) \leq 1$, for every $v_i \in V, (i = 1, 2, ..., n)$,

(ii) $E \subseteq V \times V$ where $\mu_2 : V \times V \to [0, 1]$ and $\nu_2 : V \times V \to [0, 1]$, are such that
$\mu_2(v_i, v_j) \leq (\mu_1^n(v_i) \bullet \mu_1^n(v_j))$
$\nu_2(v_i, v_j) \leq (\nu_1^n(v_i) \bullet \nu_1^n(v_j))$,
denotes the degree of membership and non-membership of an edge $(v_i, v_j) \in E$ respectively, where, $0 \leq \mu_2(v_i, v_j) + \nu_2(v_i, v_j) \leq 1$, for every $(v_i, v_j) \in E$.

Note 2.2: If $n = 1$, then the IFG is a type 1 IFG which is the product IFG, if $n = 2$, then the IFG is called a type 2 IFG, if $n = 3$, then the IFG is called a type 3 IFG and so on .

III. PRELIMINARIES

Definition 3.1: [3] An IFG $G : (V, E)$ is said to be a *strong* IFG if $\mu_2(v_i, v_j) = min(\mu_1(v_i), \mu_1(v_j))$ and $\nu_2(v_i, v_j) = max(\nu_1(v_i), \nu_1(v_j))$, $\forall (v_i, v_j) \in E$.

Definition 3.2: [3] An IFG $G : (V, E)$ is said to be a *complete* IFG if $\mu_2(v_i, v_j) = min(\mu_1(v_i), \mu_1(v_j))$ *and* $\nu_2(v_i, v_j)$=$max(\nu_1(v_i), \nu_1(v_j))$, $\forall v_i, v_j \in V$.

Definition 3.3: [3] A *path* P in an IFG is a sequence of distinct vertices $v_1, v_2, ..., v_n$ such that either one of the following condition is satisfied.

(i) $\mu_{2ij} > 0$ *and* $\nu_{2ij} = 0$ for some i *and* j.

(ii) $\mu_{2ij} = 0$ *and* $\nu_{2ij} > 0$ for some i *and* j.

Definition 3.4: [3] The *$\mu-$strength* of a path $P = v_1, v_2, ..., v_n$ is defined as min$(\mu_2(v_i, v_j))$ for all i and j and is denoted by S_μ.
The *$\nu-$strength* of a path $P = v_1, v_2, ..., v_n$ is defined as max$(\nu_2(v_i, v_j))$ for all i *and* j and is denoted by S_ν.

Note 3.1: If same edge possesses the value of both $\mu-$strength and $\nu-$strength, then it is the strength of the path P. In other words, the strength of a path is defined to be the weight of the weakest edge of the path. That is the strength of a path is denoted by (S_μ, S_ν).

Definition 3.5: Let $G : (V, E)$ be an IFG. The *$\mu-$strength of the paths* connecting any two vertices v_i, v_j is defined as max(S_μ) and is denoted by μ_{2ij}^∞. The *$\nu-$strength of the paths*

connecting any two vertices v_i, v_j is defined as $\min(S_\nu)$ and is denoted by ν^{∞}_{2ij}.

Note 3.2: If same edge possesses both the $\mu-$strength and $\nu-$strength values, then it is the strength of the strongest path P and it is denoted by $S_P = (\mu^{\infty}_{2ij}, \nu^{\infty}_{2ij})$ for all $i, j = 1, 2, ..., n$.

Definition 3.6: An edge (v_i, v_j) is said to be a *strong edge* in an IFG, $G = (V, E)$, if $\mu_{2ij} \geq \mu^{\infty}_{2ij}$, $\nu_{2ij} \leq \nu^{\infty}_{2ij}$.

Definition 3.7: A path is said to be a *strong path* in $G : (V, E)$ if it consists of only strong edges.

Definition 3.8: [7] The *order* of an IFG $G = (V, E)$ is defined to be $O(G) = (O_\mu(G), O_\nu(G))$ where

$$O_\mu(G) = \sum_{v_i \in V} \mu_1(v_i)$$

$$O_\nu(G) = \sum_{v_i \in V} \nu_1(v_i)$$

Definition 3.9: [7] The *size* of an IFG is defined to be $S(G) = (S_\mu(G), S_\nu(G))$

$$S_\mu(G) = \sum_{v_i, v_j \in V} \mu_2(v_i, v_j)$$

$$S_\nu(G) = \sum_{v_i, v_j \in V} \nu_2(v_i, v_j)$$

Definition 3.10: [7] The *degree* of a vertex v_i is defined by $d(v_i) = (d_\mu(v_i), d_\nu(v_i))$ where

$$d_\mu(v_i) = \sum_{v_i \neq v_j} \mu_2(v_i, v_j)$$

$$d_\nu(v_i) = \sum_{v_i \neq v_j} \nu_2(v_i, v_j)$$

Definition 3.11: [3] The *complement* of an IFG $G = (V, E)$ is an IFG $\bar{G} = (\bar{V}, \bar{E})$, where

(i) $\bar{V} = V$
(ii) $\bar{\mu}_{1i} = \mu_{1i}$ and $\bar{\nu}_{1i} = \nu_{1i}$, for all $i = 1, 2, ..., n$.
(iii) $\bar{\mu}_{2ij} = min(\mu_{1i}, \mu_{1j}) - \mu_{2ij}$ and $\bar{\nu}_{2ij} = max(\nu_{1i}, \nu_{1j}) - \nu_{2ij}$, for all $i, j = 1, 2, ..., n$.

Definition 3.12: [3] Consider the two IFGs $G_1 = (V_1, E_1)$ and $G_2 = (V_2, E_2)$. An *isomorphism* between two IFGs G_1 and G_2, denoted by $G_1 \cong G_2$,is a bijective map $I : V_1 \to V_2$ which satisfies

$$I(v_i) = v'_i, v_i \in V$$

$$\mu_1(v_i) = \mu'_1(I(v_i)), \nu_1(v_i) = \nu'_1(I(v_i)), \forall v_i \in V$$

$$\mu_2(v_i, v_j) = \mu'_2(I(v_i), I(v_j)) \text{ and}$$

$$\nu_2(v_i, v_j) = \nu'_2(I(v_i), I(v_j)), \forall v_i, v_j \in V.$$

Definition 3.13: A *homomorphism* between two IFGs $G_1 = (V_1, E_1)$ and $G_2 = (V_2, E_2)$ is defined as $H : V_1 \to V_2$ is a map which satisfies

$$H(v_i) = v'_i, v_i \in V$$

$$\mu_1(v_i) \leq \mu'_1(H(v_i)), \nu_1(v_i) \geq \nu'_1(H(v_i)), \forall v_i \in V_1$$

$$\mu_2(v_i, v_j) \leq \mu'_2(H(v_i), H(v_j)) \text{ and}$$

$$\nu_2(v_i, v_j) \geq \nu'_2(H(v_i), H(v_j)), \forall v_i, v_j \in V.$$

Definition 3.14: A *weak isomorphism* between two IFGs $G_1 = (V_1, E_1)$ and $G_2 = (V_2, E_2)$ is defined as $I : V_1 \to V_2$ is a bijective homomorphism that satisfies

$$\mu_1(v_i) = \mu'_1(I(v_i)), \ \nu_1(v_i) = \nu'_1(I(v_i)), \forall v_i \in V.$$

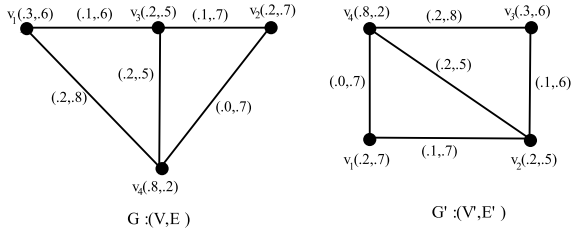

Fig. 1. G_1 is isomorphic to G_2

Definition 3.15: A *co-weak isomorphism* between two IFGs $G_1 = (V_1, E_1)$ and $G_2 = (V_2, E_2)$ is defined as $I : V_1 \to V_2$ is a bijective homomorphism that satisfies

$$\mu_2(v_i, v_j) = \mu'_2(I(v_i), I(v_j)) \text{ and}$$

$$\nu_2(v_i, v_j) = \nu'_2(I(v_i), I(v_j)), \forall v_i, v_j \in V_1$$

Definition 3.16: An *automorphism* of an intuitionistic fuzzy graph $G : (V, E)$ is an isomorphism of $G : (V, E)$ to itself.

IV. Properties of Isomorphism on Intuitionistic Fuzzy Graphs

Theorem 4.1: For any two isomorphic IFG their order and size are same.

Proof: If $h : G \to G'$ is an isomorphism between the IFG G and G' with the underlying sets V and V' respectively then
$\mu_1(v_i) = \mu'_1(h(v_i))$ and $\nu_1(v_i) = \nu'_1(h(v_i))$, $\forall v_i \in V$.
$\mu_2(v_i, v_j) = \mu'_2(h(v_i), h(v_j))$ and
$\nu_2(v_i, v_j) = \nu'_2(h(v_i), h(v_j))$, $\forall v_i, v_j \in V$.
we know that

$$order(G_\mu) = \sum_{v_i \in V} \mu_1(v_i) = \sum_{v_i \in V} \mu'_1(h(v_i)) = order(G'_\mu)$$

$$order(G_\nu) = \sum_{v_i \in V} \nu_1(v_i) = \sum_{v_i \in V} \nu'_1(h(v_i)) = order(G'_\nu)$$

$$size(G_\mu) = \sum_{v_i,v_j \in V} \mu_2(v_i, v_j)$$
$$= \sum_{v_i,v_j \in V} \mu_2'(h(v_i), h(v_j))$$
$$= size(G_\mu')$$

$$size(G_\nu) = \sum_{v_i,v_j \in V} \nu_2(v_i, v_j)$$
$$= \sum_{v_i,v_j \in V} \nu_2'(h(v_i), h(v_j))$$
$$= size(G_\nu')$$

■

Corollary 4.1: Converse of the above theorem need not be true.

Example 4.1: Here, $O_\mu(G)$ = 1.2, $O_\nu(G)$ = 1.8, $S_\mu(G)$ = .4, $S_\nu(G)$ = 1.5, $O_\mu(G')$ = 1.2, $O_\nu(G')$ = 1.8, $S_\mu(G')$ = .4, $S_\nu(G')$ = 1.5.

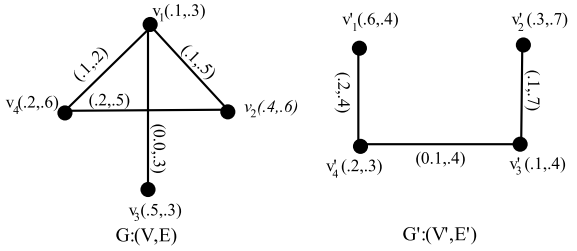

Fig. 2. Graphs of same order and size but not isomorphic

Remark 4.1: If the IFGs are weak isomorphic then their order are same. But the IFGs are of same order need not be weak isomorphic.

Example 4.2:

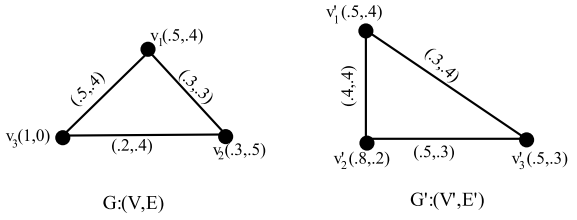

Fig. 3. Graphs of same order but not weak isomorphic

Remark 4.2: If the IFGs are co-weak isomorphic then their size are same. But the IFGs are of same size need not be co-weak isomorphic.

Example 4.3:

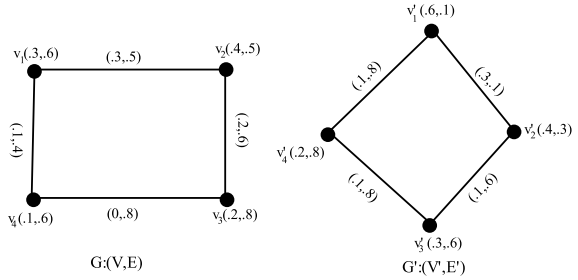

Fig. 4. Graphs of same size but not co-weak isomorphic

Theorem 4.2: If G and G' are isomorphic IFGs then the degrees of their vertices are preserved.

Proof: Let $h : V \to V'$ be an isomorphism of G and G'. By the definition of an isomorphism,
$\mu_2(v_i, v_j) = \mu_2'(h(v_i), h(v_j)), \forall v_i, v_j \in V$.
$\nu_2(v_i, v_j) = \nu_2'(h(v_i), h(v_j)), \forall v_i, v_j \in V$.

$$d_\mu(v_i) = \sum_{v_i \neq v_j} \mu_2(v_i, v_j)$$
$$= \sum_{v_i \neq v_j} \mu_2'(h(v_i), h(v_j))$$
$$= d_\mu[h(v_i)]$$

$$d_\nu(v_i) = \sum_{v_i \neq v_j} \nu_2(v_i, v_j)$$
$$= \sum_{v_i \neq v_j} \nu_2'(h(v_i), h(v_j))$$
$$= d_\nu(h(v_i))$$

■

Corollary 4.2: Converse of the above theorem need not be true.

Example 4.4: Consider the two graphs $G : (V, E)$ and $G' : (V', E')$ which preserving the degree of vertices but G and G' are not isomorphic.

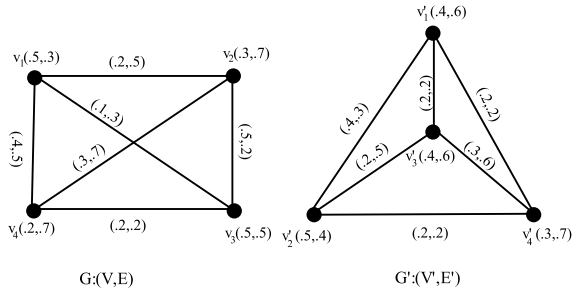

Fig. 5. Graphs preserving the degree of the vertices but not isomorphic

Theorem 4.3: Isomorphism between IFG is an equivalence relation.

Proof: Let $G : (V, E)$, $G' : (V', E')$, $G'' : (V'', E'')$ be IFGs.
(i) Reflexive:

Consider the identity map $h : V \to V$, such that

$$h(v_i) = v_i, \forall v_i \in V \tag{1}$$

This h is bijective map satisfying

$$\mu_1(v_i) = \mu_1(h(v_i)) \tag{2}$$

$$\nu_1(v_i) = \nu_1(h(v_i)), \forall v_i \in V \tag{3}$$

$$\mu_2(v_i, v_j) = \mu_2(h(v_i), h(v_j)) \tag{4}$$

$$\nu_2(v_i, v_j) = \nu_2(h(v_i), h(v_j)), \forall v_i, v_j \in V \tag{5}$$

Hence h is an isomorphism of an IFG onto itself.
(ii) Symmetric:
Let $h : V \to V'$,

$$h(v_i) = v_i', v_i \in V \tag{6}$$

be an isomorphism of G onto G' satisfying,

$$\mu_1(v_i) = \mu_1'(h(v_i)), \nu_1(v_i) = \nu_1'(h(v_i)), \forall v_i \in V \tag{7}$$

$$\mu_2(v_i, v_j) = \mu_2'(h(v_i), h(v_j)) \ and \tag{8}$$

$$\nu_2(v_i, v_j) = \nu_2'(h(v_i), h(v_j)), \forall v_i, v_j \in V \tag{9}$$

from equation (6) we have $h^{-1}(v_i') = v_i, \forall v_i' \in V$,
Therefore,

$$\mu_1(h^{-1}(v_i')) = \mu_1'(v_i'), \nu_1(h^{-1}(v_i')) = \nu_1'(v_i'), \forall v_i' \in V' \tag{10}$$

$$\mu_2(h^{-1}(v_i'), h^{-1}(v_j')) = \mu_2'(v_i', v_j') \ and \tag{11}$$

$$\nu_2(h^{-1}(v_i'), h^{-1}(v_j')) = \nu_2'(v_i', v_j'), \forall v_i', v_j' \in V' \tag{12}$$

which implies $h^{-1} : V' \to V$ is a bijective map and $G' \cong G$.
(iii) Transitive:
Let $h : V \to V'$ and $g : V' \to V''$ be two isomorphisms of the IFGs G onto G' and G' onto G'' respectively.
Then we have to prove that $g \circ h$ is a one $-$ one onto map from V to V'',
where $(g \circ h)(v_i) = g(h(v_i)), \forall v_i \in V$.
As h is an isomorphism, we have, $h(v_i) = v_i', \forall v_i \in V$.

$$\mu_1(v_i) = \mu_1'(h(v_i)), \nu_1(v_i) = \nu_1'(h(v_i)), \forall v_i \in V \tag{13}$$

$$\mu_2(v_i, v_j) = \mu_2'(h(v_i), h(v_j)) \ and \tag{14}$$

$$\nu_2(v_i, v_j) = \nu_2'(h(v_i), h(v_j)), \forall v_i, v_j \in V \tag{15}$$

using equation (6)

$$\mu_1(v_i) = \mu_1'(v_i'), \nu_1(v_i) = \nu_1'(v_i') \tag{16}$$

$$\mu_2(v_i, v_j) = \mu_2'(v_i', v_j') \ and \tag{17}$$

$$\nu_2(v_i, v_j) = \nu_2'(v_i', v_j') \tag{18}$$

As g is an isomorphism from V' to V'', we have,
$g(v_i') = v_i'', v_i' \in V'$ and

$$\mu_1'(v_i') = \mu_1''(g(v_i')), \nu_1'(v_i') = \nu_1''(g(v_i')), \forall v_i' \in V' \tag{19}$$

$$\mu_2'(v_i', v_j') = \mu_2''(g(v_i'), g(v_j')) \ and \tag{20}$$

$$\nu_2'(v_i', v_j') = \nu_2''(g(v_i'), g(v_j')), \forall v_i', v_j' \in V' \tag{21}$$

from equations (16) and (19) and using $h(v_i) = v_i', v_i \in V$, we get

$$\mu_1(v_i) = \mu_1'(v_i') = \mu_1''(g(v_i')),$$
$$\mu_1(v_i) = \mu_1''(g(h(v_i))), \forall v_i \in V$$
$$\nu_1(v_i) = \nu_1'(v_i') = \nu_1''(g(v_i')),$$
$$\nu_1(v_i) = \nu_1''(g(h(v_i))), \forall v_i \in V$$

from equations (17), (18), (20) and (21), we get

$$\begin{aligned}\mu_2(v_i, v_j) &= \mu_2'((v_i'), (v_j')) \\ &= \mu_2''(g(v_i'), g(v_j')) \ , \forall v_i', v_j' \in V' \\ &= \mu_2''(g(h(v_i)), g(h(v_j))), \forall v_i, v_j \in V \\ \nu_2(v_i, v_j) &= \nu_2'((v_i'), (v_j')) \\ &= \nu_2''(g(v_i'), g(v_j')) \ , \forall v_i', v_j' \in V' \\ &= \nu_2''(g(h(v_i)), g(h(v_j))), \forall v_i, v_j \in V\end{aligned}$$

Therefore $g \circ h$ is an isomorphism between G and G''. Hence isomorphism between IFGs is an equivalence relation. ■

V. Properties of Isomorphism on Strong Intuitionistic Fuzzy Graphs

Theorem 5.1: If $G \cong G'$ then G is a strong IFG if and only if G' is also a strong IFG .

Proof: Let $G = (V, E)$ and $G' = (V', E')$ be an IFG. If $G \cong G'$ then there exists an isomorphism $I : V \to V'$, which is bijective that satisfies

$$\mu_1(v_i) = \mu_1'(I(v_i)), \nu_1(v_i) = \nu_1'(I(v_i)), \forall v_i \in V \tag{22}$$

$$\mu_2(v_i, v_j) = \mu_2'(I(v_i), I(v_j)) \ and \tag{23}$$

$$\nu_2(v_i, v_j) = \nu_2'(I(v_i), I(v_j)), \forall v_i, v_j \in V \tag{24}$$

G is a strong IFG if and only if

$$\mu_2(v_i, v_j) = min(\mu_1(v_i), \mu_1(v_j)),$$
$$\nu_2(v_i, v_j) = max(\nu_1(v_i), \nu_1(v_j)), \forall (v_i, v_j) \in E$$

if and only if

$$\mu'_2(I(v_i), I(v_j)) = min(\mu'_1(I(v_i)), \mu'_1(I(v_j)))$$
$$\nu'_2(I(v_i), I(v_j)) = max(\nu'_1(I(v_i)), \nu'_1(I(v_j))), \forall (v_i, v_j) \in E$$

if and only if

$$\mu'_2(v_i', v_j') = min(\mu'_1(v_i'), \mu'_1(v_j'))$$
$$\nu'_2(v_i', v_j') = max(\nu'_1(v_i'), \nu'_1(v_j')), \forall (v_i', v_j') \in E'$$

if and only if G' is also a strong IFG. ■

Theorem 5.2: If G is co-weak isomorphic with a strong IFG G', then G is also a strong IFG.

Proof: If G is co-weak isomorphic with G', then there exists a co-weak isomorphism $I : V \to V'$ which is bijective that satisfies

$$\mu_1(v_i) \leq \mu_1'(I(v_i)), \ \nu_1(v_i) \geq \nu_1'(I(v_i)), \forall v_i \in V \tag{25}$$

$$\mu_2(v_i, v_j) = \mu_2'(I(v_i), I(v_j)) \ and \tag{26}$$

$$\nu_2(v_i, v_j) = \nu_2'(I(v_i), I(v_j)), \forall v_i, v_j \in V \tag{27}$$

Since G_2 is a strong IFG, we've

$$\mu'_2(I(v_i), I(v_j)) = min(\mu'_1(I(v_i)), \mu'_1(I(v_j)))$$
$$\nu'_2(I(v_i), I(v_j)) = max(\nu'_1(I(v_i)), \nu'_1(I(v_j))), \forall v_i, v_j \in V$$

Now we consider,

$$\begin{aligned} min(\mu'_1(I(v_i)), \mu'_1(I(v_j))) &= \mu'_2(I(v_i), I(v_j)) \\ &= \mu_2(v_i, v_j) \\ &\leq min(\mu_{1i}, \mu_{1j}) \\ &\leq min(\mu'_1(I(v_i)), \mu'_1(I(v_j))), \forall (v_i, v_j) \in E \\ \Rightarrow \mu_2(v_i, v_j) &= min(\mu_{1i}, \mu_{1j}), \forall (v_i, v_j) \in E \end{aligned}$$

Now,we consider,

$$\begin{aligned} max(\nu'_1(I(v_i)), \nu'_1(I(v_j))) &= \nu'_2(I(v_i), I(v_j)) \\ &= \nu_2(v_i, v_j) \\ &\leq max(\nu_{1i}, \nu_{1j}) \\ &\leq max(\nu'_1(I(v_i)), \nu'_1(I(v_j))), \forall (v_i, v_j) \in E \\ \Rightarrow \nu_2(v_i, v_j) &= max(\nu_{1i}, \nu_{1j}), \forall (v_i, v_j) \in E \end{aligned}$$

Hence G is a strong IFG. ■

Theorem 5.3: $G = (V, E)$ is a strong IFG if and only if $\bar{G}$ =$(\bar{V}, \bar{E})$ is also a strong IFG

Proof: G is a strong IFG if and only if

$$\mu_2(v_i, v_j) = min(\mu_1(v_i), \mu_1(v_j)),$$
$$\nu_2(v_i, v_j) = max(\nu_1(v_i), \nu_1(v_j)), \forall (v_i, v_j) \in E$$

if and only if

$$\bar{\mu}_2(v_i, v_j) = \begin{cases} 0, & \forall (v_i, v_j) \in E \\ min(\mu_{1i}, \mu_{1j}), & \forall (v_i, v_j) \notin E \end{cases}$$

$$\bar{\nu}_2(v_i, v_j) = \begin{cases} 0, & \forall (v_i, v_j) \in E \\ max(\nu_{1i}, \nu_{1j}), & \forall (v_i, v_j) \notin E \end{cases}$$

Hence,

$$\bar{\mu}_2(v_i, v_j) = min(\mu_1(v_i), \mu_1(v_j)),$$
$$\bar{\nu}_2(v_i, v_j) = max(\nu_1(v_i), \nu_1(v_j)), \forall (v_i, v_j) \in \bar{E}$$

if and only if $\bar{G} = (\bar{V}, \bar{E})$ is a strong IFG. ■

Theorem 5.4: If $G = (V, E)$ is an IFG then

$$S_\mu(G) + S_\mu(\bar{G}) \leq 2 \sum_{v_i \neq v_j} \mu_2(v_i, v_j)$$
$$S_\nu(G) + S_\nu(\bar{G}) \leq 2 \sum_{v_i \neq v_j} \nu_2(v_i, v_j).$$

Proof: By definition, order of G = order of $\bar{G}$. That is

$$O_\mu(G) = O_\mu(\bar{G}),\ O_\nu(G) = O_\nu(\bar{G})$$

$$\mu_2(v_i, v_j) \leq min(\mu_1(v_i), \mu_1(v_j)), \tag{28}$$

$$\nu_2(v_i, v_j) \leq max(\nu_1(v_i), \nu_1(v_j)), \forall (v_i, v_j) \in E \tag{29}$$

$$\bar{\mu}_2(v_i, v_j) = min(\mu_{1i}, \mu_{1j}) - \mu_{2ij}, \forall v_i, v_j \in V \tag{30}$$

$$\mu_2(v_i, v_j) + \bar{\mu}_2(v_i, v_j) = min(\mu_{1i}, \mu_{1j}) \tag{31}$$

Also,

$$\bar{\mu}_2(v_i, v_j) \leq min(\mu_{1i}, \mu_{1j}) \tag{32}$$

From equation(28),(31) and (32), we get

$$\begin{aligned} min(\mu_{1i}, \mu_{1j}) &= \mu_2(v_i, v_j) + \bar{\mu}_2(v_i, v_j) \\ &\leq 2\ min(\mu_{1i}, \mu_{1j}), \forall v_i, v_j \in V \\ \mu_2(v_i, v_j) + \bar{\mu}_2(v_i, v_j) &\leq 2\ min(\mu_{1i}, \mu_{1j}), \forall v_i, v_j \in V \end{aligned}$$

Taking summation on both sides, weget

$$\begin{aligned} \sum_{v_i, v_j \in V} \mu_2(v_i, v_j) + \sum_{v_i, v_j \in V} \bar{\mu}_2(v_i, v_j) \\ \leq\ 2 \sum_{v_i, v_j \in V} min(\mu_{1i}, \mu_{1j}) \end{aligned}$$

By the definition of size, we get

$$\begin{aligned} S_\mu(G) + S_\mu(\bar{G}) &\leq 2 \sum_{v_i, v_j \in V} min(\mu_{1i}, \mu_{1j}) \\ &= 2 \sum_{v_i, v_j \in V} \mu_2(v_i, v_j) \end{aligned}$$

Now,

$$\bar{\nu}_2(v_i, v_j) = max(\nu_{1i}, \nu_{1j}) - \nu_{2ij}, \forall v_i, v_j \in V \tag{33}$$

$$\nu_2(v_i, v_j) + \bar{\nu}_2(v_i, v_j) = max(\mu_{1i}, \mu_{1j}) \tag{34}$$

Also,

$$\bar{\nu}_2(v_i, v_j) \leq max(\nu_{1i}, \nu_{1j}) \tag{35}$$

From equation(29),(34) and (35), we get

$$\begin{aligned} max(\nu_{1i}, \nu_{1j}) &= \nu_2(v_i, v_j) + \bar{\nu}_2(v_i, v_j) \\ &\leq 2\ max(\nu_{1i}, \nu_{1j}), \forall v_i, v_j \in V \\ \nu_2(v_i, v_j) + \bar{\nu}_2(v_i, v_j) &\leq 2\ max(\nu_{1i}, \nu_{1j}), \forall v_i, v_j \in V \end{aligned}$$

Taking summation on both sides, we get

$$\begin{aligned} \sum_{v_i, v_j \in V} \nu_2(v_i, v_j) + \sum_{v_i, v_j \in V} \bar{\nu}_2(v_i, v_j) \\ \leq\ 2 \sum_{v_i, v_j \in V} max(\mu_{1i}, \mu_{1j}) \end{aligned}$$

By the definition of size, we get

$$\begin{aligned} S_\nu(G) + S_\nu(\bar{G}) &\leq 2 \sum_{v_i, v_j \in V} max(\mu_{1i}, \mu_{1j}) \\ &= 2 \sum_{v_i, v_j \in V} \nu_2(v_i, v_j). \end{aligned}$$

■

VI. Conclusion

This paper presents the basic definitions and some properties of isomorphism on strong IFG. We have shown that if $G : (V, E)$ is a strong IFG then its complement is also strong IFG and vice-versa. We've also given the boundary conditions for $\mu-$ size and $\nu-$ size of an IFG. The main motivation of this paper is to encourage IFG researchers to pursue similar ideas in the field in order to advance the use of IFGs in all other fields.

ACKNOWLEDGMENT

The authors would like to thank the University Grants Commission, New Delhi, India for its financial support to Minor Research Project F. MRP - 3365/ 10 (MRP/UGC - SERO) dated 23rd July 2010 and to UGC Research Award No. F. 30 - 1/ 2009 (SA - II) dated 2nd July 2009.

REFERENCES

[1] K. Atanassov, *Intuitionistic Fuzzy Sets:Theory and Applications*, Springer Physica-Verlag, Berlin, 1999.

[2] Bondy,JA and Murthy, U.S.R. *Graph Theory with Applications*, American Elseiver Publishing Co., Newyork, 1976.

[3] M.G. Karunambigai and R. Parvathi, *Intuitionistic Fuzzy Graphs*, Journal of Computational Intelligence, Theory and Applications, Vol. 20, 139-150, 2006.

[4] A. Nagoor Gani and V.T Chandarasekaran, *A First Look at Fuzzy Graph Theory*, by the Allied Publishers Pvt.Ltd, 2010.

[5] A. Nagoor Gani and J. Malarvizhi, *Isomorphism Properties on Strong Fuzzy Graphs*, International Journal of Algorithms, Computing and Mathematics, Vol 2, Number 1, 2009.

[6] A. Nagoor Gani and J. Malarvizhi, *Isomorphism on Fuzzy Graphs*, International Journal of Computational and Mathematical Sciences, 2:4 2008

[7] A. Nagoor Gani and S. Shajitha Begum, *Degree, Order and Size in Intuitionistic Fuzzy Graphs*, International Journal of Algorithms, Computing and Mathematics, Vol 3, Number 3, 2010.

[8] R. Parvathi and M.G. Karunambigai, *Operations on Intuitionistic Fuzzy Graphs*, Proceedings of FUZZ-IEEE 2009, South Korea, 1396-1401, 2009.

[9] A. Shannon , K. Atanassov, *A First Step to a Theory of the Intuitionistic Fuzzy Graphs*, Proc. of the First Workshop on Fuzzy Based Expert Systems (D. akov, Ed.), Sofia, 59-61,1994.

[10] Shannon A., Atanassov K., *Intuitionistic Fuzzy Graphs from α, β and $(\alpha; \beta)$-Levels*, Notes on Intuitionistic Fuzzy Sets, Vol. 1, No. 1, 32-35, 1995.

2011 IEEE International Conference on Fuzzy Systems
June 27-30, 2011, Taipei, Taiwan

Fuzzy Controller Based Output Power Leveling Enhancement for a Permanent Magnet Synchronous Generator

Abdul Motin Howlader, Naomitsu Urasaki, Shantanu Chakraborty, Atsushi Yona and Tomonobu Senjyu
Department of Electrical and Electronics Engineering
University of the Ryukyus
Okinawa, Japan
E-mail: urasaki@tec.u-ryukyu.ac.jp

Dr. Ahmed Y. Saber
Senior Power System Engineer - R&D Department
Operation Technology, Inc.
CA, USA
E-mail: aysaber@ieee.org

***Abstract*—Due to irregular wind velocity, the output power of a wind turbine generator system (WTGS) is fluctuated. There are many methods to propose to generate smooth output power of a wind turbine. For example, energy storage devices, electric double layer capacitors, flywheels are well-known. But these methods are required a significant extra cost for installation and maintenance. In recent years, some researches have been conducted to generate smooth output power by using inertia or by controlling kinetic energy of a wind turbine. The major benefit of this method, it does not require extra energy storage to generate smooth output power. So, it can reduce of a system cost significantly. But this method is reduced output power radically at the steady wind velocity as compare with maximum power point tracking (MPPT) control method. To overcome this problem, this paper is proposed a fuzzy controller based output power smoothing method by controlling kinetic energy of a wind turbine. The generator electrical speed is controlled by the proposed method that helps to generate efficient smooth output power at different wind speeds. The proposed method is compared with conventional method and MPPT control method. The effectiveness of the proposed method is verified by MATLAB SIMULINK with *SimPowerSystems* and *Fuzzy Logic Toolbox*.**

Keywords-wind turbine generator system; power leveling; kinetic energy; inertia; fuzzy controller.

I. INTRODUCTION

Due to crisis of fossil fuels (e.g. coal, oil, gas) and to reduce the emission of CO_2, the world is going to achieve safe, clean and economical energy. In recent years, wind turbine conversion systems (WTCS) have received increasing attention in order to lack of fossil fuels [1]. Especially, variable speed wind turbine (VSWT) system with a power electronics interface has attracted interest. The use of permanent magnet synchronous generator (PMSG) also have increased [2]. Because PMSG has simple structure and high efficiency, it is expected that more large size wind turbine generator (WTG) systems will adapt it. Currently, WTCS using PMSG generally uses AC-DC-AC methods. WTG system using the method does not need to synchronize the rotational speed of the WTG with power system frequency. Moreover, the gearbox can be omitted resulting in lower costs. However, wind energy has a drawback of having only 1/800 gm/cm^3 density as compared with water energy and it is not constant, and wind turbine output power is proportional to the cube of wind speed. As a result, the generated power of WTG is fluctuated. A wind farm with many WTG has a tendency of smoothing output power. Various methods have been utilized to generate smooth wind power, including the use of ultra capacitors [3], superconducting magnetic energy storage (SMES) [4], flywheel energy storage system (FESS) [5], storage batteries, aqua electrolyze fuel cell, and backup generator. Each method has its advantages and disadvantages. The high frequency charge and discharges affect the efficiency of the lead-acid battery thereby shortening its life. SMES and capacitor are very expensive. Aqua electrolyze with fuel cell system is very large. Back-up generator requires operational cost.

Among various control methods for a stand-alone WTGS output power control such as output power smoothing by using pitch angle control or the inertia of wind turbine [2,6,7]. The inertia stores kinetic energy during acceleration of a wind turbine at high wind velocity. It releases kinetic energy during deceleration of a wind turbine at low wind velocity. This phenomenon helps to generate smooth output power of a wind turbine. When wind velocity is fluctuated, the inertia power smoothing technique is effective. This method can generate efficient output power as compared with MPPT control method. On the other hand, when wind velocity moves to steady state, this method reduced output power rapidly as compared with MPPT control method. So, the total system efficiency is decreased at different wind velocities. It is important to overcome this problem.

This paper represents a fuzzy-controller-based output power smoothing method of a WTGS with a PMSG using the inertia. The fuzzy controller system adjust the integral/averaging time (T) at different wind speeds. In a conventional control system, the integral/averaging time (T=6s) remains constant. So, the final outcomes of the controller such as reference electrical speed for WTGS becomes more adjustable by using proposed method. It helps to generate smooth and efficient output power at different wind velocities. The proposed method is compared with conventional and MPPT control methods. The effectiveness of the proposed method is verified by MATLAB SIMULINK environment.

978-1-4244-7316-8/11/$26.00 ©2011 IEEE

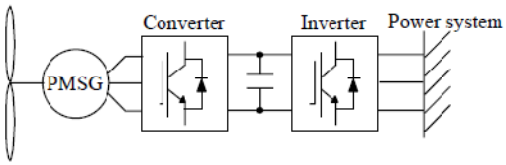

Fig. 1 Gearless wind generation system using PMSG

II. WIND TURBINE CONVERSION SYSTEM

A. System configuration

The system configuration of a WTG system is shown in Fig. 1. Wind power energy is obtained from the wind turbine. It is sent to PMSG. Due to generate maximum power and smoothing power, the rotational speed of PMSG are controlled by the generator-side converter. Here, PMSG output power is supplied to the power system through a generator-side converter and grid-side inverter.

B. Wind turbine model

The input power of wind turbine P_{wind} is expressed as

$$P_{wind} = \frac{1}{2}\rho\pi R_o^2 V_w^3 \quad (1)$$

where R_o is the wind turbine blade radius, V_w is the wind speed and ρ is air density. The wind turbine input torque T_{wind} can be described as

$$T_{wind} = \frac{\lambda}{\omega_w} P_{wind} = \frac{1}{2}\rho\pi R_o^3 V_w^2 \quad (2)$$

where ω_w is the angular velocity of wind turbine and λ is the tip speed ratio, which can be defined as $\lambda = \frac{R_0 \omega_w}{V_w}$. The wind turbine output power P_w and windmill output torque T_w are given by the following equations:

$$P_w = \frac{1}{2} C_p(\lambda,\beta)\rho\pi R_o^2 V_w^3 \quad (3)$$

$$T_w = \frac{1}{2} C_p(\lambda,\beta)\rho\pi R_o^3 V_w^2 / \lambda \quad (4)$$

where β is pitch angle. The wind turbine power coefficient C_p is defined by the following equation :

$$C_p = 0.22\left(\frac{116}{\Gamma} - 0.4\beta - 5\right)\exp^{-\frac{12.5}{\Gamma}} \quad (5)$$

$$\Gamma = \frac{1}{\frac{1}{\lambda + 0.08\beta} - \frac{0.035}{\beta^3 + 1}} \quad (6)$$

The motion equation of wind turbine is expressed as:

$$T_w = J_w \frac{d\omega_w}{dt} + T_{lw} \quad (7)$$

where J_w is the wind turbine inertia and T_{lw} is the load torque which corresponds to the input torque of generator. Input

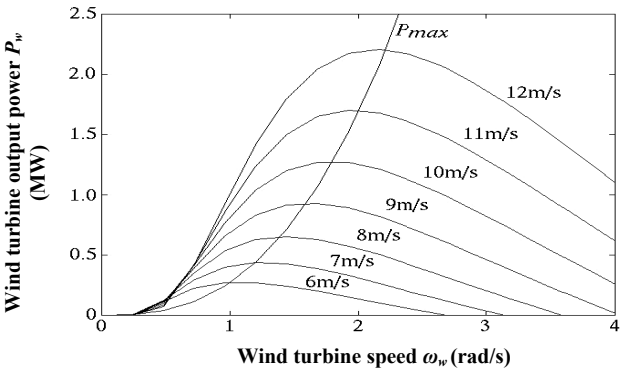

Fig. 2. Wind turbine output power characteristics.

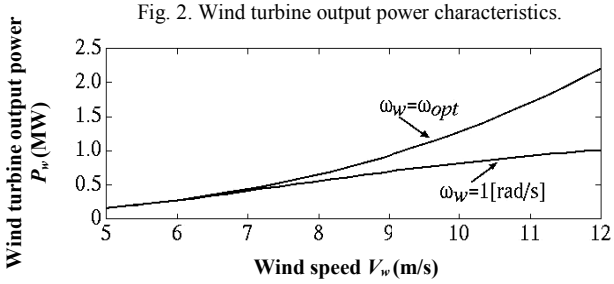

Fig. 3. Wind speed Vs. wind turbine output power characteristics.

power to the generator P_{in} is expressed as

$$P_{in} = -T_{lw}\omega_g \quad (8)$$

where ω_g is the angular velocity of the generator. The output power of generator P_g is expressed as:

$$P_g = -T_e\omega_g \quad (9)$$

where T_e is the generator electric torque.

C. Maximum power point tracking control system

From equations (3) and (5), the wind turbine output power characteristics are described in Fig. 2, from which it can be realized that, for any particular wind speed, there is a rotational speed ω_{opt}, called the optimum rotational speed, which generates the maximum power P_{max}. In this way, the MPPT control for each wind speed increases the energy generation in variable speed wind generation (VSWG) system. The optimum rotational speed ω_{opt} is calculated by differentiating C_p with respect to ω_w. Therefore, ω_{opt} is approximated by

$$\omega_{opt} = 0.2V_w - 0.2 \quad (10)$$

If $\omega_w = \omega_{opt}$, the wind turbine maximum output power P_{max} can be obtained. Fig. 3 shows the simulation results of wind speed versus wind turbine output power characteristics for fixed speed operation and variable speed operation with the MPPT control, where ω_w = 1rad/s is optimum rotational speed for V_w =6 m/s. In case of fixed speed operation, it is clear that energy loss for wind turbine is increased as the distance from 6 m/s. The MPPT control is applied when wind speed V_w is smaller than the rated wind speed $V_{w\text{-}ref}$. If wind speed V_w is greater than the rated wind speed $V_{w\text{-}ref}$, then the output power of

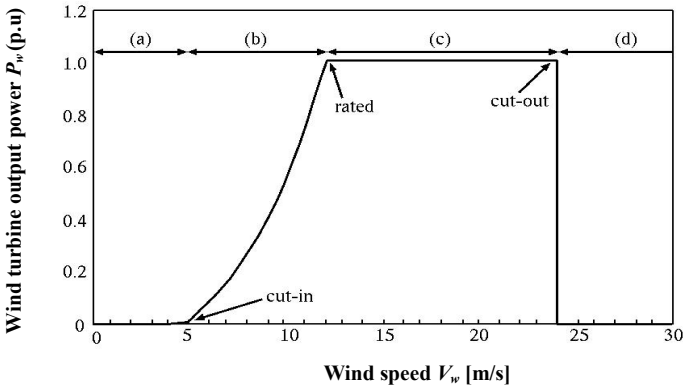

Fig. 4. Pitch angle control law.

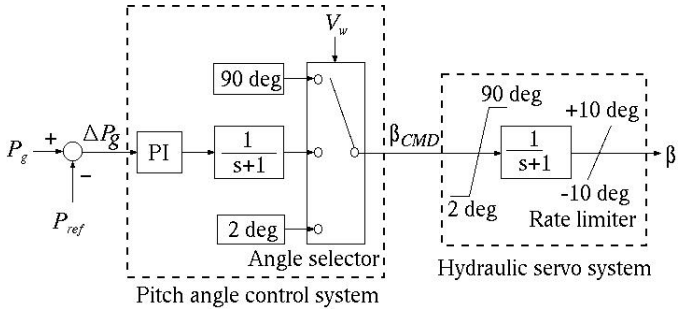

Fig. 5. Pitch angle control system.

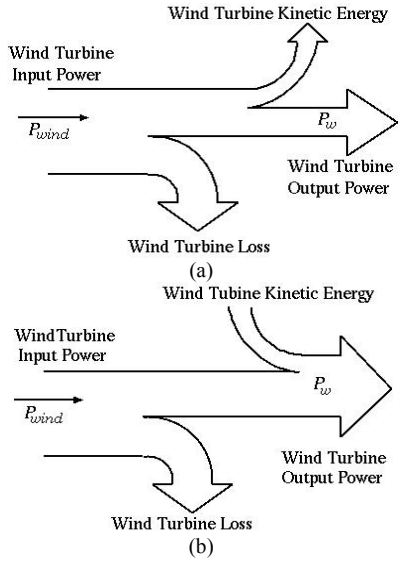

Fig. 6. Power flow (a) acceleration, (b) deceleration.

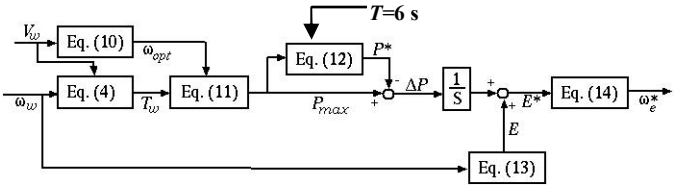

Fig. 7. Conventional power leveling control system.

PMSG is controlled by the pitch angle control system. Pitch angle β is controlled according to the pitch angle control law shown in Fig. 4. For example, in Fig. 4 (a) wind speed range is P_w = 0 pu so that pitch angle is fixed at β= 90° because the energy of the wind turbine is smallest at 90°, (b) is P_w = 0 pu to P_w = 1 pu so that pitch angle is fixed as β = 2°, (c) is P_w = 1 pu so that pitch angle β is selected to keep wind turbine output P_w = 1 pu, and finally, (d) is P_w = 0 pu so that pitch angle is fixed at β = 90° for safety reasons.

Fig. 5 shows the pitch angle control system that resolves pitch angle β, where output power error ΔP_g is used as input into PI controller. Actually, the pitch angle control system includes a hydraulic servo system. The system has nonlinear characteristics, but it is able to make first-order lag system. Therefore, in this paper it is simulated by a first-order lag system where the time constant is 1 s. Moreover, the pitch angle β is limited by a limiter in the range of 2°-90°, and the maximum rate of change is ±10°/s.

III. Output Power Smoothing Control

WTG system output power smoothing is controlled by the both charge and discharge of the kinetic energy in response to the wind speed. The charging stage is occurred when the wind turbine rotational speed accelerates at high wind speed, while discharge follows the deceleration of the wind turbine at low wind speed. Fig. 6 shows the power flow diagram for a WTG system.

A. Conventional power smoothing control system

The conventional output power smoothing control system is shown in Fig. 7. First, wind turbine maximum output power, P_{max} is calculated by

$$P_{\max} = T_w \omega_{opt} \tag{11}$$

Next, the average value of the wind turbine maximum output power is calculated as

$$P^* = \frac{1}{T}\int_{t-T}^{t} P_{\max} dt \tag{12}$$

where t denotes the present time and T is the averaging time. The difference ΔP, between the maximum output power and the average value of maximum output power is calculated. The $\int \Delta P dt$ gives the wind turbine storing and restoring energy. Wind turbine kinetic energy, E, is determined as

$$E = \frac{1}{2} J_{eq} \omega_w^2. \tag{13}$$

where J_{eq}= generator inertia (J_g) + wind turbine inertia (J_w) is equivalent inertia. The wind turbine speed command, ω_w^*, is determined from kinetic energy command, E^* (sum of $\int \Delta P dt$ and E), as

$$\omega_w^* = \sqrt{\frac{2E^*}{J_{eq}}} \tag{14}$$

The generator electrical speed reference ω_e^* for the proposed method, is determined from gear ratio, R_n, and the number of pole pairs p, as

$$\omega_e^* = R_n \omega_w^* p \quad (15)$$

and for the MPPT

$$\omega_e^* = R_n \omega_{opt} p \quad (16)$$

In this paper, the gear ratio R_n is set as 1 because a gearless PMSG is considered.

B. Fuzzy Controller based power leveling control system

The averaging time T in Eq. (12) is one of the key component for the conventional output power smoothing control. When the averaging time becomes large, the output power of the WTG system is reduced and generates smooth output power. In case of the small averaging time, the output power of the WTG system tends to generate same power as the MPPT control system with fluctuation. If the wind velocity is fluctuated in any region, the averaging time will be large to generate smooth output power. On the other hand, when the wind velocity remains steady, the averaging time can be small to generate same power as MPPT control system. But wind velocity for a particular region can be both fluctuated and steady state. So, adjustment is required for the averaging time to achieve maximum efficiency from this power leveling method. Fig. 8 shows the characteristic between the averaging time and the output power of a WTG system. The dotted line is shown the maximum output power of a WTG system during a simulation time. The conventional method output power is moved to the maximum power when the averaging time becomes smaller. From this figure (Fig. 8), it can be realized that a constant averaging time can be decreased the system efficiency at different wind speeds. The conventional power smoothing control method using inertia or controlling kinetic energy is always measured by a constant averaging time.

So, an adaptive averaging time is necessary to improve overall performance of conventional power smoothing method (instead of constant averaging time) for a WTG system. It can be implemented by a fuzzy controller. The wind velocity and fluctuation of wind velocity are online determined an averaging time. The fluctuation of wind velocity is calculated by the first derivative of wind speed. It is an input of fuzzy controller. Another input of fuzzy controller is wind velocity.

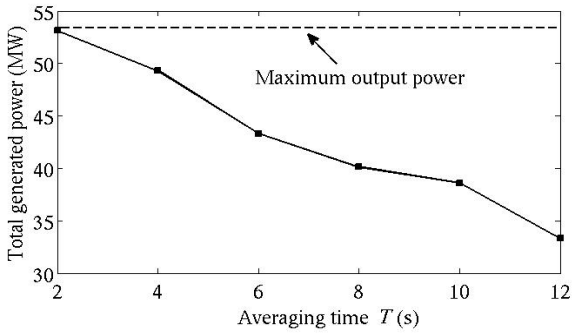

Fig. 8. Averaging time Vs. total generated power characteristics.

Depending on inputs, the fuzzy controller generates a averaging time (T) as an output. The fuzzy membership functions and fuzzy rules are shown in Fig. 9.

The fuzzy rules depict that when the change of wind velocity is large, the averaging time is set to large value. In contrast, the averaging time is small value, when the change of wind velocity is small. In case of wind velocity, when the wind velocity is very large, the averaging time is set to large value. The averaging time is set to small value, when the wind velocity becomes small.

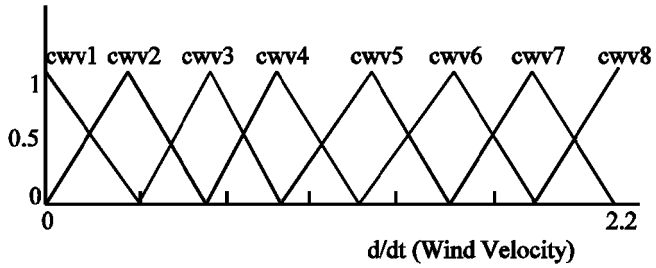

(a)

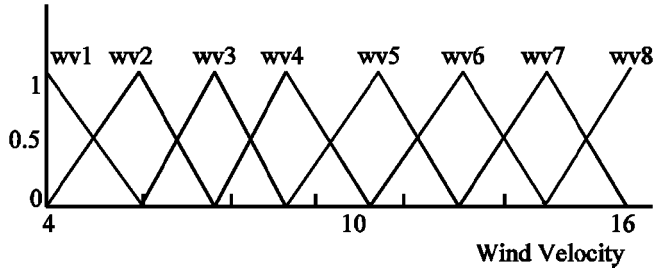

(b)

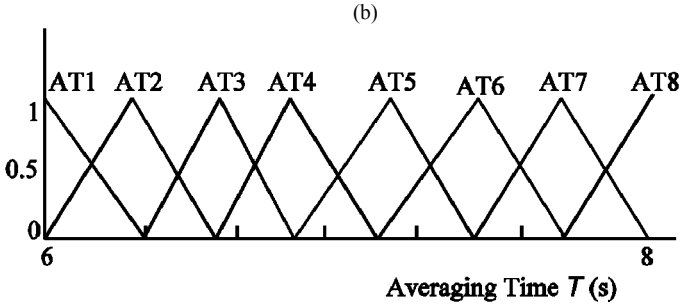

(c)

cwv = Change of wind velocity
wv = Wind velocity
AT=Averaging time

		d/dt(V_w)							
		cwv1	cwv2	cwv3	cwv4	cwv5	cwv6	cwv7	cwv8
V_w	wv1	AT1	AT1	AT1	AT1	AT1	AT2	AT2	AT3
	wv2	AT1	AT1	AT1	AT1	AT2	AT2	AT2	AT3
	wv3	AT1	AT1	AT1	AT1	AT2	AT2	AT3	AT3
	wv4	AT1	AT1	AT1	AT1	AT2	AT3	AT3	AT4
	wv5	AT1	AT1	AT1	AT2	AT2	AT3	AT4	AT4
	wv6	AT1	AT1	AT2	AT2	AT3	AT3	AT5	AT6
	wv7	AT1	AT2	AT3	AT4	AT5	AT5	AT6	AT7
	wv8	AT2	AT3	AT4	AT5	AT6	AT7	AT7	AT8

(d)

Fig. 9. Fuzzy membership functions (a) & (b) Input membership functions (c) Output membership functions and (d) Fuzzy rules

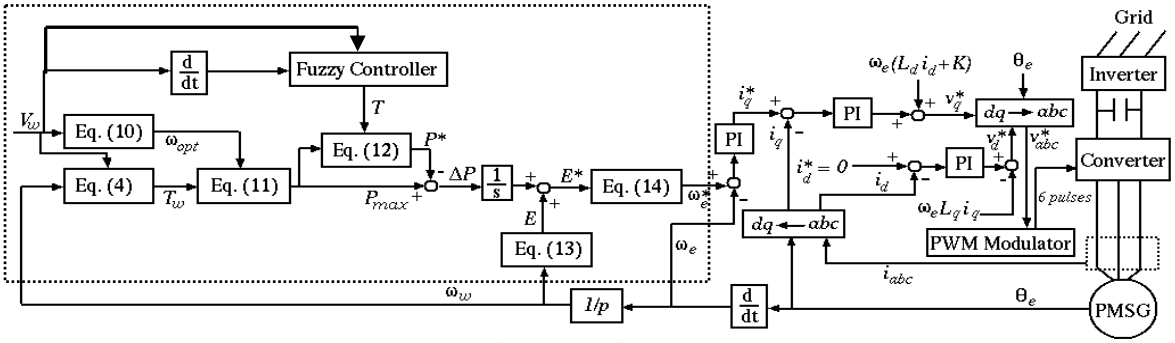

Fig. 10. Control system.

IV. SIMULATION RESULTS

The entire control system of power smoothing method is shown in Fig. 10. The dotted block represents the proposed power smoothing control system. The effectiveness of the proposed fuzzy controller based method is evaluated by the simulation results. The MPPT control method, conventional power smoothing method, and proposed fuzzy based output power smoothing method are compared in this simulation. Simulation parameters of a wind turbine, PMSG, and power converter are shown in Table 1.

The wind velocity is shown in Fig. 11(a). This wind velocity data has significant fluctuation and speed. The Fig. 11(b) and 11(c) are input and output of fuzzy control. From Fig. 11(d), it is observed that the WTGS speed fluctuates significantly. As seen in Fig. 11(e), as the wind velocity increases, the turbine rotational speed accelerates thereby transforming the wind energy into wind turbine kinetic energy.

TABLE 1. Simulation parameters.

Parameters of windmill	
Blade radius	R_o = 41 m
Air density	ρ = 1.205 kg/m^3
Gear ratio	R_n = 1
Equivalent inertia	J_{eq} = 8000 kg.m^2
Rated wind speed	$V_{w\ rated}$ = 12 m/s
Averaging time (conventional method)	T = 6 s
Parameters of PMSG	
Rated power	$P_{g\ rated}$ = 2 MW
Number of poles pair	p = 80
Stator resistance	R_a = 0.1 Ω
Inductance	L = 0.005 H
Field flux	K = 10.68 V.s/rad
Rotational damping	D = 0
Parameters of power converter	
PWM carrier frequency	f_p = 10 kHz
Rated DC-link voltage	$V_{dc\ rated}$ = 7.1 kV

Similarly, as the wind velocity decreases, a discharge of the wind turbine kinetic energy occur, through decrease in turbine rotational speed. Fig. 11(f) shows a comparison of the generator electric torque. The power smoothing method decreases the fluctuation of electric torque significantly as compare with MPPT.

This contributes the reduction of mechanical stress of generator. Fig. 11(g) shows the pitch angle of the wind turbine. Fig. 11(h) shows a comparison of generated output power from the PMSG. From this figure, the proposed method generates smooth output power with high efficiency as compared with conventional method. Both methods are compared with MPPT control method. The conventional method reduced output power significanty when wind velocity becomes steady as compare with MPPT control method.

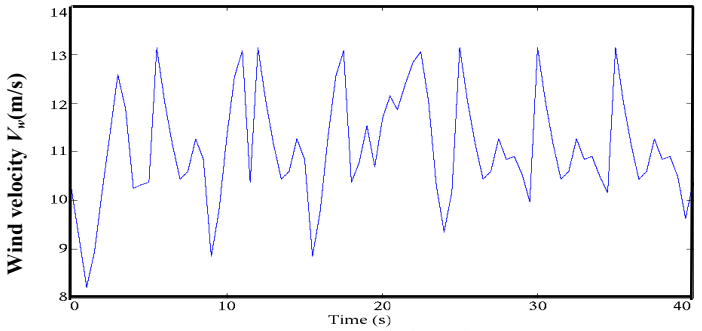

(a) Wind speed

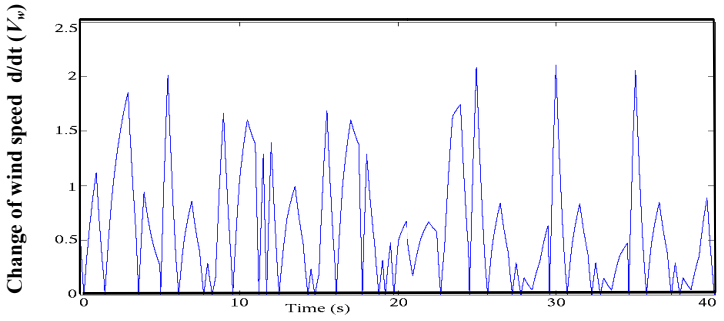

(b) Derivative of wind speed

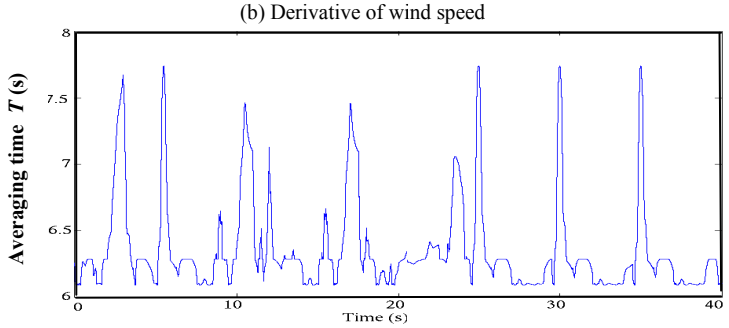

(c) Averaging time

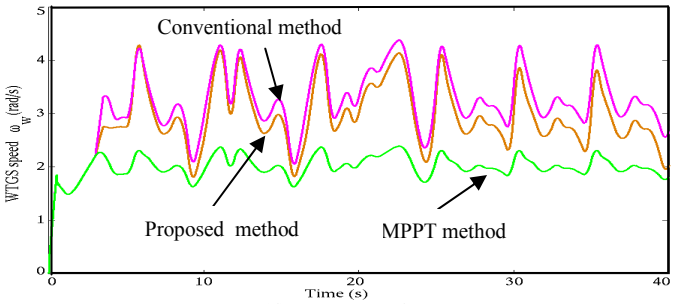

(d) WTGS speed

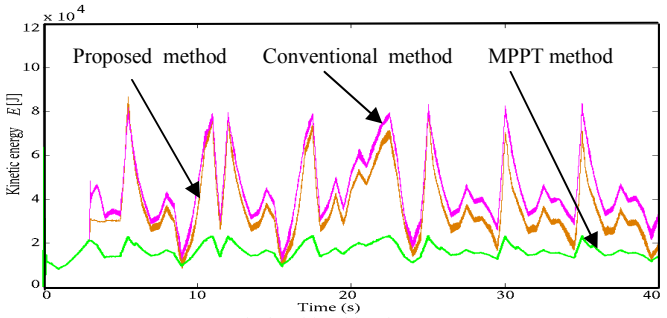

(e) Wind turbine kinetic energy

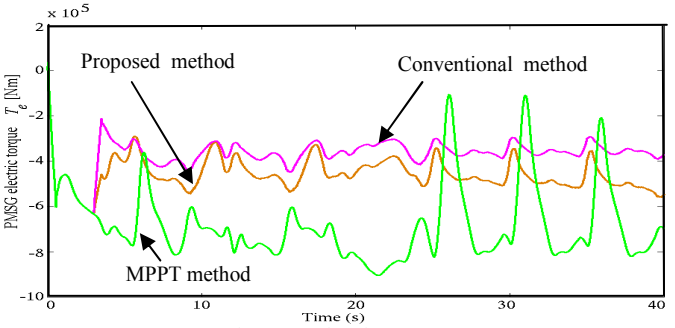

(f) PMSG electric torque

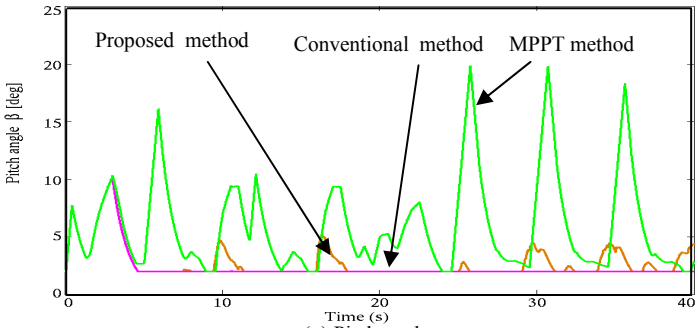

(g) Pitch angle

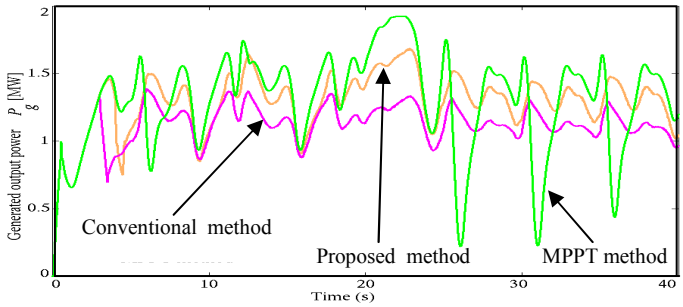

(h) Output power

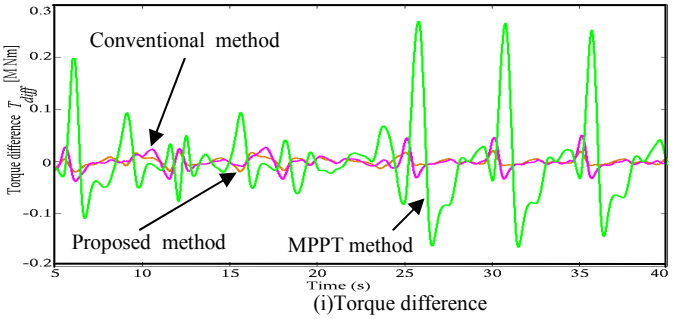

(i)Torque difference

Fig. 11 Simulation results

Fig. 11(i) shows the torque difference which is smoothed extensively as compare with MPPT control method. So, it is possible to mitigate the mechanical stress of the shaft in WTCS.

V. CONCLUSION

A fuzzy controller based output power smoothing method of a wind turbine has been proposed in this paper. It is simulated by using an adaptive averaging or integral time which depends on wind velocity and fluctuation of wind velocity. The conventional system is simulated by a constant averaging time (T=6s). If it is lower than 6s, the generated power will be fluctuated like MPPT method. Alternatively, if it is above than 6s, the performance will be more degraded. The propose method is compared with both conventional method and MPPT control method. The fuzzy based propose method can adjust the averaging time and generates efficient output power smoothing. From the simulation results, the overall performance are improved by using our proposed method.

REFERENCES

[1] A. D. Hansen, and L. H. Hansen, "Wind Turbine Concept Market Penetration over 10 Years (1994-2004)," *Wind Energy*, vol. 10, issue. 1, pp. 81-97, January/February 2007.

[2] D. Sato, and H. Saitoh, "Smoothing Control of Wind Farm Output by Using Kinetic Energy of Variable Speed Wind Power Generators," *T. IEE Japan*, vol. 129-B, no. 5, pp. 580-590, 2009. (in Japanese)

[3] Abbey, C. and Joos, G., "Supercapacitor energy storage for wind energy applications," *IEEE Trans. on Industry Application*, vol. 43, no. 3, pp. 769-776, May-June 2007.

[4] Kinjo, T., Senjyu, T. Urasaki, N., and Fujita, H., "Terminal-voltage and output-power regulation of wind-turbine generator by series and parallel compensation using SMES," *IET Proc. Generation, Transmission & Distribution*, vol. 153, no. 3, pp. 276-282, May 2006.

[5] Lilia Jerbi, Lotfi Krichen, and Abderrazak Ouali, "A fuzzy logic supervisor for active and reactive power control of a variable speed wind energy conversion system associated to a flywheel storage system," *Electric Power Systems Research*, vol. 79, no. 6, pp 919-925, June 2009.

[6] Abdul Motin Howlader, Naomitsu Urasaki, Atsushi Yona, Tomonobu Senjyu, Chul-Hwan Kim, and Ahmed Yousuf Saber, "Output power leveling of a wind generation system using inertia of a wind turbine," *International Journal of Emerging Electric Power Systems*, vol. 10, no. 4, Article 5, 2009.

[7] Senjyu T., Sakamoto R., Urasaki N., Funabashi T., Fujita H., and Sekine H., "Output power leveling of wind turbine generator for all operating regions by pitch angle control," *IEEE Trans. on Energy Conversion*, vol. 21, no. 2, pp. 467-475, June 2006

2011 IEEE International Conference on Fuzzy Systems
June 27-30, 2011, Taipei, Taiwan

Important Issues To Be Considered In Developing Fuzzy Cognitive Maps

Costas Neocleous
Department of Mechanical Engineering
Cyprus University of Technology, Lemesos, Cyprus
costas.neocleous@cut.ac.cy

Christos Schizas
Department of Computer Science
University of Cyprus,
Nicosia, Cyprus
schizas@ucy.ac.cy

Maria Papaioannou
Department of Computer Science
University of Cyprus, Nicosia, Cyprus
cs03pm2@ucy.ac.cy

***Abstract*—The formalism of fuzzy cognitive maps as used for the modeling of various dynamical systems is presented with a critical point of view. Various issues related to terminology, concepts, sensitivities, time dependence, iteration procedures, and stability, are systematically considered with critical mind, aiming at making the overall system models be more realistic and useful, and to initiate discussions that can lead to clarifications and to uniformities. Emphasis is given to applications in social, political, economic and engineering systems.**

Keywords-fuzzy cognitive maps.

I. INTRODUCTION

Fuzzy cognitive maps (FCM) have been used to model dynamical systems in diverse fields, such as in computer science (knowledge representation, reasoning, inference, robotics, adaptation, learning, classification,) engineering (controls, robotics, adaptation), production systems (planning), management (decision making, game theory, logistics), medical/health systems (diagnostics, classification), economic/financial systems, education, environment/ecology, social/political/military systems (policy making, social dynamics, conflict resolution) [1-11].

An FCM is a system of interrelated (interconnected) concepts, also found in literature with many other names such as characteristics, factors, parameters, attributes, states, events, actions, values, goals, trends, components, resources. These concepts embed the dynamical cause-effect relationships that model a specific domain of interest.

The strength (or degree of effectiveness) of the interconnecting relations among the various concepts is governed by the degree that a concept *i* affects a concept *j*. These are called by different names in the literature such as sensitivity, weights, causality, etc. Many a times, for better appraisal of the relevant dynamics, they are graphically represented. In this formalism, the concepts are connected through directed graphs. The intensity of the interrelationships is not clearly known, and not agreed by all concerned. Thus, suitable membership functions may be used. By using appropriate systematic process it is possible to estimate the effect of a change in a specific state (concept) on any other concept (or set of concepts) of the system.

Once the parameters have been identified and initialized, the system is allowed to evolve through appropriate simulation procedures. When and if ultimately the system settles, a researcher/user can observe the effects of a change of one factor on the intensity of another. It is pointed that a modeled system may not quasi-settle to finite states, but rather may go through a limit cycle, or even exhibit chaotic behaviour [12, 13].

The work reported here is mainly involved with a critical examination of some various issues related to terminology, concepts, sensitivities, time dependence, iteration procedures, and stability, in relation to proper functioning of the FCMs, aiming at making the overall system models be more realistic and useful. Ultimately, it is hoped to initiate discussions that can lead to clarifications and to uniformities.

Emphasis is given to applications in social, political, economic and engineering systems.

II. THE FCM SYSTEM

An FCM system of n interrelated concepts, which are connected by causal relations, here called sensitivities, may be represented with the following system of equations.

Let the sensitivity relating the changes in the activation of a concept C_j to changes in the activation of a concept C_i be defined by:

$$s_{ij} \equiv \frac{\partial C_j}{\partial C_i} \tag{1}$$

The total accumulated change in the activation of concept C_j due to changes in concepts C_i is then given by:

$$\delta C_j = \sum_{i,i\neq j}^{n} \frac{\partial C_j}{\partial C_i}\delta C_i = \sum_{i,i\neq j}^{n} s_{ij}\delta C_i \quad (2)$$

where,

C is the activation strength of the concept of interest.

s_{ij} is the sensitivity (weight) as defined in equation 1. The way sensitivity is defined here, it implies that it is a measure on how much a change in the current standing of concept C_i affects the changes in the standing of concept C_j.

In discrete time form the above equation becomes:

$$C_j(t+\delta t) = C_j(t) + \delta C_j = C_j(t) + \sum_{i=1}^{n} s_{ij}\left(\delta C_i\right) \quad (3)$$

and in iterative form can be implemented by:

$$C_j(k+1) = C_j(k) + \sum_{i,i\neq j}^{n} s_{ij}\left(C_i(k) - C_i(k-1)\right) \quad (4)$$

where k is the iteration counter.

In most of the published literature, it is more common to represent the FCM systems in a different form, as shown in equation 5.

$$A_j(k+1) = f\left(A_j(k) + \sum_{i,i\neq j}^{n} w_{ij}A_i(k)\right) \quad (5)$$

or,

$$A_j(k+1) = f\left(\sum_{i,i\neq j}^{n} w_{ij}A_i(k)\right) + A_j(k) \quad (6)$$

where,

A is the activation strength of the concept C.

w_{ij} is the weight (sensitivity)

f is a transformation (smoothening) function, usually of sigmoid form.

The above equation is also found in different variants, such as [5]:

$$A_j(k+1) = f\left(A_j(k)\sum_{i,i\neq j}^{n} w_{ij}A_i(k)\right) - d_j A_j(k) \quad (7)$$

where d_j is a decay factor.

It is pointed here that the suggested approach of equation 4 is different than the approach that is followed by most FCM implementations of equation 5 in two important respects:

i) The weights (sensitivities) are defined differently, as previously explained, and

ii) No smoothening activation function f has been used.

The updating is done quasi-statically and interactively until the system evolves to settlement specified by desired boundaries. Any changes in the various concepts affect either directly or indirectly all the other concepts of the system.

III. Important Considerations When Building FCM

The important aspects to be considered when building and implementing FCMs for systems simulations may be organized as follows:

A. Terminology/Nomenclature

B. Model dynamics

C. Concept identification and initial values

D. Sensitivity identification

E. Smoothening functions

F. Time dependence

In the following exposition, these areas are critically examined. Suggestions for improved FCMs are made wherever possible. The various points that are raise are clarified with appropriate examples. It is hoped that discussions will be initiated that can lead to clarifications and to uniformities.

A. Considerations on terminology and nomenclature.

In the relevant literature there have been different names for different features of FCM. The most diversified nomenclature proposed is for the concepts. The numerous terms that have been used for the concepts are mainly reflecting the application at hand. The most common names given are the following: *Concepts, Characteristics, Factors, Parameters, Attributes, States, Events, Actions, Values, Goals, Trends, Components, Resources.* This is not surprising, and it is not a serious problem when it comes to specific applications. For the fundamental theory though, it creates unnecessary confusions, and it is better to adopt a single term. To this end, we propose the adoption of the term ACTION CONCEPTS, as this term encompasses to a large extend those listed before, and is appropriate for many applications in social sciences, engineering and medicine.

Concerning the notation used, there doesn't seem to be a serious problem by using either A for the activations or action concepts (AC), or C for the concept values. As for the interconnecting strengths, we believe that using the symbol s for sensitivity is better than using w for weights, which are more commonly used for the synaptic weights of the neural network paradigms. The term sensitivity will more easily guide the user to establish more realistic values for the interconnecting strengths.

B. Dynamical modeling.

The most commonly used formalism for describing the system dynamics for an FCM are those shown in equation 5, and the occasional variant expressed in equation 6.

We believe that the form of system dynamics as proposed in equation 4 is more appropriate for two main reasons.

i) It is more compatible with the mathematical expression for finite differentials, and

ii) It does not need to use the smoothening function f, that is quite arbitrary, and poorly or even totally unjustified. Of course if one still wants to use a squashing function with equation 4, then it should be modified as shown in equation 8.

$$C_j(k+1) = f\left(C_j(k) + \sum_{i,i\neq j}^{n} s_{ij}\left(C_i(k) - C_i(k-1)\right)\right) \quad (8)$$

C. Establishing the types of action concepts and their initial values.

With respect to this aspect, there is hardly any disagreement that the important AC that need to be incorporated in an FCM system will have to be identified by highly knowledgeable persons (experts in the field(s)). However, there are certain important issues/questions to be raised. Namely,

i) How certain are we that those AC are indeed the most influential and the most appropriate ones to capture the system dynamics? Maybe it is desirable to assign a degree of certainty (or ignorance) to each AC, that will somehow be embedded in the system. Certainly, the more the experts, the better is the realistic model.
ii) Are these AC constant during the whole period of simulation, or some vanish and others may emanate? This is a problem specific issue that needs to be tackled when a specific system is being modeled. However, the relevant equations and algorithms have to be reformulated.
iii) How independent to each other are? The FCM model to a certain extend, captures this interdependence.

Another important issue in relation to the ACs is how and in what scale to establish the initial values of the ACs in the system under study. For socio-economic-political systems, in the systems that we have simulated, we have adopted a scaling from 0 to 100%.

Thus, it seems that there is some room for improvements in this aspect. It is definitely advantageous to receive information from very many different experts, and if needed to get the weight average from their propositions.

Also, it would be most beneficial if a methodology is being developed that will enable a user to check and verify the relevance of the various ACs and their initial values.

D. Establishing the values of the sensitivities connecting the ACs.

This is one of the most crucial aspects of building FCMs. The comments made in *section C* are also valid for this issue.

In addition, there are also some important aspects such as:

i) Do all the experts have same understanding of the terms that are being used? To this end we propose that the sensitivity is defined by equation 1, that specifies the differential contribution of a change in AC i to a change in AC j. For example, for a social system, a 100% increase (doubling) say in nationalism, to how much (%) is it estimated that the risk of conflict will be?
ii) How certain/fuzzy are they, and how to fuzzify/defuzzify them?
iii) Can these relationships be learned? This can be done, provided there is available a large database of passed cases/examples, as is usually the case with some medical system applications.
iv) How to handle conflicting or even mutually exclusive values proposed by the different experts?
v) Who can be considered as an expert? On what basis? Should they be weighted? Should they be eliminated depending on how well they predict?
vi) Can the sensitivities be extracted through automated procedures, e.g. NEFCLASS?

E. Smoothening (or squashing) functions

To us, the use of squashing functions, especially in sociopolitical systems, is quite artificial and not properly justified. In the system we propose there is no such need. In certain systems though, such as in controls, they may serve the purpose that they were meant, i.e to confine the various values to manageable levels.

F. Time dependence

We think that this is one of the most important aspects that has not been given proper attention. Certain observations are being made that will enable us to find ways to tackle this issue:

i) The various AC have different time responses when they are given a certain sudden change (input). Some respond slowly, others faster. For instance, a new law that makes the learning of a foreign language imperative will affect the students' attitudes many years later. Also, there may be a dead time before a system responds to a certain input. Thus, not only is the time constant (exponential time) important, but also the dead time. Some argue that the logistic sigmoid serves this purpose, but this is not the case, because the response in the functionals f that are used for the sigmoids, is instant.
ii) How can time dependencies be incorporated in an FCM?
iii) In what kind of problems and FCM models are the time dependent issues most important?
iv) How about the problems of synchronization that may be important in real systems? How are they captured in a simplistic iterative method?

Considering the above, then for better representation of real system dynamics, each expert could give also information on the dead time and the time constant associating an AC i to an AC j. Such information will also make the understanding of the problem better, thus enabling a better model of the system of interest.

ACKNOWLEDGMENT

This research is partly supported by the University of Cyprus, the Cyprus University of Technology, and the Cyprus Research Promotion Organization.

REFERENCES

[1] A. Andreou, N. Mateou, and G. Zombanakis, "The Cyprus puzzle and the Greek-Turkish arms race: Forecasting developments using geneticallly evolved fuzzy cognitive maps", Journal of Defence and Peace Making, vol. 14, pp. 293-310, 2003.
[2] P. Groumpos, "Fuzzy cognitive maps: Basic theories and their application to complex systems", Springer Berlin/Heidelberg, 2010.
[3] P. Hanafizadeh, and R. Aliehyaei, "The application of fuzzy cognitive map in soft system methodology", Systemic Practice and Action Research, vol. 1, pp. 1-30, 2010.
[4] K. Lee, and H. Kim, "A fuzzy cognitive map-based bi-directional inference mechanism: An application to stock investment analysis", Intelli-

gent Systems in Accounting, Finance & Management, 6, pp. 41-57, 1997.
[5] N. Mateou, C. Stylianou, and A. Andreou, "Hybrid fuzzy cognitive map modeler", Soft Computing as Transdisciplinary Science and Technology, vol. 29, pp. 851-862, 2005.
[6] C. Neocleous, C. Schizas, and C. Yenethlis, "Application of fuzzy cognitive maps to the political-economic problem of Cyprus" Proceedings of the International Conference on Fuzzy Sets and Soft Computing in Economics and Finance, St Petersburg, pp. 340-349, June 17-20, 2004.
[7] V. Niskanen, "Application of fuzzy linguistic cognitive maps to prisoner's dilemma", ICIC International, pp. 139-152, 2005.
[8] E. Papageorgiou, P. Spyridonos, D. Glotsos, C. Stylios, P. Ravazoula, G. Nikiforidis, and P. Groumpos, "Brain tumor characterization using the soft computing technique of fuzzy cognitive maps", Applied Soft Computing, 8(1), pp. 820-828, 2008.
[9] C. Stylios, and P. Groumpos, "Fuzzy cognitive maps in modeling supervisory control systems", Journal of Intelligent and Fuzzy Systems, vol. 8, pp. 83-98, 2000.
[10] C. Stylios, and P. Groumpos, "Modeling complex systems using fuzzy cognitive maps", IEEE Transactions on Systems, Man, and Cybernetics Part A: Systems and Humans, vol. 34, pp. 155-162, 2004.
[11] A. Tsadiras, and K. Margaritis, "Using certainly neurons in fuzzy cognitive maps", Neural Network World, Prague, pp.719-728, 1996.
[12] Y. Boutalis, T. Kottas, and M. Christodoulou, "Adaptive estimation of fuzzy cognitive maps with proven stability and parameter convergence", IEEE Transactions on Fuzzy Systems, vol. 17, no. 4, pp. 874-889, 2009.
[13] Y. Boutalis, T. Kottas, and M. Christodoulou, "On the existence and uniqueness of solutions for the concept values in fuzzy cognitive maps", Proceedings of 47th IEEE Conference on Decision and Control, Cancun, Mexico, pp. 98-104, 2008.

2011 IEEE International Conference on Fuzzy Systems
June 27-30, 2011, Taipei, Taiwan

A Fall Detection Study on the Sensors Placement Location and a Rule-Based Multi-Thresholds Algorithm Using Both Accelerometer and Gyroscopes

Jerene Jacob, Tam Nguyen, Donald Y.C. Lie
Dept. of Electrical and Computer Engineering Texas Tech University (TTU)
Lubbock, TX 79401 USA
Email: donald.lie@ttu.edu

Steven Zupancic, J. Bishara, Andrew Dentino, and Ron E. Banister
Texas Tech University Health Sciences Center (TTUHSC), Texas Tech University,
Lubbock, TX 79415 USA

Abstract -- **Falls are dangerous among the elderly population and are a major health concern. Many investigators have reported the use of accelerometers for fall detection. In addition, the use of miniature gyroscopes has also been reported to be able to detect falls, but the effects of sensor placement on the back of a person have not been studied thoroughly. In this paper we present a simple solution for effective fall detection using both an accelerometer and two gyroscopes placed, as a single unit, on three different positions along the thoracic vertebrae (i.e., T-4, T-7, and T-10). Results indicated that T-10 was not a good location for the gyroscope placement for fall detection. However, both T-4 and T-7 were suitable, with the results for T-4 being slightly better. Using a simple rule-based multi-thresholds algorithm that utilizes the recorded resultant gravitational acceleration, angular change, angular velocity, and angular acceleration, we were able to successfully detect all 60 falls and differentiate between falls and activities of daily living (ADL) with no false positives on young volunteers. More testing data is needed, especially for backward falls, to test the robustness of our simple algorithm and to improve the sensor portability for future trial studies on geriatric populations.**

Keywords: accelerometer, activities of daily living (ADL), fall detection, gyroscope, T-4, sensor.

I. INTRODUCTION

Unfortunately, falls are very common among the elderly population, which can lead to high health care costs and mortality [1-3]. After a serious fall has occurred, the fear of future falling can also tax a heavy psychological toll on the patient, leading to functional declines and even eventually limit the person to be placed in an institution for the elderly [4]. Numerous researchers have performed fall detection using body-worn accelerometers [5-7]. Several accelerometer-based fall detection reports use simple threshold values to differentiate between falls and activities of daily living (ADL) for patients. These systems mostly rely on a single threshold value to detect whether an activity is considered as a fall or simply an ADL, therefore are prone to false positives. In addition, an accelerometer-only system cannot measure movements with constant velocities and is limited in its use for serious gait analysis for potential fall *prevention* for any individual patient. Similarly, research has been conducted where gyroscopes were used to detect falls [8-9]. This kind of system has been able to clearly distinguish between falls and ADL using simple threshold-based algorithms, as well as providing more info on gaits. Therefore, we have used both an accelerometer and a gyroscope and placed them together at the same location of a person's back for robust fall detection. Most of the reported accelerometers have been placed near the trunk or the thigh region [5-7] and gyroscopes have usually been placed on the anterior aspect of the trunk [8-9]. Since our interest lies on fall detection of the elderly, it is expected that they would rather have a device on their backs than on the front on their chests [10]. Commercially available systems are available (e.g., SwayStar™ [11]) and are rather effective for gait analysis and with very high resolution (<0.01 degree/sec). However, this system is expensive and not FDA-approved. We hope the devices and algorithms we developed can be used eventually as a low-cost alternative to gait and risk of fall analysis.

II. SENSORS BASICS

Finding a suitable location for the placement of both an accelerometer and gyroscopes as an integrated unit is important, as a single fall-detection sensor can be more wearable and the readings can cross-check each other to better distinguish falls vs. ADL. During our testing three places were considered as regions of interests: T-4, T-7 and T-10 in the thoracic vertebrae as shown in Fig. 1. The sensors were built with commercially available components. The accelerometer used is Freescale semiconductor's MMA7341LC, which has a selectable range of +/-3g or +/-11g. In this work the accelerometer is set to +/-11g. The gyroscopes used are the LPR530AL dual axis gyroscope (pitch and roll) and the LY530ALH single axis gyroscope (yaw); both have a sensitivity of +/- 300 °/sec and are from the ST Microelectronics.

978-1-4244-7316-8/11/$26.00 ©2011 IEEE

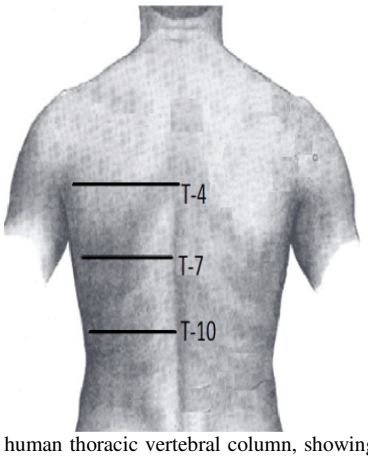

Figure 1: A view of the human thoracic vertebral column, showing regions of interest for sensor placement [12]

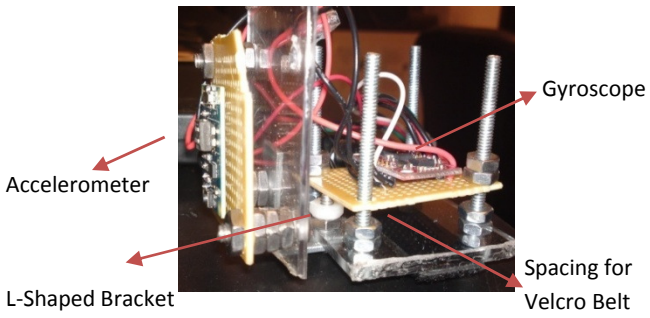

Figure 2: The device that contains the gyroscope and accelerometer sensors with a fixture used in this study. The entire device is 11 cm x 10 cm x 13 cm and weights 0.4 lb, and it can be easily mounted on a person's back.

III. METHODOLGY

Team members volunteered to perform the fall trials. They were asked to fall certain ways (e.g., face first, left side, right side) multiple times per condition to improve the statistical power. The same team members also performed ADL wearing the same sensors shown in Fig. 2.The falls were conducted using three team members falling onto two large stacked 4" thick therapy mats. The team members ranged from 22 to 28 years of age. Each test was repeated five times. Both the gyroscope data and the accelerometer data were collected from the sensors using the National Instruments NI-DAQ™ USB 6009. Matlab™ was used as the main program for both gathering the data as well as data processing. To conduct the fall tests, data was continuously read with the NI-DAQ™ at a sampling rate of 1 kHz. Similarly, ADL were also recorded using the sensors shown in Fig. 2. Since the main idea was to select an optimal location for the placement of the sensors for fall detection, all tests were conducted for all three regions where the sensors are placed (i.e., T-4, T-7 and T-10) and then analyzed. The tests conducted were similar to those reported by Bourke (6,9). In this prototype study, sensors are not tested on any geriatric cohort.

IV. RESULTS

Using the data recorded from the accelerometer and the gyroscopes, a simple rule-based multi-thresholds algorithm was developed to calculate the gravitational acceleration, the angular velocity and the angular acceleration (i.e., the derivative of angular velocity) recorded by the sensors. All these three parameters were calculated for all fall and ADL as shown in Fig. 3. Note that during falls and ADL only the peak values are plotted here. The use of the peak values is important because sometimes the peak value may not always happen during the exact time of the fall but may be occurring slightly afterwards. For example, the accelerometer might record a high value when the subject is about to sit down but the gyroscope will record a high value when the subject is fully upright on the chair. We have, therefore, allowed a freedom of 300ms across the peaks of the accelerometer and gyroscope data. For example if we detect a peak in the accelerometer data at 3.4 s, we will check the gyroscope data between 3.1 to 3.7 seconds to detect a peak in the gyroscope data and vice-versa.

The results from the falls and ADL are shown in Figure 3. We have recorded data from several different falls: falling forward (FF), falling sideways (FS), falling forward knee flexion (FF KF), falling sideways to the right (FSR), and falling sideways to the left (FSL). For ADL we have recorded when the subject is sitting down in a chair, when standing up, and when walking with a norm speed. Looking at the data we can clearly see that T-10 is the worst location for the sensors placement, since there is a large overlap between the highest recorded values for ADL and the lowest recorded values for falls. T-7 and T-4 regions can be used since from the recorded data we can distinguish falls from ADL; however, when we examine the highest recorded values of ADL vs. the lowest recorded values of falls, T-4 sensors data generally exhibits a slightly larger separation with better distinction. For example, the lowest recorded value of falls by the gyroscope was 2.74 rad/sec and of the highest recorded ADL was 2.5 rad/sec when sensors are placed at the T-4 region, while for the T-7 region the highest recorded value of the ADL was 2.34 rad/sec and the lowest value of falls was 2.38 rad/sec. Therefore, T-4 should be close to the optimal location when we place both the integrated 3D gyroscope with the 3D accelerometer at the back for fall detection.

From the data collected, the minimum threshold values for falls were determined for the case of T-4 placement. The equations used to calculate the resultant gravitational acceleration, angular velocity, angular acceleration and total angular change are given below.

$$Resultant\ Gravitational\ Acc. = \sqrt{A_x{}^2 + A_y{}^2 + A_z{}^2}$$

$$Resultant\ Angular\ Velocity = \sqrt{x^2 + y^2 + z^2}$$

$$Resultant\ Angular\ Acc. = \sqrt{(\frac{d}{dt}x)^2 + (\frac{d}{dt}y)^2 + (\frac{d}{d}(z)^2}$$

$$Total\ Angular\ Change = \sum\sqrt{x^2 + y^2 + z^2}$$

The threshold values are set as 2.73g for the accelerometer, 2.74 rad/sec for the resultant angular velocity and 0.04 rad/sec^2 for the resultant angular acceleration. Using these threshold values we were able to distinguish between falls and ADL successfully. From Fig.4, one can see that the data of ADL(i) did not exceed any threshold values (red dashed lines), so it cannot be classified as a fall. For ADL(ii) and Fall(i) shown in Fig. 4, one can see that their angular acceleration are close to each other. Since we also calculate the thresholds of the resultant gravitational acceleration and the resultant angular velocity, and that ADL(ii) only has its angular acceleration close to its threshold, it can not be classified as a fall.

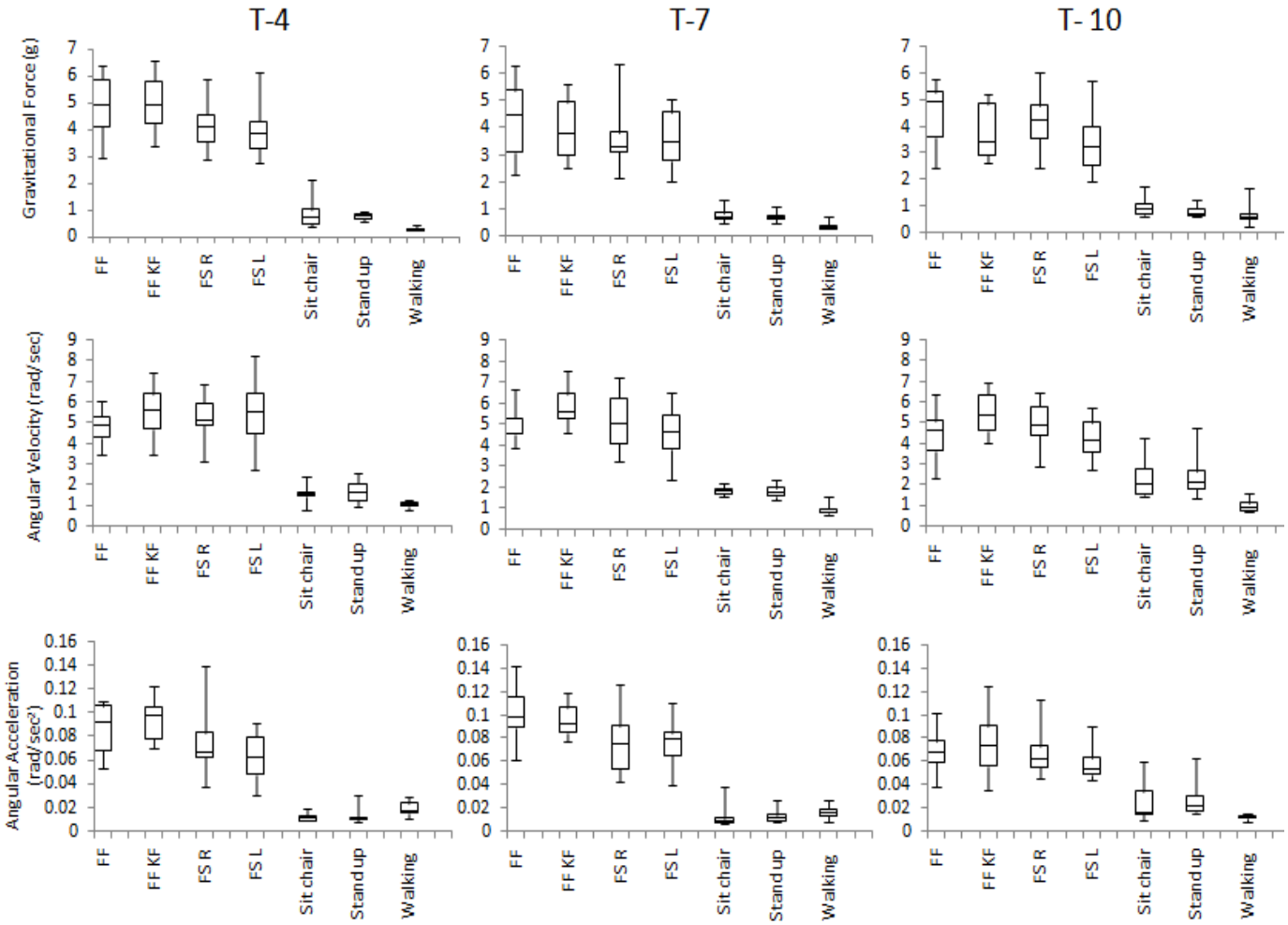

Figure 3: Box plots showing the peak values of measured acceleration, angular velocity and angular acceleration at T-4, T-7 and T-10 for different falls and ADL. FF: Falling Forward, FS: Falling Sideways, KF: Knee Flexion, R: Right, L: Left. The upper edge of each box indicates the 75th percentile of the data value and the lower edge of the box plot indicates the 25th percentile of the data value. The line inside each box indicates the median. The ends of the vertical lines indicate the maximum and the minimum values of each dataset (i.e., the data range).

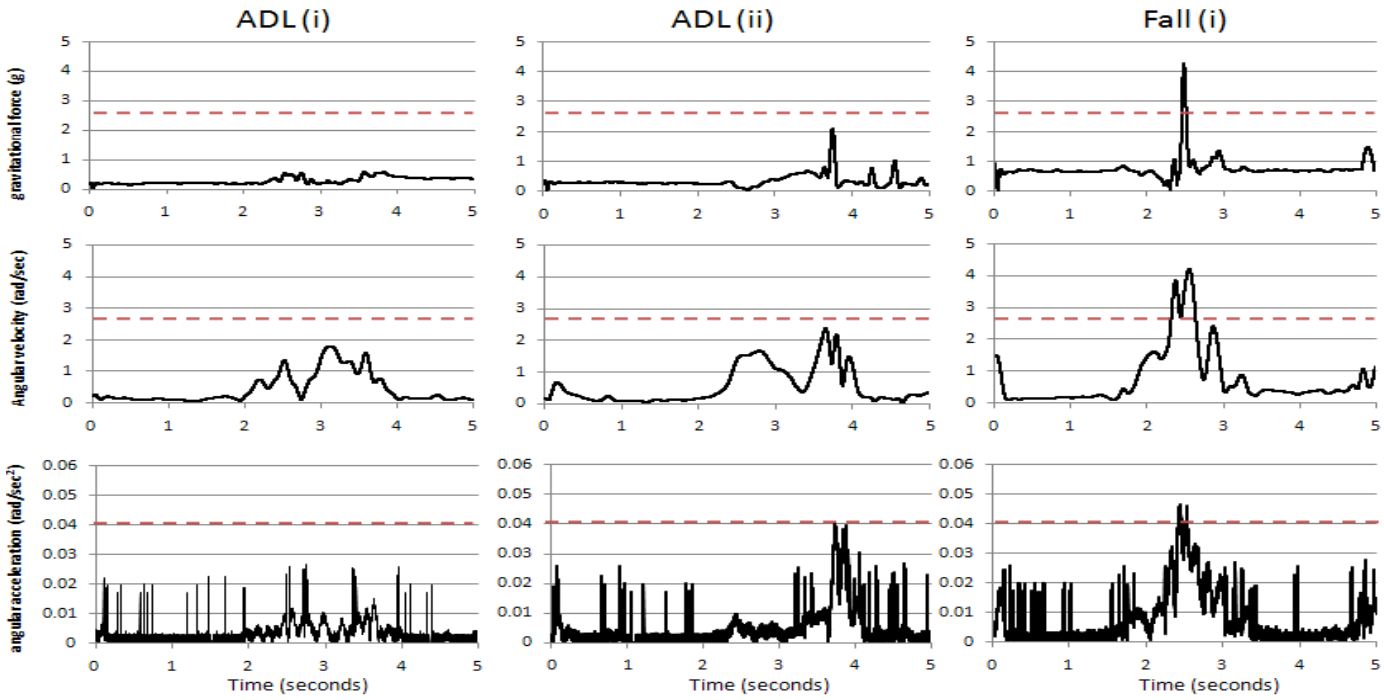

Figure 4: The resultant gravitational acceleration, angular velocity and angular acceleration from several ADL cases. (Left): ADL(i), an ADL that did not exceed any thresholds; (MIDDLE): ADL(ii): an ADL that has only the angular acceleration close to the threshold; and (RIGHT): Fall (i). Note if the sensor data exceeds all three threshold values, it will automatically be classified as a fall.

Note in our initial algorithm, if *all three thresholds* are exceeded, it will automatically be classified as a fall. However, after considering an actual fall case where the sensed data only exceed two threshold value but not three thresholds, we have improved our algorithm by using additional thresholds from the angular changes from the gyroscope data. Fig. 5 shows a flowchart of our simple but effective thresholds-based fall detection algorithm. Note here we also used the total angular change threshold and the thresholds of each axial angular orientation (i.e., the 3 angular changes in the individual axes) in our fall detection algorithm. Here the threshold value for the resultant total angular change was set to be 31° (i.e., "Th4" in Fig, 5). To detect a person falling, a threshold value of -21° in the y-axis is used (i.e., "Th6" in Fig, 5). Similarly, after taking the absolute value of the data from the X-axis, a threshold value of 25° was set (i.e., "Th5" in Fig, 5) and the threshold for angular change in the Z-axis was 21° (i.e., "Th7" in Fig, 5). In this manner, we were able to successfully detect all falls. It needs to be noted that angular change should be used along with other thresholds from the angular acceleration and gravitational force experienced by the sensors. For example, there was one fall case where angular change did not go above any of the threshold values; however, using the entire set of the 4 threshold values, all 60 falls were successfully detected within 2 seconds with no false positives, as will be explained next.

Let us look at these realistic scenarios we encountered: there is one measured fall data that has a peak value of 2.7g, below the gravitational acceleration threshold value of (2.73g); and there is a 2nd fall data that has a peak value of 2.7rad/sec, below the angular velocity threshold of 2.74rad/sec. If we consider a total of 60 falls, and calculate the fall detection sensitivity for this 1st case (Table I, 1st row), we can see that if we use the accelerometer threshold only we will miss detecting this 1st fall and achieve 98.33% sensitivity. Similarly if we use the angular velocity as the only threshold we will miss detecting the 2nd fall and achieve 98.33% sensitivity. Now if we use both the gravitational acceleration and the angular velocity thresholds, the fall detection sensitivity will drop even further because now two falls are not detected since they do not pass both of the two threshold values (i.e., sensitivity of 96.33% in Table I). However, if we take into accounts of the gravitational acceleration, angular velocity, angular acceleration and total angular change as the threshold values (i.e., Th1, Th2, Th3, Th4), and if we consider an event as a fall where as long as three out of the four thresholds have been exceeded, we are able to achieve 100 percent sensitivity as shown in Table 1. Similarly, if we use four out of seven threshold values, we can achieve 100 percent sensitivity as well. Using this simple algorithm that considers all 7 thresholds as shown in Fig. 5, 100 percent specificity is obtained for these 60 falls. More fall data is needed to improve the robustness of the threshold values selection and specificity.

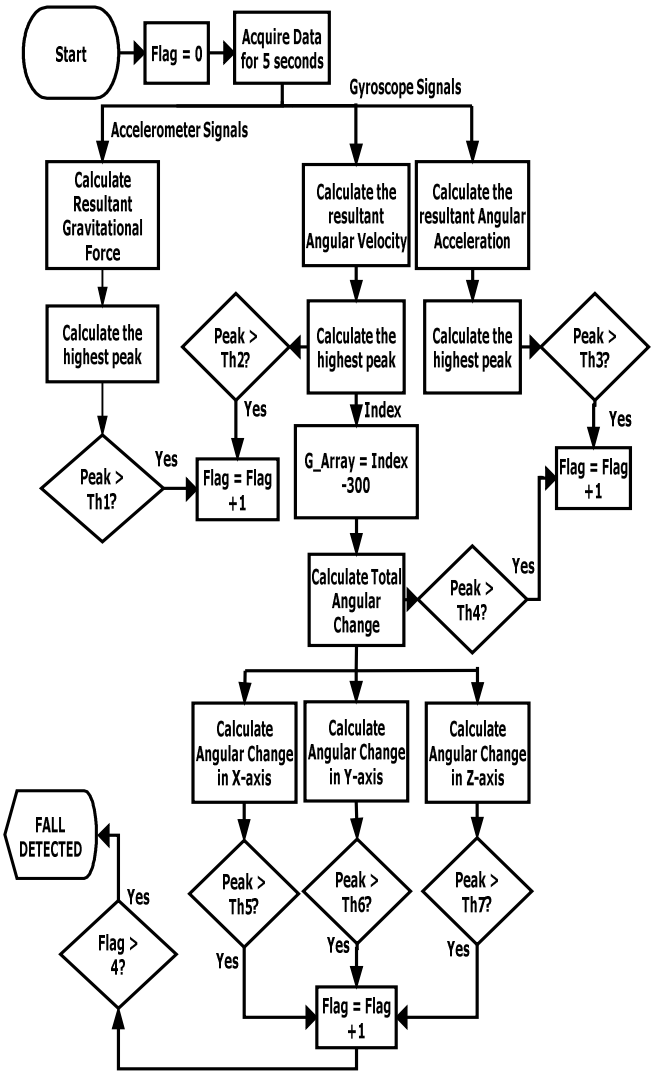

Figure 5: A flowchart of our rule-based multi-thresholds algorithm for fall detection. Th1: accelerometer threshold; Th2: angular velocity threshold; Th3: angular acceleration threshold; Th4: total angular change threshold; Th5: angular change in the X-axis threshold; Th6: angular change in the Y-axis threshold; Th7: Angular change in the Z-axis threshold.

Table I: Fall detection sensitivity percentage obtained using our simple rule-based multi-thresholds algorithm from sensors mounted at T-4.

Different Thresholds to Classify Falls	**Sensitivity (%)**
Accelerometer (Th1) only	98.33
Angular velocity threshold (Th2) only	98.33
Angular acceleration threshold (Th3) only	100
Two thresholds together (Th1, Th2)	96.66
Two thresholds together (Th2,Th3)	98.33
Three thresholds out of four (Th1, Th2, Th3, Th4)	100
Four thresholds out of seven (Th1, Th2, Th3, Th4, Th5, Th6, Th7)	100

V. CONCLUSION AND FUTURE WORK

Placing both the 3-D accelerometer and 3-D gyroscope sensors in different locations on a person's back, we were able to find a suitable location for the concurrent placement of our sensors close to the T-4 region. We also developed a simple thresholds-based algorithm by calculating the gravitational force, the resultant angular velocity, the resultant angular acceleration, etc. In this manner, all 60 falls were successfully detected and with no false positives. In our fall detection algorithm we use the threshold values from the gravitational force, angular velocity and angular acceleration along with the resultant angular change and the angular change of each individual axis. If an event exceeds 4 or more threshold values, then the event will be classified as a fall. Using this simple algorithm we have accomplished a sensitivity of 100 percent with no false positives on young volunteers. Table II shows the summary of our prototype system's preliminary test results on young volunteers compared with other fall detection systems reported.

Presently, the system collects 5 seconds of data and the analysis is later done in MatLab™. This data analysis can be further improved by using real-time software like LABVIEW™ and with wireless transmission and smaller fixture size. It can also be improved by creating an adaptive algorithm along with a height and weight profile to automatically calculate the necessary threshold values for each individual. Therefore, more data needs to be collected, including additional falls (especially backwards falling data that is lacking here in this work) and other activities of daily living. Please note that younger subjects were used in this present work as proxies for older persons as a study limitation. After the data collected on young volunteers demonstrates our sensors and algorithms are effective and robust, we will start conducting testing on a more appropriate cohort using our system.

Table II: Summary and comparison of our system with other fall detection systems.

Paper	Accelero-meter	Gyro-scope	Specificity (%)	Fall Dataset	Placement of sensors
[6]	2	0	100	240	Trunk and Thigh
[8]	2	2	92	70	Chest and Thigh
[9]	0	1	100	240	Sternum
[13]	1	1	96.7	60	Chest
This Work	1	2	100	60	Both on T-4 at back

ACKNOWLEDGMENT

The authors thank our team members for their kind support of performing falls and other tasks. The authors are indebted to the funding support and guidance from Texas Instruments (TI).

REFERENCES

[1] M. E. Tinetti, M. Speechley, and S. F. Ginter, "Risk factors for falls among elderly persons living in the community," N. Eng. J. Med., vol. 319, pp. 1701-1707, 1988

[2] J. Askham, E. Glucksman, P. Owens, C. Swift, A. Tinker, and G. Yu, "Home and leisure accident research: A review of research on falls among elderly people," International Journal of Geriatric Psychiatry, Vol.6, Issue 11, Pg 825, 1990

[3] Centers for Disease Control and Prevention, National Center for Injury Prevention and Control. Web–based Injury Statistics Query and Reporting System (WISQARS) [online]. Accessed December 30, 2010

[4] B.J. Vellas, S.J. Wayne, L.J. Romero, R.N. Baumgartner, and P.J. Garry, "Fear of falling and restriction of mobility in elderly fallers", Age and Ageing 1997;26:189–193

[5] N. Noury, P. Barralon, G. Virone, P. Boissy, M. Hamel, and P. Rumeau , "A smart sensor based on rules and its evaluation in daily routines," Proc. 25th Annual Int'l Conf. of IEEE EMBS, Cancun, Mexico, pp. 3286–3289, Sept 2003

[6] A.K. Bourke, J.V. O'Brien, G.M. Lyons, "Evaluation of a threshold-based tri-axial accelerometer fall detection algorithm. Gait and Posture", 26:194–199, 2007

[7] B. Najafi *et al.* "Ambulatory system for human motion analysis using a kinematic sensor: monitoring of daily physical activity in the elderly", IEEE Trans Biomed Eng 2003; 50: 711–23

[8] Q. Li , J.A. Stankovic, M.A. Hanson, A.T. Barth, J. Lach, and G. Zhou, "Accurate, Fast Fall Detection Using Gyroscopes and Accelerometer-Derived Posture Information", Proc. Sixth Int'l Workshop on Wearable and Implantable Body Sensor Networks, p.138-143, June 03-05, 2009

[9] A.K. Bourke and G.M. Lyons, "A threshold-based fall-detection algorithm using a bi-axial gyroscope sensor" Med. Eng. Phys., 30:84-90, 2008

[10] G. Wu. "Distinguishing fall activities from normal activities by velocity characteristics", J Biomech 2000;33(11):1497–500

[11] Balance International Innovations "SwayStar™" 15th Sept. 2010. http://www.b2i.info/web/index.htm

[12] Henry, Gray. Surface anatomy of the back. 1918. Gray's Anatomy of the Human Body, Pg.1303. Lea & Febiger Philadelphia.

[13] Hwang, J.Y. *et al*. "Development of Novel Algorithm and Real-time monitoring Ambulatory system using Bluetooth module for fall detection in the elderly", Proc. 26th Annual Int'l Conf. of the IEEE-EMBS. San Francisco, CA, USA. September 1-5, 2004

2011 IEEE International Conference on Fuzzy Systems
June 27-30, 2011, Taipei, Taiwan

A Fuzzy Representation for Non-additive Weights of AHP

Shin-ichi Ohnishi
Faculty of Engineering
Hokkai-Gakuen University
Sapporo, Japan
ohnishi@eli.hokkai-s-u.ac.jp

Takahiro Yamanoi
Faculty of Engineering
Hokkai-Gakuen University
Sapporo, Japan
yamanoi@eli.hokkai-s-u.ac.jp

Hideyuki Imai
Graduate School of Information Science and Technology
Hokkaido University
Sapporo, Japan
imai@ist.hokudai.ac.jp

***Abstract* - AHP (Analytic Hierarchy Process) has been widely used in a domain of decision making, and there are a lot of extensions using fuzzy measure and integrals. In the previous research, we propose a kind of sensitivity analyses for AHP or fuzzy measure AHP, because it often occurs that data of AHP loses its reliability. In other words a comparison matrix there in does not always have enough consistency. Also in these cases, the authors propose one representation for weights using results from the sensitivity analysis. In this paper we refine fuzzy weights representation for fuzzy measure AHP. It can show how results of (fuzzy) AHP have fuzziness when the comparison matrix does not have relatively good consistency.**

Keywords-decision making; AHP; fuzzy measure; fuzzy sets; sensitivity analysis

I. INTRODUCTION

The AHP was proposed by Saaty, T.L. in 1977 [2], [3], and it has been widely used in a field of decision making since it includes the natural feelings of human. Normalized eigenvector that corresponds to a Frobenius root of comparison matrix is usually used as weight.

On the other hand, fuzzy measure AHP [4], an extension of the normal AHP, allows us to obtain two types of decisions by use of fuzzy measure. Substitutive and complementary properties are considered in the method.

However, it often occurs that data of fuzzy measure AHP loses its reliability, because a comparison matrix does not always have consistency. The consistency of a comparison matrix A is usually measured by the following consistency index

$$\text{C.I.} = \frac{\lambda_A - n}{n-1} \tag{1}$$

where n is the order of matrix A, and λ_A is its Frobenius root. In these cases, it is very important to investigate how components of a pairwise comparison matrix influence on its consistency or on weights. The sensitivity analysis[5] is useful to investigate them. In this study, the authors apply a sensitivity analysis for fuzzy measure AHP that some of the present authors have proposed before [6]. It evaluates a fluctuation of the consistency index and weights, when a comparison matrix is perturbed. Moreover, we suppose that answers from a decision-maker have ambiguous or fuzziness in these cases. Therefore, it is natural for the weights to be represented by fuzzy sets. Then, we refine the representation by use of results from the sensitivity analysis and fuzzy sets operations.

II. NON-ADDITIVE WEIGHTS OF AHP

Since the weights of criteria in AHP are normalized as their sum becomes 1, it can be regarded as additive measure similar to the probability measure. Because of the additive property of the weights, substitutive and complementary evaluations are not considered in the normal AHP. The substitutive evaluation prefers an alternative that is particularly excellent, and the complementary evaluation prefers one with as few defects as possible. Further, reversals of priority orders can occur due to the addition of a similar criterion.

Meanwhile, with fuzzy measure AHP[4], we can obtain two types of decisions using the possibility measure and the necessity measure that are non-additive fuzzy measure. Substitutive and complementary decisions are considered in it. Results from the normal AHP can be regarded as the midway evaluation between substitutive and complementary. Moreover, the reversals of the priority orders due to the addition of a similar criterion are mitigated.

Let x_i and $\boldsymbol{w}=(w_i)$ $(i=1,\ldots, n)$ denote criteria and their weights, y_p $(p=1,\ldots,m)$ be the alternatives, and $f_p(x_i)$ be a weight of x_i with respect to y_p. In the normal AHP the weight $\boldsymbol{w}$ is normalized as their sum of components becomes 1. But in fuzzy measure AHP, $\boldsymbol{w}$ is considered to be possibility measure (or necessity measure). Therefore, w_i is regarded as the degree of importance expressed by possibility (or necessity) measure of the i-th criterion. Weight $\boldsymbol{w}$ is eigenvector as in normal AHP, however the conditions are $0 \leqq w_i \leqq 1$, and $\exists i$, $w_i=1$. Weights $f_p(x_i)$ only satisfy $0 \leqq f_p(x_i) \leqq 1$. When w_i takes q values $r_1 < r_2 < \ldots < r_q = 1$, we can make a set A_l such as

$$A_l = \{x_i \mid w_i \geq r_l\}, \quad (l = 1,\ldots,q) \tag{2}$$

Thus, the basic probability assignment of A_l becomes

$$m(A_l) = r_l - r_{l-1} \tag{3}$$

where $r_0=0$. The upper limit expectation E^* based on possibility measure and the lower limit expectation E_* based on necessity measure are found as follows

$$E_p^* = \sum_l^q m(A_l) \max_{x \in A_l} f_p(x), \quad (4)$$

$$E_{*p} = \sum_l^q m(A_l) \min_{x \in A_l} f_p(x). \quad (5)$$

Accordingly, the most preferable alternatives are

$$y^* = \{y_p \mid \max_p E_p^*\},$$

$$y_* = \{y_p \mid \max_p E_{*p}\}.$$

If a decision-maker desires a substitutive decision, then y^* is acceptable. And if he or she prefers a complementary decision, y_* is acceptable.

It should be noted that weights of alternatives y^* and y_* in fuzzy measure AHP are not fuzzy value but crisp, although fuzzy measure is used.

III. Sensitivity Analyses

When we actually use AHP, it often occurs that a comparison matrix is not consistent or that there is not great difference among the overall weights of the alternatives. In these cases, it is very important to investigate how components of the pairwise comparison matrix influence on its consistency or on the weights. To analyse how results are influenced when a certain variable has changed, we can use sensitivity analysis.

In this study, we use a method that some of the present authors have proposed before. It evaluates a fluctuation of the consistency index and the weights when the comparison matrix is perturbed. It is useful because it does not change a structure of the data.

Since the pairwise comparison matrix is a positive square matrix, Perron-Frobenius theorem holds [1]. From Perron-Frobenius theorem, following theorem about a perturbed comparison matrix holds.

Theorem 1 *Let $A = (a_{ij})$, $(i, j = 1, \ldots, n)$ denote a comparison matrix and let $A(\varepsilon) = A + \varepsilon D_A$, $D_A = (a_{ij} d_{ij})$ denote a matrix that has been perturbed. Let λ_A be the Frobenius root of A, $\boldsymbol{w}$ be the eigenvector corresponding to λ_A, and $\boldsymbol{v}$ be the eigenvector corresponding to the Frobenius root of A'. Then, a Frobenius root $\lambda(\varepsilon)$ of $A(\varepsilon)$ and a corresponding eigenvector $\boldsymbol{w}(\varepsilon)$ can be expressed as follows*

$$\lambda(\varepsilon) = \lambda_A + \varepsilon \lambda^{(1)} + o(\varepsilon), \quad (6)$$

$$\boldsymbol{w}(\varepsilon) = \boldsymbol{w} + \varepsilon \boldsymbol{w}^{(1)} + \boldsymbol{o}(\varepsilon), \quad (7)$$

where

$$\lambda^{(1)} = \frac{\boldsymbol{v}' D_A \boldsymbol{w}}{\boldsymbol{v}' \boldsymbol{w}}, \quad (8)$$

$\boldsymbol{w}^{(1)}$ is an n-dimension vector that satisfies

$$(A - \lambda_A I)\boldsymbol{w}^{(1)} = -(D_A - \lambda^{(1)} I)\boldsymbol{w}\ , \quad (9)$$

where $\boldsymbol{o}(\varepsilon)$ denotes an n-dimension vector in which all components are $o(\varepsilon)$.

About a fluctuation of the consistency index, following corollary can be obtained from Theorem 1.

Corollary 1 *Using appropriate g_{ij}, we can represent the consistency index* C.I.(ε) *of the perturbed comparison matrix $A(\varepsilon)$ as follows*

$$\text{C.I.}(\varepsilon) = \text{C.I.} + \varepsilon \sum_i^n \sum_j^n g_{ij} d_{ij} + o(\varepsilon). \quad (10)$$

To see g_{ij} in the equation (10) in Corollary 1, how the components of a comparison matrix impart influence on its consistency can be found.

A. Analysis for weights of normal AHP

About the fluctuation of the weights, following corollary also can be obtained from Theorem 1.

Corollary 2 *Using appropriate $h_{ij}^{(k)}$, we can represent the fluctuation $\boldsymbol{w}^{(1)} = (w_k^{(1)})$ of the weight* (*i.e. the eigenvector corresponding to the Frobenius root*) *as follows*

$$w_k^{(1)} = \sum_i^n \sum_j^n h_{ij}^{(k)} d_{ij}. \quad (11)$$

From the equation (7) in Theorem 1, the component that has a great influence on weight $\boldsymbol{w}(\varepsilon)$ is the component which has the greatest influence on $\boldsymbol{w}^{(1)}$. Accordingly, from Corollary 2, how components of a comparison matrix impart influence on the weights, can be found, to see $h_{ij}^{(k)}$ in the equation (11).

Calculations or proofs of these theorem and corollaries are shown in [8].

B. Analysis for fuzzy measure AHP

About the fluctuation of the basic probability assignment, following corollary also can be obtained from corollary 2..

Corollary 3 *Using appropriate $e_{ij}^{(k)}$, we can represent the fluctuation $m(A_l)^{(1)}$ of the basic probability assignment as follows*

$$m(A_l)^{(1)} = \sum_i^n \sum_j^n e_{ij} d_{ij} + o(\varepsilon) \quad (12)$$

(Proof)

Let $\boldsymbol{w}(\varepsilon) = (w(\varepsilon)_i)$, $(\max w(\varepsilon)_i = 1)$ be the eigenvector that corresponds to the Frobenius root of the perturbed comparison matrix $A(\varepsilon)$. It is possible to replace the elements as arranged the order from the smallest. When $w(\varepsilon)_i$ takes q values $r(\varepsilon)_1 < r(\varepsilon)_2 < \ldots < r(\varepsilon)_q = 1$, from formula (2) the basic probability assignment is

$$m(A_l)(\varepsilon) = r(\varepsilon)_l - r(\varepsilon)_{l-1} \quad (13)$$

$$r(\varepsilon)_0 = 0, \quad (l = 1,...,q)$$

and from Corollary 2, it can be expressed as

$$m(A_l)(\varepsilon) = m(A_l) + \varepsilon \sum_i^n \sum_j^n (h_{ij}^{(l)} - h_{ij}^{(l-1)}) d_{ij} + o(\varepsilon) \qquad (14)$$

However, different from the proof of corollary 2 of normal AHP, we should be careful that the standard of the calculation of $h^{(l)}_{ij}$ is w_t=0, where t is satisfied max $w_i = w_t$.

(Q.E.D)

Following theorem can be obtained from the process of fuzzy measure AHP and Corollary 3.

Theorem 2 *Let $A = (a_{ij})$, $(i, j = 1,..., n)$ be a comparison matrix and E^*_p $(p= 1,...,m)$ be the overall weight of the p-th alternative be. Let E^*_p (ε) denote weight of the p-th alternative based on a perturbed comparison matrix $A(\varepsilon) = A+ \varepsilon D_A$, $D_A=(a_{ij}d_{ij})$. Then using appropriate $z_{ij}^{(p)}$, weights $E^*_p(\varepsilon)$ is represented as*

$$E^*_p(\varepsilon) = E^*_p + \varepsilon \sum_i^n \sum_j^n z_{ij}^{(p)} d_{ij} + o(\varepsilon). \qquad (15)$$

(Proof)
Let $f_p(x_i)$ denote weight of the criterion x_i of alternative p. From equation (4) and Corollary 3, the upper limit expectation (substitutive evaluation value) becomes as follows.

$$E^*_p(\varepsilon) = E^*_p + \varepsilon \sum_i^n \sum_j^n \{\sum_l^q (h_{ij}^{(l)} - h_{ij}^{(l-1)}) \max_{x \in A_l} f_p(x)\} d_{ij} + o(\varepsilon) \qquad (16)$$

Accordingly, the fluctuation part of the weight of the alternatives is also expressed by the linear combination of d_{ij}.
(Q.E.D)

From Theorem 2, the component of the comparison matrix that has the greatest influence on weight $E^*_p(\varepsilon)$ can be found. In a complementary case, evaluation also becomes possible with a similar way.

IV. Fuzzy Weights Representations

It often occurs that data of fuzzy measure AHP loses its reliability, when a comparison matrix has not so good consistency (i.e. 0.1<C.I.<0.2). In these cases, we consider that components of a comparison matrix of criteria have fuzziness, because they are results from fuzzy judgement of a decision-maker. Therefore weights could be treated as fuzzy sets. Here, to represent fuzziness of weights of alternatives, we use L-R fuzzy number.

The multiple of coefficients $g_{ij}z_{ij}^{(p)}$ found in Corollary 1 and Theorem 2 is considered as the influence concerned with a_{ij} from the fluctuation of the consistency index.

Since g_{ij} is always positive, if the coefficient $z_{ij}^{(p)}$ is positive, the real weight of alternative p is considered as bigger than E^*_p, and if $h_{ij}^{(k)}$ is negative, the real weight of criterion k is considered as smaller. Therefore, a sign of $z_{ij}^{(p)}$ represents a direction of a spread of the fuzzy number. Of course the absolute value $g_{ij}|z_{ij}^{(p)}|$ represents the amount of the influence.

On the other hand, C.I. becomes bigger then the judgement becomes fuzzier.

Consequently, multiple C.I. $g_{ij}|z_{ij}^{(p)}|$ can be regarded as a spread of a fuzzy weight $\widetilde{E}^*_p$ concerned with a_{ij}.

Definition (fuzzy weights for fuzzy measure AHP) *Let E^*_p be the crisp weight of alternative p in fuzzy measure AHP using possibility measure. g_{ij}, $z_{ij}^{(p)}$ denote the coefficients found in Corollary* 1 *and Theorem* 2 and C.I. *denotes consistency index of the comparison matrix of the criteria. When* C.I.<0.2 *holds, a fuzzy weight $\widetilde{E}^*_p$ is defined by*

$$\widetilde{E}^*_p = (E^*_p, l_p, r_p)_{LR} \qquad (17)$$

where

$$l_p = \text{C.I.} \sum_i^n \sum_j^n s(-, z_{ij}^{(p)}) g_{ij} |z_{ij}^{(p)}|, \qquad (18)$$

$$r_p = \text{C.I.} \sum_i^n \sum_j^n s(+, z_{ij}^{(p)}) g_{ij} |z_{ij}^{(p)}|, \qquad (19)$$

$$s(+, z) = \begin{cases} 1 & (z > 0), \\ 0 & (z \le 0), \end{cases}$$

$$s(-, z) = \begin{cases} 0 & (z > 0), \\ 1 & (z \le 0). \end{cases}$$

We can calculate the fuzzy weights of alternatives in fuzzy measure AHP using Definition 1. They show how the result from fuzzy measure AHP has fuzziness. In a complementary case, it is also possible to represent with a similar way.

And this definition can be used when weights of the alternatives with respect to criterion is also fuzzy number weights, even if comparison matrices of alternatives do not have enough consistency.

V. Conclusions

We propose one representation of the weights of fuzzy measure (non–additive weight) AHP by use of fuzzy sets and the result of the sensitivity analysis. It will be useful for case for the cases that consistency of a comparison matrix is not so good. It was refined from our old representation. It can show not only how to represent weights, but also how the result from the fuzzy measure AHP has fuzziness, especially when some bad consistency exists.

References

[1] M. Saito, An Introduction to Linear Algebra. Tokyo University Press, 1966.

[2] T. L. Saaty, "A scaling method for priorities in hierarchical structures," J. Math. Psy., 15(3), pp. 234-281, 1977.

[3] T. L. Saaty, The Analytic Hierarchy Process. McGraw-Hill, New York, 1980.
[4] T. Terano, K. Asai and M. Sugeno, An Introduction to Applied Fuzzy System. Ohm-sha, Tokyo, 1989.
[5] Y. Tanaka, "Recent advance in sensitivity analysis in multivariate statistical methods," J. Japanese Soc. Comp. Stat., 7(1), pp. 1-25, 1994.
[6] S. Ohnishi, H. Imai and M. Kawaguchi, "Evaluation of a stability on weights of fuzzy analytic hierarchy process using a sensitivity analysis," J. Japan Soc. for Fuzzy Theory and Sys., 9(1), pp. 140-147, 1997.
[7] S. Ohnishi and H. Imai, "Evaluation for stability of fuzzy decision making using a sensitivity analysis," 1998 Conference of the NAFIPS, U.S.A, pp. 86-90, August 1998.
[8] S. Ohnishi, H. Imai and T. Yamanoi, "Weights representation of analytic hierarchy process by use of sensitivity analysis," Proceedings of the conference IPMU'2000, II, pp. 801-806, 2000.
[9] S. Ohnishi, H. Imai and T. Yamanoi, "Weights representation of fuzzy decision making by use of sensitivity analysis," Proceedings of the conference IPMU'2002, pp. 39-42, 2002.
[10] S. Ohnishi, H. Imai and T. Yamanoi, "A fuzzy weights representation for inner dependence AHP," Journal of Advanced Computational Intelligence and Intelligent Informatics, Vol. 15, No.3, in press.

2011 IEEE International Conference on Fuzzy Systems
June 27-30, 2011, Taipei, Taiwan

A Social Cognitive Framework of Knowledge Contribution in the Online Community

Fan-Chuan Tseng
Department of Business and Management
National University of Tainan
Tainan, Taiwan
misfctseng@gmail.com

Feng-Yuan Kuo
Department of Information Management
National Sun Yat-Sen University
Kaohsiung, Taiwan
kuofengyang@gmail.com

***Abstract*—In recent years, knowledge management has become an important issue for many organizations to boost their intellectual capital and business performance. Rather than the emphasis of system functions, a social cognitive model is proposed to examine the associations among members' cognition, interpersonal relationships, and their knowledge contribution behavior. The research results demonstrate that the online members' outcome expectancy, personal efficacious beliefs, as well as the strength of online ties among online peers, have positive and direct influence on their knowledge contribution behavior. Moreover, the mediating effects of outcome expectancy and self-efficacy are both significantly proved on members' engagement in knowledge contribution.**

Keywords-knowledge contribution, outcome expectancy, self-efficacy, knowledgecontribution satisfaction, strength of ties

I. INTRODUCTION

An online community, established and developed through information and computer technology, is composed of individuals with the same goals or similar needs. This new type of interpersonal networks have impact on activities like retrieving and using of community resources, taking collective actions, seeking emotional comfort, and developing working strategies [1, 2]. Even though the benefit of knowledge management has been widely recognized, information technology is not a solution to all problems. Behavior of learning and knowledge sharing has to be interactively adjusted among personal beliefs and the environment [3, 4]. knowledge management is not an objective and individual phenomenon in an organization [5], but is embedded in the close connection among individuals, environment and behaviors that are constantly under the influence of social background, system regulations and interpersonal interactions [3, 6, 7].

The purpose of this research expects to demonstrate the reciprocal relationships among individuals' cognition and affection toward knowledge contribution engagement. In this paper, we focus on the social cognitive and interpersonal relationship perspectives to explore individuals' outcome expectation toward online knowledge community participation, personal efficacious beliefs and satisfaction in knowledge contribution, as well as members' relational ties emerged in the online environment, where the knowledge contribution behavior further arises.

II. THEORETICAL BACKGROUND AND RESEARCH HYPOTHESES

A. Outcome Expectancy

According to Vroom's expectancy theory, the reason why an individual takes certain action is not just because of his special likes, but also depends on his judgment on the possibility of expected results [8]. An outcome expectation indicates the judgment of the likely consequences that one specific action will produce [9]. The attractiveness and expectancy of goal attainment would affect an individual's determination and promise to achieve certain goals, by making effort to fulfill the goal and would not give up easily [10]. Behavior of knowledge contribution comes from the expectation and satisfaction with extrinsic rewards and reciprocal relationships [11]. Only when they are certain that sharing can create other benefits, like monetary rewards, respect from others, or contribute to maintaining reciprocal relationships with others will knowledge sharing be smoothly processed. People think that they can actually fulfill some kind of expectation and benefits through the sharing and reuse of knowledge, they will be encouraged to participate in related activities [12], such as acquiring new knowledge, getting recreation and entertainment, enhancing interpersonal communication, promoting professional skills, and enhancing closeness of family.

According to perspective of public good, an individual's willingness to share knowledge with others is considered to be the collective benefits of the social community but not their own profits [3, 13]. Through sharing and solving other people's problems, one feels pleasant and recognizes the value of oneself. Besides, the "perceived enjoyment" (PE) has a significant influence on the willingness to use work-related information systems [14]. In terms of knowledge contribution of online communities, the sharing and communication of both information resources and knowledge skills not only help with

978-1-4244-7316-8/11/$26.00 ©2011 IEEE

the execution of tasks, but the contents and process of the sharing may also include interactive pleasure and emotional support [1, 15]. Finally, self-actualization – the highest level in Maslow's hierarchy of need theory, refers to how an individual does what he wants to do, demonstrates the inner potentials, equips oneself with creativity and adjustability, faces challenge and grows aggressively according to self-awareness [16]. Bandura argues that how an individual considers an activity with rewarding values derives from self- satisfaction after actualizing his personal achievement, which is even more meaningful than substantial monetary rewards [17]. Hendriks [18] and Andriesses [19] argue that the actualization of personal achievement and values is the primary factor of the willingness to knowledge sharing.

From all of the above discussion about one's outcome expectancy of altruistic good, hedonic expectancy, and value of self-actualization, the first hypothesis can be raised from this research:

H1: The outcome expectancy of knowledge contribution has a direct and positive influence on knowledge contribution behavior.

B. Self-Efficacy

The concept of self-efficacy refers to the judgment on one's capabilities for completing specific task, further affecting what kind of strategic move to plan, how much efforts to put in, the persistence when they encounter obstacles and adversities, the capability of recovery and the feasibility of achieving anticipated objectives. Many studies have proved the significant effect of self-efficacy on the performance in various settings, such as workplace, health management, and educational development. Caprara and others [20] have demonstrated the influence of teachers' self-efficacy beliefs on their satisfaction with teaching and students' learning achievement. In terms of related researches on self-efficacy and knowledge management, Bock & Kim [21] point out that an individual's judgment on whether he can make the expected contribution is a key issue that affects how he processes knowledge management activities in an organization. When organizational employees think they have the ability to contribute to better performance and target achievement, they hold a more positive and affirmative attitude toward knowledge contribution.

In the discourse of social cognitive theories, Bandura further points out that outcome expectancy is an important factor that affects on whether certain behavior can produce certain results, and the levels of efficacy belief are different for the anticipation of behavioral outcome [17]. People with higher self-efficacy believe that their action can lead to good results; therefore, it is positive and stimulating in actual action to achieve the desired outcome. In the field of information management, the relationship between self-efficacy and outcome expectancy is verified that people with higher self-efficacy expect to use ICT to increase other people's recognition in one's ability, enhance one's sense of achievement with work, and have chances of getting a job promotion [22, 23]. Then, the outcome expectancy has a significant influence and explanation to the intention of utilizing information systems.

Based on the above-mentioned argument concerning how self-efficacy affects the behavior and the relationship between individual's self-efficacy and outcome expectancy, we raise the following two hypotheses:

H2: The self-efficacy of knowledge contribution has a direct and positive influence on knowledge contribution behavior.

H3: The self-efficacy of knowledge contribution has a direct and positive influence on the outcome expectancy of knowledge contribution.

C. Knowledge Contribution Satisfaction

User satisfaction indicates that how individuals compare the actual performance of a service or product with prior expectation. When they feel satisfied with the service or product, he can be prompted to continue to use it. Alavi et al. [24] indicate that satisfaction is a useful indicator to evaluate learning effectiveness derived from instructions and assistance from other users. Within the realm of knowledge management practice, the facilitation of individuals' satisfaction with knowledge management also becomes a critical cognitive dimension to evaluate the state of organizational knowledge management [25, 26]. An individual's perceived knowledge satisfaction, instead of the objective assessment of knowledge effectiveness, constitutes an essential element of one's access to the resources and the personal commitment to greater knowledge contribution for the reciprocal or future exchange within their social group [27, 28]. Accordingly, we propose the following hypothesis,

H4: The user satisfaction with online knowledge community has a direct and positive influence on knowledge contribution behavior.

Individuals' satisfaction derived from the successful experience can increase their self-efficacy perception from a sense of personal fulfillment, reflecting the degree to how well they feel capable of completing the specific task [17]. Based on the positive perceptions and self-efficacy beliefs toward the learning program and expected outcome of ICT utilization [29-31], our study also attempts to examine the relationship between satisfaction and self-efficacy regarding knowledge contribution in the online community. Thus, the hypothesis is proposed as follows,

H5: The user satisfaction with online knowledge community has a direct and positive influence on knowledge contribution self-efficacy.

D. Online Ties

According to social capital theory, the establishment and maintenance of social relations help individuals obtain the power to get resources available with his identity as a member of the social network [32-34]. Granovetter [35] identifies the social relations as strength of ties, which reflect intensified, emotionally oriented and reciprocal relationship, continue to

Identify applicable sponsor/s here. *(sponsors)*

offer reliable support and speed up the flow of information to resolve the conflicts, crisis, or uncertainties that the members face in the social environment [36, 37]. The mutual experience, goal-setting, resources exchange and emotional support among members can invoke creativity and learning efficiency, as well as boost the production and application of intellectual capital [38]. Through the special properties of online environment which is unconfined by space or time and facilitated by ICT, members of the online community not only know other peers, they also realize under what circumstance can they win resources like the support of their peers, coordination, cooperation, and mutual learning [39, 40]. Moreover, Coleman [41] emphasizes the forming of social capital comes from the structural obligations, expectations, and trustworthiness among members in a closed social network. Due to the mutual benefits or sense of responsibility within the group, online community members with closer community recognition, mutual trust and obligation awareness are more willing to express their feelings and opinions toward something with no conservation.

To conclude the aforementioned points, we assume in this research that members of online communities form their social recognition as well as relationships, and have an influence on their knowledge contribution behavior as well as high expectancy on the reward generated from participating in the activities of knowledge contribution.

H6: The online ties of knowledge community members have a direct and positive influence on their knowledge contribution behavior.

H7: The online ties of knowledge community members have a direct and positive influence on their outcome expectancy of knowledge contribution.

Through the collective faith that social interaction contributes to sharing, community members put together their knowledge, skills and resources to provide mutual support among members, form alliance, collaborate mutually to solve problems and promote living qualities [42]. With collective social persuasion, the level of an individual's self-efficacy can be affected. Through the establishment and maintaining of relationships between social members, the vicarious experience produced by the social models further make them realize the possibility of fulfillment toward the behaviors [43-45]. Accordingly, we assume that the strength of ties among members of an online knowledge community would affect how an individual judges whether he has the ability to contribute knowledge, resources or experience. So we come up with the following hypothesis:

H8: The online ties of online knowledge community members have a direct and positive influence on their knowledge contribution self-efficacy.

In the context of interpersonal relationships, individuals develop beliefs and values as a major source of happiness as well as a buffer against conflicts [46]. The expressive interaction increases group partners' feelings of relationship satisfaction and commitment to remain in the relationship [47]. Since the sense of belonging in the online community encourages participants' collective actions to create and share instrumental resources or emotional support [48], their satisfaction with accessibility and adequacy of needed knowledge can be reinforced [25, 49]. Thus, this study proposes the following hypothesis:

H9: The online ties of knowledge community members have a direct and positive influence on their satisfaction with online knowledge community.

According to the previous literature review, our research model is depicted as Figure 1.

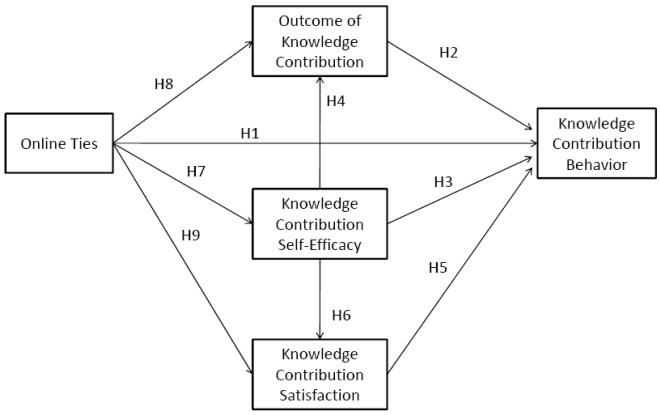

Figure 1: Research Model

III. RESEARCH DESIGN AND DATA ANALYSIS

A. Participants and Data Collection

This study focuses on a teachers' professional online learning community, the biggest web-based KMS for the teacher professional community in Taiwan. Practically, teachers need to upgrade their domain knowledge and teaching skills in order to work effectively with their students [50, 51]. The teacher communities of practice may facilitate professional collaborations and enhance better understanding about teachers' teaching practices, frustration, needs, and desires [52].

For this study, we adopt a survey methodology to collect and analyze empirical data. The operational definition and its references for the research model is demonstrated in Table 1. The instrument was examined by three senior members to examine the construct validity in ease of understanding, logical consistencies, and context fitness. The questionnaire was placed on the web site for members' voluntary participation. 433 survey responses were received, with 22 being discarded owing to their incomplete answers. The remaining 411 questionnaires were brought into further examination and analysis.

Table 1: Operational Definitions of Constructs

Construct	Operational definition	Sources
Outcome expectancy of knowledge contribution	An individual's outcome expectation of contributing knowledge in the online knowledge community, such as helping others, increasing one's own happiness and enjoyment, demonstrating the competence, gaining other's recognition, and achieving the desired goal.	Wasko & Faraj, 2005; (Kankanhalli, Tan, & Wei, 2005; Davis et al., 1992; Sun & Zhang, 2006 ; Maslow, 1954; Tickle, 2001, 2005; Woods, 2002
Knowledge contribution self-efficacy	An individual's judgment on his ability in executing knowledge contribution in the online knowledge community.	Bandura ,1989, 1997, 2002; Chan and Cheng, 2004; Smith, Kass, Rotunda, & Schneider 2006
Knowledge contribution satisfaction	An individual's perceptual evaluation of knowledge contribution, reflecting members' motives when engaging in the .online knowledge community.	Becerra-Fernandez and Sabherwal, 2001; Kulkarni, Ravindran, and Freeze, 2006-7
Online ties	The strength of relationships linking individuals with other members in the online knowledge community.	Hansen, 1999 ; BarNir & Smith, 2002; Jenssen & Koenig, 2002
Knowledge contribution behavior	The behavior that an individual contributes his/her resources, knowledge, experience, or emotional support to other members in the online knowledge community.	Morahan-Martin and Schumacher, 2003; Wasko and Faraj, 2000, 2005; Wellman & Gulia, 1999

B. *Measurement Instrument*

The measurement items (see the appendix) are developed on the basis of literature discussed above.

1) Outcome expectancy of knowledge contribution: Three aspects of outcomes are considered in terms of altruism, enjoyment, and self-actualization, indicating that online members expect to provide teaching resources and opinions to help solve other members' problem. By contributing their valuable knowledge or experience, people believe they will feel pleasant, interesting, and accomplished with the professional development.

2) Knowledge contribution of self-efficacy: To measure the online community members' confidence in contributing knowledge, we develop eight items to assess the level of subjects' beliefs in sharing their teaching practices, resources, and personal experiences with other members in the online knowledge community.

3) Knowledge contribution satisfaction: According to Bhattacherjee (2001), the concept of satisfaction is measured via three items to assess if the online members feel satisfied and content while contributing their knowledge with others. Furthermore, they would like to recommend this online community to their friends.

4) Online ties: Three items are adopted to examine their reciprocal identification from complete unknown stranger to good partners with common goals or interests. We suppose that more strength of ties can lead to more knowledge contribution.

5) Knowledge contribution behavior: As for the knowledge contribution behavior in the online knowledge community, we develop five items to measure the discussion, upload teaching resources, experience, or skills, as well as share their own emotional stories and express the concern or encourage to other members.

C. *Data Analysis and Resultss*

In this study, the structural equation analysis — partial least square (PLS), is used to test the research hypotheses. The first step in PLS is to assess the measurement reliability and validity by Confirmatory Factor Analysis (CFA). The internal consistency, convergent validity, and discriminant validity are examined. As a result, the factor loadings of each item is greater than 0.5 [53]. The CR value exceeds the generally recommended threshold values of 0.7 [54]. Finally, the square root of average variance extracted [55] is compared with the correlations among constructs [56]. All square roots of Ave values are greater than the correlations between pairs of constructs. Thus, all the constructs and items meet the requirement of internal reliability, convergent validity, and discriminant validity.

Table 2: CFA Results for Reliability and Validity of Measurement Items

Construct	Original items	Mean	SD	Factor loading	Cronbach's alpha	Composite reliability	Average variance extracted
Online ties	Ra1	3.88	2.33	0.91	0.80	0.88	0.73
	Ra2	2.27	2.22	0.70			
	Ra3	3.76	2.20	0.93			
Outcome expectancy of knowledge contribution	Al	4.74	1.24	0.89	0.87	0.92	0.79
	He	5.22	1.21	0.87			
	Sf	4.83	1.17	0.90			
Knowledge contribution self-efficacy	Se1	6.24	1.81	0.82	0.94	0.95	0.69
	Se2	6.15	1.88	0.86			
	Se3	5.82	1.85	0.88			
	Se4	6.27	1.79	0.82			
	Se5	5.74	2.07	0.80			
	Se6	6.03	1.87	0.84			
	Se7	6.09	1.87	0.82			
	Se8	6.46	1.77	0.81			
Knowledge contribution satisfaction	Ksa1	5.04	1.17	0.90	0.89	0.93	0.82
	Ksa2	5.42	1.27	0.89			
	Ksa3	5.14	1.21	0.93			
Knowledge contribution behavior	Kcb6	3.76	1.80	0.88	0.93	0.95	0.78
	Kcb7	3.45	1.96	0.84			
	Kcb8	3.53	1.85	0.93			
	Kcb9	2.94	1.71	0.86			
	Kcb10	3.45	1.84	0.91			

Table 3: Discriminant validity for the research constructs

Construct	OT	OE	KCSE	KSA	KCB
OT	0.85				
OE	0.35	0.89			
KCSE	0.40	0.61	0.83		
KSA	0.27	0.70	0.52	0.91	
KCB	0.43	0.43	0.47	0.36	0.88

OT = Online tie; OE = Outcome expectancy of knowledge contribution; KCSE = Knowledge contribution self-efficacy; KSA = Knowledge contribution satisfaction KCB = Knowledge contribution behavior

Diagonal elements represent the square root of AVE for each construct; off diagonal elements are correlations among constructs.

After assessing the validity and reliability of the research construct, we continue to use PLS to test hypotheses by measuring the relationship between constructs. As demonstrated in Figure 2, except for the relationship between individuals' satisfaction and their knowledge contribution behavior (H4), the other three paths (H1, H2, and H6) are significant. The R^2 value shows that outcome expectancy, self-efficacy, satisfaction, and online members' strength of ties account for 31.7% of the variance in knowledge contribution behavior. Furthermore, the path between self-efficacy and outcome expectancy is also supported (H3); while individuals' satisfaction and their online ties with other members are both significant to influence their self-efficacious belief in knowledge contribution (H5 and H8). Finally, online ties in this study are proved to have significant influence on online members' outcome expectancy and self-efficacy in the realm of knowledge contribution.

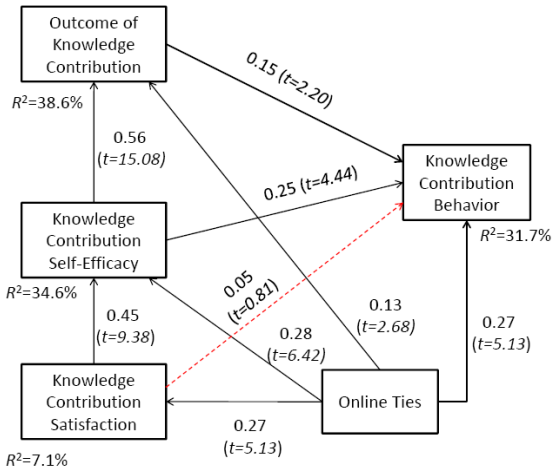

Figure 2: Results of model test

IV. Discussion and Clusion

In recent years, knowledge economy has emerged as an important issue for many organizations to establish the online community as internal or inter-organizational platforms of knowledge management. By using the existing human resources and intellectual capital to strength organizational members' interpersonal connection, knowledge management help increase resource-sharing, promote task-execution, boost learning, evoke knowledge innovations, and promote organizational performance [57-59]. Although the benefit of knowledge management has been emphasized via the utilization of information and computer technologies (ICTs), it is not a total solution to all knowledge management practices. Actually, the formation and application of knowledge is embedded in people's everyday activities, involving a knowing and understanding state of mind, as well as a process that focuses on the relationships among members.

In this paper, we propose a social cognitive framework of knowledge management to understand the associations among online members' outcome expectancy, self-efficacy, satisfaction regarding knowledge contribution, the strength of online ties, and individuals' knowledge contribution behavior. The hypotheses tested in this study are all supported, with the exception of people's satisfaction with their knowledge contribution in the online community. Consistent with the studies of Watson and Hewett [12], Andriesses [19], as wll as Bock et al., [11], as people think they can achieve some expectation and benefits in terms of the collective good, perceived enjoyment, and self-actualization, they are more willing to participant in knowledge management activities. Online members' perception of self-efficacy also plays an important role in determining one's behavior and outcome expectancy of knowledge contribution. The more beliefs that one can provide the instrumental resources or emotional support to help others, the more knowledge they would like to contribute, with the positive evaluation of good results that their knowledge contribution can lead to.

Although online members' satisfaction with knowledge contribution does not significantly influence their knowledge contribution behavior, it is consistent with Bandura's social cognition perspective that satisfaction derived from the successful experience can increase people's self-efficacy perception, indicating they can feel capable of completing one specific task. In this study, self-efficacy reflects a stronger mediating effect to influence online members' outcome expectancy and participation of knowledge contribution. Finally, the development of social relationships among online knowledge community members is proven to help them get potential resources and reliable support with one's identity as a member of the social network. It is useful to speed up the flow of information to resolve the conflicts, crisis, or uncertainties that online members face in their social settings [36]. Furthermore, the mutual experience, goal-setting, resources exchange and emotional support among members can increase creativity and learning performance, as well as enhance the production and application of intellectual capital [38].

Our research results support the view that knowledge management is not confined to only system functions. Instead of an illusionary space where people may meet without face-to-face interaction, learning and sharing derived from knowledge contribution has to be reciprocally adjusted among personal cognition and the environment. Therefore, the online members' outcome expectation, efficacious beliefs, satisfactory perception, and the strength of online ties are critical to the success in knowledge management practices.

REFERENCES

[1] B. Wellman, "An Electronic Group in Virtually a Social Network," in The Culture of the Internet, S. Kiesler, Ed. Hillsdale, NJ: Lawrence Erlbaum, 1997.

[2] H. Rheingold, The Virtual community: homesteading on the electronic frontier. New York: Harper Perennial, 1993.

[3] M. M. Wasko and S. Faraj, ""It Is What One Does": Why People Participate and Help Others in Electronic Communities of Practice," Journal of Strategic Information Systems, vol. 9, pp. 155-173, 2000.

[4] A. Kankanhalli, B. C. Y. Tan, and K.-K. Wei, "Contributing Knowledge to Electronic Knowledge Repositories: An Empirical Investigation," MIS Quarterly, vol. 29, pp. 113-143, 2005.

[5] M. Alavi, T. R. Kayworth, and D. E. Leidner, "An Empirical Examination of the Influence of Organizational Culture on Knowledge Management Practices," Journal of Management Information Systems, vol. 22, pp. 191-224, 2005-6.

[6] S. M. Miranda and C. S. Saunders, "The Social Construcion of Meaning: An Alternative Perspective on Information Sharing," Information Systems Research, vol. 14, pp. 87-106, 2003.

[7] J. B. Thomas, S. W. Sussman, and J. C. Henderson, "Understanding trategic Learning? Linking Organizational Learning, Knowledge Management, and Sensemaking," Organization Science, vol. 12, pp. 331-345, 2001.

[8] V. H. Vroom, Work and motivation. New York: John Wiley & Sons, 1964.

[9] A. Bandura, Social Foundations of Thought and Action. Englewood Cliffs, NJ: Prentice-Hall, 1986.

[10] J. R. Hollenbeck and H. J. Klein, "Goal commitment and the goal-setting process: problems, prospects, and proposals for future research," Journal of Applied Psychology, vol. 72, pp. 212-220, 1987.

[11] G.-W. Bock, R. W. Zmud, Y.-G. Kim, and J.-N. Lee, "Behavioral Intention Formation in Knowledge Sharing: Examining the Roles of Extrinsic Motivators, Social-Psychological Forces, and Organizational Climate," MIS Quarterly, vol. 29, pp. 87-111, 2005.

[12] S. Watson and K. Hewett, "A Multi-Theoretical Model of Knowledge Transfer in Organizations: Determinants of Knowledge Contribution and Knowledge Reuse," Journal of Management Studies, vol. 43, pp. 141-173, 2006.

[13] M. M. Wasko and S. Faraj, "Why should I share? examining social capital and knowledge contribution in electronic networks of practice," MIS Quarterly, vol. 29, pp. 35-57, 2005.

[14] F. D. Davis, R. P. Bagozzi, and P. R. Warshaw, "Extrinsic and Intrinsic Motivation to Use Computers in the Workplace," Journal of Applied Social Psychology, vol. 22, pp. 1111-1132, 1992.

[15] B. Daniel, R. A. Schwier, and G. McCalla, "Social Capital in Virtual Learning Communities and Distributed Communities of Practice," Canadian Journal of Learning and Technology, vol. 29, pp. 113-139, 2003.

[16] A. H. Maslow, Motivation and Personality. New York: Haper & Row, 1954.

[17] A. Bandura, Self-Efficacy: The Exercise of Control. New York: W. H. Freeman and Company, 1997.

[18] P. Hendriks, "Why share knowledge? the influence of ICT on the motivation for knowledge sharing," Knowledge and Process Management, vol. 6, pp. 91-100, 1999.

[19] J. H. E. Andriessen, "To share or not share, that is the question: Conditions for the willingness to share knowledge," 2006.

[20] G. V. Caprara, C. Barbaranelli, P. Steca, and P. S. Malone, "Teacher's self-efficacy beliefs as determinants of job satisfaction and students' academic achievement: a study at the school level," Journal of School Psychology, vol. 44, pp. 473-490, 2006.

[21] G. W. Bock and Y. G. Kim, "Breaking the Myths of Rewards: An Exploratory Study of Attitudes About Knowledge Sharing," Information Resource Management Journal, vol. 15, pp. 14-21, 2002.

[22] D. R. Compeau and C. A. Higgins, "Computer Self-Efficacy: Development of a Measure and Initial Test," MIS Quarterly, vol. 19, pp. 189-211, 1995.

[23] D. R. Compeau, C. A. Higgins, and S. Huff, "Social Cognitive Theory and Individual Reactions to Computing Technology: A Longitudinal Study," MIS Quarterly, vol. 23, pp. 145-158, 1999.

[24] M. Alavi, B. C. Wheeler, and J. S. Valacich, "Using IT to reengineer business education: an exploratory investigation of collaborative tele-learning," MIS Quarterly, vol. 19, pp. 293-313, 1995.

[25] C.-S. Ong and J.-Y. Lai, "Measuring user satisfaction with knowledge management systems: scale development, purification, and initial test," CyberPsychology & Behavior, vol. 23, pp. 1329-1346, 2007.

[26] I. Becerra-Fernandez and R. Sabherwal, "Organizational knowledge management: A contingency perspective," Journal of Management Information Systems, vol. 18, pp. 23-55, 2001.

[27] M. Ma and R. Agarwal, "Through a glass darkly: information design, identity verification, and knowledge contribution in online communities," Information Systems Journal, vol. 18, pp. 42-67, 2007.

[28] M. Givertz and C. Segrin, "Explaining personal and constraint commitment in close relationships: the role of satisfaction, confliect responses, and relational bond," Journal of Social and Personal Relationships, vol. 22, pp. 757-775, 2005.

[29] O. Lopez-Fernandez and J. L. Rodriguez-Illera, "Investigating unversity students' adaptation to a digital learner course portfolio," Computer & Education, vol. 52, pp. 608-616, 2009.

[30] K.-S. Hong, "Relationships between students' and instructional variables with satisfaction and learning from a web-based course," Internet and Higher Education, vol. 5, pp. 267-281, 2002.

[31] J.-K. Lee and W.-K. Lee, "The relationship of e-Learner's self-regulatory efficacy and perception of e-Learning environmental quality," Computers in Human Behavior, vol. 24, pp. 32-47, 2008.

[32] A. Portes, The Economic Sociology of Immigration. . New York: Russell Sage, 1995.

[33] A. Portes, "Social Capital: Its Origins and Applications in Modern Sociology," Annual Review of Sociology, vol. 22, pp. 1-24, 1998.

[34] P. Bourdieu and J.-C. Passeron, Reproduction in Education, Society, Culture. Beverly Hills, CA.: Sage, 1977.

[35] M. S. Granovetter, "The strength of weak ties," American Journal of Sociology, vol. 78, pp. 1360-1380, 1973.

[36] D. Krackhardt and R. N. Stern, "Informal Networks and Organizational Crises: an Experinmental Simulation," Social Psychology Quarterly, vol. 51, pp. 123-140, 1988.

[37] R. E. Nelson, "The Strength of Strong Ties: Social Networks and Intergroup Conflict in Organizations," Adademy of Management Journal, vol. 32, pp. 377-401, 1989.

[38] J. Nahapiet and S. Ghoshal, "Social capital, intellectual capital, and organizational advantage," Academy of Management Review, vol. 23, pp. 242-266, 1998.

[39] C. R. Leana and H. J. van Buren III, "Organizational Social Capital and Employment Practices," Academy of Management Review, vol. 24, pp. 538-555, 1999.

[40] K. H. Williams, "Social networks, social capital, and the use of information and communications technology in socially excluded communities: a study of community groups in Manchester, England," University of Michigan, 2005.

[41] J. S. Coleman, "Social Capital in the Creation of Human Capital," American Journal of Sociology, vol. 94, pp. S95-S121, 1988.

[42] A. Bandura, " Exercise of human agency through collective efficacy," Current Directions in Psychological Science, vol. 9, pp. 75-78, 2000.

[43] D. H. Lindsley, D. J. Brass, and J. B. Thomas, "Efficacy-Performance Spirals: A Multi-level Perspective," Academy of Management Review, vol. 20, pp. 645-678, 1995.

[44] C. B. Gibson, "Do They Do What They Believe They Can? Group Efficacy and Group Effectiveness Across Tasks and Cultures," Academy of Management Journal, vol. 42, pp. 138-152, 1999.

[45] D. F. Baker, "The Development of Collective Efficacy in Small Task Groups," Small Group Research, vol. 32, pp. 451-474, 2001.

[46] A. J. Martin and M. Dowson, "Interpersonal relationships, motivation, engagement, and achievement: yields for theory, current issues, and

educational practice," Review of Educational Research, vol. 79, pp. 327-365, 2009.

[47] S. Sprecher, S. Metts, B. Burleson, E. Hatfield, and A. Thompson, "Domains of expressive interaction in intimate relationships: associations with satisfaction and commitment," Family Relations, vol. 44, pp. 203-210, 1995.

[48] H. Bressman, J. Birkenshaw, and R. Nobel, "Knowledge Transfer in International Acquisitions," Journal of International Business Studies, vol. 30, pp. 439-462, 1999.

[49] U. R. Kulkarni, S. Ravindran, and R. Freeze, "A knowledge management success model: theoretical development and empirical validation," Journal of Management Information Systems, vol. 23, pp. 309-347, 2006-7.

[50] M. Cochran-Smith and S. L. Lytle, "Relationships of knowledge and practice: teacher learning in communities," in Review Research in Education, vol. 24, A. Iran-Nejad and C. D. Pearson, Eds. Washington, DC: American Educational Research Association, 1999.

[51] M. W. McLaughlin, "Sites and Sources of Teachers' Learning," in Developing Teachers and Teaching Practice: International Research Perspectives, C. Sugure and C. Day, Eds. London: Routledge, 2002.

[52] J. M. Carroll, C. W. Choo, D. R. Dunlap, P. L. Isenhour, S. T. Kerr, A. MacLean, and M. B. Rosson, "Knowledge Management Support for Teachers," Educational Technology, Research and Development, vol. 51, pp. 42-64, 2003.

[53] J. B. E. M. Steenkamp and H. C. M. Van Trijp, "The Use of LISREL in Validating Marketing Constructs," International Journal of Research in Marketing, vol. 8, pp. 283-299, 1991.

[54] J. C. Nunnally and I. H. Bernstein, Psychometric Theory, 3rd ed. ed. New York: McGraw-Hill, 1994.

[55] T. H. Davenport and L. Prusak, Working knowledge. Boston: Harvard Business School Press, 1998.

[56] W. W. Chin, "The partial least square approach to structural equation modeling," in Modern Methods for Business Research, G. A. Marcoulides, Ed. Mahway, NJ: Lawrence Erlbaum Assoicates, 1998, pp. 295-336.

[57] P. Hildreth, C. Kimble, and P. Wright, "Communities of Practice in the Distributed International Environment," Journal of Knowledge Management, vol. 4, pp. 27-38, 2000.

[58] B. Kogut and A. Metiu, "Open Source Software Development and Distributed Innovation," Oxford Review of Economic Policy, vol. 17, pp. 248-264, 2001.

[59] G. von Krogh, S. Spaeth, and K. R. Lakhani, "Community, Joining, and Specialization in Open Source Software Innovation: A Case Study, Research Policy," in Open Source Software Development, 2003.

APPENDIX

Outcome expectancy of knowledge contribution

1. As the online community members need teaching resources, I provide what I have to them.
2. As the online community members need suggestion for teaching,, I will provide what I have to them.
3. As the online community members express their emotion, I will response and encourage them.
4. It is joyful for me to contribute knowledge in SCTNet.
5. It is pleasant for me to contribute knowledge in SCTNet.
6. It is interesting for me to contribute knowledge in SCTNet.
7. Contributing knowledge in SCTNet can enhance my professional capabilities and development.
8. Contributing knowledge in SCTNet can enhance my professional capabilities and development.
9. Contributing knowledge in SCTNet can help increase my concentration and enthusiasm for teaching.
10. Contributing knowledge in SCTNet can help release my frustrations and stresses of teaching.

Kowledge contribution slf-efficacy

1. I have confidence in contributing my teaching experience with other SCTNet members.
2. I have confidence in contributing my teaching resources with other SCTNet members.
3. I have confidence in sharing my emotion with other SCTNet members.
4. Even I have different opinions from other SCTNet members, I have confidence in keeping discussion on related issues.
5. Even my opinion may be an offense to other SCTNet members, I have confidence in keeping discussion on related issues.
6. I have confidence in sharing my success or joyfulness with other SCTNet members, rather than worrying that it is regarded as show off.
7. I have confidence in sharing my failure or frustration with other SCTNet members, rather than worrying that I may be ridiculed.
8. I have confidence in engaging the knowledge contribution activities in SCTNet.

Knowledge contribution satisfaction

1. I feel satisfied with contributing knowledge in SCTNet.
2. I will recommend SCTNet to my friends.
3. I am content to contribute knowledge in SCTNet.

Oline ties

1. Is there any SCTNet member with whom I contribute knowledge?

   Yes. Our relationship varies from totally unknown stranger to the partner in the same camp.
2. Is there any discussion group member with whom I contribute knowledge?

   Yes. Our relationship varies from totally unknown stranger to the partner in the same camp.
3. On the whole, is there any SCTNet member with whom we share our knowledge to each other?

   Yes. Our relationship varies from totally unknown stranger to the partner in the same camp.

Knowledge contribution behavior

1. I often respond to the topics discussed in SCTNet.
2. I often upload my teaching resources to SCTNet.
3. I often contribute my teaching experience, knowledge or skill in SCTNet.
4. I often share my emotion in SCTNet.
5. I often express my concern or encourage to other SCTNet members.

2011 IEEE International Conference on Fuzzy Systems
June 27-30, 2011, Taipei, Taiwan

Fuzzy Clustering of Large-Scale Data Sets Using Principal Component Analysis

Olfa Arfaoui
National Engineering School of Tunis
BP. 37, Le Belvédère 1002 Tunis, Tunisia
olfa.arfaoui@yahoo.fr

Minyar Sassi
National Engineering School of Tunis
BP. 37, Le Belvédère 1002 Tunis, Tunisia
minyar.sassi@enit.rnu.tn

***Abstract*—To effectively exploit large-scale data sets using a limited storage space, it is necessary to find a special treatment which reduces them. There are certain methods with this intention. We can quote clustering method. However, this method proves its limits in the case of large-scale data sets. In this paper, we propose to reduce the workspace using the Principal Component Analysis (PCA). We work with fuzzy clustering of a data set in which users don't know the optimal number of clusters to be generated. We proved the effectiveness of the pre-processing use of this technique before any clustering operation.**

Keywords-Clustering; Fuzzy Logic; Principal Component Analysis; Sampling; Data Compression.

I. INTRODUCTION

The evolution of the data processing and storage technologies and tools involved an explosion of available data. This phenomenon was reinforced by the awakening of the decision makers of the potential knowledge value which contain their databases (DB). Nevertheless, the available large data don't bring any appreciation in absence of exploration and analysis methods. In this case, the installation of treatments tools to clarify the available knowledge in these data is fundamental and represents one of the major stakes of the Knowledge Discovery from Database (KDD).

The reduction of the space of description and the number of data are two dual approaches which bring brief replies to this problem. We often gather them under name "reduction of dimensions". Their objective is to select or extract an optimal subset from characteristics and/or objects for a fixed criterion. By eliminating non relevant or redundant information according to the criterion used, these approaches make it possible to reduce the size of the data set according to its two dimensions to make it more representative to a given problem.

They have the following objectives: (1) simplify the data visualization and comprehension; (2) reduce the storage space; (3) reduce the time of training and use, and (4) identify the relevant factors.

Several works were proposed in the literature to seek and improve the Data Mining methods among which we quote the Information Retrieval (IR), the data querying, the clustering, the Formal Concept Analysis (FCA) etc.

In this work, we focus ourselves on fuzzy clustering of large-scale data sets.

Several works improve this method while proving its performances in the management of the large-scale data sets that on the determination of the optimal number of clusters.

However, these solutions are insufficient to ensure a good clustering of the large-scale datasets, in which the data can have hundred attributes or variables and make the clustering in this space extremely difficult.

The Principal Component Analysis (PCA) permits to solve these problems while putting in considerations the following objectives: (1) represent observations moreover than 2 variables into 2 or 3 dimensions; (2) reduce dimension in a relevant way while guaranteeing a minimal loss of information.

The new variables obtained have the following characteristics: (1) they are ordered according to the information which it restores of the initial variables; (2) they are not linearly correlated between them.

The rest of the paper is organized as follows: section 2 presents some works on the clustering large data sets. Section 3 presents our approach for fuzzy clustering of large-scale data sets while using the PCA. Section 4 presents experimentation and evaluates the approach. Section 5 concludes the paper and presents the future work.

II. CLUSTERING OF LARGE DATA SETS

When we treat large datasets, the problem of the resources always emerges. In our case, the traditional clustering techniques have important complexities, so, it is not obvious to apply them to large datasets, because they are so enormous that we cannot store it in memory. A solution consists of applying compression technique to prevent that these kind of datasets exceeds the memory space.

For this, several techniques and approaches were applied to the methods and existing algorithms to deal with the problem of the clustering in the large datasets, we divided them into data reduction and dimension reduction techniques.

For data reduction, several researchers studied the concept of sampling and data compression [9], [10], [11], [12], [13], [14], [15], [16]. Table 1 presents a comparative study of these approaches.

978-1-4244-7316-8/11/$26.00 ©2011 IEEE

TABLE I. COMPARATIVE STUDY OF LARGE DATA SETS CLUSTERING ALGORITHMS

Name	Type	Inputs	Used techniques (sampling or compression)	Optimized for
CURE	Hierarchical	*X+C+* Number of representatives	Sampling	Large Data sets
CLARANS	Partition-based clustering	*X+C+* Maximum number of the nearest	Sampling	Spatial data sets
GEFFCM	Partition-based clustering	*X+C*	Sampling	Large Data sets
Single pass k Means	Partition-based clustering	$X+C+V_i$	Compression	Large Data sets
Single pass fuzzy C-Means	Partition-based clustering	*X+C+P*	Compression	Large Data sets
WEFCM	Partition-based clustering	*X*	Compression	Large Data sets

Were X is the data set, C is the number of clusters, V the initial centers and P the sampling data.

The majority of the algorithms presented above are interesting, but they present some limits. Although they solve the problem of the clustering of large datasets, they require also the number of clusters like input parameter. However WEFCM (Weighted Enhance Fuzzy C-Means) [19] presents a good automatic system of clustering while provides the optimal number of clusters. Based on this point, and since this algorithm allows only the data reduction, we will associate to him a dimension reduction procedure. This is to facilitate the clustering of large-scale datasets.

The principle of this algorithm is as follow: suppose we intend to cluster a large data sets present on a disk. We can only load a certain percentage of the data based on the available memory allocation. If we load 1% of the data into memory at a time then we have to do it 100 times to scan through the entire data set. We call each such data access a Partial Data Access (PDA). The number of partial data accesses will depend on how much data we load each time.

In this algorithm, after the first PDA, data is clustered into c partitions using EFCM [8]. Then the data in memory is condensed into c weighted points and clustered with new points loaded in the next PDA. These points are calculated by summing the membership of examples in a cluster. In each PDA new singleton points are loaded into memory and clustered along with the past c weighted points obtained from the previous clustering. It is called Partial Data Clustering (PDC). After clustering these new singleton points along with the past c weighted points, they are condensed again into c new higher weighted points and clustered with examples loaded in the next PDA. This continues until all the data has been scanned once.

The evaluation of the clustering with WEFCM is done globally and locally. So, it uses the following measures:

Global Weighted Separation-Compactness: given a cluster scheme $C=\{C_1,C_2,...,C_c\}$ for a data set $X=\{x_1,x_2,...,x_N\}$, let $C'=\{C_{pj}\,|\,C$ and C_{pj} is not singleton, $j=1,2,...,k$ where $k=|C'|\}$, the global weighted separation-compactness, WSC, of a cluster scheme C is given equation (1).

$$WSC=\frac{k^2}{c}\frac{\left(\sum_{j=1}^{c}\min_{1\le k\le c}\left\{\left\|v_j-v_k\right\|^2\right\}/c\right)}{\sum_{j=1}^{k}\left(\sum_{x_i\in C_{pj},x_i\neq v_j}w_i\mu_j(x_i)^2\left\|x_i-v_j\right\|^2/\sum_{x_i\in C_{pj},x_i\neq v_j}w_i\mu_j(x_i)^2\right)} \quad (1)$$

where $\mu_j(x_i)$ is the membership degree of data x_i to j^{th} cluster and w_i the weight of a data [19].

Then, the objective of WEFCM algorithm is to find the cluster scheme which solves:

$$\max_{2\le c\le\sqrt{N}}\left\{\max_{\Omega_C}\{WSC\}\right\} \quad (2)$$

Where Ω_C denotes all of the candidate cluster schemes for a certain number of clusters c.

We still use the measures of separation and compactness to evaluate individual clusters (except singleton).

Local Weighted Separation-Compactness: given a cluster scheme $C=\{C_1,C_2,...,C_c\}$ for a dataset $X=\{x_1,x_2,...,x_N\}$, for each $C_j\in C$, if C_j is not singleton, the local weighted separation-compactness of C_j, denoted as wsc_j, is given by equation (3) [19].

$$wsc_j=(\min_{1\le j\le c,k\neq j}\left\|v_j-v_k\right\|^2)\times\left(\frac{\sum_{x_i\in C_j,x_i\neq v_j}w_iu_j(x_i)^2}{\sum_{x_i\in C_j,x_i\neq v_j}w_iu_j(x_i)^2\left\|x_i-v_j\right\|^2}\right) \quad (3)$$

Thus, the "worst" cluster is the one with the least wsc_j value.

Procedure 1 *Weighted Merge-based Process* [19]

Step 1:	Build the array $C^*=\{C^*_1,C^*_2,...,C^*_c,C^*_{c+1}\}$, such that each v^*_j is the center of cluster $C^*_j\in C^*$.
Step 2:	Calculate *wsc* value for each C^*_j in C^*,
Step 3:	Delete the center of cluster with the least *wsc* value from C^*, recalculate the cluster centers. Store the new cluster scheme $C=\{C_1,C_2,...,C_c\}$.

Procedure 2 *Recalculate the cluster centers* [19]

Step 1:	Choose the nearest center v^*_j for each element $x_i\in X$, and group x_i into cluster C^*_j whose center is v^*_j.
Step 2:	Calculate the data median for each C^*_j as the new center for it; denote it as v_j, output the cluster scheme $C=\{C_1,C_2,...,C_c\}$.
Step 3:	If $(C^*\neq C)$ and maximum step is not reached, go to step1.
Step 4:	Output C.

Let p the fraction of data loaded in each PDA, d the number of PDA's required by WEFCM and $1\le r\le d$.

WEFCM follows the following steps [19]:

Step 1:	The first PDA. Applying the EFCM clustering algorithm.
Step 2:	**Repeat** Clustering will be applied on singleton points freshly loaded in the d^{th} PDA along with c_{opt} weighted points obtained after condensation from the $(d-1)^{th}$ PDA. So, there will be $n_d + c$ points in the memory for clustering using EFCM by taking in account of weighted local and global measures. **Until** r=d.

However, data used in clustering can have hundreds attributes or variables. Clustering in such space of high dimensionality is extremely difficult. The calculation of similarity becomes very expensive.

Another problem can occur in a space of high dimension, it is the presence of non relevant attributes which affect proximity measurements. In fact, this phenomenon can appear with data of low dimension, but the possibility of presence and the number of the non relevant attributes increase with the dimensionality.

There are certain techniques for dimension reduction to solve the problems above, such as the technique of selection of attributes, the reduction of dimensionality, classification under-spaces and Co-classification [17], [15].

We present, in the next section, a new algorithm for clustering large-scale data sets while using the PCA.

III. CLUSTERING OF LARGE-SCALE DATASETS USING PCA

The clustering is often used to facilitate the training and decrease the processing time. Particularly in the case when the clustering is made on the two levels.

It should be noted that the data clustering, in order to gather them in a number of representative clusters is the most used, but we can also make a scale clustering in order to reduce their number.

A. PCA Terminology

The purpose of PCA is to create one or more variables which are a linear combination of n variables. A data described by n variables belonging to R can be represented by a point in a space R with n dimensions.

The PCA allows, starting from n variables belonging to R^n, to build p $(\leq n)$ other variables, called principal components (or factorial axes), which are linear combinations of the n initial variables. Each principal component will be defined by a linear equation bringing into account the initial variables which take part in its construction.

If there are only two variables a_j and a_k, we give the graph giving a_j according to a_k and we see immediately if there is linear correlation or not. If there are more than two variables, this geometrical approach does not function any more, because we are unable to understand a space with more than 3 dimensions.

The fundamental idea of the PCA is the following one: considering the group of points in P dimensions (in this space, 1 point = 1 data), we seek to find the plan (the two-dimensional representation that we will be able to see and understand) in which the projection of the points of the cloud is least possible distorted therefore most reliable possible.

For that, we start by seeking the line Δ_1 which minimizes the squared sum of the distances between each point and the line.

This line has the property to be the direction according to which the variance of the points is biggest. Then, we look for a second line Δ_2 perpendicular to Δ_2 and have the same property; and we continue until obtaining P lines which form an orthogonal reference mark.

We note that, like any statistical method, the number of data and the number of attributes must be relatively important so that the conclusions of the PCA have a meaning;

Let take the example of data in table II which describes 10 persons by their physical characteristics and their annual average notes.

TABLE II. DATA EXAMPLE

Data	Weight	Tall	Age	Mark
1	45	1.5	13	14
2	50	1.6	13	16
3	50	1.65	13	15
4	60	1.75	15	9
5	60	1.7	14	10
6	60	1.7	14	7
7	70	1.6	14	8
8	65	1.6	13	13
9	60	1.55	15	17
10	65	1.7	14	11

B. Distances Calculation, Data Centering and Reduction

It is necessary to start by defining a distance concept between two data. So, if we take the Euclidean geometry, we could write:

$$d^2(x_i, x_j) = \sum_{k=1}^{k=P} (x_{i,k} - x_{j,k}) \quad (4)$$

Let us consider data x_4, x_5 and x_6. We have $d^2(x_4, x_5) = 2.0$, $d^2(x_4, x_6) = 5.0$ and $d^2(x_5, x_6) = 9.0$. Now if we express the talls in centimeters, the distances become: $d^2(x_4, x_5) = 27$, $d^2(x_4, x_6) = 30$ and $d^2(x_5, x_6) = 9$. It is noted that according to the unit used, data x_6 is closer to the 4th or of 5th, we use reduced centered variables to avoid this problem.

In this case, we obtain $d^2(x_4, x_5) = 2.3$, $d^2(x_4, x_6) = 2.6$ and $d^2(x_5, x_6) = 0.8$, whatever the units used.

Afterwards, we consider that the data are centered and reduced. The definition of distances given above means that all attributes have the same importance in the distance measure.

We use equation (5) to balance the attributes to have more or less importance:

$$d^2(x_1,x_2)=\sum_{k=1}^{k=P} w_k\left(x_{i,k}-x_{j,k}\right) \quad (5)$$

where a weight w_k belongs to R and balances each component of the distance for each attribute.

If all the attributes have the same importance, we take w_k all equals. We suppose here that all the attributes have the same importance and that $w_k=1$. For this the calculation of the averages and standard deviations is essential for data centering and reduction. $\bar{x}$ is the arithmetic mean of each column, it is presented by equation (6).

$$\bar{x}=\frac{1}{N}\sum_{i=1}^{N} x_i \quad (6)$$

The standard deviation is the square root of the variance; it is presented by equation (7):

$$\delta^2=\frac{1}{N}\sum_{i=1}^{N}\left(x_i-\bar{x}\right)^2 \quad (7)$$

Table III gives the average and the standard deviation of each variable (column).

TABLE III. CHARACTERISTICS OF THE GRAVITY CENTER

	Weight	Size	Age	Note
Average	58.5	1.64	13.8	12.0
Standard deviation	7.84	0.08	0.79	3.50

Once we calculate the average and the standard deviation of each column, we determine the centered and reduced coordinates of each data in a new reference mark whose origin is the gravity center and whose axes are parallel to the original ones (of the non reduced and non centered data).

Table IV presents the new centered and reduced data.

TABLE IV. DATA CENTRING AND REDUCTION

	Weight	Size	Age	Note
1	-1.72	-1.72	-1.01	0.57
2	-1.09	-0.45	-1.01	1.14
3	-1.09	0.19	-1.01	0.86
4	0.19	1.47	1.52	-0.86
5	0.19	0.83	0.25	-0.57
6	0.19	0.83	0.25	-1.43
7	1.47	-0.45	0.25	-1.14
8	0.83	-0.45	-1.01	0.29
9	0.19	-1.09	1.52	1.43
10	0.83	0.83	0.25	-0.29

Next, we suppose that we centered and reduced the data, $\overline{x_j}=0$ is the average of j^{th} column and $\sigma(x_j)=1\ \forall j\in\{1,...,P\}$.

This assumption simplifies the calculations and the notations. The N data described by their P characters can be put in the form of a matrix having N lines and P columns: one line describes a data and each column corresponds to an attribute. Let us note this matrix X.

C. Matrix Counting

To determine the principal components, we start from a square matrix. The choice of the matrix type is a parameter of the PCA. It is directly function of metric adapted to the problem.

- Covariance matrix

The covariance of two variables V_1 and V_2 is an indicator of the simultaneous variation. Covariance is positive when V_2 grows each time V_1 increases. It is negative when V_2 decrease each time V_1 increases. It is null if V_1 and V_2 are independent. Covariance and correlation are of the same sign. Covariance is function of the coefficient of correlation. It is given in equation (8).

$$Cov(V_1,V_2)=Stand\text{-}Dev\ (V_1)*Stand\text{-}Dev\,(V_2)*Cor(V_1,V_2) \quad (8)$$

Where *Cov* is the covariance, *Stand-Dev* is the standard deviation and *Cor* the correlation.

If there are homogeneous data with identical magnitude orders, then there is an Euclidean metric and we work with a covariance matrix.

With each couple (V_1,V_2), the value of each element of the matrix is that of the covariance of the couple (V_1,V_2).

- Correlation Matrix

For each couple (V_1,V_2), the value of each element of the correlation matrix is the correlation coefficient between V_1 and V_2. It is given in equation (9).

$$Cor(V_1,V_2)=Cov(V_1,V_2)/(Stand\text{-}Dev\,(V_1)*Stand\text{-}Dev\,(V2)) \quad (9)$$

If there are heterogeneous data with different magnitude orders, we work with a correlation matrix. It is given in equation (10)

$$R=\begin{pmatrix} 1 & r(a_1,a_2) & r(a_1,a_2)\ldots r(a_1,a_2) \\ & 1 & r(a_2,a_3)\ldots r(a_1,a_P) \\ & & \ddots \quad \vdots \\ & & 1 \end{pmatrix} \quad (10)$$

R is symmetric since $r(a_j,a_k)=r(a_k,a_j)$ (the left lower triangle was not indicated). For centered and reduced variables, these two matrices are equal: $R=V$.

We have the relation: $R=\frac{1}{P}X^TX$ where X^T indicates the transposed of the matrix X. The examination of the correlation matrix is interesting: it makes it possible to immediately locate the strongly correlated variables and the variables which are not correlated.

The calculation of the eigenvalues and the eigenvectors of R provide all required information.

Let we note $\lambda_i\in\{1,...,P\}$ the P eigenvalues of R ordered in a decreasing way: $\lambda_1\geq\lambda_2\geq...\geq\lambda_P$ and their P associated

eigenvectors $\vec{v}_i \quad i \in \{1,...,P\}$. R is symmetric and defined positive, its values are real and positive and its own vectors have real coordinates.

If there exists one, or many, null eigenvalues, we understand that the attributes are not linearly independent some of the others: one, or several, attributes are obtained by linear combination of the others.

Eigenvectors are unit and orthogonal two by two and form an orthonormal basis. They are the required main axes. The main axis is that associated to the biggest eigenvalue. Therefore, the q main axes are the lines whose unit vectors are the eigenvectors associated to the q biggest eigenvalues and going by G.

We obtain the principal coordinates of the data by projecting them in this space, i.e. by making the scalar product of the coordinates (centered reduced) of a data by each one of the P eigenvectors. By taking $q = 2$, we can represent the N data in the principal plan.

The data distribution in the principal plan must be realized and studied. The problem is to know if the representation in the principal plan is faithful to the initial group of data. We approach this point below.

In the rest, we give an explanation on the calculation of eigenvectors and eigenvalues of the correlation matrix.

The first question is "What are we looking for"? The answer is that we seek the directions of greater lengthening of the data group, these directions having to be orthogonal to obtain an orthogonal base.

The second question is "How to determine lengthening according to a certain direction $\vec{v}$ of the data group? We determine it by the variance according to this direction which is obtained by $V^T R V$.

The third question is "How we obtain the direction of greater lengthening? We look for the vector $\vec{V}$ which maximizes this lengthening, so which cancels the derivative of this lengthening. We seek $\vec{v}$ a vector with norm 1 which cancels $\frac{d \vec{v}^T R \vec{v}}{d \vec{v}}$. The direct calculation of this derivative don't give anything interesting, the trick consists in calculating the derivative of this same quantity divided by 1; the norm of $\vec{v}$ is 1 (by assumption); this norm is worth $\vec{v}^T R \vec{v}$; we are interested in $\vec{v}$ which cancels $\frac{(d \vec{v}^T R \vec{v})/(\vec{v}^T \vec{v})}{d \vec{v}}$. So that this derivative is null, the relation obtained is: $R \vec{v} = \left(\vec{v}^T R \vec{v} \right) \vec{v} = \lambda \vec{v}$.

Therefore, $\vec{v}$ must be an eigenvector of R associated to the eigenvalue. We must be interested in the eigenvector associated to the greatest eigenvalue. More generally, the set ordered eigenvectors according to their decreasing eigenvalues will provide the set of directions corresponding to lengthening in the decreasing order of the data group.

The matrix R is symmetric and definite positive. It has only real and positive or null eigenvalues. Moreover, eigenvectors form an orthonormal base. The rank of the eigenvalues indicates their importance. If some eigenvalues have much more important values than the others that mean that the essence of information is given by these main axes and that the others axes give little information.

On the contrary, if all the eigenvalues have approximately the same value, then no main axis can be left. The ideal situation is, when one or two eigenvalues are very important compared to the others. Notice that $\sum_{i \in \{1,...,P\}} \lambda_i = P$, the importance of an eigenvalue compared to the others is well measured by its inertia. It is given in equation (11).

$$\lambda_i = \frac{\lambda_i}{P} \tag{11}$$

λ_i is the variance along the main axis carried by the eigenvector; therefore $\vec{V}_i$ is the variance of the principal component z_i.

Also we note that the covariance matrix in principal space is diagonal: by a PCA, we obtain a representation in a data space in which the components are not linearly correlated. It is a very interesting property, knowing that projection in the principal plan deforms reality by shortening the distances (the distribution of the data in the first space).

It is necessary to be able to estimate this deformation. For that, we calculate the cosine of the angle formed by the half-line going of the origin to the initial point and the half-line going of the origin to the projection of the point in principal space, either an axis, or a plan.

We note $\theta_{i \in \{1,...,N\}, j \in \{1,...,p\}}$ the angle between the half-line passing by the origin and the initial point x_i and the main axis j. $\theta_{i \in \{1,...,N\}, j \in \{1,...,p\} \times k \in \{1,...,p\}}$ is the angle between the half-line passing by the origin and the plan formed by the main axes j and k. The square cosine of these angles is given in equation (12) and (13).

$$\cos^2 \theta_{i \in \{1,...,N\}, j \in \{1,...,p\}} = \frac{{z_{ij}}^2}{\sum_{j \in \{1,...,P\}} {x_{ij}}^2} \tag{12}$$

$$\cos^2 \theta_{i \in \{1,...,N\}, j \in \{1,...,p\} \times k \in \{1,...,p\}} = \frac{{z_{ij}}^2 + {z_{ik}}^2}{\sum_{j \in \{1,...,P\}} {x_{ij}}^2} \tag{13}$$

Where z_{ij} and z_{ik} are the coordinates on the main axes j and k of the data x_i. A square cosine lower than 0.3 indicates an important deformation (>57°).

The linear coefficient of correlation between the j^{th} initial variable x_j and the k^{th} principal component z_k is given in equation (14).

$$r_{j,k} = \vec{v}_k[j] \times \sqrt{\lambda_k} \tag{14}$$

All the axes can have their utility. To judge some, it is necessary to compare the various eigenvalues (seen above). For each one, we can measure their inertia I_j and their cumulated inertia. It is given in equation (15).

$$C_i = \sum_{j \le i} I_j \tag{15}$$

D. Dimension Reduction

The dimension reduction procedure makes it possible to reduce the number of variables of the data set while maximizing the information (variance) contained in the simplified model.

Procedure 3*Dimension Reduction by PCA*

Step 1: Data centering and reduction by using equations 6 and 7.

Step 2: Calculation of the correlation or covariance matrix using the equations 8 and 9.

Step 3: Calculation of eigenvalues and eigenvectors of the matrix.

Step 4: Sort out the eigenvalues thanks to their inertia given by the equation 11.

Step 5: Select the $K \le P$ eigenvectors and generate the whole data in a new presentations structure using the equation 15.

Step 6: Look into the correlation between the initial and the principal data using the equation 14.

This procedure will be applied to the data set in order to ensure a dimension reduction. Once reduced, WEFCM can be applied to classify the data. The new algorithm was named SR-WEFCM (Scale Reduction-Weighted Enhance Fuzzy C-Means).

E. Illustrative Example

For a better assimilation of PCA, we take again the example given above with persons and their characteristics. It is given by equation (16).

$$R = \begin{pmatrix} & Weight & Tall & Age & Mark \\ Weight & 1 & 0.37 & 0.48 & -0.56 \\ Tall & 0.36 & 1 & 0.39 & -0.32 \\ Age & 0.48 & 0.39 & 1 & -0.32 \\ Mark & -0.56 & -0.62 & -0.32 & 1 \end{pmatrix} \tag{16}$$

The eigenvalues and eigenvectors are given in equation (17).

$$\lambda_1 = 2.391, \ \vec{v}_1 = (0.5080, 0.5038, 0.4455, -0{,}5383) \tag{17}$$

$$\lambda_2 = 0.750, \ \vec{v}_2 = (0.3065, 0.4641, 0.7085, -0{,}4381)$$

$$\lambda_3 = 0.584, \ \vec{v}_3 = (-0.6593, 0.5253, 0.4712, -0{,}2593)$$

$$\lambda_4 = 0.274, \ \vec{v}_4 = (-0.4619, 0.5042, 0.2855, -0{,}6715)$$

We notice that no eigenvalue is null and we can verify that the 4 eigenvectors are unit and orthogonal two to two. We can calculate the inertia and the cumulated inertia of each eigenvalue in table V.

TABLE V. INERTIA AND CUMULATED INERTIA FOR EACH EIGENVALUE

λ	I	C
2.391	0.59775	0.59775
0.750	0.1875	0.78525
0.584	0.146	0.93125
0.274	0.0685	1.0

The data coordinates in the new reference mark are calculated as given in equation (18).

$$\begin{pmatrix} (x_{1,1} & x_{1,2} & x_{1,3} & x_{1,4})\vec{V}_1 \\ (x_{1,1} & x_{1,2} & x_{1,3} & x_{1,4})\vec{V}_2 \\ (x_{1,1} & x_{1,2} & x_{1,3} & x_{1,4})\vec{V}_3 \\ (x_{1,1} & x_{1,2} & x_{1,3} & x_{1,4})\vec{V}_4 \end{pmatrix} \tag{18}$$

For example, the coordinates of first data are: (-2,64;-0,20;-0,10; 1,04).

The data coordinates on the principal's axis are given in table VI.

TABLE VI. DATA COORDINATES IN THE NEW PRINCIPAL PLAN

Data	Coordinates
1	(-2.64, -0.20,-0.10 ,1.04)
2	(-1.94, -0.36, 0.32,-0.35)
3	(-1.44,-0.80, 0.59,-0.35)
4	(2.08,-0.08, 1.20, 0.19)
5	(0.99,-0.42, 0.30,-0.05)
6	(1.47,-0.82, 0.06, 0.56)
7	(1.32,-0.35,- 1.45, 0.41)
8	(-0.43,-0.14, -1.25,-0.67)
9	(-0.57, 2.39, 0.41,-0.07)
10	(1.17,-0.08, -0.07,-0.57)

In table VII, we calculate the correlation between initial variables and principal components.

TABLE VII. STUDY OF THE CORRELATION BETWEEN INITIAL VARIABLES AND PRINCIPAL COMPONENTS

	z_1	z_2	z_3	z_4
Weight	0.785	0.266	-0.504	-0.242
Tall	0.779	-0.403	0.402	-0.264
Age	0.689	0.611	0.360	0.150
Mark	-0.832	0.380	0.198	-0.352

We notice that: the 4 variables are strongly correlated (in absolute value) with the first main axis. The variable Mark is correlated negatively with the three other variables. And finally to estimate the deformation due to projection in the principal plan, we calculate $\cos^2$. It is given in table VIII.

TABLE VIII. ILLUSTRATION OF THE DEFORMATION DUE TO THE PROJECTION

Data	$\cos^2 \theta_{1,1}$	$\cos^2 \theta_{1,2}$	$\cos^2 \theta_{1,3}$	$\cos^2 \theta_{1,4}$
1	**0.859**	**0.005**	**0.82**	**0.82**
2	**0.916**	**0.031**	**0.94**	**0.94**
3	**0.628**	**0.195**	**0.83**	**0.74**
4	**0.745**	**0.001**	**0.75**	**0.99**
5	**0.785**	**0.142**	**0.88**	**0.79**
6	**0.690**	**0.212**	**0.87**	**0.67**
7	**0.419**	**0.030**	**0.45**	**0.93**
8	**0.084**	**0.008**	**0.09**	**0.79**
9	**0.053**	**0.919**	**0.97**	**0.08**
10	**0.804**	**0.004**	**0.80**	**0.80**

IV. EXPERIMENTATION AND EVALUATION

We evaluated in experiments the algorithm SR-WEFCM on large-scale data such as isolet5. We then carried out a comparison of the results given when we applied only WEFCM to the data and in the case when we applied SR-WEFCM.

ISOLET5 is a subset of the ISOLET (Isolated Letter Speech Recognition) set, the letter of the experiment of voice recognition. This subset was prepared in the same way that in [18]. Ten classes out of 26 (represents the letters of the alphabet) were selected by chance (this set is composed of 1559 data and 617 attributes) [18]. The optimal number of clusters for this whole data is 10.

The comparative study will be made according to tow axes: the first consists of the dimension reduction, the second will be the clustering quality.

A. Dimension Reduction

Our dimension reduction procedure using PCA produces two files: the first contains a general data analysis like columns average, their standard deviation, the values, the vectors and some other information about correlation between the initial variable and principles components. The second file contains new coordinates of each data in the new plan.

The performance and importance of the dimension reduction approach using PCA becomes clear when we examine the isolet5 data set. Thanks to this method we could reduce the variables number. After this analysis, we obtain 3 principles components instead of 617 attributes. Each principle component presents and synthesizes a set of initial variables.

During this first step, we could reduce the attributes number to a restricted number of principles components. In other word, we were aware of information quantity observed in the initial data set while tacking only few reduced principles components. We obtained the new coordinates in the new mark. The next step will be the data reduction, which means that we will apply the WEFCM clustering algorithm on the new data set.

B. Clustering Quality

We applied WEFCM and SR-WEFCM to ISOLET5, 10 is the optimal the number of clusters. The matrix of the output centers was the following one:

TABLE IX. MATRIX OF CENTERS BY WEFCM

	Variable 1	**…**	**Variable 100**	**…**
Cluster 1	-0.032180	…	0.103958	…
…	…	…	…	…
…	…	…	…	…
Cluster 10	0.074184	…	0.055395	…

We point out that each element contains 617 Attributes, and therefore we chose to represent only some attributes, and only for some clusters.

TABLE X. MATRIX OF GENERATED C ENTERS BY SR-WEFCM

	Variable 1	**Variable 2**	**Variable 3**
Cluster 1	0.216584	-0.036261	-0.000480
…	…	…	…
…	…	…	…
Cluster 10	-0.002041	0.000196	0.152780

In the same way, we drew the tables of the associated indices relating to ISOLET5.

Table VII presents the validity indices obtained when we use WEFCM clustering algorithm.

TABLE XI. VALIDITY INDICES WITH WEFCM

Number of clusters	**Validity indices**
11	0.026344
10	0.050870
9	0.046293
8	0.028907
7	0.029964
6	0.020478
5	0.017594
4	0.013673
3	0.006801
2	0.001851

As we can see, the optimal number of clusters is obtained with the biggest value of validity index.

Table VIII presents the validity indices obtained when we use SR-WEFCM clustering algorithm.

TABLE XII. VALIDITY INDICES WITH SR-WEFCM

Number of clusters	Validity indices
11	0.049331
10	0.283013
9	0.030206
8	0.044234
7	0.036985
6	0.245792
5	0.120833
4	0.022860
3	0.046677
2	0.001674

According to table VIII, the biggest value of the index corresponded to the optimal number of clusters is equal to 10.

We note that in spite of the dimension reduction, the suggested system proved its performances in the determination and the evaluation of the number of clustering.

Table IX presents the run time of both WEFCM and SR-WEFCM clustering algorithms.

TABLE XIII. RUN TIME

WEFCM	71.076442
SR-WEFCM	0.288956

The importance of our system was quite remarkable also when we examine the run time of the clustering algorithm for large-scale data set, (the isolet5 in our case). It is noticed that the difference in run time is very important, so, we can say that the reduction of large-scale data set by dimension reduction procedure involves necessarily a run time reduction.

V. CONCLUSION

Recent progress in data filing field offers new challenges to the theorists of Data Mining. One of these challenges is to manage large data sets, in which traditional algorithms and researcher's intuition have multiple difficulties.

In this direction, clustering proposes important and effective techniques of data sampling and compression in order to reduce the memory size dedicated to the data which will be classified.

So, it is possible to know, that only a small number of variables have interest. In this case, these variables can be selected and the other thrown, in order to reduce the data set dimensionality. More generally, dimension and data reduction prove to be necessary for the management of large-scale data sets.

The scale-reduction is a complex problem which has been largely studied. In this paper, we have proposed a new clustering algorithm, called SR-WEFCM, used in the case of large-scale data sets and based on, both a compression technique to reduce the data, and PCA to reduce the variables (or attributes).

With SR-WEFCM, our objective is reached. We work out an automatic clustering algorithm for large-scale data set. This is ensured through both an enhanced compression technique and validity measures which allow the evaluation of obtained clustering while giving the optimal number of clusters. It ensures a double reduction, the dimension and the data.

As future work, we propose to i) test our approaches with other large-scale data sets and ii) take into account uncertain data and keep only the data representative by using a selection variables technique.

REFERENCES

[1] J. Han and M. Kamber, Data Mining: Concepts and Techniques, San Francisco:Morgan Kaufmann Publishers, pp.105-130, 2001.

[2] T. Zhang, R. Ramakrishnan, and, M. Livny, "BIRCH: An efficient data clustering algorithm for large databases," ACM SIGMOD International Conference on Management of Data, pp. 73-84, 98, Montreal, Canada, 1996.

[3] J. McMueen, "Some methods for classiffication and analysis of multivariate observations," The Fifth Berkeley Symposium on Mathematical Statistics and Probability, pp. 81-297, 1967.

[4] J. Bezdek, Fuzzy mathematics in pattern classification, Ph.D. Dissertation, Cor-nell University, 1973.

[5] W.P.Vogt, Dictionary of statistics and methodology, A nontechnical guide for the social sciences, CA: Sage, pp. 177,1993.

[6] J. Bezdek, Chapter F6: Pattern Recognition in Handbook of Fuzzy Computation, IOP Publishing Ltd, 1998.

[7] H.Sun, "A theory on distinguishing overlapping components in mixture models," Research Report, DMI, University of Sherbrooke, n° 345, November 2003.

[8] M. Sassi, G.Touzi, and H. Ounelli, "Using Gaussians Functions to Determine Representative Clustering Prototypes," 17th IEEE International Conference on Database and Expert Systems Applications, Poland, pp. 435-439, 2006.

[9] P. Hore, L. Hall, and D. Goldgof, Single Pass Fuzzy C Means, IEEE International conference on Fuzzy Systems, pp. 847-852, 2007.

[10] P. Hore, L.Hall, and D.Goldgof, "A Cluster Ensemble Framework for Large Datasets," IEEE International Conference Systems, Manand Cybernetics, 2006.

[11] P.S Bradley and U.M. Fayyad, "Refining initial points for k-means clustering," 15th International Conference on Machine Learning, Morgan kaufmann, San Francisco, pp. 91-99, 1998.

[12] J. Vaillant, Notion de base en échantillonnage, Université des Antilles-guyanne, 1996.

[13] M. Aounallah, S. Quirion and G. Mineau, Forage distribué des données: une comparaison entre l'agrégation d'échantillons et l'agrégation de règles, 2004.

[14] P.S. Bradley, U.M. Fayyad and C.A. Reina, Scaling EM (Exepectation-Maximization) Clustering to Large DataBases, October 1998.

[15] D. P. Mercer, Clustering large datasets. Technical report, Linacre College, Octobre 2003.

[16] C.Candillier,thesis extract: " Méthodes d'Extraction de Connaissances à partir de Données (ECD) appliquées aux Systèmes d'Information Géographiques (SIG), " UFR Sciences et techniques, Université de Nante, September 2006.

[17] T.Ng. Raymond and J.Han, "CLARANS: A Method for Clustering Objects for Spatial Data Mining," IEEE Transactions on knowledge and data engeneering, vol. 14, no. 5, September/October 2002.

[18] Machine Learning Repository . Available at: http://archive.ics.uci.edu/ml/.

[19] M. Sassi, A. Grissa, "Clustering Large Data sets based on Data Compression Technique," IEEE conference on Fuzzy Systems (FUZZ-IEEE), Korea, August 20-24, pp. 396-402, 2009.

2011 IEEE International Conference on Fuzzy Systems
June 27-30, 2011, Taipei, Taiwan

Soft Subspace Clustering with Competitive Agglomeration

Lin Zhu
Institute of Image Processing and Pattern Recognition
Shanghai Jiao Tong University
Shanghai, China
Email: zhulin@sjtu.edu.cn

Longbing Cao*
Faculty of Engineering and IT, QCIS
University of Technology, Sydney
Sydney, Australia
Email: longbing.cao-1@uts.edu.au

Jie Yang
Institute of Image Processing and Pattern Recognition
Shanghai Jiao Tong University
Shanghai, China
Email: jieyang@sjtu.edu.cn

***Abstract*—In this paper, two novel soft subspace clustering algorithms, namely fuzzy weighting subspace clustering with competitive agglomeration (FWSCA) and entropy weighting subspace clustering with competitive agglomeration (EWSCA), are proposed to overcome the problems of the unknown number of clusters and the initialization of prototypes for soft subspace clustering. The main advantage of FWSCA and EWSCA lies in the fact that they effectively integrate the merits of soft subspace clustering and the good properties of fuzzy clustering with competitive agglomeration. This makes it possible to obtain the appropriate number of clusters during the clustering progress. Moreover, FWSCA and EWSCA algorithms can converge regardless of the initial number of clusters and initialization. Substantial experimental results on both synthetic and real data sets demonstrate the effectiveness of FWSCA and EWSCA in addressing the two problems.**

Keywords-subspace clustering; competitive agglomeration; fuzzy weighting subspace clustering; entropy weighting subspace clustering; optimal number of clusters

I. INTRODUCTION

Clustering has long been a hot research topic in various disciplines. It has been widely utilized as an efficient tool for data analysis and visualization in areas such as machine learning and data mining [1]. Clustering partitions the unlabeled input vectors into different groups, called clusters, such that data points within a cluster are more similar to each other than they are to those belonging to different clusters, i.e., by maximizing the intra-cluster similarity while minimizing the inter-class similarity [2]. However, clustering high dimensional data has become an emerging research field, since dimensions might have locally varying relevance for different groups of objects in high dimensional spaces [3]. For example, given a subset of data points identified in a cluster, it is possible that these points exhibit different characteristics from others when varied subsets of dimensions are observed.

The difficulty that traditional clustering algorithms encounter in dealing with high dimensional data sets inspired the invention of subspace clustering or projected clustering [4], which has been studied extensively in recent years [3-13]. The goal of subspace clustering is to locate clusters embedded in different subspaces of the original data space with their own associated dimensions. Based on the ways that the subspaces of clusters are determined, subspace clustering algorithms can be generally classified into two main categories : hard subspace clustering and soft subspace clustering [5]. Hard subspace clustering methods identify the exact subspaces for different clusters, which can be divided into bottom-up [4, 6] and top-down [7] subspace methods according to their subspace searching methods. Soft subspace clustering methods can measure the importance of each dimensionality to a particular cluster in the clustering process by automatically assigning different weightings to different dimensions of clusters embedded in subspaces. In this paper, we focus on soft subspace clustering. Many different soft subspace clustering algorithms have been proposed recently [8-13] and the resulting algorithms can be grouped into two main categories [9, 11]: fuzzy weighting subspace clustering (FWSC) and entropy weighting subspace clustering (EWSC). The final partition of both the FWSC and EWSC approaches assumes that the number of clusters is known prior to clustering. However, this is rarely the case and the optimal number of clusters is hard to determine.

In order to deal with the above problem for traditional clustering algorithms, Frigui and Krishnapuram introduced a regularization term to the original objective function of FCM and derived the fuzzy clustering with competitive agglomeration algorithm (FCA) [14]. In FCA, the initial partition has an over-specified number of clusters, which is progressively reduced until an optimum is reached. Zhang et al. revisited and reformulated the FCA algorithm from the point of view of entropy minimization, and proposed four generalized competitive clustering algorithms: RECA, SECA, CA-p and RECA-p [15]. Grira et al. presented a new algorithm, active fuzzy constrained clustering, in the categorization of image database by minimizing a competitive agglomeration cost function with fuzzy terms corresponding to pairwise constraints provided by the user [16]. Recently, Jeng et al. proposed an interval competitive agglomeration clustering algorithm, which uses the theory of competitive agglomeration for clustering the symbolic interval-values data [17]. However, all these competitive agglomeration-based clustering algorithms are applied in full dimensional space. It is anticipated that the performance of clustering can be further enhanced by including subspace selection in the clustering process.

By considering the advantages of competitive agglomeration, clustering algorithms can be rapidly converged in a few iterations regardless of the initial number of clusters, and can also converge to the same optimal partition regardless of its initialization. Inspired by this fact of competitive agglomeration, we propose two novel soft subspaces clustering

* Corresponding author: email (longbing.cao-1@uts.edu.au)

algorithms: fuzzy weighting subspace clustering with competitive agglomeration (FWSCA) and entropy weighting subspace clustering with competitive agglomeration (EWSCA). FWSCA and EWSCA not only inherit the merits of soft subspace clustering, but also receive the beneficial properties of fuzzy clustering with competitive agglomeration. Our experiment results demonstrate that FWSCA and EWSCA are generally effective in subspace clustering and can achieve superior performance over traditional soft subspace clustering and competitive agglomeration-based clustering algorithms in most cases. Furthermore, a link between FWSCA, EWSCA algorithms and FWSC, EWSC algorithms is established in Section III.A. Thus, the FWSC and EWSC algorithms are regarded as a special case of the proposed FWSCA and EWSCA algorithms. The rest of this paper is organized as follows. In Section Ⅱ, a brief overview of existing algorithms for soft subspace clustering is provided. The proposed FWSCA and EWSCA algorithms are presented and their properties are explained in Section Ⅲ. In Section Ⅳ, the clustering performances of FWSCA and EWSCA, as compared with other algorithms, on artificial and UCI data sets are reported. Finally, conclusions and future work are presented in Section Ⅴ.

II. SOFT SUBSPACE CLUSTERING

Soft clustering aims at grouping a set of given data points $X = \{x_1, x_2, \cdots x_n\} \subset R^d$ into a set of clustering prototypes $V = \{v_i,\ 1 \le i \le c\}$. Let u_{ij} denote the membership degree of x_j belonging to v_i, then we can define the fuzzy *c*-partition *U* of the given data set, i.e., $U = \{u_{ij} \mid 1 \le i \le c,\ 1 \le j \le n\}$. To discover clusters from different subspaces, it is important that a soft clustering algorithm has the capability of clustering data points in a subspace by automatically weighting features in the clustering process. Based on the importance of the *k*-th dimension on the formation of *i*-th cluster, a weighting w_{ik} is assigned to each dimension in soft subspace clustering. The subspaces of different clusters can be identified by the weight matrix $W = \{w_{ik} \mid 1 \le i \le c,\ 1 \le k \le d\}$ after clustering [11, 12].

A. Fuzzy weighting subspace clustering

Fuzzy weighting subspace clustering (FWSC) aims to find clusters from fuzzy weighting subspaces [8, 10, 12]. In all the fuzzy weighting subspace clustering algorithms, a fuzzy weight w_{ik}^m is assigned to the features of different clusters with a fuzzy weighting index m. The objective function of FWSC is generally formulated as:

$$J_{FWSC} = \sum_{i=1}^{c}\sum_{j=1}^{n} u_{ij}^2 \sum_{k=1}^{d} w_{ik}^m (x_{jk} - v_{ik})^2 \tag{1}$$

$$\text{s. t. } 0 \le u_{ij} \le 1, \sum_{i=1}^{c} u_{ij} = 1, 0 \le w_{ik} \le 1, \sum_{k=1}^{d} w_{ik} = 1.$$

By minimizing (1) using Lagrangian optimization, the updating equation for estimating center v_i, fuzzy weighting w_{ik} and membership u_{ij} can be derived.

B. Entropy weighting subspace clustering

The entropy concept, which is used to represent the certainty of dimensions in the identification of a cluster, is introduced into soft subspace clustering [9, 11, 13]. Because the weights in extended subspace clustering algorithms are controllable by entropy, these types of algorithms are referred to as entropy weighting subspace clustering (EWSC). In general, the objective function of EWSC can be defined as:

$$J_{EWSC} = \sum_{i=1}^{c}\sum_{j=1}^{n} u_{ij}^2 \sum_{k=1}^{d} w_{ik} (x_{jk} - v_{ik})^2 + \gamma \sum_{i=1}^{c}\sum_{k=1}^{d} w_{ik} \log w_{ik} \tag{2}$$

$$\text{s. t. } 0 \le u_{ij} \le 1, \sum_{i=1}^{c} u_{ij} = 1, 0 \le w_{ik} \le 1, \sum_{k=1}^{d} w_{ik} = 1.$$

The Lagrange multipliers method is also applied to minimize the objective function in (2). It can result in the equations for updating the estimations of center v_i, entropy weighting w_{ik} and membership u_{ij}. In (1) and (2), to cater for the fuzzy partition, we specify $0 \le u_{ij} \le 1$, while $u_{ij} \in \{0,1\}$ is used in the K-means framework-based FWSC [8, 10, 12] and EWSC algorithms [11, 13] for hard partition.

By observing the existing soft subspace clustering algorithms, we find that the final partition of both FWSC and EWSC is based on the assumption that the number of clusters is known prior to clustering. However, this is rarely the case, and the optimal number of clusters is difficult to determine. As a result, the clustering algorithms are sensitive to the initialization. An effective way to overcome the above problems is to extend the concept of the competitive agglomeration (CA) in FWSC and EWSC, since CA can help to determine the initialization and the number of clusters during the clustering progress.

III. SOFT SUBSPACE CLUSTERING WITH COMPETITIVE AGGLOMERATION

A. Objective function based on the theory of competitive agglomeration

How to find an "appropriate" number of clusters is an important issue for partition-based clustering. Fuzzy clustering with competitive agglomeration (FCA) was introduced to solve the problem by adding a regularization term to the cost function [14]. The regularization term can avoid overfitting of a data set with too many prototypes, make clusters compete for membership of data points, and result in the number of clusters gradually being reduced until an optimum is reached.

To incorporate the idea of competitive agglomeration into FWSC and EWSC, we add a term to agglomerate all data points into one cluster in the objective functions to generate fuzzy weighting and entropy weighting-based subspace clustering with competitive agglomeration, namely FWSCA, EWSCA, which minimize:

$$J_{FWSCA} = \sum_{i=1}^{c}\sum_{j=1}^{n} u_{ij}^2 \sum_{k=1}^{d} w_{ik}^m (x_{jk} - v_{ik})^2 - \alpha \sum_{i=1}^{c}\left[\sum_{j=1}^{n} u_{ij}\right]^2 \quad (3)$$

and

$$J_{EWSCA} = \sum_{i=1}^{c}\sum_{j=1}^{n} u_{ij}^2 \sum_{k=1}^{d} w_{ik} (x_{jk} - v_{ik})^2 + \gamma \sum_{i=1}^{c}\sum_{k=1}^{d} w_{ik} \log w_{ik} - \alpha \sum_{i=1}^{c}\left[\sum_{j=1}^{n} u_{ij}\right]^2 \quad (4)$$

under the same constraint of (1) or (2).

By comparing the objective functions (3) and (4) for FWSCA and EWSCA and those in (1) and (2) for FWSC and EWSC, the first terms of objective functions for FWSCA and EWSCA are similar to those of FWSC and EWSC. The first term of FWSCA is the sum of the squared distances to the prototypes weighted by the constrained feature weightings and fuzzy memberships; and the first term of EWSCA is the sum of the intra-cluster dispersions and the negative weight entropy. Both components allow us to control the shapes and sizes of the clusters and lead to the compact clusters. The global minimum of these components is achieved when the number of clusters c is equal to the number of data points n. The last terms of (3) and (4) are the sum of squares of the cardinalities of the clusters, which allows us to control the number of clusters. By minimizing this term, all data points are agglomerated into one cluster, as shown by Theorem 1.

Theorem 1: Given $0 \le u_{ij} \le 1$ and $\sum_{i=1}^{c} u_{ij} = 1$, the membership constraint function $f(u_{11}, u_{12}, \cdots u_{cn}) = -\sum_{i=1}^{c}\left[\sum_{j=1}^{n} u_{ij}\right]^2$ reaches its minimum, i.e. $-n^2$, when u_{ij} is equal to 1 and u_{kj} are equal to 0 for all other $k \ne i$ $(1 \le j \le n)$.

Therefore, the parameter α in (3) and (4) controls the balance between the two components in order to find an optimal number of clusters c. It should be noted that c is dynamically updated during the process of FWSCA and EWSCA. Fig. 1 shows the relationship between the objective function and the number of clusters for FWSCA and EWSCA on a synthetic data set used in Section Ⅳ. To show the dynamics of three curves simultaneously, all values are normalized into the interval [3, 15], since the optimal number of clusters and the initial number of clusters are 3 and 15, respectively. It shows that the first term of the FWSCA and EWSCA objective function increases as the number of clusters c decreases. On the other hand, the last term of the objective functions becomes smaller when the number of clusters c decreases. The dynamics of the objective function shows that, if α is properly chosen, adjacent clusters will compete for the data points; those clusters lost in competition will gradually be discarded and disappear. Consequently, an appropriate number of clusters is obtained.

B. *Fuzzy weighting subspace clustering with Competitive Agglomeration (FWSCA)*

To minimize the objective function of FWSCA in (3), we apply Lagrange multipliers and obtain the V and W updating equation based on the theorems below.

Theorem 2: Given that U and W are fixed, and $m > 1$, $\alpha > 0$, J_{FWSCA} reaches the local minimum if and only if V meets the following condition:

$$v_{ik} = \frac{\sum_{j=1}^{n} u_{ij}^2 x_{jk}}{\sum_{j=1}^{n} u_{ij}^2} \quad (5)$$

Theorem 3: Given that U and V are fixed, and $m > 1$, $\alpha > 0$, J_{FWSCA} reaches the local minimum if and only if W meets the following condition:

$$w_{ik} = \frac{1}{\sum_{s=1}^{d}\left[\frac{\sum_{j=1}^{n} u_{ij}^2 (x_{jk} - v_{ik})^2}{\sum_{j=1}^{n} u_{ij}^2 (x_{js} - v_{is})^2}\right]^{\frac{1}{m-1}}} \quad (6)$$

To obtain the updating equation u_{ij}, J_{FWSCA} is minimized with respect to U for fixed V and W, and both are set to zero. We apply Lagrange multipliers to (3) and obtain:

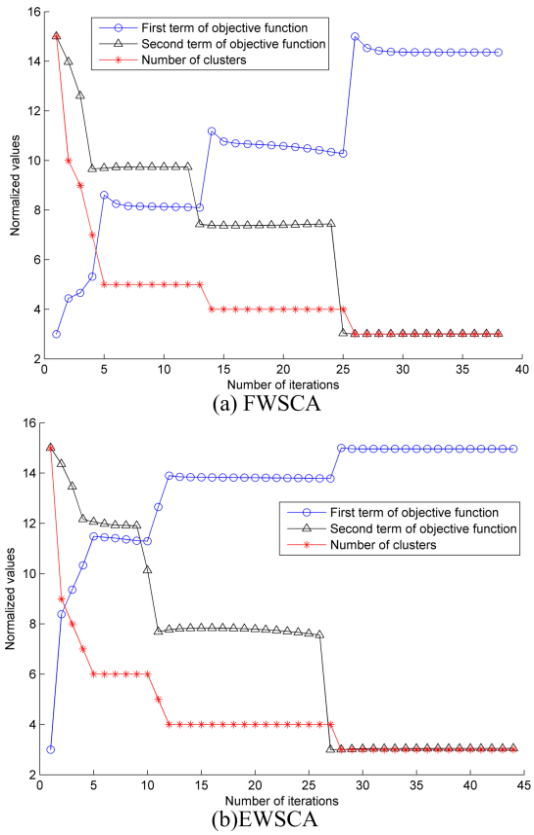

Fig. 1 The change curve of the objective function and the number of clusters. (a) FWSCA, (b) EWSCA

$$\phi(u_{ij}) = \sum_{i=1}^{c}\sum_{j=1}^{n} u_{ij}^2 \sum_{k=1}^{d} w_{ik}^m (x_{jk} - v_{ik})^2 - \alpha \sum_{i=1}^{c}\left[\sum_{j=1}^{n} u_{ij}\right]^2 - \sum_{j=1}^{n} \lambda_j^u \left(\sum_{i=1}^{c} u_{ij} - 1\right) \quad (7)$$

With (7), we can compute the optimal value of u_{ij} by setting $\partial\phi/\partial u_{ij} = 0$. These derivatives yield the following relationship:

$$\frac{\partial \phi}{\partial u_{ij}} = 2u_{ij}\left(\sum_{k=1}^{d} w_{ik}^m (x_{jk} - v_{ik})^2\right) - 2\alpha\left(\sum_{j=1}^{n} u_{ij}\right) - \lambda_j^u = 0 \quad (8)$$

The solution of (8) can be simplified by assuming that the membership values do not change significantly from one iteration to another. With this assumption, and by computing the cardinality of cluster i, $N_i = \sum_{j=1}^{n} u_{ij}$ using the membership values from previous iteration, (8) is converted to

$$u_{ij} = \frac{2\alpha N_i + \lambda_j^u}{2\left(\sum_{k=1}^{d} w_{ik}^m (x_{jk} - v_{ik})^2\right)} \quad (9)$$

Using the membership constraint $\sum_{s=1}^{c} u_{sj} = 1$, we obtain

$$\lambda_j^u = \frac{1 - \alpha \sum_{s=1}^{c}\left[N_s \Big/ \left(\sum_{k=1}^{d} w_{sk}^m (x_{jk} - v_{sk})^2\right)\right]}{\sum_{s=1}^{c}\left[1 \Big/ \left(2\sum_{k=1}^{d} w_{sk}^m (x_{jk} - v_{sk})^2\right)\right]} \quad (10)$$

Substituting (10) in (9), we obtain the following updated equation for the membership of data point x_j to center v_i after rearranging the terms.

$$u_{ij} = u_{ij}^{FCM} + u_{ij}^{Bias} \quad (11)$$

where

$$u_{ij}^{FCM} = \frac{1}{\sum_{s=1}^{c}\left[\left(\sum_{k=1}^{d} w_{ik}^m (x_{jk} - v_{ik})^2\right) \Big/ \left(\sum_{k=1}^{d} w_{sk}^m (x_{jk} - v_{sk})^2\right)\right]} \quad (12)$$

and

$$u_{ij}^{Bias} = \alpha \frac{N_i - \bar{N}_j}{\sum_{k=1}^{d} w_{ik}^m (x_{jk} - v_{ik})^2} \quad (13)$$

In (13), $\bar{N}_j$ is defined as

$$\bar{N}_j = \frac{\sum_{s=1}^{c}\left[1 \Big/ \left(\sum_{k=1}^{d} w_{sk}^m (x_{jk} - v_{sk})^2\right) N_s\right]}{\sum_{s=1}^{c}\left[1 \Big/ \left(\sum_{k=1}^{d} w_{sk}^m (x_{jk} - v_{sk})^2\right)\right]} \quad (14)$$

which is simply a weighted average of the cluster cardinalities.

The updated function (11) for FWSCA brings about several benefits. The first component in (11) is the same as that in FCM, and considers only the relative distances of a data point to all clusters. The second component contributes to the reduction of the cardinality of spurious clusters, which are discarded when their cardinality drops below a threshold. Indeed, u_{ij}^{Bias} is also a signed bias term that depends on the difference between the cardinality N_i of the cluster i and the weighted average of the cardinalities $\bar{N}_j$ from x_j. For the clusters with cardinality lower than the average value, the bias term is negative. The membership value is then decreased.

Further, α plays an important role in FWSCA in (13) for balancing the two components of (11). To make FWSCA independent of the distance measure, α should be chosen such that both terms in (11) are of the same order of magnitude [14, 16]. Thus, α should be proportional to the ratio of the two terms. In this paper, α is chosen as

$$\alpha(itr) = \tau(itr) \frac{\sum_{i=1}^{c}\sum_{j=1}^{n} u_{ij}^2 \sum_{k=1}^{d} w_{ik}^m (x_{jk} - v_{ik})^2}{\sum_{i=1}^{c}\left[\sum_{j=1}^{n} u_{ij}\right]^2} \quad (15)$$

where *itr* is an iteration index. The best choice for τ is the exponential factor defined in [16]

$$\tau(itr) = \tau_0 \exp(-|itr - itr_0| / \xi) \quad (16)$$

In our experiments, the initial value τ_0, the time constant itr_0, and ξ in (16) are set as 0.8, 10 and 20, respectively.

Finally, let us discuss the agglomeration process of FWSCA. As discussed in [16], FCA [14] discards spurious clusters whose cardinalities drop below a threshold; however the clustering is sensitive to the threshold parameter. In this paper, we investigate an alternative process to improve the agglomeration. The details of the process are given as follows.

We first compute the average cardinality of clusters at the *itr-th* iteration below.

$$Card_{avg}(itr) = \frac{\sum_{i=1}^{c}\sum_{j=1}^{n} u_{ij}}{num_of_cluster(itr)} = \frac{n}{c(itr)} \quad (17)$$

where *itr* is an iteration index, *n* is the number of data points and *c*(*itr*) is the number of clusters at the *itr-th* iteration. So the minimum cardinality threshold (*MCT*) can be defined by

$$MCT(itr) = \eta \times Card_{avg}(itr) \quad (18)$$

where η is the agglomeration threshold parameter. When the cardinality of a cluster reduces below the *MCT* at the *itr-th* iteration, we discard the cluster, and update the number of clusters. The selection of η will be discussed in the experiments in Section Ⅳ.

Next, we compute the distances between pairs of prototypes *d*(*r*), for $r = 1, \cdots, R$, $R = c(itr) \times (c(itr) - 1)/2$. If *min* is the index corresponding to the pair having the minimal distance

Procedures of FWSCA clustering algorithm

Step1. Set the maximum number of clusters c=c_{max} ($2 \le c_{max} \le n$), the fuzzy weighting index m and the agglomerate threshold parameter η, initialize the fuzzy partition $u_{ij}^{(1)}$ and fix the iterative index itr=1;
Step2. Compute the clustering centers matrix $\boldsymbol{V}(itr+1)$ using Eq.(5);
Step3. Compute the weight matrix $\boldsymbol{W}(itr+1)$ using Eq. (6);
Step4. Compute the cardinality N_i for $1 \le i \le c$;
Step5. Update $\alpha(itr)$ using Eq. (15) and Eq. (16);
Step6. Compute the partition matrix $\boldsymbol{U}(itr+1)$ using Eq. (11);
Step7. If N_i is smaller than minimum cardinality threshold (Eq. (18)) or the minimal distance between pairs of prototypes is satisfied Eq. (19) then discard the cluster;
Step8. Update the number of clusters $c(itr+1)$;
Step9. If prototype parameters are stabilized, then output the clustering result and terminate, otherwise itr=itr+1, go to Step 2.

Figure 2. Description of the proposed FWSCA algorithm

d_{min}, then we discard the cluster, and update the number of clusters when the following criterion is satisfied:

$$d_{min} < 0.2 \times \sum_{r=1}^{R} d(r) \Big/ R \tag{19}$$

where $d_{min} = \min\{d(r) \mid r = 1, \cdots, R\}$ and $\sum_{r=1}^{R} d(r) \Big/ R$ is the average distances between pairs of prototypes at the *itr-th* iteration.

Fig. 2 shows the procedure of FWSCA algorithm.

C. *Entropy weighting subspace clustering with Competitive Agglomeration (EWSCA)*

To minimize the objective function of EWSCA defined in (4), the Lagrange multipliers method is applied, and we obtain the following Theorems 4 and 5, which can help the optimization of the EWSCA procedure.

Theorem 4: Given that U and W are fixed, and $\gamma > 0, \alpha > 0$, J_{EWSCA} reaches the local minimum if and only if V meets the following condition:

$$v_{ik} = \frac{\sum_{j=1}^{n} u_{ij}^2 x_{jk}}{\sum_{j=1}^{n} u_{ij}^2} \tag{20}$$

Theorem 5: Given that U and V are fixed, and $\gamma > 0, \alpha > 0$, J_{EWSCA} reaches the local minimum if and only if W meets the following condition:

$$w_{ik} = \frac{\exp(-\sum_{j=1}^{n} u_{ij}^2 (x_{jk} - v_{ik})^2 \Big/ \gamma)}{\sum_{s=1}^{d} \exp(-\sum_{j=1}^{n} u_{ij}^2 (x_{js} - v_{is})^2 \Big/ \gamma)} \tag{21}$$

Similar to the deriving procedures of FWSCA, we obtain the updating equation u_{ij} of EWSCA:

$$u_{ij} = u_{ij}^{FCM'} + u_{ij}^{Bias'} \tag{22}$$

where

$$u_{ij}^{FCM'} = \frac{1}{\sum_{s=1}^{c} \left[\left(\sum_{k=1}^{d} w_{ik} (x_{jk} - v_{ik})^2 \right) \Big/ \left(\sum_{k=1}^{d} w_{sk} (x_{jk} - v_{sk})^2 \right) \right]} \tag{23}$$

$$u_{ij}^{Bias'} = \alpha \frac{N_i - \bar{N}_j}{\sum_{k=1}^{d} w_{ik} (x_{jk} - v_{ik})^2} \tag{24}$$

Procedures of EWSCA clustering algorithm

Step1. Set the maximum number of clusters c=c_{max} ($2 \le c_{max} \le n$), the entropy weighting index γ and the agglomerate threshold parameter η, initialize the fuzzy partition $u_{ij}^{(1)}$ and fix the iterative index itr=1;
Step2. Compute the clustering centers matrix $\boldsymbol{V}(itr+1)$ using Eq.(20);
Step3. Compute the weight matrix $\boldsymbol{W}(itr+1)$ using Eq. (21);
Step4. Compute the cardinality N_i for $1 \le i \le c$;
Step5. Update $\alpha(itr)$ using Eq. (15) and Eq. (16);
Step6. Compute the partition matrix $\boldsymbol{U}(itr+1)$ using Eq. (22);
Step7. If N_i is smaller than minimum cardinality threshold (Eq. (18)) or the minimal distance between pairs of prototypes is satisfied Eq. (19) then discard the cluster;
Step8. Update the number of clusters $c(itr+1)$.
Step9. If prototype parameters are stabilized, then output the clustering result and terminate, otherwise itr=itr+1, go to Step 2.

Figure 3. Description of the proposed EWSCA algorithm.

In (24), $\bar{N}_j$ is defined as

$$\bar{N}_j = \frac{\sum_{s=1}^{c} \left[1 \Big/ \left(\sum_{k=1}^{d} w_{sk} (x_{jk} - v_{sk})^2 \right) N_s \right]}{\sum_{s=1}^{c} \left[1 \Big/ \left(\sum_{k=1}^{d} w_{sk} (x_{jk} - v_{sk})^2 \right) \right]} \tag{25}$$

which is simply a weighted average of the cluster cardinalities.

The selection of α and the agglomeration process of EWSCA are similar to that of FWSCA. Accordingly, we describe the procedures of EWSCA as shown in Fig. 3.

D. *Convergence and computational complexity of FWSCA and EWSCA*

When (5), (6) and (11) are adopted, J_{FWSCA} will certainly converge, because FWSCA degenerates into FWSC when α takes zero, and J_{FWSCA} with $\alpha > 0$ can easily be proved to be convergent using the similar proof in [10]. Similarly, the proposed EWSCA algorithm is indeed an extension of EWSC. By employing a strategy similar to that used in EWSC [11], it can be inferred that the proposed EWSCA algorithm, at least along a subsequence, converges to either a local optimal solution or a saddle point of its objective function.

Thus, FWSC and EWSC can be regarded as special cases of FWSCA and EWSCA respectively. Consequently, FWSCA and EWSCA have the same upper bound of the computational complexity as FWSC and EWSC, i.e., $O(ncdT)$ where n denotes the number of all data points, c denotes the number of the cluster centers which varies from $\boldsymbol{c_{max}}$ to $\boldsymbol{c_{final}}$, d denotes the dimensionality of the data points, and T denotes the maximal number of iterations. As the numbers of clusters for FWSCA and EWSCA are decreased during the clustering progress, they actually require more computational time, and converge a little more slowly than FWSC and EWSC.

IV. Experiments and Evaluation

Two sets of experiments are conducted to compare the clustering results of FWSCA and EWSCA with FCA, FWSC and EWSC. All data sets are preprocessed by normalizing the feature in each dimension into the interval [0, 1]. The initial fuzzy partitions for FCA, FWSCA and EWSCA are obtained by performing the FCM algorithm in the first ten iterations respectively. Normalized mutual information (NMI) [18] and

Rand Index [19] are used to evaluate the performance of five clustering algorithms.

A. *Performance evaluation on synthetic data sets*

In this experiment, we adopt a simulated data set to examine whether FWSCA and EWSCA converge to the appropriate partition and evaluate the clustering performance of five algorithms. The data set consists of three clusters in 2-D space which satisfies the normal distribution: the centers of three clusters are (28, 22), (60, 30) and (45, 38) respectively. For the first two clusters, the number of data points per cluster is 120 and their respective covariance matrices are $\begin{bmatrix} 100 & 0 \\ 0 & 9 \end{bmatrix}$ and $\begin{bmatrix} 9 & 0 \\ 0 & 144 \end{bmatrix}$, respectively. For the last cluster centered at (45, 38), there are 140 data points and its covariance matrix is $\begin{bmatrix} 9 & 0 \\ 0 & 9 \end{bmatrix}$. Fig.4 plots this data set, which is used to test the clustering results, since the data points belonging to three clusters locate at different subspaces. In this experiment, we tried many different values of c_{max} ranging from 9 to 21, and set m=3 in FWSC and FWSCA, $\gamma = 1$ in EWSC and EWSCA, and the agglomeration threshold parameter η of 0.75 in FCA, FWSAC and EWSCA.

First, we analyze the independence of the proposed algorithms from the selection of the initial number of the clusters c_{max}. By setting different c_{max} value (9, 12, 15, 18 and 21), we reduce the number of clusters to observe whether FWSCA and EWSCA converge to the same final partition. As shown in Fig. 5 (a) and (b), we find that FWSCA and EWSCA are insensitive to the initial number of clusters; both algorithms can converge in a few iterations as long as c_{max} is higher than the optimal number of clusters.

Second, we analyze the insensitivity of FWSCA and EWSCA to the initial clustering centers. Fig. 6 (a) and (b) show the relationship between the selection of the initial clustering centers and the number of iterations. The initial clustering centers are randomly selected with c_{max} =15. The results show that both algorithms converge to the same appropriate partition regardless of the initialization of centers.

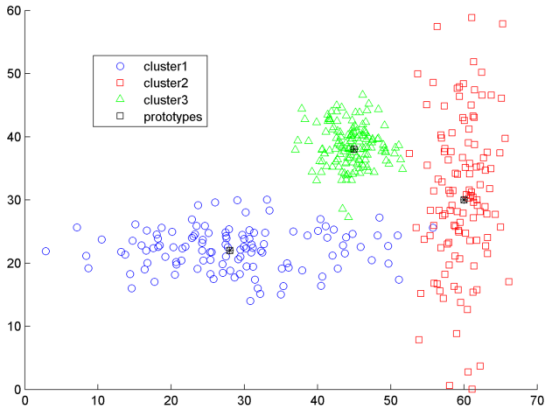

Figure 4. Synthetic data set.

Finally, we compare the clustering performance of FWSCA, EWSCA, FCA, FWSC and EWSC on the synthetic data set. Experiments are conducted by running each algorithm 20 times. The clustering results are evaluated in terms of the means and standard deviations of the NMI and Rand Index values, are shown in Table Ⅰ. From the comparison, we observe that: (1) soft subspace clustering algorithms outperform FCA, since they integrate subspace feature weighting into the clustering process. (2) FWSCA and EWSCA outperform FWSC and EWSC by achieving better and more stable results. This is due to the fact that FWSC and EWSC are sensitive to the initialization, and they can easily get into a local minimum. (3) As we discussed in Section III.D, FWSCA and EWSCA have a slightly higher average number of iterations and average CPU running time (in seconds) than FWSC and EWSC as shown in Table Ⅱ.

B. *Performance evaluation on UCI data sets*

We further evaluate the performance of FWSCA and EWSCA against FCA, FWSC and EWSC on six UCI data sets [20] as shown in Table Ⅲ. In our experience, FWSCA and EWSCA algorithms are independent of the initial number of

TABLE Ⅰ. CLUSTERING RESULTS

Dataset	FWSCA	EWSCA	FCA	FWSC	EWSC
NMI					
Mean	0.8882	**0.9110**	0.6889	0.8422	0.7710
Std	0.0001	0.0001	0.0001	0.1418	0.0332
Rand Index					
Mean	0.9611	**0.9731**	0.8572	0.9373	0.8867
Std	0.0001	0.0001	0.0001	0.0735	0.0203

TABLE Ⅱ. ITERATION NUMBER AND CPU RUNNING TIME (SECONDS)

Dataset	FWSCA	EWSCA	FCA	FWSC	EWSC
Iterations number					
Mean	31.10	46.75	74.00	26.50	34.10
Std	6.55	5.08	0.50	8.70	5.36
Running time					
Mean	0.0853	0.1144	0.1197	0.0327	0.0386
Std	0.0430	0.0410	0.0087	0.0176	0.0243

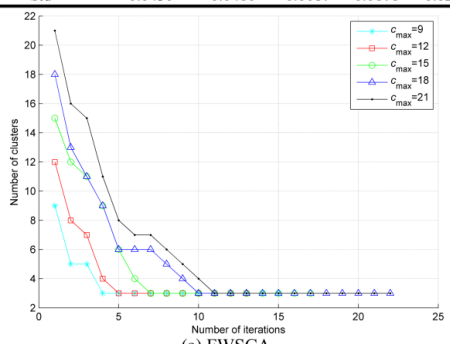

(a) FWSCA

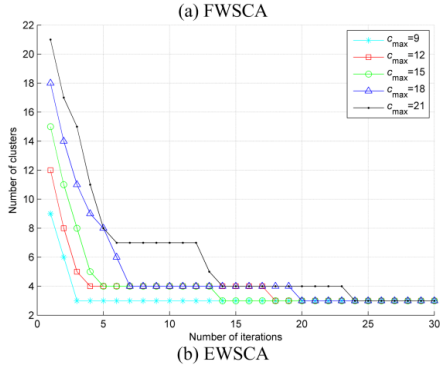

(b) EWSCA

Figure 5. The effect of reducing the number of clusters on convergence with different c_{max} values for (a) FWSCA and (b) EWSCA.

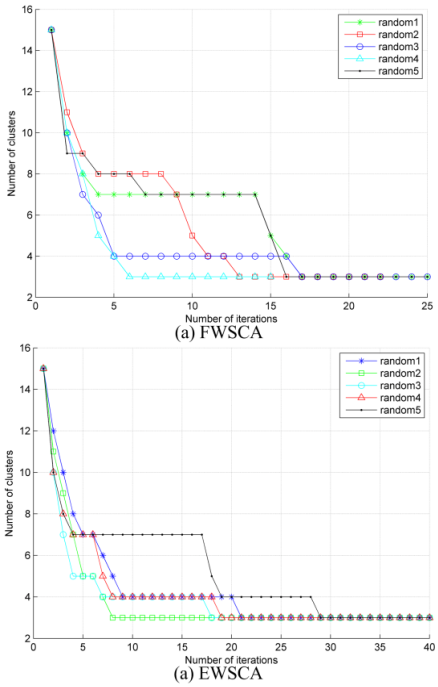

Figure 6. The effect of reducing the number of clusters on convergence with different choices of clustering centers for (a) FWSCA and (b) EWSCA.

clusters c_{max}, when c_{max} is chosen to be much larger than the expected number of clusters and the agglomerate threshold parameter η is appropriately chosen. Our proposed algorithms can produce a sequence of partitions with a decreasing number of clusters and can finally find the appropriate number of clusters. In this paper, we display the clustering results when c_{max} is chosen to be 15.

First, we test the sensitivity of FWSCA and EWSCA on the agglomeration threshold η. For all six UCI data sets, experiments are performed for different values of η ranging from 0.6 to 0.9. For each η, the percentage of 'match' is calculated on the data sets by running each algorithm 20 times. Here 'match' means that the number of clusters identified by FCA, FWSCA and EWSCA is equal to the true number of clusters in a data set. Fig. 7 presents the match percentage on datasets iris and wine for FCA, FWSCA and EWSCA, under a series of agglomeration thresholds η.

As shown in Fig. 7, the match percentage of FWSCA and EWSCA is bigger than FCA, and the effective region of FWSCA and EWSCA is wider than that of FCA. Therefore, FWSCA and EWSCA are less sensitive to η.

Second, we compare the performance of FWSCA and EWSCA against FCA, FWSC and EWSC on the six UCI data sets. We evaluate the cluster validity index NMI and Rand Index under different η values when the algorithms find the true number of clusters. Experiments are conducted by running each algorithm 20 times. The clustering results are shown in terms of mean and standard deviation of NMI and Rand Index, as in Tables Ⅳ and Ⅴ respectively. They show that EWSCA performs better than all other algorithms in most cases.

TABLE Ⅲ UCI DATA SETS USED IN THE EXPERIMENT

Data sets information	Iris	Wine	Heart	Australian	Blood	Pid
Size of data set	150	178	270	690	748	768
Number of dimensions	4	13	13	14	4	8
Number of clusters	3	3	2	2	2	2

Finally, Tables Ⅵ and Ⅶ show the average number of iterations and the average CPU running time (in seconds) of the five algorithms on the UCI data sets. We can see that the iteration numbers and CPU running time of FWSCA and EWSCA are higher than those of FWSC and EWSC. This is due to the fact that the number of clusters for FWSCA and EWSCA decreases during the clustering progress. We also find that the computational complexity of FWSCA and EWSCA is sometimes lower than FCA, since the selection of different subspaces can accelerate the clustering convergence.

In summary, experimental results on both synthetic and real data sets demonstrate that FWSCA and EWSCA have the following advantages. First, both FWSCA and EWSCA outperform the classic soft subspace clustering and competitive agglomeration-based clustering algorithms in most cases. Second, FWSCA and EWSCA can obtain the appropriate number of clusters during the clustering progress regardless of the initial number of clusters. Third, FWSCA and

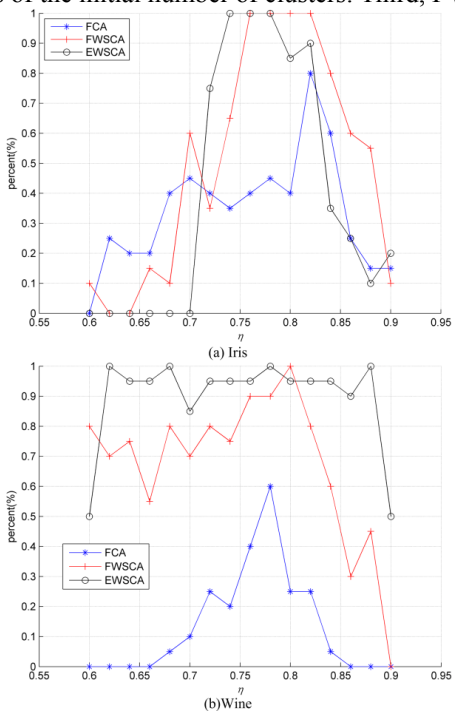

Figure 7. Percentage of the identified number of clusters by an algorithm versus the true number of clusters for different η (a) Iris and (b) Wine.

TABLE Ⅳ. CLUSTERING RESULTS IN TERMS OF NMI.

Dataset	FWSCA	EWSCA	FCA	FWSC	EWSC
Iris					
Mean	0.8623	**0.8801**	0.7433	0.8246	0.8025
Std	0.0047	0.0034	0.0026	0.1685	0.0328
Wine					
Mean	0.7586	0.8216	**0.8336**	0.7586	0.8216
Std	0.0064	0.0083	0.0053	0.0164	0.0078
Heart					
Mean	0.3438	**0.3446**	0.2671	0.3268	0.3095
Std	0.0019	0.0105	0.0090	0.0032	0.0075
Australian					
Mean	**0.3891**	0.3432	0.3228	0.3829	0.3094
Std	0.0020	0.0105	0.0157	0.0039	0.0047
Blood					
Mean	0.8587	**0.8654**	0.8287	0.8587	0.8627
Std	0.0024	0.0104	0.0048	0.0018	0.0075
Pid					
Mean	0.7798	**0.8080**	0.7608	0.7770	0.7793
Std	0.0016	0.0174	0.0138	0.0021	0.0212

TABLE V. CLUSTERING RESULTS IN TERMS OF RAND INDEX.

Dataset	FWSCA	EWSCA	FCA	FWSC	EWSC
Iris					
Mean	0.9495	**0.9575**	0.8797	0.9318	0.9132
Std	0.0023	0.0015	0.0026	0.0795	0.0605
Wine					
Mean	0.8987	0.9265	**0.9331**	0.8987	0.9215
Std	0.0013	0.0026	0.0034	0.0278	0.0196
Heart					
Mean	0.7012	**0.7102**	0.6717	0.7012	0.7063
Std	0.0024	0.0110	0.0062	0.0021	0.0036
Australian					
Mean	**0.7385**	0.6984	0.6810	0.7372	0.6691
Std	0.0137	0.0142	0.0020	0.0010	0.0090
Blood					
Mean	0.5096	**0.5191**	0.4926	0.5096	0.5154
Std	0.0011	0.0164	0.0038	0.0018	0.0224
Pid					
Mean	0.5368	0.5113	**0.5450**	0.4996	0.5242
Std	0.0017	0.0134	0.0014	0.0019	0.0154

TABLE VI. ITERATION NUMBER OF DIFFERENT ALGORITHMS

Dataset	FWSCA	EWSCA	FCA	FWSC	EWSC
Iris					
Mean	36.40	46.65	77.00	39.25	25.40
Std	7.47	12.05	2.31	19.34	2.60
Wine					
Mean	42.80	63.15	74.00	29.85	24.75
Std	2.03	8.86	2.50	3.68	3.12
Heart					
Mean	87.70	56.70	98.10	98.05	60.65
Std	6.13	24.14	4.40	3.21	9.07
Australian					
Mean	100.00	23.85	65.00	38.90	100.00
Std	2.89	12.42	3.50	3.50	3.22
Blood					
Mean	36.40	45.65	90.00	40.05	28.60
Std	1.23	6.03	2.43	2.58	3.63
Pid					
Mean	85.85	30.15	85.00	23.9	20.5
Std	1.84	12.49	1.57	2.14	2.91

TABLE VII. CPU RUNNING TIME (SECONDS) OF DIFFERENT ALGORITHMS

Dataset	FWSCA	EWSCA	FCA	FWSC	EWSC
Iris					
Mean	0.0631	0.0928	0.0938	0.0391	0.0245
Std	0.0108	0.0399	0.0078	0.0320	0.0105
Wine					
Mean	0.1051	0.1396	0.1207	0.7326	0.0245
Std	0.0267	0.0246	0.0290	0.0533	0.0044
Heart					
Mean	0.2183	0.1646	0.1714	0.0930	0.0634
Std	0.0304	0.0610	0.0287	0.0178	0.0223
Australian					
Mean	0.4012	0.1535	0.2029	0.1573	0.1587
Std	0.0346	0.0572	0.0185	0.0243	0.0360
Blood					
Mean	0.1057	0.1447	0.1711	0.0424	0.0339
Std	0.0196	0.0306	0.0329	0.0120	0.0132
Pid					
Mean	0.3042	0.1908	0.2063	0.0353	0.0290
Std	0.0296	0.0684	0.0385	0.0135	0.0094

EWSCA are insensitive to the initialization of the clusters, and can avoid trapping into the local minimum. Furthermore, although both FWSCA and EWSCA assign a weight to each dimension in the clustering process to measure the contribution of the dimension in forming a particular cluster, the experiment results show that EWSCA is better than FWSCA in most case. We attempt to merge the results of both algorithms and see if new insights do emerge in the near future.

V. CONCLUSION

Clustering algorithms face two typical challenges: the unknown number of clusters and the initialization of prototypes in the clustering. This paper has proposed two algorithms to address these problems. First, two novel objective functions have been proposed by extending the fuzzy and entropy subspace clustering objective functions, and integrating the theory of competitive agglomeration. Second, the two soft subspace clustering algorithms with competitive agglomeration, namely FWSCA and EWSCA, have been developed. Extensive experiments on artificial and UCI data sets have shown that FWSCA and EWSCA outperform the classic algorithms FCA, FWSC and EWSC in terms of identifying the number of clusters and the initialization of prototypes in the clustering.

While FWSCA and EWSCA hold great potential for soft subspace clustering, we are further enhancing them, for instance, to improve detection of the true number of clusters and the convergence speed, and to conduct a theoretical study on the sensitive parameters setting of FWSCA and EWSCA algorithms.

REFERENCES

[1] D. T. Anderson, J. C. Bezdek, M. Popescu, and J. M. Keller, "Comparing Fuzzy, Probabilistic, and Possibilistic Partitions," *IEEE Transactions on Fuzzy Systems*, vol. 18, pp. 906-918, 2010.

[2] A. K. Jain, "Data clustering: 50 years beyond K-means," *Pattern Recognition Letters*, vol. 31, pp. 651-666, 2010.

[3] E. Muller, S. Gunnemann, I. Assent, and T. Seidl, "Evaluating clustering in subspace projections of high dimensional data," VLDB 2009, pp. 1270-1281.

[4] R. Agrawal, J. Gehrke, D. Gunopulos, and P. Raghavan, "Automatic subspace clustering of high dimensional data," *Data Mining and Knowledge Discovery*, vol. 11, pp. 5-33, 2005.

[5] P. Lance, H. Ehtesham, and L. Huan, "Subspace clustering for high dimensional data: a review," *SIGKDD Explor. Newsl.*, vol. 6, pp. 90-105, 2004.

[6] C. Chun-Hung, F. Ada Waichee, and Z. Yi, "Entropy-based subspace clustering for mining numerical data," SIGKDD 1999, pp. 84-93.

[7] C. C. Aggarwal and P. S. Yu, "Finding generalized projected clusters in high dimensional spaces," SIGMOD 2000, pp. 70-81.

[8] C. Domeniconi, D. Papadopoulos, D. Gunopulos, and S. Ma, "Subspace clustering of high dimensional data," SDM 2004, pp. 517-522.

[9] Z. H. Deng, K. S. Choi, F. L. Chung, and S. T. Wang, "Enhanced soft subspace clustering integrating within-cluster and between-cluster information," *Pattern Recognition*, vol. 43, pp. 767-781, 2010.

[10] G. Gan and J. Wu, "A convergence theorem for the fuzzy subspace clustering (FSC) algorithm," *Pattern Recognition*, vol. 41, pp. 1939-1947, 2008.

[11] L. Jing, M. K. Ng, and J. Z. Huang, "An entropy weighting k-means algorithm for subspace clustering of high-dimensional sparse data," *IEEE Transactions on knowledge and data engineering*, pp. 1026-1041, 2007.

[12] E. Y. Chan, W. K. Ching, M. K. Ng, and J. Z. Huang, "An optimization algorithm for clustering using weighted dissimilarity measures," *Pattern recognition*, vol. 37, pp. 943-952, 2004.

[13] C. Domeniconi, D. Gunopulos, S. Ma, B. Yan, M. Al-Razgan, and D. Papadopoulos, "Locally adaptive metrics for clustering high dimensional data," *Data Mining and Knowledge Discovery*, vol. 14, pp. 63-97, 2007.

[14] H. Frigui and R. Krishnapuram, "Clustering by competitive agglomeration," *Pattern Recognition*, vol. 30, pp. 1109-1119, 1997.

[15] D. Zhang, S. Chen, and Z. H. Zhou, "Entropy-Inspired Competitive Clustering Algorithms," *Int J Software Informatics*, vol. 1, pp. 67-84, 2007.

[16] N. Grira, M. Crucianu, and N. Boujemaa, "Semi-supervised fuzzy clustering with pairwise-constrained competitive agglomeration," FUZZ-IEEE 2005, pp 867-872.

[17] C. C. Chuang, C. W. Tao, and J. T. Jeng, "Robust clustering algorithm for the symbolic interval-values data with outliers," FUZZ-IEEE 2009, pp. 1232-1237.

[18] A. Strehl and J. Ghosh, "Cluster ensembles - a knowledge reuse framework for combining multiple partitions," *The Journal of Machine Learning Research*, vol. 3, pp. 583-617, 2003.

[19] W. M. Rand, "Objective criteria for the evaluation of clustering methods," *Journal of the American Statistical association*, vol. 66, pp. 846-850, 1971.

[20] C. L. Blake and C. J. Merz, "UCI repository of machine learning databases," 1998.

2011 IEEE International Conference on Fuzzy Systems
June 27-30, 2011, Taipei, Taiwan

Hand Motion Recognition via Fuzzy Active Curve Axis Gaussian Mixture Models: A Comparative Study

Zhaojie Ju
Intelligent Systems & Biomedical Robotics
School of Creative Technologies
University of Portsmouth, UK
Email: zhaojie.ju@port.ac.uk

Honghai Liu
Intelligent Systems & Biomedical Robotics
School of Creative Technologies
University of Portsmouth, UK
Email: honghai.liu@port.ac.uk

***Abstract*—Unconstrained human hand motions consisting grasp motion and in-hand manipulation lead to a fundamental challenge that many algorithms have to face in both theoretical and practical development, mainly due to the complexity and dexterity of the human hand. In this paper, fuzzy active curve axis Gaussian Mixture Model (FAcaGMM) is proposed by introducing a weighting exponent on the fuzzy membership into active curve axis Gaussian Mixture Models (AcaGMM) to improve its convergence efficiency, and then FAcaGMM is used to recognize human hand motions. In addition, a comparative study of recognition methods including FAcaGMM, Time Clustering (TC), Empirical Copula (EC), GMM and HMM is presented to recognize human hand motions including both grasps and in-hand manipulations from different subjects with varying training samples.**

***Keywords*—Motion Recognition; Gaussian Mixture Models; Active Curve Axis Gaussian Mixture Models; Fuzzy Active Curve Axis Gaussian Mixture Models**

I. INTRODUCTION

Human-robot skill transfer is of great importance in order to develop advanced multifingered manipulation planning and control systems. Learning from human hand motions is preferred for human-robot skill transfer in that, unlike teleoperation-related methods, it provides non-contact skill transfer from human motions to robot motions by a paradigm that can endow artifacts with the ability for skill growth and life-long adaptation without detailed programming [1].

During the learning process, hand motion recognition is still an open problem due to the complexity and dexterity of the human hand, though it had been investigated in the past two decades. The attractiveness of applying neural network could be due to the nonlinearity of the network. Neural network approaches demonstrated its powerful grasp recognition in Glove-Talk project [2], [3]. Sato et al. [4] identified predetermined gestures in a fast and robust manner by using a neural network which has been properly trained beforehand. Support vector machine (SVM) was employed by Zoellner *et al* [5] to classify dynamic grasps in the framework of Programming by Demonstration. In addition, David *et al.* [6] used a combination of discriminative (SVM, conditional random fields) and generative approaches, Hidden Markov Model (HMMs), for the modeling and recognition of actions through motor primitives. However, the choice of the SVM kernel function has a significant effect on its performance and the best choice is application dependent. Natal *et al* [7] and Bedregal *et al* [8] developed fuzzy rule-based methods for the recognition of hand gestures, however the methods are highly dependent on a detailed previous analysis of the recognized gesture features with manual transfer involved. Note that Heumer *et al* [9] attempted to provide a performance criteria for hand grasp classification including 28 algorithms provided by Weka data mining software package. However these algorithms usually require more parameters such as finger angular speed instead of position trajectories only, they have also paid less attention to the context of intelligent robotics, for instance, real-time recognition requirement.

In addition, state of the art in human hand motion recognition can be represented by Gaussian Mixture Model (GMMs), HMM and their variants, since they are very rich in mathematical structure and hence their theoretical basis can be adopted for a wide range of applications. Calinon and Billard [10] proposed an approach to teach incrementally human gestures to a humanoid robot, which consists of projecting the movement data in a latent space and encoding the resulting signals in a GMM. Kaustubh *et al.* [11] used GMMs to classify one-handed gestures based on ultrasonic sensors, and the experiment showed simplified one-handed gestures can be recognized with a high accuracy. On the other hand, in [12], the moving hand is tracked and analyzed by Fourier descriptor (FD) from image sequences, and then the feature vector consisting the spatial and temporal features is processed by HMMs for recognition of the hand gesture. Bernardin et al. [13] presented a method using HMMs to recognize continuously executed sequences of grasping gestures. Both finger-joint angles and information about contact surfaces, captured by a data glove and tactile sensors, are used. By using the Kamakura taxonomy, most of all grasps used by humans in everyday life can be classified, increasing the system's application domain to general manipulation tasks. For 12 grasp classes, and with very little training data, a recognition accuracy of up to 89% for a single-user

978-1-4244-7316-8/11/$26.00 ©2011 IEEE

system and 95% for a multiple-user system could be reached. Ju *et al* [14] compared Time Clustering (TC) with HMMs and GMMs on the recognition rate of 13 types of different grasps. Just et al. [15] provided an empirical comparison of two state-of-the-art techniques, HMMs and Input/Output HMMs, for temporal event modeling combined with specific features on two different datasets.

Gaussian Model is confined to normal distributed clusters, so that more Gaussian components are needed for approximating the data with curve manifolds[16], [17]. In order to solve this problem, Active curve axis Gaussian Model (AcaGM), proposed by Baibo[18], is a new non-linear probability model imagined as Gaussian Model being bent at the first principal axis. Inspired from the mechanism of Fuzzy C-means (FCM) [19], in this paper, we firstly introduce a weighting exponent on the fuzzy membership into active curve axis Gaussian Mixiture Model (AcaGMM) in order to improve the efficiency of convergence and then use the proposed fuzzy active curve axis Gaussian Mixture Model (FAcaGMM) to recognize the human hand motions. In addition, a comparative study of recognition methods including FAcaGMM, Time Clustering (TC), Empirical Copula (EC), GMM and HMM is presented. This paper is organized as follows: Section II revisits the mechanism of AcaGMM. Section III proposes the FAcaGMM with an improved convergence speed. Section IV proposes the algorithm to recognize hand motions using FAcaGMM. The comparative experiments are presented in section V. Finally the paper is concluded with remarks and future work.

II. Active Curve Axis Gaussian Model

Let $\mathcal{X} = \{x_1, \cdots, x_n\}$ be a d-dimensional observed dataset of n vectors. The distribution of $\mathcal{X}$ is based on one Gaussian or bent Gaussian. First, the samples are mapped to the coordinate system determined by PCA:

$$y_i = Q \times (x_i - T) \tag{1}$$

where T and Q denote the translation vector and rotation matrix of PCA individually. Let $\mathcal{Y} = \{y_1, \cdots, y_n\}$ be the transferred coordinates of $\mathcal{X}$ by PCA. The d dimensions of $\mathcal{Y}$ are then denoted as $v = [v_1, \cdots, v_d]^T$.

Then least-squares fitting method [20] is used to fit the coordinates $[v_1, v_2]^T$, which are in $\mathcal{Y}$'s principal plane, with the standard curve which is defined as

$$y = ax^2 + b \tag{2}$$

The quadratic term coefficient a indicates the bend degree of the curve. The bigger a is, the more the principal axis bends. b is the offset of the curve. The principal axis is bent to be $y = ax^2 + b$ and the Gaussian model with the bent axis is AcaGM. An example of AcaGM is given on the left of Fig. 1.

The projective points of one sample can be thought as the points on the principal axis who have the local minimal distances with the sample. The distances between sample and points along the principal axis have zero derivatives at the sample's projective points. Given any sample $[v_{1t}, v_{2t}]^T$ which

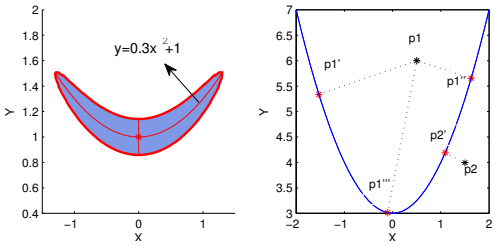

Fig. 1. AcaGM(left) and projection points on the principal curve axis(right).

is the transferred coordinates from x_t, its distance to a point $z = [z_1, z_2]^T$ on the standard curve satisfies

$$d^2 = (v_{1t} - z_1)^2 + (v_{2t} - z_2)^2$$

Using the Lagrange method, the partial derivatives to z_1 and z_2 of $d^2 - \lambda(z_2 - az_1^2 - b)$ are equal to zero,

$$(z_1 - v_{1t}) - \lambda a z_1 = 0$$

$$2(z_2 - v_{2t}) - \lambda = 0$$

Eliminate λ,

$$z_1 - v_{1t} = 2az_1(z_2 - v_{2t}) \tag{3}$$

with the standard curve equation $z_2 = az_1^2 + b$, we can solve all the real roots of this equation, which are the projective points of sample $[v_{1t}, v_{2t}]$. In the principal plane, one point may have several projection points on the principal curve axis, because bending the principal axis may cause one point locates in several different normal directions of the curve axis as shown on the right of Fig. 1. Supposing $z = [z_{1j}, z_{2j}]^T$ is the jth projective point of the sample $[v_{1t}, v_{2t}]$, the arc length of z is formulated as

$$l_j(v_{1t}) = \int_{(0,b)}^{(z_{1j}, z_{2j})} \sqrt{(dz_{1j})^2 + (dz_{2j})^2}$$

z is on the standard curve, so it satisfies $z_2 = az_1^2 + b$. So we have

$$\begin{aligned} l_j(v_{1t}) &= \tfrac{1}{2} z_{1j} \sqrt{1 + 4a^2 z_{1j}^2} \\ &+ \tfrac{1}{4|a|} \ln\left(2|a| z_{1j} + \sqrt{1 + 4a^2 z_{1j}^2}\right) \end{aligned} \tag{4}$$

The distance between the sample $[v_{1t}, v_{2t}]^T$ and its projective point z is

$$l_j(v_{2t}) = \sqrt{(v_{1t} - z_{1j})^2 + (v_{2t} - z_{2j})^2} \tag{5}$$

Then the probability density function of point x_t is the sum probability of its projective points:

$$p(x_t|\theta) = \sum_{j=1}^{J_t} \prod_{s=1}^{2} \frac{\exp(-l_j^2(v_{st})/2\Sigma_s)}{\sqrt{2\pi|\Sigma_s|}} \prod_{s=3}^{d} \frac{\exp(-v_{st}^2/2\Sigma_s)}{\sqrt{2\pi|\Sigma_s|}} \tag{6}$$

Where the parameter set $\theta = (\mu, \Sigma, C, Q, T)$; C denotes the control parameters of a standard curve $f : y = ax^2 + b$; J_t is the number of the projective points of sample x_t.

III. Fuzzy Active Curve Axis Gaussian Mixture Models

For a faster convergence speed of AcaGMMs, based on the dissimilarity function in Fuzzy C-means [21], a dissimilarity function for FAcaGMMs is defined as:

$$d_{it}^2 = \frac{1}{\alpha_i p_i(x_t|\theta_i)} \tag{7}$$

where α_i is the weight of ith component; $p_i(x_t|\theta_i)$ is from equation 6,

Compared to the standard dissimilarity function in Fuzzy C-means, the dissimilarity function defined by equation 7 consists of not only the distance but also the covariance and mixture weights, and it is in direct ratio with the exponent of the distance. The objective function is extended from Fuzzy C-means objective function as:

$$J_m(U, \mathcal{X}, \mu, \Sigma) = \sum_{t=1}^{n}\sum_{i=1}^{k}(u_{it}^m d_{it}^2) \tag{8}$$

Minimizing J_m is performed by the same u_{it} operations of FCM using

$$u_{it} = \left[\sum_{j=1}^{k}(\frac{d_{it}}{d_{jt}})^{\frac{2}{m-1}}\right]^{-1} \tag{9}$$

The new mixture weights are estimated by:

$$\alpha_i^{new} = \frac{\sum_{t=1}^{n} u_{it}^m}{\sum_{i=1}^{k}\sum_{t=1}^{n} u_{it}^m} \tag{10}$$

The parameters of curve axis (a_i, b_i) in C_i can be achieved by

$$(C_i^{new}, T_i^{new}, Q_i^{new}) = LSFM(PCA(\mathcal{X}_i')) \tag{11}$$

where

$$\mathcal{X}_i' = [w_{i1}, \cdots, w_{in}] \cdot [x_1, \cdots, x_n] \tag{12}$$

$PCA()$ is principal component analysis function for estimating the translation matrix T_i^{new} and rotation matrix U_i^{new}. $LSFM()$ is least-squares fitting method for estimating control parameters $C_i^{new} = (a, c)$ which shapes the curve axis with standard curve $y = ax^2 + b$; The centers and covariances can be computed through equations 13-15.

$$\begin{aligned}\mu_i^{new} &= (Q_i^{new})^{-1}\underbrace{[0, b, 0, \cdots, 0]^T}_{d} + T_i^{new} \\ &= (Q_i^{new})^{-1}\underbrace{[0, b, 0, \cdots, 0]^T}_{d} + \frac{\sum_{t=1}^{n} u_{it}^m x_t}{\sum_{t=1}^{n} u_{it}^m}\end{aligned} \tag{13}$$

$$\Sigma_{ie}^{new} = \frac{\sum_{t=1}^{n} u_{it}^m \bar{L}_{te}^{(i)}}{\sum_{t=1}^{n} u_{it}^m} \qquad (e = 1, 2) \tag{14}$$

$$\Sigma_{i(3-d)}^{new} = \frac{\sum_{t=1}^{n} u_{it}^m (x_t - \mu_i^{new})_{(3-d)} (x_t - \mu_i^{new})_{(3-d)}^T}{\sum_{t=1}^{n} u_{it}^m} \tag{15}$$

Where $\Sigma_{i(3-d)}$ is the covariance in the $d-3$ dimension space orthogonal to the principal plane.

With new centers and covariances, the log-likelihood expression is given by:

$$\begin{aligned}\log(\mathcal{L}(\Theta|\mathcal{X})) &= \log\left(\prod_{t=1}^{n} p(x_t|\Theta)\right) \\ &= \sum_{t=1}^{n}\log\left(\sum_{i=1}^{k}\alpha_i p_i(x_t|\theta_i)\right)\end{aligned} \tag{16}$$

where $p_i(x_t|\theta_i)$ is from equation 6.

The EM algorithm of FAcaGMMs is provided in algorithm 1 where d_{it} is obtained from equation 7.

Algorithm 1 EM algorithm of FAcaGMMs.

Require: Fix k, m and ε {k is the number of components $2 < k < n$; m is the degree of fuzziness $m > 1$; ε is a small preset real positive number}.

1: $U \leftarrow fcm(data, k)$ {Use FCM to generate matrix U satisfying equation 9}
2: **repeat**
3: **for all** i such that $1 \le i \le k$ **do**
4: $\alpha_i^{new} \leftarrow equation10$ {Compute the k fuzzy mixture weights α_i^{new} using equation 10}
5: $a_i \leftarrow equation11$
6: $\{C_i^{new}, T_i^{new}, Q_i^{new}\} \leftarrow equation11$ {Compute the k fuzzy control parameters of standard curve, translation and rotation matrices using equation 11 }
7: $\mu_i^{new} \leftarrow equation13$ {Compute the k fuzzy centers using equation 13}
8: $\Sigma_i^{new} \leftarrow equations14 - 15$ {Compute the k fuzzy covariance matrices using equations 14-15 }
9: **end for**
10: $U^{new} \leftarrow equation9$ {Upgrade the fuzzy membership using equation 9 }
11: $\log(\mathcal{L}(\Theta|\mathcal{X}))^{new} \leftarrow equation16$ {Compute the log-likelihood using equation 16}
12: **until** $\frac{\log(\mathcal{L}(\Theta|\mathcal{X}))^{new}}{\log(\mathcal{L}(\Theta|\mathcal{X}))^{old}} - 1 \le threshold$ {Stop if the relative difference of the log-likelihood between two adjacent iterations is blow the preset threshold}

An example of the comparison of AcaGMMs with fuzzy AcaGMMs in terms of the convergence speed could be seen in Fig. 2, where the overall fitnesses of these two methods are almost similar while fuzzy AcaGMMs need much less iterations. For more details about the convergence comparisons, please refer to our previous papers [22], [19].

IV. Recognition via FAcaGMM

The algorithm of equation 17 and equation 18 is constructed to recognize the testing motions. Supposing there are a attributes in the human hand motion dataset. The dissimilarity

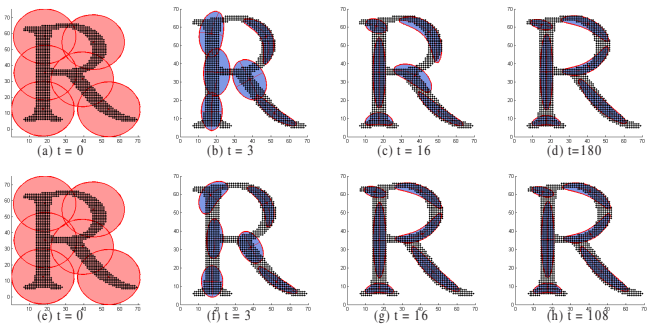

Fig. 2. A comparison of Convergence processes of AcaGMM (first row) and FAcaGMM (second row). t is the number of iterations

of the testing motion and the trained model of FAcaGMM is defined as

$$Dis = \frac{1}{a}\sum_{k=1}^{a} AvgDis^{(k)} \tag{17}$$

where k is the number of the attributes; $AvgDis^{(k)}$ is the average distance of the k^{th} attribute and is calculated by

$$AvgDis^{(k)} = \frac{1}{Cnum^{(k)}}\sum_{i=1}^{Cnum^{(k)}} |(Tmotion^{(k)}(t_i) - Center^{(k)}(i))| \tag{18}$$

where $Cnum$ is the number of the Gaussian components which is set before applying EM algorithm; $i = 1, ..., Cnum$ is the index of the Gaussian components; t_i is the time pint of i^{th} Gaussian component; $Tmotion(t_i)$ is the angle value or finger tip position of the testing hand motion at t_i; $Center(i)$ is the i^{th} model center. The corresponding motion points at the time t_i are identified according to the time points of the model centers, and then the average distances between the centers and these points which are in the same time as these FAcaGMM's centers along the dash line are calculated, as shown in the Fig 3. It calculates the average distance between testing motions and FAcaGMM centers. The testing sample is recognized as the corresponding grasp class with the minimum dissimilarity.

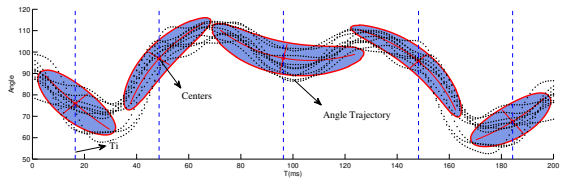

Fig. 3. An example of FAcaGMMs based in-hand manipulation motion recognition

V. Experiment

In order to evaluate the proposed algorithms, a comparative study is constructed by comparing FAcaGMM with TC, EC, GMM and HMM [14], [23]. TC is a fuzzy time-modeling approach based on fuzzy clustering and Takagi-Sugeno modeling with numerical value as output, and its details can be seen in our previous paper [14]. EC was introduced to recognize human hand motions for the first time using the proposed motion template and matching algorithm in [23]. The experiments are implemented under two scenarios a) training with various samples from single subject; b) training with various samples from multiple subjects. In this study, two datasets, 13 grasps and 10 in-hand manipulations, are employed.

A. Experiment Set-up

A fully instrumented data glove, CyberGlove from Immersion Corporation, has been employed to measure the finger joint angles during the hand movement. It can accurately transform hand and finger motions into real-time digital joint angle data by proprietary resistive bend-sensing technology. The sampling frequency of CyberGlove system in our experiments was set to 100Hz without any filter. The joint angles are measured by 22 bend sensors, which include three flexion sensors per finger, four abduction sensors, a palm-arch sensor, and sensors to measure flexion and abduction. Each sensor is extremely thin and flexible and is virtually undetectable in the lightweight elastic glove. CyberGlove is calibrated through the software from the company, and displayed by VirtualHand Studio software which converts the data into a graphical hand mirroring the subtle movements of the physical hand.

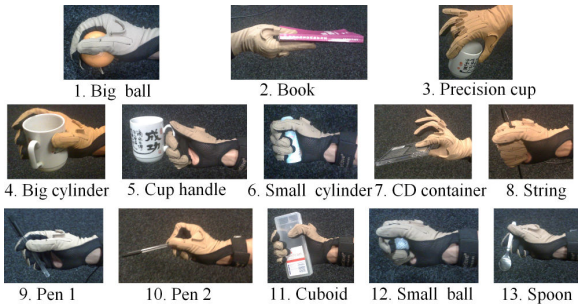

Fig. 4. Selected grasping tasks

Six (2 female, 4 male) healthy right-handed subjects volunteered for the study, their ages range from 23 to 35 with the average is 29.5 years. All subjects were trained to manipulate different objects, each grasp or in-hand manipulation is repeated 20 times for every subject. Both grasps and in-hand manipulation are considered in the study of object manipulation.

1) Grasp: According to the human hand grasp taxonomy [24], hand grasps are classified into 6 atomic different types, for instance, power grasps, precision grasps, and circular/prismatic grasps, etc. We selected 13 different grasp gestures as shown in Fig. 4 to test the algorithm recognition ability. Cup has been selected three times respectively in motions 3, 4 and 5 with different strategies. In motion 3, only three fingers are used to precisely contact the cup top; in motion 4, five fingers are laterally attached to the cup and cup handle is grasped with three fingers in motion 5.

2) In-hand Manipulation: The other dataset is for in-hand manipulation, which is much more complex than simple grasp

TABLE I
10 TYPES OF IN-HAND MANIPULATIONS

1	Open a mobile phone and then close it.
2	Screw to open a small bottle using only thumb, index finger and middle finger.
3	Pick up a coin and move it from the fingertip to the palm
4	Remove the pencil from back to front for writing, as shown in figure 5: (a) pencil walking
5	Pick up a pencil and simply rotate to write, as show in figure 5:(c) simple rotation
6	Pick up a pencil and complexly rotate to write, as show in figure 5:(d) complex rotation
7	Screw to open a big bottle using all five fingers
8	Roll a small cylinder
9	Pick up a scissor and cut paper
10	Pencil flips, as shown in figure 5:(b) pencil flips

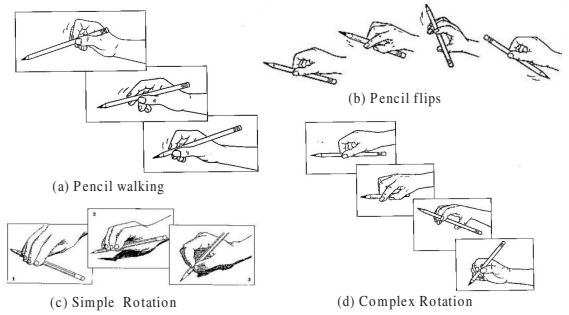

Fig. 5. Four examples of pencil in-hand manipulation

motion and associated with the most complex human motor skills. It's the ability to change the position/orientation or adjust an object within one hand. Ten types of manipulations are recorded also by Cyberglove as listed in table I, and a few examples are shown in Fig. 5.

B. Experiment 1- Training with Various Samples from Single Subject

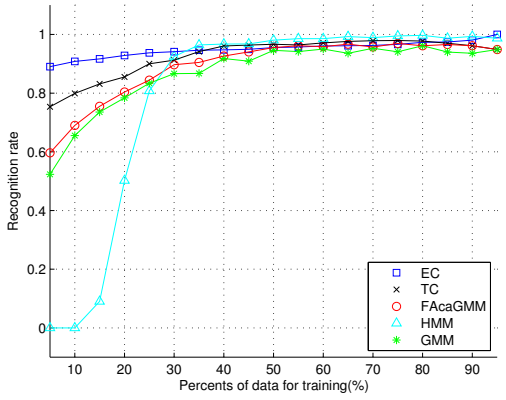

Fig. 6. Recognition results with various training percentages from single subject on grasp dataset

An empirical study was designed to evaluate sensitivity of these five methods in terms of change of the rate of training samples for the single subject. There are 13 grasp models

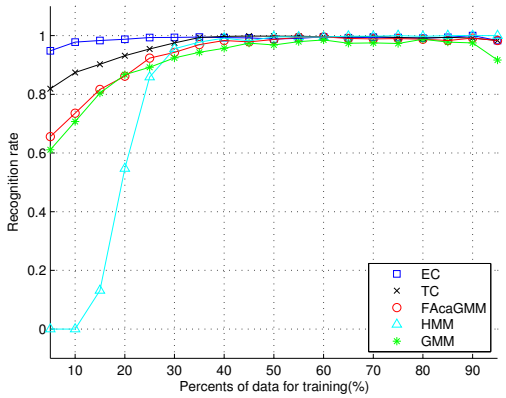

Fig. 7. Recognition results with various training percentages from single subject on in-hand manipulation dataset

and 10 in-hand manipulation models for each single subject, where each subject repeated 20 times for each motion. Each model of any subject is trained with various percentage of the data ranging from 5% to 95% from the same subject. The trained model is used to test other unused data from the same subject. The experimental results with various percentage of training data are illustrated in Fig. 6 and Fig. 7 for the two datasets. It finds that the performance of these five methods are all improved with the increase of the training datasets and their accuracies stabilize with more than 30% training data. The recognition rate of HMM improves from 0% to more than 90% when training data increase from 5 to 30 percentages and it reaches as high as that of EC with more than one third training data. Compared with GMM, FAcaGMM achieves a better result with all the various sample rates. TC stays in the middle of EC and FAcaGMM, EC presents the best overall performance among the five methods. The results demonstrate that the variation of the training samples does substantially affect performance of these methods. The increase of the training data can result in about 90, 30, 30, 20 and 10 percent increases of the recognition rates for HMM, GMM, FAcaGMM, TC, EC. It presents that HMM is sensitive to the varying training data more than any of the other four methods.

C. Experiment 2- Training with Various Samples from Multiple Subjects

Similarly an experiment was conducted to evaluate the effects of different training rates on the classifiers' performance for multiple subjects. Regarding to experiment 2, there are 13 grasp models and 10 in-hand manipulation models for all the six subjects. Each model was trained by the mixed samples from all six subjects. Each subject contributes the same amount of samples to the training data. All the other samples which are not included in the training data are used to evaluate the models trained by multiple subjects' samples. The percentage of the training data ranges from 5% to 95%

The experimental results are provided in Figs. 8 and 9 for grasp and in-hand manipulation datasets respectively. HMM

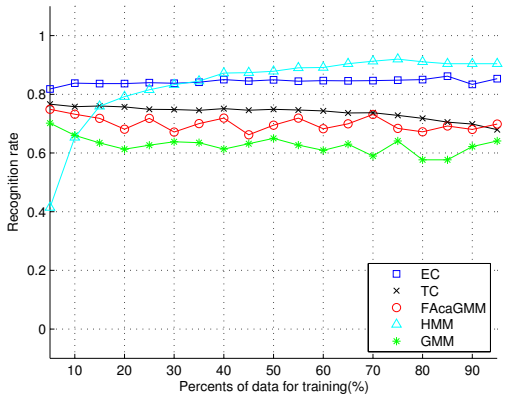

Fig. 8. Recognition results with various training percentages from multiple subjects on grasp dataset

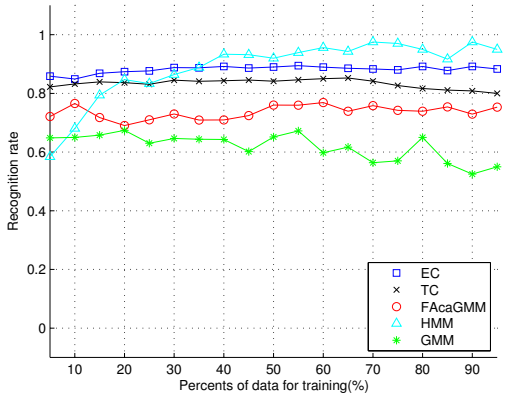

Fig. 9. Recognition results with various training percentages from multiple subjects on in-hand manipulation dataset

achieves an improvement of the recognition rate from less than 50% to 90% in terms of usage of the training samples. Different from the previous experiment results, there are no significant changes of recognition rates for the other methods with varying training samples. It is confirmed that HMM is the most sensitive method responding to varying training samples. HMM can achieve the highest accuracy with more than 40 percent training samples, but the proposed FAcaGMM, like EC and TC, outperforms HMM and GMM when the training samples are less than one fifth due to the insensitiveness to the varying percentage of the training data. FAcaGMM's performance is consistently better than GMM's thanks to the non-linear characteristic, and the Gaussian Mixture Regression (GMR) could be potentially used to generate the desired trajectory.Though TC and EC have higher recognition rate than FAcaGMM, TC is limited to the motion planning directly transfered from recognition results which are numerical values [14], and it is hard to generate desired trajectory from the dependence structure for EC [23]. FAcaGMM provides an effective solution to the applications which require abstracted patterns to store the motion features, and require an approach to generate the desired trajectory from these features.

VI. CONCLUSIONS

In this paper, we have proposed a novel FAcaGMM with a fast convergence speed, which is used to recognize human hand motions. A comparative study covering different subjects and different training samples has been conducted to compare the methods including FAcaGMM, TC, EC, GMM and HMM. Two datasets consisting of 13 different types of grasps and 10 in-hand manipulations have been employed for the algorithm evaluation. Experiment results have demonstrated that FAcaGMM consistently outperforms GMM in terms of the recognition rate because it is a component-based modeling method having the capability of modeling datasets with curve manifolds. FAcaGMM, like TC and EC, is insensitive to the varying training samples to certain extent, which means that it has advantages over practical applications, especially when requiring a fast training model process or lacking sufficient training datasets. Its performance substantially depends on the number of Gaussian components. It utilizes abstracted patterns to store the motion features, and the desired trajectory can be generated from these features. In the future work, the proposed algorithms will be applied to applications such as EMG based human motion recognition for prosthetic hands and human-robot skill transfer.

REFERENCES

[1] S. Calinon, F. Guenter, and A. Billard, "On learning, representing, and generalizing a task in a humanoid robot," *IEEE Transactions on Systems, Man and Cybernetics Part B*, vol. 37, no. 2, p. 286, 2007.

[2] S. Fels and G. Hinton, "Glove-talk: a neural network interface between a data-glove and a speech synthesizer," *IEEE Transactions on Neural Networks*, vol. 40(1), pp. 2–8, 1993.

[3] S. Fels and G. Hinton, "Glove-TalkII-a neural-network interface which maps gestures to parallel formant speech synthesizer controls," *IEEE Transactions on Neural Networks*, vol. 9, no. 1, pp. 205–212, 1998.

[4] Y. Sato, M. Saito, and H. Koike, "Real-time input of 3D pose and gestures of a user's hand and itsapplications for HCI," *Virtual Reality, 2001. Proceedings. IEEE*, pp. 79–86, 2001.

[5] R. Zöllner, O. Rogalla, J. Zöllner, and R. Dillmann, "Dynamic grasp recognition within the framework of programming by demonstration," in *The 10th IEEE International Workshop on Robot and Human Interactive Communication (Roman)*, pp. 418–423, Citeseer.

[6] D. Martinez and D. Kragic, "Modeling and recognition of actions through motor primitives," in *IEEE International Conference on Robotics and Automation*, pp. 1704–1709, 2008.

[7] R. Natal, B. Dimuro, and A. Costa, "Hand gesture recognition in an interval fuzzy approach," *TEMA Tend. Mat. Apl. Comput*, vol. 8, no. 1, pp. 21–31, 2007.

[8] B. Bedregal, A. Costa, and G. Dimuro, "Fuzzy rule-based hand gesture recognition," *International Federation for Information Processing*, vol. 217, p. 285, 2006.

[9] G. Heumer, H. Amor, M. Weber, and B. Jung, "Grasp recognition with uncalibrated data gloves-a comparison of classification methods," *Virtual Reality Conference, 2007. VR'07. IEEE*, pp. 19–26, 2007.

[10] S. Calinon and A. Billard, "Incremental learning of gestures by imitation in a humanoid robot," *Proceedings of the ACM/IEEE international conference on Human-robot interaction*, pp. 255–262, 2007.

[11] K. Kalgaonkar and B. Raj, "One-handed gesture recognition using ultrasonic Doppler sonar," in *Proceedings of the 2009 IEEE International Conference on Acoustics, Speech and Signal Processing-Volume 00*, pp. 1889–1892, IEEE Computer Society, 2009.

[12] F. Chen, C. Fu, and C. Huang, "Hand gesture recognition using a real-time tracking method and hidden Markov models," *Image and Vision Computing*, vol. 21, no. 8, pp. 745–758, 2003.

[13] K. Bernardin, K. Ogawara, K. Ikeuchi, and R. Dillmann, "A sensor fusion approach for recognizing continuous human grasping sequences using hidden Markov models," *IEEE Transactions on Robotics*, vol. 21, no. 1, pp. 47–57, 2005.
[14] Z. Ju, H. Liu, X. Zhu, and Y. Xiong, "Dynamic grasp recognition using time clustering, gaussian mixture models and hidden markov models," *Journal of Advanced Robotics*, vol. 23, pp. 1359–1371, 2009.
[15] A. Just and S. Marcel, "A comparative study of two state-of-the-art sequence processing techniques for hand gesture recognition," *Computer Vision and Image Understanding*, vol. 113, no. 4, pp. 532–543, 2009.
[16] A. Dasgupta and A. Raftery, "Detecting features in spatial point processes with clutter via model-based clustering," *Journal of the American Statistical Association*, pp. 294–302, 1998.
[17] C. Fraley and A. Raftery, "How many clusters? Which clustering method? Answers via model-based cluster analysis," *The Computer Journal*, vol. 41, no. 8, pp. 578–588, 1998.
[18] B. Zhang, C. Zhang, and X. Yi, "Active curve axis Gaussian mixture models," *Pattern Recognition*, vol. 38, no. 12, pp. 2351–2362, 2005.
[19] Z. Ju and H. Liu, "Applying fuzzy em algorithm with a fast convergence to gmms," in *Proc International Conference on Fuzzy Systems, World Congress on Computational Intelligence, Spain*, 2010.
[20] A. Björck and Å. Björck, *Numerical methods for least squares problems*. Society for Industrial Mathematics, 1996.
[21] J. C. Bezdek, *Pattern recognition with fuzzy objective function algorithms*. Kluwer Academic Publishers Norwell, MA, USA, 1981.
[22] Z. Ju and H. Liu, "A modified expectation maximization algorithm for gaussian mixture models," in *Proc 2009 UK National Workshop on Computational Intelligence, Nottingham, UK*, 2009.
[23] Z. Ju and H. Liu, "Recognizing hand grasp and manipulation through empirical copula," *International Journal of Social Robotics*, vol. 2, pp. 321–328, 2010.
[24] T. Iberall, "Human prehension and dexterous robot hands," *The International Journal of Robotics Research*, vol. 16, no. 3, p. 285, 1997.

2011 IEEE International Conference on Fuzzy Systems
June 27-30, 2011, Taipei, Taiwan

Trajectory-based Control under ZMP Constraint for the 3D Biped Walking via Fuzzy Control

Hsiu-Ming Wu, *Member, IEEE*
Opto-Mechatronics Technology Center
National Taiwan University of Science and Technology
Taipei. Taiwan, R.O.C.
email: D9307205@mail.ntust.edu.tw

Chih-Lyang Hwang, *Senior Member, IEEE*
Department of Electrical Engineering
National Taiwan University of Science and Technology
Taipei, Taiwan, R.O.C.
e-mail: chih-lyang_hwang@hotmail.com

***Abstract*—In this study, a fuzzy control policy is presented for dynamic walking of a biped robot that is modeled as a simulated five-link biped robot. Due to complex ground contact models, it is difficult to precisely model its dynamics. Besides, a spring/damper ground model and a simplified inverted pendulum model are presented to represent the ground contact relation and the approximated model of biped robots as well. Moreover, Finite State Machine (FSM) is utilized to decompose a cycle of walking gait. Under zero moment point (ZMP) constraint, each joint follows desired trajectories in each state that are generated by quintic spline curve through the model free controller (i.e., fuzzy control). In addition, its robustness is investigated by imposing pulse perturbation on torso for some directions. The results are demonstrated in simulations as well as animation and then the proposed controller is compared with a PID controller as well.**

Keywords-Biped robot; ZMP constraint; Fuzzy control; Finite state machine; PID;

I. INTRODUCTION

The biped robot possesses nonlinear dynamics and numerous degrees of freedom that are difficult to manipulate. For biped robots, it is also unavoidable to be subjected to all kinds of external disturbance (e.g. contact with ground, different ground situations). As a result, accurately modeling the dynamics of biped robot systems is quite difficult. Additionally, walking stably is also another challenge for biped robots.

A fuzzy control policy with robustness is adopted for biped walking and simultaneously a FSM approach is utilized to decompose the cycle of the walking gait. Then the biped robot system is approximated by a simplified inverted pendulum model and keeps dynamic walking based on the ZMP constraint. In summary, the contribution of this study is the development of the fuzzy control policy with robustness for the walking of the simulated 3D biped robot. The simulation and animation are done to demonstrate the validity of the proposed methodology.

A. Related Works

In recent years, the research about walking of biped robots is a popular topic. Walking stably and keeping balance are essential functions. For the dynamic walking of biped robots, ZMP analysis is an important stability criterion for dynamic walking stably [1, 2]. Recently, [3]-[5] discuss stable biped walking through direct regulation of ZMP and generate stable walking trajectories. Besides, in order to enhance walking robustness, Morimoto and Atkeson [6] use differential dynamic programming (DDP) with a minimax criterion to make the humanoid robot generate low torque for walking and insure the policy is robust. Additionally, for keeping balance, Atkeson and Stephens [7,8] investigate ankle, hip and stepping strategies to help the humanoid robot recovery under the external push. From above studies, we can get the information that ZMP control and the walking with robustness are important for biped robots. Furthermore, due to the complex nonlinear dynamics and high dimensional state space, it's quite difficult to model the biped robot precisely. In general, it has two solvable ways. One is for the use of a simplified inverted pendulum model and some studies discuss it and have verified its effectiveness. Stramigioli et al. [9] adopt a simplification of multi-body dynamics that is achieved by instantaneously reducing it to be an equivalent single inertial entity in legged robot. In [10], Goswami introduced the Reaction Mass Pendulum (RMP) and presented an extension of the inverted pendulum that modeled the rotational inertia and angular momentum of a robot through its centroidal composite rigid body. The other one is for the use of the fuzzy controller. So far, fuzzy control has already been applied into many controlled systems including bipeds [11]-[15] as well as different kinds of commercial products successfully. The reasons are that it can handle nonlinear system well and is ease of implementation.

B. Control Policies For Walking

In general, the walking process is composed of a single support phase (SS) and a double support phase (DS) for the walking phase of a biped robot. In this work, a FSM approach is presented for the walking gaits of biped robots that decompose walking gaits into different states based on SS and DS phase. In these states, a quintic spline curve is utilized to generate smooth desired trajectories of each joint. Furthermore, a simplified inverted pendulum model is used to approximate the biped robot system and the biped robot keeps balance during walking based on the ZMP constraint. Concerning a trajectory tracking of each joint, it is achieved

by fuzzy feedback control policy. An important contribution of fuzzy systems theory is to provide a systematic procedure for transforming a set of linguistic rules into a nonlinear mapping. A fuzzy control algorithm [16]-[18] consists of a set of heuristics decision rules and is regarded as an intelligent control algorithm, which is attractive in many cases where the controlled system can't be well defined or modeled. The fuzzy theory uses "IF-THEN" rules to state the relationship between the input and output of the control plan. Also, it uses the linguistic variables instead to describe the characteristics of the system.

This paper is organized as follows: in section II, the system dynamics is constructed and trajectory planning, control policies for the biped walking robot are described in section III, and the simulation and animation results demonstrate its effectiveness under the ideal situation (i.e., without any perturbations) and external disturbance in section IV. Finally, the conclusions and further works of this paper are given in section V.

II. SYSTEM DYNAMICS AND TRAJECTORY PLANNING

The system (as in Fig. 1) is a simulated 3D biped composed of five-links: one torso, two thighs, and two calves. It is a symmetric 12 DOF system including roll and pitch for each hip, pitch for a knee and roll, pitch, and yaw for each ankle on each side. Therefore it is actuated by 12 torque-controlled joints. These joints are respectively simplified as hip abduction/adduction (HAA) that is roll angle between the pelvis and the thigh, hip flex/extend (HFE) that is the pitch angle between the pelvis and the thigh, knee flex/extend (KFE) that is pitch angle between the thigh and the calf, ankle abduction/adduction (AAA) that is the roll angle between the calf and vertical, ankle flex/extend (AFE) that is pitch angle between the calf and vertical and ankle rotation (AR) that is the rotation about the calf. Furthermore, the system states position and velocity of each DOF, so it is a 24 dimensional state space. Also, the system parameters for the simulation are similar to our real humanoid robot made by Sarcos. Its weight is 78 kg, with a 50 kg torso and 14 kg legs. The legs are 0.81 m long and the center of mass is 1 m above the ground when it stands straight. The distance between the hips is 0.213 m. In addition, the biped robot will interact with the ground during walking. Therefore, considering impact with interaction is necessary. In this paper, its ground contact relation is modeled as a spring/damper ground model as following Equations (1)-(4):

$$F_z = k_z z + b_z \dot{z} \quad (1)$$

$$F_x = k_x (x - x_0) + b_x \dot{x} \quad (2)$$

$$F_y = k_y (y - y_0) + b_y \dot{y} \quad (3)$$

$$M_z = k_a (a - a_0) + b_a \dot{a} \quad (4)$$

where x_0 and y_0 are initial contact positions and a_0 is initial contact yaw angle of the foot of $Z-$ axis, k_z, k_x, k_y and k_a are spring constants, b_z, b_x, b_y and b_a are damping constants, F_z, F_x, F_y and M_z are friction force and moment respectively. According to above parameters, SDFAST software is used to generate the rigid body dynamics for the biped robot. For this study, the desired trajectories of the hip, knee and ankle joints are all generated by quintic spline curves during walking. At knot points the quintic spline curves can enforce second derivative continuity of combined curve so that smooth transition, acceleration and jerk could be ensured. Each joint is driven to its desired position through fuzzy feedback controller that is described by the following section.

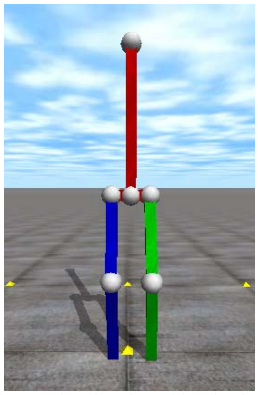

Fig. 1. Simulated 3D biped robot.

III. CONTROL POLICIES FOR BIPED ROBOT

A. Approximation Using An Inverted Pendulum Model and The ZMP Constraint

In order to simplify dynamic analysis, the biped model can be regarded as an inverted pendulum model that has been proved to be able to represent whole biped dynamics effectively. Consequently, in this study a simplified inverted pendulum model in the sagittal plane represented as Fig. 2 is described to approximate the biped robot model where forward direction is the positive X axis and above direction is positive Z axis. The height for the Center of Mass (CoM) in the walking process is assumed to be constant. From geometric relations, Equation (5) is derived where F is a net force applied on the CoM, g is the gravity acceleration and θ is the angle with vertical. Equation (6) expresses energy conservation and v is the velocity of the CoM. From Equations (5) and (6), the minimum roll distance of x direction (i.e., $x_{\min}$) is represented as Equation (7). During walking, CoM is kept within ZMP constraints via regulating the walking step and gait.

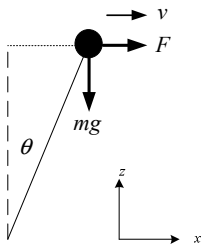

Fig.2. A simplified inverted pendulum model in the sagittal plane.

$$F/mg = \tan\theta = -x/z \tag{5}$$

$$-\int F dx = m v^2/2 \tag{6}$$

$$x_{\min} = \sqrt{x^2 - z v^2/g} \tag{7}$$

Calculating $x_{\min}$ value is to predict how far the biped system will move to. Liftoff action occurs when $x_{\min} < x_{d\min}$ where $x_{d\min}$ is a desired minimum move distance. In this paper, the value of $x_{d\min}$ is assigned as 0.07. In addition, the touchdown action occur a fixed time interval after turnaround.

B. Finite State Machine

Our proposed controllers are based on a FSM, with each state having its own trajectory for internal joint angles. A walking cycle of the human walking gait is imitated and decomposed by a FSM that is employed to plan walking gaits including eleven states. (1) WAITING (2) DS1 (double support, left leg in front) (3) LIFTOFF1 (double support, lifting right leg) (4) SSL1 (first phase of single support, left leg in stance) (5) SSL2 (second phase of single support, left leg in stance) (6) DS2 (double support, right leg in front) (7) LIFTOFF2 (double support, lifting left leg) (8) SSR1 (first phase of single support, right leg in stance) (9) SSR2 (second phase of single support, right leg in stance) (10) LAUNCH1 (squat) (11) LAUNCH2 (launch state, like DS1). These states form one cycle's walking gaits of the biped robot and transfer into other state at prescribed time or conditions described in Fig. 3 where waiting time and launch1 time are prescribed time in advance. Also, foot states and CoM velocity of Y direction are transition conditions. Besides the desired smooth trajectories generated by the quintic spline curve in each state and in any given state, the joints apply torques computed by fuzzy control in order to drive each joint to its desired local angle.

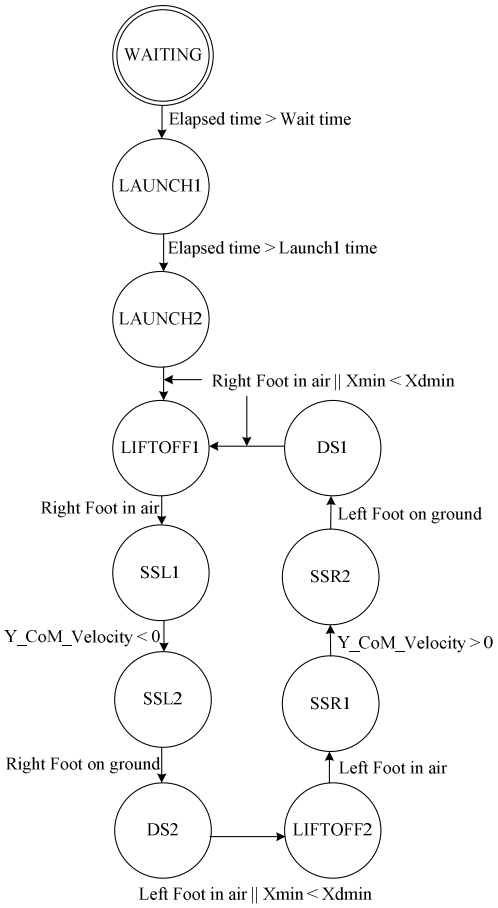

Fig. 3. FSM diagram for the biped walking.

C. Fuzzy Control Policy

The basic configuration of the fuzzy system consists of a fuzzifier, an inference engine and a defuzzifier. The fuzzifier part is to map a crisp set into a fuzzifier set. Moreover, two normalizing input scaling factors are determined. They make error and its derivative located in between -1 and 1 where error $e_i(t)$ is individual difference between desired position and actual position of each joint. Therefore, two inputs of fuzzy rule table of the *ith* subsystem are $\overline{e}_i(t) = g_{e_i} e_i(t)$ and $\dot{\overline{e}}_i(t) = g_{\dot{e}_i} \dot{e}_i(t)$, $i = 1 \sim 12$, where g_{e_i} and $g_{\dot{e}_i}$ are two normalizing input scaling factors respectively. $\overline{e}_i(t)$ and $\dot{\overline{e}}_i(t)$ are called fuzzy variables. They are quantized into the following eleven qualitative fuzzy variables: (i) Positive Huge (PH) (ii) Positive Big (PB) (iii) Positive Medium (PM) (iv) Positive Small (PS) (v) Positive Infinite (PI) (vi) Zero (ZE) (vii) Negative Infinite (NI) (viii) Negative Small (NS) (ix) Negative Medium (NM) (x) Negative Big (NB) (xi) Negative Huge (NH). The membership functions of the fuzzy variables are with triangular type as in Fig. 4 in this paper.

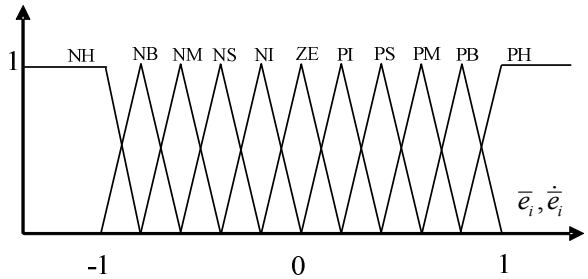

Fig. 4. Membership functions with triangular type.

In addition, the inference engine is usually composed of a series of fuzzy rules i.e., "IF-THEN" rules. The fuzzy logic subsystem *i* as in Fig. 5 performs a mapping from $X_i \in \Re^2$ to $\Re$.

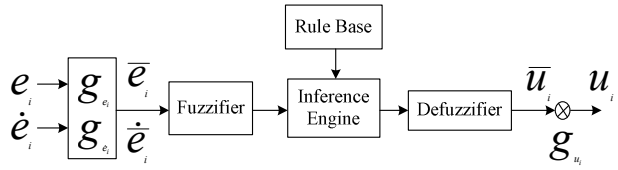

Fig. 5. Configuration of the *ith* fuzzy logic system.

There are *l* fuzzy control rules and the upper script *k* denotes the *kth* fuzzy rule:

IF $\bar{e}_i$ is $F_{1_i}^k$ and $\dot{\bar{e}}_i$ is $F_{2_j}^k$, THEN $\bar{u}_i$ is G_i^k (8)

where $\left[\bar{e}_i(t) \quad \dot{\bar{e}}_i(t)\right]^T \in X_i \subset \Re^2$, with $\bar{e}_i(t) = g_{e_i} e_i(t)$, $\dot{\bar{e}}_i(t) = g_{\dot{e}_i} \dot{e}_i(t)$, and $\bar{u}_i(t) \in V_i \subset \Re$ are the inputs and output of the fuzzy logic subsystem *i*, respectively; $F_{j_i}^k (1 \le i, j \le 2, 1 \le k \le l)$ and G_i^k are labels of sets in X_i and V_i, respectively. The parameters g_{e_i} and $g_{\dot{e}_i}$ are chosen such that $\bar{e}_i(t)$ and $\dot{\bar{e}}_i(t) \in [-1, 1]$. The fuzzy inference engine performs a mapping from fuzzy sets in $X_i \subset \Re^2$ to fuzzy sets in $V_i \subset \Re$, based upon the fuzzy IF-THEN rules in the fuzzy rule base and the compositional rule of inference. The defuzzifier part is to utilize the center-average method to get the crisp control input signal $\bar{u}_i(t)$. In summary, overall fuzzy logic system can be employed to form a look-up Table 2 that directly relates the inputs $\bar{e}_i$(t) and $\dot{\bar{e}}_i(t)$ with the output $\bar{u}_i(t)$. Also, the output $\bar{u}_i(t)$ of the look-up table ranges between from -1 and 1 that is multiplied by output scaling factor g_{u_i} to be real control output torque $u_i(t)$ as Eq. (9). Output scaling factor can be regarded as saturation limit of the actuators. Generally speaking, a larger output scaling factor is assigned, a smaller tracking error and a faster response are achieved; however, the risk of transient or oscillatory response increases after transience happen.

$$u_i(t) = g_{u_i} \bar{u}_i(t) = g_{u_i} \left[\bar{e}_i(t) + \Delta_i(t) \operatorname{sgn}(\bar{e}_i)\right], \; i = 1 \sim 12. \quad (9)$$

where $\bar{u}_i(t)$ is fuzzy variable of $u(t)$, and $\Delta_i(t) > 0 \; \forall t$ denotes the switching gain, which is related to Table 2. Furthermore, the roll torque of ankle in SS is constant. Moreover, hip roll torque needs to hold the torso up, so the desired position tracks ankle roll angles. In DS, it is occupied a very short time during the all of the walking period and then hip and ankle roll are pure torque sources (i.e., constant torques).

IV. SIMULATIONS AND DISCUSSIONS

Through the investigations of $e_i(t)$ and $\dot{e}_i(t)$ range from each joint, the control parameters g_{e_i} values are all selected as 0.01 and the $g_{\dot{e}_i}$ values respectively are selected as $\{0.009, 0.01, 0.01, 0.01, 0.005, 0.01\}$ at one side respectively such that their values are located between -1 and 1. They have the same values at another side. In addition, g_{u_i} values are assigned as $\{3500, 1300, 1700, 300, 45000, 200\}$ at one side. Also, these values are identical to another side. In general, a larger output scaling factor is assigned, a smaller tracking error and a faster response are achieved; however, the risk of transient response happens.

For ideal conditions (i.e., no any perturbations and uncertainties), the responses of each joint are illustrated in Fig. 6 that shows the responses of left hip, knee and ankle pitch angles. From these results shown, based on fuzzy controller and FSM method the responses of each joint have good trajectory tracking performance. In addition, PID controller is also applied to biped walking and it still obtains stable walking. For simplicity, these responses are omitted. However, to investigate further whether the fuzzy controller I propose has robustness, the external pulse force of 25 Newton is imposed on torso during 2.0~2.1 seconds from lateral push (i.e., positive *Y* direction) and those control parameters are the same with ones of ideal conditions. These simulation results are illustrated in Fig. 7. Moreover, Fig. 8 represents the responses under the same conditions by PID controller. It will crash at about 3 seconds. From these illustrations of the simulation results, it reveals the proposed controller is with better robustness to resist some extent disturbance and possess good performance. Except the computer simulation, it is also displayed walking of the 3D simulated biped robot using animation that reveals the proposed strategy is effective for the biped walking. In summary, they both exhibit acceptable performance under with or without uncertainty and disturbance. Further, it is also verified that the approximation of a simplified inverted pendulum model with ground contact relation for the biped robot is feasible and effective.

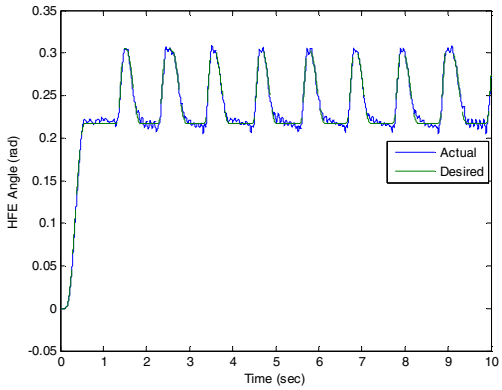

(a) The response of the hip pitch angle

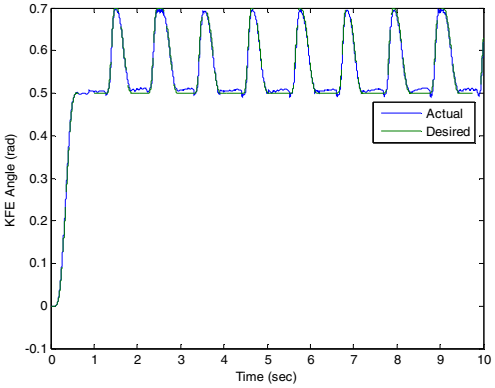

(b) The response of the knee pitch angle

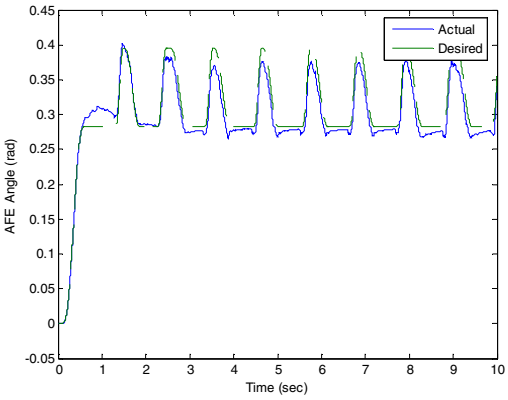

(c) The response of the ankle pitch angle

Fig. 6. The responses of internal joints in the absence of perturbation.

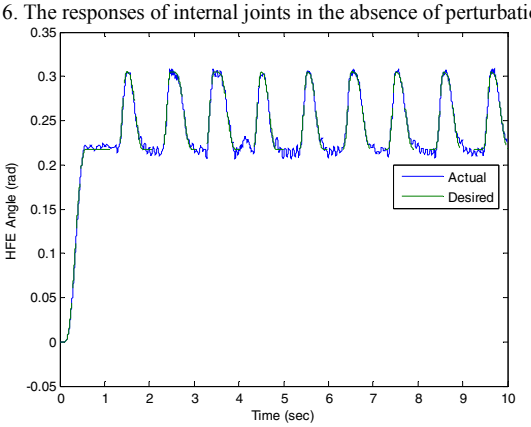

(a) The response of the hip pitch angle

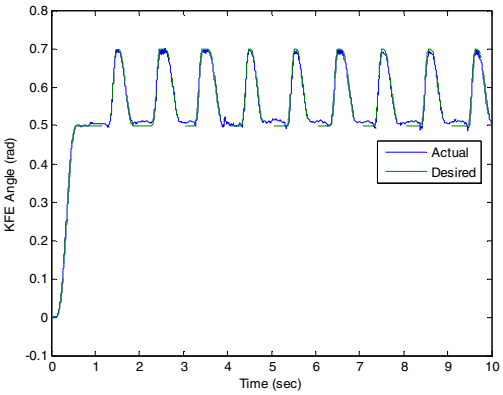

(b) The response of the knee pitch angle

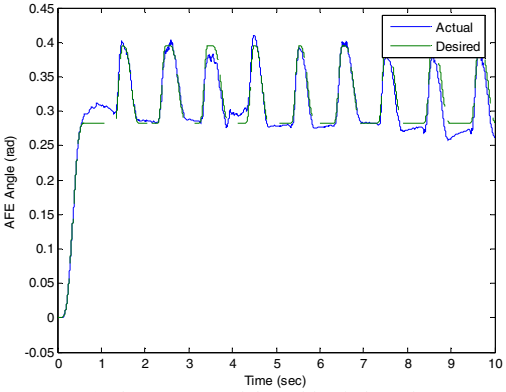

(c) The response of the ankle pitch angle

Fig. 7. The responses of joints in the presence of 25N pulse perturbation force on torso during 2~2.1 sec. by the fuzzy controller.

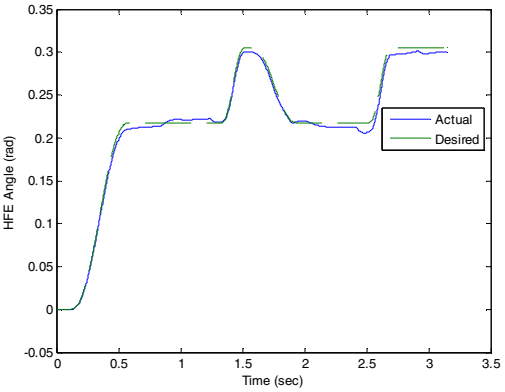

(a) The response of the hip pitch angle

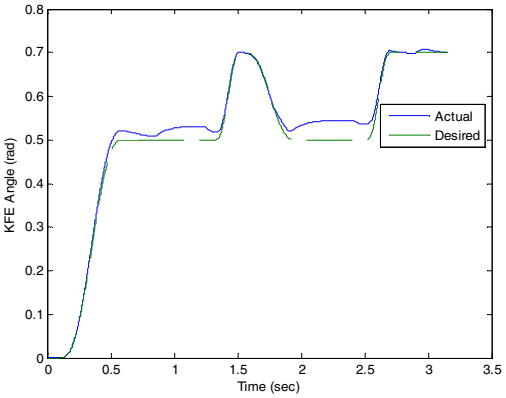

(b) The response of the knee pitch angle

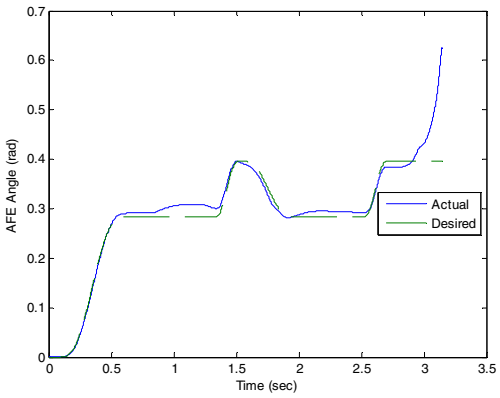

(c) The response of the ankle pitch angle

Fig. 8. The responses of Fig. 7 by the PID controller.

V. CONCLUSIONS

In this paper, the simulated 3D biped robot is considered as a simplified inverted pendulum model with ground contact relation. The fuzzy control policy and FSM approach are proposed for the periodic walking of the simulated 3D biped robot based on ZMP constraint. Under without perturbations, it has good response for the trajectory tracking on each joint. In addition, the lateral pulse perturbation force on torso is imposed to verify the robustness of the proposed controller. Finally, through the demonstration of the simulation, the responses are shown to possess good trajectory tracking as well as better robustness as compared with PID controller. Moreover, the animation also displayed that the biped robot can walk stably and periodically.

In future works, a real biped robot by the proposed control will be implemented. Additionally, it will be compared with other control strategies with respect to the robustness and performance.

ACKNOWLEDGMENT

The first author would like to appreciate the financial support from National Science Council of R.O.C. with Grant No.NSC-97-2917-I-011-101 for the Graduate Students Study Abroad Program. In addition, he also appreciates much assistance from Robotics Institute, School of Computer Science, Carnegie Mellon University, USA.

REFERENCES

[1] M. Vukobratovic, A. A. Frank, and D. Juricic, "On the stability of biped locomotion," *IEEE Transaction on Biomedical Engineering*, vol. BME-17, no. 1, pp. 25-36, Jan. 1970.

[2] K. Erbatur, and O. Kurt, "Natural ZMP Trajectories for Biped Robot Reference Generation," *IEEE Transactions on Industrial Electronics*, vol. 56, no. 3, pp. 835-845, Mar. 2009.

[3] C. Chevallereau, D. Djuoudi, and J. W. Grizzle, "Stable Bipedal Walking With Foot Rotation Through Direct Regulation of the Zero Moment Point," *IEEE Transactions on Robotics*, vol. 24, no. 2, pp. 390-401, Apr. 2008.

[4] D. Djuoudi, C. Chevallereau, and J. W. Grizzle, "A Path-Following Approach to Stable Bipedal Walking and Zero Moment Point Regulation," *IEEE International Conference on Robotics and Automation*, pp. 3597-3602, April 2007.

[5] K. Nishiwaki and S. Kagami, "High frequency walking pattern generation based on preview control of ZMP," *IEEE International Conference on Robotics and Automation*, pp. 2667-2672, May 2006.

[6] J. Morimoto and C. G. Atkeson, "Robust low torque biped walking using differential dynamic programming with a minimax criterion," *Proceedings of 5th International Conference on Climbing and Walking Robots*, pp. 453-459, 2002.

[7] C. G. Atkeson and B. Stephens, "Multiple balance strategies from one optimization criterion," *IEEE-RAS International Conference on Humanoid Robots*, pp. 57-64, Nov. 2007.

[8] B. Stephens, "Humanoid push recovery," *IEEE-RAS International Conference on Humanoid Robots*, pp. 589-595, Nov. 2007.

[9] S. Stramigioli, V. Duindam G. van Oort and A. Goswami, "Compact analysis of 3D bipedal gait using geometric dynamics of simplified models," *IEEE International Conference on Robotics and Automation*, pp. 1978-1984, May 2009.

[10] A. Goswami, "Kinematic and dynamic analogies between planar biped robots and the reaction mass pendulum (RMP) model," *IEEE-RAS International Conference on Humanoid Robots*, pp. 182-188, Nov. 2008.

[11] C. W. Tao, J. S. Taur, T. W. Hsieh, and C. L. Tsai, "Design of a Fuzzy Controller with Fuzzy Swing-Up and Parallel Distributed Pole Assignment Schemes for an Inverted Pendulum and Cart System." *IEEE Transactions on Control Systems Tech.*, vol. 16, no. 6, pp. 1277-1288, Nov. 2008.

[12] Z. Liu, Y. Zhang, and Y. Wang, "A Type-2 Fuzzy Switching Control System for Biped Robots," *IEEE Transactions on System, Man, and Cybernetics, Part C*, vol. 37, no. 6, pp. 1202-1213, Nov. 2007.

[13] S. A. A. Moosavian, M. Alghooneh, and A. Takhmar, "Stable trajectory planning, dynamics modeling and fuzzy regulated sliding mode control of a biped robot," *IEEE-RAS International Conference on Humanoid Robots*, pp. 471-476, Nov. 2007,.

[14] R. C. Luo, C. W. Tzeng, P. Z. Cheng and K. W. Lee, "Trajectory-Tracking of Nonlinear Biped Robot System Based on Adaptive Fuzzy Sliding Mode Control," *IEEE IECON*, pp. 2789-2794, Nov. 2007.

[15] C. L. Hwang, "A Trajectory Tracking of a Biped Robots Using Fuzzy-Model-Based Sliding-Mode Control," *IEEE Conference on Decision and Control*, pp. 203-208, Dec. 2002.

[16] R. E. Precup and S. Preitl, "Optimization criteria in development of fuzzy controller with dynamics," *Engineering Applications of Artificial Intelligence*, vol. 17, no. 6, pp. 661-674, Sep. 2004.

[17] K. Y. Tu, T. T. Lee and C. H. Wang, "Design of a new fuzzy suction controller using fuzzy modeling for nonlinear boundary layer," *IEEE Trans. Fuzzy Syst.,* vol. 13, no. 5, pp. 605-616, Oct. 2005.

[18] A. Sala, T. M. Guerra and R. Babuska, "Perspectives of fuzzy systems and control," *Fuzzy Sets and Syst.*, vol. 156, no. 3, pp. 432-444, Dec. 2005.

Table 1. Rule table of the *ith* fuzzy inference engine.

$\overline{e}_i$ \ $\dot{\overline{e}}_i$	PH	PB	PM	PS	PI	ZE	NI	NS	NM	NB	NH
NH	ZE	NI	NS	NM	NM	NB	NB	NB	NH	NH	NH
NB	PI	ZE	NI	NS	NM	NM	NB	NB	NB	NH	NH
NM	PS	PI	ZE	NI	NS	NM	NM	NB	NB	NB	NH
NS	PM	PS	PI	ZE	NI	NS	NM	NM	NB	NB	NB
NI	PM	PM	PS	PI	ZE	NI	NS	NM	NM	NB	NB
ZE	PB	PM	PM	PS	PI	ZE	NI	NS	NM	NM	NB
PI	PB	PB	PM	PM	PS	PI	ZE	NI	NS	NM	NM
PS	PB	PB	PB	PM	PM	PS	PI	ZE	NI	NS	NM
PM	PH	PB	PB	PB	PM	PM	PS	PI	ZE	NI	NS
PB	PH	PH	PB	PB	PB	PM	PM	PS	PI	ZE	NI
PH	PH	PH	PH	PB	PB	PB	PM	PM	PS	PI	ZE

Table 2. Look-up table of the *ith* fuzzy inference engine.

$\overline{e}_i$ \ $\dot{\overline{e}}_i$	1.0	0.8	0.6	0.5	0.2	0	-0.2	-0.5	-0.6	-0.8	-1.0
-1.0	0.0	-0.05	-0.2	-0.5	-0.7	-0.8	-0.9	-0.95	-1.0	-1.0	-1.0
-0.8	0.05	0.0	-0.05	-0.2	-0.5	-0.7	-0.8	-0.9	-0.95	-1.0	-1.0
-0.6	0.2	0.05	0.0	-0.05	-0.2	-0.5	-0.7	-0.8	-0.9	-0.95	-1.0
-0.5	0.5	0.2	0.05	0.0	-0.05	-0.2	-0.5	-0.7	-0.8	-0.9	-0.95
-0.2	0.7	0.5	0.2	0.05	0.0	-0.05	-0.2	-0.5	-0.7	-0.8	-0.9
0	0.8	0.7	0.5	0.2	0.05	0.0	-0.05	-0.2	-0.5	-0.7	-0.8
0.2	0.9	0.8	0.7	0.5	0.2	0.05	0.0	-0.05	-0.2	-0.5	-0.7
0.5	0.95	0.9	0.8	0.7	0.5	0.2	0.05	0.0	-0.05	-0.2	-0.5
0.6	1.0	0.95	0.9	0.8	0.7	0.5	0.2	0.05	0.0	-0.05	-0.2
0.8	1.0	1.0	0.95	0.9	0.8	0.7	0.5	0.2	0.05	0.0	-0.05
1.0	1.0	1.0	1.0	0.95	0.9	0.8	0.7	0.5	0.2	0.05	0.0

2011 IEEE International Conference on Fuzzy Systems
June 27-30, 2011, Taipei, Taiwan

Formation Behavior of Multiple Robots based on Tele-operation

Yuki Wagatsuma
Tokyo Metropolitan University
Tokyo, Japan
wagatsuma-yuki@sd.tmu.ac.jp

Yuichiro Toda
Tokyo Metropolitan University
Tokyo, Japan
toda-yuuichirou@sd.tmu.ac.jp

Naoyuki Kubota
Tokyo Metropolitan University
Tokyo, Japan
kubota@tmu.ac.jp

Abstract: Recently, multi-robot systems have been discussed to realize a large size of distributed autonomous system. Furthermore, multi-robot systems have been applied to various problems such as autonomous guided vehicles, soccer robots, and search and rescue system by multi-robot. This paper proposes intelligent formation behavior for the multi-robot based on sensor fusion. First, we discuss multi-agent systems and wireless network technologies. Next, we explain the hardware specification of robot and tele-operated system and wireless communication. Finally, we show experimental results, and discuss the availability of intelligent formation behavior for multi-robot.

Keywords; Multiple Robots, Formation Behaviors, Fuzzy Control, Tele-operation

I. INTRODUCTION

Recently, various types of intelligent multi-agent systems have been proposed to realize a large size of autonomous systems [1-8]. Multi-agent systems have been applied to various problems such as autonomous guided vehicles, soccer robots, and search and rescue system by multi-robot. Network robots are also assumed as one of multi-agent systems. We should discuss two different types of problems in multi-agent systems simultaneously. The first one is the relationship of each agent with its environment from individual point of view. The other is the internal relationship among agents with their outer environmental conditions from the collective point of view. Furthermore, intelligent technologies including fuzzy, neural network, and evolutionary computing, have been applied to such the intelligent systems interacting with environments [9-13]. However, the high level of integration of the collective intelligence and individual intelligence has not discussed much yet. Therefore, we proposed the formation control methods for multi-robot system, and discussed the applicability of the proposed methods in various environmental conditions [14-17]. However, we did not use multiple mobile robots in real world conditions on network technologies.

As the progress of wireless network technologies and ubiquitous computing, various types of network robots have been developed [18-21]. The research on wireless sensor networks combines three components of sensing, processing, and communicating into a single tiny device. The ubiquitous computing integrates computation into the environment. The ubiquitous computing is conceptually different from sensor network, but both aim at the same research direction. Sensor networks and ubiquitous computing have been incorporated into robotics. These researches are called network robotics and ubiquitous robotics, respectively. If the robot can receive the environmental data through the network without the measurement by sensors, the size of the robot can be easily reduced and the received environmental data are more precise because the sensors equipped in the environment are designed suitable to the environmental conditions. The available communication channels are limited under the real world conditions. Therefore, we apply different standards of network channels, e.g., ZigBee for the network communication among mobile robots, and between a host computer and mobile robots.

Furthermore, we discuss the formation behavior based on available sensing data. Next, we explain the multi-objective behavior coordination, and we propose the sensor fusion method based on various types of sensor inputs. Next, we propose monitoring system to enable environmental measurement under unknown environment by using multi-robot. Finally, we show several experimental results of the proposed method.

II. TELE-OPERATION OF MULTIROBOT

A. A Mobile Robot for Information Seeking

We developed various types of mobile robots using Bioloid [22]. The robot can perform the wireless communication by ZigBee with host computers or other robots. Figure 1 shows developed the mobile robots developed in this paper. This leader robot is controlled by the manual operation with a joystick. The first mobile robot shown in Fig.1 (a) equips a wireless camera. The size of the robot in Fig.1 (a) is 140 x 120 x 90 [mm].

The follower robot shown in Fig.1 (b) equips two cameras and a laser range finder (LRF). Furthermore, the small size of PC is attached on the robot to perform autonomous behavior by using web camera and LRF. This robot constructs a formation according to the position of the leader robot. One wireless camera is used for the expanding view area for the human operator in order to present the area surrounding the

978-1-4244-7316-8/11/$26.00 ©2011 IEEE

leader robot. Another camera is used for the target tracing behavior, and LRF is used for collision avoidance behavior. The size of the robot in Fig.1 (b) is 300 x 150 x 250 [mm]. The communication range of the wireless camera and ZigBee with the host computer is 30 [m]. ZigBee is one of the Near Field Communications (NFC) suitable to short range and high frequency communication for home appliances. Moreover, the ZigBee can form various types of network topologies such as star type, tree type and mesh type according to the aim and environmental conditions.

Table 1 shows the specification of two robots. A human operator sends a control command to the leader robot from the host computer based on images received directly from the wireless camera.

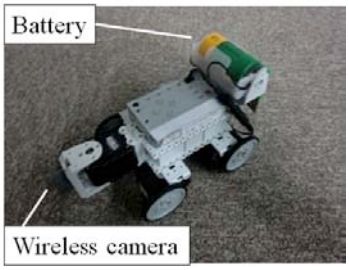

(a) A leader robot

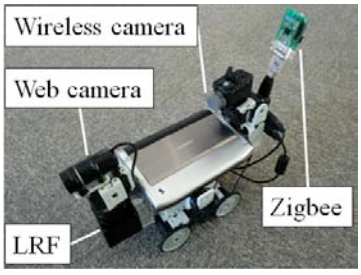

(b) A follower robot

Figure 1. Tele-operated mobile robots

TABLE I. SPECIFICATION OF TWO ROBOTS

Type	*Leader*	*Follower*
Weight	0.8kg	2.0kg
Speed	Max 1.7 m/s	Max 1.8 m/s
Sensor	Wireless camera	Wireless camera Web camera LRF
Operation method	Manual (Joystick)	Autonomous

B. Tele-operation system

We developed a human interface for the tele-operation based on graphical user interface (GUI) from the host computer. The image data of wireless camera equipped with the leader robot are transmitted to the host computer, and the operator can monitor those data (Fig.2 (a)).

The behaviors of the leader robot are based on the semi-autonomous control. Figure 2 (b) shows a snapshot of the control of the robot by the operator. The operator can navigate the leader robot by using a joystick. The collision avoidance and target trace of the follower robot with obstacles are done automatically. Therefore, the operator can focus on the monitoring of the environment with the low human load of navigation based on the semi-autonomous control mode.

Figure 2 (c) shows the user interface for the remote monitoring and remote control of three mobile robots. A view image from the leader robot is displayed in the upper on the screen, and that from the follower robot is displayed in the lower left and right. The operator can see the facing situation from the camera of the leader robot from the local point of view, while he or she can see the surrounding situation from the camera of the follower robot from the global point of view. In this way, the operator can control these mobile robots by changing the viewpoint of an operator.

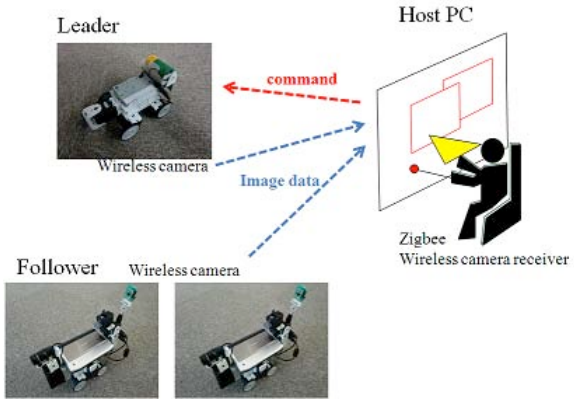

(a) The information flow in the tele-operation

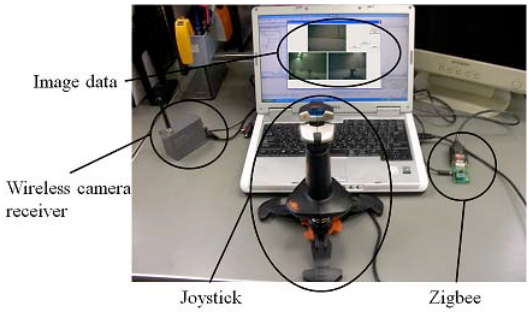

(b) The control of the pan-tilt mechanism by touch panel

(c) Camera images of tele-operated mobile robots in the monitoring display

Figure 2. Tele-operattion system

C. Formation Behaviors

The multi-robot system should update the shape of formation according to the aim of information seeking under the features of environmental conditions, e.g., unknown, dynamic, and/or unreliable. For example, we show five types of shapes of formation in Figure 3 where the number of robots is 3, the equipped sensors are camera and LRF, and blue fan-shaped area and green fan-shaped area mean the measurable ranges by LRF and wireless camera, respectively.

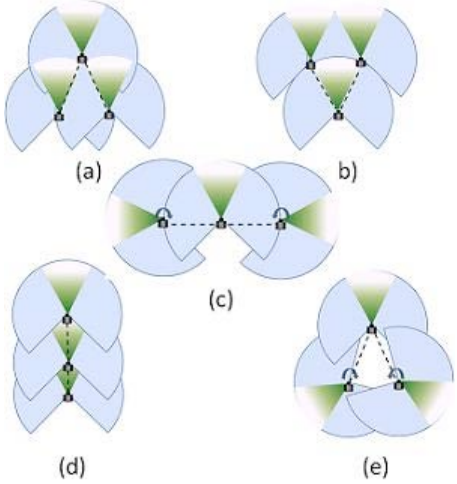

Figure 3. various type of formation

Figure 3 (a) is a basic triangular formation by three robots where one leader robot and two follower robots. The operator controls the leader, while two follower robots gather their surrounding environmental information. Figure 3 (b) shows a formation in unknown or dangerous environment where the two top followers gather the environmental information in order to detect dangerous state and others, and the operator controls the leader robot from the backward. Figure 3 (c) shows a formation of three robots arranged in a single horizontal row. This formation can gather wide range of images to display the global environmental state at a glance. Figure 3 (d) shows a formation of three robots arranged in a single tandem line in a narrow path, small space, and many obstacles. Figure 3 (e) shows a formation of three robots to observe all-around view in dynamic or changing environment when three mobile robots stop at a point. In this way, we can change the formation of robots according to the aim of information seeking under different environmental conditions. In this paper, we focus on the basic triangular formation behavior as the first step of this study.

III. FORMATION BEHAVIORS

A. Functions for Formation Behaviors

Each robot needs to understand its relative position with other robots to build the global formation shape by multiple robots. Consequently, the robot should localize the self-position relative to its neighboring robots, and share the information on position and posture with other robots. A dead-reckoning algorithm is often used to estimate the global self-position, but this method has a problem of accumulating errors in the estimation. Therefore, we use web cameras and LRF for the relative localization. The web camera image is used for relative localization, and the wireless camera image is used for remote monitoring and control by a human operator.

B. Object Detection

Various types of pattern recognition methods and image processing methods have been proposed [23-30]. We applied the continuously adaptive mean shift (CAMSHIFT) algorithm using Open CV library to extract the landmark of the leader mobile robot from the camera image of the follower mobile robot. Because the basic CAMSHIFT algorithm updates the target template sequentially, it is difficult to trace a target landmark if the mobile robot fails to recognize the current target template.

(a) Leader robot (b) follower robot

Figure 4. Landmarks used for visual tracking

In order to detect and identify other robots, we use landmark identifiers based on combination of two different colors (Fig.4). We use a steady-state genetic algorithm (SSGA) for object detection as one of search methods, because SSGA can easily obtain feasible solutions through environmental changes with low computational cost. SSGA simulates a continuous model of the generation, which eliminates and generates a few

of individuals in a generation (iteration). A template is composed of numerical parameters of $g_{i,1}$, $g_{i,2}$, $g_{i,3}$, and $g_{i,4}$. The number of individuals is G. One iteration is composed of selection, crossover, and mutation. The worst candidate solution is eliminated ("Delete least fitness" selection strategy), and is replaced with the candidate solution generated by the crossover and the mutation. We use the elitist crossover and adaptive mutation. The elitist crossover randomly selects one individual and generates an individual by combining genetic information from the randomly selected individual and the best individual. Next, the following adaptive mutation is performed to the generated individual,

$$g_{i,j} \leftarrow g_{i,j} + \left(\alpha_j + \frac{f_{\max} - f_i}{f_{\max} - f_{\min}} + \beta_j \right) \cdot N(0,1) \qquad (1)$$

where f_i is the fitness value of the ith individual, $f_{\max}$ and $f_{\min}$ are the maximum and minimum of fitness values in the population; $N(0,1)$ indicates a normal random variable with a mean of zero and a variance of one; α_j and β_j are the coefficients ($0 < \alpha_j < 1.0$) and offset ($\beta_j > 0$), respectively. In the adaptive mutation, the variance of the normal random number is relatively changed according to the fitness values of the population.

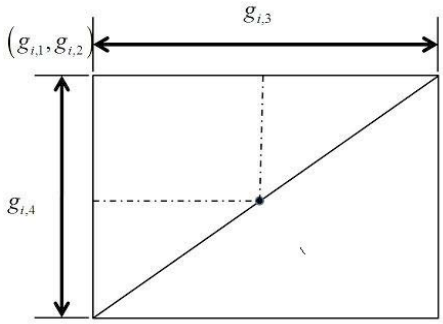

Figure 5. A candidate solution for object detection

The template of each candidate solution is evaluated as the sum of local evaluations in small subareas shown in Fig.6. Each subarea is evaluated by different weights in the following;

$$f_i = \sum_{a=1}^{n_1} \sum_{b=1}^{n_2} \sum_{c=1}^{n_3} M_{a,b,c} C_{a,b,c} \qquad (2)$$

where $C_{a,b,c}$ and $M_{a,b,c}$ are the number of pixels of the cth color in the subarea (a,b), and its evaluation weight. We can perform the search of landmarks with different color distribution. If the fitness value of the best candidate solution is higher than the predefined threshold, its corresponding template is recognized as the target landmark. The position (u,v) of the landmark in the local coordinate on the camera image is calculated as

$$(u,v) = \left(g_{b,1} + \frac{g_{b,3}}{2}, g_{b,2} + \frac{g_{b,4}}{2} \right) \qquad (3)$$

where b is the best candidate solution. The relative angle (ξ) between the moving direction of the follower robot and the position of the leader robot is calculated by

$$\xi = \tan^{-1} \left(\frac{2 \cdot u \cdot \tan \frac{\omega}{2}}{Q} \right) \qquad (4)$$

where the size of pixels on the camera image is $P \times Q$, ω is the view angle of the web camera in Fig.7. Next, we obtain the distance information (L_{leader}) by referring to the distance measured by LRF.

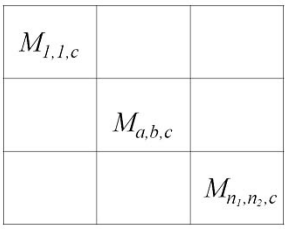

Figure 6. A template matching evaluation using subarea

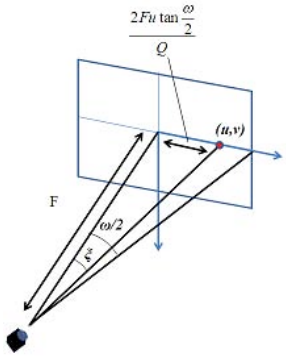

Figure 7. Estimation of the relative angle

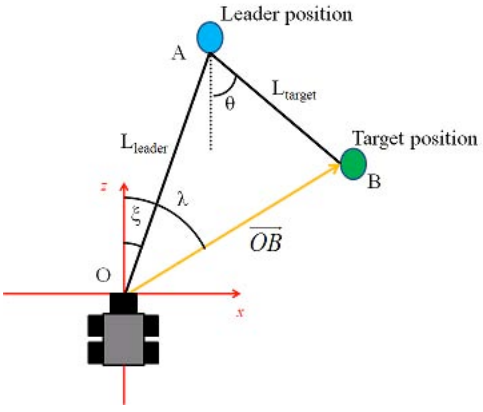

Figure 8. Estimation of the relative position

C. Multi-Objective Behavior Coordination

Various types of intelligent control methods for mobile robots have been proposed such as production rules, Bayesian networks, neural networks, fuzzy inference systems, and classifier systems [31-34]. We have applied fuzzy inference systems to represent behavior rules of mobile robots, because the behavioral rules can be designed easily and intuitively by human linguistic representations. A behavior of the robot can be represented using fuzzy rules based on simplified fuzzy inference [31]. In general, a fuzzy if-then rule is described as follows,

If x_1 is $A_{i,1}$ and ... and x_M is $A_{i,M}$
Then y_1 is $w_{i,1}$ and ... and y_N is $w_{i,N}$

where $A_{i,j}$ and $w_{i,k}$ are the Gaussian membership function for the jth input and the singleton for the kth output of the ith rule; M and N are the numbers of inputs and outputs, respectively. Fuzzy inference is performed by,

$$\mu_{A_{i,j}}(x_j) = \exp\left(-\frac{(x_j - s_{i,j})^2}{t_{i,j}^2}\right) \tag{5}$$

$$\mu_i = \prod_{j=1}^{M} \mu_{A_{i,j}}(x_j) \tag{6}$$

$$y_k = \frac{\sum_{i=1}^{R} \mu_i w_{i,k}}{\sum_{i=1}^{R} \mu_j} \tag{7}$$

where $s_{i,j}$ and $t_{i,j}$ are the central value and the width of the membership function $A_{i,j}$; R is the number of rules. Outputs of the robot are output levels of the left and right motors (N=2). Fuzzy controller is used for collision avoidance and target tracing behaviors. The inputs to the fuzzy controller for collision avoidance are the measured distance to the obstacle by LRF. The inputs to the fuzzy controller for target tracing are the estimated distance to the target point and the relative angle to the target point from the moving direction (M_i=2).

In general, a mobile robot has a set of behaviors for achieving various objectives, and must integrate these behaviors according to the environmental conditions. Therefore, we proposed the method for multi-objective behavior coordination [14,15]. The multi-objective behavior coordination can integrate outputs of several behaviors according to the time-series of perceptual information, while the original subsumption architecture selects one behavior [13]. This multi-objective behavior coordination is composed of a sensory network, behavior coordinator, and behavior weight updater. The sensory network outputs perceptual information based on sensing data and updates the parameters of sensors recursively according to the perceptual information [33]. A behavior weight is assigned to each behavior. The output is calculated by

$$y_k = \frac{\sum_{j=1}^{K} wgt_j(t) \cdot y_{j,k}}{\sum_{j=1}^{K} wgt_j(t)} \tag{8}$$

where K is the number of behaviors; $wgt_j(t)$ is a behavior weight of the jth behavior over the discrete time step t. By updating the behavior weights, the robot can take a multi-objective behavior according to the time series of perceptual information. The update amount of each behavior is calculated as follows,

$$\begin{bmatrix} \Delta wgt_1 \\ \Delta wgt_2 \\ \vdots \\ \Delta wgt_K \end{bmatrix} = \begin{bmatrix} dw_{1,1} & dw_{1,2} & \cdots & dw_{1,L} \\ dw_{2,1} & & & \\ \vdots & & \ddots & \vdots \\ dw_{K,1} & & \cdots & dw_{K,L} \end{bmatrix} \begin{bmatrix} si_1 \\ si_2 \\ \vdots \\ si_L \end{bmatrix} \tag{9}$$

where si_i is the parameter on the perceptual information; L is the number of perceptual inputs. This method can be considered as a mixture of experts if the behavior coordinator is considered as a gating network.

IV. EXPERIMENTAL RESULTS

This section shows several experimental results of the proposed method. We use one leader robot for tele-operation and two follower robots to extend the view area for the monitoring and control by human operators. The size of the experiment environment is 3,000 [mm] ×7,000 [mm] including three obstacles. The suitable distance between two robots is set at 500 [mm]. The number of candidate solutions in SSGA is 50; the number of evaluations is 1,500 (corresponding to 30 iterations of discrete generations). If the fitness value of the best candidate solution is larger than 200, its corresponding template is considered as a detected landmark, and the mobile robot traces the rear of the leader robot with the predefined relative angle.

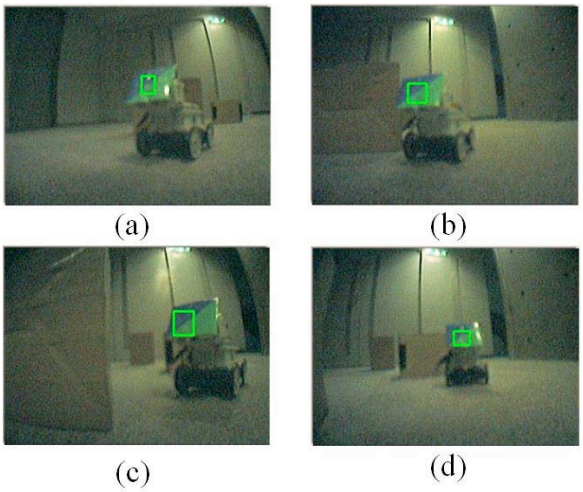

Figure 9. Follower's camera view

(e)

Figure 10. Leader's camera view

First, we show experimental results of image processing for target tracing. Figure 9 shows an experimental result of image processing by SSGA for landmark detection using camera images of the follower robot where a green frame indicates the detected landmark attached with the leader robot. Furthermore, the human operator can understand the environmental state in front of the leader robot, but this image is not enough to control the leader robot (Fig.10). On the other hand, the image from the follower robots includes the environmental state surrounding the leader robot (Fig.11 (a)-(d)). Therefore, the human operator can easily understand the situation of the leader robot, and can control the leader robot by using two types of images from the leader robot and follower robots.

Next, we show experimental results of tandem formation behavior of three robots. Figures 11 and 12 show overview of an experimental result of tele-operation and images sent from robots, respectively. In Figure 11 (d), the solid and dotted lines indicate the trajectories of the leader robot and follower robots, respectively. The follower robot traces the rear of the leader robot by extracting the landmark with keeping the suitable distance with the leader robot, while avoiding the collision with other obstacles. Figure 13 shows the change of fitness value and the degree of danger in the tandem formation behavior of second robot (Follower 1). In the experimental result, since the fitness value is larger than threshold (200) for the target tracing, the robot successfully traces the rear of the leader robot. The behavior weight is updated according to the degree of danger calculated by the minimal distance to obstacles. If the value is high, the behavior weight for collision avoidance is high. The motor output signals are calculated every 300 msec. In the experimental result, because the degree of danger is high, the follower robot tried to avoid the collision. As a result, the fitness value is not so high because the ratio of target tracing behavior is not high (Figure 11 (d).

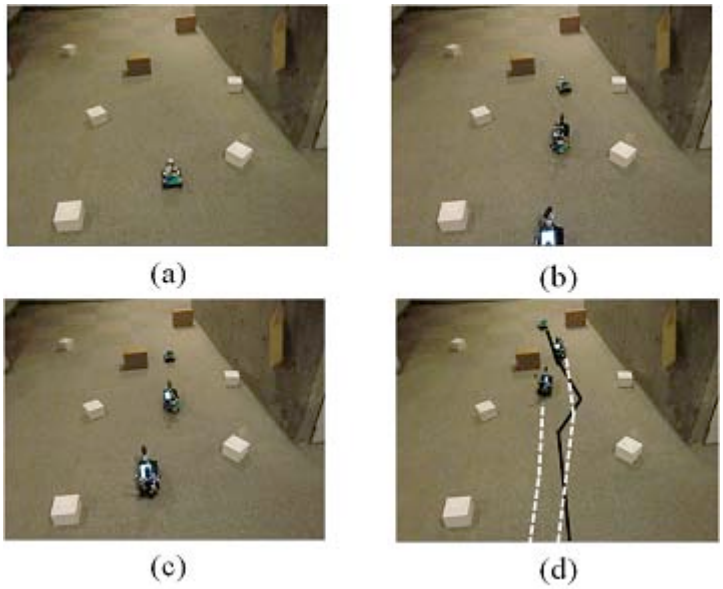

Figure 11. Appearance of line experiment

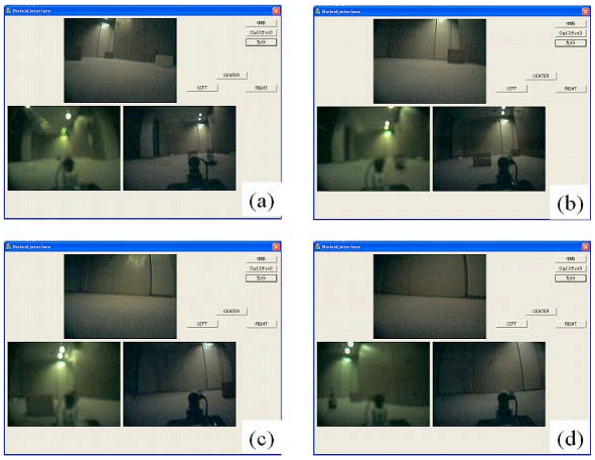

Figure 12. Images sent from robots in tandem formation behavior

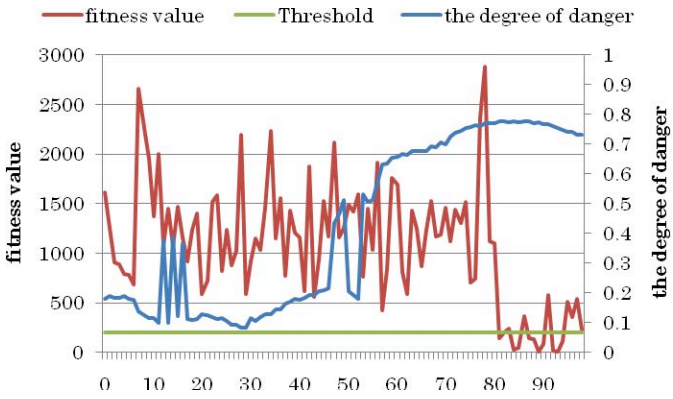

Figure 13. The change of fitness value and the degree of danger in the tandem formation behavior

Next, we show experimental results of a basic triangular formation behavior of three robots. Here we use 30 degree of relative angle to construct the shape of equilateral triangle. Figures 14 and 15 show overview of an experimental result of tele-operation and images sent from robots, respectively. In Figure 14 (d), the solid and dotted lines indicate the trajectories of the leader robot and follower robots, respectively. The follower robot traces the rear of the leader robot with suitable angle and distance. Figure 16 shows the change of fitness value and the degree of danger in the tandem formation behavior.

Figure 16 shows the change of fitness value and the degree of danger in the triangle formation behavior of second robot (Follower 1). In the experimental result, since the fitness value is larger than the threshold (200) for the target tracing, the robot successfully traces the rear of the leader robot. In this case the maximum fitness is not stable as in the tandem formation. Tandem formation always captured landmark at a front. However, triangle formation captured landmark at an angle. So the triangle formation's maximum fitness is unstable.

Finally, we compare the view areas expanded by the tandem formation behavior and basic triangular formation behavior. In case of tandem formation behavior, the image sent from the last follower robot includes the far but wide range surrounding the leader robot. On the other hand, in case of basic triangular formation behavior, the image sent from two follower robots can expand the view area of left and right sides, respectively, but these two images are not symmetrical from the position of the leader position. In this way, these two formation behaviors have one advantage and one disadvantage, respectively. In order to solve this problem, we are developing a 3D visualization method based on distance and color information.

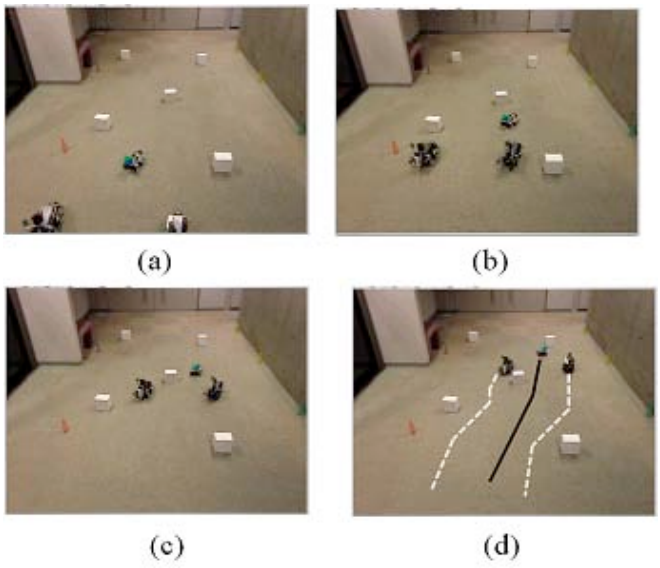

Figure 14. Appearance of line experiment

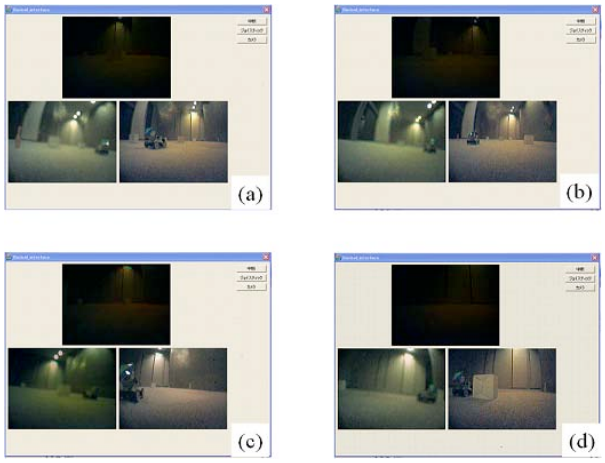

Figure 15. Leader's interface of triangle experiment

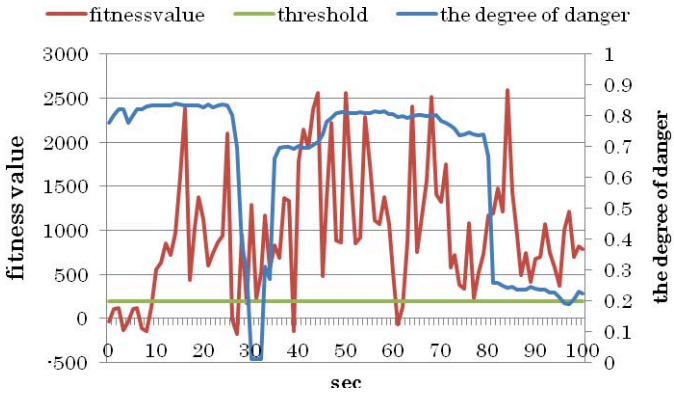

Figure 16. The change of fitness value and the degree of danger in the tandem formation behavior

V. SUMMARY

In this paper, we discussed the formation behavior of multi-robot based on sensor fusion under different environmental conditions. Furthermore, we proposed the method of image processing by a steady-state genetic algorithm for relative localization, and applied a multi-objective behavior coordination method based on fuzzy control. The experimental results showed the effectiveness of the proposed method for target tracing and collision avoidance of the Follower under the tele-operation of the Leader. However, the hybrid communication by wireless LAN, ZigBee, XBee, and Bluetooth is under development. We will propose a control method of several communication technologies. Furthermore, we discuss how to change or update the shape of a formation of three robots according to environmental conditions.

VI. REFERENCE

[1] D. Kurabayashi and K. Osagawa, Formation Transition based on Geometric Features for Multiple Autonomous Mobile Robots, Journal of the Robotics Society of Japan, Vol.23, No.3, pp.376-382, 2005.

[2] P. T. Szemes, H. Hashimoto, Fuzzy Neural Network based Mobile Agent Control for Intelligent Space, Proc. of SICE Annual Conference 2004, 2004, pp.1372-1377.

[3] G. Antonelli, F. Arrichiello, S. Chiaverini, Flocking for Multi-Robot Systems via the Null-Space-based Behavioral Control, Proc. (CD-ROM) of IEEE/RSJ International Conference on Intelligent Robots and Systems, 2008, pp. 1409-1414.

[4] C.G.Langton, C.Taylor, J.D.Farmer, S.Rasmussen, Artificial Life II, Massachusetts: Addison Wesley Publishing Company, 1992.

[5] C.G.Langton, ed., Artificial Life –An Overview, Massachusetts, The MIT Press, 1995.

[6] N.Kubota, M.Ogishi, and F.Kojima, Learning of Multiple Robots in Quasi-Ecosystem, Proc. (CD-ROM) of 2000 26th Annual Conference of the IEEE Industrial Electronics Society, pp.2105-2110, 2000.

[7] N. Moriwaki, D. Yokoi, N. Inuzaka, H. Itoh, Evolution of n-BDD Using Genetic Programming Method – a Food Chain Simulation of Evolutional Agents, Journal of the Japanese Society for artificial Intelligence, Vol. 14, No. 3, pp. 477-484, 1995.

[8] I.Kelly, O.Holland, C.Melhuish, SlugBot, A Robotic Predator in the Natural World, The 5th International Symposium on Artificial Life and Robotics, pp. 470-475, 2000.

[9] J.-S.R.Jang, C.-T.Sun, E.Mizutani, Neuro-Fuzzy and Soft Computing, Prentice-Hall, Inc., 1997.

[10] S.J.Russell, P.Norvig. Artificial Intelligence, Prentice-Hall, Inc., 1995.

[11] J. M. Zurada, R. J. Marks II, C. J. Robinson (eds.), Computational Intelligence - Imitating Life, IEEE Press, 1994.

[12] D.Kurabayashi and K.Osagawa, Formation Transition based on Geometric Features for Multiple Autonomous Mobile Robots, Journal of the Robotics Society of Japan, Vol.23, No.3, pp.376-382, 2005.

[13] R.A. Brooks, A Robust Layered Control System For A Mobile Robot, IEEE Journal Of Robotics And Automation, RA-2, April. pp. 14-23, 1986.

[14] N.Kubota, Y.Nojima, F.Kojima, and T.Fukuda, Multi-Objective Behavior Coordinate for A mobile Robot with Fuzzy Neural Networks, Proc. (CD-ROM) of IEEE-INNS-ENNS International Joint Conference on Neural Networks, 2000.

[15] N.Kubota, M.Mihara, and F.Kojima, Multi-Objective Behavior Coordination and Target Selection of Multiple Robots for Quasi-Ecosystem, Proceedings of the 1st International Conference on Fuzzy Systems and Knowledge Discovery, 2002, pp354-358.

[16] N.Kubota, N.Aizawa, "Self-Adaptation in Intelligent Formation Behaviors of Multiple Robots based on Fuzzy Control", 2009 IEEE International Conference on Fuzzy Systems (FUZZ-IEEE 2009)

[17] N.Kubota, Y.Wagatsuma "Cooperative Control of Multi-robot for Information Seeking", The 2010 International Symposium on Intelligent Systems (iFAN 2010)

[18] I. Khemapech, I. Duncan and A. Miller, A Survey of Wireless Sensor Networks Technology, Proc. of The 6th Annual PostGraduate Symposium on The Convergence of Telecommunications, Networking and Broadcasting, 2005.

[19] I. Satoh, Location-based Services in Ubiquitous Computing Environments, International Journal of Digital Libraries, Springer, 2006.

[20] D. Hafnel, W. Burgard, D. Fox, K. Fishkin, and M. Philipose, Mapping and Localization with RFID Technology, Proc. of the IEEE International Conference on Robotics and Automation, 2004.

[21] Kulyukin, et al., RFID in Robot-Assisted Indoor Navigation for the Visually Impaired, Proc. 2004 IEEE/RSJ International Conference on Intelligent Robots and Systems, 2004, pp. 1979-1984.

[22] http://www.robotis.com/xe/bioloid_jp

[23] J.C.Bezdek, J.M.Keller, R.Krishnapuram, N.R.Pal, "Fuzzy Models and Algorithms for Pattern Recognition and Image Processing", Kluwer, Dordrecht, in Press, 1999.

[24] M. S. Nixon and A. Aguado, "Feature Extraction and Image Processing", Newnes, 2002.

[25] T.Kanda, D.F.Glas,M. Shiomi,N. Hagita; "Abstracting People's Trajectories for Social Robots to Proactively Approach Customers" Int. Intell. Robot. & Commun. Labs., Adv. Telecommun. Res. Inst., Seika, Japan

[26] P.Srinivasan , J.Shi "Bottom-up Recognition and Parsing of the Human Body" Computer Vision and Pattern Recognition, 2007. CVPR '07. IEEE Conference on

[27] C.H. Chen, L.F. Pau, and P.S.P.Wang, Handbook of Pattern Recognition & Computer Vision, World Scientific Publication Co. Pte. Ltd., 1993.

[28] Mark E. Roberts, Ela Claridge, "An Artificially Evolved Vision System for Segmenting Skin Lesion Images," Proc. of 6th International Conference of Medical Image Computing and Computer-Assisted Intervention, pp. 655-662, 2003.

[29] J. Spletzer, A.K.Das, R.Fierro, C.J.Taylor,V.Kumar, and J.P.Ostrowski "Cooperative Localization and Control for Multi-Robot Manipulation" Proc. of IEEE/RSJ International Conference on Intelligent Robots and Systems, 2001.

[30] A.K.Das, R.Fierro, V.Kumar, J.P.Ostrowski, J.Spletzer, and C.J.Taylor, "A Vision-Based Formation Control Framework", IEEE Transactions on Robotics and Automation, Vol.18, No.5, pp.813-826, 2002.

[31] Lotfi A. Zadeh, Fuzzy Logic = Computing with Words, IEEE Trans. on Fuzzy Systems, Vol.4, No.2, 1996.

[32] G. J. Klir and B. Yaun (ed.), Fuzzy Sets, Fuzzy Logic, and Fuzzy Systems, World Scientific Publishing, 1996.

[33] T. Fukuda, N. Kubota, An Intelligent Robotics System Based on A Fuzzy Approach, Proceedings of The IEEE, Vol. 87, No. 9, 1999, pp. 1448-1470.

[34] T.Hastie, R.Tibshirani, and J.Friedman, The Elements of Statistical Learning: Data Mining, Inference, and Prediction, Springer-Verlag, New York, 2001.

2011 IEEE International Conference on Fuzzy Systems
June 27-30, 2011, Taipei, Taiwan

Evaluation of Pointing Navigation Interface for Mobile Robot with Spherical Vision System

Kyohei YOSHIDA, Fuminori HIBINO, Yasutake TAKAHASHI, and Yoichiro MAEDA
Dept. of Human and Artificial Intelligent Systems, Graduate School of Engineering, University of Fukui
3-9-1, Bunkyo, Fukui, Fukui, 910-8507, Japan
Email: {kyosida,fhibino,yasutake,maeda}@ir.his.u-fukui.ac.jp

***Abstract*—In human robot interaction, intuitive interface is necessary. A specific interaction device, for instance, a joystick or a teaching pendant, is not usually intuitive and needs trainings for a general user. Instruction by gesture is one of the intuitive interfaces and a potential user does not need any training for showing a gesture. Pointing is one of the simplest gestures. Hibino et. al.[1] proposed a simple human pointing recognition system for a mobile robot that has an upward directed camera and recognizes human pointing and navigate itself to the place a user is pointing by simple visual feedback control. This paper shows improvement of the method and investigates the validity and usefulness of the proposed method with questionnaire investigations with the proposed and conventional user interfaces.**

Keywords-pointing navigation interface; spherical vision system; omni-directional mobile robot

I. Introduction

Recently, robots are getting popular not only in factory environments but also in human daily life environments. Especially, entertainment robots, for instance, AIBO from Sony[2] and Nao from Aldebaran[3], attract the general people. On the other hand, more practical mobile robots becomes gradually popular, for example, rumba from iRobot[4] and SO-ZI from CCP[5], as a vacuum cleaner robot. More practical robots interacting with a general user are going to be popular in near future although the current vacuum cleaner robots work automatically without human interaction.

In human robot interaction, intuitive interface is necessary. A specific interaction device, for instance, a joystick or a teaching pendant, is not usually intuitive and needs trainings for a general user. Instruction by gesture is one of the intuitive interfaces and a potential user does not need any training for showing a gesture.

Most conventional studies related to gesture recognition assume that height of camera position is about the one of human torso[6], [7], [8]. This assumption is reasonable for a robot that is as tall as a human, however, it is not for a smaller robot like a vacuum cleaner robot for a general user, for example, rumba.

On the other hand, localization and navigation with an upward directed camera on a mobile robot has been studied[9], [10], so far. The mobile robot watches ceiling above and localizes by itself. The method has some advantages over the other vision-based localization methods. One of them is that ceiling image can be captured with less occlusion than side view. Another one is less computational cost for localization based on image processing. A ceiling image has almost only parallel and rotation transform with less magnification transform while the mobile robot moves on the flat. Therefore, visual processing can eliminate an image magnification factor. For instance, template matching needs less computational cost if it does not have to deal with the image magnification factor.

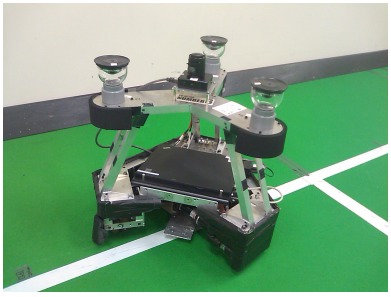

Fig. 1. Mobile Robot with a Spherical Vision System consists of an Upward Directed Fish-Eye Camera and Cameras with Omni-Mirrors

A fish-eye upward directed camera has not only same advantages with the conventional upward-directed-camera based localization methods but also wide view angle. The camera captures not only ceiling but also a human as a potential general user, simultaneously. Therefore, a robot with a fish-eye upward directed camera can localize itself with ceiling image while it recognizes a human gesture.

Hibino et. al.[1] proposed a simple human pointing recognition system for a mobile robot. The mobile robot with a fish-eye upward directed camera recognizes human pointing and navigates itself to the place the human points with a simple visual feedback controller. A human user can navigate the mobile robot intuitively by pointing at desired position on a field with his hand. However, the human pointing system proposed by Hibino et. al.[1] has low operability where the robot goes far from the user. This paper shows improvement of the proposed method with a simple visual feedback control system. Real robot experiments and questionnaire investigation with 11 persons in their twenties are conducted to show the validity and usefulness of the proposed method.

II. Mobile Robot with Spherical Vision System

Figure 1 shows an omni-directional vehicle with a spherical vision system consists of an upward-directed fish-eye camera and cameras with omni-mirrors, which we designed and built. The upward-directed fish-eye camera captures a sight upper

978-1-4244-7316-8/11/$26.00 ©2011 IEEE

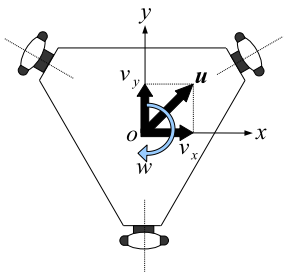

Fig. 2. Robot Coordinate

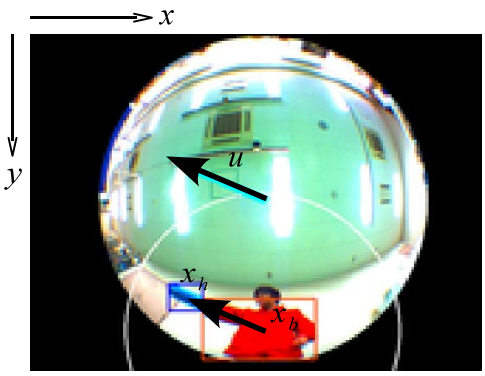

Fig. 3. Simple Visual Feedback for Navigation

than horizon while cameras with omni-mirrors capture sight lower than horizon. Height of the robot is about 50cm and the cameras capture a human surrounding the robot. The method proposed in this paper focuses on the captured images by the upward-directed fish-eye camera. Figure 7 shows captured images. For simplicity of a vision system, a human wears a red jacket and a blue glove.

Figure 2 shows a model of our omni-directional vehicle with three omni-wheels. Coordinates x and y indicate left and front directions of the robot. The robot has two omni-wheels at left and right front and the other at back. It can move toward any direction v_x, v_y including rotation w on a plane surface.

III. Recognition of Human Pointing and Navigation

Recognition of human pointing is realized with a simple algorithm. A vision system extracts red and blue regions on the captured image to recognize positions of the human torso and hand. In order to reduce hand recognition error, blue regions within a certain distance from a red/torso region (shown by white circles in Figure 7) are regarded as candidates of hand region. The largest region of them is recognized as a hand.

Navigation algorithm is designed as a simple visual feedback. The robot moves to the position so that the hand comes to the human torso region on the fish-eye camera image. The human hand comes to the torso area where the robot locates at the place human is pointing as shown in Figure 7(e). The hand position is far from the torso region when the human points with his hand at a position where the robot does not locate as shown in Figure 7(b). The intuitive idea leads to a simple visual feedback based navigation controller. The movement vector $\boldsymbol{u} = (v_x, v_y)$ for the navigation is designed by Hibino at al.[1] as followings:

$$\boldsymbol{u} = k(\boldsymbol{x}_h - \boldsymbol{x}_b) \tag{1}$$

while k, $\boldsymbol{x}_h$, and $\boldsymbol{x}_b$ are a control gain and center position vectors of the extracted human hand and torso on the captured image, respectively (see Figure 3).[1] Actually an object located at right side is projected to left side on a ceiling image and vice versa, therefore, x direction on a ceiling image is reversed when it calculate the movement vector $\boldsymbol{u}$. Furthermore, in general image processing, y coordinate is set from top to down as shown in Figure 3. We just flips y coordinate upside down in order to follow the robot coordinate shown in Figure 2. This means that upper and right directions on the camera image correspond to forward and left in the robot coordinate.

However, the controller designed by Eq.1 has low operability where the robot goes far from the user. The region of the user in the image captured by the upward-directed fish-eye camera becomes smaller if the user is farther from the robot. This means Eq.1 gives smaller movement vector when the user is farther from the robot while it is larger vector when the user is nearer to the robot. In order to compensate the length of the movement vector depending on the distance from the robot and the user, the movement vector is magnified based on the scale of the user region in the image. If the user is projected small in the image, the image is virtually magnified so that the user region in the image becomes same size of the user region projected in the image when the user is near to the robot. This means that the user size in the image is virtually kept as constant so that the length from the torso and the and of the user keeps constant if the user shows exact same pointing gesture to the robot. The concrete adaptive gain control is designed as followings:

$$\boldsymbol{u} = k\frac{f(S_{\max})}{f(S)}(\boldsymbol{x}_h - \boldsymbol{x}_b) \tag{2}$$

where S, $S_{\max}$, $f(S)$ are red region size in the current image, the red region size when the user stands nearest to the robot, and length of the vector between the red(torso) and blue(hand) regions, respectively. $\frac{f(S_{\max})}{f(S)}$ magnifies the moving vector as long as the user stands nearest to the robot. Data of relationship between the red region size and the length of vector between red and blue regions while the user is pointing horizontally as shown at bottom right in Figure 4 are collected beforehand. The data is approximated with the function Eq.3.

$$f(S) = aS^2 + bS + c \tag{3}$$

Parameters, a, b, and c, of the function $f(S)$ are tuned based on the data. Figure 4 shows the data and the function with tuned parameters. [2]

[1]Rotation speed w is fixed to zero because it is not directory related to the navigation in experiments.

[2]$a = -0.000000234337$, $b = 0.0111673$, $c = 39.9448$

IV. Performance Evaluation of Human Pointing Navigation

First of all, control performance of the proposed human pointing navigation is evaluated. Experiments are carried out on a small soccer field in order to evaluate the performance of the proposed method. Figure 5 shows a experimental setup for evaluation of human pointing and navigation. The yellow and blue regions indicate goals. A human stands on (0, 0) depicted in Figure 5 and faces the opposite side line. The human points with his right hand at one point on one of the dots depicted in Figure 5. An omni-directional mobile robot with an upward-directed fish-eye camera recognizes the human pointing and navigates itself to the pointed place. Errors between the pointed place and the robot destination are recorded.

Figure 6 shows how the robot works with human pointing. While the human does not show his hand to the robot, the robot stays around the human (Figure 6(a)). When the human points with his right hand at a certain point on the field, the robot recognizes hand and torso region on the fish-eye camera image and moves to the point successfully (Figures 6(b)(c)(d)(e)).

In order to evaluate navigation performance, error between a query point and converged location of the navigated robot is investigated. A human points at one of the dots depicted in Figure 5. The size between the dots is 0.5 [m] by 0.5 [m]. Figure 8 show the query points on the field and the final locations of the navigated robot based on the controller with adaptive gain control. Red crosses and heads of green arrows indicate the query points and the final locations of the navigated robot, respectively.

The error becomes small when the query point is close to the pointing user because pointing vector is detected large while the robot is close to the human. The controller with the adaptive gain control (Figure8) shows less errors when the robot starts from the region [-2m to 2m] horizontally. Unfortunately, the error becomes over 0.5[m] if the pointed place is over 2m from the user. The reason is that the red (torso

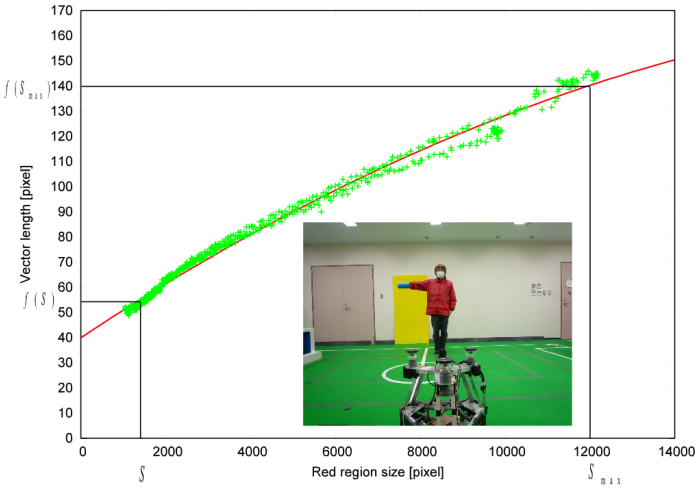

Fig. 4. Relationship between Red Region Size and Length of Vector between Red and Blue Regions

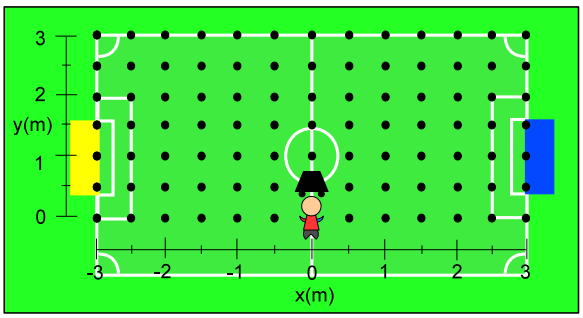

Fig. 5. Experimental Setup for Evaluation of Human Pointing Navigation

of the user) region in the image becomes too small when the robot goes far from the user to compensate the moving vector accordingly.

The errors on the right side on the field are smaller than the ones on the left side. One of the reasons is that the projection of the human right hand to the fish-eye camera image tends to be smaller while the human points left side of the field. Another reason is that the center of the torso is not proper position of origin of the moving vector as described in Eqs.1 and 2. Actually, the position of the right shoulder should be the position of the origin when the user points with his right hand. When the user points in right side, the center of the torso is close to the position of the right shoulder but it becomes far if the user points in the left side.

Figure 9 shows a comparison on the error rate between the adaptive gain control and the fixed one[1]. A user stands at [0m, 0m] on the field and point [0m, 1m] with his right hand. The robot starts to navigate to the point from one of points depicted with red crosses. It is apparent that the adaptive gain control leads the robot to more accurate point than the fixed one. The fixed gain control shows larger errors vertically because the size of vector on the projected image by the fish-eye camera, that is, $\boldsymbol{x}_h - \boldsymbol{x}_b$ in Eqs. (1) and (2), tends to be too small to lead the robot to the query point. On the other hand, the adaptive gain control compensates the effect by tuning the gain accordingly.

V. Usability Evaluation of Human Pointing Navigation

In order to evaluate usability of the proposed human pointing navigation, questionnaire investigation with 11 persons in their twenties are conducted. We prepare 4 methods for robot navigation: Pointing with fixed control gain, pointing with adaptive gain control (Figure 10(a)), a joystick control (Figure 10(b)), and a game-pad one (Figure 10(c)). A subject is asked to navigate the robot as he/she like with one of the method for about half a minute to become used to the method. After he/she becomes used to the method, he/she navigates the robot along a 2.1m by 1.5m rectangle on the soccer field for about one minute. He/she repeats the procedure for all methods. Then, he/she answers questionnaires as shown below:

- Amusement: no fun(1) - fun(5)
- Operability: hard(1) - easy(5)

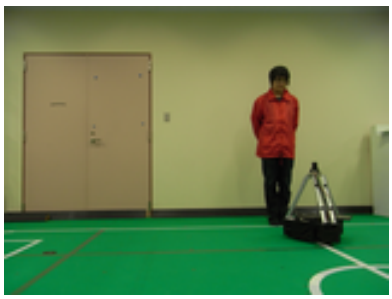

(a)

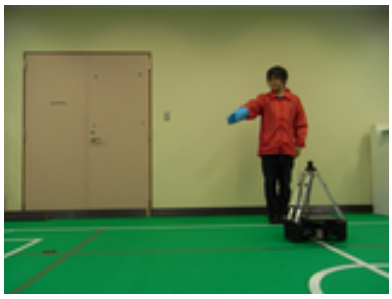

(b)

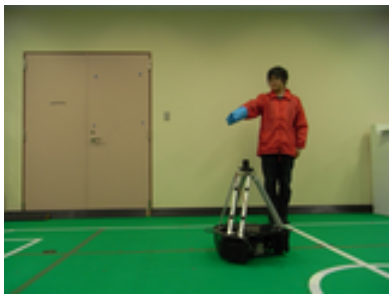

(c)

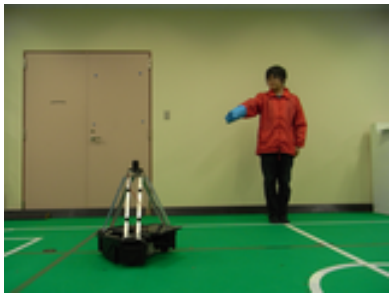

(d)

(e)

Fig. 6. Human Pointing and Navigation

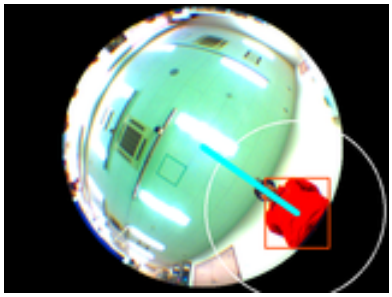

(a)

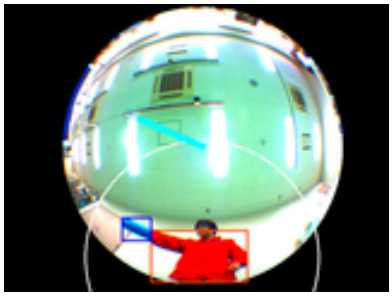

(b)

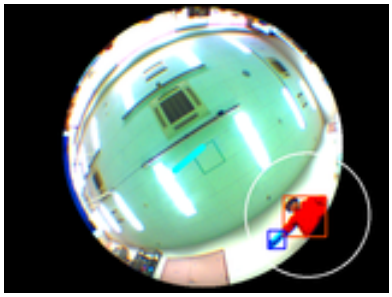

(c)

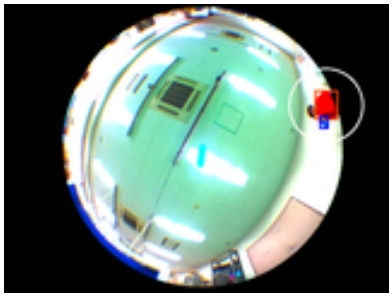

(d)

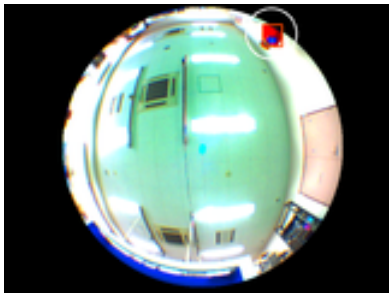

(e)

Fig. 7. Images from the Upward-Directed Fish-Eye Camera

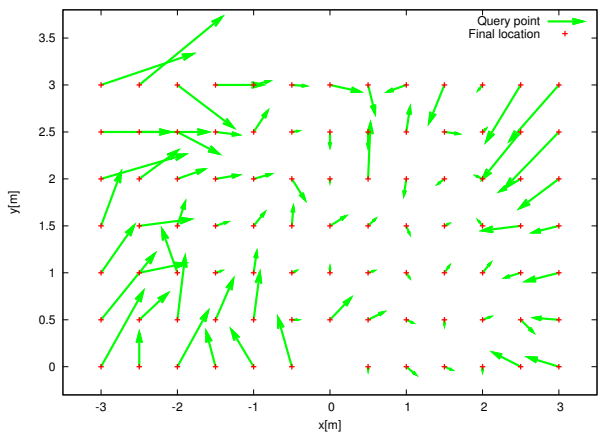

Fig. 8. Navigation Errors with Adaptive Gain Control

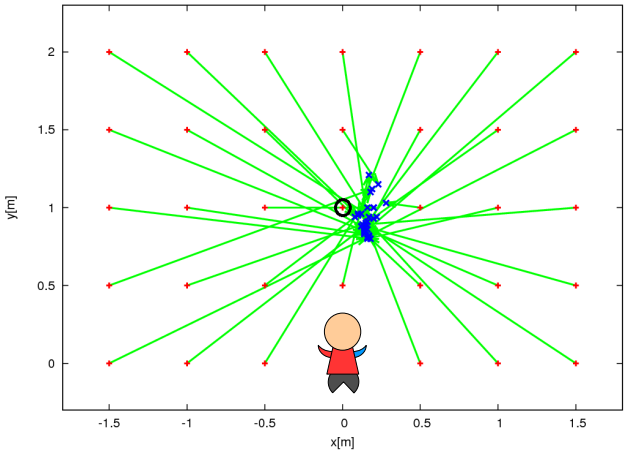

(a) adaptive gain

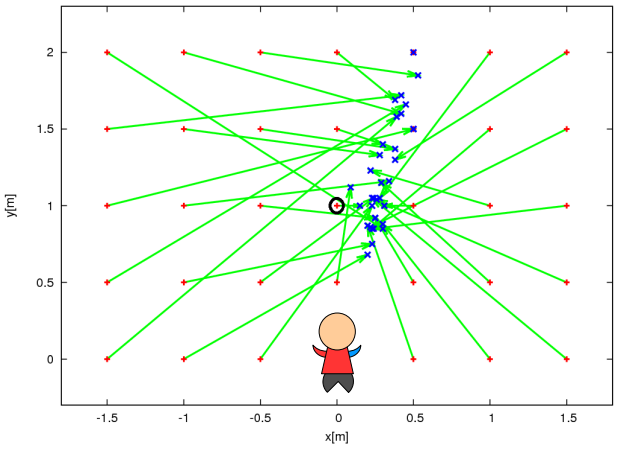

(b) fixed gain

Fig. 9. Errors with Adaptive/Fixed Gain Control during Navigation to a Fixed Point

- Favorite: dislike(1) - like(5)

Figures 11, 12, and 13 show the questionnaire results. Vertical axes indicate number of votes for each degree (from 1 to 5) of the items (amusement, operability, and favorite). The most subjects are used to the gamepad because they sometimes play computer games but not used to the joystick. They feel fun with the joystick and the pointing with fixed/adaptive control gain because of new experiences for them. They feel hard to navigate the robot with the joystick and the pointing with fixed control gain because they are not used to the joystick and the the pointing with fixed control gain makes the robot behave in different way depending on the distance from the robot to the user. On the other hand, the gamepad shows the best operability because they are used to it and the pointing with adaptive control gain shows the 2nd best. Eventually, the pointing with adaptive control gain shows the best favorite evaluation over all. The reason is that the subjects enjoy the new experience and the operability is well nevertheless they are not used to the pointing navigation interface.

VI. Conclusions and Future Work

We proposed a simple human pointing recognition system for a mobile robot and investigate the validity and usefulness with a real robot. Our mobile robot with a fish-eye upward directed camera recognizes human pointing and navigates itself to the place the human points. A human user can navigate the mobile robot intuitively by simply pointing at desired position on a field with his hand. Experimental results show that the proposed method reasonably works and the user can control and navigate the robot intuitively. Adaptive control gain works well so that it reduces the different behavior of the robot according to distance from the robot and the pointing user and increases the operability and favorite of the user.

The current method forces a potential user to wear bright and uniform color jacket and glove to detect them by simple color extraction processing on vision system. It is not convenient for him/her to wear them every time to navigate the robot. A method extracting user region on the upward directed fish-eye camera image should be developed.

At this moment, a potential user has to keep pointing at desired position until a robot reach it. As future work, the proposed method is extended so that a robot estimates direction and distance of the pointed place from a captured image of the pointing user. Nagai et al.[11] proposed a model of "joint attention" that enables a robot to look at an object which its caregiver watches. Their model trains a map from a caregiver's face camera image to an input to head direction control. A similar idea might be applicable for our purpose, that is, a mobile robot learns a map from a captured image of a pointing user to a direction and distance of the pointing place as well.

References

[1] K. Y. Y. M. Fuminori Hibino, Yasutake Takahashi, "Human pointing navigation of mobile robot with spherical vision system," in *Proceedings of Joint 5th International Conference on Soft Computing and Intelligent Systems and 11th International Symposium on Advanced Intelligent Systems*, vol. CD-ROM, 2010, pp. 217–221.
[2] "Aibo official site," http://www.sony.jp/products/Consumer/aibo/.
[3] "Aldebaran robotics, the creators of nao — aldebaran robotics," http://www.aldebaran-robotics.com/.
[4] "irobot corporation: Home page," http://www.irobot.com/.
[5] "Ccp co.,limited — so-zi robotic vacuum cleaner [in japanese]," http://www.ccp-jp.com/life/so-zi/.

(a) Pointing

(b) Joystick

(c) Game-pad

Fig. 10. User Interfaces

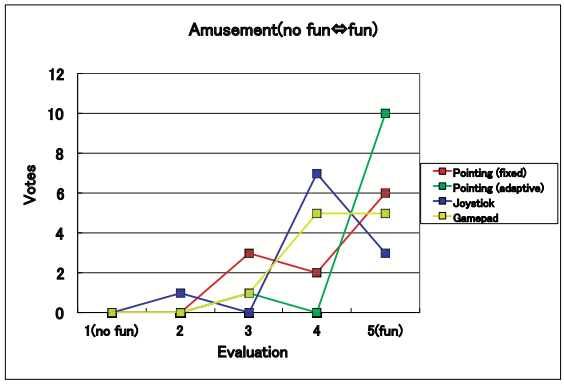

Fig. 11. Questionnaire Result: Ammusement

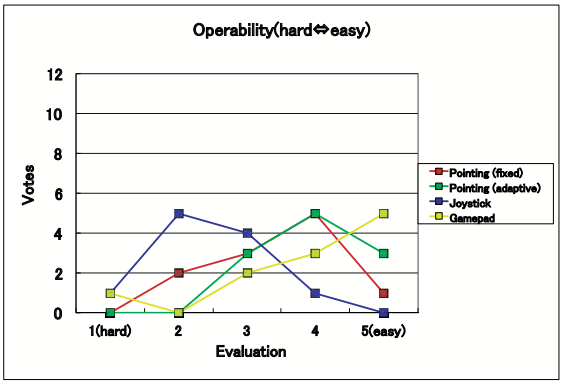

Fig. 12. Questionnaire Result: Operability

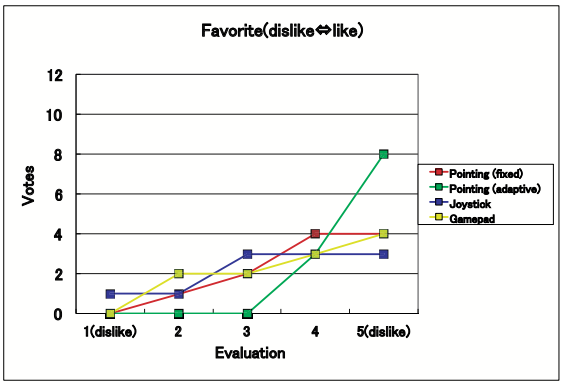

Fig. 13. Questionnaire Result: Favorite

[6] T. Nishimura, H. Yabe, and R. Oka, "A method of model improvement for spotting recognition of gestures using an image sequence," *New Generation Computing*, vol. 18, no. 2, pp. 89–101, 2000.

[7] Y. Iwai, H. Shimizu, and M. Yachida, "Real-time context-based gesture recognition using hmm and automaton," vol. 0. Los Alamitos, CA, USA: IEEE Computer Society, 1999, p. 127.

[8] N. Yoshiike and Y. Takefuji, "Object segmentation using maximum neural networks for the gesture recognition system," *Neurocomputing*, vol. 51, pp. 213–224, apr 2003.

[9] T. Fukuda, S. Ito, F. Arai, Y. Yokoyama, Y. Abe, K. Tanaka, and Y. Tanaka, "Navigation system based on ceiling landmark recognition for autonomous mobile robot-landmark detection based on fuzzy template matching (ftm)," *Intelligent Robots and Systems, IEEE/RSJ International Conference on*, vol. 2, p. 2150, 1995.

[10] W. Jeong and K. M. Lee, "Cv-slam: a new ceiling vision-based slam technique," in *2005 IEEE/RSJ International Conference on Intelligent Robots and Systems*, Aug 2005, pp. 3195–3200.

[11] Y. Nagai, M. Asada, and K. Hosoda, "Learning for joint attention helped by functional development," *Advanced Robotics*, vol. 20, no. 10, pp. 1165–1181, 2006.

2011 IEEE International Conference on Fuzzy Systems
June 27-30, 2011, Taipei, Taiwan

Fuzzy PID Controller Design for Artificial Finger based SMA Actuators

Alireza Khodayari
Mechanical Engineering Department
Islamic Azad University, Pardis Branch
Tehran, Iran
arkhodayari@ieee.org

Mohammad Mahdi Kheirikhah
Mechanical & Industrial Engineering Research Center
Islamic Azad University, Qazvin Branch
Qazvin, Iran
kheirikhah@qiau.ac.ir

Maryam Talari
Mechanical & Industrial Engineering Research Center
Islamic Azad University, Qazvin Branch
Qazvin, Iran
m63_tatlari@yahoo.com

***Abstract*— Shape Memory Alloy (SMA) wires are currently employed in robotics, as well as prosthetic limbs and medical equipment. Due to advantages such as reducing the size in the application, high power-to-weight ratio, elimination of complex transmission systems and noiseless actuation, and human–machine interface, these materials are used as actuators in the prosthesis limb. Because of hysteresis property and nonlinear behavior of SMA, control of these actuators is very complicated. In this paper, the design of control algorithms has been discussed for SMA actuators in the artificial fingers with 3 DOF, which includes PID-fuzzy controller. Gains of controllers are set so that the current applied to SMA wires has minimum overshoot and output of system has minimal time to achieve stability. The simulation results compared with actual measured data show how well the controllers decrease the overshoot and time of stability of input signal to SMA wires.**

Keywords- shape memory alloy; artificial hand; Fuzzy and Fuzzy-PID controller.

I. INTRODUCTION

Actuators are components of robot drive and caused the movement of them. Based of motion, actuators are divided in two types: linear and rotation, and based on performance they are divided in various types: electrical, hydraulic and pneumatic. Using actuators with physical characteristics of them such as weight and size has some limitation. So much activity on these systems has been carried out. In humanoid robots and artificial limbs, due to multiple active joints in limited space, need lightweight, small and powerful actuators for making large placement. SMA is used in robotics because of high ability such as reducing the size of robot and Compatibility with the human body. SMA constitutes a group of metallic materials with the ability of recovering a previous defined length or shape when stands under a thermodynamic process. The transition from one form of crystalline structure to another creates a mechanism by which the shape change occurs in SMAs. This change involves transition from a monoclinic crystal form (martensite) to an ordered cubic crystal form (austenite). The austenite phase is stable at high temperature, and the martensite is stable at lower temperatures. So, the phase transformation between the two phases, martensite and austenite, is accompanied by variations in its resistivity [1]. The typical attribute of these materials is that their parameters can't be determined by simple interpolation of properties of alloys included in the compound. superplasticity, superelasticty, acid resistance and the shape memory effect (SME) make these compounds technically important. Due to advantages such as reducing the size in the application, high power-to-weight ratio, elimination of complex transmission systems and noiseless actuation, and human–machine interface, these materials are used as actuators in the prosthesis limb [2]. Disadvantages of these materials can be cited to hysteresis property. Despite these limitations, they are used in robotic hands and biomaterials.

In recent years, much researches aimed at controlling SMA actuators have been carried out in an artificial limb. Hull and et al. presented a PI controller for obtaining the desired position in SMA actuator [3]. Neguyen presented a new development of a SMA position control system by using a self-tuning fuzzy PID controller [4]. This control algorithm is used by tuning the parameters of the PID controller thereby integrating fuzzy inference and producing a fuzzy adaptive PID controller, which can then be used to improve the control performance of nonlinear systems. Bizdoaca presented a fuzzy logic controller for a SMA tentacle robotic structure [5]. Nicu-George was investigated PI, PD, PID and fuzzy logic controllers are connected to the single link SMA actuation [6]. Ahn used a PID controller for position control of SMA actuator that the parameters of this controller obtained by genetic algorithm [7]. J.Park presented combination of compliant tendon cables and one-way shape memory alloy (SMA) wires that form a set of agonist–antagonist artificial muscle pairs for the required flexion/extension or abduction/adduction of the finger joints [8]. The performance of the proposed actuation system is demonstrated using a 4

978-1-4244-7316-8/11/$26.00 ©2011 IEEE

DOF artificial finger and for evaluation of finger's efficiency, he used PWM-PD controller.

In this paper, according to a dynamic model for an artificial finger with three degrees of freedom using the actuator of SMA [9], fuzzy-PID controller has been designed for position control of SMA actuators. Gains of controllers are carried out so that the current applied to SMA wires has minimum overshoot and output of system has minimal time to achieve stability.

II. DYNAMIC MODEL OF ROBOT

A dynamic model for an artificial finger by using properties of the SMA actuator is designed and presented [9]. This robotic finger has been designed and modeled with 3 DOF, revolute joints, SMA wires as the tendon in order to adduct each phalange of finger and springs to restore each phalanges of finger to original position. In this model, the direct and inverse kinematics of robot and robot motion equations are presented. Mechanism schematic of robot with 3 DOF, parameters and coordinate system is shown in Fig. 1. As shown in this figure, the SMA wire as an actuator after passing the pulley is connected to links of robot. When electrical current is applied in these wires, the wires are hot and after the phase changing, their lengths become shorter so the link of robot starts to turn. After removal of current, the wires are cooled gradually and return to their initial length. Torsion springs in the joints will cause the links to go to the original position.

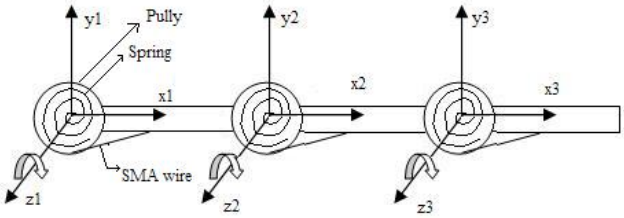

Figure 1. Mechanism schematic of robot with 3 DOF, parameters and coordinate

Kinetic of this robot with SMA actuators and thermodynamic properties of these actuators that include heat transfer, constitutive and phase transformation models are reviewed in reference [9]. Equation of motion of each robot's link by using Lagrange relations is expressed according to (1):

$$\tau_{ji} - \tau_{si} = \sum_{j=1}^{n} D_{ij}(q)\ddot{q}_i + \sum_{k=1}^{n}\sum_{j=1}^{n} c_{kj}^{i}(q)\dot{q}_k\dot{q}_j + h_i(q) + b_i(\dot{q}) \qquad \iota=1,2,3 \quad (1)$$

For each link i, D_{ij} is mass matrix, c^{i}_{kj} is waste viscose term, h_i is terms related to the gravitational potential energy and b_i is frictional force. This model is ignored from friction of joints. Also τ_{si} the torque due to tensional spring and τ_{ji} the torque applied by the SMA actuator [9].

All elements expressed in equation (1), derived according equation and tables in [9].

Dynamic model of this artificial finger simulated in MATLAB/SIMULINK, as shown in Fig. 2. The entering input to and exiting output from this model are current and angles of joints respectively.

This simulation of dynamic model consists of SMA wire heat transfer model, SMA constitutive model and SMA phase transformation model.

The results of simulation model didn't have any offset and steady error; this means that after cutting off current, joints return to their initial position. Also joints reached the desired angle without fluctuation. In addition, after applying the current, joints begin to move immediately and it means that simulation didn't have delay and system motion is perfect (close to actual conditions).

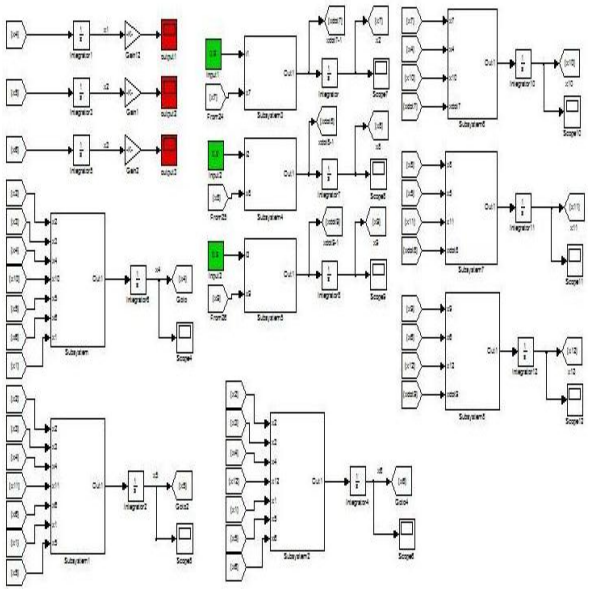

Figure 2. Simulation of dynamic model of artificial finger

III. DESIGN OF CONTROL SYSTEM

One of the most important parts of control system design is determining the appropriate controller parameters [10]. Planning system and achieving the best behavior is the definition that all the positive factors such as increased stability and reduced steady state error have been in the system.

In this paper a closed loop control method is expressed that is simulated in MATLAB /Simulation.

The design of a fuzzy-PID controller can be achieved in different ways. One way is to build a fuzzy controller with three inputs: the error (proportional action-GE), the delta error (derivative action-GCE) and the sum of the error (integral action-GIE) (see Fig. 3). The inconvenience for such a controller is that the number of rules will grow and instead of 25 rules (for system with 5 membership functions on each input), this controller will have 125 rules, making the tuning task very difficult .The solution is to divide the controller in two controllers, one that is the PD equivalent and another one

that provides the integral action. It will reduce the number of rules to 30 (see Fig. 4).

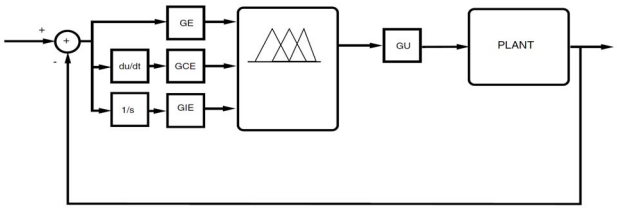

Figure 3. Fuzzy PID controller [10]

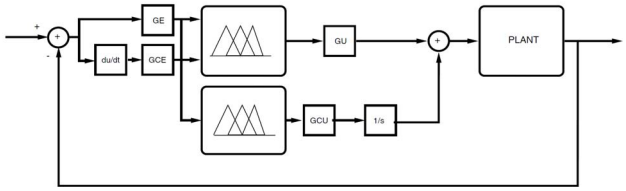

Figure 4. Fuzzy PD+I controller [10]

The use of the "gain constants" can be avoided using a more complex initialization on the fuzzy system where the inputs are not scaled and the singletons of the output are calculated using its direct relation with model values of the membership function in the antecedents, in the similar way as the rules are initialized in the training algorithm.

Further improvement will be done by trial and error, if there is no model of the plant, or via optimization, if a model is available. Using this initialization, the controller will guarantee a performance at least as good as the one provided by the linear PID controller.

Some of the typical actions in the trial-and-error procedure are to increase the impact of the proportional action when the error is very large and slightly reduces the integral action. These two actions tend to reduce the settling time and the overshoot.

In PID-fuzzy, value of desired angle is compared with the amount of feedback. Difference between these two signals is called the position error that it is input of fuzzy controller. The inputs of first fuzzy controller in each link are error (proportional action) and the delta error (derivative action) and because of fuzzy controller introduction in normal form, output is multiplied in a gain. The input of second fuzzy controller in each link is error (proportional action) and output of this controller is multiplied in a gain firstly then enters into the integral. Finally, the total outputs of both controllers are added together, current rate of SMA wire for achieving the desired angle is obtained.

In this section the structure of the fuzzy controller designed for artificial fingers, is investigated. Assuming five membership functions as Negative Big (NB), Negative Small (NS), Zero (Z), Positive Small (PS) and Positive Big (PB) on each input of the fuzzy controller and seven membership functions as Very Low (VL), Low (L), Middle Low (ML), Middle (M), Middle High (MH), High (H) and Very High (VH) in the output of the fuzzy controller. The membership functions of inputs and output, which are defined normally, are shown in Fig. 5 and Fig. 6 respectively.

To express the rules, we need to note, the negative error means that the value of position is upper than desired position and applied current must be reduced for reducing the temperature of the wire and the positive error means that the value of position is lower than desired position, so the applied current should be increased for increasing the temperature of wire. With this definition, rules of first and second fuzzy controller are shown in Table 1 and Table 2 respectively.

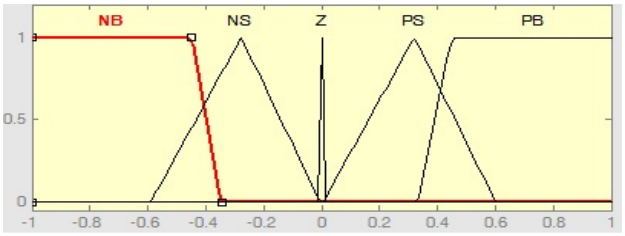

Figure 5. Membership functions for the input variables

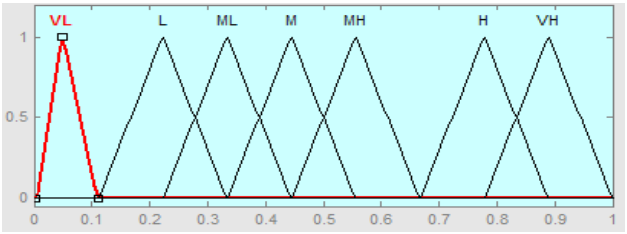

Figure 6. Membership functions for the output variable

TABLE I. RULES BASE FOR FIRST FUZZY CONTROLLER

e / de(t)	NB	NS	Z	PS	PB
NB	VL	ML	M	H	VH
NS	L	M	VL	H	VH
Z	L	M	VL	H	VH
PS	L	M	VL	H	VH
PB	L	MH	VL	L	H

TABLE II. RULES BASE FOR SECOND FUZZY CONTROLLER

e	i
NB	VL
NS	L
Z	MH
PS	H
PB	VH

Gain scheduling has been used extensively on industrial applications. The advantage of this technique is the use of liner techniques to design controllers for nonlinear systems by applying linearization around the different operating points. In this way several linear controllers are designed and "connected" to the plant according to the current operating point. Fuzzy systems offer to these techniques the advantage of integrating in one mechanism the detection of the operating point and the interpolation among the different operating points, providing a smooth nonlinear control law. It has been proved that the fuzzy controllers can be seen as smooth gain scheduling controllers [10].

We used an approach intelligent to determine gain, so that for optimization of fuzzy controller, the code is written for checking the behavior of the system to different inputs and obtaining optimal output (angle of link) in the system. Then this code has been approximated as a linear relationship for each link and is used for obtaining value of error's gain and delta error's gain.

Before entering error to fuzzy controller at the first link, a gain $GE_1(t)$ is used which is obtained by (2):

$$GE_1(t) = 1/ (Setpoint1 -3) \quad (2)$$

And before entering delta error to fuzzy controller at the first link, a gain $GCE_1(t)$ is used which is obtained by (3):

$$GCE_1(t)=1/(GE_1(t)*10) \quad (3)$$

Before entering error to fuzzy controller at the second link, a gain $GE_2(t)$ is obtained by (4):

$$GE_2(t) = 1/ (Setpoint2 -2) \quad (4)$$

And before entering delta error to fuzzy controller at the second link, a gain $GCE_2(t)$ is used which is obtained by (5):

$$GCE_2(t)=1/(GE_2(t)*10) \quad (5)$$

Before entering error to fuzzy controller at the third link, a gain $GE_3(t)$ is obtained by (6):

$$GE_3(t) = 1/ (Setpoint3 -3) \quad (6)$$

And before entering delta error to fuzzy controller at the third link, a gain $GCE_3(t)$ is used which is obtained by (7):

$$GCE_3(t)=1/(GE_3(t)*10) \quad (7)$$

The output gain of the first controller is chosen to be constant at 0.9 (GU). Maximum rate of reducing temperature in the wire is achieved with minimum current and maximum rate of increasing temperature in the wire is achieved with maximum current. Due to the overheating phenomenon in the wire, maximum applied current is 0.9A.

Also is used a gain in constant 0.001 (GCU), after exiting of output from the second fuzzy controller which decreases fluctuations in the output of system.

IV. DISCUSSION

In this section, results have been investigated by using membership functions in first and second fuzzy controller and system simulation in MATLAB.

A. Performance of PID-Fuzzy controller in position control on the first link of artificial finger

Fig. 7 shows control signal is generated by the PID-Fuzzy controller with the setpoint 12 (degrees) at the first link. Output of system to this setpoint is shown in Fig. 8.

As shown in Fig. 7 and Fig. 8, Less time to reach the desired angle and uniformity of control signal show successful performance of controller at the first link of artificial finger. Also system is not disturbed and fluctuated and its steady state error is low.

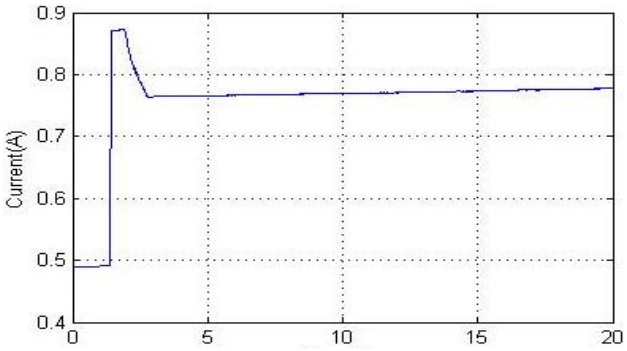

Figure 7. Output of PID-fuzzy (current) in the first link

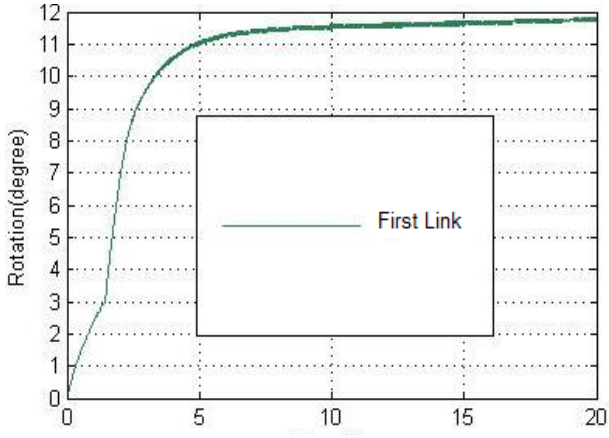

Figure 8. Output of system (rotation of link) in the first link

B. Performance of PID-Fuzzy controller in position control on the second link of artificial finger

Fig. 9 shows control signal is generated by the PID-Fuzzy controller with the setpoint 10 (degrees) at the second link. Output of system to this setpoint is shown in Fig. 10.

As shown in fig. 9 and Fig. 10, time to reach stability is acceptable and appropriate. Less time to reach the desired angle and uniformity of control signal shows successful performance of controller at the first link of artificial finger. Also system is not disturbed and fluctuated and its steady state error is low.

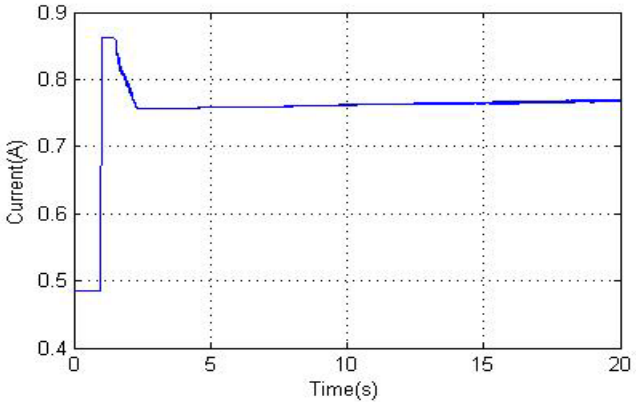

Figure 9. Output of PID-fuzzy (current) in the second link

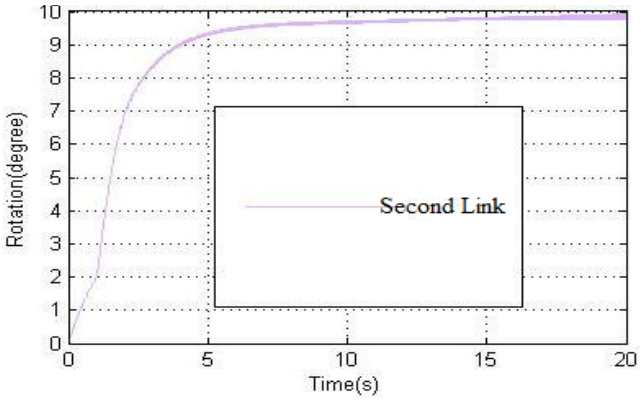

Figure 10. Output of system (rotation of link) in the second link

C. Performance of PID-Fuzzy controller in position control on the thired link of artificial finger

Fig. 11 shows control signal is generated by the PID-Fuzzy controller with the setpoint 8 (degrees) at the third link. Output of system to this setpoint is shown in Fig. 12.

As shown in Fig. 11 and Fig 12 Less time to reach the desired angle and uniformity of control signal show successful performance of controller at the first link of artificial finger. Also system is not disturbed and fluctuated and its steady state error is low.

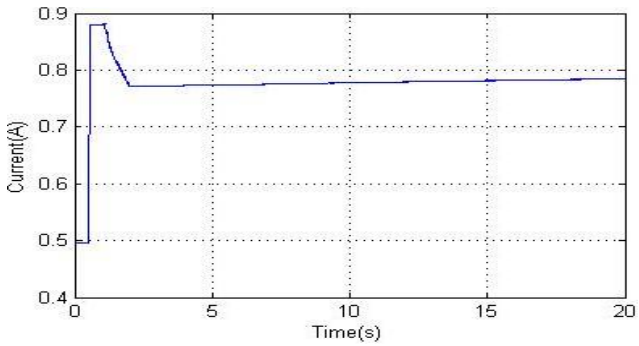

Figure 11. Output of PID-fuzzy (current) in the third link

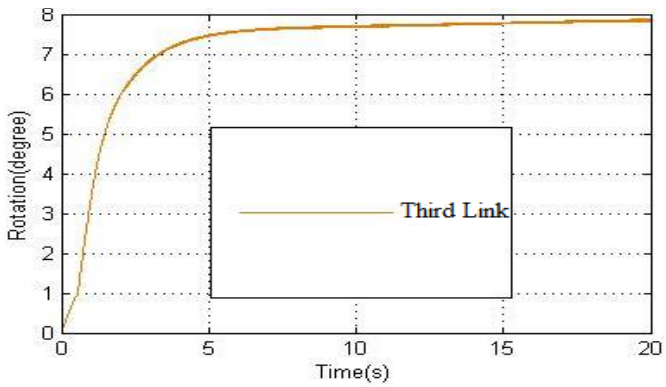

Figure 12. Output of system (rotation of link) in the third link

Results of control system which is designed to bind the model to this controller has been compared with the results of PWM-PD control system which were provided by Bundhoo [11]. Bundhoo designed a PD controller, which is designed to control the current applied to SMA actuator for arriving links of artificial fingers to desired position. Figure 13 shows output of PD controller provided by Bundhoo (apply current to the actuator in the first link).

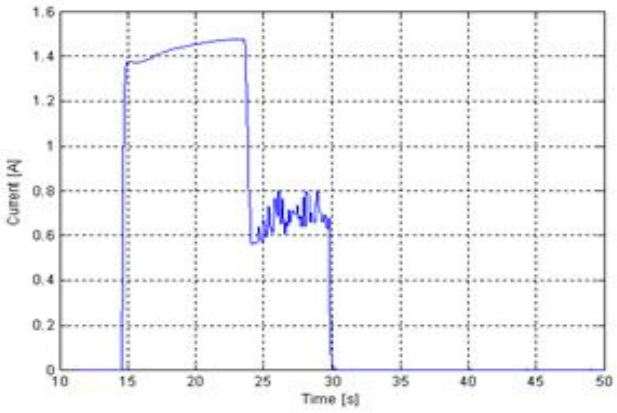

Figure 13. The current profile of the corresponding SMA actuator [11]

The obtained results in this paper with PID-fuzzy controller (first link Fig. 7) is better than Bundhoo's controller because

the overshoot and time stability of output signal in PID-fuzzy controller are smaller and less than Bundhoo's controller.

V. CONCLUSIONS

In this paper, algorithm and performance results of PID-fuzzy controller for the artificial finger with three degrees of freedom are presented. Gains of controllers are carried out so that the current applied to SMA wires has minimum overshoot and output of system has minimal time to achieve stability. Results obtained from simulation and comparison with experimental results show that the PID-fuzzy controllers have good performance in reducing the maximum overshoot and stability of time in input signal to the SMA actuators. Also this controller was able to produce reliable outputs with relatively small errors.

REFERENCES

[1] J. Wakjira, "The VT1 Shape Memory Alloy Heat Engine Design, "Blacksburg, VA, January 2001.

[2] J. P. Kyberd, C. Light, P.H. Chappell, J.M. Nightingale, D. Whatley and M. Evans, "The design of Anthropomorphic prosthetic hands: A study of the southampton hand, " Robotica 19 ,pp. 593–600, 2001.

[3] M. Sreekumar, M. Singaperumal, T. Nagarajan, M. Zoppi, R. Molfino, "Recent advances in nonlinear control technologies for shape memory alloy actuators, " Journal of Zhejiang University Science, 2007.

[4] K. Kwan Ahn and B. K. Nguyen, "Position Control of Shape Memory Alloy Actuators Using Self Tuning Fuzzy PID Controller, " International Journal of Control, Automation and Systems, vol. 4, no. 6. December 2006,

[5] N. Bizdoaca, H. Hamdan and D. Selisteanu, "Fuzzy Logic Controller for a Shape Memory Alloy Tentacle Robotic Structure, " Proceedings of the IEEE Conference on Information and Communication Technologies: from Theory to Application Damascus, Syria. April 2006.

[6] B .Nicu-George, P. Anca and B. Elvira, "Conventional Control and Fuzzy Control Algorithms for Shape Memory Alloy based Tendons Robotic Structure," Wseas Transactions on Systems and Control, Issue 2, Volume 3, February 2008.

[7] K. K. Ahn and N. B. Kha, "Modeling and Control of Shape Memory Alloy Actuators Using Preisach Model, Genetic Algorithm and Fuzzy Logic, " Science Direct, Mechatronics 18, 2008.

[8] V. Bundhoo, E. Haslam, B. Birch and E.J. Park, "A shape memory alloy based tendon-driven actuation system for biomimetic artificial fingers, part I: design and evaluation, " Cambridge University Press, March 18. 2008.

[9] M. M. Kheirikhah, A. Khodayari and M. Tatlari , "Design a New Model for Artificial Finger by Using SMA Actuators," IEEE International Conference on Robotics and Biomimetics (ROBIO2010), China, 2010.

[10] M. J. Grimble and M. A. Johnson, "Fuzzy Logic, Identification and Predictive Control", Springer, 2004.

[11] V. Bundhoo, "Design and evaluation of a shape memory alloy-based tendon driven actuation system for biomimetic artificial fingers," BEng., University of Mauritius, 2009.

2011 IEEE International Conference on Fuzzy Systems
June 27-30, 2011, Taipei, Taiwan

Fuzzy shape Classification exploiting Geometrical and Moments Descriptors

Ugo Erra
Dipartimento di Matematica e Informatica,
Università della Basilicata,
Viale Dell'Ateneo 10, Macchia Romana
85100, Potenza, Italy
email: ugo.erra@unibas.it

Sabrina Senatore
Dipartimento di Informatica
Università degli Studi di Salerno
Via Ponte Don Melillo
84084 Fisciano(SA), Italy
email: ssenatore@unisa.it

***Abstract*—In the era of data intensive management and discovery, the volume of images repositories requires effective means for mining and classifying digital image collections. Recent studies have evidenced great interest in image processing by "mining" visual information for objects recognition and retrieval. Particularly, image disambiguation based on the shape produces better results than traditional features such as color or texture. On the other hand, the classification of objects extracted from images appears more intuitively formulated as a shape classification task.**

This work introduces an approach for 2D shapes classification, based on the combined use of geometrical and moments features extracted by a given collection of images. It achieves a shape-based classification exploiting fuzzy clustering techniques, which enable also a query-by-image.

***Index Terms*—fuzzy clustering, image data mining, image retrieval.**

I. Introduction

The evolution of multimedia computing and applications has seen an explosive growth of digital images in many application domains. This development has remarkably increased the need for image recognition management and image retrieval systems that are able to effectively classify a large amount of images and to efficiently retrieve them based on their visual contents. In developing a visual content-based image retrieval system, two different approaches have been applied: one based on textual information, the other based on image content information. The choice of image features, or combinations of image features to be used for image indexing and retrieval purposes is a critical decision for the efficacy of the adopted approach.

The retrieval based on textual information considers attached textual metadata to each image in the database, then a keyword-based query may be submitted to the system to get relevant images [1]. This approach requires a preliminary annotation activity which often is laborious and time-consuming; moreover, it is a human driven process: that means similar images characteristics can be expressed by different terminologies, according to the subjective evaluation and feeling of the user, affecting the performance of the keyword-based image search. For these shortcomings, (semi-)automatic approaches have been achieved to process the image in order to get more "objective" *content-based* image properties such as color, texture, and shape.

Content-Based Image Retrieval (CBIR) systems instead characterize an image through a set of features; retrieval or classification is then performed by measuring similarity to a required query image [2] contrasting to the effort needed to annotate images. Because images can be particularly complex to manage; CBIR techniques often require a translation of high-level user perceptions into low-level image features. To cope with the so called "semantic gap" problem, these features should be consistent and invariant to remain representative for the images collection in a database.

On the other hand, the CBIR technology tries to address two intrinsic problems: (a) how to mathematically describe an image, and (b) how to assess the similarity between a pair of images based on their abstracted descriptions. Recent methodology development employs statistical and machine learning techniques in various aspects of the CBIR technology. In image classification methods, the approaches are based on learning-based and non-parametric classifiers. As been pointed out in [3], despite the large performance gap between non-parametric classifiers and state-of-the-art learning-based, the non-parametric image classification have been considerably under-valued and offer several advantages: (i) can naturally handle a huge number of classes; (ii) avoid overfitting of parameters, which is a central issue in learning based approaches; (iii) require no learning/training phase.

This work presents an approach for image classification and retrieval based on 2D shape features and extends a previous work [4] for further investigations on shape classification, through fuzzy clustering techniques.

The remainder of the paper is organized as follows. Section II gives a sketched overview of the related works in this area. Section III provides a background on the image processing for the image analysis and features extraction whereas Section IV-A introduces the fuzzy clustering algorithms exploited in this approach. Finally, Section V describes the experiments and provides the results and comparisons. Conclusions and future works close the paper.

II. Related Works

The large repository of digital information needs enhanced image acquisition technologies and computer-assisted image

978-1-4244-7316-8/11/$26.00 ©2011 IEEE

understanding tools in order to get an efficient assistance in image processing, query and retrieval. CBIR aims at efficient retrieval of relevant images form large databases exploiting automatically derived image features [5]. Popular CBIR systems are QBIC, Virage, RetrievalWare, Photobook, Chabot, VisualSeek, WebSeek, MARS system, SurfImage, Netra, and CANDID (for a complete survey, refer to[6]); almost all of these approaches are based on indexing imagery in a feature space. A feature is a certain visual property of an image, either globally for the entire image or locally for a small group of pixels. The feature extraction is often considered as a preprocessing step, which represents the inputs to subsequent image analysis tasks. These features are typically extracted from color, texture, shape and region. Particularly, shapes can be represented by their contours, i.e. a potentially large number of points from their boundaries. Shape descriptors have been used widely as features to characterize an image for classification and image retrieval tasks, such as character recognition [7], word recognition [8] and copyrighted trademark retrieval [7][9]. Like for the texture features, shape features can be used to distinguish between objects where the color feature reveals an unreliable classification due to different objects in image representation can have the same color.

Also the increasing diffusion of images compression requires challenging techniques to extract visual features [10]: sophisticated global features such as the wavelets [11] and large collection of local image descriptors as SIFT [12].

Some other techniques improve the effectiveness of image retrieval through multi-features combination [13],[14] and then, by measuring similarity to a required query image [2]. Combination of words and features characterize annotated training sets of images [8], which will be used for classification or retrieval.

The image description and the user's perception of these features evidence the imprecise nature of the retrieval which can benefit by fuzzy techniques. Fuzzy logic is suitable for expressing linguistic expression by means of fuzzy rather than crisp features values [15].

Applying fuzzy processing techniques to CBIR approaches has been extensively investigated in literature. In general, fuzzy retrieval models offer more flexibility in the representation of the terms' index, preferences among terms in a query and ranked results. In particular CBIR models take advantage by using technique based on fuzzy theory for knowledge representation, for uncertainty management, against traditional information retrieval models based on boolean, vector-based or probabilistic representation. An example is given in [16] where a fuzzy information retrieval model for textual data has been extended to implement a model in image context. In [17], fuzzy logic has been employed to interpret the overall color information of images: according to the human perception, nine classes of colors are defined as features.

A fuzzy color histogram approach in [18] allows the evaluation of similarity through fuzzy logic-based operations. In [19], instead the similarity of two images has been defined by considering the overall similarity between families of fuzzy features. More specifically, each image has been associated to a family of fuzzy features (fuzzy set) representing color, texture, and shape properties. This approach reduces the influence of inaccurate segmentation, compared with other similarity measures based on regions and with crisp-valued feature representations.

Many CBIR approaches exploit clustering for preprocessing activities [20], specifically, fuzzy techniques are widely employed in image classification methods. In [21], a method to calculate image similarity measure using fuzzy partition of the HSI color space has been presented. In particular, the fuzzy c-means (FCM) clustering algorithm [22] has been shown to provide effective partitions for image segmentation on medical images [23][24], satellite images [25][26], and so on. Some extension and modification of FCM are applied to image segmentation in infrared images domain [27]. In [28] a modified version of FCM has been proposed, to solve the problem of large-scale image retrieval and classification, even though the clustering step is performed in lower-dimension space, and image retrieval is only performed in clustered prototypes. Yet, in the most of approaches, the execution time of the clustering algorithm is a critical point, which finds a solution in [27].

III. Design of the feature space

The first step toward the shape analysis of a given image involves separating the object (or region) of interest from other non-important image structures by using an image segmentation approach. There are several approaches for the extraction of the shape from a given image based on clustering methods, histogram methods, edge detection, level set methods, graph partitioning methods and so on. In general there is no a general solution and there is always an image where an approach does not yield good result, i.e., if the foreground and background share many similar colors, an approach could give a result with parts of background labeled as foreground object. This is challenging in shapes classification because any approach must take into account this drawback. In our implementation, we adopt the k-means clustering algorithm for image segmentation which is suitable when the foreground and background colors contrast sufficiently with each other.

A shape descriptor is a set of numbers that are extracted from the region of interest in order to describe a given shape feature. Efficient shape features must present some essential properties such as identifiability, invariance, noise resistance, statistically independence and so on.

In this work, we adopt three types of such shape descriptions: geometric description, invariant moments and affine moments. The geometric features discriminate shapes with large difference. They are useful to eliminate false hits and usually are not suitable as single description, in fact they are combined with other shape descriptors to better discriminate shapes. The moment instead, represents a mathematical concept coming from the concept of moment in physics. It is used in computer vision for both contour and region of a shape. In particular, the invariant moments [29] are one of the most popular and

widely used contour-based shape descriptors. Affine moments invariants are instead features computed from moments that do not change their value in affine transformation.

In the case of geometric features, let P and A denote the shape perimeter and area, respectively. Note that perimeter and area are invariants respect to translation and rotation but when combined, they are not invariant with respect to scale. The features we adopt are:

- Eccentricity E is the measure of aspect ratio. It is defined as the ratio $E = W_{bb}/H_{bb}$ where W_{bb} and H_{bb} are, respectively, the width and height of minimal bounding rectangle of the shape.
- Rectangularity R represents how rectangular a shape is, i.e. how much it fills its minimum bounding box. It is defines as $R = A/A_{bb}$ where A_{bb} is the area of the minimum bounding rectangle.
- Compactness C is a measure that combines area with perimeter. It is defined as $C = L^2/4\pi A$.
- The value π_{gen} is a measure of the compactness of a shape respect to a circle. It is defined as $\pi_{gen} = P/W_{bb}$.

Among the region-based descriptors, invariant moments m_{pq} are the simplest and is given as:

$$m_{pq} = \sum_x \sum_y x^p y^q f(x,y) \qquad p,q = 0,1,2,\ldots$$

where $f(x,y)$ is the intensity function at position (x,y) in a 2D gray level image. In order to obtain translation invariance, the central moments μ_{pq} should be applied:

$$\mu_{pq} = \sum_x \sum_y (x-\overline{x})^p (y-\overline{y})^q f(x,y) \qquad p,q = 0,1,2,\ldots$$

where $\overline{x} = m_{10}/m_{00}$ and $\overline{y} = m_{01}/m_{00}$. Given central moments we are able to compute a set of 7 invariant moments [29], given by:

$$\begin{aligned}
I_1 &= \eta_{20} + \eta_{02} \\
I_2 &= (\eta_{20} - \eta_{02})^2 + 4\eta_{11}^2 \\
I_3 &= (\eta_{30} - 3\eta_{12})^2 + (3\eta_{21} - \eta_{03})^2 \\
I_4 &= (\eta_{30} + \eta_{12})^2 + (\eta_{21} + \eta_{03})^2 \\
I_5 &= (\eta_{30} - 3\eta_{12})(\eta_{30} + \eta_{12})[(\eta_{30} - \eta_{12})^2 - 3(\eta_{21} - \eta_{03})^2] + \\
&\quad (3\eta_{21} - \eta_{03})(\eta_{21} + \eta_{03})[(3\eta_{30} + \eta_{12})^2 - (\eta_{21} - \eta_{03})^2] \\
I_6 &= (\eta_{20} - \eta_{02})[(\eta_{30} + \eta_{12})^2 - (\eta_{21} - \eta_{03})^2] + \\
&\quad 4\eta_{11}^2(\eta_{30} + \eta_{12})(\eta_{21} + \eta_{03}) \\
I_7 &= (3\eta_{21} - \eta_{03})(\eta_{30} + \eta_{12})[(\eta_{30} - \eta_{12})^2 - 3(\eta_{21} - \eta_{03})^2] + \\
&\quad (3\eta_{12} - \eta_{03})(\eta_{21} + \eta_{03})[(3\eta_{30} + \eta_{12})^2 - (\eta_{21} + \eta_{03})^2]
\end{aligned}$$

where $\eta_{pq} = \mu_{pq}^{\gamma}$ and $\gamma = 1 + (p+q)/2$ for $p+q = 2,3,\ldots$. These moments are simple to calculate and they are invariant to translation, rotation and scaling but have an information redundancy drawback since the basis in not orthogonal[30]. From central moments with a little computational effort we are able to obtain also an affine transform invariance which includes the similarity transform and in addition to that stretching and second rotation. We adopt affine moments as defined in [31] and given as:

$$\begin{aligned}
AMI_1 &= (\mu_{20}\mu_{02} - \mu_{11}^2)/\mu_{00}^4 \\
AMI_2 &= (\mu_{30}^2\mu_{03}^2 - 6\mu_{30}\mu_{21}\mu_{12}\mu_{03} + 4\mu_{30} + \mu_{12}^3 + \\
&\quad 4\mu_{03}\mu_{21}^3 - 3\mu_{21}^3\mu_{12}^3)/\mu_{00}^{10} \\
AMI_3 &= (\mu_{20}(\mu_{21}\mu_{03} - \mu_{12}^2) - \mu_{11}(\mu_{30}\mu_{03} - \mu_{21}\mu_{12}) + \\
&\quad \mu_{02}(\mu_{30}\mu_{12} - \mu_{21}^2))/\mu_{00}^7
\end{aligned}$$

All these features are sufficient to characterize the shape of an image. The rationale behind the choice of these moments is that we are interesting in translation, rotation, scale, and projective transform invariance in order that the location, orientation, and scaling of the shape do not affect the extracted features. Further information on these approaches is discussed in [32].

IV. Unsupervised clustering techniques for the image arrangement

The clustering algorithms achieves a partitioning of given data into clusters. In general a partition holds two properties: homogeneity within the clusters (data in a cluster must be similar) and separation between clusters (data of different clusters have to be as different as possible).
The data are opportunely translated into a matrix, where each row is a characteristic vector which represents an image. In fact, the images set has been processed (as described previously) to pull out a such data matrix, whose rows and columns are respectively the collected images and the relative extracted features. Two clustering algorithms have been take into account: the well-known fuzzy C-Means (briefly FCM) algorithm [22] which takes as input the whole data set of images and the approach presented in [33] that works with more than one (sub-)set of data, trying to reconcile them in one complete final partitioning.

A. Fuzzy clustering

FCM represents the most common fuzzy clustering, particularly useful for flexible data organization. It takes as input a collection of patterns of a universe U in form of matrix and produces fuzzy partitions of the given patterns into (prefixed) c clusters.
The FCM algorithm recognizes spherical clouds of points (clusters) in a multi-dimensional data space and each cluster is represented by its center point (prototype). This process is completely unsupervised, aimed at identifying some inherent structures in a set of data.
The fuzzy version of clustering produces a more flexible partitioning of data. Precisely, each pattern (in our case, an image) is not associated exclusively to a cluster, but it can belong to more than one. After the fuzzy clustering execution, each pattern has associated a c-dimensional vector, where each cell represents the membership (in the range $[0,1]$) of that pattern to each cluster.

Compared to the crisp version, the fuzzy clustering generates a flexible partitioning, more intuitive to interpret: a pattern can have some characteristics that are natively representative of more than one cluster, and the exclusive belonging to one

cluster is a too restricted condition. In the fuzzy approach, the membership values better reveal the nature of data set and allow a clearer data analysis. Anyway, it is conceivable to assign a pattern to the cluster, whose membership is the highest.

More formally, each row of the matrix is a vector that represents an image $I \longleftrightarrow \underline{x} = (x_1, x_2, \ldots, x_h)$, where each component of vector is a value computed for a feature. The FCM algorithm aims at minimizing the objective function constituted by the weighted sum of the distances $dist_{i,k}$ between data points $\underline{x}_k = (x_{k,1}, x_{k,2}, \ldots, x_{k,h})$ and the centers (or prototypes) $\underline{v}_i = (v_{i,1}, v_{i,2}, \ldots, v_{i,h})$, according to this formula:

$$Q(U, c) = \sum_{i=1}^{c} \sum_{k=1}^{n} u_{i,k}^{m} (dist(\underline{x}_k, \underline{v}_i))^2 \quad (1)$$

where $c \geq 2$ is the number of clusters, $u_{i,k} \in$ [0,1] is the membership degree of $\underline{x}_k$ (k=1, …, n) in the i-th cluster A_i (i=1, …, c), and $m > 1$ is the fuzzifier, which controls the quantity of fuzziness in the classification process (common choice of fuzzifier is $m = 2$) and finally $dist(\underline{x}_k, \underline{v}_i)$ is:

$$dist(\underline{x}_k, \underline{v}_i) = \sqrt{(||\underline{x}_k - \underline{v}_i||^2)} \quad (2)$$

represents the euclidean distance between the data $\underline{x}_k$ and the center $\underline{v}_i$ of the i-th cluster.

In details, $U = (u_{i,k})$ is a $c \times n$ matrix of cluster memberships satisfying some constraints. In particular, M_{fc} is a family of fuzzy partition matrices:

$$M_{fc} = \left\{ U | u_{i,k} \in [0,1]; \sum_{i=1}^{c} u_{i,j} = 1; 0 < \sum_{k=1}^{n} u_{i,j} < n, \forall\, i, j \right\}, \quad (3)$$

and $V = (\underline{v}_1, \ldots, \underline{v}_c)$ is the ordered collections of cluster centers.

In our study, the data matrix is composed of n images, each one with h values, associated to the corresponding features. The FCM algorithm produces a partitioning of this collection into a prefixed number c of clusters.

The algorithm finds an optimal fuzzy partition of the data, which is carried out through an iterative optimization of (1).

Let us note the only actual parameter of this algorithm is the number c of clusters. In general, this number is not known a priori. Selecting a different number of initial clusters can effectively affect the final partitioning of the data. The problem for finding an optimal c is usually called cluster validity [34]. The objective is to find optimal c clusters that can validate the best description of the data structure. Each of these optimal c clusters should be compact and separated from other clusters. In the literature, many heuristic criteria have been proposed for evaluating fuzzy partitions; some of traditional cluster validity indexes, which have been frequently used, are Bezdek's partition coefficient (PC) [35], partition entropy (PE) [34], Xie-Beni's index [36].

B. Collaborative clustering

The clustering presented in [33] proposes an approach which takes as input two or more subsets of the reference data domain. It achieves a collaborative and proximity-based mechanism of clustering through a collaborative and highly synergistic discovery of structure in data. The collaborative clustering exploits FCM clustering to get a thorough arrangement of data, according to their different typologies of features. In other words, the subsets of features identify collections of descriptors which represent different views of the interest domain, i.e., the structure at different levels of granularity (clusters), providing a scheme of incorporating collaboration. At the end, a collection of homogeneous clusters are given that often better group the data.

More formally, let us consider a collection of patterns (objects) X whose features are described by distinct feature spaces, say $X[1], X[2], \ldots, X[p]$. Let us note X is composed by concatenating all the sub-datasets $X = X[1]X[2] \ldots X[p]$. The approach uses FCM as basic clustering technique and minimizes a objective function given in (1). As said the final outcome of this clustering is a partition matrix that reveals all details about the structure of the data set.

The collaborative clustering achieves two levels of processing:

- numeric: it involves original data sets. FCM clustering is applied to each feature spaces. The approach assumes the number of the clusters by $c_1, c_2, \ldots, c_p$ are different values. The final results are a set of partition matrices $U[1], U[2], \ldots, U[p]$.
- granular: it is based upon membership grades computed through the partition matrices. As the comparison among partition matrices is not possible (they are built with different number of the clusters), the proximity matrices are computed. Let us recall, that for two patterns x_i and x_j the proximity measure returns a number in [0,1] such that it is equal to 1 if $i = j$. Moreover, this measure is symmetric.

  Given a partition matrix $U[k], (k = 1, \ldots, p)$ the proximity between pattern "i" and "j" based on the values of their corresponding entries is [37]:

$$Prox[k](i, j) = \sum_{l=1}^{c} min(u(l, i), u(l, j)) \quad (4)$$

  The results of final consensus are reached through reconciling proximities based upon the clusters.

Thus, the performance index to optimize is described by the following formula:

$$V = \sum_{k=1}^{p} \sum_{i=1}^{N} \sum_{j=1}^{N} [Prox(U)(i, j) - Prox[k](i, j)]^2 \quad (5)$$

where $Prox(U)$ is the proximity matrices computed by Eq. (4) on the whole data set $X(= X[1]X[2] \ldots X[p])$.

The optimization of V is carried out using a standard gradient-based mechanism, thus the minimization of V proceeds over successive iterations until when the difference between two successive partition matrices is insignificant.

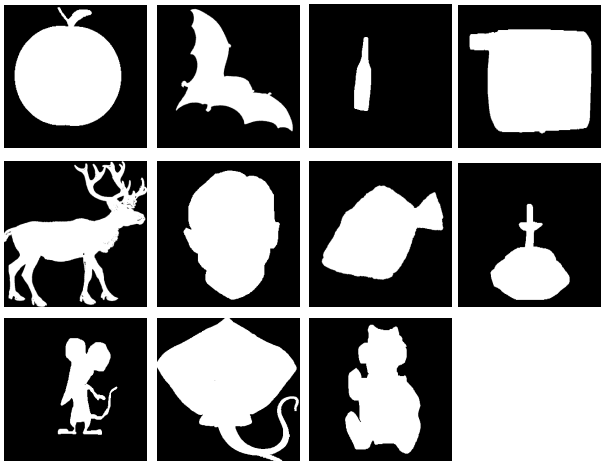

Fig. 1. Sample images representing classes of MPEG-7 CE data set used in the experiment

C. Query by Image

Query by image is a technique that involves providing the CBIR system with an example image that it will then base its search upon. The underlying search approach may vary depending on the application, but result images should all share common descriptors with the provided example. There are essentially two options in providing image: a) the user chooses an image from a given data set. b) the user draws a sketch of the image they are looking for. Both options simplifies the process of describe images with words which can arise in several mismatches during the search.

We explored query by image using as example image a shape draws by the user. For each shape, we compute the shape descriptor associated with it using the approach described in this section. Formally, given a shape descriptor s, a number c of centers v_i, and a fuzziness threshold ϵ, we use the following criteria to obstain the cluster membership. The potential cluster i is found by taking into account the minimal distance center with the shape descriptor, that is

$$i = min_{1 \leq j \leq c} \{j | dist(s, v_j)\}$$

A reference data x point belonging to the cluster i and immediately below the fuzziness threshold is obtained as

$$x_i = min_{1 \leq k \leq n} \{x_k | u_{k,i} \geq \epsilon\}$$

where, n is the size of cluster i. Then, if $dist(v_i, s) \leq dist(v_i, x_i)$, the query is in the space computed as a sphere, with radius equals to $dist(v_i, x_i)$. Then, we return all the images contained in the cluster i sorted based on euclidean distance and whose membership is above the fuzziness threshold. This ranked list represents the answer to the given query.

V. Experimental results

The testing phase consider three datasets. The first experiment considers a subset of the MPEG-7 Core Experiment Shape-1 dataset, which is frequently used to evaluate shape matching and recognition algorithms. In particular, we have used the MPEG-7 CE Shape-1 Part-B dataset [38], composed of 70 shape categories, each of which has 20 samples with in-plane rotations, articulations and occlusions. We have used eleven shape classes, considering all the twenty shape samples. The shape classes are: apple, bat, bottle, cellular phone, deer, face, flatfish, fountain, rat, ray, teddy, shown in Figure 1. The shape classes are very distinct, but the data set shows some within-class variations. All the fourteen features presented above has been exploited in the experiment: geometrical features (E,R, C, π_{gen}), invariants moments features (I_1, I_2, I_3, I_4, I_5, I_6, I_7), and affine moments features (AMI_1,AMI_2, AMI_3).

The 220×14 data matrix has been given as input to FCM. Further, we would like to get a direct association between cluster and class (i.e., each cluster is representative of a class), thus, the number of clusters is equal to the number of images categories ($c = 11$).

Then, according to the natural grouping of features, three data matrices have been built: one has the size 220×4,including only the geometrical features; a 220×7 matrix describing the invariant moments and then a 800×3 matrix representing the affine moments. These matrices have been given as an input to the collaborative clustering, setting the number of clusters c_1, c_2, c_3 to 4, 5, 3, respectively. Also in this setting configuration, $c = 11$, i.e., the number of images categories.

In the fuzzy clustering techniques, the membership of an image may be distributed on more than one clusters. Usually, an image (in general, a pattern) is associated to the cluster in which its membership is the highest. In order to emphasize the natural flexibility of the fuzzy clustering methods in the distribution of data, we have processed the dataset on crisp k-means too.

Table I synthesizes the results, showing the confusion matrix associated to this experiment for the three clustering algorithms. Each cell indeed, contains the results computed for k-means, FCM and collaborative clustering algorithms, respectively. A single value zero means all the results are zero. Let us note that many correspondences are revealed between the generated clusters (*predicted*) and the given (*actual*) images classes. The worst case is computed exploiting k-means: some classes are not well-identified; for instance the class *deer* is composed of only eight images, while the most of its images is placed in the class *ray*. Even, class *cellular phone* is completely empty and most of its images is within the class *teddy*. This emphasizes that the k-means is not suitable to cluster these data. Differently, it is evident how the FCM and collaborative provides meaningful results. In fact, some clusters look very homogeneous; most of them includes averagely about 80% of proper images. Just to give some example, on the FCM clustering, the elements of the classes represented by *bat, bottle, deer, face* are well-placed in each individual cluster (100% of individuals appear in the right cluster). This is not true any longer for the cluster concerning the class *ray*, due to some overlaps among categories. Finally, some clusters are representative of specific classes, even though a certain percentage of elements of other classes appears in them (for

instance, see the clusters representing the classes *apple, flatfish*, etc.). The classification produces improvements, exploiting the collaborative clustering, where the "uncertain" classes such as *apple* and *cellular phone* are almost completely identified.

Other two experiments have been executed on a collection of images downloaded through Google images[1]. Fig. 2 shows a sample of ten images for each considered category. The first testbed consists of a sample of 800 images, composed of five classes of about 160 images, ranked as follows: images in the range 1-160 represent bottles; in the range 161-320 there are images of guitars, then the images of apples cover the range 321-480, the motorcycles images are in 481-640 and finally the last images set consists of guns in the range 641-800. The dataset has been given as an input to the three clustering algorithms. All the clustering algorithm set the number of cluster equals to the number of images categories ($c = 5$). The k-means and the FCM work on all the features set considering a 800×14 matrix , while the collaborative clustering takes as an input three submatrices: one has the size 800×4, including only the geometrical features; a 800×7 matrix describing the invariant moments and then a 800×3 matrix representing the affine moments. The setting the number of clusters is $c_1 = 4, c_2 = 5, c_3 = 4$.

TABLE II
800DATASET: CLUSTER-BASED EVALUATION OF CLUSTERING RESULTS, FOR K-MEANS, FCM AND COLLABORATIVE CLUSTERING, RESPECTIVELY

Classes	*# Misclassified.*	*# Undecided.*	*Recall. %*	*Precision. %*
bottle	0-8-7	0-2-2	86-95-95	95-100-100
guitar	0-3-3	0-0-0	95-98-98	95-93-96
apple	0-12-12	0-0-0	89-92-94	97-100-100
motorcycle	0-5-4	0-1-0	91-96-97	77-88-90
gun	0-13-10	0-3-2	91-91-93	93-93-95

TABLE III
965DATASET: CLUSTER-BASED EVALUATION OF CLUSTERING RESULTS, FOR K-MEANS, FCM AND COLLABORATIVE CLUSTERING, RESPECTIVELY

Classes	*# Misclassified.*	*# Undecided.*	*Recall. %*	*Precision. %*
bottle	21-6-3	0-0-1	86-96-97	93-100-100
guitar	7-3-3	0-0-1	95-98-98	95-96-97
leaf	92-58-45	0-7-5	44-64-72	41-78-81
apple	94-16-14	0-2-0	41-90-91	79-92-94
motorcycle	17-22-17	0-5-4	89-86-90	57-70-78
gun	13-14-10	0-3-3	91-91-93	92-93-96

Table II shows a synthetic view of the results computed for the three algorithms. Each row provides the name of the class, the *misclassified* images, i.e. those images that appear to belong to a cluster, different by the expected one (i.e., they have the highest membership in another class), the *undecided* images, viz. all the images which membership is almost equally distributed among two or more clusters. Recall that, due to the crisp nature of the k-means algorithm, there are no resulting *undecided* images. Then a *recall* and *precision* that is evaluated for each cluster.
In fact, in order to evaluate the recall and precision inside each cluster, we define the *local recall* and the *local precision* as follows:

$$Recall = \frac{relevant\ retrieved\ images}{relevant\ images} \tag{6}$$

$$Precision = \frac{relevant\ retrieved\ images}{retrieved\ images} \tag{7}$$

where the *relevant images* are the images which are expected in a certain class, the *retrieval images* are all the (correct and incorrect) images which are returned in that cluster, while the *relevant retrieved images* are just the images that really belong to the right cluster, associated to the correct class.

From the analysis of resulting partitioning, let us note that the collaborative clustering tends to get better results in terms of recall and precision. Nevertheless, the cluster associated to the class *motorcycle* presents the lowest membership distribution, even though the most of images are well placed in the right cluster.

Last test considers the same dataset of 800 images, but adds 165 images representing *leaf*. We have choice deliberately a set composed of very heterogeneous image samples of leaf, in order to evaluate the performance of FCM and collaborative clustering algorithms in this case study. Table III shows the results for the three clustering algorithms. The introduction of the set of leaf makes the resulting partition more confused: most of misclassified data appear in cluster of apples; this is due to the different shapes of leaves: after the image processing, some leaves present rounded shapes that can be easily confused with apples. In fact, values computed for geometrical features such as Pi and compactness are close to those ones of apples. The best performance are obtained exploiting the collaborative clustering even though the recall and precision values, computed for the class *leaf* are quite low, anyway.

VI. CONCLUSION

The work presents an image classification and content-based retrieval. After an initial phase of image analysis for extracting visual shape-based features, fuzzy clustering techniques have been applied. These techniques provide a relaxed distribution of images (compared to the crisp clustering); moreover they are robust respect to an image segmentation approaches based on k-means segmentation which meet some difficulties foreground and background colors do not contrast sufficiently. The effectiveness of this approach is evaluated through recall and precision, revealing discrete performance.

Let us observe that the use of fuzzy clustering techniques which, even though requires an a-priori fixed number of clusters, avoid overfitting of parameters and does not require a learning/training phase. Moreover an image retrieval technique has been proposed through a query-by-image. As future extensions of this work we would investigates in this direction as well as introduce additional features particularly, some moments that are invariant to elastic transformations and convolution.

[1]The dataset can be downloaded at: http://www.dmi.unisa.it/people/senatore/www/dati/dataset.rar

TABLE I

CONFUSION MATRIX RELATIVE TO A SUBSET OF MPEG-7 CE SHAPE-1 PART-B DATASET FOR K-MEANS, FCM AND COLLABORATIVE CLUSTERING ALGORITHMS, RESPECTIVELY.

		ACTUAL										
		apple	bat	bottle	cell_phone	deer	face	flatfish	fountain	rat	ray	teddy
PREDICTED	apple	17-18-19	0	0	2-1-0	0	0-0-0	0	0	0	0	0
	bat	0	18-20-20	0	0	2-0-0	0	0	0	0	0	0
	bottle	0	0	11-20-20	0	0	0	0	0	0	0	0
	cell_phone	0-0-0	0	0	0-19-20	0	0	0	0	0	0	0
	deer	0	0	0	0	8-20-20	0	0	0	0	0	0
	face	3-0-0	0	0	0	0	20-20-20	2-2-0	0	1-0-0	0	0
	flatfish	0	0	0	0	0	0	17-18-20	0	0	8-2-2	0
	fountain	0	0	0	5-0-0	0	0	0	20-20-20	0	0	0
	rat	0	2-0-0	9-0-0	0	0	0	0	0	19-20-20	2-7-7	0
	ray	0	0	0	0	10-0-0	0	1-0-0	0	0	10-11-11	0
	teddy	0-2-1	0	0	13-0-0	0	0	0	0	0	0	20-20-20

Fig. 2. Some samples used for the experiments. The entire dataset is composed of 930 images subdivided in six categories; bottles, leafs, guitars, motorcycles, guns, and apples.

REFERENCES

[1] H. Lieberman, E. Rozenweig, and P. Singh, "Aria: An agent for annotating and retrieving images," *Computer*, vol. 34, pp. 57–62, 2001.

[2] D. Zhang and G. Lu, "Evaluation of mpeg-7 shape descriptors against other shape descriptors," *Multimedia Syst.*, vol. 9, no. 1, pp. 15–30, 2003.

[3] O. Boiman, E. Shechtman, and M. Irani, "In defense of nearest-neighbor based image classification," in *CVPR'08: Proceedings of the Conference on Computer Vision and Pattern Recognition*, 2008.

[4] U. Erra and S. Senatore, "Experiences with shape classification using fuzzy c-means with geometrical and moments description," in *Proceedings of 8th International Workshop on Adaptive Multimedia Retrieval*, ser. Lecture Notes in Computer Science (In press). Springer Berlin / Heidelberg, 2010.

[5] T. Gevers and A. W. M. Smeulders, "Image search engines - an overview," in *Emerging Topics in Computer Vision*. G. Medioni and S. B. Kang, Eds. Englewood, Cliffs, NJ: Prentice-Hall, 2004.

[6] R. Datta, D. Joshi, J. Li, and J. Z. Wang, "Image retrieval: Ideas, influences, and trends of the new age," *ACM Computing Surveys*, vol. 40, no. 2, pp. 1–60, 2008.

[7] S. Belongie, J. Malik, and J. Puzicha, "Shape matching and object recognition using shape contexts," *IEEE Transactions on Pattern Analysis and Machine Intelligence*, vol. 24, no. 4, pp. 509–522, 2002.

[8] T. M. Rath, R. Manmatha, and V. Lavrenko, "A search engine for historical manuscript images," in *SIGIR '04: Proceedings of the 27th annual international ACM SIGIR conference on Research and development in information retrieval*. New York, NY, USA: ACM, 2004, pp. 369–376.

[9] A. Jain and A. Vailaya, "Shape-based retrieval: A case study with trademark image databases," *Pattern Recognition*, vol. 31, pp. 1369–1390, 1998.

[10] J. A. Lay and L. Guan, "Image retrieval based on energy histograms of the low frequency dct coefficients," in *ICASSP '99: Proceedings of the Acoustics, Speech, and Signal Processing, 1999. on 1999 IEEE International Conference*. Washington, DC, USA: IEEE Computer Society, 1999, pp. 3009–3012.

[11] Y. Tian and L. Mei, "Image retrieval based on multiple features using wavelet," in *ICCIMA '03: Proceedings of the 5th International Conference on Computational Intelligence and Multimedia Applications*. Washington, DC, USA: IEEE Computer Society, 2003, p. 137.

[12] D. G. Lowe, "Object recognition from local scale-invariant features," *Computer Vision, IEEE International Conference on*, vol. 2, pp. 1150–1157 vol.2, August 1999. [Online]. Available: http://dx.doi.org/10.1109/ICCV.1999.790410

[13] J.-Y. Ha, G.-Y. Kim, and H.-I. Choi, "The content-based image retrieval method using multiple features," in *NCM '08: Proceedings of the 2008 Fourth International Conference on Networked Computing and Advanced*

Information Management. Washington, DC, USA: IEEE Computer Society, 2008, pp. 652–657.

[14] D. Zhang, "Improving image retrieval performance by using both color and texture features," in *ICIG '04: Proceedings of the Third International Conference on Image and Graphics*. Washington, DC, USA: IEEE Computer Society, 2004, pp. 172–175.

[15] R. Krishnapuram, S. Medasani, S.-H. Jung, Y.-S. Choi, and R. Balasubramaniam, "Content-based image retrieval based on a fuzzy approach," *IEEE Transactions on Knowledge and Data Engineering*, vol. 16, no. 10, pp. 1185–1199, 2004.

[16] A. Aguilera, A. Suber, L. Martinez, A. Subero, and L. Tineo, "Fuzzy image retrieval system," in *The 10th IEEE International Conference on Fuzzy Systems*, vol. 3, 2001, pp. 1247 –1250.

[17] S. Kulkami, B. Verma, P. Sharma, and H. Selvaraj, "Content based image retrieval using a neuro-fuzzy technique," in *Neural Networks, 1999. IJCNN '99. International Joint Conference on*, vol. 6, jul 1999, pp. 4304 –4308 vol.6.

[18] C. Vertan and N. Boujemaa, "Embedding fuzzy logic in content based image retrieval," in *Fuzzy Information Processing Society, 2000. NAFIPS. 19th International Conference of the North American*, 2000, pp. 85 –89.

[19] Y. Chen and J. Wang, "A region-based fuzzy feature matching approach to content-based image retrieval," *IEEE Transactions on Pattern Analysis and Machine Intelligence*, vol. 24, no. 9, pp. 1252 – 1267, sep 2002.

[20] H. Frigui, "Membershipmap: Data transformation based on granulation and fuzzy membership aggregation," *IEEE Transactions on Fuzzy Systems*, vol. 14, no. 6, pp. 885 –896, dec. 2006.

[21] M. Nachtegael, D. V. der Weken, V. D. Witte, S. Schulte, T. Mélange, and E. E. Kerre, "Color image retrieval using fuzzy similarity measures and fuzzy partitions," in *ICIP (6)*, 2007, pp. 13–16.

[22] J. C. Bezdek, *Pattern Recognition with Fuzzy Objective Function Algorithms*. Norwell, MA, USA: Kluwer Academic Publishers, 1981.

[23] L. Hall, A. Bensaid, L. Clarke, R. Velthuizen, M. Silbiger, and J. Bezdek, "A comparison of neural network and fuzzy clustering techniques in segmenting magnetic resonance images of the brain," *IEEE Transactions on Neural Networks*, vol. 3, no. 5, pp. 672 –682, sep 1992.

[24] H. Zhou, G. Schaefer, A. Sadka, and M. E. Celebi, "Anisotropic mean shift based fuzzy c-means segmentation of skin lesions," in *Proceedings of the 5th international conference on Soft computing as transdisciplinary science and technology*, ser. CSTST '08. New York, NY, USA: ACM, 2008, pp. 438–443.

[25] Z. C. Images, M. Zhang, L. O. Hall, F. E. Muller-karger, and D. B. Goldgof, "Knowledge-guided classification of coastal," *International Journal of Pattern Recognition and Artificial Intelligence*, vol. 14, pp. 200–0, 2000.

[26] W. Yao, L. Hall, D. Goldgof, and F. Muller-Karger, "Finding green river in seawifs satellite images," *International Conference on Pattern Recognition*, vol. 2, p. 2307, 2000.

[27] S. E. Jingwei, S. Eschrich, J. Ke, L. O. Hall, and D. B. Goldgof, "Fast fuzzy clustering of infrared images," in *Joint 9th IFSA World Congress and 20th NAFIPS International Conference*, 2001.

[28] L. Pengyu, J. Kebin, and Z. Peizhen, "An effective method of image retrieval based on modified fuzzy c-means clustering scheme," in *Signal Processing, 2006 8th International Conference on*, vol. 3, nov 2006.

[29] M.-K. Hu, "Visual pattern recognition by moment invariants," *Information Theory, IRE Transactions on*, vol. 8, no. 2, pp. 179 –187, february 1962.

[30] M. E. Celebi and Y. A. Aslandogan, "A comparative study of three moment-based shape descriptors," in *ITCC '05: Proceedings of the International Conference on Information Technology: Coding and Computing*. Washington, DC, USA: IEEE Computer Society, 2005, pp. 788–793.

[31] J. Flusser and T. Suk, "Pattern recognition by affine moment invariants," *Pattern Recognition*, vol. 26, no. 1, pp. 167–174, 1993.

[32] J. Flusser, B. Zitova, and T. Suk, *Moments and Moment Invariants in Pattern Recognition*. Wiley, December 2009.

[33] V. Loia, W. Pedrycz, and S. Senatore, "Semantic web content analysis: A study in proximity-based collaborative clustering," *IEEE Transactions on Fuzzy Systems*, vol. 15, no. 6, pp. 1294–1312, 2007.

[34] J. C. Bezdek, "Cluster validity with fuzzy sets," *Journal of Cybernetics*, vol. 3, p. 5872, 1974.

[35] ——, "Numerical taxonomy with fuzzy sets," *Journal of Mathematical Biology*, vol. 1-1, pp. 57–71, 1974.

[36] X. Xie and G. Beni, "A validity measure for fuzzy clustering," *IEEE Transactions on Pattern Analysis and Machine Intelligence*, vol. 13, pp. 841–847, 1991.

[37] J. C. Bezdek and J. D. Harris, "Fuzzy partitions and relations: an axiomatic basis for clustering," *Fuzzy Sets and Systems*, vol. 1, no. 2, pp. 111 – 127, 1978.

[38] "Shape data for the mpeg-7 core experiment ce-shape-1." http://www.cis.temple.edu/ latecki/TestData/mpeg7shapeB.tar.gz.

2011 IEEE International Conference on Fuzzy Systems
June 27-30, 2011, Taipei, Taiwan

Piece-wise Convex Spatial-Spectral Unmixing of Hyperspectral Imagery using Possibilistic and Fuzzy Clustering

Alina Zare
Electrical and Computer Engineering
University of Missouri
Columbia, Missouri 65211
Email: zarea@missouri.edu

Paul Gader
Computer & Information Science & Engineering
University of Florida
Gainesville, FL 32611
Email: pgader@cise.ufl.edu

***Abstract*—Imaging spectroscopy refers to methods for identifying materials in a scene using cameras that digitize light into hundreds of spectral bands. Each pixel in these images consists of vectors representing the amount of light reflected in the different spectral bands from the physical location corresponding to the pixel. Images of this type are called hyperspectral images. Hyperspectral image analysis differs from traditional image analysis in that, in addition to the spatial information inherent in an image, there is abundant spectral information at the pixel or sub-pixel level that can be used to identify materials in the scene. Spectral unmixing techniques attempt to identify the material spectra in a scene down to the sub-pixel level. In this paper, a piece-wise convex hyperspectral unmixing algorithm using both spatial and spectral image information is presented. The proposed method incorporates possibilistic and fuzzy clustering methods. The typicality and membership estimates from those methods can be combined with traditional material proportion estimates to produce more meaningful proportion estimates than obtained with previous spectral unmixing algorithms. An analysis of the utility of using all three estimates produce a better estimate is given using real hyperspectral imagery.**

***Index Terms*—hyperspectral, endmember, spectral unmixing, possibilistic, fuzzy, piece-wise convex, linear mixing, convex geometry model.**

I. Introduction

Hyperspectral images are three-dimensional data cubes that have two spatial and one spectral dimension. Hyperspectral imagers collect data about an image scene across many narrow, contiguous spectral wavelengths. As opposed to image processing, spectral information (rather than spatial information) is generally the focus in hyperspectral image analysis. *Endmember detection* and *spectral unmixing* are two major goals in hyperspectral image analysis. Endmembers are spectra that are defined by analogy to standard spectroscopy.

In standard spectroscopy, the basic elements (oxygen, nitrogen, etc.) making up a substance are identified. Each element has a unique spectral signature and the spectral properties of the substance are defined by combinations of the pure elements in the substance. Endmembers are thought of as representing the "pure" spectral signatures of the materials found in the scene. However, the analogy is not strict for several reasons. It is generally not possible to get enough resolution to identify pure elements. In addition, it may not even be useful to identify them. For example, when an intelligent system is analyzing a scene, it may only need to know where the grass, trees, concrete, water, etc. are located in a scene. Therefore, in hyperspectral image analysis applications, the endmembers represent spectra of the basic scene elements such as these. We refer to these endmembers as "pure materials" in the scene with the understanding that they may really represent the types of materials discussed above.

Spectral unmixing determines the *proportion* (or *abundance*) of each endmember found in every hyperspectral pixel. The standard model applied during hyperspectral unmixing is the linear mixing model [**?**]. In the linear mixing model, the spectral signatures in a hyperspectral scene are modeled as convex combinations of the endmember signatures. This model can be written as follows.

$$\mathbf{x}_i = \sum_{k=1}^{M} p_{ik}\mathbf{e}_k + \epsilon_i, \quad 1 \leq i \leq N \tag{1}$$

where N is the number of pixels, M is the number of endmembers, ϵ_i is an error term, p_{ik} is the abundance of endmember k in pixel i, and $\mathbf{e}_k$ is the k^{th} endmember. The abundances of this model satisfy the following constraints.

$$p_{ik} \geq 0 \quad \forall k = 1, \ldots, M \tag{2}$$

$$\textstyle\sum_{k=1}^{M} p_{ik} = 1 \tag{3}$$

Given the input hyperspectral data, $\mathbf{X}$, endmember detection estimates the spectral signatures of the endmembers, $\mathbf{E}$, and spectral unmixing determines the values of the proportions (or abundances) $\mathbf{P}$ of each endmember in every hyperspectral data point. By following this model, finding endmembers amounts to estimating the spectral signatures whose convex hull enclose the hyperspectral data.

Numerous hyperspectral unmixing methods based on the linear mixing model have been developed in the literature. Generally, these methods search for a single set of endmembers and, therefore, assume that pixels are a combination of all endmembers in the scene. However, in real hyperspectral

978-1-4244-7316-8/11/$26.00 ©2011 IEEE

data, pixels are often combinations of only a subset of the endmembers.

In this paper, an endmember extraction and spectral unmixing algorithm using fuzzy and possibilistic clustering methods is presented. The proposed method represents an input hyperspectral scene using multiple sets of endmembers with a piecewise convex representation. By estimating fuzzy membership and typicality values for each set of endmembers (i.e. a convex region) meaningful proportion values are estimated where the majority of pixels are combinations of a subset of the endmembers in the scene, some pixels may be identified as highly-mixed and combinations of most or all of the endmembers in the scene, and some pixels are identified as outliers. We refer to pixels in categories as single-region pixels,

The piece-wise convex representation for hyperspectral imagery was first developed in [**?**] and [**?**]. Endmember detection methods that incorporate spatial information include [**?**], [**?**], [**?**]. However, these methods do not employ a piece-wise convex model.

An exciting contribution of this approach is that the initial estimates of the proportions, memberships, and typicality all play important roles in defining more meaningful and realistic final proportion estimates. There are three categories of pixels: single-region pixels, overlap-region pixels, and outlier pixels.

A single-region pixel is composed of only those endmembers that are associated with one convex region. In this case, the typicality value for the convex region containing the pixel should be 1, the membership value for the corresponding region should also be 1, and the proportion values should the proportions of the endmembers associated with that convex region for the data point. Therefore, in the single convex region case, the final proportion vector will be the proportion values found for the endmembers in the convex region containing the data point.

Overlap-region pixels are convex combination of endmembers associated with two or more convex regions in the data. The typicality values for the pixel in all of the associated convex regions should be 1, the product of the membership values and the proportion vectors for each convex region will sum-to-one. This product will result in a final proportion vector for the data point with appropriate weights for all of the endmembers that compose the pixel.

In the outlier pixel case, the pixels are not convex combinations of the endmembers found in the scene. In this case, the typicality values for all convex regions should be small and tend towards zero. By using the product of the typicality, membership and proportion values, the final proportions for the outlier pixels should sum to less than one. This indicates that the pixel is not fully described by the endmembers found in the scene. This lack of information is represented directly in the final proportions rather than indirectly by large error. If only membership is used, then the proportions will still sum to one but they will certainly not be correct. Thus, the final proportion values calculated using the initial proportions, the memberships, and the typicality will represent the true level of information available in the scene.

In the following, Section 2 outlines the algorithm, Section 3 presents experimental results and Section 4 provides a discussion and conclusions.

II. Method

A. P-COMMEND

The P-COMMEND (Piece-wise Convex Multiple Model Endmember Detection) algorithm [**?**] performs alternating optimization to autonomously estimate the endmembers, $\mathbf{E}$, abundances, $\mathbf{P}$, and membership values, $\mathbf{U}$, for a given hyperspectral image. P-COMMEND iteratively minimizes the objective function in Equation **??** subject to the constraints in Equation **??**, $\sum_{i=1}^{C} u_{ij} = 1$ and $u_{ij} \geq 0$.

$$\begin{aligned} J &= \sum_{i=1}^{C}\sum_{j=1}^{N} u_{ij}^{m} \left(\mathbf{x}_j - \mathbf{p}_{ij}\mathbf{E}_i\right)\left(\mathbf{x}_j - \mathbf{p}_{ij}\mathbf{E}_i\right)^T \\ &+ \alpha \sum_{i=1}^{C} \left(M \cdot trace(\mathbf{E}_i\mathbf{E}_i^T) - 1_{1\times M}\mathbf{E}_i\mathbf{E}_i^T 1_{M\times 1}\right) \end{aligned} \tag{4}$$

where $\mathbf{x}_j$ is a $1 \times d$ vector representing the j^{th} pixel of the image, N is the number of pixels in the image, M is the number of endmembers in each convex region (or model), P_i is a $N \times M$ matrix such that $\mathbf{p}_{ij}$, is the vector of abundances associated with pixel j with respect to model i, p_{ijk} is the proportion of endmember k in pixel j with respect to model i, and $\mathbf{E}_i$ is a $M \times d$ matrix such that each row of $\mathbf{E}_i$, $\mathbf{e}_{ik}$, is a $1 \times d$ vector representing the k^{th} endmember with respect to model i. The notation $1_{S\times T}$ denotes an $S \times T$ matrix with all entries equal to 1. The multiple models compete for data $\mathbf{X}$ through a set of weights u_{ij} which represent the memberships of the data points $\mathbf{X}$ in the i^{th} model where m is the "fuzzifier" parameter controlling the degree to which the data points are shared among the models.

The first term of this objective function represents the residual error incurred by representing each spectra using the estimated endmembers, abundances and fuzzy membership values. The use of the fuzzy membership values is related to the fuzzy c-means and the Multiple Model General Linear Regression algorithms [**?**], [**?**]. The second term is related to the volume enclosed by the endmembers by representing the sum of squared distances (SSD) between the endmembers and encourages the endmembers to have a tight fit around the data. The SSD term is the same volume-related term used by ICE (Iterated Constrained Endmembrs) and SPICE (Sparsity Promoting Iterated Constrained Endmembers) for endmember detection [**?**], [**?**].

When updating membership values, the objective function is minimized subject to the constraint that all the membership values for a data point must sum to one. This results in the following update equation given abundances and endmembers,

$$u_{ij} = \frac{1}{\sum_{q=1}^{C}\left(\frac{(\mathbf{x}_j - \mathbf{p}_{ij}\mathbf{E}_i)(\mathbf{x}_j - \mathbf{p}_{ij}\mathbf{E}_i)^T}{(\mathbf{x}_j - \mathbf{p}_{qj}\mathbf{E}_q)(\mathbf{x}_j - \mathbf{p}_{qj}\mathbf{E}_q)^T}\right)^{\frac{1}{m-1}}}. \tag{5}$$

The endmembers are updated given the following equation,

$$\mathbf{E}_i = \left(\sum_j u_{ij}^m \mathbf{p}_{ij}^T \mathbf{p}_{ij} + 2\alpha D \right)^{-1} \left(\sum_j u_{ij}^m \mathbf{p}_{ij}^T \mathbf{x}_j \right) \quad (6)$$

where $D = MI_{M\times M} - 1_{M\times M}$. Finally, abundance values are updated by minimizing Equation **??** subject to the constraints in Equation **??** by using a Lagrange multiplier term and evaluating and applying the required KKT conditions to enforce Equation **??**. The resulting update equations are

$$\mathbf{p}_{ij}^T = \left(\mathbf{E}_i \mathbf{E}_i^T\right)^{-1} \left(\mathbf{E}_i \mathbf{x}_j^T - \frac{\lambda_{ij}}{2} 1_{M\times 1} \right) \quad (7)$$

and

$$\mathbf{p}_{ij}^{KKT} = max\left(\mathbf{p}_{ij}^T, 0\right) \quad (8)$$

where $\lambda_{ij} = 2\frac{1_{1\times M}\left(\mathbf{E}_i\mathbf{E}_i^T\right)^{-1}\mathbf{E}_i\mathbf{x}_j^T - 1}{1_{1\times M}\left(\mathbf{E}_i\mathbf{E}_i^T\right)^{-1}1_{M\times 1}}$.

B. FLICM

Spatial information is incorporated by encouraging neighboring pixels in the image to have similar membership values to the different convex regions. This is accomplished by adopting the spatially-smooth fuzzy c-means method, FLICM (Fuzzy Local Information C-Means), developed in [**?**]. The FLICM algorithm adds a term, G, to the objective function that influences the updates of the membership values by incorporating spatial information. The G term, adapted for use in the proposed algorithm, is shown in Equation **??**.

$$G_{ij} = \sum_{\substack{k\in N_j \\ j\neq k}} \frac{1}{d_{jk}+1} (1-u_{ik})^m \left|\left|\mathbf{x}_k - \mathbf{p}_{ik}\mathbf{E}_i\right|\right|_2^2 \quad (9)$$

where the $\mathbf{x}_j$ is the center pixel in the local window under consideration, N_j is the neighborhood around the center pixel (such as a 3x3 window), d_{ij} is the Euclidean distance in pixel space of the image indices between pixels $\mathbf{x}_j$ and $\mathbf{x}_k$. Therefore, the G term scales the influence of neighboring pixels based on their distance in the index space. Also, when a neighboring pixel has high membership in a convex region, the point under consideration is encouraged to also have a high membership in that region. G_{ij} term is updated each iteration and treated as a constant during updates to the endmembers, abundances and membership values. With the addition of G, the objective function for is shown in Equation **??**.

$$\begin{aligned} J &= \sum_{i=1}^{C}\sum_{j=1}^{N} u_{ij}^m \left(\left(\mathbf{x}_j - \mathbf{p}_{ij}\mathbf{E}_i\right)\left(\mathbf{x}_j - \mathbf{p}_{ij}\mathbf{E}_i\right)^T + G_{ij} \right) \\ &+ \alpha \sum_{i=1}^{C} \left(M \cdot trace(\mathbf{E}_i\mathbf{E}_i^T) - 1_{1\times M}\mathbf{E}_i\mathbf{E}_i^T 1_{M\times 1} \right) \end{aligned} \quad (10)$$

When incorporating FLICM into the P-COMMEND algorithm, the update equations for the endmembers and abundances remain the same as in Equations **??** and **??**. Membership updates change as shown below.

$$u_{ij} = \frac{1}{\sum_{q=1}^{C} \left(\frac{(\mathbf{x}_j - \mathbf{p}_{ij}\mathbf{E}_i)(\mathbf{x}_j - \mathbf{p}_{ij}\mathbf{E}_i)^T + G_{ij}}{(\mathbf{x}_j - \mathbf{p}_{qj}\mathbf{E}_q)(\mathbf{x}_j - \mathbf{p}_{qj}\mathbf{E}_q)^T + G_{qj}} \right)^{\frac{1}{m-1}}}. \quad (11)$$

C. PFCM Clustering

The proposed method adopts the approach presented in the PFCM (Possibilistic Fuzzy Clustering Method) [**?**]. PFCM determines both typicality and membership values for each data and every cluster.

D. Proposed Method

Incorporating FLICM and PFCM into the P-COMMEND objective function results in the objective function shown in Equation **??**.

$$\begin{aligned} J &= (1-\alpha)\sum_{i=1}^{C}\sum_{j=1}^{N} a u_{ij}^m \left(\left(\mathbf{x}_j - \mathbf{p}_{ij}\mathbf{E}_i\right)\left(\mathbf{x}_j - \mathbf{p}_{ij}\mathbf{E}_i\right)^T + G_{ij} \right) \\ &+ bt_{ij}^n \left(\mathbf{x}_j - \mathbf{p}_{ij}\mathbf{E}_i\right)\left(\mathbf{x}_j - \mathbf{p}_{ij}\mathbf{E}_i\right)^T \\ &+ \alpha \sum_{i=1}^{C} \left(M \cdot trace(\mathbf{E}_i\mathbf{E}_i^T) - 1_{1\times M}\mathbf{E}_i\mathbf{E}_i^T 1_{M\times 1} \right) \\ &+ \sum_{i=1}^{C} \gamma_i \sum_{j=1}^{N} (1-t_{ij})^n \end{aligned} \quad (12)$$

As shown in the equation above, spatial information is used in the membership terms only. In future work, incorporating this information when updating typicality will be investigated and implemented as well. The update equations for the proportions remain the same as for the P-COMMEND algorithm described in Section II A. The membership update equations remain the same shown in Equation **??**. The endmember update equation becomes as shown below.

$$\begin{aligned} \mathbf{E}_i = &\left(\sum_j (a u_{ij}^m + bt_{ij}^n) \mathbf{p}_{ij}^T \mathbf{p}_{ij} + 2\alpha D \right)^{-1} \\ &\left(\sum_j (a u_{ij}^m + bt_{ij}^n) \mathbf{p}_{ij}^T \mathbf{x}_j \right) \end{aligned} \quad (13)$$

The update equation for the typicality results the following.

$$t_{ij} = \frac{1}{1 + \left(\frac{b}{\gamma_i} \left|\left|\mathbf{x}_j - \mathbf{p}_{ij}\mathbf{E}_i\right|\right|_2^2 \right)^{\left(\frac{1}{n-1}\right)}} \quad (14)$$

The γ_i value in the above equation is set to be the mean of the $\left|\left|\mathbf{x}_j - \mathbf{p}_{ij}\mathbf{E}_i\right|\right|_2^2$ value for all of the pixels in the associated convex region. Therefore, each iteration, the γ_i value gets updated.

The final proportion values are computed by taking the production of the initial proportion values, membership and typicality for data point and convex region.

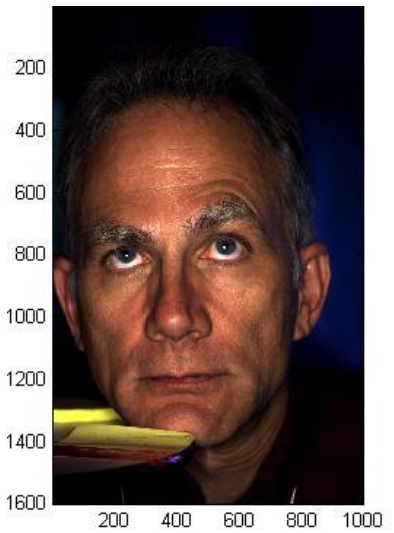

(a)

Fig. 1. Color image of hyperspectral face data used for testing.

III. Experimental Results

The proposed algorithm was tested on VIS/NIR hyperspectral face imagery. This data was collected by Norsk Elektro Optikk using their HySpex hyperspectral sensor on participants at the 2010 IEEE Workshop on Hyperspectral Image and Signal Processing: Evolution in Remote Sensing (WHISPERS10). The data contain 160 spectral bands ranging in wavelength from 410 to 990nm. An image was selected from this data set and spatially sub-sampled by selecting every 4th row and column in the image. A color image created using the hyperspectral data is shown in Figure **??**. The size of this image is 400×250 pixels.

Using the PCA algorithm, the dimensionality of the hyperspectral data was reduced from 160 dimensions to 5 dimensions. The algorithm was run on the dimensionality-reduced imagery using the following parameters: $\alpha = 0.001$, $a = 20$, $b = 0.1$, $m = 2$ and $n = 1.1$. Results are shown in the following figures.

By examining the final proportion maps shown in Figure **??**, it can be seen that an effective segmentation of the imagery is found by the method. The first convex region corresponds to skin, both shadowed and bright skin. The second convex region corresponds to the table and eyes. The third convex region corresponds to background. The fourth convex region corresponds to the shirt. The fifth convex region corresponds to hair and eyebrows.

The membership and typicality maps associated with each convex region is shown in Figure **??**.

There were several pixels of glare with a high specular reflection in the imagery. These pixels were a result of reflection from the lighting in the room on pixels in the eyes of the photographed individual. As desired, the typicality for these outliers were found by the method to be zero for all convex regions.

IV. Conclusion

By using a combination of initial proportions, typicality, fuzzy membership and fuzzy spatial information, excellent segementation and identification of endmembers in the scene is achieved. Future work will involve applying this algorithm to a large set of data. Also, parameter sensitivity and a reduction in the number of parameters will be investigated.

References

[1] N. Keshava and J. F. Mustard, "Spectral unmixing," *IEEE Signal Processing Magazine*, vol. 19, pp. 44–57, 2002.

[2] A. Zare, "Hyperspectral endmember detection and band selection using bayesian methods," Ph.D. dissertation, University of Florida, 2009.

[3] A. Zare and P. Gader, "PCE: Piece-wise convex endmember detection," *IEEE Trans. on Geoscience and Remote Sensing*, vol. 48, no. 6, pp. 2620–2632, June 2010.

[4] A. Plaza, P. Martinez, R. Perez, and J. Plazas, "Spatial/spectral endmember extraction by multidimensional morphological operators," *IEEE Trans. on Geoscience and Remote Sensing*, vol. 40, no. 9, pp. 2025–2041, Sep. 2002.

[5] D. M. Rogge, B. Rivard, J. Zhang, A. Sanchez, J. Harris, and J. Feng, "Integration of spatial-spectral information for the improved extraction of endmembers," *Remote Sensing of Environment*, vol. 110, pp. 287–303, 2007.

[6] M. Zortea and A. Plaza, "Spatial preprocessing for endmember extraction," *IEEE Trans. on Geoscience and Remote Sensing*, vol. 47, no. 11, pp. 2679–2693, 2009.

[7] A. Zare, O. Bchir, H. Frigui, and P. Gader, "Spatially-smooth piece-wise convex endmember detection," in *Hyperspectral Image and Signal Processing: Evolution in Remote Sensing (WHISPERS), 2010 2nd Workshop on*, june 2010, pp. 1 –4.

[8] J. Bezdek, *Pattern Recognition with fuzzy objective function algorithm*. Plenum Press, 1981.

[9] H. Frigui and R. Krishnapuram, "A robust competitive clustering algorithm with applications in computer vision," *IEEE Trans. on Pattern Analysis and Machine Intelligence*, vol. 21, no. 5, pp. 450–465, May 1999.

[10] M. Berman, H. Kiiveri, R. Lagerstrom, A. Ernst, R. Donne, and J. F. Huntington, "ICE: A statistical approach to identifying endmembers in hyperspectral images," *IEEE Trans. on Geoscience and Remote Sensing*, vol. 42, pp. 2085–2095, Oct. 2004.

[11] A. Zare and P. Gader, "Sparsity promoting iterated constrained endmember detection for hyperspectral imagery," *IEEE Geoscience and Remote Sensing Letters*, vol. 4, no. 3, pp. 446–450, July 2007.

[12] S. Krinidis and V. Chatzis, "A robust fuzzy local information c-means clustering algorithm," *IEEE Transactions on Image Processing*, 2010, in Press.

[13] N. Pal, K. Pal, J. Keller, and J. Bezdek, "A possibilistic fuzzy c-means clustering algorithm," *IEEE Transactions on Fuzzy Systems*, vol. 13, no. 4, pp. 517–530, Aug. 2005.

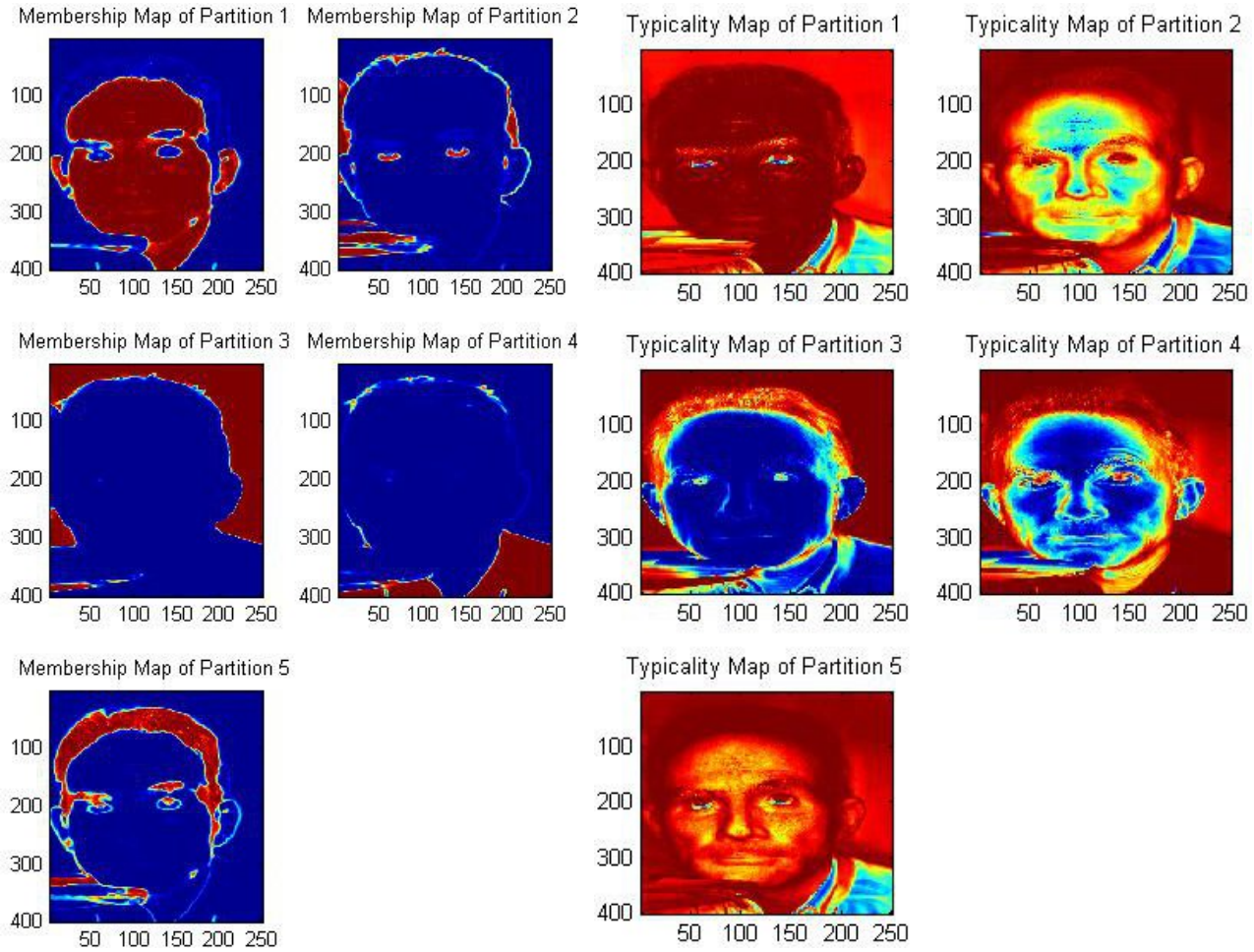

(a) Membership maps found for each convex region using the proposed method.

(b) Typicality maps found for each convex region using the proposed method.

Fig. 2.

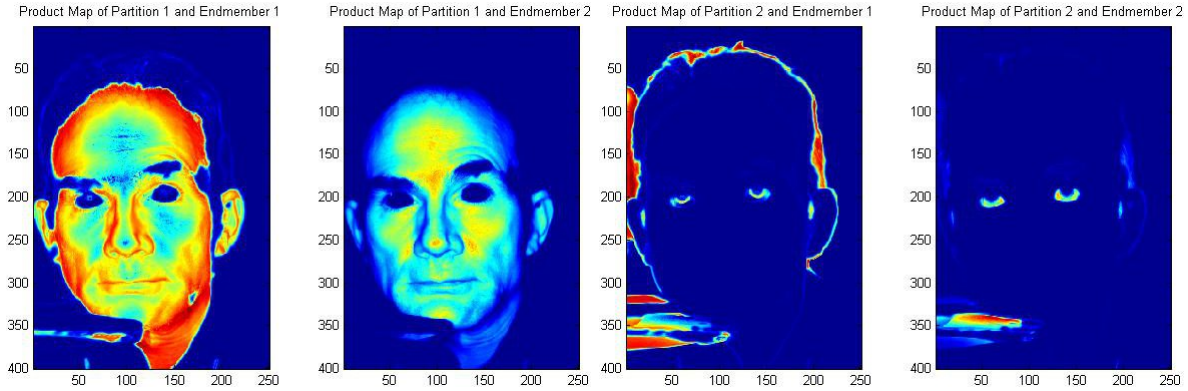

(a) Convex Region 1 (b) Convex Region 2

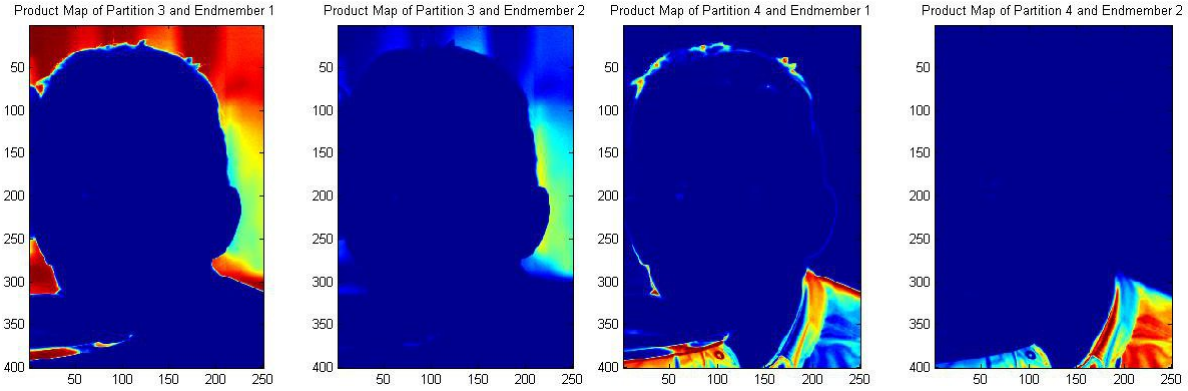

(c) Convex Region 3 (d) Convex Region 4

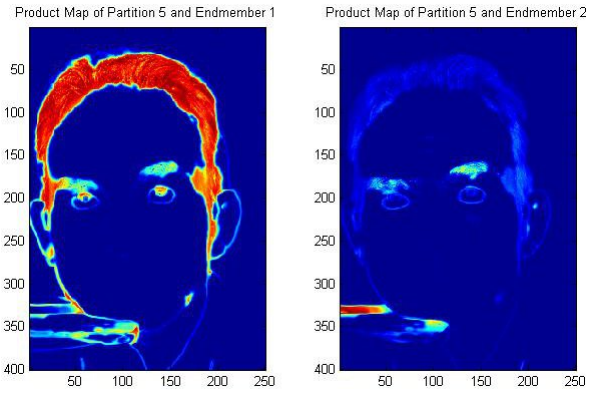

(e) Convex Region 5

Fig. 3. Final proportion maps found using the proposed method. Final proportion maps are computed using the product of the typicality, membership and initial proportion values for each convex region. Each pair of images corresponds to one convex region. Each convex region consists of two endmembers.

2011 IEEE International Conference on Fuzzy Systems
June 27-30, 2011, Taipei, Taiwan

Bio-inspired Computing of Vision- Fuzzy and Neuromorphic Processing

Woo Joon Han, Il Song Han
Korea Advanced Institute of Science and Technology
335 Gwahak-ro, Yuseong-gu, 305-701
Daejeon, Republic of Korea
woo.han@kaist.ac.kr, i.s.han@kaist.ac.kr

Abstract— **This paper describes the early vision of bio-inspired neuromorphic system enhanced by fuzzy processing, mimicking the primitive behaviour of visual cortex. The proposed bio-inspired system exhibits the biologically plausible function of mimicking the cat's visual cortex experimentation of Hubel and Wiesel. The neuromorphic implementation of vision is inspired by the directional visual signal selectivity of cortex and the CMOS spiking neuron based on Hodgkin-Huxley formalism. The membership function is introduced to improve the early vision and the improvement is demonstrated for robust applications, based on the recognition of human head figures.**

Keywords-neuromorhic; neural networks; CMOS; vision, visual cortex, simple cell, Hodgkin-Huxley formalism, membershio function

I. INTRODUCTION

There have been many works proposed recently for bio-inspired vision and neuromorphic vision devices. Although, computer vision algorithms are effective in their condition of usage, at most times, they lack the robustness of the human vision. We describe here the early vision of bio-inspired implementation of primary visual cortex, based on the neuron of Hodgkin-Huxley formalism and the visual cortex experimentation of Hubel and Wiesel. In this paper, the elements of neuromorphic implementation of visual cortex are presented with the enhanced performance by introduction of membership function.

The feasibility of bio-inspired visual signal processing is evaluated showing robustness for gray scale image and single color component image. Potential application for such system is explored in human detection in wide range of environment; passenger occupancy detection, pedestrian detection and human detection in the conference presentation. The latter environment was explored with a view to further extend it into gesture detection.

II. PRIMARY VISUAL CORTEX FUNCTION AND BIO-INSPIRED SPIKING NEURON BASED ON CMOS CIRCUIT

The physiological studies about visual cortex from the investigation of cat's striate cortex by Hubel and Wiesel have confirmed the consensus of knowledge [1], though there are many models about visual cortex. The idea on the primary visual cortex of simple cell motivated various theories of object recognition from characters to complex natural images [2]. For an idea of neural system implementation, the research on neurophysiology introduced the principles and demands of biologically plausible electronic implementation. In this paper, we employ the new way of implementing the neuromorphic VLSI for the primary visual cortex, inspired by the ideas on the primary visual cortex by Hubel and Wiesel's experimentation and the neurophysiological model of neuron by Hodgkin and Huxley [3]. The design motivation is from the well-known experimentation of simple cell in Fig. 1 by Hubel and Wiesel. The experimentation of spike burst for given static line input is aimed to mimick, while there is another experimentation of complex cell based on moving stimulus by Hubel and Wiesel.

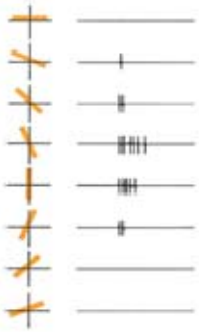

Figure 1. Response of the cat's cortex to shining a rectangular slit of light in various orientations [1].

The controlled conductance by CMOS transistors is an element of the proposed neuromorphic system, which have been studied for the biologically plausible analog-mixed neural networks [4, 5].

III. BIO-INSPIRED VISUAL INFORMATION PROCESSING AND APPLICATION TO OBJECT DETECTION

Hodgkin-Huxley (H-H) formalism is a widely adopted idea of neuron's biophysical characterisation and dynamics. The electrical equivalent circuit model of Fig. 2a is known as the empirical model of H-H formalism, which describes quantitatively the dynamics of the voltage-dependent conductance. Although the particular advantages of H-H formalism were not exhibited in neural network's tasks of

978-1-4244-7316-8/11/$26.00 ©2011 IEEE

vision or recognition yet, asynchronous spikes based on H-H formalism are considered as a principle element of high level or large scale neural computing or application system. The H-H formalism is widely of interest for its biophysical dynamics, though its complexity in computation is prohibitively high. Hence, asynchronous dynamics of the H-H formalism is adopted as the idea of neuron model.

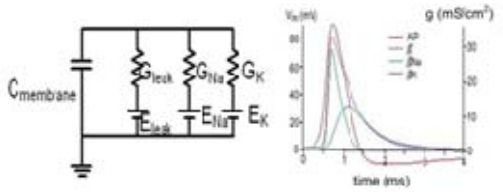

(a) (b)

Figure 2. (a) The electrical equivalent circuit of a neuron, Hodgkin-Huxley formalism (b) dynamics of asynchronous spike and refractory period vs. the membrane potential [3].

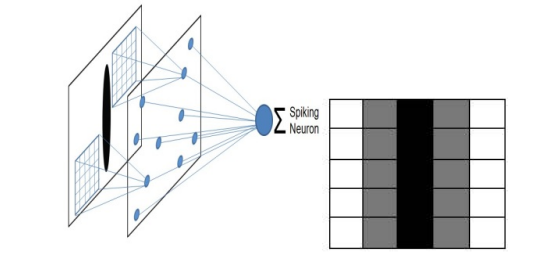

(a)

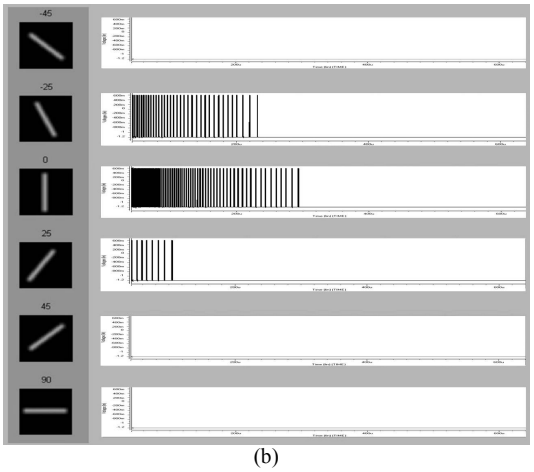

(b)

Figure 3. (a) The artificial primary visual cortex model with orientation selective synaptic weights to mimick the simple cell of visual cortex (b) the simulated spike burst of VLSI visual cortex to the stimulus in various orientations.

The tuning properties of orientation selectivity have been believed to play the key role for perception in visual cortex. As shown in Fig. 1, the tuning of specific neurons to the orientation of visual stimulus probably depends on the tuning features after passive or active learning for the earlier processing of natural image. To mimick this response, a simple model was implemented as illustrated in Fig. 3, though some modifications are likely necessary for being more plausible to the natural system. The tuned feature map (or connection) of 5 x 5 synaptic weights is used, based on the reference stimulus to match with the minor adjustment depending on the output. The tuned feature map of vertical orientation is illustrated in Fig. 3a, while the synaptic weights of Fig. 3a are in the ration of (1: -0.6: 0.1 for black : grey : white). The six types of input stimulus (50 x 50 pixels) are experimented with the feature map (as synaptic connections) and spiking neurons based on H-H formalism[4]. The spike burst output of Fig. 3b is observed through a SPICE simulation, where the neuromorphic visual cortex response mimics that of the biological spike burst of Fig. 1 from the experimentation work of Hubel and Wiesel.

The feasibility of bio-inspired neuromorphic system is demonstrated with its plausibility to primary simple cell function of visual cortex as exhibited in Fig. 3b. The tuned feature characteristics of other orientations (-45˚, 25˚) are evaluated with the consistent outcomes as expected in the original experimentation shown in Fig. 1.

The proposed bio-inspired neuromorphic system is applied to example cases for evaluating its feasibility in forming competent visual processing system with the robustness that is characteristic of animal or human vision. The previous research demonstrated the robustness to a certain application of object detection, i.e. the vehicle license plate detection. The license plate detection was investigated for the flexible detection based on the rectangle with the right angle, regardless of the aspect ratio or the whole size. It is based on the particular selective response to orientation at the right angle, i.e. presenting both components of horizontal and vertical orientation of the still image. It demonstrated the robust detection under some environmental challenges such as the shiny reflection from the nearby area of license plate, in addition to the different sizes from the various distance [5]. In this paper, the application of multi-directional selectivity on the video information is investigated further for the detection of human heads in the driving vehicle of changing background and illumination. The human torso template in Fig. 4 is applied to the head detection, as the property of rectangle was utilized in the license plate detection [5].

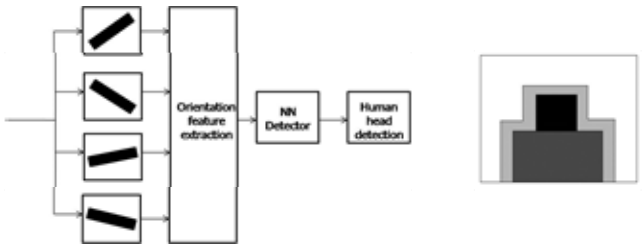

Figure 4. Neuromorphic vision for human detection, inspired by the visual cortex, and based on the neural network detector of head-torso shape.

Fig 5 shows the successful detection of the two passengers in the car. Since tests were done on an image sequence, slightly different approach could be made than when input data were still images. As seen in Fig. 5, the frame difference was made between current and previous bio-inspired directional selective processed image to decrease any orientation features that were stand-still. Although it is true that

passengers sitting in their seats rarely have any or no body movement, all human has slightest movement in their head whether that is tilting of head or changes in facial expression whereas other unwanted signals such as from the interior of car is decreased. For the orientation selectivity, the 6 simulated synaptic connections of 9 x 9 were used for the orientation feature extraction. Six were orientations were used as six different orientation, more or less, can describe the basic outline of human head while reducing the chance of other unwanted objects being detected. The orientation features extracted shows heavy density in the head area which yields the high lightened head area. And lastly, neural net detection were made resulting the yellow boxes of human heads detected, which was decided by performing 'winner takes all' approach to get strongest signal. Note that for the detection, number of human head in the input date is known, i.e. for the image shown in Fig. 5, two strongest signals were taken.

Figure 5. (from top left in anti-clockwise direction) Input image with resolution of 640 x 480, bio-inspired processing of current and previous image, torso template-based neural network detector of Fig. 4 and detection result where yellow box denotes the passenger head detected from the bio-inspired visual processing and green box denotes the detected passenger

The driving vehicle is subject to the wide range of changes in the illumination level and background. There is a difficulty of detecting every passenger due to the change in both the illumination and background when only gray image is used. Thus to improve robustness, color component of image was added during processing to improve the robustness reflecting on the fact that animals utilizes different color components to human when processing. In Fig. 6, red color component was taken to process to improve the robustness. There is a small difference; the head area became slightly lighter, and all passengers were successfully detected with the mixed combination of gray image and red-color component image. Other mixtures of color components were evaluated not suitable for the improvement of an example application, while the mixed gray image illustrated the better detection accuracy of 95% than the single red-color component image.

Figure 6. (from top left in anti-clockwise direction) The gray input image converted from the colour image, the image of red-color component extracted from the colour image, improved detection of passenger based on the combination of the gray image and the red-colour component image and imperfect detection of passenger based on the gray image converted from the colour image.

The bio-inspired processing is applied to pedestrian detection where the test image set was captured from a moving bus in London from a commericially available camera. Same approach was used for pedestrian detection such that the orientation features from the input image is extracted first and then neural network with human shape template was used to detect the human. For pedestrian detection application, especially for a vehicle, may require the detection of a pedestrian who is having certain amount of motion, e.g. running. Also there is more interest in a pedestrian moving across the field of vision as there is more likelihood of collision. Considering these points, frame differences were taken so that the detected pedestrians are those with more than certain motion as seen in Fig. 7. In Fig. 7, other pedestrians are seen other than the detected pedestrian but they were not detected since their motions were low.

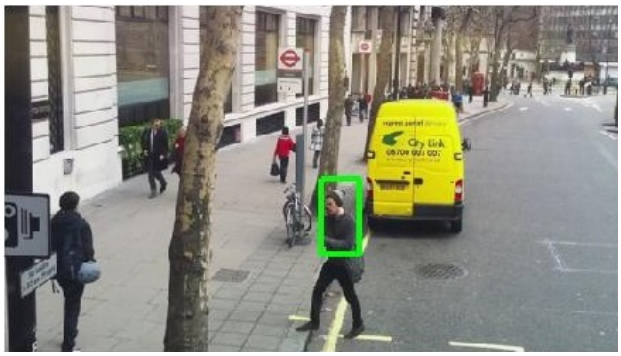

Figure 7. Pedestrian detection result where two previous frames were used in the process.

IV. FUZZY MEMBERSHIP FUNCTION TO ENHANCE DETECTION

There are some tasks demanding further processing, because of dynamic environmental changes or the limitation of template features for complex object. The detection of a presenter in the dark conference room is challenging, as there are not only the dynamic changes of illumination but also the confusing patterns from the displayed presentation. The recognition process in the neuromorphic vision is based on the winner neuron representing the regional summation after the template processing, however the exact winner location can be disturbed by multiple locations close to the maximum value (i.e. the winner). The membership function of Fig. 8 is

introduced to improve the cases of confusing illumination or complex situation of Fig. 9. The illustrated membership function is derived for 12 x 22 reference locations is based on the heuristic evaluation. The average of 12 x 22 elements from the local summation of saliency map is derived to accommodate the changes in the illumination or patterns, while the membership function of Fig. 11 is determined by four points of (average)x8, (average)x10, (average)x11, (average)x12. The action potential value is applied to the membership function, and the multiple candidate locations can be determined with revised value rather than a winner location of the maximum action potential. Several locations are suggested as the location of human head object with the processing of fuzzy membership function.

In Fig. 10, the application of fuzzy processing illustrates the improve detection of a presenter (head) than the case without the fuzzy processing, though the primitive fuzzy membership function is applied.

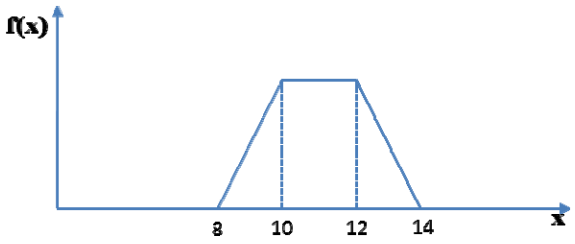

Figure 8. Membership function introduced to the neuromorphic vision

Figure 9. Effect of applying fuzzy function.

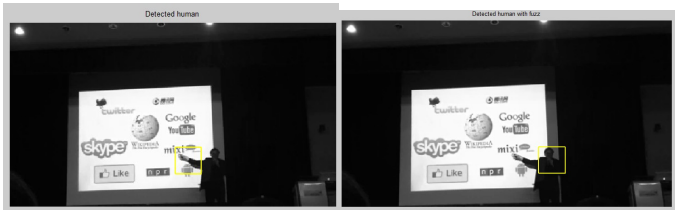

Figure 10. Enhanced human detection procedure with membership function is shown on the right and on the left shows the detection result without applying the mempership function.

V. CONCLUSION

The bio-inspired neuromorphic vision enhanced by fuzzy processing is proposed as a feasible way of mimicking the primitive function of visual cortex, with an application example of detecting human heads. The example cases successfully illustrate the bio-inspired processing with the neural network enhanced by fuzzy processing. The bio-inspired early vision is based on the neuromorphic processing of one-fourth scale of original images, while the gray-and-color mixed combination of input video image improved the robustness substantially.

The object detection in the moving vehicle or the conference room shows the successful human detection under the changing environment of illumination. The bio-inspired computing of human detection in the moving vehicle or the dark conference room demonstrated the robust vision, and the feasibility of neuromorphic vision is exhibited for various applications in the limited operation environment.

ACKNOWLEDGMENT

This research was supported by the grant from National Research Foundation of Korean Government.

REFERENCES

[1] D.H. Hubel and T.N. Wiesel, “Receptive fields of single neurons in the cat’s striate,” J. Physiol. 148, pp. 574–591, 1959.

[2] M. Risenhuber and T. Poggio, “Hierachichal models of object recognition in cortex,” Nature Neuroscience, pp. 1019-1025, 1999.

[3] M. Hausser, “The Hodgkin-Huxley theory of action potential,” Nature Neuroscience Supplement 3, pp. 1165, 2000.

[4] I. S. Han, “Mixed-signal neuron-synapse implementation for large scale neural networks,” J. Neurocomputing, pp. 1860-1867, 2006.

[5] W.J. Han and I.S. Han, “Bio-inspired visual signal processing based on neuromorphic circuit,” Proc. 10th WSEAS International Conference on Instrumentation, Measurement, Circuit and Systems, pp. 131-136, 2010.

2011 IEEE International Conference on Fuzzy Systems
June 27-30, 2011, Taipei, Taiwan

Detection of Hyperintense Regions on MR Brain Images using a Mamdani Type Fuzzy Rule-Based System

Application to the Detection of Small Multiple Sclerosis Lesions

F.X. Aymerich
[1]ESAII Department; [2]Magnetic Resonance Unit – IDI
[1]Univ. Politècnica de Catalunya; [2]Hospital Vall Hebron
[1]08034-[2]08035 Barcelona, Spain
xavier.aymerich@{[1]upc.edu; [2]idi-cat.org}

E. Montseny
ESAII Department
Universitat Politècnica de Catalunya
08034 Barcelona, Spain
eduard.montseny@upc.edu

P. Sobrevilla
Applied Mathematics II Department
Universitat Politècnica de Catalunya
08034 Barcelona, Spain
pilar.sobrevilla@upc.edu

A. Rovira
Magnetic Resonance Unit– IDI
Hospital Vall Hebron
08035 Barcelona, Spain
alex.rovira@idi-cat.org

***Abstract*—In this paper we present an algorithm for detecting hyperintense regions in brain images acquired by Magnetic Resonance Imaging. The work is part of a more general research oriented to the design of support tools that assist the healthcare experts in their research activities on brain diseases. The algorithm has been focused on the detection of small multiple sclerosis lesions in PD- and T2-weighted images. In the design of the algorithm we have considered a fuzzy approach to deal with the uncertainty and vagueness characteristic of these lesions in magnetic resonance images. The core of the work is the introduction of a Mamdani type Fuzzy Rule-Based System to optimize the detection taking into account the necessary trade-off between true and false positives in this kind of problems. Results show a very good sensitivity of the algorithm in the detection of hyperintense regions associated with small multiple sclerosis lesions, and a low false positive rate with regard the number of pixels analyzed.**

Keywords-component; fuzzy rule-based systems; fuzzy reasoning; magnetic resonance imaging; multiple sclerosis

I. INTRODUCTION

Multiple Sclerosis (MS) is a disease of the central nervous system characterized by multifocal inflammation and destruction of the myelin that encases the axons. This demyelinating process results in an inhibition of neural transmission and causes the appearance of several clinical symptoms, such as motor and sensory disturbances, paralysis or visual alterations ([1], [2], [3]). These areas of demyelination, or lesions, can be observed by magnetic resonance imaging (MRI).

Magnetic resonance imaging (MRI) is the modality of choice for clinical evaluation of MS because it provides an objective and direct assessment of the evolving pathology in multiple sclerosis [4], and it has also been recognized as a diagnostic criterion of this disease [5]. Moreover, quantitative analysis of MR images to measure and monitor lesion load and tissue volumes has become invaluable for patient follow-up and evaluation of therapies [6].

In a MRI examination, MS lesions can be visualized using different sequences. Dual acquisition of proton density (PD-) and T2-weighted images is one of the most common sequences used to evaluate MS lesion volume ([4], [6]). In these weighted images pixels belonging to MS lesions show hyperintensity, a lighter gray level in relation to its surroundings. So, the detection of MS lesions in these weighted images is based on the location of the hyperintense regions.

However, segmentation of MS lesions in PD- and T2-weighted images is a challenging task which stems from several reasons. Among them it is worth to highlight the following: MS lesions are not the only regions presenting hyperintensity within the images; detection of MS lesions in MRI involves the analysis of several images with different anatomical features, and presents a high dependence of contrast-to-noise ratio in the images; the presence of noise, partial-volume effects and motion can have significant consequences on the performance of segmentation algorithms [7].

One of the main challenges in developing an automated MS segmentation algorithm within MRI images is the minimization of false-positive. Beside aforementioned drawbacks, the presence of small MS lesions is one of the main problems to avoid false detections. The size of small lesions gives a greater weight to the boundary pixels and, consequently, the detection

This work has been partially supported by the Spanish CICYT Project TIN2007-68063

978-1-4244-7316-8/11/$26.00 ©2011 IEEE

of small MS lesions without false detections is difficult due to the presence of factors such as noise or non-homogeneities of magnetic resonance images. Therefore, the greater the sensitivity for detecting small lesions, the greater the chance of false positives.

Moreover, MS lesions are inherently fuzzy with an uncertainty component mainly in the definition of their boundaries [4]. This consideration made that some authors ([8], [9]) introduced fuzzy techniques in the design of their MS detection and segmentation algorithms.

Although some authors, [10], [11], [12], [13], have developed crisp and fuzzy algorithms for detecting MS lesions, within them false detections must be manually removed or require that the detection excludes regions below a minimum size. Then, the design of an automatic algorithm for this purpose has the risk of removing small lesions.

Thus, in order that an automatic MS lesions detection algorithm can ensure high sensitivity in the detection of hyperintense pixels, while avoiding a large number of false positives, it seems necessary to introduce a trade-off between the number of true and false positives. This trade-off may also help in the selection of optimal parameters to combine the multiple features involved in an algorithm.

Taking into account previous considerations, our research is oriented to the development of automatic algorithms for detecting small MS lesions A successful detection of these lesions would be useful to avoid manual removing of false positives using an existing MS lesion segmentation algorithm, or to be used as an starting point in the design of a new automatic MS lesion segmentation algorithm.

In this paper, we present an approach based on a *Mamdani* type *Fuzzy Rule-Based System* (*MFRBS*) [14] to design the detection step of this kind of algorithms. In our approach, we start from an algorithm developed in previous works ([15], [16]), and we introduce this fuzzy scheme to improve the design of the previous detection step using also an MRI sequence more sensitive to the presence of small lesions.

The rest of the paper is organized as follows. Section II described the system proposed in [15] for detecting multiple sclerosis small lesions. The section III outlines the proposed algorithm. The results are presented in section IV, and the last section is devoted to presenting the conclusions and future research works.

II. An Approach to MS Small Lesions Detection

Present paper, as some previous works of the authors, is part of a more general research activity oriented to a general methodology for the development of automatic algorithms oriented to offer support tools that can assist to radiologists and other healthcare professionals in the diagnosis and research activity on neurological diseases that require medical imaging.

With this aim in [15] authors developed a fuzzy-based algorithm for detecting small MS lesions in whose design it was implemented the protocol followed by the experts for detecting MS lesions. With this in mind, lesions detection was based on the location of pixels showing hyperintense behavior regarding its local neighbouring pixels. However, since the hyperintensity may also appear in regions that do not correspond to lesions, fuzzy rules were introduced allowing differentiating lesions from other hyperintense regions.

The proposed algorithm consisted of four main stages: *Preprocessing, Fuzzy characterization and evaluation of hyperintensity characteristics, Defuzzification, and Filtering of false detections*. The image database considered for the development of the system was acquired with a Spin Echo sequence (TR / TE / matrix / FOV: 2200ms / 12-80ms / 192x256 / 250mm) that provided 5mm thick slices separated 1mm.

1) Fuzzy characterization and evaluation of hyperintensity characteristics: On the images obtained from the preprocessing step, the extraction of hyperintensity due to the presence of MS small lesions was based on next definitions:

Definition 2.1
A pixel, p_{ij}, presents hyperintensity if its gray level, $g(p_{ij})$ in PD- and T2-weighted images is high enough in relation to its near surrounding.

Definition 2.2
A region, R_k, is a small MS lesion if:
i.- R_k is located within the encephalic parenchyma,
ii.- $\forall\, p_{ij} \in R_k$, p_{ij} presents hyperintensity, and
iii.- R_k is contained within a 5x5 raster window with a minimum size of 3 pixels.

Then, the *hyperintensity characterization and evaluation* was carried out considering a 9x9 raster window centered on the pixels of the MS small lesions marked by the neuroradiologists, and applying next rules:

Rule 2.1
The higher the gray level of pixels in a region, the greater its hyperintense behavior.

Rule 2.2
A pixel has hyperintense behavior if its gray level is sufficiently distinguishable from the gray levels of two adjacent pixels for a sufficiently large number of radios within a 9x9 window centered at that pixel.

Rule 2.3
A region can be associated with MS lesion if its pixels present hyperintense behavior in both PD- and T2-weighted images.

The implementation of these rules provided the values $\mu_D^{rk}(p_{ij})$ and $\mu_{T2}^{rk}(p_{ij})$, or degrees with which the pixel p_{ij} is sufficiently differentiable at each radius r_k ($1 \le k \le 8$) of the 9x9 window in PD and T2-weighted images, respectively.

Figure 1 shows the 9x9 window, $W(p_{ij})$, used by the algorithm to study the local hyperintensity behaviour of the pixel p_{ij} (black square in the image). The black lines correspond to the eight considered radius, and the gray squares under them the pixels considered.

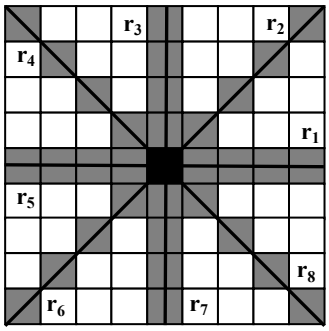

Figure 1. Example of 9x9 window considered for evaluating the hyperintensity. Gray-levels of the pixels under the eight radius (black lines), together with the gray-level of central pixel (black lines), are used for evaluating the hyperintensity of the last one.

Finally these degrees were aggregated for obtaining the membership degree of each pixel to the hyperintensity fuzzy set, $\mu_H(p_{ij})$.

2) Defuzzification and Filtering of false detections: To obtain the agrupations associated with small MS lesions we applied a defuzzification process to the membership functions previously obtained. Then, with the aim of eliminating false detections, due to hyperintense pixels do not associated with MS small lesions, a filtering process was carried out in which size, location and regional restrictions were applied:

III. Proposed Algorithm Description

The aim of the algorithm here presented is to increase lesion detection ratio obtained by our previous system, but maintaining both its general structure and the trade-off between true and false detections.

With this in mind, our approach takes into account the greater sensitivity to show small MS lesions of MRI sequences used at present in MS examinations. This greater sensitivity is mainly due to the acquisition of images with contiguous 3 mm thick sections. As Molyneux et al. showed [17], the reduction of the section thickness from 5 mm to 3 mm increases the MR-visible lesion volume by about 9%.

Next section presents the images considered in this paper. The differences introduced by the MRI acquisition parameters with regard to the previous works ([15], [16]) were taken into account in the design of the algorithm here proposed.

A. Images

The images were acquired in a Magnetom Vision 1.5T (Siemens, Erlangen, Germany) equipment using a Turbo Spin Echo (TSE) sequence that enables dual acquisition of PD and T2 weighted images with the same sequence. The acquisition was performed with interleaved contiguous 3mm-thick axial sections (TR /TE / matrix / FOV: 3000ms / 14-80ms / 256x256 / 250mm). Two blocks of 23 interleaved slices were required to cover the whole brain.

The data set considered for our study consisted of 8 T2-, PD-weighted couples of slices selected from the images obtained from two clinically definite MS patients. The selected images corresponded to axial slices associated with representative brain locations.

For having into account the aforementioned sources of problems, the half of the images showed low lesion volume and the other half high lesion load. For designing the algorithm we considered two out of the eight slices, one of a patient with reduced lesion volume, Im_R, and the other of a patient having high lesion load, Im_H

The images obtained by the TSE sequence showed some differences at contrast level regarding the images considered at previous approach. These differences were more noticeable at the PD weighted images, where the differentiation between the gray levels of parenchyma and fluid regions was lower than the appreciated at the images acquired with the SE sequence. Moreover, with the new acquisition in the case of T2-weighted images the differentiation between lesions and fluid regions is more complex in some locations due to the similarity of their gray levels.

B. Study Design

With the aim of facing up to the differentiating factors introduced by the new acquisition method, the algorithm was overhauled looking for the steps that should be modified. After the analysis carried out it was showed that, though the methodology applied for local assessment of hyperintensity should be preserved, was necessary to perform some modifications within the "*Fuzzy characterization and evaluation of hyperintensity*" stage developed at previous algorithm.

Specifically, the changes came about in the way the hyperintensity fuzzy set was obtaining throughout the radial analysis. Thus, following previous algorithm, after applying the rules 2.1 and 2.2, the degrees with which a pixel p_{ij} is sufficiently differentiable at each radius r_k ($1 \le k \le 8$) of the window $W(p_{ij})$ were obtained for PD- ($\mu_D^{r_k}(p_{ij})$) and T2- ($\mu_{T2}^{r_k}(p_{ij})$) weighted images.

Then, as shown in the gray shaded region of Figure 1, the new proposal for obtaining the hyperintensity fuzzy set was carried out by means of a *Mamdani* type *Fuzzy Rule-Based System* (*MFRBS*) which took into account previous membership functions, rules 2.1 and 2.2 and the knowledge of experts.

1) Obtaining the PD and T2 Hyperintensity Membership Functions $\mu_{H,D}$ and $\mu_{H,T2}$: According to rule 2.2, for determining the degree with which a pixel is hyperintense at both weighted images must be imposed that *for a high enough number of radii the pixel is sufficiently differentiable*. Our proposal for implementing this restriction consisted on aggregating the differentiability degrees of the pixel at each radius ($\mu_P^{r_k}(p_{ij})$ (P=PD, T2)) using an OWA operator [18], i.e.

$$\mu_{H,P}(p_{ij}) = f_{WP}\left(\mu_P^{r_1}(p_{ij}),\cdots,\mu_P^{r_8}(p_{ij})\right) \quad (1)$$

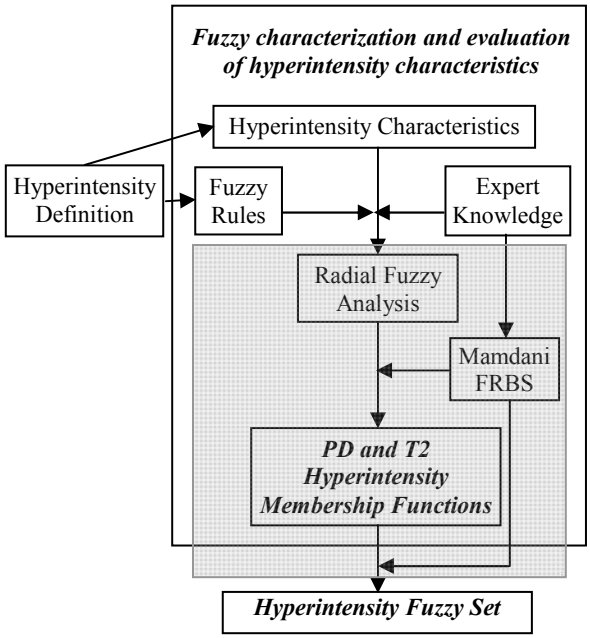

Figure 2. Gray-shaded region shows the step of the proposed algorithm that has been modified regarding the previous proposal.

To get the vectors w_P to be considered in the definition of $\mu_{H,PD}$ and $\mu_{H,T2}$ we followed the next two steps: *a) Sensitivity analysis* of $\mu_{H,PD}$ and $\mu_{H,T2}$ to the consideration of the vectors $w_P^1 = (1,0,\cdots,0)$, $w_P^2 = (0,1,0,\cdots,0)$, …, and $w_P^8 = (0,\cdots,0,1)$, which correspond to consider 1, 2, … and 8 radii respectively; *b)* Implementation of a *MFRBS* to the results of the *sensitivity analysis* to determine w_{PD} and w_{T2}.

a) Sensitivity analysis: To perform this analysis we considered the following quality indexes: Correction Factor associated with the detection level of small lesions, *CF*; Sensitivity to the Detection of pixels of small lesions, *SD*; and Efficiency for Avoiding False Positives; *EAFP*.

Since the minimum size for a region to be considered small lesion is of three pixels, if the number of pixels of a region R_k detected by the algorithm is greater or equal to 3 the region can be associated with lesion, otherwise, although it can not be considered as lesion, may be recovered as such at subsequent steps. However, a lesion would not be recovered if the algorithm did not detect any pixel of this lesion.

Taking into account previous considerations the first quality index was introduced as follows:

Definition 2.3
Let L be the set of lesions, l_i, marked by the experts at a given image I, $Alg(L)$ the set of lesions detected by the algorithm, and $N=\#(L)$. Then the *Correction factor associated with the detection level of small lesions* at I is given by

$$FC = \frac{1}{1+\sum_{i=1}^{N} \max(\overline{\chi}_{Alg(L)}(l_i), DP_{Alg(L)}(l_i))}. \quad (1)$$

where $\overline{\chi}_{Alg(L)}(l_i)$ is the complementary of the characteristic function of $Alg(L)$, and $DP_{Alg(L)}(l_i)$ is equal to 0.5 if the algorithm detects less than 3 pixels of lesion l_i and equal to 0 in other case.

This factor was considered as a weighting factor of the true positives fraction for defining the *Sensitivity to the Detection of pixels of small lesions,* as follows:

Definition 2.4
Let TP be the number of voxels in the image I detected as of lesion by experts and by our algorithm, and FN the number of image voxels detected as of lesion by experts but not by our algorithm. Then, the *Sensitivity to the Detection of pixels of small lesions* in I is given by:

$$SD = FC\,\frac{TP}{TP+FN}. \quad (3)$$

This Sensitivity index provides information regarding the possibility for detecting lesion pixels of an image and penalizes the cases of missed lesions, although some pixels of those lesions have been detected by the algorithm.

Whereas previous indexes are related to sensitivity and ability of the algorithm for correctly detecting lesion pixels, the third index focuses on its accuracy for avoiding false detections.

Definition 2.5
Given an image I, let *card* (*ICR*) be the number of pixels within the Intracraneal Region (*ICR*) of I, or number of image pixels analyzed by the algorithm. Then, the *Efficiency for Avoiding False Positives* in I is given by:

$$EAFP = 1 - \frac{FP}{card(ICR)} = 1 - \frac{FP}{TP+FN+TN+FP}. \quad (4)$$

where TN (true negatives) is the number of *ICR* image pixels neither marked by experts nor detected by the algorithm, and FP (false positives), is the number of *ICR* image pixels detected by the algorithm but unmarked by experts.

These quality indexes were evaluated on the PD- and T2-weighted images of the design database. To do it, for each pixel p_{ij} situated at position (i, j) on Im_R and Im_H, its hyperintensity values $\mu_{H,D}^k(p_{ij}) = f_{w_D^k}(\mu_D^{r1}(p_{ij}), \mu_D^{r2}(p_{ij}), \cdots, \mu_D^{r8}(p_{ij}))$ and $\mu_{H,T2}^k(p_{ij}) = f_{w_{T2}^k}(\mu_{T2}^{r1}(p_{ij}), \mu_{T2}^{r2}(p_{ij}), \cdots, \mu_{T2}^{r8}(p_{ij}))$ were obtained for the PD- and T2- weighted images, and the 8 weighting vectors, $1 \le k \le 8$. Then these values were defuzzified applying an α-cut with $\alpha = 0.5$, since for this value there is a balance between being and not be hyperintense.

The quality values obtained after the defuzzification process for the PD- and T2-weighted images are shown in tables I and II. Rows two to nine of these tables display the mean results obtained for the 8 weighting vectors for images Im_R (columns 2, 4 and 6) and Im_H (columns 3, 5 and 7).

TABLE I. VALUES OF QUALITY INDEXES FOR PD-WEIGHTED IMAGES

Vector Weights	*FC*		*SD*		*EAFP*	
	Im_R	Im_H	Im_R	Im_H	Im_R	Im_H
w^1_{PD}	1.0	1.0	1.0	1.0	0.579	0.596
w^2_{PD}	1.0	1.0	1.0	0.980	0.718	0.732
w^3_{PD}	1.0	1.0	1.0	0.961	0.809	0.819
w^4_{PD}	1.0	1.0	0.850	0.922	0.894	0.89
w^5_{PD}	0.667	1.0	0.433	0.843	0.946	0.933
w^6_{PD}	0.667	0.667	0.4	0.471	0.977	0.963
w^7_{PD}	0.4	0.333	0.16	0.137	0.993	0.985
w^8_{PD}	0.333	0.2	0.1	0.047	0.999	0.997

TABLE II. VALUES OF QUALITY INDEXES FOR T2-WEIGHTED IMAGES

Vector Weights	*FC*		*SD*		*EAFP*	
	Im_R	Im_H	Im_R	Im_H	Im_R	Im_H
w^1_{T2}	1.0	1.0	1.0	1.0	0.539	0.589
w^2_{T2}	1.0	1.0	1.0	0.980	0.674	0.720
w^3_{T2}	1.0	1.0	0.95	0.961	0.775	0.815
w^4_{T2}	1.0	1.0	0.850	0.824	0.875	0.892
w^5_{T2}	0.667	0.667	0.433	0.458	0.938	0.943
w^6_{T2}	0.5	0.4	0.275	0.235	0.974	0.973
w^7_{T2}	0.4	0.25	0.18	0.108	0.993	0.992
w^8_{T2}	0.286	0.154	0.071	0.024	0.999	0.999

In the analysis of these values was borne in mind that the best weighting vector for each weighted image ought: *1)* allow detecting a minimum of 3 pixels in all (or the maximum of) lesions, and *2)* furnish high detection level of lesion pixels but maintaining the number of false positives as small as possible.

From definitions 2.3, 2.4 and 2.5 it follows that the higher the value of *FC* the closer we will be to meet first condition, and the higher the values of *SD* and *EAFP* the more will be fulfilled condition *2)*. Moreover, the larger number of considered radii the more the restriction of lesion size will be satisfied, and the lower the possibility that correct and false detections show connectivity. As can be observed looking at tables I and II, these characteristics have significantly influence in the values of *SD* and *EAFP*, making that as the number of radii increases the first increases and the second decreases.

Given the above, the obtaining of the weighting vectors considered for defining $\mu_{H,PD}$ and $\mu_{H,T2}$ was performed using a *Mamdani type Fuzzy Rule system* because besides its high level of description, this type of system provides a natural framework for including expert knowledge in the form of linguistic rules, and possesses a high degree of freedom for selecting the most suitable fuzzification, defuzzification and inference components.

b) Application of the MFRBS for determining w_{PD} and w_{T2}: The *Knowledge Base* (*KB*) of the proposed system was obtained from experience and knowledge of experts. So, taking into account experts experience and the relationship between *FC* and *SD*, the *Data Base* (*DB*) was constituted by *SD* and *EAFP*, as input variables, and the *Adequacy* of the weighting vector as output variable. Moreover the linguistic terms, or labels, related to input and output variables were: L_{SD}={*High, Medium, Low*}, L_{EAFP}={*High, Medium, Low*} and $L_{Adequacy}$={*High, Medium, Low, Very Low*}.

For defining the membership functions associated with the linguistic labels considered for *SD* we studied the behavior of *FC* in cases where for some lesion the algorithm detected less than 3 pixels. From this study it appeared that there was a reverse proportionality factor between the increasing of lesions for which less than 3 pixels were detected by the algorithm and the value of *FC*. Furthermore, given the relationship between *FC* and *SD*, this factor made diminishing the *SD* value in the same proportion than *FC* if there are not false negatives, and at a higher rate in case of false negative detections.

In addition to previous considerations it was considered that the value of *EAFP* decreases as *FP* increases and, the greater the number of false positives the easier these pixels can present connectivity with the false positives, making that small lesions appear larger than their actual size. With the aim of avoiding this situation, we should be very restrictive in defining the membership functions associated with the variable *EAFP*

Given the above considerations, as well as the knowledge of the experts, the semantics of the linguistic variables were defined by the membership functions shown in the graphs of figure 3.

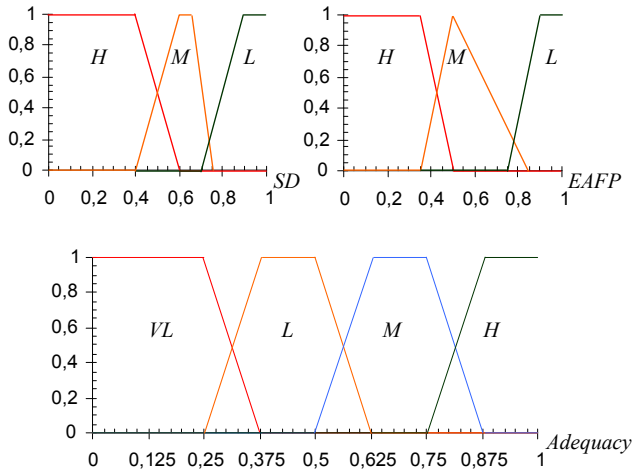

Figure 3. Membership functions of the labels associated with the input (*SD* and *ENDFP*) and output (*Adequacy*) variables.

The *Rule Base* (*RB*) considered in the *KB* was constituted by the nine linguistic rules represented by the *decision table* shown in table III.

TABLE III. DECISION TABLE OF THE KB CONSIDERED FOR DEFINING $\mu_{H,D}$ AND $\mu_{H,T2}$

Decision Table		SD		
		High	***Medium***	***Low***
EAFP	***High***	R_1:High (H)	R_4: Medium (M)	R_7: Low (L)
	Medium	R_2: Medium (M)	R_5: Low (L)	R_8: Very Low (VL)
	Low	R_3: Low (L)	R_6: Very Low (VL)	R_9: Very Low (VL)

Once the *KB* of the considered *MFRBS* was identified, we went on to define the *Inference Engine* (*IE*) which, by means of previous rules, put into effect the inference process on the system inputs.

The *IE* here considered was the classic of Mamdani, i. e. the t-norm minimum was used as conjunction and implication operators, and the mode A-FATI (first aggregate, then infer) as defuzzification interface. Finally in the *Defuzzification interface* the aggregation operator was modeled by the t-conorm maximum, while the defuzificación was carried out by the *Gravity Center* method, i.e. we considered the usually called *max-min-CG* inference engine

Tables IV and V show the results obtained by applying the proposed *MFRS* to the PD- and T2-weighted images, respectively. Having a look at these results it can be observed that for both weighted images the best performance is given for the weighting vectors that consider 4 radii (values highlighted in bold at both tables). This fact is better appreciated at figure 4 wherein blue triangles, red ellipses, green squares, black crosses, and brown triangles have been used for representing the *GC*s obtained for the weighting vectors w_P^1, w_P^2, w_P^3, w_P^4 and w_P^5, while the *GC*s obtained for the weighting vectors w_P^6, w_P^7 and w_P^8, are represented by purple ellipses. Therefore, the membership degrees of a pixel p_{ij} to the *PD* and *T2* hyperintense fuzzy sets are given by:

$$\mu_{H,P}(p_{ij}) = (0,0,0,1,0,0,0,0) \bullet \left(\mu_P^{r\sigma(1)}(p_{ij}),\ldots,\mu_P^{r\sigma(8)}(p_{ij})\right)^T . \quad (5)$$

TABLE IV. RESULTS OBTAINED APPLYING THE PROPOSED MFRBS TO THE PD-WEIGHTED IMAGES OF THE DESIGN DATABASE

	w_{PD}^k	*SD*	*EAFP*	*Rules*	*GC*
Im_R	*k*=1	1	0.579	R_2	(0.687, 0.342)
	k=2	1	0.718	R_2	(0.687, 0.179)
	k=3	1	0.809	R_1, R_2	(0.741, 0.055)
	***k*=4**	**0.85**	**0.894**	R_1	**(0.897, 0.346)**
	k=5	0.433	0.946	R_4, R_7	(0.484, 0.32)
	k=6	0.4	0.977	R_7	(0.437, 0.417)
	k=7	0.16	0.993	R_7	(0.437, 0.417)
	k=8	0.1	0.999	R_7	(0.437, 0.417)
Im_E	*k*=1	1	0.596	R_2	(0.687, 0.324)
	k=2	0.98	0.732	R_2	(0.687, 0.161)
	k=3	0.961	0.819	R_1, R_2	(0.83, 0.068)
	***k*=4**	**0.922**	**0.89**	R_1	**(0.90, 0.406)**
	k=5	0.843	0.933	R_1	(0.895, 0.331)
	k=6	0.471	0.963	R_4, R_7	(0.530, 0.256)
	k=7	0.137	0.985	R_7	(0.437, 0.417)
	k=8	0.047	0.997	R_7	(0.437, 0.417)

TABLE V. RESULTS OBTAINED APPLYING THE PROPOSED MFRBS TO THE T2-WEIGHTED IMAGES OF THE DESIGN DATABASE

	w_{T2}^k	*SD*	*EAFP*	*Rules*	*GC*
Im_R	*k*=1	1	0.539	R_2	(0.687, 0.382)
	k=2	1	0.674	R_2	(0.687, 0.235)
	k=3	0,95	0.775	R_1R_2	(0.744, 0.1)
	***k*=4**	**0.85**	**0.875**	R_1	**(0.897, 0.346)**
	k=5	0.433	0.938	R_4, R_7	(0.484, 0.320)
	k=6	0.275	0.974	R_7	(0.437, 0.417)
	k=7	0.18	0.993	R_7	(0.437, 0.417)
	k=8	0.071	0.999	R_7	(0.437, 0.417)
Im_E	*k*=1	1	0.589	R_2	(0.687, 0.332)
	k=2	0.98	0.72	R_2	(0.687, 0.177)
	k=3	0.961	0.815	R_1, R_2	(0.83, 0.165)
	***k*=4**	**0.824**	**0.892**	R_1	**(0.894, 0.291)**
	k=5	0.458	0.943	R_4, R_7	(0.515, 0.272)
	k=6	0.235	0.973	R_7	(0.437, 0.417)
	k=7	0.108	0.992	R_7	(0.437, 0.417)
	k=8	0.024	0.999	R_7	(0.437, 0.417)

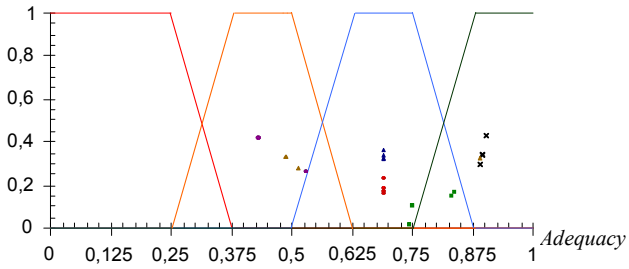

Figure 4. Gravity centers obtained applyinf¡g the proposed MFRBS. Black crosses, and brown triangles represent the GCs obtained for the weighting vectors w_P^4 and w_P^5, respectively.

2) Obtaining the Hyperintensity Membership Function μ_H: According to rule 2.3, a pixel is hyperintense if it presents hyperintense behavior at both PD- and T2-weighted images. So, for obtaining the membership degree of a pixel to the hyperintense fuzzy set, its membership degrees to the *PD* and *T2* hyperintense fuzzy sets had to be aggregated.

Given the characteristics of $\mu_{H,PD}$ and $\mu_{H,T2}$ it was considered that the aggregation operator used for defining μ_H should be a not too restrictive "logical and" (to provide similar importance to both membership functions), and ought take into account the process followed for obtaining the functions to be aggregated.

Bearing in mind the above restrictions as well as the characteristics of the lesions within the images, we studied the operators that could better adapt to them. After this study it was decided that the best operators were: the T-norms Minimum (Min) and Product (Prod), and Averaging Operator Geometric Mean (GM).

For determining which of these operators was better suited to our model we applied a *MFRBS* similar to the considered at previous step. The differences regarding previous system were at the *KB*. So, at the *DB* the linguistic variables and the membership functions associated to the output variable were modified. This change involved the modification of the *RB*.

The set of linguistic terms associated to the output variable was $L'_{Adequacy}$={High, Medium, Low}. The semantics associated with this variable, as well as the Rule Base, which were determined from the information provided by the experts, are shown at figure 5 and table VI, respectively.

The results obtained after applying the proposed *MFRBS* are shown at table VII. Moreover, for a better understanding of these results, the *GC*s obtained from the defuzzification step for the minimum, product, and geometric mean have been depicted as blue, red, and black points at figure 5.

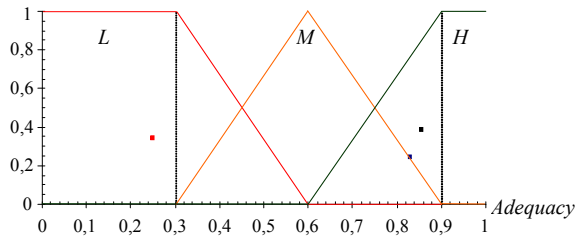

Figure 5. Membership functions of the output variable considered in the DB of the MFRBS designed for determining the aggregation operator used in the definition of the hyperintensity membership function. Blue, red and black points are the GCs obtained for the operators *Min, Prod* and *GM*, respectively.

TABLE VI. DECISION TABLE OF THE KB CONSIDERED FOR DEFINING μ_H

Decision Table		**SD**		
		High	***Medium***	***Low***
EAFP	***High***	R_1:High (H)	R_4: Medium (M)	R_7: Low (L)
	Medium	R_2: Medium (M)	R_5: Medium (M)	R_8: Low (L)
	Low	R_3: Low (L)	R_6: Low (L)	R_9: Low (L)

TABLE VII. RESULTS OBTAINED APPLYING THE PROPOSED MFRBS TO THE DESIGN DATABASE FOR OBTAINING μ_H

Operator	***FC***	***FSD***	***EAFP***	***Rules***	***GC***
Min	1	0.8	0.948	R_1	(0.835, 0.23)
Prod	0.667	0.433	0.964	R_4, R_7	(0.246, 0.345)
GM	1	0.88	0.924	R_1	(0.856, 0.376)

In analyzing the results it is appreciated that the product T-norm has clearly the worst fitting to the data, since its *Adequacy* is Low. As for the T-norm minimum, though its *Adequacy* is High, the *CG* obtained after the defuzzification is very close to *Adequacy* Medium. Therefore, since for the Geometric Mean aggregation Operator the Adequacy obtained was clearly High, the hyperintensity membership function (μ_H) was defined as:

$$\mu_H(p_{ij}) = \sqrt{\mu_{H,D}(p_{ij})\mu_{H,T2}(p_{ij})} \qquad (6)$$

IV. RESULTS

The proposed algorithm was evaluated on the 8 PD- and T2-weighted images of the data set. To do it, once the hyperintensity degrees of all the pixels were obtained using (6), we applied a 0.5-cut in order to maintain the balance between being and not be hyperintense. Then we evaluated the quality indexes *FC*, *SD*, and *EAFP*, obtaining the results shown at table VIII.

It must be emphasized that the algorithm showed a high sensitivity detecting hiperintensity regions associated with MS lesions, as can be inferred from the mean value of *SD* that appears at table VIII. In the evaluation of this value must be taken into consideration the hard penalization introduced by the *correction factor FC*. However this index showed also a high mean value (close to 1), and a minimum value of 0.5, what points out that the vast majority of pixels belonging to MS lesions were detected throughout the detection of hiperintensity within these images. Moreover, although we had a small number of false negatives, and the size of MS lesions can be very small, we checked out that all small lesions previously marked up by the experts were detected after applying the proposed algorithm.

On the other hand, the values obtained for *EAFP* indicate a low presence of false detections (*FP*) with regards to the number of pixels within the intracranial region (*card*(*ICR*)). The small difference between minimum and maximum values for this index, depicted at last column in fourth and fifth rows of table VIII, also allow us to infer that the detection of false positives showed no dependence of the different anatomical features that appear on different slides.

TABLE VIII. RESULTS OBTAINED TROUGH THE LOCAL ANALYSIS OF THE IMAGES DATABASE

	FC	***SD***	***EAFP***
Mean	0.94	0.85	0.93
σ	0.177	0.195	0.008
Minimum	0.5	0.43	0.92
Maximum	1.0	1.0	0.94

However, it must be taken into consideration that though a mean value obtained for this index is very high, this not implies necessarily that the number of FP were extremely low because *card*(*ICR*) is much greater than the possible number of *FP*. In this regard, should be noted that, although it would be desirable, in our implementation of the proposed trade-off it was not imposed that the results provided by the algorithm were free of false detections, instead it was decided to prioritize correct detections, as can be inferred from the definition of the semantic of the output linguistic variable shown in figure 3.

V. CONCLUSIONS AND FUTURE WORK

In conclusion, we have presented an algorithm to detect small hyperintense regions in PD- and T2-weighted MR images of the brain, and we have applied it to the detection of small multiple sclerosis lesions. The algorithm is designed based on a trade-off between true and false positive detections

that has been assessed by the introduction of quality indexes defined for this purpose. Then, a Mamdani type *FRBS* designed considering knowledge and experience of experts, and whose *KB* has fed on the results of the quality indexes obtained for the design images, has provided the aggregation operators defining the hyperintensity fuzzy set. Results have shown that the algorithm is very efficient detecting hyperintense regions associated with small MS lesions.

Future work will involve the introduction of new strategies for reducing false detections without removing true detections. Also the algorithm will be applied to a greater data set to achieve a better validation.

REFERENCES

[1] A. Compston and A. Coles, "Multiple sclerosis," The Lancet, vol. 359, no. 9313, pp. 1221–1231, 2002

[2] J. R. Mitchell, S. J. Karlik, D. H. Lee, and A. Fenster, "Computer-assisted identification and quantification of multiple sclerosis lesions in mr imaging volumes in the brain," J Magn Reson Imaging, vol. 4, no. 2, pp. 197–208, Mar-April 1994.

[3] M. K. Edwards and J. M. Bonnin, " White matter diseases in magnetic resonance imaging of the brain and spine," in Magn Reson. Imaging of the Brain and Spine, ed., Atlas. S. W, Raven Press, 1991, pp. 467–477.

[4] D. H. Miller, R. I. Grossman, S. C. Reingold, and H. F. McFarland, "The role of magnetic resonance techniques in understanding and managing multiple sclerosis," Brain, vol. 121, no. 1, pp. 3–24, Jan. 1998.

[5] W. I. McDonald, A. Compston, G. Edan, et al., "Recommended Diagnostic Criteria for Multiple Sclerosis: Guidelines from the International Panel on the Diagnosis of Multiple Sclerosis," Annals of Neurology, vol. 50, no. 1, pp. 121–127, 2001.

[6] D. H. Miller, M. Filippi, F. Fazekas, et al., "Role of magnetic resonance imaging within diagnostic criteria for multiple sclerosis," Annals of Neurology, vol. 56, pp. 273–278, 2004.

[7] D. L. Pham, C. Xu, and J. L. Prince, "A survey of current methods in medical image segmentation," Annual Review of Biomedical Engineering, vol. 2, pp. 315–337, 2000.

[8] M. Hasanzadeh and S. kasaei, "Multispectral brain MRI segmentation using genetic fuzzy systems," 9th Int. symposium on signal processing and its applications, pp. 1–4, Feb. 2007.

[9] P. Wang and H. Lei Wang, "A modified FCM algorithm for brain image segmentation," Int. seminar on Biom. Informat. Eng. pp. 26–29, 2008.

[10] K. Van Leemput, F. Maes, D. Vandermeulen, A. Colchester, and P. Suetens, "Automated segmentation of multiple sclerosis lesions by model outlier detection," IEEE Trans Med Imaging, vol. 20, no. 8, pp. 677–688, Aug. 2001.

[11] F. Admiraal-Behloul, D. M. J. van den Heuvel, H. Olofsen, M. J. P. van Osch, J. van der Grond et al., "Fully automatic segmentation of white matter hyperintensities in MR images of the elderly," Neuroimage, vol. 28, no. 3, pp. 607–617, Nov. 2005.

[12] B. R. Sajja, S. Datta, R. He, M. Mehta, R.K. Gupta et al., "Unified Approach for multiple sclerosis lesions segmentation on brain MRI", Ann. Biomed. Eng., vol.34, no. 1, pp. 142–151, Jan. 2006.

[13] A. Askelrod-Ballin, M. Galun, J.M. Gomori, M. Filippi, P. Valsasina, et al., "Automatic segmentation and classification of multiple sclerosis in multichannel MRI", IEEE Trans. On Biomedical Engineering, vol. 56, no. 10, pp. 2461–2469, Oct. 2009.

[14] E. H. Mamdani, "Application of fuzzy algorithms for control of a simple dynamic plant," Proc. Inst. Electr. Eng., no. 121, pp. 1585–1588, 1974.

[15] F. X. Aymerich, P. Sobrevilla, J. Capellades, E. Grivé, J. Gili et al., "Fuzzy detection of multiple sclerosis small lesions", in Proceedings of the fifth conference of the European Society for Engineering and Medicine (ESEM), pp. 197–198, 1999.

[16] F. X. Aymerich, P. Sobrevilla, E. Montseny, and J. Gili J, "Detección mediante técnicas difusas de lesiones de esclerosis múltiple en imágenes de resonancia magnética," XVIII Congreso Anual Sociedad Española de Ing. Biomédica (CASEIB), pp. 269–273, 2000 (not available in english)

[17] Molyneux P.D., Tubridy N., Parker G.J., et al., "The effect of section thickness on MR lesion detection and quantification in multiple sclerosis," AJNR Am J Neuroradiol., vol. 19, pp. 1715–1720, 1998.

[18] R. R Yager, "Families of OWA Operators," Fuzzy Sets and Systems, vol. 59, pp. 125-148, 1993.

2011 IEEE International Conference on Fuzzy Systems
June 27-30, 2011, Taipei, Taiwan

On Fuzzy Partitions for Visual Texture Modelling

J. Chamorro-Martínez and P. Martínez-Jiménez
Department of Computer Science and Artificial Intelligence,
University of Granada, Spain
email:{jesus,pedromartinez}@decsai.ugr.es

J.M. Soto-Hidalgo
Dep. of Comp. Architecture, Electronics and Elect. Tech.,
University of Córdoba, Spain
email: jmsoto@uco.es

***Abstract*—Texture is one of the most used low-level feature for image analysis and, in addition, one of the most difficult to characterize due to its imprecision. It is usual for humans to describe visual textures according to some perceptual properties like coarseness-fineness, orientation or regularity. In this paper, we propose to model the fineness property, that is the most popular one, by means of a fuzzy partition on the domain of representative fineness measures. In our study, a wide variety of measures is studied, and the partitions are obtained by relating each measure (our reference set) with the human perception of fineness. Assessments about the perception of this property are collected from pools. This information is used to analyze the capability of each measure to discriminate different fineness categories, which imposes the number of fuzzy sets of the partition. Moreover, it is used to calculate the parameters of the membership function associated to each fuzzy set.**

***Index Terms*—Coarseness, fineness, fuzzy partition, fuzzy texture, image features, texture features.**

I. Introduction

Texture is, together with color and shape, one of the most important features for image analysis. However, it is also one of the most difficult to characterize due to its imprecission [1], [2]. In fact, there is not an accurate definition for the concept of texture but some intuitive ideas, as local changes in the intensity patterns or as a set of basic items arranged in a certain way [3]. Moreover, it is usual for humans to describe visual textures according to some vague textural properties like *coarseness/fineness*, *directionality* or *regularity* [4], [5]. Thus, coarseness is related to the spatial size of texture primitives, directionality reflects if they have a dominant orientation, and regularity refers to the variation of their placement. In this framework, visual textures are described by humans using linguistic terms as *fine* (e.g. the image in figure 1(J)), *very coarse* (figure 1(I)), *irregular* (figure 1(B)) or *very directional* (figure 1(I)).

There are many measures in the literature that, given an image, capture the presence of one of these perceptual properties in the sense that the greater the value given by the measure, the greater the perception of the property [3], [4]. However, there is no perceptual relationship between the value given by these measures and the degree in which the humans perceive the texture. Thus, given a certain value calculated by applying a measure to an image, we can not give a textural interpretation (e.g. for coarseness measures, there is not an immediate way to decide whether there is a fine texture, a coarse texture or something intermediate).

To face this problem, fuzzy logic has been recently employed for representing the imprecision related to texture. In many of these approaches, fuzzy logic is usually applied just during the process, being the output a crisp result [6], [7]. Other approaches try to model the texture and its semantic by means of fuzzy sets defined on the domain of a given texture measure. In this last framework, some proposals model the texture property by means of an unique fuzzy set [8], and other approaches define fuzzy partitions providing a set of linguistic terms [9], [10].

Focusing our study in the last type of approaches, two questions need to be faced for defining properly a fuzzy partition: (i) the number of linguistic labels to be used, and (ii) the parameters of the membership functions associated to each fuzzy set (and, consequently, the kernel localization). However, these question are not treat properly in the literature. Firstly, the number of fuzzy sets are often chosen arbitrarily, without take into account the capability of each measure to discriminate between different categories. Secondly, in many of the approaches, just an uniform distribution of the fuzzy sets is performed on the domain of the measures, although is wellknown that measure values corresponding to representative labels are not distributed uniformly. In addition, from our knowledge, none of the fuzzy approaches in the literature considers the relationship between the computational feature and the human perception of texture, so the labels and the membership degrees do not necessarily will match with the human assessments.

Among all the perceptual texture properties, the *coarseness-fineness* is the most popular one, being considered as the most fundamental feature in texture analysis by some authors [10]. In fact, the presence of fineness is usually associated to the presence of texture (from this point of view, texture is defined as local variations against the idea of homogeneity). In this sense, a *fine* texture contains small texture primitives with big gray tone differences between neighbor pixels (e.g. the image in Figure 1(A)), whereas a *coarse* texture corresponds to bigger primitives formed by several pixels (e.g. the image in Figure 1(I)). By considering the importance of the *coarseness-fineness* concept and in order to explain the methodology proposed in this paper, we will focus our study on this textural property (although other properties can be easily applied in a similar way).

In this paper, we propose to model the fineness property by means of a fuzzy partition on the domain of representative

978-1-4244-7316-8/11/$26.00 ©2011 IEEE

Figure 1. Some examples of images with different degrees of fineness

fineness measures. Firstly, in order to select the number of linguistic labels, we analyze the ability of each measure to discriminate different categories of the perceptual property. For this purpose, data about the human perception of fineness is collected by means of pools. This information is also used to localize the position and size of the kernel of each fuzzy set, obtaining a fuzzy partition adapted to the human perception of fineness.

The rest of the paper is organized as follows. In section II we present our methodology to obtain the fuzzy partition. Results are shown in section III, and the main conclusions and future work are sumarized in section IV.

II. Defining Fuzzy Partitions for Texture

Given a texture property (coarseness, directionality, regularity, etc), let $\mathcal{M}$ be a measure of that property and let $\mathcal{D}_{\mathcal{M}}$ be the measure domain. The notions of fuzzy texture and fuzzy texture space are introduced as follows:

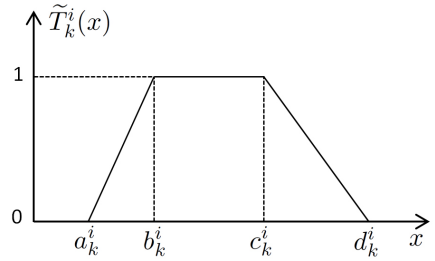

Figure 2. Trapezoidal function used for each fuzzy set $\widetilde{T}_k^i$

Definition 2.1: A fuzzy texture $\widetilde{T}$ is a linguistic label whose semantics is represented by a normalized fuzzy subset of $\mathcal{D}_{\mathcal{M}}$.

Definition 2.2: A fuzzy texture space Π is a set of fuzzy textures that defines a partition of $\mathcal{D}_{\mathcal{M}}$.

In this paper, we will focus our study on the *coarseness-fineness* property. Thus, we need to define the *coarseness-fineness* measures $\mathcal{M}$ that are used as the reference set (section II-A).

As it was pointed, there is not a clear perceptual interpretation of the value given by a coarseness-fineness measure. To face this problem, fuzzy partitions on the domain of the measures shown in section II-A are proposed. From now on, we will note Π_k the partition defined on the domain of a given fineness measure $\mathcal{M}_k$, N_k the number of fuzzy sets which compounds the partition Π_k, and $\widetilde{T}_k^i$ the i-th fuzzy set in Π_k.

In our approach, we propose to define the membership function $\widetilde{T}_k^i(x)$ for each fuzzy set $\widetilde{T}_k^i$ by using the trapezoidal function shown in Figure 2, that has the form

$$\widetilde{T}_k^i(x; a_k^i, b_k^i, c_k^i, d_k^i) = \begin{cases} 0 & x < a_k^i \quad or \quad x > d_k^i \\ \frac{x - a_k^i}{b_k^i - a_k^i} & a_k^i \leq x \leq b_k^i \\ 1 & b_k^i \leq x \leq c_k^i \\ \frac{d_k^i - x}{d_k^i - c_k^i} & c_k^i \leq x \leq d_k^i \end{cases} \tag{1}$$

This way, two questions need to be faced in order to define the fuzzy partition Π_k: (i) how many fuzzy sets will compound the partition, and (ii) how to obtain the parameter values of the membership function for each fuzzy set.

In order to answer both questions, we will analyze the ability of each measure to distinguish between different degrees of fineness. This analysis will be based on how the human perceives the fineness. To get information about human perception of fineness, a set of images covering different degrees of this property will be gathered. These images will be used to collect, by means of a pool, human assessments about the perceived fineness (section II-B)

Using the data about human perception, and the measure values obtained for each image, we will apply an iterative algorithm based on a set of multiple comparison tests, in order to obtain the number of classes (fineness degrees) that each measure can discriminate. Thus, we propose to set the number

Algorithm 1 Distinguishable clusters selection

Input:

$Part^0 = C_1, C_2, \ldots, C_n$: Initial Partition

δ: distance function between clusters

ϕ: Set of multiple comparison tests

NT: Number of positive tests to accept distinguishability

1.-Initialization

$k = 0$

$distinguishable = false$

2.- While (distinguishable = false) and (k < n)

Apply the multiple comparison tests ϕ to $Part^k$

If for each pair C_i, $C_j \in Part^k$ more than NT of the multiple comparison tests ϕ show distinguishability

$distinguishable = true$

Else

Search for the pair of clusters C_r, C_{r+1}, verifying $\delta(C_r, C_{r+1}) = \min\{\delta(C_i, C_{i+1}), C_i, C_{i+1} \in Part^k\}$

Join C_r and C_{r+1} on a cluster $C_u = C_r \cup C_{r+1}$

$Part^{k+1} = Part^k - C_r - C_{r+1} + C_u$

$k = k + 1$

3.- Output: $\widetilde{Part}_k = C_1, C_2, \ldots, C_{n-k}$

of fuzzy sets N_k in the partition Π_k as the number of classes that can be discriminated by the measure $\mathcal{M}_k$ (section II-C). In addition, the information given by the tests, will be used to define the parameter values of the membership function $\widetilde{T}_k^i(x)$ for each fuzzy set $\widetilde{T}_k^i$ (section II-D).

A. Texture measures

As mentioned in the introduction, there are many measures in the literature that, given an image, capture the fineness (or coarseness) presence in the sense that the greater the value given by the measure, the greater the perception of texture [4], [3]. In this paper, some of the most representative of these measures, that are listed in the first column of Table I, have been analyzed. It should be noticed that most of these measures were developed in the early nineties. However, they are still considered the state of the art in the characterization of the coarseness property of textures. In fact, they are achieving a growing interest due to applications in fields like image retrieval, where low level features like texture are the basis for the description of visual content (e.g. MPEG-7 descriptors) [11], [12], or for learning new concepts [13], [14]. All the coarseness-fineness measures analyzed in this paper are automatically computed from the texture image, obtaining a real value. Thus, the domain for all of them is $\mathcal{D}_{\mathcal{M}} = \mathbb{R}$.

B. Assessment collection

From now on, let $\mathcal{I} = \{I_1, \ldots, I_N\}$ be the set of N images representing fineness examples, and let $\Gamma = \{v^1, \ldots, v^N\}$ be the set of perceived fineness values associated to $\mathcal{I}$, with v^i being the value representing the degree of fineness perceived by humans in the image $I_i \in \mathcal{I}$. In this section, the way to obtain the set Γ will be described. For this purpose, firstly the image set $\mathcal{I}$ will be selected (section II-B1). After that, a poll for getting assessments about the perception of fineness will be designed (section II-B2). Finally, for a given image, the assessments of the different subjects will be aggregated (section II-B3).

1) The texture image set: A set $\mathcal{I} = \{I_1, \ldots, I_N\}$ of $N = 80$ images representative of the concept of *fineness* has been selected. Figure 1 shows some images extracted from the set $\mathcal{I}$. Such set has been selected satisfying the following properties:

1) It covers the different presence degrees of fineness.
2) The number of images for each presence degree is representative enough.
3) Each image shows, as far as possible, just one presence degree of fineness.

Due to the third property, each image can viewed as "homogeneous" respect to the fineness degree represented, i.e., if we select two random windows (with a dimension which does not "break" the original texture primitives and structure), the perceived fineness will be the same for each window (and also respect to the original image). In other words, we can see each image $I_i \in \mathcal{I}$ as a set of lower dimension images (windows) with the same fineness degree of the original one.

As we explained, given an image $I_i \in \mathcal{I}$, a fineness measure $\mathcal{M}_k$ will be applied on it. In fact, and thanks to the third property, we really can apply this measure for each subimage, assuming that the human assessment associated to that subimage will be the human assessment associated to the whole image. From now on, we will note as $m_k^{i,w}$ the result of applying the measure $\mathcal{M}_k$ to the w-th window of the image I_i.

2) The poll: Given the image set $\mathcal{I}$, the next step is to obtain assessments about the perception of fineness from a set of subjects. From now on we shall note as $\Theta^i = [o_1^i, \ldots, o_L^i]$ the vector of assessments obtained from L subjects for the image I_i. To get Θ^i, subjects will be asked to assign images to classes, so that each class has associated a perception degree of fineness. In particular, 20 subjects have participated in the poll and 9 classes have been considered. The first nine images in figure 1 show the nine representative images for each class used in this poll. It should be noticed that the images are decreasingly ordered according to the degree of fineness.

As result, a vector of 20 assessments $\Theta^i = [o_1^i, \ldots, o_{20}^i]$ is obtained for each image $I_i \in \mathcal{I}$. The degree o_j^i associated to the assessment given by the subject S_j to the image I_i is computed as $o_j^i = (9-k) * 0.125$, where $k \in \{1, \ldots, 9\}$ is the index of the class C_k to which the image is assigned by the subject.

3) Assessment aggregation: Our aim at this point is to obtain, for each image in the set $\mathcal{I}$, one assessment v^i that summarizes the assessments Θ^i given by the different subjects about the presence degree of fineness.

To aggregate opinions we have used an OWA operator guided by a quantifier [24]. Concretely, the quantifier "the most" has been employed, which allows to represent the opinion of the majority of the polled subjects. This quantifier is defined as

Table I
RESULT OBTAINED BY APPLYING THE ALGORITHM 1

Measure	N_k	Classes	$\bar{c}_5 \pm \Psi_5$	$\bar{c}_4 \pm \Psi_4$	$\bar{c}_3 \pm \Psi_3$	$\bar{c}_2 \pm \Psi_2$	$\bar{c}_1 \pm \Psi_1$
Correlation [3]	5	{1,2-4,5-6,7-8,9}	0.122±0.038	0.403±0.0272	0.495±0.0225	0.607±0.0133	0.769±0.0210
ED [15]	5	{1,2,3-5,6-8,9}	0.348±0.0086	0.282±0.0064	0.261±0.0063	0.238±0.0066	0.165±0.0061
Abbadeni [16]	4	{1,2-6,7-8,9}	-	5.672±0.2738	9.208±0.4247	11.12±0.2916	25.23±1.961
Amadasun [4]	4	{1,2-6,7-8,9}	-	4.864±0.271	7.645±0.413	9.815±0.230	19.62±1.446
Contrast [3]	4	{1,2-5,6-8,9}	-	3312±265.5	2529±295.5	1863±94.84	790.8±129.4
FD [17]	4	{1,2,3-8,9}	-	3.383±0.0355	3.174±0.0282	2.991±0.0529	2.559±0.0408
Tamura [5]	4	{1,2-6,7-8,9}	-	1.540±0.0634	1.864±0.0722	2.125±0.0420	3.045±0766
Weszka [18]	4	{1,2-6,7-8,9}	-	0.153±0.0064	0.113±0.0093	0.099±0.0036	0.051±0.0041
DGD [19]	3	{1,2-8,9}	-	-	0.020±0.0010	0.038±0.0017	0.091±0.0070
FMPS [20]	3	{1,2-8,9}	-	-	0.256±0.0477	0.138±0.0122	0.0734±0.0217
LH [3]	3	{1,2-8,9}	-	-	0.023±0.0010	0.052±0.0025	0.127±0.0096
Newsam [21]	3	{1,2-6,7-9}	-	-	0.1517±0.0425	0.2654±0.0466	0.4173±0.0497
SNE [22]	3	{1,2-8,9}	-	-	0.879±0.0182	0.775±0.0087	0.570±0.0232
SRE [23]	3	{1,2-8,9}	-	-	0.995±0.00026	0.987±0.00066	0.966±0.0030
Entropy [3]	2	{1,2-9}	-	-	-	9.360±0.124	8.656±0.301
Uniformity[3]	2	{1,2-9}	-	-	-	$1.3_{E^{-4}}$ $\pm 2.6_{E^{-5}}$	$3.9_{E^{-4}}$ $\pm 1.9_{E^{-4}}$
Variance[3]	1	-	-	-	-	-	-

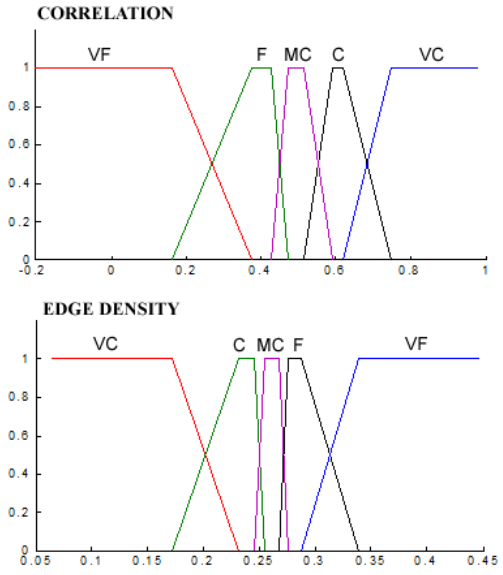

Figure 3. Fuzzy partitions for the measures Correlation and Edge Density. The linguistic labels are VC = very coarse, C = coarse, MC = medium coarse, F = fine, VF = very fine

$$Q(r) = \begin{cases} 0 & \text{if } r < a, \\ \frac{r-a}{b-a} & \text{if } a \leq r \leq b, \\ 1 & \text{if } r > b \end{cases} \quad (2)$$

with $r \in [0,1]$, $a = 0.3$ and $b = 0.8$. Once the quantifier Q has been chosen, the weighting vector of the OWA operator can be obtained following Yager [24] as $w_j = Q(j/L) - Q((j-1)/L), j = 1, 2, ..., L$. According to this, for each image $I_i \in \mathcal{I}$, the vector Θ^i obtained from L subjects will be aggregated into one assessment v^i as follows:

$$v^i = w_1 \hat{o}_1^i + w_2 \hat{o}_2^i + ... + w_L \hat{o}_L^i \quad (3)$$

where $[\hat{o}_1^i, \ldots, \hat{o}_L^i]$ is a vector obtained by ranking in nonincreasing order the values of the vector Θ^i.

C. Distinguishability Analysis of the Fineness Measures

As it was expected, some measures have better ability to represent fineness than the others. To study the ability of each measure to discriminate different degrees of fineness (i.e. how many classes can $\mathcal{M}_k$ actually discriminate), we propose to analyze each measure by applying a set of multiple comparison tests following the algorithm 1. This algorithm starts with an initial partition[1] and iteratively joins clusters until a partition in which all classes are distinguishable is achieved. In our proposal, the initial partition will be formed by the 9 classes used in our poll (where each class will contain the images assigned to it by the majority of the subjects), as δ the Euclidean distance between the centroids of the involved classes will be used, as ϕ a set of 5 multiple comparison tests will be considered (concretely, the tests of Scheffé, Bonferroni, Duncan, Tukey's least significant difference, and Tukey's honestly significant difference [25]), and finally the number of positive tests to accept distinguishability will be fixed to $NT = 3$.

From now on, we shall note as $\Upsilon_k = C_1^k, C_2^k, \ldots, C_{N_k}^k$ the N_k classes that can be discriminated by $\mathcal{M}_k$. For each C_i^k, we will note as $\bar{c}_i^k$ the class representative value. In this paper, we propose to compute $\bar{c}_i^k$ as the mean of the measure values in the class C_i^k.

Table I shows the parameters obtained by applying the proposed algorithm with the different measures considered in this paper. The second column of this table shows the N_k classes that can discriminate each measure and the third column shows how the initial classes have been grouped. The columns from fourth to eighth show the representative values $\bar{c}_r^k$ associated to each cluster.

D. The Fuzzy Partitions

In this section we will deal with the problem of defining the membership function $\mathcal{T}_k^i(x)$ for each fuzzy set $\mathcal{T}_k^i$ compounding the partition Π_k. As it was explained, the number of

[1]Let us remark that this partition is not the "fuzzy partition". In this case, the elements are measure values and the initial clusters the ones given by the pool.

Table II
PARAMETER VALUES THAT DEFINE THE MEMBERSHIP FUNCTIONS $\mathcal{T}_k^i(x)$ COMPOUNDING THE PARTITION FOR THE MEASURES OF CORRELATION AND EDGE DENSITY

(a) CORRELATION

i	a_k^i	b_k^i	c_k^i	d_k^i
1	$-\infty$	$-\infty$	0.1600	0.3758
2	0.1600	0.3758	0.4302	0.4725
3	0.4302	0.4725	0.5175	0.5937
4	0.5175	0.5937	0.6203	0.7480
5	0.6203	0.7480	∞	∞

(b) EDGE DENSITY

i	a_k^i	b_k^i	c_k^i	d_k^i
1	$-\infty$	$-\infty$	0.1711	0.2314
2	0.1711	0.2314	0.2446	0.2547
3	0.2446	0.2547	0.2673	0.2756
4	0.2673	0.2756	0.2884	0.3394
5	0.2884	0.3394	∞	∞

fuzzy sets will be given by the number of categories that each measure can discriminate (shown in Table I).

In this paper, the trapezoidal function given by equation (1) is used for defining each membership function $\widetilde{T}_k^i(x)$. In addition, a fuzzy partition in the sense of Ruspini is proposed. Figure 3 shows some examples of the type of fuzzy partition used.

To establish the value of the parameters b_k^i and c_k^i, that define the kernel of the trapezoidal membership function associated to the fuzzy set $\widetilde{T}_k^i$, we propose a solution based on the multiple comparison tests used in section II-C. As it is known, in these tests confidence intervals around the representative value of each class are calculated (being accomplished that these intervals do not overlap for distinguishable classes). All values in the interval are considered plausible values for the estimated mean. These confidence intervals are defined by the parameter $\Psi_i^k = 1.96\bar{\sigma}_i^k/\sqrt{||C_i^k||}$, with $\bar{c}_i^k$ and $\bar{\sigma}_i^k$ being the representative value and the estimated standard deviation for the class C_i^k, respectively. Table I shows the values Ψ_i^k for each measure and each class.

Based on this idea, we propose to set the center of the kernel of the membership function $\widetilde{T}_k^i(x)$ as the representative value $\bar{c}_i^k$ of the corresponding i-th class, using the information of the confidence interval to obtain the value of the parameters b_k^i and c_k^i:

$$b_k^i = \bar{c}_i^k - \Psi_i^k \qquad c_k^i = \bar{c}_i^k + \Psi_i^k \tag{4}$$

Since a fuzzy partition in the sense of Ruspini is proposed, the value of the parameters a_k^i and d_k^i is obtained as

$$a_k^i = c_k^{i-1} \qquad d_k^i = b_k^{i+1} \tag{5}$$

It should be noticed that $a_k^1 = b_k^1 = -\infty$ and $c_k^{N_k} = d_k^{N_k} = \infty$.

Figure 3 shows the graphical representation of the fuzzy partitions for the measures of correlation and ED (the ones with higher capacity to discriminate fineness classes), and Table II shows their corresponding parameters.

III. RESULTS

In this section, the fuzzy partition defined for the measure "Correlation" (showed in Figure 3) will be applied in order to analyze the performance of the proposed model.

Let's consider Figure 4(a) corresponding to a mosaic made by several images, each one with a different increasing degree of fineness. Figure 4(b-f) shows the membership degree to the fuzzy sets "very coarse", "coarse", "medium coarse", "fine" and "very fine", respectively, using the proposed model. For each pixel in the original image, a centered window of size 32×32 has been analyzed and its membership degree to each fuzzy set has been calculated. Thus, Figure 4(b) represents the degree in which the texture is perceived as "very coarse", with a white level meaning maximum degree, and a dark one meaning zero degree. It can be noticed that our model captures the evolution of the perception degrees of fineness.

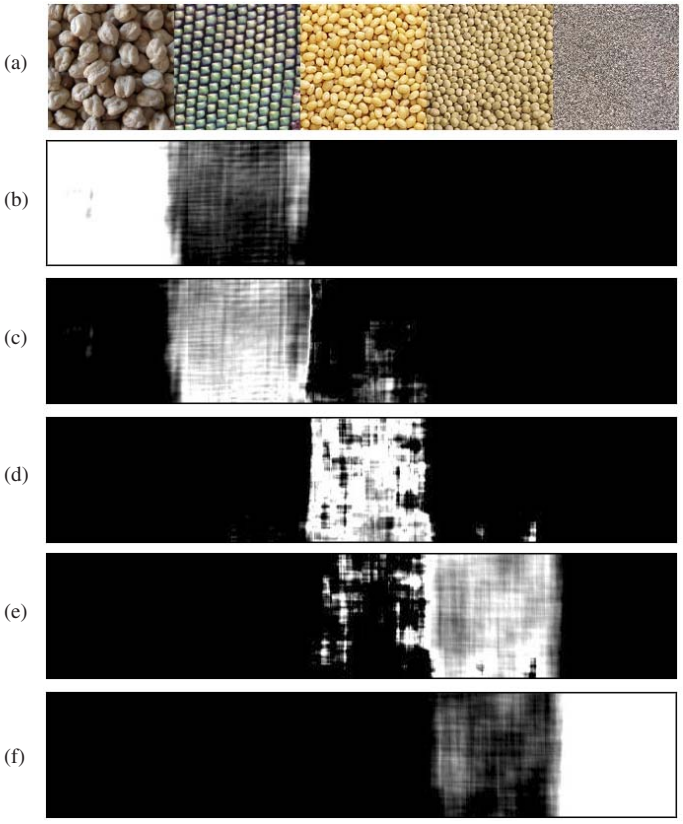

Figure 4. Results for a mosaic image. (a) Original image (b)(c)(d)(e)(f) Membership degree of each pixel to the sets "very coarse", "coarse", "medium coarse", "fine" and "very fine", respectively (the darker the pixel, the lower the membership degree).

Figure 5 presents an example where the proposed fuzzy partition has been employed for pattern recognition. In this case, Figure 5(a) shows a microscopy image corresponding to the microstructure of a metal sample. The lamellae indicates islands of eutectic, which are to be separated from the uniform light regions. The brightness values in regions of the original image are not distinct, so texture information is needed for extracting the uniform areas. This fact is showed in Figures 5(b) and 5(c), where a thersholding on the original image is displayed (homogeneous regions cannot be separated from the textured ones as they "share" brightness values). Figure 5(d) shows a mapping from the original image to its membership degree to the fuzzy set associated "very coarse". Thus, Figure 5(d) represents the degree in which the texture is perceived as "very coarse" and it can be noticed that uniform regions

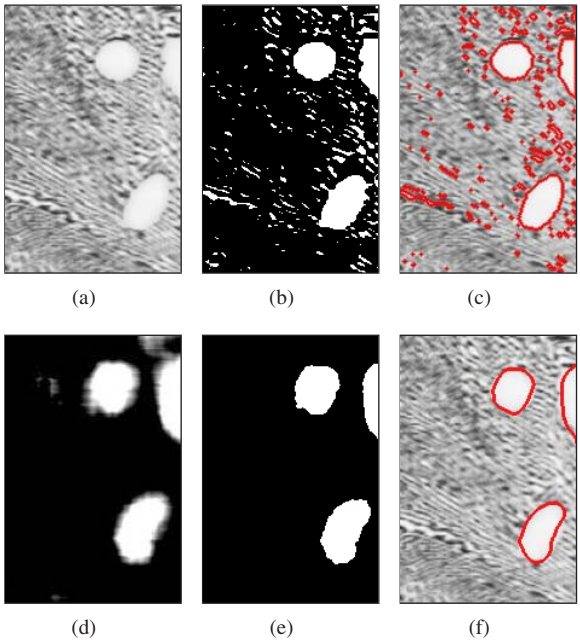

Figure 5. Example of pattern recognition (a) Original image (b) Binary image obtained by thresholding the original one (c) Region outlines of *b* superimposed on original image (d) Membership degrees to the set "very coarse" obtained with our model from the original image (e) Binary image obtained by thresholding *d* (f) Region outlines of *e* superimposed on original image.

correspond to areas with the maximum degree (bright grey levels), so if only the pixels with degree upper than 0.9 are selected (Figure 5(e)), the uniform light regions emerge with ease (Figure 5(f)).

Figure 6 presents another example of the application of the proposed fuzzy partition for pattern recognition. Figure 6(a) shows the natural image used in this example, that corresponds to a microscopic image of a Volvox (a colony of greencells). In this case, we want to separate the main colony from the background and the daughter colonies from the mother colony. As in the previous example, this can not be done by thresholding on the original image, as it is shown in Figure 6(b), so texture information is needed. Figures 6(c), 6(d) and 6(e) shows the mapping from the original image to its membership degree to the fuzzy sets "very fine", "medium coarse" and "very coarse", respectively. It can be noticed that daughter colonies in Figure 6(a) correspond to areas with high degrees of fineness, so they can be obtained by selecting the pixels with membership degree higher than 0.9 to the fuzzy set "very fine". On the other hand, the main colony can be separated from the uniform background as in the previous example (with a threshold of 0.9 in the membership degree to the fuzzy set "very coarse"), obtaining the region outlines shown in Figure 6(f)

IV. Conclusions and Future Works

In this paper, a fuzzy partition for representing the fineness concept have been proposed. The number of fuzzy sets and

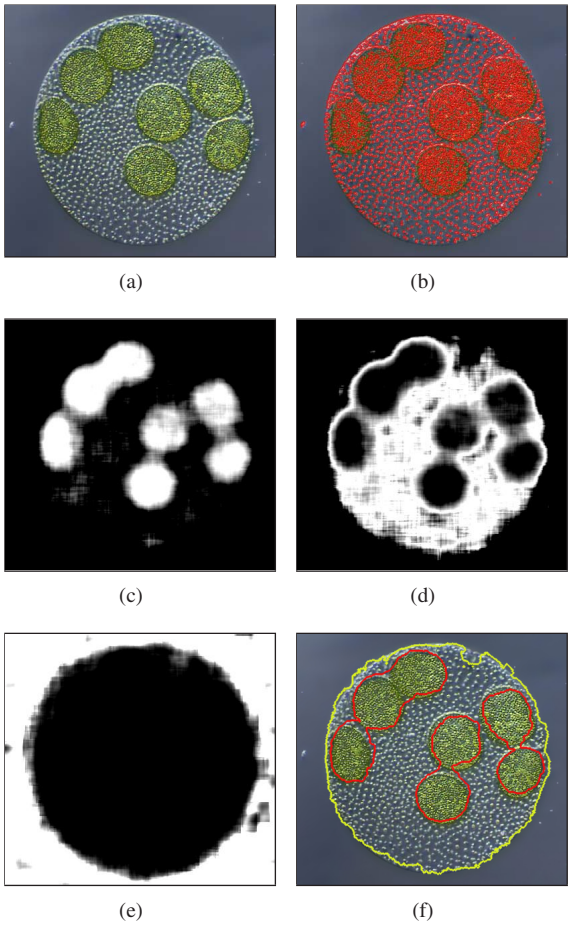

Figure 6. Results for a microscopy image. (a) Original image (b) Thresholding performed on *a* superimposed on original image (c)(d)(e) Membership degrees to the sets "very fine", "medium coarse" and "very coarse", respectively (f) Thresholding performed on *c* and *e* superimposed on original image.

the parameters of the membership functions have been defined relating fineness measures with the human perception of this texture property. Pools have been used for collecting data about the human perception of fineness, and the capability of each measure to discriminate different fineness degrees has been analyzed. The results given by our approach show a high level of connection with the human perception of fineness. As future work, the performance of the fuzzy partition will be analyzed in applications like textural classification or segmentation.

Acknowledgment

This work has been partially supported by the Spanish Government under the TIN2009-08296 and Consolider Ingenio 2010 MIPRCV (CSD2007-00018) projects.

References

[1] C. Jacobs, A. Finkelstein, and D. Salesin, "Fast multiresolution image querying," in *Proc. Computer Graphics, Annual Conference Series*, 1995, pp. 277–286.

[2] S. Belongie, C. Carson, H. Greenspan, and J. Malik, "Color- and texture-based image segmentation using expectation-maximization and its application to content-based image retrieval," in *Proc. 6th International Conference on Computer Vision*, 1998, pp. 675–682.

[3] R. Haralick, "Statistical and structural approaches to texture," *Proceedings IEEE*, vol. 67, no. 5, pp. 786–804, 1979.
[4] M. Amadasun and R. King, "Textural features corresponding to textural properties," *IEEE Transactions on Systems, Man and Cybernetics*, vol. 19, no. 5, pp. 1264–1274, 1989.
[5] H. Tamura, S. Mori, and T. Yamawaki, "Textural features corresponding to visual perception," *IEEE Trans. on Systems, Man and Cybernetics*, vol. 8, pp. 460–473, 1978.
[6] M. Hanmandlu, V. K. Madasu, and S. Vasikarla, "A fuzzy approach to texture segmentation," in *Proc. International Conference on Information Technology: Coding and Computing*, vol. 1, 2004, pp. 636–642.
[7] A. Barcelo, E. Montseny, and P. Sobrevilla, "Fuzzy texture unit and fuzzy texture spectrum for texture characterization," *Fuzzy Sets and Systems*, vol. 158, pp. 239–252, 2007.
[8] J. Chamorro-Martinez, E. Galan-Perales, J. Soto-Hidalgo, and B. Prados-Suarez, "Using fuzzy sets for coarseness representation in texture images," in *Proceedings IFSA'07*, 2007, pp. 783–792.
[9] S. Kulkarni and B. Verma, "Fuzzy logic based texture queries for cbir," in *Proc. 5th International Conference on Computational Intelligence and Multimedia Applications*, 2003, pp. 223–228.
[10] H. Lin, C. Chiu, and S. Yang, "Finding textures by textual descriptions, visual examples, and relevance feedbacks," *Pattern Recognition Letters*, vol. 24, no. 14, pp. 2255–2267, 2003.
[11] P. Wu, Y. M. Ro, C. S. Won, and Y. Choi, "Texture descriptors in mpeg-7," in *Proceedings of the 9th International Conference on Computer Analysis of Images and Patterns*, ser. CAIP '01. Springer-Verlag, 2001, pp. 21–28.
[12] B. S. Manjunath, *Introduction to MPEG-7, Multimedia Content Description Interface*, P. S. B. S. Manjunath and T. Sikora, Eds. John Wiley and Sons, Ltd., Jun 2002.
[13] B. Manjunath, J.-R. Ohm, V. Vasudevan, and A. Yamada, "Color and texture descriptors," *Circuits and Systems for Video Technology, IEEE Transactions on*, vol. 11, no. 6, pp. 703 –715, June 2001.
[14] H. Lin, C. Chiu, and S. Yang, "Finding textures by textual descriptions, visual examples, and relevance feedbacks," *Pattern Recogn. Lett.*, vol. 24, pp. 2255–2267, October 2003.
[15] J. Canny, "A computational approach to edge detection," *IEEE Transactions on Pattern Analysis and Machine Intelligence*, vol. 8, no. 6, pp. 679–698, 1986.
[16] N. Abbadeni, N. Ziou, and D. Wang, "Autocovariance-based perceptual textural features corresponding to human visual perception," in *Proc. of 15th International Conference on Pattern Recognition*, vol. 3, 2000, pp. 901–904.
[17] S. Peleg, J. Naor, R. Hartley, and D. Avnir, "Multiple resolution texture analysis and classification," *IEEE Transactions on Pattern Analysis and Machine Intelligence*, no. 4, pp. 518–523, 1984.
[18] J. Weszka, C. Dyer, and A. Rosenfeld, "A comparative study of texture measures for terrain classification," *IEEE Trans. on SMC*, vol. 6, pp. 269–285, 1976.
[19] S. Kim, K. Choi, and D. Lee, "Texture classification using run difference matrix," in *Proc. of IEEE 1991 Ultrasonics Symposium*, vol. 2, December 1991, pp. 1097–1100.
[20] H. Yoshida, D. Casalino, B. Keserci, A. Coskun, O. Ozturk, and A. Savranlar, "Wavelet-packet-based texture analysis for differentiation between benign and malignant liver tumours in ultrasound images," *Physics in Medicine and Biology*, vol. 48, pp. 3735–3753, 2003.
[21] S. Newsam and C. Kammath, "Retrieval using texture features in high resolution multi-spectral satellite imagery," in *Data Mining and Knowledge Discovery: Theory, Tools, and Technology VI, SPIE Defense and Security*, April 2004.
[22] C. Sun and W. Wee, "Neighboring gray level dependence matrix for texture classification," *Computer Vision, Graphics and Image Processing*, vol. 23, pp. 341–352, 1983.
[23] M. Galloway, "Texture analysis using gray level run lengths," *Computer Graphics and Image Processing*, vol. 4, pp. 172–179, 1975.
[24] R. Yager, "On ordered weighted averaging aggregation operators in multicriteria decisionmaking," *IEEE Trans. on SMC*, vol. 18, no. 1, pp. 183–190, 1988.
[25] Y. Hochberg and A. Tamhane, *Multiple Comparison Procedures*. Wiley, 1987.

2011 IEEE International Conference on Fuzzy Systems
June 27-30, 2011, Taipei, Taiwan

Educational System with the Android Robot SAYA and Field Trial

Takuya Hashimoto and Hiroshi Kobayashi
Department of Mechanical Engineering
Faculty of Engineering, Tokyo University of Science
Tokyo, Japan
{tak, hiroshi}@kobalab.com

Naoki Kato
Department of Mechanical Engineering
Graduate School of Engineering, Tokyo University of Science
Tokyo, Japan
kato@kobalab.com

Abstract— **Communication robots are hard to interact with humans autonomously in everyday environment due to lack of intelligence even though robots can perform certainly only in limited environments and limited situations. However, since intelligence of robots is handled by an operator, tele-operated robots are useful to investigate functions required for robots and effects of robots in real-environment. This paper proposes an educational system with a tele-operated android robot that has human-like appearance. The developed android robot, named SAYA, is able to express human-like facial expressions and performs some communicative functions with its head and eye movements, and it is utilized as a roll of a teacher in the proposed educational system. In addition, SAYA's utterances and behaviors are controlled remotely by an operator so that it is able to not only conduct the class but also interact with students. A field trial was carried out at an elementary school, and SAYA conducted the class concerning the principle of leverage as a topic of science classes while interacting with students. Also, how it affected students' interest and motivation was investigated. As results, the trial verified that some students became interested in science class more than before the trial, and its positive effects in educational field, especially elementary schools, were verified.**

Keywords-android robot; remote class system; educational robot; field trial; human-robot interaction

I. INTRODUCTION

In the last decade, various kinds of robots which offer services in daily environment through interactions with humans have been developed and studied. In the near future, robots are expected to be able to offer not only physical supports but also informative and emotional supports. For that purpose, it is very interesting to investigate what kinds of functions, mechanisms, and intelligence are required for robots, and investigate how robots should interact with human in daily environment. Thus, many kinds of communication robots have been developed and applied to not only laboratories but also our daily lives [1]-[6]. For example, the pet-type robot, named AIBO [1], was commercialized around ten years ago, and it can act in our living space. A seal type robot was also developed as a mental therapy robot and its effectiveness for elderly people was verified by being utilized in nursing-care facilities [2]. These kinds of animal-type robots interact with humans emotionally by performing endearing movements. On the other hand, humanoid-type robots have been developed, which have human-like properties such as a head and arms to express more human-like behaviors. Thus, in humanoid-type robot researches, they utilize bodily movements such as gestures, nodding, eye-orientation, and facial expressions as non-verbal behaviors to interact with humans naturally [3]-[7]. For example, Robovie [3]-[5] interacts with humans and offers informative services by utilizing its human-like physical structure, and it was actually used at real-environment such as a train station, a museum, and an elementary school. However since intelligence technologies for robots are still impractical, robots cannot interact with human autonomously even though they can perform effectively in limited environments or limited situations. On the other hand, it is expected that tele-operated robots are applicative as an interface of telecommunication system rather than autonomous robots because their intelligence is handled by human operator. That is, in tele-operated robot, an operator enables a robot to interact with human by controlling robot's behaviors and utterances remotely without advanced intelligence technologies.

In this paper, a remote class support system is proposed as a one of applications of telecommunication system in which a robot is used as an interface. Especially, android type communication robot SAYA [8][9] which has human-like appearance is utilized in the proposed system, and it can interact with humans with human-like body movements such as facial expressions, head movements, and eye-orientation. Actually, Sakamoto et al. [10] verified effectiveness of the tele-operated android robot on conveying presence of a human who was in different place rather than existing media such as a speaker or a video-conference system. To investigate its effectiveness for children in elementary schools is also interesting, because children were interested in learning with a robot and they were motivated to learn a foreign language as shown in previous research [5] in which the robot interacted with children by speaking only English. Hence, the remote class support system with the android robot SAYA is also expected to contribute to children's motivation to learn. Thus, a science class is conducted for children at an elementary school with the proposed system to investigate its effectiveness on children's interest and motivation through this trial.

The structure of this paper is as follows. In Section 2, the android robot SAYA and its communicative functions are introduced. Section 3 describes the system structure of the

Japan Society for the Promotion of Science *(JSPS)*

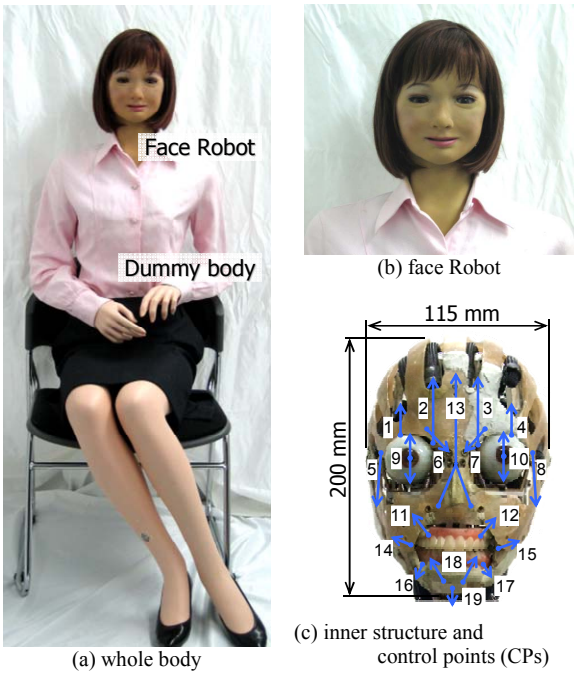

Figure 1. Android Robot SAYA

remote class support system with SAYA and the detailed content of the class. In section 4, detailed procedure of a field trial and its results are presented. In final section 5, the contributions of this research are discussed, and this paper is conluded.

II. ANDROID ROBOT SAYA

Fig. 1 shows SAYA which has been developed as one of android-type communication robots. The face robot [9][11] is mounted on a dummy body and it is highly realistic appearance. SAYA is also used as an interface of receptionist system at a university [8], which equips a speech dialogue function and some non-verbal communicative functions such as facial expressions, head movements, and eye-orientation.

A. Facial Expressions with the Face Robot

In human face-to-face communication, facial expressions are said to play a very important role as one of non-verbal communication [12]. Facial expressions are expected to contribute to realize smooth communication between humans and robots. Therefore highly realistic face robots that resembles to human-like face have been developed, and it can express facial expressions [9][11]. Almost all related studies of producing facial expressions are based on "action unit" that is defined in FACS (Facial Action Coding System) [13]. Action units express motions of mimic muscles as 44 kinds of basic motions, and there are 14 action units to express 6 typical facial expressions. Referring to these studies, 19 control points and their directions on the face robot are modeled as shown in Fig. 1(c). By combining movements of control points, various facial expressions are realized with the face robot. Fig. 2 shows examples of 6 typical facial expressions of the face robot, and the face robot succeeded in achieving high correct recognition rate of these facial expressions in previous study [9].

Figure 2. Examples of SAYA's facial expressions

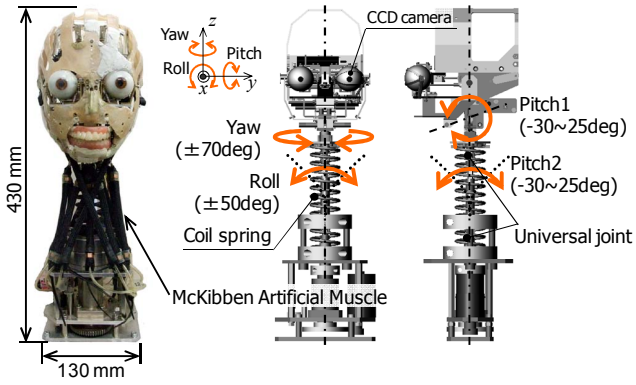

Figure 3. Mechanical structure of SAYA

In the face robot, McKibben artificial muscles are utilized to actuate control points. Since it is small, lightweight and flexible, it can be distributed to curved surfaces of the skull like human muscles.

The facial skin is formed with soft urethane resin to mimic the texture of human facial skin.

B. Eye and Head Movements

Figs. 1(b) and 3 show the internal structure of the face robot. There are 2 DOF for eye movements. Two eyeballs are linked mutually and two DC motors move both pitch and yaw rotations of eyeballs. In addition, a small CCD camera is mounted to the inside of an eyeball to obtain images of SAYA's view point. The eye orientation is also able to be controlled by extracting human skin color region from image of the CCD camera so that the face robot can track a human.

There are 4 DOF for head movements. In order to mimic flexible neck movements of a human cervical spine, we utilize a coil spring in the neck part. Furthermore, the center of rotations for pitch rotation ("Pitch1") and yaw rotation are set in the base of the head part. The forward and backward motions are realized by combining the head rotation ("Pitch1") and the neck bending ("Pitch2"). The roll-rotation, both pitch-rotations ("Pitch1" and "Pitch2") and the yaw-rotation are also actuated by McKibben artificial muscles as shown in Fig. 3.

We use electro-pneumatic regulators for controlling contraction of McKibben artificial muscle.

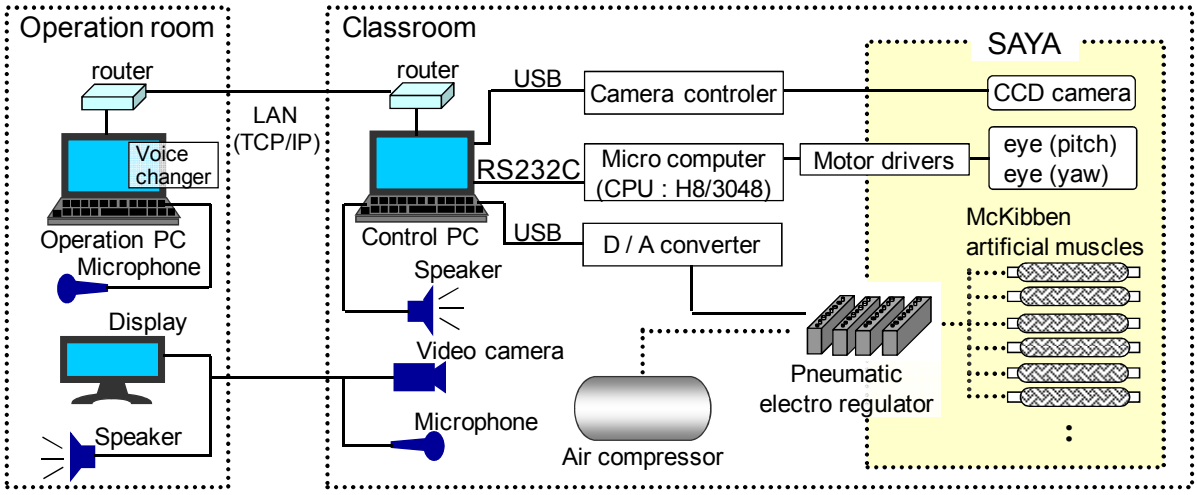

Figure 4. System configuration

III. Remote Class Support System with the Android Robot SAYA

A. System Configuration

Fig. 4 shows the system configuration of the developed remote class support system, and the android robot SAYA is utilized as the interface and it plays the role of a teacher.

In a classroom, there are SAYA, control PC, and some control equipment. An air compressor and an electro-pneumatic regulator are used to control contraction of McKibben artificial muscle. A microphone and a video camera are also used to obtain visual and sound information of a classroom.

In an operation room, one monitor is used for an operation, and the other one is used for an observation. The operator is able to monitor students' behaviors through observation monitor, and he can control SAYA's behaviors by sending commands to the control PC through the operation PC. Commands of the operation PC are delivered to the control PC through the LAN. Then, the control PC executes robot's behaviors based on received commands. For example, captured images of the SAYA's CCD camera and the video camera are transmitted to the operation PC, and the operator can observe the classroom from both viewpoints of the robot and the rearward. Then, the operator can move the SAYA's viewpoint by controlling its eye and head orientations using this visual information. As a result, SAYA is able to look around a classroom and look at a specific student.

The operator is also able to hear students from speakers and talk to students. Operator's voice is changed to women's voices through a voice-changer as SAYA's voice.

B. Interactive Behaviors

In this system, there are two operation modes that are "lecture mode" and "interaction mode".

In "lecture mode", the operator gives students explanations about slides displayed at the front of a classroom through SAYA. The operator speaks sentences that were prepared based on lecture content. SAYA's mouth is moved in synchronization with sound information of operator's voice, and SAYA looks around a classroom while talking.

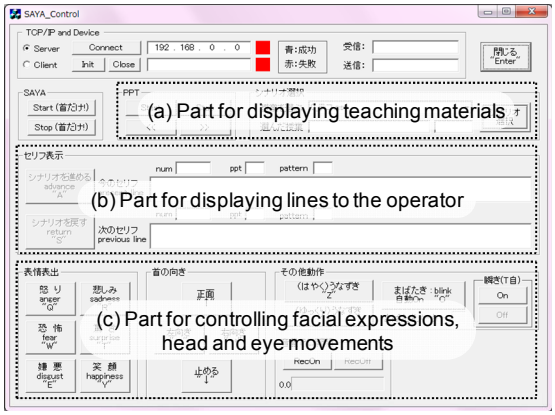

Figure 5. Operation interface

In "interaction mode", the operator controls SAYA's head and eye orientations to let SAYA look around a room and look at a student. The operator also talks to students through SAYA to answer students' talks and questions. In addition, he sometimes says short words to encourage students to concentrate on the class such as "do your best", "be quiet", "don't look away" and so on. The operator also executes to appropriate facial expressions according to its utterance. For example, when he says "be quiet", he executes facial expression "anger".

Since behaviors of SAYA consist of simple movements, the operator can execute these interactive behaviors easily. Additionally, SAYA is basically performed by tele-operation. As a result, it seems to apparently conduct the class and interact with students autonomously.

C. Operation Interface

Fig. 5 shows the operation interface for the operator. It mainly consist 3 parts: (a) part for displaying teaching materials, (b) part for displaying lines to the operator, (c) part for controlling facial expressions, head and eye movements. In

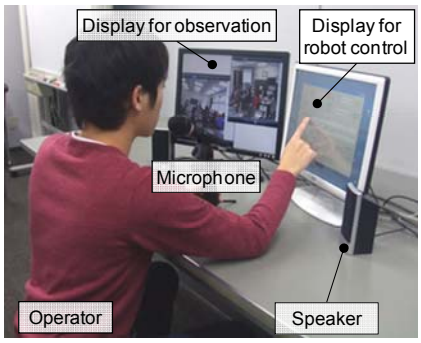

Figure 6. Operation room

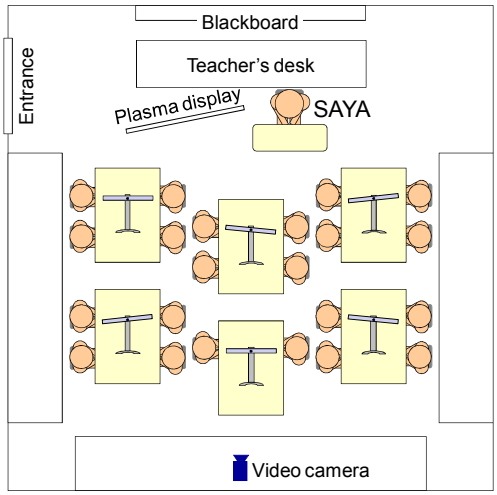

Figure 7. Experimental environment

part (a), there are some icons to change teaching materials that are displayed to a screen or a display. In part (b), lines that the operator should say are displayed in the text boxes. In part (c), there are many icons that are corresponding to robot's behaviors such as facial expressions, eye and head movements. An operator can easily control the robot by clicking these icons with a mouse or a touch panel as shown in Fig. 6.

D. *Content of Science Class*

The principle of leverage is adopted as a topic of the science class for elementary school students. This topic is said to be difficult for students because it contains both mathematical elements and experimental validations. In order to create teaching materials, science textbooks that are generally used in elementary schools are referred.

Table 1 shows the flow of the science class concerning the principle of leverage. First of all, self-introduction of the android robot SAYA is performed, and the class is opened. Then, SAYA explains the theory and mechanical advantages of leverage with some slides. In this scene, three important points of leverage are introduced. That is, a pivot point, a point of effort, and a point of load are explained. SAYA then shows familiar examples of leverage that are seen in our daily lives. For example, scissors, bottle-opener, tweezers, and so on are shown. After that, SAYA lets students experiment for discovering or confirming the principle of leverage with an experimental lever kit, and students are able to experience the

(a) experimental lever kit

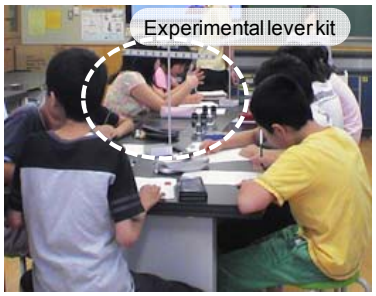

(b) photo of classroom

Figure 8. Photos of experimental environement

TABLE I. THE FLOW OF SCIENCE CLASS CONCERNING THE PRINCIPLE OF LEVERAGE

Scene	Contents
1	Self introduction of SAYA and opening the class.
2	Lecture on basic theories and mechanical advantages of leverage.
3	Lecture on familiar examples of leverage in daily lives.
4	Experiments for discovering and confirming the principle of leverage.
5	Conclusion of the class.

balancing theory of leverage. Finally, SAYA summarizes its talk and closes the class.

IV. FIELD TRIAL AT AN ELEMENTARY SCHOOL AND EVALUATION

A. *Setting*

A field trial at an elementary school was conducted to verify effectiveness of the developed educational system in actual educational fields. The trial was carried out after school, and it took about one hour. 22 students who were 10-11 years old and belonged to the fifth-grade class participated.

Fig. 7 shows experimental environment. We used a standard classroom, and we put SAYA on the front of the room as the role of a teacher. A plasma display was also put on the front of the room to display teaching-materials, and a video camera was put on the rearward to let the operator monitor the classroom. In addition, there was an experimental lever kit on each desk every four students as shown in Fig. 8.

Four students per a desk were made to sit on assigned positions. The position of each student had defined so that the operator could identify each student, and he could let SAYA look at a student and call a student's name individually.

B. *Experimental Procedure*

At the first, an experimenter let students sit down in assigned positions. He then explained the flow of this trial briefly and asked students to answer a brief questionnaire. After that, he exited the room and the operator began the science class by controlling SAYA. The science class was conducted along the scenario that had prepared based on content described in Table I. During the class, the operator sometimes talked to students. That is, the operator asked some questions or gave cautions and advices to students through

(a) SAYA explained to students and they concentrated on SAYA's talk

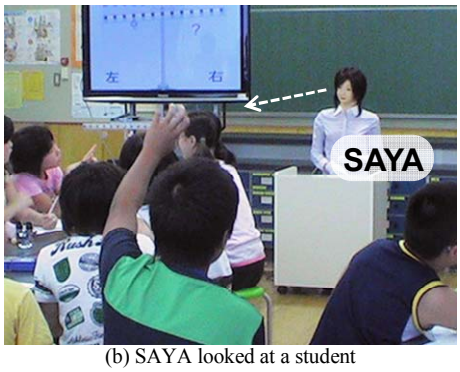

(b) SAYA looked at a student

(c) students raised their hand and attempted to answer a question

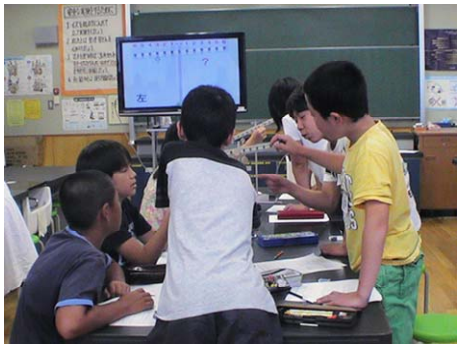
(d) students discovered and comfirmed the principle of leverage through the experiment with experimental lever kit

Figure 9. Scenes of the field trial in the elementary school

SAYA. After the class, the experimenter asked children to answer a questionnaire.

Fig. 9 shows scenes of the field trial in the elementary school. Fig. 9(a) shows the scene in which SAYA gave explanations about the leverage along the scenario, and students concentrated on hearing SAYA's talk and paid attention to the screen. SAYA sometimes looked at students and asked some questions as shown in Fig. 9(b). Fig. 9(c) shows the scene in which students raised their hand and attempted to answer a SAYA's question. In class, students experimented for discovering and confirming the principle of leverage with the experimental lever kit as shown in Fig. 9(d).

TABLE II. QUESTIONNAIRE AND RESULTS OF Q. 1 TO Q. 12

	Questionnaire	Result (ave. (s.d.))
Q.1	Are you interested in science and technology?	1.00 (0.87)
Q.5		1.36 (1.00)
Q.2	Do you prefer science classes?	0.73 (1.08)
Q.6		1.45 (0.74)
Q.3	Are you interested in robots?	1.09 (1.15)
Q.7		1.36 (1.09)
Q.4	Are you interested in a class conducted by robots?	1.27 (0.94)
Q.8		1.50 (0.96)
Q.9	Were you able to concentrate on the class more than usual?	0.55 (1.30)
Q.10	Was the class easy to understand?	1.45 (0.86)
Q.11	Do you want to participate in the class again if you have opportunity?	1.09 (1.23)
Q.12	Did SAYA answer you correctly? (yes / no)	yes: 17, no : 5

C. *Questionnaire Investigation for Evaluation*

In order to evaluate the developed educational system, the questionnaire was prepared to investigate how students' interest and motivation were affected through this experiment. Therefore, questionnaire investigations were conducted before and after the class. Tables II shows the questionnaire that consisted of 12 questions (Q.1 - Q.12). First 4 questions (Q.1 - Q.4) were used for the investigation before the class as the brief questionnaire, and last 8 questions (Q.5 - Q.12) were used after the class. Each question was evaluated on a scale of -2 to 2 except Q.12, where 2 is most positive evaluation. Only Q.12 was evaluated with "yes" or "no". Moreover, Q.1 and Q.5 (interest in science and technology), Q.2 and Q.6 (interest in science classes), Q.3 and Q.7 (interest in robots), Q.4 and Q.8 (interest in a class conducted by robots) are same question. Their results are compared to estimate the contrast of students' interest and motivation between before and after the experimental science class.

D. *Questionnaire Results*

Table II also shows averages (ave.) of Q.1 to Q.11, and numbers provided in parentheses are standard deviations (s.d.). The numbers of respondents who answered "yes" or "no" in Q.12 are also shown. In addition, Fig. 10 shows comparisons between Q.1 and Q.5, Q.2 and Q.6, Q.3 and Q.7, Q.4 and Q.8. In Tables II, we can find that students' interest and motivation were affected through this experiment. That is, evaluation

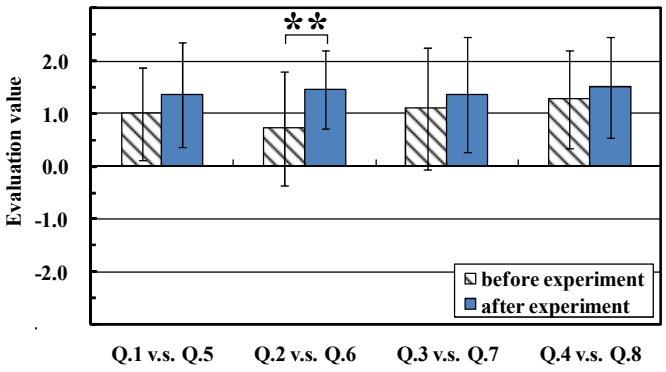

Figure 10. Comparisons between paired questions (Q.1 and Q.5, Q.2 and Q.6, Q.3 and Q.7, Q.4 and Q.8)

values of Q.1, Q.2, Q.3, and Q.4 are higher than values of Q.5, Q.6, Q.7, and Q.8 respectively. Wilcoxon signed-rank test was also applied to each pair, and its results are shown in Fig. 10. The results revealed a significant difference in the pair of Q. 2 and Q.6 ($p < .01$). Therefore, the class conducted with SAYA enhanced students' interest in science classes.

In addition, it is confirmed that concentration of students was low because evaluation value of Q.9 (concentration on the class) is relatively lower than those of other questions. The results of Q.10 and Q.11 indicate that students could understand SAYA's explanations and teaching materials easily, and students wanted to participate in the classes again. In Q.12, 17 of 22 students answered "Yes". That is, it is confirmed that the operator replied to them correctly through SAYA.

V. CONCLUSION

In this paper, a remote class support system was proposed as a one of applications of telecommunication system in which the android robot SAYA was used as an interface. SAYA has human-like appearance and can interact with humans with human-like body movements such as facial expressions, head movements, and eye-orientation. A remote control system of SAYA was also developed for the remote class support system, and this system allows an operator to control SAYA's behaviors and observe students' behaviors remotely. In addition, the principle of leverage was adopted as the topic of a science class, and the scenario of the class concerning that topic was made. Then, the science class with SAYA was carried out in an elementary school to investigate how the proposed educational system affects students' interest and motivation.

Results of field trial reveal that students came to like science class. That is, it is expected that this system enhanced students' interest in science classes. However, other students' interest and motivation (interest in science and technology, interest in robots, and interest in a class conducted by robots) were not affected significantly even though their evaluation values were higher than before the trial.

Our future work is to investigate how students' attributions (familiarity with robots, science classes, and science and technology) affect to changes of their interest and motivation through experience of the class conducted by SAYA. In addition, various topics of science classes will be prepared, and the proposed educational system should be compared with other existing media such as video-conference system. Also, it would be interesting to investigate contrasts between the proposed educational system and human teacher.

ACKNOWLEDGMENT

This research was partially supported by Japan Society for the Promotion of Science (JSPS), Grant-in-Aid for Young Scientists (Start-up), 21800058, 2009.

REFERENCES

[1] M. Fujita, "AIBO: towards the era of digital creatures", International Journal of Robotics Research, Vol. 20, No. 10, pp. 781–794, 2001.

[2] K. Wada, T. Shibata, T. Saito and K. Tanie, "Analysis of factors that bring mental effects to elderly people in robot assisted activity", Proceedings of IEEE/RSJ International Conference on Intelligent Robots and Systems, Vol. 2, pp. 1152-1157, 2002.

[3] K. Hayashi, D. Sakamoto, T. Kanda, M. Shiomi, S. Koizumi, H. Ishiguro, T. Ogasawara and N. Hagita, "Humanoid robots as a passive-social medium - a field experiment at a train station -", Proceedings of ACM/IEEE 2nd Annual Conference on Human-Robot Interaction , pp. 137-144, 2007.

[4] M. Shiomi, T. Kanda, H. Ishiguro, and N. Hagita, "Interactive Humanoid Robots for a Science Museum", IEEE Intelligent Systems, Vol. 22, No. 2, pp. 25-32, 2007.

[5] T. Kanda, T. Hirano, D. Eaton, H. Ishiguro, "Interactive Robots as Social Partners and Peer Tutors for Children: A Field Trial", Human Computer Interaction, Vol. 19, No. 1-2, pp. 61-84, 2004.

[6] T. Watanabe, M. Okubo and H. Ogawa, An Embodied Interaction Robots System Based on Speech, Proceedings of the 8th IEEE International Workshop on Robot and Human Communication (RO-MAN'99), pp. 225-230, 1999.

[7] C. Breazeal and B. Scassellati, How to build robots that make friends and influence people, Proceedings of Inteligent Robots Systems (IROS '99), pp. 858-863, 1999.

[8] T. Hashimoto and H. Kobayashi, Development of the receptionist system with an anthropomorphism face, Proceedings of the 5th Asian Symposium on Applied Electromagnetics And Mechanics, pp. 190-196, 2005.

[9] T. Hashimoto, S. Hiramatsu, T. Tsuji and H. Kobayashi, Development of the Face Robot SAYA for Rich Facial Expressions, Proceedings of SICE-ICASE International Joint Conference 2006, pp. 5423-5428, 2006.

[10] D. Sakamoto, T. Kanda, T. Ono, H. Ishiguro, N. Hagita, Android as a telecommunication medium with a human-like presence, Proceedings of the ACM/IEEE international conference on Human-robot interaction, pp. 193-200, 2007.

[11] H. Kobayashi and F. Hara, Study on face robot for active human interface-mechanisms of face robot and expression of 6 basic facial expressions, Proceedings of 2nd IEEE International Workshop on Robot and Human Communication (RO-MAN'93), pp. 276-281, 1993.

[12] A. Mehrabian, Communication without Words, Psychology Today, Vol. 2, No. 4, pp.53-55, 1968.

[13] P. Ekman, and W. V. Friesen, The Facial Action Coding System, Consulting Psychologists Press, 1978.

2011 IEEE International Conference on Fuzzy Systems
June 27-30, 2011, Taipei, Taiwan

Multimodal Gesture Recognition Based on Choquet Integral

K. Hirota[1)], H. A. Vu[1)], P. Q. Le[1)], C. Fatichah[1)], Z. Liu[1)], Y. Tang[1)], M. L. Tangel[1)], Z. Mu[1)], B. Sun[1)], F. Yan[1)], D. Masano[1)], O. Thet[1)], M. Yamaguchi[1)], F. Dong[1)], and Y. Yamazaki[2)]

[1)]Dept. of Computational Intelligence & Systems Science,
Tokyo Institute of Technology
Yokohama, Japan
{ hirota, vuanhai, phuclq, chastine, liuzhentao,tang, martin, mu, sun, yan, masano, thetoohan, yamaguchi, tou }@hrt.dis.titech.ac.jp

[2)]Dept. of Electrical, Electronic, and Information Eng.
Kanto Gakuin University
Yokohama, Japan
yamazaki@ kanto-gakuin.acwq43.jp

***Abstract*— A multimodal gesture recognition method is proposed based on Choquet integral by fusing information from camera and 3D accelerometer data. By calculating the optimal fuzzy measures for the camera recognition module and the accelerometer recognition module, the proposal obtains enough recognition rate 92.7% in average for 8 types of gestures by improving the recognition rate approximate 20% compared to that of each module. The proposed method aims to realize the casual communication from humans to robots by integrating nonverbal gesture messages and verbal messages.**

Keywords- Gesture Recognition; Sensor Fusion; Choquet Integral; Human-Robot Interaction; 3D Accelerometer

I. INTRODUCTION

Recognition of human motions is greatly needed for communication between humans and robots in social robot systems such as service robots, entertainment robots, and household robots, that need to assist human with hospitality attitude in daily life. The casual communication robotic system, e.g., mascot robot system [1, 2], has been proposed based on verbal information to assist human in living environment. As for nonverbal approaches, gesture recognition has recently become attractive research themes in the field of Human-Computer Interaction (HCI) for robotics [3], human behavior studies [4], emotion [5] and sign language [6] recognition, and virtual environment navigation [7]. Most works on the gesture recognition for HCI have been done based on visual information, in terms of Hidden Markov Models(HMM) [8], Dynamic Time Warping(DTW) [9], and Self Organizing Markov Map(SOMM) [10]. Camera based human gesture recognition system often gets moving information of body parts (hands and head) by applying skin color tracking method. It is, however, easy to have a noise effect by the object that has similar color of the skin [11]. On the other hand, application of accelerometer data to gesture recognition is an emerging technique to improve recognition performance. A wearable acceleration sensor based air writing system that recognizes the gestures of writing alphabets is proposed in [12].

A multimodal gesture recognition system is proposed in [13], where information of both 3D acceleration and image are combined based on fuzzy logic. In the study, when the similarity calculated from the acceleration recognition modules is greater than given threshold value, the recognition result from the accelerometer module is taken as the final result. In reverse, image recognition module processes the candidate gestures that come from acceleration module to get final result. They, however, have not discussed about how to decide the given threshold. So, it is difficult to use the method for other cases of gestures in general.

To improve the robustness of [13], a Choquet integral[14] based multimodal gesture recognition method is proposed, where human gestures are recognized based on the fusion of video images and 3D acceleration sensors. The Angular Metrics for Shape Similarity (AMSS) [15] algorithm is employed to evaluate the similarity between gesture templates and input data from above two modules separately. Next, the optimal fuzzy measures of Choquet integral are calculated from the training data by a hill climbing algorithm. In the fusion processing, the fused similarities are calculated from similarities of both modules by Choquet integral. Finally, the gesture with maximum fused similarity is chosen as the recognition result.

In II, the multimodal gesture recognition system based on camera and 3D accelerometers is proposed. The experiments to confirm the proposal and discussion are presented in III.

II. MULTIMODAL GESTURE RECOGNITION SYSTEM

The architecture of the proposed gesture recognition system is shown Fig. 1.

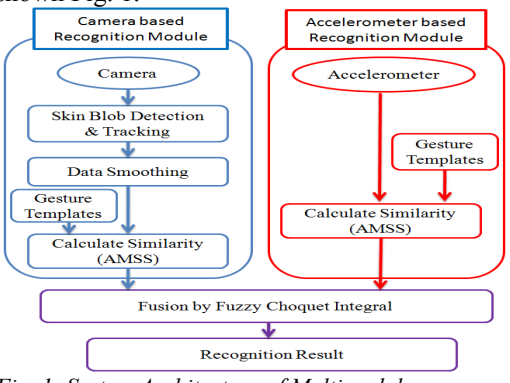

Fig. 1: System Architecture of Multimodal Gesture Recognition System

The system consists of two modules, i.e., camera based gesture recognition module and accelerometers based gesture recognition module.

A. Camera based Gesture Recognition Module

1) Skin Blob Detection and Tracking

The skin blob detection and tracking module uses the HSV color space because the HSV color space is suitable for detecting human's skin color. A pixel's color is identified as the skin color if the HSV value of this pixel exists in certain color ranges set in advance. The possible range of skin color, however, is changed according to the environment, and the final assigned range in the experiment is $2 \le H \le 14$, $65 \le S \le 180$, and $20 \le V \le 250$ by using OpenCV Library. It is confirmed that the three regions of the head and two hands parts are detected in the skin blob detection processing module.

The detected blobs are labeled from the first frame, i.e., the blobs in the left side and right side of the frame are labeled as hands, and the blob between two hands is labeled as head. From the second frame on, the nearest blob to the blob in the previous frame will be marked as the same label.

2) Feature Extraction and Data Smoothing

To recognize gestures, the 2D locations of blobs' centers are used as the features. The locations of left hand, head, and right hand are denoted as $\{x_l, y_l\}$, $\{x_h, y_h\}$, and $\{x_r, y_r\}$, respectively.

In the feature extractions part, the following two processes are done on the raw data:

a) Data Smoothing: Simple moving average of 3 adjacent points is used to smooth raw data, i.e.,

$$x_{smoothing} = (x_{i-1} + x_i + x_{i+1}) /3, \quad (1)$$

where xi stands for the raw locations of blobs.

b) Quantization: The DTW (Dynamic Time Warping) algorithm mentioned in 3.1.4 is used for recognizing gestures. The complexity of the DTW algorithm is dependent on the length of the input sequence and template sequence. The short length of sequences contributes to the performance improvement of recognition. If the distance between a point and its nearest point of the trajectory is shorter than 10 pixels, the point is ignored; otherwise the point is added to the points' sequence of trajectory.

3) Camera based Gesture Recognition by AMSS

The Dynamic Time Warping (DTW) is widely used for matching time series by calculating the optimal distance between two time series based on dynamic programming. The Angular Metrics for Shape Similarity (AMSS) [15] algorithm is used to calculate the similarity between gesture sequence and template sequence, which is a robust improvement of DTW algorithm. Instead of calculating the distance of elements in conventional DTW, the AMSS takes the cosine value of the intersection angular of two trend vectors, which is computed by neighboring element of each time series, as the distance measurement. The warping path is computed through the whole distance matrix. The similarity of two time series is calculated as the average value of accumulated value on optimal warping path.

The AMSS algorithm is based on trend vectors which are scale-invariant, so it has the power for recognizing user-independent gestures. Besides, due to its efficiency and simplicity, the AMSS algorithm is selected as the main recognition algorithm.

The recognition rate of DTW based system is greatly dependent on the quality of the reference template. Accordingly selecting reliable template is one of the important tasks in the training process. There are several methods for template selection such as random selection, minimum selection, normal selection, and multiple selection [16]. After checking from the cost performance viewpoint, minimum selection is used to select the appropriate template for the gesture recognition.

B. Accelerometer based Gesture Recognition Module

Two 3D acceleration sensors are used for capturing the motion of human's two hands.

The sequence of feature values are taken as the input of the accelerometers based gesture recognition module. The AMSS is used for measuring the similarity of input sequence and template sequences. The average similarity of the 3-axes is taken as the similarity of this module.

C. Proposed Fusion Method based on Choquet integral

The information obtained from two accelerometers and a camera is different in accuracies and frequencies. This information is processed by different preprocessing and recognition algorithms. The recognition result comes from accelerometers and camera is not additive. Thus, a Choquet integral based method is proposed for fusing the similarity of accelerometers and camera based recognition modules.

The Choquet integral is proposed by Murofushi and Sugeno[14]. Let $S^a_{i,g,t}$ denotes the similarity between the i-th training data of g-th gesture and the t-th template sequence by the accelerometers based module, and $S^c_{i,g,t}$ the similarity calculated from the camera based module. M^c_g and M^a_g stand for the fuzzy measure of camera module and the accelerometer module of g-th gesture template separately. Then, the fused similarity calculated by Choquet integral [14] is shown as

$$C_{i,g,t}\left(S^c_{i,g,t}, S^a_{i,g,t}, M^c_g, M^a_g\right) = \begin{cases} S^a_{i,g,t} + (S^c_{i,g,t} - S^a_{i,g,t}) \times M^c_g, if\,(S^c_{i,g,t} \ge S^a_{i,g,t}) \\ S^c_{i,g,t} + (S^a_{i,g,t} - S^c_{i,g,t}) \times M^a_g, if\,(S^c_{i,g,t} < S^a_{i,g,t}) \end{cases} . \quad (2)$$

The difference of similarity error between i-th training data of g-th gesture and the misrecognized gesture is calculated as

sponsor*(JSPS: Japan Society for the Promotion of Science)*

$$f\left(i,g,M_1^a,M_1^c,...,M_G^a,M_G^c\right) = \max_{k\in\{1,...,T\}}\{C_{i,g,k}\} - C_{i,g,g} \quad , \quad (3)$$

where G denotes the number of gesture, and T is the number of templates.

Then, the problem of finding the optimal fuzzy measure $\left({}^*M_1^a, {}^*M_1^c,..., {}^*M_G^a, {}^*M_G^c\right)$ from all training data can be modeled as

$$\min_{\left(M_1^a,M_1^c,...,M_G^a,M_G^c\right)} \sum_{g\in\{1,...,G\}}\sum_{i\in\{1,...,TN\}} f\left(i,g,M_1^a,M_1^c,...,M_G^a,M_G^c\right), \quad (4)$$

where TN is the number of training data for each gesture.

The optimal fuzzy measure value of both modules cannot be calculated exactly, but it can be found approximately. A hill climbing based algorithm is employed to find the optimal fuzzy measure. The algorithm is demonstrated as follows:

Step-0: Initialize $\left(M_1^a,M_1^c,M_2^a,M_2^c,...,M_G^a,M_G^c,\right)$ randomly in the range of between 0 and 1 by uniform distribution.

Step-1: Calculate the fused similarity from the two modules by equation (2), and then calculate the recognition rate from the training data.

Step-2: Preserve current parameters if the recognition rate in step 1 is better than the best training rate before.

Step-3: For each gesture *g* in {1, 2, ..., G}, similarity error of all training data is calculated by changing the parameters and one step forward and backward as in equation (3). And then the minimum of these similarity errors is found.

Step-4: If the minimum similarity error calculated in step 3 is greater than the similarity error before parameter adjustment, then it has reached to the local minimum similarity error, so exit the loop.

Step-5: Update the changes if it is less than the current error, and go back to step 1.

III. Experiment on Multimodal Gesture Recognition

A. Experimental Environment

To demonstrate the validity and applicability, the proposed method is confirmed by using the gestures from the mascot robot system. The experiments on the mascot robot system are complex and require a lot of time, therefore, the authors here did the offline experiments on eight types of gestures, which are used in the mascot robot system.

The proposed method is implemented on each of notebook PCs with Intel® Core2Duo 2.54GHz, 2GB of RAM by using Visual C++ 2008 and OpenCV 2.1 library for video processing on Windows system. Two 3D accelerometers and a web camera are used to track movements of parts of a body in experiments. The wearable accelerometers (W=45mm, D=45mm, H=20mm), manufactured by Microstone Inc.[17], are used to get three dimensional acceleration data of human body movements in (x, y, z) 3D space, and the accelerometer transmits these 3D movement data via a Bluetooth connection. Each human participant wears accelerometer on his/her wrists as shown in Fig. 5. The video sequences are captured by a Logicool Qcam(R) Connect camera mounted on a notebook PC with 30 fps rate and 320x240 pixels resolution.

Eight gestures are employed in the home party scenario experiments. Each name and description of the eight gestures is;

(G1) Toast: Raising a hand with a glass upwards from the waist level.

(G2) Throw dart: Moving a hand with a dart forward speedily from the head level.

(G3) Victory pose: From the relaxed position besides legs, the right hand is raised up to a level between the chest and the head. (This motion expresses happiness when the dart hits the target.)

(G4) Banzai pose: Both hands are first put down besides legs and then both are held right up. (This motion expresses happiness when the dart hits the target.)

(G5) Squatting with hands over the head: From the relaxed position the besides legs, both hands are put on the head and human participant squats. (This expresses disappointment when the dart loses the target.)(Fig. 2)

Fig. 2: G5 (Squatting with hands over the head). The blue, red, green lines are the trajectory of the three body parts.

(G6) Face covering: Both hands are first put down besides legs and then right hand is held at face. (This expresses sadness when the dart loses the target.) (Fig. 3)

Fig. 3: G6 (Face covering).

(G7) Guiding: From their relaxed position, the right hand beside legs is swung up to the point towards the right direction.

(G8) Bye-bye: Both hands are first put down besides legs and then right hand is waved iteratively at right side.

The eight types of gestures are performed by 6 experimenters for five times separately (240 gestures in total).

B. Training the value of fuzzy measure

The main task in the training phase is to select the proper template and to calculate the optimal fuzzy measure values for similarities fusion.

The dataset includes 240 data which is divided into a training set and a testing set for each gesture with the ratio of 3:2. As mentioned in 3.1.3, the minimum selection is used to choose the suitable template. To find the optimal fuzzy measure values, the following three steps are done;

(1) Similarity calculation: Calculate the similarities of camera and accelerometers modules separately for all of the training data.

(2) Similarity normalization: Each training data is compared to the eight templates. That is, it will get eight similarities for each input data. Then these eight similarities are normalized in the range of [0, 1], i.e., dividing by the maximum of the eight similarities.

(3) Finding optimal measure value: The algorithm illustrated in 3.3 is implemented for calculating the optimal fuzzy measures for each gesture.

Because the algorithm mentioned in 3.3 is the one relied on initial values, it is executed for many times to get the approximate global optimal fuzzy measures. The fuzzy measures which achieve best recognition rates from the training data are considered as the optimal fuzzy measures for evaluating test data.

In this experiment, the algorithm is applied for 100 times with step value of 0.05, which achieves the best recognition rate of 97.9% by the training data. Table 1 demonstrates the initial and calculated final fuzzy measures of the two modules in the training stage.

Table 1: The initial and final values of fuzzy measure

Gesture	Camera Module		Accelerometers module	
	Initial	Final	Initial	Final
G1	0.5	0.6	0.9	0.85
G2	0.3	0.4	0.9	0.6
G3	0.5	0.45	0.8	0.3
G4	0.5	0.8	0.4	0.3
G5	0.4	0.7	0.3	0.5
G6	0.4	0.25	0.1	0.75
G7	0.1	0.25	0.9	0.55
G8	0.5	0.5	0.9	0.75

C. Result of Multimodal Gesture Recognition and Discussion

The recognition result of the camera based and the accelerometers based modules are given in Table 2 and Table 3. According to Table 2, G1 (toast gesture) shows the worst result of the camera based recognition module. Because G7 (guide gesture) has the similar trajectory to G1 (Fig. 4), 10 data of G1 are misrecognized as G7 and 6 data of G7 are misrecognized as G1. For some gesture (i.e. G6) obtained better recognition result in the camera based recognition module, while some gestures (i.e. G7) got better recognition result in the accelerometers module.

Table 2: Gesture Recognition Results of camera based recognition module

Gesture	Gesture category								
	G1	G2	G3	G4	G5	G6	G7	G8	Total
G1	**18**	0	1	0	0	1	10	0	30
G2	2	**19**	0	0	0	0	9	0	30
G3	0	0	**20**	0	0	2	8	0	30
G4	0	0	5	**24**	0	1	0	0	30
G5	0	0	0	0	**30**	0	0	0	30
G6	2	0	0	0	0	**25**	3	0	30
G7	6	0	4	0	0	0	**20**	0	30
G8	0	0	1	0	0	0	1	**28**	30

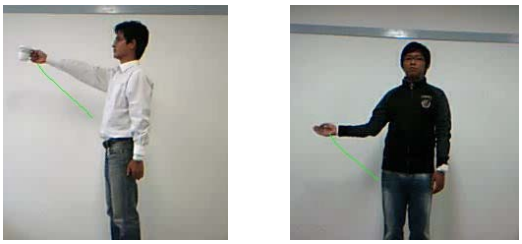

(a) G1 (toast gesture) *(b) G7(guide gesture)*

Fig. 4: The trajectories (shown in green) of G1 and G7

Table 3: Gesture Recognition Results of accelerometers based recognition module

Gestures	Gesture category								
	G1	G2	G3	G4	G5	G6	G7	G8	Total
G1	**14**	0	3	10	1	1	0	1	30
G2	0	**30**	0	0	0	0	0	0	30
G3	0	0	**9**	5	13	2	0	1	30
G4	0	0	0	**16**	14	0	0	0	30
G5	0	0	0	6	**24**	0	0	0	30
G6	0	0	4	4	7	**15**	0	0	30
G7	0	0	0	0	0	0	**30**	0	30
G8	0	0	0	0	0	0	0	**30**	30

The recognition rate of training data and test data is shown in Fig. 5. By calculating the optimal fuzzy measure of fuzzy

Choquet integral, the proposed fusion method achieves an average recognition rate of 92.7%, which is 19.4% higher than the average recognition rate of both modules. Seven of all eight gestures achieve higher recognition rate than the one of each modules. For the large difference of the both modules' recognition rate, the recognition result of G7 is affected by the recognition result of camera module so that it gets lower recognition rate than the rate of accelerometers modules. The proposed multi-modal recognition method obtains the average evaluation value of 92.7%, i.e., the highest recognition rate in the averages of all gestures.

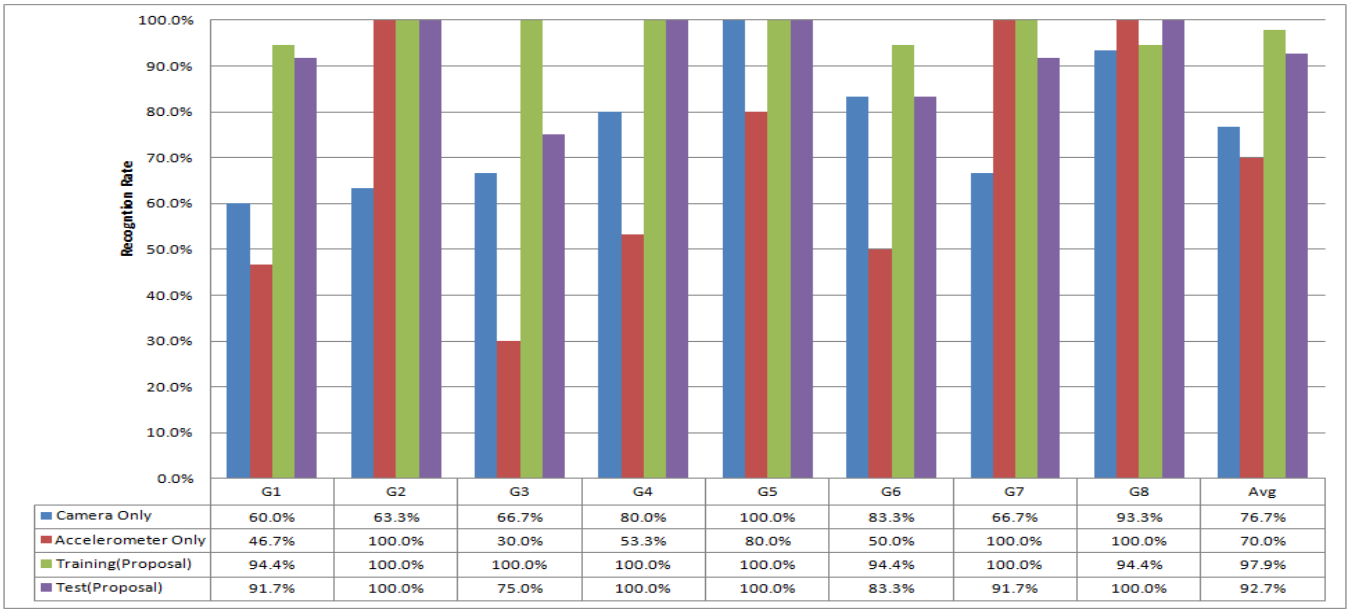

	G1	G2	G3	G4	G5	G6	G7	G8	Avg
Camera Only	60.0%	63.3%	66.7%	80.0%	100.0%	83.3%	66.7%	93.3%	76.7%
Accelerometer Only	46.7%	100.0%	30.0%	53.3%	80.0%	50.0%	100.0%	100.0%	70.0%
Training(Proposal)	94.4%	100.0%	100.0%	100.0%	100.0%	94.4%	100.0%	94.4%	97.9%
Test(Proposal)	91.7%	100.0%	75.0%	100.0%	100.0%	83.3%	91.7%	100.0%	92.7%

Fig. 5: The recognition rate of training data and test data in proposed multimodal gesture recognition system

This result confirms the practical applicability of the proposed multi-modal recognition method compared with other the recognition methods which are based on a single sensor.

IV. CONCLUSION

A Choquet integral based multimodal gesture recognition method is proposed. The proposal achieves the highest recognition rate in the 8 types of gestures. More than 92.7% of gestures are recognized as for all types of gestures, which show the proposed multimodal gesture recognition method advances to the recognition methods based on single sensor.

The proposed multimodal gesture recognition provides casual communication abilities for the Mascot Robot System, where robots assist humans in view of the home party atmosphere based on recognitions of verbal and nonverbal messages from humans. Multimodal sensing based Emotion Spaces and Fuzzy Atmosfield [18] will enable robots to help humans according to the atmosphere in all social situations by integrating verbal and nonverbal communication cues from humans and robots, such as speech, gesture, and facial expression.

References

[1] Y. Yamazaki, H. A. Vu et al., "Mascot Robot System by Integrating Eye Robot and Speech Recognition using RT Middleware and its Casual Information Recommendation", 3rd International Symposium on Computational Intelligence and Industrial Applications (ISCIIA2008), 2008, pp. 375-384.

[2] H. A. Vu, Y. Yamazaki et al., "The Interrupt of Mascot Robot System Embedded in RT Middleware Based on Fuzzy Logic", FACTA UNIVERSITATIS Series: Mechanics, Automatic Control and Robotics, 7-1, 2009,pp. 11-28.

[3] C. Shan, T. Tan et al., "Real-time Hand Tracking Using a Mean Shift Embedded Particle Filter", Journal of the Pattern Recognition Society, 2007,pp. 1958-1970.

[4] E. Huber and D. Kortenkamp, "A Behavior based Approach to Active Stereo Vision for Mobile Robots", Engineering Applications of Artificial Intelligence Journal, 1998,pp. 229-243.

[5] R. Douglas-Cowie, E. Tsapatsoulis et al., "Emotion recognition in human-computer interaction", Signal Process Magazine, IEEE 18-1, 2001,pp. 32-80.

[6] A. Vinciarelli, M. Pantic et al., "Social Signal Processing: State-of-the-Art and Future Perspectives of an Emerging Domain", ACM Multimedia, 2008,pp.1061–1070.

[7] Z. Othman, A.R. Yaakub et al., "Virtual Environment Navigation Using an Image based Approach", Student Conference on Research and Development, 2002, pp. 364-367.

[8] C. Keskin and L. Akarun, "STARS: Sign Tracking and Recognition System Using Input-Output HMMs", Patter Recognition Letters 30, 2009, pp. 1086-1095.

[9] H. Kang, C.W. Lee et al., "Recognition based gesture spotting in video games", Pattern Recognition Letters 25, 2004,pp. 1701–1714 .

[10] G. Caridakis, K. Karpouzis et al., "SOMM: Self organizing Markov map for gesture recognition", Pattern Recognition Letters 31, 2010, pp. 52–59.

[11] V. Paquin and P. Cohen, "A Vision based Gestural Guidance Interface for Mobile Robotic Platforms", HCI/ECCV, LNCS 3058, 2004,pp. 39–47.

[12] C. Amma, D. Gehrig et al., "Airwriting Recognition Using Wearable Motion Sensors", Augmented Human Conference, 2010.

[13] [13] Y. Yamazaki, H. A. Vu et al., "Gesture Recognition Using Combination of Acceleration Sensor and Images for Casual Communication between Robots and Humans", IEEE Word Congress on Computational Intelligence, 2010, pp. 18-23,.

[14] T. Murofushi and M. Sugeno, "An Interpretation of Fuzzy Measures and the Choquet Integral as an Integral with Respect to a Fuzzy Measure", Fuzzy Sets and Systems 29, 1989, pp. 201-227.

[15] T. Nakamura, K. Taki et al., "AMSS: A Similarity Measure for Time Series Data", IEICE D, 91-D-1, 2008,pp. 2579-2588.

[16] M. H. Ko, G. West et al., "Using dynamic time warping for online temporal fusion in multisensory systems", Information Fusion 9, 2008,pp. 370-388

[17] Micro Stone, MVP-RF8, http://www.microstone.co.jp/

[18] Z. Liu, F. Dong et al., "Proposal of Fuzzy Atmosfield for Mood Expression of Human-Robot Communication", International Symposium on Intelligent Systems(iFAN), 2010

2011 IEEE International Conference on Fuzzy Systems
June 27-30, 2011, Taipei, Taiwan

Emotional States Based 3-D Fuzzy Atmosfield for Casual Communication between Humans and Robots

Zhen-Tao Liu, Fang-Yan Dong, and Kaoru Hirota
Department of Computational Intelligence and Systems Science
Tokyo Institute of Technology
Yokohama, Japan
E-mail: {liuzhentao, tou, hirota}@hrt.dis.titech.ac.jp

Min Wu, Dan-Yun Li
School of Information Science and Engineering
Central South University
Changsha, P. R. China
E-mail: min@csu.edu.cn

Yoichi Yamazaki
Department of Electrical, Electronic, and Information Engineering
Kanto Gakuin University
Yokohama, Japan
E-mail: yamazaki@kanto-gakuin.ac.jp

***Abstract*—Emotional states based three-dimensional (3-D) Fuzzy Atmosfield (FA) is proposed to express the feeling between humans and robots in communication, and is built with 3-D coordinates, i.e. "friendly-hostile", "lively-calm", and "casual-formal" axes. The FA aims to be an effective tool to proceed with the communication paying attention to the atmosphere generated by individual emotional state which is calculated from bimodal communication cues namely emotional-speech and emotional-gesture by using weighted fusion and fuzzy inference. A novel emotion recognition approach is presented which consists of two steps, i.e., classification of six basic emotions for initial emotional states in the Affinity-Pleasure-Arousal emotion space, and emotional transition from prior state by using fuzzy logic. Home party enjoying demonstration confirms FA's availability empirically by questionnaires from unrelated persons of authors' group, where smooth communication between four humans and five eye robots is realized in Mascot Robot System.**

Keywords- human-robot communication; emotion recognition; emotional state; communication atmosphere; fuzzy inference

I. INTRODUCTION

Affecting computing, playing a significant role in human-robot interactions, has been paid more and more attention, where how to identify atmosphere amongst communicators as well as attitude, mood, and emotion of interlocutors, and how to provide a comfortable environment to eliminate the barriers between humans and robots, have become the main objectives for the next generation of intelligent robots.

Emotion recognition, a popular topic in recent years, has attracted increasing attention from researchers involved in a variety of discipline e.g. psychology, computer science, linguistics, neuroscience, and related disciplines [1]. Multiple channels of information during communication are used to analyze emotional states of humans including speech, facial expression, body gesture, posture, and so on [2-5]. Few studies, however, concentrate on communication atmosphere which is easily felt but hard to define, and even more difficult to evaluate, and it is never finished, static or at rest [6, 7]. In [8], human expressive communication is analyzed by exploiting interrelation between speech and gestures. A 3-D communication atmosphere is built by using audio-visual modals, where only face-to-face communications between two participants are considered in recognition [7]. Most of previous researches concentrate on analysis of personal mood without understanding the atmosphere which is composed of all emotional states of humans in the communication.

Fuzzy Atmosfield is proposed to describe mood states among communicators being generated from not only the verbal and non-verbal information of speakers, but also background music or noise. Bimodal information based emotion recognition is carried out in two steps: 1. Emotion of the interlocutor is classified on the basis of six primary emotions, i.e. "happiness", "surprise", "fear", "anger", "disgust", and "sadness", which are predetermined as the initial emotional states in Affinity-Pleasure-Arousal emotion space; 2. Emotional state's transition is executed by using fuzzy logic on speech features including volume, average frequency, and interval time. Fuzzy inference and expert rules are employed to build Fuzzy Atmosfield from individual emotion spaces, and a 3-D space defined as "friendly-hostile", "lively-calm", and "casual-formal" axes is presented to express Fuzzy Atmosfield. Experiments for Fuzzy Atmosfield are performed with four humans and five eye robots in a household environment by using Mascot Robot System. The results based on questionnaires verify availability of proposed methods.

The emotion recognition based on bimodal communication cues is mentioned in II. In III, emotional states based Fuzzy Atmosfield by using fuzzy inference and expert rules is presented. The experiments for Fuzzy Atmosfield in Mascot Robot System are given in IV.

II. EMOTION RECOGNITION BASED ON BIMODAL COMMUNICATION CUES

A. Overview of the Model's Architecture

This work was supported by Japan Society for the Promotion of Science (JSPS) KAKENHI 21300080

Emotion recognition based on bimodal information, i.e. emotional speech and gesture, is proposed to express the emotional states of interlocutors in Affinity-Arousal-Pleasure space. Fig. 1 shows the procedure of the proposed emotion recognition method, where there are two steps.

- Initial states of emotion are determined by fusing semantic cues from speech and the gestures of communicators.
- Starting from the initial/previous state of emotion, transition of emotional states in the 3-D emotion space is executed by using fuzzy inference considering the influence from features of speech.

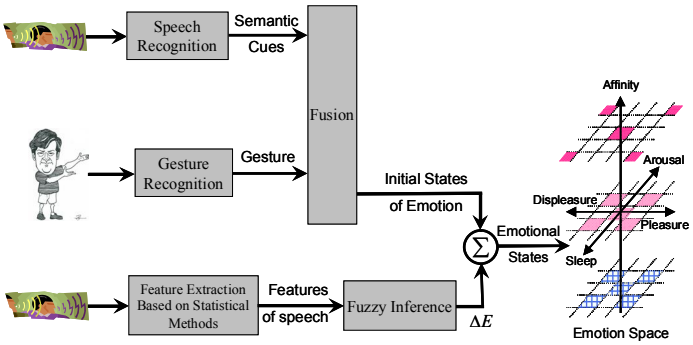

Figure 1. Emotion recognition based on bimodal information

B. *Affinity-Pleasure-Arousal Emotion Space*

A 3-D emotion space named Affinity-Pleasure-Arousal space is used to illustrate the mentality state of speakers during communication. By using the Affinity-Pleasure-Arousal plane, it is not only possible to express fixed mentality states but also to take into account rapid variations in the mentality state due to time involving communication [9], as shown in Fig. 2.

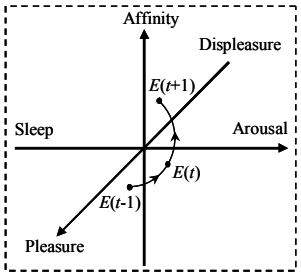

Figure 2. Emotion space expressed in 3-D axes

Affinity-Pleasure-Arousal emotion space is defined with fuzzy domains that can be indicated as

$$E = (e_{affinity},\ e_{pleasure},\ e_{arousal}),$$
$$\forall e_{affinity} \in [-1,\ 1],\ \forall e_{pleasure} \in [-1,\ 1],\ \forall e_{arousal} \in [-1,\ 1] \quad (1)$$

where $e_{affinity}$, $e_{pleasure}$, $e_{arousal}$ are the values in "affinity", "pleasure-displeasure", and "arousal-sleep" axes, respectively. The membership functions for these three axes are shown in Fig. 3.

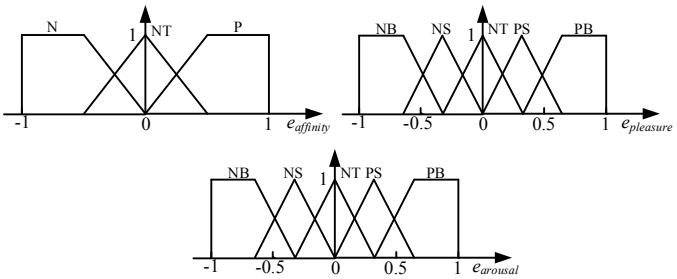

Figure 3. Membership functions for emotion space axes

C. *Semantic Cues from Emotional Speech*

Automatic speech recognition (ASR) system is developed for general robot systems by NEC Corporation in the Development Project for a Common Basis of Next-Generation Robots led by the NEDO organization. Its functions include single word speech recognition, noise canceller, sound source directional detection, speaker independent recognition and dictionary switching, i.e. it can select a specific dictionary fitting with current conversation topic. The speech recognition principle in the ASR is a word-matching search based on pre-defined dictionary.

Traditionally, research on the recognition of emotion from semantic cues of speech was focused on the discovery and utilization of emotional keywords, that is, specific words that express the speaker's emotional state [10]. To take advantage of the function of single word recognition in ASR, emotional keywords from speech are selected for emotion recognition.

Six primary emotions [11], i.e., "happiness", "surprise", "fear", "anger", "disgust", and "sadness", are employed as the initial state of emotion recognition. The contribution from any emotional keyword w to one of the six basic emotion e_i is defined as $P(e_i|w)$ which is calculated in a training phase by its frequency of occurrence under the observation of the emotion on the basis of large emotional speech corpus.

D. *Emotional Gesture Recognition*

Although semantic cues of speech, to some extent, could reflect emotional state, the variety and complexity of language makes it difficult for researchers to recognize emotional states from pure textual information. Emotional-gesture, another available modal in communication, is necessary adopted for emotion recognition, which can originate from any bodily motion or state but commonly originate from the hand or face.

A multi-modal information based hand gesture recognition system is developed by authors' group [12, 13], where emotional gestures are recognized based on multi-modal sensing, i.e., the combination of the 3-D acceleration sensor and web cameras. The gesture recognition system includes two modules, i.e. the acceleration sensor recognition module and the image recognition module. After fusing above two independent module's results, emotional gestures are recognized finally. In the same way as emotional keywords, the contribution from any gesture g to one of the six basic emotion e_i is defined as $P(e_i|g)$ which is calculated in the data training of a large gesture database.

E. Emotion Recognition by Weighted Fusion

Weighted fusion is one kind of techniques for decision-level fusion, which arrives at the final classification decision by combining the weights of individual recognition. The basic idea behind this approach is with the hypothesis that the overall recognition rate will be improved by combining pieces of evidence provided by independent sources.

Information fusion of bimodal communication cues, i.e., semantic cues of speech and gesture is executed by using weighted fusion. Through calculating the sum of each emotion probabilistic from keywords of speech and gestures, the emotion e_i, receiving the maximum of probabilistic contribution, will be output as the final recognition result of emotion, as shown in Fig. 4. If it fails to receive only one kind of emotion, then jump to the recalculate procedure.

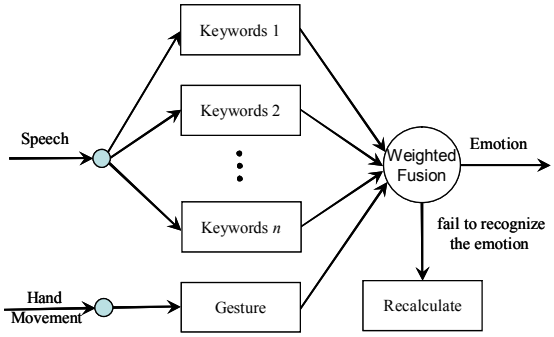

Figure 4. Emotion recognition by weighted fusion

Emotion recognition based on bimodal information outputs one of the six primary emotions as the initial coordinate in Affinity-Pleasure-Arousal emotion space, where is predetermined according to the relationship between six primary emotions and three axes of the emotion space.

F. Transition of Emotional States in Emotion Space

To recognize the real emotional states of communicators, features of speech such as volume, average frequency, and interval time are assigned to inputs for transition of emotional states. Fuzzy inference method is accepted to establish the relation-ship between voice features and the variation of three axes from previous position in Affinity-Pleasure-Arousal emotion space, as shown in Fig. 5.

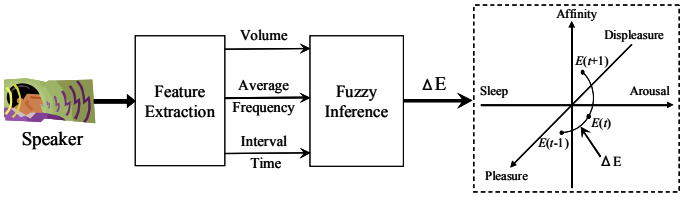

Figure 5. Emotion space of speaker using fuzzy inference

After completion of the feature extraction module, the ratio of two voices' volume, ratio of average frequency between speaker's and standard, and interval time between two utterances are used for fuzzy inference in transition of emotional states. The membership functions for these features are shown in Fig. 6.

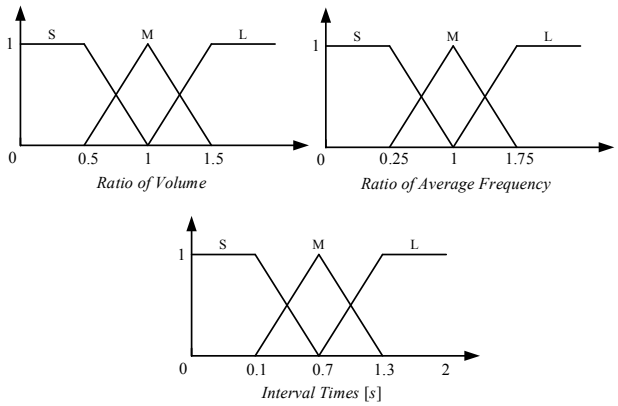

Figure 6. Membership functions for speech features

The fuzzy rules of ΔE, namely $\Delta e_{affinity}$, $\Delta e_{pleasure}$ and $\Delta e_{arousal}$ based on speech features are shown in Table I, Table II, and Table III, respectively.

TABLE I. FUZZY RULES OF $\Delta E_{AFFINITY}$

		Ratio of Average Frequency		
		S	M	L
Ratio of volume	S	N	P	P
	M	N	NT	P
	L	N	P	P

TABLE II. FUZZY RULES OF $\Delta E_{PLEASURE}$

		Ratio of Average Frequency		
		S	M	L
Ratio of volume	S	N	P	P
	M	N	NT	P
	L	N	P	P

TABLE III. FUZZY RULES OF $\Delta E_{AROUSAL}$

		Interval Time		
		S	M	L
Ratio of volume	S	NT	NT	N
	M	P	NT	N
	L	P	P	NT

To obtain the values of $\Delta e_{affinity}$, $\Delta e_{pleasure}$ and $\Delta e_{arousal}$ in Affinity-Pleasure-Arousal space, the center of gravity method is used as a defuzzification method, and then $E(t) = E(t-1) + \Delta E$.

The transfer of emotional states is one continuous process in the 3-D emotion space, as the smooth curve connecting $E(t-1)$, $E(t)$, and $E(t+1)$ in Fig 1. For instance, when the speaker stops talking, emotional state is in the process of diminishing but not at origin (neutral state).

III. FUZZY ATMOSFIELD BASED ON EMOTIONAL STATES

Fuzzy Atmosfield is invisible but it is supposed to exist by occupying space and containing energy. It reflects the mood states of communication between speakers, and affects the emotional states of humans as well. Thus, Fuzzy Atmosfield is not just a natural phenomenon, bus also one kind of "psychological field", associated with individual emotional states, background music, and noises, etc. In this paper, only emotional states are concerned.

A. *Fuzzy Atmosfield described in a 3-D Space*

Atmosfield (Atmosphere Field, i.e., atmos' field) exists in the space surrounding us. It is created in the process of communication between speakers, producing "psychological feeling" that can give influence to the process and results of humans' behavior. Due to its special characteristic of "psychological field", it could not be calculated as accurately as some physic's fields such as electrical field and magnetic field, and therefore, is defined as Fuzzy Atmosfield.

Fuzzy Atmosfield is illustrated in a 3-D space defined by "friendly-hostile", "lively-calm", and "casual-formal" axes, which is determined by questionnaires from 10 peoples on 20 different occasions [14], as shown in Fig. 7.

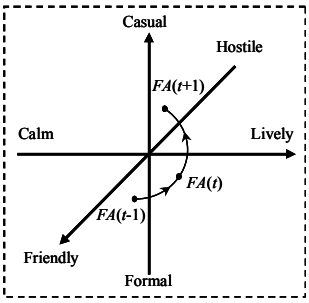

Figure 7. Fuzzy Atmosfield expressed in 3-D axes

To construct Fuzzy Atmosfield, the proposed 3-D space with fuzzy domains is described firstly as

$$FA = (a_{friendly},\ a_{lively},\ a_{casual}),$$
$$a_{friendly} \in [-1,\ 1],\ a_{lively} \in [-1,\ 1],\ a_{casual} \in [-1,\ 1] \tag{2}$$

where $a_{friendly}$, a_{lively}, a_{casual} are the values in "friendly-hostile", "lively-calm", and "casual-formal" axes, respectively. The membership functions for Fuzzy Atmosfield's axes are shown in Fig. 8.

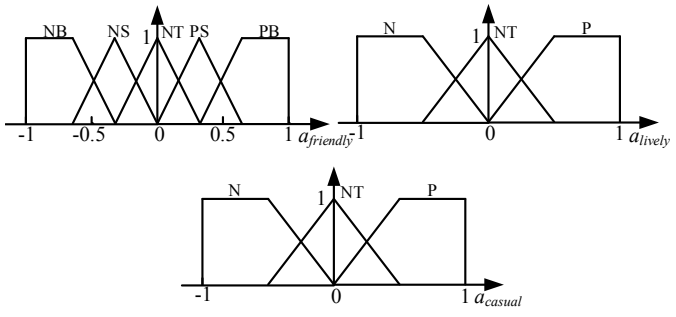

Figure 8. Membership functions for Fuzzy Atmosfield axes

B. *Scheme of Fuzzy Atmosfield*

The scheme of Fuzzy Atmosfield based on emotional states of communicators is presented as shown in Fig. 9. First of all, the emotional states of all participants in the conversation have been obtained in emotion recognition system (for humans) or emotion synthesis system (for robots). Secondly, information fusion module of emotional states is executed, where fuzzy inference is employed to express the relationship between Fuzzy Atmosfield and emotion space, and with the utilization of speaker's volume, some expert rules are arranged to realize the mapping from *n* emotion spaces to Fuzzy Atmosfield. At last, the atmosphere state is given in the 3-D Fuzzy Atmosfield.

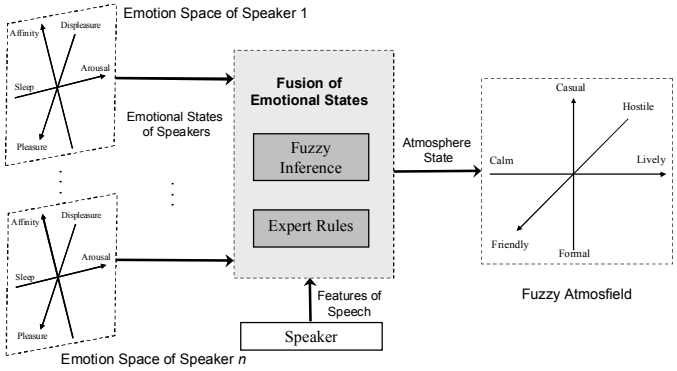

Figure 9. Scheme of Fuzzy Atmosfield

C. *Emotional states based Fuzzy Atmosfield*

As mentioned in II, Fuzzy Atmosfield is composed of individual emotion spaces. Meanwhile, the changing of atmosphere state is a continuous process as well as emotional state. In a word, at time *t*, the transfer of atmosphere state in Fuzzy Atmosfield is not only related to the atmosphere state at time *t*-1, but also the new emotional states of communicators stimulated from external environment. Therefore, the formula of Fuzzy Atmosfield can be defined as

$$FA(t) = \begin{cases} f(E_1(t),\ \cdots,\ E_n(t)),\ t = 1 \\ (1-\lambda)FA(t-1)\cdot\gamma + \lambda f(E_1(t),\ \cdots,\ E_n(t)),\ t > 1 \end{cases} \tag{3}$$

where FA is the atmosphere state in Fuzzy Atmosfield; f is the function of emotional states E at time *t*; *n* is the number of speakers involved in the communication; γ is the decreasing function of $FA(t-1)$, and γ is an undetermined function, $0 \le \gamma \le 1$; λ is the correlation factor, $0 \le \lambda \le 1$; When $t = 0$, FA is at initial state where is set beforehand.

Considering different contribution of individual emotional states to Fuzzy Atmosfield, weighted average method is accepted to construct function f in

$$f:\ \sum_{i=1}^{n} w_i \cdot defuzzy(\underset{\sim}{E}_i(t) \circ R),\ i = 1,\ 2,\ \ldots,\ n \tag{4}$$

where R is the relationship between emotion space and Fuzzy Atmosfield, which is obtained by using fuzzy inference, and 75

fuzzy rules are arranged to build R; $\underset{\sim}{E}_i(t)$ is fuzzy set of emotion space of ith communicator; the center of gravity method is used as a defuzzification method in *defuzzy*; w_i is the weight of ith emotion space contributing to the Fuzzy Atmosfield, $\forall w \in [0,\ 1]$, $\sum_{i=1}^{n} w_i = 1$. It can be illustrated as shown in Fig. 10.

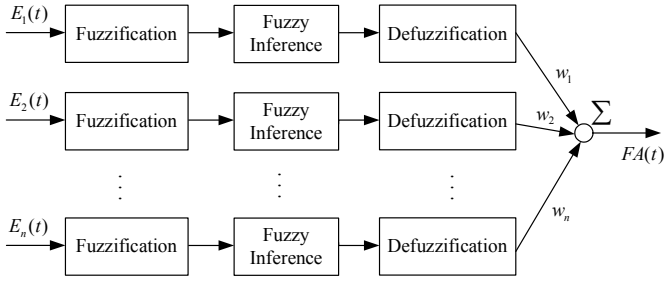

Figure 10. Flow chart from emotion spaces to Fuzzy Atmosfield

D. *The weights of* w_i

To analyze the contribution of each emotion space, the role of each participant for altering communication atmosphere should be considered, i.e., the actions such as speech, facial expression, and other body movements should be taken into account. In this paper, volume of speech is employed for computing the weights of each emotion space. At time t, w_i is calculated as

$$w_i = \frac{v_i}{\sum_{j=1}^{n} v_j},\ i = 1,2,\ \ldots,\ n,\ j = 1,2,\ \ldots,\ n \tag{5}$$

where v is the volume of speaker.

E. *The weight of* λ

Considering the influencing factors for communication atmosphere, volume of speech is used to determine the correlation factor λ in equation (3). Some expert rules are formulated by using ratio of volume $v(t)$ and $v(t-1)$ as

$$ra_{volume} = \frac{\sum_{i=1}^{n} v_i(t)}{\sum_{i=1}^{n} v_i(t-1)} \tag{6}$$

where ra_{volume} is the ratio of volume $v(t)$ and $v(t-1)$, and

$$\lambda = \begin{cases} 0, & if\ \sum_{i=1}^{n} v_i = 0 \\ \frac{1}{2} \cdot ra_{volume}, & if\ ra_{volume} < 1 \\ \frac{1}{2}, & if\ ra_{volume} = 1 \\ 1 - \frac{1}{2}\exp(-(\frac{ra_{volume} - 1}{\sigma})^2), & if\ ra_{volume} > 1 \end{cases} \tag{7}$$

where σ is an undetermined parameter.

IV. Experiments for Fuzzy Atmosfield

The proposed Fuzzy Atmosfield is evaluated by performing communication experiments with four humans and five eye robots in Mascot Robot System (MRS). The MRS is an information presentation system destined to be used mainly as an information terminal in a home environment for casual communication with humans [15]. The five eye robots include four fixed robots (placed on a TV, a darts game machine, an information terminal, and a mini-bar) and 1 mobile robot, as shown in Fig. 11.

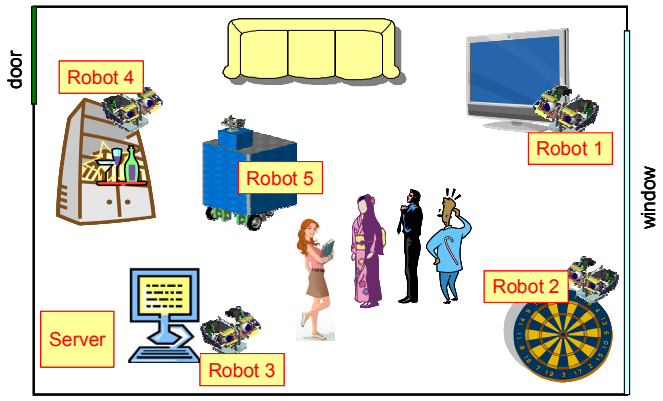

Figure 11. Household environment for humans and robots

An ideal household environment is created that is a relatively quiet place without background music or noises. Six scenarios are performed in the experiment, i.e., Scenario 1: "Greeting guests at the door", Scenario 2: "Drinking at the bar", Scenario 3: "Playing dart game", Scenario 4: "Watching TV", Scenario 5: "Checking timetable of train at the terminal computer", Scenario 6: "Farewell with guests at the door". Each scenario is designed with dialog between humans and robots, where eight types of typical human emotional gestures [11], including "Toast", "Throw dart", "Victory pose", "Banzai pose", "Put both hands on head and squat", "Put hand on one's face", "Guiding", and "Goodbye", are performed as well. Fig. 12 shows the photo and dialog of Scenario 5, where a conversation is taken place between Host, Guest 1, Guest 2, and Robot 3 (the information terminal robot).

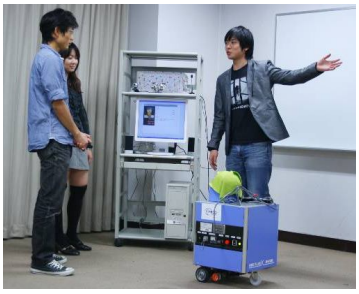

Robot 3: [Which station?]
Host: Shibuya.
Robot 3: [Trains heading out of the city?]
Host: Yamanote line. To Shinagawa.
[Display PC shows the timetable.]
Guest 1: That's just right.
Guest 2: Thank you.
Robot: You're welcome.
Host: So let's go to the door.

a) The photo of Scenario 5 b) The dialog of Scenario 5

Figure 12. The scenario 5 of "Checking timetable of train"

Emotional state of each person is obtained by proposed emotion recognition approach with high recognition rates, while robots' emotion spaces are established in expression synthesis system [9] which is developed by the authors' group.

To integrate individual emotional state of humans and robots, in the experiments, some parameters of Fuzzy Atmosfield's model are decided empirically, i.e., $\gamma = e^{0.1}$, $\sigma = 2$. The Fuzzy Atmosfield of Scenario 5 in home party is built by using proposed method, as shown in Fig. 13, where the coordinate of the sphere's center is $FA(t)$, and the diameter d which represents the variation of atmosphere state is calculated as

$$d = \min\{\frac{1}{\sqrt{3}}\sqrt{[a_{friendly}(t) - a_{friendly}(t-1)]^2 + [a_{lively}(t) - a_{lively}(t-1)]^2 + [a_{causal}(t) - a_{causal}(t-1)]^2}, 0.1\}. \quad (8)$$

The results of Fuzzy Atmosfield based on questionnaires by 10 peoples verify availability of proposed methods. Smooth communication between 4 humans and 5 eye robots in home party proceeds with harmonious atmosphere, where robots can recognize the atmosphere state in real time. And then, through classification, identification, and response, robots could adjust talking contents and tones to improve communication atmosphere.

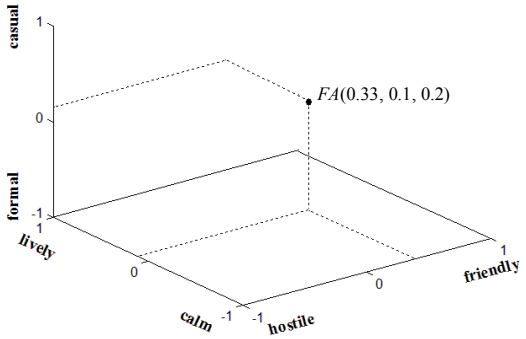

Figure 13. Fuzzy Atmosfield of Scenario 5 in home party

V. Conclusions

To express affective states during human-robot communication, the concept of Fuzzy Atmosfield is proposed, where it is composed of individual emotional states of humans and robots.

On the basis of bimodal communication cues including speech message and gesture message, first emotion classification is carried out in accordance with six basic emotions which are predetermined as the initial states in Affinity-Pleasure-Arousal emotion space; second transition of emotional state is executed by using fuzzy logic on some speech features. With the fusion idea of emotional states, Fuzzy Atmosfield is created by using fuzzy inference and expert rules. Being convenient to observe for users, a 3-D space with "friendly-hostile", "lively-calm", and "casual-formal" axes is introduced to express Fuzzy Atmosfield. Results of experiment demonstrate the availability of Fuzzy Atmosfield in a home party with smooth communication proceeded between 4 humans and 5 eye robots.

The proposed Fuzzy Atmosfield aims to realize casual communication in multi-human and multi-robot environments, not only integrating the mood expression of individuals, but also providing good guidance for robots to improve communication atmosphere by adjusting the content of speech, improving the way of communication, or playing harmonious music, and so on.

In-depth study on assignment of appropriate parameter in the model of Fuzzy Atmosfield will continue in the further researches. In addition, more verbal or non-verbal information except speech and hand gesture would be considered to construct Fuzzy Atmosfield, for example, facial expression, head movements, and other body languages. Furthermore, the background music or noise would be essential factors for Fuzzy Atmosfield.

References

[1] Z. Zeng, et al, "A Survey of Affect Recognition Methods--Audio,Visual, and Spontaneous Expressions," IEEE Transactions on Pattern Analysis and Machine Intelligence, Vol. 31, No. 1, pp. 39-58, 2009.

[2] T. L. Pao, Y. T. Chen, J. J. Lu, J. H. Yeh, and W. Y. Liao, "Detecting Emotions in Mandarin Speech," International Journal of Computational Linguistics and Chinese Language Processing, Vol. 10, No. 3, pp. 347-362, 2005.

[3] Y. Wang and L. Guan. "Recognizing Human Emotional State from Audiovisual Signals," IEEE Transactions on Multimedia, Vol. 10, No. 5, pp. 936-946, 2008.

[4] M. L. Song, et al, "A Robust Multimodal Approach for Emotion Recognition," Neurocomputing, Vol. 71, No. 10, pp. 1913-1920, 2008.

[5] M. J. Han, J. H. Hsu, and K. T. Song, "A New Information Fusion Method for Bimodal Robotic Emotion Recognition," Journal of Computers, Vol. 3, No. 7, pp. 39-47, 2008.

[6] B. Anderson, "Affective Atmospheres," Emotion, Space and Society, Vol. 2, No. 2, pp. 77-81, 2009.

[7] T. M. Rutkowski and D. P. Mandic, "Modelling the Communication Atmosphere: A Human Centered Multimedia Approach to Evaluate Communicative Situations, " AI for Human Computing, Berlin, Springer Press, pp. 155-169, 2007.

[8] C. Busso, "Multimodal Analysis of Expressive Human communication: Speech and Gesture Interplay," PhD thesis, University of Southern California, 2008.

[9] Y. Yamazaki, Y. Hatakeyama, F. Y. Dong, and K. Hirota, "Fuzzy Inference based Mentality Expression for Eye Robot in Affinity Pleasure-Arousal Space," Jounal of Advanced Computational Intelligence and Intelligent Informatics, Vol. 12, No. 3, pp. 304-313, 2008.

[10] C. H. Wu, Z. J. Chuang, and Y. C. Lin, "Emotion Recognition from Text Using Semantic Labels and Separable Mixture Models," ACM Transactions on Asian Language Information Processing, Vol. 5, No. 2, pp. 165-182, 2006.

[11] P. Ekman, "Are There Basic Emotions?" Psychological Review, Vol. 99, No. 3, pp. 550-553, 1992.

[12] Y. Yamazaki, et al, "Gesture Recognition Using Combination of Acceleration Sensor and Images for Casual Communication between Robots and Humans," IEEE World Congress on Evolutionary Computation , 2010.

[13] Y. Tang, et al, "Multimodal Gesture Recognition for Mascot Robot System Based on Choquet Integral Using Camera and 3D Accelerometers Fusion," Jounal of Advanced Computational Intelligence and Intelligent Informatics, unpublished.

[14] K. Fukuda, "Conversation Atmosphere Recognition using Fuzzy Inference on Speech Information," Master Thesis, Tokyo Institue of Technology, 2009.

[15] K. Hirota and F. Y. Dong, "Development of Mascot Robot System in NEDO project," In Proc. 4th IEEE Int. Conf. Intelligent Systems, pp. 38-44, 2008.

2011 IEEE International Conference on Fuzzy Systems
June 27-30, 2011, Taipei, Taiwan

Presence Expression using Eye Robot for Computer Go and System

Yoichi Yamazaki,
Masaya Hanada,
Makoto Motoki
Dept.Electr.Electron.&Inf. Eng.
Kanto Gakuin University
Yokohama, Japan
yamazaki@kanto-gakuin.ac.jp

Chang-Shing Lee
Dept. C.S., & Inf. Eng.
National University of Tainan
Tainan, Taiwan
leecs@mail.nutn.edu.tw

Takuya Hashimoto
Dept. Mechanical Eng.
Tokyo University of Science
Tokyo, Japan
tak@kobalab.com

Fangyan Dong,
Kaoru Hirota
Dept. C.I. & S.S.
Tokyo Institute of Technology,
Yokohama, Japan

***Abstract*— Friendly user interface is desired for robots and computer systems which support human in all areas of daily life, e.g., information service, educational system, support service for elderly, etc.. Presence expressions by eye robot is proposed, where the eye robot expressions help human to more deeply understand robot, and then effectively provide their service in its situation e.g., a personal learning program and an entertainment program. The proposed presence expression is applied a personal education system that involves the eye robot, learning contents on a laptop PC with a web camera, a wii remote (Nintendo Co.,Ltd.) for measuring attention span of a subject based on 3D accelerometer information. To estimate effects of presence expression by the eye robot, subjective questioner is performed in the personal education system. Three type of leaning programs are conducted by the system for 10 subjects with subjective questionnaires evaluated with the 3-poin scale. The results show that the proposed expressions by the eye robot help the subject to feel like one is watching and to have an uncanny impression. As a result, the system has enabled the subjects to take the program with feeling of tension. This research plans to apply computer go system, another personal educational and entertainment system, where the system realizes casual communication in the games.**

Keywords-component; communitation robotics, computer Go, presence expression, casual communication

I. INTRODUCTION

Computer systems with computational intelligence technique is helping supporting human in all areas of daily life, e.g., information service, games, educational system, support service for elderly, etc.. In these systems, e.g. e-learning system and computer game, intelligent agents are working to assess their situations and to decide actions according to personal actions and data [1] [2]. One thing these systems have in common is one-to-one interactive situations between system and human when these systems present information to human. For assisting inputs of these types of system, evolutionary robot vision approach has been proposed for face detection [3]. For assisting outputs of one-to-one interactive systems, friendly user interface is requested communication robots, interactive interfaces that can communicate with human in a natural way.

Presence expressions by eye robot is proposed, where the eye robot expressions help human to more deeply understand robot, and then effectively provide their service in its situation e.g., a individual learning program and an entertainment program. The proposed presence expression is applied a personal education system that involves the eye robot, learning contents on a laptop PC with a web camera, a wii remote (Nintendo Co.,Ltd.) for measuring attention span of a subject based on 3D accelerometer information. To estimate effects of presence expression by the eye robot, subjective questioner is performed in the personal education system. Three type of leaning programs are conducted by the system for 10 subjects with subjective questionnaires evaluated with the 3-poin scale.

II. COMUNICATION ROBOTIC SYSTEM

Friendly user interface is strongly desired for computer system that support human in all areas of daily life, e.g., information service, educational system, support service for elderly, etc.. Communication robots have been developed as interfaces that can communicate with human in a natural way. Human comprehend others including nonhuman, e.g., robots by constructing virtual model in their own mind through their interaction, where presence is important. Communication robots are media that mainly show their presence according to their own appearance. The android robot, Geminoid HI-1 that appears and behaves like a living person have represented specified personal presence by teleoperating [4]. Telenoid-R1 is designed to appear and to behave as a minimalistic human, where the Telenoid-R1 has expressed unspecified personal presence in the distance [5]. As a real application for group education system, the android SAYA is applied for a remote class system at an elementary school, where SAYA conduct the class with her effective presence by using her voice and eye contact [6].

As a casual communication interface, an eye robot have been proposed, where the eye robot interacts with human by friendly eye expressions. The eye robot is developed based on the mechanisms of the human eye [7]. Eye motions consist of eyelid motion and ocular motion. This motion set is one of the components of casual communication. The structure of the

978-1-4244-7316-8/11/$26.00 ©2011 IEEE

eyelids part and the ocular part is shown in Fig. 1. The eye robot has 2 degrees of freedom (D.O.F) for the eyelids part and 3 D.O.F for the ocular part. The eye robot covers a wider range with each motion of the eye than is possible with human eyeballs. Therefore the eye robot can sufficiently simulate a human being's eye motions. The picture of the eye robot is shown in Fig.2, where the eye robot expresses representative motions. The size of the eye robot is 130 mm in width, 80 mm in height, and 75 mm in depth. This size is inspired by the size of a five-year-old child's head.

The eye motion of eye robot is defined as the combination of eyelid motion and ocular motion. Eyelid motion and ocular motion are independent in the pleasure-arousal plane. All motions of the eyelids and eyeballs have the tendency to change according to each axis of the pleasure-arousal plane. The motions are assigned to the 25 different partitions of the pleasure-arousal plane based on psychological knowledge and results from the questionnaire survey. The eye robot realizes casual communication between human and system by expressing mentality and intention according to human action based on affinity pleasure-arousal space.

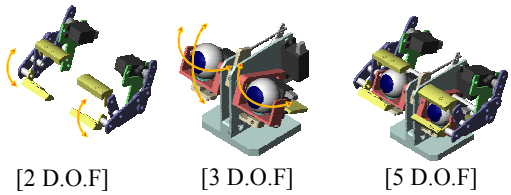

Figure 1. the structure of the robot

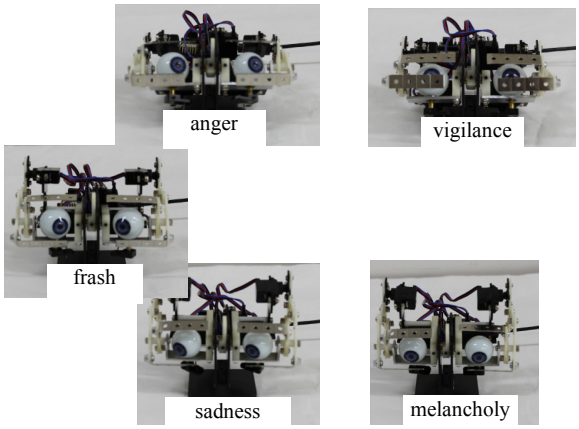

Figure 2. the representatiove motions of the eye robot

III. THE STRUCTURE OF THE ROBOTPRESENCE OF ROBOT FOR COMPUTER GO

In 2, communication robot systems are introduced, where robots assist human with expressing their presence. This type of robots can provide casual information system by combining with information system.

A. Presence expression using robotic agent for co-creation

Presence of communication robots works effectively in human-robot interaction. Presence of robots depends on their appearance, and the appropriate appearance should be selected on a case-by-case basis. In home environment, presence of robot should be restricted from the view point of size and expression manner, where space is limited and interpersonal distance is small. Presence expressions by the eye robot as a small and casual communication robot is proposed in home environment, where the presence expression encourage cooperation between human and robot system, and realize human-robot co-creation in home-use personal education system and entertainment system.

B. Individual learning system and Computer Go system

The presence expressions are applied individual learning systems and entertainment systems requiring individual learning. The presence by a robot has worked effectively in the group-learning situation [6]. In individual learning situations in home environment, robot's size and expression manner should be restricted considering the robot is on human side. In this research, the eye robot as a small and casual communication robot is used for assistant of human learner.

This individual learning system is able to be combined to entertainment systems requiring individual learning, that is computer Go system that has already developed on a CG basis [1].

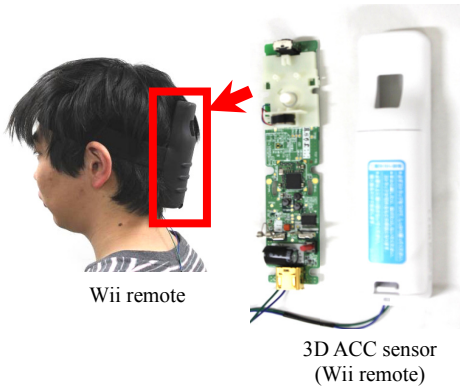

Figure 3. the 3D ACC sensor unit

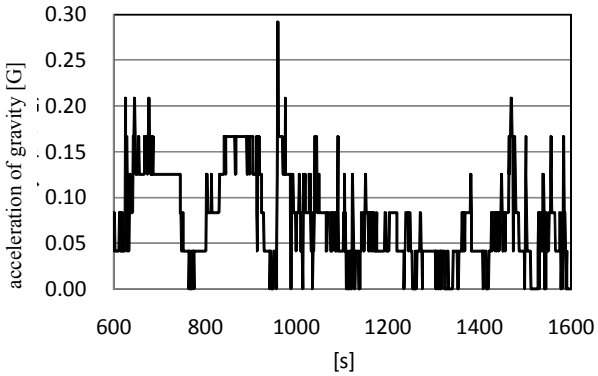

Figure 4. the sample data of ACC sensor

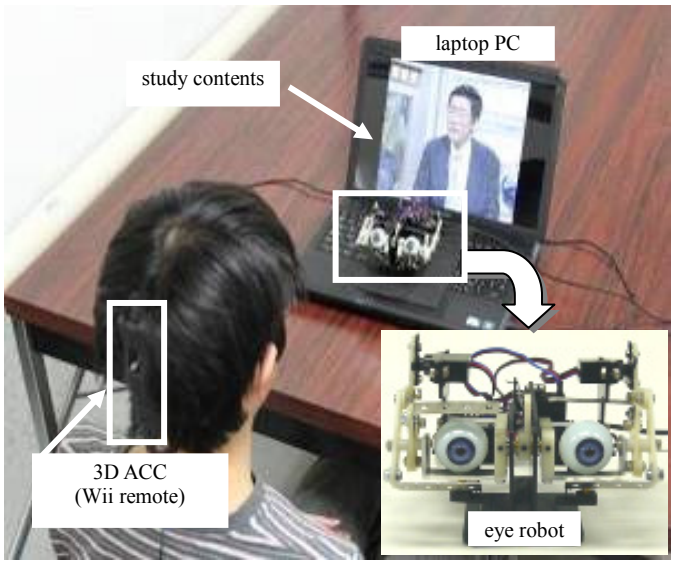

Figure 5. the expresimental situation by individual learning system

IV. INTERPERSONAL EXPERIMENTS FOR EVALUATING PRESENCE EXPRESSION

To estimate effects of presence expression by eye robot, subjective questioner is performed in personal education system. To perform effectively, memory experiments should be performed implicitly. At first psychological evaluation experiments are expressly performed in a mascot robot system environment. In the psychological evaluation experiments, memory experiments are performed implicitly.

A. Evaluation Experiments on Interactions based on Subjective Estimation

To estimate human impressions on the proposed presence expression by eye robot, interactive experiments are performed in individual learning situation by using a multimedia system. In the experiments, subjective estimations by questionnaires are conducted. In addition, attention spans are measured.

Experimental situation involves the learning contents on a laptop PC with a web camera, the eye robot, a subjective that wears wii remote (Nintendo Co.,Ltd.) for measuring his/her attention span based on 3D accelerometer information. The experiment's disposition is shown in Fig.3, and an obtained data example from accelerometer is shown in Fig.4.

To verify the influence of proposed presence expression, the following three types of action patterns are performed by the system according to the human behavior information, and compared to one another. The first pattern is that the eye robot expresses alert motion in incremental steps with voice (pattern 1: present expression with voice). The second is that the system alert with voice when a subject loses his/her consideration, but without eye robot (patter 2: voice). The third is that the system does not any alert without eye robot (pattern 3: nothing). In the experiments, these three patterns are performed in no particular order.

For the experiment, three types of the highschool-level learning contents (geography, earth science, and domestic science) are prepared, where the 30-minute learning movies are played on the PC. The procedure of the experiments is as follows;

Step1) the subject is informed about the experiment and the eye robot, and wears a wii remote on the head.

Step2) the subject start an individual learning program. The system behaves according to the attention of the subject in a predetermined one of three patterns.

Step3) after the learning program, the subject fills out a test on the learning contents. After that test, subjective questionnaires on nine items are conducted.

Step4) steps2) and 3) are repeated for the three action patterns in the same way.

The subjective questionnaires are evaluated with the 3-poin scale. The items of the subjective questionnaires are as follows;

1) Have you had the class about the learning contents?

2) Could you concentrate on the learning program?

3) Did you take the program with a feeling of tension?

4) Did you feel like one is being watched?

5) Did you feel friendly?

6) Did you feel the presence of human?

7) Did you have an uncanny impression?

8) Did you feel the learning contents interesting?

9) Was the alert done at the right time?

The subjects for the experiment are 10 engineering students.

B. Result of the Experiments

The results of the subjective estimations are shown in Fig.5. These figures show the mean values obtained for each question in the three action patterns. The subjective questionnaires are evaluated on a 3-poin scale of zero to two. Low values imply negative, and high values imply positive effect. Table I gives the average frequency of the head-nodding movement. Table II gives the average value of the attention span in the 30-minutes learning program. Table III gives the average score of the test on the learning contents, and this graph is shown in Fig. 7.

Fig. 2 shows that the pattern 1 is evaluated as the most positive on (3), (4), and (7), and the pattern 3 is the most positive on (2) and (8). Tab. I and Tab. II show the pattern 3 is the lowest, where the subject's head move less often than any others. Tab. III and Fig. 7 show that the pattern1 get most high score, but there is not so major deference.

These mean that first, the proposed expression by the eye robot shows the presence, and then the subject feel like one is watching and have an uncanny impression. As a result, the subject could take the program with feeling of tension.

On the other hand, the subjects feel no action is the fittest situation to concentrate the learning contents. And the frequency of the head movement is the lowest when the system dose nothing. But the "pattern 3: nothing" gets the lowest score in the memory test even though there is not so large deference. These result that the system has a possibility not to grasp the subject in foggy state, where the subject doesn't move his/her head, and spread his/her focus.

As all results, it have been confirmed that the proposed expression by the eye robot shows the presence in the individual learning system, and then the subject feel like the robot is watching and the subject have been able to take the program with feeling of tension.

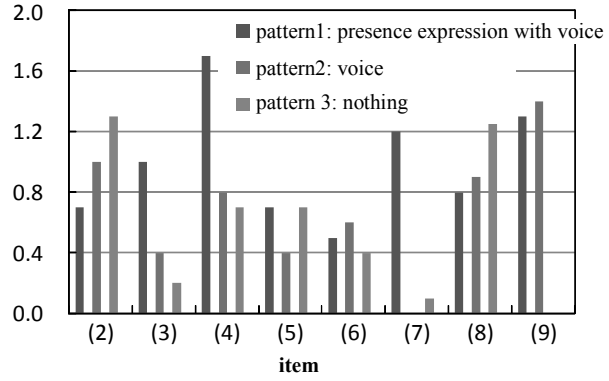

Figure 6. the score of the subjective estimation

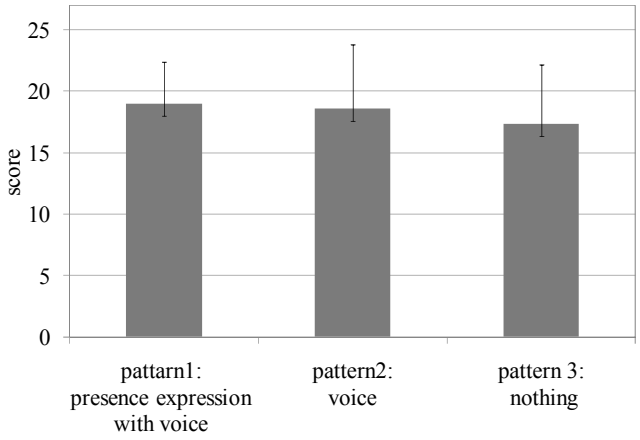

Figure 7. the score of memory test for learning contents

TABLE I. THE FREQUANCY OF THE SUBJECT'S HEAD MOBEMENT

average times		
pattern1: presence expression with voice	pattern2: voice	pattern3: nothing
8.2	6.1	5.6

TABLE II. THE ATTENTION SPAN OF THE SUBJECTS

average attention span[s]		
pattern1: presence expression with voice	pattern2: voice	pattern3: nothing
436.8	388.7	487.5

TABLE III. THE SCORE OF THE MEMORY TEST ON LEARNING CONTENTS

average score (out of 27)		
pattern1: presence expression with voice	pattern2: voice	pattern3: nothing
19.0	18.6	17.4

V. CONCLUSION

The presence expressions by eye robot is proposed, where the eye robot expressions help human to more deeply understand robot, and then effectively provide their service in its situation e.g., a personal learning program and an entertainment program. The proposed presence expression is applied a personal education system that involves the eye robot, learning contents on a laptop PC with a web camera, a wii remote (Nintendo Co.,Ltd.) for measuring attention span of a subject based on 3D accelerometer information. To estimate effects of presence expression by the eye robot, subjective questioner is performed in the personal education system. Three type of leaning programs are conducted by the system for 10 subjects with subjective questionnaires evaluated with the 3-poin scale. The results show that the proposed expressions by the eye robot help the subject to feel like one is watching and to have an uncanny impression. As a result, the system has enabled the subjects to take the program with feeling of tension.

This research plans to apply computer go system, another personal educational and entertainment system, where the system realizes casual communication in the games.

REFERENCES

[1] Hoock, J.-B., Chang-Shing Lee, et.al., "Intelligent Agents for the Game of Go," IEEE Computational Intelligence Magazine, Vol.5, No.4, pp.28-42, 2010.

[2] Acampora, G., Loia, V., Gaeta, M., "Exploring e-Learning Knowledge Through Ontological Memetic Agents," Computational Intelligence Magazine, IEEE , vol.5, no.2, pp.66-77, May 2010.

[3] A. Yorita and N. Kubota. "Multi-stage fuzzy evaluation in evolutionary robot vision for face detection," Evolutionary Intelligence vol 3 , pp. 67-78, 2010.

[4] Nishio S., Ishiguro, H. and Hagita, N., "Geminoid: Teleoperated Android of an Existing Person," Humanoid Robots: New Developments, de Pina Filho, A.C. eds., I-Tech Education and Publishing, Vienna, Austria, 2007.

[5] "Telenoid-R1," http://www.irc.atr.jp/Geminoid/Telenoid-overview.html

[6] T. Hashimoto, N. Kato, and H.i Kobayashi, "Field Trial of Android-type Remote Class Support System in Elementary School and Effect Evaluation," Proc. of IEEE International Conference on Robotics and Biomimetics (ROBIO 2009), pp. 1135-1140, 2009..

[7] Y. Yamazaki, K. Hirota, et.al., "Fuzzy Inference based Mentality Expression for Eye Robot in Affinity Pleasure-Arousal Space," Journal of Advanced Computational Intelligence and Intelligent Informatics (JACIII), Vol.12 No.3, pp.304-313, 2008.

2011 IEEE International Conference on Fuzzy Systems
June 27-30, 2011, Taipei, Taiwan

Emotion Recognition based on Human Gesture and Speech Information using RT Middleware

H. A. Vu[1], Y. Yamazaki[2], F. Dong[1], K. Hirota[1]

[1)]Dept. of Computational Intelligence & Systems Science,
Tokyo Institute of Technology
Yokohama, Japan
{vuanhai, tou, hirota }@hrt.dis.titech.ac.jp

[2)]Dept. of Electrical, Electronic, and Information Eng.
Kanto Gakuin University
Yokohama, Japan
yamazaki@ kanto-gakuin.ac.jp

Abstract— **A bi-modal emotion recognition approach is proposed for recognition of four emotions that integrate information from gestures and speech. The outputs from two uni-modal emotion recognition systems based on affective speech and expressive gesture are fused on a decision level fusion by using weight criterion fusion and best probability plus majority vote fusion methods, and the performance of classifier which performs better than each uni-modal and is helpful in recognizing suitable emotions for communication situations. To validate the proposal, fifty Japanese words (or phrases) and 8 types of gestures that are recorded from five participants are used, and the emotion recognition rate increases up to 85.39%. The proposal is able to extent to using more than other modalities and useful in automatic emotion recognition system for human-robot communication.**

Keywords- Emotion Recognition; Decision-level Fusion; Expressive Gesture; Affective Speech

I. INTRODUCTION

In the last years, emerging research in human-robot communication is daily life support robot system such as entertaintment robots system, service robot system, or household robot system. In such systems, robots communicate with humans friendlity by talking to humans and expressing the emotion [1,2] coresponding to the humans' speeches. The casual communication between humans and mutiple robots via both of humans' speech and gestures has proposed in mascot robot system [3, 4]. Recognition users' mood or emotional state is main key to determining the coressponding emotion of robots. Most of the work analizes the human emotion by verbal and non-verbal information. For instance, the emotion recognition using only speech by combining acoustic and semantic analyses [5], and the bi-modal emotion recognition using visual information from expressive face and body gestures [6]. Morerever, the most approach is fusion of both speech information and gesture information [7], also including the expressive faces [8,9].

In this work, the bi-modal emotion recognition is proposed by combining the information from speech, hands and simple body gestures. The motivation of the proposal is improve social communication between humans and robots in assist robot systems. Fisrt, the two uni-modal emotion recognition system for human's speech and gesture are performed separately. Then, at the decision-level fusion, the output of the two uni-modalities are fused by using weight criterion fusion and majority vote fusion methods. The 50 Japanese word or phrases and 8 type of gestures that are using in mascot robot system are used to perform the emotion recognition accuracy.

In II, the overview of mascot robot system is presented. In III, two uni-modal emotion recognitions based on speeches and gestures multimodal are presented; bi-modal emotion recognition on decision-level fusion is proposed. The experiments to confirm the proposal is presented in IV.

II. MASCOT ROBOT SYSTEM

The mascot robot system (MRS) is an information retrieval and recommendation system for household environments which is able to use casual communication between humans and robots through humans' speeches and gestures. In this system, the robots need to recognize human's speeches and give back the actions corresponding to semantic of requirements. Also, the emotional reactions are appeared to do friendly casual communication. The MRS is developed as a national project with the purpose of developing the Common Basis of Next-Generation Robots led by the New Energy and Industrial Technology Development Organization (NEDO 2005-2008), and now under the support from Japan Society for the Promotion of Science (JSPS 2009-2012). The construction of MRS is shown in Fig.1.

In the home environment such as living room, the fixed type robots are setup on furniture and appliances such as the TV, a dart, information retrieval monitor, drink bar, and a self-propelled type mobile robot. Each robot is controlled by a PC. The common server which controls whole system and the four fixed robots are connected using local area network, LAN cables, while the connection with the mobile robot is achieved via a wireless LAN. The overall management server controls and supervises the whole system, allowing it to coordinate the action of the whole group of robots.

In order to connect the system, the Robot Technology

978-1-4244-7316-8/11/$26.00 ©2011 IEEE

middleware (RTM) [10] is used to construct the network system which is called RTM-Network as shown in Fig.2. In RTM-Network, each robot can be viewed as a network component and each function unit of every robot is called a robot technology component (RTC).

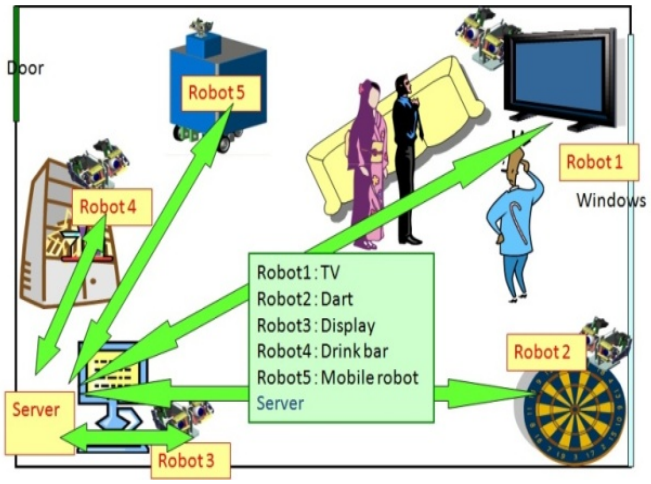

Figure 1. Mascot robot system in a home environment

Every robot is composed of a controlled PC, a microphone,a web camera, a Speech Recognition Module (SRM), a Gesture Recognition Module (GRM), and an Eye robot. The input speeches and gestures that are gotten from the microphone and web camera are processed and then indicated the recognition result on the PC display or written down the information in a log file through the RT Middleware network system. Depending on the recognition results, the eye robot expresses their corresponding emotions through designated actions, and the other actions or talking with people from five robots.

The eye robot on its part has a pair of eyeballs and eyelids. The eyeball movement is based on fuzzy control (up and down, left and right) and serves to express different emotions such as happiness, sadness, surprise, and anger. The eye robots are shown in Fig.2, the appearance of mobile eye robot is shown in Fig.3.

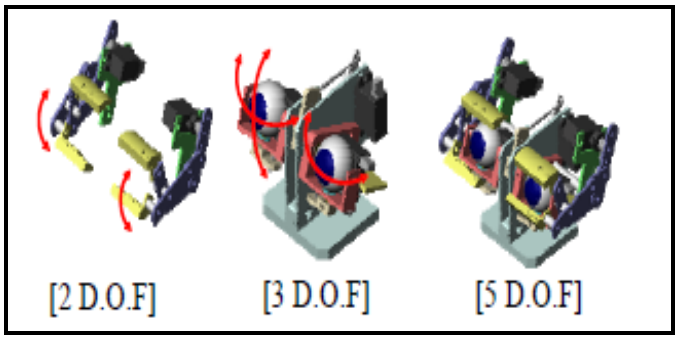

Figure 2. Structure of eye robot

Figure 3. Mobile type eye robot

A host and three guests are considered as users of the MRS. The MRS is ascertained the validity based on a typical situation scenario where the MRS performs representative function of the system. The specification of the scenario is as follows. When the users mention something to the robots that requires an affinity response (for example, "this is interesting", "we won the game", or doing banzai pose, etc...), the system searches for and subsequently provides information based on the user's speech and gestures. Communication between the user and the system is established by the user's speech and gestures to the robots and the robot's response as an emotional expression, as well as displaying information on a screen. For example, the MRS can propose cocktail recipes or provide companionship during a game of darts and reacting accordingly to the performance of the players. The MRS could also take cues from baseball games on TV and offer the user information about the players participating in the game. Futhermore, MRS presents the atmosphere of communications from emotion expresstions of humans and robots.

III. BI-MODAL EMOTION RECOGNITION

A. Uni-modal Emotion recognition

1) Uni-modal Emotion Recognition based on Speeches

To achieve the speakers' emotion based on their speeches, both acoustic analysis and semantic analysis are used in recently research. Here it is assumed that the speakers' expresstion of their emotion consists in meaningful talking words or phrases. Therefore, an approach in spotting for emotional information is needed. In order to reduce the complexity and reduce the cost of speech recognition module (SRM), in this work, free software Julius is used to recognize the human's speech under the RT middleware [10]. The RT-Middleware aims at establishing a common platform based on the distributed object technology and which would support the construction of various networked robotic systems by the integration of various network enabled robotic elements called RT-Components. The concept of the Julius based SRM is shown in Fig.4. There are two RT components to recognize humans' speech. The first component- PulseAudioInput is using a microphone to get the speech signal. The second component-pyJulius is using Python language to recognize the input speech signal. The speech based uni-modal emotion recognion is using the data that collect from 4 people using in

home party scenario in mascot robot system [3,4]. There are five emotion extract from the communicaiton in mascot robot system: happiness, sadness, supriseness, and neutral.

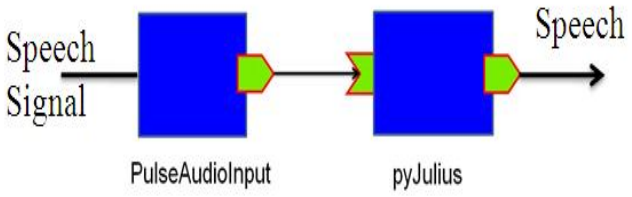

FigURE 4. RTM based speech recognition module

2) Uni-modal Emotion Recognition based on Gestures

Recognition of human emotion from body and hands movements is unresolved in non-verbal communication. In gesture based emotion recognition uni-modal, 8 types of gestures in mascot robot system [3, 4] are used to detect the corresponding emotions. Table 1 provides the list of gesture emotion categories recognized by the system.

The fuzzy Choquet integral [12] based multimodal gesture recognition method is used, where human gestures are recognized based on the fusion of video images and 3D acceleration sensors. The Angular Metrics for Shape Similarity (AMSS) [11] algorithm is employed to evaluate the similarity between gesture templates and input data from the two modules above separately. Next, the optimal fuzzy measures of the Choquet integral are calculated from the training data by a hill climbing algorithm. In the fusion processing, the fused similarities are calculated from similarities of both modules by Choquet integral. Finally, the gesture with maximum fused similarity is chosen as the recognition result. The architecture of the gesture recognition system is shown Fig.5.

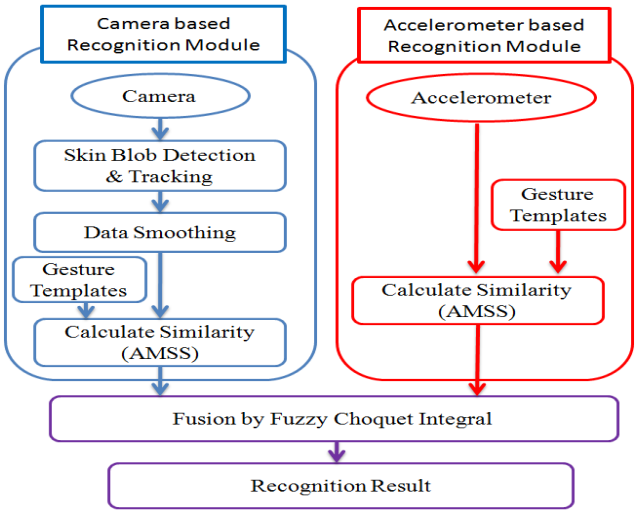

Figure 5. System Architecture of Multimodal Gesture Recognition System

a) Feature Extraction from Acceleration Data

With each gesture time series data, the maximum and minimum are calculated at first. Then the parameters of mean, variance, and mean crossing rate are calculated by:

$$mean = \sum_{k=1}^{N} sample_k / N \quad (1)$$

$$variance = \sum_{k=1}^{N} (sample_k - mean)^2 / N \quad (2)$$

$$mcr = \sum_{k}^{N-1} \mathrm{sgn}(sample_k - mean) - \mathrm{sgn}(sample_{k+1} - mean) \quad (3)$$

where N is the number of total samples of a gesture in the time series data. All of the parameters have be calculated on axis x, y, and z.

In order to indentify the gesture from the eight types of gestures, the Angular Metrics for Shape Similarity (AMSS) [11] is used for measuring the similarity of input sequence and template sequences. The average similarity of the 3-axes is taken as the similarity of this module.

b) Image Recognition Module

Gestures are also recognized by video image processing along with acceleration sensor recognition to help make decisions when the system cannot recognize the gestures from acceleration sensor which is the main part of algorithm. Video image sequences are captured while a web camera is put in front of the human within home environment background. The gesture is extracted from each frame in the stream by three main steps: skin-color detection, head and hands tracking and rules matching.

c) Skin Color Detection and Tracking

The skin detection algorithm is based on the HSV (Hue-Saturation-Value) color space with its robustness to the way that humans tend to perceive colors. Generally, a pixel's color can be considered as skin color if $h_{min} < H < h_{max}$ and $s_{min} < S < s_{max}$,where H,S, and V are the pixel's color components in the HSV color space and, h_{min}, h_{max}, s_{min}, s_{max} are the threshold values. From this operation, three regions including the head and two hands can be found as groups of skin color areas.

B. Bi-modal Emotion Recognition based on Speeches and Gestures

After describing the two uni-modal emotion recognition systems based on semantic information of speech and gestures separately, the effective bi-modal emotion recognition system based on both human's speech and gestures is proposed to do the casual communication between humans and robots. By fusing speech and gesture modalities at the decision level, the combined emotion is classified. The structure of the bi-modal emotion recognition is shown in Fig.6. In the decision level, the output is computed combining the probabilities of the two uni-modal modules. Various researches have been proposed such as sum rule, product rule, median rule, majority vote, etc.

In this work, two different approaches are used to get output emotions by combining the posterior probabilities of the two uni-modal systems. The first approach selects the emotion that received the best probabilities in the two uni-modal system. When each uni-modal system gives the output of different emotion with same probabilities, majority vote is used (in this case, the highest voting for speech based uni-modal system) to get suitable emotions. The second approach selects the emotion using the weight criterion rule. Suppose that, α is assigned as the weight of speech based uni-modal system, β is assigned as the weight of gesture based uni-modal system.

Then, the output emotion is defined by using the weight criterion rule is shown as

$$\text{Emotion (i)} = \arg\max_{i=1,2,\ldots,M} \{ \alpha p(e_i|S) + \beta p(e_i|G) \}, \quad (4)$$

where M denotes the maximum of possible emotions, $p(e_i|S)$ and $p(e_i|G)$ denote probabilities of i^{th} emotion that gotten from each speech based emotion recognition system and gesture based emotion recognition system. Cause of speech is still main language in daily communication, α and β are assigned 0.7 and 0.3 respectively.

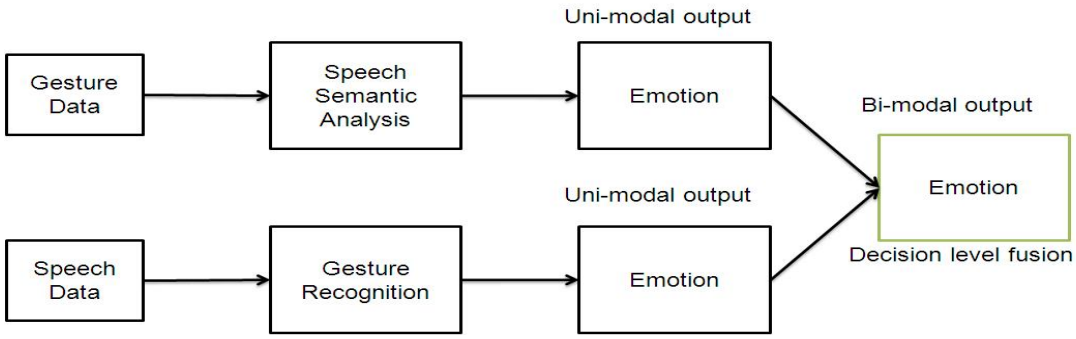

Figure 6. Bi-modal emotion recognition based on speech and gesture

Table 1. 8 types of emotional gestures recognized by the system

Happiness
(G1) **Victory pose**: From the relaxed position besides the legs, the right hand is raised up to a level between the chest and the head.
(G2) **Banzai pose**: Both hands are first put down besides legs and then both are held right up.
Sadness
(G3) **Face covering**: Both hands are first put down besides the legs and then the right hand is held at face.
(G4) **Bye-bye**: Both hands are first put down besides the legs and then the right hand is waved iteratively at right side.
Disappointment
(G5) **Squatting with hands over the head:** From the relaxed position hands besides the legs, both hands are put on the head and human participant squats.
Neutral
(G6) **Toast**: Raising a hand with a glass upwards from the waist level.
(G7) **Dart throwing**: Moving a hand with a dart forward speedily from the head level.
(G8) **Guiding**: From their relaxed position, the right hand beside legs is swung up to the point towards the right direction.

IV. EXPERIMENTS ON BI-MODAL EMOTION RECOGNITION

A. Data Collection

Five participants (4 male and 1 female) within the age range 22 - 30 took part in the recording. The participants are three different nationalities: Japanese, Chinese, and Vietnamese. Fifty (50) Japanese word and phrases, and 8 type of gestures that are used in home party scenario of mascot robot system are recorded. The sample frames of banzai pose gesture are shown in Fig.7.

Figure 7. Banzai pose gesture

B. *Emotion Recognition Results*

1) *Speech based emotion recognition*

Table 2 shows the performance of the uni-modal emotion recognition based on speech. The overall performance of this classifier is 70%. Happiness is recognized with high rate (87.67%). Sadness and Disappointment have lower rates (60.33% and 6.33% respectively).

Table 2. Confusion matrix of emotion recognition based on speeches

	Happiness	Sadness	Disappointment	Neutral
Happiness	87.67	3.33	3.33	5.67
Sadness	3.67	60.33	26.33	9.67
Disappointment	0	23.33	62.33	14.34
Neutral	7.33	13.33	11	68.34

2) *Gesture based emotion recognition*

Table 3 shows the performance of the uni-modal emotion recognition based on humans' gestures. The overall performance of this classifier is 88.5%. Disappointment is classified with the highest rate (96.67). Happiness has the lowest recognition rate of 83.33%.

Table 3. Confusion matrix of emotion recognition based on gestures

	Happiness	Sadness	Disappointment	Neutral
Happiness	83.33	0	0	16.67
Sadness	1.67	85	0	13.33
Disappointment	0	3.33	96.67	0
Neutral	5.55	5.55	0	88.89

3) *Decision-level fusion*

In daily communication, speech is still the main language to express meaningful moods and emotions. Then here the weight criterions are set 0.7 and 0.3 for speeches based uni-modal and gestures based uni-modal respectively. Table 4 shows the performance of the emotion recognition bi-modal based on both speech and gestures. The accuracy of majority vote approach is higher than that of weight criterion.

Table 4. Confusion matrix of emotion recognition based on decision-level fusion

	Weight Criterion	Majority Vote
Happiness	86.67	86.33
Sadness	63.34	80.22
Disappointment	76.63	90.67
Neutral	78.48	84.34
Overall	76.28	85.39

V. CONCLUSIONS

A bi-modal emotion recognition approach is proposed for recognition of four emotions (happiness, sadness, disappointment, and neutral) that integrates information from humans' speech and gestures. The outputs from two uni-modal emotion recognitions based on speech and gestures are fused on the decision level fusion by using weight criterion fusion and best probability plus majority vote fusion methods. The performance of the classifier was found to be better than each of the uni-modal recognition system and is more helpful in recognizing suitable emotions for communication situations. Firstly, two uni-modal emotion recognition are performed under the 50 Japanese word or phrases and 8 types of gestures that are recorded from five participants. Then, two approaches on the decision-level fusion are performed and obtained 76.28% and 85.39% respectively. The proposal is able to extent to using more than other modalities and useful in automatic emotion recognition system for human-robot communication.

References

[1]. H. Gunes, M. Piccardi, "Bi-modal emotion recognition from expressive face and body gesture", Journal of Network and Computer Applications, pp. 1334-134, 2007.

[2]. P. Bernardis, M. Gentilucci, "Speech and gesture share the same communication system", Neuropsychologia, Vol.44, pp.178-190, 2006.

[3]. Y. Yamazaki, H. A. Vu et al., "Mascot Robot System by Integrating Eye Robot and Speech Recognition using RT Middleware and its Casual Information Recommendation", 3rd International Symposium on Computational Intelligence and Industrial Applications (ISCIIA2008), 2008, pp. 375-384.

[4]. Y. Yamazaki, H. A. Vu et al., "Gesture Recognition Using Combination of Acceleration Sensor and Images for Casual Communication between Robots and Humans", IEEE Word Congress on Computational Intelligence, 2010, pp. 18-23.

[5]. H. A. Vu, Y. Yamazaki et al., "The Interrupt of Mascot Robot System Embedded in RT Middleware Based on Fuzzy Logic", FACTA UNIVERSITATIS Series: Mechanics, Automatic Control and Robotics, 7-1, 2009,pp. 11-28.

[6]. R. Douglas-Cowie, E. Tsapatsoulis et al., "Emotion recognition in human-computer interaction", Signal Process Magazine, IEEE 18-1, 2001,pp. 32-80.

[7]. Z. Liu, F. Dong et al., "Proposal of Fuzzy Atmosfield for Mood Expression of Human-Robot Communication", International Symposium on Intelligent Systems(iFAN), 2010.

[8]. A. Suzuki, T. Hoshino, and K. Shigemasu, "Measuring individual differences in sensitivities to basic emotions in faces", Cognition, Vol. 99, Issue 3, 2006, pp. 327-353.

[9]. A. I. Goldman and C. S. Sripada "Simulationist models of face-based emotion recognition", Cognition, Vol. 94, Issue 3, 2005, pp.193-213.

[10]. http://www.openrtm.org/OpenRTM-aist/html/FrontPage.html

[11]. T. Nakamura, K. Taki et al., "AMSS: A Similarity Measure for Time Series Data", IEICE D, 91-D-1, 2008,pp. 2579-2588.

[12]. T. Murofushi and M. Sugeno, "An Interpretation of Fuzzy Measures and the Choquet Integral as an Integral with Respect to a Fuzzy Measure", Fuzzy Sets and Systems 29, 1989, pp. 201-227.

2011 IEEE International Conference on Fuzzy Systems
June 27-30, 2011, Taipei, Taiwan

FCMdd-type Linear Fuzzy Clustering for Incomplete Non-Euclidean Relational Data

Takeshi Yamamoto, Katsuhiro Honda, Akira Notsu, Hidetomo Ichihashi
Department of Computer Science and Intelligent Systems
Osaka Prefecture University
1-1 Gakuen-cho, Nakaku, Sakai, Osaka 599-8531, Japan
Email: {honda, notsu, ichi}@cs.osakafu-u.ac.jp

***Abstract*—A linear fuzzy clustering model based on Fuzzy c-Medoids (FCMdd) was proposed for extracting intrinsic local linear substructures from relational data. In the same way with Non-Euclidean Relational Fuzzy (NERF) c-Means, β-spread transformation was also proved to be useful for handling non-Euclidean relational data in FCMdd-type linear clustering. In this paper, the FCMdd-type linear clustering model is further modified in order to handle incomplete data including missing values. In several numerical experiments, it is demonstrated that some pre-imputation strategies contribute to properly selecting representative medoids of each cluster.**

***Keywords*—relational clustering, linear fuzzy clustering, missing value.**

I. Introduction

Relational data analysis is an important technique for revealing intrinsic structure of relational data composed of mutual relations among objects. Besides the basic fuzzy clustering models for object-type data such as Fuzzy c-Means (FCM) [1], which is a fuzzy extension of k-Means [2], several relational fuzzy clustering models have been proposed for extracting cluster substructures from relational data. Relational Fuzzy c-Means (RFCM) [3] is the basic FCM-type relational clustering model, which can be identified with FCM when mutual relations are given by Euclidean distances. k-Medoids approach [5] is an alternative of FCM-type clustering where cluster prototypes are not given by mean vectors but are chosen from object sets. Krishnapuram *et al.* [4] extended (hard) k-Medoids to Fuzzy c-Medoids (FCMdd), in which the chosen object called "medoid" is the representative object of a cluster. FCMdd-type clustering models can easily be applied to relational data matrices without calculating cluster centroids in a intrinsic data space.

FCM-type linear fuzzy clustering models such as Fuzzy c-Lines (FCL) [6] and its variants [7] use linear-shape prototypes like lines, planes and linear varieties. Fitting lines or linear varieties to data sets, the linear clustering models perform fuzzy principal component analysis (fuzzy PCA) [8] in each cluster [9]. Haga et al. [10] proposed an FCMdd-type linear clustering model where each linear prototype is spanned by several representative "medoids".

This work was funded in part by the Ministry of Education, Culture, Sports, Science and Technology, Japan, under Grant-in-Aid for Scientific Research (20700214).

When relational data are not Euclidean, FCM-type and FCMdd-type clustering models cannot be directly applied because their algorithms are essentially designed for Euclidean data space. Hathaway and Bezdek [11] proposed non-Euclidean-type Relational Fuzzy (NERF) c-Means, in which a spreading transformation called β-spread transformation is performed in order to decrease the influences of non-Euclidean relations. Yamamoto *et al.* [12] applied the β-spread transformation to FCMdd-type linear clustering and demonstrated that a suitable data transformation is achieved by selecting proper parameter values automatically.

In [13], Hathaway and Bezdek demonstrated that the β-spread transformation is also useful for handling missing elements in relational data matrices, in which the bad influences of imputation errors are decreased by β-spread transformation. This paper demonstrates that the performance of FCMdd-type linear fuzzy clustering for incomplete relational data can also be improved by β-spread transformation through several experiments.

II. FCMdd-type Linear Clustering for Relational Data

A. FCM-type Linear Clustering

Assume that we have m dimensional observations of n samples $\boldsymbol{x}_i = (x_{i1}, \ldots, x_{im})^\top, i = 1, \ldots, n$ and that the goal is to partition the n samples into C clusters. The objective function for FCM-type clustering is defined as:

$$L_{fcm} = \sum_{c=1}^{C} \sum_{i=1}^{n} u_{ci}^{\theta} D_{ci} \tag{1}$$

where u_{ci} is the fuzzy membership degree of sample i to cluster c, and θ is the fuzzification parameter. The larger the θ, the fuzzier the membership assignment. The clustering criterion D_{ci} is the distance between sample i and the prototype of cluster c. Besides point-type prototypes in FCM, FCL used linear prototypes defined as:

$$Line_c(\boldsymbol{b}_c, \boldsymbol{a}_c) = \{\boldsymbol{x} | \boldsymbol{x} = \boldsymbol{b}_c + t\boldsymbol{a}_c; t \in R\}, \tag{2}$$

where $\boldsymbol{a}_c$ is the basis vector of the principal sub-space. The clustering criterion is calculated as:

$$D_{ci} = ||\boldsymbol{x}_i - \boldsymbol{b}_c||^2 - |\boldsymbol{a}_c^\top (\boldsymbol{x}_i - \boldsymbol{b}_c)|^2. \tag{3}$$

978-1-4244-7316-8/11/$26.00 ©2011 IEEE

The updating rules for membership u_{ci} and the cluster center $\boldsymbol{b}_c$ are derived as:

$$u_{ci} = \left[\sum_{l=1}^{C} \left(\frac{D_{ci}}{D_{li}} \right)^{\frac{1}{\theta-1}} \right]^{-1}, \tag{4}$$

$$\boldsymbol{b}_c = \frac{\sum_{i=1}^{n} u_{ci}^{\theta} \boldsymbol{x}_i}{\sum_{i=1}^{n} u_{ci}^{\theta}}. \tag{5}$$

The basis vectors $\boldsymbol{a}_c$ are the principal eigenvectors of the generalized fuzzy scatter matrix:

$$S_{fc} = \sum_{i=1}^{n} u_{ci}^{\theta} (\boldsymbol{x}_i - \boldsymbol{b}_c)(\boldsymbol{x}_i - \boldsymbol{b}_c)^{\top}. \tag{6}$$

B. FCM-type Relational Clustering

When we have relational data composed of mutual relations among samples $D = \{d_{ij}\}$, the FCM-type objective function is redefined as [3]:

$$L_{rfcm} = \sum_{c=1}^{C} \sum_{i=1}^{n} \sum_{j=1}^{n} \frac{u_{ci}^{\theta} u_{cj}^{\theta} d_{ij}^2}{2 \sum_{t=1}^{n} u_{ct}^{\theta}}. \tag{7}$$

If the mutual relation d_{ij} is given by the Euclidean distance among samples i and j, the relational clustering model is equivalent to FCM with object-type data. However, the clustering model can derive only poor results if the relational information is not Euclidean.

In order to transform a non-Euclidean matrix to one of Euclidean form, Hathaway and Bezdek [11] considered the following β-spread transformation:

$$D_{\beta} = D + \beta \times (M - I), \tag{8}$$

where I is a unit matrix and β is a suitably chosen scalar. M is a matrix whose elements are all 1. It was shown that D_{β} is Euclidean if $PD_{\beta}P$ with $P = I - (1/n)M$ is negative semi-definite, i.e., β is greater than or equal to the largest eigenvalue of PDP. In NERF, β is gradually increased from 0 to a certain value by considering the negative elements of clustering criteria because negative values of the clustering criterion signal the non-existence of Euclidean space and indicate that the current value of β should be increased so that the basic RFCM iteration can be continued.

C. FCMdd-type Linear Clustering

Assume that d_{ij} is the mutual Euclidean distance such that

$$d_{ii} = 0, d_{ij} \geq 0, d_{ij} = d_{ji}, i, j = 0, \ldots, n. \tag{9}$$

FCMdd [4] is a fuzzy extension of k-Medoids, which performs an FCM-like clustering by selecting $\boldsymbol{b}_c$ from objects $\boldsymbol{x}_i$, $i = 1, \ldots, n$. The representative objects are called 'medoids'.

Haga et al. [10] applied the idea to linear fuzzy clustering, in which two representative medoids are selected in each cluster and the prototypical line is defined as:

$$Line_c(\boldsymbol{x}_{c1}, \boldsymbol{x}_{c2}) = \{\boldsymbol{x} | \boldsymbol{x} = \boldsymbol{x}_{c1} + t(\boldsymbol{x}_{c2} - \boldsymbol{x}_{c1}); t \in R\}. \tag{10}$$

The squared Euclidean distance between object i and the prototypical line $Line_c$ is given as:

$$D_{ci} = d_{i,c1}^2 - \frac{(d_{i,c1}^2 - d_{i,c2}^2 + d_{c1,c2}^2)^2}{4 d_{c1,c2}^2}. \tag{11}$$

With fixed fuzzy memberships u_{ci}, the optimal representative medoids $\boldsymbol{x}_{c1}$ and $\boldsymbol{x}_{c2}$ in cluster c are derived by $\boldsymbol{x}_{q1}$ and $\boldsymbol{x}_{q2}$ as follows:

$$(q1, q2) = \underset{(k1,k2)}{\arg} \min_{\substack{1 \leq k1,k2 \leq n \\ k1 \neq k2}} \sum_{i=1}^{n} u_{ci}^{\theta} D_{ci}. \tag{12}$$

In order to reduce the computational cost of the combinatorial optimization problem, a simplified medoid search process was also proposed such that medoids are selected from a subset X_c of objects having large memberships as follows:

$$(q1, q2) = \underset{(k1,k2)}{\arg} \min_{\substack{\boldsymbol{x}_{k1}, \boldsymbol{x}_{k2} \in X_c \\ k1 \neq k2}} \sum_{i=1}^{n} u_{ci}^{\theta} D_{ci}, \tag{13}$$

where $X_c = \{\boldsymbol{x}_i : u_{ci} > M_{min}\}$.

This linear fuzzy clustering model was also extended to the 2-D prototype case by spanning 2-D prototypical planes using three medoids [10].

When $D = d_{ij}$ is Non-Euclidean, the clustering criterion of Eq.(11) can be negative. From the practical view point, we have no trouble in operating the conventional FCMdd-type linear clustering algorithm if all clustering criteria are not negative. Yamamoto *et al.* [12] proposed a method for automatically transforming non-Euclidean relational data with β-spread transformation when clustering criteria have negative value in FCMdd-type linear clustering. If all relational data elements satisfy triangle inequality, clustering criteria are non-negative, i.e., if triangle inequality ($d_{c1,c2} \leq d_{i,c1} + d_{i,c2}$) is satisfied, the clustering criterion D_{ci} is positive. For all objects, the following triangle inequality transformed by β-spread transformation should be satisfied.

$$d_{c1,c2} + \beta \leq d_{i,c1} + \beta + d_{i,c2} + \beta. \tag{14}$$

Then, the β should satisfy the following relation:

$$\beta \geq d_{c1,c2} - d_{i,c1} - d_{i,c2}. \tag{15}$$

and, a plausible value of $\triangle\beta$ in a iteration step is obtained as:

$$\triangle\beta = \max\{d_{c1,c2} - d_{i,c1} - d_{i,c2} - \beta\}, \tag{16}$$

where $\triangle\beta = 0$ if $\triangle\beta < 0$. Then, β is monotonically increasing.

A sample procedure including the automated β-spread transformation can be summarized as follows:

Step.1 Set $\beta = 0$. Randomly initialize the prototypical medoids (two representative objects) of each cluster.
Step.2 Calculate the clustering criteria D_{ci} .
Step.3 If there are at least one object that has $D_{ci} < 0$, update $\beta = \beta + \triangle\beta$ by Eq.(16).
Step.4 Update fuzzy memberships.

Step.5 Search medoids in each cluster.

Step.6 Repeat Steps 2-5 until a certain stopping criterion is satisfied.

III. Application to Incomplete Relational Data Including Missing Elements

In real applications, relational data matrices may have missing elements. In such cases, the FCMdd-type linear clustering algorithm should be applied after imputing the missing elements. Hathaway and Bezdek [13] demonstrated that the β-spread transformation is also useful for handling missing elements in relational data matrices, in which β-spread transformation is responsible for decreasing the bad influences of imputation errors. This paper considers the applicability of several imputation techniques used in [13] in FCMdd-type linear clustering.

Hathaway and Bezdek [13] used three imputation technique based on triangle inequality-based approximation(TIBA).

A. minimax TIBA

The triangle inequality, which Euclidean relational data always satisfy, is represented as follows:

$$d_{ij} \leq d_{ik} + d_{kj}. \tag{17}$$

Assume that an element of relational matrix $\tilde{d_{ij}}$ is missing and that it brings

$$\tilde{d}_{ij} = \tilde{d}_{ji}. \tag{18}$$

Let K_{ij} as the corresponding index set as

$$K_{ij} = \{k | d_{ik} \text{ and } d_{kj} \text{ exist}\}. \tag{19}$$

Although it is very rare that K_{ij} is empty, $\tilde{d_{ij}}$ is defined as zero value if K_{ij} is empty. For each $k \in K_{ik}$, the triangle inequality Eq.(17) is given as upper bound of $\tilde{d_{ij}}$. In minimax TIBA, missing elements are replaced with the minimum upper bound of $\tilde{d_{ij}}$:

$$\tilde{d}_{ij} = \tilde{d}_{ji} = \min_k \{d_{ik} + d_{kj}\}. \tag{20}$$

B. maximin TIBA

The triangle inequality is also represented as follows:

$$d_{ik} \leq \tilde{d}_{ij} + d_{jk} \tag{21}$$

$$d_{jk} \leq \tilde{d}_{ji} + d_{ik}. \tag{22}$$

and brings the following inequalities:

$$\tilde{d}_{ij} \geq d_{ik} - d_{jk} \tag{23}$$

$$\tilde{d}_{ji} \geq d_{jk} - d_{ik} \tag{24}$$

So, the lower bound of $\tilde{d_{ij}}$ is given as:

$$\tilde{d}_{ij} \geq |d_{ik} - d_{jk}|. \tag{25}$$

In maximin TIBA, missing elements are replaced with the maximum lower bound of $\tilde{d_{ij}}$:

$$\tilde{d}_{ij} = \tilde{d}_{ji} = \max_k \{|d_{ik} - d_{jk}|\}. \tag{26}$$

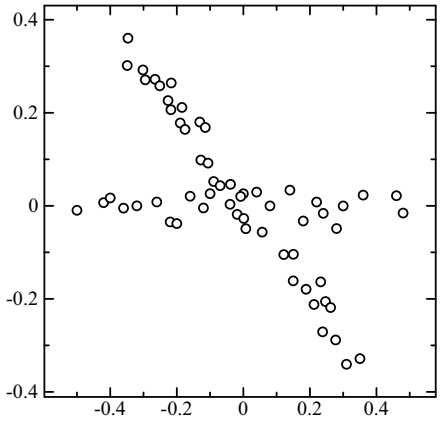

Fig. 1. 2-D plots of artificial data set

C. Average TIBA

It is also reasonable to use the complement value of the previous two imputation values. In average TIBA, the average values of minimax TIBA and maximin TIBA is used for imputing missing elements.

These imputation techniques based on triangle inequalities can be easily applied to relational clustering problems. In the next section, these three imputation approaches are compared in FCMdd-type linear clustering tasks in conjunction with β-spread transformation.

IV. Numerical Experiments

Several experimental results are shown in order to consider the applicability of the three TIBA imputation techniques in FCMdd-type linear clustering with β-spread transformation.

A. Artificial Data Set 1

First numerical experiment was performed using an artificially generated relational data set. The relational data set composed of 60 objects was generated from a 2-D data set shown in Fig. 1, in which objects form two line-shape clusters. The first relational data matrix was generated by Euclidean norm. The iterative algorithm was performed until the medoids become unchanged and the model parameters were set as $(C, \theta) = (2, 2)$. In order to demonstrate the characteristics of the algorithm, the initial memberships were given in a supervised manner, i.e., $(u_{1i}, u_{2i}) = (0.9, 0.1)$ for the first visual cluster and $(u_{1i}, u_{2i}) = (0.1, 0.9)$ for the second one.

Figure 2 shows the cluster partition (maximum membership partition) derived by FCMdd-based linear fuzzy clustering without missing elements, where objects were partitioned into two clusters of circles and times, smaller times has very fuzzy memberships, and the medoids and prototypical lines are indicated by black circles and lines, respectively. This Euclidean relational data can be successfully partitioned without β-spread transformation.

Next, incomplete relational data matrices were generated by removing a part of off-diagonal elements so that K_{ij} was not empty. In order to protect tridiagonal parts of relational

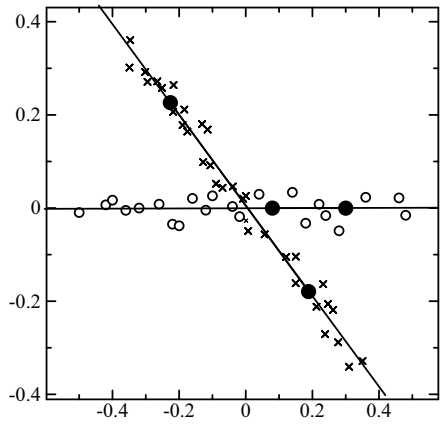

Fig. 2. Cluster partition of Euclidean data without missing elements

data, the maximum number of missing elements was set as $n^2 - 3n + 2$.

Clustering results are depicted in Fig. 3. Each approximation method could estimate cluster medoids for capturing the two visual linear prototypes until the numbers of missing elements are less than about 30%. Small crosses having ambiguous memberships increased more than complete relational data of Fig. 2. β-spread transformation performed on each approximation, e.g. minimax TIBA: $\beta = 0.04867$, maximin TIBA: $\beta = 0.044286$, average TIBA: $\beta = 0.051706$. The maximum eigenvalues of PDP were also calculated as minimax TIBA:0.053808, maximin TIBA:0.1711612, average TIBA:0.083694. This results imply that the FCMdd-type linear clustering can successfully extract linear substructures of incomplete Euclidean relational data using β-spread transformation although the three imputation technique could regenerate non-Euclidean relational matrices only.

B. Artificial Data Set 2

The second relational data matrix was generated by using L1 norm from Fig. 1. Figure 4 shows the cluster partition derived without missing elements. The linear substructures were successfully estimated by using β-spread transformation with $\beta = 0.005808$, which is much smaller than the maximum eigenvalue of PDP 0.44933. In this way, β-spread transformation plays an important role for handling non-Euclidean relational data in FCMdd-type linear clustering.

Next, incomplete relational data matrices were generated in a same manner with the Euclidean case. Clustering results were depicted in Fig. 5. Minimax TIBA and average TIBA could extract linear prototypes until the numbers of missing elements are less than about 60%, and maximin TIBA also could until about 40%. The parameters β in β-spread transformation were given as, minimax TIBA: $\beta = 0.23344$, maximin TIBA: $\beta = 0.137577$, average TIBA: $\beta = 0.165504$. The derived β values are still smaller than the maximum eigenvalues of PDP, minimax TIBA:0.655306, maximin TIBA:0.427750, average TIBA:0.619776. In this way, β-spread transformation also works well in incomplete situations.

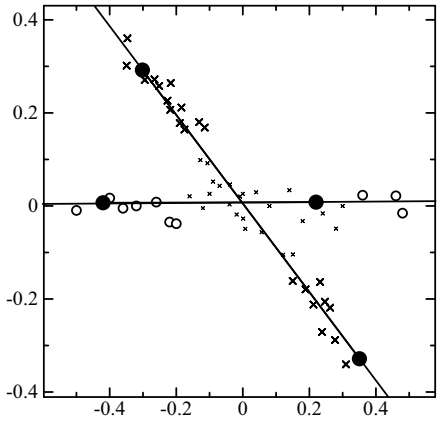

(a) minimax TIBA (# missing: 500)

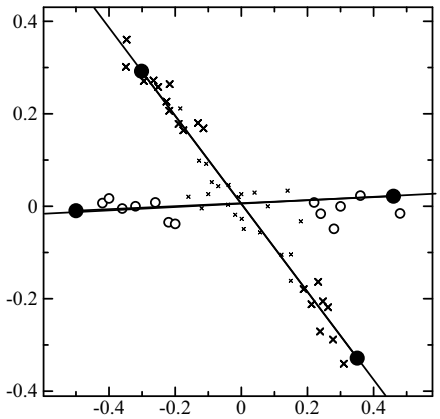

(b) maximin TIBA (# missing: 400)

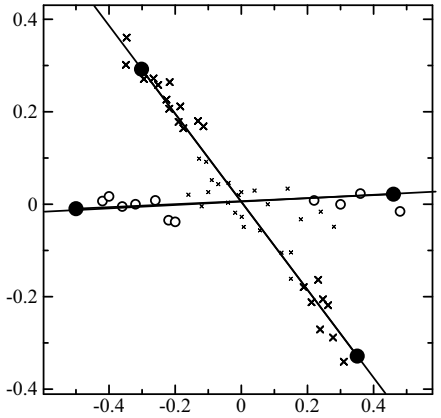

(c) average TIBA (# missing: 500)

Fig. 3. Comparison of cluster partitions from relational data imputed by three TIBA (Euclid norm)

C. Ekman's Color Similarities Data

Third, the proposed algorithm is applied to the Ekman's color similarities data [14]. The 14×14 data matrix is composed of mutual similarities among 14 different colors. In this experiment, mutual similarities s_{ij} are first transformed

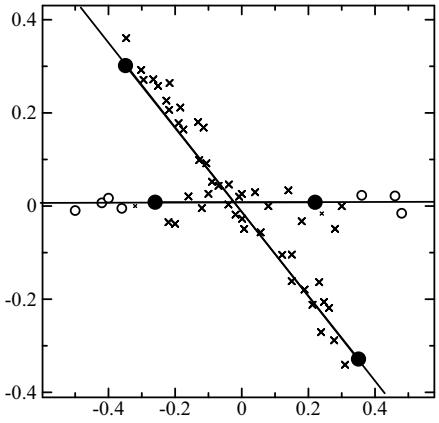

Fig. 4. Cluster partition of L1 norms without missing elements

into dis-similarity measure as follows:

$$d_{ij} = \max_{k,l} s_{kl} - s_{ij}. \tag{27}$$

In the proposed algorithm, parameters were set as $C = 2$, $\theta = 2.0$. Figure 6 shows the derived cluster partitions on the 2-D plane constructed by multi-dimensional scaling (MDS) [15]. Minimax TIBA and average TIBA derived a same cluster partition, in which colors from purple to blue belonged to the first cluster while colors from yellow, green to red belonged to another cluster. Other colors equally belonged to both classes. This cluster partition is almost similar to the case without missing elements. Maximin TIBA also derived a similar partition to the other imputation technique, but this partition was more ambiguous. The parameters β in β-spread transformation were given as, minimax TIBA: $\beta = 275.085$, maximin TIBA: $\beta = 59.776$, average TIBA: $\beta = 134.000$. The derived β values are still smaller than the maximum eigenvalues of PDP, minimax TIBA:430.8659, maximin TIBA:150.667, average TIBA:192.596. Here, maximin TIBA gave a much smaller β value than the maximum eigenvalues of PDP. It may be the reason why it derived a very ambiguous partition.

D. Rothkopf Morse Code Confusion Data

Fourth, the proposed approach is applied to the classical Rothkopf Morse code confusion data [16]. The (36 $\times$ 36) relational data is composed of confusion rates among 36 Morse code signals (26 letters and 10 digits). Before the experiment, the asymmetric relational data matrix, whose element s_{ij} represents the percentage of trials that i was identified as j, was transformed into a symmetric relational data matrix as follows:

$$d_{ij} = s_{ii} + s_{jj} - s_{ij} - s_{ji} \tag{28}$$

The model parameters were set as $C = 3$, $\theta = 2.0$. Clustering results are depicted in Fig. 7, which constructed on the 2-D plane by MDS. Minimax TIBA and average TIBA allowed with 30 % missing values or fewer. Maximin TIBA resulted in a good partition with 10 % missing values or

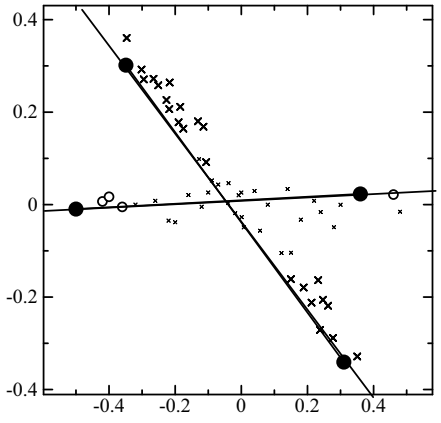

(a) minimax TIBA (# missing: 1000)

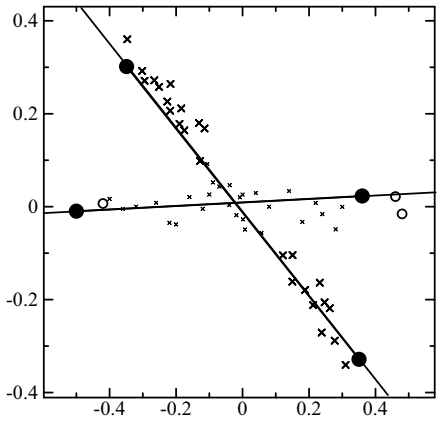

(b) maximin TIBA (# missing: 700)

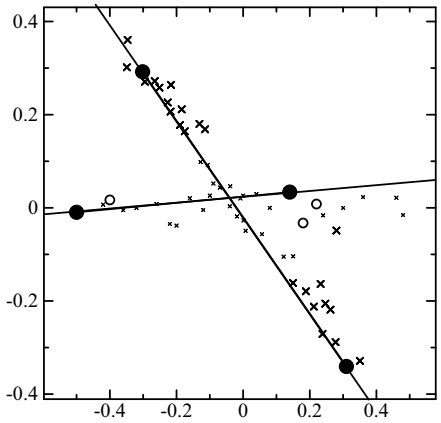

(c) average TIBA (# missing: 1100)

Fig. 5. Comparison of cluster partition from relational data imputed by three TIBA (L1 norm)

fewer. The parameters β in β-spread transformation were given as, minimax TIBA: $\beta = 226.945$, maximin TIBA: $\beta = 91.523$, average TIBA: $\beta = 0.0$. The derived β values are still smaller than the maximum eigenvalues of PDP, minimax TIBA:460.808, maximin TIBA:173.284, average TIBA:132.503. In this experiment, average TIBA was the best imputation method of the three TIBA, because average

TIBA did not need β-spread transformation. However, a similar partition was derived with β-spread transformation even when missing values were imputed by other methods.

In this way, β-spread transformation also works well with incomplete real world data.

V. Conclusion

This paper considered the applicability of β-spread transformation for handling incomplete relational data in FCMdd-type linear clustering. In numerical experiments, three imputation techniques of minimax TIBA, maximin TIBA and average TIBA were compared using two artificially generated data sets and a real one. The experimental results indicated that β-spread transformation still works well for incomplete data while minimax TIBA and average TIBA seem to be better than maximin TIBA. It is because that relational data imputed by maximin TIBA were more non-Euclidean.

A potential future work is extension to the case of multi-dimensional prototype models.

References

[1] J. C. Bezdek: *Pattern Recognition with Fuzzy Objective Function Algorithms*, Plenum Press, 1981.

[2] J. B. MacQueen, "Some methods of classification and analysis of multivariate observations," *Proc. of 5th Berkeley Symposium on Math. Stat. and Prob.*, pp. 281-297, 1967.

[3] R. J. Hathaway, J. W. Davenport and J. C. Bezdek: "Relational duals of the *c*-means clustering algorithms," *PatternRecognition*, vol. 22, no. 2, 1989, pp. 205-212.

[4] R. Krishnapuram, A. Joshi, O. Nasraoui and L. Yi: "Low-complexity fuzzy relational clustering algorithms for web mining," *IEEE Trans. Fuzzy Systems*, vol.9, no.4, pp.595-607, 2001.

[5] L. Kaufman and P. J. Rousseeuw, *Finding Groups In Data: An Introduction To Cluster Analysis*, Wiley-Interscience, 1990.

[6] J. C. Bezdek, C. Coray, R. Gunderson and J. Watson, "Detection and characterization of cluster substructure I. Linear structure fuzzy *c*-lines," *SIAM Jour. of Appl. Math.*, vol.40, no.2, pp.339-357, 1981.

[7] J. C. Bezdek, C. Coray, R. Gunderson, and J. Watson, "Detection and characterization of cluster substructure 2. Fuzzy *c*-Varieties and convex combinations thereof," *SIAM J. Appl. Math.*, vol.40, no.2, pp.358-372, 1981.

[8] Y. Yabuuchi and J. Watada, Fuzzy principal component analysis and its application, *Biomedical Fuzzy and Human Sciences*, vol. 3, pp. 83-92, 1997.

[9] K. Honda and H. Ichihashi, "Regularized linear fuzzy clustering and probabilistic PCA mixture models," *IEEE Trans. Fuzzy Systems*, vol. 13, no. 4, pp. 508-516, 2005.

[10] N. Haga, K. Honda, A. Notsu and H. Ichihashi, "Local sub-space learning by extended fuzzy *c*-medoids clustering," *International Journal of Knowledge Engineering and Soft Data Paradigms*, vol. 2, no. 2,pp. 169-181, 2010.

[11] R. J. Hathaway and J. C. Bezdek: "Nerf c-means: non-Euclidean relational fuzzy clustering," *Pattern Recognition*, vol. 27, no. 3, pp. 429-437, 1994.

[12] T. Yamamoto, K. Honda, A. Notsu and H. Ichihashi: "An FCMdd Based Linear Clustering Model for Non-Euclidean Relational Data" *Proc. of Joint 5th International Conference on Soft Computing and Intelligent Systems and 11th International Symposium on Advanced Intelligent Systems*, pp.243-247, 2010.

[13] R. J. Hathaway and J. C. Bezdek: "Clustering incomplete relational data using the non-Euclidean relational fuzzy *c*-means algorithm" *Pattern RecognitionLetters*, vol. 23, no. 1-3, 1994, pp. 151-160.

[14] G. Ekman, "Dimensions of color vision," *Journal of Psychology*, vol. 38, pp. 467-474, 1954.

[15] W. S. Torgerson, *Theory & Methods of Scaling*, Wiley, 1958.

[16] E. Z. Rothkopf, "A measure of stimulus similarity and errors in some paired-associate learning tasks," *Jour. Experimental Psychology*, vol. 53, pp.94-101, 1957.

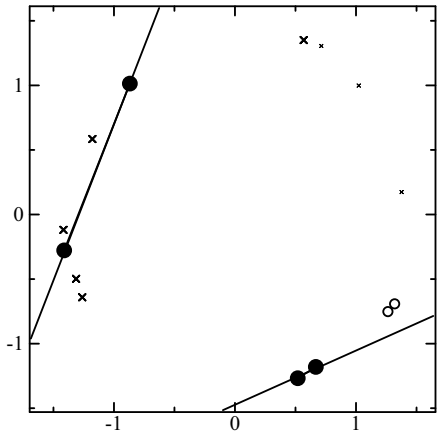

(a) minimax TIBA (# missing: 70)

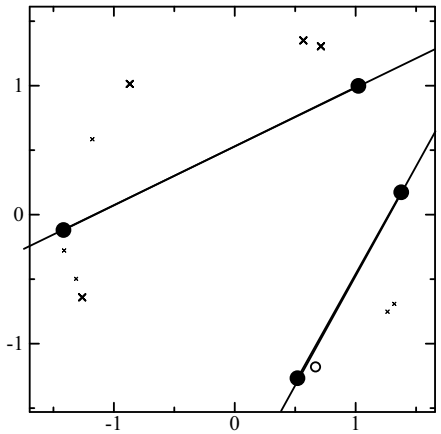

(b) maximin TIBA (# missing: 40)

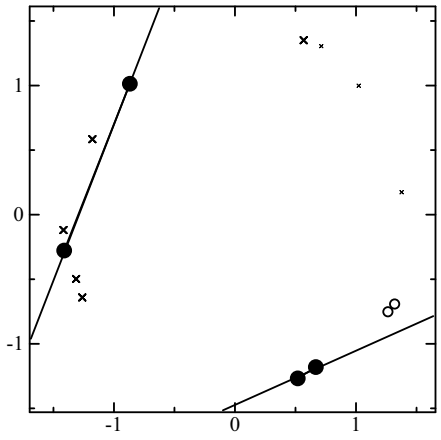

(c) average TIBA (# missing: 70)

Fig. 6. Comparison of cluster partition from incomplete Ekman's color data imputed by three TIBA

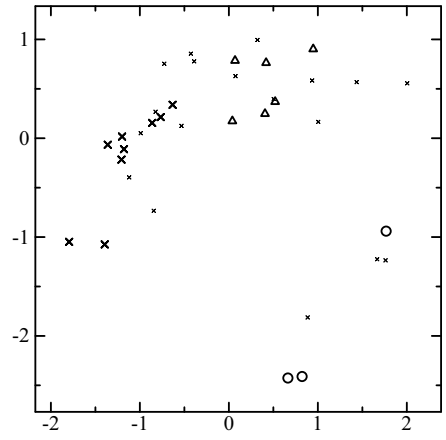

(a) minimax TIBA (# missing: 300)

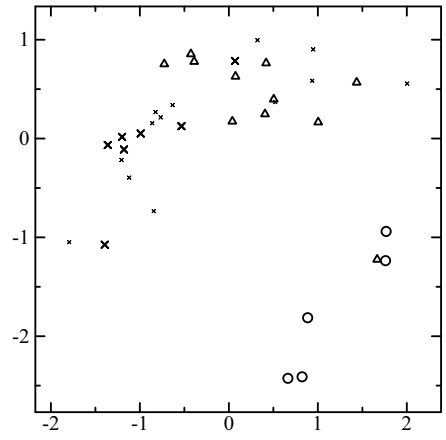

(b) maximin TIBA (# missing: 100)

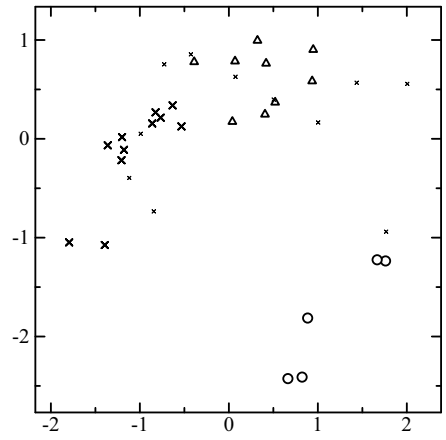

(c) average TIBA (# missing: 300)

Fig. 7. Comparison of cluster partition from incomplete Rothkopf Morse Code Confusion Data imputed by three TIBA

2011 IEEE International Conference on Fuzzy Systems
June 27-30, 2011, Taipei, Taiwan

Hybrid Objective Function of Fuzzy c-Varieties and Cross-shape Fuzzy Cluster Extraction

Daisuke Yoshida, Katsuhiro Honda, Akira Notsu, Hidetomo Ichihashi
Department of Computer Science and Intelligent Systems
Osaka Prefecture University
1-1 Gakuen-cho, Nakaku, Sakai, Osaka 599-8531, Japan
Email: {honda, notsu, ichi}@cs.osakafu-u.ac.jp

***Abstract*—This paper proposes an FCM-type clustering method for capturing cross-shape fuzzy clusters in multi-dimensional data spaces. The proposed objective function is a combination of Fuzzy c-Varieties (FCV) and cross-shape cluster extraction in 2-D space, which is an extended linear fuzzy clustering model with local coordinate rotation. FCV is responsible for finding 2-D planes, on which cross-shape prototypes exist. Each prototypical cross is estimated on the FCV prototypes. Fuzzy memberships are updated using a combined clustering criterion of distances between data samples and FCV prototypes and measures for linear clustering on the FCV prototypes with local coordinate rotation.**

***Keywords*—co-clustering, collaborative filtering, principal component analysis.**

I. Introduction

Many variants of FCM-type clustering models [1], [2], [3] have been proposed by extending the original Fuzzy c-Means (FCM) algorithm [4], which is a fuzzy counterpart of k-Means clustering [5]. If we have some structural information on cluster prototypes, we can modify the point-type prototypes of FCM by replacing with other shapes. Fuzzy c-Lines (FCL) [6] is a linear fuzzy clustering model, in which cluster prototypes are defined by lines having infinite length. Fuzzy c-Varieties (FCV) [7] extended FCL, in which cluster prototypes are defined by linear varieties such as planes and hyper-plane. These linear clustering models have close connection with local principal component analysis (local PCA) [8], [9], in which fuzzy PCA [10] is performed in each cluster based on the FCM-type alternate optimization scheme [11], [12].

Using other non-linear-shape prototypes, many FCM variants such as Fuzzy c-Spherical Shells (FCSS) [13] with circular-shape prototypes, Fuzzy c-Quadric Shells (FCQS) [14] with quadric surfaces and Fuzzy c-Rectangular Shells (FCRS) [15] with rectangular-shape prototypes have been proposed. Yoshida *et al.* [16] proposed a technique for extracting cross-shape clusters in 2-D data space by introducing local coordinate rotation in linear fuzzy clustering. Each cross-shape cluster is composed of two linear sub-clusters and is captured in a single local minor component extraction context [17] by considering coordinate rotation of one sub-cluster around intersection of two linear sub-prototypes.

This work was funded in part by the Ministry of Education, Culture, Sports, Science and Technology, Japan, under Grant-in-Aid for Scientific Research (20700214).

In this paper, the cross-shape extraction model is extended to multi-dimensional cases. In the Gaussian mixture models (GMMs) field, a combined likelihood function was proposed for capturing 2-D non-linear manifolds [18]. In the same manner, this paper proposes a combined objective function of FCV and cross-shape cluster extraction. The objective function for FCV composed of distances between data samples and 2-D plane-like prototypes is responsible for capturing 2-D planes, on which each cross-shape exists. Each cross-shape prototype is estimated in the prototypical 2-D planes. The clustering criteria for updating fuzzy memberships are given by the two criteria.

The remaining parts of this paper are organized as follows. Section II briefly reviews the FCM-type linear fuzzy clustering models and the cross-shape prototype model. Section III proposes a combined objective function. Numerical experimental result is presented in Section IV. Finally, Section V gives conclusion.

II. FCM-type Linear Fuzzy Clustering and Cross-shape cluster extraction

A. Fuzzy c-Lines and Fuzzy c-Varieties

Assume that we have n samples with m dimensional observation $\boldsymbol{x}_i = (x_{i1}, \ldots, x_{im})$, $i = 1, \ldots, n$ and the goal is to partition the samples into C clusters. The FCM algorithm uses point-type prototypes given by mean vectors $\boldsymbol{b}_c = (b_{c1}, \ldots, b_{cm})$, $c = 1, \ldots, C$ and the clustering criterion for cluster c is the squared Euclidean distance d_{ci} between sample $\boldsymbol{x}_i$ and prototype $\boldsymbol{b}_c$. The objective function to be minimized is the weighted within-sum-of-distances.

$$\begin{aligned} L_{fcm} &= \sum_{c=1}^{C}\sum_{i=1}^{n} u_{ci}^{\theta} d_{ci} \\ &= \sum_{c=1}^{C}\sum_{i=1}^{n} u_{ci}^{\theta} ||\boldsymbol{x}_i - \boldsymbol{b}_c||^2. \end{aligned} \quad (1)$$

$u_{ci} \in [0, 1]$ is the fuzzy membership degree of sample i in cluster c and follows the probabilistic constraint of $\sum_{c=1}^{C} u_{ci} = 1$. θ is the fuzzification parameter called 'fuzzifier'. Membership assignment becomes fuzzy as θ becomes large, while $\theta = 1$ reduces a crisp partition of k-Means.

The optimal cluster center for each cluster with fixed memberships u_{ci} is derived as the membership-weighted mean

978-1-4244-7316-8/11/$26.00 ©2011 IEEE

vector.

$$\boldsymbol{b}_c = \frac{\sum_{i=1}^{n} u_{ci}^{\theta} \boldsymbol{x}_i}{\sum_{i=1}^{n} u_{ci}^{\theta}}. \quad (2)$$

With fixed cluster prototypes $\boldsymbol{b}_c$, the optimal memberships satisfying the probabilistic constraint are given as

$$u_{ci} = \left[\sum_{\ell=1}^{C} \left(\frac{d_{ci}}{d_{\ell i}} \right)^{1/(\theta-1)} \right]^{-1}. \quad (3)$$

In the singular situation where some data samples are on prototypes (zero-distances), the data samples are crisply assigned to the prototypes and have zero-memberships to other clusters. These two phases of cluster prototype estimation and membership estimation are repeated until converge based on the alternate optimization scheme.

FCL replaces the point-type prototype with 1-dimensional lines defined as follows:

$$Line_c(\boldsymbol{b}_c, \boldsymbol{a}_c) = \{x | x = \boldsymbol{b}_c + \boldsymbol{a}_c t; t \subseteq R\}. \quad (4)$$

Each line is defined by two vectors of cluster center $\boldsymbol{b}_c$ and basis vector $\boldsymbol{a}_c$. The prototypical line of cluster c is to pass through its cluster center and to be spanned by basis vector $\boldsymbol{a}_c$. The clustering criteria are squared Euclidean distances between sample points and linear prototypes, and the objective function is defined as follows:

$$\begin{aligned} L_{fcl} &= \sum_{c=1}^{C} \sum_{i=1}^{n} u_{ci}^{\theta} D_{ci} \\ &= \sum_{c=1}^{C} \sum_{i=1}^{n} u_{ci}^{\theta} \left(||\boldsymbol{x}_i - \boldsymbol{b}_c||^2 - |\boldsymbol{a}_c^{\top} (\boldsymbol{x}_i - \boldsymbol{b}_c)|^2 \right). \quad (5) \end{aligned}$$

The optimal memberships u_{ci} with fixed cluster prototypes are calculated by Eq.(3) replacing the clustering criteria with $D_{ci} = ||\boldsymbol{x}_i - \boldsymbol{b}_c||^2 - |\boldsymbol{a}_c^{\top} (\boldsymbol{x}_i - \boldsymbol{b}_c)|^2$. With fixed memberships, optimal prototype estimation is achieved in a 2 step procedure. $\boldsymbol{b}_c$ is often updated in a same formula with Eq.(2). Next, basis vector estimation is reduced to fuzzy PCA [10], in which the conventional PCA procedure is performed in a fuzzy set where the fuzzy membership degree of each sample is given by u_{ci}^{θ}. The optimal basis vector of cluster c is the eigen vector corresponding to the largest eigenvalue of the following generalized fuzzy scatter matrix S_{fc}:

$$S_{fc} = \sum_{i=1}^{n} u_{ci}^{\theta} (\boldsymbol{x}_i - \boldsymbol{b}_c)(\boldsymbol{x}_i - \boldsymbol{b}_c)^{\top}. \quad (6)$$

FCV extended FCL into multi-dimensional case. Using p independent basis vectors $\boldsymbol{a}_{ck}, k = 1, \ldots, p$, p-dimensional linear varieties to be used as the prototype of cluster c is given as

$$V_c{}^p(\boldsymbol{b}_c; \boldsymbol{a}_{c1}, \boldsymbol{a}_{c2}, \ldots, \boldsymbol{a}_{cp}) = \{\boldsymbol{x} | \boldsymbol{x} = \boldsymbol{b}_c + \sum_{k=1}^{p} t_k \boldsymbol{a}_{ck}; t_k \in R\}, \quad (7)$$

and the clustering criteria are replaced with the distances between data samples and the linear varieties. The membership updating rule is Eq.(3) with the modified criteria. If cluster center $\boldsymbol{b}_c$ is also updated by Eq.(2), the basis vectors are given by the eigenvectors corresponding to the p largest eigenvalues of S_{fc}.

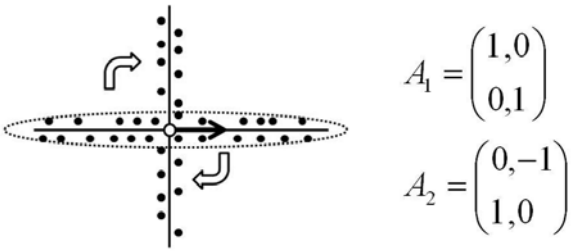

Fig. 1. Definition of prototypical cross-shape and rotation matrix

B. Cross-shape Cluster Extraction in 2-D Data Space

Yoshida *et al.* [16] proposed a technique for capturing the cross-shape substructure by using a single linear prototype. Assume that samples were drawn from a 2-D data space ($m = 2$). The cross-shape prototype of a cluster can be defined by two elements of center point and first normal vector as shown in Fig. 1 where the two lines cross at the center point.

In the model, each cross-shape cluster is further divided into two linear sub-clusters corresponding to the two component lines. The first sub-cluster memberships u_{c1i} represent the degree of belongingness to the first prototypical line whose normal vector is $\boldsymbol{a}_c$. The second ones u_{c2i} correspond to the second line whose basis vector is $\boldsymbol{a}_c$. The conventional membership value for cluster c is recovered by $u_{ci} = u_{c1i} + u_{c2i}$. In order to jointly estimate the two memberships of u_{c1i} and u_{c2i} in a single linear clustering-like procedure, vertical rotation of the second sub-cluster around the center point is considered. The local coordinate rotation matrix for the second sub-cluster is given as A_2 in Fig. 1. The distances between sample i and sub-cluster j in cluster c is given as follows:

$$D_{cji} = ||\boldsymbol{a}_c^{\top} \boldsymbol{A}_j (\boldsymbol{x}_i - \boldsymbol{b}_c)||^2 \quad (8)$$

The objective function is defined based on the minor component analysis concept [17], in which linear manifolds are formulated by normal vectors.

$$\begin{aligned} L_{cross} &= \sum_{c=1}^{C} \sum_{j=1}^{2} \sum_{i=1}^{n} u_{cji}^{\theta} D_{cji} \\ &= \sum_{c=1}^{C} \sum_{j=1}^{2} \sum_{i=1}^{n} u_{cji}^{\theta} |\boldsymbol{a}_c^{\top} \boldsymbol{A}_j (\boldsymbol{x}_i - \boldsymbol{b}_c)|^2, \quad (9) \end{aligned}$$

where the probabilistic constraint for memberships is modified as:

$$\sum_{c=1}^{C} \sum_{j=1}^{2} \sum_{i=1}^{n} u_{cji} = 1. \quad (10)$$

Fuzzy memberships for sub-clusters are given by

$$u_{cji} = \left[\sum_{\ell=1}^{C} \left(\frac{||\boldsymbol{a}_c^\top \boldsymbol{A}_j(\boldsymbol{x}_i - \boldsymbol{b}_c)||^2}{||\boldsymbol{a}_\ell^\top \boldsymbol{A}_j(\boldsymbol{x}_i - \boldsymbol{b}_\ell)||^2} \right)^{\frac{1}{\theta-1}} \right]^{-1}. \quad (11)$$

From the necessary condition for the optimality, center points of prototypical cross-shape are updated as

$$\boldsymbol{b}_c = \frac{\sum_{j=1}^{2}\sum_{i=1}^{n} u_{cji}^{\theta}(\boldsymbol{A}_j^\top \boldsymbol{a}_c \boldsymbol{a}_c^\top \boldsymbol{A}_j \boldsymbol{x}_i)}{\sum_{j=1}^{2}\sum_{i=1}^{n} u_{cji}^{\theta} \boldsymbol{A}_j^\top \boldsymbol{a}_c \boldsymbol{a}_c^\top \boldsymbol{A}_j}. \quad (12)$$

Normal vectors $\boldsymbol{a}_c$ is derived in a similar way to minor component analysis so that $\boldsymbol{a}_c$ corresponds to the smallest eigenvalue of the following modified scatter matrix:

$$\boldsymbol{S}_{fc} = \sum_{j=1}^{2}\sum_{i=1}^{n} u_{cji}^{\theta}(\boldsymbol{x}_{ci}^j - \boldsymbol{v}_c)(\boldsymbol{x}_{ci}^j - \boldsymbol{v}_c)^\top, \quad (13)$$

where x_{ci}^j and $\boldsymbol{v}_c$ are sample vector and cluster center after local coordinate rotation such that

$$\boldsymbol{x}_{ci}^j = \boldsymbol{A}_j(\boldsymbol{x}_i - \boldsymbol{b}_c), \quad (14)$$

$$\boldsymbol{v}_c = \frac{\sum_{j=1}^{2}\sum_{i=1}^{n} u_{cji}^{\theta}\boldsymbol{A}_j(\boldsymbol{x}_i - \boldsymbol{b}_c)}{\sum_{j=1}^{2}\sum_{i=1}^{n} u_{cji}^{\theta}}. \quad (15)$$

Because of coordinate rotation, samples are virtually duplicated and the scatter matrix is calculated using $2n$ objects.

III. Hybrid of FCV and Cross-shape Fuzzy Cluster Extraction

A. Active Curve Axis Gaussian Mixture Models

Zhang *et al.* [18] proposed a non-linear extension of Gaussian mixture models (GMMs) in order to deal with curve manifolds using a non-linear probability model called active curve axis Gaussian model. The non-linear Gaussian model is generated by bending the normal Gaussian model at the first principal axis in 2-D data space. Then, they modified the mixture models into multi-dimensional data space by assuming that the principal axis curves are located in 2-D planes determined by the first two eigenvectors. The modified likelihood function was defined by combining the two measures: deviations from 2-D planes and distances from principal axis on the 2-D planes. The model parameters are estimated by a generalized Expectation-Maximization (EM) algorithm.

In this paper, a similar idea of combining two criteria is performed in order to capture cross-shape clusters in multiple-dimensional data space.

B. Combination of Two Criteria and Generalized Algorithm

In this paper, FCV is combined with cross-shape cluster extraction in 2-D plane. Assume that we have n samples with m dimensional observation $\boldsymbol{x}_i = (x_{i1}, \ldots, x_{im})$, $i = 1, \ldots, n$ and the cluster prototypes are given by cross-shape composed of two lines on 2-D plane. In the FCV part, the prototypical 2-D plane in cluster c is defined by cluster center $\boldsymbol{q}_c$ and basis vectors $\boldsymbol{p}_{c1}$ and $\boldsymbol{p}_{c1}$. Then, the FCV criterion of distance between samples $\boldsymbol{x}_i$ and the 2-D plane is calculated as:

$$d_{ci}^{*} = ||\boldsymbol{x}_i - \boldsymbol{q}_c||^2 - \sum_{k=1}^{2} |(\boldsymbol{x}_i - \boldsymbol{q}_c)^\top \boldsymbol{p}_{ck}|^2. \quad (16)$$

Next, in order to consider the cross-shape cluster extraction in the 2-D plane, samples are projected on the 2-D plane as $\boldsymbol{y}_i = (y_{i1}, y_{i2})^\top$):

$$y_{ij} = \boldsymbol{p}_{cj}^\top(\boldsymbol{x}_i - \boldsymbol{q}_c), \quad j = 1, 2. \quad (17)$$

The cross-shape prototype on the 2-D plane is defined by cluster center (intersection of two lines) $\boldsymbol{b}_c$ and first normal vector $\boldsymbol{a}_c$. Then, the criterion of distance between the projected sample vector $\boldsymbol{y}_i$ and the prototypical cross is calculated as:

$$d_{ci}^{**} = ||\boldsymbol{a}_c^\top \boldsymbol{A}_j(\boldsymbol{y}_i - \boldsymbol{b}_c)||^2. \quad (18)$$

using the two criteria, the combined objective function is defined as:

$$\begin{aligned} L &= \sum_{c=1}^{C}\sum_{j=1}^{2}\sum_{i=1}^{n} u_{cji}^{\theta}(d_{ci}^{*} + d_{ci}^{**}) \\ &= \sum_{c=1}^{C}\sum_{j=1}^{2}\sum_{i=1}^{n} u_{cji}^{\theta}\Bigg(||\boldsymbol{x}_i - \boldsymbol{q}_c||^2 - \\ &\quad + \sum_{k=1}^{2} |(\boldsymbol{x}_i - \boldsymbol{q}_c)^\top \boldsymbol{p}_{ck}|^2 + ||\boldsymbol{a}_c^\top \boldsymbol{A}_j(\boldsymbol{y}_i - \boldsymbol{b}_c)||^2 \Bigg). \end{aligned} \quad (19)$$

The iterative algorithm is composed of three steps. In the first step, prototypical 2-D planes are estimated. Cluster centers $\boldsymbol{q}_c$ are calculated by Eq.(2) where $u_{ci}^{\theta} = u_{c1i}^{\theta} + u_{c2i}^{\theta}$. Basis vectors $\boldsymbol{p}_{ck}$ are given by the k-th principal eigenvector of Eq.(6) replacing $\boldsymbol{b}_c$ with $\boldsymbol{q}_c$.

In the second step, cross-shape prototypes are estimated on 2-D planes. Intersection vectors $\boldsymbol{b}_c$ are calculated by Eq.(12) replacing $\boldsymbol{x}_i$ with $\boldsymbol{y}_i$. Normal vectors $\boldsymbol{a}_c$ are given by the eigenvectors corresponding to the smallest eigenvalues of Eq.(13) replacing $\boldsymbol{x}_i$ with $\boldsymbol{y}_i$.

Then, in the third step, fuzzy memberships for sub-clusters u_{cji} are calculated as:

$$u_{cji} = \left[\sum_{\ell=1}^{C} \left(\frac{d_{ci}^{*} + d_{ci}^{**}}{d_{\ell i}^{*} + d_{\ell i}^{**}} \right)^{\frac{1}{\theta-1}} \right]^{-1}. \quad (20)$$

IV. Numerical Example

A numerical experiment was performed with an artificially generated data set composed of 80 samples. Figure 2 shows the 3-D plots of the data set including two separate cross-shape clusters. The two cross-shape clusters exist on two 2-D planes, which are mutually orthogonal as shown in Fig. 3, and the intersection areas of the two crosses have small distances for both two planes. The goal of the experiment is to capture the two cross-shape sub-structures by partitioning samples into two clusters ($C = 2$). The fuzzification parameter was set as $\theta = 2$. Figure 4 shows the clustering result derived by FCV

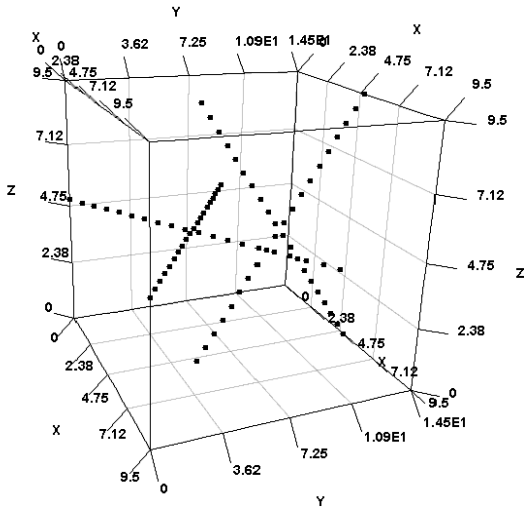

Fig. 2. 3-D plots of the data sets

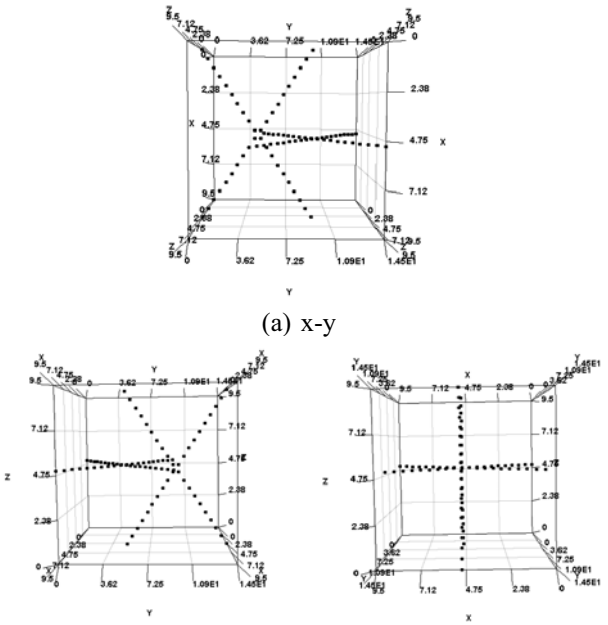

(a) x-y

(b) y-z (c) x-z

Fig. 3. Other views of Fig. 2

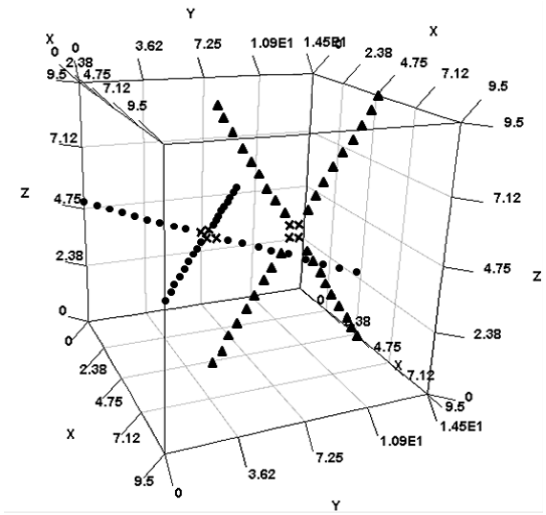

Fig. 4. Clustering result of FCV

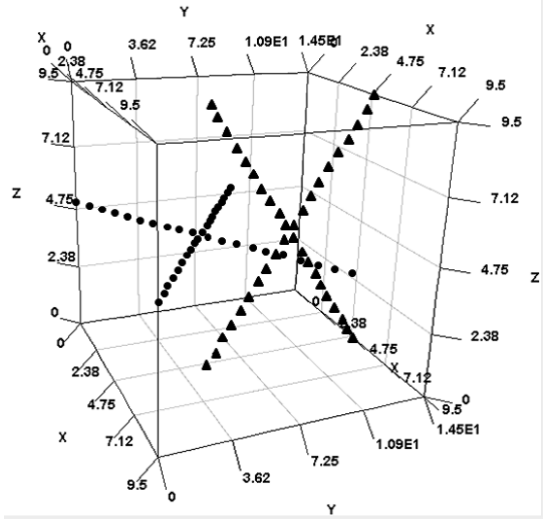

Fig. 5. Clustering result of proposed method

where circles and triangles indicate the maximum membership classification and times indicate the samples having very fuzzy memberships of $u_{ci} \in [0.4, 0.6]$. FCV is useful for capturing 2-D planes, on which cross-shape clusters exist, while it cannot reveal cross-shape substructure. Figure 5 shows the result by the proposed method where two cross-shape clusters were properly extracted. The intersection areas were also properly assigned to clusters by considering both two criteria.

Table I compares the membership degrees of the eight data points, which are described by $\times$ in the intersection of two cross-shapes in Fig. 4. The table indicates that the proposed hybrid approach made it possible to clarify the cross-shape cluster partitions by assgining more crisp memberships. In this way, the proposed hybrid objective function contributes to extraction of cross-shape substructures in multi-dimensional data space.

V. Conclusion

This paper proposed a hybrid objective function of FCV and cross-shape cluster extraction for extracting cross-shape substructures in multi-dimensional data space. The FCV part is responsible for capturing 2-D planes, on which cross-shape substructures exist, while cross-shape cluster extraction part performs linear sub-space learning with local coordinate rotation. Fuzzy memberships are estimated considering both criteria.

A possible future work is hybridization with FCM in such a way with Fuzzy c-Elliptotypes (FCE) [7] for avoiding the size problem of FCL-type linear clustering models. Another

data point		FCV		proposed method	
		Cluster1	Cluster2	Cluster1	Cluster2
Cross1	1	0.535	0.465	0.943	0.057
	2	0.550	0.450	0.947	0.053
	3	0.574	0.426	0.955	0.045
	4	0.625	0.375	0.977	0.023
Cross2	1	0.474	0.526	0.023	0.977
	2	0.465	0.535	0.045	0.955
	3	0.450	0.550	0.053	0.947
	4	0.426	0.574	0.057	0.943

TABLE I
COMPARISON OF MEMBERSHIP DEGREES IN INTERSECTION OF TWO CROSSES

potential future work is related to other shape recognition tasks. By changing rotation angles, the proposed model has ability for handling other shape prototypes.

REFERENCES

[1] F. Höppner, F. Klawonn, R. Kruse, and T. Runkler, *Fuzzy Cluster Analysis*, Jhon Wiley & Sons, 1999.

[2] J. C. Bezdek, J. Keller, R. Krisnapuram and N. R. Pal, *Fuzzy Models and Algorithms for Pattern Recognition and Image Processing*, Springer, 2005.

[3] S. Miyamoto, H. Ichihashi and K. Honda, *Algorithms for Fuzzy Clustering*, Springer, 2008.

[4] J. C. Bezdek, *Pattern Recognition with Fuzzy Objective Function Algorithms*, Plenum Press, 1981.

[5] J. B. MacQueen, "Some methods of classification and analysis of multivariate observations," *Proc. of 5th Berkeley Symposium on Math. Stat. and Prob.*, pp. 281-297, 1967.

[6] J. C. Bezdek, C. Coray, R. Gunderson and J. Watson, "Detection and characterization of cluster substructure I. Linear structure fuzzy *c*-lines," *SIAM Jour. of Appl. Math.*, vol.40, no.2, pp.339-357, 1981.

[7] J. C. Bezdek, C. Coray, R. Gunderson, and J. Watson, "Detection and characterization of cluster substructure 2. Fuzzy *c*-Varieties and convex combinations thereof," *SIAM J. Appl. Math.*, vol.40, no.2, pp.358-372, 1981.

[8] N. Kambhatla and T. K. Leen, "Dimension reduction by local principal component analysis," *Neural Computation*, vol. 9, no. 7, pp. 1493-1516, 1997.

[9] G. E. Hinton, P. Dayan, and M. Revow, "Modeling the manifolds of images of handwritten digits," *IEEE Trans. on Neural Networks*, vol. 8 no. 1, pp. 65-74, 1997.

[10] Y. Yabuuchi and J. Watada, "Fuzzy principal component analysis and its application," *Biomedical Fuzzy and Human Sciences*, vol.3, pp.83-92, 1997.

[11] K. Honda and H. Ichihashi, "Linear fuzzy clustering techniques with missing values and their application to local principal component analysis," *IEEE Trans. on Fuzzy Systems*, vol.12, no.2, pp.183-193, 2004.

[12] K. Honda and H. Ichihashi, "Regularized linear fuzzy clustering and probabilistic PCA mixture models," *IEEE Trans. on Fuzzy Systems*, vol. 13, no. 4, pp. 508-516, 2005.

[13] R. Krishnapuram, O. Nasraoui and H. Frigui, "The fuzzy *c* spherical shells algorithms: a new approach," *IEEE Trans. on Neural Networks*, vol.3, no.5, pp.663-671, 1992.

[14] R. Krishnapuram, H. Frigui and O. Nasraoui, "Fuzzy and possiblistic shell clustering algorithms and their application to boundary detection and surface approximation - Part I," *IEEE Trans. on Fuzzy systems*, vol.3, no.1, pp.29-43, 1995.

[15] F. Höppner, "Fuzzy shell clustering algorithms in image processing: fuzzy *c*-rectangular and 2-rectangular shells," *IEEE Trans. on Fuzzy Systems*, vol.5, no.4, pp. 599-613, 1997.

[16] D. Yoshida, K. Honda, A. Notsu and H. Ichihashi, "Local coordinate rotation for cross-shape cluster extraction in linear fuzzy clustering," *Proc. of Joint 5th International Conference on Soft Computing and Intelligent Systems and 11th International Symposium on Advanced Intelligent Systems*, pp.239-242, 2010.

[17] E. Oja, "Principal components, minor components and linear neural networks," *Neural Networks*, vol.5, 1992, pp.927-935.

[18] B. Zhang, C. Zhang and X.Yi, "Active curve axis gaussian mixture models," *Pattern Recognition*, vol.38, pp.2351-2362, 2005.

2011 IEEE International Conference on Fuzzy Systems
June 27-30, 2011, Taipei, Taiwan

Kernelized Fuzzy c-Means Clustering for Uncertain Data using Quadratic Penalty-Vector Regularization with Explicit Mappings

ENDO Yasunori
Dept. of Risk Eng.
University of Tsukuba
Ibaraki 305-8573, Japan

TAKAYAMA Isao
Dept. of Risk Eng.
University of Tsukuba
Ibaraki 305-8573, Japan

HAMASUNA Yukihiro
Dept. of Informatics
Kinki University
Osaka 577-8502, Japan

MIYAMOTO Sadaaki
Dept. of Risk Eng.
University of Tsukuba
Ibaraki 305-8573, Japan

***Abstract*—Recently, fuzzy c-means clustering with kernel functions is remarkable in the reason that these algorithms can handle datasets which consist of some clusters with nonlinear boundaries. However the algorithms have the following problems: (1) the cluster centers can not be calculated explicitly, (2) it takes long time to calculate clustering results. By the way, we have proposed the clustering algorithms using penalty-vector regularization to handle uncertain data. In this paper, we propose new clustering algorithms using quadratic penalty-vector regularization by introducing explicit mappings of kernel functions to solve the following problems. Moreover, we construct fuzzy classification functions for our proposed clustering methods.**

Keywords*— *clustering, kernel function, uncertain data, penalty-vector regularization, classification function, explicit mapping

I. Introduction

Clustering is one of the data classification techniques and we can classify data without any external criterion using clustering methods. One of most typical and useful clustering methods is fuzzy c-means clustering (FCM) [1] and we consider FCM in this paper.

Now, studies of clustering methods for detecting nonlinear boundary have been widely discussed and kernel trick [2], [3] is focused as a very useful tool to handle datasets which consist of some clusters with nonlinear boundaries. The kernel trick uses some function called "kernel function".

Here, we consider a mapping $\phi : \Re^p \to \Re^s$ $(p \ll s)$. The kernel function is an operator $K : \Re^p \times \Re^p \to \Re$ which satisfies $K(x, y) = \langle \phi(x), \phi(y) \rangle$. We can calculate the value of the inner product in the high-dimensional feature space with low-cost calculation by the kernel functions.

However, special problems frequently arise when we introduce kernel functions into FCM. First, the cluster centers can not be calculated directly. The reason is that the mapping ϕ can not be represented explicitly in general. The second problem is caused by the first one, that is, it takes long time to calculate clustering results. The procedure to calculate the belongingness or membership grades of each data to clusters becomes complicated. To solve the above problems, Miyamoto et al. introduced explicit mappings into kernel trick and succeeded to calculate the cluster centers directly [4].

By the way, the data we handle have uncertainties in many cases. Until now, we have two methodologies to analyze such data, deterministic and parametric ones.

In the deterministic methodology, the uncertainty introduced data is represented as an interval. Distances or dissimilarities are the most essential measures for data analysis and therefore, the measures between intervals must be defined when we handle uncertainty of data as interval. There are many kinds of such measures, e.g., Hausdorff distance. However, we have two problems when we try to classify the dataset of such data. First, we don't have any clear principle to select which measures to use. Second, we can't discuss clustering in the framework of optimization with such measures.

On the other hand, the uncertainty is represented by some probabilistic density function (PDF) in parametric methodology. In this methodology, the clustering is regarded as a method to determine some parameters of the PDF. However, the methodology have also at least one problem, that is, selection of types of PDFs.

Therefore, we have proposed and developed the concept of tolerance in Ref. [5], [6] to solve the above problems. In our concept, tolerance vectors [5] and penalty ones [6] play main role. Uncertain data is allowed to allocate any position by those vectors as far as the constraints for those vectors are satisfied and the position is derived as an optimal solution of a given objective function. Hence, we can say that this concept is in the framework of methodology of soft computing. Penalty vector is a similar concept to tolerance one and the methods using penalty vectors become more flexible than tolerance vectors because no constraint for the vectors is needed. Moreover, the concept has been developed by using kernel trick in Ref. [7]. The method can classify datasets which consist of clusters of uncertain data with nonlinear boundary.

In this paper, we try to construct new FCMs for uncertain data using quadratic penalty-vector regularization with explicit mappings of kernel functions. The proposed methods have the following advantages:

1) The method can classify datasets which consist of clusters of uncertain data with nonlinear boundaries because of kernel trick.
2) The methods can calculate clustering results at shorter

ENDO Yasunori: endo@risk.tsukuba.ac.jp
TAKAYAMA Isao: takayama@soft.risk.tsukuba.ac.jp
HAMASUNA Yukihiro: yhama@info.kindai.ac.jp
MIYAMOTO Sadaaki: miyamoto@risk.tsukuba.ac.jp

978-1-4244-7316-8/11/$26.00 ©2011 IEEE

time than the conventional methods because of explicit mappings.

Moreover, we try to construct fuzzy classification functions for our proposed clustering. Fuzzy classification functions [10] calculate the values of membership grade of arbitrary points for any cluster by handling clustering results as prototypes of supervised classification. Therefore, the functions are very useful tools to give some principle to classify new observations and we can construct the functions because kernel functions can be described as explicit mapping.

II. FCM for Uncertain Data with Regularization Term of Penalty Vectors

A. Preliminaries

First of all, we define some symbols. Each data is denoted $x_k = (x_{k1}, \ldots, x_{kp})^T \in \Re^p$ and the dataset $X = \{x_1, \ldots, x_n\}$ is given. Each cluster $C_i (i = 1, \ldots, c)$ has a cluster center $v_i = (v_{i1}, \ldots, v_{ip})^T \in \Re^p$. V means a set of cluster centers $\{v_1, \ldots, v_c\}$. A membership grade for x_k to C_i, which means belongingness of x_k to C_i, is denoted by u_{ki}. U means a partition matrix $(u_{ki})_{1 \leq k \leq n, 1 \leq i \leq c}$. Moreover, $\delta_k = (\delta_{k1}, \ldots, \delta_{kp})^T \in \Re^p$ and $w_k \in [0, +\infty)$ mean a penalty vector and a weight of the penalty vector δ_k, respectively. Δ and W mean a set of penalty vectors $\{\delta_1, \ldots, \delta_n\}$ and a set of weights $\{w_1, \ldots, w_n\}$, respectively.

B. Objective Functions

As mentioned above, a method using quadratic penalty-vector regularization has been proposed in Ref. [6] as methodology of soft computing. Here, we show the objective function of FCM using quadratic penalty-vector regularization (FCMP).

$$J_{sp}(U, \Delta, V) = \sum_{k=1}^{n} \sum_{i=1}^{c} (u_{ki})^m d_{ki} + \sum_{k=1}^{n} w_k \|\delta_{kj}\|^2, \tag{1}$$

$$J_{ep}(U, \Delta, V) = \sum_{k=1}^{n} \sum_{i=1}^{c} u_{ki} d_{ki} + \lambda^{-1} \sum_{k=1}^{n} \sum_{i=1}^{c} u_{ki} \log u_{ki} + \sum_{k=1}^{n} w_k \|\delta_{kj}\|^2. \tag{2}$$

The dissimilarity d_{ki} is the square of the norm as follows.

$$\begin{aligned} d_{ki} &= d(x_k + \delta_k, v_i) \\ &= \|x_k + \delta_k - v_i\|^2 \\ &= \sum_{j=1}^{p} (x_{kj} + \delta_{kj} - v_{ij})^2. \end{aligned} \tag{3}$$

The constraint is as follows.

$$\sum_{i=1}^{c} u_{ki} = 1, \ u_{ki} \in [0, 1], \ ^\forall k. \tag{4}$$

J_{sp} and J_{ep} are objective functions for the standard FCMP (sFCMP) and the entropy based FCMP (eFCMP), respectively. The solutions can be derived by using Lagrange multiplier.

C. Optimal Solutions and Algorithms

The optimal solutions of sFCMP are as follows:

$$\begin{cases} u_{ki} = \dfrac{(1/d_{ki})^{\frac{1}{m-1}}}{\sum_{l=1}^{c} (1/d_{kl})^{\frac{1}{m-1}}}, & (5) \\ v_i = \dfrac{\sum_{k=1}^{n} (u_{ki})^m (x_k + \delta_k)}{\sum_{k=1}^{n} (u_{ki})^m}, & (6) \\ \delta_k = \dfrac{-\sum_{i=1}^{c} (u_{ki})^m (x_k - v_i)}{w_k + \sum_{i=1}^{c} (u_{ki})^m}. & (7) \end{cases}$$

The optimal solutions of sFCMP are as follows:

$$\begin{cases} u_{ki} = \dfrac{\exp(-\lambda d_{ki})}{\sum_{l=1}^{c} \exp(-\lambda d_{kl})}, & (8) \\ v_i = \dfrac{\sum_{k=1}^{n} u_{ki} (x_k + \delta_k)}{\sum_{k=1}^{n} u_{ki}}, & (9) \\ \delta_k = \dfrac{-\sum_{i=1}^{c} u_{ki} (x_k - v_i)}{w_k + 1}. & (10) \end{cases}$$

We can construct clustering algorithms using the above optimal solutions.

Algorithm 1 (sFCMP and eFCMP):

Step 1 Set the initial values U and Δ.

Step 2 Calculate V by the optimal solution on fixing U and Δ.

Step 3 Calculate U by the optimal solution on fixing Δ and V.

Step 4 Calculate Δ by the optimal solution on fixing V and U.

Step 5 Finish the algorithm if the solutions are convergent, else go back to Step 2.

III. Kernelized FCM for Uncertain Data with Quadratic Regularization Term of Penalty Vectors Using Explicit Mappings

In this section, we try to construct FCM for uncertain data using quadratic penalty-vector regularization with explicit mappings of kernel functions (EK-FCMP). First, we describe kernelized FCM for uncertain data using quadratic penalty-vector regularization (K-FCMP). Next, we introduce explicit mappings of kernel functions into K-FCMP to construct EK-FCMP. Last, we show an algorithm of EK-FCMP.

A. Kernel Functions

First, we define some symbols to introduce kernel functions. A mapping from the pattern space to the feature space is expressed as $\phi : \Re^p \to \Re^s$ $(p \ll s)$. Each data in the feature space is denoted $\phi(x_k) = x_k^\phi = (x_{k1}^\phi, \ldots, x_{ks}^\phi)^T \in \Re^s$ and the dataset $X^\phi = \left\{x_1^\phi, \ldots, x_n^\phi\right\}$ is given. Each cluster $C_i (i = 1, \ldots, c)$ has a cluster center $v_i^\phi = (v_{i1}^\phi, \ldots, v_{is}^\phi)^T \in \Re^s$. V^ϕ means a set of cluster centers $\left\{v_1^\phi, \ldots, v_c^\phi\right\}$. A membership grade for x_k^ϕ to C_i, which means belongingness of x_k^ϕ to C_i, is denoted by u_{ki}. U means a partition matrix $(u_{ki})_{1 \le k \le n, 1 \le i \le c}$. Moreover, $\delta_k^\phi = (\delta_{k1}^\phi, \ldots, \delta_{ks}^\phi)^T \in \Re^s$ and $w_k \in [0, +\infty)$ mean a penalty vector and a weight of the penalty vector δ_k^ϕ, respectively. Δ and W mean a set of penalty vectors $\{\delta_1^\phi, \ldots, \delta_n^\phi\}$ and a set of weights $\{w_1, \ldots, w_n\}$, respectively.

Now, a kernel function $K : \Re^p \times \Re^p \to \Re$ satisfies the following relation:

$$K(x, y) = \langle \phi(x), \phi(y) \rangle \tag{11}$$

From Mercer's theorem [9], K is a continuous symmetric non-negative definite kernel iff a mapping ϕ which satisfies the above relation exists. We should notice that ϕ is not explicit.

B. Objective Functions

Kernelized fuzzy c-means clustering (K-FCM) is FCM in which a kernel function is introduced into dissimilarity. An extended K-FCM by introducing penalty vectors have been proposed in Ref. [7]. We show the objective function of the standard model J_{ksp} and the one of the entropy based model J_{ksp} of K-FCM using quadratic penalty-vector regularization (K-FCMP) as follows:

$$J_{ksp}(U, \Delta^\phi, V^\phi) = \sum_{k=1}^{n} \sum_{i=1}^{c} (u_{ki})^m d_{ki} + \sum_{k=1}^{n} w_k \|\delta_{kj}^\phi\|^2, \tag{12}$$

$$J_{kep}(U, \Delta^\phi, V^\phi) = \sum_{k=1}^{n} \sum_{i=1}^{c} u_{ki} d_{ki} + \lambda^{-1} \sum_{k=1}^{n} \sum_{i=1}^{c} u_{ki} \log u_{ki} + \sum_{k=1}^{n} w_k \|\delta_{kj}^\phi\|^2. \tag{13}$$

The dissimilarity d_{ki} between the k-th uncertain data and the i-th cluster is the square of the norm on the feature space as follows:

$$\begin{aligned} d_{ki} &= d(x_k^\phi + \delta_k^\phi, v_i^\phi) \\ &= \|x_k^\phi + \delta_k^\phi - v_i^\phi\|^2 \\ &= \sum_{j=1}^{s} (x_{kj}^\phi + \delta_{kj}^\phi - v_{ij}^\phi)^2. \end{aligned} \tag{14}$$

The constraint is as follows:

$$\sum_{i=1}^{c} u_{ki} = 1, \ u_{ki} \in [0, 1], \ {}^\forall k. \tag{15}$$

C. Optimal Solutions

We can derive the optimal solutions by using Lagrange multiplier. The optimal solutions of standard K-FCMP are as follows:

$$\begin{cases} u_{ki} = \dfrac{(1/d_{ki})^{\frac{1}{m-1}}}{\sum_{l=1}^{c} (1/d_{kl})^{\frac{1}{m-1}}}, & (16) \\ v_i^\phi = \dfrac{\sum_{k=1}^{n} (u_{ki})^m (x_k^\phi + \delta_k^\phi)}{\sum_{k=1}^{n} (u_{ki})^m}, & (17) \\ \delta_k^\phi = \dfrac{-\sum_{i=1}^{c} (u_{ki})^m (x_k^\phi - v_i^\phi)}{w_k + \sum_{i=1}^{c} (u_{ki})^m}. & (18) \end{cases}$$

The optimal solutions of entropy based K-FCMP are as follows:

$$\begin{cases} u_{ki} = \dfrac{\exp(-\lambda d_{ki})}{\sum_{l=1}^{c} \exp(-\lambda d_{kl})}, & (19) \\ v_i^\phi = \dfrac{\sum_{k=1}^{n} u_{ki} (x_k^\phi + \delta_k^\phi)}{\sum_{k=1}^{n} u_{ki}}, & (20) \\ \delta_k^\phi = \dfrac{-\sum_{i=1}^{c} u_{ki} (x_k^\phi - v_i^\phi)}{w_k + 1}. & (21) \end{cases}$$

We can formally obtain the optimal solutions as above. However, we cannot calculate v_i^ϕ and δ_k^ϕ directly by this method. The reason is that the map ϕ is not explicit and we have to use x_k, not x_k^ϕ. Therefore, Algorithm 1 cannot be adapted and the procedure of K-FCMP becomes more complicated. Hence, We introduce explicit mappings into K-FCMP to calculate v_i^ϕ directly. It is expected that introducing the explicit mappings makes the procedure more simple and makes calculation time short.

D. Optimal Solutions with Explicit Mappings of Kernel Functions

In this paragraph, we introduce explicit mappings of kernel functions [4]. As above, the kernel function K satisfies $K(x, y) = \langle \phi(x), \phi(y) \rangle = \langle x^\phi, y^\phi \rangle$. Now, we consider a kernel function with the kernel matrix $K = (K_{kl}) = (K(x_k, x_l))$. As K is a positive symmetric matrix, we can introduce a inner product $\langle x, y \rangle_K = xKy$ into $\Re^s$. We assume that $\phi : X \to \Re^n$ and $\phi(x_k) = x_k^\phi = e_k$. Here e_k is a unit vector. Because ϕ can be represented explicitly, we call ϕ using the kernel matrix K explicit mapping. Therefore, the inner product is as follows:

$$\langle e_g, e_h \rangle_K = K_{gh}. \tag{22}$$

Thus, the dissimilarity d_{ki} can be calculated as follows:

$$\begin{aligned} d_{ki} &= d(x_k^\phi + \delta_k^\phi, v_i^\phi) \\ &= d(e_k + \delta_k^\phi, v_i^\phi) \\ &= \langle e_k + \delta_k^\phi - v_i^\phi, e_k + \delta_k^\phi - v_i^\phi \rangle_K \\ &= (e_k + \delta_k^\phi - v_i^\phi)^T K (e_k + \delta_k^\phi - v_i^\phi). \end{aligned} \tag{23}$$

We can calculate the optimal solutions by using the above inner product and dissimilarity. First, we show the solutions of standard EK-FCMP (sEK-FCMP) with the explicit mappings as follows:

$$\begin{cases} u_{ki} = \dfrac{(1/d_{ki})^{\frac{1}{m-1}}}{\sum_{l=1}^{c}(1/d_{kl})^{\frac{1}{m-1}}}, & (24) \\ v_i^\phi = \dfrac{\sum_{k=1}^{n}(u_{ki})^m (e_k + \delta_k^\phi)}{\sum_{k=1}^{n}(u_{ki})^m}, & (25) \\ \delta_k^\phi = \dfrac{-\sum_{i=1}^{c}(u_{ki})^m (e_k - v_i^\phi)}{w_k + \sum_{i=1}^{c}(u_{ki})^m}. & (26) \end{cases}$$

Next, we show the solutions of entropy based EK-FCMP (eEK-FCMP) with the explicit mappings as follows:

$$\begin{cases} u_{ki} = \dfrac{\exp(-\lambda d_{ki})}{\sum_{l=1}^{c}\exp(-\lambda d_{kl})}, & (27) \\ v_i^\phi = \dfrac{\sum_{k=1}^{n} u_{ki}(e_k + \delta_k^\phi)}{\sum_{k=1}^{n} u_{ki}}, & (28) \\ \delta_k^\phi = \dfrac{-\sum_{i=1}^{c} u_{ki}(e_k - v_i^\phi)}{w_k + 1}. & (29) \end{cases}$$

E. Algorithm

Here, we construct an algorithm for EK-FCMP using the above optimal solutions with the explicit mappings as follows.

Algorithm 2 (sEK-FCMP and eEK-FCMP):

Step 1 Set the initial values U and Δ^ϕ. Generate the kernel matrix K.

Step 2 Calculate V^ϕ by the optimal solutions with the explicit mappings on fixing U and Δ^ϕ.

Step 3 Calculate U by the optimal solutions with the explicit mappings on fixing Δ^ϕ and V^ϕ.

Step 4 Calculate Δ^ϕ by the optimal solutions with the explicit mapping on fixing V^ϕ and U.

Step 5 Finish if the solutions are convergent, else go back to Step 2.

F. Fuzzy Classification Functions

Fuzzy classification functions [10] calculate the value of membership grade of an arbitrary point for any cluster by handling the clustering result as a prototype of supervised classification. Therefore, The functions are very useful tools to give some indication to classify new observations and it is significant to discuss how to construct the functions in case of the work in this paper. However, it is difficult to construct the functions because the optimal solution of the membership grades includes the term of penalty vectors and the value cannot be calculated directly. Thus, we have to consider another way to calculate the values of membership grades and we try to obtain the values by iterative optimization for an arbitrary point on the pattern space. We show a standard model algorithm to calculate the value of membership grade $u_i(x) = u_i$ of an arbitrary point $x \in \Re^p$ for the i-th cluster.

Algorithm 3:

Step 1 Suppose that a new observation x is given. Derive a cluster center set V^ϕ by Algorithm 2. Introduce $\hat{V}^\phi = \left\{ \hat{v}_i^\phi \mid \hat{v}_i^\phi = (v_{i1}^\phi, \ldots, v_{is}^\phi, 0)^T \right\}$ and generate a kernel matrix $\hat{K} \in \Re^{(n+1)\times(n+1)}$ for the new dataset $\hat{X} = \{X, x\}$. Set an initial penalty vector $\hat{\delta}^\phi \in \Re^{n+1}$ for the observation x.

Step 2 Calculate u_i by the following equation on fixing $\hat{\delta}^\phi$

$$\begin{cases} u_i = \dfrac{(1/d_i)^{\frac{1}{m-1}}}{\sum_{l=1}^{c}(1/d_l)^{\frac{1}{m-1}}}, & (30) \\ d_i = (e_{n+1} + \hat{\delta}^\phi - \hat{v}_i^\phi)^T \hat{K} (e_{n+1} + \hat{\delta}^\phi - \hat{v}_i^\phi). & (31) \end{cases}$$

Step 3 Calculate $\hat{\delta}^\phi$ by the following equation on fixing u_i.

$$\hat{\delta}^\phi = \frac{-\sum_{i=1}^{c}(u_i)^m (e_{n+1} - \hat{v}_i^\phi)}{w(x) + \sum_{i=1}^{c}(u_i)^m}. \tag{32}$$

Step 4 Finish if the solutions are convergent, else go back to Step 2.

We omit the algorithm for eEK-FCMP.

IV. Numerical Examples

We show numerical examples in Fig. 1 $\sim$ Fig. 24. The pattern space is $[0, 1] \times [0, 1]$. We use the following Gaussian kernel:

$$K(x, y) = \exp(-\beta \|x - y\|^2).$$

The parameters are as follows: $m = 1.2$, $\beta = 70$, $\lambda = 1.2$ and $w_k = 3.0$ for all k. We use the same initial values at all case.

We apply the proposed methods to three types of datasets. First, we compare the conventional and the proposed methods through the nesting dataset. Fig. 1 $\sim$ Fig. 4, Fig. 5 $\sim$ Fig. 8, Fig. 9 $\sim$ Fig. 12 and Fig. 13 $\sim$ Fig. 16 are the results by K-sFCM, K-eFCM, sEK-FCMP and eEK-FCMP, respectively. We also show the cluster centers by using kernel principal component analysis (K-PCA) [11].

Next, we apply sEK-FCMP to other two types of datasets. The clustering results are shown in Fig. 17 (double-circle dataset) and Fig. 21 (double-mass dataset). Fig. 18 and Fig. 22 show the cluster centers in the feature space. The dimension of the feature space by Gaussian Kernel is infinite so that we use the kernel principal component analysis (K-PCA) [11] to show the two dimensional Euclidean space. It became possible to show the cluster centers explicitly by our proposed methods. Fig. 19 and Fig. 20, and Fig. 23 and Fig. 24 show the fuzzy classification functions of each cluster for three types of datasets. We can classify the new given data by the classification functions.

In Table I we show the range of w_k when desirable clustering results are obtained. In the range, the larger w_k gets, the faster the algorithm converges and the clearer the shape of the fuzzy classification functions becomes. EK-FCMP, in particular the entropy based model, with the adequate w_k gives more natural results than K-FCM.

TABLE I
THE RANGE OF w_k WHEN OBTAINING DESIRABLE CLUSTERING RESULTS

sEK-FCMP ($\beta = 70, m = 1.2$)	$1.62 \leq w_k \leq 4.96$
sEK-FCMP ($\beta = 40, m = 1.2$)	None
eEK-FCMP ($\beta = 70, \lambda = 10$)	$2.52 \leq w_k \leq 5.68$
eEK-FCMP ($\beta = 40, \lambda = 5.0$)	$13.2 \leq w_k$

V. CONCLUSION

In this paper, we developed FCM for uncertain data using quadratic penalty-vector regularization by introducing explicit mappings of kernel functions. The proposed algorithm has the following features:

1) The algorithm can handle datasets which consist of some clusters with nonlinear boundary.
2) Because of explicit mappings of kernel functions, we reduce the calculation time.
3) The algorithm becomes more simple than the conventional ones.

Moreover, we construct the fuzzy classification functions.

In the forthcoming paper, we will discuss how to find appropriate parameters and apply to real data.

ACKNOWLEDGMENT

This study is partly supported by the Grant-in-Aid for Scientific Research (C) (Project No.21500212) from the Ministry of Education, Culture, Sports, Science and Technology, Japan.

REFERENCES

[1] J. C. Bezdek: *Pattern Recognition with Fuzzy Objective Function Algorithms*, Plenum, New York, 1981.
[2] V. N. Vapnik: *Statistical Learning Theory*, Wiley, New York, 1998.
[3] V. N. Vapnik: *The nature of Statistical Learning Theory*, 2nd edn., Springer, New York, 2000.
[4] S. Miyamoto, Y. Kawasaki, K. Sawazaki: *An Explicit Mapping for Fuzzy c-Means Using Kernel Function and Application to Text Analysis*, IFSA/EUSFLAT 2009, 2009.
[5] Y. Endo, R. Murata, H. Haruyama, S. Miyamoto: *Fuzzy c-Means for Data with Tolerance*, Proc. 2005 International Symposium on Nonlinear Theory and Its Applications, pp.345-348, 2005.
[6] Y. Hasegawa, Y. Endo, Y. Hamasuna: *On Fuzzy c-Means for Data with Uncertainty using Spring Modulus*, SCIS&ISIS 2008, 2008.
[7] Y. Kanzawa, Y. Endo, S. Miyamoto: *Entropy Regularized Fuzzy c-Means for Data with Tolerance introducing Penalty Term in Feature Space*, SCIS&ISIS 2008, 2008.
[8] S. Miyamoto and M. Mukaidono: *Fuzzy c-Means as a Regularization and Maximum Entropy Approach*, Proc. of the 7th International Fuzzy Systems Association World Congress (IFSA'97), Vol.2, pp.86–92, 1997.
[9] J. Mercer: *Functions of Positive and Negative Type and Their Connection with the Theory of Integral Equations*, Philosophical Transactions of the Royal Society A, 209, pp.415–446, 1909.
[10] S. Miyamoto, K. Umayahara, M. Mukaidono: *Fuzzy Classification Functions in the Methods of Fuzzy c-Means and Regularization by Entropy*, Journal of Japan Society for Fuzzy Theory and Systems Vol.10, No.3, pp.548–557, 1998.
[11] B. Schölkopf, A. Smola, and K.-R. Müller: *Nonlinear Component Analysis as a Kernel Eigenvalue Problem*, Neural Computation, Vol.10, pp.1299–1319, 1998.

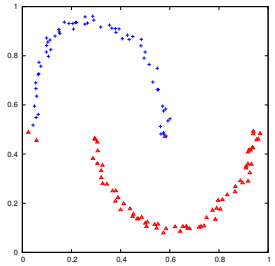

Fig. 1. K-sFCM

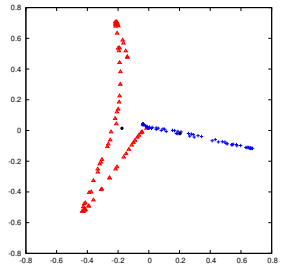

Fig. 2. K-PCA for K-sFCM

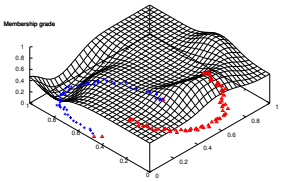

Fig. 3. The fuzzy classification function for K-sFCM (the first cluster)

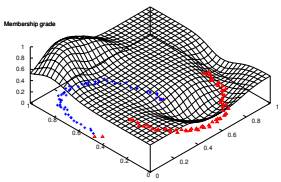

Fig. 4. The fuzzy classification function for K-sFCM (the second cluster)

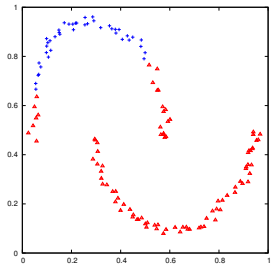

Fig. 5. K-eFCM

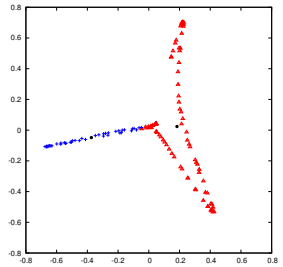

Fig. 6. K-PCA for K-eFCM

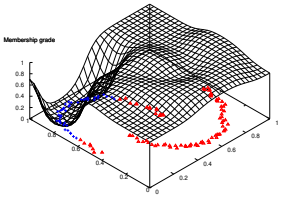

Fig. 7. The fuzzy classification function for K-eFCM (the first cluster)

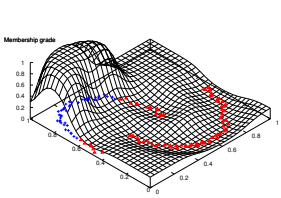

Fig. 8. The fuzzy classification function for K-eFCM (the second cluster)

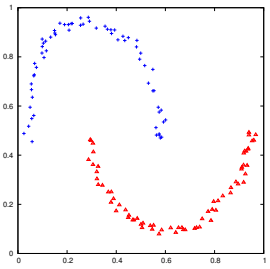

Fig. 9. sEK-FCMP

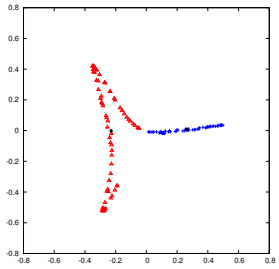

Fig. 10. K-PCA for sEK-FCMP

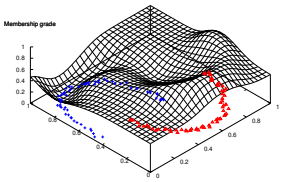

Fig. 11. The fuzzy classification function for sEK-FCMP (the first cluster)

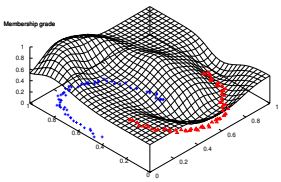

Fig. 12. The fuzzy classification function for sEK-FCMP (the second cluster)

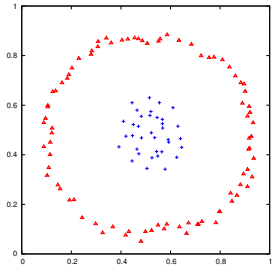

Fig. 17. sEK-FCMP

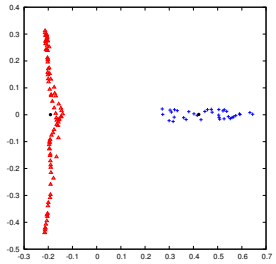

Fig. 18. K-PCA for sEK-FCMP

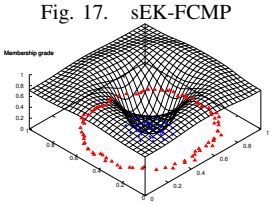

Fig. 19. The fuzzy classification function for sEK-FCMP (the first cluster)

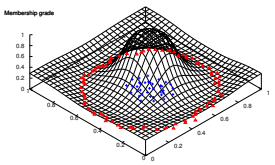

Fig. 20. The fuzzy classification function for sEK-FCMP (the first cluster)

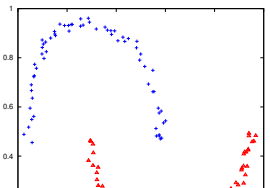

Fig. 13. eEK-FCMP

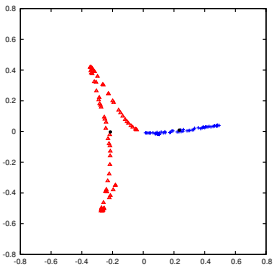

Fig. 14. K-PCA for eEK-FCMP

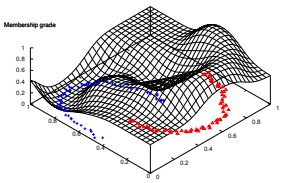

Fig. 15. The fuzzy classification function for eEK-FCMP (the first cluster)

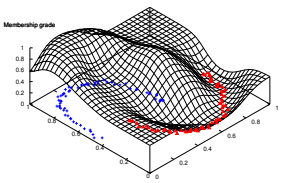

Fig. 16. The fuzzy classification function for eEK-FCMP (the second cluster)

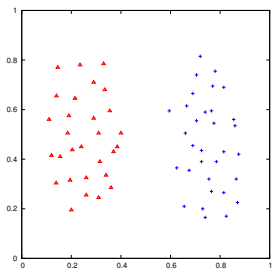

Fig. 21. sEK-FCMP

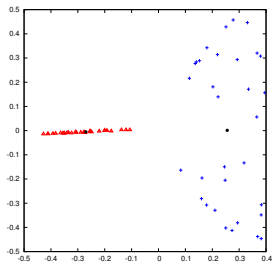

Fig. 22. K-PCA for sEK-FCMP

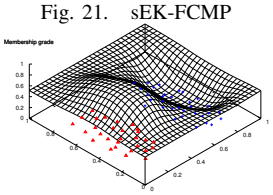

Fig. 23. The fuzzy classification function for sEK-FCMP (the first cluster)

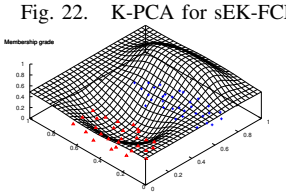

Fig. 24. The fuzzy classification function for sEK-FCMP (the second cluster)

2011 IEEE International Conference on Fuzzy Systems
June 27-30, 2011, Taipei, Taiwan

On Mahalanobis Distance Based Fuzzy c-Means Clustering for Uncertain Data Using Penalty Vector Regularization

Yukihiro Hamasuna
Department of Informatics
School of Science and Engineering, Kinki University
3-4-1 Kowakae, Higashi Osaka, Osaka 577-8502, Japan
Phone: +81-6-6721-2332 (5411);
Email: yhama@info.kindai.ac.jp

Yasunori Endo and Sadaaki Miyamoto
Department of Risk Engineering
Faculty of Sys. and Info. Eng. University of Tsukuba
1-1-1 Tennodai, Tsukuba, Ibaraki 305-8573, Japan
Phone: +81-29-853-5135; Fax: +81-29-853-5135;
email: {endo, miyamoto}@risk.tsukuba.ac.jp

***Abstract*—This paper presents Mahalanobis distance based fuzzy c-means clustering for uncertain data using penalty vector regularization. When we handle a set of data, data contains inherent uncertainty e.g., errors, ranges or some missing value of attributes. In order to handle such uncertain data as a point in a pattern space the concept of penalty vector has been proposed. Some significant clustering algorithms based on it have been also proposed. In conventional clustering algorithms, Mahalanobis distance have been used as dissimilarity as well as squared L_2 and L_1-norm. From the viewpoint of the guideline of dissimilarity, Mahalanobis distance based fuzzy c-means clustering for uncertain data should be considered. In this paper, we introduce fuzzy c-means clustering for uncertain data using penalty vector regularization as our conventional works. Next, we propose Mahalanobis distance based one. Moreover, we show the effectiveness of proposed method through numerical examples.**

***Index Terms*—fuzzy c-means clustering, penalty vector regularization, uncertain data, Mahalanobis distance.**

I. Introduction

Advanced data analysis methods are required in order to discover important properties from massive and complex databases. Data analysis method consists of supervised learning and unsupervised one. Data clustering simply called clustering is the most well-known unsupervised learning method. Clustering is a method which divides a set of objects into some groups which are referred to as clusters. Objects in same cluster are considered similar, while objects in different cluster are considered dissimilar. The method of K-means which referred to as hard c-means clustering (HCM) is the most popular clustering method [1]. Fuzzy c-means clustering (FCM) [2], [3] is an extension of HCM. In fuzzy c-means clustering, squared Euclidean distance [1]–[3], L_1-norm [4], [5] and Mahalanobis distance [6], [7] are used as dissimilarity.

By the way, each data is conventionally handled as a point in a pattern space and analyzed in clustering procedures. However, there are many cases that data contains inherent uncertainty such as errors, ranges or missing value of attributes. Typical examples of uncertain data are as follows:

- **Errors being introduced when the object is mapped from the real space to pattern space:**
  This kind of error is one of the most typical examples. A round-off error, a truncation error, and a reading error margin are introduced when we map a data from the real space to the pattern space.
- **Missing value of attributes:**
  When we handle data from the questionnaires, there are several questions which are not answered. This causes the missing value of attributes.

These uncertain data are represented by other form instead of a point [8], [9]. Even now, handling uncertain data have been actively studied in many researches [8]–[10]. This means handling uncertain data is one of the significant problems in the field of data mining.

From the viewpoint of handling uncertain data, a concept of tolerance has been proposed and formulated into clustering procedures as the constraint [11]. Moreover, clustering algorithms for data with tolerance have been also proposed [12]–[14]. In these clustering methods for data with tolerance, uncertain data is handled as data with tolerance.

In addition, the concept of penalty vector have been proposed to remove the constraint for tolerance [15], [16]. This concept is formulated on the basis of the concept of regularization such as L_2 or L_1 regularization terms. By introducing regularization terms, some fuzzy c-means clustering algorithms have been proposed [17], [18]. In these clustering algorithms, the L_1-norm [17] and the squared L_2-norm [18] are used as dissimilarity. However, Mahalanobis distance based fuzzy c-means clustering using penalty vector concept has not been discussed. From that sense, we propose Mahalanobis distance based fuzzy c-means clustering for uncertain data using penalty vector regularization.

The contents of this paper are the followings. In the second section, we denote some symbols, fuzzy c-means clustering (FCM). In the third section, we introduce the concept of penalty vector regularization. In the forth section, Mahalanobis distance based fuzzy c-means clustering for uncertain data using penalty vector regularization (FCMQS). In the fifth section, we show the effectiveness of proposed method through

978-1-4244-7316-8/11/$26.00 ©2011 IEEE

numerical examples. In the last section, we conclude this paper.

II. Preliminaries

Let a data, a cluster and its cluster center be $x = (x_{k1}, \ldots, x_{kp})^T \in \Re^p$, $(k = 1, \ldots, n)$, $C_i (i = 1, \ldots, c)$ and $v_i = (v_{i1}, \ldots, v_{ip})^T \in \Re^p$, respectively. Moreover, u_{ki} is the membership grade of x_k belonging to C_i and we denote a partition matrix $U = (u_{ki})_{1 \leq k \leq n,\ 1 \leq i \leq c}$. Here, a set of data and a set of cluster center be $X = \{x_1, \ldots, x_n\}$, $V = \{v_1, \ldots, v_c\}$, respectively.

A. Fuzzy c-Means Clustering

Fuzzy c-means clustering is based on optimizing an objective function under the constraint for membership grade.

We consider following two objective functions J_s and J_e.

$$J_s(U, V) = \sum_{k=1}^{n} \sum_{i=1}^{c} (u_{ki})^m d_{ki},$$

$$J_e(U, V) = \sum_{k=1}^{n} \sum_{i=1}^{c} \left\{ u_{ki} d_{ki} + \lambda^{-1} u_{ki} \log u_{ki} \right\}.$$

here, m and λ is fuzzified parameters.

J_s is a well-known objective function as standard fuzzy c-means clustering (sFCM) proposed by Bezdek [2] and J_e is an entropy based fuzzy c-means clustering (eFCM) [3].

The constraint for u_{ki} is as follows:

$$\mathcal{U}_f = \left\{ (u_{ki}) : u_{ki} \in [0, 1], \ \sum_{i=1}^{c} u_{ki} = 1, \ {}^{\forall} k \right\}. \quad (1)$$

The dissimilarity for clustering is generally the squared L_2-norm between each data and a cluster center:

$$d_{ki} = \|x_k - v_i\|^2 = \sum_{j=1}^{p} (x_{kj} - v_{ij})^2.$$

In addition, the L_1-norm based FCM [4], [5] Mahalanobis distance based one [6], [7] are also considered. In Mahalanobis distance based FCM, the dissimilarity is as follows:

$$d_{ki} = (x_k - v_i)^T S_i (x_k - v_i).$$

where $S_i = (S_{ijl})_{1 \leq i \leq c, 1 \leq j, l \leq p}$ is a positive definite matrix having p^2 elements. In Mahalanobis distance based FCM, S_i is handled as a variable for optimization. The set of S_i is denoted by $S = \{S_1, \ldots, S_c\}$. The constraint for S_i is as follows:

$$|S_i| = \rho_i, \ (\rho_i > 0), {}^{\forall} i. \quad (2)$$

where ρ_i is a constant and $|S_i|$ is the determinant of S_i.

B. Concept of Tolerance

In general, each data is regarded as one point and classified into clusters. However, the uncertain data should be often represented in other form, instead of a point. In the concept of tolerance, data is handled as data with tolerance $x_k + \varepsilon_k$ [11]. A tolerance vector $\varepsilon_k = (\varepsilon_{k1}, \ldots, \varepsilon_{kp})^T \in \Re^p$ is within the tolerance κ_k. A set of tolerance vector is denoted as $E = \{\varepsilon_1, \ldots, \varepsilon_n\}$. By introducing this concept, clustering algorithms for data with tolerance have been proposed [12]–[14]. A constraint for tolerance vector is as follows:

$$(\varepsilon_{kj})^2 \leq (\kappa_{kj})^2, \ (\kappa_{kj} \geq 0), {}^{\forall} k, \ j. \quad (3)$$

III. Concept of Penalty Vector Regularization

Next, we introduce a concept of penalty vector. In the above-mentioned clustering algorithms for data with tolerance, the upper bound of ε_k is constrained by (3). Therefore, those clustering algorithms can not handle the data with unknown range. Thus, we have to consider another way to handle uncertain data with unknown range. From the viewpoint of handling uncertain data with unknown range, the concept of penalty vector has been proposed [15], [16]. A penalty vector is denoted as $\delta_k = (\delta_{k1}, \ldots, \delta_{kp})^T \in \Re^p$ and a set of δ_k is $\Delta = \{\delta_1, \ldots, \delta_n\}$. In clustering algorithms by using the concept of penalty vector, the data is represented as $x_k + \delta_k$ [17], [18]. The regularization terms for penalty vector are as follows:

$$\sum_{k=1}^{n} \sum_{j=1}^{p} \omega_{kj} (\delta_{kj})^2, \quad (4)$$

$$\sum_{k=1}^{n} \sum_{j=1}^{p} \omega_{kj} |\delta_{kj}|. \quad (5)$$

where, $\omega_{kj} > 0$ is a regularization parameter.

As the generalization of (4), the quadratic term for δ_k is considered as follows [18]:

$$\sum_{k=1}^{n} \delta_k^T W_k \delta_k. \quad (6)$$

where, $W_k = (\omega_{kjl})_{1 \leq k \leq n,\ 1 \leq j, l \leq p}$ is a positive definite matrix having p^2 elements. In case that W_k is a diagonal matrix, the second term of J_s is the same as (4). In particular, the diagonal elements ω_{kjj} affect d_{ki}. The bigger ω_{kjj} is, the smaller the optimal solution δ_{kj} is. Oppositely, the smaller ω_{kjj} is, the bigger the optimal solution δ_{kj} is. Hence, we know that W_k means the uncertainty of x_k.

By using this concept, fuzzy c-means clustering for uncertain data using penalty vector regularization (FCMQ) has been constructed [18].

IV. Mahalanobis Distance Based Fuzzy c-Means Clustering for Uncertain Data Using Penalty Vector Regularization

In this section, we propose Mahalanobis distance based fuzzy c-means clustering for uncertain data using penalty vector regularization (FCMQS). The dissimilarity for proposed method is Mahalanobis distance between $x_k + \delta_k$ and v_i written as follows:

$$d_{ki} = (x_k + \delta_k - v_i)^T S_i (x_k + \delta_k - v_i).$$

If we fix S_i with unit matrix, proposed method is equivalent to FCMQ.

A. Mahalanobis Distance Based Standard Fuzzy c-Means Clustering for Uncertain Data Using Penalty Vector Regularization

First of all, we propose Mahalanobis distance based standard fuzzy c-means clustering for uncertain data using penalty vector regularization (sFCMQS). The objective function of sFCMQS is as follows:

$$J_s(U,\Delta,V,S)=\sum_{k=1}^{n}\sum_{i=1}^{c}(u_{ki})^m d_{ki}+\sum_{k=1}^{n}\delta_k^T W_k\delta_k.$$

The constraints for u_{ki} and S_i remain the same as (1) and (2). From the convexity of objective function, the constraints (1) and (2), we introduce the following Lagrangian L_s as follows:

$$L_s=J_s(U,\Delta,V,S)+\sum_{k=1}^{n}\gamma_k\left(\sum_{i=1}^{c}u_{ki}-1\right)+\sum_{i=1}^{c}\psi_i\log\frac{|S_i|}{\rho_i}.$$

where, γ_k and ψ_i are Lagrange multiplier.

The optimal solutions for u_{ki} and v_i are derived from $\frac{\partial L_s}{\partial u_{ki}}=0$ and $\frac{\partial J_s}{\partial v_i}=0$ as follows:

$$u_{ki}=\frac{\left(\frac{1}{d_{ki}}\right)^{\frac{1}{m-1}}}{\sum_{l=1}^{c}\left(\frac{1}{d_{kl}}\right)^{\frac{1}{m-1}}},\tag{7}$$

$$v_i=\frac{\sum_{k=1}^{n}(u_{ki})^m(x_k+\delta_k)}{\sum_{k=1}^{n}(u_{ki})^m}.\tag{8}$$

Next, we consider δ_k. From $\frac{\partial J_s}{\partial \delta_k}=0$, we can get

$$\sum_{i=1}^{c}(u_{ki})^m S_i(x_k+\delta_k-v_i)+W_k\delta_k=0.\tag{9}$$

We put two symbols A_k and B_k are as follows:

$$A_k=\sum_{i=1}^{c}(u_{ki})^m S_i+W_k,$$

$$B_k=\sum_{i=1}^{c}(u_{ki})^m S_i(x_k-v_i)$$

Then,

$$A_k\delta_k=B_k.$$

From above, the optimal solution for δ_k is derived as follows:

$$\delta_k=-A_k^{-1}B_k.\tag{10}$$

Last, we consider S_i. From $\frac{\partial L_s}{\partial S_i}=0$, we can get

$$\sum_{k=1}^{n}(u_{ki})^m(x_k+\delta_k-v_i)(x_k+\delta_k-v_i)^T+\psi_i S_i^{-1}=0.$$

From above,

$$S_i=-\psi_i F_i^{-1}.$$

where F_i is following:

$$F_i=\sum_{k=1}^{n}(u_{ki})^m(x_k+\delta_k-v_i)(x_k+\delta_k-v_i)^T$$

From the constraint $|S_i|=\rho_i$,

$$(-\psi_i)^p\left|F_i^{-1}\right|=\rho_i.$$

Hence,

$$-\psi_i=\left(\frac{\rho_i}{\left|F_i^{-1}\right|}\right)^{\frac{1}{p}}.$$

Finally, the optimal solution for S_i is derived as follows:

$$S_i=\left(\frac{\rho_i}{\left|F_i^{-1}\right|}\right)^{\frac{1}{p}}F_i^{-1}.\tag{11}$$

B. Mahalanobis Distance Based Entropy Based Fuzzy c-Means Clustering for Uncertain Data Using Penalty Vector Regularization

Next, we propose entropy based FCMQS (eFCMQS). The objective function of eFCMQS J_e is as follows:

$$J_e(U,\Delta,V)=\sum_{k=1}^{n}\sum_{i=1}^{c}\left\{u_{ki}d_{ki}+\lambda^{-1}u_{ki}\log u_{ki}\right\}+\sum_{k=1}^{n}\delta_k^T W_k\delta_k.\tag{12}$$

The constraints for u_{ki} and S_i remain the same as (1) and (2). By the same procedures, the optimal solutions for u_{ki}, v_i, δ_k and S_i are derived as follows:

$$u_{ki}=\frac{\exp(-\lambda d_{ki})}{\sum_{l=1}^{c}\exp(-\lambda d_{kl})},\tag{13}$$

$$v_i=\frac{\sum_{k=1}^{n}u_{ki}(x_k+\varepsilon_k)}{\sum_{k=1}^{n}u_{ki}},\tag{14}$$

$$\delta_k=-A_k'^{-1}B_k',\tag{15}$$

$$S_i=\left(\frac{\rho_i}{\left|F_i'^{-1}\right|}\right)^{\frac{1}{p}}F_i'^{-1}.\tag{16}$$

where, A_k', B_k' and $F_i'$are as follows:

$$A_k'=\sum_{j=1}^{p}u_{ki}S_i+W_k,$$

$$B_k'=\sum_{i=1}^{c}u_{ki}S_i(x_k-v_i),$$

$$F_i'=\sum_{k=1}^{n}u_{ki}(x_k+\delta_k-v_i)(x_k+\delta_k-v_i)^T$$

C. Algorithm of Proposed Method

The algorithm of FCMQS is described as Algorithm 1. Eqs. **A**, **B**, **C** and **D** used in each algorithm follow Table I.

Algorithm 1 FCMQS

FCMQS1 Set initial values and parameters.
FCMQS2 Calculate $u_{ki} \in U$ by using Equation **A**.
FCMQS3 Calculate $v_i \in V$ by using Equation **B**.
FCMQS4 Calculate $\delta_k \in \Delta$ by using Equation **C**.
FCMQS5 Calculate $S_i \in S$ by using Equation **D**.
FCMQS6 If convergence criterion is satisfied, stop. Otherwise go back to **FCMQS2**.

TABLE I
THE OPTIMAL SOLUTIONS OF FCMQS.

Algorithm	Eq. **A**	Eq. **B**	Eq. **C**	Eq. **D**
sFCMQS	(7)	(8)	(10)	(11)
eFCMQS	(13)	(14)	(15)	(16)

V. NUMERICAL EXAMPLES

In this section, we show numerical examples of FCMQ and FCMQS with Polaris data set. This data set is the star chart of Polaris and its neighboring stars. This data set consists of 51 points which are allocated in two dimensional space and should be classified into three clusters. The fuzzified parameter $m = 2.0$ for sFCMQ and sFCMQS, while $\lambda = 1.0$ for eFCMQ and eFCMQS. Moreover, $\rho_i = 1.0$ in each algorithm.

We show classification results by sFCMQ, sFCMQS, eFCMQ and eFCMQS with some parameters W_k. In Figs. 1, 4, 7, 10, 2, 5, 8, 11 and 3, 6, 9, 12, W_k^1, W_k^2, and W_k^3 are used, respectively.

$$W_k^1 = \begin{pmatrix} 2.0 & 0.0 \\ 0.0 & 2.0 \end{pmatrix}, \ ^\forall k,$$

$$W_k^2 = \begin{pmatrix} 2.0 & 0.2 \\ 0.2 & 2.0 \end{pmatrix}, \ ^\forall k,$$

$$W_k^3 = \begin{pmatrix} 2.0 & 0.2 \\ 0.2 & 1.0 \end{pmatrix}, ^\forall k.$$

From these results, δ_k obtained by sFCMQ and eFCMQ indicate the belonging cluster center, while δ_k obtained by sFCMQS and eFCMQS indicate in the same straight line through the belonging cluster center. The reason is that A_k^{-1} and S_i work as rotation matrix for B_k.

This feature is typical difference between FCMQ and FCMQS. The effectiveness of proposed algorithm is shown from these classification results.

VI. CONCLUSIONS

In this paper, we have introduced the concept of penalty vector regularization in order to handle uncertain data. Moreover, we have proposed Mahalanobis distance based Fuzzy c-Means Clustering for uncertain data using penalty vector regularization (FCMQS). The proposed method is quite different from conventional clustering methods for uncertain data from the viewpoint of handling uncertain data as data with penalty vector. Furthermore, we have verified the effectiveness of proposed methods with numerical examples.

In future works, we will consider the relation and effect between S_i and W_k. Moreover, we will show the effectiveness of our proposed method and consider the features of our proposed methods in detail through various kinds of data set. In particular, it is an important problem to reveal the cluster shapes obtained by proposed method

ACKNOWLEDGMENT

This study is partly supported by Research Fellowships of the Japan Society for the Promotion of Science for Young Scientists and the Grant-in-Aid for Scientific Research (C) (Project No.21500212) from the Ministry of Education, Culture, Sports, Science and Technology, Japan.

REFERENCES

[1] M. R. Anderberg, *Cluster Analysis for Applications*, Academic Press, New York, 1973.
[2] J. C. Bezdek, *Pattern Recognition with Fuzzy Objective Function Algorithms*, Plenum Press, New York, 1981.
[3] S. Miyamoto, M. Mukaidono, Fuzzy c-means as a regularization and maximum entropy approach, *Proc. of the 7th International Fuzzy Systems Association World Congress* (IFSA'97), Vol. 2, pp. 86–92, 1997.
[4] Jajuga K., L_1-norm based fuzzy clustering, Fuzzy Sets and Systems, Vol.39, pp. 43–50, 1991.
[5] Miyamoto S., and Agusta Y., Efficient algorithm for hard clustering and fuzzy clustering using L_1 space, Proceedings of 10th Fuzzy System Symposium, pp. 575–576, 1994.
[6] Gustafson D. E., and Kessel W. C., Fuzzy clustering with a fuzzy covariance matrix, IEEE Conference on Decision and Control including the 17th Symposium on Adaptive Processes, pp. 761–766, 1978.
[7] Höppner F, Klawonn F., Kruse R., and Runkler T., *Fuzzy Cluster Analysis*, John Wiley & Sons, Chichester, 1999.
[8] R. J. Hathaway, J. C. Bezdek, Fuzzy c-means clustering of incomplete data, *IEEE Transactions on Systems, Man, and Cybernetics, Part B : Cybernetics*, Vol. 31, No. 5, pp. 735–744, 2001.
[9] W. K. Ngai, B. Kao, C. K. Chui, R. Cheng, M. Chau, K. Y. Yip, Efficient clustering of uncertain data, *Proc. of the Sixth International Conference on Data Mining* (ICDM2006), pp. 436–445, 2006.
[10] B. Kao, S. D. Lee, D. W. Cheung, W. Ho, K. F. Chan, Clustering uncertain data using voronoi diagrams, *Proc. of Eighth IEEE International Conference on Data Mining* (ICDM2008), pp. 333–342.
[11] Y. Endo, R. Murata, H. Haruyama, S. Miyamoto, 'Fuzzy c-means for data with tolerance, *Proc. of International Symposium on Nonlinear Theory and Its Applications* (Nolta2005), pp. 345–348, 2005.
[12] R. Murata, Y. Endo, H. Haruyama, S. Miyamoto, On fuzzy c-means for data with tolerance, *Journal of Advanced Computational Intelligence and Intelligent Informatics* (JACIII), Vol. 10, No. 5, pp. 673–681, 2006.
[13] Y. Hasegawa, Y. Endo, Y. Hamasuna, S. Miyamoto, Fuzzy c-means for data with tolerance defined as hyper-rectangle, *Proc. of Modeling Decisions for Artificial Intelligence* (MDAI2007), pp. 237–248, 2007.
[14] Y. Hamasuna, Y. Endo, Y. Hasegawa, S. Miyamoto, Two clustering algorithms for data with tolerance based on hard c-means, *Proc. of 2007 IEEE International Conference on Fuzzy Systems* (FUZZ-IEEE 2007), pp. 688–691, 2007.
[15] Yasushi Hasegawa, Yasunori Endo, Yukihiro Hamasuna, On fuzzy c-means for data with uncertainty using spring modulus, Joint 4th International Conference on Soft Computing and Intelligent Systems and 9th International Symposium on advanced Intelligent Systems (SCIS & ISIS 2008), pp. 415–418, 2008.
[16] Yuchi Kanzawa, Yasunori Endo, Sadaaki Miyamoto, Entropy regularized fuzzy c-means for data with tolerance introducing penalty term in feature space, Joint 4th International Conference on Soft Computing and Intelligent Systems and 9th International Symposium on advanced Intelligent Systems (SCIS & ISIS 2008), pp. 578–581, 2008.
[17] Tomoaki Miyamoto, Yasunori Endo, Yukihiro Hamasuna, Sadaaki Miyamoto, On L_1-norm based fuzzy c-means clustering with penalty term, The 6th International Conference on Modeling Decisions for Artificial Intelligence (MDAI2009), pp. 209–220, 2009.
[18] Yasunori Endo, Yasushi Hasegawa, Yukihiro Hamasuna, Yuchi Kanzawa, Fuzzy c-means clustering for uncertain data using quadratic regularization of penalty vectors, Journal of Advanced Computational Intelligence and Intelligent Informatics (JACIII), (to be published).

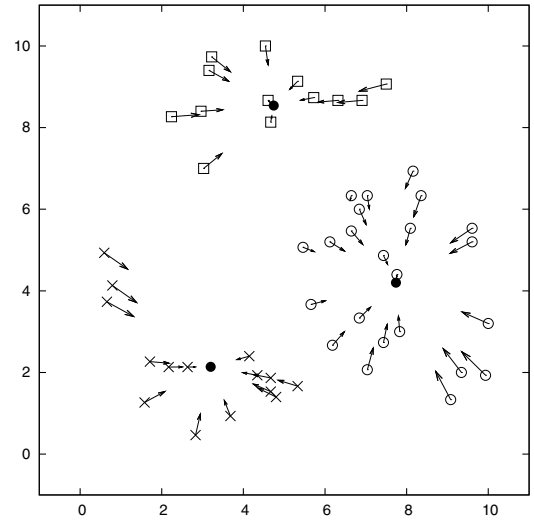

Fig. 1. Classification result 1 by sFCMQ with $\omega_{k11} = \omega_{k22} = 2.0$, $\omega_{k12} = \omega_{k21} = 0.0\ ^{\forall}k$.

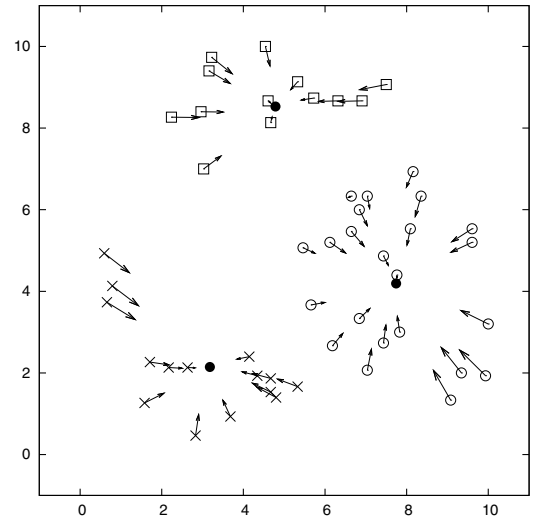

Fig. 2. Classification result 2 by sFCMQ with $\omega_{k11} = \omega_{k22} = 2.0$, $\omega_{k12} = \omega_{k21} = 0.2\ ^{\forall}k$.

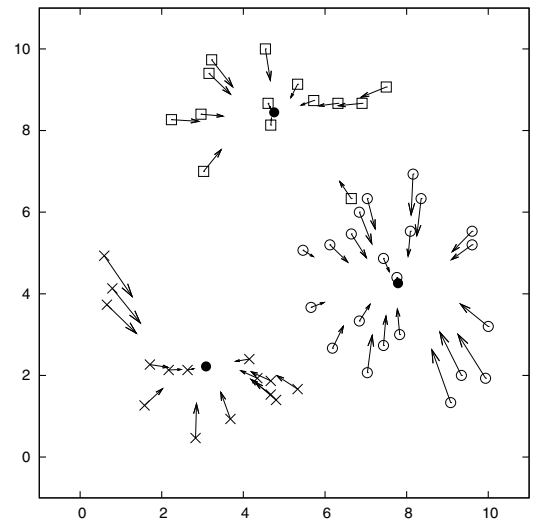

Fig. 3. Classification result 3 by sFCMQ with $\omega_{k11} = 2.0$, $\omega_{k12} = \omega_{k21} = 0.2$, $\omega_{k22} = 1.0\ ^{\forall}k$.

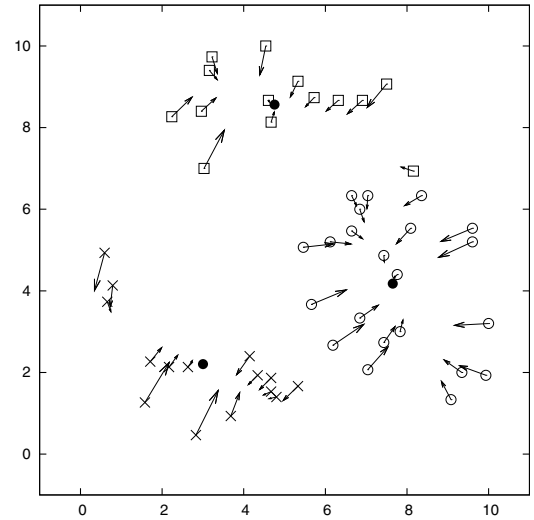

Fig. 4. Classification result 1 by sFCMQS with $\omega_{k11} = \omega_{k22} = 2.0$, $\omega_{k12} = \omega_{k21} = 0.0\ ^{\forall}k$.

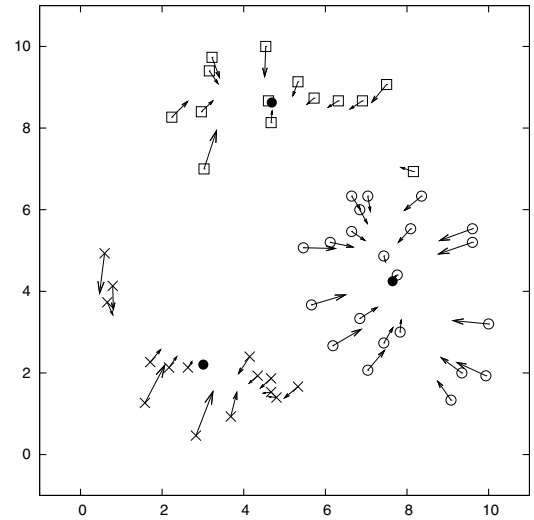

Fig. 5. Classification result 2 by sFCMQS with $\omega_{k11} = \omega_{k22} = 2.0$, $\omega_{k12} = \omega_{k21} = 0.2\ ^{\forall}k$.

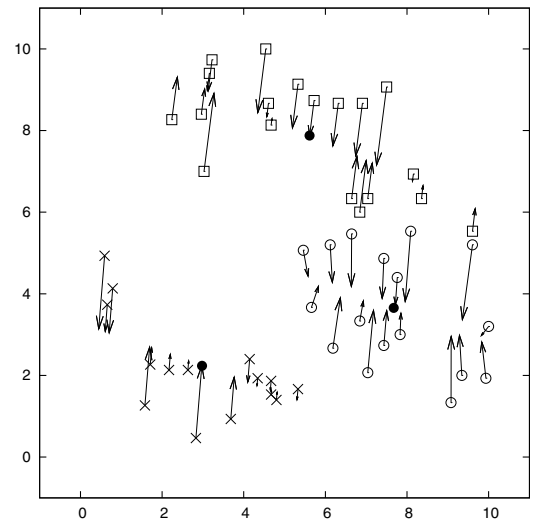

Fig. 6. Classification result 3 by sFCMQS with $\omega_{k11} = 2.0$, $\omega_{k12} = \omega_{k21} = 0.2$, $\omega_{k22} = 1.0\ ^{\forall}k$.

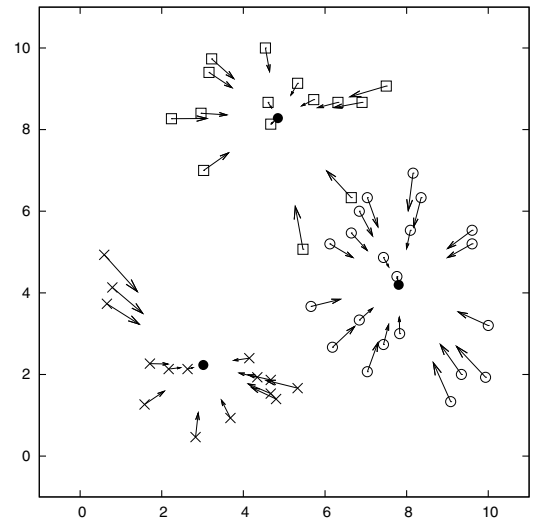

Fig. 7. Classification result 1 by eFCMQ with $\omega_{k11} = \omega_{k22} = 2.0$, $\omega_{k12} = \omega_{k21} = 0.0\ ^{\forall}k$.

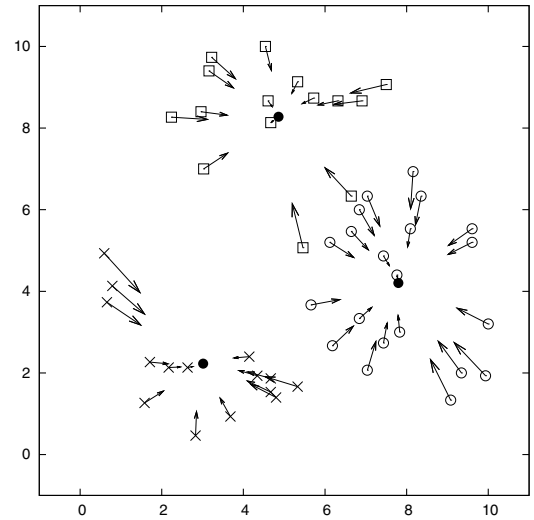

Fig. 8. Classification result 2 by eFCMQ with $\omega_{k11} = \omega_{k22} = 2.0$, $\omega_{k12} = \omega_{k21} = 0.2\ ^{\forall}k$.

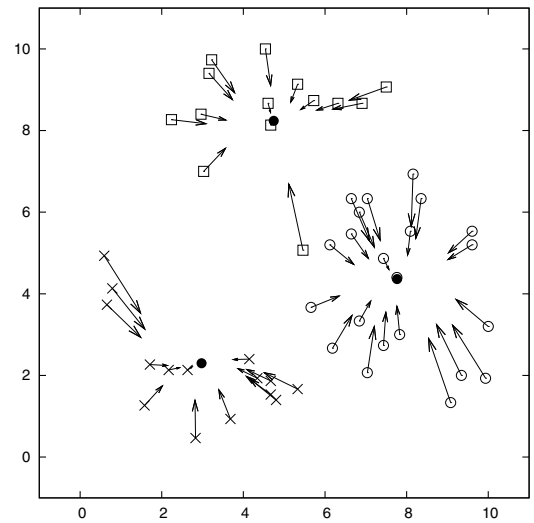

Fig. 9. Classification result 3 by eFCMQ with $\omega_{k11} = 2.0$, $\omega_{k12} = \omega_{k21} = 0.2$, $\omega_{k22} = 1.0\ ^{\forall}k$.

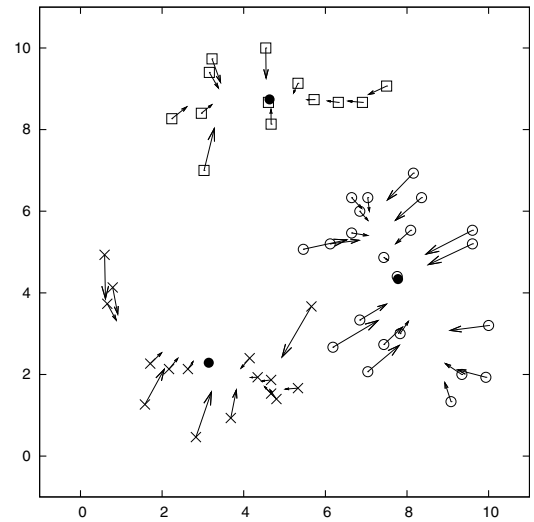

Fig. 10. Classification result 1 by eFCMQS with $\omega_{k11} = \omega_{k22} = 2.0$, $\omega_{k12} = \omega_{k21} = 0.0\ ^{\forall}k$.

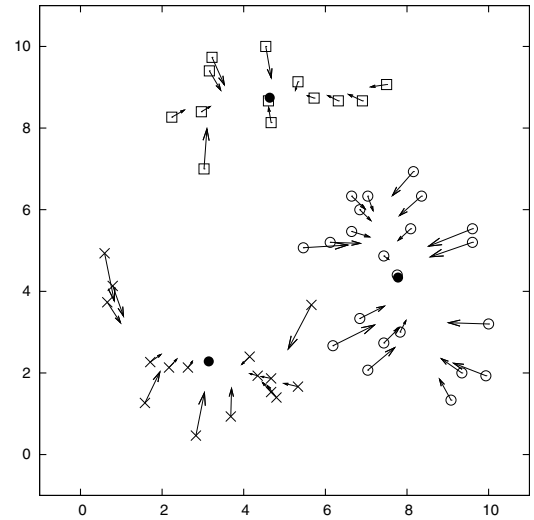

Fig. 11. Classification result 2 by eFCMQS with $\omega_{k11} = \omega_{k22} = 2.0$, $\omega_{k12} = \omega_{k21} = 0.2\ ^{\forall}k$.

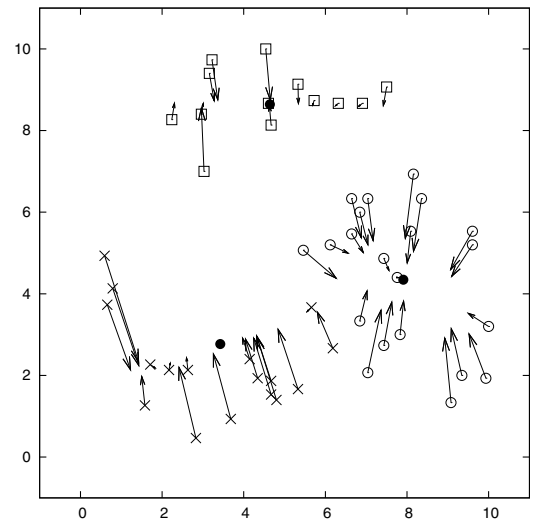

Fig. 12. Classification result 3 by eFCMQS with $\omega_{k11} = 2.0$, $\omega_{k12} = \omega_{k21} = 0.2$, $\omega_{k22} = 1.0\ ^{\forall}k$.

2011 IEEE International Conference on Fuzzy Systems
June 27-30, 2011, Taipei, Taiwan

On Hard and Fuzzy c-Means Clustering with Conditionally Positive Definite Kernel

Yuchi Kanzawa
Shibaura Institute of Technology
Tokyo, Japan 135-8548
Email: kanzawa@sic.shibaura-it.ac.jp

Yasunori Endo
University of Tsukuba
Ibaraki, Japan

Sadaaki Miyamoto
University of Tsukuba
Ibaraki, Japan

***Abstract*—In this paper, we investigate three types of c-means clustering algorithms with a conditionally positive definite kernel. One is based on hard c-means, and the others are based on standard and entropy-regularized fuzzy c-means. First, based on a conditionally positive definite kernel describing a squared Euclidean distance between data in the feature space, these algorithms are derived from revised optimization problems of the conventional kernel c-means. Next, based on the relationship between the positive definite kernel and conditionally positive definite kernel, the revised dissimilarity between a datum and a cluster center in the feature space is shown. Finally, it is shown that a conditionally positive definite kernel c-means algorithm and a kernel c-means algorithm with a positive definite kernel derived from the conditionally positive definite kernel are essentially identical to each other. An explicit mapping for a conditionally positive definite kernel is also described geometrically.**

***Index Terms*—Clustering, Fuzzy c-means, Conditionally positive definite kernel**

I. Introduction

Fuzzy c-means (FCM) clustering [1] is a well-known fuzzy clustering technique, and many FCM variants have been proposed. One of the authors has proposed an FCM algorithm based on the concept of entropy regularization [2]; this algorithm is known as the entropy-regularized FCM (eFCM) algorithm. It is a useful algorithm that is mathematically related to other techniques.

Three algorithms [3], [4] have been proposed to cluster data with nonlinear borders via nonlinear transformation from the original pattern space into a higher dimensional feature space with support vector machine (SVM) kernel functions [5]. They are the K-HCM algorithm derived from the hard c-means (HCM) algorithm, the K-sFCM algorithm derived from the standard FCM (sFCM) algorithm, and the K-eFCM algorithm derived from the eFCM algorithm. These three algorithms are known as kernel c-means (K-CM) algorithms. For kernel data analysis, an explicit mapping is unknown, whereas the inner product is known. An explicit mapping has been introduced by one of the authors, and it is used to describe the situation of kernel fuzzy c-means in higher dimensional space via kernel principal component analysis [6], [7].

In kernel data analysis, the kernel must be positive definite so that it describes the inner product between the data in the feature space. On the other hand, there exists a class of conditionally positive definite (cpd) kernel [8]. In this paper, we investigate c-means clustering algorithms with cpd kernel. First, we develop three c-means clustering algorithms with cpd kernel by solving the revised optimization problem of K-HCM, K-sFCM, and K-eFCM. Accordingly, the cpd kernel is the squared Euclidean distance between the data in the feature space. We call these three algorithms cpdK-HCM, cdK-sFCM, and cpdK-eFCM, respectively; and sum up to cpdK-CM. Next, we show how the cpd kernel is used in K-CM algorithms, with the positive definite kernel obtained by arranging the cpd kernel. Furthermore, we show the connection between the cpdK-CM algorithms and the K-CM algorithms with the positive definite kernel obtained from the cpd kernel, and we interpret a mapping from the original data space to the feature space, which is latent in the cpdK-CM algorithms. Finally, we show a numerical example of the cpdK-CM algorithms.

II. Preliminaries

In this section, we introduce three K-CM clustering algorithms with an explicit mapping from the original data space to the feature space [6],[7]

The data set $X = \{x_i \mid x_i \in \mathbb{R}^p, i \in \{1, \ldots, N\}\}$ is given. The membership by which x_i belongs to the j-th cluster is denoted by $u_{i,j}$ $(i \in \{1, \cdots, N\}, j \in \{1, \cdots, C\})$, and the set of $u_{i,j}$, denoted by $u \in \mathbf{R}^{N \times C}$, is known as the partition matrix. The constraint on u is

$$\sum_{j=1}^{C} u_{i,j} = 1 \quad (0 \leq u_{i,j} \leq 1).$$

A high-dimensional feature space used in SVM is denoted by $\mathbb{H}$, whereas the original space, which is known as the data space, $\mathbb{R}^p$. $\mathbb{H}$ may be infinite dimensional. Let the inner product be denoted by $\langle \cdot, \cdot \rangle$. The norm of $\mathbb{H}$ for an element $g \in \mathbb{H}$ is given by

$$\|g\|_{\mathbb{H}} = \sqrt{\langle g, g \rangle}. \tag{1}$$

A transformation $\Phi : \mathbb{R}^p \to \mathbb{H}$ is employed, whereby x_i is mapped into $\Phi(x_i)$. In general, Φ is not usable; however, the inner product $\langle \Phi(x), \Phi(y) \rangle$ can be expressed by a kernel function

$$\mathcal{K}(x, y) = \langle \Phi(x), \Phi(y) \rangle. \tag{2}$$

The matrix whose (i, j)-element is $\mathcal{K}(x_i, x_j)$ is denoted by K. The cluster center set in $\mathbb{H}$ is denoted by $W = \{W_1, \cdots, W_C\}$.

978-1-4244-7316-8/11/$26.00 ©2011 IEEE

An explicit function Φ corresponding to an introduced kernel function has been proposed as

$$\Phi(x_i) = e_i \tag{3}$$

with

$$\langle e_i, e_j \rangle = e_i^{\mathsf{T}} K e_j, \tag{4}$$

where $\mathbb{H} = \mathbb{R}^N$ and e_i is the k-th unit vector whose i-th component is unity and remaining components are zero. Note that $\Phi : X \to \mathbb{R}^N$, i.e., Φ is not defined on $\mathbb{R}^p$ but on finite data X.

Three K-CM algorithms with explicit mapping are obtained by solving the following optimization problem:

$$\underset{u,W}{\text{minimize}} \sum_{i=1}^{N}\sum_{j=1}^{C} u_{i,j}\|\Phi(x_i) - W_j\|_{\mathbb{H}}^2, \tag{5}$$

$$\text{subject to } \sum_{j=1}^{C} u_{i,j} = 1, \quad u_{i,j} \in \{0,1\}, \tag{6}$$

for K-HCM,

$$\underset{u,W}{\text{minimize}} \sum_{i=1}^{N}\sum_{j=1}^{C} u_{i,j}^m\|\Phi(x_i) - W_j\|_{\mathbb{H}}^2, \tag{7}$$

$$\text{subject to } \sum_{j=1}^{C} u_{i,j} = 1, \tag{8}$$

for K-sFCM, and

$$\underset{u,W}{\text{minimize}} \sum_{i=1}^{N}\sum_{j=1}^{C} u_{i,j}\|\Phi(x_i) - W_j\|_{\mathbb{H}}^2 + \lambda^{-1}\sum_{i=1}^{N}\sum_{j=1}^{C} u_{i,j}\log(u_{i,j}), \tag{9}$$

$$\text{subject to } \sum_{j=1}^{C} u_{i,j} = 1. \tag{10}$$

for K-eFCM. These algorithms are described as follows:

Algorithm 1 (K-CM): [6] [7]

STEP 1. Set $m > 1$ for K-sFCM. Set $\lambda > 0$ for K-eFCM. Set the kernel matrix K and initial partition matrix.

STEP 2. Update the cluster centers W:

$$W_j = \left(\sum_{i=1}^{N} u_{i,j}\right)^{-1} (u_{1,j}, \ldots, u_{N,j})^{\mathsf{T}}, \tag{11}$$

for K-HCM and K-sFCM, and

$$W_j = \left(\sum_{i=1}^{N} u_{i,j}^m\right)^{-1} (u_{1,j}^m, \ldots, u_{N,j}^m)^{\mathsf{T}}, \tag{12}$$

for K-eFCM.

STEP 3. Update the squared Euclidean distance between the cluster center W_j and data $\Phi(x_i)$ in the feature space:

$$d_{i,j} = (e_i - W_j)^{\mathsf{T}} K (e_i - W_j). \tag{13}$$

STEP 4. Update the membership $u_{i,j}$:

$$u_{i,j} = \begin{cases} 1 & (i = \arg\ \min_k d_{k,j}), \\ 0 & (\text{otherwise}), \end{cases} \tag{14}$$

for K-HCM,

$$u_{i,j} = 1/\sum_{k=1}^{C}\left(\frac{d_{i,j}}{d_{i,k}}\right)^{1/(m-1)}, \tag{15}$$

for K-sFCM, and

$$u_{i,j} = \frac{\exp(-\lambda d_{i,j})}{\sum_{k=1}^{C}\exp(-\lambda d_{i,k})}, \tag{16}$$

for K-eFCM.

STEP 4. If (u, W, d) converge, terminate this algorithm. Otherwise, go to STEP 2.

III. Conditionally Positive Definite Kernel c-Means

In this section, we investigate K-CM clustering algorithms with a conditionally positive definite kernel. First, we derive conditionally positive definite K-CM algorithms; thus, the conditionally positive definite kernel is the squared Euclidean distance in a feature space. Next, we show how the cpd kernel is used in a K-CM algorithm with a positive definite kernel obtained by arranging the cpd kernel. Furthermore, we determine the relation between the cpdK-CM and K-CM algorithms with a positive definite kernel obtained from a cpd kernel, and we interpret a mapping from the original data space to the feature space, which is latent in cpdK-CM algorithms. Finally, we show a numerical example of the cpdK-CM algorithms.

A. c-Means algorithms with cpd kernel

In this subsection, we develop c-means clustering algorithms with a cpd kernel by solving the revised optimization problems of K-HCM, K-sFCM, and K-eFCM; thus, the cpd kernel is the squared Euclidean distance between the data in the feature space.

The cpd kernel is defined as follows:

Definition 1 (cpd matrix): [8]

A symmetric $N \times N$ matrix K ($N \geq 2$) taking values in $\mathbb{R}$ and satisfying

$$\sum_{i=1}^{N}\sum_{k=1}^{N} \zeta_i \zeta_k K_{i,k} \geq 0 \tag{17}$$

for all $\zeta_i \in \mathbb{R}$, with

$$\sum_{i=1}^{N} \zeta_i = 0, \tag{18}$$

is said to be conditionally positive definite (cpd).

Definition 2 (cpd kernel): [8]

Let $\mathcal{X}$ be a nonempty set. A function $\tilde{\mathcal{K}} : \mathcal{X} \times \mathcal{X} \to \mathbb{R}$, which yields a conditionally positive definite Gram matrix for all $N \geq 2$, $x_1, \cdots, x_N \in \mathcal{X}$, is known as a conditionally positive definite (cpd) kernel.

A cpd kernel describes the squared Euclidean distance in a feature space as follows:

Theorem 1 (Hilbert space representation of cpd kernels): [8]

Let $\tilde{\mathcal{K}}$ be a real-valued conditionally positive definite kernel on $\mathcal{X}$, satisfying $\tilde{\mathcal{K}}(x, x) = 0$ for all $x \in \mathcal{X}$. Then, there exists a Hilbert space $\mathbb{H}$ of real-valued functions on $\mathcal{X}$ and a mapping $\Phi : \mathcal{X} \to \mathbb{H}$ such that

$$\|\Phi(x) - \Phi(x')\|_{\mathbb{H}}^2 = -\tilde{\mathcal{K}}(x, x'). \tag{19}$$

If we drop the assumption $\tilde{\mathcal{K}}(x, x) = 0$, the Hilbert space representation reads

$$\|\Phi(x) - \Phi(x')\|_{\mathbb{H}}^2 = -\tilde{\mathcal{K}}(x, x') + \frac{1}{2}(\tilde{\mathcal{K}}(x, x) + \tilde{\mathcal{K}}(x', x')). \tag{20}$$

We cannot utilize the squared Euclidean distance between the data in the feature space for K-CM (Algorithm 1) because the optimization problems (5)–(10) include the squared Euclidean distance between the data and the cluster center in the feature space. Therefore, we reformulate the K-CM optimization problems (5)–(10) into the following problems:

$$\underset{u}{\text{minimize}} \sum_{j=1}^{C} \frac{\sum_{i=1}^{N}\sum_{k=1}^{N} u_{i,j}\|\Phi(x_i) - \Phi(x_k)\|_{\mathbb{H}}^2}{\left(\sum_{t=1}^{N} u_{t,j}\right)^2}, \tag{21}$$

$$\text{subject to } \sum_{j=1}^{C} u_{i,j} = 1, \quad u_{i,j} \in \{0, 1\}, \tag{22}$$

for K-HCM,

$$\underset{u}{\text{minimize}} \sum_{j=1}^{C} \frac{\sum_{i=1}^{N}\sum_{k=1}^{N} u_{i,j}^m\|\Phi(x_i) - \Phi(x_k)\|_{\mathbb{H}}^2}{\left(\sum_{t=1}^{N} u_{t,j}\right)^2}, \tag{23}$$

$$\text{subject to } \sum_{j=1}^{C} u_{i,j} = 1, \tag{24}$$

for K-sFCM, and

$$\underset{u}{\text{minimize}} \sum_{j=1}^{C} \frac{\sum_{i=1}^{N}\sum_{k=1}^{N} u_{i,j}\|\Phi(x_i) - \Phi(x_k)\|_{\mathbb{H}}^2}{\left(\sum_{t=1}^{N} u_{t,j}\right)^2} + \lambda^{-1}\sum_{i=1}^{N}\sum_{j=1}^{C} u_{i,j}\log(u_{i,j}), \tag{25}$$

$$\text{subject to } \sum_{j=1}^{C} u_{i,j} = 1. \tag{26}$$

for K-eFCM. The form $\|\Phi(x_i) - \Phi(x_k)\|_{\mathbb{H}}^2$ in the above objective functions can be translated into $-\tilde{K}_{i,k}$ if $\tilde{K}_{i,i} = 0$, and $-\tilde{K}_{i,k} + 1/2(\tilde{K}_{i,i} + \tilde{K}_{k,k})$ otherwise, with the cpd kernel matrix $\tilde{K}$. Such optimization problems are identical to those for RHCM and RFCM [9] if the corresponding relational data matrix is $\tilde{K}$, and they are solved using the following algorithms:

Algorithm 2 (cpdK-{H,sF,eF}CM):

STEP 1. Set the fuzzifier parameter m and λ for cpdK-sFCM and cpdK-eFCM, respectively. Set the cpd kernel matrix $\tilde{K}$ and the initial membership $u_{i,j}$. Set the N-dimensional squared matrix R as

$$R_{i,k} = -\tilde{K}_{i,k} + 1/2(\tilde{K}_{i,i} + \tilde{K}_{k,k}) \tag{27}$$

STEP 2. Update the intermediate variable $w_j \in \mathbb{R}^N$ as

$$w_j = \left(\sum_{i=1}^{N} u_{i,j}\right)^{-1} (u_{1,j}, \ldots, u_{N,j})^{\mathsf{T}}, \tag{28}$$

for cpdK-HCM,

$$w_j = \left(\sum_{i=1}^{N} u_{i,j}^m\right)^{-1} (u_{1,j}^m, \ldots, u_{N,j}^m)^{\mathsf{T}}, \tag{29}$$

for cpdK-sFCM, and

$$w_j = \left(\sum_{i=1}^{N} u_{i,j}\right)^{-1} (u_{1,j}, \ldots, u_{N,j})^{\mathsf{T}}. \tag{30}$$

for cpdK-eFCM.

STEP 3. Update the intermediate variable $\tilde{d}_{i,j}$ as

$$\tilde{d}_{i,j} = (Rw_j)_i - \frac{1}{2} w_j^{\mathsf{T}} R w_j. \tag{31}$$

STEP 4. Update the membership $u_{i,j}$ as

$$u_{i,j} = \begin{cases} 1 & (i = \arg\ \min_k \tilde{d}_{k,j}), \\ 0 & (\text{otherwise}), \end{cases} \tag{32}$$

for cpdK-HCM,

$$u_{i,j} = 1/\sum_{k=1}^{C} \left(\frac{\tilde{d}_{i,j}}{\tilde{d}_{i,k}}\right)^{1/(m-1)}, \tag{33}$$

for cpdK-sFCM, and

$$u_{i,j} = \frac{\exp(-\lambda \tilde{d}_{i,j})}{\sum_{k=1}^{C} \exp(-\lambda \tilde{d}_{i,k})}, \tag{34}$$

for cpdK-eFCM.

STEP 5. If a stopping criterion is satisfied, terminate this algorithm. Otherwise, go to STEP. 2.

B. c-Means with pd kernel obtained from cpd kernel

In this subsection, we show how the cpd kernel is used in K-CM algorithms with a positive definite kernel obtained by arranging the cpd kernel. First, we show the relation between the cpd kernel and the pd kernel. Next, for K-CM (Algorithm 1) with a pd kernel obtained by reformulating the cpd kernel, we show how the cpd kernel is used to calculate the squared Euclidean distance between the data and the cluster center in the feature space.

The cpd kernel and the pd kernel have the following relation:

Theorem 2 (Connection cpd — pd): [8]

Let K be an N-dimensional symmetric matrix; $\mathbf{1} \in \mathbb{R}^N$, an N-dimensional real-valued vector whose elements are all 1; $E \in \mathbb{R}^{N \times N}$, the identity matrix; and $\eta \in \mathbb{R}^N$, a vector satisfying

$$\mathbf{1}^\mathsf{T} \eta = 1. \tag{35}$$

Then,

$$K = (E - \mathbf{1}\eta^\mathsf{T})\tilde{K}(E - \eta \mathbf{1}^\mathsf{T}) \tag{36}$$

is positive definite if and only if $\tilde{K}$ is conditionally positive definite.

Given the cpd kernel $\tilde{K}$ for a data set X, we can obtain the pd kernel

$$K = (E - \mathbf{1}\mathbf{1}^\mathsf{T}/N)\tilde{K}(E - \mathbf{1}\mathbf{1}^\mathsf{T}/N) \tag{37}$$

from Theorem 2 and use it K-CM (Algorithm 1). Then, STEP 3 of Algorithm 1 is rewritten as

STEP 3. Update the intermediate variable $\tilde{d}_{i,j}$ as

$$d_{i,j} = (e_i - W_j)^\mathsf{T} \tilde{K}(e_i - W_j) \tag{38}$$

from that

$$(E - \eta \mathbf{1}^\mathsf{T})(e_i - W_j) = (e_i - W_j). \tag{39}$$

C. Discussion

In this subsection, we show the relation between the K-CM algorithm with a pd kernel obtained from the cpd kernel and the cpdK-CM algorithm, and we geometrically interpret the explicit mapping from the data space to the feature space, hiding in cpdK-CM.

First, the updating equations (28) and (29) of the intermediate variable w_j in cpdK-CM (Algorithm 2) and the updating equations (11) and (12) of the cluster center W_j in K-CM (Algorithm 1) are identical. Next, the updating equations (32), (33), and (34) of the membership $u_{i,j}$ in cpdK-CM (Algorithm 2) and the updating equations (14), (15), and (16) of the membership $u_{i,j}$ in K-CM (Algorithm 1) are also identical. Furthermore, the updating equation of $d_{i,j}$ in K-CM (Algorithm 1) with a pd kernel obtained by reformulating the cpd kernel is expressed as Eq. (38). On the other hand, the updating equation of $\tilde{d}_{i,j}$ in cpdK-CM (Algorithm 2) can be expressed as

$$\begin{aligned} \tilde{d}_{i,j} =& (Rw_j)_i - \frac{1}{2} w_j^\mathsf{T} R w_j \\ =& \frac{1}{2}(e_i - w_j)^\mathsf{T} \tilde{K}(e_i - w_j) \end{aligned} \tag{40}$$

from $R = -\tilde{K}$, with $\tilde{K}_{i,i} = 0$. Therefore, $\tilde{d}_{i,j}$ in cpdK-CM (Algorithm 2) and $d_{i,j}$ in K-CM (Algorithm 1) with a pd kernel obtained by reformulating the cpd kernel have the following relation:

$$\tilde{d}_{i,j} = \frac{1}{2} d_{i,j}. \tag{41}$$

Comparing these relations with that between the pd kernel and the cpd kernel, cpdK-CM (Algorithm 2) for the cpd kernel $\tilde{K}$ with $\tilde{K}_{i,i} = 0$ and K-CM (Algorithm 1) for the pd kernel K with

$$K = 2(E - \mathbf{1}\eta^\mathsf{T})\tilde{K}(E - \eta \mathbf{1}^\mathsf{T}) \tag{42}$$

are identical.

Next, we geometrically interpret the explicit mapping from the data space to the feature space, hiding in cpdK-CM. Since cpdK-CM (Algorithm 2) and K-CM (Algorithm 1) with a pd kernel obtained from the cpd kernel are identical, we interpret cpdK-CM (Algorithm 2) from the geometrical interpretation of K-CM (Algorithm 1) with a pd kernel obtained from the cpd kernel.

Fig. 1 shows the feature space $\mathbb{H}$ used in K-CM (Algorithm 1). The mapping $e_i = \Phi(x_i)$ from each data x_i by an explicit mapping Φ is expressed along the i-th axis. From the updating equation of the cluster center W_j in K-CM (Algorithm 1), every cluster center W_j is in the $N-1$-dimensional subspace spanned by each data e_i. Hence $e_i - W_j$ for all $i \in \{1, \cdots, N\}$ and $j \in \{1, \cdots, C\}$ is orthogonal to $\mathbf{1}$. Therefore, it is guaranteed that $d_{i,j}$ is non-negative, even if $\tilde{K}$ is conditionally positive definite (and not positive definite) in K-CM (Algorithm 1).

IV. NUMERICAL EXAMPLE

In this section, we present an example of cpdK-CM. Fig. 2 shows 147 data points in two-dimensional space, which form doughnut-shaped and ball-shaped clusters. Such data cannot be clustered correctly using the usual HCM, sFCM, and eFCM algorithms because these clusters have a nonlinear border. Introducing the cpd kernel

$$\tilde{\mathcal{K}}(x, x') = \log(1 + \|x - x'\|_2^{0.5}), \tag{43}$$

cpdK-sFCM (Algorithm 2) with the fuzzifier parameter $m = 1.1$ yielded a successful result, as shown in Fig. 3.

V. CONCLUSION

In this paper, we investigated a hard and two fuzzy c-means clustering algorithms with a conditionally positive definite

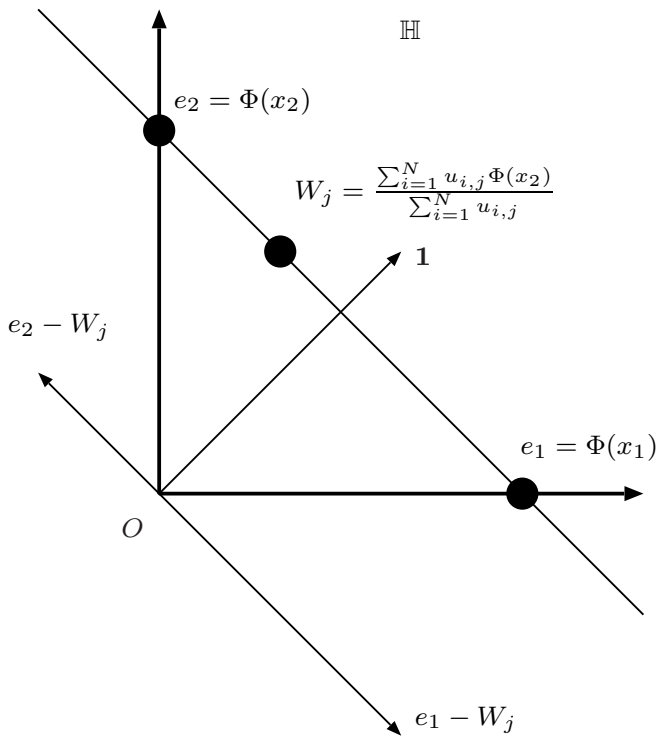

Fig. 1. Data and cluster centers in feature space $\mathbb{H}$

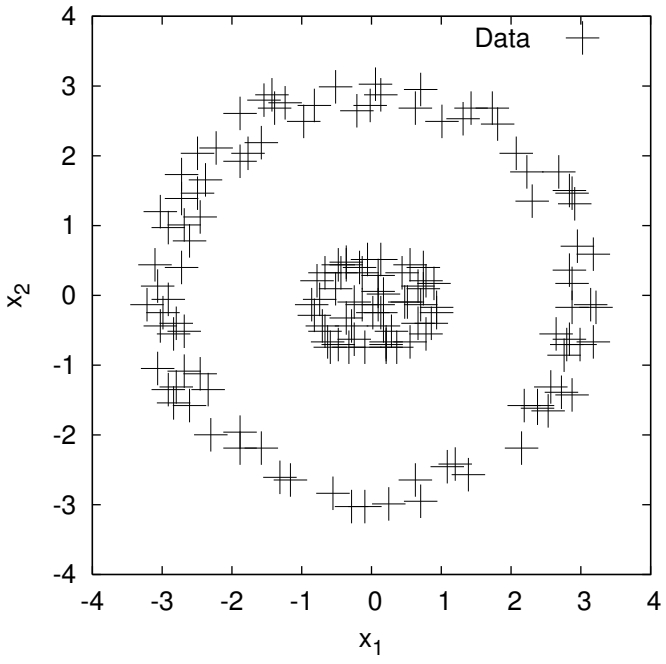

Fig. 2. Data

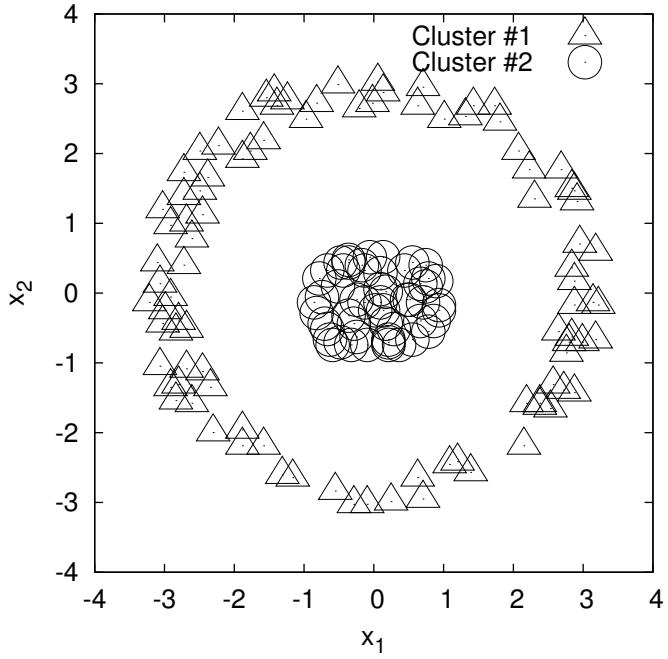

Fig. 3. Successful result ($\tilde{\mathcal{K}}(x, x') = \log(1 + \|x - x'\|_2^{0.5})$, $m = 1.1$

kernel. First, we developed c-means clustering algorithms using cpd kernel by solving the revised optimization problem of K-HCM, K-sFCM, and K-eFCM; thus, the cpd kernel is the squared Euclidean distance between the data in the feature space. Next, we showed how the cpd kernel is used in K-CM algorithms with a positive definite kernel obtained by arranging the cpd kernel. Furthermore, we showed the relation between the cpdK-CM algorithms and K-CM algorithms with a positive definite kernel obtained from the cpd kernel, and we interpreted a mapping from the original data space to the feature space, which is latent in cpdK-CM algorithms. Finally, we showed a numerical example of the cpdK-CM algorithms.

REFERENCES

[1] Bezdek, J.C.: Pattern Recognition with Fuzzy Objective Function Algorithms, Plenun, New York, (1981).

[2] Miyamoto, S. and Umayahara, K.: "Methods in Hard and Fuzzy Clustering", in: Liu, Z.-Q. and Miyamoto, S. (eds), Soft computing and human-centered machines, Springer-Verlag Tokyo, (2000).

[3] Miyamoto, S. and Nakayama, Y.: "Algorithms of Hard c-Means Clustering Using Kernel Functions in Support Vector Machines", J. Advanced Computational Intelligence and Intelligent Informatics, Vol.7, No.1, pp.19–24, 2003.

[4] Miyamoto, S. and Suizu, D.: "Fuzzy c-Means Clustering Using Kernel Functions in Support Vector Machines", J. Advanced Computational Intelligence and Intelligent Informatics, Vol.7, No.1, pp.25–30, 2003.

[5] Vapnik, V., N.: Statistical Learning Theory, Wiley, New York, 1998.

[6] Miyamoto, S., Kawasaki, Y. and Sawazaki, K.: "An Explicit Mapping for Kernel Data Analysis and Application to Text Analysis", Proc. IFSA-EUSFLAT 2009, pp.618–623, 2009.

[7] Miyamoto, S. and Sawazaki, K.: "An Explicit Mapping for Kernel Data Analysis and Application to c-Means Clustering", Proc. NOLTA 2009, pp.556–559, 2009.

[8] Schoölkopf, B: "The Kernel Trick for Distances", In Advances in Neural Information Processing System 13, MIT Press, 2001.

[9] Hathaway, R.J., Davenport, J.W. and Bezdek, J.C.: "Relational Duals of the c-means Clustering Algorithms", Pattern Recognition, Vol.22, No.2, pp.205–212, 1989.

2011 IEEE International Conference on Fuzzy Systems
June 27-30, 2011, Taipei, Taiwan

Intuitionistic Fuzzy Reasoning with Cognitive Maps

Dimitris K. Iakovidis, and Elpiniki I. Papageorgiou
Dept of Informatics and Computer Technology
Technological Educational Institute of Lamia
Lamia, Greece
dimitris.iakovidis@ieee.org, epapageorgiou@teilam.gr

***Abstract*—Fuzzy cognitive maps have proven an exceptional means to reasoning for decision support. In this paper we propose a novel approach to hesitancy-aware reasoning based on cognitive maps and intuitionistic fuzzy logic. Intuitionistic fuzzy sets are considered for the linguistic representation of both the concepts of a cognitive map and the relations defined between them. A comparative advantage of this approach over the state of the art is an intrinsic mechanism of modeling human hesitancy, as introduced in the construction of a cognitive model, and propagated through the reasoning process to a final decision. A numerical example demonstrates its effectiveness which can extend to a variety of real-world applications.**

Keywords-fuzzy cognitive maps; intuitionistic fuzzy sets; reasoning; decision support

I. INTRODUCTION

Human decisions are commonly expressed with a degree of hesitation, originating from uncertain or imperfect facts and imprecise knowledge. The theory of intuitionistic fuzzy sets (IFSs) [1] offers a sound mathematical framework to modeling hesitation through a tradeoff between the membership and the non-membership of an element to such a set.

A pioneering approach to intuitionistic fuzzy reasoning for decision support have been proposed in [3], where different forms of fuzzy propositional expressions and their relations have been investigated. In [4] Sanchez's approach to fuzzy reasoning has been extended with IFSs and applied for medical diagnosis. As an alternative to that method, a distance-based method has been proposed in [5]. Recent advances in field include an intuitionistic fuzzy Petri net model and reasoning algorithm [6], and an extension of the fuzzy cognitive map (FCM) model for intuitionistic fuzzy reasoning [7].

FCMs are fuzzy directed graphs whose nodes represent concepts which can be causally interrelated through the graph edges and describe knowledge with fuzzy logic [8]-[9]. In [7] IFSs have been used to define fuzzy relations between the concepts including the hesitancy of the experts in defining such relations during the construction of an intuitionistic FCM (iFCM). Advantages of this approach include a) capability to model the expert's hesitation in the construction of the cognitive map b) coping with incomplete or even conflicting information, c) easy construction and parameterization.

The improved results obtained with the iFCM in comparison with the conventional FCM approach on a real application for medical decision support [7] motivated us to investigate an enhanced iFCM model for decision support. This model, presented in this paper, co-evaluates human hesitancy not only in the definition of the relations between the concepts but also in the definition of the concept values. It can be considered as a generalization of the original iFCM enabling the expression of hesitancy both in the construction of cognitive models by experts and in their application by users.

The rest of this paper consists of three sections. Section II briefly describes the previous iFCM approach [7], to which we will refer to as iFCM-I, and presents the novel iFCM approach for intuitionistic fuzzy reasoning. In order to differentiate it from the previous one, we will call it iFCM-II. A numerical example that demonstrates the effectiveness of the latter one is presented in Section III, whereas the conclusions of this study are summarized in Section IV.

II. INTUITIONISTIC FUZZY COGNITIVE MAPS

A. Intuitionistic Fuzzy Sets

Given a universe of discourse E an IFS is defined as [1]

$$A=\left\{\left\langle x,\mu_A(x),\gamma_A(x)\right\rangle \middle| x\in E\right\} \quad (1)$$

where $\mu_A : E\to[0,1]$ and $\gamma_A : E\to[0,1]$ define the degree of *membership* and *non-membership*, respectively, of the element $x\in E$ to the set $A\subset E$. For every element $x\in E$ it holds that $0\le\mu_A(x)\le 1 \quad 0\le\gamma_A(x)\le 1$ and $0\le\mu_A(x)+\gamma_A(x)\le 1$. For $x\in E$, if $\gamma_A(x)=1-\mu_A(x)$, A represents a fuzzy set. The *hesitancy* of the element $x\in E$ to the set $A\subset E$ is defined as

$$\pi_A(x)=1-\mu_A(x)-\gamma_A(x) \quad (2)$$

A variety of operations over IFSs have been defined [2]. These include the summation and the multiplication of two fuzzy sets, which are defined as

$$A\oplus B=\left\{\left\langle x,\mu_A(x)+\mu_B(x)-\mu_A(x)\cdot\mu_B(x),\gamma_A(x)\cdot\gamma_B(x)\right\rangle \middle| x\in E\right\} \quad (3)$$

$$A\otimes B=\left\{\left\langle x,\mu_A(x)\cdot\mu_B(x),\gamma_A(x)+\gamma_B(x)-\gamma_A(x)\cdot\gamma_B(x)\right\rangle \middle| x\in E\right\} \quad (4)$$

B. iFCM-I

Similarly to a conventional FCM [10], iFCM-I models a decision making task as a graph [7]. Its nodes represent N concepts that sufficiently describe this task. Each concept is

This work was realized in the framework of the project DebugIT which is co-funded by the EC FP7 grant agreement n° FP7–217139. The EC, DG INFSO, is not liable for any use that may be made of the information in this document. It reflects solely the views of the authors.

modeled as a *linguistic variable* C_i, i=1,2,…N that can take linguistic values represented by fuzzy sets $\widetilde{L}_n^{C_i}$, n=1,...,l, on U_i, where U_i represents the respective universe of discourse.

The experts describe the *relations* between the concepts by if-then *rules* of the form:

"**If** a *change X* occurs in the value of concept C_j **then** a *change Y* is caused in the value of concept C_i."

where X and Y are linguistic variables quantifying the respective *change* with a linguistic value represented by a fuzzy set $\widetilde{R}_n$, on E, from $\widetilde{R} = \{\widetilde{R}_r\}$, n=1,…,r.

From each rule the *influence* of concept C_j on concept C_i is inferred as a linguistic value represented by a fuzzy set $(\widetilde{I}_n)_{ji}$ on E, from $\widetilde{I} = \{\widetilde{I}_n\}$, n=1,...,g, according to [10]. These fuzzy sets express the degree to which a concept C_j influences another concept C_i, i=1,2,…N, j=1,2,…N.

Unlike a conventional FCM, iFCM-I can model the *hesitation* of the expert to express the rule and therefore the influence among two concepts, C_i and C_j, i=1,...N, j=1,...,N. This is represented by a fuzzy set $(\widetilde{H}_n)_{ij}$, on [0,1], from $\widetilde{H} = \{\widetilde{H}_n\}$, n=1,...,h, which is subsequently used to construct a set Ω of IFSs from $\widetilde{I} \times \widetilde{H}$, defined as

$$\Omega_n = \left\{ \left\langle x, \mu_{\Omega n}(x), \gamma_{\Omega n}(x) \right\rangle \middle| x \in E \right\}, n = 1,..., \omega \le m \cdot p \qquad (5)$$

with a membership function $\mu_{\Omega n}(x) = \mu_{\widetilde{I}m}(x)$, m=1,...,g, a non-membership function $\gamma_{\Omega n}(x) = 1 - \mu_{\widetilde{I}m}(x) - \mu_{\widetilde{H}p}(x)$, p=1,...,h, and a hesitancy function $\pi_{\Omega n}(x) = \mu_{\widetilde{H}p}(x)$ as Eq.(2), where $0 \le \mu_{\Omega n}(x) \le 1$, $0 \le \gamma_{\Omega n}(x) \le 1$, $0 \le \pi_{\Omega n}(x) \le 1$.

The reasoning process with iFCM-I involves iterative calculation of the following equation until a steady state is reached [7]:

$$s_i^{k+1} = f\left(\left(2s_i^k - 1\right) + \sum_{\substack{j=1 \\ j \ne i}}^{N} \left(\left(2s_j^k - 1\right) \cdot w_{ji}^{\mu} \cdot \left(1 - w_{ji}^{\pi}\right) \right) \right) \qquad (6)$$

where $s_i^k \in [0,1]$, i=1,2,…N represent real node values at an iteration k, $w_{ji}^{\mu} \in [-1,1]$ and $w_{ji}^{\pi} \in [0,1]$ represent the influence weight and the hesitancy weight corresponding to the edge directed from node j to node I. Function f is of sigmoid form and aims to keep the node values within [0, 1]. The initial weights are estimated by defuzzification of the aggregated, linguistically expressed, influences between the concepts [10].

C. iFCM-II

The previous iFCM approach considers only the hesitancy in expression of the influence between the concepts. However, in human decision making tasks hesitancy may also be introduced in the determination of concept values, and it may also be propagated through the reasoning process to the final decision. In order to incorporate such a consideration into a concise decision making model, we propose a more general, novel, formulation of the iFCM.

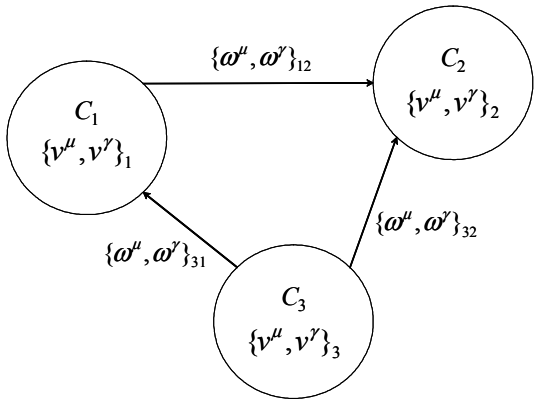

Figure 1. The proposed iFCM-II model.

The proposed approach considers that concepts C_i, i=1,2,…N are modeled as linguistic variables that can take linguistic values represented by IFSs of the form $L_n^{C_i} = \left\{ \left\langle x, v_i^{\mu}(x), v_i^{\gamma}(x) \right\rangle \middle| x \in U_i \right\}$, n=1,...,l, on U_i, where U_i represents the respective universe of discourse. Therefore, each concept is characterized by a pair $\{v^{\mu}, v^{\gamma}\}_i$ representing the membership and the non-membership to the respective IFS. Similarly, considering the use of IFSs in the description of the influence of a concept C_i to another concept C_j, a pair of membership and non-membership values $\{\omega^{\mu}, \omega^{\gamma}\}_{ji}$ can be used for the representation of this influence. This enhanced iFCM model is illustrated graphically in Fig.1. It should be noted that the pair $\{\omega^{\mu}, \omega^{\gamma}\}_{ji}$ defines an IFS as in Eq.(1), whereas in the case of iFCM-I which in turn results in $\left(w_{ji}^{\mu}, w_{ji}^{\pi}\right)$, represents a pair of weight values characterizing the influence between the concepts and not an IFS.

Having such an IFS-based representation of the concepts and the influences between the concepts, we reformulate the equation of the conventional FCM [10], which is

$$s_i^{k+1} = f\left(s_i^k + \sum_{\substack{j=1 \\ j \ne i}}^{N} s_j^k w_{ji} \right) \qquad (7)$$

so that it can be applied on IFSs, for i=1,2,…N

$$\{v^{\mu}, v^{\gamma}\}_i^{k+1} = F\left(\{v^{\mu}, v^{\gamma}\}_i^k \oplus \left(\bigoplus_{\substack{j=1 \\ j \ne i}}^{N} \left(\{v^{\mu}, v^{\gamma}\}_j^k \otimes \{\omega^{\mu}, \omega^{\gamma}\}_{ji} \right) \right) \right) \qquad (8)$$

where the arithmetic summation and multiplication of Eq.(7) have been replaced by the respective operations on IFSs defined by Eqs.(3-4), and $F(A)$ is a function defined on IFSs as

$$F(A) = \left\{ f_{\mu}(\mu_A), f_{\gamma}(\gamma_A) \right\} \qquad (9)$$

where A is an IFS, and f_{μ}, and f_{γ} are sigmoid functions such that $0 \le f_{\mu}(\mu_A) + f_{\gamma}(\gamma_A) \le 1$. In this work we consider

$$f_\mu(x) = f_\gamma(x) = \tanh(x) \tag{10}$$

It should be noted that function F is considered mainly as a means to push the system to converge to a steady state by deforming the real membership and non-membership values and not for the normalization of the real membership and the non-membership values, which by definition range in a standard interval i.e. [0, 1].

By using Eq.(4) on Eq.(8) for the calculation of the IFS multiplication, it is obtained:

$$\{v^\mu, v^\gamma\}_i^{k+1} = F\left(\{v^\mu, v^\gamma\}_i^k \oplus \left(\bigoplus_{\substack{j=1 \\ j\neq i}}^{N} \left(\{v_j^\mu \omega_{ji}^\mu, v_j^\gamma + \omega_{ji}^\gamma - v_j^\gamma \omega_{ji}^\gamma\}\right)\right)\right) \tag{11}$$

and by using Eq.(3) on the right-hand term of Eq.(9) it becomes

$$\{v^\mu, v^\gamma\}_i^{k+1} = F\left(\{v^\mu, v^\gamma\}_i^k \oplus \left\{m_{iN}, \prod_{\substack{j=1 \\ j\neq i}}^{N} \left(v_j^\gamma + \omega_{ji}^\gamma - v_j^\gamma \omega_{ji}^\gamma\right)\right\}^k\right)$$

which again due to Eq.(3) results in

$$\{v^\mu, v^\gamma\}_i^{k+1} = F\left(\left\{v_i^\mu + m_{iN} - v_i^\mu m_{iN}, v_i^\gamma \cdot \prod_{\substack{j=1 \\ j\neq i}}^{N} \left(v_j^\gamma + \omega_{ji}^\gamma - v_j^\gamma \omega_{ji}^\gamma\right)\right\}^k\right)$$

or

$$\{v^\mu, v^\gamma\}_i^{k+1} = F\left(\left\{v_i^\mu + \left(1 - v_i^\mu\right) \cdot m_{iN}, v_i^\gamma \cdot \prod_{\substack{j=1 \\ j\neq i}}^{N} \left(v_j^\gamma + \omega_{ji}^\gamma - v_j^\gamma \omega_{ji}^\gamma\right)\right\}^k\right) \tag{12}$$

where

$$m_{Ni} = \bigoplus_{\substack{j=1 \\ j\neq i}}^{N}{}^{\mu} v_j^\mu \omega_{ji}^\mu,\ i=1,2,\ldots N. \tag{13}$$

In this equation $\oplus^\mu$ represents the summation operator applied on the memberships of the IFSs in Eq.(3), i.e.

$$\mu_A \oplus^\mu \mu_B = \mu_A + \mu_B - \mu_A \mu_B. \tag{14}$$

Equation (12) can be calculated recursively for all j=1…N

$$m_{ij} = \begin{cases} v_1^\mu \omega_{1i}^\mu & j = 1 \\ m_{(j-1)i} \oplus^\mu v_j^\mu \omega_{ji}^\mu, & j > 1 \end{cases} \tag{15}$$

which due to Eq.(13) can also be expressed as

$$m_{ij} = \begin{cases} v_1^\mu \omega_{1i}^\mu & j = 1 \\ m_{(j-1)i} + v_j^\mu \omega_{ji}^\mu - m_{(j-1)i} v_j^\mu \omega_{ji}^\mu, & j > 1 \end{cases} \tag{16}$$

Obviously the complexity of Eq.(11) is higher than that of Eq.(6) and Eq.(7); however, the result obtained will be more informative since a propagated degree of hesitation will be quantifiable through the application of Eq.(2) on Eq.(11).

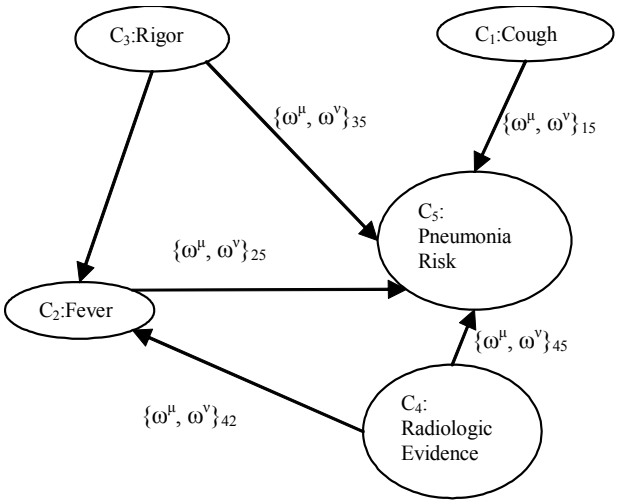

Figure 2. iFCM for pneumonia risk assessment.

The hesitancy of the proposed model at steady state is calculated from Eq.(2) by using the real membership and non-membership values. These are obtained by application of the inverse F on the decision concepts i.e. if c is a decision concept the real membership and non-membership values at the iteration K where convergence is met will be $F^{-1}\left(\{v^\mu, v^\gamma\}_c^K\right)$, which is defined as $\{f_\mu^{-1}(v^\mu), f_\gamma^{-1}(v^\gamma)\}_c^K$.

III. NUMERICAL EXAMPLE

The medical decision making task of pneumonia risk assessment, described in [11], has been considered for our case study. This is an important medical decision making task because of the serious, life threatening, adverse consequences that could occur in the critically ill patients if the pneumonia infection is misdiagnosed [12].

In order to present a numerical example that would be easily reproducible by other researchers, despite the complex IFS operations involved, we constructed a reduced version of the cognitive model presented in [11]. This iFCM model consists of only five concepts instead of 34 (Fig. 2). We demonstrate its construction and simulation for three cases, using both the iFCM-I and the iFCM-II approaches.

A. Model construction

The pneumonia risk assessment model was based on the knowledge of three expert physicians. The opinions of these experts were pooled to define the number and types of parameters/factors associated with the particular decision making task, as well as the interconnections among these parameters. The parameters have been considered as concepts of the FCM and include the symptoms of cough (C_1), fever (C2), rigor (C_3), the presence of radiological evidences of pneumonia in the patient's chest radiograph (C_4), and the risk

TABLE I. EXPERTS' OPINIONS ON INFLUENCES BETWEEN CONCEPTS

Relation ($C_i \rightarrow C_j$)	Experts' Opinions					
	***I*-1**	***H*-1**	***I*-2**	***H*-2**	***I*-3**	***H*-3**
$C_1 \rightarrow C_5$	low	v.low	low	v.low	low	low
$C_2 \rightarrow C_5$	med	v.low	med	v.low	med	v.low
$C_3 \rightarrow C_5$	low	low	med	low	med	low
$C_4 \rightarrow C_5$	high	low	med	v.low	high	v.low
$C_3 \rightarrow C_2$	med	low	low	v.low	low	v.low
$C_4 \rightarrow C_2$	high	low	v.high	med	high	low

TABLE II. RELATIONSHIPS AMONG IFCM CONCEPTS

Relation ($C_i \rightarrow C_j$)	Membership, Non-membership and Hesitancy iFCM-I / iFCM-II		
	w_{ji}^{μ} / ω_{ji}^{μ}	w_{ji}^{γ} / ω_{ji}^{γ}	w_{ji}^{π} / ω_{ji}^{π}
$C_1 \rightarrow C_5$	0.250	0.630	0.120
$C_2 \rightarrow C_5$	0.500	0.430	0.070
$C_3 \rightarrow C_5$	0.345	0.500	0.150
$C_4 \rightarrow C_5$	0.584	0.300	0.100
$C_3 \rightarrow C_2$	0.300	0.600	0.100
$C_4 \rightarrow C_2$	0.700	0.070	0.220

TABLE III. DECISION RANGES FOR CONCEPT C_5

Decision Node Values	Ranges Proposed by Physicians			
	<0.50	**0.50-0.70**	**0.70-0.85**	**>0.85**
Infection Risk	Low	Moderate	High	Very high

of infection (C_5), which is the decision concept. These concepts are well documented in the literature [12]. They represent the main variables that play an important role in the final diagnostic decision about the risk of pneumonia. For this application, the concepts take two, three, four or five possible discrete or fuzzy values [7]. For example the symptom of cough takes three fuzzy values (no cough, moderate cough, serious cough state) according to the initial patient stage. The decision concept (C_5) represents the risk of pulmonary infection and takes four fuzzy values (low, moderate, high, very high).

According to the proposed methodology (Section II.C), the opinions of three experts were pooled together to assign new if-then rules that describe the influences from concepts C_i to concepts C_j, i=1…5, j=1…5. The inferences of the rules are linguistic weights described by IFSs $\{\omega^{\mu}, \omega^{\gamma}\}_{ji}$. The linguistic weights obtained by the experts for the construction of the iFCM model are apposed in Table I. For each influence (I-E_i) between two concepts, the expert E_i, i =1,2,3 expresses his/her hesitancy (H-E_i). The linguistic values of hesitancy vary from very low (v.low) to high. The respective membership, non-membership and hesitancy values derived from Table I are common for both the iFCM-I and iFCM-II models, and they are summarized in Table II. The interpretation of the numeric risk for pneumonia infection obtained from the output concept C_5 is performed according to Table III.

In what follows, we provide three example patient cases for which we would like to assess the pneumonia risk using the constructed model for both iFCM-I and iFCM-II approaches.

B. First Case

In the first case, we consider a patient with suspected pneumonia having moderate cough (C_1=0.6), high fever (C_2=0.7), and no other information is available. Based on these data, the experts assessed the infection risk as moderate.

In iFCM-I, as noted in [7], the concepts with unknown values are set to 0.5, i.e. C_3=C_4=0.5. In iFCM-II the membership values of the respective concepts are set to zero, i.e. C_3=C_4=0. The non-membership values of these concepts are initially set to 0.5. However, the initial non-membership values do practically affect the final decision, because, as it can be noticed by the obtained results, they reach zero at convergence.

The results of the reasoning process obtained with iFCM-I (Eq. 6), at each iteration k, till convergence at a steady state are apposed in Table IV. The first row includes the initial concept values, and the last row, in boldface, indicates the concept values at steady state. The respective results with the use of the proposed iFCM-II approach are presented in Tables V and VI. We provide all concept values for validation of the results of other researchers that would like to implement our iFCM models. Table V shows that iFCM-II reaches a steady state at a numerical value that is close to the membership value obtained with iFCM-II, whereas the decisions derived

TABLE IV. FIRST CASE: REASONING USING IFCM-I

Iteration k	Concept Values Till Steady State				
	C_1	C_2	C_3	C_4	C_5
0	0.6000	0.7000	0.5000	0.5000	0.0000
1	0.6000	0.7000	0.5000	0.5000	0.5000
2	0.6000	0.7000	0.5000	0.5000	0.5342
3	0.6000	0.7000	0.5000	0.5000	0.5512
4	0.6000	0.7000	0.5000	0.5000	0.5596
5	0.6000	0.7000	0.5000	0.5000	0.5637
6	0.6000	0.7000	0.5000	0.5000	0.5657
7	0.6000	0.7000	0.5000	0.5000	0.5667
8	0.6000	0.7000	0.5000	0.5000	0.5672
9	0.6000	0.7000	0.5000	0.5000	0.5674
10	0.6000	0.7000	0.5000	0.5000	0.5676
11	0.6000	0.7000	0.5000	0.5000	0.5677
12	**0.6000**	**0.7000**	**0.5000**	**0.5000**	**0.5677**

TABLE V. FIRST CASE: REASONING USING IFCM-II

Iteration k	Concept Membership Values Till Steady State				
	C_1^{μ}	C_2^{μ}	C_3^{μ}	C_4^{μ}	C_5^{μ}
0	0.6000	0.7000	0.0000	0.0000	0.0000
1	0.5370	0.6044	0.0000	0.0000	0.4198
2	0.4908	0.5402	0.0000	0.0000	0.5713
3	0.4548	0.4931	0.0000	0.0000	0.6203
4	0.4258	0.4567	0.0000	0.0000	0.6330
5	0.4018	0.4274	0.0000	0.0000	0.6333
6	0.3815	0.4031	0.0000	0.0000	0.6295
7	0.3640	0.3826	0.0000	0.0000	0.6245
8	0.3488	0.3650	0.0000	0.0000	0.6194
9	0.3353	0.3496	0.0000	0.0000	0.6144
10	0.3233	0.3360	0.0000	0.0000	0.6097
11	0.3124	0.3239	0.0000	0.0000	0.6053
12	0.3027	0.3130	0.0000	0.0000	0.6012
13	0.2937	0.3032	0.0000	0.0000	0.5974
14	0.2856	0.2942	0.0000	0.0000	0.5938
15	0.2781	0.2860	0.0000	0.0000	0.5904
16	0.2711	0.2785	0.0000	0.0000	0.5842
17	**0.2710**	**0.2755**	**0.0000**	**0.0000**	**0.5842**

TABLE VI. FIRST CASE: REASONING USING IFCM-II

Iteration k	Concept Non-Membership Values Till Steady State				
	C_1^{γ}	C_2^{γ}	C_3^{γ}	C_4^{γ}	C_5^{γ}
0	0.30000	0.20000	0.50000	0.50000	0.50000
1	0.29131	0.08539	0.46212	0.46212	0.09794
2	0.28334	0.03348	0.43181	0.43181	0.01576
3	0.27600	0.01220	0.40683	0.40683	0.00224
4	0.26920	0.00417	0.38578	0.38578	0.00030
5	0.26288	0.00135	0.36772	0.36772	0.00004
6	0.25698	0.00042	0.35199	0.35199	0.00000
7	0.25147	0.00012	0.33814	0.33814	0.00000
8	0.24630	0.00003	0.32582	0.32582	0.00000
9	0.24144	0.00001	0.31476	0.31476	0.00000
10	0.23685	0.00000	0.30476	0.30476	0.00000
11	0.23252	0.00000	0.29566	0.29566	0.00000
12	0.22842	0.00000	0.28734	0.28734	0.00000
13	0.22453	0.00000	0.27968	0.27968	0.00000
14	0.22083	0.00000	0.27261	0.27261	0.00000
15	0.21731	0.00000	0.26605	0.26605	0.00000
16	0.21395	0.00000	0.25995	0.25995	0.00000
17	0.21075	0.00000	0.25425	0.25425	0.00000
18	**0.20768**	**0.00000**	**0.24891**	**0.24891**	**0.00000**

by both iFCM approaches, according to Table III are in agreement with the aggregated fuzzy experts' opinion i.e. moderate. The non-membership values of all the concepts of iFCM-II are monotonically decreasing. The steepest decrease is observed at the output concept C_5, whose non-membership value reaches zero after converging at a steady state. Furthermore a real hesitancy estimation can be obtained from the decision concept, which according to Section II.C where $\tanh^{-1}(0.5842)=0.6688$, is 0.3312 using Eq.(2).

C. Second Case

The second case refers to a patient with suspected pulmonary infection having moderate cough (C_1=0.6), low fever (C_2=0.3), and rigor (C_3=1). Based only on these symptoms, the experts decided that the infection risk is moderate.

The convergence of both iFCM-I and iFCM-II follows a similar pattern with the first case, so we provide a condensed graphic representation of the values till steady state in Figs. 3 and 4. The respective values of the concepts are provided in Tables VII-IX. In these tables the first rows include the initial concept values, and the last rows, appearing in boldface, indicate the concept values at steady state. Both iFCM approaches are in accordance with the experts' opinion since they both evaluate to moderate risk according to Table III. The hesitancy at the output node is where $\tanh^{-1}(0.6874)=0.8430$, is 0.1581 using Eq. (2).

TABLE VII. SECOND CASE: REASONING USING IFCM-I

Iteration k	Concept Values Till Steady State				
	C_1	C_2	C_3	C_4	C_5
0	0.6000	0.3000	1.0000	0.5000	0.0000
13	**0.6000**	**0.6290**	**1.0000**	**0.5000**	**0.6896**

TABLE VIII. SECOND CASE: REASONING USING IFCM-II

Iteration k	Concept Membership Values Till Steady State				
	C_1^{μ}	C_2^{μ}	C_3^{μ}	C_4^{μ}	C_5^{μ}
0	0.6000	0.3000	1.0000	0.0000	0.0000
16	**0.2781**	**0.5978**	**0.7616**	**0.0000**	**0.6874**

TABLE IX. SECOND CASE: REASONING USING IFCM-II

Iteration k	Concept Non-Membership Values Till Steady State				
	C_1^{γ}	C_2^{γ}	C_3^{γ}	C_4^{γ}	C_5^{γ}
0	0.30000	0.20000	0.00000	0.50000	0.50000
16	**0.21395**	**0.00000**	**0.00000**	**0.25995**	**0.00000**

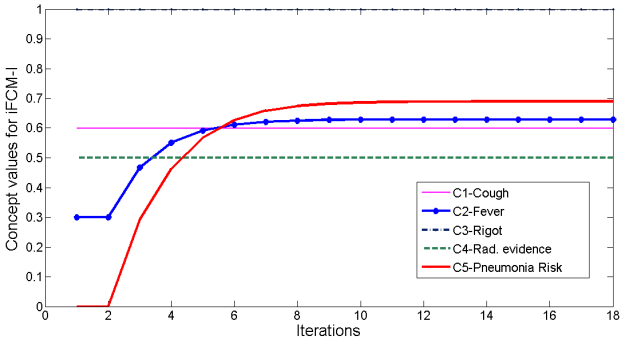

Figure 3. Convergence of iFCM-I for the second case.

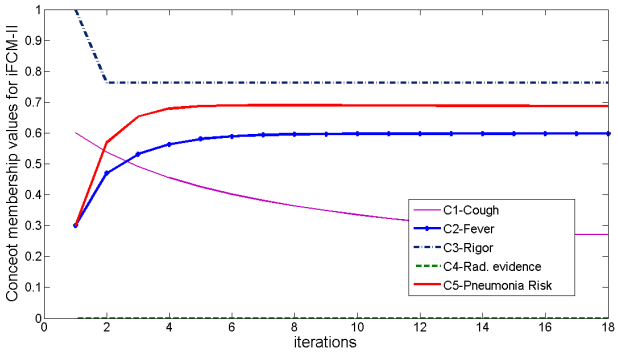

Figure 4. Convergence of iFCM-II for the second case.

D. *Third Case*

In this case, we consider a patient with low fever (C_2=0.3) and presence of radiological evidences of pneumonia (C_4=1).

TABLE X. THIRD CASE: REASONING USING IFCM-I

Iteration *k*	**Concept Values Till Steady State**				
	C_1	C_2	C_3	C_4	C_5
0	0.5000	0.3000	0.5000	1.0000	0.5000
12	0.5000	0.7337	0.5000	1.0000	0.7895

TABLE XI. THIRD CASE: REASONING USING IFCM-II

Iteration *k*	**Concept Membership Values Till Steady State**				
	C_1^{μ}	C_2^{μ}	C_3^{μ}	C_4^{μ}	C_5^{μ}
0	0.5000	0.3000	0.5000	1.0000	0.0000
15	**0.2781**	**0.7076**	**0.4621**	**0.7616**	**0.7266**

TABLE XII. THIRD CASE: REASONING USING IFCM-II

Iteration *k*	**Concept Non-Membership Values Till Steady State**				
	C_1^{γ}	C_2^{γ}	C_3^{γ}	C_4^{γ}	C_5^{γ}
0	0.3000	0.5000	0.1000	0.2000	0.5000
15	**0.2173**	**0.0000**	**0.2660**	**0.2660**	**0.0000**

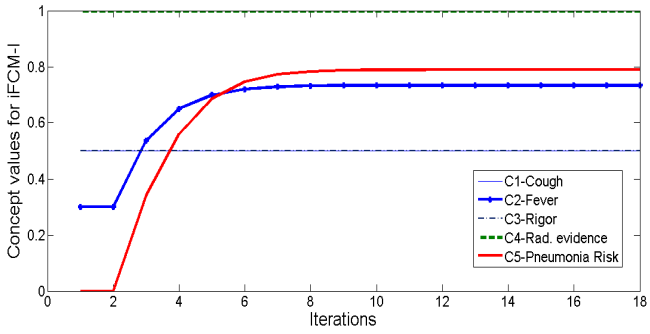

Figure 5. Convergence of iFCM-I for the third case.

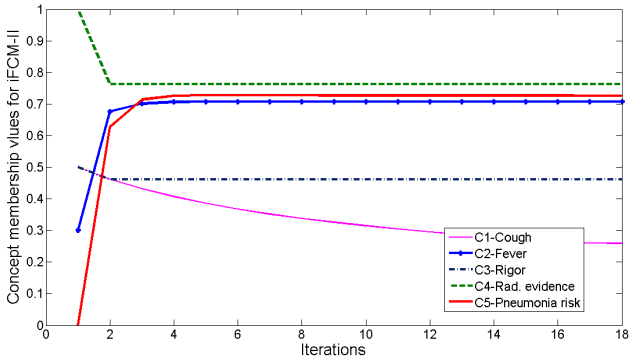

Figure 6. Convergence of iFCM-II for the third case.

There is no any information on other symptoms. According to the experts there is a high risk of this patient having pneumonia.

The convergence of both iFCM-I and iFCM-II is graphically represented in Figs. 5-6. The initial concept values and the concept values after converging at a steady state are apposed in Tables X-XII. According to Table III it can be noticed that both iFCM models result in a decision that is in agreement with the experts' opinion, i.e. high pneumonia risk. The hesitancy obtained at the decision node of iFCM-II is 0.0785 using Eq. (2), where $\tanh^{-1}(0.7266) = 0.9214$.

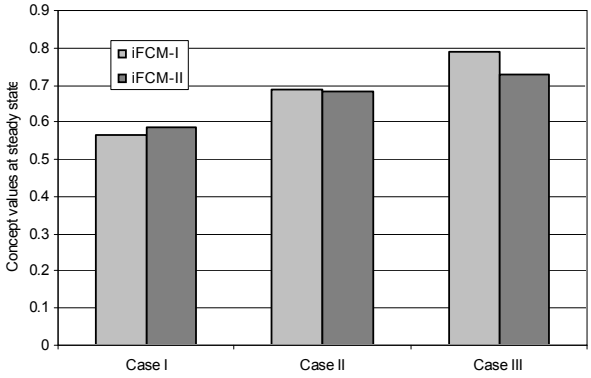

Figure 7. Comparison of the decision concept values at steady state with iFCM-I and iFCM-II for the three different patient cases presented in this study.

In the examined cases the results of both iFCM techniques are identical according to the calculated decision concepts (see Figure 7) and agree with the experts' opinion. But the advantageous point of iFCM-II technique is that it further assesses the hesitancy on concepts values and especially on decision nodes for which the physicians are interested.

IV. CONCLUSIONS

We presented a novel approach to intuitionistic fuzzy reasoning for decision support based on a novel iFCM model, which is referred to as iFCM-II. The proposed iFCM model is elegantly formulated using the mathematical formalism of IFS operations and exhibits several advantages over the previously proposed one. These include:

- It enables modelling of the uncertainty and imprecision introduced not only in the definition of the relations between the concepts of the cognitive map but also in the definition of the concept values.
- It is more general and could be used to closer approximate human decision making. It reduces to the previous iFCM model if the hesitancy in the determination of all concept values is zero.
- The output of the reasoning process may include a degree of hesitation expressed through IFS hesitancy.

The proposed iFCM-II model was applied for pneumonia risk assessment on three patient cases to demonstrate its functionality. The results showed that both iFCM-I and iFCM-II lead to decisions that are in accordance to the decisions of the experts. However, as illustrated in Fig. 7, the calculated decision concepts may exhibit differences.

Future research will focus on the application and the evolution of the proposed model towards an even improved modelling of uncertainty and human indecision.

REFERENCES

[1] K.T. Atanassov, Intuitionistic Fuzzy Sets: Theory and Applications. Studies in Fuzziness and Soft Computing, vol. 35, 1999.

[2] K.T. Atanassov, "New Operations Defined over the Intuitionistic Fuzzy Sets', *Fuzzy Sets and Systems*, vol. 61, pp. 137-142, 1994.

[3] T. Ciftcibasi, D. Altunay, "Two-Sided (intuitionistic) Fuzzy Reasoning," *IEEE Trans. Systems Man Cybernet.* Part A, vol. 28, pp. 662-677, 1998.

[4] A. De SK, Biswas A, E. Roy, "An Application of Intuitionistic Fuzzy Sets in Medical Diagnosis," *Fuzzy Sets and Systems*, vol. 117, no. 2, pp. 209-213, 2001.

[5] E. Szmidt, and J. Kacprzyk, "A Similarity Measure for Intuitionistic Fuzzy Sets and Its Application in Supporting Medical Diagnostic Reasoning," L. Rutkowski et al. (Eds.): ICAISC 2004, LNAI 3070, pp. 388–393, 2004.

[6] X.-Y. Shen, Y.-J. Lei, C.-H. Li, "Intuitionistic Fuzzy Petri Nets Model and Reasoning Algorithm," Int. Conf. Fuzzy Systems and Knowledge Discovery, pp. 119-122, 2009.

[7] D.K. Iakovidis, and E. Papageorgiou, "Intuitionistic Fuzzy Cognitive Maps for Medical Decision Making," IEEE Transactions on Information Technology in Biomedicine, vol. 15, no. 1, 2010.

[8] B. Kosko, "Fuzzy Cognitive Maps, International Journal of Man-Machine Studies," vol. 24, pp. 65-75, 1986.

[9] E.I. Papageorgiou, "A new methodology for Decisions in Medical Informatics using Fuzzy Cognitive Maps based on Fuzzy Rule-Extraction techniques", Applied Soft Computing, vol. 11, pp. 500–513, 2011.

[10] E.I. Papageorgiou, C.D. Stylios, P.P. Groumpos, "An Integrated Two-Level Hierarchical Decision Making System based on Fuzzy Cognitive Maps", IEEE Transactions on Biomedical Engineering, Vol. 50, No 12, December 2003, pp. 1326-1339.

[11] E.I. Papageorgiou, N.I. Papandrianos, G. Karagianni, G. Kyriazopoulos, D. Sfyras, "A Fuzzy Cognitive Map based Tool for Prediction of Infectious Diseases", in *Proc. FUZZ-IEEE* 2009, Korea, pp. ??/

[12] M. Langer, S. Pifferi, M. Peta, "Diagnosis of Bacterial Infection in the ICU: General Principles," *Intensive Care Medicine*, vol. 20, no. 4, pp. 1432-1238, 1994.

[13] Z. Hoare, WS Lim, "Pneumonia: Update on Diagnosis and Management", *BMJ*, vol. 332, pp. 1077-1079, 2006.

2011 IEEE International Conference on Fuzzy Systems
June 27-30, 2011, Taipei, Taiwan

Review study on Fuzzy Cognitive Maps and their applications during the last decade

Elpiniki I. Papageorgiou
Dept of Informatics and Computer Technology
Technological Educational Institute of Lamia
Lamia, Greece
epapageorgiou@teilam.gr

Abstract— **This survey work tries to review the most recent applications and trends on fuzzy cognitive maps (FCMs) at the last ten years. FCMs are inference networks, using cyclic directed graphs, for knowledge representation and reasoning. In the past decade, FCMs have gained considerable research interest and are widely used to analyze causal systems such as system control, decision making, management, risk analysis, text categorization, prediction etc. Some example application domains, such as engineering, social and political sciences, business, information technology, medicine and environment, where the FCMs emerged a considerable degree of applicability were selected Their dynamic characteristics and learning methodologies make them essential for modeling, analysis, prediction and decision making tasks as they improve the performance of these systems. A survey on FCM studies concentrated on FCM applications on diverse scientific fields is elaborated during the last decade.**

Keywords-fuzzy cognitive maps; review; applications; styling; insert (key words)

I. INTRODUCTION

This study tries to gather the recent advances and trends on FCMs, their dynamic capabilities and application characteristics in diverse scientific areas. FCM represents a system in a form that corresponds closely to the way humans perceive it. Experts of each scientific area are used to express their knowledge by drawing weighted causal digraphs. The developed model is easily understandable, even by a non-technical audience and each parameter has a perceivable meaning [1,2].

In a graphical form, the FCMs are typically signed fuzzy weighted graphs, usually involving feedbacks, consisting of nodes and directed links connecting them. The nodes represent descriptive behavioral concepts of the system and the links represent cause-effect relations between the concepts. In the context of FCM theory, the fuzzy value of a concept denotes the degree in which the specific concept is active in the general system, usually bounded in a normalized range of [0, 1]. Furthermore, the weights of the system's interrelations reflect the degree of causal influence between two concepts and they are usually assigned linguistically by experts [3]. They work by capturing and representing cause and effect relationships.

According to Codara (1998) [4], FCMs can be used for various purposes, including:

• to reconstruct the premises behind the behavior of a given agent, to understand the reasons for their decisions and for the actions the take, highlighting any distortions and limits in their representation of the situation (explanatory function);

• to predict future decisions and actions, or the reasons that a given agent will use to justify any new occurrences (prediction function);

• to help decision-makers ponder over their representation of a given situation in order to ascertain its adequacy and possibly prompt the introduction of any necessary changes (reflective function);

• to generate a more accurate description of a difficult situation (strategic function).

Essentially, a Fuzzy Cognitive Map is developed by integrating the existing experience and knowledge regarding a system. This can be achieved by using a group of human experts to describe the system's structure and behavior in different conditions. With FCM it is usually easy to find which factor should be modified and how and by this sense, an FCM is a dynamic modeling tool in which the resolution of the system representation can be increased by applying further mapping [5,6]. As simple mathematical models, FCMs represent the structured causality knowledge for qualitative and quantitative inference. The resulting fuzzy model can be used to analyze, simulate, and test the influence of parameters and predict the behavior of the system.

The main reasons someone uses the FCM approach are [7]: easy of use, easy to construct and parameterize, flexibility in representation (as more concepts/phenomena can be added and interact), low time performing, easily understandable/transparent to non-experts and lay people [8], handle with complex issues related to knowledge elicitation and management, handle with dynamic effects due to the feedback structure of the modeled system.

Furthermore, individual FCMs pertaining to a particular domain can be combined mathematically [1,2]. This means that FCMs allow for different experts and/or stakeholder views to be incorporated [9], and can provide a useful mechanism for combining information drawn from many sources to create a rich body of knowledge [10-12]. Finally, vector-matrix operations allow an FCM to model dynamic systems [1,13],

978-1-4244-7316-8/11/$26.00 ©2011 IEEE

allowing for the dynamic aspect of system behaviour to be captured [14]. Thus, FCMs have gained considerable research interest and accepted as useful methodology in many diverse scientific areas from knowledge modeling and decision making.

This work presents a survey on FCMs applications and trends in diverse scientific areas during the last decade exploring some of the most representative for each application study. The main aim of this study is to give an outline on how the FCMs increase their applications and more methodological efforts made by other researchers to enhance their applicability in different domains. It is difficult to present all the representative applications in each domain, as the number of FCM papers was extremely increased the last three years. Thus, we attempt to figure out only some of the most representative works of each domain, during the last decade.

II. FUZZY COGNITIVE MAPS AND APPLICATIONS

FCM is an efficient inference engine for modeling complex causal relationships easily, both qualitatively and quantitatively. Dickerson and Kosko (1994) used the FCM in a virtual world to model how sharks and fish hunt [15]. Parenthoen and his colleagues [16] successfully used the FCM to model the intentions and movements of a sheep dog and sheep in a virtual world.

During the past decade, FCMs played a vital role in the applications of diverse scientific areas, such as social and political sciences, engineering, information technology, robotics, expert systems, medicine, education, prediction, environment etc. Aguilar (2005) was the first who tried to gather the FCM applications in different scientific domains till 2004 [17]. In his work, most of the FCM applications were referred: administrative sciences, information analysis, popular political developments, engineering and technology management, prediction, education, cooperative man–machines, decision making and support, environmental management etc. After 2004, a large number of research studies related to methodologies for constructing or enhancing FCMs as well as innovative applications of FCMs were emerged. It is pinpointed that the number of research papers at 2010 is almost the double of the research papers presented till 2004 (see Table I). The recent applications are focused not only to the previous referred domains but to more others such as telecommunications, game theory, e-learning, virtual environments, ambient intelligence, collaborative systems. New methodologies engaged with dynamic construction of FCMs, learning procedures, fuzzy inference structures were explored to improve the performance of them.

In this work, we concentrate our effort on FCM research studies after 2000 and especially on the presentation of the main categories of them at the last ten years (2001 to 2010). In particular, we describe recent research studies after 2008 for most of the application domains.

From the number of FCM studies opposed in Table I (last access in scopus at 20 February 2011), it is observed that during the last decade (we consider the years 2000 till 2010), there is a large increase on the number of research papers related to FCMs.

TABLE I. RESEARCH STUDIES OF FCMS FOUND IN SCOPUS

Year	Number of FCM-related studies from scopus		
	Studies	*Journals & Book chapters*	*Conferences*
2000	18	8	10
2001	22	2	20
2002	7	4	3
2003	19	9	10
2004	53	15	38
2005	35	16	19
2006	50	11	39
2007	56	19	37
2008	81	21	60
2009	84	26	58
2010	(91+11 journals published in 2011) 102	50+11 Journals at 2011	41

Also, it is clearly shown that the last two years (2009-2010) the number of published papers in FCMs has been quadruple from the number of papers at the first years of decade (2000, 2001), and doubled from the papers published at 2004. Most of the research papers are related to FCMs applications and methodologies. 517 studies were accomplished during the past decade. A collection of papers with applications in various disciplines is presented in the book "Fuzzy Cognitive Maps: Advances in Theory, Methodologies, Applications and Tools edited by M. Glykas and prefaced by B. Kosko [6]. This is a significant index on FCM acceptability and applicability in research studies. Bar-chart in Figure 1 illustrates the FCM research studies for the last twenty years, including conference and journal papers, book chapters and technical reports, respectively for each year. It is clear from the chart that the FCMs have gained a considerable interest in research, which extremely increased during the last years. Furthermore, some types of typical problems solved by FCMs are modeling, prediction, interpreting, monitoring, decision making, classification, management. Paradigms of typical problems solved by FCMs are depicted in Table II.

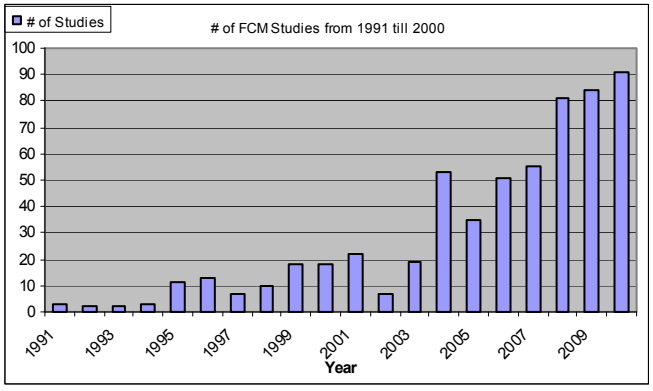

Figure 1. FCM papers during the last twenty years

TABLE II. PARADIGMS OF TYPICAL PROBLEMS SOLVED BY FCMS

Paradigm	Typical problems solved by FCMs
	Description
Control	Prediction interpreting, monitoring
Business	Planning, management, decision making, inference
medicine	Decision support, modeling, prediction, classification
robotics	Navigation, learning, prediction
environment	Knowledge representation, reasoning, stakeholders'analysis, policy making
Information technology	Modeling, analysis

A. FCM methodologies

In this section, a very short review is attempted to present the FCM methodologies and theories, depicting the estimation of their causal weights, the design and development process, the inference process etc.

As a generic model, the FCM relies on several assumptions. For example, the concepts' activation values are updated simultaneously at the same rate, and the causalities among the concepts are always in effect. However, these assumptions might not always hold, and the FCM isn't powerful or robust enough to model a dynamic, evolving virtual world. One other restriction is that use only simple monotonic and symmetric causal relations between concepts. But many real world causal relations are neither symmetric nor monotonic.

To solve these and other shortcomings and thus to improve the performance of FCMs, several methodologies were explored. Extensions to the FCMs theory are more than anything needed because of the feeble mathematical structure of FCMs and mostly the desire to assign advanced characteristics not met in other computational methodologies. Under this standpoint, some core issues are discussed and respective solutions are proposed in recent studies [18-25]; Pedryez (2010) presented the synergy of granular computing and evolutionary optimization to design efficiently FCMs, through a theoretic analysis [18]. Salmeron (2010) proposed the case of fuzzy grey cognitive maps, based on grey system theory, which is a very effective theory for solving problems within environments with high uncertainty, under discrete small and incomplete data sets [19]. Next, Iakovidis and Papageorgiou (2011) introduced the intuitionistic fuzzy sets and reasoning to handle the experts' hesitancy for decision making [20]. Also, more extensions of FCMs have been proposed, such as Rule-based FCMs [21,22], temporal FCMs [23], evolutionary multilayered FCMs [24,25] etc.

A dynamic version of FCMs, namely Dynamic Cognitive Networks, and a transformation process of cognitive maps, were proposed by Miao et al. [5,26] in order to explore the dynamic nature of concepts and to determine the strength of the cause and the cause-effect relationships as much as the degree of influence. Also, Fuzzy Cognitive Networks (FCNs) proposed as an operational extension of FCMs [27] that always reach equilibrium points in their operations especially to control unknown plants.

As another core task to design the FCMs, Song and his colleagues (2010) proposed a fuzzy neural network to enhance the learning ability of FCMs so that the automatic determination of membership functions and quantification of causalities can be incorporated with the inference mechanism of conventional FCMs. They employed mutual subsethood to define and describe the causalities in FCMs. It provides more explicit interpretation for causalities in FCMs and makes the inference process easier to understand. In this manner, FCM models of the investigated systems can be automatically constructed from data, and therefore are independent of the experts [28]. Next, Papageorgiou (2011) proposed a new methodology to design augmented FCMs combining knowledge from experts and knowledge from different data sources in the form of fuzzy rules [12].

It is worth noting that another important methodology for improving the performance of FCMs is learning algorithms. Learning methodologies for FCMs have been developed in order to update the initial knowledge of human experts and/or include any knowledge from historical data to produce learned weight matrices. The adaptive Hebbian-based learning algorithms, the evolutionary-based such as genetic algorithms and the hybrid approaches composed of Hebbian type and genetic algorithm were established to handle the task of FCM training [29,30-33]. These algorithms are the most efficient and widely used for training FCMs according to the existing literature [29,34].

B. Example Application Areas

Some example application areas were selected to present the way FCMs were applied and depicted in what follows. In Figure 2, the number of research studies accomplished in each one of the most common application domains during the last decade is depicted. At 2010, 13 application studies of FCMs were emerged in business, 12 in engineering and control, 8 in information technology, 5 in medical domain, and 6 in environment and agriculture.

1) Political and Social Sciences

FCMs emerged as a technique for modeling political and strategic issues situations and supporting the decision-making process in view of an imminent crisis. The research group of Andreou et al. proposed the use of the genetically evolved certainty neuron fuzzy cognitive map (GECNFCM) as an extension of CNFCMs aiming at overcoming the main

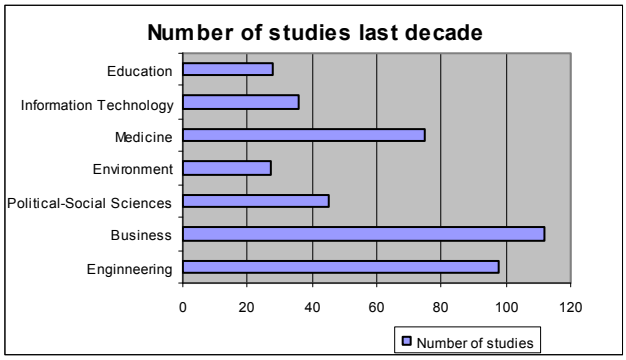

Figure 2. Number of FCM studies during the last decade (approximately +/- 5 studies per category).

weaknesses of the latter, namely the recalculation of the weights corresponding to each concept every time a new strategy is adopted [35]. That novel technique combined CNFCMs with genetic algorithms (GAs), the advantage of which lies with their ability to offer the optimal solution without a problem-solving strategy, once the requirements are defined. Using a multiple scenario analysis the value of the hybrid technique was demonstrated in the context of a model that reflects the political and strategic complexity of the Cyprus issue, as well as the uncertainties involved in it. Later, the same research group [24,36], presented the evolutionary FCMs for crisis management of the political problem of Cyprus.

An Ambient Intelligence (AmI) system, integrating aspects of psychology and social sciences, can be considered as a distributed cognitive framework composed by a collection of intelligent entities capable of modifying their behaviors by taking into account the user's cognitive status in a given time. Acampora et al. (2007), introduced a novel methodology of AmI systems' design that exploits multi-agent paradigm and a novel extension of FCMs theory benefiting on the theory of Timed Automata in order to create a collection of dynamical intelligent agents that use cognitive computing to define actions' patterns able to maximize environmental parameters as, for instance, user's comfort or energy saving [37].

Carvalho (2010) in his recent study, discussed the structure, the semantics and the possible use of FCM as tools to model and simulate complex social, economic and political systems, while clarifying some issues that have been recurrent in published FCM papers [38].

2) Medicine

At the last decade, FCMs have found important applicability in medical diagnosis and decision support [12, 39-45. In medical domain and in particular for medical decision support tasks, FCM based decision methodologies include an integrated structure for treatment planning management in radiotherapy [39], a model for specific language impairment [40], models for bladder and brain tumor characterization [41], an approach for the pneumonia severity assessment [42], and a model for the management of urinary tract infections [43]. Stylios et al. proposed FCM architectures for decision support in medicine [44].

Papakostas et al. (2007) implemented FCMs for pattern recognition tasks [45]. Froelich and Deja, 2009, proposed an FCM approach for mining temporal medical data [46]. Rodin et al. (2009) developed a fuzzy influence graph to model cell behavior in systems biology through the intracellular biochemical pathway [47]. Next, this model can be integrated in agents representing cells. Results indicate that despite individual variations, the average behavior of MAPK pathway in a cells group is close to results obtained by ordinary differential equations. The model was applied in multiple myeloma cells signaling.

3) Engineering

In this domain, FCMs found a large number of applications, especially in control and prediction. Particularly, FCMs have been used to model and support a plant control system, to construct a system for failure modes and effect analysis, to fine tune fuzzy logic controllers, to model the supervisor of a control system etc. Stylios and Groumpos, [2004] investigated the FCM for modeling complex systems and controlling supervisory control systems [48]. Papageorgiou et al. implemented learning approaches based on non-linear Hebbian rule to train FCMs that model industrial process control problems [29].

Recently, an integration of a cognitive map and a fuzzy inference engine was presented, as a cognitive–fuzzy model, targeting online fuzzy logic controller (FLC) design and self fine-tuning [49]. The proposed model was different than previous proposed FCMs in that it presents a hierarchical architecture in which the FCM process, available plant, and control objective data on represented knowledge to generate a complete FLC architecture and parameters description. Simulation results demonstrate model interpretability, which suggests that the model is scalable and offers robust capability to generate near optimal controller.

At 2010, Kottas et al. [27] presented basic theoretical results related to the existence and uniqueness of equilibrium points in FCN, the adaptive weight estimation based on system operation data, the fuzzy rule storage mechanism and the use of the entire framework to control unknown plants. The results are validated using well known control benchmarks. The same research team, at the same year, used FCN to construct a maximum power point tracker (MPPT), which may operate in cooperation with a fuzzy MPPT controller [50]. The proposed scheme outperforms other existing MPPT schemes of the literature giving very good maximum power operation of any PV array under different conditions such as changing insolation and temperature.

Beeson et al. (2010) proposed a factored approach to mobile robot map-building that handles qualitatively different types of uncertainty by combining the strengths of topological and metrical approaches [51]. This framework is based on a computational model of the human cognitive map and allows robust navigation and communication within several different spatial ontologies.

4) Business

In business, FCMs have found a great applicability. They can be used for product planning, for analysis and decision support. Some interested applications and worthy to be referred are illustrated. Jetter et al. (2006) used the concept of fuzzy front end for ideation, concept development and concept evaluation of new product development. This concept helped various problems managers who faced difficulty in early product development, as well as to systematic approaches to deal with them [52]. This approach helped in identification of market needs and technology potentials, detection and exploitation of idea sources, early stage assessment of ideas and product concepts, and successful management styles.

Yaman & Polat (2009) proposed the use of fuzzy cognitive maps (FCMs) as a technique for supporting the decision-making process in effect-based planning. With adequate consideration of the problem features and the constraints governing the method used, an FCM is developed to model effect-based operations (EBOs) [53]. In the mentioned study, the model was applied to an illustrative scenario involving military planning. Wei et al (2008) investigated the use of

fuzzy cognitive time maps for modeling and evaluating trust dynamics in the virtual enterprises [54]. Bueno & Salmeron (2008) proposed a tool for fuzzy modeling Enterprise Resource Planning selection [55]. Salmeron (2009) proposed the augmented fuzzy cognitive maps for modeling LMS critical success factors [56].

Kim and his coworkers (2008) developed a hybrid qualitative and quantitative approach, using FCMs and GAs, to evaluate forward-backward analysis of RFID supply chain [57]. The research group of Trappey et al (2010) used FCMs to model and evaluates the performance of RFID-enabled reverse logistic operations [58]. Radio frequency identification (RFID) complying with the EPCglobal (2004) Network architecture, i.e., a hardware- and software-integrated cross-platform IT framework, is adopted to better enable data collection and transmission in reverse logistic management. Inference analysis using genetic algorithms contributes to the performance forecasting and decision support for improving reverse logistic efficiency [58]. The study provided a method to predict future logistic operation states and to construct a decision support model to manage system performance based on the forecast.

Büyüközkan et al. (2009) proposed a systematic way of analyzing collaborative planning, forecasting and replenishment (CPFR) supporting factors using FCM approach [59]. Through their study, it was verified the application of FCM where interrelated variables like decision variables and uncontrollable variables were used. Xirogiannis et al. (2010) addressed the problem of designing an "intelligent" decision support methodology tool to act as a back end to financial planning [60].

One of the challenges in Risk Analysis and Management (RAM) is identifying the relationships between risk factors and risks. Lazzerini et al. (2010), proposed Extended Fuzzy Cognitive Maps (E-FCMs) to analyze the relationships between risk factors and risks [61]. The main differences between E-FCMs and conventional FCMs are the following: E-FCMs have non-linear membership functions, conditional weights, and time delay weights. Therefore E-FCMs are suitable for risk analysis as all features of E-FCMs are more informative and can fit the needs of Risk Analysis. Particularly, the work explores the Software Project Management (SPM) and discusses risk analysis of SPM applying E-FCMs.

5) Production Systems

FCM can provide an interesting solution to the issue of assessing the factors which are considered to affect the operator's reliability and can be investigated for human reliability in production systems [13]. Bertolini & Bevilacqua (2010) investigated the human reliability in production systems which act as an excellent means to study a production process and obtain useful indications on the consequences which can be determined by the variation of one or more variables in the system examined.

Lo Storto et al., (2010) presented a methodological framework to explore the cognitive processes implemented by members of a software development team to manage ambiguous situations at the stage of product requirements definition [62]. FCMs were used in the framework to elicit cognitive schemes and developed a measure of individual ambiguity tolerance. Moreover, FCMs were used to design game-based learning systems because it has the excellent ability of concept representation and reasoning [63]. A novel game-based learning model which includes a teacher submodel, a learner submodel and a set of learning mechanisms was established.

In computer vision, which is a new emerging area, there are demanding solutions for solving different problems. The data to be processed are bi-dimensional (2D) images captured from the tri-dimensional (3D) scene. The objects in 3D are generally composed of related parts that joined form the whole object. Fortunately, the relations in 3D are preserved in 2D. Hence, there are necessary ingredients to build a structure under the FCMs paradigm. FCMs have been satisfactorily used in several areas of computer vision including: pattern recognition, image change detection or stereo vision matching [64]. Pajares (2010) established a general framework of FCMs in the context of 2D images and described the performance of three applications in the three mentioned areas of computer vision.

6) Environment and Agriculture

FCMs were applied in ecology and environmental management for: modeling a generic shallow lake ecosystem by augmenting the individual cognitive maps [65], assessing local knowledge use in agroforestry management [66], modeling of interactions among sustainability components of an agro-ecosystem using local knowledge [67], predicting modeling a New Zealand dryland ecosystem to anticipate pest management outcomes [68], semi-quantitative scenario, with an example from Brazil [69]. Recently, van Vliet et al., (2010) used FCMs as a communication and learning tool for linking stakeholders and modelers in scenario studies [7]. In their recent work demonstrated the potential use of a highly participatory scenario development framework that involves a mix of qualitative, semi-quantitative and quantitative methods. Giordano, et al. (2010) proposed a methodology based on a FCM to support the elicitation and the analysis of stakeholders' perceptions of drought, and the analysis of potential conflicts [70]. The same year, Kafetzis et al. (2010) investigated two separate case studies concerned with water use and water use policy [71]. The documentation and analysis of such stakeholders' models will presumably offer insights into the use and limitations of local knowledge and management, while concurrently providing a current approach to developing appropriate strategies for process-oriented problem solving and decision making in an environmental pollution context.

In agricultrure, FCMs used to represent knowledge and assess cotton yield prediction in precision farming by connecting yield defining parameters with yield in Cotton Crop Production in Central Greece as a basis for a decision support system [72].

7) Information Technology (IT)

In information technology (IT) project management, a FCM-based methodology helps to success modeling. Current methodologies and tools used for identifying, classifying and evaluating the indicators of success in IT projects have several limitations. These could be overwhelmed by employing the FCMs for mapping success, modeling Critical Success Factors (CSFs) perceptions and the relations between them [8].

Rodriguez-Repiso et al (2007) demonstrated the applicability of the FCM methodology through a case study based on a new project idea, the Mobile Payment System (MPS) project, related to the fast evolving world of mobile telecommunications.

Xiangwei et al. (2009) analyzed and summarized common software's usability quality character system in order to find a software usability malfunction discovers and improve problems [73]. They used FCM to describe the software quality character relationship and give an integrated training arithmetic, syntax pruning arithmetic, semantic pruning arithmetic and quality relationship analysis arithmetic to the method.

An interesting tool for FCM development was presented in [74] where the FCM is defined by concepts and relationships that can change during the execution time. Using the tool, someone can design a FCM, follow the evolution of a given FCM, change FCM defined previously, etc. Furfaro et al. (2010) presented a novel method for the identification and interpretation of sites that yield the highest potential of cryovolcanic activity in Titan and introduced the theory of FCMs for the analysis of remotely collected data in planetary exploration [75].

In telecommunications, FCMs applied for distributed wireless P2P networks [76]. Peer-to-peer (P2P) technologies have raised great research interest due to a number of successful applications in wired networks. Popular commercial applications such as Skype and Napster have attracted millions of users worldwide. A novel team-centric peer selection scheme based on FCMs, which simultaneously considers multiple selection criteria in wireless P2P networks, was proposed. The main influential factors and their complex relationships for peer selection in wireless P2P networks were investigated.

TABLE III. FCM APPLICATIONS AT THE FIRST TWO MONTHS OF 2011

Research works published in 2011	**FCM applications at the first two months of 2011**	
	Application area	***Problem solving***
Kannappan et al. [80]	medicine	Classification, prediction
Papageorgiou [12]	medicine	Knowledge representation, decision making
Beena, & Ganguli [79]	Structural damage detection	learning
Song et al. [78]	Business	Classification and prediction
Hanafizadeh, P., Aliehyaei, R. [81]	Soft system	Modeling, analysis
Iakovidis & Papageorgiou [20]	medicine	Decision making, reasoning
Lee, N., Bae, J.K., Koo, C. [82]	Sales assessment	reasoning
Chytas, P., Glykas, M., Valiris, G. [834]	Business	Planning, analysis
Jetter, A., Schweinfort, W. [84]	Solar energy	Modeling, policy scenarios
A. Baykasoglu, Z.D.U. Durmusoglu, V. Kaplanoglu, [71]	Industial process control	Learning, control

Moreover, the participation of agents in FCM process [77] intends to a non-centralized detection of FCM stable state and to a modification process using asynchronous calculations. Stula et al. (2010) developed an agent-based fuzzy cognitive map (ABFCM) for injecting the concept of multi-agent system (MAS) into the FCM and the different inference algorithms in each node enabled the simulation of systems with diverse behavior concepts.

Of course, it was difficult in this study to present all the innovative and useful applications performed by FCMs and their extensions. We attempted to figure out some of the most mentioned applications emerged in the literature and to give the recent research directions of FCMs.

III. FCM APPLICATIONS AT 2011

During the first two months of year 2011, ten journal papers on FCM applications and modeling in different scientific fields were emerged. Table III includes these studies with the related application areas. So, the FCM has gradually emerged as a powerful paradigm for knowledge representation and a simulation mechanism that is applicable to numerous research and application fields. For example, Song et al. (2011) proposed a fuzzy neural network to enhance the learning ability of FCMs and incorporated the inference mechanism of conventional FCMs with the determination of membership functions. The effectiveness of this approach lies in handling the prediction of time series [78]. Beena et al. (2011) developed a new algorithmic approach for structural damage detection based on the use of FCM and Hebbian-based learning [79] and Baykasoglu et al. (2011) proposed a new training algorithm for FCMs, the Extended Great Deluge Algorithm (EGDA) [71]. Hanafizadeh and Aliehyaei applied FCMs in soft system methodology [81], Lee et al applied FCMs to sales opportunity assessment [82], Chytas et al applied FCMs to address the problems of proactive balanced scorecards [83], and Jetter et al. applied FCMs for scenario planning of solar energy [84]. Kanappan et al. [80] and Papageorgiou [12,20] applied FCMs in medical domain for classification and decision making.

IV. CONCLUSION

The Fuzzy Cognitive Map methodology has been proven through the literature a very useful approach and cognition tool to model and analyze complex dynamical systems. There is a considerable number of application studies of FCMs in different domains and the application of FCMs emerges a rapid continue. They are helpful to the decision-makers ponder over their representation of a given situation in order to ascertain its adequacy and possibly prompt the introduction of any necessary changes. It is a research challenge for applying FCMs in diverse scientific areas especially when efficient methods to quantify causalities, to adapt and learn FCMs, are proposed which might be handle with the complex tasks of each domain, thus to improve the FCM performance.

ACKNOWLEDGMENT

The DebugIT project (http://www.debugit.eu/) is receiving funding from the European Community's Seventh Framework Programme under grant agreement n° FP7–217139, which is gratefully acknowledged. The information in this document reflects solely the views of the authors and no guarantee or warranty is given that it is fit for any particular purpose.

REFERENCES

[1] B. Kosko, "Fuzzy cognitive maps", International Journal of Man-Machine Studies, vol. 24, no.1, pp. 65-75, 1986.

[2] B. Kosko, "Adaptive inference in fuzzy knowledge networks", in: D. Dubois, H. Prade, R.R. Yager (Eds.), Readings in Fuzzy Sets for Intelligent Systems, Morgan Kaufman, San Mateo, 1993.

[3] B. Kosko, "Fuzzy Thinking", 1993/1995, ISBN 0-7868-8021-X (Chapter 12: Adaptive Fuzzy Systems)

[4] Codara, L.: Le mappe cognitive. Carrocci Editore, Roma (1998).

[5] Y. Miao, Z.Q. Liu, C.K. Siew and C.Y. Miao, Dynamical cognitive network - an extension of fuzzy cognitive map, *Fuzzy Systems, IEEE Transactions on*, vol. 9, 2001, pp 760-770.

[6] G. Glykas, "Fuzzy Cognitive Maps: Theory, Methodologies, Tools and Applications", Springer Verlag, July 2010

[7] M. van Vliet, K. Kok, T. Veldkamp, "Linking stakeholders and modellers in scenario studies: The use of Fuzzy Cognitive Maps as a communication and learning tool", Futures 42 (1), 2010 pp. 1-14.

[8] L. Rodriguez-Repiso, R. Setchi, and J.L. Salmeron. Modelling IT Projects success with Fuzzy Cognitive Maps. Expert Systems with Applications 32(2) pp. 543-559. 2007.

[9] Stach W, Kurgan LA, and Pedrycz W(2010), Expert-based and Computational Methods for Developing Fuzzy Cognitive Maps, In: Glykas, M., Fuzzy Cognitive Maps: Advances in Theory, Methodologies, Tools and Applications, Springer (ISBN-10: 36-42032-19-2), 2010.

[10] E.I. Papageorgiou, N.I. Papandrianos, D. Apostolopoulos, P.J. Vassilakos, "Complementary use of Fuzzy Decision Trees and Augmented FCMs for Decision Making in Medical Informatics", Proc. of the 1st BMEI 2008, 28-30 May, Sanya, China, art. no. 4548799, pp. 888-892.

[11] E.I. Papageorgiou, C.D. Stylios, P.P. Groumpos, "Novel architecture for supporting medical decision making of different data types based on Fuzzy Cognitive Map Framework", in Proc. 28th IEEE EMBS 2007, 21-23 August, Lyon, France, Conference 2007, pp. 1192-1195.

[12] E.I. Papageorgiou, "A new methodology for Decisions in Medical Informatics using Fuzzy Cognitive Maps based on Fuzzy Rule-Extraction techniques", Applied Soft Computing, 11 (2011) 500–513.

[13] M. Bertolini and M. Bevilacqua, "Fuzzy Cognitive Maps for Human Reliability Analysis in Production Systems" Production Engineering and Management under Fuzziness Studies in Fuzziness and Soft Computing, 2010, Volume 252/2010, 381-415

[14] Y., Miao, C., Miao, X., Tao, Z., Shen, Z. Liu, "Transformation of cognitive maps", IEEE Transactions on Fuzzy Systems 18 (1), art. no. 5340662, 2010 pp. 114-124.

[15] A. Dickerson and B. Kosko, "Virtual Worlds as Fuzzy Cognitive Maps," Presence, vol. 3, no. 2, 1994, pp. 173–189.

[16] M. Parenthoen, P. Reignier, and J. Tisseau, "Put Fuzzy Cognitive Maps to Work in Virtual Worlds," Proc. 10th IEEE Int'l Conf. Fuzzy Systems, vol. 1, IEEE CS Press, 2001, p. 38.

[17] J. Aguilar, "A survey about fuzzy cognitive maps papers", International Journal of Computational Cognition, vol. 3, (2005), 27-33.

[18] W. Pedrycz, "The design of cognitive maps: A study in synergy of granular computing and evolutionary optimization", Expert Systems with Applications, 2010, in press.

[19] J. Salmeron, "Modeling grey uncertainty with Fuzzy Grey Cognitive Maps", Expert Systems with Applications 37 (2010) 7581–7588.

[20] D.K. Iakovidis, and E. Papageorgiou, "Intuitionistic Fuzzy Cognitive Maps for Medical Decision Making," IEEE Transactions on Information Technology in Biomedicine, vol. 15, no. 1, 2011.

[21] J. P. Carvalho, J. A. B. Tome, "Rule Based Fuzzy Cognitive Maps in Socio-Economic Systems", Proc. of IFSA-Eusflat 2009.

[22] Carvalho, J.P., Tomé,J.A.,"Rule Based Fuzzy Cognitive Maps - Expressing Time in Qualitative System Dynamics", Proceedings of the 2001 FUZZ-IEEE, Melbourne, Australia, 2001.

[23] H. Zhong, Chunyan Miao, Zhiqi Shenand Yuhong Feng, Temporal Fuzzy Cognitive Maps, 2008 IEEE World Congress on Computational Intelligence, June 1-6, 2008, Hong Kong, pp. 1831-1840.

[24] A.S., Andreou, N.H. Mateou and G.A Zombanakis, "Evolutionary Fuzzy Cognitive Maps: A Hybrid System for Crisis Management and Political Decision-Making", In Proc. Computational Intelligent for Modeling, Control & Automation CIMCA, Vienna, 2003, pp.732-743.

[25] A. S. Andreou, N. H. Mateou and G. A. Zombanakis, "Soft computing for crisis management and political decision making: the use of genetically evolved fuzzy cognitive maps", Soft Computing Journal, vol. 9, No. 3, 194-210, 2005, DOI: 10.1007/s00500-004-0344-0.

[26] Y., Miao, C., Miao, X., Tao, Z., Shen, Z. Liu, "Transformation of cognitive maps", IEEE Transactions on Fuzzy Systems 18 (1), art. no. 5340662, 2010 pp. 114-124.

[27] Kottas, T.L., Boutalis, Y.S., Christodoulou, M.A. Fuzzy Cognitive Networks: Adaptive network estimation and control paradigms, 2010a, *Studies in Fuzziness and Soft Computing* 247, pp. 89-134.

[28] H., Song, C., Miao, W., Roel, Z., Shen, F., Catthoor, "Implementation of fuzzy cognitive maps based on fuzzy neural network and application in prediction of time series", IEEE Transactions on Fuzzy Systems 18 (2), 2010 art. no. 5352265, pp. 233-250.

[29] E.I. Papageorgiou, C.D. Stylios & P.P. Groumpos, "Unsupervised learning techniques for fine-tuning FCM causal links", Intern. Journal of Human-Computer Studies, vol. 64, (2006), pp. 727-743.

[30] E.I. Papageorgiou, & P.P. Groumpos, "A new hybrid learning algorithm for Fuzzy Cognitive Maps learning", Applied Soft Computing, Elsevier, Vol. 5, 2005b, pp. 409-431.

[31] W. Froelich, A. Wakulicz-Deja, "Predictive Capabilities of Adaptive and Evolutionary Fuzzy Cognitive Maps - A Comparative Study", in: N.T. Nguyen and E. Szczerbicki (Eds.) Intel. Sys. for Know. Management, Springer Verlag Berlin, SCI 252, (2009b), 153–174.

[32] W. Stach, L.A. Kurgan, W. Pedrycz, M. Reformat, "Genetic learning of fuzzy cognitive maps", Fuzzy Sets and Systems, vol. 153, no. 3, pp. 371-401, 2005.

[33] D.E. Koulouriotis, I.E. Diakoulakis, D.M. Emiris and C.D. Zopounidis, Development of dynamic cognitive networks as complex systems approximators: validation in financial time series, *Applied Soft Computing*, vol. 5, 2005, pp 157-179.

[34] W. Stach, L. A. Kurgan, W. Pedrycz, "A survey of fuzzy cognitive map learning methods", In: Grzegorzewski, P., Krawczak, M., Zadrozny, S., (Eds.), Issues in soft computing: theory and applications, 2005.

[35] Andreou, A., Mateou, N.H., Zombanakis, G.: The Cyprus Puzzle and the Greek-Turkish Arms Race: Forecasting Developments Using Genetically Evolved Fuzzy Cognitive Maps. Journal of Defence and Peace Making 14, 293–310 (2003).

[36] A. S. Andreou, N. H. Mateou and G. A. Zombanakis, "Soft computing for crisis management and political decision making: the use of genetically evolved fuzzy cognitive maps", Soft Computing Journal, vol. 9, No. 3, 194-210, 2006.

[37] G. Acampora, and V. Loia, A Dynamical Cognitive Multi-Agent System for Enhancing Ambient Intelligence Scenarios, *IEEE International Conference on Fuzzy Systems* , art. no. 5277303, pp. 770-777.

[38] Carvalho, J.P., "On the semantics and the use of Fuzzy Cognitive Maps in social sciences, Proc. 2010 IEEE World Congress on Computational Intelligence, WCCI 2010 , art. no. 5584033.

[39] E.I. Papageorgiou, C.D. Stylios and P.P. Groumpos, "The Soft Computing Technique of Fuzzy Cognitive Maps for Decision Making in Radiotherapy", in book: Intelligent and Adaptive Systems in Medicine, editors: Dr. O. Haas and Prof. K. Burnham, Chapter 5, Taylor & Francis, LLC, IOPs Publications, February 2008.

[40] V.C. Georgopoulos G.A. Malandraki, and C.D. Stylios, "A fuzzy cognitive map approach to deferential diagnosis of specific language impairment", Artificial Intelligence in Medicine, 29(3), pp261-278, 2003.

[41] E.I. Papageorgiou, P. Spyridonos, P. Ravazoula, C.D. Stylios, P.P. Groumpos, & G. Nikiforidis, "Advanced Soft Computing Diagnosis Method for Tumor Grading", Artificial Intelligence in Medicine, Vol. 36, Number 1, January 2006, pp. 59-70.

[42] E.I. Papageorgiou, N.I. Papandrianos, G. Karagianni, G. Kyriazopoulos, D. Sfyras, "A fuzzy cognitive map based tool for prediction of infectious diseases", Proceeding of FUZZ-IEEE 2009, World Congress, 24-27 August 2009b, Korea, pp. 2094-2099.

[43] E.I. Papageorgiou, C. Papadimitriou, S.Karkanis, "Management uncomplicated urinary tract infections using fuzzy cognitive maps", Proc. of the 9th ITAB 2009a, pp. November 5-7, 2009, Larnaca, Cyprus, ISBN: 978-1-4244-5379-5.

[44] C.D. Stylios, V.C. Georgopoulos, Fuzzy Cognitive Maps Structure for Medical Decision Support Systems, Studies in Fuzziness and Soft Computing, 218 (2008) 151–174.

[45] G.A. Papakostas, Y.S. Boutalis, D.E. Koulouriotis, B.G. Mertzios, "Fuzzy cognitive maps for pattern recognition applications", International Journal of Pattern Recognition and Artificial Intelligence 22 (8), pp. 1461-1486, 2008.

[46] Froelich, W., Wakulicz-Deja, A. Mining temporal medical data using adaptive fuzzy cognitive maps 2009 Proceedings - 2009 2nd Conference on Human System Interactions, HSI '09, art. no. 5090946, pp. 16-23.

[47] V. Rodin, G. Querrec, P. Ballet, F. Bataille, G. Desmeulles, Jean–Francois Abgrall, Multi-Agents System to model cell signaling by using Fuzzy Cognitive Maps. Application to computer simulation of Multiple Myeloma, Proc. 2009 Ninth IEEE International Conference on Bioinformatics and Bioengineering, pp. 236-241.

[48] C.D. Stylios, and P.P. Groumpos, "Modeling Complex Systems using Fuzzy Cognitive Maps," *IEEE Transactions on Systems, Man and Cybernetics, Part A: Systems and Humans*, vol. 34, pp. 155-162, 2004.

[49] Gonzalez, J.L., Aguilar, L.T., Castillo, O. A cognitive map and fuzzy inference engine model for online design and self fine-tuning of fuzzy logic controllers, 2009 *International Journal of Intelligent Systems* 24 (11), pp. 1134-1173.

[50] Kottas, T.L. Boutalis, Y.S., Christodoulou, M.A. Fuzzy Cognitive Networks for Maximum Power Point Tracking in Photovoltaic Arrays Studies in Fuzziness and Soft Computing, 2010 (2010b), vol. 247, 231-257.

[51] P., Beeson, J., Modayil, B. Kuipers, "Factoring the mapping problem: Mobile robot map-building in the hybrid spatial semantic hierarchy", International Journal of Robotics Research vol. 29 (4), pp. 428-459.

[52] A.J.M. Jetter, "Fuzzy Cognitive Maps in engineering and technology management – what works in practice?", in: T. Anderson, T. Daim, D. Kocaoglu (Eds.), Technology Management for the Global Future: Proceedings of PICMET 2006, Istanbul, Turkey July 8–13, 2006, Portland, 2006.

[53] D. Yaman, S. Polat, "A fuzzy cognitive map approach for effect based operations: an illustrative case", Information Sciences, Volume 179, Issue 4, 1 February 2009, Pages 382-403.

[54] Z., Wei, L., Lu, Z. Yanchun, "Using fuzzy cognitive time maps for modeling and evaluating trust dynamics in the virtual enterprises", Expert Systems with Applications, 35 (4), 2008, pp. 1583-1592.

[55] S. Bueno, J.L. Salmeron, Fuzzy modeling Enterprise Resource Planning tool selection, Computer Standards & Interfaces vol.30 (2008) 137–147.

[56] Salmeron, J.L. Supporting decision makers with fuzzy cognitive maps: These extensions of cognitive maps can process uncertainty and hence improve decision making in R&D applications. 2009 Research Technology Management 52 (3), pp. 53-59.

[57] M.-C. Kim, C.O. Kim, S.R Hong, I.-H. Kwon, "Forward-backward analysis of RFID-enabled supply chain using fuzzy cognitive map and genetic algorithm", Expert Systems with Applications 35 (3), pp. 1166-1176, 2008.

[58] A.J.C. Trappey, Charles V. Trappey, Chang-Ru Wub, "Genetic algorithm dynamic performance evaluation for RFID reverse logistic management, Expert Systems with Applications: An International Journal, Vol. 37 (11), (November 2010) pp: 7329-7335.

[59] A. Baykasoglu, Z.D.U. Durmusoglu, V. Kaplanoglu, Training Fuzzy Cognitive Maps via Extended Great Deluge Algorithm with applications, *Computers in Industry*, 62 (2), pp. 187-195, *2011.*

[60] G. Xirogiannis, M. Glykas and C. Staikouras, Studies in Fuzziness and Soft Computing, 2010, Volume 247/2010, 161-200.

[61] B. Lazzerini, M. Lusine, Risk Analysis Using Extended Fuzzy Cognitive Maps 2010 International Proc. *ICICCI 2010* , art. no. 5566004, pp. 179-182

[62] Lo Storto, C. Assessing ambiguity tolerance in staffing software development teams by analyzing cognitive maps of engineers and technical managers 2010 2nd Int. Conf. on Engineering System Management and Applications, ICESMA 2010; Sharjah; April 2010.

[63] X. Luo, X. Wei, and J. Zhang, Game-based Learning Model Using Fuzzy Cognitive Map Proceeding MTDL '09 Proceedings of the first ACM international workshop on Multimedia technologies for distance learning, 2009, ISBN: 978-1-60558-757-8.

[64] G. Pajares, Fuzzy Cognitive Maps Applied to Computer Vision Tasks, Studies in Fuzziness and Soft Computing, Vol. 247, 2010, 259-289.

[65] C.O. Tan and U. Ozesmi, "A generic shallow lake ecosystem model based on collective expert knowledge", Hydrobiologia (2006) 563:125–142, 2006.

[66] M. E. Isaac, E. Dawoe, K. Sieciechowicz, "Assessing Local Knowledge Use in Agroforestry Management with Cognitive Maps", Environmental Management (2009) 43:1321–1329.

[67] D. Ramsey, and G. L. Norbury, "Predicting the unexpected: using a qualitative model of a New Zealand dryland ecosystem to anticipate pest management outcomes", Austral Ecology (2009) 34, 409–421.

[68] T. Rajaram, A. Das, "Modeling of interactions among sustainability components of an agro-ecosystem using local knowledge through cognitive mapping and fuzzy inference system", Expert Systems with Applications, (2010) in press.

[69] K. Kok, "The potential of Fuzzy Cognitive Maps for semi-quantitative scenario development, with an example from Brazil", Global Environmental Change vol. 19, (2009) 122–133.

[70] Giordano, R., Vurro, M. Studies in Fuzziness and Soft Computing, 2010, Volume 247/2010, 403-425.

[71] A. Kafetzis, Neil McRoberts and Ioanna Mouratiadou (2010) Using Fuzzy Cognitive Maps to Support the Analysis of Stakeholders' Views of Water Resource Use and Water Quality Policy Studies in Fuzziness and Soft Computing, 2010, Volume 247/2010, 383-402.

[72] E.I. Papageorgiou, Ath. Markinos, Th. Gemtos, "Soft Computing Technique of Fuzzy Cognitive Maps to connect yield defining parameters with yield in Cotton Crop Production in Central Greece as a basis for a decision support system for precision agriculture application", in book: Fuzzy Cognitive Maps, edited by M. Glykas, Springer Verlag, July 2010.

[73] Lai X., Zhou Y. and Zhang W. "Software Usability Improvement: Modeling, Training and Relativity Analysis", Proc. 2nd Int Symp on Information Science and Engineering *ISISE 2009*, art. no. 5447282, pp. 472-475.

[74] Aguilar Jose and José Contreras, The FCM Designer Tool, Studies in Fuzziness and Soft Computing, 2010, Volume 247/2010, 71-87.

[75] Furfaro, R., Kargel, J., S., Lunine, J., I., Fink, W., Bishop, M. P., 2010, Identification of Cryovolcanism on Titan Using Fuzzy Cognitive Maps, Planetary and Space Science, Volume 5, Issue 5, Pages 761–779.

[76] Li, X., Ji, H., Zheng, R., Li, Y., Yu, F.R. A novel team-centric peer selection scheme for distributed wireless P2P networks 2009 *IEEE Wireless Communications and Networking Conference, WCNC*, art. no. 4917532.

[77] M. Stula, D. Stipanicev, L. Bodrozic, Intelligent Modeling with Agent-Based Fuzzy Cognitive Map, International Journal of Intelligent Systems Volume 25, Issue 10, pages 981–1004, October 2010.

[78] Song, H.J., Miao, C.Y., Wuyts, R., Shen, Z.Q., D'Hondt, M., Catthoor, F. An extension to fuzzy cognitive maps for classification and prediction, 2011 *IEEE Transactions on Fuzzy Systems* 19 (1), art. no. 5601761, pp. 116-135.

[79] Beena, P., and Ganguli, R., "Structural Damage Detection using Fuzzy Cognitive Maps and Hebbian Learning", Applied Soft Computing, Vol. 11, No. 1, 2011, pp.1014-1020.

[80] K. Arthi. A. Tamilarasi, E.I. Papageorgiou, "Analyzing the performance of fuzzy cognitive maps with non-linear hebbian learning algorithm in predicting autistic disorder", Expert Systems with Applications, 38 (3), 2011, 1282-1292.

[81] Hanafizadeh, P., Aliehyaei, R. The Application of Fuzzy Cognitive Map in Soft System Methodology, Systemic Practice and Action Research, pp. 1-30, 2011, in press.

[82] Lee, N., Bae, J.K., Koo, C. A case-based reasoning based multi-agent cognitive map inference mechanism: An application to sales opportunity assessment, 2011 Information Systems Frontiers, pp. 1-16, in press.

[83] Chytas, P., Glykas, M., Valiris, G., A proactive balanced scorecard, 2011 International Journal of Information Management, Article in Press.

[84] Jetter, A., Schweinfort, W., Building scenarios with Fuzzy Cognitive Maps: An exploratory study of solar energy, 2011 Futures 43 (1), pp. 52-66.

2011 IEEE International Conference on Fuzzy Systems
June 27-30, 2011, Taipei, Taiwan

Nonlinear Cause-Effect Relationships In Fuzzy Cognitive Maps

Maria K. Ketipi, Dimitrios E. Koulouriotis, Evangelos G. Karakasis,
George A. Papakostas and Vassilios D. Tourassis

Department of Production and Management Engineering
Democritus University of Thrace, Greece, Xanthi GR-67100
mketipi@pme.duth.gr, jimk@pme.duth.gr, ekarakas@pme.duth.gr
gpapakos@ee.duth.gr, vtourasi@pme.duth.gr

***Abstract*—Fuzzy Cognitive Maps (FCMs) have been widely used for a plethora of applications, exploiting its ability to represent the knowledge and the dynamics of a system. The diversity of inference mechanisms, which have been proposed until nowadays, discloses the effort for an effective concept value calculation methodology. In contrast with the most research efforts which consider a linear relation of the influence that a concept exercise to another concept, in this paper a nonlinear representation of that influence is introduced. The importance which is associated with the proposed methodology is that a nonlinear cause-effect relationship strengthens the behavior of an FCM through the simulation process. The analysis of this proposal through a progressive reasoning is followed by appropriately selected problems.**

***Index Terms*—Cognitive inference, Concept influence, Generalized logistic function, Cause-effect relationships.**

I. Introduction

Knowledge representation, in a complex system, is a demanding and composite procedure. Experts, from different fields of interest, are invited to offer their knowledge and experience for the modeling of the system. Conforming to market requirements, researchers systematically use qualitative approaches for the representation of the systems. The first attempt to represent knowledge through graphs was introduced by Alexrod [1]. Specifically, Alexrod in [1] proposed the technique of Cognitive Maps (CMs) as a tool of decision making in social and political systems. Kosko in [2] enriched the CMs with fuzzy logic and proposed Fuzzy Cognitive Maps (FCM). CM, a soft computing tool, constricts its contribution to system analysis because of the binary representation of cause-effect relationships. Kosko in [2] transformed the signed directed graphs to fuzzy signed directed graphs and overcame the issues related to systems' rules about knowledge-mining. Moreover, the reliability of causal relationship matrix is increased according to [3], which resulted from the synthesis of multiple experts' knowledge. The introduction of FCMs provoked the interest of the scientific community and challenged many researchers to notice the particular field. Taber and Siegel in [4] and Taber in [5] proposed a methodology of estimating experts' credibility weight, while Kosko and Burgess in [6] developed the inference mechanism of FCMs and applied the Differential Hebbian Law for unsupervised learning. The conception of combining different FCMs was inserted by Dickerson and Kosko [7] enhancing the architectural configuration of FCMs.

To continue with, Pelaez and Bowles [8] supported the idea that various factors, such as integrity constraints and time lag, should be taken into consideration during the inference process. The introduction of these constraints was the beginning of a race, in order for dynamic (non-linear) systems to be represented using FCM. Tsadiras and Margaritis in [9] introduced Certainty Neuron Fuzzy Cognitive Maps (CNFCM), which reveal the existence of concepts' memory related to its previous states and used for the computation of its current states. Andreou et al. [10] extended the previous model by combining CNFCM and genetic algorithms in order to surpass the weaknesses lie in the recalculation of a concept's weights every time a new strategy is applied.

A dynamic version of FCM proposed by Miao et al. [11] in order to explore the dynamic nature of concepts and to determine the strength of the cause and the cause-effect relationship as much as the degree of influence. Evolutionary strategies, combined with fuzzy cognitive maps, revealed efficiency and credibility increment when applied in ambiguous and multi-stimulus situations ([12], [13], [14], [15]). An integrated research, elaborated by Koulouriotis et al. [16], combines decay mechanisms, inertial forces, diminishing effects and biases, such as synergies and conditional effects ([17]), in order to describe and comprehend nonlinear and asymmetric cause-effect relationships, achieving simultaneously controllability. Fuzzy cognitive maps have several applications, either by implementing a learning procedure ([33], [18]) or not ([19], [20], [21], [23], [22]). Finally, the participation of agents in FCM process ([24], [25], [26]) intends to a non-centralized detection of FCM stable state and to a modification process using asynchronous calculations.

In the current article, an integrated inference mechanism is presented which is based on influence modification in order to meet the requirements of dynamic systems. In section II, a concise presentation of the theoretical background of FCM is quoted, offering an introductory view and the key points of inference mechanism development. The subsequent sections deal with the presentation of the proposed methodology and

978-1-4244-7316-8/11/$26.00 ©2011 IEEE

the experimental analysis, while the concluding remarks are given in the last section.

II. Fuzzy Cognitive Maps: A theoretical background

Fuzzy Cognitive Maps (FCMs), proposed by Kosko [2], are fuzzy signed directed graphs with feedback, emphasizing both to the representation of the cause-effect relationships between concepts (i.e., positive, negative, zero) and the influence degree of this relationship expressed in linguistic values. Concretely, a FCM is a fuzzy graph which models a system and its behavior using the concepts and their relationships. A concept i indicates a state, a procedure, an event or a variable of the system and is represented with C_i $(i = 1, 2, \ldots, n)$. The directed edge between concepts C_i and C_j denotes the causality between concepts i and j and is represented with the weight w_{ij}, that can be a fuzzy value within $[-1, 1]$ or a trivalent logic within $\{-1, 0, 1\}$. There are three possible types that a weight (w_{ij}) can be distinguished in: a) positive $(w_{ij} > 0)$, which means that an increase (decrease) in the value of concept C_i leads to an increment (decrement) of value of C_j, b) negative $(w_{ij} < 0)$, which means that an increase (decrease) in the value of concept C_i leads to a decrement (increment) of value of C_j, and c) neutral $(w_{ij} = 0)$, which means that there is no relationship between C_i and C_j. The graphic illustration of the modeled system and the corresponding adjacency matrix is shown in Fig.1 and Fig.2.

A general rule for computing the value of a concept in each simulation step is the calculation of the influence caused by other concepts that are connected to the particular concept. The value A_i^{t+1} denotes the effect that concept C_i caused at time $t+1$ by other concepts [27] and is calculated by the following equation:

$$A_i^{t+1} = f\left(A_i^t + \sum_{j=1, j\neq i}^{n} A_j^t \cdot w_{ji}\right) \tag{1}$$

where, A_i^t is the value of concept C_i at time t, A_j^t is the value of concept C_j at time t, w_{ji} is the weight of the interconnection between concepts C_i and C_j, and f is a threshold function which limits the result of the multiplication in the interval [-1,1].

Tsadiras in [28] analyzed and compared different FCMs according to the type of threshold function which was implemented. After the initialization of the system by the experts and defuzzifying the inserted data, the concepts are ready to interact according to the determined relation network. The moment that a concept is activated, the other concepts, which are connected with, are influenced. The interaction between concepts continues until a fixed-point equilibrium is reached; a limit cycle is reached; or chaotic behavior is exhibited [9]. Tsadiras and Margaritis [9], developed a procedure by which the appropriate threshold function can be chosen according to concept's value and the effect influence field of definition. The interpretation of (2-4) is that a concept which is influenced by

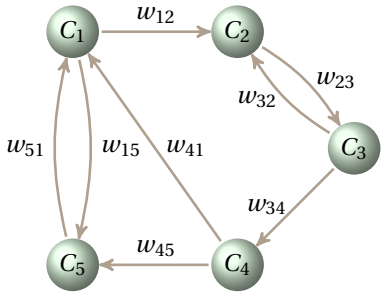

Fig. 1. A simple Fuzzy Cognitive Map

$$\mathbf{W} = \begin{array}{c} \\ \mathbf{C_1} \\ \mathbf{C_2} \\ \mathbf{C_3} \\ \mathbf{C_4} \\ \mathbf{C_5} \end{array} \begin{array}{c} \begin{array}{ccccc} \mathbf{C_1} & \mathbf{C_2} & \mathbf{C_3} & \mathbf{C_4} & \mathbf{C_5} \end{array} \\ \begin{pmatrix} 0 & w_{12} & 0 & 0 & w_{15} \\ 0 & 0 & w_{23} & 0 & 0 \\ 0 & w_{32} & 0 & w_{34} & 0 \\ w_{41} & 0 & 0 & 0 & w_{45} \\ w_{51} & 0 & 0 & 0 & 0 \end{pmatrix} \end{array}$$

Fig. 2. The Adjacency matrix of FCM

external effect can be activated to the degree that is not already activated.

$$f(A_i^t, S_i^t) = \begin{cases} A_i^t + S_i^t(1 - A_i^t), & A_i^t,\ S_i^t \geq 0 \\ A_i^t + S_i^t(1 + A_i^t), & A_i^t,\ S_i^t < 0,\ |A_i^t|, |S_i^t| \leq 1 \\ \frac{A_i^t + S_i^t}{1 - \min(|A_i^t|, |S_i^t|)}, & otherwise \end{cases} \tag{2}$$

$$A_i^{t+1} = f(S_i^t, A_i^t) \tag{3}$$

$$S_i^t = \sum_{j=1,\, j\neq i}^{n} A_j^t w_{ji} \tag{4}$$

where A_i^t is the value of concept C_i at the moment t, and S_i^t is the total influence which has applied from other concepts at moment t. The problem which arises from (4) is that S_i^t should belong within space $[-1, 1]$. The influence of the other concepts, S_i^t, has the maximum value when $|A_i^t| = 1$ and all $A_j^t,\ j = 1, \ldots, n$, have the same sign with the corresponding weight w_{ji}. So,

$$S_{i,\max} = \sum_{j=1}^{n} |A_j^t||w_{ji}| = \sum_{j=1}^{n} |w_{ji}|, \quad i = 1, \ldots, n \tag{5}$$

The maximum value of $S_{i,\max}$ can be calculated as follows:

$$S_{\max} = \max(S_{1,\max}, S_{2,\max}, \ldots, S_{n,\max}) \tag{6}$$

A new matrix w' is created which its elements w_{ji} can be calculated using the following equation:

$$w'_{ji} = \frac{w_{ji}}{S_{\max}} \tag{7}$$

Tsadiras and Margaritis [9], using (7), ensured that the influence value S_i^t will never be out of space $[-1, 1]$. Considering that the third part of (2) could possibly lead to division with

zero, Andreou et al. [29] proposed a transformation by which the absolute values of variables are replaced by their normal values. The third part of (2) transformed and acquired the form $\frac{A_i^t+S_i^t}{1-\min(A_i^t,S_i^t)}$.

Moreover, Yaman and Polat in [30] modified the third part of (2) and the one that Andreou et al. [29] proposed, inserting the mathematical expression $A_i^t + S_i^t$. In the case that the particular condition is satisfied, the sum of $A_i^t + S_i^t$ is impossible to be out of the continue space $[-1, 1]$. As it is obvious, (3) and (4) are also part of this proposition. Generally, the influence degrees are expected to be computed at the end of the determined influence durations. In the proposed methodology, links' influence duration is reduced by one unit and unit influence degree is recalculated for every step.

Finally, Koulouriotis et al. [16] proposed an enhancement on Dynamic Cognitive Networks (DCNs), combining adaptive characteristics which portraiture a dynamic system. These extensions are nonlinear and asymmetric cause-effect relationships, decaying mechanisms, inertial forces, diminishing effects and biases. Referring to nonlinear and asymmetric cause-effect relationships, Koulouriotis et al. [16] introduced a formula which is based on sigmoid function and is used for the computation of the effect that a concept A cause to a concept B (8).

$$\begin{array}{c} EFFECT = ef_{AB}\left(C_A\right) = \frac{2}{1+e^{-\alpha C_A}} - 1 \\ + \\ A \rightarrow B \end{array} \tag{8}$$

where α is a control parameter whose role is to adjust the rate of the impact that concept A exerts on B. The methodology by which authors [16] calculated the value of concept is given by (9):

$$A_i^{t+1} = \min\left(1, \max\left(\begin{array}{c} -1, A_i^t + \sum_{j=1, j\neq i, A_j^t>0}^{n} w_{ji}^{+} A_j^t \\ + \sum_{j=1, j\neq i, A_j^t<0}^{n} w_{ji}^{-} A_j^t \end{array}\right)\right) \tag{9}$$

Similarly, Koulouriotis et al. [16] imported decaying mechanisms, inertial forces, diminishing effects and biases in inference procedure, specifying the necessity of meticulously defined systems.

III. Proposed Methodology

Considering the above presentation of Fuzzy Cognitive Maps, we presume that A_j is the value of concept C_j and the weight w_{ji} indicates the relationship between concepts C_j and C_i, where $A_j, w_{ji} \in [-1, 1]$. The influence F_{ji} that a concept C_j causes to C_i is denoted with

$$F_{ji} = w_{ji} \cdot A_j, \qquad F_{ji} \in [-1, 1] \tag{10}$$

The graphic representation of (10) is illustrated in Fig.3 and reflects the linear function $y = a \cdot x$. Analytically, the vertical axis represents the influence F_{ji} that a concept C_j cause to concept C_i and the horizontal axis represents the value A_j of concept C_j. The line ϵ (red line in Fig.3) represents the linear

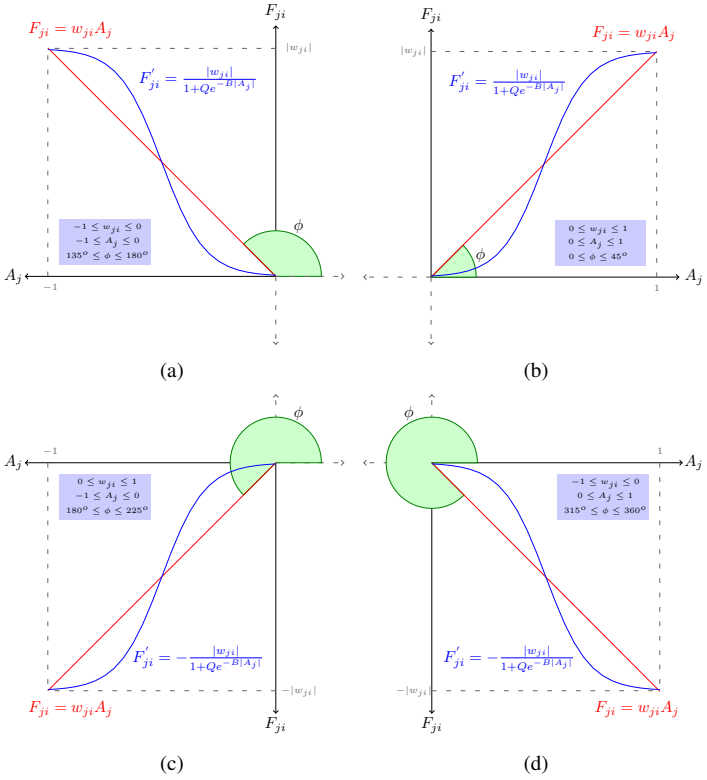

Fig. 3. The influence degree of concept C_j to C_i expressed with the generalized logistic function for a) $135^o \le \phi \le 180^o$, b) $0^o \le \phi \le 45^o$, c)$180^o \le \phi \le 225^o$, d)$315^o \le \phi \le 360^o$.

relation of F_{ji} and A_j. From the above statements, it can easily be deduced that w_{ji} is the slope of line ϵ.

$$w_{ji} = \tan(\phi) \tag{11}$$

In order for F_{ji} to belong within $[-1, 1]$, given that A_j, $w_{ji} \in [-1, 1]$, the field of definition of ϕ is $\phi \in \{[0^o, 45^o] \cup [135^o, 225^o] \cup [315^o, 360^o]\}$. Considering the current perception, the relation between influence F_{ji} and the value A_j is linear. In the present article, it is proposed a nonlinear representation of this relation, using the generalized logistic function.

$$f(x) = L + \frac{U - L}{(1 + Qe^{-B(x-M)})^{1/\nu}} \tag{12}$$

where, L is the lower asymptote, U is the upper asymptote, B is the growth rate, ν affects near which asymptote maximum growth occurs, Q depends on the value $f(0)$ and M is the time of maximum growth if $Q = \nu$.

According to the above considerations(11, 12), the influence F_{ji} that a concept C_j causes to a concept C_i, where A_j, $w_{ji} \in [-1, 1]$, can be formulated using the generalized

logistic function (12).

$$F_{ji}^{'} = \begin{cases} \frac{|w_{ji}|}{1+Qe^{-B|A_j|}}, & for \quad 0 \leq w_{ji},\, A_j \leq 1 \\ & \quad or \\ & -1 \leq w_{ji},\, A_j \leq 0 \\ -\frac{|w_{ji}|}{1+Qe^{-B|A_j|}}, & for \quad 0 \leq A_j \leq 1,\; -1 \leq w_{ji} \leq 0 \\ & \quad or \\ & -1 \leq A_j \leq 0,\; 0 \leq w_{ji} \leq 1 \end{cases} \tag{13}$$

where, $L = 0,\ U = |w_{ji}|,\ M = 0,\ \nu = 1$ and Q, B are two free parameters in order to adjust the shape of the sigmoid curve. The graphic illustration of influence $F_{ji}^{'}$, in relation to A_j, is shown in Fig.3. In the first quadrant Fig.3(a), the linear relation of F_{ji} and A_j is represented with the red line. The angle ϕ $(0 \leq \phi \leq 45^o)$ shows the space that line $F_{ji} = w_{ji}A_j$ can move in order to satisfy the limitation $0 \leq w_{ji} \leq 1$, considering (11). Moreover, the nonlinear relation of F_{ji} and A_j is represented with the generalized logistic function (sigmoid function), with upper limit $F_{ji_{max}} = |w_{ji}|$. Similarly, the other three quadrants are defined in Figs.3(b), 3(c) and 3(d), verifying the expression (13). Taking into consideration the above definitions in (13) and Fig.3, the value A_i^{t+1} of concept C_i at time $t+1$ can be computed using the following equation:

$$A_i^{t+1} = f\left(A_i^t + \sum_{j=1, j\neq i}^{n} F_{ji}^{'}(A_j^t, w_{ji})\right) \tag{14}$$

However, this methodology can be applied to every concept value computational methodology due to the fact that it not changes the methodology but the cause-effect relationship between two concepts.

The particular methodology proposes a nonlinear way to represent influence between concepts considering its appliance to dynamic systems. Essentially, the proposed methodology which is based on generalized sigmoid function, is a generalization of the concepts causal-effect relationship, which is reported in [16]. The nonlinear relationship between concepts transforms their values in such a way that results in a smoother convergence. However, this behavior might cause slower convergence to an equilibrium state. Furthermore, appropriately selected parameters (L, U, Q, B, M, ν) could lead the map to an equilibrium state even if a linear causal-effect relationship is not able to reach a stable state.

IV. Experimental Analysis

In order to apply, analyze and compare the proposed methodology, two different scenarios have been chosen which implement real-word and synthetic data.

A. Scenario 1

The first scenario [33] is referred to a simple control process in chemical industry. It comprises one tank and three valves that influence the amount of liquid in the tank. The particular procedure can be described as follows: Valves 1 and 2 pour two different liquids into the tank, producing a new liquid while a chemical reaction is triggered. When the new liquid produced reaches a specific level, measured by a sensor, valve 3 empties the tank. The FCM model is derived from the above control problem, according to a group of experts, and is illustrated in Fig.4. As we can assume from Fig.4, there are five concepts that constitute the FCM. The first concept (C_1) indicates that the amount of the liquid that Tank contains is dependent on the operational state of Valves 1, 2 and 3. Moreover, the state of Valves 1, 2 and 3 (C_1, C_2 and C_3 correspondingly) according to the predefined problem, could be closed, open or partially opened. Finally, the specific gravity of the liquid into the tank typifies the last concept (C_5). The initial values of concepts are given in matrix $A_{initial} = [0.4\ 0.7\ 0.6\ 0.7\ 0.3]$, the initial weight matrix ($W_{initial}$) is derived from the FCM of Fig.4 and the values of concepts C_1 and C_5 must be inside the ranges $0.68 \leq C_1 \leq 0.74$ and $0.74 \leq C_5 \leq 0.80$. In the current experimental analysis (Scenario 1, 2), the values of the free parameters Q and B (13) which are used in the procedure are $Q = 200$, $B = 10.5966$.

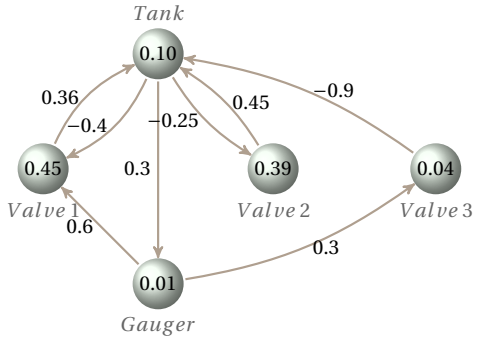

Fig. 4. The Fuzzy Cognitive Map derived from scenario 1

In [33], a linear cause-effect relationship between concepts (1) is used during the training process (Nonlinear Hebbian Learning - NHL) of the above FCM. In [33] the desired equilibrium state $A_{NHL}^1 = [0.683\ 0.7632\ 0.6538\ 0.7534\ 0.744]$ is reached and the NHL algorithm returns the updated weight matrix (W_{NHL}^1). In order for the proposed methodology to be compared with the common procedure, the above FCM is trained again with the difference that the NHL uses the proposed methodology (14) to compute the concepts values. In this case the equilibrium state $A_{prop} = [0.7108\ 0.7789\ 0.6480\ 0.7764\ 0.7660]$ is reached and the NHL algorithm returns the weight matrix W_{prop} (Fig.5). The values of concepts C_1 and C_5 which have been resulted from the aforementioned training processes are illustrated in Table I.

In order to evaluate the weight matrix W_{prop}, 1000 random initial vectors (A_{random}) are produced. These vectors are used as initial states of the FCM models which have as weighted matrices the W_{prop} and W_{NHL}^1 correspondingly. The minimum, maximum and mean values of concepts C_1 and C_5 as well as the standard deviations, which have been derived from the random examples, are presented in Table II.

By examining the mean values of Table II can be observed

TABLE I
EQUILIBRIUM STATES OF TRAINING PROCESSES

	Training Process Equilibrium State	
	Tank (C_1)	Gauger (C_5)
A^1_{NHL}	0.6830	0.7440
A_{Prop}	0.7108	0.7660

TABLE II
RANDOM EXAMPLES OF C_1,C_5

			1000 random examples			
			A^1_{NHL}		A_{Prop}	
Tank (C_1)	min	max	0.6833	0.6843	0.7106	0.7113
	Mean	St.Dev.	0.6836	1.29e-004	0.7109	1.29e-004
Gauger (C_5)	min	max	0.7447	0.7454	0.7657	0.7663
	Mean	St.Dev.	0.7450	1.53e-004	0.7660	1.24e-004

$$\mathbf{W_{prop}} = \begin{array}{c} \\ \mathbf{C_1} \\ \mathbf{C_2} \\ \mathbf{C_3} \\ \mathbf{C_4} \\ \mathbf{C_5} \end{array} \begin{array}{c} \begin{array}{ccccc} \mathbf{C_1} & \mathbf{C_2} & \mathbf{C_3} & \mathbf{C_4} & \mathbf{C_5} \end{array} \\ \begin{pmatrix} 0 & -0.2112 & -0.0417 & 0 & 0.4649 \\ 0.5362 & 0 & 0 & 0 & 0 \\ 0.5617 & 0 & 0 & 0 & 0 \\ -0.8274 & 0 & 0 & 0 & 0 \\ 0 & 0.7110 & 0 & 0.4966 & 0 \end{pmatrix} \end{array}$$

Fig. 5. The weight matrix of FCM using the proposed methodology

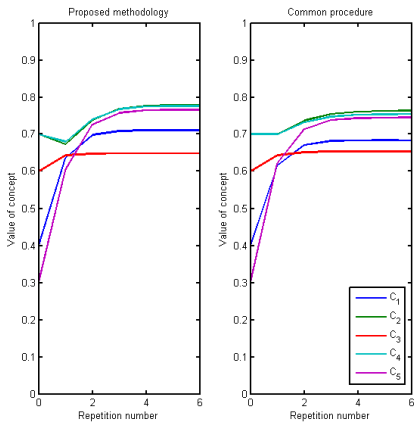

Fig. 6. Simulation process of Scenario 1

that the usage of the proposed methodology (nonlinear cause-effect relationships between concepts) in the NHL learning process leads to an equilibrium state for C_1 and C_5 very close to the midpoint of the desired bounds. It can further be concluded, from the minimum and maximum values as well as the standard deviations of 1000 random examples, that the consideration of a nonlinear cause-effect relationship between concepts leads to a FCM model as stable as the traditional methodology.

B. Scenario 2

An engine for producing scenarios with different properties (number of concepts, initial concept values, weight matrices) has been developed for the paper purposes. In order to investigate the simulation results, two different cases of the created scenarios have been selected. In the first case, the function $f(n) = \frac{1}{1+e^{-n}}$ is used as a threshold function (concept values inside the range $[0, 1]$), whereas in the second case the threshold function is $f(n) = \frac{2}{1+e^{-2n}} - 1$ (concept values inside the range $[-1, 1]$). The proposed methodology is compared with a common procedure in which (1) is used for calculating concepts values. Figures 8, 10 and 12 consist of two parts. The left part shows the simulation results of the proposed methodology while the right indicates the simulation results of (1).

In the first case, the proposed methodology presents very similar results with the common procedure (Fig.8). The initial weight matrix and the initial values of concepts which have been chosen for the simulation as much as the equilibrium state values (values of concepts) of the compared methodologies are illustrated in Fig.7 and Table III, respectively.

However, in the second case, the proposed methodology illustrates not only similar results with the common procedure, but also results which enhance its strength inference nature against the common procedure (Fig.12). The first example of the second case (when threshold function is $f(n) = \frac{2}{1+e^{-2n}} - 1$) is consisted of five concepts. The weight matrix, the initial concepts values as well as the equilibrium state of the two methodologies are presented in Fig.9 - Fig.10 and Table IV. It can be observed that although the two methodologies reach a similar equilibrium state, the proposed methodology needs more steps to finish the simulation process. Furthermore, the curves in Fig.10 follow a slightly different path to reach the final state.

Information about the initial and the equilibrium state of the second example of case two are given in Fig.11 - Fig.12 and Table V. By examining the aforementioned figures and

$$\mathbf{W_{initial}} = \begin{array}{c} \\ \mathbf{C_1} \\ \mathbf{C_2} \\ \mathbf{C_3} \\ \mathbf{C_4} \\ \mathbf{C_5} \\ \mathbf{C_6} \end{array} \begin{array}{c} \begin{array}{cccccc} \mathbf{C_1} & \mathbf{C_2} & \mathbf{C_3} & \mathbf{C_4} & \mathbf{C_5} & \mathbf{C_6} \end{array} \\ \begin{pmatrix} 0 & 0 & 0 & 0 & 0 & 0 \\ 0 & 0 & 0.1764 & 0 & 0.3342 & 0 \\ 0 & 0 & 0 & -0.1011 & 0.1729 & -0.8323 \\ -0.3024 & 0 & 0 & 0 & 0 & 0.9496 \\ -0.0973 & -0.7245 & 0.0076 & 0 & 0 & 0.3027 \\ 0 & 0.6734 & -0.0208 & 0.9459 & 0.2406 & 0 \end{pmatrix} \end{array}$$

Fig. 7. Initial weight matrix for Scenario 2 - Case 1

TABLE III
INITIAL AND EQUILIBRIUM STATE VALUES OF CONCEPTS FOR SCENARIO 2 - CASE 1

Concepts	Initial state	Equilibrium state	
	$A_{Initial}$	$A_{Proposed}$	A_{Common}
C_1	0.3569	0.5372	0.5588
C_2	0.6627	0.6416	0.6439
C_3	0.2815	0.6959	0.6882
C_4	0.2304	0.8386	0.8133
C_5	0.7111	0.8128	0.7869
C_6	0.6246	0.7781	0.7699

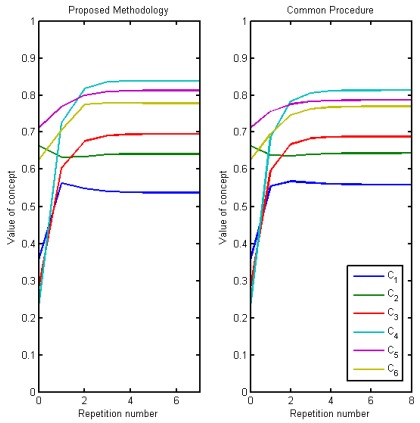

Fig. 8. Simulation process of Scenario 2 - Case 1

the corresponding table can be concluded that the selection of the threshold function leads to different results between the two methodologies. In Fig.12 can be observed that the proposed methodology reached an equilibrium fixed-point in contrast to the common procedure which reaches a limit cycle. This is feasible with an appropriate adjustment of the proposed methodology parameters (12-13). This fact, in combination with the first example of case two, highlights the enhanced, by the proposed methodology, dynamic behavior of the FCM. To continue with, the adjustable character (parameters Q, B) of the proposed influence mechanism introduce additional adaptability to similar situations.

V. CONCLUSIONS AND FUTURE WORK

Fuzzy cognitive maps are a remarkable simulation methodology primarily based on a linear cause-effect relationship between concepts. The subject of the particular research is the nonlinear representation of influence between concepts in order to achieve more effective simulation of real-world situations. The characteristics of the proposed methodology,

$$\mathbf{W_{prop}} = \begin{array}{c} \\ \mathbf{C_1} \\ \mathbf{C_2} \\ \mathbf{C_3} \\ \mathbf{C_4} \\ \mathbf{C_5} \end{array} \begin{array}{c} \begin{array}{ccccc} \mathbf{C_1} & \mathbf{C_2} & \mathbf{C_3} & \mathbf{C_4} & \mathbf{C_5} \end{array} \\ \begin{pmatrix} 0 & -0.0999 & -0.1133 & 0 & 0.9380 \\ -0.1444 & 0 & 0.1095 & 0 & 0.6938 \\ 0 & 0 & 0 & 0 & 0.0636 \\ 0 & 0 & 0.7425 & 0 & 0 \\ 0 & 0 & 0 & 0.3017 & 0 \end{pmatrix} \end{array}$$

Fig. 9. Initial weight matrix for Scenario 2 - Case 2 - Example 1

TABLE IV
INITIAL AND EQUILIBRIUM STATE VALUES OF CONCEPTS FOR SCENARIO 2 - CASE 2 - EXAMPLE 1

Concepts	Initial state	Equilibrium state	
	$A_{Initial}$	$A_{Proposed}$	A_{Common}
C_1	0.6455	0.6048	0.5646
C_2	0.2268	-0.5647	-0.5198
C_3	-0.1384	0.8955	0.8616
C_4	0.8747	0.7952	0.7527
C_5	-0.9476	0.8046	0.7506

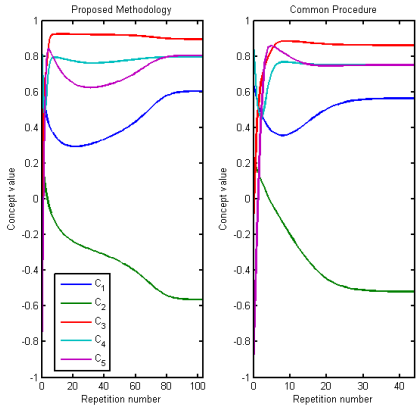

Fig. 10. Simulation process of Scenario 2 - Case 2 - Example 1

$$\mathbf{W_{prop}} = \begin{array}{c} \\ \mathbf{C_1} \\ \mathbf{C_2} \\ \mathbf{C_3} \\ \mathbf{C_4} \\ \mathbf{C_5} \end{array} \begin{array}{c} \begin{array}{ccccc} \mathbf{C_1} & \mathbf{C_2} & \mathbf{C_3} & \mathbf{C_4} & \mathbf{C_5} \end{array} \\ \begin{pmatrix} 0 & -0.4750 & -0.3156 & 0 & 0.4645 \\ 0 & 0 & -0.3722 & 0 & 0.6527 \\ -0.4407 & 0 & 0 & -0.7656 & 0 \\ 0 & 0 & 0.0968 & 0 & 0 \\ -0.2620 & 0 & 0 & 0 & 0 \end{pmatrix} \end{array}$$

Fig. 11. Initial weight matrix for Scenario 2 - Case 2 - Example 2

TABLE V
INITIAL AND EQUILIBRIUM STATE VALUES OF CONCEPTS FOR SCENARIO 2 - CASE 2 - EXAMPLE 2

Concepts	Initial state	Equilibrium state	
	$A_{Initial}$	$A_{Proposed}$	A_{Common}
C_1	-0.0978	0.7304	-
C_2	-0.5402	-0.8613	-
C_3	-0.0484	0.2923	-
C_4	-0.4572	-0.5676	-
C_5	-0.2925	-0.7408	-

which exploit experts' knowledge and experience, as well as its adjustability, highlight the enhanced inference mechanism.

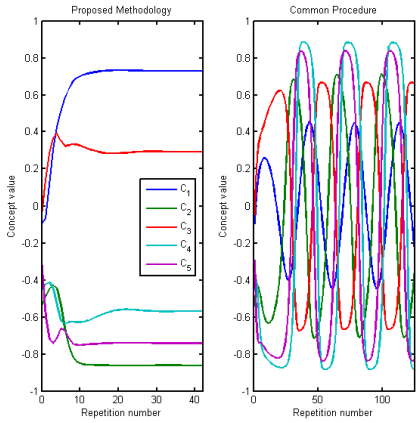

Fig. 12. Simulation process of Scenario 2 - Case 2 - Example 2

Improved learning results and randomly generated indicative examples, illustrate the ability of the proposed mechanism to converge into fixed states and efficiently manage realistic systems, even when the conventional approach falling into repeated cycle state. The proposed methodology stimulates the future research to a direction which is associated with the targeted and extensive analysis of real-world and other problems, especially when limit cycle or chaotic behavior is detected. Furthermore, the proposed methodology depends on a set of free parameters (L, U, Q, B, M, ν), thus a sensitivity analysis is going to be explored in a future work. Moreover, a thorough study of learning algorithms using the nonlinear influence mechanism in conjunction with its property of adjustability, could improve the whole process.

REFERENCES

[1] R.M. Axelrod, *Structure of decision: the cognitive maps of political elites*, Princeton University Press, Princeton, NJ; 1976.

[2] B. Kosko, Fuzzy cognitive maps, *Int. J. of Man-Machine Studies*, vol. 24, 1986, pp 65-75.

[3] B. Kosko, Hidden patterns in combined and adaptive knowledge networks, *Int. J. of Approximate Reasoning*, vol. 2, 1988, pp 377–393.

[4] W.R. Taber and M.A. Siegel, "Estimation of expert weights using fuzzy cognitive maps", *in First International Conference on Neural networks*, vol. 2, 1987, pp 19-325.

[5] W.R. Taber, Knowledge processing with Fuzzy Cognitive Maps, *Expert Systems with Applications*, vol. 2, 1991, pp 83-87.

[6] B. Kosko and J.C. Burgess, Neural Networks and Fuzzy Systems, *The Journal of the Acoustical Society of America*, vol. 103, 1998, pp 3131-3131.

[7] J.A. Dickerson and B. Kosko, Virtual Worlds as Fuzzy Cognitive Maps, *Presence*, vol. 3, 1994, pp 73-89.

[8] C.E. Pelaez and J.B. Bowles, Using fuzzy cognitive maps as a system model for failure modes and effects analysis, *Information Sciences*, vol. 88, 1996, pp 177-199.

[9] A.K. Tsadiras and G.K. Margaritis, Cognitive mapping and certainty neuron fuzzy cognitive maps, *Information Sciences*, vol. 101, 1997, pp 109-130.

[10] A.S. Andreou, N.H. Mateou and G.A. Zombanakis, The Ciprus puzzle and the Greek - Turkish arms race: Forecasting developments using genetically evolved fuzzy cognitive maps, *Defence and Peace Economics*, vol. 14, 2003, pp 293-310.

[11] Y. Miao, Z.Q. Liu, C.K. Siew and C.Y. Miao, Dynamical cognitive network - an extension of fuzzy cognitive map, *Fuzzy Systems, IEEE Transactions on*, vol. 9, 2001, pp 760-770.

[12] D.E. Koulouriotis, I.E. Diakoulakis and D.M. Emiris, "Anamorphosis of fuzzy cognitive maps for operation in ambiguous and multi-stimulus real world environments", *in IEEE International Conference on Fuzzy Systems*, Melburne, Australia, 2001, pp 1156-1159.

[13] D.E. Koulouriotis, I.E. Diakoulakis and D.M. Emiris, "Learning fuzzy cognitive maps using evolution strategies: A novel schema for modeling and simulating high-level behavior", *in Proceedings of the IEEE Conference on Evolutionary Computation, ICEC*, 2001, pp 364-371.

[14] D.E. Koulouriotis, I.E. Diakoulakis and D.M. Emiris, "A fuzzy cognitive map-based stock market model: Synthesis, analysis and experimental results", *in IEEE International Conference on Fuzzy Systems*, Melburne, Australia, 2001, pp 465-468.

[15] D.E. Koulouriotis, I.E. Diakoulakis, D.M. Emiris, E.N. Antonidakis and I.A. Kaliakatsos, Efficiently Modeling and Controlling Complex Dynamic Systems using Evolutionary Fuzzy Cognitive Maps (Invited Paper), *International Journal of Computational Cognition*, vol. 1, 2003, pp 41-65.

[16] D.E. Koulouriotis, I.E. Diakoulakis, D.M. Emiris and C.D. Zopounidis, Development of dynamic cognitive networks as complex systems approximators: validation in financial time series, *Applied Soft Computing*, vol. 5, 2005, pp 157-179.

[17] D.E. Koulouriotis, I.E. Diakoulakis and D.M. Emiris, "Realism in fuzzy cognitive maps: Incorporating synergies and conditional effects", *in IEEE International Conference on Fuzzy Systems*, Melburne, Australia, 2001, pp 1179-1182.

[18] P. Beena and R. Ganguli, Structural damage detection using fuzzy cognitive maps and Hebbian learning, *Applied Soft Computing*, vol. 11, 2011, pp 1014-1020.

[19] R. Yu and G.-H. Tzeng, A soft computing method for multi-criteria decision making with dependence and feedback, *Applied Mathematics and Computation*, vol. 180, 2006, pp 63-75.

[20] C.D. Stylios, V.C. Georgopoulos, G.A. Malandraki and S. Chouliara, Fuzzy cognitive map architectures for medical decision support systems, *Applied Soft Computing Journal*, vol. 8, 2008, pp 1243-1251.

[21] L. Beatrice and M. Lusine, "Risk analysis using Extended Fuzzy Cognitive Maps", *in 2010 International Conference on Intelligent Computing and Cognitive Informatics, ICICCI*, 2010, pp 179-182.

[22] G.A. Papakostas and D.E. Koulouriotis, Classifying patterns using Fuzzy Cognitive Maps, *Studies in Fuzziness and Soft Computing*, vol. 247, 2010, pp 291-306.

[23] G.A. Papakostas, Y.S. Boutalis, D.E. Koulouriotis and B.G. Mertzios, Fuzzy cognitive maps for pattern recognition applications, *International Journal of Pattern Recognition and Artificial Intelligence*, vol. 22, 2008, pp 1461-1486.

[24] W.R. Zhang, S.S. Chen, W. Wang and R.S. King, A cognitive map based approach to the coordination of distributed cooperative agents, *IEEE Trans. Syst. Man Cybern*, vol. 22, 1992, pp 103-113.

[25] M.A. Gadallah and A.H. Hefny, "A novel multiagent system based on dynamic fuzzy cognitive map approach", *in 10th International Conference on Intelligent Systems Design and Applications*, Cairo, Egypt, 2010, pp 254-259.

[26] M. Stula, D. Stipanicev and L. Bodrozic, Intelligent modeling with agent-based fuzzy cognitive map, *Int. J. of Intell. Syst.*, vol. 25, 2010, pp 981-1004.

[27] C.D. Stylios and P.P. Groumpos, Fuzzy Cognitive Maps in modeling supervisory control systems, *J. Intell. Fuzzy Syst.*, vol. 8, 2000, pp 83-98.

[28] A.K. Tsadiras, Comparing the inference capabilities of binary, trivalent and sigmoid fuzzy cognitive maps, *Information Sciences*, vol. 178, 2008, pp 3880-3894.

[29] A.S. Andreou, N.H. Mateou and G.A. Zombanakis, Soft computing for crisis management and political decision making: the use of genetically evolved fuzzy cognitive maps, *Soft Comput. - A Fusion of Foundations, Methodologies and Applications*, vol. 9, 2005, pp 194-210.

[30] D. Yaman and S. Polat, A fuzzy cognitive map approach for effect-based operations: An illustrative case, *Information Sciences*, vol. 179, 2009, pp 382-403.

[31] F.J. Richards, A Flexible Growth Function for Empirical Use, *Journal of Experimental Botany*, vol. 10, 1959, pp 290-301.

[32] C.D. Stylios, P.P. Groumpos, V.C. Georgopoulos, An fuzzy cognitive maps approach approach to process control systems, *J. Adv. Comput. Intell.*, vol. 3, 1999, pp 409-417.

[33] E.I. Papageorgiou, C. Stylios and P.P Groumpos, Unsupervised learning

techniques for fine-tuning fuzzy cognitive map causal links, *Int. J. Human-Computer Studies*, vol. 64, 2006, pp 727-743.

[34] E.I. Papageorgiou and P.P Groumpos, A new hybrid method using evolutionary algorithms to train Fuzzy Cognitive Maps, *Applied Soft Computing*, vol. 5, 2005, pp 409-431.

2011 IEEE International Conference on Fuzzy Systems
June 27-30, 2011, Taipei, Taiwan

Case Based Fuzzy Cognitive Maps (CBFCM) : New method for medical reasoning

Comparison study between CBFCM/FCM

Nassim Douali
Inserm UMRS 872 équipe 20
Cordeliers Research Center Paris, France
Nassim.douali@crc.jussieu.fr

Jos De Roo
Agfa HealthCare
Agfa HealthCare NV, Moutstraat 100, 9000
Gent, Belgium

Elpiniki I. Papageorgiou
Dept. of Informatics & Computer Technology
Technological Educational Institute of Lamia, Lamia
Greece
epapageorgiou@teilam.gr

Marie-Christine Jaulent
Inserm UMRS 872 équipe 20
Cordeliers Research Center Paris, France
Marie-christine.jaulent@crc.jussieu.fr

Abstract— **Doctor usually uses his experience from the clinical practice to confirm a diagnosis and to prescribe an appropriate treatment for a specific patient. The computerized medical reasoning should not only focus on existing medical knowledge but also on physician's previous experiences and new knowledge. Such knowledge and experience are vague and define uncertain relationships between facts and diagnosis. Case Based Fuzzy Cognitive Maps (CBFCM) are proposed as an evolution of Fuzzy Cognitive Maps (FCM) that allow more complete representation of knowledge since case-based fuzzy rules are introduced to improve FCM decision support systems. Semantic web is used to implement both FCM approaches. A database of 71 patients with urinary tract infections was used to perform the proposed approach. A comparative study between FCM (92%) and CBFCM (99%) was conducted and the results derived by CBFCM approach showed CBFCM to be superior to FCM.**

Keywords : Fuzzy Cognitive Maps, Rules, Decision Support Systems, Knowledge Representation, Clinical Guidelines, Semantic Web, case based reasoning.

I. INTRODUCTION

In medical practice, the doctor evokes several diagnoses but the differential diagnosis remains the major problem in medical decision making. It requires a several complementary examinations and experts review. Clinical Decision Support Systems (CDSS) are tools to improve patient safety and care processes [1,2]. Several studies and reviews have shown their effectiveness, i.e. [3,4,5,6] in the areas of diagnosis and therapy.

In a recent review, Peleg and others [7] claim that CDSS allow "*right knowledge to the right people in the right form at the right time*" [8]. The development of CDSS has two knowledge-management tasks: the possibility of integration into the care system workflow, and knowledge management for proper decision making.

CDSS models have to take into consideration issues related to patient data quality that is: incompleteness, poorly structured and sometimes unreliable data, problems associated with inaccuracies and uncertainties in Clinical Practice Guidelines (CPG). Many clinical diagnosis tasks involve reasoning under uncertainty [9]. Modeling a dynamic system can be hard in a computational sense.

The use of CDSS in urinary tract infections will reduce false diagnoses and establish a proper antibiotic regimen. FCMs have proved their efficiency in medical decision support and medical reasoning through the literature [10-14]. This paper describes and evaluates a new method to create a diagnosis model framework based on semantic web approach and Case Based Fuzzy Cognitive Maps (CBFCM). The produced results of the examined framework are compared with those obtained from FCM reasoning approach for 71 patients.

II. BACKGROUND

A. Clinical decision support system

CDSS form a significant part of the field of medical knowledge management technologies through their capacity to support the clinical process and use of knowledge, from diagnosis and investigation through treatment and long-term care. Their role and acceptance in daily clinical practice is increasing [15]. Recent studies [16] showed that CDSS can improve physician performance and accuracy, while the quality of each system may depend on the technical approach they use to model medical information.

CPG are structured documents that list a set of specific cases for which some diagnosis and therapeutic action plans are recommended with a given degree reflecting the strength of the recommendation corresponding to the level of scientific evidence. CPG include the description of the various

978-1-4244-7316-8/11/$26.00 ©2011 IEEE

alternatives and the factors that would allow establishing decisions amongst them. However, because of the sheer volume of one such CPG and the rigid structure of such guidelines, it is very difficult for the physician to apply and strictly follow the workflow presented by guidelines. Our work is directed towards the creation of a computerised system that dynamically guides the physician through the workflow and assist physicians in diagnosis of clinical forms of UTI (Urinary Tract Infection).

An empirical antimicrobial therapy well suited to the patient requires consideration of the patient treatment parameters (treatment ongoing, drug allergies...) but above all a good first diagnosis is primarily based on a clinical approach. The diagnosis is based on a notion of causality between infectious disease and clinical signs that it generates light in the field of physiological and pathological patient. In order to solve the problem of modeling medical knowledge from guidelines and to assign UTI diagnosis by handling imprecision and uncertainty, the FCMs and their extension, namely CBFCMs, are investigated. The semantic web approach was used to implement the proposed approaches.

B. *Cognitive Maps*

Cognitive Maps were introduced by R. Axelrod in 1976 to represent political and social knowledge [17]. They are directed graphs with signed edges. The nodes represent variable concepts and the arrows interconnecting concepts represent the relations between concepts. The sign attached to the head of arrows indicates the polarity of the causal relations. A positive arrow from node (concept) C1 to node C2, means C1 causally increases C2. Cognitive maps have been used to model a number of areas (political, social, business, ...).

C. *Fuzzy Cognitive Maps (FCM)*

FCMs, as an extension of cognitive maps, were developed by R. Kosko [18] to represent the causal relationship between concepts and analyze inference patterns. FCM represents knowledge in a symbolic manner, encoding the relations between the elements of a mental landscape so that the impact of these elements can be assessed. FCMs have gained considerable research interest and have been applied to many areas [Papageorgiou & Arthi, 2010].

FCM inherits the fuzzy logic properties on cognitive maps that allow predicting the change of the concepts represented in Cognitive Maps. The graphical illustration of FCM is signed directed graph with feedback, consisting of nodes and weighted interconnections. Nodes stand for concepts, variables, states that are used to describe the behavior of the system and they are connected by weighted arcs representing the causal relationships among nodes. Each concept is characterized by a fuzzy value usually ranging from [0…1] or [-1…1].

The most important element in describing the system is the determination of which a concept influences which others and with which degrees. There are three possible types of causal relationships among concepts that express the type of influence from one concept to the others. The weight of the interconnection between concept *Ci* and concept *Cj*, denoted by Wij, could be positive Wij > 0 for positive causality or could be negative causality Wij < 0 or could be null when there is no relationship between concept Ci and concept Cj , thus Wij = 0.

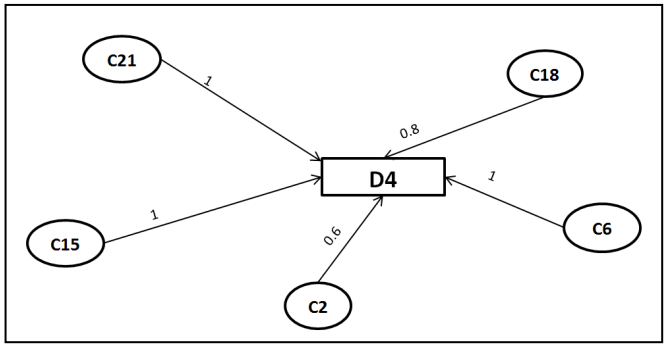

Figure 1. Representation of FCM model of acute prostatitis
(C2: Fever, C15: Vesical Uretral Reflux, C8: Vomitting, C18: Flank Pain, C19: Urine Dipstick Test, D8: Acute Prostatitis)

To get the value of a concept *Cj*, the value of each of its concepts inputs *Ci* is multiplied by the respective weight Wij which takes values in [-1..1]; then the results are added and passed by a non-linear function used to limit the range of possible output values.

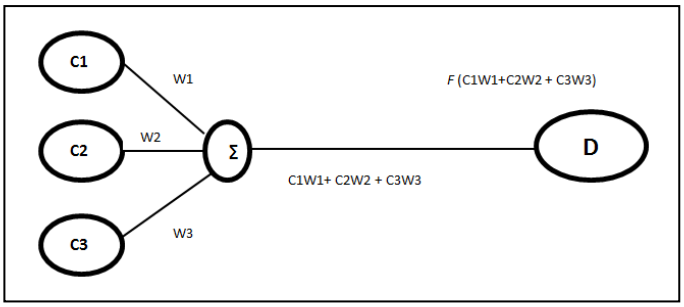

Figure 2. Graphical representation of calculating the value of the concepts of decision

So the value *Ai* for each concept *Ci* is calculated by the following rule:

$$A_i(k+1) = f(A_i(k) + \sum_{\substack{j \neq i \\ j=1}}^{N} (A_j(k) \cdot E_{ji}) \qquad (1)$$

where $A_i^{(k+1)}$ is the value of concept C_i at simulation step $k+1$, $A_j^{(k)}$ is the value of concept C_j at step k, E_{ji} is the weight of the interconnection between concept C_j and concept C_i and f is a threshold (activation) function that squashes the result of the multiplication in the interval [0, 1].

This equation indicates that a FCM is free to interact; at every step of interaction every concept has a new value. Several formulas can be used as threshold function [19], and as the interval of concept is bivalent (i.e., the concepts belong to the interval [0, 1]), we propose the function $f(x)$:

$$f(x)=1/(1+\exp(-cx)) \qquad (2)$$

where c is a real positive number and x is the value $A_i^{(k)}$ on the equilibrium point. In this work we use c=1, because this value showed best results in previous works [20].

Reasoning mechanism

The FCM inference algorithm is consisting of the following steps is used to simulate the process and give the necessary decisions about it.

(Step 1) Definition of the initial vector **A** that corresponds to the elements-concepts identified by experts' suggestions and available knowledge.

(Step 2) Multiply the initial vector **A** and the matrix **W** defined by experts by the eq. (1).

(Step 3) The resultant vector **A** at time step k is updating using Eqs. (1)–(2).

(Step 4) This new vector $\mathbf{A}^k$ is considered as an initial vector in the next iteration.

(Step 5) Steps 2–4 are repeated until $\mathbf{A}^k - \mathbf{A}^{k-1} \leq e$ = 0.001 (where e is a residual, describing the minimum error difference among the subsequent concepts) or $\mathbf{A}^k = \mathbf{A}^{k-1}$. Thus $\boldsymbol{A_f} = \mathbf{A}^k$.

In each of the case studies, an initial vector **A** is assigned (consisting of *Ai* values corresponding to each one concept *Ci*), representing the presented events at a given time of the process, and a final vector **A_f** is calculated at the steady state of the system, representing the last state that can be arrived at.

The iteration stops when a limit vector is reached, i.e., when $\mathbf{A}^k = \mathbf{A}^{k-1}$ or when $\mathbf{A}^k - \mathbf{A}^{k-1} \leq e$; where e is a residua, whose value depends on the application type (and in most applications is equal to 0.001).

1) Fuzzy Cognitive Maps extensions

FCMs are limited to the representation of simple monotonic causal relations between concepts and they do not handle the AND/OR relationships among the antecedent nodes, although they represent the causal relations between the antecedent and consequent nodes. Numerous works have been proposed to improve FCMs performances. Many extensions to the FCMs were developed, such as Extended Fuzzy Cognitive Maps (EFCMs), Rule Based Fuzzy Cognitive Maps (RBFCMs), Random Fuzzy Cognitive Maps (RFCMs), Intuitionistic FCMs, Fuzzy Grey Cognitive Maps and so on.

2) Case based reasoning:

Case-based reasoning (CBR) systems reason from experience: they solve new problems by retrieving relevant prior cases and adapting them to fit new situations. In 1988 the first case-based reasoning workshop identified theoretical foundations and fundamental issues for case-based reasoning research [20]. Case-based reasoning systems process new situations by retrieving a relevant prior case from memory, comparing that case to the new situation to determine important similarities and differences, and applying pertinent information from the old case to the new situation. Case-based reasoning has been applied to many tasks and domains, such as message classification, dispute mediation, explanation, language understanding, legal reasoning and planning.

Motivations for using case-based reasoning include: increasing efficiency in solving new problems, because relevant reasoning can be re-used rather than having to be re-derived; improving the quality of solutions; and simplifying knowledge acquisition. CBR facilitates the knowledge acquisition process because cases can be stored and used without having a perfect domain theory; case acquisition can be achieved without analyzing the interactions between individual factors in a case. Also, extensive pre-existing case libraries are available for many tasks, and those libraries can provide a starting point when building CBR systems [20].

D. Semantic web tools :

1) RDF / RDFS (Resource Description Framework / Schema)

RDF is a standard model for data interchange on the Web. RDF has features that facilitate data merging even if the underlying schemas differ, and it specifically supports the evolution of schemas over time without requiring all the data consumers to be changed. RDF extends the linking structure of the Web to use URIs (Url Resources Identifier) to name the relationship between things as well as the two ends of the link (this is usually referred to as a "triple"). The data are shown in triples:

Subject Verb/Predicate Object

These expressions are known as triples in RDF terminology. The subject denotes the resource, and the predicate denotes traits or aspects of the resource and expresses a relationship between the subject and the object. The subject is a resource identified by a URI (Uniform Resource Identifier), which is described by another resource (object) with a property (Word / Predicate). In the case problem of UTI, an example is given for the "pyelonephritis" diagnosis, where the subject "fever" has the property "symptom" for the object "pyelonephritis".

Exemple :

```
<rdf:Description about=
"http://www.spim.jussieu.fr/Pyelonephritis">
<prefixe:Symptom>Fever</prefixe:Symptom>
</rdf:Description>
```

Using this simple model, it allows structured and semi-structured data to be mixed, exposed, and shared across different applications.

2) Web Ontology Language (OWL):

The Web Ontology Language OWL is a semantic markup language for publishing and sharing ontologies on the World Wide Web. OWL is developed as an extension of RDF vocabulary. It is derived from the DAML + OIL Web Ontology Language. OWL is flexible, extendable, and decentralized because it's designed for use in the dynamic, global environment of the Web. OWL supports hierarchical relationships at their core, allowing for easy incorporation of subclasses and subproperty relationships that are essential for

managing and integrating complex data. We used in our project an ontology written in OWL, which will be described in the material.

3) Notation 3/ N3 logic:

The notation N3 is the format being developed by Tim Berners-Lee and others from the Semantic Web community. RDF / N3 is a rating given by Tim Berners Lee as an alternative to RDF / XML [30]. Notation3, or N3 is more compact and human readable than RDF / XML.

For example, the notion "The Fever is a symptom of Pyelonephritis" in RDF is represented as the triple: a subject denoting "Fever", a predicate denoting "Symptom", and an object denoting "Pyelonephritis". In N3, this is written as an RDF triple just like that:

```
:Fever :Symptom :Pyelonephritis
```

N3 language has been selected on purpose to represent medical knowledge due to its human readability and close relationship to the semantic web. Formalized medical information is represented with ontological concepts using Notation3 format. An example is given:

```
@prefix dco:
<http://www.debugit.eu/ontology/1.0/dco.owl#>.
dco:Fever dco:Symptom dco:Pyelonephritis.
```

N3 Logic is a logical platform that uses semantic web N3 as RDF syntax and expands the vocabulary of predicates. The goal of logic N3 is to give the possibility to integrate an RDF data model, logical rules and provide integrated functions that allow access and reason about data.

This allows expressing knowledge in N3 logic for a specific purpose [21]. In a rule, the premise is the subject and the conclusion is the complement (object). The sign "=>" is a common predicate expression log-rule namely implies.

An example of N3 rule is given:

If the patient is pregnant Then the diagnosis of "`PregnancyUrinaryTractInfection`" is inadequate for this patient. The main aspects of programming CBFCM approach in N3 are depicted :

```
{(?P dco:Pregnant) fl:mu 1} => {(?P
dco:PregnancyUrinaryTractInfection) fl:sigma 0}.
```

III. MATERIALS AND METHODS

A. Materials

In our project, we used 71 clinical cases to create a database of patient testing. We worked with domain ontology of Infectious Diseases DCO (DebugIT Core Ontology) [22]. DCO serve as the core component of the interoperability platform for the DebugIT project.

Inference engine:

As part of our project, we formalized the rules and we executed by an inference engine. EulerSharp [23] is an inference engine with backward-forward-backward chaining that allows the "loop-checking to ensure the processing of all data, to reason with data, queries and rules in N3". We choose Euler for historical performance[1], frequent updates[2], plugins & the ability to integrate new features[3] (built in).

B. Methods

1) Case Based Fuzzy Cognitive Maps (CBFCM)

One advantage of the FCM-based decision making is that it resembles human decision making, with its ability to perform approximate reasoning and handle incomplete information. But FCM seems to be limited to the representation of simple monotonic causal relations between concepts and could not handle the AND/OR relationships among the antecedent nodes.

In medical reasoning, many observables/factors such as painful, febrile, old, take the form of fuzzy concepts and used in FCM. These fuzzy concepts can be represented by fuzzy sets. Doctors use their academic knowledge and clinical cases already dealt with that imply a case-based reasoning and a heuristic approximate reasoning. A new method to improve results from the FCM approach is proposed by adding a system of rules based on cases. This method is developed using the tools of the semantic web. Fig3 is a graphical representation of CBFCM method:

A patient 01 represents a set of clinical parameters (C1, C2, and C3). These clinical parameters could be clinical signs, age, gender or biological results. They are used as input concepts in our CBFCM. These concepts are then processed by a set of fuzzy rules that are outcome of our case base. If the patient case is similarly of one of the cases already known then the diagnosis is confirmed by consensus; else we use our FCM algorithm to have a concept D1 for diagnosis decision.

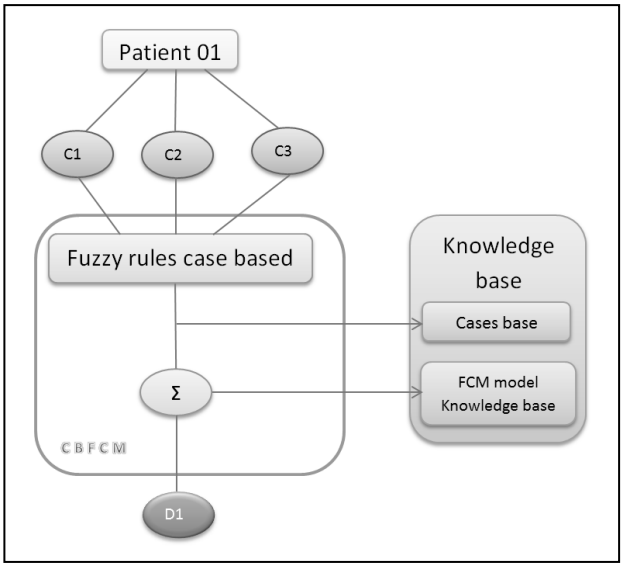

Figure 3. Diagram represents the CBFCM method

2) CBFCM Euler Plugin

To allow management of CBFCM fuzzy rules, FCM plugin for Eye[23] updated several times to change the value of a

[1] http://eulersharp.sourceforge.net/2003/03swap/dtb-2010.txt
[2] http://eulersharp.sourceforge.net/DONE
[3] http://eulersharp.sourceforge.net/2003/03swap/euler-builtins.html

fuzzy set membership (pi) and two decisions-conclusions can be arranged at the same rule.

We present in detail the steps followed for the design of our diagnosis model based CBFCM:

Extraction of clinical concepts and diagnostic:

From several CPG, we extracted clinical concepts and diagnostic concepts (all diagnoses).

Standardization of clinical concepts and diagnostic:

We have standardized, manually, concepts with the DebugIT ontology of Infectious Diseases (DCO).

Writing diagnostic rules:

The messages of CPG are as rules "*If Premise Then Conclusion*". The premise takes into account several patient parameters and it consists of several basic premises. Extracting Knowledge from CPG in fuzzy rules "If-Then". The rules are formalized as follows:

If the value of the concept *Ci* is X then the value of *Dj* is Y with a degree of influence (weight) Wij. Every relationship between a concept and a clinical diagnostic concept is defined by a membership function that determines the degree of causality between two concepts. Example, "If the urine dipstick test is negative then the diagnosis of UTI is wrong with a degree of 0.9".

In our approach, we use the knowledge from CPGs to build our cognitive maps that these rules represent the relationship between concepts and the weight of this relationship has a fuzzy value.

3) Construction of CBFCM diagnosis model

A number of medical guidelines for the diagnosis problem of UTI were formalized into CBFCM knowledge models using the approach presented in Fig.3. In order to construct our FCM model for medical decision support, the main concepts with their strengths of connections (causal influences) have to be assigned. Also a number of IF-THEN CBFCM rules were extracted to be used to improve the differential diagnosis and manage conflicts. The concepts and their relationships were extracted from CPG and each concept and clinical diagnosis contributes to a node represented in FCM.

All the concepts were defined. The relationships between these concepts and the clinical diagnosis concepts described in the CPG natural language were translated into formal language by defining the fuzzy weight of each concept. The fuzzy weights were determined using the methodology proposed in [24, 25]. These linguistic weights are initially used to describe the influence that exists between a clinical sign (concept) and a clinical diagnosis. Then, these weights are transferred to numerical weights in the range [-1,1] using the centroid defuzzification method of fuzzy logic[26].

a) CBFCM implementation in N3

To implement our algorithm for reasoning in N3, we use plugins of the inference engine EulerSharp developed in Prolog4. In Appendix B, the main aspects of programming CBFCM approach in N3 are depicted.

Our implementation method is to write rules in N3 logic for reasoning with standardized patients data using the FCM algorithm.

The CBFCM concepts are included in an ontology repository established for the project needs, namely DCO. DCO is updated continuously in order to contain all relevant clinical concepts. We worked with the DebugIT project ontologists to enrich the DCO ontology and can be used with our rules.

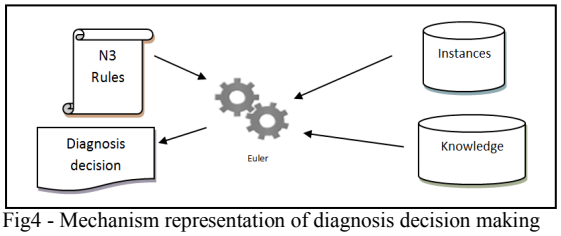

Fig4 - Mechanism representation of diagnosis decision making

Thus, based on this implementation technique, all the concepts, relationships and fuzzy rules for differential diagnosis are written in N3. Then, using the Euler plugin, the reasoning of the constructed model is accomplished, suggesting a differential diagnosis.

IV. RESULTS

The results presented here follow the steps of the methodology previously and the inference mechanism of CBFCMs (Eulersharp/plugin) [23]. The proposed methodology was validated with 71 patient cases derived from several European hospitals.

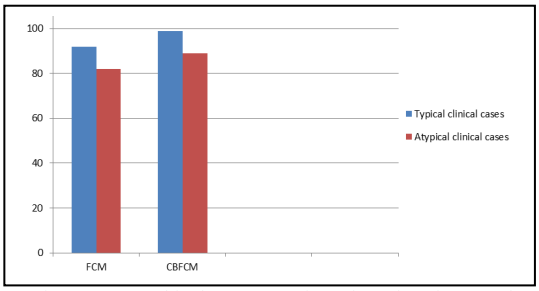

Figure 5 - Graphical representation of results of our study

Since this work is concerned by the modeling of diagnosis guidelines, the results are compared to the recommendations provided by the relevant clinical suggestions. Therefore, according to this approach, the rate of "correct" decisions, i.e. the decisions complying with the clinical diagnosis suggestions, is considered as the success rate of the compared models. The success rate of FCM approach was 92% and 99% of CBFCM approach for 71 examined patient cases. In 92%, and 99% of cases with FCM and CBFCM respectively, the answer given by our system was equivalent to the correct answers in cases involving clinical UTIs and 87%, 89% (FCM, CBFCM) in clinical cases involving other diseases (gynecological diseases, surgery ...) with urinary tract infection.

[4] http://eulersharp.sourceforge.net/2006/02swap/fcm-plugin.yap

Fig5 represent the results of corrects diagnosis given by our system.

V. DISCUSSION

The CBFCM approach allowed us to model medical knowledge of CPGs and to identify causal relationships in close as possible to the human reasoning. The use of CBFCM has enabled us to incorporate a second source of knowledge what we find beneficial to incorporate other types of knowledge. It allows us to model a simple knowledge of a medical field that is broad, complex and closely related to other areas.

The goal of our research study was threefold. First reasoning algorithms of Case Based fuzzy cognitive maps were established. Then, as a result the N3 notation and logic was used for the implementation of our cognitive maps for knowledge formalization of CPG and integration of others knowledge resources (others CPG). Finally, a patient database on which we applied the reasoning of our cognitive maps was created and tested for the model's validation.

We have implemented the knowledge bases, rules and databases in the same environment (RDF, N3, Euler..) without compatibility constraints, this is one of the advantages of using Semantic Web tools. The success rate of the proposed model giving UTI diagnosis was assigned to 99%, which shows the functionality of the model and its future usefulness in clinical practice.

CPG don't cover the whole field of community-acquired infections of the urinary tract in adults and we found a lot of information missing: the relationship between domain concepts. The rules, we have implemented, concern only the community urinary tract infections in adults. Integrating other GBPC, experts review, data mining results covering other areas of infectious diseases will allow us to improve our system.

Future work will be directed towards the construction of more dynamic systems based on the CBFCM methodology that could be integrating more sources of knowledge and data covering other areas of infectious diseases. Another part of the system is not yet developed that involves learning from the new case to enrich our knowledge base and enable close collaboration with practitioners on a daily basis.. The rules will be tested on a larger number of data and will be updated by integrating knowledge from more giuidelines/experts and data mining techniques.

VI. CONCLUSION

This under investigation study presents the results of comparison between the two reasoning methods: FCM and CBFCM. We explored the problem of modeling medical knowledge/guidelines and capturing the system's behavior for decision support of UTI diagnosis by using a new soft computing technology of CBFCMs implemented in semantic web. More specific, this work establishes a decision support tool based on CBFCM formalism for UTI diagnosis by proposing the appropriate diagnosis for each individual case.

The developed software tool calculates the diagnosis recommendations for UTIs. It receives the relevant patient state on input from the data store or a clinical information system (CIS). The simulations for test patients that are performed using the implementation of the proposed CBFCMs provide the differential diagnosis for these test patients.

The conducted study allowed us to test cognitive approaches for implementing CPG with Semantic Web tools. The advantage of this approach is to enable the sharing and reuse of knowledge from databases GBPC, experts and simplify maintenance.

This work represents a preliminary step in developing a methodology for the implementation of dynamic heterogeneous knowledge in the medical field and their use in decision support systems.

Acknowledgment

The DebugIT project (http://www.debugit.eu/) is receiving funding from the European Community's Seventh Framework Program under grant agreement n° FP7–217139, which is gratefully acknowledged. The information in this document reflects solely the views of the authors and no guarantee or warranty is given that it is fit for any particular purpose. The European Commission, Directorate General Information Society and Media, Brussels, is not liable for any use that may be made of the information contained therein.

REFERENCES

[1] Sittig DF, Wright A, Osheroff JA, Middleton B, Teich JM, Ash JS, et al. Grand challenges in clinical decision support. J Biomed Inform 2008;41(2):387–92.

[2] Balas EA, Weingarten S, Garb CT, Blumenthal D, Boren SA, Brown GD. Improving preventive care by prompting physicians. Arch Intern Med 2000;160(3):301–8

[3] Hunt DL, Haynes RB, Hanna SE, Smith K. Effects of computer-based clinical decision support systems on physician performance and patient outcomes: a systematic review. JAMA 1998; 280(15): 1339-46.

[4] Kawamoto K, Houlihan CA, Balas EA, Lobach DF. Improving clinical practice using clinical decision support systems: a systematic review of trials to identify features critical to success. BMJ 2005;330(7494):765.

[5] Garg AX, Adhikari NK, McDonald H, Rosas-Arellano MP, Devereaux PJ, Beyene J, et al. Effects of computerized clinical decision support systems on practitioner performance and patient outcomes: a systematic review. JAMA 2005;293(10):1223–38.

[6] Kucher N, Koo S, Quiroz R, Cooper JM, Paterno MD, Soukonnikov B, et al. Electronic Alerts to Prevent Venous Thromboembolism among Hospitalized Patients. N Engl J Med 2005; 352(10):969-77.

[7] Peleg M, Tu S. Decision support, knowledge representation and management in medicine. Methods Inf Med. 2006;45 Suppl 1:72-80.

[8] Schreiber G, Akkermans H, Anjewierden A, de Hoog R, Shadbolt, Nigel, Van de Velde W, Wielinga B. Knowledge Engineering and Management: The CommonKADS Methodology. Cambridge, MA: The MIT Press; 2000.

[9] Lin Lin, Paul Jen-Hwa Hu, Olivia R. Liu Sheng. A decision support system for lower back pain diagnosis: Uncertainty management and clinical evaluations. Decision Support Systems Volume 42, Issue 2, November 2006, Pages 1152-1169

[10] E.I. Papageorgiou, C.D. Stylios, P.P. Groumpos, "An Integrated Two-Level Hierarchical Decision Making System based on Fuzzy Cognitive Maps", IEEE Transactions on Biomedical Engineering, Vol. 50, No 12, December 2003, pp. 1326-1339.

[11] E.I. Papageorgiou, C.D. Stylios, P.P. Groumpos, "Novel architecture for supporting medical decision making of different data types based on

Fuzzy Cognitive Map Framework", in Proc. 28th IEEE EMBS 2007, 21-23 August, Lyon, France, Conference 2007, pp. 1192-1195.

[12] Stylios, C.D., Georgopoulos, V.C., Malandraki, G.A., Chouliara, S.: Fuzzy cognitive map architectures for medical decision support systems. Appl. Soft Comput. 8(3), 1243–1251 (2008).

[13] E.I. Papageorgiou, P. Spyridonos, P. Ravazoula, C.D. Stylios, P.P. Groumpos, & G. Nikiforidis, "Advanced Soft Computing Diagnosis Method for Tumor Grading", Artificial Intelligence in Medicine, Vol. 36, Number 1, January 2006, pp. 59-70.

[14] E.I. Papageorgiou, N.I. Papandrianos, G. Karagianni, G. Kyriazopoulos, D. Sfyras, "A fuzzy cognitive map based tool for prediction of infectious diseases", Proceeding of FUZZ-IEEE 2009, World Congress, 24-27 August 2009b, Korea, pp. 2094-2099.

[15] E.S. Berner, Clinical Decision Support Systems: Theory and Practice, Springer, 2007

[16] C.A.M. Schurink, P.J.F. Lucas, I.M. Hoepelman, and M.J.M. Bonten, "Computer-assisted decision support for the diagnosis and treatment of infectious diseases in intensive care units", The Lancet of infectious diseases, Volume 5, Issue 5, May 2005, Pages 305-312.

[17] R. Axelrod, Structure of décision: The cognitive maps of political elites. Princeton, News Jersey: Princeton University, 1976.

[18] Levi, A., & Tetlock, P. E. (1980). A cognitive analysis of Japan's 1941 decision for war. Journal of Conflict Resolution, 24, 195-211.

[19] Kosko b. (1986) Fuzzy Cognitive Maps, International Journal Man-Machine Studies, 24 :65-75.

[20] DAVID B. LEAKE. Case-based reasoning. The Knowledge Engineering Review, Vol. 9:1, 1994, 61-64.

[21] Tim Berners-Lee, Dan Connolly, Lalana Kagal, Yosi Scharf. "N3Logic: A Logical Framework For the World Wide Web". Theory and Practice of Logic Programming (2008), 8:249-269 Cambridge University Press Copyright © Cambridge University Press 2008

[22] Schober D, Boeker M, Bullenkamp J, Huszka C, Depraetere K, Teodoro D, Nadah N, Choquet R, Daniel C, Schulz S. The DebugIT core ontology: semantic integration of antibiotics resistance patterns.MEDINFO 2010 - Proceedings of the 13th World Congress on Medical Informatics

[23] Jos De Roo. Eye note. http://eulersharp.sourceforge.net/2003/03swap/eye-note.txt. (last accessed on January 9th, 2011).

[24] E.I. Papageorgiou, "A new methodology for Decisions in Medical Informatics using Fuzzy Cognitive Maps based on Fuzzy Rule-Extraction techniques", Applied Soft Computing, 11 (2011) 500–513.

[25] E.I. Papageorgiou, and A. Kannappan, "A Review Study about Fuzzy Cognitive Maps Applications", *Proc. of the International Conference on Communication and Computational Intelligence 2010,* Kongu Engineering College, Perundurai, T.N., India.27, – 29 December, 2010, pp.425-430.

[26] Y. Boutalis, T. Kottas and M. Christodoulou, Adaptive Estimation of Fuzzy Cognitive Maps with proven Stability and Parameter Convergence, IEEE Transactions on Fuzzy Systems, vol. 17, no. 4, pp. 874 - 889, Aug. 2009.

2011 IEEE International Conference on Fuzzy Systems
June 27-30, 2011, Taipei, Taiwan

Training Fuzzy Cognitive Maps by Using Hebbian Learning Algorithms: A Comparative Study

G.A. Papakostas, A.S. Polydoros, D.E. Koulouriotis and V.D. Tourassis
Department of Production and Management Engineering
Democritus University of Thrace (DUTH)
Xanthi, Greece
gpapakos@ee.duth.gr, {athapoly, jimk, vtourasi}@pme.duth.gr

***Abstract*—A detailed analysis of the Hebbian-like learning algorithms applied to train Fuzzy Cognitive Maps (FCMs) is presented in this paper. These algorithms aim to find appropriate weights between the concepts of the FCM so the model equilibrates to a desired state. For this manner, four different types of Hebbian learning algorithms have been proposed in the past. Along with the theoretical description of these algorithms, their performance in system modeling problems is investigated in this work. The algorithms are studied in a comparative fashion by using appropriate performance indices and useful conclusions about their training capabilities are experimentally derived.**

Keywords-fuzzy cognitive maps; hebbian learning; training; system modeling

I. INTRODUCTION

An increased interest about the theory and application of the Fuzzy Cognitive Maps (FCMs) [1] in engineering science is noted recently. FCMs are characterized by their ability to model the dynamics of complex systems by incorporating the casual relationships between the main concepts that describe the system. They have been used initially to model complex social and financial systems [2,3], where analytical descriptions do not exist or can not be derived.

The design of the FCMs is highly dependent on the knowledge of the experts, which define the model's concepts and their interconnections among them. This dependency may significantly affect the modeling accuracy due to the imprecise expert's knowledge.

In order to enhance the knowledge storing capabilities of the FCM models, learning algorithms that search for the best weight values of the concepts' interconnections have been proposed. Mainly, there are two categories of learning algorithms: (1) algorithms that use the Hebbian adaptation rule (Hebbian-like) [5-11] and (2) algorithms that use evolutionary optimization mechanisms (Evolutionary-like) [12-14].

Although the algorithms of the second category ensure near-optimum solutions in the weights search space, the Hebbian-like algorithms of the first category are studied in this work, due to their popularity and quick convergence to desirable FCM states.

The first usage of the Hebbian rule in learning FCMs was performed by Dickerson and Kosko [5], who proposed the *Differential Hebbian Learning* (DHL) algorithm by using the generalized Hebbian rule introduced by Oja [15]. Since there, three other types of Hebbian learning algorithms were proposed, the *Nonlinear Hebbian Learning (NHL)* [7,8], *Data-Driven Nonlinear Hebbian Learning (DD-NHL)* [9] and *Active Hebbian Learning (AHL)* [10,11] ones.

Despite of the review of the Hebbian-like learning algorithms from the literature, the main contribution of this work is the comparison of these algorithms under the same conditions. On the author's best knowledge this kind of comparison is missing from the literature, although such an analysis has to be performed whether a new algorithm is proposed.

The paper is organized, by describing shortly the fundamental theory of the FCMs in section 2, by discussing the Hebbian-like learning algorithms in section 3, by comparing the learning capabilities of the algorithms in system modeling problems in section 4 and finally, by summarizing some to useful conclusions in section 5.

II. FUZZY COGNITIVE MAPS

Fuzzy Cognitive Maps (FCMs) are fuzzy signed directed graphs with feedback [4]. They were proposed by Kosko [6] as a modeling methodology of complex systems, able to describe the casual relationships between the main factors (concepts) that determine the dynamic behaviour of a system.

In their graphical presentation, FCMs have the form of a diagram with nodes having interconnections between them, as illustrated in the following Fig. 1.

As it can be seen from Fig. 1, a FCM consists of nodes (concepts), C_i, $i=1,2,3,...,N$, where N is the total number of concepts, which are characteristics, main factors, or properties of the system being modeled. The concepts are interconnected through arcs having weights that denote the cause and effect relationship that a concept has on the others. There are three possible types of casual relationships between two concepts C_i and C_j (i) positive, meaning that an increase or decrease in the value of a cause concept results in the effect concept moving in the same direction and it is described by a positive weight W_{ij}, (ii) negative, meaning that changes in the cause and effect

978-1-4244-7316-8/11/$26.00 ©2011 IEEE

concepts take place in opposite directions, and the weight W_{ij} has negative sign and (iii) no relation, with the interconnection weight being zero. The weight value, e.g. W_{ij}, denotes the strength of how casual concept C_i causes C_j and takes values in the range [-1,1].

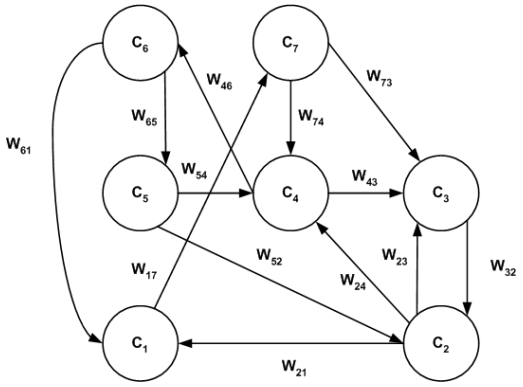

Figure 1. A simple Fuzzy Cognitive Maps

At each time, the value of each concept A_i is calculated, by summarizing the influences of all the other concepts to this and by squashing the overall impact using a barrier function f, according to the following rule

$$A_i^{(t+1)} = f\left(A_i^{(t)} + \sum_{i=1, i\neq j}^{N} W_{ji} A_j^{(t)} \right) \quad (1)$$

where A_i^{t+1} and A_i^t are the values of concept C_i at times t+1and t respectively, A_i^t the value of concept C_j at time t, W_{ji} the weight value of the interconnection with direction from concept C_j to concept C_i, and f the barrier function used to restrict the concept value into a specific range, usually in the range [0,1].

In each step, a new state of the concepts is derived according to (1) and after a number of iterations, the FCM may arrive in one of the following states: (1) a fixed equilibrium point, (2) a limited cycle and (3) a chaotic behaviour.

When the FCM arrives in a fixed equilibrium point, we can conclude that the FCM has converged and the final state corresponds to the actual system state in which the system concludes, when the initial values of concepts are applied.

The design of the FCMs is significantly based on the experience of some experts, who have the knowledge of the system being modeled and provide the weight values for the interconnection between concepts. In more flexible FCM structures these weights are being found during a learning procedure, in a similar way as in the case of neural networks training. For this reason many researchers have borrowed and adjusted algorithms from the neural network theory and proposed new learning procedures [5-9].

In the present paper, the Hebbian-like learning algorithms [5-11] is used in order to find the optimal weight set of the FCMs under investigation and their performance is compared to each other.

III. HEBBIAN LEARNING ALGORITHMS

Hebbian learning constitutes an unsupervised technique initially applied on the training of artificial neural networks [16]. The main feature of this learning rule is that the change of a synaptic is computed by taking into account the presynaptic and postsynaptic signals flow towards each processing unit (neuron) of a neural network and is defined by the following Eq.(2).

$$\Delta w_{ij} = \eta y_i(n) x_j(n) \quad (2)$$

where η is a positive constant that determines the *rate of learning* and x_j and y_i is the presynaptic and postsynaptic signals. The above rule has been modified by Oja [15] in order to solve the stability problems imposed in Eq.(2) by introducing a generalized form of the Hebbian rule called *Oja's rule*, having the following form:

$$\Delta w_{ij} = \eta y_i(n)\left(x_j(n) - y_i(n) w_{ij}(n) \right) \quad (3)$$

Based on the Oja's rule, several Hebbian like learning algorithms have been proposed in the literature, initially for the case of neural networks and recently, after appropriate modifications, for training FCMs.

A short description of the Hebbian like algorithms, having the form of Eq.(2), proposed as learning procedures that find an appropriate set of interconnection weights (connection matrix) subject to a system's requirements is presented hereafter.

A. Differential Hebbian Learning (DHL)

The DHL algorithm was the first Hebbian learning algorithm proposed by Dickerson and Kosko [5] in order to find better interconnection weights than those provided by the experts participated to the FCM design. This algorithm correlates the changes in the concept nodes of the model in order to modify their weights, according to the following Eq.(4).

$$w_{ij}^{(t+1)} = \begin{cases} w_{ij}^{(t)} + \mu_t \left(\Delta A_i^{(t)} \Delta A_j^{(t)} - w_{ij}^{(t)} \right), & \Delta A_i^{(t)} \neq 0 \\ w_{ij}^{(t)} , & \Delta A_i^{(t)} = 0 \end{cases} \quad (4)$$

where

$$\Delta A_i^{(t)} = A_i^{(t)} - A_i^{(t-1)} \quad (5)$$

Moreover, parameter μ_t refers to the learning rate which decreases with the algorithm's iteration as follows:

$$\mu_t = 0.1\left[1-\frac{t}{1.1N}\right] \quad (6)$$

where t is the current iteration and N is a constant that ensures the learning rate not to take negative values. An acceptable value of this constant is the maximum number of the algorithm's iterations.

B. Nonlinear Hebbian Learning (NHL)

The next Hebbian learning algorithm that mostly likes with the Oja's rule is the NHL proposed by Papageorgiou et al. [7], defined as:

$$w_{ij}^{(t+1)} = w_{ij}^{(t)} + \eta A_j^{(t)}\left(A_i^{(t)} - A_j^{(t)} w_{ij}^{(t)}\right) \quad (7)$$

where η is the learning rate. Besides the above basic formulation of the NHL algorithm two more extensions were introduced by Papageorgiou et al. [8], having the following forms:

$$w_{ij}^{(t+1)} = w_{ij}^{(t)} + \eta A_j^{(t)}\left(A_i^{(t)} - \mathrm{sgn}\left(w_{ij}^{(t)}\right) A_j^{(t)} w_{ij}^{(t)}\right) \quad (8)$$

where sgn(·) corresponds to the sign function that returns the sign of a quantity and it is used to maintain the sign of the corresponding weight. The last NHL form is derived by adding a weight decay parameter γ in the update rule, as follows:

$$w_{ij}^{(t+1)} = \gamma w_{ij}^{(t)} + \eta A_j^{(t)}\left(A_i^{(t)} - \mathrm{sgn}\left(w_{ij}^{(t)}\right) A_j^{(t)} w_{ij}^{(t)}\right) \quad (9)$$

In order to decrease the number of the free parameters, only the NHL version of Eq.(8) will be considered in the experimental section of the paper.

Despite of the new weight update rule of the NHL algorithm, the usage of two termination criteria [8] of the learning procedure was also a significant novel feature. These two criteria have the following form:

$$F_1 = \sqrt{\sum_{i=1}^{n}\left(OC_i^{(t)} - T_i\right)^2} \quad (10)$$

$$F_2 = \left|OC_i^{(t+1)} - OC_i^{(t)}\right| < e \quad (11)$$

where $OC_i^{(t)}$ is the i[th] output concept at iteration t and T_i the target value of the output concept, which for the case of a constrained concept lies in a range of $\left[T_i^{\min}, T_i^{\max}\right]$ takes the value $T_i = \frac{T_i^{\min} + T_i^{\max}}{2}$. The objective of the NHL learning algorithm is to find a set of interconnection weights that minimizes the cost functions F_1 and F_2 (subject to a tolerance e), so the FCM model can reach a desired state. While the first criterion shows the error of the output concepts from the desired values, the second one ensures that the FCM model equilibrates to a final state.

A short description of the processing steps of the algorithm is as follows [7]:

Step 1: For a given initial state $\mathbf{A}^o$ and weight set $\mathbf{W}^0$.

Step 2: For each iteration k.

Calculate the concept values $\mathbf{A^k}$ by using Eq.(1).

Update weights $\mathbf{W^k}$ by using Eq.(8).

Until the termination criteria F1 and F2 are met.

Step 3: Return the final weights $\mathbf{W^{final}}$.

C. Data-Drive Nonlinear Hebbian Learning (DD-NHL)

A modified version of the NHL algorithm was proposed by Stach et al. [9], which incorporated historical data of the model into the learning procedure. This algorithm called Data-Driven Nonlinerar Hebbian Learning (DD-NHL) and differs to the original NHL in two steps:

Difference 1: Instead of computing the concept values in each iteration by using Eq.(1), the concept values are provided by the historical data. These data is generated by applying the NHL algorithm [9] in a first stage.

Difference 2: The termination criterion F1 is replaced by the measuring the output concepts that lie inside the desired target values. More precisely, the candidate weight set is used to simulate the FCM model and if the output concepts equilibrated to a desired state the learning is completed (with simultaneously satisfaction of the F2 criterion), otherwise the procedure continues.

D. Active Hebbian Learning (AHL)

A common feature of the previous learning algorithms is that in each iteration the concepts of the FCM model are updated by using Eq.(1), synchronously.

The Active Hebbian Learning (AHL) algorithm considers that the concept nodes are activated asynchronously by a specific sequence. In this way the equilibrium point is reached by considering different times of nodes' activation, a mechanism that is useful in systems where the concepts are

activated based on a specific activation sequence. Moreover, unlike the previous algorithms where only the non-zero weights are being updated, in the case of the AHL algorithm all weights except those of the diagonal are updated.

Based on the AHL algorithm, the nodes of the FCM model is distinguished to *Activated* and *Activation* concepts, by the former ones being the nodes that firstly activated by causing the activation of the latter. In this case the activated concepts are updated through the following rule:

$$A_i^{(t+1)} = f\left(A_i^{(t)} + \sum_{i=1, i\neq j}^{N} W_{ji} A_j^{act(t)} \right) \quad (12)$$

where A_i are the value of the Ci activated concept and A_j^{act} the values of the activation concepts that influence the concept Ci. The weights are updated according to the following rule:

$$w_{ij}^{(t+1)} = \left(1-\gamma^{(t)}\right) w_{ij}^{(t)} + \eta^{(t)} A_i^{(t)} \left(A_j^{(t)} - w_{ij}^{(t)} A_i^{act(t)} \right) \quad (13)$$

where the learning rate η and the weight decay γ are decreased exponentially with the algorithm's iteration number (activation-simulation cycles) as follows:

$$\begin{aligned} \eta^{(t)} &= b_1 e^{(-\lambda_1 t)} \\ \gamma^{(t)} &= b_2 e^{(-\lambda_2 t)} \end{aligned} \quad (14)$$

where $0.01<b_1<0.09$, $0.1<\lambda_1<1$ and b_2, λ_2 are positive constants determined by trial and error. Furthermore, the two termination criterion of the NHL is also applied in the case of AHL in order to derive a desired equilibrium point of the FCM model.

The DHL, NHL, DD-NHL and AHL algorithms will be used to train the same FCM models that describe three different systems and their performance will be compared to each other, in the hereafter section.

IV. Comparative Study

In order to compare the performance of the previously described learning algorithms, in finding the appropriate weights set that give desired output concepts' values, two performance indices are used.

The first one (Mean Squared Error - MSE) measures the mean error between the values of the output concepts (OCs) and the desired values defined by the problem's specifications and is defined as:

$$MSE = \frac{1}{N} \sum_{n=1}^{N} \left(OC_n - T_n \right)^2 \quad (15)$$

where N is the number of the output concepts, OC_i and T_i the value the i^{th} simulated output concept and the corresponding desired value, respectively.

Furthermore, in order to measure the capability of the proposed weight set to converge to an acceptable output values when different initial states are applied (generalization capabilities), the following metric (Generalization Error – GE) is used.

$$GE = \frac{1}{NM} \sum_{k=1}^{M} \sum_{n=1}^{N} \left(OC_n^k - T_n \right)^2 \quad (16)$$

where M is the number of the different initial states.

A. Problem I

The first problem under study, is a benchmark system modeling problem commonly used in the literature [8,9]. It is a process control example consisting of one tank and three valves that control the amount of a liquid in the tank, as depicted in Fig.2.

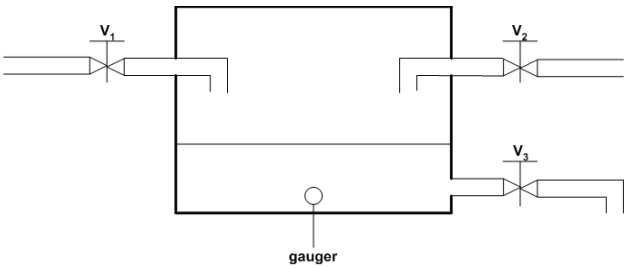

Figure 2. A simple process control problem

The main objective is to keep the height of the liquid and the specific gravity (measured by a sensor – gauger) of the liquid inside of predefined ranges. The FCM model for this process control problem consists of five concepts:

Concept 1 – C1: the amount of the liquid in the tank.

Concept 2 – C2: the state of valve 1

Concept 3 – C3: the state of valve 2

Concept 4 – C4: the state of valve 3

Concept 5 – C5: the specific gravity of the liquid in the tank

The initial weights provided by the experts are:

$$W^{initial} = \begin{bmatrix} 0 & -0.4 & -0.25 & 0 & 0.3 \\ 0.36 & 0 & 0 & 0 & 0 \\ 0.45 & 0 & 0 & 0 & 0 \\ -0.9 & 0 & 0 & 0 & 0 \\ 0 & 0.6 & 0 & 0.3 & 0 \end{bmatrix}$$

By taking into account that the constraints regarding the desired regions of the output concepts (C_1,C_5) are

$$0.68 \le A_1 \le 0.74$$
$$0.74 \le A_5 \le 0.80 \quad (17)$$

the four algorithms are applied with the settings of Table I and the following weight sets are derived in each case:

TABLE I. ALGORITHMS SETTINGS

Algorithms	Parameters
DHL	N=100, e=0.005
NHL	e=0.005, η=0.04
DD-NHL	e=0.005, η=0.04
AHL	e=0.005, b_1=0.02, b_2=0.04, λ_1=0.1, λ_2=1

$$W^{DHL} = \begin{bmatrix} 0 & -0.214 & -0.133 & 0 & 0.164 \\ 0.192 & 0 & 0 & 0 & 0 \\ 0.241 & 0 & 0 & 0 & 0 \\ -0.481 & 0 & 0 & 0 & 0 \\ 0 & 0.320 & 0 & 0.160 & 0 \end{bmatrix}$$

$$W^{NHL} = \begin{bmatrix} 0 & -0.197 & -0.017 & 0 & 0.477 \\ 0.547 & 0 & 0 & 0 & 0 \\ 0.578 & 0 & 0 & 0 & 0 \\ -0.825 & 0 & 0 & 0 & 0 \\ 0 & 0.710 & 0 & 0.5 & 0 \end{bmatrix}$$

$$W^{DD-NHL} = \begin{bmatrix} 0 & -0.244 & -0.068 & 0 & 0.445 \\ 0.515 & 0 & 0 & 0 & 0 \\ 0.557 & 0 & 0 & 0 & 0 \\ -0.839 & 0 & 0 & 0 & 0 \\ 0 & 0.690 & 0 & 0.467 & 0 \end{bmatrix}$$

$$W^{AHL} = \begin{bmatrix} 0 & -0.152 & -0.025 & 0.213 & 0.441 \\ 0.465 & 0 & 0.168 & 0.205 & 0.192 \\ 0.538 & 0.167 & 0 & 0.210 & 0.197 \\ -0.738 & 0.072 & 0.073 & 0 & 0.080 \\ 0.131 & 0.627 & 0.128 & 0.409 & 0 \end{bmatrix}$$

The initial values of the concepts used by the algorithms are A^0=[0.4 0.7 0.6 0.7 0.3], while the final state of the FCM model after applying each one of the above weight matrix is presented in the following Table II.

TABLE II. EXPERIMENTAL RESULTS – PROBLEM I

	Algorithms			
	DHL	***NHL***	***DD-NHL***	***AHL***
A1	0.645	**0.706**	**0.692**	**0.697**
A2	0.682	0.759	0.749	0.628
A3	0.634	0.656	0.645	0.654
A4	0.690	0.756	0.749	0.827
A5	0.689	**0.747**	**0.740**	**0.794**
Iterations	6	16	14	17
MSE	$5.42\text{x}10^{-3}$	$2.72\text{x}10^{-4}$	$6.05\text{x}10^{-4}$	$3.76\text{x}10^{-4}$
GE	$5.42\text{x}10^{-3}$	$2.72\text{x}10^{-4}$	$6.05\text{x}10^{-4}$	$3.76\text{x}10^{-4}$

The above table also includes some additional experimental results such as the algorithm's numbers of iterations needed to converge the algorithms, along with the two performance indices defined in Eq.(15) and Eq.(16).

In this table the bold faced concept values indicate that these outputs concepts lie inside the pre-defined range of desired values of Eq.(17). Comparing the equilibrium points of each algorithm it is deduced that only the DHL algorithm fails to converge in a desirable state, while the rest ones are behave desirable. Among those well converged algorithms the NHL shows the best performance since it equilibrates to a point that is closest to the desired central of the concept's range. This is also justified by examining the MSE value in each case. Moreover, the iterations of the algorithms are almost the same, but as the overall algorithms' execution time is concerned, it has to be mentioned that the DD-NHL algorithm is the most time consumed due to the historical data construction procedure.

Furthermore, it has to be noted that all the algorithms show a remarkable stability on the different initial concepts' state. This perceived from the GE index, which has been calculated by using 10 different random initial state vectors, which remains the same (in fact the final states are differ beyond the fifth decimal digit) with the corresponding MSE value for the case of all the algorithms.

B. Problem II

The second problem studied here, is a part of a chemical plant consisting of two tanks [10], three valves, a heating element and two thermometers and is depicted in the following Fig.3. The objective of the control system is to keep the height of the liquid in both tanks between some desired values, by simultaneously preserving the temperature of the two tanks between predefined limits.

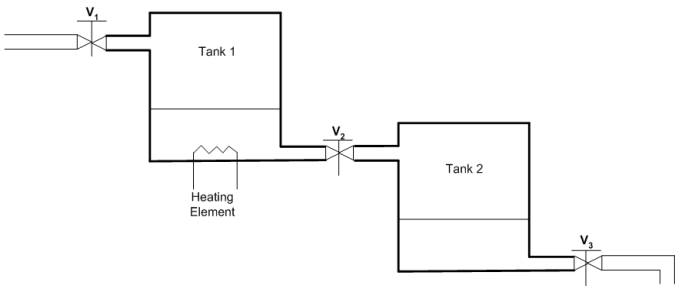

Figure 3. A chemical process control problem

The FCM model for this chemical process control problem consists of eight concepts:

Concept 1 – C1: the height of the liquid in tank 1

Concept 2 – C2: the height of the liquid in tank 2

Concept 3 – C3: the state of valve 1

Concept 4 – C4: the state of valve 2

Concept 5 – C5: the state of valve 3

Concept 6 – C6: the temperature of the liquid in tank 1

Concept 7 – C7: the temperature of the liquid in tank 2

Concept 8 – C8: the heating element operation

The initial weights provided by the experts are:

$$W^{initial} = \begin{bmatrix} 0 & 0 & 0.21 & 0.38 & 0 & 0 & 0 & 0 \\ 0 & 0 & 0 & 0.70 & 0.60 & 0 & 0 & 0 \\ 0.75 & 0 & 0 & 0 & 0 & 0 & 0 & 0 \\ -0.80 & 0.70 & 0 & 0 & 0 & 0 & 0.09 & 0 \\ 0 & -0.42 & 0 & 0 & 0 & 0 & 0 & 0 \\ 0 & 0 & 0.40 & 0 & 0 & 0 & 0 & 0.50 \\ 0 & 0 & 0 & 0.30 & 0 & 0 & 0 & 0 \\ 0 & 0 & 0 & 0 & 0 & 0 & 0.40 & 0 \end{bmatrix}$$

By taking into account that the constraints regarding the desired regions of the output concepts (C_1,C_2,C_6,C_7) are

$$\begin{aligned} 0.55 \le A_1 \le 0.75 \\ 0.75 \le A_2 \le 0.80 \\ 0.75 \le A_6 \le 0.82 \\ 0.65 \le A_7 \le 0.75 \end{aligned} \quad (18)$$

the values of the algorithm's free parameters are determined by trial and error and the applied settings are summarized in the following Table III.

TABLE III. ALGORITHMS SETTINGS

Algorithms	Parameters
DHL	N=30, e=0.005
NHL	e=0.005, η=0.03
DD-NHL	e=0.005, η=0.03
AHL	e=0.005, η=0.005, γ=0 (constant)

The resulted weight sets provided by the four Hebbian-like learning algorithms are as follows:

$$W^{DHL} = \begin{bmatrix} 0 & 0 & 0.146 & 0.262 & 0 & 0 & 0 & 0 \\ 0 & 0 & 0 & 0.483 & 0.414 & 0 & 0 & 0 \\ 0.517 & 0 & 0 & 0 & 0 & 0 & 0 & 0 \\ -0.549 & 0.551 & 0 & 0 & 0 & 0 & 0.063 & 0 \\ 0 & -0.287 & 0 & 0 & 0 & 0 & 0 & 0 \\ 0 & 0 & 0.276 & 0 & 0 & 0 & 0 & 0.365 \\ 0 & 0 & 0 & 0.207 & 0 & 0 & 0 & 0 \\ 0 & 0 & 0 & 0 & 0 & 0.276 & 0 & 0 \end{bmatrix}$$

$$W^{NHL} = \begin{bmatrix} 0 & 0 & 0.266 & 0.420 & 0 & 0 & 0 & 0 \\ 0 & 0 & 0 & 0.720 & 0.635 & 0 & 0 & 0 \\ 0.780 & 0 & 0 & 0 & 0 & 0 & 0 & 0 \\ -0.762 & 0.831 & 0 & 0 & 0 & 0 & 0.177 & 0 \\ 0 & -0.362 & 0 & 0 & 0 & 0 & 0 & 0 \\ 0 & 0 & 0.453 & 0 & 0 & 0 & 0 & 0.571 \\ 0 & 0 & 0 & 0.357 & 0 & 0 & 0 & 0 \\ 0 & 0 & 0 & 0 & 0 & 0.454 & 0 & 0 \end{bmatrix}$$

$$W^{DD-NHL} = \begin{bmatrix} 0 & 0 & 0.272 & 0.424 & 0 & 0 & 0 & 0 \\ 0 & 0 & 0 & 0.722 & 0.639 & 0 & 0 & 0 \\ 0.783 & 0 & 0 & 0 & 0 & 0 & 0 & 0 \\ -0.757 & 0.835 & 0 & 0 & 0 & 0 & 0.186 & 0 \\ 0 & -0.356 & 0 & 0 & 0 & 0 & 0 & 0 \\ 0 & 0 & 0.458 & 0 & 0 & 0 & 0 & 0.575 \\ 0 & 0 & 0 & 0.363 & 0 & 0 & 0 & 0 \\ 0 & 0 & 0 & 0 & 0 & 0.460 & 0 & 0 \end{bmatrix}$$

$$W^{AHL} = \begin{bmatrix} 0 & 0.020 & 0.224 & 0.392 & 0.019 & 0.017 & 0.017 & 0.017 \\ 0.020 & 0 & 0.022 & 0.705 & 0.609 & 0.021 & 0.021 & 0.021 \\ 0.753 & 0.021 & 0 & 0.020 & 0.021 & 0.018 & 0.018 & 0.018 \\ -0.765 & 0.805 & 0.020 & 0 & 0.022 & 0.019 & 0.107 & 0.019 \\ 0.020 & -0.385 & 0.021 & 0.022 & 0 & 0.020 & 0.020 & 0.020 \\ 0.017 & 0.021 & 0.411 & 0.019 & 0.021 & 0 & 0.018 & 0.538 \\ 0.018 & 0.022 & 0.019 & 0.314 & 0.021 & 0.018 & 0 & 0.018 \\ 0.017 & 0.021 & 0.018 & 0.019 & 0.021 & 0.411 & 0.018 & 0 \end{bmatrix}$$

The initial values of the concepts used by the algorithms are A^0=[0.480 0.570 0.580 0.680 0.580 0.590 0.520 0.580], while the final state of the FCM model after applying each one of the above weight matrix is presented in the following Table IV.

TABLE IV. EXPERIMENTAL RESULTS – PROBLEM II

	Algorithms			
	DHL	***NHL***	***DD-NHL***	***AHL***
A1	**0.640**	**0.643**	**0.645**	**0.670**
A2	0.723	**0.771**	**0.773**	0.806
A3	0.736	0.785	0.787	0.701
A4	0.813	0.876	0.877	0.730
A5	0.738	0.781	0.781	0.790
A6	0.714	**0.750**	**0.751**	0.679
A7	**0.674**	**0.702**	**0.704**	**0.703**
A8	0.729	0.768	0.768	0.679
Iterations	4	5	7	7
MSE	4.27×10^{-3}	6.46×10^{-4}	6.46×10^{-4}	6.28×10^{-3}
GE	4.27×10^{-3}	6.46×10^{-4}	6.46×10^{-4}	6.28×10^{-3}

The derived experimental results for the case of the second problem are almost the same with those of the first one. The NHL algorithm and its modified version DD-NHL, show the best performance by keeping the four output concepts inside the predefined ranges. The DHL and AHL algorithms have 50% accuracy, since they control satisfactory the two of the four outputs of the FCM model. Again, all the weight sets ensure robustness of the FCM model to the changes of the initial concepts' state as the GE index show.

C. Problem III

The third system that is being modeled by a FCM is a heat exchanger which constitutes a common part of the chemical and process industry [17]. The main objective in this case is the development of a model that simulates the behaviour of the system in order to control the water outlet temperature by adjusting the water flow rate.

The FCM model for this problem consists of five concepts:

Concept 1 – C1: the fan speed (S_f).

Concept 2 – C2: the water flow rate (F_w).

Concept 3 – C3: the water inlet temperature (T_{wi}).

Concept 4 – C4: the air inlet temperature (T_{ai}).

Concept 5 – C5: the water outlet temperature (T_{wo}).

The initial weights provided by the experts are:

$$W^{initial} = \begin{bmatrix} 0 & 0.625 & 0.75 & -0.25 & 0.625 \\ 0 & 0 & -0.75 & 0 & -0.75 \\ 0 & 0 & 0 & 0 & 0 \\ 0 & 0 & 0 & 0 & 0 \\ -0.75 & 0.125 & 0.125 & -0.75 & 0 \end{bmatrix}$$

The output concept is the water outlet temperature (C_5) which for the experimental needs has to satisfy the following constraint

$$0.74 \le A_5 \le 0.75 \tag{19}$$

The corresponding values of the algorithms' free parameters are determined by trial and error and the applied settings are summarized in the following Table III.

TABLE V. ALGORITHMS SETTINGS

Algorithms	Parameters
DHL	N=30, e=0.005
NHL	e=0.001, η=0.06
DD-NHL	e=0.001, η=0.06
AHL	e=0.01, b_1=0.05, b_2=0.02, λ_1=0.1, λ_2=1

The resulted weight sets provided by the four Hebbian-like learning algorithms are as follows:

$$W^{DHL} = \begin{bmatrix} 0.107 & 0.133 & 0.160 & -0.052 & 0.134 \\ 0 & 0.106 & -0.159 & 0 & -0.159 \\ 0 & 0 & 0.106 & 0 & 0 \\ 0 & 0 & 0 & 0.108 & 0 \\ -0.158 & 0.027 & 0.027 & -0.158 & 0.107 \end{bmatrix}$$

$$W^{NHL} = \begin{bmatrix} 0 & 0.655 & 0.729 & 0.271 & 0.736 \\ 0 & 0 & 0.009 & 0 & -0.037 \\ 0 & 0 & 0 & 0 & 0 \\ 0 & 0 & 0 & 0 & 0 \\ -0.380 & 0.651 & 0.646 & -0.368 & 0 \end{bmatrix}$$

$$W^{DD-NHL} = \begin{bmatrix} 0 & 0.653 & 0.734 & 0.241 & 0.734 \\ 0 & 0 & -0.071 & 0 & -0.106 \\ 0 & 0 & 0 & 0 & 0 \\ 0 & 0 & 0 & 0 & 0 \\ -0.414 & 0.630 & 0.624 & -0.405 & 0 \end{bmatrix}$$

$$W^{AHL} = \begin{bmatrix} 0 & 0.602 & 0.692 & -0.047 & 0.594 \\ 0.139 & 0 & -0.402 & 0.135 & -0.410 \\ 0.138 & 0.144 & 0 & 0.134 & 0.136 \\ 0.130 & 0.136 & 0.135 & 0 & 0.128 \\ -0.404 & 0.236 & 0.235 & -0.416 & 0 \end{bmatrix}$$

The initial values of the concepts used by the algorithms are A^0=[0.300 0.650 0.450 0.150 0.300], while the final state of the FCM model after applying each one of the above weight matrix is presented in the following Table VI.

TABLE VI. EXPERIMENTAL RESULTS – PROBLEM II

	Algorithms			
	DHL	***NHL***	***DD-NHL***	***AHL***
A1	0.628	0.567	0.563	0.735
A2	0.687	0.844	0.843	0.712
A3	0.662	0.845	0.840	0.718
A4	0.619	0.614	0.609	0.675
A5	0.652	**0.750**	**0.744**	**0.745**
Iterations	33	36	34	18
MSE	$8.70\text{x}10^{-3}$	$2.04\text{x}10^{-5}$	$3.57\text{x}10^{-7}$	$5.71\text{x}10^{-8}$
GE	$8.56\text{x}10^{-4}$	$5.07\text{x}10^{-6}$	$4.51\text{x}10^{-10}$	$6.09\text{x}10^{-7}$

Based on the above table it is deduced that the DHL algorithm fails to equilibrate to a desired point since the final value of the output concept lies outside the desirable range Eq. (19). On the other hand, the rest algorithms give a satisfied equilibrium state of the FCM model, especially the AHL algorithm, which gives the best output value in a shorter time (18 iterations). As far as the GE performance index is concerned, the DD-NHL algorithm shoes better generalization capabilities, since it equilibrates to the same state independently of the initial state of the model. Moreover, although the performance of the NHL algorithm is accepted, it is quite marginal.

Generally, the NHL algorithm exhibits a satisfactory behaviour since it fully controls the output concepts variations by keeping them between the system's specifications. While the DD-NHL presents similar performance, its dependency on historical data, gives them high execution time without showing significant improvement of its performance. The remaining algorithms the DHL and AHL, seem to perform worst for the three and the two problems under study respectively, but the feature of the AHL algorithm to search for new interconnections between the concepts, can help to design more reliable FCM models.

Finally, it has to be mentioned that all the Hebbian-like learning algorithms studied in this work, are dependent on some free parameters *(η, γ, e, N)*, which significantly affect the convergence and termination of the algorithms to desired FCM model's states. Therefore special attention has to be paid to the selection of these parameters.

V. CONCLUSIONS

A detailed description of the Hebbian-like learning algorithms for training FCM models was presented in the previous sections. Appropriate experiments have been

conducted in order to analyze the performance of each algorithm under the same conditions. The results show that the NHL algorithm exhibits a satisfactory behaviour with low algorithmic complexity as compared with the other similar algorithms. While the comparison of the algorithms was realized by using some performance indices, there is a need to develop a methodology that permits the comparison of the different solutions in the real system's workspace.

The dependency of the Hebbian-like algorithms on some free parameters that significantly influence their performance is a disadvantage of these algorithms, since they control not only the final equilibrium point of the model but also the successfully termination of the algorithm. A novel algorithm with less sensitivity on such parameters and with high convergence rate on desirable states remains a major target of the scientists in this field.

REFERENCES

[1] M. Glykas, "Fuzzy Cognitive Maps: Advances in theory, methodologies, tools and applications", Studies in Fuzziness and Soft Computing, vol. 247, Springer-Verlag, 2010.

[2] J. Aguilar, "A survey about fuzzy cognitive maps papers (Invited Paper)", International Journal of Computational Cognition, vol. 3, no. 2, 2005.

[3] D.E. Koulouriotis, I.E. Diakoulakis, D.M. Emiris, C.D. Zopounidis, "Development of dynamic cognitive networks as complex Systems approximators: Validation in financial time series", Applied Soft Computing, vol. 5, no. 2, 2005, pp. 157-179.

[4] B. Kosko, "Fuzzy Cognitive Maps", International Journal Man-Machine Studies, vol. 24, 1986, pp. 65-75.

[5] J.A. Dickerson and B. Kosko, "Virtual worlds as fuzzy cognitive maps", Presence, vol. 3, no. 2, 1994, pp. 173-189.

[6] A.V. Huerga, "A balanced differential learning algorithm in fuzzy cognitive maps", Int. Workshop on Qualitative Reasoning, 2002.

[7] E.I. Papageorgiou, C.D. Stylios, P.P. Groumpos, "Fuzzy cognitive map learning based on nonlinear Hebbian rule", In: T.D. Gedeon and L.C.C. Fung (Eds.): AI 2003, LNAI vol. 2903, Springer-Verlag, 2003, pp. 254-266.

[8] E.I. Papageorgiou, C.D. Stylios, P.P. Groumpos, "Unsupervised learning techniques for fine-tuning fuzzy cognitive map casual links", International Journal of Human-Computer Studies, vol. 64, no. 8, 2006, pp. 727-743.

[9] W. Stach, L. Kurgan and W. Pedrycz, "Data-driven nonlinear Hebbian learning method for fuzzy cognitive maps", IEEE Int. Conf. on Fuzzy Systems (FUZZ-IEEE), 2008, pp. 1975-1981.

[10] E.I. Papageorgiou, C.D. Stylios, P.P. Groumpos, "Active Hebbian learning algorithm to train fuzzy cognitive maps", International Journal of Approximate Reasoning, vol. 37, no. 3, 2004, pp. 219-249.

[11] E.I. Papageorgiou and P.P. Groumpos, "A weight adaptation method for fuzzy cognitive maps to a process control problem", In: M. Bubak et al. (Eds.): ICCS 2004, LNCS vol. 3037, 2004, pp. 515-522.

[12] G.A. Papakostas, Y.S. Boutalis, D.E. Koulouriotis and B.G. Mertzios, "Fuzzy cognitive maps for pattern recognition applications", International Journal of Pattern Recognition and Artificial Intelligence, vol. 22, no. 8, 2008, pp. 1461-1468.

[13] W. Stach, L. Kurgan, W. Pedrycz, M. Reformat, "Genetic learning of fuzzy cognitive maps", Fuzzy Sets and Systems, vol. 153, no. 3, 2005, pp. 371-401.

[14] E.I. Papageorgiou, K.E. Parsopoulos, C.S. Stylios, P.P. Groumpos and M.N. Vrahatis, "Fuzzy cognitive maps learning using particle swarm optimization", Journal of Intelligent Information Systems, vol. 25, no. 1, pp. 95-121, 2005.

[15] E. Oja, "Neural networks, principal components and subspaces", International Journal of Neural Systems, vol. 1, pp. 61-68, 1989.

[16] S. Haykin, "Neural networks: A comprehensive foundation", 2nd Ed., Prentice-Hall, 1999.

[17] C.D. Stylios and P.P. Groumpos, "Modeling complex systems using fuzzy cognitive maps", IEEE Trans. On Systems, Man and Cybernetics – Part A: Systems and Humans, vol. 34, no. 1,2004, pp. 155-162.

2011 IEEE International Conference on Fuzzy Systems
June 27-30, 2011, Taipei, Taiwan

Applications of Fuzzy Classification with Fuzzy C-Means Clustering and Optimization Strategies for Load Identification in NILM Systems

Yu-Hsiu Lin
Graduate Institute of Mechanical and Electrical Engineering
National Taipei University of Technology
Taipei, Taiwan
t6618001@ntut.edu.tw

Men-Shen Tsai
Graduate Institute of Automation Technology
National Taipei University of Technology
Taipei, Taiwan
mstsai@ntut.edu.tw

Chin-Sheng Chen
Graduate Institute of Automation Technology
National Taipei University of Technology
Taipei, Taiwan
saint@ntut.edu.tw

***Abstract*—Due to global warming and climate changes, it is very important to use and conserve the power energy effectively. Monitoring the electrical consumption of consumers is one of the methods that can improve the energy usage efficiency. In this paper, a Non-Intrusive Load Monitoring (NILM) system, which applies a fuzzy classifier with the Fuzzy C-Means (FCM) clustering and optimization algorithms to identify the energizing and de-energizing statuses of each appliance, is proposed. Load energizing and de-energizing transient features are extracted, and the fuzzy classifier performs load identification based on these features. A two-stage fuzzy classifier is used in this paper. For the first stage, the FCM clustering is used to coarsely determine the parameters of the fuzzy classifier. Following this stage, two optimization algorithms, Error Back-Propagation Algorithm (EBPA) and Genetic Algorithm (GA), are employed to fine tune those parameters. As the classification results obtained from different realistic experimental environments, the proposed system is confirmed that it is able to identify the operational status of each appliance.**

Keywords- Fuzzy C-Means; Genetic Algorithm; Appliance Identification; Non-Intrusive Load Monitoring; Power Signatures

I. INTRODUCTION

Due to global warming and climate changes, effectively using and conserving the electricity has become a very important issue recently. One of the approaches for restraining the global warming is to improve the energy usage efficiency by monitoring the residential and commercial electrical consumption. If each appliance is efficiently operated and managed with respect to energy policies formulated by the government, the power energy can be used and conserved effectively. Further, as the energy usage efficiency is improved, the production of greenhouse gases, such as CO_2, CFCs, and so on, can also be reduced. In order to realize these goals, the operational information of each appliance must be understood first. Traditionally, loads are monitored by attaching "smart" sensors. These sensors are able to calculate the energy consumption and transmit the information to an energy management system. Although this approach is easy to implement, it has several disadvantages, e.g., a large amount of sensors, high installation cost. Therefore, to remedy the disadvantages of the traditional load monitoring approach, several *Non-Intrusive Load Monitoring* (NILM) systems were proposed [1-12]. The NILM approach requires a voltage and/or current sensor that is installed on the main electrical panel in a household. By analyzing the power signals, the NILM system is able to identify the energy consumption information of each appliance.

This paper aims to assess the feasibility of using fuzzy classification technique with the *Fuzzy c-Means* (FCM) clustering technique and two different optimization algorithms, *Error Back-Propagation Algorithm* (EBPA) and *Genetic Algorithm* (GA), for the NILM. In this paper, a two-stage fuzzy classifier is developed. At the first stage, the FCM clustering is used to coarsely determine the parameters of the antecedent and consequent of *fuzzy If-Then rules*. In this stage, the FCM clustering constructs fuzzy rules from a training dataset; each rule corresponds to a partition of feature space that is of *universes of discourse*. Also, this stage can be seen as embedding *heuristic* knowledge into the fuzzy classifier. After this stage, the EBPA and GA are adopted to fine tune the parameters of each fuzzy rule such that the classification accuracy can be improved. The load energizing and de-energizing transient features are extracted from current waveforms that are measured at the power entering point. The fuzzy classifier performs load identification based on the features. As the results, the proposed NILM system is capable of distinguishing the energizing and de-energizing statuses of each appliance. The organization of this paper is as follows: First, the existing NILM methods and power signatures used by the methods are surveyed in Sec. II. The proposed NILM method is discussed in Sec. III. The optimization strategies employed to fine tune the parameters are expressed in Sec. IV. The realistic experiments and their results are shown in Sec. V. The conclusions are summarized in Sec. VI.

II. EXISTING NON-INTRUSIVE LOAD MONITORING SYSTEMS

Two signal processing approaches, steady-state analysis and transient analysis, for NILM have been studied in the past.

An NILM system developed by the Electric Power Research Institute (EPRI) applied steady-state approach [1]. The system uses the variations of real and reactive power as the identification signatures. A five-stage algorithm was applied to detect the operation ON/OFF status of each load. Although the system with acceptable performance had been applied to some fields, several problems were pointed out by references [2-4]. For example, the system cannot distinguish the loads with similar real and reactive power consumption. In papers [5-6], the authors indicated that the nonlinear loads not only consume real and reactive power, they also introduce harmonics to the power lines. Hence, the harmonics can be used as the features for identifying different loads. In [7], nine time-domain steady-state features were used. Combinations of the features were sequentially inputted to a 1-Nearest-Neighbor Rule recognizer in order to find the best features that result the highest recognition rate. Besides the steady-state analysis, several studies shown that the transient waveforms for different types of loads are unique due to the differences of physical characteristics [2-3, 8-9]. These studies also found that the transient waveforms have completely or partially repeated profiles. Therefore, the transient properties can also be used as the features for load identification. In [10], a load recognition scheme that applied the notion of maximum approaching degree based on fuzzy logic theory was proposed. Since this scheme does not involve any training process, the NILM system is simple in implementation. In articles [4, 11-12], several steady-state features, such as real power, reactive power, and total harmonic distortion, with the turn-on transient energy are used as the features used by different Artificial Neural Network architectures for load identification. These articles also introduced the Coefficients of Variations to validate the repeatability of turn-on transient energy for each load.

III. Proposed Non-Intrusive Load Monitoring System

In this study, the proposed NILM system that integrates transient load current feature extraction methods with *soft-computing* techniques is used to identify the energizing and de-energizing statuses of each load. The flowchart of the proposed system is shown in Figure 1.

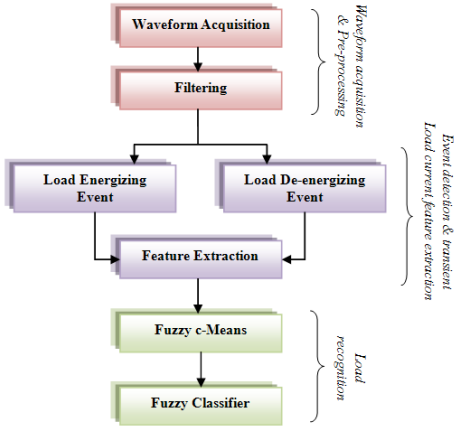

Figure 1. Flowchart of the proposed NILM System. The fuzzy classifier is optimized by optimization strategies.

Detailed descriptions of the system are described in the following sub-sections.

A. *Waveform Acquisition and Filtering*

The aim of waveform acquiring and filtering is to acquire load current waveforms and filter the high-frequency noise, respectively. The cut-off frequency of the low-pass filter of 500 Hz is used in this approach.

B. *Event Detection and Feature Extraction*

In the proposed system, the load energizing or de-energizing event of an appliance can be detected. The feature extraction process is triggered after the event is detected. Following descriptions deal with the processes of event detection and feature extraction.

1) Energizing event detection & Feature extraction:

When the *variation* of current intensity calculated using Eq. (1) is greater than a pre-specified positive threshold, α, a load energizing event is detected.

$$\Delta[I_{intensity}] = (I_{intensity})_{k+1} - (I_{intensity})_k \quad (1)$$

$$I_{intensity} = \frac{\sum_{j=1}^{N} |\, i(j) - \text{mean}(i) \,|}{N} \quad (2)$$

In Eq. (1), i(j) represents the j-th current sampling point; N is the total number of sampling points per cycle; k indicates the k-th sampling cycle; mean(i) denotes the average current value for each sampling cycle.

After the load energizing event is detected, the process for determination of transient period starts. Since the transient period may continue for certain cycles after a load is energized, a differential procedure based on the fundamental property of superposition is performed first. After this procedure, the *change rate* of current intensity is calculated using Eqs. (3) and (4). In Eq. (3), i'(t) represents a differential waveform that is obtained through the differential procedure. During this process, ΔI' is compared with a pre-specified threshold, γ. If ΔI' is less than γ for a pre-specified δ cycles, the determination of transient period terminates. Finally, the transient period, E_t, is defined as the total period of transient determination minus δ cycle time.

$$I'_{intensity} = \log\left(\sum_{j=1}^{N} (i'(j) - \text{mean}(i'))^2\right) \quad (3)$$

$$\Delta[I'_{intensity}] = \left| (I'_{intensity})_{k+1} - (I'_{intensity})_k \right| \quad (4)$$

Some load energizing current waveforms for different single and multiple load operation scenarios are shown in Figure 2. The acquired transient current waveform, i_{aq}(t), of an unidentified load is shown on the right column of these figures. In multiple load operation scenarios, all loads except the unidentified load were energized in advance.

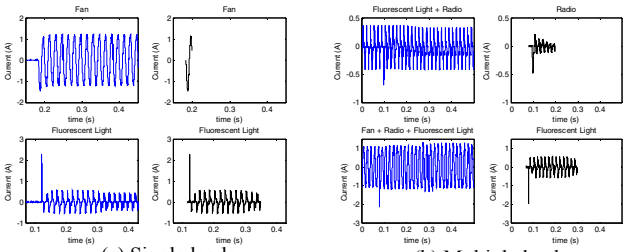

(a) Single loads. (b) Multiple loads.

Figure 2. Load current waveforms for different operation scenarios.

Feature extraction is crucial for load identification. The feature extraction process transforms an observation space into a feature space. Generally, the feature space is of much lower dimensions than the observation space. In this paper, *Crest Factor* (*C.F.*) calculated using Eq. (5) and E_t are used as the features for load energizing identification. In Eq. (5), $i_{aq}(t)$ indicates the acquired transient waveform.

$$Crest\ Factor\ (C.F.) = \frac{\max|i_{aq}(t)|}{\sqrt{\int_{E_t} {i_{aq}}^2(t)dt \Big/ E_t}} \tag{5}$$

2) De-energizing event detection & Feature extraction:

When the variation of current intensity that is obtained from Eq. (1) is less than a pre-specified negative threshold, β, a load de-energizing event is detected. Following the detection of the event, the current waveforms before and after the event are subtracted. By doing so, the load de-energizing transient waveform of an undetermined load can be acquired. For the determination of load de-energizing transient period, the transient period, E_t, is defined as one cycle.

Figure 3 shows some load de-energizing current waveforms for different single and multiple load operation scenarios. The features, *C.F.* and I_{peak}, of an acquired de-energizing transient waveform are calculated using Eqs. (5) and (6). These features are used for load de-energizing identification.

$$I_{peak} = \max|i_{aq}(t)| \tag{6}$$

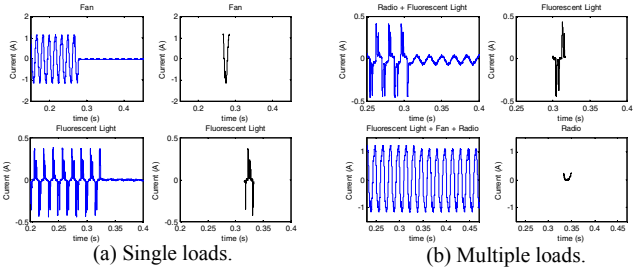

(a) Single loads. (b) Multiple loads.

Figure 3. Load current waveforms for different operation scenarios.

C. Fuzzy Classifier with Fuzzy C-Means Clustering

In this sub-section, the fuzzy classifier and the FCM clustering which is used to roughly construct the fuzzy classifier are discussed. The structure of the fuzzy classifier is shown in Figure 4. In Figure 4, the *fuzzifier* transforms the crisp input values calculated from the acquired current waveform into fuzzy sets. After this fuzzification process, the fuzzified inputs with fuzzy rules are passed to *inference engine* that combines them using a fuzzy *t*-norm operator to derive the *firing strength* of each fuzzy rule. When the firing strength of each rule is obtained, the crisp output can be calculated using a *de-fuzzifier*. Finally, this crisp output is delivered to the *decision-making unit* to determine the class of an unidentified appliance corresponding to the acquired current waveform.

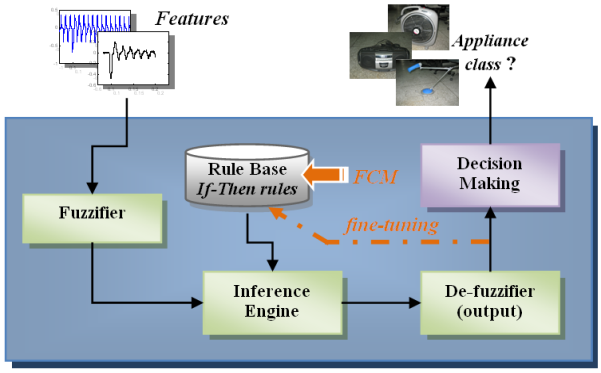

Figure 4. Structure of the fuzzy classifier.

1) Fuzzy Classifier:

A *fuzzy Rule Base* that consists of a set of fuzzy IF-THEN rules has the form shown in Eq. (7) [13]:

$$Ru^{(l)}: IF\ x_1\ is\ A_1^l\ and\ ...\ and\ x_n\ is\ A_n^l, THEN\ y\ is\ B^l \tag{7}$$

In Eq. (7), A_i^l and B^l are fuzzy sets in $U_i \subset R$ and $V \subset R$, respectively; $x=(x_1, x_2, \ldots, x_i, \ldots, x_n)^T \in U \subset R^n$ and $y \in V \subset R$ are the input and output linguistic variables of the fuzzy classifier, respectively; M is the total number of rules in the fuzzy rule base (i.e., l=1, 2, …, M).

a) Fuzzifier, Inference Engine, and De-fuzzifier:

Each fuzzy set in Eq. (7) is characterized as a *Gaussian membership function*. The center of the fuzzy set B^l in Eq. (7) is *singleton* with value of $\bar{y}^l$. By using *singleton fuzzifier*, *product inference engine* and *center average de-fuzzifier*, the fuzzy classifier can be formulated as Eq. (8). In Eq. (8), $f(x) \in V \subset R$ is the de-fuzzified output of the fuzzy classifier; $a_i^l \in$ (0, 1] are constants; $\sigma_i^l \in (0, \infty)$, $\bar{x}_i^l \in$ R, and $\bar{y}^l \in$ R are real-valued parameters.

$$f(x) = \frac{\sum_{l=1}^{M} \bar{y}^l [\prod_{i=1}^{n} a_i^l \exp(-(\frac{x_i - \bar{x}_i^l}{\sigma_i^l})^2)]}{\sum_{l=1}^{M} [\prod_{i=1}^{n} a_i^l \exp(-(\frac{x_i - \bar{x}_i^l}{\sigma_i^l})^2)]} \tag{8}$$

The Gaussian-type membership function rather than other types of membership functions is chosen in this paper for two reasons. Firstly, the total number of parameters to be tuned or evolved is small since each Gaussian membership function requires two parameters. Secondly, the Gaussian-type membership function ensures that the firing strength of each rule is always non-zero. In addition, the total number of universes of discourse for the input of the fuzzy classifier is

two. Each universe of discourse is further divided into three partitions using three Gaussian membership functions (because three-class energizing or de-energizing classification problem is considered). Thereby, the total number of fuzzy rules is nine. Thus, the feature space is partitioned into 3×3 decision regions. In this paper, the partition with the parameters of the fuzzy classifier is initialized using the FCM clustering, which will be discussed in the next sub-section.

b) Decision-Making Unit:

After the de-fuzzified output of the fuzzy classifier is calculated using Eq. (8), the output is passed to the decision-making unit to determine the class label of the input using Eq. (9). In Eq. (9), $Class^k$, an integer, denotes the pre-assigned class label of the k-th class; w is the total number of classes.

$$Class\ label = Class^j;\ j = \underset{k=1,2,\ldots,w}{\operatorname{argmin}}(|f(x) - Class^k|) \tag{9}$$

The recognition rate is one of the criteria for evaluating the performance of a classifier. In this paper, the recognition rate is defined as the number of correctly classifying the test data with the total data in the test dataset.

2) Fuzzy c-Means Clustering:

A 2-stage approach used to design the fuzzy classifier is proposed in this paper. These stages are described as follows:

- **Stage 1**. Apply the FCM clustering with the training dataset to coarsely determine the parameters of the fuzzy If-Then rules. This stage is a "heuristic" stage.
- **Stage 2**. Apply the optimization algorithms with the training dataset to fine tune the parameters determined in Stage 1.

After the fuzzy classifier with the acceptable performance is designed, it can be used to classify new patterns.

The FCM clustering is one of the partition clustering algorithms for data clustering [13, 14]. The FCM clustering algorithm allows each datum belonging to two or more clusters as the sense in *Fuzzy Logic*. The goal of the FCM clustering applied in this research is to find c *codebook prototypes*/*centroids*/*centers* in respect of the training dataset. These c cluster centers can be used to determine the parameters of each fuzzy If-Then rule. The FCM clustering procedure is summarized as follows:

- **Step 1**. For a dataset $X=\{\mathbf{x}_1, \mathbf{x}_2, \ldots, \mathbf{x}_k, \ldots, \mathbf{x}_n\}$, where $\{\mathbf{x}_k\}_{k=1}^n \in R^p$: fix $c \in \{2, 3, \ldots, (n\text{-}1)\}$, set $m \in (1, \infty)$, and initialize $U^{(0)} \in M_{fc}$. Here, $M_{fc} = \{U \in V_{cn} \mid u_{ik} \in [0, 1],\ 1 \le i \le c,\ 1 \le k \le n;\ \sum_{i=1}^{c} u_{ik} = 1, \forall k \in \{1,2,\ldots,n\}$ is true$\}$; V_{cn} is the set of real $c \times n$ matrices $U=[u_{ik}]$; u_{ik} is the membership value of $\mathbf{x}_k$ that belongs to cluster A_i.
- **Step 2**. At iteration l, where l=0, 1, 2, …: compute the c mean centers using

$$\mathbf{v}_i^{(l)} = \frac{\sum_{k=1}^{n} (u_{ik}^{(l)})^m \mathbf{x}_k}{\sum_{k=1}^{n} (u_{ik}^{(l)})^m}, 1 \le i \le c$$

.

- **Step 3**. Update $U^{(l)}$ to $U^{(l+1)}=[u_{ik}^{(l+1)}]$ using

$$u_{ik}^{(l)} = \frac{1}{\sum_{j=1}^{c} \left(\frac{\| \mathbf{x}_k - \mathbf{v}_i^{(l)} \|}{\| \mathbf{x}_k - \mathbf{v}_j^{(l)} \|}\right)^{\frac{2}{m-1}}}, 1 \le i \le c, 1 \le k \le n$$

.

- **Step 4**. If $\|U^{(l+1)} - U^{(l)}\|$ is less than or equal to a pre-determined tolerance, stop; otherwise, set l=l+1 and go to Step 2.

The cluster centers and the distribution of clusters are used in this paper. They are identified using the FCM clustering to roughly allocate the parameters of the fuzzy classifier. The *center* parameter of each Gaussian membership function, $\bar{x}_{x_i j}$, on each universe of discourse is set to the corresponding component of cluster center. Also, the *spread* parameter of each Gaussian membership function on each universe of discourse is determined using Eq. (10).

$$\sigma_{x_i j} = x'_i - \bar{x}_{x_i j};\ i=1, 2, \ldots, n, \text{ and } j=1, 2, \ldots, N_{MF} \tag{10}$$

In Eq. (10), n is the total number of universes of discourse (input variables); N_{MF} is the total number of membership functions (clusters) on each universe of discourse; x'_i is the component of a datum which belongs to cluster j with the approximate membership degree of e^{-1}. For the cases studied in this paper, n and N_{MF} are 2 and 3, respectively.

After the center and spread parameters are determined, the singleton parameters, $\{\bar{y}^l\}_{l=1}^M$, for the part of consequent of fuzzy rules can also be assigned based on the partitions and the labels of training data. After coarsely determining these parameters, they are further adjusted using the EBPA and GA.

IV. Optimizing of Fuzzy Classifier

In this section, two different types of optimization algorithms are applied to fine tune the parameters of fuzzy classifier. The gradient descent algorithm [13, 15-16] used to find the quasi-optimal structure of the fuzzy classifier of (8) according to the training dataset is discussed first.

A. Gradient Descent Algorithm Approach

Suppose that the following input-output pairs are collected: $\{(x_0^p, y_0^p)\}_{p=1}^N$, where $x_0^p \in U \subset R^n$ and $y_0^p \in V \subset R$. The goal is to design the fuzzy classifier based on these N input-output pairs. In Eq. (8), σ_i^l, $\bar{x}_i^l$, and $\bar{y}^l$ are roughly initialized based on the results of the FCM clustering. Once these parameters are specified, the quasi-optimal structure of the fuzzy classifier can be obtained. The gradient descent algorithm used for tuning the classifier's parameters is summarized as follows:

- **Step 1**. Initialize the parameters. Determine the initial parameters, $\bar{y}^l(0)$, $\bar{x}_i^l(0)$, and $\sigma_i^l(0)$, according to stage 1.
- **Step 2**. Present an input-output pair (x_0^p, y_0^p) and calculate the output associated with the inputs of the fuzzy classifier at the q-th iteration of tuning.
- **Step 3**. Update the parameters. The following updating equations are used to update the parameters:

$\bar{y}^l(q+1) = \bar{y}^l(q) - \eta \frac{f-y}{a} b^l$, where η is a tuning constant; f and y denote $f(x_0^p)$ and y_0^p, respectively; $a = \sum_{l=1}^{M} b^l$; $b^l = \prod_{i=1}^{n} \exp(-(\frac{x_i - \bar{x}_i^l}{\sigma_i^l})^2)$.

$$\bar{x}_i^l(q+1) = \bar{x}_i^l(q) - \eta \frac{f-y}{a}(\bar{y}^l(q) - f) b^l \frac{2(x_{0i}^p - \bar{x}_i^l(q))}{\sigma_i^{l2}(q)}$$

$$\sigma_i^l(q+1) = \sigma_i^l(q) - \eta \frac{f-y}{a}(\bar{y}^l(q) - f) b^l \frac{2(x_{0i}^p - \bar{x}_i^l(q))^2}{\sigma_i^{l3}(q)}.$$

- **Step 4**. Go to Step 2 with q=q+1, until $|f-y_0^p|$ is less than a pre-determined tolerance, or until the value of q equals to a pre-determined iteration.
- **Step 5**. Go to Step 2 with p=p+1 to update the parameters using next input-output pair, (x_0^{p+1}, y_0^{p+1}).
- **Step 6**. Set p=1 and re-do steps 2 to 5, until the result of the classifier is satisfactory.

B. Genetic Algorithm Approach

For the second approach, GA is used to globally search the optimal parameters. [16-18] The GA, which had been applied to different engineering optimization problems, is a global and stochastic search algorithm. Two types of operators for the GA are used: *genetic operators* and *evolution operator*. The genetic operators include *crossover* and *mutation* operators; the evolution operator comprises a *selection* operator. The flowchart of the GA used in this paper is shown in Figure 5.

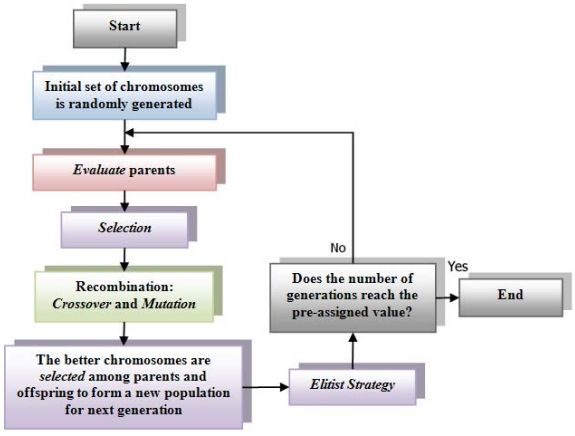

Figure 5. Flowchart of the GA.

With application of GA, the first important step is to *encode* the fuzzy classifier into the *chromosome* (*genotype* representation). In this paper, two universes of discourse are considered. Each universe of discourse is partitioned into three regions using three Gaussian membership functions. Hence, there are nine rules due to the 3×3 regions. As a result, a total of 21 parameters ($3_{\text{membership functions}} \times 2_{\text{parameters per function}} \times 2_{\text{inputs}} + 9_{\text{rules}}$) need to be adjusted. Each parameter is encoded into a binary string. The structure illustration of the chromosome is illustrated in Figure 6.

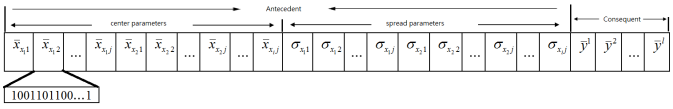

Figure 6. Representation of the chromosome.

In order to evaluate the quality of each chromosome, *fitness function* is needed. A good fitness function can gradually guide the GA to find the optimal solution. In this paper, the fitness function, the reciprocal of *mean-squared error* (MSE_{rror}), is defined as follows:

$$fitness = \frac{1}{MSError} = \frac{1}{\frac{1}{N}\sum_{p=1}^{N}[f(x_0^p) - y_0^p]^2}$$

s.t.

$$\bar{x}_{x_i(j-1)} \le \bar{x}_{x_i j} \le \bar{x}_{x_i(j+1)}$$

$$\bar{x}_{x_i j} - \rho \cdot \sigma_{x_i j} \le \sigma_{x_i j} \le \bar{x}_{x_i j} + \rho \cdot \sigma_{x_i j}$$

$$\bar{y}^l - 1 \le \bar{y}^l \le \bar{y}^l + 1$$

Note that, the boundaries of these constraints are determined based on the results of the FCM clustering; and ρ is a constant.

During *evaluation*, each chromosome must be *decoded* to the corresponding fuzzy classifier (*phenotype* representation). After each chromosome in current generation is evaluated, the *natural selection* process that mimics the process of Darwinian evolution to create populations from generation to generation is performed. In this paper, the *roulette wheel selection* is adopted; it belongs to the fitness-proportional selection. A new population with respect to the probability distribution based on fitness values is generated. The *enlarged* (μ+λ) *sampling space* is considered in this paper. With this sampling space, μ parents and λ offspring compete for survival. The μ best out of offspring and old parents are selected as the population for the next generation. The genetic operators facilitate an efficient search and guide the search into new regions. The crossover facilitates exploration, while the mutation facilitates exploitation of the search space [18]. In this paper, one-cut-point crossover and bit-wise flipping mutation operators are used. In addition, the *Elitist strategy* is also applied. This strategy ensures that the best chromosome is passed onto next generation if it is not selected via the selection process.

V. EXPERIMENTAL RESULTS

In this paper, the proposed NILM system is used to identify the operation status of each appliance. The appliances include *Fan*, *Fluorescent Light* (F.L.) and *Radio*. All the experiments in this study are executed at different realistic environments. During identification, no loads were energized or de-energized simultaneously. Experimental 1 describes the results of the appliance energizing identification; Experimental 2 describes the results of the appliance de-energizing identification. A circuit was designed to energize the appliance at different energizing phase angles. As the waveforms shown in Figures 2 and 7, the current waveforms for different types of loads are *unique* and *repeatable*.

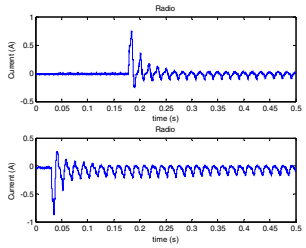

Figure 7. Current waveforms for different load energizing phase angles. The load, Radio, was energized at 73.5 degree (top) and 225 degree (bottom) at different measurement locations.

For all the experiments, 108 single load current measurements are performed. 69 of the measurements are used for training; while the remaining 39 measurements are used for testing. Additionally, 41 multiple load current measurements are used for testing as well.

A. Experimental 1: Load Energizing Classification

In this experiment, the proposed system is used to identify the energizing status of each load. The results of the fuzzy classifier with the two different optimization strategies for this load energizing classification are summarized below.

1) Fuzzy Classifier with the EBPA

In this experiment, the universes of discourse for the inputs are set to appropriate ranges according to the distribution of the training data. The feature space and the results of the FCM clustering are illustrated in Figure 8.

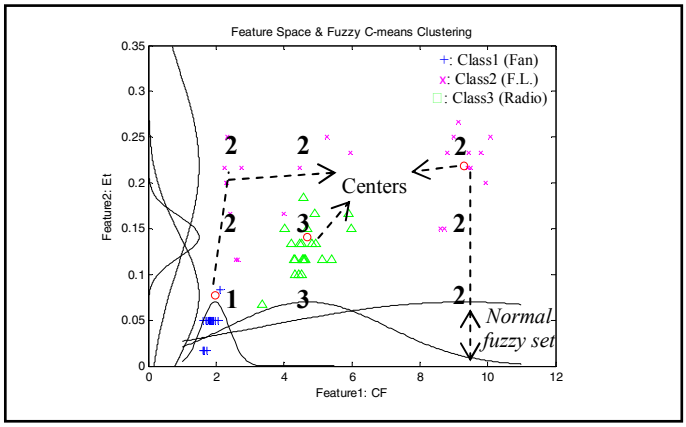

Figure 8. Feature space and fuzzy c-means clustering in Experimental 1.

In Figure 8, the interval of *CF* is [1, 11], whereas the interval of E_t is [0, 0.3]. The label of each partition is assigned according to the clusters and the training data. Analysis of the data shows that E_t has less ambiguity than *CF*. Hence, E_t is a better feature than *CF*.

The values of feature parameters, (α, γ, δ), used in this experiment are (0.03, 0.065, 10.0), respectively. These values are determined based on the past experience. The fuzziness constant, *m*, is 2; the value of *c* is 3 because this is a three-class problem. The tuning constant, η, is 0.003; the maximum training epoch is 500. The training and testing results of the fuzzy classifier with the gradient descent algorithm in this experiment are shown in Figure 9. The testing results are tabled in Table I.

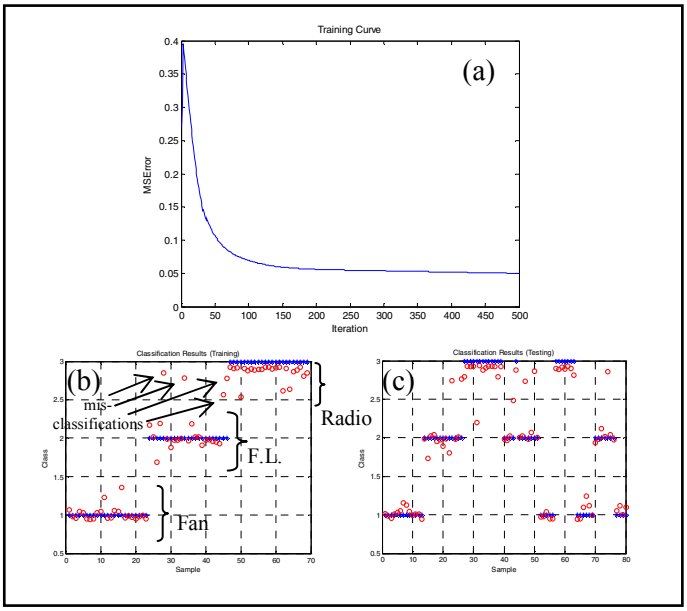

Figure 9. Training and testing results of the fuzzy classifier with the gradient descent algorithm in experimental 1. (a). Training curve. The final MSE_{rror}=0.04991; (b) Training result. The O.R.R.=94.2%; (c). Testing result. The O.R.R.=92.5%.

TABLE I. IDENTIFICATION RESULTS OF THE FUZZY CLASSIFIER WITH THE GRADIENT DESCENT ALGORITHM IN EXPERIMENTAL 1

C.M.	Single Load and Multiple Load operation		
	Fan	F.L.	Radio
Fan	28 (100%)	0 (0%)	0 (0%)
F.L.	0 (0%)	26 (83.87%)	5 (16.13%)
Radio	0 (0%)	1 (4.76%)	20 (95.24%)
O.R.R.[a] (%)	**92.5**		

O.R.R.[a]: Overall Recognition Rate

The units used in the Confusion Matrix (C.M.) table are the number of successful/unsuccessful recognizing count and percentage, respectively. From Table I, Fluorescent Light has the lowest recognition rate of 83.87%; Radio has the recognition rate of 95.24%; and Fan has the highest recognition rate of 100%. The overall recognition rate is 92.5%.

2) Fuzzy Classifier with the GA

The parameters used by the GA are as follows: The total length of each chromosome is 223. The population size and maximum generation are 50 and 200, respectively. For simplicity, the crossover and mutation rates during evolution are held constant; they are set to 0.63 and 0.07, respectively. The training and testing results of the fuzzy classifier with the GA in this experiment are shown in Figure 10. The testing results are shown in Table II.

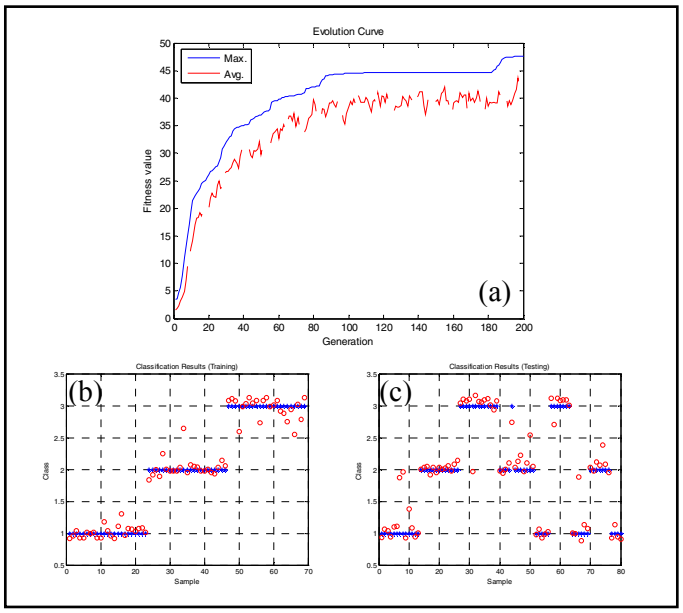

Figure 10. Training and testing results of the fuzzy classifier with the GA in experimental 1. (a). Evolution curves. The final f.v.=47.624; (b) Training result. The O.R.R.=98.55% (**+4.35%**); (c). Testing result. The O.R.R.=93.75% (**+1.25%**).

TABLE II. IDENTIFICATION RESULTS OF THE FUZZY CLASSIFIER WITH THE GA IN EXPERIMENTAL 1

C.M.	**Single Load and Multiple Load operation**		
	Fan	F.L.	Radio
Fan	25 (89.29%)	3 (10.71%)	0 (0%)
F.L.	0 (0%)	30 (96.77%)	1 (3.23%)
Radio	0 (0%)	1 (4.76%)	20 (95.24%)
O.R.R. (%)	**93.75**		

From Table II, Fan has the lowest recognition rate of 89.29%; Radio has the recognition rate of 95.24%; and Fluorescent Light has the highest recognition rate of 96.77%. The overall recognition rate is 93.75%.

B. Experimental 2: Load De-energizing Classification

In this experiment, the proposed system is used to identify the de-energizing status of each load. The feature space and the results of the FCM clustering are illustrated in Figure 11 (a). Analysis of the data shows that *CF* as well as I_{peak} is a good feature for classification. Based on the past experience, the β is set to 0.016. The tuning constant, η, is 0.01; the maximum training epoch is 500. The training and testing results of the fuzzy classifier with the gradient descent algorithm in this experiment are shown in Figure 11 (b) to (d). The testing results are tabled in Table III. The results show that he overall recognition rate is 100%.

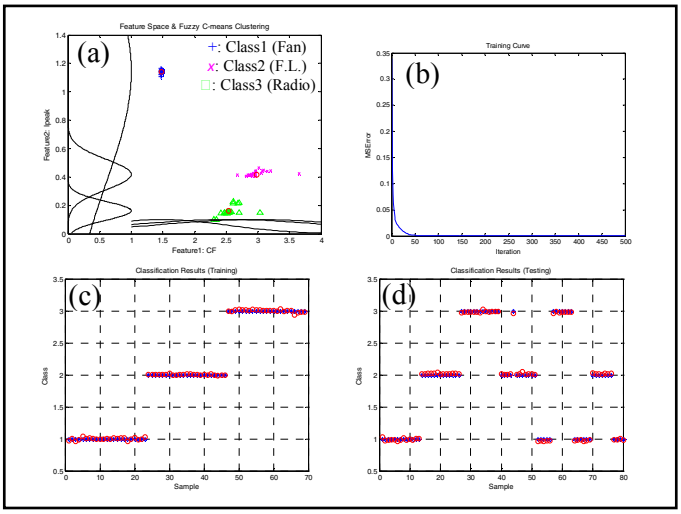

Figure 11. Training and testing results of the fuzzy classifier with the gradient descent algorithm in experimental 2. (a) Feature space and fuzzy c-means clustering in Experimental 2; (b). Training curve. The final MSE_{rror}=0.000268; (c) Training result. The O.R.R.=100%; (d). Testing result. The O.R.R.=100%.

TABLE III. IDENTIFICATION RESULTS OF THE FUZZY CLASSIFIER WITH THE GRADIENT DESCENT ALGORITHM IN EXPERIMENTAL 2

C.M.	**Single Load and Multiple Load operation**		
	Fan	F.L.	Radio
Fan	28 (100%)	0 (0%)	0 (0%)
F.L.	0 (0%)	31 (100%)	0 (0%)
Radio	0 (0%)	0 (0%)	21 (100%)
O.R.R. (%)	**100**		

VI. CONCLUSIONS

The NILM system acts an important role for effectively using and conserving the electricity. In this paper, an NILM system that integrates transient load current feature extraction methods and soft-computing techniques is proposed. The proposed system, which uses the fuzzy classifier with the FCM clustering and the two optimization algorithms as the load identifier, is capable of identifying energizing and de-energizing statuses of each load under single load and multiple load operation scenarios in different realistic environments. From the experimental results, the classification performance of the fuzzy classifier with the GA is better than the performance of the classifier with the conventional EBPA because the GA is a global search optimization algorithm. The overall recognition rates are above 92.5%. Additionally, the identification is not affected by different experimental locations. These results confirm that the proposed NILM system is able to identify the usage status of each appliance robustly.

VII. ACKNOWLEDGEMENT

This research is partially supported by National Energy Project of National Science Council, Taiwan, under the grant number NSC 99-3113-P-006-004.

REFERENCES

[1] S. Drenker and A. Kader, "Nonintrusive Monitoring of Electric Loads," *IEEE Computer Applications in Power*, vol. 12, no. 3, pp. 47-51, Oct. 1999.

[2] C. Laughman, K. Lee, R. Cox, S. Shaw, S. B. Leeb, L. Norford, and P. Armstrong, "Power Signature Analysis," *IEEE Power & Energy Magazine*, vol. 1, pp. 56-63, March/April 2003.

[3] A. Shrestha, E. L. Foulks, R. W. Cox, "Dynamic load shedding for shipboard power systems using the non-intrusive load monitor," *IEEE Electric Ship Technologies Symposium*, pp. 412-419, 20-22 April 2009.

[4] H. H. Chang, C. L. Lin, H. T. Yang, "Load Recognition for Different Loads with the Same Real Power and Reactive Power in a Non-intrusive load-monitoring System," *12th International Conference on Computer Supported Cooperative Work in Design*, pp. 1122-1127, 16-18 April 2008.

[5] A. Cole and A. Albicki, "Nonintrusive Identification of Electrical Loads in a Three-Phase Environment Based on Harmonic Content," *IEEE Conf. on Instrumentation and Measurement Technology*, vol. 1, pp. 24-29, 1-4 May, 2000.

[6] Y. Nakano, H. Murata1, K. Yoshimoto1, S. Hidaka, M. Tadokoro, and K. Nagasaka, "Non-Intrusive Electric Appliances Load Monitoring System Using Harmonic Pattern Recognition - Performance Test Results at Real Households," *4th International Conference on Energy Efficiency in Domestic Appliances and Lighting*, pp. 477-488, Jun. 2006.

[7] Takeshi Saitoh, Yuuki Aota, Tomoyuki Osaki, Ryosuke Konishi, Kazunori Sugahara, "Current Sensor based Non-intrusive Appliance Recognition for Intelligent Outlet," *The 23rd International Technical Conference on Circuits/Systems, Computers and Communications*, pp. 349-352, 11:00-12:30 Monday, July 7, 2008.

[8] S. B. Leeb, S. R. Shaw, and J. L. Kirtley Jr., "Transient Event Detection in Spectral Envelope Estimates For Nonintrusive Load Monitoring," *IEEE Trans. on Power Delivery*, vol. 10, no. 3, pp. 1200-1210, Jul. 1995.

[9] S. R. Shaw, S. B. Leeb, L. K. Norford and R. W. Cox, "Nonintrusive Load Monitoring and Diagnostics in Power Systems," *IEEE Transactions on Instrumentation and Measurement*, vol. 57, pp. 1445-1454, July 2008.

[10] S. R. Kamat, "Fuzzy logic based pattern recognition technique for non-intrusive load monitoring," *IEEE Region 10 Conference on TENCON*, Vol. 3, pp. 528-530, 21-24 Nov. 2004.

[11] H. T. Yang, H. H. Chang, C. L. Lin, "Design a Neural Network for Features Selection in Non-intrusive Monitoring of Industrial Electrical Loads," *11th International Conference on Computer Supported Cooperative Work in Design*, pp. 1022-1027, 26-28 April 2007.

[12] H. H. Chang, C. L. Lin, L. S. Weng, "Application of artificial intelligence and non-intrusive energy-managing system to economic dispatch strategy for cogeneration system and utility," *13th International Conference on Computer Supported Cooperative Work in Design*, pp.740-745, 22-24 April 2009.

[13] L. X. Wang, *A COURSE IN FUZZY SYSTEMS AND CONTROL*. Pearson Education Taiwan Ltd., 2005.

[14] Jyh-Shing Roger Jang, "Data Clustering and Pattern Recognition", available at the links for on-line courses at the author's homepage at http://www.cs.nthu.edu.tw/~jang.

[15] H. Nomura, I. Hayashi, and N. Wakami, "A learning method of fuzzy inference rules by descent method," *IEEE International Conference on Fuzzy Systems*, pp. 203-210, 1992.

[16] Chin-Teng Lin and C. S. George Lee, *Neural fuzzy systems: A neuro-fuzzy synergism to intelligent systems*. Pearson Education Taiwan Ltd., Taiwan, 2003.

[17] Mitsuo Gen and Runwei Cheng, *Genetic Algorithms & Engineering Design*. John Wiley & Sons, Inc., 1997.

[18] Chua, T.W., Tan, W.W., Non-singleton genetic fuzzy logic system for arrhythmias classification. Engineering Applications of Artificial Intelligence (2010), doi:10.1016/j.engappai.2010.10.003.

2011 IEEE International Conference on Fuzzy Systems
June 27-30, 2011, Taipei, Taiwan

Knowledge-Based Fuzzy Imbalanced Force Compensator Design for a Single Active Magnetic Bearing Suspended Rotor System

Yi Hua Fan
Department of Mechanical Engineer
Chung Yuan Christian University
Taiwan
yihuafan@cycu.edu.tw

Ying Tsun Lee
Department of Mechanical Engineer
Chung Yuan Christian University
Taiwan
at0820.cat@gmail.com

***Abstract*—A fuzzy imbalanced force estimator and feed-forward controller designed by the knowledge of rotor dynamics for a single active magnetic bearing suspended rotor system was proposed to eliminate the unbalancing vibration of rotor in the paper. The variable parameters used in the fuzzy estimator are displacement and velocity of the rotor and control current of the magnetic bearing. Based on the estimating signal, a feed-forward control system is set to suppress the unbalancing vibration. The simulation and experiment results show that the proposed estimation system could accurately estimate the unbalance force and the feed-forward control system could restrain the unbalancing vibration to improving the rotational accuracy.**

Keywords-fuzzy imbalanced force estimator, single active magnetic bearing

I. INTRODUCTION

Active magnetic bearing (AMB) is the essential part of the non-contact rotor systems and have been widely developed in industrial application, i.e., the spindle of machine tool, the linear motor, the flywheel energy store system, and the compound molecular pump, etc. By the reference [1], we know the AMB can't work stably without a control system. Thus the control system which contains position sensors and a traditional proportional-integral-derivative (PID) controller is the standard control system for the industries. Parameters of the PID controller are based on the system's dynamic model. But the system model can't obtain accurately and always keep in the same condition. Thus, in order to optimize the controller to make the system more stable, there are many researches working for the controllers with the unknown parameters of the AMB system. For the unknown parameters of the AMB rotor system with vibrating base, an adaptive back stepping controller was proposed and the results showed the bearable acceleration disturbance level was higher than PID controller [2]. The model uncertainty of the AMB system changed with the operating rotor speed, a linear parameter-varying controller was proposed for the time-varying AMB parameters [3]. Mainly vibration source of the disturbance is the unbalance force from the rotor. The Sliding mode control was applied to increase the robustness of the AMB system to reduce the disturbance response [4].

From these researches, we can find in such a non-contact rotor system the unbalance force is usually the other factor which induced the rotor system being unstable as the rotor running to the critical speed of the system, consequently, the unbalance compensation is needed. Moreover, if the unbalance force can be predicted, the parameters of the controller can be modified to control the system operating more smoothly [5]. A model based force estimator with an adaptive tuner for a single AMB suspended rotor system was proposed to eliminate the imbalance vibration in our early research [6]. These methods are frequency dependent because the synchronous reference signal generator has parameters that are dependent on the rotor spin rate, thus requiring continual adaptation as the spin rate varies or they are built on the linear model of the AMB system that there are parameters uncertain problem must be resolved. Therefore, this problem was tried to be solved by a traditional PID controller and a fuzzy feed-forward force compensator.

In recent years, fuzzy controller has been found to be one of the most popular controllers. A well designed fuzzy logic controller can handle uncertain information and used in the control of the AMB system which are having a complex time-variable mathematical model.[7-10] The fuzzy logic control system contains sets of variable functions which are fuzzy rules and membership functions. Generally these variables can be adjusted by the experiment results and try and error. By continuing adjust the fuzzy variable functions, the fuzzy logic control system can be the most effective controller to control the AMB systems.

In this paper, a knowledge-based fuzzy imbalanced force compensator system is proposed. The compensator system is established by the measurement of the displacement of the rotor, control current of the magnetic bearing and rotor speed. And the fuzzy rules and membership functions was established by the previously research which showed the feed-forward compensator could meliorate the rotational accuracy in the operational range. After building the fuzzy compensator system, the feed-forward control system is established. To verify the compensator system and the feed-forward control system, the simulation and experiment results was carried out.

978-1-4244-7316-8/11/$26.00 ©2011 IEEE

II. MODELING OF A SINGLE MAGNETIC BEARING SUSPENDED ROTOR SYSTEM

Fig.1 shows the basic structure of the single AMB system. The rotor is suspended horizontally by an AMB in the free end and a flexible coupling in the other end connected with the motor. The rotor positions in the free end are measured by two eddy-current type sensors at the magnetic bearing location. The spinning shaft is driven by the motor. Fig.2 shows the relative positions of the coupling, magnetic bearing and the mass center of rotor. Fig.2 also shows the directions of the four degrees of freedoms of the rotor and the action positions and directions of the magnetic forces (F_1 ~F_4) and the reacted forces (F_{xt}, F_{yt}) of the flexible coupling.

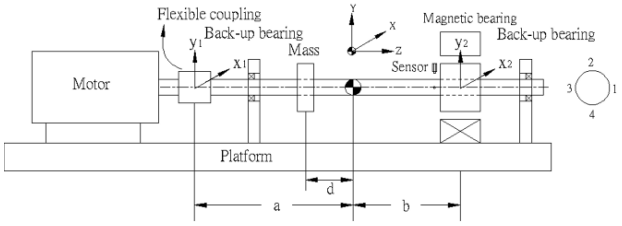

Fig.1 Structure of the single AMB system

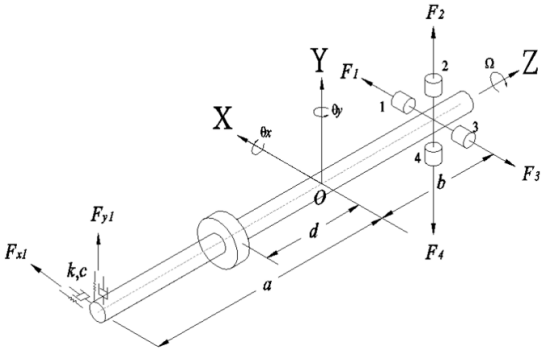

Fig.2 Geometric relationship of the single AMB system

According to the research[5], the magnetic force and the reacted forces of the flexible coupling can be expressed as:

$$F_1 - F_3 = k_i i_1 + k_{d1} x_2$$
$$F_2 - F_4 = k_i i_2 + k_{d1} y_2$$

where x_1, y_1, x_2, and y_2 are the radial displacements at the positions of flexible coupling and AMB; k_T and c_T are the equivalent stiffness and damping coefficients of the flexible coupling; k_i is the current-force coefficient and k_d is the displacement-force coefficient of AMB.

The dynamics of the system in terms of displacements in the flexible coupling and magnetic bearing locations, which can be written in matrix form as follows:

$$M\underline{\ddot{x}} + C\underline{\dot{x}} + K\underline{x} = B\underline{u} + E\underline{w} + F\underline{x}^3 + Dg$$

$$M = \begin{bmatrix} 1 & 0 & 0 & 0 \\ 0 & 1 & 0 & 0 \\ 0 & 0 & 1 & 0 \\ 0 & 0 & 0 & 1 \end{bmatrix}; C = \begin{bmatrix} c_T\beta_3 & 0 & \alpha_1 & -\alpha_1 \\ -c_T\beta_2 & 0 & -\alpha_2 & \alpha_2 \\ -\alpha_1 & \alpha_1 & c_T\beta_3 & 0 \\ \alpha_2 & -\alpha_2 & -c_T\beta_2 & 0 \end{bmatrix}$$

$$K = \begin{bmatrix} k_T\beta_3 & k_{d1}\beta_2 & 0 & 0 \\ -k_T\beta_2 & -k_{d1}\beta_1 & 0 & 0 \\ 0 & 0 & k_T\beta_3 & k_{d1}\beta_2 \\ 0 & 0 & -k_T\beta_2 & -k_{d1}\beta_1 \end{bmatrix}; B = \begin{bmatrix} -k_i\beta_2 & 0 \\ k_i\beta_1 & 0 \\ 0 & -k_i\beta_2 \\ 0 & k_i\beta_1 \end{bmatrix}; E = \begin{bmatrix} \gamma_2 & 0 \\ -\gamma_1 & 0 \\ 0 & \gamma_2 \\ 0 & -\gamma_1 \end{bmatrix};$$

$$D\begin{bmatrix} 0 \\ 0 \\ -1 \\ -1 \end{bmatrix}; \underline{x} = \begin{bmatrix} x_1 \\ x_2 \\ y_1 \\ y_2 \end{bmatrix}; \underline{u} = \begin{bmatrix} i_1 \\ i_2 \end{bmatrix}; \underline{w} = \begin{bmatrix} m_p r\Omega^2 \cos(\Omega t + \theta) \\ m_p r\Omega^2 \sin(\Omega t + \theta) \end{bmatrix};$$

$$\alpha_1 = \frac{I_p \Omega a}{IL}; \alpha_2 = \frac{I_p \Omega b}{IL};$$

$$\beta_1 = \left(\frac{b^2}{I} + \frac{1}{m}\right); \beta_2 = \left(\frac{ab}{I} - \frac{1}{m}\right); \beta_3 = \left(\frac{a^2}{I} + \frac{1}{m}\right);$$

$$\gamma_1 = \left(\frac{bd}{I} - \frac{1}{m}\right); \gamma_2 = \left(\frac{ad}{I} + \frac{1}{m}\right)$$

where m is the mass of the rotor; m_p is the eccentric mass of the rotor; θ is the angle between eccentricity and axis coordinate; I is the transverse moment inertia of the rotor; I_p is the polar moment inertia of the rotor; Ω is the rotating speed; r is the radius of the rotor; L is the length between the AMB and the flexible coupling.

The stability of the AMB system by using a PD controller and a force observer compensator was verified in the research. But the force observer design is based on the dynamic equations, and there are some model uncertainties of the flexible coupling and the nonlinearities of the magnetic bearing system, the observer would not work well for all the operation speed. And the phase of estimated force signal may be lag and the amplitude may be smaller than exact disturbance.

The control structure in this paper is showed as Fig.3. A fuzzy compensated system is used to estimate the imbalance force and disturbance and the control current is modified by the output of the fuzzy compensator. The fuzzy compensated system is built on the knowledge of rotor dynamics and doesn't need a precise mathematical model. The input signals of the proposed fuzzy mechanism are obtained from the position error and velocity of the rotor and the control current of the AMB system. And making use of the concept of the fuzzy set, the compensator signals are adjustable in varies with the response.

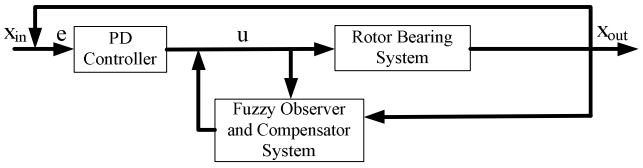

Fig.3 Control structure diagram of the single AMB system

III. DESIGN OF THE FUZZY MECHANISM

A fuzzy mechanism is constructed by the membership function and the fuzzy rules. Inputs of the fuzzy observer system proposed in this paper were established by the control current and the position of the rotor. In the fuzzy observer system, the control current and the displacement vibration signal are used to design fuzzy rules and membership functions to build up the fuzzy compensator.

The linguistic variable inputs for the fuzzy observer system are denoted as i_c and x. And the linguistic variable output is the observer force which is denoted as f. Membership functions of the input and output linguistic variables and the linguistic values for the input and output are showed as Fig.4, where the linguistic variables are labeled with "L," "M," and "S" to represent "large," "medium," and "small," respectively. The Mamdani method is used to design the membership functions of the fuzzy system. The membership bounds of the membership functions are modified from the results of the reference [5] and “try and error” results.

The fuzzy rules for the observer system are showed in table 1. There are six fuzzy linguistic values for the input linguistic variables, and three fuzzy linguistic values for the output linguistic variables. After the fuzzy observer system, the observer force is modified by a constant coefficient and feedback to the control current to make the system more stable.

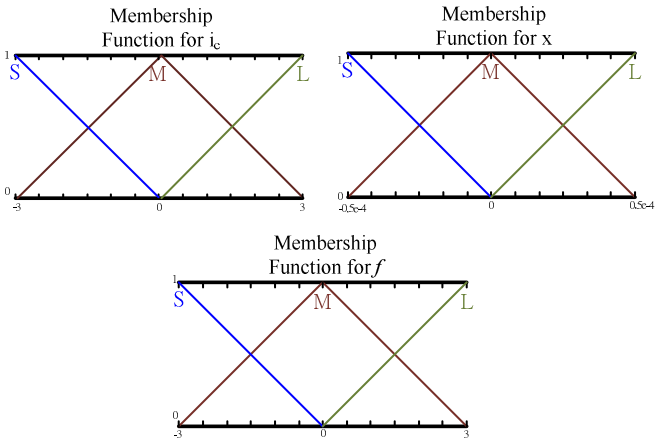

Fig.4 Membership functions of the inputs and output

Table1. Fuzzy rules

Fuzzy Rules				
		i_c		
		S	M	L
x	S	L	M	M
	M	M	M	S
	L	M	S	S

IV. SIMULATION RESULTS

The simulation program of the single AMB system is established by MATLAB. The AMB system consists by a PD controller and the fuzzy compensator as the fig.5 shows. The gain value of the PD controller and the parameters of the AMB system are shown in table 2.

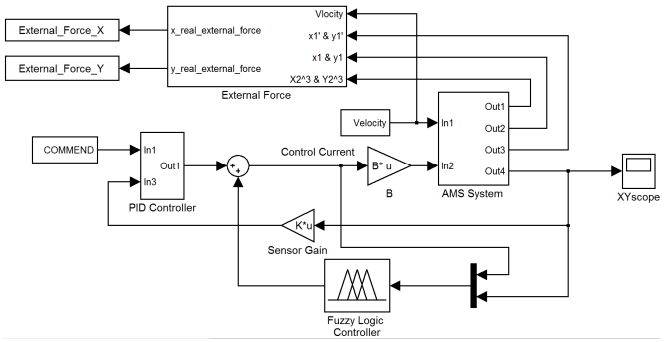

Fig.5 The AMB system established by the Simulink toolbox of the MATLAB

Table2. Parameters of the AMB system

M, the mass of the rotor	:	2.142 kg
L, length of the rotor	:	0.414 m
Mp, Eccentric mass	:	0.0013 kg
Ki, current parameter of the AMB	:	35.549
Kd, displacement parameter of the AMB:		1.423e5
Gs, Sensor gain	:	7000V/m

From the simulation of the AMB system, the disturbance force obtained by the fuzzy observer at various rotating speeds can be showed in fig. 6. With different rotating speeds of the rotor, we can see the disturbance is displayed like a harmonic signal with different magnitude and frequency. Thus, the simulation results shows the fuzzy observer system can observers the disturbance force, and the estimated results is close to the actual disturbance force of the system, even if we can’t demonstrate the system model very accurately.

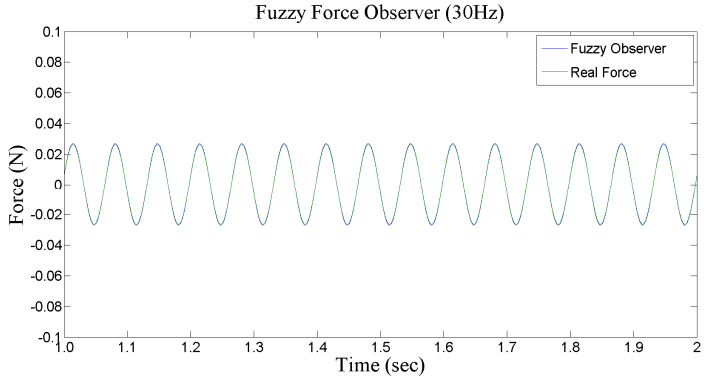

(a) 30Hz

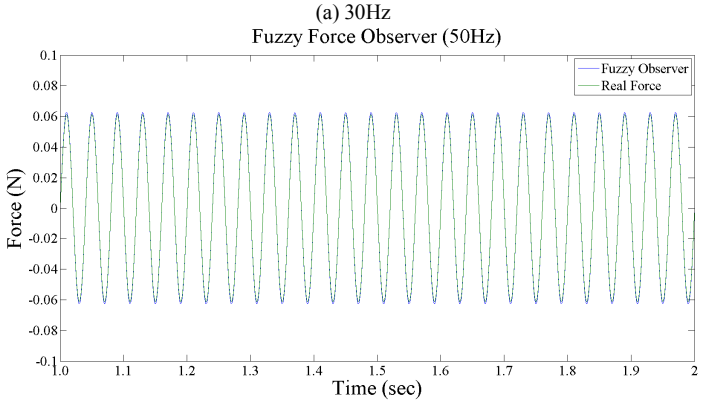

(b) 50Hz

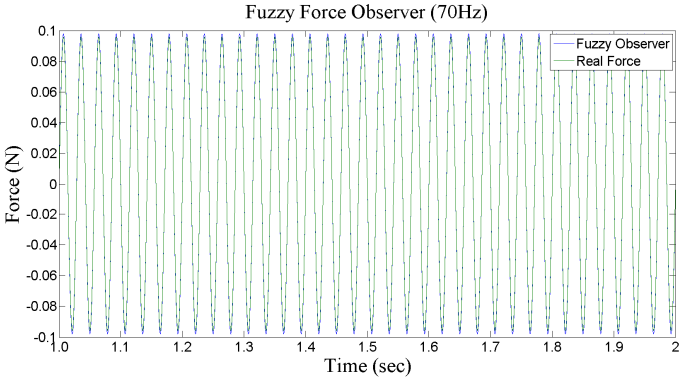

(c) 70Hz

Fig6. The observer force by the fuzzy observer system

Disturbance force from fuzzy observer will sent to the AMB system to be a compensated signal which is constructed by the disturbance force. Fig.6 shows the rotating orbits of the rotor with traditional PD controller, and fig.7 is the rotating orbits with the compensated signal. The limits of both horizontal and vertical axes in PD simulations are [100μm 100 μm]. The limits of both horizontal and vertical axes in simulations with fuzzy system are [10μm 1μm]. Simulation results show the fuzzy compensator can increase rotational accuracy in the operating range.

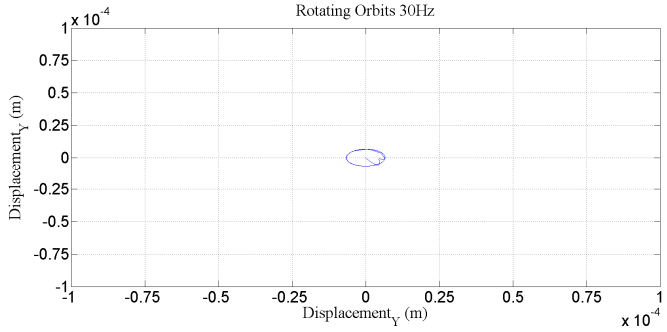

(a) 30Hz

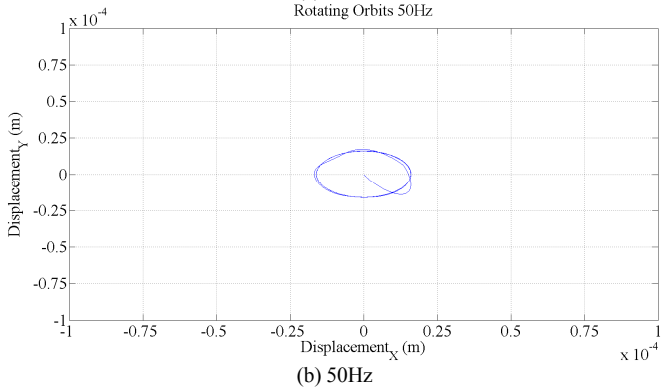

(b) 50Hz

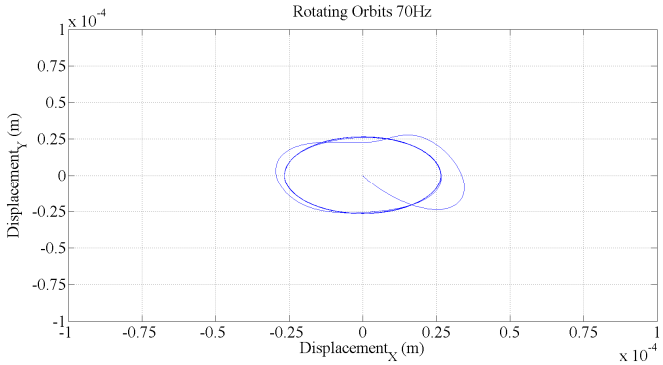

(c) 70Hz

Fig7. The rotating orbits of the AMB system with the PD controller at 30, 50 and 70 Hz

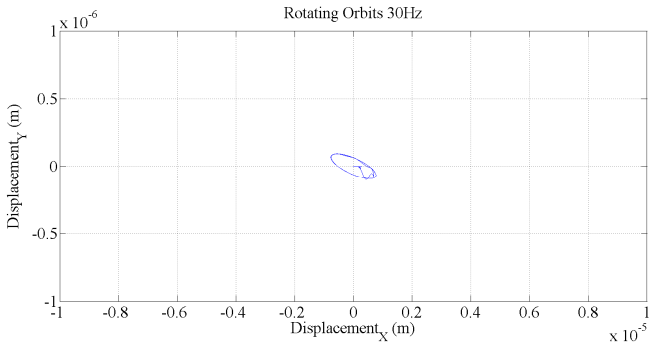

(a) 30Hz

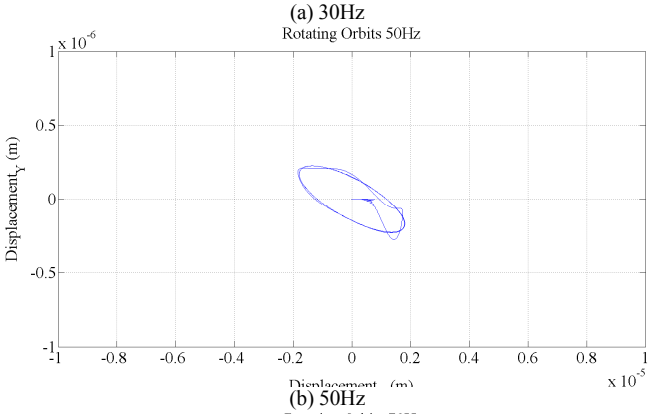

(b) 50Hz

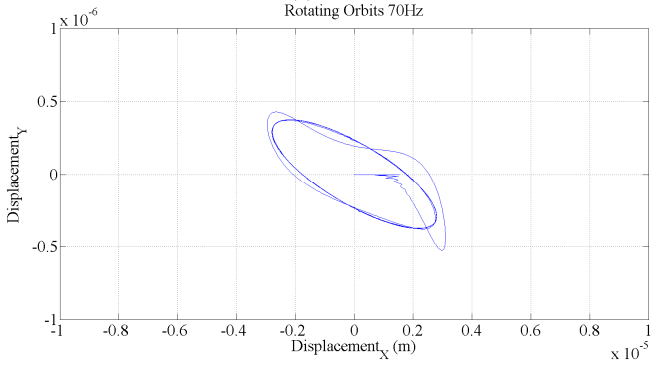

(c) 70Hz

Fig8. The rotating orbits of the AMB system with the Fuzzy system at 30, 50 and 70 Hz

V. EXPERIMENT RESULTS

To validate the compensator, a single AMB system with a flexible bearing is constructed as shown in fig.9. The fuzzy

compensator is constructed in PC and is connecting with AMB system using the XPC system. The AMB system is connected to a rotor with a flexible coupling.

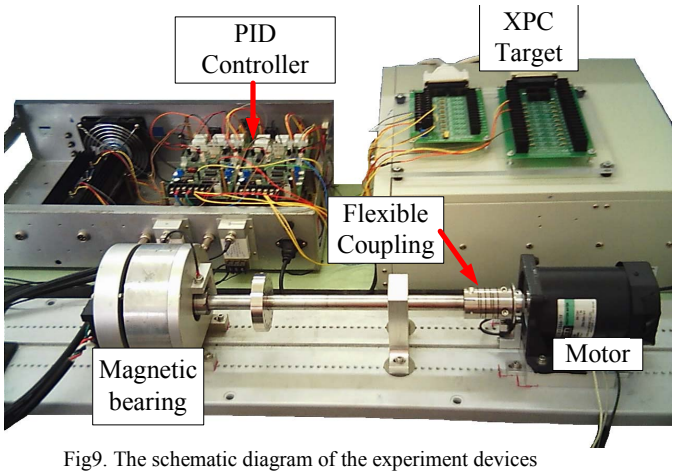

Fig9. The schematic diagram of the experiment devices

The vibrations of the shaft at the location of the AMB at several rotating speed are shown in fig.10. The rotor is controlled by a traditional PD controller with a fuzzy compensator being added to the system at 5 sec after. The blue lines in fig.10 are the average values of vibration of the shaft. The maximum peak to peak value of the vibration is approximately 5.7e-4 m ~ 7e-4 m when only using the PD controller. It demonstrates that the maximum vibration amplitude is reduced to 4.2e-4 m ~ 5.3e-4 m as the fuzzy compensator is added to the system. The average value is approximately 1.5e-4 m when only using the PD controller and is reduced to 0.9e-4 m as the fuzzy compensator added. It is obviously that the peak to peak values and the average values of the vibration are all suppressed after the fuzzy compensator is added. As the results, we can identify the valid of the fuzzy compensator system and it means that the fuzzy compensator system can make the system operating more smoothly, even if the system model is not accurate.

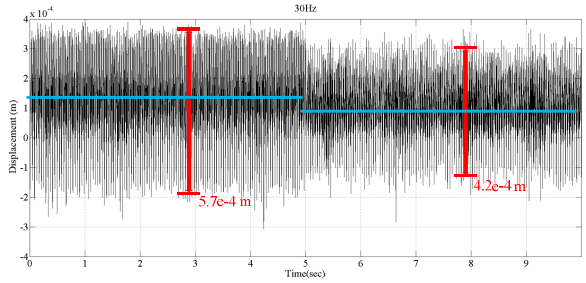

(a) 30Hz

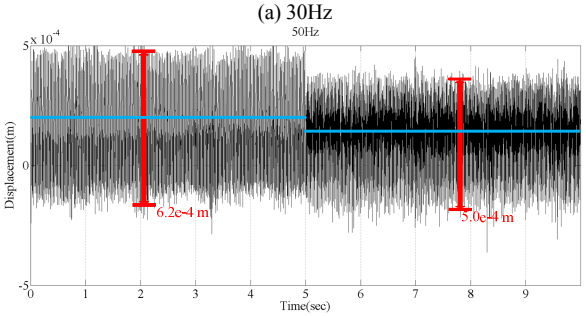

(b) 50Hz

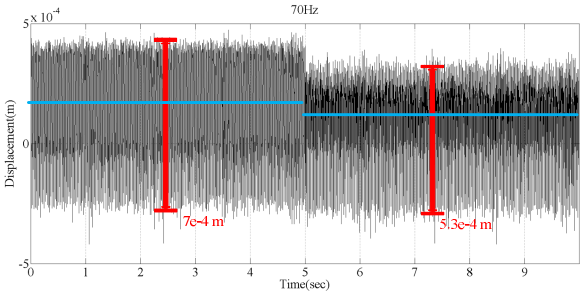

(c) 70Hz

Fig.10 The experiment results of the AMB system, fuzzy observer system is utilized after 5secs.

VI. CONCLUSION

This study demonstrates that the fuzzy force compensator applied to the single AMB system is useful for restraining the unbalancing vibration and to improve the rotational accuracy. From the results of the simulation and experiment, the fuzzy observer can works well at different operating speeds. And the fuzzy observer output can feed to the AMB system to make the system operating more smoothly. The whirling orbits of the rotor in the experiment showed it can be maintained in a small range than the traditional PD controller.

REFERENCE

[1] Earnshaw, Samuel, "On the Nature of the Molecular Forces which Regulate the Constitution of the Luminiferous Ether," Trans. Camb. Phil. Soc., vol. 7, pp. 97–112, 1842.

[2] S. Sivrioglu, "Adaptive backstepping for switching control active magnetic bearing system with vibration base," IET Control Theory Appl., vol. 1, pp. 1054-1059, 2007.

[3] B. Lu, H. Choi, G. D. Buckner and K. Tammi, "Linear Parameter-varying techniques for control of a magnetic bearing system," Control Engineering Practice, vol. 16, pp. 1161-1172, 2008.

[4] M. S. Kang, J. Lyou and J. K. Lee, "Sliding mode control for an active magnetic bearing system subject to base motion," Mechatronics, vol. 20, pp. 171-178, 2010.

[5] I. S. Cade, P. S. Keogh and M. N. Sahinkaya, "Rotor/active magnetic bearing transient control using wavlet predictive moderation," Journal of Sound and Vibration, Vol. 302, pp. 88-103, 2007.

[6] Y. H. Fan, K. Y. Chen, D. L. Weng and Y. T. Lee, "Design of adaptive compensator of force imbalance for a single active magnetic bearing suspended rotor system," Journal of Applied Physics, vol. 103, pp. 07E935-07E935-3, 2008.

[7] M. A. Arjona, R. E. Perez, E. M. Vázquez, "Convergence improvement in two-dimensional finite element nonlinear magnetic problems—a fuzzy logic approach," Finite Elements in Analysis and Design, Vol. 41, pp. 583–598, 2005.

[8] K. Y. Chen, P. C. Tung, M. T. Tsai and Y. H. Fan, "A self-tuning fuzzy PID-type controller design for unbalance compensation in an active magnetic bearing," Expert Systems with Applications, Vol. 36, pp. 8560–8570, 2009.

[9] L. T. Rekik and M. Chtourou, "FUZZY SUPERVISED NONLINEAR PID CONTROL OF A CLASS OF UNKNOWN NONLINEAR SYSTEM," Journal of Circuits, Systems, and Computers, Vol. 19, No. 8, pp. 1847-1862, 2010.

[10] N. Hachicha, B. Jarboui and P. Siarry, "A fuzzy logic control using a differential evolution algorithm aimed at modelling the financial market dynamics," Information Sciences Vol. 181, pp. 79–91, 2011.

2011 IEEE International Conference on Fuzzy Systems
June 27-30, 2011, Taipei, Taiwan

DSP-Based Cross-Coupled Synchronous Control for Dual Linear Motors via Functional Link Radial Basis Function Network

Chin-Sheng Chen
Graduate Institute of Automation Technology
National Taipei University of Technology
Taipei, Taiwan
saint@ntut.edu.tw

Po-Huan Chou
Department of Electrical Engineering
National Dong Hwa University
Hualien, Taiwan
d9623002@ems.ndhu.edu.tw

Faa-Jeng Lin
Department of Electrical Engineering
National Central University
Chungli, Taiwan
linfj@ee.ncu.edu.tw

***Abstract*—A digital signal processor (DSP)-based cross-coupled functional link radial basis function network (FLRBFN) control is proposed in this study for the synchronous control of a dual linear motors servo system which is installed in a gantry position stage. The dual linear motors servo system comprises two parallel permanent magnet linear synchronous motors (PMLSMs). First, the dynamics of the field-oriented control PMLSM servo drive with a lumped uncertainty, which contains parameter variations, external disturbance and friction force, is introduced. Then, to achieve accurate trajectory tracking performance with robustness, an intelligent control approach using FLRBFN is proposed for the field-oriented control PMLSM servo drive system. The proposed FLRBFN is a radial basis function network (RBFN) embedded with a functional link neural network (FLNN). The network structure and its on-line learning algorithms for connective weights, means and standard derivations are described in detail. Moreover, since a cross-coupled technology is incorporated into the proposed intelligent control scheme for the gantry position stage, both of the position tracking errors and synchronous errors of dual linear motors will converge to zero, simultaneously. Finally, some experimental results are illustrated to depict the validity of the proposed control approach.**

Keywords- Dual linear motors servo system, gantry position stage, functional link neural network, radial basis function network, cross-coupled technology.

I. INTRODUCTION

The high precision motion control of gantry position stages has found numerous applications in the manufacturing industries including microelectronics, aerospace, solar cell, and flat panel manufacturing and inspection [1]. In the configuration of gantry position stage, two motors are mounted on two parallel linear guides to drive a moving stage. For the machining centers with heavy type high-speed gantry position stage, though the pillars of the two side of the gantry have the same drive mechanisms, the synchronous error between the two motors is unavoidable due to non-balanced forces adding to the cross gantry and other moving parts, mechanism assembly variations and various uncertainty disturbances during the working process. The synchronous error will influence the quality of the work-pieces and even lead to stop the working process due to the over current protection. Hence, the control of the synchronous error in the gantry configuration has become a challenge with increasing demands for high-speed and high accuracy manufacture and inspection.

Over the past decade, the cross-coupled technology was majorly used in machine tools and multiple axes motion applications for the reducing of contour tracking errors [2-3]. Recently, the cross-coupled technology was incorporated into some well-know adaptive control approaches to solve the synchronous control problem and improve the control performance [2-3]. In [3], an adaptive coupling control approach had been developed for the synchronous control of multiple motion axes systems. This approach was developed to stabilize the position tracking of each axis while synchronizing its motion with the motions of the other axes. However, a linear sliding mode control (SMC) has been adopted in this synchronous strategy.

In general, intelligent control approaches such as neural and fuzzy mechanisms are dynamic model-free control techniques [4]. Therefore, many studies on neuro-fuzzy approaches for controller developments and for describing the dynamic behaviors of complex systems have been published [5]. In these approaches, the RBFN method, which took local receptive field to perform function mappings, was investigated in [6]. Because the RBFN has a simple structure, the convergence speed of the RBFN is faster than a multilayer perceptron (MLP) network. Moreover, the RBFN has similar features in the following as the fuzzy system: (i) The output value is obtained by using a weighted sum method; (ii) The number of nodes in hidden layer in the RBFN is identical to the number of if-then rules in the fuzzy system; (iii) The receptive field functions in RBFN are similar to the membership functions of the premise part in the fuzzy system. As a result, the RBFN is one of the powerful tools for the systems control development [6].

The basic idea behind an FLNN is the use of the functional links. These functional links generate nonlinear transformations of the original input space before they are fed to the network which constructs the output layer. In other words, the input

978-1-4244-7316-8/11/$26.00 ©2011 IEEE

variables can be enhanced and linear separability can be achieved in the extended space using the FLNN [7]. Moreover, the FLNN can capture nonlinear input-output relationship by the adequate set of polynomial inputs since the high order effects are incorporated in the input variables to increase the dimension of the input space. Thus, FLNN is suitable to be applied in system identifications or control applications [7].

II. Modeling of Dual Linear Motors Servo System

The dual linear motors servo system adopted in this study is composed of two 220V 5.0A 330N PMLSMs. The detailed machine model of the PMLSM, described in the synchronously rotating reference frame, can be found in [22, 23]. With the implementation of the field-oriented control, the electromagnetic force can be simplified as follows [23]:

$$F_{ei} = K_{fi} i_{qi}^{*} \tag{1}$$

$$K_{fi} = 3\pi n_{pi} \lambda_{PMi} / (2\tau_i) \tag{2}$$

where K_{fi} is the thrust coefficient; i_{qi}^{*} is the thrust current command; λ_{PMi} is the permanent magnet flux linkage; n_{pi}, which is 1, is the number of primary pole pairs; τ_i, which is 32mm, is the pole pitch; $i = y1, y2$ is to represent the y1-axis and y2-axis of the dual linear motors servo system.

The mover dynamic equation using the electromagnetic force shown in (1) is

$$F_{ei} = M_i \dot{v}_i + D_i v_i + F_{Li} + f_i(v) \tag{3}$$

where v_i is the linear velocity of the mover; M_i is the total mass of the mover; D_i is the viscous friction and iron-loss coefficient; F_{Li} is the external disturbances term; $f_i(v)$ is the friction force. Considering Coulomb friction, viscous friction and Stribeck effect, the friction force can be formulated as follows [24]:

$$f_i(v) = F_{Ci}\,\mathrm{sgn}(v_i) + (F_{Si} - F_{Ci}) e^{-(v_i / v_{si})^2}\,\mathrm{sgn}(v_i) + K_{vi} v_i \tag{4}$$

where F_{Ci} is the Coulomb friction; F_{Si} is the static friction; v_{Si} is the Stribeck velocity parameter; K_{vi} is the coefficient of viscous friction; $\mathrm{sgn}(\cdot)$ is a sign function. All the parameters in (4) are time-varying.

Curve-fitting technique based on step response of the mover position is applied here to find the model of the motor drive system. For the convenience of the controller design, the position and speed signals in the control loop are set at 1V=0.04963m and 1V=0.04963m/sec, respectively. The major system parameters are:

$$\begin{aligned} &\overline{K}_{fy1} = 195\ \text{N/A},\ \overline{M}_{y1} = 6.32\text{kg} = 0.4023\ \text{Nsec/V}, \\ &\overline{D}_{y1} = 819.4069\ \text{kg/sec} = 52.165\ \text{N/V} \end{aligned} \tag{5}$$

$$\begin{aligned} &\overline{K}_{fy2} = 195\ \text{N/A},\ \overline{M}_{y2} = 6.33\text{kg} = 0.4123\ \text{Nsec/V}, \\ &\overline{D}_{y2} = 821.4103\ \text{kg/sec} = 53.261\ \text{N/V} \end{aligned} \tag{6}$$

The overbar symbol represents the system parameter in the nominal condition. Though the electromagnetic force can be simplified as (1) via the field-oriented control mechanism, however, considering the variations of system parameters, external disturbances and friction force, the dual linear motors servo system is a nonlinear time-varying system in practical applications.

III. Proposed Cross-Coupled FLRBFN Control System

A. Strategy of Cross-Coupled Synchronous Control

Assuming that the system parameter variations, external disturbances and friction force are absent, each field-oriented control PMLSM servo drive can be formulated by rewriting (1) and (3) as follows:

$$\ddot{d}_i(t) = -\frac{\overline{D}_i}{\overline{M}_i}\dot{d}_i(t) + \frac{K_{fi}}{\overline{M}_i} i_{qi}^{*}(t) \triangleq A_{ni}\dot{d}_i(t) + B_{ni}\,u_i \tag{7}$$

where $d_i(t)$ is the position of the mover $A_{ni} = -\overline{D}_i / \overline{M}_i$; $B_{ni} = K_{fi} / \overline{M}_i > 0$; u_i is the control effort, i.e., the thrust current command. Now, considering the existence of parameter variations, external force disturbances and friction force for the single-axis field-oriented control PMLSM servo drive system, then (7) becomes

$$\begin{aligned} \ddot{d}_i(t) = {} & (A_{ni} + \Delta A_i)\dot{d}_i(t) + (B_{ni} + \Delta B_i)\,u_i + (C_{ni} + \Delta C_i)[F_{Li} \\ & + f_i(v)] = A_{ni}\dot{d}_i(t) + B_{ni}\,u_i + H_i \end{aligned} \tag{8}$$

where $C_{ni} = -1/\overline{M}_i$; ΔA_i, ΔB_i and ΔC_i denote the uncertainties introduced by system parameters M_i and D_i; H_i is named the lumped uncertainty and defined by

$$H_i \equiv \Delta A_i \dot{d}_i(t) + \Delta B_i\,u_i + (C_{ni} + \Delta C_i)[F_{Li} + f_i(v)] \tag{9}$$

Here, the lumped uncertainty is assumed to be bounded

$$|H_i| \le \rho_i \tag{10}$$

where ρ_i is a given positive constant.

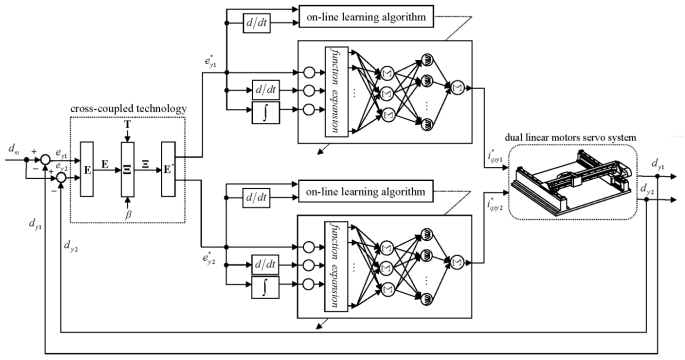

Figure 1. Configuration of cross-coupled FLRBFN control system.

In the proposed control approach, besides the position tracking of each axis, the position synchronization of two axes is considered simultaneously. First, define the position tracking error as

$$e_i = d_m - d_i \tag{11}$$

where d_m denotes the desired command. Then, the synchronous errors are defined as

$$\varepsilon_{y1} = e_{y1} - e_{y2},\ \varepsilon_{y2} = e_{y2} - e_{y1} \tag{12}$$

where ε_{y1} and ε_{y2} denote the synchronous errors of dual linear motors, respectively. If the synchronous errors show in (12) are zero, the goal of synchronous control, i.e., $e_{y1} = e_{y2}$, is achieved [3]. Rewrite (12) in the matrix form as

$$\boldsymbol{\Xi} = \mathbf{T}\mathbf{E} \tag{13}$$

where $\boldsymbol{\Xi} = \left[\varepsilon_{y1}\ \varepsilon_{y2}\right]^T$, $\mathbf{E} = \left[e_{y1}\ e_{y2}\right]^T$, and $\mathbf{T} = \begin{bmatrix} 1 & -1 \\ -1 & 1 \end{bmatrix}$ denotes the synchronous transformation matrix. Then, a cross-coupled position tacking error is defined as

$$\mathbf{E}^* = \mathbf{E} + \beta\boldsymbol{\Xi} \tag{14}$$

where $\mathbf{E}^* = \left[e_{y1}^*\ e_{y2}^*\right]^T$ and β is a positive coupled parameter. Substituting (13) into (14) yields

$$\mathbf{E}^* = \left(\mathbf{I} + \beta\mathbf{T}\right)\mathbf{E} \tag{15}$$

where $\mathbf{I}$ is a unit matrix and $\left(\mathbf{I} + \beta\mathbf{T}\right)$ is a positive defined matrix. In (15), $\mathbf{E} = \mathbf{0}$ if and only if $\mathbf{E}^* = \mathbf{0}$. It also implies that $\boldsymbol{\Xi} = \mathbf{0}$ [3]. Therefore, the control objective is to design a controller to guarantee the convergence of both the position tracking error e_i and the synchronous error ε_i to zero, simultaneously.

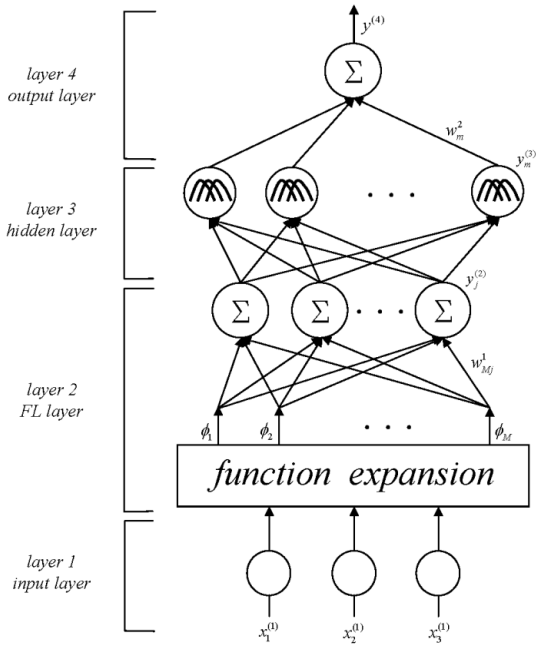

Figure 2. Structure of FLRBFN.

B. Proposed Cross-Coupled FLRBFN Control System

Not only to eliminate the synchronous error of the dual linear motors but also to guarantee the precision position tracking requirement in single axis motor, a cross-coupled FLRBFN control system shown in Fig. 1 is proposed. The four-layer neural network structure of the FLRBFN is shown in Fig. 2. Moreover, since the motions of the y1-axis and y2-axis are controlled separately, all the subscripts *i* are removed for simplicity in the following description.

1) Functional link neural network

To improve the accuracy of the function approximation, an FLNN is adopted to implement the function expansion for the proposed FLRBFN. In the function expansion of the FLNN, the basis functions such as trigonometric, Gaussian or other orthogonal polynomials are feasible. In this study, the trigonometric function is adopted since it forms a more compact representation than Gaussian function, and the sine and cosine functions can be computed more quickly. Therefore, for an input vector $\mathbf{X} = [x_1, x_2, x_3]^T$, the input variables can be separated in the enhanced space as $\boldsymbol{\Phi} = [\phi_1, \phi_2, ..., \phi_M]^T = \left[x_1, \cos(\pi x_1), \sin(\pi x_1), x_2 \cos(\pi x_2), \sin(\pi x_2), x_3, \cos(\pi x_3), \sin(\pi x_3)\right]^T$. Moreover, the output of the FLNN is given by a linear sum of the *j*th node as:

$$\hat{f}_j = \sum_M w_{Mj}^1 \phi_M(\mathbf{X}),\ M = 1, 2, \cdots, 9 \quad j = 1, 2, \cdots, k \tag{16}$$

where k is the number of the output nodes of the FLNN; $\hat{f}_j$ is the output of the FLNN; w_{Mj}^1 is the connective weight; ϕ_M is the output of function expansion.

2) Structure of FLRBFN

The structure of the FLRBFN is a three-layer RBFN embedded with an FLNN, including the input layer (layer 1), the functional link (FL) layer (layer 2), the hidden layer (layer 3) and the output layer (layer 4). To give a clear understanding, the signal propagation and the basic function of each layer are introduced in the following:

Layer 1 (input layer):

In this layer, the node output is represented as

$$y_l^{(1)} = x_l^{(1)}, \ l = 1, 2, 3 \tag{17}$$

where $x_l^{(1)}$ and $y_l^{(1)}$ are the input and output of the lth node in this layer. In this study, $x_1^{(1)}$, $x_2^{(1)}$ and $x_3^{(1)}$ are the cross-coupled position tacking error e^*, its integral $\int e^* d\tau$ and its derivative $\dot{e}^*$, respectively.

Layer 2 (FL layer):

In this layer, each node represents the outputs of the FLNN. The FLNN is designed to increase the dimensionality of the input variables and provide greater discrimination capability in the input variables space [7]. For the jth node

$$y_j^{(2)} = \hat{f}_j(y_l^{(1)}) \qquad j = 1, 2, \ldots, k \tag{18}$$

where $y_j^{(2)}$ is the output of the layer 2.

Layer 3 (hidden layer):

In this layer, the Gaussian function [8] is adopted as the receptive field function. The mathematical function of each node is

$$\Gamma_{jm}(y_j^{(2)}) = \exp\left[\frac{-\left(y_j^{(2)} - c_{jm}\right)^2}{\sigma_{jm}^2}\right], \ m = 1,2,\ldots,f \tag{19}$$

where f is the number of the hidden nodes; c_{jm} and σ_{jm} are the mean and standard derivation of the Gaussian function, respectively; $\Gamma_{jm}(y_j^{(2)})$ is the output of the receptive field function. Then, in this layer, the node output is represented as

$$y_m^{(3)} = \prod_{j=1}^{k} \Gamma_{jm}(y_j^{(2)}), \quad j = 1, 2, \ldots, k, \quad m = 1,2,\ldots,f \tag{20}$$

where $y_m^{(3)}$ is the output of the layer 3.

Layer 4 (output layer):

In the output layer, the weighted sum method is used to calculate the output of the FLRBFN. Then, the node output becomes

$$y^{(4)} = i_q = \sum_{m=1}^{f} y_m^{(3)} w_m^2 \quad m = 1,2,\ldots,f \tag{21}$$

where w_m^2 is the connective weight between the hidden layer and the output layer; $y^{(4)}$ is the output of the FLRBFN as the trust command current.

3) On-line learning algorithms

To describe the on-line learning algorithms of the FLRBFN using gradient decent method, first the energy function E is defined as

$$E = \frac{1}{2} e^{*2} \tag{22}$$

Then, the learning algorithms of connective weights, means and standard derivations are described as follows:

Layer 4:

The error term to be propagated is given by

$$\delta^{(4)} = -\frac{\partial E}{\partial y^{(4)}} = -\frac{\partial E}{\partial d}\frac{\partial d}{\partial y^{(4)}} \tag{23}$$

and the connective weight is updated by the amount

$$\Delta w_m^2 = -\eta_1 \frac{\partial E}{\partial w_m^2} = -\eta_1 \frac{\partial E}{\partial y^{(4)}}\frac{\partial y^{(4)}}{\partial w_m^2} = \eta_1 \delta^{(4)} y_m^{(3)} \tag{24}$$

The connective weight w_m^2 is updated according to the following equation:

$$w_m^2(n+1) = w_m^2(n) + \Delta w_m^2 \tag{25}$$

where the factor η_1 is the learning rate of the connective weight.

Layer 3:

The error term propagated in this layer is derived as

$$\delta_m^{(3)} = -\frac{\partial E}{\partial y_m^{(3)}} = -\frac{\partial E}{\partial y^{(4)}}\frac{\partial y^{(4)}}{\partial y_m^{(3)}} = \delta^{(4)} w_m^2 \tag{26}$$

and the update law of c_{jm} is

$$\begin{aligned} \Delta c_{jm} &= -\eta_m \frac{\partial E}{\partial c_{jm}} = -\eta_m \frac{\partial E}{\partial y^{(4)}}\frac{\partial y^{(4)}}{\partial y_m^{(3)}}\frac{\partial y_m^{(3)}}{\partial c_{jm}} \\ &= 2\eta_m \delta_m^{(3)} \frac{\left(y_j^{(2)} - c_{jm}\right)}{\sigma_{jm}^2} \prod_{j=1}^{k} \exp\left[\frac{-\left(y_j^{(2)} - c_{jm}\right)^2}{\sigma_{jm}^2}\right] \end{aligned} \tag{27}$$

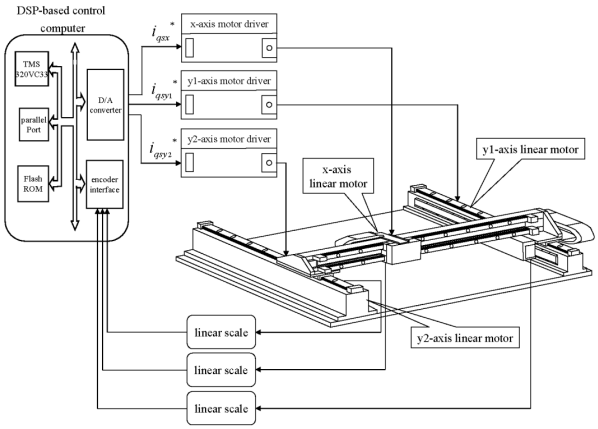

Figure 3. Block diagram of DSP-based control system.

where the factor η_m is the learning rate of the mean. The update law of σ_{jm} is

$$\begin{aligned}\Delta\sigma_{jm} &= -\eta_\sigma \frac{\partial E}{\partial c_{jm}} = -\eta_\sigma \frac{\partial E}{\partial y^{(4)}}\frac{\partial y^{(4)}}{\partial y_m^{(3)}}\frac{\partial y_m^{(3)}}{\partial \sigma_{jm}} \\ &= 2\eta_\sigma \delta_m^{(3)} \frac{\left(y_j^{(2)} - c_{jm}\right)^2}{\sigma_{jm}^3}\prod_{j=1}^{k}\exp\left[\frac{-\left(y_j^{(2)} - c_{jm}\right)^2}{\sigma_{jm}^2}\right]\end{aligned} \tag{28}$$

where the factor η_σ is the learning rate of the standard derivation. The mean c_{jm} and the standard derivation σ_{jm} of the Gaussian function are updated as follows:

$$c_{jm}(n+1) = c_{jm}(n) + \Delta c_{jm} \tag{29}$$

$$\sigma_{jm}(n+1) = \sigma_{jm}(n) + \Delta\sigma_{jm} \tag{30}$$

Layer 2:

The error term propagated in this layer is derived as

$$\begin{aligned}\delta_j^{(2)} &= -\frac{\partial E}{\partial y_j^{(2)}} = -\frac{\partial E}{\partial y^{(4)}}\frac{\partial y^{(4)}}{\partial y_m^{(3)}}\frac{\partial y_m^{(3)}}{\partial y_j^{(2)}} \\ &= \delta_m^{(3)} \frac{(-2)\left(y_j^{(2)} - c_{jm}\right)^2}{\sigma_{jm}^2}\prod_{j=1}^{k}\exp\left[\frac{-\left(y_j^{(2)} - c_{jm}\right)^2}{\sigma_{jm}^2}\right]\end{aligned} \tag{31}$$

According to (31), the connective weight is updated by the amount

$$\Delta w_{Mj}^1 = -\eta_2 \frac{\partial E}{\partial w_{Mj}^1} = -\eta_2 \frac{\partial E}{\partial y^{(4)}}\frac{\partial y^{(4)}}{\partial y_m^{(3)}}\frac{\partial y_m^{(3)}}{\partial y_j^{(2)}}\frac{\partial y_j^{(2)}}{\partial w_{Mj}^1} = \eta_2 \delta_j^{(2)} \phi_M \tag{32}$$

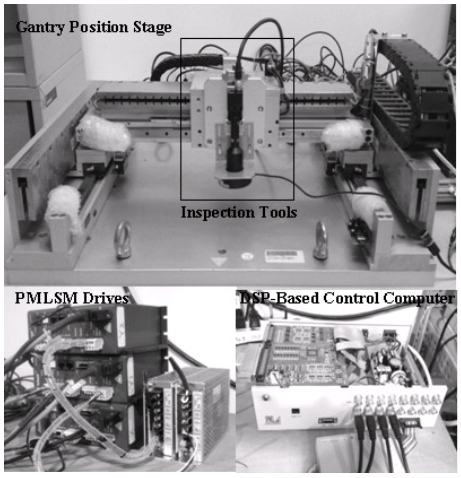

Figure 4. Photos of experimental setup.

TABLE I. EXPERIMENTAL CASES.

	reference trajectories				loads (add iron disk on the moving table)
	sinusoid		trapezoid		
	frequency	stroke	frequency	stroke	
Case 1	0.2Hz	±4*mm*	0.2Hz	4*mm*	0kg
Case 2	0.6Hz	±6*mm*	0.6Hz	6*mm*	7.32kg
Case 3	1Hz	±10*mm*	1Hz	10*mm*	10kg

where the factor η_2 is the learning rate of the connective weight in layer 2. The connective weight w_{Mj}^1 is updated according to the following equation:

$$w_{Mj}^1(n+1) = w_{Mj}^1(n) + \Delta w_{Mj}^1 \tag{33}$$

The exact calculation of the Jacobian of the system, $\partial d / \partial y^{(4)}$, is difficult to be determined due to the unknown dynamics of the PMLSM servo drive system. In this study, a linear combination of the cross-coupled position tracking error and its first derivative is adopted to approximate the Jacobian of the system in order to simplify the on-line adaption laws of the FLRBFN in practical applications as follows:

$$\delta^{(4)} \cong e^* + \dot{e}^* \tag{34}$$

IV. EXPERIMENTAL RESULTS

The block diagram of the DSP-based computer control dual linear motors servo system is shown in Fig. 3. A TMS320VC33 floating-point DSP is the core of the control computer. The photos of the experimental setup including the dual linear motors servo system installed in the gantry position stage, the motor drives and the control computer using DSP are shown in Fig. 4. To investigate the effectiveness of the proposed DSP-based control system with different test signals, strokes and load conditions, three cases as shown in Table I are

considered. The experimental results of the tracking response, control effort and tracking error of the three test conditions are shown in Fig. 5 and Fig. 6, respectively. From the results, the excellent control performance of the proposed cross-coupled FLRBFN control system under the occurrence of parameter variations and different trajectories are obvious owing to on-line learning.

V. CONCLUSIONS

The major contributions of this study are: (i) the successful development of an on-line trained FLRBFN which combines the merits of FLNN and RBFN; (ii) the successful implementation the intelligent control approach and the cross-coupled technology in a control computer which is based on a 32-bit floating-point DSP, TMS320VC33; (iii) the successful application of the cross-coupled FLRBFN control system to dual linear motors servo system to track different reference trajectories with robust control performance.

ACKNOWLEDGMENT

The authors would like to acknowledge the financial support of the National Science Council of Taiwan, R.O.C. through its grant NSC 97-2221-E-008-098-MY3.

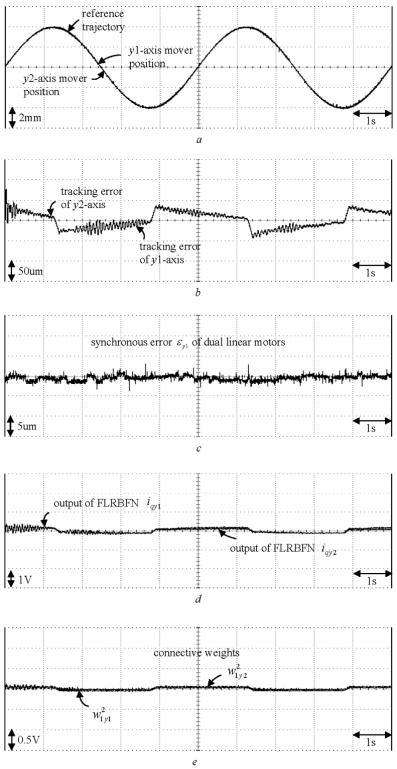

Figure 5. Experimental results of cross-coupled FLRBFN controller with for periodical sinusoidal reference trajectory: (a) Tracking responses of y1-axis and y2-axis at Case 1. (b) Tracking errors of y1-axis and y2-axis at Case 1. (c) Synchronous error of dual linear motors at Case 1. (d) Outputs of two FLRBFNs at Case 1. (e) Connective weights of two FLRBFNs at Case 1.

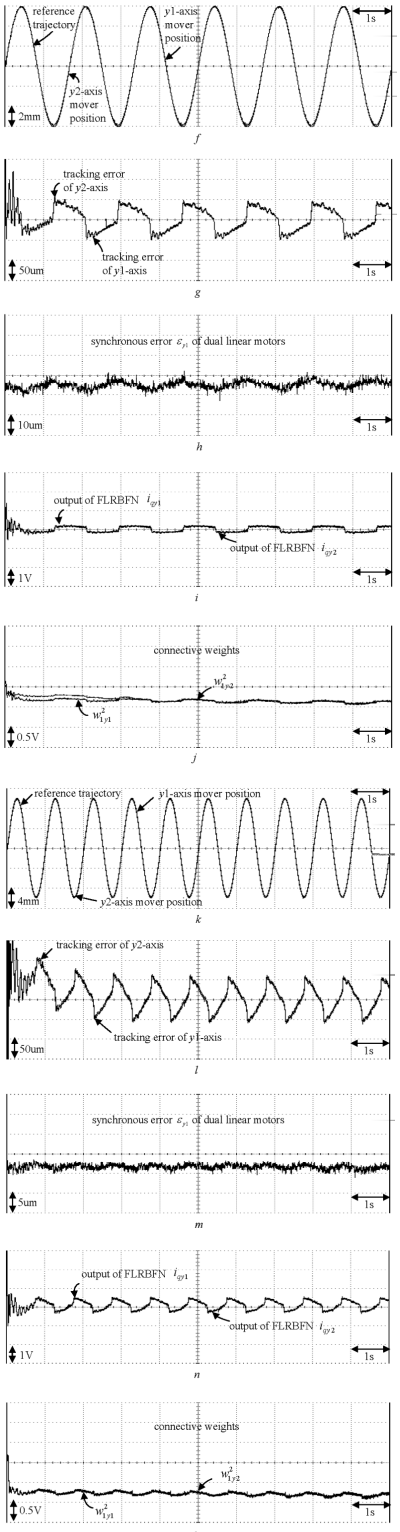

Figure 5. (Cont.) Experimental results of cross-coupled FLRBFN controller with for periodical sinusoidal reference trajectory: (f) Tracking responses of y1-axis and y2-axis at Case 2. (g) Tracking errors of y1-axis and y2-axis at Case 2. (h) Synchronous error of dual linear motors at Case 2. (i) Outputs of two FLRBFNs at Case 2. (j) Connective weights of two FLRBFNs at Case 2. (k) Tracking responses of y1-axis and y2-axis at Case 3. (l) Tracking errors of y1-axis and y2-axis at Case 3. (m) Synchronous error of dual linear motors at Case 3. (n) Outputs of two FLRBFNs at Case 3. (o) Connective weights of two FLRBFNs at Case 3.

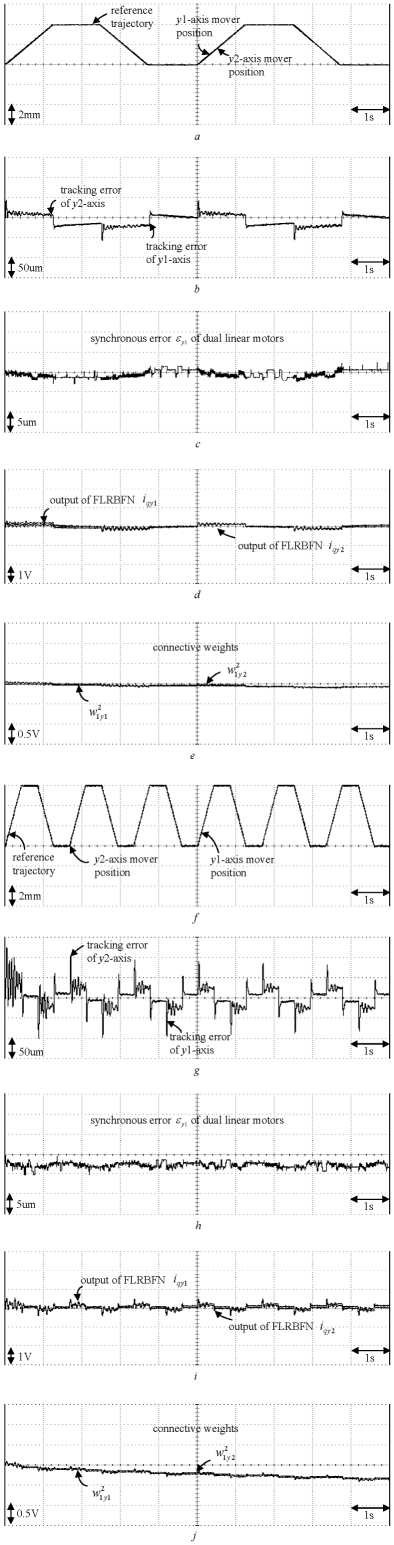

Figure 6. Experimental results of cross-coupled FLRBFN controller with for periodical trapezoidal reference trajectory: (a) Tracking responses of y1-axis and y2-axis at Case 1. (b) Tracking errors of y1-axis and y2-axis at Case 1. (c) Synchronous error of dual linear motors at Case 1. (d) Outputs of two FLRBFNs at Case 1. (e) Connective weights of two FLRBFNs at Case 1. (f) Tracking responses of y1-axis and y2-axis at Case 2. (g) Tracking errors of y1-axis and y2-axis at Case 2. (h) Synchronous error of dual linear motors at Case 2. (i) Outputs of two FLRBFNs at Case 2. (j) Connective weights of two FLRBFNs at Case 2.

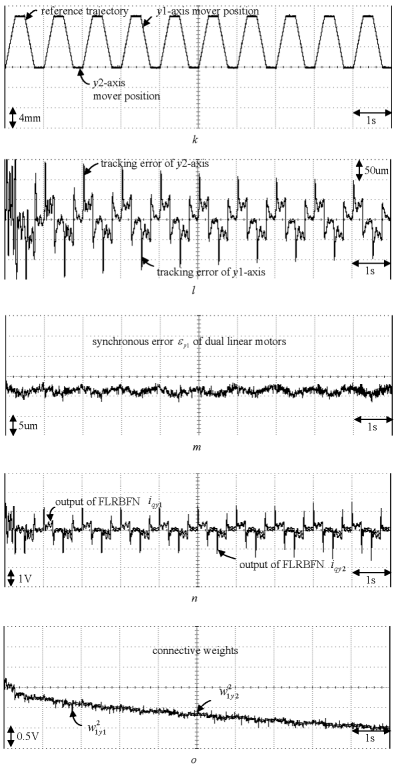

Figure 6. (Cont.) Experimental results of cross-coupled FLRBFN controller with for periodical trapezoidal reference trajectory: (k) Tracking responses of y1-axis and y2-axis at Case 3. (l) Tracking errors of y1-axis and y2-axis at Case 3. (m) Synchronous error of dual linear motors at Case 3. (n) Outputs of two FLRBFNs at Case 3. (o) Connective weights of two FLRBFNs at Case 3.

REFERENCES

[1] O. Sawodnya, H. Aschemannb, and S. Lahres, "An automated gantry crane as a large workspace robot," *Control Engineering Practice*, vol. 10, pp. 1323-1338, 2002.

[2] M. T. Yan, M. H. Lee, and P. L. Yen, "Theory and application of a combined self-tuning adaptive control and cross coupling control in a retrofit milling machine," *IEEE/ASME Trans. Mechatronics*, vol. 15, no. 2, pp. 193-211, 2005.

[3] D. Sun, "Position synchronization of multiple motion axes with adaptive coupling control," *Automatica*, vol. 39, no. 3, pp. 997-105, 2003.

[4] T. L. Chien, C. C. Chen, Y. C. Huang, and W. J. Lin, "Stability and almost disturbance decoupling analysis of nonlinear system subject to feedback linearization and feedforward neural network controller," *IEEE Trans. Neural Network*s, vol. 19, no. 7, pp.1220-1230, 2008.

[5] J. S. R. Jang, C. T. Sun, and E. Mizutani, *Neuro-fuzzy and soft computing: a computational approach to learning and machine intelligence*, Prentice-Hall, NJ, 1997.

[6] X. Hong, "Modified radial basis function neural network using output transformation," *IET Control Theory and Applications*, vol. 1, no. 1, pp. 1-8, 2007.

[7] J. C. Patra and A. C. Kot, "Nonlinear dynamic system identification using Chebyshev functional link artificial neural networks," *IEEE Trans. Syst., Man, and Cybern. B*, vol. 32, no. 4, pp. 505-511, 2002.

[8] F. J. Lin, P. H. Shen, P. H. Chou, and S. L. Yang, "TSK-type recurrent fuzzy network for DSP-based permanent magnet linear synchronous motor servo drive," *IEE Proc. Electric Power Application*, vol. 153, no. 6, pp. 921-931, 2006.

2011 IEEE International Conference on Fuzzy Systems
June 27-30, 2011, Taipei, Taiwan

An Interactive Fuzzy Satisficing Method for Multiobjective Stochastic Defensive Location Problems

Takeshi Uno
Institute of Socio-Arts and Sciences,
The University of Tokushima
1-1, Minamijosanjima-cho,
Tokushima, 770-8502, JAPAN
Email: uno@ias.tokushima-u.ac.jp

Kosuke Kato
Faculty of Applied Information Science,
Hiroshima Institute of Technology
2-1-1, Miyake, Saeki-ku,
Hiroshima, 731-5193, JAPAN
Email: k.katoh.me@it-hiroshima.ac.jp

***Abstract*—This paper extends the defensive location problem (DLP), proposed by Uno and Katagiri, considering the situations that the defender locates defensive facilities for preventing invaders from reaching some important vertices in a network. Their DLPs assumed that invaders, with a given energy, exist on a given vertex in it. On the other hand, this paper considers a new DLP that invaders' sites and energies are given uncertainly. By representing their existing vertices and energies as random variables with scenarios, the new DLP can be formulated as a multiobjective bilevel stochastic programming problem. In order to find a satisficing solution of the decision maker for the multiobjective DLP, an interactive fuzzy satisficing method with tabu search algorithm based on strategic oscillation is proposed. The efficiency of the proposed method is shown by applying it to numerical examples of the DLPs.**

***Index Terms*—Facility location, Stackelberg equilibrium, stochastic programming, multiobjective programming, tabu search.**

I. Introduction

Defensive location problem (DLP), proposed by Uno and Katagiri [12], is one of the bilevel location problems in a competitive environment. Hakimi [4] considered a bilevel location problem of commercial facilities, e.g. shops and supermarkets, on a network. His problem deals with a type of competitiveness between two decision makers (DMs) locating their own facilities, with the aim of maximizing her/his profit obtaining from their customers. For the detail of Hakimi's problem and its applications, the readers can refer to the book of Miller et al. [8]. As an extension of Hakimi's location problem, Shiode and Drezner [11] considered a problem with random demands, Uno et al [13] considered a problem with fuzzy random demands, and Yang et al [14] considered a bilevel flow interception problem. Meanwhile, O'Hanley and Church [9] considered a bilevel maximum covering problem, which is a noncompetitive type of location problem.

On the other hand, the DLP deals with another type of competitiveness between two types of decision makers, called a defender and invader. Uno and Katagiri [12] considered the situation that the defender locates defensive facilities for preventing the invaders from reaching some important sites, called cores. Examples of their DLPs are "a government of a country locates self-defense bases to prevent her/his aggressors from reaching the capital of the country," "a coach of a succor/football team locates its players to defend goal from its opponent team," etc. By representing the location region as a network and the core is a vertex in the network and the defender and the invaders as an upper and a lower DM, their DLP can be formulated as a bilevel programming problem. An example of DLPs is illustrated in Fig. 1.

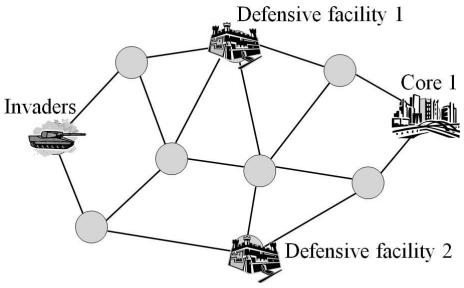

Fig. 1. An example of DLPs

Although the DLP can be expected for many situations that there are both a defender and invaders, their DLP assumed that the site of invaders is on a given vertex and their energy is a given value. This means that their DLP cannot deal with the situations that there are several vertices with several types of invaders given uncertainly, e.g., the defender locates fire stations for preventing that wildfire, which can be regarded as invaders, marching toward important sites. Then, in this paper, we consider a new DLP that invaders' sites and energies are given uncertainly. By representing their existing vertices and energies as random variables with scenarios, the new DLP can be formulated as a multiobjective bilevel stochastic programming problem. We define each objective function of the DLP as minimizing the degree of invasion for each core

978-1-4244-7316-8/11/$26.00 ©2011 IEEE

under a probability given by the defender.

In order to find a satisficing solution for the defender, we apply an interactive fuzzy satisficing method in order to find a satisficing solution for multiobjective linear fractional programming problems. As other applications of the method, Katagiri et al [6] considered multiobjective fuzzy random linear programming problems whose objectives are possibility and probability, and Kato et al [7] considered fractile criterion optimization for multiobjective stochastic integer programming problems. For applying the method to the multiobjective DLP, we need to solve minimax problems for finding M-Pareto optimal solutions, which are candidates of satisficing solutions. We propose its solution method based upon tabu search algorithm proposed by Glover [3]; for the details of algorithm, the readers can refer to the book of Reeves [10]. Since there are many M-Pareto optimal solutions, in order to solve the problem efficiently, we introduce the algorithm to the idea of strategic oscillation, suggested by Hanafi and Freville [5], by utilizing characteristics of DLPs. We show an efficiency of the method by applying it to examples of the multiobjective DLPs.

The remaining structure of this article is organized as follows: In Section 2, we formulate an extended DLP as a multiobjective bilevel stochastic programming problem. We propose an interactive fuzzy satisficing method for finding a satisficing solution of the defender in Section 3. For solving minimax problems in the method, we propose a tabu search algorithm with strategic oscillation in Section 4. In Section 5, we show the efficiency of the interactive fuzzy satisficing method by applying it to examples of the DLPs. Finally, concluding comments and future extensions are summarized in Section 6.

II. Formulation of stochastic DLP

We represent a location region as network $N = (V, E)$, where $V = \{v_1, \ldots, v_n\}$ is a set of n vertices and E is a set of edges. For edge $e \in E$, let $d(e)$ be its weight, meaning the distance between vertices with e. In the network N, there are k core vertices, denoted by $c_1, \ldots, c_k \in V$. that the defender needs to defend from the invader.

In the new DLP, first the defender locates her/his defensive facilities before a scenario is determined., and then the invaders choose sets of paths with knowing a determined scenario. The defender can locate at most one defensive facility on each vertex in V. For i-th vertex, let $q_i \in \{0, 1\}$ denote the variable such that $q_i = 1$ if a defensive facility is located on v_i and $q_i = 0$ otherwise. Then the decision vector of the DLP for the defender can be represented as $\boldsymbol{q} := (q_1, \ldots, q_n)^T$.

On the other hand, sites of the invaders are given randomly with scenarios, whose set are denoted by S. For each scenario $s \in S$, the set of the invaders' sites and their energies are given as $\Xi(s) \subseteq V$ and $\gamma(\xi), \xi \in \Xi(s)$, respectively, Let p_h^ξ be the path ξ to h-th core c_h. Then, for scenario s and h-th core, the decision vector of the DLP for the invader can be represented as $\boldsymbol{p}_h(s) = \{p_h^\xi | \xi \in \Xi(s)\}$.

We define the degree of invasion for h-th core as the following function:

$$f_h(\boldsymbol{q}, \boldsymbol{p}_h(s)|s) := \\ 0 \vee \max_{\xi \in \Xi(s)} \{\gamma(\xi) - D(p_h^\xi) - \beta \cdot W(\boldsymbol{q}, p_h^\xi)\}, \tag{1}$$

where

$$D(\boldsymbol{p}_h(s)) := \sum_{e \in p_h^\xi} d(e), \tag{2}$$

β is a given positive number meaning the capacity that a defensive facility can reduce the energy of invaders on ξ, and $W(\boldsymbol{q}, p_h^\xi)$ is the number of facilities in p_h^ξ. Equation (1) is the objective function of the invader for scenario s and h-th core. Hence the invaders have k objective function for each scenario.

On the other hand, Since the defender needs to decide her/his location before a scenario is determined, an objective function value of the defender for h-th core can be represented as a random variable whose value for each scenario s is $f_h(\boldsymbol{q}, \boldsymbol{p}_h(s)|s)$. By integrating decision vectors of the invaders for all scenarios , we represent paths to h-th core as a random path as $\bar{\boldsymbol{p}}_h$. Then, the objective function of the defender for h-th core is denoted by $\bar{f}_h(\boldsymbol{q}, \bar{\boldsymbol{p}}_h)$, Hence the defender has k objective functions.

Next we represent feasible sets of the defender and the invaders. For the defender, we set m linear constraints represented as follows:

$$A\boldsymbol{q} \leq \boldsymbol{b}, \tag{3}$$

where

$$A := (\boldsymbol{a}_1, \ldots, \boldsymbol{a}_m)^T = \begin{pmatrix} a_{11} & \ldots & a_{1n} \\ \vdots & \ddots & \vdots \\ a_{m1} & \ldots & a_{mn} \end{pmatrix}, \tag{4}$$

$$\boldsymbol{b} := (b_1, \ldots, b_m)^T, \tag{5}$$

and $a_{ij}, b_i \geq 0$ for any $i = 1, \ldots, m, j = 1, \ldots, n$. Hence the feasible set of the defender can be represented as follows:

$$SD := \{\boldsymbol{q} \in \{0, 1\}^n | \boldsymbol{A}\boldsymbol{q} \leq \boldsymbol{b}\}. \tag{6}$$

On the other hand, the feasible set of the invader for scenario $s \in S$ and h-th core can be regarded as the family of sets of paths from all vertices in $\Xi(s)$ to c_h, denoted by $SI_h(s)$. Therefore, the extending DLP can be formulated as the following stochastic bilevel programming problem:

$$\left.\begin{array}{ll} \underset{\boldsymbol{q}}{\text{minimize}} & \left(\bar{f}_1(\boldsymbol{q}, \bar{\boldsymbol{p}}_1), \ldots, \bar{f}_k(\boldsymbol{q}, \bar{\boldsymbol{p}}_k)\right)^T \\ \text{where} & \bar{\boldsymbol{p}}_1, \ldots, \bar{\boldsymbol{p}}_k \text{ solve} \\ \underset{\boldsymbol{p}_h(s)}{\text{maximize}} & f_h(\boldsymbol{q}, \boldsymbol{p}_h(s)|s), \\ & \qquad \forall s \in S, \forall h = 1, \ldots, k \\ \text{subject to} & \boldsymbol{q} \in SD, \\ & \boldsymbol{p}_h(s) \in SI_h(s), \\ & \qquad \forall s \in S, \forall h = 1, \ldots, k. \end{array}\right\} \tag{7}$$

For solving (7), we give $\sigma_h \in (0, 1]$, $h = 1, \ldots, k$ for each core, meaning the probability that the defender wants to guarantee for invasion to each core. Then, we transform

(7) to the following bilevel programming problem by using k auxiliary variables $\alpha_1(\boldsymbol{q}), \ldots, \alpha_k(\boldsymbol{q})$:

$$\left.\begin{array}{ll} \underset{\boldsymbol{q}}{\text{minimize}} & (\alpha_1(\boldsymbol{q}), \ldots, \alpha_k(\boldsymbol{q}))^T \\ \text{subject to} & Pr\left(\bar{f}_1(\boldsymbol{q}, \bar{\boldsymbol{p}}_1) \leq \alpha_1(\boldsymbol{q})\right) \geq \sigma_1, \\ & \qquad \vdots \\ & Pr\left(\bar{f}_k(\boldsymbol{q}, \bar{\boldsymbol{p}}_k) \leq \alpha_k(\boldsymbol{q})\right) \geq \sigma_k, \\ \text{where} & \bar{\boldsymbol{p}}_1, \ldots, \bar{\boldsymbol{p}}_k \text{ solve} \\ \underset{\boldsymbol{p}_h(s)}{\text{maximize}} & f_h(\boldsymbol{q}, \boldsymbol{p}_h(s)|s), \\ & \qquad \forall s \in S, \forall h = 1, \ldots, k \\ \text{subject to} & \boldsymbol{q} \in SD, \\ & \boldsymbol{p}_h(s) \in SI_h(s), \\ & \qquad \forall s \in S, \forall h = 1, \ldots, k. \end{array}\right\} \quad (8)$$

III. Interactive fuzzy satisficing method

For h-th core, $h = 1, \ldots, k$, we provide a satisfaction level of the defender for each objective function as the following linear membership function:

$$\mu_h(\alpha_h(\boldsymbol{q})) = \begin{cases} 1, & \alpha_h(\boldsymbol{q}) \leq \alpha_h^1, \\ \dfrac{\alpha_h(\boldsymbol{q}) - \alpha_h^1}{\alpha_h^0 - \alpha_h^1}, & \alpha_h^1 \leq \alpha_h(\boldsymbol{q}) \leq \alpha_h^0, \\ 0, & \alpha_h^0 \leq \alpha_h(\boldsymbol{q}), \end{cases} \quad (9)$$

where α_h^1 means the infimum of k-th objective function value satisfying the defender sufficiently, and α_h^0 the supremum of that no satisfying her/him.

For estimating all satisfaction levels for objective functions simultaneously, we use the concept of M-Pareto optimal solutions.

Definition 1: $\boldsymbol{q}^*$ is called an M-Pareto optimal solution to (8) if and only if there does not exist another $\boldsymbol{q}$ such that $\mu_h(\alpha_h(\boldsymbol{q})) \geq \mu_h(\alpha_h(\boldsymbol{q}^*))$ for all $h = 1, \ldots, k$ and $\mu_{h'}(\alpha_{h'}(\boldsymbol{q})) \neq \mu_{h'}(\alpha_{h'}(\boldsymbol{q}^*))$ for at least one $h' \in \{1, \ldots, k\}$.

Interactive fuzzy satisficing method is a method to find a satisficing solution among a set of M-Pareto optimal solutions by utilizing information of M-Pareto optimal solutions computed on the way of this method. We propose the interactive fuzzy satisficing method to the multi-objective DLPs in order to find a satisficing solution for the defender among a set of M-Pareto optimal solutions. Let $(\bar{\mu}_1, \ldots, \bar{\mu}_k)$ be a k-tuple of reference membership levels of membership functions $\mu_1, \ldots, \mu_k$, respectively.

Interactive fuzzy satisficing method for the stochastic DLPs

Step 1: Set membership function (9) for each $h = 1, \ldots, k$ by giving α_h^1 and α_h^0.

Step 2: Set initial reference membership levels $(\bar{\mu}_1, \ldots, \bar{\mu}_k) = (1, \ldots, 1)$.

Step 3: For the given $(\bar{\mu}_1, \ldots, \bar{\mu}_k)$, solve the following corresponding minimax problem:

$$\left.\begin{array}{ll} \underset{\boldsymbol{q}}{\text{minimize}} & \max\limits_{h=1,\ldots,k}\{\bar{\mu}_h - \mu_h(\alpha_h(\boldsymbol{q})) \\ & \qquad + \rho \sum\limits_{l=1}^{k} (\bar{\mu}_l - \mu_l(\alpha_l(\boldsymbol{q})))\} \\ \text{subject to} & Pr\left(\bar{f}_1(\boldsymbol{q}, \bar{\boldsymbol{p}}_1) \leq \alpha_1(\boldsymbol{q})\right) \geq \sigma_1, \\ & \qquad \vdots \\ & Pr\left(\bar{f}_k(\boldsymbol{q}, \bar{\boldsymbol{p}}_k) \leq \alpha_k(\boldsymbol{q})\right) \geq \sigma_k, \\ \text{where} & \bar{\boldsymbol{p}}_1, \ldots, \bar{\boldsymbol{p}}_k \text{ solve} \\ \underset{\boldsymbol{p}_h(s)}{\text{maximize}} & f_h(\boldsymbol{q}, \boldsymbol{p}_h(s)|s), \\ & \qquad \forall s \in S, \forall h = 1, \ldots, k \\ \text{subject to} & \boldsymbol{q} \in SD, \\ & \boldsymbol{p}_h(s) \in SI_h(s), \\ & \qquad \forall s \in S, \forall h = 1, \ldots, k, \end{array}\right\} \quad (10)$$

where ρ is a sufficiently small positive number.

Step 4: If the defender is satisfied by the given solution of (10), then it is a satisficing solution of the defender. Otherwise, ask the defender to update $(\bar{\mu}_1, \ldots, \bar{\mu}_k)$ by considering the current membership function values, and return to Step 3.

The following theorem introduces an important relationship between (8) and (10).

Theorem 1: (i) If $\boldsymbol{q}^* \in SD$ is an optimal solution of (10) with some $(\bar{\mu}_1, \ldots, \bar{\mu}_k)$, then $\boldsymbol{q}^*$ is also an M-Pareto optimal solution of (8).
(ii) If $\boldsymbol{q}^* \in SD$ is an M-Pareto optimal solution of (8), then there exists $(\bar{\mu}_1, \ldots, \bar{\mu}_k)$ such that $\boldsymbol{q}^*$ is an optimal solution of (10).

Proof: (i) if $\boldsymbol{q}^*$ is not an M-Pareto optimal solution of (8), then there exist a solution $\boldsymbol{q}$ such that $\mu_h(\alpha_h(\boldsymbol{q})) \geq \mu_h(\alpha_h(\boldsymbol{q}^*))$ for all $h = 1, \ldots, k$ and $\mu_{h'}(\alpha_{h'}(\boldsymbol{q})) \neq \mu_{h'}(\alpha_{h'}(\boldsymbol{q}^*))$ for at least one $h' \in \{1, \ldots, k\}$. This means that $\boldsymbol{q}$ is better than $\boldsymbol{q}^*$ for (10) with any $(\bar{\mu}_1, \ldots, \bar{\mu}_k)$, and then this contradicts the optimality of $\boldsymbol{q}^*$.

(ii) if there does not exist $(\bar{\mu}_1, \ldots, \bar{\mu}_k)$ such that $\boldsymbol{q}^*$ is an optimal solution of (10), then for any $(\bar{\mu}_1, \ldots, \bar{\mu}_k)$, there exist a solution $\boldsymbol{q}$ such that $\bar{\mu}_h - \mu_h(\alpha_h(\boldsymbol{q})) \leq \bar{\mu}_h - \mu_h(\alpha_h(\boldsymbol{q}^*))$ for all $h = 1, \ldots, k$ and $\bar{\mu}_{h'} - \mu_{h'}(\alpha_{h'}(\boldsymbol{q})) \neq \bar{\mu}_{h'} - \mu_{h'}(\alpha_{h'}(\boldsymbol{q}^*))$ for at least one $h' \in \{1, \ldots, k\}$. This contradicts that $\boldsymbol{q}^* \in SD$ is an M-Pareto optimal solution of (8). ■

At Step 3 in the above method, we need to find an optimal solution of (10) for updated reference membership levels. In the next section, we propose an efficient solution method for (10).

IV. Tabu search based on strategic oscillation

First, we consider the complexity to solve (10) strictly. For each location $\boldsymbol{q} \in SD$, we need to compute its objective

function values. This means that for each scenario $s \in S$, we need to find the k sets of paths $\boldsymbol{p}_1(s), \ldots, \boldsymbol{p}_k(s)$ so as to minimize $f_1(\boldsymbol{q}, \boldsymbol{p}_1(s)|s), \ldots, f_k(\boldsymbol{q}, \boldsymbol{p}_k(s)|s)$ among all sets of paths from vertices in $\Xi(s)$ to cores $c_1, \ldots, c_k$. We can utilize a version of Warshall-Floyd Algorithm [1] to find such k sets of paths at a polynomial time. However, since the number of defensive locations is 2^n, solving (10) strictly needs enormous computational times for large-scale DLPs. Therefore, we propose an efficient solution method for (10) based upon tabu search algorithm with strategic oscillation.

The tabu search is one of local search methods, which replicates movement from a current solution $\boldsymbol{q}^{\mathrm{now}}$ to a next solution $\boldsymbol{q}^{\mathrm{next}}$. In the proposed method, we define a move as adding/subtracting one to/from an element of $\boldsymbol{q}^{\mathrm{now}}$, and a neighborhood of $\boldsymbol{q}^{\mathrm{now}}$, denoted by $\mathcal{N}(\boldsymbol{q}^{\mathrm{now}})$, as the set of all solutions that can be transferred by only one move from it. From $\mathcal{N}(\boldsymbol{q}^{\mathrm{now}})$, $\boldsymbol{q}^{\mathrm{next}}$ is chosen as the best solution in the sense of a given criterion, e.g. objective function value. However, without modification, a circulation of certain chosen moves may occur on the way of search, and then it only can examine a limited local area. Then, for cases that a move is chosen in the search, the tabu constraint for its opposite move is activated for given tenure, called the tabu tenure and denoted by T_1. Then the activated moves are forbidden to choose, called tabu, even if the moves make the objective function value of (10) best in $\mathcal{N}(\boldsymbol{q}^{\mathrm{now}})$. Tabu are memorized in a tabu list through the search.

Although the tabu search method has the advantage of finding several local optimal solutions efficiently, the feasible set of (10) is generally wide and there are many local optimal solutions in the feasible set. Then, we introduce the concept of strategic oscillation for finding various types of local optimal solutions. The following function, meaning the degree of feasibility for $\boldsymbol{q}$, plays an important role in the strategic oscillation:

$$r(\boldsymbol{q}) := \max_{i=1,\ldots,m} \{\boldsymbol{a}_i \cdot \boldsymbol{q} - b_i\} \tag{11}$$

Tabu search algorithm with strategic oscillation for the stochastic DLPs

- Step 0: Generate the initial searching matrix $\boldsymbol{q}^{\mathrm{now}}$, and initialize the tabu list and other parameters. If $\boldsymbol{q}^{\mathrm{now}} \in SD$, then go to Step 4.
- Step 1: Move $\boldsymbol{q}^{\mathrm{now}}$ to $\boldsymbol{q}^{\mathrm{next}}$ by decreasing an element of $\boldsymbol{q}^{\mathrm{now}}$ for the aim of increasing $r(\boldsymbol{q}^{\mathrm{next}})$ as much as possible. This step is repeated until it is satisfied $r(\boldsymbol{q}^{\mathrm{next}}) \geq 0$, that is $\boldsymbol{q}^{\mathrm{next}} \in SD$.
- Step 2: Move $\boldsymbol{q}^{\mathrm{now}}$ to $\boldsymbol{q}^{\mathrm{next}}$ for the aim of improving the objective function value of (10). This step is repeated at a given tenure, denoted by $T_2 > 0$.
- Step 3: Move $\boldsymbol{q}^{\mathrm{now}}$ to $\boldsymbol{q}^{\mathrm{next}}$ by decreasing an element of $\boldsymbol{q}^{\mathrm{now}}$ for the aim of increasing $r(\boldsymbol{q}^{\mathrm{next}})$ as much as possible. This step is repeated until $r(\boldsymbol{q}^{\mathrm{next}})$ is less than a given value, denoted by r_{low}.
- Step 4: Move $\boldsymbol{q}^{\mathrm{now}}$ to $\boldsymbol{q}^{\mathrm{next}}$ by increasing an element of $\boldsymbol{q}^{\mathrm{now}}$ for the aim of improving the objective function value of (10). This step is repeated until one step short of $r(\boldsymbol{q}^{\mathrm{next}}) < 0$.
- Step 5: Do the same operations as Step 2.
- Step 6: Move $\boldsymbol{q}^{\mathrm{now}}$ to $\boldsymbol{q}^{\mathrm{next}}$ by increasing an element of $\boldsymbol{q}^{\mathrm{now}}$ for the aim of improving the objective function value of (10) without the feasibility of (10). This step is repeated until $r(\boldsymbol{q}^{\mathrm{next}})$ is more than a given value, denoted by r_{upp}.
- Step 7: If the iteration count of the algorithm reaches a given number, denoted by T_3, then terminate. Otherwise, return to Step 1.

V. Numerical experiments

This section shows the efficiency of the method introduced in the previous sections by applying to a given numerical example of the stochastic multiobjective DLP. We consider the DLP on network $N = (V, E)$, where V and E have $n = 100$ vertices and 1000 edges, respectively, and there are $k = 3$ cores in V. For each edge $e \in E$, w_e is given a value in $\{1, \ldots, 100\}$ randomly.

For the defender, the capacity of the defensive facility is $\beta = 30$, and there are the following $m = 30$ constraints: for (4), each a_{ij}, $i = 1, \ldots, m$ and $j = 1, \ldots, n$, is given as a value in $\{1, \ldots, 100\}$ randomly, and

$$b_i = \theta_i \cdot \sum_{j=1}^{n} a_{ij}, \tag{12}$$

where θ_i, $i = 1, \ldots, m$ is a given value in $[0.1, 0.3]$ randomly. For (8), we set $\sigma_h = 0.7$, $h = 1, 2, 3$.

For the invaders, we give $s = 3$ scenarios each of whose possibilities is given randomly. For each scenario, their sites, number of vertices, and their initial energies are given in N, $\{1, \ldots, 3\}$, and $[100, 300]$, randomly and respectively.

For the tabu search algorithm in Section IV, we set $T_1 = 20$. In Steps 2 and 4 of the algorithm with strategic oscillation, we set $T_2 = 7$ and $T_3 = 100$, respectively.

For the interactive fuzzy satisficing method in Section III, at Step 0, we define three membership functions μ_1, μ_2, μ_3 whose parameters are $(\alpha_1^L, f_1^U) = (30, 90)$, $(\alpha_2^L, f_2^U) = (40, 120)$, and $(\alpha_3^L, f_3^U) = (60, 200)$, respectively. In this example of the DLP, we assume that the defender regards that c_3 is the most important, c_2 is the second, and c_1 is the last. Then, the defender thinks that she/he hopes to improve μ_3 even if μ_1 and μ_2 are worse, and similarly to improve μ_2 even if μ_1 is worse. TABLE I shows computational results for applying the method to the example of DLP, where we obtain them computed by Dell Studio XPS 8100 (CPU: Inter^R CORE^{TM} i7-860 2.80GHz $\times$ 2, RAM: 6.00GB).

In TABLE I, for the satisfaction levels of the M-Pareto optimal solution obtained at Iteration 1, the defender decreased $\bar{\mu}_1$ and $\bar{\mu}_2$ in order to improve the value of μ_3 at Iteration 2. Then, the defender can obtain the solution improving the value of $\bar{\mu}_3$. However, the solution did not satisfy the defender,

TABLE I
COMPUTATIONAL RESULTS

Iteration	1	2	3	4
$\bar{\mu}_1$	1.0	0.7	0.7	0.7
$\bar{\mu}_2$	1.0	0.9	0.8	0.8
$\bar{\mu}_3$	1.0	1.0	1.0	0.95
$\mu_1(f_1(\boldsymbol{q}^*, \boldsymbol{p}^*))$	0.564	0.356	0.475	0.501
$\mu_2(f_2(\boldsymbol{q}^*, \boldsymbol{p}^*))$	0.570	0.595	0.532	0.570
$\mu_3(f_3(\boldsymbol{q}^*, \boldsymbol{p}^*))$	0.558	0.680	0.747	0.727
CPU Time (seconds)	57.24	54.68	60.77	60.70

because the values of μ_1 for its solution is too bad. Then, at Iteration 3, the defender reduced $\bar{\mu}_2$ a little. Although the values of μ_1 for its solution is recovered, that of μ_2 is too bad. Then, the defender reduced $\bar{\mu}_3$ a little at Iteration 4. As a result, the defender obtained a satisficing solution and the method is terminated.

VI. CONCLUSION

In this paper, we have proposed a new location problem by considering a multiobjective DLP with invaders whose sites are given randomly. By representing a location region as a network, we have formulated the DLP as a stochastic multiobjective bilevel programming problem. For finding its satisficing solution of the defender, we have proposed an interactive fuzzy satisficing method with tabu search algorithm with strategic oscillation. Its efficiency has been shown by applying the proposed method for examples of the DLP.

For the proposed DLP, both the capacity of defensive facilities and the energy of invaders are given determinate values. However, it is often cases that these data include vagueness and ambiguity. Considering the DLP representing these data as fuzzy random variables [6], [13], which can be formulated as a fuzzy random programming problem, is an important future research.

REFERENCES

[1] T. H. Cormen, C. E. Leiserson, R. L. Rivest, *Introduction to algorithms*. MIT Press, 1990.

[2] Z. Drezner, *Competitive Location Strategies for Two Facilities*. Regional Science and Urban Economics, vol.12, vol.3, pp.485-493, 1982.

[3] F. Glover, *Future Paths for Integer Programming and Links to Artificial Intelligence*. Computers & Operations Research, vol.5, pp.533-549, 1986.

[4] S. L. Hakimi, *On Locating New Facilities in a Competitive Environment*. European Journal of Operational Research, vol.12, pp.29-35, 1983.

[5] S. Hanafi, A. Freville, *An Efficient Tabu Search Approach for the 0-1 Multidimensional Knapsack Problem*. European Journal of Operational Research, vol.106, pp.659-675, 1998.

[6] H. Katagiri, M. Sakawa, K. Kato, I. Nishizaki, *Interactive Multiobjective Fuzzy Random Linear Programming: Maximization of Possibility and Probability*. European Journal of Operational Research, vol.188, no.2, pp. 530-539, 2008.

[7] K. Kato, M. Sakawa, H. Katagiri, C. Perkgoz, *An interactive fuzzy satisficing method based on fractile criterion optimization for multiobjective stochastic integer programming problems*. Expert Systems with Applications, vol.37, no.8, pp.6012-6017, 2010.

[8] T. C. Miller, T. L. Friesz, R. L. Tobin, *Equilibrium Facility Location on Networks*, Springer Verlag, Berlin, 1996.

[9] J. R. O'Hanley, R. L. Church, *Designing Robust Coverage Networks to Hedge against Worst-Case Facility Losses*. European Journal of Operational Research, vol.209, no.1, pp.23-36, 2011.

[10] C. R. Reeves, ed., *Modern Heuristic Techniques for Combinatorial Problems*. Blackwell Scientific Press, Oxford, 1993.

[11] S. Shiode, Z. Drezner, *A Competitive Facility Location Problem on a Tree Network with Stochastic Weights*. European Journal of Operational Research, vol. 149, no. 1, pp.47-52, 2003.

[12] T. Uno, H. Katagiri, *Single- and Multi-Objective Defensive Location Problems on a Network*. European Journal of Operational Research, vol.188, no.1, pp.76-84, 2008.

[13] T. Uno, H. Katagiri, K. Kato, *A Stackelberg Location Problem on a Tree Network with Fuzzy Random Demands*. Advances in Intelligent Decision Technologies (eds: G. Phillips-Wren, L.C. Jain, K. Nakamatsu, R.J. Howlett), pp.581-588, Springer, 2010.

[14] J. Yang, M. Zhang, B. He, C. Yang, *Bi-level programming model and hybrid genetic algorithm for flow interception problem with customer choice*. Computers & Mathematics with Applications, vol.57, no.11-12, pp.1985-1994, 2009.

2011 IEEE International Conference on Fuzzy Systems
June 27-30, 2011, Taipei, Taiwan

Robust Speed-Controlled Permanent Magnet Synchronous Motor Drive using Fuzzy Logic Controller

Gunawan Dewantoro
Graduate Institute of Automation and Control
National Taiwan University of Science and Technology
Taipei, Taiwan
gunawan_dewantoro@yahoo.com

Yong-Lin Kuo
Graduate Institute of Automation and Control
National Taiwan University of Science and Technology
Taipei, Taiwan
kuo@mail.ntust.edu.tw

***Abstract*—The Permanent Magnet (PM) Synchronous Motor is ideal in the field of the low power high performance servo, since it is controllable and its vigorous performance is excellent. However, the variations of moment inertia, load torque, and motor internal parameters have been a major difficulty to deal with speed control. This paper investigates the fuzzy logic controller based speed control for a vector-controlled PM synchronous motor drive. The fuzzy logic is based on the speed error and change of speed error measured between the actual motor speed and the reference speed. The robust control performance of the fuzzy logic controller is evaluated for various operating conditions using the parameters of a prototype PM synchronous motor and compared to that of conventional PI controller. The design and application of the fuzzy logic controller are considered and discussed.**

Keywords - fuzzy logic controller; permanent magnet synchronous motor; vector control ; robustness

I. INTRODUCTION

Fuzzy logic can be regarded as a mathematical approach based on intelligent reasoning, probability theory, and multi-valued logic to mimic the human nature in inferring problems. The theoretical development of fuzzy logic has gone through significantly and there have been numerous applications of this mathematical framework to a variety of fields [1]-[3]. In control system, fuzzy logic is considered as an alternative for classical control theory in the control of complex nonlinear plants where accurate mathematical modeling is difficult, if not impossible [2]. At present, fuzzy logic speed controller is renowned with its superior performance in the research community worldwide. It has been demonstrated by various publications with diversity of industrial drive applications such as high performance dc drives [4], vector controlled induction motor [5]-[7], permanent magnet (PM) Synchronous Motor [8]-[12], brushless dc motor [13] and switched reluctance motor [14]. It has been suggested that fuzzy controllers are more robust to plant parameter changes than classical PI controllers. The merit of fuzzy logic control as compared to conventional control approach resides in the fact that there is no need of mathematical models to deal with a problem, but skill is required to create the rules in a particular fuzzy logic controller [1].

Brushless ac servo drives using PM synchronous motor are increasingly utilized in high-performance positioning systems such as in robotics due to their excellent characteristics compared to dc motor or ac induction motor drives. Many researches have been studied the comparison between the operation of drive with speed control by fuzzy logic and PI techniques. Then the main conclusion verified that fuzzy logic control determines superior performance [6], [7], [12]. Vector control is typically used in these drives to improve the dynamic response. However, the papers are focused on the speed performance while only load torque varies. In this paper, a fuzzy logic controller for a vector-controlled PM synchronous motor drive is investigated. It is applied to the speed control with variation of moment inertia, stator resistance, and load torque. As in all variable-controlling schemes, the very ultimate goal is to minimize error between the desired and actual value. Therefore, the error and change of error measured between the actual motor speed and the reference speed are applied to a fuzzy logic adaptation mechanism. This intelligent behavior will force the system to behave a more satisfactory performance than that of conventional PI controller. The robustness to parameters variation of the fuzzy logic controller is evaluated by simulation for various operating conditions using the parameters of a prototype PM synchronous servo drive. The design and implementation of the fuzzy logic controller are considered and discussed.

II. MODELING OF PERMANENT MAGNET SYNCHRONOUS MOTOR DRIVE

A. Drive Configuration

Fig. 1 shows a block diagram of a typical vector-controlled PM synchronous motor drive. The PM synchronous motor is fed by a current-controlled voltage-source pulse width modulated (PWM) inverter. The motor phase currents waveforms are imposed by current controllers having reference input signals generated from rotor position sensor signals. The synchronous motor is thus fed with sinusoidal currents having phase and frequency locked to the rotor position. As a result, synchronism is obtained for all speeds. The motor currents are decomposed into i_d and i_q components which are respectively flux and torque components in the rotor-based d-q coordinates

978-1-4244-7316-8/11/$26.00 ©2011 IEEE

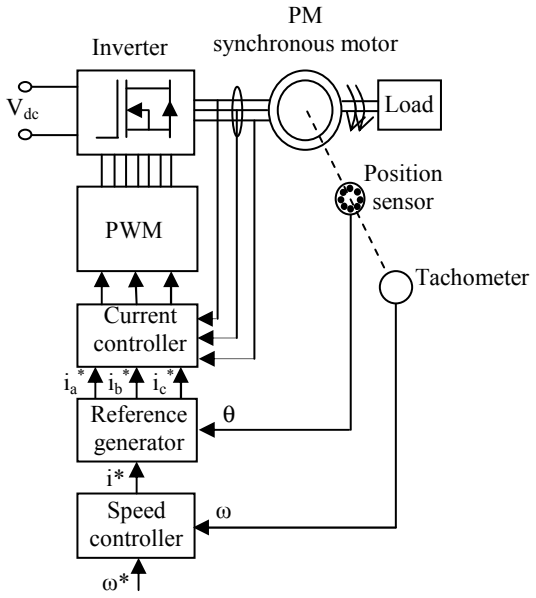

Fig.1 Vector-controlled PM synchronous motor drive

system. Maximum torque is obtained with i_d = 0 which corresponds to the case when the rotor and stator fluxes are perpendicular. The operation of the drive is then similar to that of a current-controlled dc motor.

B. Mathematical Model in d-q frame

In synchronous rotating d-q frame, one might decouple the flux-producing current (I_d) and torque-producing current (I_q). When I_{ds} constant, PM Synchronous Motor might be treated the same as dc motor. Hereafter, the modeling will be conducted in d-q frame. The electrical equation for the PM synchronous motor can be written as

$$V_d = R_s i_d + L_d \frac{\mathrm{d}i_d}{\mathrm{d}t} - \omega_s L_q i_q \quad (1)$$

$$V_q = R_s i_q + L_q \frac{\mathrm{d}i_q}{\mathrm{d}t} + \omega_s \left(L_d i_d + \psi_f\right) \quad (2)$$

By taking Laplace transformation, one might yield

$$\frac{i_d(s)}{V_d(s) + \omega_s L_q i_q(s)} = \frac{1}{(R_s + L_d s)} = \frac{1/R_s}{(\tau_s s + 1)} \quad (3)$$

$$\frac{i_q(s)}{V_q(s) - \omega_s \left(L_d i_d(s) + \psi_f\right)} = \frac{1}{\left(R_s + L_q s\right)} = \frac{1/R_s}{(\tau_s s + 1)} \quad (4)$$

where R_s is the stator resistance, L_d is the direct-axis inductance, L_q is the quadrature-axis inductance, ω_s is the electrical angular speed, ψ_f is the rotor-stator flux linkage, and $\tau_s = \frac{L_d}{R_s} = \frac{L_q}{R_s}$.

The electromechanical torque equation can be expressed as

$$T = \frac{3}{2} p\left[\psi_f i_q + \left(L_d - L_q\right) i_d i_q\right] \quad (5)$$

Since in the case of PM Synchronous Motor, L_d=L_q, (5) can be simplified as

$$T = \frac{3}{2} p \psi_f i_q = k_T i_q \quad (6)$$

The Laplace transformation of (6) is

$$\frac{T(s)}{i_q(s)} = \frac{3}{2} p \psi_f = k_T \quad (7)$$

where p = number of pole pairs.
The dynamic equation is

$$T - T_L = J \frac{d\omega}{dt} + B\omega \quad (8)$$

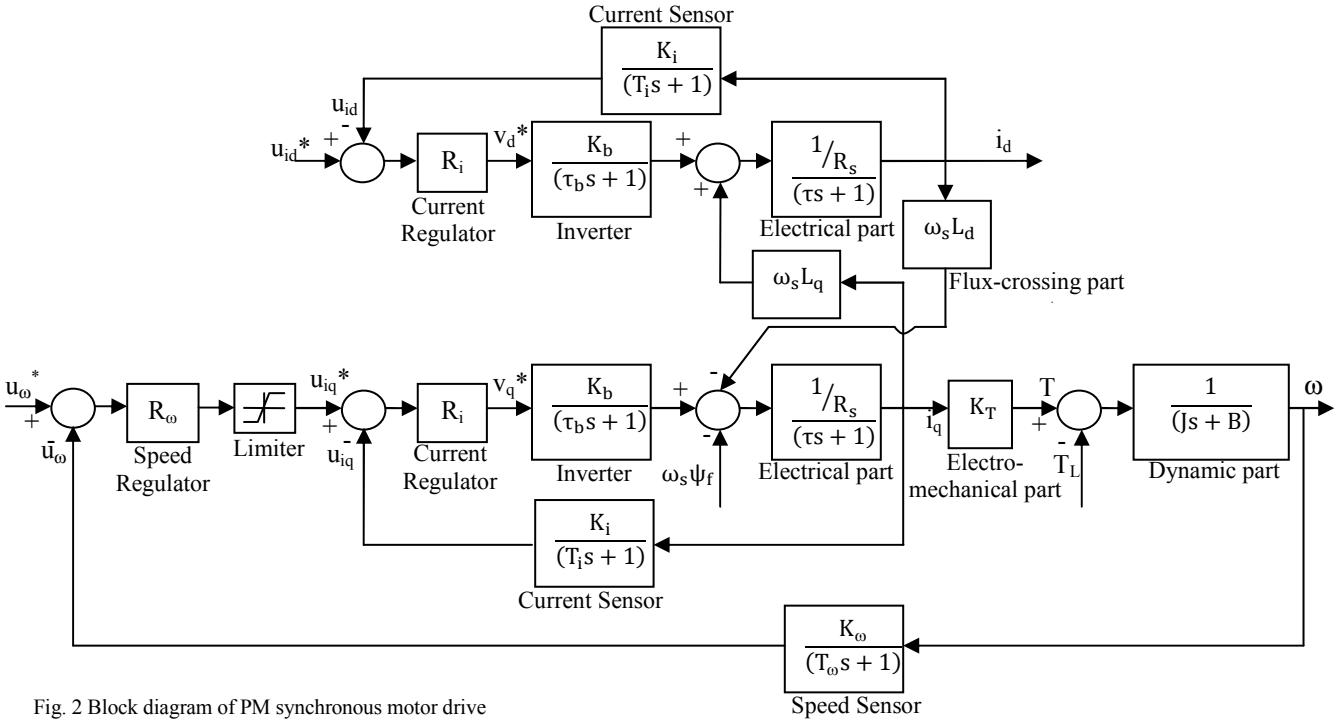

Fig. 2 Block diagram of PM synchronous motor drive

Laplace transformation is taken on (8), yield

$$\frac{\omega(s)}{T(s)-T_L} = \frac{1}{(Js+B)} \tag{9}$$

where, T_L is load torque, J = moment inertia, and B = friction coefficient

C. Block Diagram

An equivalent block diagram can be established according to (1)-(9) as shown in Fig. 2. This drive configuration also contains the transfer functions of speed sensor, current sensor, and inverter. A limiter is aimed to limit the maximum current fed to motor drive for safety concern.

III. Design of Fuzzy Logic Controller

Fig. 3 shows a simplified block diagram of speed control system based on a fuzzy logic controller. This controller has two inputs, namely speed error eω and change in speed error ceω, and one output ci_q* which represents the change in quadrature reference current i_q*.

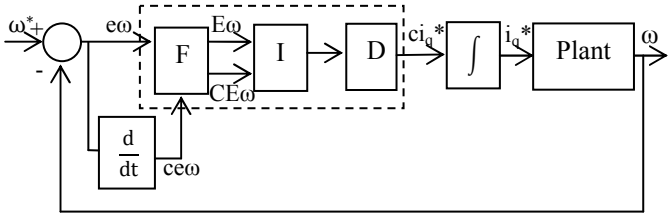

Fig. 3 Diagram block of fuzzy logic speed control scheme

The speed error and change of error are evaluated at instantaneous time as:

$$e\omega = \omega^* - \omega \tag{10}$$

$$ce\omega = \frac{de\omega}{dt} \tag{11}$$

where ω* is the reference speed, and ω is the actual speed. As shown in Fig. 3, the fuzzy logic controller consists of three phases: fuzzification (F), inference (I), and defuzzification (D).

In the first phase, the crisp variables eω and ceω are transformed into fuzzy variables Eω and CEω using triangular membership functions shown in Fig. 4. The universes of discourse of the input fuzzy variables, Eω and CEω, are respectively [-10,10] and [-1.2,1.2]. Whereas, the universe of discourse of the output variable CI_q^* is [-8,8]. For convenience, per-unit scaling factors are utilized to normalize all universe of discourse to [-1,1]. Each universe of discourse is then divided into seven fuzzy sets: NL (Negative Large), NM (Negative Medium), NS (Negative Small), Z (Nearly Zero), PS (Positive Small), PM (Positive Medium), PL (Positive Large). Each fuzzy variable is a member of the subsets with a degree of membership μ varying between 0 (nonmember) and 1 (full member). For example, the degree of membership of element x in fuzzy set Y of the universe of discourse X is expressed as $\mu_Y(x)$ with $0 \le \mu_Y(x) \le 1$

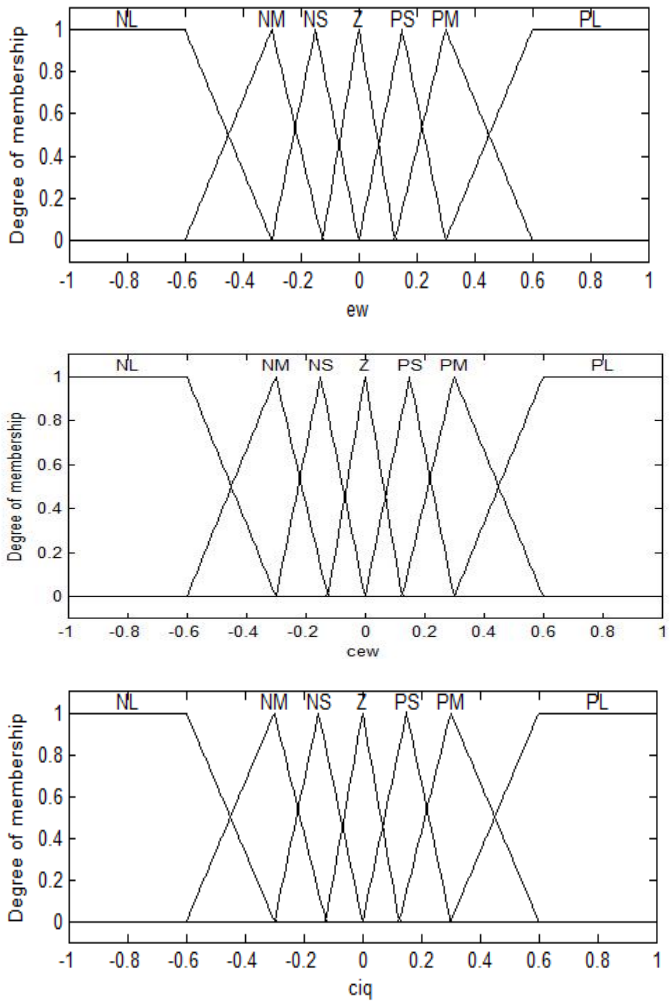

Fig. 4 Membership functions of Eω, CEω, and CI_q^*

In the second phase, in order to determine the controller output from the measured system variables, a fuzzy relation matrix is established. The fuzzy relation matrix gives a relationship between fuzzy set characterizing controller inputs and fuzzy set characterizing controller outputs. The fuzzy variables Eω and CEω are thus processed by an inference engine that performed a set of control rules contained in a (7x7) rule base as shown in Fig. 5.

CEω \ Eω	NL	NM	NS	Z	PS	PM	PL
NL	NL	NL	NL	NL	NM	NS	Z
NM	NL	NL	NL	NM	NS	Z	PS
NS	NL	NL	NM	NS	Z	PS	PM
Z	NL	NM	NS	Z	PS	PM	PL
PS	NM	NS	Z	PS	PM	PL	PL
PM	NS	Z	PS	PM	PL	PL	PL
PL	Z	PS	PM	PL	PL	PL	PL

Fig. 5 Fuzzy control rules

These 7 fuzzy sets of input and output have been chosen to give adaptability during the decision inference. The control rules are formulated using the knowledge of the PM synchronous motor behavior and the experience of control engineers. Each rule is assigned in the form shown in the following example: IF (Eω is Positive Medium) AND (CEω is Negative Large) THEN (CI_q^* is Negative Small). Different inference algorithms can be utilized to produce the fuzzy set values for the output fuzzy variable CI_q^*. In this study, the max-min inference algorithm is utilized in which the membership degree of CI_q^* is equal to the maximum of the minimum between Eω and CEω membership degrees:

$$\mu[(CIq*)_k] = max\,[min\,\{\mu(E\omega_i), \mu(CE\omega_j)\}] \qquad (12)$$

for $1 \le i \le n, 1 \le j \le n$

In the third phase, the inference output variable CI_q^* is transformed back into a crisp value ci_q^*. Various defuzzification algorithms have been proposed in many literatures. Here, the Mamdani centroid defuzzification algorithm is utilized in which the crisp value is calculated as the center gravity of the membership function of CI_q^*:

$$ci_q^* = \frac{\int \mu(CI_q^*) CI_q^* dCI_q^*}{\int \mu(CI_q^*) dCI_q^*} \qquad (13)$$

The reference current i_q^* for the vector control system is obtained by integrating ci_q^*:

$$i_q^* = \int ci_q^*\, dt \qquad (14)$$

IV. Simulation Results

The control performance of the prescribed fuzzy logic controller was evaluated by simulation using a test drive system with the following parameters: P = 1 kW, V_d = 300 V, R_s = 1.4 Ω (including power switch equivalent resistance), L_s = 9.5 mH, J_{min} = 0.03 kgm^2, J_{max} = 0.23 kgm^2, B = 0.4E-3 kgm^2/s.

The parameters that vary are the system moment of inertia, stator resistance, and load torque. To evaluate the effectiveness of the proposed scheme, the step response of the speed control system is obtained for the varying parameters for two cases: (a) conventional PI controller, (b) fuzzy logic controller. All of the approaches described above were simulated in the Simulink environment.

A. Conventional PI Controller

For this study, the PI coefficients for current controller and speed controller are K_p=1 T_i = 0.2, and K_p = 0.8 T_i =0.5, repectively. The obtained results for these cases are presented in Fig. 6.

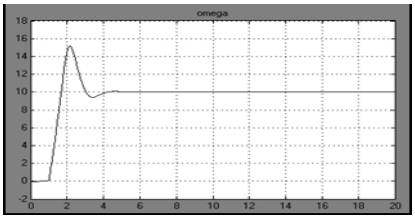

(a)

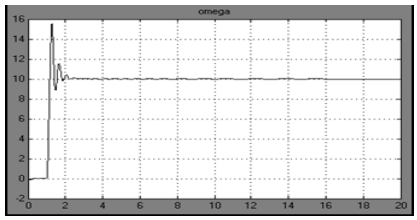

(b)

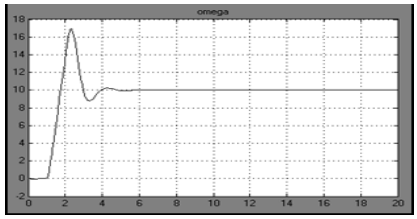

(c)

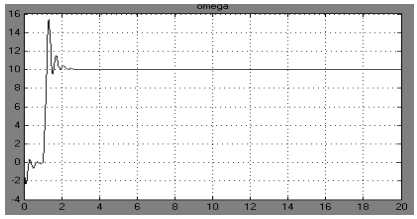

(d)

Fig. 6. Response of the system with PI speed controller
(a) J=0.03 kgm^2 (b) J=0.23 kgm^2 (c) R_s=2.8 Ω (d) T_L=3 Nm

Fig. 6(a) and 6(b) demonstrate the system response with minimum and maximum moment inertia, respectively. It is obvious that the change of moment inertia influences greatly the system performance. As shown in Fig. 6(c), the variation of stator resistance also hurts the overall performance, particularly the extent of overshoot. Fig. 6(d) also shows undesirable ripples when an additional load torque is attached to the PM synchronous motor.

B. Fuzzy Logic Controller

The obtained results for the fuzzy logic based scheme are presented in Fig. 7.

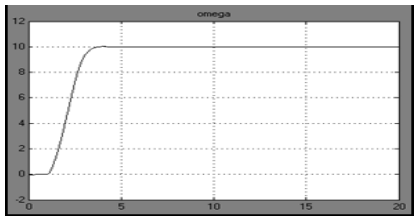

(a)

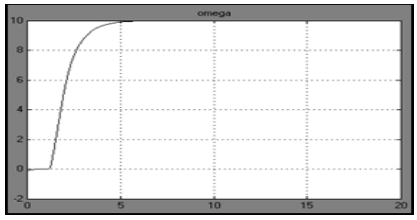

(b)

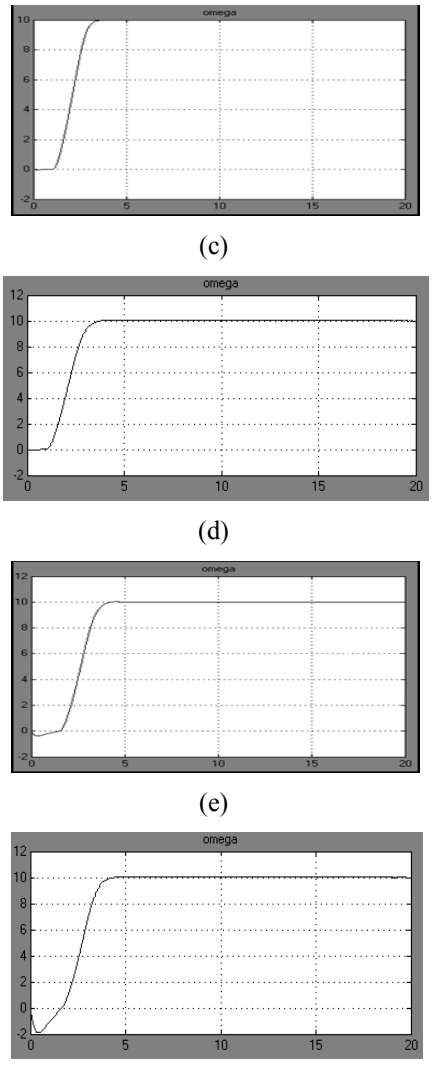

Fig. 7. Response of the system with fuzzy logic controller
(a) J=0.03 kgm^2 (b) J=0.23 kgm^2 (c) R_s=2.8 Ω (d) R_s=4.2 Ω
(e) T_L=3 Nm (f) T_L=6 Nm

Fig. 7(a) and 7(b) show the system response with minimum and maximum moment inertia, respectively. It is shown that the variation of moment inertia affects slightly in the fact that the system response in maximum moment inertia is a little bit more sluggish. However this influence does not hurt the overall performance. As shown in Fig. 7(c) and 7(d), the variation of stator resistance up to 200% is not an issue for fuzzy logic controller. And finally, Fig. 7(3) and 7(f) no longer shows undesirable ripples which occurs for that of PI controller.

V. CONCLUSION

A fuzzy logic control scheme has been studied for the speed control of a vector-controlled PM synchronous motor drive. Speed error and change of speed error measured between the actual motor speed and the reference speed were used as the fuzzy inputs. The simulation results have confirmed the efficiency and robustness of the fuzzy logic controller against the varying moment inertia, stator resistance, and load torque. Due to its simplicity and effortlessness, this scheme is applicable to industrial environment using conventional microprocessor.

REFERENCES

[1] E.H. Mamdani, "Application of fuzzy algorithms for control of simple dynamic plant," Proc. IEE, vol. 121, no. 12, pp. 1585-1588, Dec. 1974.

[2] T. Tagaki and M. Sugeno, "Fuzzy identification of systems and its applications to modeling and control," IEEE Trans. Systems, Man and Cybernetics, vol. SMC-15, pp. 116-132, Jan/Feb 1985.

[3] J. Maiers and Y.S. Sherif, "Applications of fuzzy set theory," IEEE Trans. Systems, Man and Cybernetics, vol. SMC-15, pp. 175-189, Jan/Feb 1985

[4] J. N. Lygouras, P. N. Botsaris, J. Vourvoulakis, V. Kodogiannis, "Fuzzy logic controller implementation for a solar air-conditioning system," Applied Energy 84, vol. 20, pp. 1305-1318, 2007.

[5] V. Kumar, R. R. Joshi, "Hybrid controller based intelligent speed control of induction motor," *Journal of Theoretical and Applied Information Technology*, pp. 71-75, 2005.

[6] H. A. F. Mohamed, W. P. Hew, "A fuzzy logic vector control of induction motor," in *Proc. TECON 2000*, vol. 3, pp. 324-328.

[7] M. N. Uddin, T. S. Radwan, M. A. Rahman, "Performances of fuzzy logic based indirect vector control for induction motor drive," *IEEE Trans. On Industry Applications*, vol. 38, pp. 1219-1225, Sept./Oct. 2002.

[8] A. Karakaya, E. Karakas, "Performance analysis of PM synchronous motors using fuzzy logic and self tuning fuzzy PI speed controls," *The Arabian Journal for Science and Engineering*, vol. 33, pp. 153-177, Apr. 2008.

[9] A. G. Aissaoui, M. Abid, H. Abid, A. Tahour, A. K. Zeblah, "A fuzzy logic controller for synchronous machine," *Journal of Electrical Engineering*, vol. 58, pp. 285-290, 2007.

[10] M. N. Uddin, T. S. Radwan, M. A. Rahman, G. H. George, "Fuzzy logic based position control of permanent magnet synchronous motor," in *Canadian Conference on Electrical & Computer Engineering*, vol. 1, pp. 93-97, 2000.

[11] T. Pham-Dinh, T. Nguyen-Thanh, "Fuzzy speed controller for rotor flux oriented control of permanent magnet synchronous machine," in *Proc. ISEE 2007*, pp. 72-78, Oct 2007.

[12] İ. Güney, Y. Oğuz, F. Serteller, "Dynamic behaviour model of permanent magnet synchronous motor fed by PWM inverter and fuzzy logic controller for stator phase current, flux and torque control of PMSM," in *Proc. IEMDC'01*, pp. 479-485, 2001.

[13] R. N. Tuncay, Z. Erenay, M. Yilmaz, Ö.Ustun, "Rapid control prototyping approach to fuzzy speed control of brushless DC motor," in *Proc. ELECO'03*, Dec 2003.

[14] M. G. Rodrigues, W. I. Suemitsu, P. Branco, J. A. Dente, L. G. B. Rolim, "Fuzzy logic control of a switched reluctance motor," in *Proc. ISIE'97*, vol. 2, pp. 527-531, Jul. 1997.

2011 IEEE International Conference on Fuzzy Systems
June 27-30, 2011, Taipei, Taiwan

Possibilistic Regression Analysis by Support Vector Machine

Pei-Yi Hao
Department of Information Management.
National Kaohsiung University of Applied Sciences, Kaohsiung, Taiwan, R.O.C.
e-mail: haupy@cc.kuas.edu.tw

***Abstract*—Support vector machines (SVMs) have been very successful in pattern recognition and function estimation problems for crisp data. This paper proposes a new method to evaluate interval linear and nonlinear regression models combining the possibility and necessity estimation formulation with the principle of SVM. For data sets with crisp inputs and interval outputs, the possibility and necessity models have been recently utilized, which are based on quadratic programming approach giving more diverse spread coefficients than a linear programming one. The SVM also uses quadratic programming approach whose advantage in interval regression analysis is to be able to perform interval nonlinear regression analysis by constructing an interval linear regression function in a high dimensional feature space. The proposed algorithm is a attractive approach to modeling nonlinear interval data, and is model-free method in the sense that we do not have to assume the underlying model function for interval nonlinear regression model with crisp inputs and interval output. Experimental results are then presented which indicate the performance of this algorithm.**

Keyword: Interval regression analysis, possibility and necessity models, Support vector machines (SVMs), Support vector regression machines, Quadratic programming.

I. INTRODUCTION

Regression analysis is to find a crisp relationship between the dependent and independent variables and to estimate a variance of measurement error. If a phenomenon under consideration is not governed by random variables but is governed by possibility variables, it is more natural to seek a fuzzy functional relationship for the given data being fuzzy or crisp. That is to say, the vague phenomenon where it is not assumed to follow randomness should be modeled by a fuzzy functional relationship. Fuzzy regression analysis can be classified into two categories; the first is possibilistic regression analysis based on possibility concepts and the second is least squares method for minimizing errors between the given outputs and the estimated outputs. Possibilistic regression derives new estimators by dealing directly with models formulated in a possibility context. Possibilistic regression analysis was first proposed by Tanaka et al. [1] where a fuzzy linear system was used as a regression model. Since membership functions of fuzzy sets are often described as possibility distributions, this approach is usually called possibilistic regression analysis [2,3].

Support vector machines (SVMs) have been very successful in pattern recognition and function estimation problems for crisp data [5,6]. Jeng *et al*. [7] first proposed the support vector interval regression networks (SVIRNs) for interval regression analysis by utilizing the ε -insensitive support vector regression (ε -SVR) in [5,6]. Hwang *et al*. [8] proposed the support vector interval regression machine (SVIRM) to evaluate the interval regression model combining the possibility estimation formulation and the property of central tendency with the principle of ε -SVR. Hao proposed a v-support vector interval regression network (v-SVIRN) to evaluate interval linear and nonlinear regression models for crisp input and output data [9]. As it is difficult to select an appropriate value of the insensitive tube width in ε -SVR, the v-SVIRN alleviates this problem by utilizing a new parametric-insensitive loss function. The v-SVIRN automatically adjusts a flexible parametric-insensitive zone of arbitrary shape and minimal size to include the given data. For a priori chosen v, v is an upper bound on the fraction of training errors and a lower bound on the fraction of support vectors. Hence, the selection of v is more intuitive.

In this paper, we propose a new method to evaluate interval linear and nonlinear regression models combining the possibility and necessity estimation formulation with the principle of support vector learning approach. The SVM approach allows us to perform interval nonlinear regression analysis by constructing an interval linear regression function in a high-dimensional feature space. Hence, the proposed algorithm is a very attractive approach to model nonlinear interval data. This algorithm is model-free method in the sense that we do not have to assume the underlying model function for interval nonlinear regression model with crisp inputs and interval output. This model-free method turns out to be a promissing method which has been attempted to treat interval nonlinear regression model.

II. A REVIEW OF PREVIOUS WORKS

A. Interval Regression Formulation Unifying the Possibility and Necessity Models

For a data set with crisp inputs and interval outputs, we can consider two interval regression models, i.e., the possibility and necessity models. In this section, we review the unified QP approach [4] to obtain the possibility and necessity models

978-1-4244-7316-8/11/$26.00 ©2011 IEEE

simultaneously. In this unified approach, we assume for simplicity that the center coefficients of the possibility regression model and necessity regression model are same.

Suppose that we are given training data $\{(\mathbf{x}_1, Y_1),...,(\mathbf{x}_n, Y_n)\}$, where $\mathbf{x}_i = (1, x_{i1},..., x_{im})^t$ is the i-th input vector, $Y_i = (y_i, e_i)$ is the corresponding interval output that consists of a center y_i and a radius e_i. For this data set, the possibility and necessity estimation models are denoted as

$$Y^*(\mathbf{x}_i) = A_0^* + A_1^* x_{i1} + \cdots A_m^* x_{im} \qquad i = 1,..., n \tag{1}$$

$$Y_*(\mathbf{x}_i) = A_{*0} + A_{*1} x_{i1} + \cdots A_{*m} x_{im} \qquad i = 1,..., n \tag{2}$$

where the interval coefficients A_i^* and A_{*i} are denoted as $A_i^* = (a_i^*, c_i^*)$ and $A_{*i} = (a_{*i}, c_{*i})$, respectively. The estimated interval $Y^*(\mathbf{x}_i)$ by the possibility model always includes the observed interval Y_i, whereas the estimated interval $Y_*(\mathbf{x}_i)$ by the necessity model should be included in the observed interval Y_i. We can denote the interval coefficients and as

$$A_i^* = (a_i, c_i + d_i) \text{ and } A_{*i} = (a_i, c_i)$$

which satisfies the condition $A_{*i} \subseteq A_i^*$, $i = 0,1,...,m$, since c_i and d_i are assumed to be nonnegative. Therefore, by interval arithmetic the possibility model $Y^*(\mathbf{x}_i)$ and the necessity model $Y_*(\mathbf{x}_i)$ can be written as

$$Y^*(\mathbf{x}_i) = (\mathbf{a}^t \mathbf{x}_i, \mathbf{c}^t |\mathbf{x}_i| + \mathbf{d}^t |\mathbf{x}_i|) \tag{3}$$

$$Y_*(\mathbf{x}_i) = (\mathbf{a}^t \mathbf{x}_i, \mathbf{c}^t |\mathbf{x}_i|) \tag{4}$$

The two objective functions in the possibility and the necessity models are assumed as follows:

$$\min \ J_P = \sum_{i=1}^{n} (\mathbf{c}^t |\mathbf{x}_i| + \mathbf{d}^t |\mathbf{x}_i|) : \text{Possibility model} \tag{5}$$

$$\max \ J_N = \sum_{i=1}^{n} \mathbf{c}^t |\mathbf{x}_i| : \text{Necessity model} \tag{6}$$

The objective function of the unified model can be obtained by the combination of these two objective functions. The combination of two functions yields the following:

$$\min \ J_P - J_N = \sum_{i=1}^{n} \mathbf{d}^t |\mathbf{x}_i| . \tag{7}$$

Then, the objective function in the unified approach by QP can be assumed as the following quadratic function:

$$J = \sum_{i=1}^{n} \left(\mathbf{d}^t |\mathbf{x}_i|\right)^2 = \mathbf{d}^t \left(\sum_{i=1}^{n} |\mathbf{x}_i|^t |\mathbf{x}_i| \right) \mathbf{d} \tag{8}$$

Therefore, interval regression analysis [4] is to determine the interval coefficients A_i^* and A_{*i}, i=1,…,m that minimize the aforementioned objective function and satisfy inclusion relations $Y^*(\mathbf{x}_i) \subseteq Y_i \subseteq Y_*(\mathbf{x}_i)$. This problem can be described as the following QP problem:

$$\min_{\mathbf{a},\mathbf{c},\mathbf{d}} \quad J = \mathbf{d}^t \left(\sum_{i=1}^{n} |\mathbf{x}_i|^t |\mathbf{x}_i| \right) \mathbf{d} + \xi(\mathbf{a}^t \mathbf{a} + \mathbf{c}^t \mathbf{c})$$

$$\text{subject to} \begin{cases} \mathbf{a}^t x_i + \mathbf{c}^t |x_i| + \mathbf{d}^t |x_i| \geq y_i + e_i \\ \mathbf{a}^t x_i - \mathbf{c}^t |x_i| - \mathbf{d}^t |x_i| \leq y_i - e_i \\ \mathbf{a}^t x_i + \mathbf{c}^t |x_i| \leq y_i + e_i \\ \mathbf{a}^t x_i - \mathbf{c}^t |x_i| \geq y_i - e_i, \ i = 1,..., n \\ \mathbf{c} \geq 0, \ \mathbf{d} \geq 0 \end{cases} \tag{9}$$

where ξ is a significantly small positive number, and so leads the influence of $\xi(\mathbf{a}^t \mathbf{a} + \mathbf{c}^t \mathbf{c})$ to be negligible.

III. Estimization of Possibility and Necessity Models by Support Vector Machines

In this section, we propose a new method to evaluate interval linear and nonlinear regression models combining the possibility and necessity estimation formulation with the principle of SVM.

A. Interval Linear Regression

We first propose how to get solutions for interval linear regression models by implementing SVM approach for crisp-input interval-output data. Suppose that we are given training data $\{(\mathbf{x}_1, Y_1),...,(\mathbf{x}_N, Y_N)\}$, where $\mathbf{x}_i = (x_{i1},..., x_{im})^t$ is the i-th input vector, $Y_i = (y_i, e_i)$ is the corresponding interval output that consists of a center y_i and a radius e_i. For this data set, the possibility and necessity estimation models are denoted as

$$Y^*(\mathbf{x}_i) = B^* + W_1^* x_{i1} + \cdots W_m^* x_{im} \qquad i = 1,..., N \tag{10}$$

$$Y_*(\mathbf{x}_i) = B_* + W_{*1} x_{i1} + \cdots W_{*m} x_{im} \qquad i = 1,..., N \tag{11}$$

where the interval coefficients W_i^* and W_{*i} are denoted as $W_i^* = (w_i^*, c_i^*)$ and $W_{*i} = (w_{*i}, c_{*i})$, respectively. Besides, the interval bias coefficients B^* and B_* are denoted as $B^* = (b^*, d^*)$ and $B_* = (b_*, d_*)$, respectively. The estimated interval $Y^*(\mathbf{x}_i)$ by the possibility model always includes the observed interval Y_i, whereas the estimated interval $Y_*(\mathbf{x}_i)$ by the necessity model should be included in the observed interval Y_i. We can denote the interval coefficients as

$$W_i^* = (w_i, c_i + a_i) \text{ and } W_{*i} = (w_i, c_i) \tag{12}$$

which satisfies the condition $W_{*i} \subseteq W_i^*$, $i = 0,1,...,m$, since c_i and a_i are assumed to be nonnegative. Similarly, we can denote the interval bias coefficients as

$$B^* = (b, d + k) \text{ and } B_* = (b, d) \tag{13}$$

which satisfies the condition $B_* \subseteq B^*$, since d and k are assumed to be nonnegative. Therefore, by interval arithmetic the possibility model $Y^*(\mathbf{x}_i)$ and the necessity model $Y_*(\mathbf{x}_i)$ can be written as

$$\begin{aligned} Y^*(\mathbf{x}_i) &= W_1^* x_{i1} + \cdots W_m^* x_{im} + B^* \\ &= \left(\langle \mathbf{w} \cdot \mathbf{x} \rangle + b, \langle \mathbf{c} \cdot |\mathbf{x}| \rangle + d + \langle \mathbf{a} \cdot |\mathbf{x}| \rangle + k\right) \end{aligned} \tag{14}$$

and

$$\begin{aligned} Y_*(\mathbf{x}_i) &= W_{*1} x_{i1} + \cdots W_{*m} x_{im} + B_* \\ &= \left(\langle \mathbf{w} \cdot \mathbf{x} \rangle + b, \langle \mathbf{c} \cdot |\mathbf{x}| \rangle + d\right) \end{aligned} \tag{15}$$

The problem of finding the **w**, **c**, **a**, b, d and k that satisfies the inclusion relation $Y^*(\mathbf{x}_i) \supseteq Y_i \supseteq Y_*(\mathbf{x}_i)$ is equivalent to the following constrained optimization problem:

$$\min_{\mathbf{a},\mathbf{c},\mathbf{d}} \quad J = \frac{1}{2}\|\mathbf{w}\|^2 + \frac{C_1}{2}\left(\|\mathbf{c}\|^2 + d\right) + \frac{C_2}{2}\left(\|\mathbf{a}\|^2 + k\right)$$

$$\text{subject to} \begin{cases} \langle \mathbf{w} \cdot \mathbf{x}_i \rangle + b + \langle \mathbf{c} \cdot |\mathbf{x}_i| \rangle + d + \langle \mathbf{a} \cdot |\mathbf{x}_i| \rangle + k \geq y_i + e_i \\ \langle \mathbf{w} \cdot \mathbf{x}_i \rangle + b - \langle \mathbf{c} \cdot |\mathbf{x}_i| \rangle - d - \langle \mathbf{a} \cdot |\mathbf{x}_i| \rangle - k \leq y_i - e_i \\ \langle \mathbf{w} \cdot \mathbf{x}_i \rangle + b + \langle \mathbf{c} \cdot |\mathbf{x}_i| \rangle + d \leq y_i + e_i \\ \langle \mathbf{w} \cdot \mathbf{x}_i \rangle + b - \langle \mathbf{c} \cdot |\mathbf{x}_i| \rangle - d \geq y_i - e_i, \; i = 1, \ldots, n \\ k, d \geq 0 \end{cases} \tag{16}$$

The weight coefficient $C_1, C_2 > 0$ determines the tradeoff between model complexity, which is characterized by $\|\mathbf{w}\|^2$, and the vagueness of the possibility and the necessity models, which is characterized by $\left(\|\mathbf{c}\|^2 + d\right)$ and $\left(\|\mathbf{a}\|^2 + k\right)$, respectively. We can find the solution of this optimization problem given by Eq. (18) in dual variables by finding the saddle point of the Lagrangian:

$$\begin{aligned} L = {} & \frac{1}{2}\|\mathbf{w}\|^2 + \frac{C_1}{2}\left(\|\mathbf{c}\|^2 + d\right) + \frac{C_2}{2}\left(\|\mathbf{a}\|^2 + k\right) \\ & - \sum_{i=1}^{N} \alpha_{1i}\left(\langle \mathbf{w} \cdot \mathbf{x}_i \rangle + b + \langle \mathbf{c} \cdot |\mathbf{x}_i| \rangle + d + \langle \mathbf{a} \cdot |\mathbf{x}_i| \rangle + k - y_i - e_i\right) \\ & - \sum_{i=1}^{N} \alpha_{2i}\left(-\langle \mathbf{w} \cdot \mathbf{x}_i \rangle - b + \langle \mathbf{c} \cdot |\mathbf{x}_i| \rangle + d + \langle \mathbf{a} \cdot |\mathbf{x}_i| \rangle + k + y_i - e_i\right) \\ & - \sum_{i=1}^{N} \alpha_{3i}\left(-\langle \mathbf{w} \cdot \mathbf{x}_i \rangle - b - \langle \mathbf{c} \cdot |\mathbf{x}_i| \rangle - d + y_i + e_i\right) \\ & - \sum_{i=1}^{N} \alpha_{4i}\left(\langle \mathbf{w} \cdot \mathbf{x}_i \rangle + b - \langle \mathbf{c} \cdot |\mathbf{x}_i| \rangle - d - y_i + e_i\right) \\ & - \mu d - \gamma k \end{aligned} \tag{17}$$

where $\alpha_{1i}, \alpha_{2i}, \alpha_{3i}, \alpha_{4i}, \mu$, and γ are nonnegative Lagrange multipliers. Differentiating L with respect to **w**, **c**, **a**, b, d, and k, and setting the result to zero, we obtain:

$$\partial L / \partial \mathbf{w} = 0 \Rightarrow \mathbf{w} = \sum_{i=1}^{N} (\alpha_{1i} - \alpha_{2i} + \alpha_{3i} - \alpha_{4i}) \mathbf{x}_i \,, \tag{18}$$

$$\partial L / \partial \mathbf{c} = 0 \Rightarrow \mathbf{c} = \frac{1}{C_1} \sum_{i=1}^{N} (\alpha_{1i} + \alpha_{2i} - \alpha_{3i} - \alpha_{4i}) |\mathbf{x}_i| \,, \tag{19}$$

$$\partial L / \partial \mathbf{a} = 0 \Rightarrow \mathbf{a} = \frac{1}{C_2} \sum_{i=1}^{N} (\alpha_{1i} + \alpha_{2i}) |\mathbf{x}_i| \,, \tag{20}$$

$$\partial L / \partial b = 0 \Rightarrow \sum_{i=1}^{N} (\alpha_{1i} - \alpha_{2i} - \alpha_{3i} + \alpha_{4i}) = 0 \,, \tag{21}$$

$$\partial L / \partial d = 0 \Rightarrow \sum_{i=1}^{N} (\alpha_{1i} + \alpha_{2i} - \alpha_{3i} - \alpha_{4i}) = C_1 - \mu \leq C_1 \,, \tag{22}$$

$$\partial L / \partial k = 0 \Rightarrow \sum_{i=1}^{N} (\alpha_{1i} + \alpha_{2i}) = C_2 - \gamma \leq C_2 \,, \tag{23}$$

Substituting Eqs. (18)-(23) into (17), we obtain the following dual problem

$$\begin{aligned} \max \; & \frac{-1}{2} \sum_{i=1}^{N} \sum_{j=1}^{N} (\alpha_{1i} - \alpha_{2i} - \alpha_{3i} + \alpha_{4i})(\alpha_{1j} - \alpha_{2j} - \alpha_{3j} + \alpha_{4j}) \langle \mathbf{x}_i \cdot \mathbf{x}_j \rangle \\ & - \frac{1}{2C_1} \sum_{i=1}^{N} \sum_{j=1}^{N} (\alpha_{1i} + \alpha_{2i} - \alpha_{3i} - \alpha_{4i})(\alpha_{1j} + \alpha_{2j} - \alpha_{3j} - \alpha_{4j}) \langle |\mathbf{x}_i| \cdot |\mathbf{x}_j| \rangle \\ & - \frac{1}{2C_2} \sum_{i=1}^{N} \sum_{j=1}^{N} (\alpha_{1i} + \alpha_{2i})(\alpha_{1j} + \alpha_{2j}) \langle |\mathbf{x}_i| \cdot |\mathbf{x}_j| \rangle \\ & + \sum_{i=1}^{N} (\alpha_{1i} - \alpha_{2i} - \alpha_{3i} + \alpha_{4i}) y_i . + \sum_{i=1}^{N} (\alpha_{1i} + \alpha_{2i} - \alpha_{3i} - \alpha_{4i}) e_i . \end{aligned}$$

subject to (24)

$$\begin{aligned} & \sum_{i=1}^{N} (\alpha_{1i} - \alpha_{2i} - \alpha_{3i} + \alpha_{4i}) = 0 \,, \\ & \sum_{i=1}^{N} (\alpha_{1i} + \alpha_{2i} - \alpha_{3i} - \alpha_{4i}) \leq C_1 \\ & \sum_{i=1}^{N} (\alpha_{1i} + \alpha_{2i}) \leq C_2 \,, \\ & \alpha_{1i}, \alpha_{2i}, \alpha_{3i}, \alpha_{4i} \geq 0. \end{aligned}$$

As for the pair (**w**,**c**,**a**,b,d,p), it is easy to find that

$$\mathbf{w} = \sum_{i=1}^{N} (\alpha_{1i} - \alpha_{2i} + \alpha_{3i} - \alpha_{4i}) \mathbf{x}_i \,,$$

$$\mathbf{c} = \frac{1}{C_1} \sum_{i=1}^{N} (\alpha_{1i} + \alpha_{2i} - \alpha_{3i} - \alpha_{4i}) |\mathbf{x}_i| \,,$$

and $$\mathbf{a} = \frac{1}{C_2} \sum_{i=1}^{N} (\alpha_{1i} + \alpha_{2i}) |\mathbf{x}_i| \,.$$

While parameters b, d and k can be determined from the Karush-Kuhn-Tucker (KKT) conditions:

$$\alpha_{1i} \left| \left(\langle \mathbf{w} \cdot \mathbf{x}_i \rangle + b\right) + \left(\langle \mathbf{c} \cdot |\mathbf{x}_i| \rangle + d\right) + \left(\langle \mathbf{a} \cdot |\mathbf{x}_i| \rangle + p\right) - y_i - e_i \right| = 0 \tag{25}$$

$$\alpha_{2i} \left| -\left(\langle \mathbf{w} \cdot \mathbf{x}_i \rangle + b\right) + \left(\langle \mathbf{c} \cdot |\mathbf{x}_i| \rangle + d\right) + \left(\langle \mathbf{a} \cdot |\mathbf{x}_i| \rangle + p\right) + y_i - e_i \right| = 0 \tag{26}$$

$$\alpha_{3i} \left| -\left(\langle \mathbf{w} \cdot \mathbf{x}_i \rangle + b\right) - \left(\langle \mathbf{c} \cdot |\mathbf{x}_i| \rangle + d\right) + y_i + e_i \right| = 0 \tag{27}$$

$$\alpha_{4i} \left| \left(\langle \mathbf{w} \cdot \mathbf{x}_i \rangle + b\right) - \left(\langle \mathbf{c} \cdot |\mathbf{x}_i| \rangle + d\right) - y_i + e_i \right| = 0 \tag{28}$$

For some $\alpha_{3i}, \alpha_{4j} > 0$, the second factor in Eqs. (27) and (28) has to vanish. Hence, b and d can be computed as follows:

$$b=\frac{1}{2}\begin{pmatrix}-\langle \mathbf{w}\cdot\mathbf{x}_i\rangle-\langle \mathbf{w}\cdot\mathbf{x}_j\rangle-\langle \mathbf{c}\cdot|\mathbf{x}_i|\rangle+\langle \mathbf{c}\cdot|\mathbf{x}_j|\rangle\\ +y_i+y_j+e_i-e_j\end{pmatrix}, \tag{29}$$

$$d=\frac{1}{2}\begin{pmatrix}-\langle \mathbf{w}\cdot\mathbf{x}_i\rangle+\langle \mathbf{w}\cdot\mathbf{x}_j\rangle-\langle \mathbf{c}\cdot|\mathbf{x}_i|\rangle-\langle \mathbf{c}\cdot|\mathbf{x}_j|\rangle\\ +y_i-y_j+e_i+e_j\end{pmatrix}, \tag{30}$$

for some $\alpha_{3i},\alpha_{4j}>0$.

Once bias b and d is computed, we can determine the bias k from the Karush-Kuhn-Tucker (KKT) conditions. For some $\alpha_{1i},\alpha_{2j}>0$, the second factor in Eqs. (25) and (26) has to vanish. Hence, bias k can be computed as follows:

$$k=-\langle \mathbf{w}\cdot\mathbf{x}_i\rangle-b-\langle \mathbf{c}\cdot|\mathbf{x}_i|\rangle-d-\langle \mathbf{a}\cdot|\mathbf{x}_i|\rangle+y_i+e_i, \tag{31}$$

$$k=\langle \mathbf{w}\cdot\mathbf{x}_j\rangle+b-\langle \mathbf{c}\cdot|\mathbf{x}_j|\rangle-d-\langle \mathbf{a}\cdot|\mathbf{x}_j|\rangle-y_j+e_j, \tag{32}$$

for some $\alpha_{1i},\alpha_{2j}>0$.

Therefore, the possibility model $Y^*(\mathbf{x}_i)$ and the necessity model $Y_*(\mathbf{x}_i)$ constructed by the proposed approach are given as follows:

$$Y^*(\mathbf{x})=\begin{pmatrix}\sum_{i=1}^{N}(a_{1i}-\alpha_{2i}-\alpha_{3i}+\alpha_{4i})\langle \mathbf{x}\cdot\mathbf{x}_i\rangle+b,\\ \sum_{i=1}^{N}(a_{1i}+\alpha_{2i}-\alpha_{3i}-\alpha_{4i})\langle|\mathbf{x}|\cdot|\mathbf{x}_i|\rangle+d\\ +\sum_{i=1}^{N}(a_{1i}+\alpha_{2i})\langle|\mathbf{x}|\cdot|\mathbf{x}_i|\rangle+k\end{pmatrix} \tag{33}$$

$$Y_*(\mathbf{x})=\begin{pmatrix}\sum_{i=1}^{N}(a_{1i}-\alpha_{2i}-\alpha_{3i}+\alpha_{4i})\langle \mathbf{x}\cdot\mathbf{x}_i\rangle+b,\\ \sum_{i=1}^{N}(a_{1i}+\alpha_{2i}-\alpha_{3i}-\alpha_{4i})\langle|\mathbf{x}|\cdot|\mathbf{x}_i|\rangle+d\end{pmatrix} \tag{34}$$

B. Extension to the Interval Nonlinear Regression Model

Next, we will consider how to get solutions for interval nonlinear regression models. The basic idea is that an interval nonlinear regression function could be achieved by simply mapping the input patterns $\mathbf{x}_i$ by Φ: $R^n \rightarrow F$ into a high-dimensional feature space F, and then applying the interval linear regression algorithm in that space [5,6,12]. A key property of the proposed algorithm is that the only quantities that we need to compute are inner products, of the form $\langle \mathbf{x}_i\cdot\mathbf{x}_j\rangle$ and $\langle|\mathbf{x}_i|\cdot|\mathbf{x}_j|\rangle$. The algorithm would only depend on the data through inner products in F, i.e. on functions of the form $\langle \Phi(\mathbf{x}_i)\cdot\Phi(\mathbf{x}_j)\rangle$ and $\langle \Phi(|\mathbf{x}_i|)\cdot\Phi(|\mathbf{x}_j|)\rangle$. The functional form of mapping Φ does not need to be known since it is implicitly defined by the choice of kernel function $k(\mathbf{x},\mathbf{y})\equiv\langle \Phi(\mathbf{x})\cdot\Phi(\mathbf{y})\rangle$. Therefore, it is enough to know and use $k(\mathbf{x}_i,\mathbf{x}_j)=\langle \Phi(\mathbf{x}_i)\cdot\Phi(\mathbf{x}_j)\rangle$ and $k(|\mathbf{x}_i|,|\mathbf{x}_j|)=\langle \Phi(|\mathbf{x}_i|)\cdot\Phi(|\mathbf{x}_j|)\rangle$ instead of defining $\Phi(\bullet)$ explicitly. The well-used kernels for the regression problem are given as follows:

$k(\mathbf{x},\mathbf{y})=(\langle \mathbf{x}\cdot\mathbf{y}\rangle+1)^d$: Polynomial kernel of degree d;

$k(\mathbf{x},\mathbf{y})=\exp\left(\frac{-\|\mathbf{x}-\mathbf{y}\|^2}{2\sigma^2}\right)$: Gaussian RBF kernel;

$k(\mathbf{x},\mathbf{y})=\tanh(k\langle \mathbf{x}\cdot\mathbf{y}\rangle+\theta)$: Sigmoid kernel.

Hence, by replacing $\langle \mathbf{x}_i\cdot\mathbf{x}_j\rangle$ and $\langle|\mathbf{x}_i|\cdot|\mathbf{x}_j|\rangle$ with $k(\mathbf{x}_i,\mathbf{x}_j)$ and $k(|\mathbf{x}_i|,|\mathbf{x}_j|)$, respectively, we obtain the dual quadratic optimization problem given by Eq. (26). Here, we should note that the constraints are not changed.

$$\begin{aligned}\max\ & \frac{-1}{2}\sum_{i=1}^{N}\sum_{j=1}^{N}(\alpha_{1i}-\alpha_{2i}-\alpha_{3i}+\alpha_{4i})(\alpha_{1j}-\alpha_{2j}-\alpha_{3j}+\alpha_{4j})k(\mathbf{x}_i,\mathbf{x}_j)\\ &-\frac{1}{2C_1}\sum_{i=1}^{N}\sum_{j=1}^{N}(\alpha_{1i}+\alpha_{2i}-\alpha_{3i}-\alpha_{4i})(\alpha_{1j}+\alpha_{2j}-\alpha_{3j}-\alpha_{4j})k(|\mathbf{x}_i|,|\mathbf{x}_j|)\\ &-\frac{1}{2C_2}\sum_{i=1}^{N}\sum_{j=1}^{N}(\alpha_{1i}+\alpha_{2i})(\alpha_{1j}+\alpha_{2j})k(|\mathbf{x}_i|,|\mathbf{x}_j|)\\ &+\sum_{i=1}^{N}(\alpha_{1i}-\alpha_{2i}-\alpha_{3i}+\alpha_{4i})y_i.+\sum_{i=1}^{N}(\alpha_{1i}+\alpha_{2i}-\alpha_{3i}-\alpha_{4i})e_i.\end{aligned}$$

subject to (35)

$$\sum_{i=1}^{N}(\alpha_{1i}-\alpha_{2i}-\alpha_{3i}+\alpha_{4i})=0,$$

$$\sum_{i=1}^{N}(\alpha_{1i}+\alpha_{2i}-\alpha_{3i}-\alpha_{4i})\le C_1$$

$$\sum_{i=1}^{N}(\alpha_{1i}+\alpha_{2i})\le C_2,$$

$$\alpha_{1i},\alpha_{2i},\alpha_{3i},\alpha_{4i}\ge 0.$$

By using different kernel functions $k(\mathbf{x},\mathbf{y})$, one can construct different learning machines with arbitrary types of nonlinear regression functions in the input space [5,6,12]. Therefore, the possibility model $Y^*(\mathbf{x}_i)$ and the necessity model $Y_*(\mathbf{x}_i)$ constructed by the proposed approach are given as follows:

$$Y^*(\mathbf{x})=\begin{pmatrix}\sum_{i=1}^{N}(a_{1i}-\alpha_{2i}-\alpha_{3i}+\alpha_{4i})k(\mathbf{x},\mathbf{x}_i)+b,\\ \sum_{i=1}^{N}(a_{1i}+\alpha_{2i}-\alpha_{3i}-\alpha_{4i})k(|\mathbf{x}|,|\mathbf{x}_i|)+d\\ +\sum_{i=1}^{N}(a_{1i}+\alpha_{2i})k(|\mathbf{x}|,|\mathbf{x}_i|)+k\end{pmatrix} \tag{36}$$

and

$$Y_*(\mathbf{x})=\begin{pmatrix}\sum_{i=1}^{N}(a_{1i}-\alpha_{2i}-\alpha_{3i}+\alpha_{4i})k(\mathbf{x},\mathbf{x}_i)+b,\\ \sum_{i=1}^{N}(a_{1i}+\alpha_{2i}-\alpha_{3i}-\alpha_{4i})k(|\mathbf{x}|,|\mathbf{x}_i|)+d\end{pmatrix} \tag{37}$$

Kernel representations offer an alternative solution by projecting the data into a high dimensional feature space to increase the computational power of the interval linear regression algorithm. The use of interval linear regression model in the dual representation makes it possible to perform this step implicitly. By replacing the inner product with an appropriately chosen "kernel" function, one can implicitly perform a nonlinear mapping to a high dimensional feature space without increasing the number of tunable parameters [13,14]. Another attraction of the kernel method is that the learning algorithms can largely decoupled from the specifics of the application area, which must simply be encoded into the design of an appropriate kernel function. Hence, the problem of choosing an architecture for an interval regression model is replaced by the problem of choosing a suitable kernel. Several kernels have been developed by other researchers for discrete structures such as text and bio-sequences [15,16], indicating that the proposed approach is not restricted only to input spaces that are subsets of the Euclidean space.

IV. Numerical Example

In this section, we use one data set, crisp inputs-interval outputs shown in Table I. This data is taken from Tanaka and Lee [4]. The proposed SVM approaches are applied to this data set from an illustrative point of view.

TABLE I. Crisp Input-Interval Output Data

No.	1	2	3	4	5	6	7	8
x	1	2	3	4	5	6	7	8
Y	[15,30]	[20,37.5]	[15,35]	[25,60]	[25,55]	[40,65]	[55,95]	[70,100]

We first consider interval linear regression analysis. The interval linear model for this data is assumed as

$$Y(\mathbf{x}) = B + W \cdot \mathbf{x}$$

Applying the proposed SVM approach to the given data set, we obtain the possibility model $Y^*(\mathbf{x})$ and the necessity model $Y_*(\mathbf{x})$ as

$$Y^*(\mathbf{x}) = (10.7813,9.5833) + (7.9167,29.1667)x$$

$$Y_*(\mathbf{x}) = (10.7813,0.6250) + (7.9167,3.6458)x$$

Here, we set C_1=700 and C_2=400, respectively. We now introduce Tanaka and Lee's results to compare and evaluate both methods for the linear case

$$Y^*(\mathbf{x}) = (7.3111,11.856) + (8.371,2.462)x$$

$$Y_*(\mathbf{x}) = (7.311,0.168) + (8.371,0.514)x$$

We can see the interval coefficients are similar. A detailed comparison will be made later in Table II by using a measure of fitness. Fig. 1 illustrates the results for the proposed linear model. The solid line explains the fitted regression line for center. The two dash and dotted lines explain the fitted possibility and necessity models, respectively. As seen from Fig. 1, the proposed interval linear regression method works fairly well.

We now apply the proposed nonlinear method to analyze this data set. At first glance over Fig. 1, the nonlinear regression model looks appropriate for these data. Hence, we apply interval nonlinear regression method to this data set. Here, we use a Gaussian kernel for estimating the interval nonlinear model. Here, we set C_1=1, C_2=100000, and σ=0.08, respectively. Fig. 2 illustrates the results for the proposed nonlinear model.

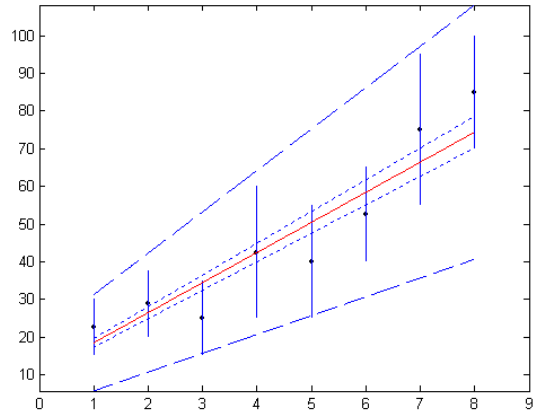

Figure 1. Linear interval regression model obtained by the proposed approach.

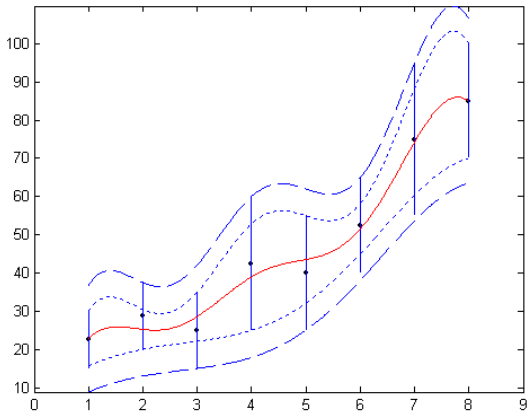

Figure 2. Linear interval regression model obtained by the proposed approach with Gaussian kernel.

As in Fig. 1, the solid line explains the fitted regression curve for center. The two dash and dotted curves explain the fitted possibility and necessity models, respectively. As seen from Fig. 2, we know that the interval nonlinear model looks more appropriate for this particular data set, and the proposed nonlinear algorithm performs well, too.

We now consider a measure of fitness to evaluate both the proposed methods and the methods of Tanaka and Lee's. We briefly review the measure of fitness (for details, see [4]). In the case of the linear model, the measure of fitness for the i-th data $\varphi_Y(\mathbf{x}_i)$ is defined as

$$\varphi_Y(\mathbf{x}_i) = \frac{\langle \mathbf{c} \cdot \mathbf{x}_i \rangle + d}{\langle \mathbf{c} \cdot \mathbf{x}_i \rangle + d + \langle \mathbf{a} \cdot \mathbf{x}_i \rangle + k}$$

which indicates how closely the possibility output for the i-th input approximates the necessity output for the ith input. Here, the denominator and the numerator represent the spreads of the estimated intervals $Y^*(\mathbf{x}_i)$ and $Y_*(\mathbf{x}_i)$, repectively. Then, the measure of fitness for all data φ_Y is defined as

$$\varphi_Y = \frac{1}{n}\sum_{i=1}^{n}\varphi_Y(\mathbf{x}_i) = \frac{1}{n}\sum_{i=1}^{n}\frac{\langle \mathbf{c} \cdot \mathbf{x}_i \rangle + d}{\langle \mathbf{c} \cdot \mathbf{x}_i \rangle + d + \langle \mathbf{a} \cdot \mathbf{x}_i \rangle + k}$$

Where n is a sample size and $0 \le \varphi_Y \le 1$. We can also define $\varphi_Y(\mathbf{x}_i)$ and φ_Y for nonlinear model by using the corresponding spreads of the estimated intervals $Y^*(\mathbf{x}_i)$ and $Y_*(\mathbf{x}_i)$. The larger the value of φ_Y, the better the model is fitting the data.

Table II shows the obtained $\varphi_Y(\mathbf{x}_i)$ and φ_Y for the linear model and the quadratic model of Tanaka and Lee's, and the proposed linear and nonlinear models. We can observe that the values of $\varphi_Y(\mathbf{x}_i)$ in the proposed nonlinear models are much larger than those in the linear and quadratic models of Tanaka and Lee's. Also, the summary measure of fit for all data φ_Y is greater for the nonlinear model as compared to the linear model. In particular, the nonlinear model with Gaussian kernel has the largest value $\varphi_Y = 0.5699$. Thus, the measure of fit indicates that the nonlinear model is providing the best fit to the given data compared to the other models. As a whole, the proposed interval regression and model selection methods work fairly well.

TABLE II. OBTAINED $\varphi_Y(\mathbf{x}_i)$ AND φ_Y FOR NUMERICAL DATA

No.(i)	$\varphi_Y(\mathbf{x}_i)$		
	linear		Gaussian kernel
	Tanaka's approach	Proposed approach	Proposed approach
1	0.0476	0.0900	0.5125
2	0.0713	0.1005	0.4284
3	0.0889	0.1076	0.4750
4	0.1025	0.1128	0.6613
5	0.1133	0.1168	0.6197
6	0.1221	0.1198	0.4895
7	0.1295	0.1223	0.6761
8	0.1356	0.1244	0.6967
φ_Y	0.1013	0.1118	0.5699

V. CONCLUSION

Through numerical experiments, we realize that the proposed algorithms derive the satisfying solutions and are the attractive approaches to modeling the data with crisp inputs and interval output. In particular, we realize that we can use these algorithms successfully when a linear model is inappropriate. One of advantages of these algorithms is that we do not need to assume the underlying structure for the interval nonlinear regression model used in this paper. The algorithms combine generalization control with a technique to address the curse of dimmensionality. The main formulation results in solving a global quadratic optimization problem with linear constraints. Hence, this is not a computationally expensive way. In fact, this quadratic optimization problem can be solved easily by such computer software as Matlab, Mathematica, and so on.

In this paper, we deal with estimating interval nonlinear regression model combining the possibility and necessity estimation formulation with the principle of SVM for crisp inputs and interval output dataset. In future work, we intend to devise algorithms for estimating interval nonlinear regression model with interval inputs and interval output, without assuming the underlying structure. Furthermore, we will devise algorithms for estimating fuzzy nonlinear regression model with fuzzy inputs and fuzzy output.

ACKNOWLEDGMENT

This research work was supported in part by the National Science Council Research Grant NSC 99-2221-E-151 -058 -.

REFERENCES

[1] H. Tanaka, S. Uejima, and K. Asai, "Linear regression analysis with fuzzy model," IEEE Trans. Syst. Man, Cybern., vol. 12, pp. 903–907,1982.

[2] H. Tanaka, "Fuzzy data analysis by possibilistic linear models," Fuzzy Sets Syst., vol. 24, pp. 363–375, 1987.

[3] H. Tanaka and J. Watada, "Possibilistic linear systems and their application to the linear regression model," Fuzzy Sets Syst., vol. 27, pp. 275–289, 1988.

[4] H. Tanaka and H. Lee, "Interval regression analysis by quadratic programming approach," IEEE Trans. Fuzzy System. vol. 6, no. 4, pp. 473-481, 1998.

[5] V. Vapnik, The Nature of Statistical Learning Theory. Berlin, Germany: Springer-Verlag, 1995.

[6] A. J. Smola and B. Schölkopf, "A tutorial on support vector regression,"NeuroCOLT, NeuroCOLT2 Tech. Rep., 1998.

[7] J.-T. Jeng, C.-C. Chuang, and S.-F. Su, "Support vector interval regression networks for interval regression analysis," Fuzzy Sets Syst., vol. 138, pp. 283–300, 2003.

[8] C. Hwang, D. H. Hong, and K. H. Seok, "Support vector interval regression machine for crisp input and output data," Fuzzy Sets and Systems, vol. 157, pp. 1114-1125, 2006.

[9] P.-Y. Hao, "Interval regression analysis using support vector networks," Fuzzy Sets and Systems, vol. , pp. , 2009.

[10] H. Ishibuchi, H. Tanaka, "Several formulations of interval regression analysis," Proc. Sino-Japan Joint Meeting on Fuzzy Sets and Systems, Beijing, China, 1990, pp. B2–2.

[11] G. Peters, "Fuzzy linear regression with fuzzy intervals," Fuzzy Sets and Systems, vol. 63, pp. 45-54, 1994.

[12] H. Drucker, C. Burges, L. Kaufman, A. Smola, and V. N. Vapnik, "Support vector regression machines," In Advances in Neural Information Processing Systems 9, vol. 9, pp. 155-161. The MIT Press, 1996.

[13] B. Schölkopf, C. J. C. Burges, and A. J. Smola, Advances in Kernel Method - Support Vector Learning, MIT Press, Cambridge, MA, 1999.

[14] N. Cristianini and J. Shawe-Taylor, An Introduction to Support Vector Machines, Cambridge University Press, 2000.

[15] A. Ben-Hur and W. S. Noble, "Kernel methods for predicting protein-protein interactions," Bioinformatics, vol. 21, suppl. 1, pp. i38-46, 2005.

[16] H. Saigo, J.-P. Vert, N. Ueda, and T. Akutsu, "Protein homology detection using string alignment kernels," Bioinformatics, vol. 20, no. 11, pp. 1682-1689, 2004.

2011 IEEE International Conference on Fuzzy Systems
June 27-30, 2011, Taipei, Taiwan

Cognitive Simulation-Based on Knowledge Evolution in Fuzzy Discrete Event Systems

Paul-Antoine Bisgambiglia
University of Corsica and
CNRS UMR SPE 6134
Quartier Grossetti, Bat 018
France, Corte 20250
Email: bisgambiglia@univ-corse.fr

Paul Antoine Bisgambiglia
University of Corsica and
CNRS UMR SPE 6134
Quartier Grossetti, Bat 018
France, Corte 20250
Email: bisgambi@univ-corse.fr

Jean-Sebastien Gualtieri
University of Corsica and
CNRS UMR SPE 6134
Quartier Grossetti, Bat 018
France, Corte 20250
Email: gualtieri@univ-corse.fr

***Abstract*—Discrete event systems (DES) theory has been developed and widely used to study the behavior of complex systems. In this paper, from a formalism based on this theory (DEVS), we propose to present a formal approach for taking into account the knowledge evolution. Indeed, knowledge is not static; it can evolve in time, or during the simulation. Few tools offer to take into account these developments, which may have a significant impact on the validity of results. To deal this knowledge, we suggest adding a lifespan to the modeled data, the latter is used to define the validity degree of knowledge; it is a kind of confidence measure.**

***Keywords*—DES; FDES; DEVS; fuzzy sets; knowledge; modeling; simulation**

I. Introduction

In this article we will present works that aim to improve the knowledge consideration in numerical models.

The process of modeling and simulation (M&S) can be divided into three phases (Figure 1):

(1) the acquisition of knowledge about the system, and proposing hypotheses;

(2) model the system based on the proposed assumptions to simplify it and make it executable by computer;

(3) simulate the model to validate and confirm the hypotheses.

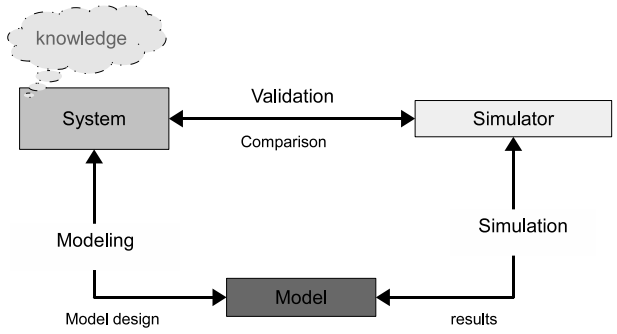

Figure 1. Modeling and simulation (MS) process

These three phases are more or less based on the need to correctly represent, i.e. in a legible and understandable, the knowledge. This knowledge can come from field observations and laboratory. They can be inferred or learned from an expert, etc. It is therefore important to identify any issues arising. What types of knowledge are needed to realize a good model? How to represent and express them? How to take into account their evolution?

Knowledge can be defined as a system for explaining the relationship between thoughts and objects. Knowledge representation amounts to establishing a correspondence between the studied system and a symbolic representation that can be processed by a computer: our model (see Figure 1). The cognitive sciences are the source of the work on knowledge; they have contributed to the development of multiple theoretical approaches [1]. Philosophers, psychologists, linguists, sociologists, computer scientists, mathematicians seek to analyze and represent knowledge. The ambition is to allow to the computer to use when calculating the same type of information that man. The difficulty of validating the information gained is the fact that we do not control the knowledge of an individual but an expression of that knowledge. The representation problem arises and causes problems of understanding, representation, expression and communication. This problem has led us to use fuzzy logic [2], [3], [4] because it allows to represent and manipulate imperfect knowledge (imprecise and uncertain). Methodological tools it offers can take into account the information so gradually, expressed in natural language, that is to say, very close to the mode of reasoning and expression of the human being. These properties are very interesting.

Recently, to deal imperfect knowledge in our models, we proposed several extensions that couple the computational intelligence methods with the DEVS formalism. iDEVS [5] is based on fuzzy set theory [2], it can simulate systems with imprecise parameters. DEVFIS to represent the FIS as a DEVS model [6]. Articles [7], [8] introduce a high-level language, based on the MDA approach and fuzzy logic for the specification of DEVS models. The experience gained during this work led us to think, and see, differently, some stages of the knowledge representation, and in particular the modeling phase. Generally modeling is defined as a step for creating a simplified representation (equation, experience, black box) of the studied system: a model (Figure 1). (1) A model is

978-1-4244-7316-8/11/$26.00 ©2011 IEEE

an accurate or simplified description of the system in its environment. This definition is most commonly used. It is illustrated in Figure 1, which details the steps of modeling and simulation.

We want to propose an alternative definition, more focused on cognition: (2) "a model does not describe the system, but a state of knowledge, knowledge gained from the study or observation of system". This interpretation seems more consistent with the presented knowledge definition. The work presented thereafter, will be based on the definition (2). In this paper, our objectives are to introduce the concept of cognitive simulation, and explain and elaborate our modeling approach. We can define cognition as a process of complex information, such as reasoning, decision making, etc. A cognitive process is to acquire information about its environment, and relates everything to do with knowledge. Unlike a classical simulation, which evolves over time a model based on static knowledge, we propose the concept of cognitive simulation [9], [10], [11]: it aims to take into account the knowledge evolution over time. A state of knowledge may vary depending on the expert who utters (interpretability problem), it can also vary over time and become less relevant (temporality or confidence problems), it is knowledge that we can describe as dynamics.

In the first section, we present the general framework of the discrete event systems (DES) theory, then the DEVS formalism. In the second part, we detail the mechanisms to implement to apply our approach to cognitive simulation. Before concluding and presenting the limitations and perspectives of our work, in the last part, we will describe a sample application.

II. Discrete Event Modeling

Modeling and simulation (M&S) have emerged as essential tools for analyzing the behavior of complex systems. Several methods have been proposed to improve the analysis process. These proposals attempt to achieve more realistic models, relatively simple and highly flexible. Our interest focuses on DEVS (Discrete Event System Specification [12]) is a formalism for modeling systems based on the DES theory [13].

A. DES and FDES

A Discrete Event System (DES) is a discrete-state, event-driven dynamical system in which the state space is described by a discrete set, and states evolve in terms of asynchronous occurrence of discrete events over time [13]. In DES theory, states, events and transition functions have crisp values and they are defined as: a DES can be modeled by a five-tuple [13], [14], [15]:

$$G = (S, \Sigma, \delta, \lambda, s_0) \tag{1}$$

where:

- S: is the set of states;
- Σ: is the set of events containing detectable (i.e. an event is detectable if it produces a measurable change in the system output) and undetectable events, which are generally fired asynchronously;
- $\delta : S \times \Sigma \to S$ is the state transition function;
- $\lambda : S \times \Sigma \to \Sigma_d$ is the output function, where Σ_d and Σ_{ud} are the set of detectable and undetectable events, respectively $\Sigma = \Sigma_d \cup \Sigma_{ud}$;
- and, s_0 is the initial state vector whose elements are zero or one.

Actually, DESs represent many technological and engineering systems such as communication networks, computer networks, manufacturing systems, transportation systems, natural systems, and more. So far, many modeling approaches of DESs have been proposed and developed, including the notably finite automata [13], [16], fuzzy automata [17], [18], Petri nets [13], [19], DEVS formalism [12].

DES theory is used to model systems that cannot be described by differential or difference equations. However, dynamic models that cannot be easily represented by the ordinary and classical approaches might be modeled by sequences of events recording significant qualitative changes in the state of the system. Although DES theory has been applied in many engineering fields, it is not adequate for all fields. Recently, in order to make it possible to effectively represent deterministic uncertainties and vagueness as well as human subjective observation and judgment inherent to many real-world problems especially those in complex systems, several works introduce the concept of fuzzy states and fuzzy events, and generalize (crisp) discrete event systems (DES) to fuzzy DES (FDES). Fuzzy discrete event systems (FDESs) were proposed recently by [20], [14], [21], which may better cope with the real-world problems with fuzziness, impreciseness, and subjectivity such as those in biomedicine.

In summary in [20], [14], [21], a fuzzy DES is represented by a fuzzy automaton:

$$\widetilde{G} = (\widetilde{S}, \widetilde{\Sigma}, \widetilde{\delta}, \widetilde{s}_0) \tag{2}$$

where $\widetilde{S}$, $\widetilde{\Sigma}$, $\widetilde{\delta}$, $\widetilde{s}_0$ are fuzzy extensions of the crisp S, Σ, δ, s_0 respectively. Formally:

- $\widetilde{S}$ is a set of fuzzy states $\widetilde{s}$, where $\widetilde{s}$ is represented by a vector over $[0, 1]$;
- $\widetilde{\Sigma}$ is a set of fuzzy events $\widetilde{\alpha}$, where $\widetilde{\alpha}$ is represented by a matrix over $[0, 1]$;
- $\widetilde{\delta} : \widetilde{S} \times \widetilde{\Sigma} \to \widetilde{S}$ is a transition function, where $\widetilde{\delta}(\widetilde{s}, \widetilde{\alpha}) = \widetilde{s} \circ \widetilde{\alpha}$;
- and, $\widetilde{s}_0$ is the initial state.

The integration of fuzzy information and the definition of FDES is a plus to improve the knowledge processing. This is a first step towards defining approaches to cognitive simulations. However, data to be processed (imprecise or uncertain) can occur at all levels of the system (see equation 1), their proper representation and their inclusion is a major issue. Despite this, most approaches only take into account that the vagueness or uncertainty of the states and/or system events. Inputs and the knowledge evolution over time are often omitted. We propose to extend the DEVS formalism for the inclusion of such information.

B. DEVS formalism

For several years our team working on the DEVS formalism [22], we work to develop and expand this M&S tool. This formalism provides a formal foundation to M&S that combines the advantages of a simulation-based approach with the rigor of a formal methodology. DEVS formalism is based on a mathematical paradigm with well-defined concepts of coupling of components, hierarchical, modular model construction, support for discrete event approximation of continuous systems and support of object-oriented paradigms. The DEVS formalism is based on the definition of two types of components: atomic models and coupled models.

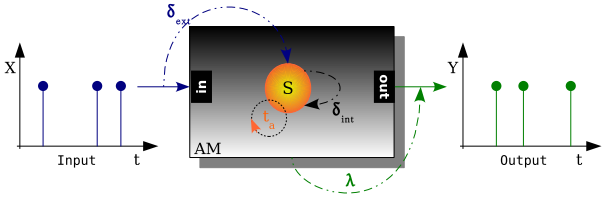

Figure 2. Behavior of atomic DEVS model

The atomic model (eq. 3) provides an autonomous description of the behavior of the system, defined by states, input/output functions and transition functions (see Figure 2). The coupled model is a composition of atomic models and/or coupled models. It is modular and presents a hierarchical structure which enables the creation of complex models from basic models.

Atomic DEVS model:

$$AM :< X, Y, S, t_a, \delta_{ext}, \lambda, \delta_{int} > \quad (3)$$

where:

- X: is the set of input events, is characterized by a couple (port, time, value), where the port means the input on which the event occurs, the time is the date of occurrence of the event, it is blank for internal events, and the value symbolizes the data from the event;
- Y: is the set of output events;
- S: is the set of partial or sequential states, which includes the state variables;
- $t_a : S \rightarrow \mathrm{T}^{\infty}$: is the time advance function which is used to determine the lifespan of a state;
- $\delta_{ext} : Q \times X \rightarrow S$: is the external transition function which defines how an input event X changes a state of the system, where $Q = \{(s, t_e) | s \in S,\ t_e \in (\mathrm{T} \cap [0, t_a(s)])\}$ is the set of total states, and t_e is the elapsed time since the last event;
- $\lambda : S \rightarrow Y^{\iota}$: is the output function where $Y^{\iota} = Y \cup \{\iota\}$ and $\iota \notin Y$ is a silent event or an unobserved event. This function defines how a state of the system generates an output event, when the elapsed time reaches to the lifetime of the state;
- $\delta_{int} : S \rightarrow S$: is the internal transition function which defines how a state of the system changes internally, when the elapsed time reaches to the lifetime of the state.

Every state S is associated with a lifetime t_a, which is defined by the time advance function. When an event receives an input event X, the external transition function δ_{ext} is triggered. This function uses the input event, the current state and the time elapsed since the last event in order to determine what the next model's state is. If no events occur before the time specified by the time advance function for that state, the model activates the output function λ (providing outputs Y), and changes to a new state determined by the internal transition function δ_{int}.

The DEVS models are executed by abstract simulators that are independent from the models themselves. Consequently, separated concerns between models and implementations of simulation can be achieved and enhance the verification of each layer independently. DEVS is a popular method to simulate a variety of systems. However, since its introduction by Zeigler in [12], significant efforts were taken to adapt this formalism to different fields and situations. The many proposed extensions [23], [24], [25], [26], [5], [6], proved its ability to extend and openness. In this large niche, we look towards the issue of knowledge evolution over time.

C. Proposal

As for the extension from DES to FDES, there are extensions to the DEVS formalism to deal fuzzy data, but they only address the uncertainty associated with events or states transitions [23], [26]. As used, the models are the result of the expression of imperfect knowledge and static over time. As we present them, they are not based on knowledge of an individual but on the expression of such knowledge, that is to say, on a state of knowledge, state variable over time.

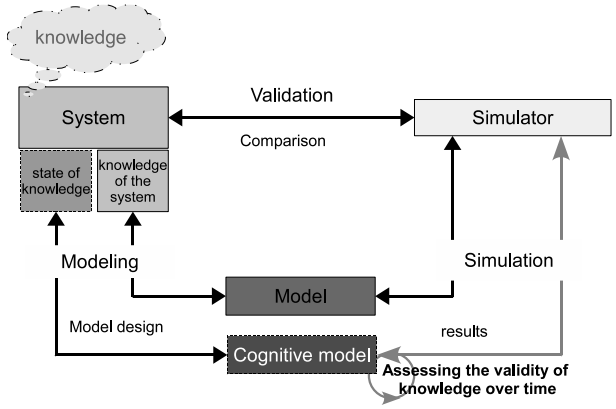

Figure 3. Integration of our cognitive model in MS process

Using Figure 3, we want to introduce the differences between the classic approach of M&S, presented in the introduction, and our approach. Between the cognitive model and the simulator, we added an evaluation mechanism that can evolve during the simulation the validity of the model parameters (eq. 3). Our approach makes sense, if we consider

that to give correct results must be taken into account in the models, the evolution and validity of data.

For example, a transport company that uses a predictive model to estimate the cost of its investments will not fix the price of a Brent barrel in advance. The evolution of the price of Brent is greatly influenced by complex factors: consumption, geopolitics, etc. Consider its price as imprecise can execute the model taking into account possible fluctuations in the price. Failing to have an accurate result, from our method, the company may have a tool for decision-making. Our proposal does not provide accurate results, it even adds to the imprecision of knowledge, but the results thus obtained allow having a broad estimate that has a good chance of being correct. We can consider this as a tool for decision support.

III. DEVS Cognitive approach

From the DEVS formalism, which is based on the DES theory, we propose a cognitive simulation approach to knowledge representation whose validity may decrease over time. Such data or information are not based on supposed knowledge of the expert, but are inferred from the knowledge expression. They are subjective, subject to human interpretation, and their relevance may vary. The information we want to take into account, can be likened to adding a confidence measure in the expert knowledge.

A. Cognitive DEVS models

We start from a simple observation, knowledge expressed and validated at a time t can, and is often the case; loses its relevance over time. To represent this loss of information, we propose to define a mechanism to data control and integrate it into the atomic DEVS model. Our goal is to extend the DEVS formalism to take into account what we call dynamic data. During the simulation, as data may lose their relevance and precision, we add a knowledge evaluation function called (Γ), during the simulation, it assessed the validity of data models and transforms some data to imprecise interval. This transformation, which can be seen as a fuzzification, will be performed by a new function added in the atomic DEVS model.

B. iDEVS method

The integration mechanism is based on our previous work, they aim to represent and manipulate imprecise data in DEVS models [27], [5]. The mechanism is simple and intuitive; we defined a new data type (a class), which allows to represent and to manipulate a fuzzy interval (Fuzzy Set) as an integer or a float. It is possible to perform calculations: basic operations (+, -, *, /) or implement functions (sin, cos, log). With the advantages of object-oriented programming (OOP), the use of our data type is transparent to the user. For example, let an integer A, and a fuzzy interval B, A+A = an integer, A+B = a fuzzy interval, B+A = a fuzzy interval, and B+B = a fuzzy interval. This is possible thanks to operator overloading to the right and left. Our data type is used to represent imprecision in various forms described in Figure 4.

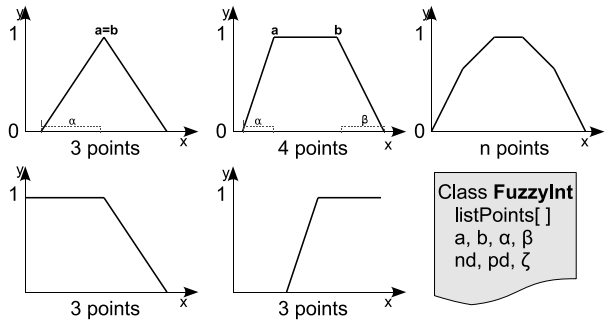

Figure 4. Example of imprecise data described from our class

Our data structure consists of a list of point (type (x, y)), 4 points defining the kernel (a and b) and the support (ψ and ω). We also added the left and right radius: $\alpha = a - \psi$ and $\beta = \omega - b$, and a linguistic label. Added to this, different coefficients to represent the validity of the information (pd), its necessity (nd), and so on. We also added a temporality variable (lifespan τ) which is evaluated and used to define the validity degree. The addition of this new information can describe the state of knowledge.

C. Operation method

We offer two application modes:

(1) a classic data (crisp) will be transformed into imprecise data (fuzzy interval), and we add a validity coefficient, a coefficient of necessity, and a lifespan. Interval support ($\omega - \psi$) or fuzzification coefficient (radius) is fixed by the user. All data are transformed into an object of $FuzzyInt$ type, in order to add our coefficients. During the first transformation, there is really no fuzzification, that is to say, that we do not add imprecision, the aim of the transformation is to add the coefficients, e.g. a value $A = 5$, will be transformed into interval $I_A = [5; 5; 5; 5]$, then depending on the validity degree and the simulation time, the bounds of the interval I_A will grow;

(2) imprecise data is tested and evaluated. Depending on its lifespan, its validity coefficient is decreased, and its support is increased (see Table I). In conclusion, we add the imprecision when data validity is low.

Table I
Proposed changes in the validity degree based on the simulation time

Simulation time (%)	0 to 40	50 to 60	70 to 100 %
Validity degree	1 to .6	.5 to .4	.3 to 0.0
Fuzzification data	$n \times 1$	$n \times 2$	$n \times 3$, a-1, b+1

D. Cognitive function

These two modes are grouped in a function added in our atomic DEVS model:

For state (S):

If S is imprecise, then we evaluate the lifespan of S compared to simulation time (lifespan equal simulation time minus current time), and we update the validity degree and the interval radius with the correlation table (Tab I).

Else, we transform S (fuzzification) using data from the user; the default fuzzification radius is 1.

For input (X):

If X is imprecise, then we evaluate the lifespan of X compared to simulation time, and we update the validity degree and the interval radius with the correlation table (Tab I).

Else, we transform X (fuzzification) using data from the user; the default fuzzification radius is 1.

Algorithm 1 Cognitive function algorithm

```
Γ(Q, X):
    N = Q (state) or X (input);
    if type(N) == fuzzy interval:
        N.update(N.listPoints = newList, N.to = SIM_TIME –
c_Time, N.pd = tab[N.to]) ;
    else
        N.fuzzification(data_user);
end;
```

In Table I we present an example of evolution of the state of knowledge. When the simulation advances of 10 %, decreases the validity degree of 0.1. Depending on the data validity, we increase the imprecision. It is the user to give the fuzzification data. By default, if the validity degree is above 0.7, we do not change; between 0.5 and 0.6 we double the interval radius, and under 0.4, we are tripling the interval radius and we are moving from a triangular representation ($a = b$) to a trapezoidal representation ($a \neq b$).

E. Integration into DEVS

Our cognitive function may be launched either in simulation algorithms, either directly in the atomic models. Its integration in the simulation part implies modification in the simulation algorithms. The method loses its genericity, because it will only work with a specific algorithm. In this case, add a line of code to run this function before launch the external transition function (δ_{ext}). We chose to integrate in the modeling part, at the level of atomic models. The function is called and then executed in the code of the external transition function. This is the first thing that must be δ_{ext}. Thus, it is not necessary to modify the simulation algorithms, and our method can be deployed in existing DEVS environments. So we keep the genericity of the approach.

F. Atomic Cognitive DEVS model

Our atomic cognitive model has the same features as the classic atomic DEVS model. Almost all functions have the same role, and the same behavior. Level simulation algorithms, their sequence is identical. The equation 4 describes our atomic model. The elements identified as being imprecise are described by a tilde. The additional element that appears is the function Γ, it defines the knowledge behavior over time.

Atomic cognitive model:

$$AcM := < \tilde{X}, \tilde{Y}, \tilde{S}, t_a, \delta_{ext}, \Gamma, \lambda, \delta_{int} > \quad (4)$$

with $\tilde{X}$, $\tilde{Y}$ and $\tilde{S}$ are a fuzzy extensions of the crisp X, Y, S, and where:

- $\tilde{X} \supset X$: is the set of input events, is characterized by a couple (port, $\widetilde{time}$, $\widetilde{value}$), where:
  - the $\widetilde{port}$ means the input on which the event occurs;
  - the $\widetilde{time}$ is the date of occurrence of the event, it can be imprecise, that is to say, defined as an object of $\widetilde{FuzzyInt}$ type. It is blank for internal events;
  - and, the $\widetilde{value}$ symbolizes the imprecise data from the event;
- $\tilde{Y} \supset Y$: is the set of output events, if one element of the model is imprecise, the outputs are imprecise;
- $\tilde{S} \supset S$: is the set of partial or sequential states, which includes the state variables. States are not directly imprecise, the state variables can be of $FuzzyInt$ type;
- $t_a : S \rightarrow \mathrm{T}^{\infty}$: is the time advance function which is used to determine the lifespan of a state. The lifetime of the state may not be accurate, in this case solutions have been proposed in [27], [28], [5];
- $\delta_{ext} : Q \times \tilde{X} \rightarrow \tilde{S}$: is the external transition function which defines how an input event $\tilde{X}$ changes a state of the system. In our model δ_{ext} has the same objectives and a new role, which is to trigger the function Γ;
- Γ : is our cognitive function, it allows to control and assess the confidence we have in information (see 1);
- $\lambda : \tilde{S} \rightarrow \tilde{Y}^{\iota}$: is the output function. This function defines how a state of the system generates an output event, when the elapsed time reaches to the lifetime of the state. In the case of imprecise data, it is used to send additional information such as membership degrees;
- $\delta_{int} : \tilde{S} \rightarrow \tilde{S}$: is the internal transition function which defines how a state of the system changes internally, when the elapsed time reaches to the lifetime of the state.

This model takes into account imprecise data, it is by no means a general proposal detailing the fuzzy DEVS model. To generalize it to fuzzy information (imprecision and uncertainty), one should take into account the uncertainties associated with the transition functions, the state changes, and events.

IV. Case study

To illustrate the interest of our approach, we propose to present a pedagogic example of application. We will present the difference in results between a traditional model and a model that performs our cognitive function.

The system is simple, a random generator (I) sends digital information (time, value) to two summer (adder) (A and B) responsible for adding the input value with a value stored in state variables. The summer A has a classical behavior, B run our cognition function. Two output models (O_1 and O_2) to print the results. In Model A, there is no distinction between knowledge of the system and state of knowledge. By cons, this is the case in Model B. For the latter, knowledge defined the

model behavior, that is to say, the addition of an input and a state variable. The state of the knowledge is characterized by the fuzzification of the value of state variable.

Table II
MODELS A AND B SIMULATION RESULTS

time	input	Output A	Output B
0	0	0	$[-2; 0; 0; 2]$
1	5	5	$[2; 5; 5; 8]$
8	2	7	$[2; 7; 7; 12]$
11	6	13	$[5; 13; 13; 21]$
27	3	16	$[4; 15; 17; 28]$
32	7	23	$[7; 21; 25; 39]$
40	2	25	$[5; 22; 28; 25]$
45	8	33	$[9; 29; 37; 57]$
50	5	38	$[10; 33; 43; 66]$

Table II presents the simulation results of the models A and B. We can see that the vagueness increases much during the simulation; this is due to the loss of data validity.

Model A makes only an addition of the input value with the value stored as a state variable. For example, at time 27: 13+3 = 16.

Before each addition, model B evaluates the lifespan of its state variable, and updates its validity degree, then it converts input value to imprecise variable and finally, adds its imprecise state variable with the imprecise input data. For example, at time 27: state model is [5;13;13;21], pd=1, τ=30, after its evaluation, we get [2;12;14;24], pd=0,3 and τ=3. The input data is transformed (fuzzification) [2;3;3;4] the lifespan is 23 (Simulation final time minus current time 50-27), validity degree is set at 1. The result is well [4;15;17;28], pd= 1 (max(0,3;1)) and τ=3 (min(3;23)).

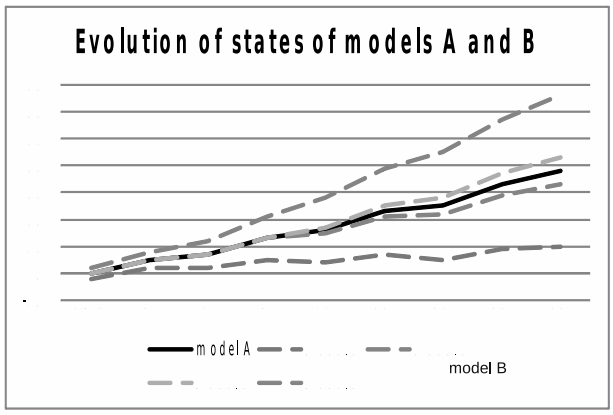

Figure 5. Models A and B state variables evolution

For this example, we chose to use the max operator for operations between validity degrees, and the min operator for the operations between lifespan. Curve 5 shows that the imprecision increases over time, and the results obtained from the classical model are bordered by the results of the cognitive model.

We are aware that the proposed case study is limited, its purpose is to validate the theoretical approach on a simple and concrete case. As shown by the example, and as one might expect, over time the imprecision of the data increases. All the advantages of this method are not clearly exposed from this application, we will soon propose other implementations. We can still highlight the originality of our approach, few studies focus on the impact of knowledge evolution over time, and therefore on the simulation results.

V. CONCLUSION

In this paper, from a formalism based on DES theory (DEVS) and a method for modeling imprecision (iDEVS), we presented a formal approach for taking into account the knowledge evolution: from our point of view, knowledge is not static, it can evolve in time, or during the simulation. To take into account this knowledge, we added a lifespan to the modeled data, the latter is used to define the validity degree of knowledge. It is a kind of confidence measure.

This work has as main objective to take into account the evolution over time of the knowledge validity, that is to say, a state of knowledge and a confidence measure. A mechanism of control and fuzzification was added at the atomic models of DEVS formalism (Atomic Cognitive DEVS model). The integration of this mechanism can respond to our problems while retaining all the properties of the DEVS formalism.

This work complements our research in the fields of FDES. They should be seen in a broader context, which aims to develop a multi-modeling framework for the study of complex systems, and more particularly a fuzzy toolbox for DES [29], [6].

Our approach is in validation phase, and it has to be improved to take into account to the problems of combinatorial explosion associated with the use of some mathematical operators in interval arithmetic. Another avenue of reflection is to study the impact of the operator used in operations between the validity degrees (pd). We propose three methods max, min, average, but we have not evaluated their impact in real situations. Finally, returning to Figure 3, and complete our reflection, we believe that the traditional model may be regarded as derived from necessary knowledge, and not necessarily sufficient. The cognitive model rather describes a possible behavior of the system. This reflection allows us to do a parallel with the possibility theory [30], [31], [32], and a link between possibility measure and necessity. We plan thus to complete our approach from the development of possibility theory.

REFERENCES

[1] B. Russell, *Introduction to Mathematical Philosophy*. 1993.
[2] L. Zadeh, "Fuzzy sets," *Information Control*, vol. 8, pp. 338–353, 1965.
[3] L. A. Zadeh, "Fuzzy logic," *Computer*, vol. 21, no. 4, pp. 83–93, 1988.
[4] D. Dubois and H. Prade, "Fuzzy set in approximate reasoning," *part 1, Fuzzy set and Systems, vol 40*, 1993.
[5] P.-A. Bisgambiglia, E. de Gentili, P. Bisgambiglia, and J.-F. Santucci, "idevs: new method to study inaccurate systems," in *Proceedings of the The Annual IEEE International Conference on Fuzzy Systems, Jeju Island (Korea)* (IEEE, ed.), IEEE, 8 2009.

[6] P.-A. Bisgambiglia, L. Capocchi, P. Bisgambiglia, and S. Garredu, "Fuzzy Inference Models For Discrete EVent Systems," in *Proceedings of the 2010 IEEE World Congress on Computational Intelligence (WCCI 2010) - IEEE International Conference on Fuzzy Systems (FUZZ-IEEE), Barcelona (SPAIN)* (IEEE, ed.), IEEE, 7 2010.

[7] S. Garredu, P.-A. Bisgambiglia, E. Vittori, and J. Santucci, "Towards the definition of an intuitive specification language," in *Proceedings of the International Modeling and Simulation Multiconference (IMSM) - Conceptula Modeling Simulation (CMS)* (SCS, ed.), pp. 187–192, 2 2007.

[8] S. Garredu, P.-A. Bisgambiglia, E. Vitttori, and J. Santucci, "A new approach to describe devs models using both uml state machine diagrams and fuzzy logic," in *Proceedings of the 2010 International Mediterranean and Latin American Modelling Multiconference, I3M 2010, Fez, (Maroco)* (EMSS, ed.), EMSS, 10 2010.

[9] P. Cacciabue, F. Decortis, B. Drozdowicz, M. Masson, and J.-P. Nordvik, "COSIMO: A cognitive simulation model of human decision making and behavior in accident management of complex plants," vol. 22, no. 5, pp. 1058 – 1074, 1992.

[10] P. Mayenobe, L. Trassoudaine, T. Bellet, and H. Tattegrain-Veste, "Cognitive simulation of driver and cooperative driving assistance," in *Proceedings of Intelligent Vehicle Symposium*, vol. 1, p. 234, IEEE, 2002.

[11] A. Das and W. Stuerzlinger, "A cognitive simulation model for novice text entry on cell phone keypads," in *Proceedings of the 14th European conference on Cognitive ergonomics: invent! explore!*, ECCE '07, (New York, NY, USA), pp. 141–147, ACM, 2007.

[12] B. P. Zeigler, H. Praehofer, and T. G. Kim, *Theory of Modeling and Simulation, Second Edition*. 2000.

[13] C. Cassandrass and S. Lafortune, *Introduction to Discrete Event Systems*. 1999.

[14] F. Lin and H. Ying, "Modeling and control of fuzzy discrete event systems," vol. 32, no. 4, pp. 408 – 415, 2002.

[15] E. Kilic, C. Karasu, and K. Leblebicioglu, "Fault diagnosis with dynamic fuzzy discrete event system approach," vol. 3949, pp. 117 – 124, 2005.

[16] J. Thistle, "Supervisory control of discrete event systems,"

[17] W. G. Wee and K. S. Fu, "A formulation of fuzzy automata and its applications as a model of learning systems," *IEEE transaction on SSC*, vol. 5, pp. 215–223, 1969.

[18] M. Doostfatemeh and S. C. Kremer, "New directions in fuzzy automata," *International Journal of Approximate Reasoning*, vol. 38, pp. 175–214, 2005.

[19] L. Holloway, B. Krogh, and A. Giua, "A suvery of petri net methods for controlled discrete event systems,"

[20] F. Lin and H. Ying, "Fuzzy discrete event systems and their observability," in *Proceedigns of IFSA World Congress and 20th NAFIPS International Conference, Vancouver, (Canada)* (IEEE, ed.), vol. 3, pp. 1271 – 1276, 2001.

[21] F. Lin, H. Ying, R. D. MacArthur, J. A. Cohn, D. Barth-Jones, and L. R. Crane, "Decision making in fuzzy discrete event systems," *Inf. Sci.*, vol. 177, pp. 3749–3763, September 2007.

[22] B. P. Zeigler, T. G. Kim, and H. Praehofer, *Theory of Modeling and Simulation*. Orlando, FL, USA: Academic Press, Inc., 2000.

[23] Y. Kwon, H. Park, S. Jung, and T. Kim, "Fuzzy-DEVS Formalisme : Concepts, Realization and Application," *Proceedings AIS 1996*, pp. 227–234, 1996.

[24] N. Giambiasi and S. Ghosh, "Min-Max-DEVS: A new formalism for the specification of discrete event models with min-max delays," pp. 616–621, 13th European Simulation Symposium, 2001.

[25] L. Ntaimo and B. P. Zeigler, "Expressing a forest cell model in parallel DEVS and timed cell-DEVS formalisms," Proceedings of the 2004 Summer Computer Simulation Conference, 2002.

[26] S. Sheikh-Bahaei, J. Liu, M. Jamshidi, and P. Lino, "An intelligent discrete event approach to modeling, simulation and control of autonomous agents," vol. 10, no. 4, pp. 337 – 348, 2004.

[27] P.-A. Bisgambiglia, E. de Gentili, P. Bisgambiglia, and J. Santucci, "Fuzzy simulation for discrete events systems," in *Proceedings of the 2008 IEEE World Congress on Computational Intelligence (WCCI 2008) - IEEE International Conference on Fuzzy Systems (FUZZ-IEEE)*, pp. 688–694, 06 2008.

[28] P.-A. Bisgambiglia, E. de Gentili, P. Bisgambiglia, and J. Santucci, "Discrete events system simulation-based defuzzification method," in *Proceedings of The 14th IEEE Mediterranean Electrotechnical Conference (MELECON)*, pp. 132–138, 05 2008.

[29] P.-A. Bisgambiglia, E. de Gentili, P. Bisgambiglia, and J.-F. Santucci, "Fuzz-idevs: Towards a fuzzy toolbox for discrete event systems," in *Proceedings of the SIMUTools'09, Rome (Italie)* (ACM, ed.), SIMUTools, 3 2009.

[30] L. Zadeh, "Fuzzy sets as a basics for a theroy of possibility," *Fuzzy Sets and Systems*, pp. 3–28, 1978.

[31] D. Dubois and H. Prade, "Representation and combination of uncertainty with belief functions and possibility measures," *Comput. Intell*, no. 4, pp. 244–264, 1988.

[32] D. Dubois, H. T. Nguyen, and H. Prade, "Possibility theory, probability and fuzzy sets : Misunderstandings, bridges and gaps," pp. 343–438, 2000.

2011 IEEE International Conference on Fuzzy Systems
June 27-30, 2011, Taipei, Taiwan

A Fuzzy Tool for the Validation of Individual Risk Premia in High-Technology Venture Valuation

The Application of a Novel Framework to Convert FCMs into Rule-Based Fuzzy Systems

Ralf Salomon
Department of Computer Science
and Electrical Engineering
University of Rostock,
D-18051 Rostock, Germany
ralf.salomon@uni-rostock.de

Peter Heydebreck
inno Germany AG
D-76133 Karlsruhe, Germany
p.heydebreck@inno-group.com

Lars Krüger
engage - Key Technology Ventures AG
D-18057 Rostock, Germany
l.krueger@engage-ventures.com

Abstract **- Venture valuation is an essential technique in economics. Depending on the reason for a valuation, there are several methods applicable. It becomes even more complex when it comes to the valuation of companies that possess mainly intangible assets and whose success lies in the future. In this article a further step towards a Fuzzy Method is presented and discussed that allows the determination of a relevant parameter for a widely used valuation method. We focus on the application of a novel methodological framework to convert Fuzzy Cognitive Maps into Fuzzy rule-based Inference Systems. We demonstrate the principal feasibility and elucidate a method to optimize the functionality**.

Key Words *Fuzzy Cognitive Map, Fuzzy Inference Systems, Fuzzy Rules, High-Technology Ventures, Company Valuation, Risk-adequate Discount Rate*

I. INTRODUCTION

A. Background

There is a substantial need with key decision makers for support instruments that are robust, reliable, and above all, applicable in business real life. Particularly in the Venture Capital world, decisions that are based on unreliable or even wrong information can lead to significant losses of the invested money. This is particularly essential when it comes to valuing a young high-technology venture before an investment transaction. The inherent peculiarities of small high-technology ventures in venture capital transactions are analyzed exemplarily in [16].

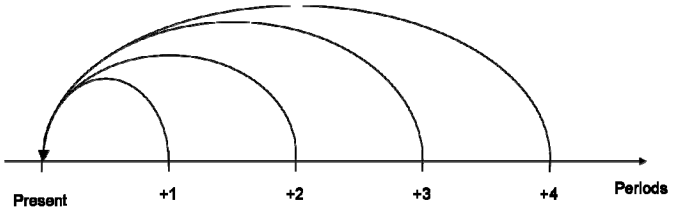

Figure 1: Principle of Future-Oriented Valuation Methods

Due to the lack of historic data, the existence of mainly tangible assets and the limited comparability to grown mature companies even in the same industry field, there is a need for specific valuation methods for young high-technology companies. A concept that has experienced a broad acceptance with practitioners in the recent years is based on the time-value-of-money concept. The main feature of Discounted Cash Flow Methods (DCF) is its future-oriented approach to valuation, i.e., prospective earnings determine the current value of the company (Fig. 1). The formal expression is shown in Equation 1. The present value *PV* of a company is the result of the added cash-flow *CF,* discounted by the discount rate *r,* the company is going to earn in the next *i* periods (Equation 1).

$$PV = \sum_{n=1}^{i} \frac{CF_i}{(1+r)^i}$$

Equation 1: Presented Value - Discounted Cash-Flow Method

The future development of a young high-technology company is, however, risky. Until now, no basic principle on how to consider the company or entrepreneurial risk in the context of company valuation has achieved acceptance.

One of the most popular methods with practioners is the so-called *Risk Premium Method*. This approach implies that the discount rate *r* consists of two components: the prime rate and an additive risk premium. The former can be relatively distinctly derived from, for example, the rate of return of risk-free fixed income assets (e.g. government bonds). The latter, however, is one the most disputed component in scientific literature on company valuation. In fact, there has not been a distinct, clear, and practicable method for exactly determining the risk premium, particularly when it comes to High-Technology Ventures. Usually, the chosen risk premia largely depends on subjective assessments of the valuer. Hence, an objective traceability is not fully given. Current research on this obvious deficit is agile, though; the aim of higher objectivity has not attained yet [3].

Obviously, the need for models and methods that can cope with uncertain prospective developments is big. Fuzzy techniques have already shown that they can be capable to

978-1-4244-7316-8/11/$26.00 ©2011 IEEE

manage uncertainty and map it to formal computable structures. So, the application of Fuzzy techniques and concepts to this field is self-evident.

B. State-of-the-Art

The use of Fuzzy techniques to model relevant parameters in Finance has not been a major issue. Certain approaches have been presented, e.g., the use of fuzzy numbers to model uncertainty with investment decisions [4] or fuzzy interval methods in investment risk appraisal [5]. Takagi-Sugeno probabilistic fuzzy systems have also been used to identify relevant states of financial markets [19]. Modeling of risk has also been touched, for example when it comes to investment project risk appraisal [6]. The widely used *Capital Asset Pricing Model* (CAPM) was as well enhanced by Fuzzy concepts to model risk-return-relations under uncertainty [8], [9]. A further specific application of a Fuzzy CAPM in Insurance was presented in [7].

Besides adopting conventional Finance models with Fuzzy aspects, there have only been little advances in developing practical tools that play out the strengths of Fuzzy theory in modeling and making complex real-world systems manageable. Particularly, describing the relationship between risk and return in Venture Capital Investment has obviously been rarely touched by scientific literature. Hence, there is only a relatively small number of articles that directly deals with this issue. In [10] for example, a novel risk warning control method was presented that allows the comparison of different investment objects on the basis of risk-return-characteristics.

It becomes obvious that there is no explicit Fuzzy method that can help determine the relevant parameters for the DCF-model in the context of *High-Technology Venture* (HTV) Valuation.

C. Aim of this paper

In this article we want to discuss a novel approach to a risk-adequate company valuation. It shall allow a clear and traceable determination of the risk premium upon the basis of individual company characteristics. Essentially, our approach is based upon more realistic assumptions and does not demanding historic and comprehensive statistic data. To realize these ambitious goals, we make use of a novel method allowing the use of *Fuzzy Cognitive Maps* (FCM) as a knowledge capturing and representation tool and, in addition, as a starting point from which a rule-based *Fuzzy Inference System* (FIS) can be methodically clear derived from. As a result a crisp value for the parameter risk premium r_{rp} can be obtained.

D. Contribution

This article represents a significant further development of our original approach. The methodological fundament was presented and discussed in [1]. Therein, the initial model was established that uses verbal expert knowledge to assess the influence of specific factors on the risk of young HTVs. *Fuzzy Cognitive Maps* (FCM) were used for knowledge capturing and representation. Moreover, the FCMs can be used as the fundament for the development of rule-based *Fuzzy Inference Systems* (FIS). A first attempt to apply this technique in the context of high-technology venture valuation was presented in [2] and [3]. The aim was to obtain a crisp parameter upon the basis of qualitative expert knowledge. Besides the starting points for further research we showed the principal feasibility of this approach.

One of the major weak points of our method was the limited accuracy and efficacy of the initial model describing the relationship between the individual company's characteristics and the inherent risk. We primarily used not fully empirically proven factors. By founding our model on the findings of statistical meta-analysis, we could present in [11] a model that realistically maps the influence factors onto the company risk. Key to this enhancement is the number and the relevance of the factors that was statistically proven by 131 single quantitative studies on this issue.

In this article a further leap ahead is presented. Besides the enhanced economic model the focus is laid on the underlying Fuzzy Inference Systems and their rule bases. A particular focus is laid on the rule definition and rule base optimization of the final FIS. The result is a far more realistic behavior of the underlying model. Thus, our model provides the principal and technical fundament for a practicable decision making tool in venture capital investments, particularly focusing on high-technology ventures in the early stage.

E. Structure

After the introduction in Section 1, the preliminaries of the used methodological framework are presented in Section 2. The novel approach is elucidated in Section 3. Besides the basics of the underlying economic model, the rule base is being optimized. Simulation outputs before and after optimization are also depicted in this Section. Subsequently, the results and further research needs are discussed in Section 4.

II. PRELEMINARIES

The detailed presentation of the methodical framework in [1], [2] is used as a conceptual fundament. Hence, in this article, only the main features of the underlying method are cursorily presented.

A. Interpretation of Nodes and Edges

The shortages of conventional FCM are overcome by transformation using the specifically developed method presented in [1]. The major assumption of the novel framework is that there is no central rule base that represents the causal relations between the nodes. In contrast, it is assumed that each causal link can be represented by a standardized rule base. A causal link of the causal strength w_{ij} between two nodes C_i and C_j depicted by an arrow in an FCM is represented by a rule-based Fuzzy Inference System FIS_{ij} (see Figure 2). Hence, each causal link in an FCM can be translated into a corresponding single-input-single-output Fuzzy Inference System. By applying this procedure, every highly-individual FCM can be translated into a network of Fuzzy Inference Systems.

The authors thank *engage - Key Technology Ventures* for material and intellectual support.

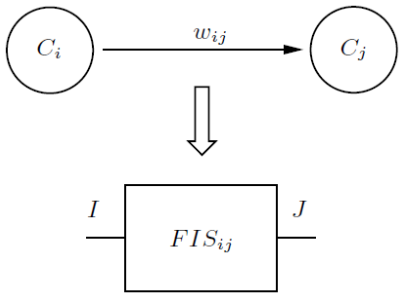

Figure 2: Representation of a single Causal Link by an FIS

B. *Multiple Causal Inputs*

To cope with multiple causal inputs, a method for combining multiple causal inputs is proposed being similar to the aggregation operator *A* proposed by Khan and Khor [17], [18]. Initially, all incoming edges are transformed to individual FIS according to the causal weight associated to them.

Thereby, the incoming signals can be weighted according to their (assumed) importance (Fig. 3). Usually, the signals are all treated equally. The outgoing signal represents the combined causal effect of the preceding cause nodes on the following effect node.

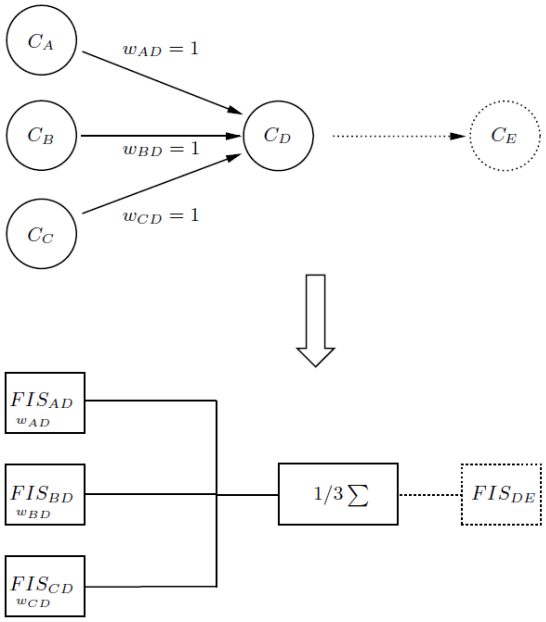

Figure 3: Interpretation of Multiple Causal Links

C. *Rule-Based Causality*

Each of these causalities is represented by a specific rule-based Fuzzy Inference System. The type of causality (positive or negative) as well as its strength is expressed by a specific rule base. The rule base is made for a single-input-single-output-Fuzzy Inference System. On the one hand, this decreases the calculation power needed to calculate a whole network of FIS. On the other hand, it reduces the risk of rule explosion.

The input and output parameters of the FIS correspond with the level of activation of the actual node. They are represented by *I*, whereas *J* denotes the output parameter level of activation of the effect node. Both parameters are defined on the basic set $X_{I,J} = [-1; 1] \in R$. An input signal $I = 1.0$ stands for the highest activation of the actual concept. It can correspond with the highest growth of the underlying concept. In contrast to that, an input value $I = -1.0$ expresses the highest activation of the node in the negative sense; it corresponds with the largest decline of the actual concept. The parameters *I* and *J* can take 21 parameter values each. Every step at 0.1 is represented by a parameter value. The output signal *J* equals the value of the concept node Cj and is, thus, possibly the input signal *I* of a successive FIS.

Each parameter is mapped onto a Fuzzy Set. The corresponding membership function is bell-shaped or Gaussian. This form of membership function provides a more realistic modeling of the underlying concept values and their corresponding membership degrees. At the outer borders of a fuzzy set, bell-shaped membership functions allow for a less harsh end and beginning of the membership. But, the closer the value gets to center c of the fuzzy number, the stronger the membership degree grows. This non-linearity corresponds with the real-world understanding of fuzzy observations (Fig. 4).

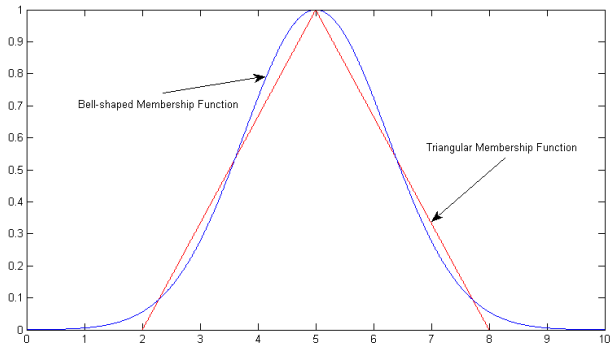

Figure 4: Triangular vs. Gaussian Membership Function

The set of membership functions representing the input and output parameter *I* and *J* is shown in Fig. 5.

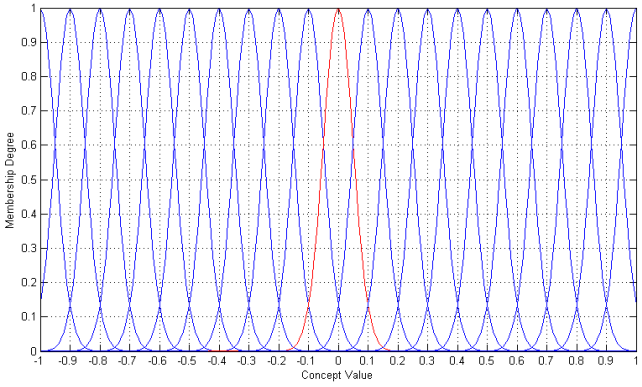

Figure 5: Membership Functions of the Parameters *I* and *J*

Next, the causal linkage between the two parameters has to be defined. To model (non-linear and non-symmetric) causality a specified rule base is designed. Each causality, and hence each causal strength is represented by a specific rule base. The IF-part of the rule consists of only one input *I*. This signal equals the fuzzy number of the concept node value C_i. Due to the discretization in steps of 0.1, the rule base is limited to a reasonable number of rules. Correspondingly, the THEN-part of the rule also consists of only one de-fuzzified output signal *J*. To determine the individual rule bases, the general understanding of the causal relationship between input and output parameter has to be highlighted. A positive causal relationship between C_i and C_j means that if C_i increases (less/ much) then C_j also increases (less/ much). A positive causal relation that has the causal strength $w_{ji} < 1$ leads, thus, to a weakened increase of C_j in case C_i increases. This weakening effect grows the lower the causal strength is.

For example, a concept value of $C_i = 1.0$ may lead only to a concept value $C_j = 0.2$. The same holds true for a decline when there is a positive causal relation. An exemplary rule base representing a positive causal strength $w = 1.0$ and the corresponding output profile is shown in Figure 5 and Figure 6, respectively. Analogue to this example there are specific rule bases for all possible causal weights *w*, $w \in [-1; 1]$. In the herein proposed methodological framework there is a total of 11 specific rule bases (increment of causality is 0.2, ranging from -1 to 1).

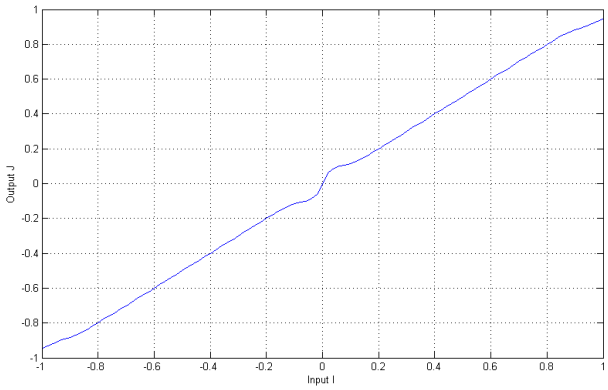

Figure 6: Output Profile of the FIS for Causality $w_{ij} = 1.0$

D. Crisp Output

To eventually obtain a crisp output, a specified component is needed: a final FIS_f. Its purpose is to take all directly preceding causal links and to 'calculate' a final output value. The input value is obtained by aggregating all incoming causal links (inputs) by using the aggregation operator (Figure 3). Its value ranges from +1 (highest increase) to -1 (highest decrease). The input value is mapped onto the corresponding output value by a specific rule base depending on the actual context. By applying this methodological framework it is possible to describe and model any complex system and its behavior by means of FCMs. Subsequently, this model of a complex system can be analyzed quantitatively, that means, a crisp value is returned.

Rule1:	IF	$I = -1.0$	THEN	$J = -1.0$
Rule2:	IF	$I = -0.9$	THEN	$J = -0.9$
Rule3:	IF	$I = -0.8$	THEN	$J = -0.8$
Rule4:	IF	$I = -0.7$	THEN	$J = -0.7$
Rule5:	IF	$I = -0.6$	THEN	$J = -0.6$
Rule6:	IF	$I = -0.5$	THEN	$J = -0.5$
Rule7:	IF	$I = -0.4$	THEN	$J = -0.4$
Rule8:	IF	$I = -0.3$	THEN	$J = -0.3$
Rule9:	IF	$I = -0.2$	THEN	$J = -0.3$
Rule10:	IF	$I = -0.1$	THEN	$J = -0.2$
Rule11:	IF	$I = 0$	THEN	$J = 0$
Rule12:	IF	$I = 0.1$	THEN	$J = 0.1$
Rule13:	IF	$I = 0.2$	THEN	$J = 0.2$
Rule14:	IF	$I = 0.3$	THEN	$J = 0.3$
Rule15:	IF	$I = 0.4$	THEN	$J = 0.4$
Rule16:	IF	$I = 0.5$	THEN	$J = 0.5$
Rule17:	IF	$I = 0.6$	THEN	$J = 0.6$
Rule18:	IF	$I = 0.7$	THEN	$J = 0.7$
Rule19:	IF	$I = 0.8$	THEN	$J = 0.8$
Rule20:	IF	$I = 0.9$	THEN	$J = 0.9$
Rule21:	IF	$I = 1.0$	THEN	$J = 1.0$

Figure 7: Rule Base for Causality $w_{ij} = 1.0$

III. Application

A. Basic Assumptions

For presenting a novel method to determine a relevant parameter for venture valuations, it is necessary to model the relationship between this parameter r_{rp} and the influencing factors. Referring to [4] and [12], the main factors are listed in Table 1.

Table 1: Significant Meta-Factors of Succes [12]

Metafactor	N	K	ρ	Expl. Var	X_S
Market Scope	1,046	10	0.21	100%	78
Industry Experience	423	4	0.11	100%	2
Marketing Experience	381	3	0.11	100%	2
Financial Resources	638	6	0.12	100%	14
Firm Age	1,890	15	0.16	87%	157
Patent Protection	453	5	0.11	100%	157
Size of Founding Team	332	5	0.13	100%	6
Supply Chain Integration	604	6	0.23	89%	41

N…aggregate sample size
K…number of correlation in the underlying studies that build the metafactor
ρ…estimate of the real population correlation
X_S…critical number of null-studies

Using these factors as the conceptual starting point, five experts were asked to construct an FCM upon these factors and weigh the causal interrelations between them. The result is depicted in Fig. 8.

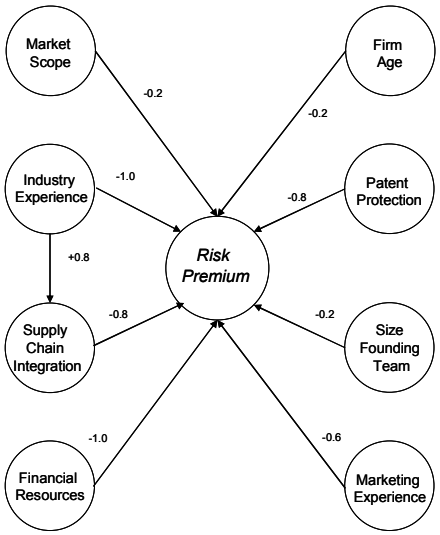

Figure 8: Expert FCM

The corresponding adjacency matrix E_{fin} is given by:

$$E_{fin} = \sum_{n=1}^{k} a_k E_{ij}^k = \begin{pmatrix} 0 & 0 & 0 & 0 & 0 & 0 & 0 & 0 & -0.6 \\ 0 & 0 & 0.8 & 0 & 0 & 0 & 0 & 0 & -1.0 \\ 0 & 0 & 0 & 0 & 0 & 0 & 0 & 0 & -0.8 \\ 0 & 0 & 0 & 0 & 0 & 0 & 0 & 0 & -1.0 \\ 0 & 0 & 0 & 0 & 0 & 0 & 0 & 0 & -0.2 \\ 0 & 0 & 0 & 0 & 0 & 0 & 0 & 0 & -0.8 \\ 0 & 0 & 0 & 0 & 0 & 0 & 0 & 0 & -0.2 \\ 0 & 0 & 0 & 0 & 0 & 0 & 0 & 0 & -0.6 \\ 0 & 0 & 0 & 0 & 0 & 0 & 0 & 0 & 0 \end{pmatrix}$$

B. *Fuzzy Inference System and Rule Base*

According to the methodological framework discussed in [1], this FCM can be converted into a network of FIS. To eventually obtain a crisp value a final FIS is designed. Its position in the network of FIS is analogue to the configuration in Fig. 3. The final FIS maps the aggregated auxiliary parameter R onto the output parameter r_{rp} that is the crisp output. The design of the final FIS is of particular relevance as it transforms the model's causal relationships into one final crisp output. To obtain a realistic behavior the underlying relationship is modeled according to empirical findings on the relationship between risk and return rates and risk premia, respectively.

We conduct the process of Fuzzy Engineering as described by Kosko [14]. For constructing the rule base, we lean on the findings on different high technology ventures and corresponding return rates and risk premia that were observed in the recent past by Achleitner [13]. According to the used methodology, the input parameter of the final FIS_{f} consists of the aggregated antecedent causal inflows in the parameter *Risk Premium*. It integrates all impacting factors into one single figure.

Corresponding to the general understanding of nodes and their concept values the values R can take range in the interval -1 to 1. Thus, $X_R = [-1; 1] \subseteq R$. The observed risk premium r_{rp} in the Early-Stage sector scatters between 10% p.a. and 75% p.a. whereas about 50% of the values lie in the interval between 20% p.a. and 50% p.a. Thus, $X_{\text{rrp}} = [10; 75] \subseteq R$. Consequently, this distribution can be a guideline for determining the membership functions' form and position for representing the risk premia. The empirically observed risk premia concentrates in the interval [20; 45]. The borders of this interval represent the upper 75-quartile and the lower 25-quartile of the empirical distribution. This is modelled by using asymmetrically bell-shaped membership functions.

The modeling of the concentration of risk premia in the interval [25; 50] is supported by centring the membership functions stepwise at every five percent (20%, 25%, 30%, as well as, 40%, 45%, 50%). Outside this interval, the membership functions are centred at every ten percent (10%, 20% and 50%, 60%, 70%).

The median r_{rp} = 35% is depicted by a special form of the bell-shaped curve. It rather covers an interval than representing a single fuzzy value. Here, the Fuzzy Number $\tilde{r}_{\text{rp}}$ = 35 stands for the interval between r_{rp} = 30 and r_{rp} = 40. This should strengthen modelling the risk premia's concentration around the median. The lower and upper borders of the interval, namely the return rates r_{rpl} =10% and r_{rpu} = 75% are represented by triangular membership functions. Thus, a clear and distinct border is modelled guaranteeing that there are no risk premia smaller than 10% p.a. or greater than 75% p.a. The resulting membership functions are shown in Fig.9. A detailed description of this process can be found in [4].

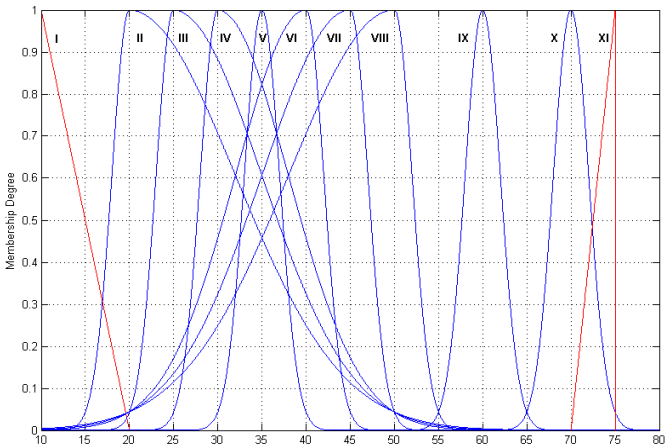

Figure 9: Membership Functions Representing the Empirically Observed Risk Premia

C. *First Results*

The simulation was carried out using the Fuzzy Logic Toolbox (Version V2.2.5 R2007a) for Matlab™(Version R 2007a). The Fuzzification is realized by singleton sets. The

Implication is carried out by using the *Min*-method. The *Max*-method is used as the aggregation operator. The *Center-of-Gravity*-method is used for de-fuzzification. In Fig. 10 the obtained preliminary output profile is depicted.

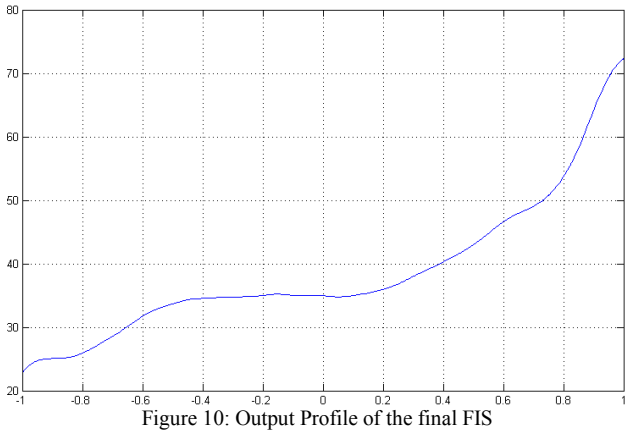

Figure 10: Output Profile of the final FIS

The depicted output profile fundamentally corresponds with the empirical findings of [12]. Below neutral point R = 0, the increase of the risk premium r_{rp} is rather slow. Beyond the point R = 0, the increase of r_{rp} is above-average denoting the tendency to increase the risk premia when the risk rises especially above a normal level. However, the mapping is still to be improved. Particularly, the peaks and unevenness of the output profile is to be bettered.

D. Rule Base Optimization

Not every rule is needed to approximate an arbitrary continuous function. The *Fuzzy Representation Theory* states that a Fuzzy Systems only needs to cover the extrema of the approximant *f* (Fig. 11).

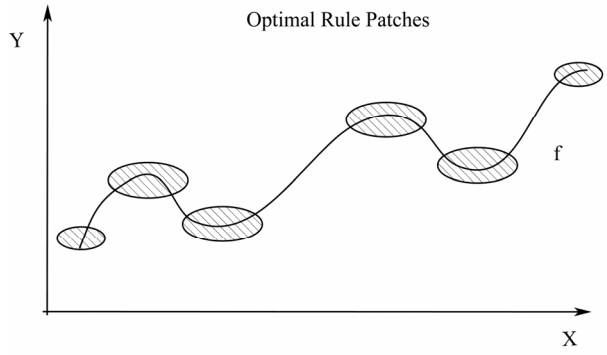

Figure 11: Rule Patches covering Extrema of the Approximant *f*

A proof of this theorem, made by Watkins [15], even states that two rules covering the turning points are sufficient to fully approximate the function. This, however, requires the exact knowledge about the function's shape. Despite of any theoretical limitations, this theorem gives a clear hint where to begin with rule optimization.

Table 2: Rule Base Covering the Extrema

Rule1	*IF*	R= -1.0	*THEN*	r_{rp} = 10%
Rule2	*IF*	R= 0	*THEN*	r_{rp} = 35%
Rule3	*IF*	R= 1.0	*THEN*	r_{rp} = 75%

1) Rules Covering the Extrema

The rule base optimization with the FIS rule base starts with a rule coverage at the extremes (-1.0; 10%), (1.0; 75%) and at the point (0; 35%) (Table 2). The resulting output profile can be seen in Fig. 12. However, the transitions are still too abrupt and the mapping is far too symmetrical. It does not yet possess the targeted shape and mapping compared to the preliminary output profile in Fig. 10.

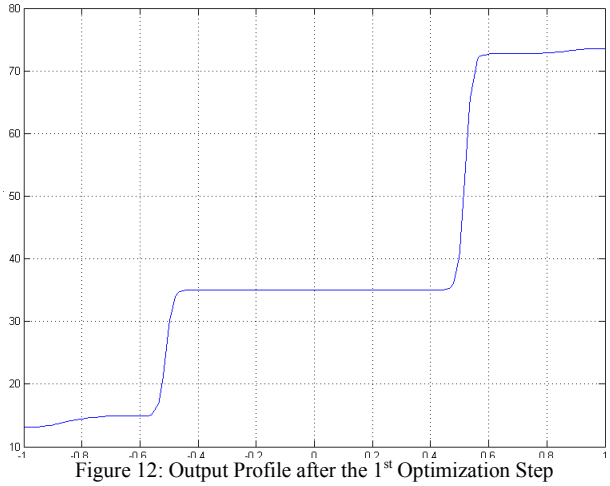

Figure 12: Output Profile after the 1st Optimization Step

2) Rules Covering the Extrema and the right-hand Side

($R > 0$). The rule base is enlarged by seven rules covering the right-hand side beyond $R = 0$ (Table 3). This results in a clearly smoother increase of r_{rp} when R rises over $R = 0$. The left-hand side $R < 0$ is still characterized by a too harsh, step-wise increase of r_{rp} (Fig. 13).

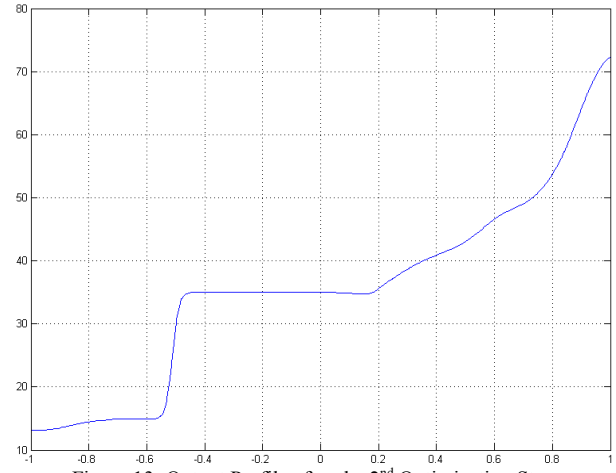

Figure 13: Output Profile after the 2nd Optimization Step

Table 3: Rule Base 2nd Optimization Step

Rule1	*IF*	R= -1.0	*THEN*	r_{rp} = 10%
Rule2	*IF*	R= 0	*THEN*	r_{rp} = 35%
Rule3	*IF*	R= 0.2	*THEN*	r_{rp} = 40%
Rule4	*IF*	R= 0.4	*THEN*	r_{rp} = 45%
Rule5	*IF*	R= 0.5	*THEN*	r_{rp} = 50%
Rule6	*IF*	R= 0.6	*THEN*	r_{rp} = 50%
Rule7	*IF*	R= 0.7	*THEN*	r_{rp} = 60%
Rule8	*IF*	R= 0.8	*THEN*	r_{rp} = 75%
Rule9	*IF*	R= 0.9	*THEN*	r_{rp} = 75%
Rule10	*IF*	R= 1.0	*THEN*	r_{rp} = 75%

3) Rule covering the Extrema and both Sides

Consequently, this next step mainly focuses on the rule coverage of the left-hand side (R < 0). Particularly, the peak at R = -0:2 and the slight trough at R ≈ 0.2 disrupt the continuity needed for the intended output profile. By deleting rules on the left-hand side of the mapping (R < 0) the peak at R ≈ -0.2 is lessened. The same holds true for the slight trough at R ≈ 0:2 which is mainly due to the added rule number seven (Fig. 14).

Table 4: Rule Base 3rd Optimization Step

Rule1	*IF*	R= -1.0	*THEN*	r_{rp} = 10%
Rule2	*IF*	R= -0.9	*THEN*	r_{rp} = 10%
Rule3	*IF*	R= -0.7	*THEN*	r_{rp} = 25%
Rule4	*IF*	R= -0.5	*THEN*	r_{rp} = 30%
Rule5	*IF*	R= -0.2	*THEN*	r_{rp} = 30%
Rule6	*IF*	R= 0	*THEN*	r_{rp} = 35%
Rule7	*IF*	R= 0.2	*THEN*	r_{rp} = 40%
Rule8	*IF*	R= 0.3	*THEN*	r_{rp} = 45%
Rule9	*IF*	R= 0.4	*THEN*	r_{rp} = 50%
Rule10	*IF*	R= 0.5	*THEN*	r_{rp} = 50%
Rule11	*IF*	R= 0.6	*THEN*	r_{rp} = 60%
Rule12	*IF*	R= 0.7	*THEN*	r_{rp} = 75%
Rule13	*IF*	R= 0.8	*THEN*	r_{rp} = 75%
Rule14	*IF*	R= 0.9	*THEN*	r_{rp} = 75%
Rule15	*IF*	R= 1.0	*THEN*	r_{rp} = 75%

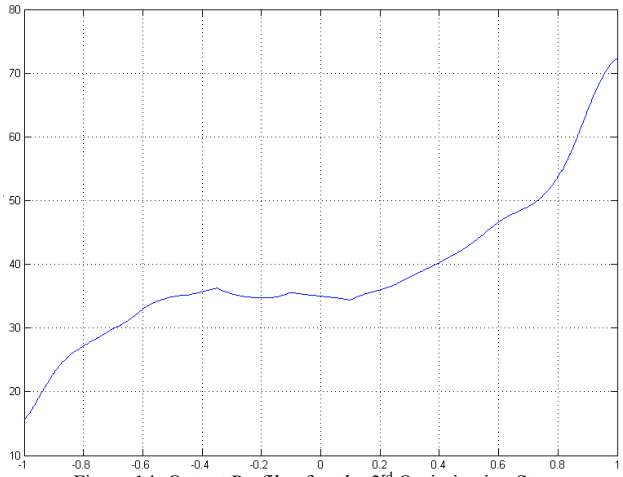

Figure 14: Output Profile after the 3rd Optimization Step

4) Optimal Rule Base

By reducing the rules on the left-hand side as well as on the right-hand side to finally twelve (Table 5), the behaviour of the mapping of R to r_{rp} is optimal. It is attained that there is a nearly monotonic growth of r_{rp} when R increases. But the increase of growth rate of r_{rp} depends on the actual value of R. The higher R grows, the stronger becomes the increase of r_{rp}

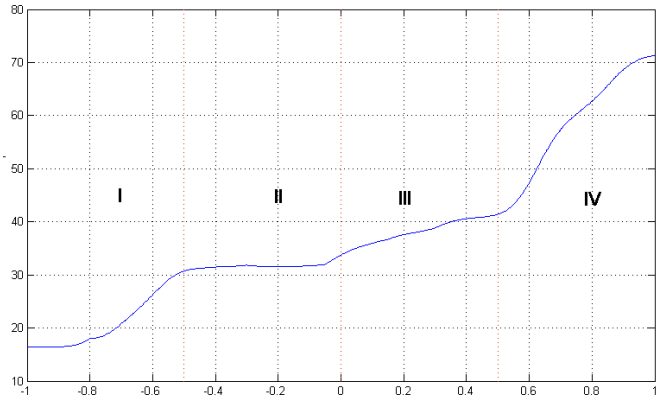

Figure 15: Simulation Results: Output Profile after Rule-Base Optimization

This optimal profile (Fig. 15) is the result of the optimized rule base (Table 5). This profile can be subdivided into four sections denoting the different behaviour of the FIS depending on the actual height of the aggregated risk R.

Table 5: Optimized Rule Base

Rule1	*IF*	R= -1.0	*THEN*	r_{rp} = 10%
Rule2	*IF*	R= -0.7	*THEN*	r_{rp} = 10%
Rule3	*IF*	R= -0.5	*THEN*	r_{rp} = 20%
Rule4	*IF*	R= -0.4	*THEN*	r_{rp} = 25%
Rule5	*IF*	R= -0.2	*THEN*	r_{rp} = 25%
Rule6	*IF*	R= -0.1	*THEN*	r_{rp} = 30%
Rule7	*IF*	R= 0	*THEN*	r_{rp} = 30%
Rule8	*IF*	R= 0.1	*THEN*	r_{rp} = 40%
Rule9	*IF*	R= 0.2	*THEN*	r_{rp} = 40%
Rule10	*IF*	R= 0.4	*THEN*	r_{rp} = 45%
Rule11	*IF*	R= 0.7	*THEN*	r_{rp} = 60%
Rule12	*IF*	R= 1.0	*THEN*	r_{rp} = 75%

Section I. In Section I, the risk parameter is below -0.5. Obviously, the risk is significantly smaller than usual. This is also expressed by a rather slow growth of the risk premium r_{rp} in the interval [-1; 0:8). In the range -0:8 < R ≤ -0:5, however, the risk premium r_{rp} grows stronger than in the preceding sector. This denotes the positive relationship between risk and risk premium even in cases that appear to be lesser risky than normal.

Section II. The second section is characterized by an almost constant mapping of the risk parameter R to the risk premium r_{rp}. This signifies the vague understanding of risk being only somewhat smaller than usually observed. The interval -0.5 < R < 0 stands for the wider range of high-

technology ventures whose risk is, at most, normal. But their risk profile not justifies yet a significant abatement of the risk premium r_{rp}.

Section III. Closely before *R* becomes zero or positive, the return rate r begins to grow steadily. This indicates that in case the high-technology venture appears to be more risky than average the required return rate r is used as a compensation for every unit risk that is taken more. This nearly linear relationship spans over the whole section III ($0 < R < 0{:}5$).

Section IV. After the risk parameter *R* has grown above 0.5, the growth of r_{rp} becomes above-average. This signifies that when a high-technology venture appears to be significantly riskier than the average ($R > 0{:}5$), the growth of the return rate r is no longer linear. It nearly becomes exponential. This is due to the fact that an investor only engages in a more-then-usual risky venture if there is an exceptional risk premium. Summing up, by optimizing the rule base, amore realistic behaviour of our model could be attained.

IV. DISCUSSION

In prior articles [1], [2], [3], [4], the principal feasibility of our approach was presented and discussed. In this article, we presented a further development of the approach. In detail, it comprises an enhanced economic model based upon statistically proven factors. Moreover, an optimized rule base was proposed. By these features, a way was demonstrated how to validate the risk premium, the most disputed component in DCF-valuation methods. Besides these promising results, there is still a lot of work to be done.

The herein proposed rule base is built and optimized manually. The conceptual basis for this is the theorem elaborated by Watkins [15]. Hence, future research will be focused on integrating learning algorithms to build the final rule base. This can lead to an even more objective rule base and even more realistically modeled system behavior. One suitable approach has already been identified: in [11] genetic algorithms are used to build and to optimize the rule base. The combination of our methodological framework with genetic algorithms for rule base building seems promising since genetic algorithm, as bio-inspired optimization methods in general, does not demand for an exact mathematical model. This feature significantly alleviates the application in the here presented context in which exact are intentionally avoided.

An improvement of the modeling of the economic relationships and the determination of the relevant factors is out of the scope of this article. The authors will look out for advancements on this topic. The herein used model provides the flexibility to adapt changing parameters and concepts.

ACKNOWLEDGMENT

L. Krueger wishes to thank *engage – Key Technology Ventures AG* for material and intellectual support.

REFERENCES

[1] L. Krueger, K2F – A Novel Framework for Converting Fuzzy Cognitive Maps into Rule-Based Fuzzy Inference Systems", in Lecture Notes on Artificial Intelligence and Soft Computing, L. Rutkowski et al. (Eds), Vol.6113, Pt. 1, 2010, pp. 128-135

[2] L. Krueger, M. Klofstem, P. Heydebreck et al. "A Fuzzy Cognitive Map-based Approach to the Determination of appropriate Discount Rates for the Valuation of High-Technology Ventures in the Early Stages of Venture Capital Investments", in: Proceedings of the 14th International Business Information Management Association Conference IBIMA, June 23-23, 2010, Istanbul, Turkey

[3] L. Krueger, M. Klofsten, P. Heydebreck " K2F – A Methodical Framework to use Fuzzy Cognitive Maps for the Determination of adequate Discount Rate in Venture Valuations", in Communications of the IBIMA, in press Jan 2011

[4] L. Krueger, P. Heydebreck, R. Salomon et al. "Validation of Subjectively Determined Risk Premia in High-Technology Ventures Investments using a Novel Framework for Converting Fuzzy Cognitive Maps into Rule-Based Fuzzy Inference Systems", 2011, unpublished

[5] R. Simonelli "Fuzziness in Valuing Financial Instruments by Certainty Equivalents", in European Journal of Operational research, 2001, Vol. 135, Is. 2, 201l, pp. 296-302

[6] A. Serguieva "Fuzzy Interval Methods in Investment Risk Appraisal", in: Fuzzy Sets and Systems, Vol. 142, Is. 3, 2004, pp. 443-466

[7] B. Rebiasz "Fuzziness and Randomness in Investment Project Risk Appraisal", in: Computer Operations Research, Vol. 34, Is.1, 2007, pp. 199-210

[8] L.-H. Lai "Underwriting Systamtic Risk and Profit Margin in Fuzzy CAPM and ICAPM Models: The Case of Aviation Coverage", in: Contemporary Management Research, Vol. 5, No. 4, 2009, pp. 387-396

[9] S.K. Blatt et al. "Capital Asset Pricing Modell under Fuzzy Information", in: Proceedings of the Annual Conference of the Administrative Sciences Association of Canada, ASAC Conference June 14-17, 2003, Halifax, Nova Scotia, Canada

[10] Hasuike, T. et al. "Multiobjective Random Fuzzy Portfolio Selection Problems based on CAPM", in: Systems, Man and Cybernetics 2009, Oct. 11-14, 2009, San Antonio,TX, USA

[11] O. Cordon, F. Herra, P. Villar, "Generating the Knowledge Base of a Fuzzy Rule-Based System by the Genetic Learning of the Data Base", in: IEEE Transactions on Fuzzy Systems, Vol. 9 Is. 4, 2001, pp. 667-674

[12] Song, M. Podoynitsyna K., van der Bij H., J. Halman, „Success Factors in New Ventures. A Meta Analysis", in: Journal of Product Innovation Management, 25, 2008, pp. 7-27

[13] A. Achleitner, E. Nathusius "Venture Valuation and Venture Capital Financing " (German), in: Business Studies (Wirtschafts-wissenschaftliches Studium), No.3, 2004, pp. 134-139

[14] B. Kosko, "Fuzzy Engineering", Prentice Hall, 1997, New Jersey

[15] F.A. Watkins "The Representation Problem for Additive Fuzzy Systems", in Proceedings of the IEEE FUZZ-95, Vol. 1, pp.117-122, 1995

[16] M. Klofsten, M. Jonsson, J. Simon, „Supporting the Pre-Commercialisation Stages of Technology-based Firms: the Effects of Small-Scale Venture Capital", in: International Journal of Venture Capital, Vol. 1, Is. 1, 1999, pp. 43-52

[17] M.S. Khan and S.W. Khor "Framework for Fuzzy Rule-Based Cognitive Maps", Lecture Notes in Computer Science, (2004), 454-463

[18] M.S. Khan A. Chong, M. Quaddus "Fuzzy Cognitive Maps and Intelligent Decision Support - A Review", Journal of Systems Research and Information Science, 26, (2004), 257-268

[19] J. van den Berg, U. Kaymak, W.M. van den Bergh „Financial Markets Analysis by using a probabilistic Fuzzy Modelling Approach", in: International Journal of Approximate Reasoning, Vol. 35, Is.3, (2004), 291-305

2011 IEEE International Conference on Fuzzy Systems
June 27-30, 2011, Taipei, Taiwan

Soft-Core Implementation for Centre of Slice Area Average Defuzzifier

Antonio Hernández Zavala
Electronics Department
Unidad profesional interdisciplinaria en Ingeniería y Tecnologías Avanzadas – Instituto Politécnico Nacional
Distrito Federal, México
anhernandezz@ipn.mx

Oscar Camacho Nieto, Cornelio Yáñez Márquez
Microelectronics Department
Centro de Investigación en Computación – Instituto Politécnico Nacional
Distrito Federal, México
{oscarc, cyanez}@cic.ipn.mx

***Abstract*—Fuzzy systems are broad used for the decision making task given its capability of extract knowledge from an expert and translate it into rules that define described system. Implementations are made according to speed requirements of the problem, for the case of critical real time systems hardware is the best choice. One important issue on fuzzy systems is the final step, defuzzifier, when computed fuzzy data is turned into crisp data. There are many different defuzzifier methods from which most used for hardware purposes are Center Of Gravity and Mean Of Maxima. This work presents hardware implementation for Center of Slice Area Average defuzzifier, for digital soft-core implementation; its main advantages are reduction on resource consumption and reduction of calculation time without loss of accuracy.**

Keywords: Soft Computing, Fuzzy Systems, Digital Systems, Discrete Numbers, Defuzzification

I. INTRODUCTION

Fuzzy systems are broad used for the decision making task given its capability of extract knowledge from an expert and translate it into rules that define described system providing better results than conventional controllers. Examples of successful implementations for fuzzy systems are: automatic parking car [1], nuclear reactors [2], robotics [3], function approximation [4], physics experiments [5], database Querying [6] among others.

A rule based fuzzy system is a special type of fuzzy systems that use fuzzy numbers as data for processing. It is constructed of four basic blocks known as: Fuzzifier, rule base, inference and defuzzifier. First and last blocks are used as interface between real world values and fuzzy values at input and output respectively. Rule base contains acquired knowledge from an expert that is managed by inference stage according to data retrieved from fuzzifier stage and delivers its result to defuzzifier stage.

Implementations for fuzzy systems are made according to speed requirements of the problem, for the case of critical real time systems where response time is crucial in order to keep a safe system operation, hardware is the best choice to provide high processing speed.

One important issue on fuzzy systems is the final step, defuzzifier, when computed fuzzy data is turned into crisp data. There are different forms for defuzzifiers satisfying different precision and speed requirements, even though, Center Of Gravity method COG and Mean Of Maxima MOM are the most used on hardware.

COG is proved to be more accurate than MOM, but it requires much more calculations [7], [10]. On this paper a defuzzifier method called Center of Slice Area Average Defuzzifier COSAA [8] is implemented in hardware, it is based on α-levels for membership functions representation and uses discrete numbers which make it fit better into digital computers. As results, it reduces execution time of Center Of Gravity COG, without loss of accuracy as Mean Of Maxima MOM and even with hardware resources reduction.

Paper is organized as follows: in order to implement efficient digital circuit is necessary to make some digital considerations as presented in Section II. Generalities for defuzzifiers are covered on Section III. Soft Core implementation for Center of Slice Area Average Defuzzifier is presented on Section IV. Results are shown in section V. Finally conclusions and future work are considered in Section VI.

II. CONSIDERATIONS FOR DIGITAL IMPLEMENTATION OF FUZZY SYSTEMS

Real world systems use precise units that can be grouped into a crisp universe where all elements are well defined. In contrast, fuzzy values are grouped into membership functions that belong to a linguistic variable where limits are defined, but not the elements.

Commonly in fuzzy systems, there is a range of values for result of operations that belongs to [0, 1] representing truth values, where 0 means no membership, and 1 is complete membership. Another form to represent membership values is using integer numbers, this case is best suited for digital implementations because floating point operations consume much more time and resources. For this case, results are considered on [0, *I*] interval, where *I* is an integer represented by equation 1, where *m* is the number of bits used for resolution [8].

978-1-4244-7316-8/11/$26.00 ©2011 IEEE

$$I = 2^m - 1 \quad (1)$$

A. Linguistic Variables

Let us consider A be a linguistic variable, the k number of membership functions to define A is given by equation 2 and is graphically expressed on Figure 1.

$$A = \{A_0, A_1, A_2, \ldots, A_K\} \quad (2)$$

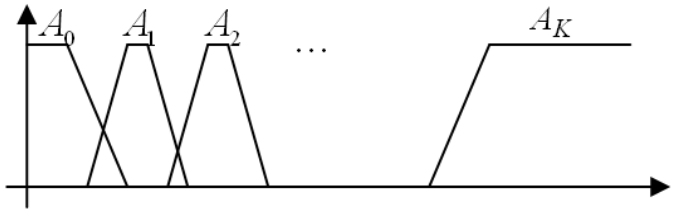

Figure 1. Membership functions for linguistic variable A

B. Membership Functions

To represent membership functions there are mainly two approaches, on the first, a membership function is represented trough a membership value for each element on input universe, it means that for a better output resolution is necessary to use a higher bit number, so while more resolution is gained, more values must be computed independently of the membership value number that modify truth universe.

The second approach is to use $\alpha - levels$ [9] or $\alpha - cuts$ [10] for membership values representation, on this case, a membership function is decomposed on a set of vectors that contain for each membership value, the interval on which the function is true. This approach allows the use of any shape for membership functions and does not take care of input resolution.

Let M be a membership function, with $x_i \in X; i = 0,1,\ldots,J$; where J is the number of points in x axis given by $J=2^n-1$, n is the number of bits used for input space representation.

Each $\alpha - level$ is defined by the following four parameters:

1. M is the name of the membership function;
2. i is the weight index, is at most equal to I and represents membership value in M;
3. α_0^i is the initial point for the interval with i as membership value.
4. α_f^i is the final point for the interval with i as membership value.

Figure 2 shows the representation of a membership function M represented by I number of $\alpha - levels$. The whole M membership function is now defined by the set of all its $\alpha - levels$ over input universe X, values for m and n depend on the number of bits used for each universe and can be different, better if $m<n$, usually 5 or 6 bits are suitable for membership universe m, and while more bits are used for crisp universe is a better resolution.

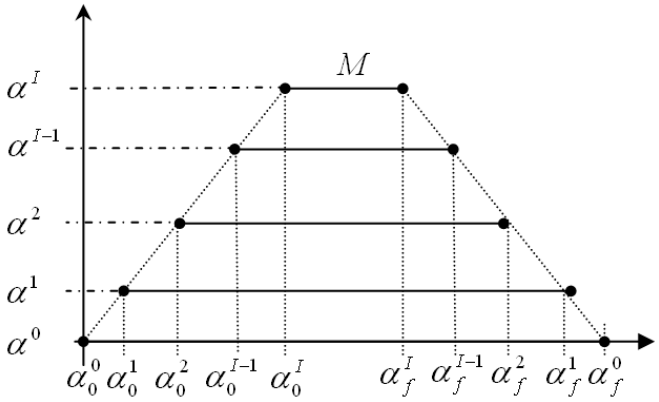

Figure 2. Discretization of a trapezoidal membership function into I number of $\alpha - levels$

C. Rule-base and Inference

The fuzzy system is dedicated to infer from fuzzy input data which is the most suitable fuzzy output it must deliver. Rule-base that contains knowledge acquired from an expert is expressed with rules in the form of Mamdani as on equation 3.

$$R_s: \text{IF x is } A_i \text{ AND y is } B_j \text{ THEN z is } C_k \quad (3)$$

where x and y are input variables, z is output variable, A_i, B_j and C_k are linguistic values for variables A and B at input and C at output.

Membership degree values for x and y inputs are used to calculate antecedent part of rule, realizing an intersection with both input membership values, commonly this is computed by some t-norm operation as on equation 4.

$$\mu_{C_k}(z) = T\left(\mu_{A_i}(x), \mu_{B_j}(y)\right) \quad (4)$$

When all rules are evaluated, only those membership functions that contribute to final result are joined by the use of an or t-conorm as on equation 5, obtaining a unified membership function made of those output membership functions whose maximum membership value is greater then zero, this resultant function is called aggregated membership function

$$\mu_C(z) = S((\mu_{C_0}(z)), \ldots, (\mu_{C_k}(z))) \quad (5)$$

An example for aggregated function is the one from Figure 3. There is a case for an $\alpha - level$ based fuzzy system with two inputs with four membership functions each, and one output with five membership functions, all trapezoidal. When two inputs $x=119$ and $y=374$ are evaluated, there are four activated rules, when they are aggregated, they turn into a unified shape represented with 512 values for universe of discourse and 32 membership values. Functions 0 and 5 do not contribute to final result, on behalf, functions 1, 2 and 3 do, with 13, 25 and 9 as membership values respectively.

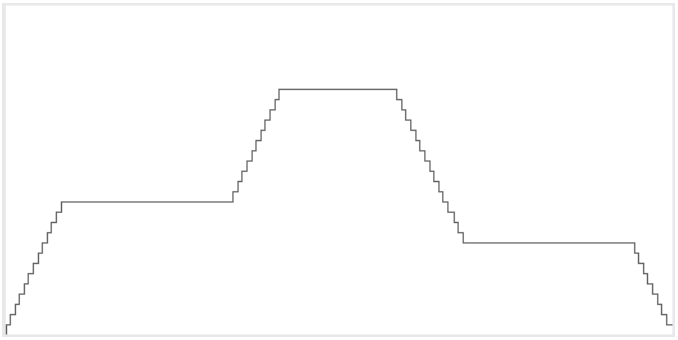

Figure 3. Aggregated membership function for *x=119* and *y=374*.

III. DIGITAL DEFUZZIFIERS

Final step on a fuzzy system is defuzzifier; it calculates the final result out of aggregated membership function, by computing only one crisp value that best represent desired output. There are many defuzzifier methods satisfying different precision and speed requirements, traditional methods are Center of Gravity COG and Mean of Maxima MOM, others are presented as Plateau Average PA [11], and Trapezoid Median Average [12].

As it has been proved on literature that COG is the best defuzzifier, many authors use it as ideal for testing, obtaining deviations from their methods with respect to COG [7], [10]. The intention then is to obtain a defuzzifier as good as COG but that is more suitable for digital implementations avoiding excessive calculation time elapsed by COG.

A. Mean of Maxima Defuzzifier

For calculation of Mean of Maxima defuzzifier MOM (equation 6), it is only necessary to know which was the highest membership value on aggregated function and obtain the middle point of that level as result, it is very simple, that is why it is fast, but does not consider rest of function so changes here are like big increases or decreases for final output, being unstable, but is well suited for many applications.

$$z_{MOM} = \sum_{j=1}^{l} \frac{w_j}{l} \tag{6}$$

B. Center of Gravity Defuzzifier

Center Of Gravity defuzzifier COG realization requires calculating the whole area and determining where its weighted midpoint is. As it uses all elements from input universe, it requires $r=2^n-1$ iterations according to number of bits used for input universe as on equation 7. This defuzzifier is preferred by most authors because of its accuracy and easiness for implementation.

$$z_{COG} = \frac{\sum_{i=1}^{k} x_i \times \mu(x_i)}{\sum_{i=1}^{k} \mu(x_i)} \tag{7}$$

C. Centre of Slice Area Average Defuzzifier

To work efficiently with a $\alpha - level$ based aggregated membership function Centre of Slice Area Average defuzzifier COSAA is used. On this case it requires at most *I* iterations according to membership values resolution as on (1).

COSAA is defined by 8, where upper part calculates summation of midpoints for all $\alpha - levels$, to calculate midpoint of each level do not require complex operations, it uses only addition, subtraction and right shift to realize division by 2. the only required division is made at endpoint with α_{MAX} . Operating description is graphically expressed on Figure 4 where *I* is equal to 4, i.e. two bits are used. Midpoints for each level are calculated and accumulated to finally obtain the average result indicated as COSAA.

$$z_{COSAA} = \frac{\sum_{i=0}^{\alpha_{\max}} \left(\frac{\left(x_f^{\alpha_i} - x_0^{\alpha_i} \right)}{2} + x_0^{\alpha_i} \right)}{\alpha_{\max}} \tag{8}$$

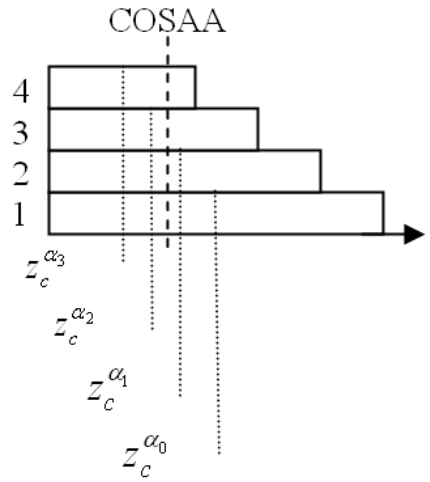

Figure 4. Center of Slice Area Average Defuzzifier operation.

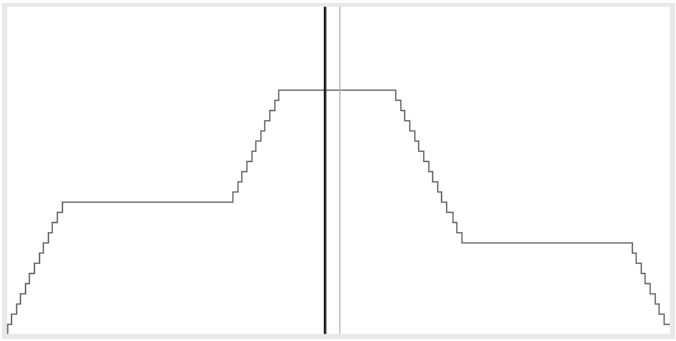

Figure 5. Defuzzifier results for inputs *x=119* and *y=374*, outputs are COG=243, MOM=255 and COSAA=244.

As example of defuzzifiers presented, there is a case for a $\alpha - level$ based fuzzy system with two inputs with four

membership functions each, and one output with five membership functions, all trapezoidal, represented on universes of 512 values (9-bit) for universe of discourse and 32 membership values (5-bit). Inputs are *x=119* and *y=374*, output results are COG=243, MOM=255 and COSAA=244 as on Figure 5.

IV. HARDWARE IMPLEMENTATION OF COSAA

Centre of Slice Area Average Defuzzifier Hardware implementation is based on equation (8) and is presented on Figure 8. Aggregated membership function resultant from previous stage is loaded into two ROM memories that contain the complete description of the function in terms of its $\alpha - levels$. Height index k for each $\alpha - level$ is given by memory address, and the contents are the initial point α_0^k on MEM_32x8 block, and final point α_f^k on MEM_32x8_FINAL. Five bits are used for membership resolution obtaining 32 levels, for that reason, memories are 32 deep, 8-bit wide.

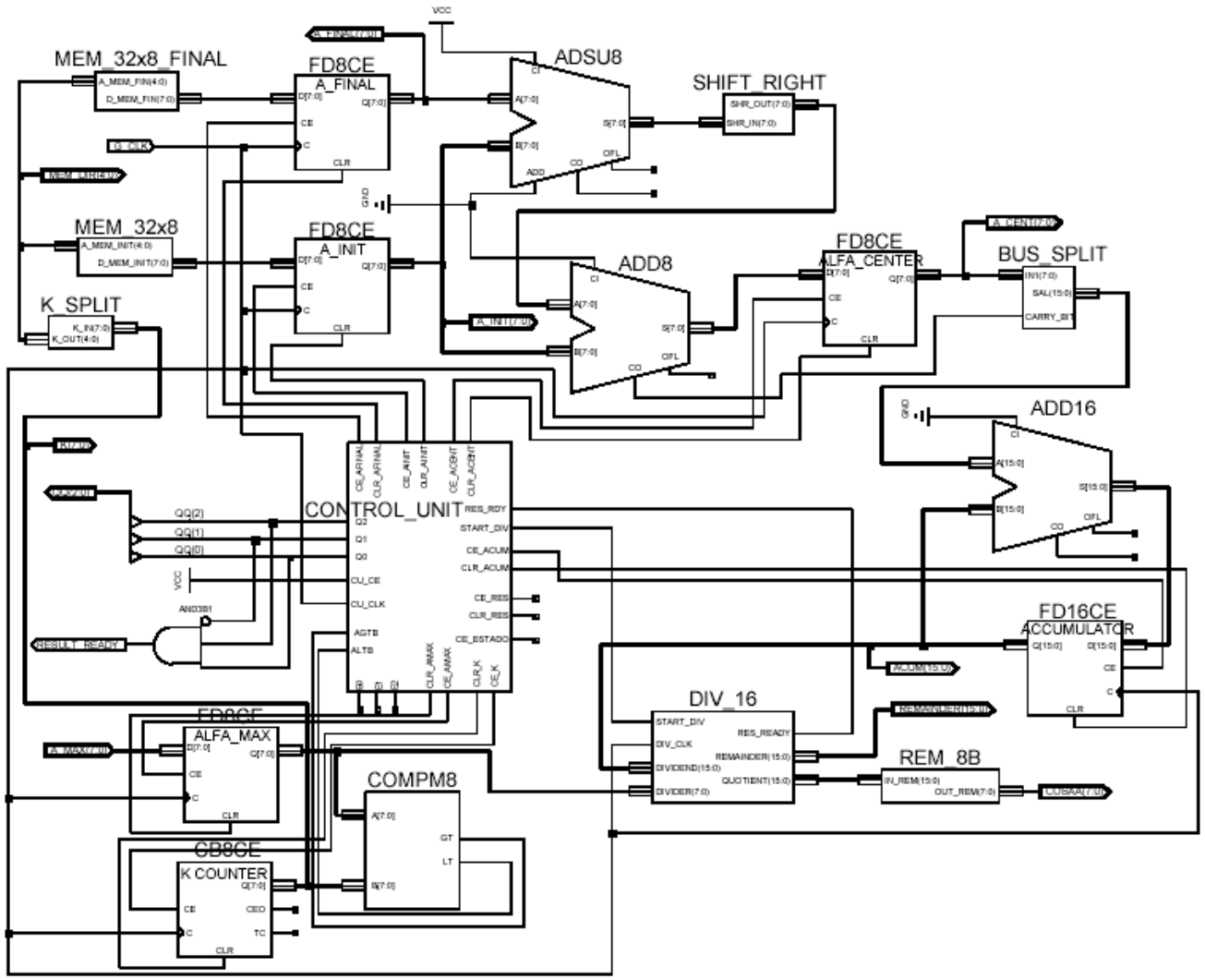

Figure 6. Hardware realization for Centre of Slice Area Average defuzzifier. There can be identified five 8-bit registers FD8CE that are D-type flip-flops and are used to store values of α_0^k (A_INIT), α_f^k (A_FINAL), α_C^k (ALFA_CENTER), α_{MAX} (ALFA_MAX) and Accumulator respectively labelled.

There can be identified four 8-bit registers (FD8CE) that are D-type flip-flops used to store values for α_0^k (A_INIT), α_f^k (A_FINAL), α_C^k (ALFA_CENTER), α_{MAX} (ALFA_MAX) and a 16 bit register for accumulator.

To calculate the center of a level as on upper part from Equation 8, ADSU8 is used as an 8-bit subtractor to realize the α_f^k - α_0^k part, division by two is performed by SHIFT_RIGHT unit; ADD8 realizes the summation of offset to obtain the center of evaluated level that will be now stored on its correspondent ALFA_CENTER register.

BUS_SPLIT is an 8 to 16 bit conversion block that drive α_C^k calculated value as input for ADD16 that is a 16 bit

adder used to realize summation among calculated value and previous values stored on accumulator register.

An 8-bit counter CB8CE labeled K_COUNTER, is used as pointer for each $\alpha - level$ address on both memories. COMPM8 is a magnitude comparator used for iteration control procedure between α_{MAX} and K. The procedure of calculate midpoints for all levels is repeated until *ALTB* signal from comparator goes high that is the moment when *k* is equal to α_{MAX} and is the appropriated moment to start division. The completion of division algorithm requires about 50 clock cycles to obtain a 16-bit result that is converted to 8-bit value trough REM_8B block. Result is available when RESULT_READY signal goes high and remains there until next COSAA calculation overwrite final value.

V. RESULTS

A. Simulation Results

This methodology was first implemented on a C++ Builder simulator on which every stage was constructed according to methodology presented. Simulation is realized for a fuzzy system with two inputs with four membership functions each, one output with five membership functions and 16 rules at rule base, for an easy visualization of universe spaces they are discretized at 32 $\alpha - levels$ i.e. 5 bits for *y* axis (membership universe), and 256 values, i.e. 8 bits for *x* axis (input universe).

Table I presents some test cases realized for three defuzzifiers, there is shown the result and elapsed time.

TABLE I. SOME TESTS REALIZED FOR THE SYSTEM.

x	y	Defuzz	Result	Time us
10	63	COSAA	23	2.23
10	63	COG	33	13.40
10	63	MOM	9	1.95
10	157	COSAA	65	2.23
10	157	COG	70	22.346
10	157	MOM	63	1.95
43	215	COSAA	128	2.23
43	215	COG	128	32.68
43	215	MOM	127	1.95
75	229	COSAA	176	2.79
75	229	COG	160	49.34
75	229	MOM	191	2.51
109	109	COSAA	86	3.35
109	109	COG	107	70.67
109	109	MOM	63	2.69
146	117	COSAA	132	3.07
146	117	COG	132	71.79
146	117	MOM	127	3.07
216	216	COSAA	214	2.23
216	216	COG	204	18.15
216	216	MOM	245	2.23

B. Soft-Core Implementation Results

Hardware for COSAA was constructed from logical gate design using Xilinx tools for FPGA design over a Spartan 3 XC3S400-5FG320 device that has 400,000 logic gates. Execution results for COSAA hardware are shown on Figure 7 and Figure 8 using the set of $\alpha - levels$ that describes aggregated function.

G_CLK is the global clock signal for the system; *QQ* is the 3-bit state counter, it iterates from states1 to 3 until all levels are evaluated, this is controlled by *K* counter until its value reaches α_{MAX} (*A_MAX)* value as last level to evaluate. *MEM_DIR* is the current address index of the memory that contains α_0^k (*A_INIT)* and α_f^k (*A_FINAL)* values, the calculation of α_C^k is presented on *A_CENT* and its summation is stored on *ACUM*.

When all levels are calculated system goes to state 4 where it starts the final division between *ACUM* and *A_MAX* and wait there until division completion that is the moment to go to state 5 where result ready signal (*RESULT_READY)* is activated indicating that final result can be read from *COSAA* as integer and it will be available until next division is started on state 4.

On Table II there are resources consumed by final implementation of COSAA defuzzifier, it can be noticed that it uses few circuitry and delay times are considered for a combinatory array. Calculation of COSAA from an aggregated membership function requires 129 clock cycles to provide final result, considering that division uses almost 50 clock cycles, then it takes about 80 clock cycles to calculate the summation of all levels. To make this function more efficient it maybe must consider another type of division that is faster, but maybe hardware complexity increases.

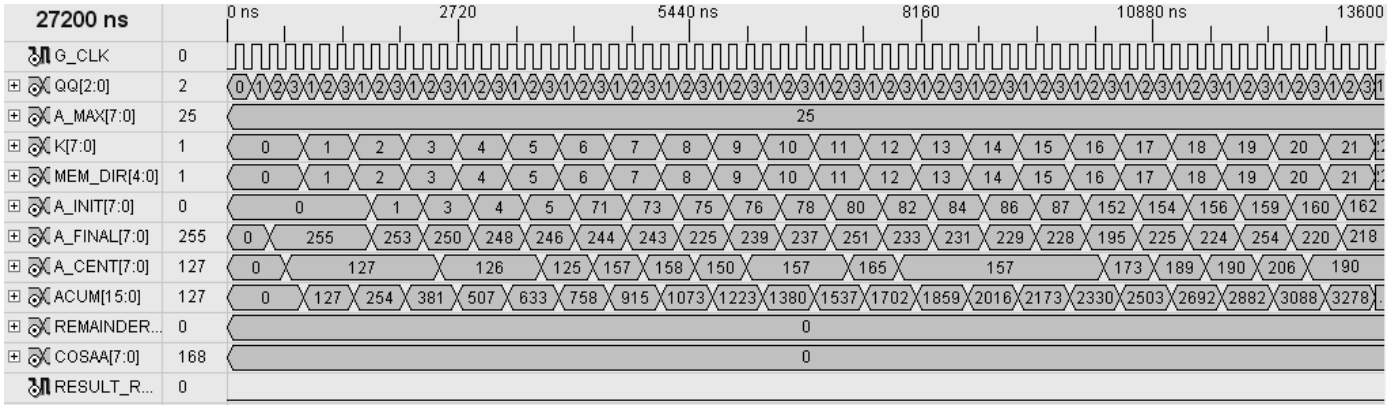

Figure 7. Simulation results for COSAA hardware implementation, the calculation of each level stored on memory is realized using *K* as index pointer until it is equal to *A_MAX* on state 4 where it starts to calculate final division for average. Final result is presented on state 5 where *RESULT_READY* signal is activated.

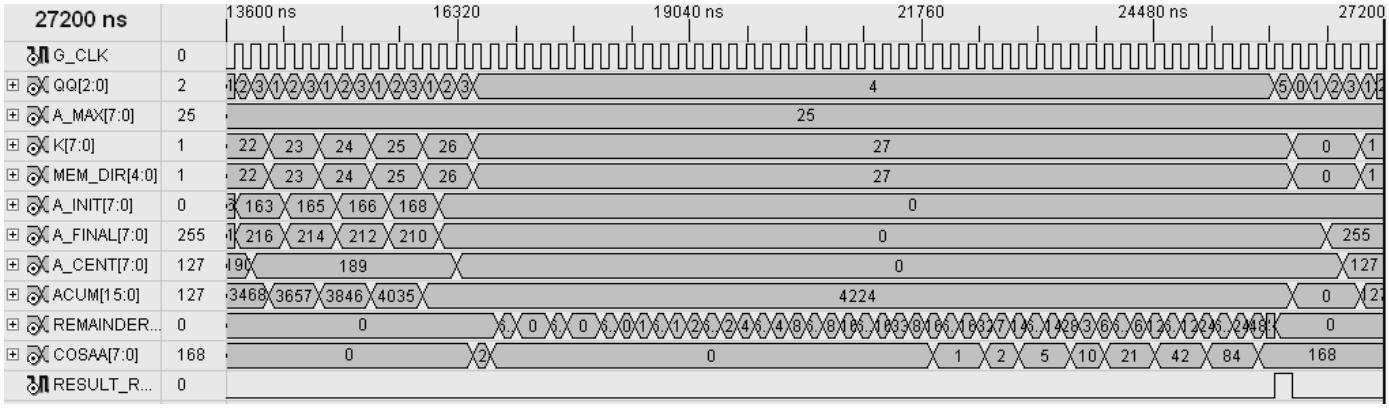

Figure 8. Simulation results for COSAA hardware implementation (Continued from Figure 17)

TABLE II. HARDWARE RESOURCES CONSUMED BY IMPLEMENTATION OF COSAA DEFUZZIFIER. TOTAL DELAY IS CONSIDERED JUST FOR A COMBINATORY CIRCUIT THAT DO NOT ITERATE.

Operation	Logic Gates	Logic Levels	I/O used	Total Delay us	Delay Logic	Delay Route
COSAA	972	14	124	26	41%	59%

VI. CONCLUSIONS

Center of Slice Area Average (COSAA) Defuzzification reduces considerably calculation time consumed by Center of Gravity (COG) that uses at least $2^n - 1$ iterations. The new method proposed has a maximum iteration number equal to the *I* number of $\alpha - levels$ and is proportional to the number of bits used to quantify membership space, being COSAA as fast as MOM.

About precision, COSAA competes with COG and is much better than MOM, versatility can be added by use of different aggregation methods.

The $\alpha - level$ method used for representing fuzzy systems with integer numbers, can be implemented easily over any binary computer system using simple operations such as additions and shifting, avoiding time consuming operations such as multiplications and divisions obtaining a reduction on calculation time, and a more flexible and efficient approach for fuzzy systems realization.

ACKNOWLEDGMENT

Authors would like to thank ICYTDF project 243/2010 and SIP-IPN Project 200110465 for their support.

REFERENCES

[1] M. Sugeno, K. Murakami. "An experimental study of fuzzy parking control using a model car". In Industrial Applications of Fuzzy Control, North-Holland, Amsterdam. 125-138, 1985.

[2] J. A. Bernard. “Use of rule-based system for process control”. IEEE Control Systems Magazine, Vol. 8, No. 5. 3-13, 1988.

[3] E. H. Ruspini. “Reactive Fuzzy Control of Autonomous Robots”. Industrial Applications of Fuzzy technollogy in the world, Hirota, Sugeno Eds., World Scientific. 1995.

[4] R. Lovassy, L. Koczy, L. Gal, “Function Approximation Capability of a Novel Fuzzy Flip-Flop Based Neural Network,” Proc. of the International Joint Conference on Neural Networks, pp. 1900-1907, 2009.

[5] D. Falchieri, A. Gabrielli, E. Gandolfi, M. Masetti. “Design of very high speed cmos fuzzy processors for applications in high energy physics experiments”. Seventh International Conference on Microelectronics for Neural, Fuzzy, and Bio-Inspired Systems. 284-291, 1999

[6] C. Tudore, S. Bumbaru, L. Dimitriu, “Relative Aggregation Operator in Database Fuzzy Quering,”The Annals of “Dunarea de Jos” Unniversity of Galati, Fascicle III, pp.39-44, 2005.

[7] T. Runkler, “Selection of Appropriate Defuzzification Methods Using Application Specific Properties”. IEEE Transactions on Fuzzy Systems, Vol. 5, Issue 1. 72-79, 1997.

[8] A. Hernández Zavala, O. Camacho Nieto, I. Batyrshin, “Center of Slice Area Average Defuzzifier for Digital Implementations of Fuzzy Systems,” Proc. of International Conference on Artificial Intelligence, pp. 97-102, 2010.

[9] K. Uehara, M. Fujise. “Fuzzy inference based on families of a-level Sets”. IEEE Transactions on Fuzzy Systems, Vol. 1, No. 2. 111-124, 1993.

[10] G. Bojadziev, M. Bojadziev. “Fuzzy Sets, Fuzzy Logic, Applications”, Advances in Fuzzy Systems – Applications and Theory Vol. 5, World Scientific Publishers. 1995.

[11] S.S. Lancaster, M.J. Wierman, “Empirical study of defuzzification”, Conference of the North American Fuzzy Information Processing Society. 121- 126, 2003.

[12] A. Banaiyan, S. M. Fakhraie, H. R. Mahdiani. “Cost-performance co-analysis in VLSI implementation of existing and new defuzzification methods”. International Conference on Computational Intelligence for Modelling, Control and Automation Vol. 1. 828 – 833. 2005.

2011 IEEE International Conference on Fuzzy Systems
June 27-30, 2011, Taipei, Taiwan

Fuzzy Integral-based Composite Facial Expression Generation for a Robotic Head

Bum-Soo Yoo, Se-Hyoung Cho and Jong-Hwan Kim
Department of Electrical Engineering
KAIST
Daejeon, Republic of Korea
{bsyoo, shcho, johkim}@rit.kaist.ac.kr

***Abstract*—Conventional methods produced composite facial expressions by interpolating the representative facial expressions under the assumption that the transitions between facial expressions are linear. Considering the nonlinear property, this paper proposes a fuzzy integral-based method for generating composite facial expressions. Fuzzy measures represent the relationship among emotions and the partial evaluation of current emotion state is obtained from a predefined error function of the ideal basic emotion states and the current emotion state. Fuzzy integral of the partial evaluation with respect to fuzzy measures is employed to globally evaluate the current emotion state for generating composite facial expressions. The effectiveness of the proposed method for generating composite facial expressions is demonstrated through the experiments with a robotic head with 19 degrees of freedom, developed in RIT Laboratory, KAIST.**

Keywords: Facial expression generation, choquet integral, λ-fuzzy measure, robotic head, diamond pairwise comparison method.

I. Introduction

Nowadays, robots have been used in many areas. Robots can guide people in a museum or play with children [1], [2]. It is expected that robot can be developed as a sociable partner in the future [3]. Considering the symbiosis between robots and humans, it is unavoidable for robots to interact with humans. In this sense, there have been many researches on human robot interaction (HRI) [4]- [6].

When robots interact with humans, robots should imitate the human's interaction because human can interact naturally with robots without additional education or knowledge. Facial expressions play an important role in human's interaction. According to Mehrabian, only 7% of information is delivered by language, 38% of information is delivered by paralanguage like voice and 55% of information is delivered by non-verbal communication like facial expressions and gestures [7], [8]. Therefore, facial expression is an important mean in communication.

There have been many researches on how to generate natural facial expressions. For example, linear dynamic affect-expression model and simple recurrent network were developed to generate facial expressions dynamically [9], [10]. Fuzzy rule based system was applied to generate facial expressions [11]. Grizard and Lisetti used three-levels architecture by adapting psychological theory and Lin and Huang used anatomical theory for generating facial expressions [12], [13].

However, researches on composite facial expressions have not been much progressed. To generate composite facial expressions, relationship among emotions should be considered. According to the psychologist Ekman, happiness is a positive emotion, surprise is a neutral emotion and anger, disgust, fear and sadness are negative emotions [14]. Therefore, both anger and disgust are very similar and they often appear together. However, being happy and disgust at the same time is highly unlikely produced. To generate more natural facial expressions, relationship between emotions should be considered. In addition, each emotion has its own main features in facial expressions. Happiness is chiefly expressed by stretching a mouth and surprise is mainly expressed by raising a forehead and eyebrows. When composite facial expressions are generated, each emotion is expressed separately in some parts of face such that they are produced in a big picture. Conventional methods for generating the composite facial expressions used the linear interpolation of the representative facial expressions under the assumption that the transitions between facial expressions are linear. Thus, linear interpolation method cannot generate natural facial expressions.

In this paper, fuzzy integral and fuzzy measure are used to generate natural composite facial expressions. The fuzzy measure deals with the ambiguity of the crisp set. Emotion state can be represented by the fuzzy measures because the relationship among them are ambiguous such that people cannot easily tell how much a subject is in a happy state, sad state, etc. Thus, the fuzzy measures are employed to represent the relationship among emotions. The partial evaluation of current emotion state is obtained from a predefined error function of the ideal basic emotion states and the current emotion state. Fuzzy integral of the partial evaluation with respect to fuzzy measures is employed to globally evaluate the current emotion state for generating composite facial expression by separately actuating the parts of a robotic face. The effectiveness of the proposed method for generating composite facial expressions is demonstrated through the experiments with a robotic head with 19 degrees of freedom, developed in RIT Laboratory, KAIST.

The rest of this paper is organized as follows. In Section II, the generation process of composite facial expressions is proposed based on the fuzzy measure and fuzzy integral.

978-1-4244-7316-8/11/$26.00 ©2011 IEEE

Simulation and experimental results are presented in Section III. Finally, concluding remarks follow in Section IV.

II. Generation of Facial Expression

A. Composite Facial Expressions

According to the psychologist Ekman, human's basic emotions are anger, disgust, fear, happiness, sadness and surprise. Emotions are represented by facial expressions. When two emotions are mixed, facial expression is not produced with the average value. Each emotion is expressed separately in parts of face, and composite facial expressions are produced in a big picture [14]. Expressed parts in composite facial expressions are summarized in Table I. In several composite facial expressions, the expressed parts are exchangeable. For example, when fear and surprise are mixed, surprise can be expressed in a mouth and fear can be expressed in eyes, eye brows, and eye lids.

B. Fuzzy Measure and Fuzzy Integral

In this paper, Sugeno λ-fuzzy measure is used to reflect the relationship among emotions and the Choquet fuzzy integral is used to generate facial expressions. The fuzzy measure is defined in the following [15].

Definition 1: A fuzzy measure on the set X of symbols is a set function $g : P(X) \rightarrow [0,1]$ satisfying the following axioms;

i) $g(\varnothing) = 0, g(X) = 1$;

ii) $A \subset B \subset X$ implies $g(A) \leq g(B)$.

The Sugeno λ-fuzzy measure satisfies the following [16]:

$$g(A \cup B) = g(A) + g(B) + \lambda g(A)g(B). \tag{1}$$

TABLE II
Meaning of Fuzzy Measure

Fuzzy measure property	λ	ξ	Symbol relation
$g(A \cup B) > g(A) + g(B)$	$+\infty$	0	Negative correlation
	$\vdots$	$\vdots$	
$g(A \cup B) = g(A) + g(B)$	0	0.5	Independent
	$\vdots$	$\vdots$	
$g(A \cup B) < g(A) + g(B)$	-1	1	Positive correlation

In (1), g represents the fuzzy measure, λ represents the interaction degree, and ξ is a normalized value of λ. If λ is positive, $g(A \cup B) > g(A) + g(B)$, which means that $g(A \cup B)$ is overestimated and hence A and B have a negative correlation.

The Choquet fuzzy integral is defined in the following [17].

Definition 2: Let h be a mapping from finite set X to [0,1]. For $x_i \in X, i = 1, 2, \ldots, n$, assume $h(x_i) \leq h(x_{i+1})$ and $E_i = \{x_i, x_{i+1}, \ldots, x_n\}$. The Choquet fuzzy integral of h over X with respect to the fuzzy measure g is define as

$$\int_X h \circ g = \sum_{i=1}^{n} (h(x_i) - h(x_{i-1}))g(E_i), \; h(x_0) = 0. \tag{2}$$

In (2), fuzzy measure g should be calculated for all the power sets of X and partial evaluation values h are calculated from a predefined error function of the ideal basic emotion states and the current emotion state of a robot.

C. Diamond Pairwise Comparison

Six symbols are used because the number of human's basic emotions is six. Without fuzzy measure identification method, it is hard to identify $2^6 - 2 = 62$ fuzzy measures. Diamond pairwise comparison method is used to reflect the relationship among emotions [18]. Every two pair should be compared with the diamond pairwise comparison. In Fig. 1(a), one point in the diamond is marked. The Diamond can be translated to the coordinate axis on the right-hand side in Fig. 1(b) which X-axis represents sv_i and Y-axis represents I_{ij}. sv_i means the relative importance between two symbols. I_{ij} is the parameter to represent whether two symbols are positive relations or negative relations, which can be replaced with ξ_{ij}. ξ_{ij} is the normalized value and it can sufficiently express the relationship among emotions. The meaning of ξ is summarized in Table II. In this paper, ξ_{ij} is used instead of I_{ij}.

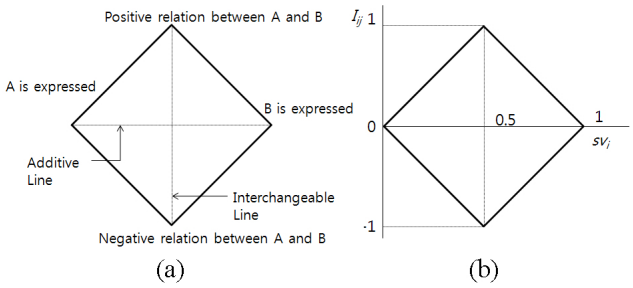

Fig. 1. Diamond pairwise comparison

$$sv_i + sv_j = 1, \; c_{ij} = sv_i / sv_j \tag{3}$$

c_{ij} is calculated from sv_i through (3). c_{ij} means the relative importance between two elements. If sv_i is more important, c_{ij} is greater than one and if sv_j is more important, c_{ij} is smaller than one. From C matrix in (4), the normalized eigenvector of maximum eigenvalue is the weight vector on each symbol. It will be changed by combining with information about relationship among emotions. Based on Table I, face consist of four parts, i.e. eye lids and eye brows, mouth and jaw, eyes, and neck. Each part has different weight so that there are four C matrices and four weight vectors.

$$C = \begin{pmatrix} c_{11} & c_{12} & \cdots & c_{16} \\ c_{21} & c_{22} & \cdots & c_{26} \\ \vdots & \vdots & \ddots & \vdots \\ c_{61} & c_{62} & \cdots & c_{66} \end{pmatrix} \tag{4}$$

D. Hierarchical Structure

A dissimilarity graph is obtained from the interaction degrees ξ_{ij}. Two closest clusters in the dissimilarity graph are merged through a step-by-step process until only one

TABLE I
EXPRESSED PARTS IN COMPOSITE FACIAL EXPRESSIONS

Emotion	expressed part	Emotion	expressed part
Anger	eyes, eye brows, eye lids	Disgust	mouth
Anger	eyes, eye brows, eye lids	Fear	mouth
Anger	eyes, eye brows, upper eye lids	Happiness	mouth, lower eye lids
Anger	eyes, eye brows, eye lids	Sadness	mouth
Anger	eyes, eye brows, eye lids	Surprise	mouth
Disgust	eyes, eye brows, upper eye lids	Fear	mouth, lower eye lids
Disgust	eyes, eye brows, eye lids	Happiness	mouth
Disgust	eyes, eye brows, upper eye lids	Sadness	mouth, lower eye lids
Disgust	eyes, eye brows, upper eye lids	Surprise	mouth, lower eye lids
Fear	eyes, eye brows, upper eye lids	Happiness	mouth, lower eye lids
Fear	mouth	Sadness	eyes, eye brows, eye lids
Fear	mouth	Surprise	eyes, eye brows, eye lids
Happiness	mouth	Sadness	eyes, eye brows, eye lids
Happiness	mouth	Surprise	eyes, eye brows, eye lids
Sadness	mouth	Surprise	eyes, eye brows, eye lids

cluster remains. Dissimilarity between two clusters, G_p and G_q, means the average distance in difference to the others except G_p and G_q, which is calculated as follows:

$$D_{G_p,G_q} = \frac{\Sigma_{G_r \in \mathfrak{G}, G_r \neq G_p, G_r \neq G_q} [\xi_{G_p,G_r} - \xi_{G_q,G_r}]^2}{|\mathfrak{G}| - 2} \quad (5)$$

where $\mathfrak{G}$ is the set of all clusters and $|\mathfrak{G}|$ is the number of clusters in that stage. If the difference of dissimilarity is smaller than a certain threshold, more than three symbols can be merged at the same time. Large threshold will generate a simplified hierarchical structure and small threshold will generate a complex but accurate hierarchical structure. Note that 0.1 is used as a threshold in this paper. The interaction degree graph from ξ_{ij} is shown in Fig. 2 and the dissimilarity graph from the interaction degree graph is shown in Fig. 3.

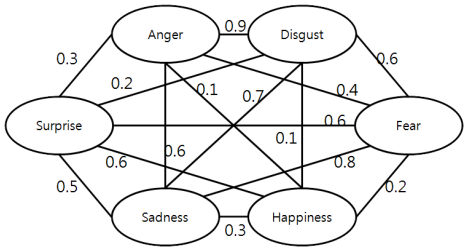

Fig. 2. Interaction degree graph

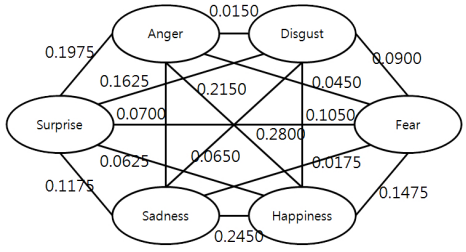

Fig. 3. Dissimilarity graph

In Fig. 4, the hierarchical structure from the dissimilarity graph and the four weight vectors from pairwise comparison matrices C are combined to produce the fuzzy measures of all sets.

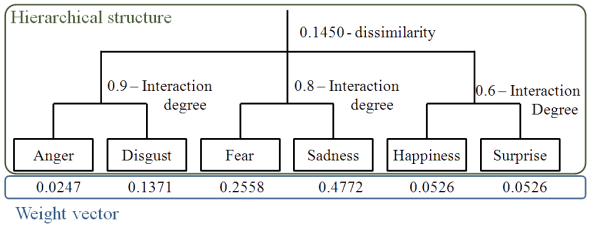

Fig. 4. A hierarchical structure

E. Fuzzy Measure Identification

ϕ_s transformation is used to get fuzzy measures $g(A)$. ϕ_s transformation is defined as follows [19]:

$$\phi_s : [0,1] \times [0,1] \rightarrow [0,1] \quad (6)$$

$$\phi_s(\xi, u) = \begin{cases} 1 & \text{if } \xi = 1 \text{ and } u > 0 \\ 0 & \text{if } \xi = 1 \text{ and } u = 0 \\ 1 & \text{if } \xi = 0 \text{ and } u = 1 \\ 0 & \text{if } \xi = 0 \text{ and } u < 1 \\ \frac{s^u - 1}{s - 1} & \text{other cases} \end{cases} \quad (7)$$

where $s = \frac{(1-\xi)^2}{\xi^2}$. Fuzzy measure $g(A)$, where $A \subset X$, is calculated as follows:

$$g(A) = \phi_s(\xi_R, \sum_{B \subset R} u_B^R) \quad (8)$$

where R means root level set and ξ_R is the dissimilarity degree in root level and B is upper level set. Weights in upper level are calculated as follows:

$$u_C^B = \begin{cases} w_i & \text{if } |C| = 1 \text{ and } i \in A \\ 0 & \text{if } |C| = 1 \text{ and } i \notin A \\ \phi_s^{-1}(\xi_B, \phi_s(\xi_C, \sum_{D \subset C} u_D^C) \times T_C^B) & \text{other cases} \end{cases} \quad (9)$$

where $w_i, i \in C$, is the weight in lower level and $\phi_s^{-1}(\xi, u)$ is the inverse function of $\phi_s(\xi, r)$. Weights in lower level should be changed to weights in upper level. In this paper, the hierarchical structure has only two levels so that ξ_C is an interaction degree in a lower level and ξ_B is a dissimilarity degree in an upper level. T_C^B is a conversion ratio from lower-level to upper-level which is defined as follows:

$$T_C^B = \frac{\phi_s(\xi_B, \sum_{D \in C} w_D^C)}{\phi_s(\xi_C, \sum_{D \in C} w_D^C)} \tag{10}$$

where

$$u_C^B = \begin{cases} w_i & \text{if } |C| = 1 \\ \sum_{D \in C} w_D^C & \text{other cases} \end{cases} \tag{11}$$

where $w_i, i \in C$, is a weight from pairwise comparison matrix C.

F. Partial Evaluation

Partial evaluation values are obtained from the emotion state of robot. Let the current emotion state vector $X = [x_1; x_2; \ldots; x_6]^T$, where each of $x_i, i = 1, 2, \ldots, 6$ is between 0 and 1. The emotion state is represented by six parameters and each parameter represents each emotion, i.e. $x_1, x_2, \ldots, x_6$ means anger, disgust, fear, happiness, sadness, and surprise, respectively.

Let $S_i = \{s_{i1}; s_{i2}; \ldots; s_{i6}\}^T, i = 1, 2, \ldots, 6$ be the ideal emotion state vector. The ideal emotion state means that the corresponding emotion is fully activated. Ideal emotion states parameter $s_{ij}, i = 1, 2, \ldots, 6$ and $j = 1, 2, \ldots, 6$ is calculated as follows:

$$s_{ij} = \begin{cases} 0 & \text{if } i \neq j \\ 1 & \text{if } i = j. \end{cases} \tag{12}$$

For example, anger is fully activated when emotion state is $S_1 = \{1; 0; 0; 0; 0; 0\}^T$. Current emotion state should be close to S_i to activate i-th emotion. $E = \{E_1; E_2; \ldots; E_6\}$ is a distance matrix containing the every distance from current emotion state vector to the ideal emotion state vectors, which is calculated as follows:

$$\begin{pmatrix} E_1 \\ E_2 \\ \vdots \\ E_5 \\ E_6 \end{pmatrix} = \begin{pmatrix} I - |S_1 - X| \\ I - |S_2 - X| \\ \vdots \\ I - |S_5 - X| \\ I - |S_6 - X| \end{pmatrix} \tag{13}$$

where $E_i = \{e_{i1}; e_{i2}; \ldots; e_{i6}\}^T$ is a size six matrix and $I = \{1; 1; 1; 1; 1; 1\}^T$.

Each e_{ij} has a different importance in E_i. For example, when anger expression is generated, anger parameter is more important than other parameters. Therefore, e_{ii} is multiplied to E_i to get partial evaluation vector H_i such that $H = \{H_1; H_2; \ldots; H_6\}$ is a calculated as follows:

$$\begin{pmatrix} H_1 \\ H_2 \\ \vdots \\ H_5 \\ H_6 \end{pmatrix} = \begin{pmatrix} e_{11} \times E_1 \\ e_{22} \times E_2 \\ \vdots \\ e_{55} \times E_5 \\ e_{66} \times E_6 \end{pmatrix} \tag{14}$$

where $H_i = \{h_{i1}; h_{i2}; \ldots; h_{i6}\}^T$ is a size six matrix. Every H_i and fuzzy measures from Fig. 4 are globally integrated by the Choquet integral. Each $H_i, i = 1, 2, \ldots, 6$ is evaluated and the largest output of the Choquet integral is selected with the Choquet integral output.

III. Simulation and Experimental Results

A. Parameter Setting

People see the relationship among emotions differently. 20 subjects were asked to fill out the interaction degree graphs. 20 types of hierarchical structures were produced and 5 subjects generated the same type of hierarchical structure as shown in Fig. 4, which was used in this experiment.

Based on Table I, pairwise comparison matrix C was produced. If i-th emotion was more important than j-th emotion, six times of relative weight was assigned to sv_i. Weight vectors in each part were shown in Table III.

TABLE III
Weight vectors on each part

	Mouth and jaw	Eye lids and eye brows	Eyes	Neck
Anger	0.0247	0.4771	0.2547	0.1666
Disgust	0.1371	0.0860	0.2069	0.1666
Fear	0.2558	0.0461	0.1059	0.1666
Happiness	0.4772	0.0247	0.2058	0.1666
Sadness	0.0526	0.1831	0.1569	0.1666
Surprise	0.0526	0.1831	0.0702	0.1666

B. Robotic Head

Robotic head's width, height, length, weight are 16cm, 26cm, 25cm, and 2.85kg, respectively. It can receive three-dimensional images through a stereo camera. Facial movements are controlled by 15 servo motors and neck's movements are controlled by 4 DC motors. Thus, it has 19 degrees of freedom. Three servo motors move jaw left and right, up and down, forward and backward. Four servo motors can push and pull the end of upper lip and lower lip. Two servo motors can move the eyes left and right, up and down. Four servo motors control the eye brows left and right, up and down, and two servo motors control the eye lids up and down. Neck is controlled by four DC motors. To sustain strong torque, harmonic drives are also used together with the DC motors. Each of the three DC motors rotates the head along the yaw, pitch and roll axes, respectively and the last one is to add one more degree of freedom to the pitch axis for nodding. Note that robotic head's movements are designed based on the facial action coding system (FACS) [20]. Normally, to maximize degrees of freedom, many robotic heads contains only mechanical structure in robotic heads and other modules

such as control module and motor module are placed near the robotic heads. Lots of wires are used to convey motors force from motor module to mechanical structure. However, the robotic head used in this experiment is designed to contain every module in its head. Thus, it does not have many degrees of freedom. However, it has good expandability.

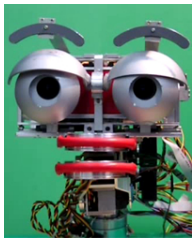

Fig. 5. Robotic head

The robotic head is controlled by digital signal processors (DSP) and electrically programmable logic devices (EPLD). Because DSP does not have enough counters, it is supported by EPLD to count the encoder's output.

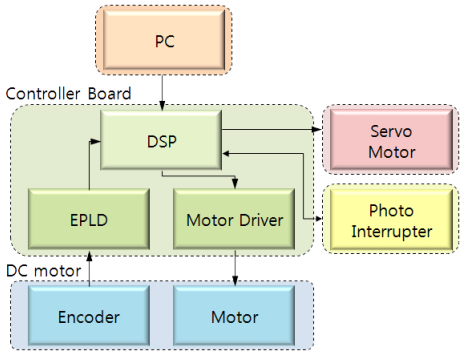

Fig. 6. Control circuit diagram

C. Simulation Results

Initial emotion state was set as $\{Anger, Disgust, Fear, Surprise, Sadness, Surprise\} = \{x_1, 0.09, 0.14, 0.10, 0.11, 0.65\}$ and the anger parameter x_1 was increased from zero to one to observe the variation of the composite facial expression. In the initial state, surprise was dominant.

In Fig. 7, X-axis is for the anger parameter and Y1-axis is for the normalized motor output value and Y2-axis shows the selected emotion. When the anger parameter was zero, surprise was selected in all the four parts because the surprise parameter value was much larger than the other parameter values. As the anger parameter value was increased, surprise was still selected in some initial time period but the normalized motor output value was decreased because the anger parameter moved far from zero to one. When the anger parameter value was continuously increased, eye brows and eye lids chose anger even though its value was smaller than that of the surprise parameter. When the anger parameter value was the same as the surprise parameter value, mouth, jaw and neck expressed

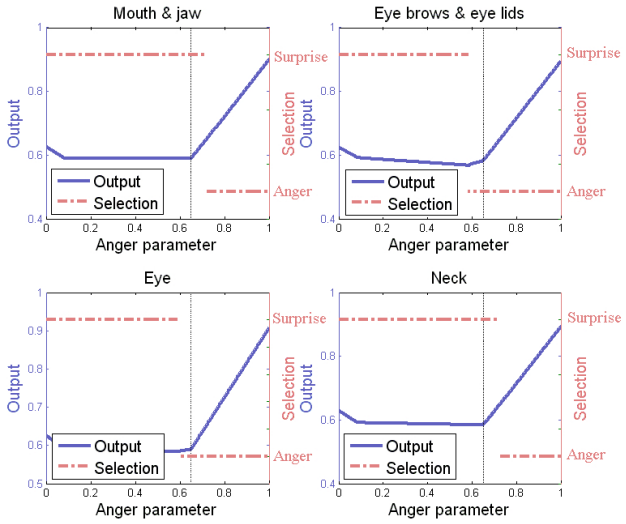

Fig. 7. Transition from surprise to anger

surprise and eyes, eye brows and eye lids expressed anger. Thus, the composite facial expression was generated. If the anger parameter value was increased more, all the four parts selected anger and the output became much larger. However, since the emotion state vector in this simulation could not be the ideal emotion state vector of anger S_1, the output could not reach the maximum value. Note that similar result for generating various composite facial expressions could be obtained for the other case, for example, by increasing the disgust parameter value when the anger was dominant.

D. Experiments

Ekman's six basic emotions were generated and shown to 12 subjects. Facial expressions were generated by random order and subjects who had not seen the robotic head before were surveyed. The result was shown in Table IV.

TABLE IV
A SURVEY ON BASIC EXPRESSIONS

	Correct	Wrong	Percentage
Anger	9	3	75%
Disgust	9	3	75%
Fear	10	2	83%
Happiness	12	0	100%
Sadness	12	0	100%
Surprise	12	0	100%

As the Table IV shows, most of people could distinguish every basic facial expression except anger and disgust. These two emotions were quite similar that some subjects got confused in distinguishing them.

Fifteen composite facial expressions were generated by random order and shown to 10 subjects. The result was shown in Table V. People could not easily distinguish composite facial expressions. The reason was that some composite facial expressions were not familiar and hard to be identified. For example, being disgust and happiness together was unlikely generated in

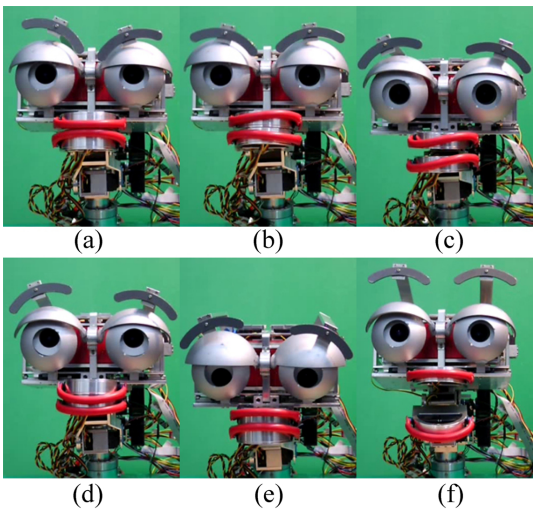

Fig. 8. Six basic emotions. (a) Angry (b) Disgust (c) Fear (d) Happiness (e) Sadness (f) Surprise

a normal life. Even if this facial expression was well generated, subjects could not easily recognize it. However, most subjects could identify familiar composite facial expressions easily, i.e. anger and disgust, happiness and surprise, etc.

TABLE V
A SURVEY ON COMPOSITE FACIAL EXPRESSIONS

	Anger	Disgust	Fear	Happiness	Sadness
Anger	x	x	x	x	x
Disgust	8	x	x	x	x
Fear	5	2	x	x	x
Happiness	5	3	2	x	x
Sadness	9	4	4	6	x
Surprise	4	7	3	9	4

Other reason was that some facial movements could not be generated by the developed robotic head. Happiness was mainly expressed by stretching a mouth and naso-labial folds. Robotic head did not have wrinkles so that it could not produce some facial movements. This point made subjects hard to identify the generated facial expressions. Easily and hardly recognizable facial expressions by the subjects are shown in Fig. 9 and Fig. 10, respectively.

Among the composite facial expressions, several familiar composite facial expressions were generated by the linear interpolation method and showed to 10 subjects. Only facial expressions with easily recognizable were generated because it is not important to generate facial expressions with unlikely produced in normal life. Table VI shows the result of comparison. The percentage of correct answers of linear interpolation method was lower than that of fuzzy integral-based method. Because characteristics of each emotion were disappeared by the linear interpolation, fewer people could recognize them.

Fig. 11 shows the composite facial expressions generated by the linear interpolation method. The linear interpolation method could generate continuous facial expressions transitions. However, it could not express the characteristics of each

TABLE VI
A COMPARISON WITH LINEAR INTERPOLATION METHOD AND FUZZY INTEGRAL-BASED METHOD

Facial expression	Anger and disgust	Anger and sadness	Happiness and surprise
Linear interpolation	6	5	5
Fuzzy integral-based	8	9	9

emotion in composite facial expressions. Thus, compared to Fig. 9(b) and Fig. 10(b), it become more difficult to identify which emotions are expressed in composite facial expressions.

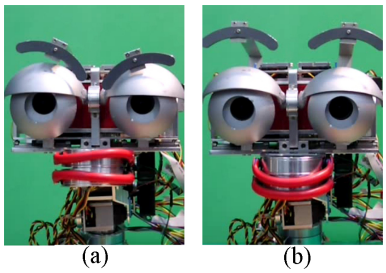

Fig. 9. Easily recognizable expressions. (a) Anger and disgust (b) Happiness and surprise

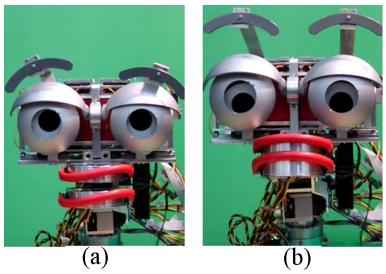

Fig. 10. Hardly recognizable expressions. (a) Happiness and fear (b) Surprise and sadness

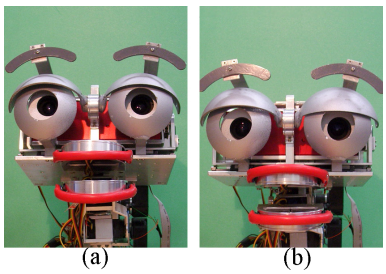

Fig. 11. Facial expressions from linear interpolation method. (a) Happiness and surprise (b) Surprise and sadness

IV. CONCLUSION

In this paper, a fuzzy integral-based generation method of composite facial expressions was proposed and demonstrated its effectiveness through the experiment with the developed robotic head. Fuzzy measures reflected the relationship among

emotions and the partial evaluation of current emotion state was obtained from a predefined error function. The Choquet fuzzy integral of the partial evaluation with respect to fuzzy measures was employed for generating composite facial expressions by separately actuating the parts of a robotic face. Experimental results showed that basic facial expressions were successfully generated and identified by the subjects. Composite facial expressions were also generated and some of them were hard to be identified, however, some familiar facial expressions were easily identified. It also showed that people could easily recognize the composite facial expressions generated by fuzzy integral-based method.

In future research, one microphone and one speaker will be added to the robotic head. Proper sound will be produced with the generation of facial expressions. Then people can recognize robot's facial expressions easily with sound.

ACKNOWLEDGEMENT

This research was supported by Basic Science Research Program through the National Research Foundation of Korea (NRF) funded by the Ministry of Education, Science and Technology (2011-0000321).

REFERENCES

[1] F. Faber, M. Bennewitz, C. Eppner and A. Görög, "The humanoid museum tour guide Robotinho," in IEEE Int. Symp. Robot and Human Interactive Communication, Toyama International Conference Center, Japan, 2009, pp. 891-896.

[2] G. Castellano., A. Pereira and P. W. McOwan, "Detecting user engagement with a robot companion using task and social interaction-based features," in Proc. IEEE Int. Conf. Multimodal Interfaces, Massachusetts, USA, 2009, pp. 119-126.

[3] C. L. Breazeal, "Social interactions in HRI: the robot view," IEEE Trans. Syst. Man Cybern. C, Appl. Rev, vol. 34, no. 2, pp. 181-186, May. 2004.

[4] C. L. Breazeal, Designing Sociable Robots, Cambridge, MA:MIT Press, 2002.

[5] T. Hashimoto, S. Hitramatsu, T. Tsuji and H. Kobayashi, "Development of the face robot SAYA for rich facial expressions," in Proc. SICE-ICASE Int. Joint Conf., Busan, Korea, 2006, pp. 5423-5428.

[6] R. Beira *et al.*, "Design of the Robot-Cub(iCub) head," in Proc. IEEE Int. Conf. Robotics and Automation, Florida, USA., 2006, pp. 94-100.

[7] A. Mehrabian, Nonverbal Communication, Aldine-Atherton, 1972.

[8] A. Mehrabian, Communication without words, Psychology Today, vol. 2, no. 4, pp. 53-56, 1968.

[9] J.-W. Park, W.-H. Kim, W.-H. Lee, W.-H. Kim and M.-J. Chung, "Lifelike facial expression of mascot-type robot based on emotional boundaries," in Proc. IEEE Int. Conf. Robotics and Biomimetics, Guilin, China, 2009, pp. 830-835.

[10] Y. Matsui, M. Kanoh, S. Kato, T. Nakamura and H. Itoh, "Evaluating a model for generating interactive facial expressions using simple recurrent network," in Proc. IEEE Int. Conf. Syst. Man Cybern., Texas, USA., 2009, pp. 1639-1644.

[11] T. Bui, D. Heylen, M. Poel and A. Nijholt, "Generation of facial expressions from emotion using a fuzzy rule based system," in Proc. 14th Australian Joint Conf. Artificial Intelligence, D. Corbett, M. Stumptner and M. Brooks, Eds., Adelaide, Australia, 2003. pp. 83-94.

[12] A. Grizard and C. Lisetti, "Generation of facial emotional expressions based on psychological theory," in Proc. 1rst Wrks. Emotion and Computing, 29th Annu. Conf. Artificial Intelligence, Bremen, Germany, 2006.

[13] C.-C. Lin and H.-P. Huang, "Design of a face robot with facial expression," in Proc. IEEE Int. Conf. Robotics and Biomimetics, Guilin, China, 2009, pp. 492-497.

[14] P. Ekman and W. Friesen, Unmasking the face: A Guide to Recognizing Emotions From Facial Expressions, Englewood Cliffs, NJ: Prentice Hall, 1975.

[15] M. Sugeno, "Theory of fuzzy integrals and its applications," Ph.D. dissertation, Tokyo Institute of Technology, 1974.

[16] M. Sugeno, "Fuzzy measures and fuzzy integrals - a survey," Fuzzy Automata and Decision Processes, M.M. Gupta, G.N. Saridis and B.R. Gaines, eds. Amsterdam, North Holland, 1977, pp.89-102.

[17] M. Grabisch, H.-T. Nguyen and E.-A. Walker, Fundamentals of uncertainty Calculi, with Applications to Fuzzy Inference, Boston, MA: Kluwer, 1995.

[18] E. Takahagi, "A fuzzy measure identification method by diamond pairwise comparisons and ϕ_s transformation," J. Fuzzy Optimization Decision Making, vol. 7, pp. 219-232, 2008.

[19] Y. Narukawa and V. Torra, "Fuzzy measure and probability distribution: distorted probabilities," IEEE Trans. Fuzzy Syst., vol.13, pp. 617-629, Oct. 2005.

[20] P. Ekman and W. Friesen, Facial Action Coding System: A Technique for the Measurement of Facial Movement, Palo Alto, CA: Consulting Psychologists Press, 1978.

2011 IEEE International Conference on Fuzzy Systems
June 27-30, 2011, Taipei, Taiwan

Comparing Soft Clusters and Partitions

Derek T. Anderson, James M. Keller, Ozy Sjahputera and James C. Bezdek
Electrical and Computer Engineering
University of Missouri
Columbia, MO, USA
andersondt@missouri.edu, kellerj@missouri.edu, sjahputerao@missouri.edu and jcbezdek@gmail.com

Mihail Popescu
Health Management and Informatics
University of Missouri
Columbia, MO, USA
popescum@missouri.edu

***Abstract*—Previously, we presented a method for comparing soft partitions (i.e. crisp, probabilistic, fuzzy and possibilistic) to a known crisp reference partition. Many of the classical indices that have been used with outputs of crisp clustering algorithms were generalized so that they are applicable for candidate partitions of any type. In particular, focus was placed on generalizations of the Rand index. In this article, we extend our prior work by (1) investigating the behavior of the soft Rand for comparing non-crisp, specifically possibilistic, partitions and (2) we demonstrate how the possibilistic Rand and visual assessment of (cluster) tendency (VAT) algorithm can be used to discover the number of actual clusters and coincident clusters for outputs from the possibilistic c-means (PCM) algorithm.**

Keywords; cluster validity; possibilistic Rand index; comparing soft partitions; cluster correspondence.

I. INTRODUCTION

Let $O = \{o_1,\ldots,o_n\}$ denote n objects. When each object in O is represented by a (column) vector $\mathbf{x}$, the set $X = \{\mathbf{x}_1,\ldots,\mathbf{x}_n\} \subset \Re^p$ is an *object data representation* of O. When each object in $o_i \in O$ has a *physical label*, O is a set of *labeled data*; otherwise, O is unlabeled. Let integer c denote the number of classes, $1 < c < n$. Clustering in unlabeled data is the assignment of one of four types of labels to each object in O. The label vectors of the objects are the columns of c-partitions of O, which are sets of (cn) values $\{u_{ik}\}$ that can be conveniently arrayed as $(c \times n)$ matrices, say $U = [u_{ik}]$. The three sets are:

$$M_{pcn} = \left\{ U \in \Re^{cn} : u_{ik} \in [0,1] \forall\, i,k;\ 0 < \sum_{k=1}^{n} u_{ik}\ \forall\, i \right\}, \quad (1a)$$

$$M_{fcn} = \left\{ U \in M_{pcn} : \sum_{i=1}^{c} u_{ik} = 1 \forall\, k \right\}, \quad (1b)$$

$$M_{hcn} = \left\{ U \in M_{fcn} : u_{ik} \in \{0,1\} \forall i,k \right\}, \quad (1c)$$

where M_{pcn} (1a) are possibilistic c-partitions, M_{fcn} (1b) are fuzzy or probabilistic c-partitions, and M_{hcn} (1c) are crisp or hard c-partitions. It is convenient to have a single name for the set M_{pcn}-M_{hcn}, which contains the fuzzy, probabilistic, and possibilistic c-partitions of O. We call M_{pcn}-M_{hcn} the *soft c-partitions* of O.

Clustering algorithms map $X \subset \Re^p \mapsto M_{pcn}$. Let $CP = \{U_i: 1 \le i \le N\}$ denote N different *candidate partitions* of a fixed object set O that may arise as a result of clustering X with one algorithm at various values of its parameters; or more generally, with different algorithms, each with its own parameters. Which $U \in CP$ best explains and represents the (unknown) structure in O? In [1,2], we introduced one way to answer this question through the use of a *comparison index,* s(U,V). Applications of our prior approach include:

A1. s(U,V): V $(r \times n)$ is a *reference partition* that purports to represent the "true cluster structure" in O. s(U,V) measures the extent to which U's in CP recover or retrieve the true clusters in O, and hence, the sizes of U and V are equal. Retrieval rates are called *resubstitution error rates* when U and V are crisp, r = c, and s is a measure that counts matches between the columns in U and V.

A2. s(U,U'): U is a partition of O found with clustering algorithm A. Perturb each $\mathbf{x}_k$ or r_{ij} with zero mean, unit variance noise, and obtain U', a clustering of the perturbed data. s(U, U') measures the sensitivity of A to perturbations of the data.

A3. s(U,U'): U, U' are partitions of O found with clustering algorithms A and A'. s(U, U') measures the agreement between the two algorithms about clusters in O.

A4. s(U,U'): U, U' are partitions of O found by successive iterations of clustering algorithms. s(U, U') measures the change in similarity due to the next iteration, and hence, can be used as a stopping criterion for iterative methods.

A5. s(U,V): Prediction of V given U, or U given V (regression).

In [1,2], our experiments focused on A1. We <u>never</u> have an external reference partition in a real clustering situation which, by definition, involves unlabeled data. So, why do this at all? Well, the only way you can evaluate *any* clustering algorithm before using it in a real situation is to see how well it recovers "true but unknown" reference partitions. If nothing else, good recovery rates on data with "known" cluster structure at least provide some psychological reassurance that the clustering algorithm *can* sometimes recover "good clusters".

978-1-4244-7316-8/11/$26.00 ©2011 IEEE

In this article, we extend our prior work by exploring the behavior of the soft Rand for comparing non-crisp, specifically possibilistic, partitions. We also demonstrate how the possibilistic Rand index and visual assessment of (cluster) tendency (VAT) algorithm can be coupled in order to estimate the number of clusters and identify coincident clusters found by the possibilistic c-means (PCM) algorithm [3,4]. This work supports the claim [4] that coincident clusters found by PCM can be advantageous. We demonstrate that by over specifying the number of clusters, one can address important different clustering tasks.

II. BACKGROUND

A. Prior Work

Let $U \in M_{hm}$ and $V \in M_{hcn}$ be crisp partitions of O. U and V need not possess the same number of clusters. The four classical combinations for pairs of objects from $O \times O$ in clusters of U and V are: (i) paired in U and V; (ii) not paired in U nor in V; (iii) paired in V but not in U; and (iv) paired in U but not in V [5]. The comparison of U to V with a similarity measure s begins with the $r \times c$ contingency matrix $N = UV^T$ shown in Table 1 that contains counts of the number of occurrences of each of the four types over the n(n-1)/2 distinct, unordered pairs in $O \times O$. Entry n_{ij} is the number of objects common to classes U_i and V_j.

Table 1. The contingency matrix N.

		Partition V (V_j = row j of V)				
	Class	V_1	V_2	…	V_c	Sums
Partition U (U_i = row i of U)	U_1	n_{11}	n_{12}	…	n_{1c}	$n_{1\bullet}$
	U_2	n_{21}	n_{22}	…	n_{2c}	$n_{2\bullet}$
	⋮	⋮	⋮		⋮	⋮
	U_r	n_{r1}	n_{r2}	…	n_{rc}	$n_{r\bullet}$
	Sums	$n_{\bullet 1}$	$n_{\bullet 2}$	…	$n_{\bullet c}$	$n_{\bullet\bullet} = n$

The building blocks of many similarity measures for s(U,V) are the four equations (2a)-(2d). These four equations simply count the number of occurrences among the n(n-1)/2 pairs of each of the four types of unordered pairs.

$$a = \frac{1}{2}\sum_{i=1}^{r}\sum_{j=1}^{c} n_{ij}(n_{ij}-1) \tag{2a}$$

$$b = \frac{1}{2}\left(\sum_{j=1}^{c} n_{\bullet j}^2 - \sum_{i=1}^{r}\sum_{j=1}^{c} n_{ij}^2\right) \tag{2b}$$

$$c = \frac{1}{2}\left(\sum_{i=1}^{r} n_{i\bullet}^2 - \sum_{i=1}^{r}\sum_{j=1}^{c} n_{ij}^2\right) \tag{2c}$$

$$d = \frac{1}{2}\left(n^2 + \sum_{i=1}^{r}\sum_{j=1}^{c} n_{ij}^2 - \left(\sum_{i=1}^{r} n_{i\bullet}^2 + \sum_{j=1}^{c} n_{\bullet j}^2\right)\right) \tag{2d}$$

Formula (2a) is the number paired in U and V, formula (2d) is the number paired in neither U nor V, formula (2b) is the number paired in V, not U, and formula (2c) is the number paired in U, not V.

The sums (a+d) and (b+c) are usually interpreted, respectively, as (the total number of) agreements and disagreements between U and V. In [1], we tabulate a [non-exhaustive] list of 14 coefficients that have been proposed for s(U,V) based on functions of a, b, c and d; Sokal and Sneath [6] list many others. In this note, the only index we consider is Rand's index [7], the classical form of which is

$$s_r(U,V) = (a+d)/(a+b+c+d). \tag{3}$$

B. Generalizing $s_r(U,V)$ when U and/or V are soft partitions

Rand's index first appeared in Sokal and Michener in 1958, where it was called a simple matching coefficient [8]. Rand reintroduced this function in 1971 [7], and the literature has consistently referred to it as "Rand's Index" since then. The resurgence of Rand's index in bioinformatics [9-12] has renewed interest in generalizing it, along with some of the other comparison indices based on the elements in Table 1, to various non-crisp cases. Specifically, we mention the papers (in chronological order) of Campello [13], Frigui et al. [14], Brower [15], Hullermeier and Rifqi [16], and Anderson et al. [1,2]. All of these papers generalize the Rand index to the case of U and/or V being fuzzy partitions of the n objects.

In [1,2], we provide generalizations for 14 comparison indices. It begins with the construction of the contingency matrix as $N = UV^T$. We showed that a modification is needed to accommodate the case when U and/or V are possibilistic. In the possibilistic case, we can have

$$\sum_{i=1}^{r} n_{i\bullet} > n, \text{ or } \sum_{j=1}^{c} n_{\bullet j} > n. \tag{4}$$

One or both of the terms $\sum_{i=1}^{r} n_{i\bullet}^2$ and $\sum_{j=1}^{c} n_{\bullet j}^2$ can make d in (2d) relatively large and negative. Depending on b in (2b) and c in (2c), the (soft) Rand index can result in $s_r(U,V) < 0$ or > 1. To remedy this, we scale N with

$$\phi = n/\sum_{i=1}^{r} n_{i\bullet} \tag{5}$$

or

$$\varphi = n/\sum_{j=1}^{c} n_{\bullet j}. \tag{6}$$

Since

$$\sum_{i=1}^{r} n_{i\bullet} = \sum_{j=1}^{c} n_{\bullet j}, \tag{7}$$

$\varphi = \phi$. Our normalized generalization [1] is

$$s_{r*}(U,V) = N^* = \phi UV^T = [n/\sum_{i=1}^{r} n_{i\bullet}]UV^T. \tag{8}$$

An advantage of this scaling is that when U and V are crisp, fuzzy or probabilistic partitions, ϕ=1, thus $N^* = N = UV^T$. This

shows that *ANY* index based on only the elements of Table 1 will reduce to the original index when U and V are both crisp partitions of the n objects; and otherwise, they will be valid soft generalizations of those indices. Moreover, for possibilistic partitions, the normalization produces index values in [0,1].

III. Comparing Non-Crisp Partitions

In [1,2], we explored A1, which measures the extent to which U's in CP recover or retrieve the true clusters in O. Our initial experiments did not contain any analysis of non-crisp to non-crisp partition comparison. In this section, we demonstrate non-crisp experiments, specifically for case A3, using the fuzzy c-means (FCM) algorithm [17] and the PCM [3,4]. We discuss the behavior of the measure.

Candidate fuzzy partitions are generated by the FCM using the *fcm* function from the MATLAB Fuzzy Logic Toolbox with the fuzzifier q = 2, maximum number of iterations MAXIT = 100, objective function error EPS = 1e-5 and random partition initialization. The PCM partitions are generated using our MATLAB implementation of the algorithm with the fuzzifier q = 2, MAXIT = 100, EPS = 0.001 and a FCM-based initialization. As discussed by Krishnapuram and Keller in [3,4], we re-estimated the parameters η_i (i.e. the value that determines the distance at which the membership value of a point in a cluster becomes 0.5) for each cluster at every iteration. The data sets are made up of different numbers of Gaussian clouds. The number of clouds and their parameters are provided with the discussion for each data set.

Example 1. Our analysis begins with data set 1 (D1), the scatterplot of which is shown in the uppermost view in figure 1. The images of the partition matrices shown in figure 1 are color coded, using a jet colormap, to assist visual interpretation. The value displayed, [0,1], ranges from blue to red, and passes through the colors cyan, yellow, and orange.

FCM is applied twice to D1 using different random initializations at c = 3, resulting in the terminal partitions $U_{f,1}$ and $U_{f,2}$. The images of these two fuzzy partitions in the middle views of figure 1 suggest that $U_{f,1} = U_{f,2}$, up to a relabeling (the data points are sorted by cluster to aid visual analysis, which is possible because we synthetically generated X). And this is the case. Putting U = V equation (8) we have

$$U = V \Rightarrow s_{r*}(U,U) = s_{r*}(V,V) = s_{r*}(U,V) \qquad (9)$$

In view of this, it is not surprising to find that $s_{r*}(U_{f,1},U_{f,1}) = s_{r*}(U_{f,2},U_{f,2}) = s_{r*}(U_{f,1},U_{f,2}) = 0.97$. The converse, which would be a useful result, does not follow. That is, we cannot conclude from $s_{r*}(U_{f,1},U_{f,1}) = s_{r*}(U_{f,2},U_{f,2}) = s_{r*}(U_{f,1},U_{f,2})$ that U = V.

Next, the PCM is applied twice with different random initializations and c = 3 ($U_{p,1}$ and $U_{p,2}$). The two partition matrices are shown in the bottom view of figure 1. We find $s_{r*}(U_{p,1},U_{p,1}) = s_{r*}(U_{p,2},U_{p,2}) = s_{r*}(U_{p,1},U_{p,2}) = 0.59$. We will explain why s_{r*} is considerably less than 1 after the next example.

Example 2. Data set 2 (D2) is shown in figure 2. The main difference between D2 and D1 is that clusters in D1 are visually more compact and well separated. FCM and PCM are

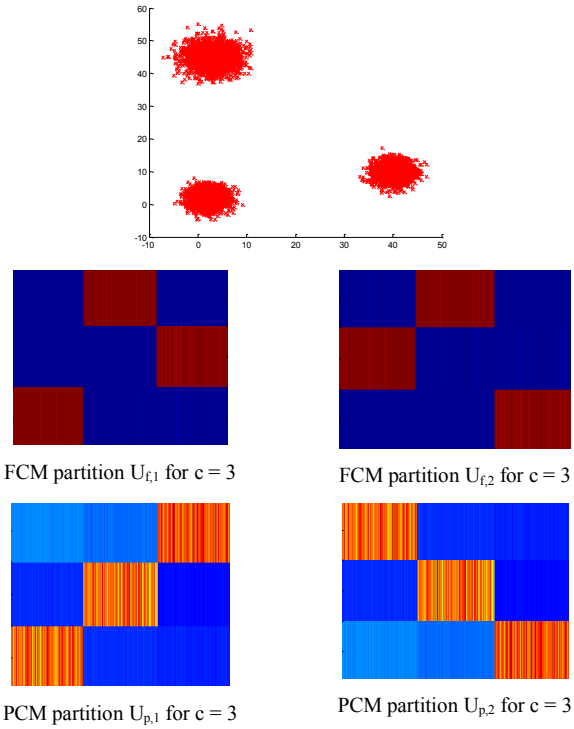

FCM partition $U_{f,1}$ for c = 3 — FCM partition $U_{f,2}$ for c = 3

PCM partition $U_{p,1}$ for c = 3 — PCM partition $U_{p,2}$ for c = 3

Fig. 1. Data set 1 (D1) and corresponding FCM and PCM partitions. D1 is made up of three Gaussian clouds, each with 2000 samples, means of $[2\ 2]^T$, $[40\ 10]^T$, $[3\ 45]^T$ and standard deviations of 2, 2 and 3 respectively. The four candidate partitions are shown in order to visually compare and contrast D1 to data set 2 (D2), figure 2.

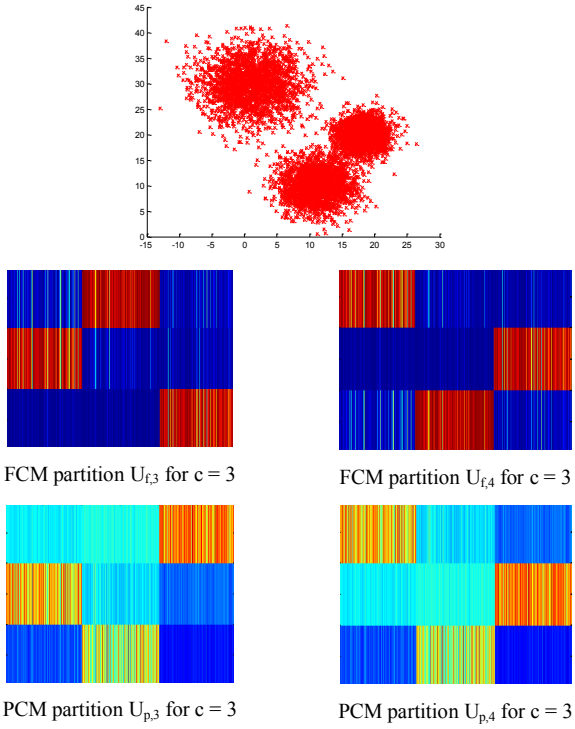

FCM partition $U_{f,3}$ for c = 3 — FCM partition $U_{f,4}$ for c = 3

PCM partition $U_{p,3}$ for c = 3 — PCM partition $U_{p,4}$ for c = 3

Fig. 2. Data set 2 (D2) and corresponding FCM and PCM partitions. D2 is made up of three Gaussian clouds, each with 2000 samples, means of $[10\ 10]^T$, $[18\ 20]^T$, $[1\ 30]^T$ and standard deviations of 3, 2 and 4 respectively.

each applied twice with random initialization for FCM (and hence, equal initializations for PCM) with c = 3. The images of the four terminal partitions discovered by these two algorithms again suggest that the fuzzy partitions are equal, and the PCM partitions are equal, and they are. Thus, in accordance with (9), $s_{r*}(U_{f,3},U_{f,4}) = s_{r*}(U_{f,3},U_{f,3}) = s_{r*}(U_{f,4},U_{f,4}) = 0.80$; and $s_{r*}(U_{p,3},U_{p,4}) = s_{r*}(U_{p,3},U_{p,3}) = s_{r*}(U_{p,4}, U_{p,4}) = 0.57$.

Examples 1 and 2 suggest that the *softer* the partition, the lower the $s_{r*}(U,V)$ value. For crisp partitions, Rand proved [7] that $s_r(U,U) = 1$, thus $s(V,V) = 1$ and $0 \le s(U,V) \le 1$. Entry n_{ij} in the contingency matrix is the number of objects common to clusters U_i and V_j. We calculated it as follows:

$$n_{ij} = \sum_{k=1}^{n} \left(U_{i,k} * V_{j,k} \right). \qquad (10)$$

If the partitions are crisp, then $U_{i,k} * V_{j,k}$ is in {0,1}, i.e. a value of 1 when the k^{th} data point belongs to the i^{th} cluster in U and the j^{th} cluster in V. When the values $U_{i,k}$ and $V_{j,k}$ are fuzzy and in particular less than 1, the membership values result in even smaller products. Our formulation of the contingency matrix leads to interesting behavior for the four counting formulae, (2a)-(2d), as well as the Rand ratio (a+d)/(a+b+c+d). The most interesting component is the effect on equations (2b) and (2c), i.e. the disagreements.

In order for the Rand to obtain a value of 1, the disagreement cases (2b) and (2c) must be zero. However, from equation (10), we see that as the partitions become *softer*, the support in agreements decreases and evidence in disagreements rises. This means that the Rand ratio will decrease because the value (2b)+(2c) is increasing. This is what we observe for FCM in D1 for U1 and U2 and in D2 for U5 and U6. In D1, the (2a)-(2d) values are: a=5747176, b=249975, c=249975 and d=11749871. In D2, we find that a=4039502, b=1997238, c=1997242 and d=9963017. What we observe is that the (2a) and (2d) values are less for D2 versus D1 (where D2 produces softer partitions than those for D1). We also notice that the (2b) and (2c) values are higher for D2 versus D1, making the ratio (a+d)/(b+c), i.e. (agreements)/(disagreements), for D1 (a+d)/(b+c) = 35 and (a+d)/(b+c) = 3.51 for D2.

The following normalization is proposed in order to address this behavior,

$$s'_{r*}(U,V) = s_{r*}(U,V) / \max(s_{r*}(U,U) , s_{r*}(V,V)) \qquad (11)$$

This normalization is proposed because $0 \le s_{r*}(U,V) \le \max(s_{r*}(U,U), s_{r*}(V,V))$. In the case of a crisp U or V, the normalization is 1 and the scaling reduces to Rand's result.

IV. Visual Assesment of (Cluster) Tendency

The problem of determining whether clusters are present as a step prior to *actual* clustering is called assessment of cluster tendency (algorithm 1).

The visual assessment of (cluster) tendency (VAT) algorithm [18] can be used to help discover if there are clusters in a given data set. The basic concept behind VAT (algorithm 1) is that objects are reordered and the reordered matrix of pair-wise object dissimilarities is displayed as an intensity image.

Algorithm 1: *Visual Assessment of (Cluster) Tendency (VAT)*

0. Input: An nxn matrix of dissimilarities $[R_{pq}]$

1. Set K = {1,2,…,n} ; I = J = Ø; P[0] = (0, …, 0).

2. Select $(i,j) \in \underset{p \in K, q \in K}{\arg\max} \{R_{pq}\}$.

   Set P(1) = i; I = {i}; and J = K – {i}.

3. For r=2,…,n:

   Select $(i,j) \in \underset{p \in I, q \in J}{\arg\min} \{R_{pq}\}$.

   Set P(r) = j;

   Replace $I \leftarrow I \cup \{j\}$ and $J \leftarrow J - \{j\}$.

   Next r.

4. Obtain the ordered dissimilarity matrix $\tilde{R}$ using the ordering array P as: $\tilde{R} = R_{P(i)P(j)}$, for $1 \le i,j \le n$.

5. Display the reordered matrix $\tilde{R}$.

Clusters may be indicated by dark blocks of pixels along the matrix diagonal. While VAT is used herein for analysis, clustering in ordered dissimilarity data (CLODD [19] and p-specVAT [20]) can be used to address the partitioning and validity questions by automatically creating partitions from the VAT image and providing a validity measure of each partition. In algorithm 1, R_{pq} is the dissimilarity of objects p and q and the vector P is the permuted indices of the n objects.

V. Comparing Possibilistic Partitions

In [21], Barni et al. remarked that the PCM has the undesirable tendency to produce coincidental clusters. In [4], Keller and Krishnapuram responded by providing additional insight into the inner workings of the PCM. In particular, they explained both the importance and behavior of the scaling parameters, η_i, and the fuzzifier, q. They also discussed how PCM can find c good clusters from a data set that may have more than c clusters. On the other hand, if the data set has less than c clusters, PCM can still potentially find c good clusters, some of which may be identical. However, how does one algorithmically discover the number of clusters in O as well as say that two clusters are equal?

Discovering the number of actual clusters. It is sometimes helpful to categorize clustering into three different tasks. In the previous section, the problem of *assessing cluster tendency* was briefly discussed. The FCM and PCM algorithms are examples of the second class of clustering problems, *actual clustering*. The third class is *cluster validity*. First, we may use a validity index, v(U), e.g. Dunn's index [22] or the Davies-Bouldin's index [23]. One generally varies an algorithm parameter, e.g. the number of clusters (c), the fuzzifier (q), etc., and v(U) is used to identify a trend such as the maximum or minimum or

Algorithm 2: *Simultaneous Discovery of the Number of Actual Clusters and Coincident Clusters Found by the PCM*

0. Overspecify the number of clusters (c) and obtain a terminal partition U from the PCM

1. Generate the similarity matrix S (c × c) from U

$$S_{pq} = s'_{r*}(V_p, V_q) \text{ for } \forall p,q \in \{1,\ldots,c\}$$

$$V_p = \begin{bmatrix} U_{p,1} & \cdots & U_{p,n} \\ \max_{k\neq p}\left(U_{k,1}\right) & \cdots & \max_{k\neq p}\left(U_{k,n}\right) \end{bmatrix} \quad (2\times n)$$

$$V_q = \begin{bmatrix} U_{q,1} & \cdots & U_{q,n} \\ \max_{k\neq q}\left(U_{k,1}\right) & \cdots & \max_{k\neq q}\left(U_{k,n}\right) \end{bmatrix} \quad (2\times n)$$

2. Generate the dissimilarity matrix D from S via 1 - S_{pq}

3. Run VAT on D

Visually identify the *actual* number of clusters

4. Clusters in D are coincident clusters in the PCM algorithm

"the big jump". The second group of methods use comparison indices, s(U,V), that compare pairs of partitions. Examples of this group include the crisp Rand [7] and our generalized Rand index [1-2]. If U and V are both in CP (and hence, both obtained by algorithmic means), s(U,V) is an internal criterion, and otherwise, we call it an external criterion.

Since c is unknown in real clustering situations, it is not generally possible to know that it has been overspecified. However, the problem domain often suggests a maximum plausible value for c, and this knowledge can be used to make a realistic overspecification. For example, if you are segmenting MRI images of the brain with c-means clustering, there will certainly not be more than 8 or 10 meaningful regions, so taking c at, say, 15, is a reasonable guess at overspecification.

However, each approach makes certain assumptions and therefore operates ideally for data sets with particular profiles, e.g. VAT and its relationship to single linkage [24]. Even more critical to PCM, these approaches do not solve the cluster correspondence problem. If one of the above methods is used to discover the number of *actual* clusters, there is no guarantee that PCM will find the c unique clusters (due to coincident clusters).

Since the inception of the PCM algorithm, a few extensions have been presented that attempt to avoid coincident clusters. In [25], Timm et al. add a penalizing term to the PCM objective function in order to help repel cluster prototypes. Additionally, de Caceres et al. present an improved way to estimate the cluster bandwidths, which in return appears to help keep prototypes from converging to similar spots [26].

Cluster correspondence (or registration) problem. A naive approach to cluster correspondence is to *directly* compare clusters, i.e. according to some distance of clustering algorithm parameters (i.e. prototypes, covariance matrices, etc.). It is

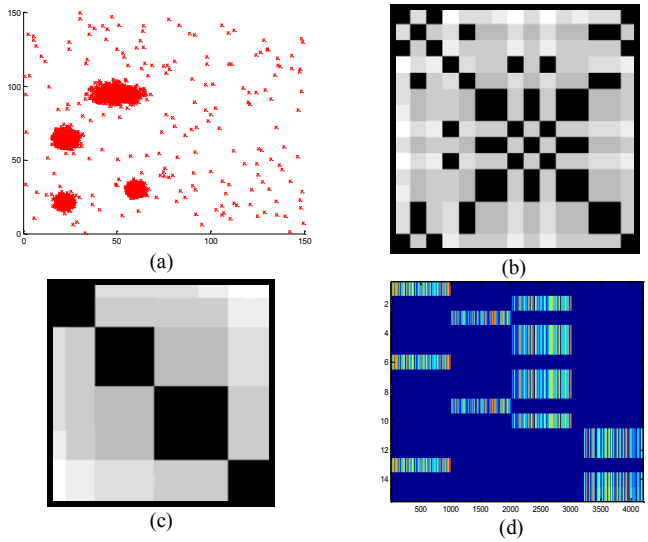

Fig. 3. Data set 3 (D3) and results from algorithm 2. D3 is four Gaussian clouds, each with 1000 samples, means of $[22\ 22]^T$, $[60\ 30]^T$, $[23\ 65]^T$, $[50\ 95]^T$ and standard deviations of 2, 2, 3 and (6,3) respectively. A set of 200 random points are included. (a) is the object data, (b) is the unordered dissimilarity matrix D for c = 15, (c) is the VAT reordering of D showing 4 clusters, and (d) is the possibilistic partition matrix (15 × n) that clearly shows which of the original clusters are coincident. We see that between 3,000 and 3,200 there are 200 objects (noise) that do not belong strongly to any particular cluster.

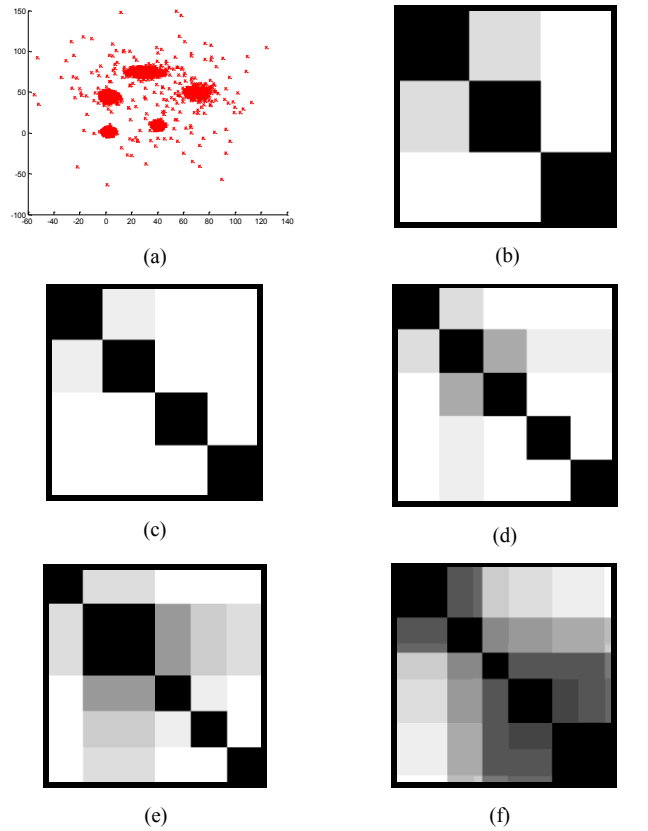

Fig. 4. Data set 4 (D4) and results from algorithm 2. D4 is five Gaussian clouds and noise; ($[2\ 2]^T$, 900, 2), ($[40\ 10]^T$, 500, 2), ($[3\ 45]^T$, 1000, 3), ($[30\ 75]^T$, 1200, (6,3)), and ($[70\ 50]^T$, 250, 6) for (mean, number of samples, standard deviation). There are 200 random noise points. In (b) c = 3, (c) c = 4, (d) c = 5, (e) c = 6, and in (e) c = 25.

possible that this approach might work for a limited number of scenarios. One example from the area of computer vision is the color space CIELAB. This space is designed around approximating human perception. Namely, this space makes it possible to interpret distance to a degree and therefore make reasonable working assumptions regarding merging criteria. An example of this is the mean shift clustering algorithm [27]. In [27], CIELAB space is exploited to *merge* mean shift prototypes for image region segmentation and filtering. However, this overly simplistic approach is not theoretically well founded and should not be relied upon in general.

Simultaneous discovery of the number of actual clusters and coincident clusters found by the PCM. Algorithm 2 begins with the overspecification of c. After PCM has terminated, the measure s'_{r*} is used to compare clusters and VAT is used in order to visually discover the number of *actual* clusters and coincident clusters simultaneously. This algorithm supports the claim [4] that coincident clusters are not a shortcoming of PCM. However, s'_{r*} is defined for partitions not clusters. How is it that cluster p can be compared to cluster q in the same partition?

In algorithm 2, a set of possibilistic partitions, $\{V_1, \ldots, V_c\}$, are built (where c is the number of clusters in U). The idea is to generate a possibilistic partition ($2 \times n$) for each cluster that contains the membership of every data point in cluster p ($1 \times n$) and the maximum membership value of each data point in the remaining set of clusters ($1 \times n$), i.e. for all $q \neq p$. The value S_{pq} is the similarity, [0,1], between clusters p and q based on the possibilistic partitions V_p and V_q. Next, VAT is used on the dissimilarity matrix D, $D_{pq} = 1 - S_{pq}$, to visually discover the *actual* number of clusters in O and subsequently coincident clusters. Figures 3 and 4 demonstrate this approach.

In figure 3(a), O contains four *actual* clusters and random noise. Figure 3(b) is the dissimilarity matrix D for c = 15. Figure 3(c) is the VAT reordering of D, $D_{pq} = 1 - S_{pq}$. Figure 3(c) indicates that there are four *actual* clusters in O and that each *actual* cluster is associated with multiple clusters found by the PCM. Figure 3(d) is the PCM partition matrix. In figure 3(d), rows are clusters and columns are data points (15×4200). The first 1,000 data points belong to clusters {1, 6, 13} and the second 1,000 data points belong to {3, 9}. The next 1,000 data points belong to clusters {2, 4, 5, 7, 8, 10}. The next 200 data points are the random noise and they do not have a strong membership in any cluster. Finally, the last 1,000 data points belong to clusters {11, 12, 14, 15}.

In figure 4, O contains five *actual* clusters. When the number of clusters is underspecified, i.e. c = 3 in figure 4(b) and c = 4 in figure 4(c), PCM finds a subset of the *actual* clusters. However, the VAT image shows that there are three and four clusters respectively and that there are no coincident clusters. The same story is true for figure 4(d), i.e. c = 5 and no coincident clusters. However, when the number of clusters is over specified to PCM (c > 5), e.g. figures 4(e) and 4(f), algorithm 2 identifies the correct answer, five *actual* clusters. We also discover that each *actual* cluster is accounted for by one or more clusters returned by PCM (coincident clusters). Even one step further, we know which clusters from the PCM map to an *actual* cluster in O.

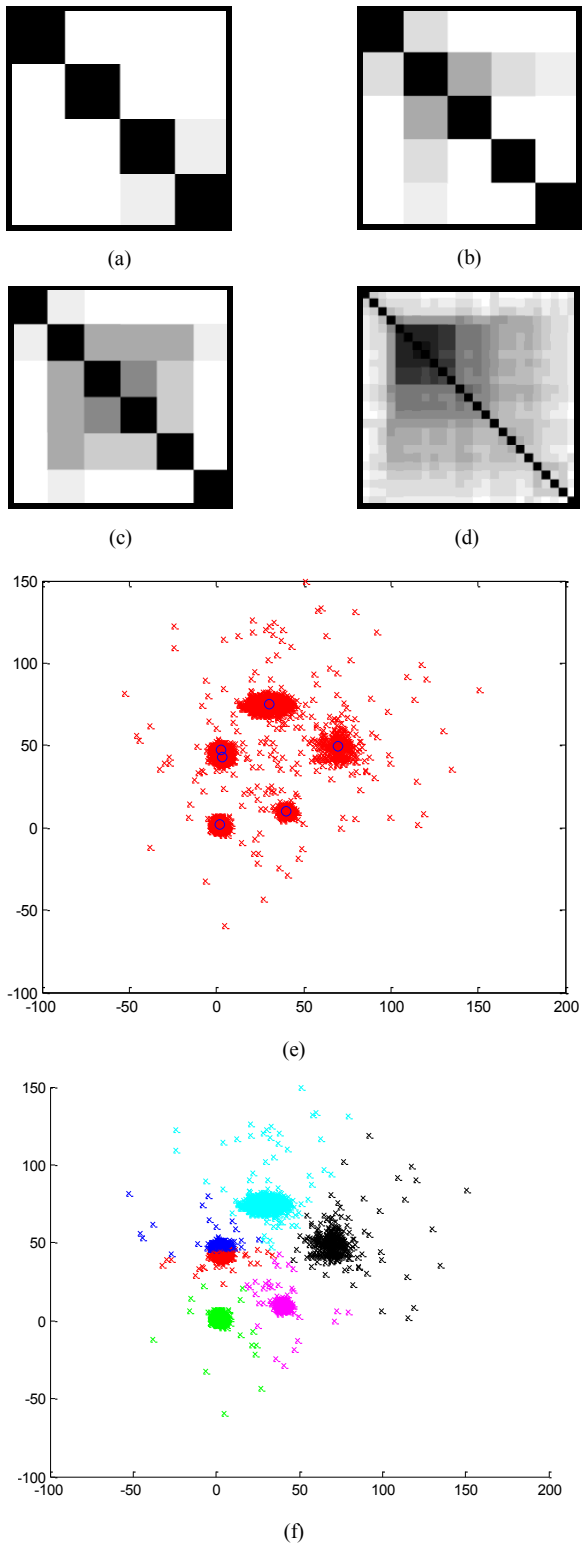

Fig. 5. Data set 5 (D5), which is generated using the same parameters used to generate D4 in figure 4, and the results from algorithm 2. However, in this experiment the FCM algorithm is used in place of the PCM. In (a) c = 4, (b) c = 5, (c) c = 6 and in (d) c = 25. In (e), the locations of the prototypes found in (c) are shown as blue circles. In (f), the FCM (c=6) membership matrix is hardened and each cluster is color coded.

These experiments demonstrate that when the number of clusters is underspecified to the PCM, algorithm 2 does not identify the correct *actual* number of clusters (instead some value smaller than it). The difficulty is that in a true clustering scenario, we do not know the answer. For example, in figure 4(b), c = 3, we would not know if the PCM found the correct number of clusters using algorithm 2. When we attempt c = 4, i.e. figure 4(c), we still are unaware if we have found the correct number of clusters. It is not until the specified c is greater than the *actual* number of clusters that we begin to get an indication of the correct number of *actual* clusters. This is the moment in which coincident clusters becomes an advantage. As c is steadily increased, i.e. algorithm 2 is run for c = 2, c = 3, etc., we eventually notice a *leveling off* in terms of the number of clusters discovered by algorithm 2. Therefore, we recommend testing a range of values for c in algorithm 2 in order to identify the *actual* number of clusters in O. In addition, different initializations can (and often do) lead to different clusterings. Therefore, we recommend running the PCM multiple times, e.g. 10, per c value. For each c, the user should select the largest value for the number of clusters found by algorithm 2.

On a final note, we demonstrate the result of algorithm 2 for FCM instead of PCM (figure 5). We see that when c is less than the number of *actual* clusters, i.e. figures 5(a) and 5(b), the VAT images show that the number of *actual* clusters is c. However, when c is overspecified, i.e. figures 5(c) and 5(d), the VAT image continues to indicate that the number of actual clusters is c. We are therefore unable to identify the *actual* number of clusters and the cluster correspondences via algorithm 2. Figure 5(e) is the scatterplot of D5 along with the locations of the prototypes. What we see is that when c is overspecified, the FCM tends to splits clusters. This is not the same behavior as the PCM, which produces coincident clusters. That is, coincident clusters in the PCM will have very similar rows in the membership matrix.

VI. CONCLUSIONS

In this article, we extended our prior work by exploring the behavior of the soft Rand for comparing non-crisp partitions. We also demonstrated how the possibilistic Rand and visual assessment of (cluster) tendency (VAT) algorithms can be used to simultaneously discover the number of *actual* clusters and coincident clusters found by the PCM. Our approach supports the claim [4] that coincident clusters are not a shortcoming of the PCM.

In future work, we will investigate how to extend the soft Rand to comparing partitions acquired across different data sets, e.g. samples drawn from the same underlying process. At the moment, our generalization of the Rand requires that U and V share the same object data set, O; however they need not possess the same number of clusters, $r \neq c$. We will explore next how to extend our approach to cases such as (1) temporal data sets, (2) clustering in unloadable data sets, and (3) the comparison of clustering discoveries found across potentially disjoint (sample) data sets. Namely, case (3) will investigate the question, "how similar are the clustering discoveries in data set A to data set B using clustering algorithms C and D"?

VII. ACKNOWLEDGEMENT

D. Anderson, J. Keller and M. Popescu would like to acknowledge support from ARO grant 57940-EV and LWI grant LWI-101-022.

REFERENCES

[1] D. T. Anderson, J. C. Bezdek, M. Popescu and J. M. Keller, "Comparing Fuzzy, Probabilistic, and Possibilistic Partitions," in *IEEE Transactions on Fuzzy Systems*, 18 (5), 906-918, 2010.

[2] D. T. Anderson, J. C. Bezdek, J. M. Keller and M. Popescu, "A comparison of five fuzzy Rand indices," *Intl. Conf. on Info. Processing and Management of Uncertainity in Knowledge-Based Systems*, Germany, 446-454, 2010.

[3] R. Krishnapuram and J. M. Keller, "A Possibilistic Approach to Clustering," *IEEE Transactions on Fuzzy Systems*, 1 (2), 98-110, 1993.

[4] R. Krishnapuram and J. M. Keller, "The Possibilistic C-Means Algorithm: Insights and Recommendations," *IEEE Transactions on Fuzzy Systems*, 4 (3), 385-393, 1996.

[5] L. Hubert and P. Arabie, Comparing partitions, *J. Classification*, 2, 193-218, 1985.

[6] P. Sneath and R. Sokal, *Numerical Taxonomy - The Principles and Practice of Numerical Classification*, W. H. Freeman, San Francisco, CA, 1973.

[7] W. Rand, "Objective criteria for the evaluation of clustering methods," *JASA*, 66 (336), 846-850, 1971.

[8] R. Sokal and C. Michener, "A Statistical Method for Evaluating Systematic Relationships," The University of Kansas Scientific Bulletin 38, 1409-1438, 1958.

[9] F. Duan and H. Zhang, "Correcting the loss of cell-cycle synchrony in clustering analysis of microarray data using weights," *Bioinformatic*s, 20 (11), 1766-1771, 2004.

[10] A. Thalamuthu, I. Mukhopadhyay, X. Zheng and G. Tseng, "Evaluation and comparison of gene clustering methods in microarray analysis," *Bioinformatic*s, 22 (19), 2405-2412, 2006.

[11] D. Wong, F. Wong and R. Wood, "A multi-stage approach to clustering and imputation of gene expression profiles," *Bioinformatic*s, 23 (8), 998-1005, 2007.

[12] Z. Yu, H. Wong and H. Wang, "Graph-based consensus clustering for class discovery from gene expression data," *Bioinformatic*s, 23 (21), 2888-2896, 2007.

[13] R. Campello, "A fuzzy extension of the Rand index and other related indexes for clustering and classification assessment," *Patt. Recog. Letters*, 28, 833-841, 2007.

[14] H. Frigui, C. Hwang and F. Rhee, "Clustering and aggregation of relational data with applications to image database categorization, *Pattern Recognition*, 40, 3053 – 3068, 2007.

[15] R. Brower, "Extending the Rand, adjusted Rand, and Jaccard indices to fuzzy partitions," *J. Intell. Inf. Systems*, 32, 213-235, 2009.

[16] E. Hullermeier and M. Rifqi, "A fuzzy variant of the Rand index for comparing clustering structures," *Proc. IFSA*, Portugal, 1-6, 2009.

[17] J. C. Bezdek, Pattern Recognition with Fuzzy Objective Function Algoritms, Plenum Press, New York, 1981.

[18] J. Bezdek and R. Hathaway, "VAT: A Tool for Visual Assessment of (Cluster) Tendency," Proc. of the Intl. Joint Conf. on Neural Networks, 2225-2230, 2002.

[19] T. C. Havens, J. C. Bezdek, J. M. Keller and M. Popescu, "Clustering in ordered dissimilarity data," *Int. J. Intelligent Systems*, 24 (5), 504-528, 2009.

[20] L. Wang, X. Geng, J. C. Bezdek, C. Leckie and R. Kotagiri, "Enhanced visual analysis for cluster tendency assessment and data partitioning," *IEEE TKDE*, 22 (10), 1401-1414, 2010.

[21] M. Barni, V. Cappellini and A. Mecocci, "Comments on 'A Possibilistic Approach to Clustering'," *IEEE Transactions on Fuzzy Systems*, 4 (5), 393-396, 1996.

[22] J. Dunn, “A fuzzy relative of the ISODATA process and its use in detecting compact wellseparated clusters,” *J. Cybern*., 3 (3), 32–57, 1974.

[23] D. Davies and D. Bouldin, “A cluster separation measure,” *IEEE Trans. Pattern Anal. Mach. Intelligence*, 1, 224–227, 1979.

[24] T. Havens, J. C. Bezdek, J.M. Keller, M. Popescu and J.M. Huband, “Is VAT really single linkage in disguise?,” *Ann. Mathematics and Artificial Intelligence*, 55 (3), 237-251, 2009.

[25] H. Timm, C. Borgelt, C. Doring, and R. Kruse, "An extension to possibilistic fuzzy cluster analysis", in *Fuzzy Sets and Systems*, 147, 3-16, 2004.

[26] M. de Caceres, F. Olvia, and X. Font, "On relational possibilistic clustering," in *Pattern Recognition*, 39, 2010-2024, 2006.

[27] D. Comaniciu and P. Meer, "Mean Shift: A Robust Approach Toward Feature Space Analysis," *IEEE Trans. Pattern Anal. Mach. Intelligence*, 24 (5), 603–619, 2002.

2011 IEEE International Conference on Fuzzy Systems
June 27-30, 2011, Taipei, Taiwan

An Adaptive Hybrid Data Fusion Based Identification of Skeletal Muscle Force with ANFIS and Smoothing Spline Curve Fitting

Parmod Kumar, C. H. Chen, Anish Sebastian, Madhavi Anugolu, Chandrasekhar Potluri, Amir Fassih, Yimesker Yihun, Alex Jensen, Yi Tang, Steve Chiu, Ken Bosworth, D. S. Naidu and Marco P. Schoen
Measurement and Control
Engineering Research Center
College of Science and Engineering
Idaho State University
Pocatello, ID 83209, USA
Email: kumaparm@isu.edu, chenchen@isu.edu, sebaanis@isu.edu, anugmadh@isu.edu, potlchan@isu.edu, fassamir@isu.edu, yihuyime@isu.edu, jensalex@isu.edu, mrtang_42@hotmail.com, chiustev@isu.edu, boswkenn@isu.edu, naiduds@isu.edu, schomarc@isu.edu

Jim Creelman and Alex Urfer
Department of Physical and Occupational Therapy
Idaho State University
Pocatello, ID 83209, USA
Email: creejame@isu.edu, urfealex@isu.edu

***Abstract*—Precise and effective prosthetic control is important for its applicability. Two desired objectives of the prosthetic control are finger position and force control. Variation in skeletal muscle force results in corresponding change of surface electromyographic (sEMG) signals. sEMG signals generated by skeletal muscles are temporal and spatially distributed that result in cross talk between adjacent sEMG signal sensors. To address this issue, an array of nine sEMG sensors is used with a force sensing resistor to capture muscle dynamics in terms of sEMG and skeletal muscle force. sEMG and skeletal muscle force are filtered with a nonlinear Teager–Kaiser Energy (TKE) operator based nonlinear spatial filter and Chebyshev type-II filter respectively. Multiple Takagi-Sugeno-Kang Adaptive Neuro Fuzzy Inference Systems (ANFIS) are obtained using sEMG as input and skeletal muscle force as output. Outputs of these ANFIS systems are fitted with smoothing spline curve fitting. To achieve better estimate of the skeletal muscle force, an adaptive probabilistic Kullback Information Criterion (KIC) for model selection based data fusion algorithm is applied to the smoothing spline curve fitting outputs. Final fusion based output of this approach results in improved skeletal muscle force estimates.**

Keywords – sEMG; TKE; ANFIS; KIC

I. INTRODUCTION

In the United States, 1.6 million people lived with amputations during 2005 [1]. This increase reflects on the war effects in Afghanistan and Iraq since 2003 [2]. During the same period of time, the fields of prosthetic design and development research for prosthesis has received increased attention. Precise and timely control of prosthesis is critical for its applicability, which necessitates the replacement of conventional algorithms by intelligent systems and decision methods. Therefore, a natural means of interface between the user and prosthesis is required. sEMG signals from skeletal muscles are a convenient means for users who do not want to deal with additional surgeries and regular hygiene problems. sEMG signals are simply electric voltages ranging between -5 and +5 [mV] which can be recorded on the skin surface of a hand amputee's forearm. Skeletal muscles generate a base sEMG even without a limb movement which changes with different movements and applied forces. This makes sEMG signals useful for position and force control of prosthesis. Presently available prosthetic hands have no tactile or proprioceptive feedback for grasping and only user's direct vision as a sensory feedback is available for its position control. Afore mentioned reasons cause 30–50% of the upper extremity amputees to choose not to use their prosthetic hand on a regular bases [3-4].

Effective grasping of any object requires the knowledge of force and its feedback. Since the hand amputee uses only sEMG signals collected from skeletal muscles, there is no hand force information directly available. sEMG is a measure of the nervous excitation that ultimately is responsible for activating the skeletal muscles, which in turn generate the finger forces with the help of the link kinematics of human hand. Therefore, a model or estimation scheme is needed for the dynamic estimation of skeletal muscle force from sEMG

978-1-4244-7316-8/11/$26.00 ©2011 IEEE

signals. There have been numerous efforts in this direction and some of the recent are evident in the research work of [5-10].

The present work proposes a novel scheme of skeletal muscle force identification using sEMG signals. An array of nine sEMG sensors is used to record sEMG signals and skeletal muscle force signals recorded with a force sensing resistor from the arm of a healthy subject, which respectively is explained in detail in Section II and III. Eight Takagi-Sugeno-Kang ANFIS with different membership functions each with a rule base of ten are designed. The training of each ANFIS is done using a hybrid optimization method with zero error tolerance and 40 epochs. Each of the force signals simulated using these ANFIS and measured force signals are applied to a smoothing spline curve fitting method. Figure 1 shows the flow chart of the proposed approach. Final estimated force signal shows good match with the measured signal. This approach is tested on two different data sets of 45 and 60 seconds duration and the results seem promising. The paper is organized in eight sections. Present section follows the experimental set-up and then signal processing, ANFIS modeling, smoothing spline curve fitting, data fusion, results and discussion and conclusion and future work is presented respectively.

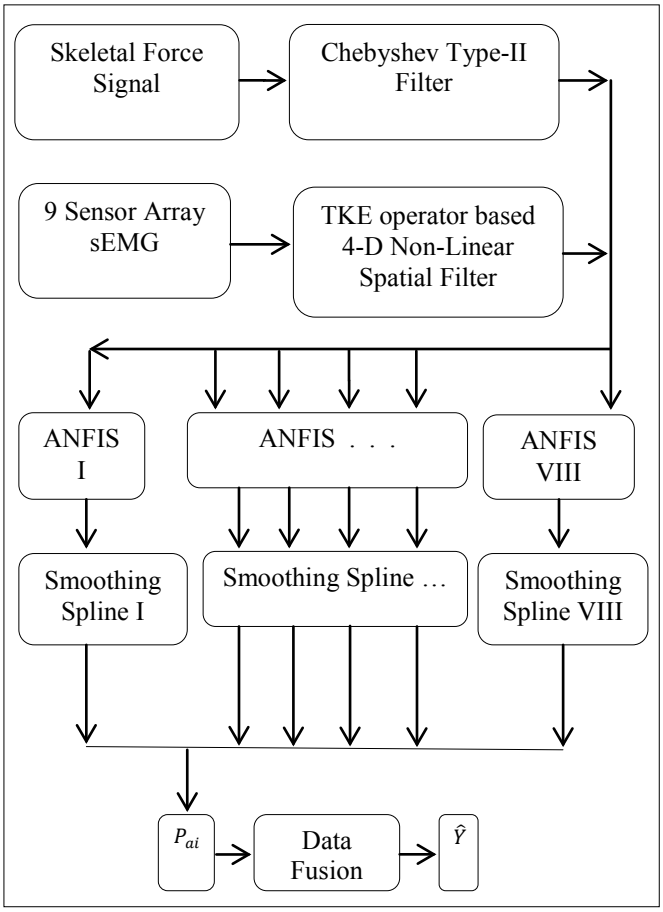

Figure 1. Flow chart of the approach used in this research work.

II. EXPERIMENTAL SET-UP

Based on the set-up of a sEMG sensor array in [11], an experiment set-up was developed using DELSYS® Bagnoli-16 EMG system with nine DE-3.1 sEMG sensors to capture sEMG signals from skeletal muscles. Here, the array involves nine sensors covering four directional spatial distributions of the sEMG signal. The middle three sEMG sensors were attached directly on the skin surface above the motor point of the flexor digitorum superficialis muscle (FDS) which controls the flexion of the ring finger. Appropriate sEMG electrode attachment point for the flexion of the ring finger was identified using a wet probe muscle stimulator at the FDS (RICH-MAR, HV 1000).

Prior to placing the sEMG sensors, the skin surface of the subject was prepared according to International Society of Electrophysiology and Kinesiology (ISEK) protocols. The thumb movement was restricted in this experiment using a thumb splint. However, the corresponding force data was captured using NI ELVIS™ with Interlink™ Electronics FSR 0.5" circular force sensor. Experimental set-up is shown in Figure 2, where 9 sensors are shown on a healthy subject forearm, holding a stress ball for force measurements. The sEMG and finger force data was collected at a sampling rate of 2000 Hz using LabVIEW™ in conjunction with DELSYS® Bagnoli-16 EMG and NI ELVIS™. With this experimental set-up we conducted several experiments of 30 seconds, 45 seconds and 60 seconds durations.

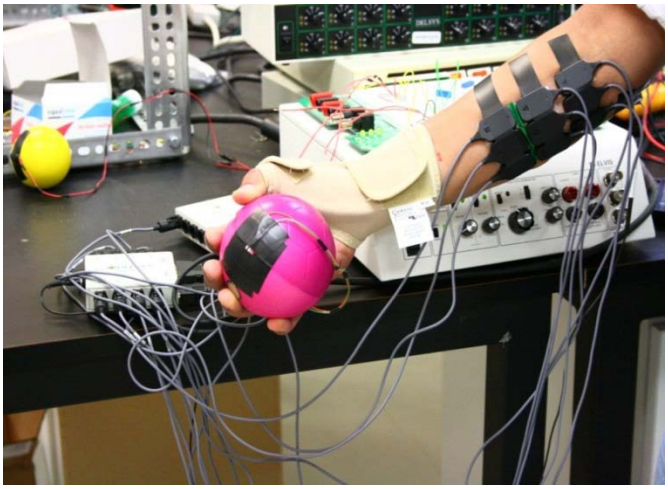

Figure 2. Experiment set-up.

III. SIGNAL PROCESSING

The recorded sEMG signal is filtered using nonlinear spatial filtering for multichannel surface EMG. As given in [12], this nonlinear spatial filter is derived from "Nonlinear Teager-Kaiser Energy (TKE) Operator." As given in [11], the

TKE operator in the time domain on sEMG signal is defined by Equation (1).

$$\Psi[x(n)] = x^2(n) - x(n+1) * x(n-1). \quad (1)$$

Here, Ψ is the TKE operator and $x(n)$ is the time domain sEMG signal. Based on the TKE operator, the four-dimensional nonlinear spatial filter is given by Equation (2).

$$\Psi_{d,4}[x(m,n)] = 4 * x^2(m,n) - x(m-1,n) * x(m+1,n) - x(m,n-1) * x(m,n+1) - x(m-1,n+1) * x(m+1,n-1) - x(m-1,n-1) * x(m+1,n+1). \quad (2)$$

Figure 3 shows a comparison between the measured and nonlinear spatial filtered sEMG signals.

A Chebyshev type II infinite impulse response (IIR) low pass filter with a 550 Hz pass band frequency is used to filter the skeletal muscle force signal. Figure 4 shows the comparison between the measured and Chebyshev type II filtered skeletal muscle force signal.

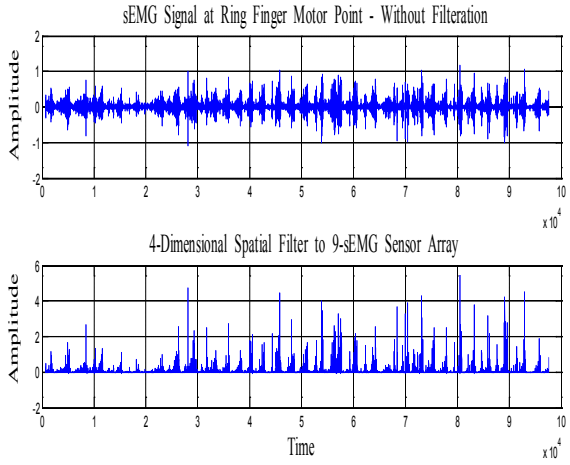

Figure 3. sEMG signal from ring finger.

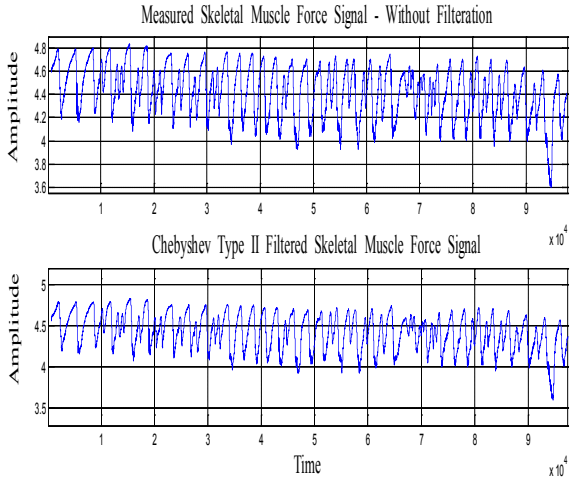

Figure 4. Skeletal muscle force signal from ring finger.

IV. ANFIS MODELING

In 1965 professor Lofti A. Zadeh introduced the concept of "*Fuzzy Sets*", which are sets with imprecise amplitudes [12]. Dr. Zadeh stated that the "*membership*" in a fuzzy set is a matter of degree and not a matter of affirmation or denial. For last four decades, this proposal has gained recognition as an important point in the evolution of modern concept of imprecision and uncertainty [12]. This innovation represents a paradigm shift from the classical sets or the crisp sets to "*Fuzzy Sets*" [12].

Fuzzy set and fuzzy logic theory can be used to capture the natural phenomenon of the imprecision and uncertainty [12]. The membership function is the characteristic of fuzzy set, which is a function whose range is an ordered membership set within the closed unit interval [12].

A crisp set which is a collection of distinct objects is defined in a way to partition objects in a given domain of discourse into two groups: members and non-members [12]. On the other hand, a fuzzy set can be formed by assigning a membership value (which represents the degree to which an object belongs to a fuzzy set) to each object in the interval of 0 to 1 [12]. Fuzzy membership functions can be of different forms such as triangular, trapezoidal, pi, bell and Gaussian form.

Fuzzy Inferance System (FIS) in fuzzy logic can be used to model a system which is an inference system based on empirical knowledge based linguistic rules [13]. The fuzzy inference system is composed of five steps: fuzzification of the input variables, application of the fuzzy operator (AND or OR) in the precedent, implication from the precedent to the subsequent, aggregation of the subsequents across the rules, and defuzzification. In the fuzzification process, the membership values coming from quantitative measurements are converted to linguistic values based on the membership functions [13].

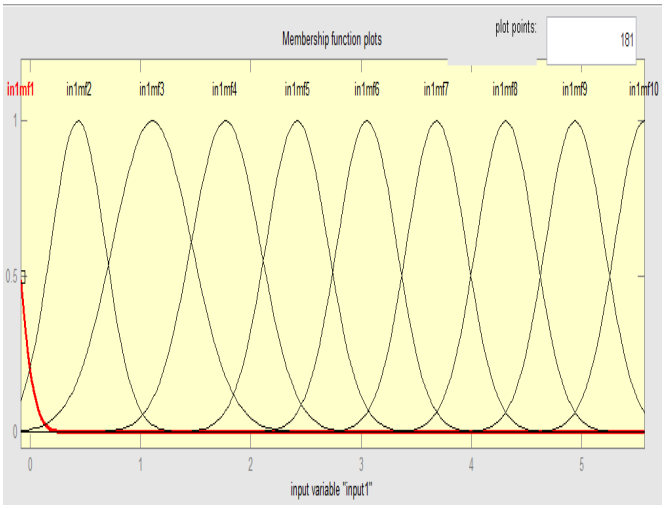

Figure 5. Gaussian membership functions for sEMG.

Figure 5 shows the plot of Gaussian membership functions for fuzzification of sEMG. The process of fuzzification followed by IF .. AND.. THEN ..OR ELSE type control or relation/estimation rules [13]. The output of the rules is computed as a max-min composition [13]. In the defuzzification process, the output of the rules has to be converted to a crisp value [13].

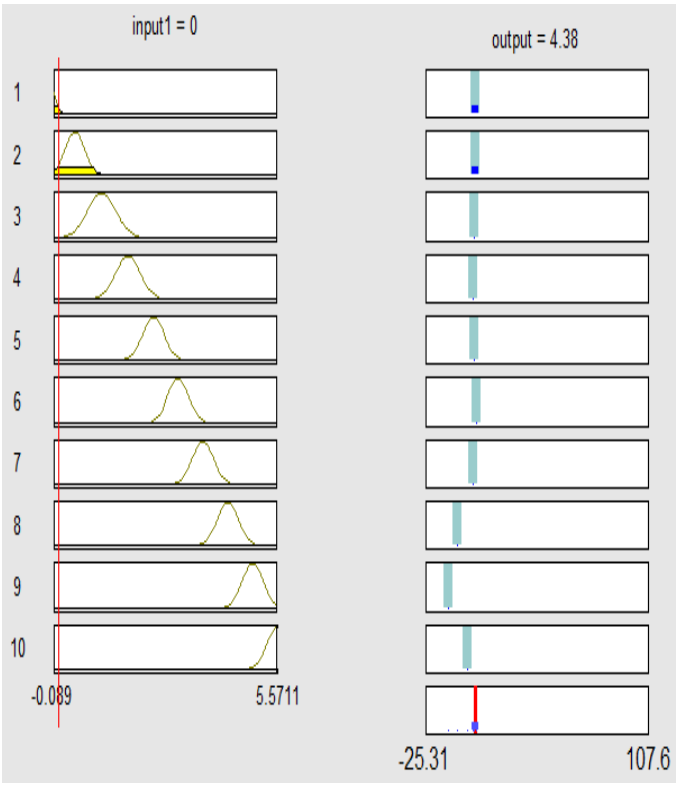

Figure 6. Illustration of ANFIS inference mechanism.

TABLE I. MEMBERSHIP FUNCTIONS

S. No.	Membership Function
1.	Gaussian (GAUSSMF)
2.	Gaussian combination (GAUSS2MF)
3.	Difference between two sigmoidal membership functions (DSIMF)
4.	Generalized bell-shaped (GBELLMF)
5.	Π-shaped (PIMF)
6.	Product of two sigmoidally shaped membership functions (PSIMF)
7.	Trapezoidal-shaped (TRAPMF)
8.	Triangular-shaped (TRIMF)

Using eight different membership functions types we designed eight single-output Sugeno-type adaptive neuro-fuzzy inference systems (ANFIS) using a grid partition on the data. The output membership function in each of these is linear. Each ANFIS has ten rules and connection type is 'And' with a weight of 1. For the 'And' method 'product' and for 'Or' method 'probabilistic' types are used for each ANFIS. Deffuzification is achieved using weighted average (wtaver) from each rule. Figure 6 shows the rules for ANFIS with Gaussian membership functions and illustrate the ANFIS inference mechanism. The membership functions used are tabulated in Table 1.

A Gaussian function is given by $f(x;\sigma,c) = e^{\frac{-(x-c)^2}{2\sigma^2}}$ for some real constants c and $\sigma > 0$, and $e = 2.718$. Gaussian combination membership function (GAUSS2MF) depends on the c and σ parameters [14]. The sigmoidal membership function is given as $f(x;a,c) = \frac{1}{1+e^{-a(x-c)}}$ and depends on the two parameters a and c. The difference between two sigmoidal membership function (DSIMF) which is the difference between two sigmoidal functions depends on the four parameters a_1, c_1, a_2, and c_2 [14]. Generalized bell-shaped membership function (GBELLMF) is given as $f(x;a,b,c) = \frac{1}{1+\left|\frac{x-c}{a}\right|^{2b}}$ and depends on three parameters a, b, and c where parameter a and b decide the width of the curve and parameter c locates the center, usually $b > 0$ [14]. Pi-shaped membership function (PIMF) is given by

$$f(x;a,b,c,d) = \begin{pmatrix} 0, & x \le a \\ 2\left(\frac{x-a}{b-a}\right)^2, & a \le x \le \frac{a+b}{2} \\ 1-2\left(\frac{x-b}{b-a}\right)^2, & \frac{a+b}{2} \le x \le b \\ 1, & b \le x \le c \\ 1-2\left(\frac{x-c}{d-c}\right)^2, & c \le x \le \frac{c+d}{2} \\ 2\left(\frac{x-d}{d-c}\right)^2, & \frac{c+d}{2} \le x \le d \\ 0, & x \ge d \end{pmatrix}, \quad \text{and}$$

evaluated at the points given by vector x. The "feet" of the curve is determined by parameters a and d whereas parameters b and c decides its "shoulders" [14]. The Product of two sigmoidally shaped membership functions (PSIMF) is simply the products of two sigmoidal functions as given before. The trapezoidal shaped membership function (TRAPMF) is given by

$$f(x;a,b,c,d) = \begin{pmatrix} 0, & x \le a \\ \frac{x-a}{b-a}, & a \le x \le b \\ 1, & b \le x \le c \\ \frac{d-x}{d-c}, & c \le x \le d \\ 0, & d \le x \end{pmatrix}$$ which depends on

four scalar parameters a, b, c, and d. The triangular shaped membership function (TRIMF) is given by

$$f(x;a,b,c) = \begin{pmatrix} 0, & x \le a \\ \frac{x-a}{b-a}, & a \le x \le b \\ \frac{c-x}{c-b}, & b \le x \le c \\ 0, & c \le x \end{pmatrix}$$ which depends on the scalar parameters a, b and c [14].

V. Smoothing Spline Curve Fitting

MATLAB® Curve Fitting Toolbox™ is a useful tool for fitting curves and surfaces to acquired data [15]. It can be used to do exploratory data analysis, preprocessing and post-processing of the data, comparing candidate models, and for removing outliers [15]. Weights for each smoothing spline curve fit are calculated by subtracting the ANFIS output from the measured skeletal muscle force output. A graphical user interface is used to fit the smoothing spline curve to each output from eight ANFIS with respective weights. Smoothing spline which is a piecewise polynomial computed from a smoothing parameter (p) of 0.92 is fitted to each of eight outputs of ANFIS. Smoothing parameter (p) is a number between 0 and 1. Change in the value of p from 0 to 1 results in the change in smoothing spline. For $p = 0$ the smoothing spline is a least-square straight-line approximation to the data whereas for $p = 1$ it gives the "natural" cubic spline interpolant to the data [15].

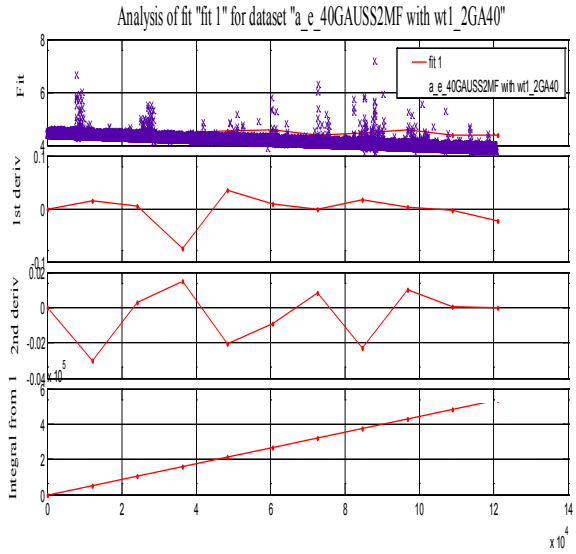

Figure 7. Analysis results for smoothing spline curve fitting to the output of ANFIS with Gaussian membership function.

For the specified weight (w_i) and smoothing parameter (p) a smoothing spline s is formed which minimizes the parameter J given by Equation (3).

$$J = p\sum_i w_i(y_i - s(x_i))^2 + (1-p)\int(\frac{d^2s}{dx^2})^2 dx, \qquad (3)$$

where x_i and y_i are predictor and response data respectively. The smoothing parameter p should be chosen to make the error $E(s) = \sum_i w_i(y_i - s(x_i))^2$ and roughness $\int(\frac{d^2s}{dx^2})^2 dx$ small. In this work the smoothing parameter p is chosen as 0.92 [15]. Figure 7 shows the analysis results for smoothing spline curve fitting to the output of ANFIS with Gaussian membership function.

VI. Data Fusion

Data fusion of multiple outputs of smoothing spline curve fittings is done by assigning a particular probability to each individual output [16]. This method gives good estimation of the skeletal muscle force. The goodness of the fit of each smoothing spline output can be measured using System Identification (SI) model fit value which is given by Equation (4).

$$FIT = [1 - |Y - \hat{Y}|/|Y - \bar{Y}|] * 100 \qquad (4)$$

In Equation (4) Y is measured, $\hat{Y}$ is estimated and $\bar{Y}$ is mean output signal. The model selection criterion used in this paper is Kullback Information Criterion (KIC) which has shown to perform well for sEMG sensor data fusion [7-10]. The sum of two directed divergences, which is the measure of the models dissimilarity, is known as Kullback's symmetric or J-divergence [17], as given by Equation (5).

$$KIC(p_i) = \frac{n}{2}logR_i + \frac{(p_i+1)n}{n-p_i-2} - n\psi\frac{(n-p_i)}{2}) + g(n), \qquad (5)$$

where $g(n) = n * log(n/2)$.

The fusion algorithm as given by [16] is applied for data fusion of the outputs of eight smoothing spline curve fit outputs which are obtained from eight different ANFIS models:

(I) Find smoothing spline curve fit outputs $M_1, M_2, \ldots, M_k$ for k number of outputs.

(II) Compute the residual square norm

$R_i = \|Y - \Phi_i\,\hat{\Theta}_i\|^2 = \|Y - \hat{Y}\|^2$,
where $\hat{\Theta}_i = \{\Phi_i{}^T\Phi_i\}^{-1}\Phi_i{}^T Y$, and

$$\Phi = \begin{bmatrix} Y_p^T & u_p^T & Y_{p-1}^T & \ldots & u_1^T \\ Y_{p+1}^T & u_{p+1}^T & Y_p^T & \ldots & u_2^T \\ \vdots & \vdots & \vdots & \ddots & \vdots \\ Y_{n-1}^T & u_{n-1}^T & Y_{n-2}^T & \ldots & u_{n-p}^T \end{bmatrix}.$$

(III) Calculate the model criteria coefficient using Equation (5).

(IV) Compute the model probability $p(M_i|Z) = \frac{e^{-l_i}}{\sum_{j=1}^{k1} e^{-l_j}}$, where l is model selection criterion, i.e. $KIC(p_i)$.

(V) Compute the fused model output $\hat{Y}_f = \sum_{i=1}^{k1} p(M_i|Z)\hat{Y}_i$.

(VI) Compute the overall model from $\hat{Y}_f$ and skeletal muscle force data.

Here all the computation from step (II) to (VI) is adaptive i.e. the residual square norm, $KIC(p_i)$, model probability

$p(M_i|Z)$, and fused model output $\hat{Y}_f$ are being updated with time or for each data point. Figure 8 shows the flow chart for fusion of outputs and adaptive probability of KIC.

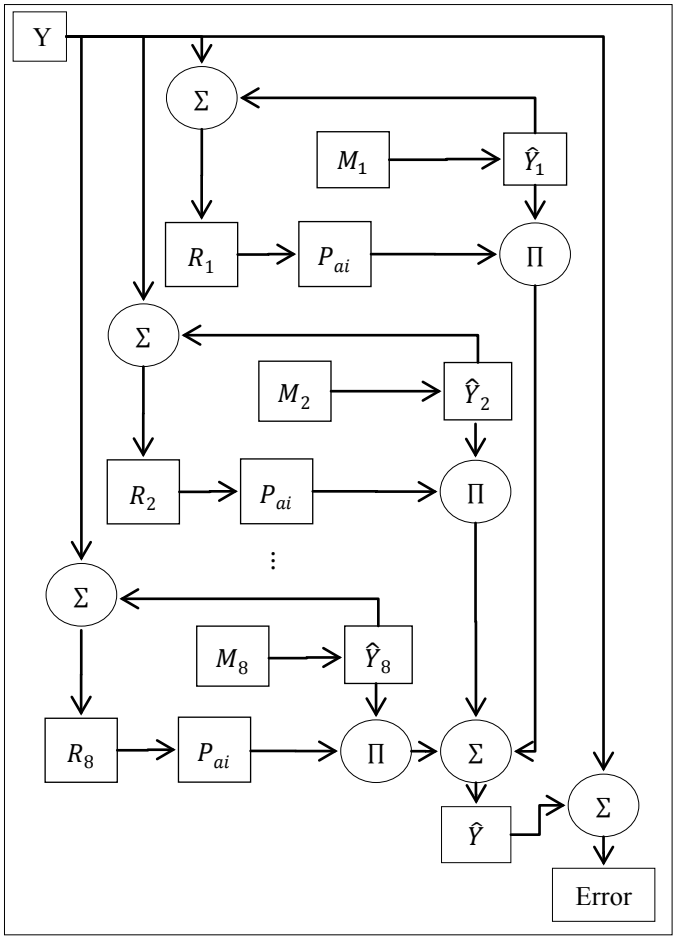

Figure 8. Flow chart for fusion of outputs and adaptive probability.

VII. Results and Discussion

The proposed method gives good estimation of the skeletal muscle force. A data set of 45 seconds is used to estimate the output. Figure 9 shows the measured and estimated skeletal muscle force using this method.

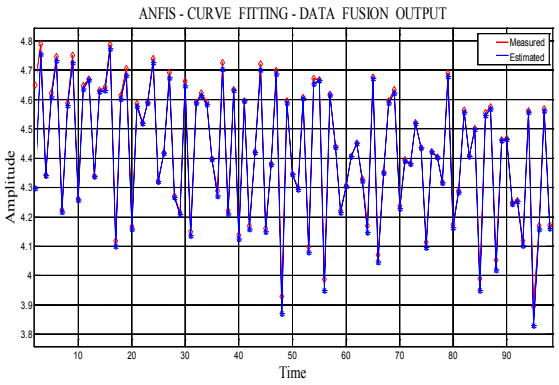

Figure 9. Plot of measured and proposed method estimated skeletal muscle force.

Figures 10 and 11 are the validation plots for 45 seconds and 60 seconds of data sets respectively. All of these three plots show a very close follow up of the measured signal by the estimated signal using this approach. Figure 12 shows the percentage error between the measured force signal and estimated finger force signal for 45 seconds of data set. The percentage error reduced to the lower values and the maximum percentage error value is 1.7 percent. The mean fit value between the measured and estimated output is 91.3 percent.

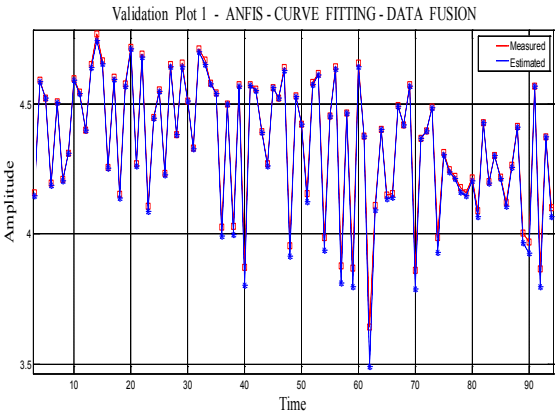

Figure 10. Validation plot 1 using different data set.

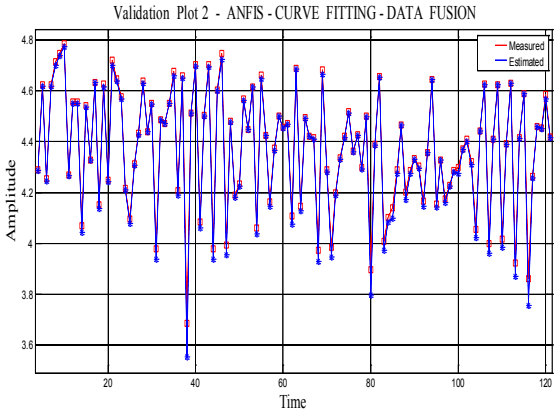

Figure 11. Validation plot 2 using different data set.

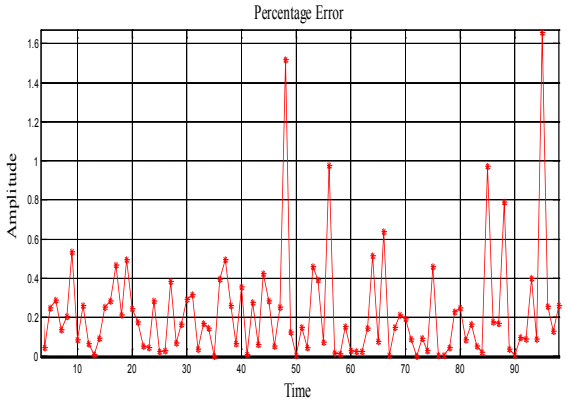

Figure 12. Percentage error plot.

Figure 13 shows the percentage error plot for different data set of 60 seconds duration. Percentage error reduced to lower values and the maximum percentage error value is 3.7 percent. The mean fit value between the measured and estimated output is 40 percent. The mean fit value for another 45 seconds of data set is 73 percent.

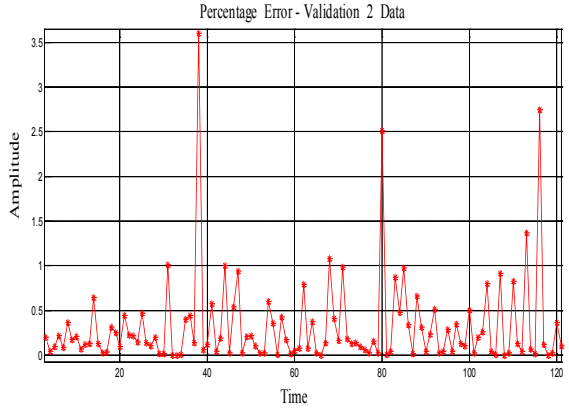

Figure 13. Percentage error plot for 60 seconds data set.

VIII. Conclusion and Future Work

Using sEMG and skeletal muscle force as input and output data, eight ANFIS were designed and tested. Output of these ANFIS were fitted with smoothing spline curve fit and resultant outputs were fused using a KIC based data fusion algorithm. This approach has been validated using two separate data sets. Results are promising and show good estimation of skeletal muscle force which can be applied to design, application and improvement of prosthetic hands for amputees.

Future work will address the improvement of data collection techniques, sEMG sensor design, use of this approach for finger angles and stiffness estimation from sEMG signals. Different modeling techniques with this approach and combined probability of different model selection criteria such as Akaike Information Criterion (AIC), Kullback Information Criterion (KIC) and the Bayesian Information Criterion (BIC) together will give improved results.

Acknowledgment

This research was sponsored by the US Department of the Army, under the award number W81XWH-10-1-0128 awarded and administered by the U.S. Army Medical Research Acquisition Activity, 820 Chandler Street, Fort Detrick MD 21702-5014. The information does not necessarily reflect the position or the policy of the Government, and no official endorsement should be inferred. For purposes of this article, information includes news releases, articles, manuscripts, brochures, advertisements, still and motion pictures, speeches, trade association proceedings, etc.

References

[1] K. Ziegler-Graham, E. J. MacKenzie, P. L. Ephraim, T. G. Travison, and R. Brookmeyer, "Estimating the Prevalence of Limb Loss in the United States - 2005 to 2050," Archives of Physical Medicine and Rehabilitation, vol. 89, pp. 422-429, March 2008.

[2] P. O'Connor. (2009, February 15). Iraq war vet decides to have second leg amputated [Online]. Available: http://www.columbiamissourian.com/stories/2009/02/15/soldier-who-lost-leg-iraq-may-lose-other/

[3] D. J. Atkins, D. C. Y. Heard, and W. H. Donovan, "Epidemiologic overview of individuals with upper-limb loss and their reported research priorities," Journal of Prosthetics and Orthotics, vol. 8, No. 1, pp. 2-11, 1996.

[4] D. H. Silcox, M. D. Rooks, R. R. Vogel, and L. L. Fleming, "Myoelectric prostheses. A long-term follow-up and a study of the use of alternate prostheses," The Journal of Bone and Joint Surgery, vol. 75-A, No. 12, pp. 1781–1789, December 1993.

[5] P. K. Artemiadis and K. J. Kyriakopoulos, "EMG-based position and force control of a robot arm: Application to teleoperation and orthosis," *in Conf. Rec. 2007 IEEE/ASME Int. Conf. on Advanced Intelligent Mechatronics,* Zurich, pp. 1-6, September 2007.

[6] P. K. Artemiadis and K. J. Kyriakopoulos, "EMG-Based Position and Force Estimates in Coupled Human-Robot Systems: Towards EMG-Controlled Exoskeletons," in *Experimental Robotics*, *Springer Tracts in Advanced Robotics*, vol. 54, Berlin Heidelberg: Springer-Verlag, 2009, pp. 241-250.

[7] P. Kumar, C. Potluri, A. Sebastian, S. Chiu, A. Urfer, D. S. Naidu, and M. P. Schoen, "A Adaptive Multi Sensor Data Fusion with Hybrid Nonlinear ARX and Wiener-Hammerstein Models for Skeletal Muscle Force Estimation," in *Proc. The 14th World Scientific and Engineering Academy and Society (WSEAS) International Conference on Systems*, Corfu Island, Greece, 2010, July 22-24.

[8] P. Kumar, A. Sebastian, C. Potluri, A. Urfer, D. S. Naidu, and M. P. Schoen, "Towards Smart Prosthetic Hand: Adaptive Probability Based Skeletal Muscle Fatigue Model," in *Conf. Rec. 32nd Annual International Conference of the IEEE Engineering in Medicine and Biology Society*, Buenos Aires, Argentina, Aug. 31 – Sept. 4, 2010.

[9] P. Kumar, C. Potluri, A. Sebastian, S. Chiu, A. Urfer, D. S. Naidu, and Marco P. Schoen, "Adaptive Multi Sensor Based Nonlinear Identification of Skeletal Muscle Force," *WSEAS Transactions on Systems*, vol. 9, Issue 10, pp. 1051-1062, October 2010.

[10] P. Kumar, C. Potluri, M. Anugolu, A. Sebastian, J. Creelman, A. Urfer, S. Chiu, D. S. Naidu, and M. P. Schoen, "A Hybrid Adaptive Data Fusion with Linear and Nonlinear Models for Skeletal Muscle Force Estimation," in *Proc. 5th Cairo International Conference on Biomedical Engineering*, Cairo, Egypt, Dec. 16-18, 2010.

[11] P. Zhou, N. L. Suresh, M. M. Lowery, and W. Z. Rymer, "Nonlinear Spatial Filtering of Multichannel Surface Electromyogram Signals During Low Force Contractions," *IEEE Transactions on Biomedical Engineering*, vol. 56, No. 7, pp. 1871-1879, July 2009.

[12] A. Celikyilmaz, and I. B. Turksen, *Modeling Uncertainty with Fuzzy Logic: With Recent Theory and Applications*. Berlin Heidelberg: Springer-Verlag, 2009, pp. 11-50.

[13] J. Espinosa, J. Vandewalle, and V. Wertz, *Fuzzy Logic, Identification and Predictive Control*. Springer-Verlag London Limited, 2005.

[14] *MATLAB® Fuzzy Logic Toolbox™ User's Guide*. The MathWorks, Inc. 2010.

[15] *MATLAB® Curve Fitting Toolbox™ User's Guide*. The MathWorks, Inc. 2010.

[16] H. Chen and S. Huang, "A Comparative study on Model Selection and Multiple Model Fusion," in *Proc. 7th International Conference on Information Fusion*, New Orlean, USA, July 25-28, 2005, pp. 820-826.

[17] A. K. Seghouane, and M. Bekara, "A Small Sample Model Selection Criterion Based on Kullback's symmetric Divergence," *IEEE Transactions on Signal Processing*, vol. 52, No. 12, pp. 3314-3323, 2004.

2011 IEEE International Conference on Fuzzy Systems
June 27-30, 2011, Taipei, Taiwan

A Functional-Link based Interval Type-2 Compensatory Fuzzy Neural Network for Nonlinear System modeling

Jyh-Yeong Chang
Department of Electrical and Control Engineering, National Chiao-Tung University
Hsin-Chu, Taiwan, R.O.C.
jychang@mail.nctu.edu.tw

Yang-Yin Lin
Department of Electrical and Control Engineering, National Chiao-Tung University
Hsin-Chu, Taiwan, R.O.C.
oliver.yylin@gmail.com

Ming-Feng Han
Department of Electrical and Control Engineering, National Chiao-Tung University
Hsin-Chu, Taiwan, R.O.C.
ming0901@gmail.com

Chin-Teng Lin
Department of Electrical and Control Engineering, National Chiao-Tung University
Hsin-Chu, Taiwan, R.O.C.
ctlin@mail.nctu.edu.tw

***Abstract*—In this paper, the Functional-Link based Interval Type-2 Compensatory Fuzzy Neural Network (FLIT2CFNN) is a six –layer structure, which combines compensatory fuzzy reasoning method, and the consequent part is combined the proposed functional-link neural network with interval weights. The compensatory fuzzy reasoning method uses adaptive fuzzy operations of neuro-fuzzy systems that can make the fuzzy logic system more adaptive and effective. Initially, there is no rule in the FLIT2CFNN. A FLIT2CFNN is constructed using concurrent structure and parameter learning. The advantages of this learning algorithm are that it converges quickly and the obtained fuzzy rules are more precise. All of the antecedent part parameters and compensatory degree values are learned by gradient descent algorithm. Several simulation results show that the FLIT2CFNN achieves better performance than other feedforword type-1 and type-2 FNNs.**

Keywords- type-2 fuzzy systems, Compensatory, structure learning, on-line fuzzy clustering.

I. INTRODUCTION

Fuzzy neural networks have been successful in a variety of area. However, most of fuzzy neural networks handle nonlinear system or time-varying modeling that its popular issue of research. In recent years, studies on dealing with optimize fuzzy membership function and defuzzification scheme have drawn attention [1-3], and adjust the parameter of fuzzy membership functions and defuzzification functions to adaptive network. Unfortunately, for optimize fuzzy logic reasoning and select optimal fuzzy operators, only static fuzzy operators are often used to make fuzzy reasoning. Such that the conventional neural fuzzy system can only adjust fuzzy membership functions by using fixed fuzzy operations such as Min and Max, the compensatory neural fuzzy system [4] with adaptive fuzzy reasoning is more effective and adaptive than the conventional neural fuzzy system with non-adaptive fuzzy reasoning.

In the typical TSK-type neural fuzzy network (TSK-type NFN), which is a linear polynomial of input variables. Nevertheless, the traditional TSK-type neural fuzzy network does not take full advantage of the mapping capabilities that may be offered by the consequent part. However, the multilayer neural network has such disadvantages as slower convergence and greater computational complexity. Therefore, this studied uses the functional link neural network (FLNN) [5-6] to the consequent part of the fuzzy rules. The consequent part of the proposed FLNN model is a nonlinear combination of input variables, which differs from the other existing models [1-3,7]. Moreover, using the functional expansion can effectively increase the dimensionality of the input vector, so the hyper-planes generated by the FLNN will provide a good discrimination capability in input data space.

All of the aforementioned FNNs only use type-1 fuzzy sets. Recently, studies on type-2 FLSs have paid close attention [8,9] and a complete theory of type-2 have been developed in [10]. Type-2 FLS are extensions of type-1 FLS, where the membership value of a type-2 fuzzy set is a type-1 fuzzy number. The type-1 fuzzy set cannot directly deal with these uncertainties. Because the membership functions of type-2 fuzzy systems are themselves fuzzy, they supply a powerful framework to represent and handle such types of uncertainties. Successful applications of type-2 FLS include area of signal processes [11] and control [12]. Therefore, the purpose of this paper is to develop a self –evolving type-2 FNN with compensatory-based fuzzy logic reasoning and functional-link-based in the consequent part. The network is called a Functional-Link based Interval Type-2 Compensatory Fuzzy Neural Network (FLIT2CFNN).

The rest of this paper is organized as follows. Section II describes the FLIT2CFNN structure. Section III introduces structure and parameter learning in a FLIT2CFNN. Section IV simulates nonlinear system identification problems. Finally, Section V draws conclusions.

978-1-4244-7316-8/11/$26.00 ©2011 IEEE

II. FLIT2CFNN STRUCTURE

In this section, the structure of Functional-Link based Interval Type-2 Compensatory Fuzzy Neural Network (FLIT2CFNN) is introduced. Figure 1 shows the structure of FLT2CFNN, which has a six-layer. This six-layer network realizes an interval type-2 fuzzy system whose consequent part is a nonlinear combination of functional expansion of input variables, i.e., functional-link based. The detailed mathematical functions of FLT2CFNN are introduced as following below.

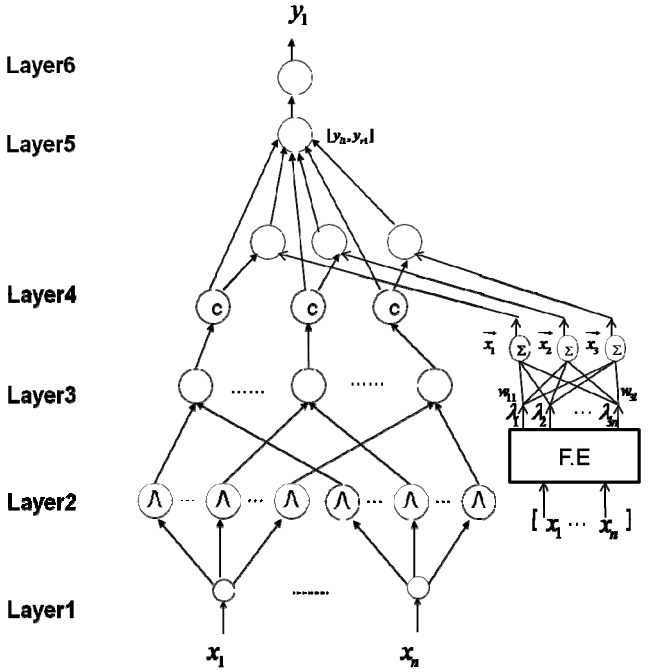

Fig.1. Structure of the FLIT2CFNN

Layer 1 (input layer): The inputs are crisp values. Only the current states $x(t)$ are fed as inputs to this layer. Note that there is no weights to be adjusted in this layer.

Layer 2 (MF Layer): Each node in this layer defines an interval type-2 membership function (MF). We use a Gaussian primary MF having a fixed standard deviation (STD) and an uncertain mean that takes on values in $[m_1, m_2]$ (Fig. 2), i.e., That is, the output $\tilde{A}_j^i$ of each node can be represented as an interval $[\overline{\mu}_j^i, \underline{\mu}_j^i]$.

$$\mu_{\tilde{A}_j^i} = \exp\{-\frac{1}{2}(\frac{x_j - m_j^i}{\sigma_j^i})^2\} \equiv N(m_j^i, \sigma_j^i; x_j),\ m_j^i \in [m_{j1}^i,\ m_{j2}^i] \quad (1)$$

The footprint of uncertainty (FOU) of this MF can be represented as a bounded interval in terms of upper MF, $\overline{\mu}_{\tilde{A}_j^i}$, and lower MF, $\underline{\mu}_{\tilde{A}_j^i}$,

where

$$\overline{\mu}_{\tilde{A}_j^i}(x_j) = \begin{cases} N(m_{j1}^i, \sigma_j^i; x_j), & x_j < m_{j1}^i \\ 1, & m_{j1}^i \le x_j \le m_{j2}^i \\ N(m_{j2}^i, \sigma_j^i; x_j), & x_j > m_{j2}^i \end{cases} \quad (2)$$

and

$$\underline{\mu}_{\tilde{A}_j^i}(x_j) = \begin{cases} N(m_{j2}^i, \sigma_j^i; x_j), & x_j \le \dfrac{m_{j1}^i + m_{j2}^i}{2} \\ N(m_{j1}^i, \sigma_j^i; x_j), & x_j > \dfrac{m_{j1}^i + m_{j2}^i}{2} \end{cases} \quad (3)$$

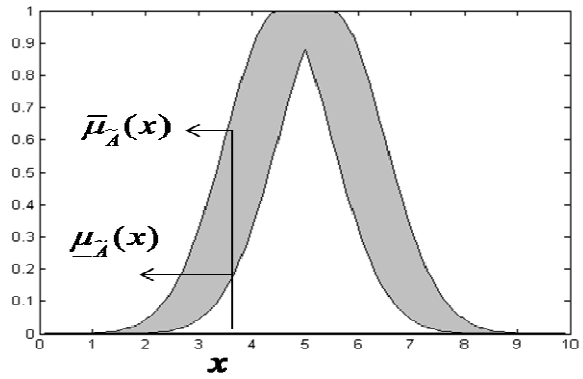

Fig.2. An interval type-2 fuzzy set with an uncertain mean.

Layer 3 (Spatial Firing layer): Each node performs a fuzzy meet operation on inputs from layer 2 using an algebraic product operation to obtain the spatial firing strength. The output of a rule node is a firing strength, F^i, which is an interval type-1 fuzzy set. The firing strength is computed as follows (Liang and Mendel,2000)

$$F^i = [\overline{f}, \underline{f}] \quad i = 1 \sim M, \quad (4)$$

where

$$\overline{f}_i = \prod_{j=1}^{n} \overline{\mu}_{\tilde{A}_j^i} \quad \text{and} \quad \underline{f}_i = \prod_{j=1}^{n} \underline{\mu}_{\tilde{A}_j^i} \quad (5)$$

and M is total number of rules.

Layer 4 (Compensatory Firing layer): Each node in this layer performs a compensatory fuzzy operation mentioned in [4], and derives if-condition matching of fuzzy rules. As a result, the compensatory firing function of inference node is

$$\varphi^i = [\overline{\varphi}, \underline{\varphi}], \quad i = 1, \cdots, M \quad (6)$$

where

$$\overline{\varphi}^i = \left(\prod_j^n \overline{f}_j^i\right)^{(1-\gamma_i + \frac{\gamma_i}{n})}, \quad \underline{\varphi}^i = \left(\prod_j^n \underline{f}_j^i\right)^{(1-\gamma_i + \frac{\gamma_i}{n})} \quad (7)$$

Here, the $\gamma_i \in [0,1]$ is called compensatory degree. The purpose of tuning γ_i is to increase the adaptability of fuzzy operation.

Layer 5(Consequent and Output processing layer): Each rule node in layer 3 has its own corresponding consequent node in layer 4.The output of each node is an interval type-1 fuzzy set , denoted by $[w_l^i\ ,\ w_r^i]$, if function-link neural network is used, then the link is existent.

$$[w_l^i\ ,\ w_r^i]=[c_0^i-s_0^i,\ c_0^i+s_0^i]+\sum_{k=1}^{L}[c_k^i-s_k^i,c_k^i+s_k^i]\cdot\lambda_k \quad (8)$$

That is,

$$w_l^i=\sum_{k=0}^{L}c_k^i\lambda_k-\sum_{k=0}^{L}|\lambda_k|s_k^i \quad (9)$$

where $\lambda_0=1$, and L=3n

$$w_r^i=\sum_{k=0}^{L}c_j^i\lambda_j+\sum_{k=0}^{L}|\lambda_k|s_k^i \quad (10)$$

Here λ_k is the functional expansion of input variables. The functional expansion uses a trigonometric polynomial basis function, given by $[x_1\ sin(\pi x_1)\ cos(\pi x_1)\ x_2\ sin(\pi x_2)\ cos(\pi x_2)]$ for two-dimensional input variables.

For output processing, the output y_l *and* y_r can be computed by using KM procedure [10]. In that procedure, the consequent part weights should be re-arranged in ascending order. According to [13], the relationship between $y_l\ , y_r, \tilde{y}_l,$ and $\tilde{y}_r$ is

$$\boldsymbol{y}_l=Q_l\tilde{\boldsymbol{y}}_l \text{ and } \boldsymbol{y}_r=Q_r\tilde{\boldsymbol{y}}_r \quad (11)$$

where Q_l and Q_r are $M\times M$ permutation matrices. Re-order the f^i accordingly and call them g^i. The outputs y_l and y_r can be computed as follows

$$y'_l=\frac{\sum_{i=1}^{L}\overline{g}^i y_l^i+\sum_{i=L+1}^{M}\underline{g}^i y_l^i}{\sum_{i=1}^{L}\overline{g}^i+\sum_{i=L+1}^{M}\underline{g}^i} \quad (12)$$

and

$$y'_r=\frac{\sum_{i=1}^{R}\underline{g}^i y_r^i+\sum_{i=R+1}^{M}\overline{g}^i y_r^i}{\sum_{i=1}^{R}\underline{g}^i+\sum_{i=R+1}^{M}\overline{g}^i} \quad (13)$$

Layer 6 (Output layer): The node in this layer computes the output linguistic variable y by defuzzification operation. The output of layer 5 is an interval set as a result of computing average of y'_l and y'_r. Hence, the defuzzified output is

$$y=\frac{y'_l+y'_r}{2} \quad (14)$$

III. FLIT2CFNN LEARNING

In this section, the FLIT2CFNN simultaneously uses on-line two types of learning algorithm, the structure and parameter learning. There are no rules in the FLIT2CFNN initially. The rules are created dynamically and automatically as learning proceeds upon receiving on-line incoming training data by performing the structure and parameter learning processes. All of free parameters are learned by following learning as a rule is generated. The details of structure learning and parameter learning are introduced in the rest of this section.

A. Structure learning

The first task in structure learning is conducted to decide whether or not to extract a new rule from training data as well as the number of fuzzy sets on the universal of discourse of each input variable. A previous study [2] used the rule firing strength as a criterion for type-1 fuzzy rule generation. This idea is extended to type-2 fuzzy rule generation criteria in a FLIT2CFNN. The firing strength is an interval in the FLIT2CFNN so that the center of interval is computed as

$$f_c^i=\frac{1}{2}(\overline{f}^i+\underline{f}_i) \quad (15)$$

The firing strength center then serves as a rule generation criterion. That is, for each piece of incoming data $\vec{x}=(x_1,\ldots,x_n)$, find

$$I=\arg\max_{1\le i\le M(t)} f_c^i(\vec{x}) \quad (16)$$

where $M(t)$ is the number of existing rules at time t. If $f_c^I(\vec{x})\le\phi_{th}$, then a new rule is generated, where $\phi_{th}\in(0,1)$ is a pre-specified threshold that decays during the learning process.. The threshold decides the number of input clusters generated in FLIT2CFNN.

Once a new fuzzy set is generated, the initial uncertain means and widths of the corresponding new type-2 fuzzy sets are assigned as

According to the notation in Eq. (1), the initial uncertain mean m_j^i and standard deviation σ_j^i for the new interval type-2 fuzzy set in input variable x_j are

$$m_j^i\in[x_j-0.1,\ x_j+0.1] \quad (17)$$

$$\sigma_j^i=\sigma_{fix} \quad (18)$$

B. Parameter Learning

The parameter learning phase occurs concurrently with the structure learning phase. For each incoming data, all of free parameters in the FLIT2CFNN are tuned, whether a newly generated rules or formerly existent. When we consider the single output case for clarity, our goal to minimize the error function is defined as

$$E(t)=\frac{1}{2}[y(t)-y^d(t)]^2=\frac{1}{2}e^2(t) \quad (19)$$

where $y(t)$ and $y_d(t)$ denote real and desired outputs, respectively. The Karnik-Mendel iterative procedure for computing y_l and y_r in Eqs. (12) and (13) has a premise that y_l^i and y_r^i are re-arranged in ascending order.

Since the FLIT2CFNN training process, the consequent part parameters change, and the corresponding rule orders change accordingly. It is necessary to know the specific site of antecedent and consequent parameters for updating the parameters. According to this mapping, (12) and (13) are expressed by $\tilde{\boldsymbol{y}}_l$ and $\tilde{\boldsymbol{y}}_r$, i.e., with the consequent values arranged in the original rule order despite their changes during the parameter learning process. Based on this original rule-ordered expression, the consequent part parameters are tuned using Kalman filter algorithm [14]. The compensatory degree weights and the antecedent part parameters are tuned using the gradient descent algorithm, and it is expressed as

$$w_i(t+1) = w_i(t) - \eta \frac{\partial E}{\partial w_i}, \tag{20}$$

where w can be expressed as $m_{j1}, m_{j2}, \sigma, \gamma$, *and* η is a learning coefficient. Details of the learning algorithm can be found in [13].

IV. SIMULATIONS

To demonstrate the ability of FLIT2CFNN to evolve, the following nonlinear system is described by the difference equation [1-2]

$$y_d(t+1) = \frac{y_d(t)}{1+y_d^2(t)} + u^3(t) \tag{21}$$

The training patterns are generated with $u(t) = \sin(2\pi t/100)$, $t = 1, \cdots, 200$. The inputs of FLIT2CFNN are $y_d(t)$ and $u(t)$, and the desired output is $y_d(t+1)$. Performance is evaluated using root-mean-square-error (RMSE)

$$RMSE = \sqrt{\frac{1}{200}\sum_{k=1}^{200}[y(t+1) - y^d(t+1)]^2} \tag{22}$$

where $y(t)$ is the output of FLIT2CFNN. Learning coefficient η is set to be 0.075. During the training process, the three rules are generated. Training is performed for 500 iterations. Table I shows that the performance of the FLIT2CFNN contains the network size, training and test RMSEs. Figure 3 shows the outputs of the plant and the IT2RFNN for these test inputs. The performance of FLIT2CFNN is compared with that of type-1and type-2 FNNs, including SONFIN[2] and Feedforward type-2 FNN, where the former parameter learning are learned by hybrid learning of Kalman filter algorithm and gradient descent, and the latter free parameters are tuned by gradient descent method. The results show that the FLIT2CFNN achieves smaller test errors than the other feedforward networks.

TABLE I. PERFORMANCE OF FLIT2CFNN AND OTHER FEEDFORWARD SYSTEM

Model	SONFIN	FEEDFORWARD TYPE-2 FNN	FLIT2CFNN
Rule number	10	6	3
Parameter number	70	72	66
Iterations	250	250	250
RMSE	0.0075	0.0082	0.0035

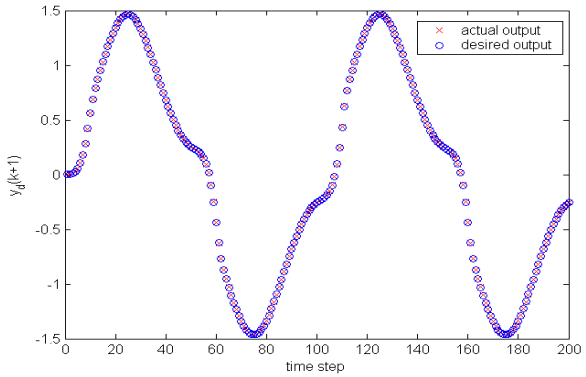

Fig.3. Output of the nonlinear system (O) and FLIT2CFNN (X).

This example is also considered the noise resistance ability of an FLIT2CFNN. Assumed that the measure y^d output contains noise. The added noise is artificially generated and is uniformly distributed in [-2.5, 2.5]. There are 20 Monte-Carlo realizations. On average, three rules are generated for the FLIT2CFNN. Fig. 4 shows one learning result of the 20 realizations, showing that the FLIT2CFNN output does not change as violently as the actual noisy output. This result verifies the FLIT2CFNN's noise resistance abilities. Table II shows the performance of FLIT2CFNN with noise. For comparison, the self-evolving type-1 system, SONFIN[2] and the Feedforward type-2 FNN are compared to the same problem. These results show that the FLIT2CFNN learning performance is better than the SONFIN and Feedforward type-2 FNN learning performance when there is noise.

TABLE II. PERFORMANCE OF FLIT2CFNN AND OTHER FEEDFORWARD SYSTEM WITH NOISE STATE

Model	SONFIN	FEEDFORWARD TYPE-2 FNN	FLIT2CFNN
Rule number	10	6	3
Parameter number	70	72	66
Train RMSE	0.13	0.142	0.128
Test RMSE	0.095	0.088	0.066

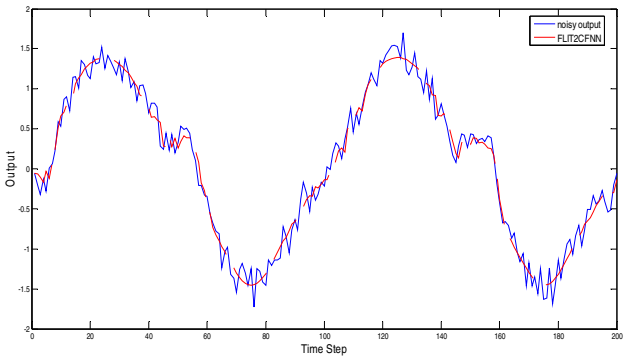

Fig.4. Online learning results of the FLIT2CFNN when noise appears in the measured data

V. CONCLUSIONS

This paper proposes a functional-link-based Interval Type-2 Compensatory Fuzzy Neural Network (FLIT2CFNN) structure for nonlinear system modeling and resistance noise ability. To achieve optimize type-2 fuzzy logic reasoning, the compensatory operation is chosen. The FLIT2CFNN model can automatically construct and adjust free parameters by performing online structure/parameter learning schemes concurrently. Moreover, the rule-ordered Kalman filter algorithm helps tune the consequent parameters online and improves learning accuracy. Except that the FoU in FLIT2CFNN helps handle the numerical uncertainty associated with system inputs and outputs. Therefore, the FLIT2CFNN has the potential to achieve better performance than type-1 fuzzy systems when dealing with noisy data. The proposed FLIT2CFNN can efficiently handle nonlinear system and good performance is achieved.

REFERENCES

[1] C.J. Lin and C. T. Lin, "An ART-Based Fuzzy Adaptive Learning Control Network" *IEEE Transactions on Fuzzy Systems,* vol. 5, no. 4, pp.477-496 Nov. 1997.J. Clerk Maxwell, A Treatise on Electricity and Magnetism, 3rd ed., vol. 2. Oxford: Clarendon, 1892, pp.68–73.

[2] F. Juang and C. T. Lin, "An On-Line Self-Constructing Neural Fuzzy Inference Network and Its Applications," *IEEE Transactions on Fuzzy Systems*, vol. 6, no.1, pp. 12-31, Feb. 1998

[3] F. J. Lin, C. H. Lin, and P. H. Shen, "Self-Constructing Fuzzy Neural Network Speed Controller for Permanent-Magnet Synchronous Motor Drive," *IEEE Transactions on Fuzzy Systems*, vol. 9, no. 5, pp. 751-759, Oct. 2001.

[4] Y. Q. Zhang and A. Kandel, "Compensatory Neurofuzzy Systems with Fast Learning Algorithms," *IEEE Transactions on Neural Networks*, vol. 9, no. 1, pp. 83-105, Jan. 1998.

[5] Y. H. Pao, Adaptive Pattern Recognition and Neural Networks, MA: Addison-Wesley, 1989.

[6] J. C. Patra, R. N. Pal, B. N. Chatterji, and G. Panda, "Identification of nonlinear dynamic systems using functional link artificial neural networks," *IEEE Trans. on Syst., Man, and Cybern.*, vol. 29, Apr. 1999.

[7] T. Lin and C. F. Juang, "An adaptive neural fuzzy filter and its applications," *IEEE Trans. Syst., Man, Cybern. B, Cybern.*, vol. 27, no. 4, pp. 635–656, Aug. 1997.

[8] N. N. Karnik, J. M. Mendel, and Q. Liang, "Type-2 fuzzy logic systems," *IEEE Trans. Fuzzy Syst.*, vol. 7, no. 6, pp. 643–658, Dec. 1999.

[9] J. M. Mendel and R. I. John, "Type-2 fuzzy sets made simple," *IEEE Trans. Fuzzy Syst.*, vol. 10, no. 2, pp. 117–127, Apr. 2002.

[10] J. M. Mendel, Uncertain Rule-Based Fuzzy Logic System: Introduction and New Directions. Upper Saddle River, NJ: Prentice-Hall, 2001.

[11] Q. Liang and J. M. Mendel, "Equalization of nonlinear time-varying channels using type-2 fuzzy adaptive filters," *IEEE Trans. Fuzzy Syst.*, vol. 8, no. 5, pp. 551–563, Oct. 2000.

[12] H. Hagras, "A hierarchical type-2 fuzzy logic control architecture for autonomous mobile robots," *IEEE Trans. Fuzzy Syst.*, vol. 12, no. 4, pp. 524–539, Aug. 2004.

[13] J. M. Mendel, "Computing derivatives in interval type-2 fuzzy logic system," *IEEE Trans. On Fuzzy Systems*, vol. 12. no. 1, pp. 84-98, Feb.2004.

[14] C.F. Juang and Y. W. Tsao, "A self-evolving interval type-2 fuzzy neural network with on-line structure and parameter learning," *IEEE Trans. Fuzzy Systems*, vol. 16, no. 6, pp. 1411-1424, Dec. 2008.

2011 IEEE International Conference on Fuzzy Systems
June 27-30, 2011, Taipei, Taiwan

Infrared Image Segmentation using Enhanced Fuzzy C-Means Clustering for Automatic Detection Systems

SITANSHU GUPTA
Department of Electronics and Communication Engineering,
National Institute of Technology, Allahabad
Allahabad -211004, India
Email: sitanshu.08@gmail.com

ASIM MUKHERJEE
Department of Electronics and Communication Engineering,
National Institute of Technology, Allahabad
Allahabad -211004, India
Email: asimmkj@yahoo.co.in, asimmkj@mnnit.ac.in

***Abstract*-This paper proposes Enhanced Fuzzy C-means technique (EFCM) based infrared image segmentation and its broad application in Automatic detection systems. The EFCM based image segmentation is able to approximate the exact number of clusters present in the image. EFCM based segmentation is applied on various infrared images that can be used for automatic detection systems and compared with widely used clustering techniques such as K-means and EM. Clustering performance has been compared in terms of well-proven and widely accepted validation indices, Global Silhouette Index and Separation Index. The segments or clusters obtained from above mentioned clustering methods have been assessed visually. Automatic Detection Systems based on EFCM can help in reducing complexities present in conventional systems.**

Keywords: EFCM, K-means, EM, GS, SI.

I. INTRODUCTION

Clusters are the collection of similar objects such that each group or cluster is homogeneous; that is, objects belonging to the same group are similar to each other. Each group or cluster should be different from other clusters; that is, objects belonging to one cluster should be different from the objects of other clusters. Clustering technique [1] can be hard or fuzzy. A hard clustering algorithm assigns each data point to a particular cluster during its operation and in its output. A fuzzy clustering method allocates a degree of membership to each data point depending on its association with several other clusters.

Automatic Detection Systems, on which proposed technique can be used, are those that can control any process, weather forecast or detect diseases with the help of infrared images. These systems are discussed in Section-4 of this paper.

This paper is organized in four sections. An overview of the existing clustering algorithms is given in Section-2. The proposed technique is explained in Section-3. In Section-4, we present the simulation results of all the clustering techniques, including the proposed EFCM technique. Moreover, a comparison between the cluster quality of all clustering techniques is made. Finally, we present our conclusion in the last section.

II. AN OVERVIEW OF SOME CLUSTERING BASED SEGMENTATION TECHNIQUES

Some of the widely used clustering techniques are K-means Clustering [2], FCM Clustering [3], Gath-Geva Clustering [4] and EM Clustering [5].

K-means clustering algorithm was proposed by Forgy and MacQueenin in 1967. It is one of the simplest unsupervised clustering algorithms, which has been widely used in various applications. It groups data into a fixed number of clusters where the centroid of one cluster is placed as far away as possible from another. Each data point in a cluster is associated to the nearest centroid. The Expectation Maximization (EM) clustering algorithm is based on the statistical model that uses the finite Gaussian mixtures model. This clustering algorithm utilizes the K-means initialization in which a fixed number of clusters are obtained through K-means clustering. Then the cluster parameters (weights, means and co-variances) are re-computed until a desired convergence value is achieved. In infinite mixture model, all attributes are assumed to be independent random variables. The Probabilistic Clustering technique [6] objects at fitting a fixed k-component Gaussian mixture model (GMM) to the data set. It assesses the probability of the components of a GMM such that whole data set can be categorized into components with high probability. This clustering algorithm employs the basic Expectation-Maximization Algorithm. Fuzzy C-Means (FCM) clustering was developed by Dunn in 1973 and later improved by J. C. Bezdek in 1981. FCM is frequently used in pattern recognition. In this technique, data points are bound to each cluster by means of membership functions, which give degree of association with each cluster. A data point is assigned to that cluster with which it is highly associated i.e. degree or membership is highest.

III. ENHANCED FUZZY C-MEANS CLUSTERING ALGORITHM (EFCM)

The FCM algorithm [3] could not identify the optimum number of clusters required, which is a major drawback. To overcome this drawback, a modified and improvised algorithm EFCM is presented in this paper. This algorithm has the capability to find the optimum number of clusters.

A. The Algorithm

The EFCM algorithm has four important steps:

1) Generation of subsets.
2) Estimation of optimum number of clusters.

1) Generation of subsets:

Fuzzy c-means (FCM) is a method of clustering which allows one piece of data to belong to two or more clusters. It is based on minimization of the following objective function:

$$J_m = \sum_{i=1}^{N}\sum_{j=1}^{C} u_{ij}^{m} \| x_i - c_j \|^2, \qquad 1 \le m \le \infty \quad (1)$$

where m is any real number greater than 1, u_{ij} is the degree of membership of x_i in the cluster j, x_i is the ith of d-dimensional measured data, c_j is the d-dimension center of the cluster, C is no. of cluster, and ||*|| is any norm expressing the similarity between any measured data and the center. Fuzzy partitioning is carried out through an iterative optimization of the objective function shown above, with the update of membership u_{ij} by:

$$u_{ij} = \frac{1}{\sum_{k=1}^{C}\left(\frac{\| x_i - c_j \|}{\| x_i - c_k \|}\right)^{\frac{2}{m-1}}} \quad (2)$$

and the cluster centers c_j are given by:

$$c_j = \frac{\sum_{i=1}^{N} u_{ij}^{m} x_i}{\sum_{i=1}^{N} u_{ij}^{m}} \quad (3)$$

This iteration will stop when $\max_{ij}\{| u_{ij}^{k+1} - u_{ij}^{k} |\} < \in$, where $\in$ is a termination criterion between 0 and 1, whereas k is the iteration step. This procedure converges to a local minimum or a saddle point of J_m.

The algorithm comprises of four steps:

1. Initialize the $U = [u_{ij}]$ matrix. It represents $U^{(0)}$.
2. At k-step: calculate the centers vectors $Ce^{(k)}=[c_j]$ with $U^{(k)}$ using equation 3 given above, assuming $C=2$ initially.
3. Update $U^{(k)}$, $U^{(k+1)}$ using equation 2 mentioned above.
4. *If* $|| U^{(k+1)} - U^{(k)} || < \in$ *then STOP; otherwise return to step 2.*

In this manner, the algorithm iteratively converges on the most optimum cluster centers.

2) Estimation of Optimum number of Clusters:

Determine the optimum number of clusters, C using validity measure Global Silhouette Index (GS) [7,8] defined in Section 3.2. GS value is calculated for various number of clusters (*n=1,2,...20*). Value of n for which GS is maximum is assigned to C . Form optimum number of clusters C using the Steps 2 to13. These are the required clusters for an infrared image.

B. Cluster Quality Measure

1) Global Silhouette Index

GS is calculated as shown below:

$$GS = \frac{1}{c}\sum_{m=1}^{c} S_m \quad (4)$$

S_m is calculated as:

$$S_m = \frac{1}{N_m}\sum_{i=1}^{N_m} s(i), \quad (5)$$

where N_m is number of data points in m^{th} cluster and $s(i)$ is :

$$s(i) = \frac{b(i) - a(i)}{\max\{a(i), b(i)\}}, \quad (6)$$

where $a(i)$ is the average distance between the i^{th} sample and all of the samples included in X_m (m^{th} cluster); '*max*' is the operator, and $b(i)$ is the minimum average distance between the i^{th} sample and all of the samples clustered in X_k ($k = 1,\ldots, c;\ k \neq m$). From this formula it follows that $-1 \le s(i) \le 1$. For a good cluster GS value should be near to 1.When $s(i)$ is close to 1, one may infer that the i^{th} sample has been "well-clustered ", i.e. it was assigned to an appropriate cluster. When $s(i)$ is close to zero, it suggests that the i^{th} sample could also be assigned to the nearest neighboring cluster.

2) Separation Index (SI) [9]

It uses a minimum-distance separation for partition validity. A lower value of *SI* indicates a better partition. For good quality clusters *SI* should have the least possible value.

$$SI = \frac{\sum_{m=1}^{c}\sum_{j=1}^{n}(\mu_{jm})^2 \| \overline{\mathbf{x}^j} - \bar{z}_m \|^2}{n.\min_{k,m} \| \bar{z}_k - \bar{z}_m \|^2} \quad (7)$$

where,

$\bar{z}_m$ is the m^{th} cluster center,

μ_{jm} is the membership of data point j in cluster m.

$$\mu_{jm} \in \{0,1\};\ 1 \le j \le n;\ 1 \le m \le c$$

$$\sum_{m=1}^{c} \mu_{jm} = 1$$

IV. RESULTS

The widely used clustering algorithms discussed above are tested on various synthetic and natural infrared images. Simulations are done using MATLAB on a PC with 2GB RAM, using a 2.00 GHz processor. Prior to the experiments, no pre-processing was done on these images. RGB features are used in clustering. The effectiveness of clusters is compared in terms of GS and SI values of cluster formed.

Example 1: In this example we deal with an infrared image of a boiler. Fig.1 shows why four is chosen as an optimum number of clusters. Table 1 shows the performance of different clustering techniques. Table 2 shows the clusters formed by different clustering techniques. From Table 2 we can easily visualize that the yellow part (1^{st} cluster) which shows the hot water part is segmented properly using EFCM.

Example 2: Here we are concerned with an infrared image showing breast cancer. Yellow part shows the cancer prone area in the breast. Fig. 2 shows how the optimum number of cluster is four. Table 3 shows the performance of different clustering techniques used in this paper. Table 4 shows the clusters formed by different clustering methods. From this table we can see that cancer prone part (3^{rd} cluster) is removed properly using EFCM. Validity of number of clusters can be assessed visually.

Example 3: In this example we consider segmentation of an infrared image taken at Tromso satellite station showing advancing of bloom. Yellow and red part shows warmer water and advancement of bloom. Here five is chosen as the optimum number of clusters. From Table 6 we can see that the red region (1^{st} cluster) is completely separated from the image.

A. Comparison of performance

The results of infrared image segmentation indicate that EFCM is successful in segmenting the image properly with optimum number of clusters. The Global Silhouette Index value of EFCM is the best in most of the cases. Results show that EFCM could retrieve most of the clusters properly. The cluster centers in case of Fuzzy C-means are widely separated. It is able to retrieve all the basic clusters, giving less redundant clusters. The disadvantage with Fuzzy C-Means is that it cannot find out the optimum number of clusters. K-means result is also good but the most important disadvantage of K-means is that it generally does not give proper clusters in the first run. This is due to random selection of cluster centers which results in consumption of more time while dealing in large images. EM results are not better than that of EFCM and K-means.

B. Practical Application

The main aim of the paper is to propose a technique which can be conveniently used in automatic detection systems. Here, the phrase "Detection Systems" is concerned with systems like detection of hot water level in boilers, detection of geographical features on any planet or even on unreachable areas of earth, weather forecasting systems and medical systems. Systems related to the examples mentioned above are described below:

1) Detection of water level in a boiler: Infrared images work on the principle of temperature sensing. They map a temperature range to various colors. This detection system takes the infrared image of the boiler and uses EFCM technique to segment the image properly for optimum number of clusters. For each cluster, average R, G, B value is calculated and corresponding temperature of that color is obtained from predefined scale. Then it compares the predefined temperature of water (i.e. 100^{o}C) with the temperature of various clusters and finds out the required cluster. Next step is to check the height of water level in boiler which is proportional to the height of color in the required cluster (1^{st} cluster) . Now water supply can be controlled on the basis of height of color. Real time implementation of this system can reduce the complexity of conventional boiler control system designs.

2) Detection of breast cancer: Medical thermal imaging (MII) can indicate life threatening diseases like breast cancer in their developing states, earlier than anatomical examinations. This type of detection system takes the infrared image, processes it for EFCM, calculates the average R, G, B values and obtains corresponding temperatures as described earlier. Subsequently, it checks for a predefined temperature region of the affected area to obtain the required cluster. From the cluster, affected area can be easily visualized. In Example 2 yellow color (3^{rd} cluster) shows the cancer prone area which is faithfully separated.

3) Detection of Geographical Features: Example 3 shows the infrared image taken at Tromso Satellite station. This image shows the bloom. Advancement of red color can give the information about direction of movement of bloom and its intensity. Usually satellite sends the whole image (very large data) to earth station. The large amount of data to be transmitted is very likely to be corrupted by noise. So it is better to send only required information which is depicted in red color (1^{st} cluster) in this case. If the satellite is equipped with EFCM processor then it will take the image, cluster it properly as shown in Table 6, and send only red color image to the earth station which is very small volume of data as compared to the amount of data required to represent the entire image. Continuous tracking of red color can give information about the advancement and intensity of bloom. This system can help in reducing the quantity of data transferred from the satellite to earth station because we can send only the required part of the image to earth.

TABLE 1
PERFORMANCE OF DIFFERENT CLUSTERING METHODS

Original image Optimum number of clusters=4	Clustering Methods	GS	SI
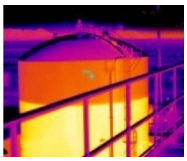	K-Means	.7800	.0221
	EM	.5786	.0554
	EFCM	.7914	.0210

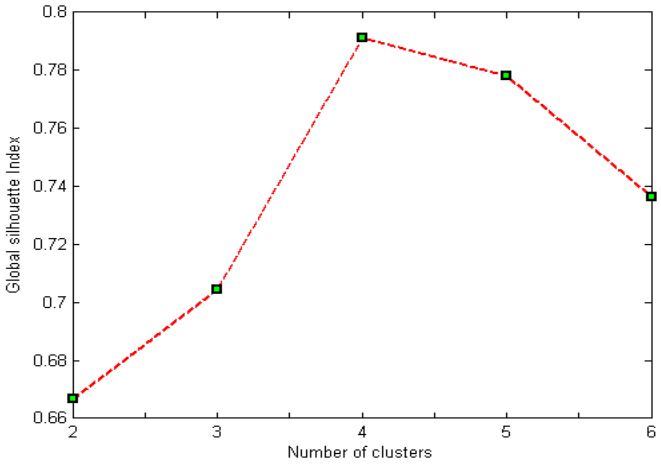

Fig. 1: Variation of GS with the number of clusters

TABLE 2
CLUSTERS OF INFRARED BOILER IMAGE FORMED BY DIFFERENT CLUSTERING TECHNIQUES

Clustering Method	1st Cluster	2nd Cluster	3rd Cluster	4thCluster
K-means		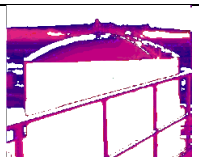	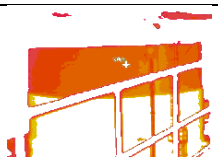	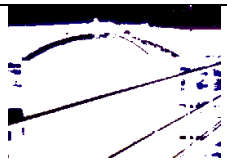
EM		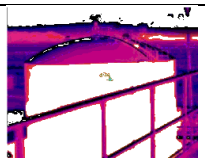	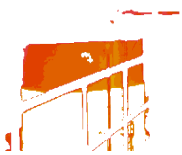	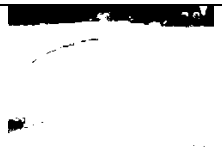
EFCM		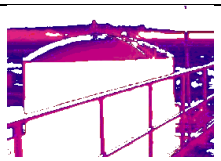	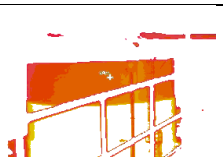	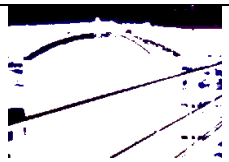

TABLE 3
PERFORMANCE OF DIFFERENT CLUSTERING METHODS

Original image Optimum number of clusters=4	Clustering Methods	GS	SI
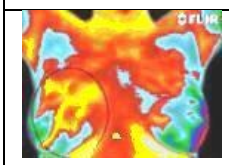	K-Means	.7097	.0347
	EM	.7094	.1122
	EFCM	.7128	.0317

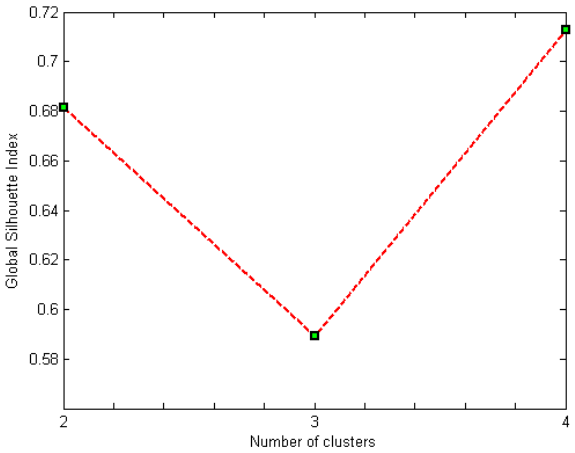

Fig. 2: Variation of GS with the number of clusters

TABLE 4
CLUSTERS OF INFRARED BREAST CANCER IMAGE FORMED BY DIFFERENT CLUSTERING TECHNIQUE

Clustering Method	1st Cluster	2nd Cluster	3rd Cluster	4thCluster
K-means	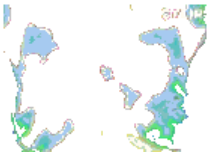	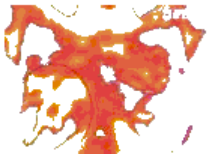		
EM	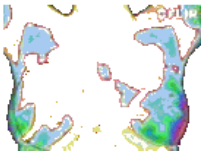	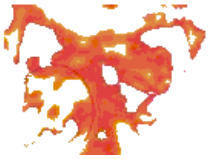		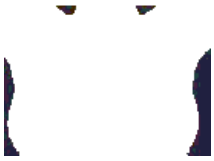
EFCM	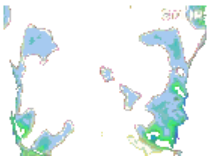			

TABLE 5
PERFORMANCE OF DIFFERENT CLUSTERING METHODS

Original image Optimum number of clusters=5	Clustering Methods	GS	SI
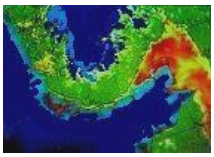	K-Means	.6480	.0256
	EM	.4031	.1913
	EFCM	.6498	.0263

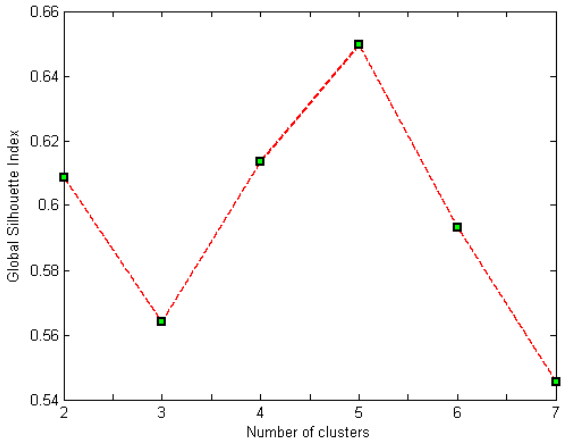

Fig.3: Variation of GS with the number of clusters

TABLE 6
CLUSTERS OF INFRARED GEOGRAPHICAL IMAGE FORMED BY DIFFERENT CLUSTERING TECHNIQUES

Clustering Method	1st Cluster	2nd Cluster	3rd Cluster	4thCluster	5thCluster
K-means	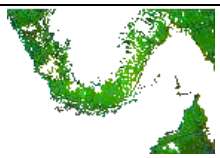	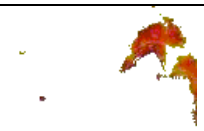	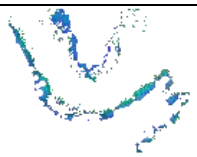		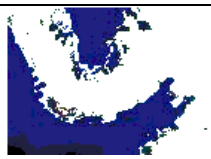
EM	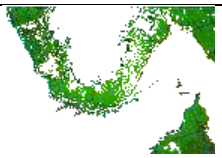	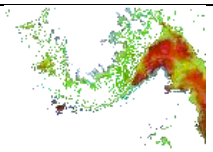	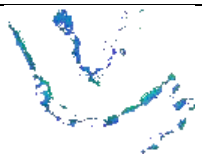	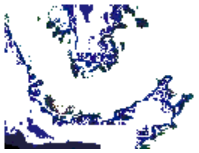	
EFCM	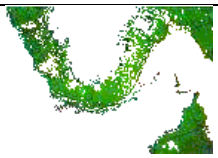	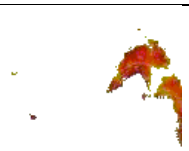	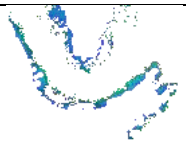		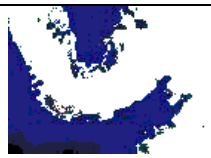

V. CONCLUSION

In this paper, we present EFCM based infrared image segmentation. We have applied some well-known clustering techniques, viz., K-Means, EM for the segmentation of colored images and compared their performance in terms of Global Silhouette Index and Separation Index that they achieve. We have obtained that EFCM was able to estimate the number of clusters accurately. Its performance on the basis of GS and SI is better than other techniques used for comparison. Hence this technique can be preferably used for the Automatic Detection Systems. Automatic Detection Systems described in this paper can make data transfer much faster and easier (in Example 3), can reduce the size and complexity of conventional control systems for boiler (in Example 1) and can even detect the very dangerous and rare diseases that cannot be easily diagnosed in early stages.

ACKNOWLEDGMENT

The authors would like to thank Mr. Sayed Atif Ali, undergraduate student at National Institute of Technology Allahabad, India, for helping to revise the paper thoroughly.

REFERENCE

[1] A. K. Jain, M.N. Murthy, P.J. Flynn, "Data Clustering: A Review", *ACM Computing Surveys*, Vol. 31,No. 3,September 1999.

[2] J.A. Hartigon and M.A. Wong,"*A K-means clustering algorithm*". Appl. Stat., 28, 126-130,1979.

[3] M. Razaz,"*A fuzzy C-means clustering placement algorithm*" ,.Circuits and Systems, 1993., ISCAS '93, 1993 *IEEE International Symposium*, 3-6 May 1993 Page(s): 2051 -2054 vol.3.

[4] J. Abonyi, R. Babuska, F. Szeifert, "Modified Gath-Geva Clustering for Identification of Takagi-Sugeno Fuzzy Models", *IEEE Trans. on Systems, Man, and Cybernetics-partB: cybernetics*, Vol.32, no5, October 2002.

[5] A.P. Dempster, N.M. Laird, and D.B. Rubin, "*Maximum likelihood from incomplete data via the EM algorithm*",*J.RoyStat.Soc. B*, Vo. 39, pp.1-38, 1977.

[6] G. M. Tao, A .Tan, M.Hanmandlu, "*The Model-Selection Problem*", submitted to *IEEE Trans. on Fuzzy Systems.*

[7] P.J. Rousseeuw, "*Silhouettes: a graphical aid to the interpretation and validation of cluster analysis*", J. Comp App. Math, Vol. 20, 1987, pp. 53-65.

[8] N. Bolshakova and F. Azuaje, "*Clustering validation techniques for genome expression data*", Genomic signal processing, Vol. 83, Issue 4, April 2003, pp. 825-833.

[9] A.M Bensaid, L.O.Hall, J.C. Bezdek, L.P. Clarke, M.L. Silbiger, J.A.Arrington, and R.F. Murtagh. "*Validity-guided (Re) Clustering with applications to image segmentation*", *IEEE Transactions on Fuzzy Systems*, 4:112-123, 1996.

2011 IEEE International Conference on Fuzzy Systems
June 27-30, 2011, Taipei, Taiwan

Image-Correlation Data Association with Global Uncertainty Techniques

Stephen C. Stubberud
Department of Advanced Technology
Oakridge Technology
San Diego, CA, USA
scstubberud@ieee.org

Kathleen A. Kramer
Department of Engineering
University of San Diego
San Diego, CA, USA

***Abstract*—A data association technique for target tracking that uses image correlation is enhanced by incorporating uncertainty. The approach uses fuzzy logic to simplify the mapping of the uncertainty to a usable construct to adjust the image generation based on the uncertainty of the measurements. The application of the uncertainty mapping for two methods is developed. The first technique varies the size of the image based on uncertainty. The second modifies the phase variation range that is used to generate the elements in the tile. The techniques are compared to the baseline image correlation technique in a baseline target-tracking example.**

Keywords- Data fusion; data association; image correlation; fuzzy logic application; uncertainty.

I. INTRODUCTION

In data fusion applications, one of the most important steps in the process is the data association step [1, 2]. No matter the estimation algorithm or application, a technique to determine which measurements or observations are related to existing fusion estimates or each other is necessary. In target tracking, the standard method for data association is the chi-squared metric. This measure, based on the Mahalanobis distance, is a weighted measure that is used to compare two Gaussian random variables and is usually applied to kinematic distances. It is not easily applied to non-kinematic information, non-Gaussian distributions, or different data formats, e.g., classification and kinematics.

Another approach to data association was developed using image correlation [3]. In that effort, kinematic and classification over time was mapped to an image representation. Using this approach, a representation of the target track attributes over time, referred to as a tile, is generated. This windowed association technique, similar in concept of association to the ND-assignment problem [4], uses a phase-only filter (POF) image correlation score. While the technique of [3] had promise, it did not rely on the phase information that is the foundation of the POF. A better implementation using a phase-based tile was developed in [5, 6] that compared favorably when compared to the chi-squared metric. While the chi-square metric incorporates uncertainty, the phase-based tile approaches previously developed did not. In this work, two separate techniques to incorporate uncertainty into the association score are developed.

The first technique to incorporate uncertainty alters the size of the tile elements used for the image correlation based upon the uncertainty. Here, this is incorporated into the association and the effect on the resulting association of changing the size of the tile elements based on the uncertainty is observed. The second technique incorporates uncertainty by using phase variation mappings. Both techniques require the ability to map the variations based on the size of the uncertainties. A fuzzy logic process based the fuzzy data association technique of [7, 8] is employed by each of the two techniques in order to map the uncertainty. The application of the rescaling is global in that the entire tile is affected for each attribute based on all of the uncertainties in the time window. This is in contrast to techniques that change each measurement based on its uncertainty.

In Section 2, the image correlation technique using a phase-tile is presented. This is followed in Section 3 by an overview of tile generation. The development of the fuzzy logic used to map the uncertainty into the function that will vary the size of different attribute in the tile and the phase variation for each attribute is discussed in Section 4. Section 5 presents the technique to be used for tile size variation. The application of the fuzzy logic technique for the mapping of the phase variation is presented in Section 6. Section 7 provides a comparison of the techniques with two different tracking examples.

II. PHASE ONLY FILTER IMAGE CORRELATION

The 2-D image correlation problem has several approaches. The standard 2-dimensional image correlation function is defined by the 2-D convolution sequence

$$h(x,y)=\sum_{n=1}^{N}\sum_{m=1}^{M} g(m,n) f(x-n,y-m) \qquad (1)$$

As with most straightforward mathematical techniques, the function is a computational bottleneck and memory intensive. The operational computations are $O(n^4)$ flops where n is the number of pixels along an edge (assuming a square image). The resulting image will have four times the pixels. A more efficient approach is to utilize the frequency domain implementation. This requires three 2-D fast Fourier transforms

978-1-4244-7316-8/11/$26.00 ©2011 IEEE

(FFTs) and one pixel-by-pixel multiplication of the two transformed images. The resulting algorithm is given as

$$\begin{aligned}&\sum\sum f^*(x,y) * f(x+X, y+Y) = \\ &\sum\sum F^*(k_x,k_y) F(k_x,k_y) e^{-j(k_x X + k_y Y)} \\ &= \mathbf{F}^{-1}\left\{\left|F(k_x,k_y)\right|^2\right\}\end{aligned} \tag{2}$$

for autocorrelation, and

$$\begin{aligned}&\sum\sum g^*(x,y) * f(x+X, y+Y) \\ &= \sum\sum G^*(k_x,k_y) F(k_x,k_y) e^{-j(k_x X + k_y Y)} \\ &= \mathrm{Re}\left\{\mathbf{F}^{-1}\left\{G^*(k_x,k_y) F(k_x,k_y)\right\}\right\}\end{aligned} \tag{3}$$

for cross-correlation.

Mathematically, the FFT was an improvement, but early implementers of image correlation used specific optical hardware, referred to as an optical correlator, to provide the calculations since large images could take significant computing power. Figure 1 shows the functional flow for such a device.

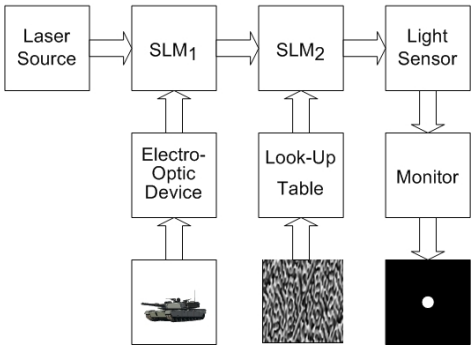

Figure 1. Function flow for optical correlator device providing image correlation

The physical limitations of the optical correlators did not exactly produce the correlation functions of Eqs. 2 and 3. Instead, the input signal became amplitude normalized such that primarily only the phase information was transmitted. The resulting equations became a phase-only filter (POF) given by

$$\begin{aligned}&\sum\sum G^*(k_x,k_y) \frac{F(k_x,k_y)}{\left|F(k_x,k_y)\right|} e^{-j(k_x X + k_y Y)} \\ &= \mathrm{Re}\left\{\mathbf{F}^{-1}\left\{G^*(k_x,k_y) \frac{F(k_x,k_y)}{\left|F(k_x,k_y)\right|}\right\}\right\}\end{aligned} . \tag{4}$$

As discussed in [10], the phase contained the most information of the image for comparison. As such the POF inadvertently became a powerful image correlation algorithm.

It is also worth noting that Eq. (4) is not commutative. Thus, if we change the order of the images in the cross-correlation problem, a different correlation will result.

III. Tile Generation

Each feature of a pattern for a given target report is comprised of an element of the tile comprised of a contiguous *n* x *n* pixel set. This set will be referred to as a sub-tile. In previous work [5], the size of the sub-tile for phase attribute matching has set to 20 pixels along each edge. This was determined to be a size that provided enough information in the frequency and phase based tiles for comparisons. These subtiles will not be fixed in size for one variant application. For the amplitude mapping approach, each attribute is assigned a region of interest or operational constraint. For example, a given pattern of data association is measured at two separate times. Position is given in terms of latitude and longitude. The third feature is the tracked altitude of the target. The fourth feature represents the measured vehicle speed. The final feature is the target heading. These values are tabulated in Table 1.

The POF correlation technique relies upon the majority of the image information being found within the phase components of the image. In contrast, the amplitude tile, first discussed in [3], uses amplitude variation to compare information. In [12], a phase representation was developed and compared well against the amplitude technique. Each attribute is mapped into a sub-tile that is defined as

$$f(x,y) = \sin(\omega x + \phi)\sin(\omega y + \phi). \tag{5}$$

TABLE I. Track Reports for Data Association

Feature	Lat. (deg.)	Long. (deg)	Altitude (m)	Speed (m/s)	Heading (deg.)
Scan 1	32	27	2500	100	45
Scan 2	32.6	25.6	3000	100	187

The frequency is different for each attribute or feature. For each frequency used, the value of each attribute is expressed by the phase component. The region of interest for the phase of each attribute value in Eq. (5) is mapped linearly between 0^o and 180^o. When the pattern from Table 1 is mapped into a phase tile, the result is a two-scan image that is depicted in Figure 2. The region of interest for the features is defined between 30^o and 35^o for latitude, 25^o and 28^o for the target's longitude, an altitude range between 0 and 4000 meters, a speed between 0 and 200 m/s, and a heading between 0^o and 360^o.

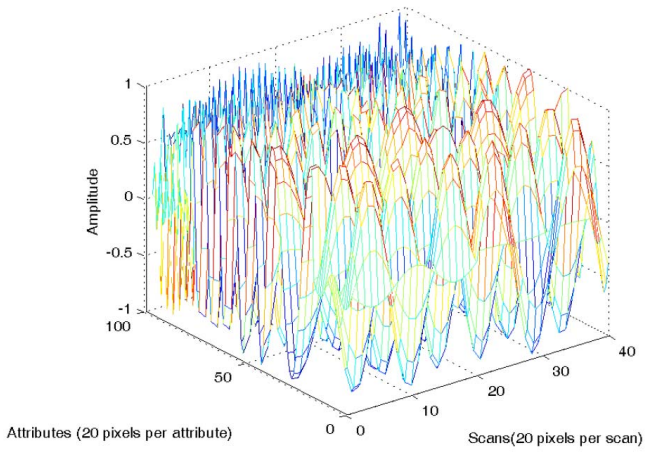

Figure 2. Two-scan image of phase tile for example data reports.

A. *Normalization*

The correlation function created by the POF provides a visual correlation peak that is easily understood. The function, however, does vary based on the amount of energy in the images. While this function is computationally complex, the optical correlator has it built-in via the physics and architecture. The energy variation means that comparisons require a normalization implementation. The approach used in this investigation is to compute the autocorrelation peaks of both images using the POF

$$\max\left(\max\left(POF(f(x,y),f(x,y)\right),\max(POF(g(x,y),g(x,y))\right) \quad (6)$$

and to find the maximum autocorrelation of both images. This value is used to divide the values of all of the points in the cross-correlation function.

IV. Fuzzy Logic Mapping of Uncertainty

In [7], a fuzzy logic approach to the data association problem was developed. There, the technique used multi-layered fuzzy logic to create a score by implementing a linguistic interpretation of the chi-squared metric. It looked at closeness based on the weighted distance between the two track elements. It also looked at the overlap of the error ellipses [11]. In this approach, a similar view of the error ellipses is used. Instead of using complex mathematical distances which would be adverse to the simplicity of the image correlation technique, a basic fuzzy logic approach is developed to adjust the tile creation based on the uncertainty ellipse size and orientation.

The first variable to be mapped is that of the orientation of the error ellipses. The fuzzy memberships are defined as five potential angles of the error ellipse relative to the longitude (x-axis). As seen in Figure 3, the memberships are 0^o, 45^o, 90^o, 135^o, 180^o. The alignments provide two inputs to the fuzzy decision process described in Figure 4. The first is a weighting factor that is generated using the crisp value of the antecedent functions. These weights are used in the defuzzification process of the second defuzzification step in Figure 4. The output of the first fuzzy logic function is used to modify the the range of values that defined the consequence membership functions in the defuzzification step of the second fuzzy logic function.

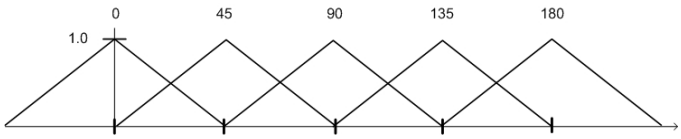

Figure 3. The antecedant triangular membership functions used to determine the alignment of the uncertainty ellipses

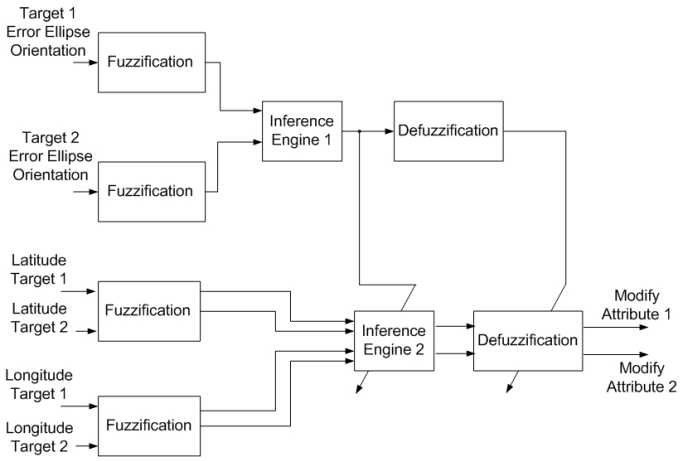

Figure 4. The fuzzy logic process to vary the tile generation used in image correlation track association process

The second input is the different rules that are activated from the inference engines in Tables 2 and 3 which relate to longitude component of the target track (or the x-axis) or the latitude component of the track (x-axis). These rules from the first stage determine vary the inputs to the inference engine the second stage (Table 4). The variations in the inputs are defined in Table 5. The input A indicates the average size of the minor or major axes of the uncertainty ellipse of Track 1 and B indicates the average of minor or major axes of Track 2. The table also indicates that multiple instantiations of the fuzzy inference engine are used in several cases.

The second process is based on the size of the axis of interest of the uncertainty ellipse. The actual uncertainty in the directions of latitude and longitude are mapped to membership functions in Figure 5. The elements of the membership functions are *small*, *medium_one*, *medium_two*, and *large*. Since the uncertainty measure is global, i.e., averaged over the entire time window, the results will affect all of the time subtiles of the entire attribute similarly. The proposed inference engine, defined in Table 4, varies depending on the alignment rule from the first step. If multiple instantiations are desired, then the output of each instantiation is weighted by the noted factor in Table 5. An NA indicates that those

rules are not used and result in a zero value for that component. The terms Maj and Min in the table refer to the major and minor axes of the uncertainty ellipses, respectively.

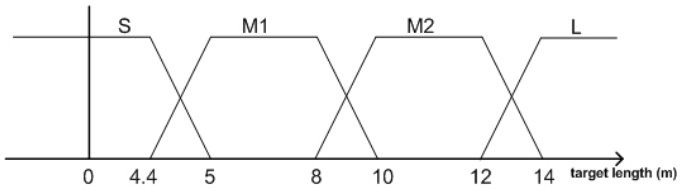

Figure 5. The antecedant triangular membership functions used to determine the size of the uncertainty ellipses axis

To simplify the development shown, the association score is generated on only the position data. The extension to include velocity would simply repeat the process on the velocity measures and uncertainties.

TABLE II. INFERENCE ENGINE MAJOR AXIS ALIGNMENT OF COVARIANCE EFFECT ON LANGITUDE (X-AXIS)

	0	**45**	**90**	**135**	**180**
	1	2	3	2	1

TABLE III. INFERENCE ENGINE MAJOR AXIS ALIGNMENT OF COVARIANCE EFFECT ON LATITUDE (Y-AXIS)

	0	**45**	**90**	**135**	**180**
	3	2	1	2	3

TABLE IV. INFERENCE ENGINE OF AVERAGED ALIGNED ERROR COVARIANCE AXIS SIZES

		B			
		Small	***Medium1***	***Medium2***	***Large***
A	***Small***	1	2	3	4
	Medium1	2	3	4	5
	Medium2	3	4	5	6
	Large	4	5	6	7

V. ATTRIBUTE PIXEL RESIZING BASED ON UNCERTAINTY

In image correlation, two images can have a noticeable difference, but, if the difference is a small percentage of the overall difference, then the images can still be highly correlated. In target tracking, if a component of the track has a large uncertainty, then the any effective difference between that component and the same component for a track or measurement to which it is being associated is reduced. The seven potential modifications will take the height of each subtile for a given attribute from 20 pixels down to 2 pixels. This is a reduction of 3 pixels for each rule. This means the consequence membership functions becomes as seen in Figure 6.

TABLE V. ALIGNMENT EFFECTS ON THE COVARIANCE INFERENCE ENGINE AND PROCESS

Alignment		**Wt.**	**Component**							
Tgt 1	**Tgt 2**		***A1***	***B1***	***A2***	***B2***	***A3***	***B3***	***A4***	***B4***
1	1	1	Maj	Maj	NA	NA	NA	NA	NA	NA
1	2	0.5	Maj	Min	Maj	Min	NA	NA	NA	NA
1	3	1	Maj	Min	NA	NA	NA	NA	NA	NA
2	1	0.5	Maj	Maj	Maj	Maj	NA	NA	NA	NA
2	2	0.25	Maj	Maj	Maj	Min	Min	Maj	Min	Min
2	3	0.5	Maj	Min	Min	Min	NA	NA	NA	NA
3	1	1	Min	Maj	NA	NA	NA	NA	NA	NA
3	2	0.5	Min	Maj	Min	Min	NA	NA	NA	NA
3	3	1	Min	Min	NA	NA	NA	NA	NA	NA

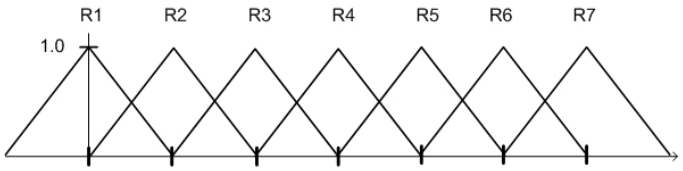

Figure 6. The consequence triangular membership functions used to determine the reduction in the attribute pixel size

The result of this approach is that large uncertainty has a lesser effect on the correlation score. This implies that the attributes (or elements of the track) with small differences relative to the uncertainty should be mapped into similar phases rather than different phases. Thus, rather than a linear mapping, the mapping should be non-linear in order to better represent attributes that effectively or near match, given the measurement uncertainty.

VI. INCORPORATING UNCERTAINTY AS A QUANTIZATION OF THE PHASE SEPARATION

The second approach to incorporating uncertainty is to vary the phase difference used in generating the subtiles. As seen in Figure 7, the linear range of values is reduced as the uncertainty becomes larger. This implies that the variation in the phase for small changes becomes less for very uncertain tracks than when the uncertainty is smaller. Thus, the association score in the former case would be greater as occurs in the chi-squared metric. The consequence function is the same as that seen in Figure 6. The defuzzified value is used to reduce the phase range.

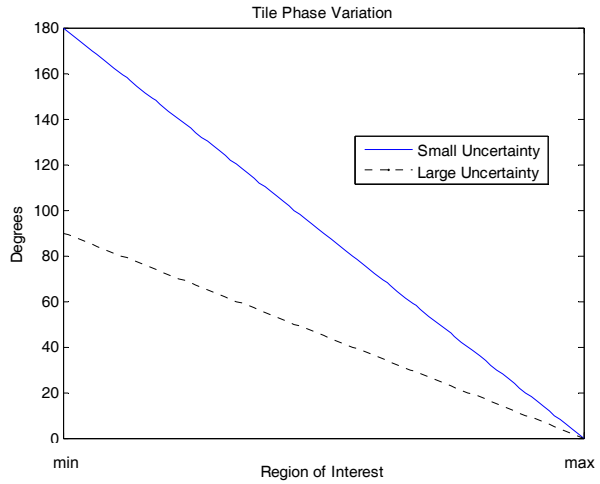

Figure 7. An example of the change in range of the phase variation based on track uncertainty

VII. EXAMPLE AND RESULTS

A scenario with two targets and three sensor systems was generated to compare the standard to the two techniques that incorporate uncertainty in a global manner. The two targets' trajectories are depicted in Figure 8 where the target on the bottom is considered Target 1 and that on top is considered Target 2. The sensor locations were chosen so that nearly parallel measurements (based on the uncertainty ellipses) were generated (Sensors 1 and 2) as the targets moved further along and nearly perpendicular target measurements were generated. These are considered extremes in target tracking and provide a good baseline.

The three sensors platforms, which are stationary throughout the scenario, are also shown in Figure 8. The three sensors are identical range-bearing sensors, i.e., a radar or active sonar, each with Kalman filter kinetic target tracking systems on them. As noted previously, the target tracks are associated with only the position data for this effort.

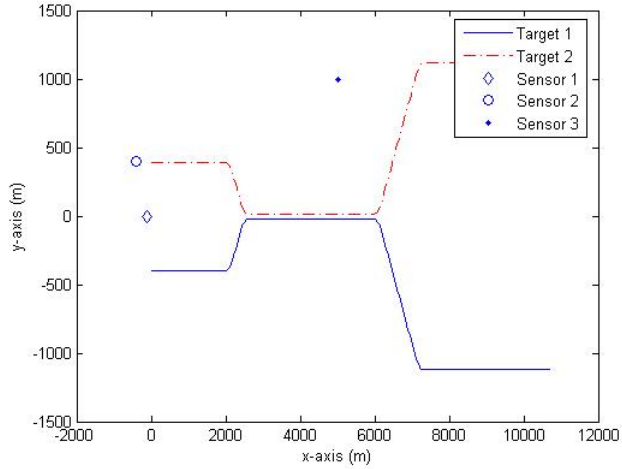

Figure 8. Example scenario with two targets and three sensors

The association scores of the track of Target 1 produced by the tracker of Sensor 1 compared to the two tracks of Sensor 2 are seen in Figures 9-11. Figure 9 depicts the association results of the original correlation technique without uncertainty. The results as in past efforts [7, 8] provide the ability to discern the two targets. In Figure 10, the uncertainty approach using the global resizing of the height of each attribute based on the average uncertainty is shown. In this case, the early portion of the track association does significantly better than without the uncertainty. At the end of the trajectory, the results are similar. This is due to the affects of the larger cross-range error of the sensor reports as the target gets further from the sensors. The cross-range error, especially for Sensor 1, is primarily in the direction of the y-axis. This is where the difference between the two targets exists in position. Figure 11 shows that the phase modification based uncertainty has a greater, and overall better, effect on the association scoring.

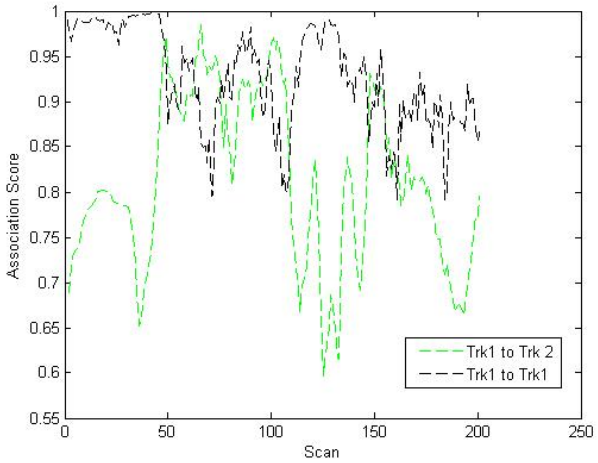

Figure 9. Association results for Sensor 1 and Sensor 2 without incorporating uncertainty

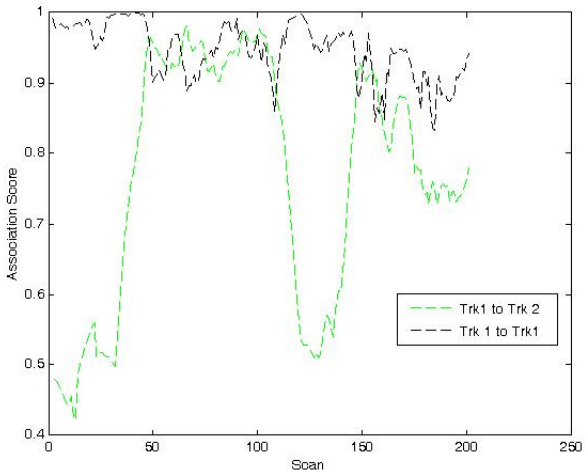

Figure 10. Association results for Sensor 1 and Sensor 2 incorporating global resizing

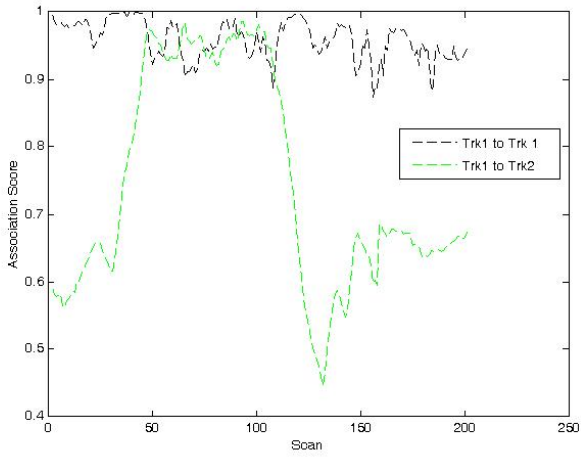

Figure 11. Association results for Sensor 1 and Sensor 2 incorporating phase modification based uncertainty

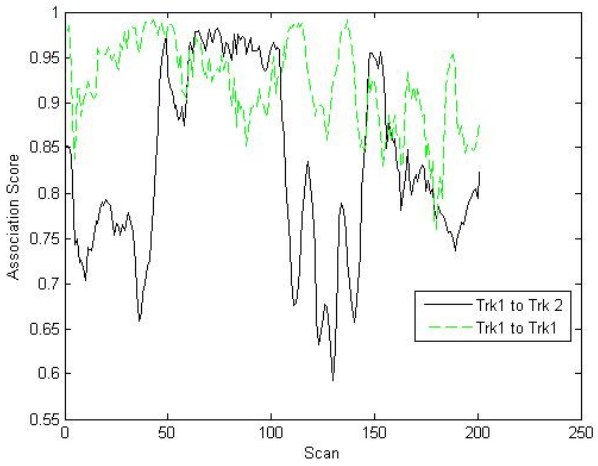

Figure 12. Association results for Sensor 1 and Sensor 3 without incorporating uncertainty

Figures 12-14 show the same comparisons as above but between Track 1 from Sensor 1 and both Tracks from Sensor 3. Similar results are obtained. The main differences that are seen are a result of the placement of the Sensor 3, which is perpendicular to Sensor 1 but closer to the end of the trajectory of the targets.

VIII. CONCLUSIONS

In this paper, two new approaches to incorporate uncertainty into the tile generation technique using fuzzy logic were introduced and demonstrated to provide significant improvement in the association scores. The use of fuzzy logic was able to provide the algorithm with less complex process to make the adjustments to the parameters used in the tile generation than if a full model of the process were developed.

Each technique was a global one in that the entire attribute component of the tile was changed based on the fuzzy system output. Future efforts are to show that by modifying only the input to the fuzzy system, the time component of each attribute can be changed with better results while allowing the fuzzy system to remain unchanged.

As this work continues, tracking system with different sensors types, e.g., bearing-only sensors, will be considered. This will demonstrate the total effectiveness of the uncertainty incorporation. Another adaptation to the techniques is to explore the incorporation of non-Gaussian uncertainties. By not limiting the association routine, it will become an effective tool with new tracking systems such as the particle filter.

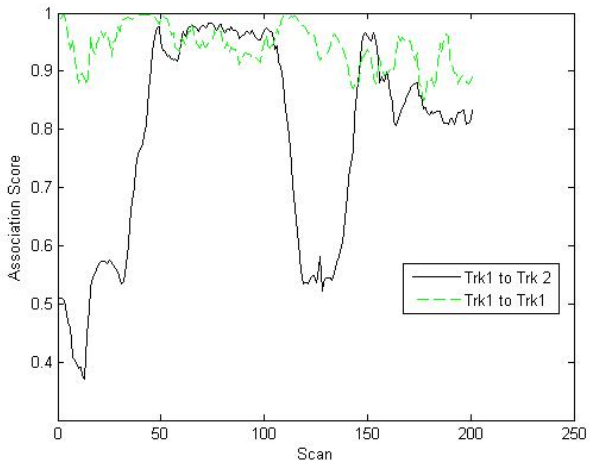

Figure 13. Association results for Sensor 1 and Sensor 3 incorporating global resizing

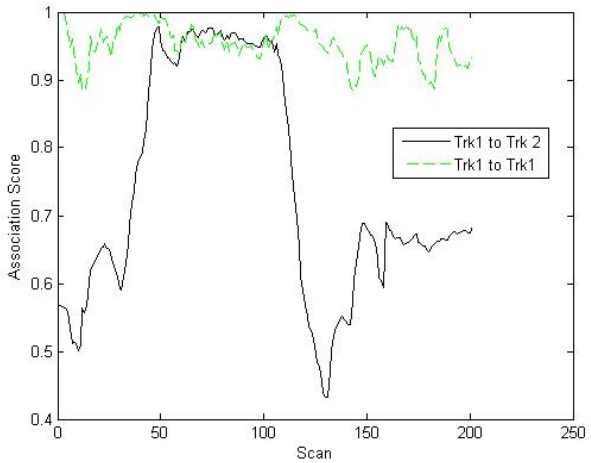

Figure 14. Association results for Sensor 1 and Sensor 3 incorporating phase modification based uncertainty

REFERENCES

[1] D. Hall, & J. Llinas, The Handbook of Multisensor Data Fusion, CRC Press: Boca Raton, 2001.

[2] S. Blackman and R. Popoli, Design and Analysis of Modern Tracking Systems, Artech House: Norwood, 1999.

[3] C.J. Stanek, B. Javidi, and P.Yanni, "Performance assessment of frequency plane filters applied to track association and sensor registration," Proc. of SPIE, Vol. 5094, Orlando, April 2003, pp. 323-328.

[4] A.B. Poore and A. J. Robertson III, "A new Lagrangian relaxation based algorithm for a class of multidimensional assignment problems," Computational Optimization and Applications, vol. 8, 1997, pp. 129-150.

[5] S. C. Stubberud and K. A. Kramer, "Phase vs. amplitude: analysis of optically-based correlation for track association," Proceedings of the IEEE International Conference of Systems Engineering: Coventry, Sepember 2009, pp. 429-433.

[6] S. C. Stubberud and K. A. Kramer, "Effects of measurement unobservability on neural extended Kalman filter tracking," Proc. of SPIE, vol. 7336, Signal Processing, Sensor Fusion, and Target Recognition XVIII: Orlando, April 2010, pp. 733605.1-15.

[7] Stubberud, S. C., Kramer, K. (2006). Data Association for Multiple Sensor Types Using Fuzzy Logic. *IEEE Transactions on Instrumentation and Measurement, 55*(6), 2292-2303.

[8] S.C.Stubberud and K.A. Kramer, Target data association using a fuzzy-logic based approach," in Sensor and Data Fusion, I-Tech: Vienna, 2009, pp. 35-56.

[9] Symmetric phase only filtering, NASA webpage: http://www.grc.nasa.gov/WWW/OptInstr/Wernet_Web/ SPOF.html, 2005, accessed February 2011.

[10] B.V.K.V. Kumar, A. Mahalanobis, and R.D. Juday, Correlation Pattern Recognition, Cambridge University Press: Cambridge, 2005.

[11] S. Blackman, Multiple-target tracking with radar applications, Artech House: Norwood, 1986.

2011 IEEE International Conference on Fuzzy Systems
June 27-30, 2011, Taipei, Taiwan

A Non-Singleton Interval Type-2 Fuzzy Logic System for Universal Image Noise Removal using Quantum-Behaved Particle Swarm Optimization

Daoyuan Zhai, Minshen Hao, Jerry M. Mendel
Signal and Image Processing Institute
Ming Hsieh Department of Electrical Engineering
University of Southern California
Los Angeles, CA, 90089-2564, USA
daoyuanzhai@gmail.com, minshenhao@gmail.com, mendel@sipi.usc.edu

***Abstract*—Removing Mixed Gaussian and Impulse Noise (MGIN) is considered to be very important in the domain of image restoration, but it is a somewhat more challenging topic than removing pure Gaussian or impulse noise. Therefore, relatively fewer works have been published in this area. This paper proposes a Non-Singleton Interval Type-2 (IT2) Fuzzy Logic System (FLS) for MGIN removal, explains how it can be designed based on a Quantum-behaved Particle Swarm Optimization algorithm, and shows that it provides both quantitatively and visually much better results compared to other often-used non-fuzzy techniques as well as its Type-1 and singleton IT2 counterparts.**

I. Introduction

Noises introduced into digital images during acquisition and/or transmission stages can be adequately modeled by either Additive Gaussian White Noise (AGWN), impulse noise, or Mixed Gaussian and Impulse Noise (MGIN) [28], [51].

AWGN, which is inadvertently introduced to an image during its acquisition stage, can be modeled as adding to each image pixel a value from a zero-mean Gaussian distribution. An ideal filter for removing AWGN would be able to smooth pixels within a distinct local region of an image without reducing the sharpness of the edges of that region. A Gaussian filter, which is a linear filter, can smooth noise out very efficiently; but, it does this at the price of significant edge blurring. To overcome this drawback, some nonlinear filters have been proposed [50], [64] that focus on using local measures of an image to detect the edges and smooth them less than other parts of the image.

Impulse noise, generally caused by transmission errors, can be modeled by randomly replacing a portion of the pixels with random pixels, while leaving the remaining pixels unchanged. The filters specifically developed for AWGN removal do not work well on impulse noise, because these filters consider the impulse noise pixels as edges, and preserve them. Different kinds of filters that aim at removing impulse noise have therefore been proposed, and were summarized by Yildirim et al. [74] as follows: 1) standard median filter [24], [65], which replaces the center pixel of a filtering window with the median value of all pixels in that window, has decent performance in terms of noise removal, but it also blurs image details like thin lines even at a low noise level; 2) modified versions of the median filter, e.g., weighted and center-weighted median filters [37], [75], [76], which give more weights to certain pixels in the filtering window, gain improved performance in terms of preserving image details at the cost of reduced noise removal capability; 3) approaches based on impulse detectors, which aim at deciding whether the center pixel of the filtering window has been corrupted by noise or not, e.g., [2], [7]–[12], [15], [19], [26], [36], [53], [59], [60], [63], [67], [72], [77], [80], [83]; 4) other mean-filter-based approaches [1], [29], [42] also exhibited good performance, but at the price of high computational expenses; 5) many different approaches based on soft computing methodologies [6], [13], [49], [55], [56], [58], [66], [74], [79], along with a number of nonlinear filters [39], [54], [57], [61], [68], [71], [78] that integrate the desired features of some of the aforementioned filters.

MGIN often occurs when an already corrupted image is transmitted over a noisy communication channel [25], [51]; and, is modeled by first adding AWGN and then impulse noise into the images. The study of MGIN removal is considered to be more general and challenging than that of pure AWGN or impulse noise removal; therefore, relatively fewer works have been published in this area, e.g., 1) Ma et al. developed a Structure-Adaptive Hybrid Vector Filter (SAHVF) [43] that employs a quad-tree decomposition to assess activities in different regions of the image, in order to choose a noise removal filter among a set of *ad hoc* approaches such as Peer Group Filter (PGF) [35], Adaptive Nearest Neighbor Filter (ANNF) [52], and Structure Weighted Average Filter (SWAF); 2) Garnett et al. [25] introduced a Rank Order Absolute Differences (ROAD) method that first focuses on impulse detection, and then uses a bilateral Gaussian filter to suppress noise; 3) Yang and Wu [73] first use an Impulse Proportion Adaptive Median Filter (IPAMF) to remove impulse noise, and then a Block-Matching 3-Dimensional (BM3D) DCT filter [16] to clean up AWGN.

Two types of criteria are often used to evaluate the performances of noise removal filters: quantitative measures, such as Mean Square Error (MSE) and Peak Signal-Noise Ratio

978-1-4244-7316-8/11/$26.00 ©2011 IEEE

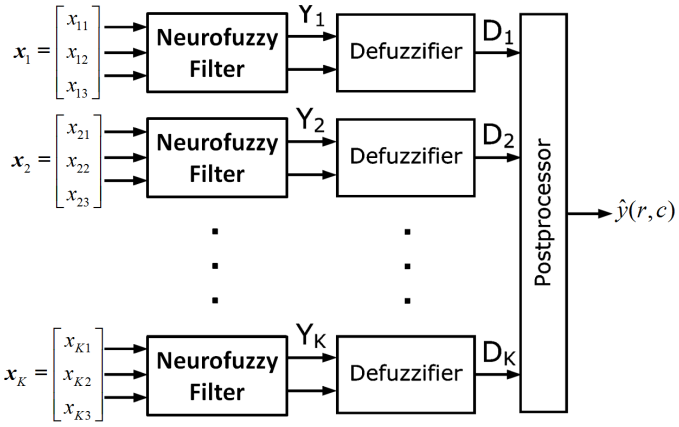

Fig. 1. Overview of the complete IT2 FLS composed by K neurofuzzy filters [74].

(PSNR), and visual quality of the restored image. It is generally very difficult for a filter to produce both quantitatively excellent and visually satisfactory outputs. Regarding MGIN removal, Yang and Wu's IPAMF+BM3D approach yields the best results from a visual quality perspective; while in the domain of pure impulse noise removal, an approach based on Interval Type-2 (IT2) TSK Fuzzy Logic System (FLS) [45], recently introduced by Yildirim et al. [74], has significantly exceeded all other filters in terms of quantitative measures.

Based on the framework proposed by Yildirim et al. [74], this paper develops a Non-Singleton (NS) IT2 FLS[1] [45], uses it jointly with the BM3D DCT filter, and shows that this new approach, referred to in the sequel as NS-IT2+BM3D, enables the highly corrupted images in MGIN environment to achieve excellent visual quality and exceptionally good quantitative results.

The rest of the paper is organized as follows: Section II presents the overview of the complete FLS, the detailed structure of its building blocks, namely, the neurofuzzy filters, and how a training image set can be generated and used by a Quantum-behaved Particle Swarm Optimization (QPSO) algorithm to find the "optimal" set of design parameters for each neurofuzzy filter; Section III demonstrates the improved performance of our NS-IT2 FLS by comparing it against several other techniques as well as its T1 and singleton IT2 counterparts; Section IV draws conclusions for the paper.

II. Noise Removal based on Fuzzy Logic System

A. Neurofuzzy filters

Our complete IT2 FLS has the general structure as depicted in Fig. 1. It is composed of K neurofuzzy filters, each of which can be viewed as a sub-FLS, and has the same structure,

[1]Compared to Singleton FLSs, NS FLSs allow users to account for the uncertainties associated with the input measurements. Note that NS FLSs based on Gradient Descend Methods have been well studied in [45], but were never widely applied due to their extremely complicated gradient formulas. This paper shows how Quantum-behaved Particle Swarm Optimization algorithm enables designers to achieve "optimal" NS IT2-FLSs without having to derive the gradient formulas.

$x(r-1,c-1)$	$x(r-1,c)$	$x(r-1,c+1)$
$x(r,c-1)$	$x(r,c)$	$x(r,c+1)$
$x(r+1,c-1)$	$x(r+1,c)$	$x(r+1,c+1)$

Fig. 2. Filtering window for neurofuzzy filters, where r and c are the indices of rows and columns, respectively, e.g., $x(r,c)$ is the luminance value of the pixel located at row r and column c [74].

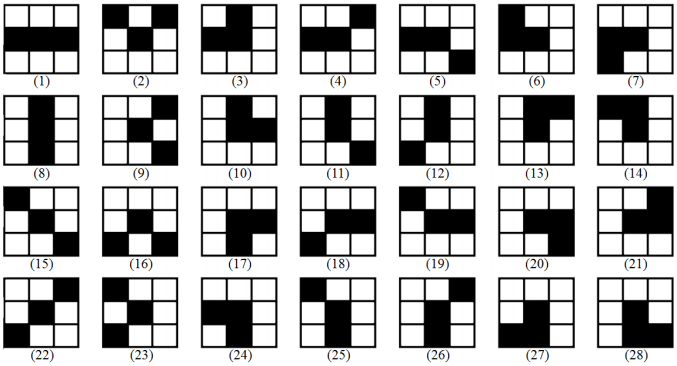

Fig. 3. 28 possible pixel topologies for the neurofuzzy filters [74].

i.e., the same number of antecedents, the same number of rules, and so on; but each uses a different input data set obtained from the given noisy image, and, therefore, has different design parameters. Each data set is obtained by shifting a 3×3 filtering window (see Fig. 2) through all pixels (excluding boundary pixels) in the image. Each time the window centers at a pixel, three of the nine pixels in the filtering window are selected to form an input vector, $\boldsymbol{x}_i = [x_{i1} \;\; x_{i2} \;\; x_{i3}]^T \; (i = 1, \ldots, K)$, for the i^{th} neurofuzzy filter.

Observe, in Fig. 3, that there are a total of 28 possible combinations of any three pixels in a filtering window, i.e., there can be at most $K = 28$ neurofuzzy filters. To give a specific example, assume we are focusing on the 7^{th} neurofuzzy filter that corresponds to pixel topology (7) in Fig. 3, and assume that the filtering window is centered at the pixel located at row r and column c (see Fig. 2), then the input vector for this neurofuzzy filter at this location is $\boldsymbol{x}_7 = [x_{71} \;\; x_{72} \;\; x_{73}]^T = [x(r+1,c-1) \;\; x(r,c-1) \;\; x(r,c)]^T$. The output of this neurofuzzy filter is an interval of numbers of the noise-free luminance value at location (r,c), $Y_7(r,c) = [\underline{y}_7(r,c), \bar{y}_7(r,c)]$. How the neurofuzzy filter actually obtains such an interval of numbers is described in details in Section II-B. A point-value for pixel (r,c), $D_7(r,c)$, is then computed, as:

$$D_7(r,c) = \frac{\underline{y}_7(r,c) + \bar{y}_7(r,c)}{2} \tag{1}$$

Similar operations are carried out by all other neurofuzzy filters, each using an input vector obtained based on the corresponding pixel topology. This leads to K defuzzified values, $D_1(r,c), D_2(r,c), \ldots, D_K(r,c)$. A post-processor block takes these defuzzified values and performs the following

computations to obtain the final estimation, $\hat{y}(r,c)$, of the noise-free luminance value at location (r,c):

$$D_{AV}(r,c) = \frac{1}{K}\sum_{i=1}^{K} D_i(r,c) \tag{2}$$

$$\hat{y}(r,c) = \begin{cases} 0 & \text{if } D_{AV}(r,c) < 0 \\ 255 & \text{if } D_{AV}(r,c) > 255 \\ \text{round}[D_{AV}(r,c)] & \text{otherwise} \end{cases} \tag{3}$$

It is worth of mentioning that all the neurofuzzy filters can be computed in parallel to save computation time.

B. Non-singleton Interval Type-2 Fuzzy Logic System

1) Structure: Type-2 (T2) FSs [46], [47], [81] have been shown to be more capable of modeling uncertainties than are T1 FSs. As a special case of T2 FSs, IT2 FSs have been widely used in FLS design for various applications [3], [4], [20], [44], [48]. On the other hand, a Non-Singleton (NS) FLS [45] allows users to take into consideration the uncertainties embedded in the input measurements, and gives the users more degree of design freedom by modeling input values as FSs instead of crisp numbers.

In this paper, we build each of the neurofuzzy filters mentioned in Section II-A as a T1 NS IT2 FLS, where the input values are modeled as T1 FSs[2]. Without loss of generality, assume we are focusing on the i^{th} $(i = 1, 2, \ldots, K)$ neurofuzzy filter, and want to use it to obtain an interval estimation, $Y_i(r,c)$, of the pixel value at location (r,c). Recall that the input vector is $\boldsymbol{x}_i = [x_{i1}\ \ x_{i2}\ \ x_{i3}]$, which is obtained by collecting three pixel values in the filtering window based on the corresponding topology. Our proposed NS IT2 FLS is based on N rules that take the following forms:

Rule 1: IF $\tilde{X}_{i1}$ is $\tilde{F}_{i1}^1$ and $\tilde{X}_{i2}$ is $\tilde{F}_{i2}^1$ and $\tilde{X}_{i3}$ is $\tilde{F}_{i3}^1$
THEN y_i is $\tilde{G}_i^1$

$\cdots$

Rule N: IF $\tilde{X}_{i1}$ is $\tilde{F}_{i1}^N$ and $\tilde{X}_{i2}$ is $\tilde{F}_{i2}^N$ and $\tilde{X}_{i3}$ is $\tilde{F}_{i3}^N$
THEN y_i is $\tilde{G}_i^N$

where the consequent of each rule, $\tilde{G}_i^k$ $(k = 1, \cdots, N)$, is an IT2 FS whose centroid [33], [45] is the interval $[y_{il}^k, y_{ir}^k]$; and each antecedent, $\tilde{F}_{ij}^k$ $(j = 1, 2, 3$ and $k = 1, \cdots, N)$, is an IT2 FS described by a *Lower Membership Function* (LMF) and an *Upper Membership Function* (UMF) that have the following forms, respectively $(u \in X)$:

$$\underline{\mu}_{ij}^k(u) = \begin{cases} N(\overline{m}_{ij}^k, \sigma_{ij}^k; u) & \text{if } u \le \frac{\underline{m}_{ij}^k + \overline{m}_{ij}^k}{2} \\ N(\underline{m}_{ij}^k, \sigma_{ij}^k; u) & \text{if } u > \frac{\underline{m}_{ij}^k + \overline{m}_{ij}^k}{2} \end{cases} \tag{4}$$

[2]The input values can be further modeled as IT2 FSs, which will give the system even more degrees of design freedom, and has the potential to gain additional improvements for the performance. Since this paper is the first attempt to develop a NS IT2 FLS in the domain of image processing, and only has limited space, we only focus on the T1 NS IT2 FLS here, and will study the IT2 NS IT2 FLS in the future.

$$\overline{\mu}_{ij}^k(u) = \begin{cases} N(\underline{m}_{ij}^k, \sigma_{ij}^k; u) & \text{if } u < \underline{m}_{ij}^k \\ 1 & \text{if } \underline{m}_{ij}^k \le u \le \overline{m}_{ij}^k \\ N(\overline{m}_{ij}^k, \sigma_{ij}^k; u) & \text{if } u > \overline{m}_{ij}^k \end{cases} \tag{5}$$

where, e.g., $N(\underline{m}_{ij}^k, \sigma_{ij}^k; u) = \exp[-\frac{1}{2}(u - \underline{m}_{ij}^k/\sigma_{ij}^k)^2]$. Examples of the three antecedent IT2 FSs of the k^{th} rule are depicted by the gray areas in Fig. 4, that are called *Footprints Of Uncertainty* (FOU).

The input T1 FS, $\tilde{X}_{ij}$ $(j = 1, 2, 3)$, for the corresponding antecedent has the following MF $(u \in X)$:

$$\mu_{ij}^k(u) = N(x_{ij}, \sigma_{\tilde{X}_{ij}}^k; u) \tag{6}$$

where the mean of the MF is the actual crisp input value x_{ij}. Examples of the three input T1 FSs are depicted by the dotted lines in Fig. 4.

2) Inference Engine: Details regarding the above rule-based inference system can be found in [45], Chapter 11. This section briefly reviews all the necessary steps of the computations.

First, the firing interval for every antecedent in each rule, $[\underline{f}_{ij}^k, \overline{f}_{ij}^k]$ $(j = 1, 2, 3$ and $k = 1, 2, \ldots, N)$, needs to be computed, where $\underline{f}_{ij}^k$ $(\overline{f}_{ij}^k)$ corresponds to the maximum value of the fuzzy intersections between the LMF (UMF) of $\tilde{F}_{ij}^k$ and the MF of X_{ij}, respectively:

$$\underline{f}_{ij}^k = \max_{u \in X} \left\{ \min \left[\underline{\mu}_{ij}^k(u), \mu_{ij}^k(u) \right] \right\} \tag{7}$$

$$\overline{f}_{ij}^k = \max_{u \in X} \left\{ \min \left[\overline{\mu}_{ij}^k(u), \mu_{ij}^k(u) \right] \right\} \tag{8}$$

An example of the fuzzy intersections between $\underline{\mu}_{ij}^k(u)$ $[\overline{\mu}_{ij}^k(u)]$ and μ_{ij}^k for the k^{th} rule are depicted by the heavy dashed (solid) lines in Fig. 4, where the corresponding $\underline{f}_{ij}^k$ and $\overline{f}_{ij}^k$ values are also labeled.

Once the firing interval of each antecedent becomes available, the firing interval for each rule, $[f_{il}^k, f_{ir}^k]$ $(k = 1, 2, \cdots, N)$, is obtained as follows:

$$f_{il}^k = \min_{j \in \{1,2,3\}} \underline{f}_{ij}^k \tag{9}$$

$$f_{ir}^k = \min_{j \in \{1,2,3\}} \overline{f}_{ij}^k \tag{10}$$

Finally, the Karnik-Mendel (KM) algorithm [33], [45] or the Enhanced KM (EKM) algorithm [69] is used to compute the following two values:

$$\underline{y}_i(r,c) = \min_{f^k \in [f_{il}^k, f_{ir}^k]} \frac{\sum_{k=1}^N f^k y_{il}^k}{\sum_{k=1}^N f^k} \tag{11}$$

$$\overline{y}_i(r,c) = \max_{f^k \in [f_{il}^k, f_{ir}^k]} \frac{\sum_{k=1}^N f^k y_{ir}^k}{\sum_{k=1}^N f^k} \tag{12}$$

which are the desired outputs of the i^{th} neurofuzzy filter, namely, $Y_i(r,c)$ at location (r,c).

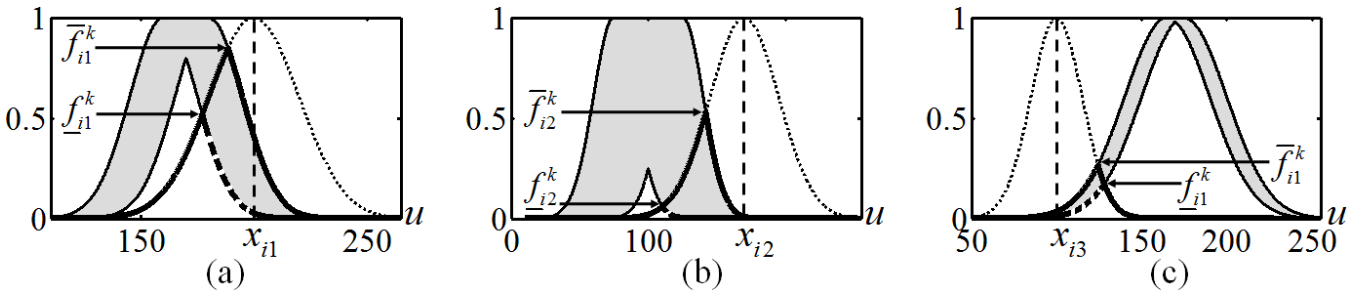

Fig. 4. An example of the LMFs and UMFs, $\underline{\mu}_{ij}^k(u)$ and $\overline{\mu}_{ij}^k(u)$, of the three antecedent IT2 FSs, $\tilde{F}_{ij}^k$ $(j = 1, 2, 3)$; the MFs, $\mu_{ij}^k(u)$, of the corresponding input T1 FSs , $\tilde{X}_{ij}$ $(j = 1, 2, 3)$; and, the fuzzy intersections between $\underline{\mu}_{ij}^k(u)$ $[\overline{\mu}_{ij}^k(u)]$ and μ_{ij}^k $(j = 1, 2, 3)$, where (a) $j = 1$; (b) $j = 2$; (c) $j = 3$.

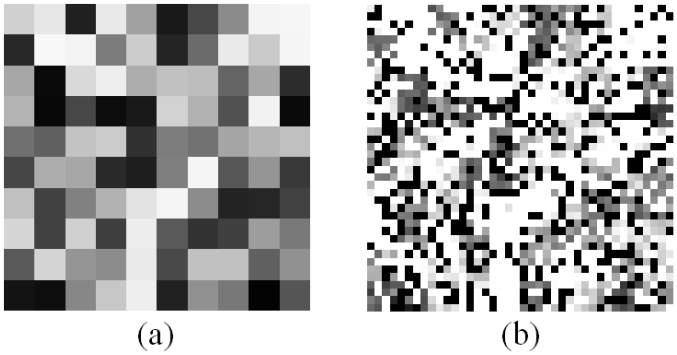

Fig. 5. Training image set: (a) original image, and (b) image corrupted by 30% AWGN and 50% impulse noise.

For the above i^{th} sub-system, each antecedent IT2 FS has three parameters, $\underline{m}_{ij}^k$, $\overline{m}_{ij}^k$ and σ_{ij}^k, each input T1 FS has one parameter, $\sigma_{\tilde{X}_{ij}}^k$, and each consequent has two parameters, y_{il}^k and y_{ir}^k; therefore, there are $3 \times (3 + 1) + 2 = 14$ parameters for each rule. We chose the number of rules[3] to be $N = 3^3 = 27$; consequently, the total number of parameters of each neurofuzzy filter is $N \times 14 = 378$.

C. Training Image Set

The training image set, which is used to tune the parameters of the neurofuzzy filters, consists of an original clean image and its corrupted version, and is artificially generated by a computer. The original image, depicted in Fig. 5(a), is 40×40 pixels and is divided into $10 \times 10 = 100$ boxes, i.e., each box contains $4 \times 4 = 16$ pixels. Pixels in each box have the same luminance value, an 8-bit integer uniformly distributed between 0 and 255.

The corrupted image was obtained by adding MGIN to the original one. The noise level was carefully chosen because it has important impact on the performance of the entire system. After extensive simulations, we used 30% AWGN and 50% impulse noise to contaminate the clean image, and depict the corrupted output in Fig. 5(b).

[3] N is chosen based on extensive simulations, where we tried to find an "optimal" number that provided satisfactory results and yet did not consume too much computation time.

To train the i^{th} neurofuzzy filter, the filtering window shifted through all pixel locations (excluding the boundary pixels), i.e., $r = 2, 3, \ldots, R-1$ and $c = 2, 3, \ldots, C-1$, where R and C are the total number of rows and columns of the pixels in the given image; and a set of input vectors, $\boldsymbol{x}_i$, is collected. Then the rule-based inference system produce a set of $D_i(r, c)$ values ($r = 2, 3, \ldots, R-1$ and $c = 2, 3, \ldots, C-1$), which can be viewed as the i^{th} neurofuzzy filter's estimation of the original pixel values at corresponding locations. Note that all the neurofuzzy filters were trained independently; therefore, the post-processer block was not involved in this stage. The "optimal" set of design parameters is obtained by optimizing the Mean Square Error (MSE) of the estimated pixel values:

$$MSE = \frac{1}{(R-2)(C-2)} \sum_{r=2}^{R-1} \sum_{c=2}^{C-1} [D_i(r, c) - y(r, c)]^2 \quad (13)$$

where $y(r, c)$ is the original noise-free pixel value at (r, c).

Comment: A reviewer of this paper suggested that it is not very clear whether different images would need different training images. In response, we want to point out that only one training image set (as shown in Fig. 5) is needed to obtain a NS IT2 FLS that is universally applicable to all different images.■

D. Particle Swarm Optimization

Different techniques can be employed to tune the parameters of the above neurofuzzy filters (NS IT2 FLSs), e.g., *gradient-based* methods [5], [21] proposed by Liang and Mendel [40], [45]. The analytical forms of the gradients of such a NS IT2 FLS that has this many parameters and nonlinear computations are quite complicated, making the computer implementation very difficult. In fact, this has been the main reason that has prevented NS T2 FLSs from becoming widely used. Also, the performance of the system can suffer significantly if the solution quickly falls into a local minimum, which can easily occur when gradient-based methods are used.

In recent years, *population-based random optimization* techniques, such as *Particle Swarm Optimization* (PSO) [34], *Genetic Algorithm* (GA) [27] and *evolutionary programming* (EP) [22], have been widely applied to T1 FLS designs [14], [18], [23], [30]–[32], [41]. In this paper, we utilize the PSO

algorithm, because it is computationally fast, is the easiest to implement; and, as will be seen in Section III, it enables our system to provide very good results.

1) Quick Review: The standard PSO algorithm, first introduced by Kennedy and Eberhart [34], is briefly reviewed in this section[4].

Let M denote the swarm (population) size, where each particle in the swarm represents a possible solution to the optimization problem; n denote the dimensionality of the search space; and, G denote the total number of generations (iterations) of the optimization process.

Each particle i ($i = 1, 2, \ldots, M$) has three inherent attributes: 1) a current position $\underline{X}_i = (X_{i,1}, X_{i,2}, \ldots, X_{i,n})$ in the search space; 2) a current velocity $\underline{V}_i = (V_{i,1}, V_{i,2}, \ldots, V_{i,n})$; and 3) a personal best (*pbest*) position (the position that produces the minimal value in the history of the particle) $\underline{P}_i = (P_{i,1}, P_{i,2}, \ldots, P_{i,n})$, i.e.:

$$\underline{P}_i(t+1) = \begin{cases} \underline{P}_i(t) & \text{if } f_{obj}(\underline{X}_i(t+1)) \geq f(\underline{P}_i(t)) \\ \underline{X}_i(t+1) & \text{if } f_{obj}(\underline{X}_i(t+1)) < f(\underline{P}_i(t)) \end{cases} \tag{14}$$

where $t = 1, 2, \ldots, G-1$ is the index of generation.

In each generation, each particle updates its velocity as follows ($j = 1, 2, \ldots, n$; $i = 1, 2, \ldots, M$):

$$V_{i,j}(t+1) = w \cdot V_{i,j}(t) + c_1 \cdot r_{1,i}(t)[P_{i,j}(t) - X_{i,j}(t)] + c_2 \cdot r_{2,i}(t)[P_{g,j}(t) - X_{i,j}(t)] \tag{15}$$

where, e.g., $X_{i,j}(t)$ is the j^{th} element of position of the i^{th} particle in the t^{th} generation; c_1 and c_2 are two constants called *acceleration coefficients*; $r_{1,i}(t)$ and $r_{2,i}(t)$ are two random variables uniformly distributed in the interval $[0, 1]$; w is called *inertia weight* that is usually set to decrease linearly from 0.9 to 0.4 during the course of the search process to help PSO reach convergence; and, $\underline{P}_g(t)$ denotes the global best (*gbest*) position found in the history of the entire swarm, i.e. ($i = 1, 2, \ldots, M$):

$$\underline{P}_g(t) = \arg\min_{\underline{P}_i(t)} f_{obj}(\underline{P}_i(t)) \tag{16}$$

At the end of each generation, a new position of a particle can be obtained, as:

$$\underline{X}_i(t+1) = \underline{X}_i(t) + \underline{V}_i(t) \tag{17}$$

2) Quantum-Behaved Particle Swarm Optimization: Despite its exceptionally good performance on many different problems, Van den Bergh [17] has shown that the PSO algorithm does not guarantee global optimization; therefore, ever since its debut in 1995, many variations and modifications of the PSO algorithm have been proposed to enhance its performance [38], [62], [82].

Recently, Sun et al [62], [70] proposed a Quantum-behaved PSO (QPSO) algorithm that, theoretically, guarantees optimal solution in the search space, and, they have shown that, in practice, the QPSO algorithm indeed provides better results for many widely-used benchmark tests than does the standard PSO algorithm. Therefore, this particular version of the PSO algorithm is our choice. Its pseudo-code is [70]:

initialize $\underline{X}_i(1)$ ($i = 1, \ldots, M$) randomly[5]
set $\underline{P}_i(1) = \underline{X}_i(1)$ ($i = 1, \ldots, M$)
for $t = 1$ to $G - 1$ **do**
  calculate $\underline{m}(t) = \frac{1}{M} \sum_{i=1}^{M} \underline{P}_i(t)$
  $\underline{P}_g(t) = \arg\min f_{obj}(\underline{P}_i(t))$
  for $i = 1$ to M **do**
    if $f(\underline{X}_i(t)) < f(\underline{P}_i(t))$ **then**
      $\underline{P}_i(t) = \underline{X}_i(t)$
    end if
    for $j = 1$ to n **do**
      η =rand(0,1)
      $\underline{P}_{i,j}(t+1) = \eta \times \underline{P}_{i,j}(t) + (1-\eta) \times \underline{P}_{g,j}(t)$
      u =rand(0,1)
      if rand(0,1)> 0.5 **then**
        $\underline{X}_{i,j}(t+1) = \underline{P}_{i,j}(t+1) - \beta |m_j(t) - \underline{X}_{i,j}(t)| \ln \frac{1}{u}$
      else
        $\underline{X}_{i,j}(t+1) = \underline{P}_{i,j}(t+1) + \beta |m_j(t) - \underline{X}_{i,j}(t)| \ln \frac{1}{u}$
      end if
    end for
  end for
end for

It can be seen that the QPSO algorithm differs from the PSO algorithm mainly in two ways: 1) instead of using (14), the best personal position of each particle is updated by taking a weighted average of its previous best personal and the global positions:

$$\underline{P}_{i,j}(t+1) = \eta \times \underline{P}_{i,j}(t) + (1-\eta) \times \underline{P}_{g,j}(t) \tag{18}$$

where η is a random variable uniformly distributed in $(0, 1]$; and 2) instead of using (17), the location of each particle is updated as:

$$\underline{X}_{i,j}(t+1) = \underline{P}_{i,j}(t+1) \pm \beta |m_j(t) - \underline{X}_{i,j}(t)| \ln \frac{1}{u} \tag{19}$$

where $m(t)$ is the average best personal positions of the entire swarm and u is also a random variable uniformly distributed in $(0, 1]$. Note that (19) was developed based on the solution of the Schrödinger equation, which is why the algorithm has the prefix "Quantum-behaved".

III. Benchmark Testing

Four widely used benchmark images (see Fig. 6) were chosen to test the performance of the above NS-IT2 FLS in comparison to median filter, Wiener filter, Gaussian filter, ROAD [25], and IPAMF+BM [73]. We also tested the T1 and singleton-IT2 counterparts of the proposed NS-IT2 FLS, as

[4]Please distinguish the notations and labeling in this section from those in the previous section, as they are completely independent and denote different things here.

[5]$\underline{X}_i(1)$ ($i = 1, 2, \ldots, M$) are randomly initialized, because extensive simulations [62] have shown that the initial values of the locations have little impact on the convergence of the QPSO algorithm.

TABLE I
MSEs OF DIFFERENT APPROACHES FOR THE FOUR BENCHMARK IMAGES (BABOON, PENTAGON, BOAT, AND BRIDGE) CORRUPTED BY 30% AWGN AND 30%, 50%, AND 70% IMPULSE NOISE, RESPECTIVELY

Approach	Baboon			Pentagon			Boat			Bridge		
	30%	50%	70%	30%	50%	70%	30%	50%	70%	30%	50%	70%
Median Filter	5943.3	7173.5	10269	6163.7	7241.8	9933.5	6042.5	7231.7	10330	5934.5	7260.2	10682
Wiener Filter	4015.6	3358.7	3221.9	4026.1	2962.0	2376.2	4271.4	3531.3	3303.8	4861.2	4468.2	4401.1
Gaussian Filter	5321.1	5942.5	6902.4	5445.4	5605.1	6058.1	5676.3	6167.6	7003.4	6152.7	6899.4	7934.6
ROAD	3085.3	4210.3	5378.9	3285.7	4898.9	5571.4	2844.0	3928.6	4965.4	2878.8	3935.2	4953.4
IPAMF+BM3D	5953.0	6720.1	9461.9	6575.0	7542.3	9214.9	6069.0	6753.1	8591.7	5991.6	8096.1	11506
T1 FLS	1936.6	2213.8	2571.6	1850.7	1800.4	1813.6	2124.6	2383.2	2779.2	2817.3	3338.4	4006.4
Singleton IT2	1699.0	2062.8	2498.5	1433.5	1503.3	1600.0	1874.0	2214.4	2637.5	2479.2	3055.4	3737.2
NS IT2	1633.7	2041.7	2547.7	1242.3	1335.5	1502.8	1778.8	2124.1	2565.6	2481.9	3013.3	3595.0
T1+BM3D	1698.7	1747.2	1916.3	1493.7	1257.4	1121.4	1742.9	1810.5	2066.0	2512.0	2844.1	3343.1
Singleton-IT2+BM3D	1391.1	1541.9	1819.1	1013.4	916.49	889.19	1431.6	1594.9	1902.5	2125.9	2510.9	3045.7
NS-IT2+BM3D	1362.2	1532.1	1847.1	854.63	757.72	771.88	1367.1	1518.1	1816.2	2157.4	2473.0	2885.8

an effort to see whether modeling the inputs as FSs is indeed helpful. Three different levels of MGIN were generated for the test: 30% AWGN with 30%, 50%, and 70% impulse noise, respectively[6].

The MSEs of the above techniques for the four images under different noise levels are summarized in Table I, where one can observe that, quantitatively, the fuzzy logic family (T1, singleton-IT2, and NS-IT2 FLSs) significantly out-performed the other techniques. In addition, after extensive simulations, it was found that the performance of the fuzzy logic family can be greatly enhanced when used jointly the with BM3D[7] DCT filter [16], which is a fast way to remove the residual AWGN after the FLS process. The MSEs of such joint approaches between fuzzy logic family and BM3D are also given in Table I, where one can observe that the NS-IT2+BM3D approach generally out-performs other techniques and its T1 and singleton-IT2 counterparts, with noticeable improvements, except in two cases, image "Baboon" with 70% impulse noise

[6]Due to page limit, we only tested a limited number of different noise levels; therefore, it remains as an open issue how much noise must be present before the NS IT2 FLS provides a significant improvement over the singleton IT2 FLS.

[7]The implementations of the BM3D filter has been generously made available online by its authors [16]. But since it is just a complement to our technique and is not the focus of this paper, the details of BM3D are not provided here.

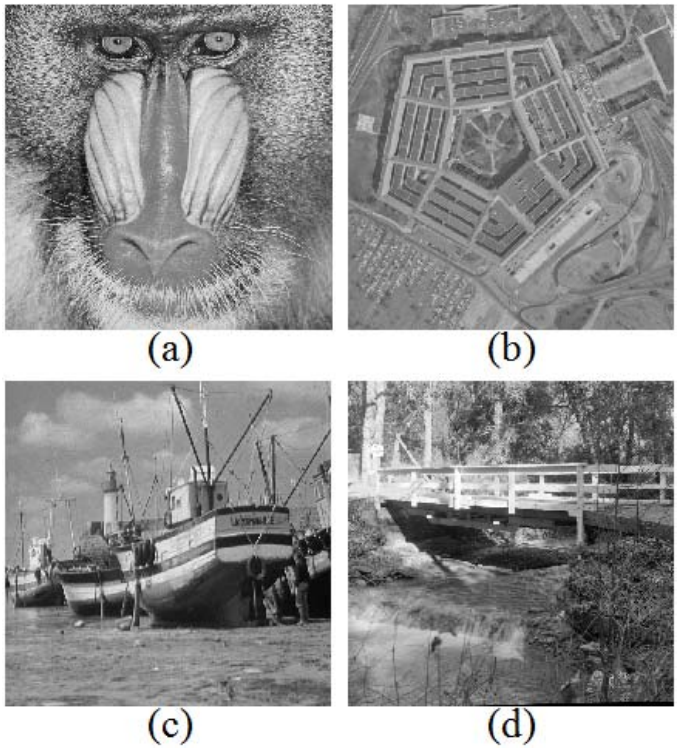

Fig. 6. Four benchmark test images: (a) baboon; (b) pentagon; (c) boat; (d) bridge.

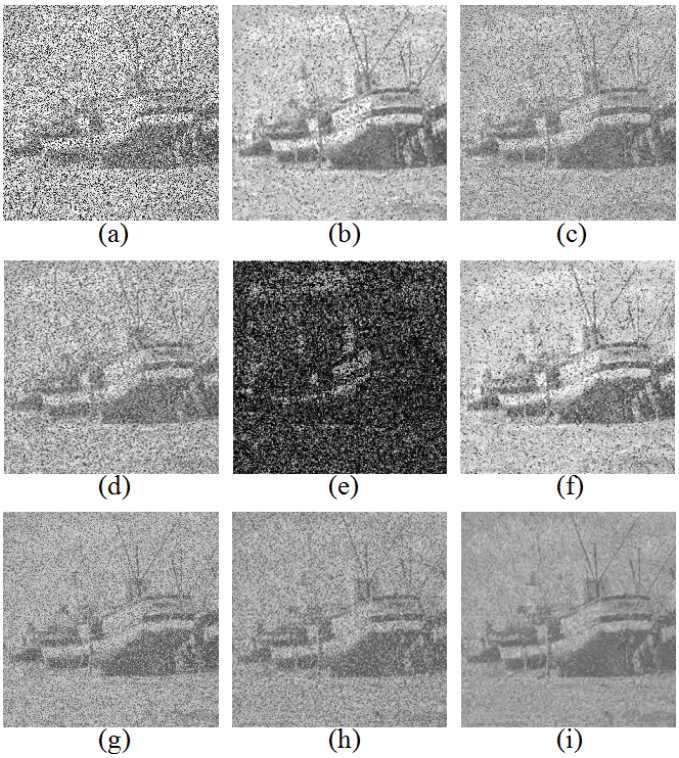

Fig. 7. (a) Image "boat" corrupted by 30% AWGN and 50% impulse noise; and its restored versions based on (b) median filter; (c) Wiener filter; (d) Gaussian filter; (e) ROAD; (f) IPAMF+BM3D; (g) T1+BM3D; (h) singleton-IT2+BM3D; (i) NS-IT2+BM3D

TABLE II
AVERAGE MSES OF THE FOUR BENCHMARK IMAGES FOR DIFFERENT APPROACHES UNDER 30% AWGN AND 30%, 50%, AND 70% IMPULSE NOISE, RESPECTIVELY

	30%	50%	70%
Median Filter	6021.0	7226.8	10303
Wiener Filter	4293.6	3580.1	3325.8
Gaussian Filter	5648.9	6153.7	6974.6
ROAD	3023.5	4243.3	5217.3
IPAMF+BM3D	6147.2	7277.9	9693.6
T1 FLS	2182.3	2434.0	2792.7
Singleton IT2	1871.4	2209.0	2618.3
NS IT2	1784.2	2128.7	2552.8
T1+BM3D	1861.8	1914.8	2111.7
Singleton-IT2+BM3D	1490.5	1641.0	1914.1
NS-IT2+BM3D	1435.4	1570.2	1830.2

and "Bridge" with 30% impulse noise, where the singleton-IT2+BM3D has slightly better results. To give an overview of these results, the average MSEs of the four images are summarized in Table II, where we can observe that the NS-IT2+BM3D always out-performs other techniques in terms quantitative measures.

Fig. 7 presents the image "boat" corrupted by 30% AWGN and 50% impulse noise and its restored versions based on the above techniques. Observe that the NS-IT2+BM3D appear to give the best visual restoration. Similar results were obtained for other images and under other noise levels.

IV. CONCLUSION

This paper presented a NS-IT2 FLS framework for removing MGIN from digital images. Using only one set of artificially generated training images, the design parameters of the system were tuned by a QPSO algorithm which allowed us to avoid using complex gradient-descent methods. The paper showed that the proposed technique yields both quantitatively and visually much better results compared to several widely-used non-fuzzy noise removal filters. Also, by introducing more degrees of design freedom into the system, the NS-IT2 FLS has also been shown to out-perform its T1 and singleton-IT2 counterparts.

REFERENCES

[1] E. Abreu, M. Lightstone, S. K. Mitra, and K. Arakawa. A new efficient approach for the removal of impulse noise from highly corrupted images. *IEEE Trans. on Image Processing*, 5(6):1012–1025, June 1996.

[2] I. Aizenberg, C. Butakoff, and D. Paily. Impulsive noise removal using threshold Boolean filtering based on the impulse detecting functions. *IEEE Signal Processing Letter*, 12(1):63–66, 2005.

[3] L. Astudillo, O. Castillo, and L. T. Aguilar. Intelligent control for a perturbed autonomous wheeled mobile robot: a type-2 fuzzy logic approach. *Journal of Nonlinear Studies*, 14(3):37–48, 2007.

[4] P. Baguley, T. Page, V. Koliza, and P. Maropoulos. Time to market prediction using type-2 fuzzy sets. *Journal of Manufacturing Technology Management*, 17(4):513–520, 2006.

[5] D. Bertsekas. *Nonlinear Programming*. Athena Scientific, Belmont, Massachusetts, second edition, 1999.

[6] E. Besdok, P. Çivicio glu, and M. Alçi. Impulsive noise suppression from highly corrupted images by using resilient neural networks. *Lecture Notes in Computer Science*, 3070:670–675, 2004.

[7] E. Besdok and M. E. Yüksel. Impulsive noise rejection from images with jarque-berra test based median filter. *International Journal of Electronics and Communications*, 59(2):105–109, 2005.

[8] R. H. Chan, C. Hu, and M. Nikolova. An iterative procedure for removing random-valued impulse noise. *IEEE Signal Processing Letter*, 11(12):921–924, 2004.

[9] J. Y. Chang and J. L. Chen. Classifier augmented median filter for image restoration. *IEEE Trans. on Instrumentation and Measurement*, 53(2):351–356, 2004.

[10] T. Chen, K. K. Ma, and L. H. Chen. Tri-state median filter for image denoising. *IEEE Trans. on Image Processing*, 8(12):1834–1838, 1999.

[11] T. Chen and H. R. Wu. Adaptive impulse detection using center-weighted median filters. *IEEE Signal Processing Letter*, 8(1):1–3, 2001.

[12] T. Chen and H. R. Wu. Space variant median filters for the restoration of impulse noise corrupted images. *IEEE Trans. on Circuits and Systems*, 48(8):784–789, 2001.

[13] Y. S. Choi and R. Krishnapuram. A robust approach to image enhancement based on fuzzy logic. *IEEE Transactions on Image Processing*, 6(6):808–825, June 1997.

[14] O. Cordon, F. Gomide, F. Herrera, F. Hoffmann, and L. Magdalena. Ten years of genetic fuzzy systems: current framework and new trends. *Fuzzy Sets and Systems*, 141(1):5–31, 2003.

[15] V. Crnojevic, V. Senk, and Z. Trpovski. Advanced impulse detection based on pixel-wise MAD. *IEEE Signal Processing Letter*, 11(7):589–592, 2004.

[16] K. Dabov, A. Foi, V. Katkovnik, and K. Egiazarian. Image denoising by sparse 3D transform-domain collaborative filtering. *IEEE Trans. on Image Processing*, 16(8):2080–2095, August 2007.

[17] F. Van den Bergh. *An analysis of particle swarm optimizer*. PhD thesis, University of Pretoria, Pretoria, South Africa, 2001.

[18] L. dos Santos Coelho and B. M. Herrera. Fuzzy identification based on a chaotic particle swarm optimization approach applied to a nonlinear yo-yo motion system. *IEEE Trans. on Industrial Electronics*, 54(6):3234–3245, 2007.

[19] H.-L. Eng and K.-K. Ma. Noise adaptive soft-switching median filter. *IEEE Trans. on Image Processing*, 10(2):242–251, February 2001.

[20] H. Rhee F. C. Uncertainty fuzzy clustering: insights and recommendations. *IEEE Computational Intelligence Magazine*, 2(1):44–56, 2007.

[21] R. Fletcher. *Practical Methods of Optimization*. Wiley, Hoboken, New Jersey, second edition, 2000.

[22] L. J. Fogel. Evolutionary programming in perspective: the top-down view. In J. M. Zurada, R. J. Marks II, and C. J. Robinson, editors, *Computational Intelligence: Imitating Life*. IEEE Press, Piscadaway, NJ, 1994.

[23] A. Fowler, A. M. Teredesai, and M. De Cock. An evolved fuzzy logic system for fire size prediction. In *Proc. of The 28th North American Fuzzy Information Processing Society Annual Conference (NAFIPS 2009)*, pages 1–6, Cincinnati, OH, 2009.

[24] M. Gabbouj, E. J. Coyle, and N. C. Gallager. An overview of median and stack filtering. *Circuits, Systems, and Signal Processing*, 11(1):7–45, 1992.

[25] R. Garnett, T. Huegerich, and C. Chui. A universal noise removal algorithm with an impulse detector. *IEEE Transactions on Image Processing*, 14(11):1747–1754, November 2005.

[26] R. Garnett, T. Huegerich, C. Chui, and W. He. A universal noise removal algorithm with an impulse detector. *IEEE Trans. on Image Processing*, 14(11):105–109, 2005.

[27] D. E. Goldberg. *Genetic Algorithms in search Optimization and Machine Learning*. Addison-Wesley, Reading, Massachusetts, 1989.

[28] R. Gonzalez and R. E. Woods. *Digital Image Processing*. Prentice Hall, Upper Saddle River, New Jersey, third edition, 2007.

[29] W. Y. Han and J. C. Lin. Minimum-maximum exclusive mean filter to remove impulse noise from highly corrupted images. *Electronic Letters*, 33(2):124–125, 1997.

[30] F. Hoffmann. Evolutionary algorithms for fuzzy control system design. *Proceedings of the IEEE*, 89(9):1318–1333, 2001.

[31] C. F. Juang. A tsk-type recurrent fuzzy network for dynamic systems processing by neural network and genetic algorithms. *IEEE Trans. on Fuzzy Systems*, 10(2):155–170, 2002.

[32] C. F. Juang, C. M. Hsiao, and C. H. Hsu. Hierarchical cluster-based multispecies particle-swarm optimization for fuzzy-system optimization. *IEEE Trans. on Fuzzy Systems*, 18(1):14–26, 2010.

[33] N. N. Karnik and J. M. Mendel. Centroid of a type-2 fuzzy set. *Information Sciences*, 132:195–220, 2001.

[34] J. Kennedy and R. Eberhart. Paticle swarm optimization. In *Proceedings of IEEE International Conference on Neural Networks*, pages 1942–1948, Perth, WA , Australia, 1995.

[35] C. Kenney, Y. Deng, B. S. Manjunath, and G. Hewer. Peer group image enhancement. *IEEE Transactions on Image Processing*, 6(2):326–334, February 2001.

[36] V. V. Khryashchev, I. V. Apalkov, A. L. Priorov, and P. S. Zovanarev. Image denoising using adaptive switching median filter. In *IEEE Internation Conference on Image Processing*, pages 117–120, Genoa, Italy, 2005.

[37] S. J. Ko and Y. H. Lee. Center weighted median filters and their applications to image enhacement. *IEEE Trans. on Circuits and Systems*, 38(9):984–993, 1991.

[38] R. A. Krohling and L. dos Santos Coelho. Coevolutionary particle swarm optimization using gaussian distribution for solving constrained optimization problems. *IEEE Trans. on Systems, Man, and Cybernetics, Part B: Cybernetics*, 36(6):1407–1416, 2006.

[39] C.-S. Lee, Y.-H. Kuo, and P.-T. Yu. Weighted fuzzy mean filter for image processing. *Fuzzy Sets and Systems*, 89(2):157–180, 1999.

[40] Q. Liang and J. M. Mendel. Interval type-2 fuzzy logic systems: Theory and design. *IEEE Trans. on Fuzzy Systems*, 8:535–550, 2000.

[41] B. D. Liu, C. Y. Chen, and J. Y. Tsao. Design of adaptive fuzzy logic controller based on linguistic-hedge concepts and genetic algorithms. *IEEE Trans. on Systems, Man, and Cybernetics, Part B: Cybernetics*, 31(1):32–53, 2001.

[42] W. Luo. An efficient detail-preserving approach for removing impulse noise in images. *IEEE Signal Processing Letters*, 13(7):413–416, July 2006.

[43] Z. Ma, H. R. Wu, and B. Qiu. An robust structure adaptive hybrid vector filter for color image restoration. *IEEE Transactions on Image Processing*, 14(12):1900–2001, December 2005.

[44] P. Melin, J. Urias, D. Solano, M. Soto, M. Lopez, and O. Castillo. Voice recognition with neural networks, type-2 fuzzy logic and genetic theory. *Information Sciences*, 13(2):108–116, 2006.

[45] J. M. Mendel. *Uncertain Rule-Based Fuzzy Logic Systems: Introduction and New Directions*. Prentice-Hall, Upper Saddle River, NJ, 2001.

[46] J. M. Mendel and R. I. John. Type-2 fuzzy sets made simple. *IEEE Trans. on Fuzzy Systems*, 10(2):117–127, 2002.

[47] J. M. Mendel, F. Liu, and D. Zhai. Alpha-plane representation for type-2 fuzzy sets: theory and applications. *IEEE Trans. on Fuzzy Systems*, 17(5):1189–1207, 2009.

[48] J. M. Mendel and D. Wu. *Perceptual Computing: Aiding People in Making Subjective Judgements*. Wiley-IEEE Press, Hoboken, New Jersey, 2010.

[49] S. Morillas, V. Gregori, G. Peris-Fajarne, and P. Latorre. A fast impulsive noise color image filter using fuzzy metrics. *Real-Time Imaging*, 11(5):417–428, 2005.

[50] P. Perona and J. Malik. Scale-space and edge detection using anisotropic diffusion. *IEEE Trans. on Pattern Analysis and Machine Intelligence*, 12(5):629–639, May 1990.

[51] K. N. Plataniotis and A. N. Venetsanopoulos. *Color Image Processing and Applications*. Springer, Heidelberg, Germany, first edition, 2000.

[52] K. N. Plataniotis, S. Vinayagamoorthy, D. Androutsos, and A. N. Venetsanopoulos. An adaptive nearest neighbor multichannel filter. *IEEE Transactions on Circuits and Systems for Video Technology*, 6(6):699–703, December 1996.

[53] G. Pok, Y. Liu, and A. S. Nair. Selective removal of impulse noise based on homogeneity level information. *IEEE Trans. on Image Processing*, 12(1):85–92, 2003.

[54] S. M. M. Rahman and M. K. Hasan. Wavelet-domain iterative center weighted median filter for image denoising. *Signal Processing*, 83(5):1001–1012, 2003.

[55] F. Russo. Fire operators for image processing. *Fuzzy Sets and Systems*, 103(2):265–275, 1999.

[56] F. Russo. Noise removal from image data using recursive neuro-fuzzy filters. *IEEE Transactions on Instrumentation and Measurement*, 49(2):307–314, April 2000.

[57] F. Russo. Impulse noise cancellation in image data using a two-output nonlinear filter. *Measurement*, 36:205–213, 2004.

[58] F. Russo and G. Ramponi. A fuzzy filter for image corrupted by impulse noise. *IEEE Signal Processing Letters*, 3(6):168–170, June 1996.

[59] S. Schulte, M. Nachtegael, V. De Witte, D. Van der Weken, and E. E. Kerre. A fuzzy impulse noise detection and reduction method. *IEEE Trans. on Image Processing*, 15(5):1153–1162, May 2006.

[60] B. Smolka and A. Chydzinski. Fast detection and impulsive noise removal in color images. *Journal of Real-Time Image Processing*, 11(4):389–402, 2005.

[61] B. Smolka, K. N. Plataniotis, A. Chydzinski, M. Szczepanski, A. N. Venetsanopulos, and K. Wojciechowski. Self-adaptive algorithm of impulsive noise reduction in color images. *Pattern Recognition*, 35(8):1771–1784, 2002.

[62] J. Sun, W. B. Xu, and B. Feng. A global search strategy of quantum-behaved particle swarm optimization. In *Proc. of 2004 IEEE Conference on Cybernetics and Intelligent Systems*, pages 111–116, 2004.

[63] T. Sun and Y. Neuvo. Detail-preserving median based filters in image processing. *Pattern Recognition Letter*, 15(4):341–347, 1994.

[64] C. Tomasi and R. Manduchi. Bilateral filtering for gray and color images. In *Proc. of IEEE International Conference on Computer Vision*, Bombay, India, 1998.

[65] S. E. Umbaugh. *Computer Vision and Image Processing: A Practical Approach using CVIPTools*. Prentice Hall, Upper Saddle River, NJ, 1998.

[66] D. Van De Ville, M. Nachtegael, D. Van der Weken, E. E. Kerre, W. Philips, and I. Lemahieu. Noise reduction by fuzzy image filtering. *IEEE Transactions on Fuzzy Systems*, 11(4):429–436, August 2003.

[67] Z. Wang and D. Zhang. Progressive switching median filter for the removal of impulse noise from highly corrupted images. *IEEE Trans. on Circuits and Systems*, 46(1):78–80, 1999.

[68] P. S. Windyga. Fast impulsive noise removal. *IEEE Transactions on Image Processing*, 10(1):173–179, 2001.

[69] D. Wu and J. M. Mendel. Enhanced Karnik - Mendel algorithms. *Information Sciences*, 17(4):923–934, 2009.

[70] M. Xi, J. Sun, and W. Xu. An improved quantum-behaved particle swarm optimization algorithm with weighted mean best position. *Applied Mathematics and Computation*, 205:751–759, 2008.

[71] H. Xu, G. Zhu, H. Peng, and D. Wang. Adaptive fuzzy switching filter for images corrupted by impulse noise. *Pattern Recognization Letters*, 25(15):1657–1663, November 2004.

[72] N. Yamashita, M. Ogura, J. Lu, H. Sekiya, and T. Yahagia. Random valued impulse noise detector using level detection. In *IEEE International Symposium on Circuits and Systems*, pages 6292–6295, Kobe, Japan, 2005.

[73] J.-X. Yang and H.-R. Wu. Mixed Gaussian and uniform impulse noise analysis using robust estimation for digital images. In *16th International Conference on Digital Signal Processing*, pages 1–5, Santorini-Hellas, 2009.

[74] M. T. Yildirim, A. Bastürk, and M. E. Yüksel. Impulse noise removal from digital images by a detail-preserving filter based on type-2 fuzzy logic. *IEEE Transactions on Fuzzy Systems*, 16(4):920–928, 2008.

[75] L. Yin, R. Yang, M. Gabbouj, and Y. Neuvo. Weighted median filters: A tutorial. *IEEE Trans. on Circuits and Systems II*, 43(3):157–192, 1996.

[76] O. Yli-Harja, J. Astola, and Y. Neuvo. Analysis of the properties of median and weighted median filters using threshold logic and stack filter representation. *IEEE Trans. on Signal Processing*, 39(2):395–410, 1991.

[77] S. Q. Yuan and Y. H. Tan. Impulse noise removal by a global-local noise detector and adaptive median filter. *Signal Processing*, 86(8):2123–2128, 2006.

[78] M. E. Yüksel. A hybrid neuro-fuzzy filter for edge preserving restoration of images corrupted by impulse noise. *IEEE Trans. on Image Processing*, 15(4):928–936, April 2006.

[79] M. E. Yüksel and A. Bastürk. Efficient removal of impulse noise from highly corrupted digital images by a simple neuro-fuzzy operator. *International Journal of Electronics and Communications*, 57(3):214–219, 2003.

[80] M. E. Yüksel and E. Besdok. A simple neuro-fuzzy impulse detector for efficient blur reduction of impulse noise removal operators for digital images. *IEEE Trans. on Fuzzy Systems*, 12(6):854–865, December 2004.

[81] D. Zhai and J. M. Mendel. Uncertainty measures for general type-2 fuzzy sets. *Information Sciences*, In Press.

[82] Z. H. Zhan, J Zhang, Y. Li, and H. S.-H. Chung. Adaptive particle swarm optimization. *IEEE Trans. on Systems, Man, and Cybernetics, Part B: Cybernetics*, 39(6):1362–1381, 2009.

[83] S. Zhang and M. A. Karim. A new impulse detector for switching median filters. *IEEE Signal Processing Letter*, 9(11):360–363, 2002.

2011 IEEE International Conference on Fuzzy Systems
June 27-30, 2011, Taipei, Taiwan

Fuzzy Folksonomy-based Index Creation for e-Learning Content Retrieval on Cloud Computing Environments

Wen-Chung Shih
Department of Applied Informatics and Multimedia, Asia University
Taichung, 41354, Taiwan
wjshih@asia.edu.tw

Chao-Tung Yang
Department of Computer Science
Tunghai University
Taichung, 40704, Taiwan
ctyang@thu.edu.tw

Shian-Shyong Tseng*
Department of Applied Informatics and Multimedia, Asia University
Taichung, 41354, Taiwan
sstseng@asia.edu.tw

***Abstract*—Due to the trend of individualization and adaptation of e-Learning, more and more SCORM-compliant teaching materials are developed by institutes and individuals in different sites. Also, cloud computing environments are emerging as powerful infrastructures to support e-Learning applications. Therefore, how to rapidly retrieve SCORM-compliant documents on cloud computing environments has become an important issue. Creating an index from folksonomies has been investigated in previous researches; however, the involved uncertainty has not been addressed. This paper focuses on the fuzzy index creation problem for learning content retrieval. A bottom-up approach to constructing the fuzzy index is proposed. The index creation method has been implemented, and a synthetic learning object repository has been built on a Hadoop cloud platform to evaluate the proposed approach. Experimental results show that this method can increase precision of retrieval.**

Keywords- Folksonomy; Fuzzy Sets; Information retrieval; e-Learning; Cloud computing

I. INTRODUCTION

Due to the advances in information technologies and the requirements of courseware, more and more teachers are able and willing to design their own teaching materials and make them accessible on the Web [1-3]. In addition, a growing number of large-scale projects aim to construct learning content repositories [4, 5]. For example, in 2002, the National Science Council of Taiwan approved a resolution on the "National Science and Technology Program for e-Learning," planning to spend $120 million within a five-year period [6]. These educational contents are mainly based on Sharable Content Object Reference Model (SCORM) [7], which has become a popular standard for creating sharable and reusable teaching materials for e-Learning. With the popularization of e-Learning, how to find and reuse these existing materials becomes an important issue.

Cloud computing systems [8, 9] are transparent resource-sharing infrastructures, which can overcome the limitations in traditional e-Learning platforms, such as scalability, interoperability, availability, etc. Also, Cloud computing technologies provide possibilities for supporting innovative applications of e-Learning. For example, a medical college can provide students with three-dimensional simulation of human body anatomy using high performance cloud computing systems, which is beyond the ability of traditional e-Learning platforms. Therefore, more and more effort has gone into the field of e-Learning cloud, using cloud technologies in the context of e-Learning.

With the promising development of e-Learning cloud, there will be a great demand to find desired teaching materials from multiple repositories in the e-Learning cloud. A traditional approach is to implement a meta-search engine on top of these distributed repositories [10]. When the meta-search engine receives a query, it distributes the query to the local repositories, and then collects the returned results and presents them to users. However, this traditional approach doesn't consider characteristics of SCORM and cloud computing to speed up the retrieval process. For example, SCORM-compliant documents are associated with nine categories of metadata. When processing a query with a restrictive filter, such as "documents about insects," the meta-searching approach will search the whole databases.

We classify the schemes of content retrieval into static and dynamic ones according to the adaptability of the retrieved results. For static CR, the retrieved result only depends on the query, independent of users and contexts. Dynamic CR can be further divided into personalized, context-aware and other schemes, according to the factors that are considered by the adaptive mechanisms of CR. To support context-aware CR, the teaching materials stored in the repositories have to be organized according to their contextual information, in order for efficient retrieval. However, it is almost impossible to request experts to annotate all these contents with suitable context-aware metadata. Therefore, content annotation based on folksonomies and automatic techniques in a collaborative way is a promising solution.

In well-known folksonomy applications, such as del.icio.us (http://del.icio.us/), Flickr (http://www.flickr.com), etc., folksonomies are organized into a flat structure, which consists of several catagories named by user-defined tags. This flat organization is suitable for users to manage their preferences. However, when the size of repositories gets larger and larger, a hierarchical organization becomes a better choice to organize the contents. To bridge the gap of the two structures, we formulate this index creation problem and

978-1-4244-7316-8/11/$26.00 ©2011 IEEE

propose a bottom-up approach to constructing an index from existing folksonomies according to the similarity between tags, which considers metadata and structural information of the teaching materials annotated by the tags [11]. Furthermore, creating an index from folksonomies often involves uncertainty. For example, which tags are associated with which categories. Therefore, a fuzzy representation is proposed to address this issue. The index creation method has been implemented, and a synthetic learning object repository has been built to evaluate the proposed approach. Experimental results show that this method can increase precision of retrieval.

The contributions can be summarized as follows. First of all, we propose a fuzzy folksonomy-based method for index creation, which can reduce the effort required in subsequent work of location-aware content retrieval. With this method, the heavy burden of experts for manually developing concept hierarchy can be significantly alleviated. Second, a similarity function is proposed to increase the precision of folksonomy fusion, which considers more characteristics of learning contents, including metadata and structural information of the teaching materials annotated by the tags. Next, a self-organizing mechanism can designed to balance the number of documents annotated by the tags, which can increase the performance of indexing structures. Finally, the proposed method is implemented and the built index is evaluated. Experimental results reveal that this method can improve the performance of retrieval.

The rest of this work is organized as follows. In Section II, we review the preliminaries and previous work on related researches. Then, the problem is formulated in Section III. Next, the method of index creation is described in Section IV. Section V illustrates experimental results. Finally, the concluding remarks are given in Section VI.

II. PRELIMINARIES AND RELATED WORK

In this section, we review previous research related to this work. First, the SCORM model is introduced. Then, methods of information retrieval are described. Finally, we review methods of ontology building, which is related to index creation.

A. Sharable Content Object Reference Model (SCORM)

To share and reuse teaching materials, several standards have been proposed recently. Among these, SCORM (http://www.adlnet.org/) is the most popular standard for learning contents. It was proposed by the U.S. Department of Defense's Advanced Distributed Learning (ADL) organization in 1997. This standard consists of several specifications developed by IEEE LTSC (Learning Technology Standards Committee, http://ltsc.ieee.org/wg12/), IMS (Instructional Management System, http://www.imsproject.org/), AICC (Aviation Industry CBT Committee, http://www.aicc.org/), etc. The SCORM specifications are a composite of several specifications developed by international standards organizations. In a nutshell, SCORM is a set of specifications for developing, packaging and delivering high-quality education and training materials whenever and wherever they are needed [12, 13]. In SCORM, content packaging scheme is proposed to package the learning objects into standard teaching materials. The content packaging scheme defines a teaching materials package consisting of four components: 1) Metadata, which describes the characteristics or attributes of this learning content; 2) Organizations, which describe the structure of the teaching material; 3) Resources, which denote the physical files linked by each learning object within the teaching material; and 4) the (Sub) Manifest, which describes this teaching material, consisting of itself and other teaching materials. SCORM Metadata refers to the IEEE's Learning Object Metadata (LOM), and describes the attributes of teaching materials. IEEE LOM v1.0 includes nine categories: General, LifeCycle, Meta-Metadata, technical, educational, rights, relation, annotation, and classification.

Su et al. proposed a level-wise approach to SCORM content management [14]. In this two-phase scheme, structural information is considered. Also, both general and specific Learning Objects can be retrieved according to requests of users. However, the design of this structure doesn't consider its usability in ubiquitous learning environments.

There have been numerous studies on Structured Document Retrieval [15, 16]. Researches showed that structured searching can increase precision. Previous work mainly addresses XML and SGML documents. Besides, XML Query Languages, such as XIRQL, XQL, etc., were proposed. However, intra-document structural modeling is not suitable for SCORM-compliant documents.

B. Search Engine Technologies

Inverted file indexing has been widely used in information retrieval [17-20]. An inverted file is used for indexing a document collection to speed up the searching process. The structure of an inverted file consists of two components: the vocabulary and the posting list. The vocabulary is composed of all distinct terms in the document collection. For each term, a list of all the documents containing this term is stored. The set of all these lists is called the posting list. However, the structure of a document is not considered in this model.

Storage requirements of inverted indices [21] have been evaluated based on B+-tree and posting list. Five strategies of the index term replication were discussed. This approach is extended to analyze the storage requirement of the proposed approach in this proposal. In [22], 11 different implementations of ranking-based text retrieval systems using inverted indices were presented, and their time complexities were also investigated.

The meta-search approach has been studied in the context of distributed information retrieval [10]. This approach consists of Query Distribution and Result Merging phases. Furthermore, the Document Retrieval problem is divided into two sub-problems: Database Selection problem and Document Selection problem. However, Distributed indexing is not suitable for common cloud architectures. Also, distributed information retrieval is less efficient in searching.

The use of ontologies to overcome the limitations of keyword-based search has been put forward as one of the motivations of the Semantic Web since its emergence in the late 1990s. One way to view a semantic search engine is as a tool that gets formal ontology-based queries from a client,

executes them against a knowledge base, and returns tuples of ontology values that satisfy the query. In this view, the information retrieval problem is reduced to a data retrieval task. While this conception of semantic search brings key advantages already, our work aims at taking a step beyond.

A purely Boolean ontology-based retrieval model makes sense when the whole information corpus can be fully represented as an ontology-driven knowledge base. But, there are well-known limits to the extent to which knowledge can be formalized this way. Boolean search does not provide clear ranking criteria, without which the search system may become useless if the retrieval space is too big.

C. Ontology Building Approaches

We review ontology building approaches because its construction process is similar to index creation in concept. Traditionally, ontology building mainly depends on the contribution of domain experts in the knowledge creation activity. Metadata extraction and merging is carried out manually by domain experts. Many tools have been developed for ontology developers to access ontologies, browse them, edit them, and propose modifications. However, some drawbacks do exist. This process is time-consuming and arduously. For this reason, recent researches turned to automatic and semiautomatic (as opposed to manually) ontology construction and maintenance. Automatic techniques for building and integrating ontologies have been studied for many years by the artificial intelligence community. More recently, several techniques specifically aimed at learning ontologies from text corpora or database repositories were proposed. Well-known research approaches to ontology building include [23]:

- Dictionary-based approach [24]: constructs the hierarchy of concepts based on a traditional dictionary, which presents the related concepts of words, including synonyms, etymology, etc.
- Conceptual clustering [25]: Concepts are grouped according to a semantic distance between each other to generate hierarchical relations.
- Association rules mining [26]: The frequency of an association of terms is computed in the text repositories. If the frequency of the association is close to the occurrence of individual terms, the association is transformed in an ontological relation.
- Formal concept analysis [23]: is a method for representation, analysis and management of data and knowledge. It can be used to build a hierarchy of terms and associated relations.

In [8], a fuzzy ontology extraction algorithm was proposed for adaptive e-learning. Folksonomies have not been widely applied to the subject of index creation. Although folksonomies are not formal models for knowledge representation, the collaborative wisdom of resource categorization can be a good start point from which effective indices can be built.

III. Problem Formulation

Before the index creation problem is described, some concepts and models are introduced. First, a level-wise structural model of learning contents is presented, which is intended to model the semantic features of different levels of a structural learning content.

Definition. Content Package (CP)

A Content Package represents a structural learning content, such as a SCORM-compliant teaching material. It is a rooted tree. The leaf node represents textual content, which is characterized by a feature vector = $<w_1, w_2, \ldots, w_n>$, where n is the size of the vocabulary and the weighting scheme is the widely used TF-IDF (Term Frequency – Inverse Document Frequency) [17, 19]. Internal nodes represent structural information of this teaching material. Each Content Package is associated with two types of attributes:

- Level j feature vector, L_j, $(0 < j < Height)$

where L_j = Average of feature vectors of nodes at level j, and Height is the height of the rooted tree;

- Metadata, $\{M_k \mid k = 1 \text{ to } m, m \text{ is the number of metadata}\}$.

A folksonomy is a user generated taxonomy used to categorize and retrieve web content such as Web pages, photographs and Web links, using user-defined labels called tags. Typically, a folksonomy has a flat structure, which consists of several user-defined categories. The folksonomic tagging is intended to make a body of information increasingly easy to search, discover, and navigate over time. One well-known website using folksonomic tagging is del.icio.us. In this work, fuzzy folksonomies are modeled as follows. The proposed model is based on Zadeh's theory of fuzzy sets [27].

Definition. Fuzzy Folksonomy

A fuzzy folksonomy defined by a user is a triple of (T, I, R), where T is a fuzzy set of tags, I is a fuzzy set of content packages and R is a fuzzy relation on $T \times I$. We say that tag t is related to a content package i if i is annotated by t. Each tag is associated with two types of attributes, which are derived from content packages annotated by this tag.

- Level j feature vector, L_j, $(0 < j < Height)$

where L_j = the average of the level j feature vectors of content packages annotated by the tag, and *Height* is the height of the rooted tree;

- Metadata, $\{M_k \mid k = 1 \text{ to } m, m \text{ is the number of metadata}\}$

where the value of M_k is defined by the most frequent M_k value of the content packages annotated by the tag.

The following example illustrates this definition. Figure 1 depicts two folksonomies defined by users A and B, respectively. The folksonomy of user A can be represented by

$T = \{t_1, t_2\}$

$I = \{i_1, i_2, i_3, i_4\}$

$R = \{(t_1, i_1), (t_1, t_2), (t_1, i_3), (t_2, i_1), (t_2, i_4)\}$

where i_1, i_2, i_3 and i_4 are content packages.

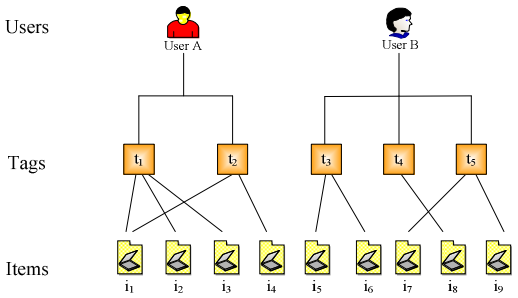

Figure 1. The folksonomy of user A

In the field of computer science, ontology is a data model that represents a set of concepts within a domain and the relationships between those concepts. It is used to understand the objects within that domain. However, there has not been a commonly acceptable definition for ontologies. The following definitions describe ontology-like indices referred to in this paper. First, the relations, general and specific, are stated.

Definition. General

A tag *a* is more general than a tag *b* if the set of teaching materials annotated by *a* includes those annotated by *b*.

Next, we define the index.

Definition. Index

An index is considered to be a rooted tree. The nodes represent concepts in the domain, and the edges represent relations between nodes. A parent node *p* is more general than its child node *c*. Each node is associated with a feature vector, which characterizes the semantic meaning of this concept.

Based on the definitions above, the index creation problem is stated as follows.

Definition. The Fuzzy Folksonomy-based Index Creation Problem (FICP)

Given a collection of content packages and corresponding folksonomies, generate an index. The objective is to improve performance of learning content retrieval.

IV. FUZZY FOLKSONOMY-BASED INDEX CREATION

Our idea to solve the FICP problem is based on the heuristic that existing folksonomies generated by users can be a good starting point from which to construct a location-aware index. While most folksonomies are organized into flat structures, we plan to build hierarchical indices to better organize the learning content. To bridge the gap of the two structures, folksonomies and indices, we propose a bottom-up approach to construct an index from existing folksonomies according to the similarity between tags, which considers metadata and structural information of the teaching materials annotated by the tags.

We design an algorithm to merge two folksonomies into one which is used for subsequent information retrieval. The idea is to make decisions of tag merging according to the similarity of the two tags. The main difficulty is how to choose a suitable similarity function for SCORM-compliant teaching materials, which are characterized by textual content, metadata and structural information. Here, a similarity measure for two tags, *a* and *b*, is proposed:

$$Sim(a,b) = (1-\beta)\sum_{i=0}^{Height}\alpha_i \times Sim_i(a,b) + \beta \times Sim_M(a,b) \quad (1)$$

where the sum of $_i$ is equal to one, and 0< <1. The parameter, $_i$, is used to adjust the weighting of level-wise content vector. The parameter is used to adjust the weighting of metadata similarity. The similarity function consists of two parts:

- Sim_i: level i similarity function, which is *cosine* function, 0< i < *Height*. The similarity between two vectors $v_k = <k_1, k_2, \ldots, k_{|V|}>$ and $v_p = <p_1, p_2, \ldots, p_{|V|}>$ is measured by the following formula:

$$sim_i = \frac{\sum_{i=1}^{|V|} k_i \times p_i}{\sqrt{\sum_{i=1}^{|V|} k_i^2} \times \sqrt{\sum_{i=1}^{|V|} p_i^2}} \quad (2)$$

- Sim_M: Metadata similarity function, which is (the number of matched attributes) / (the number of all attributes).

The Folksonomy-based Index Creation Algorithm consists of two steps: initializing the master folksonomy and iteratively merging tags of the other folksonomy into the master folksonomy, listed as follows.

Algorithm. Fuzzy Folksonomy-based Index Creation Algorithm (AlgFFIC)

Input:

F_1, F_2: the two folksonomies to be merged
Th_sim: the threshold for comparing similarity
sim: the similarity function

Output:

F: the merged folksonomy

Step 1. Initialization
  1.1 Each tag of F_1 and F_2 is represented by the average of its related teaching materials.
  1.2 F_1 is assigned as the Master folksonomy, M.
Step 2. for each tag t in F_2
  2.1 calculate the similarity of t and each tag of M.
  2.2 let *t_close* be the closest tag in M to t.
  2.3 if the *sim*(t, *t_close*) > *Th_sim* then
      add the tag t into *t_close*
    else
      add tag t into M as a new tag

Step 1 of the ***AlgFFIC*** algorithm evaluates attributes of the input folksonomies. Also, one of the input folksonomy is assigned as the Master folksonomy, which serves as the base for other tags to join. Next, tags of the other folksonomy are merged into the Master folksonomy one after another in Step 2. Finally, a merged folksonomy is generated.

In Step 2.3, a threshold, *Th_sim*, is set to decide whether to merge the tag or construct a new tag. When the similarity is greater than the threshold, the two tags are merged. Otherwise, a new tag is constructed in the master folksonomy for the dissimilar tag from the other folksonomy.

V. IMPLEMENTATION

In this experiment, we have implemented a cloud portal for query submission and results presentation. In addition, results are shown with estimated transmission time. The corpus is composed of synthetic SCORM-compliant documents. The experiments investigate searching performance in terms of query processing time.

A. Prototype Design

A folksonomy-based information retrieval system is implemented to evaluate the proposed method, as shown in Figure 2. The objective is to increase precision by folksonomy-based semantic search, and to reduce search time by folksonomy-based indexing. The phase of constructing a concept hierarchy is based on the proposed method, in order to alleviate the heavy burden of experts and knowledge engineers. This framework consists of three phases. In the concept hierarchy construction phase, users' folksonomies are merged into a hierarchy, which can be referred by the index creation phase. A bottom-up method is designed to organize teaching materials located in different repositories, according to the generated index. A global index is then created to facilitate semantic search. Finally, users' queries are submitted in the search phase, and desired teaching materials are retrieved fast and precisely.

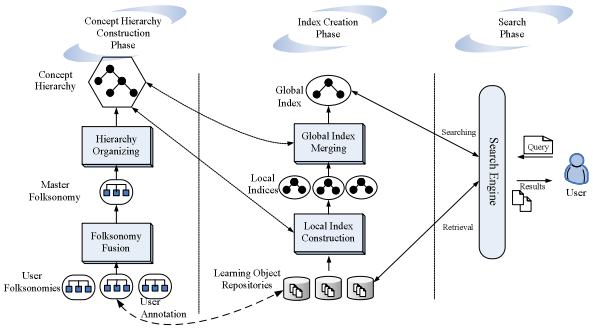

Figure 2. The overview of a folksonomy-based information retrieval system

A Cloud computing test-bed has been built by the High Performance Computing Lab. of Tunghai University, Taichung, Taiwan, using Hadoop. The summary of the nodes is shown in Figure 3.

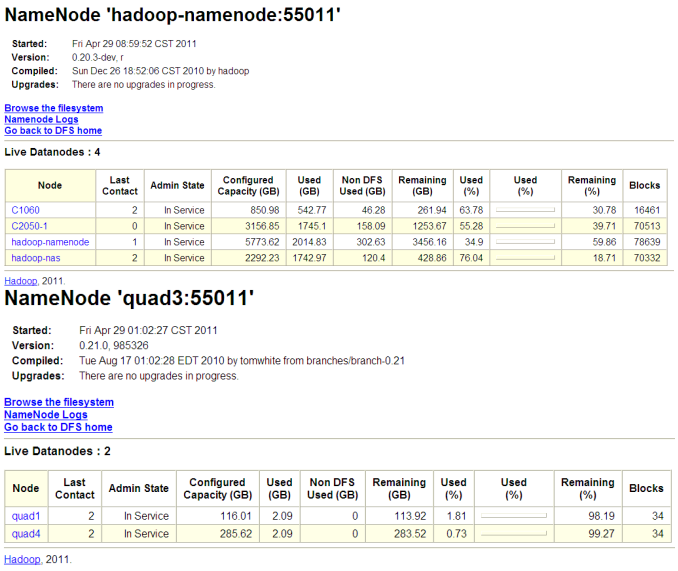

NameNode 'hadoop-namenode:55011'

Started: Fri Apr 29 08:59:52 CST 2011
Version: 0.20.3-dev, r
Compiled: Sun Dec 26 18:52:06 CST 2010 by hadoop
Upgrades: There are no upgrades in progress.

Browse the filesystem
Namenode Logs
Go back to DFS home

Live Datanodes : 4

Node	Last Contact	Admin State	Configured Capacity (GB)	Used (GB)	Non DFS Used (GB)	Remaining (GB)	Used (%)	Used (%)	Remaining (%)	Blocks
C1060	2	In Service	850.98	542.77	46.28	261.94	63.78		30.78	16461
C2050-1	0	In Service	3156.85	1745.1	158.09	1253.67	55.28		39.71	70513
hadoop-namenode	1	In Service	5773.62	2014.83	302.63	3456.16	34.9		59.86	78639
hadoop-nas	2	In Service	2292.23	1742.97	120.4	428.86	76.04		18.71	70332

Hadoop, 2011

NameNode 'quad3:55011'

Started: Fri Apr 29 01:02:27 CST 2011
Version: 0.21.0, 985326
Compiled: Tue Aug 17 01:02:28 EDT 2010 by tomwhite from branches/branch-0.21
Upgrades: There are no upgrades in progress.

Browse the filesystem
NameNode Logs
Go back to DFS home

Live Datanodes : 2

Node	Last Contact	Admin State	Configured Capacity (GB)	Used (GB)	Non DFS Used (GB)	Remaining (GB)	Used (%)	Used (%)	Remaining (%)	Blocks
quad1	2	In Service	116.01	2.09	0	113.92	1.81		98.19	34
quad4	2	In Service	285.62	2.09	0	283.52	0.73		99.27	34

Hadoop, 2011.

Figure 3. The node summary of the cloud test-bed

B. Evaluation

Two synthetic LORs are used in this experiment. The first LOR contains 1,200,000 SCORM-compliant documents, which are converted from Web pages related to educational domains. After stop-word cleansing, there remains 2,570,623 distinct index terms. The size of this LOR is around 20 GB. The other LOR contains 2,400,000 SCORM-compliant documents, which are converted from technical papers related to computer science domains. After stop-word elimination, there remains 4,730,384 distinct index terms. The size of this LOR is around 40 GB. We have implemented two algorithms for this experiment. The first algorithm is a traditional meta-searching approach, named DIR (Distributed Information Retrieval). The other is the approach using the proposed approach, named CIR (Cloud Information Retrieval).

Figure 4 presents the running time of two implementations for different numbers of query terms on LOR 1. In the three cases, CIR performs better than DIR. Figure 5 presents similar results on LOR 2. The main reason may be that CIR using the proposed approach can effectively speed the searching processing.

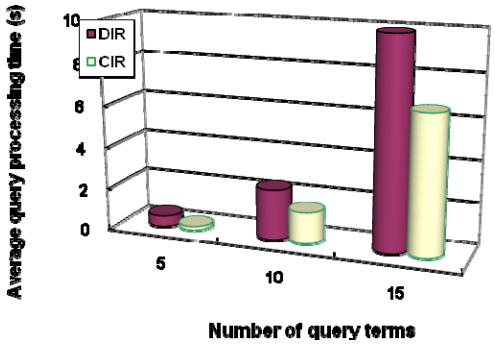

Figure 4. The running time for different numbers of query terms on LOR 1

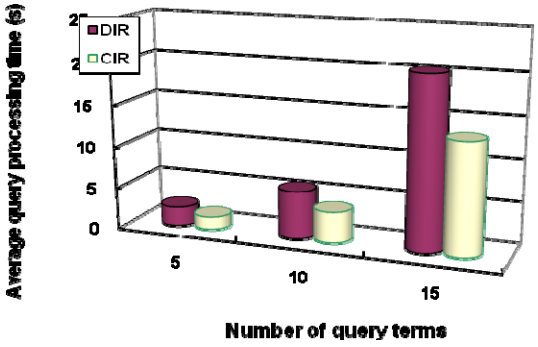

Figure 5. The running time for different numbers of query terms on LOR2

VI. CONCLUSIONS

This paper describes a fuzzy folksonomy-based approach to index creation for learning content retrieval. We divide the index creation problem into two sub-problems: folksonomy fusion and hierarchy organizing. The former problem is solved by merging tags according to a similarity function, which considers textual, metadata and structural information of teaching materials. Experimental results show the effectiveness of this approach. This folksonomy-based approach is characterized by a time-saving development process, minimal involvement of experts and high performance of information retrieval.

Learning content retrieval includes many important and challenging issues. After the study of this work, the future work will address the possibility of complementing traditional ontologies with folksonomies. In addition, it is a promising way to use Expert Systems technologies to facilitate the searching process.

ACKNOWLEDGMENT

This research was partially supported by National Science Council of Republic of China under the number of NSC97-2511-S-468-004-MY3, NSC98-2511-S-468-004-MY3, NSC98-2511-S-468-002 and NSC99-2511-S-468-003.

REFERENCES

[1] A. D. Iorio, A. A. Feliziani, S. Mirri, P. Salomoni, and F. Vitali, "Automatically Producing Accessible Learning Objects," *Journal of Educational Technology & Society,* vol. 9, pp. 3-16, 2006.

[2] R. Lanzilotti, C. Ardito, M. F. Costabile, and A. D. Angeli, "eLSE Methodology: a Systematic Approach to the e-Learning Systems Evaluation," *Journal of Educational Technology & Society,* vol. 9, pp. 42-53, 2006.

[3] J. L. Sierra, A. Fernández-Valmayor, M. Guinea, and H. Hernanz, "From Research Resources to Learning Objects: Process Model and Virtualization Experiences," *Journal of Educational Technology & Society,* vol. 9, pp. 56-68, 2006.

[4] C.-C. Kiu and C.-S. Lee, "Ontology Mapping and Merging through OntoDNA for Learning Object Reusability," *Journal of Educational Technology and Society,* vol. 9, pp. 27-42, 2006.

[5] A. Kassahun, A. Beulens, and R. Hartog, "Providing Author-Defined State Data Storage to Learning Objects," *Journal of Educational Technology & Society,* vol. 9, pp. 19-32, 2006.

[6] ELNP, "National Science and Technology Program for e-Learning." vol. 2007, 2002.

[7] SCORM, "Sharable Content Object Reference Model (SCORM)." vol. 2006: Advanced Distributed Learning, 2004.

[8] R. Y. K. Lau, D. Song, Y. Li, T. C. H. Cheung, and J.-X. Hao, "Toward a Fuzzy Domain Ontology Extraction Method for Adaptive e-Learning," *IEEE Transactions on Knowledge and Data Engineering,* vol. 21, pp. 800-813, 2009.

[9] N. Leavitt, "Is Cloud Computing Really Ready for Prime Time?," *IEEE Computer Magazine,* vol. 42, pp. 15-20, 2009.

[10] C. Yu, K. L. Liu, W. Meng, Z. Wu, and N. Rishe, "A Methodology to Retrieve Text Documents from Multiple Databases," *IEEE Transactions on Knowledge and Data Engineering,* vol. 14, pp. 1347-1361, 2002.

[11] W.-C. Shih and S.-S. Tseng, "Folksonomy-based Indexing for Location-aware Retrieval of Learning Contents," in *The 5th IEEE International Conference on Wireless, Mobile, and Ubiquitous Technology in Education (WMUTE 2008)*, Beijing, China, 2008, pp. 143-147.

[12] E. D. Nitto, L. Mainetti, M. Monga, L. Sbattella, and R. Tedesco, "Supporting Interoperability and Reusability of Learning Objects: The Virtual Campus Approach," *Educational Technology & Society,* vol. 9, pp. 33-50, 2006.

[13] J.-M. Su, S.-S. Tseng, W. Wang, J.-F. Weng, J. T. D. Yang, and W.-N. Tsai, "Learning Portfolio Analysis and Mining for SCORM Compliant Environment," *Educational Technology & Society,* vol. 9, pp. 262-275, 2006.

[14] J. M. Su, S. S. Tseng, C. Y. Wang, Y. C. Lei, Y. C. Sung, and W. N. Tsai, "A Content Management Scheme in SCORM Compliant Learning Object Repository," *Journal of Information Science and Engineering,* vol. 21, pp. 1053-1075, 2005.

[15] A. Trotman, "Searching structured documents," *Information Processing and Management,* vol. 40, pp. 619-632, 2004.

[16] A. Trotman, "Choosing Document Structure Weights," *Information Processing and Management,* vol. 41, pp. 243-264, 2005.

[17] R. Baeza-Yates and B. Ribeiro-Neto, *Modern information retrieval*. New York: ACM Press, 1999.

[18] A. Mittal, P. V. Krishnan, and E. Altman, "Content Classification and Context-Based Retrieval System for E-Learning," *Journal of Educational Technology & Society,* vol. 9, pp. 349-358, 2006.

[19] G. Salton and M. J. McGill, *Introduction to Modern Information Retrieval*. New York: McGraw & Hill, 1983.

[20] I. H. Witten, A. Moffat, and T. C. Bell, *Managing gigabytes: compressing and indexing documents and images*, 2nd ed. ed. San Francisco, California: Morgan Kaufmann, 1999.

[21] Y. K. Lee, S.-J. Yoo, K. Yoon, and P. B. Berra, "Index structures for structured documents," in *the 1st ACM international conference on digital libraries*, 1996, pp. 91-99.

[22] B. B. Cambazoglu and C. Aykanat, "Performance of query processing implementations in ranking-based text retrieval systems using inverted indices," *Information Processing and Management,* vol. 42, pp. 875-898, 2006.

[23] S.-S. Weng, H.-J. Tsai, S.-C. Liu, and C.-H. Hsu, "Ontology construction for information classification," *Expert Systems With Applications,* vol. 31, pp. 1-12, 2006.

[24] L. Khan and F. Luo, "Ontology Construction for Information Selection," in *the 14th IEEE internation conference on tools with artificial intelligence*, Washington DC, 2002, pp. 122-127.

[25] A. Hotho, A. Maedche, and S. Staab, "Ontology-based Text Clustering," in *the IJCAI-2001 workshop text learning: Beyond supervision*, Seattle, 2001.

[26] A. Maedche and S. Staab, "Ontology Learning for the Semantiv Web," *IEEE Intelligent Systems,* vol. 16, pp. 72-79, 2001.

[27] L. A. Zadeh, "Fuzzy Sets," *J. Information and Control,* vol. 8, pp. 338-353, 1965.

2011 IEEE International Conference on Fuzzy Systems
June 27-30, 2011, Taipei, Taiwan

Relationship between Intuitionistic Fuzzy Similarity Measures

Leila Baccour and Adel M. Alimi
REGIM: REsearch Group on Intelligent Machines, University of Sfax
National Engineering School of Sfax (ENIS)
BP 1173, Sfax, 3038, Tunisia
Telephone:(+216)74–274088
Email: leila.baccour@ieee.org
adel.alimi@ieee.org

Robert I. John
Center for Computational Intelligence
De Montfort University
The Gateway, Leicester LE1 9BH
Telephone: (44) 116 2078491
Email: rij@dmu.ac.uk

***Abstract*—Numerous similarity measures between intuitionistic fuzzy sets are proposed in literature using different approaches. In this paper, relationship between some existing intuitionistic fuzzy similarity and distance measures are investigated. These relations are paramount for the choice of a similarity or a distance measure and its application for any research topic.**

***keywords*—Similarity measures, distance measures, intuitionistic fuzzy sets**

I. Introduction

Intuitionistic fuzzy set (IFSs) [1], [2] which are generalizations of fuzzy sets [3] are showed in [4] to be similar to vague sets proposed by Gau and Buehrer [5] and demonstrated in [6] to be equivalent to interval valued fuzzy sets [7]. These theories were the subject of operators' propositions. Similarity and distance measures between IFSs are widely studied and discussed. Chen [8], [9] proposed measures of similarity between vague sets. Hong and Kim [10] demonstrated that these measures are not effective in some cases and proposed to rectify them by giving another similarity measure. Fan and Zhangian [11] proposed an intuitionistic fuzzy similarity measure (IFSM) which resolves some problems of the precedent measures but still contains some counter intuitive cases [12]. Dengfeng and Chuntian [13] proposed some intuitionistic fuzzy similarity measures (IFSMs) and applied them to pattern recognition. However, Mitchell showed in [14] some counter intuitive cases of these measures and proposed an IFSM to solve their weakness by adopting a statistical viewpoint. Other IFSMs are proposed in [15], [16].

In addition to IFSMs, many measures of distances between IFSs are proposed. Szmidt and Kacprzyk [17] proposed Hamming and Euclidean distances based on a geometric interpretation of IFSs. Wang and Xin [18], proposed other distance measures and applied them to pattern recognition showing that the found results are similar to those proposed in [15]. Hung and Yung [19] proposed IFSMs based on Hausdorff distance. The same authors proposed some distance measures and IFSMs in [20] based on L_p metric. More details about IFSMs and distance measures between IFSs are presented in [21], [22].

In section two, we present IFSs definition followed by the definition of distance measures and similarity measures between IFSs from literature. Therefore, we provide relationship between them.

II. Intuitionistic Fuzzy Sets and Interval Valued Fuzzy Sets

A. Definition 1

An intuitionistic fuzzy set A in a discourse universe X is defined in [1] as:
$A = \{\langle x, \mu_A(x), \nu_A(x)\rangle \,|x \in X\}$ where $\mu_A(x) : X \to [0,1]$ and $\nu_A(x) : X \to [0,1]$ with the condition $0 \leq \mu_A(x) + \nu_A(x) \leq 1 \ \forall \ x \in X$.
The numbers $\mu_A(x)$, $\nu_A(x)$ denote respectively the degrees of membership and of non-membership of the element $x \in X$ to A. Also, μ_A and ν_A are called respectively truth membership function and false membership function.
In addition to membership and non-membership functions, a function of hesitancy or uncertainty of x to A denoted by $\pi_A(x)$ must be taken into consideration. $\pi_A(x)$ is computed as:
$\pi_A(x) = 1 - \mu_A(x) - \nu_A(x)$ with $0 \leq \pi_A(x) \leq 1$

B. Definition 2

In [7], an interval-valued fuzzy set in a universe X is a mapping $A : X \to$ Int([0,1])
$x \longmapsto [\underline{A}(x), \overline{A}(x)] \subseteq [0,1]. \ \forall x \in X.$
where Int([0, 1]) is the set of all closed subintervals of [0, 1].

C. Notations

We note IFSs(X) the set of all IFSs in X and we use μ_A , ν_A and π_A instead of $\mu_A(x_i)$, $\nu_A(x_i)$ and $\pi_A(x_i)$ respectively, $\forall x_i \ \in \ A$, $\forall A \ \in$ IFSs(X).

III. Intuitionistic Fuzzy Distance Measures Proposed in Literature

In this section, we present some distance measures, existing in literature, between tow IFSs A and B.

978-1-4244-7316-8/11/$26.00 ©2011 IEEE

A. Definition 1

Atanassov [2] proposed the following distance measures:

- Hamming Distance

$$H(A,B) = \frac{1}{2n}\sum_{i=1}^{n} |\mu_A - \mu_B| + |\nu_A - \nu_B| \quad (1)$$

- Euclidean Distance

$$E(A,B) = \sqrt{\frac{1}{2n}\sum_{i=1}^{n} (\mu_A - \mu_B)^2 + (\nu_A - \nu_B)^2} \quad (2)$$

- [2] present these distances using the max operator

$$J_1(A,B) = \max_i |\mu_A(x_i) - \mu_B(x_i)| \quad (3)$$

J_1 defines the Hamming distance between fuzzy sets

$$J_2(A,B) = \max_i |\nu_A(x_i) - \nu_B(x_i)| \quad (4)$$

$$J(A,B) = \frac{1}{2}(J_1(A,B) + J_2(A,B)) \quad (5)$$

B. Definition 2

Szmidt and Kacprzyk [17] interpreted the precedent measures (1, 2) by a geometric perspective. Thus, they concluded that the hesitation degree must be taken into consideration to compute Euclidean and hamming distances and proposed these measures.

- Hamming Distance

$$\begin{aligned} l_{IFS}(A,B) &= \frac{1}{2n}\sum_{i=1}^{n} |\mu_A - \mu_B| + |\nu_A - \nu_B| \\ &+ |\pi_A - \pi_B| \end{aligned} \quad (6)$$

- Euclidean Distance

$$q_{IFS}(A,B) = \frac{1}{\sqrt{2n}} \times \sqrt{\sum_{i=1}^{n} (\mu_A - \mu_B)^2 + (\nu_A - \nu_B)^2 + (\pi_A - \pi_B)^2} \quad (7)$$

C. Definition 3

In the real space $\mathbb{R}$, for any two intervals $A = [a_1, a_2]$ and $B = [b_1, b_2]$, the Hausdorff distance $H(A,B)$ is defined as:

$$Hd(A,B) = \max\{|a_1 - b_1|, |a_2 - b_2|\} \quad (8)$$

Based on the definition of $H(A,B)$, Hung and Yang [19] proposed Hausdorff distance between two subintervals $I_A(x_i) = [\mu_B(x_i), 1 - \nu_B(x_i)]$ and $I_B(x_i) = [\mu_B(x_i), 1 - \nu_B(x_i)]$, $i = 1, 2, \ldots, n$ of the IFSs A and B defined in [0,1] by this formula:

$$d_{Hd}(A,B) = \frac{1}{n}\sum_{i=1}^{n} max(|\mu_A - \mu_B|, |\nu_A - \nu_B|) \quad (9)$$

Using the $d_{Hd}(A,B)$ definition, the authors proposed some similarity measures between IFSs in [19].

D. Definition 4

Grzegorzewski [23] proposed the following formulas for Euclidean and hamming distances for IFSs based on Hausdorff metric.

- Hamming Distance

$$l_h(A,B) = \frac{1}{n}\sum_{i=1}^{n} max(|\mu_A - \mu_B|, |\nu_A - \nu_B|) \quad (10)$$

- Euclidean Distance

$$q_h(A,B) = \sqrt{\frac{1}{n}\sum_{i=1}^{n} max((\mu_A - \mu_B)^2, (\nu_A - \nu_B)^2)} \quad (11)$$

E. Definition 5

Wang and Xin [18] showed by examples, that the normalized Euclidean distance (7) may not classify patterns in some cases and proposed the following distance measures:

$$\begin{aligned} d_1(A,B) &= \frac{1}{n}\sum_{i=1}^{n}\left[\frac{|\mu_A - \mu_B| + |\nu_A - \nu_B|}{4}\right] \\ &+ \frac{1}{n}\sum_{i=1}^{n}\left[\frac{\max(|\mu_A - \mu_B|, |\nu_A - \nu_B|)}{2}\right] \end{aligned} \quad (12)$$

$$d_2^p(A,B) = \frac{1}{\sqrt[p]{n}}\sqrt[p]{\sum_{i=1}^{n} (\varphi_\mu(x_i) + \varphi_\nu(x_i))^p} \quad (13)$$

where $\varphi_\mu(x_i) = |\mu_A - \mu_B|/2$, $\varphi_\nu(x_i) = |\nu_A - \nu_B|/2$ and p is a positive integer.

IV. Intuitionistic Fuzzy Similarity Measures Proposed in Literature

In this section, we present similarity measures between two IFSs A and B from literature, we recall that similarity measures $s(A,B)$ and distance measures $d(A,B)$ are dual concepts, so, if $s(A,B)$ is a similarity measure between IFSs A and B, then $d(A,B) = 1 - s(A,B)$ and inversely $s(A,B) = 1 - d(A,B)$.

A. Definition 1

In their paper, Hong and Kim [10] proposed the following similarity measure:

$$S_H(A,B) = 1 - \frac{\sum_{i=1}^{n} |\mu_A - \mu_B| + |\nu_A - \nu_B|}{2n} \quad (14)$$

S_H can not distinguish positive difference from negative difference, so some counter cases exist for S_H [12]. For example, if $A = \{(x, 0, 0)\}$ and $B = \{(x, 0.3, 0.5)\}$ then $S_H(A,B) = 0.6$ which is not reasonable. An example of another type of counter intuitive is given in [12]: If $A = \{(x, 1, 0)\}$, $B = \{(x, 0, 0)\}$ and $C = \{(x, 0.5, 0.5)\}$ then, $S_H(A,B) = S_H(C,B) = 0.5$.

B. Definition 2

In [11] the following measure are presented:

$$S_L(A,B) = 1 - \frac{\sum_{i=1}^{n} |S_A(x_i) - S_B(x_i)|}{4n} - \frac{\sum_{i=1}^{n} |\mu_A - \mu_B| + |\nu_A - \nu_B|}{4n} \quad (15)$$

where $S_A(x_i) = \mu_A - \nu_A$ and $S_B(x_i) = \mu_B - \nu_B$.

C. Definition 3

Dengfeng and Chuntian [13] proposed the following similarity measure between IFSs.

$$S_d^p(A,B) = 1 - \frac{1}{\sqrt[p]{n}} \sqrt[p]{\sum_{i=1}^{n} |\varphi_A(x_i) - \varphi_B(x_i)|^p} \quad (16)$$

here:

$$\varphi_A(x_i) = \frac{\mu_A(x_i) + 1 - \nu_A(x_i)}{2}$$

and

$$\varphi_B(x_i) = \frac{\mu_B(x_i) + 1 - \nu_B(x_i)}{2}$$

with $1 \leq p < +\infty$

Mitchell [14], Liang and Shi [15] present some counter-intuitive cases for S_d^p which are existing because S_d^p does not verify the property condition (P2) of similarity measures defined as:

$(P2)$ $S(A,B) = 1$ if and only if $A = B$

As an example [12], the computed similarity S_d^p (16) using the sets $A = \{(x, 0.1, 0.1)\}$ and $B = \{(x, 0.5, 0.5)\}$ with $p = 1$, is $S_d^1(A,B) = 1$.

D. Definition 4

In [15] some similarity measures are given, we present below one of them.

$$S_e^p(A,B) = 1 - \frac{1}{\sqrt[p]{n}} \times \sqrt[p]{\sum_{i=1}^{n} (\varphi_{\mu_{AB}}(x_i) + \varphi_{\nu_{AB}}(x_i))^p} \quad (17)$$

where

$$\varphi_{\mu_{AB}}(x_i) = \frac{|\mu_A - \mu_B|}{2}$$

and

$$\varphi_{\nu_{AB}}(x_i) = \left| \frac{1 - \nu_A}{2} - \frac{1 - \nu_B}{2} \right|$$

make the use of two end points of the subintervals in IFSs.

E. Definition 5

Hung and Yang [20] defined the L_p distance between two intervals $I_A(x_i) = [\mu_A, 1-\nu_A]$ and $I_B(x_i) = [\mu_B, 1-\nu_B]$, $i = 1, 2, \ldots, n$ as:

$$d_p(I_A(x_i), I_B(x_i)) = (|\mu_A - \mu_B|^p + |\nu_A - \nu_B|^p)^{1/p},\ p \geq 1$$

In consequence, the distance $L_p(A,B)$ between A and B is defined as:

$$L_p(A,B) = \frac{1}{n} \sum_{i=1}^{n} d_p(I_A, I_B) \quad (18)$$

Then, the authors proposed some similarity measures based on L_p metric, we present the following measure from them:

$$S_l^p(A,B) = \frac{2^{\frac{1}{p}} - L_p(A,B)}{2^{\frac{1}{p}}} \quad (19)$$

F. Definition 6

In [24] the authors gave a generalization of measures between fuzzy sets proposed in [25] and presented the following measures between IFSs.

$$S_{pk2}(A,B) = 1 - \frac{1}{2} \left(\max_i |\mu_A - \mu_B| + \max_i |\nu_A - \nu_B| \right) \quad (20)$$

$$S_{pk3}(A,B) = 1 - \frac{\sum_{i=1}^{n} |\mu_A - \mu_B| + |\nu_A - \nu_B|}{\sum_{i=1}^{n} (|\mu_A + \mu_B| + |\nu_A + \nu_B|)} \quad (21)$$

V. Relationship between the Presented Measures

- The Hausdorff distance (9) is the same of the Hamming distance (10). So we have:

$$d_{Hd}(A,B) = l_h(A,B) \quad (22)$$

  We mention that this measure should be the Hausdorff distance because it is the generalization of the Hausdorff distance between crisp sets.

- If we replace $\pi_A(x_i)$ and $\pi_B(x_i)$ with their formulas in $l_{IFS}(A,B)$ (6) we find that $H(A,B) \leq l_{IFS}(A,B) \leq 2H(A,B)$ where H(A,B) has the equation (1). It is obvious that $H(A,B) \leq l_{IFS}(A,B)$, thus we show below that $l_{IFS}(A,B) \leq 2H(A,B)$

  Proof:

$$\begin{aligned} l_{IFS}(A,B) &= \frac{1}{2n} \sum_{i=1}^{n} |\mu_A - \mu_B| + |\nu_A - \nu_B| \quad (23) \\ &+ |1 - \mu_A - \nu_A - 1 + \mu_B + \nu_B| \\ &\leq \frac{1}{2n} \sum_{i=1}^{n} |\mu_A - \mu_B| + |\nu_A - \nu_B| \\ &+ |\mu_B - \mu_A| + |\nu_B - \nu_A| \\ &\leq \frac{1}{2n} \sum_{i=1}^{n} 2|\mu_A - \mu_B| + 2|\nu_A - \nu_B| \\ &\leq \frac{1}{n} \sum_{i=1}^{n} |\mu_A - \mu_B| + |\nu_A - \nu_B| \quad (24) \end{aligned}$$

Then

$$H(A,B) \leq l_{IFS}(A,B) \leq 2H(A,B) \tag{25}$$

■

If we examine the formulas (23, 25) we can remark that the measure definition l_{IFS} is very close to that of $H(A,B)$.

- In the sections (III-A, III-B, III-D), we presented three different definitions of Hamming and euclidean distance measures from literature. If we examine measures S_H (14), S_L (15) and d_1(12) we remark that they are related on intuitionistic fuzzy Hamming distance measure H (1), d_1 is on relation with Hamming distance l_h (10) in addition of H. In the same way, formulas d_2^p (13) and S_l^p (19) depend on the power p, if p=1, all these formulas can be written using Hamming distances H and l_h. So, we can write formulas S_H (14), S_L (15) as follows:
  - $S_H(A,B)$(14) is a dual concept of $H(A,B)$(1), so it can be written as:

$$S_H(A,B) = 1 - H(A,B) \tag{26}$$

  - $S_L(A,B)$ (15) is on relation with $H(A,B)$(1), we have:

$$\begin{aligned} S_L(A,B) &= 1 - \frac{\sum_{i=1}^{n} |S_A(x_i) - S_B(x_i)|}{4n} \\ &- \frac{1}{2} H(A,B) \end{aligned} \tag{27}$$

    where $S_A(x_i)$ and $S_B(x_i)$ are defined in section IV-B.
  - d_1 is on relation with Hamming distances H and l_h as:

$$d_1(A,B) = \frac{1}{2}\left(H(A,B) + l_h(A,B)\right) \tag{28}$$

  - if p=1 and from (22, 28), the similarity measures d_2^p(13), S_l^p(19) are written as:

    *

$$d_2^1(A,B) = \sqrt{H(A,B)} \tag{29}$$

    *

$$S_l^1(A,B) = 1 - H(A,B) \tag{30}$$

- The IFSM S_e^p (17) is the dual concept of the distance measure d_2^p(13). It is easy to find in (17) that:

$$\varphi_{\nu_{AB}}(x_i) = \left| \frac{1-\nu_A}{2} - \frac{1-\nu_B}{2} \right|$$

$$\varphi_{\nu_{AB}}(x_i) = \left| \frac{\nu_A - \nu_B}{2} \right|$$

Thus:

$$S_e^p(A,B) = 1 - \frac{1}{\sqrt[p]{n}} \sqrt[p]{\sum_{i=1}^{n} \left(\frac{|\mu_A - \mu_B|}{2} + \frac{|\nu_A - \nu_B|}{2} \right)^p}$$

So we have the equality:

$$S_e^p = 1 - d_2^p \tag{31}$$

Despite the different interpretations of the measures (17), (13), they lead to the same formula.
When p=1, from (31, 29) we have:

$$S_e^1(A,B) = 1 - \sqrt{H(A,B)} \tag{32}$$

- The IFSM S_d^p (16) can be written as:

$$\begin{aligned} S_d^p(A,B) &= 1 - \frac{1}{\sqrt[p]{n}} \sqrt[p]{\sum_{i=1}^{n} \frac{|\mu_A - \mu_B + \nu_B - \nu_A|}{2}} \\ &\leq 1 - \frac{1}{\sqrt[p]{n}} \sqrt[p]{\sum_{i=1}^{n} \frac{|\mu_A - \mu_B| + |\nu_B - \nu_A|}{2}} \\ &\leq S_e^p \\ &\leq 1 - d_2^p \end{aligned}$$

- The measure S_{pk2} (20) presented in section IV-F is the dual concept of the distance J (5), Thus:

$$S_{pk2}(A,B) = 1 - J(A,B) \tag{33}$$

- The measure S_{pk3} (21) presented in section IV-F is written as:

$$S_{pk3(A,B)} = 1 - \frac{2nH(A,B)}{\sum_{i=1}^{n} |\mu_A + \mu_B| + |\nu_A + \nu_B|} \tag{34}$$

VI. Concluding Remarks

We showed that some measures are on relationship with the Hamming distance. Despite the different interpretations of distance measures or similarity measures, some of them are equal such as S_e^p (17) and d_2^p (13). In addition, the similarity measure $S_H(A,B)$ (14) is demonstrated to have some counter intuitive cases. So, from the equality (26), we deduce that all the following formula measures having close relation with the Hamming distance $H(A,B)$ (1) have the same counter intuitive cases of S_H:
d_1 (12), d_2^p (13), S_e^p (17), S_d^p (16), l_{IFS} (6) and S_{pk3} (21).

Acknowledgment

The authors would like to acknowledge the financial support of this work by grants from General Direction of Scientific Research (DGRST), Tunisia, under the ARUB program.

References

[1] K. Atanassov, "Intuitionistic fuzzy sets," *Fuzzy Sets Systems*, vol. 20, no. 1, pp. 87–96, 1986.
[2] ——, *Intuitionistic fuzzy sets*, Springer, Ed. Heidlberg, 1999.
[3] L. Zadeh, "Fuzzy sets," *Inform. Control*, vol. 8, pp. 338–356, 1965.
[4] H. Bustince and P. Burillo, "Vague stes are intuitionistic fuzzy sets," *Fuzzy sets Systems*, vol. 79, no. 3, pp. 403–405, 1996.
[5] W. L. Gau and D. Buehrer, "Vague sets," *IEEE Trans. Syst. Man Cybernet. 23*, vol. 2, pp. 610–614, 1993.
[6] G. Deschrijver and E. E. Kerre, "On the relationship between some extensions of fuzzy set theory," *Fuzzy sets and systems*, vol. 133, pp. 227–235, 2003.
[7] R. Sambuc, "Fonctions ϕ-floues. application à l'aide au diagnostic en pathologie thyroidienne," Ph.D. dissertation, Univ. Marseille, France, 1975.
[8] S. M. Chen, "Measures of similarity between vague sets," *Fuzzy Sets Systems*, vol. 74, no. 2, pp. 217–223, 1995.
[9] ——, "Similarity measures between vague sets and between elements," *IEEE Trans. Syst. Man Cybernet*, vol. 27, no. 1, pp. 153–158, 1997.

[10] D. H. Hong and C. Kim, "A note on similarity measures between vague sets and between elements," *Inform. Science*, vol. 115, pp. 83–96, 1999.
[11] L. Fan and X. Zhangian, "Similarity measures between vague sets," *J. Software 12*, vol. 6, pp. 922–927, 2001.
[12] L. Yanhong, L. O. David, and Q. Zhen, "Similarity measures between intuitionistc fuzzy (vague) sets: A comprative analysis," *Pattern Recognition Letters*, vol. 28, pp. 278–285, 2007.
[13] L. Dengfeng and C. Chuntian, "New similarity measure of intuitionistic fuzzy sets and application to pattern recognitions," *Pattern Recognition Letters*, vol. 23, pp. 221–225, 2002.
[14] H. B. Mitchell, "On the dengfeng-chuntian similarity measure and its application to pattern recognition," *Pattern Recognition Letters*, vol. 24, pp. 3101–3104, 2003.
[15] Z. Liang and P. Shi, "Similarity measures on intuitionistic fuzzy sets," *Pattern Recognition Letters*, vol. 24, pp. 2687–2693, 2003.
[16] C. Zhang and H. Fu, "Similarity measures on three kinds of fuzzy sets," *Pattern Recognition Letters*, vol. 27, pp. 1307–1317, 2006.
[17] E. Szmidt and J. Kacprzyk, "Distances between intuitionistic fuzzy sets," *Fuzzy sets Systems*, vol. 114, no. 3, pp. 505–518, 2000.
[18] W. Wang and X. Xin, "Distance measure between intuitionistic fuzzy sets," *Pattern Recognition Letters*, vol. 26, pp. 2063–2069, 2005.
[19] W.-L. Hung and M.-S. Yang, "Similarity measures of intuitionistic fuzzy sets based on hausdorff distance," *Pattern Recognition Letters*, vol. 25, pp. 1603–1611, 2004.
[20] ——, "Similarity measures of intuitionistic fuzzy sets based on l_p metric," *Approximate Reasoning*, vol. 46, pp. 120–136, 2007.
[21] L. Baccour and A. M. Alimi, "A comparison of some intuitionistic fuzzy similarity measures applied to handwritten arabic sentences recognition," in *IEEE International Conference on Fuzzy Systems, FUZZ-IEEE'2009, ICC Jeju Island, Korea, August 20-24, pp. 1389–1392*, 2009.
[22] L. Baccour, S. Kanoun, V. Maergner, and A. M. Alimi, "An application of intuitionistic fuzzy information for handwritten arabic word recognition," in *proc. Notes on IFS, the twelfth International Conference on Intuitionistic Fuzzy Sets ICIFS'2008, Sofia Bulgaria, vol. 14, no. 2, pp. 67–72*, 2008.
[23] P. Grzegorzewski, "Distances between intuitionistic fuzzy sets and/or interval-valued fuzzy sets based on the hausdorff metric," *Fuzzy sets and systems*, vol. 148, pp. 319–328, 2004.
[24] W.-L. Hung and M.-S. Yang, "On similarity measures between intuitionistic fuzzy sets," *International journal of intelligent systems*, vol. 23, pp. 364–383, 2008.
[25] C. Pappis and I. Karacapilidis, "A comparative assessment of measures of similarity of fuzzy values," *Fuzzy sets and systems*, vol. 56, pp. 171–174, 1993.

2011 IEEE International Conference on Fuzzy Systems
June 27-30, 2011, Taipei, Taiwan

Decomposition of Term-Document Matrix Representation for Clustering Analysis

Jianxiong Yang
Graduate School of Information, Production and Systems
Waseda University
Kitakyushu, Japan
leoworldplus@yahoo.co.jp

Junzo Watada
Graduate School of Information, Production and Systems
Waseda University
Kitakyushu, Japan
junzow@osb.att.ne.jp

Abstract— **Latent Semantic Indexing (LSI) is an information retrieval technique using a low-rank singular value decomposition (SVD) of term-document matrix. The aim of this method is to reduce the matrix dimension by finding a pattern in document collection with concurrently referring terms. The methods are implemented to calculate the weight of term-document in vector space model (VSM) for document clustering using fuzzy clustering algorithm. LSI is an attempt to exploit the underlying semantic structure of word usage in documents. During the query-matching phase of LSI, a user's query is first projected into the term-document space, and then compared to all terms and documents represented in the vector space. Using some similarity measure, the nearest (most relevant) terms and documents are identified and returned to the user. The current LSI query-matching method requires computing the similarity measure about the query of every term and document in the vector space. In this paper, the Maximal Tree Algorithm is used within a recent LSI implementation to mitigate the computational time and computational complexity of query matching. The Maximal Tree data structure stores the term and document vectors in such a way that only those terms and documents are most likely qualified as the nearest neighbor to the query will be examined and retrieved. In a word, this novel algorithm is suitable for improving the accuracy of data miners.**

Keywords-Fuzzy clustering; data mining; LSI; SVD.

I. INTRODUCTION

Data mining [1] is a technique to obtain some patterns of knowledge from a depository or a data base. This technique enables us to find and describe structural patterns in data collection as a tool for helping to explain the data patterns and make predictions from them. Generally, data mining tasks are divided into two major steps: (1) predictive tasks which aim to forecast the value of a particular attribute based on the values of other attributes and (2) descriptive tasks which aim to derive patterns (correlations, trends, clusters, trajectories, and anomalies) [2]. Clustering is a method to re-organize automatically a large data collection by partitioning a set data, so the objects in the same cluster are more similar to one another than to objects in other clusters. Especially, document clustering aims to re-organize a large text data collection. In the field of Information Retrieval (IR), document clustering is used to automatically group the document that belongs to the same topic in order to provide user's browsing of retrieval results [3]. Some experimental evidences show that IR application can benefit from the use of document clustering [4]. Document clustering has always been used as a tool to improve the performance of retrieving and navigating large data.

The clustering methods can be classified into two groups: hierarchical method and partitioning method. Partitioning clustering can be classified into hard clustering and overlapping clustering (fuzzy clustering). Any given document has a possibility to contain multiple subjects or categories. This issue aims to use a fuzzy clustering approach, which enables us to include a document in multiple clusters. The method is different from hard clustering method, which a document only belongs to one cluster, not more. The hard clustering assumes well defined boundary among the clusters.

While grouping or clustering of documents, the problem is a very huge number of terms or words are contained in the full text vector space. Many lexical matching at term grade are inaccurate. Sometimes, a word has ambiguously several meaning or some words have synonymously the same meaning, and these cause results in the selection of irrelevant documents. Therefore, this research uses an Information Retrieval approach of Latent Semantic Index (LSI). In this method, the documents are projected onto a small subspace of this vector space and are clustered. So, there is creation of new abstract vector space is capable of capturing contents of important documents in order [3].

The remaining of this paper is written as follows. Section 2 clarifies the research in the past. Section 3 is spent to give the preliminary knowledge on fuzzy clustering. In Section 4, a sufficient and necessary process is shown for the vector space model and LSI. In Section 5, we present an exemplified algorithm of this method. Finally, some concluding remarks are given in Section 6.

978-1-4244-7316-8/11/$26.00 ©2011 IEEE

II. LITERATURE REVIEW

2.1 LSI Timeline

In 1964, H. Borko and M. Bernick [5] described and tested factor analysis technique first. They report the results of a series of experiments in the techniques of automatic document classifications. Two different classification schedules are compared along with two methods of automatically classifying documents into categories. It is concluded that, while there is no significant difference in the predictive efficiency between Bayesian and Factor Score methods. Automatic document classification is enhanced by the use of a factor-analytically-derived classification schedule. Approximately 55 percent of the documents was automatically and correctly classified. Their experiments provide the information on the effectiveness of techniques for automatic document classification. In the approach to the problem the authors' began by using the computer to help gather data about a representative set of technical documents. In the initial analysis all the content words used in the abstracts of the document were counted and arranged by frequency of occurrence. A limited number of high-frequency words were manually selected to constitute an authority list for use in automatically indexing documents. Every document in the sample was automatically indexed using these terms [5].

In 1988, Furnas *et al*. published a seminal paper on LSI technique. They introduced a new method for automatic indexing and retrieval, implicit higher-order structure in the association of terms with documents is modeled to improve estimates of term-document association, and therefore the detection of relevant documents on the basis of terms found in queries. Singular-value decomposition is used to decompose a large term by document matrix into 50 to 150 orthogonal factors from which the original matrix can be approximated by linear combination; both documents and terms are represented as vectors in a 50 to 150-dimensioal space. Queries are represented as pseudo-documents vectors formed from weighted combinations of terms, and documents are ordered by their similarity to the query. Initial tests find this automatic method very promising [6].

Dumais and Nielsen first used LSI to assign articles to reviewers in 1992. The 117 manuscripts submitted for the Hypertext'91 Conference were assigned to members of the review committee, using a variety of automated methods based on information retrieval principles and Latent Semantic Indexing. Fifteen reviewers provided exhaustive ratings for the submitted abstracts, indicating how well each abstract matched their interests. The automated methods do a fairly good job of assigning relevant papers for review, but they are still somewhat poorer than assignments made manually by human experts and substantially poorer than an assignment perfectly matching the reviewers' own ranking of the papers. A new automated assignment method called "n of 2 n" achieves better performance than human experts by sending reviewers more papers than they actually have to review and then allowing them to choose part of their review load themselves [7].

Landauer etc. got patent granted for the cross-lingual application of LSI in 1994. This search was stimulated by the earlier examples of thermodynamics which arose from the attempt to understand the limits of steam engines, and by Shannon's channel capacity theory. These examples suggested that the computer could be characterized in a similar way. The earlier prototypes had derived optimum performance limits in a way which transcended particular technologies and design choices. Scientists and engineers take pride in the ability to do back-of-the-envelope calculations, to quickly reach to the critical aspects without encumbering details. Yet, in this field of ultimate physical limits of information handling, the quick and dirty approaches have turned out to be wrong in a remarkably consistent way. All of the first answers have been misleading [8].

Foltz first use LSI for grading essays in 1995. While the CHI conference focuses on issues of the interactions between humans and computers, it also addresses issues of interactions between humans and more primitive information systems, such as conference proceedings. Over the past two years, the CHI conference committee has tried to improve the usability of the conference proceedings by improving the index. For CHI'92 and '93, the proceedings had no keyword index. This can be due to the fact that generating an index is both a time consuming process and difficult to do well. For CHI'94 and '95, an information retrieval method was used for indexing that permitted both automating the indexing and developing a better index to the CHI proceedings [9].

From 1998 through 2000, an R&D program was conducted to apply a key technology, Latent Semantic Indexing (LSI), to provide superior advanced search capabilities. During this period, several federal agencies were engaged to explore applications of this technology of particular interest to the US Intelligence Community. From 2001 through 2002, a complete software framework was implemented to facilitate the use of this technology in Text Analytics applications.

In 2005, EBSCO Publishing (EBSCO, Content Analyst Company) has announced the release of Executive Daily Brief (EDB), a result of a partnership with the Content Analyst Company. EDB combines Content Analyst's Concept Search with the variety of content offered by EBSCO, to create a customizable business information monitoring and alert service.

EDB is designed to enable users to search for conceptually-related content by entering phrases, paragraphs, or entire articles into a search box. EDB then intuitively finds and retrieves the relevant information. EDB actually "trains" itself as it operates, creating a more intelligent search with each use. Users set up customized folders on topics or projects of their own choosing. EDB monitors more than 10,000 business sources each day and automatically places relevant articles into the appropriate project folders for review, based upon example documents, emails, or articles that the user places in each folder.

EDB's content repository includes business journals, current articles, and real-time business news from a variety of information sources. Along with EDB's own content resources, users may customize EDB's content by exposing other sources of data to the Concept Search, such as pertinent company documents and intranet resources.

2.2 Challenges to LSI

Early challenges to LSI focused on scalability and performance. LSI requires relatively high computational performance and memory in comparison to other information retrieval techniques. However, with the implementation of modern high-speed processors and the availability of inexpensive memory, these considerations have been largely overcome. Real-world applications involving more than 30 million documents that were fully processed through the matrix and SVD computations are not uncommon in some LSI applications.

Another challenge to LSI has been the alleged difficulty in determining the optimal number of dimensions to use for performing the SVD. As a general rule, fewer dimensions allow for broader comparisons of the concepts contained in a collection of text, while a higher number of dimensions enable more specific (or more relevant) comparisons of concepts. The actual number of dimensions that can be used is limited by the number of documents in the collection. Research has demonstrated that around 300 dimensions will usually provide the best results with moderate-sized document collections (hundreds of thousands of documents) and perhaps 400 dimensions for larger document collections (millions of documents). However, recent studies indicate that 50-1000 dimensions are suitable depending on the size and nature of the document collection.

Checking the amount of variance in the data after computing the SVD can be used to determine the optimal number of dimensions to retain. The variance contained in the data can be viewed by plotting the singular values(SV) in a scree plot. Some LSI practitioners select the dimensionality associated with the knee of the curve as the cut-off point for the number of dimensions to retain. Others argue that some quantity of the variance must be retained, and the amount of variance in the data should dictate the proper dimensionality to retain. Seventy percent is often mentioned as the amount of variance in the data that should be used to select the optimal dimensionality for recomputing the SVD.

III. Clustering analysis

Clustering is useful in several exploratory pattern-analysis, grouping, decision-making, and machine-learning situations, including data mining, document retrieval, image segmentation, and pattern classification. However, in many such problems, there is little prior information (e.g., statistical models) available about the data, and the decision-maker must make as few assumptions about the data as possible. It is under these restrictions that clustering methodology is particularly appropriate for the exploration of interrelationships among the data points to make an assessment (perhaps preliminary) of their structure.

The term “clustering” is used in several research communities to describe methods for grouping of unlabeled data. These communities have different terminologies and assumptions for the components of the clustering process and the contexts in which clustering are used. Thus, we face a dilemma regarding the scope of this survey. The production of a truly comprehensive survey would be a monumental task given the sheer mass of literature in this area. The accessibility of the survey might also be questionable given the need to reconcile very different vocabularies and assumptions regarding clustering in the various communities.

Fuzzy clustering methods partition a set of data into a number of overlapping clusters based on the distance in a metric space between the data points and the cluster prototypes. Various clustering algorithms can be used depending on the assumed structure of the identification data and the model type one wants to obtain [11]. A clustering method that has proven suitable for the identification of TS fuzzy models is the GK fuzzy clustering algorithm [12]. Unlike the popular fuzzy -means algorithm [13], the GK algorithm employs an adaptive distance norm in order to detect clusters of different geometric shapes in the data set.

Each cluster in the product space of the input/output data represents a rule in the rule base. The goal is to establish the fuzzy antecedents $\boldsymbol{A_i}$. These are defined by the fuzzy clusters found in the data. If desired, univariate membership functions $\boldsymbol{u_{i,j}}$ can be obtained by projections onto the various input variables $\boldsymbol{x_j}$ spanning the cluster space. The details are described by [11] and [14].

IV. Vector Space Model and LSI

4.1 Latent Semantic Indexing

Latent Semantic Indexing(LSI) is an indexing and retrieval method that uses a mathematical technique called Singular Value Decomposition (SVD) to identify patterns in the relationships between the terms and concepts contained in an unstructured collection of texts. LSI is based on the principle that words tend to have similar meanings in the same context. It requires relatively high computational performance and large memory in comparison to other information retrieval techniques [15]. A key feature of LSI is its ability to extract the conceptual content of texts by establishing associations among those terms which occur in similar contexts.

Latent Semantic Indexing can be able to correlate semantically terms in a collection of texts. The method was first applied to texts at Bell Laboratories in the late 1980s, also called Latent Semantic Analysis (LSA), which can uncover the underlying latent semantic structure in the usage of words in a body of texts and extract the meaning of the text in response to user queries, commonly referred to as concept searches. Queries, or concept searches, depend on a set of documents which have undergone LSI will return results that are similar in meaning to the search criteria even if the results do not share specific words with the search criteria [16].

4.2 Singular Value Decomposition

In linear algebra, the singular value decomposition (SVD) is an important factorization of a rectangular real or complex matrix, with many applications in signal processing and statistics. Suppose **A** is an m×n matrix whose entries come from a space, which is either the space of real numbers or the space of complex numbers. Then there exists a factorization of the form

$$A = \mathrm{U}\sum\mathrm{V}^{\mathrm{T}} \qquad (1)$$

where **U** is an m×m unitary matrix, the matrix **A** is an m×n diagonal matrix with nonnegative real numbers on the diagonal, and $\mathbf{V}^{\mathbf{T}}$ is an n×n unitary matrix, denotes the conjugate transpose of **V**. Such a factorization is called the singular value decomposition of **A**. The diagonal entries $\mathbf{\Sigma_{ij}}$ of **Σ** are known as the singular values of **A**. It's shown in Figure 1:

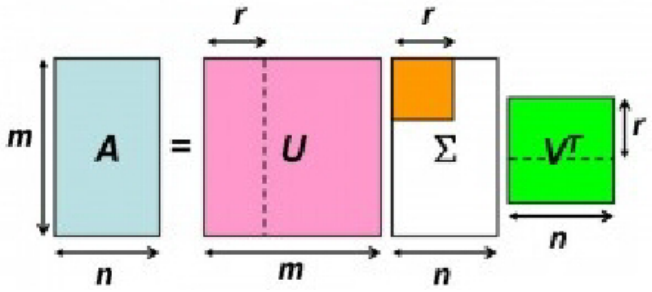

Figure 1. The singular value decomposition

For obtaining simplified vector space, we just need pick up the non-zero singular values of **Σ**. The rank-**r** is the amount of non-zero singular values of **Σ**.

A common usage is to place the singular values in descending order. In this case, the diagonal matrix **Σ** is uniquely determined by **A**.

So we obtain the followed new equation(2) and Figure 2:

$$A = \mathrm{U}_r \sum_r V_r^T \qquad (2)$$

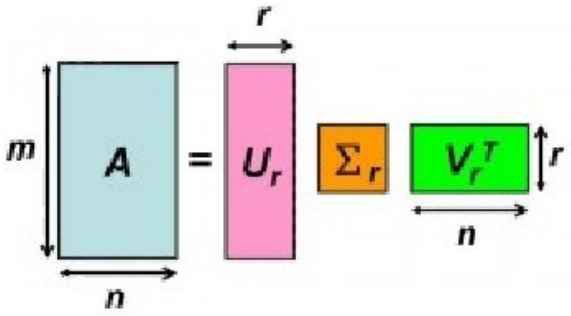

Figure 2. The simplified SVD

4.3 An Example of SVD

This example has terms 1, 2, 3, 4 and 5 as follows:
Term 1 appear 1, 0, 0, 0 times in document 1, 2, 3, 4;
Term 2 appear 0, 0, 0, 4 times in document 1, 2, 3, 4;
Term 3 appear 0, 3, 0, 0 times in document 1, 2, 3, 4;
Term 4 appear 0, 0, 0, 0 times in document 1, 2, 3, 4;
Term 5 appear 2, 0, 0, 0 times in document 1, 2, 3, 4.

Factor matrix A, that is, term-document matrix **A** is shown in matrix 3:

$$A = \begin{array}{c} \begin{matrix} t_1 & t_2 & t_3 & t_4 & t_5 \end{matrix} \\ \begin{pmatrix} 1 & 0 & 0 & 0 & 2 \\ 0 & 0 & 3 & 0 & 0 \\ 0 & 0 & 0 & 0 & 0 \\ 0 & 4 & 0 & 0 & 0 \end{pmatrix} \end{array} \begin{matrix} d_1 \\ d_2 \\ d_3 \\ d_4 \end{matrix} \qquad (3)$$

Step 1:

Calculate the interactive matrix (4).

$$A \cdot A^T = \begin{pmatrix} 1 & 0 & 0 & 0 & 2 \\ 0 & 0 & 3 & 0 & 0 \\ 0 & 0 & 0 & 0 & 0 \\ 0 & 4 & 0 & 0 & 0 \end{pmatrix} \cdot \begin{pmatrix} 1 & 0 & 0 & 0 \\ 0 & 0 & 0 & 4 \\ 0 & 3 & 0 & 0 \\ 0 & 0 & 0 & 0 \\ 2 & 0 & 0 & 0 \end{pmatrix}$$

$$= \begin{pmatrix} 1 & 0 & 0 & 0 & 2 \\ 0 & 16 & 0 & 0 & 0 \\ 0 & 0 & 9 & 0 & 0 \\ 0 & 0 & 0 & 0 & 0 \\ 2 & 0 & 0 & 0 & 4 \end{pmatrix} \qquad (4)$$

Step 2:

We calculate the eigenvalues and singular vectors of $\boldsymbol{A \cdot A^T}$. The non-zero singular eigenvectors are shown by descending as:

λ_1=16, λ_2=9, λ_3=5.

The non-zero singular values are obtained in the following:

δ_1=4, δ_2=3, $\delta_3=\sqrt{5}$, the rank-**r** of non-zero singular matrix **Σ** is 3.

So, the eigenvectors are in the following:

$$v_1 = \begin{pmatrix} 0 \\ 1 \\ 0 \\ 0 \\ 0 \end{pmatrix}, \quad v_2 = \begin{pmatrix} 0 \\ 0 \\ 1 \\ 0 \\ 0 \end{pmatrix}, \quad v_3 = \begin{pmatrix} \sqrt{0.2} \\ 0 \\ 0 \\ 0 \\ \sqrt{0.8} \end{pmatrix}.$$

So the singular value matrix **Σ** and the term decomposition matrix **V** are shown as:

$$\sum_r = \begin{pmatrix} 4 & 0 & 0 \\ 0 & 3 & 0 \\ 0 & 0 & \sqrt{5} \end{pmatrix};$$

$$V^T{}_r = \begin{pmatrix} 0 & 1 & 0 & 0 & 0 \\ 0 & 0 & 1 & 0 & 0 \\ \sqrt{0.2} & 0 & 0 & 0 & \sqrt{0.8} \end{pmatrix}.$$

Step 3:

Calculating the document decomposition matrix U.

$$u_1 = \frac{1}{\delta_1} A v_1 = \begin{pmatrix} 0 \\ 0 \\ 0 \\ 1 \end{pmatrix},$$

$$u_2 = \frac{1}{\delta_2} A v_2 = \begin{pmatrix} 0 \\ 1 \\ 0 \\ 0 \end{pmatrix},$$

$$u_3 = \frac{1}{\delta_3} A v_3 = \begin{pmatrix} 1 \\ 0 \\ 0 \\ 0 \end{pmatrix},$$

$$U_r = \begin{pmatrix} 0 & 0 & 1 \\ 0 & 1 & 0 \\ 0 & 0 & 0 \\ 1 & 0 & 0 \end{pmatrix}.$$

So if we want to analyze the attribute of document, we just need calculate the document decomposition matrix U_r.

V. ACCIDENT CASE CLUSTERING BASED ON LSI

Latent semantic analysis employs information retrieval to explore latent semantics and attributes of accident cases. So, we use latent semantic method to analyze a large number of accidents data. This analysis has the following steps: build the primary matrix, execute singular value decomposition, purse similarity analysis of accident cases and obtain the results clustering.

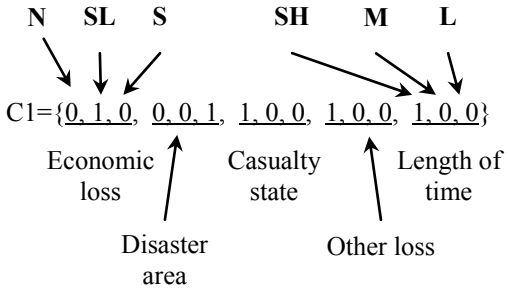

Figure 3. The description of accident attributes

TABLE I. SAMPLE DATA

No.	Attribute				
	Economic loss	*Disaster area*	*Casualty state*	*Other loss*	*Length of time*
C1	SL	S	N	N	SH
C2	N	N	S	S	SH
C3	SL	S	S	N	SH
C4	N	SL	S	S	SH
C5	S	S	S	N	SH
C6	S	SL	SL	SL	L
C7	SL	S	SL	N	M
C8	N	S	S	N	L

TABLE II. THE PRIMARY MATRIX

	C1	C2	C3	C4	C5	C6	C7	C8
Economic loss : N	0	1	0	1	0	0	0	1
Economic loss : SL	1	0	1	0	0	0	1	0
Economic loss : S	0	0	0	0	1	1	0	0
Disaster area : N	0	1	0	0	0	0	0	0
Disaster area : SL	0	0	0	1	0	1	0	0
Disaster area : S	1	0	1	0	1	0	1	1
Casualty state : N	1	0	0	0	0	0	0	0
Casualty state : SL	0	0	0	0	0	1	1	0
Casualty state : S	0	1	1	1	1	0	0	1
other loss : N	1	0	1	0	1	0	1	1
other loss : SL	0	0	0	0	0	1	0	0
other loss : S	0	1	0	1	0	0	0	0
Length of time : SH	1	1	1	1	1	0	0	0
Length of time : M	0	0	0	0	0	0	1	0
Length of time : L	0	0	0	0	0	1	0	1

5.1 Establishing Primary Matrix

In our accident database, all the data include 5 attributes: (1) economic loss, (2) disaster area, (3) casualty state, (4) other loss and (5) length of time. Every attribute has 3 serious grades which economic loss, disaster area, casualty state and other loss are **N**(nothing), **SL**(slight) and **S**(serious), and length of time is **SH**(short), **M**(middle) and **L**(long). For example, the accident case 1 has slight economic loss, serious disaster area, no casualty state, no other loss and short length of time. If the any attribute of an accident case has any grade, then this grade is "1", or else it is "0". It may denote the expression shown in Figure 3.

Table I recorded eight accident cases from the National Institute of Technology Evaluation (NITE). So we can transform it to a primary matrix as shown in Table II.

5.2 Singular Value Decomposition

In Table II, we have eight cases with five attributes. These create a 15x8 matrix, so we use Matlab to decompose singular value and obtain decomposed matrix **U**, **Σ** and $\mathbf{V^T}$. We chose the non-zero singular values of **Σ** to build $\mathbf{U_r}$, $\mathbf{\Sigma_r}$ and $\mathbf{V^T_r}$ which are shown in matrices 5, 6 and 7, respectively.

$$U_r = \begin{pmatrix} -0.39071 & 0.32158 \\ -0.29845 & -0.56435 \\ -0.46969 & 0.15712 \\ -0.30411 & -0.56933 \\ -0.43633 & 0.037314 \\ -0.10217 & -0.034567 \\ -0.30819 & 0.47413 \\ -0.38615 & -0.043407 \end{pmatrix} \quad (5)$$

$$\sum_r = \begin{pmatrix} 4.3642 & 0 \\ 0 & 2.8161 \end{pmatrix} \quad (6)$$

$$V_r = \begin{pmatrix} -0.22655 & -0.41799 \\ -0.26777 & 0.33835 \\ -0.12346 & 0.000975 \\ -0.068385 & -0.2004 \\ -0.093093 & -0.21445 \\ -0.4563 & 0.33619 \\ -0.089526 & 0.11419 \\ -0.094028 & 0.15609 \\ -0.43422 & -0.34894 \\ -0.4563 & 0.33619 \\ -0.02341 & -0.012275 \\ -0.13807 & -0.40257 \\ -0.43527 & -0.21933 \\ -0.070618 & 0.16837 \\ -0.11189 & -0.027689 \end{pmatrix} \quad (7)$$

5.3 The Clustering Of Accident Cases

At first, we calculate the cosine of any two accident cases in 2-Dimensional semantic space. If the cosine of these two cases is "1", the angle of two case vectors is 0-degree, that is, the two cases are the same else cosine is "0" these two cases are not the same. All of the values are shown in Table III.

From the data of Table III, we use the similarity measure data shown in Table III, to build the maximal tree. First, we pick all the vertices for which relation values are not less than 0.9. Thus, the vertices {1, 3}, {1, 7},{2, 4}, {3, 5}, {3, 8}, {5, 6}, {5, 8}, and {6, 8} are selected output. We connect these vertices by their similarity value to build the initial cluster tree, as shown in Figure 4.

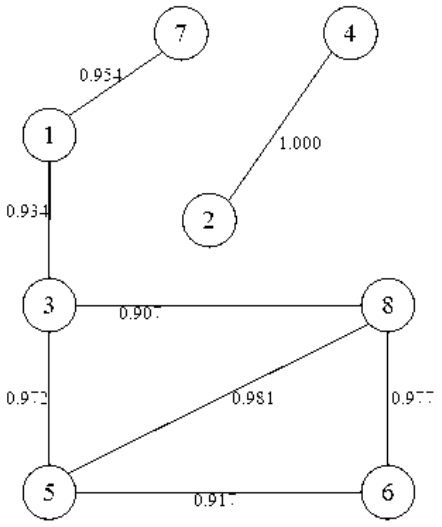

Figure 4. The initial cluster tree

The maximal tree cannot have a circuit because any two vertices have only one maximal relation. Thus, we must remove the edge of minimum value in a circuit. The edge {3, 8}, and {5, 6} should be removed. The next cluster tree is shown in Figure 5.

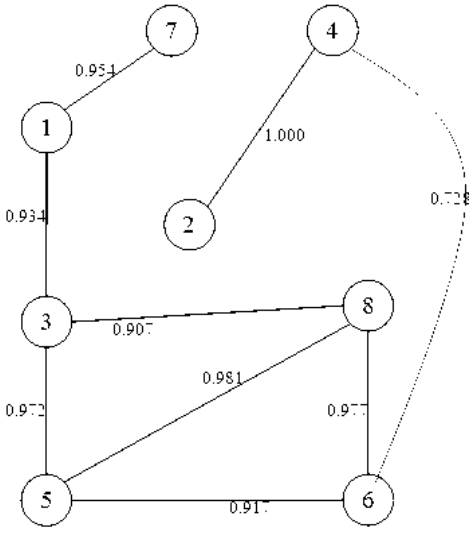

Figure 5. The clustering tree

TABLE III. FUZZY SIMILARITY DATA

	1	2	3	4	5	6	7	8
1	1							
2	-0.20082	1						
3	0.93383	0.16291	1					
4	-0.19676	0.99999	0.16699	1				
5	0.82342	0.39052	0.97192	0.39433	1			
6	0.52771	0.72615	0.79565	0.72899	0.91652	1		
7	0.95362	-0.4864	0.78282	-0.48278	0.61441	0.24753	1	
8	0.69629	0.56331	0.90698	0.56673	0.98062	0.97712	0.44792	1

However vertices 2 and 4 are not included in group{1, 3, 5, 6, 7, 8}. We thus need to connect add the two groups of vertices, {2,4} and {1,3,5,6,7,8} and connect vertices with maximum similarity value between the two groups. The similarity values are 0.782 for {4, 6}. So, all the vertices are connected. The cluster tree is shown in Figure 6.

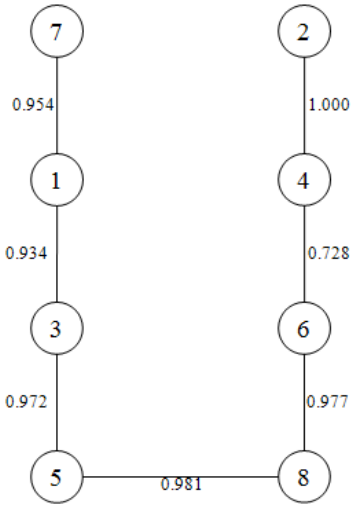

Figure 6. The Maximal Tree

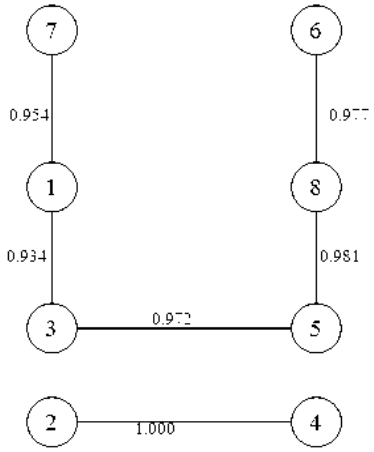

Figure 7. The clustering by λ=0.900

At last, we get a Maximal Tree, which each side has a weight "r_{ij}". By the Threshold-λ, we remove all the sides which have weight $r_{ij}<\lambda$. In the remaining vertexes, any connected vertexes are the same cluster [10].

If we select a high similarity value of λ=0.900, based on the clustering tree, we delete all the sides whose similarity value of λ blew 0.900. So the cases 1, 3, 5, 6, 7 and 8 are similar in the same group, and the Cases 2 and 4 are similar in the same group. It is shown in Figure 7. In addition, if we wish to extract some accident cases, we just need to embed the equivalent example data of these cases in the data set. If any ones can be clustered to a group with the equivalent example data according to the threshold λ, it must be a useful data element which we want [10].

VI. Application of LSI

LSI is used to realize automated document categorization. Several experiments have demonstrated a number of successful correlations between the way LSI and humans' process and effectively categorized text [17]. Document categorization is the assignment of documents to one or more predefined categories based on their similarity to the conceptual content of the categories [18]. LSI uses template documents to establish the conceptual basis for each category. During the process of categorization, the concepts contained in the documents categorized are compared to the concepts contained in the template items, and a category or categories are assigned to the documents based on the similarities between the concepts they contain and the concepts that are contained in the template documents.

LSI can realize effectively dynamic clustering based on the conceptual content of documents can also be accomplished using LSI. Clustering is a way to group documents based on their conceptual similarity to each other without using template documents to establish the conceptual basis for each cluster. This is useful when dealing with an unknown collection of unstructured text.

LSI is not restricted only to working with words. It can also process arbitrary character strings. Any object if it can be expressed in text can be represented in an LSI vector space. For example, texts with MEDLINE abstracts have shown that LSI is able to effectively classify genes based on conceptual modeling of the biological information contained in the titles and abstracts of the MEDLINE citations [19].

LSI has proven to be a useful solution to a number of conceptual matching problems [20][21]. The technique has been shown to capture key relationship information, including causal, goal-oriented, and taxonomic information [22].

VII. CONCLUSIONS

The latent semantic indexing (LSI) methodology for information retrieval has applied the singular value decomposition to identify an eigenfunction for a large matrix, whose cells represent the occurrence of terms(conditions) within documents. This methodology was used to rank text documents and data clustering, based on their relevance to a topic. In this paper, we proposed the method that integrated the Latent Semantic Indexing (LSI) concept to our document clustering. This involves the use of Singular Value Decomposition (SVD) which creates a new abstract and uses a way of finding simplified document collection in matrix representation, so that it could identify the terms and documents which are similar. The considered synthetic and real-world examples demonstrated the improved mining properties due to the befitting cluster and the algorithms capability of determining a suitable similarity degree of clusters in the data.

REFERENCES

[1] Y. Lei, V. Uren, and E. Motta, "SemSearch: A Search Engine for the Semantic Web," Proc. 15th Int'l Conf. Managing Knowledge in a World of Networks (EKAW '06), pp. 238-245, 2006.

[2] PN Tan, M.S., V Kumar, Introduction to Data Mining. Pearson International ed. 2006: Pearson Education, Inc.

[3] M.A. Hearst, a.J.O.P. "Reexamining the cluster hypothesis". 1996: In Proceeding of SIGIR '96.

[4] Jardine, N.a.v.R., C.J., The Use of Hierarchical Clustering in Information Retrieval. Information Storage and Retrieval. Vol. 7. 1971.

[5] H. Borko, S. Monica, "Automatic Document Classification Part II . Additional Experiments", Journal of the ACM (JACM) JACM Homepage archive, Volume 11 Issue 2, pp. 138-151. April 1964.

[6] G. W. Furnas, S. Deerwester, S. T. Dumais, T. K. Landauer, R. A. Harshman, L. A. Streeter, and K. E. Lochbaum, "Information retrieval using a singular value decomposition model of latent semantic structure", In SIGIR '88: Proceedings of the 11th annual international ACM SIGIR conference on Research and development in information retrieval (1988), pp. 465-480.

[7] S.T. Dumais and J. Nielsen, "Automating the Assignment of Submitted Manuscripts to Reviewers", Proceedings of the ACM SIGIR'92 15th International Conference on Research and Development in Information Retrieval (Copenhagen, Denmark, 21–24 June 1992), pp.233–244.

[8] R.Landauer, "Zig-zag path to understanding [physical limits of information handling]", Physics and Computation, 1994. PhysComp '94, Proceedings., Workshop on , Issue Date: 17-20, Nov 1994, pp. 54-59

[9] Peter W. Foltz, Improving human-proceedings interaction: indexing the CHI index, CHI '95 Conference companion on Human factors in computing systems, pp.101-102.

[10] J.X Yang, J. Watada; "Efficient data mining method based on Fuzzy Clustering", Proceedings, International Symposium on Management Engineering, Aug. 2010, Japan, Kitakyusyu, pp.242-249.

[11] R. Kruse F, R. Höppner, F. Klawonn, and T. Runkler, Fuzzy Cluster Analysis. New York: Wiley, 1999.

[12] D. E. Gustafson andW. C. Kessel, "Fuzzy clustering with a fuzzy covariance matrix," in Proc. IEEE CDC, San Diego, CA, 1979, pp. 761–766.

[13] J. C. Bezdek, Pattern Recognition With Fuzzy Objective Functions.New York: Plenum, 1981.

[14] R. Babuˇska, Fuzzy Modeling for Control. Boston, MA: Kluwer , 1998

[15] Karypis, G., Han, E., "Fast Supervised Dimensionality Reduction Algorithm with Applications to Document Categorization and Retrieval", Proceedings of CIKM-00, 9th ACM Conference on Information and Knowledge Management, 2000, pp. 12 - 19.

[16] JX Yang, J Watada; "Wise search engine based on LSI", 2010 Autonomous Agents and Multiagent Systems (AAMAS2010), May. 2010, Canada, Toronto, Workshops-ADMI, pp.127-137.

[17] Landauer, T., et al., "Learning Human-like Knowledge by Singular Value Decomposition: A Progress Report", M. I. Jordan, M. J. Kearns & S. A. Solla (Eds.), Advances in Neural Information Processing Systems 10, Cambridge: MIT Press, 1998, pp. 45–51.

[18] Bradford, R., An Empirical Study of Required Dimensionality for Large-scale Latent Semantic Indexing Applications, Proceedings of the 17th ACM Conference on Information and Knowledge Management, Napa Valley, California, USA, 2008, pp. 153–162.

[19] Homayouni, Ramin, Heinrich, Kevin, Wei, Lai, Berry, Michael W., Gene Clustering by Latent Semantic Indexing of MEDLINE Abstracts, August 2004, pp. 104–115.

[20] Ding, C., A Similarity-based Probability Model for Latent Semantic Indexing, Proceedings of the 22nd International ACM SIGIR Conference on Research and Development in Information Retrieval, 1999, pp. 59–65.

[21] Bartell, B., Cottrell, G., and Belew, R., Latent Semantic Indexing is an Optimal Special Case of Multidimensional Scaling, Proceedings, ACM SIGIR Conference on Research and Development in Information Retrieval, 1992, pp. 161–167.

[22] Graesser, A., and Karnavat, A., Latent Semantic Analysis Captures Causal, Goal-oriented, and Taxonomic Structures, Proceedings of CogSci 2000, pp. 184–189.

2011 IEEE International Conference on Fuzzy Systems
June 27-30, 2011, Taipei, Taiwan

Visual-Based Guiding Method for Unmanned Helicopter Approaching to Landmark

[1]Kuo-Hsien Hsia
Dept. of Management Information System
Far East Univ.
Tainan, Taiwan, R.O.C.
E-mail: khhsia@cc.feu.edu.tw

[2]Shao-Fan Lien
Graduate School of Engr. Sci. & Tech.
Nat'l Yunlin Univ. of Sci. & Tech.
Yunlin County, Taiwan, R.O.C.
E-mail: g9510801@yuntech.edu.tw

[3]Juhng-Perng Su
Dept. of Electric. Engr.
Nat'l Yunlin Univ. of Sci. & Tech.
Yunlin County, Taiwan, R.O.C.
E-mail: sujp@yuntech.edu.tw

***Abstract*—This paper proposes an image-guided method for estimating the position of an AUH (autonomous unmanned helicopter) from one captured landmark image. The proposed method is intended for application as auxiliary information for the guidance of an AUH during approach of a landmark based landing. The relation between the camera position and landmark image can be analyzed by projective geometry with the provision of sufficient landmark features. ANFIS is utilized for establishing the mapping relation and establishing a fuzzy model for efficient camera position estimation. The proposed method provides a highly accurate method of AUH guidance during landmark approach.**

Keywords-camera position estimation; visual-based guiding; ANFIS; incomplete landmark image

I. INTRODUCTION

Unmanned aerial vehicles (UAVs) are very useful systems for aerial photography, gas pollution detection or military applications. UAVs could potentially replace human beings in the completion of many difficult tasks. Because of their ubiquitous uses, the theories and applications of UAV systems have become popular contemporary research topics. There are many types of UAVs with different functions. Generally UAVs can be divided into two major categories, fixed-wing type and rotary-wing type. The fixed-wing UAVs can carry out long-distance and high-altitude reconnaissance missions. However, flight control of fixed-wing UAVs is not easy in low-altitude conditions. Conversely, rotary-wing UAVs can hover in low-altitude while conducting surveys, photography or other investigations. Consequently in some applications, the rotary-wing type UAV is more useful than the fixed-wing UAV. One common type of rotary-wing type UAVs is the AUH (Autonomous Unmanned Helicopter). AUHs have characteristics that include of 6-DOF flight dynamics, VTOL (vertical taking-off and landing) and the ability to hover. These attributes make them ideal for aerial photography or investigation in areas that limit maneuverability.

In recent years, there has been a lot of research interested in a more intelligent design of autonomous controllers for controlling the basic flight modes of unmanned helicopters [1] – [3]. The controller design for AUHs requires multiple sensor feedback signals for sensing states of motion. One of the basic flight mode controls of unmanned helicopters is landing. The most commonly used sensors are IMU (Inertial Measurement Unit) and GPS (Global Positioning System). The IMU provides three-axis angular velocity, and the GPS provides three-axis position information. For landing control, the height and pose of an unmanned helicopter are very important. There is a statement in [4] that the desired downward velocity is proportional to the square of the height. However, GPS error can range up to 6 meters [5]. This is much larger than the size of small unmanned helicopters and the landmark, both of which are usually measured in centimeters. Such large erroneous GPS measurements weaken the accurately landing ability of small unmanned helicopters. This paper will focus on the development of a position estimation method for that provides greater accuracy of position information for the guidance of unmanned helicopters during the approach to the landmark. The schematic diagram is shown in Fig. 1.

One of the guiding sensors is an image system which is usually collocated with IMU and GPS in the outdoor environment. The image system has been used on vehicles for navigation, obstacle avoidance or position estimation. In [6], the algorithm to extract the edge of the runway for computing the position of airplane was proposed. In [7] – [9], the image-guided methods with two or more images for guiding the RC unmanned helicopter approaching to the landmark are discussed. It is obvious that multiple-camera measurement system is an effective and mature method. However, the

This work was supported in part by the National Science Council, Taiwan, R.O.C., under Grant No. NSC99-2221-E-269-020.

978-1-4244-7316-8/11/$26.00 ©2011 IEEE

payload of the small unmanned helicopters has to be considered. Hence the image system is the smaller the better. In [10] and [11], image sequences are used to estimate the position of an unmanned helicopter. We developed a method for estimating the camera position from only a single image. Based on the estimated information, the unmanned helicopter can be guided to land autonomously.

The parking apron of a helicopter is in the shape of circle with an 'H' inside it. There are some recognition algorithms designed for recognizing the 'H' of the landmark [12], [13]. For the purpose of landing small unmanned helicopters autonomously and safely, the relative position between the small unmanned helicopter and the landmark has to be considered. Consequently, we propose a method for estimating the camera position from a single image. Referring to Fig. 1, when the unmanned helicopter is approaching the landmark, the camera position can be described by R, θ and Q.

Obviously, the measurement of spatial information from one image is very difficult. However, the relation between the camera position and landmark image can be analyzed by projective geometry. The proposed method for estimating the camera position from one image is illustrated in Fig. 2. In this method, we select sufficient features of the landmark image which can be related to the camera position. The mapping relation established by projective geometry is very complicated and the amount of data is substantial. Therefore the database is divided into four parts so as to reduce the size of the database by considering which quadrant the "center" of the landmark image is located in. The ANFIS is utilized for learning the database and establishing a fuzzy model of the mapping relation.

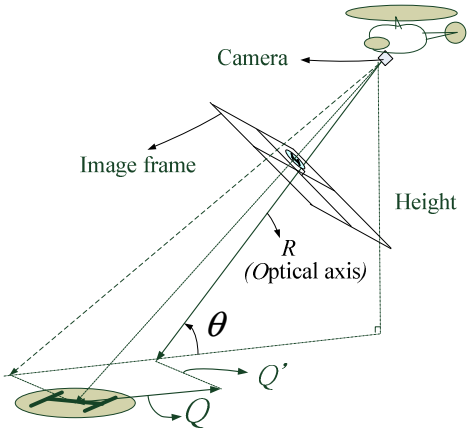

Fig. 1. The AUH approaching to landmark.

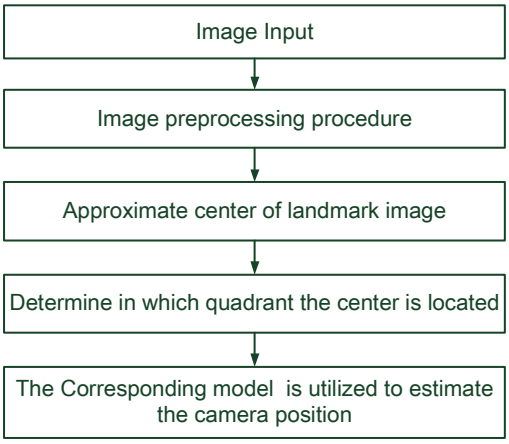

Fig. 2. The method of camera position estimation from landmark image.

In Fig. 2, the four major processes of the method are illustrated. The first step is "Image preprocessing procedure". In this procedure, the captured landmark picture is preprocessed into a clear and intact shape, and the binary image is computed to decrease the computation time. The second step is "Computing the approximate center of the landmark image". Since the landmark image is seriously deformed, the label 'H' on the landmark is employed for calculating the projection of the landmark center. The third step is "Determine in which quadrant the center is located". In this step, the approximate center is used to represent the location of landmark image. The last step is "Estimate the camera position with corresponding model". The camera position can be estimated quickly using the fuzzy model obtained by the ANFIS.

In the section of experimental results, different deformation cases of the landmark image are considered. Distortions that occur when the camera is at different shooting positions are simulated. The simulation is helpful for observing landmark image features. Moreover, the basic rectangle of the landmark image, corner detection, and the calculation of approximate center of landmark are demonstrated in the experimental results. The training results of ANFIS and camera position estimation results are demonstrated at the end of this paper.

II. Analysis of Image Features Via Projective Geometry

In this research, we consider the case of an unmanned helicopter approaching a landmark during landing. Fig. 3 illustrates the projection of the landmark diameter and the relation between the camera and the landmark. The landmark can be projected onto the image frame through the camera center [14]. The most obvious feature of the landmark is the diameter. The projection of the landmark diameter can be divided into vertical and horizontal directions. The projection cases specific to vertical direction and horizontal direction will be discussed in the following subsections.

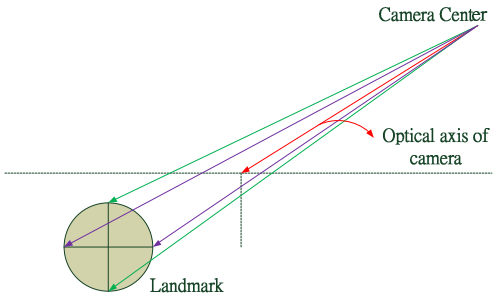

Fig. 3. The center projection of the landmark.

A. Landmark image features projection in the horizontal direction

We will first consider the projection case of the horizontal diameter. In Fig. 4, the plane π is perpendicular to the optical axis, and π is located somewhere on the optical axis. Here, π is equivalent to the image frame. In addition, form Fig. 4, the landmark diameter is projected onto π and the projection of the landmark radius r is $\hat{m}$ and $\hat{n}$ in the vertical and the horizontal directions, respectively. The geometric projection relation between landmark radius r and $\hat{m}$, $\hat{n}$ is shown as Fig. 4. The distance P and B are

$$P = \sqrt{R^2 + H^2}\ , \tag{1}$$

$$B = \sqrt{(Q+P)^2 + H^2}\ , \tag{2}$$

respectively. Where H is the altitude of camera and R is the distance from the camera center to the ground.

To analyze the projection relations in Fig. 4, three regions, named Ψ_1, Ψ_2 and Ψ_3, in the shape of triangle, are employed. They are shown as colored regions in Figs. 5, 6, and 7, respectively. Consider the case of Fig. 5, region Ψ_1 is a triangle with several angles in it. The angles could be computed with trigonometric functions. The derivation of the angles are (3) and (4) .

$$\begin{cases} \alpha_1 = \tan^{-1}\left((Q'+r)/B\right) \\ \alpha_2 = \tan^{-1}\left(Q'/B\right) \\ \alpha_3 = \tan^{-1}\left((Q'-r)/B\right) \end{cases} \tag{3}$$

$$\begin{cases} \beta_2 = \alpha_1 - \alpha_2 \\ \beta_1 = \alpha_1 - \alpha_2 - \beta_2 \end{cases} \tag{4}$$

Next, the region Ψ_2 is shown in Fig. 6. There are three angles γ_1, γ_2 and γ_3 in this region. The derivation of the angles is (5). Similarly, B' can be computed with trigonometric functions and γ_1, γ_2, γ_3.

$$\begin{cases} \gamma_1 = \tan^{-1}\left((Q+P)/H\right) \\ \gamma_2 = 90 - \theta \\ \gamma_3 = \gamma_1 - \gamma_2 \end{cases} \tag{5}$$

Finally, the third region Ψ_3 is illustrated in Fig. 7. In this figure, the projections of the landmark radius r are $\hat{m}$ and $\hat{n}$ which can be obtained by (6) and (7).

$$\begin{cases} Q'_{proj} = B' * \tan^{-1}(\alpha_2) \\ e = B' * \tan^{-1}(\alpha_3) \\ f = B' * \tan^{-1}(\alpha_1) \end{cases} . \tag{6}$$

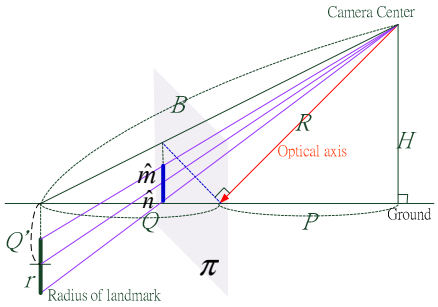

Fig. 4. The center projection of the landmark image features in horizontal direction.

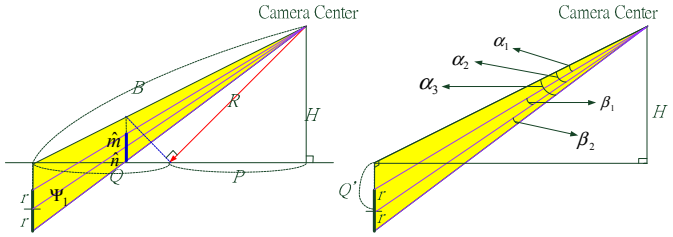

Fig. 5. Image features analysis in region Ψ_1. (a)The region Ψ_1 referring to Fig. 4. (b) The important angles α_1, α_2, α_3 and β_1, β_2 in region Ψ_1.

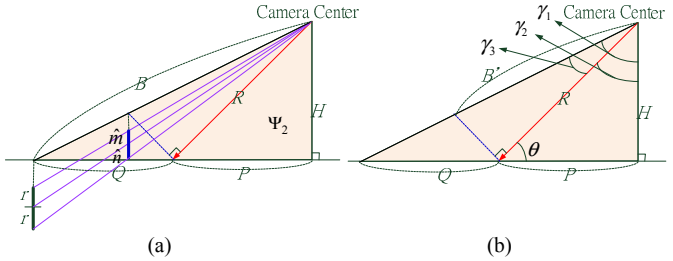

Fig. 6. Image features analysis in region Ψ_2. (a)The region Ψ_2 referring to Fig. 4. (b) The important angles γ_1, γ_2 and γ_3 in region Ψ_2.

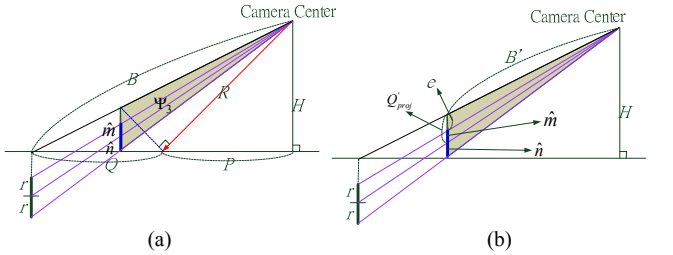

Fig. 7. Image features analysis in region Ψ_3. (a)The region Ψ_3 referring to Fig. 4. (b) The landmark radius r, and its projections $\hat{m}$ and $\hat{n}$.

$$\begin{cases} \hat{m} = Q'_{proj} - e \\ \hat{n} = f - Q'_{proj} \end{cases} . \quad (7)$$

B. Landmark image features projection in the vertical direction

In the case of landmark image features projections in the vertical direction, the geometric analyses will be more complicated than those of the horizontal case. However, the projection of the image features can be obtained by similar methods. In Fig. 8, the landmark radius is projected onto the plane π and form g_5, g_6.

The projective geometry illustrated in Fig. 8 will be discussed in terms of five distinct regions. One of them is named Ω_1, and as shown in Fig. 9, is a triangle. Three of them are triangles containing the vertical red lines individually, named Ω_2, Ω_3, and Ω_4, as shown in Fig. 10. And the last is a ladder-shaped region, named Ω_5, as shown in Fig. 11.

Consider the colored region Ω_1 shown in Fig. 9(a). Many useful quantities including angles and line segments can be computed from the region Ω_1. From Fig. 9(b), the angles obtained by (8) can be used to compute the line segments in Figs. 9(c) and 9(d) by equations (9)-(11).

$$\begin{cases} \omega_1 = \tan^{-1}\left((P+Q+r)/H\right) \\ \omega_2 = \omega_1 - \gamma_2 \\ \omega_6 = \tan^{-1}\left((P+Q-r)/H\right) \\ \omega_3 = \omega_1 - \omega_6 \\ \omega_7 = \tan^{-1}\left((P+Q)/H\right) \\ \omega_4 = \omega_1 - \omega_7 \\ \omega_5 = \omega_1 - \omega_6 - \omega_4 \\ \omega_8 = \omega_6 - \gamma_2 \end{cases} . \quad (8)$$

$$\begin{cases} e_3 = R * \tan(\omega_2) \\ e_4 = R * \tan(\omega_8) \\ e_5 = R * \tan(\omega_8 + \omega_5) \\ e_1 = e_5 - e_4 \\ e_2 = e_3 - e_5 \end{cases} . \quad (9)$$

$$\begin{cases} k_1 = \sqrt{(P+Q+r)^2 + H^2} \\ k_2 = \sqrt{(P+Q)^2 + H^2} \\ k_3 = \sqrt{(P+Q-r)^2 + H^2} \end{cases} \quad (10)$$

$$\begin{cases} u_1 = \sqrt{R^2 + e_3^2} \\ u_2 = \sqrt{R^2 + e_5^2} \\ u_3 = \sqrt{R^2 + e_4^2} \end{cases} . \quad (11)$$

From the triangles Ω_2, Ω_3, Ω_4 in Fig. 10 and the results obtained from equations (9)-(11), one can obtain q_1, q_2 and q_3 by (12).

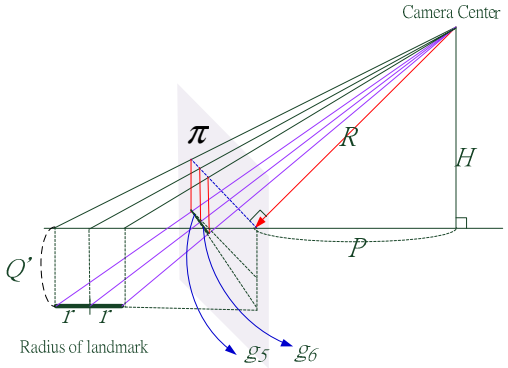

Fig. 8. The center projection of the landmark image features in vertical direction.

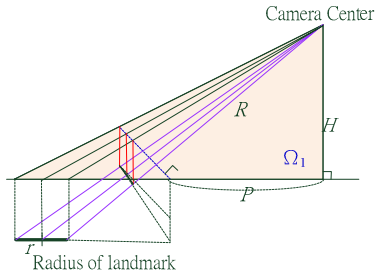

(a)

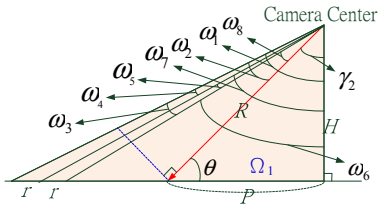

(b)

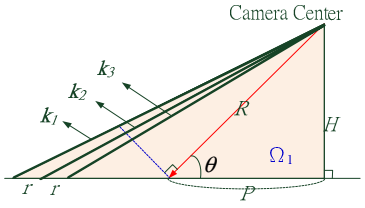

(c)

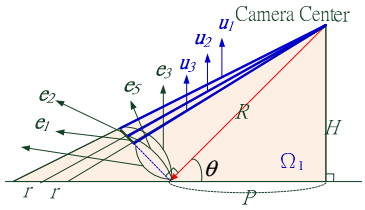

(d)

Fig. 9. Image features analysis in region Ω_1. (a) The region Ω_1 referring to Fig. 8. (b) The important angles ω_1- ω_8 in region Ω_1. (c) The important lines k_1- k_3 in region Ω_1. (d) Other important features.

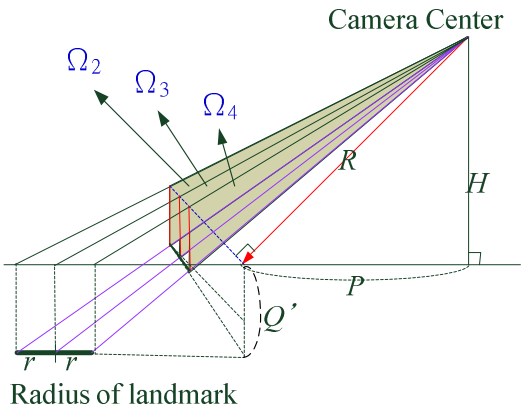

(a)

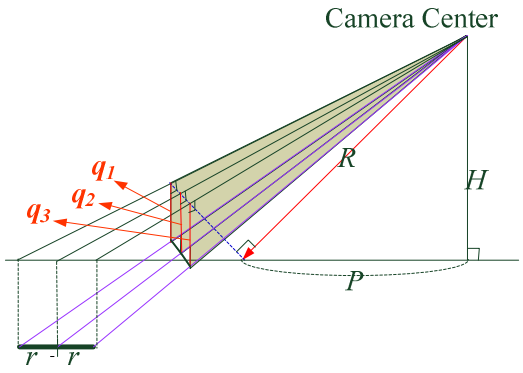

(b)

Fig. 10. Image features analysis in regions Ω_2, Ω_3, Ω_4. (a) The regions Ω_2, Ω_3, Ω_4 referring to Fig. 8. (b) The important line segments q_1-q_3 in regions Ω_2, Ω_3, Ω_4.

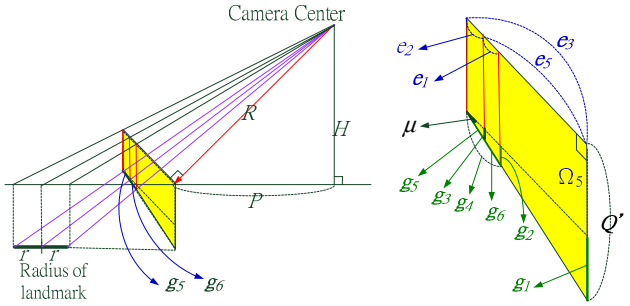

(a) (b)

Fig. 11. Image features analysis in plane Ω_5. (a) The region Ω_5 referring to Fig. 8. (b) Features g_5, g_6 in region Ω_5.

$$\begin{cases} q_1 = u_1(Q'/k_1) \\ q_2 = u_2(Q'/k_2) \\ q_3 = u_3(Q'/k_3) \end{cases}. \tag{12}$$

Then we discuss the third part, as in Fig. 11, the projection of the landmark radius g_5 and g_6 are included in Ω_5. The derivation of g_5 and g_6 is shown in (13).

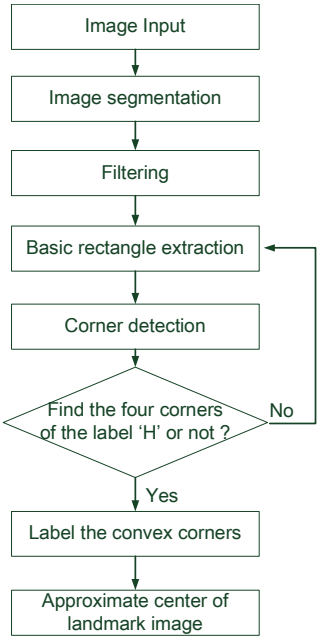

Fig. 12. The Image feature extraction procedure.

$$\begin{cases} g_1 = Q' - q_1 \\ g_2 = q_3 - q_1 \\ g_3 = q_2 - q_1 \\ g_4 = \sqrt{(e_1 + e_2)^2 + g_2^2} \\ g_5 = \sqrt{e_2^2 + g_3^2} \\ g_6 = g_4 - g_5 \end{cases}. \tag{13}$$

III. IMAGE FEATURES EXTRACTION

The procedure of image feature extraction is illustrated in Fig. 12. There are three major parts in this procedure. They are "*Image preprocessing procedure*", "*Corner detection and approximate center computing*" and "*Landmark image feature extraction*". Details about the three parts are discussed below.

A. Image preprocessing procedure

The landmark image features can be obtained by image preprocessing [15]. There are three major parts in this algorithm. The first part is image segmentation, including thresholding and filtering for segmenting the approximate landmark image in the frame. Thresholding is a fundamental tool for segmentation of an image when objects and background pixels can be distinguished by their grey level values. When an image is segmented into a binary image, analysis and computing become far easier. The second technique used for image pre-processing is morphological image processing, which is utilized to obtain more complete and clear edges of the target image. Erosion and dilation are the commonly used operations of morphological image processing [16]. The third part is landmark image extraction, including "Recursive connected labeling algorithm", "Basic rectangle computing" and "Major axis and minor axis computing". A connected labeling algorithm is usually used for multiple

objects labeling in image. But this process is not necessary in this paper since only a signal landmark image is considered.

B. Corner detection and approximate center computing

A corner detection algorithm is utilized for detecting the four corners of the label 'H' of the landmark. There are many different corner detection algorithms developed for locating feature points. One of the common corner detection algorithms is Harris corner detector [17]. The main principle of Harris corner detector is to use the Gaussian filter to detect the corners response of each pixel in the image. Gaussian filter can not only enhance the significant corners, but also remove the undesirable corners. Moreover, it can reduce the probability of misjudgment. Although the Harris corner detector is a very useful tool, it requires a lot of computing time. Therefore the corner detection operations are applied only for the basic rectangle to reduce computation time.

Further, the procedure is developed to locate the approximate center of the landmark image. The procedure is described as follows.

STEP 1 Detect the corners of the image in the basic rectangle.

STEP 2 Detect the convex corners of the label 'H'.

STEP 3 Label the convex corners and extracted the four corners of the label 'H'.

STEP 4 Find the intersection of the diagonals, and designate these coordinates as the approximate center of the landmark image.

C. Landmark image feature extraction

From section II, we know that the deformation of a landmark image is unavoidable. Even so, the projection relation can be analyzed via the proposed method. The projections of the landmark radius in vertical and horizontal directions are g_5, g_6, $\hat{m}$, and $\hat{n}$, respectively. Fig. 13(a) is an example of the image of the landmark. The white part is obviously a deformed circle. Fig. 13(b) is a sketch map showing the features of the landmark image.

IV. Database Construction and ANFIS Structure

ANFIS (Adaptive Neuro-Fuzzy Inference Systems) is a very high efficiency learning algorithm. Its learning effect is equivalent to that of NNs (neural network), but the requisite learning time is substantially lower. Consequently, ANFIS is employed in this paper for learning the mapping relation between the landmark and camera position.

The input of the ANFIS are g_5, g_6, e_5, $\hat{m}$, $\hat{n}$, q_2, and d. The output of ANFIS are θ, R and Q. The amount of the training data is very large. Since the center of the landmark image will only appear in one of the quadrants, the database is then split into four parts depending on the quadrant location of the estimated center so to reduce the quantities of training data required. They are "the landmark image located at the first quadrant", "the landmark image located at the second quadrant", "the landmark image located at the third quadrant" and "the landmark image located at the fourth quadrant".

Four ANFIS named "$ANFIS_{First_Quadrant}$", "$ANFIS_{Second_Quadrant}$", "$ANFIS_{Third_Quadrant}$" and "$ANFIS_{Fourth_Quadrant}$" are established by the corresponding database. The ANFIS for all databases is called "$ANFIS_{cam_estimation}$" and its structure is illustrated in Fig. 14. The structure of any one of these ANFIS's is illustrated in Fig. 15.

V. Experimental Results

The experimental results of the proposed method for camera position estimation are discussed in this section. The features are not easily extracted from a deformed landmark image. Fig. 16 shows some simulation results of the projection of the landmark under different conditions. The intersection of optical axis of the camera system and ground is set to be at (0,

(a)

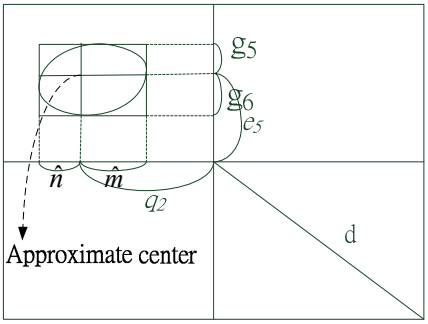

(b)

Fig. 13. The features of landmark image. (a) The captured landmark image. (b) The selected features of landmark image and the approximate center.

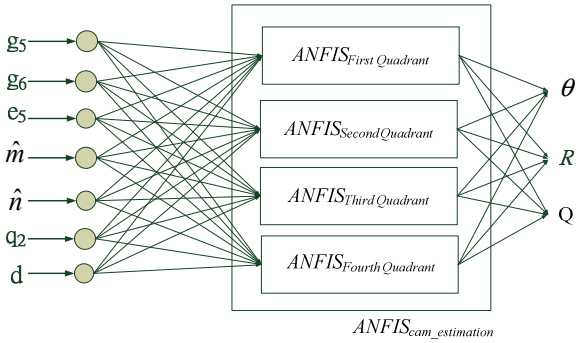

Fig. 14. The structure of the $ANFIS_{cam_estimation}$.

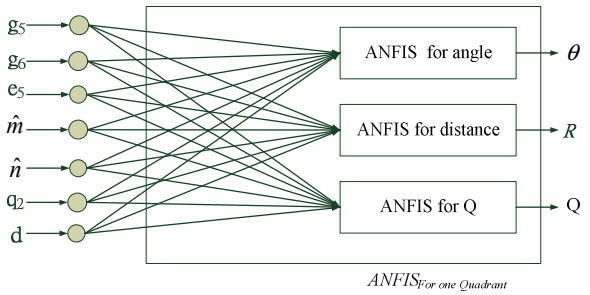

Fig. 15. The structure of one ANFIS in "$ANFIS_{cam_estimation}$"

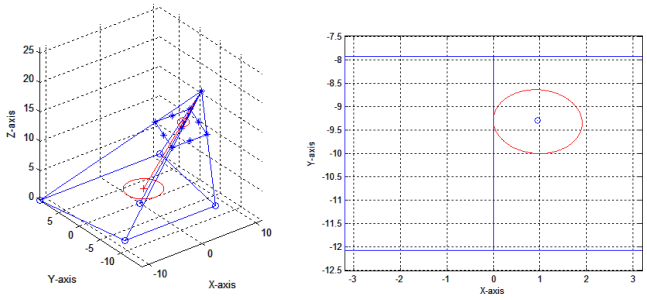

(a)

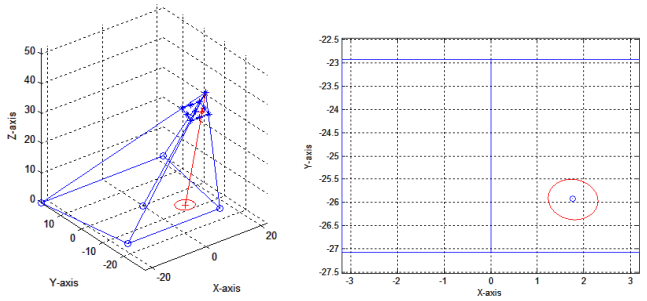

(b)

Fig. 16. The simulations of the projection of the landmark. (a) The camera system at R=30, θ=30° and the landmark position at (3,3). (b) The camera system at R=60, θ=30° and the landmark position at (10,-7)

0). For example, Fig. 16(a) shows the relations of a randomly set camera system and the landmark, and the corresponding projection of the landmark and the center is shown in Fig. 16(b). Similarly, Fig.16(c) and (d) show the camera position at R=60 , θ =30° and the center of landmark at (10, -7). The deformation of the landmark image is obvious.

A. Image processing and feature extraction results

Consider the image shown in Fig. 17, in our simulations, the landmark diameter is 3cm and the size of the image is 320 by 240 pixels. For example, Fig. 17(a) is an obtained real image, and Fig. 17(b) is the binary image and the basic rectangle of landmark. The order statistics filter [18] is utilized for obtaining the clear landmark image. The computed major and minor axis of basic rectangle are 71.70 and 58.47, respectively. Fig. 17(c) shows the corner detection result and approximate center.

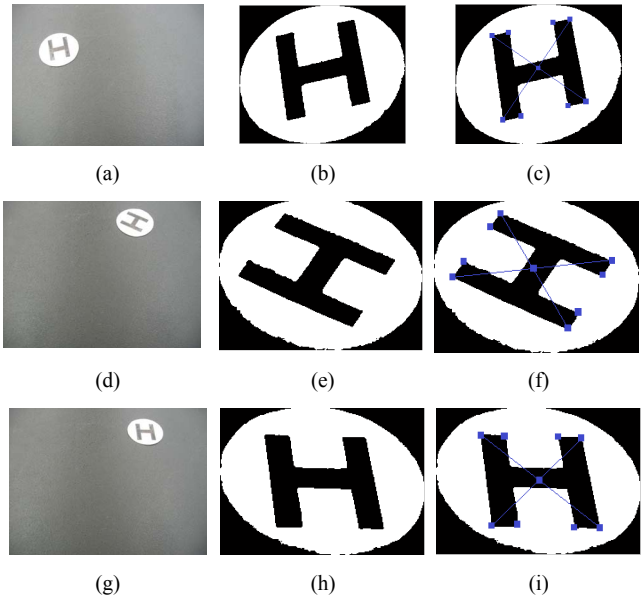

(a) (b) (c) (d) (e) (f) (g) (h) (i)

Fig. 17. The simulations of the image processing and feature extraction results. (a) The test image 1. (b) The binary image and the basic rectangle of test image 1. (c) the corner detection and approximate center of test image 1. (d) The test image 2. (e) The binary image and the basic rectangle of test image 2. (f) the corner detection and approximate center of test image 2. (g) The test image 3. (h) The binary image and the basic rectangle of test image 3. (i) the corner detection and approximate center of test image 3.

TABLE I. IMAGE FEATURES THAT EXTRACTED FROM FIG. 16

Image No.	Image Features					
	g_5	g_6	e_5	$\hat{m}$	$\hat{n}$	q_2
Test image1	32.55	22.70	37.33	28.41	37.83	77.29
Test image2	22.27	22.23	82.36	29.44	30.31	53.68
Test image3	20.64	21.11	80.48	28.50	29.00	60.38

Similarly, the other features in Fig. 17 are collated in TABLE I. By reviewing this data we can see that the simulation results demostrate that the proposed image proccess method can extract landmark image features. Furthermore the corner detection algorithm will not be affected by the rotation or deformation of a landmark image. The landmark image is clear therefore the features are easily extracted.

B. Camera position estimating results

The ANFIS training data is generated by geometric computation and then classified into four parts to reduce the training time and the structure of ANFIS. This paper considers the practical application of an AUH approaching a landmark. The research does not examine extreme situations. Therefore the training range of R is from 20cm to 300cm. The training range of θ is from 55° to 90°. The training RMSE (root mean squared error) of R, θ and Q in $ANFIS_{First_Quadrant}$ are 0.1325, 0.1433 and 0.1654, respectively. The training RMSE of R, θ

TABLE II. THE ESTIMATION RESULTS OF CAMERA POSITION

Data No.	Camera Position			Estimating Error		
	R (cm)	θ	Q (cm)	R (cm)	θ	Q (cm)
1	33	65	10	0.124	-0.145	0.216
2	45	78	19	0.217	0.204	0.145
3	59	57	21	-0.194	0.174	-0.164
4	65	81	45	-0.154	-0.134	0.201
5	106	84	50	0.198	0.165	0.169
6	124	59	54	-0.119	0.214	0.176
7	154	81	14	0.132	-0.175	0.203
8	169	71	35	0.211	0.132	-0.164
9	201	84	44	-0.209	-0.198	-0.170
10	284	65	95	-0.174	0.181	0.198

and Q in $ANFIS_{Second_Quadrant}$ are 0.1026, 0.2053 and 0.1461, respectively. The training RMSE of R, θ and Q in $ANFIS_{Third_Quadrant}$ are 0.1271, 0.0971 and 0.0745, respectively. The training RMSE of R, θ and Q in $ANFIS_{Fourth_Quadrant}$ are 0.0925, 0.1033 and 0.0754, respectively. Some of the estimation results of camera position are illustrated in TABLE II. In TABLE II, 10 data sets are employed to verify the fuzzy model. The average absolute error of R is 0.1732cm, the average absolute error of θ is 0.1722°, and the average absolute error of Q is 0.1806cm.

VI. CONCLUSIONS

For the guidance of an AUH during its landmark approach, we proposed a visual-based guidance method for camera position estimation. This method can estimate the camera position via select landmark features. The designed method can reduce the image process procedure. More importantly, the image features can be extracted from a deformed landmark image. The simulation results show that the basic rectangle and the label 'H' are very helpful for computing the image features.

In addition, the size of established database is very large. To reduce the quantities of training data and thereby speed up the ANFIS training the database is split into four parts. The ANFIS established an approximate fuzzy model to replace the complex projective relationship between the camera and landmark. In practical applications, this method can provide the position information required by an AUH for accurate guidance during approach to a landmark.

REFERENCES

[1] Z. Fang, J. Wu, and P. Li, "Control System Design and Flight Testing for a Miniature Unmanned Helicopter," Proceedings of the 7th World Congress on Intelligent Control and Automation, Chongqing, pp. 2315–2319, June 2008.

[2] X. Guo, W. Sun, Z. Li and L. Ren, "The Flight Control Design of Mini Unmanned Helicopter on Sliding Mode Control," Chinese Control and Decision Conference, China, pp. 3245–3248, May 2010.

[3] P. Song, G. Qi and K. Li, "The Flight Control System Based On Multivariable PID Neural Network For Small-Scale Unmanned Helicopter," International Conference on Information Technology and Computer Science, Kiev, vol. 1, pp. 538–541, July 2009.

[4] T. J. Ross, Fuzzy Logic with Engineering Applications, Wiley, 2010.

[5] GPS 18 Technical Specifications, Revision D, Garmin International, USA, June 2005.

[6] H.-U. Doehler and B. Korn, "Robust position estimation using images from an uncalibrated camera," Digital Avionics Systems Conference, USA, vol. 2, pp. 9.D.2–1–9.D.2–7, October 2003.

[7] C. Xu, L. Qiu, M. Liu, B. Kong and Y. Ge, "Stereo Vision Based Relative Pose and Motion Estimation for Unmanned Helicopter Landing," IEEE International Conference on Information Acquisition, China, pp. 31-36, August 2006.

[8] W. Bagen, J. Hu and Y. Xu, "A Vision-Based Unmanned Helicopter Ship Board Landing System," International Congress on Image and Signal Processing, Tianjin, China, pp. 1-5, October 2009.

[9] A. Johnson, J. Montgomery and L. Matthies, "Vision Guided Landing of an Autonomous Helicopter in Hazardous Terrain," IEEE International Conference on Robotics and Automation, Varcelona, Spain, pp. 3966-3971, April 2005.

[10] A. Cesetti, E. Frontoni, A. Mancini, P. Zingaretti and S. Longhi, "A Single-Camera Feature-Based Vision System for Helicopter Autonomous Landing," International Conference on Advanced Robotics, Munich, Germany, pp. 1-6, June 2009.

[11] B. Yuan and Y. Hao, "A Method of Vision-Based State Estimation of an Unmanned Helicopter," International Conference on Wireless Communications Networking and Mobile Computing, Chengdu, pp. 1-4, September 2010.

[12] G. F. Nsogo, K. Kith, B. J. van Wyk and M. A. van Wyk, "Robust Helipad Detection Algorithm," IEEE Africon Conference, pp.1–6, Namibia, September 2007.

[13] Y. Fan, S. Haiqing and W. Hong, "A Vision-Based Algorithm for Landing Unmanned Aerial Vehicles," International Conference on Computer Science and Software Engineering, vol. 1, pp.993-996, China, December 2008.

[14] R. Hartley and A. Zisserman, Multiple View Geometry in computer vision, Cambridge University Press, 2003.

[15] D. A. Forsyth and J. Ponce, Computer Vision: A Modern Approach, Prentice Hall, 2002.

[16] L. G. Shapiro and G. C. Stockman, Computer Vision, Prentice Hill. 2001.

[17] M. Nixon and A. Aguado, Feature Extraction & Image Processing, Amsterdam Academic, Boston, 2008.

[18] S. Peltonen, M. Gabbouj and J. Astola, "Nonlinear Order Statistic Filter Design: Methodologies," International Symposium on Image and Signal Processing and Analysis, pp. 102–107, Croatia, June 2001.

2011 IEEE International Conference on Fuzzy Systems
June 27-30, 2011, Taipei, Taiwan

On the Type-1 and Type-2 Fuzziness Measures for Thresholding MRI Brain Images

R. Rajesh
Technology Development Centre
Network Systems and Technologies
Technopark, Thiruvananthapuram - 695581
Email: kollamrajeshr@ieee.org

N. Senthilkumaran, J. Satheeshkumar,
B. Shanmuga Priya, C. Thilagavathy, K. Priya
Department of Computer Applications
Bharathiar Universisty, Coimbatore - 641046, India
Email: jsathee@rediffmail.com

***Abstract*—The result of image thresholding is not always satisfactory due to the disturbing factors like vagueness, non-uniform illumination etc and to overcome these problems recently various researchers have proposed fuzzy image thresholding. The linear index of fuzziness for type-1 fuzzy sets by Zenzo et. al. and measure of ultrafuzziness for type-2 fuzzy sets by Tizhoosh has difficulties in handling MRI brain images with one level of gray value as background and other two levels of grayness as white matter and gray matter. Hence this paper proposes new modified thresholding measures for MRI brain images using type-1 and type-2 fuzzy sets. The results show the effectiveness of the proposed modified thresholding measures.**

***Index Terms*—type-1 fuzzy sets, type-2 fuzzy sets, thresholding, ultrafuzziness**

I. Introduction

Image thresholding, considered as the simplest form of segmentation, is an important task in most of the image processing applications. Lot of research work has already been appeared on robust thresholding techniques [1], [2], [3]. Recently fuzzy set theory have been used extensively in image thresholding [4], [7], [8], [9], [10], [11], [12], [13] due to the ability of fuzzy logic in handling ambiguity/vagueness in the presence of disturbing factors like non-uniform illumination, vagueness etc.

Fuzzy thresholding techniques can be classified into four categories [4] based on the way in which it is applied. They are namely (a) fuzzy clustering using fuzzy c-means, probabilistic c-means etc. (b) rule-based approaches (c) fuzzy geometrical approaches using spatial image information and geometrical measures(compactness, area coverage etc.) (d) information-theoretical approach by minimizing/maximizing measures of fuzziness (index of fuzziness, fuzzy entropy, fuzzy divergence etc.). Due to the simplicity and high speed of information-theoretical approach [7], [8], [9], [10], [11] it has been mostly used for image thresholding.

The linear index of fuzziness for type-1 fuzzy sets by Zenzo et. al. [11] and measure of ultrafuzziness for type-2 fuzzy sets by Tizhoosh [4] has difficulties in handling (we mean thresholding) MRI brain images. Here the difficulties in thresholding are due to the presence of 3 levels of grayness in MRI images, one level of gray value as background and other two levels of grayness as white matter and gray matter. Hence this paper proposes new modified thresholding measures for MRI brain images using type-1 and type-2 fuzzy sets. The results show the effectiveness of the proposed modified thresholding measures.

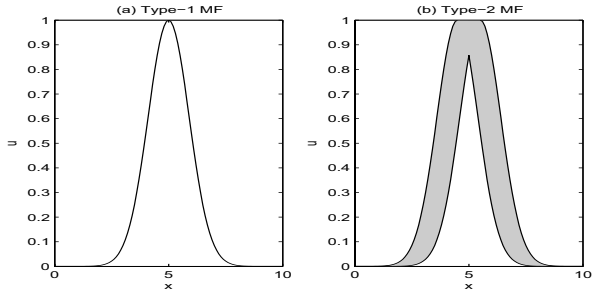

Fig. 1. Gaussian membership function with variance=0.9 of (a) type-1 with mean=5 (b) type-2 with uncertain means mean1=4.5, mean2=5.5

This paper is organized as follows. Section II deals with measure of fuzziness and section III introduces modified measures of fuzziness. Section IV presents the experimental results and section V concludes the paper.

II. Measure of fuzziness

A. Type-1 fuzzy sets

A type-1 fuzzy set A in X is defined by a type-1 membership function $\mu_A(x)$ given by

$$A = \{(x, \mu_A(x)) | x \in X\} \tag{1}$$

Figure 1a shows the Gaussian membership function of type-1 fuzzy set with variance = 0.9 and mean = 5.

The linear index of fuzziness [11] for an $M \times N$ image subset $A \subseteq X$ with L gray levels $g \in [0, L-1]$ can be given by

$$\gamma_l(A) = \frac{2}{MN} \sum_{g=0}^{L-1} h(g) \times \min[\mu_A(g), 1 - \mu_A(g)] \tag{2}$$

where h(g) is the histogram. $\mu_X(g)$ is the membership function and can be defined by the standard S-function, Huang & Wang function, triangular membership function, LR type fuzzy number etc..

978-1-4244-7316-8/11/$26.00 ©2011 IEEE

B. Type-2 fuzzy sets

Even though the application of T1 FS has seen success in all applications[5], [6], since it introduction by Zadeh in 1965, it has limited capabilities to directly model and minimize the effect of uncertainties [14], [15], [16], [17], [18]. This is due to the fact that T1 FS does not have measure of dispersion to capture more about linguistic uncertainties as equivalent to that of probability density function (pdf) [1] having variance as a measure of dispersion about the mean. In late 1975, Zadeh introduced the concept of type-2 fuzzy sets (T2 FS). T2 FS are described by membership functions (MFs) that are characterized by more parameters than MFs for T1 FSs and hence T2 FSs provide more degrees of freedom to handle uncertain environments [14]. Type-2 fuzzy sets are characterized by fuzzy membership functions that are three-dimensional with membership grade as a fuzzy set in [0, 1] rather than two dimensional membership functions with crisp number in [0, 1] as membership grade as in the case of T1 FS.

A type-2 fuzzy set ($\tilde{A}$) is given by

$$\tilde{A} = \{((x,u), \mu_{\tilde{A}}(x,u))|\ \forall x \in X,\ \forall u \in J_x \subseteq [0,1]\} \quad (3)$$

where $0 \leq \mu_{\tilde{A}}(x,u) \leq 1$ is a type-2 membership function. $\tilde{A}$ can also be expressed as

$$\tilde{A} = \int_{x\in X} \int_{u\in J_x} \mu_{\tilde{A}}(x,u)/(x,u), \qquad J_x \subseteq [0,1] \quad (4)$$

A more practical definition for a type-2 fuzzy set can be given as

$$\begin{aligned} \tilde{A} \quad = \quad & \{(x, \mu_U(x), \mu_L(x))|\ \forall x \in X, \\ & \mu_L(x) \leq \mu(x) \leq \mu_U(x), \mu \in [0,1]\} \end{aligned} \quad (5)$$

Figure 1b shows the Gaussian membership function of type-2 fuzzy set with variance = 0.9 and uncertain means 4.5 & 5.5.

The ultrafuzziness [4] $\tilde{\gamma}$ for an $M \times N$ image subset $\tilde{A} \subseteq X$ with L gray levels $g \in [0, L-1]$ can be given by

$$\gamma_l(A) = \frac{2}{MN} \sum_{g=0}^{L-1} h(g) \times [\mu_U(g) - \mu_L(g)] \quad (6)$$

where h(g) is the histogram, $\mu_{\tilde{A}}(g)$ is the membership function, $\mu_U(g) = [\mu_A(g)]^{1/\alpha}$ is the upper membership values, $\mu_L(g) = [\mu_A(g)]^{\alpha}$ is the lower membership value and $\alpha \in (1,2]$.

III. Introducing Modified fuzziness measure

A. Modified index of fuzziness for type-1 fuzzy sets

The modified index of fuzziness for an $M \times N$ image subset $A \subseteq X$ with L gray levels $g \in [0, L-1]$ can be given by

$$\gamma_m(A) = \frac{2}{MN} \sum_{g=0}^{L-1} h(g) \times \mu_A(g) \times (1 - \mu_A(g)) \quad (7)$$

[1]pdfs usually require infinite number of moments. Since it is very difficult to determine all the moments, we make use of only first two moments namely mean and variance(measure of dispersion about mean)

where h(g) is the histogram. $\mu_A(g)$ is the membership function and can be defined by the standard S-function, Huang & Wang function, triangular membership function, LR type fuzzy number etc..

B. Modified measure of ultra fuzziness for type-2 fuzzy sets

The modified ultrafuzziness $\tilde{\gamma}$ for an $M \times N$ image subset $\tilde{A} \subseteq X$ with L gray levels $g \in [0, L-1]$ can be given by

$$\gamma_m(A) = \frac{2}{MN} \sum_{g=0}^{L-1} h(g) \times \mu_L(g) \times [\mu_U(g) - \mu_L(g)] \quad (8)$$

where h(g) is the histogram, $\mu_{\tilde{A}}(g)$ is the membership function, $\mu_U(g) = [\mu_A(g)]^{1/\alpha}$ is the upper membership values, $\mu_L(g) = [\mu_A(g)]^{\alpha}$ is the lower membership value and $\alpha \in (1,2]$.

IV. Experiments and results for thresholding brain images

Image thresholding using type-1 fuzzy sets is done by thresholding with the minimum/maximum fuzziness obtained by shifting the membership function, defined over the image histogram, along the grey level range. Similarly, image thresholding using type-2 fuzzy sets can be done by thresholding with the minimum/maximum ultrafuzziness obtained by shifting the membership function, defined over the image histogram, along the grey level range.

Magnetic resonance images have three levels of grayness inherent in it. One level of gray value can be seen as background and other two levels of grayness can be seen as white matter and gray matter. Fig. 2 shows the white and gray matter in the brain slice. Due to the presence of 3 levels of greyness in MRI images, it is very difficult to threshold. Normal thresholding for two levels of greyness (namely separating background and foreground) will not work properly for MRI images.

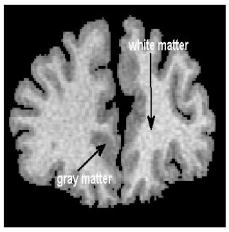

Fig. 2. White matter and gray matter corresponding to a brain slice

Several brain images have been experimented and here we show only the results of three slices of brain. Fig. 3 show the orginal brain slices and Fig. 4 show the corresponding preprocessed images.

Linear index of fuzziness (of type1) is calculated using eqn.2 and modified index of fuzziness (of type1) is calculated using eqn.7. Fig.5 show the plot of linear index of fuzziness and modified index of fuzziness corresponding to the preprocessed images (fig.4). It can be seen from the first image of Fig.5 that modified fuzziness index gives a threshold, $T_2 = 166$ for PImage1, which gives a much better thresolding result which can be seen from the first images

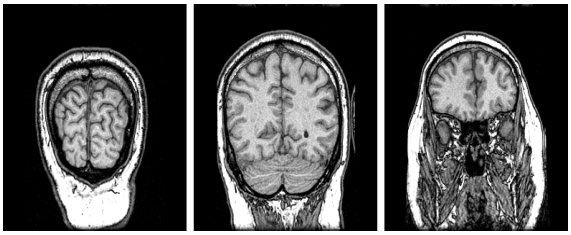

Fig. 3. Orginal images (from left) (a) Image1, (b) Image2, and (c) Image3

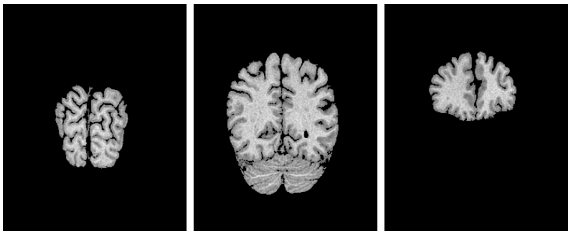

Fig. 4. Preprocessed images corresponding to Fig. 3 (from left) (a) PImage1, (b) PImage2, and (c) PImage3

of Fig.6 and Fig.7. Modified fuzziness index of PImage2 and PImage3, as seen in the second and third images of Fig.5, shows two twists corresponding to gray and white matter in the images. But such twists cannot be seen in the linear index of fuzziness of PImage2 and PImage3, as seen in the second and third images of Fig.5. The threshold values corresponding to the secondary twist helps to separate (and hence threshold) white matter. The thresholding results corresponding to the thresholds thus obtained (Fig.7) performs better than the linear thresholds (Fig.6) (Please see the second and third images of corresponding figures).

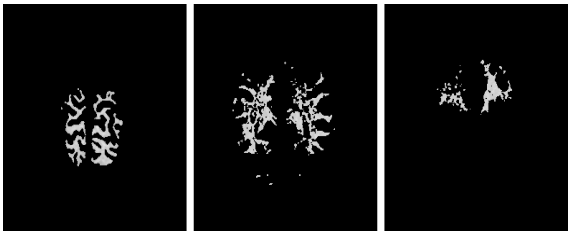

Fig. 6. Thresholded images with threshold obtained from fuzziness index of type1. Thresholded (a) PImage1 with T=176, (b) PImage2 with T=199, and (c) PImage3 with T=199

Ultrafuzziness (of type2) is calculated using eqn.6 and modified index of fuzziness (of type2) is calculated using eqn.8. Fig.8 show the plot of ultrafuzziness and modified ultrafuzziness corresponding to the preprocessed images (fig.4).

Modified ultrafuzziness shows two twists corresponding to

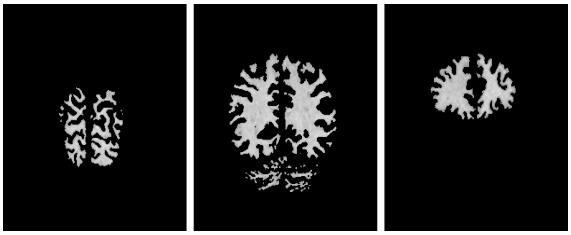

Fig. 7. Thresholded images with threshold obtained from modified fuzziness index of type1. Thresholded (a) PImage1 with T=166, (b) PImage2 with T=165, and (c) PImage3 with T=147

TABLE I
THRESHOLDS FOR THE IMAGES

	PImage1	PImage2	PImage3
Type-1	176	199	199
mType-1	166	165	147
Type-2	176	199	150
mType-2	156	150	133

gray and white matter in the images. The threshold values corresponding to the secondary twist helps to separate (and hence threshold) white matter. It can be seen from the figures that modified ultrafuzziness gives a thresholding result which is much better than the threshold of ultrafuzziness and it clear from the images of Fig.9 and Fig.10.

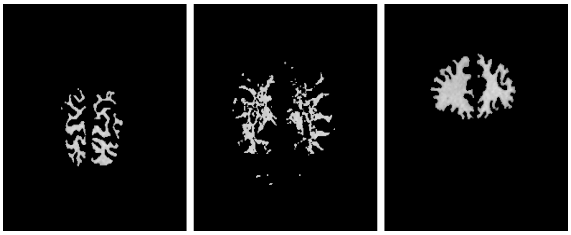

Fig. 9. Thresholded images with threshold obtained from ultrafuzziness of type2. Thresholded (a) PImage1 with T=176, (b) PImage2 with T=199, and (c) PImage3 with T=150

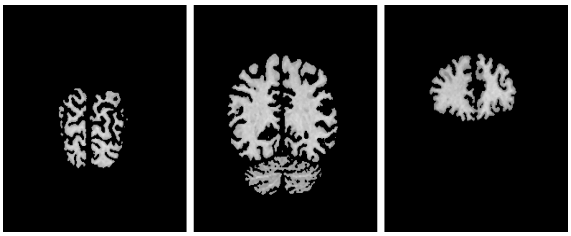

Fig. 10. Thresholded images with threshold obtained from modified ultrafuzziness of type2. Thresholded (a) PImage1 with T=156, (b) PImage2 with T=150, and (c) PImage3 with T=133

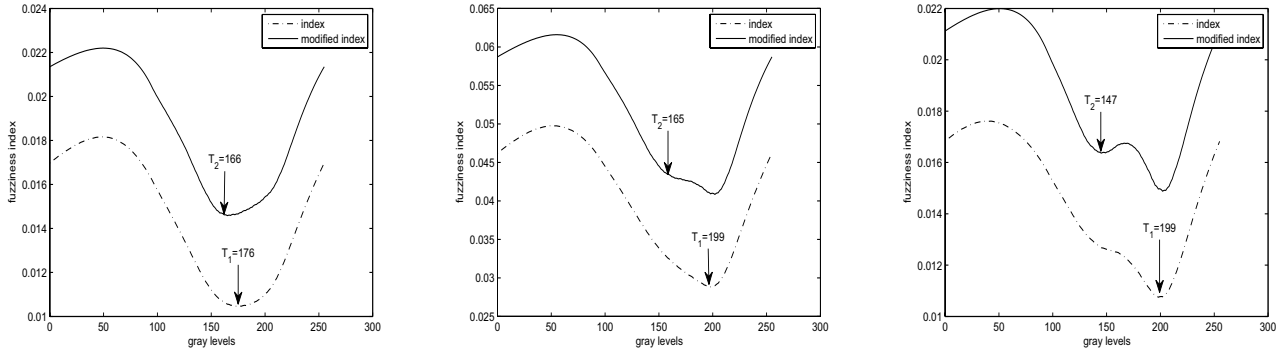

Fig. 5. Fuzziness index (of type1) and modified fuzziness index (of type1) for the images (from left) (a) PImage1, (b) PImage2, and (c) PImage3

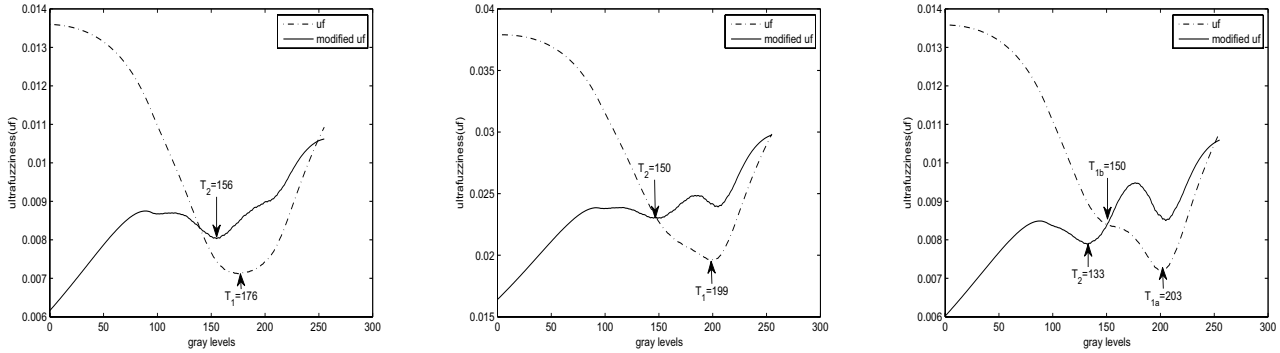

Fig. 8. Ultrafuzziness and modified ultrafuzziness for the images (from left) (a) PImage1, (b) PImage2, and (c) PImage3

V. Conclusion

Due to the difficulties in handling MRI brain images with one level of gray value as background and other two levels of grayness as white matter and gray matter, the paper has presented modified index of fuzziness for type1 fuzzy sets and modified ultrafuzziness for type2 fuzzy sets for thresolding brain images. The results have shown the effectiveness of the proposed modified thresholding measures.

Acknowledgment

This research is supported by University Grants Commission, India through a major research project grant (UGC F. No. 33-62/2007 (SR) dated 28th Feb 2008). N. Senthilkumaran, Thilagavathy, K. Priya and Shanmuga Priya are currently doing Ph.D in Bharathiar University.

References

[1] K.C. Lin, Fast image thresholding by finding the zeros of the first derivative of between class variance, Mach. Vis. Appl. 13 (5-6) (2003) 254-262.

[2] P.L. Rosin, Unimodel thresholding, Pattern Recognition 34 (11) (2001) 2083-2096.

[3] L. Snidaro, G.L. Foresti, Real-time thresholding with Euler numbers, Pattern Recognition Lett. 24 (9-10) (2003) 1543-1554

[4] H.R. Tizhoosh, Image thresholding using type II fuzzy sets, Pattern Recognition Lett. 38 (2005) 2363-2372.

[5] P. Balamurugan, R. Rajesh, Fuzzy Logic Approach using Guided Gray Level Coherence Features for Greenery and Non-Greenery Image Classification, Far East Journal of Experimental and Theoretical Artificial Intelligence, ISSN: 0974-3261, vol. 2(1), pp. 47-58, 2008

[6] R. Rajesh, M.R. Kaimal, T-S Fuzzy Model with Nonlinear Consequence and PDC Controller for a Class of Nonlinear Control Systems, Applied Soft Computing Journal, Elsevier (ISSN: 1568-4946), vol. 7(3), pp. 772-782, June 2007.

[7] L.K. Huang, M.J. Wang, Image thresholding by minimizing the measure of fuzziness, Pattern Recognition 28 (1995) 41-51.

[8] N.R. Pal, D. Bhandarai, D.D. Majumder, Fuzzy divergence, probability measure of fuzzy events and image thresholding, Pattern Recognition Lett. 13 (1992) 857-867.

[9] H.R. Tizhoosh, H. Haubecker, Fuzzy image processing: an overview, in: B. Jahne, H. Haubecker, P. Geibier (Eds.), Handbook on computer vision and applications, Academic Press, Boston, 1998.

[10] Q. Wang, Z. Chi, R. Zhao, Image thresholding by maximizing the index of nonfuzziness of the 2-D grayscale histogram, Computer Vision Image understanding 85 (2) (2002) 100-116.

[11] S.D. Zenzo, L. Cinque, S. Levialdi, Image thresholding using fuzzy entropies, SMC 28(1) (1998) 15-23.

[12] S.K. Pal, C.A. Murthy, Fuzzy thresholding: mathematical framework bound functions and weighted moving average technique, Pattern Recognition Lett. 11 (1990) 197-206.

[13] N. Senthilkumaran, R. Rajesh, "Edge Detection Techniques for Image Segmentation - A Survey of Soft Computing Approaches", International Journal of Recent Trends in Engineering, Academy Publisher (Finland), Issue. 1, Vol. 1, No. 2, June 2009

[14] J.M. Mendel, Uncertain Rule-based fuzzy logic systems, Prentice-Hall, Englewood Cliffs, NJ, 2001.

[15] J. M. Mendel and R. I. Bob John, Type-2 fuzzy sets made simple, IEEE Trans. on Fuzzy Systems, vol. 10, pp. 117-127, April 2002.

[16] Q. Liang and J. M. Mendel, Interval type-2 fuzzy logic systems: theory and design, IEEE Trans. on Fuzzy Systems, Vol. 8, pp. 535-550, Oct. 2000.

[17] N. N. Karnik, J. M. Mendel and Q. Liang, Type-2 fuzzy logic systems, IEEE Trans on Fuzzy Systems, vol. 7, pp. 643-658, Dec. 1999.

[18] N. N. Karnik and J. M. Mendel, Centroid of a type-2 fuzzy set, Information Sciences, vol. 132, pp. 195-220, 2001.

2011 IEEE International Conference on Fuzzy Systems
June 27-30, 2011, Taipei, Taiwan

A Fast Algorithm for Mining Frequent Closed Itemsets over Stream Sliding Window

Show-Jane Yen
Dept. of Computer Science & Information Engineering
Ming Chuan University
Taipei, Taiwan
sjyen@mail.mcu.edu.tw

Cheng-Wei Wu
Dept. of Computer Science & Information Engineering
National Cheng Kung University
Taipei, Taiwan
silvemoonfox@hotmail.com

Yue-Shi Lee
Dept. of Computer Science & Information Engineering
Ming Chuan University
Taipei, Taiwan
leeys@mail.mcu.edu.tw

Vincent S. Tseng
Dept. of Computer Science & Information Engineering
National Cheng Kung University
Taipei, Taiwan
tsengsm@mail.ncku.edu.tw

Chaur-Heh Hsieh
Dept. of Computer & Communication Engineering
Ming Chuan University
Taipei, Taiwan
hsiehch@mail.mcu.edu.tw

***Abstract*—Mining frequent patterns refers to the discovery of the sets of items that frequently appear in a transaction database. Many approaches have been proposed for mining frequent itemsets from a large database, but a large number of frequent itemsets may be discovered. In order to present users fewer but more important patterns, researchers are interested in discovering frequent closed itemsets which is a well-known complete and condensed representation of frequent itemsets. In this paper, we propose an efficient algorithm for discovering frequent closed itemsets over a data stream. The previous approaches need to do a large number of searching operations and computations to maintain the closed itemsets when a transaction is added or deleted. Our approach only performs few intersection operations on the transaction and the closed itemsets related to the transaction without doing any searching operation on the previous closed itemsets. The experimental results show that our approach significantly outperforms the previous approaches.**

Keywords-frequent closed itemsets; data stream; sliding window; data mining;

I. INTRODUCTION

Mining frequent itemsets [1, 4, 8] from a transaction database is a fundamental task to several data mining applications. The problem of discovering frequent itemsets in database is stated as follows: Given a finite set of *items* $I = \{a_1, a_2, \ldots, a_m\}$, a *transaction* t is a set of items which were purchased by a customer at the same time. A *transaction database* D contains a set of transactions and each transaction is given a unique identifier (TID). An *itemset* $X = \{i_1, i_2, \ldots, i_k\}$ ($i_j \in I$, $1 \le j \le k$) is a set of k distinct items, where k is the *length of* X. The *support count* of X is denoted as $SC(X)$ and defined as the number of transactions which contain X. The *support* of X is defined as the ratio of $SC(X)$ to the total number of transactions in D. An itemset is said to be *frequent* if its support is no less than a user specified threshold *min_sup* which is called *minimum support*. The problem of mining frequent itemsets from a database D is to discover all the itemsets whose supports are no less than *min_sup*. For example, suppose the *min_sup* is set to be 40% for the transaction database in Table I, that is, the *minimum support count* is 40% × 5 = 2.

TABLE I. TRANSACTION DATABASE

TID	Item Bought
t_1	C,D
t_2	A,B
t_3	A,B,C
t_4	A,B,C
t_5	A,C,D

Therefore, the frequent itemsets and their support counts are {A}:4, {B}:3, {C}:4, {D}:2, {AB}:3, {AC}:3, {BC}:2, {CD}:2 and {ABC}:2.

Several algorithms [1, 4, 9] have been proposed for mining frequent itemsets from transaction databases. But they mainly focused on static database and did not consider applications that involve data streams. A *transaction data stream* is an ordered sequence of transactions that comes in a timely order. Mining frequent itemsets over data streams is an important technique which is essential to a wide range of applications such as network traffic analysis, web click stream mining, on-line transaction analysis and many other important tasks. However, mining frequent patterns from data streams poses many challenges because data comes continuously, unbounded and usually with high speed. Furthermore, data distribution in a stream usually changes with time such that the status of itemsets may be changed (from frequent to infrequent or from infrequent to frequent). Hence, how to efficiently capture all the frequent itemsets over a data stream without information loss is a big challenge.

There are lots of works [2] in developing efficient algorithms for mining frequent itemsets from a data stream. But they often discover a large number of frequent itemsets and present too many redundant patterns to users. It is widely recognized that the larger the set of frequent itemsets is, the more the processing cost is required. In other words, the performance of the algorithms may be degraded when a database contains lots of frequent itemsets or a low threshold is used. In order to present users fewer but more important patterns, one of the solutions is to mine only the *frequent closed itemsets* [6, 8, 10]. Closed itemsets are the itemsets that have no proper supersets with the same support. Non-closed itemsets are regarded as redundant [6, 8, 10]. A closed itemset

978-1-4244-7316-8/11/$26.00 ©2011 IEEE

is said to be frequent if its support is no less than *min_sup*. For example, the frequent closed itemsets in Table I are {A}:4, {C}:4, {AB}:3, {AC}:3, {CD}:2 and {ABC}:2. In this example, itemset {B} is non-closed since its support is the same as {AB}. This implicitly indicates that {B} will not appear in a transaction without {A} and hence the whole information about {B} is included in {AB}.

It is well known that frequent closed itemset provides users not only condensed but also complete information about frequent itemsets. In general, the number of frequent closed itemsets is much less than the number of frequent itemsets, that is, the set of frequent closed itemsets is a small subset of the set of frequent itemsets. Besides, a complete set of frequent closed itemsets can be used to uniquely derive all frequent itemsets and supports without losing any information [8].

Recently, some methods for mining frequent closed itemsets over a data stream were presented. Chi et al. proposed the *Moment* algorithm [3] to incrementally update the frequent closed itemsets over a data stream. They use a tree like structure, called *CET Tree (Closed Enumerate Tree)*, to maintain a dynamically selected set of itemsets. Each node in the CET Tree represents an itemset with different node type. Whenever a transaction arrives or leaves, the nodes in the CET Tree are inserted, deleted or updated according to their node types. However, exploration of frequent closed itemsets and node type checking are time-consuming, especially when the minimum support is low. Furthermore, in order to maintain frequent closed itemsets, Moment needs to maintain a large number of nodes representing non-closed itemsets. A huge number of such non-closed nodes may require a lot of memory space when the transactions in a stream contain many frequent closed itemsets.

NewMoment [7] was recently proposed by Li et al.. It uses a tree structure, called *NewCET Tree*, to maintain the information of frequent closed itemsets. Each node in *NewCET Tree* consists of a frequent closed itemset and its support count. The search space and the memory consumption of NewMoment are much smaller than that of Moment, since there is no non-closed node in NewCET Tree. Besides, it adopts a bit-sequence technique to improve time efficiency for exploration of frequent closed itemsets. Both Moment and NewMoment relies on a depth-first, Apriori-like technique to construct their structures. When minimum support is low, the two algorithms may become inefficient, since they must enumerate a large number of candidate itemsets, which is very time-consuming.

Although Moment and NewMoment show good performance in [3, 7], they generally use a fixed support threshold to discover closed itemsets in data stream. In other words, the minimum support threshold needs to be pre-defined before mining and it cannot be changed during the mining process. However, in a data stream, data distribution of frequent closed itemsets usually changes with time such that users often need to alter support thresholds to obtain desired mining results.

To interactively present frequent closed itemsets to users online based on any minimum support threshold, Jing et al. proposed an algorithm *CFI-Stream* [5] to maintain the complete set of closed itemsets over data stream. The experiments in [5] show that CFI-Stream achieves a better performance than Moment in terms of time and space, particularly at lower minimum support. CFI-Stream uses a lexicographical ordered tree, called *DIU Tree* (*DIrect Update Tree*), to maintain all the closed itemsets and their supports such that any frequent closed itemset can be efficiently obtained based on any minimum support threshold. Comparing with Moment-based algorithm [3, 7], CFI-Stream is much more efficient and flexible when the minimum support is changed. However, the computational cost of CFI-Stream is very expensive since CFI-Stream uses a *candidate generate-and-test mechanism* to update closed itemsets. The mechanism is described as follows. When a transaction which contains k distinct items is added to (or deleted from) the database, CFI-Stream needs to *generate* $(2^k - 1)$ subsets (i.e., candidate closed itemsets) for the transaction. To *test* whether a candidate is closed or not, in the worst case, CFI-Stream needs to search all its supersets by traversing parts of DIU Tree. In other words, CFI-Stream requires to search from the DIU Tree $(2^k - 1)$ times for a transaction with k distinct items, which seriously degrades the performance of CFI-Stream.

II. PRELIMINARIES

In this section, we introduce some preliminaries for mining frequent closed itemsets over a data stream. A *data stream DS* = $<t_1, t_2,\ldots,t_t>$ is a continuous sequence of transactions in a timely order. A transaction-sensitive sliding window [2] is denoted as W, which captures the latest w transactions from a data stream. When a new transaction arrives to W, it would be added into W if the current number of transactions in W is less than w. Otherwise, if the current number of transactions in W is equal to w, then the oldest transaction would be expired from W and the new transaction would be added to W. The *support count* of an itemset X in W is denoted as $SC_W(X)$, and defined as the number of transactions which contain X in W. The *support* of X in W is defined as the ratio of $SC_W(X)$ to the total number of transactions in W. An itemset X in W is said to be *frequent* if $SC_W(X)$ is no less than $min_sup \times |W|$. The function f takes a set of transactions T in W as an input and returns an itemset which is the result of the intersection of all the transactions in T. The function g takes an itemset Y as an input and returns a set of transactions in W, which contain Y. The function $C_W(X)$ takes an itemset X as an input and returns an itemset which is the intersection of all the transactions in W belong to $g(X)$, that is, $f(g(X))$. For any itemset X, $C_W(X)$ is called *the closure of X* in W. The support of X in W is the same as the support of $C_W(X)$ since X and $C_W(X)$ in W appear in the same transactions.

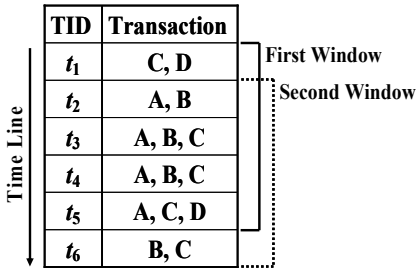

Figure 1. Transaction-sensitive sliding window

Definition 1. An itemset X is called a *closed itemset* in W if and only if $C_W(X) = X$.

$C_W(X) = X$ means that there is no proper superset of X with the same support as X. Therefore, X is a closed itemset. If $C_W(X) \neq X$, then the support of X is same as the support of its superset $C_W(X)$, that is, X is not a closed itemset. For example, Figure 1 shows a transaction-sensitive sliding window when the window size is set to 5. The first window W_1 consists of the transactions from t_1 to t_5. When a new transaction t_6 arrives to the window, the oldest transaction t_1 is expired from the window. The second window W_2 consists of the transactions from t_2 to t_6. In the first window W_1, $g(\{B\}) = \{t_2, t_3, t_4\}$ is a set of all the transactions which contain {B}. $C_{W1}(\{B\}) = f(g(\{B\})) = f(\{t_2, t_3, t_4\}) = t_2 \cap t_3 \cap t_4 = \{AB\} \cap \{ABC\} \cap \{ABC\} = \{AB\}$ is the closure of {B}. In the first window, {B} is not a closed itemset, since $C_{W1}(\{B\}) = \{AB\} \neq \{B\}$.

Definition 2. An itemset X is a *frequent closed itemset* in W if and only if $X = C_W(X)$ and $SC_W(X)$ is no less than *min_sup*.

Problem Statement. Given a transaction-sensitive sliding window size w, the problem is to efficiently find the complete set of frequent closed itemsets from the most recent w transactions over *a data stream* based on any user-specified *min_sup*.

In the following, we list some important properties about closed itemsets, which are intuitive and widely used in the previous literature [6, 8, 10].

Property 1. If $C_W(X) = Y$, then $SC_W(X) = SC_W(Y)$.

Rationale: If $C_W(X) = Y$, then $g(X) = g(Y)$. Therefore, $SC_W(X) = SC_W(Y)$.

Property 2. If $C_W(X) = Y$, then $C_W(Y) = Y$.

Rationale: Since $C_W(X) = Y$, $g(X) = g(Y)$. $C_W(Y) = f(g(Y)) = f(g(X)) = C_W(X) = Y$.

Property 3. X is closed if and only if $SC_W(X) > SC_W(Z)$, for all itemset Z, $Z \supset X$.

Rationale: If X is closed in W, then $C_W(X) = X$, that is, $C_W(X) \neq Z$ for all $Z \supset X$. Therefore, some transactions which contain X do not contain Z, that is, $SC_W(X) > SC_W(Z)$.

Property 4. If $X \subseteq Y$, then $g(Y) \subseteq g(X)$ and $C_W(X) \subseteq C_W(Y)$.

Property 5. $f(g(X)) \cap f(g(Y)) = f(g(X) \cup g(Y))$.

Theorem 1. For any two closed itemset X and Y, if $(X \cap Y) = S$ and $S \neq \varnothing$, then S is a closed itemset.

Rationale: To prove S is closed, we need to show that $C_W(S) = S$, that is, $C_W(S) \subseteq S$ and $S \subseteq C_W(S)$. If $X \cap Y = S$, then $g(X) \subseteq g(S)$ and $g(Y) \subseteq g(S)$ (Property 4). Therefore, $(g(X) \cup g(Y)) \subseteq g(S)$. According to Property 4 and Property 5, $C_W(S) = f(g(S)) \subseteq (f(g(X) \cup g(Y)) = (f(g(X) \cap f(g(Y)) = (C_W(X) \cap C_W(Y)) = (X \cap Y) = S$. That is, $C_W(S) \subseteq S$. According to Property 2, we have $S \subseteq C_W(S)$.

III. CLOSTREAM ALGORITHM

In this section, we first introduce our structures and then describe the CloStream algorithm in detail. The algorithm consists of two sub-procedures: CloStream+ and CloStream—. CloStream+ is used to update closed itemsets when a transaction arrives to the window, while deletion operation is used to update closed itemsets when a transaction leaves from the window. We use two data structures, called Closed Table and Cid List, to maintain the information of closed itemsets over a data stream. The details of the structures are described as follows.

Closed Table consists of three fields: *Cid*, *CItemset* and *SC*. Each closed itemset (CItemset) X is assigned a unique closed itemset identifier (Cid) which is a non-zero positive integer, and its support count (SC) is also recorded in a Closed Table. Each record in a Closed Table is denoted as (c, X, SC(X)), where c, X and SC(X) are the values of Cid, CItemset and SC. Given a Cid c of an itemset, the itemset and its support count can be directly retrieved from the Closed Table. Initially, the first record in a Closed Table is set to (0, *null*, 0).

Cid List consists of two fields: *Item* and *Cidset* field. The Cidset for an item i_p is denoted as *cidset*(i_p) which is a set of Cids of closed itemsets containing item i_p. Table II and Table III show the Closed Table and Cid List after the five transactions in Figure 1 arrive to the first window. In Table III, cidset(B) = {2, 3}, since item B is contained in the two closed itemsets {AB} and {ABC}, and their Cids are 2 and 3, respectively.

TABLE II. ORIGINAL CLOSED TABLE

Cid	CItemset	SC
0	null	0
1	{CD}	2
2	{AB}	3
3	{ABC}	2
4	{C}	4
5	{ACD}	1
6	{A}	4
7	{AC}	3

TABLE III. THE ORIGINAL CIDLIST

Item	Cidset
A	{2, 3, 5, 6, 7}
B	{2, 3}
C	{1, 3, 4, 5, 7}
D	{1, 5}

A. *CloStream*$^+$

In this subsection, we describe the procedure *CloStream*$^+$. Let t_A be a new transaction, D_B be the set of the transactions in the current window, and $D_U = D_B \cup \{t_A\}$ be the set of the transactions in the next window after adding t_A. $SC_{DB}(X)$ and $SC_{DU}(X)$ are the support counts of the itemset X in D_B and D_U, respectively. $C_{DB}(X)$ and $C_{DU}(X)$ are the closures of X in D_B and D_U, respectively. The sets of all the closed itemsets in D_B and D_U are denoted as C_{DB} and C_{DU}, respectively.

When a transaction $t_A = \{i_1, i_2, ..., i_k\} (i_j \in I, 1 \leq j \leq k)$ arrives to D_B, we observe that the support count of t_A is increased by one

but the support count of t_A's supersets would not be increased. According to Property 3, t_A must be a closed itemset in D_U. Besides, only the supports of the subsets of t_A would be increased and thus only the subsets of t_A would be changed from non-closed to closed.

According to Theorem 1, the closed subsets of t_A in D_U can be obtained by performing intersection operations on t_A and all the closed itemsets in D_B. However, this process is very time-consuming, since the number of closed itemsets in D_B may be very large and there may be many closed itemsets without common items with t_A. In order to avoid performing a large number of invalid intersections, CloStream$^+$ uses a Cid List and a *SET function* to find those closed itemsets which at least have a common item with t_A, that is, the intersections of the closed itemsets and t_A are not empties.

The SET function is defined as follows: SET($\{t_A\}$) = cidset(i_1) $\cup$ ... $\cup$ cidset(i_k), where cidset(i_j) ($1 \leq j \leq k$) is the cidset for item i_j in Cid List. Each Cid in SET($\{t_A\}$) represents a closed itemset which has at least a common item with t_A. Therefore, a lot of intersection operations can be reduced, since CloStream$^+$ only performs intersection operations on t_A and those closed itemsets whose Cids are in SET($\{t_A\}$).

By performing intersection operations on t_A and every closed itemsets whose Cids are in SET($\{t_A\}$), we can obtain the closed subsets of t_A in D_U. In order to update the supports of the closed subsets of t_A in D_U, we can find their closures in D_B for each of them. The support counts of them in D_U are equal to the support counts of their closures in D_B increasing by one. CloStream$^+$ uses a temp table, which is denoted as $Temp_A$, to store the closed subsets of t_A and their closures in D_B when a transaction t_A is added. $Temp_A$ is a hash structure and consists of two fields: *UItemset* and *Closure_Id*. Each record in $Temp_A$ is denoted as (S, t), where S is a closed itemset which needs to be updated and t is the identifier of the closure of S. In the following, we describe the algorithm for CloStream$^+$ in details.

As t_A is added to the current window, t_A is closed in D_U and then we put t_A into $Temp_A$. Initially, the Closure_Id of t_A is set to 0. To obtain the closed itemsets which need to be updated, CloStream$^+$ performs intersection operations on t_A and each closed itemset whose Cid i is in SET($\{t_A\}$). Let an itemset whose Cid is i be denoted as CT[i]. For an itemset S = $t_A \cap$ CT[i] ($i \in$ SET($\{t_A\}$)), S is closed in D_U according to Theorem 1. If S is not in $Temp_A$, then S is put into Temp$_A$ and its current Closure_Id is i, since CT[i] is a superset of S and may be the closure of S. Otherwise, the current Closure_Id of S, say, t, is replaced with i if SC_{DB}(CT[i]) is greater than SC_{DB}(CT[t]). This is because CT[t] is not the closure of S and CT[i] may be the closure of S.

After performing intersection operations on t_A and each closed itemset whose Cid is in SET($\{t_A\}$), all closed itemsets which need to be updated and the Cids of their closures in D_B are stored in $Temp_A$. CloStream$^+$ uses the information in $Temp_A$ to update the Closed Table and Cid List. For each record (u, c) in Temp$_A$, if u equals to CT[c], then SC_{DU}(CT[c]) is increased by 1 since u is originally closed in D_B. Otherwise, u is a new closed itemset and assigned a unique Cid n.

TABLE IV. THE CLOSED TABLE AFTER AFTER ADDING t_6

Cid	CItemset	SC
0	null	0
1	{CD}	2
2	{AB}	3
3	{ABC}	2
4	{C}	5
5	{ACD}	1
6	{A}	4
7	{AC}	3
8	{BC}	3
9	{B}	4

TABLE V. THE CIDLIST AFTER ADDING t_6

Item	Cidset
A	{2, 3, 5, 6, 7}
B	{2, 3, 8, 9}
C	{1, 3, 4, 5, 7, 8}
D	{1, 5}

CloStream$^+$ adds a new record with Cid = n, CItemset = S, and SC_{DU} = (SC_{DB}(CT[c]) + 1) to the Closed Table. Besides, identifier n is also added into the cidsets for the items that contained in u in Cid List.

After dealing with all records in $Temp_A$, the information of all the closed itemsets in D_U are maintained in the Closed Table and Cid List, and the allocated memory space for $Temp_A$ can be released. All frequent closed itemsets can be obtained by scanning Closed Table once.

B. A Running Example for CloStream$^+$

After adding t_1, t_2, t_3, t_4 and t_5 into the first window in Figure 1, the Closed Table and Cid List are shown in Table II and III, respectively. As t_6 = {BC} arrives, ({BC}, 0) is put into $Temp_A$. Then CloStream$^+$ performs intersection operations on each closed itemset whose Cid is in SET({BC}) = {1, 2, 3, 4, 5, 7}. The intersection of t_6 and CT[1] = {CD} is {C}. Because {C} does not exist in $Temp_A$, the record ({C}, 1) is put into $Temp_A$. Next, the intersection of t_6 and CT[2] = {AB} is {B}. Because {BC} does not exist in $Temp_A$, the record ({BC}, 2) is also put into $Temp_A$. Next, the intersection of t_6 and CT[3] = {ABC} is {BC}. Since {BC} exists in $Temp_A$ along with its current Closure_Id 0, we compare SC_{DB}(CT[3]) with SC_{DB}(CT[0]). Because SC_{DB}(CT[3]) is greater than SC_{DB}(CT[0]), the Closure_Id of {BC} is replaced with 3. CloStream$^+$ uses the same way to deal with the other Cids which belong to SET({BC}). Finally, the content of $Temp_A$ is shown in Table VI, which includes all closed itemsets in t_6 after adding t_6 and the identifiers of their closures before adding t_6.

CloStream$^+$ uses $Temp_A$ to update Closed Table and Cid List. In $Temp_A$, the first record is ({BC}, 3), since {BC} is not equal to CT[3], CloStream$^+$ assigns 8 as a Cid for {BC} and SC_{DU}({BC}) = SC_{DB}(CT[3]) + 1. Cid 8 is then added into cidset(B) and cidset(C) respectively. The next record in $Temp_A$ is ({C}, 4). Because {C} equals to CT[4], which means that {C} is closed in the first window, the support count of CT[4]={C} is increased by 1. For the last record ({B}, 2), since {B} is not equal to CT[2], which means that {B} is a new closed itemset, CloStream$^+$ assigns 9 as a Cid for {B} and SC_{DU}({B}) = SC_{DB}(CT[2]) + 1.

TABLE VI. TEMP$_A$

UItemset	Closure_Id
{BC}	3
{C}	4
{B}	2

Besides, Cid 9 is added into the cidset(B). Finally, the updated Closed Table and Cid List are shown in Table IV and Table V, respectively.

C. CloStream⁻

In this subsection, we describe the procedure *CloStream*⁻. Let t_D be the oldest transaction in the current window W, D_B be the original set of transactions, and $D_D = D_B - \{t_D\}$ be the set of the transactions after deleting t_A from D_B. $SC_{DB}(X)$ and $SC_{DU}(X)$ are the support counts for the itemset X in D_B and D_D, respectively. The closures of X in D_B and D_D are denoted as $C_{DB}(X)$ and $C_{DD}(X)$, respectively. The sets of closed itemsets in D_B and D_D are denoted as C_{DB} and C_{DD}, respectively.

Whenever a transaction $t_D = \{i_1, i_2, ..., i_k\}(i_j \in I,\ 1 \le j \le k)$ is deleted from the database D_B, only the support counts of the subsets of t_D will be decreased by one, that is, only the subsets of t_D may be changed from closed to non-closed. Therefore, CloStream⁻ first find out the closed subsets of t_D in D_B and then determine which closed subsets of t_D will turn out to be non-closed. The closed subsets of t_D in D_B can be obtained by performing intersection operations on t_D and all the closed itemsets in C_{DB} according to Theorem 1.

However, it is very time-consuming to perform a large number of intersections, since there is a large number of closed itemsets in D_B. In order to avoid performing a lot of invalid intersections, CloStream⁻ also uses Cid List and computes the SET function to obtain the closed itemsets which have at least a common item with t_D.

CloStream⁻ uses a temp table, called $Temp_D$, to store the information about closed subsets of t_D in D_B, which consists of a triple: *DItemset*, *Closure_Id* and *HS*. Suppose that each record in $Temp_D$ is denoted as (S, c, h), in which S is a closed subsets of t_D, c is an identifier of the closure of S in D_B, and h is the identifier of a closed superset of S, which is not contained in t_D and whose support is the largest among the supports of all the supersets of S. HS is used to check if S is closed in D_D. If $SC_{DD}(S) = SC_{DD}(CT[h])$, then S is non-closed in D_D, since there is a superset CT[h] with the same support as S. For a closed superset Z of S ($Z \subset t_D$), $SC_{DD}(Z)$ must not be equal to $SC_{DD}(S)$, since the support counts of S and Z are decreased by one simultaneously after deleting t_D. In the following, we describe the algorithm for CloStream⁻ in details.

As t_D is deleted from the database, CloStream⁻ puts t_D into $Temp_D$ since t_D is a closed itemset in D_B. The Closure_Id and HS of t_D are set to zeros. To obtain the closed subsets of t_D in D_B, CloStream⁻ performs intersection operations on t_D and each closed itemset CT[i] whose cid i is in SET($\{t_D\}$). Suppose that $S = t_D \cap$ CT[i], then S is a closed subset in D_B according to Theorem 1. If S is not in $Temp_D$, then (S, i, *0*) is put into $Temp_D$, since CT[i] may be the closure of S. Otherwise, if S exists in $Temp_D$ with Closure_Id = c and HS = h, there are two cases need to be considered. Case 1: if $SC_{DB}(CT[i])$ is greater than $SC_{DB}(CT[c])$, then CT[i] may be the closure of S but CT[c] is not (Property 3). In this case, (S, c, h) is replaced with (S, i, c). Case 2: if $SC_{DB}(CT[i])$ is not greater than $SC_{DB}(CT[c])$ but greater than $SC_{DB}(CT[h])$, then (S, c, h) is replaced with (S, c, i). Otherwise, the record (S, c, i) remains unchanged.

After performing intersection operations on t_D and each closed itemset whose Cid is in SET($\{t_D\}$), each closed subset S of t_D which need to be updated and its closure c in D_B are stored in $Temp_D$. According to Definition 1, CT[c] = S. CloStream⁻ uses the identifier c to find S in Closed Table and decreases the support count of S by 1. After finding all the closed itemsets which need to be updated and updating their support counts, CloStream⁻ then determines which closed itemsets become non-closed.

For each record (S, c, h) in $Temp_D$, if $SC_{DD}(CT[c]) = SC_{DD}(CT[h])$, then S becomes non-closed in D_D since there is a superset CT[h] with the same support as S. CloStream⁻ removes the information of CT[c] from the Closed Table and Cid List. Notice that if $SC_{DD}(CT[c]) = 0$, the information of CT[c] is also be removed. After processing all the records in $Temp_D$, the information of the closed itemsets after deleting t_D is maintained in the updated Closed Table and Cid List, and the allocated memory space for $Temp_D$ can be released. By scanning Closed Table once, frequent closed itemsets and their supports in D_D can be obtained.

TABLE VII. THE CLOSED TABLE AFTER AFTER DELETING t_1

Cid	CItemset	SC
0	null	0
2	{AB}	3
3	{ABC}	2
4	{C}	4
5	{ACD}	1
6	{A}	4
7	{AC}	3
8	{BC}	3
9	{B}	4

TABLE VIII. THE CIDLIST AFTER DELETING t_1

Item	Cidset
A	{2, 3, 5, 6, 7}
B	{2, 3, 8, 9}
C	{3, 4, 5, 7, 8}
D	{5}

D. A Running Example for CloStream⁻

Suppose D_B is the set of the transactions after adding t_6 into Table I.The Closed Table and Cid List are shown in Table IV and Table V, respectively. When t_1 is deleted from D_B, t_1 is put into DItemset of $Temp_D$ since t_1 is a closed itemset in D_B. The values of Closure_Id and HS are set to zeros. In order to efficiently obtain all the closed subsets of t_1, CloStream⁻ performs intersection operations on t_1 = {CD} and each closed itemset whose cid is in SET({CD}) = {1, 3, 4, 5, 7, 9}.

The intersection of t_1 and CT[1] = {CD} is {CD}. We find that {CD} exists in $Temp_D$ with Closure_Id = 0 and HS = 0. The record ({CD}, 0, 0) is replaced with ({CD}, 1, 0) since $SC_{DB}(CT[1])$ is greater than $SC_{DB}(CT[0])$. Next, the intersection of t_1 and CT[3] = {ABC} is {C}. Since {C} does not exist in $Temp_D$, the record ({C}, 3, 0) is put into $Temp_D$.

The intersection of t_1 and CT[4] = {C} is {C}. We find that {C} exists in $Temp_D$ with Closure_Id = 3 and HS = 0. Because SC_{DB}(CT[4]) is greater than SC_{DB}(CT[3]), the Closure_Id of {C} is replaced with 4. Besides, the HS of {C} is replaced with 3, since C_{DB}(CT[3]) is greater than SC_{DB}(CT[0]). Therefore, the current Closure_Id and HS of {C} are 4 and 3, respectively.

The next Cid in SET({CD}) is 5. The intersection of t_1 and CT[5] = {ACD} is {CD}, and {CD} exists in $Temp_D$ with Closure_Id = 1 and HS = 0. Because SC_{DB}(CT[5]) is not greater than SC_{DB}(CT[1]) but greater than SC_{DB}(CT[0]), only the value of HS is updated as 5.

After performing intersection operations on t_1 and all the closed itemsets whose Cids are in SET({CD}), the content of $Temp_D$ is shown in Table IX. CloStream⁻ then decreases support counts of {CD}and {C} by one from Closed Table.

In Table IX, the first record is ({CD}, 1, 5). Since SC_{DD}(CT[1]) = SC_{DD}(CT[5]), CT[1] = {CD} turns out to be non-closed after deleting t_1. For the second record ({C}, 4, 7), CT[4] = {C} is still closed in D_D, since SC_{DD}(CT[4]) ≠ SC_{DD}(CT[7]). After processing all the records in $Temp_D$, the updated Closed Table and Cid List are shown in Table VII and Table VIII. By scanning Closed Table once, all the frequent closed itemsets in D_D and their support counts can be obtained.

TABLE IX. $TEMP_D$

DItemset	Closure_Id	HS
{CD}	1	5
{C}	4	7

IV. EXPERIMENTAL RESULTS

In this section, we evaluate the performance of our CloStream algorithm and compare it with the three famous algorithms CFI-Stream, Moment and NewMoment. The experiments are performed on a 1.83 GHz Intel Core 2 Duo Processor with 2 Gigabyte memory, and running on Windows Vista. CloStream and CFI-Stream were coded in Java language. Moment [3] and NewMoment [7] are provided by their authors and coded in C++ language. To evaluate the performance of these algorithms, we generate a synthetic dataset T10I4D10100 from IBM data generator [1]. The parameters are described as follows: D is the total number of transactions; T is average transaction size; I is the average size of maximal potential frequent itemsets; N (=2000) is the number of distinct items. Besides, a real-world dataset BMS-Web-View-1 was downloaded from FIMI Repository [11], where I = 497, T = 2.5 and D = 59,602. The maximum length of the transactions in BMS-Web-View-1 is 267.

Fig. 2(a) shows the loading time of the first window for the four algorithms on the dataset T10I4D10100 under different minimum supports as the size of sliding window is set to 10K. From Fig. 2(a), we can see that the execution times for Moment and NewMoment increase as the minimum support decreases, since the lower the minimum support is, the larger the search space is for Moment and NewMoment. On the other hand, the execution times for CFI-Stream and CloStream are not affected by different minimum supports, since CFI-Stream and CloStream maintain all the closed itemsets in their structures. When *min_sup* is less than 0.06%, CloStream outperforms Moment and NewMoment, and the performance gap significantly increases as the minimum support decreases.

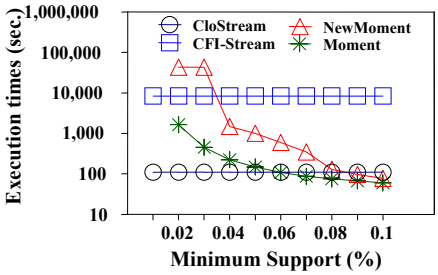

(a) Times for loading the first window

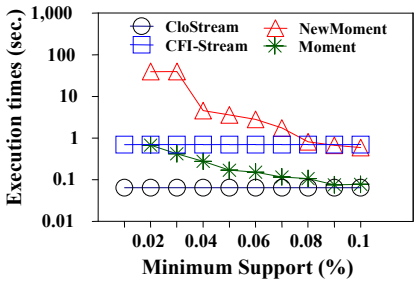

(b) Times for sliding 100 consecutive windows

Figure 2. Execution times on dataset T10I4D10100 for the four algorithms

When *min_sup* is high, Moment and NewMoment run slightly faster than CloStream since they only generates frequent closed itemsets, but CloStream generates all the closed itemsets. In Fig. 2(a), CFI-Stream runs slower than CloStream about 100 times, since CFI-Stream needs to generate all the subsets (i. e., candidate closed itemsets) for each transaction and search all the supersets for each candidate from DIU Tree to check if the candidate is closed. In other words, a transaction of length k will lead CFI-Stream to generate (2^k - 1) candidates and search from DIU-Tree (2^k - 1) times. Therefore, CFI-Stream is unfavorable to deal with long transactions.

Fig. 2(b) shows the average execution times for the four algorithms after sliding 100 consecutive windows on the dataset T10I4D10100 under different minimum supports. From Fig. 2(b), we can see that CloStream runs faster than Moment and CFI-Stream about 10 times when *min_sup* = 0.02%, and outperforms NewMoment about 100 times when *min_sup* is less than 0.03%, since Moment, NewMoment and CFI-Stream need to search their structure to determine which itemsets are closed. However, whatever the transactions are added or deleted, our CloSream algorithm only needs to do some intersection operations without doing any searching operations on the previous closed itemsets.

Fig. 3(a) shows the loading time of the first window for the algorithms Moment, NewMoment and CloStream on the real dataset BMS-Web-View-1 under different minimum supports as the size of sliding window is set to 10K. Since the maximum length of the transactions in this dataset is 267, CFI-Stream needs to enumerate (2^{267}-1) candidates and search from DIU Tree over 100 billion times. The performance for CFI-Stream is much worse than the three algorithms. Therefore, we only

compare the performance of our CloStream with Moment and NewMoment on this dataset. From Fig. 3(a), we can see that CloStream runs faster than Moment and NewMoment over 100 times when *min_sup* is less than 0.03% and 0.06%, respectively. Particularly, when *min_sup* is less than 0.03%, Moment runs out of memory, since it not only captures lots of non-closed nodes in CET-Tree but also maintains all frequent closed itemsets in CET-Tree and hash table. Although NewMoment is able to run when *min_sup* is less than 0.05%, it requires more than 2.5 hours.

Fig. 3(b) shows the average execution times for the three algorithms over 100 consecutive windows on dataset BMS-Web-View-1 under different minimum supports. From Fig. 3(b), we can see that CloStream significantly outperforms NewMoment and runs faster than Moment when *min_sup* is less than 0.04%. Although NewMoment uses less memory space than Moment, it requires a long execution time. Particularly, when *min_sup* = 0.05%, the total execution time of NewMoment for sliding 100 consecutive windows is over (100 × 1,000) = 100,000 seconds, while CloStream only takes about (0.1 × 100) = 10 seconds under the same threshold.

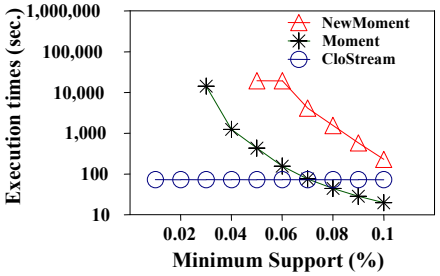

(a) Times for loading the first window

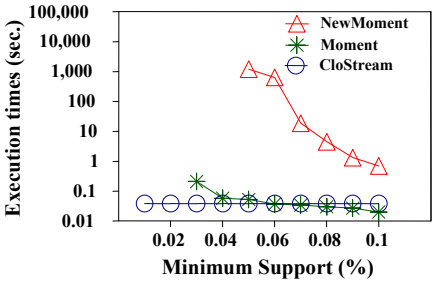

(b) Times for sliding 100 consecutive windows

Figure 3. Execution times on the real-world dataset BMS-Web-View-1 for the three algorithms

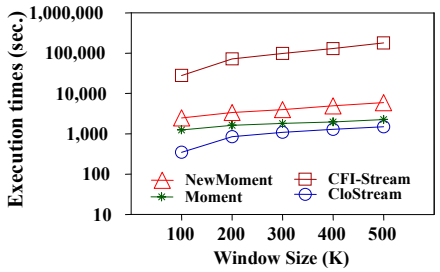

Figure 4. Scalability for the four algorithms under various sliding window sizes

Fig. 4 shows the execution times of the four algorithms for loading the first window under different sliding window sizes on dataset T5I4. In this experiment, the size of sliding window is increased from 100K to 500K and the minimum supports for Moment and NewMoment are set to 0.005%. From Fig 4 we can see that CloStream outperforms the other three algorithms and has a good scalability for large dataset.

V. CONCLUSIONS

In this paper, we propose a novel algorithm CloStream to discover frequent closed itemsets over stream sliding windows. We use Cid List and the SET function to find the closed itemsets which have the common items with the added or deleted transaction. Different from the previous approaches which need to take a lot of time to search from a tree structure, CloStream only needs to do the intersections on the closed itemsets which return from the SET function and the added or deleted transaction without searching from our proposed structures. Besides, all the frequent closed itemsets can be obtained online based on any user-specified thresholds. The experimental results also show that our CloStream algorithm outperforms the three famous algorithms CFI-Stream, Moment and NewMoment on both synthetic datasets and real-world dataset.

REFERENCES

[1] R. Agrawal, R. Srikant, "Fast Algorithm for Mining Association Rules," in Proc. of Int'l Conf. on Very Large Data Bases, pp. 487-499, 1994.

[2] J. Chang, Y. Ke, W. Ng, "Research Issues in Data Stream Association Rule Mining," Knowledge and Information Systems (KAIS), vol 16, issue 1, pp. 1–27, 2008.

[3] Y. Chi, H. Wang, P. Yu and R. Muntz, "Catch the moment: maintaining closed frequent itemsets over a data stream sliding window," Knowledge and Information Systems (KAIS), vol. 10, issue 3, pp. 265–294, 2006.

[4] J. Han, J. Pei, Y. Yin and R. Mao, "Mining frequent patterns without candidate generation: a frequent-pattern tree approach," Data Mining and Knowledge Discovery (DMKD), vol. 8, issue 1, pp. 53–87, 2004.

[5] N. Jiang and L. Gruenwald, "CFI-Stream: mining closed frequent itemsets in data streams," in Proc. of ACM SIGKDD Int'l Conf. on Knowledge Discovering and Data Mining, pp. 592–597, 2006.

[6] C. Lucchese, S. Orlando and R. Perego, "Fast and Memory Efficient Mining of Frequent Closed Itemsets," IEEE Transactions on Knowledge and Data Engineering (TKDE), vol. 18, issue 1, pp. 21–36, 2006.

[7] H. F. Lee, C. C. Ho and S. Y. Lee, "Incremental updates of closed frequent itemsets over continuous data streams," Expert System with Applications (ESWA), vol. 36, issue 2, pp. 2451-2458, 2009.

[8] N. Pasquier, Y. Bastide, R. Taouil and L. Lakhal, "Generating a Condensed representation for Association Rules," Journal of Intelligent Information Systems (JIIS), vol. 24, issue 1, pp. 29–60, 2005.

[9] S. J. Yen, Y. S. Lee, C. K. Wang, J. W. Wu and L. Y. Ouyang, "The Studies of Mining Frequent Patterns Based on Frequent Pattern Tree," in *Proc. of Int'l Conf. on* Pacific-Asia Conference on Knowledge Discovery and Data Mining (PAKDD), pp. 398–416, 2009.

[10] M. J. Zaki and C. J. Hsiao, "Efficient Algorithms for Mining Closed Itemsets and Their Lattice Structure," IEEE Transactions on Knowledge and Data Engineering (TKDE), vol. 17, issue 4, pp. 462–478, 2005.

[11] Frequent Itemset Implantation Repository (FIMI), http://fimi.cs.helsinki.fi/

2011 IEEE International Conference on Fuzzy Systems
June 27-30, 2011, Taipei, Taiwan

Neuro-Fuzzy System Design Using Differential Evolution with Local Information

Chin-Teng Lin[1,2], Ming-Feng Han[1], Yang-Yin Lin[1], Shih-Hui Liao[1], Jyh-Yeong Chang[1]
[1]Department of Electrical and Control Engineering, National Chiao Tung University, Taiwan
[2]Brain Research Center and Department of Electrical Engineering
ctlin@mail.nctu.edu.tw, u9712828.ece97g@nctu.edu.tw, oliver.yylin@gmail.com, lia0622@gmail.com, jychang@mail.nctu.edu.tw

***Abstract*—This paper proposes a differential evolution with local information for TSK-type neuro-fuzzy system optimization. The differential evolution with local information consider neighborhood between each individual to keep the diversity of population. An adaptive parameter tuning based on 1/5th rule is used to trade off between local search and global search. For structure learning algorithm, the on-line clustering algorithm is used for rule generation. The structure learning algorithm generates a new rule which compares the firing strength. Initially, there is no rule in neuro-fuzzy system model. The rules are automatically generated by fuzzy measure. For parameter learning, the parameters are optimized by differential evolution algorithm. Finally, the proposed neuro-fuzzy system with novel differential evolution model is applied in chaotic sequence prediction problem. Results of this paper demonstrate the effectiveness of the proposed model.**

Keywords- Evolution Algorithm; Neuro-Fuzzy System; Fuzzy System; Differential Evolution Optimization.

I. INTRODUCTION

To train the parameters in designing a neuro-fuzzy system (NFS), many papers had used Backpropagation (BP). The BP is a powerful training technique that can be applied to networks with a forward structure. Since the steepest descent approach is used in BP training to minimize the error function, the algorithms may reach the local minima very quickly and never find the global solution. The aforementioned disadvantages lead to suboptimal performance, even with a favorable neural fuzzy network topology. One major optimization category as evolutionary algorithm (EA) [1-3] for global solution in NFS has been proposed. These algorithms are heuristic and stochastic. They involve populations of individuals with a specific behavior similar to a biological phenomenon, like crossover or mutation. Genetic NFS [4-7] is a well-known case which design FSs using genetic algorithms (GAs).

Another evolutionary algorithms category for FS design, called particle swarm optimization (PSO), appears to be better than the backpropagation algorithm. It is an evolutionary computation technique that was developed by Kennedy and Eberhart in 1995 [8]. The underlying motivation for the development of PSO algorithm is the social behavior of animals, such as bird flocking, fish schooling and swarm theory. PSO has been successfully applied to many optimization problems, such as feedforward neural network design [9-11] in control problems, with improved performance over GAs.

A differential evolution algorithm (DE), similar to GA, has emerged as a robust numerical optimization algorithm and has been successfully applied to solve various difficult optimization problems [12-14]. The basic strategy employs the difference of two randomly selected individuals as the source of random variations for a third individual. In [15-16], the researcher has proposed a modified differential evolution (MODE) for an adaptive neural fuzzy network (ANFN-MODE). This MODE provides a cluster-based mutation scheme to prevent the algorithm from being trapped in local optima of the search space. However, a DE that lacks the diversity and adaptive parameter tuning is often to affect the proformace[14].

This study proposes DE using local information (DELI) for TSK-type NFS optimization. The DELI consider neighborhood between each individual to keep the diversity of population. An adaptive parameter tuning based on 1/5th rule is used to tradeoff between local search and global search. An online learning algorithm, consisting of structure learning and parameter learning, is proposed to construct the NFS automatically. The structure learning algorithm generates a new rule which compares the fire strength. Initially, there is no rule in NFS model. The rules are automatically generated by fuzzy measure. The parameter learning algorithm is based on DELI to tune the free parameters in the NFS. To investigate the effectiveness of the proposed NFS-DELI, it is applied to dynamic system identification. The proposed NFS-DE model shows effectiveness results in simulations**.**

This paper is organized as follows. Section II describes the basic structure and function for NFS. Section III introduces the rule generation and parameter optimization algorithm in DELI. Section IV presents NFS design results of DELI and its performance comparisons with other evolutionary algorithms. Finally, Section V draws conclusions.

II. THE STRUCTURE OF NFS

A four-layered NFS is shown in Fig. 1, which is comprised of the input, membership function, rule, and output layers. The signal propagation and the basic functions in each layer are described as follows.

Layer 1—Input layer: No computation is done in this layer. Each node in this layer, which corresponds to one input

variable, only transmits input values to the next layer directly. That is

$$O^{(1)} = z_i . \tag{1}$$

Where i =1,2…*n* are the input variables of the NFS.

Layer 2—Membership function layer: Each node in this layer is a membership function that corresponds one linguistic label of one of the input variables in Layer 1. In other words, the membership value which specifies the degree to which an input value belongs to a fuzzy set is calculated in Layer 2

$$O^{(2)} = \mu_{ij} = \exp\left({-(z_i - m_{ij})^2} \Big/ {\sigma_{ij}^2} \right). \tag{2}$$

Where i =1,2…*n,* j=1,2…M, m_{ij} and σ_{ij} are respectively, the center (or mean) and the width (or variance) of the Gaussian membership function of input variable. M is number of rules.

Layer 3—Rule layer: A node in this layer represents a fuzzy logic rule and performs precondition matching of a rule. Here, we use the AND operation for each Layer 2 node

$$O^{(3)} = R_j = \prod_{i=1}^{n} \mu_{ij} . \tag{3}$$

The output of a layer 3 node represents the firing strength of the corresponding fuzzy rule.

Layer 4—Output layer: Each node in this layer corresponds to one output variable. The node integrates all of the actions recommended by layers 4 and acts as a defuzzifier with

$$O^{(4)} = y = \frac{\sum_{j=1}^{M} R_j \left(\sum_{i=1}^{l} s_{ij} z_i + s_{0j} \right)}{\sum_{j=1}^{M} R_j} . \tag{4}$$

In this paper, the consequent part use a TSK type which linear combination of TSK parameters S_{ij} and input variables.

III. Learning Algorithms of the NFS

This section describes the basic concepts of two types of learning algorithm. Section III-A describes the rule generation based on-line clustering algorithm for structure learning. Section III-B describes the DELI algorithm for parameter optimization.

A. Using on-line clustering algorithm for rule generation

The first task in structure learning is to decide when to generate a new rule. In many study, an on-line cluster algorithm is used to neuro-fuzzy system for generating fuzzy rule [2-5]. Fig.2. shows a detailed flow chart for this online procedure. Initially, there is no rule in NFS. For first incoming data, NFS generates a first fuzzy rule. The mean of membership function set the value of first incoming data, the variance of membership function set initial value. The weights set value randomly between the ranges. After first incoming data, the firing strength is calculated by Layer 3. A maximum firing strength in Layer 3 has to compare with a threshold which pre-specified threshold between 0 and 1. If the maximum firing strength is smaller than threshold, then a new rule is generated. Next step is to assign the value of mean, variance, and weights for the new rule. Repeating the above process for every incoming piece of training data generates new rules, until the iteration is termination.

B. Differential evolution with local information (DELI)

The DELI learning algorithm consists of three major phases: the initialization phase, the DE operator phase, and the parameter tuning phase.

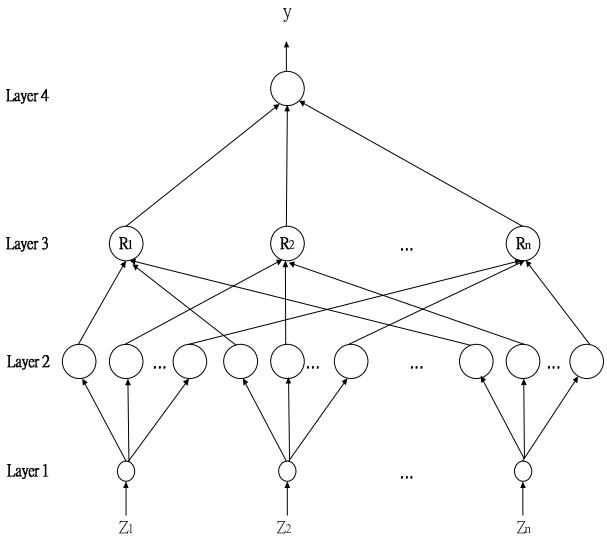

Fig. 1. Architecture of the NFS.

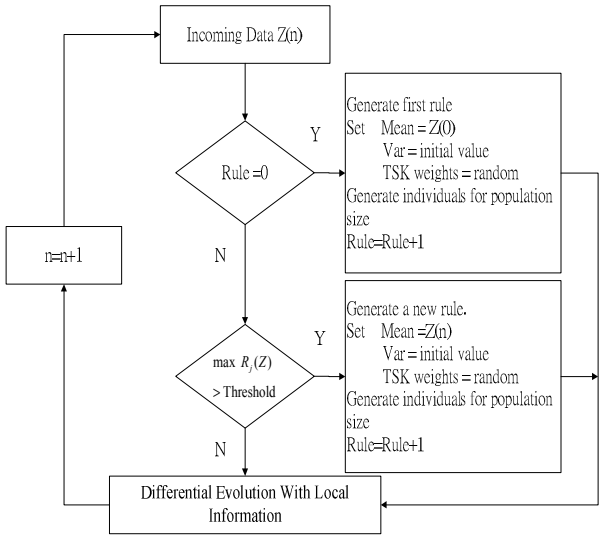

Fig. 2. The flow chart for on-line procedure.

In the initialization phase, every individual is consisted of mean, variance, and TSK weights. An individual is a neuro-fuzzy system in this paper. The detailed individual structure is shown in Fig.2. Before the DELI learning algorithm is applied, every individual must be created randomly. For evaluation of

performance, we adopt a fitness function to evaluate the performance of each individual as follows:

$$fitness = \sqrt{\frac{1}{N}\sum_{i=1}^{N}(y_i - \bar{y}_i)^2}\ , \tag{5}$$

where y_i represents the model output of the ith data, $\bar{y}_i$ the desired output of the ith data, and N the number of the training data.

For DE operator phase, first operation is mutation operator. A mutated individual is generated according to the following equation:

$$\begin{aligned} v_g = &(1-\alpha)(x_1 + (1-F)(x_2 - x_3) + F(x_{local} - x_1)) \\ &+ \alpha(x_1 + (1-F)(x_2 - x_3) + F(x_{gbest} - x_1)) \end{aligned}, \tag{6}$$

where F, commonly known as the scaling factor, α is a control factor, x_{gbest} is the best fitness value up to now in the population and x_{local} is the local best fitness value that consider the neighborhood of individual. Three individuals (x_1, x_2, and x_3) are randomly selected in population for operation.

Second operation is crossover operator which mutated individual v_i and random individual x_i generate the offspring. If a random number smaller than crossover probability, the mutated individual v_i is selected for the element of offspring. Else, random individual x_i is selected. Finally, better individuals based on fitness function values are reserved to the next generation.

To prevent the DE from being trapped in the local optima of the search space, an adaptive parameter tuning is used in this paper. This scheme uses 1/5th rule to increase the search capability. The basic concept of 1/5th rule is derived from the Evolution Strategies [17-18]. The short description of the 1/5th rule is present in Figure 3.

1. perform the DELI for a number G of generations:
   - keep F constant during this period.
   - count the number N of better Gbest during this period.

2. determine an estimate of success probability P

   P = N/G

3. change F according to

$$F = \begin{cases} F/\beta & \text{if P>1/5} \\ F\cdot\beta & \text{if P<1/5} \\ F & \text{if P>1/5} \end{cases} \quad ,0 < \beta < 1$$

Fig. 3. The 1/5th code in DELI.

IV. Simulation Results

The time-series prediction problem used in this example is the chaotic Mackey–Glass time series, which is generated from the following differential equation:

$$\frac{dx(t)}{dt} = \frac{0.2x(t-\tau)}{1+x^{10}(t-\tau)} - 0.1x(t) \tag{7}$$

where τ > 17. In this paper, the parameter τ = 30, and x(0) = 1.2. Four past values are used to predict x(t), and the input–output data format is given by

$$[x(t-24), x(t-18), x(t-12), x(t-6) \mid x(t)]$$

A total of 1000 patterns are generated from t = 124 to 1123, where the first 500 patterns are used to train, and the last 500 are used to test. A total of 50 runs are performed for statistical analysis. As in the previous study [11], a first-order TSK-type FS is used. In DELI, the threshold μth is set to 0.011 α is set to 0.4, β is set to 0.9. Fig. 4 shows the average best-so-far training RMSE for each evaluation. DELI have better fitness value and learning capability. Table 1 shows the average training and test RMSEs over 50 runs. Comparison of GA, PSO , DE , MODE[15] , HGAPSO[11], DELI, the proposed DELI have a good performance. Fig. 5 shows the desired output (blue line) and actual output (red line) of DELI.

The result shows the best prediction output of DELI.

V. Conclusions

This paper proposed a DELI for dynamic system identification. The DELI is simple evolution algorithm with neighborhood information, and keeps the diversity in population. DELI with 1/5th rule parameter tuning scheme tradeoff between local search and global search during evolution to effectively find a good solution for parameter optimization. An online cluster algorithm is used for rule generation. The experimental results demonstrate that the DELI obtains a smaller RMSE value than other algorithm for dynamic system identification.

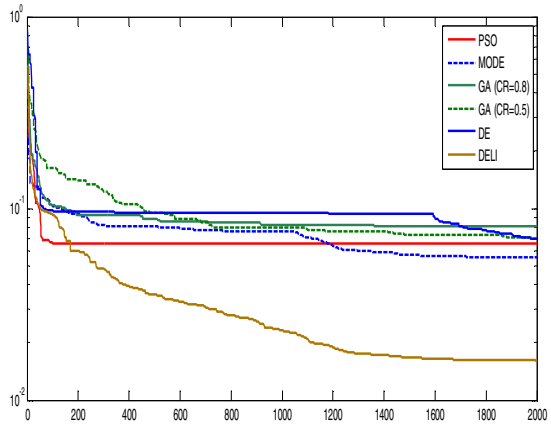

Fig. 4. Training RMSEs at each performance evaluation for DELI and other algorithms.

Table1. Performance of the DELI and other algorithms for the chaotic sequence prediction problem.

	GA	PSO	DE	HGAPSO[11]	MODE[15]	DELI
Rule number	4	4	4	4	4	4
Training RMSE	0.081	0.066	0.069	0.035	0.041	0.016
Testing RMSE	0.090	0.077	0.072	0.047	0.053	0.020

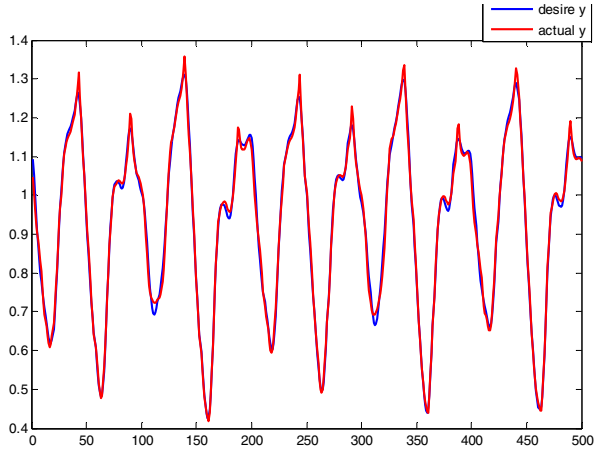

Fig. 5. Results of the DELI-optimized NFS in simulation.

REFERENCES

[1] C. T. Lin and C. S. G. Lee, Neural Fuzzy Systems: *A Neuro-Fuzzy Synergism to Intelligent System*. Englewood Cliffs, NJ: Prentice-Hall, 1996

[2] O. Cordon, F. Herrera, F. Hoffmann, and L. Magdalena, *Genetic Fuzzy Systems*. Singapore: World Scientific, 2001.

[3] E. Sanchez, T. Shibata, and L. A. Zadeh, *Genetic Algorithms and Fuzzy Logic Systems: Soft Computing Perspectives*. Singapore: World Scientific, 1997.

[4] C. F. Juang, "A TSK-type recurrent fuzzy network for dynamic systems processing by neural network and genetic algorithms," *IEEE Trans. Fuzzy Syst.*, vol. 10, no. 2, pp. 155–170, Apr. 2002.

[5] C. F. Juang, "Combination of on-line clustering and Q-value based GA for reinforcement fuzzy system design," *IEEE Trans. Fuzzy Syst.*, vol. 13, no. 3, pp. 289–302, Jun. 2005.

[6] C. H. Chou, "Genetic algorithm-based optimal fuzzy controller design in the linguistic space," *IEEE Trans. Fuzzy Syst.*, vol. 14, no. 3, pp. 372–385, Jun. 2006.

[7] F. Hoffmann, D. Schauten, and S. Holemann, "Incremental evolutionary design of TSK fuzzy controllers," *IEEE Trans. Fuzzy Syst.*, vol. 15, no. 4, pp. 563–577, Aug. 2007.

[8] J. Kennedy and R. Eberhart, "Particle swarm optimization," in Proc. IEEE Int. Conf. Neural Netw., Dec., 1995, pp. 1942–1948.

[9] C. F. Juang, "A hybrid of genetic algorithm and particle swarm optimization for recurrent network design," *IEEE Trans. Syst., Man, Cybern. B, Cybern.*, vol. 34, no. 2, pp. 997–1006, Apr. 2004.

[10] K. D. Sharma, A. Chatterjee, and A. Rakshit, "A hybrid approach for design of stable adaptive fuzzy controllers employing Lyapunov theory and particle swarm optimization," *IEEE Trans. Fuzzy Syst.*, vol. 17, no. 2, pp. 329–342, Apr. 2009.

[11] C. F. Juang, C. M. Hsiao, and C. H. Hsu," Hierarchical Cluster-Based Multispecies Particle-Swarm Optimization for Fuzzy-System Optimization," *IEEE Trans. Fuzzy Syst.*, vol. 18, no. 1, pp. 14–26, Feb. 2010.

[12] R. Storn, "System design by constraint adaptation and differential evolution," *IEEE Trans. Evol. Comput.*, vol. 3, no. 1, pp. 22–34, Apr. 1999.

[13] K. V. Price, R. M. Storn, and J. A. Lampinen, *Differential Evolution: A Practical Approach toGlobal Optimization*. Berlin,Germany: Springer- Verlag, 2005.

[14] J. Liu and J. Lampinen, "A fuzzy adaptive differential evolution algorithm," *Soft Comput.—A Fusion Found., Methodol. Appl.* vol. 9, no. 6, pp. 448–642, 2005.

[15] C.H Chen, CJ Lin, and CT Lin, "Nonlinear System Control Using Adaptive Neural Fuzzy Networks Based on a Modified Differential Evolution" *IEEE Trans. Syst. Man Cybern. Part C*. 2009, pp. 459–473.

[16] C. T. Lin, and M. F. Han, "Differential Evolution based Optimization of Locally Recurrent Neuro-Fuzzy System for Dynamic System Identification," The 17th National Conference on Fuzzy Theory and its Applications, pp. 702-707, 2010.

[17] Thomas Bäck, T., & Schwefel, H.-P., "Evolution strategies I: Variants and their computational implementation," *Genetic Algorithms in Engineering and Computer Science*, pp. 111-126. 1995.

[18] Beyer, H.-G., & Schwefel, H.-P, "Evolution strategies: A comprehensive introduction," *Natural Computing,* 3-52, 2002.

2011 IEEE International Conference on Fuzzy Systems
June 27-30, 2011, Taipei, Taiwan

Stability Analysis and Synthesis of Markovian Jump Nonlinear Systems with Incomplete Transition Descriptions via Fuzzy Control

Min Kook Song
Department of Electrical and Electronic Engineering, Yonsei University, Shinchon-Dong, Seodaemum-Gu, Seoul, Korea
Email: MinKookSong@gmail.com

Jin Bae Park
Department of Electrical and Electronic Engineering, Yonsei University, Shinchon-Dong, Seodaemum-Gu, Seoul, Korea
Email: jbpark@yonsei.ac.kr

Young Hoon Joo
School of Electronic and Information Engineering, Kunsan National University, Kunsan, Chonbuk, 573-701, Korea
Email: yhjoo@kunsan.ac.kr

***Abstract*—This paper is concerned with exploring an extended approach for the stability analysis and synthesis for Markovian jump nonlinear systems (MJNLSs) with incomplete transition descriptions via fuzzy control. In this paper, not all the elements of the rate transition matrices (RTMs) are assumed to be known. By fully considering the properties of the RTMs and the convexity of the uncertain domains, sufficient criteria of stability and stabilization are obtained. The proposed stability conditions are much less conservative than most of the existing results and stabilization conditions with a mode-dependent fuzzy controller are derived for Markovian jump fuzzy systems (MJFSs) in terms of linear matrix inequalities (LMIs). Finally, illustrative numerical examples are provided to demonstrate the effectiveness of the proposed approach.**

***Index Terms*—Markovian fuzzy systems, partially known transition matrix, linear matrix inequality**

I. Introduction

Markovian jump nonlinear systems (MJNLSs) are a class of multi-modal systems in which the transitions among different modes are governed by a Markov chain. The studies of these systems are motivated by the powerful modeling capability of Markov chains in practical applications, and many useful results have been obtained, see [2]-[6] for instance. However, in most of the studies, complete knowledge of the mode transitions is required as a prerequisite for analysis and synthesis of MJNLSs. This means that the transition probabilities (TPs) of the underlying Markov chain are assumed to be completely known.

To relax the assumption that all the TPs are known, a new concept for Markovian jump linear systems (MJLSs) with partially unknown TPs was proposed in [17] and a series of studies have been carried out [18]-[20]. Meanwhile, as two extreme cases, the so-called switched systems under arbitrary switching [18]-[20] and the conventional Markov jump systems was covered in the framework. However, although the works laid a conceptual foundation for analysis and synthesis of MJLSs, the proposed approach still have room for improvement in terms of conservatism. In fact, the properties of the transition rate matrix (RTM) has not been fully used. And most of existing results are dedicated to the MJLSs, while few results are available for the control design of Markovian jump nonlinear systems (MJNLSs).

In this paper, a new approach will be explored for the analysis and synthesis of MJNLSs with incomplete description of their transitions via fuzzy control. The proposed systems are more general and because it includes the completely known or unknown transition probabilities. Using the properties that the sum of each row is zero in a RTM, together with the convexity of the uncertain domains, necessary and sufficient conditions for the stability analysis and stabilization synthesis problems are first derived. The stabilization condition is expressed in terms of linear matrix inequalities (LMIs), which can be solved efficiently via existing LMI-optimization techniques.

II. Problem Formulation and Preliminaries

Given the probability space $(\Omega, \mathbb{F}, \mathbb{P})$: and consider continuous-time and discrete-time MJLNS , which can be described by the following fuzzy models :

$$\begin{aligned} R_i\text{: IF } & z_1(t) \text{ is } \Gamma_{i1} \text{ and } \cdots \text{ and } z_p(t) \text{ is } \Gamma_{ip} \\ \text{THEN } & \dot{x}(t) = A_{0i}(\eta(t))x(t) + B_i(\eta(t))u(t) \end{aligned} \quad (1)$$

where $x(t) \in \mathbb{R}^n$ constitutes the state vector, $u(t) \in \mathbb{R}^m$ is the control input, $R_i, i \in \mathcal{I}_R = \{1, 2, \cdots, r\}$, denotes the ith fuzzy rule, $z_h(t), h \in \mathcal{I}_P = \{1, 2, \cdots, p\}$, is the hth premise variable, Γ_{ih}, $(i, h) \in \mathcal{I}_R \times \mathcal{I}_P$, is the fuzzy set of $z_h(t)$ in R_i, the system matrices of the ith rule are denoted by $(A_{0i}, B_i$, which are assumed known and some constant matrices of compatible dimensions. The stochastic process $\{\eta(t), t \geq 0\}$(respectively, the Markovian chain $\eta(k), k \geq 0$), taking values in a finite space state denoted by $\mathbb{T} = \{1, 2, \cdots, \mathcal{N}\}$. The random form process $\eta(t)$ is a continuous-time has the following mode transition probabilities :

$$\mathbf{Pr}(\eta(t + \Delta t) = s | \eta(t) = l) = \begin{cases} \lambda_{ls}\delta + o(\Delta), s \neq l \\ 1 + \lambda_{ls}\delta + o(\Delta), s = l \end{cases}$$

where $\Delta > 0$, $\lim_{\Delta \to 0}(o(\Delta t)/\Delta t) = 0$ $(l, s \in \mathbb{T}, l \neq s)$ denotes the switching rate from mode l at time t to mode s at

time $t+\Delta t$, and $\lambda_{ll}=-\sum_{s=1,s\neq l}\lambda_{ls}$ for all $l\in\mathbb{T}$. Hence, the rate transition matrix (RTM) in the Markov process is given by

$$\Lambda=\begin{bmatrix}\lambda_{11} & \lambda_{12} & \cdots & \lambda_{1\mathcal{N}}\\ \lambda_{21} & \lambda_{22} & \cdots & \lambda_{2\mathcal{N}}\\ & & \ddots & \\ \lambda_{\mathcal{N}1} & \lambda_{\mathcal{N}2} & \cdots & \lambda_{\mathcal{N}\mathcal{N}}\end{bmatrix} \tag{2}$$

The set $\mathbb{T}$ contains $\mathcal{N}$ modes of system (1) for $\eta(t)=l\in\mathbb{T}$, the system matrices of the lth modes are denoted by $(A_{0i,l},B_{i,l})$, which are real known with appropriate dimensions.

In addition, the transition rates or probabilities of the Markov chain in this paper are considered to be partially known, namely, some elements in matrix Λ or 1 are time-invariant but unknown. We denote

$$\mathbb{T}_{\mathbb{K}}^{l}=\{s:\text{if }\lambda_{ls}\text{ is known}\} \tag{3}$$

$$\mathbb{T}_{\mathbb{UK}}^{l}=\{s:\text{if }\lambda_{ls}\text{ is unknown}\} \tag{4}$$

Moreover, if $\mathbb{T}_{\mathbb{K}}^{l}\neq 0$, it is described as

$$\mathbb{T}_{\mathbb{K}}^{l}=\left\{\mathbb{E}_{1}^{l},\cdots,\mathbb{E}_{m}^{l}\right\},\quad 1\leq m\leq\mathbb{N} \tag{5}$$

where $\mathbb{E}_{m}^{l}$ represents the mth element with the index $\mathbb{E}_{m}^{l}$ in the lth row of matrix Λ. In the continuous-time case, when λ_{ll} is unknown, it is necessary to provide a lower bound $\lambda_{d}^{(l)}$ for it and we have $\lambda_{d}^{(l)}<-\lambda_{\mathbb{E}}^{(l)}$. Let the mode at t be l. Using the center-average defuzzifer, product inference, and singleton fuzzifier, (1) is inferred as

$$\dot{x}(t)=\sum_{i=1}^{r}\theta_{i}(z(t))\left(A_{0i}\left(\eta(t)\right)x(t)+B_{i}(\eta(t))u(t)\right) \tag{6}$$

where $\theta_{i}(z(t))=w_{i}(z(t))/\sum_{i=1}^{r}w_{i}(z(t))$, $w_{i}(z(t))=\prod_{h=1}^{p}\mu_{\Gamma_{ih}}(z_{h}(t))$, and $\mu_{\Gamma_{ih}}(z_{h}(t))$: $U_{z_{h}}\subset\mathbb{R}\rightarrow\mathbb{R}_{[0,1]}$ is the membership function of $z_{h}(t)$ on the compact set $U_{z_{h}}$. Some basic properties are $\theta_{i}(z(t))\geq 0$ and $\sum_{i=1}^{r}\theta_{i}(z(t))=1$.

Throughout this paper, it is assumed that state $x(t)$ or $x(k)$ are available and the mode $\eta(t)$ or $\eta(k)$ are not available for feedback control. For each possible value of $\eta(t)=l$ or $\eta(k)=l,l\in\mathbb{T}$ in the succeeding discussion, for the convenience of notations, we will denote

$$A_{0i,l}(t)=\sum_{i=1}^{r}\theta_{i}(z(t))A_{0i}(\eta(t))$$

$$B_{i,l}(t)=\sum_{i=1}^{r}\theta_{i}(z(t))B_{i}(\eta(t))$$

In this paper, we will derive the stochastic stability criteria for system (1) when the transition rates or probabilities are partially known, and to determine the feedback gains $K_{j}(j\in\mathcal{I}_{r})$ such that the resulting closed-loop system is stochastically stable via the mode-independent fuzzy controller

$$\begin{aligned}R_{i}&\text{: IF }z_{1}(t)\text{ is }\Gamma_{i1}\text{ and }\cdots\text{ and }z_{p}(t)\text{ is }\Gamma_{ip}\\ &\text{THEN }u(t)=K_{j}(\eta(t))x(t),\quad j\in\mathcal{I}_{R}\end{aligned}$$

whose defuzzified output is given by

$$\begin{aligned}u(t)&=\sum_{j=1}^{r}\theta_{j}(z(t))K_{j}(\eta(t))x(t)\\ &=K_{j,l}(t)x(t)\end{aligned} \tag{7}$$

With the mode-independent fuzzy control law (7), the overall closed-loop MJFS when $\eta(t)=l$, $l\in\mathbb{T}$ can be written as

$$\dot{x}(t)=\left(A_{0i,l}\left(t\right)+B_{i,l}(t)K_{j,l}(t)\right)x(t) \tag{8}$$

Let $x(t,x_{0},\eta_{0})$ denote the trajectory of the state $x(t)$ from the initial state $x(0)=x_{0}$ and the initial mode $\eta(0)=\eta_{0}$.

III. Stability analysis and Stabilization

In this section, a stochastic stability condition for system (1) will be developed when the transition rates or probabilities are partially unknown, and a state feedback fuzzy controller will be designed for the MJFSs (8) such that the closed-loop systems are stochastically stable. First, we provide the following previous stability results for MJFSs when the transition rates or probabilities are partially unknown:

Lemma 1: System (1) is stochastically stable if and only if there exist matrices $Q_{l}=Q_{l}^{T}\succ 0$, $Q_{s}=Q_{s}^{T}\succ 0$, $l,s\in\mathbb{T}$ such that

$$A_{0i,l}^{T}(t)Q_{l}+Q_{l}A_{0i,l}(t)+\sum_{s=1}^{\mathbb{N}}\lambda_{ls}Q_{s}<0 \tag{9}$$

Let us first give the stability result for the unforced system ($u(t)\equiv 0$). The following theorem presents a necessary and sufficient condition on the stochastic stability of the considered system with partially known transition rates.

Theorem 1: Consider the unforced MJFS (1) with $u(k)=0$ and known transition probabilities. The corresponding system is stochastically stable if there exist matrices $P_{i,l}\succ 0$, $i\in\mathcal{I}_{r}$, $l,s\in\mathbb{T}$,

$$\begin{aligned}&A_{0i,l}^{T}P_{i,l}+P_{i,l}A_{0i,l}+\mathcal{P}_{\mathbb{K}}^{l}-\sum_{s\in\mathbb{T}_{\mathbb{K}}^{l}}\lambda_{ls}P_{i,s}<0\\ &\qquad\forall s\in\mathbb{T}_{\mathbb{UK}}^{l},\text{if }\ l\in\mathbb{T}_{\mathbb{K}}^{l}\end{aligned} \tag{10}$$

$$\begin{aligned}&A_{0i,l}^{T}P_{i,l}+P_{i,l}A_{0i,l}+\mathcal{P}_{\mathbb{K}}^{l}+\lambda_{d}^{l}P_{i,l}\\ &-\lambda_{d}^{s}P_{i,s}-\sum_{s\in\mathbb{T}_{\mathbb{K}}^{l}}\lambda_{ls}P_{i,s}<0\\ &\qquad\forall s\in\mathbb{T}_{\mathbb{UK}}^{l},\text{if }\ l\in\mathbb{T}_{\mathbb{UK}}^{l}\end{aligned} \tag{11}$$

where λ_{d}^{l} is a given lower bound for the unknown diagonal element.

Proof: We consider the proof into two cases, that is $l\in\mathbb{T}_{\mathbb{K}}^{l}$ and $l\in\mathbb{T}_{\mathbb{UK}}^{l}$.

1) Case I: $l\in\mathbb{T}_{\mathbb{K}}^{l}$ It should be noted that one has $\sum_{s\in\mathbb{T}_{\mathbb{K}}^{l}}\lambda_{ls}\leq 0$. Since $\sum_{s\in\mathbb{T}_{\mathbb{K}}^{l}}\lambda_{ls}=0$ measn the elements in the i^{th} row of the transition rates are known, we only need to consider $\sum_{s\in\mathbb{T}_{\mathbb{K}}^{l}}\lambda_{ls}<0$ here. Now we rewrite the left-hand side of (9) as

$$\begin{aligned}\Theta_l &= A_{0i,l}^T P_{i,l} + P_{i,l} A_{0i,l} + \mathcal{P}^l \\ &= A_{0i,l}^T P_{i,l} + P_{i,l} A_{0i,l} + \mathcal{P}_{\mathbb{K}}^l + \sum_{s\in\mathbb{T}_{\mathbb{UK}}^l} \hat{\lambda}_{ls} P_{i,s} \\ &= A_{0i,l}^T P_{i,l} + P_{i,l} A_{0i,l} + \mathcal{P}_{\mathbb{K}}^l - \lambda_{\mathbb{K}}^l \sum_{s\in\mathbb{T}_{\mathbb{UK}}^l} \frac{\hat{\lambda}_{ls}}{-\lambda_{\mathbb{K}}^l} P_{i,s}\end{aligned}$$

where $\mathcal{P}^l = \sum_{s=1}^{\mathcal{N}} \lambda_{ls} P_s$ and the elements $\hat{\lambda_{ls}}$, $s \in \mathbb{T}_{\mathbb{UK}}^l$ are unknown. Since we have $0 \leq \frac{\hat{\lambda}_{ls}}{-\lambda_{\mathbb{K}}^l} \leq 1$ and $\sum_{s\in\mathbb{T}_{\mathbb{UK}}^l} \frac{\hat{\lambda}_{ls}}{\lambda_{\mathbb{K}}^l} = 1$, we know that

$$\Theta_l = \sum_{s\in\mathbb{T}_{\mathbb{UK}}^l} \frac{\hat{\lambda}_{ls}}{-\lambda_{\mathbb{K}}^l} \left[A_{0i,l}^T P_{i,l} + P_{i,l} A_{0i,l} + \mathcal{P}_{\mathbb{K}}^l - \lambda_{\mathbb{K}}^l P_{i,s}\right]$$

Therefore, for $0 \leq \hat{\lambda}_{ls} \leq -\lambda_{\mathbb{K}}^l$, $\Theta_l < 0$ is equivalent to $A_{0i,l}^T P_{i,l} + P_{i,l} A_{0i,l} + \mathcal{P}_{\mathbb{K}}^l - \lambda_{\mathbb{K}}^l P_{i,s} < 0$, $\forall s \in \mathbb{T}_{\mathbb{UK}}^l$, which implies that, in the presence of unknown elements $\hat{\lambda}_{ls}$, the system stability is ensured if and only if (10) holds.

2) CaseII : $\hat{\lambda}_{ii}$ is unknown, $\hat{\lambda}_{\mathbb{K}}^l \geq 0$ and $\hat{\lambda}_{ll} \leq -\lambda_{\mathbb{K}}^l$. Also, we consider $\hat{\lambda}_{ll} < -\lambda_{\mathbb{K}}^l$ since if $\hat{\lambda}_{ll} = -\lambda_{\mathbb{K}}^l$, then the i_{th} row of the transition rates matrix is completely known. Now, the left-hand side of the stability condition in (9) can be rewritten as

$$\begin{aligned}\Theta_l &= A_{0i,l}^T P_{i,l} + P_{i,l} A_{0i,l} + \mathcal{P}^l \\ &= A_{0i,l}^T P_{i,l} + P_{i,l} A_{0i,l} + \mathcal{P}_{\mathbb{K}}^l + \hat{\lambda}_{ii} P_{i,l} + \sum_{s\in\mathbb{T}_{\mathbb{UK}}^l, s\neq l} \hat{\lambda}_{ls} P_{i,s} \\ &= A_{0i,l}^T P_{i,l} + P_{i,l} A_{0i,l} + \mathcal{P}_{\mathbb{K}}^l + \hat{\lambda}_{ii} P_{i,l} \\ &+ \left(-\hat{\lambda}_{ll} - \lambda_{\mathbb{K}}^l\right) \sum_{s\in\mathbb{T}_{\mathbb{UK}}^l, s\neq l} \frac{\hat{\lambda}_{ls}}{-\hat{\lambda}_{ll} - \lambda_{\mathbb{K}}^l} P_{i,s}\end{aligned}$$

Likewise, since we have $0 \leq \hat{\lambda}_{ls}/(-\hat{\lambda}_{ll} - \lambda_{\mathbb{K}}^l) \leq 1$ and $\sum_{s\in\mathbb{T}_{\mathbb{UK}}^l, s\neq l} \frac{\hat{\lambda}_{ls}}{(-\hat{\lambda}_{ll} - \lambda_{\mathbb{K}}^l)} = 1$, we know that

$$\begin{aligned}\Theta_l = \sum_{s\in\mathbb{T}_{\mathbb{UK}}^l, s\neq l} \frac{\hat{\lambda}_{ls}}{-\hat{\lambda}_{ll} - \lambda_{\mathbb{K}}^l} &\left[A_{0i,l}^T P_{i,l} + P_{i,l} A_{0i,l} + \mathcal{P}_{\mathbb{K}}^l \right. \\ &\left. + \hat{\lambda}_{ii} P_{i,l} - \hat{\lambda}_{ii} P_{i,s} - \lambda_{\mathbb{K}}^l P_{i,s}\right]\end{aligned}$$

which means that $\Theta_l \leq 0$ is equivalent to $\forall s \in \mathbb{T}_{\mathbb{UK}}^l$, $s \neq l$

$$A_{0i,l}^T P_{i,l} + P_{i,l} A_{0i,l} + \mathcal{P}_{\mathbb{K}}^l + \hat{\lambda}_{ii} P_{i,l} - \hat{\lambda}_{ii} P_{i,s} - \lambda_{\mathbb{K}}^l P_{i,s} \quad (12)$$

As $\hat{\lambda}_{ll}$ is lower bounded by λ_d^l, we have

$$\lambda_d^l \leq \hat{\lambda}_{ll} \leq -\lambda_{\mathbb{K}}^l$$

which implies that $\hat{\lambda}_{ll}$ may take any value between $[\lambda_d^l, -\lambda_{\mathbb{K}}^l + \epsilon]$ for some $\epsilon < 0$ arbitrarily small. Then $\hat{\lambda}_{ll}$ can be further written as a convex combination

$$\hat{\lambda}_{ll} = -\alpha\lambda_{\mathbb{K}}^l + \alpha\epsilon + (1-\alpha)\lambda_d^l$$

where α takes values arbitrarily in $[0, 1]$. Thus (12) holds if and only if $\forall s \in \mathbb{T}_{\mathbb{UK}}^l$, $s \neq l$

$$A_{0i,l}^T P_{i,l} + P_{i,l} A_{0i,l} + \mathcal{P}_{\mathbb{K}}^l - \lambda_{\mathbb{K}}^l P_{i,l} + \lambda_{\mathbb{K}}^l P_{i,s} - \lambda_{\mathbb{K}}^l P_{i,s} + \epsilon(P_{i,l} - P_{i,s}) \leq 0 \quad (13)$$

and

$$A_{0i,l}^T P_{i,l} + P_{i,l} A_{0i,l} + \mathcal{P}_{\mathbb{K}}^l + \lambda_d^l P_{i,l} - \lambda_d^l P_{i,s} - \lambda_{\mathbb{K}}^l P_{i,s} < 0 \quad (14)$$

simultaneously hold. Since ϵ is arbitrarily small, (13) holds if and only if

$$A_{0i,l}^T P_{i,l} + P_{i,l} A_{0i,l} + \mathcal{P}_{\mathbb{K}}^l - \lambda_{\mathbb{K}}^l P_{i,l} < 0 \quad (15)$$

which is the case in (14) when $s = l$, $s \in \mathbb{T}_{\mathbb{UK}}^l$. Hence (12) is equivalent to (11). Therefore, in the presence of unknown elements in the transition rates matrix, one can readily conclude that the system is stable if and only if (10) and (11) hold for $l \in \mathbb{T}_{\mathbb{K}}^l$ and $l \in \mathbb{T}_{\mathbb{UK}}^l$, respectively. ■

Now let us consider the stabilizing controller design in the presence of unknown elements in the transition rates matrix. The following theorem presents a sufficient criterion for the existence of a mode-dependent stabilizing controller of the form in (7).

Theorem 2: Consider the system (1) with partially known transition rates. If there exist matrices $X_{i,l} > 0$ and $Y_{i,l}$, $i, j \in \mathcal{T}_r$ $l \in \mathbb{T}$, Z and a positive scalar μ such that

$$\Upsilon_{ii,ls} < 0, \quad i \in \mathcal{I}_r, \forall s \in \mathbb{T}_{\mathbb{UK}}^l, \text{ if } l \in \mathbb{T}_{\mathbb{K}}^l \quad (16)$$

$$\frac{1}{r-1}\Upsilon_{ij,ls} + \frac{1}{2}\left(\Upsilon_{ij,ls} + \Upsilon_{ji,ls}\right) < 0 \quad (17)$$
$$i \neq j \in \mathcal{I}_r, \forall s \in \mathbb{T}_{\mathbb{UK}}^l, \text{ if } l \in \mathbb{T}_{\mathbb{K}}^l$$

$$\Xi_{ii,ls} < 0 \quad i \in \mathcal{I}_r, \forall s \in \mathbb{T}_{\mathbb{UK}}^l, \text{ if } l \in \mathbb{T}_{\mathbb{UK}}^l \quad (18)$$

$$\frac{1}{r-1}\Xi_{ii,ls} + \frac{1}{2}\left(\Xi_{ij,ls} + \Xi_{ji,ls}\right) < 0 \quad (19)$$
$$i \neq j \in \mathcal{I}_r, \forall s \in \mathbb{T}_{\mathbb{UK}}^l, \text{ if } l \in \mathbb{T}_{\mathbb{UK}}^l$$

where, $\Upsilon_{ij,ls}, \Xi_{ij,ls}$ are shown at the top of the next page,

$$\mathcal{X}_{\mathbb{K}}^l = \text{diag}\left[X_{\mathbb{K}_1}, \cdots, X_{\mathbb{K}_{m_l}}\right] \quad (20)$$

$$\mathcal{T}_{\mathbb{K}}^l = \left[\sqrt{-\lambda_{l\mathbb{K}_1}} X_{i,l}, \cdots, \sqrt{-\lambda_{l\mathbb{K}_{m_l}}} X_{i,l}\right] \quad (21)$$

and $\forall e \in \{1, 2, \cdots, m_l\}$, K_e is described in (7), $K_e \neq l$, then there exists a mode-dependent stabilizing controller of the form in (7) such that the closed-loop system is stochastically stable. Moreover, if the LMIs in (16)- (19) have solutions, a fuzzy controller gain is give by

$$K_j = Y_{j,l} Z^{-1} \quad (22)$$

Proof: Consider the system (1) with the control input (7) and replace $A_{0i,l}$ by $A_{0i,l} + B_{i,l}K_{j,l}$ in (10) and (11), respectively. Then if $l \in \mathbb{T}_{\mathbb{K}}^l$, performing a congruence transformation to (10) by $P_{i,l}^{-1}$, we can obtain

$$\begin{aligned}&\left(A_{0i,l} + B_{i,l}K_{j,l}\right) P_{i,l}^{-1} + P_{i,l}^{-1} \left(A_{0i,l} + B_{i,l}K_{j,l}\right)^T \\ &+ P_{i,l}^{-T} \mathcal{P}_{\mathbb{K}}^l P_{i,l}^{-1} - P_{i,l}^{-T} \left(\sum_{s\in\mathbb{T}_{\mathbb{K}}^l} \lambda_{ls} P_{i,s}\right) P_{i,l}^{-1}\end{aligned} \quad (25)$$

Setting $X_{i,l} = P_{i,l}^{-1}$, $Y_{i,l} = K_{j,l}Z$ and considering (21). Applying the lemma 3, one can obtain that (25), then the lth

$$\Upsilon_{ij,ls}=\begin{bmatrix} -Z-Z^T & Z^TA_{0i,l}^T+Y_{j,l}^TB_{i,l}^T+X_{i,l} & Z^T & 0 & 0 \\ * & -\mu^{-1}X_{i,l}+\pi_{ll}X_{i,l} & 0 & \mathcal{T}_{\mathbb{K}}^l & \sqrt{-\lambda_{\mathbb{K}}^l}X_{i,l} \\ * & * & -\mu X_{i,l} & 0 & 0 \\ * & * & * & -\mathcal{X}_{\mathbb{K}}^l & 0 \\ * & * & * & * & -X_{i,s} \end{bmatrix} \tag{23}$$

$$\Xi_{ij,ls}=\begin{bmatrix} -Z-Z^T & Z^TA_{0i,l}^T+Y_{j,l}^TB_{i,l}^T+X_{i,l} & Z^T & 0 & 0 \\ * & -\mu^{-1}X_{i,l}+\pi_{d}X_{i,l} & 0 & \mathcal{T}_{\mathbb{K}}^l & \sqrt{-\lambda_{d}^l-\lambda_{\mathbb{K}}^l}X_{i,l} \\ * & * & -\mu X_{i,l} & 0 & 0 \\ * & * & * & -\mathcal{X}_{\mathbb{K}}^l & 0 \\ * & * & * & * & -X_{i,s} \end{bmatrix} \tag{24}$$

inequality of (10) holds for some matrices $X_{i,l}=X_{i,l}^T>0$ if and only if there exist a scalar $\mu>0$ and a matrix Z such that (26), at the top of page.

By Schur complement, we can obtain that (26) is equivalent to (27). In a similar way, if $s\in\mathbb{T}_{\mathbb{UK}}^l$, (18) and (19) can be worked out from (11). (10)-(11) will be satisfied in Theorem 1 such that the closed-loop system (8) is stochastically stable. Meanwhile, due to $Y_{i,l}=K_{j,l}Z$, the desire controller gain is given by (22). ■

IV. SIMULATIONS

In this section, we present an numerical example to demonstrate the effectiveness of the proposed results. Consider a single-link robot arm in, in which the dynamic equation is given by

$$\ddot{\theta}(t)=-\frac{MgL}{J}\sin(\theta(t))-\frac{D(t)}{J}\dot{\theta}(t)+\frac{1}{J}u(t) \tag{28}$$

where $\theta(t)$ is the angle position of the arm, and $u(t)$ is the control input. M is the mass of the payload. J is the moment of inertia, g is the acceleration of gravity, L is the length of the arm, and $d(t)$ is the coefficient of viscous friction. The values of parameters g and L are given by $g=9.81$ and $L=0.5$. It is assumed that the parameter $D(t)=D=2$ is time invariant, and the parameters M and J have four different modes at shown in Table 1. Let $x_1(t)=\theta(t)$ and $x_2(t)=\dot{\theta}(t)$. Under the condition $-179.4270<\theta(t)<179.4270$, the nonlinear term $\sin(\theta(t))$ can be exactly represented as

$$\sin(\theta(t))=h_1(x_1(t))\cdot x_1(t)+h_2(t)(x_1(t))\cdot\beta\cdot x_1(t) \tag{29}$$

with $\beta=10^{-2}/\pi$, where $h_1(x_1(t))$, $h_2(x_1(t))\in[0,1]$, and $h_1(x_1(t))+h_2(x_1(t))=1$. By solving the equations, the membership functions $h_1(x_1(t))$ and $h_2(x_1(t))$ are obtained as follows:

$$h_1(x_1(t))=\begin{cases}\frac{\sin(x_1(t))-\beta\cdot x_1(t)}{x_1(t)\cdot(1-\beta)}, x_1(t)\neq 0\\ 1, x_1(t)=0.\end{cases} \tag{30}$$

$$h_2(x_1(t))=\begin{cases}\frac{x_1(t)-\sin(x_1(t))}{x_1(t)\cdot(1-\beta)}, x_1(t)\neq 0\\ 0, x_1(t)=0.\end{cases} \tag{31}$$

It can be seen from the above equations that $h_1(x_1(t))=1$ and $h_2(x_1(t))=0$, when $x_1(t)$ is about 0 rad, and $h_1(x_1(t))=0$ and $h_2(x_1(t))=1$, when $x_1(t)$ is about π rad or $-\pi$ rad. Then the nonlinear Markovian system (28) can be represented by the following T–S fuzzy model:

Plant Rule 1 :
IF $x_1(t)$ is "about 0 rad," THEN
$\dot{x}(t)=A_{1,l}x(t)+B_{1,l}u(t)$
Plant Rule 2 :
IF $x_1(t)$ is "about π rad or $-\pi$ rad," THEN
$\dot{x}(t)=A_{2,l}x(t)+B_{2,l}u(t)$

where

$$x(t)=\begin{bmatrix}x_1(t)\\x_2(t)\end{bmatrix}, A_{1,1}=\begin{bmatrix}0 & 1\\ -gl & -D\end{bmatrix},$$
$$A_{1,2}=\begin{bmatrix}0 & 1\\ -gL & -0.8D\end{bmatrix}, A_{1,3}=\begin{bmatrix}0 & 1\\ -gL & -0.5D\end{bmatrix},$$
$$A_{1,4}=\begin{bmatrix}0 & 1\\ -gL & -0.4D\end{bmatrix}, A_{2,1}=\begin{bmatrix}0 & 1\\ -\beta gL & -D\end{bmatrix}$$
$$A_{2,2}=\begin{bmatrix}0 & 1\\ -\beta gL & -0.8D\end{bmatrix}, A_{2,3}=\begin{bmatrix}0 & 1\\ -\beta gL & -0.5D\end{bmatrix},$$
$$A_{2,4}=\begin{bmatrix}0 & 1\\ -\beta gL & -0.4D\end{bmatrix},$$
$$B_{1,1}=B_{2,1}=\begin{bmatrix}0\\1\end{bmatrix}, B_{1,2}=B_{2,2}=\begin{bmatrix}0\\0.8\end{bmatrix}$$
$$B_{1,3}=B_{2,3}=\begin{bmatrix}0\\0.5\end{bmatrix} B_{1,4}=B_{2,4}=\begin{bmatrix}0\\0.4\end{bmatrix}$$

TABLE I
MODES OF THE PARAMETERS M, AND J

Mode l	M	J
1	1	1
2	1.25	1.25
3	2	2
4	2.5	2.5

The two cases for the transition rates matrix are considered in Table 2. The proposed theorem 2 is to design a mode-independent fuzzy controller such that the closed-loop system is stochastically stable with partially unknown transition

$$\begin{bmatrix} -Z-Z^T & Z^T\left(A_{0i,l}+B_{i,l}K_{j,l}\right)^T+X_{i,l} & Z^T \\ * & -\mu^{-1}X_{i,l}+X_{i,l}^T\mathcal{P}_{\mathbb{K}}^l X_{i,l}-X_{i,l}^T\left(\sum_{s\in\mathbb{T}_{\mathbb{K}}^l}\lambda_{ls}P_{i,s}\right)X_{i,l} & 0 \\ * & * & -\mu X_{i,l} \end{bmatrix}<0 \tag{26}$$

$$\Upsilon_{ij,ls}=\begin{bmatrix} -Z-Z^T & Z^TA_{0i,l}^T+Y_{j,l}^TB_{i,l}^T+X_{i,l} & Z^T & 0 & 0 \\ * & -\mu^{-1}X_{i,l}+\pi_{ll}X_{i,l} & 0 & \mathcal{T}_{\mathbb{K}}^l & \sqrt{-\lambda_{\mathbb{K}}^l}X_{i,l} \\ * & * & -\mu X_{i,l} & 0 & 0 \\ * & * & * & -\mathcal{X}_{\mathbb{K}}^l & 0 \\ * & * & * & * & -X_{i,s} \end{bmatrix}<0 \tag{27}$$

probabilities. With the choice of $\mu = 0.2$, we can obtain the following controller gain matrices by solving (16)-(19) in Theorem 2:

Case I

$$K_{1,1}=\begin{bmatrix}-4.7256\\-6.2890\end{bmatrix}^T, K_{1,2}=\begin{bmatrix}-4.8434\\-6.1849\end{bmatrix}^T$$
$$K_{2,1}=\begin{bmatrix}-7.1346\\-93.1655\end{bmatrix}^T, K_{2,2}=\begin{bmatrix}-7.1646\\-8.8974\end{bmatrix}^T$$
$$K_{3,1}=\begin{bmatrix}-5.4878\\-10.0789\end{bmatrix}^T, K_{3,2}=\begin{bmatrix}-5.4967\\-10.1987\end{bmatrix}^T$$
$$K_{4,1}=\begin{bmatrix}-7.1648\\-13.1846\end{bmatrix}^T, K_{4,2}=\begin{bmatrix}-7.1649\\-14.7868\end{bmatrix}^T$$

Case II

$$K_{1,1}=\begin{bmatrix}-3.1648\\-5.1464\end{bmatrix}^T, K_{1,2}=\begin{bmatrix}-3.1684\\-6.1879\end{bmatrix}^T$$
$$K_{2,1}=\begin{bmatrix}-0.7978\\-2.4798\end{bmatrix}^T, K_{2,2}=\begin{bmatrix}-0.4798\\-2.4987\end{bmatrix}^T$$
$$K_{3,1}=\begin{bmatrix}-14.1654\\-19.7934\end{bmatrix}^T, K_{3,2}=\begin{bmatrix}-14.4684\\-21.4987\end{bmatrix}^T$$
$$K_{4,1}=\begin{bmatrix}-6.7913\\-13.2890\end{bmatrix}^T, K_{4,2}=\begin{bmatrix}-5.8434\\-13.1201\end{bmatrix}^T$$

TABLE II
DIFFERENT TRANSITION PROBABILITIES MATRICES

Case I	1	2	3	4
1	-0.5	?	0.3	?
2	?	-0.6	?	0.3
3	0.2	0.3	?	?
4	?	?	0.3	?
Case II				
1	-0.7	?	0.1	0.1
2	?	-0.4	0.1	?
3	0.5	0.3	?	?
4	?	?	0.4	?

Figures 1-2 show the result of the changing between modes during the simulation with the initial mode at mode 1. Applying the fuzzy controller (7) with the above gain matrices, the state response and control inputs of the closed-loop system are shown in figures under given initial condition

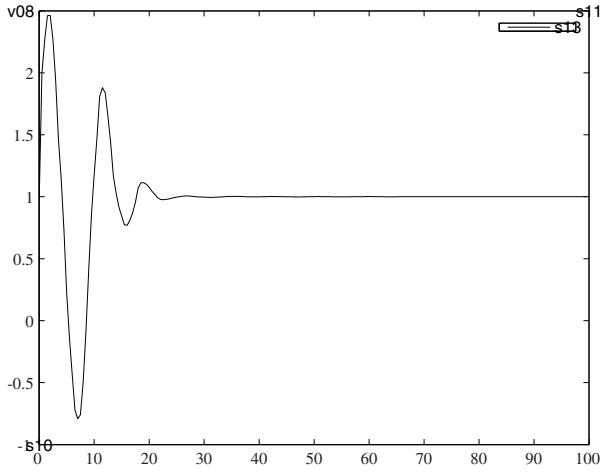

Fig. 1. The trajectories of states x_1

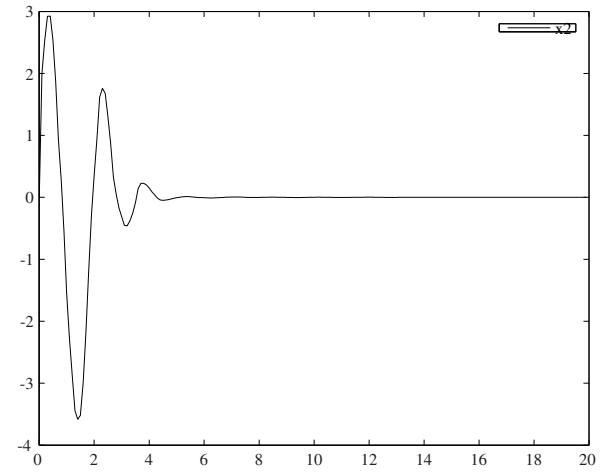

Fig. 2. The trajectories of states x_2

$x_0 = [0.5\pi, -2]^T$. It is seen from the curves in Figures 1-2 that, despite the partially unknown transition rates, the designed controllers stabilize the system (28) effectively.

V. Conclusion

In this paper, we have revisited the analysis and synthesis problems of Markov jump nonlinear system with incomplete transition descriptions via fuzzy control. Necessary and sufficient criteria are obtained for MJFSs by fully exploiting the properties of the transition rates matrix and the transition probabilities matrix. The conservatism of the approach developed previously, which only leads to sufficient conditions for the system, is reduced by the newly developed approach. The proposed stabilization conditions with a mode-dependent fuzzy controller are derived for Markovian jump fuzzy systems in terms of LMIs, which can be solved readily by using existing LMI optimization techniques. Finally, numerical examples have verified the theoretical results given in the paper.

Acknowledgment

References

[1] H. Kopka and P. W. Daly, *A Guide to LaTeX*, 3rd ed. Harlow, England: Addison-Wesley, 1999.

[2] Y. Ji and H. J. chizeck, "Controllability, stabilizability, and continuous-time Markovian jump linear quadratic control," *IEEE Trans. Automat. Control*, vol 35, no 7, pp. 777-788, 1990.

[3] J. Xiong, J. Lam, H. Gao, and D. W. Ho, "On robust stabilization of Markovian jump systems with uncertain switching probabilities", *Automatica*, vol 41, no 5, pp. 897-903, 2005.

[4] O. L. V. Costa, M. D. Fragoso, and R. P. Marques, "Discrete-time Markovian jump linear systems," *London: Springer- Verlag*, 2005.

[5] J. L. Xiong, J. Lam, H. J. Gao, and W. C. Daniel, "On robust stabilization of Markovian jump systems with uncertain switching probabilities," *Automatica*, vol. 41, no. 5, pp. 897-903, 2005.

[6] L. Zhang, Y. Shi, T., Chen, and B. Huang, "A new method for stabilization of networked control systems with random delays", *IEEE Trans. Autom. Control*, vol. 50, no. 8, pp. 1177-1181, 2005.

[7] K. Tanaka and M. Sano, "A robust stabilization problem of fuzzy control systems and its application to backing up control of a truck-trailer," *IEEE Trans. Fuzzy Syst.*, vol. 2, no. 2, pp. 119-134, 1994.

[8] Y. Y. Cao and P. M. Frank, "Analysis and synthesis of nonlinear time-delay systems via fuzzy control approach," *IEEE Trans. Fuzzy Syst.*, vol. 8, no. 2, pp. 200-211, 2000.

[9] Y. Y. Cao and P. M. Frank, "Stability analysis and synthesis of nonlinear time-delay systems via linear Takagi-Sugeno fuzzy models," *Fuzzy Sets Syst.*, vol. 124, no. 2, pp. 213-229, 2001.

[10] T. M. Guerra and L. Vermeiren, "LMI-based relaxed nonquadratic stabilization conditions for nonlinear systems in the Takagi.Sugenos form," *Automatica*, vol. 40, no. 5, pp. 823-829, 2004.

[11] N. S. D. Arrifano and V. A. Oliveira, State feedback fuzzy-modelbased control for Markovian jump nonlinear systems, Controle Automacao: Revista da Sociedade Brasileira de Automacao, vol. 15, no. 3, pp. 279-290, 2004.

[12] S. Natache, N. S. D. Arrifano and V. A. Oliverira, "Robust H_∞ fuzzy conrol approach for a class of markovian jump nonlinear systems," *IEEE Trans. Fuzzy Syst.*, vol. 13, no. 6, pp. 738-754, 2006.

[13] N. S. D. Arrifano and V. A. Oliveira "State feedback fuzzy-model-based control for Markovian jump nonlinear systems," *Controle Automacao: Revista da Sociedade Brasileira de Automacao*, vol. 15, no. 6, pp. 279, 2004.

[14] S. Nguang,W. Assawinchaichotge, and P. Shi, "Robust H_∞ control design for fuzzy singularly perturbed systems with Markovian jumps: an LMI approach," *IET Control Theory and Applications*, vol 1, no. 4, pp. 893-908, 2007

[15] H. N. Wu, and K. Y. Cai, "Robust fuzzy control for uncertain discrete-time nonlinear Markovian jump systems without mode observations", *Information sciences.*, vol. 177, no. 6, pp. 1509-1522, 2007.

[16] H. J. Kushner, "Stochastic Stability and Control", *New York: Academic*, 1967.

[17] L. X. Zhang and E. K. Boukas, "Stability and stabilization of Markovian jump linear systems with partly unknown transition probability," *Automatica*, vol. 45, no. 2, pp. 463-468, 2009.

[18] L. X. Zhang and E. K. Boukas, "H_∞ control for discrete-time Markovian jump linear systems with partly unknown transition probabilities," *Int. J. Robust Nonlin. Control*, vol. 19, no. 5, pp. 868-883, 2009.

[19] L. X. Zhang and E. K. Boukas, "H_∞ control of a class of extended Markov jump linear systems," *IET Control Theory Appl.*, vol. 3, no. 7, pp. 834-842, 2009.

[20] L. X. Zhang, E. K. Boukas, and J. Lam, "Analysis and synthesis of Markov jump linear systems with time-varying delays and partially known transition probabilities," *IEEE Trans. Autom. Control*, vol. 53, no. 10, pp. 2458-2464, 2008.

[21] L. Sheng and M. Gao, "Stabilization for markovian jump nonlinear systems with partly unknown transition probabilities via fuzzy control," *Fuzzy Sets and Systems*.

2011 IEEE International Conference on Fuzzy Systems
June 27-30, 2011, Taipei, Taiwan

A Testicular Tubule Evaluation Method by Ultrasonic Array Probe

Yuya Takashima[1], Kei Kuramoto[1),2)], Syoji Kobashi[1),2)], Yutaka Hata[1),2)], Tomomoto Ishikawa[3)],

[1)] Graduate School of Engineering, University of Hyogo, Hyogo, Japan
er11u017@steng.u-hyogo.ac.jp

[2)] WPI Immunology Frontier Research Center, Osaka University, Osaka, Japan

[3)] Ishikawa Hospital, Hyogo, Japan

Abstract— **This paper describes a testicular tubules evaluation using 1.0MHz ultrasonic array probe. In this system, we evaluate a diameter of testicular tubules. We employ an ultrasonic array probe with the center frequency of 1.0MHz. We employ evaluation index that cumulative relative frequency of amplitude values. In the experiment, we employ 24 nylon lines as the testicular tubules. Amplitude of large nylon line echo is larger than that of small nylon echo. For the evaluation, we calculate cumulative relative frequency amplitude of acquisition data. Fuzzy if-then rules are made by the cumulative relative frequency of large and small lines. We evaluate a rate of large lines among all lines by using the fuzzy MIN-MAX center-of-gravity method. In this experiment, the proposed method successfully evaluated the rate of the large lines. We changed the rate of large lines in 24 nylon lines, and tested our method 20 times for each rate. We evaluated the rate with 5.77 % in mean absolute error.**

Keywords-medical system; ultrasonic; cumulative relative frequency; azoospermia; testicular tubule.

I. INTRODUCTION

Azoospermia is the term used when there is a complete absence of sperm in the ejaculate. Fifteen-20% of infertile men turn out to be azoospermia. Azoospermia is caused by two problems; a production problem which is called non-obstructive azoospermia (NOA) and a deliver problem which is called obstructive azoospermia (OA). The development of intracytoplasmic sperm injection (ICSI) opened a new era in the field of assisted reproduction and revolutionized the assisted reproductive technique protocols of couples with male factor infertility [1]. Fertilization and pregnancies can be obtained with spermatozoa recovered not only from the ejaculate, but seminiferous tubules.

The ideal technique of sperm extraction from testicle for NOA would be minimally invasive and avoid destruction of testicular function without compromising the chance of retrieval adequate numbers of spermatozoa to perform ISCI. Schlegel et al. have successfully developed the techniques with the assistance of an operating microscope as Micro-TESE [2]. The testicle can be inspected for the presence of a spermatogenically active region of normal seminiferous tubules (Diameter: 0.250mm~0.300mm), which containing many developing germ cells. Those tubules are usually larger and more opaque than tubules without sperm production, and therefore easily distinguishable from sclerotic tubules that are much smaller in diameter (Diameter: <0.150mm). In almost all patients in whom micro-TESE was successful we could identify focal spermatogenesis in dilated and opaque seminiferous tubules surrounded by shrunken tubules or fibrous tissue [3], [4].

The determination of factors that can predict successful sperm retrieval (SR) procedure can offer realistic expectations for both the couple and the physician because SR rate is at most 50% even after the introduction of micro-TESE. Additionally, the operation is high cost and physically large burden for patients. Retrospectively, we examined the differences between SR success and failure group in FSH, LH, testosterone, testicular volume and age. So far, no one could foretell about the presence of a spermatogenic focus inside an NOA testis. Therefore, we request the system that noninvasive measures the tubules heterogeneity in the testicle before micro-TESE procedure [5], [6].

In our study, we propose a testicular tubule evaluation system with a 1.0MHz ultrasonic array probe. We can noninvasively evaluate it by the ultrasonic array probe. We employ two different diameter nylon fishing lines as a small tubule and large tubule. We calculate the cumulative relative frequency of amplitude values. From the difference of the frequency of amplitude values, we derive fuzzy IF-THEN rules and make a fuzzy MIN-MAX center-of-gravity method. We then evaluate the rate of large line among all lines by the method. In our experimental results, mean absolute error was 5.77 %.

II. PRELIMINARIES

In this section, we describe the ultrasonic array probe and the experimental system used here. Fig. 1 shows the system of our ultrasonic array probe (ISL Inc., ISL1938). It consists of 32 elements in line. Center frequency of the array probe is 1.0 MHz, and each element interval is 1.5 mm. As shown in Fig. 1, a combination ultrasonic is generated by applying a voltage to several elements. The applied voltage shifts for 1 element distance [7].

978-1-4244-7316-8/11/$26.00 ©2011 IEEE

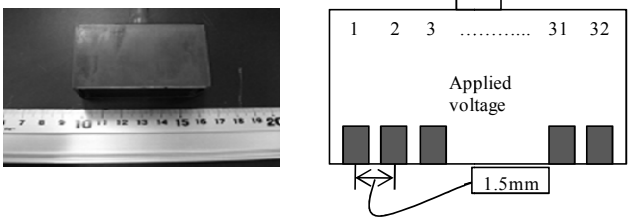

(a) Ultrasonic array probe (b) The structure

Figure 1. The system of 1.0MHz ultrasonic array probe.

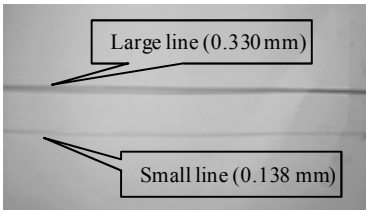

Figure 2. Large fishing line and small fishing line.

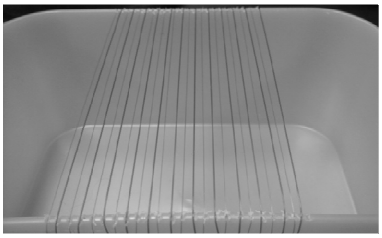

Figure 3. Object that line up 24 fishing line.

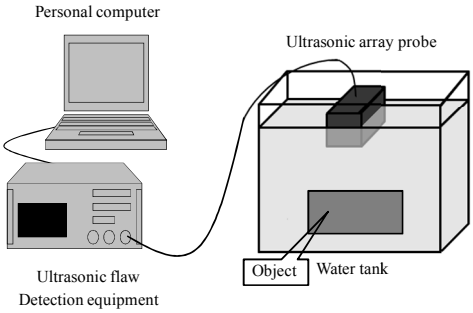

Figure 4. Ultrasonic data acquisition system.

In our experiment, we employ two different diameter nylon fishing lines as shown in Fig. 2, we employ these lines as the object. The diameter of small line is 0.138 mm and that of large line is 0.330 mm. Here, it is noted that testicular larger diameter ranged fro m 0.25 to 0.30 mm and smaller one is 0.15 mm. Fig. 3 shows the phantom of it. It line up 24 fishing lines in parallelism. The ultrasonic data acquisition system is shown in Fig. 4. Fig. 5 shows the data acquisition method. The sampling interval is 500 ms. The ultrasonic data are provided to a personal computer through the ultrasonic array probe.

III. LARGE LINE EVALUATION

A. *Outline of the procedure*

Our method consists of five steps. Firstly, we acquire the waveforms from the probes, and extract the data in the nylon lines. Secondly, we calculate the amplitude values. Thirdly, we calculate cumulative relative frequency of amplitude values. Fourthly, we apply the fuzzy-if then rules from cumulative

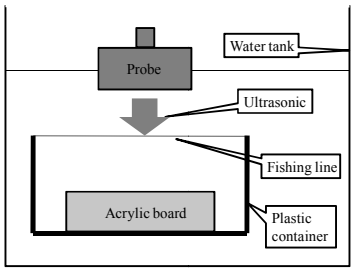

(a) Slice view

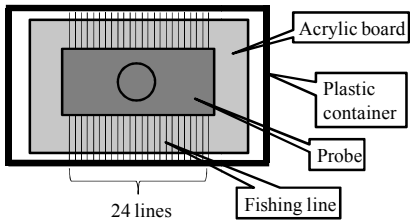

(b) Top view

Figure 5. Ultrasonic data acquisition method.

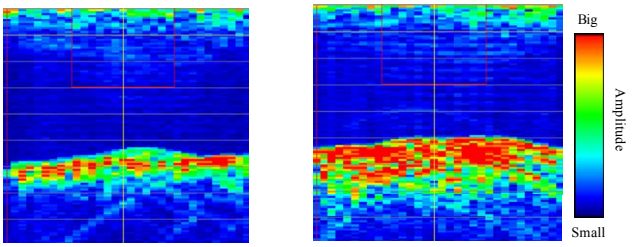

(a) 24 small lines (b) 24 large lines

Figure 6. Examples of ultrasonic data (B-mode).

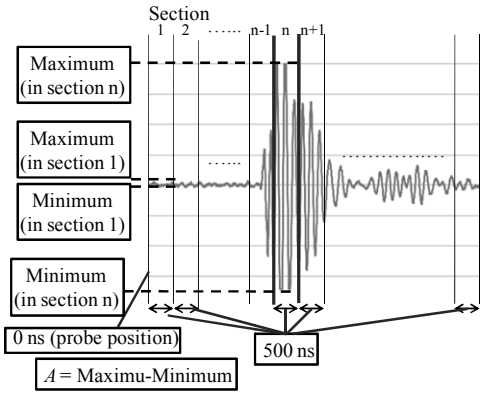

Figure 7. Calculation Amplitude

relative frequency of particular amplitude. Finally, we calculate the rate of large line among all lines by the fuzzy MIN-MAX center-of-gravity method.

B. *Calculation of cumulative relative frequency of amplitude*

Fig. 6 shows an example of ultrasonic data. As shown in Fig. 6, the rate of big amplitudes in the large lines is larger than that of the small lines. We use the difference of the distribution of the amplitude values for evaluating the rate of large line.

We employ the cumulative relative frequency of amplitude to compare the rate of the big amplitudes. We extract the waves of the interval 500 ns as shown in Fig. 7. We then calculate

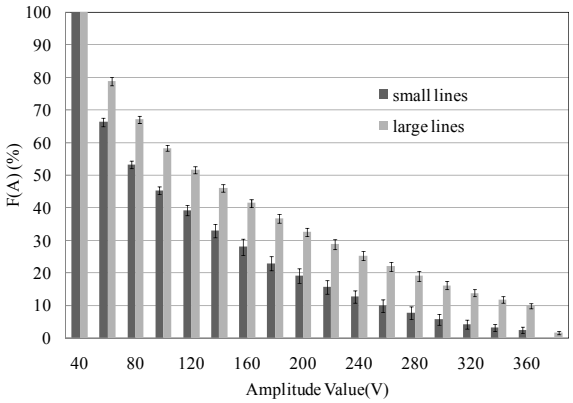

Figure 8. Average of cumulative relative frequency

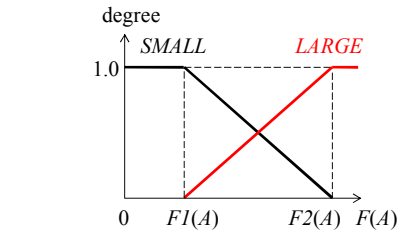

(a) Input membership functions.

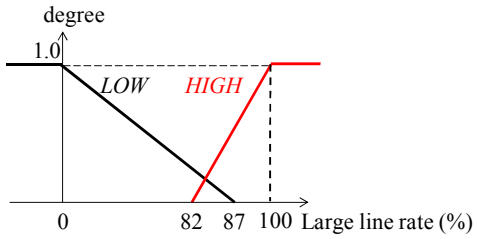

(b) Output membership functions.

Figure 9. Fuzzy membership functions.

peak to peak value in amplitude in every interval. In Fig. 7, the notation A denotes peak to peak value. We calculate cumulative relative frequency from relative frequency from 40 V to 400 V at the interval of 20 V. The cumulative relative frequency is calculated by (1).

$$F(A) = \sum_{X=A}^{400} f(X) \tag{1}$$

Here, the notation $F(A)$ denotes cumulative relative frequency of amplitude of A, and $f(A)$ denotes relative frequency. We show the average of $F(A)$ of 20 times of 24 small and 24 large lines in Fig. 8. As shown in Fig. 8, cumulative relative frequency of large lines is larger than that of small lines.

C. Evaluation of rate of large line

We evaluate a rate of large line in mixed lines using fuzzy inference. From Fig. 8, we obtain knowledge of the cumulative relative frequency of amplitude as follows.

Knowledge 1: The cumulative relative frequency of large line is larger than that of small lines at same amplitude value.

TABLE I. Fuzzy IF-THEN Rules

Input			Output
$F(80)$	$F(180)$	$F(200)$	Large line rate
SMALL	*SMALL*	*SMALL*	*LOW*
SMALL	*SMALL*	*LARGE*	*LOW*
SMALL	*LARGE*	*SMALL*	*LOW*
SMALL	*LARGE*	*LARGE*	*HIGH*
LARGE	*SMALL*	*SMALL*	*LOW*
LARGE	*SMALL*	*LARGE*	*HIGH*
LARGE	*LARGE*	*SMALL*	*HIGH*
LARGE	*LARGE*	*LARGE*	*HIGH*

TABLE II. Values of $F1(A)$ and $F2(A)$.

$A(V)$	$F1(A)$	$F2(A)$
80	53.22	66.98
180	22.85	36.75
200	19.02	32.51

Knowledge 2: When amplitude value is 180, the cumulative relative frequency has the largest difference between small lines and large lines.

Knowledge 3: When amplitude value is 80, the cumulative relative frequency has the 2nd largest difference between small lines and large lines.

Knowledge 4: When amplitude value is 200, the cumulative relative frequency has the 3rd largest difference between small lines and large lines.

These knowledge are converted into eight fuzzy IF-THEN rules. The fuzzy IF-THEN rules are derived as shown in Table I. "*LOW*", "*HIGH*", "*SMALL*" and "*LARGE*" are fuzzy linguistic values, and these values are defined by fuzzy membership functions as shown in Fig. 9. The notations $F1(A)$ and $F2(A)$ denote $F(A)$ of 24 large lines and $F(A)$ of 24 small lines, respectively. To determine these values, we acquire ultrasonic data 20 times for each line set, and we calculate the average values. We show the values of $F1(A)$ and $F2(A)$ in Table II. The fuzzy IF-THEN rules are expressed by fuzzy MIN-MAX center-of-gravity method [8]. We determine a value of center of gravity as the rate of large line among all lines.

IV. Experimental Results

We acquired ultrasonic waves by 32 elements of the ultrasonic array probe. We used eight kinds of phantoms. These are lined up from large and small lines in total 24. We acquired 20 times ultrasonic waveforms for each object. Table III shows average of the calculated large line rate and truth large line rate

TABLE III. Object and evaluation result

Object		Large line rate(%)	
N_S	N_L	evaluation result	truth
24	0	2.84	0.00
23	1	14.33	4.17
20	4	19.55	16.67
16	8	27.99	33.33
12	12	49.33	50.00
8	16	66.94	66.67
4	20	93.60	83.33
0	24	86.25	100.00

(*truth* = N_L / (N_S + N_L) × 100 %). The notation N_S denotes number of small lines, and N_L denotes number of large lines.

Fig. 10 shows the result. The continuous line shows our evaluation result, and the dotted line shows the true value. As shown in this figure, the rate of large line is increased by the increment of the number of large line and our result accords with the truth value. The mean absolute error was then 5.77 %. The correlation coefficient the obtained was 0.98.

V. CONCLUSION

In our study, we proposed a testicular tubules evaluation system with a 1.0MHz ultrasonic array probe. We employed two different diameter nylon fishing lines as a small tubule and large tubule. In the preliminary experiment, we analyzed the difference of cumulative relative frequency of amplitude from the obtained ultrasonic data, and we found the difference of the distribution of the amplitude values. From these results, eight fuzzy IF-THEN rules were derived. The rate of large line was evaluated by fuzzy MIN-MAX center of gravity method. As the result, the evaluated rate of large line increases according to the increment of the number of large line. Then the correlation coefficient was 0.98. The experiments were done with 1.0 MHz ultrasonic waves. This experimental results suggested the high possibility to determine the larger diameter testicular tubule under the assumption that the characteristics of human testicular tubule is similar to that of the fishing line.

In the future, we will add the other indexes for optimize the fuzzy membership functions. Additionally we do experiment with the model being nearer to the living body and we experiment with the higher frequency ultrasonic waves than 1.0 MHz ultrasonic waves.

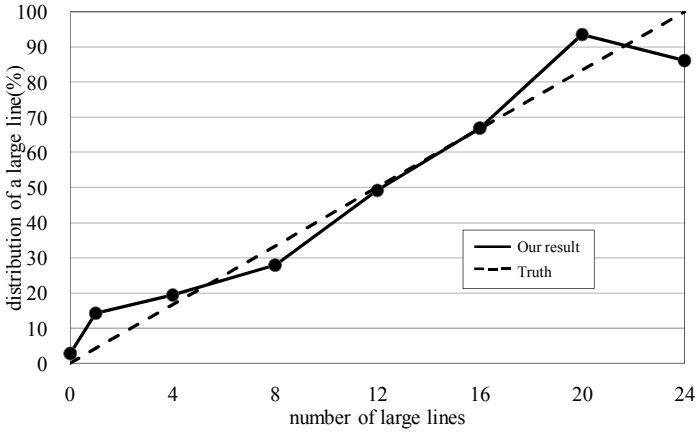

Figure 10. Result of large line rate.

REFERENCES

[1] G. Palermo, H. Joris, P. Devroey, A. C. Van Steirteghem, "Pregnancies after intracytoplasmic injection of single spermatozoon into an oocyte," Lancet 1992 vol.340, pp. 17–18.

[2] P. N. Schlegel, P. S. Li, "Microdissection TESE: spermatozoa retrieval in non-obstructive azoospermia," Hum Reprod Update 1998 vol.4, pp. 439.

[3] T. Ishikawa, R. Nose, K. Yamaguchi, K. Chiba, and M. Fujisawa, "Learning curves of microdissection testicular sperm extraction for non-obstructive azoospermia," Fertil Steril in press, pp. 1008-11, August 2010.

[4] T. Ishikawa, and M. Fujisawa, "Microdissection testicular sperm extraction for non-obstructive azoospermia: The assessment of serum hormone levels before and after procedure." Japanese Journal of Reproductive Endocrinology, vol. 14, pp.15-20, 2009.

[5] A. Ramkumar, A. Lal, D. A. Paduch, and P. N. Schlegel,"AN Ultrasonically Actuated Silicon-Microprobe-Based Testicular Tubule Assay," IEEE Transactions on biomedical engineering, vol. 56, pp. 2666-74, November 2009.

[6] J. L. Giffin, S.E.Franks, J. R. Rodariguez-Sosa, A. Hahnel, and P. M. Bartlewski, "A Study of Morphological and Haemodynamic Determinants of Testicular Echotexture Characteristics in the Ram," Exp Biol Med,pp. 794-801,2009 July.

[7] M. Nakamura, Y.T. Kitamura, T. Yanagida, S. Kobashi, K. Kuramoto, and Y. Hata, "Free placement trans-skull doppler system with 1.0MHz array ultrasonic probe," Proc. of 2010 IEEE Int. Conf. on Systems, Man and Cybernetics, pp. 1370-1374, 2010.

[8] E. A. Mamdani, "Application of fuzzy algorithm for control of simpledynamic plant," Proc. IEEE, Vol. 121, No. 12, 1974, pp. 1552-1558.

2011 IEEE International Conference on Fuzzy Systems
June 27-30, 2011, Taipei, Taiwan

Fuzzy RASP Determination by 1kHz Ultrasonic Probe for Total Hip Arthroplasty

Naomi Yagi
Yoshitetsu Oshiro, Osamu Ishikawa
Ishikawa Hospital
2-150 Bessho, Bessho-cho, Himeji, Hyogo,
671-0221, Japan
naomi.yagi@ieee.org

Yutaka Hata*
Graduate School of Engineering, University of Hyogo
2167, Shosha, Himeji, Hyogo,
671-2280, Japan
*WPI Immunology Frontier Research Center, Osaka University,
Osaka, Japan

Nao Shibanuma
Kobe Kaisei Hospital
3-11-15 Shinohara Kitamachi, Nada-Ku, Kobe, Hyogo,
657-0068, Japan

***Abstract*—This paper describes an effective system of selecting most suitable rasp for the patients. We suggest the ultrasonic system with a single ultrasonic probe. Firstly, we make a knock to the upper point of the rasp inserted with a hammer which has the trigger signals. We detected the acoustic signals with the knocking signals. An ultrasonic probe is fixed in the upper side of the rasp with a built-in magnet. A personal computer got the acoustic data. In the surgery, the surgeon tries to adapt for the patient from the small size rasp to the larger size rasp in turn. There is a correlation between the degree of tightening and the attenuation time of acoustic signal for the knocked sound by a hammer when inserting the rasp. The higher tightened degree implies shorter attenuation period. At the present time, the surgeon's experience chooses the suitable rasp. Therefore, we suggest the rasp determination system which selects the suitable rasp by fuzzy inference which dynamically corresponds for each patient. As the result, we successfully determined the suitable rasp in comparison to the results obtained from the practical surgery. We could indicate the indexes in order to judge how degree the rasp fits in the clinical treatment.**

Keywords— fuzzy inference, ultrasonic system, suitable rasp, total hip Arthroplasty (THA)

I. INTRODUCTION

A joint replacement consists in replacing a damaged joint with a prosthesis. In the orthopedic surgery, the arthritic or dysfunctional joint surface is replaced with an orthopaedic prosthesis [1]. Total hip arthroplasty (THA), which rebuilds the damaged hip joint with some implants, is operated to treat the hip joint diseases such as osteoarthritis, etc. The THA implants mainly consist of cup, liner, head and stem that play a role of acetabulum, hip cartilage, head of femur, and femur, respectively. The principal complication after THA is dislocation [2]. The primal mechanisms of dislocation are impingement of the femoral heck on the cup liner, impingement of the femur on the pelvis, and spontaneous dislocation due to excessive external force against muscular force. For example a hip joint that is affected by osteoarthritis may be replaced entirely with a prosthetic hip. This would involve replacing both the acetabulum, hip socket, and the head and neck of the femur. The purpose of this procedure is to relieve pain, to restore range of motion and to improve walking ability, thus leading to the improvement of muscle strength.

Joint replacement surgery is becoming a more common practice [3] [4]. The prosthetic implant used in hip replacement consists of different parts, the acetabular cup, the femoral component and the articular interface. The femoral component is the component that fits in the femur. The use of cementless femoral implants for total hip arthroplasty has increased in popularity over the last few decades [5]. Numerous implant designs based on different views concerning implant fixation are currently available. Bone is removed and the femur is shaped to accept the femoral stem with attached prosthetic femoral head or ball. Options exist for different patients and indications. Correct selection of the prosthesis is important [6], [7]. The selection of the optimum size and type of implant to fit the anatomical characteristics of the individual patient is important in order to avoid postoperative complications such as dislocation or loosening [8]-[10]. Regardless of implant design, primary stability of the cementless femoral implants in the femoral canal must be achieved at the time of operation and is really important for osseointegration, long-term fixation and clinical success [11]-[13].

The surgeon's experience in choosing the rasp size to be implanted is fundamental to achieve good fixation. However, especially for complicated cases, there is still the risk that the stem size chosen might be unsuitable. To solve the problem, References [14] and [15] described the mechanical stability at the time of implantation. Moreover, in order to do more quantitative evaluation and analysis, we propose how to select the most suitable stem for the patients by using the ultrasonic system in our study. The fuzzy inference which dynamically

978-1-4244-7316-8/11/$26.00 ©2011 IEEE

corresponds for each patient is able to solve the problem of the Individual difference. As the results, we were able to select the suitable rasp with higher accuracy.

II. Total Hip Arthroplasty

Hip fractures occur as a result of major or minor trauma. In elderly patients with bones weakened by osteoporosis, relatively little trauma, even walking, may result in a hip fracture. The hip is made of a ball and a socket joint, linking the dome at the head of the femur and the cup in the pelvic bone. A total hip prosthesis is surgically implanted to replace the damaged bone within the hip joint.

Then a metal ball and a metal stem are inserted in the femur and a plastic socket is placed in the enlarged pelvis cup as shown in Fig. 1. The artificial components are fixed in place. The muscles and tendons are then replaced against the bones and the incision is closed.

Figure 1. Total Hip Arthroplasty

Each patient has each various bone in the hip. So the surgeon has to find the most suitable rasp for the patient while operating. In the present situation, there are some differences of selecting the suitable rasp. Therefore, we propose the determination system of selecting the suitable rasp for the patient.

III. Measurement System

We show our system in Fig. 2. The center frequency of the single ultrasonic probe is 1,000Hz. The acquired ultrasonic waveform is analyzed by a personal computer.

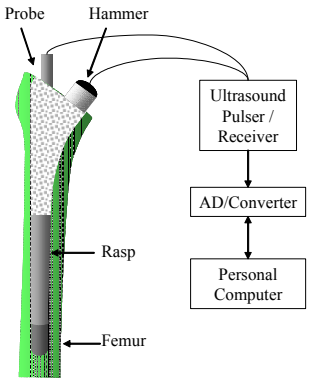

Figure 2. Measument System

At first, we make a knock to the upper point of the rasp inserted with a hammer which has the trigger signals. By using the knocking signals, we measured the acoustic signals. The microphone for measuring (10mmΦ) is fixed in the upper side of the rasp with a built-in magnet. The acoustic data is changed to the digital data by the AD converter (Picoscope ADC-212/100), and is sent to the personal computer.

A. Experimental Materials

In the clinical treatment, one of the indexes to judge how degree the rasp fits for the patient is the knocked sound by a hammer when inserting the rasp. The surgeon recognizes that the dull knocked sound means the loose fixed. From the physical opinion, in the case of loose fixing, the attenuation time of amplitude is long because the acoustic energy continues to transmit into the rasp. On the other side, in the case of tight fixing, the attenuation time of amplitude is short because the acoustic energy transmits from the rasp to the external fixed object and is absorbed on the early stage.

At first, we do envelope processing to the positive area of the acoustic wave as shown in Fig. 3. In this figure, we define the maximum of the attenuation value as A_{max} and the time at that time as T_{max}. A_{10} is A_{max} / 10. After the time of T_{max}, we define the time as T_{10} when the value is less than A_{10}.The attenuation time is obtained by (1). We estimate the degree of fixing by using this derived attenuation time.

$$T_{ATT} = T_{10} - T_{max} \quad (1)$$

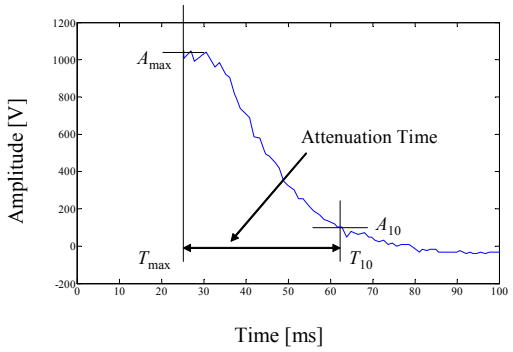

Figure 3. Measument System

B. Fuzzy Inference

We propose a fuzzy evaluation system with two features, the attenuation time and the difference time. The difference time defines as the time between the attenuation time of the rasp and that of the one size smaller rasp. From the obtained coefficients, Knowledge 1, 2, 3 and 4 are derived.

Knowledge 1: The tight fixing has the short attenuation time.
Knowledge 2: The tight fixing has the short difference time.
Knowledge 3: The attenuation time depends on the fixed degree.
Knowledge 4: The difference time depends on the fixed degree.

These are converted to the following fuzzy if-then rules.

Rule 1: IF *Attenuation time* is *Short* THEN the degree of fixing is High.
Rule 2: IF *Difference time* is *Short* THEN the degree of fixing is High.

The fuzzy if-then rules are represented by the fuzzy membership functions as shown in Fig. 4.

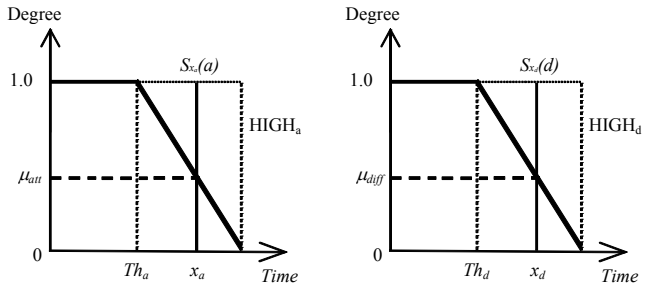

(a) Attenuation Time (b) Difference Time

Figure 4. Fuzzy membership function

In this figure, the notations, Th_a and Th_d denote thresholds of *Attenuation Time* and *Difference Time*, respectively. The notation Th_a is determined as the time which is the standard deviation being shorter than the mean of the attenuation time. The notation Th_d is determined as the time which is the standard deviation being shorter than the mean of the difference time. Two fuzzy degrees, μ_{att} and μ_{diff} are calculated by (3) and (4).

$$\mu_{att}(x,y) = \min(S_{x_a}(a), HIGH_a) \quad (3)$$

$$\mu_{diff}(x,y) = \min(S_{x_d}(d), HIGH_d) \quad (4)$$

The fuzzy singleton functions $S_{x_a}(a)$ and $S_{x_d}(d)$ are defined by (5) and (6).

$$S_{x_a}(a) = \begin{cases} 1 & \text{if } a = x_a \\ 0 & \text{otherwise} \end{cases} \quad (5)$$

$$S_{x_d}(d) = \begin{cases} 1 & \text{if d} = x_d \\ 0 & \text{otherwise} \end{cases} \quad (6)$$

TABLE I. THRESHOLD OF FUZZY MEMBERSHIP FUNCTION (SUBJECT1)

	Attenuation Time MF Th_a	Difference Time MF Th_d
Rasp 4	30.61	-
Rasp 5	23.22	2.21
Rasp 6	18.91	4.73
Rasp 7	18.91	-1.73
Rasp 8	14.75	-0.41
Rasp 9	18.51	-2.57
Rasp 10	-	-

TABLE II. THRESHOLD OF FUZZY MEMBERSHIP FUNCTION (SUBJECT2)

	Attenuation Time MF Th_a	Difference Time MF Th_d
Rasp 4	-	-
Rasp 5	-	-
Rasp 6	-	-
Rasp 7	20.13	-
Rasp 8	17.42	-0.08
Rasp 9	20.79	-2.45
Rasp 10	-	-

TABLE III. THRESHOLD OF FUZZY MEMBERSHIP FUNCTION (SUBJECT3)

	Attenuation Time MF Th_a	Difference Time MF Th_d
Rasp 4	-	-
Rasp 5	23.19	-
Rasp 6	18.53	2.95
Rasp 7	19.41	-2.09
Rasp 8	17.30	-0.13
Rasp 9	-	-
Rasp 10	-	-

TABLE IV. THRESHOLD OF FUZZY MEMBERSHIP FUNCTION (SUBJECT4)

	Attenuation Time MF Th_a	Difference Time MF Th_d
Rasp 4	-	-
Rasp 5	-	-
Rasp 6	18.60	-
Rasp 7	20.52	-0.38
Rasp 8	15.74	0.73
Rasp 9	-	-
Rasp 10	-	-

TABLE V. THRESHOLD OF FUZZY MEMBERSHIP FUNCTION (SUBJECT5)

	Attenuation Time MF Th_a	Difference Time MF Th_d
Rasp 4	28.44	-
Rasp 5	25.48	2.17
Rasp 6	21.88	2.93
Rasp 7	-	-
Rasp 8	-	-
Rasp 9	-	-
Rasp 10	-	-

TABLE VI. THRESHOLD OF FUZZY MEMBERSHIP FUNCTION (SUBJECT6)

	Attenuation Time MF Th_a	Difference Time MF Th_d
Rasp 4	27.50	-
Rasp 5	24.58	2.15
Rasp 6	20.51	3.00
Rasp 7	20.64	-0.27
Rasp 8	16.39	0.19
Rasp 9	19.72	5.28
Rasp 10	-	-

TABLE VII. THRESHOLD OF FUZZY MEMBERSHIP FUNCTION (SUBJECT7)

	Attenuation Time MF Th_a	Difference Time MF Th_d
Rasp 4	30.94	-
Rasp 5	28.42	2.01
Rasp 6	22.59	3.80
Rasp 7	23.04	-0.62
Rasp 8	16.65	2.69
Rasp 9	-	-
Rasp 10	-	-

TABLE VIII. THRESHOLD OF FUZZY MEMBERSHIP FUNCTION (SUBJECT8)

	Attenuation Time MF Th_a	Difference Time MF Th_d
Rasp 4	27.50	-
Rasp 5	23.19	6.04
Rasp 6	19.13	2.95
Rasp 7	19.82	-1.27
Rasp 8	-	-
Rasp 9	-	-
Rasp 10	-	-

After consideration of the thresholds on these tables above, the threshold of the attenuation time MF Th_a is more adaptable than that of the difference time MF Th_d. Therefore, we calculate the adaptable ratio (=0.823) and put the adaptable ratio to the fuzzy membership functions. The total degree μ_{fix} is calculated by (7).

$$\mu_{fix} = \mu_{att}(x) * ratio + \mu_{diff}(x) * (1 - ratio) \qquad (7)$$

IV. EXPERIMENTAL RESULTS

We applied our proposed system to 8 total hip arthroplasty patients. The result of the fixed rasp size and the analyzed rasp size was shown in TABLE IX. The attenuation time measured in the practical surgery is showed in Fig. 5. In this figure, the horizontal-axis means the size of the rasp and the vertical-axis means the attenuation time.

By using our proposed method, we were able to select the suitable rasp of 7 patients. As concerns Subjects 1 and 7, there are two sizes of the determined rasp. Because these subjects have the fixed rasp which is one size larger than the rasp with the shortest attenuation time, it is left out of consideration that the determined rasp has two types which are the fixed size rasp and the one size smaller rasp. As concerns Subjects 2 and 5, we were not able to select the suitable rasp because the difference time is relatively large as shown in Fig. 5. As the result, the effectiveness of selecting the suitable rasp is 87.5%.

TABLE IX. RESULT OF RASP SIZE

	Fixed Size	Determined Size
Subject 1	10	9 or 10
Subject 2	9	-
Subject 3	8	8
Subject 4	8	8
Subject 5	6	5 or 6
Subject 6	9	9
Subject 7	8	7 or 8
Subject 8	7	7

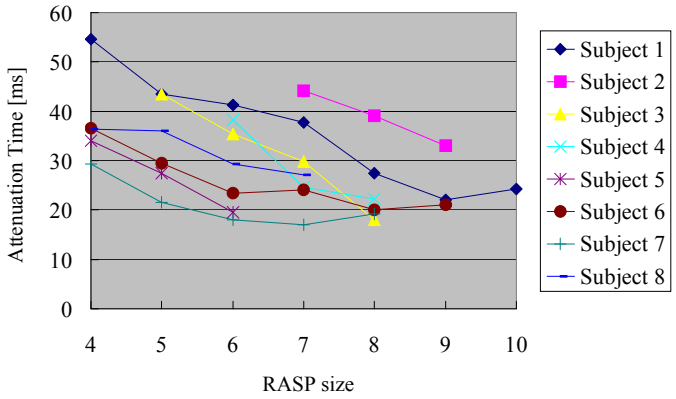

Figure 5. Rasp data in the practical surgery

V. CONCLUSIONS

In this paper, we have proposed a rasp determination system for total hip arthroplasty patients. The acquired ultrasonic waveform with the single ultrasonic probe with the center frequency 1,000Hz is analyzed by a personal computer. At first, we make a knock to the upper point of the rasp inserted with a hammer which has the trigger signals. By using the knocking signals, we measured the acoustic signals. The ultrasonic probe for measuring is fixed in the upper side of the rasp with a built-in magnet. The acoustic data is changed to the digital data by the AD converter and is sent to the personal computer. In the surgery, the surgeon tries to adapt for the patient from the small size rasp to the larger size rasp in turn. Therefore, our system which selects the best suitable rasp by using the attenuation time is superior for surgeons and patients of total hip arthroplasty.

As the result, we successfully determined the suitable rasp in comparison to the results obtained from the practical surgery.

It is thought the indexes in order to judge how degree the rasp fits in the clinical treatment.

It remains as future works to consider the much better effective method and to apply the method to total hip arthroplasty patients.

REFERENCES

[1] A .Sansom, J. Donovan, C. Sanders, P. Dieppe, J. Horwood, I. Learmonth, S. Williams, R. Gooberman-Hill, "Routes to total joint replacement surgery: patients' and clinicians' perceptions of need," Arthritis Care Res (Hoboken), vol. 62, no. 9, pp. 1252-1257, Sep 2010.

[2] G. E. Lewinnek, J. L. Lewis, R. Tarr, C. L. Compere, and J. R. Zimmerman, "Dislocations after total hip-replacement arthroplasties," J Bone Joint Surg Am, vol. 60, no. 2, pp. 217-220, 1978.

[3] W. J. Maloney, T. Schmalzried, W. H. Harris, "Analysis of longterm cemented total hip arthroplasty retrievals," Clin. Orthop. Relat. Res., pp. 70-78, 2002.

[4] E. Schneider, C. Kinast, J. Eulenberger, D. Wyder, G.Eskilsson, S. M. Perren,. "A comparative study of the initial stability of cementless hip prostheses," Clin. Orthop. Relat. Res., pp. 200-209, 1989.

[5] R. K. Sinha, D. S. Dungy, H. B. Yeon, "Primary total hip arthroplasty with a proximally porous-coated femoral stem,"J Bone Joint Surg Am, vol. 86-A, pp. 1254-1261, 2004.

[6] M. Lannocca, E. Varini, A. Cappello, L. Cristofolini, E. Bialoblocka, "Intra-operative evaluation of cementless hip implant stability: A prototype device based on vibration analysis," Medical Engineering & Physics 29, pp. 886-894, 2007.

[7] E. Varini, L. Cristofolini, F. Traina, M. Viceconti, A. Toni, "Can the rasp be used to predict intra-operatively the primary stability that can be achieved by press-fitting the stem in cementless hip arthroplasty," Clinical Biomechanics 23, pp. 408-414, 2008.

[8] D. D. D'lima, A. G. Urquhart, K. O. Buehler, R. H. Walker, C. W. Colwell, "The effect of the orientation of the acetabular and femoral components on the range of motion of the hip at different head-neck ratios," J Bone Joint Surg, vol. 82-A, no. 3, pp. 315-321, 2000.

[9] S. L. Delp, A. V. Komattu, R. L. Wixson, "Superior displacement of the hip in total joint replacement: Effects of prosthetic neck length, neck-stem angle, and anteversion angle on the moment-generating capacity of the muscles," J Orthopaedic Res, vol. 12, no. 6, pp. 860-870, 1994.

[10] F. Pierchon, G. Pasquier, A. Cotton, C. Fontaine, J. Clarisse, A. Duquennoy, "Causes of dislocation of total hip arthroplasty," J Bone Joint Surg, vol. 76-B no. 1, pp.45-48, 1994.

[11] T. Albrektsson, PI. Branemar, HA. Hansson, J. Lindstrom, "Osseointegrated titanium implants. Requirements for ensuring a long-lasting, direct bone-to-implant anchorage in man," Acta Orthop Scand , vol. 52, pp.155-170, 1981.

[12] J. J. Callaghan, C. S. Fulghum, R. R. Glisson, S. K. Stranne, "The effect of femoral stem geometry on interface motion in uncemented porous-coated total hip prostheses. Comparison of straight-stem and curved-stem designs," J Bone Joint Surg Am, vol. 74, pp.839-848, 1992.

[13] P. S. Nourbash, W. G. Paprosky, "Cementless femoral design concerns. Rationale for extensive porous coating," Clin Orthop Relat Res, pp.189-199, 1998.

[14] N. Shibanuma, K. Nagamune, Y. Hata, T. Nishiyama, H. Tateishi, and M. Kurosaka, "Evaluation of the stability of a femoral stem using ultrasound," Proc. of the 53rd Annual Meeting of the Orthopaedic Research Society, p.1733, 2007.

[15] N. Shibanuma, Y. Hata, T. Nishiyama, T. Fujishiro, H. Tateishi, and M. Kurosaka, "Determination of Total Hip Arthroplasty Stem Stability by Intraoperative Measurement Using an Acoustic Testing Technique," Proc. of the 54rd Annual Meeting of the Orthopaedic Research Society, p.1842, 2008.

2011 IEEE International Conference on Fuzzy Systems
June 27-30, 2011, Taipei, Taiwan

A Fuzzy Logic Approach to Predict Human Body Weight Based on AR Model

Hideaki Tanii[1)], Hiroshi Nakajima[2)], Naoki Tsuchiya[2)]
Kei Kuramoto[1), 3)], Syoji Kobashi[1), 3)], Yutaka Hata[1), 3)].

1) Graduate School of Engineering
University of Hyogo
Hyogo, Japan
er11u022@steng.u-hyogo.ac.jp

2) OMRON Corporation
Kyoto, Japan

3) WPI Immunology Frontier
Research Center
Osaka University
Osaka, Japan

***Abstract*—This paper proposes a body weight prediction method using autoregressive (AR) model and Fuzzy-AR model. First, we employ 6 persons body weight change data of 365 days. AR model predicts body weight of a day from these time-series data. We calculate an order of AR model for each person by Akaike's Information Criterion. In the experiment, we predicted body weight change of next day for those subjects. The AR model obtained 0.798 in correlation coefficient between predicted and truth values. Second, we propose a Fuzzy-AR model that predicts body weight of next *p* days from last *p* days, where *p* is the order of AR model. In this method, we propose a Fuzzy-AR model with the fuzzy membership function using last *p* days data. In the experiment, the Fuzzy-AR model obtained 0.558 in correlation coefficient on 2 subjects.**

Keywords- healthcare system; autoregressive model; prediction model; time-series data; body weight.

I. INTRODUCTION

Generally, the health care system provides healthcare services, including screening examinations, prenatal care and infectious disease control. Currently, busy lifestyles including hard work in daily business rise in chronic disease. In this situation, health care system for healthy people receives much considerable attentions. Reference [1] pointed that *"More than 1 billion people in the world are overweight, and at least 300 million of those are clinically obese. Without action, more than 1.5 billion people are expected to be overweight by 2015."* Thus, human body weight control is very important in the world.

In this paper, we consider a personal telehealth system to control body weight of the individual. In this system, it collects the daily weight data and analyzes them. It finally gives an advice to control it. In Ref. [1], this system is the following goal, i.e., *"Empower individuals and patients to better manage their health by providing them with information regarding their fitness and health through personal medical devices and services."*

In this paper, we propose a prediction method of body weight of next day using autoregressive (AR) model [2]-[4]. Next, we predict body weight change for next plural days using Fuzzy-AR model [5]-[8]. Thus, we predict body weight change using AR model and Fuzzy-AR model. We employ 6 subjects the body weight change data. The 6 subjects of AR parameters are calculated from Yule-Walker equation, and the order of AR model is determined by Akaike's Information Criterion. As the result, the correlation coefficient between the predicted and truth values is 0.798 on the 6 subjects. Next, using the order of AR model, we find the cycle of body weight change. The cycle is used as the order, *p*, of the Fuzzy-AR model proposed here. Fuzzy-AR model with fuzzy membership function predicts body weights of next *p* days from the time-series data of last *p* days. We compare the prediction accuracy using AR model with that using Fuzzy-AR model. As the result, Fuzzy-AR model obtained higher correlation coefficient.

II. PREDICTION METHOD BY AR MODEL

We predict body weight change of a day by AR model. The AR model is defined by (1).

$$y(t) = \sum_{i=1}^{p} a(i)x(t-i) + u(t) \tag{1}$$

Here, the notation $y(t)$ denotes a predicted value of time t, $x(t)$ does a measured value, $a(i)$ does AR parameter, u (t) does white noise, and p does the order. AR parameter, $a(i)$, is calculated by using Yule-Walker equation defined by (2).

$$\begin{pmatrix} R(0) & R(1) & \cdots & R(p-1) \\ R(1) & R(0) & \cdots & R(p-2) \\ \vdots & \vdots & \ddots & \vdots \\ R(p-1) & R(p-2) & \cdots & R(0) \end{pmatrix} \begin{pmatrix} a(1) \\ a(2) \\ \vdots \\ a(p) \end{pmatrix} = \begin{pmatrix} R(1) \\ R(2) \\ \vdots \\ R(p) \end{pmatrix} \tag{2}$$

Here, the notation $R(i)$ denotes auto covariance function. Moreover, the order, p, is determined on the basis of Akaike's Information Criterion (*AIC*) [9], [10]. In our experiment, the order, p, is determined from the time-series data of 365 days. That is, we vary p from 1 to 365, and then calculate the value of *AIC* by (3).

$$AIC = -2\ln(L) + 2k \tag{3}$$

Table I
Subjects Data

Subject	Sex	Age	Range of body weight change (kg)	Height (cm)
A	Male	35	66.6 ~ 71.1	180.0
B	Male	35	68.7 ~ 79.4	173.0
C	Male	39	74.8 ~ 88.3	176.0
D	Male	36	60.6 ~ 65.2	157.0
E	Male	41	95.6 ~ 105.0	175.0
F	Male	36	65.3 ~ 69.1	174.5

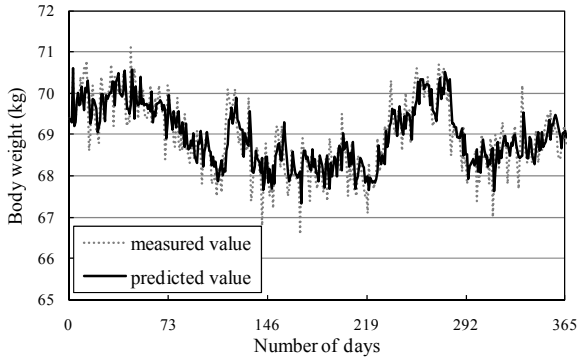

Figure. 1 Prediction result in subject A

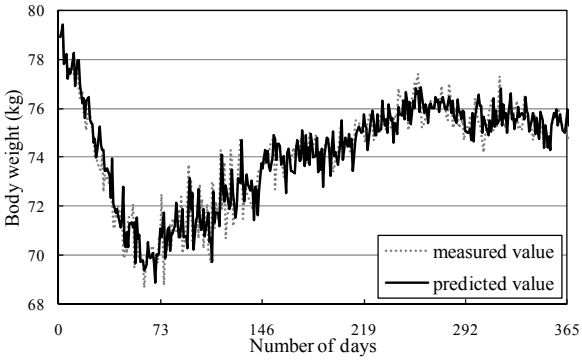

Figure. 2 Prediction result in subject B

Here, L denotes maximum likelihood and k does number of free parameter. Maximum likelihood, L, is changed by p. The order of AR model is determined as p with the minimum AIC during [1, 365]. We predict body weight of next day from time-series data of last p days.

III. Prediction Results of One Day

In our experiment, we employed body weight data while 365 days of 6 subjects in Table I. We predicted their body weight change by AR model. We evaluated our prediction results by using correlation coefficient between predicted values and truth values. We tested AR model 5 times and calculated the mean and the standard deviation (SD).

Fig. 1 shows prediction result of subject A. Subject A has rapid body weight change during [109, 117]. From Fig. 1, we can see that AR model predicted this rapid change. Fig. 2 shows prediction result of subject B. Subject B has body weight change of about 10 kg during about 2 months. From Fig. 2, we can see that AR model predicted this change. Fig. 3 shows the prediction result of subject C. Subject C has slowly decreasing body weight data. In Fig. 3, AR model predicted this slow change. Fig.4 shows the prediction result of subject D. Subject D has decreasing body weight data in short term. From

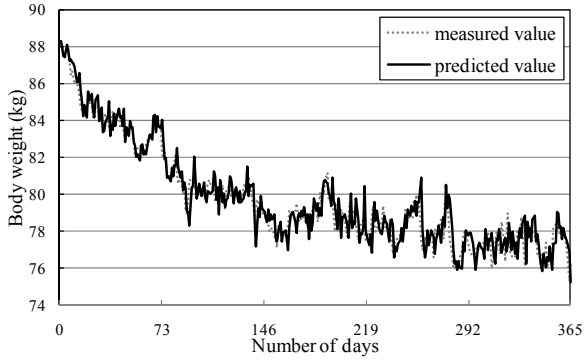

Figure. 3 Prediction result in subject C

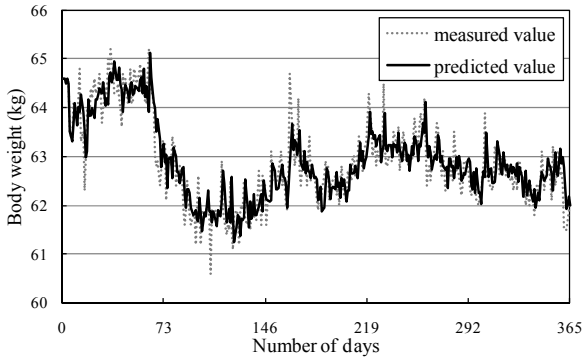

Figure. 4 Prediction result in subject D

Fig. 4, we can see that AR model predicted this change in short term. Fig.5 shows the prediction result of subject E. Subject E has rapidly body weight change during about 10 days. From Fig. 5, we can see that AR model predicted this change during about 10 days. Fig.6 shows prediction result of subject F. Subject F has rapid body weight change during a few days. From Fig. 6, AR model then did not predict this rapid change during a few days.

Table II shows the mean ± SD of correlation coefficient and the determined order of AR model. We obtained 0.798 ± 0.073 in the average.

IV. Prediction Method by Fuzzy-AR Model

The orders of AR model are different from person to person. The order would represent a cycle of body weight of individuals. By calculating the order, p, we will predict body weight change of next p days.

To find the weight cycle, we employ 100 subjects and determine the order for each subject. All subjects are ranged from 24 to 79 years old (male: 87 and female: 13). Fig. 7 shows histogram of the orders. In Fig.7, the peak frequency is 3 or 7 and their neighbors. Also, 14 is larger than its neighbors. From these results, we consider that the frequency is 7 days as the highest peak and 3 days as the second. Especially some persons have 14 days. We propose a Fuzzy-AR model with a fuzzy membership function. The fuzzy membership function defined from the order, p, where the order is individually determined as the highest frequency of the AR model. The notation t_x denotes the current point. Fuzzy-AR model is defined by (4).

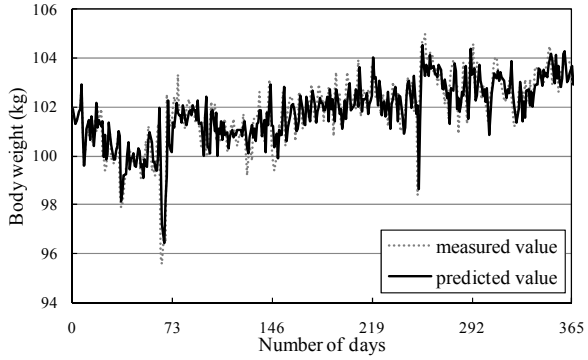

Figure. 5 Prediction result in subject E

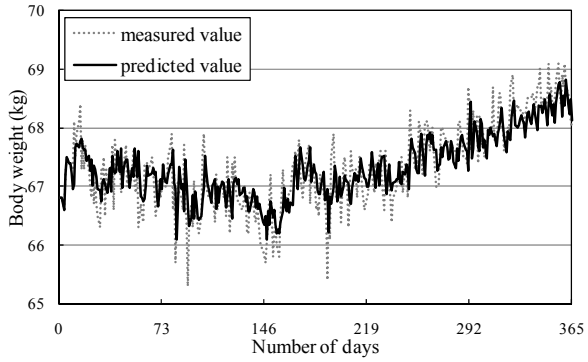

Figure. 6 Prediction result in subject F

Table II
Prediction Results

Subject	Order of AR model *p*	Correlation coefficient
A	8	0.734 ± 0.014
B	9	0.872 ± 0.015
C	3	0.906 ± 0.013
D	7	0.807 ± 0.013
E	10	0.734 ± 0.033
F	8	0.733 ± 0.013
Average	-	0.798 ± 0.073

$$y(t_x + d) = \sum_{i=1}^{p} a(i)x(t_x + d - i) + u(t) + \mu_w(d) \qquad (4)$$

Here, $x(t)$ means the measured values when $t < t_x$, and does the predicted values when $t \geq t_x$. The notation d denotes a predicted day parameter during $1 \leq d \leq p$. The notation $\mu_w(d)$ is fuzzy membership function defined by (5). We calculate minimal (W_{min}) and maximal (W_{max}) weights from the last p days data from t_x.

$$\mu_w(d) = \frac{x(t_x - p + d) - W_{\min}}{W_{\max} - W_{\min}} \qquad (5)$$

Fig. 8 shows an example of fuzzy membership function with p = 3. Also, Fig. 9 shows an example of fuzzy membership function with p = 7.

V. Prediction Results of *P* Days

In this experiment, we first employed subject C and subject D in Table I. We consider 6 days body weight change data of subject C because the order is 3. Fuzzy membership function was made by body weight data from 1st to 3rd days, and we predicted those from 4th to 6th days. We compare the prediction results of Fuzzy-AR model with AR model. In AR model, we use body weights from 1st to 3rd days. Furthermore, we extracted 14 days body weight change data of subject D because the order is 7. Fuzzy membership function was made by body weight data from 1st day to 7th day, and we predicted next 7 days. We compare the prediction results of Fuzzy-AR model with AR model. In AR model, we use body weight of last 7 days. We evaluated these prediction results by correlation coefficient between predicted values and truth values. We tested these models 100 times and calculated the mean and SD.

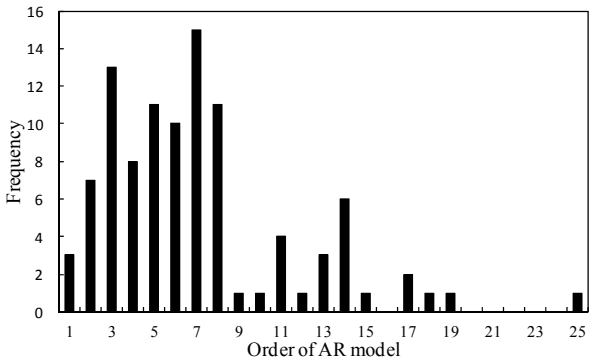

Figure. 7 Histogram of order of AR model

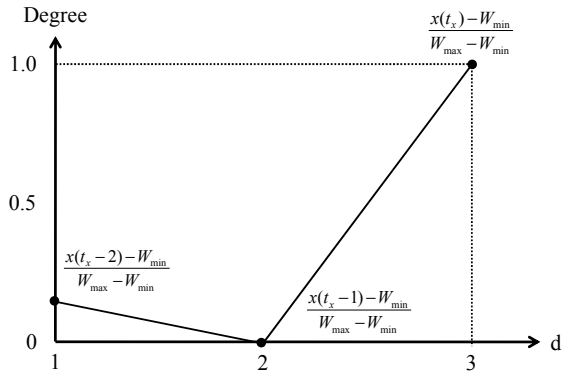

Figure. 8 Example of fuzzy membership function (p = 3)

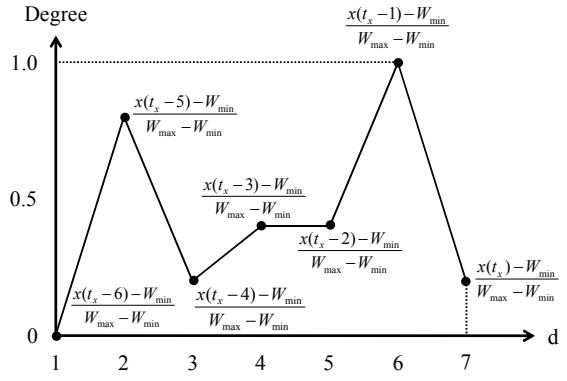

Figure. 9 Example of fuzzy membership function (p = 7)

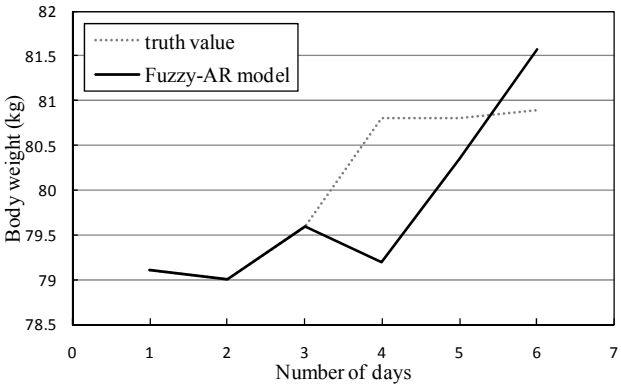

Figure. 9 Prediction result using Fuzzy-AR model in subject C

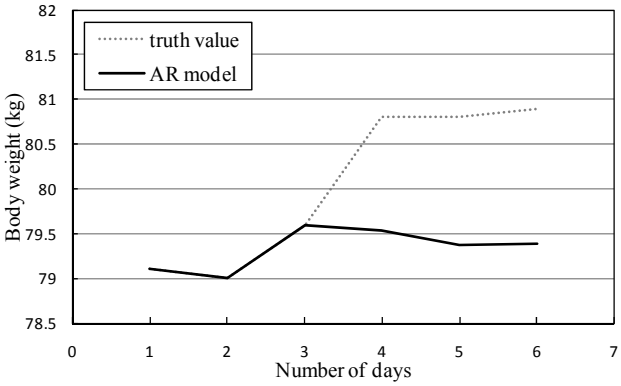

Figure. 10 Prediction result without using AR model in subject C

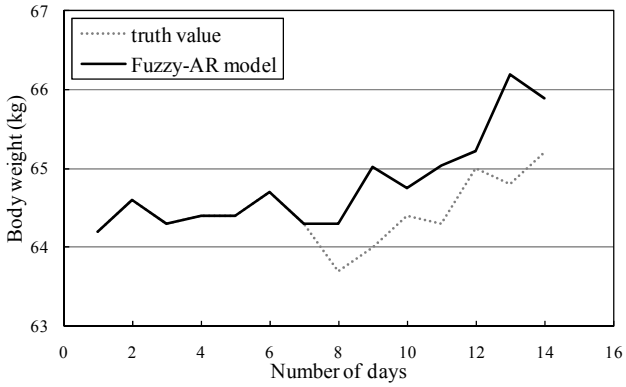

Figure. 11 Prediction result using Fuzzy-AR model in subject D

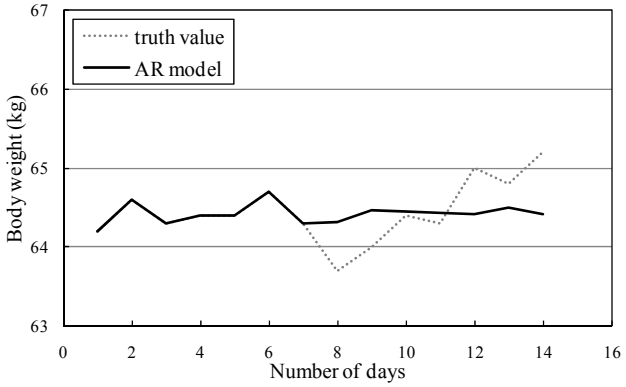

Figure. 12 Prediction result without using AR model in subject D

Fig. 9 shows prediction result using Fuzzy-AR model in subject C. The correlation coefficient was 0.571 ± 0.413. Fig. 10 shows prediction result using AR model in subject C. The correlation coefficient was 0.232 ± 0.615. Fig. 10 shows prediction result using Fuzzy-AR model in subject D. The correlation coefficient was 0.542 ± 0.187. Fig. 11 shows prediction result using AR model in subject D. The correlation coefficient was 0.176 ± 0.341. Thus, the accuracy using Fuzzy-AR model is higher than that using AR model.

VI. CONCLUSIONS

In our study, we predicted body weight change based on AR model. We predicted body weight change of 6 subjects by AR model. We tested AR model 5 times and calculated the mean of correlation coefficient. As a result, the AR model obtained 0.798 ± 0.073 in correlation coefficient between predicted and measured values. Next, we determined body weight change cycle from 100 persons data. Then, the peak frequency is 7 days. Next, we propose a Fuzzy-AR model for body weight data from last p days, where p is the order of AR model, and we predicted next p days. As a result of 2 subjects, Fuzzy-AR model obtained 0.558 ± 0.317 in correlation coefficient. This value was higher than AR model (0.204 ± 0.497). Thus, Fuzzy-AR model accurately predicted body weight change of next 3 or 7days than AR model.

In the future, we will improve prediction accuracy by considering the other attributes such as calories and athletics.

REFERENCES

[1] Continua Health Alliance home page, http://www.continuaalliance.org/index.html

[2] J. Wang and T. Zhang, "Degradation prediction method by use of autoregressive algorithm," IEEE ICIT, pp. 1-6, April 2008.

[3] F. M. Bennett, D. J. Christini, H. Ahmed, K. Lutchen, J. M. Hausdorff, N. Oriol, "Time series modeling of heart rate dynamics," Computers in Cardiology, p.273, September 1993.

[4] W. Gersch and T. Brotherton, "AR model prediction of time series with trends and seasonalities: A contrast with Box-Jenkins modeling," Decision and Control including the Symposium on Adaptive Processes, vol 19, p.988, December 1980.

[5] R. Palaniappan, P. Reveendran, S. Nishida, N. Saiwaki, "Evolutionary fuzzy ARTMAP for autoregressive model order selection and classification of EEG signals," Systems, Man, and Cybernetics, vol 5, p. 3682, October 2000.

[6] J. Liu, J. Mo, S. Pourbabak, "Human cardiovascular system identification and application using a hybrid method of auto-regression and neuro-fuzzy inference systems," Machine Learning and Cybernetics, vol 7, p.4107, August 2004.

[7] B. S. Chen, S. C. Peng, K. C. Wang, "Traffic Modeling, Prediction, and Congestion Control for High-Speed Networks: A Fuzzy AR Approach," IEEE Transaction on Fuzzy Systems, vol 8, pp. 491-508, October 2000.

[8] N. Watanabe, "A Fuzzy Rule Based Time Series Model," Fuzzy Information, vol 2, p.936, June 2004.

[9] H. Akaike, "A new look at the statistical model identification," IEEE Transactions, vol 19, pp. 716-723, December 1974.

[10] R. Shibata, " Selection of the order of an autoregressive model by Akaike's information criterion," Biometrika, vol 63, pp. 117-126, June 1975.

2011 IEEE International Conference on Fuzzy Systems
June 27-30, 2011, Taipei, Taiwan

Consideration of Invasion, Intrusion, and Consciousness in Biomedical Sensing with Uncertainty

Hiroshi Nakajima, Naoki Tsuchiya
Omron Corporation
Core Technology Center
9-1 Kizugawadai, Kizugawa City,
Kyoto 619-0280 JAPAN
Hiroshi_Nakajima@ieee.org

Yutaka Hata
University of Hyogo
Graduate School of Engineering
Himeji City, Hyogo, 671-2280 JAPAN
hata@ieee.org

Abstract— **Both burden of human and performance of sensing technology should be carefully considered in bioinstrumentation. The article proposes the ideas of invasion, intrusion, and consciousness in biomedical sensing to improve its comfort and performance. Consideration of the three concepts is very important to realize burden-reduction of human. They also save sensing accuracy when sensing targets and sensor heads are influenced by invasion, intrusion, or consciousness during sensing. Realizing noninvasive, nonintrusive, and unconscious sensing requires solutions against uncertainty in sensory signals and estimation models. Sensory signals from these sensing methods might superimpose various types of signals besides target one. Target signals would be appropriately extracted by the causal analysis-based model. Case studies were investigated by considering the method and experimental results were reported in the article.**

Keywords-component; Biomedical sensing, Fuzzy Logic, Noninvasive, Nonintrusive, Unconscious, Uncertainty information processing, Causal Analysis, Hierarchical Knowledge Representation

I. INTRODUCTION

There have been noticed many kinds of problems related to our healthy, social, and environmental issues during the new decades of 21st century. Among them, aging society will make rapid progress especially in advanced nations. Medical crisis has also become clear. Environmental issues centering global warming would have some impacts on our live body. Through these rapid changes close to our daily life and health, it has been much more important for us to know about our human body by bioinstrumentation than ever.

For instance, metabolic syndrome which is caused by life style habit has been immediately paid attention to. Even though the cause would be individual's life style, the result is quite serious from obesity through hypertension and diabetes to cardiovascular events like brain and cardiac infraction and complication [1][2]. The most important and effective against the disease is to change the life style of diet, exercise, and sleep. However, it is very hard for the patients and the preliminary group of the disease to change their life styles which have been continued for a long time. In order to change the life style, it is effective for them to notice the status of their body condition based on the measurements of their vital signs and life styles. Continuation of the measurements would be the key to success in changing lifestyle habit. For this reason, bioinstrumentation and lifestyle measurement without invasion, intrusion and consciousness in daily life would be required besides the indices such as Electrocardiograph (ECG) and blood pressure (BP) sensed in the medical field.

In the article, the importance of idea of invasion, intrusion, and consciousness in bioinstrumentation is studied and discussed. The realized biomedical sensing methods which consider the idea are introduced and surveyed for considering the uncertainty in the sensing methods.

The rest of the article is organized as follows; Section II studies the bioinstrumentation from the views of invasion, intrusion, and consciousness. Section III introduces the biomedical sensing methods which are for visceral fat estimation and heart rate monitoring as the case studies. The methods employ the causal analysis with hierarchical knowledge against uncertainty which is caused by restrictions of reducing invasion, intrusion, and consciousness. Discussions follow the introductions and experimental results. Section IV concludes the article with summaries.

II. RELATIONSHIP BETWEEN LIVING BODY AND SENSING

Physical and mental pain and restraint of patients should be eliminated or minimized during bioinstrumentation with accurate sensing results. It is the motif of reducing invasion, intrusion, and consciousness. Fig. 1 shows the overview of bioinstrumentation. Various types of sensory signals from the living body are obtained via sensory head. The signals are accumulated into the database to put them to practical use of medical and healthcare by feeding back some effects the patients. Besides them, the database is used in the medical science and engineering to develop the new evidences and the new solutions.

978-1-4244-7316-8/11/$26.00 ©2011 IEEE

In this section, invasion, intrusion, and consciousness in biomedical sensing are studied and discussed from the views of both human burden and technology performance. Invasion has been studied more than intrusion and consciousness so far. However, latter two issues are also important idea to provide different meanings and values from invasion to realize comfortable and accurate biomedical sensing method.

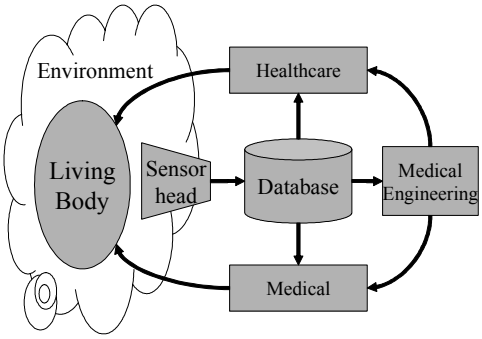

Figure 1. Overview of Bioinstrumentation

A. Invasion

Invasion levels can be defined by distance between sensory head and sensing target or location of them. According to [3], there are five invasion level of biomedical sensing as follows;

1. A catheter is inserted into body to send transmitter to a sensor head.
2. A sensor head is implanted to send sensory signals via fixed line.
3. A sensor head is implanted to send sensory signals via wireless communication.
4. A sensor head is contacted on skin of the body to detect signals.
5. A sensor head is not contacted on skin of the body to detect signals.

As mentioned above, the invasion levels are defined by the positional relationship between sensory head and live body. Even though the invasion level is low according to the definitions above, a CT scan that is non contact sensing requires X-ray exposure which is serious invasive. This case should be treated as high invasion. Thus, definition could be changed according to the development of sensing technology and consideration of influence to human body.

Compared with invasion, intrusion and consciousness sensing are new ideas in biomedical but important for both of sensing accuracy and human comfort.

B. Intrusion

Nonintrusion is important idea for sensing daily life activity. ECG and BP are very important physical indices used in medical and healthcare. The indices can be measured in just in hospital and clinic. It is strongly required to monitor for 24 hours to detect defect condition of body in daily life. However, it is impossible to monitor ECG in daily life in the case of using ordinary ECG equipment. A Holter electrocardiographic monitor has been realized for gathering the ECG signals and an ambulatory blood pressure monitor for accumulating blood pressure signals for 24 hours. Although the equipment could be used for sensing live body, it is far from non-intrusion. The user has to use contacted sensory head and to carry on the equipment. There has not been clearly defined but some levels would be discussed on intrusion.

C. Consciousness

Consciousness or realization to be sensed would have some influence to the sensing signals. White coat hypertension and masked hypertension [4] are examples for understating the importance of unconsciousness sensing. Not just for these serious cases, other examples can be easily pointed out with considering consciousness such as video and image sensing. Long and continuous sensing for 24 hours requires unconsciousness. Besides them, unconsciousness helps for users not to forget the measurement.

Through these definitions and observations on invasion, intrusion, and unconsciousness, some discussions on influences to patients and live bodies and to measurements.

D. To Living Body

It is strongly required to reduce and to eliminate burden, pain, and damage both physically and mentally to live bodies and patients. According to the definitions of invasion level, the level is decided by distance and location between sensor head and body. However, even though X-ray CT scan is non contact sensing, it gives serious impact of X-ray exposure on a living body. Implant sensing requires surgery whose invasion level is quite high, but intrusion is very low when the sensor could be used for a long time without any invasion. Additionally, a patient who is implanted a sensor into could feel unconscious with the sensor. As these discussions, invasion is not the only perfect prerequisite in biomedical sensing. Intrusion and consciousness should be also considered for realizing the effective and efficient bioinstrumentation.

E. To Measurements

Sensing performance would be generally sophisticated according to higher invasion level. However, invasion sometimes brings negative results in sensing. Contact between a sensor head and live body makes energy exchange among them to possibly cause unstable sensing. For example, huge sensor head of clinical thermometer realizes good fitting with body however it takes body temperature. Like the examples pointed out in intrusion section, it would be very hard to keep the ideal situation of the patient such as in daily life activities with high intrusion. Besides, unconscious sensing might bring good results with the sensing performance as discussed in consciousness section.

F. Uncertainty

Realization of biomedical sensing without invasion, intrusion, and consciousness would bring some uncertainty in the sensing mechanism. Sensor signals superimpose not just target but other kinds or noises. Besides extraction of target

signal, it is also required to compose causal structures which explain sensing principles well.

The article proposes causal analysis method against the problems to be solved discussed above. Causality plays an important role for solving the uncertainty discussed above because it is the basis of human's understandings and also machine could handle with it; i.e., it is transparent among humans and machines mutually. It brings powerful solution which improves observability and controllability of the target system.

III. CASE STUDIES

In this section, two applications to biomedical sensing with considering the sensing issues described in the previous section are described.

A. Visceral Fat Area Estimation

Entering the 21st century, declining birthrate and a growing proportion of elderly people have developed into more serious social problems especially in advanced nations. Not only solving the problem of labor power reduction but also extending healthy life expectancy is the important challenge which should be socially addressed. In terms of the issues, primary prophylaxis has been recognized as an important activity to prevent life style related diseases. Currently, the waist circumference and blood sugar, neutral fat or quantities of cholesterol in the blood are measured for the primary screening whether the person is metabolic syndrome at the medical checkup. Generally, it has been clarified that over-accumulation of visceral fat causes several life-style related diseases. X-ray CT or MRI is currently the gold standard in medical field but it causes serious invasion of X-ray exposure. An accurate and safe measurement of the visceral fat accumulation status is desired in medical field. In responding to the invasion problem, simple, accurate, and safe equipment of visceral fat estimation has been proposed based on bioelectrical impedance analysis (BIA) [5-7, 14] with considering low invasion. As shown in Fig. 2 and 3, body compositions depend on individuals and have complicated mixture. A patient in Fig. 2 accumulates much visceral fat and low subcutaneous one. On the other hand, we can see much subcutaneous fat and low visceral one in Fig. 3.

1) Measurement Principles and sensing

There are three types of composition which are visceral fat, subcutaneous fat, and lean body. Lean body is not fat and internal organs, muscles, and bones. Each area can be calculated by image processing technology applied to the image of cross sectional area gotten by a CT scan or an MRI as shown in Fig. 2.

Visceral fat area can be calculated by (1) which is the measurement principle of VF.

$$VFA = CSA - SFA - LBA \tag{1}$$

where *VFA* is visceral fat area, *CSA* all cross sectional area, *SFA* subcutaneous area, and *LBA* lean body area. In the sensing, two types of bioelectrical impedance and the abdominal shape at umbilical level are measured. As in (1), each area of *CSA*, *SFA*, and *LBA* will derive *VFA*. The strategy of the measurement is as follows;

1. *CSA* could have high correlation with the abdominal shape information.
2. SFA could be estimated by the abdominal shape and the internal abdominal impedance.
3. LBA could have inverse correlation with the total body impedance.

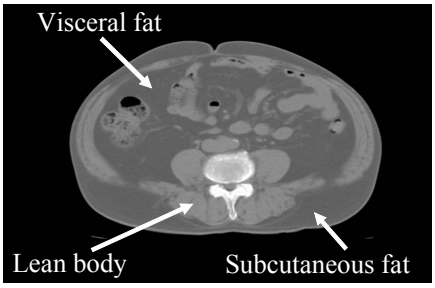

Figure 2. Cross sectional area image at umbilical level

Firstly, let us consider about the abdominal shape information. In a medical checkup, waist circumference is used to diagnose metabolic syndrome. However, it brings less information about the abdominal shape. The shape estimation performance could be improved by using the measurements of the width *a* and the depth *b* at abdominal level as shown in Fig. 3, instead of waist circumference. These variables are used in calculating *CSA* and *SFA*.

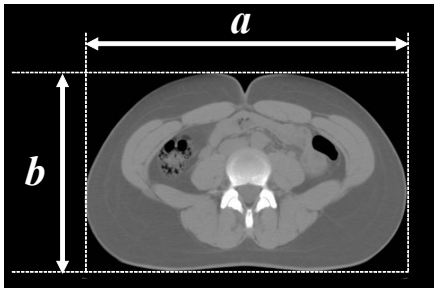

Figure 3. Body shape measurement

In order to measure the total body impedance, the electrodes for turning on electricity are placed on the back of both hands and the instep of both feet with the subjects lying on their back. Eight electrodes for the measurement are placed on surroundings of the waist circumference at umbilical level. These electrodes are placed on the trunk, paired in intervals of 9 cm, centered at the umbilicus with *250 μA* with *50 kHz*. The total body impedance can be obtained as Z_T. Regarding the abdominal surface impedance, the eight electrodes are classified into groups of four. In each group, the electricity is impressed using one electrode, and the impedances of the abdominal surface are obtained by the other electrode as Z_S.

2) Causal Structure Design

Fig. 4 illustrates the causality of *VFA* estimation considering the relationship between the sensory variables and the measurement principle. The left and the right are the sensory variables and the principle measurement respectively. According to the causal structure, we prepare the variables which are the candidates for constructing the causality. By using the selected variables, multi linear regression was employed to acquire the estimation model. In this step, we carefully considered about nature of the model without over-fitting, multicollinearity, and some other difficulties; especially keeping the notion of the measurement principle. We finally derived the estimation model denoted by the equation (2).

$$\widetilde{A}_{VF4} = \alpha_1 a + \alpha_2 b^2 + \alpha_3 Z_S \sqrt{a^2 + b^2} + \alpha_4 / Z_T + \varepsilon \quad (2)$$

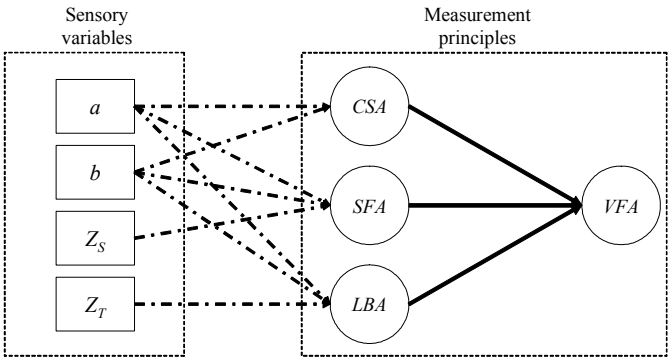

Figure 4. Causality between the sensory variables and the measurement principle

In order to extract the causality for estimating VFA, we designed the following development steps;

1. Preparation of variables according to the measurement principles
2. Selection of the variables by applying AIC and VIF on the sample dataset

In the first step, we prepared the candidates of the variables as possible as used in the estimation equation. The idea here is that the candidates should bring some information about VFA estimation and be understandable from the point view of the measurement principles shown in the Fig. 4. The prepared variables are listed in the table 1.

The second step is the suitable variables selection as a set of them. We employed two different criteria to realize the legitimate model for VFA estimation. Our consideration was to realize both promised performance and transparency according to the measurement principle. The first is the accuracy and simplification of the model without over-fitting to the sample dataset. The second is multicollinearity which causes some difficulties in the estimation results. The problem is caused by an almost linear relationship among dependent variables in the regression model. Akaike Information Criterion (AIC) [8] and Variance Inflation Factor (VIF) [9] are the employed criteria for former and later considerations. The criteria are given by the (3) and (4), respectively.

$$AIC = n\log(2\pi\hat{\sigma}_e^{\,2}) + \frac{1}{\hat{\sigma}^2}\sum_{i=1}^{n}\{y - (\alpha_1 x_1 + \cdots + \alpha_m x_m + \varepsilon)\}^2 + 2(m+2) \quad (3)$$

where m and n is the numbers of independent variables and data respectively, y a dependent variable, $x_i (i = 1,2,...,m)$ independent variables, $\alpha_i (i = 1,2,...,m)$ coefficient terms, ε error term, $\hat{\sigma}_e$ the standard deviation of estimation errors.

$$VIF_i = 1/(1 - R^2{}_i) \quad (4)$$

where R_i is the multiple correlation coefficient between the independent variable $x_i (i = 1,2,...n)$ and the rest of $(n-1)$ variables.

3) Experimental Dataset

We designed the experimental data set by using the three variables of gender, age, and waist circumference which is substituted to for VFA because it could not be used in the recruiting phase. The number of subject is 180 (90 males + 90 females) who were 22 to 80 years old (mean is 49.95) and had from 65.8 to 120 cm of their waist circumferences (the mean 90.09). All of the subjects are measured by both the proposed method and a CT scan as reference values.

4) Experimental Results and Discussions

The results were as follows; the correlation coefficient 0.88, the errors mean -1.38, and the errors standard deviation 27.28. The scatter diagrams of the proposed instrument and the CT scan and waist circumferences and the CT scan are shown in Fig. 5 and 6, respectively. The correlation coefficient between waist circumferences and CT scans is 0.77.

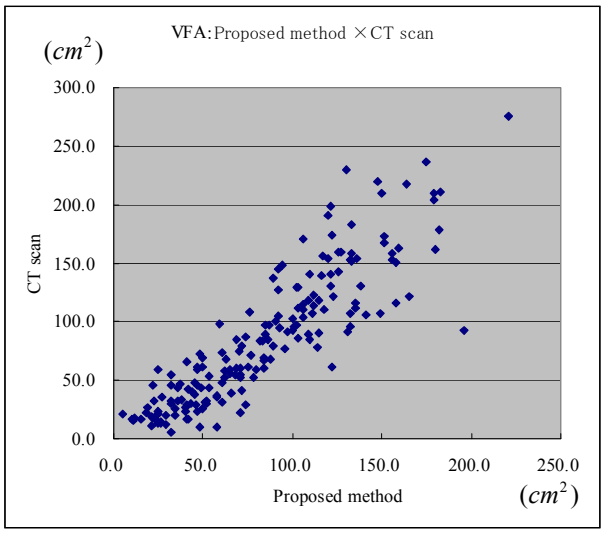

Figure 5. VFA: the proposed method vs. CT scan

As the results, visceral fat areas estimated by the proposed method achieved high correlation with ones by the CT scan. Waist circumference which is used in a medical checkup works

well but the estimation accuracy is lower than the proposed method. Besides, it cannot differentiate VF from subcutaneous one and lean body in principle. According to the scatter diagrams, the method estimates stably from small to huge size of visceral fat volume. Difference plot shown in Fig. 7 would also suggest this nature but is has a tendency of slightly lower estimation as VF goes large. The correlation coefficients of females' VFA and males' are 0.913 and 0.862 respectively. The difference between them is statistically non significance ($p = 0.114$).

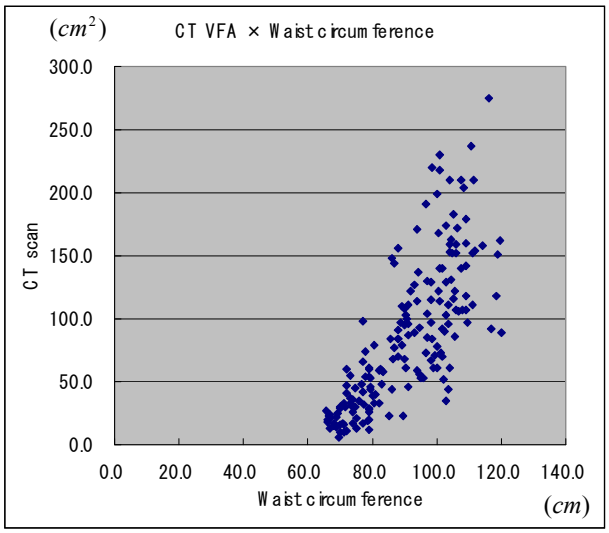

Figure 6. Waist circumference vs. CT scan

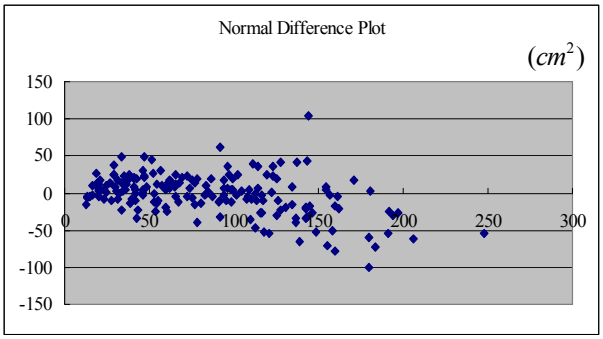

Figure 7. Normal difference plot

B. Heart Rate Estimation

Among vital-signals, heart rate (HR) provides important information of humans' health transit [10] such as an early stage of cardiac disease. It would be pretty important for us to continuously measure our heart rate to know the changes in our daily life. In addition, the variability of heart rate transit provides information of autonomic nerve activity [11]. Through these discussions, it might be clarified that continuous heart rate monitoring in daily life is quite important.

Currently, in a medical domain, an electrocardiography (ECG) is the gold standard system for measuring heart rate transit correctly. However, ECG requires subjects to be put electrodes on and is high intrusive. It is strongly preferred to be sensed in daily life without invasion, intrusion, and unconsciousness. In response to the requirements, heart rate monitoring equipment by using an air pressure sensor (APS) has been developed [11-13].

1) System Configuration

The equipment measures body pressure variability via an air pressure sensor, and extracts heart rate variability from the obtained pressure variability. Fig. 8 shows the system architecture of the equipment. Heart beats are detected and the heart rate variability is calculated by using detected heart beat intervals.

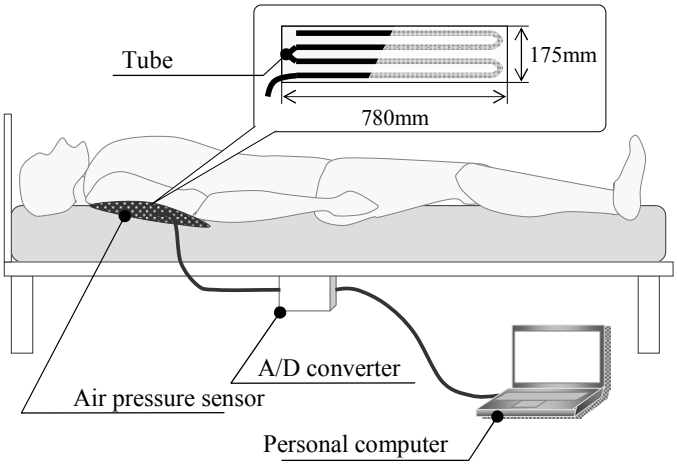

Figure 8. Heart rate extraction equipment

2) Causal Structure Transformation

Heart rate will be estimated as follows; heart beat locations which are R-waves are decided from the changes of the signal caused by heart beat, R-R interval can be calculated by using the R-waves, then heart rate is calculated by using R-R intervals. The causality is designed by considering the similarity between electrocardiograms and air pressure sensors.

Firstly, the conceptual causality by using ECG was designed as shown in Fig. 9. ECG extracts R-waves τ_R from the electrical change caused by heart rate *HR* and calculate heart rate from their RR intervals τ_{RR}.

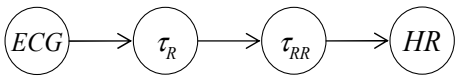

Figure 9. The conceptual causality for HR extraction via ECG

In the next step, the causality was divided into two parts. Because the process of calculating heart rate from RR interval τ_{RR} can be generalized, it was considered as independent causality, which allows the decomposition of the causality as shown in Fig. 10.

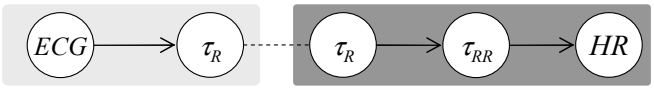

Figure 10. Decomposition of conceptual causality for ECG

Then, the original causality should be modified according to the development equipment. The aforementioned heart rate extraction equipment using an air pressure sensor measures pressure change caused by body movement *MV* and respiration *RSP* as well as heart beat *HB*. The conceptual causality considering the nature is depicted as shown in Fig. 11, which indicates that only *HB* is extracted from the pressure change, and *HR* is calculated by τ_{RR} in the same manner as ECG.

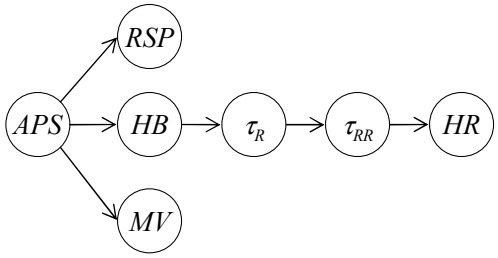

Figure 11. The conceptual causality for HR extraction via APS

The causality shown in Fig. 11 will be decomposed to the partial causalities as shown in Fig. 12 because in the structure, the process of calculating *HR* from τ_{RR} can be generalized. That is, the causality modification caused by the equipment replacement is limited to the process of extracting τ_R from the air pressure sensor.

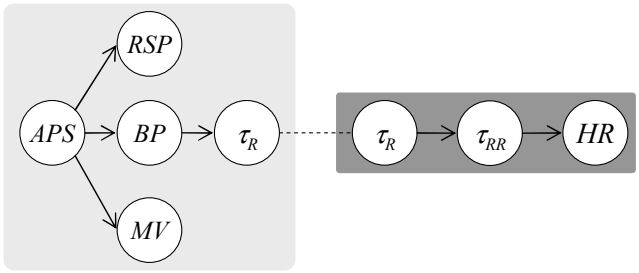

Figure 12. Decomposition of conceptual causality for HR extraction equipment via APS

As shown in Fig.12, τ_R should be extracted according to the changes of waves from the signals which superimpose not only *BP*, but *RSP* and *MV*. It is difficult to determine the precise position of R-waves τ_R by autocorrelation function and peak detection method. We developed formulate knowledge about heart beat by using fuzzy logic [12-14]. In the method, moving averages of pressure changes are calculated and smoothened. Then, the fuzzy logic based on the knowledge about τ_{RR} is applied to the smoothened pressure changes to extract *BP*.

3) Experimental Dataset

In the study, we use the dataset which is obtained from seven healthy male subjects by concurrently measuring pressure changes in body with the equipment shown in Fig 8 and the electrocardiogram from an ECG.

4) Experimental Results and Discussions

In this experiment, we compare the method with autocorrelation functions and peak detection and one with fuzzy logic. TABLE I shows correlations between heart rate changes that obtained from the ECG and those that obtained from the heart rate extraction equipment with an air pressure sensor.

The result indicates that the method with fuzzy logic achieved higher performance for all of the subjects. In particular, the correlation to ECG for the subject *E* is 0.991, which is extremely high. The improvement of the performance is realized by conducting minimum arrangement via consideration for sensors' characteristics based on experts' knowledge.

TABLE I. HR EXTRACTION PERFORMANCE VIA APS

Subjects	**Attributes**		**Correlation coefficient**	
	Height [cm]	***Weight [kg]***	***Developed method***	***AC function***
A	**175**	**76**	**0.973**	**0.703**
B	**171**	**68**	**0.807**	**0.389**
C	**165**	**50**	**0.754**	**0.621**
D	**171**	**56**	**0.872**	**0.699**
E	**180**	**92**	**0.972**	**0.658**
F	**172**	**55**	**0.844**	**0.677**
G	**170**	**62**	**0.737**	**0.346**
Mean	**172**	**65.6**	**0.851**	**0.585**

C. Discussions on both studies

In the case of visceral fat estimation, the sensing requires intrusion but invasion level is quite low compared with X-ray CT scan which is used in medical field as the gold standard. According to the causality development, the method used knowledge and statistical approach for realizing good performance.

As the case in heart rate estimation, it realizes noninvasive, nonintrusive, and unconscious sensing for heart rate monitoring of body on the bed. The method requires highly sophisticated signal extraction from multiple superimposed original sensory data.

Both cases prove that the causal analysis with hierarchical knowledge and causal analysis method works well against uncertainty in biomedical sensing.

IV. SUMMARIES AND CONCLUSIONS

This article discusses the importance of the ideas of intrusion and consciousness besides invasion in biomedical sensing. The problems to be solved in such noninvasive, nonintrusive, and unconscious sensing is to extract target signals and estimation model from uncertainty information.

Hierarchical knowledge and causal analysis methods are studied and applied to the two biomedical sensing case studies of visceral fat estimation and heart rate monitoring. The former considers noninvasive but intrusive and conscious and the latter realized noninvasive, nonitrusive, and unconscious biomedical sensing. Uncertainties in the both applications are investigated with the knowledge and causal analysis. The article has discussed on the ideas of invasion, intrusion, and consciousness in the biomedical sensing with considering uncertainty and provided the case studies and their experimental results. Biomedical sensing methods would be more sophisticated by considering the notions of the three points in the future.

REFERENCES

[1] The Examination Committee of Criteria for 'Obesity Disease' in Japan, "Japan society of the study of obesity: new criteria fot 'Obesity disease in Japan," Japanease Circulation Society Journal, Vol. 66, pp.987-992, 2006.

[2] NIPPON DATA 80 Reasearch Group, "Risk assessment chart for death from cardiovascular disease based on a 19-year follo-up study of Japanese representative population – NIPPON DATA 80-," Japanese Circulation Society Journal, Vol. 70, 1249-1255, 2006.

[3] K. Yamagoe and T. Togawa, "1.4 Perticularity of Bioinstrumentation and Sensing Method," Biomedical Sensors and Instruments, Corona Publishing Co.,Ltd. 2000 (In Japanese).

[4] Franz H. Messerli and Delia Cotiga, "Masked hypertension and white-coart hyptertension – Therapic navigation between Scylla and Charybdis," Jouranal of the American College of Cardiology, Vol.46, No.3, pp.516-517, 2005.

[5] T. Shiga, Y. Oshima, H. Kanai, M.Hirata, K. Hosoda, and K. Nakao, "A simple measurement method of visceral fat accumulation by bioelectrical impedance analysis," *ICEBI 13th*, 2007.

[6] M. Yoneda, H. Tasaki, N. Tsuchiya, H. Nakajima, T. Hamaguchi, S. Oku, and T. Shiga, "A study of bioelectrical impedance analysis methods for practical visceral fat estimation," *IEEE International Conference on Granular Computing 2007*, pp. 622-627, 2007.

[7] M. Yoneda, H. Tasaki, N. Tsuchiya, H. Nakajima, T. Hamaguchi, S. Oku, and T. Shiga, "Development of visceral fat estimation model based on bioelectrical impedance analysis method," *Journal of Japan Society for Fuzzy Theory and Systems*, Vol. 20, No. 1, 2008 (in Japanese).

[8] H. Akaike, "A new look at the statistical model identification," *IEEE Trans on Automatic Control*, Vol. AC-19, No. 6, pp. 716-723, 1974.

[9] P. Armitage, G. Berry, and J.N.S. Matthews, "Statistical Methods in Medical Research", Wiley-Blackwell, pp. 358-360 (2001)

[10] R. I. Kitney and O. Rompelman, "The study of heart-rate variability," *Clarendon Press*, Oxford, 1980.

[11] H. Kobayashi, K. Ishibashi, and H. Noguchi, "Heart rate variability; an index for monitoring and analyzing human autonomic activities," *Applied Human Science*, Vol. 18, No. 2 pp.53-59, 1999.

[12] Y. Hata, Y. Kamozaki, T. Sawayama, K. Taniguchi, and H. Nakajima, "A heart pulse monitoring system by air pressure and ultrasonic sensor systems," *IEEE SMC International Conference on System of Systems Engineering 2007*, pp. 1-5, 2007.

[13] H. Yamaguchi, H. Nakajima, K. Taniguchi, S. Kobashi, K. Kondo, and Y. Hata, "Fuzzy detection system of behavior before getting out of bed by air pressure and ultrasonic sensors," *IEEE International Conference on Granular Computing 2007*, pp. 114-119, 2007.

[14] N. Tsuchiya, M. Yoneda and H. Nakajima,"Causal-effect structure transformation based on hierarchical representation for biomedical sensing," *World Review of Science, Technology and Sustainable Development 2010*, Vol. 7, No.1/2 pp. 116 – 129, 2010.

2011 IEEE International Conference on Fuzzy Systems
June 27-30, 2011, Taipei, Taiwan

Load Forecasting using Fuzzy Wavelet Neural Networks

Mahdi Amina
School of Electronics & Computer Science
University of Westminster
London, United Kingdom
mahdiamina@gmail.com

Vassilis S. Kodogiannis
School of Electronics & Computer Science
University of Westminster
London, United Kingdom
kodogiv@wmin.ac.uk

Abstract—Load forecasting is an important component for power system energy management system. Precise load forecasting helps the electric utility to make unit commitment decisions, reduce spinning reserve capacity and schedule device maintenance plan properly. This paper presents the development of a novel fuzzy wavelet neural network model and validates its prediction on the short-term electric load forecasting of the Power System of the Greek Island of Crete. In the proposed scheme, a wavelet neural network has replaced the classic TSK model in the consequent part, while subtractive clustering has been applied to the definition of fuzzy rules. The forecasting error statistical results, corresponding to the minimum and maximum load time-series, indicate that the proposed load forecasting model provides more accurate forecasts, compared to conventional neural networks models.

Keywords- Load forecasting; power systems, fuzzy wavelet networks neural networks.

I. INTRODUCTION

Load forecasting is an important component for power system energy management system. Precise load forecasting helps the electric utility to make unit commitment decisions, reduce spinning reserve capacity and schedule device maintenance plan properly. Besides playing a key role in reducing the generation cost, it is also essential to the reliability of power systems. The system operators use the load forecasting result as a basis of off-line network analysis to determine if the system might be vulnerable. If so, corrective actions should be prepared, such as load shedding, power purchases and bringing peaking units on line. Since in power systems the next days' power generation must be scheduled every day, day-ahead short-term load forecasting (STLF) is a necessary daily task for power dispatch. Its accuracy affects the economic operation and reliability of the system greatly. Under-prediction of STLF leads to insufficient reserve capacity preparation and, in turn, increases the operating cost by using expensive peaking units. On the other hand, over-prediction of STLF leads to the unnecessarily large reserve capacity, which is also related to high operating cost.

In spite of the numerous literatures on STLF published since 1960s, the research work in this area is still a challenge to the electrical engineering scholars because of its high complexity. How to estimate the future load with the historical data has remained a difficulty up to now, especially for the load forecasting of holidays, days with extreme weather and other anomalous days. With the recent development of new mathematical, data mining and artificial intelligence tools, it is potentially possible to improve the forecasting result. With the recent trend of deregulation of electricity markets, STLF has gained more importance and greater challenges [1].

The research approaches of short-term load forecasting can be mainly divided into two categories: statistical methods and computational intelligence (CI) methods. In statistical methods, equations can be obtained showing the relationship between load and its relative factors after training the historical data, while CI methods try to imitate human beings' way of thinking and reasoning to get knowledge from the past experience and forecast the future load. Regression is one of most widely used statistical techniques. For load forecasting regression methods are usually employed to model the relationship of load consumption and other factors such as weather, day type and customer class. Engle *et al.* [2] presented several regression models for the next day load forecasting. Their models incorporate deterministic influences such as holidays, stochastic influences such as average loads, and exogenous influences such as weather. Time series approach is based upon the assumption that the data has some internal structure such as autocorrelation, trend or seasonal variation. Most commonly used classical time series methods are ARMA (autoregressive moving average), ARIMA (autoregressive integrated moving average), ARMAX (autoregressive moving average with exogenous variables), and ARIMAX (autoregressive integrated moving average with exogenous variables). Fan and McDonald [3] and Cho *et al.* [4] described implementations of ARIMAX models for load forecasting.

The interest in applying neural networks to electric load forecasting began in 1990. Neural Networks (NN) have parallel and distributed processing structures. As for the STLF problem, the multilayer perceptron (MLP) network is the most widely used one. With the ability to approximate any continuous nonlinear function, the MLP network has very good mapping (forecasting) abilities. Peng *et al*. presented a search procedure for selecting the training cases for ANNs to recognize the relationship between the weather changes and load shape. It utilizes a neural network algorithm that includes a combination of linear and non-linear terms which map past load and temperature inputs to the load forecast output. The single forecast output is the total daily load [5]. Lu *et al*. used a similar feed-forward neural network incorporating the previous

978-1-4244-7316-8/11/$26.00 ©2011 IEEE

load demands, day of week, hour of day and temperature information for load forecasting [6]. Papalexopoulos *et al.* proposed the inclusion of additional input variables such as a seasonal factor and a cooling/heating degree into a single neural network [7]. An alternative technique for load forecasting using recurrent high order neural networks was considered in Kariniotakis *et al.* [8]. This type of neural network is supposed, in theory, to approximate very accurately any non-linear function, with exponential error convergence to zero [9]. Based on an interpolation procedure, the method gives superb results in training; in testing, however, the results are rather disappointing. The lack of generalization can be explained by the fact that the specific method needs an enormous number of training patterns in order to create a satisfactory input/output mapping. In this work, the training data set was created from the whole year of 1994 and the testing set for the first four months of 1995. The relatively small training data set had, as a consequence, the poor performance of the recurrent high order neural network model, despite its perfect training phase.

Many attempts by researchers have been made to improve load-forecasting process in many worldwide regions. Khan and Abraham [10] used a hybrid of neural network and fuzzy logic to forecast the load in Czech Republic. They found that hybrid fuzzy neural network and radial basis function networks are the best candidates for the analysis of the load in Czech Republic. Another study by Kodogiannis and Anagnostakis [11] discussed the development of improved neural-network-based short-term electric load-forecasting models for the power system of the Greek island of Crete. The performance was evaluated through a simulation study, using metered data provided by the Greek Public Power Corporation. Their results indicated that the load-forecasting models developed provided more accurate forecasts than the conventional methods.

NN models basically use the sigmoid activation function in neurons. However, the sigmoid function is not orthogonal, and the energy of the sigmoid function is limitless, and this leads to slow convergence. Wavelet function is a waveform that has limited duration and an average value of zero. The integration of the localization properties of wavelets and the learning abilities of NN shows advantages of Wavelet neural networks (WNN) over NN in complex nonlinear system modeling. A WNN that uses wavelet functions have been proposed by researchers for solving approximation and classification problems [12]. In this paper we present a methodology that follows the time series approach. In our case a novel fuzzy wavelet neural network traces previous load patterns and predicts a load pattern using recent load data without using weather information for modeling. The developed system identifies the load model, which reflects the stochastic behavior of the hourly load demand for the island of Crete in Greece. The balance of this paper contains also a comparative study of various other prediction techniques used to develop the STLF for the power system of Crete.

II. THE SHORT-TERM LOAD FORECASTING PROBLEM

This section is dealing with the application of the developed STLF models on the power system of the island of Crete. Public Power Corporation of Greece is the main provider of the electric power in Crete. Although the island has a population of around 600.000, during summer its total population is almost doubled due to the high tourist season. The island's electric system can be considered as small-scale one; hence serious damages could be suffered by small disturbances-overload. Thermoelectric power stations in two areas, Chania and Heraklion provide the necessary power. The later in Chania is composed of 4 (wind-turbine) units with total power of 202.5 MW. The former in Heraklion is composed of 12 (gas-turbine) units with total power of 192.9 MW. The objective of STLF is to predict the 24 hourly loads of the next day. Here, a modular-constructed forecasting system is proposed, where 24 neural blocks with a single output have to be developed and trained separately to represent the 24 hourly loads respectively. The outline of the proposed architecture is illustrated in Fig. 1.

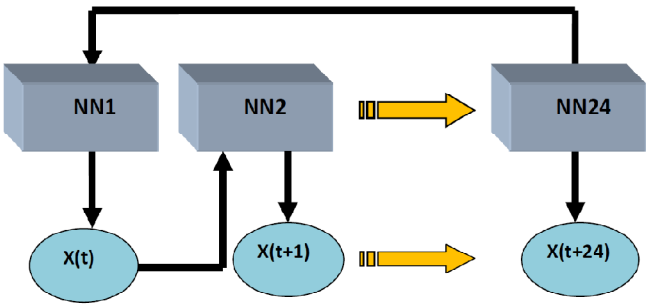

Figure 1. Proposed modular architecture for the STLF problem

Each neural block is fed by its previous. Hence, step-by-step, 24-hour load prediction can be obtained. In this work, the training data set was created from the whole year of 1994 and the testing one for the first four months of 1995. Both training and testing sets were classified into 24 time series, each one corresponds to a different daily hour. Therefore, for each neural block, the following non-linear load model is proposed for one-hour ahead forecasting:

$$x(t) = F\{ x(t-24l), x(t-k), x(t-24l - k) \}$$
$$l = 1,...,p \qquad k = 1,...,q \tag{1}$$

where p and q indicate the number of previous days and hours respectively. The main objective of the proposed system is the development of sufficiently accurate blocks representing the individual hourly loads. The investigation of a novel fuzzy wavelet neural network (FWNN) for system modelling has been carried out for the prediction of all 24h, each one trained separately, one for each hour. In the proposed scheme, a wavelet neural network has replaced the classic TSK model in the consequent part usually found in neuro-fuzzy schemes, while subtractive clustering has been applied to the definition of fuzzy rules. An assumption has been made in the case of black-outs, which occurred during the whole year. All the zero load values have been removed from both training and testing sets, and were replaced by the mean value of the preceding and subsequent load value. Eq. (1) is used to provide the input variables to the individual blocks. According to Eq. (1), the

requested load is forecast using not only the load data of previous days, but also the forecast load data for the same day at previous time steps. In the following sections, only results that correspond to hours with the maximum (14:00 h) and minimum (02:00 h) load consumption are illustrated.

III. MODELLING USING FWNN

A. Wavelet Neural Networks

Wavelet techniques can offer added insight and performance in data analysis situations where Fourier techniques have previously been used. The idea of using wavelets in neural networks has been proposed by Zhang and Benveniste [13]. The fundamental of WNN is looking for a series of appropriate wavelet basis functions in wavelet space. This process can be realised by iteration computation of wavelet basis function, which is to make the energy function minimized. To design a WNN, the main work is to design network structure, to determine the number of nodes in the middle layer, and to choose the wavelet basis function and the learning algorithm of weights training. Compared to the multilayer perceptron neural network (MLP), WNNs provide some advantages, such as the learning efficiency and the structure transparency. However, the problem of basis function networks is also led by it. Due to the crudeness of the local approximation, a large number of basis function units have to be employed to approximate a given system. In order to take advantage of the local capacity of the wavelet basis functions while not having too many hidden units, in this paper we propose an alternative type of WNN which has been influenced from related neuro-fuzzy architectures. The architecture of the proposed multiplication wavelet neural network-linear coefficients weights (LCW-MWNN) is shown in Fig. 2 [14].

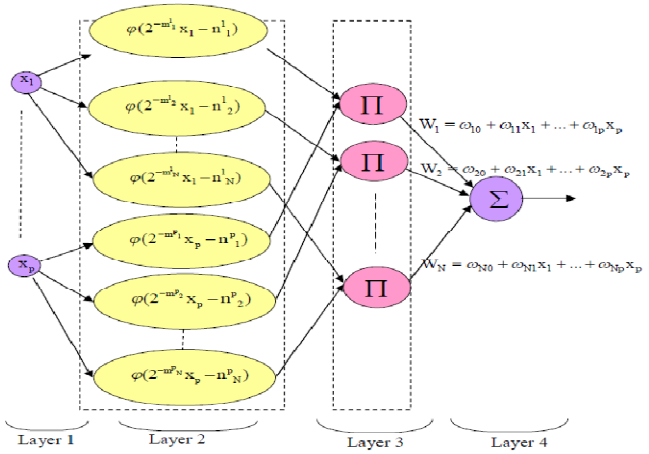

Figure 2. LCW-MWWN architecture

Referring to Fig. 2, Layer 1 accepts the input variables which are in form of $X_j = [x_{j1}, x_{j2}, ..., x_{jp}]^T$, while Layer 2 is used to calculate the wavelet "membership" values. In this layer, each node performs a membership function and acts as an element for membership degree calculation, where a wavelet function is adopted as the membership function. Generally, a WNN approximates any desired signal $y(t)$ by generalising a linear combination of a set of daughter wavelets $\varphi_{m,n}(t)$ which are generated by step sizes dilation and translation m and n from a mother wavelet with either of the forms below:

$$\varphi_{m,n} = \varphi\left(\frac{t-n}{m}\right) \qquad (2)$$
$$\varphi_{m,n} = \varphi(2^{-m}t - n)$$

where $m > 0$. The mother wavelet in the proposed Layer 2 is in the form of $\varphi_{m,n} = \varphi\left(\frac{t-n}{m}\right)$. The wavelet function adopted in this layer, is a modified differentiable version of Morlet wavelet

$$\varphi(x) = \cos(2\pi\beta x)e^{-\frac{x^2}{\upsilon}} \qquad (3)$$

Therefore, the mother wavelet of Eq. 2 from the i^{th} wavelet node connection to the p^{th} input data is expressed as

$$\varphi_{m^p_i, n^p_i}(x^p_j) = 2\pi\beta\left(\frac{x^p_j - n^p_i}{m^p_i}\right)e^{\frac{-\left(\frac{x^p_j - n^p_i}{m^p_i}\right)^2}{\upsilon}} \qquad (4)$$

This wavelet is derived from a function that is proportional to the cosine function and Gaussian probability density function. The nodes of Layer 3 are regarded as the "wavelet" rules in association to the fuzzy rules in a neuro-fuzzy architecture. The number of the "wavelet" membership functions for each input variable is equal to the number of "wavelet" inference rules. These units are fixed, meaning that no modifiable parameter is associated with them. The multiplicative inference (Larsen product operator) has been used, thus the output of this inference layer is given by

$$\phi_i(x_j) = \prod_{p=1}^{P} \varphi_{m^p_i, n^p_i}(x_j), \qquad p=1,2,..P \;\; j=1,2,..N \;\; i=1,2,..C \qquad (5)$$

The proposed approach differs from the conventional fuzzy rule table approaches. In those models, an input space is divided into $K_1 \times K_2 \times .... \times K_n$ fuzzy subspaces, where K_p, $p = 1,2,..,n$ is the number of fuzzy subsets for the p^{th} input variable. There is a fuzzy rule for each of these subspaces. The main drawback of that approach is that the number of fuzzy rules increases exponentially with respect to the number of inputs n. The structure of the output Layer 4, has been designed in the form of a local model $f(x_1, x_2, ..x_p)$, identical to the output layer appeared in *Takagi-Sugeno-Kang* (TSK) defuzzification schemes. For modelling of dynamic processes, TSK schemes possess an excellent interpretation, which is superior to most, if not all, alternative approaches. Usually $f(x_1, x_2, ..x_p)$ is a polynomial in the input variables x_p but it can be any function as long as it can appropriately describe the output of the model within the fuzzy region specified by the antecedent of the rule. When $f(x_1, x_2, ..x_p)$ is a first-order polynomial, the resulting fuzzy inference system is called a

first-order Sugeno fuzzy model. Thus, the output of Layer 4 is given as

$$y = \sum_{i=1}^{C} \left(w_{i0} + w_{i1} x_1 + \ldots + w_{ip} x_p \right) \phi_i(x) \qquad (6)$$

where, the network output is calculated as a weighted sum of the outputs of the local linear models and ϕ_i is interpreted as the operating point dependent weighting factor (i.e. output of Layer 3). Low time consumption is an advantage of this system. The Sugeno-type system is usually used when we operate on numerical (crisp) data. This system can be viewed as switching regression model or mixture of local experts. The scale and translation parameters and local linear model parameters are randomly initialised at the beginning and are optimized by using the Extended Kalman Filter algorithm.

B. Fuzzy EM-based Clustering

An effective approach to the identification of complex non-linear systems is the partitioning of the available data into subsets and approximation each subset by a simple model. This aim is furnished by gathering the objects are more similar to each other in one cluster. The term "similarity" in many cases considered as a *distance norm* from a data vector to a prototype object called as centre. While most classical clustering algorithms assign each datum to exactly one cluster, thus forming a crisp partition of the given data, fuzzy clustering allows for degrees of membership, to which the transitions of the subsets are gradual rather than abrupt (soft membership). Here clustering is based on Expectation Maximization in which the similarity should be understood as the probability that a data belongs to a specific Density. The Density parameter estimation is sought by the algorithm along with partitioning of the data.

Clustering algorithms typically require the user to pre-specify the number of cluster centers and their initial locations; the locations of the cluster centers are then adapted in a way such that these can better represent a set of data points covering the range of data behavior. Fuzzy Subtractive approach is a fast, one pass algorithm for estimating the number of clusters and clusters centers in a set of data. The subtractive clustering method assumes each data point is a potential cluster centre and calculates a measure of the likelihood that each data point would define the cluster centre, based on the density of surrounding data points. For better results it is recommended that normalization of each point into a unit hyper-box would make each dimension to be identical. The algorithm starts by finding the first large cluster, and then goes to find the second, etc [15]. The algorithm is represented in the following lines:

• *Selects the data point with the highest potential to be the first cluster centre. It is done by introducing a potential measure at data point* x_j *, defined as*

$$Pot_j = \sum_{k=1}^{N} \exp\left(-\frac{\left\| x_j - x_k \right\|^2}{(r_a / 2)^2}\right) \quad j = 1,\ldots,N \qquad (7)$$

Where r_a *is a positive constant representing a neighborhood radius and* $\left\| x_j - x_k \right\|^2$ *is the square of Euclidean distance between* x_j *and* x_k *. Hence, a data point will have a high density value if it has many neighbouring data points. After calculating the potential for each vector, the one with the higher potential is selected as the first cluster centre* x_{c1} *.*

• *Removes all data points in the vicinity of the first cluster centre (as determined by radii of all data points to the newly selected cluster centre), in order to determine the next data cluster and its centre location. The first cluster centre* x_{c1} *is chosen as the point having the largest density value* Pot_{c1} *. Next, the density measure of each data point* x_j *is revised as follows:*

$$Pot_j = Pot_j - Pot_{c1} \exp\left(\frac{\left\| x_j - x_{c1} \right\|^2}{(r_b / 2)^2}\right) \qquad (8)$$

Usually the r_b *variable is taken to be as* $1.5 r_a$ *. The process of acquiring new cluster centre is based on potential value in relation to an acceptance threshold* $\overline{\varepsilon}$ *, rejection threshold* $\underline{\varepsilon}$ *, and the relative distance criterion. A data point with the potential greater than the acceptance threshold is directly accepted as a cluster centre. The acceptance of a data point with a potential between the upper and the lower thresholds depends on the relative distance equation, defined as*

$$\frac{d_{min}}{r_a} + \frac{Pot_k}{Pot_1} \geq 1 \qquad (9)$$

where d_{min} *is the shortest distance between the candidate cluster centre and all previously found cluster centers. If Eq. 9 is greater than 1, then the associated x will be considered as a new cluster centre.*

• *Iterates on this process until a sufficient number of clusters is attainted. Since the algorithm is fixed and does not rely on any randomness, the results are fixed. However, we can test the effect of the four parameters, namely, acceptance ratio* $\overline{\varepsilon}$ *, reject ratio* $\underline{\varepsilon}$ *, cluster radius* r_a *and squash factor* r_b *These parameters have influence on the number of clusters and error performance measures. Large values of* $\overline{\varepsilon}$ *and* $\underline{\varepsilon}$ *will result in small number of rules. Conversely small values of* $\overline{\varepsilon}$ *and* $\underline{\varepsilon}$ *will increase the number of clusters. A large value of* r_a *generally result in fewer clusters that lead to a coarse model. A small value of* r_a *can produce excessive number of clusters that may result in an over-defined system.*

IV. CB-FWNN SCHEME

This paper presents a clustering based FWNN (CB-FWNN) that follows an "ANFIS structure" and its details are illustrated in Fig. 3. However significant differences against ANFIS have been considered in the proposed modeling structure. In many fuzzy and neuro-fuzzy models, the kernel of the fuzzy system

is the fuzzy knowledge base that consists of the input–output data points of the system interpreted into linguistic fuzzy rules. The consequent parts of TSK-type fuzzy IF–THEN rules are represented by either a constant or a function. Generally, the function is a linear combination of the input variables plus a constant term. TSK-type systems cannot, in general, model complex processes with desired accuracy using a certain number of rules. These systems do not have localizability; instead model the global features of the process, and their convergence is generally slow. The consequent part of these TSK-types fuzzy networks do not provide full mapping capabilities, and, in the case of modeling of complex nonlinear processes, may require a high number of rules in order to achieve the desired accuracy. Increasing the number of the rules leads to an increase in the number of neurons in the hidden layer of the network. In addition, in such TSK-schemes, the gradient decent method is usually used to train the non-linear antecedent parameters. However in the proposed structure instead of a linear function, a novel Linear Combination Multiplication Weight Wavelet Neural Network (LCW-MWNN) has been utilized. The specific model integrated two learning schemes; Weighted Least Square as well as the classic gradient descent (GD) learning algorithms. However, GD scheme is characterized by slow convergence training speed. Hence, in this study, the scale and translation parameters and local linear model parameters which have been randomly initialized at the beginning are optimized by using the Extended Kalman Filter algorithm.

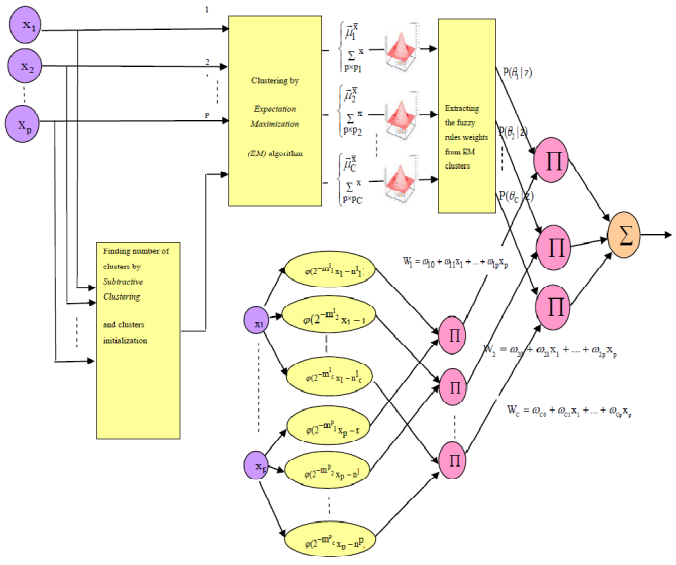

Figure 3. CB-FWNN proposed structure

In order to design the CB-FWNN structure, we assume initially, that one cluster in the input-output space corresponds to one potential fuzzy logic rule. Then the first step in structure learning is the determination of the number of fuzzy sets in the universal of discourse of each input variable [16]. In this research, the number of clusters are determined by subtractive clustering based on the training data as described earlier and remain constant throughout. Once the number of clusters defined, then the layout of the desired CB-FWNN can be sketched. At the consequence section, different scales of wavelet-neurons $\varphi_{x^p}(m_i^p, n_i^p)$ assigned for every dimension of the input. Although the number of different scales/ translation allocated to each dimension is fixed, each of inputs can be associated with different scales/translations. Knowing the optimum number of clusters, the number of different scales which each input dimension is going to be decomposed then can be determined, while the known number of clusters could assist in the determination of the number of fuzzy rules c as well as to the number of unknown parameters at the antecedent section. CB-FWNN's output is formulated as,

$$\begin{aligned}\hat{y}_j &= \sum_{i=1}^{C} \gamma_i(X_j) W_i(X_j) \phi_i(X_j) \\ &= \sum_{i=1}^{C} \gamma_i(X_j) W_i(X_j) \prod_{p=1}^{P} \varphi_{m_i^p, n_i^p}(x_j) \\ &= \sum_{i=1}^{C} W_i(X_j) \gamma_i(X_j) \left(\prod_{p=1}^{P} \cos\left(2\pi\beta\left(\frac{x_j^p - n_i^p}{m_i^p}\right)\right) e^{\frac{-\left(\frac{x_j^p - n_i^p}{m_i^p}\right)^2}{\upsilon}}\right)\end{aligned} \tag{10}$$

The conditional density $p(y \mid x)$ is a mixture of Gaussians functions at the output of clustering sub-unit therefore the regression problem is re-formulated also as

$$\begin{aligned}\hat{y}_j &= f(x) = E[y_j \mid x_j] \\ &= \int_y y_j p(y_j \mid x_j) dy = \frac{\int y_j p(x_j, y_j) dy}{p(x_j)} \\ &= \sum_{i=1}^{C} \frac{[W_i \phi_i(x_j)] p(x_j \mid \theta_i) p(\theta_i)}{p(x_j)} = \sum_{i=1}^{C} W_i \times P(\theta_i \mid x_j)[\phi_i(x_j)]\end{aligned} \tag{11}$$

where $\phi_i(x_j)$ is related to the i^{th} from c LCW-MWNN outputs, and the j^{th} input vector. $W_i(X_j)$ is the linear combination weight and $P(\theta_i \mid X_j)$ is the probability that the i^{th} Gaussian component is generated by the input vector X_j as depicted in the following equation, which replaces γ in eq. 10.

$$P(\theta_i \mid x_j) = \frac{\frac{P(\theta_i)}{(2\pi)^{p/2}\sqrt{|\Sigma_i|}} \exp\left(-\frac{1}{2}(x_j - \mu_i)^T (\Sigma_i)^{-1} (x_j - \mu_i)\right)}{\sum_{i=1}^{C} \frac{P(\theta_i)}{(2\pi)^{p/2}\sqrt{|\Sigma_i|}} \exp\left(-\frac{1}{2}(x_j - \mu_i)^T (\Sigma_i)^{-1} (x_j - \mu_i)\right)} \tag{12}$$

The final output based on dynamics of the proposed structure is derived by merging Eqs. 10 and 11 and have the following form

$$\hat{y}_j = \sum_{i=1}^{C} W_i(X_j) \times P(\theta_i \mid X_j) \left(\prod_{p=1}^{P} \cos\left(2\pi\beta\left(\frac{x_j^p - n_i^p}{m_i^p}\right)\right) e^{\frac{-\left(\frac{x_j^p - n_i^p}{m_i^p}\right)^2}{\upsilon}}\right) \tag{13}$$

The cluster parameters in this proposed scheme are estimated with the use of Expectation Maximization algorithm, while the Wavelet Neural Network parameters have been modified by Extended Kalman Filter and Weighted Least Square. The

choice of EM algorithm is justified by the fact that this approach avoids numerical instabilities encountered in Gradient Decent algorithm and presents an improved learning convergence.

V. RESULTS

This section presents the results and the statistics of forecasts obtained from the application of the developed STLF models on the power system of the island of Crete. Case studies for the proposed methods were carried out for a 24-hour load forecasting. The complete results for the STLF problem, for the hours with minimum and maximum load consumption, are illustrated in Table 1. Training has been conducted using power load data for 1994 (365 data points), while testing has been evaluated using data from the 4 first months of 1995.

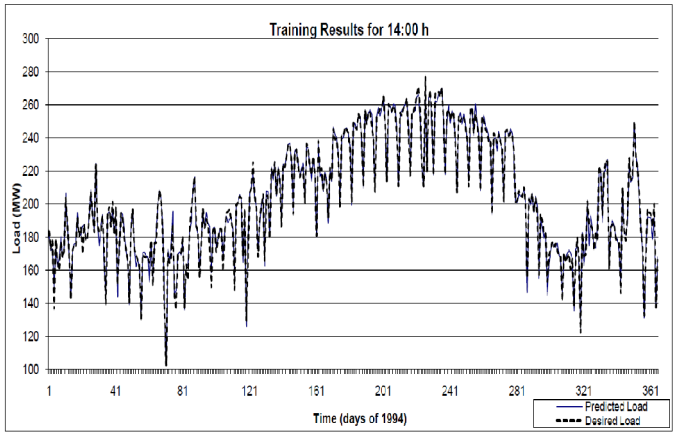

Figure 4. Training performance for max load

An obvious advantage of the proposed modular architecture is that, since the complete system consists of 24 neural blocks, each one with a single output, training is easier and faster compared to traditional neural approaches, which treat the output as a 24x1 vector. After many trials, it has been found that only two previous time load parameters are necessary for the proposed CB-FWNN to achieve an acceptable performance.

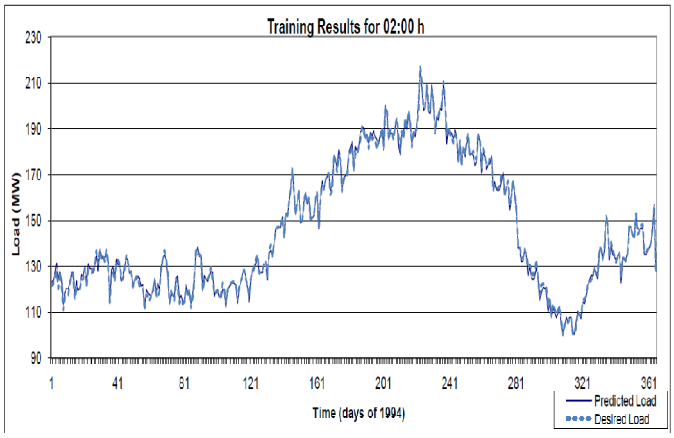

Figure 5. Training performance for min load

Fig. 4 and 5 illustrate the training performances on both minimum and maximum power consumption cases. Table I summarizes the various performance indices. The regression coefficient (R^2) is often used as an overall measure of the prediction attained. It measures the fraction of the variation about the mean that is explained by a model. The higher the value ($0 \le R^2 \le 1$), the better is the prediction by the model. The FWNN scheme developed herein was found to yield high level agreement with experimental observations for the test data set. The values of the coefficient of determination (R^2), as shown in Table I, indicate a very good fit of the experimental data from the FWNN-based approach.

TABLE I PERFORMANCE INDICES

Statistical index	Testing Data sets	
	14:00	02:00
Coefficient of determination (R^2)	0.9804	0.9654
Root mean square error (RMSE)	4.9492	2.6664
Mean absolute relative error (MARE) (%)	2.0481	1.3029
Mean Square Error	24.4943	7.1099
Standard error of prediction (SEP) (%)	2.7021	2.0324
Bias factor (B_f)	1.0089	1.0052
Accuracy factor (A_f)	1.0205	1.0131
Deviation	4.9492	2.6664

However, R^2 is a suitable criterion for model comparison on the assumption that the error is normally distributed and not dependent on the mean value. In fact, the distribution of the error is not clearly known, so this term must be used with caution, particularly in non-linear regression models and hence additional indices must be employed for model comparison.

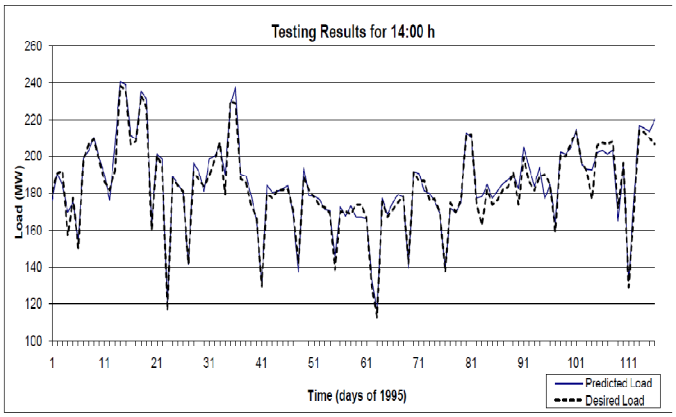

Figure 6. Testing performance for max load

The RMSE index is calculated between the desired and output values and then averaged across all data and it can be used as an estimation of the goodness of fit of the models. It can also provide information about how consistent the model would be in the long run. The MARE term provides information on how close forecasts or predictions are to the eventual outcomes. The SEP index is determined as the relative deviation of the

mean prediction values and it has the advantage of being independent on the magnitude of the measurements. Based on this index, the FWNN scheme achieved again a very good performance. The usual measures of goodness-of-fit for model comparison in many applications is performed by calculating in addition to squared correlation coefficient (R^2) the bias (B_f) and accuracy (A_f) indices [17]. Models describing predictions with B_f in the range of $\{0.9-1.05\}$ could be considered good, in the range of $\{0.7-0.9\} || \{1.06-1.15\}$ are considered acceptable, while for $\{<0.7 \;||\; >1.15\}$ are considered unacceptable. Bias factor is a multiplicative factor that compares model predictions and is used to determine whether the model over- or under-predicts the power consumption. A B_f greater than 1.0 indicates that a growth model is fail-dangerous.

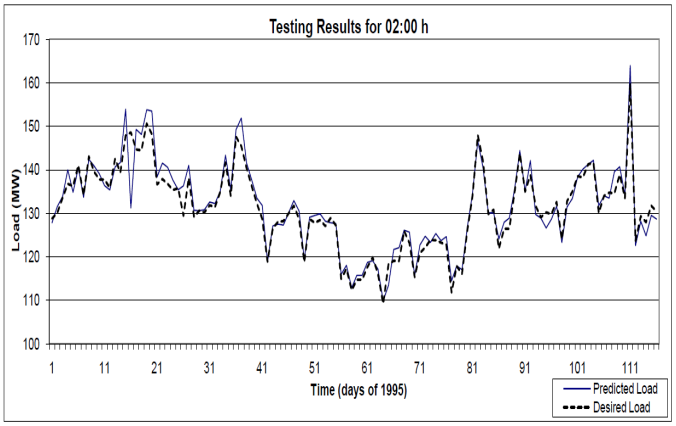

Figure 7. Testing performance for min load

Conversely, a B_f less than 1.0 generally indicates that a growth model is fail-safe, i.e. observed generation times were larger than predicted values, so that predicted values give a margin of safety. Perfect agreement between predictions and observations would lead to B_f of 1. The accuracy factor (A_f), is a simple multiplicative factor indicates the spread of results about the prediction. A value of 1 indicates that there is perfect agreement between all the predicted and measured values. Table I also shows the bias and accuracy factor values obtained for the two testing cases. Figs. 6 and 7 illustrate the testing performances for both cases. In order to evaluate the goodness of the current performance of the proposed FWNN scheme, a comparison against traditional neural networks using the same datasets has been made [11]. For the maximum load consumption, the MARE indices for MLP and RBF networks were 11.967 and 2.792 respectively, while for the minimum load case, the relevant values were 2.734 and 1.35. This comparison reveals the superiority of the proposed CB-FWNN scheme.

VI. CONCLUSIONS

This paper presented the development of a novel fuzzy wavelet neural network model and validated its prediction on the short-term electric load forecasting of the Power System of the Greek Island of Crete. In the proposed scheme, a wavelet neural network has replaced the classic TSK model in the consequent part, while subtractive clustering has been applied to the definition of fuzzy rules. The forecasting error statistical results, corresponding to the minimum and maximum load time-series, indicate that the proposed load forecasting model provides more accurate forecasts, compared to conventional neural networks models such as MLP and RBF. It should be noted that the proposed structures differ from the usual time-series prediction models since they include only loads for both previous times and previous days for hourly load forecasting. In a future work, the present approach will be enhanced by using additional load and weather information such as illuminations level, temperature, humidity, wind direction and industrial load.

REFERENCES

[1] F. Gao, X. Guan, X.-R. Cao, A., Papalexopoulos, "Forecasting power market clearing price and quantity using neural network method", Power Engineering Society Summer Meeting, Vol. 4, 2000, pp. 2183-2188.

[2] R.F. Engle, C. Mustafa and J. Rice, "Modelling Peak Electricity Demand", Journal of Forecasting, vol. 11, no. 3, 1992, pp. 241–251.

[3] J.Y. Fan and J.D. McDonald, "A Real-Time Implementation of Short-Term Load Forecasting for Distribution Power Systems", IEEE Transactions on Power Systems, Vol. 9, 1994, pp. 988–994

[4] M.Y. Cho, J.C. Hwang and C.S. Chen, "Customer Short-Term Load Forecasting by using ARIMA Transfer Function Model", Proceedings of the International Conference on Energy Management and Power Delivery, Vol. 1, No. 1, 1995, pp.317–322.

[5] M. Peng, N.F. Hubele and G.G. Karady, "Advancement in the Application of Neural Networks for Short-Term Load Forecasting", IEEE Transactions on Power Systems, Vol. 7, No. 1, 1992, pp. 250–257.

[6] Lu, C.N., Wu, H.T., Vemuri, S., "Neural network based short term load forecasting", IEEE Transactions on Power Systems, Vol. 8, No. 1, 1993, pp. 337-342.

[7] Papalexopoulos, A., How, S., Peng, T.M., "An implementation of a neural network based load forecasting model for the EMS", IEEE/PES 1994 Winter Meeting, 1994, pp. 207-209.

[8] Kariniotakis, G.N., Kosmatopoulos, E., Stavrakakis, G., "Load forecasting using dynamic high-order neural networks", Proceedings of IEEE-NTUA Joint International Power Conference, 1993, pp. 801-805.

[9] Kosmatopoulos, E., Polycarpou, M., Christodoulou, M., Ioannou, P., "High-order neural network structures for identification of dynamical systems", IEEE Transactions on Neural Networks, Vol. 6, No. 2, 1995, pp. 422-432.

[10] M.R. Khan, A. Abraham, "Short term load forecasting models in Czech Republic using soft computing paradigms", International Journal of Knowledge-Based Intelligent Engineering Systems, Vol. 7, No. 4, 2003, pp. 172–179.

[11] V.S. Kodogiannis, E.M. Anagnostakis, "A study of advanced learning algorithms for short-term load forecasting", Engineering Applications of Artificial Intelligence Journal, Vol. 44, No. 9, 1999, pp. 159–173.

[12] Y.C. Pati, P.S Krishnaprasad, "Analysis and synthesis of feed-forward neural networks using discrete affine wavelet transformations", IEEE Transactions on Neural Networks, Vol. 4, 1993, pp. 73–85.

[13] Q. Zhang, A. Benveniste, "Wavelet Networks", IEEE Trans. Neural Networks, Vol. 3, No. 6, 1992, pp. 89-98.

[14] M. Amina, E.Z. Panagou, V.S. Kodogiannis, G.-J.E. Nychas, "Wavelet Neural Networks for modelling high pressure inactivation kinetics of Listeria monocytogenes in UHT whole milk", Chemometrics and

intelligent laboratory systems, Elsevier, Vol. 103, No. 2, 2010, pp. 170-183.

[15] A. Priyono, M. Ridwan, A. J. Alias, R. Atiq, K. Rahmat, A. Hassan, M. Ali, and M. Alauddin, "Generation Of Fuzzy Rules With Subtractive Clustering", Jurnal Teknologi (D), Vol. 43, 2005, pp. 143-153.

[16] C.-J. Lin and C.-H. Chen, "Identification and prediction using recurrent compensatory neuro-fuzzy systems", Fuzzy Sets and Systems, Vol. 150, 2005, pp. 307-330

[17] T. Ross, "Indices for performance evaluation of predictive models in food microbiology", J Appl Microbiol, Vol. 81, 1996, pp. 501-508.

2011 IEEE International Conference on Fuzzy Systems
June 27-30, 2011, Taipei, Taiwan

Fuzzy Modelling Using a New Compact Fuzzy System: A Special Application to the Prediction of the Mechanical Properties of Alloy Steels

Qian Zhang and Mahdi Mahfouf
Department of Automatic Control and Systems Engineering
The University of Sheffield
Sheffield, UK
qian.zhang@sheffield.ac.uk, m.mahfouf@sheffield.ac.uk

***Abstract*—In high-dimensional modelling cases, a fuzzy modelling approach based on the grid-partitioning of fuzzy sets always meets great challenges, as it cannot avoid the problem of introducing a huge number of fuzzy rules. To tackle this issue, a new grid-partitioning based fuzzy modelling paradigm is proposed in this paper to construct a compact fuzzy system by including 'short fuzzy rules', in which only a few but strategic premises are used. In the proposed approach, the generation of fuzzy rules is data-orientated, a consideration which can greatly reduce the computational complexity. A new framework for fuzzy reasoning and defuzzification is also devised, which employs some archived reference data to help choose the most suitable fuzzy rules. In material engineering, describing the behaviour of mechanical properties of alloys is often a high-dimensional modelling problem, which involves the complexity of materials' chemical composites and their underlying physical processing mechanisms. In this paper, the proposed approach was successfully applied to generate models of ultimate tensile strength of alloy steel. Compared with the standard grid-partitioning based fuzzy modelling paradigms, the new method shows an improvement in both complexity and interpretability. Compared with the clustering-based fuzzy modelling approaches, the proposed method can achieve the same accuracy level and is more transparent.**

Keywords-fuzzy; high-dimensional modelling; grid partitioning; interpretability; short fuzzy rule; alloy steel; mechanical property

I. INTRODUCTION

There are many complex real-life modelling problems for which precise physical models do not currently exist, while abundant data that represent the input-output relationships can be collected. In this situation, some forms of intelligent systems associated with data-driven techniques, such as fuzzy rule-based systems and artificial neural networks (ANNs), appear to be suitable for model construction.

The fundamental concepts related to fuzzy rule-based systems were first introduced by Zadeh [1], [2]. They are known as robust universal approximators and allow a system to be represented using an explicit knowledge representation (linguistic 'IF-THEN' rules), which can easily be understood and explained by humans to allow them to gain a deeper insight into uncertain, complex, and ill-defined systems [3]. Compared with artificial neural networks, fuzzy systems are more transparent to humans to interpret. This is the most attractive property that distinguishes fuzzy systems from other black-box modelling approaches.

Normally, data-driven fuzzy modelling can be realised via two different routes: the grid-partitioning based method or the data-clustering based method. In the first method, the grid-partitioning initially defines a number of well-distributed fuzzy sets for each variable. The corresponding fuzzy rules are then elicited based on the fixed partitioning of fuzzy sets. In this approach, the fuzzy sets are also shared by all the fuzzy rules. In contrast, the second method employs data clustering (grouping) [4] information to define both the fuzzy sets and the fuzzy rules simultaneously. In this method, one cluster is associated to one fuzzy rule; the fuzzy sets are not shared by all the rules, but each set is only mapped into one particular fuzzy rule.

Compared with the grid-partitioning based method, the data-clustering based method needs less fuzzy rules to achieve a certain accuracy level; nevertheless its fuzzy sets are not evenly and well distributed and are not consistent with human knowledge and understanding. The grid-partitioning based method produces more interpretable systems, but it cannot avoid the problem of introducing a huge number of fuzzy rules for high-dimensional modelling problems. Another problem lies in high-dimensional modelling cases where a fuzzy rule may include too many antecedent conditions, a fact that defeats the interpretability property.

In this paper, a modelling paradigm using 'short fuzzy rules' is proposed to solve the above problems, where only a few but strategic antecedent conditions (premises) are included in a 'short fuzzy rule'. This remarkably decreases the number of fuzzy rules, as one short fuzzy rule possesses more powerful generalisation ability and can cover a wider input space. On the other hand, the short expression of fuzzy rules is much easier to be understood by a human. Table 1 illustrates the comparison among different fuzzy modelling paradigms.

978-1-4244-7316-8/11/$26.00 ©2011 IEEE

TABLE I. COMPARISON OF THE PROPOSED APPROACH OF 'SHORT FUZZY RULES' WITH OTHER FUZZY MODELLING PARADIGMS

		Clustering based methods	*Grid-partitioning based methods*	*The proposed method*
Interpretability	*Number of fuzzy rules*	Good	Bad	Medium
	The length of fuzzy rules	Bad	Bad	Good
	The number of fuzzy sets	Medium	Good	Good
	The distribution of fuzzy sets	Bad	Good	Good
	General performance	Medium	Medium	Good
Accuracy		Good	Medium	Medium

The remaining parts of this paper are organised as follows. Section II introduces the fuzzy systems with short fuzzy rules. Section III describes the proposed method to generate the compact fuzzy system. In Sections IV and V, a modified fuzzy reasoning and defuzzification mechanisms and a new framework for the proposed fuzzy system are proposed. Section VI presents an experimental study relating to the modelling of the mechanical property of the alloy steel. Finally, concluding remarks are drawn in Section VII.

II. FUZZY SYSTEMS WITH SHORT FUZZY RULES

Generally, a fuzzy rule-based system consists of four fundamental components: a fuzzy rule-base, a fuzzy inference engine, a fuzzifier, and a defuzzifier. Fig. 1 shows the diagram of a fuzzy system. The central part of a fuzzy system is the knowledge-base (rule-base) consisting of fuzzy rules. A fuzzy rule is an IF-THEN statement in which some words are characterised by continuous membership functions. All other components are used to implement these rules in a reasonable and in an efficient manner. The fuzzifier represents a mapping from a real-valued point $\boldsymbol{x} \in U \subset R^i$ to a fuzzy set $\boldsymbol{A}$ in U, which is defined by a membership function $\mu_A(\boldsymbol{x})$: $\boldsymbol{A} \rightarrow [0, 1]$. In a fuzzy inference engine, fuzzy logic principles direct how to employ the fuzzy rules into a mapping from an input fuzzy set $\boldsymbol{A}$ to an output fuzzy set B. The defuzzifier is a mapping from the output fuzzy set B in $V \subset R$ to a real-valued point $y \in V$. Conceptually, the purpose of the defuzzifier is to specify a point in V that best represents B [5].

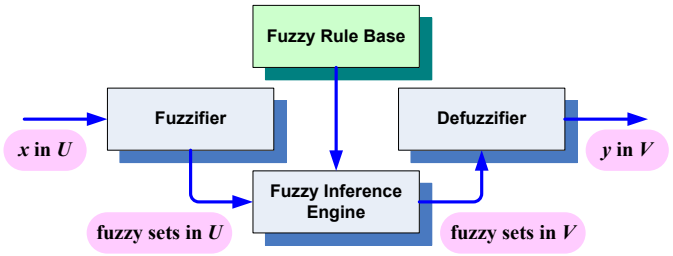

Figure 1. The basic configuration of fuzzy systems.

For an i-input 1-output system, a fuzzy rule-base could comprise the following Mamdani fuzzy rules:

Rule$_j$: IF x_1 is A_{1j} AND x_2 is A_{2j} AND … AND x_i is A_{ij}, THEN y is B_i.

where $\boldsymbol{x} = (x_1, x_2, \ldots, x_i)^T \in U$ and $y \in V$ are the input and output (linguistic) variables of the fuzzy system; A_{ij} and B_i are fuzzy sets in $U_i \subset R$ and $V \subset R$, respectively.

In some literatures [6], '*don't care*' is employed as an additional antecedent fuzzy set, which is fully compatible with any input value. Its membership function is defined as follows:

$$\forall x: \ \mu_{don't\ care}(x) = 1. \tag{1}$$

Since '*don't care*' conditions are usually omitted from the antecedent part, fuzzy rules with many '*don't care*' conditions are short and interpretable. The following shows an example of a fuzzy rule with '*don't care*' conditions:

IF x_1 is *don't care* AND x_2 is *medium* AND x_3 is *don't care*, THEN y is *large*.

If two '*don't care*' conditions are omitted, the above fuzzy rule can be shortened as follows:

IF x_2 is *medium*, THEN y is *large*.

In this paper, the number of antecedent conditions (premises) of each fuzzy rule is referred to as the rule length. In the above case, the rule length is reduced from 3 to 1 by using the '*don't care*' label.

III. GENERATION OF THE 'COMPACT FUZZY SYSTEM'

Generally, when constructing a fuzzy system, the fuzzy inference engine and the defuzzifiers are predefined. In the grid-partitioning based method, the uniformly-distributed fuzzy sets are also predefined for each variable. Thus, the primary work becomes to generating appropriate fuzzy rule-base.

In this work, the following steps are executed to elicit short fuzzy rules for the 'compact fuzzy system':

A. *Find candidate short fuzzy rules from all possible fuzzy rules*

The possible fuzzy rules include every combination of linguistic terms, although they are too many to be comprehensively evaluated. Suppose an i-input 1-output system has k linguistic terms (excluding '*don't care*') for every input variable and l linguistic terms for the output variable, the number of possible fuzzy rules could be $(k+1)^i * l$. The number of possible short fuzzy rules with rule length being 1 is $i*k*l$ and the number of possible short fuzzy rules with rule length being 2 is $\frac{i*(i-1)}{2} * k^2 * l$. In this paper, only the fuzzy rules no longer than 2 are considered.

As stated above, for a high-dimensional modelling problem, the possible short fuzzy rules may even be too many to be evaluated. In order to further decrease the number of candidate rules, it is required that only the rule that covers at least one training data point is considered as a candidate fuzzy rule.

Let $\boldsymbol{C}$ be a set of m training data $\boldsymbol{c}_n$, where $\boldsymbol{c}_n = [\boldsymbol{x}_n, y_n]^T = [x_{1n}, x_{2n}, \ldots, x_{in}, y_n]^T$ and $n = 1, 2, \ldots, m$. $Rule_j$ is regarded as a candidate short fuzzy rule, if

$$\exists n: \min\left(\mu_{A_{1j}}(x_{1n}), \mu_{A_{2j}}(x_{2n}), \ldots, \mu_{A_{ij}}(x_{in}), \mu_{B_j}(y_n)\right) > Th_1, \tag{2}$$

where 'Th_1' is a threshold value and it is set to 0.5 in this work without any loss of generality.

B. Calculate the 'confidence' value for each candidate short fuzzy rule

To estimate whether a fuzzy rule is redundant or not, an evaluation measure '*confidence*' is applied [7], [8]. In the area of data mining, it has been used for evaluating association rules in the pattern classification problem. The *confidence* of rule $\boldsymbol{A} \rightarrow B$ is defined as follows:

$$conf(\boldsymbol{A} \rightarrow B) = \frac{|C(\boldsymbol{A}) \cap C(B)|}{|C(\boldsymbol{A})|} \tag{3}$$

where $|C(\boldsymbol{A})|$ is the number of training patterns that are compatible with the antecedent $\boldsymbol{A}$, and $|C(\boldsymbol{A}) \cap C(B)|$ is the number of training patterns that are compatible with both the antecedent $\boldsymbol{A}$ and the consequent B. This *confidence* measure indicates that *conf*×100% of the training patterns that are compatible with the antecedent $\boldsymbol{A}$ are also compatible with the consequent B. In [7, 8], the *confidence* measure is extended to the fuzzy case and can be rewritten as follows:

$$conf(\boldsymbol{A} \rightarrow B) = \frac{|C(\boldsymbol{A}) \cap C(B)|}{|C(\boldsymbol{A})|} = \frac{\sum_{n=1}^{m}\left(\mathrm{N}_{\boldsymbol{A}}(\boldsymbol{x}_n) \times \mu_B(y_n)\right)}{\sum_{n=1}^{m}\mathrm{N}_{\boldsymbol{A}}(\boldsymbol{x}_n)} \tag{4}$$

where $\mathrm{N}_{\boldsymbol{A}}(\boldsymbol{x}_n)$ is the compatibility grade of the input vector $\boldsymbol{x}_n$ with the antecedent part $\boldsymbol{A} = [A_1, A_2, \ldots, A_i]^T$ of the fuzzy rule, and $\mu_B(y_n)$ is the compatibility grade of the output value y_n with the consequent part B of the rule. $\mathrm{N}_{\boldsymbol{A}}(\boldsymbol{x}_n)$ is usually defined by the minimum operator or the product operator. Such as:

$$\mathrm{N}_{\boldsymbol{A}}(\boldsymbol{x}_n) = \min\left(\mu_{A_{1j}}(x_{1n}), \mu_{A_{2j}}(x_{2n}), \ldots, \mu_{A_{ij}}(x_{in})\right) \text{ or} \tag{5}$$

$$\mathrm{N}_{\boldsymbol{A}}(\boldsymbol{x}_n) = \mu_{A_{1j}}(x_{1n}) \times \mu_{A_{2j}}(x_{2n}) \times \ldots \times \mu_{A_{ij}}(x_{in}). \tag{6}$$

In this work, these *confidence* values are also saved as the rule weights and will be further used in the defuzzification stage, as will be seen in Section IV.

C. Determine the final short fuzzy rule-base

A subset of candidate short fuzzy rules is selected as the active rule-base by taking into account the obtained *confidence* values. It is designed as the minimum subset of candidate rules which have the largest *confidence* values and can also cover all the training data. Specifically, if RS_p represent the selected rules and RU_q represent those unselected rules,

$$\min_p conf(RS_p) \geq \max_q conf(RU_q), \tag{7}$$

$$\forall n, \exists p: \min\left(\mu_{A_{ip}}(x_{1n}), \mu_{A_{2p}}(x_{2n}), \ldots, \mu_{A_{ip}}(x_{in}), \mu_{B_p}(y_n)\right) > Th_2 \tag{8}$$

where $conf(RS_p)$ is the *confidence* value of the pth short fuzzy rule RS_p; Th_2 is a threshold and a value 0.5 is used in this work without any loss of generality.

IV. Fuzzy Reasoning and Defuzzification

Because of the different rule structures of the compact fuzzy system and standard fuzzy systems, it is not appropriate to implement the traditional fuzzy reasoning and defuzzification methods directly. For a compact fuzzy system with short fuzzy rules, the following two issues should be addressed. First, a shorter rule describes a more general circumstance and a longer rule reflects a more specific situation. In a system including various rule lengths, longer rules should have higher priority to take effect. Second, among the rules with the same rule length, each makes a different level of impact on the system. This can be observed from a variety of *confidence* values for different fuzzy rules. In this work, both of the above issues are taken into account in the proposed fuzzy reasoning and defuzzification mechanism.

Suppose the product inference engine and the centre average defuzzifier [5] are employed, the system output $y(\boldsymbol{x})$ is calculated as follows:

$$y(\boldsymbol{x}) = \frac{\sum_p \mathrm{N}_{\boldsymbol{A}_p}(\boldsymbol{x}) \times b_p}{\sum_p \mathrm{N}_{\boldsymbol{A}_p}(\boldsymbol{x})} \tag{9}$$

where $\mathrm{N}_{\boldsymbol{A}p}(\boldsymbol{x})$ is the compatibility grade of the input vector $\boldsymbol{x}$ with the antecedent part $\boldsymbol{A}_p = [A_{1p}, A_{2p}, \ldots, A_{ip}]^T$ of the fuzzy rule RS_p; b_p is a representative real number of the consequent fuzzy set B_p (the centre of its membership function). $\mathrm{N}_{\boldsymbol{A}p}(\boldsymbol{x})$ is usually defined by the minimum operator or the product operator. Such as:

$$\mathrm{N}_{\boldsymbol{A}_p}(\boldsymbol{x}) = \min\left(\mu_{A_{1p}}(x_1), \mu_{A_{2p}}(x_2), \ldots, \mu_{A_{ip}}(x_i)\right) \text{ or} \tag{10}$$

$$\mathrm{N}_{\boldsymbol{A}_p}(\boldsymbol{x}) = \mu_{A_{1p}}(x_1) \times \mu_{A_{2p}}(x_2) \times \ldots \times \mu_{A_{ip}}(x_i). \tag{11}$$

By considering both the rule length and the rule weight, the above equation can be amended as follows:

$$y(\boldsymbol{x}) = \frac{\sum_p (l_{RS_p})^{conf_{RS_p}} \times \mathrm{N}_{\boldsymbol{A}_p}(\boldsymbol{x}) \times b_p}{\sum_p (l_{RS_p})^{conf_{RS_p}} \times \mathrm{N}_{\boldsymbol{A}_p}(\boldsymbol{x})}. \tag{12}$$

where l_{RSp} is the rule length of the pth short fuzzy rule RS_p, and $conf_{RSp}$ is the rule weight (*confidence* value) of RS_p.

V. A New Framework for the Compact Fuzzy System

After some initial experimental tests, it was found that the above compact fuzzy system always tends to yield a moderate prediction. The reason behind this may lie in the existing parallel fuzzy rules, which have similar or the same antecedent conditions but dissimilar consequent parts. To distinguish which rules should be applied in a certain situation, a new framework for the compact fuzzy system is proposed, as shown in Fig. 2.

The modified system will not use all the fuzzy rules including in the rule-based in the fuzzy inference engine. Only a set of relevant fuzzy rules, which is carefully selected by comparing their compatibility with the relevant reference data, will be employed into the fuzzy reasoning.

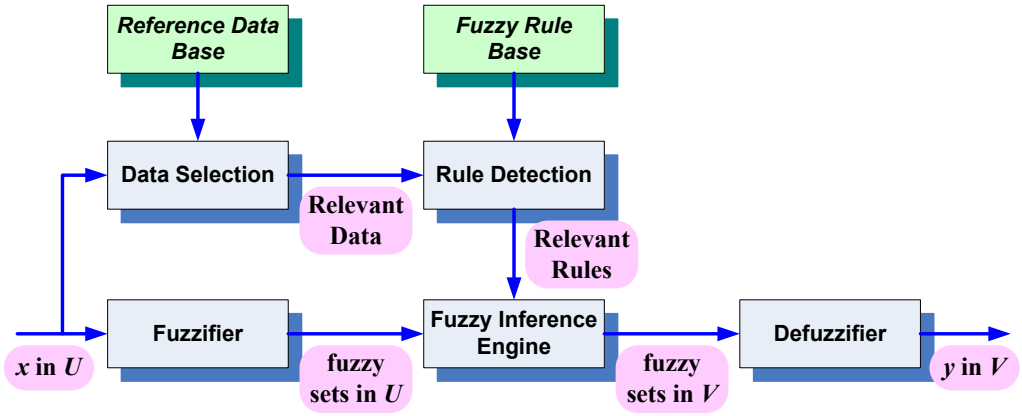

Figure 2. The diagram of the proposed fuzzy system.

Specifically, when a set of inputs $\boldsymbol{x} = [x_1, x_2, \ldots, x_i]^T$ goes into the system, it will be compared with the archived reference data set $\boldsymbol{C}_R = [\boldsymbol{c}_{R1}, \boldsymbol{c}_{R2}, \ldots, \boldsymbol{c}_{Rr}]$, where $\boldsymbol{c}_{Rr} = [\boldsymbol{x}_{Rr}, y_{Rr}]^T = [x_{1Rr}, x_{2Rr}, \ldots, x_{iRr}, y_{Rr}]^T$ and r is the number of all the reference data, and the most similar data $\boldsymbol{C}_S = [\boldsymbol{c}_{S1}, \boldsymbol{c}_{S2}, \ldots, \boldsymbol{c}_{Ss}]$ will be selected, where $\boldsymbol{c}_{Ss} = [\boldsymbol{x}_{Ss}, y_{Ss}]^T = [x_{1Ss}, x_{2Ss}, \ldots, x_{iSs}, y_{Ss}]^T$ and s is the number of the selected reference data. To estimate the similarity between $\boldsymbol{x}$ and a reference data, the Euclidean distance in the input space is calculated. If it is less than a threshold 'Th_3', the reference data are regarded as close to $\boldsymbol{x}$ and they will be selected to be used in the further fuzzy rule detection. This can be described as follows:

$$\boldsymbol{c}_R \subset \boldsymbol{C}_S, \text{ if } \sqrt{\sum_{t=1}^{i}(x_t - x_{tR})^2} < Th_3. \tag{13}$$

In general, 'Th_3' is recommended to be set as follows, without any loss of generality:

$$Th_3 = 0.15 \times \sqrt{\sum_{t=1}^{i}(x_{t\max} - x_{t\min})^2} \tag{14}$$

where $x_{t\max}$ and $x_{t\min}$ represent the maximum value and the minimum value of all the reference data in their tth dimension, respectively.

In the subsequent rule detection, the obtained relevant reference data are employed to identify the most relevant fuzzy rules $\boldsymbol{R}_S$. If a fuzzy rule R is compatible with at least one reference data to some extent, the fuzzy rule is reckoned as relevant and will be passed through fuzzy reasoning phase. This can be described as follows:

$R \subset \boldsymbol{R}_S$, if $\exists n \in [1, 2, \ldots, s]$:

$$\min\left(\mu_{A_1}(x_{1n}), \mu_{A_2}(x_{2n}), \ldots, \mu_{A_i}(x_{in}), \mu_B(y_n)\right) > Th_4, \tag{15}$$

where 'Th_4' is a threshold value and it is set to be 0.5 in this work without any loss of generality.

VI. Prediction of Mechanical Properties

In material engineering, it is crucial to establish transparent and reliable mechanical property prediction models for materials design and development [9]-[11]. But it may be 'tricky' to precisely describe the behaviour of mechanical properties using mathematical models alone due to the complexity of materials' chemical composites and their underlying physical processing mechanisms, such as hot rolling and heat treatment. Thus, developing a fast, efficient and transparent data-driven modelling framework for material property prediction is still a priority.

In the past, some prediction models relating to mechanical properties have been developed, which were mainly based on linear regression methods, artificial neural networks [12], and fuzzy systems [13]-[15]. Such linear models were only designed for specific classes of steels and specific processing routes, and are not sophisticated enough to account for more complex interactions, while neural networks are black-box techniques and the knowledge behind this kind of models cannot be understood fully. The fuzzy modelling techniques included in [13]-[15] employed data clustering information, which lead to a fuzzy rule-base which was not interpretable enough.

Particularly in this work, one of the studied mechanical properties of heat-treated alloy steels, is the Ultimate Tensile Strength (UTS), which represents a measure of the maximum load that a material can withstand. This problem is a high-dimension modelling problem and includes fifteen (15) input variables, which include the weight percentages for various chemical composites as well as the processing parameters of the heat treatment, consisting of the weight percentages for the chemical composites, namely carbon (C), silica (Si), manganese (Mn), sulphur (S), chromium (Cr), molybdenum (Mo), nickel (Ni), aluminium (Al) and vanadium (V), the test depth, the bar size, the treatment site, the quenching medium, as well as the hardening and tempering temperatures. Moreover, this problem is associated with a large amount of industrial data (3760 UTS data), which are not well-distributed and may be quantitatively redundant for training purposes. All the data are provided by Tata Steel Europe. In the following experiment, 60% of the data were used for training, and the remaining 40% were used for final testing. This experiment was repeated 20 times. Only one set of typical results out of the 20 runs is chosen and shown in the following.

For configurations, the number of fuzzy sets for each input variable was set to be 7 and the number of fuzzy sets for the output variable was set to be 15. In such a grid partitioning of input space, the number of all the possible fuzzy rules is $5.28*10^{14}$, the number of possible short fuzzy rules with rule length being 1 is 1575, and the number of possible short fuzzy

rules with rule length being 2 is 77175. By employing the proposed approach, only 214 'short fuzzy rules' were elicited.

Fig. 3 shows the prediction performance (predicted outputs against measured outputs) of the compact fuzzy model using standard fuzzy reasoning and defuzzification. It can be seen that the predictions tend to be of moderate values. Fig. 4 shows the prediction performance of the same model with the new framework introduced in Section IV and the modified reasoning and defuzzification methods proposed in Section V. For this case, the Root Mean Square Error (RMSE) based on the training data and the testing data are 40.05 MPa and 47.92 MPa, respectively. This accuracy is as good as those reported in [14], [15], which established fuzzy models via data-clustering based methods with rules including many antecedents unnecessarily.

For more details about the developed UTS model, Fig. 5 compares the fuzzy rules between a full-length one generated using data clustering techniques [14], [15] and the short ones obtained in this work. It can be seen that the full-length fuzzy rule is too complicated to be interpreted. One can also observe another disadvantage of the fuzzy system elicited from data clustering that the fuzzy sets are not evenly and well distributed. For these fuzzy rules, they can be rewritten as the following approximate linguistic rules using the linguistic hedges approach [16]:

R_1: IF Test Depth is *small* AND Size is *small medium* AND Site Number is *large* AND C is *large medium* AND Si is *medium* AND Mn is *medium small* AND S is *small* AND Cr is *medium small* AND Mo is *medium* AND Ni is *large medium* AND Al is *very small* AND V is *very small* AND Hardening Temperature is *small* AND Cooling Medium Number is *more or less large* AND Tempering Temperature is *medium large*, THEN UTS is *large medium*.

R_2: IF Mn is *large medium*, THEN UTS is *small medium*.

R_3: IF V is *small medium*, THEN UTS is *medium small*.

R_4: IF Ni is *medium* AND Hardening Temperature is *small*, THEN UTS is *small medium*.

It is clear that the linguistic fuzzy rules as R_2, R_3, and R_4, allow for a better insight into the heat-treated alloy steels process.

To verify the physical interpretation of the obtained models, Fig. 6 shows the three-dimensional response surfaces of the compact model. These surfaces are achieved by plotting two varying input variables against the output while keeping other input variables constant. The constant variables are set to the average values of the dominant steel grade, which is the 1%CrMo steel grade [17]. These plots in Fig. 6 are consistent with those variable effect plots in [17], which have been verified to follow the expected behaviour as predicted by theory and knowledge experts.

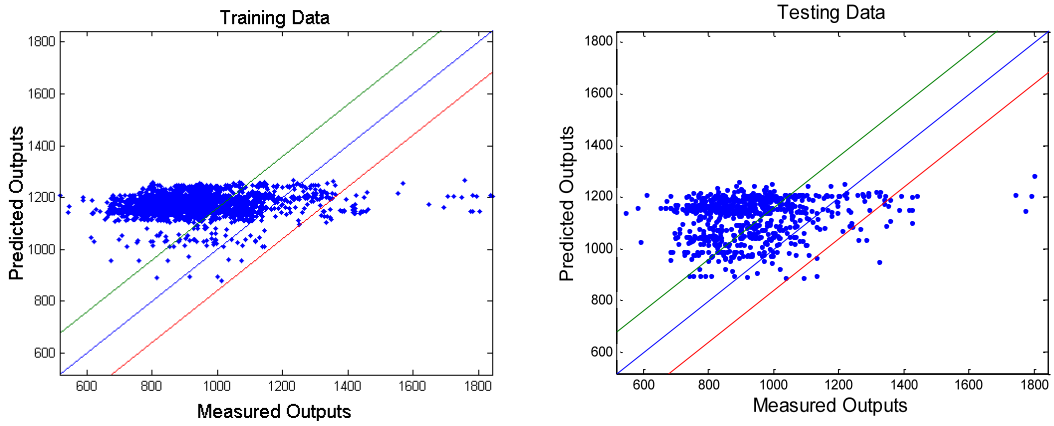

Figure 3. The UTS model's predicted outputs versus the measured outputs with the standard fuzzy reasoning and defuzzification methods.

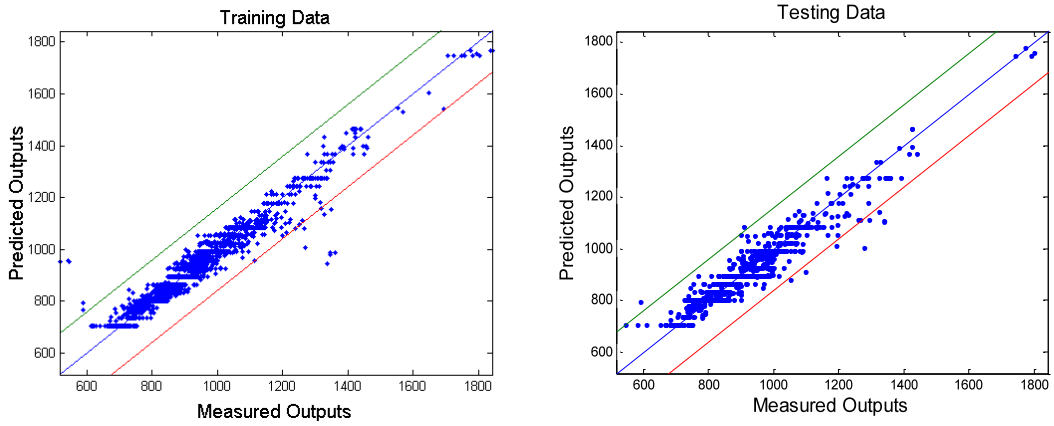

Figure 4. The UTS model's predicted outputs versus the measured outputs with the proposed system structure.

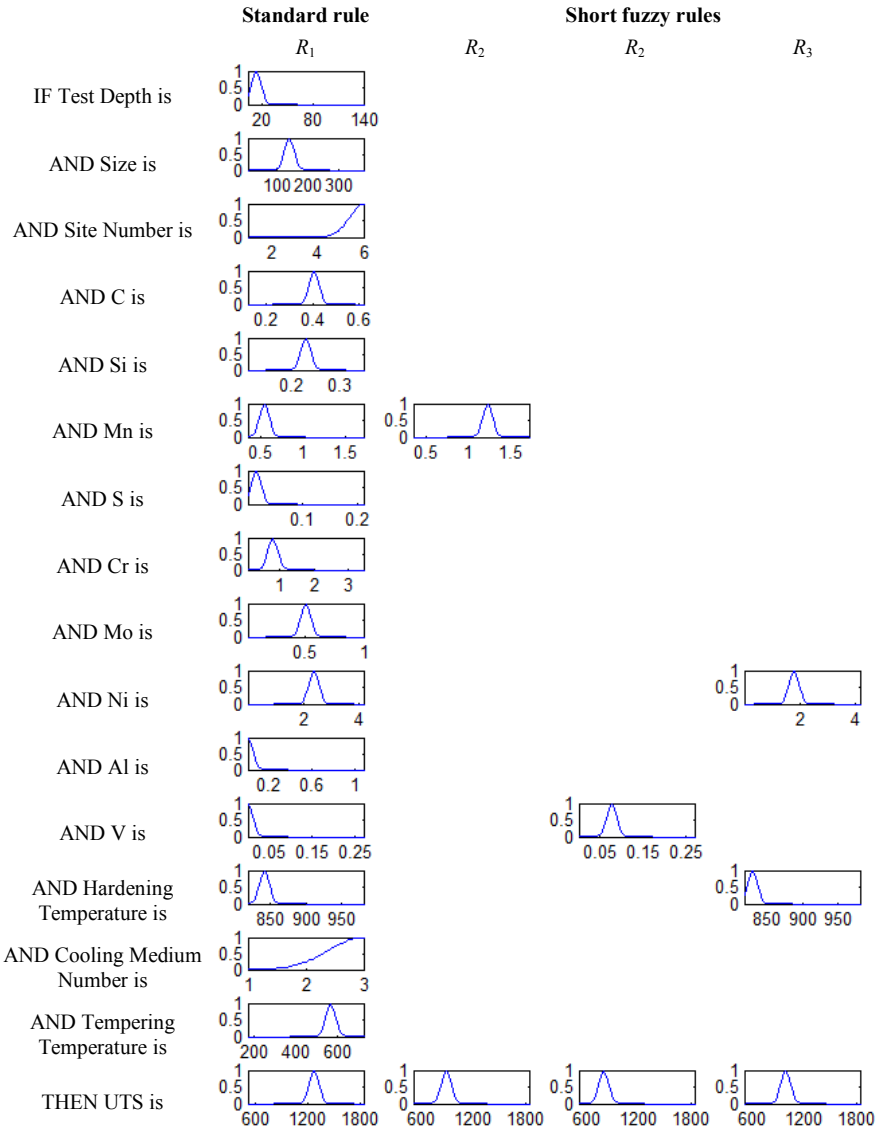

Figure 5. A comparison between a full-length and short fuzzy rules.

VII. CONCLUSION

For modelling problems, the most attractive advantage of fuzzy rule-based systems lies in their interpretability, which means that users should be able to understand a fuzzy system's behaviour by inspecting its associated rule-base. Normally, the interpretability issue involves the following widely accepted aspects: First, the number of fuzzy rules should be small enough to be comprehensible. Second, the rule premises should be simple in structure and contain only a few features (input variables). Third, the linguistic terms should be intuitively comprehensible. The form and parameters of the membership functions should correspond to the understanding of the linguistic expressions.

The grid-partitioning based fuzzy modelling approaches are considered to be more interpretable than data-clustering based ones since they include a set of well-distribution fuzzy sets. In the traditional grid-partitioning based methods, all the possible fuzzy rules in every partition are evaluated, which is time-consuming and cannot be achieved in high-dimensional modelling cases. In this work, the generation of fuzzy rules is data-orientated using 'short fuzzy rules', which can greatly reduce the number of fuzzy rules as well as the computational complexity. Among the fuzzy rules with various rule length, the shorter ones represent more general status and the longer ones deal with more specific situation. This has been fully taken into account in the reasoning and defuzzification. To identify the most appropriate fuzzy rules in a certain circumstance, a new mechanism of reference rules detection has also been developed.

The proposed approach was then successfully applied to generate models of the mechanical properties (in our case one) of alloy steels. Compared with the standard grid-partitioning based fuzzy modelling paradigms, the new method reveals an improvement in both the computational complexity and the interpretability. Compared with the clustering-based fuzzy modelling approaches, the proposed method can achieve the same accuracy level with a more transparent rule-base.

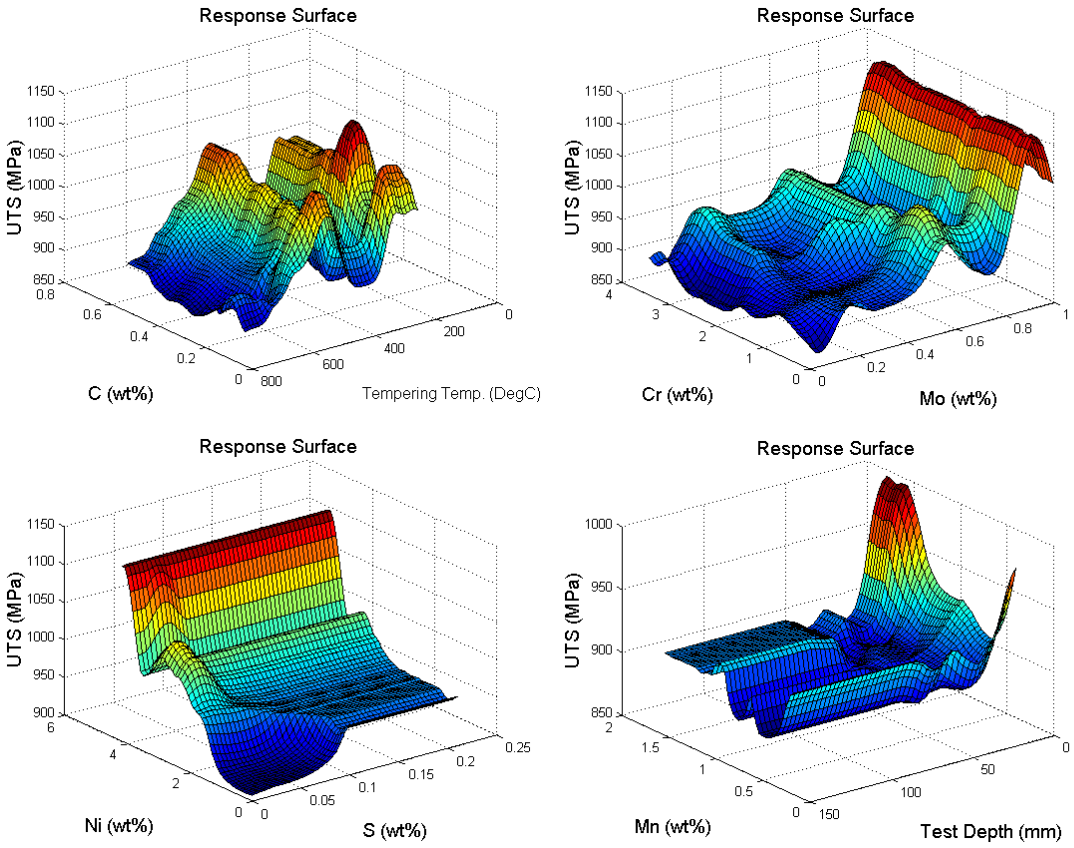

Figure 6. Response surfaces of the obtained UTS model.

In this paper, only the Mamdani-type fuzzy systems [18], which use linguistic expressions in both the antecedent and consequent parts, are considered. In the near future, the design could be extended to TSK-type fuzzy systems [19], which would replace the linguistic consequent parts of the Mamdani-type fuzzy system with deterministic forms. The authors will, also explore the possibility of extending the idea of employing short fuzzy rules within the framework of data-clustering based fuzzy modelling. It is also worth noting that the proposed framework does not include any optimisation strategy. In future, learning via effective optimisation could be embedded into the system to further improve overall accuracy while maintaining the same level of interpretability.

REFERENCES

[1] L.A. Zadeh, "Fuzzy sets," Information and Control, vol. 8, no. 3, pp. 338–353, 1965.

[2] L.A. Zadeh, "Outline of a new approach to the analysis of complex systems and decision processes," IEEE Transactions on Systems, Man, and Cybernetics, vol. 3, pp. 28–44, 1973.

[3] Q. Zhang, Nature-Inspired Multi-Objective Optimisation and Transparent Knowledge Discovery via Hierarchical Fuzzy Modelling. PhD Thesis, The Department of Automatic Control and Systems Engineering, The University of Sheffield, UK, 2008.

[4] P. Berkhin, "A survey of clustering data mining techniques," in Grouping Multidimensional Data: Recent Advances in Clustering, J. Kogan, C. Nicholas, and M. Teboulle, Eds. Berlin: Heidelberg: Springer, 2006, pp. 25–71.

[5] L.-X. Wang, A course in fuzzy systems and control. Englewood Cliffs, NJ: Prentice-Hall, 1997.

[6] H. Ishibuchi and T. Yamamoto, "Interpretability issues in fuzzy genetics-based machine learning for linguistic modelling," in Modelling with Words, J. Lawry, J. Shanahan, and A. Ralescu, Eds. Berlin: Heidelberg: Springer, 2003, pp. 209–228.

[7] T.-P. Hong, C.-S. Kuo, and S.-C. Chi, "Trade-off between computation time and number of rules for fuzzy mining from quantitative data," International Journal of Uncertainty, Fuzziness and Knowledge-Based Systems, vol. 9, pp. 587–604, 2001.

[8] H. Ishibuchi, T. Yamamoto, and T. Nakashima, "Fuzzy data mining: effect of fuzzy discretization," in Proceedings of the First IEEE International Conference on Data Mining, pp. 241–248, 2001.

[9] Q. Zhang and M. Mahfouf, "A Modified PSO with a Dynamically Varying Population and Its Application to the Multi-Objective Optimal Design of Alloy Steels," in Proceedings of the 2009 IEEE Congress on Evolutionary Computation, pp. 3241-3248, 2009.

[10] Q. Zhang and M. Mahfouf, "A nature-inspired multi-objective optimisation strategy based on a new reduced space searching algorithm - special application to the design of alloy steels," Engineering applications of artificial intelligence, vol. 23, no. 5, pp. 660–675, 2010.

[11] Q. Zhang, M. Mahfouf, J.R. Yates, C. Pinna, G. Panoutsos, S. Boumaiza, R.J. Greene, and L. de Leon, "Modeling and Optimal Design of Machining-Induced Residual Stresses in Aluminium Alloys Using a Fast Hierarchical Multiobjective Optimization Algorithm," Materials and Manufacturing Processes, vol. 26, no. 3, pp. 508-520, 2011.

[12] C.L.P. Chen, C. Yang, and S.R. LeClair, "Materials structure-property prediction using a self-architecting neural network," Journal of Alloys Compounds, vol. 279, no. 1, pp. 30–38, 1998.

[13] M.-Y. Chen and D.A. Linkens, "A systematic neuro-fuzzy modeling framework with application to material property prediction," IEEE Transactions on Systems, Man, and Cybernetics - Part B: Cybernetics, vol. 31, no. 5, pp. 781–790, 2001.

[14] Q. Zhang, and M. Mahfouf, "Mamdani-type fuzzy modelling via hierarchical clustering and multi-objective particle swarm optimisation

(FM-HCPSO)," International Journal of Computational Intelligence Research, vol. 4, no. 4, pp. 314–328, 2008.

[15] Q. Zhang, and M. Mahfouf, "A hierarchical Mamdani-type fuzzy modelling approach with new training data selection and multi-objective optimisation mechanisms: A special application for the prediction of mechanical properties of alloy steels," Applied Soft Computing, vol. 11, no. 2, pp. 2419–2443, 2011.

[16] L.A. Zadeh, "A fuzzy-set-theoretic interpretation of linguistic hedges," Journal of Cybernetics, vol. 2, pp. 4–34, 1972.

[17] J. Tenner, Optimisation of the Heat Treatment of Steel Using Neural Networks, PhD Thesis, The Department of Automatic Control and Systems Engineering, The University of Sheffield, UK, 1999.

[18] E.H. Mamdani and S. Assilian, "An experiment in linguistic synthesis with a fuzzy logic controller," International Journal Man-Machine Studies, vol. 7, pp. 1–13, 1975.

[19] T. Takagi and M. Sugeno, "Fuzzy identification of systems and its applications to modeling and control," IEEE Transaction Systems, Man and Cybernetics, vol. 15, no. 1, pp. 116–132, 1985.

2011 IEEE International Conference on Fuzzy Systems
June 27-30, 2011, Taipei, Taiwan

Agent Simulation for Contents Evaluation with User Models for Hierarchical Knowledge Relations

Kiyota Hashimoto
School of Humanities and Social Sciences
Osaka Prefecture University
Sakai, Japan
hash@lc.osakafu-u.ac.jp

Kazuhiro Takeuchi
Faculty of Information and Communication Engineering
Osaka Electro-Communication University
Neyagawa, Japan
takeuchi@isc.osakac.ac.jp

***Abstract*—To construct an appropriate e-learning system, it is inevitable to evaluate it by testing it with real human learners, but it naturally implies some sacrifices on the part of learners. To minimize the risk, some computational simulative evaluations are desirable. In this paper, we propose a multi-layered multi-agent simulation model for learner's growth through using an e-learning system. As a typical example of complex learning objects, we employ the task of learning presentation skills for which we are constructing a comprehensive learner support system and learners' data, and the knowledge model and learner growth model are prototypically proposed. By a preparatory experiment, our attempt, though it is still in its fancy, is shown to be on the right track.**

Keywords- contents evaluation; agent simulation; multi-layered knowledge model; hierarchical knowledge relations; awareness promotion

I. INTRODUCTION

With more need for customized tutoring or learning support with information and communication technology, more and more e-learning systems have been developed and utilized for various types of topics. They are supposedly developed deliberately with preceding analyses of the topic, the targeted learners, and the expected functions and user interfaces, but their effectiveness has been measured only when they are used by real human learners. It is true that the real value of any system is known only in the real situations, but as much risk of inappropriateness or failure should be avoided as possible, though we admit that the complete displacement of human trials is impossible.

To evaluate e-learning systems without real human learners, it may well be useful to employ an agent simulation. However, we face at least three fundamental issues:

- Knowledge and skill of many complicated, and often very abstract, tasks to be learned by human learners contains different levels of knowledges. Thus modeling such a complex system is not trivial, let alone implementing an agent system.
- Learner's knowledge and skill is in definition incomplete and often contains incorrect parts, which has also to be modeled.
- Learning steps contains continuous revisions, corrections, and refinements of prior knowledge and skill. So adequate model of growth has also to be modeled.

To tackle these issues, we will take a synthetic approach with an inter-related knowledge structure of complex tasks. As a typical example of complex learning objects, we employ the task of learning presentation skills for which we are constructing a comprehensive learner support system and learners' data, and we propose a multi-layered multi-agent simulation model for learner's growth through using an e-learning system. Though our attempt is still in its infancy, a preparatory experiment seems to show our attempt to be on the right track.

The organization of this paper is as follows. In section II, we describe our ongoing project to construct a comprehensive learner support system for English presentation, particularly for the purpose of presenting knowledge models assumed in the system. In section III, we propose a prototypical multi-layered multi-agent simulation model, and in section IV we conduct a preparatory experiment to evaluate our model.

II. PRESENTATION LEARNING SUPPORT

A. Overview of the relevant system

Based on the recognition above, we are currently developing a comprehensive learner support system for basic presentation in English [1]. It consists of several modules including digital contents of preliminary tutorials, an interactive aide for organizing a presentation and its corresponding slides, semi-automatic evaluation estimation, and a online review of recorded presentations, with a multimedia learner corpus of presentation. The overview of our system is shown in Fig.1.

B. Underlying Learner Model

As a learner support system, our system assumes a basic meta-cognitive model of presentation preparation and exercise similar to that of writing process designed by Hayes and Flower [2], and our model is shown in Fig. 2.

978-1-4244-7316-8/11/$26.00 ©2011 IEEE

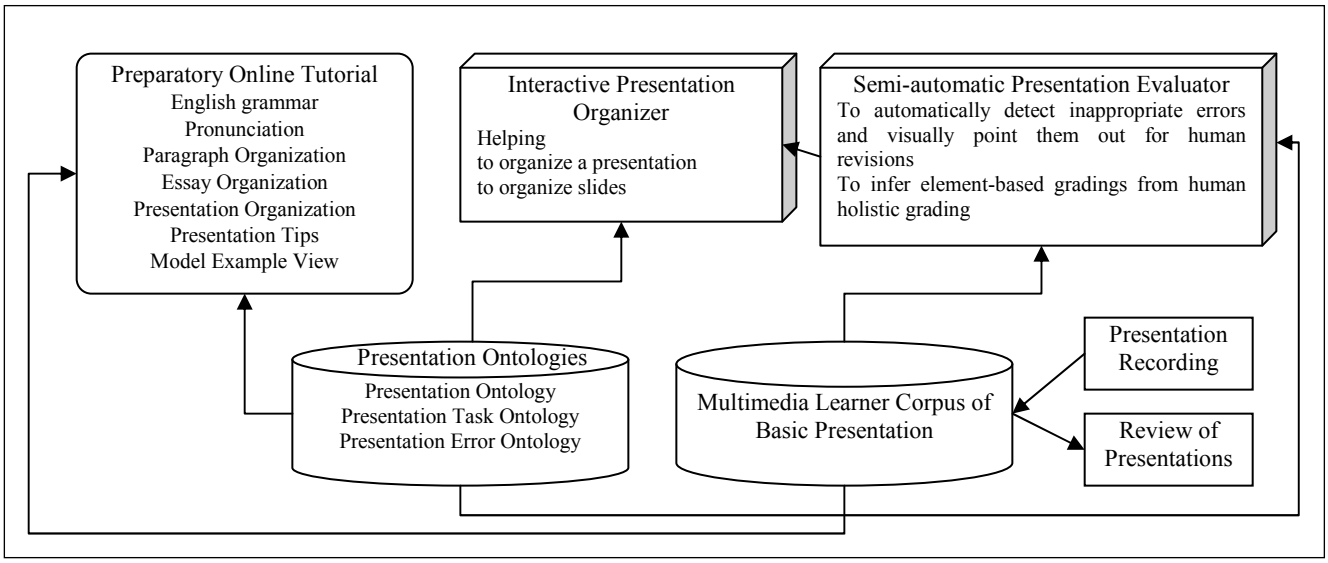

Figure.1 Overview of our prototypical learning support system of Basic Presentation

Based on the Hayes and Flower model, we added a performance section and clarified the status of strategies in the long-term memory. With this model, what any learner support system for presentation should promote is clear. In order for learners to acquire presentation strategies in their long-term memory, the skill choosing the proper writing style, speaking style, visual aids, and performance style, together with the feature of the chosen topic and the tendency of the audience, should be fostered in the way to stimulate their self-awareness. When preparing the presentation itself, three processes are to be effectively supported again by letting them be aware of what they are doing and what are to be improved.

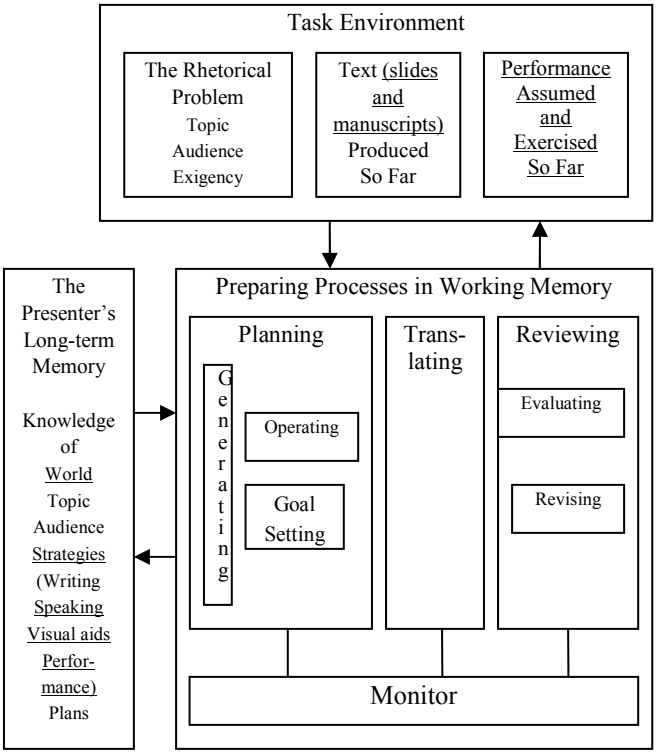

Figure 2 Our tentative model of the presentation preparation process

C. *Presentation Style Factors*

Presentation, whether it is oral or written, is delivered for a particular communicative purpose, which is to determine what and how to be delivered—content and style. A communicative purpose can be analyzed into different aspects. Let us call these aspects style factors. As each style factor affects what and how to be delivered, they have to be deliberately considered. Numerous books on presentation preparation emphasize the consideration of style factors, though each calls style factors differently, and we classify them as in Table 1.

With the decisions on style factors, oral and slide contents are to made not only on what to be delivered but also how to

TABLE 1 STYLE FACTORS

Factors	Examples
Topical (Genre)	inorganic chemistry, English literature ... (Note that the topical factor can be very much specific.)
Media	newspaper, textbook, oral presentation...
Targeted reader/ audience	laypeople, professionals ...
Purpose	persuasion, explanation ...
Intention	formal, informal or friendly ...
Time	the length of presentation

deliver it. Preparation for discussion is also affected. In other words, all the other aspects of presentation preparation and delivery are decided along the line of the choices of the appropriate style factors for the presentation. Particularly, all the linguistic style elements like shown in Figure 3 which manifest the choices are heavily affected.

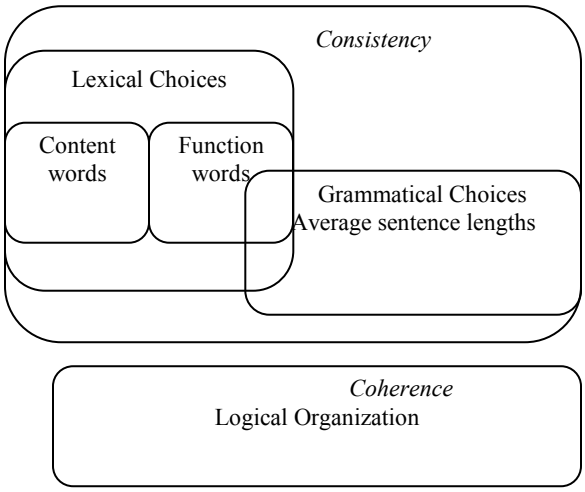

Figure 3 Linguistic Style Elements

D. Rhetorical Structure

The actual content of a presentation is then represented as a series of spoken sentences constituting a logical organization. One of the best known logical organization is that of paragraph, but a more fine-grained relation between sentences is needed, and a number of theories and frameworks have been proposed [4], of which Rhetorical Structure Theory, originally proposed by Mann and Thompson [5-9] is the most popular.

In the RST framework, the discourse structure of a text is considered to be coherent and thus capable of being be basically represented as a single-rooted tree with a set of directed graphs. Each directed graph is labeled for its rhetorical relation. Originally 23 relations were proposed [10], but the exact number proposed varies among researchers. Based on various proposals, we constructed a revised rhetorical relations of RST for presentation as shown in Table 2 [11].

It is important to note that the adequate sequence of rhetorical relations varies according to the purpose, targeted audience, and intention of the presentation. So, though it is difficult at this stage to reveal an quantitative correspondence between them, styles factors and rhetorical relations are related.

E. Learners' Presentation Samples

We have been constructing a multimedia learner corpus of English basic presentation (MLCP), part of which is to be employed as learning data in this paper. MLCP contains more than three hundred English presentations by learners [12]. The collected presentations vary in topic and in purpose, but all have common structure of five paragraphs, and common targeted audience, i.e. peer learners. The common structure is schematized as in Fig. 4, which is originally hinted by the idea of basic five paragraph essays. As shown, each slide roughly corresponds to a paragraph.

- Title and its corresponding slide
- Introduction and its corresponding slide
- Three supports and their corresponding slide
- Conclusion and its corresponding slide

As learning data for the experiment to be described later, we manually tagged rhetorical structure relations to the transcribed oral speech for 100 presentations. To facilitate the experiment, however, we manually added the style factors to them, which is not included in MLCP.

MLCP contains human evaluations of each presentations, which is considered to represent the growth level of the presenter.

TABLE 2 OUR REVISED RHETORICAL RELATIONS OF RST

EDU(Elementary Discourse Unit): Semantically clausal segments

A rhetorical relation is basically based on the surface structure and is assigned 0 or 1 according to the logical validity.

The Set of Rhetorical Relations for our purpose

Name	Description	Order of N&S
Background	Satellite provides background information to the nucleus	S before N
Contrast	Applies to two nuclei that contrast each other	
Elaboration	Satellite elaborates the information in the nucleus	N before S
*Elaborative Example	Satellite exemplifies the information in the nucleus	N before S
Enablement	Information in the satellite enables the audience to perform action in nucleus	N before S
Evidence	Satellite provides evidence to the statement in the nucleus	N before S
Justify	Satellite justifies the nucleus	
Motivation	Satellites motivates the reader to perform the action in the nucleus	
List	Listed nuclei	S before N
Sequence	Multiple nuclei that follow each other in sequence	
Solutionhood	Satellite is the problem; Nucleus provides the solution.	N before S
Summary	Short summary or paraphrase of the previous span	
*Supra-textual Cue	Cue for an action on the part of the audience.	
*Orphaned	Any other orphaned nucleus, to be connected to the nearest dominating nucleus (* indicates that the item is newly introduced here)	

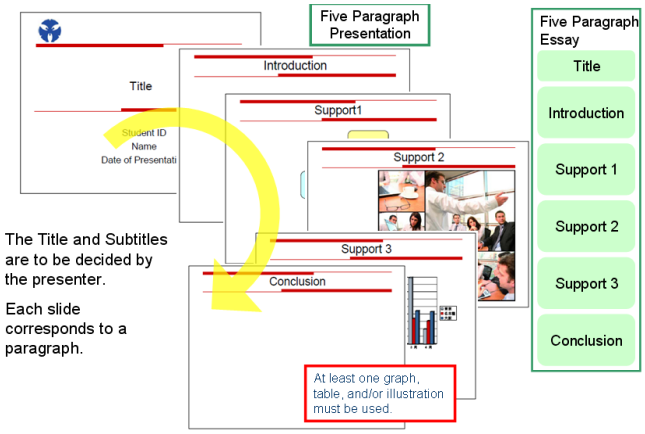

Figure 4 Correspondence between presentation slides and basic five paragraph essay

III. MULTI-LAYERED MULTI-AGENT MODEL OF LEARNER

According to our developing e-learning system for English presentation and learners' data described in the previous section, we constructed a multi-layered multi-agent model of learner in learning English presentation skills.

A. A Multi-Layered Model of Relevant Knowledges

When preparing a presentation, one should first analyze and determine style factors. According to style factors, he constructs what is to be presented, i.e. contents, and it is constructed as oral speech and slides. As noted previously, style factors do affect contents. For example, if the topic is technical while the audience is assumed to have little prior knowledge on the topic, then it should be supposed that the contents should contain comprehensible definitions and a fair amount of examples for easy understanding. Then, the actual speech and slides reflects the determination of style factors and the construction of contents. It is difficult to make a rigorous model for this kind of relationship, but a restricted part of the relationship can be stated fairly simply. In this paper, as a prototypical restricted model, we prepared a set of simple relations between the technical complexity of topics and the knowledge level of the targeted audience like the following.

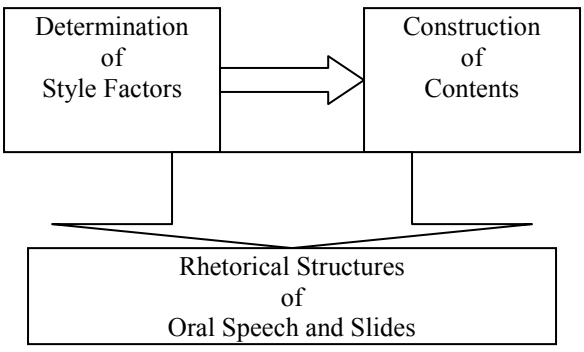

Figure 5 Primitive Multi-Layered Model

- The more technical the topic is, the more comprehensible definitions and examples (including metaphorical ones) are needed.
- The more abstract the topic is, the more metaphorical elaborations are needed.
- If the targeted audience have some prior knowledge, then the definitions usually come first. On the contrary, if not, then they may not.

At the same time, some style factors like purpose and intention both directly and indirectly (i.e., through the determination of contents) affect the sequence of rhetorical relations.

Note here that humans have each knowledge on style factors, contents, and rhetorical relations at different levels, and have additional knowledge on relations among them, which is why the model adopted here, roughly shown in Fig. 5, is called a multi-layered model of relevant knowledges.

B. A Multi-Agent Model

Each pieces of knowledges in the multi-layered model can be considered to an agent with a limited knowledge and reasoning rules. In other words, The body of knowledges of a human can be considered to a set of agents.

As for the relationship between style factors and contents, we only focus on the degree of necessity of definitions and examples, and the *style factor agents* are supposed to have one reasoning that require the corresponding construction of contents. Because it is beyond the scope of this paper, we assume that the construction of contents is the mere reflection of the determination by style factor agents; in other words, we do not deal with the actual contents, and the construction of contents is a set of the number of words (expressions, to be more exact) with definitions and the number of examples, both of which are determined by style factor agents, together with some other pieces of contents like causes and conclusions.

As for the rhetorical relations, we assume each rhetorical relation is implemented as an agent with simple reasoning of the order between nucleus and satellites.

C. A Learner Model Reflecting Growth Stages

The two notions of "multi-layered" and "multi-agent" are considered to constitute a human knowledge of a complex skill, and if they are constructed idealistically, it is a model of the perfected body of related knowledges. We assume as a zero hypothesis that the perfected body of related knowledges can in fact be constructed for some types of e-learning systems including that for English presentation, though we admit that it is not the case with every kind of possible e-learning systems. If we have a perfected body of related knowledges, then *a learner model at a particular growth stage* is to be constructed as an imperfect, often incorrect, body of related knowledges, and let's suppose so.

Then, a model for a particular growth stage constitute a set of agents at multi-layers whose reasoning is unstably probabilistic or just inert as shown in Fig. 6.

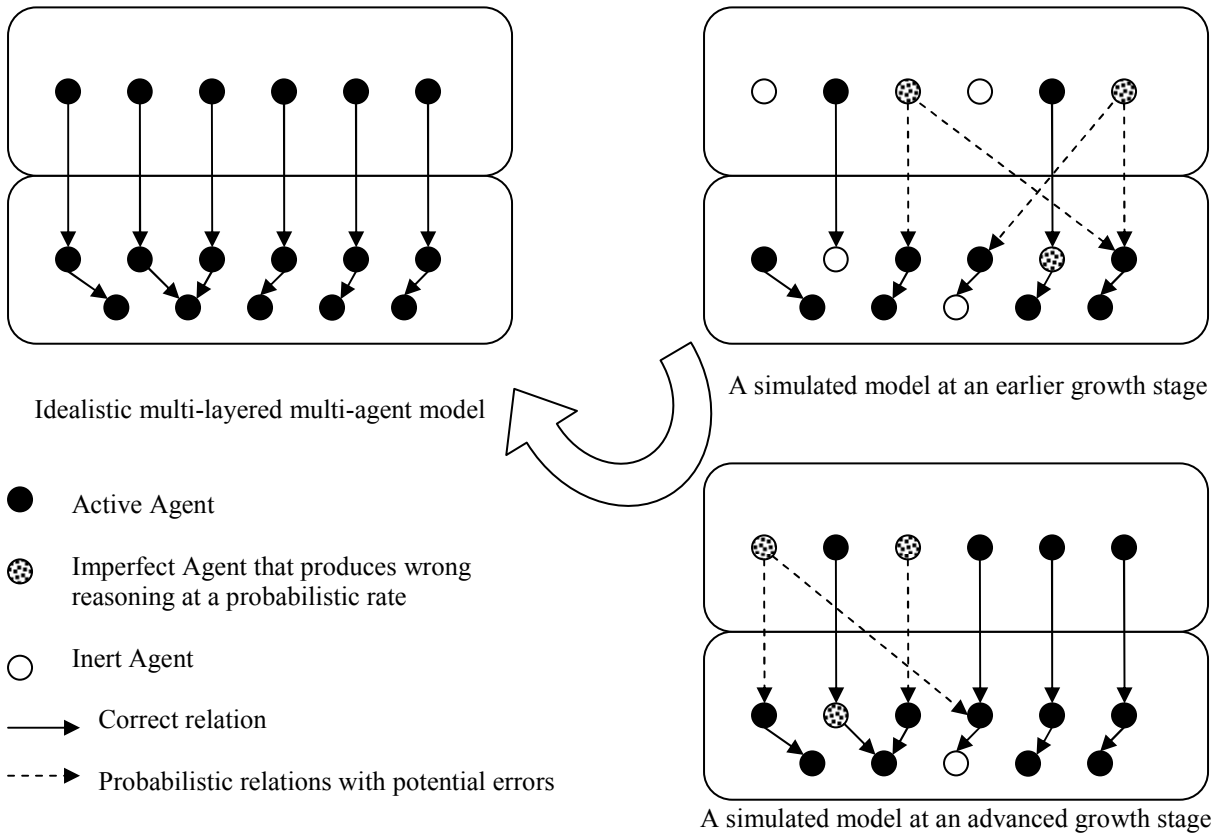

Figure 6 A Multi-Layered Multi-Agent Learner Model at Different Growth Stages

For convenience, each agent belongs to one of the two layers in Fig. 6, and in learner's model, agents are categorized as one of the three conditions.

- Active Agent
- Imperfect Agent that produces wrong reasoning at a probabilistic rate
- Inert Agent

Active agents requires other agents related to it to make a particular action, while imperfect agents may or may not do so to other agents that may or may not be related to it. Inert Agent does nothing. Then growth is considered to have more active agents than the previous stage.

IV. PROTOTYPICAL EXPERIMENT

Based on the model we described in the previous section, we conducted a prototypical experiment to evaluate our model.

Each agent has a set of two rules, one of which is inherent reasoning and the other of which is the request to other agents to a particular action. At the rhetorical relation layer, actions are categorized into the following two actions:

- To require another rhetorical relation agent to follow
- To require a particular type of sentence.

The experiment consists of two phases. The first phase is the stage to statistically learn the condition of each agent and the relations between agents from the data that represent a particular growth stage. A growth stage is judged with the evaluation value of presentations in MLCP. In this paper, we set four growth stages according to the evaluation value. So we will obtain (at least) four models each of which represents one of the four growth stage. Let us call each g_1, g_2, g_3, g_4. The second phase is the stage in which the set of agents whose conditions are learned for a particular growth stage re-learn for the next growth stage. Let us call each g_i^{i+1}. Then compare g_i^{i+1} with g_{i+1}. If g_i^{i+1} is the same or very similar to g_{i+1}, then it may well be considered that our model represents a growth stage from which it can learn to the next stage.

In average, each presentation consists of 15 sentences, and each learning set consists of 50 presentations. We admit that this size of the learning sets is not so large, and so we employed an SVM method, due to its perseverance to the small size of learning data sets.

As for style factor agents, we just implemented four, each of which may send their requests to the rhetorical relation layer. In this paper, we skipped the contents layer, simply because there is no data dedicated to the contents layer in the current MLCP while the data of leaner's speeches can be considered to

be the result of the construction of the contents at least for our experiment here.

Each style factor agents get an input from the meta data of each presentation whether its targeted audience is prepared or not, and whether the topic is technical or not. Then they may make inherent reasoning to send the preset request, and look for another agent to receive their request.

As for rhetorical relation agents, we just picked up four: background, elaboration, elaborative example, and solutionhood. Because the prepared style factor agents have to do with background and elaborative example, the expected result is that only the relations between style factor agents and *background* and *elaborative example* rhetorical relation agents are related.

The learning process has two stages: one for distinguishing the existence of relations from no relation, which distinguishes active and imperfect agents from inert agents, and the other for distinguishing the high probability of relations and the low probability of relations, which distinguishes active from imperfect agents.

The results of the second phase is shown in Table 3.

TABLE 3 THE RESULTS OF THE SECOND PHASE LEARNING RATE

	○ v. ●	○ v ⊛	⊛ v. ●
g_1^2 v. g_2	83.4%	75.8%	82.3%
g_2^3 v. g_3	52%	37.4%	64.7%
g_3^4 v. g_4	91.2%	62.3%	86.1%

As Table 3 shows, the comparison between g_2^3 and g_3 is low. This is because the third level is inherently intermediate and such an intermediate level of learners have relatively unstable conditions with unstable tendencies to use correct patterns. However, the comparisons between g_1^2 and g_2 and between g_3^4 and g_4 are relatively high, which indicates that our multi-layered multi-agent learner model can represent growth stages.

V. CONCLUDING REMARKS

In this paper, for the purpose of computational evaluation of e-learning systems for complex skills, we proposed a multi-layered multi-agent learner model which can trace growth stages. The result of the prototypical experiment indicates that our model in fact represents growth stages. It is quite primitive, but this model opens up a possibility to computational learner simulation, and it leads to minimize the risk of learner's sacrifice to be exposed to imperfect e-learning systems.

ACKNOWLEDGEMENT

This study is supported by KAKENHI (22520576).

REFERENCES

[1] K. Hashimoto and K. Takeuchi, "Prototypical Development of Awareness Promoting Learning Support System of Basic Presentation," Proc. of 2nd ISAC, 291-298, 2010.

[2] J. R. Hayes and L. Flower, "Identifying the organization of writing processes," L.W. Gregg and E.R. Steinberg (eds.) Cognitive Processes in Writing, New Jersey: Lawrence Erlbaum Associates, 1980.

[3] D. R. Garrison and N. D. Vaughan, Blended Learning in Higher Education: Framework, Principles, and Guidelines, New York: Jossey-Bess, 2007.

[4] T. Groza, S. Handschuh, T. Clark, S. Buckingham Shum, and A. de Waard, A Short Survey of Discourse Representation Models, Proc. of 8th International Semantic Web Conference, Workshop on Semantic Web Applications in Scientific Discourse. Lecture Notes in Computer Science, Springer Verlag: Berlin, 2009 .(available from http://ceur-ws.org/Vol-523Groza.pdf)

[5] W. C. Mann and S.A. Thompson, "Rhetorical Structure Theory: A Theory of Text Organization," ISI/RS-87-190, 1987.

[6] W. C. Mann and S.A. Thompson, "Rhetorical Structure Theory: Toward a Functional Theory of Text Organization," Text 8(3), 241-281, 1988.

[7] S. A. Thompson and W.C.Mann, "Rhetorical Structure Theory: A Framework for the Analysis of Texts," Papers in Pragmatics 1-1, 79-105, 1992.

[8] Taboada, M. and W.C. Mann (2006) Rhetorical Structure Theory: Looking Back and Moving Ahead, Discourse Studies 8(3), 423-459

[9] Taboada, M. and W.C. Mann (2006b) Applications of Rhetorical Structure Theory, Discourse Studies 8(4), 567-588.

[10] N. Nicholas, Problems in the Application of Rhetorical Structure Theory to Text Generation, Unpublished M.Eng. Sc. Thesis, University of Melbourne., 1994.

[11] K. Hashimoto, K. Takeuchi, "Rhetorical Structure Ontology for Representing Learner's Presentations with Potential Textual Inconsistencies and Imperfections," ICIC Express Letters 5-5, 1649-1654, 2011.

[12] K. Hashimoto, K. Takeuchi, "Multimedia Learner Corpus of Foreigner's Basic Presentation in English with Evaluations," Proc. of International Conference on Educational and Information Technology, Vol.2, 469-473, 2010.

2011 IEEE International Conference on Fuzzy Systems
June 27-30, 2011, Taipei, Taiwan

Giving Awareness of Maturity by Capability Assessment

Yi-Ling Kuo
National University of Tainan
Tainan, Taiwan
egmilkcherry@gmail.com

Yu Nakamura
Masayuki Sakoda
Hiroshi Tsuji
Osaka Prefecture University
Osaka, Japan
tsuji@cs.osakafu-u.ac.jp

Chang-Shing Lee
National University of Tainan
Tainan, Taiwan
leecs@mail.nutn.edu.tw

***Abstract*—Based on knowledge management and the spiral learning model for E-Learning, this paper proposes an interactive system, SPIral Capability Enhancement (SPICE) support system, to define two subjects: *Human Education* and *Information Security.* A student can review his situation on the subject to get feedback to evaluate his own capabilities based on comparisons. Basic idea of the proposed system originates in the pineapples of Capability Maturity Model Integration (CMMI) to allow the organizations and the systems to do the personal learning. This paper also discusses the possibility to adopt fuzzy markup language (FML) to infer the capability of maturity model which let the teachers as well as students know their capability of maturity model.**

Keywords: E-Learning; Knowledge Management; CMMI; FML

I. INTRODUCTION

The present education system not only achieves the goal of education but also promotes student's study level. During learning process, we first have to clarify our sub-goal as well as final goal to learn and then achieve the pre-defined goals. However, teachers and learners cannot discuss with each other in any time after class, so students have sometimes difficulties in clearly finding their achievement level to the met final goal. For instance, currently teachers cannot fully obtain the level that students have learned in the class. On the other hand, students cannot share their own advices on the subject with each other. In order to make teachers much understand students' performance level, developing a computerized assessment system is important to not only provide students with after-school teaching aid but also to facilitate teachers and officials to entirely track the students' learning process [4]. If there is a system which can achieve the above-mentioned purposes, students with the low-level understanding on the subject can learn more from such as a system. Therefore, such a system with the function of sharing learning feedback with each other is highly expected to make teachers save their reviewing time assisting students after class.

This paper proposes a spiral capability enhancement learning model to solve the above-mentioned problems. In this proposed model, the steps about how to use the developed system for students are as follows: Students (1) select the subject that they studies, (2) review themselves what they are able to do or what they understands, (3) and input their advices via the learning system to be able to share with other students. After that, the developed system shows students' learning level which have been achieved. According to the proposed model, students are able to not only review but also improve themselves through the feedback of the developed system. In this way, the involved students are capable of assisting with other students with lower maturity level and promoting their learning maturity level to the next higher one.

In this paper, the principles of Capability Maturity Model Integration (CMMI) are introduced to the SPICE [5, 6], and we called the CMMI-based spiral capability enhancement support. The main topic of this paper focuses on two SPICE applications, including human education management and information security management. Additionally, this paper also introduces the fuzzy inference mechanism to the developed system. From the simple simulation results, the proposed approach is feasible for students and teachers to understand the maturity level via the proposed CMMI-based SPICE system.

The remainder of the paper is organized as follows. Section II describes the spiral capability enhancement support system (SPICE). Section III introduces the application for human education management of SPICE system. Section IV introduces another application for the information security management of SPICE system. The simulation results of fuzzy markup language (FML) are demonstrated in Section V. Finally, conclusions are drawn in Section VI.

II. WHAT IS SPICE

A. Overview of SPICE

Fig. 1 shows the overview of the SPICE. In the model, first, a teacher analyzes the purposes of the course and divides to some circumstantial capabilities. Then he defines some maturity with them and registers to the learning system. On the other hand, a student who reviews his learning and inputs his situation with defined capabilities. At the same time, he also discloses know-how, means how he did or what he did, to the system in order to share among students. Then, the learning system judges his maturity with his inputs and defines maturity, and shows him it with what has been failed to achieve upper level and know-how given by other students. According to SPICE message, he has chance to improve himself to skill-up with these feedbacks. In this model, students repeat these three steps and can spiral up themselves

978-1-4244-7316-8/11/$26.00 ©2011 IEEE

step by step. To efficiently enhance students' maturity level, it is needed to notify them their own current learning state to make students know how to do next in order to step into the next maturity level. Therefore, in this section, based on our previous work [5], the CMMI-based SPICE is introduced.

CMMI is an evaluating process method for software developing organizations [1]. It is specialized in software developing process, and currently it has been used in various fields, including national projects [2], corporate governance, and security policy. Table I shows the maturity level of CMMI is quantified with five levels. According to the definition of five maturity levels of CMMI, organizations can realize what is needed to further improve the organizational maturity. By introducing these five maturity levels to the CMMI-based SPICE, the students can promote their learning maturity level by following the defined maturity levels. The CMMI-based SPICE is an improved version of SPICE and it is easy to customize evaluation items and questions.

TABLE I. MATURITY LEVEL IN CMMI

Maturity	Stage meaning
1	Initial
2	Managed
3	Defined
4	Quantitatively Managed
5	Optimizing

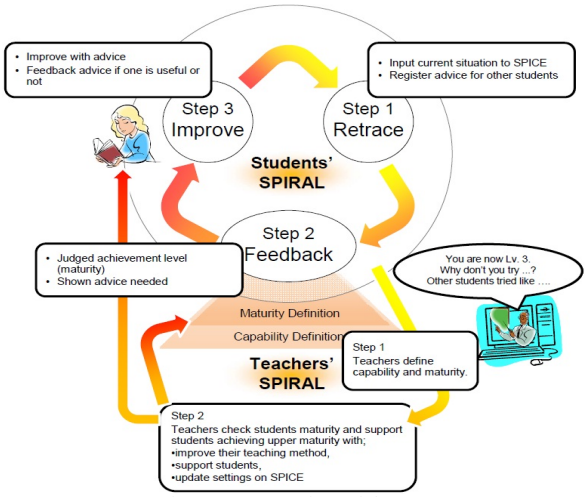

Figure 1. Overview of the SPICE.

B. *Structure of SPICE*

The SPICE is developed based on the maturity model of the knowledge management engineering, which is shown in Fig. 3. It operates as follows: (1) The manager extracts, defines, classifies, and then systemizes the process in order to further define the knowledge base for each application domain; (2) The defined and classified data are stored into the maturity model knowledge base to make manager acquire them; (3) The organizations and users can supervise and evaluate the current process of the activities via the system, and then stored the current activities' situation into the organization present condition management database; (4) The system also can diagnose the users' learning maturity level and how to promote to the next level, and then the diagnosis is stored into the practice know-how advice base. With the help of the SPICE, the manager and staff of the organizations can understand their own learning maturity level.

Take Fig. 2 for an example to describe the system. It is the system's screenshot to describe that there are two subjects, including human education and information security. In this figure, it indicates that the system can provide the taking-course students' list, analysis of the students' learning, and the learning maturity level of the students for the teachers.

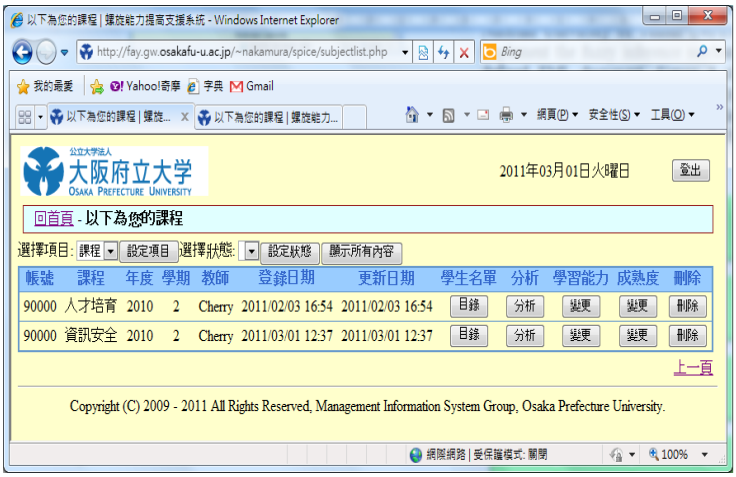

Figure 2. Screeshot showing teachers' courses.

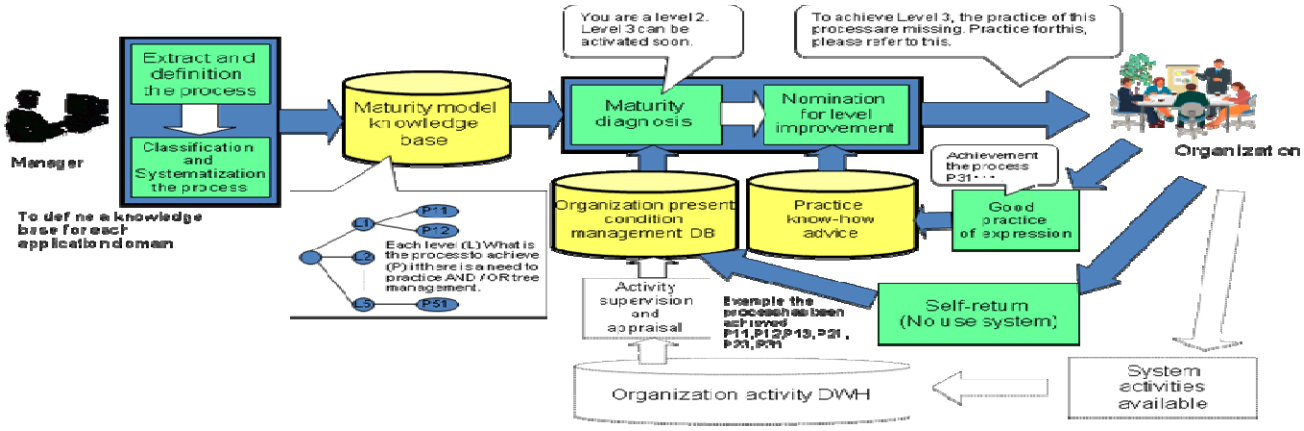

Figure 3. Process of developing the SPICE.

III. APPLICATION FOR HUMAN EDUCATION MANAGEMENT

A. Goal

The present education system should not only achieve the goal of education but also promote students' themselves study. It is necessary to clarify the achieving goal and then further attain the pre-defined goal. Therefore, five definitions of the subject human education, including technical capabilities, leadership, autonomy, cooperativeness, and responsibility, are defined in the SPICE system. With these definitions provided by the system, the teachers and students can continuously learn and share achieved goal. It is hoped that the proposed system will make as a reference for other education units in the future.

B. CMMI-based Human Education Definitions

In this application domain, according to the principles of CMMI [1], five definitions for the human education, including technical capability, leadership, autonomy, cooperativeness, and responsibility, from level 1 to level 5 are set up. Table II lists the detailed information of each definition for each level.

Following the five capability lists, we define five levels for each capability, for instance, in the technical capabilities: (L1) new technology is studied; (L2) one or more new technology is studied; (L3) new technology can by guided to others; (L4) the technology which represents the company has been developed; (L5) it continues to develop the new technology which represents the company.

Defining maturity levels as mentioned above enables teachers to understand the students learn capability and how many students on the level. Following the capability list that we define in human education subject, the students are easy to know how to achieve the level and how to step up. In addition, it is possible to refer other high-level student's advice to enhance the learn capability, the student can share knowledge with each other. Until now, we have already proposed 50 advices of human education subject. The other hand, teacher can reduce the time to educate student after school. Example interfaces are shown in Figure 4 and Figure 5.

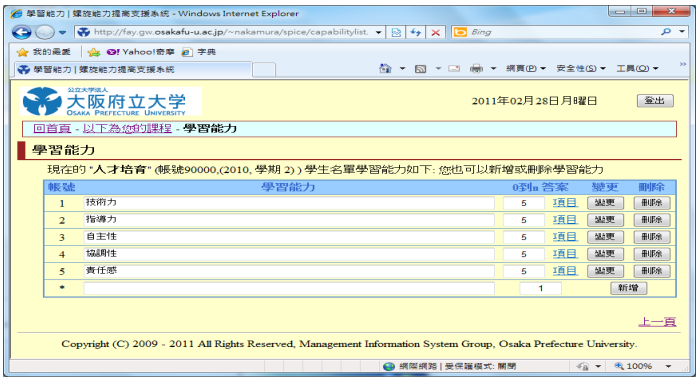

Figure 4. Form for defining questions to evaluate human education.

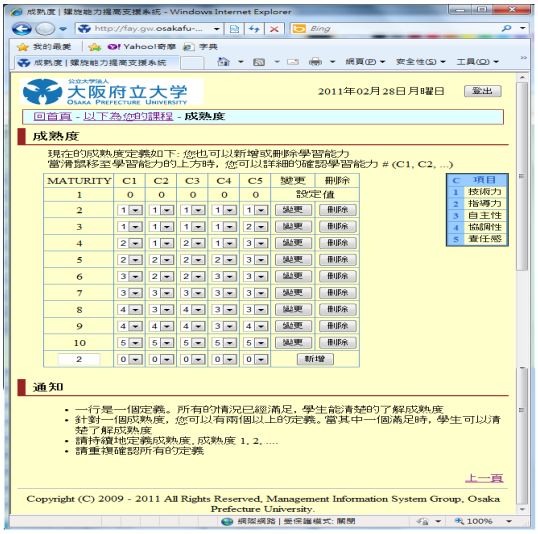

Figure 5. Form for defining maturity of human education.

We also set up the ten maturities for the subject. *Maturity 1* means that students do not register the subject, so each capability value is 0. When students register the subject, they can input their learn capability and advice how they achieve to next level, that can be the advice to other students.

TABLE II. EXAMPLE OF MATURITY MODEL: HUMAN EDUCATION

Level	Technical Capabilities	Leadership	Autonomy	Cooperativeness	Responsibility
L5	The new technologies have been continuously developed by the people in the organizations.	The guided people in the organization could become one truly leader.	The people in the organization could train their employees to have the autonomy in the organization.	The imitation person it negotiates, can adjust work	The action which is responsibility social natural environment is taken
L4	The new technologies have been developed by the people in the organizations.	The guided people in the organization could propose to organize one new team and recombine the teams.	The people in the organization could check the risk of the organization in advance and take all of the possible measures.	Can do the adjustment of work also the company internal some post	The internal policy of company, it plans the conduct which is responsibility, it is possible to execute
L3	New technologies could be guided other involved people in the organizations.	The guided people in the organization could become the leadership of other more than two teams.	The people in the organization could negotiate with the people in other organizations and plan a new proposal.	You can adjust work between the team	It is possible to carry out responsibility of the team
L2	One or more new technologies are studied by the people in the organizations.	The guided people in the organization could become a leader of their own teams.	The people in the organization could set the goal to evaluate themselves each half of year.	It can adjust work inside the team	It has responsibility for own speech
L1	New technology is studied by the people in the organizations.	The people in the organization are under the guided stage.	The people in the organization could accomplish the delivered jobs automatically.	The people in the organization could finish the assigned jobs under guidance.	Still, it is rearing stage

IV. APPLICATION FOR INFORMATION SECURITY MANAGEMENT

A. Goal

Information security has gradually become one of the most important factors in the current organizations. If the internal and external information of the organizations can work well and effectively, it will enhance the whole organizations' information security to increase the organizations' work efficiency and employees' work performance [10].

Defining some capability for information security subject of SPICE system, we hope that the paper's performance will make as a reference case for other administrative units to introduce the information security in the future.

B. CMMI-based Security Management Definition

As example, we set up five maturity levels and seven capability list in information security subject shown in Table III. The basic idea is referred from Capability Maturity Model Integration (CMMI) for software developing organization [1] is an evaluating method of progress.

We set up seven capability lists for the maturity model, such as information security, personal information, data encryption, data backup, idle machinery, antivirus software, and private information. Following the seven capability list, we define five levels for each capability, for instance, in the information security: (L1) organizations don't have any information security, (L2) organization conclude the information security, but never to implement, (L3) organization conclude the information security and to implement, (L4) organization conclude the information security by themselves, and regularly to self-criticism, (L5) provide other organization to instruct the information security. Until now, we have already collected 70 advices of information security subject.

The SPICE system interfaces of information security subject are shown in Figure 6 and Figure 7.

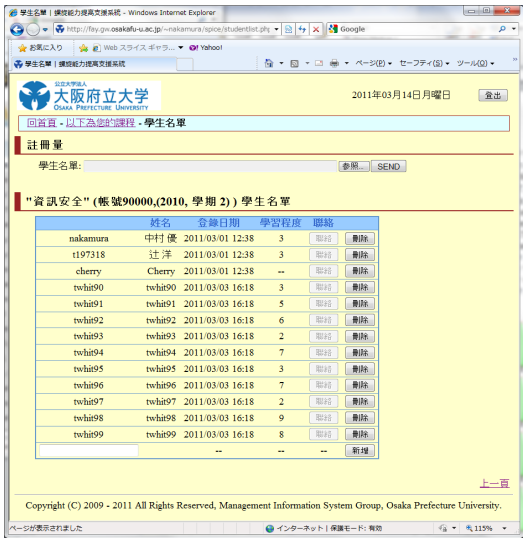

Figure 6. Form for student list of information security.

Figure 7. Form for subject analysis of information security.

TABLE III. EXAMPLE OF MATURITY MODEL: INFORMATION SECURITUY

Level	Information Security	Personal Information	Data Encryption	Data Backup	Idle Machinery	Antivirus Software	Private Information
L5	Provide other organization to instruct the information security	The computer is automaticity to turn off, when leave the computer for a long time	Use SSL(Secure Sockets Layer) to data encryption, and turn off computer when leave the seat	Regularly copy the date into CD	Don't have any idle machinery of company	Keep on the best condition everyday	Data Encryption the private information
L4	Organization conclude the information security by themselves, and regularly to self-criticism	The password is not easy to guess(Not name, birthday, phone, number plate)	Use SSL(Secure Sockets Layer) to data encryption	Regularly data backup of memory, USB drive and hard discs	Before sell and recycle, the data already delete of the idle machinery	Drawing off the web line immediately, when the computer is poisoned, and delete it	Never send the private information by e-mail
L3	Organization conclude the information security and to implement	The employee autonomy and regularly to change the password	Before mail, any information are encryption	The employee autonomy to data backup	Follow the regulation to sell and recycle the idle machinery	Buy the antivirus software to set up	Never open the private information on public computer
L2	Organization conclude the information security, but never to implement	The boss required to change the password	Mail the personal information are encryption	The boss required to data backup	Sell and recycle the idle machinery	Set up the antivirus software from internet	Security to store up the private information
L1	Organizations don't have any information security	Never change personal password	Mail the information that no be encryption	Never data backup	No properly to deal with the idle machinery	No antivirus software to set up of computer	No security to store up the private information

V. FUTURE PERSPECTIVE BASED ON FUZZY MARKUP LANGUAGE

As future perspective, let us combine our previous fuzzy inference model with FML to describe the knowledge base and rule base of the Spiral Capability Enhancement Support System. Figure 8 shows the structure for Human Education of the Spiral Capability Enhancement Support System.

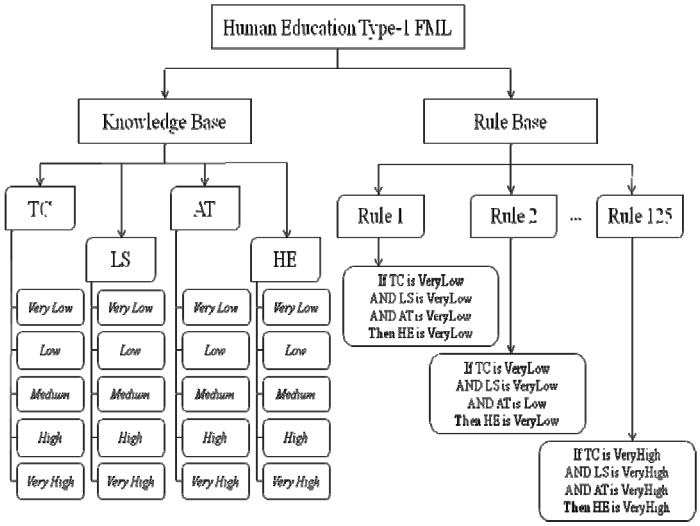

Figure 8. Membership functions of the fuzzy variables TC, LS, AT, and HE.

FML is a fuzzy-based markup language that manages fuzzy concepts, fuzzy rules, and a fuzzy inference engine [3, 8, 9].

There are three input fuzzy variables Technical Capabilities (TC), Leadership (LS), and Autonomy (AT) as well as one output fuzzy variable Human Education (HE) defined for the fuzzy reasoning mechanism. For fuzzy variable TC, LS, AT and HE, there are five linguistic terms are defined, including VeryLow, Low, Medium, High and VeryHigh. The brief descriptions of TC, LS, AT and HE are mentioned as follows:

- *TC:* The Technical Capabilities of company that develops new technology.
- *LS*: Leadership capabilities of team, including responsibility.
- *AT*: To accomplish the schedule of team, including negotiation with other company.
- *HE*: It represents the term relation strength. Based on the values of the *TC*, *LS*, and *AT*. *HE* is the inferred term relation strength of the term pair.

Herein, a FML editor, developed by the Ontology Application & Software Engineering (OASE) Laboratory, National University of Tainan (NUTN), Taiwan, will be used to implement the fuzzy inference mechanism based on the pre-defined FML document. Figure 9 shows the example membership functions of the fuzzy variables TC, LS, AT and HE. Figure 10 shows the structure of the adopted rule-based fuzzy inference mechanism. Table IV lists the adopted fuzzy rules.

Figure 9. Membership functions of the fuzzy variables TC, LS, AT, and HE.

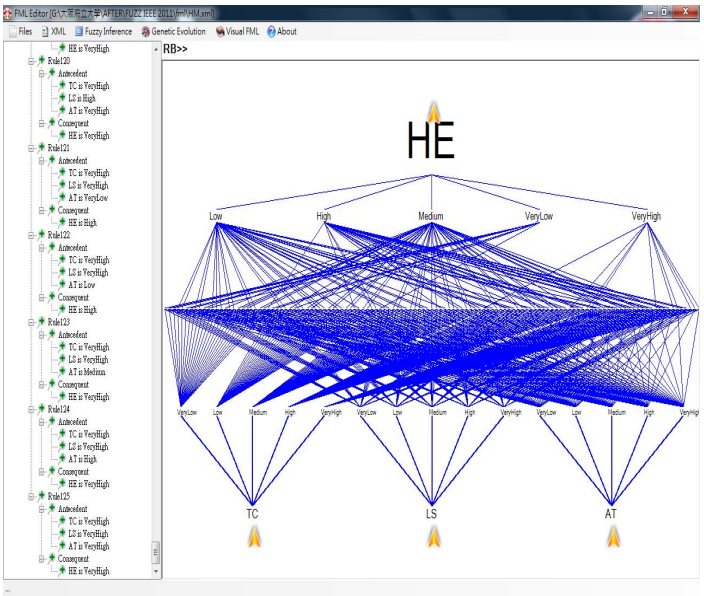

Figure 10. Structure of the adopted rule-based fuzzy inference mechanism.

TABLE IV. ADOPTED FUZZY RULES

Rule No	Fuzzy Variable				Rule No	Fuzzy Variable			
	TC	LS	AT	HE		TC	LS	AT	HE
1	VL	VL	VL	VL	69	M	H	H	H
2	VL	VL	L	VL	70	M	H	VH	H
3	VL	VL	M	VL			…		
4	VL	VL	H	L	96	H	VH	VL	M
5	VL	VL	VH	L	97	H	VH	L	H
		…			98	H	VH	M	H
36	L	M	VL	L	99	H	VH	H	VH
37	L	M	L	L	100	H	VH	VH	VH
38	L	M	M	L			…		
39	L	M	H	M	121	VH	VH	VL	H
40	L	M	VH	M	122	VH	VH	L	H
		…			123	VH	VH	M	VH
66	M	H	VL	L	124	VH	VH	H	VH
67	M	H	L	M	125	VH	VH	VH	VH
68	M	H	M	M					

VL: VeryLow, L: Low, M: Medium, H: High, VH: VeryHigh

VI. CONCLUSION

In this paper, a CMM-based E-Learning system has been proposed and applied spiral capability enhancement learning model as a new learning model. In this model, a student has chance to review himself what or how he learned, to get feedbacks from the learning system, and to improve himself with these feedbacks to enhance his capability. At the same time, a teacher is allowed to check students' achievement level and can ameliorate a way to teach.

This paper proposes the fuzzy markup language (FML) to apply to apply to human education and information security. In the future, we hope to refer the method of expert to define the genetic fuzzy markup language (GFML), and to devise the distinct rules that refer to other organizations.

ACKNOWLEDGMENT

The authors would like to thank the involved classmate of Osaka Prefecture University (OPU) and National University of Tainan (NUTN) for their joining this research project. The authors also would like to thank the National Science Council of Taiwan for financially supporting this international NSC99-2622-E-024-003-CC3.

REFERENCES

[1] M. B. Chrissis, M. Konrad and S. Shrum: "CMMI for Development, Version 1.2" http://www.sei.cmu.edu/cmmi/ tools/dev/download.cfm (Accessed on Mar 14, 2011)

[2] M. Sakoda, Y. Wada, H. Tsuji and K. Seta: "Social Network Service with Maturity Level for Science Teachers", Proc. of IEEE International Conference on Systems, Man and Cybernetics, pp. 1718–1723, Texas, USA, 2009.

[3] G. Acampora and V. Loia, "Fuzzy Control Interoperability and Scalability for Adaptive Domotic Framework," IEEE Transactions on Industrial Informatics, vol. 1, no. 2, pp. 97–111, 2005.

[4] M. H. Wang, Z. R. Yan, C. S. Lee, P. H. Hung, Y. L. Kuo, H. M. Wang, and B. H. Lin, "Apply fuzzy ontology to CMMI-based ASAP assessment system, " 2010 IEEE World Congress on Computational Intelligence (IEEE WCCI 2010), Barcelona, Spain, Jul. pp. 18-23, 2010.

[5] Y. Nakamura and H. Tsuji: "Spiral Capability Enhancement Support System". Aware Computing (ISAC), 2010 2nd International Symposium on Aware Computing(ISAC 2010), Tainan,Taiwan Nov. pp. 233-238, 2010.

[6] Y. Nakamura, H. Tsuji and Y. Majima: "General Purpose E-Learning Engine Based on Capability Maturity Model Integration and SECI Model" Japan-Cambodia Joint Symposium on Information Systems and Communication Technology(JCAICT 2011), pp. 121-122, 2011.

[7] C. S. Lee, M. H. Wang, and J. J. Chen, "Ontology-based Intelligent Decision Support Agent for CMMI Project Monitoring and Control, " International Journal of Approximate Reasoning, vol. 48, no. 1, PP. 62-76, 2008.

[8] C. S. Lee, M. H. Wang, G. Acampora, C. Y. Hsu, and H. Hagras, "Diet assessment based on type-2 fuzzy ontology and fuzzy markup language," International Journal of Intelligent System, vol. 25, no. 12, pp. 1187-1216, Dec. 2010.

[9] C. S. Lee, M. H. Wang, S. J. Yen, Y. J. Chen, C. W. Chou, G. Chaslot, J. B. Hoock, A. Rimmel, and H. Doghmen, "An ontology-based fuzzy inference system for computer Go applications," (SCIE) International Journal of Fuzzy Systems, vol. 12, no. 2, pp. 103-115, Jun. 2010.

[10] C. S. Lee, Y. L. Kuo, Y. L. Wang, H. T. Liang, Y. W. Lin, Y. L. Chen, M. H. Wang, and M. Y. Ju, "A Study on CMMI-Based Information Security Management System" Journal of National University of Tainan, vol. 44, no. 2, pp. 61-88, Oct. 2010.

2011 IEEE International Conference on Fuzzy Systems
June 27-30, 2011, Taipei, Taiwan

Medical Care System Evaluation Based On DEA Of Prefectures In Japan

Kenji Fukuoka
Department of Computer Science and Intelligent Systems
Osaka Prefecture University
Osaka, Japan
fukuoka@mis.cs.osakafu-u.ac.jp

Shingo Aoki
Department of Computer Science and Intelligent Systems
Osaka Prefecture University
Osaka, Japan
aoki@cs.osakafu-u.ac.jp

Yukie Majima
Faculty of Liberal Arts and Science
Osaka Prefecture University
Osaka, Japan
majima@las.osakafu-u.ac.jp

***Abstract*— In order to reveal disparity and its cause in medical care among Japanese prefectures, this paper describes how DEA works as follows: (1) DEA/BCC model estimates the disparity between prefectures, (2) "RM-DEA using Cone-Ratio approach" estimates the cause of the disparity, and (3) Improved MF-DEA (Multi-Frontier based DEA) model estimates the disparity between eastern and western Japan. This paper also illustrates three numerical experiments.**

Keywords; Data Envelopment Analysis, Medical Service.

I. INTRODUCTION

Nowadays the shortage of medical employees connects with the regional and medical disparity, and it becomes a bigger problem. Especially the shortage of medical doctor is reported by Ministry of Health [1], and that of nurse is done by Japan Medical Association [2]. As these countermeasures, the analysis is done in Japan Medical Association Research Institute [3] (JMARI), and the committee relating to the medical employees is held also by the organization in the Japan[4]. Thus, the concern about the shortage of medical employees is higher and higher.

However, not only the number of employees but also the enhancement of equipment is critical to offer the better medical service. Therefore, the above-mentioned evaluation by only employee's data is insufficient in order to consider "anytime, anywhere, anyone, equally [5]" which is the medical ideal in Japan. And the regional and medical disparity should be considered by data including employees' and equipment's information. There is a similar analysis in JMAR, while the analysis is not carried out by the overall evaluation used multiple data items, and which item is prime cause of the disparity is not investigated. Then this paper intends to examine these disparity and its cause by using the multiple data, the number of medical employees and that of medical equipment. In this case, a relative evaluation method corresponding to the multiple inputs and outputs is necessary.

Recent years, in order to examine the efficiency of medical and other public services, a nonparametric method, Data Envelopment Analysis (DEA), is often used [5]. DEA is a method that can relatively compare ratios of the input and the output. This relative comparison and the comparative evaluation are basis in DEA.

Then the purpose of this paper is to evaluate the medical care system of prefecture in Japan and to reveal the regional and medical disparity by BCC (Banker-Charnes-Cooper) model. And "Restricted Multipliers DEA model using Cone-Ratio approach (RM-DEA) [6]" is applied in order to find out the weakness and the strength of prefecture. In addition, the medical disparity between western and eastern Japan is examined by the improved Multi-Frontier based DEA (MF-DEA) [7].

II. THE PROBLEM OF MEDICAL CARE SYSTEM EVALUATION IN CONVENSIONAL METHOD

Medical care system is evaluated by one ratio in a lot of researches. And most researches use the ratio to the number of patients. Hereafter, this method is regarded as the conventional method. Now, there are the following six data items: the number of doctors, nurses, high priced medical equipment, beds, ICU beds, and hospitals in inhabitable area (Hospital density). Then doctor and nurse items indicate medical employees. Bed, ICU bed, and high priced medical equipment item indicate equipment. The data item of hospital density shows geographical factor. For example, this factor indicates time to go to hospital. Here, prefectures can be evaluated in each data compared with the ratio value.

TABLE I. EXAMPLE:THE RATIO OF EACH ITEM

Prefecture	Ratio value per 100,000 patients		
	Doctor	Nurse	Bed
Hokkaido	208.8	947.4	1830.7
Aomori	150.2	709.2	1286.6
Iwate	185.2	735.1	1382.3
Miyagi	190.8	661.1	1162.1
Akita	187.6	728.7	1394.1
Yamagata	179.2	718.6	1161.1
:	:	:	:

However, there is not evaluation reached by all six items. Medical service can not be evaluated by one data item such as the number of doctors. The number of the doctors and nurses may be the most important in the hospital management but no medical employees can work in the place where there are no

978-1-4244-7316-8/11/$26.00 ©2011 IEEE

medical facilities. Conversely, even if there are some medical employees, a necessary medical service cannot be offered without the necessary equipment. Therefore, medical service should be evaluated by multiple data items which show the number of medical employees and the enhancement of medical facilities equipment.

TABLE II. DATA SET

Data items	Data sources
The number of doctors	Hospital Report
The number of nurses	Hospital Report
The number of expensive equipments	Survey of Medical Institutions
The number of beds	Survey of Medical Institutions
The number of Icu beds	Survey of Medical Institutions
The number of hospitals	Survey of Medical Institutions
Inhabitable area	Social life statistics index
The numberof patients	Survey of Medical Institutions

III. OUTLINE OF DATA ENVELOPMENT ANALYSIS

DEA was proposed by A. Charnes et al. in 1978 as a method for management analysis. It is applied in various fields such as data mining, prospect for bankruptcy or so.

Evaluated objects, namely DMUs (Decision Making Units) are hospital, bank, electricity company or prefecture, for example. And each DMU is characterized by multi-inputs and multi-outputs. Then DMU which have smaller inputs and larger outputs is regarded as more efficient. Management efficiency is evaluated by efficiency value. Then efficient DMU has efficiency value as 1, inefficient DMU has it as less than 1. Efficiency value is calculated based on line called efficiency frontier which is formed by efficient DMUs [8, 9].

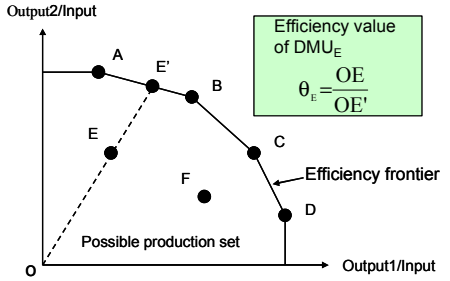

Fig. 1. Efficiency frontier and efficiency value of DMU_E

Here, Fig. 1 is prepared to signify how to evaluate DMU. Each axis indicates outputs divided by input. Therefore, DMU which is far from origin is more efficient. Four $DMU_{A,B,C,D}$ have no difference of superiority or inferiority, and they are equally efficient. The efficient frontier is formed with these efficient DMUs. Moreover, four $DMU_{A,B,C,D}$ get efficiency value 1 since they are located on the efficiency frontier. And other DMU $DMU_{E,F}$ is judged to be inefficient, their efficiency values are calculated at ratio of distance to the efficient frontier. As an example, the way to calculate the efficiency value of inefficient DMU_E is described. This time, the efficiency value of DMU_E is calculated by distance to efficiency frontier. In a word, the efficiency value is calculated from OE / OE' by ratio of the distance from origin to Point E' and origin to point E. Here, E' shows ideal state that DMU_E can reach by improvement of production activity.

IV. ANALYSIS METHODS

A. BCC Model

There are some models in DEA as the analytic model. And there are two analytic types called input-oriented type and output-oriented type. Here, output-oriented BCC model is explained since it is utilized in this paper. BCC model assumes the harvest variable of the scale. Moreover, the output-oriented type premises the current input, and obtains maximum output which is expected.

Assuming that there are *n DMUs* (DMU_1, DMU_2, ..., DMU_k, ..., DMU_n), and DMU_k is characterized by *m* inputs and *s* outputs. Then DMU_k has input expressed as $x_{1k},\ldots,x_{mk}$ and output expressed as $y_{1k},\ldots, y_{sk}$. Here the efficiency value is shown by calculating following linear algorithm.

$$\begin{aligned} \max \quad & \theta_k \\ s.t. \quad & \sum_{j=1}^{n} x_{ij}\lambda_{jk} \le x_{ik} \qquad (i = 1,2,\ldots, m) \\ & -\sum_{j=1}^{n} y_{rj}\lambda_{jk} + \theta_k y_{rk} \le 0 \quad (r = 1,2,\ldots, s) \\ & \sum_{j=1}^{n} \lambda_{jk} = 1 \\ & \lambda_{jk} \ge 0 \ , \ \theta : free \ , \ j = 1,2,\ldots, n \end{aligned}$$

About the optimal solution θ_k^* calculated by the formula (1), there is $\theta_k^* \ge 1$ and an efficiency value is expressed as $1/\theta_k^*$ at this time. When $1/\theta_k^* = 1$, DMU_k is evaluated to be efficient. And when $\theta_k^* \le 1$, DMU_k is evaluated to be inefficient.

B. RM-DEA model using Cone-Ratio approach

RM-DEA limits input and output items in an evaluation axis by restricting the variable weights, then the method can include subjective information. However, this method has the problem that the optimal solution cannot be obtained when the restricting condition is strong.

Therfore, in order to avoid this problem in the previous study, the evaluation method which gives distortion in the search direction by using a valuing level $0<\alpha_r \le 1$ (r=1,2;·;s) is proposed.

At this time, the formula is shown below. And α_r is any number decided by the evaluator and shows valuing level to the *r*-th output item.

$$\begin{aligned} \max \quad & \theta_k \\ s.t. \quad & \sum_{j=1}^{n} x_{ij}\lambda_{jk} \le x_{ik} \qquad (i = 1,2,\ldots, m) \\ & -\sum_{j=1}^{n} \frac{1}{\alpha_r} y_{rj}\lambda_{jk} + \theta_k y_{rk} \le 0 \quad (r = 1,2,\ldots, s) \\ & \sum_{j=1}^{n} \lambda_{jk} = 1 \\ & \lambda_{jk} \ge 0 \ , \ \theta : free \ , \ j = 1,2,\ldots, n \end{aligned}$$

The *r*-th output item is evaluated most at $\alpha_r = 1$, and the more α_r approaches *0*, the more the *r*-th output item is disregarded. Therefore, the efficiency value can be calculated when α of the item that the evaluator wants to value is set as 1 and α of other items is set as any value in the range of *0* and *1*. As a result in the previous study, the items which are the strength and weakness in DMU are able to be found by the change of the efficiency value when valuing level of the item is changed.

Next, Above-mentioned way to find is concretely explained by using 5 as sample data. When valuing level is given to the output item y_3, Table 3 shows the results. And the strength and weakness of each DMU are found.

TABLE III. RESULT IN VALUING Y_3

DMU	Efficiency value			
	α=1.0	α=0.8	α=0.5	α=0.3
1	0.86	0.73	0.70	0.70
2	0.92	0.74	0.46	0.39
3	1.00	0.95	0.91	0.91
4	1.00	1.00	1.00	1.00
5	1.00	0.94	0.93	0.93

Table 3 shows efficiency value when the valuing level of y_3 is set to 1, and the valuing level of other output items is set as 1, 0.8, 0.5, and 0.3. At this time the valuing level of the output item other than y_3 is α in this table.

In Table 3, DMU_4 did not show a decrease in the efficiency value even if the valuing level of the output item other than y_3 becomes small. The output item y_3 is the strength of DMU_4.

On the other hand, DMU_2 show a great decrease in the efficiency value, when the valuing level of the output item other than y_3 becomes small. Therefore, the output item y_3 is the extreme weakness of DMU_2.

Thus this paper finds out the strong and weak items in each prefecture by the change of the efficiency value when valuing level of the item is changed.

C. *Improved MF-DEA*

The previous study proposed MF-DEA which assigns frontier to each group, and gathering evaluation based on each frontier leads to multi-evaluation. Moreover, position in the group or relation with other groups can be considered if multiple efficiency values are compared. Fig. 2 shows the frontier formed by MF-DEA in the case of two groups.

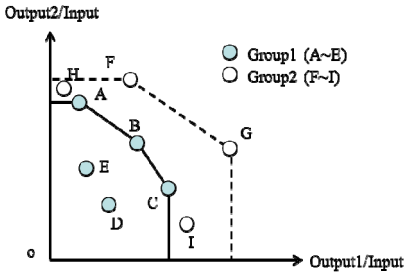

Fig. 2. Frontier formed by MF-DEA

Next, the formula of MF-DEA is described. There are *p* groups here. Group1 consists of α DMUs chosen optionally, group2 consists of β DMUs chosen optionally, and group p consists of γ DMUs.

$$\min \quad \theta_k$$

$$s.t. \quad \theta_k x_{ik} \geq \sum_{a=1}^{\alpha} x_{ia}\lambda_a^1 + \sum_{b=1}^{\beta} x_{ib}\lambda_b^2 + \cdots + \sum_{p=1}^{\gamma} x_{ip}\lambda_p^p \qquad (i = 1,2,\ldots,m)$$

$$y_{rk} \leq \sum_{a=1}^{\alpha} y_{ra}\lambda_a^1 + \sum_{b=1}^{\beta} y_{rb}\lambda_b^2 + \cdots + \sum_{p=1}^{\gamma} y_{rp}\lambda_p^p \qquad (r = 1,2,\ldots,s)$$

$$\theta_k = \theta_k^1 + \theta_k^2 + \cdots + \theta_k^p$$

$$\theta_k^a x_{ik} \geq \sum_{a=1}^{\alpha} x_{ia}\lambda_a^1 \qquad \theta_k^b x_{ik} \geq \sum_{b=1}^{\beta} x_{ib}\lambda_b^2 \qquad \cdots \qquad \theta_k^p x_{ik} \geq \sum_{p=1}^{\gamma} x_{ip}\lambda_p^p$$

$$y_{rk} \leq \sum_{a=1}^{\alpha} y_{ra}\lambda_a^1 \qquad y_{rk} \leq \sum_{b=1}^{\beta} y_{rb}\lambda_b^2 \qquad \cdots \qquad y_{rk} \leq \sum_{p=1}^{\gamma} y_{rp}\lambda_p^p$$

$$\sum_{a=1}^{\alpha} \lambda_a^1 = \sum_{b=1}^{\beta} \lambda_b^2 = \quad \cdots \quad = \sum_{p=1}^{\gamma} \lambda_p^p = 1$$

$$\theta \ : \ free \qquad \lambda_a^1 \geq 0 \qquad \lambda_b^2 \geq 0 \qquad \cdots \qquad \lambda_p^p \geq 0$$

Here, θ_k^p indicates efficiency value based on group *p*, and then DMU_k is evaluated from *p* viewpoints. Objective function θ_k which is sum of the efficiency value based on each viewpoint does not have any particular meaning. Here, efficiency value based on each group is shown in Table 4 by 9 DMUs data in Fig. 2.

TABLE IV. RESULT IN MF-DEA

Group	DMU	Efficiency value based on each frontier	
		Group1	Group2
1	A	1	0.85
	B	1	0.8
	C	1	0.7
	D	0.55	0.4
	E	0.7	0.45
2	F	1.2	1
	G	1.3	1
	H	1.05	0.9
	I	1.1	0.7

Then all group1's efficiency value based on group2 and all group2's efficiency value based on group1 are remarkable. The former values are less than 1 and the latter values are over 1. This means that DMUs in group1 exists outside the frontier of group 2 and DMUs in group2 exists inside the frontier of group1. In other words, the frontier of group2 covers that of group1. The relation between frontiers can also be considered by an efficiency value in Table 4. When the former and latter values are various, they have relation as union of set. This means that these frontiers cross.

However, relation between frontiers cannot completely be considered by efficiency values. As an example, there are six DMUs which have one input and two outputs. And Table 5 shows the result. Then, all group1's efficiency value based on group2 and all group2's efficiency value based on group1 are remarkable. Because the former and latter values are various, they have relation as union of set. Therefore these frontiers cross. However, the figure cannot be uniquely determined because there are two possible cases shown in Fig. 3 and Fig. 4.

The relation between frontiers can be almost considered by only efficiency values of efficient DMUs in belonging group. However, in the case of Table 5, the relation between frontiers cannot be uniquely determined due to different interpretations on inefficient DMU_D.

TABLE V. EXAMPLE:RESULT IN MF-DEA

Group	DMU	Efficiency value based	
		Group1	Group2
1	A	1	1.1
	B	1	1.25
	C	1	1.5
	D	0.6	0.8
2	E	1.2	1
	F	1.3	1

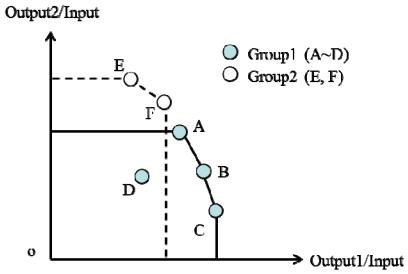

Fig. 3. Case1

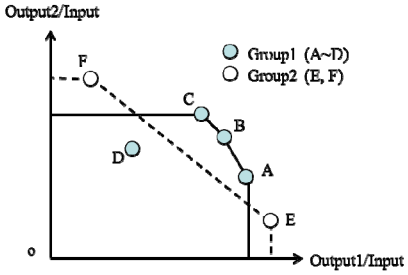

Fig. 4. Case2

Then, this paper pushes up inefficient DMUs to the frontier of its own group intentionally in order to solve this problem. Now, DMU_D moves to the frontier and then the arrival point is regarded as point D'. Here, the correction data is shown below. θ_k^* is the optimal solution calculated by BCC model.

$$x_{ik}^{+} = x_{ik} \qquad (i = 1,2,..m)$$
$$y_{rk}^{+} = \theta_k^* y_{rk} \quad (r = 1,2,..s)$$

And when MF-DEA is applied to these correction data in Fig. 5, Table 6 shows the result. Hereafter, improved MF-DEA indicates what MF-DEA is applied to these correction data.

$DMU_{D'}$'s efficiency value based on group2 is remarkable, and then this value is more than 1. $DMU_{D'}$ in group 1 exists outside the frontier of group2. Therefore the relation between frontiers is shown as Fig. 5. Finally, the figure can be uniquely determined from Table 5.

TABLE VI. EXAMPLE:RESULT IN IMPROVED MF-DEA

Group	DMU	Efficiency value based	
		Group1	Group2
1	A	1	1.1
	B	1	1.25
	C	1	1.5
	D'	1	1.2
2	E	1.2	1
	F	1.3	1

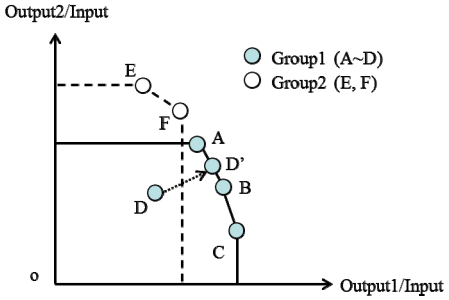

Fig. 5. Relation between frontiers in TABLE V

Thus this paper examines the relation between frontiers by using improved MF-DEA. This time position in the group is not considered. The frontier is regarded as the characteristics of its own group, and the difference between groups is described from the relation.

V. NUMERICAL EXPERIMENTS

A. Experimental conditions

Then this paper evaluates the medical care system by the following three experiments:

I. Experiment1 evaluates the medical care system based on the efficiency value, which is calculated by DEA. This time, BCC model is applied in order to notice output items. Finally, the result in this experiment compares with that in the conventional method.

II. "RM-DEA using Cone-Ratio approach" is able to find out data items which show strength and weakness. For that, there are the following three patterns in the previous study:

a) The valuing level α of one output item is set as 1, and those of other output items are set as 0.8.

b) The valuing level α of one output item is set as 1, and those of other output items are set as 0.5.

c) The valuing level α of one output item is set as 1, and those of other output items are set as 0.3.

Experiment2 applies these patterns to every six output items and especially examines the cause of medical disparity. Here, the cause indicates data items which show the weakness of prefecture. conventional method.

III. Experiment3 makes the analysis by improved MF-DEA in order to examine medical disparity between two big regions named western and eastern Japan. Eastern Japan has total 18 prefectures including Hokkaido, Tohoku region, Kanto region and four prefectures (Niigata, Yamanashi, Nagano and Shizuoka). Western Japan has 29 prefectures of the rest. Moreover, the result in MF-DEA is not placed due to the limitation of the page space. Therefore, the comparison between the result in MF-DEA and improved MF-DEA is performed in this paper.

B. Experimental data

Data set (Table 2) in II is used. The number of DMUs is forty-seven, and each DMU has the following two inputs and six outputs:

◆Inputs

Input1 : The number of patients

Input2 : The amount of investment

◆Output

Output1 : The number of doctors

Output2 : The number of nurses

Output3 : The number of expensive equipment

Output4 : The number of beds

Output5 : The number of ICU beds

Output6 : Hospital density.

C. Experimental Result

1) Experiment 1

Table 7 shows the result in BCC model and the conventional method. Here, "The ranking of rate per 100,000 patients" indicates the results in the conventional method, and the value indicates ranking in each item. Then "score" indicates the efficiency value in BCC model, "rank" indicates the ranking in "score".

TABLE VII. RESULT IN EXPERIMENT1

DMU	Ranking of rate value per 100,000 patients						BCC model	
	Doctor	Nurse	Bed	ICU	Equip	Density	score	rank
Hokkaido	25	8	4	9	6	47	1.000	1
Aomori	47	32	30	22	20	42	0.779	45
Iwate	43	27	25	45	12	42	0.850	35
Miyagi	39	39	38	10	30	39	0.795	43
Akita	41	28	24	37	37	39	0.839	39
Yamagata	45	31	39	33	43	34	0.689	47
Fukushima	42	22	23	14	24	45	0.850	36
Ibaraki	30	35	28	29	16	42	0.861	32
Tochigi	18	37	34	33	28	33	0.853	34
Gunma	16	20	26	43	22	25	0.883	29
Saitama	32	45	41	27	40	32	0.826	41
Chiba	23	44	43	21	39	41	0.847	37
Tokyo	1	47	47	7	46	10	1.000	1
Kanagawa	7	46	45	12	47	15	0.942	24
Niigata	46	30	37	44	30	46	0.744	46
Toyama	20	14	11	47	6	23	0.976	20
Ishikawa	8	4	7	29	1	15	1.000	1
Fukui	22	17	16	5	8	9	1.000	1
Yamanashi	19	33	22	39	34	3	0.926	26
Nagano	21	21	33	7	19	37	0.908	28
Gifu	44	43	44	14	27	28	0.792	44
Shizuoka	26	38	32	3	26	30	0.931	25
Aichi	31	40	46	33	45	37	0.878	30
Mie	40	42	40	25	36	24	0.812	42
Shiga	13	24	36	25	44	14	0.839	38
Kyoto	3	23	20	23	35	4	1.000	1
Oosaka	5	34	35	4	41	8	1.000	1
Hyogo	24	41	42	16	41	29	0.853	33
Nara	4	25	21	37	15	1	1.000	1
Wakayama	14	36	29	18	10	5	0.970	21
Tottori	11	15	19	24	23	2	1.000	1
Shimane	9	12	15	41	37	7	0.990	19
Okayama	6	18	18	2	17	26	1.000	1
Hiroshima	35	29	31	36	32	26	0.828	40
Yamaguchi	34	13	12	40	17	20	1.000	1
Tokushima	17	16	8	18	4	6	1.000	1
Kagawa	33	26	27	10	9	10	1.000	1
Ehime	38	19	17	17	21	20	0.910	27
Kochi	12	2	1	20	2	13	1.000	1
Fukuoka	10	10	13	5	32	31	1.000	1
Saga	37	11	14	32	28	18	0.868	31
Nagasaki	27	9	9	27	24	17	0.951	22
Kumamoto	29	7	6	46	14	34	1.000	1
Oita	15	5	5	31	2	19	1.000	1
Miyazaki	35	6	10	41	11	22	0.951	23
Kagoshima	28	3	2	13	5	34	1.000	1
Okinawa	2	1	3	1	13	10	1.000	1

2) Experiment 2

Table 8 shows only the result when doctor item is given valuing level due to the limitation of the page space. Table 9 extracts "Change from BCC" in the time when each item is given valuing level. Symbol (△) indicates the increase from efficiency value at BCC, and symbol (▼) indicates decrease. And the value beside a symbol indicates the degree of the change.

TABLE VIII. RESULT IN EXPERIMENT2

DMU	BCC(α=1)		α=0.8		α=0.5		α=0.3		Change from BCC	
	score	rank	score	rank	score	rank	score	rank	±score	±rank
Hokkaido	1.000	1	0.909	18	0.779	29	0.779	29	▼0.22	▼28
Aomori	0.779	45	0.628	46	0.525	47	0.525	47	▼0.253	▼2
Iwate	0.850	35	0.730	40	0.660	42	0.660	42	▼0.189	▼7
Miyagi	0.795	43	0.724	42	0.667	40	0.667	40	▼0.128	△ 3
Akita	0.839	39	0.783	35	0.779	30	0.779	30	▼0.059	△ 9
Yamagata	0.689	47	0.628	46	0.621	45	0.621	45	▼0.068	△ 2
Fukushima	0.850	36	0.724	42	0.657	43	0.657	43	▼0.192	▼7
Ibaraki	0.861	32	0.785	34	0.712	37	0.712	37	▼0.148	▼5
Totigi	0.853	34	0.797	29	0.797	26	0.797	26	▼0.055	△ 8
Gunma	0.883	29	0.815	27	0.807	24	0.807	24	▼0.075	△ 5
Saitama	0.826	41	0.766	38	0.748	32	0.748	32	▼0.077	△ 9
Chiba	0.847	37	0.788	33	0.774	31	0.774	31	▼0.073	△ 6
Toukyou	1.000	1	1.000	1	1.000	1	1.000	1	0.000	0
Kanagawa	0.942	24	0.942	15	0.942	14	0.942	14	0.000	△ 10
Niigata	0.744	46	0.673	45	0.601	46	0.601	46	▼0.143	0
Toyama	0.976	20	0.935	16	0.921	15	0.921	15	▼0.054	△ 5
Ishikawa	1.000	1	0.972	11	0.950	11	0.950	11	▼0.049	▼10
Fukui	1.000	1	0.956	13	0.946	12	0.946	12	▼0.054	▼11
Yamanashi	0.926	26	0.877	21	0.875	18	0.875	18	▼0.05	△ 8
Nagano	0.908	28	0.828	25	0.794	27	0.794	27	▼0.113	△ 1
Gihu	0.792	44	0.695	44	0.638	44	0.638	44	▼0.153	0
Shizuoka	0.931	25	0.789	32	0.723	35	0.723	35	▼0.208	▼10
Aichi	0.878	30	0.821	26	0.821	22	0.821	22	▼0.057	△ 8
Mie	0.812	42	0.804	28	0.804	25	0.804	25	▼0.008	△ 17
Shiga	0.839	38	0.839	23	0.839	21	0.839	21	0.000	△ 17
Kyouto	1.000	1	1.000	1	1.000	1	1.000	1	0.000	0
Oosaka	1.000	1	1.000	1	1.000	1	1.000	1	0.000	0
Hyougo	0.853	33	0.793	30	0.792	28	0.792	28	▼0.061	△ 5
Nara	1.000	1	0.973	10	0.945	13	0.945	13	▼0.055	▼12
Wakayama	0.970	21	0.839	23	0.821	23	0.821	23	▼0.149	▼2
Tottori	1.000	1	1.000	1	1.000	1	1.000	1	0.000	0
Shimane	0.990	19	0.975	9	0.975	9	0.975	9	▼0.014	△ 10
Okayama	1.000	1	1.000	1	1.000	1	1.000	8	0.000	▼7
Hiroshima	0.828	40	0.726	41	0.666	41	0.666	41	▼0.162	▼1
Yamaguchi	1.000	1	0.972	11	0.966	10	0.966	10	▼0.033	▼9
Tokushima	1.000	1	0.910	17	0.886	17	0.886	17	▼0.113	▼16
Kagawa	1.000	1	1.000	1	1.000	1	1.000	1	0.000	0
Aiti	0.910	27	0.769	37	0.737	33	0.737	33	▼0.173	▼6
Kouchi	1.000	1	0.945	14	0.903	16	0.903	16	▼0.097	▼15
Fukuoka	1.000	1	1.000	1	1.000	1	1.000	1	0.000	0
Saga	0.868	31	0.747	39	0.726	34	0.726	34	▼0.141	▼3
Nagasaki	0.951	22	0.792	31	0.721	36	0.721	36	▼0.23	▼14
Kumamoto	1.000	1	0.903	19	0.863	19	0.863	19	▼0.137	▼18
Ooita	1.000	1	0.885	20	0.850	20	0.850	20	▼0.149	▼19
Miyazaki	0.951	23	0.776	36	0.709	37	0.709	37	▼0.241	▼14
Kagoshima	1.000	1	0.857	22	0.709	39	0.709	39	▼0.29	▼38
Okinawa	1.000	1	1.000	1	1.000	1	1.000	1	0.000	0

TABLE IX. CHANGE OF RANKING IN EACH ITEM

DMU	Change of ranking					
	Doctor	Nurse	Bed	ICU	Equip	Denisty
Hokkaido	▼28	0	0	▼9	0	▼35
Aomori	▼2	△ 7	△ 8	△ 18	△ 16	0
Iwate	▼7	△ 2	△ 7	▼11	△ 16	▼8
Miyagi	△ 3	△ 2	△ 1	△ 30	△ 8	△ 3
Akita	△ 9	△ 16	△ 16	△ 8	▼6	▼3
Yamagata	△ 2	△ 4	△ 1	△ 6	△ 1	0
Fukushima	▼7	△ 10	△ 13	△ 16	△ 9	▼8
Ibaraki	▼5	▼3	△ 5	△ 2	△ 8	▼6
Totigi	△ 8	▼8	▼6	▼6	▼6	▼7
Gunma	△ 5	△ 1	0	▼15	▼1	▼1
Saitama	△ 9	▼4	△ 3	△ 18	▼1	△ 10
Chiba	△ 6	▼7	▼6	△ 21	▼7	▼2
Toukyou	0	0	0	0	0	0
Kanagawa	△ 10	▼6	▼8	△ 13	▼14	△ 13
Niigata	0	△ 14	△ 2	▼1	△ 5	0
Toyama	△ 5	△ 3	△ 5	▼25	△ 5	▼5
Ishikawa	▼10	0	▼12	▼25	0	▼14
Fukui	▼11	▼14	▼10	0	0	▼9
Yamanashi	△ 8	▼5	0	▼12	▼5	△ 18
Nagano	△ 1	△ 1	▼7	△ 15	△ 5	▼9
Gihu	0	▼3	▼3	△ 23	△ 9	△ 9
Shizuoka	▼10	▼14	▼9	△ 16	▼7	▼9
Aichi	△ 8	△ 8	0	△ 6	△ 8	▼2
Mie	△ 17	△ 5	△ 6	△ 17	△ 15	△ 22
Shiga	△ 17	△ 4	▼7	△ 2	▼9	△ 21
Kyouto	0	▼24	▼20	▼21	▼25	0
Oosaka	0	0	0	0	▼13	0
Hyougo	△ 5	▼3	▼6	△ 21	▼4	△ 5
Nara	▼12	▼39	▼30	▼38	▼24	0
Wakayama	▼2	▼25	▼20	▼7	△ 3	△ 9
Tottori	0	0	0	0	0	0
Shimane	△ 10	△ 3	△ 5	▼14	▼15	△ 10
Okayama	▼7	▼19	▼19	0	▼15	▼22
Hiroshima	▼1	△ 11	△ 7	△ 3	△ 1	△ 13
Yamaguchi	▼9	0	0	▼28	▼11	▼12
Tokushima	▼16	▼22	▼18	▼14	▼10	▼6
Kagawa	0	0	0	0	0	0
Aiti	▼6	△ 6	△ 5	△ 8	△ 6	△ 8
Kouchi	▼15	0	0	▼16	0	▼15
Fukuoka	0	0	0	0	0	▼21
Saga	▼3	△ 12	△ 6	▼1	▼12	△ 13
Nagasaki	▼14	△ 4	△ 5	▼13	▼11	△ 1
Kumamoto	▼18	0	0	▼41	0	▼28
Ooita	▼19	▼12	▼11	▼33	▼9	▼23
Miyazaki	▼14	△ 9	△ 5	▼20	△ 6	▼3
Kagoshima	▼38	0	0	▼17	▼12	▼32
Okinawa	0	0	▼15	0	▼19	▼13

3) Experiment 3

The tracery in Table 10 indicates the efficiency value based on belonging group, other parts indicate the efficiency value based on each group. The marking parts (*) indicate the result in CCR model as a reference because the efficiency value is not able to be calculated by cancellation error through calculation process.

TABLE X. RESULT IN EXPERIMENT3

Group	DMU	Efficiency value based on each criterion		
		Eastern Japan	Western Japan	All Japan
Eastern Japan	Hokkaido	1.000	1.388	1.000
	Aomori	1.000	0.893	0.870
	Iwate	1.000	0.868	0.850
	Miyagi	1.000	0.936	0.906
	Akita	1.000	0.839	0.839
	Yamagata	1.000	0.878	0.876
	Fukushima	1.000	0.864	0.850
	Ibaraki	1.000	0.988	0.933
	Totigi	1.000	0.903	0.886
	Gunma	1.000	0.910	0.883
	Saitama	1.000	1.053	0.949
	Chiba	1.000	1.017	0.955
	Toukyou	1.000	1.755	1.000
	Kanagawa	1.000	0.970	0.942
	Niigata	1.000	1.030	0.947
	Yamanashi	1.000	0.926	0.926
	Nagano	1.000	0.923	0.908
	Shizuoka	1.000	0.963	0.931
Western Japan	Toyama	*1.961	1.000	1.000
	Ishikawa	*1.704	1.000	1.000
	Fukui	*1.844	1.000	1.000
	Gihu	1.185	1.000	0.995
	Aichi	1.702	1.000	1.000
	Mie	2.674	1.000	1.000
	Shiga	1.778	1.000	1.000
	Kyouto	2.936	1.000	1.000
	Oosaka	1.593	1.000	1.000
	Hyougo	1.422	1.000	1.000
	Nara	1.975	1.000	1.000
	Wakayama	2.096	1.000	1.000
	Tottori	1.754	1.000	1.000
	Shimane	*1.738	1.000	1.000
	Okayama	*2.249	1.000	1.000
	Hiroshima	1.159	1.000	1.000
	Yamaguchi	*2.505	1.000	1.000
	Tokushima	*1.938	1.000	1.000
	Kagawa	3.833	1.000	1.000
	Aiti	2.063	1.000	1.000
	Kouchi	*1.505	1.000	1.000
	Fukuoka	1.895	1.000	1.000
	Saga	1.648	1.000	1.000
	Nagasaki	1.237	1.000	1.000
	Kumamoto	1.746	1.000	1.000
	Ooita	1.460	1.000	1.000
	Miyazaki	1.394	1.000	1.000
	Kagoshima	1.191	1.000	1.000
	Okinawa	2.480	1.000	1.000

D. Discussion

1) Experiment 1

BCC model and conventional method evaluate the medical care system. And these results are compared. As mentioned in II, it is difficult to apply superiority or inferiority to prefectures in consideration of plural items. For example, Kagawa and Toyama of "Ranking of rate value per 100,000 patients" in Table 7 are remarkable. Toyama's ranking in items other than the hospital density and ICU bed item is higher place than Kagawa's ranking. However, Toyama's ranking is the lowest place in ICU beds item. Then, superiority or inferiority between these prefectures is not able to be evaluated. Thus, the difference between prefectures cannot be examined because there are no absolute standards in medical fields. Then according to score in Table 7, 18 prefectures are judged to be efficient because these efficiency values are 1. Therefore, these prefectures have the better medical care system.

Next, efficient prefectures are shown by using the map of Japan as Fig 6. At this time, the tracery indicates efficient prefectures. Then, because there are a lot of efficient prefectures in Kyushu and Shikoku region, these regions have the better medical care system in the whole region.

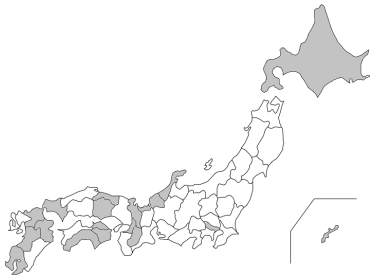

Fig. 6. Result in BCC model

On the other hand, Table 7 shows that Tohoku region has a lot of prefectures, such as Yamagata, Aomori, Miyagi, Akita, Fukushima, and Iwate whose efficiency value is low. In Fig. 6, while the other regions have at least one efficient prefecture, there is no efficient prefecture in Tohoku region. Therefore, the medical care system in Tohoku region is inferior to that in other region.

2) Experiment 2

When "valuing level α" is given to each item, the efficiency value almost is changed. If a DMU shows great decrease in the efficiency value when the valuing level of an output item is given, the output item is the weakness. However, this great decrease is clearly not defined. Therefore, this paper evaluates the weakness from "Change of ranking" in table 9. Here, "Change of ranking" indicates "±rank" of "Change from BCC" in table 8. Moreover, the strength is evaluated by "change of ranking", too.

In Table 9, let us focus on Tokyo, Tottori, and Kagawa. These prefectures did not show a decrease in the ranking, if the valuing level is given to every six output items. Here it is said that the medical care system is offered to the patient because these three prefectures do not have the weakness in any output item.

Next, Hokkaido prefecture is remarkable. When ICU bed item and hospital density item are strongly valued, these ranking decreased. Especially, 28 places are dropped in doctor item and 35 places are dropped in the hospital density item. This means that these items are weakness in this prefecture compared with other prefectures. Therefore, firstly hospital density item should be improved from the degree of ranking drop and secondly doctor item should be improved. Conversely, there was no change from 1st place when nurse, bed, and the high priced medical equipment item are strongly valued. This means that these items are the strength in this prefecture compared with other prefectures. In this way, while experiment1 is not able to find out the weakness and the strength, experiment2 is able to do those.

Miyagi is remarkable. In this case, the up of ranking happens in all items. In these ranking up, the degree of the up is the smallest in bed item. Subsequently, the degree is the second in nurse item. This means that there are a lot of prefectures where these two items are the strength compared with other items. In other word, these items are the weakness of Miyagi. Therefore, firstly bed item should be improved from the degree of ranking up and then nurse item should be improved.

3) Experiment 3

The medical disparity between western and eastern Japan is described by the relation between frontiers. Let us denote efficiency value based on each criterion as follows to simplify the discussion.

Efficiency value based on All Japan : θ

Efficiency value based on Eastern Japan : θ^E

Efficiency value based on Western Japan: θ^W

In Table 10, all prefectures in western Japan are remarkable, then θ^E is higher than θ^W . From this result, the prefectures in western Japan exist outside the frontier of eastern Japan. Therefore, the frontier of western Japan exists outside that of eastern Japan.

Next, all prefectures in eastern Japan are remarkable. θ^W is higher than θ^E in most prefectures, while θ^E is higher than θ^W in the following five prefectures: Hokkaido, Saitama, Chiba, Tokyo and Niigata prefectures. This result shows that most prefectures in western Japan exist outside the frontier of eastern Japan, these five prefectures exist outside the frontier of western Japan and these frontiers cross here.

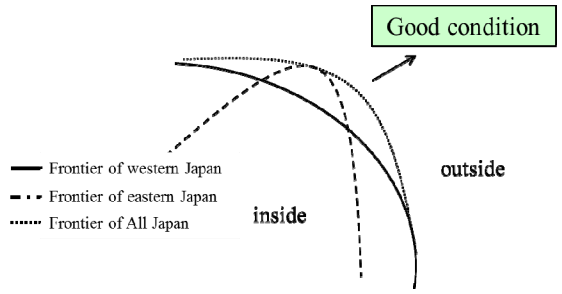

Fig. 7. Image of frontiers

As the result, the relation among frontiers is shown as Fig. 7. Therefore, western Japan has better medical care system than eastern Japan because the frontier of western Japan almost covers that of eastern Japan except for a part. Conversely, the medical care system of eastern Japan almost is inferior to that of western Japan, and there are few efficient prefectures in eastern Japan as shown Table 7. That is why, it is necessary to improve the medical care system in the entire eastern Japan.

VI. CONCLUSION

In order to evaluate the medical care system and to reveal the regional and medical disparity, this paper has applied three kinds of methods to the data published by Ministry of Health. The conventional method, ratio-comparison per 100,000 patients, could not evaluate the medical care system in each prefecture. However, the medical disparity between prefectures can have been examined by BCC model this time. And its cause has been found out by "Restricted Multipliers DEA model using Cone-Ratio approach". In addition, the regional relation between western and eastern Japan has been examined by the improved MF-DEA.

As future works, it is necessary to examine the medical disparity in a smaller region, secondary medical region, than prefecture and to reveal the disparity in a prefecture. In addition, the selection of input and output items needs to be rethought because there are a lot of data which show medical employees and equipment else.

REFERENCES

[1] Ministry of Health, Vision of securing medical treatment of safety and hope, June 2008.

http://www.mhlw.go.jp/shingi/2008/06/s0618-8.html

[2] Japan Medical Association, About the nursing staff's shortage and uneven distribution, and the measures, January 2008.

http://dl.med.or.jp/dl-med/teireikaiken/20080116_1.pdf

[3] Kouichiro Mori, Working paper of JMARI "Shortage and uneven distribution of doctor by secondary medical region" No.216, June 2010.

[4] Ministry of Health, "The seventh measure concerning supply and forecast of nursing member , ", Feb 2010.

http://www.mhlw.go.jp/shingi/2005/s0522-6.html

[5] Yasufumi Kita, "Review of Efficiency Analysis of Productivity in Health Care Services," Kawasaki medical welfare society, Vol.19 No.1, pp.25-34, 2009.

[6] R. Gejima, K. Inoue, S. Yamasaki, and S. Aoki, DEA evaluation method with subjective viewpoint, The institute of System, Control and information engineers, pp.399-400, 2010.

[7] Akio Naito, K. Inoue, and S. Aoki, Data Envelopment Analysis for evaluating universities by group relationship, Control and information engineers, pp.283-284, 2010.

[8] Charnes, A., Cooper, W. W. and Rhodes, E. L. (1978), Measuring the Efficiency of Decision Making Units.European Journal of Operational Research, Vol. 2, pp. 42, 1978.

2011 IEEE International Conference on Fuzzy Systems
June 27-30, 2011, Taipei, Taiwan

Structured DEA Model Considering Relation among Input and Output Elements

Shingo Yamasaki
Department of Computer Science and Intelligent Systems
Osaka Prefecture University
Osaka, Japan
yamasaki@mis.cs.osakafu-u.ac.jp

Shingo Aoki
Department of Computer Science and Intelligent Systems
Osaka Prefecture University
Osaka, Japan
aoki@cs.osakafu-u.ac.jp

***Abstract*- Data Envelop Analysis (DEA) is method for evaluating management efficiency of DMU (Decision Making Unit). DEA can analyze DMU's characteristic of data by assigning variable weight to each input and output elements. However the more the number of input and output elements is, the more complex assigning weight is. So, there is a problem that when the number of input and output elements is so large, it is difficult to analyze DMU's characteristics. This paper proposed new DEA model considering relation among input and output elements in order to analyze DMU's characteristics more easily. This model can limit assigned weights. Therefore, above problem can be solved. The power of the proposed method is examined by applying data set of Japanese professional baseball player's result in 2010.**

Keywords*. *Data Envelop Analysis, Linear Programming, Decision Making Unit,

I. INTRODUCTION

Data Envelopment Analysis (DEA) is a method for evaluating management efficiency of DMU (Decision Making Unit). Now Application of DEA is spreading, for example Universities, hospital, professional sport player and so on[1]. And it is expected that DEA will develop further. DEA has two characteristic as follows. (1) evaluates DMU by using multi-input and multi-output data. (2) can analyze DMU's characteristic of data by assigning variable weights to each element of input and output elements. However, the more the number of input and output elements is, the more non-zero weights are[2]. So, if the number of input and output elements are so large, it is difficult to analyze characteristics of DMU[3]. There is another problem of DEA. DMU is evaluated without considering relation among input and output elements. Therefore, the efficiency value of DMU is not necessarily correct.

This study proposes structured DEA method that is considering relation among input and output elements to solve above problems. Then the power of the proposed method is examined by applying data set of Japanese professional baseball player's result in 2010.

II. DATA ENVELOPMENT ANALYSIS

A. Outline of DEA

DEA was proposed by A. Charnes et al. in 1978 as a method for management analysis. The applicable field of DEA is wide such as data mining or prospect of bankruptcy[4][5].

DEA regards each DMU as production function that produces output by input. Then the efficiency of DMU is calculated compared with other DMUs relatively[6]. There are two characteristics DEA has; (1) weights are assigned to each input and output data and virtual input and output are generated. These weights are not fix but variable so that each DMU can employ suitable weight to be evaluated better. (2) common index for evaluation is shown as efficiency value. The efficient DMU gets efficiency value as one. On the other hand, inefficient DMU gets efficiency value less than one.

Assuming that there are n DMUs and each DMU is characterized by m input and s output. Then the DMU K has input expressed as x_{1k}, K, x_{mk} and output expressed as y_{1k}, y_{sk}. Here the efficiency value is shown by calculating following linear programming .

$$\begin{aligned} \max \quad & \sum_{r=1}^{s} u_r y_{rk} \\ \text{S.t} \quad & -\sum_{r=1}^{s} v_i x_{ij} + \sum_{r=1}^{s} u_r y_{rj} \le 0 \ (j = 1,2,3...,n) \\ & \sum_{r=1}^{s} v_i x_{ij} = 1 \\ & v_i \ge 0 \ (i = 1,2,3...,n) \quad u_r \ge 0 \ (r = 1,2,3...,n) \end{aligned} \tag{1}$$

Above formula signifies that weights are assigned to input of DMU K to make it as one. Then DEA controls the efficiency value of other DMUs does not exceed over one based on the weights for DMU K. Objective function has the role for maximizing output of remarkable DMU. Moreover, it is possible to analyze strong points of each DMU by weights. That is because input and output are considered in evaluation when the weights have value.

B. Problem of DEA

1) Problem of increasing input and output elements

DEA can analyze characteristics of DMU more multipronged from optimal weights as the number of input and output elements increase. However, increase of them causes

problem about analyzing characteristics of DMU. Generally, if input and output elements are so large, the number of DMU evaluated efficiency is also large. In this case, it is difficult to compare DMUs from their efficiency values. Moreover, non-zero weights which are actually used for evaluation increases. In other words, input and output elements which are characteristic of DMU increase. Then, it is difficult to understand strong characteristics of DMU.

Table I shows example of a result when input and output elements are so large (DMU:10 input:6 output:9). All DMU in this result are evaluated efficiency. So, it is impossible to compare DMUs by efficiency values. Moreover, Non-zero weights of DMU10 are 14 in 15. Because non-zero weights are too large, analyst can't understand strong characteristics of DMU3.

2) Problem of relation among inputs and outputs elements

Generally, analyst considers relation among input and output elements when he evaluates DMUs. However, DEA evaluates DMU regarding input and output elements as not having relation each other at all. So, the relation doesn't reflect in calculation even if there are strong relations among input and output elements. efficiency value of DMU is not necessarily correct.

Ⅲ. PROPOSED METHOD

This paper points out two problems of DEA in section Ⅱ. Then, this paper proposes structured DEA for solving them. This model makes structure of DMU and defined component of structure as group of related input and output elements. Structure shows relation among components and total efficiency of DMU. It is possible to evaluate each component by calculating efficiency value. And total efficiency value is calculated by efficiency value of components.

A. Structure of DMU

The structure of this study is constructed according to the following procedure.

Step1 is "Making component". Component is evaluated aspect of DMU and made by making input and output elements which related to an evaluated aspect to same group. It is defined that input elements set of Component K is X_k, output elements set is Y_k. And its efficiency value is θ_k. θ_k is calculating by (1) formula.

Step2 is "Adding middle layer and connecting components". If there is evaluated aspect that is composed of some component which are made in Step1, new component that is called middle layer added to the structure. Middle layer has some outputs which are efficient values of some component that compose middle layer. At the end, connect middle layer and total efficiency are connected based on their relation.

The example of the structure is shown as Figure 1. Now, there are four components, Component A ~ Component D and Middle Layer1. Arrow in Figure 1 shows that a middle layer at arrow's head is composed of component at arrow's tail. For example, Middle Layer 2 is composed of Component C, and Component D.

B. Calculating efficiency

Efficiency value of component is calculated by formula (1). It is impossible to calculate efficiency value of middle layer and total efficiency, because they don't have input elements. Then their efficiency value is calculated by formula (2) as follows.

$$\begin{aligned} \max \quad & \sum_{r=1}^{s} u_r y_{rk} \\ \text{S.t} \quad & \sum_{r=1}^{s} u_r y_{rj} \le 0 \ (j = 1,2,3...,n) \\ & x_i = 1 \ (i = 1,2,3...,n) \\ & v_i \ge 0 \ (i = 1,2,3...,n) \quad u_r \ge 0 \ (r = 1,2,3...,n) \end{aligned} \tag{2}$$

This formula is based on formula (1) and different point is that formula(2) assumes input value is 1. Therefore, all DMU's input value is equal. So, formula (2) calculates efficiency value by only relative comparison of output. Output elements of the middle layer are efficiency values of components that compose the middle layer. Equally, Efficiency value of total efficiency is calculated by formula (2).

Proposed method can overcome the problem of relation among inputs and outputs elements by calculating efficiency value in each component. Efficiency value of each component is calculated with only inputs and outputs which have relation. And, inputs and outputs which don't have relation aren't used for calculation together. Therefore, proposed method can evaluate as considering relation among inputs and outputs elements.

Table I Example of result when inputs and outputs elements are so large

DMU	effieicincy value	weights						weights								
		input1	input2	input3	input4	input5	input6	output1	output2	output3	output4	output5	output6	output7	output8	output9
DMU1	1	0.779	0.802	0.095	0.401	0	0.275	0.584	0	0.153	0	0.014	0.181	0.000	0	0
DMU2	1	0.990	0	0	0.509	0	0.656	1.244	0	0	0	0	0	0	0	0
DMU3	0.9242011	1.291	0.036	0.007	0	0.142	0.696	0.962	0.038	0.157	0.214	0.254	0.657	0.081	0.000	0
DMU4	1	0.662	0.892	0.041	0	0.173	0.378	0.705	0.202	0.043	0	0.007	0.367	0.000	0.00104	0.001
DMU5	1	0.701	1.125	0	0.225	0.041	0.240	0.753	0.253	0	0.059	0	0.216	0.000	0	0
DMU6	1	1.209	0.644	0	0.108	0.022	0.314	0.894	0.278	0	0.231	0.103	0.267	0.083	0.000	0
DMU7	1	0.625	0.191	2.546	0	0	0.026	1.373	0.571	0	0	0	0	0	0	0
DMU8	1	0.269	0.400	1.966	0	0.164	0	0.829	0.546	0.079	0	0.216	0	0	0	0
DMU9	1	0.979	0.400	0	0	0	0	1.024	0	0	0	0	0	0	0	0
DMU10	1	0.524	0.680	0.030	0.071	0.188	0.710	0.583	0.201	0	0.037	0.168	0.548	0.20663	0.140	0.140

Now, calculation example by using Figure1 is shown as follow. First, efficiency value of Component A ~ Component D is calculated by formula (1). Next, efficiency value of Middle Layer1 is calculated by formula (2) using $\theta_A, \theta_B, \theta_C$ as outputs. Middle Layer2 calculated as well as Middle Layer1 using θ_C, θ_D. At the end, Total Efficiency value is calculated by formula (2) using θ_1, θ_2.

C. *Analyzing result*

Analyzing result in traditional method is done with optimal weights. On the other hand, proposed method can overcome the problem that it is difficult to understand strong characteristics of DMU by using efficiency values of components and middle layers for analyzing result.

In proposed method, if efficiency value of Component K is 1, the evaluation of Component K is superior to the other DMUs. So, Component K is considered to be characteristic of the DMU. Oppositely, if efficiency value of Component K is low, Component K isn't considered to be characteristic of the DMU.

In analyzing DMUs as stated above, analyst can get characteristics of each DEA without using optimal weights. Therefore, it isn't caused problem in proposed method, when the input and output elements are so large. Moreover, proposed method can compare DMUs whose efficiency values are 1 by efficiency values of each component.

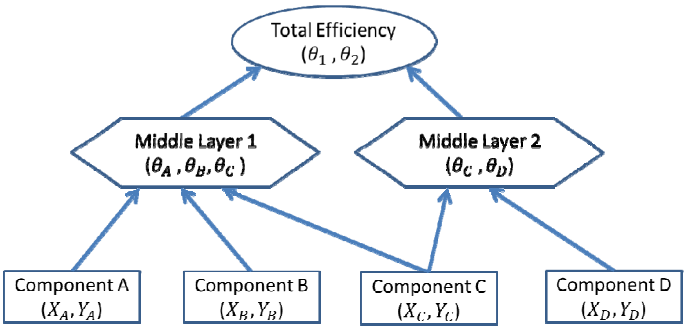

Fig. 1 Example of the structure

IV. NUMERICAL EXPERIMENTS

A. *Experimental conditions and data*

In order to examine utility of proposed method, Proposed method is applied to data set of 61 Japanese professional baseball player's result in 2010. There are 6 input and 9output elements as follows.

- Input
  (1) Total plate appearance
  (2) Number of strikeout
  (3) Number of failing stolen bases
  (4) Number of ground into double plays
  (5) Number of error
  (6) Total Defense opportunity

- Output
  (1) Number of hits
  (2) Number of caught stealing
  (3) Number of homerun
  (4) Number of run batted in
  (5) Number of Stolen Bases
  (6) Number of assists
  (7) Number of putouts
  (8) Number of double plays
  (9) Number of sacrifice bunts

From above input and output elements, considering input and output elements, we made five components and two middle layers as follows.

<Component 1> Bat Control

Input: (1),(2),(4) Output:(1)

<Component 2> Stolen Bases

Input: (3) Output :(5)

<Component 3> Sacrifice Bunts

Input: (1),(2),(4) Output:(9)

<Component 4> Slugging

Input: (1),(2),(4) Output:(3) (4)

<Component 5> Defense

Input: (5),(6) Output:(2) (6) (7) (8)

<Middle Layer 1>Technique of hitting

Input : 1 Output: efficiency of Component_1,2,3.

<Middle Layer 2>Offense

Input : 1 Output: efficiency of Middle Layer_1,
efficiency of Component_4

From above component and middle layer, the structure of Baseball player is constructed as Fig. 2.

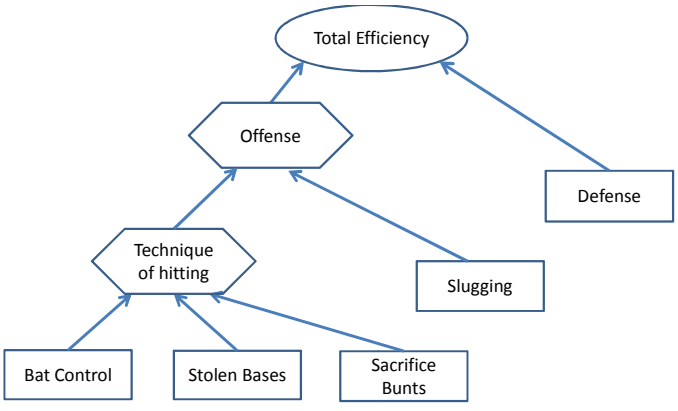

Fig. 2 Structure of Baseball Player

B. *Results*

The results is shown in Table Ⅱ. For example, DMU1 has efficiency as 0.918 in Total Efficiency, 0.918 in Technique of hitting and 0.537 in Defense.

C. *Disucussion*

1) Result of Traditional and Proposed methods

The efficiency value of the traditional method is calculated by formula(1). Table Ⅲ shows a part of the result of traditional method. It is shown that all DMU exclude only DMU60 have the efficiency value as 1 by traditional method. In this case, it is difficult for analyst to understand difference of DMUs by the efficiency value.

One of the reasons of it is increasing input and output elements. The other is assigning weights without considering relation among input and output elements. For example, DMU1's weight of input(3) is non-zero value, but weight of output(5) is zero. Input(3) and output(5) should be calculated together, because they have relation. Thus, calculation without considering relations makes DMU efficiency in the appearance, but analyst doesn't know whether DMU1 is real efficiency or inefficiency.

In proposed method, assigning weights are limited by making component. So, proposed method can evaluate considering relation among input and output elements. In the result of proposed method, number of DMU which has the efficiency value as 1 is fewer than the result of the traditional method. DMU1 has efficiency as 1 in traditional method but in proposed method efficiency as 0.918. Proposed method could find DMU1 is inefficiency, though analyst doesn't know in traditional method.

Weights have value 13 of 15 input and output elements in DMU3. Therefore, DMU3 is analyzed that it has characteristics overall. However, it is difficult for analyst to understand detail of characteristics, for example which elements is most superior or inferior. Proposed method can analyze detail of characteristics by the efficiency of each Component or Middle Layer. If DMU has high efficiency value of Component or Middle Layer, it is superiority. Oppositely, if DMU has low efficiency value of Component or Middle Layer , it is inferiority.

In this case, it is easy for analyst to understand characteristics of DMU3 by proposed method. Fig. 3 shows the structure and efficiency value of DMU3. The result based on

proposed method writes in structure figure like Fig.3, it is possible to understand characteristics of DMU just one look.

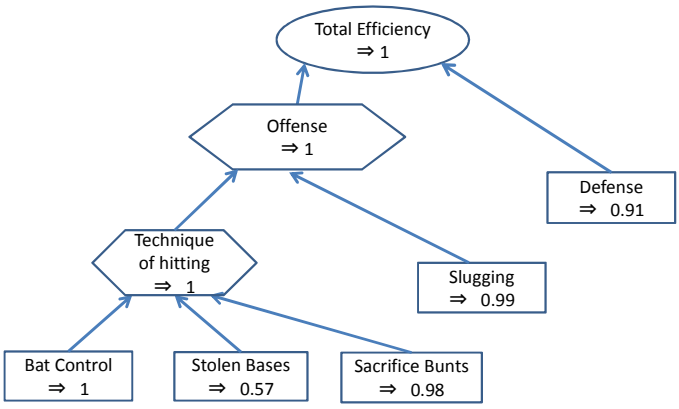

Fig. 3 Structure and Efficiency Value of DMU 3

For instance in Fig. 3, the efficiency value of Offense is 1, so DMU3 has superiority on Offense. The reason why Offense is superiority is found by the efficiency of its lower component. In this case, the reason is that the efficiency value of Technique of hitting is 1. Moreover, DMU3 has high efficiency value of Sacrifice Bunts and Slugging. So, Sacrifice Bunts and Slugging is also characteristics of DMU3. Like this, proposed method can analyzes characteristics of DMU which is difficult to understand by weights based traditional methods.

Table II a part of the result of proposed method

DMU	Total effieicincy value	efficiency value of component						
		Offense	Slugging	Technique of hitting	Stolen Bases	Sacrifice Bunts	Bat Control	Deffense
DMU1	0.918	0.918	0.894	0.918	0.476	0.761	0.918	0.537
DMU2	1	1	1	0.94	0.500	0.743	0.940	0.905
DMU3	1	1	0.987	1.000	0.571	0.985	1	0.905
DMU4	1	1	1	0.887	0.476	0.793	0.887	1
DMU5	1	1	1	0.863	0.643	0.680	0.863	0.748
DMU6	1	1	1	1	1	0.993	1	0.834
DMU7	1	1	0.875	1	0.5	0.905	1	0.666
DMU8	1	0.885	0.706	0.885	0.286	0.777	0.885	1.000
DMU9	1	1	0.686	1	0.841	0.675	1	0.879
DMU10	1	0.991	0.961	0.991	0.476	0.962	0.991	1

Table III a part of the result of traditional method

DMU	effieicincy value	weights						weights								
		Input(1)	Input(2)	Input(3)	Input(4)	Input(5)	Input(6)	Output(1)	Output(2)	Output(3)	Output(4)	Output(5)	Output(6)	Output(7)	Output(8)	Output(9)
DMU1	1	0.779	0.802	0.095	0.401	0	0.275	0.584	0	0.153	0	0.014	0.181	0.197	0	0
DMU2	1	0.990	0	0	0.509	0	0.656	1.244	0	0	0	0	0	0	0	0
DMU3	1	1.291	0.036	0.007	0	0.142	0.696	0.962	0.038	0.157	0.214	0.254	0.657	0.078	0.081	0
DMU4	1	0.662	0.892	0.041	0	0.173	0.378	0.705	0.202	0.043	0	0.007	0.367	0.235	0	0.001
DMU5	1	0.701	1.125	0	0.225	0.041	0.240	0.753	0.253	0	0.059	0	0.216	0.178	0	0
DMU6	1	1.209	0.644	0	0.108	0.022	0.314	0.894	0.278	0	0.231	0.103	0.267	0.060	0.083	0
DMU7	1	0.625	0.191	2.546	0	0	0.026	1.373	0.571	0	0	0	0	0	0	0
DMU8	1	0.269	0.400	1.966	0	0.164	0	0.829	0.546	0.079	0	0.216	0	0	0	0
DMU9	1	0.979	0.400	0	0	0	0	1.024	0	0	0	0	0	0	0	0
DMU10	1	0.524	0.680	0.030	0.071	0.188	0.710	0.583	0.201	0	0.037	0.168	0.548	0	0.207	0.140

2) Comparison characteristics between DMUs

When the number of DMU which has efficiency value as 1 is so large, it is difficult for analyst to compare DMUs by efficiency value based traditional method. Proposed method can compare the efficiency values of same component between DMUs. So, proposed method can compare DMUs that have efficiency value as 1. For example, it is shown Comparison between DMU2 and DMU4. DMU2 and DMU4 have total efficiency value as 1.Therefore, it is impossible to compare total efficiency value. DMU4 has the efficiency value as 1 in Defense, on the contrary DMU2 has efficiency value as 0.905. From this, DMU2 is superior to DMU4 in Defense. Similarly, it is compared the efficiency value in Technique of hitting, it is found that DMU2 is inferior to DMU4 in Technique of hitting. It is possible to compare each component or middle layer. As a result, it is shown that the proposed method can compare DMUs which have efficiency value as 1.

V. CONCULUTION

This study pointed out two problems of DEA. In order to solve them, this paper proposes Structured DEA. Two problems are as follows: (1) Difficulty to understand characteristics of DMU from the optimal weights calculated by the traditional DEA, (2) DEA can't consider relation among input and output elements. Structured DEA calculates partial evaluation of DMU by input and output elements which have relation. Total evaluation is calculated by the result of partial evaluation.

The proposed method is examined by applying 61 data of Japanese baseball players. From the numerical experiments, it is found that proposed method can analyzes characteristics of DMU which is difficult to understand by weights based traditional methods and can evaluate considering relation among input and output elements.

REFERENCES

[1] K. Inoue et al. "Data envelopment analysis for evaluatig Japanese Universities", *Proc. of The Fifteenth International Symposium on Artificial Life and Robotics 2010*, pp.110-114,(2010)

[2] Charnes, A., Cooper, W. W. and Rhodes et al. (1999), "Measuring the Efficiency of Decision Making Units," *Proc. of European Journal of Operational Research,Vol.2,*pp429-444 ,(1978)

[3] T. Sueyoshi, Y. Kinase and S. Aoki, "DEA Duality on Returns to Scale in Production and Cost Analysis", Proceedings of the Sixth Asia Pacific Management Conference 2000, pp1-7, (2000)

[4] T. Sueyoshi and S. Aoki, "A use of a nonparametric statistic for DEA frontier shift: the Kruskal and Wallis rank test", *Proc. of The International Journal of Management Science, Vol.29, No.1,* pp1-18, (2001)

[5] T.Sueyoshi, K.Onishi, and Y.Kinase, "A Bench Mark Approach for Baseball Evaluation", *Proc. of European Journal of Operational Research, Vol.115*, pp.429-428,(1999)

[6] D. K. Despotis and Y. G. Smirlis, "Data Envelopment analysis with imprecise data", *Proc. of European Journal for Operational Research, Vol. 140*, pp. 24-36,(2002)

2011 IEEE International Conference on Fuzzy Systems
June 27-30, 2011, Taipei, Taiwan

Component-Based Search Engine for Blogs

Sachio Hirokawa, Chengjiu Yin, Tetsuya Nakatoh
Research Institute for Information Technology
Kyushu University
Fukuoka 812-8581, JAPAN
Email: {hirokawa,yin,nakatoh}@cc.kyushu-u.ac.jp

***Abstract*—A wrapper is a program that selectively extracts a necessary part (component) from Web pages. Automatic or semi-automatic wrapper construction is crucial to achieve a fine grained search engine for Web pages. However, this is not an easy task to achieve. This paper proposes a component-based search engine in which the content components gain a high score in the search results. Thus, the required segments for a query can be obtained without using a wrapper.**

***Index Terms*—search engine; blogs; ranking; semi-structured document**

I. INTRODUCTION

Information extraction is a necessary step for developing a Web search engine. However, web pages contain information which is not main content, for instance, online advertising, related information, website menu, navigation links, and so on. This kind of information has become the noise of creating Web search engine and decreases the accuracy of search result. Therefore, extraction of the main contents is crucial to improve the quality of blog search. A wrapper is a program that selectively extracts a necessary part (component) from Web pages. By ranking the importance of the components, we propose a component-based search engine in which the content components gain a high score in the search results. Thus, the required segments for a query can be obtained without using a wrapper.

The authors of the present paper have been working on a new search model [1], [2]. Tourism information was chosen to explain the effectiveness of the model. The blog site "Kyushu seifuku Blog" was chosen as analysis target of this research. This blog site is about the tourism information on the Kyushu area, which is published by Kyushu Tourism Promotion Organization [1]. Every blog entity on the site is composed of simple introduction and link. The details of the blog entities are open to the public on other external sites which are independent to the Kyushu Tourism Promotion Organization. We collected 1,303 blog entities and saved as html files and extracted 136,368 components from these blog.

II. RELATED WORK

A. Keyword Search for Semi-Structured Documents

There are two kinds of search engines – a vector space model based keywords search engine and semi-structured documents search engine. The vector space model is an algebraic model for representing text documents as vectors of identifiers. The first use was in the SMART Information Retrieval System [3]. According to the increase of HTML documents and XML documents, search engine for semi-structured documents are gaining attention. Moreover, it has been a big issue to integrate structure search and keyword search. For example, Seki et.al. [4] realised a faceted search for sub-structures using multiple vector space model search engines. It has become very popular to utilize vector space model to extract contents from semi-structured documents. Chidlovskii [5] described a method about information extraction from HTML/XML trees. Hu and his colleagues tried to formulate the semi-automatic construction parts as an algorithm [6]. Cooper and his colleagues proposed an indexing structure in order to achieve high query performance using semi-structured data repositories [7]. Moreover, Zhang, Ohmori and Hoshi analyzed the efficiency of keyword-based search for Hybrid XML-relational databases [8]. In order to improve the retrieval efficiency, Hatano and his colleagues proposed a method for determining fine grained results for keyword-based XML document retrieval [9].

All of these papers demonstrate how to integrate efficiently semi-structured document search into keyword document search. However, most of these approaches consider fixed XML formats which cannot deal with a variety of structures often seen in various blog sites. Each blog site provides completely different structures. Sometimes, bloggers can settle their own favorite format. So, we need structure-independent methods for blog search.

B. Blog Spams and Content Extraction

Blog sites are written in HTML. They are typical semi-structured documents. However, blog sites are not official sites. Official sites have documents with specific and clear purpose. Blogs are mixed by different purpose information such as the comments of blogger and company online advertising. Therefore it is difficult to evaluate the importance of a blog page as a single entity. We focus on the smallest plain text areas, which we call components, by which the pager is evaluated as s single entity.

One of the main difficulties in dealing with blogs is the increase of spams. There are a lot of researches about detection and the removal of the blog spam to improve the quality of search [10]. Even if we would succeed in choosing non-spam blogs, there remains a difficulty in extracting the real contents from the blog pages. Indeed, the target 1303 web pages, the present paper is analyzing, are chosen by experts of the tourism

[1] http://www.welcomekyushu.jp/

978-1-4244-7316-8/11/$26.00 ©2011 IEEE

organization. They are not spam at all. However they still contain many navigational contents and advertisements in the pages. So, we will lose the feature of the page if we use all the words that appear in the page as the index words. To separate the real contents and other is a big problem we have to face. There are a few researches in extracting the pure contents using shallow features [11], [12].

III. Component Index

In order to create a blog search engine, it is necessary to extract the useful and valuable information from that blog. A large number of blog entries are written by the blog authors, and these constitute the main contents of the blog, and represent useful and valuable information. However, the main contents are often accompanied by a large amount of noise such as online advertisements, links to other blogs, copyright notices or the comments of readers. These noise data seriously harm the extraction of the blog's primary content. The top-ranked search results might not be pertinent for the query due to these noise. This is a big problem we must overcome to realise an ideal blog search engine. If all blogs were written in the same uniform template, it would be very easy separate contents and noise. However, there are a large number of blog sites, which have different templates. Moreover, blog authors can set up personalized templates according to their individual preferences. If we cannot distinguish the main contents and other noise, all the words in the HTML page will be recognized and indexed as feature words by which search is performed. In the end, the top ranked search results might be irrelevant.

The present paper considers a different approach to realise a high quality blog search. We believe that we can distinguish enhanced blogs and thin blogs even if we do not have a complete extraction program for article contents.

In the present paper, a web page is caught as a set in a lot of small text parts, which contain no tags. In other words, we focus on the leaves of HTML-trees. We do not try to separate the contents and other parts. Instead, we introduce a score for all these components. According to this score, the weight of words in the article become high and those in other parts become low. As the result, the rich content blogs appear at the top ranking in the search result.

Fig. 1 is an article in a tourism blog. It contains the navigational links of the site ①, links to the archives ②, links to the latest contents ③, the title of the article ④, and the main contents of the article ⑤. Fig. 2 shows the web page as an html-tree, where the square boxes highlight the main contents, where square boxes represents those content text areas. We call these small text areas as "components" and realised a search engine for these components by indexing them. We used GETA system [2] to realise the search engine. Fig. 3 displays the index file of the search engine. The lines starting with "@" symbol show the indexed objects, i.e. components. For example, "@1-1" and "@1-2" represents the first and the second test area of the first HTML file (Fig. 1). Other lines display index keywords and their frequencies in the text area. The keywords with "h:" represents the id of the HTML file. The keywords with "p:" represents the X-path by which the component can be reached from the root of the HTML-tree structure. For example, the keyword "p:/html[2]/body[4]/div[1]/div[1]/h3[1]/" in the second component "@1-2" represents the X-path to the text area ④, in Fig. 1, which is the headline of the article "Huis Ten Bosh is now blooging with roses!".

[2]http://geta.ex.nii.ac.jp

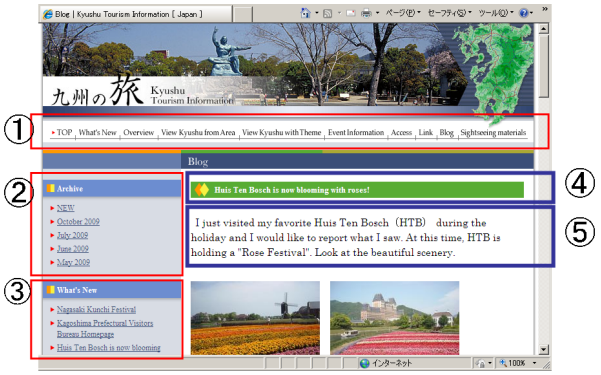

Fig. 1. A Tourism Blog

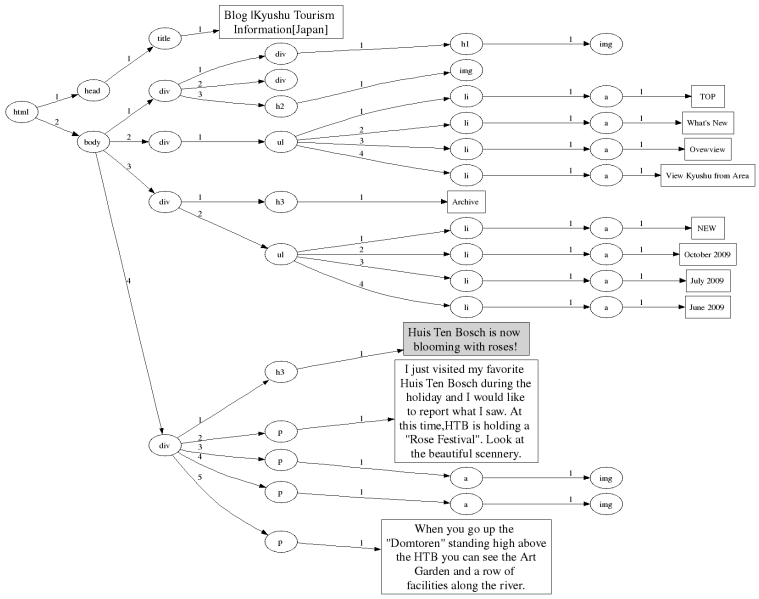

Fig. 2. HTML Tree

The anchor text that appears under the anchor tag is excluded from the components. Because the linked text is usually relevant to the other web pages, it is not useful contents to the search engine. Actually, most of them were displayed in the top, bottom, left and right of a blog page, what are links to top page, other blogs, or links to the online advertisement. Some anchor texts might correspond to internal link within the page. However, these anchor text usually contain only oe or two words. Moreover, these words appear in the text area which is the target of the link. Therefore, eliminating these

```
@1-1
1 h:1
1 p:/html[1]/head[1]/title[1]
1 Blog
1 Kyushu
1 Tourism
1 ...
@1-2
1 h:1
1 p:/html[2]/body[4]/div[1]/div[1]/h3[1]/
1 Houis
1 Ten
2 Bosh
2 is
1 ...
@1-3
1 h:1
1 p:/html[2]/body[4]/div[1]/div[2]/p[1]/
3 I
1 just
1 visit
1 ...
⋮
```

Fig. 3. Component Index

internal link anchor texts does not loose any information from the page.

IV. Component Scores

Lots of calculation methods were proposed to evaluate how important a word is to a document in a collection, such as "tf*idf" and the calculation method of SMART system [3], which are suitable long document. Comparing with the generic document, the sizes of the most of the components in this paper are a lot smaller. Therefore, "tf*idf" is not suitable these components.

We introduce the following formula for calculating the score of the components.

$$score(C_i) = NW(C_i) * depth(C_i),$$

where $NW(C_i)$ is the number of the distinct words in the component C_i and the depth $depth(C_i)$ is the length of the path to HTML tree's root. We found that the individual and detailed content is always put on the deeper nodes of the HTML tree, therefore, we use the depth to calculate the SC. On the other hand, the noise such as online advertisements is always put on the shallow nodes, which have common templates. Moreover, individual entities are written in original contents, which have rich vocabulary. The score of a web page is defined as the total scores of all the components in the page.

V. Search Results for "noodle"

We compared the SMART base standard score $S(D)$ and the component score $C(D)$ of html files D. Considering

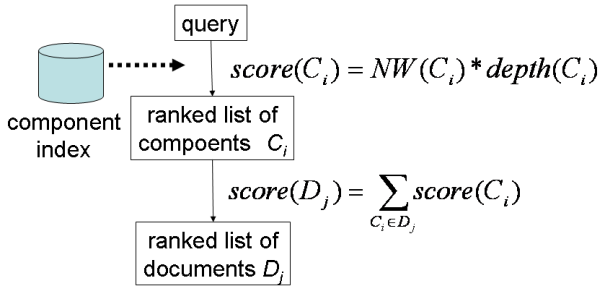

Fig. 4. Score of Components and Documents

practical situation, we conducted empirical evaluation using the following 22 keywords which are often seen in blog articles. These keywords are related to food, restaurant and gourmet.

noodle, soup, "ramen", dish, lunch, "chaashuu", vegetable, meat, pork, onion, 'sake", "udon", gourmet, chicken, fish, "soy sauce", egg, restaurant, meal, beef, rice, "tonkotsu"

For each 22 keyword w_i, firstly, we retrieved all the blog articles $D_{i,1}, \cdots, D_{i,N_i}$ that contain the keyword w_i. Secondly, we calculated the scores S-score(D_i) and C-score(D_i) together with their ranking S-rank(D_i) and C-rank(D_i). Then, we manually checked each pages $D_{i,j}$ when they have a large difference between S-rank(D_i) and C-rank(D_i). According to the limit fo space, we explain the analysis for the word "food" and 121 articles that contains the word.

Fig. 5 displays the scores of the 121 pages, where the x-axis represents the standard ranking (S-rank) and the y-axis represents the component-based ranking (C-rank) of each page. Most pages locate on the diagonal line and have almost similar rankings in S-rank and C-rank. However, there are some pages whose rankings are greatly changed. We selected top 12 pages among those pages and marked by square points. Table II displays the original data of those pages.

In the page where the ranking falls down, C-score is small. On the other hand, C-score is large for the page where the order went up. TableII displays typical components of each page which contain the query word (noodle). We see that the page where the ranking falls down (rank-descending page) contains a short sentence. We see that the page where the ranking went up is an article which contains given keyword and is written by a detailed content. It is worth-while to note that the rank-descending pages contain the query word, as shown in TableII, and that their C-score are small. This implies that short sentences shown as the snippets in TableII are the reason why those pages matches the query, as long as the components are concerned. The reason why those rank-descending pages gained high ranking in the standard ranking is not that their main contents contain the keyword but that they contain the keyword in navigation area or in left or right frames. On the other hand, the rank-ascending pages gained the high ranking because they are written with detailed contents as we can see Table II.

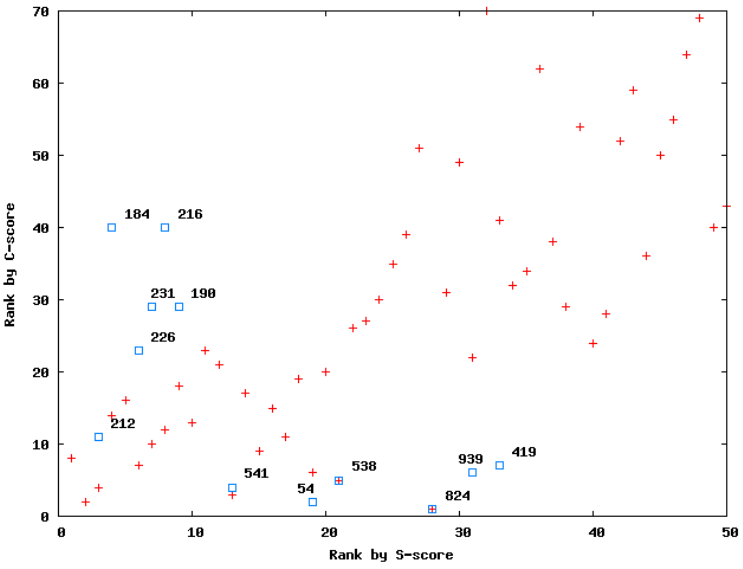

Fig. 5. Comparison of S-rank and C-rank

TABLE I
SCORE AND RANKING

HTML	S-rank	C-rank	Rank Diff	S-score	C-score
184.html	4	40	-36	0.0406	153
216.html	8	40	-32	0.0367	153
231.html	7	29	-22	0.0374	207
190.html	9	29	-20	0.0366	207
226.html	6	23	-17	0.0389	252
212.html	3	11	-8	0.0420	476
541.html	13	4	9	0.0348	880
538.html	21	5	16	0.0295	868
54.html	19	2	17	0.0309	1125
939.html	31	6	25	0.0260	830
419.html	33	7	26	0.0252	793
824.html	28	1	27	0.0272	1249

We displayed only one component in Table II. But the system already has all the components of the page and the scores of those components. So, we can display other appropriate components as snippets, which helps users to grasp the contents of the page before they actually read.

Top 6 pages (184.html, 216.html, 231.html, 190.html, 226.html, 212.html) that gained a big loss in the ranking, are in a private blog [3]. Their main articles are very short. However, they use a large area in the page for the pictures and for the links to related articles and to advertisement of affiliate (See Fig. 6).

A rank-ascending page, for example 419.html [4], contains a long sentence with the keyword and most of other contents concern personal experience and reproof of the blogger (See Fig. 7).

According to this case study, we observe that the pages which contain enhanced contents gained high ranks in the component-based ranking, while the pages whose related information is more than the article itself becomes a subordinate

[3]http://bakudankozo.blog118.fc2.com/
[4]http://blog.livedoor.jp/ukiinfo/archives/2170710.html

TABLE II
DESCENDING PAGES(−) AND ASCENDING PAGES(+)

inc/ dec	comp id	content
-	184-25	太麺の丸麺。
-	216-27	前回の麺三昧は
-	231-38	前回の麺三昧は。
-	190-25	ただ薄いか？と思いながら麺へ
-	226-22	前回の麺三昧は
-	212-81	モツ＆ちゃんぽん麺なんて最高ですね～（●＾ｏ＾●）
+	541-11	私はかなり久しぶりに来たんですが、 ランチメニューを見ると、日替わりのセット (800 円）に担々麺 (700 円)、酢豚や麻婆豆腐 （各 950 円）といった具合に、なかなか幅広い 選択肢があるようです♪
+	538-27	チャーシューも柔らかく旨みがあって 美味しいんですが、この麺と野菜の ボリュームからするとやや寂しいので、 トッピングの「細切れ豚」(100 円）を 頼むのが正解かもしれませんね
+	54-63	とり天も冷麺も大好きな私！こりゃ 参加せねばいかんでしょう
+	939-119	野菜、魚介の旨みが凝縮されてミルクの ようにコクのあるクリーミーなスープは最高。 スープに馴染んだ太麺の食感も最高。
+	419-27	坦々麺に、たっぷりのカボチャピューレと、 素揚げしたカボチャが入っています♪
+	824-25	すると、麺に絡まるんです

Fig. 6. Page with Navigational Contents(184.html)

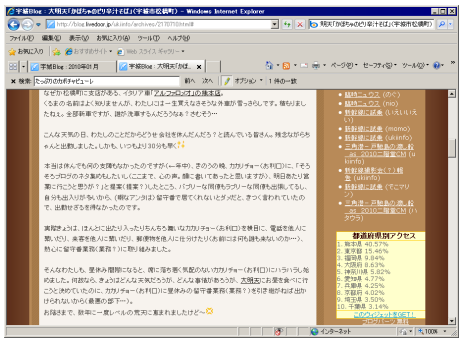

Fig. 7. Page with Rich Contents(419.html)

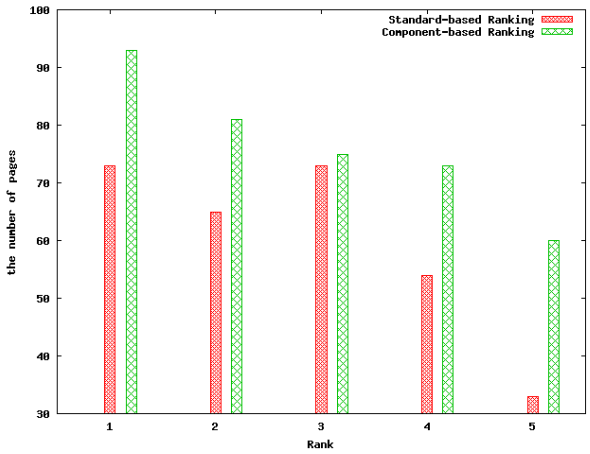

Fig. 8. User Preference of Standard Ranking and Component-based Ranking

position. This case study can be a clue for the effectiveness of the proposed ranking for detecting rich content blogs. We observed the similar pattern for other 21 cases of the keywords.

VI. Quantitative evaluation of ranking

We realised a standard search engine and a component-based search engine for 1303 blogs using GETA. We performed a quantitative evaluation of rankings using the 22 keywords as queries.

We compare the ranking of the pages in S-rank and C-rank. Actually, we constructed an experiment system for testee to select appropriate pages among

(A) top 5 pages in S-rank and

(B) top 5 pages in C-rank.

These pages are shuffled random and displayed as a search result for each query word for 22 keywords. We hide the rank of each search result. The testees do not know which page is chosen by S-rank or by C-rank. We displayed the components of the highest score as snippets in (A) and (B). Testees read the snippets and view the page, if they are interested, to choose the pages according to their preference. Fig. 8 shows the result. Component-based ranking obtained a better preference by testees in all ranks.

The total number of articles is not so large. But, those blog articles are collected from 144 sites and written different format. So, we think that this diversity supports our observation of the effectiveness of the proposed method.

VII. Conclusion and Further Work

Many people are using blogs as a means for publishing their opinions and recognize them as useful informal information sources to be searched for. However, a blog page contains various information besides the article itself. It is difficult to extract only the contents and utilize these contents, since there is no general rule to describe blog pages. In fact, blog pages have different format even if they are written in the same site. The present paper introduced a novel scoring method for a blog page focused on their components. This score and the ranking by this score succeeds to distinguish pages with enhanced articles from thin pages. Empirical evaluation are shown by constructing a search engine for tourism blogs. Effectiveness of the proposed method is confirmed through a detailed comparison of rankings of search result as well as quantitative evaluation.

We considered the leaves of an HTML-tree as components in the present paper. We excluded the anchor texts from components, since they do not contain the actual content of the page, but are links to external information. There may be other possibilities to formalize components. Inline tags, such as BR tag, and punctuation marks will be useful to characterize the real article area. Such shallow feature will improve the score as indicated in [12].

The authors appreciate the valuable comments from reviewers.

References

[1] X. Wu, S. Hirokawa, C. Yin, T. Nakatoh, Y. Tabata, Extraction and Comparison of Tourism Information on the Web, Proc. AROB2011, 2011
[2] C. Yin, T. Nakatoh, S. Hirokawa, X. Wu, J. Zeng, A proposal of search engine "XYZ" for tourism events, Proc. JCAI2010, 2010
[3] G. Salton, The SMART Retrieval System—Experiments in Automatic Document Processing, Prentice-Hall, Inc. (1971)
[4] Takahiro Seki, Taiki Wada, Yasuhiro Yamada, Nozomi Ytow and Sachio Hirokawa, Multiple Viewed Search Engine for e-Journal — a Case Study on Zoological Science, Proc. of the 12th International Conference on Human-Computer Interaction, Lecture Notes in Computer Science, Vol. 4553/2007, pp. 989-998, July 2007.
[5] Boris Chidlovskii: Information Extraction from Tree Documents by Learning Subtree Delimiters. IIWeb 2003: 3-8
[6] Jin Hu, Hedenari Kiyomitsu, Kazuhiro Ohtsuki and Junya Morishita, Operations for Retrieving a Potion from Semi-structured(in Japanese) Resources,3C-i12, DEWS2006, 2006
[7] B. F. Cooper, N. Sample, M. J. Franklin, G. R. Hjaltason and M. Shadmon," A fast index for semistructured data, " Proceedings of the 27th VLDB Conference, 2001.
[8] Liru Zhang, Tadashi Ohmori and Mamoru Hoshi, Keyword-based Search for Hybrid XML-Relational Databases (in Japanese), DEWS2008 C6-2, 2008
[9] Kenji Hatano, Hiroko Kinutani, Masatoshi Yoshikawa and Shunsuke Uemura, Determining Fine-grained Results for Keyword-based XML Document Retrieval (in Japanese), DBSJ Letters Vol.2, No.1, 2003
[10] http://airweb.cse.lehigh.edu/2008/
[11] http://search.cpan.org/dist/HTML-ExtractContent/
[12] Christian Kohlschutter, Peter Fankhauser, Wolfgang Nejdl, Boilerplate detection using shallow text features, Proc. WSDM'2010, pp.441–450, 2010

2011 IEEE International Conference on Fuzzy Systems
June 27-30, 2011, Taipei, Taiwan

Influence of the Space Segmentation and its Adaptive Automation for Reinforcement Learning

Akira Notsu, Yuki Komori, Katsuhiro Honda and Hidetomo Ichihashi
Osaka Prefecture University
1-1 Gakuencho, Nakaku, Sakai, Osaka 599-8531, JAPAN
Email:{notsu, honda, ichi}@cs.osakafu-u.ac.jp

***Abstract*—We performed a single pendulum simulation and observed the influence of the situation space segmentation pattern in reinforcement learning processes in order to propose a new adaptive automation for situation space segmentation. Usually, in real-world reinforcement learning processes, infinite states and actions and the uncertainty of the optimum solution make the learning process more difficult than the finite Markov decision process. In a numerical experiment, a single pendulum simulation is performed in order to demonstrate the influence and adaptability of the proposed method.**

***Index Terms*—reinforcement learning, space segmentation.**

I. Introduction

Reinforcement learning is a framework for a strategy to learn through trial and error according to the reward provided by the environment[1]. In reinforcement learning, if the purpose of study is set, the agent automatically determines the best way to achieve the goal.

Reinforcement learning is chiefly applied to problems in the finite Markov decision process with a finite state and a finite action. However, recently, research on methods of expressing a continuous state and a continuous action, which is more similar to the real-world situation, has progressed. Research on motion control and autonomous control of the robot has been extensive. For example, studies have examined a control problem in order to enable the robot to walk. However, in the real world, this problem is difficult, as compared with the problem in the Markov decision process, because there are an infinite number of states and actions, and it is unclear as to whether an optimum solution exists.

Q-learning[2], [3] and SARSA are typical reinforced study methods that target discrete actions. Solving a problem that has a continuous state and a continuous action requires discrimination of the continuous state and continuous action.

In the present thesis, we investigate the method of this discretization, how to divide in order to find the optimum solution faster, and the technique by which an agent can acquire the best approach to automatically divide states, and the headstand stabilization problem of the pendulum was considered.

II. Reinforcement learning

Reinforcement learning assumes that agents can visit only a finite number of states, and that when visiting a state, they will collect a numerical reward (which can be interpreted as a punishment in the case of a negative reward). Each state has a different value associated with it. Given an initial state, subsequent states are reached according to actions. The value of a given state is defined as the average reward that can be collected by selecting actions available in that state.

A. Q-learning

Q-learning is a well-known reinforcement learning technique that works by learning an action-value function that gives the expected utility of taking given action a in given state s and following a fixed policy thereafter. One advantage of Q-learning is that Q-learning can compare the expected utility Q of available actions without requiring a model of the environment (usually, the agent selects the action with the maximum expected utility).

Expected utility Q is updated iteratively. For each state s from state set S, and for each action a from action set A, we update Q-value Q that depends on current state s of the agent, action a selected by the agent, the next state s of the agent after taking action a, and reward r received by the agent after taking the action. An update is calculated by the following expression:

$$Q(s,a) \leftarrow Q(s,a) + \alpha \left[r + \gamma \max_{\acute{a} \in A(\acute{x})} Q(\acute{s},\acute{a}) - Q(s,a) \right], \tag{1}$$

where α is the learning rate and γ is the discount factor. Once Q-learning has finished, the optimal policy and the optimal value function have been found without continuously updating the policy during learning.

Q-learning algorithm:

```
procedure Q-learning
begin
  initialize Q-table Q, ∀s ∈ S, ∀a ∈ A;
  set initial state s_0 and goal state s_n;
  for cycle := 1 to MAXCYCLE do s := s_0
    while s ≠ s_n do
      a := ActionSelect(Q, s);
      r := GetReward(s, a);
      s' := GotoNextState(s, a);
      Q := UpdateQ(Q, s, a, trace);
      s := s';
    end
  end
end
```

978-1-4244-7316-8/11/$26.00 ©2011 IEEE

B. State and action space segmentation

A high-performance agent usually requires appropriately segmented state set S and action set A due to the state-space explosion of an agent. Generally, a genetic algorithm is used to search for appropriate segmentation in such individual double-loop learning. In other words, the particle swarm is a classification system in which we consider the minimization of (3) under the following condition:

$$\sum_{i=1}^{c} u_{ki} = 1, \tag{2}$$

where c is the number of clusters, and u_{ki} is called a membership function.

$$L = \sum_{i=1}^{c} \sum_{k=1}^{N} u_{ki} D\left(x_k, v_i\right), , \tag{3}$$

where N is the amount of data, c is the number of clusters, and $D\left(x_k, v_i\right)$ denotes the distance between data vector x_k and cluster center v_i, which is the difference between expected utility V and observed utility V' in the learning process.

C. Softmax Action Selection

In the present simulation, we use softmax action selection rules as an action selection policy. Softmax action selection rules rank and weight according to Q-value Q. The most common softmax method uses a Gibbs or Boltzmann distribution. This method chooses an action on the play with probability.

$$P(s,a) = \frac{\exp^{Q(s,a)/\tau}}{\sum_{\grave{a} \in A} \exp^{Q(s,\grave{a})/\tau}} \tag{4}$$

where τ is the temperature parameter. High temperatures cause (almost) all of the actions to be equiprobable, and low temperatures cause a greater difference in selection probability for actions that differ in their value estimates. If $\tau \to$ inf, then softmax action selection becomes the same as greedy action selection.

III. Single pendulum simulation

We simulated the single pendulum standing task (fig. 1). This physical calculation is performed by Runge-Kutta 4th order method.

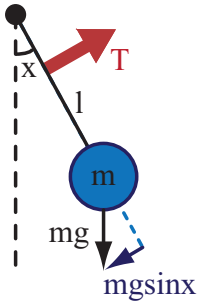

Fig. 1. Single pendulum

The following motion equation is simulated in increments of 0.05 seconds[4]:

$$m\ddot{x} = -mgl\sin x - k\dot{x} + T \tag{5}$$

where the parameters and variables are defined as follows:

- $m = 1(kg)$
- $l = 1(m)$
- $k = 0$
- $g = 9.8(m/s^2)$
- $-\pi < \theta \leq \pi$
- $-3\pi \leq \dot{\theta} \leq 3\pi$
- $-20 \leq T \leq 20$
- 1 iteration = 20 seconds
- 1 learning cycle = 0.2 seconds
- $\theta = \pi, \dot{\theta} = 0$, in the initial state
- $r_t = \frac{|x|}{\pi} - 0.5\frac{|T|}{20}$
- $\alpha = 0.25$
- $\gamma = 0.9$
- $\tau = 1$ at the first learning cycle, $\tau = 0.001$ at the last learning cycle (linearly decreasing)

A. Segmentation pattern in the state

First, we generated some patterns by dividing the state space, and a simulation was conducted.

```
procedure Q-learning with segmentation pattern
begin
  initialize Q-table Q, ∀s ∈ S, ∀a ∈ A;
  set initial state s_0;
  select dividing methods;
  for cycle := 1 to MAXCYCLE do s := s_0
    for time := 0 : 0.05 : 20
      s' := GetNextState(s, a);
      if mod(time, 0.2)==0;
        s'_r := s';
        r := GetReward(s'_r, a);
        Q := UpdateQ(Q, s_r, s'_r, a);
        a := ActionSelect(Q, s'_r);
        s_r := s'_r;
      end
      s = s';
    end
  end
end
```

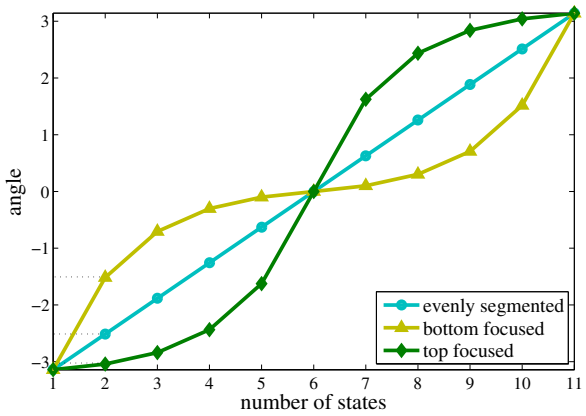

Fig. 2. dividing methods

Fig. 2 show the rate of the space segmentation. Vertical axes show the rate of the angle width (width of each segment) and horizontal axes show the angle of each segment.

For example, for "evenly segmented," the space is evenly segmented to 10 parts. for "bottom focused," the space is segmented larger around the bottom, and smaller around the top. In other words, the bottom is segmented to many parts and the agent can find difference of angle even small difference compared with the top. for "top focused," on the contrary, the top is segmented to many parts.

Other parameters and variables are defined as follows:

- 1000 episodes × 30
- θ and $\dot{\theta}$ are segmented into 10 segments
- T is segmented into six segments
- $\dot{\theta}$ and T are segmented evenly

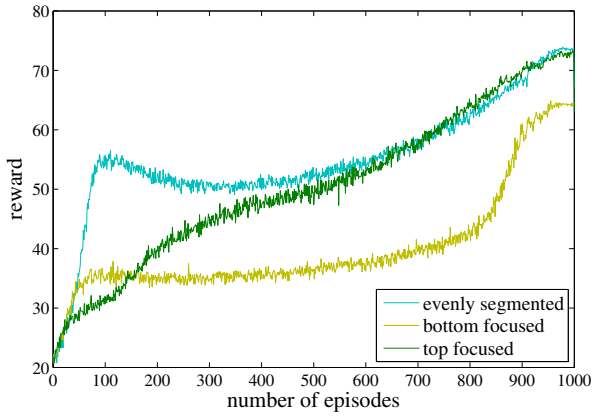

Fig. 3. comparison of the three methods

The results indicate that "evenly segmented" and "top focused" eventually provided good rewards, whereas "bottom focused" provided smaller rewards. In addition, the "bottom focused" requires more iterations than the first method in order to provide good rewards.

B. Segmentation and integration method

We investigated an automatic segmentation and integration method through simulation.

```
procedure Q-learning with segmentation and integration
begin
  initialize Q-table Q, ∀s ∈ S, ∀a ∈ A;
  set initial state s_0;
  for cycle := 1 to MAXCYCLE do s := s_0
    for time := 0 : 0.05 : 20
      s' := GetNextState(s, a);
      if mod(time, 0.2)==0;
        s'_r := s';
        r := GetReward(s'_r, a);
        Q := UpdateQ(Q, s_r, s'_r, a);
        a := ActionSelect(Q, s'_r);
        s_r := s'_r;
      end
      s = s';
    end
    if mod(cycle, FREQUENCY)==0;
      (S, Q) := Combine(S, Q);
      (S, Q) := Divide(S, Q);
  end
end
```

In this method, the space is initially evenly segmented, segmentation and integration is performed at regular cycles by the Combine(S, Q) and Divide(S, Q) functions.

The neighboring states that an average of the visited frequency is the least are integrated into a single state that has an average expected utility of the states by the Combine(S, Q) function. And the state that the visited frequency is the most is equally segmented into two states that have the same expected utility by the Divide(S, Q) function. Other expected utilities are undisturbed.

Other parameters and variables are defined as follows:

- 1000 episodes × 30
- θ and $\dot{\theta}$ are segmented into 10 segments
- T is segmented into six segments
- θ is segmented evenly, in the initial state
- $\dot{\theta}$ and T are segmented evenly

First of all, to decide how often states are combined and divided, each various episodes was combined and divided. These average rewards from 951 episodes to 1000 episodes were shown in TABLE I.

As a result, "every 200 episodes" had the best reward. So after this, we chose that the states were combined and divided every 200 episodes.

The proposed method eventually provides the best reward and the reward was increasing especially every 200 episodes, which indicates that the proposed method can be used to determine an appropriate segmentation method automatically over time.

Next, how to divide the states after the learning of "proposed method" was checked and the states were shown in fig.

TABLE I
HOW OFTEN COMBINE AND DIVIDE AND THE AVERAGE REWARD

how often combine and divide	the average reward
every 50 episodes	73.7279
every 100 episodes	77.3704
every 200 episodes	**78.3863**
every 300 episodes	76.4497
every 400 episodes	75.4669
every 500 episodes	74.6121
not combine and divide	73.2671

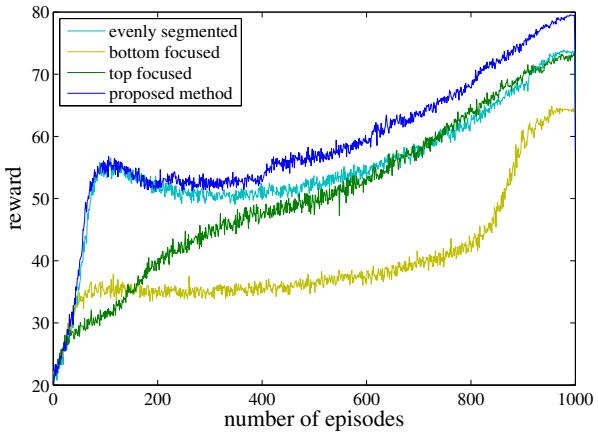

Fig. 4. comparison of the four methods

5. The result was got by average of 100 times.

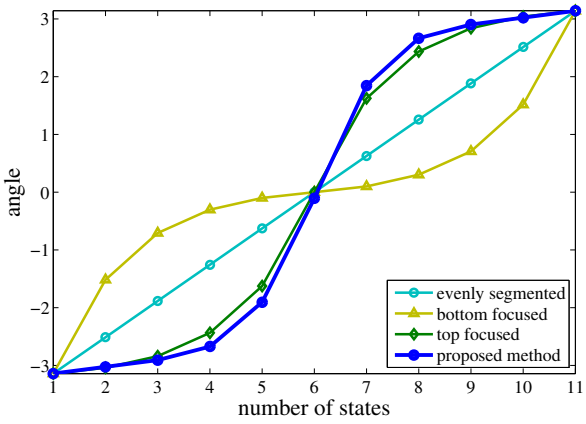

Fig. 5. final dividing methods

Following results were observed in fig. 5, "proposed method" had feature which was emphasized the feature of "top focused." In short, the top was segmented to many parts and the bottom was segmented to few parts.

Finally, the experiments with the finally segmented states of the proposed method were done from the beginning. In the experiments, the states were not combined and divided. The results were following fig. 6, 7.

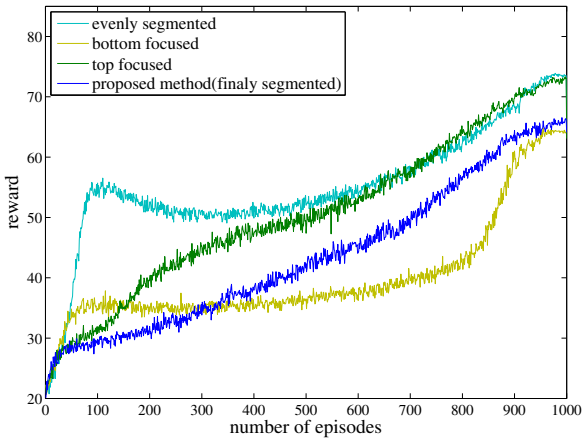

Fig. 6. results in 1000 episodes

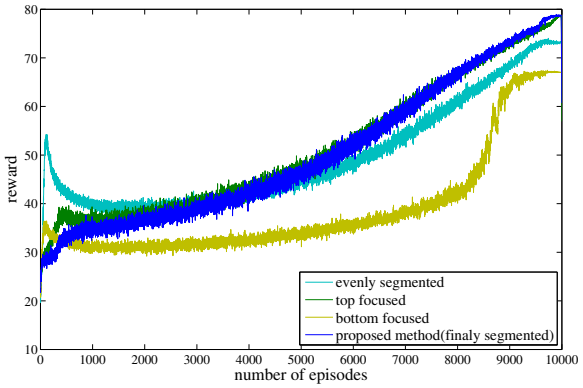

Fig. 7. results in 10000 episodes

Figures show that "1000 episodes" was not enough and "10000 episodes" was enough to get good rewards. This means the dividing way needs much time than the proposed method.

IV. Conclusion

We simulated a single pendulum simulation and observed the influence of the space segmentation and its adaptive automation for reinforcement learning. In order to divide state space, three methods were proposed, and "evenly segmented" and "top focused" got good rewards in the end episode.

The proposed method eventually provides the best reward and the reward was increasing especially every 200 episodes, which indicates that the proposed method can be used to determine an appropriate segmentation method automatically over time.

But, when the experiments with the state which were gotten by simulation were done from the beginning, the experiments needed much episodes than the proposed method to get reward at the same level. This shows that an appropriate division method is different depending on the advancement condition of study.

In the future, it is needed that a technique for integrating non-adjacent states, and expressed state space by using a function and particles, etc. In addition, more complicated experiments are also needed. For example, double pendulum simulation.

ACKNOWLEDGMENT

This work was supported in part by the Ministry of Education, Culture, Science and Technology, Japan under Grant-in-Aid for Scientific Research No. 21700242 and funded by the Ministry of Internal Affairs and Communications, Strategic Information and Communications R&D Promotion Programme.

REFERENCES

[1] R. S. Sutton, Learning to Predict by Method of Temporal Differences, Machine Learning, vol. 3, 1, pp. 9-44, 1988.
[2] T. Jaakkola, M. Jordan, and S. P. Singh, On the Convergence of Stochastic Iterative Dynamic Programming Algorithms, Neural Computation, vol. 6, pp. 341–362, 1992.
[3] C. J. C. H. Watkins, and P. Dayan, Technical Note: Q-Learning, Machine Learning, vol. 8, pp. 56–68, 1992.
[4] Y.Kashimura, A.Ueno, S.Tatsumi, A Continuous Action Space Representation by Particle Filter for Reinforcement Learning, JSAI2008, pp. 118-121, 2008
[5] J. H. Holland, and J. Reitman, Cognitive Systems Based on Adaptive Algorithms, in D. A. Waterman and F. Hayes-Roth (Eds.), Pattern Directed Inference Systems, Academic Press, 1978.
[6] J. H. Holland, K. J. Holyoak, R. E. Nisbett, and P. R. Thagard, Induction, The MIT Press, 1986.

2011 IEEE International Conference on Fuzzy Systems
June 27-30, 2011, Taipei, Taiwan

Learning with Imbalanced Datasets using Fuzzy ARTMAP-based Neural Network Models

Shing Chiang Tan
Faculty of Information Science and Technology
Multimedia University, Malaysia
sctan@mmu.edu.my

Junzo Watada
Graduate School of Information, Production and Systems
Waseda University, Japan
watada@waseda.jp

Zuwarie Ibrahim
Centre of Artificial Intelligence and Robotics (CAIRO)
University of Technology Malaysia, Malaysia
zuwairie@fke.utm.my

Marzuki Khalid
Centre of Artificial Intelligence and Robotics (CAIRO)
University of Technology Malaysia, Malaysia
marzuki@utm.my

Lee Wen Jau
ATTD Automation (APAC) Pathfinding Intel Technology
Sdn. Bhd. Kulim, Malaysia
wen.jau.lee@intel.com

Lim Chun Chew
ATTD Automation (APAC) Pathfinding Intel Technology
Sdn. Bhd. Kulim, Malaysia
chun.chew.lim@intel.com

***Abstract*—One of the main difficulties in real-world data classification and analysis tasks is that the data distribution can be imbalanced. In this paper, a variant of the supervised learning neural network from the Adaptive Resonance Theory (ART) family, i.e., Fuzzy ARTMAP (FAM) which is equipped with a conflict-resolving facility, is proposed to classify an imbalanced dataset that represents a real problem in the semiconductor industry. The FAM model is combined with the Dynamic Decay Adjustment (DDA) algorithm to form a hybrid FAMDDA network. The classification results of FAM and FAMDDA are presented, compared, and analyzed using several classification metrics. The outcomes positively indicate the effectiveness of the proposed FAMDDA network in undertaking classification problems with imbalanced datasets.**

Keywords-Data classification; imbalanced data; Adaptive Resonance Theory Neural Networks; supervised learning

I. INTRODUCTION

Many problems in modern engineering applications can be undertaken as a classification task. Over the years, various machine learning techniques have been investigated and applied to process and analyze real databases from industries. In particular, data classification is an active research field in machine learning. A classification model can be constructed by capturing associations between the input and the output variables of a dataset through a supervised learning procedure. The effectiveness of the classification model can be affected by an imbalanced dataset in which its data samples from one class exist in a large quantity (i.e., the majority class) whereas data samples with other classes are available in small quantities (i.e., the minority classes). Imbalanced datasets are commonly observed in real applications. Many real-world datasets exhibit such characteristics, for examples, in medical prognosis and diagnosis [1], vision recognition [2], credit card fraud detection [3], and bioinformatics [4]. In these applications, the occurrence of minority/rare cases is occasionally given more attention than that of the majority.

Learning with an imbalanced dataset is never an easy task. One of the main challenges is how a classification model, whereby its knowledge base is dominated by information from the majority class, is able to learn information of the minority classes accurately. The reason is that a classification model may tend to neglect information acquired from data samples with the minority classes owing to overwhelming information of the majority class. The situation becomes worse if the imbalanced dataset is large in size and has an arbitrary high complexity. From the literature, data mining and machine learning techniques such as decision trees, *k*-nearest neighbor and naïve Bayesian [5] have been employed as classification models for handling imbalanced datasets. Nevertheless, they are unable to yield satisfactory results [5]. Modifications made on these techniques (e.g., [6, 7]) are able to improve the classification performances in dealing with imbalanced datasets. In this regard, two common approaches have been adopted to construct a more effective classification model for tackling imbalanced datasets, i.e., modifications are at either the data level [6] or the algorithm level [7]. At the data level, re-sampling methods, which include methods for under sampling the instances from the majority class, over sampling the instances from the minority classes, and the use of these two methods, have been introduced. The re-sampling methods are applied to determine a good mix of samples belonging to different classes from the imbalanced dataset for achieving good classification performances. On the other hand, at the algorithm level, the learning algorithm of the classification model is modified so as to learn the characteristics of samples from the minority classes more effectively.

In this research, a supervised Adaptive Resonance Theory (ART) neural network, namely Fuzzy ARTMAP (FAM) [8], is proposed as a base classifier to handle imbalanced datasets. FAM, an incremental learning model, is able to overcome the

The Matsumae International Foundation and the Watada Lab

stability-plasticity dilemma [9]. The FAM network is *plastic* enough to absorb new information from new samples and, at the same time, is *stable* enough to retain previously learned information from being corrupted by newly learned information. An interesting feature of FAM is that it integrates fuzzy set theory [10] and the stability-plasticity characteristic of ART into a common framework, and this allows the network to encode both analog and binary input patterns (i.e., information) in the form of rectangular prototypes. The focus of this research is on evaluating the effectiveness of a variant of FAM in dealing with a large imbalanced dataset collected from a manufacturing industry. Original FAM does not have the conflict resolving capability for handling overlaps among prototypes of different classes. In this case, a Dynamic Decay Adjustment (DDA) algorithm [11] can be integrated within the supervised learning mechanism of FAM, and the resulting network is known as FAMDDA. As far as imbalanced datasets are concerned, such additional facility is helpful for FAM to adapt and distinguish information of the minority classes from those of the majority class more accurately; hence, the network is able to provide a better solution to problem under scrutiny.

The organization of this paper is as follows. Section II explains the classification models (i.e., FAM and FAMDDA) used for learning imbalanced datasets. Section III describes the indicators for assessing the performance of a classification model with imbalanced datasets. In Section IV, a case study with a large imbalanced dataset from a semiconductor manufacturing plant is carried out. The results and the associated discussion are presented. Concluding remarks are given in Section V.

II. Fuzzy ARTMAP-based Neural Networks

A. Fuzzy ARTMAP (FAM)

FAM [8] is an incremental learning neural network from the ART family. The network is capable of self-organizing and self-stabilizing information gained from training samples during supervised learning. The structure of FAM is depicted in Fig. 1. The network is constructed by a pair of fuzzy ART modules (i.e., ART_a and ART_b) that are interconnected through a map field, F^{ab}. Each ART module consists of three layers of nodes, i.e., $F_0^a(F_0^b)$ is the normalization layer wherein an $M-$dimensional input vector, $\boldsymbol{a}$, is complement-coded [8] to a $2M-$dimensional vector $\boldsymbol{A}$; $F_1^a(F_1^b)$ is the input layer wherein the nodes receive the complement-coded input vectors; $F_2^a(F_2^b)$ is the recognition layer containing recognition nodes that encode prototypes of input patterns. Note that new nodes can be created in $F_2^a(F_2^b)$ when necessary to include new information.

The learning procedure of FAM is as follows. During supervised learning, an input pattern is presented to ART_a whereas its corresponding target output is presented to ART_b. At ART_a, the input pattern is complement-coded as pattern $\boldsymbol{A}$ and then propagated to F_2^a through F_1^a. The activation of each node j in F_2^a is measured by a choice function [8]

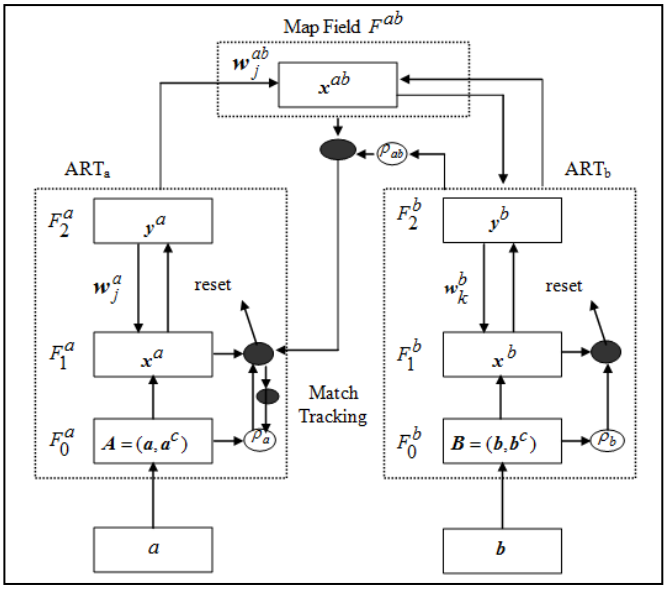

Figure 1. The network structure of Fuzzy ARTMAP.

$$T_j = \frac{\left|\boldsymbol{A} \wedge \boldsymbol{w}_j^a\right|}{\chi_a + \left|\boldsymbol{w}_j^a\right|} \tag{1}$$

where χ_a is the choice parameter and is set close to zero [8]; $\boldsymbol{w}_j^a$ the weight of node j. Based on the *winner-take-all* competition scheme, the node with the largest activation is selected as the winning node, and is denoted as node J. FAM imposes a vigilance test that measures the similarity between the winning prototype patterns, $\boldsymbol{w}_J^a$, and $\boldsymbol{A}$ against a threshold (vigilance parameter, ρ_a), as follows [8]

$$\frac{\left|\boldsymbol{A} \wedge \boldsymbol{w}_J^a\right|}{\left|\boldsymbol{A}\right|} \geq \rho_a \tag{2}$$

If the winning node fails in the vigilance test, a new search cycle for another winning node is exercised. The process of searching for a winning node is continued until the selected node is able to satisfy the vigilance test. If no such node exists, a new node is created in F_2^a to encode the input pattern. The same pattern-matching cycle takes place in ART_b using the target vector to find a winning node that encodes the target class.

Upon the identification of the winning nodes in F_2^a and F_2^b, a prediction is sent from F_2^a to F_2^b via F^{ab}. A map-field vigilance test is conducted to ascertain the prediction, i.e., [8]

$$\frac{\left|\boldsymbol{y}^b \wedge \boldsymbol{w}_J^{ab}\right|}{\left|\boldsymbol{y}^b\right|} \geq \rho_{ab} \tag{3}$$

where $\boldsymbol{y}^b$ denotes the output vector of $\boldsymbol{y}^b$; $\boldsymbol{w}_J^{ab}$ denotes the weight vector from F_2^a to F^{ab}; and ρ_{ab} is the map-field

vigilance parameter. If the map field vigilance test fails, this indicates that the winning node in F_2^a has made a wrong prediction of the target class in F_2^b; hence, a matching-tracking process [8] ensues. Parameter ρ_a, which is initially set to a user-defined baseline vigilance parameter $\overline{\rho}_a$, is now increased to

$$\rho_a = \frac{\left|\boldsymbol{A} \wedge \boldsymbol{w}_J^a\right|}{\left|\boldsymbol{A}\right|} + \delta \tag{4}$$

where δ is a small positive value. By increasing ρ_a, the current winning node in F_2^a will fail in the ART$_a$ vigilance test. A new search cycle in ART$_a$ is initiated again with a new level of ρ_a. This process is repeated until a correct prediction is made between the winning nodes in F_2^a and F_2^b. Then, FAM enters a learning phase, whereby the weight vector of the winning node in F_2^a is updated as [8]

$$\boldsymbol{w}_J^{a(new)} = \beta_a\left(\boldsymbol{A} \wedge \boldsymbol{w}_J^{a(old)}\right) + \left(1-\beta_a\right)\boldsymbol{w}_J^{a(old)} \tag{5}$$

where β_a is the learning rate of ART$_a$. The same learning process as in ART$_a$ also takes place in ART$_b$. Note that all equations in ART$_a$ are applicable to ART$_b$, but with superscript or subscript *a* replaced by *b*.

B. Fuzzy ARTMAP with the Dynamic Decay Adjustment (FAMDDA) Algorithm

The architecture of FAMDDA is the same as that of FAM. However, FAMDDA is equipped with an additional conflict-resolving facility contributed by the DDA algorithm. In this regard, the FAM learning procedure, specifically in its ART$_a$ module, is modified for resolving overlaps (conflicts) among prototypes of different classes.

In order to include the idea of infinite/finite volume as in [11] within the FAM framework, each dimension d of prototype p in the recognition layer (i.e., F_2^a) of the ART$_a$ module is given a status of S_{pd}=0 (i.e., infinite dimension) or S_{pd}=1 (i.e., finite dimension). All dimensions of a newly committed F_2^a prototype are initialized as 0. When the prototype is involved in width shrinking, the status of the selected dimension is changed to 1. In addition, a new set of *reference vector*, $\boldsymbol{w}_j^r$, is introduced to each prototype in F_2^a. Each reference vector is initialized as a zero vector. When learning takes place, besides the weight vector $\boldsymbol{w}_J^a$ [8], the reference vector of the *J*-th F_2^a winning node is also updated according to a recursive center estimation procedure [12], as follows.

$$\left(\boldsymbol{w}_J^r\right)^{new} = \left(\boldsymbol{w}_J^r\right)^{old} + \frac{1}{N_J}\left(\boldsymbol{A} - \left(\boldsymbol{w}_J^r\right)^{old}\right) \tag{6}$$

where N_J is the number of input patterns of the J-th node, $N_J = N_J + 1$.

If $\boldsymbol{x}$, which represents the weights of the $M-$dimension (or $2M-$ dimension with complement coding) winning prototype falls in the region formed by the prototype of different classes (i.e., λ), a conflict is said to occur. As such, a width shrinking procedure is executed to avoid the conflict. The width of the conflicting prototypical region is shrunk. The shrinking procedure is applied successively between the winning prototype and other conflicting prototypes. In general, three cases of width shrinking are considered [11]. First, if the existing finite dimensions of the conflicting prototype q can be shrunk without falling below a pre-set $\varepsilon_{\min}$, the one with the smallest loss in volume ($\gamma_{best,k}$) is chosen, as follows [11].

$$\gamma_{best,k} = \min\{\left|w_{qk}^r - x_k\right| : \forall 1 \le i \le n, i \ne k : \left(\frac{\lambda_{qk} - \left|w_{qk}^r - x_k\right|}{\lambda_{qk}} \le \frac{\lambda_{qi} - \left|w_{qi}^r - x_i\right|}{\lambda_{qi}}\right) \wedge \left(\lambda_{qk} \ge \varepsilon_{k,min}\right) : S_{qi}, S_{qk} = 1\} \tag{7}$$

where $\lambda_{qj} = \left|w_{qj} - w_{qj}^r\right|$ and w_{qj} represents the weight of the prototype q at dimension j. Equation (7) indicates that shrinking of an existing finite dimension is preferred for not losing the "infinite volume" of other infinite dimensions. Such idea also complies with the learning paradigm of FAM, which supports the stability property; i.e., it helps protect previously learned knowledge of FAMDDA from being washed away. However, if the first option is not satisfied, the following options are considered, i.e., either one of the remaining infinite dimensions is shrunk ($\gamma_{\max,l}$),

$$\gamma_{\max,l} = \max\left\{\left|w_{ql}^r - x_l\right| : S_{ql} = 0\right\} \tag{8}$$

or, the width of the finite dimension of the prototype q is shrunk

$$\gamma_{min,m} = \min\{\left|w_{qm}^r - x_{qm}\right| : \forall 1 \le i \le n, i \ne m : \left(\frac{\lambda_{qm} - \left|w_{qm}^r - x_{qm}\right|}{\lambda_{qm}} \le \frac{\lambda_{qi} - \left|w_{qi}^r - x_{qi}\right|}{\lambda_{qi}}\right) : S_{qi}, S_{qk} = 1\} \tag{9}$$

Equation (8) is selected if $\gamma_{\max,l} > \gamma_{\min,m}$. Upon the selection of γ_z from (7)–(9), region λ_{qk} is reduced by adjusting w_{qz}, as follows.

$$w_{qz}^{new} = \begin{cases} w_{qz}^{old} + \gamma_z & \text{if } w_{qz}^{old} < w_{qz}^r \\ w_{qz}^{old} - \gamma_z & \text{if } w_{qz}^{old} > w_{qz}^r \end{cases} \tag{10}$$

If $w_{qz} > 1$ or $w_{qz} < 0$, it is rounded as $w_{qz} = 1$ or $w_{qz} = 0$, respectively. For clarity, FAMDDA undergoes sequential learning which synchronizes the operation of the DDA algorithm with the learning process of FAM in a fast manner. In this situation, the DDA algorithm is not possible to find an optimum solution which can eliminate all conflicts within reasonable time in this sequential learning paradigm. Instead,

the proposed FAMDDA network attempts to reduce and/or avoid overlapping among prototypes of conflicting classes during its training session. The conflict-resolved prototypes and their associations obtained in the training phase are used, during the test phase, to recall a prediction when an unseen pattern is presented to ART_a.

In general, the training procedure of FAMDDA can be summarized as follows.

1. An M-dimensional input pattern $\boldsymbol{a} \in [0,1]^M$ in F_0^a is complement-coded to a $2M$-dimensional vector $\boldsymbol{A}$.
2. The input vector $\boldsymbol{A}$ is propagated from F_1^a to F_2^a through the weight vector, $\boldsymbol{w}^a$. The response of each node is computed according to the match function as in (1).
3. The prototype of node J is propagated back from F_2^a to F_1^a to participate in the vigilance test as in (2).
4. If the vigilance test fails, a new search cycle is initiated by re-visiting step 3. (The above cycle runs simultaneously in ART_b).
5. A prediction is sent from F_2^a (i.e., $\boldsymbol{w}_J^{ab}$) and from F_2^b (i.e., $\boldsymbol{y}^b$), respectively, to F^{ab}, where the map-field vigilance test as in (3) is performed.
6. If the map-field vigilance test fails, a matching-tracking procedure as in (4) is triggered. Similar to FAM, the matching-tracking procedure only affects the ART_a module of FAMDDA, and step 3 is re-visited.
7. The weight vectors $\boldsymbol{w}_J^a$ and $\boldsymbol{w}^r$ are updated according to (5)–(6). The weight vector $\boldsymbol{w}_J^b$ of the winning node in ART_b is updated using (5) by replacing superscript or subscript a with b.
8. The F_2^a nodes with different class from that of the winning node J are identified. Width shrinking of the existing conflicting nodes is initiated by considering one of the three cases as in (7)–(9).

The training session is completed when all training patterns have been presented to the network. Otherwise, the training session is continued by presenting the next pattern to the network, and step 1 is re-visited.

III. LEARNING WITH IMBALANCED DATASETS

The class distributions of an imbalanced dataset are uneven whereby most of the data samples belong to the majority class and very few data samples belong to the minority classes. Learning from such an imbalanced dataset is a challenging task especially when the database is huge and complex. For a binary classification problem, many performance indicators have been introduced, and they are based on a confusion matrix as shown in Table I.

A popular metric in pattern classification is the overall accuracy, which is the *correctly classified rate* (CCR) as shown in (11). Indeed, the CCR is suitable for assessing the performance of a classification model with balanced datasets. A tendency of a typical classification model when dealing with imbalanced datasets is that the model can be biased to classify

TABLE I. CONFUSION MATRIX

	Predicted Positive (Label=0)	**Predicted Negative (Label=1)**
Actual Positive (Label=0)	True Positive (TP)	False Negative (FN)
Actual Negative (Label=1)	False Positive (FP)	True Negative (TN)

all data samples as belonging to the majority class. In this regard, the model is likely to classify data samples from the majority class well (i.e., very high TP) but unlikely to classify data samples from the minority class efficiently (i.e., very low TN). Under this circumstance, a high CCR value can be contributed by a very high value of TP and a very low value of TN. As such the CCR is not an appropriate measure for classification performance when dealing with imbalanced datasets.

$$\mathrm{CCR} = \frac{\mathrm{TP} + \mathrm{TN}}{\mathrm{TP} + \mathrm{FP} + \mathrm{FN} + \mathrm{TN}} \tag{11}$$

From the literature, geometric mean, G-mean, is a more feasible performance indicator for imbalanced data classification. It is a nonlinear measurement, and is independent of the distribution of data samples among different classes [13]. G-mean evaluates the performance of a classification model in a fair way by considering the results of both the majority and minority classes. G-mean is expressed as follows:

$$\mathrm{G\text{-}mean} = \sqrt{\mathrm{TPR} \times \mathrm{TNR}} \tag{12}$$

where

$$\mathrm{TPR} = \frac{\mathrm{TP}}{\mathrm{TP} + \mathrm{FN}}, \ \mathrm{TNR} = \frac{\mathrm{TN}}{\mathrm{TN} + \mathrm{FP}} \tag{13}$$

TPR and TNR are the rates of TP and TN, respectively. TPR and TNP, respectively, represent the rates of the majority and minority classes being predicted correctly.

IV. CLASSIFICATION WITH A LARGE IMBALANCED DATASET

In the manufacturing industry, finished goods are normally produced in large quantities. The volume of production is a key performance index to indicate processing capacity and quality. In semiconductor as well as in other manufacturing industries, production growth from the mass production of one finished good is a target to achieve because it could bring a reduction in cost and also an increase in revenue. If the volume of production could be estimated by analyzing data from an upstream process with an intelligent system, then it could assist the production unit to identify impending yield or quality issues related to the final product. In this case, the undesirable variations from the upstream process could be identified to make improvements, and this helps to assure high product quality and efficient supply line management. Indeed, as pointed out in [14], classification is a useful way to help understand complex manufacturing processes.

A. Data Background

In this research, a case study involving the use of an encrypted dataset collected from a semiconductor company. The input and output features of the dataset are shown in Table II. The dataset comprises three input attributes where one of them is a categorical attribute whereas the other two are numerical attributes. The categorical attribute has a record of

215 values, ranging from 1A to 215A. Both numerical attributes have discrete values; the first has a range from 174610 to 299370 whereas the second from 174650 to 301770. The output class a binary number.

The dataset consists of 169910 samples, and they were divided into training and test sets. Table III summarizes the distributions of the data samples in the training and test sets. As can be seen from Table III, the data distribution in training and test sets was highly skewed. This is because in both training and test sets, the number of samples with label 0 is more than those with label 1. Indeed, the dataset exhibits a property of data imbalance, i.e., relative imbalance [15]. Thus, it was a challenging task to predict the samples from the minority class accurately.

B. Experimental Setups

Data normalization is required for use with FAM so as to mitigate the effect of category proliferation [8] during its learning process. In this case, the value of an attribute is normalized between 0 and 1 using

$$(x - \min(x))/(\max(x) - \min(x)) \qquad (14)$$

where $\min(x)$ and $\max(x)$ are respectively the lowest and the highest values of the attribute, x, in the dataset.

Data re-sampling techniques are useful for assisting a classification model in learning imbalanced datasets [15]. As such, an under sampling technique [6] was applied to select randomly a portion of training samples from the majority class in this experiment. The FAM-based networks were trained with the selected samples from the majority class together with all samples from the minority class. In this case, the numbers of samples selected from the majority class were respectively 10%, 30%, 50% and 100% of number of the samples from minority class (i.e., four ratios, namely 1:10, 3:10, 5:10 and 10:10).

The parameter settings of FAM-based networks are as follows. Original FAM used a fast training approach with $\beta = 1$; baseline vigilance of ART_a, $\bar{\rho}_a = 0.0$; choice parameter $\chi \approx 0$. As for FAMDDA, it was trained with the same parameter settings as original FAM in addition to a minimum width value, $\varepsilon_{\min} = 0.1$. In order to ascertain the stability of the classification performance, the experiment was repeated 10 times. The average results were computed using the bootstrap method [16], with the 95% confidence intervals estimated. The bootstrap method was employed because it did not rely on the assumption that the samples must be drawn from a normal distribution. In order to compare the average results between FAM and FAMDDA, a bootstrap hypothesis testing was conducted. In this case, the null hypothesis assumes the average results of FAM and FAMDDA were the same whereas the alternative hypothesis stated that the average result of FAM is lower than that of FAMDDA. The significance level α is set at 0.05. If the probability value (p-value) is lower than α, then the null hypothesis is rejected.

C. Results and Discussion

Fig. 2 compares graphically the G-mean results of the trained networks on the test set. Note that the networks were trained with samples from majority and minority classes in four different ratios. By observing Fig. 2, the FAM and FAMDDA, which were trained with a combination of majority and minority samples with a ratio 3:10, could give the highest G-mean results. Such classification results of the trained networks on the test set are presented in more details in Table IV. Even though 55% of the test samples recorded by attribute 2 (and a small portion of the test samples recorded by attribute 3) are extrapolated, both FAM and FAMDDA are able to classify the samples with good performances that exceed the extrapolation rates. In particular, the performances of FAM in terms of CCR, TPR, and G-mean are significantly lower than those from FAMDDA statistically (at the 95% confidence level). The performances of FAM and FAMDDA in terms of TNR are statistically similar. However, the latter is able to yield a slightly higher TNR by predicting more test samples from the minority class correctly. Overall, FAMDDA is able to outperform FAM in dealing with the imbalanced dataset from this problem.

In addition, despite the presence of a substantially large number of unseen samples that are different from those in the training set, the learned FAMDDA model is able to classify the unseen samples with very similar TPR (i.e., 77.57%) and TNR (i.e., 74.96%). This observation indicates that FAMDDA is able to predict equally well samples from the majority and minority classes, whereby it does not show a bias to the majority class that contains more samples.

TABLE II. AN OVERVIEW OF AN ENCRYPTED SEMICONDUCTOR DATASET

Dataset	Attribute 1 (categorical)	Attribute 2 (numerical)	Attribute 3 (numerical)	Output (numerical)
Training Set	1A to 215A	174610–261970	174650–278140	0/1
Test Set	1A to 215A	180800–299370	176670–301770	0/1
Interpolate Rate of Test Data (%)	100	44.66	93.06	100
Extrapolate Rate of Test Data (%)	0	55.34	6.94	0

TABLE III. CLASS DISTRIBUTIONS OF THE SAMPLES IN TRAINING AND TEST SETS

Dataset	Samples of the Majority Class	Samples of the Minority Class	Total Samples	Minority Rate (Minority/Total)
Training Set	44924	7469	52393	0.166
Test Set	108622	8895	117517	0.076

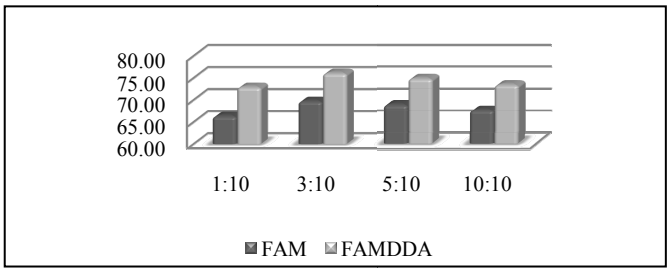

Figure 2. The G-mean results of the trained networks on the test set.

TABLE IV. PERFORMANCE COMPARISON BETWEEN FAM AND FAMDDA

Metric (%)	FAM			FAMDDA			*p*-value
	Average	Highest	Lowest	Average	Highest	Lowest	
CCR	66.04	72.62	60.85	77.36	84.02	70.74	0.000
TPR	65.31	72.42	59.53	77.57	84.92	70.06	0.000
TNR	74.70	78.25	70.13	74.96	79.07	71.05	0.425
G-Mean	69.78	73.71	66.47	76.14	78.73	74.43	0.000

TABLE V. PERFORMANCE COMPARISON WITH OTHER CLASSIFICATION METHODS

Model	CRR	TPR	TNR	G-mean
KNN	0.91	0.95	0.43	0.64
SVM-RBF	0.75	0.74	0.83	0.79
FAM (best)	0.7262	0.7242	0.7503	0.7371
FAMDDA (best)	0.8402	0.8492	0.7300	0.7873

The classification performances of FAM and FAMDDA are also compared with those results of other methods, which include K-nearest neighborhood (KNN) algorithm and support vector machines with radial basis function kernels (SVM-RBF) [17]. In this regard, the best individual classification performances of FAM and FAMDDA, which are based on the highest G-mean, are listed in Table V for comparison. KNN represents an instance-based learning algorithm whereas SVM-RBF is a kernel-based model making use of selected instances (i.e., support vectors, for which the margins between their locations and the concept boundary (hyperplane) have been maximally optimized) for performing pattern classification. Both FAM and FAMDDA could give more *balanced* results in terms of TPR and TNR as compared to KNN and thus, they could contribute to higher G-mean than the latter. The classification results of FAM are not better than SVM-RBF in terms of G-mean and CRR. On the other hand, FAMDDA could give G-mean that is compatible with that of SVM-RBF and the former has a slight advantage in performing with a higher CRR. This finding indicates the potential of FAMDDA as a useful model for learning and classifying imbalanced dataset from the semiconductor industry.

V. SUMMARY

In this paper, a variant of FAM, which has been equipped with a conflict-resolving facility, i.e., fuzzy ARTMAP with Dynamic Decay Adjustment algorithm (FAMDDA), has been proposed for undertaking learning with imbalanced datasets. It is used together with a data re-sampling technique for learning and classifying a large imbalanced dataset collected from a semiconductor company. The results and analysis showed that the proposed FAMDDA network can identify the samples from both the minority and majority classes more accurately than FAM. A benchmark study was also conducted to check on the classification performances of FAM and FAMDDA with other methods. The finding indicated that FAMDDA could serve as one of the favorable classification models in handling the imbalanced dataset problem from the semiconductor industry.

As for future work, additional experimentation should be conducted to evaluate the applicability of the proposed FAMDDA model in dealing with imbalanced datasets from different application domains. This allows validation of FAMDDA as a useful classification model for imbalanced datasets from different application domains. Besides, a long-term target in this research is to improve the classification performances, especially in terms of TPR and TNR. Hence, additional research effort will be devoted to devise more effective learning algorithms based on the existing framework for achieving this target.

ACKNOWLEDGMENT

The first author was a fellowship recipient of the Matsumae International Foundation (MIF) in 2010 for a six-month research visit to the Watada Lab. He is grateful to the MIF and the Watada Lab for providing financial supports and warm hospitality during his research stay in Japan.

REFERENCES

[1] J. Thongkam, G. Xu, Y. Zhang, and F. Huang, "Toward breast cancer survivability prediction models through improving training space," Expert Systems with Applications, vol. 36, pp. 12200–12209, 2009.

[2] M. Merler, Y. Rong, and J.R. Smith, "Imbalanced rankboost for efficiently ranking large-scale image/video collections," IEEE Conference on Computer Vision and Pattern Recognition, pp. 2607–2614, 2009.

[3] P. Juszczak, N.M. Adams, D.J. Hand, C. Whitrow, and D.J. Weston, "Off-the-peg and bespoke classifiers for fraud detection," Computational Statistics and Data Analysis , vol. 52, pp. 4521–4532, 2008.

[4] H. Wang and H. Zheng, "A bayesian approach to improving decision making in support vector machine and its application in bioinformatics," Fifth International Conference on Natural Computation ICNC '09, vol. 2, pp. 89–93, 2009.

[5] Y.-Y. Nguwi and S.-Y. Cho, "An unsupervised self-organizing learning with support vector ranking for imbalanced datasets," Expert Systems with Applications, vol. 37, pp. 8303–8312, 2010.

[6] N. Japkowicz and S. Stephen, "The class imbalance problem: a systematic study," Intelligent Data Analysis, vol. 6, pp. 429–449, 2002.

[7] X. Hong, S. Chen and C.J. Harris, "A kernel-based two-class classifier for imbalanced data sets," IEEE Transactions on Neural Networks, vol. 18, pp. 28–41, 2007.

[8] G.A. Carpenter, S. Grossberg, N. Markuzon, J. Reynolds, and D. Rosen, "Fuzzy ARTMAP: a neural network architecture for incremental learning of analog multidimensional maps," IEEE Transactions on Neural Networks, vol. 3, pp. 698–713, 1992.

[9] G.A. Carpenter and S. Grossberg, "A massively parallel architecture for a self-organizing neural pattern recognition machine," Computer Vision Graphics and Image Processing, vol. 37, pp. 54–115, 1987.

[10] L. Zadeh, "Fuzzy sets," Information and Control, vol. 8, pp. 338–353, 1965.

[11] K.-P. Huber and M.R. Berthold, "Building precise classifiers with automatic rule extraction," Proceedings of the IEEE International Conference on Neural Networks, vol. 3, pp. 1263–1268, 1995.

[12] C.P. Lim and R.F. Harrison, "An incremental adaptive network for on-line supervised learning and probability estimation," Neural Networks, vol. 10, pp. 925–939, 1997.

[13] M. Kubat, R.C. Holte and S. Matwin, "Machine learning for the detection of oil spills in satellite radar images," vol. 30, pp. 195–215, 1998.

[14] A. R. Chaturvedi, "Acquiring implicit knowledge in a complex domain," Expert Systems with Applications, vol. *6,* pp. 23–35, 1993.

[15] H. He and E.A. Garcia, "Learning from Imbalanced Data," IEEE Transactions on Knowledge and Data Engineering, vol. 21, pp. 1263-1284, 2009.

[16] B. Efron, "Bootstrap methods: another look at the jackknife," The Annals of Statistics, vol. 7, pp. 1–26, 1979.

[17] L. Ding, J. Watada, C.C. Lim, Z. Ibrahim, W.J. Lee, M. Khalid, "Building a svm-rbf-based classifier for forecasting large imbalanced dataset problem," *Proc* Int'l Symposium on Intelligent Informatics *ISII2010*, 2010.

2011 IEEE International Conference on Fuzzy Systems
June 27-30, 2011, Taipei, Taiwan

Re-Scheduling the Unit Commitment Problem in Fuzzy Environment

Bo Wang
The Graduate School of
Information, Production and Systems,
Waseda University,
Kitakyushu 808-0135, Japan
Email: bwangips@gmail.com

You Li
The Graduate School of
Information, Production and Systems,
Waseda University,
Kitakyushu 808-0135, Japan
Email: rubyli@toki.waseda.jp

Junzo Watada
The Graduate School of
Information, Production and Systems,
Waseda University,
Kitakyushu 808-0135, Japan
Email: junzow@osb.att.ne.jp

***Abstract*—The conventional prediction of future power demands are always made based on the historical data. However, the real power demands are affected by many other factors as weather, temperature and unexpected emergencies. The use of historical information alone cannot well predict real future demands. In this study, the experts' opinions from related fields are taken into consideration. To deal the uncertainty of historical data and imprecise experts' opinions, we employ fuzzy variables to better characterize the forecasted future power loads. The conventional unit commitment problem (UCP) is updated here by considering the spinning reserve costs in a fuzzy environment. As the solution, we proposed a heuristic algorithm called local convergence averse binary particle swarm optimization (LCA-PSO) to solve the UCP. The proposed model and algorithm are used to analyze several test systems. The comparisons between the proposed algorithm and the conventional approaches show that the LCA-PSO performs better in finding the optimal solutions.**

***Index Terms*—Power supply reliability, Fuzzy set theory, Unit commitment problem, Fuzzy Value-at-Risk, Local convergence averse binary particle swarm optimization, Test systems.**

I. Introduction

Most previous studies have evaluated power loads forecasted using sufficient historical data. Nevertheless, these studies have the disadvantage that: there are many factors that must be simulated or determined in order to find which factors will affect the real power loads. For example, weather, temperature and unexpected emergencies influence power consumption. As a result, the power systems are suffering from the uncertainty associated with the fact that the real power demands always deviate from forecasts [1]. Consequently, the use of historical information alone cannot predict real future demands.

In this study, the conventional methods are improved to mitigate the above shortcoming. The experts' opinions from related fields are taken into consideration to better describe the future power loads. To handle the uncertainty that arises from the use of historical data and expert opinions, it is better to treat the forecasted power loads as variables with imprecise distributions, i.e., fuzzy variables.

In actuality, fuzzy set theory is a fundamental mathematical system that describes uncertainty, and various researchers have applied it to solve power system problems. To minimize real power losses and improve the voltage profile of a given system, Rahman [4] mathematically formulated an optimal reactive power control problem in which the objective function and constraints are expressed by fuzzy sets when modeled. In Khare's paper [5], fuzzy set theory was used to capture the subjective preferences of human operators in order to model their decision-making and generate a prioritized list of emergency problems that is more acceptable to the operator. Using a multi-objective fuzzy linear programming technique, Abou El-Ela [6] proposed a multi-stage procedure that lessens the influence of different emergency conditions. The results of their experiments showed that the proposed fuzzy procedure can reduce the influence of different emergency conditions.

Employing fuzzy set theory, we take the forecasted loads as fuzzy variables. The conventional unit commitment problem (UCP) which has been commonly formulated as a complex, nonlinear, mixed-integer optimization problem [1], [2], [3] is improved here to take the spinning reserve costs in a fuzzy environment into consideration. To handle this improved UCP, we propose a local convergence averse binary particle swarm optimization (LCA-PSO), which outperforms existing algorithms.

The remainder of this paper is organized as follows: in Section 2, we briefly review previous fuzzy power system problems and introduce some basic background regarding fuzzy variables; Section 3 illustrates the improved UCP; then, Section 4 provides the LCA-PSO as the solution; the model and algorithm are exemplified by some test systems in Section 5; finally, Section 6 summarizes the conclusions.

II. Preliminaries

In this section, we preliminarily provide some basic concepts and features of fuzzy variables.

Suppose ξ is a fuzzy variable whose membership function is μ_ξ, and r is a real number. Then, the possibility, necessity and credibility of event $\xi \le r$ are expressed, respectively, as follows:

$$\mathrm{Pos}\{\xi \le r\} = \sup_{t \le r} \mu_\xi(t), \tag{1}$$

$$\mathrm{Nec}\{\xi \le r\} = 1 - \sup_{t > r} \mu_\xi(t), \tag{2}$$

978-1-4244-7316-8/11/$26.00 ©2011 IEEE

$$\mathrm{Cr}\{\xi \le r\} = \frac{1}{2}\left[\mathrm{Pos}\{\xi \le r\} + \mathrm{Nec}\{\xi \le r\}\right]. \tag{3}$$

The credibility measure is formed on the basis of the possibility and necessity measures, and in the simplest case, it is taken as their average. The credibility measure is a self-dual set function [7], *i.e.* $\mathrm{Cr}\{\xi \le r\} = 1 - \mathrm{Cr}\{\xi > r\}$. Equation (3) also results in the following:

$$\mathrm{Cr}\{\xi \le r\} = \frac{1}{2}\left[\sup_{t\le r}\mu_\xi(t) + 1 - \sup_{t>r}\mu_\xi(t)\right]. \tag{4}$$

For further information on fuzzy variables, one may refer to [7], [8] and [9].

According to [10], the VaR of an investment can be considered as the greatest value under a given confidence level. Following [11], if $\widetilde{L}_t$ denotes the fuzzy power demand of period t, in a fuzzy environment, the VaR of L_t with a confidence of $(1-\beta)$ can be written as:

$$\mathrm{VaR}_{1-\beta} = \sup\{\lambda | \mathrm{Cr}(\widetilde{L}_t \ge \lambda) \ge \beta\}, \tag{5}$$

where $\beta \in (0, 1)$.

Equation (5) tells us that the greatest value of $\widetilde{L}_t$ under confidence level $(1-\beta)$ is the largest λ.

The following numerical example illustrates the calculation of the VaR.

Example 1. *Supposing fuzzy variable* $\widetilde{L}$*=FN(1.0, 2.0), its membership function is normally distributed as* $\mu_{\widetilde{L}}(r) = \mathrm{Exp}\{-[(r-1.0)/2]^2\}$*, then let us calculate* $\mathrm{VaR}_{0.9}$.

At first, we need to calculate the credibility function of $\widetilde{L} \ge r$*. From Equation (1) and (2), we can compute the possibility and the necessity of* $\widetilde{L} \ge r$ *in the following*:

$$\begin{aligned}
\mathrm{Pos}\{\widetilde{L} \ge r\} &= \begin{cases} 1 & \mathrm{r}\le 1.0 \\ \mathrm{Exp}\{-[(r-1.0)/2]^2\}, & \mathrm{r}>1.0 \end{cases} \\
\mathrm{Nec}\{\widetilde{L} \ge r\} &= \begin{cases} 1-\mathrm{Exp}\{-[(r-1.0)/2]^2\} & \mathrm{r}\le 1.0 \\ 0 & \mathrm{r}>1.0. \end{cases}
\end{aligned} \tag{6}$$

Hence, according to Equation (3), the credibility of $\widetilde{L} \ge r$ *is written as:*

$$\mathrm{Cr}\{\widetilde{L} \ge r\} = \begin{cases} 1 - \frac{1}{2}\mathrm{Exp}\{-[(r-1.0)/2]^2\} & \mathrm{r}\le 1.0 \\ \frac{1}{2}\mathrm{Exp}\{-[(r-1.0)/2]^2\} & \mathrm{r}>1.0. \end{cases} \tag{7}$$

Therefore, making use of Equation (5), we have,

$$\mathrm{VaR}_{0.9} = \sup\{\lambda | \mathrm{Cr}(\widetilde{L} \ge \lambda) \ge 0.1\} = 2.91.$$

Recently, the measure of Value-at-Risk has been applied to many engineering problems to build fuzzy optimization models [11], [12], [13], [14], [15].

III. Modeling

From the literatures, with the purpose of providing sufficient electricity and reducing the generation cost, the UCP is solved by determining the power generation unit schedule. It is necessary to provide sufficient real power and spinning reserve in each period. However, in a market environment, the profit is also important. Therefore, the majority of the previous studies summarized the UCP as minimizing the cost function without violating the constraints.

A. The conventional UCP

1) Objective function:

$$\min F = \sum_{t=1}^{T}\sum_{i=1}^{N} u_i^t \cdot [f_i(P_i^t) + SC_i(1 - u_i^{t-1})]. \tag{8}$$

Respectively, F denotes the total cost of the power plant over the scheduling periods; T and N denote the number of considered system periods and the number of generation units, P_i^t is the power generation of unit i at time t; SC_i is the start cost of unit i; u_i^t denotes the status of unit i at time t. $f_i(P_i^t)$ is the cost function of unit i at time t, which is normally expressed by the following equation:

$$f_i(P_i^t) = a_i + b_i P_i^t + c_i (P_i^t)^2, \tag{9}$$

where, a_i, b_i and c_i are the coefficients determined by the attributes of each generation unit.

B. The improved UCP

1) Objective function: This study takes the spinning reserve cost into consideration. Then, in a fuzzy environment, the objective function is modified as follows:

$$\begin{aligned}
\min F = \sum_{t=1}^{T}\sum_{i=1}^{N} u_i^t \cdot \{&[1 - \mathrm{Pos}(Q_t > P_t)] f_i(P_i^t) \\
&+ \mathrm{Pos}(Q_t > P_t) f_i(P_i^t + R_i^t) + SC_i(1 - u_i^{t-1})\}.
\end{aligned} \tag{10}$$

P_t is the forecasted power demand of period t. If we assign a suitable value to the confidence level β, then, P_t can be calculated by Equation (5). Q_t is the real load in period t, $\mathrm{Pos}(Q_t \ge P_t)$ is the possibility that the real demand is larger than the forecasted value P_t, R_i^t is the spinning reserve of unit i at time t, and $\sum_{i=1}^{N} R_i^t = R_t$, respectively.

Remarks:

□ Supposing $\triangle P = Q_t - P_t$, if and only if $\triangle P > 0$(that is to say the real load is larger than the forecasted value), the reserve is considered to be called (even though the $\triangle P$ is sufficiently small).

□ In an uncertain environment, the power loads are fuzzy variables, and subsequently, the possibility theory can be applied to measure the chance that the spinning reserve will be called:

$$\mathrm{Pos}\{Q_t > P_t\} = \sup_{t>P_t}\mu_{\widetilde{L}_t}(t). \tag{11}$$

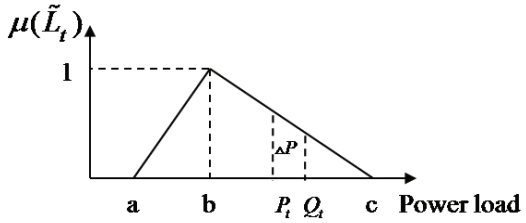

Fig. 1. The situation that spinning reserve is called

2) Constraints: The constraints are forwarded on the basis of system objective environmental demands. From the literature, they can be summarized as follows:
a). Power demand balance

$$\sum_{i=1}^{N} P_i^t u_i^t = P_t, \tag{12}$$

where P_t is the total power demand in period t.
b). Spinning reserve balance

$$\sum_{i=1}^{N} P_{max} u_i^t \geq P_t + R_t, \tag{13}$$

where R_t is the spinning reserve in period t.
c). Interval of each generation unit

$$P_{min}^i \leq P_i^t \leq P_{max}^i, \tag{14}$$

where P_{max}^i and P_{min}^i are the maximum and minimum generation capacity of unit i, respectively.
d). Unit on/off limitations

Usually, the unit state should be kept on for certain hours before it can be changed.

$$\begin{cases} T_{i,on}^t \geq T_{i,up} \\ T_{i,off}^t \geq T_{i,down} \end{cases}. \tag{15}$$

where, respectively, $T_{i,on}^t$ and $T_{i,off}^t$ are the time periods that unit i has been turned on or off. $T_{i,up}$ and $T_{i,down}$ are the minimum unit on time and maximum off time which are determined by the property of each unit.
e). Initial status of each unit

Before arranging the schedule, the unit initial status needs to be taken into consideration. That is, it is necessary to decide how many hours each unit has been committed or decommitted.

IV. The Solution

In this section, we provide the solution for the improved UCP in fuzzy environment.

UCP has been solved using various kinds of heuristic algorithm, such as genetic algorithm (GA) [16], evolutionary programming (EP) [17] and lagrangian relaxation based PSO (LRPSO) [18]. Based on these methods, Yuan [3] proposed an improved binary PSO (IPSO) algorithm, which has proven to be more effective than other approaches.

In this research, based on original PSO [19], an LCA-PSO is proposed to better solve the problem. The following is a preliminary explanation of the proposed method.
A. The fitness function of the improved UCP

Considering the spinning reserve cost and fuzzy power load, the objective function is updated as Equation (10), which is considered as the fitness function of LCA-PSO.
B. The equations update particle's position and velocity

The equations proposed in classic binary PSO [20] are employed here. The particle position is updated by the following equations:

$$v_i = w \cdot v_i + c_1 \cdot rand() \cdot (P_{best,i} - x_i) + c_2 \cdot rand() \cdot (G_{best} - x_i),$$

$$x_i = x_i + v_i, \tag{16}$$

where, v_i is the velocity of i, ω is the inertia weight, c_1 and c_2 are the learning rates generated in the interval $[0, 4]$. $rand()$ is a random number distributed in the interval $[0, 1]$. $P_{best,i}$ and G_{best} are the personal and global best among the iterations of particles, respectively. Subsequently, the position of particle i is updated by Equation (16).

Finally, the particles 0/1 states are determined by a sigmoid function $S(x)$:

$$S(x) = \frac{1}{1 + e^{-x_i}}. \tag{17}$$

C. The local convergence of PSO

It is well known that the PSO algorithm can find the optimal solution in fewer iterations than other algorithms, but may suffer from the local convergence problem. In particular, when the selection problem contains a large number of objectives, this defect of the PSO becomes more obvious. To solve this problem, Yuan [3] performed 10 trials from different initial populations and selected the smallest cost as the result. Lee [21] proposed a mutation-based PSO (MPSO) where mutations occur with given possibility. In this paper, we design the LCA-PSO by employing the escape speed (ES) and velocity modification (VM).

Escape speed: If the optimal solution cannot be updated after a specified number of time iterations, it will be considered as having fallen into local convergence. Then, each particle speed will be modified by the escape speed. The value of ES should be determined by the experiments' performances: on one hand, if the escape speed is sufficiently large, all of the particles can jump out of the current loop and resume searching in different areas; on the other hand, if the escape speed is smaller, the new optimal solution can be obtained more quickly.

Velocity modification: After the above step, each particle's velocity has been modified to an opposite direction with a random value. This is inappropriate for the future search.

Therefore, the VM is used to modify the velocity to a suitable value and in direction. In this case, a potential global optimal solution will be found.

We use the following two-dimensional Figure 2 to approximate the LCA-PSO.

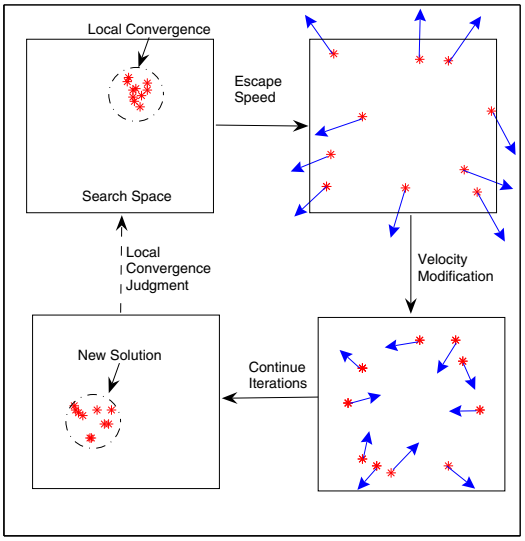

Fig. 2. Local convergence averse BPSO

Based on the above analysis, we summarize the LCA-PSO algorithm as follows:

[Step 1]. Initialize particles: Each particle contains $T \times N$ generator states, as:

$$x_i = \begin{bmatrix} u_1^1 & u_1^2 & \cdots & u_1^T \\ u_2^1 & u_2^2 & \cdots & u_2^T \\ \cdots & \cdots & \cdots & \cdots \\ u_N^1 & u_N^2 & \cdots & u_N^T \end{bmatrix}.$$

[Step 2]. Check the constraints of UCP, as mentioned in Subsection 3.2.2, part B.

[Step 3]. Solve the economic load dispatch (ELD) problem and update gray zone states for start-up cost. The concepts of ELD and gray zone have been well described in previous studies. One may refer to [3] and [22] for further information regarding these topics.

[Step 4]. Initialize personal best and global best: The personal best and global best are determined by the fitness function (10).

[Step 5]. Particle iterations: The particle positions are updated by Equation (16), and Step 2 is repeated to modify the unit states, then, new P_{best} and G_{best} are calculated.

[Step 6]. Solve the local convergence problem: If the global best cannot be improved in a given number of iterations, we consider the program to have fallen into the local convergence. Then, the aforementioned approach is used to cause the particles to jump out of current loop and to revise the particle's velocity.

[Step 7]. Following the completion of all iterations, the final global best is returned as the optimal result.

V. Exemplification using Test Systems

A. The performances of the proposed model and LCA-PSO

In this section, the proposed model and algorithm are exemplified using test systems. The 24-hour power loads are fuzzy variables evaluated from previous data and experts' opinions, as listed in Table 1. (a, b, c) denotes the triangular fuzzy variable, and FN(a, σ^2) represents a normally distributed fuzzy variable. The power demand here are measured in megawatt (MW).

TABLE I
24 Hours forecasted fuzzy power demands

Period	Power Demands	Period	Power Demands
1	(650, 700, 750)	13	(1350, 1400, 1450)
2	(700, 750, 800)	14	(1250, 1300, 1350)
3	(800, 850, 900)	15	(1150, 1200, 1250)
4	(900, 950, 1000)	16	(1000, 1050, 1100)
5	(950, 1000, 1050)	17	FN(1000, 400)
6	(1050, 1100, 1150)	18	FN(1100, 410)
7	(1100, 1150, 1200)	19	FN(1200, 410)
8	FN(1200, 440)	20	FN(1400, 430)
9	FN(1300, 420)	21	FN(1300, 400)
10	FN(1400, 400)	22	(1050, 1100, 1150)
11	FN(1450, 400)	23	(850, 900, 950)
12	FN(1500, 390)	24	(750, 800, 850)

Supposedly, the lowest and highest confidence levels provided by the grid company of VaR is 80% and 95%, respectively. Then, using Equation(5), we get the demands and reserves in real values, as listed in the following Table 2.

TABLE II
24 Hours evaluated power demands and reserves

Period	Demands	Reserves	Period	Demands	Reserves
1	730.0	15.0	13	1430.0	15.0
2	780.0	15.0	14	1330.0	15.0
3	880.0	15.0	15	1230.0	15.0
4	980.0	15.0	16	1080.0	15.0
5	1030.0	15.0	17	1019.1	11.2
6	1130.0	15.0	18	1119.4	11.3
7	1180.0	15.0	19	1219.4	11.3
8	1220.1	11.7	20	1419.4	12.1
9	1319.6	11.5	21	1319.1	11.2
10	1419.1	11.2	22	1130.0	15.0
11	1469.1	11.2	23	930.0	15.0
12	1518.9	11.1	24	830.0	15.0

Based on the above analysis, the proposed LCA-PSO is evaluated through the use of different-sized test systems (10, 20, 40, 60, 80 and 100 units), which are expanded from a 10-unit based system [17]. All of the experiments are implemented on a Dell E8500 3.16 GHz CPU with 2.96 GB of RAM.

We first tested the LCA-PSO in different systems of various unit sizes. The parameters were selected as follows: 20 particles, 500 iterations, $c_1 = 2.8$, $c_2 = 1.2$, $\omega = 1$, a maximum speed of 4.0 and a minimum speed of -7.0. For LCA-PSO, the given time iteration mentioned in Section IV was set at 20,

and this was used to evaluate whether the local convergence occurs.

Table 3 illustrates the performance of LCA-PSO by comparing the initial cost and the cost after 1000 iterations in different-sized systems. The savings are calculated as $(InitialCost - FinalCost)/InitialCost * 100\%$.

TABLE III
THE PERFORMANCE OF LCA-PSO

Unit No.	Initial Cost	Final Cost	Savings
10	602,270	570,006	5.36%
20	1,208,507	1,139,005	5.75%
40	2,420,321	2,277,396	5.91%
60	3,625,509	3,420,438	5.67%
80	4,827,049	4,554,346	5.65%
100	6,036,371	5,706,201	5.46%

From Table 3, we can find that, the LCA-PSO could result in a cost-saving of more than 5.3% amongst all of the test systems.

In Tables 4 and 5, we show an example of initial and final schedules as found by the LCA-PSO for the 10-unit test model. This illustrates the number of start-up and shut-down decisions made through the LCA-PSO optimization process.

TABLE IV
THE INITIAL SOLUTION OF LCA-PSO (COST: 602,270)

Hours \ Unit No.	0	1	2	3	4	5	6	7	8	9
1	1	1	1	1	1	0	0	1	1	0
2	1	1	1	1	1	0	0	0	0	1
3	1	1	1	1	1	0	0	0	0	0
4	1	1	1	1	1	1	1	1	1	1
5	1	1	1	1	1	1	1	0	0	0
6	1	1	1	1	1	1	1	0	0	0
7	1	1	1	1	1	0	1	1	0	0
8	1	1	1	1	1	0	1	0	0	1
9	1	1	1	1	1	0	1	0	1	1
10	1	1	1	1	1	1	1	0	0	0
11	1	1	1	1	1	1	1	0	1	0
12	1	1	1	1	1	1	1	0	0	1
13	1	1	1	1	1	1	1	0	0	0
14	1	1	1	1	1	1	1	1	1	0
15	1	1	1	1	1	1	1	0	1	1
16	1	1	1	1	1	1	1	1	1	0
17	1	1	1	1	1	1	1	0	1	1
18	1	1	1	1	1	1	1	0	0	1
19	1	1	1	1	1	1	1	0	0	1
20	1	1	1	1	1	1	1	0	0	1
21	1	1	1	1	1	1	0	1	0	1
22	1	1	1	1	1	1	0	0	0	0
23	1	1	1	1	1	0	0	0	1	0
24	1	1	1	1	1	0	0	0	0	0

B. Comparisons between LCA-PSO and other improved PSO algorithms

In this subsection, we compare the LCA-PSO with IPSO (*the best result of 10 trails was selected*) [3] and MPSO [21]. For MPSO, the mutation probability was 0.1. After 1000 iterations, the total costs and CPU time of each algorithm are listed in Tables 6 and 7.

TABLE V
THE OPTIMIZED SOLUTION OF LCA-PSO (COST: 570,006)

Hours \ Unit No.	0	1	2	3	4	5	6	7	8	9
1	1	1	0	0	1	0	0	0	0	0
2	1	1	0	0	1	0	0	0	0	0
3	1	1	0	0	1	0	0	0	0	0
4	1	1	0	0	1	0	0	0	0	0
5	1	1	0	0	1	0	0	0	0	0
6	1	1	0	1	1	0	0	0	0	0
7	1	1	0	1	1	0	0	0	0	0
8	1	1	1	1	1	0	0	0	0	0
9	1	1	1	1	1	0	0	0	0	0
10	1	1	1	1	1	1	1	0	0	0
11	1	1	1	1	1	1	1	0	0	0
12	1	1	1	1	1	1	1	1	0	0
13	1	1	1	1	1	1	1	0	0	0
14	1	1	1	1	1	1	0	0	0	0
15	1	1	1	1	1	0	0	0	0	0
16	1	1	1	1	1	0	0	0	0	0
17	1	1	1	1	1	0	0	0	0	0
18	1	1	1	1	1	0	0	0	0	0
19	1	1	1	1	1	0	0	0	0	0
20	1	1	1	1	1	1	0	1	0	0
21	1	1	1	1	1	1	0	0	0	0
22	1	1	0	0	1	1	0	0	0	0
23	1	1	0	0	1	0	0	0	0	0
24	1	1	0	0	1	0	0	0	0	0

TABLE VI
OPTIMAL RESULTS OF DIFFERENT ALGORITHMS

Unit No. \ Methods	LCA-PSO	MPSO	IPSO
10	570,006	574,905	599,782
20	1,139,005	1,152,966	1,196,029
40	2,277,396	2,323,435	2,401,728
60	3,420,438	3,451,762	3,592,585
80	4,554,346	4,691,481	4,798,427
100	5,706,201	5,864,719	5,988,264

We found that, in most of the test systems, the LCA-PSO was able to obtain better optimal solutions with less runtime cost than other approaches.

Nevertheless, compared with the CPU time used in prior work, more computation time is required to reach the final optimal solutions in this study. The reason for this could be that the objective function here is modified from Equations (8) to (10). Therefore, during each iteration, the cost was computed with respect to two options: 1. The reserve was not called (as in the conventional UC models); 2. The reserve was called. We must re-arrange different unit on/off schedules for each situation. Therefore, more time was required to obtain the optimal result.

To prove the effectiveness of LCA-PSO, we employed a 100-units test system, and Figure 3 shows the performance of each method during the 1000 iterations.

Finally, in Figure 3, it should be noted that, in the 100 units test system, the IPSO and MPSO are suffering from the local convergence problem. However, the proposed LCA-PSO could overcome the local convergence effectively, the ES and VM were quite effective in solving such unit commitment

TABLE VII
COMPARISONS OF CPU TIME (S)

Unit No. \ Methods	LCA-PSO	MPSO	IPSO
10	18.34	15.73	14.48
20	57.32	65.87	60.65
40	274.67	317.29	316.86
60	572.30	673.46	744.19
80	1068.58	1284.01	1439.51
100	1734.67	2122.44	2503.78

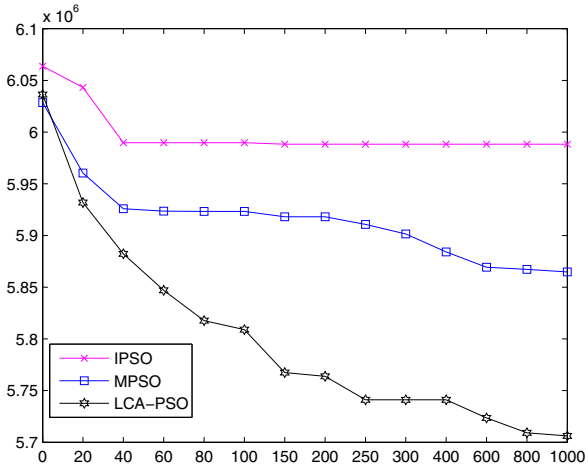

Fig. 3. Performances in a 100 unit test system

optimization problem.

VI. CONCLUSION

In this study, the fuzzy variable is used to more accurately describe the future power load while the fuzzy Value-at-Risk is employed as a technique to evaluate the power demand and reserve for each period. The conventional unit commitment model is improved by considering the possibility that the reserve is called in uncertain environment. This model can minimize the system cost by considering various constraints. To solve the problem, we proposed an LCA-PSO as the solution that has been proved to be most useful and effective by the test systems. Furthermore, comparisons with existing algorithms show that the LCA-PSO has higher performance. In addition, the proposed model can be applied to various engineering reliability control problems.

ACKNOWLEDGMENT

This research was supported by Waseda University Global COE Program "International Research and Education Center for Ambient SOC" sponsored by MEXT, Japan.

REFERENCES

[1] P. A. Ruiz, C. R. Philbrick, K. W. Cheung and P. W. Sauer, "Uncertainty management in the unit commitment problem", *IEEE Trans. On power system*, vol. 24, no. 2, pp. 642-651, 2009.

[2] A. Pathom, K. Hiroyuki, and T. Eiichi, "A hybrid LR-EP for solving new profit-based UC problem under competitive environment", *IEEE Trans. on power system*, vol. 18, no. 1, pp. 229-237, 2003.

[3] X. Yuan, H. Nie, A. Su, L. Wang and Y. Yuan, "An improved binary particle swarm optimization for unit commitment problem", *Expert Systems with applications*, vol. 36, no. 4, , pp. 8049-8055, 2009.

[4] H. A. Rahman and S. M. Shahidehpour, "A fuzzy based optimal reactive power control", *IEEE Trans. on power system*, vol. 8, no. 2, pp. 662-670, 1993.

[5] R. Khare and R. D. Christie, "Prioritizing emergency control problem with fuzzy set theory", *IEEE Trans. on power system*, vol. 12, no. 3, pp. 1237-1242, 1997.

[6] A. A. Abou El-Ela, M. A. Bishr, S. M. Allam and R.A. Ei-Sehiemy, "An emergency power system control based on the multi-stage fuzzy based procedure", *Electric Power Systems Research*, vol. 77, no 5-6, pp. 421-429, 2007.

[7] B. Liu and Y. K. Liu, "Expected value of fuzzy variable and fuzzy expected value models", *IEEE Trans. on Fuzzy Systems*, vol. 10, no. 4, pp. 445-450, 2002.

[8] S. Nahmias, "Fuzzy variable", *Fuzzy Sets and Systems*, vol. 1, no. 2, pp. 97-101, 1978.

[9] S. Wang, Y. Liu and X. Dai, "On the continuity and absolute continuity of credibility functions", *Journal of Uncertain System*, vol. 1, no. 2, pp. 185-200, 2007.

[10] D. Duffie and J. Pan, "An overview of value-at-risk", *Journal of Derivatives*, vol. 4, no. 3, pp. 7-49, 1997.

[11] S. Wang, J. Watada and W. Pedrycz, "Value-at-Risk-Based two-satge fuzzy facility location problems", *IEEE Trans. on Industrial Informatics*, vol. 5, no. 4, pp. 465-482, 2009.

[12] S. Wang and J. Watada, "Two-stage fuzzy stochastic programming with Value-at-Risk criteria", *Applied Soft Computing*, vol. 11, no. 1, pp. 1044-1056, 2011.

[13] Z. Zmeskal, "Value at risk methodology of international index portfolio under soft conditions", *International Review of Financial Analysis*, vol. 14, no. 6, pp. 263-275, 2005.

[14] B. Wang, Y. Li and J. Watada, "Fuzzy Power System Reliability Model Based on Value-at-Risk", *In: Proceedings of the 14th International Conference on Knowledge-Based and Intelligent Information and Engineering Systems*, pp. 445-453, 2010.

[15] R.A. Jabr, "Robust self-scheduling under price uncertainty using conditional value-at-risk", *IEEE Trans. on Power Systems*, vol. 20, no. 4, pp. 1852-1858, 2005.

[16] S. Kazarlis and A. Bakirtzis, "A genetic algorithm solution to the unit commitment problem", *IEEE Trans. on Power System*, vol. 11, no. 1, pp. 83-92, 1996.

[17] K. Juste, H. Kita and E. Tanaka, "An evolutionary programming solution to the unit commitment problem", *IEEE Trans. on power system*, vol. 14, no. 4, pp. 452-259, 1999.

[18] H. Balci and J. Valenzuela, "Scheduling electricity power generations using particle swarm optimization combined with the Lagrangian relaxation method", *International Journal of Applied Mathematics and Computer Science*, vol. 14, no. 3, pp. 411-421, 2004.

[19] J. Kennedy and R. C. Eberhaart, "Particle swarm optimization", *In: Proceedings of the 1995 IEEE International Conference on Neual Network, IV*, pp. 1942-1948, 1995.

[20] J. Kennedy, R. C. Eberhaart, "A Discrete Binary Version of the Particle Swarm Algorithm," *In Proceeding of IEEE International Conference on Systems, Man, and Cybernetics*, pp. 4104-4108, 1997.

[21] S. Lee, H. Park, and M. Jeon, "Binary particle swarm optimization with bit change mutation, *IEICE Trans. Fundam. Electron. Commun. Comput. Sci.*, vol. E-90A, no. 10, pp. 2253-2256, 2007.

[22] X. Yuan, A. Su, Y. Yuan, H. Nie and L. Wang, "An improved PSO for dynamic load dispatch of generators with valve-point effects", *Energy*, vol. 34,no. 1, pp. 67-74, 2009.

2011 IEEE International Conference on Fuzzy Systems
June 27-30, 2011, Taipei, Taiwan

Building a Fuzzy Multi-objective Portfolio Selection model with Distinct Risk Measurements

You Li
The Graduate School of
Information, Production and Systems,
Waseda University,
Kitakyushu 808-0135, Japan
Email: rubyli@toki.waseda.jp

Bo Wang
The Graduate School of
Information, Production and Systems,
Waseda University,
Kitakyushu 808-0135, Japan
Email: bwangips@gmail.com

Junzo Watada
The Graduate School of
Information, Production and Systems,
Waseda University,
Kitakyushu 808-0135, Japan
Email: junzow@osb.att.ne.jp

***Abstract*—Based on portfolio selection theory, this study proposes an improved fuzzy multi-objective model that can evaluate the invest risk exactly and increase the probability of obtaining the expected return. In building the model, fuzzy Value-at-Risk (VaR) is used to evaluate the exact future risk, in term of loss. The VaR can directly reflect the greatest loss of a selection case under a given confidence level. On the other hand, variance is utilized to make the selection more stable. This model can provide investors with more significant information in decision-making. To better solve this model, an improved particle swarm optimization algorithm is designed to mitigate the conventional local convergence problem. Finally, the proposed model and algorithm are exemplified by some numerical examples. Experiment results show that the model and algorithm are effective in solving the multi-objective portfolio selection problem.**

***Index Terms*—Fuzzy multi-objective portfolio selection model, fuzzy variable, fuzzy Value-at-Risk, fuzzy simulation, improved particle swarm optimization.**

I. Introduction

In finance, portfolio selection theory plays a pivotal role in decision-making for portfolio investors. As an early adopter, Markowitz [1] proposed a significant portfolio selection theory in 1952. He used the single period variance of returns as a risk measure to develop techniques for portfolio optimization. From then on, various researches have been carried on.

Security returns in conventional models are always determined by precise historical data. However, such data are not always available. On the other hand, securities are always affected by infinitive factors. It is impossible to simulate the influence of all factors well. Therefore, in today's stock markets, it is not reasonable to evaluate future security returns only based on the historical data. To make the forecasting more accuracy, the expert's opinions from related fields need to be considered. In prediction, to handle the uncertain factors wthat affect the security return and the imprecise expert's opinions, it is in reason to treat security returns as variables with imprecise distributions, i.e., fuzzy variables.

Based on fuzzy set theory, recently, various fuzzy portfolio selection models are proposed [2-9]. Among these fuzzy portfolio selection models, the most important distinction could be the risk measure method. Different techniques provide different criteria to select a portfolio. Huang [8] employed the variance of fuzzy variables as a risk measurement. As an extension of conventional variance theory, the variance of fuzzy variables can reflect an average deviation level of a selection case to the expected value in fuzzy environment. Huang [3] also developed a mean-entropy model. As a physics concept, entropy was utilized here to reduce the uncertainty of a portfolio and make the prediction easily. Li *et al.* [4] proposed a mean-variance-skewness portfolio selection model. Being combined with variance, the skewness was taken for a new risk measurement which can evaluate an average deviation level from the expected value with asymmetry fuzzy returns. Recently, Wang *et al.* [9] introduced fuzzy Value-at-Risk (VaR) to this field. The VaR can directly reflect the loss of one selection case under given confidence level. It was used as a novel risk measurement. Different from previous methods which try to make the portfolio stable, the VaR can tell investors the exact future risk in term of loss.

Nevertheless, the above [2-9] are all single-objective models based on Markowitz's principle. That is, the return and risk are compensated by each other. Some decision makers do not want to set a fixed level to return or the risk as the constraints. They want to choose the investment scheme which can maximize the profit and minimize the potential risk together. Therefore, a single optimized portfolio cannot satisfy all investors. On the other hand, sometimes portfolio optimization models are required to consider more criteria than the standard mean-variance model. Therefore, to provide comprehensive selection information for investors, recently multi-objective portfolio selections models (MOPSM) were built. From the literatures, some studies on MOPSM have been investigated. Jana *et al.* [10] proposed a multi-objective portfolio based model and added another entropy objective function to generate a well diversified asset portfolio within optimal asset allocation. In this research, a fuzzy programming technique is utilized as the solution of the multi-objective non-linear programming model. Steuer *et al.* [11] took some additional arguments of portfolio selection theory into consideration, such as: dividends, liquidity, social responsibility, amount of short selling, and so forth. This study is significant for non-standard investors to make decisions. Zhang *et al.* [12] presented a fuzzy multi-objective mean-variance-skewness model with transaction costs. The skewness of portfolio return is considered as a critical factor

978-1-4244-7316-8/11/$26.00 ©2011 IEEE

in selecting a portfolio. In order to solve the above model, a hybrid intelligent algorithm was designed by integrating simulated annealing algorithm, relevance vector machine and fuzzy simulation.

In this study, based on the property of fuzzy Value-at-Risk, we propose a mean-variance-VaR multi-objective portfolio selection model (VaR-MOPSM).

The remainder of this paper is organized as follows: Section 2 introduces some basic information on fuzzy variables. We also explain the concepts and calculations of the variance and fuzzy VaR. Section 3 illustrates the motivations behind our research. In Section 4, we briefly review previous MOPSM and build the VaR-MOPSM. The model can be solved by an improved particle swarm optimization (IPSO) introduced in Section 5. In Section 6, we apply the proposed algorithm to solve a numerical example. In order to demonstrate the effectiveness of the IPSO, we also compare it with existing methods in this Section. Finally Section 7 summarizes our conclusions.

II. Preliminaries

To make a better prediction of security returns, fuzzy set theory is employed to portfolio selection problem. In this section, we briefly review some features on fuzzy variables. The fuzzy variable is a fundamental mathematical tool to describe fuzzy uncertainty, and there are mainly three types of fuzzy variables frequently used: triangular, trapezoidal and normal distributions. Before introducing the variance and fuzzy VaR, it is necessary to review some basic knowledge on the credibility theory of fuzzy variables.

Suppose ξ is a fuzzy variable whose membership function is μ_ξ, and r is a real number. Then, the possibility, necessity and credibility of event $\xi \leq r$ are expressed, respectively, as follows:

$$\mathrm{Pos}\{\xi \leq r\} = \sup_{t \leq r} \mu_\xi(t), \tag{1}$$

$$\mathrm{Nec}\{\xi \leq r\} = 1 - \sup_{t > r} \mu_\xi(t), \tag{2}$$

$$\mathrm{Cr}\{\xi \leq r\} = \frac{1}{2}\left[\mathrm{Pos}\{\xi \leq r\} + \mathrm{Nec}\{\xi \leq r\}\right]. \tag{3}$$

The credibility measure is formed on the basis of the possibility and necessity measures, and in the simplest case, it is taken as their average. The credibility measure is a self-dual set function [13], *i.e.* $\mathrm{Cr}\{\xi \leq r\} = 1 - \mathrm{Cr}\{\xi > r\}$. Equation (3) also results in the following:

$$\mathrm{Cr}\{\xi \leq r\} = \frac{1}{2}\left[\sup_{t \leq r} \mu_\xi(t) + 1 - \sup_{t > r} \mu_\xi(t)\right]. \tag{4}$$

For further information on fuzzy variables, one may refer to [13], [14] and [15].

A. Expected value

The most general definition of expected value of fuzzy variable was given by Liu and Liu [13].

Let ξ be a fuzzy variable. Then the expected value of ξ is defined by:

$$\mathrm{E}[\xi] = \int_0^{+\infty} \mathrm{Cr}\{\xi \geq r\}\mathrm{d}r - \int_{-\infty}^{0} \mathrm{Cr}\{\xi \leq r\}\mathrm{d}r. \tag{5}$$

B. Variance

The variance of a fuzzy variable provides a measure of the spread of the distribution around its expected value. A small value of variance indicates that the fuzzy variable is tightly concentrated around its expected value; and a large value of variance indicates that the fuzzy variable has a wide spread around its expected value. Therefore, the variance can be used to represent the level of risk in a fuzzy system.

If the fuzzy variable has a finite expected value, according to Liu and Liu [13], its variance is defined as:

$$\mathrm{V}[\xi] = \mathrm{E}[(\xi - e)^2] \tag{6}$$

C. Value-at-Risk

The Value-at-Risk (VaR) of an investment is the likelihood of the greatest loss with a given confidence level [17], [18]. Following Wang *et al.* [16], if $\widetilde{L_t}$ denotes the fuzzy power demand of period t, then, in a fuzzy environment, the VaR of L_t with a confidence of $(1-\beta)$ can be written as:

$$\mathrm{VaR}_{1-\beta} = \sup\{\lambda | \mathrm{Cr}(\widetilde{L_t} \geq \lambda) \geq \beta\}, \tag{7}$$

where $\beta \in (0, 1)$.

Equation (7) tells us that the greatest value of $\widetilde{L_t}$ under confidence level $(1-\beta)$ is the largest λ.

Recently, the measure of Value-at-Risk has been applied to many engineering problems to build fuzzy optimization models [19], [20], [21], [22].

III. Motivations

As we mentioned in Section I, the most important distinction of the portfolio selection models could be the risk measure methods. Investor probability obtains quite different optimal results with different methods. In Table I below, we list the risk measurements in detail which have been applied to fuzzy portfolio selection problem.

The risk measurements listed in Table I can be sorted into two types. The first type includes mean-risk, mean-variance, mean-semivariance, entropy and mean-variance-skewness which find the optimal solutions by minimizing the risk measure functions, thus maximizing the stability of a portfolio. However, these evaluation methods do not focus on the exact risk of future loss, which is significant to investors. The second type is fuzzy VaR. Using fuzzy VaR as the risk measurement, investors can assign different confidence levels and then use the model to gain how much return they can

TABLE I
THE COMPARISONS OF THE FUZZY VAR AND EXISTING RISK MEASUREMENTS

Methods Name	Risk Measure Function	Purpose
Mean-risk [23]	$\mathrm{Cr}\{b - (x_1\xi_1 + x_2\xi_2 + ... + x_n\xi_n) \geq r\} \leq \alpha(r)$	Describe the credibility values of the bad events,which should lower than the given tolerance levels
Mean-variance [2]	$\mathrm{V}[x_1\xi_1 + x_2\xi_2 + ... + x_n\xi_n] \leq r$	Reflects an average deviation level from the expected value, which is limited by the given vale
Mean-semivariance [5]	$\mathrm{H}[x_1\xi_1 + x_2\xi_2 + ... + x_n\xi_n] \leq r$	Measures only the lower deviation from the expected return
Entropy optimization [3]	$\mathrm{SV}[x_1\xi_1 + x_2\xi_2 + ... + x_n\xi_n] \leq r$	Minimize the entropy can reduce the uncertainty of a portfolio and make the prediction easily
Mean-variance-skewness [4]	$\mathrm{V}[x_1\xi_1 + x_2\xi_2 + ... + x_n\xi_n] \leq \alpha$ $\mathrm{S}[x_1\xi_1 + x_2\xi_2 + ... + x_n\xi_n] \geq \beta$	Reflects an average deviation level from the expected value with asymmetry fuzzy returns
Fuzzy Value-at-Risk [9]	$\mathrm{VaR}_{1-\beta} = \sup\{\lambda \mid \mathrm{Cr}(\mathcal{L} \geq \lambda) \geq \beta\}$	Directly reflect the loss of one selection case under given confidence level

expect and how much future loss they may suffer in the worst case scenario. Nevertheless, the VaR cannot enhance the stability of a portfolio which may not make the selection case trusted.

To the best of our knowledge, the conventional multi-objective portfolio selection models were built based on the first type of risk measurements. That is to say, all of the existing MOPSMs only focus on enhancing the stability of a selection case from different aspects, but the exact risk in term of loss is not considered.

In this study, we proposed a MOPSM based on both types risk measure methods: variance is utilized to evaluate the portfolio stability while fuzzy VaR is applied to measure the exact future risk. Therefore, the obtained selection result could be more helpful in decision making.

IV. Modeling

In this Section, we briefly review the existing multi-objective portfolio selection models and then provide our model. Some notations are given as follows:

x_i: Proportion invested on security i, $i = 1, 2, ..., n$.

ξ_i: The fuzzy return of security i.

E: The expected return of a selection case.

V: The variance of a selection case.

S: The skewness of a selection case.

$(1 - \beta)$: The confidence level of Value-at-Risk.

$\mathrm{VaR}_{1-\beta}$: The VaR of a selection case under confidence level $(1 - \beta)$.

Cr: The credibility functions of fuzzy variables.

L: The loss functions of selection cases, defined as $L = -(x_1\xi_1 + x_2\xi_2 + ... + x_n\xi_n)$.

In the conventional MOPSM, the objective considered was to maximize the investment return and minimize several risk measure functions at the same time. Thus, it can be summarized as:

$$\begin{cases} \max\ \mathrm{E}[x_1\xi_1 + x_2\xi_2 + ... + x_n\xi_n] \\ \min\ \mathrm{V}[x_1\xi_1 + x_2\xi_2 + ... + x_n\xi_n] \\ \min\ \text{-S}[x_1\xi_1 + x_2\xi_2 + ... + x_n\xi_n] \\ \text{Subject to} \\ \quad x_1 + x_2 + ... + x_n = 1; \\ \quad x_i \geq 0,\ i = 1, 2, ..., n. \end{cases} \tag{8}$$

If we quantify the skewness function of model (8) by risk measurements mentioned in Table I, some other existing fuzzy portfolio selection models can be obtained.

In this study, we retain the Markowitz mean-variance selection principle; however, the fuzzy VaR is considered as another risk measure method. In this case, the proposed VaR-MOPSM can be described as:

$$\begin{cases} \max\ \mathrm{E}[x_1\xi_1 + x_2\xi_2 + ... + x_n\xi_n] \\ \min\ \mathrm{V}[x_1\xi_1 + x_2\xi_2 + ... + x_n\xi_n] \\ \min\ \mathrm{VaR}_{1-\beta} = \sup\{\lambda \mid \mathrm{Cr}(\mathcal{L} \geq \lambda) \geq \beta\} \\ \text{Subject to} \\ \quad x_1 + x_2 + ... + x_n = 1; \\ \quad x_i \geq 0,\ i = 1, 2, ..., n. \end{cases} \tag{9}$$

V. Solution

The VaR-MOPSM is a complex nonlinear optimization problem which cannot be solved by linear programming methods or simplex algorithms. Therefore, in this section, we provide a fuzzy simulation based multi-objective PSO algorithm to get the solutions.

A. Fuzzy simulation

In Section II, we have introduced the calculation of expected value, fuzzy variance and VaR of single fuzzy variable. However, we are required to deal with a series of different distributed fuzzy variables, such as $\xi = (\xi_1, \xi_2 ... \xi_n)$. It is impossible to solve the problem as $\mathrm{V}[x_1\xi_1 + x_2\xi_2 + ... + x_n\xi_n]$ or $\mathrm{VaR}_{1-\beta} = \sup\{\lambda | \mathrm{Cr}(\xi \geq \lambda) \geq \beta\}$ from the above definitions. The fuzzy simulation developed by Liu and Liu [13] plays a pivotal role in solving the above problem. Employing this technique, the theoretical calculation of fuzzy VaR can be briefly summarized as follows:

Suppose $\xi_i = (\xi_1, \xi_2, ..., \xi_n)$ is a continuous fuzzy variables with support $\prod_{i=1}^{n}[a_i^L, a_i^U]$, where a_i^L and a_i^U are the lower and upper supports of ξ_i. We first divide each fuzzy variable into l parts and then approximate the membership function μ_{ξ_i} by a sequence of discrete fuzzy vectors ζ_i^r which can be constructed as:

$$\zeta_i^r = a_i^L + \frac{r}{l}(a_i^U - a_i^L), \tag{10}$$

where, l and r are integers, and $0 \leq r \leq l$.

Second, the loss variable $\mathcal{L} = -(x_1\xi_1 + x_2\xi_2 + ... + x_n\xi_n)$ can be simulated by the fuzzy vectors ζ_i^r.

Third, on the basis of the approximate membership function of $\mathcal{L}$, the credibility function $\mathrm{Cr}\{\mathcal{L} \geq \lambda\}$ can be calculated by equation (4).

Finally, we can obtain an approximate values of variance and fuzzy VaR by equation (6) and (7) .

Therefore, the larger the value of l, the more exact the result will be, but the longer the computation time will be. We can conclude that the value of l should be set specially to different optimization problems. For more about this methods, you may refer to [4], [16] and [28].

B. Improved particle swarm optimization algorithm

The PSO algorithm was initially proposed by Kennedy [24] in 1995. It has been widely used and demonstrated its effectiveness in a variety of fields; refer to [9], [25], [26] and [27] for details.

1) Improving conventional PSO to mitigate the local convergence problem: It is well known that the PSO algorithm can find the optimal solution in fewer iterations than other algorithms, but may suffer from the local convergence problem. To overcome the above problem and better solve the multi-objective model, we improve the original PSO algorithm by the escape speed (ES) and particle restart position (PRP).

ES: If the optimal solution cannot be updated after a fixed number of iterations, then it will be considered as having fallen into local convergence. Then, each particle's speed will be modified by the escape speed. If the escape speed is sufficiently large, all the particles can jump out of their current loops and restart searching in different areas.

PRP: After the particle speed has been modified by the escape speed, the particles will be distributed randomly. For most of the selection problems, there should be a constraint on the search space; for example, in our problem, each position value belongs to the range (0,1). Then, the particle restart position is generated by the edge value of the search space.

2) The evaluation method of the multi-objective problem: To solve the multi-objective model, the following researches have been done:

Find the ideal Pareto solution. Pareto solutions are those for which improvement in one object can only occur with the worsening of at least one other objective. If we optimize each object (expected value or variance or VaR) without considering others, the ideal Pareto solution can be created. Such processes can be summarized as follows:

Scenario I: the expected return is considered as the unique object, then, the proposed model (9) degenerate to the following:

$$\begin{cases} \max\ \mathrm{E}[x_1\xi_1 + x_2\xi_2 + ... + x_n\xi_n] \\ \text{Subject to} \\ \quad x_1 + x_2 + ... + x_n = 1; \\ \quad x_i \geq 0,\ i = 1, 2, ..., n. \end{cases} \tag{11}$$

Scenario II: the variance is considered as the unique object, then, model (9) is revised to:

$$\begin{cases} \min\ \mathrm{V}[x_1\xi_1 + x_2\xi_2 + ... + x_n\xi_n] \\ \text{Subject to} \\ \quad x_1 + x_2 + ... + x_n = 1; \\ \quad x_i \geq 0,\ i = 1, 2, ..., n. \end{cases} \tag{12}$$

Scenario III: the fuzzy VaR is considered as the unique objective, then,

$$\begin{cases} \min\ \mathrm{VaR}_{1-\beta} = \sup\{\lambda | \mathrm{Cr}(\mathcal{L} \geq \lambda) \geq \beta\} \\ \text{Subject to} \\ \quad x_1 + x_2 + ... + x_n = 1; \\ \quad x_i \geq 0,\ i = 1, 2, ..., n. \end{cases} \tag{13}$$

The revised models (11), (12), (13) are single object optimization problem which can be easily solved by simplex methods. Supposedly, these models results in E_{max}, V_{min} and VaR_{min}, then, the ideal Pareto solution is considered as (E_{max}, V_{min}, VaR_{min}).

In model (7), if one selection case i produces the result of (E_i, V_i, VaR_i), the fitness value (FV) of portfolio i is considered as the distance between the ideal Pareto solution and optimal solution i, which can be obtained by the following equation (14).

$$\mathrm{FV}(i) = \sqrt{(\mathrm{E}_{max} - \mathrm{E}_i)^2 + (\mathrm{V}_{min} - \mathrm{V}_i)^2 + (\mathrm{VaR}_{min} - \mathrm{VaR}_i)^2} \tag{14}$$

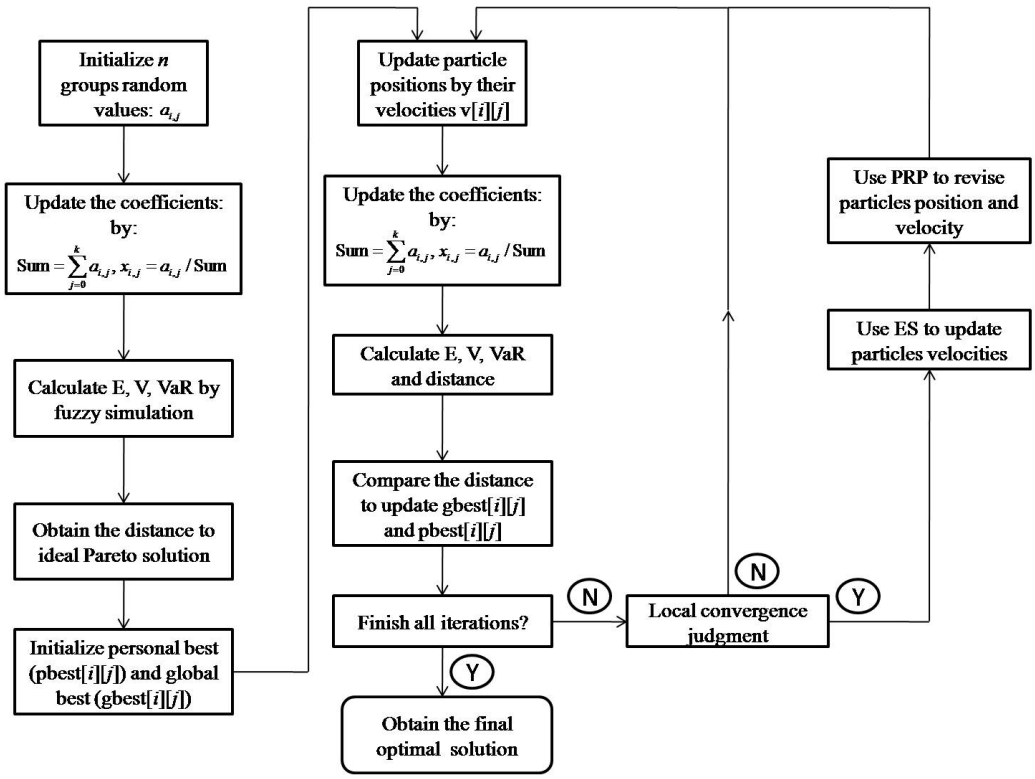

Fig. 1. The flow chart of IPSO

Therefore, the smaller the distance is, the better the optimal solution will be.

We use Figure 1 above to illustrate the IPSO.

VI. Numerical example

In this section, the proposed model and algorithm are exemplified by the following numerical example.

Example: Suppose that there are ten securities whose returns are independent triangular or normally distributed fuzzy variables, as given in Table II. The confidence level of fuzzy Value-at-Risk is set as 0.9, that is $\beta = 0.1$.

TABLE II
Security returns

Security No.	Return	Security No.	Return
1	(-0.8, 0.4, 2.0)	6	$N(0.9, 1.7^2)$
2	(-0.7, 0.6, 1.8)	7	$N(0.6, 1.0^2)$
3	(-1.1, 0.6, 2.8)	8	$N(0.8, 1.4^2)$
4	(-1.6, 0.9, 3.2)	9	$N(0.7, 1.1^2)$
5	(-1.4, 0.8, 3.9)	10	$N(1.1, 1.9^2)$

Then, apply these data to model (9), we get the following selection problem.

$$\begin{cases} \max \ \mathrm{E}[x_1\xi_1 + x_2\xi_2 + ... + x_{10}\xi_{10}] \\ \min \ \mathrm{V}[x_1\xi_1 + x_2\xi_2 + ... + x_{10}\xi_{10}] \\ \min \ \mathrm{VaR}_{0.9} = \sup\{\lambda | \mathrm{Cr}(\mathcal{L} \geq \lambda) \geq 0.1\} \\ \text{Subject to} \\ \quad x_1 + x_2 + ... + x_{10} = 1; \\ \quad x_i \geq 0, \ i = 1, 2, ..., 10. \end{cases} \tag{15}$$

Now, we use the IPSO algorithm to get the optimal solutions. All of the following experiments were implemented on a personal computer: Dell E8500 3.16 GHz CPU with RAM 2.96 GB.

A. The performance of IPSO

We first applied IPSO to solve model (15). After 100 iterations, the optimal fitness value (FV) is 0.146, and the capital should be allocated as Figure 2 shows, the numerical value of the selection is (0.00; 0.47; 0.00; 0.00; 0.52; 0.00; 0.00; 0.01; 0.00; 0.00).

From the numerical data provided in this Example, we may find security 2 is overlapped by security 3. However, from the selection result, only security 2 is considered as an invest proportion. The reason is: The VaR and variance of security 2 is smaller than those of security 3, when compute the distance to ideal Pareto solution, security 2 performs better.

B. Comparisons with other algorithms

Some existing approaches have been proposed to solve fuzzy portfolio optimization problems, such as genetic algorithms (GA) [3], [4] and simulated annealing algorithm

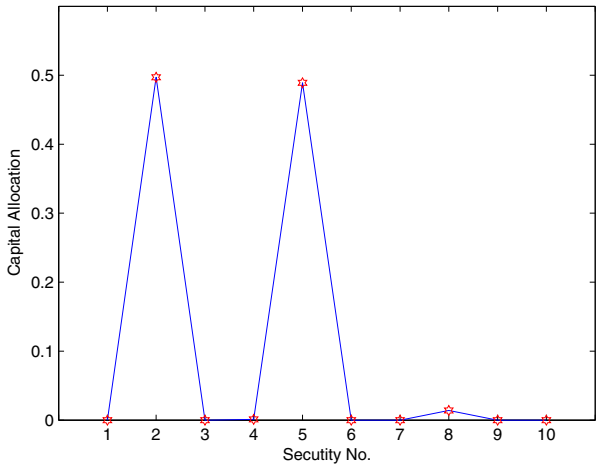

Fig. 2. Optimal solution of IPSO (Capital allocations)

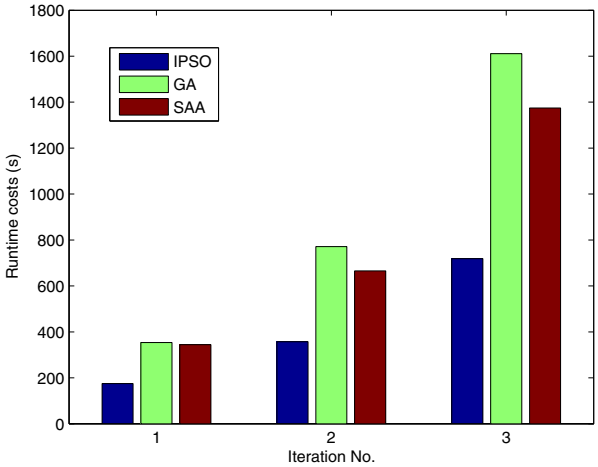

Fig. 4. Optimal solutions of different approaches

(SAA) [7]. In this study, we first revised the fitness functions of GA and SAA to solve the multi-objective portfolio selection problem. Then, the proposed IPSO is compared with other approaches from two aspects: the optimal solutions and runtime cost.

1) Solutions comparisons: The IPSO, GA and SAA are applied to solve the above numerical example. For GA, the crossover and mutation probability is set as 0.8 and 0.05, the Chromosome number is 20. The temperature reduction coefficient of SAA is selected as 0.984. The following Figure 3 shows the optimal process of each method during the 100 times iterations.

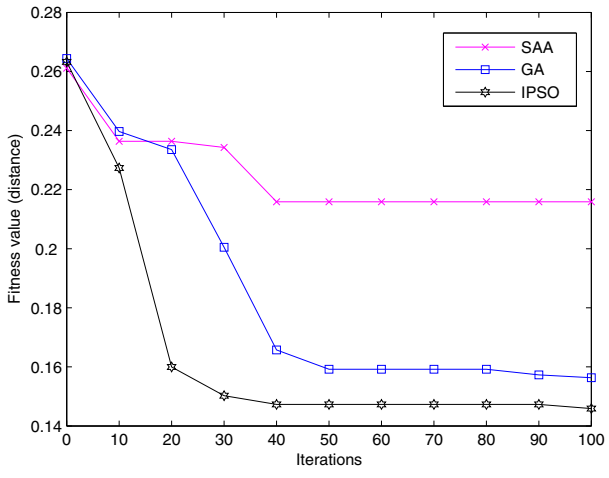

Fig. 3. Optimal solutions of different approaches

From the Figure 3, we can conclude that: the proposed IPSO can mitigate the local convergence problem very well and find better solutions than other methods.

2) Runtime comparisons: The runtime costs (50, 100, 200 iterations) of each algorithm are depicted in Figure 4.

From the comparisons results in Figures 3 and 4, we can conclude that the proposed IPSO has better performance than GA and SA for our VaR-MOPSM.

C. Discussion on the optimal results of VaR-MOPSM with previous MOPSMs

Here, we provide more explanations on the effectiveness of VaR-MOPSM by linguistic analysis.

Because the risk measurements of the existing portfolio selection models are quite different, each method produces varying criteria to select a portfolio, so comparisons among the selection results of different models may not be very meaningful. However, it is important to note that, investors clearly understand the purposes of the first type risk measurements (provided in Section III), such as mean-variance, mean-semivariance or entropy; minimize these values can improve the selection. However, they cannot identify the potential risk included in these numerical values. For instance, in the conventional MOPSM, if the risk level r is modified from 1.6 to 1.7, then the investors will obtain a selection case with higher expected return and risk. However, it is quite difficult for them to determine how much higher the future risk becomes, so they cannot balance the higher expected return with the higher risk. As a result, investors cannot clearly determine the parameters and evaluate the results of these models. Based on the above analysis, the existing MOPSMs are not sensitive in measuring the future risk. In our VaR-MOPSM, on the other hand, investors can determine the confidence levels as they wish, and any change in these values will be directly reflected by the greatest loss obtained from the fuzzy VaR. Therefore, from this perspective, the multi-objective portfolio selection model with the fuzzy VaR can provide more effective information for investors and help them make decisions more easily.

VII. Conclusion

In this paper, we built a novel multi-objective fuzzy portfolio selection model (VaR-MOPSM) which takes the expected value, Value-at-Risk and variance as the criteria to evaluate a selection case. Applying this model, investors can well balance the future return with the potential loss, and therefore make more proper decisions. The model is formed as a non-linear complicated multi-objective optimization problem, which cannot be solved by linear programming methods or simplex algorithms. To solve the VaR-MOPSM, a fuzzy simulation based improved particle swarm optimization algorithm (IPSO) was designed as the solution. The proposed model and algorithm were exemplified by some numerical experiments. From the experiments' results and discussion on the optimal results of VaR-MOPSM with previous approaches, we concluded that: 1. the VaR-MOPSM is more helpful for general investors in decision-making; 2. the IPSO can mitigate the local convergence very well; 3. IPSO is more effective in solving the multi-objective than other existing approaches. The VaR-MOPSM model proposed in this paper is also applicable to various investment or engineering problems.

Acknowledgment

This research was supported by Waseda University Global COE Program "International Research and Education Center for Ambient SOC" sponsored by MEXT, Japan.

References

[1] H. Markowitz, "Portfolio selection", *Journal of Finance*, vol. 7, no. 1, pp. 77-91, 1952.

[2] J. Watada, "Fuzzy portfolio selection and its application to decision making", *Tatra Mountains Math. Publication*, vol. 13, no. 4, pp. 219-248, 1997.

[3] X.Huang, "Mean-entropy models for fuzzy portfolio selection", *IEEE Transactions on Fuzzy Systems*, vol. 16, no. 4, pp. 1096-1101, 2008.

[4] X. Li, Z. Qin and S. Kar, "Mean-variance-skewness model for portfolio selection with fuzzy returns", *European Journal of Operational Research*, vo1. 202, no. 1, pp. 239-247, 2009.

[5] X.Huang, "Mean-semivariance models for fuzzy portfolio selection", *Journal of Computational and Applied Mathematics*, vol. 217, no. 1, pp. 1-8, 2008.

[6] X. Huang, "Risk curve and fuzzy portfolio selection", *Computers and Mathematics with applications*, vol. 55, no. 6, pp. 1102-1112, 2008.

[7] X. Li, Y. Zhang, H. Wong and Z. Qin, "A hybrid intelligent algorithm for portfolio selection problem with fuzzy returns", *Journal of Computational and Applied Mathematics*, vo1. 223, no. 2, pp. 264-278, 2009.

[8] X.Huang, "Portfolio selection with fuzzy returns", *Journal of Intelligent and Fuzzy Systems*, vol. 18, no. 4, pp. 383-390, 2007.

[9] B. Wang, S. Wang and J. Watada, "Fuzzy portfolio selection based on Value-at-Risk", *In Proceeding of the 2009 IEEE International Conference on System, Man and Cybernetics*, pp. 1840-1845, 2009.

[10] P. Jana, T.K. Roy and S.K. Mazumder, "Multi-objective possibilistic model for portfolio selection with transaction cost", *Journal of Computational and Applied Mathematics*, vol. 228, no. 1, pp. 188-196, 2009.

[11] R. E. Steuer, Y. Qi and M. Hirschberger, "Multiple Objectives in Portfolio Selection", Journal of Financial Decision Making, vol. 1, no. 1, 2005.

[12] Y. Zhang, X. Li, H. Wong and L. Tan, "Fuzzy multi-objective portfolio selection model with transaction cost", *In Proceeding of the 2009 IEEE International Conference on Fuzzy System*, pp. 273-278, 2009.

[13] B. Liu and Y. K. Liu, "Expected value of fuzzy variable and fuzzy expected value models", *IEEE Transaction on Fuzzy Systems*, vol. 10, no. 4, pp. 445-450, 2002.

[14] S. Nahmias, "Fuzzy variable", *Fuzzy Sets and Systems*, vol. 1, no. 2, pp. 97-101, 1978.

[15] S. Wang, Y. Liu and X. Dai, "On the continuity and absolute continuity of credibility functions", *Journal of Uncertain System*, vol. 1, no. 2, pp. 185-200, 2007.

[16] S. Wang, J. Watada and W. Pedrycz, "Value-at-Risk-Based two-satge fuzzy facility location problems", *IEEE Transactions on Industrial Informatics*, vol. 5, no. 4, pp. 465-482, 2009.

[17] D.Duffie and J.Pan, "An overview of value-at-risk", *Journal of Derivatives*, vol. 4, no. 3, pp. 7-49, 1997.

[18] P. Jorion, *Value at Risk: The New Benchmark for Managing Financial Risk*, McGraw-Hill, 2006.

[19] S. Wang and J. Watada, "Two-stage fuzzy stochastic programming with Value-at-Risk criteria", *Applied Soft Computing*, vol. 11, no. 1, pp. 1044-1056, 2011.

[20] Z. Zmeskal, "Value at risk methodology of international index portfolio under soft conditions", *International Review of Financial Analysis*, vol. 14, no. 6, pp. 263-275, 2005.

[21] B. Wang, Y. Li and J. Watada, "Fuzzy Power System Reliability Model Based on Value-at-Risk", *In: Proceedings of the 14th International Conference on Knowledge-Based and Intelligent Information and Engineering Systems*, pp. 445-453, 2010.

[22] R.A. Jabr, "Robust self-scheduling under price uncertainty using conditional value-at-risk", *IEEE Transactions on Power Systems*, vol. 20, no. 4, pp. 1852-1858, 2005.

[23] X. Huang, "Risk curve and fuzzy portfolio selection", *Computers and Mathematics with applications*, vol. 55, no. 6, pp. 1102-1112, 2008.

[24] J. Kennedy and R. C. Eberhaart, "Particle swarm optimization", *In: Proceedings of the 1995 IEEE International Conference on Neual Network*, IV, pp. 1942-1948, 1995.

[25] K. D. Sharma, A. Chatterjee and A. Rakshit, "A Hybrid Approach for Design of Stable Adaptive Fuzzy Controllers Employing Lyapunov Theory and Particle Swarm Optimization", *IEEE Transactions on Fuzzy Systems*, vol. 17, no. 2, pp. 329 - 342, 2009.

[26] Y. Jiang, T. Hu, C. Huang and X. Wu, "An improved particle swarm optimization algorithm", *Applied Mathematics and Computation*, vol. 193, no. 1, pp. 231-239, 2007.

[27] L. Zhao and Y. Yang, "PSO-based single multiplicative neuron model for time series prediction", *Expert Systems with Applications*, vol. 36, no. 2, pp. 2805-2812, 2009.

[28] B. Liu, *Foundation of Uncertainty Theory: an Introduction to its Axiomatic Foundations*, Springer-Verlag Berlin Heidelberg New York, 2004.

2011 IEEE International Conference on Fuzzy Systems
June 27-30, 2011, Taipei, Taiwan

Statistic Test on Fuzzy Portfolio Selection Model

Pei-Chun Lin
Graduate School of Information, Production and System
Waseda University
Kitakyushu, Japan
peichunpclin@gmail.com

Junzo Watada
Graduate School of Information, Production and System
Waseda University
Kitakyushu, Japan
watada@waseda.jp

Berlin Wu
Department of Mathematical Sciences
National Chengchi University
Taipei, Taiwan
berlin@nccu.edu.tw

***Abstract*—Markowitz's mean-variance model is based on probability distribution functions which have known or were assumed as some kinds of probability distribution functions. When our data are vague, we can't know the underlying distribution functions. The objective of our research was to develop a method of decision making to solve portfolio selection model by statistic test. We used central point and radius to determine the fuzzy portfolio selection model and statistic test. Empirical studies were presented to illustrate the risk of fuzzy portfolio selection model with interval values. We can conclude that it is more explicit to know the risk of portfolio selection model. According to statistic test, we can get a stable expected return and low risk investment in different choose *K*.**

Keywords-*Portfolio selection, Optimization, fuzzy probability distributions, fuzzy statistics and data analysis*

I. INTRODUCTION

Portfolio selection model has been well developed on the basis of a mean-variance approach proposed by Markowitz [10, 11, 13], who combines probability theory and optimization theory to analyze the behavior of economic agents. The key principle of the mean-variance model is to use the expected return of a portfolio as the investment return and the variance of the expected returns of the portfolio as the investment risk. Most of existing portfolio selection models is based on probability theory. Also some researches on the mean-variance portfolio selection problem have been studied by Sharpe [17], Merton [12], Perold [15], Pang [14], Voros [20] and Best [1, 2]. In order to analyze uncertain phenomena in real world, research works have applied multivariate data analysis to investigate some portfolio selection problems such as Wang et al.[29] propose a new real options analysis approach by combing binomial lattice-based model with fuzzy random variable. Zhang et al. [32] proposed a model to transform the forecasted uncertain values evaluated by experts into some normal fuzzy numbers. Tanaka and Guo [18, 19] proposed two kinds of portfolio selection models based on fuzzy probabilities and exponential possibility distributions, respectively. Wang and Zhu [28], Lai et al. [6] constructed interval programming models of portfolio selection. Zhang and Wang [30] and Zhang et al. [31] discussed the portfolio selection problem based on the (crisp) possibilistic mean and variance when short sales are not allowed on all risky assets. Watada [24], Ramaswamy [16] and Leon et al. [7] discussed portfolio selection using fuzzy decision theory. Usually the works did not consider any kind of probability distribution function with fuzzy random variables. From this point of view, the objective of this paper is to apply the concept of distribution function and fuzzy random variables in the portfolio selection model.

In order to find the probability distribution function in continuous fuzzy data, we have to take the concept of fuzzy statistic into consideration. Such fundamental statistics as mean, median and mode are useful measurements in illustrating some characteristics of a sample distribution. More research works should place focus on the fuzzy statistical analysis and applications in engineering, medical and social science fields. Wu and Hwang [22] proposed fuzzy statistical testing method to discuss the stationary of Taiwan short-term money demand function; Wu and Cheng [25] identified a model structure through qualitative simulation; Casalino, et al. [3], Esogbue and Song [5], Wu [23], and Wu and Sun [26] demonstrated the concepts of fuzzy statistic and applied them to social survey; Wu and Tseng [27] use fuzzy regression method of coefficient estimation to analyze Taiwan monitoring index of economic. All above-mentioned studies dealt with problems by means of central point values. Pei-Chun Lin, et al. [8] defined a new weight function, by means of fuzzy numbers defined with central point and radius. Moreover, Pei-Chun Lin, et al. [9] also purposes a method to recognize the underlying distribution function using central point and radius. It gives us more information about original fuzzy data.

The objective of this paper is to define a fuzzy portfolio selection model and decision by statistic test. In the first step, we need to find out the probability distribution function for each parameter. When we know the distribution function of each parameter, we can easily calculate the expected return and variance. Those values can enable us to define a fuzzy portfolio selection model. Moreover, we give a decision by statistic test. It give us a explicit risk in investment.

The rest of the paper consists of the following. Section 2 gives the brief review of related studies. The main method is described in section 3. Section 4 illustrates empirical studies with interval values to show that fuzzy portfolio selection model with statistic test. Finally, the concluding remarks and the topics of further studies are addressed in Section 5.

978-1-4244-7316-8/11/$26.00 ©2011 IEEE

II. NOTATIONS AND PRELIMINARY DEFINITIONS

A. Fuzzy Numbers

In a standard formulation of the portfolio selection, literatures revealed that the authors pervert to use LR-type fuzzy numbers [4] to deal with problems.

Definition 1 A fuzzy number $A = [a, b, c, d]$ is called trapezoidal with tolerance interval $[b, c]$, left width $L = b - a$ and right width $U = d - c$ if its membership function has the following form:

$$\mu_A(x) = \begin{cases} 1 - \dfrac{b-t}{L} & if \;\; b - L \le t \le b, \\ 1 & if \;\; b \le t \le c, \\ 1 - \dfrac{t-c}{U} & if \;\; c \le t \le c + U, \\ 0 & otherwise \end{cases}$$

and we give the notation as $A \equiv (b, c, L, U)$.

Definition 2 Especially, if $b = c$, we have a triangular fuzzy number $B = [a, b, d]$, the left width $L = b - a$ and right width $U = d - b$. Its membership function is written in the following form:

$$\mu_B(x) = \begin{cases} 1 - \dfrac{b-t}{L} & if \;\; b - L \le t \le b, \\ 1 & if \;\; t = b, \\ 1 - \dfrac{t-b}{U} & if \;\; b \le t \le b + U, \\ 0 & otherwise \end{cases}$$

and we give the notation as $B \equiv (b, L, U)$.

Definition 3 An interval value is denoted as $A = [a, b]$ with central point $o = \frac{a+b}{2}$ and radius $l = \frac{b-a}{2}$. We give the notation as $A \equiv (o, l)$.

Moreover, two operations on LR-type fuzzy numbers, namely fuzzy addition and scalar multiplication, are given as follows.

Definition 4 Let $A_1 = (a, b, c, d)$ and $A_2 = (\bar{a}, \bar{b}, \bar{c}, \bar{d})$ be any two fuzzy numbers and λ be any real number. Then

(a) $A_1 + A_2 = (a + \bar{a}, b + \bar{b}, c + \bar{c}, d + \bar{d})$.

(b) $\lambda A_1 = (\lambda a, \lambda b, \lambda c, \lambda d)$, $\forall\, \lambda \ge 0$.

When we have those fuzzy numbers, we need some statistic methods to deal with those data. We introduce a statistic test in the following subsection.

B. Statisitc Analysis

In statistics often functions of observations are important [21]. An example is the sample mean $\overline{x}_n$ of n observations $x_1, x_2, \dots, x_n$ of a stochastic quantity.

For a sample $X_1, X_2, \dots, X_n$ of a normally distributed stochastic quantity $X \sim N(\mu, \sigma^2)$ a statistic for the hypothesis $H_0: \mu = \mu_0$ is

$$T = \frac{\overline{X}_n - \mu_0}{\frac{S_n}{\sqrt{n}}} \tag{1}$$

and the acceptance region A for T under probability δ for an error of the first type is

$$A = \left\{ t \in \mathbb{R} : \; |t| = \left| \frac{\overline{X}_n - \mu_0}{\frac{S_n}{\sqrt{n}}} \right| \le t_{n-1;1-\frac{\delta}{2}} \right\}, \tag{2}$$

where $\overline{X}_n$ is the sample mean of data, S_n is the sample standard deviation of data and $t_{n-1;1-\frac{\delta}{2}}$ is the $(1 - \frac{\delta}{2})$-fractile of the *t*-distribution with *n-1* degrees of freedom.

When we have those information above, we have prepare all prior knowledge for dealing with portfolio selection problem. Now, we give a briefly statement with Markwitz's portfolio selection model in the following subsection.

C. Markwitz's Portfolio Selection Model

Markowitz's mean-variance model is based on probability distribution where uncertainty is equated with randomness [10, 11, 13]. That is, the rate of return on the ith asset, r_i, will be regarded as a random variable.

Consider a market with n risky assets. An investor's position in this market is described by a portfolio $\mathbf{x} = (x_1, x_2, \dots, x_n)'$, where the ith component x_i represents the proportion invested in asset i. The return vector on portfolio $\mathbf{x}$ is described by $\mathbf{r} = (r_1, r_2, \dots, r_n)'$, where r_i represents the return rate of asset i. In conventional mean-variance methodology for portfolio selection, r_i is regarded as a random variable, $\forall\, i = 1,2, \dots, n$. Assume $\bar{\mathbf{r}} = (\overline{r_1}, \overline{r_2}, \dots, \overline{r_n})'$ and $V = (\sigma_{ij})_{n \times n}$ be the expected return vector and covariance matrix, respectively. The return R on the portfolio $\mathbf{x}$ is given by $R = \sum_{i=1}^{n} r_i x_i$. Set $F = (1, 1, \dots, 1)'$. The objective of the investor is to choose a portfolio that maximizes the return on the investment subject to some constraints on the risk of the investment.

A mean-variance model for portfolio selection can be formulated mathematically as:

$$\left.\begin{array}{c} \max \quad \bar{\mathrm{r}}\mathrm{x} \\ \text{s.t.} \quad \sqrt{\mathrm{x}'\mathrm{V}\mathrm{x}} \le \sigma \\ \mathrm{F}'\mathrm{x} \le 1 \\ x_i \ge 0 \quad \forall\, i = 1,2, \dots, n \end{array}\right\} \tag{3}$$

where σ ($\sigma \ge 0$) represents the risk level, $\mathrm{x}'\mathrm{V}\mathrm{x} = \sum_{i=1}^{n} \sigma_{ii}{}^2 x_i{}^2 + \sum_{j=1}^{n} \sum_{i=1, i \ne j}^{n} \sigma_{ij} x_i x_j$, $\sigma_{ij} = cov(a_i, a_j)$ is covariance, a_i and a_j are random variables, $\forall\, i, j = 1,2, \dots, n$.

Here, we rewrite formula (3) clearly as following formula.

$$\left.\begin{array}{c} \max \quad \mathrm{E}(\sum_{i=1}^{n} r_i x_i) \\ \text{s.t.} \quad \sqrt{\mathrm{x}'\mathrm{V}\mathrm{x}} \le \sigma \\ \sum_{i=1}^{n} x_i \le 1 \\ x_i \ge 0 \quad \forall\, i = 1,2, \dots, n \end{array}\right\} \tag{4}$$

i.e. We need to solve the programming problem as follows.

$$\left.\begin{array}{c} \max \quad \sum_{i=1}^{n} E(r_i) x_i \\ \text{s.t.} \quad \sqrt{\mathrm{x}'\mathrm{V}\mathrm{x}} \le \sigma \\ \sum_{i=1}^{n} x_i \le 1 \\ x_i \ge 0 \quad \forall\, i = 1,2, \dots, n \end{array}\right\} \tag{5}$$

In the next section, we will give definitions of fuzzy expected return and fuzzy portfolio variance. Moreover, we will give the procedure about how to solve the fuzzy portfolio selection model by statistic test.

III. Statistic Test on Fuzzy Portfolio Selection Model

A. Fuzzy Expeced Return and Fuzzy Portfolio Variance

Suppose that there are n distinct tradable assets in the market. The terminal rate of return for asset i, denoted as r_i, $\forall\, i = 1,2,\dots,n$, is assumed as a fuzzy random variable. By the widely accepted definition, the expectation of a fuzzy random variable is a fuzzy variable. We give the following combination to express the total fuzzy return R on a portfolio $\mathbf{x}$, where $\mathbf{x} = [\mathbf{x}_1, \mathbf{x}_2, \dots, \mathbf{x}_m]$ is a $n \times m$ matrix and $\mathbf{x}_1 = (x_{1_1}, x_{1_2}, \dots, x_{1_n})'$, $\mathbf{x_2} = (x_{2_1}, x_{2_2}, \dots, x_{2_n})'$, ..., $\mathbf{x}_m = (x_{m_1}, x_{m_2}, \dots, x_{m_n})'$ are $n \times 1$ vectors.

Definition 5 Fuzzy Expected Return

Let $A_i \equiv (o_i, l_i), \forall\, i = 1,2,\dots,n$, are interval values on the probability space $(\Omega, \mathcal{F}, P)$, where o_i is random variables of central point of A_i and l_i is random variables of radius of A_i, $\forall\, i = 1,2,\dots,n$. Then the fuzzy expected returns of A_i defined as follows.

For the proportion invested in asset k_i, i.e $k = o, l$ and $i = 1,2,\dots,n$. We have $\mathbf{x} = [\mathbf{x}_o, \mathbf{x}_l]$, where $\mathbf{x}_o = (x_{o_1}, x_{o_2}, \dots, x_{o_n})'$ and $\mathbf{x}_l = (x_{l_1}, x_{l_2}, \dots, x_{l_n})'$. Hence,

$$E[R(\mathbf{x})] = diag\left(\sum_{i=1}^{n} E(o_i)x_{o_i}, \sum_{i=1}^{n} E(l_i)x_{l_i}\right).$$

Note that $\sum_{i=1}^{n} E(k_i)x_{j_i} = 0$, for $k \neq j$.

Definition 6 Fuzzy Portfolio Variance

Let $A_i \equiv (o_i, l_i), \forall\, i = 1,2,\dots,n$, are interval values on the probability space $(\Omega, \mathcal{F}, P)$. Then the fuzzy portfolio variance of $A_i, \forall\, i = 1,2,\dots,n$, are defined as follows.

$$var[R(\mathbf{x})] = diag\left(var(\sum_{i=1}^{n} o_i x_{o_i}), var(\sum_{i=1}^{n} l_i x_{l_i})\right),$$

where
$var(\sum_{i=1}^{n} o_i x_{o_i}) = \sum_{i=1}^{n} {\sigma_{o_{ii}}}^2 {x_{o_i}}^2 + \sum_{j=1}^{n}\sum_{i=1,i\neq j}^{n} \sigma_{o_{ij}} x_{o_i} x_{o_j}$, $\sigma_{o_{ij}} = cov(o_i, o_j)$, and $var(\sum_{i=1}^{n} l_i x_{l_i}) = \sum_{i=1}^{n} {\sigma_{l_{ii}}}^2 {x_{l_i}}^2 + \sum_{j=1}^{n}\sum_{i=1,i\neq j}^{n} \sigma_{l_{ij}} x_{l_i} x_{l_j}$, $\sigma_{l_{ij}} = cov(l_i, l_j), \forall\, i = 1,2,\dots,n$.

Now, let us give the models of fuzzy portfolio selection model in the following subsection.

B. Fuzzy Portfolio Selection Model

Model 1 Fuzzy Portfolio Selection Model with Interval Values

Let $A_i \equiv (o_i, l_i), \forall\, i = 1,2,\dots,n$, is interval values. The portfolio selection model with interval values is as follows.

$$\left.\begin{array}{c} \max \quad \sum_{i=1}^{n} E(o_i)x_{o_i} \\ \text{s.t.} \quad \mathbf{x}_o{}'\mathbf{V}_o\mathbf{x}_o \leq {k_1}^2 \\ \sum_{i=1}^{n} x_{o_i} \leq 1 \\ x_{o_i} \geq 0 \quad \forall\, i = 1,2,\dots,n \end{array}\right\} \tag{6}$$

$$\left.\begin{array}{c} \min \quad \sum_{i=1}^{n} E(l_i)x_{l_i} \\ \text{s.t.} \quad \mathbf{x}_l{}'\mathbf{V}_l\mathbf{x}_l \leq {k_2}^2 \\ \sum_{i=1}^{n} x_{l_i} \leq 1 \\ x_{l_i} \geq 0 \quad \forall\, i = 1,2,\dots,n \end{array}\right\} \tag{7}$$

where $\mathbf{x}_o{}'\mathbf{V}_o\mathbf{x}_o = \sum_{i=1}^{n} {\sigma_{o_{ii}}}^2 {x_{o_i}}^2 + \sum_{j=1}^{n}\sum_{i=1,i\neq j}^{n} \sigma_{o_{ij}} x_{o_i} x_{o_j}$, $\sigma_{o_{ij}} = cov(o_i, o_j)$, and $\mathbf{x}_l{}'\mathbf{V}_l\mathbf{x}_l = \sum_{i=1}^{n} {\sigma_{l_{ii}}}^2 {x_{l_i}}^2 + \sum_{j=1}^{n}\sum_{i=1,i\neq j}^{n} \sigma_{l_{ij}} x_{l_i} x_{l_j}$, $\sigma_{l_{ij}} = cov(l_i, l_j), \forall\, i = 1,2,\dots,n$.

We can solve the optimal solution for each model in (6) and (7) by choosing different values for k_i ($k_i \geq 0$), $\forall\, i = 1,2$, which is presented the tolerated risk level. We get the optimal solution vector $\mathbf{x}^* = [\mathbf{x}_o{}^*, \mathbf{x}_l{}^*]'$, where $\mathbf{x}_o{}^*$ is the optimal solution for model in (6) and $\mathbf{x}_l{}^*$ is the optimal solution for model in (7).

Moreover, when we have the solution $\mathbf{x}^* = [\mathbf{x}_o{}^*, \mathbf{x}_l{}^*]'$, we can get the total expected return

$$\mathrm{E}\big(R(\mathbf{x}^*)\big) = diag\left(\sum_{i=1}^{n} E(o_i)\mathbf{x}_o{}^*, \sum_{i=1}^{n} E(l_i)\mathbf{x}_l{}^*\right).$$

Now, we have defined the fuzzy portfolio selection model with interval values. There are many solutions in the model. It is depended on choosing the k_i, $\forall\, i = 1,2$. We give a description about how to choose the k_i, $\forall\, i = 1,2$, in the following subsection.

C. Statistic Test on Fuzzy Portfolio Selection Model

First, we give a definition of T-test with interval data.

Definition 7 T-test with interval value

For interval value $A = [a, b] \equiv (o, l)$, sample $o_1, o_2, \dots, o_n$ can be approximated as a normally distributed stochastic quantity $X_o \sim N(\mu, \sigma^2)$ and sample $l_1, l_2, \dots, l_n$ can be approximated as a normally distributed stochastic quantity $X_l \sim N(\mu, \sigma^2)$.

Statistics for each hypothesis is as follows.

$$H_0^o: \mu_o = \mu_{o_0}, \text{ for statistic } T_o = \frac{\overline{X}_{o_n} - \mu_{o_0}}{\frac{S_{o_n}}{\sqrt{n}}}, \tag{8}$$

$$H_0^l: \mu_l = \mu_{l_0}, \text{ for statistic } T_l = \frac{\overline{X}_{l_n} - \mu_{l_0}}{\frac{S_{l_n}}{\sqrt{n}}}. \tag{9}$$

The acceptance region $A_i, \forall\, i = o, l$, for T under probability δ for an error of the first type are

$$A_o = \left\{ t_o \in \mathbb{R} \middle| |t_o| = \left| \frac{\overline{X}_{o_n} - \mu_{o_0}}{\frac{S_{o_n}}{\sqrt{n}}} \right| \leq t_{n-1;1-\frac{\delta}{2}} \right\}, \tag{10}$$

$$A_l = \left\{ t_l \in \mathbb{R} \middle| |t_l| = \left| \frac{\overline{X}_{l_n} - \mu_{l_0}}{\frac{S_{l_n}}{\sqrt{n}}} \right| \leq t_{n-1;1-\frac{\delta}{2}} \right\}. \tag{11}$$

Where $t_{n-1;1-\frac{\delta}{2}}$ is the $(1-\frac{\delta}{2})$-fractile of the *t*-distribution with *n-1* degrees of freedom.

Now, we give the decision making for the fuzzy portfolio selection model by statistic test.

Definition 8 Statistic test on Fuzzy Portfolio Selection Model with interval values

According to Definition 7 and Model 1, we set up

$$K_o = \left\{ k_1 \middle| k_1 \geq 0 \text{ such that } \mu_{o_0} = \sum_{i=1}^{n} E(o_i)\mathbf{x}_o{}^* \in A_o, \text{we don't reject } H_0^o \right\},$$

$$K_l = \left\{ k_2 \middle| k_2 \geq 0 \text{ such that } \mu_{l_0} = \sum_{i=1}^{n} E(l_i)\mathbf{x}_l{}^* \in A_l, \text{we don't reject } H_0^l \right\}.$$

Moreover, we choose $K = K_o \cap K_l$, for $K_o \cap K_l \neq \emptyset$.

Hence, we get the solution of Model 1.

Now, we give the procedure of solving fuzzy portfolio selection model by statistic test in the following.

Procedure of Solving Fuzzy Portfolio Selection Model with Interval Values

Step 1. Collect the fuzzy data.

Step 2. Compute o_i *and* l_i, $\forall\, i = 1,2,\dots,n$.

Step 3. Identify the underlying distribution by simulating o_i *and* l_i.

Step 4. Calculate the parameters for the expected value, variance and covariance in model (6) and (7).

Step 5. Solve the optimization model (6) and (7) with different values for k_i, $\forall\, i = 1,2$, *respectively.*

Step 6. Calculate $K = K_o \cap K_l$ *by Definition 8.*

Step 7. Get the optimal solution $\mathbf{x}^*$ *with different* K.

Step 8. Compute the possibility distribution of total return $R(\mathbf{x}^*)$ *with different* K.

In order to illustrate our proposed effective meanings and approaches of the efficient portfolios, we exemplify a real portfolio selection problem in the following section.

IV. Empirical Studies

Example 1 We select five exchange currencies (USD, EUR, AUD, GBP and CHF) from Bank of Tokyo-Mitsubishi. Original data come from every day's closed prices from January 2010 to November 2010. There are 224 interval values in this period (*a, b*), where *a* is the minimum price and *b* is the maximum price in one day. We give some interval values in TABLEI.

TABLEI. Interval values of each exchange currency

	(*a*, *b*)			
USD	(83.4, 84.3)	(83.8, 84.4)	⋯	(83.01, 83.54)
EUR	(108.46,110.01)	(109.98,112.00)	⋯	(111.96,113.65)
AUD	(79.83, 80.82)	(80.52, 81.65)	⋯	(81.03, 82.51)
GBP	(129.54,130.47)	(130.74,131.74)	⋯	(132.69,133.48)
CHF	(83.32, 84.32)	(83.83, 84.44)	⋯	(84.27, 85.12)

First, we calculate the central point $o = \frac{a+b}{2}$ and radius $l = \frac{b-a}{2}$. We give the data in TABELII.

TABLEII. Central point o and radius l of each interval values (a, b)

	(*o*, *l*)			
USD	(83.85, 0.45)	(84.1, 0.3)	⋯	(83.275,0.265)
EUR	(109.235,0.775)	(100.99, 1.01)	⋯	(112.805,0.845)
AUD	(80.325, 0.495)	(81.085,0.565)	⋯	(81.77, 0.74)
GBP	(130.005,0.465)	(131.24, 0.5)	⋯	(133.085,0.395)
CHF	(83.82, 0.5)	(84.135,0.305)	⋯	(84.695, 0.425)

We simulate the values of o and l respectively. We get the probability distributions o and l respectively in exchange currency. We give the result in TABLEIII.

TABLEIII. Parameters of Probability Distribution Functions for Interval Values

	o	l
USD	$\mathrm{W}(29.91, 89.73)$	$\mathrm{W}(3.07, 0.51)$
EUR	$\Gamma(270.87, 0.43)$	$\Gamma(7.38, 0.09)$
AUD	$\Gamma(563.13, 0.14)$	$\Gamma(4.99, 0.11)$
GBP	$\Gamma(601.20, 0.23)$	$\Gamma(7.37, 0.10)$
CHF	$\mathrm{N}(83.95, 2.63^2)$	$\Gamma(8.97, 0.05)$

When we know the distribution function, we use moment method estimator (MME) to estimate our parameter in each distribution function. We can find out the expected values and variances by using those parameters. TABLEIV shows the results.

TABLEIV. Expected Values and Variances for Interval Values

	o_1	o_2	o_3	o_4	o_5
Expected value	88.09	116.47	78.84	138.28	83.95
Variance	13.62	50.08	11.04	31.80	6.92
	l_1	l_2	l_3	l_4	l_5
Expected value	0.46	0.66	0.55	0.74	0.45
Variance	0.03	0.06	0.06	0.07	0.02

Moreover, we give the values of $V_o = [cov(o_i, o_j)]_{5\times5}$ and $V_l = [cov(l_i, l_j)]_{5\times5}$, $\forall\, i, j = 1,2,\dots,5$ are in the following.

$$V_o = \begin{pmatrix} 13.62 & & & & \\ 0.92 & 50.08 & & & \\ 0.04 & -1.15 & 11.04 & & \\ 0.77 & 1.83 & 0.05 & 31.80 & \\ 0.32 & 0.33 & -0.64 & -0.48 & 6.92 \end{pmatrix} \text{ and}$$

$$V_l = \begin{pmatrix} 0.0257 & & & & \\ -0.0004 & 0.0602 & & & \\ -0.0008 & 0.0019 & 0.0625 & & \\ 0.0011 & 0.0029 & 0.0006 & 0.0661 & \\ 0.0001 & -0.0012 & -0.0004 & -0.0020 & 0.0236 \end{pmatrix}.$$

Now, we have all the data we need in our fuzzy portfolio selection model. We rewrite our model with estimated parameters as follows.

$$\left.\begin{array}{c} \max \quad 88.09x_{o_1} + 116.47x_{o_2} + 78.84x_{o_3} + 138.28x_{o_4} + 83.95x_{o_5} \\ \min \quad 13.62{x_{o_1}}^2 + 50.08{x_{o_2}}^2 + 11.04{x_{o_3}}^2 + 31.80{x_{o_4}}^2 + 6.92{x_{o_5}}^2 \\ +2(0.92x_{o_1}x_{o_2} + 0.04x_{o_1}x_{o_3} + 0.77x_{o_1}x_{o_4} + 0.32x_{o_1}x_{o_5} \\ -1.15x_{o_2}x_{o_3} + 1.83x_{o_2}x_{o_4} + 0.33x_{o_2}x_{o_5} \\ +0.05x_{o_3}x_{o_4} - 0.64x_{o_3}x_{o_5} - 0.48x_{o_4}x_{o_5}) \\ \text{s.t.} \quad x_{o_1} + x_{o_2} + x_{o_3} + x_{o_4} + x_{o_5} = 1 \\ x_{o_i} \geq 0 \qquad \forall\, i = 1,2,\dots,5 \end{array}\right\} \quad (12)$$

and

$$\left.\begin{array}{c} \min \quad 0.46x_{l_1} + 0.66x_{l_2} + 0.55x_{l_3} + 0.74x_{l_4} + 0.45x_{l_5} \\ \min \quad 0.03{x_{l_1}}^2 + 0.06{x_{l_2}}^2 + 0.06{x_{l_3}}^2 + 0.07{x_{l_4}}^2 + 0.02{x_{l_5}}^2 \\ +2(-0.0004x_{l_1}x_{l_2} - 0.0008x_{l_1}x_{l_3} + 0.0011x_{l_1}x_{l_4} + 0.0001x_{l_1}x_{l_5} \\ +0.0019x_{l_2}x_{l_3} + 0.0029x_{l_2}x_{l_4} - 0.0012x_{l_2}x_{l_5} \\ +0.0006x_{l_3}x_{l_4} - 0.0004x_{l_3}x_{l_5} - 0.002x_{l_4}x_{l_5}) \\ \text{s.t.} \quad x_{l_1} + x_{l_2} + x_{l_3} + x_{l_4} + x_{l_5} = 1 \\ x_{l_i} \geq 0 \qquad \forall\, i = 1,2,\dots,5 \end{array}\right\} \quad (13)$$

In fact that it is not easy to solve the model (12) and (13). In order to reduce the calculation load, we simplify the minimum goal in (12) and (13) as follows:

We set $G_1 = \min \quad 13.62{x_{o_1}}^2 + 50.08{x_{o_2}}^2 + 11.04{x_{o_3}}^2 + 31.80{x_{o_4}}^2 + 6.92{x_{o_5}}^2 + 2(0.92x_{o_1}x_{o_2} + 0.04x_{o_1}x_{o_3} + 0.77x_{o_1}x_{o_4} + 0.32x_{o_1}x_{o_5} - 1.15x_{o_2}x_{o_3} + 1.83x_{o_2}x_{o_4} + 0.33x_{o_2}x_{o_5} + 0.05x_{o_3}x_{o_4} - 0.64x_{o_3}x_{o_5} - 0.48x_{o_4}x_{o_5})$.

Hence, we have $G_1 \leq (\sqrt{13.62}x_{o_1} + \sqrt{50.08}x_{o_2} + \sqrt{11.04}x_{o_3} + \sqrt{31.80}x_{o_4} + \sqrt{6.92}x_{o_5})^2 \leq {k_1}^2$,

where k_1 ($k_1 \geq 0$) represents the tolerated risk level.

It implies that $3.69x_{o_1} + 7.08x_{o_2} + 3.22x_{o_3} + 5.64x_{o_4} + 2.63x_{o_5} \leq k_1$.

Let $G_2 = \min \quad 0.03{x_{l_1}}^2 + 0.06{x_{l_2}}^2 + 0.06{x_{l_3}}^2 + 0.07{x_{l_4}}^2 + 0.02{x_{l_5}}^2 + 2(-0.0004x_{l_1}x_{l_2} - 0.0008x_{l_1}x_{l_3} + 0.0011x_{l_1}x_{l_4} + 0.0001x_{l_1}x_{l_5} + 0.0019x_{l_2}x_3 + 0.0029x_{l_2}x_{l_4} - 0.0012x_{l_2}x_{l_5} + 0.0006x_{l_3}x_4 - 0.0004x_{l_3}x_{o_5} - 0.002x_{l_4}x_{l_5})$.

Hence, we have $G_2 \leq (\sqrt{0.03}x_{l_1} + \sqrt{0.06}x_{l_2} + \sqrt{0.06}x_{l_3} + \sqrt{0.07}x_{l_4} + \sqrt{0.02}x_{l_5})^2 \leq {k_2}^2$,

where k_2 ($k_2 \geq 0$) represents the tolerated risk level.

It implies that $0.17x_{l_1} + 0.24x_{l_2} + 0.24x_{l_3} + 0.26x_{l_4} + 0.14x_{l_5} \leq k_2$.

Therefore, we rewrite model (12) and (13) in the following.

$$\left.\begin{array}{c} \max \quad 88.09x_{o_1} + 116.47x_{o_2} + 78.84x_{o_3} + 138.28x_{o_4} + 83.95x_{o_5} \\ \text{s.t.} \quad 3.69x_{o_1} + 7.08x_{o_2} + 3.22x_{o_3} + 5.64x_{o_4} + 2.63x_{o_5} \leq k_1 \\ x_{o_1} + x_{o_2} + x_{o_3} + x_{o_4} + x_{o_5} \leq 1 \\ x_{o_i} \geq 0 \qquad \forall\, i = 1,2,\dots,5 \end{array}\right\} \quad (14)$$

and

$$\left.\begin{array}{c} \min \quad 0.46x_{l_1} + 0.66x_{l_2} + 0.55x_{l_3} + 0.74x_{l_4} + 0.45x_{l_5} \\ \text{s.t.} \quad 0.17x_{l_1} + 0.24x_{l_2} + 0.24x_{l_3} + 0.26x_{l_4} + 0.14x_{l_5} \leq k_2 \\ x_{l_1} + x_{l_2} + x_{l_3} + x_{l_4} + x_{l_5} \leq 1 \\ x_{l_i} \geq 0 \qquad \forall\, i = 1,2,\dots,5 \end{array}\right\} \quad (15)$$

We solve the model (14) and (15) by using GP-IGP (Linear and Integer Goal Programming). The result depends on the selection of $k_i, i = 1,2$. TABLEV shows the result of model (14) and TABLEVI shows the result of model (15).

TABLEV. STATISTIC TEST FOR X_O^* WITH DIFFERENT CONDITIONS k_1 AND THE RESULT OF PARAMETERS

k_1	0.5	1	1.5	2	2.5	3	3.5
$\sum_{i=1}^{5} x_{o_i}$	0.19	0.38	0.57	0.76	0.95	1	1
$\mathbf{x}_o^*$	$(0,0,0,0,.19)'$	$(0,0,0,0,.38)'$	$(0,0,0,0,.57)'$	$(0,0,0,0,.76)'$	$(0,0,0,0,.95)'$	$(0,0,0,.12,.88)'$	$(0,0,0,.29,.71)'$
$\sum_{i=1}^{n} E(o_i)\mathbf{x}_o^*$	15.96	31.92	47.88	63.84	79.80	90.63	99.65
μ_o^*	15.95	31.90	47.85	63.80	79.75	90.18	99.00
$S_{o_n}^*$	0.49	0.99	1.49	1.99	2.49	2.81	3.19
CI_o	(15.88, 16.01)	(31.77, 32.03)	(47.65, 48.05)	(63.54, 64.06)	(79.42, 80.08)	(89.81, 90.55)	(98.58, 99.42)
Decision(o)	A	A	A	A	A	R	R

k_1	4	4.5	5	5.5	6	6.5	7
$\sum_{i=1}^{5} x_{o_i}$	1	1	1	1	1	1	1
$\mathbf{x}_o{}^*$	$(0,0,0,.46,.54)'$	$(0,0,0,.62,.38)'$	$(0,0,0,.79,.21)'$	$(0,0,0,.95,.05)'$	$(0,0,0,1,0)'$	$(0,0,0,1,0)'$	$(0,0,0,1,0)'$
$\sum_{i=1}^{n} E(o_i)\mathbf{x}_o{}^*$	108.68	117.70	126.73	135.75	138.28	138.28	138.28
$\mu_o{}^*$	107.83	116.13	124.95	133.26	135.85	135.85	135.85
$S_{o_n}^*$	3.67	4.18	4.77	5.35	5.54	5.54	5.54
CI_o	(107.34, 108.31)	(115.58, 116.68)	(124.33, 125.58)	(132.55, 133.96)	(135.13, 136.58)	(135.13, 136.58)	(135.13, 136.58)
Decision(o)	R	R	R	R	R	R	R

TABLEVI. STATISTIC TEST FOR $\mathrm{X_L}^*$ WITH DIFFERENT CONDITIONS k_2 AND THE RESULT OF PARAMETERS

k_2	0.5	1	1.5	2	2.5	3	3.5
$\sum_{i=1}^{5} x_{l_i}$	0.19	0.38	0.57	0.76	0.95	1	1
$\mathbf{x}_l{}^*$	$(0,0,0,0,.19)'$	$(0,0,0,0,.38)'$	$(0,0,0,0,.57)'$	$(0,0,0,0,.76)'$	$(0,0,0,0,.95)'$	$(0,0,0,0,1)'$	$(0,0,0,0,1)'$
$\sum_{i=1}^{n} E(l_i)\mathbf{x}_l{}^*$	0.09	0.17	0.26	0.34	0.43	0.45	0.45
$\mu_l{}^*$	0.08	0.17	0.26	0.35	0.44	0.47	0.47
$S_{l_n}^*$	0.03	0.06	0.09	0.12	0.15	0.15	0.15
CI_l	(0.08, 0.09)	(0.17, 0.18)	(0.25, 0.28)	(0.34, 0.37)	(0.42, 0.46)	(0.45, 0.49)	(0.45, 0.49)
Decision(l)	A	A	A	A	A	A	A

Explain of decision with T-test.

In TABLEV, for example, when $k_1 = 2.5$, we have $\mathrm{x_o}^* = (0,0,0,0,0.95)'$. We calculate the return

$$R = \sum_{i=1}^{n} r_{o_i} x_{o_i} = r_{o_1}x_{o_1} + r_{o_2}x_{o_2} + r_{o_3}x_{o_3} + r_{o_4}x_{o_4} + r_{o_5}x_{o_5} = 0.95 * x_{o_5}.$$

Therefore, we have 224 new data.

We calculate the expected value $\mu_o{}^*$ and standard deviation $S_{o_n}^*$ by Minitab15. The results are $\mu_o{}^* = 79.75$ and $S_{o_n}^* = 2.49$. The hypothesis is $H_0^o: \mu_o = 79.80$, for statistic $T_o = \left|\frac{79.75-79.80}{\frac{2.49}{\sqrt{224}}}\right| = 0.26$. The 95% critical region is (79.42, 80.08).

Since $79.80 \in (79.42, 80.08)$, we accept the hypothesis.

The same method for $k_1 = 3$, we have $\mathrm{x_o}^* = (0,0,0,0.12,0.88)'$. The return

$$R = \sum_{i=1}^{n} r_{o_i} x_{o_i} = r_{o_1}x_{o_1} + r_{o_2}x_{o_2} + r_{o_3}x_{o_3} + r_{o_4}x_{o_4} + r_{o_5}x_{o_5} = 0.12 * x_{o_4} + 0.29 * x_{o_5}.$$

Therefore, we have 224 new data.

We calculate the expected value $\mu_o{}^*$ and standard deviation $S_{o_n}^*$ by Minitab15. The results are $\mu_o{}^* = 90.18$ and $S_{o_n}^* = 2.81$. The hypothesis is $H_0^o: \mu_o = 90.63$, for statistic $T_o = \left|\frac{90.18-90.63}{\frac{2.81}{\sqrt{224}}}\right| = 2.38$. The 95% critical region is (89.81, 90.55).

Since $90.63 \notin (89.81, 90.55)$, we reject the hypothesis.

It is the same way to calculate decision in TABLEVI.

We conclude the result as follows.

In TABLEV, we can see that when $k_1 \geq 3$, we reject the hypothesis. Moreover, we also see that we accept the hypothesis for all k_2 in TABLEVI.

That is we accept the hypothesis when $k_1 = 0.5, 1, 1.5, 2, 2.5.$

and

$$k_2 = 0.5, 1, 1.5, 2, 2.5, 3, 3.5, 4, 4.5, 5, 5.5, 6, 6.5, 7.$$

Hence, the result for $K = k_1 \cap k_2 = 0.5, 1, 1.5, 2, 2.5.$

We give the total expected return in TABLEVII. We get good total expected return when K is small.

TABLEVII. THE EXPECTED RETURN WITH DIFFERENT CONDITIONS K

K	0.5	1	1.5	2	2.5
$\sum_{i=1}^{n} E(o_i)\mathbf{x}_o{}^*$	15.96	31.92	47.88	63.84	79.80
$\sum_{i=1}^{n} E(l_i)\mathbf{x}_l{}^*$	0.09	0.17	0.26	0.34	0.43
Expected Return	(15.97, 16.05)	(31.75, 32.09)	(47.62, 48.11)	(63.50, 64.18)	(79.37, 80.23)

Suppose that we choose $K = k_1 = k_2 = 2.5$, the optimal solution of model (14) is $\mathbf{x}_o{}^* = (0,0,0,0.95)'$ and the optimal solution of model (15) is $\mathbf{x}_l{}^* = (0, 0, 0, 0, 0.95)'$.

Hence, we have our return of fuzzy vector

$$\mathbf{x}^* = [\mathbf{x}_o{}^*, \mathbf{x}_l{}^*]' = \begin{bmatrix} 0, 0, 0, 0, 0.95 \\ 0, 0, 0, 0, 0.95 \end{bmatrix}. \quad (16)$$

Moreover, we get the total expected return

$$\mathrm{E}[\mathrm{R}(\mathbf{x}^*)] = \mathrm{diag}\left(\sum_{\mathrm{i}=1}^{\mathrm{n}} E(o_i)\mathbf{x}_o{}^*, \sum_{\mathrm{i}=1}^{\mathrm{n}} E(l_i)\mathbf{x}_l{}^*\right) = \mathrm{diag}\,(79.80, 0.43). \quad (17)$$

The interval value of the total expected return resulted in (79.37, 80.23).

V. CONCLUSIONS

In this paper, we proposed a method to estimate the probability distribution function with fuzzy data. When we know the probability distribution function with fuzzy data, we can calculate the expected value, variance and covariance by using the estimated parameters of underlying distribution function. Therefore, we can solve the fuzzy portfolio selection model by statistic test. We give an empirical study by using fuzzy portfolio selection model based on statistic test in example 1. We can see that it is more explicit and meaningful to use fuzzy portfolio selection model by statistic test to estimate the maximum return because of considering more information based on vagueness, which comes from original fuzzy data. We have many choices K to decide which expected return is better and have less risk level in our model. Through this method, we also can provide not only one choice of portfolio selection but also two or more for decision makers.

We have further points to improve in the future as follows:

1. In this paper, we just use the most useful probability distribution function in industry to estimate the parameters. We can do more estimation with other probability distribution functions and compare which one gives better results in our fuzzy portfolio selection problem.
2. Moreover, if we can get the triangular fuzzy numbers or trapezoid fuzzy numbers, it will be good for us to examine fuzzy portfolio selection model with statistic test which we proposed is more explicit and easily for decision makers.

REFERENCES

[1] M.J. Best and R. R. Grauer, The efficient set mathematics when mean-variance problems are subject to general linear constrains, *Journal of Economics and Business*, Vol.42, No.2, pp.105-120, 1990.

[2] M.J. Best and J. Hlouskova, The efficient frontier for bounded assets, *Mathematical Methods of Operations Research*, Vol.52, No.2, pp.195-212, 2000.

[3] G. Casalino, F. Memola and C. Minutolo, A model for evaluation of laser welding efficiency and quality using an artificial neural network and fuzzy logic, *Proceedings of the Institution of Mechanical Engineers*, Vol.218, No.6, pp.641-646, 2004.

[4] D. Dubois, H. Prade, Systems of linear fuzzy constrains, *Fuzzy Sets and Systems*, Vol.3, No.1, pp.37-48, 1980.

[5] A. O. Esogbue and Q. Song, On optimal defuzzification and learning algorithms: theory and applications, *Fuzzy Optimization and Decision Making*, Vol.2, No.4, pp.283-296, 2003.

[6] Lai, K.K. Wang, S.Y. Xu, J.P. Zhu, S.S. Fang and Y., A class of linear interval programming problems and its application to portfolio selection, *IEEE Transactions on Fuzzy Systems*, Vol.10, No.6, pp.698-704, 2002.

[7] T. Leon, V. Liem and E. Vercher, Viability of infeasible portfolio selection problems: A fuzzy approach, *European Journal of Operational Research*, Vol.139, No.1, pp.178-189, 2002.

[8] P.-C. Lin, B. Wu and J. Watada, Kolmogorov-Smirnov Two Sample Test with Continuous Fuzzy Data, *Integrated Uncertainty Management and Applications*, AISC 68, pp. 175-186, 2010.

[9] P.-C. Lin, J. Watada and B. Wu, Database of Fuzzy Probability Distribution Function and Its Application, *The International Symposium on Innovative Management, Information & Production* (IMIP 2010), Hangzhou, China, Oct. 9-11, 2010.

[10] H. Markowitz, Portfolio selection, *Journal of Finance*, Vol. 7, No.1, pp. 77-91, 1952.

[11] H. Markowitz., *Portfolio selection: Efficient Diversification of Investments*, Wiley, New York, 1952.

[12] R.C. Merton, An analytic derivation of the efficient frontier, *Journal of Finance and Quantitative Anaysis*, September, Vol.7, No.4, pp.1851-1872, 1972.

[13] H. Markowitz., *Analysis in Portfolio Choice and Capital Markets*, Basil Blackwell, Oxford, 1987.

[14] J. S. Pang, A new efficient Algorithm for a class of portfolio selection problems, *Operational Research*, Vol.28, No.3, pp.754-767, 1980.

[15] A. F. Perold, Large-scale portfolio optimization, *Management Science*, Vol.30, No.10, pp.1143-1160, 1984.

[16] S. Ramaswamy, Portfolio Selection Using Fuzzy Decision Theory, *Working Paper of Bank for International Settlements*, No. 59, 1998.

[17] W. F. Sharpe, *Portfolio Theory and Capital Markets*, McGraw-Hill, New York, 1970.

[18] H. Tanaka and P. Guo, Portfolio selection based on upper and lower exponential possibility distributions, *European Journal of Operational Research*, Vol.114, No.1, pp.115-126, 1999.

[19] H. Tanaka, P. Guo and I. B. Turksen, Portfolio selection based on fuzzy probabilities and possibility distributions, *Fuzzy Sets and Systems*, Vol.111, No.3, pp.387-397, 2000.

[20] J. Voros, Portfolio analysis-An analytic derivation of the efficient portfolio frontier, *European Journal of Operational Research*, Vol.23, No.3, pp.294-300, 1986.

[21] R. Vertl, Statistical Methods for Non-Precise DATA. CRC, New York,1995.

[22] B. Wu and Z. Hwang, Testing for stability of Taiwan's short run money demand function: the application of fuzzy time series, *Annual Conference Proceedings of Taiwan Economic Association*. pp.169-190, 1995.

[23] B. Wu, Fuzzy statistical analysis: a new research method on the sampling survey, *Research Letters of National Chengchi University*, Vol.2, pp.65-80, 1995.

[24] J. Watada, Fuzzy Portfolio Selection and Its Applications to Decision Making, 13, *Tatra Mountains Mathematical Publication*, pp.219-248, 1997.

[25] B. Wu and M. Chen, Use of fuzzy statistical technique in change periods detection of nonlinear time series, *Applied Mathematics and Computation*. Vol.99, No.2-3, pp.241-254, 1999.

[26] B. Wu and C. Sun, Interval-valued statistics, fuzzy logic, and their use in computational semantics, *Journal of Intelligent and Fuzzy Systems*, Vol.11, No.1-2, pp.1-7, 2001.

[27] B. Wu and N. Tseng, A new approach to fuzzy regression models with application to business cycle analysis, *Fuzzy Sets and System*. Vol.130, No.1, pp.33-42, 2002.

[28] S. Y. Wang and S. S. Zhu, On fuzzy portfolio selection problems, *Fuzzy Optimization and Decision Making*, Vol.1, No.4, pp.361-377, 2002.

[29] B. Wang, S. Wang and J. Watada, Fuzzy portfolio selection based on value-at-risk, *Systems, Man and Cybernetics* (SMC2009), IEEE International Conference on 11-14 Oct., 2009.

[30] W. G. Zhang, Y. L. Wang, Using fuzzy possibilitic mean and variance in portfolio selection model, *Lecture Notes in Artificial Intelligence*, Vol.3801, pp.291-296, 2005.

[31] W. G. Zhang, W. A. Liu, Y. L. Wang, A class of possibilistic portfolio selection models and algorithms, *Lecture Notes in Computer Science*, Vol.3828, pp.464-472, 2005.

[32] H. Zhang, P.-C. Lin, B. Wu, and J. Watada, Fuzzy Valuation in Real Options Analysis, *The 25th Fuzzy System Symposium* (FSS2009) *English Section: Decision Making under Uncertain Environment*, Tsukuba, Japan, July 14-16, 2009.

2011 IEEE International Conference on Fuzzy Systems
June 27-30, 2011, Taipei, Taiwan

An Approach Based on Takagi-Sugeno Fuzzy Inference System Applied to the Operation Planning of Hydrothermal Systems

Ricardo A. L. Rabêlo
and Ricardo A. S. Fernandes
and Adriano A. F. M. Carneiro
University of São Paulo
Engineering School of São Carlos
São Carlos, São Paulo, Brazil
Email: ricardor_usp@yahoo.com.br, ricardo.asf@gmail.com, adriano@sel.eesc.usp.br

Rosana T. V. Braga
University of São Paulo
Department of Computing Science
São Carlos, São Paulo, Brazil
Email: rtvb@icmc.usp.br

***Abstract*—The operation planning in hydrothermal systems with great hydraulic participation, as it is the case of Brazilian system, seeks to determine an operation policy to specify how hydroelectric plants should be operated, in order to use the hydroelectric resources economically and reliably. This paper presents an application of Takagi-Sugeno Fuzzy Inference Systems to obtain an operation policy (PBFIS - Policy Based on Fuzzy Inference Systems) that follows the principles of the optimized operation of reservoirs for electric power generation. PBFIS is obtained through the application of an optimization algorithm for the operation of hydroelectric plants. From this optimization the relationships between the stored energy of the system and the volume of the reservoir of each plant are extracted. These relationships are represented in the consequent parameters of the fuzzy linguistic rules. Thus, PBFIS is used to estimate the operative volume of each hydroelectric plant, based on the value of the energy stored in the system. In order to verify the effectiveness of PBFIS, a computer simulation model of the operation of hydroelectric plants was used so as to compare it with the operation policy in parallel; with the operation policy based on functional approximations; and also with the result obtained through the application of the optimization of individualized plants' operation. With the proposed methodology, we try to demonstrate the viability of PBFIS' obtainment and application, and with the obtained results, we intend to illustrate the effectiveness and the gains which came from it.**

***Index Terms*—Takagi-Sugeno, Fuzzy Inference System, Operation Planning, Hydrothermal Systems, Operation Policy.**

I. Introduction

The operation planning of hydrothermal systems aims to determine an operation policy to specify how thermal and hydraulic subsystem should be operated so that the available resources for electric power generation are used efficiently. The problem of the planning is very complex due to several aspects, such as: the stochasticity of the water inflows and of the electric power market; the hydraulic interconnection of the hydroelectric plants in a cascade; the nonlinear operational characteristics of hydroelectric and thermoelectric plants; the dynamic relationship among the operation decisions taken along the whole horizon; and the transmission constraints of the electric system [1], [2], [3], [4].

In hydrothermal systems with great hydraulic participation, the operation policy seeks to replace the generation of complementary origin (thermo electrical plants, import of energy from other systems and the deficit) by hydroelectric origin generation, whenever possible [5]. Thus, in these hydrothermal systems, the operation planning has to determinate an operation policy for the reservoirs of the generation hydroelectric system as a fundamental point. The operation policy adopted in Brazilian electric power system is the Parallel Policy (PP) [6]. In this operation policy, the reservoirs are operated in parallel, which should maintain the same percent level of their useful volumes. This operation policy has its simplicity as its greatest attraction. However, it doesn't obey the principles of the optimized operation of the reservoirs for electric power generation [7], [8], [9].

To obtain an operation policy that represents the optimized behavior of the reservoirs, initially, the operation of the hydroelectric system is optimized under distinct operative conditions. With this optimization we can get a group of operation points that relate the energy stored in the hydroelectric system with the state of the reservoir of each hydroelectric plant. Figures 1 and 2 exhibit representative points of the optimized operation of some Brazilian power plants.

So that the group of operation points can be used as indicative for an operation policy, the adjustment of functions that represent the behavior of the optimized operation of the reservoirs will be necessary. Several works are related to the obtainment of operation policies, only differentiating in the employed technique for the adjustment of the points obtained relative to the optimized operation. In [10], the authors use third degree polynomial functions to adjust the points obtained with the optimization of the operation in order to obtain the operation policy. In [11], the authors make the adjustment of the points, obtaining polynomial and exponential functions to represent the operational policy whereas in [2], [12], [13], the authors use the method of the least squares in the adjustment of the polynomial, exponential and linear functions. In [14], [15],

978-1-4244-7316-8/11/$26.00 ©2011 IEEE

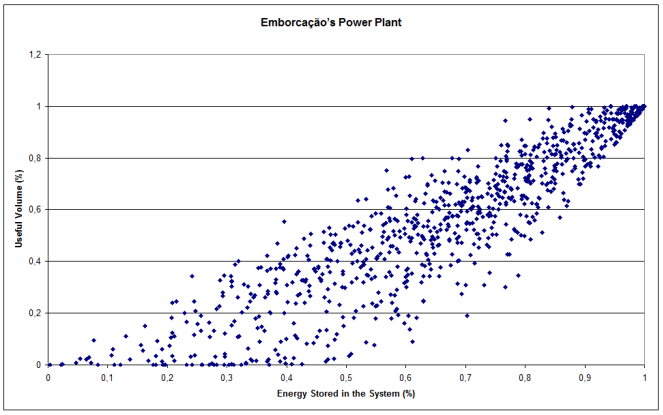

Fig. 1. Representative points of the optimized operation of Emborcação's power plant.

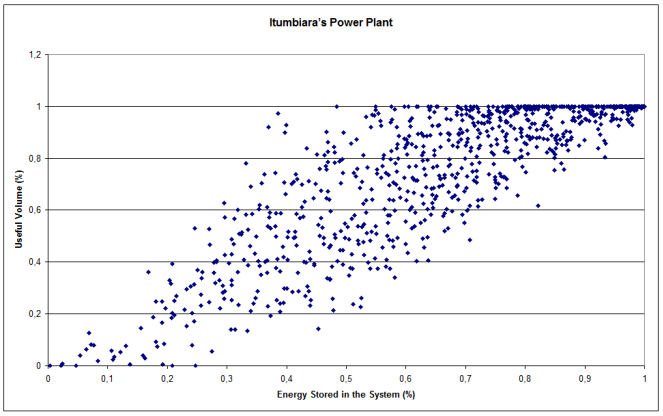

Fig. 2. Representative points of the optimized operation of Itumbiara's power plant.

Artificial Neural Networks (ANNs) are used, more specifically the SONARX model, for the obtainment of an operation policy that follows the principles of the optimized operation.

This paper presents an application of Takagi-Sugeno (TS) Fuzzy Inference Systems [16], responsible for obtaining an operation policy (PBFIS - Policy Based on Fuzzy Inference System) that represents the optimized operation of reservoirs for electric power generation [17]. The parametric functions in the consequents of the TS fuzzy rules and the adjustment easiness starting from a set of input and output data makes the TS fuzzy inference systems be related to the functions approximation task [18]. So as to illustrate the effectiveness of PBFIS, it was evaluated comparatively with the Parallel Policy (PP); with the operation policy based on functional approximations that use polynomial and exponential functions (policy based on polynomial and exponential functions - PBPEF), obtained through the method of the least squares; and also with the results obtained through the optimization of the operation of hydroelectric plants. Hence, we try to demonstrate the viability of the obtainment and application of PBFIS, as well as the energy gain that came from it.

Section 2 presents the problem of the operation planning of hydrothermal systems focusing on the adopted planning horizon, the mathematical formulation, and the operation policy for hydroelectric systems, besides presenting the hydroelectric system used in the case studies of this paper. In the Section 3, some foundations of the Takagi-Sugeno fuzzy inference system are presented, as well as the proposed fuzzy system. Section 4 brings the application of the operation policy for the chosen hydroelectric system, emphasizing the main results of the case studies. Section 5 presents the discussions of the work, followed by Section 6, in which the conclusions and final observations of the work are presented as a whole.

II. OPERATION PLANNING OF HIDROTHERMAL SYSTEMS

A. Hydroelectric System

Figure 3 illustrates the hydroelectric system used in the case studies of this paper. This system is composed of some hydroelectric plants of the Brazilian system. It is pinpointed that the chosen hydroelectric system can be characterized as a complex system, because it contains interlinked plants in parallel and in cascade.

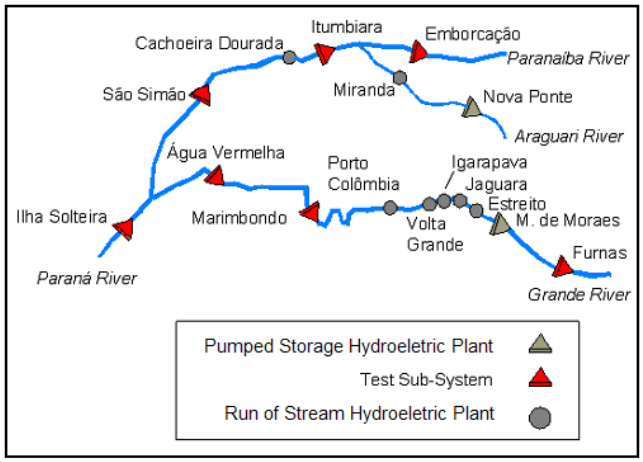

Fig. 3. Hydroelectric system used.

B. Planning Horizon

In this paper, the operation planning was adopted with five-year horizons (monthly discretized), but considering the individualized representation of the hydroelectric plants. The simplification of the composite representation of the system makes the hydroelectric generating system not be used in the most possible efficient way, once the equivalent reservoir of energy doesn't get to represent the individual operative characteristics of the plants. Thus, the individualized representation of each hydroelectric plant is important.

C. Mathematical Formulation

The operation planning of hydrothermal systems, with individualized representation of the hydroelectric plants and with

deterministic water inflows can be formulated according to the following optimization problem:

$$\min \quad \sum_{t=1}^{T} CVP_t \cdot 0,5 \cdot \Phi(D_t - H_t)^2 + V(x_T) \quad (1)$$

$$s.a. \quad E_t = D_t - H_t, \quad (2)$$

$$H_t = \sum_{i=1}^{N} k_i \cdot hl(x_{i,t}^{med}, u_{i,t}) \cdot min[u_{i,t}, q_{i,t}^{max}], \quad (3)$$

$$x_{i,t} = x_{i,t-1} + \\ +(y_{i,t}^{inc} + \sum_{k \in \Omega_i} u_{k,t} - u_{i,t} - x_{i,t}^{evap}) \cdot [\tfrac{\Delta t_t}{10^6}], \quad (4)$$

$$u_{i,t} = q_{i,t} + v_{i,t}, \quad (5)$$

$$x_{i,t}^{min} \leqslant x_{i,t} \leqslant x_{i,t}^{max}, \quad (6)$$

$$u_{i,t}^{min} \leqslant u_{i,t} \leqslant u_{i,t}^{max}, \quad (7)$$

$$q_{i,t}^{min} \leqslant q_{i,t} \leqslant q_{i,t}^{max}, \quad (8)$$

$$x_{i,0} \text{ given}, \quad (9)$$

onde:

- T: number of intervals of the planning horizon;
- N: number of hydroelectric plants;
- CVP: coefficient of present value;
- E_t: total thermal generation [MW];
- H_t: total hydroelectric generation [MW];
- D_t: demand (electric energy market) [MW];
- $x_{i,t}$: volume stored in the reservoir i at the end of the interval t [hm^3]. The values of the initial volumes of the reservoirs are given;
- $x_{i,t}^{med}$: medium volume stored in the reservoir i in the interval t [hm^3];
- $x_{i,t}^{evap}$: volume evaporated in the reservoir i in the interval t t[hm^3];
- $hl_{i,t}$: net water head of the plant i in the interval t [m];
- $y_{i,t}^{inc}$: incremental water inflow to the reservoir of the plant i in the interval t [m^3/s];
- $q_{i,t}$: turbinated flow of the plant i in the interval t [m^3/s];
- $u_{i,t}$: flow release of the plant i in the interval t [m^3/s];
- $v_{i,t}$: spill flow of the plant i during the interval t [m^3/s];
- $x_{i,t}^{max}$, $x_{i,t}^{min}$: maximum and minimum limits of stored volume for the reservoir of the plant *i* at the end of interval *t* [hm^3];
- $u_{i,t}^{max}$, $u_{i,t}^{min}$: maximum and minimum limits of the flow release for the plant *i* in the interval *t* [m^3/s];
- $q_{i,t}^{max}$, $q_{i,t}^{min}$: maximum and minimum limits of turbinated flow for the plant *i* in the interval *t* [m^3/s];
- Δt_t: number of seconds in the interval t [s];
- Ω_i: group of indexes of the plants immediately upstream of plant i.

The objective function is composed of two terms, which represent the operational cost during the horizon planning (Φ) and the future costs associated with the final storage condition from hydroelectric plants to reservoirs (V). As the Brazilian system is a hydrothermal system greatly predominant of hydraulic origin generation, for our purposes, complementary generation system is being used by an equivalent thermoelectric plant that substitutes all non-hydraulic system [19]. Thus, the operational cost is represented by a single cost function of non-hydraulic sources. Future cost is a terminal condition used in the optimization models of the operation to balance the use of water during the planning horizon and its future use [20].

The equality (2) represents the constraints towards the electric power demand in the interval t. The total hydraulic generation of the hydroelectric system is represented by equation (3), given by the sum of the hydraulic production functions of each hydraulic plant. The equation (4) represents the water balance in the reservoir. The output flow of the plant corresponds to the flow released and is equivalent to the sum of the turbinated flow with the spilled flow and it is represented in equation (5). The constraints (6) and (7) represent the storage and the released flow limits of the hydroelectric plants. The limits presented in these inequations vary in time, because these reflect the operational restrictions of the plant and other restrictions associated with the multiple use of water, such as: irrigation, control of floods, navigation, etc. Restriction (8) represents the minimum and maximum limits of turbinated flow, which can be associated with physical restrictions of the plant itself or electric restrictions.

D. Hydroelectric Systems Operation Policy

The operation policies for hydroelectric systems are present in several stages of the operation planning of hydrothermal systems. They are necessary in the aggregation procedure for obtainment of the equivalent reservoir [21], [22], in the simulation of the operation to disaggregate the goals of hydraulic generation of the equivalent reservoir among all the plants [10], and for the evaluation of the performance of the hydroelectric system in several conditions [23], [24]. Additionally, operation policies are also used in the expansion planning of the Brazilian hydrothermal system.

The operation policies for hydroelectric systems try to determine the amount of electric power produced by each one of the plants, through the definition of the storage state of each reservoir. The operation policy can be understood as a group of operation rules, one to each plant (or reservoir) of the system, which defines how these plants will be operated in a coupled way. To implement the coupling in the operation of hydroelectric systems, a global parameter is defined, denominated coupling factor of the operation among the plants, denoted by λ_t. The coupling factor represents the percentage of storage of the system in a certain interval t, and it is calculated (Equation 10) as the proportion between the energy stored in the system (ESS_t) and the maximum energy stored in the system (ESS^{max}), resulting in the values in the interval: $0 \leq \lambda_t \leq 1$.

$$\lambda_t = \frac{ESS_t}{ESS^{max}} \quad (10)$$

With the value of λ, the volume of each reservoir can be determined by the following equation:

$$x_{i,t}(\lambda_t) = x_{i,t}^{min} + f_i(\lambda_t) \cdot (x_{i,t}^{max} - x_{i,t}^{min}) \quad (11)$$

Where:

- $x_{i,t}(\lambda_t)$: operative volume of plant *i* in the interval *t*;
- $f_i(\lambda_t)$: operation rule of the reservoir of plant *i* as function of the parameter λ_t. It expresses the rules of emptying/filling of the reservoir together with the other reservoirs of the hydroelectric system.

III. TAKAGI-SUGENO FUZZY INFERENCE SYSTEMS

The fuzzy inference systems are based on production rules that make use of the linguistic variables [25] to execute a process of decision making. The operation of fuzzy inference systems can be divided in three stages: fuzzification, inference procedures and defuzzification.

In the fuzzy inference systems, usually, crisp (or precise) inputs are considered resulting from observations or measurements. Because of that, it is necessary to make a conversion (fuzzification) of those data for the fuzzy input sets. This way, the fuzzification is a mapping of the domain of the crisp input variable for the fuzzy domain, to attribute linguistic values (vague or qualitative descriptions) defined by membership functions to the entrance variables. The inference procedure is responsible for processing the fuzzy input data together with the production rules, so as to infer the contributions in the fuzzy output of the inference system. A typical production rule of Takagi-Sugeno fuzzy inference model is: if *x* is *F* and *y* is *G*, then, $z = f(x, y)$, where *F* and *G* are fuzzy sets and f is a polynomial function of x and y. The inference procedure in the Takagi-Sugeno model, specifically, consists of obtaining all the individual contributions z_i coming from each one of the fired rules. After this stage, we should combine all of the individual contributions to get the final answer z. Thus, the numeric output is calculated directly by the sum of the outputs pondered by the degree of fired of each rule (μ_i). Therefore, the defuzzification process is unnecessary [26]. This model was proposed as an effort to develop a systematic approach so as to generate fuzzy rules starting from a group of input and output data [27].

The fuzzy inference systems implemented have as input linguistic variable the ESS, defined in the group of linguistic terms (Very Low, Low, Medium, High and Very High)(Figure 4).

In this paper, we specialized for each one of the 7 plants (Figure 3), a Takagi-Sugeno fuzzy inference system. Each TS system is composed of 5 disjunctive inference rules. The syntax of the rules base of the fuzzy systems implemented is represented by the following linguistic conditional declarations:

- Rule 1: If (ESS *é Very Low*), Then $z_1 = f_1(ESS) = a_1 \cdot ESS + b_1$
- Rule 2: If (ESS *é Low*), Then $z_2 = f_2(ESS) = a_2 \cdot ESS + b_2$
- Rule 3: If (ESS *é Medium*), Then $z_3 = f_3(ESS) = a_3 \cdot ESS + b_3$
- Rule 4: If (ESS *é High*), Then $z_4 = f_4(ESS) = a_4 \cdot ESS + b_4$

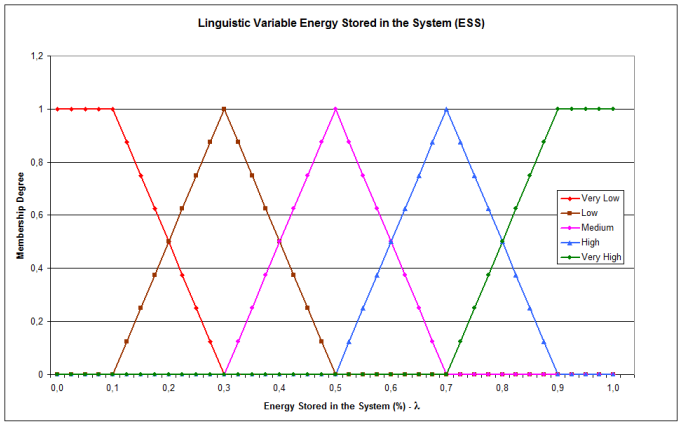

Fig. 4. Input linguistic variable representing the energy stored in the system.

TABLE I
PARAMETERS OF THE CONSEQUENTS OF THE PRODUCTION RULES OF THE FUZZY INFERENCE SYSTEM TO THE PLANT OF EMBORCAÇÃO.

i	ESS	a	b
1	Very Low	$0,5272$	$-0,0188$
2	Low	$0,8928$	$-0,1013$
3	Medium	$1,0796$	$-0,1776$
4	High	$1,2216$	$-0,2690$
5	Very High	$1,4516$	$-0,4533$

- Rule 5: If (ESS *é Very High*), Then $z_5 = f_5(ESS) = a_5 \cdot ESS + b_5$

With the optimization of the hydroelectric system operation, we obtain a set of operation points, which relate the stored energy of the hydroelectric system to the operative volume of each reservoir. For each one of the 5 rules that compose each fuzzy system, linear regression is applied at the points belonging to its activation domain, using the known input/output points, in order to determine the parameters (a_i, b_i) of each one of the $(5 \cdot N)$ polynomial functions relative to the consequent of *N* fuzzy systems (N = 7). Tables I, II and III present the parameters of the consequents of the fuzzy production rules relative to the policy proposed for some reservoirs of the hydroelectric system used.

With the determination of the 70 parameters of the consequents of the linguistic rules (a_i, b_i), the fuzzy system can be put to operation. In the particular matter, the TS fuzzy inference system *i* determines the operation rule of the plant *i* of the hydroelectric system:

$$f_i(\lambda) = \frac{\sum_{j=1}^{5}(z_j \cdot \mu_j)}{\sum_{j=1}^{5}\mu_j};\ i = 1,...,\ N \qquad (12)$$

IV. CASE STUDIES

In this paper, a computer model was used to simulate the operation of hydroelectric systems, so as to allow the performance evaluation of the proposed operation policy (PBFIS). The simulation model used is part of a computer tool that has been developed by the authors for the accomplishment

TABLE II
PARAMETERS OF THE CONSEQUENTS OF THE PRODUCTION RULES OF FUZZY INFERENCE SYSTEM FOR TO THE PLANT OF ITUMBIARA.

i	ESS	a	b
1	Very Low	$1,4329$	$-0,0757$
2	Low	$1,4357$	$-0,0744$
3	Medium	$1,0728$	$0,0724$
4	High	$0,9702$	$0,1341$
5	Very High	$0,4968$	$0,5114$

TABLE III
PARAMETERS OF THE CONSEQUENTS OF THE PRODUCTION RULES FUZZY INFERENCE SYSTEM TO SÃO SIMÃO'S PLANT.

i	ESS	a	b
1	Very Low	$2,5578$	$0,1792$
2	Low	$0,7766$	$0,5879$
3	Medium	$0,1661$	$0,8414$
4	High	$0,1414$	$0,8584$
5	Very High	$0,1008$	$0,8924$

of studies related to the operation planning of hydrothermal systems. The tool comprehends, besides the simulation model, a model of optimization of the hydrothermal systems operation [28]. The optimization model is used to determine the optimized operation of reservoirs and is inspired in algorithms of optimization designed for the operation planning of hydrothermal systems [29], [30]. It should be stressed that the authors applied a development process (UML Components) [31] based on software components [32] for the construction of the computer models, in order to guide the development of the tool.

The simulation of the operation intends to verify how a hydroelectric system would behave in case it were submitted to certain operation conditions (electric power market, operation policies, operative restrictions, initial volume, etc.). Thus, to make the comparison among the proposed policy (PBFIS), the policy based on polynomial and exponential functions (PBPEF), and the parallel policy (PP); the simulations of the operation are accomplished under the same operation conditions. Therefore, the differences of behavior in the operation of the hydroelectric system will only result from the policies used.

A. Operation Conditions

Five case studies were realized, with the intention of accomplishing a comparison among the three operation policies implemented in the simulation model, under several hydrological conditions. The goal of hydraulic generation (or electric power market) is said to be equal to the hydraulic generation provided by the operation optimization model, for the periods of the report from 1936 to 1941; 1951 to 1956; 1971 to 1976; 2000 to 2005 and with data of LTA (Long Term Average). The natural water inflow corresponds to the flows verified for the same periods of the report. The month of May was adopted (beginning of the dry period for the hydrographic basin of the Brazilian southeastern system) as the beginning month for all case studies. For additional comparisons, the optimization of the hydroelectric system operation was accomplished with water inflows really occurred in the periods, in order to obtain the solution with the perfect knowledge of the water inflows for the whole planning horizon. We emphasize that the solution obtained through the optimization model corresponds to the superior performance limit in the use of the hydroelectric generation resources. We considered in all the case studies that the initial volume stored in the reservoirs were the same as the operative maximum volume.

B. Results

1) Volume Stored in the Reservoirs: Figures 5 and 6 exhibit the trajectories of reservoirs' useful volume of some plants of the hydroelectric system considered for test. A differentiated behavior can be observed for each plant's reservoir, in which the oscillation of the reservoirs' volume is made in function of its positioning in the cascade. In the figures, one can visualize that the more upstream reservoir (Emborcação) presents a smaller storage level during the planning horizon. The plant of Itumbiara, in the intermediate position, presented a medium storage level, while the plants of São Simão downstream, presents lower emptying level (higher storage level).

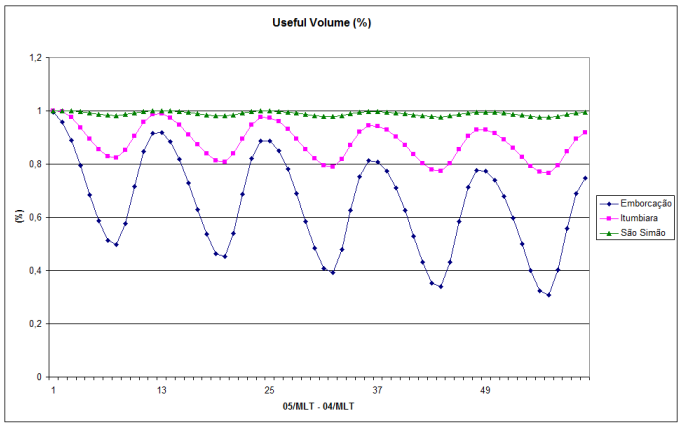

Fig. 5. Trajectories of useful volume in some reservoirs of the hydroelectric system for MLT.

With PBFIS, the downstream plants, whenever possible, remain full, so as to maintain high productivity and, thus, value the water that goes by them. As the energy stored at a plant is valued by the productivity of all downstream plants, the net water head of the plant more downstream, for instance, affects the stored energy of all plants of the cascade. Therefore, the consequent parameters of the fuzzy inference system are adjusted to prioritize higher storage levels in the upstream to the downstream reservoirs in the cascade of plants.

2) Deficit of Energy Stored in the System: Figure 7 illustrates the deficit path of stored energy (in %) in the system for the simulations of the operation accomplished with the three implemented policies, using the LTA. The deficit of energy stored in the system is calculated as the subtraction between the value of the stored energy resulting through the optimized solution, and the values of the stored energy resulting from the

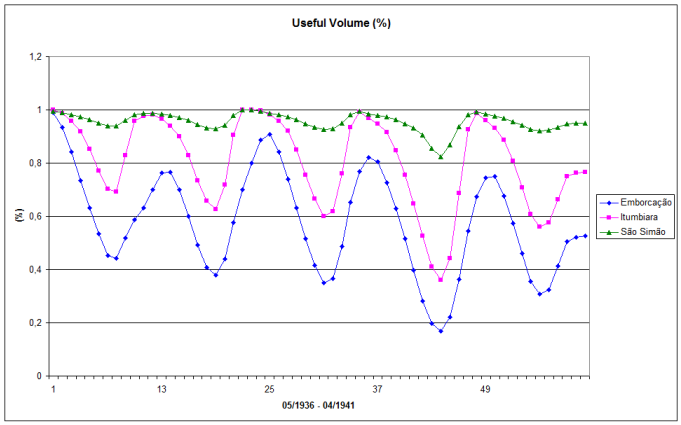

Fig. 6. Trajectories of useful volume in some reservoirs of the hydroelectric system 1936 to 1941.

application of operational policies implemented in the simulation model. A more severe emptying of the group of reservoirs can be noticed when using the parallel policy, followed by a less rigorous emptying when using PBPEF, and an even less accentuated emptying using PB, what implicates a larger efficiency in the use of generation hydroelectric resources, through the proposed policy (PBFIS).

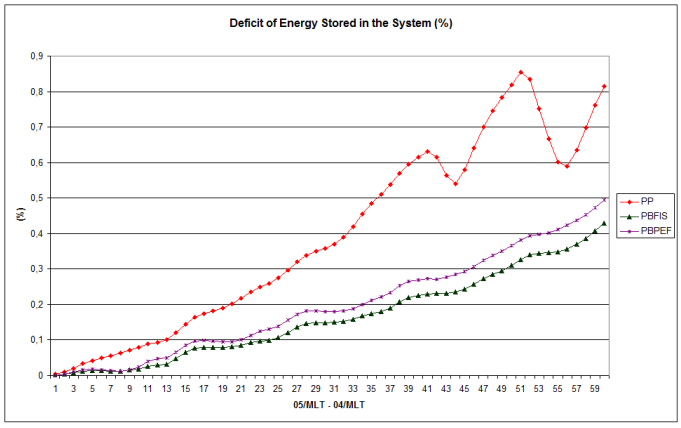

Fig. 7. Trajectories of the deficit of energy stored in the system for MLT.

Table IV allows the reader an additional comparison, in order to verify the efficiency of each operation policy with the optimized solution numerically. Considering the planning horizon involving the years 1936 - 1941, 1951 - 1956, 1971 - 1976, 2000 - 2005 and LTA (05 years of medium flows), we can confirm the greatest efficiency supplied by the proposed policy when compared with the parallel policy, in the use of generation hydroelectric resources. It is noteworthy that when compared with PBPEF, PBFIS only presents more reduced levels of stored energy (or a higher stored energy deficit) in the horizon from 1971 to 1976.

In Figure 8, we can verify the best use of generation hydroelectric benefits, for the proposed policy, where it is noticed that the emptying of the reservoirs is much more

TABLE IV
AVERAGE OF ENERGY STORED IN THE SYSTEM [MW].

Planning Horizon	PP	PBPEF	PBFIS	Optimal Solution
1936-1941	27865.83	29773.74	32299.55	34824.86
1951-1956	24232.82	26817.27	28851.86	38375.47
1971-1976	14329.13	27517.44	26544.69	33470.54
2000-2005	18151.44	21761.86	25847.11	29761.31
LTA	17171.52	25950.09	27437.61	34991.9

intense when the parallel policy and the PBPEF are employed. It may be emphasized that although, during the whole planning horizon, the proposed policy has always presented lower deficit values of energy stored in the system, confirming that this policy needs to use less water to meet the same electric energy market. Additionally, at the end of the planning horizon, we can see that the parallel policy and PBPEF do not get to reach the storage levels obtained by the proposed policy.

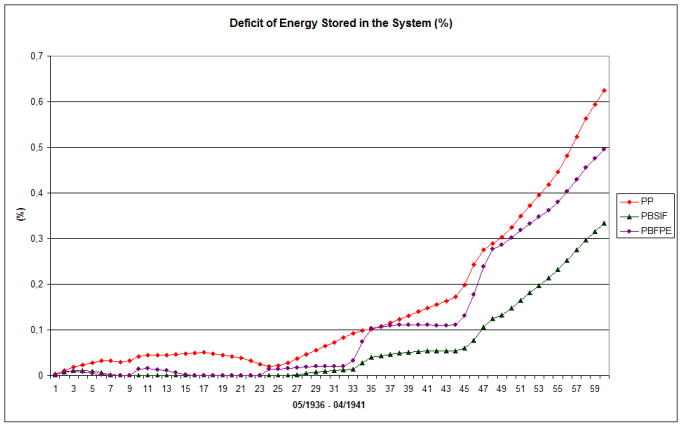

Fig. 8. Trajectories of the deficit of energy stored in the system 1936 to 1941.

Based on the trajectories of deficit of the energy stored in the system, it can be affirmed that, in most case studies accomplished, the simulation of the operation using the proposed policy maximize the hydroelectric benefits of the generation hydrothermal system, as it assists the same market of electric energy, using less water stored in the reservoirs of the plants. Again, at the end of the planning horizon, it is observed that the parallel policy does not get to maintain the close storage levels of the established storage levels for PBFIS and PBPEF. On the contrary, the parallel policy gets to the end of the simulation with more reduced storage levels in the reservoirs, making reliability and the cost of the operation extremely damaged in the continuous operation of the system. Therefore, PBFIS and PBPEF allow the simulation of the hydroelectric system operation to be solid with the continuous operation of the system, since the hydroelectric system does not stop being operated with the end of the planning horizon.

When using the representative operation points of the optimized operation of the reservoirs, the proposed policy (PBFIS) tries to present a differentiated behavior for each reservoir of

plants of hydroelectric system. With the specialization of a fuzzy inference system for each plant, the operation of each one reflects the role that it plays in the hydroelectric system, in agreement with its location in the cascade. Therefore, hydroelectric system is capable of maintaining higher levels of stored energy.

It should be taken into account that the comparisons made with the optimized solution took the optimization with previous knowledge of affluences (optimal absolute), characterizing it as an extremely rigorous pattern. Therefore, the solutions obtained with the simulation model of the operation and the several implemented policies should present a large or smaller degree of sub-optimality.

V. DISCUSSIONS

The proposed operation policy was compared, through some case studies, in the hydroelectric plants of the southeastern Brazilian system, with the policy of parallel operation and with the policy based on functional approximation that uses polynomial and exponential functions. Most results evidenced the efficiency of the proposed policy, taking into account the deficit trajectories and the average of energy stored in the system as parameters. These parameters were obtained by the simulation of the hydroelectric system operation. Regarding the energy stored in the system, the results illustrated that the proposed policy needs less hydraulic resources under the same operation conditions of the parallel policy and PBPEF.

Thus, it is verified that the proposed policy can assure a more reliable and economical supply of the electric power. Economical because the proposed policy needs less hydraulic generation resources than the parallel policy and PBPEF. Reliable because the proposed policy allows the operation of the hydroelectric system with superior storage levels in the reservoirs, reducing the possibility of hydraulic deficits of the hydrothermal generation system. Therefore, the potentiality of the proposed policy can be evidenced in the use of the hydraulic resources turned to electric energy generation.

Additionally, at the end of all planning horizons, it was observed that the parallel policy does not manage to equal the levels of stored energy of the hydroelectric system with the established levels for PBFIS and for PBPEF. Therefore, the proposed policy, besides maximizing the benefits of the generation hydroelectric resources during the planning horizon, still guarantees a larger reliability and a smaller cost of the hydrothermal generation system operation in the continuity of the operation of the hydroelectric system, when arriving at the end of the planning horizon with higher levels of water stored in the reservoirs.

VI. CONCLUSIONS

By the found results, the operation policy based on the Takagi-Sugeno fuzzy inference system establishes a different behavior for the group of reservoirs, so as to maximize the energy stored in the system during the simulation of the hydroelectric system operation. This behavior is obtained through the specific operation for each reservoir, in the agreement with its position in the cascade. With the predominant influence of the quota effect, the plants whose reservoir volume does not have great influence on the energy stored in the hydroelectric system have emptying priority. On the other hand, the plants whose operative volume of the reservoir has great influence on the system's stored energy present filling priority. As the energy stored in a hydroelectric system is valued by the productivity of the downstream plants, the parameter of the fuzzy rule consequents prioritize higher storage levels in the reservoirs from upstream to downstream in the cascade of plants. Thus, the knowledge of the volume oscillations, in the function of the positioning in the cascade, is represented through the fuzzy production rules.

When opting for a fuzzy inference system to determine the operative volume of each hydroelectric plant, we obtained an action/control strategy that can be monitored and interpreted, even from the language viewpoint. It should be emphasized that, as future works, some improvements can still be investigated in relation to parameters of the fuzzy inference system, mainly in the adjustment of the membership functions, the number of rules and the consequents of the rules employing techniques like Artificial Neural Networks of Genetic Algorithms.

VII. THANKS

The authors would like to thank Prof. Dr. Ivan Nunes da Silva of Universidade of São Paulo (Engineering School of São Carlos, Electric Engineering Departament). The authors also thank the financial support of the SEFAZ-PI and FAPESP.

REFERENCES

[1] H. Duran, C. Puech, J. Diaz, and G. Sanchez, "Optimal Operation of Multireservoir Systems using an Aggregation-decomposition Approach," *IEEE Transactions on Power Apparatus and Systems*, vol. PAS-104, no. 8, pp. 2086–2092, 1985.

[2] G. C. Cruz Jr and S. Soares, "Non-Uniform Composite Representation Hydroelectric Systems for Long-Term Hydrothermal Scheduling," *IEEE Transactions on Power Systems*, vol. 11, no. 2, pp. 702–707, 1996.

[3] P. T. Leite, A. A. F. M. Carneiro, and A. C. P. L. F. Carvalho, "Energetic Operation Planning Using Genetic Algorithms," *IEEE Transactions on Power Systems*, vol. 17, no. 1, pp. 173–179, 2002.

[4] C. E. Zoumas, A. G. Bakirtzis, J. B. Theocharis, and V. Petridis, "A genetic algorithm solution approach to the hydrothermal coordination problem," *IEEE Transactions on Power Systems*, vol. 19, no. 2, 2004.

[5] Z. Yu, F. T. Sparrow, and B. H. Bowen, "A new long-term hydro production scheduling method for maximizing the profit of hydroelectric systems," *IEEE Transactions on Power Systems*, vol. 13, no. 1, pp. 66 – 71, February 1998.

[6] T. C. Marques, M. A. Cicogna, and S. Soares, "Assessment of energy availability of hydro system under different operation policies," *Proceedings of IEEE Power Tech*, 2005.

[7] E. G. Read, "Economic Principles of Reservoir Operation I: Perfect Foresight," *CBER Working Paper, College of Business Administration, University of Tennessee*, 1982.

[8] R. Sacchi, J. S. Nazareno, M. A. A. Castro, D. Silva Filho, and A. A. F. M. Carneiro, "Economics principles of the hidrothermal power systems operation," in *IX Symposium of Specialists in Electric Operational and Expansion Planning*, 2004.

[9] S. Sjelvgren, S. Anderson, and T. S. Dillon, "Optimal operations planning in a large hydro-thermal power system," *IEEE Transactions on Power Apparatus and Systems*, vol. 102, no. 11, pp. 3644 – 3651, November 1983.

[10] S. Soares and A. A. F. M. Carneiro, "Reservoir Operation Rules for Hydroelectric Power System Optimization," in *Athens Power Tech, 1993. APT 93. Proceedings. Joint International Power Conference*, vol. 2, 1993.
[11] A. A. F. M. Carneiro and M. Kadowaki, "Operation rules for great hydrolectric system in cascade (in portuguese)," in *Brazilian Conference of Automatic*, 1996.
[12] G. Cruz Jr and S. Soares, "Non-parallel composite representation of hydroelectric systems for long-term hydrothermal scheduling," in *IEEE Power Industry Computer Applications Conference*, 1995, pp. 566–571.
[13] G. C. Cruz Jr and S. Soares, "General Composite Representation of Hydroelectric Systems," in *Power Industry Computer Applications, 1999. PICA'99. Proceedings of the 21st 1999 IEEE International Conference*, 1999, pp. 177–182.
[14] R. Sacchi, A. A. F. M. Carneiro, and A. F. R. Araújo, "Operation policies for hydropower systems: Using the unsupervised sonarx neural network," *IEEE - Power Systems Conference & Exposition*, 2004.
[15] ——, "A rbf network trained by the sonarx model and applied to obtain the operation policies of the hydropower systems," in *8th Brazilian Symposium on Artificial Neural Networks*, 2004.
[16] T. Takagi and M. Sugeno, "Fuzzy identification of systems and its applications to modeling and control," *IEEE Trans. Syst., Man, Cybern.*, vol. 15, pp. 116–132, 1985.
[17] S. Soares and A. A. F. M. Carneiro, "Optimal Operation of Reservoirs for Electric Generation," *IEEE Transactions on Power Delivery*, vol. 6, no. 3, pp. 1101–1107, 1991.
[18] J. M. Mendel, *Uncertain Rule-Based Fuzzy Logic Systems: Introduction and New Directions*. Prentice Hall, 2001.
[19] S. J. Huang, "Enhancement of hydroelectric generation scheduling using ant colony system based optimization approachs," *IEEE Transactions on Energy Conversion*, vol. 16, pp. 296–301, 2001.
[20] L. Martinez and S. Soares, "Comparison between closed-loop and partial open-loop feedbackcontrol policies in long term hydrothermal scheduling," *IEEE Transactions on Power Systems*, vol. 17, no. 2, pp. 330–336, 2002.
[21] N. V. Arvanitidis and J. Rosing, "Composite Representation of a Multireservoir Hydroelectric Power System," *IEEE Transactions on Power Apparatus and Systems*, vol. PAS-89, no. 2, pp. 319–326, 1970.
[22] ——, "Optimal Operation of Multireservoir Systems Using a Composite Representation," *IEEE Transactions on Power Apparatus and Systems*, vol. PAS-89, no. 2, pp. 327–335, 1970.
[23] J. A. Gonzalez, "Probabilistic production costing modeled with ampl," *IEEE Transactions on Power Systems*, vol. 17, no. 2, 2002.
[24] E. Silva and E. Finardi, "Parallel Processing applied to the Planning of Hydrothermal Systems," *IEEE Transactions on Parallel and Distributed Systems*, pp. 721–729, 2003.
[25] L. A. Zadeh, "The Concept of a Linguistic Variable and its Application to Approximate Reasoning -I," *Information Sciences*, vol. 8, no. 3, pp. 199–249, 1975.
[26] H. J. Zimmermann, *Fuzzy Set Theory – and its Applications*. Kluwer Academic Publishers, 2001.
[27] T. J. Ross, *Fuzzy Logic with Engineering Applications*. Wiley, 2004.
[28] R. A. L. Rabelo, A. A. F. M. Carneiro, and R. T. V. Braga, "Component-based development applied to energetic operation planning of hydrothermal power systems," in *Proceedings of IEEE Bucharest PowerTech*, 2009.
[29] M. F. Carvalho and S. Soares, "An Efficient Hydrothermal Scheduling Algorithm," *IEEE Transactions on Power Systems*, vol. 2, no. 3, pp. 537–542, 1987.
[30] A. A. F. M. Carneiro, S. Soares, and P. S. Bond, "A Large Scale of an Optimal Deterministic Hydrothermal Scheduling Algorithm," *IEEE Transactions on Power Systems*, vol. 5, no. 1, pp. 204–211, 1990.
[31] J. Cheesman and J. Daniels, *UML components*. Addison-Wesley Boston, 2001.
[32] C. Szyperski, *Component Software - Beyond Object Oriented Programming*. Addison-Wesley, 2002.

2011 IEEE International Conference on Fuzzy Systems
June 27-30, 2011, Taipei, Taiwan

Fuzzy Cognitive Maps In Estimating The Repercussions Of Oil/Gas Exploration On Politico-economic Issues In Cyprus

Costas Neocleous
Department of Mechanical Engineering
Cyprus University of Technology,
Lemesos, Cyprus
costas.neocleous@cut.ac.cy

Christos Schizas
Department of Computer Science
University of Cyprus
Nicosia, Cyprus
schizas@ucy.ac.cy

Maria Papaioannou
Department of Computer Science
University of Cyprus
Nicosia, Cyprus
cs03pm2@ucy.ac.cy

***Abstract*—Some important politico-economic dynamics, in relation to different scenarios involving the finding and exploitation of oil/gas in the exclusive economic zone of Cyprus, have been modeled and examined through the use of suitable fuzzy cognitive maps. In the interrelated dynamics, various important dynamical parameters have been taken into account, reflecting the interests of the republic of Cyprus, as well as the interests of the Greek and Turkish Cypriot communities. In some respects these interests are antagonistic, while in others could be cooperative. The interests of other countries involved in the Cyprus politico-economic problem have also been taken into account. These are primarily Greece, Turkey, United Kingdom, USA, Russia, Israel and the European Union. The main parameters involved in the interrelated dynamics are nationalism, religiousness, knowledge of history, level of educational development, tourism, unemployment, external debt, oil extraction, Anatolian settlers, and the general interests of the countries involved and those of the two communities. The system that has been developed can be used to study the effects of a change in any parameter or a combination of parameters, on the growth and stability of the remaining parameters. Different scenarios on the effects on economies, politics and military involvement have been implemented, observed and appraised.**

Keywords-fuzzy cognitive maps; Cyprus problem; politico-economic modeling.

I. INTRODUCTION

Cyprus is a small island in the Eastern Mediterranean. It has about 900,000 inhabitants. The population consists of approximately 78% Greek-Cypriots, 18% Turkish-Cypriots and the remaining 4% of Armenian, Maronite and Latin-Cypriots. Turkish and Greek Cypriots lived mostly harmoniously for almost five centuries. Since the early 1960s and more intensely after July 1974 when Turkey invaded the island, there have been political problems between the two dominant communities. Turkey occupies about one third of the territory of the Republic of Cyprus, and is systematically changing the social fabric by bringing Anatolian settlers into the island. This creates thrifts and conflicts among the genuine inhabitants.

The dynamics involved for the security and stability of the island, as well as the economic development, are related to the interests of both the Greek-Cypriot and the Turkish-Cypriot communities. Theses dynamics have been influenced largely by the strategic position of the island, being at the Eastern Mediterranean, where many conquerors and civilizations spread their influence (Greek, Roman, Byzantine, Arabs, Francs, Venetians, Crusaders, Ottomans, Turks, and English). The historical roots of the two communities forged them to be both cooperative and antagonistic. Also, the interests of other countries involved in the problem played a significant role in the politico-economic developments. These are primarily Greece, Turkey and the United Kingdom.

The accession in 2004 of Cyprus into the European Union, as well as the recent political – social unrest in the wider Mediterranean neighborhood (Tunisia, Egypt, Libya, Syria and Jordan) has made the involvement of Europe, USA, Russia and Israel to be highly important influential-dynamical factors.

In this work, an attempt to model the dynamics of the problem, using a fuzzy cognitive map-like (FCM) approach has been made. More specifically, the main parameters involved in the interrelated dynamics are:

- The overall interests of the Republic of Cyprus,
- The economic welfare of both communities,

- The risk of conflict between the two major communities,
- The importance of oil/gas exploration,
- The unemployment,
- The level of tourism, and
- The general interests (political, economic, military) of the countries mentioned previously and the interests of the two dominant communities.

A cognitive map is a set of cause-effect relationships that model the interrelationships among specific concepts (also identified as characteristics, factors, parameters, attributes, states, actions, values, goals, trends, events, components, resources etc). By using an appropriate systematic process it is possible to estimate the effect of a change in the state of a specific concept on any other concept (or set of concepts) of the system. The concepts are related through directed graphs. The intensity of the interrelationships among them is not clearly known, and thus, suitable membership functions may be used. Different fuzzy cognitive map paradigms have been proposed [2, 3, 4, 5, 6, 7], and different application areas have been investigated [8, 9, 10, 11, 12, 13]. In most of the applications each concept is related to the other concepts through appropriate degrees of effectiveness (also called sensitivity, weights, causality). Once the parameters have been identified and initialized, the system is allowed to grow through proper simulation. When the system settles, a researcher can observe the effects of a change in the state of one factor on the intensity of change in another.

The work reported here is mainly involved with an effort to apply an FCM variant to the dynamics of the Cyprus problem, aiming at getting some useful insight on the effectiveness and interactivity of the important contributing parameters, primarily the importance of the oil/gas exploration in the future events in Cyprus. Also, it may be used as a study tool for exploring complicated economic-political dynamics through the use of computing simulations.

II. THE FCM SYSTEM

Computationally intelligent systems have largely been inspired by natural or real life systems. A general observation is that dynamical systems in nature as well as political-economical-social systems, in which the parameters are characterized by causal relations, tend to reach quasi-steady states. That is, after interacting with each other, the parameters may reach equilibrium, cyclic behavior, or chaotic oscillation. The parameters of a system change iteratively their values, as a response to the first change(s) that happen in the system. Also, in real systems, an adaptive evolutionary behavior is usually observed, something that is not captured in the classic FCM paradigms.

In the present study, a slightly different approach from the established FCM formalism is adopted.

Consider an FCM system of n interrelated concepts (parameters), which are connected by causal relations, here called sensitivities. The sensitivity relating the changes in the activation of a concept C_j to changes in the activation of a concept C_i is defined by:

$$s_{ij} \equiv \frac{\partial C_j}{\partial C_i} \tag{1}$$

Thus, the total accumulated change in the activation of concept C_j due to changes in concepts C_i is given by:

$$\delta C_j = \sum_{i,i\neq j}^{n} \frac{\partial C_j}{\partial C_i} \delta C_i = \sum_{i,i\neq j}^{n} s_{ij} \delta C_i \tag{2}$$

where,

C is the activation strength of the concept of interest.

s_{ij} is the sensitivity (weight).

It is a measure on how much a change in the current standing of concept C_i affects the changes in the standing of concept C_j.

In discrete time form the above equation becomes:

$$C_j(t+\delta t) = C_j(t) + \delta C_j = C_j(t) + \sum_{i=1}^{n} s_{ij} \left(\delta C_i\right) \tag{3}$$

and in iterative form has been implemented by:

$$C_j(k+1) = C_j(k) + \sum_{i,i\neq j}^{n} s_{ij} \left(C_i(k) - C_i(k-1)\right) \tag{4}$$

where,

k is the iteration counter.

It is pointed here that this approach is different than the approach that is followed by most FCM implementations in two respects:

i) The weights (sensitivities) are defined differently, as previously explained, and

ii) No smoothening activation function, such as the logistic has been used.

The updating is done quasi-statically and interactively until the system evolves to settlement specified by desired boundaries. Any changes in the various concepts affect either directly or indirectly all the other concepts of the system.

III. THE FCM CONCEPTS

For the study presented here, 42 influencing parameters (concepts) have been used. These are shown in Table 1.

It should be mentioned that these factors are difficult to quantify. Also they are not fully agreed by every person involved in the analysis and decision. Some form of fuzzy approximation may be employed, using persons having good knowledge (experts) and extensive experience (politicians). Furthermore, each one of them embodies a general state (and associated trend), as it is commonly employed and understood. For instance by the term "General welfare of the Republic of Cyprus" we mean a state that has characteristics of prosperity, political stability, social development, high quality of life, etc. The initial starting values are also shown in Table 1. These have been estimated by the experts, and given as the average of their suggestions.

Three knowledgeable persons have been asked to suggest the various sensitivities that were used to update the various concepts as per Equation 4. Obviously, there are discrepancies between the values given by each person. This is indicatively

shown in Figure 1, where the values given by three persons are displayed in colours. The green colour shows a non-relationship ($s_{ij} = 0$). The blue numbers are positive sensitivities, and the red negative.

The average of the sensitivities that have been used are as shown in Table 2.

IV. Results and conclusions

The effects of finding and exploring oil and/or gas, on various political, economic and military issues and parameters - based on the average sensitivity values from the three experts (Figure 1) - are shown in Figures 2, 3, 4. In these figures, the horizontal axis shows the initial (starting) values of the concept "IMPORTANCE OF FINDING AND EXPLOITATION OF OIL/GAS", from 0% to 100%, i.e from no natural gas available, to the highest possible. In the vertical axis, the resulting percentage changes in various parameters and factors of interest, which are due to natural gas exploration variations, are shown. These values are obtained after evolution and settling to stable values of the FCM model. The initial values used, other than those of oil/gas, are those displayed in Table 1.

Due to the constraint of having to maintain a reasonably short paper, only three major areas of interest are presented, namely the economic and political effects as well as the military interests. In all the cases examined, the concept C38 (importance of oil/gas exploration) was sequentially initialized to starting values of: 0%, 15%, 30%, 45%, 60%, 75%, and 100%. The exact absolute values are not that important, but rather the relative changes that indicate trends, and can serve as guidance to decision makers, and for better appraisal of the system dynamics.

The various changes and associated trends have been investigated for the following areas of concern:

- Effects on the economic interests of USA, Russia, UK, Israel, Greece, Turkey and Europe.
- Effects on the military interests of USA, UK, Israel, Greece and Turkey.
- Effects on various economic characteristics of the Republic of Cyprus.
- Effects on nationalism of the two communities and the risk of conflict between them.

The FCM model has shown interesting and somewhat expectable trends and effects based on the scenarios studied. However, by closely observing the various trends, some notably interesting observations and conclusions may be made. Specifically, the model predicts that the Turkish Cypriot community and Greek Cypriot community will benefit approximately equally from the prospects of finding and exploiting any natural gas/oil, even though the potential oil/gas fields are located in the south-eastern zone of the Republic, whereas most of the Turkish Cypriot population lives in the north of the island. This of course depends on whether the exploitation is done through peaceful operations. In fact, another relevant observation made, is that any oil/gas exploitation increases the risk of conflict between the two communities. Thus, the situation becomes strongly politically influenced.

As expected the military interests of the countries mentioned, are increasing as the prospects for oil/gas exploitation increase. This increase is also nonlinear, resulting at even more interest, as more natural gas may be exploited (Figure 4). It is also observed that Turkey will show the greatest increase in military interests, followed by Greece.

Also, a very interesting observation can be made concerning the growth of nationalism in the two communities (Figure 3). It is noted that the model predicts a significant increase in the nationalism of the Greek Cypriots, but even higher for the Turkish Cypriot community.

However, it should once again be pointed out that the model is based on what the three experts considered as important parameters, and influencing sensitivities, that may not necessarily agreed by all, and that they may be incomplete and vague. In order to make the model more reliable, one has to get more expert opinions (from politicians, journalists, historians, authoritative analysts etc). Also, results from large scale public opinion research may be incorporated into the system.

Despite that, the proposed FCM model is a highly useful tool for quick explorations, for better understanding of the dynamics involved, for more sound decisions, and for building a basis for more complicated scenarios. However, further explorations are needed to verify the credibility and to fine-tune the various parameters and processes.

Acknowledgment

This research is partly supported by the University of Cyprus, the Cyprus University of Technology, and the Cyprus Research Promotion Organization.

References

[1] A. Andreou, N. Mateou, and G. Zombanakis, "The Cyprus puzzle and the Greek-Turkish arms race: Forecasting developments using geneticall-ly evolved fuzzy cognitive maps", Journal of Defense and Peace Making, vol. 14, pp. 293-310, 2003.

[2] P. Groumpos, "Fuzzy Cognitive Maps: Basic Theories and Their Application to Complex Systems", Springer Berlin/Heidelberg, 2010.

[3] P. Hanafizadeh, and R. Aliehyaei, "The application of fuzzy cognitive map in soft system methodology", Systemic Practice and Action Research, vol. 1, pp. 1-30, 2010.

[4] B. Kosko, "A dynamic systems approach to machine intelligence", Neural Networks and Fuzzy Systems, 2nd ed., Prentice Hall, London, 1992.

[5] B. Kosko, "Fuzzy cognitive maps", International Journal of Man-Machine Studies, vol. 24, pp. 65-75, 1986.

[6] D. Koulouriotis, I. Diakoulakis, D. Emiris, E. Antonidakis, and I. Kaliakatsos, "Efficiently modeling and controlling complex dynamic systems using evolutionary fuzzy cognitive maps", International Journal of Computational Cognition, vol. 1, pp. 41-65, 2003.

[7] N. Mateou, C. Stylianou, and A. Andreou, "Hybrid fuzzy cognitive map modeler", Soft Computing as Transdisciplinary Science and Technology, vol. 29, pp. 851-862, 2005.

[8] C. Neocleous, C. Schizas, and C. Yenethlis, "Application of Fuzzy Cognitive Maps to the Political-Economic Problem of Cyprus", Proceedings of the International Conference on Fuzzy Sets and Soft Computing in Economics and Finance, St Petersburg, pp. 340-349, June 17-20, 2004.

[9] E. Papageorgiou, P. Spyridonos, D. Glotsos, C. Stylios, P. Ravazoula, G. Nikiforidis, and P. Groumpos, "Brain tumor characterization using the soft computing technique of fuzzy cognitive maps", Applied Soft Computing, 8(1), pp. 820-828, 2008.
[10] C. Stylios, and P. Groumpos, "Fuzzy cognitive maps in modeling supervisory control systems", Journal of Intelligent and Fuzzy Systems, vol. 8, pp. 83-98, 2000.
[11] C. Stylios, and P. Groumpos, "Modeling complex systems using fuzzy cognitive maps", IEEE Transactions on Systems, Man, and Cybernetics Part A: Systems and Humans, vol. 34, pp. 155-162, 2004.
[12] E. Papageorgiou, Ath. Markinos, and Th. Gemtos, "Fuzzy cognitive map based approach for predicting yield in cotton crop production as a basis for decision support system in precision agriculture application", Applied Soft Computing, in press.
[13] E. Papageorgiou, N. Papandrianos, G. Karagianni, and D. Sfyras, "Fuzzy cognitive map based approach for assessing pulmonary infections", Lecture Notes in Computer Science/LNAI 5722, pp. 109-118, 2009.

TABLE 1
THE VARIOUS INFLUENCING PARAMETERS THAT HAVE BEEN STUDIED
(GC = GREEK CYPRIOT, TC = TURKISH CYPRIOT)

	CONCEPT	INITIAL VALUES
C1	General welfare/standing of the Republic of Cyprus	50%
C2	Economic welfare of GC community	50%
C3	Economic welfare of TC community	30%
C4	Economic welfare of Greece	20%
C5	Economic welfare of Turkey	20%
C6	Greek Cypriot Nationalism	50%
C7	Turkish Cypriot Nationalism	50%
C8	Christian religiousness	50%
C9	Islamic religiousness	50%
C10	Knowledge of Greek language by the TC community	50%
C11	Knowledge of Turkish language by the GC community	50%
C12	Educational level of the GC community	50%
C13	Educational level of the TC community	50%
C14	Knowledge of Turkish history by the GC community	50%
C15	Knowledge of Greek history by the TC community	50%
C16	Political interests of Europe	50%
C17	Political interests of USA	50%
C18	Political interests of Russia	40%
C19	Political interests of UK	50%
C20	Political interests of Israel	50%
C21	Political interests of Greece	60%
C22	Political interests of Turkey	60%
C23	Economic interests of Europe	50%
C24	Economic interests of USA	50%
C25	Economic interests of Russia	50%
C26	Economic interests of UK	50%
C27	Economic interests of Israel	50%
C28	Economic interests of Greece	50%
C29	Economic interests of Turkey	60%
C30	Military interests of Israel	50%
C31	Military interests of Greece	50%
C32	Military interests of Turkey	50%
C33	Military interests of UK	50%
C34	Military interests of USA	50%
C35	Interests of Anatolian settlers	50%
C36	Level of tourism in the GC community	50%
C37	Level of tourism in the TC community	50%
C38	Importance of Oil/gas exploration	---
C39	Unemployment in Republic of Cyprus	50%
C40	Unemployment in TC community	50%
C41	External debt of Republic of Cyprus	50%
C42	Risk of conflict between the two communities	50%

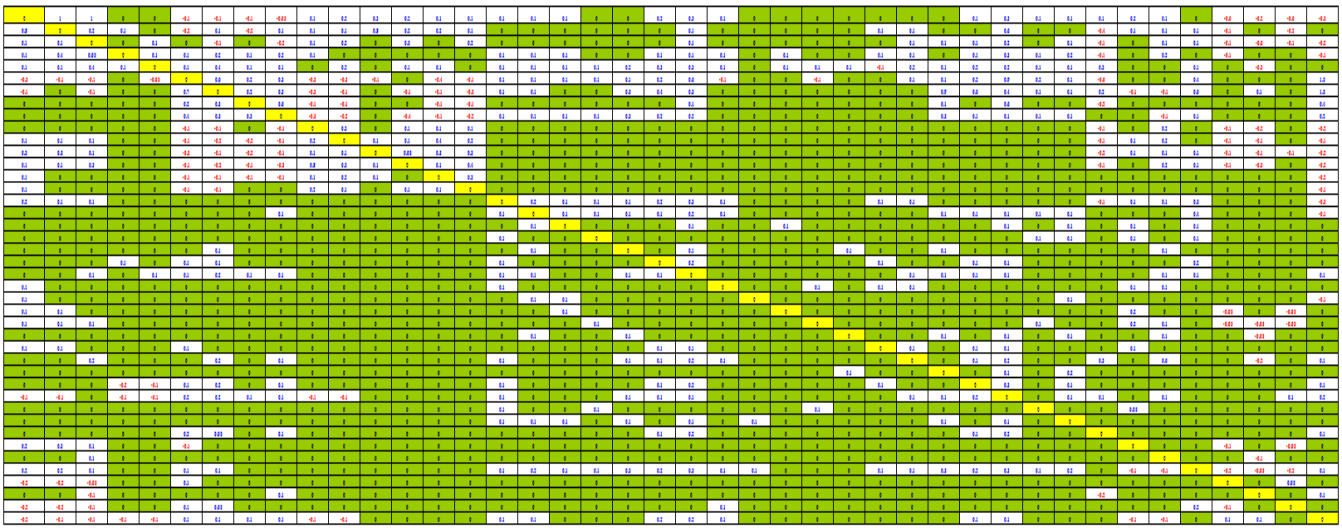

(a) Sensitivities given by person #1

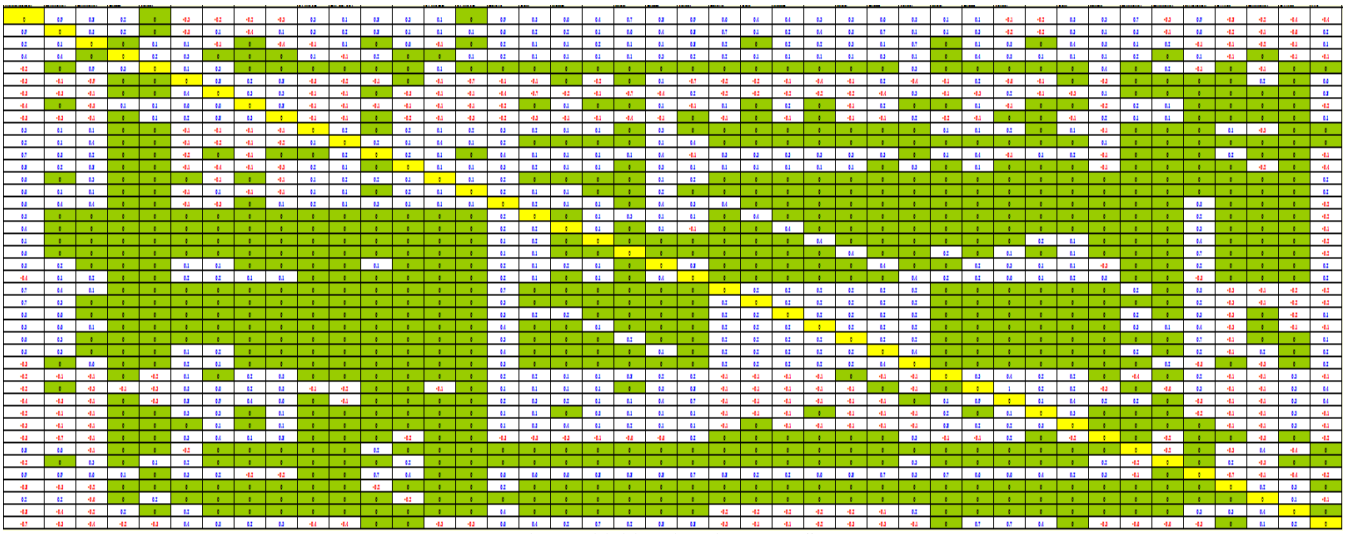

(b) Sensitivities given by person #2

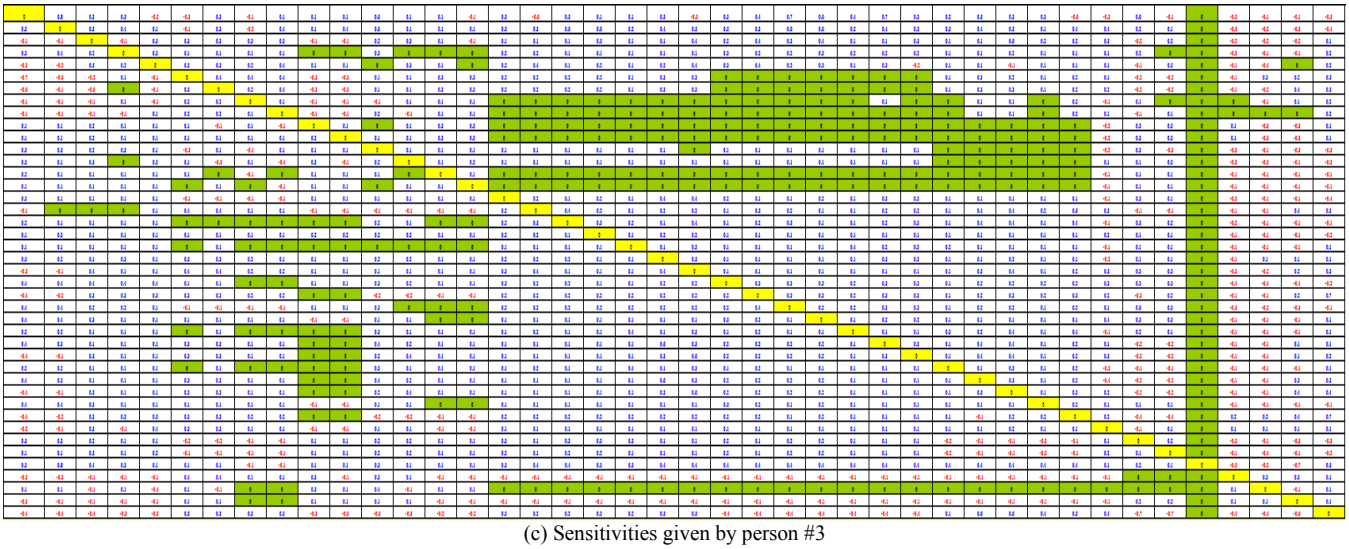

(c) Sensitivities given by person #3

Figure. 1. The sensitivities suggested by three different experts.

TABLE 2
THE AVERAGE OF THE SENSITIVITIES

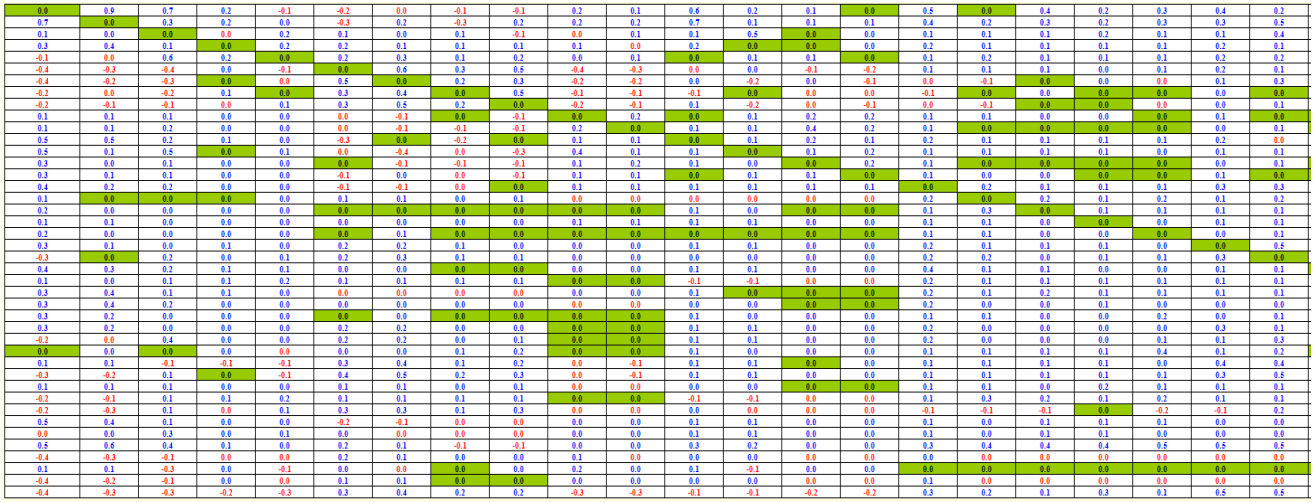

(a) Sensitivities for concepts 1 to 21

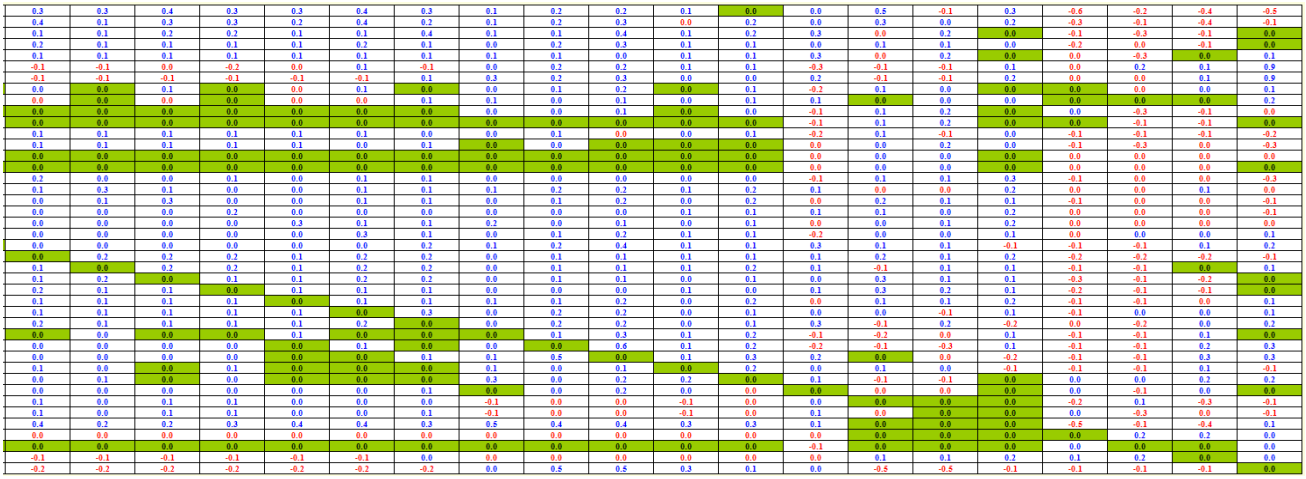

(b) Sensitivities for concepts 22 to 42

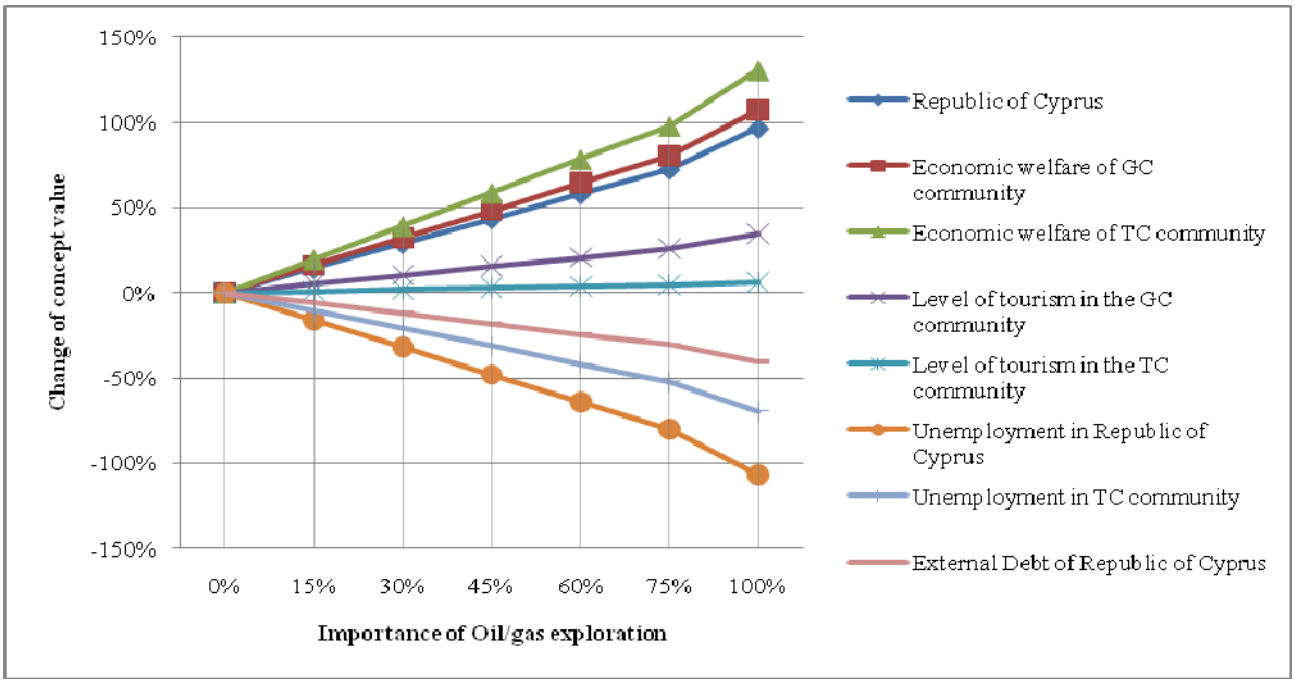

Figure 2. Effects on various economic parameters/issues, based on the average sensitivity values.

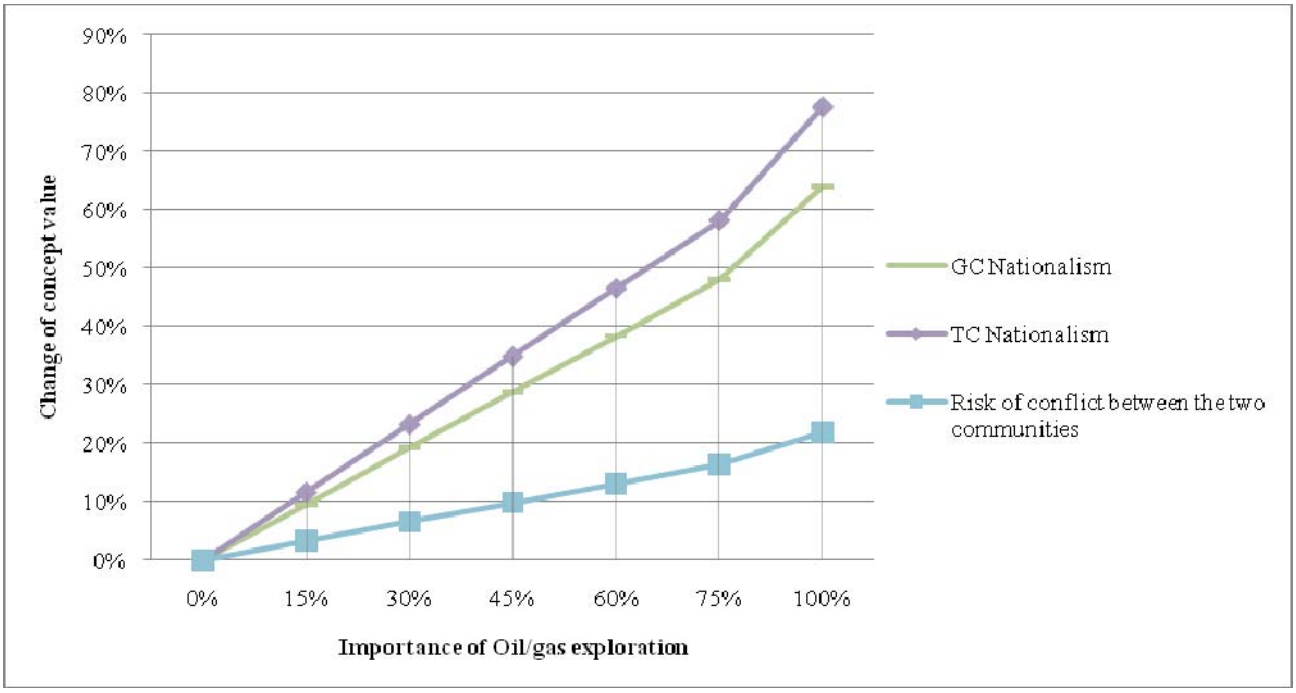

Figure 3. Effects on various political issues based on the average sensitivity values.

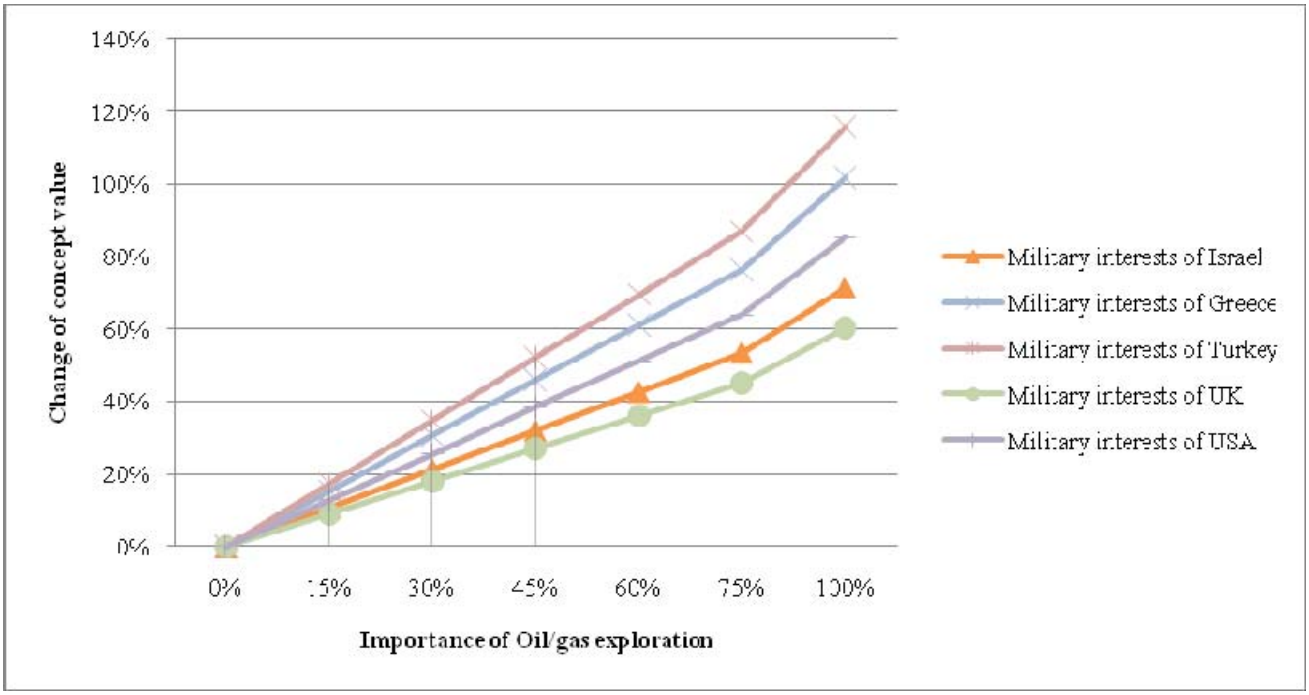

Figure 4. Effects on various military issues, based on the average sensitivity values.

2011 IEEE International Conference on Fuzzy Systems
June 27-30, 2011, Taipei, Taiwan

The Picked and Placed Control of the Objects for a Pneumatic X-Y Servo Platform by Integrating Image Processing Techniques and a Fuzzy Sliding Mode Controller Design

Hong-Ming Chen
department of Electronic Engineering
Chien-kuo Technology University
Chang-hua City, Taiwan, R.O.C.
steven@ctu.edu.tw

Yi-Ping Shyu, Chun-Sheng Shen, Hong-Jia Yang
department of Electronic Engineering
Chien-kuo Technology University
Chang-hua City, Taiwan, R.O.C.
vmupung@yahoo.com.tw

***Abstract*—In this paper, integrated a image processing techniques and a fuzzy sliding mode control design for a pneumatic X-Y servo platform system was proposed to realize the picked and placed control of the objects. The key feature of this control scheme is by means of immediately modulated the boundary layer sliding surface and fuzzy function design to improve the steady state error of time response effect. Then, use the image pattern recognition technique to determine the loading and unloading object positions, and drive the Z axis device to active the picking and placing control of the objects to obtain automatic loading-unloading device performance. The validity of the proposed control scheme is verified through practical testing on an experimental pneumatic cylinder X-Y axis servo system device and CCD video camera. In the cases of the step position command input, the test results show that the proposed control scheme and object image pattern recognition technique are capable of reaching the picking and placing precision control of the object.**

Keywords- image processing; fuzzy sliding mode control; pneumatic; pattern recognition; picking and placing control

I. INTRODUCTION

Recently, due to the technological advance, the pneumatic system has been extensively applied in automation fields and automatic production machines. Such as optical electrical industry, medicine industry, packing industry, and foodstuff industry, which production process always needs the pneumatic system convert the compressed air to the mechanical energy power. Owing to the air is easy acquired, low polluted, high-speed activity, and provided a large effective power energy, the pneumatic systems are always adopted in many automation industries. Sometimes, the picked and placed control of the objects for the production process are needed in many automation equipment applications, the pneumatic servo position control is still more considerable. To automatic accurate the picked and placed objects, the image recognized technique are often been addressed. In this paper, the image recognized technique and fuzzy sliding mode controller design are integrated to realize the picked and placed objects control for a pneumatic x-y table system.

However, the pneumatic air is compressible, and the pneumatic system has many nonlinear characteristics, such as the mass flow rate parameters variable and the servo valve dead zone problems [1], there have many challenges in designing a controller for the pneumatic servo control system. To reach a better precision control, there are many nonlinear control strategies have been proposed to deal with the pneumatic servo system, for examples, sliding mode control [1][2], fuzzy control[3], and iterative learning control [4],[5],[6]. Due to its robustness against parameter variations and external disturbance, sliding mode control has been an effective means for controlling nonlinear systems with uncertainties [2]. The traditional sliding mode control always design a boundary layer of the sliding surface to eliminate undesired chattering control input [2]. However, there have some problems to be solved, such as the chattering can be made negligible if the width of the boundary layer is chosen large enough, the guaranteed tracking precision will deteriorate if the available control boundary layer width is limited. For the purpose of obtaining the high tracking accuracy, a thin boundary layer is required. And others, the most commonly used design is the linear sliding surface defined by polynomials with repeat roots [2]. Such sliding surfaces are short of sufficient adjustable free parameters, especially in lower order systems.

In this paper, we designed a switching boundary layer and with adjustable parameters free sliding surface of the sliding mode control scheme [1] for the pneumatic cylinder position servo control system to realize and improve the regulating and tracking control performances. To realize the picking and placing precision control of the objects, the image recognized technique was adopted to identify the pattern position, through the video camera, NI-8252 interface card, and LabVIEW vision and motion builder assistance, the objects pattern center point will be recognized. To accomplish the picked and placed of the objects option, an experimental pneumatic cylinder X-Y axis servo system device is constructed. The proposed

978-1-4244-7316-8/11/$26.00 ©2011 IEEE

controller and the process measuring data were all implement by Pentium IV PC through an NI-6024E interface card with RTW Window target tool box of the Matlab Simulink software designed. Through the test results show that the proposed control scheme is capable of improving the tracking precision of the pneumatic cylinder position control, and for the objects pattern image recognized help, the precision control of picking and placing of the objects with pneumatic system has been come true. The paper is organized as follows: Section 2 a pneumatic cylinder servo system modeling will be constructed, and Section 3 a main control law, fuzzy sliding mode controller design, is also described. Section 4 a pattern image recognized system will be formed with pneumatic servo platform. Experimental results are presented in Section 5, and conclusions are drawn in Section 6.

II. PNEUMATIC CYLINDER SERVO SYSTEM MODELLING

Consider a pneumatic cylinder position servo system which mainly consists of a servo valve and a pneumatic cylinder. Fig.1 shows the structure of pneumatic servo system, the upper portion is a proportional servo valve which actuate the below cylinder with the compressed air flowing into the chamber by the spool displacement X_v of servo valve, hence the pneumatic cylinder can be arrived at any desire position. In general, the response of servo valve is faster than the response of pneumatic cylinder, the orifice area will be proportional to the control input, u, which can be considered as $A_o = K_a K_v u$, where K_a is constant of valve displacement, and K_v is gain constant of valve spool displacement. According to Mocloy & Martin [7],[8] proposed the fluid compressible mass flow rate through the orifice store in chamber can be given by

$$\dot{M}_a = C_{da} C_{ma} A_{oa} P_s \Big/ \sqrt{T_s} \tag{1}$$

$$\dot{M}_b = -C_{db} C_{mb} A_{ob} P_b \Big/ \sqrt{T_b} \tag{2}$$

where, C_{da} and C_{db} are left and right chamber's discharge coefficient respectively, C_{ma} and C_{mb} are left and right chamber's mass flow parameter respectively, A_{oa} and A_{ob} are left and right chamber's orifice area respectively, P_s and P_b are left and right chamber's upstream stagnation pressure respectively, T_s and T_b are left and right chamber's upstream stagnation temperature respectively. However, the mass flow parameters of C_{ma} and C_{mb} have the following calculation:

If $\frac{P_{vc}}{P_o^*} > \left(\frac{2}{\gamma+1}\right)^{\gamma/(\gamma-1)} \approx 0.528$, the C_{ma} and C_{mb} indicate as

$$C_m = \sqrt{\frac{2\gamma}{R(\gamma+1)}\left\{\left(\frac{P_{vc}}{P_o^*}\right)^{2/\gamma} - \left(\frac{P_{vc}}{P_o^*}\right)^{(\gamma+1)/\gamma}\right\}}$$

where, P_{vc} and P_o^* are the orifice static pressure and upstream stagnate pressure respectively, R is the gas parameter, and γ is the ratio of specific heat. If $\frac{P_{vc}}{P_o^*} \le \left(\frac{2}{\gamma+1}\right)^{\gamma/(\gamma-1)} \approx 0.528$, than

$$C_m = \left(\frac{2}{\gamma+1}\right)^{\gamma/(\gamma-1)} \sqrt{\frac{2\gamma}{R(\gamma+1)}} \approx 0.0405 .$$

Fig.2 shows the relationship between of C_m parameter value and $\frac{P_{vc}}{P_o^*}$ value. It can be shown that the C_m parameter is alternated when the orifice gas flow rate decreased. Applying the Law's Conservation of energy [9]

$$\sum \dot{M}_{in} h'_{in} - \sum \dot{M}_{out} h'_{out} + \left\{\frac{dQ}{dt} - \frac{dW}{dt}\right\} = \frac{dE}{dt} \tag{3}$$

where, $\dot{M}_{in}, \dot{M}_{out}$ are mass flow rate of entering the control volume and leaving out the control volume respectively, h'_{in}, h'_{out} are enthalpy of entering the control volume and leaving out the control volume respectively, Q is rate of heat transfer into the chamber, W is kinetic energy for the moving position, E is total of internal energy of the chamber, Eq.(3) can be written as

$$C_p \dot{M}_a T_a - P_a \frac{dV_a}{dt} + \frac{dQ}{dt} = \frac{d}{dt}\left(C_v \rho_a V_a T_a\right) \tag{4}$$

where, C_v is the specific heat value of the air beside constant volume, P_a is the pressure of left chamber, assuming no heat flow in to control volumes, then dQ/dt is small can be ignored, we have

$$\frac{dP_a}{dt} = \frac{\gamma R T_a}{A_a y}\dot{M}_a - \frac{\gamma P_a}{y}\frac{dy}{dt} \tag{5}$$

where, A_a is the cross-sectional area of the left chamber, and y is the displacement of cylinder moving. With the similar procedures to the right chamber of cylinder, we have

$$\frac{dP_b}{dt} = -\frac{\gamma R T_b}{A_b(l-y)}\dot{M}_b + \frac{\gamma P_b}{(l-y)}\frac{dy}{dt} \tag{6}$$

where, l is maximum displacement of pneumatic cylinder, A_b is the cross-sectional area of the right chamber, and P_b is pressure of right chamber. Then the pneumatic cylinder motion equation can be obtained as follows [8],

$$P_a A_a - P_b A_b - b\frac{dy}{dt} - F_f \,\mathbf{sgn}(\dot{y}) - F_L = m\frac{d^2 y}{d^2 t} \tag{7}$$

where, b is damping coefficient, F_f is force due to friction, and F_L is force due to external loading. Substituting (5),(6) into (7) can be obtained as follows

$$\frac{d^3 y}{d^3 t} = \frac{\gamma R}{m}\left[\frac{T_a}{y}\dot{M}_a + \frac{T_b}{1-y}\dot{M}_b\right] - \frac{\gamma}{m}\left[\frac{A_a P_a}{y} - \frac{A_b P_b}{1-y}\right]\frac{dy}{dt} - \frac{b}{m}\frac{d^2 y}{d^2 t} - \frac{\dot{F}_f}{m}\mathbf{sgn}(\dot{y}) - \frac{\dot{F}_L}{m} \tag{8}$$

Then, Substituting (1),(2) into (8),

$$\frac{d^3 y}{d^3 t} = -\frac{\gamma}{m}\left[\frac{A_a P_a}{y} - \frac{A_b P_b}{1-y}\right]\frac{dy}{dt} - \frac{b}{m}\frac{d^2 y}{d^2 t} - \frac{\dot{F}_f}{m}\mathbf{sgn}(\dot{y}) - \frac{\dot{F}_L}{m} + \frac{\gamma R C_d C_m K_a K_v}{m}\left[P_s\sqrt{T_a} - P_b\sqrt{T_b}\right]u \tag{9}$$

where, u is control input, Eq.(9) is a real model of the pneumatic position control system, it's shown that the model is a nonlinear and coefficient variable system. In the Section 3, a multi-variable design sliding surface with switching

boundary later of sliding mode control scheme will be developed to deal with the pneumatic servo system and improving the tracking precision.

III. FUZZY SLIDING MODE CONTROLLER DESIGN

To highlight the main point of the design sliding mode control, we consider the following simple nth-order SISO nonlinear uncertain system [2]:

$$y^{(n)} = f(y, \dot{y}, \ldots, y^{(n-1)}, t) + g(y, \dot{y}, \ldots y^{(n-1)})u \tag{10}$$

where $u, y \in R$, are the input and output, respectively; $f, g: R^n \to R$ are smooth functions. Assume that f is not completely known but can be written as $f = \hat{f} + \Delta f$, where $\hat{f}$ is the nominal part and Δf is the uncertain part which is bounded by a known function F, i.e., $|\Delta f(\mathrm{x}, t)| \le F(\mathrm{x}, t)$, where $\mathrm{x} := [x_1, x_2, \ldots, x_n]^T = \left[y, \dot{y}, \ldots, y^{(n-1)}\right]^T$, and the control gain $g(\mathrm{X})$ is unknown but confined in certain constant range; i.e. $0 < \beta^{\min} \le g(x) \le \beta^{\max}$. where $\beta^{\min}, \beta^{\max}$ are given constants, time-varying or state-dependent functions.

The control object is to find a continuous sliding control u such that the output y of (10) will approximately track a desired signal, y_d, which is assumed to be nth-order continuously differentiable and all of its derivatives are uniformly bounded, i.e., $\lim_{t\to\infty} y(t) = y_d(t)$. Given the tracking error $e(t) := y(t) - y_d(t)$, For any $\lambda_m > 0$, where $m = 1, \ldots, n$, the generalized error as

$$s(t) = \left(\frac{d}{dt} + \lambda_1\right)\left(\frac{d}{dt} + \lambda_2\right)\cdots\left(\frac{d}{dt} + \lambda_m\right)\xi_e(t) \tag{11}$$

where $\xi_e(t) = \int^t e(\tau)d\tau$, the integral of tracking error. Eq. (11) provides a useful transformation so that the original n^{th}-order tracking problem can be transformed into an equivalent 1^{st}-order stabilization problem in s variable. Differentiating s with respect to t and adding the term $\lambda_{n+1}s$ yields

$$\begin{aligned}\dot{s} + \lambda_{n+1}s &= \left(\frac{d}{dt} + \lambda_1\right)\cdots\left(\frac{d}{dt} + \lambda_n\right)\left(\frac{d}{dt} + \lambda_{n+1}\right)\xi_e(t)\\ &= e^{(n)}(t) + c_1 e^{(n-1)}(t) + \cdots + c_{n+1}\xi_e(t)\\ &= f(x) + g(x)u - x_d^{(n)}(t) + c_1 e^{(n-1)}(t) + \cdots + c_{n+1}\xi_e(t)\\ &= \hat{f} + \Delta f + c_1 e^{(n-1)}(t) + \cdots c_{n+1}\xi_e(t) - x_d^{(n)}(t) + g(x)u\end{aligned} \tag{12}$$

where $c_1 = \lambda_1 + \lambda_2 + \cdots + \lambda_{n+1}$, and $c_{n+1} = \lambda_1\lambda_2\cdots\lambda_{n+1}$. Multiplying s in the both sides of Eq.(12), we have

$$\begin{aligned}s\dot{s} &= -\lambda_{n+1}s^2 + [\hat{f} + \Delta f + c_1 e^{(n-1)} + \cdots + c_{n+1}\xi_e - x_d^{(n)} + gu]s\\ &= -\lambda_{n+1}s^2 + [\hat{f} + \Delta f + \hat{w} + gu]s\end{aligned} \tag{13}$$

where $\hat{w} = c_1 e^{(n-1)} + \cdots + c_{n+1}\xi_e - x_d^{(n)}$. The feedback control u for Eq. (13) was designed as

$$u = G(\hat{u} + v) \tag{14}$$

where $G := \frac{1}{\sqrt{\beta^{\min}\beta^{\max}}}$, $\hat{u} = -\hat{f} - \hat{w}$, $v = -Ksat(\frac{s}{\Phi})$. Clearly, $0 < \beta^{-1} \le gG \le \beta$, and $0 < \beta^{-1} \le (gG)^{-1} \le \beta$, where $\beta = \sqrt{\beta^{\max}/\beta^{\min}}$. Whenever $|s| \ge \Phi$, where Φ is the width of the boundary layer, the following result can be obtained

$$s\dot{s} \le -\lambda_{n+1}s^2 - \left(gGK - \left|1 - gG\right|\left|\hat{f} + \hat{w}\right| - \left|\Delta f\right|\right)|s| \tag{15}$$

If we choose K as follows,

$$K \ge \beta(\eta + F) + (\beta - 1)\left|\hat{f} + \hat{w}\right| \tag{16}$$

where $\eta > 0$, then Eq.(15) becomes

$$s\dot{s} \le -\lambda_{n+1}s^2 - \eta|s| \tag{17}$$

Using the Lyapunov function candidate

$$V(s) = \tfrac{1}{2}s^2, \tag{18}$$

it can be shown that, whenever $|s| \ge \Phi$,

$$\dot{V} \le -\lambda_{n+1}s^2 - \eta|s|. \tag{19}$$

This ensures that any trajectory starting from any initial point will reach the boundary layer, $\forall|s| \le \Phi$, in finite time. Consequently, the guaranteed tracking precision will be

$$|e(t)| \le \frac{\Phi}{\lambda_1\lambda_2\cdots\lambda_n} \tag{20}$$

whenever $|s| \le \Phi$.

For smoothness (to reduce chattering) of the control input signal, larger width of the boundary layer is preferred. However, for better tracking accuracy, a boundary layer with smaller width is required [1]. In this paper, the concept of varying width of the boundary layer is proposed, which takes simultaneously the advantages of both the smoothness of the control inputs and the better tracking accuracy. First, let $\Phi = \Phi(|e|)$ and the control input (14) is rewritten as follows

$$v = -Ksat\left(\frac{s}{\Phi(|e|)}\right) \tag{21}$$

We let Φ_1 and Φ_2 are two different boundary layers, $0 < \Phi_2 < \Phi_1$, and ε_1 and ε_2 are two different error, $0 < \varepsilon_2 < \varepsilon_1$. For the relationship of absolute error, $|e|$, and boundary layer Φ are shown in (22)

$$\begin{cases} |e| \ge \varepsilon_1, & \Phi = \Phi_1 \\ \varepsilon_2 \le |e| \le \varepsilon_1, & \Phi = \Phi_a \\ |e| \le \varepsilon_2, & \Phi = \Phi_2 \end{cases} \tag{22}$$

$$\Phi_a = \Phi_2 + \left(\frac{|e| - \varepsilon_2}{\varepsilon_1 - \varepsilon_2} \right) (\Phi_1 - \Phi_2)$$

Therefore, if the initial state is outside the boundary layer, $|s| \ge \Phi_1$, it will be attracted to the boundary layer of sliding surface. Furthermore, if the absolute value of the tracking error is smaller than ε_1, the boundary layer is changed from Φ_1 to Φ_a, and when the absolute value of the tracking error is smaller than ε_2, the boundary layer is fixed at Φ_2, such that the tracking precision and the chattering of the control input signal are improved significantly.

Remark: The widths Φ_1, Φ_2 of boundary layer can be determined, respectively, as follows.

(1). By trial-and-error, the width of the boundary layer Φ is decreased till a visible Chattering of the control input signal occurs and then set $\Phi = \Phi_1$.

(2). A positive constant error ε_1 and ε_2 are used to define the switching threshold of the tracking error such that the width of the boundary is continuously changed from the Φ_1 to the smaller value Φ_2, which is a small enough that the chattering of the control input does not happen and the tracking error precision will be improved.

For $n = 2$ and $\lambda = 1$, the guaranteed tracking error bounds are depicted in Fig. 3, where the real-line region represents the error bound of the proposed sliding mode control with varying boundary layer, while the desh-line region represents that of the conventional sliding mode control with fixed boundary layer. Obviously, the guaranteed steady-state tracking error by using the proposed sliding mode control with switching boundary layer is effectively reduced as shown in Fig. 3.

In section 2, the pneumatic cylinder position system model is a three-order nonlinear system, let

$$f_m(y, \dot{y}, \ddot{y}) = -\frac{\gamma}{m}\left[\frac{A_a P_a}{y} - \frac{A_a P_a}{1-y}\right]\frac{dy}{dt} - \frac{b}{m}\frac{d^2y}{d^2t} - \frac{\dot{F}_f}{m}\mathrm{sgn}(\dot{y}) - \frac{\dot{F}_L}{m} \tag{23}$$

$$g_m(y, \dot{y}, \ddot{y}) = \frac{\gamma R C_d C_m K_a K_v}{m}\left[P_s\sqrt{T_a} - P_b\sqrt{Tb}\right] \tag{24}$$

Then, the system model can be rewritten as follows

$$\overset{(3)}{y} = f(y, \dot{y}, \ddot{y}) + g(y, \dot{y}, \ddot{y})u \,. \tag{25}$$

Let the tracking error be $e(t) = y(t) - y_d(t)$, and $\overset{(3)}{e} = \overset{(3)}{y} - \overset{(3)}{y_d}$, the error equation can be obtained as follows

$$\begin{aligned} \overset{(3)}{e} &= f(\mathbf{y}) + g(\mathbf{y})u - \overset{(3)}{y_d} \\ &= \hat{f}(\mathbf{y}) - \overset{(3)}{y_d} + \Delta f(\mathbf{y}) + g(\mathbf{y})u \end{aligned} \tag{26}$$

Defined the generalized error as

$$\begin{aligned} s &= \left(\frac{d}{dt} + \lambda_1\right)\left(\frac{d}{dt} + \lambda_2\right)\left(\frac{d}{dt} + \lambda_3\right)\int e d\tau \\ &= \dddot{e} + a_1\ddot{e} + a_2\dot{e} + a_3\int e dt \end{aligned} \tag{27}$$

where, $a_1 = (\lambda_1 + \lambda_2 + \lambda_3)$, $a_2 = (\lambda_1\lambda_2 + \lambda_2\lambda_3 + \lambda_1\lambda_3)$, $a_3 = \lambda_1\lambda_2\lambda_3$, we have

$$\begin{aligned} \dot{s} + \lambda_4 s &= \left(\frac{d}{dt} + \lambda_1\right)\left(\frac{d}{dt} + \lambda_2\right)\left(\frac{d}{dt} + \lambda_3\right)\left(\frac{d}{dt} + \lambda_4\right)\int e d\tau \\ &= \overset{(3)}{e} + b_1\ddot{e} + b_2\dot{e} + b_3 e + b_4\int e dt \\ &= \hat{f}(\mathbf{y}) + g(\mathbf{y})u + \Delta f(\mathbf{y}) - \overset{(3)}{y}_d + b_1\ddot{e} + b_2\dot{e} + b_3 e + b_4\int e dt \end{aligned} \tag{28}$$

where, $b_1 = \lambda_1 + \lambda_2 + \lambda_3 + \lambda_4$, $b_2 = \lambda_1\lambda_2 + \lambda_2\lambda_3 + \lambda_3\lambda_4 + \lambda_1\lambda_4 + \lambda_1\lambda_3 + \lambda_2\lambda_4$, $b_3 = \lambda_1\lambda_2\lambda_4 + \lambda_2\lambda_3\lambda_4 + \lambda_1\lambda_3\lambda_4 + \lambda_1\lambda_2\lambda_3$, $b_4 = \lambda_1\lambda_2\lambda_3\lambda_4$,

The feedback control u was designed as

$$u = G(\hat{u} + \hat{v}_f) \tag{29}$$

where, $\hat{u} = -\hat{f}(\mathbf{y}) - \hat{w}$, $\hat{v}_f = -K \cdot fuzzy\left(\frac{s}{\Phi(|e|)}\right)$. In this paper, we change the conventional sliding mode controller's saturation function $v = -Ksat(\frac{s}{\Phi})$ replaced by $\hat{v}_f = -K \cdot fuzzy\left(\frac{s}{\Phi(|e|)}\right)$. Fig. 4 shows the conventional linear saturation function, if it is replaced by the fuzzy function as shown in Fig. 5, it will improve the precision control performance. For the input output membership function are all design by the triangle function as shown as Fig. 6 and Fig. 7. The fuzzy rules of the input output function are proportional relationship as following:

input={NVB, NB, NM, NS, ZE, PS, PM, PB, PVB}

output={NVB, NB, NM, NS, ZE, PS, PM, PB, PVB}

where NVB= Negative Very Big, NB = Negative Big, NM = Negative Medium, NS = Negative Small, ZE = Approximately Zero, PS = Positive Small, PM = Positive Medium, PB = Positive Big, PVB= Positive Very Big.

We choose

$$K \ge \beta(\eta + M) + (\beta - 1)\left|\hat{f} + \hat{w}\right| \tag{30}$$

where, $\eta > 0$, satisfying the inequality:

$$s\dot{s} \le -\lambda_4 s^2 - \eta|s| \tag{31}$$

IV. Image Pattern Recognized System and Pneumatic Servo Platform Constructed

The image pattern recognized system and pneumatic servo platform structure shows as Fig. 8. In the pneumatic platform system above has built a CCD video camera to recognize the objects pattern. The pneumatic servo platform moving control is following the captured image pattern shape center point coordinates by CCD camera with IEEE 1394E transmission line and PCI-8252 interface card to PC. The digital image

signal can be calculated the object pattern center point coordinates by LabVIEW software design program. Then, passing the calculated objects pattern center point coordinates which can be looked as a position command of the pneumatic cylinder to the fuzzy sliding mode controller which design by Matlab Simulink program, and through the NI-6024E AD/DA card with servo valve to drive the cylinder to control the pneumatic cylinder moving position. All of the X-Y axis cylinder position feedback signals are adopted by linear scale resistance. In the end point of the X-Y axis cylinder, there have a vertical Z-axis can be moved up and down, and the end point of vertical Z-axis have sucking disc vacuum device which can be accomplished the objects loading and unloading. So, the picked and placed precision control of the objects for a pneumatic X-Y servo platform by integrating image pattern recognized and fuzzy sliding mode controller design can be achieved. For the image pattern recognized scheme process can be shown in Fig. 9. First, the object pattern image will be captured by CCD video camera. Second, mask the image with threshold method and filter the noise image, then detect the pattern edges of the image. Third, using geometric template matching method recognized the picking object. And, the last step is calculating and sending out the object shape center point coordinate by gravity method.

V. Experimental Results and Discussion

The following parameters of sliding mode controller in practical test as:

$$a_1 = 0.5, a_2 = 50, a_3 = 0.5, b_1 = 0.008, b_2 = 0.11, b_3 = 1.5, \beta = 1.8,$$
$$\eta = 0.05, M = 0, \Phi_1 = 10, \Phi_2 = 0.1, \varepsilon_1 = 0.1, \varepsilon_2 = 0.05, G = 2$$

This paper, using Matlab/Simulink software design the variable boundary layer of fuzzy sliding mode controller, and adopt the LabVIEW software with vision and motion builder to recognize the object pattern image and calculate the object pattern center point coordinate from CCD video camera. Thus the precision control of the picked and placed of the objects for the pneumatic servo platform system can be achieved. In the experimental test, there are four different shape objects, which have triangle, circle, squire, and trapezoid in the pneumatic servo platform shown as in Fig. 10-(1), we can accurately pick the squire shape object and precisely place to the circle object location. The detail process is shown in Fig. 10-(2) to Fig. 10-(5). In Fig. 10-(6) to Fig. 10-(11) shows the trapezoid shape object has been precisely picked and accurately placed it to the triangle shape object location. All of these picked and placed actions are driven by the X-Y axis pneumatic cylinder servo platform and CCD video camera. Fig. 11 shows the X axis pneumatic cylinder position control response, and the tracking error response is shown in Fig. 12. Identically, the Y axis pneumatic cylinder position control response and tracking error response are shown in Fig. 13 and Fig. 14. From the X axis and Y axis tracking error results show that the tracking errors are approximately smaller than ±0.5mm.

VI. Conclusions

In this paper, we propose a variable boundary layer of fuzzy sliding mode controller scheme for the pneumatic cylinder X-Y axis servo platform system to realize precision position control. And apply CCD video camera to capture the object pattern image and recognize its center point coordinate position technique to provide the picked and placed of the objects performance.

References

[1] H. M. Chen, J. C. Renn, and J. P. Su, "Sliding mode control with varying boundary layers for an electro-hydraulic position servo system," International Journal of Advance Manufacture Technology, Vol. 26, No. 2, pp. 117-123, July 2005.

[2] J-J. E. Slotine and W. Li, "Applied nonlinear control," Prentice-Hall, Englewood Cliffs, NJ, 1991.

[3] P. Korondi and J. Gyeviki, "Robust position control for a pneumatic cylinder," 12th International Power Electronics and Motion Control Conference, pp. 513-518, Sept. 2006.

[4] P. Righettiniand and H. Giberti, "A nonlinear controller for trajectory tracking of pneumatic cylinders**,** Advanced Motion Control," 7th International Workshop, pp.396-401, July 2002.

[5] C. K. Chen and J. Hwang, "Iterative learning control for Position Tracking of a Pneumatic," Proceedings of the 2004 IEEE International Conference on Control Applications, Taipei, Taiwan, September 2004.

[6] D. C. Gross and K. S. Rattan, "Pneumatic cylinder trajectory tracking control using a feed-forward multilayer neural network," National Aerospace and Electronics Conference, 1997, Vol.2, pp.777-784, July 1997.

[7] D. Mccloy, "Control of Fluid Power:Analysis and Design," 2nd Edition, 1983

[8] Movloy and Martin, "Control of Fluid Power," 2nd Edition., Ellis Horwood Limited, 1980.

[9] J. N. Zheng, "Design and Control for the Pneumatic Cylinder Precision Positioning under Vertical Loading," National Cheng Kung University Department of Mechanical Engineering, 2005

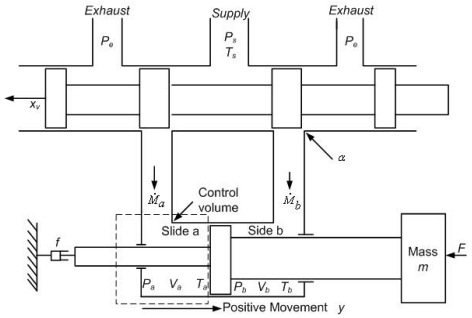

Fig. 1 The pneumatic cylinder servo system.

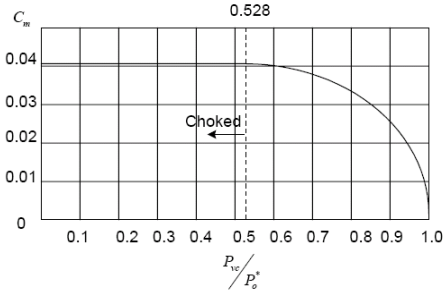

Fig. 2 The C_m parameter value varying with the ratio of pressure.

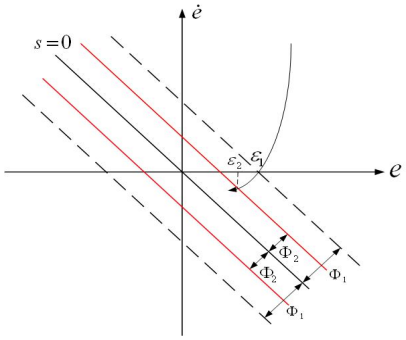

Fig. 3 The variable boundary layer of sliding surface.

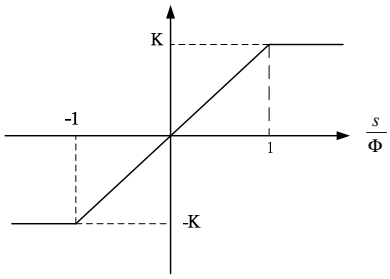

Fig. 4 The sliding mode conventional saturation function.

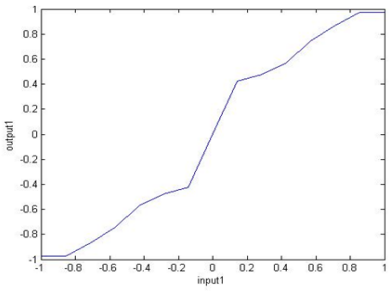

Fig. 5The Fuzzy saturation function.

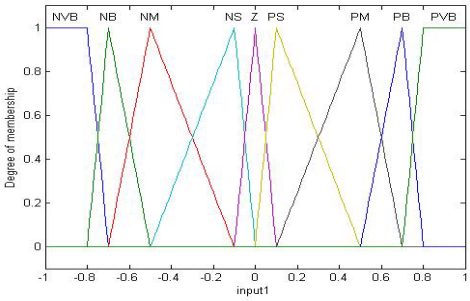

Fig. 6 The fuzzy input membership function.

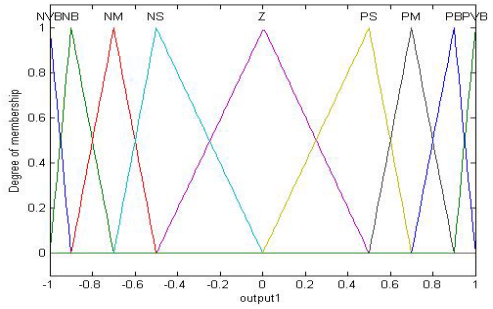

Fig. 7 The fuzzy output membership function.

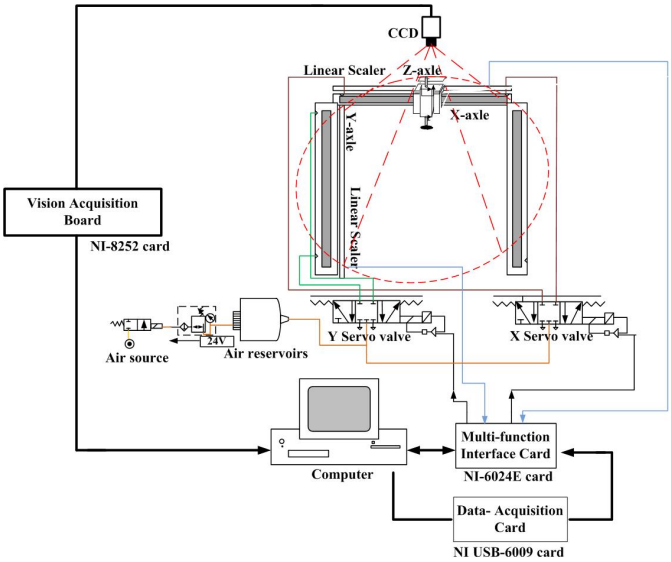

Fig. 8 The pneumatic cylinder servo control with image pattern recognition system diagram

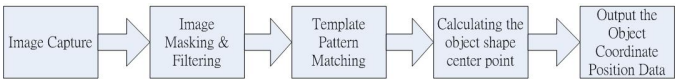

Fig 9 The object pattern image recognition process flow chart

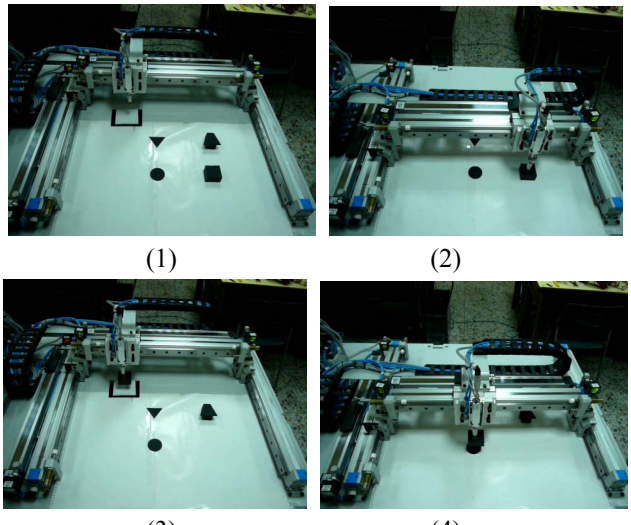

(1) (2)

(3) (4)

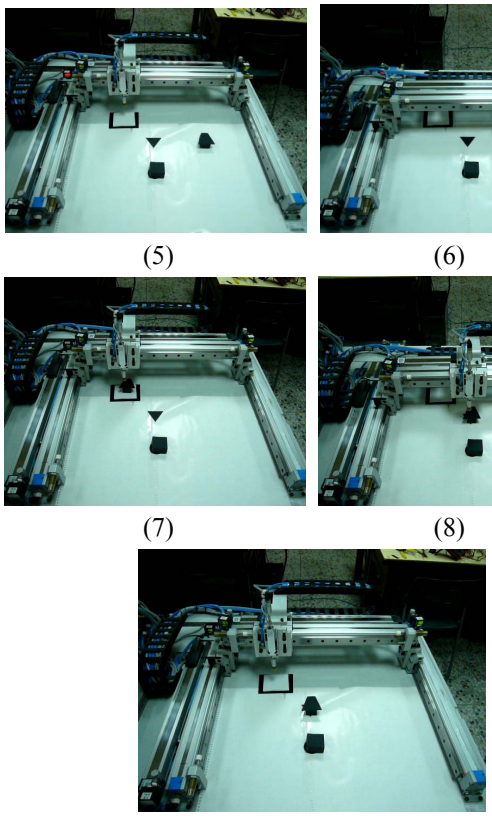

Fig. 10 The picked and placed control of the objects for the pneumatic cylinder servo system action diagram.

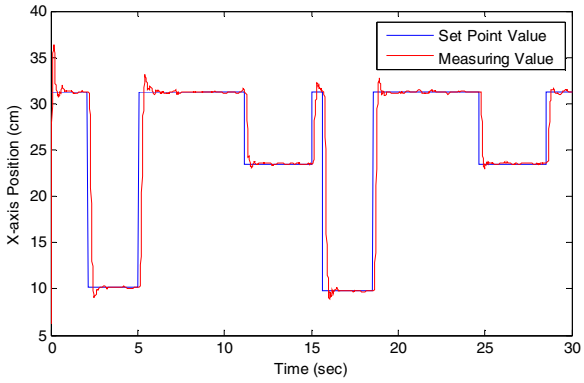

Fig. 11 The X-axis pneumatic cylinder response diagram.

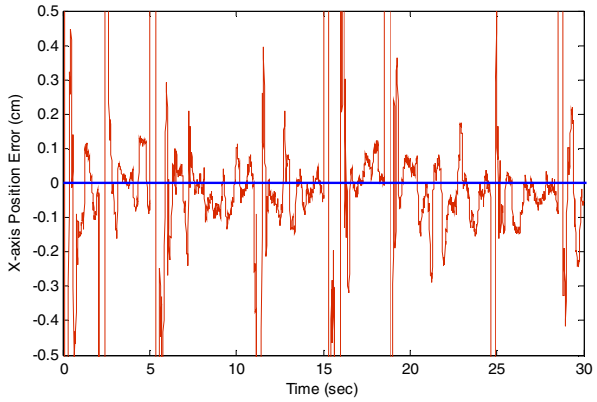

Fig. 12 The X-axis pneumatic cylinder tracking error response diagram.

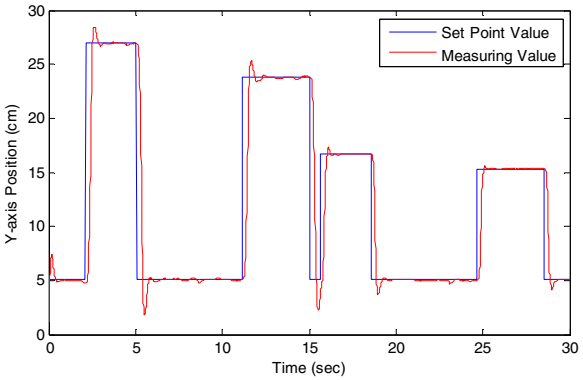

Fig. 13 The Y-axis pneumatic cylinder response diagram.

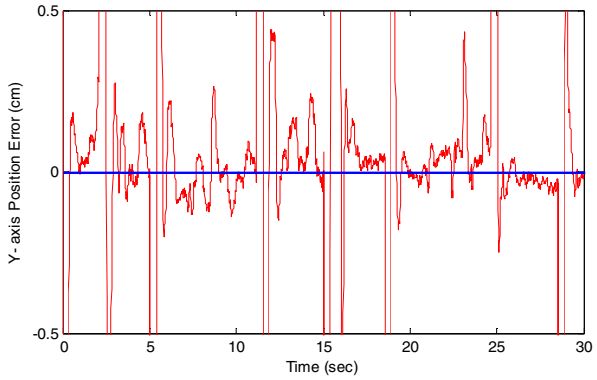

Fig. 14 The Y-axis pneumatic cylinder tracking error response diagram.

2011 IEEE International Conference on Fuzzy Systems
June 27-30, 2011, Taipei, Taiwan

The Dynamic Measurement System Design for Stewart Platform by Using Digital Image Processing Method

Ker-Wei, Yu
Department of Marine Engineering
National Kaohsiung Marine University
Kaohsiung, Taiwan, R.O.C.
kwyu@mail.nkmu.edu.tw

Yu-Quan, Zhou
Department of Marine Engineering
National Kaohsiung Marine University
Kaohsiung, Taiwan, R.O.C.

***Abstract*—In this study, the digital image processing method in the dynamic measurement system for Stewart platform is investigated. The measured signals of the platform based on the digital image processing method represent as the feedback signal of control system. In the study, the accuracy of control system is reasonable by capturing the image information of platform by using the digital image processing method and getting the detail of platform action directly.**

Keywords-digital image process; Stewart Platform; sensor

I. INTRODUCTION

In recent years, the parallel link manipulators, namely, Stewart platform, have attracted much attention and many studies have been done on the dynamic analysis and/or controller design of the parallel link manipulators. The Stewart platform is a mechanical device with six extensible legs mounted on a level surface in three pairs, crossing over to three mounting points on a top plate. Devices placed on the top plate can be moved in the six degrees of freedom (6 DOF) in which it is possible for a freely-suspended body to move. These are the three linear movements x, y, z (lateral, longitudinal and vertical), and the three rotations pitch, roll, & yaw [1]. Because of its unique capability, the platforms have been employed in many control engineering applications such as simulator shakers, robotic manipulators, etc. [2, 3, 4]

Traditionally, the displacement sensor, namely, linear voltage differential transmitter (LVDT), is used to determine the length of the six extensible legs. The gyro compass are also widely been used to evaluate the dynamic of Stewart platform. In recent year, the Force/torque (F/T) sensors have widely been used in measuring inertia force of Stewart platform [5], monitoring forces of variable directions and intensity [6] and as a component of force feedback controller [7, 8]. In a sensor application, the friction, backlash and other nonlinearities at the passive spherical joints of the Stewart platform will affect the measurements in unpredictable ways.

Digital image processing is the use of computer algorithms to perform image processing on digital images. As a subcategory or field of digital signal processing, digital image processing has many advantages over analog image processing. It allows a much wider range of algorithms to be applied to the input data and can avoid problems such as the build-up of noise and signal distortion during processing.

Many of the techniques of digital image processing, or digital picture processing as it often was called, were developed in the 1960s at the Jet Propulsion Laboratory, Massachusetts Institute of Technology, Bell Laboratories, University of Maryland, and a few other research facilities, with application to satellite imagery, wire-photo standards conversion, medical imaging, videophone, character recognition, and photograph enhancement. The cost of processing was fairly high, however, with the computing equipment of that era. That changed in the 1970s, when digital image processing proliferated as cheaper computers and dedicated hardware became available. Images then could be processed in real time, for some dedicated problems such as television standards conversion. As general-purpose computers became faster, they started to take over the role of dedicated hardware for all but the most specialized and computer-intensive operations.

With the fast computers and signal processors available in the 2000s, digital image processing has become the most common form of image processing and generally, is used because it is not only the most versatile method, but also the cheapest. In this research, the digital camera is used to replace the traditional sensor due to its Advantages by using the image processing method to determine the motion of the platform dynamic.

The remainder of this article is organized as follows: The basic methodologies of the digital image processing which used in this research are discussed in Section 2. In Section 3 shows some experimental results on a realistic Stewart platform by using proposed method. Finally, some conclusions are made in Section 4.

II. MAIN METHODOLOGIES

The charge-coupled device (CCD) is a device for the movement of electrical charge, usually from within the device to an area where the charge can be manipulated, for example conversion into a digital value. Often the device is integrated with an image sensor, such as a photoelectric device to produce

978-1-4244-7316-8/11/$26.00 ©2011 IEEE

the charge that is being read, thus making the CCD a major technology for digital imaging. Although CCDs are not the only technology to allow for light detection, CCDs are widely used in professional, medical, and scientific applications where high-quality image data are required.

The RGB format images capture from the Stewart platform by CCDs are transfer into YUV format. The YUV is a color space typically used as part of a color image pipeline. It encodes a color image or video taking human perception into account, allowing reduced bandwidth for chrominance components, thereby typically enabling transmission errors or compression artifacts to be more efficiently masked by the human perception than using a "direct" RGB-representation. In this research, the algorithms of RGB formatted image transfer into YUV formatted image as follows:

Define

$$R, G, B, Y \in [0, 1].$$

$$U \in [-0.436, 0.436].$$

and

$$V \in [-0.615, 0.615]$$

$$\begin{bmatrix} Y \\ U \\ V \end{bmatrix} = \begin{bmatrix} 0.299 & 0.587 & 0.114 \\ -0.147 & -0.289 & 0.436 \\ 0.615 & -0.515 & -0.100 \end{bmatrix} \begin{bmatrix} R \\ G \\ B \end{bmatrix} \quad (1)$$

The YUV model defines a color space in terms of one luminance (Y) and two chrominance (UV) components. The platform dynamic is determined by the luminance component as the marker position with cyber action system. The coordinate of the platform is shown in Fig 1.

The 6 DOF of the platform are calculated as follows:

Step 1. Find the center O_0 of the platform and calculate the displacement of X, Y, and Z axis.

$$O_0 = \left(\frac{x_2 + x_3}{2}, \frac{y_2 + y_3}{2}, \frac{z_2 + z_3}{2} \right) = (x_i, y_i, z_i) \quad (2)$$

where

$$x_i = \frac{x_2 + x_3}{2},\ y_i = \frac{y_2 + y_3}{2}, \text{ and } z_i = \frac{z_2 + z_3}{2} \quad (3)$$

Step 2. Find the center O_1 of the marker position A to B and the center O_2 of the marker position A to C. Calculate the angles of α, β, and γ, respectively.

$$O_1 = (x_j, y_j, z_j) = \left(\frac{x_1 + x_2}{2}, \frac{y_1 + y_2}{2}, \frac{z_1 + z_2}{2} \right), \quad (4)$$

$$O_2 = (x_k, y_k, z_k) = \left(\frac{x_1 + x_3}{2}, \frac{y_1 + y_3}{2}, \frac{z_1 + z_3}{2} \right). \quad (5)$$

Such that

$$\gamma = \tan^{-1}\left(\frac{z_i - z_j}{y_i - y_j} \right) = \tan^{-1}\left(\frac{z_3 - z_1}{y_3 - y_1} \right) \quad (6a)$$

$$\beta = \tan^{-1}\left(\frac{z_i - z_k}{x_i - x_k} \right) = \tan^{-1}\left(\frac{z_2 - z_1}{x_2 - x_1} \right) \quad (6b)$$

$$\alpha = \tan^{-1}\left(\frac{x_i - x_j}{y_i - y_j} \right) = \tan^{-1}\left(\frac{x_3 - x_1}{y_3 - y_1} \right) \quad (6c)$$

The marker positions are captured by using three CCDs from fixed X, Y, and Z axis.

III. Experimental Results

The equipment used in the experiment consists of three CCDs form Logic Inc., Taiwan, Borland C++ builder 6, and the software of Microsoft DirectX9.0 SDK, namely GraphEdit. The frame size is 352×288 with 30 frames per second in YUV420 formatted. The pictures captures from three CCDs are synchronizing by GraphEdit and then find the marker positions. The graphical user interface (GUI) is shown as Fig 2.

In Fig 2, the three frame of Stewart platform shown below in the graphical user interface are x axis, y axis, and z axis, respectively. The three white points in the edge of the Stewart platform are marker positions. Those RGB based frames are transfer into YUV formatted by using equation (1) and then the motion of the platform are calculate by using equations (2)-(6). The real time output is shown as Fig 3. In the Fig3, the input signals of the x, y, and z axis are sine wave, respectively. The image processing output signals of the platform and the input commands are almost identical

The non-cyclical movement of the ship will be used as input signal. The sea trial data of the rolling angle from a small yacht and the Stewart platform output are shown as Fig 4 and Fig 5, respectively. The pitching angle of the same yacht and the Stewart platform output are shown as Fig 6 and Fig 7,

respectively. The image processing output signals of the platform and the input commands are almost identical.

IV. CONCLUSION

In this paper, the dynamic measurement system of Stewart platform based on image processing method has been proposed. The traditional sensor of the platform has been replaced by the proposed method and significantly improves the system performance. Based on the experiment results shown as above, the proposed image processing method has the potential to become one of the candidates of the Stewart platform sensor.

The advantage of the proposed method is more cheaply than traditional sensor, i.e., gyro. However, the image processing based sensor could not properly measure the torque on the platform. The disadvantage just mention restricts the possibility which be apply to the platform control system.

REFERENCES

[1] D., Stewart, "A Platform with Six Degrees of freedom," *Proceedings Institute of Mechanical Engineers*, Vol. 180, pp. 371-386, 1965.

[2] R.F., Boian, M., Bouzit, G.C., Burdea and J.E., Deutsch, "Dual Stewart Platform Mobility Simulator," *Engineering in Medicine and Biology Society, Conference Proceedings, 26th Annual International Conference,* Vol. 7, pp. 4848-4857, 2004.

[3] D.C., Yang, and T. W., Lee, "Feasibility Study of a Platform Type of Robotic Manipulators, From a Kinematic Viewpoint," *Journal of Mechanisms, Transmissions and Automation in Design,* Vol. 106, pp. 191-198, 1984.

[4] D., Garagic, and K., Srinivasan, "Contouring Control of Stewart Platform Based Machine Tools, *American Control Conference*, Vol. 4, pp. 3831-3838, 2004.

[5] D.,Diddens, D.,Reymaerts, "Design of a Ring-shaped Three-axis Micro Force/Torque Sensor," *Sensors and Actuators*, Vol. 46, pp. 225-232, 1995.

[6] E. O., Doebelin, "*Measurement systems applications and design*," McGraw Hill, New York, 1985.

[7] M., Girone G., Burdea, "A Stewart Platform-Based System for Ankle Telerehabilitation," *Special Issue on Personal Robotics, Autonomous Robots*, Vol. 10, pp. 203-212, 2001.

[8] B., Shivanand, R. Ranganath and A. Ghosal "A Near-singular, Flexure Jointed, Moment Sensitive Stewart Platform Based Force-Torque Sensor," *Proceedings of 13th National Conference on Mechanisms and Machines*, pp.12-13, 2007.

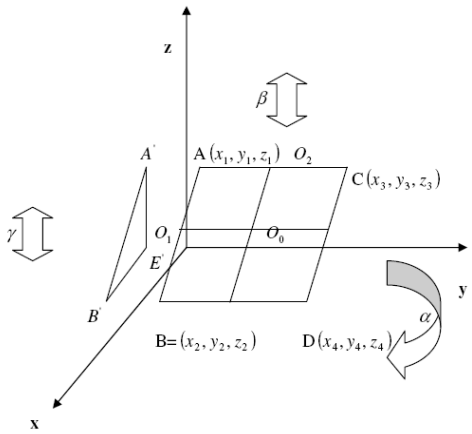

Figure 1. The coordinate of the platform.

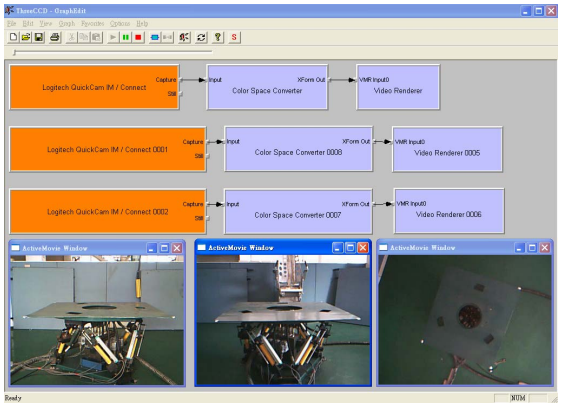

Figure 2. The graphical user interface.

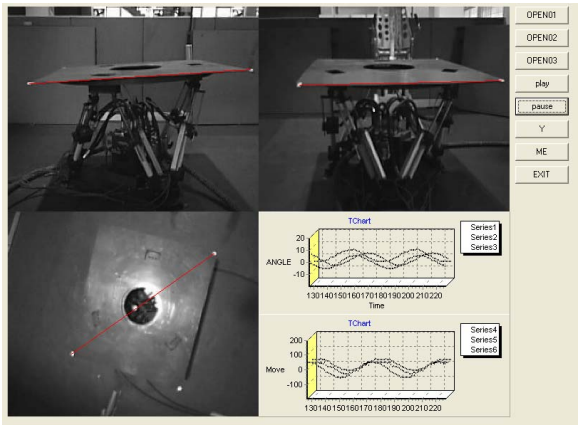

Figure 3. The real time output of the proposed algorithm.

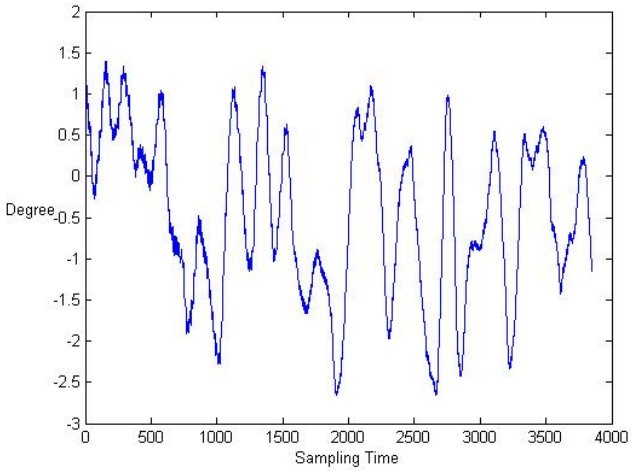

Figure 4. The rolling data of a small yacht.

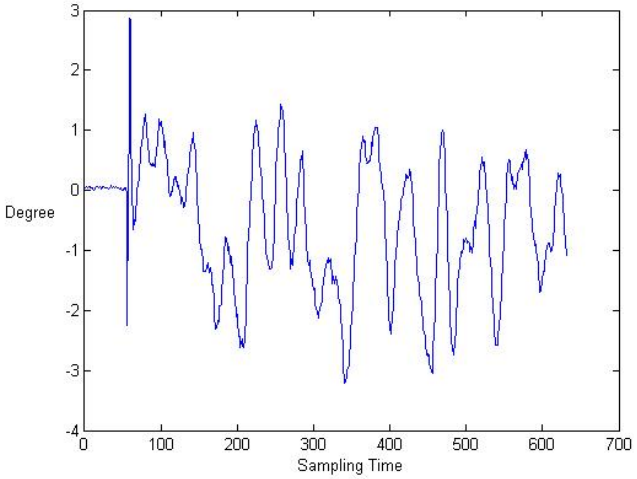

Figure 5. The rolling output based on proposed measurement method.

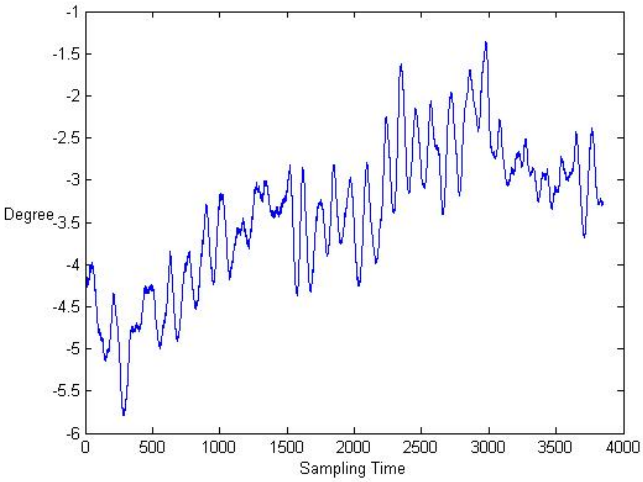

Figure 6. The pitching data of a small yacht.

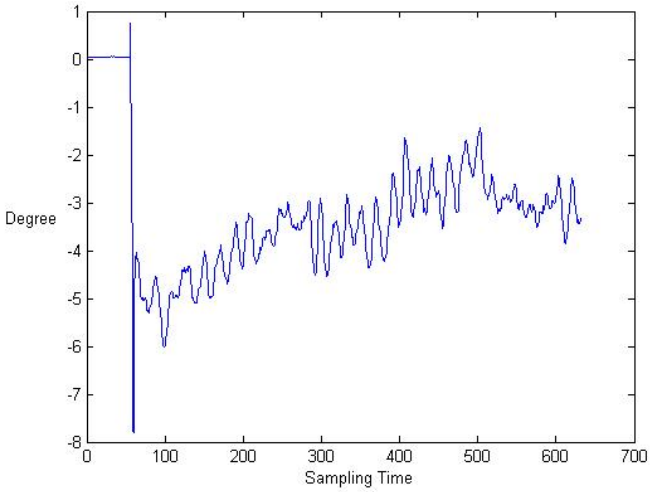

Figure 7. The pitch output based on proposed measurement method.

2011 IEEE International Conference on Fuzzy Systems
June 27-30, 2011, Taipei, Taiwan

Orientation Control of Hovercraft Systems via an SMFLC and Image-Guided Techniques

Chun-Chieh, Wang
Department of Electronic Engineering
Chienkuo Technology University
Changhua City, Taiwan, R.O.C.
jasonccw@ctu.edu.tw

***Abstract*—This paper is concerned with the control of a hovercraft vessel using a sliding mode fuzzy logic control and image-guided techniques. Firstly, we introduce the R/C hovercraft type vessel dynamics. Secondly, the sliding mode fuzzy logic control (SMFLC) is proposed in this paper. A significant feature is that the transient response during the reaching phase has been remarkably improved by the proposed control. Finally, an image-guided technique is presented. To illustrate the effectiveness of the proposed method, we choose the R/C hovercraft vessel as the experimental system. Simulation results showed good responses via the proposed techniques.**

Keywords-R/C hovercraft vessel, Sliding mode fuzzy logic control, Orientation control, Image-guided technique

I. INTRODUCTION

There was extensive research on nonlinear control in connection with the design of autopilots for high-performance aircraft in the early 1950s. In the last few years, the regulation of a ship vessel, by means of two independent thrusters located at the aft, has received sustained attention [1][2][3][4][5]. Nevertheless, position control of an underactuated vehicle is a difficult problem in general. Especially, if the friction is not existent in the environment, an underactuated vehicle often drifts in the direction without actuation. To cite an instance, it is difficult to control positions of such vehicles as a satellite, a hovercraft, and an airship unless sufficient numbers of thruster or torquer are available. Since a large motion leads to inherent nonlinear dynamics, a nonlinear control method is necessary for their position control.

Variable structure control was initiated in Russia by many researchers, like Barbashin [6], Utkin [7], Emelyanov [8]. The control scheme has successfully been applied to many engineering problems including automatic flight control, chemical processes, helicopter stability augmentation systems, electric motors, robots, etc. Variable structure control law is deliberately changed according to some defined rules which depend on the state of the system. The scheme has been mainly considered for continuous-time systems in the form of sliding mode control.

Sliding mode control is known to be very robust against parameter variations and external disturbances and has been widely accepted as an efficient method for tracking control of uncertain nonlinear systems. It has been shown to be able to achieve 'perfect' performance in principle in the presence of parameter uncertainties, bounded external disturbance, etc [9]. However, in order to account for the presence of parameter uncertainties and bounded disturbances, a discontinuous switching function is inevitably incorporated into the control law to achieve so-called sliding condition [10]. Due to imperfect switching in practice it will raise the issue of chattering, which is usually undesirable. To suppress chattering, a continuous approximation of the discontinuous sliding control is usually employed in the literature. Though, the chattering can be made negligible if the width of the boundary layer is chosen large enough, the guaranteed tracking precision will deteriorate if the available control bandwidth is limited. To reach a better compromise between small chattering and good tracking precision in the presence of parameter uncertainties, various compensation strategies have been proposed. For example, integral sliding control [11], [12], [13], sliding control with time-varying boundary layers [5] etc., were presented. Alternatively, applying so-called reaching law approach, Gao et al. [14] proposed sliding controllers such that the trajectories are forced to approach the sliding surface faster when they are far away from the sliding surface. This approach seems to be an efficient method capable of increasing the approaching speed to the sliding surface. However, the behavior of the system dynamics, governed by the transformed first-order equation, can only be predicted through the measurement of the generalized error. Hence the transient response during the reaching phase may not be remarkably improved.

In this work, it is concerned with the control of a hovercraft vessel using an SMFLC and image-guided techniques. The effectiveness of the newly developed control scheme will be demonstrated through the control of the R/C hovercraft vessel. The simulation results validate the superiority and practicality of the proposed method for the orientation control of hovercraft systems.

II. HOVERCRAFT TYPE VESSEL DYNAMICS

We employ an R/C hovercraft (356 mm×212 mm×142 mm) shown in Fig. 1 on a planar ground as the system to be controlled. This model is based on that used in the recent work

978-1-4244-7316-8/11/$26.00 ©2011 IEEE

of Tanaka *et al.* [4]. Fig. 2 shows the hovercraft type vehicle (HTV) model and its coordinate system, where

α : angle of the vehicle
d : distance between the gravity and fans
β : angle between the gravity and fans
m : mass of the vehicle
I : inertia of the vehicle
u_R : force of right side fan
u_L : force of left side fan

Then the HTV dynamics are represented as

$$\begin{aligned} \ddot{x} &= \frac{\cos\alpha}{m} u_1 \\ \ddot{y} &= \frac{\sin\alpha}{m} u_1 \\ \ddot{\alpha} &= \frac{d\sin\beta}{I} u_2 \end{aligned} \tag{1}$$

where $u_1 = u_R + u_L$ and $u_2 = u_R - u_L$. [14]

In this simulation, $\beta = \pi/4$, $m = 0.1$, $I = 0.5$ and $d = 0.1$. Since the control purpose is $\lim_{t\to\infty} y = 0$ and $\lim_{t\to\infty} \alpha = 0$, that is, x is not a controlled variable, the controlled object is described as

$$\begin{aligned} \ddot{y} &= \frac{\sin\alpha}{m} u_1 \\ \ddot{\alpha} &= \frac{d\sin\beta}{I} u_2 \end{aligned} \tag{2}$$

III. FUZZY VARIABLE STRUCTURE CONTROL

Consider a simple n^{th} -order SISO nonlinear system

$$y^{(n)} = f(t, y, ..., y^{(n-1)}) + g(t, y, ..., y^{(n-1)})u \tag{3}$$

Assume that $f = \hat{f} + \Delta f$, where $\hat{f}$ is the known part and Δf is the uncertain part, which includes the internal noise bounded in in $|\Delta f| \le F$. The object is to find a sliding control u such that the output y of (3) will approximately track a desired signal, y_d which is assumed to be n^{th} -order continuously differentiable and all of its derivatives are uniformly bounded. Given the tracking error

$$e(t) = y(t) - y_d(t) \tag{4}$$

Figure 1. Hovercraft type vehicle

For any $q > 0$, define the following transformation

$$s(t) = \left(\frac{d}{dt} + q\right)^{n-1} e(t) \tag{5}$$

Then

$$\dot{s} = \hat{f} + \hat{w} + u \tag{6}$$

where

$$\hat{w} = \sum_{k=1}^{n-1} \binom{n-1}{k-1} e^{(k)} \lambda^{n-k} - y_d^{(n)} \tag{7}$$

An n^{th} -order tracking problem can be transformed into an equivalent 1st-order stabilization problem. It is easy to show that the control law

$$u = \frac{1}{g}\left(\hat{u} + u_f\right) \tag{8}$$

with

$$\begin{cases} \hat{u} = -\hat{f} - \hat{w} \\ u_f = -\Gamma_f sat\left(\dfrac{s}{\Phi}\right) \end{cases} \tag{9}$$

will result in a closed-loop system satisfying the reaching condition:

$$s\dot{s} \le -\eta|s|, \forall |s| \ge \Phi , \tag{10}$$

Provided $\Gamma_f \ge F + \eta$, for some $\eta > 0$. u_f is the output of the FLC. Each fuzzy rule of a FSMC can be expressed as

$$\text{Rule}^i : \text{if } s = LS^i, \text{then } u_f = LU^i.$$

where LS^i is a linguistic value of s in the i-th fuzzy rule.

This controller ensures that starting from any initial state the error trajectory will reach the boundary layer, $|s| \le \Phi$ in finite time.

IV. IMAGE-GUIDED TECHNIQUE [15]

To obtain the relative locations of the landmark and the hovercraft, an image-guided search algorithm is used to find the center of the landmark and the moving vector. These procedures for image processing are shown in Fig. 3.

A. Image Preprocessing

The image preprocessing includes binarization and filtering with the aim of distinguishing the object from the background. To reduce the amount of data, the three-dimensional RGB-image information is transformed into a one-dimensional colour axis. Unfortunately, the regulation of the threshold value usually produces noise.

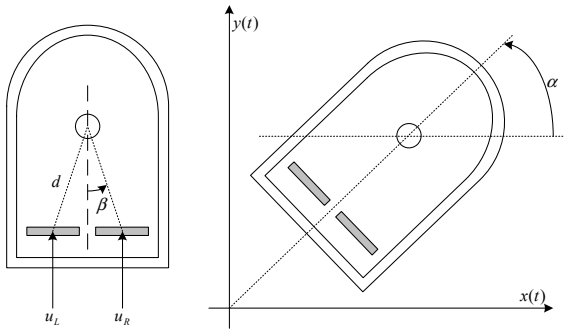

Figure 2. The HTV model and its coordinate system

To improve the image quality, the median and area filters will be used to reduce this noise.

B. Moving-Target Detection

1) Sobel filter

To detect the edge of a binarized picture, a Sobel filter is the most common tool and is very useful. The following two matrices are used as the filter operators:

$$G_x = \begin{bmatrix} -1 & 0 & 1 \\ -2 & 0 & 2 \\ -1 & 0 & 1 \end{bmatrix} \tag{11}$$

$$G_y = \begin{bmatrix} 1 & 2 & 1 \\ 0 & 0 & 0 \\ -1 & -2 & 1 \end{bmatrix}, \tag{12}$$

where G_x and G_y are used for edge detection in the x-direction and the y-direction, respectively. These two 3×3 convolution masks are applied to each pixel. The result of each convolution is treated as a vector representing the edge through the current pixel. If the magnitude of the sum of these two orthogonal vectors is greater than any user-specified threshold, the pixel is marked in black as an edge. Otherwise, the pixel is set to white.

2) Moving-edge detection

To extract the background automatically, a large enough number of successive structures must be available for processing. The procedures for moving-edge detection are shown in Fig. 4. First, three successive structures (I_t , I_{t+1} , I_{t+2})will be taken from CCD, and then the differences $D[I_{t+2} - I_{t+1}]$ and $D[I_{t+1} - I_t]$ can be calculated. The Logical AND operation can be used to evaluate the difference product. Hence, the moving vector of I_{t+1} can be obtained.

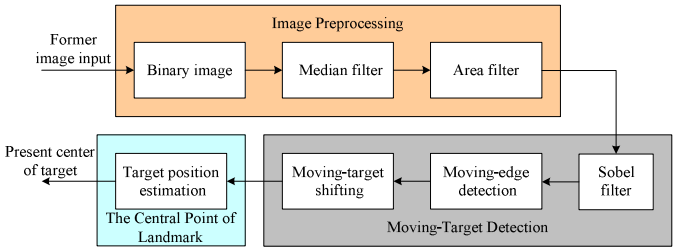

Figure 3. Procedures for image processing

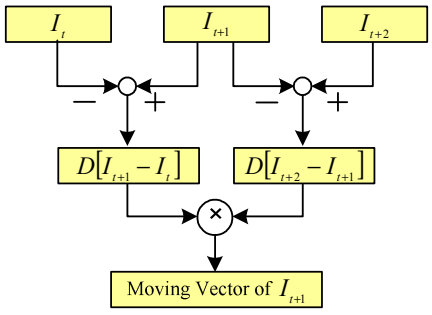

Figure 4. Moving-edge detection

3) Moving-target shifting

As shown in Fig. 5, to overcome image-delay, the moving-target shifting method will be used to get the new landmark *M2*. By comparing $D[I_{t+2} - I_{t+1}]$ with *M1*, the shift values X_d and Z_d can be estimated as follows.

$$\begin{cases} X_d = (C1 - C2) + (A1 - A2) \\ Z_d = (B1 - B2) + (D1 - D2) \end{cases} \tag{13}$$

C. The Central Point of Landmark

In this article, 0 and 1 gray-level images are regarded as the background and the landmark, respectively. If the maximum and minimum values of projection are found on the x-axis and z-axis, respectively, then the center point can be obtained (see Fig. 6).

V. Simulation Results

According to the notations given above, we take $\hat{f}_y = 0$, $\hat{w}_y = \lambda_y \dot{e}_y - \ddot{y}_d$, $\hat{f}_a = 0$, and $\hat{w}_a = \lambda_a \dot{e}_a - \ddot{\alpha}_d$. Initial values are chosen as $(x_0, y_0, \alpha_0) = (1,1,-1.5)$. By setting the parameters as $\Phi_y = 1$, $\lambda_y = 7$, $\Phi_a = 15$, and $\lambda_a = 25$.

The input and output membership functions are shown in Figs. 7 and 8, respectively. The simulation results of [4] are shown in Fig. 9. Figs. 10 and 11 indicate the time responses of the y-axis track and the angle of the vehicle under the proposed control scheme, respectively.

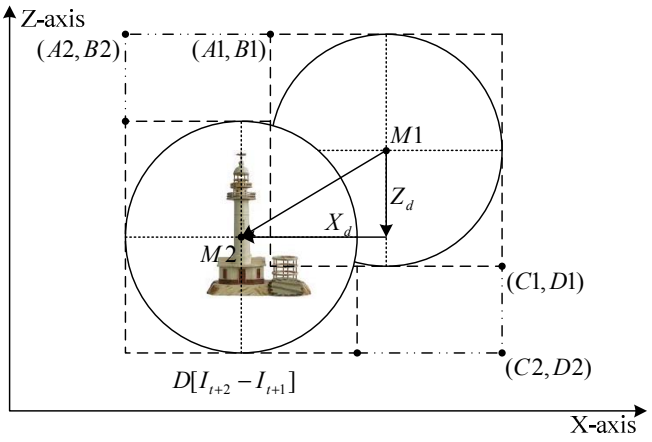

Figure 5. Moving-target shifting

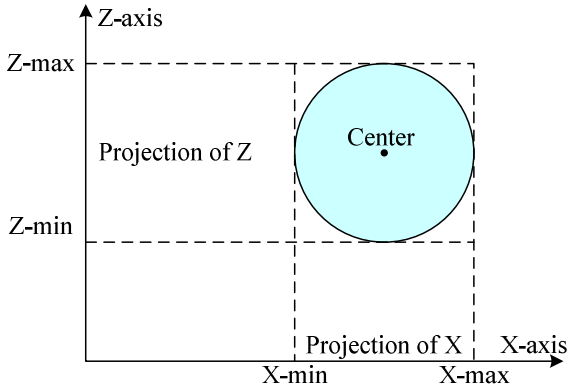

Figure 6. Central point of the landmark

The corresponding control action is shown in Fig. 12 (solid line: force of right side fan; dotted line: force of left side fan). The trajectories are evidently better than those of [3].

VI. CONCLUSION

We have presented an SMFLC scheme and image-guided techniques in this article for a hovercraft vessel. The proposed control scheme has shown to be capable of improving the transient response as well as the steady state response. To illustrate the effectiveness of the proposed method, we choose the R/C hovercraft vessel as the experimental system. The simulation results validate the superiority and practicality of the proposed method for the orientation control of hovercraft systems.

REFERENCES

[1] H. Seguchi and T. Ohtsuka, "Nonlinear receding horizon control of an RC hovercraft," *Proceedings of the 2002 IEEE International Conference on Control Applications*, Glasgow, Scotiand, U.K., pp. 1076-1081, September, 2002.

[2] K. Tanaka, M. Iwasaki, and H.O. Wang, "Switching control of an R/C hovercraft: stabilization and smooth switching," *IEEE Trans. On Systems, Man, And Cybernetics-Part B:Cybernetics*, Vol. 31, No. 6, pp. 853-863, December 2001.

[3] K. Tanaka, M. Iwasaki, and H.O. Wang, "Stable switching fuzzy control and its application to a hovercraft: type vehicle," *Proceedings of the 9th IEEE International Conference on Fuzzy Systems*, San Antonio, TX, USA, pp. 804-809, 2000.

[4] M. Young, The Technical Writer's Handbook. Mill Valley, CA: University Science, 1989.

[5] Y. Soneda and T. Ohtsuka, "Nonlinear moving horizon state estimation for a hovercraft with continuation/GMRES method," *Proceedings of the 2002 IEEE International Conference on Control Applications*, Glasgow, Scotiand, U.K., pp. 1088-1093, September, 2002.

[6] E.A. Barbashin and E.I. Geraschenko, "On speeding up sliding modes in automatic control systems (in Russian)," *Differentzialniye Uravneniya*, Vol. 1, pp. 25-32, 1965.

[7] V.I. Utkin, *Sliding Modes in Control and Optimization*, Springer-Verlag, 1992.

[8] S.V. Emelyanov, "Binary control systems," *International Research Institute for Management Sciences*, Vol. 1, 1985.

[9] J.J. Slotine, E. and W. Li, *Applied Nonlinear Control*, Prentice-Hall: Englewood Cliffs, NJ, 1991.

[10] V.I. Utkin, "Survey paper-variable structure systems with sliding modes," *IEEE Trans. Automat. Contr.* Vol. 22, No. 2, pp. 212-222, 1997.

[11] I.C. Baik, K.H. Kim, H.S. Kim, G.W. Moon, and M.J. Youn, "Robust nonlinear speed control of PM synchronous motor using boundary layer integral sliding control with sliding load torque observer," *IEEE PESC'96 Record*, pp.1242-1247, 1996.

[12] J.H. Lee, J.S. Ko, S.K. Chun, J.J. Lee, and M.J. Youn, "Design of continuous sliding mode controller for BLDDM with prescribed tracking performance," *Conference Record, IEEE PESC'92*, pp.770-775, 1992.

[13] T.L. Chern and Y.C. Wu, "Design of brushless DC position servo systems using integral variable structure approach," *IEE Proceedings - Electr. Power Appl*. Vol. 140, pp. 27-34, 1993.

[14] W. Gao and J.C. Hung, "Variable structure control of nonlinear systems: a new approach," *IEEE Trans. on Indust. Elect.* Vol. 40, pp. 45-55, 1993.

[15] C.C. Wang, C.F. Lien, K.H. Hsia, and J.P. Su, "Image-Guided Searching for Landmark," *International Journal of Artificial Life and Robotics*, vol. 14, pp.95-100, 2009.

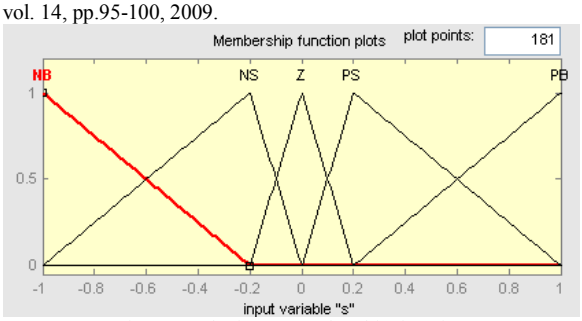

Figure 7. The input membership function

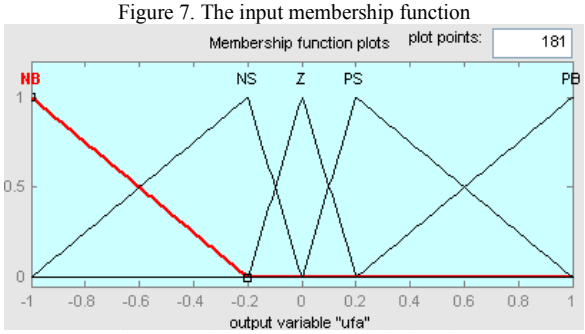

Figure 8. The output membership function

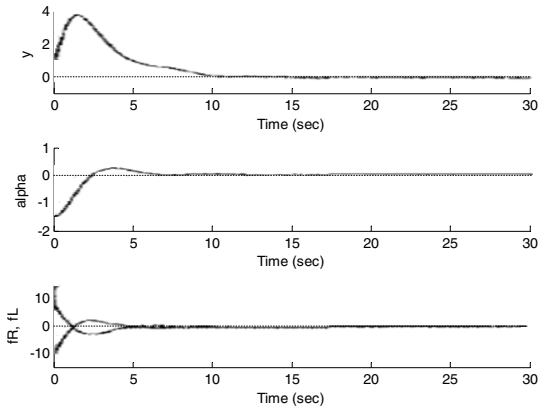

Figure 9. The simulation results of [3]

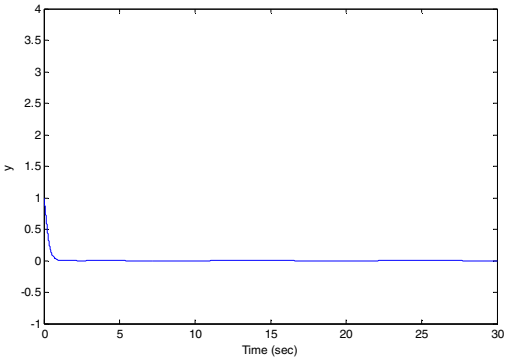

Figure 10. The response of $y(t)$ via the proposed method

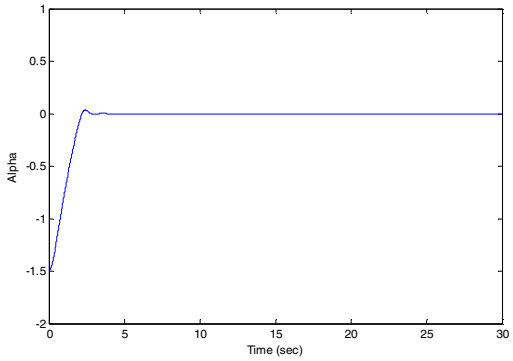

Figure 11. The response of $\alpha(t)$ via the proposed method

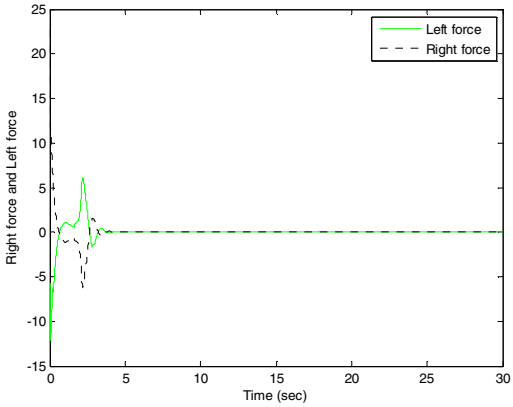

Figure 12. The forces of right and left side fans via the proposed method

2011 IEEE International Conference on Fuzzy Systems
June 27-30, 2011, Taipei, Taiwan

PSO-based Estimation for Gaussian Blur in Blind Image Deconvolution Problem

Yang-Chih Lai, Chih-Li Huo, Yu-Hsiang Yu
Department of Electrical Engineering
National Dong Hwa University
Hualien, Taiwan
E-mail: m9823046@ems.ndhu.edu.tw

Tsung-Ying Sun, *IEEE*, *Member*
Department of Electrical Engineering
National Dong Hwa University
Hualien, Taiwan
E-mail: sunty@mail.ndhu.edu.tw

***Abstract*—This study focuses on Gaussian blur estimation for blind image deconvolution (BID) problem. In BID problem, it only uses blurred image and less information of point spread function (PSF) to restore the received the blurred image. Due to restore the received image, the first step is to identify the proper PSF model. The received image does not uniquely define the PSF. Nevertheless these are many applications where the received image have been blurred either by an unknown or a partially know PSF. Therefore, this paper choose Gaussian blur image for further research, which utilized the particle swarm optimization algorithm to search for the unknown PSF. The objective function for searching the parameters of PSF is based on edge detection and image morphology. It can identify the parameters of PSF exactly. Finally, the feasibility and validity of proposed algorithm are demonstrated by several simulations.**

Keywords-Gaussian Blur, Blind Image Deconvolution, Point Sparead Function, Particle Swarm Optimization, Wiener filter, Edge Detector

I. INTRODUCTION

The objective of image restoration is to reconstruct the original scene from a degraded observation which is commonly blurred by a point spread function (PSF). However, the PSF is usually unavailable a prior in many applications, the recovery process becomes a blind image deconvolution (BID) problem. It has also taken a lot attention in many different technical areas, for example photography, medical imaging, astronomical imaging, and so forth.

Referring to the classification [1], BID approaches could be classified into two chief categories according to the stage of blur identifying:

1) A priori blur identification methods: With this approach, the PSF is identified separately from the original image, and later used in combination with one of the classical image restoration algorithms in order to restore the original image. Generally, a parametric blur model may be used.

2) Joint identification methods: With this approach, most of they use an alternating approach to estimate original image and the PSF rather than truly finding the joint solution.

Initially, D. Kundur and D. Hatzinakos proposed the restoration procedure involves recursive filtering of the blurred image to minimize a convex cost function blindly. The feasibility has been confirmed when it is applied on a scene consists of a finite support object against a uniformly black, grey, or white background [2], [3]. After that, different advanced conditions for BID and shortcomings in conventional methods have been addressed and improved respectively. For instance, since the requirement of a hard-decision on whether the blur satisfies a parametric form before their formulations in these algorithms, the precondition inhibits the incorporation of parametric blur knowledge domain into the restoration schemes [4]. The recursive soft-decision approach is therefore proposed by K.H. Yap and el al. Further, they proposed a computational reinforced learning scheme to overcome the drawbacks of conventional methods, for instance, inter-domain dependency and falling into a local solution [5]. C. Vural and el al. thought that conventional methods require either a special parametric PSF form or complex computation; hence, they proposed a non-linear adaptive filtering to minimum dispersion of image. Because this method does not impose constraints on the phase of the blur, its implementation is easy for real applications [6].

Recently, aiming at seek a higher quality of restoration; several evolutionary techniques have been introduced, for example genetic algorithm [7] and evolutionary algorithm [8]. The feasibility and benefits are verified by simulation results in [7], [8]. Most of these algorithms belong to a priori blur identification method because the parameters of blur model are suitably committed to the evolutionary learning. In the preliminary studies, we have utilized particle swarm optimization (PSO) to tackle different issues about BID problem [14], [15]. In [16], we have observed that the edge of a blurred image is thicker than that of an original image. Therefore, following this observation, the edge of a restoration with implied a well estimation for unknown PSF will be presented using PSO in this study. Each particle of PSO presents a probable PSF and evolutes according to the objective function which designed based on edge detection of its restoration.

This paper is organized as follows: Section II introduces the fundamental of blind image deconvolution. Section III is the description of the proposed method. PSO and edge detector used in this work describes first. And then presents

This work was partly supported by Grant NSC 99-2221-E-259-002-MY3, National Science Council, Taiwan, R.O.C.

the objective function and how PSO is used to seek the parameters of PSF. Section IV presents the simulation and results. The conclusion and future works are described in Section V.

II. BLIND IMAGE DECONVOLUTION

The BID problem is an advanced image restoration problem because the received image does not uniquely define the convolved signals. Nevertheless these are many applications where the received images have been blurred either by an unknown or a partially known PSF. Generally speaking, BID must consider three key issues: blur model, PSF estimation, and image restoration. In this section, a brief explanation about blur model and image restoration used in this work is given as following.

A. Blur Model

In many image applications, blurring procedure is modeled by a two-dimensional (2D) linear convolution as following [1]:

$$g(x,y) = f(x,y) * h(x,y) \tag{1}$$

where $g(x, y)$, $f(x, y)$, $h(x, y)$ denote the observed blurred image, original image, and point spread function (PSF), respectively. In (1), $f(x, y)$ and $h(x, y)$ are unavailable information in advance. Therefore, restore the origin image $f(x, y)$ requires the deconvolution of the degraded image $g(x, y)$ from the $h(x, y)$.

The general model of degradation function for Gaussian blurred images is presented as following [9]:

$$h(m,n) = K \exp\left\{-\frac{(m^2+n^2)}{2\sigma^2}\right\} \tag{2}$$

where m and n present the horizontal and vertical space of $h(\cdot)$. K is a normalization constant to ensure the summation of $h(\cdot)$ matrix is one. σ is the standard deviation for the magnitude distribution of $h(\cdot)$.

B. Wiener Filter

The Wiener filter is a image restoration technique for the deconvolution with a priori known PSF. The Wiener filter is usually applied in the frequency domain. Given a blurred image $g(x, y)$, one takes the Discrete Fourier Transform (DFT) to obtain $G(u, v)$. The original image spectrum is estimated by taking the product of $G(u, v)$ with the Wiener filter $W(u, v)$:

$$F(u,v) = G(u,v)W(u,v) \tag{3}$$

The inverse DFT is then used to obtain the original image from its spectrum. The Wiener filter can be stated as follow:

$$W(u,v) = \frac{H^*(u,v)}{|H(u,v)|^2 + \rho} \tag{4}$$

where H(u, v) denote Fourier transform of the PSF. Since the $W(u, v)$ have the possibility to produce the pulse while the $|H(u, v)|^2$ approaches zero. Hence, in (4) adopted ρ to prevent this situation. The ρ value supposes too slightly, is unable to improve the pulse situation effectively; the ρ value supposes too large, will cause $W(u, v)$ to be too small, and will cause the recover image effect variation. After many experiments of the simulation proved that the ρ value about 0.0005 may obtain a good recovered image.

III. PSF IDENTIFICATION

This section will first present the optimization tool for PSF. Next, the difference between an original image and a blurred image is analyzed by edge detection process respectively. The design of objective function is explained as follows. The final subsection presents the procedure of the proposed algorithm.

A. Particle Swarm Optimization

The PSO is a population-based optimization technique that was proposed by Eberhart and Kennedy [10] in 1995. PSO simulates the behavior of bird flocking. The population is referred to as a *swarm*. The particles examine fast convergence to local and/ or global optimal position(s) over a small number of generations. In PSO, each particle represents a potential solution to the optimization task. All particles can find possible solving repeatedly. Each particle moves to a new position according to the new velocity which includes its previous velocity, the past best solution and global best solution. Therefore, when a particle discovers a new probable solution, other particles will move to it for exploring the region with more depth in the process [11].

A swarm in PSO consists of a number of particles. Each particle represents a potential solution to the optimization task. All of the particles iteratively discover the probable solution. Each particle moves to a new position according to the new velocity which includes its previous velocity, and the moving vectors according to the past best solution and global best solution. The best solution is then kept; each particle accelerates in the directions of not only the local best solution but also the global best position. If a particle discovers a new probable solution, other particles will move closer to it in order to explore the region with more depth [11]. In general, there are three attributes, the particles' current position p_i, current velocity v_i and local best position Pb_i, for particles in the search space to present their features. Each particle in the swarm is iteratively updated according to the aforementioned attributes. Assuming that the cost function J is to be minimized so that the particles contain N dimensions, the new velocity of every particle is updated by

$$\begin{aligned} v_i(t+1) = wv_i(t) &+ c_1 \times r_1\left[Pbest_i(t) - p_i(t)\right] \\ &+ c_2 \times r_2\left[Gbest(t) - p_i(t)\right] \end{aligned} \tag{5}$$

For all $i \in 1, \cdots, N$, v_i is the velocity of the i th particle, the w, c_1 and c_2 denote the acceleration coefficients, r_1 and r_2 are elements from two uniform random sequences in the range (0, 1), and t is the number of generations. The new position of a particle is calculated as follow:

$$p_i(t+1) = p_i(t) + v_i(t+1) \tag{6}$$

The past best position of each particle is updated by:

$$Pb_i(t+1)=\begin{cases} P_i(t+1) & \text{,if } f(Pb_i(t))>f(p_i(t+1)) \\ Pb_i(t) & \text{,otherwise} \end{cases} \quad (7)$$

and the best position *Gb* found from all particles in its search dimension during the previous three steps is defined as:

$$Gb(t+1)=\arg\min_{Pb_i} f(Pb_i(t+1)) \quad (8)$$

B. Edge Detector

The edge detector [12] employed in this paper is based on a set of filters obtained from a basis filter d_0 and through successive rotations depicted as Fig. 1. The other filters were obtained by rotating basis filter with bicubic interpolation and by angles multiple of 45^o. Designating by d_θ the filters of the set presented as

$$g_\theta(x)=d_\theta * x \quad (9)$$

The output of the edge detector is given by a combination of those filters' outputs through an L_2 norm

$$f(x)=\sqrt{\sum_{\theta\in\Theta} g_\theta(x)^2} \quad (10)$$

where Θ denote the set of filter orientations under consideration.

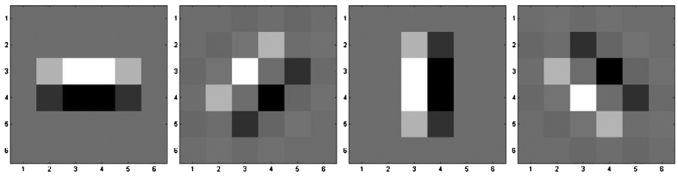

Figure 1. Set of edge detection filters, in the four orientations that were used. The leftmost filter is the basis filter d_0

As an example of the detector's operation, Fig. 2 shows the edges that were extracted from the "Cameraman" image by the proposed edge detector.

Figure 2. Edges of "Cameraman" by the proposed edge detector

C. Object Function

In this study, the proposed objective function is based on the results of edge detection for blurred image and recover image respectively. Many observations of image after edge operation are shown as Fig. 3. The observed blurred image presents thick curve of edge as Fig. 3 (a). However, the edge of correct restored image shown as Fig. 3 (b) presents thin curve and the mean brightness of image is bright. Fig. 3 (c) shows the edge of an over-recovered image. Although the edge mean brightness is also bright, it exhibits the existence of the unnecessary ringing phenomenon. Therefore, based on the comparison of difference information of image edge curve, a suitable objective function could be possible defined to distinguish different situations of image.

(a)

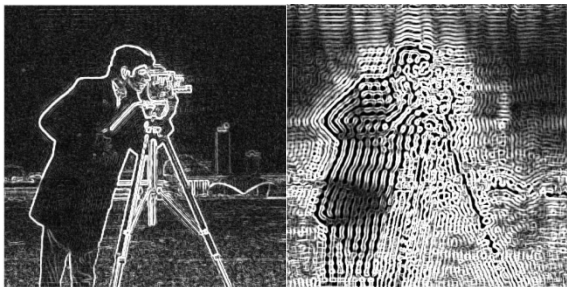

(b) (c)

Figure 3. The edge detector of Cameraman image (a) The edge of blurred image (b) The edge of correct restored image (c) The edge of over-recovered image

The main profile of a blurred image could be obtained following below:

$$\hat{g}=f(g)-\frac{1}{n}\sum f(g) \quad (11)$$

where g is blurred image; $f(g)$ is the blurred image after edge detection via (10); n is the total amount of image pixels. The obtained $\hat{g}$ will convert to binary image and its opposition processing. And then, we can obtain the *essential* edge and *non-essential* edge of blurred image as shown in Fig. 4(a) and (b) respectively. With the concept of morphology, the erosion followed by dilation tends to smooth an image, to break narrow joins, and to remove thin protrusions, as shown in Fig.4(c) (d). The value of the blurred image through edge detection filled the *essential* edge and *non-essential* edge as below:

$$\begin{cases} ged = f(g)\times ed \\ gned = f(g)\times ned \end{cases} \quad (12)$$

where *ed* is *essential* edge of blurred image; *ned* is *non-essential* edge of blurred image.

For each stage of the restored image through edge detection, also made the same blurred image with the *essential* edge and *non-essential* edge part information as below:

$$\begin{cases} xed_i = f(x_i)\times ed \\ xned_i = f(x_i)\times ned \end{cases} \quad (13)$$

where $f(x_i)$ denote the edge detection of the i^{th} estimation image.

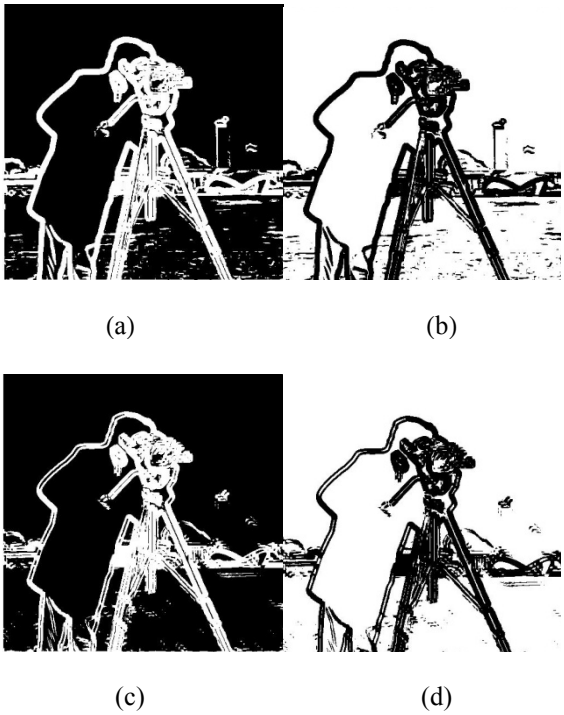

(a) (b)

(c) (d)

Figure 4. (a) The white place is the essential edge (b) The white place is the non-essential edge. The erosion followed by a dilation of (c) essential edge (d) non essential edge

The relationship between the blurred image and the i^{th} estimation image can be obtained as below:

$$\begin{cases} ered_i = xed_i - ged \\ erned_i = xned_i - gned \end{cases} \quad (14)$$

Then, (*ERed & ERned*) refers to only take information of the edge (*ered & erned*), as follows:

$$\begin{aligned} E\mathrm{Re}d &= \{ered \mid ered \neq 0\} \\ ERned &= \{erned \mid erned \neq 0\} \end{aligned} \quad (15)$$

Through the concept of entropy [13], [14] to calculate the diversity of the edge as following:

$$\begin{cases} Hed = -\sum_{i=1}^{m} P(E\mathrm{Re}d_i)\log P(E\mathrm{Re}d_i) \\ Hned = -\sum_{i=1}^{m} P(ERned_i)\log P(ERned_i) \end{cases} \quad (16)$$

where $P(ERed_i)$ and $P(ERned_i)$ are the distribution probability of the $ERed_i$ and $ERned_i$ respectively. Therefore, the objective function is set as (17), the large objective value shows that the restored image is more clear.

$$J = Hed - Hned \quad (17)$$

D. Framework of the Proposed Algorithm

The framework of the proposed algorithm is shown as Fig. 5, and each step is explained as follows:

a) Receive a blurred image *g* which is convoluted by (1).

b) Initial the particles of PSO randomly.

c) Applying Wiener filter on each particle to restore estimated images by (3) and (4).

d) The values of objective function are calculated on each estimated image.

e) Pb and Gb are selected by (7) and (8).

f) Particles move according to (5) and (6).

g) To check the size of PSF particles average velocity is less than the threshold value (this paper set the threshold value is one) or not. If it isn't done, then redo the step (c) to step (g). Otherwise, the learning is terminated.

Eventually, the optimal PSF could be obtained from final *Gb* which is able to generate the restored image with the best of objective function

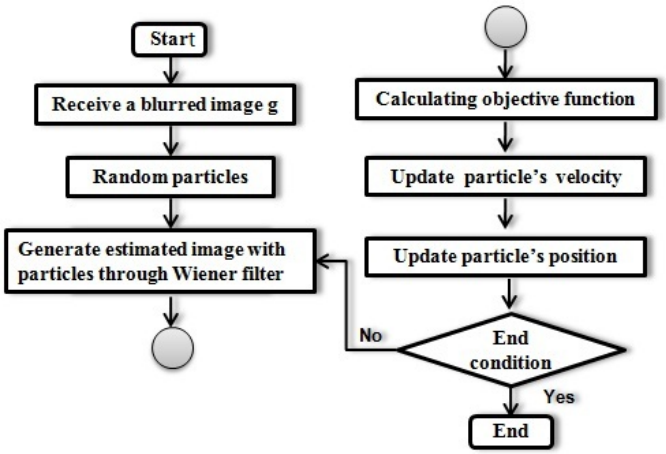

Figure 5. The flowchart of proposed algorithm

IV. EXPERIMENTAL RESULT

For the simulation design, two popular benchmarks, Lena and Cameraman, are the original images which are shown in Fig. 6 (a) and (b) respectively and with the size 512×512. The PSF size is the only knowledge a prior, besides a degraded image.

(a) (b)

Figure 6. The original image (a)Cameraman (b) Lena

The measurement of restoration quality commonly uses the Peak Signal-to-Noise Ratio (PSNR) of the image as below:

TABLE I. ESTIMATION PSF OF RESTORE LENA

Lena									
NO.	PSF of Gaussian blur		Identify of PSF for Gaussian blur				PSNR(db) of blurred image	PSNR(db) of estimation image	
	Size	σ	Size		σ			Avg.	Std.
			Avg.	Std.	Avg.	Std.			
1	5	3	5.3333	1.8257	4.4773	1.4472	77.4935	82.1522	3.3066
2	7	3.5	7.0667	0.2537	4.7291	1.4152	75.6562	80.1690	1.8435
3	9	4	9.9667	1.9384	4.6593	1.4007	74.4668	77.2082	2.9095

TABLE II. ESTIMATION PSF OF RESTORE CAMERAMAN

Cameraman									
NO.	PSF of Gaussian blur		Identify of PSF for Gaussian blur				PSNR(db) of blurred image	PSNR(db) of estimation image	
	Size	σ	Size		σ			Avg.	Std.
			Avg.	Std.	Avg.	Std.			
1	5	3	5.3333	1.8257	4.4346	1.3870	77.3059	83.0344	3.6688
2	7	3.5	7.0667	0.2537	4.5743	1.4676	74.6235	80.3489	2.5050
3	9	4	9.9333	1.7407	4.4366	1.3325	73.0687	76.8471	3.2187

$$PSNR = 10\log_{10}\frac{\sum_{i=1}^{M}\sum_{j=1}^{N}255^2}{\sum_{i=1}^{M}\sum_{j=1}^{N}(f(i,j)-\hat{f}(i,j))^2} \quad (18)$$

where f, $\hat{f}$, M and N denote the original image, restored image, image width and image length respectively. Here three simulations involve different PSF size (5×5, 7×7, and 9×9) and standard deviation (3, 3.5, and 4), the proposed algorithm are implemented for over 30 independent runs. The results are summarized in TABLE I and TABLE II. In each table, the "Avg." means the average PSNR value of estimated image of all runs; and the "Std." presents the standard deviation of PSNR of estimated image of all runs. When the result has smaller Std., it means the algorithm has robust and stability.

From Fig. 7 to Fig. 12, the blurred images and estimated images restored by the proposed algorithm are labeled by (a) and (b) respectively. These figures are contrasted for three different PSF size and standard deviation with two benchmarks. From these figures, it could be observed that the detail of the restorations is quite clear and the estimated results of the restorations approximate to the original image in Fig. 6. Although the proposed method was unable to find the correct standard deviation of PSF, it did not have to the result affects too greatly.

(a) (b)

Figure 7. (a)The received degraded Cameraman, PSF size: 5×5, σ: 3.
(b) Estimation image and PSF size: 5×5, σ: 4.2476

(a) (b)

Figure 8. (a) The received degraded Lena, PSF size: 5×5, σ: 3.
(b) Estimation image and PSF size: 5×5, σ: 4.1038

(a) (b)

Figure 9. (a) The received degraded Cameraman, PSF size: 7×7, σ: 3.5.
(b) Estimation image and PSF size: 7×7, σ: 3.5532

(a) (b)

Figure 10. (a) The received degraded Lena, PSF size: 7×7, σ: 3.5.
(b) Estimation image and PSF Size: 7×7, σ: 3.5591

(a) (b)

Figure 11. (a) The received degraded Cameraman, PSF size: 9×9, σ: 4.
(b) Estimation image and PSF Size: 9×9, σ: 4.1908

(a) (b)

Figure 12. (a) The received degraded Lena, PSF size: 9×9, σ: 4.
(b) Estimation image and PSF Size: 9×9, σ: 4.2907

V. .CONCLUSION

To aim the higher quality of blind restoration, this paper presents an algorithm that use PSO to explore the unknown PSF and deploys edge information to design the objective function. Moreover, it associates Wiener filter to restore the estimated image. From simulation results, as general-purposed in parameter definition, high quality restoration is demonstrated.

The proposed algorithm can identify and recover the image only for Gaussian Blind Image, not for real BID problem. The future work, we will study for identifying each kind of blur situation. So that it can identify encounter all the possible with photograph.

VI. REFERENCE

[1] P. Campisi and K. Egiazarian, *Blind image deconvolution theory and applications*, CRC Press,2006.

[2] D. Kundur and D. Hatzinakos, "A novel blind deconvolution scheme for image restoration using recursive filtering," *IEEE Trans. on Signal Processing*, vol. 46, no. 2, pp. 375-390, 1998.

[3] D. Kundur and D. Hatzinakos, "Blind image deconvolution," *IEEE Signal Processing Magazine*, pp. 43-64, 1996.

[4] K. H. Yap, L. Guan, and W. Liu, "A recursive soft-decision approach to blind image deconvolution," *IEEE Trans. on Signal Processing*, vol. 51, no. 2, pp. 515-526, 2003.

[5] K. H. Yap and L. Guan, "A computational reinforced learning scheme to blind image deconvolution," *IEEE Trans. on Evolutionary Computation*, vol. 6, no. 1, pp. 2-15, 2002.

[6] C. Vural and W. A. Sethares, "Blind image deconvolution via dispersion minimization," *Digital Signal Processing*, vol. 16, pp. 137-148, 2006.

[7] M. E. Moghaddam, "Out of focus blur estimation using genetic algorithm," in *Proc. 15th International Conf. on Systems, Signals and, Image Processing*, pp. 417-420, IWSSIP 2008.

[8] S. Gabarda and G. Cristobal, "An evolutionary blind image deconvolution algorithm through the pseudo-Wigner distribution," *Journal of Visual Communication & Image Pepresentation*, vol. 17, pp. 1040-1052, 2006.

[9] Fen Chen; J. Ma, "An Empirical Identification Method of Gaussian Blur Parameter for Image Deblurring," *IEEE Trans. on Signal Processing*, vol.57, no.7, pp.2467-2478, July 2009.

[10] J. Kennedy and R. Eberhart "Particle Swarm Optimization," in *Proc. IEEE intl. Conf. Neural Networks,* pp. 1942-1948, 1995.

[11] V. G. Gudise and G. K. Venayagaoorthy, "Comparison of particle swarm optimization and backpropagation as training algorithms for neural networks," in *Proc. IEEE Swarm Intelligence Symposium*, pp.110-117, 2003.

[12] Almeida, M.S.C.; Almeida, L.B.; , "Blind and Semi-Blind Deblurring of Natural Images," *IEEE Trans. on Image Processing,* vol.19, no.1, pp.36-52, Jan. 2010.

[13] R. C. Gonzalez and R. E. Woods, *Digital Image Processing*, Prentice Hall, 2002.

[14] T. Y. Sun, C. C. Liu, Y. P. Jheng, J. H. Jheng, S. T. Hsieh, "Blind Image Deconvolution via Particle Swarm Optimization with Entropy Evaluation," in *Proc. the eighth International Conference on Intelligent Systems Design and Applications*, pp. 265-270, Kaohsiung City, Taiwan, Nov. 26-28, 2008.

[15] T. Y. Sun, S. J. Ciou, C. C. Liu, and C. L. Huo, "Out-of-Focus Blur Estimation for Blind Image Deconvolution: Using Particle Swarm Optimization," in *Proc. 2009 International Conference on Systems, Man and Cybernetics*, pp. 1627-1632, San Antonio, Texas, USA, Oct. 14-18, 2009.

[16] Y. C. Lai, M. C. Yang, and T. Y. Sun, "Gaussian blurred blind image deconvolution using particle swarm optimization," in *Proc. 18th National Conf. on Fuzzy Theory and its Applications*, Hualien, Taiwan, Dec. 20

2011 IEEE International Conference on Fuzzy Systems
June 27-30, 2011, Taipei, Taiwan

Fuzzy Integrals For The Aggregation Of Confidence Measures In Speech Recognition

Julie Mauclair, Laurent Wendling, David Janiszek
LIPADE, University of Paris Descartes
Paris, France
Email: {julie.mauclair,laurent.wendling,david.janiszek}@parisdescartes.fr

***Abstract*—This paper presents a study on merging confidence measures using fuzzy logic. Instead of the previous approaches using the notion of probability, we propose to observe the uncertainty of the recognition hypotheses and the notion of possibility thanks to fuzzy reasoning. Four different confidence measures are developed, coming from different parts of a speech recognizer. Various merging methods are studied to improve the performance of the confidence measures. The methods are evaluated in terms of Confidence Error Rate (CER) and in terms of their Detection Error Tradeoff (DET) curves on a French broadcast news corpus. They are compared to some fuzzy logic aggregation techniques among which the technique based on the Choquet Integral yields to a significant improvement in terms of CER.**

***Keywords*—fuzzy logic, confidence measures, speech recognition, feature aggregation**

I. Introduction

Confidence measures are used in various applications of speech processing [1]. When used with a threshold, a confidence score associated to an hypothesis can lead to the acceptation or rejection of that hypothesis [2]. Confidence measures can also be used to select hypothesis that will increase the amount of training data needed for acoustic models [3]. They can also guide the confirmation strategy in dialog systems [4] and can be used for language identification [5]. In speech recognition, confidence measures give an estimation about the correctness of a given hypothesis. To provide such estimations, many parts of the speech recognition system can be helpful as they can provide an indication about the reliability of the system.

One way to take advantage of the quality of each measure is to find the most performant combination method. Designers often choose between the techniques available and the techniques they know best by simply making an educated guess. A tempting approach is to combine several decision rules, based on various representations and classification schemes, instead of electing only one rule. The expected outcome of an aggregation is a more robust final decision, that will improve the classification ability of a single confidence measure. Well-known operators applying this scheme include the quasi-arithmetic means, the weighted minimum and maximum, and the ordered weighted averaging [6]. Other techniques such as Support Vector Machines (SVM), neural networks and Gaussian Mixture Models (GMM), can also be used to merge scores [7].

However, none of these families of operators can take the possible interactions between the constituents of the aggregation into account. The Choquet integral is then considered because it makes it possible for such interactions to generalize many aggregation operators by choosing specific fuzzy measures such as weighted arithmetic means, ordered weighted averages, order statistics, and median [8], [9], [10]. Fuzzy integrals, and the Choquet integral in particular, have been successfully used as fusion operators in various applications of pattern recognition [11] . The aim of the paper is then to explore how fuzzy integrals and the selection of measures can improve the confidence annotation of recognition hypotheses in speech processing.

In this paper, we will first present the different confidence measures developed for our study. The third section will describe the various aggregation methods which are taken as baselines. In section IV, the two fuzzy logic systems which are used for the experiments are presented. In section V, the corpora used will be detailed along with the evaluation metrics. Some results for each merging method will also be described. Finally, section VI presents how the measures can be selected to improve the results.

II. Confidence measures

Let us consider a set of N recognized words $\{w_1, \ldots, w_N\}$. Each word w can be associated with a confidence measure $m(w)$ defined with the properties:

Property 1:
The measure should be in the usual domain $[0, 1]$ and the measure should be interpretable as the probability that the word w is correct.

Property 2:
As a consequence of the latter property, the correct recognition rate on the emitted words is given by the following approximation:

$$\frac{1}{N}\sum_{i=1}^{N} m(w_i) \approx \text{CWRR} \quad (1)$$

where CWRR is the Correct Word Retained Rate (deletions are not taken into consideration).

978-1-4244-7316-8/11/$26.00 ©2011 IEEE

A. Acoustic measure (AC)

The acoustic measure is based on the comparison of the acoustic likelihood provided by the speech recognition system for a given hypothesis and the one provided by an unconstrained phone loop model defined in [12]:

$$m^*_{ac}(w) = \frac{1}{N_f(w)}[\log P(Y|\lambda_C) - \log P(Y|\lambda_L)] \quad (2)$$

where w is the recognized word with N_f frames, Y is the sequence of acoustic observations, $P(Y|\lambda_C)$ is the acoustic score given by the recognizer model, and $P(Y|\lambda_L)$ is the acoustic score given by an unconstrained phone loop.
This measure is then normalized using a sigmoid-like transformation.

$$m_{ac}(w) = \frac{\exp\left(\frac{m^*_{ac}(w)-\mu}{\sigma}\right) + a}{\exp\left(\frac{m^*_{ac}(w)-\mu}{\sigma}\right) + 1} \quad (3)$$

where μ, σ are the mean and the standard deviation of the initial acoustic measure on a training corpus and $a = 2 * \text{CWRR} - 1$ (for an approximation of the second property defined at the begining of this section).
The value of this measure for a word w will be noted $m_{AC}(w)$.

B. Language Model Back-off Based measure (LMBB)

This measure was previously defined in [12]. It uses the back-off behavior of the language model (LM) to define the confidence score that is associated to a word.
A given word recognized with a given left context is associated with the highest order of n-grams seen in the training corpus concerning this word and this context. For a quadrigram LM, the order can be as high as 4, or it can be 0 if out-of-vocabulary words can be processed.
For example, if the sequence of words 'it is the ninth time' is recognized using a quadrigram model and if the quadrigram [is the ninth time] was observed in the training corpus, 'time' will be associated with the order 4. But if this quadrigram has never been observed, whereas the trigram [the ninth time] has, 'time' will be associated with the order 3, and so on, all the way down to order 1 (or 0 if out-of-vocabulary words can be processed).

It is well known that an error occurring in a word has an impact on the correctness of the words located in the immediate context of this erroneous word. According to this, and assuming that the LM back-off behavior is an acceptable criterion to predict the correctness of a word, our measure considers the LM back-off behavior of the left and right neighbors of a word, in addition to the highest order of n-grams this word is associated with on a training corpus.

So, each recognized word is associated with a triplet corresponding to its class.

In order to reduce the number of classes, each word of a recognized hypothesis is finally associated with a three component label:

1^{st} symbol: -, =, or + when the order of its left neighbor is respectively lower than, equal to, or higher than the order of the considered word,

2^{nd} symbol: the highest order of observed n-grams associated to the given word

3^{rd} symbol: -, =, or + when the order of its right neighbor is respectively lower than, equal to, or higher than the one of the considered word.

By comparing a set of automatic transcriptions with words labeled with these triplets, to a manual transcription of the same set of sentences, the misrecognition rate is computed [1] for each triplet on a training set. This rate is the number of substitutions and insertions divided by the number of recognized words. The misrecognition rate for a given class will later be used as the confidence measure for words labeled with that triplet when processing test data. Indeed, in [12], we showed that there is a correlation between the triplets and the error rate those words are associated with.
The value of this measure for a word w will be noted $m_{LMBB}(w)$.

C. Word posterior probability measure (WP)

Word posterior probabilities can be computed from N-best lists, word-lattices [13] or confusion networks [1], [14]. Roughly, the word posterior probability is the ratio of the *a posteriori* probability of a word and the sum of the *a posteriori* probabilities of all its alternatives. These *a posteriori* probabilities result from a combination of values given by acoustic and language models. Thus, word posteriors can be seen as a summarization of acoustic scores, linguistic scores and the search space topology. In N-best lists, the word posterior probability of a word is approximated with the ratio of the sum of the *a posteriori* probabilities of the occurrences of this word in the N hypotheses in a given position, and the sum of all the *a posteriori* probabilities of occurrences of words in this same position, including occurrences of the given word. In both word lattice and confusion network based approaches, the word posterior probability can be seen as a generalization of the N-best approach, where word-segmentations and search space depth are better considered.

Unfortunately, this measure is affected by pruning heuristics reducing the size of pruned word lattices generated during the recognition process. In practice, the use of this measure can therefore be biased. To overcome this problem, a decision tree can be trained to transform the posterior probabilities into better confidence scores [13].
In this paper, we use a confusion network based approach, directly derived from [15] to compute word posteriors. The value of this measure for a word w will be noted $m_{WP}(w)$.

D. Word posterior probability mapped measure (MAP)

An analysis showed the tendancy of the WP confidence measure to overestimate the probabilities of correct recognition as it was also described in [14]. This is due to the fact that

[1] In this paper, we use 'misrecognition rate' to refer to insertions and substitutions errors only, whereas 'word error rate' refers to the common metric including insertions, substitutions *and deletions*; this distinction is needed when studying recognized words only. The misrecognition rate equals 1-CWRR, the Correct Word Retained Rate previoulsy mentioned.

the lattices used as the basis for the posterior estimation only represent part of the posterior distribution and a significant amount of the probability mass "is missing" as we have explained in the previous section. Therefore, a piecewise linear mapping function is used in order to make this measure more discriminant. The coefficients are computed on a specific training set used for the parameters of the confidence measures and led to a new measure called MAP.
The value of this measure for a word w will be noted $m_{MAP}(w)$.

By aggregating the word posterior probability with other confidence measures which are not affected by the search space size, the performance of the word posterior probability should be improved.

III. Aggregation methods : baselines

We have four measures that come from different parts of the speech recognizer. In order to get the best of each measure, several merging techniques are studied. Various classifiers and aggregation techniques have been computed in order to compare their performance against fuzzy systems.

A. Arithmectic mean

One combination that can be a baseline is a simple arithmetic mean between all the features.

B. Linear least square regression

To take into account the quality of each measure, a simple linear interpolation can be used to fit a predictive model of the word correctness as in the equation:

$$y = \sum_{i=1}^{n} \alpha_i x_i + \alpha_0 \tag{4}$$

The method of the least squares is used to estimate the values of the interpolation parameters on the MTrain data set (see section V-C).
Various combination using the four measures or only three of them are tried.

C. Multi-Layer Perceptron (MLP)

A Multi-Layer Perceptron with two hidden layers is trained with backpropagation. Each measure gets one input node and there is one ouput node.

IV. Fuzzy logic systems

In general, uncertainty in the probability theory is seen in terms of occurrences of known facts. In a speech recognition task, what is known is whether the recognition hypothesis is correct or not. Probability is useful when dealing with serial events that require an enumeration notion of uncertainty but is not very useful when the uncertainty is about the degree of accomplishment of a known situation [16]. Indeed, when applying confidence measures to speech recognition, what we want to know is mainly about the degree of correctness that is associated with the recognition hypotheses. Fuzzy logic systems are therefore relevant for this task because they use the notion of uncertainty from the point of view of "possibility".

Fuzzy logic systems use a set of fuzzy rules to map a number of fuzzy inputs to fuzzy outputs. They allow the classification of fuzzy variables thanks to "if ... then" rules [17].

A. Possibility measures

In [18], the authors express the transformation between probability and possibility by:
Let C be the set composed of $c_1, c_2, ..., c_n$, $p_i = P(c_i)$ be the probability measures of each element of the set C where $p_1 \geq p_2 \geq ... \geq p_n$, and $\pi_i = \Pi(c_i)$ be the possibility measures on the set C, then the optimal solution is :

$$\forall i = 1, n, \pi_i = \sum_{j=i}^{n} p_j \tag{5}$$

This transformation is then used to compute the possibility measures from the scores given by the four experts. Various aggregation techniques can be used to get the final confidence score. In this article, the normalised conjonctive, the disjonctive and the adaptative fusions are computed.

B. Fuzzy Integrals

Let us denote by $X = \{D_1, \ldots, D_n\}$ the set of n decision rules (DR), and $\mathcal{P}$ the power set of X, i.e. the set of all subsets of X.
Definition 1 *A* fuzzy measure *or* capacity, μ, *defined on X is a set function* $\mu : \mathcal{P}(X) \longrightarrow [0, 1]$, *verifying the axioms:*

$$\mu(\emptyset) = 0, \mu(X) = 1 \tag{6}$$

and

$$A \subseteq B \Longrightarrow \mu(A) \leqslant \mu(B) \tag{7}$$

Fuzzy measures generalize additive measures, by replacing the additivity axiom by a weaker one (monotonicity). Fuzzy measures embed particular cases including probability measure, possibility and necessity measures, or belief and plausibility functions.
In our context of decision rule fusion, $\mu(A)$ represents the importance, or the degree of trust in the decision provided by the subset A of DRs. The next step in building a final decision, is to combine the partial confidence degree according to each DR into a global confidence degree, taking those weights into account.

1) The Choquet Integral: The Choquet integral was first introduced in the capacity theory [19], [20].

Definition 2 *Let* μ *be a fuzzy measure on X. The* discrete Choquet *integral of* $\vec{\phi} = [\phi_1, \ldots, \phi_n]^t$ *with respect to* μ, *noted* $\mathcal{C}_\mu(\vec{\phi})$, *is defined by:*

$$\mathcal{C}_\mu(\vec{\phi}) = \sum_{j=1}^{n} \phi_{(j)}[\mu(A_{(j)}) - \mu(A_{(j+1)})] \tag{8}$$

where $(.)$ *is a permutation on the source indexes, such as* $(i) \leq (j) \Rightarrow \phi(i) \leq \phi(j)$*. Also,* $A_{(j)} = \{(j), \ldots, (n)\}$ *represents the* $[j..n]$ *associated criteria in increasing order and* $A_{(n+1)} = \emptyset$*.*

Determining the Fuzzy Measure

There are several methods to determine the most adequate fuzzy measure to be used for a given application and the most straightforward learning approach is based on optimization techniques. The aim is to find the fuzzy measure that best minimizes a criterion on the training set, such has the square error. Considering $(x^k, y^k), k = 1, \ldots, l$, l learning samples where $x^k = [x_1^k, \ldots, x_n^k]^t$ is a n-dimensional vector, and y^k the expected global evaluation of object k, the fuzzy measure can be determined by minimizing [8]:

$$E^2 = \sum_{k=1}^{l} (\mathcal{C}_\mu(x_1^k, \ldots, x_n^k) - y^k)^2 \tag{9}$$

This criterion can be put under a quadratic program form and solved by the Lemke method. Nevertheless the method requires at least $n!/[(n/2)!]^2$ learning samples. When little data is available, matrices may be ill-conditioned, causing a bad behaviour of the algorithm. To cope with the above problems, "heuristic" algorithms were developed.

To our knowledge, the algorithm providing the best approximation was proposed by Grabisch in [11]. It assumes that in the absence of any information, the most reasonable way to aggregate the partial matching degrees is to compute the arithmetic mean on all the inputs. This aggregation using Choquet Integral will be later noted m_{CI}.

The fuzzy measures used in the Choquet Integral method can also be computed thanks to possibility measures (see section IV-A). This aggregation will be later noted m_{CF}.

2) The Sugeno Integral: A Sugeno-type fuzzy inference system has already been proved to be a good classifier [21]. This system was used in [22] with good results on a Spanish speech database. This database was collected via land telephone lines (sampled at 8kHz). On the continous speech database (consisting of 9405 words) the Equal Error Rate went from 22.85 with an MLP down to 22.05 when using a Sugeno-type fuzzy inference system.

For our experiments, the number of input variables corresponds to the four confidence measures and the ouput will be the value of the resulting confidence measure.

Determining the Fuzzy Measure

In this paper, the same kind of Sugeno Integral that was used in [22] is computed, using grid partitioning, and yielded to 16 rules. The generalized bell membership function is used for the fuzzification of the scores given by the speech recognizer. This method of aggregation, using the Sugeno Integral, will later be called m_{SI}.

3) Behavioural Analysis of the Aggregation:

Important Index

The importance index is based on the definition proposed by Shapley in game theory [23]. Its application in the context of fuzzy measures was made by Murofushi and Soneda [24]. It is defined for a fuzzy measure μ and a rule i as:

$$\sigma(\mu, i) = \frac{1}{n} \sum_{t=0}^{n-1} \frac{1}{\binom{n-1}{t}} \sum_{\substack{T \subseteq X \setminus i \\ |T|=t}} [\mu(T \cup i) - \mu(T)] \tag{10}$$

It can be interpreted as an average value of the marginal contribution $\mu(T \cup i) - \mu(T)$ of the decision rule i alone in all combinations.

The measure using the importance index will be noted m_{II}.

Interaction Index

Another useful index in order to apprehend the degree of interaction between decision rules was also introduced by Murofushi and Soneda [24]. The interaction value between the rules i and j, to the presence of elements of the combination $T \subseteq X \setminus ij$ is computed as:

$$(\Delta_{ij}\mu)(T) = \mu(T \cup ij) + \mu(T) - \mu(T \cup i) - \mu(T \cup j) \tag{11}$$

Extending this criteria on every subsets of $T \subseteq X \setminus ij$, an evaluation of the interaction between DRs i and j is :

$$I(\mu, ij) = \sum_{T \subseteq X \setminus ij} \frac{(n-t-2)!t!}{(n-1)!} (\Delta_{ij\mu})(T) \tag{12}$$

This index gives an idea of the complementarity or competitiveness that exist beween measures. A positive interaction between two rules means that the decision rule is discriminative power is increased when used with th second decision rule. Thus, this index will later by used to select measures in order to obtain an aggregation of complementary measures.

V. Experiments

Experiments have been carried out on the ESTER corpus. ESTER is an evaluation campaign of French broadcast news transcription systems which started in 2003 and completed in January 2005 [25]. The recognition system used for those experiments is the LIUM (Laboratoire d'Informatique de l'Université du Maine) system [26]. It is based on the CMU Sphinx 3.3 decoder. Some features were added to the Sphinx decoder, such as acoustic models adaptation using Speaker Adaptative Training (SAT) method or word-lattice rescoring to get a quadrigram language model. More details about the system can be found in [26]. The LIUM system reached the second position of the campaign with an official 23.6% word error rate.

A. Resources

The vocabulary used by the LIUM system contained about 65K words. Acoustic and language models were trained using the official training corpus of the ESTER evaluation campagn. Trigram language model was used during the first two passes processed by the recognizer, while the quadrigram language model was used for the last pass corresponding to a word-lattice rescoring. The word posteriors are computed from these

word-lattices, using acoustic scores from adapted acoustic models and linguistic scores from the 4-gram language model.

B. Training parameters for confidence measures

The parameters that are used to compute the LMBB measure, the AC measure and the MAP measure are estimated from a specific corpus composed of 4h of manually annotated broadcast news from ESTER. This corpus is independent of the training corpus of acoustic and language models and of the training set later refered as MTrain.

C. Corpora used to evaluate the merging techniques

Three corpora are used for the evaluation of the various merging techniques studied in this paper. They come from the official test of the ESTER broadcast news corpus which consists of 10h of continuous speech. Those corpora are noted MTrain, MDev and MTest. MDev is used as a validation set for the MLP and the Sugeno-type fuzzy system. In order to be consistent when defining the test set in an experiment, the choice of the data that are used in this test set (MTest) should be recorded after the data used in the training set. Therefore, MTest is defined by choosing the last 3h30 of the official ESTER test corpus. 3h30 of speech in this database correspond to an approximate amount of 31000 words. It has led to the choice of radio channels that are not contained in MTrain or MDev. As a summary MTrain is composed of 1h of Radio Classique, 1h of France Inter, 1h of France Info and 30 mins of Radio France International (RFI). MDev is composed of 1h of France Culture, 1h of France Info, 1h of France Inter and 30 mins of RFI. MTest is composed of 1h of RFI and 2h30 of Radio Television Marocaine (RTM) and is not a part of MTrain or MDev.

D. Evaluation Metrics

In those experiments, the Confidence Error Rate (CER)[27] is used to assess the relevance of a confidence measure to assess the correctness of a word. The CER is the total number of false accepts and false rejects divided by the total number of hypothesis for a given threshold. It gives an estimation of the classification ability of a confidence measure. The threshold that has led to the minimum CER on MTrain is used when computing the CER on the test set MTest.

Some Detection Error Tradeoff (DET) curves are also shown in order to compare the fuzzy logic techniques used in this article. Those DET curves present the two types of error : the false alarms and the false rejections. In the paper written by Martin [28], the authors show that the DET curve form of presentation is relevant to any detection task where a tradeoff of error types is involved. Thanks to the DET curves, performances of confidence measures in terms of their capabilities to validate correct hypotheses and reject false alarms are evaluated.

E. Single Measures

Table I shows the different measures developed in this paper. The best single measures are the WP measure and the MAP measure which have obtained a CER score of 17.88 on MTest. The mapping technique between the WP measure and the MAP measure preserves the CER score as the piecewise linear transformation does not affect the distribution from the optimal threshold. Those measures alone are relevant to assess the correctness of a word and have a CER which is much lower than the rate of the emitted words that are incorrect (17% on MTrain and 22.3% on MTest). By adding measures that are not affected by pruning heuristics, the aim is then to find the best combination that will lead to a better performance in terms of classification.

TABLE I
RESULTS IN TERMS OF CER FOR THE SINGLE CONFIDENCE MEASURES

Confidence Measure	MTrain (%)	MTest (%)
Incorrect emitted words	17	22.3
WP	14.65	**17.88**
MAP	14.65	**17.88**
AC	16.04	22.18
LMBB	16.05	22.17

F. Results after merging

Several combinations of the four measures were tried. To compare the different techniques, some baselines are computed, which are a simple arithmetic mean, a linear regression between the four single measures, and a MLP.

In order to take advantage of the uncertainty notion from the possibility theory, various fuzzy systems are tried to aggregate the four confidence measures.

Figure 1 illustrates how the Choquet Integral method computes the weights used by the fusion process (section IV). Every path of the lattice leads to a part of the plan where every single measure is associated with a weight p. Depending on which measure is the highest for the current word, it will lead to a different linear interpolation merging the four measures.

For example, let us consider a word w and its four scores coming from each confidence measures. For this word w, we have:

$$m_{WP}(w) < m_{MAP}(w) < m_{AC}(w) < m_{LMBB}(w) \quad (13)$$

The final score $m_{CI}(w)$ that will be associated to that word is:

$$\begin{aligned} & m_{WP}(w) * (p(\{1234\}) - p(\{234\})) \\ +& m_{MAP}(w) * (p(\{234\}) - p(\{34\})) \\ +& m_{AC}(w) * (p(\{34\}) - p(\{4\})) \\ +& m_{LMBB}(w) * p(\{4\}) \end{aligned} \quad (14)$$

Table II summarizes the results of the various combination techniques. The fusions on possibillity measures do not perform well. Every other technique outperforms the arithmetic mean and the linear regression and is more relevant to assess the correctness of a word. As the training corpus is substantial,

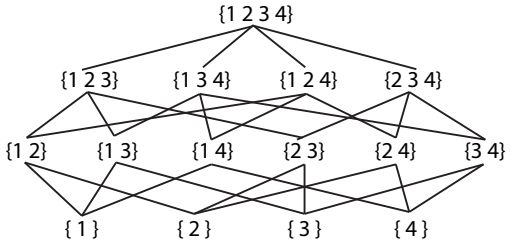

Fig. 1. Lattice for 4 measures. Each path is associated with a weight processed by the Choquet Integral technique on MTrain. {1}, {2}, {3}, {4} corresponds respectively to the weights associated to the WP, MAP, AC and LMBB measure.

TABLE II
RESULTS IN TERMS OF CER FOR THE VARIOUS MERGING TECHNIQUES.

Aggregated Measure	MTrain (%)	MTest (%)
Arithmetic mean	14.18	17.61
MLP	13.87	**17.44**
Linear Regression m_{LR}	13.92	17.55
Normalised conjonctive fusion	16.04	22.16
Disjonctive fusion	16.04	22.15
Adaptative fusion	16.04	22.17
Sugeno Integral m_{SI}	13.72	**17.44**
Choquet Integral with possibility measures	14.72	21.16
Choquet Integral m_{CI}	13.90	**17.49**

the Choquet Integral does not perform better than the Sugeno Integral but they lead to a good performance in terms of CER.

VI. SELECTION OF THE MEASURES

In order to understand the correlation between the different measures and to better aprehend which measure is important in the aggregation and which one is not, their important index and their interaction index can be good indicators. Those indexes are provided by the Choquet lattice and as the Sugeno and Choquet Integrals are very close in terms of the CER score, they will be used with the Choquet Integral to observe the relevance of selecting measures.

The important index is described in section IV-B3. It describes the correlation between the score given by a measure and the correctness of a word. All the important indexes are computed for each confidence measure and are detailed in table III.

TABLE III
IMPORTANCE INDEX OF THE FOUR MEASURES

Confidence measure	Importance Index
WP	0.517512
MAP	1.930417
AC	0.536041
LMBB	1.016030

The first merging technique simply consists in a linear interpolation of the four measures with the importance indexes used as coefficients. The resulting measure is :

$$m_{II}(w) = \frac{0.517512 m_{WP} + 1.930417 m_{MAP} + 0.536041 m_{AC} + 1.01630 m_{LMBB}}{4} \quad (15)$$

The interaction index described in section IV-B3 is also computed on our data. The results are shown in table IV.

TABLE IV
INTERACTION INDEX OF THE FOUR MEASURES

	WP	MAP	AC	LMBB
WP	0.000000	-0.255104	0.041425	-0.776167
MAP	-0.255104	0.000000	-0.418659	-1.405465
AC	0.041425	-0.418659	0.000000	0.102432
LMBB	-0.776167	-1.405465	0.102432	0.000000

The idea to select the measures that will be kept in the aggregation is to look for the measure associated with the weakest important index and for which the interaction index is lower than the average interaction index.

This led to the results shown in table V.

TABLE V
RESULTS IN TERMS OF CER FOR THE AGGREGATION USING SELECTED MEASURES

Aggregated Measure	MTrain (%)	MTest (%)
Choquet Integral (4 measures)	13.90	**17.49**
Linear regression with important indexes m_{II}	13.82	**17.34**
Choquet Integral (3 measures)	13.98	18.22
Choquet Integral (2 measures)	13.91	**17.20**

Those results show the relevance of the use of important indexes. By using them as coefficients in a simple linear regression, the resulting measure outperforms the results of a MLP and of the two fuzzy systems based on the Choquet and the Sugeno integrals.

Selecting the measures that will be used in the aggregation shows a good performance and leads to the best performance in terms of CER when using only two measures with the Choquet Integral.

The DET curve (see figure 2) confirms that, by selecting only two measures for the Choquet Integral, we obtain a relevant aggregation in terms of its ability to reject false alarms. The aggregation of three measures seems to obtain good results for the validation of correct hypotheses.

VII. DISCUSSION AND CONCLUSIONS

This paper presents how fuzzy logic is relevant in measuring the confidence in a speech processing application.

For applications where the interesting aspect of the confidence measure is its classification ability, the CER improvement is important. For example, one might want a confidence measure that is well able to detect incorrect words in order to increase the amount of training data for the acoustic models in an unsupervised way. According to the CER, the fuzzy logic techniques prove to be very efficient and combine the best of the various individual confidence measures involved on each data subset. Compared to a standard MLP, fuzzy integrals and the Choquet Integral in particular can provide a semantic

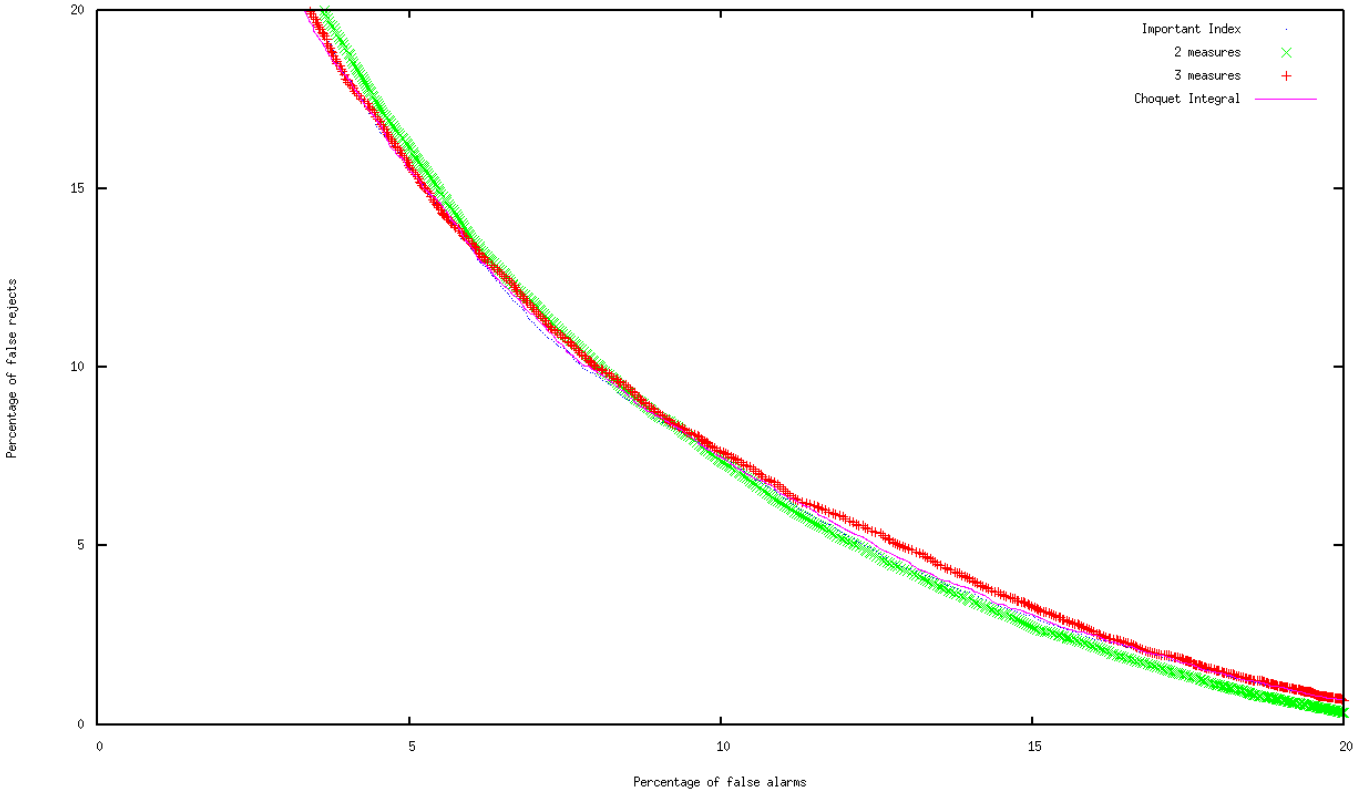

Fig. 2. DET curve for the Choquet Integral with 4, 3 and 2 measures and with the linear regression with important indexes.

interpretation and understanding of the problem. The Choquet integral technique, by selecting only two measures, improves the CER by 4.10% compared to the CER obtained by the best single confidence measure. From DET curves, the selection of the measures has also proven to increase the discriminative ability of confidence measures and to be worthwhile.

In future works, other methods using fuzzy logic will be explored.

REFERENCES

[1] H. Jiang, "Confidence measures for speech recognition: a survey," *Speech Communication Journal*, vol. 45, pp. 455–470, 2005.

[2] D. Charlet, G. Mercier, and D. Jouvet, "On combining confidence measures for improved rejection of incorrect data," in *Proc. of Eurospeech, European Conference on Speech Communication and Technology*, Aalborg, Danemark, September 2001.

[3] F. Wessel and H. Ney, "Unsupervised training of acoustic models for large vocabulary continous speech recognition," *IEEE Transactions on Speech and Audio Processing*, vol. 13, pp. 23–31, 2005.

[4] R. San-Segundo, B. Pellom, K. Hacioglu, W. Ward, and J. Pardo, "Confidence measures for spoken dialogue systems," in *Proc. of ICASSP, International Conference on Acoustics, Speech, and Signal Processing*, Salt Lake City, USA, May 2001.

[5] F. Metze, T. Kemp, T. Schaaf, T. Schultz, and H. Soltau, "Confidence measure based language identification," in *Proc. of ICASSP, International Conference on Acoustics, Speech, and Signal Processing*, Istanbul, Turkey, June 2000.

[6] R. Yager, "On ordered weighted averaging aggregation operators in multicriteria decisionmaking," in *IEEE Transactions on Systems, Man and Cybernetics*, February 1988, pp. 183–190.

[7] R. Zhang and A. Rudnicky, "Word level confidence annotation using combinations of features," in *Proc. of Eurospeech, European Conference on Speech Communication and Technology*, Aalborg, Danemark, Septembre 2001, pp. 2105–2108.

[8] M. Grabisch and N. J.M., "Classification by fuzzy integral - performance and tests," in *Fuzzy Sets and Systems, Special Issue on Pattern Recognition*, 1994, pp. 255–271.

[9] M. Grabisch, "The application of fuzzy integrals in multicriteria decision making," in *European Journal of Operational Research*, 1996, pp. 445–456.

[10] J.-L. Marichal, "Aggregation of interacting criteria by means of the discrete choquet integral," in *Physica-Verlag GmbH*, 2002, pp. 224–244.

[11] M. Grabisch, "A new algorithm for identifying fuzzy measures and its application to pattern recognition," in *IEEE International Conference on Fuzzy Systems*, 1995, pp. 145–150.

[12] J. Mauclair, Y. Estève, S. Petit-Renaud, and P. Deléglise, "Automatic detection of well recognized words in automatic speech transcriptions," in *LREC, Language Resources and Evaluation*, Genoa, Italy, May 2006.

[13] G. Evermann and P. Woodland, "Posterior probability decoding, confidence estimation and system combination," in *Speech Transcription Workshop*, 2000.

[14] G. Evermann and P. Woodland, "Large vocabulary decoding and confidence estimation using word posterior probabilities," in *Proc. of ICASSP, International Conference on Acoustics, Speech, and Signal Processing*, Istanbul, Turkey, June 2000.

[15] H. Mangu, E. Brill, and S. A., "Finding consensus in speech recognition: Word error minimization and other applications of confusion networks," *Computer Speech and Language*, vol. 14, no. 4, pp. 373–400, 2000.

[16] M. Laviolette and J. Seaman Jr., "The efficacy of fuzzy representations of uncertainty," *IEEE Transactions on Fuzzy Systems*, vol. 2, no. 1, p. 415, February 1994.

[17] J. Mendel, "Fuzzy logic systems for engineering: a tutorial," *Proceedings of the IEEE*, vol. 83, no. 3, pp. 345–377, March 1995.

[18] D. Dubois, H. Prade, and S. Sandra, "On possibility/probability transformations," in *Proc. of the Fourth IFSA Conference*, Seoul, Korea, 1993, pp. 103–112.

[19] G. Choquet, "Theory of capacities," in *Annales de l'Institut Fourier*, 1953, pp. 131–295.

[20] T. Murofushi and M. Sugeno, “A theory of fuzzy measures : representations, the choquet integral, and null sets,” in *Journal of Mathematical Analysis and Applications*, 1991, pp. 532–549.

[21] J.-S. R. Jang, “ANFIS: Adaptative-network-based fuzzy inference system,” *IEEE Transactions on systems, man and cybernetics*, vol. 23, no. 3, pp. 665–685, May/June 1993.

[22] G. Hernandez-Abrego, G. Hernandez, and J. Marino, “Fuzzy reasoning in confidence evaluation of speech recognition,” *IEEE International Workshop on Inteligent Signal Processing WISP’99*, September 1999.

[23] L. Shapley, “A value for n-person games,” in *Contributions to the Theory of Games, Annals of Mathematics Studies*, 1953, pp. 307–317.

[24] T. Murofushi and S. Soneda, “Techniques for reading fuzzy measures(III): interaction index,” in *Proc. of the 9th Fuzzy System Symposium*, Sapporo, Japan, May 1993, pp. 693–696.

[25] S. Galliano, E. Geoffrois, D. Mostefa, K. Choukri, J. Bonastre, and G. Gravier, “The ESTER phase II evaluation campaign for the rich transcription of french broadcast news,” in *Proc. of Eurospeech, European Conference on Speech Communication and Technology*, Lisbon, Portugal, September 2005.

[26] P. Deléglise, Y. Estève, S. Meignier, and T. Merlin, “The LIUM speech transcription system: a CMU Sphinx III-based system for french broadcast news,” in *Proc. of Eurospeech, European Conference on Speech Communication and Technology*, Lisbon, Portugal, September 2005.

[27] F. Wessel, K. Macherey, and R. Schlüter, “Using word probabilities as confidence measures,” in *Proc. of ICASSP, International Conference on Acoustics, Speech, and Signal Processing*, Seattle, USA, Mai 1998, pp. 225–228.

[28] A. Martin, G. Doddington, T. Kamm, M. Ordowski, and M. Przybocki, “The DET curve in assessment of detection task performance,” in *Proc. of Eurospeech, European Conference on Speech Communication and Technology*, Rhodes, Greece, September 1997, pp. 1895–1898.

2011 IEEE International Conference on Fuzzy Systems
June 27-30, 2011, Taipei, Taiwan

Active Tracking Using Intelligent Fuzzy Controller And Kernel-Based Algorithm

Moteaal Asadi Shirzi
Assistant Supervisor and Administrative Manager of Control Laboratory, University of Tehran
Tehran, Iran
Moteaalasadi@gmail.com

M.R. Hairi-Yazdi
Associate Professor and Supervisor of Control Laboratory, University of Tehran
Tehran, Iran
Myazdi@ut.ac.ir

***Abstract*—This paper introduces a practical system by combining an Intelligent Fuzzy Controller and vision processing algorithm to obtain an efficient active tracker. Target tracking performance is heavily dependent on a good blend of vision algorithm and control. Because of performance and computational complexity, many visual tracking algorithms cannot be linked with control systems in the real-time tracking. Robustness and speed are the bottlenecks of current visual tracking algorithms. Here, the target's visual model is used along with a kernel-based searching algorithm and a motion detection module to predict the target position. A model update is also incorporated to recognize when the target's appearance is changing due to variations in its position. An Intelligent Fuzzy Controller (IFC) is also synthesized to reach control performance objectives. The IFC used in this tracking system not only helps to track the target accurately in different situations, but also tries to find the target's presence after track loss. Additionally, the parallel processing technique has also been deployed to provide the desired accuracy and speed in real-time tracking. The idea has been implemented in an active camera system to track moving targets.**

Keywords- Intelligent Fuzzy Control, Kernel-Based Object Tracking, Active Tracking, Vision

I. INTRODUCTION

With the rapid enhancement of computational power, object tracking has been an active research area in the computer vision in recent years. It plays an important role in robot tracking, monitoring and surveillance systems, virtual sport, human-computer interfaces [1], vision-based control, smart rooms, military and driver assistance, astronomy and medical science. There are three common approaches that are widely used in object tracking. One is based on Kalman filter or extended the Kalman filter [2]. The Kalman filter assumes that the probability distributions of the states are Gaussian. Another is mean shift [3], [4] which is a robust non-parametric method for climbing density gradients to find the peak of probability model. Third, particle filter as a widely used approach in object tracking is well suited to estimate state of non-linear, non-Gaussian dynamic systems [5], [6]. Tracking under the constraint of low computational complexity presents a challenge in the real time tracking applications.

Recent years have witnessed rapidly growing use of fuzzy control systems in engineering applications. The numerous successful applications of fuzzy control have sparked a flurry of activities in the analysis and design of fuzzy control systems [7]. Stability and robustness are the two major points where the active tracking system presented can benefit from fuzzy controller [8]. Use of different fuzzy rules, depending on situations such as velocity and dimension of target, results in a more efficient controller to track the target. In addition, the tracker can detect the target's presence after track loss by running suitable fuzzy rules. Selecting the appropriate fuzzy rules is a complicated process. Thus, to implement these rules, an intelligent module has been used that runs special fuzzy rules with regard to situations. Therefore, the fuzzy controller is adaptive and the rules change in fuzzy engine intelligently.

In this paper, the target's visual model is used along with a kernel-based searching algorithm and a motion detection module to predict the target position. A model update is also incorporated to recognize when the target's appearance is changing due to variations in its position. An Intelligent Fuzzy Controller (IFC) is also synthesized to reach control performance objectives. In case of target track loss, a search algorithm sweeps the space in the vicinity of last target position to recover the lost target. Additionally, the parallel processing technique has also been deployed to provide the desired accuracy and speed in real-time tracking. The idea has been applied to an active camera system.

II. PROBLEM DEFENITION

The main goal is to track a dynamic target using a camera with two degrees of freedom in pan and tilt directions. This research centers on the tracking of two types of objects. The first type includes objects that are close to the camera such as faces of people. The active camera tracks people's faces regardless of whether they are approaching the camera or moving away from it or turning their heads. This example is expandable to a variety of objects that move around the camera. Sudden and rapid changing of targets aspect and their surroundings is one of the most important properties of them. The environment of target may be cluttered with other objects. Therefore, it is very important that the active camera be able to determine changes and differentiate between objects. The second type includes targets at long distances from the active

978-1-4244-7316-8/11/$26.00 ©2011 IEEE

camera, such as an aircraft. These objects have small aspect in the camera with a small rate of changes. A small unsuitable movement of the active camera causes large tracking errors for distanced objects. Accuracy is therefore crucial.

III. General Operation

Figure 1 shows the schematic of operation of the active camera. Each of pan or tilt angles uses the same operation that is mentioned in figure 1. There are four major modules: The Intelligent Fuzzy Controller (IFC) module makes the appropriate control signal for plant due to errors. The Active Camera module is the sensors, digital camera and motors of the active camera transform the control signal to physical movements in pan and tilt movements. The vision box recognizes the selected dynamic target that must be tracked. In fact, the main goal is to keep the object in the center of the camera. The distance between object and center of the camera is determined as the error, figure 2. The filter box checks the output data coming from the vision box. Filter box uses some rational rules to reject idle data latest In case of target loss, the suitable fuzzy rules runs and an intelligent local search algorithm sweeps the scene in the vicinity of last target position.

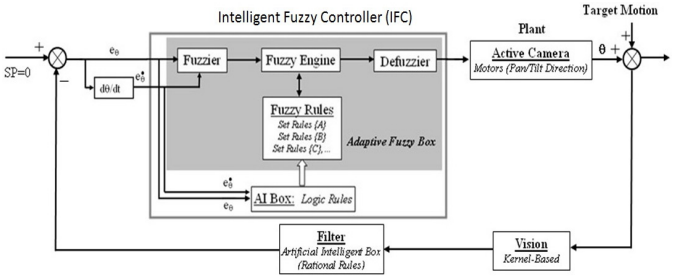

Figure1. The schematic of general operation

IV. Vision Box

As mentioned, vision box recognizes the object and calculates the distance between object and the center of screen camera. This distance transforms to the two angle errors, Δθtilt and Δθpan.

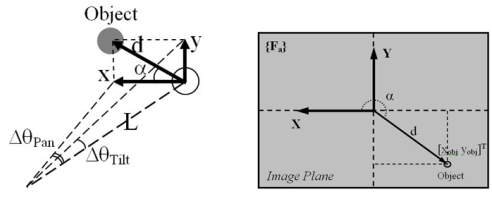

Figure2. $\Delta\theta_{Tilt}$ and $\Delta\theta_{pan}$ are calculated from the distance of the object and the center of screen camera

Δθtilt and Δθpan are calculated from equation (1). In this formula, L is a constant value to normalize Δθtilt and Δθpan.

$$\Delta\theta_{pan} = d\ Sin\alpha / L$$
$$\Delta\theta_{tilt} = d\ Cos\alpha / L \qquad (1)$$

Vision box uses various techniques to recognize and track objects. Following, briefly introduces these techniques.

V. Mean Shift

Recently, the mean shift algorithm was employed for object tracking, measuring the similarity between consecutive frames based on Bhattacharyya coefficient [9]. A major limitation of the mean shift tracker is that it uses one object model to track the target during the entire tracking process. Hence, it fails to track the target as it undergoes severe deformations and rotations. To achieve robust tracking, model updates should be considered. The adaptive Kalman filter can be used to filter the object kernel histogram and obtain the optimal estimate of the object mode [10]. Another problem is also experienced with mean shift tracker. It cannot track objects apart for more than the size of the target model between two consecutive frames. This means that if the camera is unable to capture the target movement between these two frames, it virtually fails to track it. An extension of mean shift algorithm employs spatiograms (instead of histograms) which improves the performance of the mean shift tracker under wild rotations of the target [9]. However, it does not solve the second problem mentioned previously. Thorough global template search for the target is not a practical solution as it burdens the computer in real-time. More importantly, it is not suitable for real time tracking because of the controller stability issues that can result from erratic sampling rates. However, use of spatiogram has one evident advantage over histograms due to the integration of distance information that helps distinguish between different objects of similar color distribution.

Target Representation

To characterize the target, first a feature space is chosen. The reference target model is represented by its pdf (probability density function), q, in the feature space. For instance, the reference model can be chosen to be the color pdf of the target. In the subsequent frame, a target candidate is defined at location y, characterized by the pdf p(y). To satisfy low computation cost imposed by real time processing, discreet densities or m-bin histograms should be used. Thus:

$$\hat{q} = \{\hat{q}_u\}_{u=1\ldots m} \qquad \sum_{u=1}^{m} \hat{q}_u = 1$$
$$\hat{p}(y) = \{\hat{p}_u\}_{u=1\ldots m} \qquad \sum_{u=1}^{m} \hat{p}_u = 1 \qquad (2)$$

Target model

A target is represented by an ellipsoidal region on the image. To eliminate the influence of different target dimensions, all targets are first normalized to unit circle. Let $\{x_i\}_{i=1\cdots n_h}$ be the normalized pixel locations of the target region in the current frame. The probability of feature u in the target model is calculated from:

$$\hat{q}_u = C\sum_{i=1}^{n} k\left(\|x_i\|^2\right)\delta\left[b(x_i) - u\right] \qquad (3)$$

Where b(xi) is the index of the bin at the pixel location Xi and δ is the *Kronecker delta function* and k is an isotropic kernel profile. The presence of such a kernel function assigns more weight to central pixels and reduces the effect of

peripheral pixels. The constant, C, is computed by using the fact that the sum of all probabilities over the *histogram* is one. Figure 3 shows an example of *kernel histogram* construction.

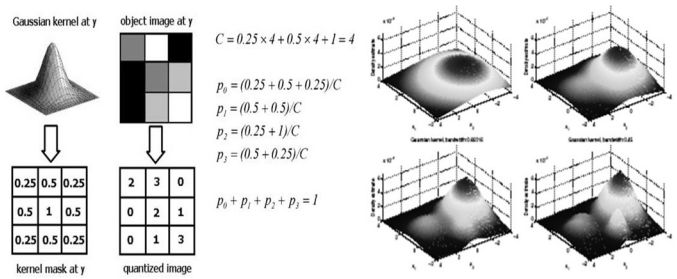

Figure3. Example of kernel histogram construction,
Multi-bandwidth density estimate on 2D artificial Gaussian mixture data.

Target Candidates

Let $\{x_i\}_{i=1\cdots n_h}$ be the normalized pixel locations of target candidate, centered at y in the current frame. The probability of feature u in the target candidate is given by:

$$\hat{P}_u(y) = C_h \sum_{i=1}^{n_h} k\left(\left\|\frac{y - x_i}{h}\right\|^2\right)\delta\left[b(x_i) - u\right] \tag{4}$$

Where h is the bandwidth (number of pixels in the region) of target candidate and C_h can be calculated the same as C_h The similarity function ρ is defined by the *Bhattacharyya coefficient* as:

$$\rho(y) = \sum_{u=1}^{m} \sqrt{\hat{P}_u(y).\hat{q}_u} \tag{5}$$

Target localization

Localization maximizes the similarity function between the two probability density functions. The search for new target location starts at the location y_0 of the target in the previous frame. The Taylor expansion of ρ(y) around ρ(y_0) yields:

$$\rho(y) \approx \frac{1}{2}\sum_{u=1}^{m}\sqrt{\hat{P}_u(\hat{y}_0).\hat{q}_u} + \frac{1}{2}\sum_{u=1}^{m}\hat{P}_u(\hat{y})\sqrt{\frac{\hat{q}_u}{\hat{P}_u(\hat{y}_0)}} \tag{6}$$

Taking the partial derivative of ρ(y) with respect to y and setting it to zero results in the mean shift equation. In this procedure, the kernel is recursively moved from the current location y0 to the new location y_1, therefore:

$$\hat{y}_1 = \frac{\sum_{i=1}^{n_h} x_i.w_i.g\left(\left\|\frac{\hat{y}_0 - x_i}{h}\right\|^2\right)}{\sum_{i=1}^{n_h} w_i.g\left(\left\|\frac{\hat{y}_0 - x_i}{h}\right\|^2\right)} \tag{7}$$

Where,

$$g(x) = -k'(x)$$

Kernels of Epanechnikov profile are typically used, i.e.:

$$k(x) = \begin{cases} \frac{1}{2}c_d^{-1}(d+2)(1-x) & if\ x \le 1 \\ 0 & otherwise \end{cases} \tag{8}$$

Where C_d is the volume of unit d-dimensional sphere and d is the dimension of the state space (2 in this case) [5]. In this case, derivative of the kernel profile, g(x), is constant and equation (7) reduces to:

$$\hat{y}_1 = \frac{\sum_{i=1}^{n_h} x_i.w_i}{\sum_{i=1}^{n_h} w_i} \tag{9}$$

'Hence, the mean shift algorithm calculates the similarity function for the target model and target candidate in subsequent frames and then, estimates the location of the target candidate using (9). This process is repeated until the similarity function goes up and the estimated location of the target changes less than a desirable threshold.

Target model update

Updating the target model during the tracking process is important if this process is to sustain for a long period of time. The generic target model update procedure can take on the following form:

$$q_{t+1} = c \cdot \left(q_t + f\left(\rho\left(q_t, p_t\right), \alpha, \ldots\right) \cdot p_t\right) \tag{10}$$

Where c is an arbitrary constant that is usually one; f is a function of the similarity, ρ, between the current target model and candidate model; α,… are other visually extractable elements such as the perimeter of object in pixel. In (11), f is taken as an exponential function as follows:

$$f = e^{-a[1-\rho(q_t, p_t)]} \tag{11}$$

Where a is the update rate and was taken as 10. In this paper an update function also is used in a similar fashion. The function has the advantage of having the least effect on target model when the similarity function is obtained too low. Hence, even if the target suddenly is buried in scene clutter the updating procedure will have no significant effect on the previous target model and it still holds the visual characteristics of last-seen target.

VI. FILTER

The vision module produces the error value. It is possible that this module produces idle error value, especially when the active camera loses the object or when the environment is very complex and vision module makes mistake in recognizing the object. Some simple logic laws are used in the filter module to check and eliminate the idle error value.

Any target in the real world such as airplane, missile, the human face or anything that the active tracker wants to track, has a continuous movement. It means that targets could not be vanished and appeared in other place immediately. So the big change in error value could not be acceptable and the filter assumes it as an idle error value and eliminates it from the data. In addition, velocity and acceleration of the object are also continuous. The filter part the big error value is replaced with the value that calculates from this formula:

$$\begin{aligned} &if\left(\Delta\theta_{pan}^{t_i} > \alpha_{pan}\right) \Rightarrow \Delta\theta_{pan}^{t_i} = 0.5\left(\Delta\theta_{pan}^{t_{i-1}} + \frac{\Delta\theta_{pan}^{t_{i-2}} + \Delta\theta_{pan}^{t_{i-3}}}{2}\right) \\ &if\left(\Delta\theta_{tilt}^{t_i} > \alpha_{tilt}\right) \Rightarrow \Delta\theta_{tilt}^{t_i} = 0.5\left(\Delta\theta_{tilt}^{t_{i-1}} + \frac{\Delta\theta_{tilt}^{t_{i-2}} + \Delta\theta_{tilt}^{t_{i-3}}}{2}\right) \end{aligned} \tag{12}$$

Where α_{pan} =10o and α_{tilt} =7o. If the active camera couldn't find the target, the search algorithm is operated. In other case, if the vision box loses the target, it produces a null value. This situation happens when the target hides behind other objects. For example, when an airplane goes behind clouds, the vision module can't recognize the position of the target. Thus it produces null value. The logic law that is used here is that the target continues its motion according to its last velocity and acceleration. In this case, filter module estimates the position for the target with the same velocity and acceleration of the target before it disappeared and produces a proximate error value.

$$if\ (\Delta\theta_{pan}^{t_i} > null) \Rightarrow \Delta\theta_{pan}^{t_i} = \Delta\theta_{pan}^{t_{i-1}},\ if\ (\Delta\theta_{tilt}^{t_i} > null) \Rightarrow \Delta\theta_{tilt}^{t_i} = \Delta\theta_{tilt}^{t_{i-1}} \quad (13)$$

Other task of the filter module is to find the lost target. By following human behavior the suitable logic law can be extracted for the active tracker when the tracker loses the target. Actually, when the active tracker loses the target, first it tracks the estimated position proportional to the velocity and acceleration of the target. But if it fails to find the target, the search algorithm is activated. For finding the lost target, first the active camera searches around the target's lost position and it gradually increases the radius of the search area with increasing the rotation pan and tilt angles.

VII. Intelligent Fuzzy Controller

Fuzzy logic is a powerful albeit somehow controversial technique. It permits control without extensive knowledge of the equations of the process and it represents in a very effective way the human reasoning methods [11]. A fuzzy control designer is inevitably faced with two questions: How does one determine the shape of the fuzzy sets, and how many sets are necessary and sufficient? [12] There are some different ways to determine the shape of the fuzzy sets in a controller, based on expert experience and control engineering knowledge, based on the operator's control actions, based on a fuzzy model of the process and based on learning [13].

While non-adaptive fuzzy control has proven its value in some applications, it is sometimes difficult to specify the rule-base for some plants. Additionally, the need could arise to tune the rule-base parameters if the plant changes. This provides the motivation for intelligent fuzzy control, where the focus is on the automatic on-line synthesis and tuning of fuzzy controller parameters [32]. There are several techniques for determining and tuning the fuzzy rules that have some strength and weaknesses which make them suitable for a specific situation. The *Intelligent Fuzzy Controller (IFC)* uses collections of fuzzy rules that each of them is efficient for a specific situation. Fuzzy laws are selected by using intelligent laws in accordance to the situation of the target. Some of these intelligent rules are as follows:

- Distanced targets need high accuracy to be tracked. Every change of the pan and tilt angles at the active camera causes large changes in vision area of the active camera at faraway. Therefore a small unsuitable movement of the active camera causes large tracking errors for faraway targets.
- Because the image of close targets in the camera move quickly and randomly, these targets could be tracked with less accuracy but with higher tracking velocity. High accuracy tracking may result in losing the target.

Three collections of different fuzzy set rules are used in the IAFC:

1. For targets with very slow velocity that are near the camera or faraway targets with slow velocity: if $\Delta\theta_{pan} < 4.5^{deg/sec}$ and if $\Delta\theta_{tilt} < 2.5^{deg/sec}$ the IAFC uses fuzzy set rules that are mentioned at figure 4.
2. For faraway targets with high velocity or near targets with medium velocity, if $4.5 < \Delta\theta_{pan} < 8^{deg/sec}$ and if $2.5 < \Delta\theta_{tilt} < 4.5^{deg/sec}$, the IAFC uses figure 5 fuzzy set laws.
3. For near targets with fast velocity: if $\Delta\dot{\theta}_{pan} > 8^{deg/sec}$ and if $\Delta\theta_{tilt} > 4.5^{deg/sec}$, the IAFC uses figure 6 fuzzy set laws.

Actually the tracker has been run frequently with variety of fuzzy rules. The suitable values and fuzzy laws are selected by considering the results of system operation. Changes in Pan Direction are more than tilt direction because objects generally move horizontally, so the signal controls are stronger for pan direction. For example there is a special collection laws for a target that is near the active camera and has high velocity. For this, accuracy is not very important. The main objective of the active tracker is to avoid losing the target. High accuracy in tracking the target causes losing the target, especially when the direction of target changes instantaneously. But if the velocity of the target is low, active camera can be more accurate in tracking by using other collection of fuzzy laws.

Angle Pan $\alpha=\Delta\theta_{pan}$ Tilt $\beta=\Delta\theta_{tilt}$	Angular Velocity $\dot{\alpha}$ Velocity $\dot{\beta}$	Controller Signal for Pan Direction	Controller Signal for Tilt Direction
Low (-)	Low (-)	High	Medium High
	Zero (·)	Medium High	Medium High
	High (+)	Zero	Zero
Medium Low	Low	High	Medium High
	Zero	Medium High	Medium High
	High	Zero	Zero
Zero (·)	Low	Medium High	Medium High
	Zero	Zero	Zero
	High	Medium Low	Medium Low
Medium High	Low	Zero	Zero
	Zero	Medium Low	Medium Low
	High	Low	Medium Low
High (+)	Low	Zero	Zero
	Zero	Medium Low	Medium Low
	High	Low	Medium Low

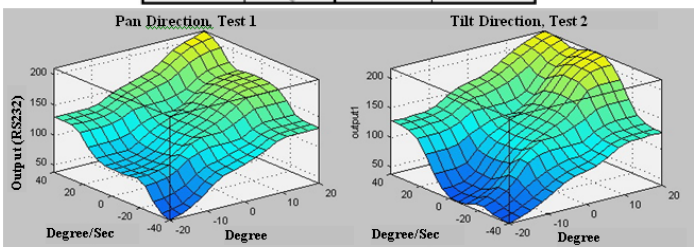

Figure 4. Selected fuzzy rules for targets with very slow velocity that are near the camera or faraway targets with slow velocity. In this case camera has fast motion, but accuracy is not much important. So, the main purpose of fuzzy rules is that the camera doesn't lose the target. Fuzzy rules produce strong commands to reduce big errors.

Angle Pan $\alpha=\Delta\theta_{pan}$ Tilt $\beta=\Delta\theta_{tilt}$	Angular Velocity $\dot{\alpha}$ Velocity $\dot{\beta}$	Controller Signal for Pan Direction	Controller Signal for Tilt Direction
Low (-)	Low (-)	Very High	High
	Zero (·)	High	Medium High
	High (+)	Zero	Zero
Medium Low	Low	High	Medium High
	Zero	Medium High	Medium High
	High	Zero	Zero
Zero (·)	Low	High	Medium High
	Zero	Zero	Zero
	High	Low	Medium Low
Medium High	Low	Zero	Zero
	Zero	Medium Low	Medium Low
	High	Low	Medium Low
High (+)	Low	Zero	Zero
	Zero	Low	Medium Low
	High	Very Low	Low

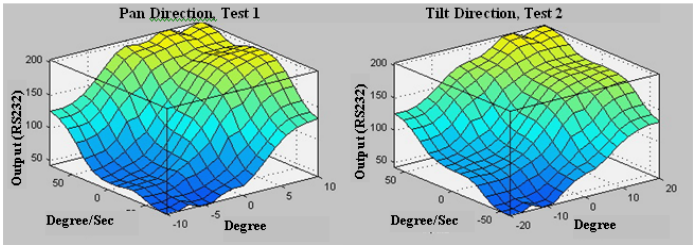

Figure 5. Selected fuzzy rules for faraway targets with fast velocity or near targets with medium velocity. In this case fuzzy rules prepare commands that cause camera tracks targets with moderate accuracy and velocity.

Angle Pan $\alpha=\Delta\theta_{pan}$ Tilt $\beta=\Delta\theta_{tilt}$	Angular Velocity $\dot{\alpha}$ Velocity $\dot{\beta}$	Controller Signal for Pan Direction	Controller Signal for Tilt Direction
Low (-)	Very Low	Very very High	Very High
	Low (-)	Very High	Very High
	Zero	High	High
	High (+)	Zero	Zero
	Very High	Low	Low
Medium Low	Very Low	Very High	Very High
	Low (-)	High	High
	Zero	Medium High	Medium High
	High (+)	Zero	Zero
	Very High	Low	Low
Zero (·)	Very Low	Very High	Very High
	Low (-)	High	High
	Zero	Zero	Zero
	High (+)	Low	Low
	Very High	Very Low	Very Low
Medium High	Very Low	High	High
	Low (-)	Zero	Zero
	Zero	Medium Low	Medium Low
	High (+)	Low	Low
	Very High	Very Low	Very Low
High (+)	Very Low	High	High
	Low (-)	Zero	Zero
	Zero	Low	Low
	High (+)	Very Low	Very Low
	Very High	Very very Low	Very Low

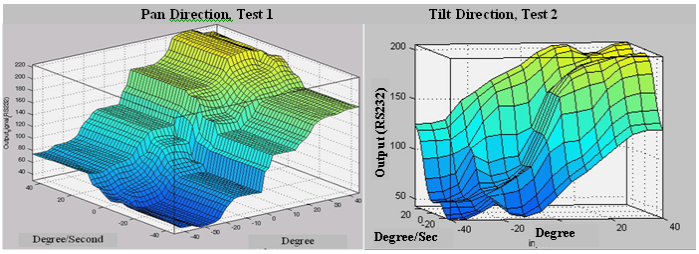

Figure 6. Selected fuzzy rules for near targets with fast velocity. In this case tracking does not need high velocity pan and tilt directions. But it needs to track targets accurately. So, Fuzzy rules produce commands that cause high accurate movement.

Owing to the interconnection of vision and control system, the optimization problem of active tracking is rather nontrivial. For instance, if robustness of tracking algorithm implies more latency, the control system would become unstable. Whereas, high overshoot of the closed loop system will cause the vision processing program to lose sight of the target.

VIII. Implementation And Experimental Results

To achieve an automatic target tracker, motion detection, target tracking and IFC must be combined. To link these two components, computers have been parallelized by the UDP protocol for communications. The vision processor extracts the target's position from the image streams delivered by the camera and packages the data to be sent over the predefined UDP sockets. On the other end, the Matlab ® sits in wait for the UDP packets, calculates the control signals by the fuzzy controller and relays commands to this active camera. The camera could track different objects such as human face or body excellently in both tilt and pan directions. Because of some unknown hardware flaws, sometimes, delays occurred in the tracker. This problem usually is solved because of the robustness of fuzzy controller. Details of active tracker and connections are shown in figure-7.

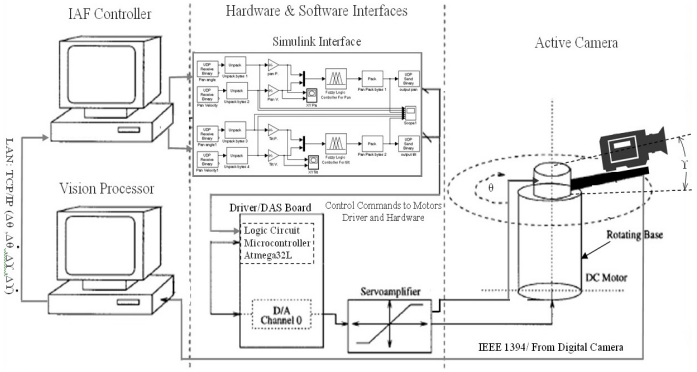

Figure7. The schematic of hardware and software of active camera

To assemble the active tracker, vision processor and fuzzy controller are each implemented on two separate computers. This way allows each portion to usurp full computation power of its own processor.

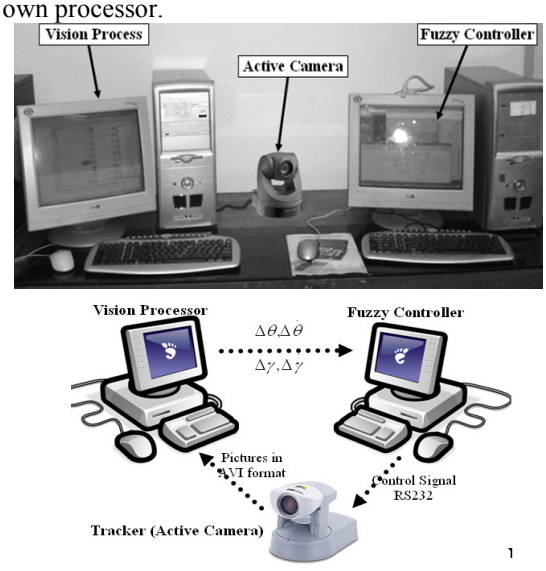

Figure 8. Using the parallel processing, the computational load is divided between two computers and delay times can decrease

Two different experiments are considered to test the fuzzy controller and vision algorithm. In the first experiment, the active camera tracks a black spot on a rotating circular plate which paces back and forth between two limits. The real position of the black spot is:

$$\theta = \tan^{-1}(\frac{r}{l})\sin(\omega t) \quad , \quad \alpha = \tan^{-1}(\frac{r}{l})\cos(\omega t) \qquad (14)$$

Where θ is the pan angle and α is the tilt angle; r refers to the radius of rotation of the black spot and l is distance between the active camera and the circular plate; ω represents the angular velocity of plate and finally t denotes time.

In addition, the normal mean-shift algorithm and a conventional PID controller are developed for comparing by the operation of the IFC and considering of effectiveness of the proposed method precisely. Figure 9, 10 and 11 shows the results in terms of angle of camera and outputs from vision and controller that the active camera has tracked. Figure 9, 10 displays the operation of the normal mean-shift algorithm and a conventional PID controller beyond the IFC algorithm.

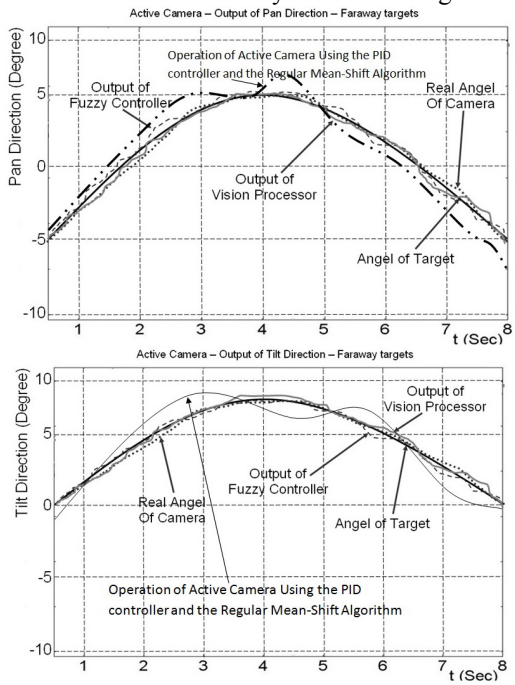

Figure9. Tracking the target with circular path(w=0.4rad/sec). These figures show that the operation of the IFC is better than the operation of the normal mean-shift algorithm and a conventional PID controller

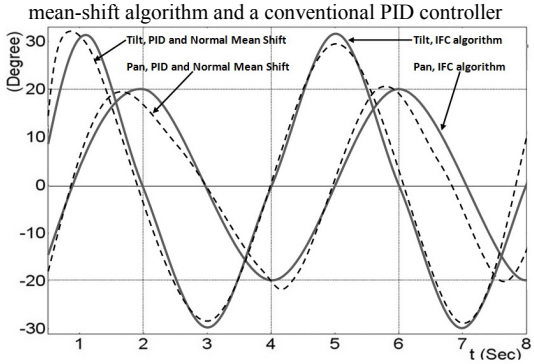

Figure10. Comparison the operation of the IFC and the operation of the normal mean-shift algorithm and a PID controller. The IFC algorithm decreases errors in the active tracker.

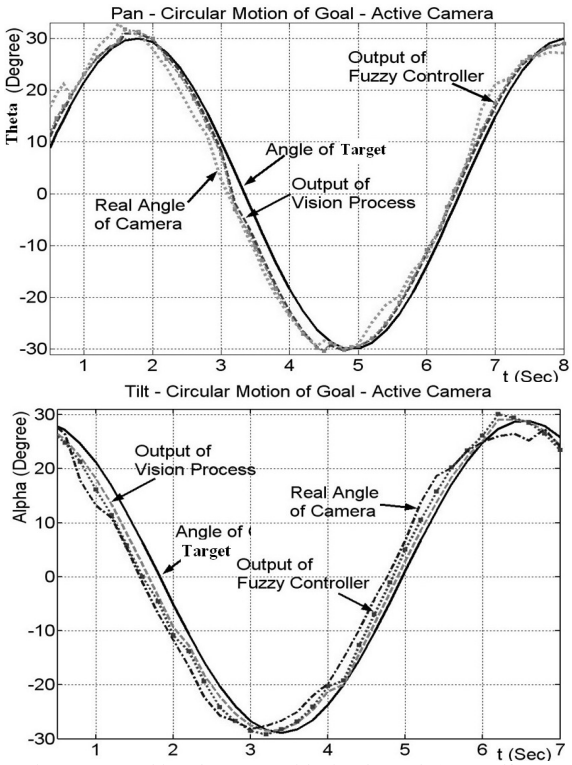

Figure11. Tracking the target with circular path (w=1rad/sec).

In the second experiment, a person with a constant velocity, moves around the camera and camera track his face. Figure 12, 13 shows the results of this experiment in the same way.

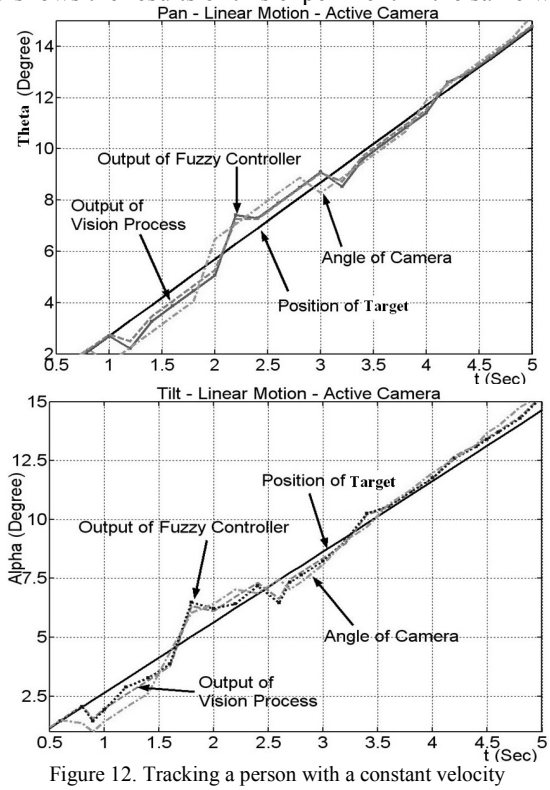

Figure 12. Tracking a person with a constant velocity

Figure13. The pictures show the operation of the vision processor box too

Figure 14 Shows the result of the tracking the faraway targets with high velocity

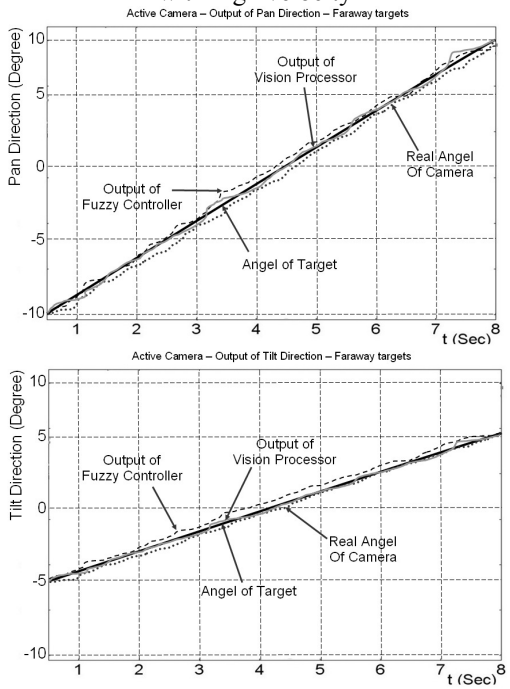

Figure 14. Tracking the faraway targets with high velocity

I. CONCLUSION

A new combination of vision and control have been presented with a new algorithm allowing a robust and accurate detection of moving objects for a small cost in memory consumption and computational complexity that allow us to use ordinary computers and cameras instead of expensive and high performance computers and vision facilities. Although the set faces to delays especially in vision process box and connections (LAN), the IFC usually solves delay problems. In addition, considering the operation of the normal mean-shift algorithm and a conventional PID controller shows that the IFC has better performance. In fact, using the IFC helps the active tracker to miss targets less than the active cameras which use the normal mean-shift algorithm and a conventional PID controller. Undoubtedly, the set can improve by using of more fuzzy rules sets for more different situations and objects.

REFERENCES

[1] F. Xu, J. Cheng, C. Wang, "Real Time Face Tracking Using Particle Filtering and Mean Shift", IEEE, International Conference on Automation and Logistics, ISBN: 978-1-4244-2502-0, pages: 2252 - 2255, 2008

[2] J. Gao, A. Kosaka, A. Kak, "A multi-Kalman filtering approach for video tracking of human-delineated objects in cluttered environments", Robot Vision Lab, Purdue University, Computer Vision and Image Understanding, Volume 102, Issue 3, Page 259-264, 2006

[3] A. Birchfield, S.T. Rangarajan, "Spatiograms versus histograms for region-based tracking", IEEE conference on computer vision and pattern recognition (CVPR), pages: 1158 –1163, vol. 2, 2005

[4] D. Comaniciu,V. Ramesh,"Kernel-based object tracking", IEEE Transactions on Pattern Analysis and Machine Intelligence, VOL. 25, NO. 5, Pages: 564-577, 2003

[5] F. Gustafsson, F. Gunnarsson, N. Bergman, U. Forssell, J. Jansson, R. Karlsson and P.J. Nordlund, "Particle Filters for Positioning Navigation and Tracking", IEEE Transactions On Signal Processing, pages: 494 – 499, 2002

[6] Z. Wang, X. Yang, S. Yu, "CamShift guided particle filter for visual tracking", Institute of Image Communication and Information Processing", Shanghai Jiao Tong University, Pattern Recognition Letters Journal, Elsevier, Volume 30 , Issue 4, ,2008

[7] K. Tanaka, H. Wang, "Fuzzy Control Systems Design and Analysis: A Linear Matrix Inequality Approach", John Wiley & Sons, 2001

[8] A. Mustafa, M. Asadi Shirzi, M.R. Hairi Yazdi, "Active Tracking Using Kernel-Based Vision Processor and Robust Fuzzy Control", Advances in Intelligent Systems Research, Vol. 3, Page 273-280, JCIS 2006

[9] N. Song Peng , J. Yang, Z. Liu , "Mean shift blob tracking with kernel histogram filtering and hypothesis testing", Pattern Recognition Letters, Elsevier, Volume 26, Issue 5 , Pages 605-614 , 2005

[10] H. YungCheng , J.N. Hwang, "Adaptive particle sampling and adaptive appearance for multiple video object tracking", Volume 89 Issue 9, Signal Processing Journal, Elsevier, 2009

[11] J.E. Naranjo, C. González, R. García, T. de Pedro, "Adaptive Fuzzy Control for Inter-Vehicle Gap Keeping" ,IEEE, intelligent transaction systems, Volume 4, No. 3, Pages 132-142, 2003

[12] Jan Jantzen, "A Robustness Study of Fuzzy Control Rules", Technical University of Denmark ,Department of Automation, pages31–36, 1998

[13] Massa, Ruffin, Tison, Lallemand, "A complete method for efficient fuzzy modal analysis", Journal of Sound and Vibration, Elsevier, Volume 309, Issues 1-2, Pages 63-85, 2008

[14] T. Hayakawaa, H. Ishii b, K. Tsumurac, "Adaptive quantized control for nonlinear uncertain systems", Systems & Control Letters, Elsevier, Volume 58, Pages 625-632, 2009

[15] K. Chougdali, M. Jedra, N. Zahid, "Kernel relevance weighted discriminant analysis for face recognition", Pattern Analysis & Applications , 2010

2011 IEEE International Conference on Fuzzy Systems
June 27-30, 2011, Taipei, Taiwan

An Interval Type 2 Fuzzy Approach to Multilevel Image Segmentation

Debanga Raj Neog*
Indian Institute of Technology
Guwahati, India
debanga@iitg.ernet.in

Muhammad Amjad Raza
Hanyang University
Korea
amjadraza@fuzzy.hanyang.ac.kr

Frank Chung-Hoon Rhee
Hanyang University
Korea
frhee@fuzzy.hanyang.ac.kr

***Abstract*—In this paper, an interval type 2 (IT2) fuzzy entropy based approach is used to compute optimum thresholds for multistage gray scale image segmentation. By finding the maximum IT2 fuzzy entropy of the gray scale image, the optimum thresholds are computed. A termination criterion for multistage segmentation is also proposed based on the range of computed entropy values of the images. Several experimental results are shown to demonstrate the performance of our proposed algorithm which outperforms type 1 (T1) fuzzy based methods.**

Keywords—Interval type2 (IT2) fuzzy sets, Footprint of uncertainty (FOU), Fuzzy membership function, Ultrafuzziness.

I. INTRODUCTION

Finding the optimal threshold is a critical step in gray scale image segmentation. Gray scale image segmentation is based on the pixel properties of the image and determining the appropriate threshold can be very challenging. In literature there exist several threshold based image segmentation techniques. According to the information exploitation, threshold techniques have been categorized as histogram shape based, clustering based, entropy based, object attribute based and spatial based [1]-[8].

Several fuzzy based methods have also been proposed. Those methods include fuzzy clustering for finding the optimal threshold and maximum entropy gray level computation to distinguish between the foreground and background [4], [9], [10]. Optimal threshold for separation of the background and object exists at the deepest valley of bimodal histogram of the image [11]. However, it is difficult to obtain optimal threshold when distribution of histogram is complex. To cope with this problem, fuzzy entropy was proposed to quantify the vagueness in images [12]. Huang *et al*. introduced a fuzzy approach to the Shannon entropy and concluded that the gray level point where the fuzziness is minimum; is the optimal threshold [13]. Information theoretic approach was used to maximize (minimize) the image information on basis of fuzziness or crispness [14]. This approach is very simple and commonly used for finding the optimal threshold. Rhee *et al*. proposed a numerical method to quickly locate the optimal threshold using fuzzy sets [15].

Type 2 fuzzy sets have been shown to better handle uncertainties than conventional type 1 fuzzy sets [16]. The ability of type 2 fuzzy sets to represent and manage the uncertainty that exists in a fuzzy set allows us to model various uncertainties, which cannot be appropriately managed by type 1 fuzzy sets [17]. Tizhoosh introduced a threshold technique based on type 2 fuzzy sets (i.e., ultrafuzzy sets) [18]. In this paper, we address two problems associated with automatic multilevel image segmentation of gray level images. The first problem is to calculate optimal threshold for segmentation. In doing so, we propose a new segmentation method that incorporates interval type 2 (IT2) fuzzy sets. This is achieved by modeling Gaussian interval type 2 (IT2) fuzzy membership functions using embedded type2 fuzziness [19]. Our goal is to decide whether a pixel belongs to the background or foreground. In this case, measurements of uncertainty can be considered as entropy, index of fuzziness and index of non fuzziness. We obtain the optimal threshold by maximizing the amount of ultrafuzziness. A membership value is then assigned to each pixel depending on its distance from the background and foreground center using some parameterized type 1 fuzzy membership function. Based on the membership values we find the threshold by maximizing the index of ultrafuzziness. The second one is to determine the optimum number of thresholds for an image in the segmentation process. Theoretically, there are as many objects in a gray level image as there are gray levels present in the image, but practically it is very difficult to segment it based on the relevant information present. Furthermore, we propose a termination criterion, which calculates and segments objects based on image entropy information. The concept of this termination criterion is based on segmenting the image in different levels using a tree structure and there is no restriction on the number of objects to be segmented.

The remainder of this paper is organized as follows. Section II contains the brief background of IT2 fuzzy sets and membership function generation used in thresholding. In Section III, our proposed segmentation algorithm and termination criterion are discussed. In Section IV, experimental results and discussion for bimodal and multi stage image segmentation are presented to show the effectiveness of our proposed method. Finally, Section V gives the conclusions.

II. BACKGROUND

A. Interval Type 2 Fuzzy sets (IT2 FS)

When we represent uncertainty for a fuzzy set with an interval type 2 fuzzy set, the primary membership J_x' of a

*Worked at Hanyang University as Research Intern

978-1-4244-7316-8/11/$26.00 ©2011 IEEE

sample x' can be represented as a membership interval with all secondary grades of the primary memberships equaling to one [20]. We define this interval as the footprint of uncertainty (FOU).

An interval type 2 fuzzy set $\tilde{\mathbf{A}}$ can be represented as

$$\tilde{\mathbf{A}} = \left\{ \left((\mathbf{x}, u), \mu_{\tilde{\mathbf{A}}}(\mathbf{x}, u) \right) \mid \forall \mathbf{x} \in \mathbf{A}, \forall u \in J_{\mathbf{x}} \subseteq [0,1], \mu_{\tilde{\mathbf{A}}}(\mathbf{x}, u) = 1 \right\} \quad (1)$$

Fig. 1 illustrates an example of an interval type 2 fuzzy set where the gray shaded region indicates the FOU. In the figure, the membership value for a 1-dimensional sample x' is represented by the interval between upper ($\overline{\mu}_{\tilde{A}}(x')$) and lower ($\underline{\mu}_{\tilde{A}}(x')$) membership [20]. Therefore, each x' has a primary membership interval as

$$J_{x'} = \left[\underline{\mu}_{\tilde{A}}(x'), \overline{\mu}_{\tilde{A}}(x') \right], \quad (2)$$

and the vertical slice of x' is shown in Fig. 1(b), where the secondary grade for the primary membership of each x' equals one, according to the property of interval type-2 fuzzy sets.

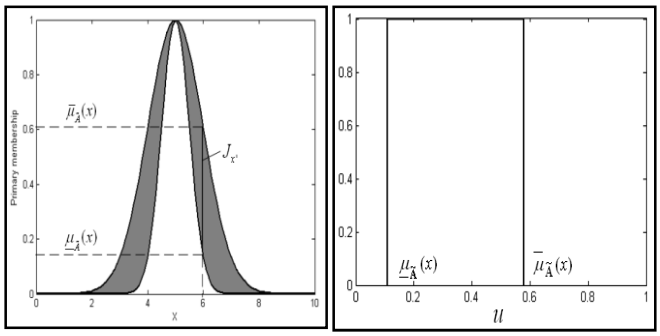

(a) (b)

Fig. 1. Illustration of an interval type-2 fuzzy set: (a) interval type-2 fuzzy set (b) vertical slice on x'.

B. Membership Function Generation

Our main concern of this research is to see whether IT2 fuzzy sets can properly handle uncertainties in comparison to T1 and non fuzzy techniques. Fuzziness depends upon the choice of membership function. Fig. 2 shows examples of membership functions used for measurement of fuzziness in an image. In this paper, we consider Gaussian membership functions (see Fig. 3) and model IT2 membership functions using linguistic hedges (see Fig. 4). Existing methods also used linguistic hedges to create IT2 fuzzy membership functions [21], [22]. The linguistic hedges were obtained by conducting experiments to create the FOU, where the values of linguistic hedges depend on statistical properties of the histogram. It is observed that different membership functions exhibit different segmentation results depending upon the gray level distribution of an image.

Let I denotes an image of size $M \times N$ having L numbers of gray levels and $i(x,y)$ is the gray level of pixel at (x,y) in I. Let $\mu_I(i(x,y))$ denotes the membership value of pixel $i(x,y)$ in image I, then we can define fuzzy image set as

$$I = \{ i(x,y), \mu_I(i(x,y)) \}, \quad (3)$$

where $0 \le \mu_I(i(x,y)) \le 1, \quad x = 0,...,M-1$ and $y = 0,...,N-1$.

Let $h(g)$ denotes the histogram of an image I. For a given threshold value T, the average levels (center) of the background and object, represented by μ_0 and μ_1, respectively, can be calculated by (4) and (5).

$$\mu_0 = \sum_{g=0}^{T} g\,h(g) \Big/ \sum_{g=0}^{T} h(g) \quad \text{if} \quad i(x,y) \le T \quad (4)$$

and

$$\mu_1 = \sum_{g=T+1}^{L-1} g\,h(g) \Big/ \sum_{g=T+1}^{L-1} h(g) \quad \text{if} \quad i(x,y) > T, \quad (5)$$

The following definitions of fuzziness (entropy) were used to construct type 1 and type 2 fuzzy membership functions [19].

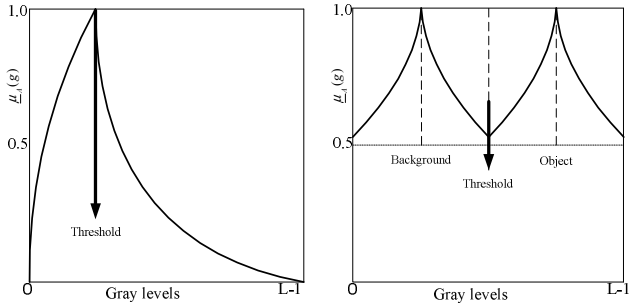

(a) (b)

Fig.2. Two types of membership functions (a) proposed by Tizhoosh .(b) Proposed by Huang .

Definition 1: A general fuzziness measure of a type 1 fuzzy set I, $f(I)$, can be defined as

$$f(I) = k\left(\sum_{i=1}^{N} q(\mu_I(i(x,y)))\right), \quad (6)$$

where k is monotonically increasing function from R^+ to R^+ and q:[0,1]→ R^+ is a function associated with each $i(x,y)$. N is the total number of elements in I. Additionally,

(1) $q(0) = q(1) = 0$;
(2) $q(0.5)$ is a unique maximum of q;
(3) q must be monotonically increasing on [0,0.5] and monotonically decreasing on [0.5,1].

Every pixel in input image should belong to either background or object to some degree of membership depending upon the gray level values.

The type 1 fuzzy membership function $\mu_l(g)$, g is the gray level, is defined as

$$\mu_I(g)=\begin{cases}1.5-\dfrac{1}{1+e^{-\frac{1}{2}\left(\frac{g-\mu_0}{\sigma}\right)^2}} & \text{if } g_{\min}\le g\le T\\ 1.5-\dfrac{1}{1+e^{-\frac{1}{2}\left(\frac{g-\mu_1}{\sigma}\right)^2}} & \text{if } g_{\max}\ge g> T,\\ 0 & \text{otherwise}\end{cases} \tag{7}$$

where $\sigma = |g_{max}-g_{min}|/2\log(1/TOL)$ is the standard deviation and TOL is suitably selected as 0.01. The minimum and maximum occurring non zero gray levels in an image I are denoted as g_{min} and g_{max}, respectively.

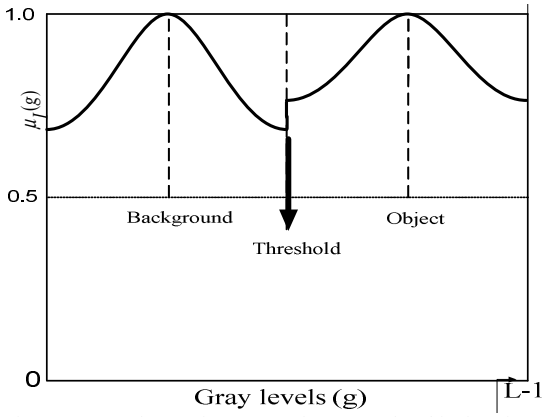

Fig.3. Proposed Gaussian Type 1 fuzzy membership function.

Definition 2: The fuzziness definition of an IT2 fuzzy set $F_{\tilde{A}}$ is the union of the fuzziness of all its embedded type 1 fuzzy sets $\mu_I(g)$, i.e.

$$F_{\tilde{A}} \equiv \bigcup_{\forall \mu_I(g)} f(\mu_i(g)) = [f_l(\tilde{A}), f_r(\tilde{A})], \tag{8}$$

where $f_l(\tilde{A})$ and $f_r(\tilde{A})$ are the minimum and maximum of fuzziness for all $\mu_I(g)$, i.e.

$$f_l(\tilde{A}) = \min_{\forall \mu_I(g)} f(\mu_I(g)) \tag{9}$$

and

$$f_r(\tilde{A}) = \max_{\forall \mu_I(g)} f(\mu_I(g)), \tag{10}$$

Here we provide a simple proof to show that our proposed IT2 MF shown in Fig. 4 follows the above definition. For that we need to show that

$$f_l(\tilde{A}) = \bar{\mu}(g) \tag{11}$$

and

$$f_r(\tilde{A}) = \begin{cases}\underline{\mu}(g); 0.5 \notin [\underline{\mu}(g), \bar{\mu}(g)]\\ 0.5 \text{ otherwise}\end{cases}, \tag{12}$$

Proof: According to definition 1, the fuzziness of a particular gray level g is determined by its deviation from 0.5, the value where it is maximally fuzzy. Membership values that approach 0 or 1 become less fuzzy. The minimum of fuzziness $f_l(\tilde{A})$ is achieved when every value $\mu_I(g)$ is as far away as possible from 0.5 and is satisfied by $\bar{\mu}(g)$ for all gray levels in (11). Similarly, $f_r(\tilde{A})$ is achieved when every $\mu_I(g)$ is as close as possible to 0.5 and is satisfied by $\underline{\mu}(g)$ for all gray levels. When $0.5 \in [\underline{\mu}(g), \bar{\mu}(g)]$, we set $f_r(\tilde{A}) = 0.5$. Therefore, (12) is satisfied.

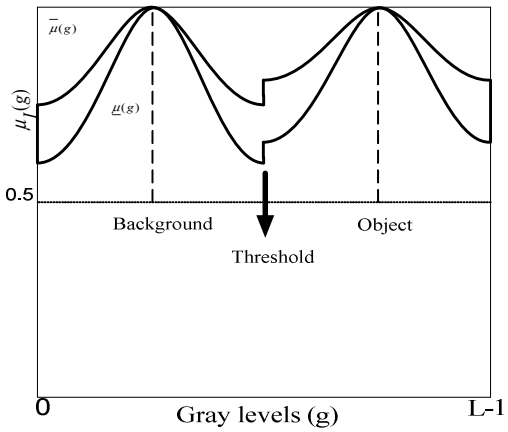

Fig. 4. Modified IT2 modeling of proposed membership function

The upper and lower membership degrees $\bar{\mu}(g)$ and $\underline{\mu}(g)$ can be obtained by linguistic hedges such as deaccentuation and accentuation

$$\bar{\mu}(g) = [\bar{\mu}(g)]^{1/\alpha} \tag{13}$$

And

$$\underline{\mu}(g) = [\underline{\mu}(g)]^{\alpha}, \tag{14}$$

where $\alpha \in (1,2]$[18].

A measure for IT2 ultrafuzziness can be modified for an image as follows

$$\tilde{\gamma}(\tilde{A}) = \frac{1}{MN}\sum_{g=0}^{L-1} h(g)[\bar{\mu}(g) - \underline{\mu}(g)], \tag{15}$$

where h(g) is the histogram of image I [23].

The measure of ultrafuzziness $\tilde{\gamma}(\tilde{A})$ should satisfy following four conditions [24]

(1) *Minimum ultrafuzziness:* $\tilde{\gamma}(\tilde{A}) = 0$ if $\mu_I(g)$ is a type 1 fuzzy set $\forall g \in X\ \bar{\mu}(g) = \underline{\mu}(g)$

(2) *Equal ultrafuzziness:* $\tilde{\gamma}(\tilde{A}) = \tilde{\gamma}(\tilde{\tilde{A}})$

(3) *Reduced ultrafuzziness:* $\tilde{\gamma}(\tilde{A}) \ge \tilde{\gamma}(\tilde{A}')$ if $\tilde{A}'$ is a crisper version of $\tilde{A}$

(4) *Maximum ultrafuzziness:* $\tilde{\gamma}(\tilde{A}) = 1$ if
$\forall g \in X \ \bar{\mu}(g) - \underline{\mu}(g) = 1$

When the ultrafuzziness measure for each gray level is computed, these results in a bell shaped curve [15]. We now need to find the gray level that corresponds to the maximum ultrafuzziness (i.e., optimum gray level g_{opt}).

III. PROPOSED ALGORITHM

Following are the steps involved to describe our proposed multilevel algorithm that includes a termination criterion.

Step 1 *Compute Ultrafuzziness*
Compute IT2 fuzzy entropy of input gray scale image at each gray level using (15) as shown in Fig. 5.

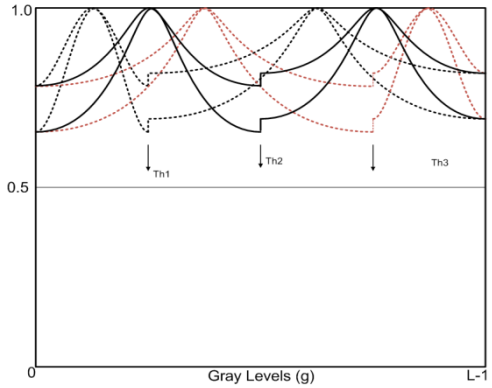

Fig. 5. IT2 MF shifted over gray level histogram range to find maximum fuzziness gray level point. (Shown for proposed Gaussian Membership Function)

Step 2 *Selecting Optimum Threshold*
Compute optimum threshold gray level g_{opt} at which the ultrafuzziness is maximized by selecting the gray level corresponding to the minimum of the computed entropy curve in the interval.

Step 3 *Extensions to Multilevel Thresholding*:
Background and foreground threshold images are obtained based on g_{opt} obtained in Step 2. The foreground may have more than one significant objects and an iterative segmentation approach can be applied to separate foreground into two or more regions by computing another g_{opt} (as in Step 2) in the sections of histogram, obtained after each level of segmentation. For determining the number of times we need to compute threshold for a given image, we use a termination criterion based on the shape of entropy curve.

Step 4 *Termination Criterion*
The termination criterion used in our experiments is obtained from the entropy values computed for a particular section of the histogram during the multilevel threshold procedure. The experiments on the synthetic images show that the thresholded regions of the image have reduced the ultrafuzziness. Since the entropy curve shows the overall ultrafuzziness measure trend for the entire image or sub images, we introduce the termination criterion factor τ as

$$\tau = \frac{\Delta E^{(i)}}{\Psi^{(i)}} \times 255, \qquad (16)$$

where $\Delta E^{(i)}$ denotes the total number of pixels and $\Psi^{(i)} = E_{\max} - E_{\min}$ corresponds to the section of the histogram obtained at the i^{th} level of thresholding.

We start our termination algorithm by segmenting the original image and observing the τ-values for the section of original histogram that is obtained at each level of thresholding. For each level, we compare the current τ-value with the τ-value of the previous level. If we observe saturation in the τ-value in a particular node of a segmenting tree as shown in Fig.6, we stop branching from that particular node. This process is continued until we reach a level where all the possible paths become saturated.

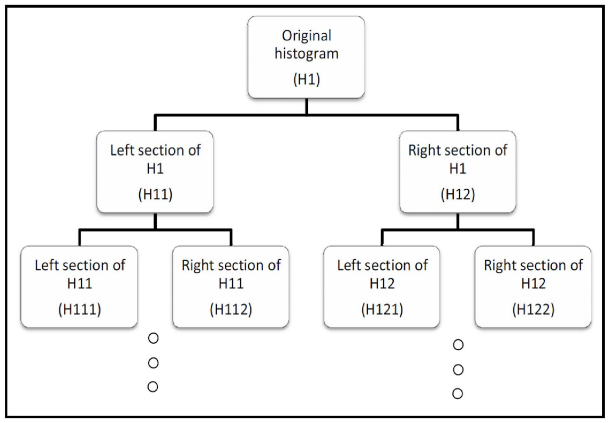

Fig.6. The numbering nomenclature that is used to denote different sections of the image histogram constructed as a tree.

Summary of termination criterion
Let H denotes the histogram of the input image I.
Step 1 Perform the first level segmentation with g_{opt}.
Step 2 Calculate τ as defined in (16) for the first level, based on entropy values.
Step 3 Create right and left histogram sections H_R and H_L about g_{opt} of image histogram H.
Step 4 Calculate τ_r and τ_l , where τ_r and τ_l are τ-values for right and left sections of histogram H.
Step 5 Compare τ_r and τ_l for the i^{th} level segmentation with τ-value of parent histogram H for the $(i-1)^{th}$ threshold.
Step 6 **IF** abs(τ_r-τ)< *TOL* **THEN** Stop thresholding H_R
ELSE Assign H_R as H and return to Step 3
IF abs(τ_l-τ)<*TOL* **THEN** Stop thresholding H_L
ELSE Assign H_R as H and return to Step 3

The above procedure automatically calculates the number of significant objects present in the input image. The tolerance value considered for our experiments is 0.01.

IV. EXPERIMENTAL RESULTS

In this section, experimental results are presented to illustrate the effectiveness of our proposed algorithm. We have

used Gaussian Membership function as our choice of parameterized function as described in Section II.B. The input images used in our experiments are shown in Fig.7.

The results of IT2 fuzzy based segmentation are presented in Fig. 8, 9, and 10. Segmented regions are shown with different gray levels. Performance comparison of type 1 and IT2 approaches have been performed by using ground truth image (mask). In general, to evaluate and compare image segmentation algorithms, masks are visually generated by different subjects as in [18] and [25]. Our masks follow this method and have already been used in [26]. A measure of performance η can be used to compare the results for a particular threshold stage as

$$\eta = 100 \times \frac{|M_1 \cap I_1| + \ldots + |M_n \cap I_n|}{|I_1| + \ldots + |I_n|}, \tag{17}$$

where, I_i and M_i denote the i^{th} class pixels in the original image and mask, respectively, after n multilevel threshold levels.

Fig. 8 shows that the g_{opt} obtained using the IT2 approach gives us better results than the T1 approach. In Table I optimal threshold g_{opt} for type 1 and IT2 fuzzy entropies for some images along with comparison of performances in percentage are listed. Table II shows multilevel threshold results in terms of g_{opt}. The number of threshold levels is determined by the proposed termination criterion. In Table V, the comparison of results obtained by using two different membership functions is shown.

It is to be noted that our proposed algorithm is different from Tizhoosh algorithm in respect to the MF generation method. We have compared our algorithm results with Tizhoosh results and concluded that our proposed MF gives satisfactory results. The second major contribution is automatic selection of number of thresholds based on the information of the IT2 fuzziness of the given image.

Results of Termination Criterion:

Experiments on a synthetic image

Fig.11 shows a synthetically generated image. The entropy curves are also shown along with the segmented images. We conducted experiments on the synthetic image to illustrate our termination criterion, which is based on the normalized range of entropy of the image. The normalization is performed with respect to the number of pixels present in the region of image that corresponds to the subinterval of interest in the histogram.

From Table III, we can observe that the τ-value decreases as the information in the subinterval decreases. We can utilize this information to determine the termination point of the segmentation process with the optimum threshold. We normalize with respect to the number of pixels since it performs better than normalizing with the gray levels. We define the images produced after 3 levels of segmentation in all possible ways, as shown in Fig.11. The experiments performed using synthetic image show that the segmentation steps that should be taken on the basis of above criterion are: 1, 2 and 5 as shown in Table VI.

The results of the termination criterion for the s2 real image are presented in Table IV and we can observe the validity of our termination criterion.

To calculate the efficiency of our multilevel proposed scheme we have calculated the recognition rate based on the masks shown in Fig.12. For this, Gaussian MF and Tizhoosh's MF using linguistic hedges are compared. The results are presented in Table V. The results show that using linguistic hedges from the histograms give desirable results.

Fig. 7. Input images used for experimental results- row1 from left to right block, table, s5; row2 left to right London, s2, s3; row3 from left to right cameraman, Lena and wolf; row4 is baseball.

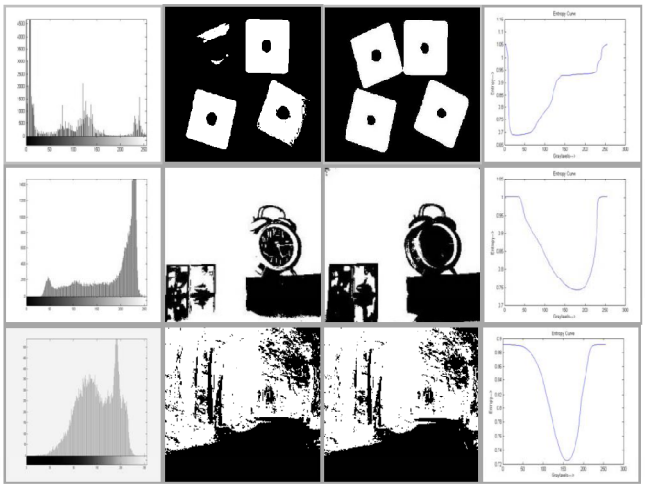

(a) (b) (c) (d)

Fig. 8.Segmentation results of images block, table, and s5 showing row wise left to right column (a) shows histograms (b) shows T1 result (c) shows IT2 result and (d) shows IT2 entropy curve.

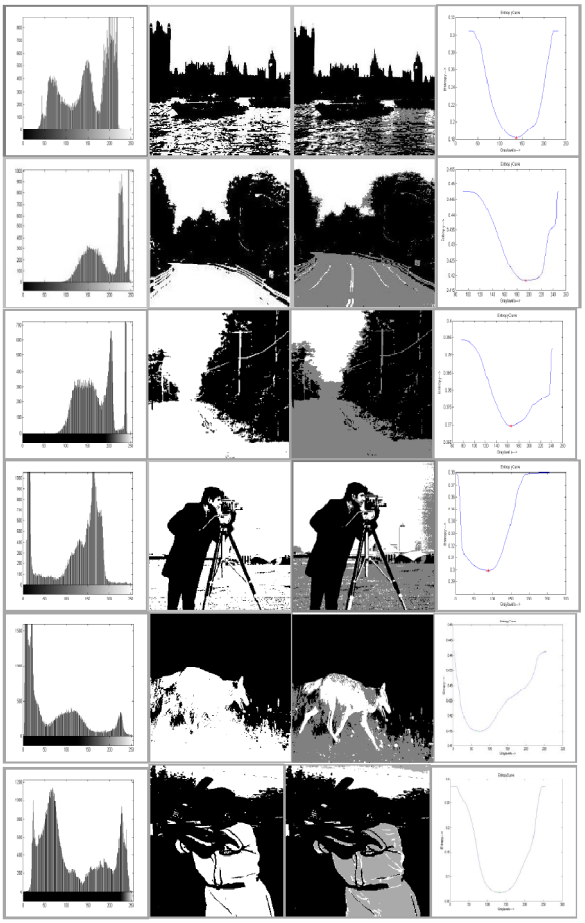

(a) (b) (c) (d)

Fig. 9. IT2 based two stage thresholding of images London, s2, s3, cameraman, wolf, and baseball (top to bottom) columns showing (a) input image histogram, (b) stage1thresholding, (c) stage2thresholding, and (d) IT2 entropy curve.

(a) (b) (c)

Fig. 10. IT2 based five stage thresholding for Lena from left to right column showing (a) input image (b) segmented image using proposed method and (c) segmented image by S. Arora et al. [27]

TABLE I
PERFORMANCE MEASURE COMPARISON OF T1 AND IT2 FUZZINESS

Image	T1		IT2	
	g_{opt}	*% performance*	g_{opt}	*% performance*
Block	110	97.97	50	99.42
Table	161	89.33	182	94.34
s5	154	79.80	159	82.76

TABLE II
OPTIMAL THRESHOLD IN MULTILEVEL IMAGE

Images g_{opt}	London	s2	s3	Camera man	Lena	Wolf	Baseball
level 1	141	194	167	59	112	71	137
level 2	158	235	214	147	158	162	197
level 3	-	-	-	-	186	-	-

TABLE III
τ-VALUES NORMALIZED BY NUMBER OF PIXELS FOR SYNTHETIC IMAGE (TABLE FOLLOWS THE TREE DIAGRAM SHOWN IN FIG.6)

Levels								
Level 1	11.7							
Level 2	5.4				7.7			
Level 3	5.2		1.7		2.4		1.9	
Level 4	5.1	1	1.4	1.2	1.2	1.7	1.9	0.3

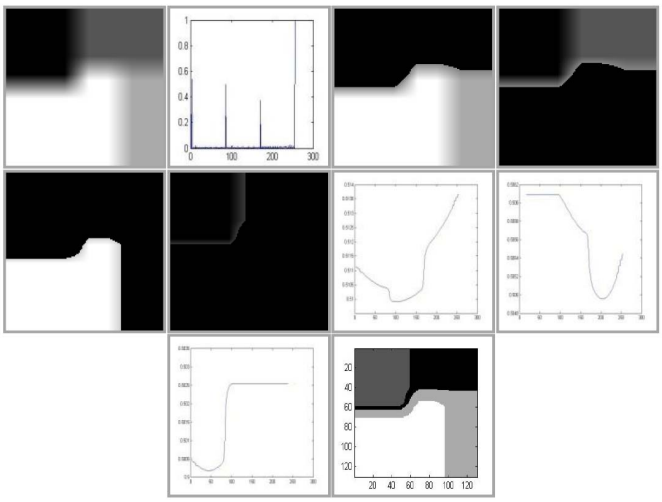

Fig. 11. IT2 based two stage thresholding for a synthetic image showing (a) input synthetic image (b) histogram of input image (c) stage1 thresholding (showing right histogram region) (d) stage1 thresholding (showing left histogram region) (e)stage 2 thresholding (right histogram region) (f) stage 2 thresholding (left histogram region) (g) entropy curve for stage 1 thresholding (h) entropy curve for stage 2 thresholding (right histogram) (i) entropy curve for stage 2 thresholding (left histogram) (j) overall segmented image.

TABLE IV
τ-VALUES NORMALIZED BY NUMBER OF PIXELS FOR S2 REAL IMAGE WITH SEGMENTATION LEVELS

Level	H111	H11	H112	H1	H121	H12	H122
Level 1	12.23						
Level 2	11.64				1.06		
Level 3	5.96		1.59		1.05		0.92

TABLE V
TABLE SHOWING THE CLASSIFICATION RATE COMPARISON OF PROPOSED GUASSIAN MF AND TIZHOOSH MF

Method	S2 Image	S3 Image
Proposed Gaussian MF	93.5 %	92.7 %
Tizhoosh MF	93.0 %	89.6 %

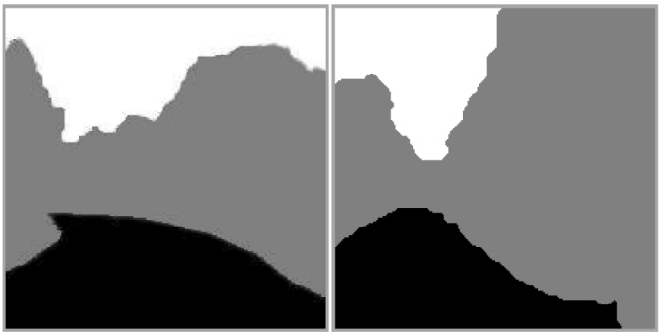

(a) (b)

Fig. 12. Shows masks used to calculate recognition rate to compare our proposed hedge based MF with Tizhoosh MF. (a) Mask for input image s2 (b) mask for input image s3.

TABLE VI
DIFFERENT POSSIBLE COMBINATIONS OF SEGMENTED PARTS OF AN IMAGE

Step No.	Combinations
1	Original Image H1
2	H11 &H12
3	H111 &H112 &H12
4	H11 &H121 &H122
5	H111 &H112 &H121 &H122
6	H1111 &H1112 &H121 &H122
7	H111 &H1121 &H1122 &H121 &H122
8	H111 &H112 &H1211 &H1212 &H122
9	H111 &H112 &H121 &H1221 &H1222

V. CONLUSION

We have successfully implemented IT2 fuzzy entropy based image segmentation by incorporating Gaussian membership functions. Our proposed algorithm performs multistage image segmentation successfully by using a termination criterion, which is based on the range of entropy values for a particular image and its thresholded sub-images. The experimental results show that the termination criterion along with Gaussian MF can be effectively used for thresholding of gray scale images with an improved recognition rate. Our future work is focused on a fast and more robust method. Moreover we are currently working on computing the value of linguistic hedges automatically based on the statistical properties of the image histogram.

REFERENCES

[1] M. Sezgin and B. Sankur, "Survey over image thresholding techniques and quantitative performance evaluation," *Journal of Electronic Imaging*, vol. 13, no. 1, pp. 146-165, Jan. 2004.

[2] A. Rosenfeld and P. De La Torre, ''Histogram concavity analysis as an aid in threshold selection," *IEEE Transactions on Systems, Man, and Cybernetics*, vol. SMC-13, pp.231–235, 1983.

[3] M. Sezan, "A peak detection algorithm and its application to histogram-based image data reduction," *Computer Vision, Graphics, and Image Processing*, vol. 49, no 1, pp. 36-51, 1990.

[4] N. Ramesh, J. H Yoo, and I. K. Sethi, "Thresholding based on histogram approximation," *IEE Proc. Vision, Image and Signal Processing,* vol. 142, no. 5, pp. 271–279, 1995.

[5] T. W. Ridler and S. Calvard, "Picture thresholding using an iterative selection method," *IEEE Transactions on Systems, Man, and Cybernetics*, vol. SMC-8, no. 8, pp. 630–632, 1978.

[6] N. Otsu, "A threshold selection method from gray-level histograms," *IEEE Transactions on Systems, Man, and Cybernetics,* vol. SMC-9, no. 1, pp. 62–66, 1979.

[7] D. Lloyd, "Automatic target classification using moment invariant of image shapes," *Technical Report, RAE IDN AW126*, Farnborough, UK Dec. 1985.

[8] J. Kittler and J. Illingworth, "On threshold selection using clustering criteria," *IEEE Transactions on Systems, Man, and Cybernetics*, vol. SMC-15, no. 5, pp. 652–654, 1985.

[9] C. Jawahar, P. Biswas, and A. Ray, "Investigations on fuzzy thresholding based on fuzzy clustering," *Pattern Recognition,* vol. 30, no. 10, pp. 1605–1613, 1997.

[10] J. Kapur, P. Sahoo, and A. Wong, "A new method for gray-level picture thresholding using the entropy of the histogram," *Computer Vision, Graphics, and Image Processing*, vol. 29, no 3, pp. 273-285, 1985.

[11] R. Gonzalez and R. Woods, "Digital Image Processing," Addison-Wesley Publishing Co. Inc., 1993.

[12] T. Pun, "A new method for gray-level picture thresholding using the entropy of the histogram," *Signal Processing*, vol. 2, no 3, pp. 223-237, 1980.

[13] L. Huang and M. Wang, "Image thresholding by minimizing the measures of fuzziness," *Pattern Recognition*, vol. 28, no. 1, pp. 41-51, 1995.

[14] S. Zenzo, L. Cinque, and S. Levialdi, "Image thresholding using fuzzy entropies," *IEEE Transactions on Systems, Man, and Cybernetics*, vol. SMC-28, no. 1, pp. 15-23, 1998.

[15] F. Rhee and Y. Shin, "A fast numerical method for finding Optimal threshold for image segmentation," *IEEE International Conference on Fuzzy systems*, vol. 2, pp. 984-989, 2003.

[16] J. Mendel, "Type-2 Fuzzy Sets: Some Questions and Answers," *IEEE Neural Networks Society Newsletter*, vol. 1, pp. 10-13, August 2003.

[17] F. Rhee, "Uncertain fuzzy clustering: insights and recommendations," *IEEE Computational Intelligence Magazine,* vol. 2, no. 1, Feb. 2007.

[18] H. Tizhoosh, "Image thresholding using type II fuzzy sets," *Pattern Recognition*, vol. 38, no. 12, pp. 2363-2372, Dec. 2005.

[19] D. Wu and J. Mendel, "Uncertainty measures for interval type-2 fuzzy sets," *Information Sciences*, vol. 177, no. 23, pp. 5378-5393, Dec. 2007.

[20] J. Mendel, "Uncertain Rule-Based Fuzzy Logic Systems: Introduction and New Directions," Prentice Hall, 2001.

[21] J. Mendel and H. Wu, "Type-2 fuzzistics for nonsymmetric interval type-2 fuzzy Sets: forward problems," *IEEE Transactions on Fuzzy Systems*, vol. 15, no. 5, pp. 916-930, Oct. 2007.

[22] B. Choi and F. Rhee, "Interval type-2 fuzzy membership function generation methods for pattern recognition," *Information Sciences*, vol. 179, no. 13, pp. 2102-2122, June 2009.

[23] P. Burillo and H. Bustince, "Entropy on intuitionistic fuzzy sets and on interval-valued fuzzy sets," *Fuzzy Sets and Systems*, vol. 78, no. 3, pp. 305-316, March 1996.

[24] A. Kaufmann, "Introduction to the Theory of Fuzzy Subsets, Fundamental Theoretical Elements," vol. 1, Academic Press, New York, 1975.

[25] S. Alpert, M. Galun, R. Basri, and A. Brandt, "Image segmentation by probabilistic bottom-up aggregation and cue integration," *IEEE Conference on Computer Vision and Pattern Recognition*, pp. 1-8, 2007.

[26] F. Rhee, K. Choi, and B. Choi, "Kernel approach to possibilistic C-means clustering," *International Journal of Intelligent Systems*, vol. 24, no. 3, pp. 272-292, March 2009.

[27] S. Arora, J. Acharya, A. Verma, and P. Panigrahi, "Multilevel thresholding for image segmentation through a fast statistical recursive algorithm," *Pattern Recognition Letters*, vol. 29, no. 2, pp. 119-125, Jan. 2008.

2011 IEEE International Conference on Fuzzy Systems
June 27-30, 2011, Taipei, Taiwan

Navigation System of Mobile Robot in an Uncertain Environment Using Type-2 Fuzzy Modelling

Sittichok Junratanasiri
Computer Engineering Department,
Faculty of Engineering, Chiang Mai University,
Chiang Mai, Thailand
dsi_4@hotmail.com

Sansanee Auephanwiriyakul
Computer Engineering Department,
Faculty of Engineering, Chiang Mai University,
Chiang Mai, Thailand
sansanee@ieee.org

Nipon Theera-Umpon
Electrical Engineering Department,
Faculty of Engineering, Chiang Mai University,
Chiang Mai, Thailand
nipon@ieee.org

***Abstract*—A navigation system of a mobile robot in an uncertain environment is one of a popular research area. There are both static and dynamic obstacles in an uncertain environment. If a robot finds a static obstacle, it can select a safe path very easily. However, a dynamic obstacle can move very randomly in the global map. Hence, in this paper, we propose a navigation system in an uncertain environment focusing on dynamic obstacles for a mobile robot. The future position of a dynamic obstacle is modeled using a fuzzy vector. The dangerous region of that obstacle is then computed. Then the free road candidates are computed based on those dangerous regions found. Then the best free road is selected. Finally, the interval type-2 fuzzy logic system is utilized to compute the velocity and angular velocity of a mobile robot. The experiment results show that our navigation system worked in an uncertain environment, i.e., an environment with an obstacle with stable velocity and angular velocity, an environment with an obstacle with random velocity, and an environment with several obstacles with both condition.**

Keywords-interval type-2 fuzzy logic; uncertain environment; fuzzy collision region;collision prediction, obstacle avoidance

I. INTRODUCTION

One of the popular research areas in robot navigation system is to navigate in an unknown or partially unknown dynamic environment. There are both static and dynamic obstacles with uncertainty in position, velocity and angular speed in the dynamic environment. There are several cause of uncertainty, e.g., limitation of the perception system, an incorrect or incomplete data from sensor, and etc. Usually, the navigation algorithm needs to have abilities to avoid collision with obstacles, to fine free road to the goal, and self-localization. A dynamic obstacle position prediction is needed in obstacle avoidance algorithm. To predict future position of a dynamic obstacle, the estimation of the position and velocity of each object are needed.

There are several research works on modeling the motion of the obstacles and dangerous region with uncertainty using a probabilistic distribution [1 – 3]. Then a collision prediction technique is added to improve local path planning algorithm. However, in [1, 3], only linear velocity obstacles are modeled.

In [4, 5], the potential field method is used for obstacle avoidance in robot navigation. The optimal and minimum occupancy path is generated. In [6], the flexible vector field is used for obstacle avoidance. The path found by [6] is shorter than the one from [4]. However, both navigation methods cannot find a good path if there are dynamic obstacles in the scene. In [7], they use radial-basis-function-neural network to predict the movement of the obstacle. However, the movement of the obstacle has to fall into one of the patterns that the system is trained on.

Type-1 fuzzy logic has been used in robotic navigation and control [2, 4, 8 – 11]. Because the system is able to control nonlinear, ill-defined problem and can make a decision under uncertainty environment. Recently, a type-2 fuzzy logic becomes a popular method in controlling a robot [12 – 14] when the fuzzy membership function is hard to define.

This paper presents an autonomous robot navigation algorithm for a mobile robot working in a dynamic environment. In particular, the velocity, angular velocity and position uncertainties of an obstacle are modeled using fuzzy membership functions. Also, the dangerous region computed from future collision region of each obstacle is modeled using a fuzzy vector. After, all dangerous regions are found, the best path is computed. Then the type-2 fuzzy logic system is used to controlled velocity and angular velocity of a robot.

II. INTERVAL TYPE-2 FUZZY LOGIC SYSTEMS

In interval type-2 fuzzy logic system [15], the crisps inputs are mapped into type-2 fuzzy singleton shown in fig. 1. The upper ($\overline{f}$) and lower ($\underline{f}$) membership function is computed. Suppose there are M rules and there are two inputs and one output for each rule. Each rule is in the form of: "If x_1 is F_1 and x_2 is F_2 then y is G" where F_1, F_2 and G are interval type-2 fuzzy sets in linguistic terms of antecedents and consequent, respectively. The minimum t-norm is used to combine the upper and lower membership values of antecedents as shown in Fig. 2 whereas the maximum t-conorm is utilized to aggregate outputs from all rules that are fired. In order to get crisp output, the type reduction and defuzzification is needed.

978-1-4244-7316-8/11/$26.00 ©2011 IEEE

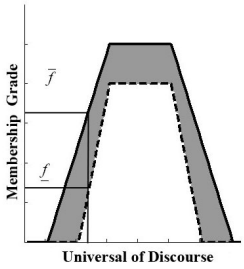

Figure 1. Interval singleton type-2 fuzzy logic system

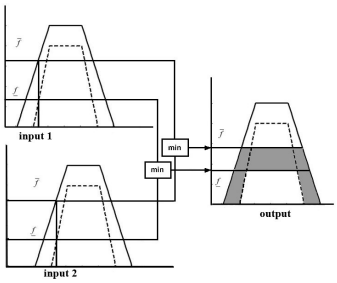

Figure 2. Inputs and antecedent operator for an interval single type-2 fuzzy logic system.

III. MODEL OF UNCERTAINTY ENVIRONMENT

A. Mobile Robot

In this paper we assume that the robot is a circle with center in (x_R, y_R) when the robot axis is (X_R, Y_R) and Y_R is the orientation of the robot. Whereas the counter clockwise is the positive direction and the angle range of this coordinates is [0, 180]. We assume that the robot can see within the range of *vis*.

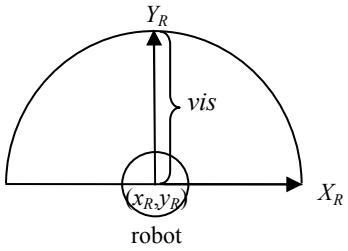

Figure 3. The robot is a circle with centre in (x_R, y_R) and (X_R, Y_R) is Robot axis.

B. Obstacle Modelling

There are both static and dynamic obstacles in an uncertain environment. The mobile robot moves through the environment with its perception setting. In real environment, the position of a static obstacle does not change. We directly use information from the perception system. Hence, the dangerous region in this case is the position of the static obstacle. But dynamic obstacle can change its position with a random move. Therefore, a fuzzy membership function is used to describe the uncertainty in position, velocity, and angular velocity of dynamic obstacles. For simplicity, we assume that the mobile robot can move faster than a dynamic obstacle in this environment. We also assume that the shape of each obstacle is circular. Fig. 4 shows a mobile robot moving in a dynamic environment and a dynamic obstacle *i* is detected by this robot. The dangerous region is the predicted collision region in the future.

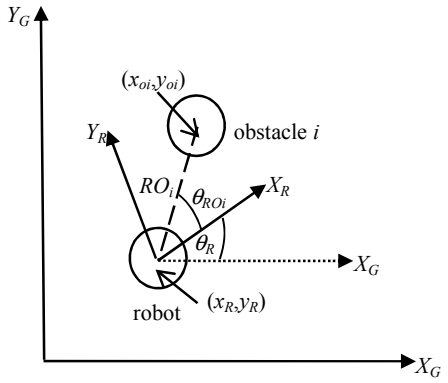

Figure 4. A dynamic obstacle i is detected

To predict a collision region, we need to estimate the position of a dynamic obstacle. Suppose that the current center of the dynamic obstacle *i* is $(xo_i(t_c), yo_i(t_c))$. It is computed based on the global map (X_G, Y_G) at time t_c. The center point can be expressed as:

$$xo_i(t_c) = x_R(t_c) + RO_i \cos(\theta_R(t_c) + \theta_{ROi}(t_c)) \quad (1)$$

$$yo_i(t_c) = y_R(t_c) + RO_i \sin(\theta_R(t_c) + \theta_{ROi}(t_c)) \quad (2)$$

where RO_i denotes the distance between the center of the obstacle *i* and the robot, θ_{ROi} is the relative angle of its center and the robot and $\theta_R(t_c)$ denotes the orientation angle of the robot relative to the global map at time t_c.

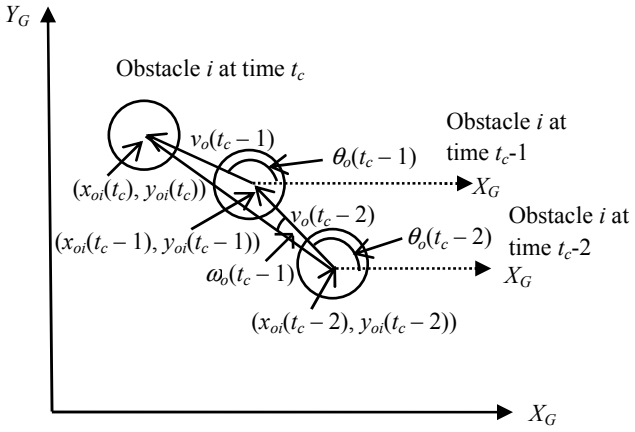

Figure 5. The velocity of obstacle i at time $t_c - 1$ and $t_c - 2$ and angular velocity of obstacle i at time $t_c - 1$

Fig. 5 shows the velocity, angular velocity and angle relative with the global map of a dynamic obstacle *i* at time $t_c - 1$ and $t_c - 2$. If there is an information of the position of a dynamic obstacle at time $t_c - 1$ and t_c, the velocity $v_o(t_c - 1)$ can be calculated. The angular velocity $\omega_o(t_c - 1)$ can be computed if the position of the dynamic obstacle at time $t_c - 2$, $t_c - 1$ and t_c are known.

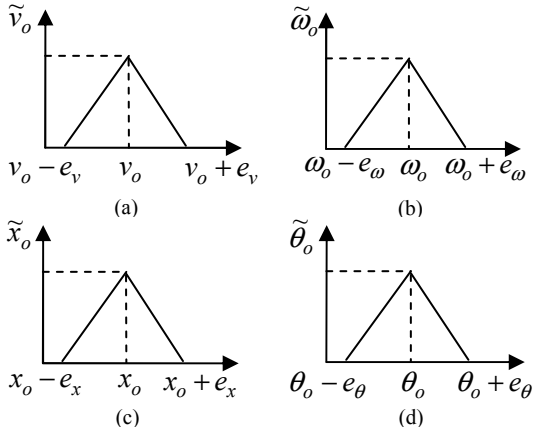

Figure 6. Fuzzy membership function of (a) velocity, (b) angular velocity, (c) position in x or y axis (d) angle relative with global map and

To get the better trend of the direction and magnitude of the velocities, the velocity $v_o(t_c)$ and angular velocity $\omega_o(t_c)$ of dynamic obstacle i are obtained from the calculation of three previous times (t_c-1, t_c-2 and t_c-3), i.e.,

$$v_o(t_c) = \lambda_1 v_o(t_c-1) + \lambda_2 v_o(t_c-2) + \lambda_3 v_o(t_c-3) \quad (3)$$

$$\omega_o(t_c) = \lambda_1 \omega_o(t_c-1) + \lambda_2 \omega_o(t_c-2) + \lambda_3 \omega_o(t_c-3) \quad (4)$$

where λ_1, λ_2 and λ_3 are weight parameters. In the experiment, we set the parameters to 0.5, 0.3 and 0.2 respectively.

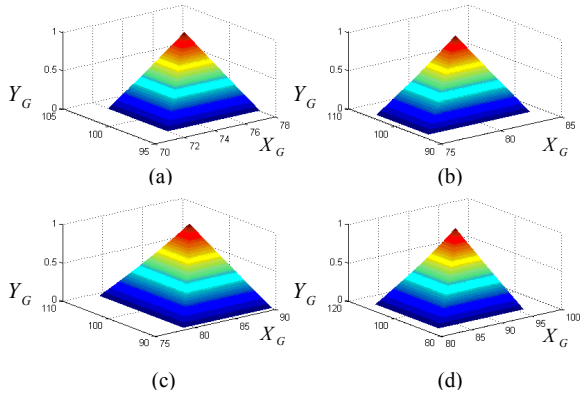

Figure 7. Fuzzy vector ($\tilde{x}_{oi}$, $\tilde{y}_{oi}$) at time (a) t_c+1, (b) t_c+2, (c) t_c+3 and(d) t_c+4

Since there are uncertainty in velocity (v_o) and angular velocity (ω_b) of each dynamic obstacle, we model the uncertainty with triangular fuzzy membership functions for both velocities shown in figures 6(a) and (b). We also model the position and the angle (θ_o) of each dynamic obstacle relative with the global map with triangular fuzzy membership functions shown in figures 6(c) and (d).

The fuzzy sets $\tilde{v}_{oi}, \tilde{\omega}_{oi}$ denote velocity and angular velocity fuzzy sets, whereas $(\tilde{x}_{oi}, \tilde{y}_{oi})$ denotes a position fuzzy vector and $\tilde{\theta}_{oi}$ denotes orientation fuzzy set of dynamic obstacle i. We can computed the position fuzzy vector at time t' by

$$\tilde{x}_{oi}(t') = \tilde{x}_{oi}(t_c) + \left(\tilde{v}_{oi}(t_c)\cos\left(\tilde{\theta}_{oi}(t_c) + \tilde{\omega}_{oi}(t_c)\Delta t\right)\right)\Delta t \quad (5)$$

$$\tilde{y}_{oi}(t') = \tilde{y}_{oi}(t_c) + \left(\tilde{v}_{oi}(t_c)\sin\left(\tilde{\theta}_{oi}(t_c) + \tilde{\omega}_{oi}(t_c)\Delta t\right)\right)\Delta t \quad (6)$$

$$t' = t_c + \Delta t \quad (7)$$

To make the calculation of equations (5) and (6) simple, the lower and upper bound of the support and the core of each fuzzy set is used to compute the lower and upper bound of the support and the core of $\tilde{x}_{oi}$ and $\tilde{y}_{oi}$ in equations (5) and (6). Fig. 7 shows the fuzzy vector ($\tilde{x}_{oi}$, $\tilde{y}_{oi}$) at time t_c + 1 to t_c + 4. Then the dangerous region is computed by extending the support of the fuzzy vector ($\tilde{x}_{oi}$, $\tilde{y}_{oi}$) at time t' with the radius of obstacle i as shown in fig. 8.

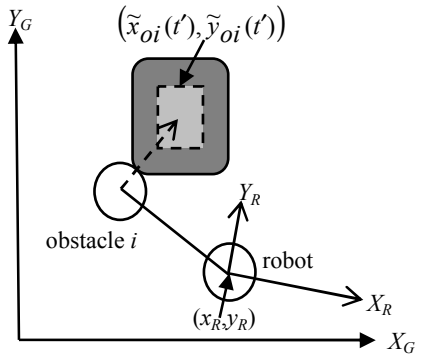

Figure 8. The gray area inside the solid line is the dangerous region whereas the one inside the dashed line is computed from the support of a fuzzy vector ($\tilde{x}_{oi}$, $\tilde{y}_{oi}$).

IV. COLLISION PREDICTION TECHNIQUE

The collision prediction technique is used to predict the dangerous region (a collision region for dynamic obstacles). Since the dangerous region is a fuzzy vector, the predicted collision time is assumed to be a triangular fuzzy set $\tilde{t}_{col}$ with parameter (*Tcola*, *Tcolb*, *Tcolc*) as shown in fig. 9. The lower bound of the support of $\tilde{t}_{col}$ (*Tcola*) is assumed to be the first predicted collision time, whereas the upper bound of the support of that (*Tcolc*) is the last predicted collision time.

The distance between the robot and the obstacle at time $\tilde{t}_{col}$ is

$$\widetilde{disRO}_i(\tilde{t}_{col}) = \sqrt{\left(x_R(\tilde{t}_{col}) - \tilde{x}_{oi}(\tilde{t}_{col})\right)^2 + \left(y_R(\tilde{t}_{col}) - \tilde{y}_{oi}(\tilde{t}_{col})\right)^2} \quad (8)$$

For simplicity, we use the lower bound of the support $(\underline{\tilde{x}}_{oi}, \underline{\tilde{y}}_{oi})$, the core $(\hat{\tilde{x}}_{oi}, \hat{\tilde{y}}_{oi})$ and the upper bound of the support $(\overline{\tilde{x}}_{oi}, \overline{\tilde{y}}_{oi})$ of fuzzy vector ($\tilde{x}_{oi}$, $\tilde{y}_{oi}$) to compute the lower bound ($\underline{\widetilde{disRO}_i}(\tilde{t}_{col})$) and upper bound ($\overline{\widetilde{disRO}_i}(\tilde{t}_{col})$)

of the support and the core ($\widehat{\widetilde{disRO}}_i(\tilde{t}_{col})$) of $\widetilde{disRO}_i(\tilde{t}_{col})$. Hence, the equation (8) will be

$$\widetilde{\widetilde{disRO}}_i(\tilde{t}_{col}) = \sqrt{\left(x_R(\tilde{t}_{col}) - \underline{\tilde{x}}_{oi}(\tilde{t}_{col})\right)^2 + \left(y_R(\tilde{t}_{col}) - \underline{\tilde{y}}_{oi}(\tilde{t}_{col})\right)^2} \quad (9)$$

$$\widehat{\widetilde{disRO}}_i(\tilde{t}_{col}) = \sqrt{\left(x_R(\tilde{t}_{col}) - \hat{\tilde{x}}_{oi}(\tilde{t}_{col})\right)^2 + \left(y_R(\tilde{t}_{col}) - \hat{\tilde{y}}_{oi}(\tilde{t}_{col})\right)^2} \quad (10)$$

$$\underline{\widetilde{disRO}}_i(\tilde{t}_{col}) = \sqrt{\left(x_R(\tilde{t}_{col}) - \overline{\tilde{x}}_{oi}(\tilde{t}_{col})\right)^2 + \left(y_R(\tilde{t}_{col}) - \overline{\tilde{y}}_{oi}(\tilde{t}_{col})\right)^2} \quad (11)$$

Suppose that δ is the shortest distance between the robot and the obstacle. Then, to find $\tilde{t}_{col}$, we can set

$$\widetilde{disRO}_i(\tilde{t}_{col}) = \delta \quad (12)$$

For simplicity, to find *Tcola*, *Tcolb* and *Tcolc* of $\tilde{t}_{col}$, we need to solve equations 13, 14 and 15 respectively with the Leap-frogging Newton's method [16].

$$\left(x_R(\tilde{t}_{col}) - \underline{\tilde{x}}_{oi}(\tilde{t}_{col})\right)^2 + \left(y_R(\tilde{t}_{col}) - \underline{\tilde{y}}_{oi}(\tilde{t}_{col})\right)^2 - \delta^2 = 0 \quad (13)$$

$$\left(x_R(\tilde{t}_{col}) - \hat{\tilde{x}}_{oi}(\tilde{t}_{col})\right)^2 + \left(y_R(\tilde{t}_{col}) - \hat{\tilde{y}}_{oi}(\tilde{t}_{col})\right)^2 - \delta^2 = 0 \quad (14)$$

$$\left(x_R(\tilde{t}_{col}) - \overline{\tilde{x}}_{oi}(\tilde{t}_{col})\right)^2 + \left(y_R(\tilde{t}_{col}) - \overline{\tilde{y}}_{oi}(\tilde{t}_{col})\right)^2 - \delta^2 = 0 \quad (15)$$

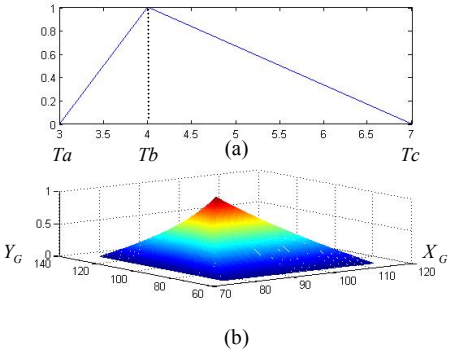

Figure 9. (a) $\widetilde{\Delta t}$ of obstacle *i* (b) the predicted fuzzy vector($\tilde{x}_{oi}$, $\tilde{y}_{oi}$) at time $\tilde{t}_{col}$ of obstacle *i*

Then, we can compute Δt in equation (7). Since $\tilde{t}_{col}$ is a triangular fuzzy set, $\widetilde{\Delta t}$ will be a triangular fuzzy set with parameter (*Ta*, *Tb*, *Tc*) as shown in fig. 9(a). The fuzzy vector ($\widetilde{x}_{oi}$, $\widetilde{y}_{oi}$) at time $\tilde{t}_{col}$ (shown in fig. 9(b)) can be computed from equations (5) and (6). Again, for simplicity, we use the lower bound, the upper bound of the support and the core of the input fuzzy sets to compute the lower bound, the upper bound of the support and the core of $\widetilde{x}_{oi}$ and $\widetilde{y}_{oi}$ in equations (5) and (6).

V. NAVIGATION PLANNING

When all dangerous regions are calculated by collision prediction technique, the robot needs to find the free road that does not intersect with any dangerous regions. In this paper, the finding process is divided into finding the free road candidate (ϕ_{RC}) according to the axis X_R from free sector (all safe regions in global map) and choosing the best free road (ϕ_{RS}) using a costing function.

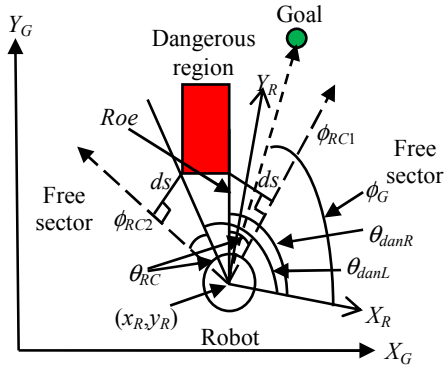

Figure 10. Finding free road candidate when there is 1 obstacle in the path to the goal

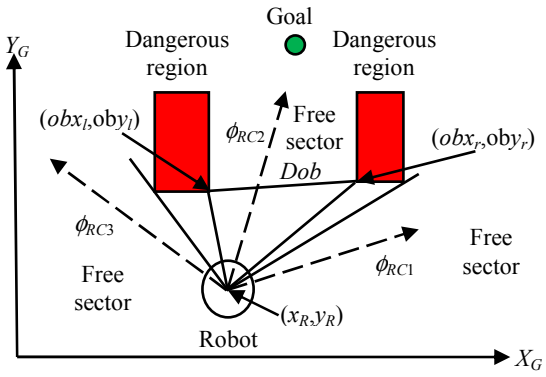

Figure 11. Finding free road candidate when robot moves through a narrow free sector

1) *Finding the free road candidate*

The location of the goal is the important factor in the finding the free road candidate. Hence, this process is as follows

a) If the goal position (ϕ_G) according to the axis X_R is located in the free sector (not in the dangerous region) and there is no collision with any obstacle in between, then $\phi_{RC} = \phi_G$

b) If the goal position (ϕ_G) is not located in the free sector or is inside the free sector and there is a collision with any obstacle in between (shown in fig. 10), then

$$\theta_{RC} = \sin^{-1}\left(\frac{ds}{ROe}\right) \quad (16)$$

where *ds* is the shortest distance between the dangerous region and the choosing path and RO_e is the shortest distance between the dangerous region and the center of the robot. Suppose that

θ_{danR} and θ_{danL} and are the angles from the axis X_R to the right and left boundaries of the dangerous region, respectively. Then we can compute free road candidate on the right (ϕ_{RC1}) and the left (ϕ_{RC2}) free road by

$$\phi_{RC1} = \theta_{danR} - \theta_{RC} \quad (17)$$

$$\phi_{RC2} = \theta_{danL} + \theta_{RC} \quad (18)$$

c) If the path to the goal is in the free sector that is narrow (shown in fig. 11), then we need to compute the movable distance (*Dob*), i.e.,

$$Dob = \sqrt{(obx_l - obx_r)^2 + (oby_l - oby_r)^2} \quad (19)$$

where (obx_l,oby_l) and (obx_r,oby_r) are the left and right boundaries of the left and right dangerous region, respectively. Let the safe width (*Rs*) is bigger than the diameter of the robot, and suppose that *Dob* > *Rs*, then this path is safe. Hence, we can find ϕ_{RC} according to case *a* or *b*.

2) Danger estimation

After the free road candidate ϕ_{RC} is computed and the robot moves following the path ϕ_{RC}, we need to estimate if there is a collision or not. Let $(x_{ro_{near}}, y_{ro_{near}})$ be the center of the nearest dangerous region located in the chosen sector. We can compute $(x_{ro_{near}}, y_{ro_{near}})$ using equations (5) and (6). Let v_R is the velocity of the robot. Then we can compute the position of the robot (x_R, y_R) at time T_{nc} (collision time) using

$$x_R(T_{nc}) = x_R + (v_R \cos(\theta_R + \phi_{RC}))\Delta T_{nc} \quad (20)$$

$$y_R(T_{nc}) = y_R + (v_R \sin(\theta_R + \phi_{RC}))\Delta T_{nc} \quad (21)$$

where ΔT_{nc} is the different time between the current and the collision time. However, T_{nc} is computed using the same method as in section IV. But since we only need this information to estimate the danger in the future of the chosen path, we will use only the core of the nearest dangerous region. Then we can estimate danger (*Dv*) of ϕ_{RC} by

$$Dv(\phi_{RC}) = \begin{cases} 1 & \Delta T_{nc} < T_{safe} \\ \dfrac{T_{ignore} - \Delta T_{nc}}{T_{ignore}} & T_{safe} \le \Delta T_{nc} < T_{ignore} \\ 0 & \Delta T_{nc} \ge T_{ignore} \end{cases} \quad (22)$$

where T_{safe} is the grace period of the stopping time of the robot, T_{ignore} is the threshold of the system.

3) Selection the best free road

The best free road must be the one with the shortest and the safest one. Hence the cost function is

$$COST(\phi_{RC}) = k_1 \cdot \Delta(\phi_{RC}, \phi_G) + k_2(Dv(\phi_{RC})) \quad (23)$$

where $\Delta(\phi_{RC}, \phi_G)$ is the difference between ϕ_{RC} and ϕ_G, k_1 and k_2 are the weight parameters. In the experiment, we set k_1 and k_2 to 0.5 and 1, respectively. Then the best free road ϕ_{RS} is the one that give the lowest $COST(\phi_{RC})$.

VI. DESIGN OF INTERVAL TYPE-2 FUZZY LOGIC

There are several researches on utilizing interval type-2 fuzzy logic as a tool to control mobile robot including the works done by [17 – 19]. Most of those research results show that the intreval type-2 fuzzy logic controller provide better results than type-1 fuzzy logic controller. Hence, in our experiment, we choose to use the interval type-2 fuzzy logic to control our mobile robot.

There are 3 inputs, i.e., D_{angle}, D_v and v_R. D_{angle} is the difference between ϕ_{RS} and Y_R, i.e., $D_{angle} = \Delta(\phi_{RS}, 90)$ as shown in fig.12. There are 2 outputs, i.e., velocity controller parameter (CV_R) and angular velocity controller parameter (CA_R). All of the membership functions utilized in the experiments are manually picked.

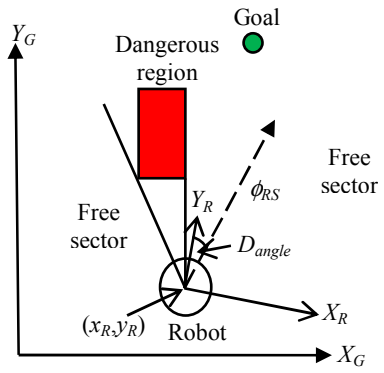

Figure 12. Example of D_{angle}

Figures 13, 14 and 15 show the interval type-2 membership functions of D_{angle}, D_v and v_R. The interval type-2 membership functions of (CV_R) and (CA_R) are shown in figures 16 and 17. The rules used for computing CV_R and CA_R are shown in tables I and II, respectively.

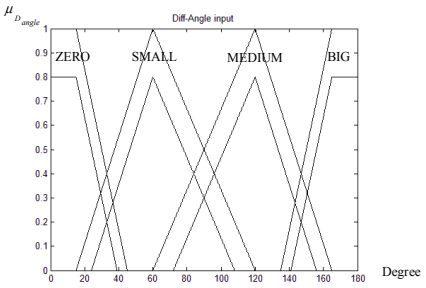

Figure 13. D_{angle} membership functions

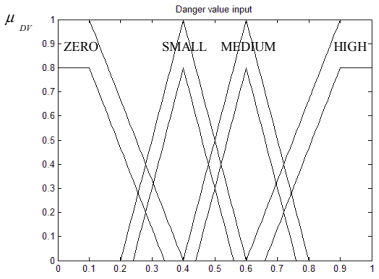

Figure 14. *Dv* membership functions

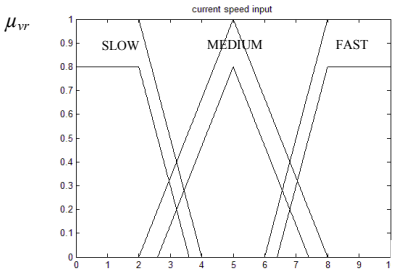

Figure 15. v_R membership functions

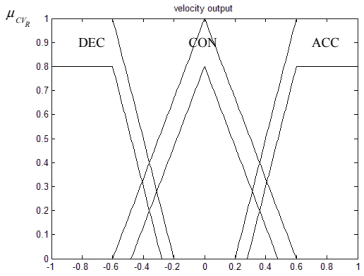

Figure 16. CV_R membership functions

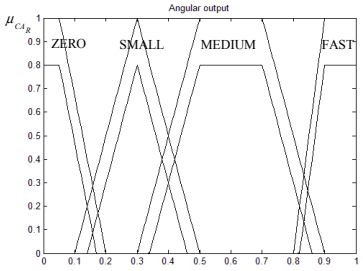

Figure 17. CA_R membership functions

Let ccv_R and cca_R are the defuzzified values of CV_R and CA_R. The velocity and angular velocity of the time $t_c + 1$ is computed by

$$v_R(t_c+1) = v_R(t_c) + ccv_R \cdot \alpha \qquad (24)$$

$$\omega_R(t_c+1) = \begin{cases} cca_R \cdot \omega_{RMAX} & d_{angle} > 0 \\ -cca_R \cdot \omega_{RMAX} & d_{angle} < 0 \end{cases} \qquad (25)$$

where α is the weight parameter and ω_{RMAX} is the maximum angular velocity. Both v_R and ω_R cannot exceed v_{RMAX} and ω_{RMAX}.

TABLE I. FUZZY RULE BASE

	rule base of control velocity			
	Input variable			*Output variable*
rule	D_{angle}	Dv	v_R	CV_R
1	ZERO - BIG	MEDIUM,HIGH	FAST	DEC
2	ZERO - MEDIUM	HIGH	MEDIUM	DEC
3	MEDIUM	MEDIUM	MEDIUM	DEC
4	BIG	SMALL - HIGH	MEDIUM	DEC
5	BIG	HIGH	SLOW,FAST	DEC
6	ZERO	ZERO	MEDIUM	CON
7	ZERO	MEDIUM	MEDIUM	CON
8	ZERO	HIGH	SLOW	CON
9	SMALL	SMALL,MEDIUM	MEDIUM	CON
10	SMALL	MEDIUM,HIGH	SLOW	CON
11	SMALL,MEDIUM	ZERO,SMALL	FAST	CON
12	MEDIUM	ZERO,SMALL	MEDIUM	CON
13	MEDIUM	SMALL - HIGH	SLOW	CON
14	BIG	ZERO	MEDIUM,FAST	CON
15	BIG	ZERO - MEDIUM	SLOW	CON
16	ZERO	ZERO	FAST	ACC
17	ZERO	ZERO,SMALL	SLOW,MEDIUM	ACC
18	ZERO	MEDIUM	SLOW	ACC
19	SMALL	ZERO,SMALL	SLOW	ACC
20	SMALL	ZERO	MEDIUM	ACC
21	MEDIUM	ZERO	SLOW	ACC

TABLE II. FUZZY RULE BASE

	rule base of control angular velocity			
	Input variable			*Output variable*
rule	D_{angle}	Dv	v_R	CA_R
1	ZERO	ZERO – HIGH	SLOW – FAST	ZERO
2	SMALL	ZERO	SLOW	ZERO
3	SMALL	ZERO - HIGH	MEDIUM ,FAST	SMALL
4	SMALL	SMALL - HIGH	SLOW	SMALL
5	MEDIUM	ZERO - HIGH	SLOW,FAST	MEDIUM
6	MEDIUM	ZERO - MEDIUM	MEDIUM	MEDIUM
7	MEDIUM	HIGH	MEDIUM	FAST
8	BIG	ZERO – HIGH	SLOW- FAST	FAST

VII. SIMULATION RESULTS

In the experiment, we set v_{RMAX} to 10, ω_{RMAX} is set to [-1, 1], and $ccv_R \times \alpha$ is [-5, 5]. The diameters of the robot and each dynamic obstacle are 10, whereas *vis* is set to 75.

A. Unknown dynamic obstacles with stable velocity and angular velocity

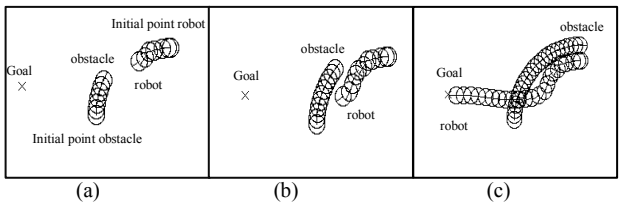

Figure 18. The robot moves to the goal and obstacle moves from bottom to top of the global map (a) both leave from initial, (b) robot decides to avoid obstacle, and (c) robot reaches the goal.

In this scenario, we do not have any information of obstacle. In fig. 18, we set the velocity and angular velocity of the obstacle to 6.3 and – 0.07 radius per time step. Fig. 18(a) shows the robot and obstacle in their starting point and their path. Fig18(b) shows the robot making a decision to avoid the obstacle based on the proposed method. Then the robot moves very fast to the goal once the obstacle is out of sight of the robot (shown in fig. 18(c)).

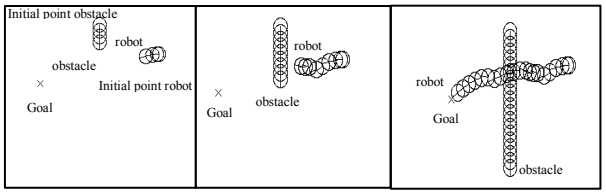

Figure 19. The robot moves to the goal and obstacle moves from top to bottom of the global map (a) both leave from initial, (b) robot decides to avoid obstacle, and (c) robot reaches the goal.

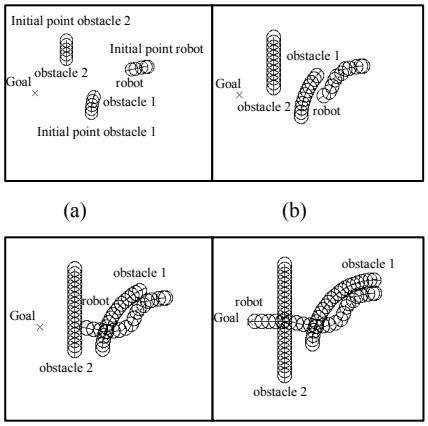

Figure 20. The robot moves to the goal and two obstacles are in the global map (a) robot and obstacles are in the starting point, (b) robot decides to avoid the first obstacle, (c) robot decides to avoid the second obstacle and (d) robot reaches the goal.

Fig. 19 shows the experiment result when the velocity and angular velocity of the obstacle is 7 and 0. Fig. 20 shows the experiment result when there are 2 obstacles with the same setting as in figures 18 and 19.

B. Unknown Dynamic obstacle with unstable velocity and angular velocity

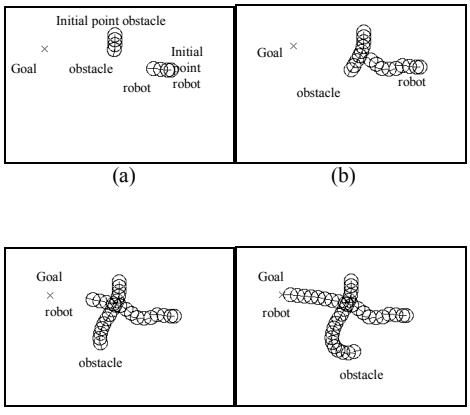

Figure 21. The robot moves to the goal and obstacle moves from top to bottom of the global map (a) robot and obstacles are in the starting point, (b) robot decides to wait for the obstacle to move, (c) the obstacle passes the robot and (d) the robot reaches to goal

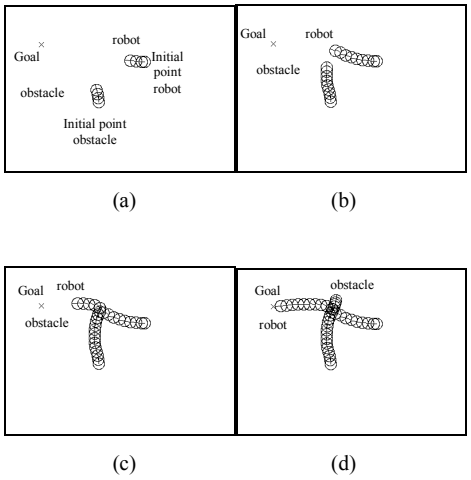

Figure 22. The robot moves to the goal and obstacle moves from bottom to top of the global map (a) robot and obstacles are in the starting point, (b) robot decides to move pass the obstacle, (c) the robot passes the obstacle and (d) the robot reaches to goal

In this experiment, the obstacle moves with random velocity and angular velocity. However, we assume that the robot will move faster than the obstacle. In Fig. 21, the robot decides to wait for the obstacle and then moving towards the goal. Whereas, in Fig. 22, the robot can move pass the obstacle without colliding with the obstacle.

VIII. CONCLUSION

In this work, we propose a navigation system in an uncertain environment (focusing on dynamic obstacle) for a mobile robot. We model the dangerous region for each obstacle by computing it future position fuzzy vector. Then the free road candidates are computed based on those dangerous regions. The best free road is selected based on the shortest and the safest path. Finally the interval type-2 fuzzy logic system is utilized to compute the velocity controller and angular velocity controller of the mobile robot. These parameters are utilized to compute the velocity and angular velocity of the mobile robot. The experiment results show that the mobile robot can find the shortest and safest path in the global map in an uncertain environment, i.e., an environment with an obstacle with stable velocity and angular velocity, an environment with an obstacle with random velocity, and an environment with several obstacles with both condition.

REFERENCES

[1] Jun Miura and Yoshiaki Shirai, "Modeling Motion Uncertainty of Moving Obstacles for Robot Motion Planning" *2000 IEEE Int. Conf. on Robotics and Automation, pp. 2258-2263.*

[2] Y. Gao and S.D. Sun, "A collision predict based local path planning of Mobile Robots", *2009 International Asia Conference on Informatics in Control, Automation and Robotics*", pp.185-190

[3] C. Fulgenzi, A. Spalanzani and C. Laugier, "Dynamic Obstacle Avoidance in uncertain environment combining PVOs and Occupancy Grid", *Proceedings of IEEE International Conference on Robotics and Automation*, 2007

[4] N.C. Tsourveloudis, K.P. Valavanis and T. Hebert, "Autonomous Vehicle Navigation Utilizing Electrostatic Potential Fields and Fuzzy Logic", *IEEE Transactions on Robotics and Automation*, Vol. 17, No. 4, August 2001

[5] H. Seki, S. Shibayama, Y. Kamiya and M. Hikizu, "Practical Obstacle Avoidance Using Potential Field for a Nonholonmic Mobile Robot with Rectangular Body", *ETFA 2008*, pp. 326 – 332.

[6] Y.J. Cho, J.P. Hong and K.W. Park, "Obstacle Avoidance using Active Window and Flexible Vector Field with a Laser Range Finder", *International Conference on Control, Automation and Systems 2007*, Oct. 17-20, 2007 in COEX, Seoul, Korea

[7] Y. Li, C. Li and R. Song, "A new hybrid algoritm of dynamic obstacle avoidance based on dynamic rolling planning and RBFNN", *Proceedings of the 2007 IEEE International Conference on Robotics and Biomimetice*, December 15-18, 2007, Sanya, China

[8] P. Rusu, E.M. Petriu, T.E. Whalen, A. Cornell and H.J.W. Spoelder, "Behavior-Based Neuro-Fuzzy Controller for Mobile Robot Navigation", *IEEE transactions on instrumentation and measurement*, Vol. 52, No. 4, August 2003

[9] R. Malhotra and A. Sarkar, "Development of a fuzzy logic based mobile robot for dynamic obstacle avoidance and goal acquisition in an unstructured environment" ,*Proceedings of the 2005 IEEE/ASME International Conference on Advanced Intelligent Mechatronics*, Monterey, California, USA, 24-28 July,2005

[10] F. Abdessermed, K. Benmahammed and E. Monacelli, "A Fuzzy-based reactive controller for a non-holonomic mobile robot", *Robotics and Autonomous Systems 47*, 2004, pp. 31-46.

[11] X. Jiang, Y. Motai and X. Zhu, "Predictive Fuzzy Control for a Mobile Robot with Nonholonomic Constraints", *Proceedings of the 2005 IEEE International Conference on Advanced Robotics, ICAR '05*, 18-20 July, 2005

[12] S. Nurmaini and S.Z.M. Hashim, "An Embedded Fuzzy Type-2 Controller Based Sensor Behavior for Mobile Robot", *2008 International Conference on Intelligent Systems Design and Applications*, 26-28 November, 2008.

[13] P. Phokharatkal and S. Phaiboon, "Mobile Robot Control Using Type-2 Fuzzy Logic System", *Proceedings of the 2004 IEEE Conference on Robotics, Automation and Mechatronics*, Singapore, 1-3 December, 2004

[14] J.Figueroa, J.Posada, J. Soriano, M. Melgarejo and S. Rolas, "A type-2 fuzzy logic controller for tracking mobile object in the context of robotic soccer games", *IEEE International Conference on fuzzy System,* 2005

[15] J.M. Mendel, "Uncertain Rule-Based Fuzzy Logic Systems: Introduction and New Direction", University of Southern California Los Angeles, CA

[16] A.B. Kasturiarachi, "Leap-frogging Newton's method", *Internation Journal of Mathematical Education in Science and Technology,* Vol.33, No.4, 2002, pp. 521-527.

[17] M. Kristic, I. Kanellakopoulos and P. Kokotovic, "Nonlinear and adaptive control design", Wiley-Interscience, 1995.

[18] H. Hagras, "Type-2 Fuzzy Logic Controllers: A Way Forward for Fuzzy Systems in Real World Environments", inWCCI 2008 Plenary/Invited Lectures, LNCS 5050, J.M. Zurada et al. Eds., Berlin Heidelberg : Springer-Verlag, 2008, pp 181-200.

[19] R. Martinez, A. Rodriguez. O. Castillo, P. Melin, and L. T. Aguilar, "Optimization of Type-2 Fuzzy Logic Contrllers for Mobile Robots Using Evolutionary Methods", *2009 IEEE International Conference on Systems, Man, and Cybernetics,* San Antonio, USA, October 2009, pp. 4764 – 4769.

2011 IEEE International Conference on Fuzzy Systems
June 27-30, 2011, Taipei, Taiwan

Multi-attribute Decision Making Models under Interval Type-2 Fuzzy Environment

Weize Wang and Xinwang Liu
School of Economics and Management
Southeast University
Nanjing, Jiangsu 210096, China
Email: weizew@gmail.com, xwliu@seu.edu.cn

***Abstract*—Interval type-2 fuzzy sets, each of which is characterized by the footprint of uncertainty, are a very useful means to depict the decision information in the process of decision making. In this article, we investigate the decision making problems in which all the information provided by the decision maker is expressed as interval type-2 fuzzy decision matrix where each of the elements is characterized by interval type-2 fuzzy set, and the information about attribute weights is partially known, which may be constructed by various forms. We first utilize the average centroid measure to calculate the average centroid of each attribute value and construct the average centroid matrix of the interval type-2 fuzzy decision matrix. Based on the average centroid matrix and the given attribute weight information, we establish some optimization models to determine the weights of attributes. Furthermore, we develop a procedure to identify the best alternative(s). Finally, we give an illustrative example.**

***Keywords*—Interval type-2 fuzzy sets (IT2 FSs); average centroid matrix; multi-attribute decision making (MADM); incomplete information.**

I. Introduction

Multi-attribute decision making (MADM) problems are widespread in real life decision situations. A MADM problem is to find the most desirable alternative(s) from a set of n feasible alternatives $X = \{x_1, x_2, \ldots, x_n\}$ according to the decision information about attribute weights and attribute values. First of all, the decision maker generally need to determine the importance degrees of a set of m attributes $G = \{g_1, g_2, \ldots, g_m\}$, that is to say, the decision maker need to provide their preference information about attribute weights (for convenience, let the weight vector of attributes be $\omega = (\omega_1, \omega_2, \ldots, \omega_m)^T$, where $\omega_j \geqslant 0, j = 1, 2, \ldots, m$ and $\sum_{j=1}^{m} \omega_j = 1$). In general, the provided attribute weight information may be constructed in the following forms [1], [2], for $i = j$,

1) A weak ranking: $\{\omega_i \geqslant \omega_j\}$;
2) A strict ranking: $\{\omega_i - \omega_j \geqslant \delta_i (> 0)\}$;
3) A ranking with multiples: $\{\omega_i \geqslant \delta_i \omega_j\}, 0 \leqslant \delta_i \leqslant 1$;
4) An interval form: $\{\delta_i \leqslant \omega_i \leqslant \delta_i + \varepsilon_i\}, 0 \leqslant \delta_i < \delta_i + \delta_i \leqslant 1$;
5) A ranking of differences: $\{\omega_i - \omega_j \geqslant \omega_k - \omega_l\}$, for $j \neq k \neq l$.

The estimation of the attribute values plays an important role in MADM. In the process of decision making, the information about attribute values is usually uncertain or fuzzy due to the increasing complexity of the socio-economic environment and the vagueness of inherent subjective nature of human thinking. Many methods have been presented for handling fuzzy MADM problems based on traditional type-1 fuzzy sets (T1 FSs) [3]. Hwang and Yoon [4] presented the technique for order preference by similarity to ideal solution (TOPSIS) method for handling MADM problems. Chen [5] presented a method for handling fuzzy MADM problems based on the similarity measure between T1 FSs. Chen and Hwang [6] presented some methods for handling fuzzy MADM problems. Chen [7] extended the TOPSIS method to present a method to handle group decision-making problems in a fuzzy environment. Chen [8] presented a method to evaluate the rate of aggregative risk in software development using the T1 FS theory in the fuzzy group decision-making environment. Wang and Lin [9] presented a fuzzy multi-criteria group decision-making approach to select configuration items for software development. Li [10] constructed some novel mathematical programming models for fuzzy MADM problems under uncertainty and proposed corresponding solving methods. Wang and Parkan [11] presented a method for handling MADM problems based on the fuzzy preference information of alternatives. Wang and Parkan [12] presented a general MADM approach for integrating subjective preferences and objective information. Yager and Xu [13] presented a continuous ordered weighted geometric operator and its application to decision making. Tsabadze [14] presented a method for fuzzy aggregation based on group expert evaluations. Wang and Chang [15] presented an application of TOPSIS in evaluating initial aircraft training under a fuzzy environment. Wu and Chen [16] presented a maximizing deviation method for group MADM under the linguistic environment. Li [17] developed a compromise ratio methodology for fuzzy multi-attribute group decision making (MAGDM). Hua et al. [18] presented an approach for MADM problems with incomplete information. Fu [19] presented a fuzzy optimization method for multi-criteria decision making. Lin and Wu [20] presented a causal analytical method for group decision-making in the fuzzy environment. Tsai and Wang [21] presented a computing coordination based fuzzy group decision-making method for web service oriented architectures.

Similar to the transition from ordinary sets to T1 FSs [22], when the circumstances are so fuzzy that we have trouble determining the membership grade even as a crisp number

978-1-4244-7316-8/11/$26.00 ©2011 IEEE

in $[0,1]$, we use type-2 fuzzy sets (T2 FSs) [23], [24]. The T2 FSs are now very well established [25] are gaining more and more in popularity [26], [27], [28], [29]. It is known that T2 FSs let us model and minimize the effects of uncertainties in rule-based fuzzy logic systems [22]. The majority of the contributions in the field use interval type-2 fuzzy sets (IT2 FSs) (a particular kind of T2 FSs) which maintain the uncertainty modelling properties of general T2 FSs but reduce the computational efforts that are needed to aggregate them. If we can use IT2 FSs [30] for handling fuzzy decision-making problems, then there is room for more flexibility due to the fact that IT2 FSs provide more flexibility to present uncertainties than traditional T1 FSs. In recent years, some authors have applied the IT2 FS theory to the field of decision making. Wu and Mendel [31], [32] presented a method using the linguistic weighted average and IT2 FSs for handling fuzzy multiple criteria hierarchical group decision-making problems, Wu and Mendel's fuzzy multiple criteria hierarchical group decision making method is to make decisions by means of aggregating the opinions of decision-makers. Wu [33] proposed a novel weighted average as a computing with words engine for MADM, and proposed perceptual reasoning as a computing with words engine for multi-objective decision making. Chen and Lee [34] presented a new method for handling fuzzy multiple criteria hierarchical group decision-making problems based on arithmetic operations and fuzzy preference relations of IT2 FSs. Chen and Lee [35] presented an interval type-2 fuzzy TOPSIS method to handle fuzzy MAGDM problems based on IT2 FSs, and use some examples to illustrate the fuzzy MAGDM process of the proposed method. Chen and Lee [36] presented a new method to handle fuzzy MAGDM problems based on the ranking values and the arithmetic operations of IT2 FSs.

In this paper, we shall focus our attention on the issue of MADM under interval type-2 fuzzy environment where all the information provided by the decision makers is characterized by IT2 FSs and the information about the attribute weights is partially known, which may be constructed by the various forms described above. To do that, the remainder of this paper is organized as follows. In Section II, we give a review of basic concepts and average centroids related to IT2 FSs. Section III presents the considered problem and utilizes the average centroid measure to calculate the average centroid of each attribute value and constructs the average centroid matrix of the interval type-2 fuzzy decision matrix. Based on the average centroid matrix and the given attribute weight information, we establish some optimization models to determine the weights of attributes. Section IV develops an approach to MADM under interval type-2 fuzzy environment, the approach uses the obtained attribute weights and the average centroid matrix of the interval type-2 fuzzy decision matrix to get the overall average centroids of alternatives and the ranking of all the given alternatives. Section V provides a practical example to illustrate the developed approach, and finally, we conclude the paper in Section VI.

II. Preliminaries

Definition 1. [23], [24] A T2 FS $\tilde{A}$ in the universe of discourse X can be represented by a type-2 membership function $\mu_{\tilde{A}}$, shown as follows:

$$\tilde{A} = \{((x,u), \mu_{\tilde{A}}(x,u)) \mid \forall x \in X, \forall u \in J_x \subseteq [0,1]\} \quad (1)$$

where $0 \leqslant \mu_{\tilde{A}}(x,u) \leqslant 1$. The T2 FS $\tilde{A}$ also can be represented as follows:

$$\begin{aligned}\tilde{A} &= \int_{x\in X}\int_{u\in J_x} \mu_{\tilde{A}}(x,u)/(x,u) \\ &= \int_{x\in X}\left[\int_{u\in J_x} \mu_{\tilde{A}}(x,u)/u\right]\Big/x \end{aligned} \quad (2)$$

where x is the primary variable, $J_x \subseteq [0,1]$ is the primary membership of x, u is the secondary variable, and $\int_{u\in J_x} \mu_{\tilde{A}}(x,u)/u$ is the secondary membership function at x. $\int\int$ denotes the union over all admissible x and u. For discrete universes of discourse, $\int$ is replaced by $\sum$.

Definition 2. [30] Let $\tilde{A}$ be a T2 FS in the universe of discourse X represented by the type-2 membership function $\mu_{\tilde{A}}(x,u)$. If all $\mu_{\tilde{A}}(x,u) = 1$, then $\tilde{A}$ is called an IT2 FS. An IT2 FS can be regarded as a special case of a T2 FS, shown as follows:

$$\tilde{A} = \int_{x\in X}\int_{u\in J_x} 1/(x,u) = \int_{x\in X}\left[\int_{u\in J_x} 1/u\right]\Big/x \quad (3)$$

where x is the primary variable, $J_x \subseteq [0,1]$ is the primary membership of x, u is the secondary variable, and $\int_{u\in J_x} 1/u$ is the secondary membership function at x.

Note that (3) means $\tilde{A} : X \to \{[a,b] : 0 \leqslant a \leqslant b \leqslant 1\}$. Uncertainty about $\tilde{A}$ is conveyed by the union of all of the primary memberships, called the footprint of uncertainty of $\tilde{A}$ (FOU($\tilde{A}$)), i.e.,

$$\mathrm{FOU}(\tilde{A}) = \bigcup_{x\in X} J_x \quad (4)$$

In this paper, we present a method to use IT2 FSs for handling fuzzy MADM problems, where the reference points and the heights of the upper and the lower membership functions of IT2 FSs are used to characterize IT2 FSs. A trapezoidal IT2 FS $\tilde{A}$ is shown in Fig. 1. The FOU is shown as the shaded region. It is bounded by an upper membership function (UMF) and a lower membership function (LMF), both of which are T1 FSs.

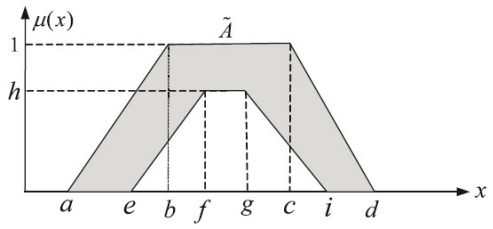

Fig. 1. The nine points to determine a FOU. (a,b,c,d) determines a normal trapezoidal UMF, (e,f,g,i,h) determines a trapezoidal LMF with height h.

Definition 3. [37] The centroid $C(\tilde{A})$ of an IT2 FS $\tilde{A}$ is the union of the centroids of all its embedded T1 FSs A_e, i.e.,

$$C(\tilde{A}) \equiv \bigcup_{\forall A_e} c(A_e) = [c_l(\tilde{A}), c_u(\tilde{A})], \tag{5}$$

where $\bigcup$ is the union operation, and

$$c_l(\tilde{A}) = \min_{\forall A_e} c(A_e) \tag{6}$$

$$c_u(\tilde{A}) = \max_{\forall A_e} c(A_e) \tag{7}$$

$$c(A_e) = \frac{\sum_{i=1}^{N} x_i \mu_{A_e}(x_i)}{\sum_{i=1}^{N} \mu_{A_e}(x_i)} \tag{8}$$

It has been shown [38], [37], [39] that $c_l(\tilde{A})$ and $c_u(\tilde{A})$ can be expressed as

$$c_l(\tilde{A}) = \frac{\sum_{i=1}^{L} x_i \overline{\mu}_{\tilde{A}}(x_i) + \sum_{i=L+1}^{N} x_i \underline{\mu}_{\tilde{A}}(x_i)}{\sum_{i=1}^{L} \overline{\mu}_{\tilde{A}}(x_i) + \sum_{i=L+1}^{N} \underline{\mu}_{\tilde{A}}(x_i)} \tag{9}$$

$$c_u(\tilde{A}) = \frac{\sum_{i=1}^{R} x_i \underline{\mu}_{\tilde{A}}(x_i) + \sum_{i=R+1}^{N} x_i \overline{\mu}_{\tilde{A}}(x_i)}{\sum_{i=1}^{R} \underline{\mu}_{\tilde{A}}(x_i) + \sum_{i=R+1}^{N} \overline{\mu}_{\tilde{A}}(x_i)} \tag{10}$$

Switch points L and R, as well as $c_l(\tilde{A})$ and $c_u(\tilde{A})$ are computed by iterative Karnik-Mendel Algorithms [38], [37], [40].

Centroid-based ranking method: First compute the average centroid for each IT2 FS $\tilde{A}_i$:

$$c(\tilde{A}_i) = \frac{c_l(\tilde{A}_i) + c_u(\tilde{A}_i)}{2}, i = 1, 2, \ldots, N \tag{11}$$

and then sort $c(\tilde{A}_i)$ to obtain the rank of $\tilde{A}_i$.

The ranking method can be viewed as a generalization of Yager's first ranking method for T1 FSs [41] to IT2 FSs.

III. Some models for determining attribute weight

For a MADM problem, let $X = \{x_1, x_2, \ldots, x_n\}$ be a finite set of alternatives and $G = \{g_1, g_2, \ldots, g_m\}$ be a finite set of attributes, and suppose that the decision maker provides the attribute weight information expressed in the forms $1) - 5)$ (see Section I). For convenience, we denote by H the set of the known information about attribute weights given by the decision maker. Let $\tilde{R} = (\tilde{A}_{ij})_{n\times m}$ be an interval type-2 fuzzy decision matrix, where $\tilde{A}_{ij}$ is an IT2 FS, provided by the decision maker for the alternative $x_i \in X$ with respect to the attribute g_j, $1 \leqslant i \leqslant n$, $1 \leqslant j \leqslant m$.

In the situations where the information about attribute weights is completely known, that is, the weight vector $\omega = (\omega_1, \omega_2, \ldots, \omega_m)^T$ of the attributes $g_k (k = 1, 2, \ldots, m)$ can be completely determined in advance, then based on the interval type-2 fuzzy decision matrix $\tilde{R} = (\tilde{A}_{ij})_{n\times m}$, Lee and Chen [36] can utilize the fuzzy ranking method and the arithmetic operations between IT2 FSs to handle fuzzy MADM problems.

However, the information about attribute weights provided by the decision maker is usually incomplete because that the increasing complexity of the socio-economic environment makes it less and less possible for the decision maker to consider all relevant aspects of a problem [1], [2]. How to utilize the interval type-2 fuzzy decision matrix and the known weight information to find the most desirable alternative(s) is an interesting and important issue, which is worth paying attention to.

In the following, we establish some optimization models to determining the weights of attributes.

As interpreted in Section II, the average centroid $c(\tilde{A})$ of an IT FS $\tilde{A}$ can reflect the magnitude of $\tilde{A}$. As a result, we utilize the average centroid function c to define the following concept.

Definition 4. Let $\tilde{R} = (\tilde{A}_{ij})_{n\times m}$ be the interval type-2 fuzzy decision matrix, then the average centroid matrix of $\tilde{R} = (\tilde{A}_{ij})_{n\times m}$ is defined as

$$C = (c_{ij})_{n\times m}$$

where $c_{ij} = c(\tilde{A}_{ij})$ is the average centroid of $\tilde{A}_{ij}$, $1 \leqslant i \leqslant n$, $1 \leqslant j \leqslant m$.

Based on the average centroid matrix, we express the overall average centroid value of each alternative as:

$$c_i(\omega) = \sum_{j=1}^{m} \omega_j c_{ij}, i = 1, 2, \ldots, n. \tag{12}$$

Obviously, the greater the value $c_i(\omega)$, the better the alternative x_i. When we only consider the alternative x_i, then a reasonable vector of attribute weights $\omega = (\omega_1, \omega_2, \ldots, \omega_m)^T$ should be determined so as to maximize $c_i(\omega)$, and thus, we establish the following optimization model:

$$\begin{aligned} (\mathrm{M}-1)\ & max\ c_i(\omega) \\ & s.t.\quad \omega = (\omega_1, \omega_2, \ldots, \omega_m)^T \in H, \\ & \qquad \omega_j \geqslant 0, j = 1, 2, \ldots, m, \sum_{j=1}^{m} \omega_j = 1. \end{aligned}$$

By solving the model $(\mathrm{M}-1)$, we get the optimal solution $\omega^{(i)} = (\omega_1^{(i)}, \omega_2^{(i)}, \ldots, \omega_m^{(i)})^T$ corresponding to the alternative x_i. However, in general, in the process of determining the weight vector $\omega = (\omega_1, \omega_2, \ldots, \omega_m)^T$, we need to consider all the alternatives $x_j (j = 1, 2, \ldots, n)$ as a whole. Thus, we construct a combined weight vector as follows:

$$\begin{aligned} \omega &= w_1\omega^{(1)} + w_2\omega^{(2)} + \cdots + w_n\omega^{(n)} \\ &= \begin{pmatrix} \omega_1^{(1)} & \omega_1^{(2)} & \cdots & \omega_1^{(n)} \\ \omega_2^{(1)} & \omega_2^{(2)} & \cdots & \omega_2^{(n)} \\ \vdots & \vdots & \vdots & \vdots \\ \omega_m^{(1)} & \omega_m^{(2)} & \cdots & \omega_m^{(n)} \end{pmatrix} \begin{pmatrix} w_1 \\ w_2 \\ \vdots \\ w_n \end{pmatrix} \\ &= \Omega w \end{aligned} \tag{13}$$

where

$$\Omega = \begin{pmatrix} \omega_1^{(1)} & \omega_1^{(2)} & \cdots & \omega_1^{(n)} \\ \omega_2^{(1)} & \omega_2^{(2)} & \cdots & \omega_2^{(n)} \\ \vdots & \vdots & \vdots & \vdots \\ \omega_m^{(1)} & \omega_m^{(2)} & \cdots & \omega_m^{(n)} \end{pmatrix}$$

and $w = (w_1, w_2, \ldots, w_n)^T$ is an undetermined nonnegative vector satisfying the condition:

$$ww^T = 1 \tag{14}$$

Let $\bar{c}_i = (c_{i1}, c_{i2}, \ldots, c_{im})(i = 1, 2, \ldots, n)$, then the average centroid matrix C can be expressed as $C = (\bar{c}_1, \bar{c}_2, \ldots, \bar{c}_n)^T$. By (12) and (13), we have

$$c_i(\omega) = \sum_{j=1}^{m} \omega_j c_{ij} = \bar{c}_i \omega = \bar{c}_i \Omega w, i = 1, 2, \ldots, n \tag{15}$$

To determine the combined weight vector $\omega = (\omega_1, \omega_2, \ldots, \omega_m)^T$, we should make all the overall average centroid values $c_i(\omega)(i = 1, 2, \ldots, n)$ as greater as possible, which means to maximize the following vector $c(\omega) = (c_1(\omega), c_2(\omega), \ldots, c_n(\omega))$ under the condition (14). In order to do that, we establish the following multiple objective optimization model:

$$\begin{aligned} (\mathrm{M}-2)\ & max\ c(\omega) = (c_1(\omega), c_2(\omega), \ldots, c_n(\omega)) \\ & s.t.\quad ww^T = 1. \end{aligned}$$

By the equal weighted summation method, the model $(\mathrm{M}-2)$ can be transformed into a single objective optimization model:

$$\begin{aligned} (\mathrm{M}-3)\ & max\ c(\omega)c(\omega)^T \\ & s.t.\quad ww^T = 1. \end{aligned}$$

Let $f(w) = c(\omega)c(\omega)^T$, then by (15), we have

$$f(w) = c(\omega)c(\omega)^T = w^T(C\Omega)^T(C\Omega)w \tag{16}$$

Let $S = (C\Omega)^T(C\Omega)$, then $S^T = (C\Omega)^T(C\Omega) = S$, i.e., S is a real symmetrical matrix. Moreover, $C \geqslant 0$. Therefore, S is a nonnegative definite matrix.

Here, we introduce two useful theorems:

Theorem 1. *[42] Let $B = (b_{ij})_{n\times n}$ be a real symmetrical matrix, i.e.,$B^T = B$, then*

$$\max \frac{x^T B x}{x^T x} = \lambda_{max} \tag{17}$$

where λ_{max} is the largest eigenvalue of B, and x is a nonzero vector.

Theorem 2. *[42] Let $B = (b_{ij})_{n\times n}$ be a real irreducible nonnegative matrix, then*

1) *B has a largest eigenvalue λ_{max}, which is also a unique eigenvalue of B.*
2) *Let $v = (v_1, v_2, \ldots, v_n)^T$ be the eigenvector of λ_{max}, then all $v_j > 0\,(j = 1, 2, \ldots, n)$, i.e., v is a positive eigenvector.*

By Theorems 1 and 2, we know that $f(w)$ has a largest value $\max f(w)$, which is also the largest eigenvalue $\bar{\lambda}_{max}$ of S. $w = (w_1, w_2, \ldots, w_n)^T$ is the eigenvector of $\bar{\lambda}_{max}$, where $\bar{\lambda}_{max}$ is unique, and all $w_i > 0\,(i = 1, 2, \ldots, n)$. After normalizing the eigenvector w, we can utilize (13) to derive the weight vector ω.

IV. An approach to multi-attribute decision making under interval type-2 fuzzy environment

Based on the analysis in Section III, interval type-2 fuzzy MADM with incomplete attribute weight information may be performed via the following steps.

1) Obtain the normalized decision matrix. In general, attributes can be classified into two types: benefit attributes and cost attributes. In other words, the attribute set G can be divided into two subsets: G_1 and G_2, where G_k $(k = 1, 2)$ are the subset of benefit attributes and cost attributes, respectively. Furthermore, $G_1 \cup G_2 = G$ and $G_1 \cap G_2 = \emptyset$, where $\emptyset$ is empty set. Since the m objectives may be measured in different ways, the decision matrix $\tilde{R}$ needs to be normalized besides all the attributes $g_j(j = 1, 2, \ldots, m)$ are of the same type. In this paper we choose the following normalization formula to update the decision matrix $\tilde{R}$:

$$\tilde{A}_{ij} = \begin{cases} \tilde{A}_{ij} & j \in G_1 \\ \tilde{A}_{ij}^c & j \in G_2 \end{cases} \tag{18}$$

   where $\tilde{A}_{ij}^c$ is the complement of $\tilde{A}_{ij}$. Hence, we obtain the normalized decision matrix $\tilde{R} = (\tilde{A}_{ij})_{n\times m}$.
2) Calculate the average centroid matrix $C = (c_{ij})_{n\times m}$ of the normalized decision matrix $\tilde{R} = (\tilde{A}_{ij})_{n\times m}$.
3) Utilize the model $(\mathrm{M}-1)$ to get the optimal weight vectors $\omega^{(i)} = (\omega_1^{(i)}, \omega_2^{(i)}, \ldots, \omega_m^{(i)})^T (i = 1, 2, \ldots, n)$ corresponding to the alternatives $x_i\,(i = 1, 2, \ldots, n)$, and construct the weight matrix Ω.
4) Calculate the normalized eigenvector $w = (w_1, w_2, \ldots, w_n)^T$ of the matrix $(C\Omega)^T(C\Omega)$.
5) Utilize (13) to derive the weight vector $\omega = (\omega_1, \omega_2, \ldots, \omega_m)^T$.
6) Utilize (12) to get the overall average centroid values $c_i(\omega)(i = 1, 2, \ldots, n)$ of the alternatives $x_i\,(i = 1, 2, \ldots, n)$.
7) Rank the alternatives $x_i\,(i = 1, 2, \ldots, n)$ based on the average centroids $c_i(\omega)(i = 1, 2, \ldots, n)$, and then select the most desirable one(s).
8) End.

V. Illustrative example

Table I shows the linguistic terms "Very Low" (VL), "Low" (L), "Medium Low" (ML), "Medium" (M), "Medium High" (MH), "High" (H), "Very High" (VH) and their corresponding IT2 FSs, respectively. In addition, the corresponding average centroids of IT2 FSs are given in Table I (see Reference [43]).

Assume that there are three cars to be evaluated with four attributes "Safety", "Price", "Appearance" and "Performance". Let X be the set of alternatives, where $X = \{x_1, x_2, x_3\}$, and let G be the set of attributes, where $G = \{g_1, g_2, g_3, g_4\}$. Assume that the decision-maker use the linguistic terms shown in Table I to represent the evaluating values of the alternatives with respect to different attributes, respectively, as shown

TABLE I
LINGUISTIC TERMS AND THEIR CORRESPONDING IT2 FSS.

Linguistic terms	IT2 FSs $\left(\tilde{A}\right)$	$c\left(\tilde{A}\right)$
Very Low (VL)	((0, 0, 0.14, 1.97), (0, 0, 0.05, 0.66,1))	0.47
Low (L)	((0, 0, 0.64,2.63), (0, 0, 0.09, 0.99,1))	0.67
Medium Low (ML)	((0.59, 2.00, 3.25, 4.41), (2.29, 2.70, 2.70, 3.21, 0.42))	2.59
Medium (M)	((3.59, 4.75, 5.50, 6.91), (4.86, 5.03, 5.03, 5.14, 0.27))	5.19
Medium High (MH)	((5.38, 7.50, 8.75, 9.81), (7.79, 8.22, 8.22, 8.81, 0.45))	7.9
High (H)	((7.37, 9.41, 10, 10), (8.72, 9.91, 10, 10, 1))	9.3
Very High (VH)	((8.68, 9.91, 10, 10), (9.61, 9.97, 10, 10, 1))	9.69

TABLE II
THE LINGUISTIC TERMS OF IT2 FSS $\tilde{A}$ AND $\tilde{A}^c$.

The linguistic terms of $\tilde{A}$	The linguistic terms of $\tilde{A}^c$
VL	VH
L	H
ML	MH
M	M
MH	ML
H	L
VH	VL

follows:

$$\tilde{R} = \begin{pmatrix} \text{MH} & \text{H} & \text{VH} & \text{VH} \\ \text{H} & \text{MH} & \text{H} & \text{H} \\ \text{VH} & \text{VH} & \text{M} & \text{H} \end{pmatrix}$$

If the information about attribute weights is completely known in advance, here, we suppose that the weight vector $\omega = (0.25, 0.15, 0.25, 0.35)^T$, then we first utilize the average centroid measure [43] and the weighted mean to handle the above problem, which needs the following steps:

1) Considering that the attributes are the benefit attributes except to the attribute "Price" (g_2), then based on the formula (18) and Table II, the decision matrix $\tilde{R}$ can be updated to the following normalized matrix.

$$\tilde{R} = \begin{pmatrix} \text{MH} & \text{L} & \text{VH} & \text{VH} \\ \text{H} & \text{ML} & \text{H} & \text{H} \\ \text{VH} & \text{VL} & \text{M} & \text{H} \end{pmatrix} \tag{19}$$

2) Based on Table I, we can get the average centroid matrix $C = (c_{ij})_{n\times m}$ of the normalized decision matrix $\tilde{R}$ as follows:

$$C = \begin{pmatrix} 7.9 & 0.67 & 9.69 & 9.69 \\ 9.3 & 2.59 & 9.3 & 9.3 \\ 9.69 & 0.47 & 5.19 & 9.3 \end{pmatrix} \tag{20}$$

3) Utilize the weight vector $\omega = (0.25, 0.15, 0.25, 0.35)^T$ and the ith line values $c_{ij}\,(j = 1, 2, 3, 4)$ of the average centroid matrix C to derive the overall average centroids c_i of the alternatives $x_i\,(i = 1, 2, 3)$:
$c_1 = \sum_{j=1}^{4} \omega_j c_{1j} = 7.8895$,
$c_2 = \sum_{j=1}^{4} \omega_j c_{2j} = 8.2835$,
$c_3 = \sum_{j=1}^{4} \omega_j c_{3j} = 7.0455$.
4) Rank the alternatives $x_i\,(i = 1, 2, 3)$ based on the average centroids $c_i\,(i = 1, 2, 3)$: $x_2 \succ x_1 \succ x_3$, and then the most desirable car is x_2.

The decision maker may, however, provide the information about attribute weights with value ranges or order relations as described in Section I because that a decision may be made under time pressure and lack of knowledge, or the decision maker has limited attention and information processing capabilities. For example, the information about attribute weights, given by the decision maker, may be as follows:

$$H = \{0.2 \leqslant \omega_3 \leqslant 0.5,\, \omega_3 - \omega_2 \geqslant \omega_4 - \omega_1,\, \omega_3 - \omega_2 \geqslant 0.1,\, \omega_4 \geqslant \omega_1\}$$

As presented in Section I, many approaches have been developed to dealing with the decision making problems based on IT2 FS theory, however, all of them are not suitable to handle this case, in the following, we will select the best car following the procedure proposed in this paper:

1) Obtain the normalized decision matrix $\tilde{R}$, i.e., (19).
2) Based on Table I, we can get the average centroid matrix $C = (c_{ij})_{n\times m}$ of the normalized decision matrix $\tilde{R}$, i.e., (20).
3) Utilize the model $(\mathrm{M}-1)$ to get the optimal weight vectors $\omega^{(i)} = (\omega_1^{(i)}, \omega_2^{(i)}, \omega_3^{(i)}, \omega_4^{(i)})^T (i = 1, 2, 3)$ corresponding to the alternatives $x^i(\ i = 1, 2, 3)$:
$\omega^{(1)} = (0.05, 0.05, 0.5, 0.4)^T$,
$\omega^{(2)} = (0.225, 0.05, 0.5, 0.225)^T$,
$\omega^{(3)} = (0.2, 0.05, 0.3, 0.45)^T$.
and construct the weight matrix

$$\Omega = \begin{pmatrix} 0.05 & 0.225 & 0.2 \\ 0.05 & 0.05 & 0.05 \\ 0.5 & 0.5 & 0.3 \\ 0.4 & 0.225 & 0.45 \end{pmatrix}$$

then

$$(C\Omega)^T (C\Omega) = \begin{pmatrix} 210.6289 & 208.2285 & 214.1800 \\ 208.2285 & 205.9309 & 211.9237 \\ 214.1800 & 211.9237 & 218.5783 \end{pmatrix}$$

4) Calculate the normalized eigenvector w of the matrix $(C\Omega)^T(C\Omega)$: $w = (0.3325, 0.3289, 0.3386)^T$.
5) Utilize (13) to derive the weight vector ω:

$$\begin{aligned} \omega &= \Omega w \\ &= \begin{pmatrix} 0.05 & 0.225 & 0.2 \\ 0.05 & 0.05 & 0.05 \\ 0.5 & 0.5 & 0.3 \\ 0.4 & 0.225 & 0.45 \end{pmatrix} \begin{pmatrix} 0.3325 \\ 0.3289 \\ 0.3386 \end{pmatrix} \\ &= (0.1583, 0.0500, 0.4323, 0.3594)^T. \end{aligned}$$

6) Utilize (12) to get the overall average centroid values $c_i\,(i = 1, 2, 3)$ of the alternatives $x_i\,(i = 1, 2, 3)$:
$c_1 = \sum_{j=1}^{4} \omega_j c_{1j} = 8.9556$,

$c_2 = \sum_{j=1}^{4} \omega_j c_{2j} = 8.9645$,
$c_3 = \sum_{j=1}^{4} \omega_j c_{3j} = 7.1435$.

7) Rank the alternatives $x_i\,(i = 1, 2, 3)$ based on the average centroids $c_i (i = 1, 2, 3) : x_2 \succ x_1 \succ x_3$, and then the most desirable car is also x_2.

VI. Conclusion

We have investigated the MADM problems under interval type-2 fuzzy environment, and developed an approach to handling the situations where the attribute values are characterized by IT2 FSs, and the information about attribute weights is partially known. We have constructed the average centroid matrix of the interval type-2 fuzzy decision matrix, and established some optimization models to determine the attribute weights. Then we have utilized the obtained attribute weights to get the overall average centroid values of the alternatives, and then find their ranking and select the most desirable one. All these procedures have been illustrated by a decision making problem regarding the selection of cars. In the future, we will apply the developed procedures to some other fields such as medical diagnosis, pattern recognition, machine learning and market prediction, supply chain management, etc.

Acknowledgment

This work has been supported by the Natural Science Foundation of China Project under Grant No. 70771025.

References

[1] S. H. Kim, S. H. Choi, and J. K. Kim, "An interactive procedure for multiple attribute group decision making with incomplete information: Range-based approach," *Eur. J. Oper. Res.*, vol. 118, no. 1, pp. 139–152, 1999.

[2] S. H. Kim and B. S. Ahn, "Interactive group decision making procedure under incomplete information," *Eur. J. Oper. Res.*, vol. 116, no. 3, pp. 498–507, 1999.

[3] L. A. Zadeh, "Fuzzy sets," *Inform. Contr.*, vol. 8, no. 3, pp. 338–353, 1965.

[4] C. Hwang and K. Yoon, *Multiple attribut decision making: Methods and applications*. Berlin, Heidelberg: Springer, 1981.

[5] S. M. Chen, "A new approach to handling fuzzy decision-making problems," *IEEE Trans. Syst. Man Cybern.*, vol. 18, no. 6, pp. 1012–1016, 1988.

[6] S. J. Chen and C. L. Hwang, *Fuzzy multiple attribute decision making: Methods and applications*. Berlin: Springer-Verlag, 1992.

[7] C.-T. Chen, "Extensions of the TOPSIS for group decision-making under fuzzy environment," *Fuzzy Sets Syst.*, vol. 114, no. 1, pp. 1–9, 2000.

[8] S.-M. Chen, "Fuzzy group decision making for evaluating the rate if aggregative risk in software development," *Fuzzy Sets Syst.*, vol. 118, no. 1, pp. 75–88, 2001.

[9] J. Wang and Y.-I. Lin, "A fuzzy multicriteria group decision making approach to select configuration items for software development," *Fuzzy Sets Syst.*, vol. 134, no. 3, pp. 343–363, 2003.

[10] D.-F. Li, "An approach to fuzzy multiattribute decision making under uncertainty," *Inf. Sci.*, vol. 169, no. 1-2, pp. 97–112, 2005.

[11] Y.-M. Wang and C. Parkan, "Multiple attribute decision making based on fuzzy preference information on alternatives: Ranking and weighting," *Fuzzy Sets Syst.*, vol. 153, no. 3, pp. 331–346, 2005.

[12] ——, "A general multiple attribute decision-making approach for integrating subjective preferences and objective information," *Fuzzy Sets Syst.*, vol. 157, no. 10, pp. 1333–1345, 2006.

[13] R. R. Yager and Z. S. Xu, "The continuous ordered weighted geometric operator and its application to decision making," *Fuzzy Sets Syst.*, vol. 157, no. 10, pp. 1393–1402, 2006.

[14] T. Tsabadze, "A method for fuzzy aggregation based on group expert evaluations," *Fuzzy Sets Syst.*, vol. 157, no. 10, pp. 1346–1361, 2006.

[15] T.-C. Wang and T.-H. Chang, "Application of TOPSIS in evaluating initial training aircraft under a fuzzy environment," *Expert Syst. Appl.*, vol. 33, no. 4, pp. 870–880, 2007.

[16] Z. Wu and Y. Chen, "The maximizing deviation method for group multiple attribute decision making under linguistic environment," *Fuzzy Sets Syst.*, vol. 158, no. 14, pp. 1608–1617, 2007.

[17] D.-F. Li, "Compromise ratio method for fuzzy multi-attribute group decision making," *Appl. Soft. Comput.*, vol. 7, no. 3, pp. 807–817, 2007.

[18] Z. Hua, B. Gong, and X. Xu, "A DS-AHP approach for multi-attribute decision making problem with incomplete information," *Expert Syst. Appl.*, vol. 34, no. 3, pp. 2221–2227, 2008.

[19] G. Fu, "A fuzzy optimization method for multicriteria decision making: An application to reservoir flood control operation," *Expert Syst. Appl.*, vol. 34, no. 1, pp. 145–149, 2008.

[20] C.-J. Lin and W.-W. Wu, "A causal analytical method for group decision-making under fuzzy environment," *Expert Syst. Appl.*, vol. 34, no. 1, pp. 205–213, 2008.

[21] M.-J. Tsai and C.-S. Wang, "A computing coordination based fuzzy group decision-making for web service oriented architecture," *Expert Syst. Appl.*, vol. 34, no. 4, pp. 2921–2936, 2008.

[22] J. M. Mendel, *Uncertain Rule-Based Fuzzy Logic Systems: Introduction and New Directions*. Upper-Saddle River, NJ: Prentice-Hall, 2001.

[23] L. A. Zadeh, "The concept of a linguistic variable and its application to approximate reasoning - I," *Inf. Sci.*, vol. 8, no. 3, pp. 199–249, 1975.

[24] J. M. Mendel and R. I. B. John, "Type-2 fuzzy sets made simple," *IEEE Trans. Fuzzy Syst.*, vol. 10, no. 2, pp. 117–127, 2002.

[25] J. M. Mendel, "Advances in type-2 fuzzy sets and systems," *Inf. Sci.*, vol. 177, no. 1, pp. 84–110, 2007.

[26] N. N. Karnik and J. M. Mendel, "Applications of type-2 fuzzy logic systems to forecasting of time-series," *Inf. Sci.*, vol. 120, no. 1-4, pp. 89–111, 1999.

[27] J. M. Mendel and D. Wu, *Perceptual Computing: Aiding People in Making Subjective Judgments*. Piscataway, NJ: Wiley-IEEE Press, 2010.

[28] N. N. Karnik and J. M. Mendel, "Operations on type-2 fuzzy sets," *Fuzzy Sets Syst.*, vol. 122, no. 2, pp. 327–348, 2001.

[29] F. Liu and J. M. Mendel, "Aggregation using the fuzzy weighted average as computed by the Karnik-Mendel Algorithms," *IEEE Trans. Fuzzy Syst.*, vol. 16, no. 1, pp. 1–12, 2008.

[30] J. M. Mendel, R. I. John, and F. Liu, "Interval type-2 fuzzy logic systems made simple," *IEEE Trans. Fuzzy Syst.*, vol. 14, no. 6, pp. 808–821, 2006.

[31] D. Wu and J. M. Mendel, "Aggregation using the linguistic weighted average and interval type-2 fuzzy sets," *IEEE Trans. Fuzzy Syst.*, vol. 15, no. 6, pp. 1145–1161, 2007.

[32] ——, "Corrections to "aggregation using the linguistic weighted average and interval type-2 fuzzy sets"," *IEEE Trans. Fuzzy Syst.*, vol. 16, no. 6, pp. 1664–1666, 2008.

[33] D. Wu, "Intelligent systems for decision support," Ph.D. dissertation, 2009.

[34] S.-M. Chen and L.-W. Lee, "Fuzzy multiple criteria hierarchical group decision-making based on interval type-2 fuzzy sets," *IEEE Trans. Syst. Man Cybern. A, Cybern.*, vol. 40, no. 5, pp. 1120–1128, 2010.

[35] ——, "Fuzzy multiple attributes group decision-making based on the interval type-2 TOPSIS method," *Expert Syst. Appl.*, vol. 37, no. 4, pp. 2790–2798, 2010.

[36] ——, "Fuzzy multiple attributes group decision-making based on the ranking values and the arithmetic operations of interval type-2 fuzzy sets," *Expert Syst. Appl.*, vol. 37, no. 1, pp. 824–833, 2010.

[37] J. M. Mendel, *Uncertain Rule-Based Fuzzy Logic Systems: Introduction and New Directions*. Upper Saddle River, NJ: Prentice-Hall, 2001.

[38] N. N. Karnik and J. M. Mendel, "Centroid of a type-2 fuzzy set," *Inf. Sci.*, vol. 132, no. 1-4, pp. 195–220, 2001.

[39] J. M. Mendel and H. Wu, "New results about the centroid of an interval type-2 fuzzy set, including the centroid of a fuzzy granule," *Inf. Sci.*, vol. 177, no. 2, pp. 360–377, 2007.

[40] D. Wu and J. M. Mendel, "Enhanced Karnik–Mendel Algorithms," *IEEE Trans. Fuzzy Syst.*, vol. 17, no. 4, pp. 923–934, 2009.

[41] R. R. Yager, "Ranking fuzzy subsets over the unit interval," vol. 17. Proceedings of the IEEE Conference on Decision and Control, 1978, pp. 1435–1437.

[42] R. A. Horn and C. R. Johnson, *Matrix analysis*. Cambridge: Cambridge University Press, 1990.

[43] D. Wu and J. M. Mendel, "A comparative study of ranking methods, similarity measures and uncertainty measures for interval type-2 fuzzy sets," *Inf. Sci.*, vol. 179, no. 8, pp. 1169–1192, 2009.

2011 IEEE International Conference on Fuzzy Systems
June 27-30, 2011, Taipei, Taiwan

A Fuzzy Toolbox for the R Programming Language

Christian Wagner and Simon Miller
Horizon Digital Economy Research /
Intelligent Modelling and Analysis Research Group
University of Nottingham
Nottingham, U.K.
{christian.wagner, s.miller}@nottingham.ac.uk

Jonathan M. Garibaldi
Intelligent Modelling and Analysis Research Group
University of Nottingham
Nottingham, U.K.
jmg@cs.nott.ac.uk

***Abstract*—In this paper, we describe the main functionality of an initial version of a new fuzzy logic software toolkit based on the R language. The toolkit supports the implementation of several types of fuzzy logic inference systems and we discuss and present several aspects of its capabilities to allow the straightforward implementation of type-1 and interval type-2 fuzzy systems. We include source code examples and visualizations both of type-1 and type-2 fuzzy sets as well as output surface visualizations generated using the R toolkit. Finally, we describe the significant benefits of relying on the R language as a language which is employed across several research disciplines (thus enabling access to fuzzy logic tools to a variety of researchers), outline future developments and most importantly call for contributions, comments and feedback to/on this open-source software development effort.**

Keywords; fuzzy inference software; type-1 fuzzy inference; type-2 fuzzy infererence; open-source software; Matlab; R

I. INTRODUCTION

Since its introduction in 1965 [1], fuzzy logic has become widely popular, both as a specific field of research, as well as a tool for the modeling of and computation with data applied in a myriad of disciplines, from the arts, over medical sciences to industrial control. The vast majority of current applications of fuzzy logic are based on type-1 fuzzy logic.

While the research interest in type-2 fuzzy logic has steadily grown in the last 10 years, the number of applications is still very limited. In particular, the majority of existing applications are mostly confined to applications that are research-led, frequently by members of the fuzzy logic research community, rather than third party applications entirely conceived and implemented for example by practitioners in other fields and industry.

It is a well-known phenomenon in computing that an essential criterion for the adoption of a new method or algorithm, the availability of software implementing said algorithm is essential. Analogously, we believe that for the more widespread adoption and application of non-classical fuzzy logic systems (such as non-stationary, interval type-2 and general type-2 fuzzy systems), the provision of free, widely available, open-source software is essential. As part of this paper, we are introducing an open-source software package based on the R language which is approaching the release of its first version.

This work was partly funded by the RCUK's Horizon Digital Economy Research Hub grant, EP/G065802/1.

R is a free, open-source language and importantly, is already used widely across disciplines (from Computer Science to Social Sciences - such as Political Science). As such, providing freely accessible software to employ non-classical fuzzy systems as part of an R package will allow practitioners and researchers from a wide range of areas to make use of the research developed by the fuzzy logic research community who in turn can incorporate the potentially vast amount of feedback and real-world deployment information into their research.

The paper is intended both to introduce the R fuzzy logic toolbox as well as an invitation to the fuzzy community, particularly the type-2 community, to join with the development effort, give feedback and recommendations.

The paper is structured as follows. Section II provides basic background information on the current availability of packages for the development of non-classical fuzzy logic applications as well as the R language in general. Subsequently, Section III describes the R toolbox and reviews some of the currently available functionality. Section IV provides some sample plots of non-classical fuzzy logic membership functions as well as control surfaces, demonstrating the graphical capabilities of the toolbox. Finally, Section V discusses the current development of the toolbox and describes the planned long-term development.

II. BACKGROUND

The use of toolboxes for implementing type-1 fuzzy systems is widespread owing to the availability of such software to facilitate development. Perhaps the most well known of these is the Fuzzy Logic Toolbox provided for MATLAB® (The Mathworks, Inc.) which allows users to create type-1 fuzzy inference systems using MATLAB® command-line functions or a graphical user interface (GUI) [2].

Currently, there is a lack of toolboxes available for creating other types of fuzzy systems including, in particular, type-2 fuzzy systems. We should note that a several researchers (e.g. J. Mendel) and research groups have opened their source code and made it accessible, however the use of source code still requires in-depth familiarity with the material in question (i.e. non-classical fuzzy logic systems) and thus does not fulfill the same role as toolkits in terms of making the material easily accessible for people from a variety of backgrounds.

Castro et al. have previously demonstrated a toolbox for MATLAB® that provides tools for the development of interval

978-1-4244-7316-8/11/$26.00 ©2011 IEEE

type-2 fuzzy systems [3] which provides a GUI interface similar to that of the MATLAB® Fuzzy Logic Toolbox [2]. While the toolbox allows the implementation of interval type-2 fuzzy systems using MATLAB®, it, being based on the proprietary MATLAB® is restricted in terms of its availability (MATLAB® is subject to license fees) as well as its user base (MATLAB® is predominantly used as part of the physical sciences and engineering). These restrictions as well as the limitation to interval type-2 fuzzy logic limit the adoption potential of the existing MATLAB® based toolbox and currently it is difficult to find examples of its more widespread adoption.

The toolbox introduced as this paper is based on/around the freely available R platform/language. As noted, R offers the advantage of not only being freely available but importantly that it, as a language is accessible to people from a large variety of backgrounds. This in particular should facilitate the experimentation with fuzzy logic and the research and investigation into new problem domains.

Further, the advantage of high-level specialist mathematical languages such as R and MATLAB® is that, in contrast to low-level languages such as C or Java, they provide built-in primitives for representing and manipulating vectors and matrices, which can be used to directly represent and manipulate fuzzy sets. In addition, these languages provide comprehensive built-in graphical capabilities for 2D and 3D plotting, which can be used to visualize fuzzy sets.

R itself is an open-source language and environment for statistical computing and graphics, similar to the S language and environment originally developed at Bell Laboratories (formerly AT&T, now Lucent Technologies) by John Chambers and colleagues. It is a mature, open-source language which is actively maintained by the community. R is similar to MATLAB® in that it is a generic programming environment within which mathematical and statistical techniques are implemented [4]. R is an integrated suite of software facilities for data manipulation, calculation and graphical display, including effective data handling and storage facilities, a suite of operators for calculations on arrays and matrices, a large integrated collection of intermediate tools, graphical facilities for display either on-screen or on hardcopy, and a well-developed, simple and effective programming language which includes conditionals, loops, user-defined recursive functions and input and output facilities. R can be easily extended via packages. (Text adapted from [4]). R is freely downloadable from the main R Project repository [4], and can easily be installed on many platforms including popular versions of Microsoft Windows, Apple Mac OS X and Linux.

In this paper we present a fuzzy logic toolbox for the programming language R that includes tools for creating type-1, non-stationary [5], interval type-2 [6] and zSlices based general type-2 fuzzy systems [7]. At the present stage, the toolbox is in the final stages of development in preparation for the release of its first version. In particular, features such as the general type-2 aspects are being completed, documentation material is being added. This paper aims to encourage the research community to engage and provide feedback and suggestions for the final release. In the following sections, we provide a high level view of some of the features that are currently included.

III. TOOLKIT FEATURES

The R toolkit has several similarities with the MATLAB® toolbox. This is natural as both toolkits/toolboxes implement established fuzzy logic concepts and algorithms. The similarity between both approaches however has the distinct advantage of greatly facilitating the use of either toolkit for authors familiar with the other one.We proceed by illustrating the similarities based on fundamental fuzzy logic concepts between both toolkits in III.A, followed by a basic overview of some of the currently implemented features in terms of type-1 fuzzy logic in III.B and interval type-2 fuzzy logic in III.C.

Non-stationary fuzzy systems and zSlices based general type-2 fuzzy systems' functionality has largely been included in the toolkit but as part of this paper we will focus on the features of "standard" type-1 and interval type-2 fuzzy systems. We are addressing some features of non-classical fuzzy logic systems in Section IV, in particular demonstrating the visualization capabilities of the current toolkit in terms of 3D set visualizations.

A. Similarity between R and MATLAB® toolkits.

As noted, the R toolkit has been designed to maximize the transparency for people who are already familiar with the parameters and specification of fuzzy sets and systems while also making it easy to learn for people who are new to the area. Incidentally, the command line interface employed in the R language results in a high similarity compared to the command line interface operation of the MATLAB® Fuzzy Logic Toolbox. However, while the R language offers many similar functions to MATLAB® and add-on toolboxes (termed 'packages' in R), the language is a development of the S language and not a 'clone' of MATLAB®. Hence, it has detailed syntactic differences from MATLAB®, as summarized in [8].

For example, in MATLAB®, the command:

```
x = [ 1, 2, 3];
```

creates a vector of length 3, while the equivalent in R is:

```
x = c(1, 2, 3) or   x <- c(1, 2, 3)
```

(these two forms of assignment operator are not completely identical, and the latter version is preferred in the R community). Similarly, the MATLAB® command:

```
x = [ 1, 2, 3; 4, 5 6];
```

creates a matrix of 2 rows by 3 columns, while the equivalent in R for this is:

```
x = rbind(c(1,2,3), c(4,5,6))
```

While there are syntactic difference between R and MATLAB®, in terms of the scope of the implementation the current state of the R toolkit is comparable to the MATLAB® Fuzzy Logic Toolbox in terms of type-1 fuzzy logic, however, the R toolkit further addresses more complex types of fuzzy logic such as interval and general type-2 fuzzy logic. For the

majority of the type-1 functionality, one can establish a direct mapping between the functions provided in the R package and those in the MATLAB® Fuzzy Toolbox as is expected because of the underlying fundamental fuzzy logic theory concepts).

The main functions necessary to create and perform fuzzy inference in Mamdani-style are supplied within the package (note that Sugeno / TSK style inference is not currently supported). A wide variety of forms of membership functions are supported similar to those currently provided by MATLAB®. Additionally, currently the common forms of conjunction, disjunction, implication and aggregation operators are supported (including, minimum, maximum, product and probabilistic OR), as well as Mamdani inference and popular forms of defuzzification as further detailed below.

To illustrate the creation of a complete FLC using the R toolkit we have provided a comparison between implementing a completed fuzzy inference system (FIS) in both MATLAB® and using the R toolkit. The example is based on the 'tipper' example provided as part of the MATLAB® Fuzzy Logic Toolbox documentation. The complete source code to set up the example for both MATLAB® and R is provided in Section VI.A and VI.B respectively. Note the expected high similarity between the constructions of a fuzzy inference system in both platforms. Each example also demonstrates the output capabilities, specifically (we use the R notation here):

- *showfis(fis)*
  Produces a summary of the constructed FIS.
- *showrule(fis)*
  Prints the rules of the specific FIS.
- *evalfis(c(1,2), fis)*
  Evaluates the given FIS using the specified input values.
- *evalfis(rbind(c(3,5), c(2,7)), fis)*
  Evaluates the given FIS for the specified set of inputs.
- *gensurf(fis)*
  Produces the control surface (visualisation) for the given FIS.

Overall, the R toolkit is aimed to generally providing at least the same set of features as are offered as part of the MATLAB® Fuzzy Logic Toolbox. As an open-source toolkit, it is hoped that in the medium and long term the overall feature richness and functionality of the toolkit will be increased through open access and contribution. This could potentially also include further components that employ the provided toolkit, such as a Graphical User Interface (GUI) which could further facilitate the implementation of FLCs in particular for users who are not familiar with the implementation of FLCs and/or have no programming background or interest. Further, it is expected that several community-centred "flavours" of the R toolkit will be developed in time (for example for medical applications, applications in economy, etc.).

In the following Sections we describe some of the basic aspects of creating type-1 and interval type-2 fuzzy systems using the toolkit.

B. Type-1 fuzzy logic features.

As part of describing the type-1 functionality we give examples of the basic membership functions currently supported before briefly reviewing the inference and defuzzification operations.

1) Membership Functions.

a) Triangular

Triangular membership functions are created by providing the left, right and center points of the membership function. For example, the source code snippet below produces the membership function depicted in Figure 1.

```
x <- 1:10
y <- trimf(x,c(2,5,8))
```

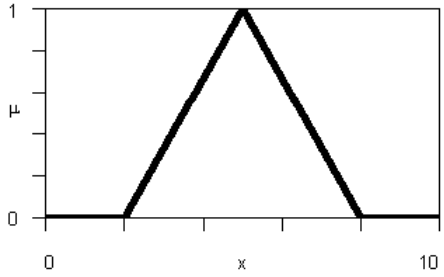

Figure 1 An example of a triangular type-1 membership function produced using the R toolkit.

b) Trapezoidal

For trapezoidal sets, four values describing the left and right slopes of the trapezoid are used to create the membership function. For example, the source code snippet below produces the membership function depicted in Figure 2.

```
x <- 1:10
y <- trapmf(x,c(2,4,6,8))
```

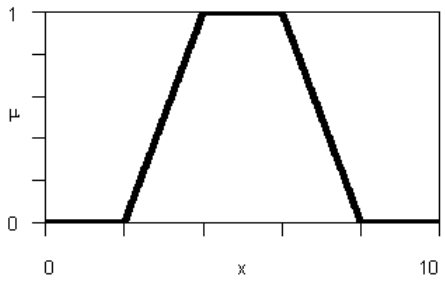

Figure 2 An example of a trapezoidal type-1 membership function produced using the R toolkit.

c) Gaussian

To create a Gaussian membership function the centre of the Gaussian and Sigma (describing the curve) are required. For example, the source code snippet below produces the membership function depicted in Figure 3.

```
x <- 1:10
y <- gaussmf(x,c(2,5))
```

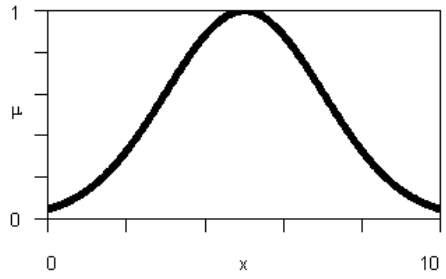

Figure 3 An example of a Gaussian type-1 membership function produced using the R toolkit.

d) Sigmoidal

Sigmoidal membership functions are created using two values representing the centre and width of the slope. For example, the source code snippet below produces the membership function depicted in Figure 4.

x <- 1:10

y <- sigmf(x,c(2,5))

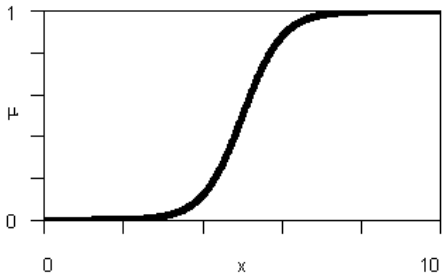

Figure 4 An example of a sigmoidal type-1 membership function produced using the R toolkit.

2) Inference Mechanisms.

The inference mechanisms provided as part of the R toolkit are comparable to those provided by the MATLAB® Fuzzy Logic Toolbox. Specifically, during the rule specification, each rule can be associated with a given weight and the logical connective (AND or OR) can be specified. Considering the 'tipper' example provided in Section VI, we have the example rule specification:

rules= rbind(c(1,1,1,1,2), c(2,0,2,1,1), c(3,2,3,1,2))

The example defines three rules where each rule is described by five parameters (in our example). The parameters are specified analogous to the MATLAB® Fuzzy Logic Toolbox as follows (adopted from [9]) , where *m* is the number of inputs and *n* is the number of outputs:

- The first parameter is the index number for the membership function associated with input 1.
- The second is the index number for the membership function associated with input 2, and so on.
- The next *n* parameters work the same way for the outputs.
- Parameter *m* + *n* + 1 is the weight associated with that rule (typically 1) and parameter *m* + *n* + 2 specifies the connective used (where AND = 1 and OR = 2).

3) Defuzzification Methods.

The following defuzzification methods are currently available as part of the R toolkit:

a) Centroid

This method takes the centre of the area of a membership function on the x-axis.

b) Bisector

Bisector splits the set into two sections of equal area, and takes the vertical that separates the two sections.

c) Mean of maximum

Mean of maximum (MOM) uses the mean value of all discrete x coordinates associated with the maximum membership for the given output set.

d) Smallest of maximum

Smallest of maximum (SOM) uses the smallest value of all discrete x coordinates associated with the maximum membership for the given output set.

e) Largest of maximum

Largest of maximum (LOM) uses the largest value of all discrete x coordinates associated with the maximum membership for the given output set.

Having considered the basic features for type-2 FISs as part of the R toolkit, we proceed to briefly review the currently available interval type-2 features.

C. Interval type-2 fuzzy logic features.

The features available in terms interval type-2 fuzzy systems as part of the R toolkit are briefly summarized below. Specifically, we address the available membership functions in Section III.C.1, followed by the inference capabilities in Section III.C.2 and the type-reduction/defuzzification methods in III.C.3.

1) Membership Functions.

a) Triangular

Type-2 triangular membership functions are created by providing the width of the footprint of uncertainty (FOU), and the left, right and center points of the membership function. For example, the source code snippet below produces the membership function depicted in Figure 5.

x <- 1:10

y <- tri2mf(x,c(1,2,5,8))

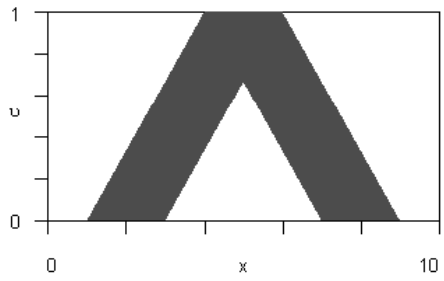

Figure 5 An example of a triangular interval type-2 membership function produced using the R toolkit.

b) Trapezoidal

For type-2 trapezoidal sets, 5 values are required: the width of the FOU, the x coordinate of the leftmost point of the lower membership function, the x coordinate of the rightmost lower membership function, the gradient of the left slope and the gradient of the right slope. For example, the source code snippet below produces the membership function depicted in Figure 5.

x <- 1:10

y <- trapmf2(x, c(1,3,7,1,1))

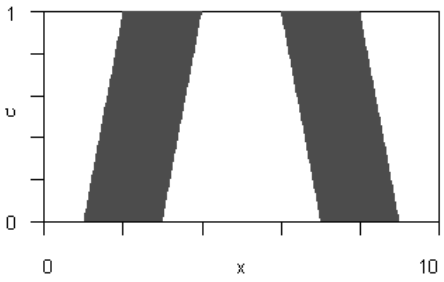

Figure 6 An example of a trapezoidal interval type-2 membership function produced using the R toolkit.

c) Gaussian

To create a Type-2 Gaussian membership function two values of the standard deviation describing the lower and upper membership functions as well as the centre of the Gaussian are required. For example, the source code snippet below produces the membership function depicted in Figure 7.

x <- 1:10

y <- gausst2mf(x,c(1,1.5,5))

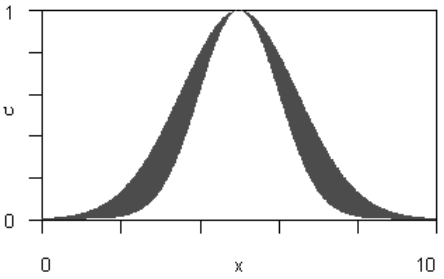

Figure 7 An example of a Gaussian interval type-2 membership function produced using the R toolkit.

2) Inference Mechanisms.

The inference mechanisms are identical to those described in Section III.B.2 for type-1 fuzzy systems but applied to interval type-2 fuzzy sets as described for example in [10].

3) Type-Reduction and Defuzzification.

Type-reduction is currently conducted based on the Karnik-Mendel iterative procedure [11]. The type-reduced set is finally defuzzified by computing the average of its endpoints as in [10].

IV. Sample Visualisations

One of the strengths of R and similar languages is the powerful set of visualization features available. We provide both sample visualizations of linguistic variables (and membership functions) in Section IV.A as well as a comparison of output surface visualizations between the MATLAB and R implementations for the 'tipper' example in Section IV.B.

For all visualizations, the R environment supports a variety of formats for both soft-copy and hard-copy output. The precise details of any implementation depend on the underlying operating system, but in most platforms the production of *jpeg* or *png* graphical formats and *postscript* of Adobe® *pdf* formats is supported.

A. Linguistic Variable and Membership Function Visualisation.

The current R toolkit contains a series of functions for plotting membership functions. Figure 8 and Figure 9 depict examples of visualizing the linguistic variable "Temperature" based on the three linguistic labels *cool*, *warm* and *hot*. The linguistic labels are represented by Gaussian Type-1 and Interval Type-2 membership functions in Figure 8 and Figure 9 respectively.

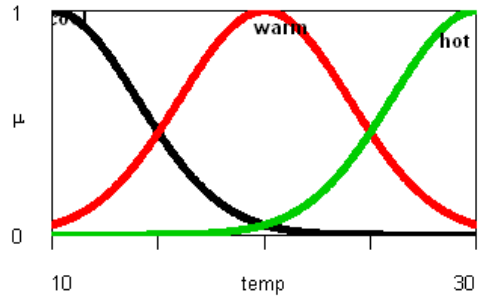

Figure 8 An example of the plotting of multiple type-1 membership functions using the R toolkit.

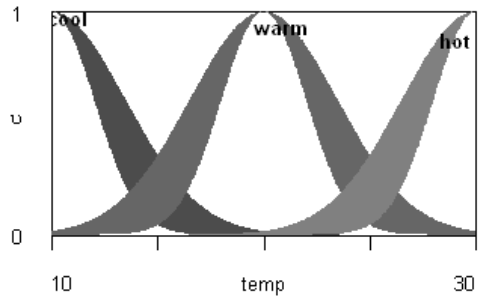

Figure 9 An example of the plotting of multiple interval type-2 membership functions using the R toolkit.

By utilizing the recently released `RGL` library, it is possible to create three dimensional plots of both interval type-2 and general type-2 membership functions. Examples of both are includes as part of Figure 10 and Figure 11 respectively.

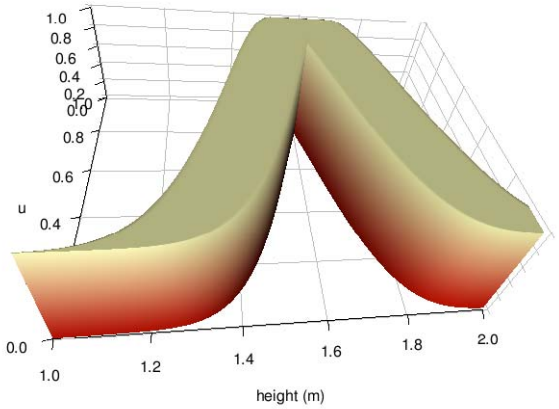

Figure 10 An example of a interval type-2 Gaussian membership function produced using the R toolkit. (shown in 3D)

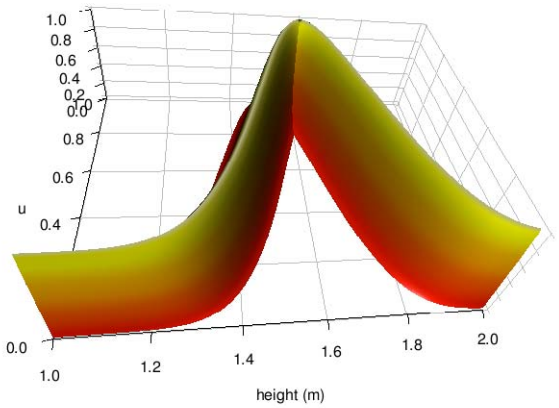

Figure 11 An example of a general type-2 Gaussian membership function produced using the R toolkit.

As well as the visualization of membership functions, the R toolkit also supports the visualization of output surfaces as shown in the following Section.

B. Output Surface Plots

For FIS featuring two input variables and one output variable, the R toolkit supports the generation of a visualization of the output surface using the function `gensurf` (as shown in VI.B).

In order to allow the comparison in terms of visualization between the MATLAB® and R implementations we provide the output surfaces produced for the 'tipper' example (see Appendices) in Figure 12 and Figure 13 respectively.

Note: The control surfaces are shown from a slightly different viewpoint, however the visualization capability of the R toolkit is clearly demonstrated which is the primary aim in this section.

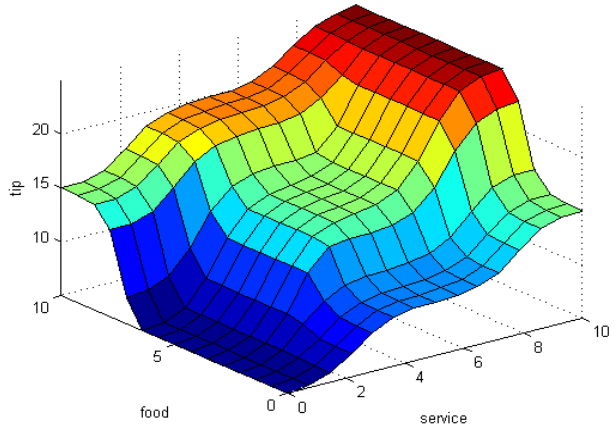

Figure 12 The control surface of the 'tipper' example produced using the MATLAB®.

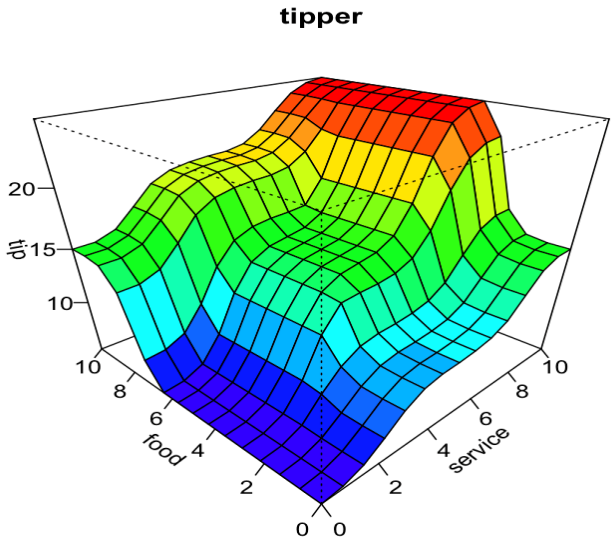

Figure 13 The similar control surface of the 'tipper' example produced using the R toolkit.

V. Conclusions and Future Work

As part of this paper we have given a brief introduction to a Fuzzy Logic toolkit based on the R language. We have provided a brief overview as well as source code samples of the currently available features within the toolkit. Specifically, we have described the functionality in terms of type-1 and interval type-2 fuzzy logic systems and provided examples of the visualization capabilities of the toolkit for type-2 fuzzy systems in general.

The current toolkit already supports other variations of fuzzy systems, including non-stationary fuzzy sets and the basics for zSlices based general type-2 fuzzy systems. We are aiming to complete these and other features and to include appropriate documentation materials before the free release of the toolkit. The open nature of the R language means that the package will be available to be freely expanded by other authors and contributors after its release and additional features such as TSK inference can easily be included.

The purpose of the paper is to get feedback and suggestions from our peers on the current approach, its functionality and applicability, and to gather information on similar efforts that may be underway in order to avoid duplication of work.

R is an ideal choice of language for such a toolbox as it is freely available and used by a wide variety of researchers from a variety of research fields: creating a tool in R will provide a generic infrastructure for a wide range of users and will hopefully lead to an increase in the uptake of fuzzy logic systems (of all flavours).

The result of this work will be an open source toolkit that can be used freely, placing the tools required to create these types of fuzzy system into the hands of all researchers interested in adopting a fuzzy approach.

Acknowledgment

We would like to thank the reviewers for providing a series of helpful and constructive comments and suggestions for the further development of the toolkit.

References

[1] L.A. Zadeh, "Fuzzy sets", Information and Control, 8 (3), 1965, pp. 338—353.

[2] MATLAB Fuzzy Logic Toolbox http://www.mathworks.com/products/fuzzylogic/ (live on 28th Feb 2011)

[3] J.R. Castro, O. Castillo, P. Melin, "An Interval Type-2 Fuzzy Logic Toolbox for Control Applications", Proceedings of the International conference of Fuzzy Systems, pp. 1-6, July 2007, London, UK.

[4] R Development Core Team; "R: A Language and Environment for Statistical Computing", *R Foundation for Statistical Computing*, Vienna, Austria, ISBN: 3-900051-07-0, URL: http://www.R-project.org, 2011.

[5] J.M. Garibaldi, M. Jaroszewski, S. Musikasuwan; "Nonstationary Fuzzy Sets", *IEEE Transactions on Fuzzy Systems*, 16(4): 1072-1086, 2008.

[6] J.M. Mendel, R.I. John and F. Liu, "Interval Type-2 Fuzzy Logic Systems Made Simple," *IEEE Transactions on Fuzzy Systems*, 14: 808-821, 2006.

[7] C. Wagner and H. Hagras, "Towards general type-2 fuzzy logic systems based on zSlices," IEEE Transactions Fuzzy Systems, vol. 18, no. 4, pp. 637-660, August 2010.

[8] D. Hiebeler; "MATLAB/R Reference", URL: http://cran.r-project.org/doc/contrib/Hiebeler-matlabR.pdf (live on 28th Feb 2011)

[9] MATLAB® Fuzzy Logic Tool™ 2 Users'Guide, The MathWorks, Inc., Natick, USA, March 2010.

[10] J. Mendel, Uncertain Rule-Based Fuzzy Logic Systems: Introduction and New Directions. Upper Saddle River, NJ, Prentice Hall, 2001.

[11] N. N. Karnik and J. M. Mendel, "Centroid of a type-2 fuzzy set," Inform. Sci., vol. 132, pp. 195–220, 2001.

VI. Appendices

A. *The tipper example in MATLAB®.*

The source code is based on the example provided in the tipper application example provided in the MATLAB® Fuzzy Logic Toolbox 2 users' guide.

```
a=newfis('tipper');
a=addvar(a,'input','service',[0 10]);
a=addvar(a,'input','food',[0 10]);
a=addvar(a,'output','tip',[0 30]);

a=addmf(a,'input',1,'poor','gaussmf',[1.5 0]);
a=addmf(a,'input',1,'good','gaussmf',[1.5 5]);
a=addmf(a,'input',1,'excellent','gaussmf',[1.5 10]);

a=addmf(a,'input',2,'rancid','trapmf',[-2 0 1 3]);
a=addmf(a,'input',2,'delicious','trapmf',[7 9 10 12]);

a=addmf(a,'output',1,'cheap','trimf',[0 5 10]);
a=addmf(a,'output',1,'average','trimf',[10 15 20]);
a=addmf(a,'output',1,'generous','trimf',[20 25 30]);

ruleList=[ ...
1 1 1 1 2
2 0 2 1 1
3 2 3 1 2 ];
a=addrule(a,ruleList);

showfis(fis)
showrule(fis)

evalfis([1 2], a)
evalfis([3 5; 2 7], a)
gensurf(a)
```

B. *The tipper example using the R toolkit.*

The complete R Fuzzy code for the same example as provided for MATLAB®.

```
fis= newfis('tipper')

fis= addvar(fis, 'input', 'service', c(0,10))
fis= addvar(fis, 'input', 'food', c(0,10))
fis= addvar(fis, 'output', 'tip', c(0,30))

fis= addmf(fis, 'input', 1, 'poor', 'gaussmf', c(1.5,0))
fis= addmf(fis, 'input', 1, 'good', 'gaussmf', c(1.5,5))
fis= addmf(fis, 'input', 1, 'excellent', 'gaussmf', c(1.5,10))
```

```
fis= addmf(fis, 'input', 2, 'rancid', 'trapmf', c(0,0,1,3))
fis= addmf(fis, 'input', 2, 'delicious', 'trapmf', c(7,9,10,10))

fis= addmf(fis, 'output', 1, 'cheap', 'trimf', c(0,5,10))
fis= addmf(fis, 'output', 1, 'average', 'trimf', c(10,15,20))
fis= addmf(fis, 'output', 1, 'generous', 'trimf', c(20,25,30))

rules= rbind(c(1,1,1,1,2), c(2,0,2,1,1), c(3,2,3,1,2))
fis= addrule(fis, rules)

showfis(fis)
showrule(fis)

evalfis(c(1,2), fis)
evalfis(rbind(c(3,5), c(2,7)), fis)
gensurf(fis)
```

2011 IEEE International Conference on Fuzzy Systems
June 27-30, 2011, Taipei, Taiwan

A Comparison of Non-stationary, Type-2 and Dual Surface Fuzzy Control

Naisan Benatar, Uwe Aickelin and Jonathan M. Garibaldi *Member, IEEE*
School of Computer Science
University of Nottingham
Email: [nxb,uxa,jmg]@cs.nott.ac.uk

***Abstract*—Type-1 fuzzy logic has frequently been used in control systems. However this method is sometimes shown to be too restrictive and unable to adapt in the presence of uncertainty. In this paper we compare type-1 fuzzy control with several other fuzzy approaches under a range of uncertain conditions. Interval type-2 and non-stationary fuzzy controllers are compared, along with 'dual surface' type-2 control, named due to utilising both the lower and upper values produced from standard interval type-2 systems. We tune a type-1 controller, then derive the membership functions and footprints of uncertainty from the type-1 system and evaluate them using a simulated autonomous sailing problem with varying amounts of environmental uncertainty. We show that while these more sophisticated controllers can produce better performance than the type-1 controller, this is not guaranteed and that selection of Footprint of Uncertainty (FOU) size has a large effect on this relative performance.**

Keywords: Interval Type-2 Fuzzy, Robot Boat control, Fuzzy Control, Non-stationary

I. Introduction

Fuzzy controllers use the principles of fuzzy sets and fuzzy logic to automate system controllers. The underpinning technique of fuzzy logic was originally introduced by Zadeh in his seminal paper [1]. In this paper, various types of fuzzy set are used including: type-0 which are identical to crisp sets; type-1 where membership is a continuous real value in $[0, 1]$; and type-2 in which the membership values are themselves type-1 fuzzy sets. The complexity of the sets increases from type-0 to type-2 as the number of dimensions is increased accordingly. Type-1 fuzzy logic has been applied extensively to a range of real-world problems due to the ease with which it can be applied. It has been applied successfully to areas including robotic control, fuzzy decision making and fuzzy classifier systems. However, a number of issues are known to exist in the application of type-1 in problem domains which require decision making in the presence of uncertainty [2]. It is suggested in [3] that such type-1 fuzzy systems have no capacity for modelling uncertainty, which limits their application to more complex real-world problems.

Type-2 fuzzy logic has been proposed as a solution to overcome some of the limitations experienced when using type-1 systems. In contrast to type-1 systems, type-2 systems contain membership functions which in themselves are type-1 fuzzy sets. This adds an extra layer of dimensionality to the system which is postulated to assist in the process of coping with uncertainty in the problem domain. However, this addition of an additional dimension is not without its problems. As a result, additional computational overhead is incurred when implementing type-2 control, which has limited the applicability of type-2 systems to the classical problems solved by type-1 systems, including robotic controllers. This has become less of a problem due to advances in both computational processing power and available memory in computational systems. However, it may still pose a problem when applying type-2 systems to lightweight embedded systems. A more complete overview of interval type-2 fuzzy logic can be found in both [4] and [5].

It has been shown, for example in [6], that type-2 systems can outperform type-1, potentially due to the fact that type-2 fuzzy sets have this 'extra' dimension. There has been some investigation into the reasons underpinning the improved performance of type-2 in comparison with type-1 systems. However, such investigations have been limited in scope. It is also uncertain if improved tuning of type-2 sets or alternative approaches might provide equally good performance without the computational overhead experienced in the application of a full type-2 system.

In conventional type-2 controllers, two control surfaces are obtained, one from the lower bound of interval type-2 defuzzification and one from the upper bound. Due to memory constraints or performance constraints, it is common to implement type-2 fuzzy controllers by calculating the control surface offline, by simply taking the mean of the lower and upper bound value returned by the controller, and then by downloading the resulting surface as a look-up table [7]. In this paper, Birkin and Garibaldi outlined a novel formulation of a controller which maintains the lower and upper control surfaces separately, and then switches dynamically between the surfaces. If the average of the lower and upper control surfaces is used, this novel controller reduces to a 'conventional' interval type-2 controller. Other dynamic combinations are also possible, such that some of the additional information available from an interval type-2 system is maintained in order to be utilised by the controller. This is termed a 'dual-surface' (interval) type-2 controller.

Non-stationary (NS) fuzzy sets, as described in [8] and [9], have been proposed to model variability in human decision making, and may offer a method to alleviate some of the issues raised by the application of type-2 sets. NS fuzzy sets are a relatively new development in the field and are based on the principles of type-1 systems. The 'non-stationary' component refers to variations made to the membership functions defined

978-1-4244-7316-8/11/$26.00 ©2011 IEEE

in a type-1 system. A NS fuzzy set uses perturbations of standard T1 membership functions to produce several slightly different membership function on each iteration through the system. These can then be processed iteratively in the inference system and outputs aggregated, such as by majority vote or mean. NS fuzzy sets have the potential to cope with uncertainty in a problem domain while limiting the additional computational overhead. However, the current extent of comparisons between the different fuzzy controllers is somewhat limited.

It is clear that both theoretical and practical comparisons must be performed in order to understand the differences between the three different fuzzy systems. In this paper we use a simulated autonomous sailing problem (SASP) to examine the practical differences between the different fuzzy control mechanisms. The SASP forms an ideal test-bed for a number of reasons. Firstly, control of an autonomous robot is a challenging problem containing decision making in an uncertain environment. Secondly, this problem involves the interplay between a simulated boat and a dynamic environment, in which data from both the boat and environment are inherently noisy. The amount of uncertainty present in the SASP is an important factor in this application selection. Fuzzy controllers have been researched within the domain of autonomous sailing, especially the application of type-1 controllers, including [10]. In particular, [11] used a type-1 fuzzy system to control an autonomous boat of 1m in length around a predefined course using an attached state machine to handle situations such as tacking (upwind navigation through side to side movement). In this paper it is shown that while the fuzzy controller performed well downwind, it struggled to perform in upwind/tacking scenarios. Fuzzy controllers are not the only method used in the control of autonomous sailing boats. PID controllers [12], and neuro-endocrine approaches [13] have also been successfully applied to navigation problems. Proportional Integral (PI) controllers are also indicated as suitable control mechanisms for autonomous sail boat navigation.

The aim of this paper is to provide a comparison between a number of alternative controllers, including a Proportional-Integral (PI) controller, a type-1 and a conventional interval type-2 controller, when applied to the SASP. We investigate changes in the behaviour of the controllers upon the application of environmental noise, in our case, changes in simulated wind direction. We use a simulator termed 'Tracksail' to perform our experiments (see Section III-A). Performing the experiments in simulation has the distinct advantage that experimental set-ups can be precisely replayed and repeated, allowing for the comprehensive analysis of the different techniques. We examine differences between controllers through the resultant control surfaces and by statistical analysis of the experimental results.

This paper is organised as follows: Section II describes the components of the fuzzy systems that are under test along with a PI controller that was used as a control. Section III outlines the environment and experimental set-up used to make the comparison. This is followed by Section V which presents the results obtained, followed by Section VI which discusses the implications of these results and draws some conclusions. Finally, Section VII outlines some avenues for potential future work.

II. Fuzzy Robot Control

A. Design Decisions

Stelzer's work on fuzzy sailboats [14], [11] is used as a basis for our controller design. Several changes were necessary due to lack of data about our boat model which were used in the paper to determine some of the parameters, such as *rate of turn* and *heeling* of the boat. Error was retained as the difference between current and desired directions in degrees as shown in Equation 1 while an additional input, change in error has been added to the system. This is defined as the change in the error since the previous iteration of the controller as shown in Equation 2.

$$error = Desired\ Direction - Current\ Direction \quad (1)$$

$$\Delta error = Current\ Error - Previous\ Error \quad (2)$$

Each input has five associated fuzzy sets which gives a rule base of 25 rules as shown in Table II-C. The membership functions (MFs) for the terms of the two inputs are shown in Figure 1(a), along with the output of the system which is the percentage change of the rudder of the boat characterised by singleton outputs, shown in Figure 1(f).

Horizontal perturbations of the type-1 membership functions was used to generate our non-stationary controller membership functions. The perturbation function was a horizontal movement defined by a gaussian distribution with a mean of zero. The standard deviation of the distribution was altered several times per batch of experiments to generate several different non-stationary controllers and resulted in input membership functions as shown in Figures 1(b) and 1(d). During execution, each controller would select 30 values from the above distribution to create 30 membership functions which were then processes as a standard type-1 system, the mean of the outputs from each of the 30 systems was taken to give a final output.

Interval type-2 systems in which secondary membership functions are binary instead of continuous can be visualised as a two dimensional area known as the Footprint of Uncertainty (FOU). This makes interval type-2 systems considerably more manageable than the general type-2 variety. We have derived footprints of uncertainty by starting with the simple type-1 and moving a uniform distance along the x-axis in both directions providing a lower and upper bound. This gives FOUs that are very similar in shape to the non-stationary membership functions as shown in Figures 1(c) and 1(e).

A dual surface type-2 controller is implemented to determine if improved results can be achieved through incorporating extra information, such as the upper and lower outputs as outlined in [7]. This employs the algorithm described in Figure 2 for selection of control surfaces and determination of output. This algorithm compares a user chosen metric, in this case the magnitude of the input error with a threshold value.

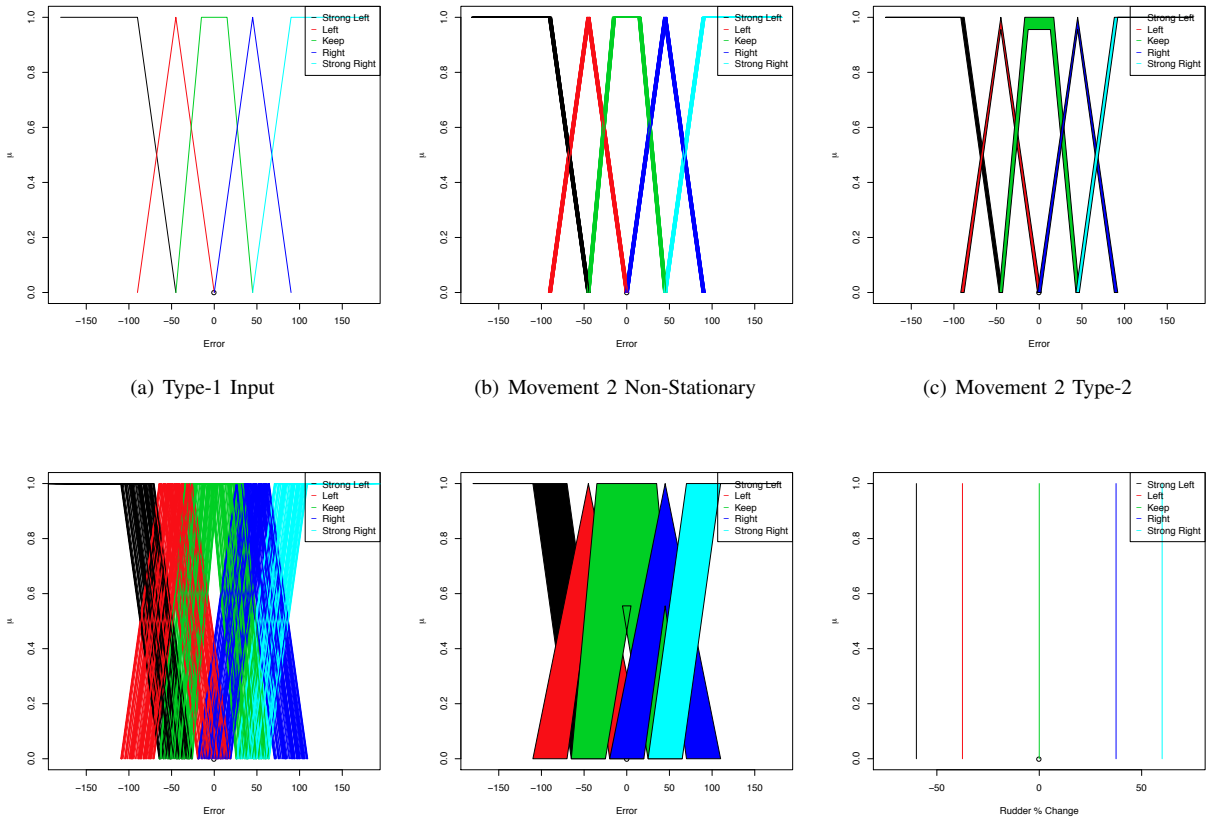

(a) Type-1 Input (b) Movement 2 Non-Stationary (c) Movement 2 Type-2

(d) Movement 20 Non-stationary (e) Movement 20 Type-2 (f) Type-1 Output Singletons

Fig. 1. Membership functions of Type-1, Type-2 and Non-stationary controllers. Unless stated these are input membership functions

```
error = control_var - set_point
diff = abs(error)
if ( diff < THRESHOLD )
   control_action = (LS + US) / 2
else
   if ( error > 0 )
      control_action = LS
   else
      control_action = US
endif
```

Fig. 2. The dual-surface control algorithm

On this basis, the final output of the system is selected from either the lower, upper or mean value. For this comparison, the original method of using the magnitude of the error in the system is retained. As with other controllers, several different threshold values are used to determine any observable effect on the system and its performance.

B. Tuning & Optimisation

While manual tuning of the original membership functions ([14] and [15]) was performed we did not specifically perform any automatic tuning for two main reasons. Firstly the intention was to ensure generality and this would not be possible were we to use a specific training data set. Secondly it would be difficult to ensure the same ámountóf tuning was performed on each different variety of fuzzy due to the different methods required to tune for example, a type-1 system compared to a type-2, which could potentially lead to unfair comparisons being made.

C. Tacking Behaviours

With respect to the application of our controllers to SASP, additional behaviours need to be defined. One drawback of using SASP for testing these controllers is the limits of the wind — no boat can sail directly into the wind. To solve this problem, higher level control was added which modifies the desired direction input to the controller. Sailing into the wind in practice requires tacking behaviour. The design of the courses for our experiments attempts to minimise this effect by setting courses which should avoid the need to tack. The main-sail on the boat is controlled by a simple set of rules that were previously developed in conjunction with the PI controller and have been shown to provide acceptable performance.

TABLE I
RULE TABLE FOR TYPE-1 CONTROLLER: ROWS SHOW *delta error* FUZZY SETS; COLUMNS SHOW *error* FUZZY SETS; SR: STRONG RIGHT; R: RIGHT; K: KEEP; L: LEFT; SL: STRONG LEFT

	Large Positive	Positive	None	Negative	Large Negative
Strong Left	sr	sr	r	r	r
Left	k	l	r	k	k
Middle	k	l	k	r	k
Right	k	k	l	r	k
Strong Right	l	l	l	sl	sl

III. EXPERIMENTAL SETUP

A. Tracksail

The simulator used for this research, Tracksail has been used previously for development and testing of autonomous sailing robotic systems [16] including the development and tuning of described PI controller. Tracksail is Java based and communicates with controllers by means of a TCP/IP socket allowing any compatible language to be used to control the boat. Each controller is linked into a common framework which provides tacking logic, sensor readings and motor change routines in addition to any other common code required. This ensures consistency between runs with different controllers.

One aim of this work is to investigate changes in the performance of type-2 controllers as the size of the FOU is varied. This is facilitated by the simulator in that it eliminates many categories of uncertainty not directly relevant to this investigation. This includes sensor noise, where the value returned by the sensor does not truly reflect the physical value that it is measuring, for example.

B. Track Configuration

Each experiment batch consists of 30 simulator runs where the tested controller will attempt to guide the boat towards a single way-point which was defined as 550 metres west of its starting point, defined by the simulator as the point (0,0). In the first batch of experiments the wind direction was fixed as 30 degrees across the boat at a fixed velocity of 7 m/s. This means that the wind will not introduce any noise in this experiment. However, we still observed minor differences between runs, potentially attributed to the timing of interacting processes and delays caused by socket processing in the software and operating system.

A series of experiments introduced wind related noise into the system at two distinct levels. Noise was defined as a specified number of wind changes per second and by the size of the arc defined by the *Max* and *Min* wind direction parameters specified in the simulator which are specified in degrees. Experiment two (medium noise) used an arc of 20° and a single wind change every five seconds, while experiment three (high noise) used a 30° arc with a wind change every three seconds.

C. Performance Metrics

Two metrics of performance were collected for all controllers. The first is the total root mean square of the error (RMSE) between the current heading compared with the desired bearing. The second metric is the time taken for the boat to complete the set course which is a straight line distance of 550 'metres'. The correlation between RMSE and time taken is not as trivial as in the case of a wheeled robot as the boat controller must balance deviating from a straight line sufficiently to capture enough wind for forward movement, against the extra time taken to perform this manoeuvre. Higher boat speeds in Tracksail can be reached when the boat is parallel to the wind, with the sail set to 90 degrees. However, if this is performed for the entire duration the boat would not reach its destination. Hence, a balance between speed and keeping on course must be found. This becomes increasingly important as noise is introduced into the wind direction variable.

IV. CONTROLLER SETUP

For reference and control purposes a tuned PI controller is included in the comparison. This controller uses the same input value (error between current and desired bearings) as well as its integral over time instead of the change in error. It uses a P-gain value of 1.7 and an I-gain value of 0.01. These values are derived in previous experiments performed by Suaze and Neal [17].

The running rate for all controllers was fixed at 1Hz. This is chosen to ensure that the more sophisticated controllers can execute a complete control loop. This low running rate may lead to lower performance than optimal as overshoot may occur with slow running controllers. However, as all controllers were subject to the same restrictions, we believe the comparison to be fair.

Five individual values were chosen for the perturbation function of the non-stationary controller, namely 0, 2, 5, 10 and 20 degrees. These values fall within the limits of plausibility for perturbation of the *error* and *delta error* inputs to the system. This provides insight as to where the true optimal value may occur. These measures will also be used to define the FOUs of the interval type-2 systems where the number refers to the width of the FOU at any flat point ($x = c$).

Numerous parameters in the interval type-2 system (and hence the dual surface controller) were fixed to ensure consistency with the type-1 system. Each experiment involves the variation of a single parameter. In the standard type-2 case we defined a parameter `movement` which defines the width of the input FOUs and in the dual surface case we used a variable threshold value with a fixed movement value of 5.

As a validation exercise we ran experiment one (low noise) with type-2, non-stationary and dual surface controllers with the parameters including movement value and threshold (where appropriate) set to zero. This is used to highlight that when upper and lower membership functions are set to be equal, the footprint of uncertainty is reduced down to type-1 sets. This confirmed that the performance is equivalent to that of the standard type-1 system. The small disparity was put down

TABLE II
RMSE AND TOTAL TIME TAKEN FOR COURSE COMPLETION AT LOW NOISE LEVELS. MEAN AND STANDARD DEVIATION OF 30 RUNS WITH BEST IN CATEGORY SHOWN IN ITALIC, BEST OVERALL CONTROLLER IN BOLD AND VALUES THAT ARE STATISTICALLY DIFFERENT FROM THE TYPE-1 CONTROLLER ARE UNDERLINED. PARAMETER REFERS TO MOVEMENT IN NS AND IT2 CASES AND THRESHOLD IN THE DS CASE

Variety	Parameter Value	Mean RMSE	Std. Dev RMSE	Mean Time	Time Std.Dev
PI	N/A	18.01	0.30	146.56	2.02
Type 1	N/A	16.32	0.17	140.80	0.66
Non Stationary	2	17.03	0.64	139.96	1.16
Non Stationary	5	*16.72*	*0.54*	***139.28***	***0.63***
Non Stationary	10	16.99	1.14	139.59	1.41
Non Stationary	20	16.74	0.55	140.07	1.10
Type 2	2	15.97	0.62	*140.42*	*1.03*
Type 2	5	*15.84*	*0.28*	140.65	1.18
Type 2	10	16.04	0.53	140.80	0.66
Type 2	20	18.94	0.57	150.03	2.69
Dual Surface	2	19.13	0.61	153.80	1.86
Dual Surface	5	19.34	1.35	150.57	3.35
Dual Surface	10	16.73	0.59	145.43	1.33
Dual Surface	25	***15.80***	***0.24***	149.10	7.22
Dual Surface	50	15.99	0.25	*142.38*	*3.59*

TABLE III
RMSE AND TOTAL TIME TAKEN FOR COURSE COMPLETION AT MEDIUM NOISE LEVELS. MEAN AND STANDARD DEVIATION OF 30 RUNS WITH BEST IN CATEGORY SHOWN IN ITALIC, BEST OVERALL CONTROLLER IN BOLD AND VALUES THAT ARE STATISTICALLY DIFFERENT FROM THE TYPE-1 CONTROLLER ARE UNDERLINED. PARAMETER REFERS TO MOVEMENT IN NS AND IT2 CASES AND THRESHOLD IN THE DS CASE

Variety	Parameter Value	Mean RMSE	Std. Dev RMSE	Mean Time	Time Std.Dev
PI	N/A	23.25	0.30	204.69	12.97
Type 1	N/A	24.47	0.76	221.34	8.46
Non Stationary	2	22.86	1.99	160.50	9.17
Non Stationary	5	22.21	4.11	172.53	23.17
Non Stationary	10	20.27	3.18	158.53	3.61
Non Stationary	20	***21.09***	***2.80***	***161.09***	***9.23***
Type 2	2	25.65	1.39	189.81	11.69
Type 2	5	20.48	3.34	178.64	20.19
Type 2	10	*19.32*	*1.28*	*168.39*	*11.24*
Type 2	20	26.00	5.31	186.87	5.34
Dual Surface	2	20.59	0.96	168.62	7.85
Dual Surface	5	23.06	5.10	181.94	19.03
Dual Surface	10	22.02	0.92	173.54	12.54
Dual Surface	25	19.75	3.84	*171.27*	*12.66*
Dual Surface	50	***18.81***	***1.61***	174.35	18.10

to operations in the system such as floating point arithmetic which are performed in different orders in the type-2 based and non-stationary systems. We are therefore satisfied that our type-2 and NS implementations are valid and correct when compared with the type-1.

A. Hypothesis

In our experiments we predict that all controllers will show a reduction in performance as the amount of noise introduced into the environment is increased. We anticipate that the performance decrease shown in type-2 systems will be less in magnitude than that of the type-1 controller due to their ability to deal with uncertainty. We also aim elucidate the influence of the size of the FOU on the overall performance of the type-2 controller. In our experiments we ascertain if controllers with larger FOU values will produce improved performances over those with smaller FOUs under higher environmental noise conditions.

V. RESULTS

From Figure 3, it can be observed that as the noise increases (left to right in the subsigures), the courses increase in deviation. This aligns with the hypothesis that increase in environmental noise will result in increasingly non-linear routes.

The results of experiment one (low noise) are shown in Table V, in which it can be observed that the standard type-2 interval controllers have variations in which the RMSE performance is shown to be significantly better than the type-1 and PI controllers. However, there is a peak in the performance increase which occurs at a FOU size of 10 after which performance reduces and drops to lower than that of the PI. A similar pattern is observed in the case of the dual surface controller. However, in this case both RMSE and time taken start off lower

than even the PI but then improves to show the best performance overall. We hypothesise that if the threshold was further increased performance would once again eventually to

TABLE IV
RMSE AND TOTAL TIME TAKEN FOR COURSE COMPLETION AT HIGH NOISE LEVELS. MEAN AND STANDARD DEVIATION OF 30 RUNS WITH BEST IN CATEGORY SHOWN IN ITALIC, BEST OVERALL CONTROLLER IN BOLD AND VALUES THAT ARE STATISTICALLY DIFFERENT FROM THE TYPE-1 CONTROLLER ARE UNDERLINED. PARAMETER REFERS TO MOVEMENT IN NS AND IT2 CASES AND THRESHOLD IN THE DS CASE

Variety	Parameter Value	Mean RMSE	Std. Dev RMSE	Mean Time	Time Std.Dev
PI	N/A	25.85	0.38	157.2	1.41
Type 1	N/A	27.43	0.93	153.61	3.53
Non Stationary	2	31.22	4.55	153.83	7.37
Non Stationary	5	22.21	4.11	172.53	23.17
Non Stationary	10	***20.27***	***3.18***	158.53	3.61
Non Stationary	20	28.69	1.35	*151.23*	*2.60*
Type 2	2	25.48	0.66	*149.70*	*2.08*
Type 2	5	*25.33*	*1.36*	150.19	2.33
Type 2	10	25.83	0.93	149.77	2.75
Type 2	20	32.72	1.92	172.37	17.31
Dual Surface	2	*24.11*	*1.15*	***141.09***	***5.76***
Dual Surface	5	28.93	7.41	152.49	10.02
Dual Surface	10	29.12	8.46	151.91	12.63
Dual Surface	25	26.09	0.84	151.26	2.56
Dual Surface	50	25.95	2.66	149.81	2.86

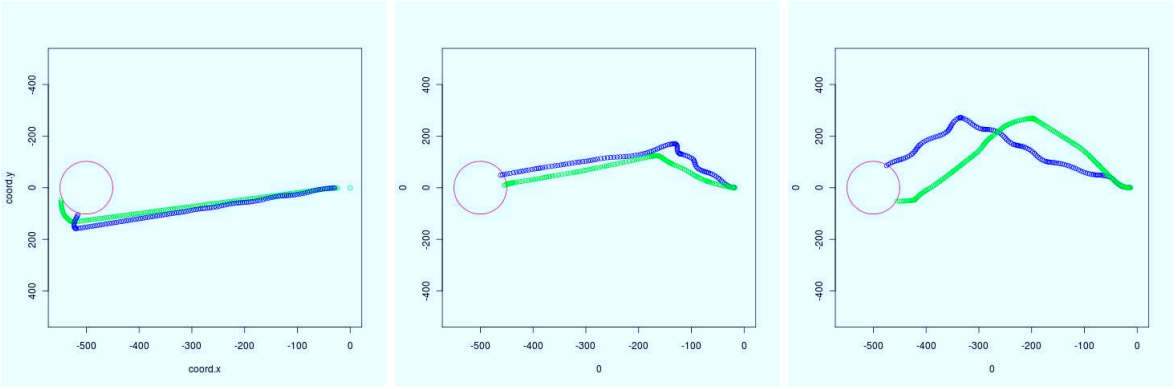

(a) Exp 1 Course Example (Low Noise) (b) Exp 2 Course Example (Medium Noise) (c) Exp 3 Course Example (High Noise)

Fig. 3. Pots of example course taken by PI (green) and Type-2 (blue) at low, medium and high noise levels. Course end point shown as a red circle.

dip below the PI performance level. In this experiment these RMSE improvements do not lead to a significant reduction in time to complete the course compared with the type-1.

Experiment two (medium noise) increases the amount of noise present in the environment with the results shown in Table reftab:Exp2. These clearly show the anticipated drop in performance with the average increase in RMSE being 5.06 and the mean increase in time being 40.2 seconds. A very similar pattern to the previous experiment can be observed in the performance values of the standard type-2 and dual surface results with a peak in performance being observed at a movement level of 10° for the interval type-2 controller, and at a threshold of 50 for the dual-surface controller. Once again it is hypothesised that a threshold greater than that tested would show a drop in performance. Overall, this experiment demonstrates that the type-2 controllers all out-perform the type-1 variety under these noise conditions.

Table V summarises the results of experiment three (high noise). The overall the performance is somewhat lower than for the previous experiment with only one configuration of the dual-surface controller obtaining statistically significant improvements over the type-1 controller, whilst none of the standard interval type-2 or non-stationary approaches achieved this (in the *time taken* metric), though the non-stationary controller did produce two cases in which the RMSE was improved significantly. The mean RMSE increase between experiments one and three were 9.57 with an average time increase of 10.4s.

Two-sided unpaired Mann-Whitney tests are used to determine any statistically significant differences between the type-1 compared against the non-stationary, type-2 and dual-surface controllers. This is performed for both RMSE and *time taken* metrics with a p-value of 0.05 being used to reject the null hypothesis. This test is also performed for the PI and type-1 controllers for all three experiments. The type-1 RMSE proved significantly lower than the PI with low noise (experiment one). For medium and high noise, it was found that the PI is significantly better (lower RMSE) than the type-1 controller. However, in the cases of the total time taken, the type-1 controller was significantly better (lower) than the PI in low and high noise, with the opposite being true for medium noise.

VI. Discussion & Conclusions

Our findings are summarised below, followed by a more detailed analysis and discussion in the following section.

- At low and high noise levels the more sophisticated controllers generally do not show a statically significant improvement when compared to the type-1 controllers. Specific controllers in each category do show this improvement however.
- At medium noise levels type-2, non-stationary and dual-surface controllers generally do exhibit statistically significant improvements on the type-1 method.
- The results difference between PI and type-1 controllers show that type-1 does improve upon the PI for the RMSE metric and improves under lower noise conditions and low and high noise conditions for the time metric.

The fact that the PI controller actually out-performed the type-1 controller in some experiments, however insignificantly, does tend towards the conclusion that some aspects of the type-1 system were not tuned optimally and that further work may be required in this regard. However, any changes required would also affect the other controllers, which have been based on this type-1. For this reason, we do not anticipate that there would be a great deal of alteration in the general ordering of the performance of the various controllers, were this to be done.

Overall, the performance of the pure type-2 controller was somewhat lower than anticipated and it failed to perform significantly better than the type-1 system in some cases, as is especially evident at low and high noise levels. One potential reason that this could be attributed to is the somewhat naïve method by which the FOUs were generated — that is by blurring a type-1 membership function in an equal distance in either direction. However, it has been shown that simple augmentations made to type-2 systems in form of the dual-surface controller can improve the results of this controller

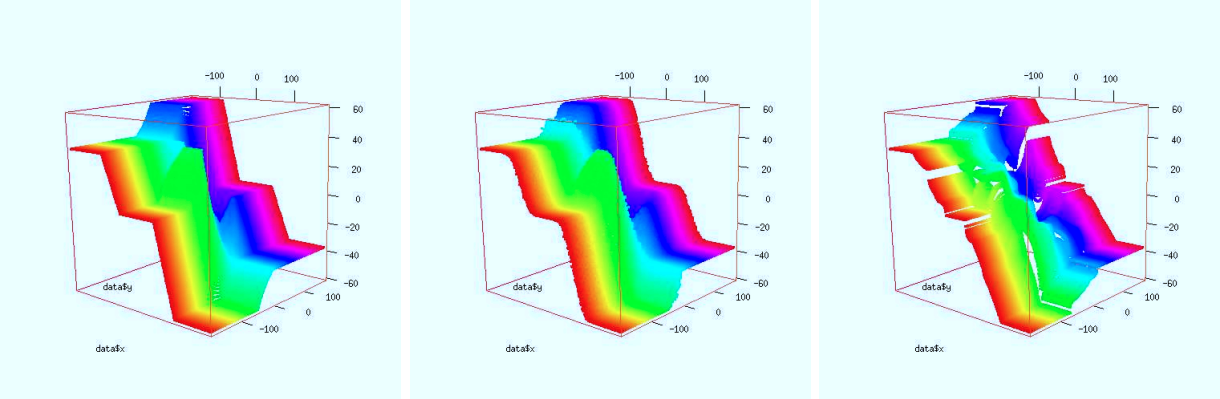

(a) Type-1 Control Surface (b) 20 Non-stationary Control Surface (c) Movement 20 Type-2 Control Surface

Fig. 4. Control Surfaces for Type-1, Type-2 (Movement=20) and Non-stationary (Movement = 20) Controllers at varying noise levels

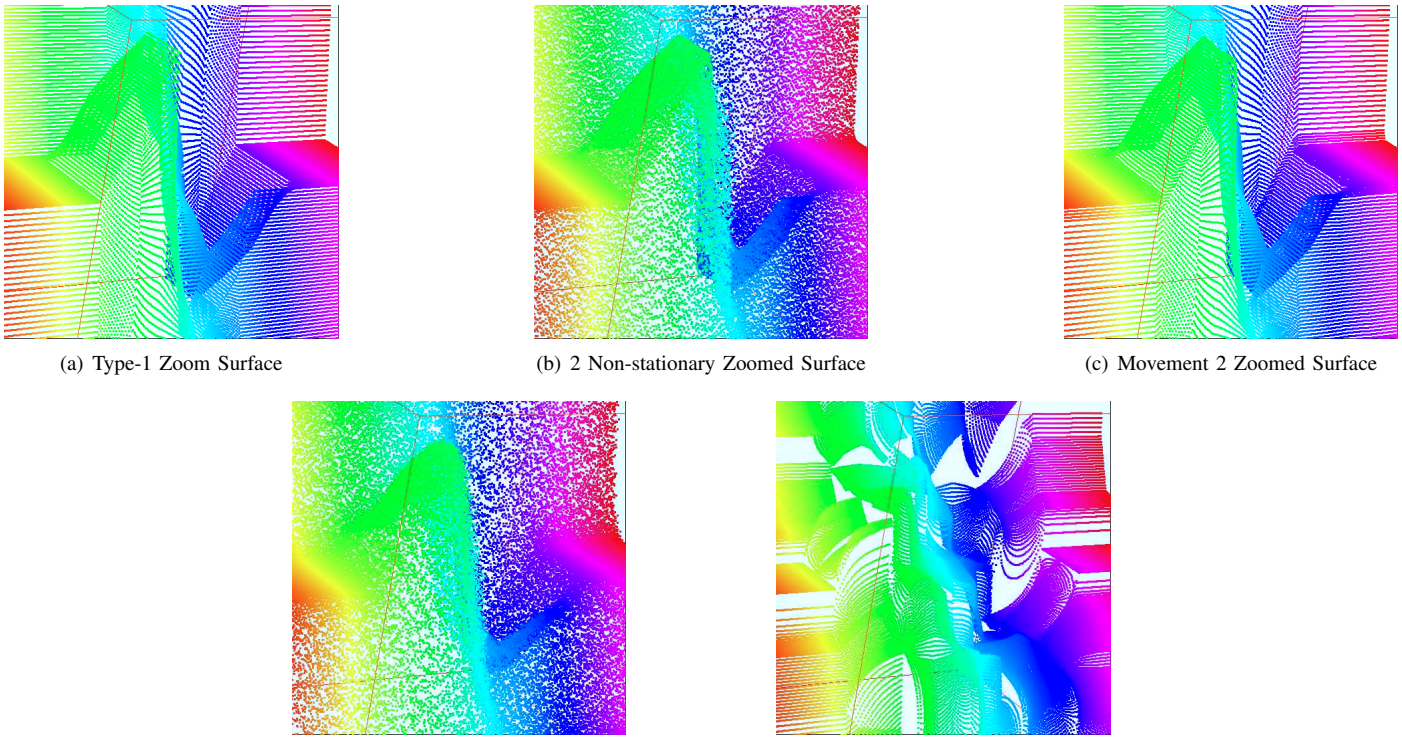

(a) Type-1 Zoom Surface (b) 2 Non-stationary Zoomed Surface (c) Movement 2 Zoomed Surface

(d) 20 Non-stationary Zoomed Surface (e) Movement 20 Type-2 Zoom Surface

Fig. 5. Zoomed view of control Surfaces for Type-1, Type-2 and Non-stationary Controllers at 2 and 20 movement

type somewhat and that if alternative methods for selection between the different outputs were investigated performance could be improved even more.

The results of the non-stationary approach in these experiments shows that in some situations that it can provide equal, or better performance than similar type-2 or dual surface controllers showing that these approaches do offer a viable alternative to type-2 systems as, even though their performance is not always fully comparable, the simplicity to implement in conjunction with the lower computational overhead does give this approach several distinct advantages.

In all of the more sophisticated controllers, the size of the movement (FOU size in type-2 based and horizontal perturbation) had a large effect of the output of the system. In almost all cases there were values selected in which performance decreased markedly. For example, using a value of 20 movement in all three experiments caused the type-2 controller to perform significantly worse than a movement of 10. When the membership functions and FOUs at these levels are observed (Figure 1) it may be suggested that in such cases the degree of overlap would cause considerably more rules to fire than occur at lower movement levels indicating that

would would either have to alter the rule-base to accommodate this or change the shape or spacing of the fuzzy sets so that this was less of a problem. This therefore implies two things. Firstly, the shape of the FOU may well be less important that its overall size or width and, secondly, that the selection of this size must be matched to the size of the uncertainty of the environment in which the controller must perform. To support the experimental work done we have also generated control surfaces for each of the described controllers. Inputs were set between -180° and 180° for both inputs and increased in 1° steps which then map to output percentages between -60% and 60%, resulting in Figure 4 and (zoomed in) Figure 5. It can be seen in the type-1 controller (Figure 4(a)) that the gradient changes are very sharply defined (causing sharp controller changes), which contrasts with both the non-stationary and type-2 controllers that are much smoother, leading to smoother controller transitions. Both varieties show a different type of smoothing with the non-stationary displaying more randomly distributed output points and the type-2 showing a more linear smoothing but both do show the same pattern that as the FOU is increased the smoothness of the transition also appears to increase.

While both of these controllers show this smoothing behaviour, it can also be observed in the type-2 surface that there seem to be artefacts in the form of white lines and areas which are not present on the other surfaces and which seem to increase in size as the footprint of uncertainties are increased. The exact nature and reason behind these artefacts are not yet fully understood but have recently been discussed and reasoned about in [18]. However the existence of these discontinuities highlights the complexity of designing and implementing type-2 fuzzy systems and shows that it is far from a trivial task. Currently available software for implementing type-2 systems is also fairly limited — while some free libraries exist many are implemented in MATLAB which is sometimes unavailable due to cost and licensing issues. There are however a great many type-1 libraries available at no charge and adaptation of one of these to create a non-stationary systems is trivial while adding the necessary code to enable type-2 is significantly harder.

In summary, these experiments show that using type-2 control can certainly give performance that exceeds that of type-1 controllers under certain environmental conditions (medium noise, in our case), whereas this performance gain is not necessarily seen in conditions wither of too low noise or too high noise. While this has long been suspected, we believe this paper provides clear experimental confirmation of this observation. We can also see that with the increase of noise this 'optimal' FOU size will increase with it and that the dual-surface controller gives a computationally inexpensive method for getting even more performance out of a type-2 system, but again careful selection of the threshold value is required to achieve these gains.

VII. Future Work

We have shown that type-2 based systems can certainly be derived from type-1 and produce performance that exceeds type-1 and PI based approaches under certain conditions, described here as a medium noise environment. Further work is required is to formalise these findings and develop a method by which noise levels can be used to generate an estimate of the FOU required for optimal performance to match the given certain conditions. For example in the above case, we would like be able to estimate an effective FOU size based on the size and frequency of the wind changes in the environment. This method could also be applied to non-stationary approaches to observe its behaviour and performance in these scenarios.

VIII. Acknowledgements

The authors thank the School of Computer Science at the University of Nottingham for supporting this work.

References

[1] L. A. Zadeh, "The concept of a linguistic variable and its application to approximate reasoning i," *Information Sciences*, pp. 199–249, 1975.

[2] D. Wu and W. W. Tan, "Interval type-2 fuzzy pi controllers: Why they are more robust," in *IEEE International Conference on Granular Computing*, 2010.

[3] J. M. Mendel and R. I. John, "Footprint of uncertainty and its importance to type-2 fuzzy sets," in *Proceedings of 6th IASTED International Conference on Artificial Intelligence and Soft Computing (ASC 2002)*, Bannf, Canada, 17 - 19 July 2002, pp. 587–592.

[4] J. M. Mendel, R. I. John, and F. Liu, "Interval type-2 fuzzy logic systems made simple," *IEEE Transactions on Fuzzy Systems*, vol. 14, 2006.

[5] N. N. Karnik, J. M. Mendel, and Q. Liang, "Type 2 fuzzy logic systems," *IEEE Transactions on Fuzzy Systems*, vol. 7, 1999.

[6] H. Hagras, "A hierachical type 2 fuzzy logic control architechture for autonomous mobile robots," *IEEE Transactions on Fuzzy Systems*, vol. 12, 2004.

[7] P. A. Birkin and J. M. Garibaldi, "A novel dual-surface type-2 controller for micro robots," in *Proceedings of FUZZ-IEEE*, 2010.

[8] J. M. Garibaldi, M. Jaroszewski, and S. Musikasuwan, "Non-stationary fuzzy sets," *IEEE Transactions on Fuzzy Systems*, vol. 16 (4), pp. 1072–1086, 2008.

[9] J. M. Garibaldi, S. Musikasuwan, and T. Ozen, "The association between non-stationary and interval type-2 fuzzy sets: A case study," in *Proceedings of the IEEE International Conference on Fuzzy Systems (FUZZ-IEEE 05), Reno, USA*, 2005, pp. 224–229.

[10] J. Abril, J. Salon, and O. Calvo, "Fuzzy control of a sailboat," *International Journal of Approximate Reasoning*, vol. 16, pp. 359–375, 1997. [Online]. Available: http://mapp1.de.unifi.it/persone/Allotta/ICAD/Abril1997.pdf

[11] R. Stelzer, T. Pröll, and R. I. John, "Fuzzy logic control system for autonomous sailboats," in *Proceedings IEEE International Fuzzy Systems Conference FUZZ-IEEE 2007*, 2007, pp. 1–6.

[12] B. Yves, "Iboat: an autonomous robot for long-term offshore operation," in *Proceedings MELECON 2010 - 2010 15th IEEE Mediterranean Electrotechnical Conference*, 2009.

[13] C. Sauzé and M. Neal, "A neuro-endocrine inspired approach to long term energy autonomy in sailing robots," in *Proceedings of TAROS (Towards Autonomous Robotic Systems)*, Bannf, Canada, 17 - 19 July 2010, pp. 255–262.

[14] R. Stelzer, "Robotic sailing: Overview," *OGAI Journal (Oesterreichische Gesellschaft fuer Artificial Intelligence)*, vol. 27, no. 2, pp. 2–3, June 2008.

[15] R. Stelzer and T. Pröll, "Autonomous sailboat navigation for short course racing," *Robotics and Autonomous Systems*, vol. 56, no. 7, pp. 604–614, July 2008.

[16] C. Sauzé and M. Neal, "Design considerations for sailing robots performing long term autonomous oceanography," in *Proceedings of The International Robotic Sailing Conference*, 2008.

[17] C. Sauzé, "Control software for a sailing robot," Master's thesis, University of Wales, Aberystwyth, 2005.

[18] D. Wu and J. Mendel, "On the continuity of type-1 and interval type-2 fuzzy logic systems," *IEEE Transactions on Fuzzy Systems*, pp. 179–192, 2011.

2011 IEEE International Conference on Fuzzy Systems
June 27-30, 2011, Taipei, Taiwan

A Perceptual Computer Based Method for Supplier Selection Problem

Shilian Han
School of Marketing and Logistics
Nanjing University of Finance and Economics
Nanjing, 210046, China

Xinwang Liu
School of Economics and Management
Southeast University
Nanjing, 210096, China

***Abstract*—The supplier selection is one of the most important components of production and logistics management for many companies. The supplier selection problem involves different kinds of words in which all of the criteria are weighted using one kind of words and the performance evaluations for all sub-criteria are another kind of words. How to aggregate these words without losing information is a very daunting task using a type-1 fuzzy set (T1 FS) approach. This paper applies a new methodology—Perceptual Computer (Per-C)—to help solve this hierarchical group multi-criteria decision making problem. The Per-C has three components: encoder, computing with words (CWW) engine and decoder. First, the interval approach (IA) is used to obtain interval type-2 fuzzy set (IT2 FS) word models for the words in a pre-specified vocabulary. Second, a linguistic weighted average (LWA) is used to aggregate all the words modeled by IT2 FSs. Finally, a centroid-based ranking method is used to rank the supplier selections, and a similarity measure is used to obtain similarities of the supplier selections. A committee of judges organized with *P* decision makers and *K* experts decides the winning supplier selection as the one with the highest ranking and least similarity to other suppliers.**

***Keywords*-interval type-2 fuzzy set (IT2 FS); perceptual computer (Per-C); supplier selection.**

I. INTRODUCTION

In today's highly competitive environment, outsourcing has become a main stream practice in global business operations [1]; hence, supplier selection is one of the most important components of production and logistics management for many companies. The selection of appropriate suppliers can help companies significantly enhance competitiveness in the market and increase customer satisfaction.

Supplier Selection is a multiple-criteria decision-making (MCDM) problem which is affected by several conflicting factors. Many methods have been proposed and used for supplier evaluation and selection [1-20].

In classical MCDM methods, the ratings and the weights of the criteria are known precisely [3-5]. In fact, human judgments including preferences are often vague, so that a judge can not estimate his preference with an exact numerical value. A more realistic approach may be to use linguistic assessments instead of numerical values to describe the desired value and important weights of criteria.

Because words can mean different things to different people, it is important to use a fuzzy set (FS) model for a word that lets us capture word uncertainty. At present, there are two possible choices, a type-1(T1) FS or an interval type-2(IT2) FS [21-23]. A large number of papers have solved the supplier selection problem using T1 FSs [2,6-20]. That using IT2 FSs as models for words is scientifically correct, whereas using a T1 FS model for a word is scientifically incorrect, follows from the following reasoning [22,24]: (1) A T1 fuzzy set A for a word is well-defined by its MFμ A (x) (x□ X) that is totally certain once all of its parameters are specified; (2) Words mean different things to different people, and so are uncertain; and, therefore, (3) it is contradiction to say that something certain can model something that is uncertain.

Lotfi Zadeh [25-27], the father of Fuzzy Logic, coined the phrase "computing with words" (CWW). He also stated he was interested in developing a computational theory of perceptions—the development of machinery for computing and reasoning with perceptions [28]. Although perceptual computing is a sub-set of CWW, it has a much longer history than CWW. Perceptual Computing used in this paper is associated with the machinery for computing and reasoning with perceptions and data. The architecture for perceptual computing is called a Perceptual Computer (Per-C), and was first used by Mendel [22, 29-30].

This paper is about how the Per-C theory can be applied to the supplier selection problem. The rest of this paper is organized as follows. Section II provides a complete description of the supplier selection problem. Section III introduces a Per-C approach for supplier selections. Section IV gives an example and obtains results using the Per-C approach. Section V draws conclusions.

II. SUPPLIER SELECTION PROBLEM STATEMENT

To achieve a company's purchasing objective, the supplier selection problem may involve n candidate suppliers, each denoted by S_i where $i = 1,\ldots,n$, from which the best supplier is chosen. A committee is organized with $P + K$ judges, where P decision makers are from cross-functional divisions within the company, each denoted by D_p where $p = 1,\ldots,P$, and where K experts are outsiders (i.e., consultants), each denoted by E_k where $k = 1,\ldots,K$. These P decision-makers come up with and decide on a list of M main criteria and l sub-criteria

The work is supported by the National Natural Science Foundation of China (NSFC) under project 70771025.

under each main criterian for supplier selection through brainstorming sessions, and give the weights of all criteria, respectively. The K experts are used to evaluate the performance scores of the sub-criteria for each supplier. The supplier evaluation problem is summarized in Fig. 1. The evaluation criteria of the problem are adopted from [10] on the basis of our literature review. Table I summarizes and defines the abbreviation that are used in Fig. 1.

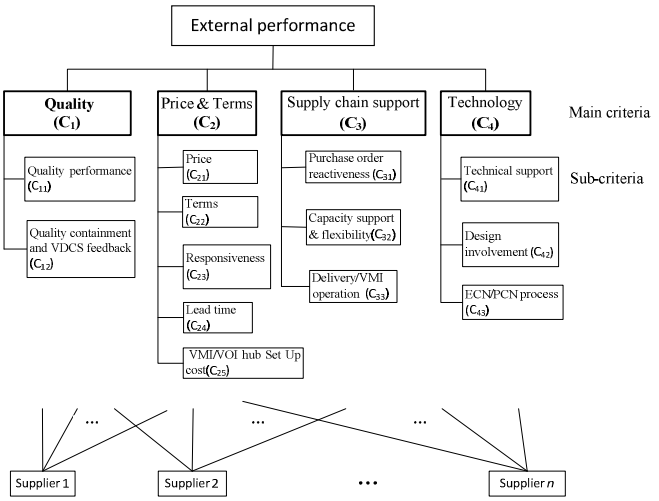

Figure 1. Hierarchical evaluating structure for supplier selections.

It is very clear from this figure that this is a multi-criteria and two-level decision making problem. At the first level each of the n suppliers is evaluated for its performance on four main criteria: Quality (C1), Price & Terms (C2), Supply chain support (C3) and Technology (C4). There are l sub-criteria $(C_{m1}, C_{m2}, \ldots, C_{ms}, \ldots, C_{ml})$ under main criterion m, where $1 \le m \le 4,\ 1 \le s \le l$, and l equals 2, 5, 3 and 3 for C1, C2, C3 and C4, respectively (see Fig. 1). The second level in this hierarchical decision making problem involves a weighted aggregation of the four main criteria for each of n suppliers.

The all sub-criteria are defined using linguistic terms represented by seven words: very poor, poor, medium poor, fair, medium good, good, and very good. The importance weights for all criteria are also defined using linguistic terms represented by seven words: very low, low, medium low, medium, medium high, high, and very high.

This paper provides a new solution method for this group multi-criteria hierarchical supplier selection problem using Perceptual Computing theory and IT2 FSs.

TABLE I. ABBREVIATIONS AND DEFINITIONS

Abbreviations	Definitions
VDCS	Vender defect correcting sheet
VMI	Vendor Managed Inventory
VOI	Vendor Owned Inventory
ECN	Engineering Change Notice
PCN	Process Change Notice

III. PER-C FOR SUPPLIERS EVALUATION

The Per-C has three components: encoder, computing with words (CWW) engine and decoder. It is depicted in Fig. 2. The encoder transforms words into IT2 FSs that activate the CWW engine. The decoder maps the output of the CWW engine into a recommendation and some accompanying data. The CWW engine maps IT2 FSs into IT2 FSs. When perceptual computing is used for the supplier evaluation problem, each of three components must be considered. Table II summarizes and defines the symbols that are used throughout the rest of this paper.

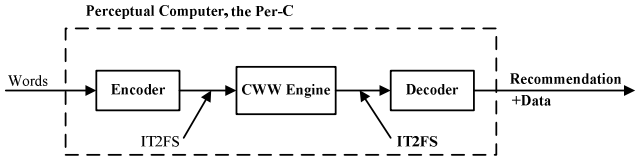

Figure 2. The Per-C that uses IT2 FS models for words [24, 30].

TABLE II. SYMBOLS AND DEFINITIONS

Symbols	Definitions
$\tilde{X}_{ms}^{k}(S_i)$	Assessment of sub-criterion s for major criterion m provided by expert k about S_i (supplier i)
$\tilde{X}_{ms}(S_i)$	Aggregation of $\tilde{X}_{ms}^{k}(S_i)$ across all K experts at S_i
$\tilde{Y}_{m}(S_i)$	Aggregation of $\tilde{X}_{ms}(S_i)$ for major criterion m across all of its sub-criteria, at S_i
$\tilde{Y}(S_i)$	Aggregation of $\tilde{Y}_{m}(S_i)$, at S_i
$\tilde{W}_{m}^{p}$	Linguistic weight assigned by decision maker p to major criterion m
$\tilde{W}_{ms}^{p}$	Linguistic weight assigned by decision maker p to sub-criterion s for major criterion m
$\tilde{W}_{ms}$	Aggregated weight across the P decision makers for sub-criterion s associated with major criterion m
$\tilde{W}_{m}$	Aggregated weight across the P decision makers for major criterion m

A. Encoder

Two codebooks are needed, one for the words that will be used by the experts and another for the weights that will be used by the decision makers. The codebook contains the words and their IT2 FS models.

1) Word FOUs: The interval approach (IA) [31] can be used to model a word using an IT2 FS. It is based on collecting interval end-point data from a group of subjects and does not require any a priori knowledge about FSs; hence, it can be used by anyone. It is a very practical method for mapping subject's data intervals into a footprint of uncertainty (FOU) for a word. The resulting FOUs are either interior, left-shoulder or right-shoulder FOUs (as in Fig. 3), and, it is the data that establishes which FOU models a word.

The IA consists of two parts, a Data Part and a Fuzzy Set (FS) Part. In the Data Part, data intervals (about where a word lies on a pre-specified scale) that have been collected from a group of subjects are pre-processed, after which data statistics are computed for the surviving intervals. In the FS part, FS uncertainty measures are established for a pre-specified triangle T1 MF [always beginning with the assumption that the FOU is an interior FOU, and, if need be, later switching to a shoulder FOU (as in Fig. 3)]. Then the parameters of the

triangle T1 MF are determined using the data statistics, and the derived T1 MFs are aggregated using union leading to an FOU for a word, and finally to a mathematical model for the FOU.

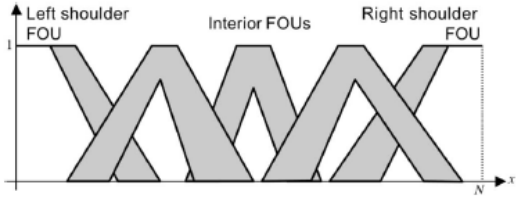

Figure 3. Left-shoulder, right-shoulder and interior FOUs, all of whose LMFs and UMFs are piecewise linear [24,31].

A word that is modeled by an interior FOU has an upper membership function (UMF) that is a trapezoid and a lower membership function(LMF) that is a triangle, but in general neither the trapezoid nor the triangle are symmetrical. A word that is modeled as a left- or right-shoulder FOU has trapezoidal upper and lower MFs; however, the legs of the respective two trapezoids are not necessarily parallel.

2) Word codebook used by experts: This codebook contains the seven words (*very poor, poor, medium poor, fair, medium good, good, very good*) and their FOUs that are used to assess some sub-criteria.

Some sub-criteria have a linguistic negative connotation, and for them, antonyms [32-34] (e. g. , "low" is the antonym of "high") are used instead of the raw words, i. e.

$$\mu_{10-\tilde{A}} = \mu_{\tilde{A}}(10-x) \tag{1}$$

where $10-\tilde{A}$ is the antonym of the IT2 FS $\tilde{A}$. Because an IT2 FS is completely characterized by its LMF ($\underline{A}$) and UMF ($\overline{A}$), each of which is a T1 FS, $\mu_{10-\tilde{A}}(x)$ above is obtained by applying antonyms of T1 FS to $\underline{A}$ and $\overline{A}$. In this paper the following sub-criteria are modeled using antonyms: trade variables, labor cost, inland transportation cost, land cost, law on investment and investment restrictions.

3) Codebook for the weights: This codebook contains the seven words (*very low, low, medium low, medium, medium high, high, very high*) and their FOUs are generated from interval data collected from domain managers and experts.

B. CWW Engine

The Linguistic Weighted Average (LWA) is used for the CWW Engine, because all the weights and ratings are modeled by IT2 FSs.

The *P+K* judges are collected together as a whole committee, so that they can interact and exchange ideas with each other. First, the evaluations of each sub-criterion are aggregated by *K* experts in the committee to get a single evaluation for it; the weights of each criterion assigned by *P* decision makers are aggregated to get a single weight for each of them. Then the aggregated sub-criteria evaluations are aggregated with the aggregated sub-criteria weights to get the four aggregated main criteria evaluations for each supplier. Finally, the aggregated main criteria evaluations are further aggregated with the aggregated weights to get the overall evaluation for each supplier.

Next, we perform four aggregations, as follows (see Table II for the definitions of symbols):

(1) Aggregation of $\widetilde{X}_{ms}^{k}(S_i)$ across the *K* experts at S_i (supplier *i)*:

$$\widetilde{X}_{ms}(S_i) = \frac{\sum_{k=1}^{K} \widetilde{X}_{ms}^{k}(S_i)}{K} \tag{2}$$

(2) Aggregation of linguistic weights $\widetilde{W}_{ms}$ and $\widetilde{W}_{m}$ $(m = 1,2,\ldots,4)$ across the *P* decision makers:

$$\widetilde{W}_{ms} = \frac{\sum_{p=1}^{P} \widetilde{W}_{ms}^{p}}{P} \tag{3}$$

$$\widetilde{W}_{m} = \frac{\sum_{p=1}^{P} \widetilde{W}_{m}^{p}}{P} \tag{4}$$

(3) Aggregation of $\widetilde{Y}_m(S_i)$ $(m = 1,2,3,4)$:

$$\widetilde{Y}_m(S_i) = \frac{\sum_{s=1}^{l} \widetilde{X}_{ms}(S_i)\widetilde{W}_{ms}}{\sum_{s=1}^{l} \widetilde{W}_{ms}} \tag{5}$$

(4) Aggregation of the overall performance $\widetilde{Y}(S_i)$ $(i = 1,2,\ldots,n)$:

$$\widetilde{Y}(S_i) = \frac{\sum_{m=1}^{4} \widetilde{Y}_m(S_i)\widetilde{W}_m}{\sum_{m=1}^{4} \widetilde{W}_m} \tag{6}$$

C. Decoder

The decoder maps the CWW Engine output FOUs into a recommendation. It computes similarity, centroid and rank. The supplier selection with the largest ranking, and with the least similarity to other suppliers will be the best suitable supplier.

1) Similarity computation: Similarity assesses the agreement between FSs. There are six similarity measures for IT2 FSs, but each of them has their drawbacks for CWW, so this paper adopts the similarity measure described in [24, 35], which is an extension of Jaccard similarity measure. In this paper, similarity, $SI[\widetilde{Y}(S_i),\widetilde{Y}(S_j)]$, is computed only for the supplier's overall performances $\widetilde{Y}(S_i)$ (i=1,2…,n), so that a judge can observe how similar the overall performances are. More specifically, $SI[(\widetilde{Y}(S_i),\widetilde{Y}(S_j)]$ is computed, as:

$$SI[\widetilde{Y}(S_i),\widetilde{Y}(S_j)] = \frac{\sum_{i=1}^{N} \min(\overline{\mu}_{\widetilde{Y}(S_i)}(x_i),\overline{\mu}_{\widetilde{Y}(S_j)}(x_i)) + \sum_{i=1}^{N} \min(\underline{\mu}_{\widetilde{Y}(S_i)}(x_i),\underline{\mu}_{\widetilde{Y}(S_j)}(x_i))}{\sum_{i=1}^{N} \max(\overline{\mu}_{\widetilde{Y}(S_i)}(x_i),\overline{\mu}_{\widetilde{Y}(S_j)}(x_i)) + \sum_{i=1}^{N} \max(\underline{\mu}_{\widetilde{Y}(S_i)}(x_i),\underline{\mu}_{\widetilde{Y}(S_j)}(x_i))} \tag{7}$$

where $\overline{\mu}_{\widetilde{Y}(S_i)}(x_i)$, $\underline{\mu}_{\widetilde{Y}(S_i)}(x_i)$ are the MF values on the UMF($\widetilde{Y}(S_i)$) and LMF($\widetilde{Y}(S_i)$), respectively.

2) Centroid computation: The centroid of an IT2 FS provides a measure of the uncertainty of such a fuzzy set [32]. Centroids, $C_{\widetilde{Y}(S_i)}$, are only computed for the supplier's overall performances $\widetilde{Y}(S_i)$ (*i*=1,2…,*n*) and provide a measure of uncertainty for each overall ranking, since all $\widetilde{Y}(S_i)$ have propagated both numerical and linguistic uncertainties through

their computations. $C_{\tilde{Y}(S_i)}$ is the union of the centroids of all of the embedded T1 FSs of $\tilde{Y}(S_i)$; $C_l(S_i)$ and $C_r(S_i)$ are the smallest and largest element of $C_{\tilde{Y}(S_i)}$, and $C_{\tilde{Y}_M(S_i)}$ is the mean of $C_{\tilde{Y}(S_i)}$, i. e.

$$C_{\tilde{Y}(S_i)} = [C_l(S_i), C_r(S_i)] \tag{8}$$

$$C_l(S_i) = \frac{\sum_{i=1}^{L} x_i \overline{\mu}_{\tilde{A}}(x_i) + \sum_{i=L+1}^{N} x_i \underline{\mu}_{\tilde{A}}(x_i)}{\sum_{i=1}^{L} \overline{\mu}_{\tilde{A}}(x_i) + \sum_{i=L+1}^{N} \underline{\mu}_{\tilde{A}}(x_i)} \tag{9}$$

$$C_r(S_i) = \frac{\sum_{i=1}^{R} x_i \underline{\mu}_{\tilde{A}}(x_i) + \sum_{i=R+1}^{N} x_i \overline{\mu}_{\tilde{A}}(x_i)}{\sum_{i=1}^{R} \underline{\mu}_{\tilde{A}}(x_i) + \sum_{i=R+1}^{N} \overline{\mu}_{\tilde{A}}(x_i)} \tag{10}$$

$$C_{\tilde{Y}_M(S_i)} = \frac{C_l(S_i) + C_r(S_i)}{2} \tag{11}$$

In equations (9) and (10), L and R are called "switch points", that are determined by KM Algorithms. Details on KM Algorithms can be found in [21, 24, 37-39].

3) Rank computation: $\tilde{Y}(S_i)$ (i=1,2…,n) in (6) are IT2 FSs; hence, the decoder must rank such IT2 FSs to find the best supplier. According to [24, 35], there are only two ranking methods for IT2 FSs; however both methods have their limitations; hence, this paper uses a simple ranking method based on the centroids of IT2 FSs proposed in [35].

First, the average centroid $C_{\tilde{Y}_M(S_i)}$ is computed for each supplier's overall performance $\tilde{Y}(S_i)$ (i=1,2…,n), using (8)-(11), and then $C_{\tilde{Y}_M(S_i)}$ are sorted to obtain the rank of $\tilde{Y}(S_i)$. Additionally, ranking bands of $\tilde{Y}(S_i)$, $r_{\tilde{Y}(S_i)}$, are computed, i. e. ,

$$r_{\tilde{Y}(S_i)} = C_{\tilde{Y}_M(S_i)} \pm \delta_{\tilde{Y}(S_i)} \tag{12}$$

where $\delta_{\tilde{Y}(S_i)}$ are the half-lengths of each centroid $C_{\tilde{Y}_M(S_i)}$ (n=1,2…,N), i. e.

$$\delta_{\tilde{Y}(S_i)} = \frac{C_r(S_i) - C_l(S_i)}{2} \tag{13}$$

IV. EXAMPLE

In this section, we use an example of a supplier selection decision to demonstrate that the Per-C approach is more appropriate than type-1 fuzzy set (T1 FS) approach. A high technology manufacturing company desires to select a suitable material supplier from three alternative suppliers (S_1, S_2, and S_3) to purchase the key components of new products. Suppose a committee of seven judges, i. e., three decision makers (D_1, D_2 and D_3) and four experts (E_1, E_2, E_3 and E_4), has been formed to determine the best of three suppliers. Table III and Table IV contain the data that will be needed in the example.

Referring to both Table III and Table IV, observe that:

(1) Quality has two sub-criteria, Price & Terms have five sub-criteria, Supply chain support has three sub-criteria, and Technology has three sub-criteria; hence, there are 13 sub-criteria all of which were established ahead of time by three decision makers.

(2) Every major criterion has three weights (in bold-face) all of which were assigned by the three decision makers using words.

TABLE III. CRITERIA WITH THEIR WEIGHTS TABLE [a]

Item	Weighting		
	D_1	D_2	D_3
Criterion1: **Quality (C_1)**	**H**	**VH**	**H**
1. Quality performance (C_{11})	MH	MH	VH
2. Quality containment and VDCS feedback (C_{12})	ML	M	MH
Criterion2: **Price & Terms (C_2)**	**MH**	**H**	**H**
1. Price (C_{21})	H	M	MH
2. Terms (C_{22})	MH	H	MH
3. Responsiveness (C_{23})	H	VH	VH
4. Lead time (C_{24})	H	M	H
5. VMI/VOI hub Set Up cost (C_{25})	M	MH	H
Criterion3: **Supply chain support (C_3)**	**M**	**H**	**VH**
1. Purchase order reactiveness (C_{31})	MH	M	MH
2. Capacity support & flexibility (C_{32})	M	MH	M
3. Delivery/VMI operation (C_{33})	MH	M	H
Criterion4: **Technology (C_4)**	**ML**	**M**	**ML**
1. Technical support (C_{41})	L	M	M
2. Design involvement (C_{42})	M	M	MH
3. ECN/PCN process (C_{43})	VL	ML	L

[a] In the 2nd and 4th column: VL=Very Low, L=Low, ML=Medium Low, M=Medium, MH=Medium High, H=High, VH=Very High (see Fig. 5)

TABLE IV. SUB-CRITERIA PERFORMANCE EVALUATION TABLE [a]

Item	Supplier 1 (S_1)				Supplier 2 (S_2)				Supplier 3 (S_3)			
	E_1	E_2	E_3	E_4	E_3	E_2	E_3	E_4	E_1	E_2	E_3	E_4
Criterion1: **Quality (C_1)**												
1. Quality performance (C_{11})	G	G	VG	MG	MG	G	G	F	VC	G	MG	G
2. Quality containment and VDCS feedback (C_{12})	G	P	F	MP	F	G	MP	MG	MP	F	MP	MG
Criterion2: **Price & Terms (C_2)**												
1. Price (C_{21})	MG	F	MP	F	G	G	MG	G	MG	G	MP	F
2. Terms (C_{22})	MP	G	F	G	MG	MP	MP	F	F	F	MG	F
3. Responsiveness (C_{23})	G	MG	F	F	MG	F	MP	MG	F	G	MP	F
4. Lead time (C_{24})	F	MP	MG	G	MP	G	F	MP	MG	F	MP	G
5. VMI/VOI hub Set Up cost (C_{25})	F	MP	MG	G	MG	F	MP	F	F	G	F	MG
Criterion3: **Supply chain support (C_3)**												
1. Purchase order reactiveness (C_{31})	G	MG	G	MP	F	MG	G	MG	P	MP	F	MP
2. Capacity support & flexibility (C_{32})	G	MG	VG	G	MP	F	F	MP	G	VG	G	G
3. Delivery/VMI operation (C_{33})	G	F	MG	G	F	G	MG	G	F	MP	MP	F
Criterion4: **Technology (C_4)**												
1. Technical support (C_{41})	G	F	MG	G	G	F	G	MG	VG	F	MG	G
2. Design involvement (C_{42})	MP	MG	F	MP	MG	F	G	MG	MP	G	F	MG
3. ECN/PCN process (C_{43})	F	MP	MG	P	G	MG	VG	MG	MG	F	F	G

[a] In the 2nd -4thcolumns: VP=Very Poor, P=Poor, MP=Medium Poor, F=Fair, MG=Medium Good, G=Good, VG=Very Good (see Fig. 4).

(3) Every sub-criterion has three weights all of which were assigned by the three decision makers using words.

(4) Every sub-criterion has four performance evaluations, which are shown for all 13 sub-criteria for the three suppliers, and, are words. The word evaluations were obtained from the four experts.

How to aggregate all of these words, although seemingly very difficult, is accomplished by using (2)-(6).

Next, we provide the details for the Encoder, CWW Engine and Decoder and how the outputs from the decoder are used to decide the final winning supplier.

Step 1: *Encoder*

As noted in Section III. A, two codebooks are needed, one for the words that will be used by the experts and the other for the weights used by the decision maker. Two codebooks contain the words and their IT2 FS models.

(1) Codebook used by experts

Seven words were used in this sub-codebook, namely *very poor, poor, medium poor, fair, medium good, good, very good*. FOUs for these words are depicted in Fig. 4. They should be obtained by collecting data from a pool of domain managers and experts and their data intervals should be mapped into word FOUs using the IA whose details can be found in [31,36]. Because this application is being used only to illustrate how a Per-C can be used for supplier evaluation, and we did not have access to domain experts, interval end-point data were not collected for these words. Instead, we adopted the codebook from [31]. Unfortunately, none of the seven words that are actually used in this paper appear in that codebook; so, each word was mapped into a word that was felt to be a synonym for it. The relationships between the terms of the sub-criteria codebook here and that of the codebook in [31] are: v*ery poor=tiny, poor=low amount, medium poor=fair amount, fair=modest amount, medium good=good amount, good=a lot, very good=huge amount.*

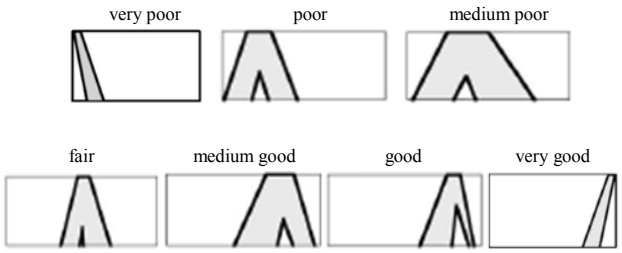

Figure 4. FOUs of the sub-criteria codebook.

For nine sub-criteria with a negative connotation [Quality containment and VDCS feedback (C_{12}), Price (C_{21}), Terms (C_{22}), Responsiveness (C_{23}), Lead time (C_{24}), VMI/VOI hub set up cost (C_{25}), Purchase order reactiveness (C_{31}), Delivery/VMI operation (C_{33}), ECN/PCN process(C_{43})], antonyms were used instead of the raw words, according to (1).

(2) Codebook for the weghts used by the decision makers

The codebook for the weights contains the seven words *very low, low, medium low, medium, medium high, high, very high*, and their FOUs that are depicted in Fig. 5. As above, we adopted each word's synonym from the codebook in [31]. i. e. *very low=very little, low=little, medium low=some, medium=medium, medium high=good amount, high=large, very high=very large*.

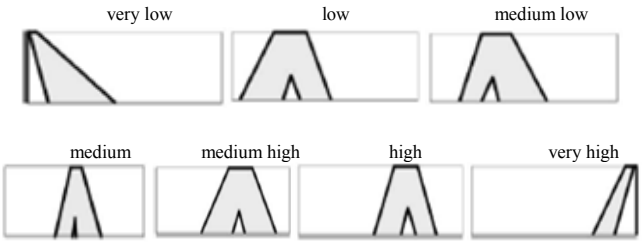

Figure 5. FOUs of the weights codebook.

Step 2: CWW Engine

The linguistic Weighted Average (LWA) was used for the CWW Engine. $\widetilde{X}_{ms}^{k}(S_i)$ (k=1,2,3,4) were aggregated by a LWA to obtain $\widetilde{X}_{ms}(S_i)$ (m=1,2,3,4; i=1,2,3), using (2); $\widetilde{W}_{ms}^{p}$ *and* $\widetilde{W}_{m}^{p}$ (p=1,2,3) were aggregated by LWAs to obtain $\widetilde{W}_{ms}$ *and* $\widetilde{W}_{m}$ (m=1,2,3,4), using (3) and (4), respectively. Each of them can be represented with 9 real numbers.

Each of the four major criteria has a LWA $\widetilde{Y}_m(S_i)$ (m=1,2,3,4; i=1,2,3) computed for it using (5). These four LWAs are then aggregated by another LWA to obtain the overall performance for each supplier, $\widetilde{Y}(S_i)$($i=1,2,3$), using (6).

Step 3: Decoder

The decoder computes the centroid, similarity and rank of the supplier's overall performance $\widetilde{Y}(S_i)(i=1,2,3)$.

(1) Centroid computation

Centroids, $C_{\widetilde{Y}(S_i)}$, and the mean of the centroid, $C_{\widetilde{Y}_M(S_i)}$, were computed for the three supplier's overall performances $\widetilde{Y}(S_i)(i=1,2,3)$ using (8)-(11).

(2) Similarity computation

Similarities, $SI(\widetilde{Y}(S_i),\widetilde{Y}(S_j))$ (i=1,2,3; j=1,2,3), between the three supplier's overall performances $\widetilde{Y}(S_i)$ (i=1,2,3) were computed using (7).

(3) Rank computation

Rankings, $r_{\widetilde{Y}(S_i)}$ (i=1,2,3), of the three suppliers were obtained from (12) and (13).

Step 4: Compute the evaluation results and decide the final winner

This section illustrates the supplier evaluation results for the three suppliers. In all figures, Supplier 1 is represented by the solid curve, Supplier 2 is represented by the dashed curve, and Supplier 3 is represented by the dotted curve. FOUs for Quality, Price & Terms, Supply chain support and Technology are depicted in Fig. 6 (a)-(d), respectively. FOUs for Overall Performance are depicted in Fig. 6 (e). Observe from Fig. 6(e) that not only is FOU ($\widetilde{Y}(S_3)$) visually well to the right of the other two FOUs, but its average centroid (which is on the horizontal axis) is also well to the right of those for Suppliers 1 and 2. FOU ($\widetilde{Y}(S_1)$) is almost the same as FOU ($\widetilde{Y}(S_2)$). So, based on ranking alone, Supplier 3 would be declared the

winner. This happens because Supplier 3 ranks first in Quality and Supply chain suport by a significant amount.

Although Supplier 3 ranks last for Technologe, its FOU is close to those of Suppliers 1 and 2, whereas FOU of Supplier 3 for Price & Terms(C_2) is also very close to those of Suppliers 1 and 2.

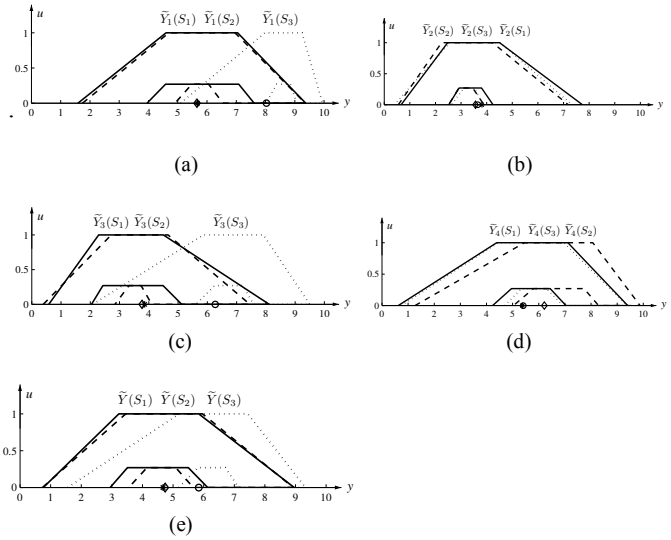

Figure 6. Aggregation results for (a) Criterion 1: Quality; (b) Criterion 2: Price & Terms; (c) Criterion 3: Supply chain support; (d) Criterion 4: Technology; and (e) Overall performances of the three suppliers. The average centroids for Suppliers A, B and C are shown in all figures by and $*, \Diamond$, and $\circ$, respectively.

Table V summarizes the similarities between $\tilde{Y}(S_1), \tilde{Y}(S_2)$ and $\tilde{Y}(S_3)$. Observe that $\tilde{Y}(S_3)$ is not very similar to either $\tilde{Y}(S_1)$ or $\tilde{Y}(S_2)$, and $\tilde{Y}(S_1)$ is very similar to $\tilde{Y}(S_2)$, so choosing Supplier 3 as the winner is further reinforced.

Table VI summarizes the centroids, average centroids, half-lengths and rankings of $\tilde{Y}(S_1), \tilde{Y}(S_2)$ and $\tilde{Y}(S_3)$. Observe that supplier 3 has the largest ranking, while it doesn't have the smallest uncertainty band about that ranking, but the uncertainty band about ranking of it is close to that of the Supplier 1 which has the smallest uncertainty band.

TABLE V. SIMILARITIES OF $\tilde{Y}$ FOR THREE COMPANIES

Supplier	$\tilde{Y}(S_1)$	$\tilde{Y}(S_2)$	$\tilde{Y}(S_3)$
$\tilde{Y}(S_1)$	1.00	0.93	0.56
$\tilde{Y}(S_2)$	0.93	1.00	0.58
$\tilde{Y}(S_3)$	0.56	0.58	1.00

TABLE VI. CENTROIDS, CENTERS OF CENTROID AND RANKING BANDS

Supplier	$\tilde{Y}(S_1)$	$\tilde{Y}(S_2)$	$\tilde{Y}(S_3)$
$C_{\tilde{Y}(S_i)}$	[3.17, 6.17]	[296, 6.52]	[4.25,7.43]
$C_{\tilde{Y}_M(S_i)}$	4.67	4.74	5.84
$r_{\tilde{Y}(S_i)}$	4.67 ± 1.50	4.74 ± 1.78	5.84 ± 1.59

The seven judges ultimately decide supplier 3 is the winner by comparing the three suppliers' overall performances and similarities between them, because supplier 3's overall performance not only has the largest ranking but it also is not similar to the other two suppliers, although the similarity is greater than 0.5 that implies more similar to than less similar to, and one may be less certain about choosing Supplier 3 as the winner.

In summary, the Per-C can consider scenarios with different numbers of judges; hence, one can evaluate the robustness of the final decision.

All the computations were implemented using Matlab software under MS Windows platform. Some basic routines can be found in the personal website of Mendel (http://sipi.usc.edu/~ mendel/software).

V. CONCLUSIONS

In order to enhance competitiveness in the market and increase customer satisfaction, the supplier selection problem for companies is very important. This paper applies a new methodology —Perceptual Computer (Per-C)—to help solve the supplier selection problem. This problem is a hierarchical group multi-criteria decision making problem in which a committee of seven (or more) judges has to decide which of three (or more) suppliers will be chosen. The Per-C has three components: encoder, CWW engine and decoder. During its design the concepts of an antonym and codebooks were needed. Without the LWA it would not have been possible to do what the Per-C has been able to do. The Per-C used the IA to obtain an IT2 FS FOU for a word; it used the LWA to aggregate all the words modeled by IT2 FSs; it used a centroid-based ranking method to rank competing suppliers; and, it also used a Jaccard similarity measure to obtain similarities of the computing suppliers.

REFERENCES

[1] T. L.Ya, L. L. Chia, C. Y. Hsiao and H. T. Gwo, "A novel hybrid MCDM approach for outsourcing vendor selection: A case study for a semiconductor company in Taiwan," *Expert Systems with Applications*, vol. 37, pp. 4796–4804, 2010.

[2] C. Chen, C. Lin and S. Huang, "A fuzzy approach for supplier evaluation and selection in supply chain management," *International Journal of Production Economics*, vol. 102, pp. 289–301, 2006.

[3] T. C. Chen, T. L. Ching and F. H. Sue, " A fuzzy approach for supplier evaluation and selection in supply chain management," *Int. J. Production Economics*, vol. 102, pp. 289–301, 2006.

[4] M. Delgado, J. L.Verdegay, and M. A. V ila, "Linguistic decision-making models," *International Journal of Intelligent Systems*, vol. 7, pp. 479–492, 1992.

[5] C. L. Hwang and K. Yoon, *Multiple Attributes Decision Making Methods and Applications*. Springer, New York, 1981.

[6] A. Sarkar and P. K. J. Mohapatra, "Evaluation of supplier capability and performance: A method for supply base reduction," *Journal of Purchasing and Supply Management*, vol. 12, pp. 148–163, 2006.

[7] L. R. Florez, "Strategic supplier selection in the added-value perspective: A CI approach," *Information Sciences*, vol. 177, pp. 1169–1179, 2007.

[8] F. T. S. Chan and N. Kumar, "Global supplier development considering risk factors using fuzzy extended AHP-based approach," *OMEGA – International Journal of Management Science*, vol. 35, pp. 417–431, 2007.

[9] C. Kahraman, U. Cebeci and Z. Ulukan, "Multi-criteria supplier selection using fuzzy AHP," *Logistics Information Management*, vol. 16, pp. 382–394, 2003.

[10] L. Y. Jiann, N. C. Huan, H. T. Gwo and H. Y. Ruey, "Vendor selection by integrated fuzzy MCDM techniques with independent and interdependent relationships," *Information Sciences*, vol. 178, pp. 4166–4183, 2008.
[11] C. S. Chia, "A performance evaluation model by integrating fuzzy AHP and fuzzy TOPSIS methods," *Expert Systems with Applications*, in press, 2010.
[12] E. Bottani and A. Rizzi, "An adapted multi-criteria approach to suppliers and products selection – An application oriented to lead-time reduction," *International Journal Production Economics*, vol. 111, pp. 763–781, 2008.
[13] V. Jain, M. K. Tiwari and F. T. S. Chan, "Evaluation of the supplier performance using an evolutionary fuzzy-based approach," *Journal of Manufacturing Technology Management*, vol. 15, pp. 735–744, 2004.
[14] A. Amid, S. H. Ghodsypour and C. O'Brien, "Fuzzy multiobjective linear model for supplier selection in a supply chain," *International Journal of Production Economics*, vol. 104, pp. 394–407, 2006.
[15] M. Bevilacqua, F. E. Ciarapica and G. Giacchetta, "A fuzzy-QFD approach to supplier selection," *Journal of Purchasing and Supply Management*, vol. 12, pp. 14–27, 2006.
[16] C. K. Kwong, W. H. Ip and J. W. K. Chan, "Combining scoring method and fuzzy expert systems approach to supplier assessment: A case study," *Integrated Manufacturing Systems*, vol. 13, pp. 512–519, 2002.
[17] S. Önüt, S. S. Kara and E. Isik. "Long term supplier selection using a combined fuzzy MCDM approach: A case study for a telecommunication company," *Expert Systems with Applications*, vol. 36, pp. 3887–3895, 2009.
[18] M. Sevkli, "An application of the fuzzy ELECTRE method for supplier selection," *International Journal of Production Research*, Vol. 48, pp. 3393–3405, 2010.
[19] G. Ali Montazer*, H. Q. Saremi and M. Ramezani, "Design a new mixed expert decision aiding system using fuzzy ELECTRE III method for vendor selection," *Expert Systems with Applications*, vol. 36, pp. 10837–10847, 2009.
[20] A. Sanayei, S. F. Mousavi and A. Yazdankhah, "Group decision making process for supplier selection with VIKOR under fuzzy environment," *Expert Systems with Applications*, vol. 37, pp. 24–30, 2010.
[21] J. M. Mendel, Uncertain Rule-Based Fuzzy Logic System: Introduction and New Directions, Prentice-Hall, Upper Saddle River, NJ, 2001.
[22] J. M. Mendel, "Fuzzy sets for words: a new beginning," Proc. FUZZY-IEEE 2003, St. Louis, MO, pp. 37-42, 2003.
[23] J. M. Mendel, "Type-2 fuzzy sets and systems: an overview," IEEE Computational Intelligence Magazine, vol. 2, pp. 20-29, Feb. 2007.
[24] J. M. Mendel and D. Wu, Perceptual Computing: Aiding People in Making Subjective Judgments, Wiley-IEEE Press, 2010.
[25] L. A. Zadeh, "Fuzzy logic=computing with words," IEEE Trans. on Fuzzy Systems, vol. 4, pp. 103-111, 1996.
[26] L. A. Zadeh, "From computing with numbers to computing with words—from manipulation of measurements to manipulation of perceptions," IEEE Trans. on Circuits and Systems-1, Fundamental Theory and Applications, vol. 4, pp.105-119, 1999.
[27] L. A. Zadeh, "Toward human level machine intelligence—is it achievable? The need for a new paradigm shift," IEEE Computational Intelligence Magazine, vol. 3, pp. 11-22, 2008.
[28] L. A. Zadeh, "A new direction in AI-Toward a computational theory of perceptions," AI Magazine, vol. 22, no. 1, pp. 73-84, Spring 2001.
[29] J. M. Mendel, "An architecture for making judgments using computing with words," Int. J. Appl. Math. Comput. Sci. , vol. 12, no. 3, pp. 325-335, 2002.
[30] J. M. Mendel, "Computing with words and its relationships with fuzzistics," Information Sciences, vol. 177, pp. 998-1006, 2007.
[31] F. Liu and J. M. Mendel, "Encoding words into interval type-2 fuzzy sets using an interval sets," IEEE Trans. on Fuzzy Systems, vol. 16, pp. 1503-1521, December 2008.
[32] A. D. Soto and E. Trillas, "On antonym and negate in fuzzy logic," International Journal of Intelligent Systems, vol. 17, pp. 295-303, 1999.
[33] C. S. Kim, D. S. Kim and J. S. Park, "A new fuzzy resolution principle based on the antonym," Fuzzy Sets and Systems, vol. 113, pp. 299-307, 2000.
[34] L. A. Zadeh, "Toward a generalized theory of uncertainty (GTU) – An outline," Information Science, vol. 172, pp. 1-40, 2005.
[35] D. Wu and J. M. Mendel, "A comparative study of ranking methods, similarity measures and uncertainty measures for interval type-2 fuzzy sets," Information Sciences, vol. 179, no. 8, pp. 1169-1192, 2009.
[36] F. Liu and J. M. Mendel, "Aggregation using the fuzzy weighted average, as computed by the KM Algorithms," IEEE Trans. on Fuzzy Systems, vol. 16, pp. 1-12, February 2008.
[37] D. Wu and J. M. Mendel, "Enhanced Karnik-Mendel algorithms," Proc. NAFIPS 2007, San Diego, CA, June 2007.
[38] D. Wu and J. M. Mendel, "Enhanced Karnik-Mendel algorithms," IEEE Trans. On Fuzzy Systems, vol. 17, no. 4, pp. 923-934, 2009.
[39] N. N. Karmik and J. M. Mendel, "Centroid of a type-2 fuzzy set," Information Science, vol. 132, no. 1-4, pp. 195-220, 2001.

2011 IEEE International Conference on Fuzzy Systems
June 27-30, 2011, Taipei, Taiwan

Type-2 Fuzzy Functional Inference Method

Hirosato Seki
Dept. Technology Management
Oaska Institute of Technology
Osaka, Japan
e-mail: h_seki@ieee.org

Masaharu Mizumoto
Dept. Engineering Informatics
Osaka Electro-Communication University
Osaka, Japan
e-mail: mizumoto3003@yahoo.co..jp

***Abstract*—This paper proposes a *type-2 fuzzy functional inference method* which extends fuzzy sets of the antecedent parts to type-2 fuzzy sets. This paper next explains that the type-2 fuzzy functional inference method can be classified to the three models: Model 1 is most common method, and Model 2 is a special case of Model 1. We show that the inference results of both Models 1 and 2 can be easily obtained from the area of fuzzy sets of the consequent parts and center of gravity. Moreover, we state that Model 3 can obtain different results compared with the simplified fuzzy inference method and T–S inference method.**

***Index Terms*—Type-2 fuzzy inference, fuzzy functional inference method, internval type-2 fuzzy sets, fuzzy function, T–S inference method.**

I. Introduction

Since Mamdani [1] applied the concept of fuzzy inference to steam engine experimental device, relevant research and applications have been executed in various fields. Especially, researches on the T–S inference method [2], [3], which is widely used as fuzzy control method and so on, are reported in many papers.

Although the antecedent parts of the T–S inference method are fuzzy sets, the consequent parts are functions. However, it may be completely natural that the consequent parts are also fuzzy. From this reason, Seki and Mizumoto [4], [5] have proposed a *fuzzy functional inference method* in which the consequent parts of the T–S inference method is generalized to fuzzy functions, and shown the equivalence [6]–[15] between the fuzzy functional inference method and the weighted T–S inference method.

On the other hand, Type-2 fuzzy inference model [16]–[19] also has the structure, in which the antecedent parts and consequent parts are fuzzy sets. Type-2 fuzzy inference model has achieved a great success in the various fields.

In this paper, we poropose a *type-2 fuzzy functional inference method* which extends fuzzy sets of the antecedent parts of fuzzy functional inference method to type-2 fuzzy sets. Firstly, we state Model 1 in which the antecedent parts and consequent parts are type-2 fuzzy sets and fuzzy function, respectively. Secondly, we state Model 2 where the antecedent parts and consequent parts are type-1 fuzzy sets and fuzzy function, respectively. And, this paper show that the Model 2 is equivalent to the type-2 TSK fuzzy model, if fuzzy function of consequent parts of Model 2 is limited to a fuzzy function of linear expression. Thirdly, we state Model 3 in which the antecedent parts and/or consequent parts are interval value, respectively. Moreover, we calarify that Model 3 can obtain different results compared with the simplified fuzzy inference method and the T–S inference method.

II. Fuzzy Inference Methods

In this section we review the min–max–gravity method, product–sum–gravity method, T–S inference method, and fuzzy functional inference method.

A. Min–Max–Gravity method

We firstly explain the *min–max–gravity method* as *Mamdani's fuzzy inference method* [1] for the fuzzy inference form (see Fig. 1). The rules of the min–max–gravity method are given as follows:

$$\text{Rule } R_i = \begin{cases} x_1 = A_i^1, x_2 = A_i^2, \ldots, x_n = A_i^n \\ \longrightarrow y = B_i \end{cases} \tag{1}$$

where $x_1, x_2, \ldots, x_n$ are variables of the antecedent part, $A_i^1, A_i^2, \ldots, A_i^n$ fuzzy sets, B_i fuzzy sets of the consequent part, $i = 1, 2, \ldots, M$ and M is the total number of rules.

Each inference result B_i' which is infered from the fact "$x_1^0, x_2^0, \ldots, x_n^0$" and the fuzzy rule "$A_i^1, A_i^2, \ldots, A_i^n \longrightarrow B_i$" is given in the following.

The degree of fitness, h_i, of the fact "$x_1^0, x_2^0, \ldots, x_n^0$" to the antecedent parts "$A_i^1, A_i^2, \ldots, A_i^n$" is given as

$$h_i = \min\{A_i^1(x_1^0), A_i^2(x_2^0), \ldots, A_i^n(x_n^0)\} \tag{2}$$

Thus, the inference result B_i' is given as

$$B_i'(y) \quad = \quad \min\{h_i, B_i(y)\} \tag{3}$$

The final consequence B' of (1) is aggregated from B_1', B_2', $\ldots$, B_M' by using the max. Namely,

$$B'(y) = \max\{B_1'(y), B_2'(y), \ldots, B_M'(y)\} \tag{4}$$

The representative point y_0 for the resulting fuzzy set B' is obtained as the center of gravity of B':

$$y_0 = \frac{\int y \cdot B'(y) dy}{\int B'(y) dy} \tag{5}$$

978-1-4244-7316-8/11/$26.00 ©2011 IEEE

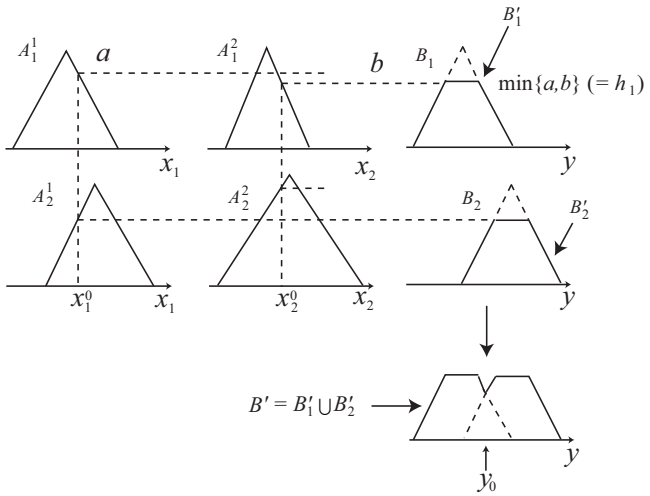

Fig. 1. Min–Max–gravity method.

B. Product–Sum–Gravity method

We secondly explain a fuzzy inference method called *product–sum–gravity method* [20]–[23] for the fuzzy inference form (see Fig. 2). The rules of the product–sum–gravity method are also given as (1).

Each inference result B_i' which is infered from the fact "$x_1^0, x_2^0, \ldots, x_n^0$" and the fuzzy rule "$A_i^1, A_i^2, \ldots, A_i^n \longrightarrow B_i$" is given in the following.

The degree of fitness, h_i, of the fact "$x_1^0, x_2^0, \ldots, x_n^0$" to the antecedent parts "$A_i^1, A_i^2, \ldots, A_i^n$" is given as

$$h_i = A_i^1(x_1^0) \cdot A_i^2(x_2^0) \cdots A_i^n(x_n^0) \tag{6}$$

where $\cdot$ stands for the algebraic product. Thus, the inference result B_i' is given as

$$\begin{aligned} B_i'(y) &= A_i^1(x_1^0) \cdots A_i^n(x_n^0) \cdot B_i(y) \\ &= h_i \cdot B_i(y) \end{aligned} \tag{7}$$

The final consequence B' of (1) is aggregated from $B_1', B_2', \ldots, B_M'$ by using the algebraic sum $(+)$. Namely,

$$B'(y) = B_1'(y) + B_2'(y) + \cdots + B_M'(y) \tag{8}$$

The representative point y_0 for the resulting fuzzy set B' is obtained as the center of gravity of B':

$$y_0 = \frac{\int y \cdot B'(y) dy}{\int B'(y) dy} \tag{9}$$

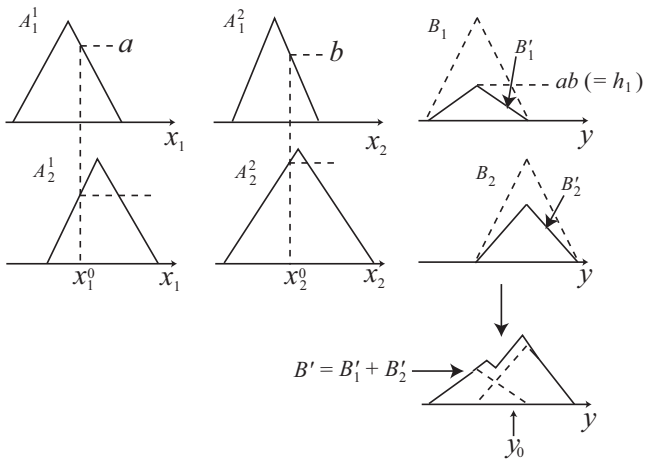

Fig. 2. Product–sum–gravity method.

C. T–S Inference Method

We thirdly explain the *T–S inference method* [2], [3].

Rules in the T–S inference method are constituted as

$$\text{Rule } R_i = \begin{cases} x_1 \text{ is } A_i^1,\ x_2 \text{ is } A_i^2,\ \ldots,\ x_n \text{ is } A_i^n \\ \longrightarrow y = f_i(x_1, x_2, \ldots, x_n) \end{cases} \tag{10}$$

where $x_1, x_2, \ldots, x_n$ are variables of the antecedent part, $A_i^1, A_i^2, \ldots, A_i^n$ fuzzy sets, and $f_i(x_1, x_2, \ldots, x_n)$ functions of the consequent part, $i = 1, 2, \ldots, M$ and M is the total number of fuzzy rules. The inference result y_0 for inputs $x_1^0, x_2^0, \ldots, x_n^0$ is given as

$$y_0 = \frac{\displaystyle\sum_{i=1}^{M} h_i f_i(x_1^0, x_2^0, \ldots, x_n^0)}{\displaystyle\sum_{i=1}^{M} h_i}, \quad h_i = \prod_{j=1}^{n} A_i^j(x_j^0) \tag{11}$$

where h_i is the degree of the ith rule.

The T–S method becomes the simplified fuzzy inference method when function $f_i(x_1, x_2, \ldots, x_n)$ in the consequence part is a constant.

D. Fuzzy Functional Inference Method

Although the antecedent parts of the conventional T–S inference method are fuzzy sets, the consequent parts are function. However, this structure is hard to understand from the different of antecedent parts and consequent parts. Rather, it may be completely natural that the consequent parts are also fuzzy.

In this subsection, we review a *fuzzy functional inference method* [4], [5] in which the consequent parts of the T–S inference method are generalized to fuzzy function. This method can make it easier to understand the structure of rules compared with the ordinary T–S inference method.

The rules in the fuzzy functional inference method are constituted as

$$\text{Rule } R_i = \begin{cases} x_1 \text{ is } A_i^1,\ x_2 \text{ is } A_i^2,\ \ldots,\ x_n \text{ is } A_i^n \\ \longrightarrow y = F_i(x_1, x_2, \ldots, x_n) \end{cases} \tag{12}$$

where $x_1, x_2, \ldots, x_n$ are variables of the antecedent part, $A_i^1, A_i^2, \ldots, A_i^n$ fuzzy sets, and $F_i(x_1, x_2, \ldots, x_n)$ are fuzzy functions.

Since the consequent parts $F_i(x_1, x_2, \ldots, x_n)$ constitutes fuzzy sets, the final output y_0 of the fuzzy functional inference method should be obtained from Mamdani type fuzzy inference method. For example, the inference result y_0 is obtained

as follows when the product–sum–gravity method is used (See Fig. 2).

Given the rules of (12), inputs $x_1^0, x_2^0, \ldots, x_n^0$ and each antecedent part $A_1^i, A_2^i, \ldots, A_n^i$, the degree h_i is obtained as (6), and the inference result $F_i(x_1^0, x_2^0, \ldots, x_n^0)'$ of each fuzzy rule is obtained as

$$F_i(x_1^0, x_2^0, \ldots, x_n^0)'(y) = h_i \cdot F_i(x_1^0, x_2^0, \ldots, x_n^0)(y) \quad (13)$$

where $\cdot$ is the algebraic product.

The final output F' of (12) is obtained by the summation of each inference result $F_i(x_1^0, x_2^0, \ldots, x_n^0)'$ as in (8). Namely,

$$\begin{aligned} F'(y) &= F_1(x_1^0, x_2^0, \ldots, x_n^0)'(y) + \cdots \\ &\quad + F_M(x_1^0, x_2^0, \ldots, x_n^0)'(y) \end{aligned} \quad (14)$$

The representative point y_0 of conclusion F' is obtained as follows:

$$y_0 = \frac{\int y \cdot F'(y) dy}{\int F'(y) dy} \quad (15)$$

III. Type-2 Fuzzy Functional Inference Method

In this section, we poropose a *type-2 fuzzy functional inference method* which extends fuzzy sets of the antecedent parts of fuzzy functional inference method to type-2 fuzzy sets. Rules of the type-2 fuzzy functional inference method are constructed as follows:

$$\text{Rule } R_i = \left\{ \begin{array}{l} x_1 \text{ is } \tilde{A}_i^1,\ x_2 \text{ is } \tilde{A}_i^2,\ \ldots,\ x_n \text{ is } \tilde{A}_i^n \\ \longrightarrow y = F_i(x_1, x_2, \ldots, x_n) \end{array} \right. \quad (16)$$

where $x_1, x_2, \ldots, x_n$ are variables of the antecedent part, $\tilde{A}_i^1, \tilde{A}_i^2, \ldots, \tilde{A}_i^n$ $(i = 1, 2, \ldots, M)$ type-2 fuzzy sets, and $F_i(x_1, x_2, \ldots, x_n)$ are fuzzy functions.

Given input $x_1^0, x_2^0, \ldots, x_n^0$, the degree $H(x_1^0, x_2^0, \ldots, x_n^0)$ is obtained by the extension principle as

$$H_i(x_1^0, x_2^0, \ldots, x_n^0) = \tilde{A}_1^1(x_1^0) * \tilde{A}_2^i(x_2^0) * \cdots * \tilde{A}_n^i(x_n^0) \quad (17)$$

where the operation $*$ is t-norm or average operation [5].

The inference result F' is obtained as follows:

$$F' = S_{i=1}^M H_i(x_1^0, x_2^0, \ldots, x_n^0) * F_i(x_1^0, x_2^0, \ldots, x_n^0) \quad (18)$$

where S is t-conorm, and the operation $*$ is t-norm or average operation, as used in the product–sum–gravity method, min–max–gravity method, and so on. For example, the inference result F' obtained by using the product–sum–gravity method, is given as follows:

$$\begin{aligned} F' &= \sum_{i=1}^M H_i(x_1^0, x_2^0, \ldots, x_n^0) \cdot F_i(x_1^0, x_2^0, \ldots, x_n^0) \\ &= \sum_{i=1}^M F_i'(x_1^0, x_2^0, \ldots, x_n^0) \end{aligned} \quad (19)$$

where $\cdot$ is the algebraic product.

The representative point y_0 of conclusion F' is obtained as follows:

$$y_0 = \frac{\int y \cdot F'(y) dy}{\int F'(y) dy} \quad (20)$$

The representative point y_0 is easily obtained from the area of fuzzy sets of the consequent parts and center of gravity by using the product–sum–gravity method [4], [5].

Note that it is possible to apply the *min–max–gravity method* by replacing algebraic product and algebraic sum with min and max, respectively, in (19).

IV. Property of type-2 fuzzy functional inference method

The type-2 fuzzy functional inference method can be considered as the following three models as well as the type-2 fuzzy logic systems [17].

- Model 1: Antecedent parts are type-2 fuzzy sets, and consequent parts are fuzzy function (see section III).
- Model 2: Antecedent parts are type-1 fuzzy sets, and consequent parts are fuzzy function (see subsection II-D).
- Model 3: Antecedent parts and/or consequent parts are interval value.

In this section, we discuss the property of the type-2 fuzzy functional inference method.

A. Model 1

Model 1 has the structure in which the antecedent parts and consequent parts are type-2 fuzzy sets and fuzzy function, respectively. The inference results of the conventional type-2 inference systems are obtained by using extension principle and type-reduction. However, the inference results of the type-2 fuzzy functional inference method are obtained from each area of (19) and its center of gravity if the additive fuzzy functional inference method [5] is used.

Therefore, we consider the type-2 fuzzy functional inference method in the case of using the product–sum–gravity method. By using the product–sum–gravity method, the inference result F_i' can be obtained as (19).

At first, let the area and the center of gravity of $F_i'(x_1^0, x_2^0, \ldots, x_n^0)$ of (19) be $S_i'(x_1^0, x_2^0, \ldots, x_n^0)$ and $f_i'(x_1^0, x_2^0, \ldots, x_n^0)$, respectively.

We use the following symbol for short:

$$F_i' = F_i'(x_1^0, x_2^0, \ldots, x_n^0) \quad (21)$$

$$f_i' = f_i'(x_1^0, x_2^0, \ldots, x_n^0) \quad (22)$$

$$S_i' = S_i'(x_1^0, x_2^0, \ldots, x_n^0) \quad (23)$$

From [4] and [5], the inference result y_0 of (20) of the type-2 fuzzy functional inference method can be transformed

to

$$
\begin{aligned}
y_0 &= \frac{\int y \cdot F_i'(x)(y)dy}{\int F_i'(x)(y)dy} \\
&= \frac{\int y \cdot \{F_1'(y) + \cdots + F_M'(y)\}dy}{\int \{F_1'(y) + \cdots + F_M'(y)\}dy} \\
&= \frac{\int y \cdot F_1'(y)dy + \cdots + \int y \cdot F_M'(y)dy}{\int F_1'(y)dy + \cdots + \int F_M'(y)dy} \\
&= \frac{S_1' \cdot f_1' + \cdots + S_M' \cdot f_M'}{S_1' + \cdots + S_M'} \qquad (24)
\end{aligned}
$$

From (24), it turns out that the inference reult y_0 of the type-2 fuzzy functional inference method is obtained from the area S_i' and the center of gravity f_i' of each inference result F_i', in case of an additive fuzzy inference method, which uses the addition as in (19) in the aggregation of each inference result.

Remark 1: In (18), the relation of (24) holds as long as the addition is used in the aggregation, even if instead of using algebraic product, min is used to the operation. Because the area, form and center of gravity of F_i' parts only change. □

B. Model 2

Model 2 has the structure in which the antecedent parts and consequent parts are type-1 fuzzy sets and fuzzy function, respectively. The rules of Model 2 are given as (12). The rules of Model 2 is equivalent to that of the type-2 TSK fuzzy system [17], when fuzzy function is limited to fuzzy function of linear expression, i.e., the rules are constructed as follows:

$$
\text{Rule } R_i = \left\{ \begin{array}{l} x_1 \text{ is } A_i^1,\ x_2 \text{ is } A_i^2,\ \ldots,\ x_n \text{ is } A_i^n \\ \longrightarrow y = C_i^0 + C_i^1 x_1 + C_i^2 x_2 + \cdots C_i^n x_n \end{array} \right. \qquad (25)
$$

where $x_1, x_2, \ldots, x_n$ are variables of the antecedent part, and $A_i^1, A_i^2, \ldots, A_i^n$ and $C_i^1, C_i^2, \ldots, C_i^n$ are type-1 fuzzy sets. Therefore, it turns out that Model 2 is extended version of the type-2 TSK fuzzy system.

As well as Model 1, the representative point y_0 of Model 2 is obtained from the area of fuzzy sets of the consequent parts and center of gravity (See [4], [5] for detail).

C. Model 3

Researches on fuzzy inference used interval-valued fuzzy sets are reported in [16]–[19], [24], [25]. Finally, we state a *interval type-2 fuzzy functional inference method* (IT2 fuzzy functional inference method) as Model 3.

Model 3 has the structure in which the antecedent parts and/or consequent parts are interval value.

We shall consider the following simple example (See Fig. 3).

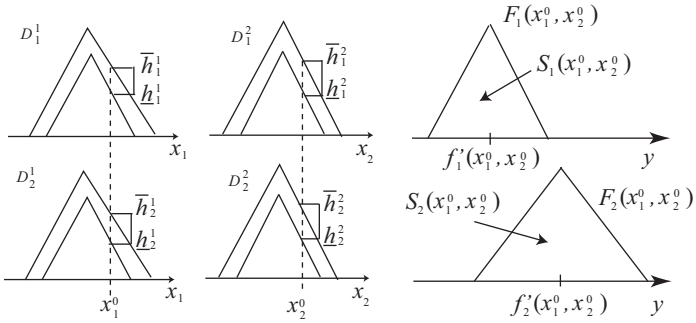

Fig. 3. Type-2 fuzzy functional inference method of Model 3.

$$
\text{Rule } 1: x_1 \text{ is } \tilde{D}_1^1, x_2 = \tilde{D}_1^2 \longrightarrow y = F_1(x_1, x_2) \qquad (26)
$$

$$
\text{Rule } 2: x_1 \text{ is } \tilde{D}_2^1, x_2 = \tilde{D}_2^2 \longrightarrow y = F_2(x_1, x_2) \qquad (27)
$$

where $\tilde{D}_j^i$'s are IT2 fuzzy sets, and $F_i(x_1, x_2)$'s are fuzzy functions.

Given input x_1^0 and x_2^0, the jth degree in the ith input x_i^0 is given as interval value as follows:

$$
\tilde{D}_i^j(x_i^0) = [\underline{h}_i^j, \bar{h}_i^j] \qquad (28)
$$

where $\underline{h}_i^j$ and $\bar{h}_i^j$ represent lower and upper of membership function, respectively.

The inference results of Model 3 are also obtained from the area and center of gravity as (24). That is,

$$
y = \frac{[\underline{h}_1^1\underline{h}_1^2, \bar{h}_1^1\bar{h}_1^2] \cdot S_1 f_1' + [\underline{h}_2^1\underline{h}_2^2, \bar{h}_2^1\bar{h}_2^2] \cdot S_2 f_2'}{[\underline{h}_1^1\underline{h}_1^2, \bar{h}_1^1\bar{h}_1^2] + [\underline{h}_2^1\underline{h}_2^2, \bar{h}_2^1\bar{h}_2^2]} \qquad (29)
$$

where $S_i(= S_i(x_1^0, x_2^0))$ and $f_i'(= f_i'(x_1^0, x_2^0))$ are the area and center of gravity of fuzzy sets of the consequent part, respectively. In the following discussion, we use $y_i = S_i f_i' = S_i(x_1^0, x_2^0) \cdot f_i'(x_1^0, x_2^0)$ $(i = 1, 2)$ for short.

From (17) and (18), we obtain the following inference results.

$$
\begin{aligned}
y &= \frac{[\underline{h}_1^1\underline{h}_1^2, \bar{h}_1^1\bar{h}_1^2] \cdot y_1 + [\underline{h}_2^1\underline{h}_2^2, \bar{h}_2^1\bar{h}_2^2] \cdot y_2}{[\underline{h}_1^1\underline{h}_1^2, \bar{h}_1^1\bar{h}_1^2] + [\underline{h}_2^1\underline{h}_2^2, \bar{h}_2^1\bar{h}_2^2]} \\
&= \frac{[y_1\underline{h}_1^1\underline{h}_1^2 + y_2\underline{h}_2^1\underline{h}_2^2, y_1\bar{h}_1^1\bar{h}_1^2 + y_2\bar{h}_2^1\bar{h}_2^2]}{[\underline{h}_1^1\underline{h}_1^2 + \underline{h}_2^1\underline{h}_2^2, \bar{h}_1^1\bar{h}_1^2 + \bar{h}_2^1\bar{h}_2^2]} \\
&= \left[\frac{y_1\underline{h}_1^1\underline{h}_1^2 + y_2\underline{h}_2^1\underline{h}_2^2}{\bar{h}_1^1\bar{h}_1^2 + \bar{h}_2^1\bar{h}_2^2}, \frac{y_1\bar{h}_1^1\bar{h}_1^2 + y_2\bar{h}_2^1\bar{h}_2^2}{\underline{h}_1^1\underline{h}_1^2 + \underline{h}_2^1\underline{h}_2^2} \right] \qquad (30)
\end{aligned}
$$

where algebraic product and algebraic sum are used as operations.

Note that the following relation holds for interval $X = [a, b]$, $Y = [c, d]$.

$$
X \cdot Y = [\min\{ac, ad, bc, bd\}, \max\{ac, ad, bc, bd\}] \qquad (31)
$$

$$
X/Y = [a, b] \cdot [1/d, 1/c] \qquad (32)
$$

The represetative point y_0 of (30) is given as the average of inference result y, i.e., it is obtained as (33), as shown at the top of the next page.

Since the inference result obtained from the above IT2 fuzzy functinoal inference method, is expressed as a function

$$
\begin{aligned}
y_0 &= \frac{1}{2}\left(\frac{y_1\underline{h}_1^1\underline{h}_1^2+y_2\underline{h}_2^1\underline{h}_2^2}{\bar{h}_1^1\bar{h}_1^2+\bar{h}_2^1\bar{h}_2^2}+\frac{y_1\bar{h}_1^1\bar{h}_1^2+y_2\bar{h}_2^1\bar{h}_2^2}{\underline{h}_1^1\underline{h}_1^2+\underline{h}_2^1\underline{h}_2^2}\right)\\
&= \frac{1}{2}\left(\frac{(y_1\underline{h}_1^1\underline{h}_1^2+y_2\underline{h}_2^1\underline{h}_2^2)(\underline{h}_1^1\underline{h}_1^2+\underline{h}_2^1\underline{h}_2^2)+(y_1\bar{h}_1^1\bar{h}_1^2+y_2\bar{h}_2^1\bar{h}_2^2)(\bar{h}_1^1\bar{h}_1^2+\bar{h}_2^1\bar{h}_2^2)}{(\bar{h}_1^1\bar{h}_1^2+\bar{h}_2^1\bar{h}_2^2)(\underline{h}_1^1\underline{h}_1^2+\underline{h}_2^1\underline{h}_2^2)}\right)\\
&= \frac{1}{2}\left(\frac{y_1(\underline{h}_1^1\underline{h}_1^2)^2+(y_1+y_2)(\underline{h}_1^1\underline{h}_1^2\underline{h}_2^1\underline{h}_2^2)+y_2(\underline{h}_2^1\underline{h}_2^2)^2++y_1(\bar{h}_1^1\bar{h}_1^2)^2+(y_1+y_2)(\bar{h}_1^1\bar{h}_1^2\bar{h}_2^1\bar{h}_2^2)+y_2(\bar{h}_2^1\bar{h}_2^2)^2}{(\bar{h}_1^1\bar{h}_1^2+\bar{h}_2^1\bar{h}_2^2)(\underline{h}_1^1\underline{h}_1^2+\underline{h}_2^1\underline{h}_2^2)}\right)
\end{aligned}
\tag{33}
$$

of the square, it can obtain different results compared with the conventional fuzzy inference methods. This is the reason computation of the inference results of the IT2 fuzzy functional inference method, is inverted by division of the numerator and the denominator in interval as (32).

Remark 2: In (30), the inference results can not be obtained by (32), if $\underline{h}_1^1\underline{h}_1^2+\underline{h}_2^1\underline{h}_2^2$ or $\bar{h}_1^1\bar{h}_1^2+\bar{h}_2^1\bar{h}_2^2$ are 0. □

V. Conclusion

In this paper, we have porposed type-2 fuzzy functional inference method which extends fuzzy sets of the antecedent parts to type-2 fuzzy sets. This paper has explained that the type-2 fuzzy functional inference method can be classified to the three Models. Model 1 is most common method, and Model 2 is a special case of Model 1. We have shown that the inference results of both Models 1 and 2 can be easily obtained from the area of fuzzy sets of the consequent parts and center of gravity. Moreover, we have stated that Model 3 can obtain different results compared with the conventional fuzzy inference methods. However, Model 3 requires cautious use when the firing level becomes 0.

Further studies are required to apply the type-2 fuzzy functional inference methods to real systems.

References

[1] E. H. Mamdani, "Application of fuzzy algorithms for control of simple dynamic plant," Proc. IEE, vol. 121, no. 12, pp. 1585–1588, 1974.

[2] M. Sugeno, "An introductory survey of fuzzy control," *Inf. Sci.*, vol. 36, pp. 59–83, 1985.

[3] T. Takagi and M. Sugeno, "Fuzzy identification of systems and its Applications to modeling and control," *IEEE Transactions on Systems, Man, and Cybernetics*, vol. SMC-15, no. 1, pp. 116–132, 1985.

[4] H. Seki and M. Mizumoto, "Fuzzy functional inference method," *Proc. 2010 IEEE World Congress on Computational Intelligence, FUZZ-IEEE 2010*, pp.1643–1648, Barcelona, Spain, July 2010.

[5] H. Seki and M. Mizumoto, "Additive fuzzy functional inference methods," *Proc. 2010 IEEE International Conference on Systems, Man, and Cyberntics*, Istanbul, Turkey, October 2010.

[6] J. R. Jang and C. T. Sun, "Functional equivalence between radial basis function networks and fuzzy inference systems," *IEEE Transactions on Neural Networks*, vol. 4, no. 1, pp. 156–159, 1993.

[7] K. J. Hunt, R. Haas, and M. Brown, "On the functional equivalence of fuzzy inference systems and spline-based networks," *Int. J. Neural Syst.*, vol. 6, no. 2, pp. 171–184, 1995.

[8] M. Mizumoto, "Product–sum–gravity method = fuzzy singleton-type reasoning method = simplified fuzzy reasoning method," *Proc. 1996 IEEE International Conference on Fuzzy Systems*, vol. 3, pp. 2098–2102, New Orleans, USA, 1996.

[9] J. M. Benitez, J. L. Castro, and I. Requena, "Are artifical neural networks black boxes?," *IEEE Transactions on Neural Networks*, vol. 8, no. 5, pp. 1156–1164, September 1997.

[10] J. L. Castro, C. J. Mantas, and J. M. Benitez, "Interpretation of artifical neural networks by means of fuzzy rules," *IEEE Transactions on Neural Networks*, vol. 13, no. 1, pp. 101–116, January 2002.

[11] E. Kolman and M. Margaliot, "Are artificial neural networks white boxes?," *IEEE Transactions on Neural Networks*, vol. 16, no. 4, pp. 844–852, July 2005.

[12] C. J. Mantas and J. M. Puche, "Artificial neural networks are zero-order TSK fuzzy systems," *IEEE Transactions on Fuzzy Systems*, vol. 16, no. 3, pp. 630–643, June 2008.

[13] H. Seki, H. Ishii, and M. Mizumoto, "On the generalization of single input rule modules connected type fuzzy reasoning method," *IEEE Transactions on Fuzzy Systems*, vol. 16, no. 5, pp. 1180–1187, October 2008.

[14] H. Seki and M. Mizumoto, "On the equivalence of single input type fuzzy inference methods," *Proc. 2009 IEEE International Conference on Systems, Man, and Cybernetics*, pp. 692–697, San Antonio, Texas, USA, October 2009.

[15] H. Seki, H. Ishii, and M. Mizumoto, "On the monotonicity of fuzzy-inference methods related to T–S inference method," *IEEE Transactions on Fuzzy Systems*, vol. 18, no. 3, pp.629–634, June 2010.

[16] N. N. Karnik, J. M. Mendel and Q. Liang, "Type-2 fuzzy logic systems," *IEEE Trans. Fuzzy Syst.*, vol. 7, no. 6, pp. 643–658, 1999.

[17] Q. Liang and J. M. Mendel, "An introduction to type-2 TSK fuzzy logic systems," in *Proc. 1999 IEEE Int. Conf. Fuzzy Syst.*, vol. 3, pp. 1534–1539, 1999.

[18] Q. Liang and J. M. Mendel, "Interval type-2 fuzzy logic systems: theory and design," *IEEE Trans. Fuzzy Syst.*, vol. 8, pp. 535–550, 2000.

[19] J. M. Mendel, *Uncertain rule-based fuzzy logic systems: introduction and new directions*, Upper Saddle River, NJ: Prentice-Hall, 2001.

[20] M. Mizumoto, "Fuzzy controls under various fuzzy reasoning methods," *Inf. Sci.*, vol. 45, pp. 129–151, 1988.

[21] M. Mizumoto, *Fuzzy controls under product–sum–grvity method and new fuzzy control methods*, Fuzzy Control Systems (ed. A. Kandel and G. Langholz), CRC Press, pp. 275–294, 1993.

[22] B. Kosco, *Neural Networks and Fuzzy Systems*, Prentice Hall, 1992.

[23] B. -G. Hu, G. K. I. Mann, and R. G. Gosine, "A systematic study of fuzzy PID controllers—function-based evaluation approach," *IEEE Transactions on Fuzzy Systems*, vol. 9, no. 5, pp. 699–712, October 2001.

[24] H. Bustince and P. Burillo, "Mathematical analysis of interval-valued fuzzy relations: application to approximate reasoning," *Fuzzy Sets and Systems*, vol. 113, no. 2, pp. 205–219, 2000.

[25] H. Bustince, "Indicator of inclusion grade for interval-valued fuzzy sets. application to approximate reasoning based on interval-valued fuzzy sets," *International Journal of Approximate Reasoning*, vol. 23, no. 3, pp. 137–209, 2000.

2011 IEEE International Conference on Fuzzy Systems
June 27-30, 2011, Taipei, Taiwan

On Extension of Consequent Parts of T–S Inference Model

Hirosato Seki
Dept. of Technology Management
Osaka Institute of Technology
Osaka, Japan 535-8585
Email: h_seki@ieee.org

Masaharu Mizumoto
Dept. of Engineering Informatics
Osaka Electro-Communication University
Osaka, Japan 572-8530
Email: mizumoto3003@yahoo.co.jp

***Abstract*—This paper discusses the extension of consequent parts of T–S inference model. First, it proposes an extended T–S inference model in which the coefficients of consequent parts of the fuzzy rules are extended from constants to functions. It also shows the property of the proposed model from the point of view of the equivalence and the monotonicity, by using simplified model of the proposed model.**

***Index Terms*—Fuzzy inference, Takagi–Sugeno (T–S) fuzzy inference model, Single Input Connected (SIC) fuzzy inference model, Equivalence, Monotonicity.**

I. Introduction

The fuzzy inference models have powerful capability in nonlinear systems, control, and so on since Zadeh introduced fuzzy sets and Mamdani [1] applied the concept of fuzzy inference to a steam engine experimental device. Especially, researches on the T–S inference model [2], which are widely used as fuzzy control method and so on, are reported in many papers.

The extention of the consequent parts of the T–S model is very difficult. For example, the single input connected fuzzy inference model (SIC model) by Hayashi et al. [4]–[6] can be transformed to the extended simplified fuzzy inference model [3].

From this reason, in this paper, we first propose an extended T–S inference model in which the coefficients of consequent parts of the fuzzy rules are extended from constants to functions, and show that this model can obtain complex inference results.

Second, we consider the extended simplified fuzzy inference model as a simple model of extended T–S inference model. As previously stated, the SIC model can be transformed to the extended simplified fuzzy inference model [3]. However, the extended simplified fuzzy inference model can not be generally transformed to the SIC model, and the equivalence conditions between the extended simplfiied fuzzy inference model and the SIC model were not shown. Therefore, we discuss the equivalence conditions of these models.

Finally, we show the monotonicity [6]–[8] of the extended simplified fuzzy inference model by using the equivalence conditions.

II. Fuzzy Inference Models

In this section we review the T–S inference model [2] and SIC model [4]–[6].

A. T–S Inference Model

Rules in the Takagi–Sugeno (T–S) inference model [2] are constituted as

$$\text{Rule } R_j = \begin{cases} x_1 = A_j^1,\ x_2 = A_j^2,\ \ldots,\ x_n = A_j^n \\ \longrightarrow y = a_0^j + a_1^j x_1 + \cdots + a_n^j x_n \end{cases} \tag{1}$$

where $x_1, x_2, \ldots, x_n$ are variables of the antecedent part, $A_j^1, A_j^2, \ldots, A_j^n$ fuzzy sets, $a_0^j + a_1^j x_1 + \cdots + a_n^j x_n$ functions of consequent part, and a_i^j's are real number. The inference result y^0 for inputs $x_1^0, x_2^0, \ldots, x_n^0$ is given as

$$y^0 = \frac{\sum_{j=1}^{M} h_j (a_0^j + a_1^j x_1^0 + \cdots + a_n^j x_n^0)}{\sum_{j=1}^{M} h_j}, \quad h_j = \prod_{i=1}^{n} A_j^i(x_i^0) \tag{2}$$

where h_j is the degree of the jth rule and M is the total number of the fuzzy rules.

Example 1: We first consider the following T–S rules as a simple example.

$$\begin{array}{l} x_1 = A_1^1, x_2 = A_1^2 \longrightarrow y = 0.45 - 0.2x_1 + 0.35x_2 \\ x_1 = A_1^1, x_2 = A_2^2 \longrightarrow y = -0.1 - 0.2x_1 - 0.1x_2 \\ x_1 = A_1^1, x_2 = A_3^2 \longrightarrow y = 0.05 - 0.2x_1 + 0.25x_2 \\ x_1 = A_2^1, x_2 = A_1^2 \longrightarrow y = 0.4 - 0.3x_1 + 0.35x_2 \\ x_1 = A_2^1, x_2 = A_2^2 \longrightarrow y = -0.15 - 0.3x_1 - 0.1x_2 \\ x_1 = A_2^1, x_2 = A_3^2 \longrightarrow y = -0.3x_1 + 0.25x_2 \\ x_1 = A_3^1, x_2 = A_1^2 \longrightarrow y = 0.25 + 0.1x_1 + 0.35x_2 \\ x_1 = A_3^1, x_2 = A_2^2 \longrightarrow y = -0.3 + 0.1x_1 - 0.1x_2 \\ x_1 = A_3^1, x_2 = A_3^2 \longrightarrow y = -0.15 + 0.1x_1 + 0.25x_2 \end{array} \tag{3}$$

where fuzzy sets, as shown in Fig. 1, are used. From (2), the inference result of (3) is obtained as shown in Fig. 2. □

B. Single Input Connected (SIC) Fuzzy Inference Model

We briefly review the single input connected fuzzy inference model (SIC model) by Hayashi et al. [4]–[6]. The SIC model has n rule modules, and the final inference result is obtained by the weighted average of the degrees of the antecedent part

978-1-4244-7316-8/11/$26.00 ©2011 IEEE

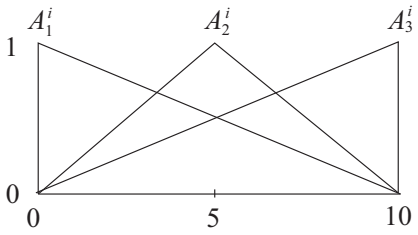

Fig. 1. Fuzzy sets.

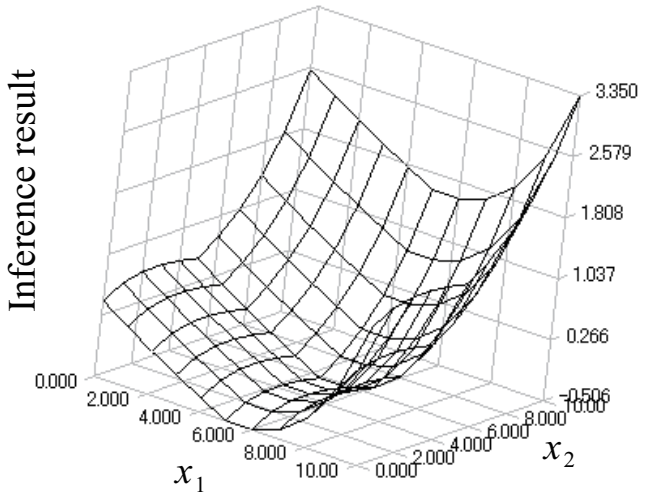

Fig. 2. Inference result by the T–S model of (3).

and consequent part of each rule module. The rule modules of the SIC model are given as

$$\begin{aligned}
&\text{Rules-1} : \{x_1 = A_j^1 \longrightarrow y_1 = y_j^1\}_{j=1}^{m_1} \\
&\qquad\vdots \\
&\text{Rules-}i : \{x_i = A_j^i \longrightarrow y_i = y_j^i\}_{j=1}^{m_i} \\
&\qquad\vdots \\
&\text{Rules-}n : \{x_n = A_j^n \longrightarrow y_n = y_j^n\}_{j=1}^{m_n}
\end{aligned} \tag{4}$$

where Rules-i stands for the ith single input rule module, the ith input item x_i is the sole variable of the antecedent part of the Rules-i, and y_i stands for the variable of its consequent part. A_j^i means the fuzzy set of the jth rule of the Rules-i, y_j^i is real value of consequent part, $i = 1, 2, \ldots, n$, $j = 1, 2, \ldots, m_i$, and m_i is the number of rules in Rules-i.

The degree of the antecedent part in the jth rule of Rules-i is obtained by (5) for input x_i^0.

$$h_j^i = A_j^i(x_i^0) \tag{5}$$

The final inference result y_0 is given as follows by using degrees of antecedent part and consequent part from each rule module.

$$\begin{aligned}
y_0 &= \frac{\sum_{j=1}^{m_1} h_j^1 y_j^1 + \cdots + \sum_{j=1}^{m_n} h_j^n y_j^n}{\sum_{j=1}^{m_1} h_j^1 + \cdots + \sum_{j=1}^{m_n} h_j^n} \\
&= \frac{\sum_{i=1}^{n}\sum_{j=1}^{m_i} h_j^i y_j^i}{\sum_{i=1}^{n}\sum_{j=1}^{m_i} h_j^i}
\end{aligned} \tag{6}$$

III. Extension of Coefficients of Consequent Parts in T–S Inference Model

In this section, we propose an extended T–S inference model in which the coefficients of consequent parts of the fuzzy rules are extended from constants to functions. The rules of proposed model are obtained as follows.

$$\text{Rule } R_j = \left\{ \begin{array}{l} x_1 = A_j^1,\ x_2 = A_j^2,\ \ldots,\ x_n = A_j^n \longrightarrow \\ y = a_0^j(\boldsymbol{x}) + a_1^j(\boldsymbol{x})x_1 + \cdots + a_n^j(\boldsymbol{x})x_n \end{array} \right. \tag{7}$$

where $x_1, x_2, \ldots, x_n$ are variables of the antecedent part, $A_j^1, A_j^2, \ldots, A_j^n$ fuzzy sets, and $a_i^j(\boldsymbol{x})$'s are functions of coefficients of consequent part, where $a_i^j(\boldsymbol{x})$ is accorded a considerable degree. The inference result y^0 for inputs $x_1^0, x_2^0, \ldots, x_n^0$ is given as

$$y^0 = \frac{\sum_{j=1}^{M} h_j(a_0^j(\boldsymbol{x}) + a_1^j(\boldsymbol{x})x_1^0 + \cdots + a_n^j(\boldsymbol{x})x_n^0)}{\sum_{j=1}^{M} h_j} \tag{8}$$

where h_j is obtained in the same way as the conventional T–S inference model.

Example 2: We consider the rules of (9) of an extended T–S inference model, as a simple extension of (3), which is shown at the bottom of the next page, where fuzzy sets of Fig. 1 are used. From (8), the inference result of (9) is obtained as shown in Fig. 3. From the result, we can find out that the above extended T–S model can obtain complex inference results. □

IV. Property of extended T–S Inference Model by Using Equivalence

Generally speaking, decision of the coefficient functions of the proposed T–S model is very difficult. Therefore, in this section, we discuss the extended simplified fuzzy inference model which reduce a part of the functions of the consequent parts to real number, as a simple version of extended T–S model.

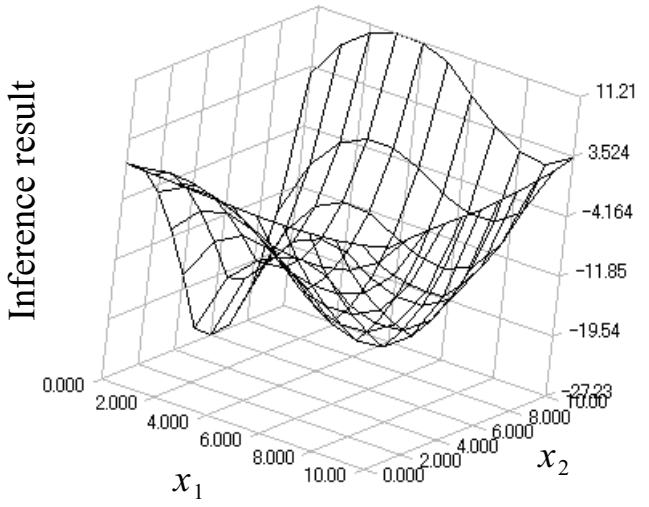

Fig. 3. Inference result by the extended T–S model of (9).

A. Equivalence

Reference [3] has shown that the SIC model can be transformed to the simplified fuzzy inference model which extends the coefficients of consequent parts to a compatibility function, but not vice versa. Therefore, we first show that the extended simplified fuzzy inference model can be transformed to the SIC model under a condition.

In order to distinguish subscript j of Rules-i in (4), j_i is used, and thus (4) is rewritten as

$$\text{Rules-}i : \{x_i = A^i_{j_i} \longrightarrow y_i = y^i_{j_i}\}_{j_i=1}^{m_i} \tag{10}$$

We can obtain the following rules of the extended simplified fuzzy inference model which corresponds to (10) of the rules of the SIC model [3]:

$$\begin{aligned} &x_1 = A^1_{j_1}, x_2 = A^2_{j_2}, \ldots, x_n = A^n_{j_n} \\ \longrightarrow y = &\frac{\sum_{j_i=1}^{m_1} h^1_{j_i}}{\sum_{i=1}^{n}\sum_{j_i=1}^{m_i} h^i_{j_i}} \cdot y^1_{j_1} + \cdots + \frac{\sum_{j_i=1}^{m_n} h^n_{j_i}}{\sum_{i=1}^{n}\sum_{j_i=1}^{m_i} h^i_{j_i}} \cdot y^n_{j_n} \end{aligned} \tag{11}$$

where $j_i = 1, 2, \ldots, m_i$.

Now, we consider the rules of the extended simplified fuzzy inference model as follows.

$$x_1 = A^1_1, x_2 = A^2_1 \longrightarrow y = f_1(x_1, x_2) = a \tag{12}$$
$$x_1 = A^1_1, x_2 = A^2_2 \longrightarrow y = f_2(x_1, x_2) = b \tag{13}$$
$$x_1 = A^1_2, x_2 = A^2_1 \longrightarrow y = f_3(x_1, x_2) = c \tag{14}$$
$$x_1 = A^1_2, x_2 = A^2_2 \longrightarrow y = f_4(x_1, x_2) = d \tag{15}$$

Suppose that the rules of the SIC model corresponding to (12)–(15) are given as

$$\begin{aligned} \text{Rules-1} &= \begin{cases} x_1 = A^1_1 \longrightarrow y_1 = y^1_1 \\ x_1 = A^1_2 \longrightarrow y_1 = y^1_2 \end{cases} \\ \text{Rules-2} &= \begin{cases} x_2 = A^2_1 \longrightarrow y_2 = y^2_1 \\ x_2 = A^2_2 \longrightarrow y_2 = y^2_2 \end{cases} \end{aligned} \tag{16}$$

Then, according to (10) and (11), (17)–(20), which are shown at the bottom of the next page, can be deduced from (16). From the correspondence of (12)–(15) and (17)–(20), we have the following relations:

$$\frac{\sum_{j_i=1}^{m_1} h^1_{j_i}}{\sum_{i=1}^{n}\sum_{j_i=1}^{m_i} h^i_{j_i}} \cdot y^1_1 + \frac{\sum_{j_i=1}^{m_n} h^2_{j_i}}{\sum_{i=1}^{n}\sum_{j_i=1}^{m_i} h^i_{j_i}} \cdot y^2_1 = a \tag{21}$$

$$\frac{\sum_{j_i=1}^{m_1} h^1_{j_i}}{\sum_{i=1}^{n}\sum_{j_i=1}^{m_i} h^i_{j_i}} \cdot y^1_1 + \frac{\sum_{j_i=1}^{m_n} h^2_{j_i}}{\sum_{i=1}^{n}\sum_{j_i=1}^{m_i} h^i_{j_i}} \cdot y^2_2 = b \tag{22}$$

$$\frac{\sum_{j_i=1}^{m_1} h^1_{j_i}}{\sum_{i=1}^{n}\sum_{j_i=1}^{m_i} h^i_{j_i}} \cdot y^1_2 + \frac{\sum_{j_i=1}^{m_n} h^2_{j_i}}{\sum_{i=1}^{n}\sum_{j_i=1}^{m_i} h^i_{j_i}} \cdot y^2_1 = c \tag{23}$$

$$\frac{\sum_{j_i=1}^{m_1} h^1_{j_i}}{\sum_{i=1}^{n}\sum_{j_i=1}^{m_i} h^i_{j_i}} \cdot y^1_2 + \frac{\sum_{j_i=1}^{m_n} h^2_{j_i}}{\sum_{i=1}^{n}\sum_{j_i=1}^{m_i} h^i_{j_i}} \cdot y^2_2 = d \tag{24}$$

$$\begin{aligned}
&x_1 = A^1_1, x_2 = A^2_1 \longrightarrow y = 0.45 - 0.2x_1 + 0.35x_2 \\
&x_1 = A^1_1, x_2 = A^2_2 \longrightarrow y = -0.1(-0.2x_1 + 5)x_1 - (0.1x_2 - 10)x_2 \\
&x_1 = A^1_1, x_2 = A^2_3 \longrightarrow y = 0.05 - 0.2x_1 + 0.25x_2 \\
&x_1 = A^1_2, x_2 = A^2_1 \longrightarrow y = 0.4 - 0.3x_1 + 0.35x_2 \\
&x_1 = A^1_2, x_2 = A^2_2 \longrightarrow y = -0.15 - (0.3x_1 - 10)x_1 - 0.1x_2 \\
&x_1 = A^1_2, x_2 = A^2_3 \longrightarrow y = (-0.3x_1 - 2)x_1 + (0.25x_2 + 1)x_2 \\
&x_1 = A^1_3, x_2 = A^2_1 \longrightarrow y = 0.25 + 0.1x_1 + 0.35x_2 \\
&x_1 = A^1_3, x_2 = A^2_2 \longrightarrow y = -0.3 + 0.1x_1 - 0.1x_2 \\
&x_1 = A^1_3, x_2 = A^2_3 \longrightarrow y = -0.15 + 0.1x_1 + 0.25x_2
\end{aligned} \tag{9}$$

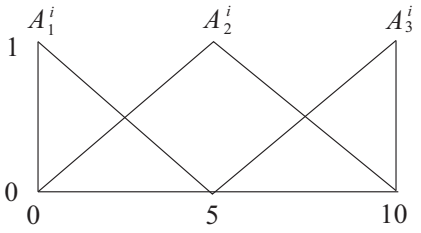

Fig. 4. Fuzzy sets with fuzzy partition.

From (21)–(24), the relation (25) is obtained

$$a + d = b + c \tag{25}$$

Under the conditions of (25), the rules of the SIC model of (16) can be obtained if $\frac{\sum_{j_i=1}^{m_1} h_{j_i}^1}{\sum_{i=1}^{n}\sum_{j_i=1}^{m_i} h_{j_i}^i}$, $\frac{\sum_{j_i=1}^{m_1} h_{j_i}^2}{\sum_{i=1}^{n}\sum_{j_i=1}^{m_i} h_{j_i}^i}$, y_1^1, y_2^1, y_1^2, and y_2^2 of (21)–(24) are fixed.

Example 3: We consider an example of the rules of the SIC model used in [3] as follows:

$$\text{Rules-1} = \begin{cases} x_1 = A_1^1 \longrightarrow y_1 = 1 \\ x_1 = A_2^1 \longrightarrow y_1 = 2 \\ x_1 = A_3^1 \longrightarrow y_1 = 1 \end{cases}$$

$$\text{Rules-2} = \begin{cases} x_2 = A_1^2 \longrightarrow y_2 = 1 \\ x_2 = A_2^2 \longrightarrow y_2 = 3 \\ x_2 = A_3^2 \longrightarrow y_2 = 5 \end{cases} \tag{26}$$

where fuzzy sets A_1^i, A_2^i, A_3^i $(i = 1, 2)$ in Fig. 4 are used. The inference results of (26) by the SIC model are obtained as shown in Fig. 5.

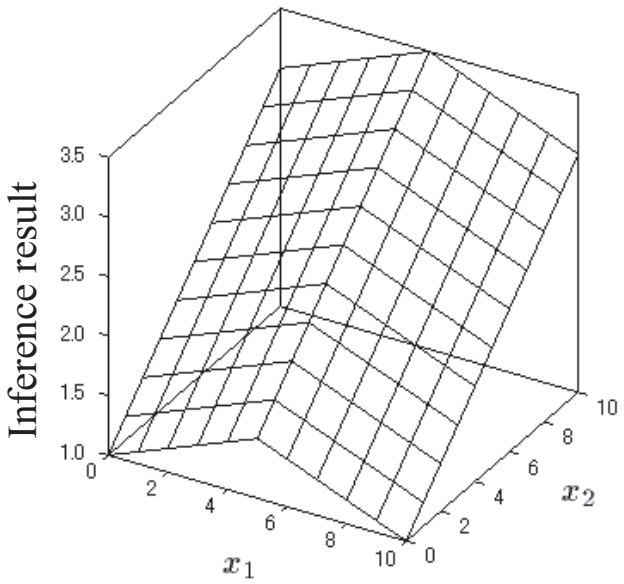

Fig. 5. Inference result by the SIC model of (26).

On the other hand, based on the above discussion, we obtain the rules of the extended simplified fuzzy inference model as (27), as shown at the bottom of the next page.

Note that $y_1^1 = 1, y_2^1 = 2, y_3^1 = 1$, and $y_1^2 = 1, y_2^2 = 3, y_3^2 = 5$ from (26), and the functional coefficients are as follows because fuzzy sets of antecedent parts constitute fuzzy

$$x_1 = A_1^1, x_2 = A_1^2 \longrightarrow y = \frac{\sum_{j_i=1}^{m_1} h_{j_i}^1}{\sum_{i=1}^{n}\sum_{j_i=1}^{m_i} h_{j_i}^i} \cdot y_1^1 + \frac{\sum_{j_i=1}^{m_n} h_{j_i}^2}{\sum_{i=1}^{n}\sum_{j_i=1}^{m_i} h_{j_i}^i} \cdot y_1^2 = a \tag{17}$$

$$x_1 = A_1^1, x_2 = A_2^2 \longrightarrow y = \frac{\sum_{j_i=1}^{m_1} h_{j_i}^1}{\sum_{i=1}^{n}\sum_{j_i=1}^{m_i} h_{j_i}^i} \cdot y_1^1 + \frac{\sum_{j_i=1}^{m_n} h_{j_i}^2}{\sum_{i=1}^{n}\sum_{j_i=1}^{m_i} h_{j_i}^i} \cdot y_2^2 = b \tag{18}$$

$$x_1 = A_2^1, x_2 = A_1^2 \longrightarrow y = \frac{\sum_{j_i=1}^{m_1} h_{j_i}^1}{\sum_{i=1}^{n}\sum_{j_i=1}^{m_i} h_{j_i}^i} \cdot y_2^1 + \frac{\sum_{j_i=1}^{m_n} h_{j_i}^2}{\sum_{i=1}^{n}\sum_{j_i=1}^{m_i} h_{j_i}^i} \cdot y_1^2 = c \tag{19}$$

$$x_1 = A_2^1, x_2 = A_2^2 \longrightarrow y = \frac{\sum_{j_i=1}^{m_1} h_{j_i}^1}{\sum_{i=1}^{n}\sum_{j_i=1}^{m_i} h_{j_i}^i} \cdot y_2^1 + \frac{\sum_{j_i=1}^{m_n} h_{j_i}^2}{\sum_{i=1}^{n}\sum_{j_i=1}^{m_i} h_{j_i}^i} \cdot y_2^2 = d \tag{20}$$

TABLE I
RULES OF EXTENDED SIMPLIFIED FUZZY INFERENCE MODEL IN TABLE FORM

		x_2			
		A_1^2	A_2^2	$\cdots$	A_n^2
x_1	A_1^1	$f(x_1,x_2)_{(1,1)}$	$f(x_1,x_2)_{(1,2)}$	$\cdots$	$f(x_1,x_2)_{(1,n)}$
	A_2^1	$f(x_1,x_2)_{(2,1)}$	$f(x_1,x_2)_{(2,2)}$	$\cdots$	$f(x_1,x_2)_{(2,n)}$
	$\vdots$	$\vdots$	$\vdots$		$\vdots$
	A_m^1	$f(x_1,x_2)_{(m,1)}$	$f(x_1,x_2)_{(m,2)}$	$\cdots$	$f(x_1,x_2)_{(m,n)}$

partition.

$$\frac{\sum_{j_i=1}^{m_1} h_{j_i}^i}{\sum_{i=1}^{n}\sum_{j_i=1}^{m_i} h_{j_i}^i} = \frac{1}{2} \tag{28}$$

From (27), the extended simplified fuzzy inference model can obtain the same result of the SIC model as shown in Fig. 5.

In the case of (27), considering the elicitation process of (25), the equivalence conditions between the extended simplified fuzzy inference model and SIC model are obtained as follows:

$$f_1(x_1,x_2) + f_5(x_1,x_2) = f_2(x_1,x_2) + f_4(x_1,x_2) \tag{29}$$
$$f_2(x_1,x_2) + f_6(x_1,x_2) = f_3(x_1,x_2) + f_5(x_1,x_2) \tag{30}$$
$$f_4(x_1,x_2) + f_8(x_1,x_2) = f_5(x_1,x_2) + f_7(x_1,x_2) \tag{31}$$
$$f_5(x_1,x_2) + f_9(x_1,x_2) = f_6(x_1,x_2) + f_8(x_1,x_2) \tag{32}$$

□

(25) and (29)–(32) show that two diagonal sums of rules in table form should be equal.

Therefore, as the generalization of the above results, we have the following Theorem regarding the equivalence between the extended simplified fuzzy inference model and the SIC model.

Theorem 1: In the extended simplified fuzzy inference model, when the rules of the extended simplified fuzzy inference model are given in table form, as shown in Table I, and the following conditions are satisfied, the inference result is equal to that of the SIC model.

$$\begin{aligned} &f(x_1,x_2)_{(i,j)} + f(x_1,x_2)_{(i+1,j+1)} \\ &= f(x_1,x_2)_{(i+1,j)} + f(x_1,x_2)_{(i,j+1)} \end{aligned} \tag{33}$$

B. Monotonicity

It is important that inference results have the property of monotonicity; this is necessary when fuzzy inference is applied to evaluation problems, engineering problems, etc. However, deriving the monotonic conditions of the fuzzy inference model is very difficult [7], [8]. In this subsection, we show the monotonicity of extended simplified fuzzy inferece model by using equivalence conditions as shown in previous subsestion.

We have the following Theorem regarding the monotonicity of the extended simplified fuzzy inference model.

Theorem 2: For the extended simplified fuzzy inference model, the inference results monotonically increase, if the antecedent parts and consequent parts of each input item are monotonically increasing, and the fuzzy sets constitute fuzzy partitions, when the condition (33) is satisfied. □

proof: Inference result y^0 of the extended simplified fuzzy inference model becomes as follows from (11):

$$y^0 = \frac{\sum_{j=1}^{M}\left\{h_j\left(\frac{y_{j_1}^1\sum_{j_i=1}^{m_1} h_{j_i}^1}{\sum_{i=1}^{n}\sum_{j_i=1}^{m_i} h_{j_i}^1} + \cdots + \frac{y_{j_n}^n\sum_{j_i=1}^{m_n} h_{j_i}^n}{\sum_{i=1}^{n}\sum_{j_i=1}^{m_i} h_{j_i}^n}\right)\right\}}{\sum_{j=1}^{M} h_j} \tag{34}$$

$$\begin{aligned}
x_1 = A_1^1, x_2 = A_1^2 &\longrightarrow y = f_1(x_1,x_2) = 0.5\cdot y_1^1 + 0.5\cdot y_1^2 = 1 \\
x_1 = A_1^1, x_2 = A_2^2 &\longrightarrow y = f_2(x_1,x_2) = 0.5\cdot y_1^1 + 0.5\cdot y_2^2 = 2 \\
x_1 = A_1^1, x_2 = A_3^2 &\longrightarrow y = f_3(x_1,x_2) = 0.5\cdot y_1^1 + 0.5\cdot y_3^2 = 3 \\
x_1 = A_2^1, x_2 = A_1^2 &\longrightarrow y = f_4(x_1,x_2) = 0.5\cdot y_2^1 + 0.5\cdot y_1^2 = 1.5 \\
x_1 = A_2^1, x_2 = A_2^2 &\longrightarrow y = f_5(x_1,x_2) = 0.5\cdot y_2^1 + 0.5\cdot y_2^2 = 2.5 \\
x_1 = A_2^1, x_2 = A_3^2 &\longrightarrow y = f_6(x_1,x_2) = 0.5\cdot y_2^1 + 0.5\cdot y_3^2 = 3.5 \\
x_1 = A_3^1, x_2 = A_1^2 &\longrightarrow y = f_7(x_1,x_2) = 0.5\cdot y_3^1 + 0.5\cdot y_1^2 = 1 \\
x_1 = A_3^1, x_2 = A_2^2 &\longrightarrow y = f_8(x_1,x_2) = 0.5\cdot y_3^1 + 0.5\cdot y_2^2 = 2 \\
x_1 = A_3^1, x_2 = A_3^2 &\longrightarrow y = f_9(x_1,x_2) = 0.5\cdot y_3^1 + 0.5\cdot y_3^2 = 3
\end{aligned} \tag{27}$$

From Reference [3] and the equivalence condition, as shown in this paper, we can transform the inference results of extended simplified fuzzy inference model from (34) into

$$
\begin{aligned}
y^0 &= \frac{\sum_{j_i=1}^{m_1} h_{j_i}^1}{\sum_{i=1}^{n}\sum_{j_i=1}^{m_i} h_{j_i}^i} \cdot \frac{\sum_{j_1=1}^{m_1} h_{j_1}^1 y_{j_1}^1}{\sum_{j_1=1}^{m_1} h_{j_1}^1} + \cdots \\
&\quad + \frac{\sum_{j_n=1}^{m_n} h_{j_n}^n}{\sum_{i=1}^{n}\sum_{j_i=1}^{m_i} h_{j_i}^i} \cdot \frac{\sum_{j_n=1}^{m_n} h_{j_n}^n y_{j_n}^n}{\sum_{j_n=1}^{m_n} h_{j_n}^n} \\
&= \frac{\sum_{i=1}^{n}\sum_{j=1}^{m_i} h_j^i y_j^i}{\sum_{i=1}^{n}\sum_{j=1}^{m_i} h_j^i} \qquad (35)
\end{aligned}
$$

(Confer [3] for detail of proof). (35) is equal to the inference results of the SIC model of (6). Reference [6] has shown that the monotonicity of SIC model is satisfied, if the antecedent parts and consequent parts of each input item are monotonically increasing, and the fuzzy sets constitute fuzzy partitions. Therefore, Theorem 2 holds. □

Note that the monotonicity of the extended T–S inference model can be also argued as well as the extended simplified fuzzy inference model, if the consequent functions are positive value and monotonically increasing, the antecedent parts are monotonically increasing, and the fuzzy sets constitute fuzzy partitions.

V. Conclusion

In this paper, we proposed an extended T–S inference model in which the coefficients of consequent parts of the fuzzy rules are extended from constants to functions.

To decide the coefficient functions of the model is generally vry difficult. However, we showed an example of the coefficient functions and its property, by using simplified model of this model.

We have also shown the equivalence conditions between the extended simplified fuzzy inference model and the SIC model. Since the SIC model is applied to PID control, etc., and good results are obtained, the proposed model will be also useful. Moreover, we clarified to obtain the monotonicity condition of this model easily, by using the above equivalence conditions.

Since the number of the parameters of the general proposed model, as shown in (7), is large compared with the conventional T–S inference model, it may obtain good results in various fields. However, how to select and optimization of its parameters should be investigated.

Further studies are required to find out other applicative coefficient functions, and to apply this model to real systems.

References

[1] E. H. Mamdani, "Application of fuzzy algorithms for control of simple dynamic plant," Proc. IEE, vol. 121, no. 12, pp. 1585–1588, 1974.

[2] T. Takagi and M. Sugeno, "Fuzzy identification of systems and its applications to modeling and control," *IEEE Trans. Syst., Man, Cybern.*, vol. SMC-15, no. 1, pp. 116–132, 1985.

[3] H. Seki and M. Mizumoto, "On the equivalence of fuzzy inference methods: part 1, basic concept and definition" *IEEE Trans. on Fuzzy Sust.*, submitted.

[4] K. Hayashi, A. Otsubo, S. Murakami, and M. Maeda, "Realization of nonlinear and linear PID controls using simplified indirect fuzzy inference method," *Fuzzy Sets Syst.*, vol. 105, pp.409–414, 1999.

[5] K. Hayashi, A. Otsubo, and K. Shiranita, "Improvement of conventional method of PI fuzzy control," *IEICE Trans. Fundamentals*, vol.E84-A, no.6, pp.1588–1592, June 2001.

[6] H. Seki, H. Ishii, and M. Mizumoto, "On the monotonicity of single input type fuzzy reasoning methods," *IEICE Trans. on Fundamentals*, vol.E90-A, no.7, pp.1462–1468, July 2007.

[7] J. M. Won, S. Y. Park, and J. S. Lee "Parameter conditions for monotonic Takagi–Sugeno-Kang fuzzy system," *Fuzzy Sets Syst.*, vol.132, pp.135–146, 2002.

[8] H. Seki, H. Ishii, and M. Mizumoto, "On the monotonicity of fuzzy-inference methods related to T–S inference method," *IEEE Trans. Fuzzy Syst.*, vol. 18, no. 3, pp. 629–634, June 2010.

2011 IEEE International Conference on Fuzzy Systems
June 27-30, 2011, Taipei, Taiwan

Optimization of Gaussian Fuzzy Membership Functions and Evaluation of the Monotonicity Property of Fuzzy Inference Systems

Kai Meng Tay
Faculty of Engineering
Universiti Malaysia Sarawak, Sarawak
Malaysia
kmtay@feng.unimas.my

Chee Peng Lim
School of Computer Sciences
University of Science Malaysia
Malaysia

***Abstract*—In this paper, two issues relating to modeling of a monotonicity-preserving Fuzzy Inference System (FIS) are examined. The first is on designing or tuning of Gaussian Membership Functions (MFs) for a monotonic FIS. Designing Gaussian MFs for an FIS is difficult because of its spreading and curvature characteristics. In this study, the *sufficient conditions* are exploited, and the procedure of designing Gaussian MFs is formulated as a constrained optimization problem. The second issue is on the testing procedure for a monotonic FIS. As such, a testing procedure for a monotonic FIS model is proposed. Applicability of the proposed approach is demonstrated with a real world industrial application, i.e., Failure Mode and Effect Analysis. The results obtained are analysis and discussed. The outcomes show that the proposed approach is useful in designing a monotonicity-preserving FIS model.**

Keywords-Fuzzy Inference System, monotonicity property, Gaussian membership functions, sufficient conditions, monotonicity testing

I. INTRODUCTION

Many real-world systems abide the monotonicity property between the input(s) and output(s) of a system. Consider an Fuzzy Inference System (FIS), $y = f(x_1, x_2, \dots, x_i, \dots, x_n)$, that fulfils the condition of monotonicity between its output, y, with respect to its input, x_i. The output monotonically increases or decreases as the input increases, i.e., $f(x_1, x_2, \dots, x_i^1, \dots, x_n) \leq f(x_1, x_2, \dots, x_i^2, \dots, x_n)$ or $f(x_1, x_2, \dots, x_i^1, \dots, x_n) \geq f(x_1, x_2, \dots, x_i^2, \dots, x_n)$, respectively, for $x_i^1 < x_i^2$. The monotonicity property is an additional qualitative information/ knowledge that can be exploited to obtain an interpretable and optimized FIS model [1]. The importance of this line of study has been highlighted in a number of recent publications [1-8]. But, there are only a few articles that address the problem of designing a monotonicity-preserving FIS model [2]. A useful foundation of the study is the *sufficient conditions*, which comprise a set of mathematical conditions derived with the assumption that $dy/dx_i \geq 0$ or $dy/dx_i \leq 0$, for the monotonic increasing or decreasing condition, respectively, via *partial differentiation* and the *quotient rule* [3].

This paper attempts to address two issues related to modeling of a monotonicity-preserving FIS model. A common issue in FIS modeling is how fuzzy Membership Functions (MFs) are designed and tuned. One of the difficulties of designing Gaussian MFs is because of their spreading and curvature characteristics [4]. Although the *sufficient conditions* have been adopted as the condition for designing MFs [2, 5-7], it is not clear how a good MF design should be. In [9], the use of computing with words in risk assessment has been reviewed, and it has been highlighted that designing MFs is a crucial problem. Thus, in this paper, the *sufficient conditions* are further extended, and applied to designing Gaussian MFs. As the design of Gaussian MFs is formulated as a constrained optimization problem, the extended *sufficient conditions* are used as the hard constraint for optimization. An objective function is also used to compare a set of candidates (Gaussian MFs) with other available information. In addition, a Genetic Algorithm (GA) is deployed to provide a solution for the optimization problem.

The second issue is how the monotonicity property of an FIS model can be measured or evaluated. From the literature, a monotonicity measure of data in neural network modeling was introduced by Daniels and Velikova [10]. However, the monotonicity measure in FIS modeling receives little attention. Thus, a method to measure the degree of fulfillment of the monotonicity property of an FIS model is proposed. The monotonicity measure is important because the exact condition(s) for an FIS to satisfy the monotonicity property is unknown, and the mathematical proof of monotonicity is difficult [8]. There is a possibility for an FIS to be monotonic even when the *sufficient conditions* are not fulfilled. Hence, the proposed monotonicity measure is useful to give an indication whether the designed FIS model is monotonic in practice. The effectiveness of our proposed techniques is demonstrated using a real industrial application, i.e., Failure Mode and Effect Analysis (FMEA) with an FIS-based Risk Priority Number (RPN) [11-12] model. This is a typical example for FIS-based risk assessment models [9] that require the monotonicity property [11].

This paper is organized as follows. In section II, a review on Gaussian MFs, FIS models, and the *sufficient conditions* are presented. In section III, the proposed technique for optimizing Gaussian fuzzy MFs is explained. In section IV, the proposed technique to measure the monotonicity property is described.

978-1-4244-7316-8/11/$26.00 ©2011 IEEE

In section V, experimental results are presented and discussed. Finally, concluding remarks are given in section VI.

II. Background of Gaussian Fuzzy Sets, Fuzzy Inference Systems, and the Sufficient Conditions

A. Gaussian Fuzzy Sets

A Gaussian MF (see Fig. 1) can be represented as

$$\mu_G(x; c, \sigma) = e^{-[x-c]^2/2\sigma^2} \quad (1)$$

where c is the center of the fuzzy set, and σ parameterizes the width of the fuzzy set. The α-cut of a fuzzy set is a crisp set that contains all the elements of the universe set X that have a membership grade equals to or greater than α, where $1 \geq \alpha > 0$ (Note that a Gaussian MF is a non-zero MF). Based on the α -cut of a fuzzy set, the width of the fuzzy set, W_α, is determined. From Fig. 1, W_α is ac or cb, which can be determined by (2).

$$W_\alpha = ac = cb = \sqrt[2]{(-\ln \alpha)(2\sigma^2)} \quad (2)$$

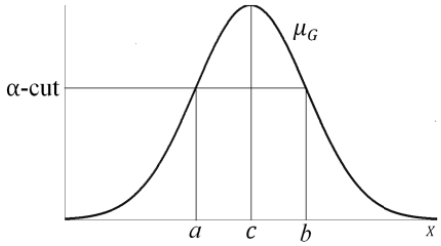

Figure 1. A Gaussian membership function

B. Fuzzy Inference Systems

The fuzzy production rules for an n-input FIS model, where $n > 0$, can be represented as follows.

$R^{j_1,j_2,\ldots,j_n}$:

$If\ (x_1 is\ A_1^{j_1}) AND\ (x_2 is\ A_2^{j_2}) \ldots AND (x_n is\ A_n^{j_n}),$
$THEN (y\ is\ B^{j_1,j_2,\ldots,j_n}) \qquad 1 \leq j_i \leq M_i.$

The AND operator in the rule antecedent part is the product function. For the x_i domain, its MFs are $\mu_i^1(x_i)$, $\mu_i^2(x_i)$, …, and $\mu_i^{n_i}(x_i)$. The upper and lower limits for the universe of discourse of x_i are $\overline{x_i}$ and $\underline{x_i}$, respectively. The output is obtained by using the weighted average of a representative value, $b^{j_1,j_2,\ldots,j_n}$ with respect to its compatibility grade, as in (3).

$$y = \frac{\sum_{j_n=1}^{j_n=M_n} \ldots \sum_{j_2=1}^{j_2=M_2} \sum_{j_1=1}^{j_1=M_1} \left(\mu_1^{j_1}(x_1) \times \mu_2^{j_2}(x_2) \times \ldots \times \mu_n^{j_n}(x_n) \times b^{j_1,j_2,\ldots,j_n}\right)}{\sum_{j_n=1}^{j_n=M_n} \ldots \sum_{j_2=1}^{j_2=M_2} \sum_{j_1=1}^{j_1=M_1} \left(\mu_1^{j_1}(x_1) \times \mu_2^{j_2}(x_2) \times \ldots \times \mu_n^{j_n}(x_n)\right)} \quad (3)$$

where $b^{j_1,j_2,\ldots,j_n}$ is the representative value of $B^{j_1,j_2,\ldots,j_n}$, i.e., $b^{j_1,j_2,\ldots,j_n} = Rep\,(B^{j_1,j_2,\ldots,j_n})$. This value represents the overall location of the MF. It can be obtained via defuzzification, or be represented by the point whereby the membership value is 1.

C. Sufficient Conditions

The first derivative of an FIS model, as in (3), returns a weighted addition series. The *sufficient conditions* assume that all the components in the weighted addition series are always *greater than or equal to* zero, or *less than* or *equal to* zero. Two conditions can be derived [3], as follows.

Condition 1. At the rule antecedent part, $(d\mu_i^p(x)/dx)/\mu_i^p(x) \geq (d\mu_i^q(x)/dx)/\mu_i^q(x)$, where $p > q$. Note that $(d\mu(x)/dx)/\mu(x)$ is the ratio between the rate of change in the membership degree and the membership degree itself. The derivative of a Gaussian MF with respect to x is $G'(x) = -((x-c)/\sigma^2)G(x)$. Note that $(d\mu(x)/dx)/\mu(x)$ for a Gaussian MF, i.e., $(G'(x)/G(x))$, returns a linear function, i.e. $E(x) = G'(x)/G(x) = -(1/\sigma^2)x + (c/\sigma^2)$.

Condition 2. At the rule consequent part, $b^{j_1,j_2,\ldots j_i=p,\ldots,j_n} - b^{j_1,j_2,\ldots j_i=q,\ldots,j_n} \geq 0$ or $b^{j_1,j_2,\ldots j_i=p,\ldots,j_n} - b^{j_1,j_2,\ldots j_i=q,\ldots,j_n} \leq 0$ for $dy/dx_i \geq 0$ or $dy/dx_i \leq 0$, respectively. This condition suggests that a monotonic rule base is required.

III. Optimization of Fuzzy Membership Functions

A. Extension for ***Condition 1***

Conditions 1 and **2** can be included as part of the FIS modeling process [2, 5-7]. **Condition 1** is an inequality that can be used to check the validity of Gaussian MF design i.e., a fuzzy partition. **Condition 2** can be used to check the validity of the rules in a monotonic FIS model. In this paper, the focus is on **Condition 1**.

In this work, $\left(d\mu_i^p(x)/dx\right)/\mu_i^p(x))$ is viewed as a projection of the Gaussian MFs, which allows the MFs to be visualized. As an example, two Gaussian MFs, $G_1 = e^{-[x-c_1]^2/2\sigma_1{}^2}$ and $G_2 = e^{-[x-c_2]^2/2\sigma_2{}^2}$, where $c_1 < c_2$, are considered. Their $G'(x)/G(x)$ ratios are $E_1(x) = -(1/\sigma_1{}^2)x + (c_1/\sigma_1{}^2)$ and $E_2(x) = -(1/\sigma_2{}^2)x + (c_2/\sigma_2{}^2)$, respectively. To satisfy **Condition 1,** $E_1(x) \leq E_2(x)$ is required for the defined universe of discourse. Hence, (4) and (5) are required.

$$E_1\left(\underline{x_i}\right) \leq E_2\left(\underline{x_i}\right) \quad (4)$$

$$E_1(\overline{x_i}) \leq E_2(\overline{x_i}) \quad (5)$$

B. Optimization of Gaussian Membership Functions

In this paper, the proposed extension for **Condition 1** (from section III(*A*)) is further exploited to be part of a Gaussian MF design process. It acts as the constraint for an optimization problem. For an input domain, x_i with n_i Gaussian MFs, the Gaussian MFs are parameterized by c_1, c_2, …, c_{n_i} and σ_1, σ_2, …σ_{n_i}. The design of the Gaussian MFs is formulated as a constrained optimization problem, as follows.

An objective function, $f(c_1, c_2, \ldots, c_{n_i}, \sigma_1, \sigma_2, \ldots, \sigma_{n_i})$, is optimized subjected to constraints as follow.

$\#\ 1.\ E_q\left(\underline{x_i}: c_q, \sigma_q\right) \le E_{q+1}\left(\underline{x_i}: c_{q+1}, \sigma_{q+1}\right)$ for $q = 1,2, \dots n_{i-1}$

$\#2.\ E_q\left(\overline{x_i}: c_q, \sigma_q\right) \le E_{q+1}\left(\overline{x_i}: c_{q+1}, \sigma_{q+1}\right)$ for $q = 1,2, \dots n_{i-1}$

Constraints #1 and #2 are the conditions of feasible Gaussian MFs design for a monotonic FIS model. The search process can be achieved by various optimization techniques, e.g., a non-linear programming technique, GA, particle swarm optimization, or harmonic search.

C. A Case Study on Failure Mode and Effect Analysis

Failure Mode and Effect Analysis (FMEA) is a popular problem prevention methodology that can be interfaced with many engineering and reliability models [11]. FMEA uses a Risk Priority Number (RPN) model to evaluate the risk associated with each failure mode [11]. The RPN model considers three risk factors, i.e., severity (S), occurrence (O), and detect (D), and produces an RPN score ($RPN = g_{RPN}(S, O, D)$) [11]. The three input factors are estimated by the domain experts in accordance with the scale from "1" to "10" based on a set of commonly agreed evaluation criteria, which are presented with the scale tables [11].

In this paper, the focus is on designing an FIS-based RPN model [11-12] that satisfies the monotonicity property. The FIS-based RPN model considered S, O, and D as the inputs and the RPN as the output. The Gaussian MFs of S, O, and D are generated from the respective scale tables. As an example, Table 1 shows the scale table of S, which is used in a semiconductor manufacturing plant. There are 5 linguistic terms; each is represented by a Gaussian MF. The relationship between S, O, and D and the RPN are expressed with a set of fuzzy If-Then rules.

Table 1. The scale table for Severity

Rank	Linguistic Terms	Criteria	Lower Limit	Mid-point	Upper Limit
10	Very High (Liability)	Failure will affect safety or compliance to law.	9.5	10	-
9~8	High (Reliability / reputation)	Customer impact. Major reliability excursions.	7.5	8.5	9.5
7~6	Moderate (Quality / Convenience)	Impacts customer yield. Wrong package/par/marking.	5.5	6.5	7.5
5~2	Low (Special Handling)	Yield hit, Cosmetic.	1.5	3.5	5.5
1	None (Unnoticed)	Unnoticed.	-	1	1.5

In our previous work [5-6, 11], it has been demonstrated that an effective FIS-based RPN model should satisfy the monotonicity property. This is because the input attributes (i.e., the S, O, and D ratings) are defined in such a way that the higher the rating, the more critical the situation is. The output (i.e., the RPN score) is a measure of the failure risk. The monotonicity property is important to allow a valid comparison among all failure modes to be made.

D. Gaussian MFs Design

A qualitative scale table usually consists of several partitions, each with some criteria. Each partition can have different width, and it can be represented using three points, i.e., the lower limit, the mid-point, and the upper limit. The width of the n partition, $W^n_{partition}$, is defined as follows:

$$W^n_{partition} = upperlimit^n - midpoint^n = midpoint^n - lowerlimit^n \quad (6)$$

As an example, the scale table of S (Table 1) consists of five partitions, i.e., 1, 2-5, 6-7, 8-9, and 10. The lower limit, the mid-point, and the upper limit for the second partition ($n = 2$), i.e., 2-5, are 1.5, 3.5, and 5.5, respectively, while $W^2_{partition}$ is 2.

In this paper, we attempt to search for a set of Gaussian MFs with their widths nearest to the widths of the partitions in the scale table. The width of a Gaussian MFs can be defined using (2) with $\alpha = 0.5$ [13-14]. The issue is on how to formulate a useful objective function. In this paper, the investigation is focused on formulating an objective function, as in (7). It is a measure of total similarity of the generated MFs corresponding to the partitions of scale table. We further assume that $c_1, c_2, \dots, c_{n_i}$ are mid-points for these partitions which need not to be optimized.

$$f\left(c_1, c_2, \dots, c_{n_i}, \sigma_1, \sigma_2, \dots, \sigma_{n_i}\right) = f\left(\sigma_1, \sigma_2, \dots, \sigma_{n_i}\right) = \sqrt[2]{\sum_{n=1}^{n=n_i}\left(W^n_{partition} - W^n_{\alpha}\right)^2} \quad (7)$$

E. Genetic Algorithm

The problem formulated can be solved using a GA, a population-based stochastic optimization technique. Each potential solution set, in the form of $\left(\sigma_1, \sigma_2, \dots, \sigma_{n_i}\right)$, is represented as an individual. The GA is used to search for the solution set with the best fitness value.

Figure 2 shows the general procedure of the GA. The hard constraints, i.e., constraints #1 and #2, are considered as penalties of the GA objective function to be minimized, as in (8). We attempt to minimize (7), which is part of the GA objective function.

$$GA\ Objective\ function = W_{penalty} \times \left(\begin{cases} 0\ if\ constraints\ \#1 \text{ and } \#2\ fulfilled \\ 1\ if\ constraints\ \#1 \text{ and } \#2\ not\ fulfilled \end{cases}\right) + f\left(\sigma_1, \sigma_2, \dots, \sigma_{n_i}\right) \quad (8)$$

```
%Note: Initialize variable
    Initial population (each individual is σ1, σ2, ..., σni)
    While stopping criteria is not triggered
    {
    Evaluate each individual with (8)
    Record the best individual sets
    Crossover
    Mutation
    Evaluate the stopping criteria
    }
```

Figure 2. Pseudo-code of the proposed GA-based MFs optimization model

IV. A MEASURE FOR THE MONOTONICITY PROPERTY

From the literature, the measure of the degree of monotonicity for a data set, D is defined by (9) [10]. The aim is to represent the monotonic relationship using a numerical value from 0 to 1. A value close to 1 indicates an increasing monotonic relationship among data. A value near to 0 indicates a decreasing monotonic relationship among data. A value near to 0.5 indicates no monotonic relationship among data.

$$Degree\ of\ monotonicity = \frac{\#\ Monotone\ pairs(D)}{\#Comparable\ pairs\ (D)} \tag{9}$$

In this paper, fulfillment of the monotonicity property of an FIS model is measured by comparing the output pairs of an FIS model. Instead of indicate the monotonic increasing or decreasing relationship of a data set as in [10], an index that indicates whether an FIS model observes the monotonicity property is proposed. The procedure is as follows.

Let $y = f(\bar{x})$ be represented by an n-dimension matrix y_{x_k}. y_{x_k} is the output of $f(x_k)$, correspond to a input(s) vector, x_k=[x_1, $x_2, \dots, x_n$], $k = 1,2, \dots n$. The test procedure test is as follows.

(A) Determine the upper and lower limits of the universe of discourse for input(s), i.e., x_k, and denote them as $\bar{x}_k$ and $\underline{x_k}$, respectively.

(B) Divide x_k into n_k^t divisions. The grid size of x_k, $gs_k = \left(\bar{x}_k - \underline{x_k}\right)/n_k^t$. $y_{x_1,x_2,\dots,x_n}$ is denoted as a $n_1^t \times n_2^t \times \dots \times n_n^t$ matrix.

(C) Compare $y_{x_{k=1,2,3\dots n,k\neq i},\underline{x_i}+gs_i\times m_i}$ and $y_{x_{k=1,2,3\dots n,k\neq i},\underline{x_i}+(gs_i+1)\times m_i}$, $m_i = 0,1,2,\dots,n_i^t - 1$, with a function denoted as $monotone\left(y_{x_{k=1,2,3\dots n,k\neq i},\underline{x_i}+gs_i\times m_i}\right)$. Equation (10) or (11) is adopted for a monotonic increasing or decreasing relationship, respectively.

$$monotone\left(y_{x_{k=1,2,3\dots n,k\neq i},\underline{x_i}+gs_i\times m_i}\right) = \begin{cases} 1 & if\ y_{x_{k=1,2,3\dots n,k\neq i},\underline{x_i}+gs_i\times m_i} \leq y_{x_{k=1,2,3\dots n,k\neq i},\underline{x_i}+(gs_i+1)\times m_i} \\ 0 & if\ y_{x_{k=1,2,3\dots n,k\neq i},\underline{x_i}+gs_i\times m_i} > y_{x_{k=1,2,3\dots n,k\neq i},\underline{x_i}+(gs_i+1)\times m_i} \end{cases} \tag{10}$$

$$monotone\left(y_{x_{k=1,2,3\dots n,k\neq i},\underline{x_i}+gs_i\times m_i}\right) = \begin{cases} 1 & if\ y_{x_{k=1,2,3\dots n,k\neq i},\underline{x_i}+gs_i\times m_i} \geq y_{x_{k=1,2,3\dots n,k\neq i},\underline{x_i}+(gs_i+1)\times m_i} \\ 0 & if\ y_{x_{k=1,2,3\dots n,k\neq i},\underline{x_i}+gs_i\times m_i} < y_{x_{k=1,2,3\dots n,k\neq i},\underline{x_i}+(gs_i+1)\times m_i} \end{cases} \tag{11}$$

(D) Obtain the $Monotone\ index$ between y and x_i for an FIS model using (12).

$$Monotone\ index = \frac{\sum_{m_n=1}^{m_n=n_n^t} \dots \sum_{m_1=1}^{m_1=n_1^t} \sum_{m_i=1}^{m_i=n_i^t-1} \left(monotone\left(y_{x_{k=1,2,3\dots n,k\neq i},\underline{x_i}+gs_i\times m_i}\right)\right)}{\sum_{m_n=1}^{m_n=n_n^t} \dots \sum_{m_1=1}^{m_1=n_1^t} \sum_{m_i=1}^{m_i=n_i^t-1} (1)} \tag{12}$$

In short, first, all possible comparable sets of y and x_i are generated. The number of the monotonic pairs is counted. The degree of monotonicity is obtained with (12). As an example, the monotonicity property between S and the RPN for an FIS-based RPN can be measured as follows.

Comparable points in the form of [S,O,D] are generated. Examples of comparable points are [1,1,1] and [2,1,1], [2,1,1] and [3,1,1],…, [9,1,1] and [10, 1,1], …, [1,1,2] and [2,1,2,], …and finally [9, 10, 10] and [10, 10, 10]. The RPN scores for [1,1,1] ($g_{RPN}(1,1,1)$) and [2,1,1] ($g_{RPN}(2,1,1)$) are compared, and their fulfillment of monotonicity ($g_{RPN}(1,1,1) \leq g_{RPN}(2,1,1)$) are checked. The same goes to other comparable points. In this study, a total of 900 comparable points are generated between S and the RPN. The same procedure can be applied to O and the RPN, as well as D and the RPN. In total, there are 2700 (3×900) comparable points that have been generated for evaluation of the monotonicity property in the study.

V. EXPERIMENTAL RESULT AND DISCUSSIONS

Figure 3 depicts the objective function versus the number of generations of the GA. Figure 4 depicts the optimized Gaussian MFs of S using the best individual after 300 iterations. Figure 5 depicts the projection of the Gaussian MFs using **Condition 1**. From the results, it is obvious that the proposed techniques can be used to automatically generate a set of optimized Gaussian MFs, which are able to fulfill **Condition 1.** From Figure 4, it can be observed that the width of each Gaussian MF is close to the scale table of S.

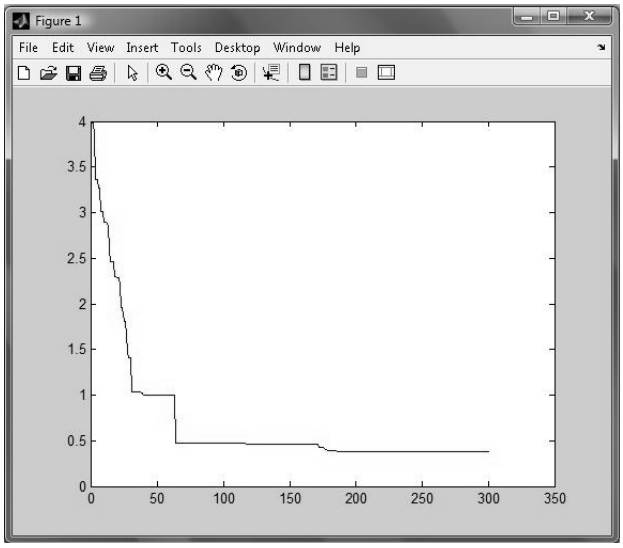

Figure 3 Objective function versus the number of generations of the GA-based MFs design procedure

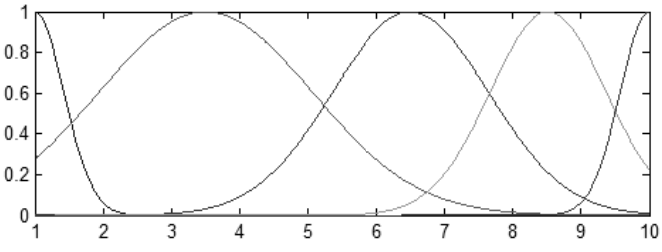

Figure 4 Projection of the MFs for Severity

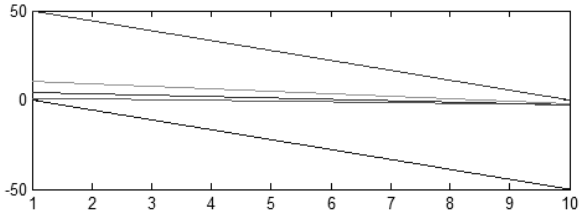

Figure 5 Optimized MFs for Severity.

Table 2 shows the scale table of D of the FIS-based RPN model. There are 6 linguistic terms, each is represented by a Gaussian MF.

Table 2 The scale table for Detect

Rank	Linguistic Terms	Criteria	Lower Limit	Mid-point	Upper Limit
10	Extremely Low	No Control available.	9.5	10	-
9	Very Low	Controls probably will not Detect	8.5	9	9.5
8~7	Low	Controls may not Detect excursion until reach next functional area.	6.5	7.5	8.5
6~5	Moderate	Controls are able to Detect within the same functional area	4.5	5.5	6.5
4~3	High	Controls are able to Detect within the same machine/module.	2.5	3.5	4.5
2~1	Very High	Controls will Detect excursions before next lot is produced. Prevent excursion from occurring	-	1	2.5

Figure 6 depicts the optimized Gaussian MFs for scale table D using the best individual after 300 iterations. From Figure 6, it can be seen that the width of each of Gaussian MF is close to the scale table of D. Figure 7 depicts the projection of the MFs using **Condition 1.**

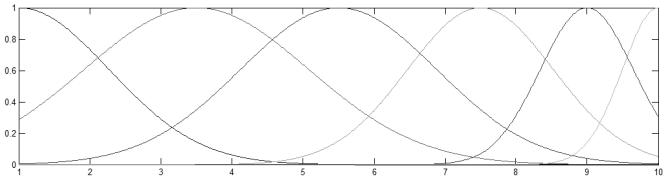

Figure 6 Projection of the MFs for Detect.

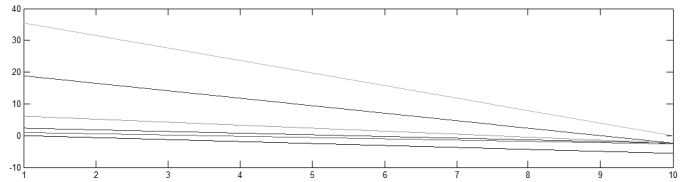

Figure 7 Optimized MFs for Detect.

In order to validate the Gaussian MFs designed using the proposed techniques, a data set collected from a real semiconductor manufacturing process, i.e., the test handler process, is used for experimentation. Figures 8 and 9 depict the surface plots of the RPN versus S and O, while D is kept at 10 and 1, respectively. Note that monotonic surface plots are obtained.

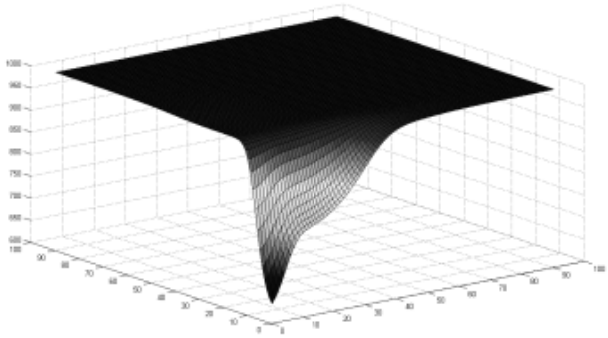

Figure 8 RPN versus S and O for the test handler process, while D=10

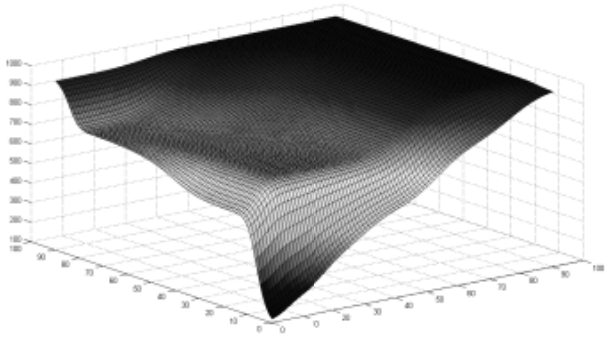

Figure 9 RPN versus S and O for the test handler process, while D=1

However, it is not straightforward to evaluate the monotonicity relationship between the RPN and S, O, and D. The surface plot may not be an effective method in this regard. As such, we propose to test the monotonic relationship using procedure in section IV. Here, comparable points are generated, and the *degree of monotonicity* is obtained. The results are summarized in Table 3. As can be seen, the *degree of monotonicity* is 1. This vindicates the monotonic increasing relationships between the RPN and S, O, and D. In another words, the monotonicity property is guaranteed.

Table 3 The scale table for Severity

Data set	#Comparable pairs	#Monotone pairs	Degree of monotonicity
Test handler	2700	2700	1

VI. SUMMARY

In this paper, the monotonicity property of an FIS model has been investigated, and a novel technique for designing

Gaussian MFs for a monotonic FIS model has been proposed. The technique shows how a set of Gaussian MFs can be generated from a qualitative scale table. The proposed technique is useful, as it allows the Gaussian MFs design procedure for a monotonic FIS model to be automated. The proposed method can be applied to various FIS modeling problems that involve a qualitative scale table, e.g., assessment and decision problems, as well as education assessment problem [7].

On the other hand, the use of a monotonicity measure in FIS modeling has been proposed in this paper. The usefulness of the proposed techniques has been demonstrated with a real industrial case study, i.e., an FIS-based RPN model for FMEA. Promising results have been obtained.

For further work, the use of other α values can be examined. Besides, other techniques such as nonlinear programming, particle swam optimization, and harmony search can be adopted for optimization purposes. Applicability of the monotonic FIS models to other domains, e.g. education assessment, can be investigated too.

ACKNOWLEDGMENT

The financial support provided by a Fundamental Research grant (No. FRGS/02(10)/752/2010(38)) and USM RU Grant (No. 814089) for this work is highly appreciated.

REFERENCES

[1] E.V. Broekhoven and B.D. Baets, "Only Smooth Rule Bases Can Generate Monotone Mamdani–Assilian Models Under Center-of-Gravity Defuzzification," *IEEE Trans. Fuzzy Syst*., vol.17, no.5, pp.1157-1174, 2009.

[2] V.S. Kouikoglou and Y.A. Phillis, "On the monotonicity of hierarchical sum-product fuzzy systems," *Fuzzy Sets Syst*., vol.160, no.24, pp.3530-3538, 2009.

[3] J.M. Won, S.Y. Park, and J.S. Lee, "Parameter conditions for monotonic Takagi-Sugeno-Kang fuzzy system," *Fuzzy Sets Syst*., vol.132, no.2, pp.135-146, 2002.

[4] P. Lindskog and L. Ljung, "Ensuring monotonic gain characteristics in estimated models by fuzzy model structures," *Automatica*, vol.36, no.2, pp.311-317, 2000.

[5] K.M. Tay and C.P. Lim, "On the Use of Fuzzy Inference Techniques in Assessment Models: Part I: Theoretical Properties," *Fuzzy Optim Decis Making*, vol.7, no.3, pp.269-281, 2008.

[6] K.M. Tay and C.P. Lim, "On the Use of Fuzzy Inference Techniques in Assessment Models: Part II: Industrial Applications," *Fuzzy Optim Decis Making*, vol.7, no.3, pp.283-302, 2008.

[7] K.M. Tay and C.P. Lim. "A Fuzzy Inference System-Based Criterion-Referenced Assessment Model," *Expert Syst. Appl*., vol.38, no.9, pp. 11129-11136, 2011.

[8] H. Seki, H. Ishii, and M. Mizumoto, "On the Monotonicity of Fuzzy-Inference Methods Related to T–S Inference Method," *IEEE Trans. Fuzzy Syst*, vol.18, no3, pp.629–634, 2010.

[9] J. Liu, L. Martínez, H. Wang, R.M. Rodríguez and V. Novozhilov, "Computing with words in risk assessments," *Int. J. Comput. Int. Sys.*, vol.3, no.4, pp. 396-419, 2010.

[10] H. Daniels and M. Velikova, "Monotone and partially monotone neural network," *IEEE Trans. Neural Netw.*, vol.21, no.6, pp.906-917, 2010.

[11] K.M. Tay and C.P. Lim, "Enhancing the Failure Mode and Effect Analysis methodology with Fuzzy Inference Techniques," *J. Intell. Fuzzy Syst.*, vol.21, no.1-2, pp.135-146, 2010.

[12] J.B. Bowles and C.E. Peláez, "Fuzzy logic prioritization of failures in a system failure mode effects and criticality analysis," *Reliab. Eng. Syst. Safe*., vol.50, no.2, pp. 203-213, 1995.

[13] J.S.R. Jang, C.T. Sun, and E. Mizutani, Neural-Fuzzy and soft Computing. Prentice-Hall,1997.

[14] C.T. Lin and C.S. Greoge Lee, Neural-fuzzy systems: a Neural-fuzzy synergirm to intelligent systems. Prentice-Hall,1996.

2011 IEEE International Conference on Fuzzy Systems
June 27-30, 2011, Taipei, Taiwan

Refinement CTIN for General Type-2 Fuzzy Logic Systems

Long Thanh Ngo
Department of Information Systems
Faculty of Information Technology
Le Quy Don Technical University, Hanoi, Vietnam
Email: ngotlong@gmail.com

***Abstract*—Triangulated irregular network (TIN) has been used for representing general type-2 fuzzy sets and gained some results of reducing computational complexity. In general, TIN-based algorithms are still complex and difficulty to deploy in applications. So, an approach based on refinement constraint TIN (CTIN) for representing general type-2 fuzzy set is proposed. The paper deals with the use CTIN in general type-2 fuzzy logic systems (GT2FLS). Operations are developed for general type-2 fuzzy sets. A T2FLS is designed and implemented in comparing previous approaches under an application of robot navigation.**

***Index Terms*—Type-2 Fuzzy Sets, Type-2 Fuzzy Logic Systems, Type-2 Fuzzy Inference, Geometric Representation**

I. Introduction

Type-2 fuzzy logic systems has widely been used in many applications. Almost applications are limited by computational complexity of general T2FLS. Recently, these are many researches arising from reduction the complexity of these systems that depend on representation of type-2 fuzzy sets. There are many approaches to representation of type-2 fuzzy sets. The point-based representation [5], [6], [7], [8] has proposed with operations and computation of type-2 fuzzy sets and systems. Mendel et al [9], [10] proposed the representation based on embedded fuzzy sets, vertical slices. Starczewski [17] introduced a method for complexity reduction of operations on triangular type-2 fuzzy sets. For the this purpose, Coupland et al [2] proposed geometric method for representation type-1 and interval type-2 fuzzy sets, new algorithms for various operations on type-1 and type-2 fuzzy sets and for defuzzification. Coupland et al [3], [4] presented new techniques using upper and lower surfaces for performing logical operations on type-2 fuzzy sets with considering computational speed and accuracy. In [14], [15], authors proposed an approach to TIN-based geometric representation of type-2 fuzzy sets with or without using upper and lower surfaces. Hagras et al [20], [21], [22] proposed an approach to representation of type-2 fuzzy sets using zSlices that be able to gap interval type-2 fuzzy sets and general type-2 fuzzy sets. A similar approach to representation of type-2 fuzzy sets was proposed by Mendel et al [11], [12] based on α - plane representation.

The paper introduces an approach to representation of general type-2 fuzzy sets, called ϵ_u-approximation. A constrained TIN representing T2FS is triangulated from set of points set that satisfy ϵ_u-approximate criterion. This representation is the basis for designing algorithms of general type-2 fuzzy logic systems. This approach is considered under two respects: computational speed and accuracy. An computational process of general type-2 FLSs (GT2FLS) involving fuzzification, inference process, aggregation and defuzzification are proposed in comparing with previous methods. Computation for GT2FLS is able to deploy in real time applications. Because geometric algorithms are only computed at vertices of TIN based on operations of interval type-2 fuzzy sets. Experimental results are shown in comparisons on speed and accuracy with other approaches. The paper also discusses the feasibility of proposed algorithms by implementing RCTIN-based type-2 fuzzy logic systems under avoidance behavior of robot navigation with reported runtime tables.

The paper is organized as follows: II presents an overview on type-2 fuzzy sets and inference, ϵ-approximation representation of type-2 fuzzy sets; III introduces ϵ_u-approximate representation and applications to operations involving meet and join under minimum, negation; IV presents a general T2FLS involving sub-processes such as fuzzification, inference process, aggregation and defuzzification. V introduces implementation and discussion of the feasibility under the experimentation of robot navigation; V is conclusion and future works.

II. Geometric Representation for General Type-2 Fuzzy Sets

A. Type-2 Fuzzy Sets

A type-2 fuzzy set in X is denoted $\tilde{A}$, and its membership grade of $x \in X$ is $\mu_{\tilde{A}}(x,u), u \in J_x \subseteq [0,1]$, which is a type-1 fuzzy set in [0, 1]. The elements of domain of $\mu_{\tilde{A}}(x,u)$ are called primary memberships of x in $\tilde{A}$ and memberships of primary memberships in $\mu_{\tilde{A}}(x,u)$ are called secondary memberships of x in $\tilde{A}$.

Definition 2.1: A $type-2\ fuzzy\ set$, denoted $\tilde{A}$, is characterized by a type-2 membership function $\mu_{\tilde{A}}(x,u)$ where $x \in X$ and $u \in J_x \subseteq [0,1]$, i.e.,

$$\tilde{A} = \{((x,u), \mu_{\tilde{A}}(x,u)) | \forall x \in X, \forall u \in J_x \subseteq [0,1]\} \quad (1)$$

or

$$\tilde{A} = \int_{x \in X} \int_{u \in J_x} \mu_{\tilde{A}}(x,u))/(x,u), J_x \subseteq [0,1] \quad (2)$$

in which $0 \leq \mu_{\tilde{A}}(x,u) \leq 1$.

978-1-4244-7316-8/11/$26.00 ©2011 IEEE

At each value of x, say $x = x'$, the 2-D plane whose axes are u and $\mu_{\tilde{A}}(x', u)$ is called a $vertical\ slice$ of $\mu_{\tilde{A}}(x, u)$. A *secondary membership function* is a vertical slice of $\mu_{\tilde{A}}(x, u)$. It is $\mu_{\tilde{A}}(x = x', u)$ for $x \in X$ and $\forall u \in J_{x'} \subseteq [0, 1]$, i.e.

$$\mu_{\tilde{A}}(x = x', u) \equiv \mu_{\tilde{A}}(x') = \int_{u \in J_{x'}} f_{x'}(u)/u, J_{x'} \subseteq [0, 1] \quad (3)$$

in which $0 \leq f_{x'}(u) \leq 1$.

In manner of embedded fuzzy sets, a type-2 fuzzy sets [9] is union of its type-2 embedded sets, i.e

$$\tilde{A} = \sum_{j=1}^{n} \tilde{A}_e^j \quad (4)$$

where $n \equiv \prod_{i=1}^{N} M_i$ and $\tilde{A}_e^j$ denoted the j^{th} type-2 embedded set of $\tilde{A}$, i.e.,

$$\tilde{A}_e^j \equiv \{\left(u_i^j, f_{x_i}(u_i^j)\right), i = 1, 2, ..., N\} \quad (5)$$

where $u_i^j \in \{u_{ik}, k = 1, ..., M_i\}$.

Let $\tilde{A}, \tilde{B}$ be type-2 fuzzy sets whose secondary membership grades are $f_x(u), g_x(w)$, respectively. Theoretic operations of type-2 fuzzy sets such as union, intersection and complement are described [6] as follows:

$$\mu_{\tilde{A} \cup \tilde{B}}(x) = \mu_{\tilde{A}}(x) \sqcup \mu_{\tilde{B}}(x) = \int_u \int_v (f_x(u) \star g_x(w))/(u \vee w) \quad (6)$$

$$\mu_{\tilde{A} \cap \tilde{B}}(x) = \mu_{\tilde{A}}(x) \sqcap \mu_{\tilde{B}}(x) = \int_u \int_v (f_x(u) \star g_x(w))/(u \star w) \quad (7)$$

$$\mu_{\tilde{A}}(x) = \mu_{\neg \tilde{A}}(x) = \int_u (f_x(u))/(1 - u) \quad (8)$$

where $\vee$, $\star$ are t-cornorm, t-norm, respectively. Type-2 fuzzy sets are called an interval type-2 fuzzy sets if the secondary membership function $f_{x'}(u) = 1\ \forall u \in J_x$.

B. Delaunay Triangulation

A *topographic surface* σ is the image of a real bivariate function f defined over a domain D in the Euclidean plane, as

$$\sigma = \left\{(x, u, f(x, u))\middle|(x, u) \in D\right\} \quad (9)$$

A polyhedral model is the image of a piecewise-line function f described on a partition of D into polygonal regions $\{T_1, ..., T_k\}$ and the image of f over each region $T_i (i = 1, ..., k)$ is a planar patch. If all of T_is $(i = 1, .., k)$ are triangles then the polyhedral model is called a $Triangulated\ Irregular\ Network$ (TIN). Hence, σ may be represented approximately by a TIN, as

$$\sigma \tilde{=} \sum_{i=1}^{k} \left\{(x, u, f_i(x, u))\middle|(x, u) \in T_i\right\}, \bigcup_{i=1}^{k} T_i \equiv D \quad (10)$$

where f_is $(i = 1, ..., k)$ are planar equations.

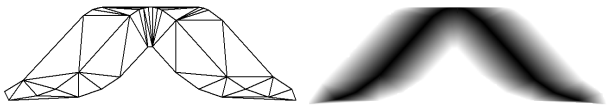

Fig. 1. Example of representation of a type-2 Gaussian fuzzy sets

The $Delaunay\ triangulation$ of a set V of points in IR^2 is a subdivision of the convex hull of V into triangles having their vertices at points of V, and such that triangles are as much aquiangular as possible. More formally, a triangulation τ of V is a Delaunay triangulation if and only if, for any triangle t of τ, the circumcircle of t does not contain any point of V in its interior. This property is called the $empty\ circle\ property$ of the Delaunay triangulation.

C. Geometric Representation of Type-2 Fuzzy Sets

In [15], geometric representation of type-2 fuzzy sets is presented as an approach based on TIN. Concept of ε-approximation set is used to approximately discretize the membership grades of type-2 fuzzy sets into triangular patches. ϵ-approximation is defined as follows:

Definition 2.2: A type-2 fuzzy set is called ϵ-approximation set, denoted $\tilde{A}^*$, of $\tilde{A}$ in continuous domain D if

$$\|\mu_{\tilde{A}}(x, u) - \mu_{\tilde{A}^*}(x, u)\| \leq \varepsilon, (x, u) \in D \quad (11)$$

The theorem on representation of a type-2 fuzzy set referenced as *Approximation Theorem* is presented as follows:

Theorem 2.1 (Approximation Theorem): Let $\tilde{A}$ be type-2 fuzzy set with membership grade $\mu_{\tilde{A}}(x, u)$ in continuous domain D. There exists a type-2 fuzzy set with membership grade is a TIN $T_{\tilde{A}}$, denoted $\tilde{A_T}$, so that $\tilde{A_T}$ is ϵ-approximation set of $\tilde{A}$, i.e,

$$\|\mu_{\tilde{A}}(x, u) - \mu_{\tilde{A_T}}(x, u)\| < \epsilon, \ \ \forall (x, u) \in D. \quad (12)$$

Fig. 1 is the TIN consisting of 36 vertices and 48 faces that represents approximately of Gaussian type-2 fuzzy sets with $\epsilon = 0.1$. The primary membership function is a Gaussian with fixed deviation and mean $m_k \in [m_1, m_2]$ and the secondary membership function is a triangular membership function that its apex is at the Gaussian function with mean $(m_1 + m_2)/2$. At the point (x, u) that its color is darker, the value of $\mu_{\tilde{A}}(x, u)$ is closer 1.0, otherwise $\mu_{\tilde{A}}(x, u)$ is closer 0.0.

III. Refinement CTIN Based Type-2 Fuzzy Sets

TIN-based representation of type-2 FS gives nice results, but computational complexity is still large. To gain more effective computational method, refinement constrain triangulated irregular network (CTIN) is proposed to represent a general T2FS. This section introduces the approach to representation using refinement CTIN and applications to operations of T2FS.

A. Representation of T2FSs Using Refinement CTIN

TIN is formed from set of points in the 3-dimensional space with satisfying Delaunay criterion, called Delaunay triangulation. CTIN is TIN satisfying Delaunay criterion with each input segment appears as an edge of triangulation. Input of CTIN is a planar straight line graph (PSLG). A PSLG is a set of vertices and segments that satisfies two constraints. First, for each segment contained in a PSLG, the PSLG must also contain the two vertices that serve as endpoints for that segment. Second, segments are permitted to intersect only at their endpoints. Fig. (2) depicts an example of PSLG with 13 vertices and 9 segments.

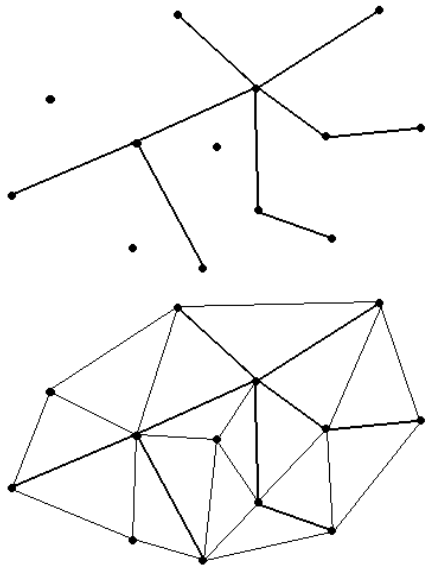

Fig. 2. An example of PSLG and its CTIN

To represent a type-2 fuzzy set using CTIN, a PSLG is approximately retrieved from type-2 fuzzy set $\tilde{A}$. The following is some definitions of ε_u criterion that points out how to retrieve a PSLG.

Definition 3.1 (ε_u approximation): On α-cut plane at z level of the type-2 fuzzy set $\tilde{A}$, the point $P'_{(x,u')} \in \alpha$ is called a ε_u-approximate point of $P_{(x,u)} \in \alpha$ if $\|u - u'\| < \varepsilon$.

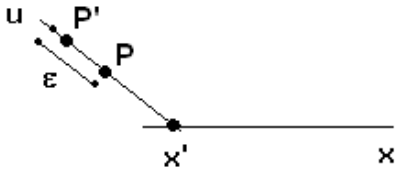

Fig. 3. The P' point is ε_u-approximate point of P.

Let type-2 fuzzy set $\tilde{A}$ and $n+1$ α-planes at levels $\{z_i = \frac{i}{n}, i = 0, 1, ..., n\}$. A contour at the level z_i of $\tilde{A}$, denoted $\tilde{Z}_i$, is a poly-line that involves its vertices on α-plane z_i. A contour $\tilde{Z}_i, (i = 0, 1, ..., n)$ is called ε_u-approximate contour of type-2 fuzzy set $\tilde{A}$ if each point $P'_{(x,u')} \in \tilde{Z}_i$ is also ε_u-approximate point of $P_{(x,u)} \in \tilde{A}$ at the level z_i. Thence, an ε_u-approximate type-2 fuzzy set is described as follows:

Definition 3.2 (ε_u-approximate T2FS): A type-2 fuzzy set $\tilde{A}'$ is called ε_u-approximate type-2 fuzzy set at n levels of $\tilde{A}$ if $n+1$ its contours $(Z_0, Z_1, ..., Z_n)$ are ε_u-approximate contour of $\tilde{A}$.

At each level k of $\tilde{A}$, contour Z_k is an interval type-2 fuzzy set, thus upper (lower) contour, denoted UC_k (LC_k), is upper (lower) bound segments of the contour. In case of $k = 0$, UC_0 (LC_0) is upper (lower) membership function (UMF/LMF) of interval type-2 fuzzy set that is an overlap of the FOU of $\tilde{A}$.

Definition 3.3: (Refinement CTIN) A TIN representing $\tilde{A}$ is called *refinement CTIN* of $\tilde{A}$ at K levels, denoted $T_{\tilde{A}}$, if $T_{\tilde{A}}$ is generated from PSLG involving set of vertices V and set of segments L, in which $\forall v \in V$ be ε_u-approximate points and L is set of segments extracted from K ε_u-approximate contours of $\tilde{A}$.

Hence, a general type-2 fuzzy set is able to be represented by a refinement CTIN as the following theorem.

Theorem 3.1: Let $\tilde{A}$ be a type-2 fuzzy set with continuous membership grade $\mu_{\tilde{A}}(x)$ in continuous domain D and enough small ε_u. These exists *refinement* CTIN that represents $\tilde{A}$ with ε_u-approximation at K levels.

Proof:

Call $T_{\tilde{A}}$ is refinement CTIN that is generated from a PSLG with set of vertices V and set of segments L extracted from $\tilde{A}$ at K levels. Suppose that exists a point $P_{(x_p,u_p,z_p)}$ on $T_{\tilde{A}}$ not to satisfy ε_u-approximate criteria. Thus P is belong to one of α-planes $Z_0, Z_1, ..., Z_{K-1}$. $T_{\tilde{A}}$ is refinement CTIN then P is inside the edge (for example v_iv_j) of $T_{\tilde{A}}$. Denote $P_0(x_{P_0}, u_{P_0}, z_{P_0})$ be the point on the edge v_iv_j that distance to respective point of $\tilde{A}$ in u-axis is maximum, i.e.

$$\{\| u_{P_0} - u \|\} \rightarrow max, z_{P_0} = \mu_{\tilde{A}}(x_{P_0}, u) \qquad (13)$$

Note that P_0 is able to coincide with P. Call t_k, t_l are two adjacent triangles of v_iv_j. The edge v_iv_j is split into two sub-edge v_iP_0 and P_0v_j, so t_k, t_l are divided into four sub-triangle. According to supposition, $\mu_{\tilde{A}}(x)$ is continuous in domain D then distance from the respective point P' of P in new edge v_iP_0 or P_0v_j of $T_{\tilde{A}}$ to respective point on $\tilde{A}$ is closer than P, i.e.

$$\| u_{P'} - u \| < \| u_P - u \|, z_P = z_P = \mu_{\tilde{A}}(x_P, u) \qquad (14)$$

If these still exists a point P inside edges v_iP_0 or P_0v_j that not to satisfy ε_u-approximation then the edge is split into sub-edges as above way. The end of each splitting step, the P is closely moved to respective point of $\tilde{A}$. Because of the continuousness of $\mu_{\tilde{A}}(x)$, these no exists any point inside sub-edge that not to satisfy ε_u-approximation after the limited incremental splitting steps. ■

Example: Let $\tilde{A}$ be Gaussian type-2 fuzzy set with $I = 5$ levels, i.e. $z_i = i/I, i = 0, 1, .., I$. Upper (lower) membership

functions at each level are described as follows:

$$f_U^i(x) = (0.9 + \frac{0.1(I-i)}{I})e^{(-\frac{x^2}{2(\sigma_1 - i*(\sigma_1-\sigma_2)/(2I))^2})}$$
$$f_L^i(x) = (0.9 - \frac{0.1(I-i)}{I})e^{(-\frac{x^2}{2(\sigma_2 + i*(\sigma_1-\sigma_2)/(2I))^2})} \quad (15)$$

Fig. 4 is to describe CTIN based type-2 fuzzy set that represent $\tilde{A}$ as the formula (15).

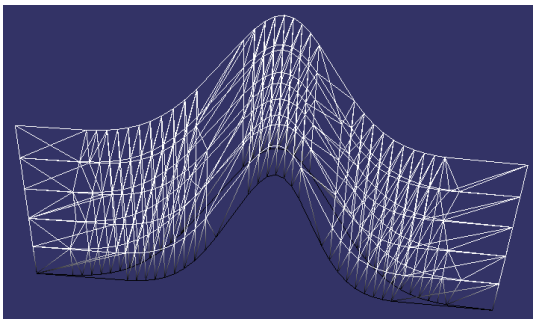

Fig. 4. Example of ε_u approximate representation of $\tilde{A}$

B. Operations

Theoretic operations of type-2 fuzzy sets are described as formulations (6)-(8). Arcording to [6], operations of n type-2 fuzzy sets are computed using max t-conorm and min t-norm as follows:

Join operation:

$$\mu_{\sqcup_{i=1}^n F_i}(\theta) = \begin{cases} \wedge_{i=1}^n \mu_{F_i}(\theta) & \theta < \upsilon_1 \\ \wedge_{i=k+1}^n \mu_{F_i}(\theta) & \upsilon_k \le \theta < \upsilon_{k+1}, 1 \le k < n \\ \vee_{i=1}^n \mu_{F_i}(\theta) & \theta > \upsilon_n \end{cases} \quad (16)$$

Meet operation:

$$\mu_{\sqcap_{i=1}^n F_i}(\theta) = \begin{cases} \vee_{i=1}^n \mu_{F_i}(\theta) & \theta < \upsilon_1 \\ \wedge_{i=1}^k \mu_{F_i}(\theta) & \upsilon_k \le \theta < \upsilon_{k+1}, 1 \le k < n \\ \wedge_{i=1}^n \mu_{F_i}(\theta) & \theta \ge \upsilon_n \end{cases} \quad (17)$$

in which $\wedge$ is a t-norm and $\vee$ is a t-conorm, υ_i is a value such that $\mu_{F_i}(\upsilon_i)$ is at the apex of $\mu_{F_i}(x)$, $i = 1, ..., n$.

Suppose that $\tilde{A}_i (i = 1, ..., n)$ are ε_u type-2 fuzzy sets based on refinement CTIN with L levels. Call V_i is vertices of $\tilde{A}_i$ and $V = \cup_{i=1}^n V_i$. Join (meet) operations of n type-2 fuzzy sets $\tilde{A}_i$ using max t-conorm and min t-norm are described as the following theorem.

Theorem 3.2: Let $\tilde{A}_i (i = 1, .., n)$ be ε_u type-2 fuzzy sets based on refinement CTIN with L levels. Call I_k is set of intersection points between k^{th}-level contours of $\tilde{A}_i$. Join (meet) operation of $\tilde{A}_i$, called $\tilde{B}$, is computed according to the formula (16) ((17) for meet operation) at $v \in V \cup (\cup_{k=0}^K I_k)$. B is ε_u type-2 fuzzy sets based on refinement CTIN with L levels.

The following is the algorithm for computing join, meet operations using max t-conorm, min t-norm of n refinement CTIN-based type-2 fuzzy sets.

Algorithm 3.1 (Join/Meet Operations): .
Input: n RCTIN-based type-2 fuzzy sets $\tilde{A}_i$, $(i = 1, ..., n)$.
Output: $\tilde{B} = \sqcup_{i=1}^n \tilde{A}_i$ ($\tilde{B} = \sqcap_{i=1}^n \tilde{A}_i$ for meet operation).

1) For each level $k = \overline{0, L}$.
   a) Compute I_k set of intersection points of k^{th} contours of $\tilde{A}_i$.
   b) For each $v \in I_k$
      If $v \notin \tilde{A}_i$ then insert v into the $\tilde{A}_i$'s TIN.
2) For each level $k = \overline{0, L}$.
   For each vertex $v \in V$ belong to k^{th} contour
   a) Compute vertex $v' \in \tilde{B}$ of join (meet) operation according to (16) or (17).
   b) If v' is not a vertex of $\tilde{A}_i$s then reject v'.
   c) Otherwise add v' into $V_{\tilde{B}}^k$, i.e. set of vertices at k^{th} level of $\tilde{B}$.
3) Triangulate set of vertices $V_{\tilde{B}} = \cup_{k=0}^L V_{\tilde{B}}^k$ with PSLG (segments in $V_{\tilde{B}}^k$).

Example: Let $\tilde{A}_1, \tilde{A}_2$ be two RCTIN-based fuzzy sets described as the formula (15) with $m_1 = 1.0, m_2 = 1.5, \sigma_{11} = 0.4, \sigma_{12} = 0.3, \sigma_{21} = 0.5, \sigma_{22} = 0.3$. Fig. (5) show results of join/meet operations.

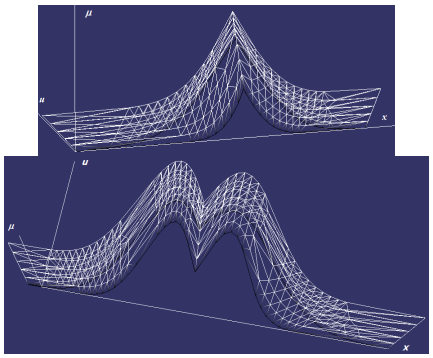

Fig. 5. Example of join/meet operations.

IV. Refinement CTIN Based Type-2 Fuzzy Logic Systems

A. Rule base and fuzzifier

Fig. 6 shows the structure of a RCTIN-based type-2 FLS. The difference from general type-2 FLS contains only geometric defuzzification in the output processing block.

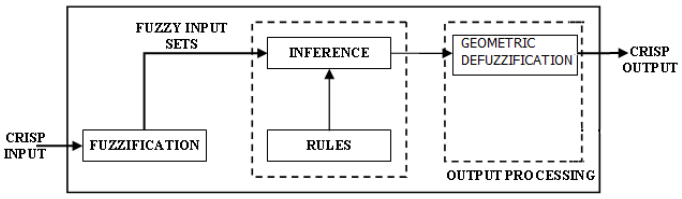

Fig. 6. The structure of RCTIN based type-2 fuzzy logic systems

The singleton fuzzifier maps the crisp input into a RCTIN-based type-2 fuzzy set. We consider only singleton fuzzification, for which the input fuzzy set has only a single point of

nonzero membership. The "IF-THEN" rules has the form, for l^{th} rule, as follows:

R^l : IF x_1 is $\tilde{F}_1^l$ and x_2 is $\tilde{F}_2^l$ and ... and x_p is $\tilde{F}_p^l$ THEN y is $\tilde{G}^l$

where: x_is are inputs; $\tilde{F}_i^l$s are antecedent sets (i=1, 2, ..., p); $\tilde{G}^l$ is the output.

Example: Consider the RCTIN-based type-2 fuzzy set that described as the formula (15). Using singleton fuzzifier at $x = 0.8$, output of the fuzzifier is a RCTIN-based type-2 fuzzy set as the Fig. 7.

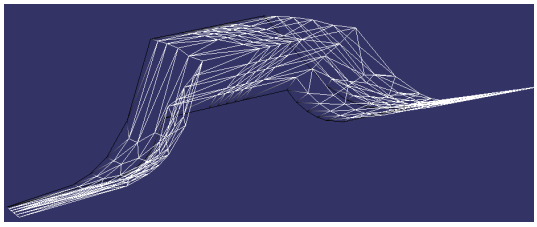

Fig. 7. Example on output of fuzzifier

B. Inference Engine

Inference engine combines rules and gives a mapping from input type-2 fuzzy sets to output type-2 fuzzy sets. Multiple antecedents in rules are connected by the meet operation. The membership grades in the input sets are combined with those in the output sets using the $sup-star$ composition. To do this one needs to find meets and joins of type-2 sets, as well as compositions of type-2 relations. Note that mentioned type-2 fuzzy sets are RCTIN-based type-2 fuzzy sets.

The output of the inference engine is a RCTIN-based type-2 fuzzy set. We do defuzzification by finding its geometric centroid, that is described more detail in the next section.

The following is the inference processing of RCTIN-based type-2 FLS:

Consider a RCTIN-based type-2 FLS having p inputs, $x_1 \in X_1, x_2 \in X_2, ..., x_p \in X_p$, and one output $y \in Y$. Suppose that it has M rules where the l^{th} rule has the form

$$R^l \text{ : IF } x_1 \text{ is } \tilde{F}_1^l \text{ AND ... AND } x_p \text{ is } \tilde{F}_p^l \text{ THEN } y \text{ is } \tilde{G}^l. \tag{18}$$

This rule represents a RCTIN-based type-2 fuzzy relation between the input space $X_1 \times X_2 \times ... \times X_p$ and the output space Y of the FLS. The membership function of this type-2 relation is denoted as $\mu_{\tilde{F}_1^l \times ... \times \tilde{F}_p^l \to \tilde{G}^l}(x, y)$, where $\tilde{F}_1^l \times ... \times \tilde{F}_p^l$ denotes the Cartesian product of $\tilde{F}_1^l$, ..., $\tilde{F}_p^l$, and $x = \{x_1, x_2, ..., x_p\}$.

When an input $\mathbf{x}'$ is applied, the composition of the fuzzy set $\tilde{X}'$ to which $\mathbf{x}''$ belongs and the rule R^l is found by using the extended sup-star composition

$$\mu_{\tilde{X}' \circ \tilde{F}_1^l \times ... \times \tilde{F}_p^l \to \tilde{G}^l}(y) = \sqcap_{x \in \tilde{X}'} [\mu_{\tilde{X}'}(x) \sqcap \mu_{\tilde{F}_1^l \times ... \times \tilde{F}_p^l \to \tilde{G}^l}(x, y)] \tag{19}$$

We denote $\tilde{X}' \circ \tilde{F}_1^l \times ... \times \tilde{F}_p^l \to \tilde{G}^l$ as $\tilde{B}^l$, the output set corresponding to the l^{th} rule. We use singleton fuzzification and the product or minimum implication, inference process of rule l^{th} is described as follows:

Fig. 8. Centroid computations of $\tilde{A}$ by partitioning the space of uncertainty

$$\begin{aligned} \mu_{\tilde{B}^l}(y) &= \mu_{\tilde{F}_1^l}(x_1) \sqcap \mu_{\tilde{F}_2^l}(x_2) \sqcap ... \sqcap \mu_{\tilde{F}_p^l}(x_p) \sqcap \mu_{\tilde{G}^l}(y) \\ &= \mu_{\tilde{G}^l}(y) \sqcap [\sqcap_{i=1}^p \mu_{\tilde{F}_i^l}(x_i)] \end{aligned} \tag{20}$$

The output sets of rules are combined in a type-2 fuzzy set by using $join$ operation, i.e.

$$\mu_{B'}(y) = \sqcup_{i=1}^K \mu_{\tilde{B}^i}(y) \tag{21}$$

in which K is number of fired rules and $\mu_{\tilde{B}^i}(y)$ is output of i^{th} fired rule.

Consider a vertex v of the TIN that represents output RCTIN-based type-2 fuzzy set of l^{th} rule. Suppose that v belongs to Z_k contour. After inference process, abscissa x, z of v are no change, abscissa u of v is computed as follows:

If $u_v = max_u\{\mu_{\tilde{G}}(x_v, u)\}$ then

$$u'_v = u_v \star [max_y\{Z^k_{\tilde{F}_1}(x_1)\} \star ... \star max_y\{Z^k_{\tilde{F}_1}(x_1)\}] \tag{22}$$

If $u_v = min_u\{\mu_{\tilde{G}}(x_v, u)\}$ then

$$u'_v = u_v \star [min_y\{Z^k_{\tilde{F}_1}(x_1)\} \star ... \star min_y\{Z^k_{\tilde{F}_1}(x_1)\}] \tag{23}$$

The algorithm for inference engine is described as follows:

Algorithm 4.1 (Inference engine): .

Input: $n+1$ RCTIN-based type-2 fuzzy sets $\tilde{A}_i, \tilde{G}$, ($i = 1, ..., n$).

Output: RCTIN-based type-2 fuzzy set $\tilde{G}$ is output of inference process.

1) For each contour $Z_k, k = \overline{0, L}$.
   a) For each vertex v is on the Z_k
   b) if v belongs to upper surface, i.e $u_v = max_u\{\mu_{\tilde{G}}(x_v, u)\}$
      computing u'_v as the formula (22).
   c) otherwise
      computing u'_v as the formula (23).

C. Defuzzification

Defuzzification is the most complex process of theoretic type-2 fuzzy logic systems. This section is described a defuzzification based on finding center of gravity of the space of uncertainty.

Let V_i with center of gravity $cog_i = (x_{ci}, y_{ci}, z_{ci})$ and mass m_i $(i = 1, \ldots, P)$ are objects in three-dimensions space. The gravity center of the system of massive objects is computed as follows:

$$\mathbf{c} = \frac{\sum_{i=1}^P \mathbf{cog}_i * m_i}{\sum_{i=1}^P m_i} \tag{24}$$

If mass density of objects is equilateral then equation (24) is rewritten as follows:

$$\mathbf{c} = \frac{\sum_{i=1}^P \mathbf{cog}_i * V_i * md}{\sum_{i=1}^P V_i * md} = \frac{\sum_{i=1}^P \mathbf{cog}_i * V_i}{\sum_{i=1}^P V_i} \tag{25}$$

where V_is are volumes of massive objects and dm is their mass density.

Let $\tilde{A}$ be RCTIN-based type-2 fuzzy set that contains N vertices $v_k (k = 1, \ldots, N)$ and M faces $f_k (k = 1, \ldots, M)$. In order to compute the center of gravity of the uncertainty space of $\tilde{A}$, $T_{\tilde{A}}$ is divided into 3-dimensional patches based on triangles of TIN. For each triangle, we make a triangular prism in which its vertices are the three vertices of the triangle and the three points of these vertices are projected on 2-dimensional plane (x, u). Next, triangular prisms are also divided into three tetrahedrons. Hence, the TIN of $\tilde{A}$ is divided into $3M$ tetrahedrons. Let t_k with center of gravity $c_k = (x_k, u_k, y_k)$ and volume V_k is the k^{th} tetrahedrons $(k = 1, \ldots, 3M)$. Because mass density of tetrahedrons is equilateral, the center of gravity of system of tetrahedrons is computed by using 25 as follows:

$$\mathbf{c} = \frac{\sum_{i=1}^{3M} \mathbf{c}_i * V_i}{\sum_{i=1}^{3M} V_i} \tag{26}$$

For a tetrahedron with vertices $\mathbf{v}_1 = (v_{11}, v_{12}, v_{13})$, $\mathbf{v}_2 = (v_{21}, v_{22}, v_{23})$, $\mathbf{v}_3 = (v_{31}, v_{32}, v_{33})$, and $\mathbf{v}_4 = (v_{41}, v_{42}, v_{43})$, the volume is computed using a dot product (.) and a cross product ($\times$), yielding

$$\mathbf{V} = \frac{|(\mathbf{v}_1 - \mathbf{v}_4).((\mathbf{v}_2 - \mathbf{v}_4) \times (\mathbf{v}_3 - \mathbf{v}_4))|}{6} \tag{27}$$

Algorithm 4.2 (Defuzzification): .
Input: $T_{\tilde{A}}$ is a T2FS.
Output: $fDefuzz$ is output value.
For each triangle t_k of $T_{\tilde{A}}$

1) Make triangular prism with with six vertices: v_1, v_2, v_3, $v_{1'}, v_{2'}, v_{3'}$ in which abscissa y of $v_{1'}, v_{2'}, v_{3'}$ is zero.
2) Divide the triangular prism into three tetrahedrons in which their vertices are $(v_{1'}, v_1, v_2, v_3)$, $(v_{1'}, v_2, v_{2'}, v_3)$ and $(v_{1'}, v_3, v_{2'}, v_{3'})$.
3) Compute centroid of each tetrahedron.
4) Compute volume of each tetrahedron as equation (27).
5) Compute centroid of the space of uncertainty of $\tilde{A}$ as equation (26).
6) Abscissa $fDefuzz = x$ of the centroid is the output of type-reduction and defuzzification.

V. Experimental Results

A. Comparisons

Algorithms are experimented to get comparisons in runtime and accuracy between the proposed method and previous methods. On runtime, the proposed representation is compared with TIN-based representation [15]. All of algorithms are implemented on Laptop HP DV9500 Core 2 Duo T7500 RAM 2GB with statistics summarised in the following table.

TABLE I
Sum of cumulative time of 100 replications (in seconds)

	Meet	Join	Negation	Inference
TIN-based representation	2.278	2.293	0.003	1.880
The proposed method	0.0118	0.0205	0.000015	0.0128

On the manner of accuracy, the proposed method (RCTIN) is compared with zSlice-based representation [18], [19]. I is number of slices/contours of a zSlice type-2 fuzzy sets or RCTIN type-2 fuzzy sets. Results on accuracy, summarised in the table II, show that RCTIN type-2 fuzzy sets accurately represent the original type-2 fuzzy sets in case primary and secondary membership grades is piece-wise linear functions.

TABLE II
Comparison on errors in representation

I	3	5	10	50	100
zSlice (triangle)	0.0251	0.0156	0.0075	0.0015	0.00075
RCTIN (triangle)	0.0	0.0	0.0	0.0	0.0
zSlice (Gaussian)	0.0623	0.0374	0.0187	0.00374	0.00187
RCTIN (Gaussian)	0.0039	0.0023	0.0012	0.00023	0.00012

B. Problems

We implement RCTIN-based type-2 fuzzy logic systems with collision avoidance behavior of robot navigation. The fuzzy logic systems have two inputs: the extended fuzzy directional relation [23] and range to obstacle, the output is angle of deviation (AoD). The behavior is experimented in comparisons between type-1 FLS and RCTIN-based general type-2 FLS. The fuzzy rule has the form as following:

IF FDR is $\tilde{A}_i$ AND Range is $\tilde{B}_i$ THEN AoD is $\tilde{C}_i$
where $\tilde{A}_i$, $\tilde{B}_i$, $\tilde{C}_i$ are type-2 fuzzy sets of antecedent and consequent, respectively.

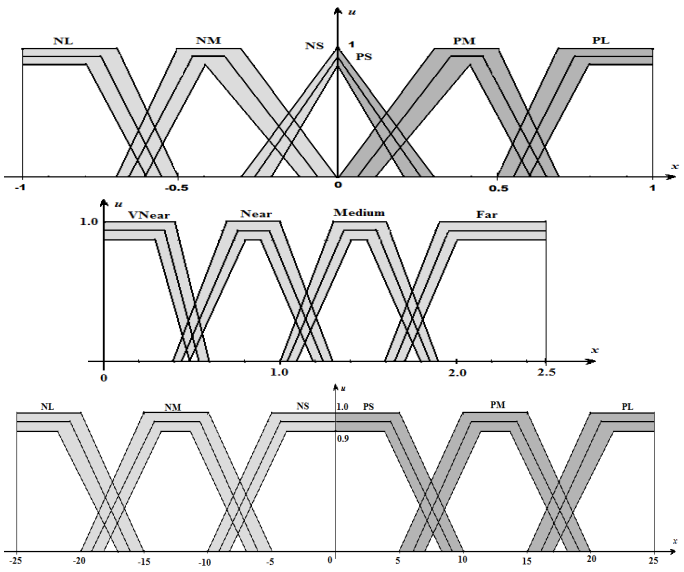

Fig. 9. Membership grades of CA behavior.

The fuzzy directional relation has six linguistic values (NLarge, NMedium, NSmall, PSmall, PMedium and PLarge). The range from robot to obstacle is divided in three subsets: VNear, Near, Medium and Far. The output of fuzzy if-then is a linguistic variable representing for angle of deviation, has six linguistic variables the same the fuzzy directional relation with the different membership functions. Linguistic values are

general type-2 fuzzy subsets that membership functions are described in Fig. 9. Membership grades are general type-2 fuzzy sets with vertical slide is triangular in which $z = 0$ for all points on upper/lower MF and $z = 1$ for all points on middle MF. For type-1 behavior, linguistic variables of inputs and output are the same type-2 behavior and their membership functions are upper MF of type-2 membership functions. RCTIN-based type-2 fuzzy subsets are triangulated at 5 levels. The rule-base is described in the table III.

TABLE III
THE RULE BASE OF COLLISION AVOIDANCE BEHAVIOR

FDR	Range	AoD	FDR	Range	AoD
NS	VN	PL	PS	VN	NL
NS	N	PL	PS	N	NL
NS	M	PM	PS	M	NM
NS	F	PS	PS	F	NS
NM	VN	PM	PM	VN	NM
NM	N	PM	PM	N	NM
NM	M	PM	PM	M	NM
NM	F	PS	PM	F	NS
NL	VN	PM	PL	VN	NM
NL	N	PM	PL	N	NM
NL	M	PS	PL	M	NS
NL	F	PS	PL	F	NS

RCTIN-based type-2 FLS is tested on whole of input spaces that is discretized with step of 0.1 in which $FDR \in [-1, 1]$ and $Range \in [0.5, 2.5]$. Fig. 10 shows inference surface of avoidance behavior based on RCTIN Type-2 FLS. Results is summarized as follows:

TABLE IV
EXPERIMENTAL RESULTS OF AVOIDANCE BEHAVIOR

	Type-1 FLS	RCTIN Type-2 FLS
Number of discretized points	441	441
Run-time (in milliseconds) for all of discretized input space	92	524
Minimum AoD	-21.111	-20.54
25%-tile AoD	-4.405	-4.676
Median AoD	-3.889	0
75%-tile AoD	4.222	5.591
Maximum AoD	18.359	18.058
Mean AoD	-0.7178	-0.3172

VI. CONCLUSION

An approach to RCTIN-based representation of generalized type-2 fuzzy sets is presented with implementations of avoidance behavior. The basis for this approach is ε_u representation of type-2 membership grades. Geometric operations involving join under minimum, meet under minimum, negation, inference and defuzzification are developed base on this representation. Geometric computation of RCTIN-based general type-2 fuzzy logic system are implemented under avoidance behavior of robot navigation. Results in comparisons with previous approach show that the proposed approach considerably reduce computational complexity.

The next goal is to implement the general type-2 FLS in applications under other hardware such as FGPA or embedded systems. And other approach is to use RCTIN for intelligent systems such as ANFIS or TSK fuzzy logic systems.

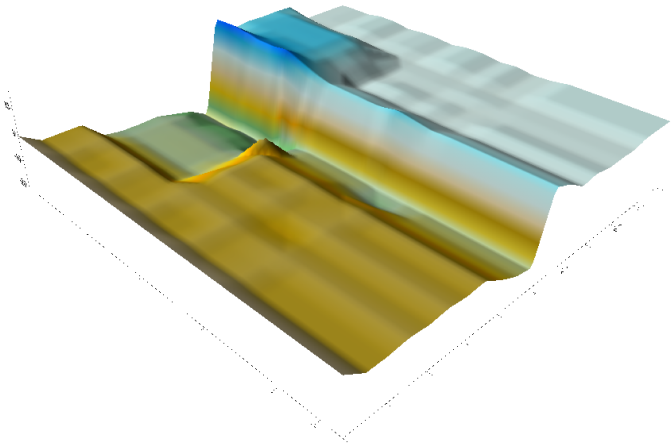

Fig. 10. Inference Surface of Type-2 avoidance behavior

ACKNOWLEDGMENT

This paper is sponsored by Vietnam's National Foundation for Science and Technology Development (NAFOSTED), Grant No 102.012010.12.

REFERENCES

[1] L. P. Chew (1989), "Constrained Delaunay Triangulations", *Algorithmica* 4(1),pp. 97-108.

[2] S. Coupland, R. John (2007), "Geometric Type-1 and Type-2 Fuzzy Logic System", *IEEE Trans. on Fuzzy Systems*, 15(1), pp. 3 - 15.

[3] S. Coupland, R. John (2008), "New geometric inference techniques for type-2 fuzzy sets", *International Journal of Approximate Reasoning*, 49(1), pp. 198-211.

[4] S. Coupland, R. John (2008), "A Fast Geometric Method for Defuzzification of Type-2 Fuzzy Sets", *IEEE Trans. on Fuzzy Systems*, Vol. 16, No.4, pp. 929-941.

[5] N. Karnik, J.M. Mendel and Liang Q. (1999), "Type-2 Fuzzy Logic Systems", *IEEE Trans. on Fuzzy Systems*, 7(6), pp. 643-658.

[6] N. Karnik and J.M. Mendel (2001), "Operations on Type-2 Fuzzy Sets", *Fuzzy Sets and Systems*, 122, pp.327-348.

[7] N. Karnik and J.M. Mendel (2001), "Centroid of a Type-2 Fuzzy Set", *Information Sciences*, 132, pp. 195-220.

[8] Liang Q. and J.M. Mendel (2000), "Interval Type-2 Fuzzy Logic Systems: Theory and Design", *IEEE Trans. on Fuzzy Systems*, 8(5), pp. 535-550.

[9] J.M. Mendel and R. I. John (2002), "Type-2 Fuzzy Sets Made Simple", *IEEE Trans. on Fuzzy Systems*, 10(2), pp. 117-127.

[10] J.M. Mendel , John R. I., Feilong Liu (2006), "Interval Type-2 Fuzzy Logic Systems Made Simple", *IEEE Trans. on Fuzzy Systems*, 14(6), pp. 808-821.

[11] J. M. Mendel, F. Liu, D. Zhai (2009), -Plane Representation for Type-2 Fuzzy Sets: Theory and Applications, *IEEE Trans. on Fuzzy Systems*, 17(5), pp. 1189-1207.

[12] Jerry M. Mendel (2010), Comments on -plane representation for type-2 fuzzy sets: theory and applications, *IEEE Trans. on Fuzzy Systems*, 18(1), pp. 229-230.

[13] Feilong Liu (2008), An efficient centroid type-reduction strategy for general type-2 fuzzy logic system , Information Sciences, Vol. 178(9), PP. 2224-2236.

[14] Long Thanh Ngo, Long The Pham, Phuong Hoang Nguyen, K.Hirota (2007), On approximate representation of type-2 fuzzy sets using triangulated irregular network, *Foundations of Fuzzy Logic and Soft Computing, Lecture Notes in Computer Science*, LNCS 4529, Springer, pp. 584-593.

[15] Long Thanh Ngo, Long The Pham, Phuong Hoang Nguyen, K.Hirota (2009), Refinement geometric algorithms for type-2 fuzzy set operations, *Proceedings, IEEE-FUZZ 09,*, pp. 866-871.

[16] J.R. Shewchuk (2002), *Delaunay Refinement Algorithms for Triangular Mesh Generation*, *Computational Geometry: Theory and Applications* 22(1-3):21-74.

[17] Janusz T. Starczewski (2009), Efficient triangular type-2 fuzzy logic systems, *International Journal of Approximate Reasoning*, Vol. 12, No.5, pp. 799-811.

[18] H. Hagras(2004), A Hierarchical Type-2 Fuzzy Logic Control Architecture for Autonomous Mobile Robots, *IEEE Trans. on Fuzzy Systems*, Vol. 12, No.4, pp. 524-539.

[19] H. Hagras(2007), Type-2 FLCs: A new Generation of Fuzzy Controllers, IEEE Computational Intelligence Magazine, Vol. 2, No. 1, pp 30-43.

[20] C. Wagner, H. Hagras(2008), zSlices :Towards Bridging the Gap between Interval and General Type-2 Fuzzy Logic, *Proceedings, IEEE-FUZZ 08,*, pp. 489 - 497.

[21] C. Wagner, H. Hagras (2009), General Type-2 Fuzzy Logic Control based on zSlices, *Proceedings, IEEE-FUZZ 09,*, pp. 718-725.

[22] C. Wagner, H. Hagras (2010), Toward General Type-2 Fuzzy Logic Systems Based on zSlices, *IEEE Trans. on Fuzzy Systems*, Vol. 18, No.4, pp. 637-660.

[23] L. T. Ngo, L. T. Pham, P. H. Nguyen. Extending fuzzy directional relationship and applying for mobile robot collision avoidance behavior, International Journal of Advanced Computational Intelligence & Intelligent Informatics, Vol. 10 No.4, 2006

[24] P. Matsakis, L. Wendling, A New Way to Represent the Relative Position of Areal Objects, PAMI (IEEE Trans. on Pattern Analysis and Machine Intelligence), vol. 21, no. 7, pp. 634-643, 1999.

[25] M. Skubic, P. Matsakis, G. Chronis, J. Keller, Generating Multi-level Linguistic Spatial Descriptions from Range Sensor Readings Using the Histogram of Forces, Autonomous Robots, vol. 14, no. 1, pp. 51-69, 2003.

[26] S. Greenfield, F. Chiclana, S. Coupland, R. John, The collapsing method of defuzzification for discretised interval type-2 fuzzy sets, Information Sciences, Vol.179, No. 13, 2009

2011 IEEE International Conference on Fuzzy Systems
June 27-30, 2011, Taipei, Taiwan

On a Strengthening Connective for Flexible Database Querying

Patrick Bosc, *Member*, *IEEE*, and Olivier Pivert
Irisa-Enssat
University of Rennes 1
Lannion, France
{bosc, pivert}@enssat.fr

***Abstract*—In most of query languages, conjunctive and disjunctive combinations of conditions remain the usual way for aggregation. Fuzzy query languages also offer trade-off operators, such as means in order to compensate between elementary conditions. In this paper, we investigate a new type of condition basically founded on the interaction between two predicates, thus enriching the panoply of tools the user is provided with and enhancing the power of query languages.**

***Index Terms*—Databases, fuzzy queries, fuzzy connectives.**

I. Introduction

Query languages based on fuzzy sets include a wide range of connectives, among which conjunction/disjunction and their weighted version, mean operators and quantified statements such as "most of $P_1, \ldots, P_n$" where P_i is a fuzzy condition. So doing, preferences are introduced at a double level: i) atomic fuzzy predicates which allow for stating that some values are preferred to others, and ii) connectors which permit to specify that some terms are more important than others or can be compensated by others.

Here, we would like to focus on an operator that has a counterpart in natural language, for which an interpretation is proposed in the context of information selection/retrieval in a database querying process. More precisely, it connects two predicates P_1 (or X *is* A) and P_2 (or Y *is* B) and it writes as follows: "P_1 *all the more as* P_2". A typical example of such a condition is: "find second hand cars that are all the cheaper as their mileage is high". The idea is to express a reinforcement of P_1 as P_2 is more and more satisfied. This obviously defines a new type of condition based on a sophisticated interaction between the two predicates involved, which are not interchangeable. One originality lies in the fact that the connector "all the more as" is by nature non commutative as are the connectors "and possibly" [1] or "then" [2] proposed earlier by other authors. Let us notice that "P_1 *all the more as* P_2" does not make sense in the Boolean context where there is no graduality in the satisfaction of a Boolean predicate, whereas this notion is at the heart of the interpretation of this type of new condition.

We consider an interpretation according to which "P_1 *all the more as* P_2" basically depends on P_1 and is not a matter of "joint" satisfaction of the predicates P_1 and P_2 as it is the case when an implication-based approach is taken. Indeed, if the gradual rule [3] "$P_2 \Rightarrow_{R-i} P_1$" is used ($\Rightarrow_{R-i}$ denoting an R-implication [4]), the truth value obtained may be high although P_1 is weakly satisfied (it suffices that the level of satisfaction of P_1 attains that of P_2 to get full satisfaction). We rather start with the idea that if the grade of satisfaction for P_1 is low, the grade of satisfaction of "P_1 *all the more as* P_2" must also be low. Our approach to interpreting the condition "P_1 *all the more as* P_2" consists in strengthening P_1 more and more as P_2 is more and more satisfied. We consider that "P_1 *all the more as* P_2" reduces to P_1 when P_2 is false and becomes "*very* P_1" when P_2 is true.

We situate our proposal as an enrichment of the SQLf query language [5]. As a consequence, the new condition is associated with a single truth value taken in the unit interval, which makes it possible to compose it with usual predicates (atomic or not).

The rest of the paper is structured as follows. Some basic notions about fuzzy predicates and queries are first recalled in Section 2. Then, different ways for strengthening a predicate are presented in Section 3. Section 4 is devoted to a detailed study of the new type of predicate "P_1 *all the more as* P_2". In Section 5, an inclusion operator derived from *all the more as* is suggested as well as its use in some advanced SQLf queries. The conclusion summarizes the contributions of the paper and draws some lines for future works.

II. Reminders on fuzzy predicates and queries

Regular sets allow for the definition of Boolean predicates. In an analogous way, gradual predicates (or conditions) can be associated with fuzzy sets [6] aimed at describing classes of objects with vague boundaries. Often, elementary fuzzy predicates correspond to adjectives of the natural language, such as *young*, *tall*, *cheap* or *well-paid*. A fuzzy predicate P can be modeled as a function μ_P (usually of triangular or trapezoidal shape) from one (or several) domain(s) X to the unit interval [0, 1]. The degree $\mu_P(x)$ represents the extent to which element x satisfies the vague predicate P (or equivalently the extent to which x belongs to the fuzzy set of objects which match the fuzzy concept P). An elementary fuzzy predicate can also compare two attributes using a gradual comparison operator such as *more or less equal*.

It is possible to alter the meaning of a given predicate using a modifier which is generally associated with an adverb (e.g., *very*, *more or less*, *relatively*). For instance, *very cheap* is more

978-1-4244-7316-8/11/$26.00 ©2011 IEEE

restrictive than *cheap* and *fairly high* is less demanding than *high*. The meaning of the predicate *mod* P (where *mod* is a modifier) may be defined in a compositional way and different approaches have been advocated, among which: $\mu_{modP}(x) = (\mu_P(x))^n$ (see [7]]).

Atomic and modified predicates can be involved in compound predicates which go far beyond those used in regular queries. Conjunction (resp. disjunction) is interpreted by means of a triangular norm $\top$ (resp. co-norm $\perp$), for instance the minimum (resp. the maximum). As to negation, it is interpreted as: $\forall x, \mu_{\neg P}(x) = 1 - \mu_P(x)$. Weighted conjunction and disjunction as well as weighted means or OWA can be used to assign a different importance to each of the predicates (see [8], [4] for more details).

The operations from the relational algebra can be straightforwardly extended to fuzzy relations by considering fuzzy relations as fuzzy sets on the one hand and by introducing fuzzy predicates in the appropriate operations on the other hand. Indeed, a fuzzy relation is designed as a fuzzy subset of a Cartesian product of domains. Thus, any such fuzzy relation r can be seen as made of weighted tuples, denoted by μ/t, where μ expresses the extent to which tuple t belongs to the relation, i.e., is compatible with the concept conveyed by r. As an illustration, we give the definition of the fuzzy selection hereafter, where "cond" denotes a fuzzy predicate built according to what was said above:

$$\mu_{sel(r,cond)}(t) = \top(\mu_r(t), \mu_{cond}(t)).$$

The language called SQLf described in [5] extends SQL so as to support fuzzy queries and it serves as a background in the rest of the paper.

III. Strengthening Operators

A. Introduction

As mentioned previously, the basis for interpreting the condition "P_1 *all the more as* P_2" is to strengthen predicate P_1 depending on the satisfaction of predicate P_2. In particular, when P_2 is true (degree equal to 1), the final satisfaction will be that of *very* P_1. So, we will look at various ways to move from P to *very* P along with their compliance with the following three common sense properties:

S1: $\forall(x,\ y),\ \mu_P(x) \geq \mu_P(y) \Rightarrow \mu_{very\ P}(x) \geq \mu_{very\ P}(y)$,
S2: *core*(*very* P) $\subseteq$ *core*(P),
S3: $\forall x,\ ((\mu_P(x) \in]0,\ 1[\Rightarrow \mu_{veryP}(x) < \mu_P(x)) \wedge$
$(\mu_P(x) \in \{0,\ 1\} \Rightarrow \mu_{very\ P}(x) \leq \mu_P(x)))$.

In other words, property S1 states that the strengthening operator *very* does not change the ordering of elements, property S2 tells that *very* P is at least as demanding as P for the elements that are completely in agreement with predicate P, and property S3 imposes that for any element which somewhat (except fully) satisfies predicate P, predicate *very* P is strictly less satisfied (there is a true strengthening).

B. Different strengthening approaches

1) Use of a triangular norm: A well known way for reinforcing a predicate P is to define:

$$\mu_{very\ P}(x) = \mu_{\top^n(P)}(x)$$

where $\top$ stands for a non idempotent triangular norm. For instance, with the product and Łukasiewicz' norm, one gets respectively:

$$\mu_{very\ P}(x) = \mu_{P^n}(x) = (\mu_P(x))^n$$
$$\mu_{very\ P}(x) = \mu_{P^n}(x) = max(n \cdot \mu_P(x) - n + 1,\ 0).$$

In such a framework, the interpretation of the statement "X *is* A *all the more as* Y *is* B" applying to an element t, denoted by $atma(A,\ B)(t)$, will be such that:

$$atma(A,\ B)(t) = f_1(A,\ B,\ n,\ t) = \mu_{A^n}(t) \text{ if } \mu_B(t) = 1$$

with n a given powering coefficient.

The satisfaction of properties S1-S3 by this strengthening method is now examined:

S1: if $\mu_P(x) \geq \mu_P(y)$ then $\mu_{P^n}(x) \geq \mu_{P^n}(y)$ due to the monotonicity of norms with respect to both arguments, then $\mu_{very\ P}(x) \geq \mu_{very\ P}(y)$
S2: if $\mu_P(x) = 1$ then $\mu_{P^n}(x) = \top(1,\ \ldots,\ 1) = 1$ due to the fact that 1 is a neutral element of any norm, and we have $core(P) = core(very\ P)$,
S3: when $\mu_P(x) = 0, \mu_{\top^n(P)}(x) = \mu_P(x) = 0$; when $\mu_P(x) = 1, \mu_{\top^n(P)}(x) = \mu_P(x) = 1$; when $\mu_P(x) \in]0,\ 1[$, the strict inferiority of $\mu_{\top^n(P)}(x)$ with respect to $\mu_P(x)$ is not necessarily satisfied by a triangular norm $\top$, except if $\top$ is Archimedean; in such a case, by definition it is ensured that $\top(y,\ y) < y$ for any $y \in]0,\ 1[$ (see [4]). Then, we have: $\top(y,\ \ldots,\ y) = \top^n(y) < y$ and $\mu_{very\ P}(x) = \mu_{\top^n(P)}(x) < \mu_P(x)$ when $\mu_P \in]0, 1[$.

So, we can conclude that if an Archimedean norm ($\top$) is used (for instance the product), the strengthening mechanism defined as $\mu_{very\ P}(x) = \mu_{\top^n(P)}(x)$ complies with all three desired properties.

2) Translation: A second approach to reinforcing a predicate is to translate its membership function. If P is an increasing (resp. a decreasing) predicate, the translation is to the right (resp. left). In the more general case of a predicate P with a trapezoidal membership function, two translations take place, to the right for its increasing part and to the left for its decreasing part. For an increasing predicate P (situation considered later on), one has the following formula:

$$\mu_{very\ P}(x) = \mu_P(x - \tau)$$

where τ is a positive value (shift). Then, the interpretation of the statement "X *is* A *all the more as* Y *is* B" applying to an element t will be such that:

$$atma(A,\ B)(t) = f_2(A,\ B,\ \tau,\ t) = \mu_A(t - \tau) \text{ if } \mu_B(t) = 1$$

with τ a given magnitude of the translation.

Such a mechanism satisfies properties S1-S3 due to the monotonicity of P and the very nature of a translation.

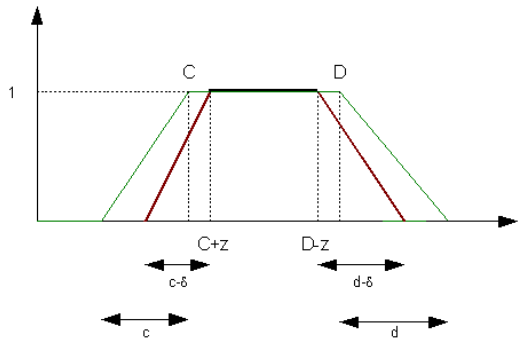

Fig. 1. Principle of the erosion operation

3) Erosion: The last strengthening technique considered here to build *very* P from P is called erosion [9] and it relies on the idea of a semantic proximity between the initial and the modified (reinforced) predicates. It makes use of a proximity relation E between two (numeric) values x and y which is reflexive and symmetric, and the quantity $\mu_E(x, y)$ can be viewed as a degree of approximate equality of x and y. This quantity can be defined as:

$$\mu_E(x,\ y) = \mu_Z(x - y)$$

which depends only on the difference between x and y. The parameter Z, called a tolerance indicator, is a fuzzy subset of the real line centered in 0 which has a trapezoidal membership function whose core is $[-z,\ z]$ and whose support is $[-z - \delta,\ z + \delta]$, denoted by $(-z,\ z,\ -\delta,\ \delta)$. So doing, the degree produced by $\mu_Z(x - y)$ evaluates the extent to which $(x - y)$ is close to 0 (according to Z). In other words, z is the maximal difference for which x and y are considered completely "approximately equal" and $z + \delta$ is the difference over which x and y are "not at all approximately equal". Using this proximity relation E parameterized by Z, a fuzzy set (or a predicate) P may be eroded into *very* P as follows:

$$\mu_{very P}(x) = \mu_{P \ominus Z}(x)$$

where $\ominus$ denotes Minkowski's difference defined as [10]:

$$\mu_{F \ominus Z}(r) = inf_s(\mu_Z(r - s) \rightarrow_{Gd} \mu_F(s)),$$

where $\rightarrow_{Gd}$ is the so-called Gödel implication ($p \rightarrow_{Gd} q) = 1$ if $p \leq q$, q otherwise). Then, the interpretation of the statement "X is A all the more as Y is B" applying to an element t will be such that:

$$atma(A,\ B)(t) = f_3(A,\ B,\ Z,\ t) = \mu_{A \ominus Z}(t) \text{ if } \mu_B(t) = 1$$

with Z a given tolerance indicator for the erosion.

Fig. (1) illustrates the behavior of the erosion operator acting on a fuzzy predicate P whose trapezoidal membership function is $(C,\ D,\ c,\ d)$. Of course, one must have $z \leq \frac{D-C}{2}$, $\delta \leq c$ and $\delta \leq d$. If z (resp. δ) equals 0, the core (resp. support) of the initial predicate remains unchanged. Such a strengthening operator satisfies Properties S1-S3 due to the nature of the erosion operator which corresponds to a difference in terms of membership functions (cf. Fig. (1)). Let us notice that erosion may modify the core and/or the support of the initial predicate, while translation does reduce both and the composition using any triangular norm leads to a reinforced predicate (*very P*) with the same core and support as the initial one (*P*).

IV. The connector "all the more as"

A. Axioms for this connector

We now review a bunch of axioms that can serve as a reasonable basis for defining the predicate "X *is* A *all the more as* Y *is* B". The following properties will act as a mandatory requirement for any definition of the connector "all the more as":

A1: decreasing monotonicity in the second argument, i.e.:

$$\mu_B(t.Y) > \mu_B(t'.Y) \wedge \mu_A(t.X) = \mu_A(t'.X) \Rightarrow atma(A,\ B)(t) \leq atma(A,\ B)(t'),$$

A2: increasing monotonicity in the first argument, i.e.:

$$\mu_A(t.X) > \mu_A(t.X) \wedge \mu_B(t.Y) = \mu_B(t'.Y) \Rightarrow atma(A,\ B)(t) \geq atma(A,\ B)(t'),$$

A3: when X is not at all A, "Y *is* B" has no effect, i.e.:

$$\mu_A(t.X) = 0 \Rightarrow \forall \mu_B(t.Y),\ atma(A,\ B)(t) = 0,$$

A4: when Y is not at all B, the value of "X *is* A *all the more as* Y *is* B" is that of "X *is* A", i.e.:

$$\mu_B(t.Y) = 0 \Rightarrow \forall \mu_A(t.X),\ atma(A,\ B)(t) = \mu_A(t.X),$$

A5: when "Y *is* B" is somewhat satisfied, the value of the statement "X *is* A *all the more as* Y *is* B" must result in an effective strengthening of "X *is* A" (except for the extreme truth values 0 and 1), i.e.:

$$(\mu_A(t.X) \in]0, 1[\ \wedge\ \mu_B(t.Y) > 0) \Rightarrow atma(A,\ B)(t) < \mu_A(t.X).$$

B. A plausible definition

As mentioned before, the interpretation of the statement "X *is* A *all the more as* Y *is* B" will have two extreme points: $\mu_A(t.X)$ when $\mu_B(t.X)$ is false and $\mu_{very A}(t.X)$ when $\mu_B(t.X)$ is completely satisfied. We suggest a linear transition between these two states, which has the advantage of being general for the three families of strengthening operators evoked before. This choice leads to the following definition of the connector "all the more as":

$$atma(A,\ B)(t) = (\mu_{very\ A}(t.X) - \mu_A(t.X)) \cdot \mu_B(t.Y) + \mu_A(t.X). \quad (1)$$

Let us remark that, in the particular case of the use of the norm product (strengthening of type 1), it could also be possible to have the following definition:

$$atma(A,\ B)(t) = (\mu_A(t.X))^{((n-1)\cdot\mu_B(t.Y)+1)} = (\mu_A(t.X))^{\mu_B(t.Y)+1} \text{ for } n = 2.$$

Example 1. Let us consider the relation *secondhandcars*(#*c*, *brand*, *name*, *year*, *price*, *mileage*, *horsepower*) with the tuples:

$t_1 = \langle$13, Ford, Focus, 2005, 6000, 40000, 75$\rangle$,
$t_2 = \langle$264, Renault, Clio, 2002, 4000, 130000, 75$\rangle$,
$t_3 = \langle$59, Toyota, Prius, 2006, 15000, 90000, 115$\rangle$,
$t_4 = \langle$508, Peugeot, 307, 2004, 5500, 100000, 110$\rangle$,
$t_5 = \langle$4, Ford, Mondeo, 2005, 6000, 125000, 110$\rangle$,
$t_6 = \langle$78, Renault, Megane, 2006, 7000, 110000, 110$\rangle$,
$t_7 = \langle$112, Nissan, Primera, 2008, 16000, 30000, 130$\rangle$

and the query looking for cars whose horsepower is less than 120 and whose price is all the cheaper as their mileage is high. The predicates "cheap" and "high" are assumed to be defined as follows:

$$\mu_{cheap}(p) = \begin{cases} 1 \text{ if } p \leq 5,000, \\ 0 \text{ if } p \geq 7,500, \\ \text{linear in-between,} \end{cases}$$

$$\mu_{high}(m) = \begin{cases} 0 \text{ if } m \leq 80,000, \\ 1 \text{ if } m \geq 120,000, \\ \text{linear in-between.} \end{cases}$$

Clearly, the seventh car does not qualify for the query since its horsepower exceeds the limit imposed by the user. With the first type of strengthening, the grades obtained by the first six cars are:

0.6/t_1, 1/t_2, 0/t_3, 0.72/t_4, 0.36/t_5, 0.08/t_6 with the product and n = 2,
0.6/t_1, 1/t_2, 0/t_3, 0.7/t_4, 0.2/t_5, 0.05/t_6 with Łukasiewicz' norm and n = 2,
0.6/t_1, 1/t_2, 0/t_3, 0.656/t_4, 0.216/t_5, 0.056/t_6 with the product and n = 3,
0.6/t_1, 1/t_2, 0/t_3, 0.6/t_4, 0/t_5, 0.05/t_6 with Łukasiewicz' norm and n = 3.

If a translation (to the left since the predicate is decreasing) is used to define *very cheap*, the grades are:

0.6/t_1, 1/t_2, 0/t_3, 0.6/t_4, 0.2/t_5, 0.05/t_6 with τ = 100,
0.6/t_1, 0.6/t_2, 0/t_3, 0.4/t_4, 0/t_5, 0.05/t_6 with τ = 200.

Last, with an erosion to reinforce *cheap*, the grades obtained are:

0.6/t_1, 1/t_2, 0/t_3, 0.73/t_4, 0.33/t_5, 0.05/t_6 with Z = (0, 0, 0, 100),
3 0.6/t_1, 1/t_2, 0/t_3, 0.68/t_4, 0.42/t_5, 0.05/t_6 with Z = (0, 100, 0, 0).

As can be seen, the results may significantly depend on the type of strengtening used as well as of the parameters chosen for a given type. $\diamond$

C. Compliance with the axioms

In this subsection, we show that, if the strengthening mechanism used to reinforce "X is A" complies with Properties S1-S3 (see Section III) in expression (1), Axioms A1-A5 are satisfied.

A1: Let us take two tuples t and t' such that: i) $\mu_A(t.X) = \mu_A(t'.X)$ and ii) $\mu_B(t.Y) > \mu_B(t'.Y)$. We have:

$$\begin{aligned} &atma(A,\ B)(t) - atma(A,\ B)(t') \\ &= (\mu_{very\ A}(t.X) - \mu_A(t.X)) \cdot \mu_B(t.Y) + \mu_A(t.X) - \\ &\quad (\mu_{very\ A}(t'.X) - \mu_A(t'.X)) \cdot \mu_B(t'.Y) - \mu_A(t'.X) \\ &= (\mu_{very\ A}(t.X) - \mu_A(t.X)) \cdot (\mu_B(t.Y) - \mu_B(t'.Y)). \end{aligned}$$

The first term is negative or equal to 0 due to the validity of Property S3 and the second one is positive according to the hypotheses stated above. So, we have:

$atma(A,\ B)(t) - atma(A,\ B)(t') \leq 0$, i.e.:
$atma(A,\ B)(t) \leq atma(A,\ B)(t')$

and Property A1 holds.

A2: Let us take two tuples t and t' such that: i) $\mu_A(t.X) > \mu_A(t'.X)$ and ii) $\mu_B(t.Y) = \mu_B(t'.Y)$. We have:

$$\begin{aligned} &atma(A,\ B)(t) - atma(A,\ B)(t') \\ &= (\mu_{very\ A}(t.X) - \mu_A(t.X)) \cdot \mu_B(t.Y) + \mu_A(t.X) - \\ &\quad (\mu_{very\ A}(t'.X) - \mu_A(t'.X)) \cdot \mu_B(t'.Y) - \mu_A(t'.X) \\ &= (\mu_{very\ A}(t.X) - \mu_{very\ A}(t'.X)) \cdot \mu_B(t.Y) + \\ &\quad (\mu_A(t.X) - \mu_A(t'.X)) \cdot (1 - \mu_B(t.Y)). \end{aligned}$$

From Axiom S1, we have:

$$\begin{aligned} \mu_A(t.X) > &\mu_A(t'.X)) \Rightarrow \\ &\mu_{very\ A}(t.X) \geq \mu_{veryA}(t'.X) \end{aligned}$$

and the first term of the sum is positive or equal to 0. The first term of the product is positive according to the hypotheses made above and the second term is positive or equal to 0. It follows that the previous expression yields a result that is positive or equal to 0, so:

$atma(A,\ B)(t) - atma(A, B)(t') \geq 0$, i.e.:
$atma(A,\ B)(t) \geq atma(A, B)(t')$

and Property A2 holds.

A3: Let us consider a tuple t such that $\mu_A(t.X) = 0$. Due to the validity of S3, one has $\mu_{very\ A}(t.X) = 0$. Then:

$$\begin{aligned} &atma(A,\ B)(t) = \\ &\quad (\mu_{very\ A}(t.X) - \mu_A(t.X)) \cdot \mu_B(t.Y) + \mu_A(t) = 0. \end{aligned}$$

A4: Let us now take a tuple t such that $\mu_B(t.Y) = 0$. We have:

$$\begin{aligned} &atma(A,\ B)(t) \\ &\quad = (\mu_{very\ A}(t.X) - \mu_A(t.X)) \cdot \mu_B(t.Y) + \mu_A(t) \\ &\quad = \mu_A(t). \end{aligned}$$

A5: Let us consider a tuple t such that: i) $\mu_A(t.X) \in]0, 1[$ and ii) $\mu_B(t.Y) > 0$. We have:

$$\begin{aligned} &atma(A,\ B)(t) = \\ &\quad (\mu_{very\ A}(t.X) - \mu_A(t.X)) \cdot \mu_B(t.Y) + \mu_A(t) \end{aligned}$$

where $(\mu_{very\ A}(t.X) - \mu_A(t.X))$ is strictly negative, then $(\mu_{very\ A}(t.X) - \mu_A(t.X)) \cdot \mu_B(t.Y)$ as well. Consequently $atma(A, B)(t) < \mu_A(t.X)$ and Axiom A5 holds.

Finally, it turns out that the strengthening approaches previously proposed (composition with an Archimedean norm, translation, erosion) are convenient for the interpretation of the statement "*X is A all the more as Y is B*". When applied to a tuple t of a relation r, the preceding predicate is defined as follows:

- with an Archimedean norm $\top$:
$$atma(A,\ B)(t) = f_1(A,\ B,\ n,\ t)$$
$$= (\mu_{\top^n(A)}(t.X) - \mu_A(t.X)) \cdot \mu_B(t.Y) + \mu_A(t.X),$$
- with a translation of magnitude $\tau > 0$ to the right applying to an increasing initial predicate A:
$$atma(A,\ B)(t) = f_2(A,\ B,\ \tau,\ t)$$
$$= (\mu_A(t.X - \tau) - \mu_A(t.X)) \cdot \mu_B(t.Y) + \mu_A(t.X),$$
- with the erosion operator associated with indicator $Z = (-z,\ z,\ -\delta,\ \delta)$:
$$atma(A,\ B)(t) = f_3(A,\ B,\ Z,\ t)$$
$$= (\mu_{A \ominus Z}(t.X) - \mu_A(t.X)) \cdot \mu_B(t.Y) + \mu_A(t.X).$$

D. The connector "all the less as"

By analogy with the operator "all the more as", one may think of a predicate "*X is A all the less as Y is B*". In such a case, one will not reinforce but weaken condition A (from "A" to "more or less A"). The interpretation is based on the fact that one is all the less demanding on the fact that X is A as the condition "*Y is B*" is more and more satisfied, similarly to the interpretation of "*X is A all the more as Y is B*" where one is all the more demanding on the fact that X is A as the condition "*Y is B*" is more and more satisfied. The generic formulation of the degree of satisfaction of the condition "*X is A all the less as Y is B*" is then given by:

$$atla(A,\ B)(t) =$$
$$(\mu_{more\ or\ less A}(t.X) - \mu_A(t.X)) \cdot \mu_B(t.Y) + \mu_A(t.X).$$

By analogy with the strengthening case, this expression will have three instantiations, namely:

- with an Archimedean co-norm $\perp$:
$$atla(A,\ B)(t) = f'_1(A,\ B,\ n,\ t)$$
$$= (\mu_{\perp^n(A)}(t.X) - \mu_A(t.X)) \cdot \mu_B(t.Y) + \mu_A(t.X),$$
- with a translation of magnitude $\tau > 0$ to the left applying to an increasing initial predicate A:
$$atla(A,\ B)(t) = f'_2(A,\ B,\ \tau,\ t)$$
$$= (\mu_A(t.X + \tau) - \mu_A(t.X)) \cdot \mu_B(t.Y) + \mu_A(t.X),$$
- with the dilation operator associated with indicator $Z = (-z,\ z,\ -\delta,\ \delta)$:
$$atla(A,\ B)(t) = f'_3(A,\ B,\ Z,\ t)$$
$$= (\mu_{A \oplus Z}(t.X) - \mu_A(t.X)) \cdot \mu_B(t.Y) + \mu_A(t.X),$$
where $\oplus$ denotes the addition of fuzzy numbers.

Example 2. Let us consider the relation *secondhandcars* introduced in Example 1 with the following extension:

$t_8 = \langle 19,$ Ford, Focus, 2005, 6000, 80000, $75\rangle$,
$t_9 = \langle 21,$ Renault, Clio, 2002, 6000, 60000, $75\rangle$,
$t_{10} = \langle 132,$ Citroen, C1, 2006, 4000, 50000, $60\rangle$,
$t_{11} = \langle 75,$ Peugeot, 307, 2004, 7500, 50000, $90\rangle$,
$t_{12} = \langle 57,$ Opel, Astra, 2008, 10000, 55000, $115\rangle$

and the query looking for cars whose horsepower is more than 55 and whose price is all the less cheap as their mileage is low. The predicate *cheap* is defined as in Example 1, and *low* as follows:

$$\mu_{low}(m) = \begin{cases} 1 \text{ if } m \leq 50,000, \\ 1 \text{ if } m \geq 70,000, \\ \text{linear in-between.} \end{cases}$$

If we assume that the weakening is done using a translation (to the right in this case) whose magnitude is $\tau = 100$, we have to compute for each tuple t:

$$(\mu_{more\ or\ less\ cheap}(t.price - \tau) -$$
$$\mu_{cheap}(t.price)) \cdot \mu_{low}(t.mileage) + \mu_{cheap}(t.price)$$

which leads to:

0.6/t_8 since $\mu_{low}(80000) = 0, \mu_{cheap}(6000) = 0.6,$
$\mu_{more\ or\ less\ cheap}(6000) = 1,$
0.8/t_9 since $\mu_{low}(60000) = 0.5, \mu_{cheap}(6000) = 0.6,$
$\mu_{more\ or\ less\ cheap}(6000) = 1,$
1/t_{10} since $\mu_{low}(50000) = 1, \mu_{cheap}(4000) = 1,$
$\mu_{more\ or\ less\ cheap}(4000) = 1,$
0.4/t_{11} since $\mu_{low}(50000) = 1, \mu_{cheap}(7500) = 0,$
$\mu_{more\ or\ less\ cheap}(7500) = 0.4,$
0/t_{12} since $\mu_{low}(55000) = 0.75, \mu_{cheap}(10000) = 0,$
$\mu_{more\ or\ less\ cheap}(10000) = 0.$

By the way, it is worth noticing that the approach chosen for the interpretation of "price *is* cheap *all the less as* mileage *is* low" is not equivalent to "price *is all the cheaper as* mileage *is not* low", which is not quite surprizing. For tuple t_9, this second interpretation would lead to the grade 0.4 ($(0.2 - 0.6) * 0.5 + 0.6$) instead of 0.8.$\diamond$

V. A derived implication and its application to database querying

A. Deriving an implication from "all the more as"

Let us come back to the expression of the predicate "*X is A all the more as Y is B*" and the reinforcement of predicate A using an Archimedean norm $\top$:

$$atma(A,\ B)(t) = f_1(A,\ B,\ n,\ t)$$
$$= (\mu_{\top^n(A)}(t.X) - \mu_A(t.X)) \cdot \mu_B(t.Y) + \mu_A(t.X).$$

One may observe that this formula rewrites:

$$(\top^n(q) - q) \cdot p + q$$

letting $p = \mu_B(t.Y), q = \mu_A(t.X)$. This latter formula may be calculated for any two quantities p and q of the unit interval.

Let us now define:

$$I_{(\top,\, n)}(p,\, q) = \begin{cases} 1 \text{ if } p = 0, \\ (\top^n(q) - q) \cdot p + q \text{ otherwise,} \end{cases}$$

where $\top$ denotes a non idempotent norm. Operator $I_{(\top,\, n)}$ complies with the following four properties:

- $\forall q,\, p_1 < p_2 \Rightarrow I_{(\top,\, n)}(p_1,\, q) \geq I_{(\top,\, n)}(p_2,\, q)$ since the term $(\top^n(q) - q)$ is negative,
- $\forall p,\, q_1 < q_2 \Rightarrow I_{(\top,\, n)}(p,\, q_1) \leq I_{(\top,\, n)}(p,\, q_2)$ since $I_{(\top,\, n)}(p,\, q_2) - I_{(\top,\, n)}(p,\, q_1) = (q_2 - q_1) \cdot (1 - p)) + (\top^n(q_2) - \top^n(q_1)) \cdot p$, where $(q_2 - q_1) > 0$ and $(\top^n(q_2) - \top^n(q_1)) \geq 0$ from Axiom S1,
- $\forall q,\, I_{(\top,\, n)}(0,\, q) = 1$ — by definition
- $\forall p,\, I_{(\top,\, n)}(p,\, 1) = 1$ since $I_{(\top,\, n)}(p,\, 1) = (\top^n(1) - 1) \cdot p + 1 = 1$.

So, this operator satisfies four of the most cited (see e.g., [4]) properties of fuzzy implications. The fact that $(1 \Rightarrow_f q = q)$ does not hold, but instead $(1 \Rightarrow_f q = \top^n(q))$ (for instance q^n with the product), may be considered acceptable in view of a "reinforcement-based implication", which could be seen as a new type of fuzzy implication, in addition to R-implications and S-implications in particular (see [3]).

B. Application to inclusion queries

We now tackle queries calling on an inclusion. For instance, consider the fuzzy relation *Profile* whose schema is (*emp, skill*) describing the skills possessed by the employees of a company along with a given level (between 0 and 1). The query looking for the employees whose set of skills is included in that associated with John writes:

select *emp* **from** *Profile* **where** emp $\neq$ "John"
group by *emp* **having set**(*skill*) **included-in**
(**select** *skill* **from** *Profile* **where** *emp* = "John")

in an SQL-like language (e.g., SQLf) equipped with a gradual operator (*included-in*) aimed at assessing the extent to which a fuzzy set is included in another. Usually, the interpretation of the inclusion operator is founded on an implication:

$$E \subseteq F \Leftrightarrow \forall x \in X,\, x \in E \Rightarrow x \in F$$

which, for the query above, should be extended with a fuzzy implication (denoted by $\rightarrow_f$) as:

$$deg(E \subseteq F) = min_{x \in X}\, \mu_E(x) \rightarrow_f \mu_F(x).$$

Different semantics of the inclusion are obtained depending on the family of fuzzy implication taken. An R-implication naturally extends the usual implication in the sense that if E is included in F according to Zadeh ($\forall x \in X,\, \mu_E(x) \leq \mu_F(x)$) the maximal degree (1) is returned, while an S-implication leads to a more demanding type of inclusion where full satisfaction is reached when the support of E is included in the core of F. Of course, the use of $I_{(\top,\, n)}$ gives birth to a third kind of semantics, more demanding than S-implications, for which 1 is obtained only when q = 1. Here, an element x of X must be in F all the more as it is in E according to the behavior of the connective *all the more as* at the heart of implication $I_{(\top,\, n)}$.

Example 3. With the following extension of relation *Profile*:

1/⟨John, A⟩, 0.7/⟨John, B⟩, 0.3/⟨John, C⟩,
0.6/⟨Peter, A⟩, 1/⟨Peter, B⟩, 0.1/⟨Peter, D⟩,
0.1/⟨Mary, A⟩, 0.2/⟨Mary, B⟩, 0.4/⟨Mary, C⟩,
0.9/⟨Jebediah, A⟩, 1/⟨Jebediah, C⟩

the results of the previous query are:

- with Gödel implication ($p \rightarrow_{Gd} q = 1$ if $p \leq q$, q otherwise): {0.3/Mary, 0.3/Jebediah}
- with Kleene-Dienes implication ($p \rightarrow_{KD} q = max(1 - p,\, q)$): {0.7/Peter, 0.6/Mary, 0.3/Jebediah} ,
- with $I_{(\top,\, n)}$ using $\top(x,\, y) = x.y$ and $n = 2$: {0.216/Mary, 0.09/Jebediah}. ⋄

VI. Conclusion

In this paper, we have proposed a new connective that gives birth to a new semantics for the aggregation of two predicates. The new predicate obtained writes "*X is A all the more as Y is B*" and the idea is to use a predicate B to reinforce predicate A into *very* A. The strengthening operates in a linear way, i.e., A applies when B is false and when B is true the result is μ_{veryA}. Strengthening A using a composition via an Archimedean norm, a translation or an erosion operation turns out to be appropriate to guarantee that reasonable properties hold for the new predicate "*X is A all the more as Y is B*". Such a predicate can be used in selection operations, but it may also serve as a basis for defining an implication operator. So, we are provided with a means to define a new type of inclusion conveying the notion of reinforcement. This work opens several perspectives, especially that of implementing the new selection and inclusion operator in the SQLf language.

References

[1] G. Bordogna and G. Pasi, "A fuzzy query language with a linguistic hierarchical aggregator," in *Proc. of ACM Symposium on Applied Computing (SAC'96)*, 1994, pp. 184–187.

[2] D. Dubois and H. Prade, "Using fuzzy sets in flexible querying: Why and how," in *Proc. of the International Conference on Flexible Query-Answering Systems (FQAS'96)*, 1996, pp. 89–103.

[3] B. Bouchon-Meunier, D. Dubois, L. Godo, and H. Prade, "Fuzzy sets and possibility theory in approximate and plausible reasoning," in *Fuzzy Sets in Approximate Reasoning and Information Systems*, D. D. J.C. Bezdek and H. Prade, Eds. Kluwer Academic Publishers, 1999, pp. 15–190.

[4] J. Fodor and R. Yager, "Fuzzy-set theoretic operators and quantifiers," in *Fundamentals of Fuzzy Sets*, D. Dubois and H. Prade, Eds. Kluwer Academic Publishers, 1999, pp. 125–193.

[5] P. Bosc and O. Pivert, "SQLF: a relational database language for fuzzy querying," *IEEE Transactions on Fuzzy Systems*, vol. 3, pp. 1–17, 1995.

[6] L. Zadeh, "Fuzzy sets," *Information and Control*, vol. 8, pp. 338–353, 1965.

[7] B. Bouchon-Meunier and J. Yao, "Linguistic modifiers and imprecise categories," *International Journal of Intelligent Systems*, vol. 7, pp. 25–36, 1992.

[8] D. Dubois and H. Prade, "Weighted minimum and maximum operations in fuzzy set theory," *Information Sciences*, vol. 39, pp. 205–210, 1986.

[9] P. Bosc, A. Hadjali, and O. Pivert, "Empty versus overabundant answers to flexible relational queries," *Journal of Fuzzy Sets and Systems*, vol. 159, pp. 1450–1467, 2008.

[10] D. Dubois and H. Prade, "Inverse operations for fuzzy numbers," in *Proc. of IFAC Symposium on Fuzzy Information, Knowledge Representation and Decision Analysis*, 1983, pp. 391–395.

2011 IEEE International Conference on Fuzzy Systems
June 27-30, 2011, Taipei, Taiwan

Studying the Behavior of a Multiobjective Genetic Algorithm to design Fuzzy Rule-Based Classification Systems for Imbalanced Data-Sets

Pedro Villar
Dept. of Software Engineering
University of Granada
Granada, Spain
Email: pvillarc@ugr.es

Alberto Fernández
Dept. of Computer Science
University of Jaén
Jaén, Spain
Email: alberto.fernandez@ujaen.es

Francisco Herrera
Dept. of Computer Science and
Artificial Intelligence
University of Granada
Granada, Spain
Email: herrera@decsai.ugr.es

***Abstract*—This paper studies the behavior of a multiobjective Genetic Algorithm for jointly performing a feature selection and granularity learning for Fuzzy Rule-Based Classification Systems in the scenario of imbalanced data-sets. We refer to imbalanced data-sets when the class distribution is not uniform, a situation that it is present in many real application areas.**

We consider two different measures, one for the precision of the model and other for its complexity as the two objectives to optimize. In one previous approach, we aggregate these two measures in a single-objective Genetic Algorithm, and thus, a multiobjective approach of that Genetic Algorithm would yield a set of models with different trade-off between high accuracy and low complexity rather than a unique model, provided by the single-objective Genetic Algorithm. The experimental analysis, carried out over a wide range of imbalanced data-sets, shows that our approach is able to obtain a set of models with good trade-off between the two objectives considered but it is an open problem how to select the solution with best prediction ability from the whole set of solutions obtained.

***Index Terms*—Fuzzy Rule-Based Classification Systems, imbalanced data-sets, Multiobjective Genetic Algorithms, feature selection, granularity level.**

I. Introduction

Fuzzy Rule Based Classification Systems (FRBCSs) are considered a very useful tool in the framework of computational intelligence, since they provide a very interpretable model for the end user [1]. An FRBCS presents two main components: the Inference System and the Knowledge Base (KB). The KB is composed of the Rule Base (RB) constituted by the collection of fuzzy rules, and of the Data Base (DB), containing the membership functions of the fuzzy partitions associated to the linguistic variables. The composition of the KB of an FRBCS directly depends on the problem being solved. If there is no expert information about the problem under solving, an automatic learning process must be used to derive the KB from examples.

The problem of imbalanced data-sets [2] for binary classification occurs when the number of instances for each class are very different between them, which can lead to a good classification of the majority class and a poor accuracy on the minority examples. Furthermore, the less representative class is usually the one which has more interest from the point of view of the learning task [3]. We must stress the importance of imbalanced data-sets, since such type of data appears in most of the real domains of classification such as medical diagnosis, finances, bioinformatics, image recognition and so on. The good behavior of FRBCS when dealing with imbalanced data-sets has been recently analyzed in [4].

Unfortunately, the use of FRBCSs in problems that presents a high number of features can originate RBs with a large number of rules, thus presenting a low degree of interpretability and a possible overfitting (the error over the training data-set is very low but the FRBCS present a significative decrease on the prediction ability). This problem can be addressed from a feature selection process that reduces the number of features used by the FRBCS.

On the other hand, the number of labels per linguistic variable (granularity) is an information that has not been considered to be relevant for the majority of FRBCS learning methods. The usual way to proceed involves choosing a number of linguistic terms for each linguistic variable, which is normally the same for all of them (the most used values are the odd numbers between 3 and 7). This operation mode to choose the granularity level is not always appropriate since it has a significant influence on the FRBCS performance. The fuzzy partition granularity of a linguistic variable can be viewed as a sort of context information with a major influence in the FRBCS behavior. Considering a specific label set for a variable, some labels can result irrelevant, that is, they can contribute nothing and even can cause confusion. In other cases, it would be necessary to add new labels to appropriately differentiate the values of the variable. The high influence of granularity in fuzzy modeling has analyzed in [5] and some approaches for automatic learning of the KB in fuzzy modeling and fuzzy classification include the granularity learning [6], [7]. In a previous work [8], we analyze the influence of granularity learning in the performance of FRBCSs for imbalanced data-sets, and the results obtained show that a significant improvement in the classification ability is possible just by learning an adequate number of labels per variable although the complexity of the model was lightly increased.

978-1-4244-7316-8/11/$26.00 ©2011 IEEE

In [9], we proposed a Genetic Algorithm (GA) for jointly perform a feature selection and a granularity learning, considering a classical FRBCS learning method to derive the RB, the Chi et al.'s approach [10]. The main objective of that method was to obtain FRBCS for imbalanced data-sets with high prediction ability joint with a significative reduction of the model complexity in order to increase the FRBCS interpretability. To achieve that purpose, we considered two measures, one for the model accuracy and the other for the model complexity. We aggregated this two measures as the final fitness value of a standard generational GA (single objective). Therefore, the obtained models will have priority on high accuracy or low complexity depending on the relative weights of each measure in the final fitness function. As we were interested in the model with best prediction ability (highest value for the accuracy measure over the test data set), we tested various possibilities for these weighting factors, but the more adequate values are strongly dependent on the data-set considered. The results of that proposal were very promising but there were two drawbacks:

- Selecting the weighting factors. We proposed concrete values that obtained the best average in prediction ability of all the executions tested, but each data-set has its own optimal values.
- The GA provide only one solution. In some cases, designers are more interested in FRBCS with very low complexity rather than the highest prediction ability and it is necessary several executions of the GA with different weighting factors for obtaining the FRBCS desired.

It seems logical that these drawbacks can be avoided considering the two values of the fitness function as separate objectives in a Multiobjective Genetic Algorithm (MGA), that generate a set of FRBCSs with different trade-off between models with high accuracy (and normally, high complexity) and models with low complexity (and normally, low accuracy). The advantages of this approach are the elimination of parameters (weighting factors) and the extended set of different solutions obtained in one simple run.

In this paper we study the behavior of a multiobjective version of the GA presented in [9], using the well known Non dominated Sorting Genetic Algorithm (NSGA-II) [11]. In the analysis of results we will study the set of solutions obtained, with special regard to the relationship between the accuracy measure for the training data set and the accuracy measure for the test data set, in order to analyze the possible overfitting. This study can help us to deal with a new problem that appears with this multiobjective approach, the difficulty of determining the prediction ability (accuracy measure for the test data set) from the whole set of solutions obtained, as we will comment in the comparison of this approach with other methods that provide only one solution. There are some recent proposals that use a multiobjective GA for designing Fuzzy systems in classification and regression [12], [13], [14], [15], but these approaches only analyzes the prediction ability in one or a few solutions of the whole set of solutions provided.

We have selected a large collection of imbalanced data-sets from KEEL data-set repository[1] [16] for developing our experimental analysis. In order to deal with the problem of imbalanced data-sets we will make use of a preprocessing technique, the "Synthetic Minority Over-sampling Technique" (SMOTE) [17], to balance the distribution of training examples in both classes.

This paper is organized as follows. First, Section II and Section III introduce, respectively, the preliminary concepts of FRBCSs and imbalanced data-sets used in this paper. Next, in Section IV we will expose our proposal, a MGA for feature selection and granularity learning. Section V describes the experimental study and finally, in Section VI, some conclusions will be pointed out.

II. Fuzzy Rule Based Classification Systems

Any classification problem consists of m training patterns $x_p = (x_{p1}, \ldots, x_{pn})$, $p = 1, 2, \ldots, m$ from M classes where x_{pi} is the ith attribute value ($i = 1, 2, \ldots, n$) of the p-th training pattern.

In this work we use fuzzy rules of the following form for our FRBCSs:

$$\text{Rule } R_j: \text{ If } x_1 \text{ is } A_{j1} \text{ and } \ldots \text{ and } x_n \text{ is } A_{jn} \text{ then Class = } C_j \text{ with } RW_j \quad (1)$$

where R_j is the label of the jth rule, $x = (x_1, \ldots, x_n)$ is an n-dimensional pattern vector, A_{ji} is an antecedent fuzzy set, C_j is a class label, and RW_j is the rule weight [18]. We use triangular MFs as antecedent fuzzy sets.

In order to build the RB, we have chosen a classical and simple FRBCS, following the same scheme as our previous works [4], [19], [8], [9]: the Chi *et al.*'s rule generation method [10]. This FRBCS design method is an extension of the well-known Wang and Mendel method [20] to classification problems.

III. Basic concepts on imbalanced data-sets

Learning from imbalanced data is an important topic that has recently appeared in the Machine Learning community [2]. We refer to imbalanced data when the class distribution is not uniform. In this situation, the number of examples that represents one of the classes of the data-set (usually the concept of interest) is much lower than that of the other classes.

Standard classifier algorithms have a bias towards the majority class, since the rules that predicts the higher number of examples are positively weighted during the learning process in favor of the accuracy metric. Consequently, the instances that belongs to the minority class are misclassified more often than those belonging to the majority class [21].

We will use the imbalance ratio (IR) [22] as a threshold to categorize the different imbalanced scenarios, which is defined as the ratio of the number of instances of the majority class and the minority class. We consider that a data-set presents a high degree of imbalance when its IR is higher than 9 (less than 10% of positive instances).

[1] http://www.keel.es/dataset.php

In a previous work on this topic [4], we analysed the cooperation of some preprocessing methods with FRBCSs, showing a good behavior for the oversampling methods, specially in the case of the SMOTE methodology [17]. We will employ in this contribution the same SMOTE algorithm in order to deal with imbalanced data-sets. In short, its main idea is to form new minority class examples by interpolating between several minority class examples that lie together. Thus, the overfitting problem is avoided and causes the decision boundaries for the minority class to spread further into the majority class space.

Most of proposals for automatic learning of classifiers use some kind of accuracy measure like the classification percentage over the example set. However, these measures can lead to erroneous conclusions working with imbalanced data-sets since it doesn't take into account the proportion of examples for each class. So, in this work we use the Area Under the Curve (AUC) metric [23], which can be defined as

$$AUC = \frac{1 + TP_{rate} - FP_{rate}}{2} \tag{2}$$

where TP_{rate} is the percentage of positive cases correctly classified as belonging to the positive class and FP_{rate} is the percentage of negative cases misclassified as belonging to the positive class.

IV. Multiobjective Genetic Algorithm for Feature Selection and Granularity Learning

The proposed method is a multiobjective approach of a genetic process for the DB learning that allows us to select a set of variables (feature selection) and learn an adequate number of labels for each selected variable (granularity learning), that was proposed in [9]. The possible values considered for the granularity are taken from the set $\{2, \ldots, 7\}$. Once the granularity for each selected feature is determined, the DB is built. Uniform partitions with triangular membership functions are considered due to its simplicity. Next, we use a quick method that derives the fuzzy classification rules and then the whole KB is obtained. We must recall from a previous section that the RB learning algorithm used in this work is the method proposed in [10], that we have called the Chi et al.'s rule generation method.

We denote our proposal as MGA-FS-GL (Multiobjective GA for Feature Selection and Granularity Learning). The main purpose of MGA-FS-GL is to obtain a set of FRBCSs with different trade-off between good accuracy and reduced complexity taking the feature selection and granularity learning as a base. We have used the well known Non dominated Sorting Genetic Algorithm (NSGA-II [11]) as MGA scheme. Next, we describe the main components of MGA-FS-GL.

A. Encoding the DB

For a classification problem with *N* variables, each chromosome will be composed of two parts to encode the relevant variables and the number of linguistic terms for variable (i.e. the granularity):

- Relevant variables (C_V): the selected features are stored in a binary coded array of length N. In this array, an 1 indicates that the correspondent variable is selected for the FRBCS.
- Granularity level (C_G): the number of labels per variable is stored in an integer array of length *N*. The possible values are taken from the set $\{2, \ldots, 7\}$.

If v_i is the bit that represents whether the variable i is selected and g_i is the granularity of variable i, a representation of the chromosome is shown next:

$$C_V = (v_1, v_2, \ldots, v_N) \quad C_G = (g_1, g_2, \ldots, g_N) \quad C = C_V C_G$$

It would be possible to merge both parts considering only an integer array, for example, including the value 1 as a placeholder for not using the variable. We use the two parts coding scheme to assign the same importance to both parts and to make easy the possibility of removing features as the mutation on the first part of the chromosome changes a selected variable for a non selected variable.

B. Initial Gene Pool

The initial population is composed of six groups with a different number of selected variables. Let g be the cardinality of the significant term set for the C_V part, in our case $g = 6$, corresponding to the six possibilities for the number of labels $(2 \ldots 7)$. The generation of the initial population is described below:

- In the first group all the chromosomes have all the features selected that is, $C_V = (1, 1, 1, \ldots, 1)$. It is composed of $g+10$ chromosomes. The first g individuals have the same granularity in all its variables. For each granularity level, one individual is created. In the second 10 chromosomes the granularity level is randomly selected.
- The next four groups have the same structure than the first group but each one of them with a different percentage of randomly selected variables (75%, 50%, 25% and 10%). So, each group has $g+10$ chromosomes (16 in our case).
- The last group is composed for the remaining chromosomes, and all of their components are randomly selected.

The minimum number of individuals is the sum of the chromosomes of the five first groups: $(g + 10) \times 5$ (80 for our proposal). We try to cover a wide zone of the search space with this population.

C. Evaluating the chromosome

There are three steps that must be done to evaluate each chromosome:

- Generate the DB using the information contained in the chromosome. For all the selected variables ($v_i = 1$), a uniform fuzzy partition with triangular membership functions is built considering the number of labels of that variable (g_i).
- Generate the RB by running the the Chi et al.'s method.
- Calculate the two measure values of the resultant FRBCS:
  - Accuracy measure: AUC metric over the training data-set (AUC_{Tr}).
  - Complexity measure: the sum of the granularity levels of all the selected variables (denoted by Ng

in the following). By using this values as complexity measure, as an example, the following situations are considered equivalent:

- Selection of 6 features of granularity 2
- Selection of 4 features of granularity 3
- Selection of 3 features of granularity 4
- Selection of 2 features of granularity 6

Finally, MGA-FS-GL considers two objectives to be minimized:

- $1 - AUC_{Tr}$ (as accuracy objective)
- Ng/N (as complexity objective)

D. Genetic operators

1) Crossover: The crossover works in the two parts of the chromosome at the same time. Therefore, an standard crossover operator is applied over C_V and C_G. This operator performs as follows: a crossover point p is randomly generated and the two parents are crossed at the p-th variable (the possible values for p are $\{2, \ldots, N\}$). The crossover is developed this way in the two chromosome parts, C_V and C_G, thereby producing two meaningful descendants.

2) Mutation: . Two different operators are used, each one of them acting on different chromosome parts. A brief description of them is given below:

- *Mutation on* C_V: As this part of the chromosome is binary coded, a simple binary mutation is developed, flipping the value of the gene.
- *Mutation on* C_G: The mutation operator selected for C_G performs a slight change in the selected variable. Once a granularity level is randomly selected to be muted, a local modification is developed by changing the number of labels of the variable to the immediately upper or lower value (the decision is made at random). When the value to be changed is the lowest (2) or highest one (7), the only possible change is developed.

V. Experimental study

We will study the performance of MGA-FS-GL employing a large collection of imbalanced data-sets with different imbalance ratio (IR). We divide the data-sets in two main groups:

- Data-sets with high imbalance :$IR > 9$
- Data-sets with low imbalance :$IR < 9$

Specifically, we have considered forty-four data-sets with different IR (twenty-two of each group) from KEEL data-set repository [16], which are publicly available on the corresponding web-page (http://www.keel.es/dataset.php), including general information about them. Table I show these data-sets, where we denote the number of examples (#Ex.), number of attributes (#Atts.), class name of each class (minority and majority), class attribute distribution and IR. This table is in ascendant order according to the IR. For the sake of obtaining binary imbalanced problems, the positive and negative classes are defined as the joint of one or more classes, which are specified in column *Class* of Table I separated by a semicolon. In order to reduce the effect of imbalance, we will employ the SMOTE preprocessing method [17] for all our experiments, considering only the 1-nearest neighbor to generate the synthetic samples, and balancing both classes to the 50% distribution.

To develop the different experiments we consider a *5-folder cross-validation model*, i.e., 5 random partitions of data with a 20%, and the combination of 4 of them (80%) as training and the remaining one as test. For each data-set we consider the average results of the five partitions. The data partitions used in this paper can be found in KEEL-dataset repository [41].

The configuration for the FRBCS is presented in Table II being "Conjuction operator" the operator used to compute the compatibility degree of the example with the antecedent of the rule and the operator used to compute the compatibility degree and the rule weight. This parameter selection has been carried out according to the results achieved by the Chi et al.'s method in our former studies on imbalanced data-sets [4]:

TABLE II
Configuration for the FRBCS

Conjunction operator:	Product T-norm
Rule Weight:	Penalized Certainty Factor [18]
Fuzzy Reasoning Method:	Winning Rule

The specific parameters setting for the GA of MGA-FS-GL is listed below, being N the number of variables:

- Number of evaluations: $1000 \cdot N$
- Population Size: 100 individuals
- Crossover Probability P_c : 1.0
- Mutation Probability P_m : 0.2

The final result of MGA-FS-GL is a set of non dominated solutions i.e., none of them is better than another in the two objectives. This set is called the *Pareto front*. The usual way to analyze the results of a classification model in machine learning involves a comparison among the obtained model and the models obtained for other learning methods used in the specialized literature, including an statistical analysis of various measures being the prediction ability (in our case, the AUC_{Tst}) the main one. So, only one solution for each data-set is used in the comparison. In the case of a cross-validation scheme, it is used the mean of the unique solution obtained for each combination of training set/test set.

Therefore, it is difficult to show, in the previous way, the results of MGA-FS-GL because there are not five solutions for each data-set but five sets of non dominated solutions and the cardinality of that sets (Pareto fronts) is usually different. Thus, it is not possible to establish a comparison among the five sets of FRBCSs obtained for each data-set due to the different number of non dominated solutions and it is not possible to compare one solution (obtained for the reference models) opposite to a set of solutions. A possible way to deal with this problem was proposed in [12], where three different non dominated solutions were selected from the whole Pareto fronts and then, these models can be used as individual solutions for comparison with classical methods:

- The best solution for the accuracy objective (greatest value in AUC_{Tr}), named best accuracy (BA)

TABLE I
SUMMARY DESCRIPTION FOR IMBALANCED DATA-SETS

Data-set	#Ex.	#Atts.	Class (min., maj.)	%Class(min.; maj.)	IR
Data-sets with Low Imbalance (IR 1.5 to 9)					
Glass1	214	9	(build-win-non_float-proc; remainder)	(35.51, 64.49)	1.82
Ecoli0vs1	220	7	(im; cp)	(35.00, 65.00)	1.86
Wisconsin	683	9	(malignant; benign)	(35.00, 65.00)	1.86
Pima	768	8	(tested-positive; tested-negative)	(34.84, 66.16)	1.90
Iris0	150	4	(Iris-Setosa; remainder)	(33.33, 66.67)	2.00
Glass0	214	9	(build-win-float-proc; remainder)	(32.71, 67.29)	2.06
Yeast1	1484	8	(nuc; remainder)	(28.91, 71.09)	2.46
Vehicle1	846	18	(Saab; remainder)	(28.37, 71.63)	2.52
Vehicle2	846	18	(Bus; remainder)	(28.37, 71.63)	2.52
Vehicle3	846	18	(Opel; remainder)	(28.37, 71.63)	2.52
Haberman	306	3	(Die; Survive)	(27.42, 73.58)	2.68
Glass0123vs456	214	9	(non-window glass; remainder)	(23.83, 76.17)	3.19
Vehicle0	846	18	(Van; remainder)	(23.64, 76.36)	3.23
Ecoli1	336	7	(im; remainder)	(22.92, 77.08)	3.36
New-thyroid2	215	5	(hypo; remainder)	(16.89, 83.11)	4.92
New-thyroid1	215	5	(hyper; remainder)	(16.28, 83.72)	5.14
Ecoli2	336	7	(pp; remainder)	(15.48, 84.52)	5.46
Segment0	2308	19	(brickface; remainder)	(14.26, 85.74)	6.01
Glass6	214	9	(headlamps; remainder)	(13.55, 86.45)	6.38
Yeast3	1484	8	(me3; remainder)	(10.98, 89.02)	8.11
Ecoli3	336	7	(imU; remainder)	(10.88, 89.12)	8.19
Page-blocks0	5472	10	(remainder; text)	(10.23, 89.77)	8.77
Data-sets with High Imbalance (IR higher than 9)					
Yeast2vs4	514	8	(cyt; me2)	(9.92, 90.08)	9.08
Yeast05679vs4	528	8	(me2; mit,me3,exc,vac,erl)	(9.66, 90.34)	9.35
Vowel0	988	13	(hid; remainder)	(9.01, 90.99)	10.10
Glass016vs2	192	9	(ve-win-float-proc; build-win-float-proc, build-win-non_float-proc,headlamps)	(8.89, 91.11)	10.29
Glass2	214	9	(Ve-win-float-proc; remainder)	(8.78, 91.22)	10.39
Ecoli4	336	7	(om; remainder)	(6.74, 93.26)	13.84
Yeast1vs7	459	8	(vac; nuc)	(6.72, 93.28)	13.87
Shuttle0vs4	1829	9	(Rad Flow; Bypass)	(6.72, 93.28)	13.87
Glass4	214	9	(containers; remainder)	(6.07, 93.93)	15.47
Page-blocks13vs2	472	10	(graphic; horiz.line,picture)	(5.93, 94.07)	15.85
Abalone9vs18	731	8	(18; 9)	(5.65, 94.25)	16.68
Glass016vs5	184	9	(tableware; build-win-float-proc, build-win-non_float-proc,headlamps)	(4.89, 95.11)	19.44
Shuttle2vs4	129	9	(Fpv Open; Bypass)	(4.65, 95.35)	20.5
Yeast1458vs7	693	8	(vac; nuc,me2,me3,pox)	(4.33, 95.67)	22.10
Glass5	214	9	(tableware; remainder)	(4.20, 95.80)	22.81
Yeast2vs8	482	8	(pox; cyt)	(4.15, 95.85)	23.10
Yeast4	1484	8	(me2; remainder)	(3.43, 96.57)	28.41
Yeast1289vs7	947	8	(vac; nuc,cyt,pox,erl)	(3.17, 96.83)	30.56
Yeast5	1484	8	(me1; remainder)	(2.96, 97.04)	32.78
Ecoli0137vs26	281	7	(pp,imL; cp,im,imU,imS)	(2.49, 97.51)	39.15
Yeast6	1484	8	(exc; remainder)	(2.49, 97.51)	39.15
Abalone19	4174	8	(19; remainder)	(0.77, 99.23)	128.87

- The solution with the worst value for the accuracy objective (lowest value in AUC_{Tr}). So, the one with the less value for the complexity objective, named best interpretability (BI)
- The solution with the intermediate value for both objectives, named intermediate (I)

Therefore, these chosen solutions can be considered a brief sample of the whole set of solutions with different trade-off between accuracy and interpretability. Table III present the detailed results for these three selected solutions, showing the expected trend in the prediction ability: the most accurate solutions present certain overfitting. The intermediate solutions have a better behavior, since they present a good prediction ability (AUC_{Tst} lightly worse than the previous) and better interpretability (less number of rules) than the previous. The solutions with best interpretability have a very poor prediction ability since they are models with very few number of rules (normally, with only one feature selected).

One way to obtain more accurate solutions with good interpretability is to choose the FRBCS with at least two variables selected, and with the lowest value for the complexity measure. In fact, it would be easy to change MGA-FS-GL to ignore the models with only one selected feature, reducing the search space. However, we think that it is interesting to obtain these models as they provide information on what is the most relevant variable and, in some data-sets, the solution with best interpretability present a good prediction ability (*Yeast6, Yeast2vs4*) and the best prediction ability in one case (*Yeast05679vs4*).

Now, We will compare these solutions of MGA-FS-GL with the models obtained for the following methods:

- The method proposed in [9] (denoted GA-FS-GL). The single objective GA version of MGA-FS-GL where the fitness function is the weighted aggregation of the two objective values.

TABLE III
DETAILED TABLE OF RESULTS FOR THE SELECTED SOLUTIONS OF MGA-FS-GL

Dataset	Best-Accuracy			Intermediate			Best-Interpretability			#Non-Dom.
	Auc_{Tr}	Auc_{Tst}	#Rules	Auc_{Tr}	Auc_{Tst}	#Rules	Auc_{Tr}	Auc_{Tst}	#Rules	
Data-Sets with Low Imbalance (1.5 <= IR < 9)										
Glass1	83.14	62.85	79.20	72.86	65.93	33.20	49.75	48.31	1.60	10.40
Ecoli0vs1	98.70	95.66	62.80	84.40	86.58	12.40	66.34	66.22	2.00	6.20
Wisconsin	99.94	52.25	400.60	94.61	90.30	249.80	46.57	45.88	2.80	12.60
Pima	88.35	66.50	527.20	78.02	69.30	242.80	58.24	56.94	1.80	15.00
Iris0	99.63	99.50	9.20	95.38	93.50	5.20	88.00	88.00	2.00	4.80
Glass0	85.64	71.75	99.60	74.12	72.32	27.80	50.00	50.00	3.00	7.20
Yeast2	74.42	69.86	319.60	69.81	68.46	94.00	55.31	54.30	2.20	10.20
Vehicle2	98.12	86.64	798.60	86.21	81.62	397.60	49.86	49.77	1.80	12.20
Vehicle1	94.62	67.09	823.20	73.96	64.67	397.20	50.11	50.44	1.20	18.00
Vehicle3	94.82	60.77	829.80	73.04	65.25	448.60	50.00	50.00	1.60	17.80
Haberman	73.68	55.02	63.20	65.58	61.50	14.40	51.64	46.75	2.20	11.00
Glass0123vs456	99.29	78.67	105.20	89.35	87.42	29.00	47.24	47.23	4.20	11.40
Vehicle0	98.47	84.23	818.00	87.59	85.60	306.80	50.00	50.00	6.00	16.40
Ecoli1	94.31	84.88	132.80	80.60	78.57	31.00	75.70	75.57	2.00	10.00
New-Thyroid2	99.31	96.63	39.60	91.01	92.66	12.40	76.56	77.14	2.00	7.20
New-Thyroid1	99.93	93.45	47.00	92.50	88.06	11.40	76.55	76.83	2.00	7.60
Ecoli2	95.14	84.77	155.60	87.69	84.74	32.20	49.84	46.73	4.40	10.40
Segment0	99.41	97.62	801.60	88.31	87.90	496.60	52.06	51.73	3.00	12.60
Glass6	98.59	84.23	107.20	94.45	86.80	53.80	64.88	66.22	2.00	9.80
Yeast3	94.79	91.41	334.80	83.41	83.40	79.80	61.37	60.94	2.00	8.20
Ecoli3	95.93	89.65	154.80	88.87	89.62	21.40	79.23	79.03	2.00	9.00
Page-Blocks0	89.74	87.27	292.20	81.17	80.04	48.80	49.93	49.82	2.40	12.00
Mean	93.45	80.03	318.26	83.31	80.19	138.46	59.05	58.54	2.46	10.91
Data-Sets with High Imbalance (IR >= 9)										
Yeast2vs4	95.20	86.86	205.80	90.34	89.04	25.40	82.32	81.96	2.00	8.80
Yeast05679vs4	90.96	73.72	248.40	83.42	76.17	95.00	79.60	79.54	2.00	11.60
Vowel0	99.92	95.55	698.40	95.42	93.99	278.80	49.99	50.00	1.20	17.20
Glass016vs2	83.73	58.52	95.00	70.91	60.64	31.60	49.93	50.00	2.00	12.80
Glass2	83.63	55.83	96.00	60.61	55.96	51.40	49.94	50.00	2.20	10.60
Ecoli4	98.62	89.81	110.20	85.86	78.88	15.80	49.92	49.69	4.00	11.00
shuttle0vs4	99.98	99.10	32.00	99.66	99.11	7.80	50.00	49.58	1.40	5.60
yeastB1vs7	86.98	67.21	210.60	72.20	71.48	34.60	61.79	60.61	2.00	12.00
Glass4	99.38	86.43	114.00	82.27	78.77	38.20	16.92	16.93	3.00	11.20
Page-Blocks13vs4	99.30	94.30	133.60	79.86	80.49	95.20	50.00	50.00	2.00	8.80
Abalone9-18	79.59	73.24	131.40	55.79	54.91	3.20	50.00	50.00	2.80	8.40
Glass016vs5	98.57	83.43	120.00	94.57	87.57	77.40	50.00	50.00	3.20	14.20
shuttle2vs4	100.00	89.18	24.60	81.35	76.80	5.00	49.59	50.00	4.00	7.80
Yeast1458vs7	86.14	64.84	284.80	71.97	64.41	60.00	60.98	61.74	2.00	12.60
Glass5	98.90	73.90	100.00	88.61	77.20	27.40	56.95	57.56	4.40	10.40
Yeast2vs8	89.00	70.55	136.20	74.52	73.52	24.60	50.39	44.82	2.20	9.60
Yeast4	90.14	85.15	318.40	83.41	81.15	53.00	49.94	49.86	4.00	10.40
Yeast1289vs7	84.99	74.45	233.80	66.05	64.96	42.60	59.55	60.56	2.00	11.00
Yeast5	96.94	92.81	281.80	90.13	89.41	56.40	51.19	50.52	3.00	6.80
Yeast6	93.05	88.06	229.40	87.92	88.04	16.60	86.76	86.83	2.00	6.40
Ecoli0137vs26	97.72	70.45	148.60	90.53	81.54	23.80	50.05	50.00	3.00	10.00
Abalone19	80.09	62.56	267.20	69.92	67.93	63.00	55.19	55.09	2.00	9.20
Mean	92.40	78.91	191.83	80.70	76.91	51.22	55.04	54.79	2.56	10.29
All Data-Sets										
Global	92.93	79.47	255.05	82.00	78.55	94.84	57.05	56.66	2.51	10.60

- The original Chi et al.'s method [10], where a previous definition for the DB is needed, normally by the use of uniform fuzzy partitions with the same number of labels in all the variables. Therefore, it is necessary to choose a number of labels, being the usual values employed for any standard FRBCS approach in the specialized literature 3, 5 and 7 labels per variable. According to this fact, we include these three possibilities in the experimental study. In the latter, we will refer these methods as G3-Chi, G5-Chi, G7-Chi, respectively.
- The method proposed in [8] (denoted GA-GL), that uses a single objective GA (similar to the used in GA-FS-GL) only for granularity learning.
- C4.5 [24], a method of reference in the field of classification with imbalanced data-sets [25], [22].

All the previous methods have all the variables selected except GA-FS-GL, that includes a feature selection in the same way as MGA-FS-GL. The FRBCS approaches (GA-FS-GL, GA-GL, G3-Chi, G5-Chi and G7-Chi) have the same configuration as MGA-FS-GL (Table II)

Table IV shows the mean of the AUC and the number of rules (NR) for the different groups of data-sets (Low imbalance, High Imbalance and all of them). There are three lines for MGA-FS-GL, corresponding with the three solutions selected: best accuracy (BA), intermediate (I) and best interpretability (BI).

As can be observed in Table IV for all the data-sets, the single objective version of the genetic learning process described (GA-FS-GL) presents the best results. Its prediction ability is better than the other methods except for GA-GL. A GA designed only for granularity learning (GA-GL) obtains the best results in prediction ability but with a high increase of the number of rules (less interpretability). Regarding to the complexity of the models (lower NR), GA-FS-GL presents

TABLE IV
AVERAGE TABLE OF RESULTS IN AUC_{Tr}, AUC_{Tst} AND NUMBER OF RULES (NR) FOR THE DIFFERENT DEGREES OF IMBALANCE

Algorithm	Low Imbalance			High Imbalance			All Data-sets		
	AUC_{Tr}	AUC_{Tst}	NR	AUC_{Tr}	AUC_{Tst}	NR	AUC_{Tr}	AUC_{Tst}	NR
G3-Chi	86.03	82.14	124.70	85.09	80.52	68.67	85.56	81.33	96.69
G5-Chi	91.60	81.43	276.93	89.56	78.76	160.20	90.58	80.10	218.56
G7-Chi	93.95	74.40	387.18	93.66	74.90	272.02	93.81	74.65	329.60
GA-GL	92.03	84.20	177.41	91.33	81.98	82.36	91.68	83.09	129.89
GA-FS+GL	85.77	83.53	26.98	85.33	80.91	12.79	85.55	82.22	19.89
C4.5	95.00	86.09	26.05	95.93	78.25	22.45	95.46	82.17	24.25
MGA-FS+GL(BA)	93.45	80.03	318.26	92.40	78.91	191.83	92.93	79.47	255.05
MGA-FS+GL(I)	83.31	80.19	138.46	80.70	76.91	51.22	82.00	78.55	94.84
MGA-FS+GL(BI)	59.05	58.54	2.46	55.04	54.79	2.56	57.05	56.66	2.51

the lesser number of rules, except for the solution with best interpretability of MGA-FS-GL, that presents the worse value for the prediction ability. The improvement of GA-FS-GL in the number of rules is even better in the group of data-sets with high imbalance, demonstrating its suitability to the framework of imbalanced data-sets.

Anyway, None of the three selected solutions of MGA-FS-GL obtain better results on AUC_{Tst} than the obtained with GA-FS-GL (considering the weighting factors proposed in [9]). However, MGA-FS-GL provide models with very good prediction ability in each Pareto front. If we chose the solutions with best AUC_{Tst} for each set of non dominated solutions, the global mean of the AUC_{Tst} for all the data-sets would be 86.32, significantly higher than those obtained with GA-FS-GL and the other methods used for comparison. Hence, MGA-FS-GL performs very well, but the unsolved problem is to find these solutions with the best prediction ability as they occupy different positions along the Pareto front of each data-set. This situation is represented in Figure 1 where the Pareto fronts obtained for MGA-FS-GL in the first partition of four problems are showed (including also the AUC_{Tst} of each non dominated solution). There are different "types" of behavior among the data-sets regarding to the values of AUC_{Tst}:

- In some cases, the values of AUC_{Tst} follow the same trend as AUC_{Tr} (Vowel0). In such data-sets, the trade-off between accuracy and interpretability is also fulfilled for the AUC_{Tst} and the final user can choose the most suitable FRBCS (depending on his preferences) assuming that AUC_{Tr} is similar to the prediction ability in all models. Unfortunately, this situation occurs only in a few data-sets.
- Many data-sets present overfitting, the AUC_{Tst} is then increased from the FRBCS with best AUC_{Tr} to an optimal value from which descends again. This point corresponds to a particular combination of weights in GA-FS-GL, which is specific for each data-set. Therefore, finding this value is a difficult problem to solve. In some cases there are a great overfitting in the solutions with best AUC_{Tr} (Wisconsin) while in other cases the overfitting is lesser and there is a smooth decrease of the AUC_{Tst} from the optimal value (Ecoli3).
- Finally, in other cases, the AUC_{Tst} follows a chaotic behavior (Glass4). So, the data fracture between the training set and the test set is very high and it is impossible to determine the solution with best prediction ability.

As most of the data-sets belong to one of the last two "types", we recommend using GA-FS-GL when the main purpose is to obtain only one model with high prediction ability (and not much complexity), unless there are some evidence to establish that the problem belongs to the first category of the previously described. MGA-FS-GL is particulary useful when many solutions with different trade-off between accuracy and interpretability is required, but it is very difficult to find the solution with best prediction ability, as that measure can not be used in the learning process. Moreover, it is difficult to know the behavior of the accuracy measure in the test data set (compared with the known behavior in training data set), that it would be valuable for selecting the most adequate solution if we were interested, for example, in a solution with a minimum degree of interpretability.

VI. CONCLUSIONS

This contribution analyzes the behavior of a multiobjective version of a previously proposed Genetic Algorithm to design FRBCS for imbalanced data-sets. The genetic learning process is used for feature selection and granularity learning, which is combined with an efficient fuzzy classification rule generation method to obtain the complete KB of the FRBCS.

The proposed approach obtains a set of FRBCSs with different trade-off between accuracy and interpretability in which to find the model with the best prediction ability generally is non evident.

ACKNOWLEDGMENT

This work has been supported by the Spanish ministry of science and technology under project TIN2008-06681-C06-01

REFERENCES

[1] H. Ishibuchi, T. Nakashima, and M. Nii, *Classification and modeling with linguistic information granules: Advanced approaches to linguistic Data Mining*. Springer–Verlag, 2004.

[2] N. V. Chawla, N. Japkowicz, and A. Kolcz, "Editorial: special issue on learning from imbalanced data sets," *SIGKDD Explorations*, vol. 6, no. 1, pp. 1–6, 2004.

[3] M. Mazurowski, P. Habas, J. Zurada, J. Lo, J. Baker, and G. Tourassi, "Training neural network classifiers for medical decision making: The effects of imbalanced datasets on classification performance," *Neural Networks*, vol. 21, no. 2–3, pp. 427–436, 2008.

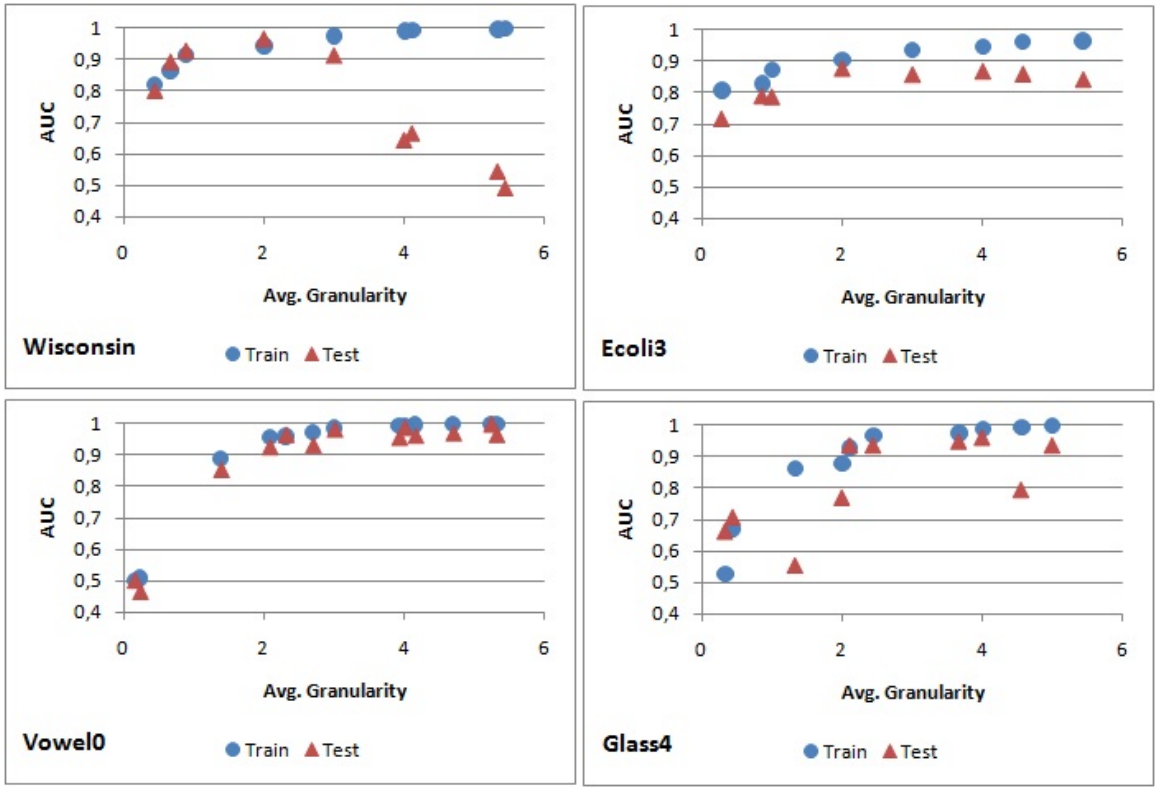

Fig. 1. Pareto fronts

[4] A. Fernández, S. García, M. J. del Jesus, and F. Herrera, "A study of the behaviour of linguistic fuzzy rule based classification systems in the framework of imbalanced data–sets," *Fuzzy Sets and Systems*, vol. 159, no. 18, pp. 2378–2398, 2008.

[5] O. Cordón, F. Herrera, and P. Villar, "Analysis and guidelines to obtain a good uniform fuzzy partition granularity for fuzzy rule–based systems using simulated annealing," *International Journal of Approximate Reasoning*, vol. 25, no. 3, pp. 187–215, 2000.

[6] ——, "Generating the knowledge base of a fuzzy rule–based system by the genetic learning of the data base," *IEEE Transactions on Fuzzy Systems*, vol. 9, no. 4, pp. 667–674, 2001.

[7] O. Cordón, F. Herrera, L. Magdalena, and P. Villar, "A genetic learning process for the scaling factors, granularity and contexts of the fuzzy rule–based system data base," *Information Sciences*, vol. 136, pp. 85–107, 2001.

[8] P. Villar, A. Fernández, and F. Herrera, "A genetic learning of the fuzzy rule–based classification system granularity for highly imbalanced data–sets," in *2009 IEEE International Conference on Fuzzy Systems (FUZZ–IEEE09)*, 2009, pp. 1689–1694.

[9] ——, "A genetic algorithm for feature selection and granularity learning in fuzzy rule-based classification systems for highly imbalanced data-sets," in *13th International Conference on Information Processing and Management of Uncertainty in Knowledge-Based Systems (IPMU2010)*, 2010, pp. 741–750.

[10] Z. Chi, H. Yan, and T. Pham, *Fuzzy algorithms with applications to image processing and pattern recognition*. World Scientific, 1996.

[11] K. Deb, S. Agrawal, A. Pratab, and T. Meyarivan, "A fast and elitist multiobjective genetic algorithm: NSGA–II," *IEEE Transactions on Evolutionary Computation*, vol. 6, no. 2, pp. 182–197, 2002.

[12] R. Alcalá, P. Ducange, F. Herrera, B. Lazzerini, and F. Marcelloni., "A multiobjective evolutionary approach to concurrently learn rule and data bases of linguistic fuzzy rule-based systems," *IEEE Transactions on Fuzzy Systems*, vol. 17, no. 5, pp. 1106–1122, 2009.

[13] F. M. M. Antonelli, P. Ducange and B. Lazzerini, "Learning concurrently partition granularities and rule bases of mamdani fuzzy systems in a multi-objective evolutionary framework," *International Journal of Approximate Reasoning*, vol. 50, no. 7, pp. 1066–1080, 2009.

[14] P. Ducange, B. Lazzerini, and F. Marcelloni, "Multi-objective genetic fuzzy classifiers for imbalanced and cost-sensitive datasets," *Soft Computing*, vol. 14, no. 7, pp. 713–728, 2010.

[15] P. Pulkkinen and H. Koivisto, "A dynamically constrained multiobjective genetic fuzzy system for regression problems," *IEEE Transactions on Fuzzy Systems*, vol. 18, no. 1, pp. 161–177, 2010.

[16] J. Alcalá-Fdez, A. Fernández, J. Luengo, J. Derrac, S. García, L. Sánchez, and F. Herrera, "KEEL data-mining software tool: Data set repository, integration of algorithms and experimental analysis framework," *Journal of Multi-Valued Logic and Soft Computing*, vol. in press, 2011.

[17] N. V. Chawla, K. W. Bowyer, L. O. Hall, and W. P. Kegelmeyer, "SMOTE: Synthetic minority over–sampling technique," *Journal of Artificial Intelligent Research*, vol. 16, pp. 321–357, 2002.

[18] H. Ishibuchi and T. Yamamoto, "Rule weight specification in fuzzy rule–based classification systems," *IEEE Transactions on Fuzzy Systems*, vol. 13, pp. 428–435, 2005.

[19] A. Fernández, M. J. del Jesus, and F. Herrera, "Hierarchical fuzzy rule based classification systems with genetic rule selection for imbalanced data–sets," *International Journal of Approximate Reasoning*, vol. 50, pp. 561–577, 2009.

[20] L. X. Wang and J. M. Mendel, "Generating fuzzy rules by learning from examples," *IEEE Transactions on System, Man and Cybernetics*, vol. 25, no. 2, pp. 353–361, 1992.

[21] G. M. Weiss, "Mining with rarity: a unifying framework," *SIGKDD Explorations*, vol. 6, no. 1, pp. 7–19, 2004.

[22] A. Orriols-Puig and E. Bernadó-Mansilla, "Evolutionary rule–based systems for imbalanced datasets," *Soft Computing*, vol. 13, no. 3, pp. 213–225, 2009.

[23] J. Huang and C. X. Ling, "Using AUC and accuracy in evaluating learning algorithms," *IEEE Transactions on Knowledge and Data Engineering*, vol. 17, no. 3, pp. 299–310, 2005.

[24] J. R. Quinlan, *C4.5: Programs for Machine Learning*. San Mateo–California: Morgan Kaufmann Publishers, 1993.

[25] G. E. A. P. A. Batista, R. C. Prati, and M. C. Monard, "A study of the behaviour of several methods for balancing machine learning training data," *SIGKDD Explorations*, vol. 6, no. 1, pp. 20–29, 2004.

2011 IEEE International Conference on Fuzzy Systems
June 27-30, 2011, Taipei, Taiwan

On the Cooperation of Interval-Valued Fuzzy Sets and Genetic Tuning to Improve the Performance of Fuzzy Decision Trees.

José Antonio Sanz and Humberto Bustince
Department of Automatica y Computacion
Universidad Publica de Navarra
Pamplona, 31006 Spain
Emails: {joseantonio.sanz, bustince}@unavarra.es

Alberto Fernández
Department of Computer Science
University of Jaén
Jaén, 23071 Spain
Email: alberto.fernandez@ujaen.es

Francisco Herrera
Department of Computer Science
and Artificial Intelligence
University of Granada
Granada, 18071 Spain
Email: herrera@decsai.ugr.es

***Abstract*—Fuzzy decision trees are widely employed to face classification problems since they combine the high interpretability given by the decision tree and the capability of management of the uncertainty inherent to fuzzy logic.**

However, the success of fuzzy systems in general depends, to a large degree, on the choice of the membership functions. For this reason, we propose to model the linguistic labels by means of Interval-Valued Fuzzy Sets to take into account the ignorance related to their definition. On the other hand, we define an evolutionary method to tune the shape of the Interval-Valued Fuzzy Sets looking for the best ignorance degree that each Interval-Valued Fuzzy Set represents.

In this contribution, we will make use of the fuzzy ID3 algorithm as a base technique from which to apply our methodology. The experimental study shows how our methodology enhances the performance of the base fuzzy decision tree. Furthermore, we compare our approach with respect to four state-of-the-art fuzzy decision trees and C4.5 as a representative algorithm for crisp decision trees. The goodness of our proposal is tested on a large collection of data-sets and it is supported by an exhaustive statistical analysis.

***Keywords*—Linguistic Fuzzy Rule-Based Classification Systems, Interval-Valued Fuzzy Sets, Ignorance functions, Tuning, Fuzzy Decision Tree, Classification.**

I. Introduction

Classification problem is one of the most studied problems in machine learning and data mining [1]. In order to face this task, a classifier needs to be induced by means of a learning algorithm. The classifier is a model encoding a set of criteria that allows a data instance to be assigned to a particular class depending on the value of certain variables. Different kinds of models, such as fuzzy rule-based classification systems or Fuzzy Decision Trees (FDTs), can be used to represent classifiers.

Specifically, FDTs are a suitable solution to face classification problems due to the good synergy between the handling of the uncertainty provided by fuzzy logic [2] and the good interpretability given by decision trees [3]. Among the large number of techniques proposed in the specialized literature for designing FDTs [4], [5], the fuzzy ID3 algorithm [6] is widely employed since it is a popular and efficient method to construct a FDT [7].

In fuzzy systems, like FDTs, the definition of the membership functions used to represent the linguistic labels is truly significant. When defining the fuzzy partitions, either through expert knowledge or homogeneously over the input space, it is possible to have an ignorance degree (lack of information) which makes their definition difficult. The theory of Interval-Valued Fuzzy Sets (IVFSs) [8] has proved to be a suitable tool to model this ignorance [9]. Specifically, we have shown that the use of IVFSs is useful to improve the performance of fuzzy rule-based classification systems [10].

In this contribution, we propose to model the linguistic labels of the classifier by means of IVFSs. To do so, we use a new parametrized construction method of IVFSs that starts from the fuzzy sets composing the knowledge base of the system. The length of each IVFS is proportional to the degree of ignorance related to the definition of the corresponding membership function, which is measured using weak ignorance functions. We must point out that we introduce the IVFSs after the induction process and we study their influence in the fuzzy reasoning mechanism, which has to be modified to take into account this modeling of the linguistic labels. As a result, a good management of the uncertainty is provided for the system while its interpretability is maintained.

Additionally, we propose the definition of an evolutionary methodology that allows to compute the optimal ignorance degree that each IVFS represents. To do so, we modify the parameters used in the IVFSs construction method to weight the degree of ignorance and consequently, we tune the length of the IVFSs. In this manner, the membership functions will be fine-tuned leading to an improvement of the performance of the system in a general framework.

The aim of our study is to show the goodness of our proposed methodology using the fuzzy ID3 algorithm as the base technique. To do so, we will compare our approach with respect to both the base FDT and with four state-of-the-art FDTs, namely the simple pattern tree [11], a look-ahead approach [12], the FDT proposed by Janikow in [13] and a method which fuzzifies the Gini index [14]. Furthermore, we will also compare our methodology with C4.5 [15]

978-1-4244-7316-8/11/$26.00 ©2011 IEEE

as a reference algorithm of crisp decision trees. In order to obtain well-founded conclusions, we have considered 20 numerical data-sets from the KEEL data-set repository [16] (http://www.keel.es/dataset.php). The measure of performance is based on accuracy rate and the study is supported by the proper statistical analysis, as suggested in the literature [17], [18], [19].

The work is arranged as follows: Section II provides some preliminary concepts of IVFSs and also describes the generation of IVFSs employing weak ignorance functions. The induction process of the fuzzy ID3 algorithm together with the modifications carried out in the reasoning mechanism, due to the use of IVFSs, are shown in Section III. In Section IV we describe in detail our methodology to tune the membership functions by means of GAs and the evolutionary method is also explained. Then, the experimental study is presented in Section V and we finish the work with some concluding remarks in Section VI.

II. Linguistic Labels Modeled by means of Interval-Valued Fuzzy Sets

In this work we propose to model the linguistic labels by means of IVFSs in order to take into account the ignorance related to the definition of the membership functions.

In this section, we remind some theoretical concepts which are necessary to understand the remainder of this contribution. Then, we define the construction method of IVFSs starting from given fuzzy sets in which we employ weak ignorance functions to measure the ignorance associated with the definition of the membership functions. Finally, we present our new methodology to model the linguistic labels by means of IVFSs.

A. Preliminaries

Let us denote by $L([0,1])$ the set of all closed subintervals in $[0,1]$, that is,

$$L([0,1]) = \{\mathbf{x} = [\underline{x}, \overline{x}] | (\underline{x}, \overline{x}) \in [0,1]^2 \text{ and } \underline{x} \leq \overline{x}\}.$$

We also denote $0_L = [0,0]$ and $1_L = [1,1]$.

Definition 1: An interval-valued fuzzy set (IVFS) [20], [21] (or interval type 2 fuzzy set) A on the universe $U \neq \emptyset$ is a mapping $A : U \to L([0,1])$, such that

$$A(u_i) = [\underline{A}(u_i), \overline{A}(u_i)] \in L([0,1]), \text{ for all } u_i \in U.$$

We denote by $\mathcal{FS}(U)$ the set of all fuzzy sets on U and by $\mathcal{IVFS}(U)$ the set of all IVFSs on U. We also denote by W the length of the interval under consideration, that is

$$W(A(u_i)) = \overline{A}(u_i) - \underline{A}(u_i).$$

To order the IVFSs we use the order relation defined by Xu and Yager [22]. Using this relationship on $L([0,1])$ is easy to see that the smallest element of $L([0,1])$ is 0_L and the largest is 1_L.

We will now recall the extension of t-norms and t-conorms in $[0,1]$ (see [23]) to IVFSs [20], [24].

Definition 2: A function $\mathbf{T} : (L([0,1]))^2 \to L([0,1])$ is said to be an *interval-valued t-norm* (IV t-norm) if it is commutative, associative, increasing in both arguments (with respect to the order $\mathbf{x} \leq_L \mathbf{y}$ if and only $\underline{x} \leq \underline{y}$ and $\overline{x} \leq \overline{y}$), and has the neutral element 1_L. In the same way, a function $\mathbf{S} : (L([0,1]))^2 \to L([0,1])$ is said to be an *interval-valued t-conorm* (IV t-conorm) if it is commutative, associative, increasing, and has the neutral element 0_L.

Definition 3: a) An IV t-norm is said to be *t-representable* if there are two t-norms T_a and T_b in $[0,1]$ so that $\mathbf{T}(\mathbf{x},\mathbf{y}) = [T_a(\underline{x},\underline{y}), T_b(\overline{x},\overline{y})]$ for all **x, y** $\in L([0,1])$.
b) An IV t-conorm is said to be *s-representable* if there are two t-conorms S_a and S_b in $[0,1]$ so that $\mathbf{S}(\mathbf{x},\mathbf{y}) = [S_a(\underline{x},\underline{y}), S_b(\overline{x},\overline{y})]$ for all **x, y** $\in L([0,1])$.

We will use $\mathbf{T}_{T_a,T_b}$ to denote the t-representable IV t-norm that can be represented by T_a and T_b as defined above. Similarly, a specific s-representable IV t-conorm will be denoted $\mathbf{S}_{S_a,S_b}$.

In this work we only use t-representable IV t-norms and s-representable IV t-conorms.

Let $[\underline{x}, \overline{x}]$, $[\underline{y}, \overline{y}]$ be two intervals in $\mathbb{R}$ so that $\underline{x} \leq \underline{y}$ and $\overline{x} \leq \overline{y}$, the rules of interval arithmetic employed in this contribution are as follows:

- Addition: $[\underline{x}, \overline{x}] + [\underline{y}, \overline{y}] = [\underline{x} + \underline{y}, \overline{x} + \overline{y}]$.
- Subtraction: $[\underline{x}, \overline{x}] - [\underline{y}, \overline{y}] = [\underline{x} - \overline{y}, \overline{x} - \underline{y}]$.
- Multiplication: $[\underline{x}, \overline{x}] * [\underline{y}, \overline{y}] = [\underline{x} * \underline{y}, \overline{x} * \overline{y}]$.
- Division: $[\underline{x}, \overline{x}]/[\underline{y}, \overline{y}] = [\underline{x}/\overline{y}, \overline{x}/\underline{y}]$ assuming $0 < \underline{y}$.

We defined a weak ignorance function from the concept of ignorance function given in [9] as follows:

Definition 4: A weak ignorance function [25] is a mapping

$$g : [0,1] \to [0,1]$$

that satisfies:

(g1) $g(x) = g(1-x)$ for all $x \in [0,1]$;
(g2) $g(x) = 0$ if and only if $x = 0$ or $x = 1$;
(g3) $g(0.5) = 1$.

Example 1: $g(x) = 2 \cdot \min(x, 1-x)$ is a weak ignorance function.

B. Construction of Interval-Valued Fuzzy Sets of Fixed Length From a Fuzzy Set

Our aim in this section is to construct an IVFS starting from any given fuzzy set. To do so, we define a function G parametrized by δ and γ, which satisfy a determined set of properties. These properties allow to obtain intervals in such a way that their length is proportional to the ignorance degree and the initial membership degree is within the interval.

Proposition 1: Let $\delta, \gamma \in [0,1]$ with $\delta \geq \gamma \geq \delta \cdot x$. The function

$$\begin{aligned} &G : [0,1]^4 \to L([0,1]) \text{ given by} \\ &G(x,y,\delta,\gamma) = [x \cdot (1 - \delta \cdot y), x \cdot (1 - \delta \cdot y) + \gamma \cdot y)] \end{aligned} \tag{1}$$

satisfies the following properties:

1) $x \in G(x,y,\delta,\gamma)$;
2) $W(G(x,y,\delta,\gamma)) = \gamma \cdot y$;

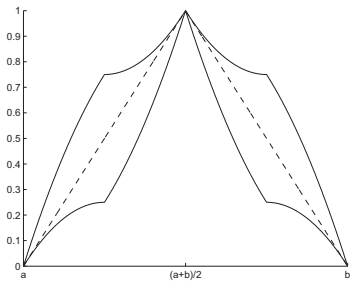

Fig. 1: Initial constructed IVFS.

3) If $x = 0$, then $G(0, y, \delta, \gamma) = [0, \gamma \cdot y]$;
4) If $y = 0$, then $G(x, 0, \delta, \gamma) = [x, x]$;
5) If $\delta = \gamma$, then:

$$\underline{G}(x, y, \delta, \delta) + \overline{G}(1 - x, y, \delta, \delta) = 1$$
$$\overline{G}(x, y, \delta, \delta) + \underline{G}(1 - x, y, \delta, \delta) = 1.$$

According to the previous proposition, we define Theorem 1 as the new construction of IVFSs.

Theorem 1: Let $A \in \mathcal{FS}(U)$. If for each $u_i \in U$ we take $g(A(u_i))$, $\delta(u_i)$, $\gamma(u_i) \in [0, 1]$, then the set

$$\begin{aligned} &A_{IV} = \{(u_i, A_{IV}(u_i)) | u_i \in U\} \text{ where} \\ &A_{IV}(u_i) = G(A(u_i), g(A(u_i)), \delta(u_i), \gamma(u_i)) \end{aligned} \tag{2}$$

is an IVFS on U.

C. Modeling Linguistic Labels by means of Interval-Valued Fuzzy Sets

In this section, we describe our methodology to generate linguistic labels modeled by means of IVFSs starting from given fuzzy sets.

We use the initial fuzzy sets (dashed line in Fig. 1 whose expression is shown in Eq. (3)) as the base to construct the IVFSs (solid line in Fig. 1) by means of Theorem 1. In the initial construction of the IVFSs, we consider the middle degree of ignorance. Therefore, we initialize $\delta(u_i) = \gamma(u_i) = 0.5$ for all $u_i \in U$ since, according to Theorem 1, the minimum value of both parameters is 0 and the maximum is 1.

$$\mu_A(u_i) = \begin{cases} 0, & \text{if } u_i \leq a, \\ \frac{2}{b-a}(u_i - a), & \text{if } a \leq u_i \leq \frac{a+b}{2} \text{ and } b \neq a, \\ \frac{2}{a-b}(u_i - b), & \text{if } \frac{a+b}{2} \leq u_i \leq b \text{ and } b \neq a, \\ 0, & \text{if } b \leq u_i, \end{cases} \tag{3}$$

III. Fuzzy ID3 with Interval-valued Fuzzy Sets

In this section, we describe the induction process of the fuzzy ID3 algorithm and then we introduce our methodology, that is, the construction of the IVFSs and the modifications carried out both in the computation of the relative frequencies and in the reasoning mechanism.

A. Fuzzy ID3 Induction

Let the universe of objects be described by n attributes $A = A^{(1)}, ..., A^{(n)}$. An attribute $A^{(k)}$ takes m_k values of fuzzy subsets $A_1^{(k)}, A_2^{(k)}, ..., A_{m_k}^{(k)}$. There are a total of N training instances. Based on the attributes, an object is classified into *m* classes $C_1, C_2, ..., C_m$. We use the symbol M(·) to denote the cardinality of a given fuzzy set. The key to the fuzzy ID3 algorithm is to select the expanded attribute, which can be performed in the following steps [7]:

(1) For each attribute value (fuzzy subset) $A_i^{(k)}, (i = 1, 2, ..., m_k)$, to compute its relative frequencies with respect to class $C_j, (j = 1, 2, ..., m)$:

$$p_i^{(k)}(j) = \frac{M(A_i^{(k)} \cap C_j)}{M(A_i^{(k)})} \tag{4}$$

(2) For each attribute value (fuzzy subset) $A_i^{(k)}, (i = 1, 2, ..., m_k)$, to compute its fuzzy classification entropy:

$$Entr_i^{(k)} = \sum_{j=1}^{m} -p_i^{(k)}(j) log(p_i^{(k)}(j)), \tag{5}$$

(3) To compute the average fuzzy classification entropy of the *k*th attribute:

$$E_k = \sum_{i=1}^{m_k} \frac{M(A_i^{(k)})}{\sum_{j=1}^{m_k} M(A_j^{(k)})} Entr_i^{(k)}. \tag{6}$$

(4) Select such an integer k_0, that

$$E_{k_0} = \arg \min_{1 \leq k \leq n} (E_k) \tag{7}$$

With a given evidence significance level α, a truth level threshold β and being A the set of attributes of the problem, the induction process consists of the following steps [6]:

(1) Execute the α-cut of the set of fuzzified examples with the evidence significant level.
(2) Measure the average fuzzy classification entropy associated with each attribute and select the attribute with the smallest average fuzzy classification entropy as the root decision node.
(3) Delete all empty branches of the decision node. For each nonempty branch of the decision node, compute the relative frequencies of all objects within the branch into each class. If the relative frequency of one class is above the given threshold β, terminate the branch as a leaf. Otherwise, do further research if an additional attribute will further partition the branch (i.e. generate more than one nonempty branch). If yes, select the attribute with the smallest average fuzzy classification entropy as a new decision node from the branch. If not, terminate this branch as a leaf. At the leaf, each class will has its relative frequency.
(4) Repeat step 3 for all newly generated decision nodes until no further growth is possible (i.e. all the attributes have been used), the decision tree then is complete.

B. Fuzzy ID3 with Interval-Valued Fuzzy Sets: A New Fuzzy Reasoning Method

The fuzzy sets composing the data base of the FDT, generated by the algorithm previously described, are created homogeneously over the input space. These fuzzy sets are employed as the starting point to construct the IVFSs using the construction method presented in Section II-C.

The modeling of the linguistic labels by means of IVFSs implies two main modifications. The relative frequencies of the classes in each leaf must be elements of $L([0,1])$. To do so, we compute the relative frequencies (Eq. (4)) associated with the lower and the upper bounds respectively. On the other hand, the reasoning mechanism, used to classify novel examples, is adapted as follows:

In a FDT, a path is the connection from the root node to each leaf. Suppose that the FDT contains *l* leaves, consequently *l* paths ($Path^i, i = 1, 2, ..., l$). For each leaf, the path *i* has N_i nodes ($Path^i_1$, $Path^i_2$, ...,$Path^i_{N_i}$). Let *e* be an example to be classified in one of the *m* classes. We must recall that each node is modeled by means of an IVFS, therefore, $Path^i_k(e_k) = [\underline{Path^i_k}(e_k), \overline{Path^i_k}(e_k)] \in L([0,1])$ with $k = 1, ..., N_i$. The *interval-valued fuzzy reasoning mechanism* follows the following 4 key steps:

- To compute the matching degree between each path and the new example. We apply a t-representable IV t-norm as the conjunction among the nodes in each path.

$$M_i = \mathbf{T}_{T_a,T_b}([\underline{Path^i_1}(e_1), \overline{Path^i_1}(e_1)], ...,$$

$$[\underline{Path^i_{N_i}}(e_{N_i}), \overline{Path^i_{N_i}}(e_{N_i})]) =$$

$$[T_a(\underline{Path^i_1}(e_1), ..., \underline{Path^i_{N_i}}(e_{N_i})),$$

$$T_b(\overline{Path^i_1}(e_1), ..., \overline{Path^i_{N_i}}(e_{N_i}))], i = 1, 2, ..., l$$

- To compute the certainty of each class in each leaf. We apply a t-representable IV t-norm to weight the matching degree of the example along the paths with the relative frequencies of the leaves.

$$Cert^i_j = \mathbf{T}_{T_c,T_d}([\underline{M_i}, \overline{M_i}], [\underline{p_i}(j), \overline{p_i}(j)]) =$$

$$[T_c(\underline{M_i}, \underline{p_i}(j)), T_d(\overline{M_i}, \overline{p_i}(j))], j = 1, ..., m, i = 1, ..., l$$

- To compute the total certainty of each class. We employ the interval addition to aggregate certainties of the same class in all the paths.

$$Total_Certainty_j = \sum_{i=1}^{l} [\underline{Cert^i_j}, \overline{Cert^i_j}], j = 1, ..., m$$

- Classify the example in the class which maximizes the total certainty following the relationship presented below.

For any interval $[\underline{x}, \overline{x}]$, $[\underline{y}, \overline{y}]$ on $\mathbb{R}$, we use the following relationship based on the score and accuracy functions given in [22] (see Subsection II-A): let $s([\underline{x}, \overline{x}]) = \underline{x} + \overline{x}$ and $s([\underline{y}, \overline{y}]) = \underline{y} + \overline{y}$ be the scores of $[\underline{x}, \overline{x}]$ and $[\underline{y}, \overline{y}]$ respectively. Let $h([\underline{x}, \overline{x}]) = \overline{x} - \underline{x}$ and $h([\underline{y}, \overline{y}]) = \overline{y} - \underline{y}$ be the accuracy degrees of $[\underline{x}, \overline{x}]$ and $[\underline{y}, \overline{y}]$ respectively. Then

- If $s([\underline{x}, \overline{x}]) < s([\underline{y}, \overline{y}])$, then $[\underline{x}, \overline{x}] < [\underline{y}, \overline{y}]$;
- If $s([\underline{x}, \overline{x}]) = s([\underline{y}, \overline{y}])$, then
  a) If $h([\underline{x}, \overline{x}]) = h([\underline{y}, \overline{y}])$, then $[\underline{x}, \overline{x}] = [\underline{y}, \overline{y}]$;
  b) if $h([\underline{x}, \overline{x}]) < h([\underline{y}, \overline{y}])$, then $[\underline{x}, \overline{x}] < [\underline{y}, \overline{y}]$.

IV. Genetic Tuning of the Linguistic Labels

Membership functions, which are usually obtained by normalization process or defined by experts, remains fixed during the induction process. Consequently, they could not be perfectly adapted to the context of each problem. To solve this problem, it can be appropriate to carry out a post-processing tuning step in which membership functions are tuned leading to a better adaptation of the system to the specific problem we are dealing with.

The optimization post-processing step is often performed by means of a GA. The hybridization between fuzzy logic and GAs leads to Genetic Fuzzy Systems (GFSs) [26], which are basically fuzzy systems augmented by learning processes based on evolutionary computation. GFS approaches are usually divided into two processes, tuning and learning. Specifically, the genetic tuning process consists of automatically selecting the best system parameters for improving the performance of the initial model without modifying the rule base.

In the remainder of this section we will first introduce the tuning approach of the linguistic labels and then we will describe in detail the evolutionary model for tuning the membership functions.

A. Ignorance Weighting Factor Tuning

The initial set-up of the linguistic labels, which are modeled by IVFSs, could not be well-suited for the specific problem we are dealing with. Therefore, it seems necessary to tune the shape of each IVFS, which is determined by the parameters employed in the IVFSs construction method (Section II-B).

As we have introduced in Subsection II-C, we consider the middle degree of ignorance for the initial construction of all the IVFSs ($\delta = \gamma = 0.5$). However, the ignorance degree can vary depending on the linguistic label, since the amount of available information to define each fuzzy term may not be the same.

Therefore, we propose the application of a genetic tuning step in which we adapt the parameters δ and γ (see Theorem 1), keeping the restriction $\delta \geq \gamma \geq \delta \cdot x$. Consequently, the amount of ignorance that each IVFS represents will vary depending on how the membership function suits the problem.

Fig. 2 depicts the behaviour of the proposed tuning approach. The original IVFS is shown in light gray whereas its final shape (afterwards the genetic tuning) is depicted in dark gray. We observe that the shape of the final IVFS is thinner than that of the initial IVFS.

B. Evolutionary Model

In order to apply the genetic tuning, we will consider the use of CHC algorithm [27]. This algorithm is a classical evolutionary model which presents a good trade-off between

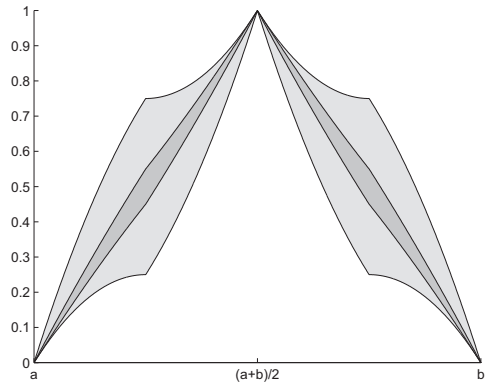

Fig. 2: Ignorance weighting factor genetic tuning. The final values of the parameters are: $\delta = 0.1$, $\gamma = 0.1$.

diversity and convergence, being a good choice in complex problems. The components needed to design this process are explained below:

1) *Coding Scheme:* A real coding is considered. Let us consider the following number of labels per variable: $(m^1, m^2, ..., m^n)$, with n being the number of variables. δ and $\gamma \in [0, 1]$ represent the genes used to encode the parameters which weight the degree of ignorance. Then, the representation of the chromosome is as follows:

$$C_{ET} = (\delta_{11}, \gamma_{11}, ..., \delta_{1m^1}, \gamma_{1m^1}, \delta_{21}, \gamma_{21}, ..., \delta_{2m^2}, \gamma_{2m^2}, ..., \delta_{n1}, \gamma_{n1}, ..., \delta_{nm^n}, \gamma_{nm^n})$$

Therefore, the chromosome length is equal to two times the number of variables times the number of linguistic labels.
2) *Chromosome Evaluation:* The fitness function is the classification accuracy.
3) *Initial Gene Pool:* The initial pool is obtained initializing three individuals having all of the genes with values of 0, 0.5 and 1, corresponding with the situations of minimum, middle and maximum degree of ignorance respectively. The remaining individuals will have initialized all the genes randomly in their respective domains.
4) *Crossover Operator:* We consider the Parent Centric BLX (PCBLX) operator, which is based on the BLX-α. We consider the incest prevention mechanism, checking and modifying an initial threshold, in order to apply the PCBLX operator.
5) *Restarting approach:* When the threshold value is lower than zero, all the chromosomes are regenerated at random in their respective domains. Furthermore, the best global solution found is included in the population to increase the convergence of the algorithm as in the elitist scheme.

V. Experimental Study

This study is oriented towards analysing the goodness of our evolutionary tuning method applied to the FDT generated by the fuzzy ID3 algorithm. To do so, we develop an experimental analysis in which we compare our methodology with respect to several state-of-the-art FDTs and also with C4.5.

In this section, we present the experimental set-up in first place. Next, we briefly describe the FDTs for the comparison together with the parameters employed in the study. Then we introduce the statistical tests used and finally, we present the results together with the corresponding analysis.

A. Experimental Set-Up

We have selected a wide benchmark of 20 numerical data-sets selected from the KEEL data-set repository [16], which are publicly available on the corresponding web page [1] including general information about them, partitions for the validation of the experimental results and so on. Table I summarizes the properties of the selected data-sets, showing for each data-set the number of examples (#Ex.), the number of attributes (#Atts.) and the number of classes (#Class.). We must point out that the *magic, page-blocks, ring* and *shuttle* data-sets have been stratified sampled at 10% in order to reduce their size for training. In the case of missing values, (*cleveland* and *wisconsin*), those instances have been removed from the data-set.

TABLE I: Summary Description for the employed data-sets.

Id.	Data-set	#Ex.	#Atts.	#Class.
app	Appendicitis	106	7	2
bal	Balance	625	4	3
bup	Bupa	345	6	2
cle	Cleveland	297	13	5
eco	Ecoli	336	7	8
gla	Glass	214	9	6
hab	Haberman	306	3	2
hea	Heart	270	13	2
iri	Iris	150	4	3
mag	Magic	1,902	10	2
new	New-Thyroid	215	5	3
pag	Page-blocks	548	10	5
pim	Pima	768	8	2
rin	Ring	740	20	2
shu	Shuttle	2,175	9	7
tae	Tae	151	5	3
tit	Titanic	2,201	3	2
win	Wine	178	13	3
wis	Wisconsin	683	9	2
yea	Yeast	1484	8	10

A *5-folder cross-validation model* was considered in order to carry out the different experiments. That is, we split the data-set into 5 random partitions of data, each one with 20% of the patterns, and we employ a combination of 4 of them (80%) to train the system and the remaining one to test it. Furthermore, the process was repeated 3 times using a different seed to obtain a sample of 15 results, which have been averaged for each data-set.

[1] http://www.keel.es/dataset.php

B. Fuzzy Decision Trees for Comparison and Parameters Set-Up

In this work, we have considered four FDTs in order to compare our methodology with respect to different approaches of the literature. Next, we briefly describe each FDT together with their specific configuration values:

- The first approach fuzzifies the Gini index [14]. This method uses the SLIQ decision tree as the base algorithm, which uses the Gini index as the split measure, and fuzzifies its decision boundaries during the tree induction. The configuration is as follows:
  - Number of labels per variable: 3 labels.
  - Threshold = 0.85.
  - Maximum number of patterns in a leaf: 5% of the number of patterns.
  - Maximum depth: number of attributes.
- The second approach is the look-ahead method [12]. This method attempts to establish a decision node by analyzing both a split measure and the classifiability of instances that are split along branches of the node. The specific values of its configuration are:
  - Number of labels per variable: 3 labels.
  - Split measure: Information Gain.
  - Number of neighbours: 3.
  - Weighting factor: 1.
- The third proposal is the FDT proposed by Janikow in [13]. This is a classical FDT widely employed in the specialized literature whose configuration is as follows:
  - Number of labels per variable: 3 labels.
  - Conjunction operator: product T-norm.
- Finally, we have selected the simple pattern tree algorithm [11]. This approach, instead of constructing one tree, whose leaves have a probability distribution expressing the membership of each class, constructs one tree per class using aggregation and similarity functions. We have chosen the following configuration:
  - Aggregation functions: min and max operators.
  - Similarity function: the similarity related with the root mean square error.
  - Number of labels per variable: 3 labels.

The specific configuration for the fuzzy ID3 algorithm with and without IVFSs (presented in Table II) and the ones of the selected FDTs in this work, have been selected experimentally since they provide the best performance for each method. Regarding the genetic tuning process presented in Section IV, it employs populations composed by 50 individuals, 30 bits per gen in order to perform the *gray* codification and the number of evaluations is 5.000 times the number of attributes.

C. Statistical Tests for Performance Comparison

In this work, we use some hypothesis validation techniques in order to give a statistical support to the result analysis. We will use a non parametric test, because the initial conditions that guarantee the reliability of the parametric tests cannot be fulfilled [17], [18]. We employ the Wilcoxon rank test [28] as non parametric statistical procedure to make comparisons between two algorithms; we use the Friedman aligned ranks test [29] to detect statistical differences among a group of results and the Holm post-hoc test [30] to find the algorithms that reject the equality hypothesis with respect to a selected control method.

These tests are suggested in the studies presented in [17], [18], [19], where its shown that their use in the field of machine learning is highly recommended. A complete description of the test and software for its use can be found on the website: http://sci2s.ugr.es/sicidm/.

TABLE II: Parameter specification for the FDTs.

Fuzzy ID3
Number of labels per variable: 3 labels
Conjunction operator: product t-norm
Evidence significance level = 0.4
Truth level threshold = 0.95
Fuzzy ID3 with IVFSs
Ignorance function: $2 \cdot \min(x, 1-x)$
Conjunction operator: product IV t-norm
δ = 0.5
γ = 0.5

D. Analysis of the Behaviour of the Evolutionary Tuning Method.

Table III shows the classification accuracy provided by our methodology and the different approaches considered in this work, specifically:

- F-ID3_IVFS_ET: the fuzzy ID3 algorithm with IVFSs and the evolutionary tuning method.
- F-ID3: the standard fuzzy ID3 algorithm.
- SPT: the simple pattern tree algorithm.
- LA: the look-ahead approach with the information gain heuristic.
- Fgini: the approach in which authors fuzzify the Gini index.
- Janikow: the classical FDT.
- C4.5: the well known decision tree.

Results are grouped in pairs for training and test, where the best global result for each data-set is stressed in **bold-face**.

From the results of Table III, it can be observed that our methodology enhances the performance of the fuzzy ID3 algorithm in most of the data-sets. Furthermore, the goodness of our evolutionary tuning model is shown since it increases the initial performance of the fuzzy ID3 algorithm in such a way that the results obtained by the remaining FDTs are clearly outperformed, as it achieves the best global performance and provides the best performance in 11 of the 17 data sets. This situation is confirmed in Fig. 3, where the rankings of the different approaches are presented, showing that the best ranking is provided by our evolutionary tuning method.

In order to detect significant differences among the results of the different approaches, we carry out the Friedman aligned rank test. This test obtains a p-value near to zero (0.004),

TABLE III: Results in Train (Tr.) and Test (Tst) achieved by the different decision trees.

Data	F-ID3_IVFS_ET		F-ID3		SPT		LA		Janikow		Fgini		C4.5	
Set	$Tr.$	Tst	$Tr.$	Tst	$Tr.$	Tst	$Tr.$	Tst	$Tr.$	Tst	$Tr.$	Tst	$Tr.$	Tst
App	93.16	86.80	90.57	84.94	80.19	80.22	91.27	84.85	89.39	**86.84**	80.19	80.22	90.09	84.98
Bal	96.60	**90.72**	91.72	90.08	78.96	77.92	90.32	88.32	91.72	90.08	89.40	88.64	89.72	77.28
Bup	79.93	**67.25**	61.52	58.26	63.99	60.29	79.78	61.74	60.65	58.84	88.62	66.67	83.84	66.09
Cle	93.18	**55.88**	87.29	53.87	53.87	53.88	94.69	49.83	97.64	50.50	89.06	53.19	83.41	51.82
Eco	82.14	77.69	80.21	76.80	67.11	66.67	80.73	75.90	77.98	76.79	89.88	77.39	91.74	**78.28**
Gla	77.57	60.80	60.17	52.80	60.40	57.52	85.86	68.24	75.12	64.04	46.26	43.02	91.94	**68.73**
Hab	79.90	72.87	75.08	71.90	75.98	74.17	78.43	73.52	74.51	72.88	79.90	**74.83**	76.06	72.22
Hea	94.81	78.52	93.52	**79.26**	81.57	75.19	98.43	75.93	98.52	78.52	90.93	72.96	92.96	**79.26**
Iri	98.83	96.00	93.07	95.33	97.17	**98.67**	97.50	96.00	95.67	96.00	83.67	83.33	97.83	93.33
Mag	82.75	78.91	95.50	78.28	78.12	78.23	86.40	78.44	78.52	77.55	79.98	77.18	87.22	**79.81**
New	97.79	**94.88**	79.80	91.16	91.86	91.63	96.05	93.95	86.05	85.58	93.49	93.02	98.37	91.16
Pag	95.03	94.16	92.67	92.15	92.97	91.24	95.67	93.79	93.75	92.51	91.70	91.24	98.95	**95.07**
Pim	83.56	**76.43**	92.84	75.77	76.20	74.34	88.25	73.57	77.54	74.34	85.38	75.78	85.81	74.09
Rin	97.09	**90.81**	79.95	49.59	80.78	78.11	94.76	77.03	95.00	90.14	88.55	84.86	97.13	82.70
Shu	97.74	97.98	98.74	90.57	92.72	92.64	97.72	97.33	83.31	83.31	99.46	99.49	99.66	**99.54**
Tae	70.86	**58.95**	63.40	54.99	55.30	48.99	71.36	53.61	68.38	57.61	56.28	50.34	78.15	54.99
Tit	78.33	**78.33**	78.33	**78.33**	77.64	77.78	**78.33**	**78.33**	78.33	78.33	67.37	66.65	78.48	77.78
Win	100.00	**98.87**	99.59	97.75	91.85	89.33	98.45	92.11	100.00	97.71	94.10	90.40	99.02	94.90
Wis	98.28	96.04	90.63	94.58	96.85	96.20	96.85	95.02	98.43	**96.49**	94.40	93.56	98.43	95.03
Yea	63.01	**57.41**	95.90	55.46	35.56	34.16	62.99	51.29	46.60	44.54	21.38	20.95	82.18	55.80
Mean	88.03	**80.46**	81.02	76.09	76.45	74.86	88.19	77.94	83.35	77.63	80.50	74.19	90.05	78.64

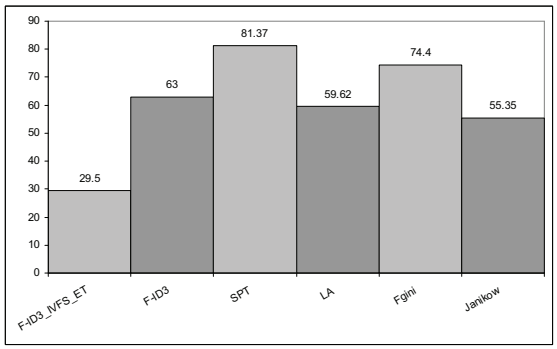

Fig. 3: Rankings of the different fuzzy decision trees.

which implies that there are significant differences between the results. For this reason, we can apply a post-hoc test to compare our methodology against the remaining FDTs. Specifically, a Holm test is applied, which is presented in Table IV. The statistical analysis reflects that all of the FDTs considered in this study are outperformed by our approach.

TABLE IV: Holm test to compare the evolutionary tuning method with all the FDTs. The evolutionary tuning model is used as the control method.

i	Algorithm	z	p	α/i	Hypothesis ($\alpha = 0.05$)
5	SPT	4.74	2.15E-6	0.01	Rejected for F-ID3_IVFS_ET
4	Fgini	4.10	4.05E-5	0.0125	Rejected for F-ID3_IVFS_ET
3	F-ID3	3.07	0.002	0.017	Rejected for F-ID3_IVFS_ET
2	LA	2.76	0.006	0.025	Rejected for F-ID3_IVFS_ET
1	Janikow	2.37	0.018	0.05	Rejected for F-ID3_IVFS_ET

Regarding C4.5, the results presented in Table III also show that our evolutionary tuning approach achieves a significant global improvement. A Wilcoxon test (Table V) will help us to make a pairwise comparison between both approaches. We can observe that the null hypothesis of equivalence is rejected in favour of the evolutionary tuning method with a high level of confidence.

TABLE V: Wilcoxon Test to compare the C4.5 algorithm (R^+) against the evolutionary tuning method (R^-).

Comparison	R^+	R^-	Hypothesis ($\alpha = 0.05$)	p-value
C4.5 vs. F-ID3_IVFS_ET	44	166	Rejected for F-ID3_IVFS_ET	0.023

VI. Conclusion

In this work we have proposed a methodology to improve the performance of FDTs by means of IVFSs and a post-processing genetic tuning step. To do so, we have modeled the linguistic labels by means of IVFSs to take into account the ignorance related to the definition of the membership functions. The degree of ignorance is weighted by two parameters and, in this manner, the shapes of the IVFSs are determined. This parametrization allows us to analyse the most appropriate set-up of the IVFSs partitions by means of a post-processing genetic tuning step. In this manner, we compute the best ignorance degree that each IVFS represents.

The experimental study has shown the quality of our approach since, applied to the FDT generated by the fuzzy ID3 algorithm, allows to outperform both the results of the base FDT and the ones of several state-of-the-art FDTs. We must highlight that our proposed approach also enhances the results of a reference algorithm in data mining like C4.5. The results obtained with this methodology allow us to determine, with the corresponding statistical support, that the proposed synergy is very useful to solve classification tasks.

ACKNOWLEDGMENT

This work was supported in part by the Spanish Ministry of Science and Technology under projects TIN2008-06681-C06-01 and TIN2010-15055.

REFERENCES

[1] E. Alpaydin, *Introduction to Machine Learning*, 2nd ed. The MIT Press, Cambridge, 2010.

[2] L. A. Zadeh, "Fuzzy sets," *Information and control*, vol. 8, no. 3, pp. 338–353, 1965.

[3] R. Kothari and M. Dong, *Decision Trees for Classification: A Review and Some New Results*. World Scientific, Singapore, 2000.

[4] K. A. Crockett, Z. Bandar, J. Fowdar, and J. O'Shea, "Genetic tuning of fuzzy inference within fuzzy classifier systems," *Expert Systems*, vol. 23, no. 2, pp. 63–82, 2006.

[5] C. Olaru and L. Wehenkel, "A complete fuzzy decision tree technique," *Fuzzy Sets and Systems*, vol. 138, no. 2, pp. 221–254, 2003.

[6] Y. Yuan and M. J. Shaw, "Induction of fuzzy decision trees," *Fuzzy Sets and Systems*, vol. 69, no. 2, pp. 125–139, 1995.

[7] X.-Z. Wang, D. S. Yeung, and E. C. C. Tsang, "A comparative study on heuristic algorithms for generating fuzzy decision trees," *IEEE Transactions on Systems, Man and Cybernetics - Part B*, vol. 31, no. 2, pp. 215–226, 2001.

[8] R. Sambuc, "Function ϕ-flous, application a l'aide au diagnostic en pathologie thyroidienne," Ph.D. dissertation, University of Marseille, 1975.

[9] H. Bustince, M. Pagola, E. Barrenechea, J. Fernandez, P. Melo-Pinto, P. Couto, H. R. Tizhoosh, and J. Montero, "Ignorance functions. An application to the calculation of the threshold in prostate ultrasound images," *Fuzzy Sets and Systems*, vol. 161, no. 1, pp. 20–36, 2010.

[10] J. Sanz, A. Fernández, H. Bustince, and F. Herrera, "Improving the performance of fuzzy rule-based classification systems with interval-valued fuzzy sets and genetic amplitude tuning," *Information Sciences*, vol. 180, no. 19, pp. 3674–3685, 2010.

[11] Z. Huang, T. Gedeon, and M. Nikravesh, "Pattern trees induction: A new machine learning method," *IEEE Transactions on Fuzzy Systems*, vol. 16, no. 4, pp. 958–970, 2008.

[12] M. Dong and R. Kothari, "Look-ahead based fuzzy decision tree induction," *IEEE Transactions on Fuzzy Systems*, vol. 9, no. 3, pp. 461–468, 2001.

[13] C. Z. Janikow, "Fuzzy decision trees: issues and methods," *IEEE Transactions on Systems, Man, and Cybernetics, Part B: Cybernetics*, vol. 28, no. 1, pp. 1–14, 1998.

[14] B. Chandra and P. P. Varghese, "Fuzzifying gini index based decision trees," *Expert Systems with Applications*, vol. 36, no. 4, pp. 8549–8559, 2009.

[15] J. Quinlan, *C4.5: Programs for Machine Learning*. San Mateo-California: Morgan Kaufmann Publishers, 1993.

[16] J. Alcalá-Fdez, A. Fernández, J. Luengo, J. Derrac, S. García, L. Sánchez, and F. Herrera, "KEEL data-mining software tool: Data set repository, integration of algorithms and experimental analysis framework," *Journal of Multiple-Valued Logic and Soft Computing*, vol. 17, no. 2-3, pp. 255–287, 2011.

[17] J. Demšar, "Statistical comparisons of classifiers over multiple data sets," *Journal of Machine Learning Research*, vol. 7, pp. 1–30, 2006.

[18] S. García and F. Herrera, "An extension on "statistical comparisons of classifiers over multiple data sets" for all pairwise comparisons," *Journal of Machine Learning Research*, vol. 9, pp. 2677–2694, 2008.

[19] S. García, A. Fernández, J. Luengo, and F. Herrera, "Advanced nonparametric tests for multiple comparisons in the design of experiments in computational intelligence and data mining: Experimental analysis of power," *Information Sciences*, vol. 180, no. 10, pp. 2044–2064, 2010.

[20] H. Bustince, E. Barrenechea, and M. Pagola, "Generation of interval-valued fuzzy and atanassov's intuitionistic fuzzy connectives from fuzzy connectives and from k_α operators: laws for conjunctions and disjunctions, amplitude," *International Journal of Intelligent Systems*, vol. 23, no. 6, pp. 680–714, 2008.

[21] J. Mendel and R. I. John, "Type-2 fuzzy sets made simple," *IEEE Transactions on Fuzzy Systems*, vol. 10, no. 2, pp. 117–127, 2002.

[22] Z. Xu and R. Yager, "Some geometric aggregation operators based on intuitionistic fuzzy sets," *International Journal of General Systems*, vol. 35, no. 4, pp. 417–433, 2006.

[23] G. Beliakov, A. Pradera, and T. Calvo, *Aggregation Functions: A Guide for Practitioners. What is an aggregation function.* San Mateo-California: Studies In Fuzziness and Soft Computing, Springer, 2007.

[24] G. Deschrijver, C. Cornelis, and E. Kerre, "On the representation of intuitionistic fuzzy t-norms and t-conorms," *IEEE Transactions on Fuzzy Systems*, vol. 12, no. 1, pp. 45–61, 2004.

[25] J. Sanz, A. Fernández, H. Bustince, and F. Herrera, "A genetic tuning to improve the performance of fuzzy rule-based classification systems with interval-valued fuzzy sets: Degree of ignorance and lateral position," *International Journal of Approximate Reasoning*, vol. In press, doi: 10.1016/j.ijar.2011.01.011, 2011.

[26] F. Herrera, "Genetic fuzzy systems: Taxonomy, current research trends and prospects," *Evolutionary Intelligence*, vol. 1, no. 1, pp. 27–46, 2008.

[27] L. Eshelman, *Foundations of Genetic Algorithms*. Morgan Kaufman, 1991, ch. The CHC adaptive search algorithm: How to have safe search when engaging in nontraditional genetic recombination, pp. 265–283.

[28] D. Sheskin, *Handbook of parametric and nonparametric statistical procedures*, 2nd ed. Chapman & Hall/CRC, 2006.

[29] J. L. Hodges and E. L. Lehmann, "Ranks methods for combination of independent experiments in analysis of variance," *Annals of Mathematical Statistics*, vol. 33, pp. 482–497, 1962.

[30] S. Holm, "A simple sequentially rejective multiple test procedure," *Scandinavian Journal of Statistics*, vol. 6, pp. 65–70, 1979.

2011 IEEE International Conference on Fuzzy Systems
June 27-30, 2011, Taipei, Taiwan

A Two-Step Approach of Feature Construction for a Genetic Learning Algorithm

David García, Antonio González and Raúl Pérez
Departamento de Ciencias de la Computación e I.A.
CITIC-UGR University of Granada (Spain)
Email: {DGarcia, A.Gonzalez,Raul_Perez}@decsai.ugr.es

***Abstract*—Traditionally, fuzzy rule based models work with a fixed set of features to describe a particular problem. Our proposal is to use feature construction by means of functions in order to obtain new variables that allow us to get more information about the problem. In particular, we propose the use of previously defined functions over the input variables in the antecedent of the rules. This let us to know if a combination of variables is able to provide us with more information than each one of them separately. In addition, we use a structure that helps us to manage and also restrict the number of functions under consideration by the learning algorithm. We also present a new model of rule in order to represent this kind of knowledge by extending a basic learning fuzzy rule-based model. Finally, we show the experimental study associated with this work.**

***Keywords*—Genetic Fuzzy Systems, Feature Construction, Iterative Learning Approach, Classification.**

I. Introduction

One of the most important areas in the development of applications based on fuzzy logic has been and is the design of fuzzy rule-based systems. In the literature different types of fuzzy rules have been used for different applications. The most common ones are the linguistic rule [1] and the TSK rule [2]. The first one presents a traditional model of rule whose antecedent and consequent is composed of linguistic variables. The second one proposed a model based on rules whose antecedent is composed of linguistic variables and the consequent is represented by a function of the input variables, frequently a linear function. A very well known extension of the linguistic rule is the DNF rule in which each input variable takes as a value a set of linguistic terms whose members are joined by a disjunctive operator, whilst the output variable remains an usual linguistic variable with a single value associated. Another types of extensions of fuzzy rules have been proposed, such as rules with weights, rules with double consequent, relational rules, etc. Each one of these different types of rules have been proposed with the idea of improving the system accuracy or to improve the system interpretability or both of them.

Traditionally, in fuzzy rule-based systems the number of variables in the antecedent is fixed, so now we want to explore the way to include new variables in the antecedent that result as a combination of the existing ones in order to improve the system description. That means that we need to apply feature construction techniques.

Many papers have been written regarding feature construction. In [3] a method is proposed in order to reduce the set of features by means of arithmetics expression trees that work only with numerical attributes. They focused the importance of making a feature selection before doing the feature construction. This is because the construction of new variables is more efficient after reducing the initial searching space. In other works as [4] feature construction is used in order to create new attributes that will be the input data for another algorithm. The process of obtaining the new features is optimized by means of genetic algorithms. On the other hand, as shown in [5], feature construction is proposed for searching effective features sets that improves the quality of recognition methods. This is obtained using the composition of fuzzy relations.

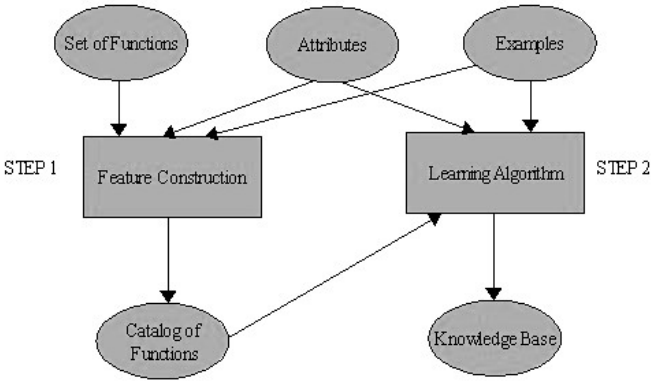

Fig. 1. Rule extraction process

In general, our proposal consists of incorporating new attributes in the learning process for obtaining an improved knowledge of the problem. In concrete, we can describe our proposal as a process with two steps: the first one is oriented to construct new attributes from the combination of the initial attributes by a set of predetermined functions. An information measurement is defined for evaluating the relevance of each new attribute. This step finishes returned the set of the best attributes that we call *catalog*. The second step takes the catalog and the training example set for obtaining a knowledge base that solves the learning problem. Figure 1 shows a graphical representation of the mentioned steps as far as the tasks taken into account in each one of them.

Next section shows a brief introduction about the rule

978-1-4244-7316-8/11/$26.00 ©2011 IEEE

model we propose. Section III explains the feature construction step showing a pseudo code with the algorithm used to obtain the most relevant features and the inference process. The fourth section describes the most relevant details of the learning algorithm NSLV, and the necessary changes done in order to extract fuzzy rules with functions in the antecedent. Section V shows the experimental results obtained as well as the study related to these results. Finally, last section is devoted for conclusions and future work related to this study.

II. Fuzzy Rules with Functions in the Antecedent

In this section we introduce the use of a new model of rule that can include functions as a component of the antecedent. First of all we will remind the linguistic fuzzy model of rules.

Linguistic rules present the following structure:

IF X_1 is A_1 and X_2 is A_2 and $\ldots$ and X_n is A_n

THEN Y is B

where $X_1, X_2, \ldots, X_n$ are the antecedent variables defined on the universes $U_1, U_2, \ldots, U_n$, and Y is the consequent variable defined on the universe V. $A_1, A_2, \ldots, A_n$ and B are fuzzy subsets defined on the respective universes.

We want to improve the capacity of knowledge representation of fuzzy models allowing that a function can be included as part of the description of a rule. To extend the rule model is easy since that a function can be considered like other variable. So, let's consider the following rule:

IF X_1 is A_1 and $SUM\{X_1, X_2\}$ is A_3

THEN Y is B

where $SUM(X_1, X_2)$ would be defined as $X_1 + X_2$ and A_3 is a fuzzy value that belongs to the function's domain.

We can interpret that $Z = SUM(X_1, X_2)$, being Z a linguistic variable defined on a fuzzy domain where A_3 is a fuzzy label that is member of that domain. Therefore, to work with functions in the antecedent of the rule does not modify the traditional inference process of the linguistic rules.

Let's suppose the following variables X_i, X_j, are defined in a fuzzy bounded domain $U_i = [inf_i, sup_i]$ and $U_j = [inf_j, sup_j]$ respectively. The range for the resultant variable Z, that represent the function $f(X_i, X_j)$, will depend on the operation selected in each case, but in general, it could be defined as $[min_{x_i \in U_i, x_j \in U_j} f(x_i, x_j), max_{x_i \in U_i, x_j \in U_j} f(x_i, x_j)]]$. For this range, we consider a fixed number of uniformly distributed linguistic labels in order to define the domain of the new variable (in this work, this value is fixed to five).

Below we show an example of the reasoning to obtain the domain for a new variable obtained by applying a function over two input variables.

Given variables X_1 and X_2, with the fuzzy domain shown in Fig. 2(a) and Fig. 2(b) respectively, we can define the domain of the resultant variable $Z_3 = SUM(X_1, X_2)$ as is shown in Fig. 2c.

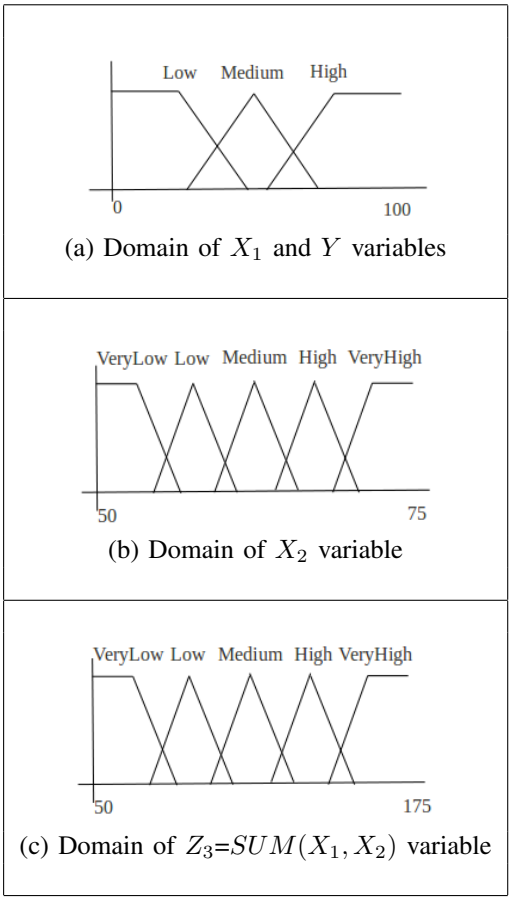

(a) Domain of X_1 and Y variables

(b) Domain of X_2 variable

(c) Domain of Z_3=$SUM(X_1, X_2)$ variable

Fig. 2. Domains associated to the variables of the example

Now we can show an example of the particular type of rules we are using:

IF X_1 is Low and $SUM\{X_1, X_2\}$ is $Medium$

THEN Y is $Medium$

where Y is the consequent variable that takes values on the same fuzzy domain as X_1 (Fig. 2(a)).

III. Step 1: Feature Construction

The first step of the learning process tries to find a set of new attributes that allow us to acquire more information about the problem. As it is shown in Figure 1, the input of this step consists in the initial variables set (V), the training example set (E) and a set of predetermined functions (F). The new variables are constructed applying the functions over some of the input variables. Although the general model could work with any kind of functions, from now on we will only work with binary functions, that is, functions over two variables. The relevance of each new attribute is evaluated using an information measure on the examples from the training set. The following code describes the process:

- FOREACH **f** in **F**
  - FOREACH subset **S** of **V**
    - $info(f(S), E)$ is a measure of the relevance of the f function with S variables, calculated on the training set.
    - IF $(info(f(S), E)) > k$, being k a threshold that establishes the minimum value for a function to be selected.
      - $f(S)$ is added to the final set of new attributes.
- RETURN the set of new attributes.

We take F as a set of previously defined (by an expert) functions. For each one of these functions we consider a subset of the input variables set. In order to know the relevance degree of the function over the set of examples we use an information measure. This measure is detailed below [6], [7]:

$$\rho(X,Y) = \frac{I(X,Y)}{H(X,Y)} \tag{1}$$

where

$$I(X,Y) = \sum_x \sum_y -p(x,y)\ log_2(\frac{p(x)p(y)}{p(x,y)}) \tag{2}$$

and H(X,Y) is the Shannon entropy over two variables, defined as

$$H(X,Y) = \sum_x \sum_y -p(x,y)\ log_2\ p(x,y). \tag{3}$$

The ρ measure estimates the dependence between two generic variables X and Y in the following way: values of $\rho(X,Y)$ close to zero determine a high degree of independence of both variables, whereas values close to one demonstrate a high degree of functional dependency between them. This is the expression we calculate:

$$\rho(Z_k,Y) = \frac{I(Z_k,Y)}{H(Z_k,Y)} \tag{4}$$

where $Z_k = f_k(X_i, X_j)$ is the particular function to be evaluated and Y is the classification measure. In these expressions, Z_k is a new variable.

Once we have this information measure we compare it with a threshold (k) that establishes the minimum value for a function to be selected. The comparison method is explained as follows. We consider the value M_I as the maximum information given by any possible initial variable and it is defined by:

$$M_I = max_p(\rho(X_p,Y)), \forall p \in \{1..n\} \tag{5}$$

being **n** the number of initial variables and **Y** the classification variable. Then, the comparison expression would be:

$$\rho(Z_k,Y) > \alpha * M_I \tag{6}$$

being $\alpha \in [0,1]$ and $k = \alpha * M_I$ the threshold. For the experimental study we considered $\alpha = 0.9$.

So, if the function's information measure exceeds the established threshold, this new variable is added to the final set of new attributes. Finally, this set of new attributes is returned at the end of the process.

The output of the previous algorithm is used to define a new structure that we will call catalog of functions (CF). In a formal way it is an index set where each entry is a relevant function to be consider by the learning algorithm. For a given *i*, *j*, *r*, we define a catalog entry as a three-position vector where the first and the second values make reference to the variables involved in the function (that is, the index of the variables in the chromosome) and the last one is the function applied to these variables. An illustrative example for the previous given values would be $f_r(X_i, X_j)$. By this way, we will be able to associate to this function an integer representing the index of the function in the catalog. This integer can be described by means of the expression $\beta(i,j,k)$ because it is ordered in the catalog. Now we can define the new proposed model of fuzzy rules as follows:

IF X_1 is $A_1 \wedge \ldots \wedge X_n$ is $A_n \wedge \{\wedge_{(i,j,k)\in H} f_k(X_i, X_j)$ is $E_k\}$

THEN Y is B

where A_i are the antecedent values, B is the consequent value and $H \subseteq CF$ is an index subset defining the specific function participating in the rule. We also define $Z_{\beta(i,j,k)} = f_k(X_i, X_j)$, as a new variable resulting of applying the function f_k over the variables (X_i, X_j). On the other hand, $E_1, \ldots, E_k$ are fuzzy values for $Z_1, \ldots, Z_k$.

As we have been managing an extended version of this kind of rules (**DNF rules**), we are able to assign a set of values from its domains to each antecedent variable, so now the new rule definition is

IF X_1 is $\tilde{A_1} \wedge \ldots \wedge X_n$ is $\tilde{A_n} \wedge \{\wedge_{(i,j,k)\in H} f_k(X_i, X_j)$ is $\tilde{E_k}\}$

THEN Y is B

with $\tilde{A_i}$ being a set of fuzzy values on universe U and $\tilde{E_i}$ a set of fuzzy values defined on a fuzzy domain. From now on, we will refer to this kind of rules as Fuzzy Functional Rules (**FFR**). It is important to mention that the new variables Z_i will have their own domain depending on the domains of the variables involved in the function. That is, it only has sense to apply the functions to compatible variables (taking into account the units).

Our model includes a weight for each rule. This weight, a value in [0, 1], is interpreted as a measure of its prediction capability. In the inference process, the weight of each rule modifies the adaptation to the example with the antecedent of the rule by means of a product operation. The winner rule is the one that obtains the highest value in this adaptation process.

IV. Step 2: Learning Algorithm

Our goal is to design a learning algorithm capable to obtain a knowledge base that better represents our problem. We think that the inclusion of functions in the antecedent of the rules can increase the amount of information about the set of examples we are working with. In order to do that we will take as a base algorithm the learning algorithm of fuzzy rules NSLV. Now we are going to describe the behavior of NSLV as well as the extension of this algorithm that is able to include new features, NSLV-F.

A. The learning algorithm NSLV

NSLV[8] is a genetic fuzzy rule learning algorithm that use a sequential covering strategy [9]. This strategy reduces the problem of learning a disjunctive set of rules to a sequence of simpler problems, each requiring that a single conjunctive rule be learned.

SEQUENTIAL-COVERING(T,A,E,D)

- Learned-rules ← {}
- Rule ← LEARN-ONE-RULE(T,A,E)
- while PERFORMANCE(Rule,E) $>$ D, do
  - Learned-rules ← Learned-rules + Rule
  - E ← E-examples correctly classified by Rule
  - Rule ← LEARN-ONE-RULE(T,A,E)
- Learned-rules ← sort Learned-rules accord to PERFORMANCE over E
- return Learned-rules

where T is the target attribute, A is the attribute set, E is the set of examples and D is a threshold.

The sequential covering algorithm reduces the problem of learning a disjunctive set of rules to a sequence of simpler problems, each requiring that a single conjunctive rule be learned.

NSLV uses a genetic algorithm (GA) to implement the **LEARN-ONE-RULE** procedure. The input of this **GA** is a target attribute, representing the consequent variable, the complete set of antecedent variables and the set of examples, and the output is a single rule that covers at least some of the examples. The criteria for selecting the best rule in NSLV is based on obtaining a single rule that covers many of the positive examples and few of the negative examples. The idea is formulated through the consistency and completeness conditions for a rule [10]. The final criterium is the product of a consistency measure by the a completeness measure.

Therefore, each individual of the population represents a complete rule. NSLV uses a DNF model of rule and therefore each variable takes as value a set of linguistic terms whose members are joined by a disjunctive operator. The genetic algorithm represents each DNF rule by three different elements or levels (Fig. 3):

- *The variable level*. This level contains a gene for each predictive variable involved in the problem. Each gene represents a real value that it is interpreted as the relevance degree of a predictive variable on the rule. Furthermore, a special gene is added in this level that it is interpreted as activation threshold, that is, the variables which associated genes have values less than the threshold are not considered in the antecedent of the rule. Therefore, the use of this level allow us to develop an embedded feature selection process [11].
  Two genetic operators are used in this level, two points crossover and real uniform mutation. The generation of this level in the initial population is based on information measure obtained from the training set. This measure permits to establish an initial relevance degree of each variable in the problem. The obtained values are used for all individual of population on this level. The activation threshold is randomly generated between the maximun and mininum value of the initial relevance degree obtained. A more detailed description can be found in [12].
- *The value level*. It is composed of the sequence of assignments to the predictive variables, where each assignment variable/value is represented by a binary string. The complete level is composed by concatenation of the binary strings representing the assignments variable/values for all input variables. The assignment of a certain variable will appear in the description of the rule if the value of its associated gene in the variable level permits to be considered to the variable relevant for this rule.
  We use a binary representation and two genetic operators on this level, two points crossover and binary uniform mutation. The generation of this level in the initial population is the following: known the consequent value (generated previously in the consequent level), an example of this class is selected. The more specific antecedent for this example is obtained and it is used for coding the individual. This process is repeated for all individuals of the population.
- *The consequent level*. It codes the value of the classification variable of the rule. This level is composed by one gene that is represented by a integer value.
  The integer uniform mutation is the unique genetic operator considered on this level and in the initial population this level is randomly generated.

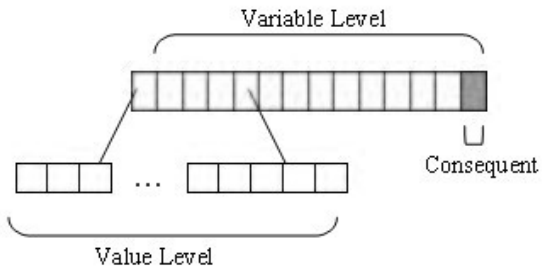

Fig. 3. A rule representation in NSLV

NSLV uses a steady state genetic algorithm. In this case, the selection process is the following: two individuals of the

population are selected, the crossover operators on levels are applied between them obtaining two new individuals. The mutation operators are used for modifying the new individuals. They are evaluated and interchanged by the two worst individuals of the population. Therefore, in each generation of the genetic process only two new individuals are generated and evaluated.

B. NSLV-F: A genetic learning algorithm of fuzzy functional rules

In the current section we explain the changes made in the latest version of NSLV in order to be able to learn FFR. Basically we need to modify the learning algorithm code so it is possible to learn this new type of rules. Thus, the first change takes place in one's own representation of each rule. In this way, we have created a new substructure called function level that encodes the active functions that appear in the rule.

The function level. This level represents from the total set of functions, those that are part of the antecedent of the rule. The individual keeps the same number of levels that the older version apart from this new one. The maximum number of functions that can be included in a single rule is defined by a parameter. In the experiments we have considered up to 10 functions in each rule. This function level use an integer coding where 0 indicates no function considered and any other positive value will refer to the index of the function in the catalog (Fig. 4).

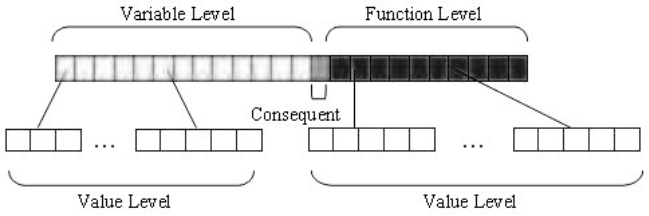

Fig. 4. A rule representation in NSLV-F

Paying attention to genetic operators, we keep the same operators for variables, antecedent values and consequent values used in NSLV. As the function level uses an integer codification, we use two points crossover and a mutation operators for integer coding. The mutation operation defined for this level has associated a probability. This probability establishes if one value of the structure is modified (in the experimental study this value has been set to **0,2**). When the previous fact occurs, a position of the level is randomly selected. If that position has zero value a new random value is generated for selecting a new function of the Catalog. If the position has a different value from zero, then zero value is assigned to that position.

As now we have a new value level associated to the function level which uses a binary coding, we also define the same two genetic operators that were defined for the value level associated to the variable level. That is, two points crossover and binary uniform mutation.

In the initial population all individuals start having the genes of their function level with zero value. That means that at the beginning of the genetic process no functions are considered in the chromosome.

V. Experimental Study

In this section we compare the behavior of the new learning algorithm with respect to the base algorithm NSLV. We also compare it with other classical fuzzy rule learning algorithms. The experimental study was performed on 9 databases of the UCI Repository of Machine Learning Databases and Domain Theories [13] and also on Tao database [14].

TABLE I describes the previously mentioned databases, where each row represents the number of examples (#E), variables (#V), continuous variables (#C), nominal variables (#N), classes (#Cl) and missing values (M).

TABLE I
Database used in the experimental study.

Database	#E	#V	#C	#N	#Cl	M
bpa	345	6	6	0	2	No
brd	106	11	4	7	7	No
h-c	303	13	6	7	2	Yes
irs	150	4	4	0	3	No
pim	768	8	7	1	2	No
son	208	60	60	0	2	No
tao	888	2	2	0	2	No
trf	748	4	4	0	2	No
wdbc	569	30	30	0	2	No
wpbc	198	33	33	0	2	Yes

We have considered in all databases five uniformly distributed linguistic labels to define the domain of the continuous variables. In both algorithms, we use the missing values treatment described in [15]. The results have been obtained by ten-fold cross validation, using the same partition for all algorithms. Parameter ***m*** determines the minimum number of individuals in the population that must be in a class. In all experiments, this value was fixed to $\frac{|pop|}{|cl|+1}$, where $|pop|$ is the size of the population and $|cl|$ is the number of classes. The size of the population was fixed to 100.

First of all we are going make a brief description of the functions considered by the algorithm in the experimental study.

A. Functions

In this empirical part we have taken into account only three possible functions:

- SUM (X_i,X_j), defined as X_i + X_j
- PRODUCT (X_i,X_j) defined as X_i * X_j
- SUBT_ABS (X_i,X_j) defined as $|X_i - X_j|$.

The adding and subtract functions will not be considered with variables with non compatible units. It would not have sense to consider the $SUM(X_1, X_2)$ where X_1 and X_2 measure time and weight respectively. It is important to remark that the domain of the new variables generated will

TABLE II
RESULTS OBTAINED FOR TRAINING.

	NSLV	NSLV-F
bpa	66.9 (2)	71.2 (1)
brd	94.7 (1)	86.6 (2)
h-c	91.2 (2)	92.1 (1)
irs	96.8 (2)	97 (1)
pim	80.2 (2)	80.3 (1)
son	90.4 (2)	96.6 (1)
tao	82.4 (2)	85.9 (1)
trf	77.1 (1)	77 (2)
wdbc	95.8 (2)	97.1 (1)
wpbc	80.1 (1)	79.5 (2)
Rnk	1.7	1.3
Pos	2	1

TABLE III
RESULTS OBTAINED FOR TEST.

	NSLV	NSLV-F
bpa	56.7 (2)	59.9 (1)
brd	55.6 (2)	57.5 (1)
h-c	77.8 (2)	78.4 (1)
irs	94 (2)	94.6 (1)
pim	72.6 (2)	74.8 (1)
son	69.1 (2)	73.9 (1)
tao	81.6 (2)	85.1 (1)
trf	75.9 (2)	76 (1)
wdbc	93.6 (2)	95.6 (1)
wpbc	74.2 (2)	77.3 (1)
Rnk	2	1
Pos	2	1

TABLE IV
RESULTS OBTAINED FOR RULES.

	NSLV	NSLV-F
bpa	6.1 (1)	8.9 (2)
brd	19.2 (1)	20.1 (2)
h-c	11.4 (1)	13.3 (2)
irs	4 (2)	3.4 (1)
pim	12.8 (1)	13.3 (2)
son	9.9 (2)	9.3 (1)
tao	3.4 (1)	4.1 (2)
trf	3.4 (2)	3 (1)
wdbc	4.5 (1)	5 (2)
wpbc	3.4 (2)	3.3 (1)
Rnk	1.4	1.6
Pos	1	2

TABLE V
A RULE SET FROM TAO DATABASE

IF SUM(var0,var1) IS {High or Very High}
THEN class IS C1 Weight=0.884278

IF var0 IS {Very Low or Low or Medium} AND
SUM(var0,var1) IS {Very Low or Low}
THEN class IS C0 Weight=0.908361

IF var0 IS {Very High}
THEN class IS C1 Weight=1

also be divided into five uniformly distributed linguistic labels.

B. Comparing NSLV with NSLV-F

We have focused our study in the following indicators: accuracy on training set (Training), accuracy on test set (Test) and number of rules (Rules).

Training and Test figure the accuracy of the learned model. On the other hand, Rules define the size and the interpretabilitiy of the knowledge base.

To perform the comparison was used Bonferroni-Dunn test [16]. It establishes that two classifiers have differences if they differ in at least one critical distance. This distance depends on the number of databases, the number of learning algorithms to compare and a critical value q_α, with error α. In that case we took 0.05, $q_\alpha = 1.960$. Finally, for 10 databases and two classifiers, the critical distance (CD) is **0,619**.

The results are shown in TABLE II, TABLE III and TABLE IV. The first column indicates databases evaluated. The second and the third columns represent the results for NSLV and NSLV-F algorithms respectively. First row shows indicators evaluated and the last one contains the value estimated for Bonferroni-Dunn test.

As we can see, there are significant differences in test (TABLE III). This means that NSLV-F improves the accuracy with respect to NSLV. Another important fact is that the results obtained for Training (TABLE II) and Rules (TABLE IV) have no significant differences, so the number of learned rules are approximately the same and they cover almost the same number of examples. Anyway, the improvement obtained in the Test results could be due to the greater ability to generalize of NSLV-F. The inclusion of new variables created by input variables combinations (by means of functions), allow us to obtain more general rules that increase the prediction capacity of the model.

TABLE V shows a rule set obtained by NSLV-F from Tao database. This database is a synthetic problem composed by two real predictive variables, $var0$ and $var1$, and two classes, $C0$, $C1$. We can see that the knowledge base is composed by three rules and it only uses $var0$ and a combination of both initial variables SUM($var0$, $var1$). The point is that the variable $var1$ does not appear alone in any rule. So that, we would be able to conclude that, in this particular case, the new variable SUM($var0$, $var1$) makes possible to obtain more general rules or even gives more information that the variable $var1$ on its own. So we find one of the main reasons why this new model is proposed.

C. Comparing NSLV-F with other fuzzy rule learning algorithms on accuracy

In this section we compare NSLV-F with other well-known fuzzy rule learning algorithms. We have used KEEL platform [17] and for all algorithms we have used the recommendation settings by KEEL. The fuzzy algorithms are the following:

- Fuzzy Ishibuchi99 [18]: Its genetic algorithm handles each fuzzy rule as an individual, and a fitness value is assigned to each rule. It uses linguistic values with

TABLE VI
COMPARING NSLV-F WITH OTHER FUZZY RULE-BASED ALGORITHMS

	GP	GAP	Ishibushi	Chi	SAP	NSLV-F
bpa	55.32 (6)	60.82 (2)	58.25 (4)	57.87 (5)	63.49 (1)	59.9 (3)
brd	55.09 (3)	56.9 (2)	51.72 (5)	43.9 (6)	54 (4)	57.5 (1)
h-c	78.17 (2)	73.49 (5)	77.87 (3)	50.77 (6)	76.88 (4)	78.4 (1)
irs	86.66 (6)	90.66 (5)	95.33 (1.5)	92.6 (4)	95.33 (1.5)	94.6 (3)
pim	73.58 (3)	73.83 (2)	68.75 (6)	73.05 (4)	72.53 (5)	74.8 (1)
son	70.69 (2)	61.07 (6)	61.59 (5)	61.74 (4)	69.14 (3)	73.9 (1)
tao	82.82 (4)	76.15 (6)	81.19 (5)	84.36 (3)	86.91 (1)	85.1 (2)
trf	76.46 (3)	76.19 (5)	76.2 (4)	77.28 (1)	76.47 (2)	76 (6)
wdbc	93.15 (3)	81.89 (5)	92.56 (4)	95.06 (2)	71.17 (6)	95.6 (1)
wpbc	76.83 (4)	88.23 (1)	76.35 (5)	69.6 (6)	80.91 (2)	77.3 (3)
Rank	3.6	3.9	4.25	4.1	2.95	2.2

fixed membership functions as antecedent fuzzy sets, so a linguistic interpretation of each fuzzy rule is easily obtained.

- Fuzzy GAP [19]: It classifies an instance as a result of a quadratic combination of its features. The weights of such combination are fitted as a quadratic discriminant. An instance is classified with the class that has the better value for the quadratic combination of its features.
- Fuzzy SAP [19]: A Simulated Annealing algorithm is used to learn a fuzzy classifier. For each hypothesis, the number of labels and number of rules must be given. In same way, as it is possible to manage any combination of conjunction and/or disjunctions in the antecedent part of a fuzzy rule, a maximum deep tree size must be given too. Those parameters are, in conjunction with Simulated Annealing typical parameters, of capital importance in the evolution of this method.
- Fuzzy GP [20]: Combining genetic programming operators with Simulated Annealing Search to evolve fuzzy rule based classifiers.
- Fuzzy Chi-RW: This algorithm takes as base algorithm the Chi et al. [21] but adding weights to rules. The algorithm is an adapted version of Wang-Mendel algorithm[22] for classification problems.

In TABLE VI appears the result of comparison with the fuzzy methods mentioned before. In this case, for 10 databases and 6 classifiers, the critical distance is **1.05**. Bonferroni test reveals that there are significant differences in test parameter and that NSLV-F has the best result, being significantly better than GP, Chi and Ishibushi. There are not significant differences with the rest of the algorithms.

VI. CONCLUSIONS AND FUTURE WORK

In this work we have presented a learning algorithm that introduces the concept of feature construction by using functions as a way of creating new attributes. The basic idea is to consider not only the knowledge given by the input variables but also the knowledge that can be extracted from the combination of these input variables. In order to do that we combine the variables by using some previously defined functions. These functions will be managed by means of a structure that will also contain the most promising ones taking into account an information measure. A new model of rule has been also proposed in order to represent this kind of knowledge. In addition, we took as basic algorithm a learning fuzzy rule-based one and we extended it to obtain this new model. Finally, the experimental results show that our proposal gives us the possibility of finding more general rules and also increases the prediction capability of the model. Our purpose is to go on improving the current model in order to consider more functions in the future that could give us better results. Anyway, this is an initial approximation and it will be necessary to go on searching for other functions that allow us to improve the accuracy and efficiency of the process.

ACKNOWLEDGMENT

This work is partially supported by the projects P09-TIC-04813.

REFERENCES

[1] E. H. Mamdani, S. Assilian, "An experiment in linguistic synthesis with fuzzy logic controller". *International Journal of Man-Machine Studies*, vol. 1, pp.1-13, 1975.
[2] T. Takagi, M. Sugeno, "Fuzzy identification of systems and its application to modeling and control". *IEEE Transactions on systems, Man and Cybernetics*, vol. 15, pp. 116-132, 1985.
[3] K. Drodz, H. Kwasnicka, "Feature Set Reduction by Evolutionary Selection and Construction". *Lecture Notes in Computer Science 6071 LNAI (PART2)*, pp. 140-149, 2010.
[4] R. Alfred, "Optimizing Feature Construction Process for Dynamic Aggregation of Relational Attributes". *Journal of Computer Science* 5 (11), pp. 864-877.
[5] H. A. Gvenir, M. akir, "Voting features based classifier with feature construction and its application to predicting financial distress". *J.Expert Systems with Applications* 37 (2), pp. 1713-1718.
[6] S. Kullback, *Information Theory and Statistics*, Gloucester, Mass, 1978.
[7] L. Wehenkel, "On uncertainty measures used for decision tree induction", *Proc. of IPMU'96*, pp. 413-418, 1996.
[8] A. González, R. Pérez, "Improving the genetic algorithm of SLAVE", *Mathware & Soft Computing*, 16, pp. 59-70, 2009.
[9] T. Mitchell, *Machine Learning*. Ed. MacGraw-Hill, 1997.
[10] A. González, R. Pérez ,"Completeness and consistency conditions for learning fuzzy rules". *Fuzzy Sets and Systems*, vol. 96, pp. 37-51, 1998.
[11] A. González, R. Pérez, "An analysis of the scalability of an embedded feature selection model for classification problems". *Proceedings of the Information Processing and Management of Uncertainty on Knowledge-Based Systems IPMU 2006*, pp. 1949-1956, 2006.
[12] A. González, R. Pérez, "Selection of Relevant Features in a Fuzzy Genetic Learning Algorithm". *IEEE Transactions on System, Man, and Cybernetics Part B*, vol. 31(3), pp. 417-425, 2001.
[13] A. Asuncion, D.J. Newman, "UCI Machine Learning Repository" Irvine, CA: University of California, School of Information and Computer Science, 2007. Available: http://www.ics.uci.edu/ mlearn/MLRepository.html.

[14] E. Bernardó-Mansilla, X. Llorá, J. Garrel (2002) XCS and gale: "A comparative study of two learning classifier". *In: P. Lanzi, W. Stolzman, S. Wilson (eds) Advances in Learning Classifier Systems, LNCS, vol. 2321*. Springer, Heidelberg, pp. 115-132.

[15] A. González, R. Pérez, "SLAVE: to genetic learning system based on an iterative aproach". *IEEE Transaction on Fuzzy System*, vol. 27 (2), pp. 176-19, 1999.

[16] O. Dunn,"Multiple Comparisons among means". *Journal of the American Stadistical Association*, 1961.

[17] Alcalá J. et al, 2009. KEEL: A Software Tool to Assess Evolutionary Algorithms to Data Mining Problems. Soft Computing 13:3 307-318

[18] Ishibuchi, H. et al, 1999. Performance evaluation of fuzzy classifier systems for multidimensional pattern classification problems. IEEE Transactions on Systems, Man, and Cybernetics, Part B: Cybernetics 29:5 pp. 601-618.

[19] Sánchez, L. and Couso, I., 2001. Combining GP Operators With SA Search To Evolve Fuzzy Rule Based Classifiers. Information Sciences 136:(1-4), pp 175-192.

[20] Otero, J. and Sánchez, L., 2006. Induction of descriptive fuzzy classifiers with the Logitboost algorithm. Soft Computing 10:9, pp 825-835.

[21] Chi, Z., Wu, J., Yan, H., Handwritten Numeral Recognition Using Self-Organizing Maps and Fuzzy Rules. *Pattern Recognition*, 28:1, pp. 59-66, 1995.

[22] Wang, L. X., Mendel, J. M., Generating Fuzzy Rules by Learning from Examples. *IEEE Transaztiond on Systems, Man and Cybernetics*, 22:6, pp. 1414-1427, 1992.

2011 IEEE International Conference on Fuzzy Systems
June 27-30, 2011, Taipei, Taiwan

Using The Adaboost Algorithm For Extracting Fuzzy Rules From Low Quality Data: Some Preliminary Results

Ana M. Palacios
Departamento de Informática
Universidad de Oviedo, Spain
email: palaciosana@uniovi.es.

Luciano Sánchez
Departamento de Informática
Universidad de Oviedo, Spain
email: luciano@uniovi.es

Inés Couso
Departamento de Estadística e I.O. y D.M
Universidad de Oviedo, Spain
email: couso@uniovi.es

***Abstract*—When the Adaboost algorithm is used for extracting fuzzy rules from data, each rule is regarded as a weak learner, and knowledge bases as assimilated to ensembles. In this paper we propose an extension of this framework for obtaining fuzzy rule-based classifiers from imprecise data. In the new approach, the mentioned search of the best rule at each iteration is carried out by a genetic algorithm with a fuzzy fitness function. The instances will be assigned fuzzy weights, however each fuzzy rule will be associated to a crisp number of votes.**

***Index Terms*—Genetic Fuzzy Systems, Low Quality Data, Boosting**

I. Introduction

Boosting algorithms combine different classifiers for obtaining an ensemble that performs better than any of its components [1]. These algorithms repeatedly invoke a learning algorithm to successively generate a committee of simple, inaccurate classifiers. Each time a new simple classifier is added to this ensemble, the examples in the training set are re-weighted so that future classifiers will focus on the most difficult examples, and a voting strength is assigned to the classifier. The number of votes a classifier is given depends on the confidence in its classification accuracy, as measured on the training set.

Fuzzy Rule Based Classification Systems (FRBCS) can also be regarded as ensembles, where each fuzzy rule is matched to one of the mentioned simple classifiers. When an appropriate reasoning scheme is used, it has been shown that the mechanism used for obtaining the output of a FRBCS, given an input value, can be assimilated to a voting process [2], and the voting strength of each simple classifier is the product of the compatibility between the antecedent of the corresponding fuzzy rule and the degree of certainty of its consequent. This interpretation has been used before, and the Adaboost algorithm has been applied to the learning of fuzzy rules from data [3][4][5], in combination with a Genetic Algorithm (GA). The resulting learning algorithm is a Genetic Fuzzy System (GFS) that shares certain properties with Iterative Rule Learning approaches [6]. Furthermore, after the work of Friedman [7], this process has been regarded as a forward stepwise estimation of the statistical parameters defining a logit transform of a Generalized Additive Model, giving rise to the LogitBoost algorithm [7] and its genetic extension for learning FRBCS from data [8]. The use of boosting techniques for learning fuzzy rules from data is therefore a well known technique, whose main virtues are a fast learning and accurate results, but this use is not free from problems. The first drawback of the employment of Adaboost for learning FRBCS is in the use of a voting-based inference, that makes the linguistic interpretation of the Knowledge Base (KB) harder. This problem was addressed in [9], where a new algorithm was proposed for which the degrees of confidence in the consequents of the rules were iteratively adjusted until the results produced by a "winner-takes-all" type of inference were similar to that of voting. Nevertheless, there are other difficulties that are still open. A second issue with the application of Adaboost to the learning of fuzzy rules lies in the requirements imposed to the data, that must be precisely perceived: being based in Generalized Additive Models, Adaboost or Logitboost can cope with random uncertainty, but they are not able to process data when a combination of epistemic and random uncertainties is present [10]. Because of these reasons, this paper contains a new proposal for applying the Adaboost algorithm for learning FRBCS from low quality data [11], including both problems with imprecisely perceived features and problems with a partial lack of knowledge about the class labels attributed to some instances.

The organization of this work is as follows: the following section, briefly introduces the Adaboost algorithm, describes the type of fuzzy classifiers that are boosted and recall a method for boosting descriptive fuzzy rule bases [12]. In Section 3, we propose an extension of this algorithm for interval and fuzzy data. In Section 4 some properties of the proposed algorithms are evaluated on a number of data sets and compared to that of other GFS for low quality data. In Section 5 some concluding remarks and future works are discussed.

II. Adaboost and fuzzy rule based classifiers

At this point we introduce the basic notation employed throughout the paper. Let $\mathbf{X}$ be the feature space, and let $\mathbf{x}$ be a feature vector $\mathbf{x} = (x_1, \ldots, x_n) \in \mathbf{X}$. Let p be the number of classes. The training set is a sample of m classified examples

978-1-4244-7316-8/11/$26.00 ©2011 IEEE

$(\mathbf{x}_i, y_i)$, where $\mathbf{x}_i \in \mathbf{X}$, $1 \leq y_i \leq p$, $1 \leq i \leq m$.

The KB of the FRBCS comprises N rules. The antecedents of the rules are logical combinations of fuzzy logic asserts, whose degrees of truth are modeled by N fuzzy subsets $A^j \in \mathcal{F}(\mathbf{X})$, forming a fuzzy partition $\mathcal{A} = \{A^j\}_{j=1\ldots N}$ of the feature space. A fuzzy rule based classifier is therefore defined by means of a fuzzy relationship defined on $\mathcal{A} \times \{1, \ldots, p\}$. Values of this relationship describe the degrees of compatibility among the fuzzy subsets of the feature space collected in $\mathcal{A}$, and each of the classes. In other words, for every antecedent A^j there are p numbers between 0 and 1 that represent the confidence in the assertion "All elements in the fuzzy set A^j belong to class number k". Values close to 1 indicate "high confidence," and values close to 0 denote "absence of knowledge about the assertion."

In this paper, we will translate the former fuzzy relationship into linguistic statements by combining p terms

$$\text{compatibility}(A^j, c_k) = s_k \quad k = 1, \ldots p,$$

into a single sentence, as follows:

$$\text{if } \mathbf{x} \text{ is } A^j \text{ then truth}(c_1) = s_1^j \text{ and } \cdots \text{ and truth}(c_p) = s_p^j.$$

The antecedents A^j are decomposed in a Cartesian product of fuzzy sets defined over each feature, $A^j = A_1^j \times A_2^j \times \ldots \times A_n^j$, thus the rules are

$$\begin{gathered}\text{if } x_1 \text{ is } A_1^j \text{ and } \ldots \text{ and } x_n \text{ is } A_n^j \\ \text{then truth}(c_1) = s_1^j \text{ and } \cdots \text{ and truth}(c_p) = s_p^j.\end{gathered}$$

An instance $\mathbf{x}$ is assigned to the class

$$\arg\max_{k=1,\ldots,p} \bigvee_{j=1}^{N} A^j(\mathbf{x}) \wedge s_k^j \tag{1}$$

where "$\wedge$" is the product and "$\vee$" is the arithmetic sum, so called "maximum voting scheme" [13].

A. The Adaboost algorithm

Let us define a set $\{g^1, g^2, \ldots, g^N\}$ of simple, but possibly unreliable binary classifiers. Boosting consists in combining these low quality classifiers (so called "weak hypotheses" in the boosting literature) with a voting scheme to generate an overall classifier that performs better than any of its individual constituents alone. It has been shown that a fuzzy rule can be regarded as a particular case of a weak hypothesis, and a fuzzy rule base can be interpreted as a weighted combination of weak hypotheses.

Weak hypotheses take feature values as input and produce both a class number as well as a degree of confidence in the given classification. In two-classes problems, these two outputs are encoded by a single real number, $g^j(\mathbf{x}) \in \mathbf{R}$, whose sign is interpreted as the label of $\mathbf{x}$ and whose absolute value is interpreted as the confidence in the classification. The higher this value the more confidence is given to the classification. AdaBoost is intended to produce a linear threshold of all hypotheses:

$$\text{sign}\left(\sum_{j=1}^{N} \alpha^j g^j(\mathbf{x})\right). \tag{2}$$

Observe that Adaboost can operate with any learning algorithm that generates a confidence rated classifier on a given weighted data set. There are different algorithms for assigning the number of votes to a weak hypothesis, and for adjusting the weights of the examples. For example, in confidence-rated Adaboost [15] the number of votes of the weak hypothesis g^h is given by the value α^h that minimizes the following function:

$$Z(\alpha) = \sum_{i=1}^{m} w_i \exp(-\alpha y_i g^h(\mathbf{x}_i)) \tag{3}$$

and the weights w_i of the examples are updated according to

$$w_i \leftarrow w_i \exp(-\alpha^h y_i g^h(\mathbf{x}_i))/v \tag{4}$$

where v is a normalization factor such that $\sum w_i = 1$. There are analytical approximations and heuristics that may replace this formula in specific problems.

B. Boosting fuzzy rules in binary problems

For the sake of simplicity, we restrict the discussion for the time being to two-classes problems $y_i \in \{-1, 1\}$. The space of weak hypotheses is, in this case, the product space of the fuzzy partition and the class labels, $\mathcal{A} \times \{-1, 1\}$. Given the results in the preceding subsection, the fitness of a fuzzy rule is

$$\text{fitness}(\text{ if } \mathbf{x} \text{ is } A^j \text{ then } c^j) = \sum_i w_i \exp(-y_i c^j A^j(\mathbf{x}_i)) \tag{5}$$

and the number of votes of this rule is the value of α minimizing the following expression [14]:

$$Z(\alpha) = \sum_i w_i \exp(-\alpha y_i A^j(\mathbf{x}_i)). \tag{6}$$

$Z(\alpha)$ is convex except for the case in which the rule antecedent does not cover any negative examples; for avoiding this and other numerical instabilities, a term that penalizes large values of α is added

$$Z(\alpha) = \sum_i w_i \exp(-\alpha y_i A^j(\mathbf{x}_i)) + \sum_{i:A^j(\mathbf{x}_i)=0} w_i \exp(|\alpha\epsilon|) \tag{7}$$

where ϵ is determined by hand.

The weights w_i of all the instances are recalculated each time a new weak learner is added to the ensemble. The weights of correctly classified instances are lowered, and these of misclassified examples are increased, using the expression that follows:

$$w_i \leftarrow \frac{w_i \exp(-\alpha^j y_i A^j(\mathbf{x}_i))}{\sum_i w_i \exp(-\alpha^j y_i A^j(\mathbf{x}_i))} \tag{8}$$

Notice, that an instance is never completely removed unless $\alpha^j \to \infty$, which is prevented by the penalty term in eq. (7).

C. Boosting fuzzy rules in multiclass problems

We have mentioned that the space of weak hypothesis in two-classes problems is $\mathcal{A} \times \{c_1, c_2\}$. That is to say, the j-th iteration of the learning algorithm searches for a pair (A^j, c^j), which are parameters of the rule

$$\text{if } \mathbf{x} \text{ is } A^j \text{ then } c^j, \tag{9}$$

for which the fitness value is maximum. This value was defined in Eq. (5), which we rewrite here as follows:

$$\begin{aligned}\text{fitness}(\text{if } \mathbf{x} \text{ is } A^j \text{ then } c^j) = \\ \sum_{i:y_i=c^j} w_i \exp(A^j(\mathbf{x}_i)) \\ +\sum_{i:y_i\neq c^j} w_i \exp(-A^j(\mathbf{x}_i)).\end{aligned} \tag{10}$$

Once the pair (A^j, c^j) maximizing this fitness function is found, the rule is assigned a number of votes s^j (see Eq. (6)), thus its final linguistic writing is:

$$\text{if } \mathbf{x} \text{ is } A^j \text{ then truth}(c^j) = s^j. \tag{11}$$

For extending this scheme to multiclass problems [3] the initial problem is transformed into p binary problems, where the instances of the k-th binary problem are re-labelled:

$$y_i^{(p)} = \begin{cases} 1 & y_i = p \\ -1 & y_i \neq p. \end{cases} \tag{12}$$

The solution of the k-th problem comprises fuzzy rules with this form:

$$\begin{aligned}&\text{if } x_1 \text{ is } A_1^j \text{ and } \ldots \text{ and } x_n \text{ is } A_n^j \\ &\text{then tr(class} = c_k) = s_1^{jk} \text{ and tr(class} \neq c_k) = s_{-1}^{jk}.\end{aligned} \tag{13}$$

These rules can be replaced by their equivalent p-classes consequents, by substituting the "class $\neq c_k$" label with the corresponding set of class labels of the multi-class problem, i.e.

$$\begin{aligned}&\text{if } x_1 \text{ is } A_1^j \text{ and } \ldots \text{ and } x_n \text{ is } A_n^j \text{ then} \\ &\text{tr}(c_1, \ldots, c_k, \ldots, c_p) = (s_{-1}^{jk}, \ldots, s_{-1}^{jk}, s_1^{jk}, s_{-1}^{jk}, \ldots, s_{-1}^{jk}).\end{aligned} \tag{14}$$

III. An extension of the Adaboost algorithm to learn fuzzy rule based classifiers from low quality data

We will represent the epistemic uncertainty in the data by means a nested set of confidence intervals, that provide us with the same information about the unknown value as a possibility distribution for which the α-cuts of its associated fuzzy membership function are confidence intervals with level $1-\alpha$, as explained in [11]. Representing the imprecision by means of sets of possible values implies that the output of the FRBCS might not be completely determined and generally speaking, it will be a fuzzy subset of the class labels. From the foregoing it can be deduced that the fitness of a rule should also be a set, however extending Eq. 5 is not trivial. Different decisions can be taken that influence the accuracy of the method and also its computational cost.

Let us use an illustrative example for introducing the problems that arise when we regard the computation of the output of an FRBCS for imprecise data as a voting-based committee. Suppose that we are given the KB that follows:

if $x < 1.5$ then truth(class is A)= 0.4 and truth(class is B)= 0.8
if $x \in [1, 2]$ then truth(class is A)= 0.8 and truth(class is B)= 0.1
if $x > 2$ then truth(class is A)= 0.2 and truth(class is B)= 0.6

and the input is

$x \in [1.2, 1.8]$.

If we determine first the set of compatibilities of each rule with the imprecise example and then add the sets of votes, the situation is as follows:

Rule	Votes for class 'A'	Votes for class 'B'
Rule # 1:	{0,0.4}	{0,0.8}
Rule # 2:	0.8	0.1
Rule # 3:	0	0
Total	{0.8, 1.2}	{0.1, 0.9}

In words, the output of the classifier is the set of classes {A,B}, because we cannot state that any element of {0.8, 1.2} is higher than any element of {0.1, 0.9} neither the opposite. However, this course of reasoning will not always produce the most specific answer. Observe that, if the actual value of x is between 1.2 and 1.5, rules 1 and 2 are true, thus the number of votes of classes 'A' and 'B' are 1.2 and 0.9. If the value of x is between 1.5 and 1.8, the number of votes are 0.8 and 0.1. In either case, the object should have been assigned the class 'A'.

With this example we have shown that regarding a KB as an ensemble is not immediate when the data are imprecise: the most specific output of the classifier, when the input is a crisp set, is the set of classes

$$\text{class}(\overline{X}) = \{\arg \max_{k=1\ldots p} \sum_{j=1}^{N} A^j(x) s_k^j \mid x \in \overline{X}\}. \tag{15}$$

However, if we regard the KB as an ensemble of weak classifiers, where each one of them is assigned a set-valued, number of votes, the output is the set

$$\text{bclass}(\overline{X}) = \operatorname*{notdom}_{k=1\ldots p} \left\{ \bigoplus_{j=1}^{N} s_k^j \odot \{A^j(x) \mid x \in \overline{X}\} \right\} \tag{16}$$

where the operator "notdom" means

$$\operatorname*{notdom}_{k=1\ldots p}\{V_k\} = \{q \mid V_q \preceq V_r, r = 1, \ldots, p\} \tag{17}$$

and the precedence between set-valued votes is

$$A \prec B \iff a < b \text{ for all } a \in A, b \in B \tag{18}$$

$$A \parallel B = \neg((A \prec B) \vee (B \prec A)) \tag{19}$$

$$A \preceq B = (A \prec B) \vee (A \parallel B). \tag{20}$$

Observe that

$$\text{class}(\overline{X}) \subseteq \text{bclass}(\overline{X}) \tag{21}$$

but the equality does not hold, in general.

If the data is fuzzy, the situation is similar. The most specific output of the classifier is the fuzzy set whose membership function is as follows:

$$\begin{aligned}\text{class}(\widetilde{X})(t) = \quad &\max\{\alpha \mid \\ &t = \arg\max_{k=1\ldots p} \textstyle\sum_{j=1}^{N} A^j(x) s_k^j \\ &\text{and } \widetilde{X}(x) \geq \alpha\}.\end{aligned} \tag{22}$$

In case we regard the KB as an ensemble of weak classifiers, where each one of them is assigned a fuzzy number of votes, the output is in turn the fuzzy set

$$\text{bclass}(\widetilde{X})(t) = \max\{\alpha \mid t \in \text{bclass}([\widetilde{X}]_\alpha)\}. \tag{23}$$

Summarizing, when the data is imprecise, the most voted option of the ensemble is not known but our information about it is a normal fuzzy set. If the KB is furthermore regarded as an ensemble, thus the number of votes of each rule are independently computed, the fuzzy set describing the result of the classification is a superset of the result given by Eq. (22). This loss of specificity in the view of a KB as an ensemble has to be taken into account in the definition of the fitness function.

A. Fitness of a rule with interval or fuzzy data

We propose to generalize the fitness function in Eq. (10) to interval-valued data with the set-valued function that follows, which is based on the bounds given in Eq. (16):

$$\begin{aligned}&\overline{\text{fitness}}_{\{(\overline{\mathbf{x}}_i,\overline{y}_i)\}}(\text{if } \mathbf{x} \text{ is } A^j \text{ then } c^j) = \\ &\quad \oplus_{i:\overline{y}_i=c^j} \overline{w}_i \odot \{\exp(A^j(x)) \mid x \in \overline{\mathbf{x}}_i\} \oplus \\ &\quad \oplus_{i:\overline{y}_i\cap c^j=\emptyset} \overline{w}_i \odot \{\exp(-A^j(x)) \mid x \in \overline{\mathbf{x}}_i\} \oplus \\ &\oplus_{i:\overline{y}_i\neq c^j,\, \overline{y}_i\cap \overline{c}^j\neq\emptyset} \overline{w}_i \odot \{\exp(\{A^j(x), -A^j(x)\}) \mid x \in \overline{\mathbf{x}}_i\}\end{aligned} \tag{24}$$

Observe that we allow the use of set valued weights $\overline{w}_i$. In turn, applying the extension principle, the same function can be extended to fuzzy data. The membership function of the fuzzy fitness of a rule is

$$\begin{aligned}&\widetilde{\text{fitness}}_{\{(\widetilde{\mathbf{x}}_i,\widetilde{y}_i)\}}(\text{if } \mathbf{x} \text{ is } A^j \text{ then } c^j)(t) = \\ &\max\{\alpha \mid t \in \overline{\text{fitness}}_{\{([\widetilde{\mathbf{x}}_i]_\alpha,[\widetilde{y}_i]_\alpha)\}}(\text{if } \mathbf{x} \text{ is } A^j \text{ then } c^j)\},\end{aligned} \tag{25}$$

where t is a real number.

B. Issues with the fitness of a rule in multiclass problems

When extending the procedure seen in Section II-C for solving multi-class problems, the intermediate binary sets of data might contain unlabeled instances. Let us explain this with an illustrative example.

Consider the imprecise dataset that follows, comprising three crisp examples with set-valued labels. It is remarked that, in this context, an instance labelled "$\{c_1, c_2\}$" means that we are sure that the true class of the object is not c_3, but this knowledge cannot be further precised:

$(x_1, y_1) = (1, \{c_1, c_2\})$
$(x_2, y_3) = (2, \{c_1, c_3\})$
$(x_3, y_3) = (3, \{c_2, c_3\})$.

Following the procedure described in Section II-C, this dataset will be decomposed in three binary problems. Let us generalize that procedure to imprecise instances by using the most specific set of labels that is compatible with the data, as follows:

Problem # 1
$(1, \{1, -1\})$
$(2, \{1, -1\})$
$(3, -1)$

Problem # 2
$(1, \{1, -1\})$
$(2, -1)$
$(3, \{1, -1\})$

Problem # 3
$(1, -1)$
$(2, \{1, -1\})$
$(3, \{1, -1\})$

Each one of these three datasets has two elements whose classes are $\{-1, 1\}$ and therefore the fitness does not depend on how they are labelled: for instance, for Problem # 1, no matter which rule between

$$\text{if x=1 then t(class = 1)=}s_1^{1,1}$$

and

$$\text{if x=1 then t(class} \neq \text{ 1)=}s_{-1}^{1,1}$$

is chosen, the same fitness is obtained (see Eq. 24).

In this case, a learning algorithm which is only guided by the optimization of the fitness function can produce any KBs formed by selecting one rule from each line that follows. We have grayed out the rules that do not appear in an arbitrary selection, whose merging will be studied later.

Problem # 1
if x=1 then t(class = 1)=$s_1^{1,1}$ $\approx$ if x=1 then t(class $\neq$ 1)=$s_{-1}^{1,1}$
if x=2 then t(class = 1)=$s_1^{2,1}$ $\approx$ if x=2 then t(class $\neq$ 1)=$s_{-1}^{2,1}$
if x=3 then t(class $\neq$ 1)=$s_{-1}^{3,1}$

Problem # 2
if x=1 then t(class = 2)=$s_1^{1,2}$ $\approx$ if x=1 then t(class $\neq$ 2)=$s_{-1}^{1,2}$
if x=2 then t(class $\neq$ 2)=$s_{-1}^{2,2}$
if x=3 then t(class = 2)=$s_1^{3,2}$ $\approx$ if x=3 then t(class $\neq$ 2)=$s_{-1}^{3,2}$

Problem # 3
if x=1 then t(class $\neq$ 3)=$s_{-1}^{1,3}$
if x=2 then t(class = 3)=$s_1^{2,3}$ $\approx$ if x=2 then t(class $\neq$ 3)=$s_{-1}^{2,3}$
if x=3 then t(class = 3)=$s_1^{3,3}$ $\approx$ if x=3 then t(class $\neq$ 3)=$s_{-1}^{3,3}$

The merging of the selected rules is

if x=1 then t(1,2,3)=($s_1^{1,1}$+$s_{-1}^{1,3}$,$s_1^{1,2}$+$s_{-1}^{1,3}$,0)
if x=2 then t(1,2,3)=($s_1^{2,1}$+$s_{-1}^{2,2}$,0,$s_{-1}^{2,2}$+$s_1^{2,3}$)
if x=3 then t(1,2,3)=($s_{-1}^{3,3}$,$s_{-1}^{3,1}$+$s_1^{3,2}$+$s_{-1}^{3,3}$,$s_{-1}^{3,1}$).

Observe that the result of this arbitrary selection has assigned a non-null degree confidence to the class c_1 in the third rule, which obviously is not the best possible KB for this problem. We realize that there are other selections that achieve the objective, but our point is showing that there is a chance that the committee does not contain the proper rules unless the unlabeled instances in the intermediate problems are removed, as follows:

Problem # 1
if x=3 then t(class $\neq$ 1)=$s_{-1}^{3,1}$

Problem # 2
if x=2 then t(class $\neq$ 2)=$s_{-1}^{2,2}$

Problem # 3
if x=1 then t(class $\neq$ 3)=$s_{-1}^{1,3}$

whose merging is:

if x=1 then t(1,2,3)=($s_{-1}^{1,3}$,$s_{-1}^{1,3}$,0)
if x=2 then t(1,2,3)=($s_{-1}^{2,2}$,0,$s_{-1}^{2,2}$)
if x=3 then t(1,2,3)=(0,$s_{-1}^{3,1}$,$s_{-1}^{3,1}$).

Notwithstanding, if the unlabeled instances are removed then additional problems with the decomposition in binary problems will appear. Since the pruned individual problems do not longer contain information about where the removed instances were located, it may happen that the corresponding areas of the feature space are covered at the same time by different rules that negatively interact between themselves. This problem also happens with Iterative Rule Learning (IRL) algorithms [12], where it is solved by a simplification stage that it is not a part of the boosting algorithm. Therefore, we have decided to simplify the search and not to generate the intermediate datasets when working with multiclass problems, and propose instead to define the fitness of a rule with multiple consequents as a vector of values, and to define a lexicographic ordering between them. The fitness function we propose is as follows:

$$\begin{aligned}
&\overline{\text{fitness}}_{\{(\overline{\mathbf{x}}_i,\overline{y}_i)\}}(\text{if } \mathbf{x} \text{ is } A^j \text{ then } (c_1,\ldots,c_p)) = \\
&\Big(\textstyle\bigoplus_{\overline{y_i}=c_1} \overline{w}_i \odot \exp(\{A^j(x) \mid x \in \overline{\mathbf{x}}_i\}) \oplus \\
&\textstyle\bigoplus_{c_1 \in \overline{y}_i, c_1 \neq \overline{y}_i} \overline{w}_i \odot \\
&\qquad \exp(\{-A^j(x), A^j(x) \mid x \in \overline{\mathbf{x}}_i\}) \oplus \\
&\textstyle\bigoplus_{c_1 \notin \overline{y}_i} \overline{w}_i \odot \exp(\{-A^j(x) \mid x \in \overline{\mathbf{x}}_i\}), \\
&\quad \vdots \\
&\textstyle\bigoplus_{\overline{y_i}=c_p} \overline{w}_i \odot \exp(\{A^j(x) \mid x \in \overline{\mathbf{x}}_i\}) \oplus \\
&\textstyle\bigoplus_{c_p \in \overline{y}_i, c_p \neq \overline{y}_i} \overline{w}_i \odot \\
&\qquad \exp(\{-A^j(x), A^j(x) \mid x \in \overline{\mathbf{x}}_i\}) \oplus \\
&\textstyle\bigoplus_{c_p \notin \overline{y}_i} \overline{w}_i \odot \exp(\{-A^j(x) \mid x \in \overline{\mathbf{x}}_i\})\Big).
\end{aligned} \tag{26}$$

In turn, the lexicographic precedence between two crisp fitness vectors $A = (a_1, \ldots, a_p)$ and $B = (b_1, \ldots, b_p)$ is as follows: let us first define two permutations of the set $\{1, \ldots, p\}$, denoted $(k_1^a, \ldots, k_p^a)$ and $(k_1^b, \ldots, k_p^b)$, such that $a_{k_1^a} \geq \ldots \geq a_{k_p^a}$ and $b_{k_1^b} \geq \ldots \geq b_{k_p^b}$. Then,

$$\begin{aligned}
&A \prec B \iff \exists m \in \{1,\ldots,p\} \mid \\
&\quad (a_{k_q^a} = b_{k_q^b})\ \forall q \in \{1,\ldots,m-1\} \wedge (a_{k_m^a} > b_{k_m^b}).
\end{aligned} \tag{27}$$

The extension of both the fitness function and the lexicographic ordering to fuzzy values results from applying the extension principle and from replacing the comparisons between real numbers with a suitable fuzzy ranking. The expression of the fitness function, in the general case, is as follows:

$$\begin{aligned}
&\widetilde{\text{fitness}}_{\{(\widetilde{\mathbf{x}}_i,\widetilde{y}_i)\}}(\text{if } \mathbf{x} \text{ is } A^j \text{ then } (c_1,\ldots,c_p))(t) = \\
&\quad \overline{\max}\{\alpha \mid t \in \\
&\quad \overline{\text{fitness}}_{\{([\widetilde{\mathbf{x}}_i]_\alpha,[\widetilde{y}_i]_\alpha)\}}(\text{if } \mathbf{x} \text{ is } A^j \text{ then } (c_1,\ldots,c_p))\},
\end{aligned} \tag{28}$$

where t denotes a p-dimensional vector of real values.

C. Assignment of weights to the consequent part

The extension of Eq. (7) to set-valued data and multiclass problems consists in assigning to the k-th class in the consequent of the rule a confidence equal to the value of α_k minimizing the set-valued function Z^k defined as follows:

$$\begin{aligned}
&\overline{Z}^k_{\{(\overline{\mathbf{x}}_i,\overline{y}_i)\}}(\alpha) = \\
&\quad \{ \textstyle\oplus_{i:c_k=\overline{y}_i} \overline{w}_i \odot \exp(-\alpha A^j(x)) \oplus \\
&\quad \textstyle\oplus_{i:c_k\notin\overline{y}_i} \overline{w}_i \odot \exp(\alpha A^j(x)) \oplus \\
&\quad \textstyle\oplus_{i:c_k\neq\overline{y}_i,\, c_k\in\overline{y}_i} \overline{w}_i \odot \exp(\{-\alpha A^j(x), \alpha A^j(x)\}) \\
&\quad \mid x \in \overline{\mathbf{x}}_i\}.
\end{aligned} \tag{29}$$

A numerical stabilization term

$$\bigoplus_{i:A^j(x)=0\ \forall x\in\overline{\mathbf{x}}_i} \overline{w}_i \exp(|\alpha\epsilon|) \tag{30}$$

with a suitable value of ϵ can also be added, if needed.

The extension of Eq. (29) to fuzzy data is as follows:

$$\widetilde{Z}^k_{\{(\widetilde{\mathbf{x}}_i,\widetilde{y}_i)\}}(\gamma)(t) = \max\{\alpha \mid t \in \overline{Z}^k_{\{([\widetilde{\mathbf{x}}_i]_\alpha,[\widetilde{y}_i]_\alpha)\}}(\gamma)\}. \tag{31}$$

In both the set-valued and fuzzy cases, the values of α_k can be found with a greedy algorithm that uses a precedence operator between fuzzy sets. However, this optimization is not as efficient as the Brent search used in the crisp version of the algorithm. Since the optimization must be launched each time a fitness value is computed, in this paper we have decided to approximate the value of α_k by the center of the set

$$\overline{\alpha}_k = \log(1 - E_k) - \log(E_k) \tag{32}$$

where E_k is a normalized weighted sum of the compatibilities of the antecedent of the j-th rule with the elements of the dataset whose class does not match the k-th term in the consequent:

$$\begin{aligned}
E_k = K \odot \Big(&\textstyle\bigoplus_{\{i:c_k\notin\overline{y}_i\}} \overline{w}_i \odot \{A^j(x) \mid x \in \overline{\mathbf{x}}_i\} \oplus \\
&\bigoplus_{\{i:c_k\neq\overline{y}_i \wedge c_k\in\overline{y}_i\}} \overline{w}_i \odot \{\{0, A^j(x)\} \mid x \in \overline{\mathbf{x}}_i\}\Big)
\end{aligned} \tag{33}$$

The normalization factor K is the inverse of the upper bound of the normalized weighted sum of the compatibilities of the antecedent of the j-th rule with all the elements of the dataset:

$$K = (\sum_i \max\{\overline{w}_i\} \cdot \max\{A^j(x) \mid x \in \overline{\mathbf{x}}_i\})^{-1}. \tag{34}$$

D. Assignment of weights to the examples

After the j-th rule is added, the weights of the instances are recomputed as follows:

$$\overline{w}'_i = \bigcup_{x\in\overline{\mathbf{x}}_i} w'_i(x) \tag{35}$$

where $w'_i(x) =$

$$K' \odot \overline{w}_i \odot \begin{cases} c_k = \overline{y}_i & \exp(-\alpha_k A^j(x)) \\ c_k \notin \overline{y}_i & \exp(\alpha_k A^j(x)) \\ \text{else} & \exp(\alpha_k A^j(x) \odot \{-1, 1\}) \end{cases} \tag{36}$$

and K' is a crisp normalization factor such that $\max \oplus_i \overline{w}'_i = 1$.

E. Some details of the genetic algorithm

Adaboost depends on a procedure that fits a weak learner to the weighted training set. If the vector-valued fitness we have proposed in this paper is to be used, learning a weak classifier reduces to finding the antecedent A^j that optimizes the fitness function explained in section III-B, with respect to the lexicographic ordering defined in the same section. Since all possible values of the fitness can be compared between themselves, implementing this criterion amounts to redefining the meaning of the operator "less than" ($<$) in an ordinary GA; there is no need to use multicriteria techniques [16], thus we have used instead a standard generational scheme with a tournament-based selection.

Details of this algorithm can be found in [3]. Let us recall for the convenience of the reader the only part in this GA besides the fitness function (whose explanation has occupied most of this paper) which departs from a standard implementation: the coding of the fuzzy memberships.

Descriptive fuzzy rules are coded by an integer, which is the index j of the antecedent A^j in $\mathcal{A}$. This integer is encoded in turn, by a sequence of n numbers that refer to labels of the linguistic terms in the underlying fuzzy partitions. In addition to linguistic labels describing subsets of the domain of each variable, such as "LOW" and "HIGH", each linguistic variable includes a wild card label "ANY VALUE", with a membership degree of 1 across the entire universe of discourse.

The linguistic expression of a fuzzy rule that contains a wild card can be simplified, as illustrated by the following example: assume a classification problem with two features (weight,height), where height=$\{$low,high$\}$ and weight=$\{$light, heavy$\}$. The two linguistic variables are extended with a wild card term such that height=$\{$low, high, anyvalue$\}$ and weight=$\{$light, heavy, anyvalue$\}$. If the rule antecedent is described by "anyvalue$\times$heavy", the linguistic expression

if height is anyvalue and weight is heavy then t(1,2)=(0.4,0.8)

is simplified to

if weight is heavy then t(1,2)=(0.4,0.8).

This property of the genetic representation allows it to code general rules that only refer to a subset of all possible features, thus enabling the boosting algorithm to take advantage of feature selection.

The last rule is coded by the sequence (3,2), as "anyvalue" is the third linguistic term in the first linguistic variable, and "heavy" is the second term in the second linguistic variable. Observe that the class labels in the rule consequent are not part of the genetic codification, neither the confidences degrees in the consequents are.

IV. Numerical results

In this section we include the first results of the implementation of Adaboost for learning fuzzy rules from low quality data, applied to the imprecise datasets "Diagnosis of the Dyslexic" [17] and "Athletics at Oviedo University" [18]. We include first a brief description of these datasets and then we discuss the compared results of the application of the new method to these problems.

A. Description of the datasets and experimental settings

The datasets "Diagnosis of the Dyslexic" and "Athletics at the Oviedo University", have been introduced in [19] and [20], respectively, and are available in the data set repository of keel-dataset (http://www.keel.es/datasets.php) [21], [22]. The names, the number of examples (Ex.), number of attributes (Atts.), the classes (Classes) and the fraction of patterns of each class (%Classes) for each dataset are displayed in Table I. Observe that the proportions of the different patterns are intervals, because the class labels of some instances are imprecise.

TABLE I
SUMMARY DESCRIPTIONS OF DATASETS WITH META-INFORMATION.

Dataset	Ex.	Atts.	Classes	%Classes
B200mlI	19	4	2	([0.47,0.73],[0.26,0.52])
B200mlP	19	5	2	([0.47,0.73],[0.26,0.52])
Long	25	4	2	([36,64],[36,64])
BLong	25	4	2	([36,64],[36,64])
100mlI	52	4	2	([0.44,0.63],[0.36,0.55])
100mlP	52	4	2	([0.44,0.63],[0.36,0.55])
B100mlI	52	4	2	([0.44,0.63],[0.36,0.55])
B100mlP	52	4	2	([0.44,0.63],[0.36,0.55])
Dyslexic-12-12	65	12	3	([0.32,0.43],[0.32,0.52], [0.12,0.30])
Dyslexic-11-01	65	11	3	([0.43,0.53],[0.23,0.35], [0.12,0.30])
Dyslexic-11-12	65	11	3	([0.32,0.43],[0.32,0.52], [0.12,0.30])

All the experiments have been run with a population size of 100, probabilities of crossover and mutation of 0.9 and 0.1, respectively, and limited to 150 generations. The fuzzy partitions of the labels are uniform and their size is 5. All the imprecise experiments were repeated 100 times with bootstrapped resamples of the training set. Each partition of test contains 1000 tests.

B. Differences in accuracy

The compared accuracies between the proposed algorithm (Boosting_LQD) and other GFS capable of extracting rules from low quality data (GFS [23] and MR_GFS [24]) data are shown in Table II. The results are expressed by means of intervals, that are our best bounds about the mean values of the test error. These intervals are defined by the expression

$$\overline{\text{error}} = \left\{ \frac{1}{m} \sum_{i=1}^{m} e_i \mid e_i \in \overline{e}_i \right\} \tag{37}$$

where

$$\overline{e}_i = \begin{cases} 0 & \text{bclass}(\overline{x}_i) = \overline{y}_i \text{ and } \#(\overline{y}_i) = 1, \\ 1 & \text{bclass}(\overline{x}_i) \cap \overline{y}_i = \emptyset, \\ \{0,1\} & \text{else.} \end{cases} \tag{38}$$

The method "Boosting_LQD" shows a better performance than the remaining classifiers, in both binary problems (Athletics datasets) and multiclass (Dyslexic datasets). Observe that MR_GFS could not be applied to the multiclass datasets in this paper because a suitable matrix of costs was not given for

TABLE II
BEHAVIOUR OF "GFS", "MR_GFS" AND "BOOSTING_LQD" IN SEVERAL DATASETS OF ATHLETICS AND DYSLEXIA.

Dataset	GFS	MR_GFS	Boosting_LQD
100mlI	[0.176,0.378]	[0.178,0.380]	[0.170,0.376]
100mlP	[0.176,0.360]	[0.188,0.367]	[0.180,0.358]
Long	[0.321,0.590]	[0.288,0.557]	[0.231,0.499]
BLong	[0.326,0.625]	[0.286,0.586]	[0.219,0.519]
B100mlI	[0.172,0.369]	[0.188,0.385]	[0.158,0.356]
B100mlP	[0.160,0.349]	[0.161,0.350]	[0.161,0.350]
B200mlI	[0.232,0.473]	[0.178,0.418]	[0.171,0.415]
B200mlP	[0.262,0.480]	[0.215,0.433]	[0.188,0.406]
Athletics mean	[0.228,0.453]	[0.210,0.434]	[0.184,0.409]
Dyslexic-12-12	[0.386,0.557]	N/A	[0.376,0.530]
Dyslexic-11-01	[0.445,0.573]	N/A	[0.447,0.567]
Dyslexic-11-12	[0.528,0.690]	N/A	[0.458,0.595]
Dyslexic mean	[0.453,0.606]	N/A	[0.427,0.564]
Global mean	[0.340,0.529]	N/A	[0.305,0.486]

these datasets. The good behavior of the algorithm in the binary problems "Long", "BLong", "B200mlI" and "B200mlP" was remarkable, as shown in the graphs of the dispersion of the results of the 100 bootstrap tests, that have been plotted in Figures 1 to 3. In these Figures, the horizontal coordinate measures the fraction of errors of the boosting algorithm, and the vertical coordinate measures the same parameter in the counterpart algorithm. Each filled circle represents a case where the boosting algorithm was the best choice, and the squares mean the opposite result. A blank circle or square means a tie (or a difference with is not significant) between both algorithms. Those figures where there is a high density of filled circles in the upper left part signal cases where the dispersion of the results is compatible with a statistically significant improvement of the bound, and those cases where the cloud is near the diagonal or in the lower, right part display situations where the differences, if exist, are not significant.

In multiclass problems there is a substantial improvement in the datasets "Dyslexic-11-12" (Figure 4) and "Dyslexic-12-12" and a slight improvement in "Dyslexic-11-01" (Figure 5). By comparing the results obtained by the boosting algorithm in "Dyslexic-12-12" and "Dyslexic-11-12" we detect that the removal of the imprecision in the input values (dataset "Dyslexic-11-12") indeed lowers the performance of the algorithm, supporting a result already found in [17]. Moreover, the boosting algorithm show us that the imprecise outputs of that dataset are significant for determining the weights of the instances and the confidences in the consequents.

V. CONCLUDING REMARKS

In this paper we have proposed a new extension of the Adaboost algorithm for learning fuzzy rule based classifiers from interval-valued or fuzzy data. Fuzzy rules were regarded as weak learners and knowledge bases as ensembles. The number of votes of a weak learner was identified with the degree of confidence of its corresponding consequent. Both the objective function of the Adaboost algorithm and the weights of the instances were assigned interval or fuzzy values, however the number of votes each weak learning is assigned

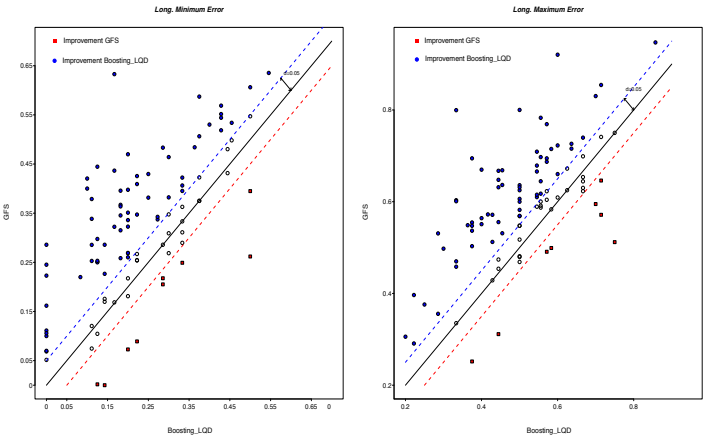

Fig. 1. Behaviour of "GFS" and "Boosting_LQD" respect to the dataset Long. **Left figure:** Lower bounds. **Right figure:** Upper bounds.

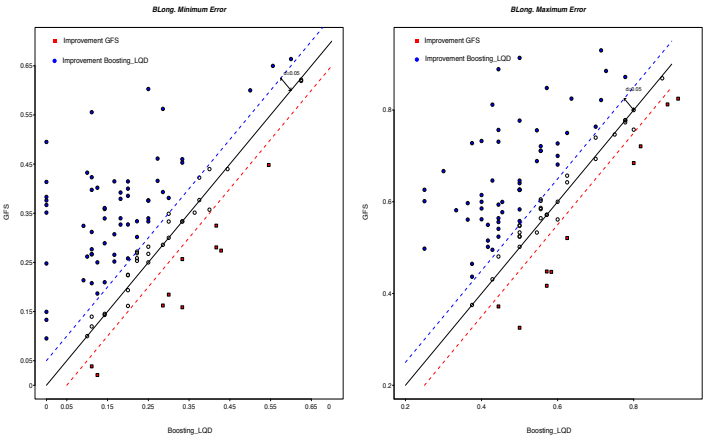

Fig. 2. Behaviour of "GFS" and "Boosting_LQD" respect to the dataset BLong. **Left figure:** Lower bounds. **Right figure:** Upper bounds.

has been designed to be a crisp number thus the classifier does not introduce uncertainty of its own.

The results of the new algorithm have been compared to that of previous genetic algorithms for low quality data. The results prove that this technique is fast, its accuracy is competitive and the number of rules in the knowledge base is not higher than that of the alternatives. On the other hand, it uses a voting-based inference, whose linguistic quality is not the best, and the performance gain is not highly relevant for multiclass problems.

ACKNOWLEDGEMENTS

This study has been supported by the Spanish Ministry of Science and Technology and by European Fund FEDER (project TIN2008-06681-C06-04) and by the Principado de Asturias, PCTI 2006-2009.

REFERENCES

[1] Freund, Y., Schapire, R. Experiments with a new boosting algorithm. In Machine Learning, Proc. 13th International Conference, 148-156 (1996)
[2] Kuncheva, L. I. Fuzzy Classifier Design. Springer-Verlag, NY, (2000).

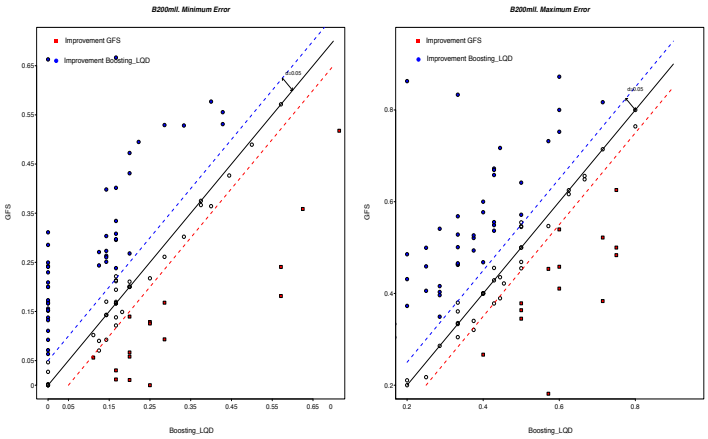

Fig. 3. Behaviour of "GFS" and "Boosting_LQD" respect to the dataset B200mII. **Left figure:** Lower bounds. **Right figure:** Upper bounds.

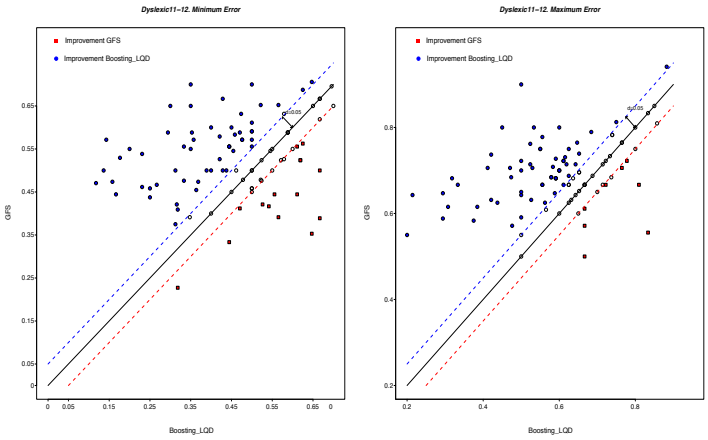

Fig. 4. Behaviour of "GFS" and "Boosting_LQD" respect to the dataset Dyslexic11-12. **Left figure:** Lower bounds. **Right figure:** Upper bounds.

[3] Del Jesus, M. J., Junco, L., Hoffmann, F., Sánchez, L., Induction of Fuzzy Rule Based Classifiers with Evolutionary Boosting Algorithms. IEEE Transactions in Fuzzy Sets. 12(3) 296-308 (2004)

[4] Hoffmann, F., Boosting a Genetic Fuzzy Classifier. in Proc. Joint 9th IFSA World Congress and 20th NAFIPS International Conference, vol. 3, (Vancouver, Canada), pp. 1564-1569 (2001)

[5] Junco, L., Sánchez, L. Using the Adaboost algorithm to induce fuzzy rules in classification problems, Proc. ESTYLF 2000, Sevilla, 297-301. (2000)

[6] González, A., Herrera, F., Multi-stage genetic fuzzy systems based on the iterative rule learning approach. Mathware and Soft Computing 4(3), 233-249 (1997).

[7] Friedman, J., Hastie, T., Tibshirani, R. Additive Logistic Regression: a Statistical View of Boosting, Annals of Statistics 28(2), 337-374. (2000).

[8] Otero, J., Sánchez, L. Induction of descriptive fuzzy classifiers with the Logitboost algorithm. Soft Computing 10(9) 825-835 (2006)

[9] Sánchez, L. Otero. J., Boosting fuzzy rules in classification problems under single-winner inference. International Journal of Intelligent Systems 22(9) 1021-1035. (2007)

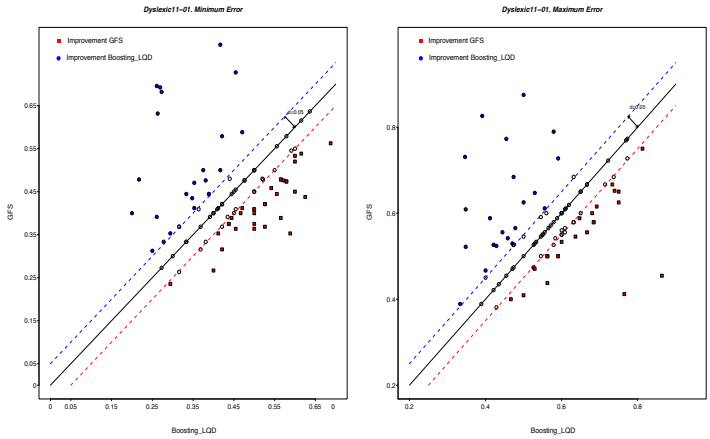

Fig. 5. Behaviour of "GFS" and "Boosting_LQD" respect to the dataset Dyslexic11-01. **Left figure:** Lower bounds. **Right figure:** Upper bounds.

[10] Dubois, D., Guyonnet, D. Risk-informed decision-making in the presence of epistemic uncertainty. International Journal of General Systems 40 (2) 145-167 (2011)

[11] Sánchez, L., Couso, I., Advocating the use of Imprecisely Observed Data in Genetic Fuzzy Systems. IEEE Transactions on Fuzzy Systems 15 (4), 551-562 (2007)

[12] Cordón, O., del Jesus, M. J., Herrera, F. A proposal on reasoning methods in fuzzy rule-based classification systems. International Journal of Approximate Reasoning 20(1), 21-45. (1999).

[13] Ishibuchi, H., Nakashima, T. and Morisawa, T., Voting in fuzzy rule-based systems for pattern classification problems. Fuzzy Sets and Systems, vol 103, no. 2, 223-239, (1999).

[14] Schapire, R., Singer, Y. Improved Boosting Algorithms Using Confidence-rated Predictions. Machine Learning 37(3): 297-336. (1999)

[15] Schapire, R. E. Theoretical views of Boosting and Applications. Lecture Notes in Artificial Intelligence, Vol. 1720, pp 13 - 25. (1999).

[16] Sánchez, L., Couso,I., Casillas, J. Modeling vague data with genetic fuzzy systems under a combination of crisp and imprecise criteria Proceedings of the First IEEE Symposium on Computational Intelligence in Multi-Criteria Decision-Making (MCDM 2007), 30-37 Honolulu, Hawaii, USA (2007)

[17] Palacios, A., Sánchez, L., Couso, I. Diagnosis of dyslexia with low quality data with genetic fuzzy systems. International Journal on Approximate Reasoning 51, 993-1009 (2010)

[18] Palacios, A. Sánchez, L., Couso, I. Future performance modelling in athletism with low quality data-based GFSs. Journal of Multivalued Logic and Soft Computing 17 (2-3) 207-228 (2011)

[19] Palacios, A. Sánchez, L. Couso, I. Diagnosis of dyslexia from vague data with Genetic Fuzzy Systems. International Journal of Approximate Reasoning 51. 993-1009 (2010)

[20] Palacios, A. Sánchez, L. Couso, I. Future performance modeling in athletism with low quality data-based GFSs. Journal of Multiple-Valued Logic and Soft Computing, 17. 207-228. (2011)

[21] Alcalá, J., Fernández, A., Luengo, J., Derrac, J., García, S., Sánchez, L., Herrera, F. KEEL Data-Mining software tool: data set repository, integration of algorithms and experimental analysis framework. Journal of Multivalued Logic and Soft Computing 17 (2-3) 255-287 (2011)

[22] Alcalá-Fdez, J., Sánchez, L., García, S., del Jesus, M.j., Ventura, S., Garrell, J. M., Otero, J., Romero, C., Bacardit, J., Rivas, V. M., Herrera, F. KEEL: A software tool to assess evolutionary algorithms to data mining problems Soft Computing 13 (3) 307-318 (2009)

[23] Palacios, A., Sánchez, L., Couso, I. Extending a simple cooperative-competitive learning fuzzy classifier to low quality datasets. Evolutionary Intelligence 2 (1-2), 73-84 (2010)

[24] Palacios, A., Sánchez, L., Couso, I. Linguistic Cost-Sensitive Learning of Genetic Fuzzy Classifiers for Imprecise Data. International Journal on Approximate Reasoning. In Press. (2011)

2011 IEEE International Conference on Fuzzy Systems
June 27-30, 2011, Taipei, Taiwan

Checking Orthogonal Transformations and Genetic Algorithms for Selection of Fuzzy Rules based on Interpretability-Accuracy Concepts

M. Isabel Rey
INDOMAUT S.L.
Pol. Ind. San Cristóbal
47012 Valladolid, SPAIN
Email: i.rey@indomaut.com

Marta Galende
CARTIF Centro Tecnológico ⋆
47151 Boecillo (Valladolid), SPAIN
Email: margal@cartif.es
gresai@cartif.es

Gregorio I. Sainz †,⋆ Maria J. Fuente †
Dpt. of Systems Engineering and Control †
School of Industrial Engineering
University of Valladolid
47011 Valladolid, SPAIN
Email: gresai@eis.uva.es maria@autom.uva.es

***Abstract*—Fuzzy modeling is one of the most known and used techniques in different areas to emulate the behavior of systems and processes. In most cases, as in data-driven fuzzy modeling, these fuzzy models reach a high performance from the point of view of accuracy, but from other points of view, such as complexity or interpretability, the models can present a poor performance.**

Several approaches are found in the specialized literature to reduce the complexity and improve the interpretability of the fuzzy models. Here, a post-processing approach is taken into account via the definition of the rules selection criterion that aims to choose the most relevant rules according to the well-known accuracy-interpretability trade-off. This criterion is based on Orthogonal Transformations, here the QRP transformation is taking into consideration, and its parameters are tuned genetically. The main objective is to check the true significance, drawbacks and advantages the firing matrix of the rules, that is the foundation of the most usual approaches based on orthogonal transformations for the complexity reduction of the fuzzy models.

A neuro-fuzzy system, FasArt (Fuzzy Adaptive System ART based), and several case studies, data sets from the KEEL Project Repository, are used to tune and check this approach. This neuro-fuzzy system generates Mamdani fuzzy rule based systems (FRBSs), each with its own particularities and complexities from the point of view of fuzzy sets and rule generation. NSGA-II is the MOEA tool used to tune the criterion parameters based on accuracy-interpretability ideas.

***Index Terms*—Fuzzy Systems, Interpretability, Accuracy, Rule Selection, Orthogonal Transformations, Genetic Algorithm**

I. Introduction

Fuzzy modeling is one the most known approaches for a wide range of problems. Data-driven rule based fuzzy models have been used in several and very different scientific and technical areas [1], [2], [3], [4], [5].

In general, the fuzzy models taken into consideration in real world applications have been data-driven and rule based fuzzy models due to their advantages: easy use and performance. This performance has usually been evaluated on the basis of the accuracy of the models, thus minimizing the error between the real output an the estimated output generated by the fuzzy models. But other aspects have not been taken into consideration: complexity, interpretability, etc. Some of them are base principles of fuzzy logic but these fuzzy models used them as simple mathematical tools, losing their original fuzzy meaning.

Complexity is a very usual index or measure, and it is a problem in data-driven rule based fuzzy models, so the reduction of this complexity permits important aspects of the fuzzy models to be improved, gaining a better performance for these models. The question is the way in which this complexity reduction must be carried out [6], [7], [8], [9], [10], [11].

Here, the complexity reduction is carried out based on Orthogonal Transformations and accuracy-interpretability trade-off, as this approach has traditionally been focused in most works [12]. The goal of this work is a postprocessing approach to simplify a rule-based fuzzy model based on a simple $Criterion\ of\ selection$ that is tuned by a genetic approach, and, in this way, checks the possibilities and drawbacks of this type of approach.

The paper is organized as follows: first, in Section II, a brief description of alternative points of view about fuzzy modeling, interpretability and accuracy are given. Also in this section, a brief description of orthogonal transformation and, specially, QR decomposition with column pivoting - QRP, are given, and finally, several complexity and interpretability measures are proposed. In Section III, a $Criterion$ to select the best rules is described. In Section IV the methodology used in this work is described. Some experimental studies are carried out and the main results obtained are discussed in Section V. Finally, in Section VI, the most interesting conclusions obtained from this work are set out.

II. Fuzzy Modeling: Accuracy vs.Interpretability

Initially, two well known modeling approaches to generate fuzzy rules are described in the technical and scientific literature [13], [14], [15]:

1) *Precise Fuzzy Modeling*, whose main goal is to obtain as much accuracy as possible. In general, the models generated have a good accuracy but a low level of interpretability. This modeling is popular with data-driven knowledge but expert knowledge is also considered.

978-1-4244-7316-8/11/$26.00 ©2011 IEEE

2) *Linguistic Fuzzy Modeling*, these models have a good level of interpretability but poor accuracy. Here, knowledge from experts and from data guide the modeling process.

Both approaches have their own drawbacks and advantages, but there are several ways to deal with the generation of fuzzy systems whose performance includes an adequate accuracy-interpretability trade-off:

- Algorithms take into account the idea of accuracy-interpretability during the generation of the fuzzy system. i.e genetic fuzzy systems [14], [16].
- Orthogonal transformations where the interpretability is improved by complexity reduction rules [12], [17], [18], [19].

The orthogonal transformations, used traditionally, permit relevant simplifications, but the loss of accuracy is also very high. In most of the usual works about this topic and approach, the accuracy-interpretability is not truly involved, and, in addition, the experimental work is not sufficient to reach relevant conclusions.

These orthogonal transformations are used for rule selection/reduction in fuzzy modeling in two approaches [12]: the range-revealing approach (Singular Value Decomposition (SVD) or QRP) and those that evaluate the individual contributions of the rules (Orthogonal Least Squares (OLS)).

In this work, range-revealing methods are used, so the fuzzy model can be written as a linear regression problem [19]:

$$y = P * \theta + e \tag{1}$$

SVD is used to determine the effective rank of the rule firing matrix (P). This can be expressed as:

$$p_i(x) = \frac{\prod_{j=1}^{N} A_{ij}(x_j)}{\sum_{k=1}^{M} \prod_{j=1}^{N} A_{kj}(x_j)} \tag{2}$$

where $x = [x_1, .., x_N]^T$ is the input vector, $A_{i1}, ...A_{iN}$ are fuzzy sets defined in the antecedent space and M is the number of rules of the fuzzy model. The most important rules are those whose singular values are higher.

The QRP approach can produce a rule ordering without an rank estimation. Here, QRP is directly applied to P, obtaining a permutation matrix [20]: The QR decomposition of P is given by $P * \Pi = Q * R$, where $\Pi \in \Re^{M*M}$ is a permutation matrix, $Q \in \Re^{N*M}$ has orthogonal columns and $R \in \Re^{M*M}$ is upper triangular, such that

$$R = \begin{bmatrix} R_{11} & R_{12} \\ 0 & R_{kk} \end{bmatrix} \tag{3}$$

The diagonal values of *R* are called $R-values$ $(|R(kk)|)$ [17], which track the singular values $\sigma(P)$, so the most active and least redundant rules are those whose R-values are higher [19] in the original fuzzy rule space.

III. Rule Selection Based on QRP Transformations and Genetic Algorithm: a $Criterion$

The objective of this work is to try to check the orthogonal transformations, in this case QRP. To reach this goal, a simple $Criterion$ is defined in order to address the post-processing rule selection based on the relevance of each rule, then some conclusions about orthogonal transformations can be reached. In this case QRP and its R-values, in decreasing order, have been considered for this approach.

The main problem in the use of orthogonal transformations for rule ordering and selection is the selection $Criterion$. The goal of this work is to select rules automatically based on the percentage of R-values associated with the selected rules. This selection must be guided by a good trade-off between accuracy and interpretability.

A. Rule Selection: a $Criterion$

In order to address the post-processing rule selection, with the aim of reducing the complexity of the fuzzy model while preserving most of its accuracy, the next $Criterion$ has been proposed:

Given a fuzzy rule model whose complexity is to be reduced by rule selection, the rules to be taken into consideration in the new fuzzy model are those rules associated to R-values whose aggregation is greater than a threshold value, β. In this way, most of the behavior (and variability) of the rules is theoretically preserved:

Given a set of n fuzzy rules, each one associated with an R-value, and given R_{norm_i} the normalized R-value of the rule i, such that

$$R_{norm_i} = \frac{R - values_{Rule_i}}{\sum_{j=1}^{j=n} R - values_{Rule_j}}$$

then

$$Rule_1, .., Rule_k \in ReducedModel$$

if

$$\sum_{i=1}^{i=k} R_{norm_i} \geq \beta, \quad k \leq n$$

where

$$\beta = \textit{Percentage of information (rules)}$$

B. Accuracy and Interpretability Measures

The accuracy and interpretability measures considered in this work are defined in [21]. The $accuracy$ of the model is measured through its Mean Squared Error (MSE) (Eq. 4):

$$MSE = \frac{1}{N} \sum_{i=1}^{N} (Y_i - Y_i')^2 \tag{4}$$

The $interpretability$ measure is a set of simple indexes based on similarity and complexity. In both cases, a lower value has a positive influence on reducing the complexity

and improving the interpretability of the fuzzy models. These indexes are:

- *Compactness* or *Number of rules*.
- *Similarity* amongst rules.
- *Redundancy* of the fuzzy rule set.
- *Incoherency* of rules.
- *Completeness* or *No-Coverage*.

¿From these indexes, the function to measure the interpretability is (Eq. 5)

$$\begin{aligned} Inter_C = ArithmeticMean(\\ \lambda_{nr} * RuleNumber_{nor}, \lambda_s * Similarity_{nor}, \\ \lambda_r * Redundancy_{nor}, \lambda_i * Incoherency_{nor}, \\ \lambda_{nc} * NoCoverage_{nor}) \\ \lambda_j \in (0,1) \end{aligned} \quad (5)$$

Here, λ_j = 1 because it gives equal weight to all indexes, and the normalization is (Eq. 6):

$$Index_{nor} = \frac{Index_{Current} - Index_{Original}}{Index_{Current}} \quad (6)$$

C. Genetic Algorithm and Neuro-Fuzzy Systems

A genetic algorithm and a neuro-fuzzy system are used in this work to check and analyze the proposal.

The well-known multi-objective evolutionary algorithm NSGA-II [22] is taken into account in this work. Two fitness functions from MSE and $Inter_C$ are used to reach a fuzzy model with a good accuracy-interpretability trade-off. A third fitness is used to penalize smaller R-values corresponding to less active and more redundant rules, such that,

$$Penalty_{R-values} = \sqrt[n]{\prod_{i=1}^{n} 1 - R_{norm_i}} \quad (7)$$

and a restriction is imposed to ensure an adequate percentage of information (rules).

Neuro-Fuzzy systems are very popular approaches to generate fuzzy rule based systems, taking advantage of the learning capacity of Artificial Neural Networks (ANN) and the explanatory capacity of Fuzzy Logic. In this work, the neuro-fuzzy system FasArt [23], [24] has been used, which is a neuro fuzzy system based on the Adaptive Resonance Theory (ART). FasArt introduces an equivalence between the activation function of each FasArt neuron and a membership function. In this way, FasArt is equivalent to a Mamdani fuzzy rule-based system with: Fuzzification by single point, Inference by product, and Defuzzification by average of fuzzy set centers. A full description of this model can be found in [23] and [24].

IV. Tuning the $Criterion$: Methodology

The methodology of this work is focused on tuning the *Criterion of selection* proposed in III-A and its parameter (β). To reach this goal, the methodology used is made up of four general steps:

1) *Initial model generation.*
   For each data set to be considered, two cases of fuzzy models are generated by FasArt: compact and complex.
2) *Tuning of the $Criterion$, β parameter, by MOEA for each fuzzy model*
   This is based on the accuracy-interpretability trade-off and the R-values associated of the fuzzy rules.
   The β parameter is tuned for each fuzzy model data set, in three representative points of the Pareto Front ([6]):
   - The most interpretable model: Best $Inter_C$ (BI).
   - The most accurate model: Best Acc (BA).
   - The balanced interpretability-accuracy model: Balanced $Inter_C - Acc$ (BIA).

   Here, the multi-objetive genetic algorithm uses the three fitness functions of Eq. 8 and the restriction of Eq. 9:

$$\begin{aligned} max(Accuracy) = min(MSE) \\ max(Interpretability) = min(Inter_C) \\ max(Penalty) = max(Penalty_{R-values}) \end{aligned} \quad (8)$$

$$\beta \in [60\% - 85\%] \quad (9)$$

   The fitness functions involve the accuracy-interpretability trade-off and penalize smaller R-values, which correspond to less active and more redundant rules. The restriction is imposed to preserve an adequate percentage of information (rules). In this work, a first run of the MOEA with the two first functions was carried out in order to estimate the restriction range of Eq. 9.
3) *Generalization of $Criterion$: Generation of the β parameter from $\beta_i's$.*
   Taking into consideration the particular tuning obtained for each fuzzy model, a general range of β is carried out for cross-validation:

```
for Criterion = 1 do
  for Model = Compact:Complex do
    for Accur-Interpret Point=BI:BA:BIA do
      for N datasets do
        All possible combinations of 2/3 of data set, each one with its β (β'_i s), are done: β's training.
        For each combination, the mean and median are done, obtaining new β's (2*num-combination).
        MSE and Inter_C are calculated with these new β's, for 2/3 and the remaining 1/3: β's test.
        The mean of MSE and Inter_C are done.
        The best accuracy (min(MSE)) and the best interpretability (min(Inter_C)) are selected and each one has a β associated obtaining two c.
        The final β is obtained to find the mean/median of these two β's. This midpoint gives a good accuracy-interpretability trade-off .
      end for
    end for
  end for
end for
```

TABLE I
DATA SETS FROM KEEL PROJECT

data sets	Variables	Records
Plastic Strength (PLA)	3	1650
Quake (QUA)	4	2178
Electrical Maintenance (ELE)	5	1056
Abalone (ABA)	9	4177
Stock prices (STP)	10	950
Weather Ankara (WAN)	10	1609
Weather Izmir (WIZ)	10	1461
Mortgage (MOR)	16	1049
Treasury (TRE)	16	1049

4) *Checking the $Criterion$: Accuracy and interpretability based on the $Criterion$ and its parameter β.*

```
for Criterion = 1 do
  for Model = Compact:Complex do
    for Accur-Interpret Point=BI:BA:BIA do
      for datasets = 1 to N do
        Calculation of MSE and Inter_C
      end for
    end for
  end for
  Analysis of results
end for
```

V. EXPERIMENTS: RESULTS AND ANALYSIS

The proposal described in previous sections is checked using nine data sets from the KEEL project [1] (Table I) [25], [26].

In accordance with the methodology described in section IV:

1) Two types of base fuzzy models are generated by FasArt for each data set: Model1-Compact and Model2-Complex.
2) MOEA has been run using several options and the best results (based on best MSE and $Inter_C$) have been obtained combining the three fitness functions formulated in Eq. 8 with the restriction of Eq. 9.
   In this work, all the *genetic operators* are used in their default options:
   - Tournament without replacement for selection. Tournament size $= 2$.
   - Simulated binary for crossover. Crossover probability $= 0.9$.
   - Polynomial for mutation. Mutation probability $= 0.1$.

   From here, the β's obtained for MOEA for each data set are shown in Table II.
   These β's of Table II are used to tune a general β by cross validation, as described in point 3 of section IV, then the best accuracy and interpretability are obtained for the β's shown in Table III.
   The final value of β, so the final tuning of the $Criterion$, is obtained by taking the mean/median of these two β's in order to obtain a compromise between the best accuracy point and the best interpretability point. The final β's are shown in Table IV.
3) MSE and $Inter_C$ are calculated for nine data sets, selecting the percentage of R-values corresponding to the final β's (Table IV).

[1] http://sci2s.ugr.es/keel/data setss.php

TABLE II
PERCENTAGE OF β OBTAINED FOR MOEA WITH THREE FITNESS FUNCTIONS AND RESTRICTION $\beta \in [60\% - 85\%]$ (%)

Model1	Best $Inter_C$	Balanced $Inter_C - Acc$	Best Acc
PLA1	63.6	68.7	70.9
QUA1	61.8	63.7	68.2
ELE1	79.1	75.3	84.0
ABA1	78.0	68.7	74.4
STP1	72.5	76.7	82.4
WIZ1	67.3	66.2	74.8
WAN1	64.3	67.8	68.8
MOR1	69.8	74.0	78.8
TRE1	68.7	72.6	78.4
Model2	$BestInter_C$	$BalancedInter_C - Acc$	$BestAcc$
PLA2	69.0	68.7	70.5
QUA2	64.5	64.1	63.1
ELE2	66.3	72.0	81.0
ABA2	63.1	63.0	66.0
STP2	74.8	72.3	72.8
WIZ2	64.6	66.7	67.8
WAN2	61.6	63.4	63.9
MOR2	74.0	74.5	76.2
TRE2	68.8	74.1	79.0

TABLE III
PERCENTAGE OF β OBTAINED FOR THE BEST MSE AND THE BEST $Inter_C$ (%)

Model1	Best $Inter_C$	Balanced $Inter_C - Acc$	Best Acc
Best MSE	72.1	73.3	78.8
Best $Inter_C$	65.7	68.0	72.6
Model2	Best $Inter_C$	Balanced $Inter_C - Acc$	Best Acc
Best MSE	69.6	72.2	74.6
Best $Inter_C$	64.6	65.4	66.9

TABLE IV
FINAL β'S (%)

	Best $Inter_C$	Balanced $Inter_C - Acc$	Best Acc
Model1	68.9	70.7	75.7
Model2	67.1	68.8	70.8

To see the results obtained for MSE and $Inter_C$ with their indexes of accuracy and interpretability, each study case is done with the new β's and the results are shown in the following subsections.

A. Performance of the Fuzzy Models

Table V summarizes the main performance aspects of the base fuzzy models generated. The indexes shown in the tables are the squared error for training (MSE_{tra}) and the test (MSE_{tst}), the rule number (RN), the similarity (S), the redundancy (R), the incoherency (I) and the percentage of completeness (C).

The performance of these base fuzzy models are matched with Wang & Mendel Models in [6]. In general, the complex models show a higher accuracy, while the compact models have a similar performance in some cases, and in others are a little more accurate or a little worse (see Table VI). The highlighted values mean that the performance (NR/MSE) in the FasArt models is greater than in Wang & Mendel.

TABLE V
PERFORMANCE OF THE FASART FUZZY MODELS

Model	MSE_{tra}	MSE_{tst}	RN	S	R	I	$C(\%)$
PLA1	6.553	6.553	14	0.204	0	0	100
PLA2	2.498	2.498	143	0.144	0.001	0.008	100
QUA1	0.071	0.071	20	0.225	0	0.005	90.4
QUA2	0.040	0.040	310	0.255	2e-4	0.002	100
ELE1	158937	158938	25	0.212	0	0.007	100
ELE2	55102	55103	145	0.291	0.008	0.001	97.6
ABA1	8.861	8.861	36	0.342	0	0.005	100
ABA2	5.176	5.176	305	0.330	4e-4	0.001	100
STP1	3.948	3.948	15	0.266	0	0	100
STP2	0.432	0.432	165	0.187	0	3e-4	100
WIZ1	15.208	15.208	26	0.317	0	0	100
WIZ2	3.737	3.737	118	0.377	0	0	100
WAN1	19.516	19.514	32	0.285	0	0	100
WAN2	4.060	4.044	391	0.358	0	0	100
MOR1	0.146	0.146	30	0.338	0	0	100
MOR2	0.071	0.071	101	0.290	4e-4	4e-4	100
TRE1	0.234	0.234	23	0.306	0	0	100
TRE2	0.138	0.138	62	0.288	0	0	100

TABLE VI
WANG & MENDEL [6] VS NEURO-FUZZY SYSTEMS.

Compact	Wang & Mendel [27]			FasArt (Model 1)		
Models	RN	MSE_{tra}	MSE_{tst}	RN	MSE_{tra}	MSE_{tst}
PLA	14.8	6.868	7.114	14	6.553	6.553
QUA	53.6	0.0516	0.0534	20	**0.071**	**0.071**
ELE	65	115212	115868	25	**158937**	**158938**
ABA	68	16.814	16.844	36	8.861	8.861
STP	122.8	18.148	18.084	15	3.948	3.948
WIZ	104.8	13.888	14.736	26	**15.208**	**15.208**
WAN	156	32.126	32.786	32	19.516	19.514
MOR	77.6	1.97	1.946	30	0.146	0.146
TRE	75	3.272	3.262	23	0.234	0.234

Complex	Wang & Mendel [6]			FasArt (Model 2)		
Models	NR	MSE_{tra}	MSE_{tst}	NR	MSE_{tra}	MSE_{tst}
PLA	14.8	6.868	7.114	**143**	2.498	2.498
QUA	53.6	0.0516	0.0534	**310**	0.040	0.040
ELE	65	115212	115868	**145**	55102	55103
ABA	68	16.814	16.844	**305**	5.176	5.176
STP	122.8	18.148	18.084	**165**	0.432	0.432
WIZ	104.8	13.888	14.736	**118**	3.737	3.737
WAN	156	32.126	32.786	**391**	4.060	4.044
MOR	77.6	1.97	1.946	**101**	0.071	0.071
TRE	75	3.272	3.262	62	0.138	0.138

Thus, these fuzzy models can be simplified in order to reach better and less complex fuzzy models using a more adequate accuracy-interpretability trade-off based on this proposal.

B. Reducing the complexity of the Fuzzy Models: Results and Analysis

The analysis of the results is organized according to the compact base fuzzy models and the complex base fuzzy models. In both cases, the values of MSE and $Inter_C$ with their indexes are presented.

1) Compact Models: Table VII shows the averaged results obtained by the characteristic models considered in this work over 5 runs for each case study considered. Specifically, the table shows the mean squared error for the test, MSE_{tst}, and the mean of the proposed index $Inter_C$, for each one of the three characteristic models taken into account: BI, BIA and BA. The first line shows the initial/original model (I) and the second line shows the improved model performance (F).

Tables VIII, IX and X show the mean values of some individual indexes for the final β's: the mean squared error for training (MSE_{tra}) and testing (MSE_{tst}), the mean rule number (RN), the mean similarity (S), the mean redundancy (R), the mean incoherency (I) and the mean percentage of completeness ($C\%$).

These tables show that the interpretability is always improved, while the accuracy is only improved sometimes. This is because the selection of rules with orthogonal transformations is done by removing the rules whose R-values are smaller, but

TABLE VII
PERFORMANCE OF THE IMPROVED COMPACT FUZZY MODELS

	Best $Inter_C$		Balanced $Inter_C - Acc$		Best Acc	
Model1	MSE_{tst}	$Inter_C$	MSE_{tst}	$Inter_C$	MSE_{tst}	$Inter_C$
PLA1(I)	6.553	0.241	6.553	0.241	6.553	0.241
PLA1(F)	12.589	0.152	12.589	0.152	12.256	0.155
QUA1(I)	0.071	0.265	0.071	0.265	0.071	0.265
QUA1(F)	0.051	0.188	0.044	0.190	0.045	0.199
ELE1(I)	158938	0.244	158938	0.244	158938	0.244
ELE1(F)	992076	0.132	749610	0.137	641352	0.152
ABA1(I)	8.861	0.269	8.861	0.269	8.861	0.269
ABA1(F)	10.916	0.190	9.521	0.194	8.070	0.202
STP1(I)	3.948	0.253	3.948	0.253	3.948	0.253
STP1(F)	14.162	0.153	13.538	0.156	13.538	0.156
WIZ1(I)	15.208	0.263	15.208	0.263	15.208	0.263
WIZ1(F)	103.700	0.173	100.041	0.177	88.800	0.182
WAN1(I)	19.514	0.257	19.514	0.257	19.514	0.257
WAN1(F)	60.108	0.172	57.658	0.176	27.359	0.181
MOR1(I)	0.146	0.268	0.146	0.268	0.146	0.268
MOR1(F)	5.045	0.162	4.106	0.161	3.707	0.167
TRE1(I)	0.234	0.261	0.234	0.261	0.234	0.261
TRE1(F)	3.987	0.135	3.839	0.137	3.288	0.149

TABLE VIII
RESULTS OBTAINED WITH COMPACT FASART BEST $Inter_C$ β=68.9 %

Model1	MSE_{tra}	MSE_{tst}	RN	S	R	I	$C(\%)$
PLA1(I)	6.553	6.553	14.00	0.204	0.000	0.000	100
PLA1(F)	12.586	12.589	8.00	0.187	-	-	100
QUA1(I)	0.071	0.071	20.00	0.225	0.000	0.005	90.4
QUA1(F)	0.051	0.051	7.80	0.365	-	0.000	81.7
ELE1(I)	158937	158938	25.00	0.212	0.000	0.007	100
ELE1(F)	861883	992077	11.00	0.213	-	0.000	99.1
ABA1(I)	8.861	8.861	36.00	0.342	0.000	0.005	100
ABA1(F)	10.944	10.916	15.40	0.411	-	0.009	89.8
STP1(I)	3.948	3.948	15.00	0.266	0.000	0.000	100
STP1(F)	13.787	14.162	5.80	0.280	-	-	90.0
WIZ1(I)	15.208	15.208	26.00	0.317	0.000	0.000	100
WIZ1(F)	101.24	103.70	10.20	0.333	-	-	85.8
WAN1(I)	19.516	19.514	32.00	0.285	0.000	0.000	100
WAN1(F)	60.101	60.108	11.60	0.371	-	-	87.4
MOR1(I)	0.146	0.146	30.00	0.338	0.000	0.000	100
MOR1(F)	4.993	5.045	9.00	0.368	-	-	86.0
TRE1(I)	0.234	0.234	23.00	0.306	0.000	0.000	100
TRE1(F)	3.829	3.987	6.80	0.291	-	-	91.1

TABLE IX
RESULTS OBTAINED WITH COMPACT FASART BALANCED $Inter_C - Acc$ β=70.7 %

Model1	MSE_{tra}	MSE_{tst}	RN	S	R	I	$C(\%)$
PLA1(I)	6.553	6.553	14.00	0.204	0.000	0.000	100
PLA1(F)	12.586	12.589	8.00	0.187	-	-	100
QUA1(I)	0.071	0.071	20.00	0.225	0.000	0.005	90.4
QUA1(F)	0.044	0.044	8.00	0.368	-	0.000	81.7
ELE1(I)	158937	158938	25.00	0.212	0.000	0.007	100
ELE1(F)	700522	749610	11.80	0.208	-	0.000	99.5
ABA1(I)	8.861	8.861	36.00	0.342	0.000	0.005	100
ABA1(F)	9.521	9.521	16.00	0.414	-	0.008	89.8
STP1(I)	3.948	3.948	15.00	0.266	0.000	0.000	100
STP1(F)	13.359	13.538	6.00	0.285	-	-	90.4
WIZ1(I)	15.208	15.208	26.00	0.317	0.000	0.000	100
WIZ1(F)	97.331	100.041	10.60	0.334	-	-	85.8
WAN1(I)	19.516	19.514	32.00	0.285	0.000	0.000	100
WAN1(F)	57.762	57.658	12.40	0.372	-	-	87.8
MOR1(I)	0.146	0.146	30.00	0.338	0.000	0.000	100
MOR1(F)	4.090	4.106	10.00	0.369	-	-	89.5
TRE1(I)	0.234	0.234	23.00	0.306	0.000	0.000	100
TRE1(F)	3.735	3.839	7.00	0.289	-	-	91.1

TABLE X
RESULTS OBTAINED WITH COMPACT FASART BEST Acc β=75.7 %

Model1	MSE_{tra}	MSE_{tst}	RN	S	R	I	$C(\%)$
PLA1(I)	6.553	6.553	14.00	0.204	0.000	0.000	100
PLA1(F)	12.230	12.256	8.20	0.188	-	-	100
QUA1(I)	0.071	0.071	20.00	0.225	0.000	0.005	90.4
QUA1(F)	0.045	0.045	9.00	0.366	-	0.000	82.0
ELE1(I)	158937	158938	25.00	0.212	0.000	0.007	100
ELE1(F)	561249	641352	13.60	0.211	-	0.000	99.7
ABA1(I)	8.861	8.861	36.00	0.342	0.000	0.005	100
ABA1(F)	8.202	8.070	18.00	0.401	-	0.007	89.8
STP1(I)	3.948	3.948	15.00	0.266	0.000	0.000	100
STP1(F)	13.359	13.538	6.00	0.285	-	-	90.4
WIZ1(I)	15.208	15.208	26.00	0.317	0.000	0.000	100
WIZ1(F)	87.841	88.800	12.20	0.323	-	-	88.3
WAN1(I)	19.516	19.514	32.00	0.285	0.000	0.000	100
WAN1(F)	27.809	27.359	14.20	0.368	-	-	90.9
MOR1(I)	0.146	0.146	30.00	0.338	0.000	0.000	100
MOR1(F)	3.594	3.707	11.00	0.373	-	-	90.4
TRE1(I)	0.234	0.234	23.00	0.306	0.000	0.000	100
TRE1(F)	3.147	3.288	8.20	0.301	-	-	91.1

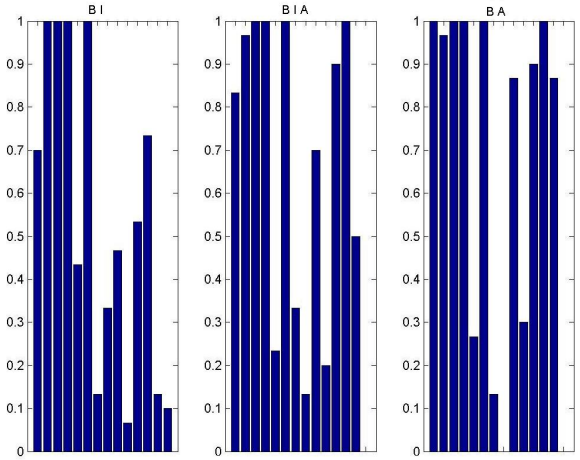

Fig. 1. Selected Rules for MOEA in PLA1

these R-values provide accuracy to the system, as can be seen in Figure 1.

This table shows the rules selected by MOEA in the case of a data set (in this example PLA1 with 14 rules) for the three points (BI, BA and BIA). In the x-axis are the rules from highest to lowest importance (from left to right), as the R-values, and the vertical axis is the percentage of times that MOEA selects each rule. Thus, 0.5 means that a rule has been selected for 50% of the time.

Figures 2, 3 and 4 show similar selections for Model1 with other data sets. In all cases, it can be seen that the rules associated to small R-values are selected, even in the best Acc point.

2) Complex Models: Table XI shows the averaged results obtained by the characteristic models considered in this work over 5 runs for each case study considered. As compact models, the table shows the mean squared error for the test, MSE_{tst}, and the mean of the proposed index $Inter_C$, for each one of the three points: BI, BIA and BA.

The first line shows the initial/original model (I) and the second line shows the improved model performance (F) for

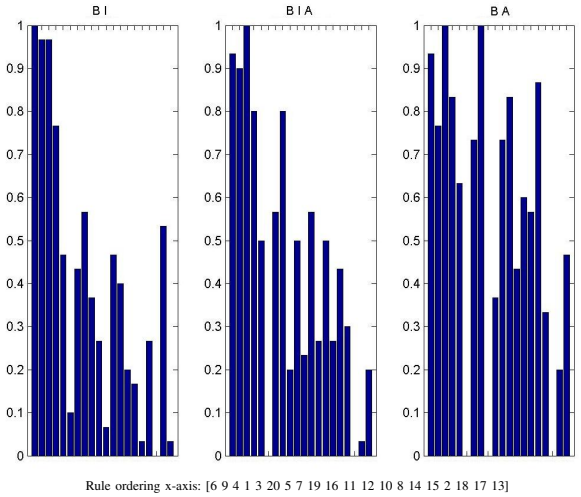

Fig. 2. Selected Rules for MOEA in QUA1

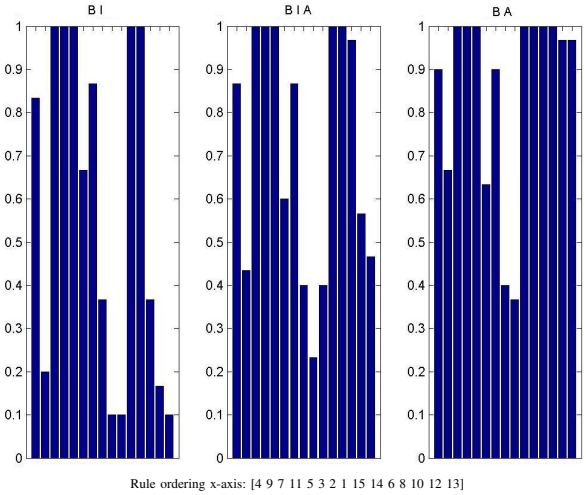

Fig. 3. Selected Rules for MOEA in STP1

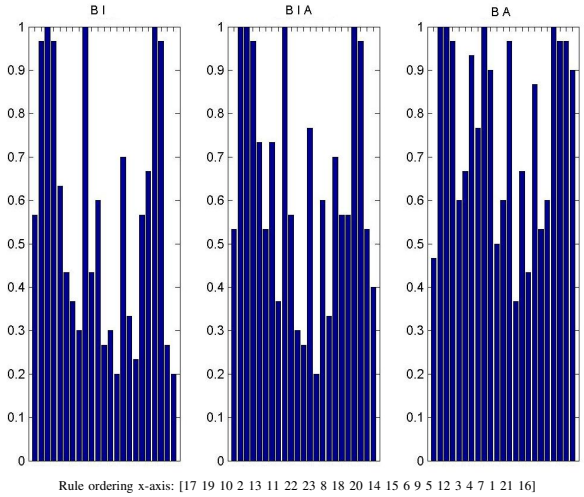

Fig. 4. Selected Rules for MOEA in TRE1

TABLE XI
PERFORMANCE OF THE IMPROVED COMPLEX FUZZY MODELS

	Best $Inter_C$		Balanced $Inter_C - Acc$		Best Acc	
Model2	MSE_{tst}	$Inter_C$	MSE_{tst}	$Inter_C$	MSE_{tst}	$Inter_C$
PLA2(I)	2.498	0.231	2.498	0.231	2.498	0.231
PLA2(F)	8.471	0.081	8.355	0.083	8.391	0.088
QUA2(I)	0.040	0.251	0.040	0.251	0.040	0.251
QUA2(F)	0.051	0.115	0.045	0.118	0.039	0.121
ELE2(I)	55103	0.265	55103	0.265	55103	0.265
ELE2(F)	1079317	0.100	1063736	0.103	1035999	0.123
ABA2(I)	5.176	0.266	5.176	0.266	5.176	0.266
ABA2(F)	6.669	0.157	6.686	0.161	6.715	0.166
STP2(I)	0.432	0.238	0.432	0.238	0.432	0.238
STP2(F)	12.957	0.131	12.529	0.132	11.793	0.135
WIZ2(I)	3.737	0.275	3.737	0.275	3.737	0.275
WIZ2(F)	18.279	0.175	17.644	0.177	17.326	0.180
WAN2(I)	4.044	0.272	4.044	0.272	4.044	0.272
WAN2(F)	9.992	0.147	9.866	0.146	9.298	0.149
MOR2(I)	0.071	0.258	0.071	0.258	0.071	0.258
MOR2(F)	3.622	0.146	3.458	0.149	3.311	0.153
TRE2(I)	0.138	0.258	0.138	0.258	0.138	0.258
TRE2(F)	3.916	0.158	3.713	0.158	3.138	0.161

TABLE XII
RESULTS OBTAINED WITH COMPLEX FASART BEST $Inter_C$ β=67.1 %

Model2	MSE_{tra}	MSE_{tst}	RN	S	R	I	C(%)
PLA2(I)	2.498	2.498	143.00	0.144	0.001	0.008	100
PLA2(F)	8.538	8.471	38.20	0.137	0.001	0.000	100
QUA2(I)	0.040	0.040	310.00	0.255	0.000	0.002	100
QUA2(F)	0.050	0.051	89.40	0.260	0.000	0.002	97.5
ELE2(I)	55102	55103	145.00	0.291	0.008	0.001	97.6
ELE2(F)	910201	1079317	39.20	0.188	0.011	0.001	97.2
ABA2(I)	5.176	5.176	305.00	0.330	0.000	0.001	100
ABA2(F)	6.570	6.669	120.40	0.339	0.001	0.001	95.0
STP2(I)	0.432	0.432	165.00	0.187	0.000	0.000	100
STP2(F)	12.654	12.957	55.20	0.254	-	0.002	93.6
WIZ2(I)	3.737	3.737	118.00	0.377	0.000	0.000	100
WIZ2(F)	18.037	18.279	36.60	0.424	-	-	86.0
WAN2(I)	4.060	4.044	391.00	0.358	0.000	0.000	100
WAN2(F)	8.575	9.992	134.00	0.357	-	-	96.4
MOR2(I)	0.071	0.071	101.00	0.290	0.000	0.000	100
MOR2(F)	3.090	3.622	37.40	0.320	0.001	0.000	96.2
TRE2(I)	0.138	0.138	62.00	0.288	0.000	0.000	100
TRE2(F)	4.054	3.916	22.80	0.321	-	-	90.0

TABLE XIII
RESULTS OBTAINED WITH COMPLEX FASART BALANCED $Inter_C - Acc$ β=68.8 %

Model2	MSE_{tra}	MSE_{tst}	RN	S	R	I	C(%)
PLA2(I)	2.498	2.498	143.00	0.144	0.001	0.008	100
PLA2(F)	8.418	8.355	40.00	0.136	0.001	0.000	100
QUA2(I)	0.040	0.040	310.00	0.255	0.000	0.002	100
QUA2(F)	0.049	0.045	93.80	0.259	0.000	0.001	97.5
ELE2(I)	551024	55103	145.00	0.291	0.008	0.001	97.6
ELE2(F)	859980	10637365	41.20	0.192	0.012	0.001	97.2
ABA2(I)	5.176	5.176	305.00	0.330	0.000	0.001	100
ABA2(F)	6.569	6.686	125.80	0.339	0.001	0.001	95.0
STP2(I)	0.432	0.432	165.00	0.187	0.000	0.000	100
STP2(F)	11.898	12.529	57.20	0.252	-	0.002	93.9
WIZ2(I)	3.737	3.737	118.00	0.377	0.000	0.000	100
WIZ2(F)	17.303	17.644	38.40	0.425	-	-	86.4
WAN2(I)	4.060	4.044	391.00	0.358	0.000	0.000	100
WAN2(F)	7.894	9.866	139.60	0.352	-	-	97.9
MOR2(I)	0.071	0.071	101.00	0.290	0.000	0.000	100
MOR2(F)	2.994	3.458	39.00	0.322	0.001	0.000	96.3
TRE2(I)	0.138	0.138	62.00	0.288	0.000	0.000	100
TRE2(F)	3.780	3.713	23.80	0.317	-	-	91.0

TABLE XIV
RESULTS OBTAINED WITH COMPLEX FASART BEST Acc β=70.8 %

Model2	MSE_{tra}	MSE_{tst}	RN	S	R	I	C(%)
PLA2(I)	2.498	2.498	143.00	0.144	0.001	0.008	100
PLA2(F)	8.362	8.391	42.20	0.134	0.001	0.000	100
QUA2(I)	0.040	0.040	310.00	0.255	0.000	0.002	100
QUA2(F)	0.040	0.039	99.40	0.258	0.000	0.001	97.5
ELE2(I)	55102	55103	145.00	0.291	0.008	0.001	97.6
ELE2(F)	790187	1035999	43.20	0.189	0.011	0.002	97.2
ABA2(I)	5.176	5.176	305.00	0.330	0.000	0.001	100
ABA2(F)	6.576	6.715	132.80	0.336	0.001	0.001	95.4
STP2(I)	0.432	0.432	165.00	0.187	0.000	0.000	100
STP2(F)	11.003	11.793	59.80	0.254	-	0.002	94.2
WIZ2(I)	3.737	3.737	118.00	0.377	0.000	0.000	100
WIZ2(F)	16.882	17.326	40.40	0.421	-	-	86.5
WAN2(I)	4.060	4.044	391.00	0.358	0.000	0.000	100
WAN2(F)	7.379	9.298	146.40	0.349	-	-	98.1
MOR2(I)	0.071	0.071	101.00	0.290	0.000	0.000	100
MOR2(F)	2.808	3.311	41.00	0.319	0.001	0.000	96.3
TRE2(I)	0.138	0.138	62.00	0.288	0.000	0.000	100
TRE2(F)	3.194	3.138	24.80	0.316	-	-	91.2

these three characteristic models.

Tables XII, XIII, XIV show the mean and individual values for some indexes considered for the final β's: the mean squared error for training (MSE_{tra}) and testing (MSE_{tst}), the mean rule number (RN), the mean similarity (S), the mean redundancy (R), the mean incoherency (I) and the mean percentage of completeness (C%).

These tables show that the interpretability is always improved, while the accuracy is only improved for one data set and for the best Acc point. This is normal because complex models have an original high precision.

However, the accuracy is also reduced by the rule selection, and this is connected with orthogonal transformations: the firing matrix used to obtain the R-values only takes into account the antecedents of the rules. Thus, there are important rules for the accuracy of the system which are removed. These rules can correspond to small R-values and Figures 1, 2, 3 and 4 show these drawbacks: rules with small R-values are selected by the MOEA to provide accuracy and to obtain a good interpretability-accuracy trade-off.

3) Global Analysis: In general, the results show the advantages and some of the drawbacks obtained when orthogonal transformation are applied to the firing matrix of the fuzzy rule based model: a high reduction of the complexity, so the levels of interpretability under fuzzy criteria are increased (see Tables VII and XI).

However, on the other hand, the model accuracy is decreased in most of the cases. This reduction of the accuracy can be highly relevant due to the hard simplification achieved by orthogonal transformations. This happens, even taking into consideration the most relevant rules based on their $R{-}values$. The cause for this is: some of the rules removed correspond to the smaller R-values, or those near to zero, and these R-values correspond to non active and redundant rules. Redundant rules, however, can significantly contribute to the output system.

This can be shown by looking at the selection of rules that MOEA carries out according to the restrictions commented in point 2 of section IV: although smaller R-values are penalized, the algorithm continues to select some of the small R-values, to provide the system with accuracy (see Figures 1 to 4).

VI. CONCLUSIONS

This work deals with the complexity reduction of fuzzy models via Orthogonal Transformations, QRP: The goal is to check the limitations of the traditional application of this type of transformation to the firing matrix of a fuzzy model. In

order to check this, a $Criterion$ for fuzzy rule selection has been defined based on R-values, and its parameter has been tuned by a MOEA. This tuning has been carried out taking into consideration the accuracy-interpretability trade-off.

In all cases, interpretability has been improved considerably. The number of rules is always reduced, to 70% in some cases, and the rest of the indexes defined to measure the interpretability are also reduced in most cases.

However, in most cases, there is a loss of accuracy. This is due to the fact that orthogonal transformations for rule reduction are usually based on a firing matrix (P) involving the rule antecedent [19], [12]. The rules associated with the smaller R-values are removed because they are considered not relevant, but these rules usually provide a better accuracy.

In this work, the R-values for rule selection are obtained from the firing matrix (P). The results show that this matrix is not sufficient for this selection of rules because the rules associated with the small R-values are removed, and some of these rules can be important to obtain a good accuracy.

Future work is focused on a more realistic *"firing matrix"*, or index-values for rule selection, considering other elements of the fuzzy models such as the inference mechanism or consequents.

ACKNOWLEDGMENT

This work was supported by the Spanish Ministry of Science and Innovation under grant no. DPI2009-14410-C02-02.

REFERENCES

[1] H. Wu and J. Mendel, "Classification of battlefield ground vehicles using acoustic features and fuzzy logic rule-based classifiers," *IEEE Transactions on Fuzzy Systems*, vol. 15, no. 1, pp. 56–72, February 2007.

[2] J. Garibaldi and T. Ozen, "Uncertain fuzzy reasoning: A case study in modelling expert decision making," *IEEE Transactions on Fuzzy Systems*, vol. 15, no. 1, pp. 16–30, February 2007.

[3] R. John and P. Innocent, "Modeling uncertainty in clinical diagnosis using fuzzy logic," *IEEE Transactions on Systems, Man and Cybernetics – Part B: Cybernetics*, vol. 35, no. 6, pp. 1340–1350, December 2005.

[4] A. Konar, *Computational Intelligence: Principles, techniques and applications*. Springer-Verlag, Berlin, 2005.

[5] F. Karray and C. d. De Silva, *Soft Computing and Intelligent Systems Design. Theory, Tools and Applications*. Addison Wesley, 2004.

[6] M. Gacto, R. Alcalá, and F. Herrera, "Integration of an index to preserve the semantic interpretability in the multi-objective evolutionary rule selection and tuning of linguistic fuzzy systems," *IEEE Transactions on Fuzzy Systems*, vol. 18, no. 3, pp. 515 – 531, 2010.

[7] H. Ishibuchi and Y. Nojima, "Discussions on interpretability of fuzzy systems using simple examples," *Proc. of 13th IFSA World Congress and 6th Conference of EUSFLAT*, pp. 1649–1654, 2009.

[8] J. Alonso, L. Magdalena, and G. González-Rodríguez, "Looking for a good fuzzy system interpretability index: An experimental approach," *International Journal of Approximate Reasoning*, vol. 51, no. 1, pp. 115 – 134, December 2009.

[9] C. Mencar and A. Fanelli, "Interpretability constraints for fuzzy information granulation," *Information Sciences*, vol. 178, no. 24, pp. 4585 – 4618, December 2008.

[10] S.-M. Zhou and J. Gan, "Low-level interpretability and high-level interpretability: a unified view of data-driven interpretable fuzzy system modelling," *Fuzzy Sets and Systems*, vol. 159, pp. 3091 – 3131, 2008.

[11] M. Gacto, R. Alcalá, and F. Herrera, "Interpretability of linguistic fuzzy rule-based systems: An overview of interpretability measures," *Information Sciences*, vol. in press, 2011.

[12] M. Setnes and R. Babuska, "Rule base reduction: Some comments on the use of orthogonal transforms," *IEEE Transactions on Systems, Man, and Cybernetics, Part C: Applications and Reviews*, vol. 31, no. 2, pp. 199 – 206, May 2001.

[13] F. Herrera, "Genetic fuzzy systems: Taxonomy, current research trends and prospects." *Evolutionary Intelligence*, vol. 1, pp. 27 – 46, 2008.

[14] R. Alcalá, J. Alcalá-Fdez, J. Casillas, O. Cordón, and F. Herrera, "Hybrid learning models to get the interpretability-accuracy trade-off in fuzzy modeling," *Soft Computing*, vol. 10, no. 9, pp. 717 – 734, 2006.

[15] J. Casillas, O. Cordón, F. Herrera, and L. Magdalena, *Accuracy Improvements in Linguistic Fuzzy Modelling*, ser. Studies in Fuzziness and SoftComputing. Berlin Heildelberg: Springer-Verlag, 2003, vol. 129, ch. Accuracy Improvements to Find the Balance Interpretability-Accuracy in Fuzzy Modeling: An Overview, pp. 3–24.

[16] O. Cordón, F. Herrera, F. Hoffmann, and L. Magdalena, *Genetic Fuzzy Systems: Evolutionary Tuning and Learning of Fuzzy Knowledge Bases*, ser. Advances in Fuzzy Systems - Applications and Theory. Singapore.: World Scientific, 2001, vol. 19.

[17] S.-M. Zhou, J. Garibaldi, R. John, and F. Chiclana, "On constructing parsimonious type-2 fuzzy logic systems via influential rule selección," *IEEE Transactions on Fuzzy Systems*, vol. 17, pp. 654 – 667, 2009.

[18] A. Lotfi, M. Howarth, and J. Hull, "Orthogonal rule-based systems: selection of optimum rules," *Neural Comput Appl*, vol. 9, pp. 4–11, 2000.

[19] J. Yen and L. Wang, "Simplifying fuzzy rule-based models using orthogonal transformation methods," *IEEE Transactions on Systems, Man and Cybernetics. Part B: Cybernetics*, vol. 29, no. 1, pp. 13–24, February 1999.

[20] G. H. Golub and C. F. Van Loan, *Matrix computations*. The Johns Hopkins University Press, 1996 (Third edition).

[21] M. Galende-Hernández, G. Sainz-Palmero, and M. Fuente-Aparicio, "Complexity reduction and interpretability improvement for fuzzy rule systems based on simple interpretability measures and indices by bi-objective evolutionary rule selection," *Soft Computing*, 2010. In review.

[22] K. Deb, A. Pratap, S. Agarwal, and T. Meyarivan, "A fast and elitist multiobjective genetic algorithm: NSGA-II," *IEEE Transacions on Evolutionary Computation*, vol. 6, no. 2, pp. 182–197, April 2002.

[23] J. Cano Izquierdo, Y. Dimitriadis, E. Gómez Sánchez, and J. López Coronado, "Learnning from noisy information in FasArt and Fasback neuro-fuzzy systems," *Neural Networks*, vol. 14, no. 4-5, pp. 407–425, May 2001.

[24] G. Sainz Palmero, Y. Dimitriadis, J. Cano Izquierdo, E. Gómez Sánchez, and E. Parrado Hernández, "ART based model set for pattern recognition: FasArt family," in *Neuro-fuzzy pattern recognition*, H. Bunke and A. Kandel, Eds. World Scientific Pub. Co., December 2000, ch. 1, pp. 147–177.

[25] J. Alcalá-Fdez, L. Sánchez, S. García, M. J. del Jesus, S. Ventura, J. M. Garrell, J. Otero, C. Romero, J. Bacardit, V. M. Rivas, J. C. Fernndez, and F. Herrera, "KEEL: a software tool to assess evolutionary algorithms for data mining problems," *Soft Computing - A Fusion of Foundations, Methodologies and Applications*, vol. 13, no. 3, pp. 307 – 318, Febraury 2009.

[26] J. Alcalá-Fdez, A. Fernandez, J. Luengo, J. Derrac, S. García, L. Sánchez, and F. Herrera, "Keel data-mining software tool: Data set repository, integration of algorithms and experimental analysis framework," *Journal of Multiple-Valued Logic and Soft Computing*, vol. in press, 2010.

[27] L.-X. Wang and J. Mendel, "Generating fuzzy rules by learning from examples," *IEEE Transactions on Systems, Man and Cybernetics*, vol. 22, no. 6, pp. 1414–1427, November/December 1992.

2011 IEEE International Conference on Fuzzy Systems
June 27-30, 2011, Taipei, Taiwan

A Hierarchical Genetic Fuzzy Rule-Based Classifier for High-Dimensional Classification Problems

Dimitris G. Stavrakoudis[a], Ioannis Z. Gitas[b], and John B. Theocharis[a]
[a]Department of Electrical and Computer Engineering
[b]School of Forestry and Natural Environment
Aristotle University of Thessaloniki
Thessaloniki, Greece
{jstavrak@auth.gr; igitas@for.auth.gr; theochar@eng.auth.gr}

***Abstract*—This paper proposes a novel Hierarchical Genetic Fuzzy Rule-Based Classification System (HGFRBCS), targeted at effectively handling high-dimensional classification tasks. A hierarchical fuzzy rule base comprises rules with linguistic terms from a multi-granular fuzzy sets database, whereby lower levels define thicker granularities of the input space fuzzy partition. The proposed system is developed through sequential repeating steps: in each step a fuzzy rule base is created using a given granularity. Subsequently, the best performing rules are inserted in the hierarchical rule base and the process is repeated again, considering a thicker granularity. The whole process is coordinated by a boosting scheme, which localizes new rules in uncovered regions of the feature space. Comparative results for various real-world high-dimensional classification problems indicate the effectiveness of the proposed methodology.**

Fuzzy rule-based classification system (FRBCS); hierachical fuzzy partitions; genetic fuzzy systems

I. INTRODUCTION

The interpretational properties of Genetic Fuzzy Rule-Based Classification Systems (GFRBCSs) [1] have rendered them useful tools in the field of data mining over the past two decades [2]. In particular, linguistic FRBCSs [3]–[4] have the most intuitive representation, comprising rules with linguistic terms from a common fuzzy sets database. Their main drawback is a possible loss in accuracy when dealing with complex classification tasks, resulting from the inflexibility introduced by the discretization of the input space into a fixed number of fuzzy sets with predefined membership functions.

In order to increase classification accuracy, a hierarchical framework for building FRBCSs has been recently proposed [5]–[6]. This approach applies a two-level methodology. In the first level, a fuzzy rule base is created with an initial fuzzy set database. Poorly performing rules are removed from the rule base and replaced by rules defined in a thicker fuzzy partition granularity. In the second level, a genetic rule selection procedure is performed, which selects the best cooperating rules from the hierarchical rule base (HRB). However, the rule extraction algorithm (REA) considered in this approach results in the generation of a high number of fuzzy rules, as the results in [6] indicate. Another drawback of the approach is that it does not consider any feature reduction procedure, resulting in fuzzy rules with a complex linguistic structure when dealing with high-dimensional classification problems.

Another HGFRBCS has been previously proposed in [7], whose HRB structure resembles the philosophy followed by the herein proposed system. In this approach, an initial pool of candidate fuzzy rules is considered, defined in fuzzy partitions with different granularities. Subsequently, a genetic rule selection procedure selects the best cooperating rules, in order to form the final HRB. The main drawback of this approach lies in the creation of the initial pool of fuzzy rules, which is performed by considering the complete rule base for each fuzzy partition granularity, rendering the procedure ineffective in high-dimensional problems.

In this paper we propose a HGFRBCS which aims at producing compact yet high-performing HRBs in high-dimensional classification tasks. The basic idea is to repeatedly invoke a rule base extraction algorithm (RBEA), each time considering a fuzzy partition of thicker granularity. Fuzzy rules that increase the HRB's performance are maintained, whereas the rest are disregarded. In order for new rules to be created in uncovered regions of the feature space, we consider a boosting scheme that penalizes previously well covered patterns, so that new valuable rules will be localized in uncovered or mixed regions of the feature space. As the basic RBEA we consider a GFRBCS from a previous contribution of ours [8], which has been proven to generate compact rule bases, with low computational requirements.

The rest of the paper is organized as follows. Section II summarizes some of the basic concepts that will be used throughout the paper. In Section III we provide a brief description of the basic RBEA. Section IV details the framework for building the hierarchical fuzzy rule base. Experimental results for a number of high-dimensional classification problems are reported in Section V and the paper concludes in Section VI with some final remarks.

II. PRELIMINARIES

This section introduces the notation that will be used in the rest of the paper, along with a description of the proposed system's fuzzy inference mechanism implementation and the boosting algorithm considered.

978-1-4244-7316-8/11/$26.00 ©2011 IEEE

A. Fuzzy Reasoning

We consider a classification problem defined in an N-dimensional feature space $\boldsymbol{x} = [x_1, \ldots, x_N] \in \Re^N$ and an M-dimensional class space $\boldsymbol{C} = \{C_1, \ldots, C_M\}$ and a set of Q labeled patterns $E = \{(\boldsymbol{x}^p, c^p),\ p = 1, \ldots, Q\}$. The proposed FRBCS comprises a number of linguistic DNF fuzzy rules, having the form:

$$R_k\text{: IF } x_1 \text{ is } A_1^k \text{ and} \cdots x_N \text{ is } A_N^k \text{ THEN } y \text{ is } C^k \text{ with } r^k, \quad (1)$$

where each input variable x_i takes as a value a set of linguistic terms $A_i^k = \{L_i^1 \text{ or } \cdots \text{ or } L_i^{\ell_k}\}$ joined by a disjunctive operator, whereas the output variable (y) is one of the class labels $C^k \in \boldsymbol{C}$. We will also consider that some input variables in each rule may be absent, which, in fuzzy terms, has the meaning of a "don't care" fuzzy set (a fuzzy set with a unity membership grade for its entire universe of discourse). For the sake of simplicity, in the rest of the paper we will refer to an input variable (feature) x_i as *active* when the fuzzy clause "x_i is A_i^k" is present in the rule and as *inactive* in the opposite case. Moreover, each fuzzy rule includes a certainty degree $r^k \in [0,1]$ which represents the confidence of the classification in the class label of the consequent (C^k). This certainty degree is calculated in our proposal through

$$r^k = \sum_{p|c^p = C^k} \mu^k(\boldsymbol{x}^p) \Big/ \sum_{p=1}^{Q} \mu^k(\boldsymbol{x}^p), \quad (2)$$

where $\mu^k(\boldsymbol{x}^p)$ is the degree of compatibility between an example and the antecedent part of a fuzzy rule (also known as matching degree). This matching degree is calculated as follows:

$$\mu^k(\boldsymbol{x}^p) = \bigwedge_{i=1}^{N} \left\{ \bigvee_{q=1}^{\ell_k} \mu_{L_i^q}(x_i^p) \right\}, \quad (3)$$

where $\mu_{L_i^q}(x_i^p)$ is the membership grade of each linguistic term participating in the formulation of ith variable's fuzzy value, and $\wedge$ and $\vee$ denote the AND and OR operators, respectively. The AND operator is implemented conventionally through the minimum operator, whereas the OR operator is implemented through the bounded sum, defined for two membership values a and b as:

$$\text{bs}(a,b) = \min(1, a+b) \quad (4)$$

With this choice, the composite fuzzy set is mathematically equivalent to a trapezoidal fuzzy set, having a far more reasonable interpretation than the one provided by the usually selected maximum operator, which results in taking the envelop of neighboring membership functions.

Since the proposed system implements a HRB, the linguistic terms A_i^k in each rule are defined in a fuzzy partition of a certain granularity. Hence, a hierarchical database (HDB) of fuzzy sets is defined, comprising S hierarchy levels with respective granularities $G(t)$, $t = 1, \ldots, S$. All linguistic terms participating in one rule are restricted to belong to the same hierarchy level.

Finally, we use the so-called maximum voting scheme in order to classify a given feature vector $\boldsymbol{x}^p$, defined as:

$$C_{\max} = \arg\max_{j=1,\ldots,M} \sum_{R^k | C^k = j} \mu^k(\boldsymbol{x}^p) \cdot r^k \quad (5)$$

B. Boosting Scheme

As mentioned in the introduction, the proposed system iteratively calls a RBEA, considering each time a fuzzy partition of thicker granularity. In order to localize new rules in uncovered regions of the feature space, we need a mechanism which will penalize previously covered examples. Such a framework can be provided by the so-called boosting algorithms. AdaBoost [9] is the most well-known boosting algorithm and its main idea is to combine a set of low quality classifiers (called weak hypotheses in the boosting literature) with a voting scheme, in order to generate an overall classifier that performs better than any of its constituents alone. In the context of FRBCSs, each fuzzy rule can be regarded as a simple but partial (in terms of overall classification performance) classifier. Assuming a training patterns set $E_{\text{trn}} = \{e^p = (\boldsymbol{x}^p, c^p),\ p = 1, \ldots, Q\}$, the AdaBoost algorithm assigns a weight w^p to each one of the Q training patterns, all initialized with a unity value $w^p = 1$. Each time a new rule R^k is inserted in the HRB, AdaBoost computes the error $E(R^k)$ of the rule, taking into consideration the examples' previous weights and their matching degrees:

$$E(R^k) = \frac{\sum_{p|c^p = C^k} w^p \mu^k(\boldsymbol{x}^p)}{\sum_{p=1}^{Q} w^p \mu^k(\boldsymbol{x}^p)}. \quad (6)$$

Incorrectly classified patterns retain their former weights, whereas the weights of correctly classified patterns are reduced by a factor $\beta^k(\boldsymbol{x}^p)$:

$$w^p \leftarrow \begin{cases} w^p, & \text{if } C^k \neq c^p \\ w^p \cdot \beta^k(\boldsymbol{x}^p), & \text{if } C^k = c^p. \end{cases} \quad (7)$$

The factor

$$\beta^k(\boldsymbol{x}^p) = \left(\frac{E(R^k)}{1 - E(R^k)} \right)^{\mu^k(\boldsymbol{x}^p)} \quad (8)$$

depends on the current rule's error and its matching degree with the pth pattern. Effectively, examples that are classified correctly and match the rule antecedent are down-weighted, whereas misclassified or uncovered examples maintain their original weights.

We should note that there is an important difference between fuzzy rules and the notion of the weak hypothesis in the boosting literature. The weak hypothesis is assumed to be a low performing classifier that, however, covers the whole feature space. On the contrary, a fuzzy rule is a local model, covering only a specific subspace of the feature space.

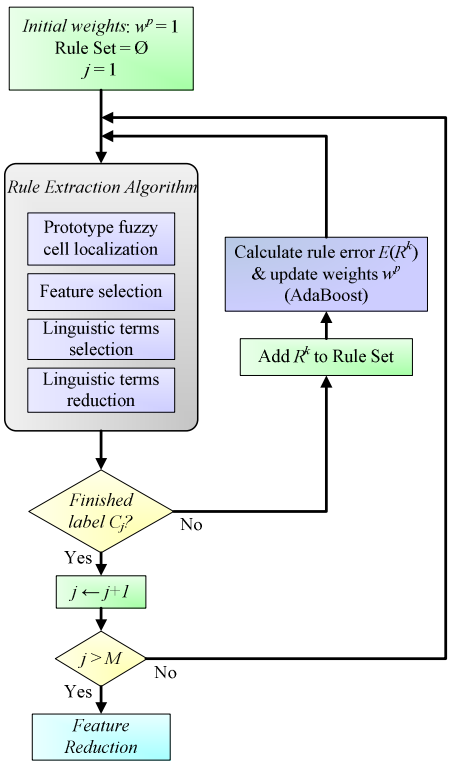

Figure 1. Outline of FaIRLiC's learning algorithm.

Therefore, under the AdaBoost philosophy, classifiers that are created at later stages handle mostly uncovered regions of the feature space, but are allowed to also (correctly) classify previously down-weighted patterns. In FRBCSs this is generally an undesirable behavior, since superfluous fuzzy rules with high overlapping may be produced. To that extent, special provision must be made to avoid such phenomena when applying the AdaBoost algorithm in the derivation of GFRBCSs.

III. Rule Base Extraction Algorithm

In a previous work [8], we introduced the so-called Fast Iterative Rule-Based Linguistic Classifier (FaIRLiC), a GFRBCS designed under the Iterative Rule Learning (IRL) approach [1]. This system is characterized by the compact rule base structure it produces, the overall good classification accuracy attained and the relatively low time requirements of its learning algorithm. Due to these attributes it has been selected here as the basic RBEA of the proposed system. In the rest of this section, we provide a brief description of FaIRLiC. A more comprehensive description can be found in the aforementioned reference.

An outline of FaIRLiC's learning algorithm is depicted in Fig. 1. FaIRLiC constructs a FRBCS comprising DNF rules in the form of (1), with a fuzzy partition of a certain granularity, selected by the designer. Following the IRL approach, the system is constructed through repeated invocation to a rule extraction algorithm, each time returning the best fuzzy rule found under the current distribution of the training examples. This distribution is controlled by the AdaBoost algorithm presented in Section II.B. Hence, each time a new rule is added to the final rule base, the weights of correctly covered examples are down-weighted and subsequent invocation to the algorithm concentrate on uncovered patterns.

The rule extraction algorithm is performed in four successive steps: a) prototype fuzzy cell localization, b) feature selection, c) linguistic terms selection and d) linguistic terms reduction. The first step initializes the algorithm by selecting the most promising single linguistic term for each input variable. Given these terms, the second step performs a genetic feature selection procedure. After having selected the relevant features of the rule, a genetic algorithm (GA) in the third step identifies the DNF-type linguistic terms that will be included in its antecedent part, for each active feature. The final step is a simple deterministic one, which corrects the fuzzy rule from extending to empty subspaces of the feature space. Specifically, for each active input variable we remove one fuzzy term at a time (if there are more than two) and accept that change if the classification performance does not decrease. The inner fuzzy sets of a contiguous block of linguistic terms are never removed, in order to avoid the creation of intermittent composite fuzzy sets.

Throughout FaIRLiC's rule extraction algorithm we evaluate extensively a feature selection oriented metric, the so-called Feature Partition Vector (FPV). The FPV quantifies the degree to which each feature can correctly classify each one of the training examples, independently from other features. This metric is used in order to localize the initial linguistic terms (first step) in the most informative region of the equivalent input variable, as well as for the initialization of the population and the application of special genetic operators in the second step. Moreover, a modified coverage fitness function is considered for the GAs in the second and third steps, which explicitly discourages new rules to cover previously well-covered examples.

Similarly to the SLAVE algorithm [10], we learn one class label at a time, with no particular order being assumed. When no more useful rules can be produced for the class under consideration, the algorithm proceeds to the next class label. Two conditions are considered to judge if the algorithm should proceed to the next class label:

- The new rule's fitness value is zero (in either the feature selection or the linguistic terms selection steps), which signifies the inability of the rule extraction algorithm to find a new useful rule.
- The classification performance of the rule base obtained so far does not increase more than a pre-specified threshold on a validation set of examples. Accordingly, our initial set of labeled patterns is split into three disjoint sets: the training, the validation, and the testing ones.

As a final step, we perform a deterministic feature reduction step, which is similar to the linguistic terms reduction one. Specifically, for each rule we inactivate one input variable at a time and observe the performance of the system in the training and validation sets. If these performances do not degrade and the rule's consequent does not change, we accept

Initialization: $w^p = 1$; $a^{NPR} = a_{\text{init}}^{NPR}$; HRB = Ø
for hierarchy level $t = 1$ to S
  call FaIRLiC($G(t)$, w^p)
  find promising rules set $R_{pr}(t)$
  for $k = 1$ to $|R_{pr}(t)|$
    insert kth rule into HRB
    if *validation performance increases*
      update weights w^p
    else
      remove kth rule from HRB
    endif
  endfor
  adjust a^{NPR}
endfor
Perform rule reduction
Perform feature reduction

Figure 2. An outline of the proposed methodology.

the chance. Moreover, since removing a feature results in a generalization of the rule, we also assure that the overlapping between rules describing the same class label does not increase.

IV. Iterative Hierarchical Framework

Here we introduce the Hierarchical Rule-Based Linguistic Classifier (HiRLiC), which is a framework for building HGFRBCSs. As mentioned in the introduction, HiRLiC repeatedly calls a RBEA (the FaIRLiC algorithm), each time considering a fuzzy partition of thicker granularity. Since FaIRLiC considers DNF-type rules in the form of (1), one might suggest to select a very fine granularity of the input space and then request FaIRLiC to implicitly identify the required granularity for each rule, by selecting the appropriate linguistic terms to be joined by the OR disjunctive operator. However, in an N-dimensional classification problem with each input variable being partitioned into ℓ fuzzy sets, plus the "don't care" (inactive feature) fuzzy set, the search space for simple linguistic rules is $(\ell+1)^N$. The actual search space is much larger if we consider the DNF type of the fuzzy rules. As the dimensionality of the feature space increases, the search space of the problem increases exponentially, thus degrading the effectiveness of FaIRLiC's GA-driven learning algorithm.

To overcome the aforementioned problem, HiRLiC decomposes the problem into smaller, easier to tackle sub-problems. Through AdaBoost, the algorithm initially concentrates in uncovered regions of the feature space, allowing the mixed areas in the borders of neighboring classes to be handled in a later stage, when a finer partition will be available and most of the easily discriminated patterns will have been practically removed (their weight values will be close to zero). When seen under this scope, HiRLiC employs a higher-level IRL methodology: just as FaIRLiC repeatedly calls a rule extraction algorithm and uses the (local) AdaBoost weights to localize new rules in uncovered regions of the feature space, so does HiRLiC iteratively invoke a RBEA in different hierarchy levels, using the (global) AdaBoost weights as the control mechanism. To that extent, HiRLiC is able to effectively handle the large search space, thus increasing its base weak learner's, that is FaIRLiC's, classification accuracy.

TABLE I. Summary Description of the Datatsets

Dataset	Patterns	Features	Classes
Ionosphere	351	34	2
Libras	360	90	15
Optdigits	5620	64	10
Satimage	6435	36	6
Sonar	208	60	2
Spambase	4601	57	2
Wdbc	569	30	2
Texture	5500	40	11
KorAgro	2706	53	8
KorWet	1219	53	5
KorWhole	3925	53	13
Thasos	1000	198	6

An outline of the HiRLiC learning methodology is given in Fig. 2. Initially we consider and empty HRB and the AdaBoost algorithm assigns unity weights to the training patterns. The designer selects the number S of the hierarchy levels to be considered, along with the respective granularities of the fuzzy partitions $G(t)$, $t = 1,\ldots,S$. For each hierarchy level t, the FaIRLiC algorithm is executed, producing fuzzy rules defined in a fuzzy partition with $G(t)$ granularity, as shown in Fig. 1. The only difference is that instead of initializing FaIRLiC's AdaBoost weights with unity values (top box in Fig. 1) we provide a copy HiRLiC's (global) current weight values.

Obviously, the most crucial point is the selection of the rules to be inserted in the HRB and the ones that will be rejected. We cannot rely solely on the classification accuracy of the HRB, since rules describing currently unhandled class labels will always increase its classification accuracy. In particular, we want to (at least initially) promote confident rules, that is, rules covering a high number of positive examples and a low number of negative ones. Therefore, we propose the use of the negative to positive examples ratio (*NPR*), which is simply defined as the ratio of the fuzzy number of positive examples n^+ to the fuzzy number of negative ones n^-. For the kth fuzzy rule, describing the C^k class label, these numbers are defined, respectively, as:

$$n^+ = \sum_{p|c^p=C^k} \mu^k(\boldsymbol{x}^p), \tag{9}$$

$$n^- = \sum_{p|c^p\neq C^k} \mu^k(\boldsymbol{x}^p). \tag{10}$$

If the *NPR* of a rule is lower than a threshold value a^{NPR}, then this rule is considered to be a *promising* one and it is inserted into the respective rule set of promising rules $R_{pr}(t)$. Generally, we should be stricter in the initial steps, where coarse granularities are considered, and relax this restriction as the algorithm proceeds to lower levels of the hierarchy. To achieve this, the designer chooses an initial threshold value $a_{\text{init}}^{NPR} < 1$ and this threshold increases linearly for subsequent hierarchy levels, achieving a unity value in the last (S) level. Hence, the threshold value at level t is expressed as:

$$a_t^{NPR} = a_{\text{init}}^{NPR} + (1 - a_{\text{init}}^{NPR})\frac{t-1}{S-1}. \tag{11}$$

TABLE II. RESULTS OBTAINED BY FAIRLIC

Dataset	P (%)	# R	GU	#F/R	T (s)
Ionosphere	84.80	3.63	3.97	1.43	1.40
Libras	41.02	20.33	40.63	2.62	14.58
Optdigits	75.85	12.10	27.23	3.23	38.05
Satimage	80.04	8.67	17.00	2.60	24.60
Sonar	67.80	4.43	9.87	2.21	1.98
Spambase	82.09	2.30	10.63	4.73	7.12
Wdbc	90.40	2.17	2.50	1.16	1.30
Texture	82.96	12.87	21.00	2.80	33.78
KorAgro	61.28	9.53	23.50	3.66	22.17
KorWet	76.51	7.27	13.67	2.56	7.72
KorWhole	59.02	15.30	28.70	4.05	47.33
Thasos	81.30	6.23	12.77	2.11	11.13
Average	**73.59**	**8.74**	**17.62**	**2.76**	**17.60**

P (%) = Testing performance (%); # R = number of rules; GU = number of features globally used; # F/R = average number of features per rule.

TABLE III. RESULTS OBTAINED BY HIRLIC

Dataset	P (%)	HD	# R	GU	#F/R	T (s)
Ionosphere	90.31	3.63	6.67	10.30	1.85	9.80
Libras	51.41	6.90	27.90	53.40	2.88	114.08
Optdigits	82.00	6.93	26.20	43.77	3.53	275.56
Satimage	83.36	6.83	17.67	26.53	2.81	212.42
Sonar	69.92	4.60	7.87	21.07	3.23	14.96
Spambase	87.82	3.50	5.10	16.30	4.36	49.54
Wdbc	93.13	2.43	3.67	5.27	1.55	9.89
Texture	86.22	6.90	22.60	26.70	2.93	306.10
KorAgro	69.35	6.53	19.90	31.23	3.35	157.22
KorWet	81.11	4.77	10.30	18.60	2.46	52.30
KorWhole	63.88	6.77	28.53	34.60	3.72	347.14
Thasos	83.60	5.63	11.40	25.13	2.53	98.53
Average	**78.51**	**5.45**	**15.65**	**26.08**	**2.93**	**137.30**

P (%) = testing performance (%); HD = hierarchy depth; # R = number of rules; GU = number of features globally used; # F/R = average number of features per rule.

After creating the rule set $R_{pr}(t)$, we insert each one of the rules into the HRB (one at a time), in the order of their creation. If the classification performance of the HRB on the validation set of examples increases with the insertion of a rule, then this rule is accepted and HiRLiC's AdaBoost weights are updated (see Fig. 2), according to (6)–(8). Otherwise the rule is rejected. Through this procedure, only rules that cooperate well with the previous HRB are inserted into the final model.

Note that all available S hierarchy levels are evaluated. Nevertheless, it is acceptable that no rules with a certain granularity $G(t)$ will be inserted in the final model. Hence, the final system utilizes only the necessary levels of the hierarchical fuzzy sets database. We should also remark, that easily discriminated classes with broad coverage will be generally handled first, which in general will result in faster execution of the FaIRLiC algorithm in later steps.

Finally, before exporting the final HRB, we perform two deterministic rule base refinement procedures, namely, rule reduction and feature reduction, as shown in Fig. 2. The features reduction algorithm is the same as the one performed at the end of FaIRLiC's algorithm (see Section III), whereas rule reduction is a similar procedure which removes one rule at a time and accepts the change if both the training and validation performance rates do not degrade. Arguably, the objectives pursued by these procedures have already been achieved in previous steps to a large extent. Indeed, for the datasets considered in our experimental setup, the average decrease in the numbers of rules and features per rule was 9.74 % and 5.07 %, respectively. Nevertheless, their application is advocated by their practically negligent computational requirements.

V. EXPERIMENTAL STUDY

In order to analyze the performance of the proposed methodology we considered 12 real-world experiments with a medium to high number of features. Table I summarizes the most important characteristics of these datasets. The first 7 datasets are from the UCI repository [11], whereas the Texture dataset is from the ELENA project [12]. The last four are remote sensing classification tasks from satellite imagery. In particular, a multispectral IKONOS image was acquired from an area surrounding Lake Koronia in northern Greece. Advanced higher order spectral and spatial features were subsequently derived from the initial four bands of the image, resulting in a total of 53 features. In order to conduct additional studies from the quality of the ecosystem point of view, the area was carefully segmented into two zones: the agricultural (KorAgro) and the wetland (KorWet) ones. For the sake of completeness, the whole (original) dataset is also considered (KorWhole) here. A detailed description of these datasets can be found in [13]–[14]. Finally, the Thasos dataset was obtained from a hyperspectral Hyperion image (level 1 radiometric product), covering a part of Thasos, Greece's most northerly island [15]. It comprises a total of 198 features in the visible near infrared (VNIR) (400–1000 nm) and shortwave infrared (900–2500 nm) range of the electromagnetic spectrum.

To develop the different experiments we consider a 5-fold cross-validation model, that is, 5 random partitions with 20 % of the data and the combination of 4 of them (80 %) as training and the remaining 20 % as testing. Due to the computational requirements of FaIRLiC and HiRLiC, the training partitions were further split into two equal parts, resulting in the final training and validation partitions. Moreover, we performed six independent runs on each partition, using different random seeds, since GAs are stochastic processes. In each case, the average results over these 30 runs are given.

The parameters used for FaIRLiC are the same as the ones proposed in [8], either when running it independently or as a part of HiRLiC's learning algorithm. When FaIRLiC is tested as a standalone classifier, we use 9 fuzzy sets per input variable, as a reasonable number of fuzzy sets used in many GFRBCSs of the respective literature. In applying HiRLiC, we consider $S = 7$ hierarchy levels with odd granularities from 3 to 15, that is, $\boldsymbol{G} = \{3, 5, 7, 9, 11, 13, 15\}$. The initial *NPR* threshold for HiRLiC was set to $a_{\text{init}}^{NPR} = 0.2$, so that at the first iteration (3 fuzzy sets per input variable) a rule is inserted into the promising rule set only if its negative examples are fewer than 20 % of its positive ones. The two systems were coded in C++ and all experiments were conducted on an Intel Core 2 Quad Q9650 at 3.0 GHz.

TABLE IV. COMPARISON OF VARIOUS GFRBCSS

Dataset	SGERD				Ishibuchi-GCCL				2SLAVE-2				HiRLiC			
	P(%)	*# R*	*GU*	*# F/R*	*P(%)*	*# R*	*GU*	*# F/R*	*P (%)*	*# R*	*GU*	*# F/R*	*P (%)*	*# R*	*GU*	*# F/R*
Ionosphere	72.10	2.00	3.60	2.00	87.18	81.00	32.20	2.56	88.89	4.80	12.00	2.77	90.31	6.67	10.30	1.85
Libras	41.73	20.00	27.40	2.00	19.53	39.20	78.60	6.66	57.60	49.60	89.60	11.79	51.41	27.90	53.40	2.88
Optdigits	55.20	21.00	21.20	1.98	40.18	82.60	59.40	5.94	76.96	63.20	63.80	7.54	82.00	26.20	43.77	3.53
Satimage	77.01	12.80	14.20	2.00	74.50	71.00	35.40	2.58	84.27	53.60	36.00	10.22	83.36	17.67	26.53	2.81
Sonar	72.59	3.00	4.00	2.00	65.80	58.40	53.20	3.82	64.66	6.40	29.20	6.21	69.92	7.87	21.07	3.23
Spambase	69.72	2.40	4.20	2.00	71.65	76.20	53.40	6.94	85.74	19.40	44.80	4.51	87.82	5.10	16.30	4.36
Wdbc	91.42	3.60	5.40	2.00	91.22	59.60	26.20	1.68	93.69	5.40	14.80	3.37	93.13	3.67	5.27	1.55
Texture	69.40	16.20	16.00	2.00	66.33	80.80	36.20	2.62	87.18	33.40	40.00	9.99	86.22	22.60	26.70	2.93
KorAgro	60.98	11.23	12.83	1.95	50.92	62.60	46.80	4.02	59.14	17.30	43.50	6.60	69.35	19.90	31.23	3.35
KorWet	73.28	6.70	7.93	1.94	69.09	58.40	43.20	4.36	80.35	11.17	34.13	5.71	81.11	10.30	18.60	2.46
KorWhole	47.00	17.50	17.43	1.99	40.66	71.60	50.00	4.57	50.89	25.60	46.63	7.12	63.88	28.53	34.60	3.72
Thasos	75.21	7.50	12.37	2.00	–	–	–	–	80.18	15.77	87.30	7.44	83.60	11.40	25.13	2.53
Average	**67.14**	**10.33**	**12.21**	**1.99**	**61.55**	**67.40**	**46.78**	**4.16**	**75.80**	**25.47**	**45.15**	**6.94**	**78.51**	**15.65**	**26.08**	**2.93**

P (%) = Testing performance (%); # R = number of rules; GU = number of features globally used; # F/R = average number of features per rule.

We will first compare the average results obtained by FaIRLiC and HiRLiC, which are shown in Tables II and III, respectively. These tables include – for each dataset – the testing classification accuracy, the number of rules, the average number of globally used features, the number of features per rule, and the runtime of each algorithm in seconds. The term globally used features is used to express the number of features being evaluated by the whole rule base, that is, the features that appear at least once in any rule of the system. Table III also includes the average hierarchy depth of HiRLiC, meaning the average number of hierarchy levels that are actually being utilized by at least one rule of the rule base. The last row of each table reports the respective average values for all datasets considered.

From the performance point of view, HiRLiC outperforms FaIRLiC in all datasets, with the additional performance gain ranging from 2.12 % (Sonar) to 10.39 % (Libras). In most cases, HiRLiC's classification performance is more than 3 % higher that FaIRLiC's ones. This fact proves the fulfillment of our primary objective, which was to increase the classification ability of the base classifier. From the model simplicity point of view, the number of features per rule have marginally increased, while the rule base size increased, subsequently resulting in a higher number of globally used features. However, observing the feature and class space dimensionality of each dataset, we can argue that the obtained HRBs are generally compact, retaining their former interpretability properties to a considerable degree. Obviously, the time requirements of HiRLiC's learning algorithm is multiple of FaIRLiC's ones, since the former repeatedly invokes the latter. Nevertheless, FaIRLiC's learning is fast enough to maintain the HiRLiC's execution times to an acceptable level, especially if we take under consideration the high number of training patterns for most of the datasets.

To validate HiRLiC's performance, we compared it against three other GFRBCSs of the literature, namely, the SGERD [16], Ishibuchi's GCCL [17] and 2SLAVE-2 [10] systems, tested using the Keel software package [18]. The number of fuzzy sets per input variable for 2SLAVE-2 was set to 9, as we have done with FaIRLiC. For Ishibuchi's GCCL we tested granularities from 3 to 9 (the maximum allowed in the Keel software) fuzzy sets per input variable and we finally chose a granularity value of 5, as it achieved the highest classification accuracy in the vast majority of the considered datasets. The rest of the parameters for these three systems were set to the respective values proposed by the authors.

In Table IV we present a comparison of HiRLiC with the three aforementioned GFRBCSs. The results for Ishibuchi's GCCL in the Thasos dataset are missing because the method was unable to produce any useful rules (zero number of rules was obtained) for this dataset. Performance-wise, HiRLiC was found to clearly outperform SGERD and Ishibuchi's GCCL, as well as 2SLAVE-2 in most cases, although the difference with the latter is smaller. However, 2SLAVE-2 resulted in significantly more complex rule bases, with a higher number of features per rules and number of rules than HiRLiC. Ishibuchi's GCCL resulted in fuzzy rule bases with high number of rules, whereas the structure of SGERD is overall approximately equivalent to FaIRLiC's one (see Table II), although the former attained lower classification accuracies in most datasets. From this comparative analysis, we can conclude that HiRLiC results in high performing rule-based classifiers, maintaining a reasonably compact rule base structure at the same time.

VI. CONCLUSION

This paper presented a novel framework for developing hierarchical GFRBCSs, targeting at increasing the classification accuracy of the obtained model. HiRLiC is constructed through an iterative process, by repeated invocations to a basic RBEA, each time considering a fuzzy partition of thicker granularity. A boosting algorithm is responsible for focusing the algorithm towards the uncovered or highly mixed regions of the feature space. The rules provided by the RBEA are evaluated by the HRB and are included in the final model only if they are confident and increase the system's performance. Extensive experimental analysis on various real-world high-dimensional classification tasks has proved the proposed methodology's ability to increase the classification accuracy of the system, maintaining at the same time a reasonably compact structure.

REFERENCES

[1] O. Cordón, F. Herrera, F. Hoffmann, and L. Magdalena, *Genetic Fuzzy Systems: Evolutionary Tuning and Learning of Fuzzy Knowledge Bases*. Singapore: World Scientific, 2001.

[2] O. Cordón, F. Gomide, F. Herrera, F. Hoffmann, and L. Magdalena, "Ten years of genetic fuzzy systems: current framework and new trends," *Fuzzy Sets Syst.*, vol. 141, no. 1, pp. 5–31, 2004.

[3] H. Ishibuchi, T. Nakashima, and M. Nii, *Classification and Modeling with Linguistic Information Granules: Advanced Approaches to Linguistic Data Mining*. Springer, 2004.

[4] M. J. Gacto, R. Alcala, and F. Herrera, "Interpretability of Linguistic Fuzzy Rule-Based Systems: An Overview of Interpretability Measures." *Inf. Sci.*, in press, 2011. DOI: 10.1016/j.ins.2011.02.021.

[5] A. Fernandez, M. J. del Jesus, and F. Herrera, "Hierarchical fuzzy rule based classification systems with genetic rule selection for imbalanced data-sets," *Int. J. Approx. Reasoning*, vol. 50, no. 3, pp. 561–577, 2009.

[6] A. Fernandez, M. J. del Jesus, and F. Herrera, "Analysing the Hierarchical Fuzzy Rule Based Classification Systems with Genetic Rule Selection," *4th Int. Workshop on Genetic and Evolutionary Fuzzy Systems (GEFS)*, pp. 69–74, 2010.

[7] H. Ishibuchi, K. Nozaki, N. Yamamoto, and H. Tanaka, "Selecting Fuzzy If-Then Rules for Classification Problems Using Genetic Algorithms," *IEEE Trans. Fuzzy Syst.*, vol. 3, no. 3, pp. 260–270, 1995.

[8] D. Stavrakoudis, G. Galidaki, I. Gitas, and J. Theocharis, "A Fast Iterative Rule-Based Linguistic Classifier for Hyperspectral Remote Sensing Tasks", *Proc. 5th Int. Workshop on Genetic and Evolutionary Fuzzy Systems (GEFS)*, pp. 25–30, 2011.

[9] Y. Freund and R. Schapire, "Experiments with a new boosting algorithm," in *Proc. 13th Int. Conf. Machine Learning*, pp. 148–156, 1996.

[10] A. González and R. Pérez, "Selection of relevant features in a fuzzy genetic learning algorithm," *IEEE Trans. Syst. Man Cybern., Part B-Cybern.*, vol. 31, no. 3, pp. 417–425, 2001.

[11] A. Asuncion and D. Newman, "UCI machine learning repository," Irvine, CA: Dept. Inf. Comput. Sci., Univ. California, 2007. [Online]. Available: http://www.ics.uci.edu/~mlearn/MLRepository.html

[12] C. Aviles-Cruz, A. Gurin-Dugu, J. L. Voz, and D.Van Cappel, "Databases, Enhanced Learning for Evolutive Neural Architecture," Tech. Rep. R3-B4-P, 1995. [Online]. Available: http://www.dice.ucl.ac.be/neural-nets/Research/Projects/ELENA/elena.htm.

[13] D. G. Stavrakoudis, J. B. Theocharis, and G. C. Zalidis, "A multistage genetic fuzzy classifier for land cover classification from satellite imagery, " *Soft Comput.*, in press, 2011. DOI: 10.1007/s00500-010-0666-z.

[14] D. G. Stavrakoudis, J. B. Theocharis, and G. C. Zalidis, "A Boosted Genetic Fuzzy Classifier for land cover classification of remote sensing imagery," *ISPRS-J. Photogramm. Remote Sens.*, in press, 2011. DOI: 10.1016/j.isprsjprs.2011.01.010.

[15] D. G. Stavrakoudis, G. N. Galidaki, I. Z. Gitas, and J. B. Theocharis, "Enhancing the interpretability of genetic fuzzy classifiers in land cover classification from hyperspectral satellite imagery," in *2010 Int. Conf. Fuzzy Systems (IEEE-FUZZ)*, Barcelona, pp. 1277–1284, 2010.

[16] E. G. Mansoori, M. J. Zolghadri, and S. D. Katebi, "SGERD: A Steady-State Genetic Algorithm for Extracting Fuzzy Classification Rules From Data," *IEEE Trans. Fuzzy Syst.*, vol. 16, no. 4, pp. 1061–1071, 2008.

[17] H. Ishibuchi, T. Nakashima, T. Murata, "Performance evaluation of fuzzy classifier systems for multidimensional pattern classification problems," *IEEE Trans. Syst. Man Cybern. Part B-Cybern.*, vol. 29, no. 5, pp. 601–618, 1999.

[18] J. Alcalá-Fdez, L. Sánchez, S. García, M. J. del Jesus, S. Ventura, J. M. Garrell, J. Otero, C. Romero, J. Bacardit, V. M. Rivas, J. C. Fernández, and F. Herrera, "KEEL: A Software Tool to Assess Evolutionary Algorithms to Data Mining Problems," *Soft Comput.*, vol. 13, no. 3, pp. 307–318, 2009. Software available online: http://www.keel.es

2011 IEEE International Conference on Fuzzy Systems
June 27-30, 2011, Taipei, Taiwan

A New Approach to Handle High Dimensional and Large Datasets in Multi-objective Evolutionary Fuzzy Systems

Michela Antonelli, Pietro Ducange, Francesco Marcelloni
Dipartimento di Ingegneria dell'Informazione: Elettronica, Informatica, Telecomunicazioni
University of Pisa
Pisa, Italy
{m1.antonelli, p.ducange, f.marcelloni@iet.unipi.it}

***Abstract*—In the framework of multi-objective evolutionary fuzzy systems (MOEFSs), the search space grows as the number of features of the dataset increases, leading to a slow and possibly difficult convergence of the evolutionary algorithm. Furthermore, mainly due to the fitness evaluation, datasets with a large number of instances require very high computational costs. In this paper, we propose a co-evolutionary approach to generate sets of Mamdani fuzzy rule-based systems (MFRBSs) with different trade-offs between accuracy and interpretability. We aim to deal with high dimensional and large datasets and to learn together the rule base (RB) and the membership function parameters. To reduce the search space, we perform the multi-objective evolutionary learning of the RB by selecting reduced sets of rules and conditions from a previously generated RB. Further, to lessen the computational costs, during the multi-objective evolutionary learning process, periodically, a single-objective genetic algorithm evolves a population of reduced training sets. We show the preliminary results obtained by applying our approach to two real world high dimensional and large regression datasets.**

Keywords: multi-objective evolutionary fuzzy systems; high dimensional datasets; large datasets; regression problems

I. INTRODUCTION

Two main approaches can be exploited to design fuzzy rule-based systems (FRBSs): i) to elicit the knowledge from a human expert and ii) to extract this knowledge from available information (typically, input-output samples). In complex application domains, with a large quantity of information sources, the first approach is difficultly applicable. Thus, the second approach is often the unique alternative.

Several techniques have been proposed in the literature to generate FRBSs from available data [1]-[3]. Among these techniques, multi-objective evolutionary fuzzy systems (MOEFSs) have been successfully used in the last years to generate sets of FRBSs with different trade-offs between accuracy and interpretability [4][5]. MOEFSs exploit multi-objective evolutionary algorithms (MOEAs) to perform the learning [6][7] or the selection [8] of rules, and the tuning of the data base (DB) [9], with a prefixed DB and rule base (RB), respectively. Further, the most recent works describe approaches to concurrently learn [10]-[13] or select [14]-[16] rules together with some elements of the DB, such as the membership function (MF) parameters and the granularities.

In real word applications, we often have to manage high-dimensional and large datasets. Let us consider, for instance, some applications such as environmental monitoring, traffic control or weather forecasting. Here, a large amount of sensors is typically used, thus generating data characterized by a large number of features. Further, if the sampling frequency is high, the resulting datasets comprise a very large amount of instances.

Dealing with high dimensional and large datasets is a challenge topic in the context of MOEFSs [4]. A high number of dimensions increases the search space, especially in rule learning approaches, thus affecting the performance of the evolutionary algorithm in terms of convergence and solution quality. A large number of instances, as mentioned in [4] and confirmed by the experimental results discussed in several papers [10]-[12], makes the computation of the fitness very time-consuming, thus hindering the full exploitation of the evolutionary process by obliging to limit the number of iterations.

Four main approaches have been followed to reduce these drawbacks in MOEFSs: i) to use data reduction techniques, such as feature selection [17][18] and instance selection [19][20], ii) to exploit parallel evolutionary algorithms [19][21], iii) to use some fitness approximation approaches [22], and iv) to exploit ad-hoc modified MOEAs [23][24].

In this contribution, we introduce a novel approach to generate sets of Mamdani FRBSs (MFRBSs) with different trade-offs between accuracy and RB complexity from high dimensional and large datasets. We aim to concurrently learn the RBs and the parameters of MFs in the same multi-objective evolutionary process.

To reduce the search space in the generation of the rules, we exploit the RB generation method recently introduced by us in [24]: RBs are determined by selecting a reduced number of rules and conditions during the evolutionary process from a previously generated RB. In [24], we used the Wang and

978-1-4244-7316-8/11/$26.00 ©2011 IEEE

Mendel algorithm [1] and denoted the approach as two-level rule selection (2LRS): at the first level we select the rules and at the second level we select the conditions. In contrast with the RB learning process exploited in our previous works [7][10]-[12], the 2LRS approach allows considerably reducing the search space, especially when the number of features is high, though preserving some good characteristics of a learning approach (actually, once determined the rule at the first level, at the second level the selection of conditions appears more similar to a learning than a selection process). We experimentally verified that the new approach allows the specific MOEA used in the experiments, namely (2+2)M-PAES, to rapidly converge to a set of solutions with trade-offs between accuracy and complexity comparable to the ones computed by the RB learning process of our previous works. In particular, we experimentally verified that the (2+2)M-PAES with the 2LRS approach achieves after 50000 evaluations Pareto front approximations comparable to the ones achieved by the (2+2)M-PAES with the rule learning after 300000 evaluations.

Further, to deal with large datasets, we integrate the 2LRS in our co-evolutionary model proposed in [20]. Here, during the execution of the MOEA, periodically, a single-objective genetic algorithm (SOGA) evolves a population of reduced training sets (RTSs).

We have aim to verify whether the co-evolutionary approach allows generating a set of MFRBSs that are statistically equivalent to those generated using the overall training set (OTS). In order to prove the positive behaviour of the new co-evolutionary approach, we show some preliminary results on two real world high dimensional and large datasets.

The paper is organized as follows: Section II briefly describes the MFRBSs and introduces some notation. In Section III, we describe the co-evolutionary approach aimed at concurrently selecting training instances and performing multi-objective evolutionary learning of MFRBSs. Finally, Section IV shows the experimental results and Section V draws some final conclusions.

II. MAMDANI FUZZY SYSTEMS

Let $\mathbf{X} = \{X_1, ..., X_f, ..., X_F\}$ be the set of input variables and X_{F+1} be the output variable. Let U_f, with $f = 1, ..., F+1$, be the universe of the f^{th} variable. Let $P_f = \left\{A_{f,1}, ..., A_{f,T_f}\right\}$ be a strong fuzzy partition of T_f fuzzy sets on variable X_f. An MFRBS is composed of M rules expressed as:

$$R_m: \quad \textbf{IF } X_1 \textbf{ is } A_{1,j_{m,1}} \textbf{ AND } \ldots \textbf{ AND } X_F \textbf{ is } A_{F,j_{m,F}} \quad \textbf{THEN } X_{F+1} \textbf{ is } A_{F+1,j_{m,F+1}} \ (m = 1, ..., M) \tag{1}$$

The RB of an MFRBS can be completely described by a matrix $J \in \mathbb{N}^{M \times (F+1)}$, where the generic element $j_{m,f}$, with $m \in \{1, ..., M\}$ and $f \in \{1, ..., F+1\}$, indicates that fuzzy set $A_{f,j_{m,f}}$ has been selected for variable X_f in rule R_m. We use the product and the centre of gravity method as AND logical operator and defuzzification method, respectively.

We adopt triangular fuzzy sets $A_{f,j}$ defined by the tuple $(a_{f,j}, b_{f,j}, c_{f,j})$, where $a_{f,j}$ and $c_{f,j}$ correspond to the left and right extremes of the support of $A_{f,j}$, and $b_{f,j}$ to the core. Since we use strong fuzzy partitions, we assume that $a_{f,1} = b_{f,1}$, $b_{f,T_f} = c_{f,T_f}$, and for $j = 2, \ldots, T_f - 1$, $b_{f,j} = c_{f,j-1}$ and $b_{f,j} = a_{f,j+1}$.

To take the "don't care" condition into account, a new fuzzy set $A_{f,0}$ $(f = 1, ..., F)$ is added to all the F input partitions P_f. This fuzzy set is characterized by an MF equal to 1 on the overall universe. The terms $A_{f,0}$ allow generating rules which contain only a subset of the input variables.

Given a set of N input observations $\mathbf{x}_n = [x_{n,1}, ..., x_{n,F}]$, with $x_{n,f} \in \Re$, and the set of the corresponding outputs $x_{n,F+1} \in \Re$, $n = 1, ..., N$, we aim to generate a set of MFRBSs with different trade-offs between accuracy and interpretability. As regards MFRBS interpretability, several definitions can be found in the literature [25][26]. In particular, MFRBS interpretability can be analyzed in terms of RB complexity and DB integrity. In this work, the DB integrity is ensured by using strong fuzzy partitions with a low level of granularity. Thus, for the sake of simplicity, we measure the interpretability in terms of only RB complexity.

III. THE PROPOSED APPROACH

In this work, we exploit both the effectiveness of the 2LRS in managing high dimensional datasets and the efficacy of the evolutionary training set selection (TSS) in reducing the computational complexity when dealing with large datasets. To this aim, we follow the same approach that we have described in [20], in which a co-evolutionary algorithm has been proposed to perform both the TSS and the multi-objective evolutionary RB learning. Unlike in [20], however, we adopt the 2LRS in place of the RB learning.

A. The Co-Evolutionary Algorithm

Fig. 1 shows the execution flow of the co-evolutionary algorithm by using the UML activity diagram notation. In the activity diagram, rectangles represent data objects, rounded rectangles represent activities and diamonds are used as decision and merge points. The algorithm handles two populations: the KB population, aimed at performing the 2LRS and the MF parameter learning, and the reduced training set (RTS) population, aimed at performing the TSS.

First of all, we apply the WM algorithm to the OTS to generate the set of candidate rules. We assume that the linguistic variables are uniformly partitioned with T_f fuzzy sets. Then, TSS is fulfilled by means of an SOGA while the 2LRS and the MF parameter learning are carried out by applying the (2+2)M-PAES algorithm.

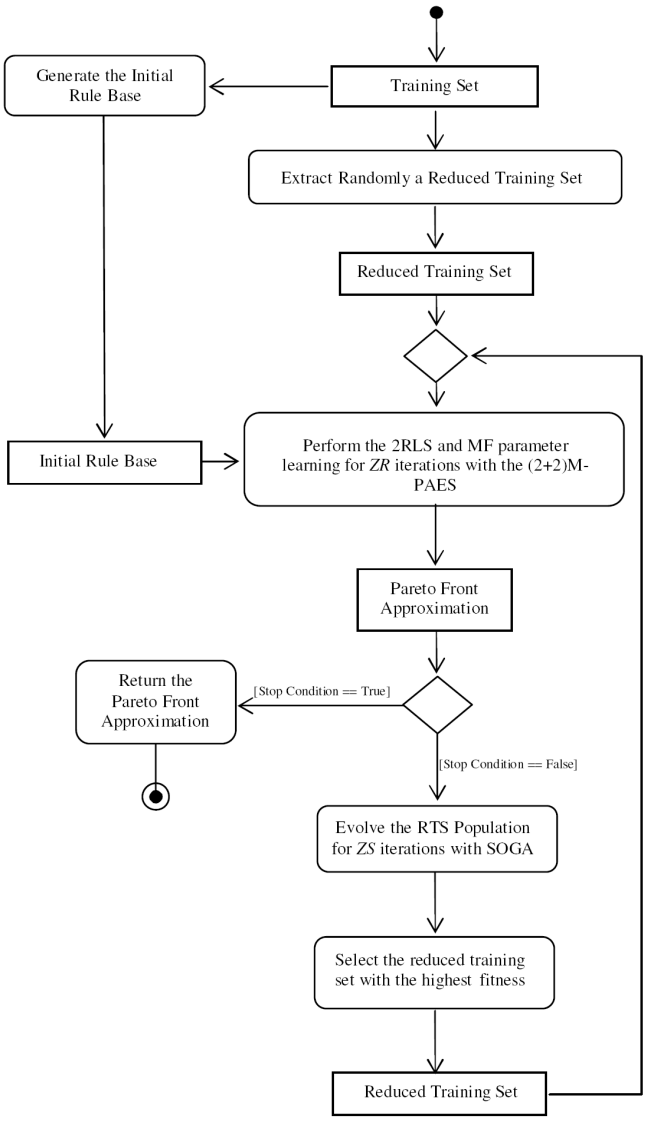

Figure 1. Activity diagram of the co-evolutionary apprach

The SOGA and (2+2)M-PAES are cyclically executed one after the other. The RTS population evolves for a fixed number *ZS* of fitness evaluations in order to search for an RTS which is a good representative of the OTS. Thus, the RTS is used in the (2+2)M-PAES to perform the multi-objective 2LRS and MF parameters learning with different trade-offs between accuracy and RB complexity. (2+2)M-PAES is executed for a fixed number *ZR* of RB fitness evaluations. The resulting approximated Pareto front (set of non-dominated MFRBSs with different accuracy-complexity tradeoffs) is used in the execution of the SOGA to calculate the fitness function.

At the end of its execution, our algorithm returns a set of non-dominated MFRBSs in the complexity-accuracy plane. Even though several stop conditions can be considered, we terminate the execution of our algorithm when a prefixed number of KB fitness evaluations have been performed. In this way, we are able to carry out comparisons with different techniques using the same number of KB fitness evaluations.

In the following, we introduce and discuss the 2LRS and the MF parameters learning, including their coding and the mating operators. Finally, we introduce the MOEA exploited in the evolutionary process.

B. The Multi-objective Evolutionary Two-Level Rule Selecion and MF Learning

The 2LRS and the MF parameters learning are carried out by (2+2)M-PAES, which determines an approximation of the optimal Pareto front by concurrently minimizing the MSE and the RB complexity.

The MSE is calculated as:

$$MSE = \frac{1}{2 \cdot |E|} \sum_{l=1}^{|E|} \left(F(x^l) - y^l \right)^2$$

where $|E|$ is the size of the dataset, $F(x^l)$ is the output obtained from the MFRBS when the *l-th* input pattern is considered, and y^l is the desired output. RB complexity is measured as sum of the conditions which compose the antecedents of the rules included in the RB. Thus, low values of complexity correspond to RB characterized by a low number of rules and a low number of input variables really used in each rule.

We indicate with J_{WM} and M_{WM} the RB generated by applying the WM algorithm to the OTS and the number of rules of this RB, respectively. We recall that the antecedent of each candidate rule has one condition for each linguistic variable, since the WM algorithm performs no selection of the conditions. Further, especially when dealing with large and high dimensional datasets, the WM algorithm could generate RBs composed by a huge number of rules. For this reason, in order to generate compact and interpretable RBs, we fix the maximum number M_{MAX} of rules which can compose the RB. Further, the minimum number of rules that must be present in the RB is fixed by the user-defined parameter M_{MIN}.

We exploit a chromosome C^{KB} composed of two parts (C_1^{KB}, C_2^{KB}), which define the RB and the positions of the centroids of each fuzzy set in each linguistic variable, respectively. The C_1^{KB} part of the chromosome is a vector of M_{MAX} pairs $\mathbf{p}_m = (k_m, \mathbf{v}_m)$, where $k_m \in [0,...,M_{WM}]$ identifies the index of the rule in J_{WM} selected for the current RB and $\mathbf{v}_m = [v_{m,1},...,v_{m,F}]$ is a binary vector which indicates, for each condition in the rule, if the condition is present or corresponds to a don't care. In particular, if $k_m = 0$, the m^{th} rule is not included in the RB. In this way we manage to generate RBs with a lower number of rules than M_{MAX}. Further, if $v_{m,f} = 0$, the f^{th} condition of the m^{th} rule is replaced by a don't care condition; otherwise it remains unchanged.

As regards C_2^{KB}, since we adopt strong fuzzy partitions with, for $j = 2, \ldots, T_f - 1$, $b_{f,j} = c_{f,j-1}$ and $b_{f,j} = a_{f,j+1}$, in order to define each fuzzy set of the partition it is sufficient to fix the positions of the cores $b_{f,j}$ along the universe U_f of the f^{th} variable (we normalize each variable in [0,1]). Since $b_{f,1}$ and b_{f,T_f} coincide with the extremes of the universe, the partition of each linguistic variable X_f is completely defined by $T_f - 2$ parameters. Finally, C_2^{KB} consists of $F+1$ vectors of $T_f - 2$ real numbers: the f^{th} vector contains the $\left[b_{f,2},...,b_{f,T_f-1}\right]$ cores which define the positions of the MFs for the linguistic variable X_f.

To ensure a good integrity level of the MFs, in terms of order, coverage and distinguishability, $\forall j \in [2, T_f - 1]$, we force $b_{f,j}$ to vary in the definition interval $\left[b_{f,j} - \frac{b_{f,j} - b_{f,j-1}}{2}, b_{f,j} + \frac{b_{f,j+1} - b_{f,j}}{2}\right]$.

The evolutionary process is performed by means of the (2+2)M-PAES proposed in [7], where both crossover and mutation operators are independently applied to each part of the chromosome. In particular we apply the one-point crossover to the C_1^{KB} part and the BLX-α crossover, with α = 0.5, to the C_2^{KB} part.

Let s_1 and s_2 be two selected parent chromosomes. The common gene for the one point crossover is chosen by extracting randomly a number in $[1, \rho_{MAX} - 1]$, where ρ_{MAX} is the maximum number of rules in s_1 and s_2. The crossover point is always chosen between two rules and not within a rule. When we apply the one-point crossover to the RB part, we can generate an RB with one or more pairs of equal rules. In this case, we simply eliminate one of the rules from each pair setting the correspondent k_m to zero. This allows us to reduce the total number of rules.

As regards the mutation, for the C_1^{KB} part we have defined three operators. The first step of each operator is to randomly select a pair $\mathbf{p}_m$, i.e. a rule, in the chromosome. The first operator replaces the value of k_m in the selected pair with an integer value randomly generated in $[1,...,M_{WM}]$. The second operator removes a rule from the RB by setting k_m of the selected pair to zero. Finally, the third operator modifies the antecedent $\mathbf{v}_m$ of the selected rule by complementing each gene $v_{m,f}$ with a probability equal to P_{cond} ($P_{cond} = 2/F$ in the experiments). After applying the three mutation operators, we remove the duplicate rules in the RB.

The mutation operator applied to C_2^{KB}, first, randomly chooses a variable X_f, $f \in [1, F+1]$, and a fuzzy set $j \in [2, T_f - 1]$ and then replaces the value of $b_{f,j}$ with a value randomly chosen within the definition interval of $b_{f,j}$.

The crossover operators are independently applied to C_1^{KB} and C_2^{KB} with probabilities P_{c1}^{KB} and P_{c2}^{KB}, respectively. As regards mutation, the first, second and third operators are applied to C_1^{KB} with probabilities P_{add}^{KB}, 0.1- P_{add}^{KB}, and P_{mod}^{KB}, respectively. Finally, the mutation operator is applied to C_2^{KB} with probability P_{m2}^{KB}.

C. The Single-objective Training Set Selection

We split the OTS into *B* disjoint blocks: each block contains *I=N/B* instances randomly extracted from the OTS. Each RTS consists of *K* blocks. Thus, in the SOGA we exploit a chromosome C^{TS} which codifies the *K* blocks included in the RTS: each gene is an integer which varies from 1 to *B* and represents the index of the block selected to be included in the RTS.

The aim of the evolutionary process is to find the *K* blocks which are the best representatives of the OTS. We measure the degree *DR* of representativeness as follows. First, for each solution C_i^{KB} ($i = 1,..., N^{KB}$, where N^{KB} is the number of solutions contained into the (2+2)M-PAES archive), we compute the MSE/2 by using the OTS and the RTSs codified in all chromosomes C_j^{TS} ($j = 1,..., N^{TS}$, where N^{TS} is the number of individuals in the SOGA population). We refer to these MSEs as $MSE_i / 2$ and $MSE_{i,j} / 2$, respectively. Then, we compute:

$$DR_j = \frac{1}{N^{KB}} \sum_{i=1}^{N^{KB}} \frac{|\, MSE_i / 2 - MSE_{i,j} / 2 \,|}{\max\left(MSE_i / 2, MSE_{i,j} / 2\right)}. \quad (2)$$

The lower the value of DR_j, the more the RTS encoded in C_j^{TS} achieves performance similar to the OTS.

In order to perform the optimization of the TSS population, we exploit a classical SOGA. We start with a randomly generated initial population P_0. At each iteration *t*, the fitness function DR_j of each individual *j* is evaluated and individuals are selected for reproduction by using the roulette wheel selection. To generate the offspring population Q_t of N^{TS} individuals both one-point crossover and mutation are used. The mutation operator, when selected, randomly chooses a gene in [1, *K*] and changes the value of the gene with an integer randomly chosen in the interval [1, *B*].

The one-point crossover could generate descendants with one or more pairs of genes which have the same value. This corresponds to have duplicate blocks in the *K* blocks which compose the RTS. If this occurs, we change randomly the value of one of the equal genes so as to eliminate duplicate blocks. In the experiments, we executed the one-point

crossover and the mutation operators with probabilities P_c^{TS} and P_m^{TS}, respectively.

The new population P_{t+1} coincides with Q_t except for the worst 5% individuals which are replaced with the best 5% individuals of P_t (in practice, we use an elitist strategy where the worst individuals of the offspring population are replaced with the best individuals of the parent population with a percentage of 5%).

IV. Experimental Results

The method has been tested on two regression problems (available at http://sci2s.ugr.es/keel/category.php?cat=reg#sub2), namely Elevators and Ailerons. As shown in Table I, the datasets are characterized by a high number of both input variables and input/output patterns.

We compare the results obtained by the proposed co-evolutionary approach (denoted as PAES-SOGA(10%)), which uses the 10% of the OTS, with the ones obtained by executing the (2+2)M-PAES with the 2LRS on the OTS (denoted as PAES). We performed a five-fold cross validation and executed each fold six trials with different seeds (thirty trials in total).

Table II shows the values used for the parameters of PAES and of PAES-SOGA(10%) in the experiments. These parameters have been obtained after a long experimentation. In particular, the choice of the probability values derives from an accurate analysis carried out to balance exploitation and exploration during the evolutionary process.

As stopping condition, we use the maximum number of evaluations. This number of evaluations is fixed to 50000 for both the algorithms. In the case of PAES-SOGA(10%) we consider as total number of evaluations the ones performed on the RTS.

Since the generation of the RBs is based on the selection of rules and conditions from the initial RB computed by the WM algorithm, in Table III we show the mean values $\overline{MSE_{TR}/2}$ and $\overline{MSE_{TS}/2}$, and the standard deviations σ_{TR} and σ_{TS} of the MSE/2 computed on the training and test sets, respectively, and the mean number $\overline{R}$ and the standard deviation σ_R of the rules of the MFRBSs generated by the WM algorithm.

In order to analyze the effectiveness of the evolutionary process when the RTSs are used in place of the OTSs, we adopt the hypervolume indicator, computed by using the MSE/2 calculated on the OTS for both PAES and PAES-SOGA(10%). Thus, for the PAES-SOGA(10%), we re-compute the MSE/2 of the solutions contained in the final archive by using the OTS in place of the RTS. The new values of MSE/2 might make some solution dominated by other solutions in the archive. Thus, before computing the indicator, we select the non-dominated solutions so as to generate again a Pareto front approximation.

TABLE I. Datasets Used in the Experiments

Dataset name	Number of patterns	Number of input variables
Elevators (ELV)	16599	18
Ailerons (AIL)	13750	40

TABLE II. Values of the Parameters Used in the Experiments

Parameter		Value
AS	(2+2)M-PAES archive size	64
N^{TS}	SOGA population size	32
ZS	Number of evaluations in the SOGA for each cycle	64
ZR	Number of evaluations in the (2+2)M-PAES block	640
T_f	Number of fuzzy sets in each variable X_f, f	3
M_{MIN}	Minimum number of rules	5
M_{MAX}	Maximum number of rules	30
P_{c1}^{KB}	Probability of applying the crossover operator to C_1^{KB}	0.2
P_{c2}^{KB}	Probability of applying the crossover operator to C_2^{KB}	0.5
P_{m1}^{KB}	Probability of applying the mutation to C_1^{KB}	0.1
P_{add}^{KB}	Probability of applying the first mutation operator to C_1^{KB}	0.07
P_{mod}^{KB}	Probability of applying the third mutation operator to C_1^{KB}	0.7
P_{m2}^{KB}	Probability of applying the mutation operator to C_2^{KB}	0.2
P_c^{TS}	Probability of applying the crossover operator to C^{TS}	0.1
P_m^{TS}	Probability of applying the mutation operator to C^{TS}	0.01
I	Number of instances in a block	5

TABLE III. Average Results Achieved by the WM Algorithm

	$\overline{MSE_{TR}/2}$ (σ_{TR})	$\overline{MSE_{TS}/2}$ (σ_{TS})	$\overline{R}$ (σ_R)
ELV	1.584E-5 (0.024E-5)	1.596E-5 (0.076E-5)	537.7 (11.9)
AIL	3.19E-8 (0.19E-8)	3.26E-8 (0.23E-8)	1116.8 (51.3)

The hypervolume indicator, whose features and properties have been discussed in detail in [27], measures the hypervolume of the portion of the objective space that is weakly dominated by a Pareto front approximation. The computations of the hypervolume were performed using the performance assessment package provided in the PISA toolkit [28]. In this package, the value of the indicator is normalized in [0,1] and lower values are associated with better performances.

The analysis of the box plots, shown in Figs. 2 and 3, suggests that in both datasets the hypervolumes of the Pareto front approximations generated by the PAES-SOGA(10%) and PAES are quite similar. This is also confirmed by the results of the Wilcoxon signed-rank test [28] executed with significance level α = 0.05. Indeed, the two distributions of the hypervolumes associated with the two algorithms result to be statistically equivalent. This means that the evolutionary process, in terms of both exploration and exploitation, is not affected by using the RTSs rather than the OTS.

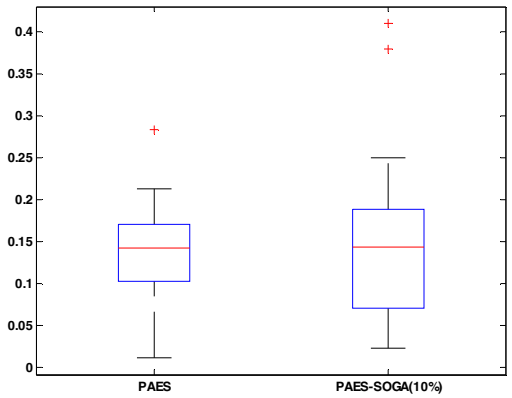

Figure 2. Box plots of the hypervolume indicators for the ELV dataset

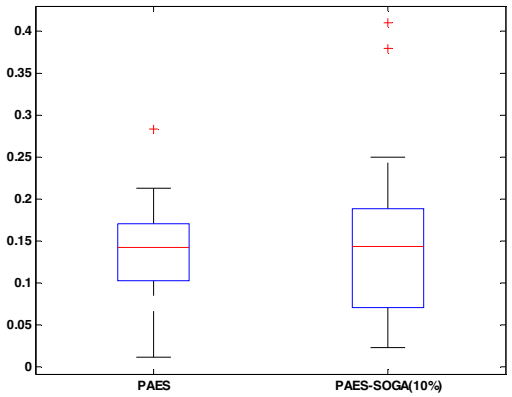

Figure 3. Box plots of the hypervolume indicators for the AIL dataset

To evaluate the MFRBSs generated by PAES and PAES-SOGA(10%) in terms of accuracy and complexity, we applied the procedure introduced in [10]. This procedure analyzes the mean and standard deviation of three representative points of the approximated Pareto front on the plane complexity-MSE/2, namely the first (the most accurate and complex), the median and the last (the least accurate and complex). This three points are referred as FIRST, MEDIAN and LAST, respectively. From an operative point of view, for each of the thirty trails, first we order the solutions of the approximated Pareto front for increasing MSE/2 values, then, we calculate the average values and the corresponding standard deviations over the thirty trials, of the MSE/2 and complexity values related to the three points for both the training and test sets.

In Figures 4 and 5, we plot the average values of the three points for ELV and AIL datasets, respectively, both on the training and test sets. We observe that there do not exist substantial differences between the training and test sets. This highlights that both the algorithms do not suffer from the overfitting problem. This result is particularly significant for PAES-SOGA(10%) which uses an RTS for most of the evolutionary optimization process. Further, though the solutions generated by PAES-SOGA(10%) are characterized by approximately the same MSE/2 as the ones generated by PAES, they result to be generally less complex.

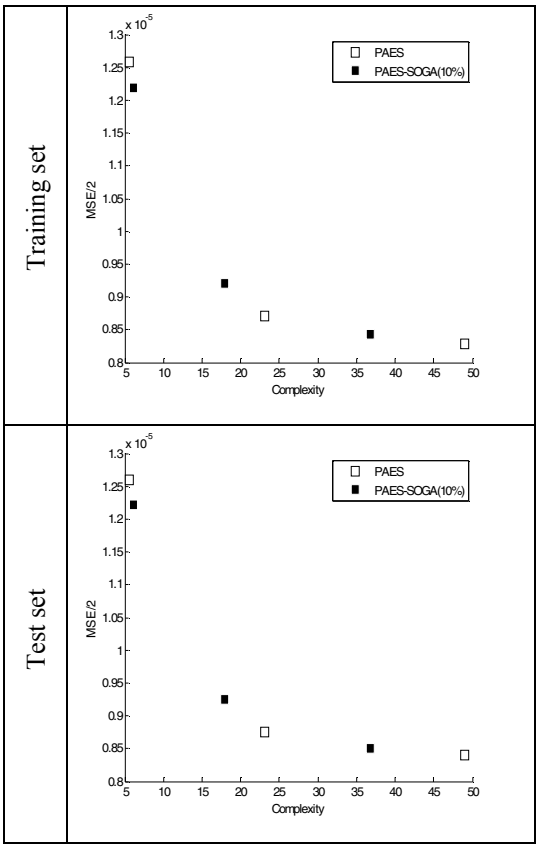

Figure 4. Average values of the FIRST, MEDIAN and LAST solutions for the ELV dataset

Tables IV and V show the mean values and the standard deviations of the MSE/2 on both the training ($\overline{\text{MSE}_{\text{TR}}/2}$ and σ_{TR}) and test ($\overline{\text{MSE}_{\text{TS}}/2}$ and σ_{TS}) sets, the average complexity ($\overline{\text{COMP}}$ and σ_{COMP}), the average number of rules ($\overline{\text{RULES}}$ and σ_{RULES}) and the average number of input variables used in the final KBs ($\overline{\text{VARS}}$ and σ_{VARS}). A careful analysis of these tables confirms the great similarity of the two Pareto front approximations generated by PAES and PAES-SOGA(10%).

In order to assess if there exist statistical differences among the MSE/2 corresponding to the FIRST, MEDIAN and LAST solutions generated by the PAES-SOGA(10%) and PAES, we applied the Wilcoxon signed-rank test with 95% confidence (columns **W-t$_{\text{TR}}$** and **W-t$_{\text{TS}}$**).

The interpretation of the **W-t$_{\text{TR}}$** and **W-t$_{\text{TS}}$** columns are as follows:

* represents the best result (the most accurate);

\+ means that the best result has better performance than that of the corresponding row;

= means that the best result has performance comparable to that of the corresponding row.

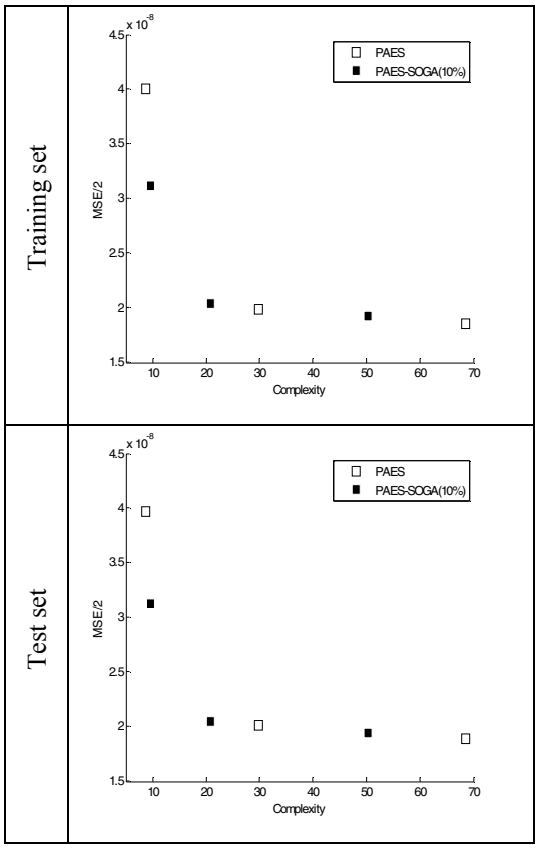

Figure 5. Average values of the FIRST, MEDIAN and LAST solutions for the AIL dataset

The results of the test confirm that choosing a specific solution in a Pareto front approximation generated by PAES is not different from choosing a corresponding solution in a Pareto front approximation obtained by the PAES-SOGA(10%), at least in terms of MSE/2. Also, typically, the solutions generated by the PAES-SOGA(10%) are characterized by a lower complexity.

TABLE IV. AVERAGE RESULTS ACHIEVED BY THE DIFFERENT MOEAS IN CORRESPONDENCE TO THE FIRST, MEDIAN AND LAST SOLUTIONS FOR THE ELV DATASET

		$\overline{MSE_{TR}/2}$ (σ_{TR})	W-t_{TR}	$\overline{MSE_{TS}/2}$ (σ_{TS})	W-t_{TR}	$Comp$ (σ_{Comp})	R (σ_R)
FIRST	PAES-SOGA(10%)	0.843E-5 (0.040E-5)	=	0.856E-5 (0.053E-5)	=	41.5 (14.9)	10.9 (2.5)
	PAES	0.824E-5 (0.049E-5)	*	0.846E-5 (0.053E-5)	*	48.1 (13.1)	11.4 (2.3)
MEDIAN	PAES-SOGA(10%)	0.899E-5 (0.087E-5)	=	0.915E-5 (0.090E-5)	=	20.5 (6.2)	9.0 (2.0)
	PAES	0.867E-5 (0.045E-5)	*	0.882E-5 (0.051E-5)	*	23.1 (5.4)	9.4 (1.8)
LAST	PAES-SOGA(10%)	1.233E-5 (0.110E-5)	=	1.253E-5 (0.121E-5)	=	5.3 (1.4)	5.0 (0.0)
	PAES	1.231E-5 (0.171E-5)	*	1.250E-5 (0.155E-5)	*	5.9 (3.9)	5.0 (0.0)

Finally, by analyzing the execution times of the two algorithms, we realized that using an RTS that contains the 10% of the overall training set allows us to save on average the 86% of the execution time.

TABLE V. AVERAGE RESULTS ACHIEVED BY THE DIFFERENT MOEAS IN CORRESPONDENCE TO THE FIRST, MEDIAN AND LAST SOLUTIONS FOR THE AIL DATASET

		$\overline{MSE_{TR}/2}$ (σ_{TR})	W-t_{TR}	$\overline{MSE_{TS}/2}$ (σ_{TS})	W-t_{TR}	$Comp$ (σ_{Comp})	R (σ_R)
FIRST	PAES-SOGA(10%)	1.92E-8 (0.10E-8)	=	1.94E-8 (0.11E-8)	=	50.3 (31.7)	7.9 (1.75)
	PAES	1.85E-8 (0.09E-8)	*	1.89E-8 (0.11E-8)	*	68.5 (49.5)	9.2 (2.4)
MEDIAN	PAES-SOGA(10%)	2.04E-8 (0.15E-8)	=	2.05E-8 (0.18E-8)	=	20.7 (13.8)	6.2 (0.9)
	PAES	1.99E-8 (0.18E-8)	*	2.02E-8 (0.19E-8)	*	29.7 (19.2)	6.9 (1.0)
LAST	PAES-SOGA(10%)	3.12E-8 (0.77)	*	3.13E-8 (0.82E-8)	*	9.6 (11.7)	5.0 (0.1)
	PAES	4.00E-8 (2.57E-8)	=	3.97E-8 (2.46E-8)	=	8.7 (9.8)	5.0 (0.0)

V. CONCLUSION

In this paper, we have proposed a novel approach to deal with high dimensional and large datasets in the framework of multi-objective evolutionary learning of Mamdani Fuzzy Rule-based Systems (MFRBSs) with different trade-offs between accuracy and interpretability.

The proposed algorithm is based on a co-evolutionary approach which allows us to concurrently perform an evolutionary training set selection (TSS) and a multi-objective evolutionary learning of the rule base (RB) and of the membership functions parameters. The RB is built by selecting first a reduced number of rules from a previously generated rule base, and then a reduced number of conditions for each selected rule. In this way, we are able to improve the convergence ability of the learning process in terms of speed and quality of the generated solutions. Furthermore, the evolutionary TSS allows us to save considerable execution time.

We experimented our method (PAES-SOGA) on two real world regression problems, characterized by a high number of both input variables and input/output patterns. The obtained results have been compared with the ones obtained by the same learning method applied using the overall dataset (PAES). By using statistical tests, we have shown that the Pareto front approximations are statistically equivalent in terms of the hypervolume indicator and three representative points. Furthermore, though the PAES-SOGA uses a reduced training set, the algorithm does not suffer from overfitting. Finally, we have observed that, the use of a training set containing the 10% of the overall training set allows us on average to save the 86% of the execution time needed when the overall training set is used.

REFERENCES

[1] L.X Wang, and J.M. Mendel, "Generating fuzzy rules by learning from examples," IEEE Trans. Syst. Man. Cybern., vol. 22, n. 6, pp. 1414–1427, 1992.

[2] O. Cordón, M.J. del Jesus, F. Herrera, and M. Lozano, "MOGUL: a methodology to obtain genetic fuzzy rule-based systems under the iterative rule learning approach," Int. J. Intell. Syst., vol. 14, n. 11, pp. 1123–1153, 1999.

[3] J. Casillas, O. Cordón, and F. Herrera, "COR: a methodology to improve ad hoc data-driven linguistic rule learning methods by inducing cooperation among rules," IEEE Trans. Syst. Man. Cybern., vol. 32, pp. 526–537, 2002.

[4] F. Herrera, "Genetic fuzzy systems: taxonomy, current research trends and prospects," Evolutionary Intelligence, vol. 1, pp. 27–46, 2008.

[5] H. Ishibuchi, and Y. Nojima, "Multiobjective genetic fuzzy systems," Computational Intelligence, vol.1, C.L Mumford and L.C. Jain, Ed. Berlin: Springer, 2009, pp 131–173.

[6] P. Ducange, B. Lazzerini, and F. Marcelloni, "Multi-objective Genetic Fuzzy Classifiers for Imbalanced and Cost-sensitive Datasets," Soft Computing, vol. 14, n. 10, pp. 713–728, 2010.

[7] M. Cococcioni, P. Ducange, B. Lazzerini, and F. Marcelloni, "A Pareto-Based Multi-objective Evolutionary Approach to the Identification of Mamdani Fuzzy Systems," Soft Computing, vol. 11, n. 11, pp. 1013–1031, 2007.

[8] H. Ishibuchi, and T. Yamamoto, "Fuzzy Rule Selection by Multi-Objective Genetic Local Search Algorithms and Rule Evaluation Measures in Data Mining," Fuzzy Sets and Systems, vol. 141, pp. 59–88, 2004.

[9] A. Botta, B. Lazzerini, F. Marcelloni, and D. Stefanescu, "Context Adaptation of Fuzzy Systems Through a Multi-Objective Evolutionary Approach Based on a Novel Interpretability Index," Soft Computing, vol. 13, n. 5, pp. 437–449, 2009.

[10] R. Alcalá, P. Ducange, F. Herrera, B. Lazzerini, and F. Marcelloni, "A Multi-objective Evolutionary Approach to Concurrently Learn Rule and Data Bases of Linguistic Fuzzy Rule-Based Systems," IEEE Trans. Fuzzy. Syst., vol. 17, n. 5, pp 1106–1122, 2009.

[11] M. Antonelli, P. Ducange, B. Lazzerini, and F. Marcelloni, "Multi-objective evolutionary learning of granularity, membership function parameters and rules of Mamdani fuzzy systems," Evolutionary Intelligence, vol. 2, n. 1-2, pp. 21–37, 2009.

[12] M. Antonelli, P. Ducange, B. Lazzerini, and F. Marcelloni, "Learning Concurrently Partition Granularities and Rule Bases of Mamdani Fuzzy Systems in a Multi-objective Evolutionary Framework," Int. J. Approx. Reason., vol. 50, n. 7, pp. 1066–1080, 2009.

[13] P. Pulkkinen and H. Koivisto, "A Dynamically Constrained Multiobjective Genetic Fuzzy System for Regression Problems," IEEE Trans. Fuzzy. Syst., vol. 18, n. 1, pp. 161–177, 2010.

[14] R. Alcalá, M.J. Gacto, F. Herrera, and J. Alcalá-Fdez, "A Multi-objective Genetic Algorithm for Tuning and Rule Selection to Obtain Accurate and Compact Linguistic Fuzzy Rule-Based Systems," Int. J. Uncertain. Fuzz., vol. 15, n. 5, 2007, pp. 539–557.

[15] M.J. Gacto, R. Alcalá, and F. Herrera, "Adaptation and Application of Multi-Objective Evolutionary Algorithms for Rule Reduction and Parameter Tuning of Fuzzy Rule-Based Systems," Soft Computing, vol. 13, n. 5, pp. 419–436, 2009.

[16] M. J. Gacto, R. Alcala, and F. Herrera, "Integration of an Index to Preserve the Semantic Interpretability in the Multi-Objective Evolutionary Rule Selection and Tuning of Linguistic Fuzzy Systems," IEEE Trans. Fuzzy. Syst., vol. 18, n.3, pp. 515-531, 2010.

[17] J. Casillas, O. Cordón, M.J. del Jesus, and F. Herrera, "Genetic feature selection in a fuzzy rule-based classification system learning process, " Information Sciences, vol. 136, pp.135–157, 2001.

[18] O. Cordón, and A. Quirin, "Comparing Two Genetic Overproduce-and-choose Strategies for Fuzzy Rule-based Multiclassification Systems Generated by Bagging and Mutual Information-based Feature Selection", International Journal of Hybrid Intelligent Systems, vol. 7, pp.45–64, 2010

[19] Y. Nojima and H Ishibuchi, "Effects of data reduction on the generalization ability of parallel distributed genetic fuzzy rule selection," in: Proc. of 9th International Conference on Intelligent Systems Design and Applications, Pisa (Italy), 30 Nov. – 2 Dec., 2009, pp. 96-101.

[20] M. Antonelli, P. Ducange, F. Marcelloni, "Exploiting a Coevolutionary Approach to Concurrently Select Training Instances and Learn Rule Bases of Mamdani Fuzzy Systems," in: Proc. of the WCCI 2010 International Conference, Barcelona (Spain), 18 – 23 Jul., 2010, pp. 1366–1372.

[21] M.A. de Vega, J.M Bardallo, F.A. Marquez, and A. Peregrin, "Parallel Distributed Two-level Evolutionary Multiobjective Methodology for Granularity Learning and Membership Functions Tuning in Linguistic Fuzzy Systems," in: Proc. of 9th International Conference on Intelligent Systems Design and Applications, Pisa (Italy), 30 Nov. –2 Dec., 2009, pp. 134–139

[22] M. Cococcioni, B. Lazzerini, and F. Marcelloni, "On reducing computational overhead in multi-objective genetic Takagi–Sugeno fuzzy systems," Applied Soft Computing, vol. 11, n. 1, pp. 675–688, 2011.

[23]] R. Alcalá, M.J. Gacto, F. Herrera, "A Fast and Scalable Multi-Objective Genetic Fuzzy System for Linguistic Fuzzy Modeling in High-Dimensional Regression Problems," IEEE Transactions on Fuzzy Systems doi: 10.1109/TFUZZ.2011.2131657, in press (2011)

[24] M. Antonelli, P. Ducange, B. Lazzerini, F. Marcelloni, "Multi-objective Evolutionary Generation of Mamdani Fuzzy Rule-Based Systems based on Rule and Condition Selection," in: Proc. of 5th IEEE International Workshop on Genetic and Evolutionary Fuzzy Systems, Paris (France), 11 – 15 Apr., 2011, in press.

[25] J. M. Alonso, L. Magdalena, and G. González-Rodríguez, "Looking for a good fuzzy system interpretability index: an experimental approach," Int. J. Approx. Reason., vol. 51, n. 1, pp. 115–134, 2009.

[26] S. M. Zhou, and J. Q. Gan, "Low-level interpretability and high-level interpretability: a unified view of data-driven interpretable fuzzy system modelling," Fuzzy Sets and Systems, vol. 159, pp. 3091–3131, 2008.

[27] E. Zitzler, L. Thiele, M. Laumanns, C.M. Fonseca, and V.G. de Fonseca, Performance assessment of multiobjective optimizers: An analysis and review," IEEE Transactions on Evolutionary Computation, vol. 7, n. 2, pp. 117–132, 2003.

[28] S. Bleuler, M. Laumanns, L. Thiele, E. Zitzler, "PISA –platform and programming language independent interface for search algorithms," in: C.M. Fonseca et al. (Eds.), Evolutionary Multi-Criterion Optimization (EMO 2003), LNCS, vol. 2632, pp. 494–508, Springer-Verlag, Heidelberg, 2003.

2011 IEEE International Conference on Fuzzy Systems
June 27-30, 2011, Taipei, Taiwan

Generalized Stabilizing Controllers for Fuzzy Systems via Circle Criterion – LMI and SOS

Ji-Chang Lo
Mechanical Engineering
National Central University
Jhong-Li, Taiwan
Email: jclo@cc.ncu.edu.tw

You-Ting Lin
Mechanical Engineering
National Central University
Jhong-Li, Taiwan

Wei-Cheng Liao
Mechanical Engineering
National Central University
Jhong-Li, Taiwan

***Abstract*—We investigate a generalized control problem via the Circle criterion borrowed from system theory; the generalized controller can be cast into existing canonical controllers depending on parameterizations. We first show a fuzzy version of the Circle criterion and then provide a synthesis result based on the Circle criterion, establishing closed-loop stabilizability for state-feedback controllers. In this paper, we show how to incorporating the membership information by approximating the cone of copositive matrices via SOS that is solvable by SOSTOOLS. Finally the validity and applicability of the approach are illuminated by examples.**

***Index Terms*—Stabilizing controllers; Circle criterion; TS fuzzy models; Linear matrix inequality (LMI); Sum of Squares (SOS); Exact solutions**

I. Introduction

OVER the decades, a large number of important results on stabilization have been derived for TS fuzzy models, which rely on the existence of a common P matrix to a quadratic Lyapunov function [1]. In a broader view, a fuzzy system may have nonlinear functions (such as parameter uncertainties, saturating inputs) involved in the model. How to tackle such problem becomes the focus of this paper. Motivated by the above mentioned nonlinearity involved in a fuzzy model and the literature on system theory [2], [3], [4], [5], [6] and references therein, we investigate a unified approach to synthesize stabilizing controllers for nonlinear fuzzy systems via system criteria. The multivariate circle criterion has been used to graphically analyze the robust stability of a fuzzy feedback linearization regulator [7]. Furthermore the circle criterion and the related Popov criterion have suggested ways to study the stability of Mamdani-type fuzzy control systems with a linear plant [8], [9], [10], [11]. While most existing papers use Mamdani-type fuzzy systems, when applying the circle criterion via graphical analysis, is for stability test, we focus on T-S fuzzy control models. Equipped with the system criteria in order to profit from the advantage of convex optimization, we propose a generalized controller, which unifies all existing controllers, for T-S fuzzy control systems, aiming at synthesizing stabilizing controllers such that the corresponding closed-loop fuzzy system is asymptotically stable. Although various control laws have been studied in the fuzzy literature, there exist no reports showing, via the generalized controller, the subtle relations among all stabilizing control laws.

This work was supported in part by the National Science Council of the ROC under grant NSC-98-2221-E-008-110.

Genetically, stability/stabilization of a fuzzy control problem is a copositive problem since checking positivity of the fuzzy matrix-valued polynomial in μ ($-\sum_i \sum_j \mu_i \mu_j M_{ij} > 0$) involves copositive matrices $-M_{ij}$, known to be NP-hardness. To avoid the NP-hardness, a solution to this problem was proposed by Parrilo [12] who showed that one can approximate the copositive cone to a given accuracy by a sufficiently large set of LMIs (therefore, only sufficient condition is shown.) Following the developments [13], [14], [15], [16], [17], we, via SOS, investigate copositive relaxation searching for existence of an SOS decomposition assuring exactness of solution to fuzzy PD-LMIs. Under this relaxation, the search for a bounded degree d, indicating exactness, can be efficiently performed and cast as an SOS program, establishing the use of SOS decomposition to solve the LMI formulations.

The organization of this paper is as follows. Section II rederives a fuzzy version of the Circle theorems expressed in an LMI formulation. In section III, a state feedback controller falling out of the general setting is addressed. The mechanism involved demonstrates that a unified treatment aiming at solving the absolute stability problems is addressed. An illustrative example is considered in Section V and concluding remarks are made in Section VI.

Notations: The symbol $\star$ is used for the transposed elements in a symmetric matrix, and $M < 0$ means a negative-definite symmetric matrix M. The notations Y_μ and $Y_{\mu\mu}$ stand for $\sum_{i=1}^r \mu_i Y_i$ and $\sum_{i=1}^r \sum_{j=1}^r \mu_i \mu_j Y_{ij}$, where $\mu_i \geq 0$ and $\sum_{i=1}^r \mu_i = 1$. The indices $i, j = 1, 2, \cdots, r$ (number of fuzzy rules) are used throughout this paper. ! denotes factorial for combinatoric expression. Let $\mathcal{K}(h)$, where h is the degree of a polynomial in μ, be the set of r-tuple defined below:

$$\mathcal{K}(h) = \{(k_1\ k_2\ \cdots\ k_r) : k_1 + k_2 + \cdots + k_r = h,$$

$$\forall k_i \in I^+(non - negative\ integers), i = 1, 2, \cdots, r\}.$$

Since the number of rules in the fuzzy rule base is r, the number of elements in $\mathcal{K}(h)$ is given by $J(h) = (r + h - 1)!/(h!(r-1)!)$. To ease the presentation, we adopt the short

978-1-4244-7316-8/11/$26.00 ©2011 IEEE

hand notations displayed below:

$$\begin{aligned} k &= k_1 k_2 \cdots k_r \\ \mu^k &= \mu_1^{k_1}\mu_2^{k_2}\cdots\mu_r^{k_r} \\ \pi(k) &= (k_1!)(k_2!)\cdots(k_r!). \end{aligned}$$

$$\mathcal{C}_{ii}^k(h) = \frac{(h!)k_i(k_i-1)}{\pi(k)},\ \mathcal{C}_{ij}^k(h) = \frac{(h!)k_ik_j}{\pi(k)}.$$

II. The Circle Criterion

We first state the Circle criterion and then study the synthesis of a state feedback controller. To facilitate the presentation, we assume that the readers are familiar with the basic fuzzy setup consisting of r fuzzy rules whose consequent parts are characterized by local Takagi-Sugeno type linear models. Then by using a standard fuzzy inference method – singleton fuzzifier, product fuzzy inference and weighted average defuzzifier, the inferred fuzzy model of interest, after normalization, is described by the following nominal (closed-loop) fuzzy system

$$\left[\begin{array}{c} \dot{x} \\ z \end{array}\right] = \left[\begin{array}{cc} \mathcal{A}_\mu & -\mathcal{B}_\mu \\ \mathcal{C}_\mu & -\mathcal{D}_\mu \end{array}\right]\left[\begin{array}{c} x \\ \phi(z,\cdot) \end{array}\right] \tag{1}$$

where $x \in R^n$, $\phi(z,\cdot) \in R^m$, $z \in R^m$ and $\mu_i \geq 0$ are the state vector, time-varying nonlinearity, controlled output, and grade of membership, respectively. The "$\cdot$" in the function $\phi(z,\cdot)$ means either the continuous-time t or the discrete-time k. $\mathcal{A}_i$, $\mathcal{B}_i$, $\mathcal{C}_i$, and $\mathcal{D}_i$ are real constant matrices of appropriate dimensions. It is noted that the negative signs in front of $\mathcal{B}_\mu$ and $\mathcal{D}_\mu$ are due to the negative feedback connection in system theory. Although the signs can be absorbed into the matrices, we keep the negative signs to signal the trait of absolute stability. We assume $(\mathcal{A}_i, \mathcal{B}_i)$ is completely controllable and $(\mathcal{A}_i, \mathcal{C}_i)$ is completely observable. To understand the Circle criterion

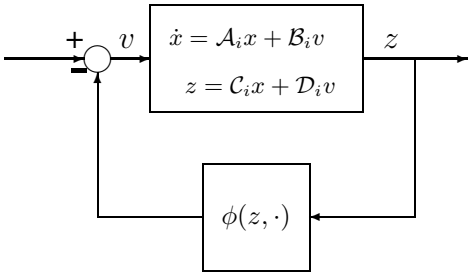

Fig. 1. Fuzzy local subsystem with nonlinear feedback connection.

borrowed from absolute stability, we need to introduce the nonlinear structure of the feedback connection ϕ depicted in Figure 1. The following definition is useful to this aim.

Definition 1 (Nonlinear Connection): Let $K_{\min} = diag(\alpha_1,\cdots,\alpha_m)$ and $K_{\max} = diag(\beta_1,\cdots,\beta_m)$ be two given diagonal matrices, the nonlinearity is characterized by the following sector bounded set $\Phi_c = \{\phi(z,\cdot) : R^m \times R^+ \rightarrow R^m$ such that $(\phi - K_{\min}z)'(\phi - K_{\max}z) \leq 0.\}$, where R^+ denotes positive real numbers for the continuous-time space over $[0.\infty)$.

The function $\phi(z,\cdot)$ defined above represents a memoryless, possibly time-varying nonlinearity. It is assumed that $\phi(z,\cdot)$ satisfies the Lipschitz condition $||\phi(z_1,\cdot)-\phi(z_2,\cdot)|| \leq L||z_1 - z_2||$ for all $(z_1,\cdot)$ and $(z_2,\cdot) \in R^m \times R^+$, where the positive constant L is called the Lipschitz constant. Moreover, it is sectorly bounded as defined in Definition 1.

Remarks:

1) For the scalar case $m = 1$, the sector condition characterizing Φ_c is equivalent to the more familiar SISO condition $\alpha_1 z \leq \phi \leq \beta_1 z$.
2) In this paper we interpret the nonlinear connection ϕ as a nonlinear term in local submodels representing unmodel dynamics. However, if ϕ were energy bounded external disturbance ($w \in L_2$), the setting (1) would be a typical H_∞ problem.

Given the definition, we establish the following theorem for the continuous-time systems.

Theorem 1 (Continuous Circle): The nominal system (1) is asymptotically stable if there exists a $\mathcal{P} > 0$ satisfying

$$M_i = \left[\begin{array}{ccc} \mathcal{A}_i'\mathcal{P} + \mathcal{P}\mathcal{A}_i & -\mathcal{P}\mathcal{B}_i + \mathcal{C}_i\bar{K}' & \mathcal{C}_i' \\ -\mathcal{B}_i'\mathcal{P} + \bar{K}\mathcal{C}_i & -I - (\bar{K}\mathcal{D}_i + \star) & -\mathcal{D}_i' \\ \mathcal{C}_i & -\mathcal{D}_i & 2K_1 \end{array}\right] < 0 \tag{2}$$

where $K_1 = (K_{\min}'K_{\max} + \star)^{-1} < 0$ and $\bar{K} = (K_{\min} + K_{\max})/2$.

Proof: Using a quadratic Lyapunov function $V(t) = x'\mathcal{P}x$ to show that the system (1) is asymptotically stable, we derive a stability condition for the following inequality

$$\dot{V} - (\phi - K_{\min}z)'(\phi - K_{\max}z) < 0. \tag{3}$$

We know in passing that the second term in (3) is negative by Definition 1. That is to say satisfaction of (3) implies

$$\dot{V} < (\phi - K_{\min}z)'(\phi - K_{\max}z) \leq 0$$

and the underlying systems is stable absolutely. The problem under study is referred to as the absolute stability problem, also known as the Luré problem. To continue the stability proof, it is straightforward to verify the following identity

$$\begin{aligned} & \dot{V} - (\phi - K_{\min}z)'(\phi - K_{\max}z) \\ = \ & x'(\mathcal{A}_\mu'\mathcal{P} + \mathcal{P}\mathcal{A}_\mu)x - \phi'\mathcal{B}_\mu'\mathcal{P}x - x'\mathcal{P}\mathcal{B}_\mu\phi \\ - \ & \phi'\phi + \phi' K_{\max}\mathcal{C}_\mu x \\ + \ & x'\mathcal{C}_\mu' K_{\min}'\phi - \phi' K_{\max}\mathcal{D}_\mu\phi \\ - \ & \phi'\mathcal{D}_\mu' K_{\min}'\phi - x'\mathcal{C}_\mu' K_{\min}' K_{\max}\mathcal{C}_\mu x \\ - \ & \phi'\mathcal{D}_\mu' K_{\min}' K_{\max}\mathcal{D}_\mu\phi \\ + \ & \phi'\mathcal{D}_\mu' K_{\min}' K_{\max}\mathcal{C}_\mu x + x'\mathcal{C}_\mu' K_{\min}' K_{\max}\mathcal{D}_\mu\phi \\ = \ & \left[\begin{array}{c} x \\ \phi \end{array}\right]' M_\mu \left[\begin{array}{c} x \\ \phi \end{array}\right] \end{aligned}$$

where the matrix M_μ is defined below

$$\begin{aligned} M_\mu = & \left[\begin{array}{cc} \mathcal{A}_\mu'\mathcal{P} + \mathcal{P}\mathcal{A}_\mu & -\mathcal{P}\mathcal{B}_\mu + \mathcal{C}_\mu\bar{K}' \\ -\mathcal{B}_\mu'\mathcal{P} + \bar{K}\mathcal{C}_\mu & -I - (\bar{K}\mathcal{D}_\mu + \star) \end{array}\right] \\ & - \left[\begin{array}{c} \mathcal{C}_\mu' \\ -\mathcal{D}_\mu' \end{array}\right] \frac{(K_{\min}'K_{\max} + \star)}{2} \left[\begin{array}{cc} \mathcal{C}_\mu & -\mathcal{D}_\mu \end{array}\right]. \end{aligned} \tag{4}$$

A sufficient condition ensuring (3) is $M_\mu < 0$. To recast $M_\mu < 0$ into a feasibility problem solvable by convex algorithms, performing the Schur complement on $M_\mu < 0$ and factoring out $\sum_{i=1}^{r} \mu_i$ yields the sufficient condition LMI (2). ■

III. Generalized Stabilizing Controllers

Having established the working theorems, we are ready to consider stabilization problems concerning absolute stability. To begin, setting up a T-S fuzzy model

$$\begin{bmatrix} \dot{x} \\ z \\ y \end{bmatrix} = \begin{bmatrix} A_\mu & -B_{1\mu} & B_{2\mu} \\ C_{1\mu} & -D_{11\mu} & D_{12\mu} \\ C_{2\mu} & -D_{21\mu} & 0 \end{bmatrix} \begin{bmatrix} x(\cdot) \\ \phi(z,\cdot) \\ u(\cdot) \end{bmatrix} \tag{5}$$

where $y \in R^q$ is the measured output, u is the control input, and all other variables are as in (1). A measured output variable y is a system variable that can be measured or through which the system influences its environment while a controlled output z is a system variable that can be controlled by some control scheme but not necessarily measurable.

To stabilize the T-S fuzzy model, we consider a generalized controller inspired by [5]

$$\begin{bmatrix} \dot{\hat{x}} \\ u \end{bmatrix} = \begin{bmatrix} F_{\mu\mu} & G_\mu & S_\mu \\ N_\mu & J & 0 \end{bmatrix} \begin{bmatrix} \hat{x} \\ y \\ u \end{bmatrix} \tag{6}$$

where F_{ij}, G_i, S_i, N_i and J are generalized parameters of appropriate dimensions. The generalized controller above has a nice merit encompassing the dynamic output feedback controller, the observed-state feedback controller and the state feedback controller.

To describe a state feedback controller, simply neglect the dynamic part of (6) by setting $F_{\mu\mu} = 0$, $G_\mu = 0$, $S_\mu = 0$, $J = 0$, and letting $\hat{x} = x$. Such control depends only on the fuzzy blending of the state x, known as a static (memoryless) state feedback (fuzzy) control or a PDC controller in fuzzy community.

Substituting the controller (6) into the open loop system (5), we have the closed-loop system displayed below.

$$\begin{bmatrix} \dot{\overline{x}} \\ z \end{bmatrix} = \begin{bmatrix} \mathcal{A}_{\mu\mu} & -\mathcal{B}_{\mu\mu} \\ \mathcal{C}_{\mu\mu} & -\mathcal{D}_{\mu\mu} \end{bmatrix} \begin{bmatrix} \overline{x} \\ \phi(z,\cdot) \end{bmatrix} \tag{7}$$

where

$$\bar{x} = \begin{bmatrix} x \\ \hat{x} \end{bmatrix}$$

$$\mathcal{A}_{\mu\mu} = \sum_{i=1}^{r}\sum_{j=1}^{r} \mu_i\mu_j \begin{bmatrix} A_i + B_{2i}JC_{2j} & B_{2i}N_j \\ G_iC_{2j} + S_iJC_{2j} & F_{ij} + S_iN_j \end{bmatrix}$$

$$\mathcal{B}_{\mu\mu} = \sum_{i=1}^{r}\sum_{j=1}^{r} \mu_i\mu_j \begin{bmatrix} B_{1i} + B_{2i}JD_{21j} \\ G_iD_{21j} + S_iJD_{21j} \end{bmatrix}$$

$$\mathcal{C}_{\mu\mu} = \sum_{i=1}^{r}\sum_{j=1}^{r} \mu_i\mu_j \begin{bmatrix} C_{1i} + D_{12i}JC_{2j} & D_{12i}N_j \end{bmatrix}$$

$$\mathcal{D}_{\mu\mu} = \sum_{i=1}^{r}\sum_{j=1}^{r} \mu_i\mu_j (D_{11i} + D_{12i}JD_{21j}).$$

Having established the closed-loop system (7) with the generalized controller (6) embedded, our investigation is performed on the basis of this setting and then derive the corresponding results for stabilization analysis and controller synthesis.

A. State Feedback Synthesis - LMI

A corollary characterizing state feedback controller synthesis fall out immediately by simplifying the generalized controller (6) to a state feedback controller $u = \sum_{i=1}^{r} \mu_i N_i x = N_\mu x$.

Corollary 1 (State Feedback Ctr, LMI): The closed-loop system (7) is asymptotically stable for all $\phi(z,\cdot) \in \Phi_c$ if, given $K_{\min}$ and $K_{\max}$, there exists a feasible solution $(Q > 0, \mathbf{N}_j)$ satisfying (8) where $K_1 = (K'_{\min}K_{\max} + \star)^{-1} < 0$, $\bar{K} = (K_{\min} + K_{\max})/2$, and $\mathbf{N}_j = N_jQ$.

Proof: The proof is straightforward, given Theorem 1. ■

Noting that the PD-LMIs (4) is a matrix-valued polynomial of degree 1 (a.k.a. affine) in μ, and $\sum_{i,j=1}^{r} \mu_i\mu_j M_{ij}$, where M_{ij}, at the top of next page, is defined in (8), is of degree 2 (a.k.a. quadratic) in μ.

IV. Sum of Squares

Applying Lyapunov-based quadratic stability to the aforementioned fuzzy control system (7), Corollary 1 is shown to bear the following form

$$M_{\mu\mu} < 0 \tag{9}$$

By applying matrix-valued Pólya's Theorem [18], [19], [20], (9) leads to

$$(\sum_{i=1}^{r} \mu_i)^d M_{\mu\mu} < 0 \tag{10}$$

The PD-LMIs (10) comprise of infinitely many LMIs, thus being a feasibility problem of infinite dimensions. We need to obtain a set of convex finite-dimensional LMI conditions associated to PD-LMIs (10) so that the relaxation becomes a finite-dimensional problem. The proposed methodology is formally stated below.

Theorem 2 (Exact Solutions for QS): Given $K_{\min}$ and $K_{\max}$. The closed-loop T-S fuzzy control system (7) is quadratically stabilizable by a state feedback PDC control (6) if and only if there exist matrices $\mathbf{N}_j$, $j = 1, 2, \ldots, r$; $Q = Q' > 0$ and a sufficient large $d > 0$ such that

$$\sum_{k \in \mathcal{K}(d+2)} H^k \mu^k < 0 \tag{11}$$

where

$$H^k = \sum_{i=1}^{r} C_{ii}^k(d) M_{ii} + \sum_{i=1}^{r-1}\sum_{j=i+1}^{r} C_{ij}^k(d)(M_{ij} + M_{ji})$$

and M_{ij} is defined in (8).

Proof: See Theorem 1 in [21] and Lemma 1 in [15]. ■

For Theorem 2, the challenge lies on how the above conditions can be verified. To this end, we seek help from SOS. The details are documented in [13] whilst the corresponding

$$M_{ij} = \begin{bmatrix} A_iQ + B_{2i}\mathbf{N}_j + \star & \star & \star \\ -B_{1i}' + \bar{K}(C_{1i}Q + D_{12i}\mathbf{N}_j) & -I - (\bar{K}D_{11i} + \star) & \star \\ (C_{1i}Q + D_{12i}\mathbf{N}_j) & -D_{11i} & 2K_1 \end{bmatrix} < 0 \tag{8}$$

LMI details are documented in [14]. We emphasize that the homogeneous polymomially parameter-dependent (HPPD) function (11) takes the membership μ into accounts, yielding less conservative results.

A. State Feedback Synthesis - SOS

Therefore, by deliberately working on polynomials consisting of basis monomials, the negated condition in Theorem 2 can be relaxed to the existence of SOS decomposition. Under this relaxation, the search for a bounded degree $2d+4$ can be efficiently solved. The SOS program is therefore formally stated below.

Corollary 2 (State Feedback Ctr, SOS): Given $K_{\min}$ and $K_{\max}$. There exist a matrix $Q = Q' > 0$ and a PDC controller (6) solving (9) if and only if for each $k \in \mathcal{K}(d+2)$ and a sufficiently large $d > 0$ there exist matrices $\mathbf{N}_j$, $j = 1, 2, \ldots, r$, $Q = Q' > 0$ such that

$$-v_1' \left(\sum_{k \in \mathcal{K}(d+2)} (H^k + \phi_1 I) x^{2k} \right) v_1 \text{ is SOS}$$
$$v_2' \left((Q - \phi_2 I) x^{2k} \right) v_2 \text{ is SOS}$$

ϕ_1 and ϕ_2 are sufficiently small positive constants and v_1, v_2 are vectors independent of x.

Proof: The proof is readily obtained from Theorem 2 and the copositive statement following Theorem 2. ■

V. An Example

A. Inverted pendulum on a cart

Consider the problem of balancing and swinging up of an inverted pendulum on a cart [6]. The system is approximated by the following two-rule model:

$$\text{IF } x_1 \text{ is about } 0 \text{ THEN } \dot{x} = A_1 x + B_1 v$$
$$\text{IF } x_1 \text{ is about } \pm\frac{\pi}{2} \text{ THEN } \dot{x} = A_2 x + B_2 v$$

where

$$A_1 = \begin{bmatrix} 0 & 1 \\ \frac{g}{\frac{4l}{3} - aml} & 0 \end{bmatrix}, B_1 = \begin{bmatrix} 0 \\ \frac{-\mu a}{\frac{4l}{3} - aml + b_1} \end{bmatrix}$$
$$A_2 = \begin{bmatrix} 0 & 1 \\ \frac{2g}{\pi(\frac{4l}{3} - aml\beta^2)} & 0 \end{bmatrix}, B_2 = \begin{bmatrix} 0 \\ \frac{-\mu a\beta}{\frac{4l}{3} - aml\beta^2 + b_2} \end{bmatrix}$$

and $\beta = \cos(88^\circ)$. Membership functions for Rule 1 and Rule 2 are given as follows:

$$p_1 = \cos(x_1), \;\; p_2 = 1 - p_1.$$

The control objective is to balance the inverted pendulum for the approximation range $x_1 \in [-\pi/2, \pi/2]$. The saturation function ϕ is given by

$$\phi = \begin{cases} u & if \; |u| \le 0.1 \\ 0.1 + 0.5(u - 0.1) & if \; u > 0.1 \\ -0.1 - 0.5(-u - 0.1) & if \; u < -0.1 \end{cases}$$

To demonstrate the superiority of SOS technique as opposed to LMI method, a comparison study for feasibility is conducted. Two varying parameters b_1 and b_2 are inserted into input matrices for feasibility test and the results are obtained for $d = 0$ and shown in Figures 2-3 respectively. It is crystal clear that SOS method can explore more solution space than LMI scheme.

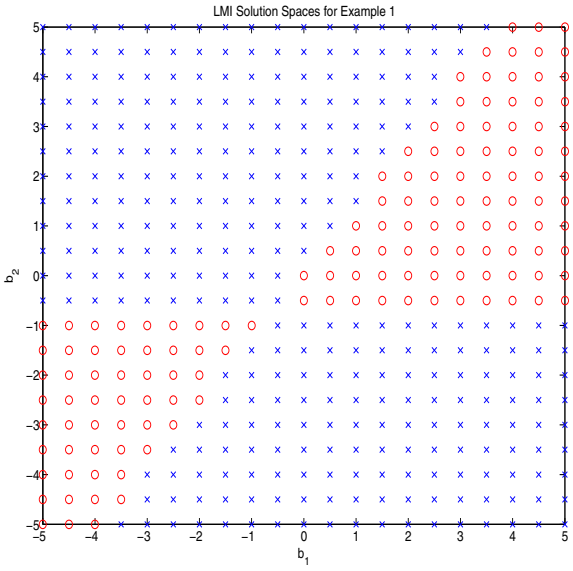

Fig. 2. LMI feasibility test

VI. Conclusion

A feedback stabilization problems involving absolute stability is presented. The Circle criterion borrowed from absolute stability is applied to derive LMI and SOS test conditions. Both results are shown, validating that the feasibility via SOS is much less conservative than that of LMIs scheme. A protruding feature of the SOS approach is that NO slack variables are involved and the membership functions are considered.

References

[1] K. Tanaka and H. Wang, *Fuzzy Control Systems Design: A Linear Matrix Inequality Approach*. New York, NY: John Wiley & Sons, Inc., 2001.

[2] W. Haddad and D. Bernstein, "Explicit construction of quadratic Lyapunov functions for the small gain, positive, circle and Popov theorems and their application to robust stability. Part I: continuous-time theory," *Int'l J. of Robust and Nonlinear Control*, vol. 3, pp. 313–339, 1993.

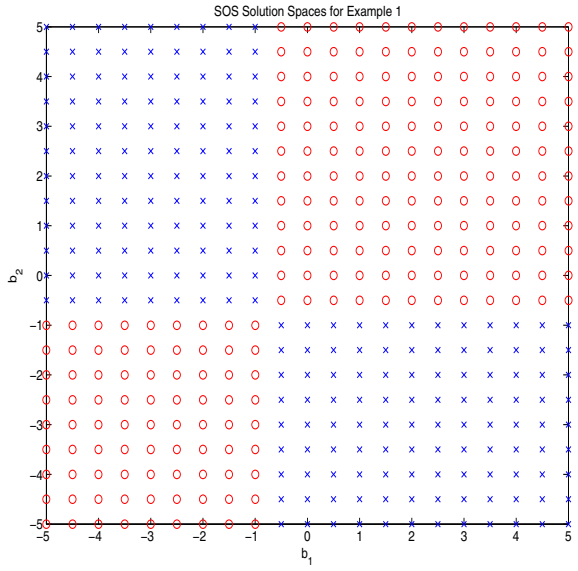

Fig. 3. SOS feasibility test, $d = 0$

[3] ——, "Explicit construction of quadratic Lyapunov functions for the small gain, positive, circle and Popov theorems and their application to robust stability. Part II: discrete-time theory," *Int'l J. of Robust and Nonlinear Control*, vol. 4, pp. 249–265, 1994.

[4] C. Pittet, S. Tarbouriech, and C. Burgat, "Stability regions for linear systems with saturating controls via circle and Popov criteria," in *Proc. of the 36th IEEE Conf. on Decision & Control*, San Diego, CA., Dec. 1997, pp. 4518–4521.

[5] ——, "Output feedback synthesis via the circle criterion for linear systems subject to saturating inputs," in *Proc. of the 37th IEEE Conf. on Decision & Control*, Tampa, FL., Dec. 1998, pp. 401–406.

[6] Y. Cao and Z. Lin, "Robust stability analysis and fuzzy-scheduling control for nonlinear systems subject to actuator saturation," *IEEE Trans. Fuzzy Systems*, vol. 11, no. 1, pp. 57–67, Feb. 2003.

[7] H. Kang, C. Kwon, H. Lee, and M. Park, "Robust stability analysis and design method for the fuzzy feedback linearization regulator," *IEEE Trans. Fuzzy Systems*, vol. 6, no. 4, pp. 464–472, Nov. 1998.

[8] K. Ray and D. Majumder, "Application of circle criterion for stability analysis of SISO and MIMO systems associated with fuzzy logic controller," *IEEE Trans. Syst., Man, Cybern.*, vol. 14, no. 2, pp. 345–349, Mar./Apr. 1984.

[9] C. M. Haissig, "Tuning fuzzy feedback controllers using the circle criterion," in *Proc. of the 1996 IEEE International Conference on Control application*, Dearborn, MI, Sept. 1996, pp. 15–18.

[10] R. Guerra, G. Schmitt-Braess, R. Haber, A. Alique, and J. Alique, "Using circle criteria for verifying asymptotic stability in PI-like fuzzy control systems: application to the milling process," *IET Control Theory & Appl.*, vol. 150, no. 6, pp. 619–627, Nov. 2003.

[11] A. Kandel, Y. Luo, and Y. Zhang, "Stability analysis of fuzzy control systems"," *Fuzzy Set and Systems*, vol. 105, pp. 33–48, 1999.

[12] P. Parrilo, *Structured Semidefinite Programs and Semialgebraic Geometry Methods in Robustness and Optimization*. Caltech, Pasadena, CA.: PhD thesis, 2000.

[13] J. Lo and M. Liu, "Exact solutions to fuzzy PD-LMIs via SOS," in *The 2010 World Congress on Computational Intelligence; FUZZ-IEEE International Conference on Fuzzy Systems*, Barcelona, SP, July 2010, pp. 1352–1357.

[14] J. Lo and J. Wan, "Studies on LMI relaxations for fuzzy control systems via homogeneous polynomials," *IET Control Theory & Appl.*, vol. 4, no. 11, pp. 2293–2302, Nov. 2010.

[15] V. Montagner, R. Oliveira, and P. Peres, "Convergent LMI relaxations for quadratic stabilization and H_∞ control of Takagi-sugeno fuzzy systems," *IEEE Trans. Fuzzy Systems*, no. 4, pp. 863–873, Aug. 2009.

[16] A. Kruszewski, A. Sala, T. M. Guerra, and C. Ariño, "A triangulation approach to asymptotically exact conditions for fuzzy summations," *IEEE Trans. Fuzzy Systems*, vol. 17, no. 5, pp. 985–994, Oct. 2009.

[17] G. Chesi, "On the non-conservatism of a novel LMI relaxation for robust analysis of polytopic systems," *Automatica*, vol. 44, no. 11, pp. 2973–2976, 2008.

[18] C. Scherer, "High-order relaxations for robust LMI problems with verifications for exactness," in *Proc. of the 42th IEEE CDC*, Maui, Hawaii, Dec. 2003, pp. 4652–4657.

[19] ——, "Relaxations for robust linear matrix inequality problems with verification for exactness," *SIAM J. Matrix Anal.Appl.*, vol. 27, no. 2, pp. 365–395, 2005.

[20] R. Oliveira and P. Peres, "Stability of polytopes of matrices via affine parameter-dependent Lyapunov functions: Asymptotically exact LMI conditions," *Linear Algebra and its Applications*, vol. 405, pp. 209–228, 2005.

[21] V. Montagner, R. Oliveira, and P. Peres, "Necessary and sufficient LMI conditions to compute quadratically stabilizing state feedback controller for Takagi-sugeno systems," in *Proc. of the 2007 American Control Conference*, July 2007, pp. 4059–4064.

2011 IEEE International Conference on Fuzzy Systems
June 27-30, 2011, Taipei, Taiwan

T-S Fuzzy Systems Approach to Approximation and Robust Controller Design for General Nonlinear Systems

Qing Gao
Department of Automation
USTC-CityU Joint Advanced Research Center,
Suzhou 215123, P. R. China
Email: gaoking@mail.ustc.edu.cn

Xiao-Jun Zeng
School of Computer Science
University of Manchester
Manchester M13 9PL, U.K.
Email: x.zeng@manchester.ac.uk

Gang Feng
Department of Manufacturing Engineering and
Engineering Management
City University of Hong Kong
83 Tat Chee Avenue, Hong Kong
Email: megfeng@cityu.edu.hk

Yong Wang
Department of Automation
University of Science and Technology of China
Hefei 230026, P. R. China
Email: yongwang@ustc.edu.cn

***Abstract*—A novel approach to control of general nonlinear system based on T-S fuzzy model is presented in this paper. Firstly, it is shown that a general nonlinear system can be approximated by a generalized T-S fuzzy model to arbitrary degree of accuracy on any compact set. And the basic idea of the proposed approach is to stabilize the general nonlinear system by solving a robust stabilization problem of the developed T-S fuzzy system with the approximation errors as the uncertainty term. Then using a piecewise Lyapunov function, robust semi-global stabilization and generalized $\mathscr{H}_2$ control of the general nonlinear system are formulated in the form of linear matrix inequalities. Finally, an example is provided to demonstrate the effectiveness of the proposed approaches.**

***Index Terms*—Approximation, General nonlinear systems, Piecewise Lyapunov functions, T-S fuzzy model, Robust Control.**

I. Introduction

Takagi and Sugeno (T-S) type fuzzy models [1] have been widely studied recently and proved to be one of the most powerful approaches to nonlinear control [2]-[5]. This model describes a nonlinear system by a group of fuzzy IF-THEN rules in the form of local linear or affine models which are smoothly connected by fuzzy membership functions. And this structure provides a basis for systematic stability analysis and controller design of T-S fuzzy control systems in view of powerful conventional control theory.

In the past decades, a large volume of works on theoretical results of stability analysis and controller synthesis of T-S fuzzy systems have been published. Readers can refer to the survey paper [6] and the references therein for details. By using the direct Lyapunov method, it is shown that stability analysis and controller design of T-S fuzzy systems can be facilitated by searching for a common quadratic Lyapunov function [7]. In order to reduce the conservatism of common quadratic Lyapunov function based approaches, some results based on piecewise quadratic and fuzzy Lyapunov functions have been proposed [8]-[16].

T-S fuzzy models have been shown to be universal function approximators in the sense that they are able to approximate any smooth nonlinear functions to arbitrary degree of accuracy in any convex compact region [17]-[19]. However, it is shown in [19] that the *commonly used* linear or affine T-S fuzzy models, where the control variables are not included in the premise variables are only able to approximate *affine nonlinear systems* to any degree of accuracy on any compact set. This implies that only the stabilization problem of *affine nonlinear systems* can be solved based on the *commonly used* T-S fuzzy models. In other words, to deal with more general nonlinear systems, a more general T-S fuzzy dynamic model should be employed.

Recently, some results on control design of more general nonlinear systems based on modified T-S fuzzy models have appeared in literature [20]-[22]. To describe conventional general nonlinear system approximately, the authors in [21] analyzed T-S fuzzy model with state variables and control variables contained in the conditional part of fuzzy rules, with each local model describes the dynamics of one state variable or control variable. The authors in [22] also analyzed the case that the control vector is a part of premise variables. However, only Mamdani-type fuzzy models were considered. Thus many fuzzy rules need to be used in these methods to describe global nonlinear systems and the construction of controllers is also very complex.

In this paper, we investigate the controller synthesis of general nonlinear systems based on a class of generalized T-S

978-1-4244-7316-8/11/$26.00 ©2011 IEEE

fuzzy models, which are proved to be universal approximators. It is shown that the stabilization problem of a general nonlinear system can be solved as robust stabilization problems of a generalized T-S fuzzy system with the approximation errors as the uncertainty term. It is also noted that with the control variables included in the conditional part of fuzzy rules, the two mainly used control schemes, say, the normally parallel distributed compensation and the local compensation [2], [6], [8], can not be applied due to the logic conflicts between antecedences and consequences. Thus a dynamic state feedback controller is employed instead. Based on a piecewise Lyapunov function, it is shown that the robust semi-global stabilization and generalized $\mathscr{H}_2$ controller design results can be obtained based on the feasible solutions of a set of linear matrix inequalities that are numerically efficient with commercially available software.

The rest of this paper is structured as follows. The section II is devoted to the description of the generalized T-S fuzzy models and the proof of its universal approximation property. In section III and IV, the robust semi-global stabilization and generalized $\mathscr{H}_2$ control design results of the nonlinear system will be presented respectively. Simulation results will be provided in section V to demonstrate the effectiveness of the proposed approaches. Conclusions will be given in section VI.

Notations. The notations used in this paper are fairly standard. The notation $\star$ is used to indicate the terms that can be induced by symmetry. For example, $\begin{bmatrix} A & B^T \\ B & C \end{bmatrix} = \begin{bmatrix} A & \star \\ B & C \end{bmatrix}$. "$T$" represents vector or matrix transpose. $\mathbf{I}_n$ and $\mathbf{0}_{m\times n}$ are used to denote the $n \times n$ identity matrix and the $m \times n$ zero matrix, respectively. The subscripts n and $m \times n$ are omitted when the size is not relevant or can be determined from the context. The notation $l_2[0, N]$ will be used for discrete-time vector-valued functions, i.e., $z_d : [0, N] \to \Re^k \in l_2[0, N]$ if $\sum_{t=1}^{N} z_d^T(t)z_d(t) < \infty$. The l_2- norm is defined as $||z_d(t)||_2 = \sqrt{\sum_{t=1}^{N} z_d^T(t)z_d(t)}$ and the $l_\infty-$ norm is defined as $||z_d(t)||_\infty = \sqrt{\sup_t\{z_d^T(t)z_d(t)\}}$.

II. Generalized T-S Fuzzy Model and Universal Function Approximation

Let us consider a general nonlinear system described by the following equation,

$$x(t + 1) = G(x(t), u(t)), \tag{1}$$

where $x(t) = [x_1(t), ..., x_n(t)]^T \in X = \prod_{i=1}^{n} X_i \subset \Re^n$ with $x_0 = [0, ..., 0]^T \in X$ and $u(t) = [u_1(t), ..., u_m(t)]^T \in U = \prod_{j=1}^{m} U_j \subset \Re^m$ with $u_0 = [0, ..., 0]^T \in U$. Throughout the paper, it is always assumed that the origin is the equilibrium of the system, that is, $G(0, 0) = 0$, and $G(x, u)$ is a continuously differentiable function on $X \times U$. Further it is assumed that $X \times U = \prod_{i=1}^{n}[\underline{x}_i, \bar{x}_i] \times \prod_{j=1}^{m}[\underline{u}_j, \bar{u}_j]$ is a compact set on $\Re^n \times \Re^m$.

Our objective is to develop an approach to control of such general nonlinear systems via a way of Takagi-Sugeno (T-S) fuzzy modelling. For this purpose, we consider to approximate the nonlinear systems by the following class of generalized T-S fuzzy models at first,

Plant rule $\mathcal{R}^l$:

IF $x_1(t)$ is μ_1^l AND ... AND $x_n(t)$ is μ_n^l ; $u_1(t)$ is ν_1^l AND ... AND $u_m(t)$ is ν_m^l

$$\textbf{THEN} \quad x(t+1) = A_l x(t) + B_l u(t); l \in \mathscr{L} := \{1, ...r\} \tag{2}$$

where $\mathcal{R}^l$ denotes the lth rule, r the total number of rules, μ_i^l and ν_j^l the fuzzy sets, $x(t) \in \Re^n$ the state vector, $u(t) \in \Re^m$ the input vector, and $[A_l, B_l]$ the matrices of the lth local model.

Under the center-average defuzzifier, product inference and singleton fuzzifier, the T-S fuzzy system in (2) can be expressed as follows,

$$x(t + 1) = F(x(t), u(t)), \tag{3}$$

with

$$\begin{cases} F(x, u) = \sum_{l=1}^{r} \mu_l(x, u)[A_l x(t) + B_l u(t)], \\ \mu_l(x, u) = \frac{\prod_{i=1}^{n} \mu_i^l(x_i) \prod_{j=1}^{m} \nu_j^l(u_j)}{\sum_{l=1}^{r} \prod_{i=1}^{n} \mu_i^l(x_i) \prod_{j=1}^{m} \nu_j^l(u_j)}, \end{cases} \tag{4}$$

where $\mu_l(x, u)$ are so-called normalized fuzzy membership functions satisfying $\mu_l(x, u) \geq 0$ and $\sum_{l=1}^{r} \mu_l(x, u) = 1$ [8].

Remark 2.1. In the commonly used T-S fuzzy model, which is referred as "the standard T-S fuzzy model" in [19], the control variable u is not included in the conditional part of the rule. It has been shown in [19] that the commonly used T-S fuzzy model, where the control variable u is not included in the premise part of the rule, are only able to approximate affine nonlinear systems. Thus, to represent the more general nonlinear systems given in (1), a more general T-S fuzzy model, such as those given in (2) or (3) is needed. These models are referred to be the generalized T-S fuzzy model in this paper.

Before giving the main results of this section, we first introduce a lemma.

Lemma 2.1. [19] If vector value function $f(z) = [f_1(z_1, ..., z_N), ..., f_n(z_1, ..., z_N)]^T$ is continuously differentiable on $Z = \prod_{i=1}^{N}[\alpha_i, \beta_i]$ with $0 \in Z$ and $f(0) = 0$, then for $i = 1, ..., N$ the vector value function

$$G_i(z) = g_i(z_i, ..., z_N) = \begin{cases} \frac{f(0,...,z_i,z_{i+1},...,z_N) - f(0,...,0,z_{i+1},...,z_N)}{z_i}, & z_i \neq 0 \\ \frac{\partial f(0,...,0,z_{i+1},...,z_N)}{\partial z_i}, & z_i = 0 \end{cases} \tag{5}$$

is continuous on Z and

$$f(z) = \sum_{i=1}^{N} G_i(z)z_i = \sum_{i=1}^{N} g_i(z_i, ..., z_N)z_i. \tag{6}$$

Then one has the following result.

Theorem 2.1. Let a general nonlinear system be given in (1) where $G(x, u)$ on the compact set $X \times U$ is continuously

differentiable with $G(0,0) = 0$. Then, for any $\epsilon_1 > 0$ and $\epsilon_2 > 0$, there exists a T-S fuzzy model $F(x,u) = \sum_{l=1}^{r} \mu_l(x,u)[A_l x(t) + B_l u(t)]$ given in (3) such that, for any $(x,u) \in X \times U$

$$G(x,u) = F(x,u) + E(x,u), \tag{7}$$

and

$$\|E(x,u)\| \leq \epsilon_1 \|x\| \ + \epsilon_2 \|u\|. \tag{8}$$

Proof. See [23].

Remark 2.2. Noticing that $X \times U = \prod_{i=1}^{n}[\underline{x}_i, \bar{x}_i] \times \prod_{j=1}^{m}[\underline{u}_j, \bar{u}_j]$ are bounded, the norm bound of approximation error $\Delta E(x,u)$ will be as small as needed by choosing $\epsilon_1 > 0$ and $\epsilon_2 > 0$ accordingly. In other words, the fuzzy control system given in (3) can approximate the general nonlinear system (1) to any degree of accuracy.

Remark 2.3. It is noted the decomposition procedure in proof of Theorem 2.1 can be conducted both in continuous-time case and discrete-time case. Thus one can conclude that any given continuous-time general nonlinear systems satisfying the described conditions in Theorem 2.1 can also be approximated by a continuous-time generalized T-S fuzzy model to any degree of accuracy.

Remark 2.4. Based on Theorem 2.1, one can easily conclude that the stabilization of a general nonlinear system given in (1) can be solved as a robust stabilization problem of its corresponding T-S fuzzy model with the approximation errors as the uncertainty term.

III. Robust Controller Design for Nonlinear Systems

It has been shown in the previous section that a general nonlinear system described by (1) can be exactly expressed in a compact set by a T-S fuzzy model with some uncertainties as follows,

$$\begin{aligned} x(t+1) = F(x(t),u(t)) + \Delta A(x(t),u(t))x(t) \\ + \Delta B(x(t),u(t))u(t), \end{aligned} \tag{9}$$

where $F(x(t),u(t))$ is described by (4) and

$$\|\Delta A(x(t),u(t))\| \leq \epsilon_1 \quad \text{and} \quad \|\Delta B(x(t),u(t))\| \leq \epsilon_2.$$

In this section, we will develop a robust control design approach to the general nonlinear systems (1) via the way of T-S fuzzy modeling in terms of system (9) based on a piecewise Lyapunov function.

In order to facilitate the piecewise controller design, we partition the premise variable space S into crisp regions and fuzzy regions [3]. Denote those regions from the premise variable space partition as $\{S_i\}_{i \in \mathscr{I}}$ with $\mathscr{I}$ as the set of region indices.

Define $\mathscr{K}(i)$ the indices of fired rules in each region S_i, $i \in \mathscr{I}$, then the crisp regions and fuzzy regions can be defined respectively by

$$S_i := \Big\{(x(t),u(t)) | \mu_k(x(t),u(t)) = 1, k \in \mathscr{K}(i)\Big\}, \tag{10}$$

and

$$S_i := \Big\{(x(t),u(t)) | 0 \leq \mu_k(x(t),u(t)) < 1, k \in \mathscr{K}(i)\Big\}. \tag{11}$$

Based on such a partition method, the global fuzzy model (9) in each region can be rewritten by a blending of $k \in \mathscr{K}(i)$ subsystems,

$$\begin{aligned} x(t+1) = \sum_{k \in \mathscr{K}(i)} \mu_k(x,u)\Big\{(A_k + \Delta A(x,u))x(t) \\ + (B_k + \Delta B(x,u))u(t)\Big\}. \end{aligned} \tag{12}$$

In order to stabilize the nonlinear system in (12), we employ the following piecewise dynamic state feedback controller,

$$u(t+1) = F_i x(t) + G_i u(t), (x,u) \in S_i, i \in \mathscr{I}. \tag{13}$$

Then the closed-loop control system can be described by

$$\bar{x}(t+1) = \left\{ \sum_{k \in \mathscr{K}(i)} \mu_k(\bar{x}(t)) \mathcal{A}_{ki} + R \Delta E \right\} \bar{x}(t), \bar{x}(t) \in S_i, \tag{14}$$

where $\mathcal{A}_{ki} = \bar{A}_k + \bar{B}_k \bar{K}_i$ and

$$\begin{cases} \bar{x}(t) = \begin{bmatrix} x(t) \\ u(t) \end{bmatrix}, \bar{A}_k = \begin{bmatrix} A_k & B_k \\ \mathbf{0}_{m\times n} & \mathbf{0}_{m\times m} \end{bmatrix}, \\ \bar{B}_k = \begin{bmatrix} \mathbf{0}_{n\times m} \\ \mathbf{I}_m \end{bmatrix}, R = \begin{bmatrix} \mathbf{I}_n \\ \mathbf{0}_{m\times n} \end{bmatrix}, \\ \Delta E = \begin{bmatrix} \Delta_A & \Delta_B \end{bmatrix}, \bar{K}_i = \begin{bmatrix} F_i & G_i \end{bmatrix}. \end{cases}$$

In addition, we define a new set that represents all possible state transitions among regions of the closed-loop T-S fuzzy system in (14) as follows,

$$\Omega := \{(i,j) | \bar{x}(t) \in S_i, \bar{x}(t+1) \in S_j, i,j \in \mathscr{I}\}. \tag{15}$$

For a piecewise Lyapunov function candidate we consider functions of the following form:

$$V(\bar{x}(t)) = \bar{x}(t)^T P_i \bar{x}(t), \bar{x}(t) \in S_i, i \in \mathscr{I}. \tag{16}$$

Suppose the upper bound of the uncertainty ΔE is given by

$$\Delta E^T \Delta E = \begin{bmatrix} \Delta_A^T \\ \Delta_B^T \end{bmatrix} \begin{bmatrix} \Delta_A & \Delta_B \end{bmatrix} \leq \bar{\epsilon}^2 \mathbf{I}_{(m+n)}. \tag{17}$$

Then we have the following stabilization results of nonlinear system (1).

Theorem 3.1. The nonlinear system (1) can be semi-globally asymptotically stabilized by the fuzzy controller in (13), if there exist a set of positive-definite matrices $X_i, i \in \mathscr{I}$, a set of positive constants $\varepsilon_i, i \in \mathscr{I}$ and a set of matrices $Q_i, i \in \mathscr{I}$, such that the following LMIs are satisfied,

$$\begin{aligned} \begin{bmatrix} X_i & \star & \star & \star \\ A_k X_i + B_k Q_i & X_j & \star & \star \\ \bar{\epsilon} X_i & \mathbf{0} & \varepsilon_i \mathbf{I} & \star \\ \mathbf{0} & \varepsilon_i R^T & \mathbf{0} & \varepsilon_i \mathbf{I} \end{bmatrix} > 0, \\ k \in \mathscr{K}(i), (i,j) \in \Omega. \end{aligned} \tag{18}$$

Moreover, the controller gains are given by

$$\bar{K}_i = Q_i X_i^{-1}, i \in \mathscr{I}. \tag{19}$$

Proof. See [23].

IV. Robust Generalized $\mathscr{H}_2$ Controller Design For Nonlinear Systems

In this section, we will address the generalized $\mathscr{H}_2$ controller synthesis problem [11] for a general nonlinear system with disturbances, which is described by

$$x(t+1) = G(x(t), u(t)) + H(x(t), u(t))w(t), \tag{20}$$

where $w(t) \in \Re^p$ is the external disturbance and other variables are the same as those defined in (1).

Based on the approximation results presented in section II, the nonlinear system (20) can be exactly expressed in a compact set by the following T-S fuzzy model with some uncertainties,

Plant rule $\mathcal{R}^l$: IF $x_1(t)$ is μ_1^l AND ... AND $x_n(t)$ is μ_n^l ; $u_1(t)$ is ν_1^l AND ... AND $u_m(t)$ is ν_m^l **THEN**

$$\begin{cases} x(t+1) = (A_l + \Delta A)x(t) + (B_l + \Delta B)u(t) \\ \qquad\qquad + (H_l + \Delta H)w(t), \\ z(t) = C_l x(t) + D_l u(t), l \in \mathscr{L} := \{1, 2, ...r\}. \end{cases} \tag{21}$$

Then using the same controller described in (13), the same premise variable space partition method as in section III, and adopting the same definitions of symbols as in (15), the closed-loop control system consisting of (20) or (21) and (13) can be described by the following equations,

$$\begin{cases} \bar{x}(t+1) = \mathcal{A}_{ic}\bar{x}(t) + \mathcal{H}_{ic}w(t), \\ z(t) = \mathcal{C}_{ic}\bar{x}(t), \quad \bar{x}(t) \in S_i \end{cases} \tag{22}$$

where

$$\begin{cases} \mathcal{A}_{ic} = \sum\limits_{k \in \mathscr{K}(i)} \mu_k(\bar{x})\mathcal{A}_{ki}^c = \sum\limits_{k \in \mathscr{K}(i)} \mu_k(\bar{x})(\mathcal{A}_{ki} + R\Delta E), \\ \mathcal{H}_{ic} = \sum\limits_{k \in \mathscr{K}(i)} \mu_k(\bar{x})\mathcal{H}_k^c = \sum\limits_{k \in \mathscr{K}(i)} \mu_k(\bar{x})R(H_k + \Delta H), \\ \mathcal{C}_{ic} = \sum\limits_{k \in \mathscr{K}(i)} \mu_k(\bar{x})\bar{C}_k = \sum\limits_{k \in \mathscr{K}(i)} \mu_k(\bar{x})[C_k \quad D_k]. \end{cases}$$

Similar to the case of stabilization discussed in Section III, the global results on generalized $\mathscr{H}_2$ control of the model (21) would imply the semi-global results on generalized $\mathscr{H}_2$ control of the system (20) due to the restriction of a compact set for the description of (20) via (21).

We at first introduce the following definition of the generalized $\mathscr{H}_2$ control.

Definition 4.1. [12] Let a constant $\gamma > 0$ be given. The closed-loop control system (22) is said to be asymptotically stable with generalized $\mathscr{H}_2$ performance γ if both of the following conditions are satisfied,

1) The disturbance-free system is globally asymptotically stable,

2) The generalized $\mathscr{H}_2$ norm of the system, which is defined as

$$\mathscr{H}_2 := \sup_{N \in \{1,2,...\}} \Big\{ \|z_N\| : x_0 = 0, \sum_{k=0}^{N-1} (\omega_k^T(t)\omega_k(t)) \le 1 \Big\},$$

is less than γ.

Before present the generalized $\mathscr{H}_2$ controller design results, we first introduce two lemmas,

Lemma 4.1.[12] The discrete-time fuzzy system (22) is stable with generalized $\mathscr{H}_2$ performance, if there exist a set of positive-definite matrices $P_i, i \in \mathscr{I}$ such that the following matrix inequalities are satisfied,

$$\begin{cases} P_i - \dfrac{1}{\gamma^2}\bar{C}_k^T\bar{C}_k > 0, i \in \mathscr{I}, & \text{(23a)} \\ (\mathcal{A}_{ki}^c)^T P_j \mathcal{H}_k^c (\mathcal{H}_k^c P_j \mathcal{H}_k^c - \mathbf{I})^{-1} (\mathcal{H}_k^c)^T P_j \mathcal{A}_{ki}^c \\ +(\mathcal{A}_{ki}^c)^T P_j \mathcal{A}_{ki}^c - P_i < 0. & \text{(23b)} \end{cases}$$

Lemma 4.2. [24] Given matrices $\Delta E(\mu)$ satisfying

$$\begin{cases} \Delta E^T(\mu)\Delta E(\mu) \le \bar{\epsilon}^2\mathbf{I} & \forall \mu \in M, \quad \text{(24a)} \\ \Delta E^T(\mu^*)\Delta E(\mu^*) = \bar{\epsilon}^2\mathbf{I} & \mu^* \in M, \quad \text{(24b)} \end{cases}$$

there exists a set of positive-definite symmetric matrix $P_i, i \in \mathscr{I}$ such that,

$$\begin{aligned} &(A + R\Delta E)^T P_j H(\mathbf{I} - H^T P_j H)^{-1} H^T P_j (A + R\Delta E) \\ &+ (A + R\Delta E)^T P_j (A + R\Delta E) - P_i < 0, \end{aligned} \tag{25}$$

if and only if there exists a set of positive constants $\varepsilon_i, i \in \mathscr{I}$ such that the following conditions hold,

$$\begin{cases} \bar{P}_j = P_j^{-1} - HH^T - \varepsilon_i RR^T > 0, & \text{(26a)} \\ A^T \bar{P}_j^{-1} A - P_i + \dfrac{1}{\varepsilon_i}\bar{\epsilon}^2\mathbf{I} < 0. & \text{(26b)} \end{cases}$$

Suppose the upper bound of uncertainty ΔH is given by

$$\Delta H \Delta H^T \le \bar{\epsilon}_h^2 \mathbf{I}_n. \tag{27}$$

then based on Lemmas 4.1, 4.2 and the upper bounds defined in (17) , one has the following result.

Theorem 4.1. Given a constant $\gamma > 0$, the nonlinear system (20) can be semi-globally asymptotically stabilized with generalized $\mathscr{H}_2$ performance γ via the controller in (13) , if there exist a set of positive definite matrices $X_i, i \in \mathscr{I}$, a set of matrices $Q_i, i \in \mathscr{I}$ and a set of positive constants $\varepsilon_i, i \in \mathscr{I}$ such that the following LMIs are satisfied,

$$\begin{bmatrix} X_i & \star \\ \bar{C}_k X_i & \gamma^2\mathbf{I} \end{bmatrix} > 0, \tag{28}$$

$$\begin{bmatrix} X_i & \star & \star \\ \bar{\epsilon}X_i & \varepsilon_i\mathbf{I}_n & \star \\ \bar{A}_k X_i + \bar{B}_k Q_i & \mathbf{0} & \Upsilon_{kij} \end{bmatrix} > 0, \quad k \in \mathscr{K}(i), (i,j) \in \Omega, \tag{29}$$

where $\Upsilon_{kij} = X_j - R(2(H_k H_k^T + \bar{\epsilon}_h^2\mathbf{I}_n) - \varepsilon_i\mathbf{I}_n)R^T$.

Moreover, the controller gains can be determined by

$$\bar{K}_i = Q_i X_i^{-1}, i \in \mathscr{I}. \tag{30}$$

Proof. The proof is omitted here.

It follows from Theorem 4.1 that the minimum generalized $\mathscr{H}_2$ performance index γ can be obtained by the following convex optimization algorithm [25].

Algorithm 4.1: $\min_{X_i,Q_i,\varepsilon_i} \gamma^2$, subject to LMIs (28) and (29).

V. Simulation Studies

Control of the inverted pendulum is one of the benchmark examples to demonstrate novel nonlinear control approaches. It is also noted that actuator models in the inverted pendulum are often given by the hyperbolic tangent functions of control input u. To show the performance of the above controller design results, we consider the balancing problem of an inverted pendulum on a cart. The equation of motion for the pendulum are

$$\begin{aligned}\dot{x}_1 &= x_2\\ \dot{x}_2 &= \frac{g\sin(x_1) - aml x_2^2 \sin(2x_1)/2 - a\cos(x_1)v}{4l/3 - aml\cos^2(x_1)} + w\\ v &= (\arctan(u) + 0.15u) * 10^3\end{aligned}$$

where x_1 denotes the angle of pendulum from the vertical, and x_2 is the angular velocity. $g = 9.8m/s^2$ is the gravity constant, m is the mass of pendulum, M is the mass of the cart, $2l$ is the length of the pendulum and w is the disturbance. Note the input force is given by $\arctan(u) + 0.15u$ with an amplifier 1000 connected. In this simulation, we choose $m = 2.0$kg, $M = 8.0$kg, $2l = 1.0$m.

We linearize the plant around the following operating points, $(x;u) = (0;0;0)$, $(0;0;\pm 3)$, $(\pm 88^\circ;0;0)$, and $(\pm 88^\circ;0;\pm 3)$ respectively, and consider the approximation errors between the linearized local model and the original nonlinear models as norm-bounded uncertainties. By the standard discretization procedure [14] with sampling time $T = 0.01$s, we can obtain the following uncertain discrete-time dynamic T-S fuzzy model,

Plant rule $\mathcal{R}^l$: IF $|x_1|$ is μ^l And $|u|$ is ν^l **THEN**

$$\begin{cases} x(t+1) = (A_l + \Delta A)x(t) + (B_l + \Delta B)u(t), \\ \qquad\qquad + (H_l + \Delta H)w(t) \\ z(t) = C_l x(t) + D_l u(t), l \in \mathscr{L} := \{1,2,3,4\}. \end{cases}$$

where

$$\begin{aligned} A_1 = A_2 &= \begin{bmatrix} 1 & 0.01 \\ 0.1729 & 1 \end{bmatrix},\\ A_3 = A_4 &= \begin{bmatrix} 1 & 0.01 \\ 0.0036 & 1 \end{bmatrix},\\ B_1 = \begin{bmatrix} 0 \\ -2.03 \end{bmatrix}, B_2 &= \begin{bmatrix} 0 \\ -1.38 \end{bmatrix},\\ B_3 = \begin{bmatrix} 0 \\ -0.060 \end{bmatrix}, B_4 &= \begin{bmatrix} 0 \\ -0.041 \end{bmatrix},\\ C_1 = C_2 = C_3 = C_4 &= \begin{bmatrix} 0.5 & 1 \end{bmatrix},\\ H_1 = H_2 = H_3 = H_4 &= \begin{bmatrix} 0 \\ 0.01 \end{bmatrix},\\ D_1 = 0.05, D_2 = D_3 = D_4 &= 0.01. \end{aligned}$$

Suppose the upper bounds of uncertainties ΔA and ΔB are given by (17) with $\bar{\epsilon} = 0.005$. It is noted that the uncertainty $\Delta H = 0$.

By using the space partition method given in section III, the premise variable space is partitioned into six regions. The membership functions and the corresponding local regions are shown in Fig. 1.

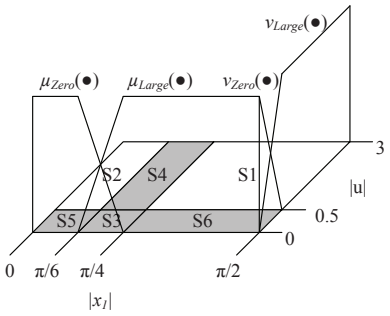

Fig. 1. MFs and the partitioned regions

By applying Algorithm 4.1, the minimum $\mathscr{H}_2$ performance $\gamma_{\min} = 0.0572$ is obtained and the corresponding controller gains are given by

$$\begin{aligned} \bar{K}_1 &= \begin{bmatrix} 0.5660 & 0.4997 & -0.0202 \end{bmatrix},\\ \bar{K}_2 &= \begin{bmatrix} 0.6613 & 0.5111 & -0.6974 \end{bmatrix},\\ \bar{K}_3 &= \begin{bmatrix} 1.1039 & 0.9744 & -1.0127 \end{bmatrix},\\ \bar{K}_4 &= \begin{bmatrix} 0.8436 & 0.7292 & -0.5135 \end{bmatrix},\\ \bar{K}_5 &= \begin{bmatrix} 0.7935 & 0.6286 & -1.0604 \end{bmatrix},\\ \bar{K}_6 &= \begin{bmatrix} 0.5673 & 0.5019 & -0.0245 \end{bmatrix}. \end{aligned}$$

To illustrate the performance of the approaches proposed in this paper, we first show the state trajectories and control input of the closed-loop system under initial condition $x(0) = (89^\circ, 0)$ in Fig. 2. It can be found that the two states converge to zero when the external disturbance $w(t) = 0$. Next we illustrate the disturbance attenuation performance. Assume zero initial conditions, Fig. 3 shows the response of the ratio $\frac{\max|z(1:\kappa)|}{\sqrt{\sum_{i=0}^{\kappa} w^T(i)w(i)}}$ of the closed-loop control system. The disturbance is $w(t) = e^{-0.02t}\sin(\pi t)$. It shows that the performance is satisfactory and the ratio $\frac{\max|z(1:\kappa)|}{\sqrt{\sum_{i=0}^{\kappa} w^T(i)w(i)}}$ is less than 0.01, which is less than the minimum disturbance attenuation level $\gamma_{\min} = 0.0572$.

A number of simulations have been conducted and it is found that the pendulum can be balanced from $x_1 \in [-89^\circ, 89^\circ]$ with guaranteed performance. Note that the control input is also bounded.

VI. Conclusions

A class of generalized T-S fuzzy models have been proposed and shown to be universal approximators to general nonlinear

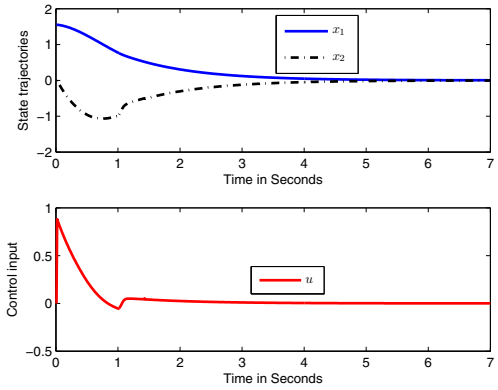

Fig. 2. State trajectories and control input

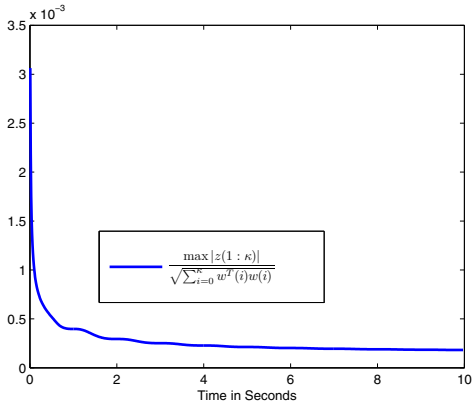

Fig. 3. Response of the ratio $\frac{\max|z(1:\kappa)|}{\sqrt{\sum_{i=0}^{\kappa} w^T(i)w(i)}}$

systems. Based on this kind of T-S fuzzy models and piecewise quadratic Lyapunov functions, approaches to stabilization and generalized $\mathscr{H}_2$ control of those general nonlinear systems have been developed. It is shown that the general nonlinear systems can be semi-globally stabilized with/without generalized $\mathscr{H}_2$ performance by solving a set of linear matrix inequalities. An example is presented to demonstrate the effectiveness of the proposed approaches. It is believed that the approaches proposed in this paper provide a new avenue to solve much more difficult control problem for general nonlinear systems.

REFERENCES

[1] T. Takagi and M. Sugeno, "Fuzzy identification of systems and its applications to modeling and control," *IEEE Transactions on Systems, Man, and Cybernetics-Part B: Cybernetics*, vol. SMC-15, no. 1, pp. 116-132, Jan./Feb. 1985.

[2] H. O. Wang, K. Tanaka, and M. F. Griffin, "An approach to fuzzy contol of nonlinear systems: stability and design issues," *IEEE Transaction on Fuzzy Systems,* vol. 4, no. 1, pp. 14-23, Feb. 1996.

[3] G. Feng, *Analysis and Synthesis of Fuzzy Control Systems: A Model-Based Approach*, CRC Press, Boca Raton, FL, 2010.

[4] B. S. Chen, C. S. Tseng, and H. J. Uang, "Robustness design of nonlinear dynamic systems via fuzzy linear control," *IEEE Transaction on Fuzzy Systems,* vol. 7, no. 5, pp. 571-585, Oct. 1999.

[5] C. S. Tseng, B. S. Chen, and H. J. Uang, "Fuzzy tracking control design for nonlinear dynamic systems via T-S fuzzy model," *IEEE Transaction on Fuzzy Systems,* vol. 9, no. 3, pp. 381-392, Jun. 2001.

[6] G. Feng, "A survey on analysis and design of model-based fuzzy control systems," *IEEE Transactions on Fuzzy Systems*, vol. 14, no. 5, pp. 676-697, Oct. 2006.

[7] K. Tanaka, and H. O. Wang, *Fuzzy control systems design and analysis: a* LMI *approach*. New York: Wiley, 2001.

[8] G. Feng, "Stability analysis of discrete time fuzzy dynamic systems based on piecewise Lyapunov functions," *IEEE Transactions on Fuzzy Systems*, vol. 12, no. 1, pp. 22-28, Feb. 2004.

[9] S. G. Cao, N. W. Rees, and G. Feng, "Analysis and design for a class of complex control systems-part I: fuzzy modeling and identification," *Automatica*, vol. 33, no. 6, pp. 1017-1028, Jun. 1997.

[10] S. G. Cao, N. W. Rees, and G. Feng, "Analysis and design for a class of complex control systems-part II: fuzzy modeling and identification," *Automatica*, vol. 33, no. 6, pp. 1029-1039, Jun. 1997.

[11] M.A. Rotea, "The generalized $\mathscr{H}_2$ control problem", *Automatica*, vol. 29, no. 2, pp. 373-385, Mar. 1993

[12] L. Wang, G. Feng and T. Hesketh, "Piecewise generalised $\mathscr{H}_2$ controller synthesis of discrete-time fuzzy systems,"*IEE Proceedings: Control Theory and Application*, vol. 151, no. 5, pp. 554-560, 2004.

[13] M. Johansson, A. Rantzer, and K. -E. Årzén, "Piecewise quadratic stability of fuzzy systems," *IEEE Transactions on Fuzzy Systems*, vol. 7, no. 6, pp. 713-722, Dec. 1999.

[14] J. Qiu, G. Feng, and J. Yang, "A new design of delay-dependent robust $\mathscr{H}_\infty$ filtering for discrete-time T-S fuzzy systems with time-varying delay," *IEEE Transactions on Fuzzy Systems*, vol. 17, no. 5, pp. 1044-1058, Oct. 2009.

[15] J. Qiu, G. Feng, and H. Gao, "Fuzzy-model-based piecewise $\mathscr{H}_\infty$ static output feedback controller design for networked nonlinear systems," *IEEE Transactions on Fuzzy Systems*, vol. 18, no. 5, pp. 919-934, Oct. 2010.

[16] J. Qiu, G. Feng, and J. Yang, "Approaches to robust $\mathscr{H}_\infty$ controller synthesis of nonlinear discrete-time-delay systems via T-S fuzzy models," Recent Advances in Intelligent Control Systems, edited by W. Yu, London: Springer, pp. 21-49, 2009.

[17] X. -J. Zeng and M. G. Singh, "Approximation theory of fuzzy systems–SISO case," *IEEE Transactions on Fuzzy Systems*, vol. 2, no. 2, pp. 162-176, May. 1994.

[18] X. -J. Zeng and M. G. Singh, "Approximation theory of fuzzy systems–MIMO case," *IEEE Transactions on Fuzzy Systems*, vol. 3, no. 2, pp. 219-235, May. 1995.

[19] X. -J. Zeng, J. A. Keane, and D. Wang, "Fuzzy systems approach to approximation and stabilization of conventional affine nonlinear systems," *In Proceedings of the 2006 IEEE International Conference on Fuzzy Systems*, Vancouver, BC, Canada, July, 2006, pp. 277-284.

[20] J. X. Dong, Y. Wang, and G. H. Yang, "Control synthesis of continuous-time T-S fuzzy systems with local nonlinear models," *IEEE Transactions on Systems, Man, and Cybernetics-Part B: Cybernetics*, vol. 39, no. 5, pp. 1245-1258, Oct. 2009.

[21] J. M. A. Márquez, A. J. B. P̃ina, and M. E. G. Arias, "A general and formal methodology to design stable nonlinear fuzzy control systems," *IEEE Transactions on Fuzzy Systems*, vol. 17, no. 5, pp 1081-1091, Oct. 2009.

[22] C. Y. Xu and Y. C. Shin, "A fuzzy inverse model construction method for general monotonic multi-input-single-output (MISO) systems," *IEEE Transactions on Fuzzy Systems,* vol. 16, no. 5, pp. 1216-1231, Oct. 2008.

[23] Q. Gao, X. -J. Zeng, G. Feng, Y. Wang, J. Qiu, "T-S Fuzzy Model Based Approximation and Controller Design for General Nonlinear Systems," *IEEE Transactions on Fuzzy Systems*, under review.

[24] J. Ma and G. Feng, "An approach to $\mathscr{H}_\infty$ control of fuzzy dynamic systems," *Fuzzy Sets And Systems*, vol. 137, no. 3, pp. 367-386, Aug. 2003.

[25] S. Boyd, L. El Ghaoui, E. Feron, and V. Balakrishnan, *Linear Matrix Inequalities in Systems and Control Theory.* Philadelphia, PA: SIAM, 1994.

2011 IEEE International Conference on Fuzzy Systems
June 27-30, 2011, Taipei, Taiwan

A Polynomial Observer Design for a Wider Class of Polynomial Fuzzy Systems

Toshiaki Seo, Hiroshi Ohtake and Kazuo Tanaka
Mechanical Engineering and Intelligent Systems
The University of Electro-Communications
Tokyo, Japan
Email: ktanaka@mce.uec.ac.jp

Ying-Jen Chen
Electrical Engineering
National Central University
Jhongli, Taiwan (R.O.C.)
Email: 93541017@cc.ncu.edu.tw

Hua O. Wang
Mechanical Engineering
Boston University
Boston, USA
Email: wangh@bu.edu

***Abstract*—This paper presents a polynomial fuzzy observer design for a wider class of polynomial fuzzy systems via a sum of squares (SOS, for brevity) approach. The proposed SOS-based framework provides a number of innovations and improvements over the existing LMI-based approaches to Takagi-Sugeno (T-S) fuzzy controller and observer designs. First, we briefly summarize previous results for a class of polynomial fuzzy systems that is more general representation of the well-known T-S fuzzy system. Next, we propose a polynomial fuzzy observer to estimate states in a wider class of polynomial fuzzy systems and derive SOS conditions to design polynomial fuzzy controllers and observers. A remarkable feature of the SOS design conditions is that they realize the so-called separation principle, that is, that a polynomial fuzzy controller and observer for this class can be separately designed without lack of guaranteeing the stability of the overall control system in addition to converging state estimation error (via the observer) to zero. The design conditions in the proposed approach can be represented in terms of SOS and are symbolically and numerically solved via the recent developed SOSTOOLS and a semidefinite program (SDP) solver, respectively. To illustrate the validity and applicability of the proposed approach, a design example is provided. The example demonstrates advantages of the SOS-based approach for the existing LMI approaches to T-S fuzzy observer designs.**

Keywords: polynomial fuzzy controller, polynomial fuzzy observer, polynomial fuzzy system, sum of squares

I. Introduction

The Takagi-Sugeno (T-S) fuzzy model-based control methodology [1], [2] has received a great deal of attention after LMI-based designs have been discussed in [3]-[4]. The fuzzy model-based control methodology provides a natural, simple and effective design approach to complement other nonlinear control techniques (e.g., [5]) that require special and rather involved knowledge.

Recently, the authors have first presented a sum of squares (SOS, for brevity) approach [6]-[11] to polynomial fuzzy control system designs. This is a completely different approach from the existing LMI approaches [2], [12]-[24]. Our SOS approach [6]-[11] provided more extensive results for the existing LMI approaches to T-S fuzzy model and control. However, to the best of our knowledge, there existed no literature on SOS-based observer designs for polynomial fuzzy systems before our previous result has been given in [25].

This paper presents SOS-based observer designs for a wider class than the class of the polynomial fuzzy systems discussed in [25]. The proposed SOS-based framework for polynomial fuzzy systems provides a number of innovations and improvements over the existing LMI approaches to T-S fuzzy observer-based control, e.g., [2], [12], [13]. First, it is known that nonlinear systems with polynomial terms can not be generally converted to globally exact T-S fuzzy models. Only local or semi-global T-S fuzzy models can be constructed for such nonlinear systems [2]. Thus, resulting control design conditions guarantee global stabilization and global state-estimation convergence only for local or semi-global models, but not always guarantee global stabilization and global state-estimation convergence for original nonlinear systems. On the other hand, it is possible to convert even nonlinear systems with polynomial terms to globally exact polynomial fuzzy models. Hence all the conditions derived here guarantee global stabilization and global state-estimation convergence for original nonlinear systems that are perfectly equivalent to polynomial fuzzy models. Secondly, even if local or semi-global T-S fuzzy models are permitted to use in practical sense, variables in polynomial terms appear in premise (part) variables of T-S fuzzy models. In polynomial fuzzy models, variables in polynomial terms do not appear in their premise parts and remain in system polynomial matrices $\boldsymbol{A}_i$ and $\boldsymbol{B}_i$ in consequence parts of polynomial fuzzy models. The difference is quite large from fuzzy observer design points of view. In general, fuzzy observer designs are not permitted to have premise variables depending on the states to be estimated. Therefore, T-S fuzzy observer designs can not be generally applied to nonlinear systems with polynomial terms. Conversely, the polynomial fuzzy observer designs proposed in this paper can be applied to even such systems. We will see these facts in the design examples later.

This paper presents an SOS-based observer design for a wider class of polynomial fuzzy systems. First, we present the previous results in [25], i.e., an observer-based design for the polynomial fuzzy systems with the polynomial matrices $\boldsymbol{A}_i$ and $\boldsymbol{B}_i$ being independent of the states $\boldsymbol{x}$ to be estimated (shortly name it as Class I). Secondly, in this paper, we newly provide an observer-based design for a wider class of polynomial fuzzy systems with the polynomial matrices

978-1-4244-7316-8/11/$26.00 ©2011 IEEE

$\boldsymbol{A}_i$ that are permitted to be dependent of the states $\boldsymbol{x}$ to be estimated (shortly name it as Class II). It should be emphasized that the design conditions derived in this paper realize the so-called separation design even for the wider class. All the design conditions discussed here are represented in terms of SOS.

It is well known that stability conditions for the T-S fuzzy system reduce to LMIs, e.g., [2]. Hence, the stability conditions can be solved numerically and efficiently by interior point algorithms, e.g., by LMI solvers. On the other hand, some kinds of control design conditions [6]-[11] for polynomial fuzzy systems reduce to SOS problems. Clearly, it is difficult to directly slove the problems by LMI solvers and the problems can be solved via the SOSTOOLS [26] and an SDP solver. Thus, SOS can be regarded as an extensive representation of LMIs. The computational method used in this paper relies on the SOS decomposition of multivariate polynomials. A multivariate polynomial $f(\boldsymbol{x}(t))$ (where $\boldsymbol{x}(t) \in R^n$) is an SOS if there exist polynomials $f_1(\boldsymbol{x}(t))$, $\cdots$, $f_k(\boldsymbol{x}(t))$ such that $f(\boldsymbol{x}(t)) = \sum_{i=1}^{k} f_i^2(\boldsymbol{x}(t))$. It is clear that $f(\boldsymbol{x}(t))$ being an SOS naturally implies $f(\boldsymbol{x}(t)) \geq 0$ for all $\boldsymbol{x}(t) \in R^n$. For more details of SOS, see [26].

The rest of the paper is organized as follows. Section II recalls a polynomial fuzzy system defined in [6]-[11] and previsou result [25]. Section III discusses an SOS-based polynomial fuzzy controller and observer design for Class II. In addition, Section IV entails a design example to demonstrate the viability of our SOS design approach.

In this paper, to save the space, we employ the following short notations with respect to matrix representation.

$\mathcal{L}\{\boldsymbol{M}\} = \boldsymbol{M}^T + \boldsymbol{M}$,

$\boldsymbol{E}_1 = diag[\epsilon_{11}\ \epsilon_{12}\ \cdots\ \epsilon_{1s}]$,

$\boldsymbol{E}_{2i}(\boldsymbol{x}) = diag[\epsilon_{2i1}(\boldsymbol{x})\ \epsilon_{2i2}(\boldsymbol{x})\ \cdots\ \epsilon_{2is}(\boldsymbol{x})]$,

where $\boldsymbol{M}$ is an arbitrary square matrix. ϵ_{1k} $(k = 1, 2, \cdots, s)$ are positive values and $\epsilon_{2ik}(\boldsymbol{x})$ $(i = 1, 2, \cdots, r,\ k = 1, 2, \cdots, s)$ are nonnegative polynomials such that $\epsilon_{2ik}(\boldsymbol{x}) > 0$ for $\boldsymbol{x} \neq \boldsymbol{0}$. ϵ_{1k} and $\epsilon_{2ik}(\boldsymbol{x})$ ($\boldsymbol{E}_1$ and $\boldsymbol{E}_{2i}(\boldsymbol{x})$) will be used as slack variables (matrices) to keep positivity of SOS conditions derived in this paper. s is the matrix size of $\boldsymbol{E}_1$ and $\boldsymbol{E}_{2i}(\boldsymbol{x})$ that are assumed to have appropriate dimensions. r is the number of fuzzy model rules.

II. Previous Results

A. Polynomial fuzzy model

This subsection II-A recalls a polynomial fuzzy system defined in [6]-[11]. Consider the following nonlinear system:

$$\dot{\boldsymbol{x}}(t) = f(\boldsymbol{x}(t), \boldsymbol{u}(t)), \tag{1}$$

where f is a smooth nonlinear function such that $f(\boldsymbol{0}, \boldsymbol{0}) = \boldsymbol{0}$. $\boldsymbol{x}(t) = [x_1(t)\ x_2(t)\ \cdots\ x_n(t)]^T$ is the state vector and $\boldsymbol{u}(t) = [u_1(t)\ u_2(t)\ \cdots\ u_m(t)]^T$ is the input vector. In [6] and [9], we proposed a new type of fuzzy model with polynomial model consequence, i.e., fuzzy model whose consequent parts are represented by polynomials. Using the sector nonlinearity concept [2], we exactly represent (1) with the following polynomial fuzzy model (2). The main difference between the T-S fuzzy model [27] and the polynomial fuzzy model is consequent part representation. The fuzzy model (2) has a polynomial model consequence.

Model Rule i:

$$\begin{aligned} &If\ z_1(t)\ is\ M_{i1}\ and \cdots\ and\ \ z_p(t)\ is\ M_{ip} \\ &then\ \dot{\boldsymbol{x}}(t) = \boldsymbol{A}_i(\boldsymbol{x}(t))\boldsymbol{x}(t) + \boldsymbol{B}_i(\boldsymbol{x}(t))\boldsymbol{u}(t), \end{aligned} \tag{2}$$

where $i = 1, 2, \cdots, r$. r denotes the number of $Model\ Rules$. $z_j(t)$ $(j = 1, 2, \cdots, p)$ is the premise variable. Note that $z_j(t)$ is assumed to be independent of the states $\boldsymbol{x}$ to be estimated. In other words, each $z_j(t)$ is a measurable time-varying quantity that may be measurable external variables, outputs and/or time. The membership function associated with the ith $Model\ Rule$ and the jth premise variable component is denoted by M_{ij}. $\boldsymbol{A}_i(\boldsymbol{x}(t)) \in \boldsymbol{R}^{n \times n}$ and $\boldsymbol{B}_i(\boldsymbol{x}(t)) \in \boldsymbol{R}^{n \times m}$ are polynomial matrices in $\boldsymbol{x}(t)$. Therefore, $\boldsymbol{A}_i(\boldsymbol{x}(t))\boldsymbol{x}(t) + \boldsymbol{B}_i(\boldsymbol{x}(t))\boldsymbol{u}(t)$ is a polynomial vector. Thus, the polynomial fuzzy model (2) has a polynomial in each consequent part.

The defuzzification process of the model (2) can be represented as

$$\dot{\boldsymbol{x}}(t) = \sum_{i=1}^{r} h_i(\boldsymbol{z}(t))\{\boldsymbol{A}_i(\boldsymbol{x}(t))\boldsymbol{x}(t) + \boldsymbol{B}_i(\boldsymbol{x}(t))\boldsymbol{u}(t)\}, \tag{3}$$

where

$$h_i(\boldsymbol{z}(t)) = \frac{\prod_{j=1}^{p} M_{ij}(z_j(t))}{\sum_{k=1}^{r} \prod_{j=1}^{p} M_{kj}(z_j(t))}.$$

It should be noted from the properties of membership functions that $h_i(\boldsymbol{z}(t)) \geq 0$ for all i and $\sum_{i=1}^{r} h_i(\boldsymbol{z}(t)) = 1$. Thus, the overall fuzzy model is achieved by fuzzy blending of the polynomial system models.

It is in general difficult to separately design a polynomial controller and a polynomial observer for (3) since $\boldsymbol{A}_i(\boldsymbol{x}(t))$ and $\boldsymbol{B}_i(\boldsymbol{x}(t))$ are dependent of the states $\boldsymbol{x}(t)$ to be estimated. Hence, as a first step, we introduce the following representation of polynomial fuzzy systems.

$$\dot{\boldsymbol{x}}(t) = \sum_{i=1}^{r} h_i(\boldsymbol{z}(t))\{\boldsymbol{A}_i(\boldsymbol{\rho}_A(t))\boldsymbol{x}(t) + \boldsymbol{B}_i(\boldsymbol{\rho}_B(t))\boldsymbol{u}(t)\}, \tag{4}$$

where (4) reduces to (3) when $\boldsymbol{\rho}_A(t) = \boldsymbol{\rho}_B(t) = \boldsymbol{x}(t)$. In general, we can consider three types of polynomial observer-based control according to three classes of polynomial fuzzy systems:

Class I: $\boldsymbol{\rho}_A(t) = \boldsymbol{\zeta}(t)$ and $\boldsymbol{\rho}_B(t) = \boldsymbol{\zeta}(t)$.

Class II: $\boldsymbol{\rho}_A(t) = \boldsymbol{x}(t)$ and $\boldsymbol{\rho}_B(t) = \boldsymbol{\zeta}(t)$.

Class III: $\boldsymbol{\rho}_A(t) = \boldsymbol{\rho}_B(t) = \boldsymbol{x}(t)$.

$\boldsymbol{\zeta}(t)$ is a measurable time-varying vector that may be measurable external variables, outputs and/or time. In other words, $\boldsymbol{\zeta}(t)$ is assumed to be independent of the states $\boldsymbol{x}(t)$ to be estimated. As we can see, Class III is the most complicated class. We have already presented a polynomial fuzzy observer design for Class I in [25]. This paper focuses on a polynomial fuzzy observer design for a wider class, i.e., for Class II. A polynomial fuzzy observer-based design for Class III will be presented in [28].

From now, to lighten the notation, we will drop the notation with respect to time t. For instance, we will employ $\boldsymbol{x}$ and $\hat{\boldsymbol{x}}$ instead of $\boldsymbol{x}(t)$ and $\hat{\boldsymbol{x}}(t)$, respectively, where $\hat{\boldsymbol{x}}(t)$ denotes the state estimated by a polynomial fuzzy observer as will be discussed later. Thus, we drop the notation with respect to time t, but it should be kept in mind that $\boldsymbol{x}$ and $\hat{\boldsymbol{x}}$ means $\boldsymbol{x}(t)$ and $\hat{\boldsymbol{x}}(t)$, respectively.

Next, we define the outputs for the polynomial fuzzy model as

$$\boldsymbol{y} = \sum_{i=1}^{r} h_i(\boldsymbol{z}) \boldsymbol{C}_i \boldsymbol{x}, \tag{5}$$

where $\boldsymbol{y} \in \mathbb{R}^q$ is the output.

B. Previous Result (Class I Observer Design [25])

This subsection presents the previous result discussed in [25].

Consider the following polynomial fuzzy system. The system matrices $\boldsymbol{A}_i$ and $\boldsymbol{B}_i$ depend on the vector $\boldsymbol{\zeta}$,

$$\begin{cases} \dot{\boldsymbol{x}} = \sum_{i=1}^{r} h_i(\boldsymbol{z}) \{ \boldsymbol{A}_i(\boldsymbol{\zeta}) \boldsymbol{x} + \boldsymbol{B}_i(\boldsymbol{\zeta}) \boldsymbol{u} \} \\ \boldsymbol{y} = \sum_{i=1}^{r} h_i(\boldsymbol{z}) \boldsymbol{C}_i \boldsymbol{x}, \end{cases} \tag{6}$$

where $\boldsymbol{y} \in \mathbb{R}^q$ denotes the output.

We design a polynomial fuzzy observer to estimate the states of (6).

$$\begin{cases} \dot{\hat{\boldsymbol{x}}} &= \sum_{i=1}^{r} h_i(\boldsymbol{z}) \{ \boldsymbol{A}_i(\boldsymbol{\zeta}) \hat{\boldsymbol{x}} + \boldsymbol{B}_i(\boldsymbol{\zeta}) \boldsymbol{u} \\ & \qquad + \boldsymbol{L}_i(\boldsymbol{\zeta}) (\boldsymbol{y} - \hat{\boldsymbol{y}}) \} \\ \hat{\boldsymbol{y}} &= \sum_{i=1}^{r} h_i(\boldsymbol{z}) \boldsymbol{C}_i \hat{\boldsymbol{x}}, \end{cases} \tag{7}$$

where $\hat{\boldsymbol{x}} \in \mathbb{R}^n$ is the sate vector estimated by the fuzzy observer and $\hat{\boldsymbol{y}} \in \mathbb{R}^q$ is estimated output calculated from $\hat{\boldsymbol{y}} = \sum_{i=1}^{r} h_i(\boldsymbol{z}) \boldsymbol{C}_i \hat{\boldsymbol{x}}$.

To stabilize the system (6) and (7), we design a polynomial fuzzy controller with the state-feedback estimated by the polynomial fuzzy observer.

$$\boldsymbol{u} = -\sum_{i=1}^{r} h_i(\boldsymbol{z}) \boldsymbol{F}_i(\boldsymbol{\zeta}) \hat{\boldsymbol{x}} \tag{8}$$

Theorem 1 provides SOS conditions to separately design the polynomial fuzzy controller (8) and the polynomial fuzzy observer (7).

Theorem 1. *[25] If there exist positive definite matrices $\boldsymbol{X}_1 \in \mathbb{R}^{n \times n}$, $\boldsymbol{X}_2 \in \mathbb{R}^{n \times n}$ and polynomial matrices $\boldsymbol{M}_i(\boldsymbol{\zeta}) \in \mathbb{R}^{p \times n}$, $\boldsymbol{N}_i(\boldsymbol{\zeta}) \in \mathbb{R}^{n \times q}$ such that (9)∼(14) are satisfied, the polynomial fuzzy controller (8) stabilizes the system (6) and the estimation error via the polynomial observer (7) tends to zero.*

$$\boldsymbol{v}_1^T (\boldsymbol{X}_1 - \boldsymbol{E}_1) \boldsymbol{v}_1 \quad is \quad SOS \tag{9}$$

$$\boldsymbol{v}_2^T (\boldsymbol{X}_2 - \boldsymbol{E}_2) \boldsymbol{v}_2 \quad is \quad SOS \tag{10}$$

$$-\boldsymbol{v}_3^T \Big(\mathcal{L}\{ \boldsymbol{A}_i(\boldsymbol{\zeta}) \boldsymbol{X}_1 - \boldsymbol{B}_i(\boldsymbol{\zeta}) \boldsymbol{M}_i(\boldsymbol{\zeta}) \} + \boldsymbol{E}_{3i}(\boldsymbol{\zeta}) \Big) \boldsymbol{v}_3 \quad is \quad SOS \tag{11}$$

$$-\boldsymbol{v}_4^T \Big(\mathcal{L}\{ \boldsymbol{X}_2 \boldsymbol{A}_i(\boldsymbol{\zeta}) - \boldsymbol{N}_i(\boldsymbol{\zeta}) \boldsymbol{C}_i \} + \boldsymbol{E}_{4i}(\boldsymbol{\zeta}) \Big) \boldsymbol{v}_4 \quad is \quad SOS \tag{12}$$

$$-\boldsymbol{v}_5^T \Big(\mathcal{L}\{ \boldsymbol{A}_i(\boldsymbol{\zeta}) \boldsymbol{X}_1 - \boldsymbol{B}_i(\boldsymbol{\zeta}) \boldsymbol{M}_j(\boldsymbol{\zeta}) \} + \mathcal{L}\{ \boldsymbol{A}_j(\boldsymbol{\zeta}) \boldsymbol{X}_1 - \boldsymbol{B}_j(\boldsymbol{\zeta}) \boldsymbol{M}_i(\boldsymbol{\zeta}) \} \Big) \boldsymbol{v}_5 \quad is \quad SOS \tag{13}$$

$$-\boldsymbol{v}_6^T \Big(\mathcal{L}\{ \boldsymbol{X}_2 \boldsymbol{A}_i(\boldsymbol{\zeta}) - \boldsymbol{N}_i(\boldsymbol{\zeta}) \boldsymbol{C}_j \} + \mathcal{L}\{ \boldsymbol{X}_2 \boldsymbol{A}_j(\boldsymbol{\zeta}) - \boldsymbol{N}_j(\boldsymbol{\zeta}) \boldsymbol{C}_i \} \Big) \boldsymbol{v}_6 \quad is \quad SOS \tag{14}$$

where $\boldsymbol{v}_1$, $\boldsymbol{v}_2$, $\boldsymbol{v}_3$, $\boldsymbol{v}_4$ $\boldsymbol{v}_5$ and $\boldsymbol{v}_6 \in \mathbb{R}^n$ denote vectors that are independent of $\boldsymbol{x}$, $\hat{\boldsymbol{x}}$ and $\boldsymbol{\zeta}$. From the solutions $\boldsymbol{X}_1$ and $\boldsymbol{M}_i(\boldsymbol{\zeta})$, we obtain polynomial feedback gains $\boldsymbol{F}_i(\boldsymbol{\zeta})$ as $\boldsymbol{F}_i(\boldsymbol{\zeta}) = \boldsymbol{M}_i(\boldsymbol{\zeta}) \boldsymbol{X}_1^{-1}$. From the solutions $\boldsymbol{X}_2$ and $\boldsymbol{N}_i(\boldsymbol{\zeta})$, we obtain polynomial observer gains $\boldsymbol{L}_i(\boldsymbol{\zeta})$ as $\boldsymbol{L}_i(\boldsymbol{\zeta}) = \boldsymbol{X}_2^{-1} \boldsymbol{N}_i(\boldsymbol{\zeta})$ as well.

Remark 1. *The conditions (9), (11) and (13) are for SOS conditions of polynomial fuzzy controller design. The conditions (10), (12) and (14) are for SOS conditions of polynomial fuzzy observer design. Thus, Theorem 1 provides SOS design conditions to separately design polynomial fuzzy controllers and observers.*

Remark 2. *If $\boldsymbol{A}_i(\boldsymbol{\zeta})$, $\boldsymbol{B}_i(\boldsymbol{\zeta})$, $\boldsymbol{L}_i(\boldsymbol{\zeta})$ and $\boldsymbol{F}_i(\boldsymbol{\zeta})$ reduce to constant matrices in (6), (7) and (8), they reduce to the ordinary T-S fuzzy model, the T-S fuzzy controller and observer, respectively. In addition, Theorem 1 reduces to the existing LMI design conditions, e.g., [13], for the T-S fuzzy controller and observer. Hence, Theorem 1 provides more general results.*

Remark 3. *Currently, sum of squares programs (SOSPs) are solved by reformulating them as semidefinite programs (SDPs). SOSTOOLS automates the conversion from SOSP to SDP and the SDP can be solved by a SDP solver [26]. At present, SOSTOOLS uses other free MATLAB add-ons such as SeDuMi [29] or SDPT3 [30] as the SDP solver. In this paper, we numerically find $\boldsymbol{X}_1$, $\boldsymbol{X}_2$, $\boldsymbol{M}_i(\boldsymbol{\zeta})$ and $\boldsymbol{N}_i(\boldsymbol{\zeta})$ satisfying the SOS conditions in Theorem 1 via SeDuMi in addition to SOSTOOLS. For more details of how to solve the SDPs using SeDuMi, see [26] and [29].*

Remark 4. *To obtain more reliable solutions for SOS conditions, we perform the following double checking throughout this paper. We first carefully check whether the command 'sossolve' find a solution without any error messages, i.e., pinf=0, dinf=0 and numerr=0, or not. If any error messages exist, we judge 'infeasible'. After getting the feasible solutions using the command 'sossolve', the 'findsos' command is employed to check the feasibility of SOS conditions by substituting solutions into SOS conditions. We also carefully check whether the command 'findsos' provides a feasibility solution or not. If the command 'findsos' returns an infeasible result, we also judge 'infeasible'. This double checking is important to have reliable solutions in the use of SOSTOOLS [26] and SeDuMi [29].*

Remark 5. *The conditions $\epsilon_{1k} > 0$, $\epsilon_{2k} > 0$, $\epsilon_{3ik}(\boldsymbol{\zeta}) > 0$ and $\epsilon_{4ik}(\boldsymbol{\zeta}) > 0$ for $\boldsymbol{\zeta} \neq 0$ can be accommodated by sum of squares optimization in a similar way as in [31].*

III. Polynomial Controller and Observer Design for Class II

In Section II-B, we discussed an observer design for the polynomial fuzzy system (6) with $\boldsymbol{A}_i(\zeta)$ and $\boldsymbol{B}_i(\zeta)$ matrices. This section presents a more complicated class, i.e., $\boldsymbol{A}_i$ depends on the state $\boldsymbol{x}$ instead of the vector $\boldsymbol{\zeta}$. Although the separation design for Class II is difficult, we derive SOS conditions to achieve it in this section. The reason will be mentioned in Remark 6.

Consider the following polynomial fuzzy system.

$$\begin{cases} \dot{\boldsymbol{x}} = \sum_{i=1}^{r} h_i(\boldsymbol{z})\{\boldsymbol{A}_i(\boldsymbol{x})\boldsymbol{x} + \boldsymbol{B}_i(\boldsymbol{\zeta})\boldsymbol{u}\} \\ \boldsymbol{y} = \sum_{i=1}^{r} h_i(\boldsymbol{z})\boldsymbol{C}_i\boldsymbol{x} \end{cases} \tag{15}$$

We design a polynomial fuzzy observer to estimate the states of (15).

$$\begin{cases} \dot{\hat{\boldsymbol{x}}} = \sum_{i=1}^{r} h_i(\boldsymbol{z})\{\boldsymbol{A}_i(\hat{\boldsymbol{x}})\hat{\boldsymbol{x}} + \boldsymbol{B}_i(\boldsymbol{\zeta})\boldsymbol{u} \\ \qquad\qquad +\boldsymbol{L}_i(\hat{\boldsymbol{x}})(\boldsymbol{y} - \hat{\boldsymbol{y}})\} \\ \hat{\boldsymbol{y}} = \sum_{i=1}^{r} h_i(\boldsymbol{z})\boldsymbol{C}_i\hat{\boldsymbol{x}} \end{cases} \tag{16}$$

To stabilize the system, we design a polynomial fuzzy controller with the state-feedback estimated by the polynomial observer.

$$\boldsymbol{u} = -\sum_{i=1}^{r} h_i(\boldsymbol{z})\boldsymbol{F}_i(\hat{\boldsymbol{x}})\hat{\boldsymbol{x}} \tag{17}$$

The difference between (17) and (8) is that (17) has the polynomial feedback gains in $\hat{\boldsymbol{x}}$ instead of those in $\boldsymbol{\zeta}$ in (8) Theorem 2 provides SOS conditions to separately design the polynomial fuzzy controller (17) and the polynomial fuzzy observer (16).

Theorem 2. *If there exist positive definite matrices $\boldsymbol{X}_1 \in \mathbb{R}^{n\times n}$, $\boldsymbol{X}_2 \in \mathbb{R}^{n\times n}$ and polynomial matrices $\boldsymbol{M}_i(\hat{\boldsymbol{x}}) \in \mathbb{R}^{p\times n}$, $\boldsymbol{N}_i(\hat{\boldsymbol{x}}) \in \mathbb{R}^{n\times q}$ satisfying (18)∼(23), the polynomial fuzzy controller (17) stabilizes the system (15) and the estimation error via the polynomial fuzzy observer (16) tends to zero.*

$$\boldsymbol{v}_1^T(\boldsymbol{X}_1 - \boldsymbol{E}_1)\boldsymbol{v}_1 \quad is \quad SOS \tag{18}$$

$$\boldsymbol{v}_2^T(\boldsymbol{X}_2 - \boldsymbol{E}_2)\boldsymbol{v}_2 \quad is \quad SOS \tag{19}$$

$$-\boldsymbol{v}_3^T\Big(\mathcal{L}\{\boldsymbol{A}_i(\hat{\boldsymbol{x}})\boldsymbol{X}_1 - \boldsymbol{B}_i(\boldsymbol{\zeta})\boldsymbol{M}_i(\hat{\boldsymbol{x}})\} + \boldsymbol{E}_{3i}(\boldsymbol{\zeta},\hat{\boldsymbol{x}})\Big)\boldsymbol{v}_3 \quad is \quad SOS \tag{20}$$

$$-\boldsymbol{v}_4^T\Big(\mathcal{L}\{\boldsymbol{X}_2\bar{\boldsymbol{A}}_i(\boldsymbol{x},\hat{\boldsymbol{x}}) - \boldsymbol{N}_i(\hat{\boldsymbol{x}})\boldsymbol{C}_i\} + \boldsymbol{E}_{4i}(\boldsymbol{x},\hat{\boldsymbol{x}})\Big)\boldsymbol{v}_4 \quad is \quad SOS \tag{21}$$

$$-\boldsymbol{v}_5^T\Big(\mathcal{L}\{\boldsymbol{A}_i(\hat{\boldsymbol{x}})\boldsymbol{X}_1 - \boldsymbol{B}_i(\boldsymbol{\zeta})\boldsymbol{M}_j(\hat{\boldsymbol{x}})\} + \mathcal{L}\{\boldsymbol{A}_j(\hat{\boldsymbol{x}})\boldsymbol{X}_1 - \boldsymbol{B}_j(\boldsymbol{\zeta})\boldsymbol{M}_i(\hat{\boldsymbol{x}})\}\Big)\boldsymbol{v}_5 \quad is \quad SOS \quad i < j \le r \tag{22}$$

$$-\boldsymbol{v}_6^T\Big(\mathcal{L}\{\boldsymbol{X}_2\bar{\boldsymbol{A}}_i(\boldsymbol{x},\hat{\boldsymbol{x}}) - \boldsymbol{N}_i(\hat{\boldsymbol{x}})\boldsymbol{C}_j\} + \mathcal{L}\{\boldsymbol{X}_2\bar{\boldsymbol{A}}_j(\boldsymbol{x},\hat{\boldsymbol{x}}) - \boldsymbol{N}_j(\hat{\boldsymbol{x}})\boldsymbol{C}_i\}\Big)\boldsymbol{v}_6 \quad is \quad SOS \quad i < j \le r \tag{23}$$

where $\bar{\boldsymbol{A}}_i(\boldsymbol{x},\hat{\boldsymbol{x}})\boldsymbol{e} = \boldsymbol{A}_i(\boldsymbol{x})\boldsymbol{x} - \boldsymbol{A}_i(\hat{\boldsymbol{x}})\hat{\boldsymbol{x}}$. $\boldsymbol{v}_1$, $\boldsymbol{v}_2$, $\boldsymbol{v}_3$, $\boldsymbol{v}_4$, $\boldsymbol{v}_5$, $\boldsymbol{v}_6$ $\in \mathbb{R}^n$ denote vectors that are independent of $\boldsymbol{x}$, $\hat{\boldsymbol{x}}$ and $\boldsymbol{\zeta}$. From the solutions $\boldsymbol{X}_1$ and $\boldsymbol{M}_i(\hat{\boldsymbol{x}})$, we obtain polynomial feedback gains $\boldsymbol{F}_i(\hat{\boldsymbol{x}})$ as $\boldsymbol{F}_i(\hat{\boldsymbol{x}}) = \boldsymbol{M}_i(\hat{\boldsymbol{x}})\boldsymbol{X}_1^{-1}$. From the solutions $\boldsymbol{X}_2$ and $\boldsymbol{N}_i(\hat{\boldsymbol{x}})$, we obtain polynomial observer gains $\boldsymbol{L}_i(\hat{\boldsymbol{x}})$ as $\boldsymbol{L}_i(\hat{\boldsymbol{x}}) = \boldsymbol{X}_2^{-1}\boldsymbol{N}_i(\hat{\boldsymbol{x}})$ as well.

Proof: Consider the estimation error, $\boldsymbol{e} = \boldsymbol{x} - \hat{\boldsymbol{x}}$, by the observer. Then, the error system with respect to $\boldsymbol{e}$ can be represented as

$$\begin{aligned} \dot{\boldsymbol{e}} &= \sum_{i=1}^{r}\sum_{j=1}^{r} h_i(\boldsymbol{z})h_j(\boldsymbol{z})\{\boldsymbol{A}_i(\boldsymbol{x})\boldsymbol{x} - \boldsymbol{A}_i(\hat{\boldsymbol{x}})\hat{\boldsymbol{x}} - \boldsymbol{L}_i(\hat{\boldsymbol{x}})\boldsymbol{C}_j\boldsymbol{e}\} \\ &= \sum_{i=1}^{r}\sum_{j=1}^{r} h_i(\boldsymbol{z})h_j(\boldsymbol{z})\{\bar{\boldsymbol{A}}_i(\boldsymbol{x},\hat{\boldsymbol{x}}) - \boldsymbol{L}_i(\hat{\boldsymbol{x}})\boldsymbol{C}_j\}\boldsymbol{e}, \end{aligned}$$

where $\bar{\boldsymbol{A}}(\boldsymbol{x},\hat{\boldsymbol{x}})\boldsymbol{e} = \boldsymbol{A}(\boldsymbol{x})\boldsymbol{x} - \boldsymbol{A}(\hat{\boldsymbol{x}})\hat{\boldsymbol{x}}$. The augmented system with the augmented vector $\boldsymbol{x}_v = \begin{bmatrix}\hat{\boldsymbol{x}}^T & \boldsymbol{e}^T\end{bmatrix}^T$ is given as

$$\begin{aligned} \dot{\boldsymbol{x}}_v &= \sum_{i=1}^{r}\sum_{j=1}^{r} h_i(\boldsymbol{z})h_j(\boldsymbol{z}) \\ &\quad\times \begin{bmatrix} \boldsymbol{A}_i(\hat{\boldsymbol{x}}) - \boldsymbol{B}_i(\boldsymbol{\zeta})\boldsymbol{F}_j(\hat{\boldsymbol{x}}) & \boldsymbol{L}_i(\hat{\boldsymbol{x}})\boldsymbol{C}_j \\ \boldsymbol{0} & \bar{\boldsymbol{A}}_i(\boldsymbol{x},\hat{\boldsymbol{x}}) - \boldsymbol{L}_i(\hat{\boldsymbol{x}})\boldsymbol{C}_j \end{bmatrix}\boldsymbol{x}_v \\ &= \sum_{i=1}^{r} h_i^2(\boldsymbol{z})\boldsymbol{G}_{ii}(\boldsymbol{x},\boldsymbol{\zeta},\hat{\boldsymbol{x}})\boldsymbol{x}_v \\ &\quad + \sum_{i=1}^{r}\sum_{i<j}^{r} h_i(\boldsymbol{z})h_j(\boldsymbol{z})\left(\boldsymbol{G}_{ij}(\boldsymbol{x},\boldsymbol{\zeta},\hat{\boldsymbol{x}}) + \boldsymbol{G}_{ji}(\boldsymbol{x},\boldsymbol{\zeta},\hat{\boldsymbol{x}})\right)\boldsymbol{x}_v \end{aligned} \tag{24}$$

where

$$\boldsymbol{G}_{ij}(\boldsymbol{x},\boldsymbol{\zeta},\hat{\boldsymbol{x}}) = \begin{bmatrix} \boldsymbol{G}_{11_{ij}}(\boldsymbol{\zeta},\hat{\boldsymbol{x}}) & \boldsymbol{G}_{12_{ij}}(\hat{\boldsymbol{x}}) \\ \boldsymbol{0} & \boldsymbol{G}_{22_{ij}}(\boldsymbol{x},\hat{\boldsymbol{x}}) \end{bmatrix},$$
$$\boldsymbol{G}_{11_{ij}}(\boldsymbol{\zeta},\hat{\boldsymbol{x}}) = \boldsymbol{A}_i(\hat{\boldsymbol{x}}) - \boldsymbol{B}_i(\boldsymbol{\zeta})\boldsymbol{F}_j(\hat{\boldsymbol{x}}),$$
$$\boldsymbol{G}_{12_{ij}}(\hat{\boldsymbol{x}}) = \boldsymbol{L}_i(\hat{\boldsymbol{x}})\boldsymbol{C}_j,$$
$$\boldsymbol{G}_{22_{ij}}(\boldsymbol{x},\hat{\boldsymbol{x}}) = \bar{\boldsymbol{A}}_i(\boldsymbol{x},\hat{\boldsymbol{x}}) - \boldsymbol{L}_i(\hat{\boldsymbol{x}})\boldsymbol{C}_j.$$

Now, consider a candidate of Lyapunov function.

$$V(\boldsymbol{x}_v) = \boldsymbol{x}_v^T \tilde{\boldsymbol{X}} \boldsymbol{x}_v, \tag{25}$$

where

$$\tilde{\boldsymbol{X}} = \begin{bmatrix} \alpha \boldsymbol{X}_1^{-1} & \boldsymbol{0} \\ \boldsymbol{0} & \boldsymbol{X}_2 \end{bmatrix}, \tag{26}$$

α is a positive value, $\boldsymbol{X}_1^{-1} \in \mathbb{R}^{n\times n}$ and $\boldsymbol{X}_2 \in \mathbb{R}^{n\times n}$ are positive definite matrices. Note that $V(\boldsymbol{x}_v) > 0$ at $\boldsymbol{x}_v \neq \boldsymbol{0}$. It is clear from Lyapunov theory that the overall control system (24) is stable if it is proved that $\dot{V}(\boldsymbol{x}_v) < 0$ at $\boldsymbol{x}_v \neq \boldsymbol{0}$.

The time derivative of $V(\boldsymbol{x}_v)$ along the trajectory of the system is obtained as

$$\begin{aligned}\dot{V}(\boldsymbol{x}_v) =& \sum_{i=1}^{r}\sum_{j=1}^{r} h_i(\boldsymbol{z})h_j(\boldsymbol{z})\boldsymbol{x}_v^T \mathcal{L}\{\tilde{\boldsymbol{X}}\boldsymbol{G}_{ij}(\boldsymbol{x},\boldsymbol{\zeta},\hat{\boldsymbol{x}})\}\boldsymbol{x}_v \\ =& \sum_{i=1}^{r} h_i^2(\boldsymbol{z})\boldsymbol{x}_v^T \mathcal{L}\{\tilde{\boldsymbol{X}}\boldsymbol{G}_{ii}(\boldsymbol{x},\boldsymbol{\zeta},\hat{\boldsymbol{x}})\}\boldsymbol{x}_v \\ &+ \sum_{i=1}^{r}\sum_{i<j}^{r} h_i(\boldsymbol{z})h_j(\boldsymbol{z})\times \\ &\boldsymbol{x}_v^T \mathcal{L}\{\tilde{\boldsymbol{X}}\left(\boldsymbol{G}_{ij}(\boldsymbol{x},\boldsymbol{\zeta},\hat{\boldsymbol{x}}) + \boldsymbol{G}_{ji}(\boldsymbol{x},\boldsymbol{\zeta},\hat{\boldsymbol{x}})\right)\}\boldsymbol{x}_v.\end{aligned}$$

If the following conditions are satisfied, $\dot{V}(\boldsymbol{x}_v) < 0$ at $\boldsymbol{x}_v \neq \boldsymbol{0}$.

$$\mathcal{L}\{\tilde{\boldsymbol{X}}\boldsymbol{G}_{ii}(\boldsymbol{x},\boldsymbol{\zeta},\hat{\boldsymbol{x}})\} < \boldsymbol{0} \tag{27}$$
$$\mathcal{L}\{\tilde{\boldsymbol{X}}\left(\boldsymbol{G}_{ij}(\boldsymbol{x},\boldsymbol{\zeta},\hat{\boldsymbol{x}}) + \boldsymbol{G}_{ji}(\boldsymbol{x},\boldsymbol{\zeta},\hat{\boldsymbol{x}})\right)\} \leq \boldsymbol{0} \quad i < j \leq r \tag{28}$$

As well as in the proof of Theorem 1, (27) can be separately rewritten as

$$\mathcal{L}\{\boldsymbol{X}_1^{-1}(\boldsymbol{A}_i(\hat{\boldsymbol{x}}) - \boldsymbol{B}_i(\boldsymbol{\zeta})\boldsymbol{F}_i(\hat{\boldsymbol{x}}))\} < \boldsymbol{0}, \tag{29}$$
$$\mathcal{L}\{\boldsymbol{X}_2(\bar{\boldsymbol{A}}_i(\boldsymbol{x},\hat{\boldsymbol{x}}) - \boldsymbol{L}_i(\hat{\boldsymbol{x}})\boldsymbol{C}_i)\} < \boldsymbol{0}. \tag{30}$$

Multiplying both side of (29) by $\boldsymbol{X}_1$ and defining a new variable $\boldsymbol{M}_i(\hat{\boldsymbol{x}}) = \boldsymbol{F}_i(\hat{\boldsymbol{x}})\boldsymbol{X}_1$, we obtain the following conditions.

$$\mathcal{L}\{\boldsymbol{A}_i(\hat{\boldsymbol{x}})\boldsymbol{X}_1 - \boldsymbol{B}_i(\boldsymbol{\zeta})\boldsymbol{M}_i(\hat{\boldsymbol{x}})\} < \boldsymbol{0} \tag{31}$$

Defining another new variable $\boldsymbol{N}_i(\hat{\boldsymbol{x}}) = \boldsymbol{X}_2\boldsymbol{L}_i(\hat{\boldsymbol{x}})$, the inequality (30) can be described as

$$\mathcal{L}\{\boldsymbol{X}_2\bar{\boldsymbol{A}}_i(\boldsymbol{x},\hat{\boldsymbol{x}}) - \boldsymbol{N}_i(\hat{\boldsymbol{x}})\boldsymbol{C}_i\} < \boldsymbol{0}. \tag{32}$$

In the same way as above, (28) can be also represented as

$$\begin{aligned}&\mathcal{L}\{\boldsymbol{A}_i(\hat{\boldsymbol{x}})\boldsymbol{X}_1 - \boldsymbol{B}_i(\boldsymbol{\zeta})\boldsymbol{M}_j(\hat{\boldsymbol{x}})\} \\ &+ \mathcal{L}\{\boldsymbol{A}_j(\hat{\boldsymbol{x}})\boldsymbol{X}_1 - \boldsymbol{B}_j(\boldsymbol{\zeta})\boldsymbol{M}_i(\hat{\boldsymbol{x}})\} \leq \boldsymbol{0},\end{aligned} \tag{33}$$

$$\begin{aligned}&\mathcal{L}\{\boldsymbol{X}_2\bar{\boldsymbol{A}}_i(\boldsymbol{x},\hat{\boldsymbol{x}}) - \boldsymbol{N}_i(\hat{\boldsymbol{x}})\boldsymbol{C}_j\} \\ &+ \mathcal{L}\{\boldsymbol{X}_2\bar{\boldsymbol{A}}_j(\boldsymbol{x},\hat{\boldsymbol{x}}) - \boldsymbol{N}_j(\hat{\boldsymbol{x}})\boldsymbol{C}_i\} \leq \boldsymbol{0}\end{aligned} \tag{34}$$

for $i < j \leq r$. It is clear from the inequality conditions (31)-(34) that $\dot{V}(\boldsymbol{x}_v) < 0$ at $\boldsymbol{x}_v \neq \boldsymbol{0}$ if the SOS conditions (18)$\sim$(23) hold.

■

Remark 6. *As we can see, Theorems 1 and 2 show that the so-called separation principle is realized, i.e., that the fuzzy polynomial controller and observer can be separately designed without lack of guaranteeing the stability of the overall control system in addition to converging state estimation error (via the observer) to zero. This is a very important point in our fuzzy polynomial controller and observer design. In particular, in Theorem 2, a key feature of realizing the separation design is that, by introducing the transformation $\bar{\boldsymbol{A}}(\boldsymbol{x},\hat{\boldsymbol{x}})\boldsymbol{e} = \boldsymbol{A}(\boldsymbol{x})\boldsymbol{x} - \boldsymbol{A}(\hat{\boldsymbol{x}})\hat{\boldsymbol{x}}$, the (2,1) element in $\boldsymbol{G}_{ij}(\boldsymbol{x},\boldsymbol{\zeta},\hat{\boldsymbol{x}})$ becomes zero element (matrix). This transformation idea leads to the successful separation design.*

IV. Design Example

Consider the following nonlinear system, where x_1 is measurable and $y = x_1$.

$$\begin{cases} \dot{x}_1 = \sin x_1 - 0.3x_2 + (x_1^2 + 1)u \\ \dot{x}_2 = -1.5x_1 - 2x_2 - x_2^3 \end{cases} \tag{35}$$

Fig. 1 shows system behaviors without inputs. It can be seen from Fig. 1 that the system is unstable.

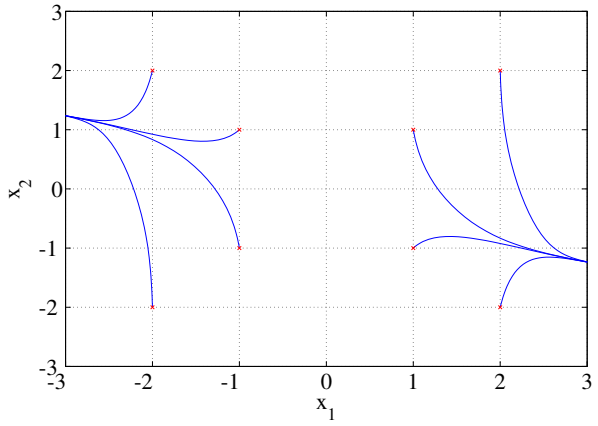

Fig. 1. System behaviors without inputs.

This system has polynomial terms $(x_1^2 + 1)u$ and x_2^3. To obtain a T-S fuzzy model, we need to assume the ranges of x_1 and x_2. Thus, the T-S fuzzy model is a local model. This means that the T-S fuzzy model stabilization and state-estimation convergence are not guaranteed for outside the ranges. The polynomial fuzzy model constructed in this example can exactly and globally represent the dynamics of the original system. Even if a local or semi-global T-S fuzzy model is permitted to use in practical sense, the premise variable vector $\boldsymbol{z}$ contain x_2 to be estimated. Hence, the previous LMI conditions mentioned above can not be applied to the nonlinear system. On the other hand, the premise variable vector $\boldsymbol{z}$ in

polynomial fuzzy model does not contain x_2 and x_2 appears in polynomial system matrices $\boldsymbol{A}_i$ in consequent parts of polynomial fuzzy models. Since the Class II design permits to have unmeasurable states in $\boldsymbol{A}_i$ matrices, it is possible to design a polynomial fuzzy observer in this example.

The dynamics of the nonlinear system can be exactly represented as the polynomial fuzzy system (15), where $r = 2$, $\boldsymbol{z} = \boldsymbol{\zeta} = y$,

$$
\begin{aligned}
&\boldsymbol{A}_1(\boldsymbol{x}) = \begin{bmatrix} 1 & -0.3 \\ -1.5 & -2 - x_2^2 \end{bmatrix}, \\
&\boldsymbol{A}_2(\boldsymbol{x}) = \begin{bmatrix} -0.2172 & -0.3 \\ -1.5 & -2 - x_2^2 \end{bmatrix}, \\
&\boldsymbol{B}_1(\boldsymbol{\zeta}) = \boldsymbol{B}_2(\boldsymbol{\zeta}) = \begin{bmatrix} y^2 + 1 \\ 0 \end{bmatrix}, \\
&\boldsymbol{C}_1 = \boldsymbol{C}_2 = \begin{bmatrix} 1 & 0 \end{bmatrix}, \\
&h_1(\boldsymbol{z}) = \frac{\sin y + 0.2172y}{1.2172y}, \\
&h_2(\boldsymbol{z}) = \frac{y - \sin y}{1.2172y}.
\end{aligned}
$$

In this example, note that

$$
\begin{aligned}
\bar{\boldsymbol{A}}_1(\boldsymbol{x}, \hat{\boldsymbol{x}})\boldsymbol{e} &= \boldsymbol{A}_1(\boldsymbol{x})\boldsymbol{x} - \boldsymbol{A}_1(\hat{\boldsymbol{x}})\hat{\boldsymbol{x}} \\
&= \begin{bmatrix} 1 & -0.3 \\ -1.5 & -2 - x_2^2 - x_2\hat{x}_2 - \hat{x}_2^2 \end{bmatrix} \begin{bmatrix} e_1 \\ e_2 \end{bmatrix},
\end{aligned}
$$

$$
\begin{aligned}
\bar{\boldsymbol{A}}_2(\boldsymbol{x}, \hat{\boldsymbol{x}})\boldsymbol{e} &= \boldsymbol{A}_2(\boldsymbol{x})\boldsymbol{x} - \boldsymbol{A}_2(\hat{\boldsymbol{x}})\hat{\boldsymbol{x}} \\
&= \begin{bmatrix} -0.2172 & -0.3 \\ -1.5 & -2 - x_2^2 - x_2\hat{x}_2 - \hat{x}_2^2 \end{bmatrix} \begin{bmatrix} e_1 \\ e_2 \end{bmatrix}.
\end{aligned}
$$

By solving the SOS conditions in Theorem 2, we have $\boldsymbol{X}_i$ $\boldsymbol{M}_i(\hat{\boldsymbol{x}})$ and $\boldsymbol{N}_i(\hat{\boldsymbol{x}})$, where the orders of $\boldsymbol{M}_i(\hat{\boldsymbol{x}})$ and $\boldsymbol{N}_i(\hat{\boldsymbol{x}})$ are two.

$$
\begin{aligned}
&\boldsymbol{X}_1 = \begin{bmatrix} 0.41696 & 0.34597e^{-6} \\ 0.34597e^{-6} & 0.50738 \end{bmatrix} \\
&\boldsymbol{X}_2 = \begin{bmatrix} 0.95521 & 0.11778e^{-5} \\ 0.11778e^{-5} & 0.61866 \end{bmatrix} \\
&\boldsymbol{M}_1(\boldsymbol{\zeta}) = \begin{bmatrix} 0.90492 \\ 0.25275e^{-5} - 0.19247e^{-11}\hat{x}_2^2 \end{bmatrix} \\
&\boldsymbol{M}_2(\boldsymbol{\zeta}) = \begin{bmatrix} 0.57747 \\ 0.22252e^{-5} - 0.19251e^{-11}\hat{x}_2^2 \end{bmatrix} \\
&\boldsymbol{N}_1(\boldsymbol{\zeta}) = \begin{bmatrix} 1.6776 \\ -0.90461 - 0.32618e^{-5}\hat{x}_2^2 \end{bmatrix} \\
&\boldsymbol{N}_2(\boldsymbol{\zeta}) = \begin{bmatrix} 0.61447 \\ -0.87404 - 0.32619e^{-5}\hat{x}_2^2 \end{bmatrix}
\end{aligned}
$$

From the solutions $\boldsymbol{X}_i$ $\boldsymbol{M}_i(\hat{\boldsymbol{x}})$ and $\boldsymbol{N}_i(\hat{\boldsymbol{x}})$, we obtain the following polynomial feedback and observer gains,

$$
\begin{aligned}
&\boldsymbol{F}_1(\hat{\boldsymbol{x}}) = \begin{bmatrix} 2.17028 + 0.31476e^{-17}\hat{x}_2^2 \\ 0.35016e^{-5} - 0.37934e^{-11}\hat{x}_2^2 \end{bmatrix} \\
&\boldsymbol{F}_2(\hat{\boldsymbol{x}}) = \begin{bmatrix} 1.38495 + 0.31482e^{-17}\hat{x}_2^2 \\ 0.34413e^{-5} - 0.37942e^{-11}\hat{x}_2^2 \end{bmatrix} \\
&\boldsymbol{L}_1(\boldsymbol{y}, \hat{\boldsymbol{x}}) = \begin{bmatrix} 1.75626 + 0.650097e^{-11}\hat{x}_2^2 \\ -1.46221 - 0.52724e^{-5}\hat{x}_2^2 \end{bmatrix} \\
&\boldsymbol{L}_2(\boldsymbol{y}, \hat{\boldsymbol{x}}) = \begin{bmatrix} 0.64328 + 0.65012e^{-11}\hat{x}_2^2 \\ -1.41280 - 0.52725e^{-5}\hat{x}_2^2 \end{bmatrix}
\end{aligned}
$$

Fig. 2 shows the control and estimation result by the designed polynomial fuzzy controller and observer, where the initial states are $\boldsymbol{x}(0) = [1\ \ 1]$ and $\hat{\boldsymbol{x}}(0) = [0\ \ 0]$. Fig. 3 shows control trajectories for same initial states as in Fig. 1. It can be seen from the figures that the designed controller stabilizes the nonlinear system and the estimation error via the polynomial fuzzy observer tends to zero.

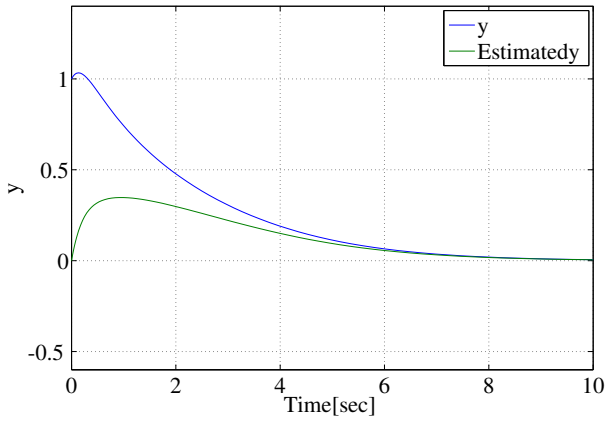

Fig. 2. Control and estimation result.

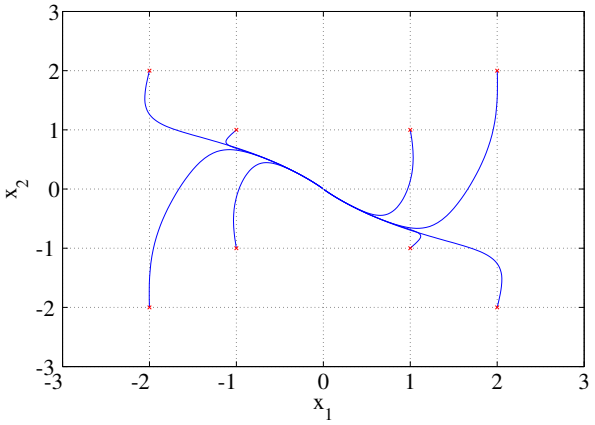

Fig. 3. Control trajectories for same initial states as in Fig. 1.

Remark 7. *Since $\boldsymbol{A}_1(\boldsymbol{x})$ and $\boldsymbol{A}_2(\boldsymbol{x})$ have unmeasurable x_2 in this design example, the Class I SOS-based observer design (Theorem 1) can not be applied to this design example. The previous LMI conditions mentioned above can not be also applied to the nonlinear system. On the other hand, since the Class II design (Theorem 2) permits to have unmeasurable states in $\boldsymbol{A}_i$ matrices, it is possible to design a polynomial fuzzy observer in this example.*

V. Conclusions

This paper has presented a sum of squares (SOS) approach to polynomial fuzzy controllers and observers for a wider class of polynomial fuzzy systems. To illustrate the validity and applicability of the proposed approach, a design example has been provided. The example has demonstrated advantages of the SOS-based approaches for the existing LMI approaches to T-S fuzzy observer designs.

Our next subjects are to derive SOS observer design conditions even for Class III [28] and to apply our observer designs to helicopter control [11].

Acknowledgment

The authors would like to thank Mr. M. Wada, UEC, for his contribution of this research.

References

[1] K. Tanaka and M. Sugeno, "Stability Analysis and Design of Fuzzy Control Systems", FUZZY SETS AND SYSTEMS 45, no. 2, pp. 135-156, 1992.

[2] K. Tanaka and H. O. Wang: Fuzzy Control Systems Design and Analysis: A Linear Matrix Inequality Approach, JOHN WILEY & SONS, INC, 2001

[3] H. O. Wang, et al., An Analytical Framework of Fuzzy Modeling and Control of Nonlinear Systems, 1995 American Control Conference, Seattle, Vol.3, pp.2272 - 2276 (1995).

[4] H. O. Wang, et al., An Approach to Fuzzy Control of Nonlinear Systems, IEEE Transactions on Fuzzy Systems, Vol.4, No.1, pp.14-23 (1996).

[5] R. Sepulcher, M. Jankovic and P. Kokotovic: Constructive Nonlinear Control, Springer, 1997

[6] K. Tanaka, H. Yoshida, H. Ohtake and H. O. Wang "A Sum of Squares Approach to Stability Analysis of Polynomial Fuzzy Systems", 2007 American Control Conference, New York, July, 2007, pp.4071-4076.

[7] K. Tanaka, H. Yoshida, H. Ohtake and H. O. Wang, " Stabilization of Polynomial Fuzzy Systems via a Sum of Squares Approach", 2007 IEEE International Symposium on Intelligent Control, pp.160-165, Singapore, October 2007.

[8] K. Tanaka, K. Yamauchi, H. Ohtake and H. O. Wang, Guaranteed Cost Control of Polynomial Fuzzy Systems via a Sum of Squares Approach, 2007 IEEE International Conference on Decision and Control, pp. 5954-5959, New Orleans, Dec. (2007)

[9] K. Tanaka, H. Yoshida, H. Ohtake and H. O. Wang, A Sum of Squares Approach to Modeling and Control of Nonlinear Dynamical Systems with Polynomial Fuzzy Systems, IEEE Transactions on Fuzzy Systems, Vol.17, No.4, pp.911-922, August 2009.

[10] K. Tanaka, H. Ohtake and H. O. Wang, Guaranteed Cost Control of Polynomial Fuzzy Systems via a Sum of Squares Approach, IEEE Transactions on Systems, Man and Cybernetics Part B, Vol.39, No.2, pp.561-567 April, 2009.

[11] K. Tanaka, T. Komatsu, H. Ohtake and H. O. Wang, Micro Helicopter Control:LMI Approach vs SOS Approach, 2008 IEEE International Conference on Fuzzy Systems, pp. 347-353, Hong Kong, June (2008)

[12] G. Feng, "A Survey on Analysis and Design of Model-Based Fuzzy Control Systems", IEEE Trans. on Fuzzy Systems, Vol.14, no.5, pp.676-697, Oct. 2006.

[13] K. Tanaka, T. Ikeda, H. O. Wang, "Fuzzy Regulators and Fuzzy Observers: Relaxed Stability Conditions and LMI-Based Designs", IEEE Transactions on fuzzy systems, VOL. 6, NO. 2, pp.250-265, 1998

[14] S. Hong and R. Langari, "Synthesis of an LMI-based Fuzzy Control System with guaranteed Optimal H^∞ Performance", *Proc. of FUZZ-IEEE'98*, Anchorage, AK, May, 1998, pp. 422-427.

[15] M. Sugeno, "On Stability of Fuzzy Systems Expressed by Fuzzy Rules with Singleton Consequents," *IEEE Transactions on Fuzzy Systems*, Vol. 7, No. 2, pp. 201-224 April, 1999.

[16] R. -J. Wang, W. -W. Lin and W. -J. Wang, Stabilizability of linear quadratic state feedback for uncertain fuzzy time-delay systems, IEEE Transactions on Systems, Man and Cybernetics, Part B, Vol. 34, No.2, pp.1288-1292 April 2004

[17] W. -J. Wang and C, -H. Sun, A relaxed stability criterion for T-S fuzzy discrete systems, IEEE Transactions on Systems, Man and Cybernetics, Part B, Vol. 34, No.5, pp.2155-2158 Oct. 2004

[18] S. -S. Chen, Y. -C. Chang, S. -F. Su, S. -L. Chung and T. -T. Lee, Robust static output-feedback stabilization for nonlinear discrete-time systems with time delay via fuzzy control approach, IEEE Transactions on Fuzzy Systems, Vol. 13, No.2, pp.263-272 April 2005

[19] A. Sala, C. Arino, Relaxed Stability and Performance Conditions for Takagi-Sugeno Fuzzy Systems With Knowledge on Membership Function Overlap, IEEE Transactions on Systems, Man, and Cybernetics, Part B, Vol.37, No.3, pp.727-732, June 2007.

[20] T. M. Guerra, A. Kruszewski and M. Bernal, Control Law Proposition for the Stabilization of Discrete Takagi-Sugeno Models, IEEE Transactions on Fuzzy Systems, Vol.17, No.3, pp.724-731, June 2009.

[21] V. F. Montagner, R. C. L. F. Oliveira and P. L. D. Peres, Convergent LMI Relaxations for Quadratic Stabilizability and H^∞ Control of Takagi-Sugeno Fuzzy Systems, IEEE Transactions on Fuzzy Systems, Vol.17, No.4, pp.863-873, August 2009.

[22] K. Tanaka, H. Ohtake and H. O. Wang: A Descriptor System Approach to Fuzzy Control System Design via Fuzzy Lyapunov Functions, IEEE Transactions on Fuzzy Systems, Vol.15, No. 3, pp.333 - 341, June 2007.

[23] H.-N Wu and H.-X. Li: New Approach to Delay-Dependent Stability Analysis and Stabilization for Continuous-Time Fuzzy Systems With Time-Varying Delay IEEE Transactions on Fuzzy Systems, Vol.e 15, No. 3, pp.482 - 493 June 2007

[24] J. -C. Lo and M. -L. Lin: Existence of Similarity Transformation Converting BMIs to LMIs, IEEE Transactions on Fuzzy Systems, Vol. 15, No.5, pp.840 - 851, Oct. 2007.

[25] K. Tanaka, H. Ohtake, M. Wada, H. O. Wang, Y.-J. Chen, Polynomial Fuzzy Observer Design: A Sum of Squares Approach, 48th IEEE conference on Decision and Control, pp. 7771 - 7776, Shanghai, China, December 16-18, 2009.

[26] S. Prajna, A. Papachristodoulou, P. Seiler and P. A. Parrilo: SOSTOOLS:Sum of Squares Optimization Toolbox for MATLAB, Version 2.00, 2004.

[27] T. Takagi and M. Sugeno, "Fuzzy Identification of Systems and Its Applications to Modeling and Control", IEEE Trans. on SMC 15, no. 1, pp.116-132, 1985.

[28] K. Tanaka, H. Ohtake and H. O. Wang, An SOS-based Observer Design for Polynomial Fuzzy Systems, 2011 IEEE Conference on Decision and Control, Orlando, FL (Submitted).

[29] J. F. Sturm: "Using SeDUMi 1.02, a MATLAB toolbox for optimization over symmetric cones", Optimization Methods and Software, vol. 11 & 12, pp.625-653, August 1999.

[30] K. C. Toh, R. H. Tutuncu and M. J. Todd, "On the implement of SDPT3 (version 3.1) - A MATLAB software package for semidefinite-quadratic-linear programming", 2004 IEEE International Conference on Computer Aided Control System Designs, pp.290-296, Sept. 2004.

[31] A. Papachristodoulou and S. Prajna, "On the construction of Lyapunov functions using the sum of squares decomposition", In Proc. 41th IEEE Conf. on Decision and Control, pp.3482-3487, Las Vega, Dec. 2002.

2011 IEEE International Conference on Fuzzy Systems
June 27-30, 2011, Taipei, Taiwan

A SVD Approach to H_∞ Decentralized Static Output Feedback Fuzzy Control Design for Nonlinear Interconnected Systems

Chung-Shi Tseng
Department of Electrical Engineering
Ming Hsin University of Science and Technology
Hsin-Feng, 30401, Taiwan
Email: cstseng@must.edu.tw

Yung-Yue Chen
Department of Electrical Engineering
National Yunlin University of Science and Technology
Douliou 64002, Taiwan
Email: chenyuyu@yuntech.edu.tw

***Abstract*—This study introduces H_∞ decentralized static output feedback fuzzy control design for nonlinear interconnected systems via T-S fuzzy models. In general, due to the interactions among subsystems, it is difficult to design an H_∞ decentralized output feedback controller for nonlinear interconnected systems. A singular value decomposition (SVD) method is proposed in this study to solve the H_∞ decentralized static output feedback fuzzy control problem. By the proposed SVD method, the problem of H_∞ decentralized static output feedback fuzzy control design for nonlinear interconnected systems is characterized in terms of solving an eigenvalue problem (EVP). This EVP can be easily solved by using a LMI-based optimization method. Finally, simulation example is given to illustrate the design procedure and robust performance of the proposed methods.**

***Keywords*—H_∞; decentralized; static output feedback; SVD; LMI; EVP.**

I. INTRODUCTION

Due to the physical configuration and high dimensionality of interconnected systems, a centralized control is neither economically feasible nor even necessary. Therefore, a decentralized control scheme is preferred in control design of the large-scale interconnected systems. In other words, the decentralized control scheme attempts to avoid difficulties in complexity of system design. In the past three decades, there are many applications of linear decentralized methodologies to spacecraft dynamics, power systems, industrial processes, transportation networks and others [1], [15]. On the other hand, there are few studies concerning with the stabilization control design for the interconnected nonlinear systems because of the complexity among them [24], [13], [14]. Due to the effects of nonlinear interconnection among subsystems, there is still no efficient way to deal with the decentralized control problem of nonlinear interconnected systems, especially for the output feedback control case.

In the past few years, there has been rapidly growing interest in decentralized fuzzy control for the nonlinear interconnected systems using T-S fuzzy model. However, most of them are state feedback cases [10], [9], [21], [22]. On the other hand, there are few studies concerned with the systematic synthesis of output feedback control design for nonlinear interconnected systems using the T-S fuzzy models [18], [19]. The output feedback control design for nonlinear systems using the T-S fuzzy models is more general and complex than the state feedback one. When dealing with output feedback control design, either a dynamic output feedback (fuzzy observer-based) case or a static output feedback case is considered. For the dynamic output feedback case, a fuzzy observer is also involved as well as the fuzzy controller [20], [8]. In other words, for the fuzzy observer-based output feedback control design, a fuzzy observer should also be involved to estimate the system states using the output information and a fuzzy controller is constructed using the estimated states. For the static output feedback case [12], [3], [4], [5], [11], [6], [23], the fuzzy controller depends on the system outputs only without the complex structures of the fuzzy observer. In general, the control design of static output feedback is more straightforward but less flexible than that of dynamic output feedback and the structure of static output feedback controller is much simpler than that of dynamic output feedback controller. This study introduces H_∞ decentralized static output feedback fuzzy control design for nonlinear interconnected systems via T-S fuzzy models. A SVD method is proposed in this study to solve the H_∞ decentralized static output feedback fuzzy control design for nonlinear interconnected systems, which can be characterized in terms of solving an EVP for each subsystem. The EVP can be easily solved by using a genetic algorithm and a LMI-based optimization method. The SVD approach provides different aspect from the linear transformation approach [12], [11] and moreover the proposed SVD method is very simple and easy to follow.

The main contributions of this paper are stated as follows: (1) The H_∞ output feedback control problem for nonlinear interconnected systems is studied via a decentralized static output feedback fuzzy controller. (2) A SVD method is proposed to solve H_∞ decentralized static output feedback fuzzy control problem which can be characterized in terms of solving an EVP for each subsystem. By the proposed SVD method, the decentralized static fuzzy control gains for each subsystem can be obtained efficiently.

The paper is organized as follows. The system description is presented in Section II. In section III, the H_∞ decentralized static feedback fuzzy control design for the nonlinear inter-

This work was supported by National Science Council under contract NSC 99-2221-E-159-024.

978-1-4244-7316-8/11/$26.00 ©2011 IEEE

connected systems is introduced. In Section IV, simulation example is provided to demonstrate the design procedures. Finally, concluding remarks are made in Section V. In what follows, $M_{[m\times n]}$ denotes a $m\times n$ matrix and $I_{[n\times n]}$ and $0_{[m\times n]}$ denote a $n \times n$ identity matrix and a $m \times n$ zero matrix, respectively. If dimensions of matrices are not particularly defined, they are of appropriate and clear dimensions.

II. SYSTEM DESCRIPTION

A T-S fuzzy dynamic model [16] has been proposed to represent locally linear input/output relations for nonlinear systems. This fuzzy dynamic model is described by fuzzy If-Then rules and will be employed here to deal with the control design problem of a nonlinear interconnected system S which is composed of N subsystems S_i $(i = 1, ..., N)$. The k^{th} rule of the fuzzy model of subsystem S_i is proposed as the following form [10], [9], [21], [22], [18], [19]:

Plant Rule k :

$$\begin{array}{ll} \textbf{If} & z_{i1}(t) \text{ is } F_{i1}^k \ldots \text{and } z_{iq_i}(t) \text{ is } F_{iq_i}^k \\ & \dot{x}_i(t) = A_{ik}x_i(t) + B_{1ik}u_i(t) \\ \textbf{Then} & \quad + \sum_{j=1, j\neq i}^{N} [A_{ijk}x_j(t)] + B_{2ik}w_i(t) \\ & y_i(t) = C_i x_i(t) \text{ for } k = 1, \ldots, L_i \end{array} \tag{1}$$

where $x_i(t) = [\ x_{i1}(t),\ \cdots,\ x_{in_i}(t)\ ]^T \in R^{n_i}$ denotes the vector of state, $u_i(t) = [\ u_{i1}(t),\ \cdots,\ u_{im_i}(t)\ ]^T \in R^{m_i}$ denotes the vector of control input, $w_i(t)$ denotes the vector of the external disturbance, $y_i(t) = [\ y_{i1}(t),\ \cdots,\ y_{ip_i}(t)\ ]^T \in R^{p_i}$ denotes the vector of output, $F_{i1}^k, ..., F_{iq_i}^k$ are the fuzzy sets, L_i is the number of If-Then rules of the subsystem S_i, the matrices A_{ik}, B_{1ik}, A_{ijk}, B_{2ik}, and C_i are of appropriate dimensions, and $z_{i1}(t), \ldots, z_{iq_i}(t)$ are the premise variables.

Remark 1: For different subsystem, the number of rules may be different. In other words, L_i can be different for different subsystem. ■

Remark 2: Since in this study the static output feedback control is considered, the premise variables $z_{i1}(t), \ldots, z_{iq_i}(t) \in y_i(t)$ with $q_i \leq p_i$ for subsystem S_i are assumed. ■

Remark 3: In this study, $C_i \in R^{p_i\times n_i}$ $(i = 1, ..., N)$ with full row rank are assumed, i.e., $rank(C_i) = p_i$. Hence, a singular value decomposition (SVD) of the output matrix C_i for the subsystem S_i can be defined as

$$C_i = U_i S_i V_i^T = U_i S_i V_i^{-1} \tag{2}$$

where

$$\begin{array}{rcl} U_i & \in & R^{p_i\times p_i} \\ S_i & = & [\ \Sigma_{i[p_i\times p_i]} \quad 0_{[p_i\times(n_i-p_i)]}\ ] \in R^{p_i\times n_i} \\ V_i & \in & R^{n_i\times n_i} \end{array}$$

and

$$\Sigma_i = diag\{\ \bar{\sigma}_{i1},\ \ \bar{\sigma}_{i2},\ \ \cdots,\ \ \bar{\sigma}_{ip_i}\ \} \in R^{p_i\times p_i}$$

with singular values $\bar{\sigma}_{i1} \geq \bar{\sigma}_{i2} \geq \cdots \geq \bar{\sigma}_{ip_i} > 0$. Note that, since U_i and V_i are orthogonal matrices, $U_i^T = U_i^{-1}$, $V_i^T = V_i^{-1}$, and then $V_i^T V_i = V_i V_i^T = V_i^{-1} V_i = V_i V_i^{-1} = I_{[n_i\times n_i]}$. ■

The overall fuzzy model of subsystem S_i can be rearranged as the following form:

$$\begin{array}{rcl} \dot{x}_i(t) & = & \sum_{k=1}^{L_i} h_k(z_i(t))\{A_{ik}x_i(t) + B_{1ik}u_i(t) \\ & & + \sum_{j=1, j\neq i}^{N} [A_{ijk}x_j(t)] + B_{2ik}w_i(t)\} \\ y_i(t) & = & \sum_{k=1}^{L_i} h_k(z_i(t))[C_i x_i(t)] \end{array} \tag{3}$$

where $\mu_k(z_i(t)) = \prod_{q=1}^{q_i} F_{iq}^k(z_{iq}(t))$, $h_k(z_i(t)) = \frac{\mu_k(z_i(t))}{\sum_{k=1}^{L}\mu_k(z_i(t))}$, $z_i(t) = [z_{i1}(t), \ldots, z_{iq_i}(t)]$, and $F_{iq}^k(z_{iq}(t))$ is the grade of membership of $z_{iq}(t)$ in F_{iq}^k $(q = 1, ..., q_i)$. It is assumed that $\mu_k(z_i(t)) \geq 0$ and $\sum_{k=1}^{L} \mu_k(z_i(t)) > 0$ for $k = 1, 2, \ldots, L_i$ for all t. Therefore, we get $h_k(z_i(t)) \geq 0$ for $k = 1, 2, \ldots, L_i$ and $\sum_{k=1}^{L_i} h_k(z_i(t)) = 1$.

The aim of this study is to propose a decentralized static output feedback fuzzy controller for nonlinear interconnected systems. Suppose the following decentralized static output feedback fuzzy controller is proposed to deal with the nonlinear interconnected subsystem S_i :

Control Rule s :

$$\begin{array}{ll} \textbf{If} & z_{i1}(t) \text{ is } F_{i1}^s \ldots \text{and } z_{iq_i}(t) \text{ is } F_{iq_i}^s \\ \textbf{Then} & u_i(t) = K_{is}y_i(t) \end{array} \tag{4}$$

for $s = 1, 2, \ldots, L_i$. The overall decentralized static output feedback fuzzy controller for the i^{th} subsystem is represented as follows:

$$\begin{array}{rcl} u_i(t) & = & \sum_{s=1}^{L_i} h_s(z_i(t))K_{is}y_i(t) \\ & = & \sum_{s=1}^{L_i} h_s(z_i(t))[K_{is}C_i x_i(t)] \end{array} \tag{5}$$

where K_{is} is the static fuzzy control gain for the s^{th} control rule and the i^{th} interconnected subsystem S_i.

After some manipulation, the i^{th} subsystem can be expressed as the following compact form:

$$\begin{array}{rcl} \dot{x}_i(t) & = & \sum_{j=1, j\neq i}^{N} \sum_{k=1}^{L_i} h_k(z_i(t)) \sum_{s=1}^{L_i} h_s(z_i(t))[\bar{A}_{iks}x_i(t) \\ & & + A_{ijk}x_j(t) + B_{2ik}w_i(t)] \end{array} \tag{6}$$

where

$$\begin{array}{rcl} \bar{A}_{iks} & = & A_{ik} + B_{1ik}K_{is}C_i \\ & = & A_{ik} + B_{1ik}K_{is}U_i S_i V_i^{-1}. \end{array}$$

III. H_∞ DECENTRALIZED STATIC OUTPUT FEEDBACK FUZZY CONTROL SYNTHESIS FOR NONLINEAR INTERCONNECTED SYSTEMS

The purpose of this study is to determine a decentralized static output feedback fuzzy controller in (5) for the system in (6) with the guaranteed H_∞ performance for all $w_i(t) \in L_2$. Let us consider the H_∞ performance for subsystem S_i as follows [18], [19], [12], [5], [11], [23]

$$\frac{\int_0^{t_f} x_i^T(t)\Psi_i x_i(t)dt}{\int_0^{t_f} w_i^T(t)w_i(t)dt} \le \rho_i^2 \tag{7}$$

or

$$\int_0^{t_f} x_i^T(t)\Psi_i x_i(t)dt \le \rho_i^2 \int_0^{t_f} w_i^T(t)w_i(t)dt \tag{8}$$

where Ψ_i is symmetric positive definite weighting matrix, t_f is terminal time of control, ρ_i is a prescribed attenuation level for the subsystem S_i. The physical meaning of (7) or (8) is that the effect of any $w_i(t) \in L_2$ on state $x_i(t)$ must be attenuated below a desired level ρ_i^2 from the viewpoint of energy, no matter what $w_i(t)$ is, i.e., the L_2 gain from $w_i(t)$ to $x_i(t)$ must be less than or equal to a prescribed value ρ_i^2. The H_∞ performance with a prescribed attenuation level is useful for a robust stabilization design without knowledge of $w_i(t)$. Thereafter, the attenuation level ρ_i^2 for each subsystem can also be minimized so that the H_∞ performance in (8) is reduced as small as possible.

Hence, if initial conditions are also considered, the H_∞ performance for subsystem S_i in (8) can be modified as follows

$$\begin{aligned} &\int_0^{t_f} x_i^T(t)\Psi_i x_i(t)dt \\ \le\ & x_i^T(0)\tilde{P}_i x_i(0) + \rho_i^2 \int_0^{t_f} w_i^T(t)w_i(t)dt \end{aligned} \tag{9}$$

where $\tilde{P}_i = (V_i^{-1})^T \bar{P}_i (V_i^{-1})$ is a symmetric positive definite weighting matrix.

For simplicity, the notation $\begin{bmatrix} M_{11} & * \\ M_{21} & M_{22} \end{bmatrix} \triangleq \begin{bmatrix} M_{11} & M_{21}^T \\ M_{21} & M_{22} \end{bmatrix}$ is adopted throughout this paper. Then, we get the following main result for the H_∞ decentralized static output feedback fuzzy control.

Theorem 1: In the nonlinear interconnected systems (6), if there exist symmetric positive matrices Q_i with

$$Q_i = \begin{bmatrix} Q_{i1[p_i \times p_i]} & 0 \\ 0 & Q_{i2[(n_i-p_i)\times(n_i-p_i)]} \end{bmatrix} \in R^{n_i \times n_i}$$

and matrices $\bar{Y}_{is}$ with

$$\bar{Y}_{is} = \begin{bmatrix} Y_{is[m_i \times p_i]} & 0_{[m_i \times (n_i-p_i]} \end{bmatrix} \in R^{m_i \times n_i}$$

such that the following LMIs

$$\begin{bmatrix} \{\bar{M}_1 + \bar{M}_1^T\} & * & * & * \\ \bar{A}_{ijk}^T & 0 & * & * \\ \bar{B}_{2ik}^T & 0 & -\rho_i^2 I & * \\ Q_i & 0 & 0 & -\Psi_{vi}^{-1} \end{bmatrix} \le 0 \tag{10}$$

hold for $i, j = 1, 2, ..., N$ $(j \ne i)$ and $k \le s = 1, 2, ..., L_i$ s.t. $h_k(\cdot) \cap h_s(\cdot) \ne \emptyset$, where

$$\begin{aligned} \bar{M}_1 &= \frac{(\bar{A}_{ik}Q_i + \bar{B}_{1ik}\bar{Y}_{is}) + (\bar{A}_{is}Q_i + \bar{B}_{1is}\bar{Y}_{ik})}{2} \\ \bar{A}_{ik} &= V_i^{-1}A_{ik}V_i \\ \bar{B}_{1ik} &= V_i^{-1}B_{1ik} \\ \bar{A}_{ijk} &= V_i^{-1}A_{ijk} \\ \bar{B}_{2ik} &= V_i^{-1}B_{2ik} \\ \Psi_{vi} &= V_i^T\Psi_i V_i = V_i^{-1}\Psi_i V_i, \end{aligned}$$

then (i) the H_∞ control performance in (9) is guaranteed for a prescribed ρ_i^2 in the case of $w_i(t) \ne 0$ and (ii) the interconnected systems S is stable in the sense of Lyapunov in the case of $w_i(t) = 0$. Moreover, the static fuzzy control gains can be obtained as

$$K_{is} = Y_{is}Q_{i1}^{-1}\Sigma_i^{-1}U_i^{-1}.$$

Proof: From (9), we obtain

$$\begin{aligned} &\int_0^{t_f} x_i^T(t)\Psi_i x_i(t)dt \\ =\ & \int_0^{t_f} \{x_i^T(t)\Psi_i x_i(t) + \frac{d}{dt}[x_i^T\tilde{P}_i x_i]\}dt \\ & + x_i^T(0)\tilde{P}_i x_i(0) - x_i^T(t_f)\tilde{P}_i x_i(t_f) \\ \le\ & x_i^T(0)\tilde{P}_i x_i(0) \\ & + \int_0^{t_f} \{x_i^T(t)\Psi_i x_i(t) + \frac{d}{dt}[x_i^T\tilde{P}_i x_i]\}dt \\ =\ & x_i^T(0)\tilde{P}_i x_i(0) \\ & + \sum_{j=1, j\ne i}^{N} \sum_{k=1}^{L_i} h_k^2(z_i(t)) \int_0^{t_f} \{x_i^T(t)\Psi_i x_i(t) \\ & + \eta^T \begin{bmatrix} \{\Psi_i & * & * \\ +\tilde{P}_i(\frac{\bar{A}_{ikk}+\bar{A}_{ikk}}{2}) & & \\ +(\frac{\bar{A}_{ikk}+\bar{A}_{ikk}}{2})^T\tilde{P}_i\} & & \\ A_{ijk}^T\tilde{P}_i & 0 & * \\ B_{2ik}^T\tilde{P}_i & 0 & -\rho_i^2 I \end{bmatrix} \eta \\ & \}dt + 2 \sum_{j=1, j\ne i}^{N} \sum_{k=1}^{L_i} h_k(z_i(t)) \sum_{k<s}^{L_i} h_s(z_i(t)) \\ & \times \int_0^{t_f} \{x_i^T(t)\Psi_i x_i(t) \\ & + \eta^T \begin{bmatrix} \{\Psi_i & * & * \\ +\tilde{P}_i(\frac{\bar{A}_{iks}+\bar{A}_{isk}}{2}) & & \\ +(\frac{\bar{A}_{iks}+\bar{A}_{isk}}{2})^T\tilde{P}_i\} & & \\ A_{ijk}^T\tilde{P}_i & -I & * \\ B_{2ik}^T\tilde{P}_i & 0 & -\rho_i^2 I \end{bmatrix} \eta \\ & \}dt + \rho_i^2 \int_0^{t_f} w_i^T(t)w_i(t)dt \end{aligned} \tag{11}$$

where $\eta^T = \left[\begin{array}{ccc} x_i^T(t), & x_j^T(t), & w_i^T(t) \end{array} \right]$. From (11), if

$$\left[\begin{array}{cc} \{\Psi_i + (V_i^{-1})^T \bar{P}_i (V_i^{-1})(\frac{\bar{A}_{iks}+\bar{A}_{isk}}{2}) & * \quad * \\ +(\frac{\bar{A}_{iks}+\bar{A}_{isk}}{2})^T (V_i^{-1})^T \bar{P}_i (V_i^{-1})\} & \\ A_{ijk}^T (V_i^{-1})^T \bar{P}_i (V_i^{-1}) & 0 \quad * \\ B_{2ik}^T (V_i^{-1})^T \bar{P}_i (V_i^{-1}) & 0 \quad -\rho_i^2 I \end{array} \right] \leq 0 \tag{12}$$

for $i, j = 1, 2, ..., N$ $(j \neq i)$ and $k \leq s = 1, 2, ..., L_i$, then we obtain

$$\begin{aligned} & \int_0^{t_f} x_i^T(t) \Psi_i x_i(t) dt \\ \leq \quad & x_i^T(0) \tilde{P}_i x_i(0) + \rho_i^2 \int_0^{t_f} w_i^T(t) w_i(t) dt. \end{aligned} \tag{13}$$

By pre-multiplying $\left[\begin{array}{ccc} V_i & 0 & 0 \\ 0 & I & 0 \\ 0 & 0 & I \end{array} \right]^T$ and post-multiplying $\left[\begin{array}{ccc} V_i & 0 & 0 \\ 0 & I & 0 \\ 0 & 0 & I \end{array} \right]$ to (12), we obtain

$$\left[\begin{array}{cc} \{V_i^T \Psi_i V_i & \\ +\bar{P}_i (V_i^{-1})(\frac{\bar{A}_{iks}+\bar{A}_{isk}}{2}) V_i & * \quad * \\ +V_i^T (\frac{\bar{A}_{iks}+\bar{A}_{isk}}{2})^T (V_i^{-1})^T \bar{P}_i\} & \\ A_{ijk}^T (V_i^{-1})^T \bar{P}_i & 0 \quad * \\ B_{2ik}^T (V_i^{-1})^T \bar{P}_i & 0 \quad -\rho_i^2 I \end{array} \right] \leq 0. \tag{14}$$

By the following definitions,

$$\begin{aligned} \bar{A}_{ik} &= V_i^{-1} A_{ik} V_i \\ \bar{B}_{1ik} &= V_i^{-1} B_{1ik} \\ \bar{A}_{ijk} &= V_i^{-1} A_{ijk} \\ \bar{B}_{2ik} &= V_i^{-1} B_{2ik} \\ \Psi_{vi} &= V_i^T(\Psi_i) V_i = V_i^{-1}(\Psi_i) V_i, \end{aligned}$$

(14) can be expressed as the following compact form

$$\left[\begin{array}{ccc} \Psi_{vi} + \bar{P}_i \bar{M}_2 + \bar{M}_2^T \bar{P}_i & * & * \\ \bar{A}_{ijk}^T \bar{P}_i & 0 & * \\ \bar{B}_{2ik}^T \bar{P}_i & 0 & -\rho_i^2 I \end{array} \right] \leq 0. \tag{15}$$

where $\bar{M}_2 = (\frac{(\bar{A}_{ik}+\bar{B}_{1ik}K_{is}U_iS_i)+(\bar{A}_{is}+\bar{B}_{1is}K_{ik}U_iS_i)}{2})$.

By pre-multiplying $\left[\begin{array}{ccc} Q_i & 0 & 0 \\ 0 & I & 0 \\ 0 & 0 & I \end{array} \right]$ and post-multiplying $\left[\begin{array}{ccc} Q_i & 0 & 0 \\ 0 & I & 0 \\ 0 & 0 & I \end{array} \right]$ to (15), we obtain

$$\left[\begin{array}{ccc} \{Q_i \Psi_{vi} Q_i + \bar{M}_3 + \bar{M}_3^T\} & * & * \\ \bar{A}_{ijk}^T & 0 & * \\ \bar{B}_{2ik}^T & 0 & -\rho_i^2 I \end{array} \right] \leq 0 \tag{16}$$

where
$\bar{M}_3 = (\frac{(\bar{A}_{ik}Q_i+\bar{B}_{1ik}K_{is}U_iS_iQ_i)+(\bar{A}_{is}Q_i+\bar{B}_{1is}K_{ik}U_iS_iQ_i)}{2})$ and

$$Q_i = \bar{P}_i^{-1} = Q_i^T > 0.$$

Note that, by the Schur complements [2], (16) is equivalent to

$$\left[\begin{array}{cccc} \{\bar{M}_3 + \bar{M}_3^T\} & * & * & * \\ \bar{A}_{ijk}^T & 0 & * & * \\ \bar{B}_{2ik}^T & 0 & -\rho_i^2 I & * \\ Q_i & 0 & 0 & -\Psi_{vi}^{-1} \end{array} \right] \leq 0. \tag{17}$$

For the simplicity of design, let

$$Q_i = \left[\begin{array}{cc} Q_{i1} & 0 \\ 0 & Q_{i2} \end{array} \right] \tag{18}$$

and then

$$\begin{aligned} & \bar{B}_{1ik} K_{is} U_i S_i Q_i \\ = \quad & \bar{B}_{1ik} K_{is} U_i \left[\begin{array}{cc} \Sigma_i & 0 \end{array} \right] \left[\begin{array}{cc} Q_{i1} & 0 \\ 0 & Q_{i2} \end{array} \right] \\ = \quad & \bar{B}_{1ik} \left[\begin{array}{cc} K_{is} U_i \Sigma_i Q_{i1} & 0 \end{array} \right] \\ = \quad & \bar{B}_{1ik} \left[\begin{array}{cc} Y_{is} & 0 \end{array} \right] = \bar{B}_{1ik} \bar{Y}_{is} \end{aligned} \tag{19}$$

where

$$\begin{aligned} Y_{is} &= K_{is} U_i \Sigma_i Q_{i1} \\ \bar{Y}_{is} &= \left[\begin{array}{cc} Y_{is} & 0 \end{array} \right]. \end{aligned}$$

By substituting (18) and (19) into (17), we obtain the following LMIs

$$\left[\begin{array}{cccc} \{\bar{M}_1 + \bar{M}_1^T\} & * & * & * \\ \bar{A}_{ijk}^T & 0 & * & * \\ \bar{B}_{2ik}^T & 0 & -\rho_i^2 I & * \\ Q_i & 0 & 0 & -\Psi_{vi}^{-1} \end{array} \right] \leq 0. \tag{20}$$

where $\bar{M}_1 = \frac{(\bar{A}_{ik}Q_i+\bar{B}_{1ik}\bar{Y}_{is})+(\bar{A}_{is}Q_i+\bar{B}_{1is}\bar{Y}_{ik})}{2}$.

If we can solve $Q_i = diag\{ \begin{array}{cc} Q_{i1}, & Q_{i2} \end{array} \}$ and $\bar{Y}_{is} = \left[\begin{array}{cc} Y_{is} & 0 \end{array} \right]$ from the above LMIs, the decentralized static fuzzy control gains can be obtained as

$$K_{is} = Y_{is} Q_{i1}^{-1} \Sigma_i^{-1} U_i^{-1}. \tag{21}$$

Therefore, the H_∞ control performance is achieved with a prescribed ρ_i^2 in the case of $w_i(t) \neq 0$. In the case of $w_i(t) = 0$, let us define a Lyapunov function for the subsystem S_i in (6) as

$$LF_i(t) = x_i^T(t) \tilde{P}_i x_i(t)$$

where $\tilde{P}_i = (V_i^{-1})^T \bar{P}_i (V_i^{-1})$ is a symmetric positive definite weighting matrix. Thus, the Lyapunov function for the overall interconnected system S can be defined as

$$LF(t) = \sum_{i=1}^{N} LF_i(t) = \sum_{i=1}^{N} \{x_i^T(t) \tilde{P}_i x_i(t)\}.$$

The time derivative of the Lyapunov function $LF(t)$ is

$$\begin{aligned}
&\frac{d}{dt}(LF(t)) \\
=\ & \sum_{i=1}^{N}\sum_{j=1,j\neq i}^{N}\sum_{k=1}^{L_i} h_k(z_i(t))\sum_{s=1}^{L_i} h_s(z_i(t)) \\
&\times\{[\bar{A}_{iks}x_i(t)+A_{ijk}x_j(t)]^T\tilde{P}_i x_i(t) \\
&+x_i^T(t)\tilde{P}_i[\bar{A}_{iks}x_i(t)+A_{ijk}x_j(t)]\} \\
=\ & \sum_{i=1}^{N}\sum_{j=1,j\neq i}^{N}\sum_{k=1}^{L} h_k(z_i(t))\sum_{s=1}^{L} h_s(z_i(t)) \\
&\times\{\bar{\eta}^T\begin{bmatrix}\tilde{P}_i\bar{A}_{iks}+\bar{A}_{iks}^T\tilde{P}_i & * \\ A_{ijk}^T\tilde{P}_i & 0\end{bmatrix}\bar{\eta}\} \\
=\ & \sum_{i=1}^{N}\sum_{j=1,j\neq i}^{N}\sum_{k=1}^{L_i} h_k^2(z_i(t)) \\
&\times\{\bar{\eta}^T\begin{bmatrix}\{\tilde{P}_i(\frac{\bar{A}_{ikk}+\bar{A}_{ikk}}{2}) & * \\ +(\frac{\bar{A}_{ikk}+\bar{A}_{ikk}}{2})^T\tilde{P}_i\} & \\ A_{ijk}^T\tilde{P}_i & 0\end{bmatrix}\bar{\eta}\} \\
&+2\sum_{i=1}^{N}\sum_{j=1,j\neq i}^{N}\sum_{k=1}^{L_i} h_k(z_i(t))\sum_{k<s}^{L_i} h_s(z_i(t)) \\
&\times\{\bar{\eta}^T\begin{bmatrix}\{\tilde{P}_i(\frac{\bar{A}_{iks}+\bar{A}_{isk}}{2}) & * \\ +(\frac{\bar{A}_{iks}+\bar{A}_{isk}}{2})^T\tilde{P}_i\} & \\ A_{ijk}^T\tilde{P}_i & 0\end{bmatrix}\bar{\eta}\} \qquad (22)
\end{aligned}$$

where $\bar{\eta}^T = [\ x_i^T(t),\quad x_j^T(t)\ ]$. From (22), if

$$\begin{bmatrix}\tilde{P}_i(\frac{\bar{A}_{iks}+\bar{A}_{isk}}{2})+(\frac{\bar{A}_{iks}+\bar{A}_{isk}}{2})^T\tilde{P}_i & * \\ A_{ijk}^T\tilde{P}_i & 0\end{bmatrix}\le 0 \qquad (23)$$

for $i,j=1,2,...,N$ $(j\neq i)$ and $k\le s=1,...,L_i$, then $\frac{d}{dt}(LF(t))\le 0$. It is easy to show that (12), which is equivalent to (10) if Q_i in (18) is specified, implies (23) and then the interconnected system S is stable in the sense of Lyapunov, if the LMIs in (10) hold. This completes the proof. ■

As mentioned, to obtain better robust performance, the attenuation level ρ_i^2 for each subsystem can be minimized so that the H_∞ performance in (9) is reduced as small as possible. Therefore, the H_∞ static output feedback fuzzy control problem for the nonlinear interconnected systems can be formulated as the following minimization problem which is also called eigenvalue problem (EVP).

$$\begin{array}{ll}\min & \sum_{i=1}^{N}\rho_i^2 \\ \text{subject to} & Q_i=Q_i^T>0,\ \bar{Y}_{is},\ \text{and (10).}\end{array} \qquad (24)$$

Remark 4: By the above formulation in (24), the attenuation level ρ_i^2 for each subsystem may not be the minimum but the sum of the attenuation level ρ_i^2, i.e., $\sum_{i=1}^{N}\rho_i^2$, is minimal, which means the formulation in (24) finds the attenuation level ρ_i^2 as small as possible for each subsystem by minimizing $\sum_{i=1}^{N}\rho_i^2$ with equal weighting for each subsystem. For the simplicity of design, one may assume $\rho_1=\rho_2=\cdots=\rho_N=\rho$. In such a case, the EVP in (24) can be simplified as follows:

$$\begin{array}{ll}\min & \rho^2 \\ \text{subject to} & Q_i=Q_i^T>0,\ \bar{Y}_{is},\ \text{and (10).}\end{array} \qquad (25)$$

■

According to the analysis above, the H_∞ decentralized static output feedback fuzzy control design is summarized as follows:

Design Procedure:

Step 1: Construct the fuzzy plant rules in (1).

Step 2: Perform the SVD for the output matrices $C_i = U_iS_iV_i^T = U_i[\ \Sigma_i\quad 0\ ]V_i^T$ $(i=1,...,N)$ in (2).

Step 3: Solve the EVP in (24) and then obtain the corresponding minimal attenuation level ρ_i^2 and the corresponding $Q_i = diag\{\ Q_{i1},\quad Q_{i2}\ \}$ and $\bar{Y}_{is} = [\ Y_{is}\quad 0\ ]$ (thus decentralized static fuzzy control gains $K_{is}=Y_{is}Q_{i1}^{-1}\Sigma_i^{-1}U_i^{-1}$ can also be obtained), simultaneously.

Step 4: Construct the H_∞ decentralized static output feedback fuzzy controller in (5).

IV. SIMULATION EXAMPLE

In this section, the stabilization problem of two interconnected systems S_1 and S_2 using the proposed decentralized static output feedback fuzzy control scheme is considered. For the subsystem S_1, a modified Lorenz's equation with input, outputs, and interconnected terms from subsystem S_2 is given by

$$S_1:\ \begin{cases}\dot{x}_{11}=-10x_{11}+10x_{12}+0.1x_{22} \\ \qquad +u_1(t)+0.1w_{11} \\ \dot{x}_{12}=28x_{11}-x_{12}-x_{11}x_{13} \\ \qquad -0.3x_{21}+0.1w_{12} \\ \dot{x}_{13}=x_{11}x_{12}-8/3x_{13}+0.05x_{21} \\ \qquad -0.01x_{22}+0.1w_{13} \\ y_{11}=x_{11} \\ y_{12}=5x_{12}+2x_{13}\end{cases} \qquad (26)$$

where external disturbance

$$\begin{aligned}&w_1(t)=[\ w_{11},\quad w_{12},\quad w_{13}\ ]^T \\ &=[\ 50\sin(10t)e^{-0.5t},\quad 50\cos(10t)e^{-t}, \\ &50[\sin(10t)+\cos(10t)]e^{-0.2t}]^T\in L_2.\end{aligned}$$

For this subsystem S_1, the modified Lorenz's equation can be exactly represented by the following two-rule fuzzy model under $x_{11}\ (=y_{11})\in[\ -\kappa_1,\quad \kappa_1\ ]$ [17].

Rule 1 : IF y_{11} is F_{11}^1

THEN $\dot{x}_1(t) = A_{11}x_1(t)+A_{121}x_2(t)+B_{111}u_1(t)+B_{211}w_1(t)$, and $y_1(t)=C_1x_1(t)$,

Rule 2 : IF y_{11} is F_{11}^2

THEN $\dot{x}_1(t) = A_{12}x_1(t)+A_{122}x_2(t)+B_{112}u_1(t)+B_{212}w_1(t)$, and $y_1(t)=C_1x_1(t)$,

where $x_1(t) = [\ x_{11},\ x_{12},\ x_{13}\ ]^T$, $y_1(t) = [\ y_{11},\ y_{12}\ ]^T$,

$$\begin{aligned} A_{11} &= \begin{bmatrix} -10 & 10 & 0 \\ 28 & -1 & -\kappa_1 \\ 0 & \kappa_1 & -8/3 \end{bmatrix}, \\ A_{12} &= \begin{bmatrix} -10 & 10 & 0 \\ 28 & -1 & \kappa_1 \\ 0 & -\kappa_1 & -8/3 \end{bmatrix}, \\ C_1 &= \begin{bmatrix} 1 & 0 & 0 \\ 0 & 5 & 2 \end{bmatrix}, \\ A_{12k} &= \begin{bmatrix} 0 & 0.1 \\ -0.3 & 0 \\ 0.05 & -0.01 \end{bmatrix}, \\ B_{11k} &= [\ 1 \quad 0 \quad 0\ ]^T, \\ \text{and } B_{21k} &= 0.1 I_{[3\times 3]}\ (k = 1, 2) \end{aligned}$$

where $F_{11}^1 = \frac{1}{2}(1 + \frac{y_{11}}{\kappa_1}) = h_1(y_{11})$, $F_{11}^2 = \frac{1}{2}(1 - \frac{y_{11}}{\kappa_1}) = h_2(y_{11})$, and $\kappa_1 = 30$.

For the subsystem S_2, a modified Duffing forced-oscillation model with input, output, and interconnected terms from subsystem S_1 is given by

$$S_2 : \begin{cases} \dot{x}_{21} = x_{22} + 0.05x_{11} - 0.01x_{12} \\ \qquad +6\cos(t) + 0.5u_2^*(t)) + 0.5w_{21} \\ \dot{x}_{22} = -x_{21}^3 - 0.1x_{22} - 0.01x_{12} + 0.04x_{13} \\ \qquad +12\cos(t) + u_2^*(t) + 0.03w_{22} \\ y_{21} = 10x_{21} \end{cases} \tag{27}$$

where external disturbance $w_2(t) = [\ w_{21},\ w_{22}\ ]^T = [\ N_1 e^{-0.5t},\ N_2 e^{-t}\ ]^T \in L_2$, where $N_1 = 200 sign[\sin(10t)]$ and $N_2 = 200 sign[\cos(10t)]$ are assumed to be periodic square wave with period $\frac{2\pi}{10}$ and magnitude ± 200. For this subsystem S_2, the modified Duffing forced-oscillation model can be exactly represented by the following two-rule fuzzy model under $x_{21}\ (= 0.1y_{21}) \in [\ -\kappa_2,\ \kappa_2\ ]$ [17].

Rule 1 : IF $0.1y_{21}$ is F_{21}^1

THEN $\dot{x}_2(t) = A_{21}x_2(t) + A_{211}x_1(t) + B_{121}u_2(t) + B_{221}w_2(t)$, and $y_2(t) = C_2x_2(t)$,

Rule 2 : IF $0.1y_{21}$ is F_{21}^2

THEN $\dot{x}_2(t) = A_{22}x_2(t) + A_{212}x_1(t) + B_{122}u_2(t) + B_{222}w_2(t)$, and $y_2(t) = C_2x_2(t)$,

where $x_2(t) = [\ x_{21},\ x_{22}\ ]^T$, $y_2(t) = y_{21}$, $u_2(t) = 12\cos(t) + u_2^*(t)$,

$$\begin{aligned} A_{21} &= \begin{bmatrix} 0 & 1 \\ 0 & -0.1 \end{bmatrix}, \\ A_{22} &= \begin{bmatrix} 0 & 1 \\ -\kappa_2^2 & -0.1 \end{bmatrix}, \\ C_2 &= [\ 10 \quad 0\ ], \\ A_{21k} &= \begin{bmatrix} 0.05 & -0.01 & 0 \\ 0 & -0.01 & 0.04 \end{bmatrix}, \\ B_{12k} &= [\ 0.5 \quad 1\ ]^T, \\ \text{and } B_{22k} &= \begin{bmatrix} 0.05 & 0 \\ 0 & 0.03 \end{bmatrix}\ (k = 1, 2) \end{aligned}$$

where $F_{21}^1 = (1 - \frac{(0.1y_{21})^2}{\kappa_2^2}) = h_1(y_{21})$, $F_{21}^2 = \frac{(0.1y_{21})^2}{\kappa_2^2} = h_2(y_{21})$, and $\kappa_2 = 50$.

Remark 5: For the simplicity of design, we can assume $\rho_1 = \rho_2 = \rho$ for these two subsystems in this example. ■

There is no efficient algorithm in Matlab [7] to solve the nonstrict LMIs in (10), therefore one may replace the diagonal zero entry in (10) by a negative value to solve the nonstrict LMIs problem in (24). Consequently, the solutions of the nonstrict LMIs in (10) can be obtained correspondingly by solving the following strict LMIs if ε^2 is small enough, for example $\varepsilon^2 \le 10^{-8}$.

$$\begin{bmatrix} \bar{M}_1 & * & * & * \\ \bar{A}_{ijk}^T & -\varepsilon^2 I & * & * \\ \bar{B}_{2ik}^T & 0 & -\rho_i^2 I & * \\ Q_i & 0 & 0 & -\Psi_{vi}^{-1} \end{bmatrix} < 0 \tag{28}$$

To obtain feasible solutions for the strict LMIs in (28), the weighting matrices Ψ_1 and Ψ_2 should be small enough. In this example, $\varepsilon^2 = 10^{-8}$ and the weighting matrices are chosen as follows

$$\Psi_1 = 5 \times 10^{-8} I_{[3\times 3]},\ \Psi_2 = 5 \times 10^{-8} I_{[2\times 2]}.$$

Then, following the **Design Procedure** in the above section, the SVD of C_1 and C_2 is given as follows:

$$\begin{aligned} C_1 &= \begin{bmatrix} 0 & 1 \\ 1 & 0 \end{bmatrix} \begin{bmatrix} 5.3852 & 0 & 0 \\ 0 & 1 & 0 \end{bmatrix} \\ &\quad \times \begin{bmatrix} 0 & 1 & 0 \\ 0.9285 & 0 & -0.3714 \\ 0.3714 & 0 & 0.9285 \end{bmatrix}^T, \\ C_2 &= [1] [\ 10 \quad 0\ ] \begin{bmatrix} 1 & 0 \\ 0 & 1 \end{bmatrix}^T. \end{aligned}$$

Solving the EVP in (25), one can obtain the corresponding minimal attenuation level $\rho_{\min}^2 = 3 \times 10^{-8}$ and

$$\begin{aligned} Q_1 &= diag\{\ Q_{11},\ Q_{12}\ \} \\ &= 10^7 \times \begin{bmatrix} 3.6452 & -0.6262 & 0 \\ -0.6262 & 0.4863 & 0 \\ 0 & 0 & 3.519 \end{bmatrix} \\ Q_2 &= diag\{\ Q_{21},\ Q_{22}\ \} \\ &= 10^6 \times \begin{bmatrix} 0.0003 & 0 \\ 0 & 1.9996 \end{bmatrix} \\ \bar{Y}_{11} &= 10^8 \times [\ -2.3573 \quad -7.0707 \quad 0\ ] \\ \bar{Y}_{12} &= 10^8 \times [\ -2.7502 \quad -3.8084 \quad 0\ ] \\ \bar{Y}_{21} &= [\ -2.0096 \times 10^6 \quad 0\ ] \\ \bar{Y}_{22} &= [\ -1.3050 \times 10^6 \quad 0\ ]. \end{aligned}$$

The decentralized static output feedback fuzzy control gains can be found as follows

$$\begin{aligned} K_{11} &= [\ -197.3995 \quad -7.4974\ ], \\ K_{12} &= [\ -113.0383 \quad -5.0066\ ], \\ K_{21} &= -713.0568,\ K_{22} = -463.0563. \end{aligned}$$

Therefore, the proposed decentralized static output feedback fuzzy controller is constructed as

$$u_i(t) = \sum_{s=1}^{2} h_s(y_{s1}) K_{is} y_i(t), \ \ (i = 1, 2).$$

Ignoring the effect of initial conditions, the H_∞ performance in this example can be written as follows

$$5 \times 10^{-8} \int_0^{t_f} x_i^T(t) x_i(t) dt \leq 3 \times 10^{-8} \int_0^{t_f} w_i^T(t) w_i(t) dt$$

which is equivalent to

$$\frac{\int_0^{t_f} x_i^T(t) x_i(t) dt}{\int_0^{t_f} w_i^T(t) w_i(t) dt} \leq 0.6$$

The following table shows the results for the different choice of ε^2 and Ψ_i, respectively.

ε^2	Ψ_i	$\rho^2_{\min}$
10^{-8}	5×10^{-8}	3×10^{-8}
10^{-9}	5×10^{-9}	3×10^{-9}
$10^{-9.5}$	$5 \times 10^{-9.5}$	9.571×10^{-10}

Remark 6: In the above example, if $\varepsilon^2 < 10^{-9.5}$, no feasible solution can be found. ■

Figs. 1-4 present the simulation results with initial conditions $(\ x_{11}(0),\ \ x_{12}(0),\ \ x_{13}(0)\ ) = (\ 5,\ \ 10,\ \ -5\ )$ and $(\ x_{21}(0),\ \ x_{22}(0)\ ) = (\ 4.5,\ \ -5\ )$. The trajectories of state variables $x_{11}(t)$, $x_{12}(t)$, and $x_{13}(t)$ are shown in Fig. 1 while the trajectories of state variables $x_{21}(t)$ and $x_{22}(t)$ are shown in Fig. 2. The control inputs $u_1(t)$ and $u_2^*(t) = u_2(t) - 12\cos(t)$ are applied at $t = 2\ (sec)$ and shown in Fig. 3 and Fig. 4, respectively. From Fig. 1 and Fig. 2, one observes that the states are very oscillating before $t < 2\ (sec)$ but all states are stabilized rapidly after the control inputs are applied. From the simulation results, the proposed H_∞ decentralized static output feedback fuzzy control scheme can solve the output feedback control problem for nonlinear interconnected systems effectively and systematically with the aid of LMI-based optimization method.

V. CONCLUSIONS

In this study, H_∞ decentralized static output feedback fuzzy control design for nonlinear interconnected systems is considered via T-S fuzzy models. Furthermore, the stability of the nonlinear interconnected systems is also guaranteed by the proposed decentralized static output feedback control scheme. A SVD method is proposed to solve the H_∞ static output feedback stabilization problem for the nonlinear interconnected systems, which can be characterized in terms of an EVP for each subsystem. By the proposed SVD method, the H_∞ decentralized static fuzzy control gains can be obtained efficiently. The proposed decentralized static output feedback fuzzy control scheme is very simple without complex control algorithms. Therefore, it is suitable for practical applications. Simulation example is given to illustrate the design procedure and robust performance of the proposed method.

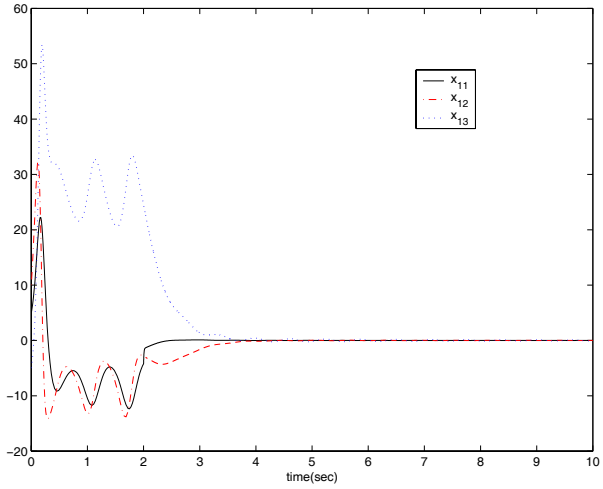

Fig. 1. The trajectories of state variables $x_{11}(t)$ (black), $x_{12}(t)$ (red), and $x_{13}(t)$ (blue).

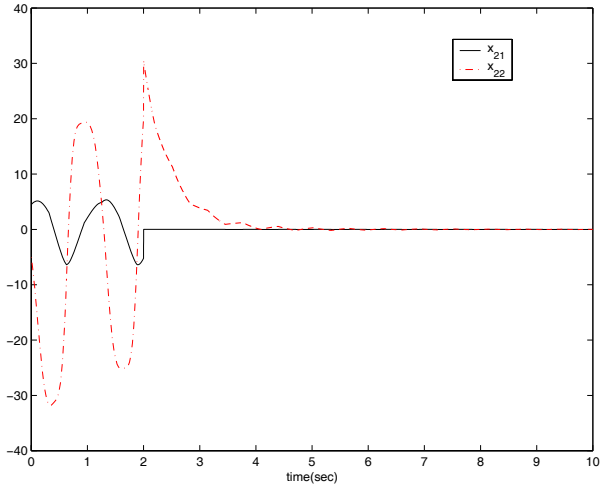

Fig. 2. The trajectories of state variables $x_{21}(t)$ (black) and $x_{22}(t)$ (red).

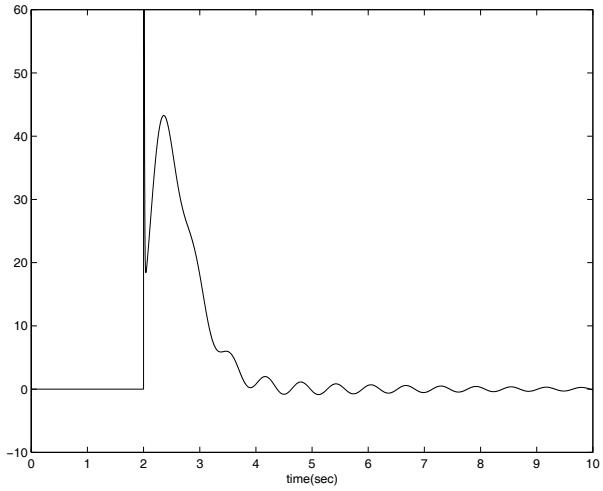

Fig. 3. The control input $u_1(t)$.

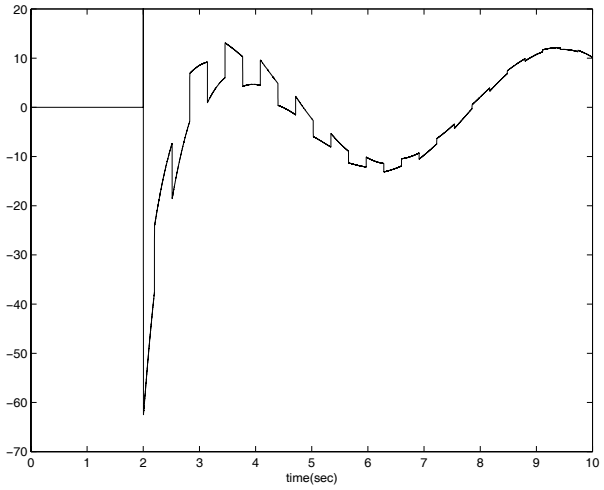

Fig. 4. The control input $u_2^*(t)$.

REFERENCES

[1] V. Bandal and B. Bandyopadhyay, "Robust Decentralized Output Feedback Sliding Mode Control Technique-Based Power System Stabiliser (PSS) for Multimachine Power System," *IET Control Theory & Applications*, vol. 1, no. 5, pp. 1512-1522, Sep. 2007.

[2] S. Boyd, L. El Ghaoui, E. Feron, and V. Balakrishnan, Linear Matrix Inequalities in System and Control Theory, *SIAM*, Philadelphia, 1994.

[3] Y.-C. Chang, S.-S. Chen, S.-F. Su, and T.-T. Lee, "Static Output Feedback Stabilization for Nonlinear Interval Time-Delay Systems via Fuzzy Control Approach," *Fuzzy Sets and Systems*, vol. 148, no. 3, pp.395-410, Dec. 2004.

[4] S.-S. Chen, Y.-C. Chang, S.-F. Su, S.-L. Chung, and T.-T. Lee, "Robust Static Output-Feedback Stabilization for Nonlinear Discrete-Time Systems with Time Delay via Fuzzy Approach," *IEEE Trans. Fuzzy Systems*, vol. 13, no. 2, pp. 263-272, April 2005.

[5] D. Huang and S. K. Nguang, "Robust H_∞ Static Output Feedback Control of Fuzzy Systems: An ILMI Approach," *IEEE Trans. Systems, Man and Cybernetics, Part B*, vol. 36, no. 1, pp. 216-222, Feb. 2006.

[6] D. Huang and S. K. Nguang, "Static Output Feedback Controller Design for Fuzzy Systems: An ILMI Approach," *Information Sciences*, vol. 177, no. 14, pp. 3005-3015, July 2007.

[7] P. Gahinet, A. Nemirovski, A. J. Laub, and M. Chilali, LMI Control Toolbox, Natick, MA: *The MathWorks*, 1995.

[8] T. M. Guerra, A. Kruszewski, L. Vermeiren, and H. Tirmant, "Conditions of Output Stabilization for Nonlinear Models in the Takagi-Sugeno's Form," *Fuzzy Sets and Systems*, vol. 157, no. 9, pp. 1248-1259, May 2006.

[9] F.-H. Hsiao, J.-D. Hwang, C.-W. Chen, and Z.-R. Tsai, "Robust Stabilization of Nonlinear Multiple Time-Delay Large-Scale Systems via Decentralized Fuzzy Control," *IEEE Trans. Fuzzy Systems*, vol. 13, no. 1, pp. 152-163, Feb. 2005.

[10] C.-L. Hwang and H.-Y. Lin, "A Fuzzy Decentralized Variable Structure Tracking Control with Optimal and Improved Robustness Design and Applications," *IEEE Trans. Fuzzy Systems*, vol. 12, no. 5, pp. 615-630, Oct. 2004.

[11] S.-W. Kau, H.-J. Lee, C.-M. Yang, C.-H. Lee, L. Hong, and C.-H. Fang, "Robust H_∞ Fuzzy Static Output Feedback Control of T-S Fuzzy Systems with Parametric Uncertainties," *Fuzzy Sets and Systems*, vol. 158, no. 3, pp. 135-146, Jan. 2007.

[12] J.-C. Lo and M.-L. Lin, "Robust H_∞ Nonlinear Control via Fuzzy Static Output Feedback," *IEEE Trans. Circuits and Systems-I: Fundamental Theory and Applications*, vol. 50, no. 11, pp. 1494-1502, Nov. 2003.

[13] S. S. Stankovic, D. M. Stipanovic, and D. D. Siljak, "Decentralized Dynamic Output Feedback for Robust Stabilization for A Class of Nonlinear Interconnected Systems," *Automatica*, vol. 43, no. 5, pp. 861-867, May 2007.

[14] S. S. Stankovic and D. D. Siljak, "Robust Stabilization of Nonlinear Interconnected Systems by Decentralized Dynamic Output Feedback," *Systems & Control Letters*, vol. 58, no. 4, pp.271-275, April 2009.

[15] A. Swamakar, H. J. Marquez, and T. Chen, "A New Scheme on Robust Observer-Based Control Design for Interconnected Systems with Application to an Utility Boiler," *IEEE Transactions on Control Systems Technology*, vol. 16, no. 3, pp. 539-547, May 2008.

[16] T. Takagi and M. Sugeno, "Fuzzy Identification of Systems and its Applications to Modeling and Control," *IEEE Trans. Syst., Man, Cybern.*, vol. 15, pp. 116-132, Jan./Feb. 1985.

[17] K. Tanaka and H. O. Wang, Fuzzy Control Systems Design and Analysis: A Linear Matrix Inequality Approach, *John Wiley & Sons, Inc.* 2001.

[18] C.-S. Tseng and B.-S. Chen, "H_∞ Decentralized Fuzzy Model Reference Tracking Control Design for Nonlinear Interconnected Systems," *IEEE Trans. Fuzzy Systems*, vol. 9, no. 6, pp. 795-809, Dec. 2001.

[19] C.-S. Tseng, "A Novel Approach to H_∞ Decentralized Fuzzy Observer-Based Fuzzy Control Design for Nonlinear Interconnected Systems," *IEEE Trans. Fuzzy Systems*, vol. 16, no. 5, pp. 1337-1350, Oct. 2008.

[20] C.-S. Tseng, "Model Reference Output Feedback Fuzzy Tracking Control Design for Nonlinear Discrete-Time Systems with Time-Delay," *IEEE Trans. Fuzzy Systems*, vol. 14, no. 1, pp. 58-70, Feb. 2006.

[21] R.-J. Wang, "Nonlinear Decentralized State Feedback Controller for Uncertain Fuzzy Time-Delay Interconnected Systems," *Fuzzy Sets and Systems*, vol. 151, no. 1, pp. 191-204, April 2005.

[22] W.-J. Wang and W.-W. Lin, "Decentralized PDC for Large-Scale T-S Fuzzy Systems," *IEEE Trans. Fuzzy Systems*, vol. 13, no. 6, pp. 779-786, Dec. 2005.

[23] H.-N. Wu, "An ILMI Approach to Robust H_∞ Static Output Feedback Fuzzy Control for Uncertain Discrete-Time Nonlinear Systems," *Automatica*, vol. 44, no. 9, pp. 2333-2339, Sep. 2008.

[24] X. G. Yan, C. Edward, and S. K. Spurgeon, "Decentralized Robust Sliding Mode Control for A Class of Nonlinear Interconnected Systems by Static Output Feedback," *Automatica*, vol. 40, no. 4, pp. 613-620, April 2004.

2011 IEEE International Conference on Fuzzy Systems
June 27-30, 2011, Taipei, Taiwan

Adaptive Fuzzy Sliding-Mode Control for a Class of Nonlinear Systems with Uncertainties

Hugang Han
Department of Management Information Science
Prefectural University of Hiroshima
Hiroshima 734-8558 , Japan
Email: hhan@pu-hiroshima.ac.jp

***Abstract*—An approach to adaptive fuzzy sliding-mode control (SMC) for a class of nonlinear dynamical systems with lumped parameter uncertainties accompanied with control input is proposed and analyzed. The approach guarantees that the system state will be uniformly ultimately bounded. Also, discussion on how to alleviate the conservativeness of the approach is provided. Finally, computer simulations illustrate the effectiveness of the control approach proposed in this paper.**

Keywords - adaptive fuzzy control; T-S fuzzy model; sliding-mode control; Uncertainties

I. Introduction

In recent years, there have been significant advances in the study of the stability analysis and controller synthesis for the so-called Takagi-Sugeno (T-S) fuzzy systems, which have been used to represent certain complex nonlinear systems. The overall model of the system is obtained by the fuzzy blending of these local models. The control design is carried out based on the fuzzy model by the so-called parallel distributed compensation (PDC) scheme [1]. For each local linear model, a linear feedback control is designed. The resulting overall controller is again a fuzzy blending of the individual linear controllers. Originally, Tanaka and his colleagues have provided certain conditions that are sufficient for the stability of the T-S fuzzy systems in the sense of Lyapunove [2]. The feedback control gain in each PDC control rule is obtained by solving certain linear matrix inequalities (LMIs).

Although a nonlinear system can be handled by a PDC controller based on the T-S fuzzy model, the control performance depends on the precision of the T-S fuzzy model. That is, if the model uncertainties between the system to be controlled and the T-S fuzzy model are significantly large, then the control performance is no longer to be as good as we expected. To compensate for the uncertainties and/or disturbances, several system design and analysis approaches have be proposed. Among the existing robust control approaches, fuzzy sliding-mode control (SMC) has been recognized as an effective robust control approach for uncertain systems. SMC is a particular type of variable structure control. Variable structure control systems are designed to derive and then constrain the system state to lie within a neighborhood of the sliding surface. There are many advantages to this approach [8]. In particular, the closed-loop response becomes totally insensitive to a particular class of uncertainties. This invariance property clearly makes the methodology an appropriate candidate for robust control. In addition, the ability to specify performance directly make SMC attractive from the design perspective. The result of Zheng *et al.* [3] is an elaborate example to illustrate that the SMC theory can be successfully applied to robust stabilization of uncertain nonlinear system with T-S fuzzy model, where uncertainties include parameter perturbation and external disturbances for which their upper-bounds are available. The ordinary T-S fuzzy model has been further extended to time-delay systems with uncertainties based on the SCM theory [4], [5]. More recently, by introducing some coordinate transformations to design a reduced-order sliding-mode dynamics, some excellent results on fuzzy sliding-mode control for nonlinear systems with uncertainties, particularly a lumped uncertainties accompanied with control input were reported [6], [7]. However, it should be pointed out that there are some limitations to the existing results. The main drawback comes to the assumption that requires the same control matrix, *i.e.,* $B_1 = B_2 = \cdots = B_r$ in the T-S fuzzy model with r rules; however, in practical applications that are a lot of cases where the control matrices are different in the T-S fuzzy model. Second, though all results showed the system state would be uniformly ultimately bounded when using some adaptive laws to deal with unknown parameters in the T-S fuzzy model, the boundedness was not mentioned further, which implies that such results are conservative.

Motivated by the aforementioned observations, in this paper we propose an adaptive SMC approach based on the T-S fuzzy model with uncertainties, trying to remove some strict assumptions on the system and alleviate the conservatism of the control results. Also, computer simulations are provided to illustrate the effectiveness of the proposed control approach.

II. Problem Description

It is now well known that T-S fuzzy models can provide an effective representation of complex nonlinear systems. Therefore, in this study, the nonlinear system under consideration is represented by T-S fuzzy models. Consider the following T-S fuzzy model:

Plant Rule i :
IF $\theta_1(t)$ is M_1^i and $\cdots$ and $\theta_p(t)$ is M_p^i,
THEN $\dot{x}(t) = A_i x(t) + B_i(x(t))\left(u(t) + \mathcal{U}_i(x(t))\right),$

978-1-4244-7316-8/11/$26.00 ©2011 IEEE

where $\theta_j^i (i = 1, 2, \cdots, r, j = 1, 2, \cdots, p)$ are variables in the antecedent; M_j^i, fuzzy sets with membership functions $\mu_{M_j^i}(\theta_j)$; $x(t) \in R^n$, system state; $u(t) \in R^m$, control input; $A_i \in R^{n\times n}$ and $B_i(x(t)) \in R^{n\times m}$, system and input matrices; $\mathcal{U}_i(x(t)) \in R^m$, lumped uncertainties including external disturbance. In this paper, we suppose that rank$(B) = m < n$. The overall fuzzy model is of the following form accordingly:

$$\dot{x}(t) = \sum_{i=1}^{r} \alpha_i(t)\big\{A_i x(t) + B_i(x(t))\left(u(t) + \mathcal{U}_i(x(t))\right)\big\}, \quad (1)$$

where

$$\alpha_i(t) = \frac{w_i(t)}{\sum_{i=1}^r w_i(t)} \geq 0, \quad \sum_{i=1}^r \alpha_i(t) = 1,$$
$$w_i(t) = \prod_{j=1}^p \mu_j^i(\theta_j(t)).$$

For the T-S fuzzy model above, we make the following assumptions.

A1: $B_i(x(t)) = B \cdot G_i(x(t))$, where $B \in R^{n\times m}$, rank$(B) = m < n$, $G_i(x(t)) \in R^{m\times m}$ is a known matrix function such that det $G_i(x(t)) \neq 0$, and of known sign; without loss of generality this sign can be taken as positive. Also, any (A_i, B) is a controllable pair.

A2: The lumped uncertainties $\mathcal{U}_i(x(t))$ are assumed to satisfy the following conditions:

$$||\mathcal{U}_i(x(t))|| \leq c_i^* + k_i^*||x(t)||, \quad (2)$$

where c_i^*, k_i^* are unknown positive constants, $||\cdot||$ denotes the Euclidean norm of a vector or a matrix.

It is noted that the T-S fuzzy model considered in this paper is significantly different from the models in this scope (see [6]-[7], for example), in which they took $B_i(x(t)) = B$ for $i = 1, 2, \cdots, r$. This implies that there is the same gain for control input $u(t)$ in each local model. Consequently, the overall fuzzy model (1) becomes

$$\dot{x}(t) = \sum_{i=1}^{r} \alpha_i(t)\big\{A_i x(t) + B\mathcal{U}_i(x(t)\big\} + Bu(t). \quad (3)$$

Although (3) has the benefit that the corresponding controllers are easier to be designed, apparently, its applications are severely restricted. Therefore, one of challenges in this paper is to design an adaptive fuzzy controller based on the T-S fuzzy model (1) towards more flexibility.

From here, unless confusion arises arguments such as t will be omitted just for notational convenience.

Letting $T_r \in R^{n\times n}$ be an orthogonal matrix such that

$$T_r A_i T_r^T = \begin{bmatrix} A_{11i} & A_{12i} \\ A_{21i} & A_{22i} \end{bmatrix} \triangleq \bar{A}_i, \quad T_r B = \begin{bmatrix} 0 \\ B_2 \end{bmatrix}, \quad (4)$$

where $A_{11i} \in R^{(n-m)\times(n-m)}$, $A_{12i} \in R^{(n-m)\times m}$, $A_{21i} \in R^{m\times(n-m)}$, $A_{22i} \in R^{(n-m)\times m}$, $B_2 \in R^{m\times m}$, and $z = T_r x$, then by pre-multiplying T_r on the both sides of (1), one obtains the following regular form.

$$\begin{aligned} \dot{z} &= \sum_{i=1}^{r} \alpha_i \left(\bar{A}_i z + \begin{bmatrix} 0 \\ B_2 \end{bmatrix} G_i\left(u + \mathcal{U}_i\right)\right) \\ &= \begin{bmatrix} \bar{A}_{11} & \bar{A}_{12} \\ \bar{A}_{21} & \bar{A}_{22} \end{bmatrix} z + \begin{bmatrix} 0 \\ B_2 \end{bmatrix} \sum_{i=1}^{r} \alpha_i G_i\left(u + \mathcal{U}_i\right), \quad (5) \end{aligned}$$

where

$$\bar{A}_{11} = \textstyle\sum_{i=1}^r \alpha_i A_{11i}, \quad \bar{A}_{12} = \sum_{i=1}^r \alpha_i A_{12i}, \quad (6)$$
$$\bar{A}_{21} = \textstyle\sum_{i=1}^r \alpha_i A_{21i}, \quad \bar{A}_{22} = \sum_{i=1}^r \alpha_i A_{22i}, \quad (7)$$

and $\mathcal{U}_i$ is a function with respect to $T_r^{-1} z$ at this point in time. Letting $z = [z_1^T \ z_2^T]^T$, where $z_1 \in R^{n-m}, z_2 \in R^m$, (5) can be transformed into

$$\dot{z}_1 = \bar{A}_{11} z_1 + \bar{A}_{12} z_2, \quad (8)$$

$$\dot{z}_2 = \bar{A}_{21} z_1 + \bar{A}_{22} z_2 + B_2 \sum_{i=1}^{r} \alpha_i G_i\left(u + \mathcal{U}_i\right). \quad (9)$$

This transformation can be accomplished for any given controllable pair (A_i, B), where B is full rank using some MATLAB commands [8].

III. Control System Design

SMC system design can be decoupled into two independent tasks. The first one is the selection of an appropriate sliding surface, which should have the property that the desired performance can be achieved while the system state remains on the sliding surface. Another task is to design a control law in order to force the system state to reach the sliding surface in spite of uncertainties in the system.

A. Sliding Surface Design

The corresponding sliding surface is chosen as follows.

$$s(t) = \bar{C} z(t) = 0 \quad (10)$$

where $\bar{C} \triangleq [-C_1 \ C_2]$ with $C_1 \in R^{m\times(n-m)}$, $C_2 = C_2^T \in R^{m\times m}$, which is positive-definite, are parameters to be designed. It follows from (10) that $z_2 = C_2^{-1} C_1 z_1$, and from (8) that

$$\dot{z}_1 = \left(\bar{A}_{11} + \bar{A}_{12} C_2^{-1} C_1\right) z_1, \quad (11)$$

which is a reduced-order $(n - m)$ sliding mode dynamics. Thus, the result of designing sliding surface can be provided as follows.

Theorem 1: Consider system (11). If there exists matrices $Q = Q^T \in R^{(n-m)\times(n-m)}$, $C_2 = C_2^T \in R^{m\times m}$, which are positive-definite, $M \in R^{m\times(n-m)}$, such that the following LMIs satisfied:

$$\begin{bmatrix} A_{11i}Q + QA_{11i}^T & M^T & A_{12i} \\ M & -C_2 & 0 \\ A_{12i}^T & 0 & -C_2 \end{bmatrix} < 0, \quad i = 1, 2, \cdots r. \quad (12)$$

then the sliding surface (10) with

$$C_1 = MQ^{-1} \quad (13)$$

will guarantee that the sliding motion in (11) is asymptotically stable.

Proof: Let us define a Lyapunov function candidate as

$$V(t) = z_1(t)^T Q^{-1} z_1(t). \tag{14}$$

Then, taking the time derivative along the state trajectory of system (11), one obtains

$$\begin{aligned}\dot{V}(t) &= z_1^T \Big(\bar{A}_{11}^T Q^{-1} + \left(C_2^{-1} C_1\right)^T \bar{A}_{12}^T Q^{-1} \\ &\quad + Q^{-1} \bar{A}_{11} + Q^{-1} \bar{A}_{12} C_2^{-1} C_1 \Big) z_1. \end{aligned} \tag{15}$$

Obviously, it follows from (15) that the sliding motion (11) is asymptotically stable, if

$$\begin{aligned}&\bar{A}_{11}^T Q^{-1} + C_1^T C_2^{-1} \bar{A}_{12}^T Q^{-1} \\ &+ Q^{-1} \bar{A}_{11} + Q^{-1} \bar{A}_{12} C_2^{-1} C_1 < 0. \end{aligned} \tag{16}$$

By pre- and post-multiplying (16) by Q, it follows that

$$Q \bar{A}_{11}^T + M^T C_2^{-1} \bar{A}_{12}^T + \bar{A}_{11} Q + \bar{A}_{12} C_2^{-1} M < 0, \tag{17}$$

where the fact that $M = C_1 Q$ is used. Due to the facts that $C_2^{-1} > 0$ and

$$\left(M - A_{12}^T\right)^T C_2^{-1} \left(M - A_{12}^T\right) \geq 0,$$

which leads to

$$M^T C_2^{-1} \bar{A}_{12}^T + \bar{A}_{12} C_2^{-1} M \leq M^T C_2^{-1} M + \bar{A}_{12} C_2^{-1} \bar{A}_{12}^T,$$

therefore, the condition for the sliding motion being asymptotical stable (17) can be replaced by the following inequality.

$$Q \bar{A}_{11}^T + \bar{A}_{11} Q + M^T C_2^{-1} M + \bar{A}_{12} C_2^{-1} \bar{A}_{12}^T < 0. \tag{18}$$

By applying the Schur complement formula to (18) and using (6), (7), it leads to LMIs (12). After all, we can conclude that the $(n-m)$ reduced-order sliding mode dynamics (11) is asymptotically stable. This completes the proof. □

Although LMIs (12) can guarantee that the sliding motion (11) is asymptotically stable, *i.e.,*

$$\bar{A}_{11} + \bar{A}_{12} C_2^{-1} C_1 < 0, \tag{19}$$

it is not taken into account how to make the state converge to 0, which is the equilibrium point in this paper, as fast as possible.

In what follows, let us consider the matter. From (11) we have

$$z_2(t) = \exp\left(A_{11} + \bar{A}_{12} C_2^{-1} C_1\right) z_2(0),$$

implying that we should find the minimum value of $A_{11} + \bar{A}_{12} C_2^{-1} C_1$ so that z_2 shrinks to 0 most rapidly. Substituting (13) into (19), it follows that

$$\bar{A}_{11} Q + \bar{A}_{12} C_2^{-1} M < 0, \tag{20}$$

which implies that the minimum values of the left side of inequality (17), then LMIs (12) lead to the minimum one of $\bar{A}_{11} + \bar{A}_{12} C_2^{-1} C_1$.

Let $R_i = R_i^T > 0$ be any given matrices, then, the minimum values of the left sides of LMIs (12) can be found by solving the following LMIs, searching the minimum value of γ.

$$\begin{aligned}&\begin{bmatrix} A_{11i} Q + Q A_{11i}^T & M^T & A_{12i} \\ M & -C_2 & 0 \\ A_{12i}^T & 0 & -C_2 \end{bmatrix} < \gamma R_i, \\ &\qquad\qquad\qquad\qquad i = 1, 2, \cdots r. \end{aligned} \tag{21}$$

Since R_i are fixed, the left sides in (21) become smaller in order to get a smaller γ. Eventually, the minimum values of the left sides can be achieved. Summarizing above, we obtain the following corollary.

Corollary 1: Consider system (11). If there exists matrices $Q = Q^T \in R^{(n-m)\times(n-m)}$, which is positive-definite, $M \in R^{m\times(n-m)}$, $C_2 = C_2^T \in R^{m\times m}$, such that the following LMIs satisfied:

$$\begin{aligned}&\min \gamma \ \texttt{subject to} \\ &\begin{cases} \texttt{LMIs } (12) \\ \texttt{LMIs } (21) \end{cases} \end{aligned} \tag{22}$$

where $R_i = R_i^T > 0$ are some given matrices with appropriate dimensions, then the sliding surface (10) with (13) will guarantee that the sliding motion in (11) is asymptotically stable with the maximum convergence rate.

LMIs (22) can be solved by using existing software packages such as `mincx` solver in the LMI Control Toolbox with MATLAB.

Regarding the LMIs in Theorem 1, we give the following remark.

Remark 1: Since $M^T C_2^{-1} M + \bar{A}_{12} C_2^{-1} \bar{A}_{12}^T > 0$, the condition for the sliding motion being asymptotical stable (17), also, can be transferred into

$$Q \bar{A}_{11}^T + \bar{A}_{11} Q + \left(M + \bar{A}_{12}^T\right)^T C_2^{-1} \left(M + \bar{A}_{12}^T\right) < 0,$$

which leads to the following LMIs by using the Schur complement formula.

$$\begin{bmatrix} A_{11i} Q + Q A_{11i}^T & M^T + A_{12i} \\ M + A_{12i}^T & -C_2 \end{bmatrix} < 0. \tag{23}$$

That is, LMIs (23) may be another solutions if LMIs (12) are infeasible, though it is difficult to say which of LMIs (12) and (23) is more feasible.

Remark 2: In case neither LMIs (12) nor (23) is feasible, it is not longer to take C_2 as a matrix variable in the LMIs, *i.e.*, we have to provide a prescribed matrix, for example an identity matrix, so that (17) turns out to be an LMI. In this case, therefore, either LMIs (12) or (23) are replaced by

$$\begin{aligned}&A_{11i} Q + Q A_{11i}^T + M^T C_2^{-1} A_{12i}^T + A_{12i} C_2^{-1} M < 0, \\ &\qquad\qquad i = 1, 2, \cdots r. \end{aligned} \tag{24}$$

B. Control Law

After designing the sliding surface so that the reduced-order sliding mode dynamics has the desired response, the next step of the SMC design procedure is to design a switching feedback control law such that the reachability of the specified sliding surface (10) is ensured.

Theorem 2: Consider the T-S fuzzy model (1) subject to the assumptions A1 and A2 provided in section II. Let us suppose that the LMIs (12), which are associated with the T-S fuzzy model by (4), are feasible and that the sliding surface is given by (10), where C_1 is given by (13) and C_2 is a solution of the LMIs. Then, the all signals involved in the closed-loop system (1) with the following control law are uniformly ultimately bounded.

$$\begin{aligned} u(t) &= -\sum_{i=1}^{r} \alpha_i \left\{ (C_2B_2)^{-1} \psi_i(t) \bar{C}\bar{A}_i z(t) + \phi_i(t) \right\} \\ &\quad - \frac{(C_2B_2)^{-1}}{\lambda_{\min}} \mu \ s(t), \end{aligned} \tag{25}$$

where $\mu > 0$, $\lambda_{\min} = \min\{\lambda(G_1), \lambda(G_2), \cdots, \lambda(G_r)\}$,

$$\psi_i(t) = \begin{cases} \frac{1}{\lambda_{\min}}, & s(t)^T \bar{C}\bar{A}_i z(t) \geq 0; \\ \frac{1}{\lambda_{\max}}, & \text{otherwise}, \end{cases} \tag{26}$$

$$\phi_i(t) = \begin{cases} \frac{\mathrm{sgn}(B_2^T C_2^T s(t))}{\lambda_{\min}} \hat{\rho}_i(t) ||G_i||, & \hat{\rho}_i(t) \geq 0; \\ \frac{\mathrm{sgn}(B_2^T C_2^T s(t))}{\lambda_{\max}} \hat{\rho}_i(t) ||G_i||, & \text{otherwise}, \end{cases} \tag{27}$$

$$\hat{\rho}_i(t) = \hat{c}_i(t) + \hat{k}_i(t) ||z(t)||, \tag{28}$$

$\lambda_{\max} = \max\{\lambda(G_1), \lambda(G_2), \cdots, \lambda(G_r)\}$, and adaptive laws are

$$\dot{\hat{c}}_i(t) = \alpha_i \gamma_{1i} \left(-\epsilon_1 \hat{c}_i(t) + ||G_i|| ||B_2^T C_2^T s(t)|| \right), \tag{29}$$

$$\dot{\hat{k}}_i(t) = \alpha_i \gamma_{2i} \left(-\epsilon_2 \hat{k}_i(t) + ||G_i|| ||B_2^T C_2^T s(t)|| ||z(t)|| \right), \tag{30}$$

where $\gamma_{1i}, \gamma_{2i}, \epsilon_1$, and ϵ_2 are positive design parameters.

Proof: From (5) and (10), we have

$$\dot{s} = \sum_{i=1}^{r} \alpha_i \left(\bar{C}\bar{A}_i z + C_2B_2G_i \left(u + \mathcal{U}_i \right) \right). \tag{31}$$

Let us define a Lyapunov function candidate as follows.

$$V(t) = \frac{1}{2} s(t)^T s(t) + \frac{1}{2} \sum_{i=1}^{r} \left\{ \gamma_{1i}^{-1} \tilde{c}_i^2(t) + \gamma_{2i}^{-1} \tilde{k}_i^2(t) \right\}, \tag{32}$$

where $\tilde{c}_i(t) = c_i^* - \hat{c}_i(t), \tilde{k}_i(t) = k_i^* - \hat{k}_i(t)$.
Using (31), the time derivative of V on any trajectory of the closed-loop system is

$$\begin{aligned} \dot{V} &= \sum_{i=1}^{r} \alpha_i \Big\{ s^T \bar{C}\bar{A}_i z + s^T C_2B_2G_i \mathcal{U}_i \\ &\quad - s^T C_2B_2G_i \frac{(C_2B_2)^{-1}}{\lambda_{\min}} \mu \ s \\ &\quad - s^T C_2B_2G_i \sum_{j=1}^{r} \alpha_j \left((C_2B_2)^{-1} \psi_j \bar{C}\bar{A}_j z + \phi_j \right) \Big\} \\ &\quad - \sum_{i=1}^{r} \gamma_{1i}^{-1} \tilde{c}_i \dot{\hat{c}}_i - \sum_{i=1}^{r} \gamma_{2i}^{-1} \tilde{k}_i \dot{\hat{k}}_i \\ &= \sum_{i=1}^{r} \sum_{j=1}^{r} \alpha_i \alpha_j \Big\{ s^T \bar{C}\bar{A}_i z + s^T C_2B_2G_i \mathcal{U}_i \\ &\quad \underbrace{- s^T C_2B_2G_i \frac{(C_2B_2)^{-1}}{\lambda_{\min}} \mu \ s}_{(I)} \\ &\quad \underbrace{- s^T C_2B_2G_i (C_2B_2)^{-1} \psi_j \bar{C}\bar{A}_j z}_{(II)} \\ &\quad \underbrace{- s^T C_2B_2G_i \phi_j}_{(III)} \Big\} \\ &\quad - \sum_{i=1}^{r} \gamma_{1i}^{-1} \tilde{c}_i \dot{\hat{c}}_i - \sum_{i=1}^{r} \gamma_{2i}^{-1} \tilde{k}_i \dot{\hat{k}}_i. \end{aligned} \tag{33}$$

Let us consider $(I) - (III)$ in (33) as follows.

$$\begin{aligned} (I) &\leq -s^T C_2B_2 \lambda_{\min} \frac{(C_2B_2)^{-1}}{\lambda_{\min}} \mu \ s \\ &= -\mu ||s||, \end{aligned} \tag{34}$$

where $\lambda_{\min} > 0$ due to the assumption *A1*. As to (II), if $s^T \bar{C}\bar{A}_j z \geq 0$, we have

$$\begin{aligned} (II) &= -s^T C_2B_2G_i (C_2B_2)^{-1} \frac{1}{\lambda_{\min}} \bar{C}\bar{A}_j z \\ &\leq -s^T C_2B_2 \lambda_{\min} (C_2B_2)^{-1} \frac{1}{\lambda_{\min}} \bar{C}\bar{A}_j z \\ &= -s^T \bar{C}\bar{A}_j z; \end{aligned} \tag{35}$$

otherwise,

$$\begin{aligned} (II) &= -s^T C_2B_2G_i (C_2B_2)^{-1} \frac{1}{\lambda_{\max}} \bar{C}\bar{A}_j z \\ &\leq -s^T C_2B_2 \lambda_{\max} (C_2B_2)^{-1} \frac{1}{\lambda_{\max}} \bar{C}\bar{A}_j z \\ &= -s^T \bar{C}\bar{A}_j z. \end{aligned} \tag{36}$$

That is,

$$(II) \leq -s^T \bar{C}\bar{A}_j z \tag{37}$$

holds in any case by virtue of switching function (26). Similarly, it follows from (27) that

$$\begin{aligned} (III) &\leq -||B_2^T C_2^T s||_1 \ \hat{\rho}_j \ ||G_j|| \\ &\leq -||B_2^T C_2^T s|| \ \hat{\rho}_j \ ||G_j||, \end{aligned} \tag{38}$$

where the fact that $||x|| \leq ||x||_1$ with x being a vector is used. Substituting (34), (37) and (38) into (33) it follows that

$$\begin{aligned}
\dot{V} &\leq \sum_{i=1}^{r}\sum_{j=1}^{r}\alpha_i\alpha_j\Big\{s^T\bar{C}\bar{A}_i z + s^T C_2 B_2 G_i \mathcal{U}_i \\
&\quad -\mu||s|| - s^T\bar{C}\bar{A}_j z - ||B_2^T C_2^T s||\ \hat{\rho}_j\ ||G_j||\Big\} \\
&\quad -\sum_{i=1}^{r}\gamma_{1i}^{-1}\tilde{c}_i\dot{\hat{c}}_i - \sum_{i=1}^{r}\gamma_{2i}^{-1}\tilde{k}_i\dot{\hat{k}}_i \\
&= -\mu||s|| + \sum_{i=1}^{r}\alpha_i\Big\{s^T\bar{C}\bar{A}_i z + s^T C_2 B_2 G_i \mathcal{U}_i \\
&\quad -s^T\bar{C}\bar{A}_i z - ||B_2^T C_2^T s||\ \hat{\rho}_i\ ||G_i||\Big\} \\
&\quad -\sum_{i=1}^{r}\gamma_{1i}^{-1}\tilde{c}_i\dot{\hat{c}}_i - \sum_{i=1}^{r}\gamma_{2i}^{-1}\tilde{k}_i\dot{\hat{k}}_i \\
&\leq -\mu||s|| + \sum_{i=1}^{r}\alpha_i\Big\{||B_2^T C_2^T s||||G_i||||\mathcal{U}_i|| \\
&\quad -||B_2^T C_2^T s||\ \hat{\rho}_i\ ||G_i||\Big\} \\
&\quad -\sum_{i=1}^{r}\gamma_{1i}^{-1}\tilde{c}_i\dot{\hat{c}}_i - \sum_{i=1}^{r}\gamma_{2i}^{-1}\tilde{k}_i\dot{\hat{k}}_i. \qquad (39)
\end{aligned}$$

Further, substituting (2), (28), and adaptive laws (29), (30) into (39), we obtain

$$\begin{aligned}
\dot{V} &\leq -\mu||s|| \\
&\quad +\sum_{i=1}^{r}\alpha_i\Big\{||B_2^T C_2^T s||||G_i||(c_i^* + k_i^*||z||) \\
&\quad -||B_2^T C_2^T s||||G_i||(\hat{c}_i + \hat{k}_i||z||)\Big\} \\
&\quad +\sum_{i=1}^{r}\alpha_i\left(\epsilon_1\tilde{c}_i\hat{c}_i - ||G_i||||B_2^T C_2^T s||\tilde{c}_i\right) \\
&\quad +\sum_{i=1}^{r}\alpha_i\left(\epsilon_2\tilde{k}_i\hat{k}_i - ||G_i||||B_2^T C_2^T s||||z||\tilde{k}_i\right) \\
&= -\mu||s|| + \sum_{i=1}^{r}\alpha_i\left(\epsilon_1\tilde{c}_i\hat{c}_i + \epsilon_2\tilde{k}_i\hat{k}_i\right). \qquad (40)
\end{aligned}$$

Since the facts that

$$\begin{aligned}
\epsilon_1\tilde{c}_i\hat{c}_i &= \frac{\epsilon_1}{2}\left(2\tilde{c}_i c_i^* - 2\tilde{c}_i^2\right) \\
&= \frac{\epsilon_1}{2}\left(-\tilde{c}_i^2 - (\tilde{c}_i - c_i^*)^2 + c_i^{*2}\right) \\
&\leq -\frac{1}{2}\epsilon_1\tilde{c}_i^2 + \frac{1}{2}\epsilon_1 c_i^{*2}, \qquad (41) \\
\epsilon_2\tilde{k}_i\hat{k}_i &\leq -\frac{1}{2}\epsilon_2\tilde{k}_i^2 + \frac{1}{2}\epsilon_2 k_i^{*2} \qquad (42)
\end{aligned}$$

hold, it yields that

$$\begin{aligned}
\dot{V} &\leq -\mu||s|| - \frac{1}{2}\sum_{i=1}^{r}\alpha_i\left(\epsilon_1\tilde{c}_i^2 + \epsilon_2\tilde{k}_i^2\right) + \varepsilon \\
&= -\mu||s|| + \varepsilon \\
&\quad -\frac{1}{2}\sum_{i=1}^{r}\alpha_i\left(\epsilon_1\gamma_{1i}\gamma_{1i}^{-1}\tilde{c}_i^2 + \epsilon_2\gamma_{2i}\gamma_{2i}^{-1}\tilde{c}_i^2\tilde{k}_i^2\right), \qquad (43)
\end{aligned}$$

where

$$\varepsilon \leq \frac{1}{2}\sum_{i=1}^{n}(\epsilon_1 c_i^{*2} + \epsilon_2 k_i^{*2}). \qquad (44)$$

Let

$$\begin{aligned}
\eta_1 &= \min\{\alpha_1\epsilon_1\gamma_{11}, \alpha_2\epsilon_1\gamma_{12}, \ldots, \alpha_r\epsilon_1\gamma_{1r}\} \qquad (45) \\
\eta_2 &= \min\{\alpha_1\epsilon_2\gamma_{21}, \alpha_2\epsilon_2\gamma_{22}, \ldots, \alpha_r\epsilon_2\gamma_{2r}\}, \qquad (46)
\end{aligned}$$

then,

$$\begin{aligned}
\dot{V} &\leq -\mu s^T s - \frac{1}{2}\sum_{i=1}^{r}\left(\eta_1\gamma_{1i}^{-1}\tilde{c}_i^2 + \eta_2\gamma_{2i}^{-1}\tilde{k}_i^2\right) + \varepsilon \\
&\leq -\eta\left\{\frac{1}{2}s^T s + \frac{1}{2}\sum_{i=1}^{r}\left(\gamma_{1i}^{-1}\tilde{c}_i^2 + \gamma_{2i}^{-1}\tilde{k}_i^2\right)\right\} + \varepsilon \\
&= -\eta V + \varepsilon, \qquad (47)
\end{aligned}$$

where

$$\eta = \min\{2\mu, \eta_1, \eta_2\}. \qquad (48)$$

From (47) we have

$$V \leq \frac{\varepsilon}{\eta} + \left(V(0) - \frac{\varepsilon}{\eta}\right)e^{-\eta t}, \qquad (49)$$

where $V(0) = V(z(t))|_{t=0}$. Since that $\eta > 0$, the second block on the right side of (49) tends to 0 when $t \to \infty$. Therefore, we can get that there exists $\mathcal{T}$ such that for $t \geq \mathcal{T}$ it satisfies

$$\|s\| \leq \tau \qquad (50)$$

where

$$\tau = \sqrt{\frac{\varepsilon}{\eta}}. \qquad (51)$$

This completes the proof. □

Remark 3: In the control law, there are two switching functions, ψ_i and ϕ_i, in which ϕ_i contains a sign function. Such a sign function usually leads to control chattering, which is undesirable in practice because it involves high control activity and further may excite unmodeled high frequency plant dynamics. Fortunately, switching function ψ_i is not around the sliding surface, $s = 0$. This implies that when the system state enters the region $||s|| \leq \tau$, the chattering phenomenon can be avoided most likely, which can be confirmed in the simulation shown later on. In case the chattering phenomenon occurs, it can be eliminated by replacing all sign functions with the so-called saturation functions [9].

C. Relaxing Conservatism

In theorem 2, it is desirable to have the largest η and the smallest τ so that the sliding mode s can shrink most quickly in a ball centered at the sliding surface $s = 0$ with radius τ. Therefore, the results obtained above are basically conservative since it took no account of the matter.

On the other hand, to our best knowledge, there is not an analytical approach to solve the optimization problem with respect

to η and τ. Therefore, the only way left to us is that we do our best to increase η and reduce τ. From (45), (46) and (48), we observe that a bigger μ, ϵ_j, γ_{ji} ($j = 1, 2, i = 1, 2, \cdots, r$), can help make η larger. At the same time, from (44) and (51) we know that a bigger ϵ_j leads to a bigger ε, further to a bigger τ. That is, there is a trade-off between making τ small and η big in terms of ϵ_j. Therefore, in order to make η big, we can do something on μ, ϵ_j, and γ_{ji} as follows.

- Choosing bigger μ, γ_{ji}. In the adaptive laws (29), (30) since γ_{ji} are free design parameters, basically they can be chosen arbitrarily large. However, there is a limit that large γ_{ji} can lead to big η_j, further to a big η due to the minimum in function in (48).
- Choosing bigger ϵ_j. As γ_{ji}, they are free design parameters in (29), (30) as well and can be chosen arbitrarily large. However, large ϵ_j will lead to a large τ at the same time. That is, we have to make a compromise between making η big and τ small in terms of ϵ_j.

Next, let us consider the problem of making τ small. As mentioned previously, since choosing small ϵ_j to make τ small is in conflict with increasing η, therefore, there is a limit on doing something about ϵ_j.

Again, let us focus on (44). Instead of (29), (30), if the adaptive laws are synthesized by

$$\dot{\hat{c}}_i(t) = \alpha_i \gamma_{1i} \left\{ -\epsilon_1 (\hat{c}_i(t) - c_{0i}) + ||G_i|| ||B_2^T C_2^T s|| \right\}, \quad (52)$$

$$\dot{\hat{k}}_i(t) = \alpha_i \gamma_{2i} \left\{ -\epsilon_2 (\hat{k}_i(t) - k_{0i}) + ||G_i|| ||B_2^T C_2^T s|| ||z|| \right\} \quad (53)$$

where γ_{ji}, and ϵ_{ji} are positive design parameters, c_{0i}, k_{0i} are a priori estimates of c_i^*, k_i^*, respectively, then (44) becomes

$$\varepsilon \leq \frac{1}{2} \sum_{i=1}^{n} \left\{ \epsilon_1 (c_i^* - c_{0i})^2 + \epsilon_2 (k_i^* - k_{0i})^2 \right\}. \quad (54)$$

From (54), we can see that the better a priori estimates for c_i^* and k_i^*, the smaller ε which further leads to a smaller τ in (51) we can get. Of course, if we do not have such knowledge about c_i^* and k_i^*, we can just put $c_{0i} = 0, k_{0i} = 0$.

IV. Simulation

Consider the well-studied example of balancing an inverted pendulum on a cart. The equations of motion for the pendulum are

$$\begin{cases} \dot{x}_1 = x_2, \\ \dot{x}_2 = \frac{g \sin(x_1) - \frac{aml x_2^2 \sin(2x_1)}{2} - a \cos(x_1)(u + \mathcal{U})}{\frac{4l}{3} - aml \cos^2(x_1)}, \end{cases} \quad (55)$$

where x_1 denotes the angle of the pendulum from the vertical; x_2, the angular velocity; u, the force applied to the cart; $g = 9.8 m/s^2$, the gravity constant; m, the mass of the pendulum; M, the mass of the cart (in kilo-Newton); $\mathcal{U}$, the lumped uncertainty, which is assumed to be $\mathcal{U} = 0.5 \cos(2\pi) + 1.5 \cos(4\pi)||x||$; $a = \frac{1}{m+M}$. We choose $m = 2.0$ kg, $M = 8.0$ kg, $l = 0.5$ m in this simulation.

The control objective is to balance the inverted pendulum. Here, Referring to [11] we approximate the system by the following two-rule T-S fuzzy model:

Plant Rule 1 : IF x_1 is $\widetilde{0}$
THEN $\dot{x} = A_1 x + B_1 (u + \mathcal{U}_1)$;

Plant Rule 2 : IF x_1 is $\pm \widetilde{\pi/2}$
THEN $\dot{x} = A_2 x + B_2 (u + \mathcal{U}_2)$,

where

$$A_1 = \begin{bmatrix} 0 & 1 \\ \frac{g}{\frac{4l}{3} - aml} & 0 \end{bmatrix}, \quad B_1 = \begin{bmatrix} 0 \\ \frac{-a}{\frac{4l}{3} - aml} \end{bmatrix},$$

$$A_2 = \begin{bmatrix} 0 & 1 \\ \frac{2g}{\pi(\frac{4l}{3} - aml\beta^2)} & 0 \end{bmatrix}, \quad B_2 = \begin{bmatrix} 0 \\ \frac{-a\beta}{\frac{4l}{3} - aml\beta^2} \end{bmatrix},$$

$\beta = \cos(88^o)$; $\widetilde{0}, \widetilde{\pi/2}$ are fuzzy sets characterized by the following membership functions:

$$\mu_{\widetilde{0}}(x_1) = \begin{cases} \cos(x_1), & -\frac{\pi}{2} \leq x_1 \leq \frac{\pi}{2} \\ 0, & \text{otherwise} \end{cases}$$

$$\mu_{\widetilde{\pi/2}}(x_1) = \begin{cases} 1 - \cos(x_1), & -\frac{\pi}{2} \leq x_1 \leq \frac{\pi}{2} \\ 0, & \text{otherwise} \end{cases};$$

$\mathcal{U}_i$ ($i = 1, 2$) is corresponding with the lumped uncertainty in the plant (55), and satisfies *A2* in section II with $c_i^* = 0.5, k_i^* = 1.5$. Regarding their estimates, $\hat{c}_i$, $\hat{k}_i$, are tuned by adaptive laws (29), and (30) with $\gamma_{1i} = \gamma_{2i} = 0.1$, $\epsilon_{1i} = \epsilon_{2i} = 0.1$, respectively.

As to the assumption *A1*, we set $B^T = [0, -1]$ and $G_1 = 0.1765, G_2 = 0.0052$ due to the facts that $B_1^T = [0, -0.1765], B_2^T = [0, -0.0052]$ in this simulation. Since B is already composed of 0 (upper part) and -1 (lower part) in the vector, there is no longer to use an orthogonal matrix T_r for B's transformation in order to get the form, $[0, B_2]^T$ in (4). By setting $C_2 = I$ and using the software package Robust Control Toolbox (MATLAB), $C_2 = -0.5$ by solving LMIs (24).

Fig. 1 depicts the response of the system state, where the solid line is x_1 and the dotted line is x_2, with initial values $x_1(0) = 87^\circ, x_2(0) = 0$ under the control law (25) where μ is set to be 0.05. The control input u, and the sliding motion s are shown in Figs. 2, 3, respectively. We observe that when system state enters around the sliding surface, the chattering phenomenon no longer exists just we claimed in Remark 3. In addition, adaptive parameters in (29) and (30) are shown in Fig. 4. From the simulation results, it can be seen that the control approach proposed in this paper works well.

V. Conclusions

An adaptive fuzzy SMC approach for a class of nonlinear dynamical systems with lumped parameter uncertainties was proposed and analyzed. In particular, the approach could deal with the T-S fuzzy model under consideration with different control matrices in the fuzzy rules. As a future work, other uncertainties including linearization error between the real system to be controlled and its T-S fuzzy model, parameter perturbations, and external disturbances will be considered in the control approach to improve its robustness.

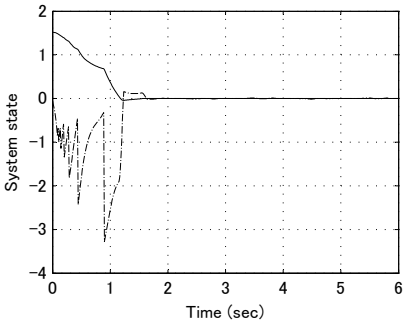

Fig. 1. System state

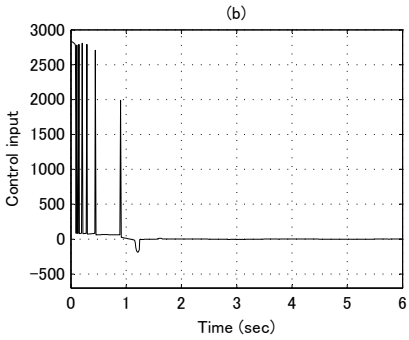

Fig. 2. Control input

REFERENCES

[1] T. Takagi, and M. Sugeno, Fuzzy identification of systems and its applications to modeling and control, *IEEE Trans. Syst., Man, Cybern.,* vol.15, pp.116-132, 1985.

[2] K. Tanaka, and M. Sugeno, Stability analysis and design of fuzzy control systems, *Fuzzy Sets Syst.,* vol.45, no.2, pp.135-156, 1992.

[3] F. Zheng, Q.-G. Wang and T. H. Lee, "Output tracking control of MIMO fuzzy nonlinear systems using variable structure control approach," *IEEE Transactions on Fuzzy Systems,* vol. 10, no. 6, pp. 686–697, 2002.

[4] C. Lin, Q.-G. Wang and T. H. Lee, "Stabilization of uncertain fuzzy time-delay systems vai variable structure control approach," *IEEE Transactions on Fuzzy Systems,* vol. 13, no. 6, pp. 787–798, 2005.

[5] D. W. C. Ho, and Y. Niu, "Robust fuzzy design for nonlinear uncertain stochastic systems via sliding-mode control," *IEEE Transactions on Fuzzy Systems,* vol. 15, no. 3, pp. 350–358, 2007.

[6] J. Zhang, P. Shi and Y. Xia, "Robust adaptive sliding-mode control for fuzzy systems with mismatched uncertainties," *IEEE Transactions on Fuzzy Systems,* vol. 18, no. 4, pp. 700–711, 2010.

[7] H. H. Choi, "Robust stabilization of uncertain fuzzy-time-delay systems using sliding-mode-control approach," *IEEE Transactions on Fuzzy Systems,* vol. 18, no. 5, pp. 979–984, 2010.

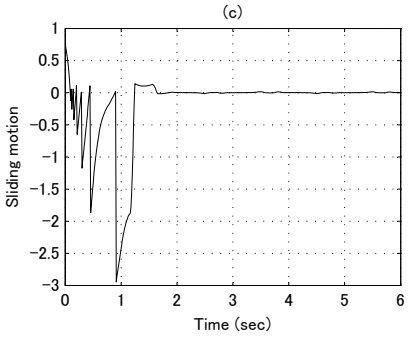

Fig. 3. Sliding motion

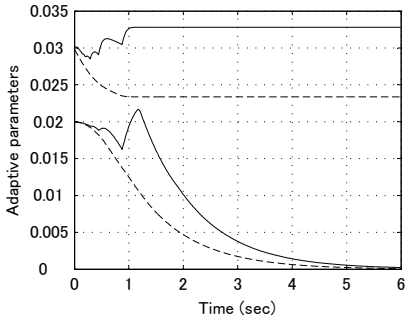

Fig. 4. Adaptive parameters

[8] C. Edwards and S. K. Spurgeon, *Sliding Mode Control: Theory and Applications,* New York: Taylor & Francis, 1998.

[9] H. Han, C.-Y. Su, and Y. Stepanenko, "Adaptive control of a class of nonlinear systems with nonlinearly parameterized fuzzy approximators," *IEEE Trans. on Fuzzy Systems,* vol. 9, no. 2, pp. 315-323, 2001.

[10] T. Hayakawa, W.M. Haddad and N. Hovakimyan "Neural network adaptive control for a class of nonlinear uncertain dynamical systems with asymptotic stability guarantees," *IEEE Trans. on Neural Networks,* vol. 19, no. 1, pp. 80–89, 2008.

[11] K. Tanaka, and H.O. Wang, *Fuzzy Control System Design and Analysis – A Linear Matrix Inequality Approach,* Wiley, New York, 2001.

2011 IEEE International Conference on Fuzzy Systems
June 27-30, 2011, Taipei, Taiwan

Mixed H_2/H_∞ Optimization with Discrete Smith Predictor for Fuzzy Decentralized Control of Nonlinear Interconnected Discrete Dynamic Systems with Large Delay

Name: Chih-Lyang Hwang, *Senior Member*, *IEEE; e-mail:* chih-lyang_hwang@hotmail.com
Department of Electrical Engineering of National Taiwan University of Science and Technology, Taiwan, R.O.C.

Abstract – **Each subsystem of a nonlinear interconnected discrete dynamic delayed system is approximated by a weighted combination of *L* pulse transfer function delayed systems (PTFDS). To deal with large time-delay of the controlled system with acceptable performance, a two-degree-of-freedom control is designed. At beginning, the H_2- norm of the difference between the transfer function of a reference model and the closed-loop transfer function of the *jth* PTFDS of subsystem *i* is minimized to obtain a suitable frequency response. In addition, the $H_\infty-$ norm of the weighted sensitivity function between the output disturbance and its corresponding output of the *jth* PTFDS is simultaneously minimized to reduce its effect. In summary, the proposed control not only accomplishes the above-mentioned optimizations but also attenuates the effect of time-delay. Furthermore the comparisons between with and without discrete Smith predictor are presented. The main contributions of this paper are three folds. First, the large nominal time-delay is compensated by a discrete Smith predictor. Secondly, the proposed control can achieve the suitable response of the closed-loop system with the attenuation of output disturbance and time-varying delay. Thirdly, an observer is not needed and the discrete controller is more suitable for the implementation.**

Keywords: **Nonlinear interconnected discrete dynamic delayed system, Decentralized control, Fuzzy linear model, H_2- optimization, $H_\infty-$ optimization, Discrete Smith predictor**.

I. INTRODUCTION

Time-delay or dead time is frequently encountered in many dynamic systems. The delay of information transmission between different subsystems, such as engine idle speed control [1], damping control in power system [2], playout or monitoring [3], an internet-based control [4], -[6] and the image processing for the dynamic target tracking of visual servo system [7], teleoperation [8]-[10], results in a time-delay system. By implementing feedback control in (especial for large) time-delay system it always results in certain restrictions on achievable system bandwidth and the maximum available gain [1]-[10]. Based on the nominal delay of each subsystem, in this paper the reduced effect of time-varying delay is achieved by Smith predictor [9]-[12].

In the past three decades, the performance properties of interconnected systems have been widely studied [12]. However, the control performance of nonlinear interconnected systems has yet received sufficient attention. Due to complicated physical configuration and high dimensionality of interconnected systems, the implementation of these systems with centralized control is neither economically plausible nor technically possible. In centralized control scheme, there are drawbacks such as the complexities in the design and debugging process. These in turn require scheduling of data collection and data storage etc. As a result, decentralized control scheme is considered a more favorable alternative for interconnected systems. However due to the inherent nonlinear interconnections among subsystems and it does not exist any efficient decentralized control scheme in dealing with interconnected nonlinear systems (e.g., the attenuation of uncertainty) [12], it needs to resort to new control scheme for such interconnected nonlinear system.

Recently, the use of fuzzy control for nonlinear systems has drawn many interests. Many successful applications have been reported in the literatures (e.g., [13], [14]). In addition, fuzzy T-S model with delayed control systems have been discussed (e.g., [15], [16]). In many of the literatures on delayed control systems, *N* linear (or bilinear) continuous-time (or discrete-time) state-space or transfer function systems for different fuzzy sets are considered. Under these circumstances, an alternative method is considered by using different pulse transfer functions with the same time delay to model the consequent parts of every subsystem. The controller design is therefore directed, simplified and more implementable. In addition, certain work does not attenuate the effect of time-delay. Facing these challenges, in this paper, we propose a controller design via mixed H_2/H_∞ optimization with discrete Smith predictor to obtain a robust and desired system performance.

Mixed H_2/H_∞ control problem has become a popular research topic in recent years [12], [17]. The response shaping based on H_2- optimization to reduce the sluggish and oscillatory effects is often adopted [18]. On the other hand, $H_\infty-$ optimization is usually used as the robust control methodology for diminishing the effect of disturbance [5], [6], [17]. As a result, the mixed H_2/H_∞ control problem is developed to robust system stability and to improve system performance [12]. Differences between this paper and previous papers [12] and [17] are described as follows: The paper in [17] did not discuss the time-delay property and its compensation; the paper in [12] discussed the controller design in the continuous time system and did not compare the

978-1-4244-7316-8/11/$26.00 ©2011 IEEE

controller with and without Smith predictor.

For an easy implementation of the proposed controller, a discrete design ([17], [19]) is considered. At the outset, a specific pulse transfer function system (PTFDS) with respect to a specific operating point is obtained by implementing the least-square parameter estimation technique. After that a nominal and large time-delay is also estimated. To enhance system performance a two-degree-of-freedom controller with discrete Smith predictor is employed to each PTFDS. Subsequently, the H_2-norm of the difference between an assigned reference model and the closed-loop transfer function of the *jth* PTFDS of subsystem *i* is minimized to attain a suitable frequency response without causing any oscillating and sluggish effects. However, the system performance may be deteriorated or even unstable due to the output disturbance caused by the interconnections among subsystems, the interactions from other PTFDSs, the error from fuzzy modeling, and/or the nonlinear time-varying uncertainties. To prevent this, the $H_\infty-$ norm of the weighted sensitivity of the *jth* PTFDS between the output disturbance and its output is minimized to reduce its effect. Moreover, a specific weighted function can be selected to reject certain mode of output disturbance or to attenuate its effect in the system frequency response. In this operation it does not need to solve the Diophantine equation; it has the computational advantage especially for low-order system.

II. Mathematical Preliminaries

A polynomial $\in \Re(z)$ is defined as $A(d)=a_{n_a}d^{n_a}+a_{n_a-1}d^{n_a-1}+...+a_0$, where a_i for $i=0,1,...,n_a$ denotes bounded coefficients, n_a stands for the system degree (i.e., if $a_{n_a}\neq 0$, $\deg\{A(d)\}=n_a$), and $d=z^{-1}$ denotes the backward shift operator (i.e., $z^{-1}y(k)\equiv y(k-1)$) or a complex variable in the z-transform. The z-transform of a discrete-time signal $y(k)$ is denoted by $Y(z^{-1})=Z\{y(k)\}$. If $a_0=1$ it is called a monotonic polynomial. The notations of $A_+(d)$ and $A_-(d)$ denote respectively the stable and unstable part of $A(d)$. The polynomial $A_+(d)$ is assumed to be monotonic to obtain a unique factorization. Define $\|G(d)\|_2=\|G(e^{-jw})\|_2=\left[\int_{-\infty}^{\infty}|G(e^{jw})|^2 dw/2\pi\right]^{1/2}$, where $G\in H_2$, the set H_2 consists of all analytic functions G in $|z|\geq 1$. A rational function $G(d)$ in H_2 is called inner if $|G(e^{-jw})|=1$ for almost all *w*, and it is outer if it has no zeros in $|z|\geq 1$. For any rational functions $G(d)$ and $H(d)$ in H_2, if $G(d)$ is inner function and $\|G(d)H(d)\|_2$ is well defined, then $\|G(d)H(d)\|_2=\|H(d)\|_2$. When a rational function multiplies by an inner function it preserves the value of the norm [12], [17]. The rational function $A_-(d)/\tilde{A}_-(d)$ is a stable, causal, and all-pass operator, i.e., $|A_-(e^{-jw})/\tilde{A}_-(e^{-jw})|=1$ for all *w*, and $\tilde{A}_-(d)=d^{n_{a-}}A_-(d^{-1})$. The notation $\|A(e^{-jw})\|_\infty=ess.\sup_w|A(e^{-jw})|$ is defined. The symbol $A_i^j(d)$ denotes a polynomial with bounded coefficients, its upper subscript *j* and lower subscript *i* respectively represent the polynomial of the *jth* PTFDS of subsystem *i*. The following lemma is given to explain the result of the minimax optimization for the *jth* PTFDS of subsystem *i*.

Lemma 1 [12], [17]: (i) The optimal $C_{2_i}^{j^*}=\left[W_i^j(d)V_i^j(d)\right]^*$, which minimizes $\|W_i^j(d)V_i^j(d)\|_\infty$, is of an all-pass form:

$$\left[W_i^j(d)V_i^j(d)\right]^*=\begin{cases}\rho_i^j\tilde{\Phi}_i^j(d)/\Phi_i^j(d), & \text{if } n_{b_{-i}}^j=n_{\phi_i}^j+1\geq 1\\ 0, & \text{if } n_{b_{-i}}^j=0\end{cases}$$

where the polynomial $\Phi_i^j(d)$ is monic and stable.

(ii) The constants ρ_i^j and $\varphi_{m_i}^j\ (1\leq m\leq n_{\phi_i}^j)$ are real and are uniquely determined by the interpolation constraints (29) as described later. Furthermore, the minimized $\|W_i^j(d)V_i^j(d)\|_\infty$ is given by

$$\min\|W_i^j(d)V_i^j(d)\|_\infty=\left\|\left[W_i^j(d)V_i^j(d)\right]^*\right\|_\infty=|\rho_i^j|.$$

III. Problem Formulation

Consider the following nonlinear interconnected discrete dynamic delayed system (NIDDDS) Σ that contains *N* subsystems Σ_i for $i=1,2,...,N$:

$$y_i(k)=f_{ii}\left[\varphi_i(k-\tau_i(k))\right]+\sum_{j=1,j\neq i}^{N}f_{ij}\left[\varphi_j(k-\tau_j(k))\right],\quad i=1,2,...,N \tag{1}$$

where $\varphi_i(k)=[y_i(k-1)\ \cdots\ y_i(k-n)\ \ u_i(k-1)\ \cdots\ u_i(k-m)]$; $y_i(k)$ and $u_i(k)$ denote the system output and the system input of the *ith* subsystem at time *k*, respectively; are the; $f_{ii}\left[\varphi_i(k-\tau_i(k))\right]$ denotes the unknown but smooth nonlinear delay function of the *ith* subsystem; $\tau_i(k)\geq 0$ is the time-varying delay of the *ith* subsystem; $f_{ij}\left[\varphi_j(t-\tau_j(k))\right]$, $j\neq i$, $i,j=1,2,...,N$, represent the smooth but unknown interconnections of the *ith* subsystem Σ_i, brought about by other subsystems Σ_m, where $m=1,...,N$, and $m\neq i$.

Based on the approximation of the fuzzy linear model [12], a fuzzy dynamic model to represent the local linear input/output relations of the *ith* subsystem (see Fig. 1) is described by the fuzzy IF-THEN rules. The *jth* rule of the fuzzy dynamic model for the *ith* subsystem Σ_i with uncertainties is expressed in the following form:

System Rule j: IF $z_{1_i}(k)$ is $M_{1_i}^j$... and $z_{\bar{m}_i}(k)$ is $M_{\bar{m}_i}^j$ THEN

$$y_i(k)=d^{\bar{\tau}_i}B_i^j(d)u_i(t)\big/A_i^j(d)+\sum_{m=1,\,m\neq i}^{N}d^{\tau_{im}(k)}B_{im}^j(d)u_m(k)\Big/A_{im}^j(d)$$
$$+\sum_{m=1,\,m\neq i}^{N}\Delta_{im}^j(u_m(k),k)+w_i(k), \qquad (2)$$

where $j=1,2,...,L$, $i=1,2,...,N$; $\bar{m}_i\le n_{a_i}^j+n_{b_i}^j+1, A_i^j(1)=1$; L is the number of IF-THEN rules; $z_{1_i}(k),...,z_{\bar{m}_i}(k)$ are premise variables, which are functions of $y_i(k-1),...,y_i(k-n)$, $u_i(k-1),...,u_i(k-m)$; $\bar{\tau}_i$ is a positive integer denoting the nominal delay of subsystem i (in this paper, it is generally several hundred); $y_i(k)$ also denotes the output from the *jth* IF-THEN rules; $d^{\bar{\tau}_i}B_i^j(d)u_i(k)\big/A_i^j(d)$ is the *jth* nominal and known PTFDS of subsystem i; $\sum_{m=1,m\neq i}^{N}d^{\tau_{im}(k)}B_{im}^j(d)u_m(d)\big/A_{im}^j(d)$ denotes the linear coupling terms; $\sum_{m=1,m\neq i}^{N}\Delta_{im}^j(u_m(k),k)$ denotes the nonlinear time-varying uncertainties, that are relatively bounded by $c_0+\sum_{i=1}^{N}c_i\|u_i(k)\|_2$, where $c_i\ge 0,\ i=0,1,...,N,$ and caused by the interconnections of other subsystems and the interactions from other PTFDSs; and $w_i(k)$ denotes the approximation error of the fuzzy model of the *ith* subsystem, e.g., time-varying delay, parameter variations. Assume that $A_i^j(d)$ and $B_i^j(d)$ for $i=1,2,...,N,\ j=1,2,...,L$ are coprime. One of main advantages of this form is that no state estimator is required; then the control design becomes simple and effective.

The output of the overall fuzzy system of the *ith* subsystem is inferred as follows:

$$y_i(k)=\sum_{j=1}^{L}\mu_i^j(k)\left\{d^{\bar{\tau}_i}B_i^j(d)u_i(k)\big/A_i^j(d)+\tilde{d}_{o_i}^j(k)\right\} \qquad (3)$$

where

$$\tilde{d}_{o_i}^j(k)=\sum_{m=1,\,m\neq i}^{N}\left\{d^{\tau_{im}(k)}B_{im}^j(d)u_m(k)\big/A_{im}^j(s)+\Delta_{im}^j(u_m(k),k)\right\}+w_i(k) \qquad (4)$$

$$\mu_i^j(k)=h_i^j(k)\Big/\sum_{j=1}^{L}h_i^j(k) \text{ and } h_i^j(t)=\prod_{m=1}^{\bar{m}_i}M_i^k(z_{i_m}(t)). \qquad (5)$$

It is assumed that

$$h_i^j(k)\ge 0,\ \sum_{j=1}^{L}\mu_i^j(k)=1 \quad \text{for } i=1,2,...,N,\ j=1,2,...,L, \text{ and } \forall k. \qquad (6)$$

It is also assumed that the fuzzy controller shares the same fuzzy sets with the fuzzy system (2).

Control Rule j: IF $z_{1_i}(k)$ is $M_{1_i}^j$... and $z_{\bar{m}_i}(k)$ is $M_{\bar{m}_i}^j$ THEN

$$u_i(k)=-S_i^j(d)y(k)\big/R_i^j(d)+T_i^j(d)r_i(k)\big/R_i^j(d)$$
$$-S_i^j(d)B_i^j(d)\left(1-d^{\bar{\tau}_i}\right)u_i(k)\Big/\left(R_i^j(d)A_i^j(d)\right) \qquad (7)$$

where the polynomials $R_i^j(d), S_i^j(d)$ and $T_i^j(d)$ are determined to achieve the control of the *jth* PTFDS of subsystem i, and the last term in (7) denotes the Smith predictor to deal with the nominal system delay. The overall fuzzy control of the *ith* subsystem is then inferred as follows:

$$u_i(k)=\sum_{j=1}^{L}\mu_i^j(k)\left\{-S_i^j(d)y(k)\big/R_i^j(d)+T_i^j(d)r_i(d)\big/R_i^j(d)\right.$$
$$\left.-S_i^j(d)B_i^j(d)\left(1-d^{\bar{\tau}_i}\right)u_i(k)\Big/\left(R_i^j(d)A_i^j(d)\right)\right\}. \qquad (8)$$

The nominal closed-loop characteristic polynomial of the *jth* PTFDS of subsystem i is also described as follows:

$$A_{c_i}^j(d)=A_i^j(d)R_i^j(d)+B_i^j(d)S_i^j(d). \qquad (9)$$

Hence, the closed-loop output response of the *ith* subsystem, i.e., $y_i(t)$, is derived from (3) and (7); i.e.,

$$y_i(k)=\sum_{j=1}^{L}\mu_i^j(k)\left\{d^{\bar{\tau}_i}B_i^j(d)\left[u_i^j(k)+u_i(k)-u_i^j(k)\right]\Big/A_i^j(d)+\hat{d}_{o_i}^j(k)\right.$$
$$=\sum_{j=1}^{L}\mu_i^j(k)\left\{d^{\bar{\tau}_i}B_i^j(d)\left[-S_i^j(d)y_i(k)+T_i^j(d)r_i(k)\right]\Big/\left[A_i^j(d)R_i^j(d)\right]\right.$$
$$\left.+\psi_i^j(k)+\hat{d}_{o_i}^j(k)\right\}$$
$$=\sum_{j=1}^{L}\mu_i^j(k)\left\{d^{\bar{\tau}_i}B_i^j(d)\left[-S_i^j(d)y_i(k)+T_i^j(d)r_i(k)\right]\Big/\left[A_i^j(d)R_i^j(d)\right]\right.$$
$$\left.+d_{o_i}^j(k)\right\} \qquad (10a)$$

where $u_i^j(k)$ denotes the control input of the *jth* PTFDS of subsystem i (i.e., (7)),

$$\psi_i^j(k)=d^{\bar{\tau}_i}B_i^j(d)\left[u_i(k)-u_i^j(k)\right]\Big/A_i^j(d),$$
$$d_{o_i}^j(k)=\hat{d}_{o_i}^j(k)+\psi_i^j(k). \qquad (10b)$$

The signal $\psi_i^j(k)$ denotes the interaction on the *jth* PTFDS of subsystem i resulting from other PTFDSs, including the error between nominal delay and time-varying delay. In summary, $d_{o_i}^j(k)$ denotes the output disturbance of the *jth* PTFDS of subsystem i caused by the interconnections stemming from other subsystems, the interactions resulting from other PTFDSs, the approximation error of fuzzy-model, and the nonlinear time-varying uncertainties. In general, the corresponding output disturbance is not small and even including various frequency components. In this situation, an effective controller is required to achieve satisfactory performance.

After some mathematical manipulations of (10a) and using (7), the following is achieved.

$$\sum_{j=1}^{L}\frac{\mu_i^j(k)A_{c_i}^j(d)}{A_i^j(d)R_i^j(d)}\left\{y_i(k)-\frac{d^{\bar{\tau}_i}B_i^j(d)T_i^j(d)}{A_{c_i}^k(s)}r_i(k)\right.$$
$$\left.-\frac{A_i^j(d)R_i^j(d)}{A_{c_i}^j(d)}d_{o_i}^j(k)\right\}=0. \qquad (11)$$

Hence, a sufficient condition for the validity of (11) is the term in the braces $\{\cdot\}$ of (11) to be equal to zero; i.e.,

$$y_i(k)=d^{\bar{\tau}_i}B_{-_i}^j(d)L_i^j(d)r_i(k)-V_i^j(d)d_{o_i}^j(k) \qquad (12a)$$

where

$$L_i^j(d)=B_{+_i}^j(d)T_i^j(d)\big/A_{c_i}^j(d),$$
$$V_i^j(d)=A_i^j(d)R_i^j(d)\big/A_{c_i}^j(d). \qquad (12b)$$

The aforementioned output disturbance is supposed to be bounded as follows (see (4), (10b)):

$$\left\| d_{o_i}^j(k) \right\|_2 \le \alpha_{0_i}^j + \sum_{m=1}^{N} \alpha_{m_i}^j \left\| u_i(k) \right\|_2 \quad (13)$$

where $\alpha_{0_i}^j$ and $\alpha_{m_i}^j$, $i, j, m = 1, 2, ..., N$ are bounded [12].

Assume that the input/output relationship between $r_i(t)$ and $\bar{y}_i^j(t)$, for a stable reference model of the *jth* PTFDS of subsystem *i*, is as follows:

$$\bar{y}_i^j(k) = d^{\bar{\tau}_i} G_i^j(d) r_i(k) / F_i^j(d) \quad (14)$$

where $G_i^j(d)$ and $F_i^j(d)$ for $i = 1, 2, ..., N, j = 1, 2, ..., L$ are coprime, and $F_i^j(d)$ is a stable monic polynomial with degree $n_{f_i}^j$. The purpose of using a reference model is to shape the response of the closed-loop of the *jth* PTFDS of subsystem *i*. For tracking a set-point, $G_i^j(1)/F_i^j(1) = 1$ is assigned.

For synthesizing the problem, two cost functions in the H_2 – norm and H_∞ – norm spaces are defined as follows [12], [17]:

$$C_{1_i}^j = \left\| d^{\bar{\tau}_i} \left[G_i^j(d)/F_i^j(d) - B_{-_i}^j(d) L_i^j(d) \right] \right\|_2 \quad \text{and} \quad C_{2_i}^j = \left\| W_i^j(d) V_i^j(d) \right\|_\infty \quad (15)$$

For $d_{o_i}^j(k) = 0$, the optimal model matching to the cost function $C_{1_i}^j$ is addressed as follows: Based on the norm-preserving property of the inner function (i.e., $\left\| e^{-jw\bar{\tau}_i} \right\| = 1 \forall w$), from eqn. (15) $C_{1_i}^j$ is reduced to the following equation:

$$C_{1_i}^j = \left\| G_i^j(d)/F_i^j(d) - B_{-_i}^j(d) L_i^j(d) \right\|_2. \quad (16)$$

At beginning, the polynomial $B_{-_i}^j(d)$ is factorized as

$$B_{-_i}^j(d) = B_{-_i}^j(d^{-1}) \cdot B_{-_i}^j(d) / B_{-_i}^j(d^{-1}) \quad (17)$$

where $B_{-_i}^j(d)/\tilde{B}_{-_i}^j(d)$ is an inner function and the remaining $\tilde{B}_{-_i}^j(d)$ is an outer function. Then

$$C_{1_i}^j = \left\| G_i^j(d)/F_i^j(d) - L_i^j(d)\tilde{B}_{-_i}^j(d) B_{-_i}^j(d)/\tilde{B}_{-_i}^j(d) \right\|_2 = \left\| B_{-_i}^j(d)/\tilde{B}_{-_i}^j(d) \left[\tilde{B}_{-_i}^j(d) G_i^j(d) / \left(F_i^j(d) B_{-_i}^j(d) \right) - L_i^j(d)\tilde{B}_{-_i}^j(d) \right] \right\|_2. \quad (18)$$

Similarly, based on the norm-preserving property of the inner function, (18) is simplified as follows:

$$\left(C_{1_i}^j \right)^2 = \left\| \tilde{B}_{-_i}^j(d) G_i^j(d) / \left(F_i^j(d) B_{-_i}^j(d) \right) - L_i^j(d)\tilde{B}_{-_i}^j(d) \right\|_2^2. \quad (19)$$

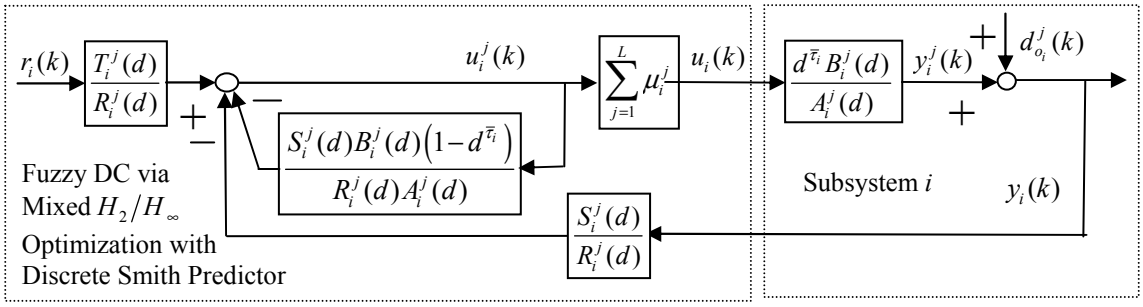

Fig.1.The overall control block diagram.

where the weighted function $W_i^j(d)$ denotes a suitable rational function for the *jth* PTFDS of subsystem *i*.

The objectives of this paper are expressed as follows (cf. Fig. 1): Search for a control function (i.e., the polynomials $R_i^j(d), S_i^j(d)$, and $T_i^j(d)$) so as to simultaneously satisfy the following two requirements: (i) For $d_{o_i}^j(k) = 0$, the cost function $C_{1_i}^j$ is minimized, (ii) The cost function $C_{2_i}^j$ is simultaneously minimized.

IV. Controller Design using Mixed H_2/H_∞ Optimization

There are two processes in the design of the decentralized fuzzy controller via mixed H_2/H_∞ optimization for the NIDDDS (1).

A. Minimization of $C_{1_i}^j$

Decomposing the first term yields

$$B_{-_i}^j(d^{-1}) G_i^j(d) / \left(F_i^j(d) B_{-_i}^j(d) \right) = \bar{F}_i^j(d)/F_i^j(d) + \bar{B}_i^j(d)/B_{-_i}^j(d) \quad (20)$$

Rewrite (20) as

$$\tilde{B}_{-_i}^j(d) G_i^j(d) = B_{-_i}^j(d) \bar{F}_i^j(d) + F_i^j(d) \bar{B}_i^j(d)$$

where $\bar{F}_i^j(d)$ and $\bar{B}_i^j(d)$ are some polynomials to be determined, which are interrelated respectively with the control polynomial $T_i^j(d)$ and the optimum value of $C_{1_i}^j$.

$$\text{or } \tilde{B}_{-_i}^j(d) G_i^j(d) - B_{-_i}^j(d) \bar{F}_i^j(d) \Big|_{d = z_1^j, ..., z_{n_{f_i}}^j} = 0 \quad (21)$$

where $z_1^j, ..., z_{n_{f_i}}^j$ are the zeros of $F_i^j(d) = 0$. Then the polynomial $\bar{B}_i^j(d)$ can be obtained from (21) by long division. Substituting (20) into (19) gives

$$\left(C_{1_i}^j \right)^2 = \left\| \bar{F}_i^j(d)/F_i^j(d) + \bar{B}_i^j(d)/B_{-_i}^j(d) - L_i^j(d)\tilde{B}_{-_i}^j(d) \right\|_2^2 \quad (22)$$

where the second term in the right hand side of (22) is

unstable, and the remaining terms are stable. By orthogonality, it follows that

$$\left(C_{1_i}^j\right)^2 = \left\| \bar{F}_i^j(d)/F_i^j(d) - L_i^j(d)\tilde{B}_{-_i}^j(d)\right\| + \left\|\bar{B}_{-_i}^j(d)/B_{-_i}^j(d)\right\|_2^2 \geq \left\|\bar{B}_i^j(d)/B_{-_i}^j(d)\right\|_2^2. \quad (23)$$

Hence, the optimal $L_i^j(d)^*$ and $C_{1_i}^{j*}$ are achieved as follows:

$$L_i^j(d)^* = \bar{F}_i^j(d)/\left(F_i^j(d)\tilde{B}_{-_i}^j(d)\right) \quad (24)$$

$$C_{1_i}^{j*} = \left\|\bar{B}_i^j(d)/B_{-_i}^j(d)\right\|_2. \quad (25)$$

Comparing (24) and (12b) and using (9) it gives

$$A_i^j(d)R_i^j(d) + B_i^j(d)S_i^j(d) = B_{+_i}^j(d)\tilde{B}_{-_i}^j(d)F_i^j(d)X_i^j(d) \quad (26)$$

$$T_i^j(d) = \bar{F}_i^j(d)X_i^j(d) \quad (27)$$

where $X_i^j(d)$ is a stable polynomial. If the reference model contains the unstable zeros of the nominal system, i.e., $G_i^j(s) = B_{-_i}^j(d)\bar{G}_i^j(d)$, for some polynomials $\bar{G}_i^j(d)$, then the perfect model matching (i.e., $C_{1_i}^{j*} = 0$) can be obtained. Then from (20) it has,

$$\bar{F}_i^j(d) = B_{-_i}^j(d^{-1})\bar{G}_i^k(s) \text{ and } \bar{B}_i^j(d) = 0. \quad (28)$$

B. Minimization of $C_{2_i}^j$

In this subsection, the task is to find the polynomials $R_i^j(d)$ and $S_i^j(d)$ such that the optimal $C_{2_i}^j$ is obtained. From previous studies [12], [17], the optimal $\left\|W_i^j(d)V_i^j(d)\right\|_\infty$ must satisfy the following interpolation constraints:

$$V_i^j(p_i^j) = 0, j = 1,2,...,n_{a_{-_i}}^j,\ 1 - V_i^j(z_i^j) = 0, j = 1,2,...,n_{b_{-_i}}^j \quad (29)$$

where $p_i^j (1 \le j \le n_{a_{-_i}}^j)$ and $z_m^j (1 \le j \le n_{b_{-_i}}^j)$ denote the zeros of $A_{-_i}^j(d)$ and $B_{-_i}^j(d)$, respectively.

Remark 1: If the inner loop of Fig. 1 disappears (e.g., [17]), then the characteristic polynomial of the closed-loop system in (9) is replaced by the following equation:

$$A_{c_i}^j(d) = A_i^j(d)R_i^j(d) + d^{\bar{\tau}_i}B_i^j(d)S_i^j(d). \quad (30)$$

Then the second interpolation constraint of (19) is modified as follows:

$$1 - V_i^j(z_i^j) = 0, j = 1,2,...,n_{b_{-_i}}^j + \bar{\tau}_i \quad (31)$$

where $z_m^j (1 \le j \le n_{b_{-_i}}^j + \bar{\tau}_i)$ denote the zeros of $d^{\bar{\tau}_i}B_{-_i}^j(d)$. The degree of $\Phi_i^j(d)$ becomes $n_{\varphi_i}^j = n_{b_{-_i}}^j - 1 + \bar{\tau}_i$, which is large especially for large time-delay system (e.g., $\bar{\tau}_i$ equals several hundred for the internet-based piezoelectric actuator driven table system). In summary, the degrees of control polynomials increase and the effect of time-delay is dominant for the control without using Smith predictor.

Based on the result of *Lemma 1* and the constraint (29), the following equation is achieved

$$V_i^j(d) = \rho_i^j W_{d_i}^j(d)A_{-_i}^j(d)\tilde{\Phi}_i^j(d)/\left[W_{n_i}^j(d)\tilde{A}_{-_i}^j(d)\Phi_i^j(d)\right] \quad (32)$$

where $W_i^j(d) = W_{n_i}^j(d)/W_{d_i}^j(d)$, $W_{n_i}^j(d)$ is a stable polynomial, and $W_{d_i}^j(d)$ contains the zeros in the region $|z| \ge 1$ for rejecting the corresponding output disturbance. In addition, the constraint (29) gives the following result:

$$W_{n_i}^j(d)\tilde{A}_{-_i}^j(d)\Phi_i^j(d) - \rho_i^j W_{d_i}^j(d)A_{-_i}^j(d)\tilde{\Phi}_i^j(d) = B_{-_i}^j(d)Q_i^j(d) \quad (33)$$

where $n_{\varphi_i}^j = n_{b_{-_i}}^j - 1$ and $n_{q_i}^j = n_{w_{n_i}}^j + n_{a_{-_i}}^j - 1$. Or, we can rewrite (33) as (34)

$$W_{n_i}^j(z_i^j)\tilde{A}_{-_i}^j(z_i^j)\Phi_i^j(z_i^j) - \rho_i^j W_{d_i}^j(z_i^j)A_{-_i}^j(z_i^j)\tilde{\Phi}_i^j(z_i^j) = 0. \quad (34)$$

By the solutions of ρ_i^j and $\Phi_i^j(d)$ for (32), the following equations are obtained from (12), (33), and (34)

$$A_{c_i}^j(d) = A_{+_i}^j(d)W_{n_i}^j(d)\tilde{A}_{-_i}^j(d)\Phi_i^j(d)B_{+_i}^j(d)\Gamma_i^j(d) \quad (35)$$

$$R_i^j(d) = \rho_i^j W_{d_i}^j(d)\tilde{\Phi}_i^j(d)B_{+_i}^j(d)\Gamma_i^j(d). \quad (36)$$

By comparing (35) and (26) and with the fact (9), one has

$$\Gamma_i^j(d) = \tilde{B}_{-_i}^j(d)F_i^j(d)\Omega_i^j(d) \quad (37)$$

$$X_i^j(d) = A_{+_i}^j(d)W_{n_i}^j(s)\tilde{A}_{-_i}^j(d)\Phi_i^j(d)\Omega_i^j(d) \quad (38)$$

where $\Omega_i^j(d)$ is a stable polynomial. Then from (35)-(38)

$$A_{c_i}^j(d) = B_{+_i}^j(d)\tilde{B}_{-_i}^j(d)F_i^j(d)A_{+_i}^j(d)W_{n_i}^j(d)\tilde{A}_{-_i}^j(d)\Phi_i^j(d)\Omega_i^j(d) \quad (39)$$

$$R_i^j(d) = \rho_i^j W_{d_i}^j(d)\tilde{\Phi}_i^j(d)B_{+_i}^j(d)\tilde{B}_{-_i}^j(d)F_i^j(d)\Omega_i^j(d). \quad (40)$$

Substituting (36), (37), and (32) into (9) yields

$$S_i^j(d) = A_{+_i}^j(d)Q_i^j(d)\tilde{B}_{-_i}^j(d)F_i^j(d)\Omega_i^j(d). \quad (41)$$

From (27) and (38), the following polynomial $T_i^j(d)$ is obtained:

$$T_i^j(d) = \bar{F}_i^j(d)A_{+_i}^j(d)W_{n_i}^j(d)A_{-_i}^j(d)\Phi_i^j(d)\Omega_i^j(d). \quad (42)$$

That is, the characteristic polynomial of the closed-loop and the control polynomials of the *jth* PTFDS of subsystem *i* for the fuzzy mixed H_2/H_∞ optimization in (15) are attained through eqns. (39)-(42).

The following theorem discusses the stability of the closed-loop interconnected system (1).

Theorem 1: Suppose the proposed controller (8) is applied to the NIDDDS (1) or an equivalent fuzzy model system (3). Suppose also the inequality (13) with the condition (43) is satisfied. Then the control system in Fig. 1 is $L_2^N -$stable.

$$\left(\Gamma_1^j\right)_{ii} = 1 - \alpha_{i_i}^j \left\|S_i^j(e^{-jw})A_i^j(e^{-jw})/A_{c_i}^j(e^{-jw})\right\|_2 > 0, \text{ for } i = 1,2,...,N, j = 1,2,...,L \quad (43a)$$

$$\Gamma_1^j(e^{-jw}) > 0 \quad (43b)$$

where $\left(\Gamma_1^j(e^{jw})\right)_{mi} = -\alpha_{m_i}^j \left\|S_i^j(e^{-jw})A_i^j(e^{-jw})/A_{c_i}^j(e^{-jw})\right\|_2$

$0 < (\Gamma_1^k)_{ii} \le 1$ and $0 \le -(\Gamma)_{ij} < 1, i \ne j$, for $i, j = 1,2,...,N$.

Proof: It can be refer to the reference [12].

C. The Proposed Control Algorithm

The design procedure of the proposed fuzzy decentralized fuzzy controller via mixed H_2/H_∞ optimization with discrete Smith predictor is as follows:

Step 1: Factorize the nominal subsystem i as $A_i^j(d) = A_{+_i}^j(d)A_{-_i}^j(d)$ and $B_i^j(d) = B_{+_i}^j(d)B_{-_i}^j(d)$.

Step 2: Assign a suitable reference model $F_i^j(d)$ and $G_i^j(d)$ for the *jth* PTFDS of subsystem *i*.

Step 3: Choose an appropriate weighted function for the second cost function (15), i.e., $W_{d_i}^j(d)$ and $W_{n_i}^j(d)$.

Step 4: Based on (21), the polynomials $\overline{F}_i^j(d)$ and $\overline{B}_i^j(d)$ are obtained. Then the optimal $C_{1_i}^{j^*} = \left\| \overline{B}_i^j(d) / B_{-_i}^j(d) \right\|_2$ is attained. If the matching condition is satisfied, then $\overline{F}_i^j(d) = \tilde{B}_{-_i}^j(d)\overline{G}_i^j(d)$ and $\overline{B}_i^j(d) = 0$.

Step 5: From (34), the scalar ρ_i^j and the polynomial $\Phi_i^j(d)$ are obtained. Then the optimal $C_{2_i}^{j^*} = \rho_i^j$ is attained. Based on the long division for (33), the polynomial $Q_i^j(d)$ is obtained.

Step 6: The characteristic polynomial of the closed-loop and the control polynomials of the *jth* PTFDS of subsystem *i*, i.e., $A_{c_i}^j(d)$, $\left\{R_i^j(d), S_i^j(d), T_i^j(d)\right\}$, for the fuzzy mixed H_2/H_∞ optimization in (15) are from (39)-(42).

VI. CONCLUSIONS

A decentralized control of nonlinear interconnected discrete dynamic systems with large delay using fuzzy mixed H_2/H_∞ optimization with discrete Smith predictor was developed. The past effort on the use of fuzzy T-S delayed control did not consider the robust tracking performance (e.g., the attenuation of uncertainty and delay, and the compensation of large delay). In this paper, a two degree-of-freedom optimization technique with discrete Smith predictor was employed to control each PTFDS. A suitable frequency response without the oscillating and sluggish phenomena was obtained. The effect of output disturbance caused by the interconnections coming from other subsystems, the approximation error of the *ith* subsystem, and the interactions resulting from other PTFDSs, was also minimized. Furthermore, the control implementation did not need to calculate the Diophantine equation. There were also computational advantages, especially for low-order system. No fuzzy observer was required; the proposed discrete controller was more suitable for the implementation. Further application to an internet-based piezoelectric actuator driven table system [17] will be progressed.

REFERENCES

[1] C. Bengea, X. Li and R. A. DeCarlo, "Combined controller-observer design for uncertain time delay systems with application to engine idle speed control," *ASME J. Dyna. Syst. Meas. & Contr.*, vol. 126, pp. 772-780, Dec. 2004.

[2] R. Majumder, B. Chaudhuri, B. C. Pal and Q.C. Zhong, "A unified Smith predictor approach for power system damping control design using remote signals," *IEEE Trans. Contr. Syst. Technol.*, vol. 13, no. 13, pp. 1063-1068, Nov. 2005.

[3] M. K. Ranganathan and L. Kilmartin, "Neural and fuzzy computation techniques for playout delay adaptation in VoIP networks," *IEEE Trans. Neural Networks,* vol. 16, no. 5, pp. 1174-1194, Sep. 2005.

[4] C. L. Hwang, L. J. Chang and Y. S. Yu, "Network-based fuzzy decentralized sliding-mode control for car-like mobile robots," *IEEE Trans. Ind. Electron.*, vol. 54, no. 1, pp. 574-585, Feb. 2007.

[5] B. Jiang, Z. Mao and P. Shi, "H_∞ – filter design for a class of networked control system via T-S fuzzy model approach," *IEEE Trans. Fuzzy Syst.*, vol. 18, no. 1, pp. 201-208, Feb. 2010.

[6] C. Huang, Y. Bai and X. Liu, "H-infinity state feedback control for networked cascade control systems with uncertain delay," *IEEE Trans. Ind. Inform.*, vol. 6, no. 1, pp. 62-72, Feb. 2010.

[7] C. L. Hwang and C. Y. Shih, "A distributed active-vision network-space approach for trajectory tracking and obstacle avoidance of a car-like wheeled robot," *IEEE Trans. Ind. Electron.,* vol. 56, no. 3, pp. 846-855, Mar. 2009.

[8] E. J. Rodr'guez-Seda, D. Lee and M. W. Spong, "Experimental comparison study of control architectures for bilateral teleoperators," *IEEE Trans. Robotics*, vol. 25, no. 6, pp. 1304-1318, Dec. 2009.

[9] C. L. Lai and P. L. Hsu, "Design the remote control system with the time-delay estimator and the adaptive Smith predictor," *IEEE Trans. Ind. Inform.*, vol. 6, no. 1, pp. 73-80, Feb. 2010.

[10] K. Natori, T. Tsuji, K. Ohnishi, A. Hace and K. Jezernik, "Time-delay compensation by communication disturbance observer for bilateral teleoperation under time-varying delay," *IEEE Trans. Ind. Electron.*, vol. 57, no. 3, pp. 1050-1059, Mar. 2010.

[11] M. Ono, H. Shibasaki, K. Matsumoto, K. Sasaki and Y. Ishida, "Discrete modified Smith predictor based on optimal control method for a plant with an integrator, *IEEE SMC2010*, pp. 630-635, 2010.

[12] C. L. Hwang and C. C. Wong, "Fuzzy mixed H_2/H_∞ optimized design of decentralized control for nonlinear interconnected dynamic delay systems," *IEEE FUZ2008*, Hong Kong, pp. 168-173, June 1st-6th, 2008.

[13] R. J. Wai, M. A. Kuo and J. D. Lee, "Design of fuzzy adaptive sliding-mode control for nonlinear two-axis inverted pendulum servomechanism," *IEEE Trans. Fuzzy Syst.*, vol. 16, no. 5, pp. 1232-1244, Oct. 2008.

[14] H. Zhang, C. Dang and C. Li, "Decentralized H_∞ filter design for discrete-time interconnected fuzzy systems," *IEEE Trans. Fuzzy Syst.*, vol. 17, no. 6, pp. 1428-1440, Dec. 2009.

[15] B. Chen, X. P. Lin, S. C. Tong and C. Lin, "Observer-based stabilization of T-S fuzzy systems with input delay," *IEEE Trans. Fuzzy Syst.*, vol. 16, no. 3, pp. 652-663, Jun. 2008.

[16] C. Peng, D. Yue, T.C. Yang and E. G. Tian, "On delay-dependent approach for robust stability and stabilization of T-S fuzzy systems with constant delay and uncertainties," *IEEE Trans. Fuzzy Syst.*, vol. 17, no. 5, pp. 1143-1156, Oct. 2009.

[17] C. L. Hwang and S. Y. Han, "Fuzzy mixed H^2/H^∞ optimization-based decentralized model reference control and application to piezo-driven XY table systems," *IEEE Trans. Fuzzy Syst.,* vol. 15, no. 2, pp. 145-160, Apr. 2007.

[18] J. Chen, S. Hara and G. Chen, "Best tracking and regulation performance under control energy constraint," *IEEE Trans. Automat. Contr.*, vol. 48, no. 8, pp. 1320-1336, Aug. 2003.

[19] J. Dong, Y. Wang and G. H. Yang, "Output feedback fuzzy controller design with local nonlinear feedback laws for discrete-time nonlinear systems," *IEEE Trans. Syst. Man & Cybern., Pt. B*, vol. 40, no. 6, pp. 1447-1459, Dec. 2010.

2011 IEEE International Conference on Fuzzy Systems
June 27-30, 2011, Taipei, Taiwan

A Hybrid Fuzzy Sliding-Mode Control for a Class of Generalized, Under-Actuated and Uncertain Nonlinear Dynamic Systems

Chih-Lyang Hwang, *Senior Member, IEEE*
Department of Electrical Engineering
National Taiwan University of Science and Technology
Taipei, Taiwan, R.O.C.
e-mail: chih-lyang_hwang@hotmail.com

Hsiu-Ming Wu, *Member, IEEE*
Opto-Mechatronics Technology Center
National Taiwan University of Science and Technology
Taipei, Taiwan, R.O.C.
e-mail: D9307205@mail.ntust.edu.tw

***Abstract*—Due to the under-actuated feature, the reference signals using the combination of the system outputs, whose number is larger than that of reference signal, are designed so that the number of control inputs and sliding surfaces is the same, and that the uncontrollable mode is indirectly controlled. Under the uncertain environment, the sliding-mode under-actuated control (SMUC) with the satisfaction of suitable condition is designed to asymptotically track the reference signal. Otherwise, a bounded tracking result is obtained for the mild condition. In this situation, an on-line fuzzy modeling for the uncertainty is employed to design a fuzzy model-based sliding-mode under-actuated control (FSMUC) to improve the system performance; e.g., the bounded tracking result of SMUC becomes an asymptotical tracking. The proposed hybrid fuzzy sliding-mode under-actuated control (HFSMUC) combining SMUC and FSMUC with a transition can be applied to a class of generalized, under-actuated and uncertain nonlinear systems, e.g., the trajectory tracking control of a differential mobile robot (DMR). Finally, the simulations of the HFSMUC system are presented to confirm the efficiency and effectiveness of the proposed control.**

Keywords-Under-actuated control system; Sliding-mode control; Fuzzy model-based adaptive control; Lyapunov stability theory;

I. INTRODUCTION

In recent years, the under-actuated systems are attractive due to these advantages: less energy consumption, less use of actuators, and less expense. The main feature for an under-actuated system is that the control objectives can be achieved merely using less actuators under certain constrained conditions. However, the controller design of an under-actuated system is a challenge problem. Furthermore, an under-actuated system in the presence of uncertainties is a difficult task. In this situation, a Hybrid Fuzzy Sliding-Mode Under-actuated Control (HFSMUC) is proposed to deal with a class of generalized, under-actuated and uncertain nonlinear dynamic systems.

In this paper, the reference signals for the controllable modes are designed to combine the signal of the uncontrollable modes so that the uncontrollable mode can be manipulated indirectly. As a result, the sliding surface can be represented as the combination of these signals to become controllable. At the same time, the number of control inputs is the same with that of sliding surfaces; then the sliding-mode under-actuated control (SMUC) is first designed. Moreover, to improve system performance the learning compensation for the system uncertainties called fuzzy sliding-mode under-actuated control (FSMUC) is designed. However, to avoid possible transient phenomenon, a hybrid fuzzy sliding-mode under-actuated control (HFSMUC) combining SMUC and FSMUC with a transition is suggested.

The main contribution of this paper is depicted as follows. Utilizing the reference signals including the uncontrollable mode makes the number of sliding surfaces equal that of control inputs. Then an HFSMUC for a class of generalized, under-actuated and uncertain nonlinear dynamic system is designed.

II. RELATED WORKS

Over the past decades, related works about under-actuated systems was proposed massively. Firstly, Lin and Mon used hierarchical fuzzy sliding-mode (HFSM) to investigate the decoupling control of a double inverted pendulum system [1]. Raimondi and Melluso [2] presented a new fuzzy adaptive motion control system including on-line extended Kalman's filter (EKF) for wheeled under-actuated cars with non-holonomic constraints. Besdies, in [3], Wai et al. proposed a cascade adaptive fuzzy sliding-mode control (AFSMC) scheme including inner and outer control loops for the stabilizing and tracking control of a nonlinear two-axis inverted-pendulum servomechanism. In 2008, Márton et al. [4] presented LQR, subspace stabilization controller and combined error metric controller for robust control of under-actuated robots compared on the classic ball and beam system. Furthermore, a closed-loop method was presented by Elliot and Gans [5] achieving full-state trajectory tracking via input-output linearization and asymptotically stable internal dynamics for the two-wheeled driven cart. In [6], Refsnes et al. presented an observer backstepping technique for slender-

978-1-4244-7316-8/11/$26.00 ©2011 IEEE

body underwater vehicles to track the desired pitch and heading angle. In addition, the papers of [7]-[9] presented a sliding mode control method respectively for a class of under-actuated mechanical systems and autonomous surface vessels. Cavdaroglu and Olgac [10] designed a desirable fixed control law to successfully accomplish the trajectory tracking of an under-actuated car-and-pendulum dynamics in the presence of multiple and independent time delays. Oryschuk et al. [11] implemented and tested the real-time control of a two-wheeled under-actuated mobile robot including test motions: translational, rotational, and uphill. In [12], neural networks and output feedback were used for a quadrotor unmanned aerial vehicle (UAV) with six DOFs which were controlled by only four control inputs.

III. PROBLEM FORMULATION

In the beginning, a class of generalized, under- actuated and uncertain nonlinear dynamic systems is expressed as follows:

$$\dot{x}_1(t) = f_1(x,t) \tag{1a}$$

$$\dot{x}_2(t) = f_2(x,t) + G(x,t)u(t) \tag{1b}$$

$$y_1(t) = H_1 x_1(t),\ y_2(t) = H_2 x_2(t) \tag{1c}$$

where $x = \begin{bmatrix} x_1(t) & x_2(t) \end{bmatrix}^T$, $x_1(t), y_1(t) \in \Re^{n-m}$ and $x_2(t), y_2(t) \in \Re^m$ are respectively denoted as the uncontrollable and controllable system state and system output, $u(t) \in \Re^m$ is the control input, and H_1, H_2 are the output gain matrices. Furthermore, the system functions are described as follows:

$$f_i(x,t) = \overline{f}_i(x) + \Delta f_i(x,t), i = 1,2 \tag{2}$$

$$G(x,t) = \overline{G}(x) + \Delta G(x,t) \tag{3}$$

where $\overline{f}_1(x) \in \Re^{n-m}$, $\overline{f}_2(x) \in \Re^m$ and $\overline{G}(x) \in \Re^{n \times m}$ denote the nominal system functions, $\Delta f_i(x,t), i = 1,2$ and $\Delta G(x,t)$ are uncertain system functions. Due to the under-actuated feature, the number of the control inputs is smaller than that of the system output, i.e., $m < n$. In summary, $y_1(t)$ and $y_2(t)$ are denoted as the uncontrollable modes and controllable modes of the system output, respectively. The tracking error is defined as follows:

$$e_i(t) = r_i(t) - y_i(t), i = 1,2. \tag{4}$$

Our problem is to design the control input for the controlled system (1)~(3) such that the system output will track a reference input (refer to Fig. 1). First, a sliding-mode under-actuated control (SMUC) is designed for the uncertainty which is not huge. In this situation, the asymptotical tracking can be obtained for the smaller uncertainty; in general, a bounded tracking result is achieved. To enhance the tracking result, a fuzzy modeling is then employed to approximate the system uncertainty such that a real-time compensation of learning uncertainty is plugged into the fuzzy sliding-mode under-actuated control (FSMUC). Finally, a combination of SMUC and FSMUC with a transition is called as hybrid fuzzy sliding-mode under-actuated control (HFSMUC). It is developed such that both advantages of SMUC and FSMUC (e.g., a better transient response of SMUC, an improved tracking performance of FSMUC) are accomplished, and that both of their disadvantages (e.g., poor tracking performance of SMUC, the transient response of FSMUC) are discarded.

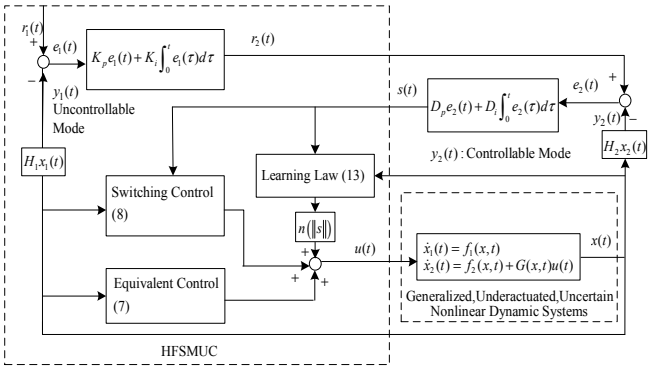

Fig. 1. Control block diagram of the overall system.

IV. FEATURES OF SLIDING SURFACE

Considering that proposed architecture is an under-actuated control system, the following sliding surface is first defined.

$$s(t) = D_p e_2(t) + D_i \int_0^t e_2(\tau)d\tau \tag{5}$$

where $D_p = diag\{d_{p1}, d_{p2}, \cdots, d_{pm}\}, D_i = diag\{d_{i1}, d_{i2}, \cdots, d_{im}\}$, $\in \Re^{m \times m}$ are constant matrices, and $s(t) \in \Re^m$. In addition, D_p and D_i are positive definite matrices, i.e., d_{pj} and $d_{ij} > 0$ for $j = 1,2,\cdots,m$. An effective reference input is assigned as follows:

$$r_2(t) = K_p e_1(t) + K_i \int_0^t e_1(\tau)d\tau \tag{6}$$

where K_p and $K_i \in \Re^{(n-m)\times(n-m)}$, their entries are chosen as $(K_p)_{jl}$ and $(K_i)_{jl} > 0 \forall j,l = 1,2,...,n-m,$ such that $r_2(t)$ is a stable reference input. The reason to design the reference signal of (6) is that the uncontrolled mode $x_1(t)$ or $y_1(t)$ should be simultaneously included into the control mode, i.e., $x_2(t)$ or $y_2(t)$, so that they are indirectly manipulated by the controllable mode. In this paper, $r_1(t) = \dot{r}_1(t) = 0$ is considered and the corresponding bounded-input-bounded-output and asymptotical tracking properties can be referred to [13], [14]. For simplicity, it is omitted.

V. CONTROLLER DESIGNS

Three design steps for the proposed controller are given as follows.

A. Sliding-Mode Under-Actuated Control

The sliding-mode under-actuated control for the controlled system (1) and (2) is designed as follows:

$$u(t) = u_{eq}(t) + u_{sw}(t) \tag{6}$$

where

$$\begin{aligned} u_{eq}(t) &= \left[D_p H_2 \bar{G}(x)\right]^{-1} \left\{ n\left(\|s(t)\|\right)\hat{W}^T(t)\Phi(z) \right. \\ &\left. + D_p\left[K_p\left(\dot{r}_1(t) - H_1\bar{f}_1(x)\right) + K_i e_1(t) - H_2\bar{f}_2(x)\right] + D_i e_2(t)\right\} \end{aligned} \tag{7}$$

$$u_{sw}(t) = \left[D_p H_2 \bar{G}(x)\right]^{-1} \left\{\Gamma_1 s(t) + \Gamma_2 s(t)/\left(\|s(t)\| + \varepsilon_b\right)\right\}/(1-\lambda) \tag{8}$$

where $D_p H_2 \bar{G}(x)$ for all $x(t)$ is nonsingular; $n\left(\|s\|\right)$ is a scalar function and here it is assigned as zero; $\hat{W}^T(t)\Phi(z)$ represents the learning compensation for system uncertainties, which will be discussed in the subsection 5B; $\Gamma_1 = diag\{\gamma_{111}, \cdots, \gamma_{1mm}\} > \delta I_m/2 > 0$ (where I_m is the unit matrix of $\Re^m$ and δ is the exponential convergent rate to the sliding surface) and $\Gamma_2 = diag\{\gamma_{211}, \cdots, \gamma_{2mm}\} > 0$ are the switching gain matrices; $\varepsilon_b \geq 0$ denotes the boundary layer of sliding surface; $\lambda > 0$ represents as the upper bound of uncertain control gain and satisfies the following inequality:

$$\left\| D_p H_2 \Delta G(x,t)\left(D_p H_2 \bar{G}(s)\right)^{-1}\right\| \leq \lambda < 1, \ \forall x(t), t. \tag{9}$$

It is assumed that the uncertain signal $K(x, u_{eq}, t)$ caused by $\Delta f_i(x,t), i = 1,2$ and $\Delta G(x,t)$ satisfying the following inequality:

$$\left\|K(x, u_{eq}, t)\right\| \leq \mu_0 + \mu_1 p(x), \ \forall x(t), u_{eq}(t), t \tag{10}$$

where

$$\begin{aligned} K(x, u_{eq}, t) &= -D_p K_p H_1 \Delta f_1(x,t) \\ &- D_p H_2 \Delta f_2(x,t) - D_p H_2 \Delta G(x,t) u_{eq}(t) \end{aligned} \tag{11}$$

$p(x)$ is a known function, and $\mu_0 \geq 0, \mu_1 \geq 0$, whose values are constrained by the stability of the closed-loop system.

B. Fuzzy Model-Based Sliding-Mode Under-Actuated Control

If the system uncertainties (10) and (11), i.e., $K(x, u_{eq}, t)$ are huge, they must be learned to compensate their effect [15]. Based on the learning model, an FSMUC is then constructed to improve system performance. First, the extension of universal approximation theory using fuzzy modeling is stated as follows [16], [17]:

Theorem 1: Suppose $z(t) \in D(z)$ (a compact subset of $\Re^n$), $K(z,t): D \times \Re^+ \to \Re^m$ is a continuous function. For an arbitrary constant $\varepsilon_0 \geq 0$, there exists an integer L (the number of membership functions) and real constant matrix $\bar{W} \in \Re^{L \times m}$, where $\|\bar{W}\| \leq W_M$, such that

$$K(z,t) = \bar{W}^T \Phi(z) + \varepsilon_K(z,t)$$

where $\Phi(z)$ denotes a known fuzzy basis function, $\|\varepsilon_K(z,t)\| \leq \varepsilon_0, \ \ \forall z(t) \in D(z)$ and $\forall t \geq 0$.

Based on the result of *Theorem 1*, the system uncertainties in a compact subset $D(z)$ and $\forall t \geq 0$, are assumed to be continuous and approximated by the following fuzzy model:

$$K(x, u_{eq}, t) = \bar{W}^T \Phi(z) + \varepsilon_K(z,t) \tag{12}$$

where $z^T(t) = \left[x^T(t) \ \ u_{eq}^T(t)\right]$, $\bar{W} \in \Re^{L \times m}$ is an unknown constant matrix which is not necessarily unique, $\|\varepsilon_k(z,t)\| \leq \varepsilon_0 \ \ \forall z(t) \in D(z)$ and $t \geq 0$. In addition, the upper bound of $\bar{W}$ is known, i.e., $\|\bar{W}\|_F \leq \bar{W}_M$, where $\|\cdot\|_F$ is the Frobenius norm.

Then the following learning laws are considered.

$$\dot{\hat{W}}(t) = \Omega \Phi(z) s^T(t) - \Omega \Psi \hat{W}(t) \tag{13a}$$

where $\hat{W}(t) \in \Re^{L \times m}$ stands for the learning weight, $\Omega = diag\{\omega_1, \cdots, \omega_L\} \in \Re^{L \times L} > 0$ is the learning matrix gain, $\Psi = diag\{\varphi_1, \cdots, \varphi_L\} \in \Re^{L \times L} > 0$ is a matrix of *e*-modification rate to ensure the boundedness of the learning weight, $\Phi(z) \in \Re^{L \times 1}$ represents the fuzzy basis function:

$$\Phi(z) = \left[1 \quad \phi_2(z) \quad \ldots \quad \phi_L(z)\right]^T \tag{13b}$$

where $\phi_j(z) = \exp\left[-\|z(t) - c_j\|^2 / \sigma_j^2\right]$, L, c_j, σ_j for j = 2, 3,…, L are known, and the centers c_j for $j = 2, 3, ..., L$ are chosen as normal distribution in the corresponding domain. Then the fuzzy model-based sliding-mode under-actuated control (FSMUC) is designed as the following equivalent control with $n\left(\|s(t)\|\right) = 1$ and the learning weight from (13).

C. Hybrid Fuzzy Sliding-Mode Under-Actuated Control

When the operating point is far away from the sliding surface, the learning law generally does not require so that the unnecessary instability and transience are avoided [15]. Although FSMUC is superior to SMUC, it is still a question when the learning law should be used. Important index for the sliding-mode control is the sliding surface. Due to the existence of system uncertainties, the operating point is always away from the sliding surface. Based on this knowledge, a scalar function $n\left(\|s\|\right)$ is designed as follows. When the norm of the sliding surfaces is inside of a defined set, the learning law (13) start; similarly, as it is outside of the other set, the learning laws shut off. For reducing the

possibility of discontinuous control input, a transition between SMUC and FSMUC is designed. Hence, we design the following scalar function:

$$n(\|s\|)=\begin{cases}0, & \text{as } \|s(t)\|>n_{s1}\\ 1, & \text{as } \|s(t)\|<n_{s2}\\ (n_{s1}-\|s(t)\|)/(n_{s1}-n_{s2}), & \text{otherwise}\end{cases} \quad (14)$$

where $n_{s1}>d_n>n_{s2}>c_n>0$. The values of d_n and c_n are respectively the upper bounds of the convergent sets of $\|s(t)\|$ for the SMUC and FSMUC. If the system uncertainties are small enough, then the value of d_n is also small enough. If the value of d_n (or the system performance) satisfies the specification, then the value of n_{s1} approaches zero, i.e., the learning laws (13) can be shut down. On the other hand, the value of d_n (or the system performance) is large, then the value of n_{s2} is away from zero, i.e., the learning law (13) nearly executes all the time. As the value of $\|s(t)\|$ is between n_{s1} and n_{s2}, the linear combination of these two conditions is obtained.

Finally, the proposed HFSMUC is summarized as follows:

Step 1: Obtain a nominal modeling of a generalized under-actuated and uncertain nonlinear dynamic system, i.e., $\bar{f}_i(x), i=1,2$ and $\bar{G}(x)$.

Step 2: Partition the uncontrollable mode (i.e., $y_1(t)$) and the controllable mode (i.e., $y_2(t)$), whose dimension is the same as that of control input $u(t)$ or sliding surface $s(t)$.

Step 3: Estimate the system uncertainty $K(x,u_{eq},t)$ such that $\mu_0+\mu_1 p(x)$ in (10) is obtained.

Step 4: Assign the suitable coefficients for the virtual reference $r_2(t)$, i.e., K_p and K_i, and the sliding surface, i.e., D_p and D_i. Then the SMUC with appropriate parameters of switching gains, i.e., Γ_1 and Γ_2, is designed.

Step 5: If the system performance is not satisfied, an on-line learning law (13) is constructed to learn the huge uncertainty, which is not tackled in a satisfactory manner by the previous SMUC. Then an FSMUC is described in (6)-(8) with $n(\|s\|)=1$ and (13).

Step 6: Besides an acceptable steady performance of an FSMUC, its transient phenomenon often occurs. In this situation, an HFSMUC is designed by the suitable selection of coefficients, i.e., n_{s1} and n_{s2} in (14) to avoid the possible transience and discontinuous control signals. Finally, the corresponding simulations are arranged to verify the effectiveness.

VI. ILLUSTRATIVE EXAMPLE

An illustrative example, namely, the trajectory tracking control of a DMR [8], is a two inputs and five states (or three outputs) under-actuated system as shown in Fig. 2 to demonstrate the validity of our proposed HFSMUC. Then the kinematic dynamic model of a DMR and the simulation results by HFSMUC are presented in the following two subsections.

A. Kinematic and Dynamic Model of a DMR

At beginning, the kinematic model of a DMR is expressed as follows:

$$\dot{x}(t)=v(t)\cos(\theta),\ \dot{y}(t)=v(t)\sin(\theta),\ \dot{\theta}(t)=\omega(t) \quad (15)$$

where the triple $(x(t),y(t),\theta(t))$ denotes the position and the orientation of the vehicle with respect to the world coordinate, and $v(t)$ and $\omega(t)$ are the linear and angular velocities of the DMR. The dynamic model is obtained by using the following relations:

$$M\dot{v}(t)-f_f(t,x)=f(t) \quad (16a)$$

$$I\dot{\omega}(t)-\tau_f(t,x)=\tau(t) \quad (16b)$$

where M is the mass of the DMR, I is the moment of inertia, $f(t)=[\tau_l(t)+\tau_r(t)]/r$ and $\tau(t)=L[\tau_l(t)-\tau_r(t)]/r$ with L being the distance between the center of mass and the wheel, $\tau_l(t)$ and $\tau_r(t)$ are the left and right wheel motor torques, and r is the radius of the rear wheel. To express the generalized form as equation (1), $x_1(t)=x(t)$, $x_2(t)=y(t)$, $x_3(t)=\theta(t)$, $x_4(t)=v(t)$ and $x_5(t)=\omega(t)$ are defined. Output gain matrices are selected as $H_1=I_3$ and $H_2=I_2$ where I_3 and I_2 respectively are 3×3 and 2×2 identity matrices. In addition, the frictional force $f_f(t,x)$ and frictional torque $\tau_f(t,x)$ are supposed to be

$$\begin{aligned}&f_f(t,x)=3\sin(tx_1)\cos(5t)+2.1x_2\sin(5tx_2)\\&-0.3x_3\cos(10tx_3)-0.2\sin(40tx_5)+0.01\sin(100tx_4)+0.2\\&\tau_f(t,x)=3x_2\cos(tx_1)\sin(10tx_3)+1.6x_2\cos(5tx_3)\\&-0.3x_2\cos(10tx_2)-0.1x_4\sin(40tx_5)+0.02x_3\sin(100tx_4)-0.3\end{aligned} \quad (17)$$

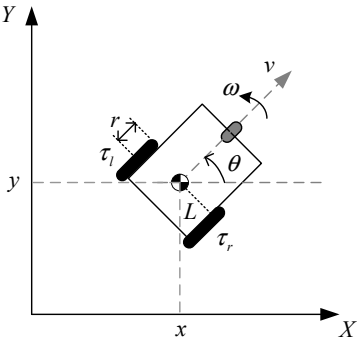

Fig. 2. Illustration of a DMR.

B. Simulation Results by HFSMUC

The simulation results by HFSMUC are considered as follows. The initial position and orientation of a DMR is selected as $\{X = 0.3m, Y = 0.1m, \theta = 1\ rad.\}$ and the physical parameters of the DMR are chosen as $M = 6.0kg$, $I = 0.157kg \cdot m^2$, $r = 0.1m$, $L = 0.25m$. The control objective is to drive the DMR from the initial position back to the origin point of the world coordinate. The above frictional force and frictional torque (17) are also considered in the simulation. The corresponding responses of the simulation are shown in Figs. 3~8. It indicates that the proposed control is effective for an under-actuate controlled system. The uncertainty and its learning uncertainty are shown in Figs. 9 and 10, which are acceptable. Moreover, the corresponding proof will be undertaken via Lyapunov stability theory in the near future.

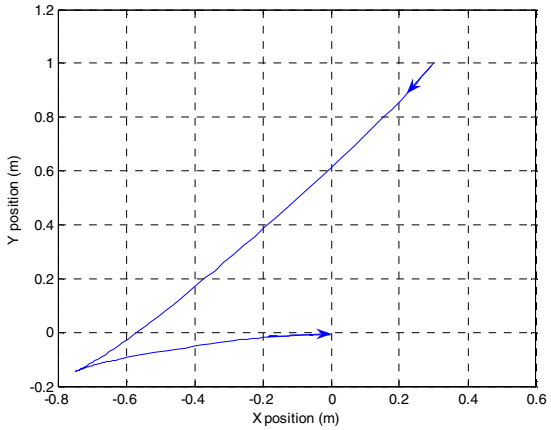

Fig. 3. The response of the DMR in the world coordinate (X, Y).

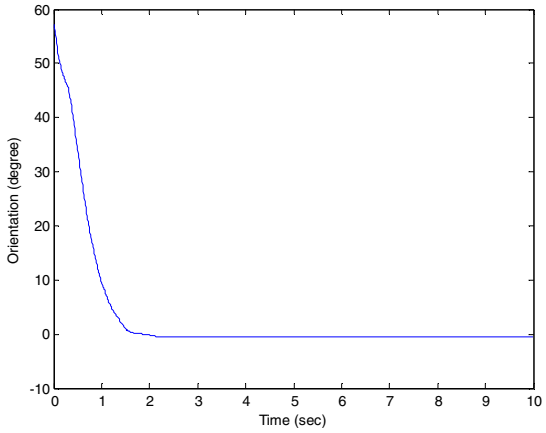

Fig. 4. The response of orientation $\theta(t)$.

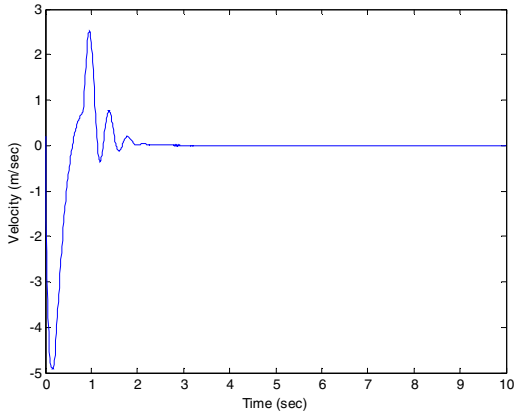

Fig. 5. The response of velocity $v(t)$.

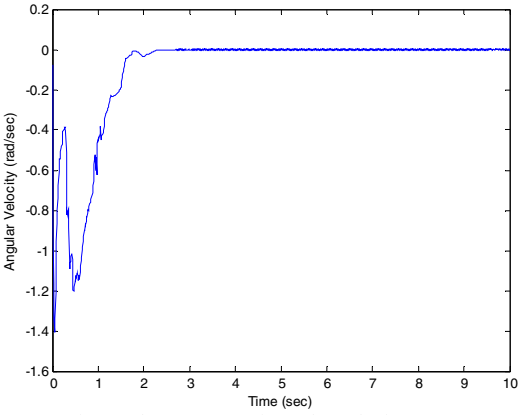

Fig. 6. The response of angular velocity $\omega(t)$.

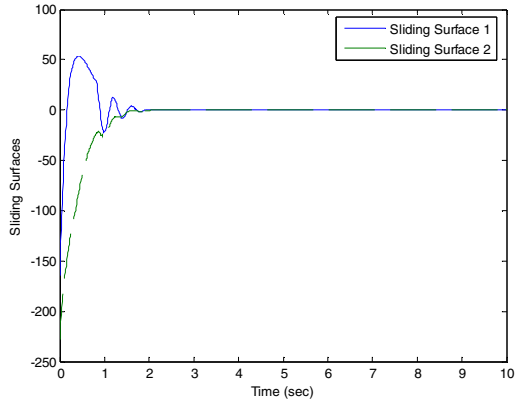

Fig. 7. The response of sliding surfaces $s(t)$.

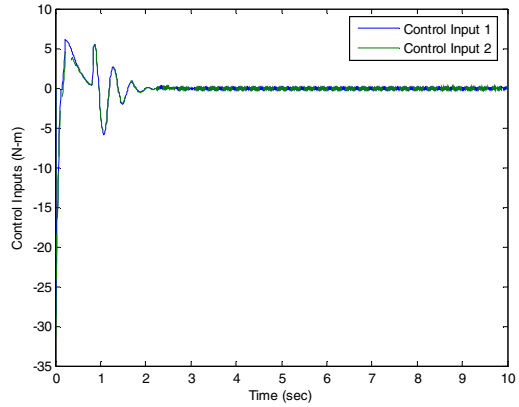

Fig. 8. The response of control inputs $\tau_l(t)$ and $\tau_r(t)$.

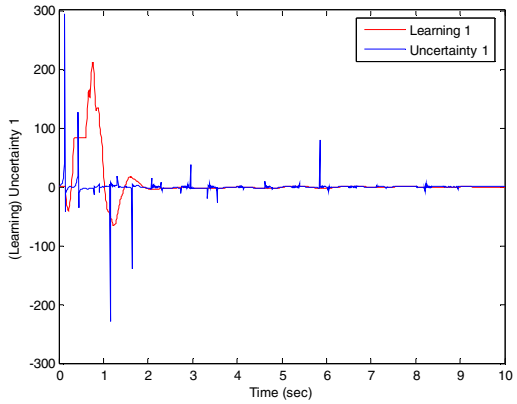

Fig. 9. Learning 1 & Uncertainty 1.

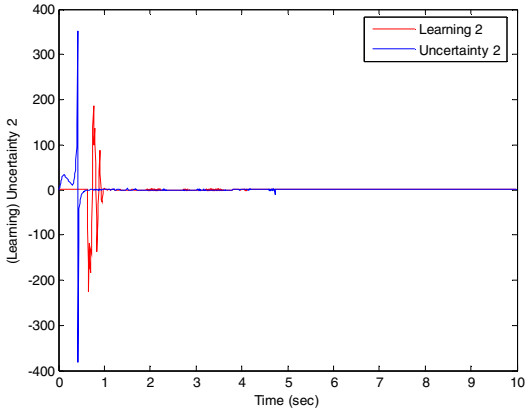

Fig. 10. Learning 2 & Uncertainty 2.

VII. CONCLUSIONS

An HFSMUC for a class of generalized under-actuated nonlinear uncertain dynamic systems is developed by the combination of SMUC and FSMUC with a transition. The proposed scheme presents both advantages of SMUC and FSMUC and simultaneous avoids the possible disadvantages coming from SMCU and FSMUC. First, the reference signals using the combination of the system outputs, whose number is larger than that of reference signal, are designed so that the number of control inputs and sliding surfaces is the same, and that the uncontrollable mode is indirectly controlled. Under the uncertain environment, the sliding-mode under-actuated control (SMUC) with the satisfaction of suitable condition is designed to asymptotically track the reference signal. Otherwise, a bounded tracking result is obtained for the mild condition. In this situation, an on-line fuzzy modeling of the uncertainty is employed to design a fuzzy sliding-mode under-actuated control (FSMUC) to improve the system performance; e.g., the bounded tracking result of previous sliding-mode control becomes an asymptotical tracking. Finally, an illustrative example: the trajectory tracking of a DMR, confirms the usefulness of the proposed HFSMUC. It is believed that the proposed control scheme can be applied to many under-actuated nonlinear uncertain dynamic systems.

REFERENCES

[1] C. M. Lin and Y. J. Mon, "Decoupling control by hierarchical fuzzy sliding-mode control," *IEEE Trans. Contr. Syst. Technol.*, vol. 13, no. 4, pp. 593-598, Jul. 2005.

[2] F. M. Raimondi and M. Melluso, "Fuzzy adaptive EKF motion control for non-holonomic and underactuated cars with parametric and non-parametric uncertainties," *IET Control Theory Appl.*, vol. 1, no. 5, pp. 1311–1321, 2007.

[3] R. J. Wai, M. A. Kuo, and J. D. Lee, "Design of cascade adaptive fuzzy sliding-mode control for nonlinear two-axis inverted-pendulum servomechanism," *IEEE Trans. Fuzzy Syst.*, vol. 16, no. 5, pp. 1232-1244, Oct. 2008.

[4] L. Márton, A. S. Hodel, Béla Lantos and J. Y. Hung, "Underactuated robot control: comparing LQR, subspace stabilization, and combined error metric approaches", *IEEE Trans. Ind. Electron.*, vol. 55, no. 10, pp. 3724-3730, Oct. 2008.

[5] J. G. Elliot and R. F. Gans, "Closed-loop control of an underactuated sheet registration device using feedback linearization and gain scheduling," *IEEE Trans. Contr. Syst. Technol*., vol. 16, no. 4, pp. 589-599, Jul. 2008.

[6] J. E. Refsnes, A. J. Sørensen and K. Y. Pettersen, "Model-based output feedback control of slender-body underactuated AUVs: theory and experiments," *IEEE Trans. Contr. Syst. Technol*., vol. 16, no. 5, pp. 930-945, Sep. 2008.

[7] R. Martinez, J. Alvarez and Y. Orlov "Hybrid sliding- mode-based control of underactuated systems with dry friction," *IEEE Trans. Ind. Electron.*, vol. 55, no. 11, pp. 3998-4003, Nov. 2008.

[8] V. Sankaranarayanan, and Arun D. Mahindrakar, "Control of a class of underactuated mechanical systems using sliding modes," *IEEE Trans. Robotics*, vol.25, no. 2, pp. 459-467, Apr. 2009.

[9] H. Ashrafiuon, K. R. Muske, L. C. McNinch and R. A. Soltan, "Sliding-mode tracking control of surface vessels," *IEEE Trans. Ind. Electron.*, vol. 55, no. 11, pp. 4004-4012, Nov. 2008.

[10] M.E. Cavdaroglu and N. Olgac, "Trajectory tracking of cart-pendulum dynamics using multiple time-delayed feedback," *IET Control Theory Appl.*, vol. 2, no. 6, pp. 458–466, 2008.

[11] P. Oryschuk, A. Salerno, A. M. Al-Husseini and J. Angeles, "Experimental validation of an underactuated two-wheeled mobile robot," *IEEE/ASME Trans. Mechatronics*, vol. 14, no. 2, pp. 252-257, Apr. 2009.

[12] T. Dierks, and S. Jagannathan, "Output feedback control of a quadrotor UAV using neural networks" *IEEE Trans. Neural Networks*, vol. 21, no. 1, pp. 50-66, Jan. 2010.

[13] C. L. Hwang, H. M. Wu and C. L. Shih, "Fuzzy sliding-mode underactuated control for autonomous dynamic balance of an electrical bicycle" *IEEE Trans. Contr. Sys. Technol.*, vol. 17, no. 3, pp. 658-670, May 2009.

[14] C. L. Hwang, H. M. Wu and C. L. Shih, "An autonomous dynamic balance of an electrical bicycle in motion using variable structure under-actuated control" *Asian Journal of Control*, vol. 13, no. 2, pp. 1-15, Mar. 2011.

[15] C. L. Hwang, H. M. Wu and C. L. Shih , "A hybrid fuzzy decentralized sliding mode under-actuated control for autonomous dynamic balance of a running electrical bicycle including frictional torque and motor dynamics and in the presence of huge uncertainty" *IEEE International Conf. on Fuzzy Systems*, pp. 1-8, July 2010.

[16] R. J. G. B. Campello, and W. C. do Amaral, "Hierarchical Fuzzy Relational Models: Linguistic Interpretation and Universal Approximation" *IEEE Trans. Fuzzy Systems*, vol. 14, no. 3, pp. 446-453, June 2006.

[17] M. G. Joo, and J. S. Lee, "A class of hierarchical fuzzy systems with constraints on the fuzzy rules" *IEEE Trans. Fuzzy Systems*, vol. 13, no. 2, pp. 194-203, April 2005.

2011 IEEE International Conference on Fuzzy Systems
June 27-30, 2011, Taipei, Taiwan

Visualization and Analytical Support of Questionnaire Free-Texts Data based on HK Graph with Concepts of Words

Daisuke Kobayashi, Tomohiro Yoshikawa and Takashi Furuhashi
Nagoya University, Japan
Furo-cho, Chikusa-ku, Nagoya 464-8601 JAPAN
Email: kobayashi@cmplx.cse.nagoya-u.ac.jp
yoshikawa@cmplx.cse.nagoya-u.ac.jp
furuhashi@cmplx.cse.nagoya-u.ac.jp

***Abstract*—A lot of companies carry out questionnaires. These questionnaires often have questions which need respondents to answer by free description. It is, however, inefficient for an analyzer to read whole texts to get outlines or classify them, or it is difficult to correctly analyze them without subjective biases. The authors have proposed "HK Graph" (Hierarchical Keyword Graph) which is a support tool for text mining. HK Graph can visualize the relationships among attributes and words with hierarchical graph structure based on frequency of co-occurrence. However, the result of HK Graph is not enough helpful for the analyzer to grasp the outlines of the texts and extract opinions from them, because it regards divided words as different ones unless they perfectly match and that makes the visualized result complicated. This paper presents a new visualization method for the HK Graph incorporating an aggregating words method based on concepts of words. An experiment is carried out by applying the proposed method to actual questionnaire data on disasters and studies the effectiveness of the proposed method.**

***Index Terms*—Text mining, HK Graph, Visualization, Questionnaire analysis, Concept.**

I. Introduction

Recently, a lot of companies often carry out questionnaires to plan marketing strategies. There are a lot of objectives in questionnaires, e.g., finding needs of products or services, predicting demand or market scale, investigating levels of customer satisfaction or images of brands, and so on. Thus, questionnaires are important information sources for companies, and effective analysis methods for them are strongly needed.

There are two types of formats in questionnaire. One is to answer from some choices or directly answer using a numerical value for a question, the other is to answer by free description. In the former case, it is easy to quantify the responses, and to apply multivariate analysis methods. It is, however, difficult to extract real opinions or impressions of respondents unless good setting of questions is done, because the respondents can respond only to the prepared questions. On the other hand, in the latter case, it is expected to extract real opinions of respondents because they can write their responses freely. However the analysis of free text data becomes difficult because numerical analysis methods can not be applied and it takes long time to aggregate and analyze them, or an analyst might be subjectively biased by same strong opinions. In many analyses of questionnaires, the analysts have to read whole text data to get outlines or manually classify them. Therefore, the demand for the support system by text mining methods for the analysis of free texts in questionnaire has been growing.

A lot of text mining methods to support the analysis of texts have been reported [1], [2], [3]. This study focuses on the approach by visualization. Analysis of free texts in questionnaires needs interactivity because a lot of grammar or syntax errors are contained in responses, and the visualization is expected to be effective for interactive analyses. There are some conventional systems to support the analysis of texts with visualization such as Key Graph [4], ACCENT [5], $KOTOBA$ network [6], and so on. Key Graph can show the relationships among words in texts based on their frequencies of co-occurrence; however, Key Graph is not designed for interactive word search. The displayed result is fixed. ACCENT and $KOTOBA$ network shows relationships of words in a form of graph structure. However, the interactivity of these methods is low because the graph has to be restructured every time a user needs to analyze further into the details.

The authors have developed Hierarchical Keyword Graph (HK Graph) [7], [8] as the support system for the analysis of texts with visualization of relationships among words. HK Graph can extract relevant words based on their co-occurrence for the words input by a user or for the groups, e.g., men and women, and visualize them as a graph structure. In addition, HK Graph can show the words as a hierarchical structure, and then a user can analyze the focused word in depth by seeing the lower layer of the word.

In HK Graph, divided words are regarded as different words except for the perfect matching ones. Therefore, synonyms such as different representation and different expression are regarded as different words even if they were used as the same meaning. Then these words are shown separately or often not presented because the frequency of appearance becomes low. In free texts of questionnaires, the representation and the

978-1-4244-7316-8/11/$26.00 ©2011 IEEE

expression of words (Hiragana/Kanji etc.) are often different in individuals. Consequently, aggregating these synonyms has been an important issue. In addition, it is difficult to grasp the outlines of the texts and extract the opinions in them when many words are presented on HK Graph, because the visualization result becomes complicated.

The aim of this paper is to consider the similarities of words in HK Graph and make it easy to grasp the outlines of texts. This paper proposes "concept" of words defined by the thesaurus, and the words are grouped based on their concepts, and then the concept and the grouped words are visualized in HK Graph. The proposed method can aggregate the words which were separately shown in the conventional HK Graph, and it is expected that the visualization of aggregated words makes it easier to grasp the outlines of the texts and extract proper features of them. This paper applies the proposed method to actual questionnaire data on disasters and studies the effectiveness of the proposed method.

II. HK Graph

In HK Graph, users can interactively analyze text data by starting to analyze the text related to the items they are interested in, and proceeding into deeper layers of words of interest shown as a keyword graph. The algorithm of HK Graph is as follows.

A. Division into Words

The first step in the algorithm of HK Graph is to divide the target texts into words by applying Cabocha[5]. Cabocha is a Japanese language morphological and paragraphic analysis tool. Unlike English, in which each word is separated by a space, it is difficult to divide Japanese text without tools like Cabocha. Applying Cabocha to the target texts, particles, symbols (punctuation, parentheses), pronouns, conjunctions and adnouns given by morphological information are regarded as noise words which are not needed for analysis, and they are deleted.

B. Selection of Base

The second step is for users to select contents to be analyzed, e.g., sex, income, age, the texts containing a certain word or sentence, the target group, and so on. If they want to grasp the outlines or the tendency of texts, they can select all texts. The selected group is called "Base." It is one of the features of HK Graph to let users give the start nodes of their interest which create the graph structure.

C. Extraction of Main-node

High co-occurrence words in the texts with the selected Base are extracted. The extracted words are called "Main-nodes." $Jaccard's$ coefficient is used as the co-occurrence value. The equation of co-occurrence is shown below.

$$Jaccard(B_i, W_j) = \frac{N(S(B_i) \cap S(W_j))}{N(S(B_i) \cup S(W_j))} \quad (1)$$

B_i is the Base i, W_j is each word divided out in II.A., $S(X)$ is the texts including the Base/word X, and $N(S)$ is the number of texts of S. Using eq.(1), the words with high co-occurrence to all Bases (All connected Main-node), those to plural Bases (Multi connected Main-node), and those to single Base (Single connected Main-node) are extracted.

D. Extraction of Sub-node

When a user wants to know more about a certain Main-node, HK Graph can extract the words which are closely related to the selected Main-node as a lower layer. The words, called "Sub-nodes," are extracted using eq.(1) where the Base is replaced with the selected Main-node. Thus in HK Graph, the words which have high co-occurrence with the focused words can be expanded as the lower layer, then a user can analyze the texts by proceeding into deeper layers of words of his/her interest.

E. Presentation of Hierarchical Keyword Graph

The image of output of HK Graph is shown in Fig.1. In this figure, B_1-B_3 are Bases, M_{a1} is All connected Main-node, M_{m121}-M_{m231} are Multi connected Main-nodes, M_{s11}-M_{s32} are Single connected Main-nodes, and S_{211}, S_{222}, etc. are Sub-nodes. A Base and Main-nodes, a Main-node and Sub-nodes are connected with their links, and the value of co-occurrence is expressed in the thickness of each link.

In this way, the relationships of the words are hierarchically presented in HK Graph. In addition, HK Graph can show the new graph starting from the presented words, either Main-nodes or Sub-nodes, as new Bases.

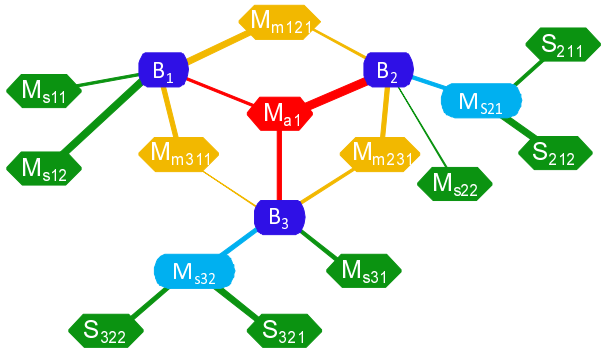

Fig. 1. Image of HK Graph

III. Proposed Method

The objective of this study is to support the analysis of free texts in questionnaires using HK Graph. However, in HK Graph, synonyms are regarded as different words, and the visualized result becomes complicated when a lot of nodes are presented as described in I. This paper considers the similarities of words in HK Graph based on their "concept" of words which are defined by the thesaurus, and proposes a method to feed back them into the visualization result with HK Graph by grouping the words based on their concepts. Moreover, the concepts are expanded using N-gram in this paper. The details of the proposed method are as follows.

A. Definition of Concept

This paper uses "Nihongo Dai-Thesaurus [9]" to define "concept." This thesaurus consists of 6 chapters. Each chapter consists of 67 sections, and each section has 1044 categories. Each category has 1-30 groups of belonging words. The small word group is the minimum unit of synonyms to be grouped. Consequently in this paper, the small word groups are defined as "concepts." Based on these concepts, the words in texts are grouped, which are called "concept groups." Each concept group is described with the label of the small word group in the thesaurus.

B. Generation of Concept Group

After the division of texts into words, it gives the label(s) of concept to each word. Concretely, each word is searched in belonging words to small word groups in the thesaurus, and the label of corresponding concept are given to the word when the word is found. Plural concepts can be given to one word because a word often has some meanings and appears in some small word groups in the thesaurus. Concept groups, in which same belonging words are, are generated based on the concept labels of words. Each concept group is shown with the corresponding label in the thesaurus.

C. Expansion of Concept Group using N-gram

Only the words in the thesaurus belong to concept groups generated in III.B. However, there are a lot of synonyms which the thesaurus does not have but shown in the texts, e.g., 'earthquake' and 'earthquake disaster,' these are originally written in Japanese, belong to the concept "earthquake," but unique nouns such as 'the Great Hanshin Earthquake' or 'a Tokai earthquake' do not belong to it. This paper expands the concept groups using N-grams [10], [11] which have been often used in the area of full-text searching. An N-gram is consist of a subsequence of n characters divided from a given sequence. In this paper, a given sequence is a word in texts (in Japanese) and a subsequence is the characters which are divided from the word. For example, in the case of N=2, from a word 'ABCDE' (each character A, B, C, D, E is a Kanji, Hiragana or Katakana), the N-grams 'AB,' 'BC,' 'CD,' 'DE,' are generated. N-grams are generated for all words presented in HK Graph, and the words which have the N-grams corresponding to those by the words in the original concept groups are put into the concept group. This expansion of concept groups can aggregate the synonyms of them which the thesaurus does not have.

D. Application to HK Graph

Words and concept groups generated in III.C. are presented in HK Graph. Concretely, as described in II.C., the high co-occurrence words in the texts with the selected Bases are extracted as Main-nodes. When 2 or more words in the extracted words belong to a same concept group, these words are aggregated into the concept group, and the label of the concept group is presented as a node in HK Graph, this paper calls these nodes "concept nodes." Links to a concept node or to Sub-nodes from a concept node are connected based on the co-occurrence values of the words belonging to the concept group. Eq.(2) shows $Jaccard's$ coefficient to calculate the co-occurrence value. The difference from eq.(1) is G_i, which is the words belonging to the concept group.

$$Jaccard(G_i, W_j) = \frac{N(S(G_i) \cap S(W_j))}{N(S(G_i) \cup S(W_j))} \quad (2)$$

IV. Experiment

A. Questionnaire Data and Division into Words

In this experiment, the proposed method was applied to 500 free texts of a questionnaire on disasters. The question of the questionnaire was "Please write your opinions or thoughts on natural disasters over 50 characters (in Japanese)." Actually, including "I don't have comments in particular" and so on, 125 respondents out of 500 wrote the responses less than 50 characters. Firstly, the text data were divided into words as described in II.A., and the words and concepts not to be needed for the analysis ('thing,' 'is,' 'there,' 'that,' and a concept "point" coming from a word 'thing') were excluded by hand. The number of N-gram N was 2. The following figures and descriptions of the results are originally written in Japanese and translated into English.

B. Study of Grasping Outline of Text

First, the easiness to grasp the outlines of texts was studied comparing with the conventional HK Graph. The conventional HK Graph was applied to the above questionnaire data, and the visualization result is shown in Fig.2 when the extracted word class was noun and the number of the presented Main-nodes was set to 100. The number of Main nodes employed here was set based on the visibility of the results. Appropriate number should be studied in the future work. Fig.3 shows the result of the proposed method with concept groups described in III.D. based on 100 words in Fig.2. Orange nodes in Fig.3 are the concept nodes.

It is slightly difficult to grasp the general outlines of the texts from Fig.2, because the number of presented words are many and the synonyms are not categorized and dispersed. On the other hand in Fig.3, main words in the texts are categorized and aggregated by the concepts, which makes it easier to grasp the outlines than Fig.2 by focusing on the concept nodes. According to the result of Fig.3, for "opinions on natural disasters," there were "Earthquake," "Flood," "Heavy rain," and they also mentioned "Environmental problem," "Broadcast" and "Prediction."

C. Study on Aggregation of Synonyms

Next, the effect of the aggregation of synonyms based on the concepts was studied. Fig.4 shows the result of the conventional HK Graph when Bases were selected as the respondents less than 40's and those more than or equal to 40's, and Fig.5 shows the result of the proposed HK Graph generated based on Fig.4. In Fig.4, 'Environmental destruction' and 'Warming temperature' are connected to the Base of the respondents less than 40's, and 'Global warming' is connected to those more than or equal to 40's. These words could be used

Fig. 2. Conventional HK Graph

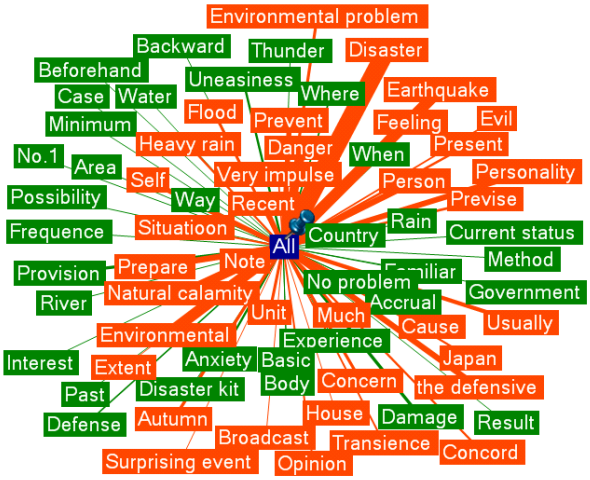

Fig. 3. Proposed method

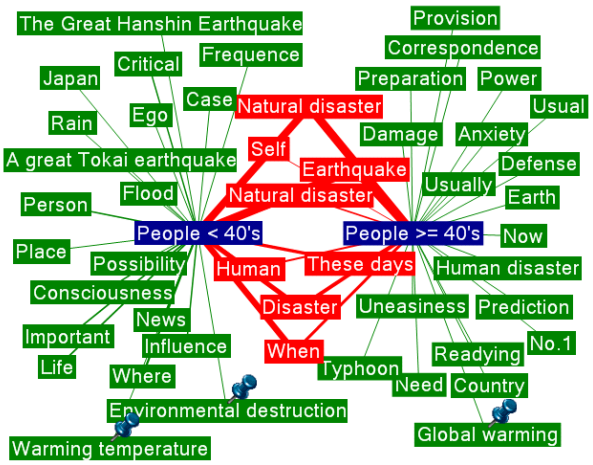

Fig. 4. Conventional HK Graph (Bases : People $<$ 40's, People $\geq$ 40's)

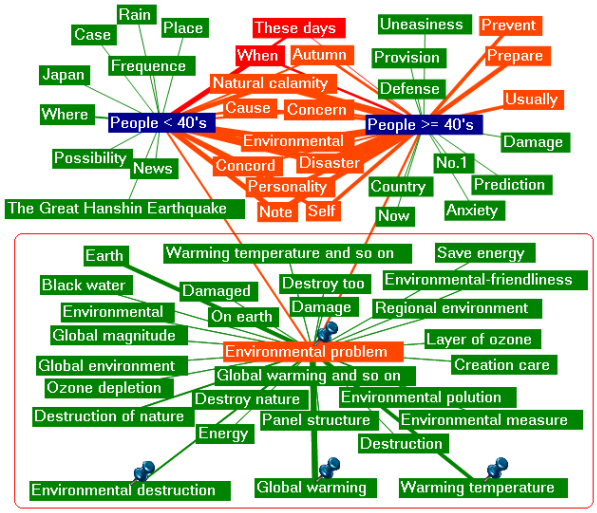

Fig. 5. Proposed method (Bases : People $<$ 40's, People $\geq$ 40's)

to describe "Environmental problem." However, these words were dealt with different words in the conventional method, then we might grasp that respondents less than 40's mentioned 'Environmental destruction' and 'Warming temperature,' and those of more than or equal to 40' did 'Global warming.' On the other hand, in the proposed method, 'Environmental destruction,' 'Warming temperature' and 'Global warming' were aggregated into the concept "Environmental problem," and this concept node was presented as All connected Main-node from both Bases. Therefore, it is found that the respondents for the wide generations had interest in environmental problem. In addition, in the proposed method, as the synonyms such as 'environmental pollution,' 'ozone depletion,' and so on, which were not presented in the conventional method because the number of the words in the texts were small, were belonging and presented as the same concept group, we can analyze more detail of the opinions on the environmental problem.

Finally, the effect of the expansion of concept groups using N-gram was studied. Fig.6(a) shows the belonging words to the concept "Earthquake" before the expansion, and Fig.6(b) shows after the expansion using N-gram as described in III.C. Extracted words in Fig.6(a) are only general words, e.g., 'Earthquake,' 'Earthquake disaster,' and so on. On the other hand, in Fig.6(b), the concept group have a lot of synonyms including the unique nouns, 'The Great Hanshin Earthquake,' 'The Chuetsu earthquake,' 'Early news about the earthquake,' and so on, by the expansion using N-gram. It gives us detail analysis on the opinions about earthquake.

V. Conclusion

This paper considered the similarities of words in HK Graph based on their "concept" of words which were defined by

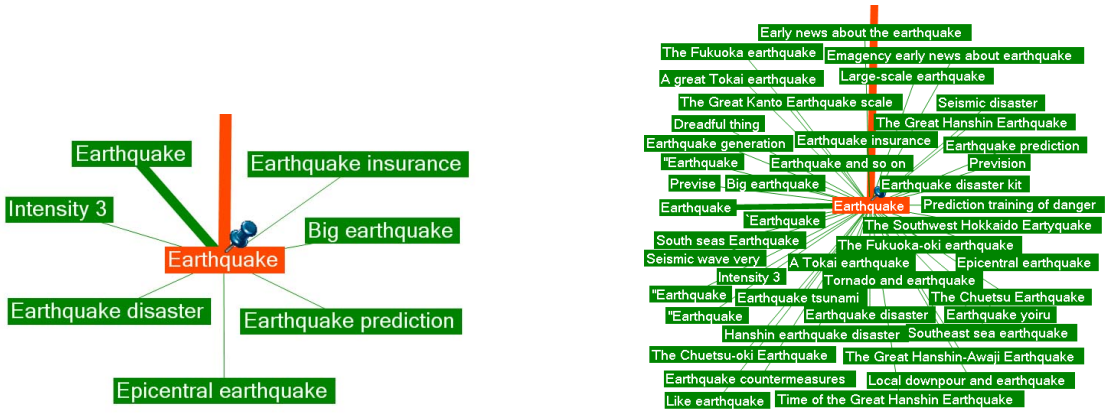

(a) Before expansion

(b) After expansion

Fig. 6. Effect of expansion of concept group

the thesaurus, and proposed a method to feed back them into the visualization result with HK Graph by grouping the words based on their concepts. This paper also proposed the expansion of concept groups using N-gram. This paper applied the proposed method to actual questionnaire data on disasters and studied the easiness to grasp the outline of texts comparing with the conventional HK Graph. It also studied the effectiveness of the aggregation of synonyms by the concept groups and the expansion of them. Future work is more study on the expansion of concept groups and the extraction of the proper concept for the word belonging to some concepts considering the meaning in the texts.

ACKNOWLEDGMENT

This work was supported by the Grant-in-Aid for Scientific Research (C) from the Ministry of Education, Culture, Sports, Science and Technology (MEXT), Japan, Grant number: 22500088.

REFERENCES

[1] B. Larsen and C. Aone, "Fast and effective text mining using linear-time document clustering," the fifth ACM SIGKDD international conference on Knowledge discovery and data mining, pp. 16-22, 1999.

[2] R. Feldman, M. Fresko, Y. Kinar, Y. Lindell, O. Liphstat, M. Rajman, Y. Schler, and O. Zamir, "Text mining at the term level," Data Mining and Knowledge Discovery, pp. 65-73, 1998.

[3] Y. Ichimura, T. Hasegawa, I. Watanabe, and M. Sato, "Text Mining : Case Studies(Special Issue : "Text Mining")," Japanese Society for Artificial Intelligence, vol. 16, no. 2, pp. 192-200, 2001.

[4] Y. Ohsawa, N.E. Benson, and M. Yachida, "KeyGraph: Automatic Indexing by Co-Occurrence Graph Based on Building Construction Metaphor," Proc. ADL, pp.12-18, 1998.

[5] K. Misue and I. Watanabe, "Visualization of keyword association for text mining," IPSJ SIG Notes, vol. 99, no. 57, pp. 65-72, 1999.

[6] M. Masaki, O. Shinobu, T. Yashuhiro, S. Masanari, I. Makoto, and F. Miki, Jireidemanabu text mining (in Japanese), Tokyo, Kyoritsu Shuppan, 2008.

[7] T. Okabe, T. Yoshikawa, and T. Furuhashi, "A proposal of analysissystem for medical incident reports using metadata and co-occurrence information," Japan Society for Fuzzy Theory and Intelligent Informatics, vol. 18, no. 5, pp. 689-700, 2006.

[8] T. Yoshikawa, Y. Uchida, T. Furuhashi, E. Hirao, and H. Iguchi, "Extraction of evaluation keywords for analyzing product evaluation in user-reviews using hierarchical keyword graph," Advanced Computational Intelligence and Intelligent Informatics, vol. 13, no. 4, pp. 457-462, 2009.

[9] T. Yamaguchi, Nihongo Dai-Thesaurus CD-ROM (in Japanese), Tokyo, Taishukan Shoten, 2006.

[10] M. Nagao and S. Mori, "A New Method of N-gram Statistics for Large Number of n and Automatic Extraction of Words and Phrases from Large Text Data of Japanese," Proc. COLING, pp.611-615, 1994.

[11] Y. Kokubu, "Full-text searching for managing a large number of documents," Information Processing and Management, vol. 42, pp. 380-389, 1999.

2011 IEEE International Conference on Fuzzy Systems
June 27-30, 2011, Taipei, Taiwan

Development of Body Mapping from Human Demonstrator to Inverted-Pendulum Mobile Robot for Imitation

Sataya TAKAHASHI*, Yasutake TAKAHASHI, and Yoichiro MAEDA
*Faculty of Engineering, University of Fukui
Graduate School of Engineering, University of Fukui
3-9-1, Bunkyo, Fukui, Fukui, 910-8507, Japan
Email: {stakahasi,yasutake,maeda}@ir.his.u-fukui.ac.jp

Takayuki NAKAMURA
Faculty of Systems Engineering, Wakayama University
Sakaetani 930, Wakayama 640-8510, Japan
Email: ntakayuk@sys.wakayama-u.ac.jp

***Abstract*—This paper addresses development of body mapping from a human demonstrator to an inverted-pendulum mobile robot for imitation. An inverted-pendulum mobile robot with torso and body links learns a dynamic kicking motion shown by a human. The robot observes the human demonstration with a camera, extracts the human region in each of images, maps the region to its own two links, estimates the link posture trajectories, and starts kicking motion learning based on the trajectory parameters for imitation. The mapping parameter gives an important role for successive imitation. A reasonable and feasible procedure of learning from observation for an inverted-pendulum robot and development of the body mapping is proposed and investigated in this paper.**

Keywords-imitation; corresponding problem; reinforcement learning; policy gradient method; inverted pendulum wheeled robot

I. INTRODUCTION

In order to develop skills, actions, behavior in a human symbiotic environment, a robot is going to learn something from behavior observation of predecessors or humans. Observation of others makes the behavior learning rapid and therefore much more efficient [1], [2], [3]. Recently, many approaches for robotics imitation have been proposed (for example, [4], [5]). It is desirable to acquire various unfamiliar behavior with some instructions from others, for example, surrounding robots and/or humans in real environment because of huge exploration space and enormous learning time to learn without any a priori knowledge. Therefore, behavior learning through observation has been more important.

However, a robot imitator does not usually share the same embodiment, for example, link configurations, constraints, dynamics, and so on, with a demonstrator. The imitator has to solve a problem of body mapping between the demonstrator and itself, so called, the correspondence problem[6], in an appropriate way. In order to avoid the problem, some conventional approaches focus not on body movement imitation but on target control imitation. For example, Bentivegna et al. [3] shows imitation of playing air hockey and marble maze. The robot does not imitate the motion of the body but the motion of the target, a paddle for the air hockey and knobs on the board for the marble maze. Another approach for the body mapping problem is to use a robot that has a similar embodiment with a demonstrator. Humanoid robots are popular for imitation of human demonstration[4], [5].They use motion capture systems to capture human body postures and map them to the body postures of a humanoid robot. They have few body mapping problems and actually it is easy to map the human body links to humanoid robot ones because the demonstrator and the imitator share similar embodiment.

For example, a dolphin imitates human motion as discussed in [6] and a child imitates a long trunk of an elephant with his/her arm. They have different embodiments with the demonstrators and show successful imitation based on mapping the body of a demonstrator to the one of the imitator The body mapping problem becomes more difficult and important if the robot imitator does not share the embodiment with a demonstrator. Therefore, an appropriate approach is necessary for the problem to realize body movement imitation learning in a human symbiotic environment.

On the other hand, two-wheeled inverted pendulum mobile robots have been developed as a realistic solution for the human symbiotic environment so far[7][8]. A inverted pendulum mobile robot has many advantages over the statically stable wheeled robots and any other biped robots. It requires a smaller amount of space to stand and stay upright than the other wheeled robots and smaller number of actuators than the conventional biped robots. Furthermore, it can easily generate more dynamic motions only by its body balancing control. The two-wheeled inverted pendulum robot has a possibility to be standard platform as a human partner robot. Most of researches regarding to the two-wheeled inverted pendulum robot focuses on the control theory for achieving stable navigation. There are few researches to realize more dynamic motions such as throwing, jumping, pushing, kicking, and so on. Takahashi et al.[9] introduced a reinforcement learning method for generating a dynamic motion such that a two-wheeled inverted pendulum robot kicks a ball far away utilizing its own body dynamics while it keeps standing. However, the learning time is too long to apply the learning method for a real mobile inverted-

978-1-4244-7316-8/11/$26.00 ©2011 IEEE

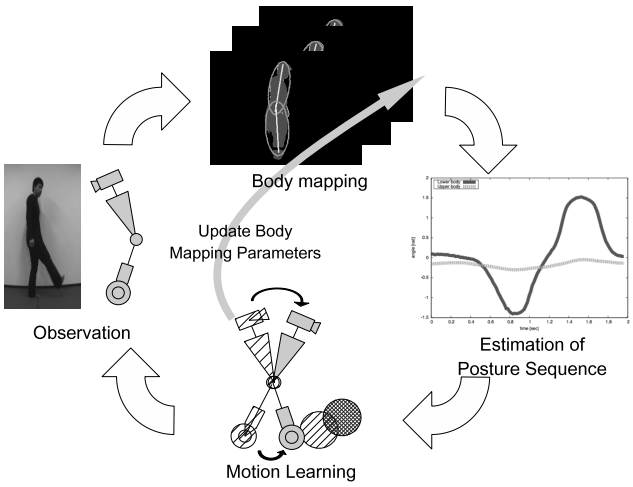

Fig. 1. Imitation Learning

pendulum wheeled robot. Furthermore, they designed initial motions by hand before learning in order to reduce unnecessary useless exploration as much as possible. In order to produce feasible initial motion for efficient learning, imitation is one of the most convincing approaches.

Tamura et al.[10] have proposed a method for recognition of demonstrator's posture for imitation based on reinforcement learning. They focus on how a two-link inverted-pendulum wheeled robot updates body mapping parameters while the demonstrator shows throwing motion after the robot learns the throwing motion. Takahashi et al.[11] investigated imitation learning performance for the two-link inverted-pendulum wheeled robot. A human demonstrator shows kicking motion and a robot learns the motion from observed data. They proposed a reasonable and feasible procedure of learning from observation for the inverted-pendulum wheeled robot. However, the body mapping parameters are tuned by hand and fixed during the imitation.

In this paper, we propose a novel learning method of body mapping parameters for imitation based on previous work[11]. A human demonstrates a ball kicking motion and a two-link inverted-pendulum mobile robot imitates the motion. Updating body mapping parameters based on gradient of evaluation of imitated motion enables the imitator to reasonably recognize demonstrator's body links for imitation and shows better performance of imitated motion than hand-tuned ones.

II. Imitation Learning

Figure 1 shows a flow of imitation learning. First, a two-link inverted-pendulum mobile robot as an imitator observes human demonstrations with a camera. A human region in the captured image is extracted and mapped to two links of the robot with a certain body mapping parameter. A sequence of link postures during the motion is estimated for imitation learning. The robot starts learning the motion from the estimated link posture sequence as initial motion parameters. After the learning, the body mapping parameter is updated based on the performance of the learned motion. This procedure repeats until the robot finds a local optimum body mapping parameter. Details of the each step are described in following sections.

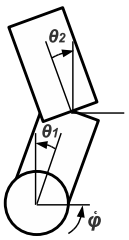

Fig. 2. Model of Two-Link Inverted-Pendulum Mobile Robot

III. Inverted Pendulum Wheeled Robot

Figure 2 shows a model of our inverted-pendulum wheeled robot. The robot body size is 20cm length, 30.5cm width, and 70cm height. The weight is 8kg including the torso, body, wheels, batteries, motors, gears, encoders, an accelerogyrometer unit, and control unit. The wheel radius is 8.5 cm and its weight is 500g each. The ball kicked by the robot is a soccer ball, roughly 22cm in diameter, and about 450g in weight. In order to perform comprehensive experiments for learning a kicking motion with the robot, we develop a computer simulation of the robot and the ball using the ODE(open dynamics engine) library.

IV. Design for Learning Kicking Motion

The kicking motion is designed with two control layers, a low-level posture controller and a posture generator. The posture controller follows a conventional torque control theory. Torque for the wheels u_1 is calculated as follows:

$$u_1 = -k_1^l(\theta_1 - \theta_d^l) - k_2^l\dot{\theta_2} - k_3^l\dot{\varphi} - k_4^l\sum(\dot{\varphi} - \dot{\varphi}_d), \qquad (1)$$

where θ_1, θ_d^l, $\dot{\varphi}$, $\dot{\varphi}_d$ are error of body angle, desired body angle, wheel angular velocity, and desired wheel angular velocity, respectively. k_1^l, k_2^l, k_3^l, k_4^l are gains for the body angle, body angular velocity, wheel angular velocity, and accumulated error of wheel angular velocity, respectively. For simplicity, torque for a joint between the body and the torso u_2 is designed as follows:

$$u_2 = -k_1^u(\theta_2 - \theta_d^u) - k_2^u\dot{\theta_2} - k_3^u\sum(\theta_2 - \theta_d^u), \qquad (2)$$

where k_1^u, k_2^u, and k_3^u are control gains.

In this work, we design the kicking motion in combination with two primitive motions (Fig.3). Each primitive motion defines the desired body and torso angles, desired wheel angular velocity, gain parameters, and a period of time. The posture generator sends the control parameters to the posture controller within the period defined by the primitive motion, one by one. The first primitive motion tries to lean forward to kick the ball and the second tries to make the robot kick the ball actually. Before and after the kicking motion, the robot controls itself to stay upright avoiding falling-down, autonomously.

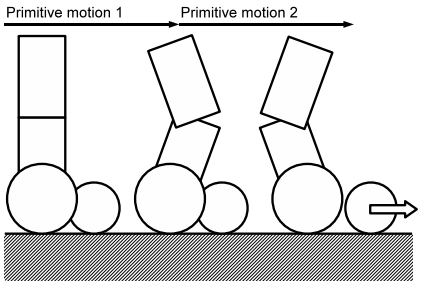

Fig. 3. Two Primitive Motions to Kick a Ball

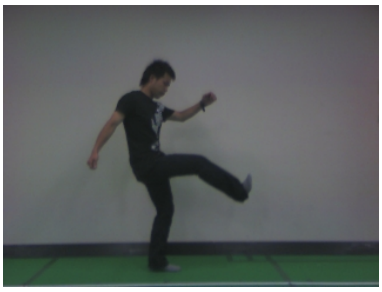

(a)

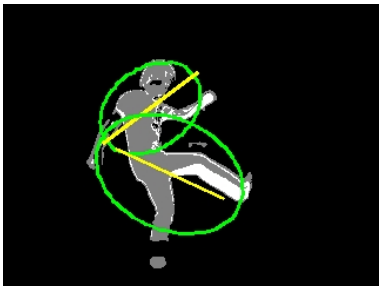

(b)

Fig. 4. View of Human Kicking Motion (a) and Upper and Lower Body Recognition (b)

V. Observation and Initial Learning Parameters

Using a camera, a robot observes a human demonstration of kicking a ball. Figure 4(a) shows a picture of observed motion of human kicking behavior. It captures pictures with 30fps and extracts regions of the human in the images with simple background subtraction and frame difference methods. Then, it estimates postures of upper and lower bodies by calculating covariances of the regions in the image. First, it divides the whole human region into two regions, upper body and lower body, with a body mapping parameter r_{bm}. The body mapping parameter r_{bm} specifies a ratio of upper and lower bodies. For example, a whole human region is divided at the center of the region when $r_{bm} = 0.5$.

Then, a region moment M_{pq} is calculated for each region:

$$M_{pq} = \sum_i \sum_j (i - i_G)^p (j - j_G)^q f(i,j) \qquad (3)$$

(i_G, j_G) is the center of the region and $f(i,j)$ is pixel value on the point (i, j) which is 1 if the point in the region, otherwise zero. The posture θ of the region (as the upper or lower body) can be calculated as:

$$\theta = \frac{1}{2} \arctan\Big(\frac{2M_{11}}{M_{20} - M_{02}}\Big) \ , \qquad (4)$$

where p and q are indexes of order of moment for x and y coordinates, respectively. Figure 4(b) shows a extracted human body region and estimated posture of upper and lower bodies.[1] Figure 5 shows a sequence of estimated postures during the observation of human kicking motion.

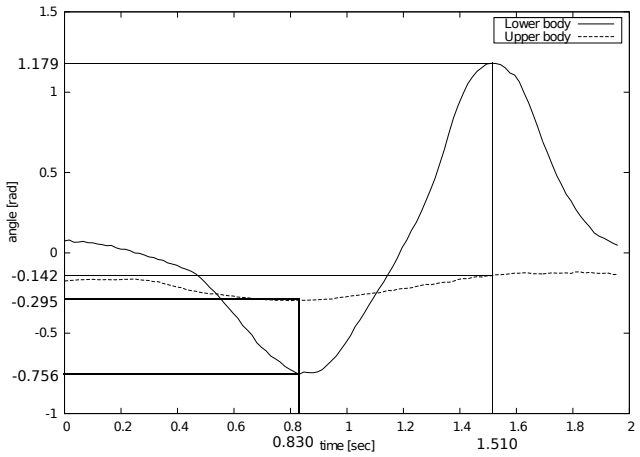

Fig. 5. Posture Estimation during Human Kicking Motion

Primitive motion parameters are initially set from the observed postures from Fig.5. In general, a human kicking motion does not consist of two primitive motions as described in Section IV. A learning robot has to extract useful parameter values from observation of human kicking motion. To be concrete, the observed human motion divided into two primitive motions for generating learning initial parameter values. A sequence of an observed trajectory is divided at points each of which lower body posture acceleration is the highest. 0.830 [sec] and 1.510 [sec] are the points to be divided from Fig.5. 0.830 [sec] and 0.680 [sec] are set as periods of time for primitive motion 1 and 2. Posture angles of lower and upper body at 0.830[sec] are -0.126 [rad] and -0.0492 [rad], respectively. Then, desired posture angles θ_d^l, θ_d^u for primitive motion 1 are set -0.126 [rad] and -0.0492 [rad]. In turn, posture angles of lower and upper body at 1.510 [sec] are -0.808 [rad] and 1.30 [rad], respectively. Then, desired posture angles θ_d^l, θ_d^u for primitive motion 2 are set 0.197 [rad] and 0.135 [rad]. Eventually, the initial parameter values with body mapping parameter $r_{bm} = 0.5$ are shown in TABLE I. The table also shows wheel angular velocity ϕ_d and initial control gains for experiments later.

The body mapping parameter r_{bm} affects not only the division of the human region into upper and lower bodies but also the estimation of body postures of the observed motion. The parameter should be tuned appropriately in order to acquire

[1]The part of ankle is failed to be extracted because the part has similar color with background. However, the effect of the extraction failure is small enough to estimate the posture of the lower body.

TABLE I
INITIAL PARAMETERS OF PRIMITIVE MOTION 1 AND 2 FROM OBSERVATION WITH BODY MAPPING PARAMETER $r_{bm} = 0.5$ AND INITIAL CONTROL GAINS

learning parameter	primitive motion 1	primitive motion 2
T [sec]	0.830	0.680
θ_d^l [rad]	-0.126	0.197
θ_d^u [rad]	-0.0492	0.0236
ϕ_d [rad/sec]	0	0
k_1^l	15.0	15.0
k_2^l	-0.3	-0.3
k_3^w	0.01	0.01
k_4^w	0.0	0.0
k_1^u	25.0	25.0
k_2^u	-0.1	-0.1
k_3^u	0.01	0.01

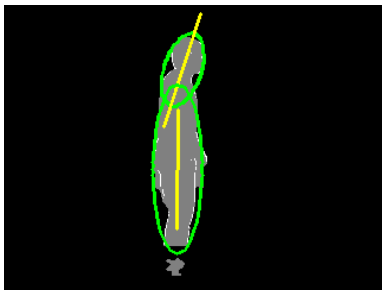

(a) $r_{bm} = 0.3$

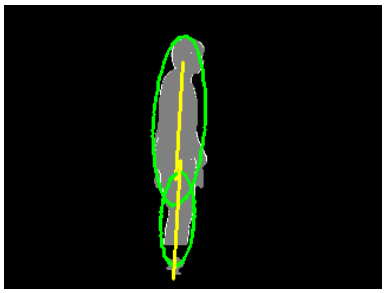

(b) $r_{bm} = 0.7$

Fig. 6. Effect of Body Mapping Parameter r_{bm}

proper initial motion parameters for imitation learning. Figure 6 shows an example. Two pictures in Fig.6 are exactly same with different body mapping parameters $r_{bm} = 0.3$ and 0.7. TABLEs II and III show extracted primitive motion parameters with body mapping parameter $r_{bm} = 0.3$ and 0.7, respectively. They indicate that different body mapping parameters on a same observed image result in different body postures of the observed motion.

VI. MOTION LEARNING

A simple policy gradient method introduced by Kohl and Stone[12] enables the posture generator to learn the kicking motion, to say more precisely, improve the control parameters of each primitive motion by trail and error. First, it has a initial control parameter and prepares a set of similar parameters by adding small disturbances. It evaluates the control parameters one by one and estimates gradient of the evaluation of the control parameters. Finally, it updates the control parameters

TABLE II
EXTRACTED PRIMITIVE MOTION PARAMETERS WITH BODY MAPPING PARAMETER $r_{bm} = 0.3$

learning parameter	primitive motion 1	primitive motion 2
T [sec]	0.896	0.674
θ_d^l [rad]	-0.0784	0.0915
θ_d^u [rad]	-0.0770	-0.0638

TABLE III
EXTRACTED PRIMITIVE MOTION PARAMETERS WITH BODY MAPPING PARAMETER $r_{bm} = 0.7$

learning parameter	primitive motion 1	primitive motion 2
T [sec]	0.830	0.714
θ_d^l [rad]	-0.285	0.288
θ_d^u [rad]	-0.0533	0.0172

according to the estimated gradient of the evaluation. The learning system repeats this procedure and updates the motion parameters to reach the local maximum of evaluation. For further details, please refer to the original paper by Kohl and Stone[12] or our previous work[11]. Figure 7 shows the

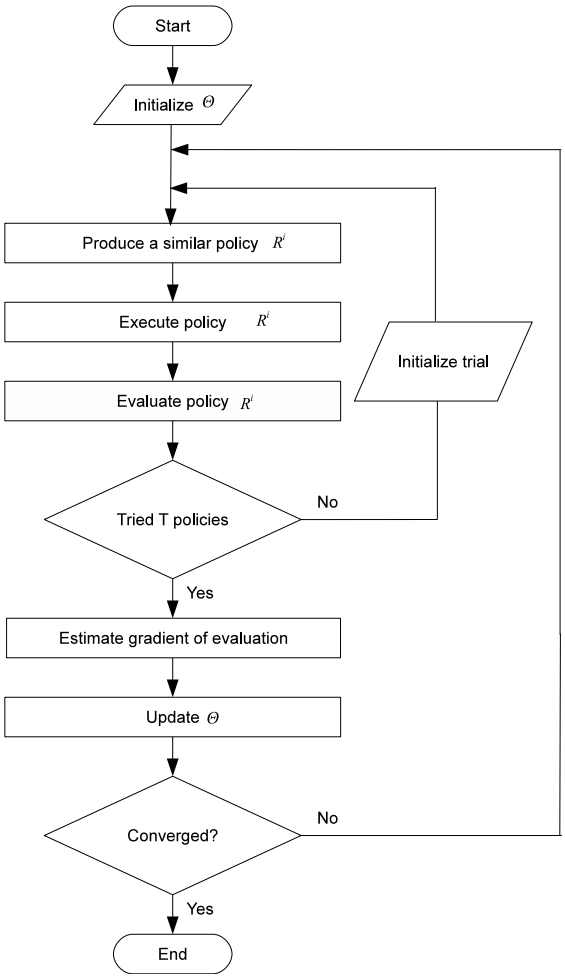

Fig. 7. Learning Procedure

learning procedure.

TABLE IV
STEP SIZE OF LEARNING PARAMETERS

learning parameter	step size
T [sec]	0.001
θ_d^l [rad]	0.01
θ_d^u [rad]	0.01
ϕ_d [rad/sec]	0
k_1	0.01
k_2	0.001
k_3	0.0001
k_4	0.00001

Each primitive motion is defined by the desired body and torso angles θ_d^l θ_d^u, the desired wheel angular velocity $\dot{\varphi_d}$, the gain parameters k_1, k_2, k_3, and k_4, and a period of time t. The learning parameters are those primitive motion parameters for each, therefore, 16 parameters in all. We determine the evaluation criterion of the kicking motion while learning process in consideration of the following points:

- Traveling distance of the robot body should be small.
- Velocity of the kicked ball should be large.
- Robot should avoid falling down by kicking the ball.

The actual evaluation is defined as follows:

$$E = \begin{cases} w_1 v_b - w_2 l_b^2 - w_f & \text{if it falls down} \\ w_1 v_b - w_2 l_b^2 & \text{else} \end{cases} \quad (5)$$

where l_b, v_b are traveling distance of the robot body during kicking motion and velocity of the kicked ball, respectively. w_1, w_2, w_f are penalty for falling down and weights and set as 2.0, 1.0, and 10.0, respectively, in the following experiments.

VII. UPDATE OF BODY MAPPING PARAMETER

Evaluation of the acquired motion $E^f(r_{bm})$ is checked after learning with body mapping parameter r_{bm}. Then, a random disturbance Δr_{bm} is added to the current body mapping parameter, estimation of sequence of upper and lower body postures and recalculation of initial motion parameters are conducted again, and motion learning is restarted. After the learning, the robot evaluates the acquired motions as $E^f(r_{bm} + \Delta r_{bm})$ and $E^f(r_{bm} - \Delta r_{bm})$. Finally, it updates the body mapping parameter to imitate the motion with higher evaluation as follows:

$$r_{bm} \leftarrow \begin{cases} r_{bm} + \Delta r_{bm} & \text{if } E^f(r_{bm} + \Delta r_{bm}) > E^f(r_{bm}) \text{ and} \\ & E^f(r_{bm} + \Delta r_{bm}) > E^f(r_{bm} - \Delta r_{bm}) \\ r_{bm} - \Delta r_{bm} & \text{if } E^f(r_{bm} - \Delta r_{bm}) > E^f(r_{bm}) \text{ and} \\ & E^f(r_{bm} - \Delta r_{bm}) > E^f(r_{bm} + \Delta r_{bm}) \\ r_{bm} & \text{else} \end{cases} \quad (6)$$

$|\Delta r_{bm}|$ is set to 0.1 in this paper.

VIII. EXPERIMENTS

A. Experiment Setup

The learning step size parameters are shown in TABLE IV. The number of deviated policies for estimating gradient of the evaluation T is set to 50 in the experiments.

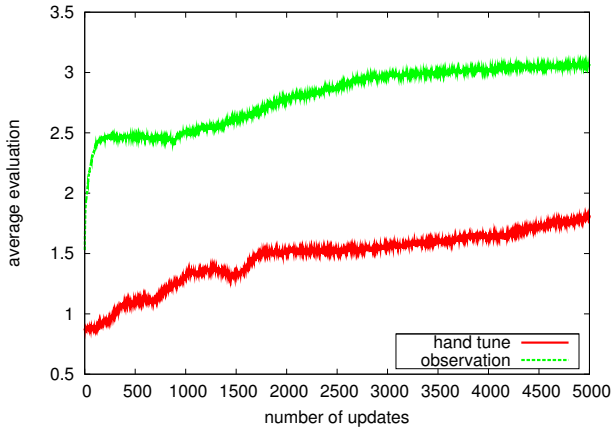

Fig. 8. Motion Evaluation during Learning with Initial Motion Parameters from Observation and Tuned by Hand

TABLE V
HAND TUNED INITIAL PARAMETERS OF PRIMITIVE MOTION 1 AND 2

learning parameter	primitive motion 1	primitive motion 2
period of time [sec]	0.500	0.500
θ_d^l [rad]	-0.052	0.052
θ_d^u [rad]	0.052	-0.052
ϕ_d [rad/sec]	0	0
k_1	15.0	15.0
k_2	-0.3	-0.3
k_3	0.01	0.01
k_4	0.0	0.0

B. Usefulness of Imitation Learning

Figure 8 shows an example sequence of motion evaluation during learning with initial motion parameters from observation and tuned by hand. Acquired kicking motion with learning from observation is twice as good as the one with hand-tuned initial motion parameters. The hand-tuned parameters are shown in Table V. This result shows usefulness of the imitation learning. Figure 9 shows an example sequence of the learned kicking motion.

C. Effect of Body Mapping Parameter

We investigated motion evaluation after learning while the body mapping parameter r_{bm} is changed gradually from 0.1 to 0.9. Figure 10 shows the result. It shows the acquired motion evaluation at $r_{bm} = 0.6$ is the best and distributed like a mountain. This means that a simple gradient method enable the imitator to find one of the best body mapping parameters by updating the parameters gradually. Figure 10 suggests that the body mapping parameter converges to the best with a simple gradient method if it starts from relatively large range (from 0.4 to 0.9) although the evaluation at $r_{bm} = 0.2$ is local maxima and it might prevent the imitator to find the best parameter value. However, a proper parameter exploration method such as simulated annealing easily avoids the local maxima.

IX. CONCLUSION

This paper addressed development of body mapping from a human demonstrator to an inverted-pendulum mobile robot

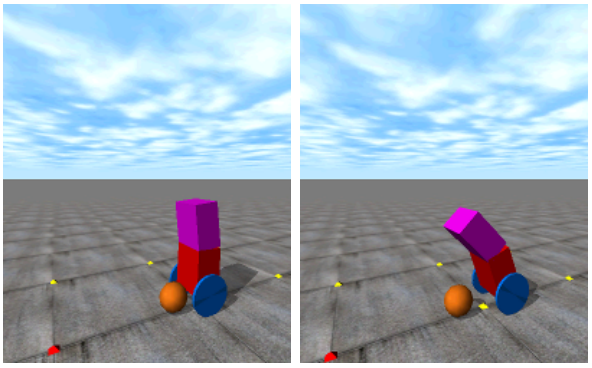

(a) 0.03 sec (b) 0.36 sec

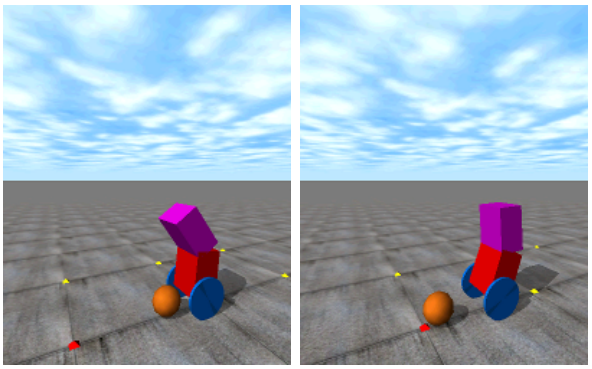

(c) 0.56 sec (d) 0.92 sec

Fig. 9. A Sequence of Ball Kicking Motion after Learning

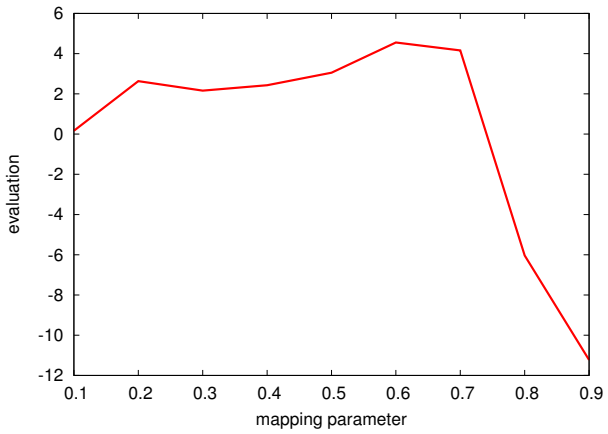

Fig. 10. Acquired Motion Evaluation with Variety of Body Mapping Parameter Values

for imitation. A human demonstrator shows kicking motion and a robot learns the motion from the observed data. In order to imitate an observed motion demonstrated by a human, the robot has to map the body of the demonstrator to its own body links. We proposed a reasonable and feasible method that enables a two-link inverted-pendulum mobile robot to learn a human motion from observation with a simple body mapping technique. Experimental results indicate that imitation gives better initial motion parameters for learning and body mapping parameter for the imitation can be updated based on the evaluation of the acquired motion after the learning. In order to show the proposed method has some generality, we are planning to apply to not only a kicking motion but also, for example, ball throwing, trapping, and so on.

ACKNOWLEDGMENT

This research was partially supported by the Ministry of Education, Science, Sports and Culture, Grant-in-Aid for Young Scientists (B), 22700201,2010.

REFERENCES

[1] S. D. Whitehead, "Complexity and cooperation in q-learning," in *Proceedings Eighth International Workshop on Machine Learning (ML91)*, 1991, pp. 363–367.

[2] B. Price and C. Boutilier, "Accelerating reinforcement learning through implicit imitatione," *Journal of Articial Intelligence Research*, vol. 19, pp. 569–629, Dec 2003.

[3] D. C. Bentivegna, C. G. Atkeson, and G. Chenga, "Learning tasks from observation and practice," *Robotics and Autonomous Systems*, vol. 47, pp. 163–169, 2004.

[4] S. Schaal, A. Ijspeert, and A. Billard, *Computational approaches to motor learning by imitation*. Oxford University Press, 2004, no. 1431, pp. 199–218.

[5] T. Inamura, Y. Nakamura, and I. Toshima, "Embodied symbol emergence based on mimesis theory," *International Journal of Robotics Research*, vol. 23, no. 4, pp. 363–377, 2004.

[6] C. L. Nehaniv and K. Dautenhahn, *The correspondence problem*. Cambridge, MA, USA: MIT Press, 2002, pp. 41–61. [Online]. Available: http://portal.acm.org/citation.cfm?id=762896.762899

[7] S. Ha, Y. Yuta, "Trajectory tracking control for navigation of self-contained mobileinverse pendulum," in *Proceedings of the IEEE/RSJ/GI International Conference on Intelligent Robots and Systems '94*, vol. 3, 1994, pp. 1875–1882.

[8] B. Browning, J. Searock, P. E. Rybski, and M. Veloso, "Turning segways into soccer robots," *Industrial Robot: An International Journal*, vol. 32, no. 2, pp. 149 – 156, 2005.

[9] Y. Takahashi, H. Nonoshita, T. Nakamura, and Y. Maeda, "Behavioral development of ball kicking motion of a two-wheeled inverted pendulum mobile robot," in *Proceedings of 2010 IEEE World Congress on Computational Intelligence*, vol. DVD-ROM, Jul 2010, pp. 830–835.

[10] Y. Tamura, Y. Takahashi, and M. Asada, "Clustering observed body image for imitation based on value system," in *Proceedings of 2010 IEEE World Congress on Computational Intelligence*, vol. DVD-ROM, Jul 2010, pp. 917–923.

[11] S. Takahashi, H. Nonoshita, Y. Takahashi, Y. Maeda, and T. Nakamura, "Inverted-pendulum mobile robot motion learning from human player observation," in *Proceedings of Joint 5th International Conference on Soft Computing and Intelligent Systems and 11th International Symposium on Advanced Intelligent Systems*, vol. CD-ROM, December 2010, pp. 211–216.

[12] N. Kohl and P. Stone, "Policy gradient reinforcement learning for fast quadrupedal locomotion," in *In Proceedings of the IEEE International Conference on Robotics and Automation*, May 2004, pp. 2619–2624.

2011 IEEE International Conference on Fuzzy Systems
June 27-30, 2011, Taipei, Taiwan

Social Interaction of Cooperative Communication and Group Generation in Multi-Agent Reinforcement Learning Systems

Kun Zhang
Dept. of System Design Engineering
Graduate School of Engineering
University of Fukui
Fukui, Japan
Email: kzhang@ir.his.u-fukui.ac.jp

Yoichiro Maeda and Yasutake Takahashi
Dept. of Human and Artificial Intelligent Systems
Graduate School of Engineering
University of Fukui
Fukui, Japan
Email: (maeda, yasutake)@ir.his.u-fukui.ac.jp

***Abstract*—Recently, researches on multi-agent systems (MAS) which autonomous agents are able to learn cooperative behavior are actively performed. It is necessary for social agents to interact each other in order to have excellent cooperative performance in MAS. But it is difficult to give appropriate coordination at the right time, not to mention the generation of group behavior. We have aimed at the group behavior generation of social agents who have excellent autonomous learning ability like human through cooperative communication between agents to acquire cooperative behavior. Social agents are able to change the environment states to individual states and communicate their cooperative behavior by sending a special signal, which can not be understood originally but could be understood by other agents through reinforcement learning (RL) after some learning processes. Furthermore, if the agents could communicate their cooperative behavior successfully, their group identity will be strengthened by exchanging rewards among them. As the learning process, social agents can get the better cooperative ability than normal reinforcement learning method through group identity. Lastly, social agents not only adjust themselves to environment but also affect other agents to generate intelligent group behavior.**

***Keywords*—Reinforcement Learning; Multi-Agent Systems; Social Interaction; Cooperative Communication; Group Generation**

I. Introduction

In multi-agent systems (MAS), massive autonomous agents are required to solve complex problems by the coordination and cooperation of other agents flexibly[1]. On the other hand, reinforcement learning (RL) is an algorithm attempts to explore a suitable behavior to maximize a performance measurement based on interacting with an environment autonomously by repeating trial and error. RL adjusts behavior to a dynamic environmental without explicit teaching signals except rewards based on evaluation of current state and action. MAS is expected that it is able to learn the cooperative behavior and the group strategy by the application of the RL to autonomous agents[2], [3].

Generally, RL is basically developed for a single agent and it is used in MAS aspect, problems such that perceptual aliasing problem, concurrent learning problem and reward distribution problem occurred[4]. In a cooperative social environment, it is effective to learn by sharing sensing information, episodes, learned policies or exchanging advice. However, one of the main problems concerned learning in a MAS environment is how to benefit from mutual interaction during the learning process[5]. It is possible to develop cooperation models to unify partial action policies to create new policies which can be optimal ones[6]. But for social agents, we believe that it is necessary to communicate the cooperative behavior and to give appropriate coordination at the right time[7]. We have aimed at the group behavior generation of social agents who have excellent autonomous learning ability like human through cooperative communication between agents to acquire cooperative behavior[8].

In this paper, social agents are able to change the environment states to individual states and communicate their states with other agents by sending a new undefined signal. For other agents, they can not understand the meaning of that signal and just take it as a new state of that agent during the learning process. After massive trial and error of RL algorithm, under the hint of this undefined signal, agents could get a better optimal policy than normal RL method. Therefore, although other agents do not know the meaning of the undefined signal, the overall identity of their behavior is to achieve the task cooperating with the signal sending agent. In other words, because both sides made similar coordinate decision, it is possible to communicate their cooperative behavior by sending a new undefined signal that can not be understood originally but could be gradually understood by other agents after some learning processes.

In addition, the agents who regularly made the similar decision have an identity of cooperation like the social identity in our human society. Based on social identity theory, these agents create an in-group or self-categorization because they have stronger organization than agents of normal RL method. Therefore, we propose a method to cause group generation by exchanging rewards as group identity among themselves. All agents not only receive rewards from the environment but

978-1-4244-7316-8/11/$26.00 ©2011 IEEE

also exchange the reward among each others based on the undefined signal hints and their decisions. It is possible for exchanging rewards among agents to reinforce the coordinative behavior autonomously when the expected actions appeared. Agents are able to acquire excellent cooperative group behavior and strength their group identity by taking reward exchanging as the social interaction strategy like human in society.

II. Social Interaction of Cooperative Communication and Group Generation

In the normal multi-agent reinforcement learning algorithm, each individual agent can only repeat trial and error through the interaction with environment. In this paper, social agents can communicate with other agents by sending an undefined special signal that can not be understood originally but could be understood by other agents after some learning processes. If the agents could communicate their cooperative behavior successfully, their group identity will be strengthened by exchanging rewards among them. Based on the group identity, group generation will be possible. The general idea of proposed Multi-agent RL systems as shown in Fig.1.

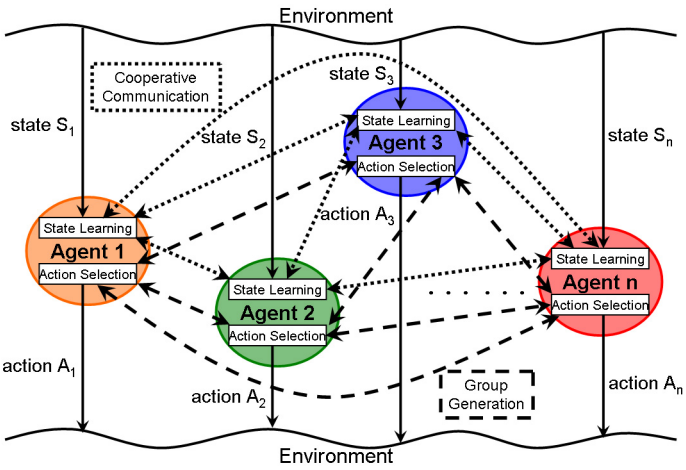

Fig. 1. Proposed Multi-agent RL systems

During the learning process, social agents can get the better cooperative ability than normal reinforcement learning method through the interaction of cooperative communication and group identity. Lastly, social agents not only adjust themselves to environment but also affect other agents to generate intelligent group behavior. Social agents will make decisions not only based on itself profit but also considering a joint profit with other agents.

A. Cooperative Communication Reinforcement Learning

For social agents, we believe that it is necessary to understand other behavior and to give appropriate coordination at the right time in MAS. In this cooperative communication reinforcement learning (CC-RL) algorithm, social agents are able to change the environment states to individual states and communicate their states with other agents by sending a new undefined signal. For other agents, they can not understand the meaning of that signal and just take it as a new states during the learning process, and try all the possible state-action strategy by trial and error using RL algorithm.

In this approach, when the target was discovered, the agent who found will change the environment state of its perception range to the state of itself, and send a special signal information (we called Help) to other agents if the task could not be achieved by itself in a dynamic environment. But other agents are uncertain this Help meaning of this special signal information and record it as a new special state S_t^n not defined in their sates. In the algorithm, S_t^n is described by a flag (0 or 1) which means a task could be achieved or not by itself.

In addition, the Help signal emerge only when an agent found target and can not achieve it. So this S_t^n information is also related to target discovering or task performing. By this way, agents can perceive other agents' states and have to adjust this new state by learning. If the overall identity of their behavior is to achieve the task cooperating with the signal sending agent, the communication of their cooperative behavior becomes possible by sending a new undefined signal.

Concretely, once the target was discovered, the agent send Help information to other agents even they are outside the range of itself perception. At the same time, other agents receive the coordinates of generated Help and compute the relative direction from itself position to Help. The emergence of Help and the relative direction will be recorded as the environment changing information like normal RL method. All the agents will perceive the signal of Help through the communication among agents if one agent found target. Therefore, this CC-RL method based on the emergence of new signal and the relative direction can partly solve the problem of incomplete perception in MAS. In Q-Learning method, Q-value is estimated on the basis of experience as follows:

Cooperative Communication Reinforcement Learning

Initialize $Q_t(S_t^e \vee S_t^n, a_t)$ arbitrarily

Repeat (for each episode)

Initialize $S_t^e \vee S_t^n$

Repeat (for each step of episode)

Observe S_t^e

Cooperative communication of individual state

Receive S_t^n from other agents

Choose a_t from $S_t^e \vee S_t^n$ using policy derived from Q-value

Take action a_t

Observe r_t and next state $S_{t+1}^e \vee S_{t+1}^n$

$Q_t(S_t^e \vee S_t^n, a_t) \leftarrow Q_t(S_t^e \vee S_t^n, a_t) + \alpha[r_t + \gamma \, max_{a \in A} \, Q_t(S_{t+1}^e \vee S_{t+1}^n, a) - Q_t(S_t^e \vee S_t^n, a_t)]$

$S_t^e \vee S_t^n \leftarrow S_{t+1}^e \vee S_{t+1}^n$

Until $S_t^e \vee S_t^n$ is terminal

---

where,

S_t^e: environment state of normal RL method,

S_t^n: the new undefined signal information state informed by other agent in current moment t. It includes the relative direction from own position to this new signal position.

The action evaluation value $w(s, b)$ becomes like in Eq.(1) in Profit Sharing method.

$$w_t(s_t^e \vee s_t^n, b) \leftarrow w_t(s_t^e \vee s_t^n, b) + f(h) \tag{1}$$

$w_t(s_t^e \vee s_t^n, b)$ is the action evaluation value when the state is $s_t^e \vee s_t^n$ and the action is b in current moment t. Reinforcement function $f(h)$ is the same as one of normal Q-Learning method. Efficient cooperative behaviors will be expected under the communication of this new signal hint among agents.

B. Group Generation Reinforcement Learning

By sending a new signal to others in the approach of CC-RL, the communication among agents is possible. But it just tells the partial information to each other not giving any evaluation for the action under this information. In our human society, if person A likes an action performed by person B, then A will praise B. The possibility of perfect action of B will be repeated in next time for the praising force. Based on this idea, we believe that if social agents want to have excellent cooperative ability like human, the agent should be praised if its action accords with the expected behavior.

In this approach, at a certain time t if the agent A_1 discovered the target but it could not achieve the task with itself power, then A_1 sent a new signal to other agents. And A_1 achieved the target with other agents A_2 and A_3 lastly, then A_1 should distribute a part of reward got from environment to A_2 and A_3 as a group reward to praise them for their help. A_2 and A_3 would receive the reward from the agent A_1 who sent a new signal information but not from the agent who did not send new signal information. Because the cooperative action of agent A_1 and agent A_2, A_3 was strengthened as the learning process, when the signal information appears in the next time, the possibility of selecting the group cooperative behavior will rise. In Q-Learning method, Q-value is estimated on the basis of experience as follows:

Group Generation Reinforcement Learning

Initialize $Q_t(S_t^e \vee S_t^n, a_t)$ arbitrarily

Repeat (for each episode)

Initialize $S_t^e \vee S_t^n$

Repeat (for each step of episode)

Observe S_t^e

Cooperative communication of individual state

Receive S_t^n from other agents

Choose a_t from $S_t^e \vee S_t^n$ using policy derived from Q-value

Take action a_t

Observe r_t and next state $S_{t+1}^e \vee S_{t+1}^n$

Distribute r_t^G among agents

$Q_t(S_t^e \vee S_t^n, a_t) \leftarrow Q_t(S_t^e \vee S_t^n, a_t) + \alpha[r_t + \beta \cdot r_t^G + \gamma \, max_{a \in A} Q_t(S_{t+1}^e \vee S_{t+1}^n, a) - Q_t(S_t^e \vee S_t^n, a_t)]$

$S_t^e \vee S_t^n \leftarrow S_{t+1}^e \vee S_{t+1}^n$

Until $S_t^e \vee S_t^n$ is terminal

---

where,

β: the rate of social interaction about group reward,

r_t^G: the group reward in current moment t.

The action evaluation value $w(s, b)$ is the same as Eq.(1) in Profit Sharing method, but reinforcement function $f(h)$ becomes as follows in Eq.(2).

$$f(h) = \alpha \cdot \gamma^h (r_t + \beta \cdot r_t^G) \tag{2}$$

For the agent of sending new signal information, it is necessary to supply a part of reward to the agents giving help and r_t^G is defined by $-\theta \cdot r_t$, and θ is the percentage of given reward as compared with r_t ($\theta \leq \theta_{lim}$). In GG-RL, the reward is re-distributed among agents, but the total reward value is not changed comparing with normal RL.

For the agents of giving cooperation, each agent will obtain a part of reward from the agent who sent signal as group reward, the reward of $\theta \cdot r_t$ is distributed by n which means the number of agents giving cooperative behavior to new signal sending agent ($n \leq n_{lim}$). Therefore, r_t^G is defined by $(\theta \cdot r_t)/n$.

In addition, the agents who regularly made the similar decision have an identity of cooperation like the social identity in our human society. Based on social identity theory, these agents create an in-group or self-categorization if they had stronger organization than agents of normal RL method. Based on group identity, we proposed group generation reinforcement learning (GG-RL) method. In GG-RL, the perfect action according with the original expected behavior will be praised through a group reward. Under the influence of group identity, group generation becomes possible.

Therefore, all agents not only receive rewards from the environment but also exchange the reward among agents to reinforce the coordinative behavior autonomously when the expected actions appeared. Agents are able to strength their group identity by taking reward exchanging as the social interaction strategy like human in society.

III. Simulation Experiments

In order to verify the effectiveness and robustness of proposed methods, we also performed the comparison prey chase simulation experiments with obstacles using Profit Sharing method. This simulation is programmed by C language with the graphic library of OpenGL executed in Linux system. The view of simulator is shown in Fig.2.

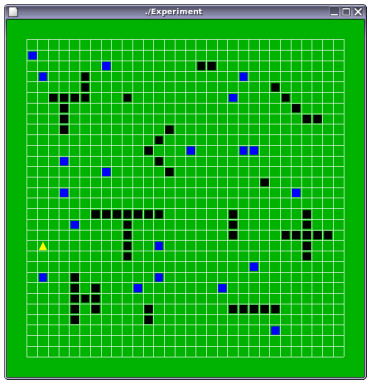

Fig. 2. The view of prey chase simulator of Exp.(1)

A. Simulation Preconditions

The preconditions of this simulation are set as follows:

- The field is composed by 30×30 grids in two dimensional environment. There are 62 obstacles in the learning environment.
- 20 hunter agents are set and represented as a square on the grid. The action and the perception ability of all agents are equal.
- Both the hunter and a prey represented as triangle agents can move in eight directions: up, down, left, right, up-right, up-left, down-right, down-left. They can stay at their current positions.
- The perception range is set 7×7 grids around itself.
- The default positions of all agents are arranged randomly and a prey agent moves always randomly.
- All hunter agents can obtain the other agents' perception information by sending new signal.
- When the prey agent becomes adjacent by three or more hunter agents, the task of chase is achieved. All the agents will return to the initial state after that.
- Hunter agent's task is to capture the prey agent as soon as possible. When the prey capturing is achieved, they will obtain the basic reward R assumed to be 100.

The parameters in this simulation are set as follows: $\gamma = 0.8$, $\lambda = 0.8$, $\alpha = 0.8$, $\beta = 1$,$\theta = 0.2$. To confirm the effectiveness of the proposed method, we performed comparison experiments with normal Profit Sharing reinforcement learning method. When an action is selected in Profit Sharing, the action is generally decided by the roulette selection of the action evaluation value added to the rule.

B. Simulation Results

We performed two simulation experiments in different conditions: Exp.(1) with only one target; Exp.(2) with 5 targets. In each experiment we compared four learning methods of RL, CC-RL and GG-RL. All of the methods are performed 5 times in this simulation, the average and deviation of simulation results are shown in result graphs.

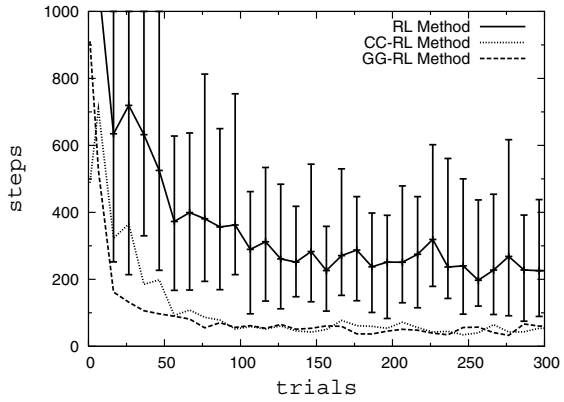

(a) Deviation of RL

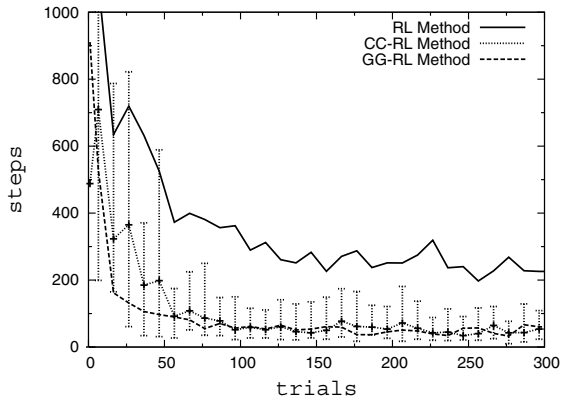

(b) Deviation of CC-RL

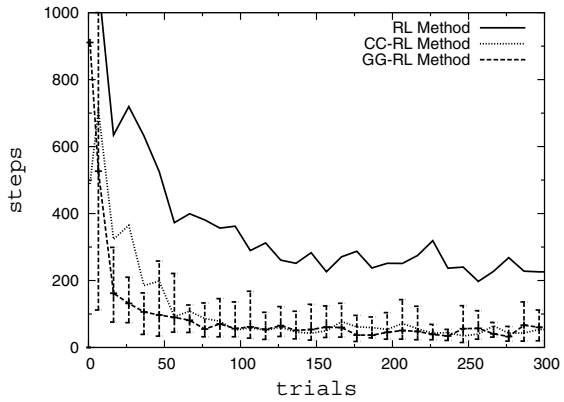

(c) Deviation of GG-RL

Fig. 3. Results of Exp.(1) with one target

Exp.(1) with only one target

In this experiment, there is only one target in the learning environment as shown in Fig.2. Vertical axis shows the steps required for capturing the prey and horizontal axis shows the trials of learning. From the average results in Fig.3(a)∼(c), we confirmed that the cooperative communication reinforcement learning (CC-RL) method obtained better results than normal

RL method, the group generation reinforcement learning (GG-RL) method obtained the best learning result than the other methods. From the deviation results in Fig.3(a)∼(c), we also confirmed that the stability of CC-RL and GG-RL methods are better than normal RL method. Furthermore, we can find that GG-RL method obtained better results than CC-RL method in the average and the deviation. That shows the exchanging group rewards among agents can reinforce the group behavior to achieve the task efficiently.

Exp.(2) with 5 targets

As a social agent, it is necessary to learn the best decision even with several targets in the complex environment. So we performed the simulation experiment with 5 targets as shown in Fig.4. The comparison experiment results of 3 methods are shown in Fig.5(a)∼(c). By these results, we found that they are similar to the results of experiment with only one target. But the degree of convergence was not as good as Exp.(1) because it is more difficult naturally to capture 5 preys than only one.

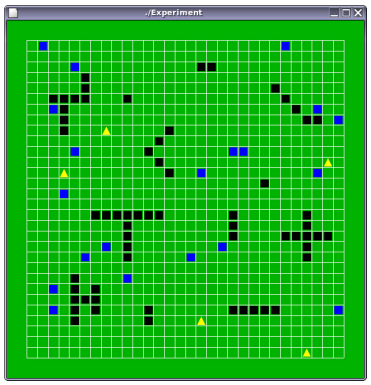

Fig. 4. Chase simulation of Exp.(2) with 5 targets

C. Individual and Group Growth

In order to distinguish the process of each individual growth, we also recorded the performance about 20 hunter agents. The growth of them is shown in Fig.6 based on catch time for preys. From this graph, we found that their performance is various after 300 trials to achieve the task. The best individual (agent 13) could get several times than the worst (agent 11) one in the achievement.

We have aimed at the generation of group behavior and recorded the interactive information among agents like Fig.7. The numbers of upside and left mean 20 agents and other numbers represent exchanging reward after 300 trials. The exchanging reward is only distributed among agent when the agents who regularly made the similar decision which means they have an identity of cooperation. Therefore, the exchanging reward represents the group identity of different agents.

In the cooperative task, all the agents maybe chose anyone to cooperate, but the agent will more likely to cooperate with the agent who holds maximum exchanging reward. For each agent, if it holds maximum exchanging reward with many agents, it will have a greater influence in these agents. From the graph of Fig.7, agent 13 holds maximum exchanging reward

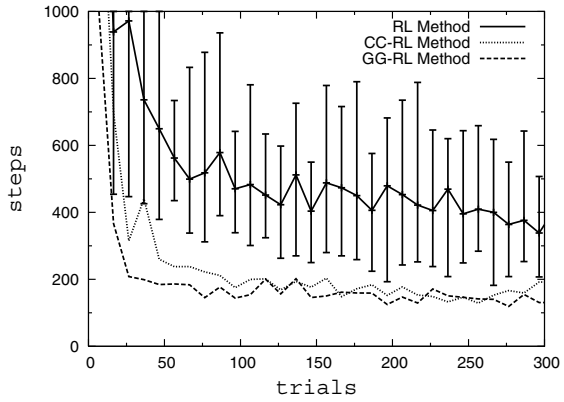

(a) Deviation of RL

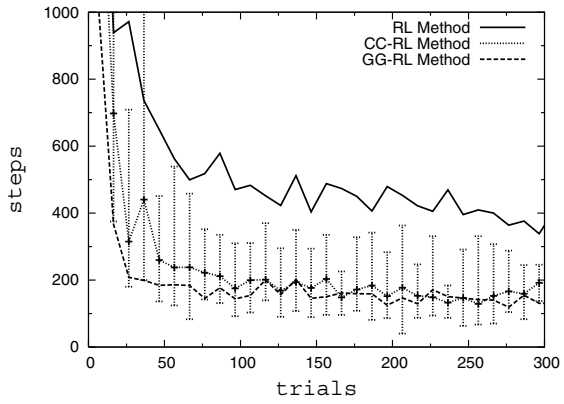

(b) Deviation of CC-RL

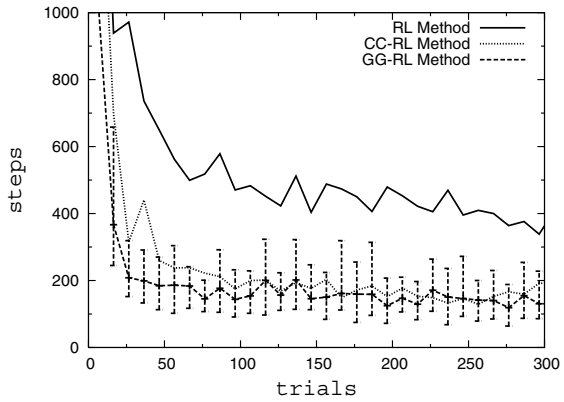

(c) Deviation of GG-RL

Fig. 5. Results of Exp.(2) with 5 targets

with other 10 agents and we defined the pair influence of agent 13 as 10. All the agents will have a pair influence value based on this idea. Lastly we can easily get the relationship of all the agents like in Fig.8. The agent having greater pair influence is represented by wider circle area filled by color. The interactive degree of each others is represented by width of connecting lines, the wider the deeper social interactive ability. Therefore, we can easily find the relationship of all the agents in the pair influence aspect. In addition, we found that agent 13 did the best performance in individual aspect and also had the greatest influence in group generation.

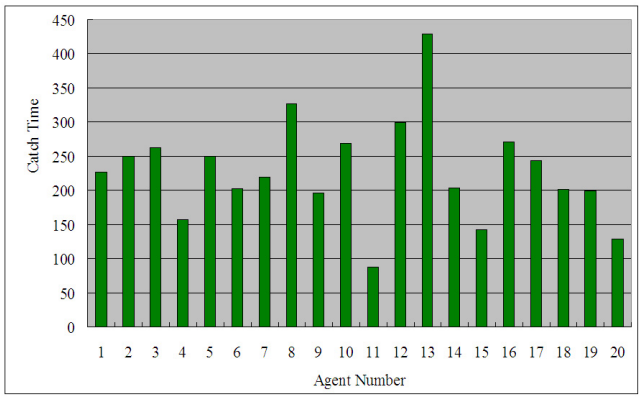

Fig. 6. Individual Growth

	1	2	3	4	5	6	7	8	9	10	11	12	13	14	15	16	17	18	19	20
1	0	350	350	160	180	190	120	430	110	170	100	220	300	130	110	130	120	150	100	120
2	350	0	320	150	170	180	190	400	190	200	80	220	400	170	90	330	100	110	110	70
3	350	320	0	150	270	160	180	200	170	170	60	220	370	180	140	310	150	140	120	60
4	160	150	150	0	140	130	160	80	130	220	60	110	70	100	120	120	140	110	90	20
5	180	170	270	140	0	270	220	210	380	160	80	260	350	110	140	180	200	200	220	110
6	190	180	160	130	270	0	200	230	80	350	100	240	190	50	60	110	160	150	100	130
7	120	190	180	160	220	200	0	290	130	240	30	210	400	70	70	140	130	140	130	130
8	430	400	200	80	210	230	290	0	140	230	100	310	570	310	100	350	370	140	120	60
9	110	190	170	130	380	80	130	140	0	170	50	130	210	100	90	90	100	60	160	90
10	170	200	170	220	160	350	240	230	170	0	40	440	330	140	140	130	110	240	140	80
11	100	80	60	60	80	100	30	100	50	40	0	110	120	50	20	70	50	40	20	20
12	220	220	220	110	260	240	210	310	130	440	110	0	510	110	100	150	230	120	190	90
13	300	400	370	70	350	190	400	570	210	330	120	510	0	450	140	380	400	120	150	80
14	130	170	180	100	110	50	70	310	100	140	50	110	450	0	40	170	200	120	90	40
15	110	90	140	120	140	60	70	100	90	140	20	100	140	40	0	120	30	90	80	50
16	130	330	310	120	180	110	140	350	90	130	70	150	380	170	120	0	150	70	70	40
17	120	100	150	140	200	160	130	370	100	110	50	230	400	200	30	150	0	100	90	60
18	150	110	140	110	200	150	140	140	60	240	40	120	120	120	90	70	100	0	140	40
19	100	110	120	90	220	100	130	120	160	140	20	190	150	90	80	70	90	140	0	40
20	120	70	60	20	110	130	130	60	90	80	20	90	80	40	50	40	60	40	40	0

Fig. 7. Group Identity Degree

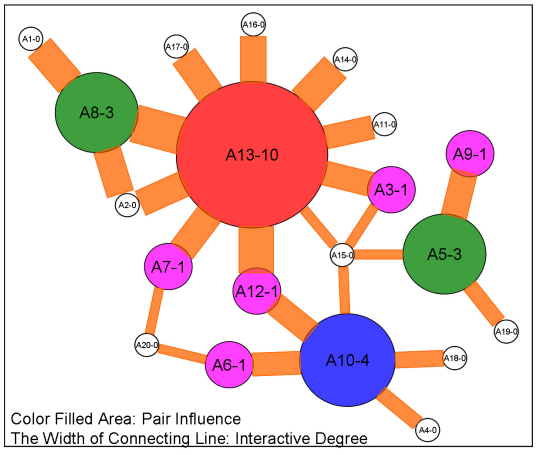

Fig. 8. Group Growth

IV. Conclusions

In this paper, we proposed CC-RL, GG-RL of multi-agent reinforcement learning methods with an excellent cooperative ability through the social interaction of cooperative communication and group generation by reward exchange which circulate among autonomous agents in MAS.

From the results of the comparison simulation between RL and CC-RL methods, we found that CC-RL method obtained the target state and individual information and could obtain the better cooperative ability than normal RL method. Although the outside of the perception range, the agent can obtain some environment states that can not be obtained from their restricted perception through the interaction with the other agents. The emergence of new undefined signal and the relative direction help the agent not only to perceive more learning states but also to get some information about the target in the task. Therefore, the communication of sending a new undefined signal accelerate their cooperative behavior.

Furthermore, we proposed GG-RL method that can give some evaluation to the action of agents by exchanging rewards. Rational re-distribution of reward causes the different learning results between CC-RL and GG-RL. Agents could encourage each other by exchanging reward. At last, the interaction among agents can be changed to the behavioral strategy communication like the human society and the autonomous cooperative group behavior of GG-RL method was best than the other methods.

At the same times, we can see the growth of 20 agents and group generation. The possibility of cooperation became very different from each other after learning. In the simulation, it is difficult to communicate more undefined signals, but it is possible to communicate and reinforce more complex behavior by proposed method. In the further works, we have a plan to add more communication modes to agents and let social agents have robust autonomous cooperative learning ability even in the competitive environment.

References

[1] M.J.Wooldridge, *An Introduction to MultiAgent Systems,* John Wiley and Sons, Ltd. England, 2002.

[2] M.J.Mataric, "Reinforcement Learning in the Multi-Robot Domain," *Autonomous Robots, 4,* pp.73-83, 1997.

[3] C.Claus, C.Boutilier, "The dynamics of reinforcement learning in cooperative multiagent systems," *AAAI/IAAI,* pp.746-752, 1998.

[4] S.Arai, "Multiagent Reinforcement Learning Frameworks : Steps toward Practical Use," *Journal of The Japanese Society for Artificial Intelligence,* Vol.16, No.4, pp.476-481, 2001.

[5] M.Tan, "Multi-Agent Reinforcement Learning: Independent vs. Cooperative Agents," *Proceedings of Tenth International Conference on Machine Learning,* pp.330-337, 1993.

[6] R.Ribeiro, A.P.Borges, F.Enembreck, "Interaction Models for Multiagent Reinforcement Learning," *Computational Intelligence for Modelling, Control and Automation, International Conference,* pp.464-469, 2008.

[7] M.Fasli, "Social Interactions in Multi-agent Systems: A Formal Approach," *2003 IEEE/WIC International Conference on Intelligent Agent Technology (IAT'03),* pp.240-246, 2003.

[8] K.Zhang, Y.Maeda, Y.Takahashi, "Group Behavior Learning in Multi-Agent Systems Based on Social Interaction among Agents," *Joint 5th International Conference on Soft Computing and Intelligent Systems and 11th International Symposium on advanced Intelligent Systems,* TH-B3-1, pp.193-198, 2010.

2011 IEEE International Conference on Fuzzy Systems
June 27-30, 2011, Taipei, Taiwan

Estimation Of Subjective Stress Via Finger Plethysmogram

Yusuke Kobashi, Genma Sano, Tsuyoshi Nakamura
Dept. of Computer Science and Engineering
Nagoya Institute of Technology
Nagoya, Japan
{kobashi, sano, tnaka}@ai.nitech.ac.jp

Masayoshi Kanoh
Dept. of Mechanics and Information Technology
Chukyo University
Toyota, Japan
mkanoh@sist.chukyo-u.ac.jp

***Abstract*—It could be very important and useful to enable human stress to be estimated on basis of quantitative values via objective analysis. There have been several approaches to estimate the stress so far. Most of them need a lot of time to measure or calculate it, and what is more, they might cause physical or mental burden for human subjects. The purpose of our study is to propose and develop a method to estimate subjective stress through a simple approach which doesn't cause much burden for users. In this paper we propose a method, which is called $\mathrm{TPA_f}$ (Turning Point Amplitude via finger plethysmogram). Original TPA is a kind of heart rate variability analysis and needs to attach sensors on his/her breast. Our experimental results indicated that it has a certain relationship between subjective stress and $\mathrm{TPA_f}$. A method based on $\mathrm{TPA_f}$ could be efficient to estimate subjective stress.**

Keywords-component; subjective stress; TPA; Face Scale (FS)

I. INTRODUCTION

Can you imagine a future society that humans and robots live together? They can talk and socialize with each other. Maybe humans and robots can understand each other through nonverbal communication. Robots can understand human feeling or emotion through his facial expression or biological signals. We consider that such a society isn't a dream or science fiction but a real society coming near future. Some studies of Human Agent Interaction(HAI) or Human Robot Interaction(HRI) focus on the communication between humans and robots. 'Palo' and 'ifbot', which are related to robot therapy, can behave based on nonverbal communication[8][9]. On the other hand, Palo and ifbot don't recognize and understand human feeling itself, of course, it is no problem from the standpoint of their design philosophy and concept. However, the near future society might require high-performance robots that have an ability to recognize human feelings or mental situation.

There have been many studies on measuring human feeling or emotions. Most of them employs subjective assessment measure, on the other hand there exist many approaches based on objective analysis. Some indexes of physiological evaluation are well known to measure human stress. For example, Immunoglobulin A type and cortisol in saliva are often used to measure the stress[1][2][3]. Stress indexes via heart rate variability (HRV) analysis is also often used [4]. The methods are very effective and useful, but there are some problems, assuming that the robots employ them to measure the stress. One problem is on sensing. In order to extract Ig. or cortisol from saliva, sensors need to be inserted in his/her mouth. HRV analysis needs to attach sensors on the breast. In daily life wearing the sensors is unnatural and it assigns a lot of burden to users. The another is on measurement time. In order to extract Ig. or cortisol from saliva, it takes only a few seconds. But HRV analysis generally takes several minutes to evaluate the electrocardiographic wave. In future daily life it would be better to employ an evaluation method based on near realtime analysis because the robots can quick respond and act according to the realtime mental situation of human.

In this study our goal is to develop a simple estimation of subjective stress which can measure the stress in near realtime. There are two kinds of subjective stress that are unconsicous and consious. People are not aware of unconsious stress existing, thus it might be important for people to care the unconsious stress in terms of medical reason. On the other hand, people could be aware of conscious stress. We consider that the conscious stress is suitable to decide and control robot behaviors for taking care of human people because users could be able to recognize the robot behaviors are due to the conscious stresses of users themselves. Unless users are aware of their stresses, they couldn't understand what the robot aims to do. The unconsicous stress to control autonomous robots would carriy a lot of risk in daily life. Our study therefore deals with consicous subjective stress. The contributions of this study to develop the estimation are as follows:

1) Proposal and development of $\mathrm{TPA_f}$ calculation via finger plethysmogram. Original TPA was developed by Yokoyama et al[5]. It could be calculated by the data of electrocardiographic wave measured for about several tens of seconds. The calculation formula of $\mathrm{TPA_f}$ is very simple, thus we could achieve near realtime processing. Furthermore, the finger plethysmogram is measured more easily than the electrocardiographic wave.
2) Investigation of a relationship between the subjective conscious stress and $\mathrm{TPA_f}$ via finger plethysmogram. $\mathrm{TPA_f}$ could have some relationship to human stress, but no experiments have been done on the relationship with conscious subjective stress so far. We employ Face Scale

978-1-4244-7316-8/11/$26.00 ©2011 IEEE

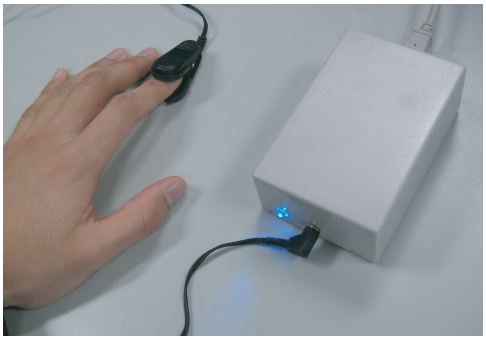

Fig. 1. Pulse sensor to measure finger plethysmogram

to measure conscious subjective stress.

II. EVALUATION INDEX OF STRESS

In this study we adopted heart rate variability (HRV) analysis via finger plethysmogram. The power spectra of heart rate variability contain the low frequency components (LF) from 0.04 to 0.15Hz and the high frequency components (HF) from 0.15 to 0.4Hz. HF is said to be mainly affected by components originated human breathing called 'Respiratory Sinus Arrhythmia (RSA)'. HF reflects the activity of the parasympathetic nerves. LF is said to be mainly affected by components originated blood pressure called 'Mayer Wave related Sinus Arrhythmia (MWSA)'. LF reflects the activity of the sympathetic nerves and parasympathetic nerves. The ratio of LF to HF reflects the activity of sympathetic nerves. It is said that the parasympathetic nerve activity becomes higher while feeling comfortable. Therefore HF is used as an index of relaxation or stress reduction. The power spectrum analysis, such as FFT, AR method and wavelet transform are generally used to calculate HF in HRV. Yokoyama et al. proposed a method which is able to estimate HF component of HRV based on local characteristics in time series[5]. Of course it has no need to use power spectrum analysis, and it is calculated by data at most of around 20-30 points. Thus the method is able to work in near real time because a calculating formula is simple. They verified that there was high correlation among the average values of HF detected with their proposed method, AR method and wavelet transform. In our study we adopted an method based on TPA (Turning Point Amplitude). TPA can be calculated in near real time, and it requires human subjects to attach sensors on their breast as mentioned in the previous section. Therefore we exploit a simple sensor to measure finger plethysmogram illustrated in Fig.1. The sensor is easier to handle than the sensors attached on the breast. In this paper $\mathrm{TPA_f}$(TPA via finger plethysmogram) is used to evaluate human stress from the objective view.

On the other hand Face Scale (FS) is a well-known index to measure human subjective feeling. FS, which is suggested by Lorish et al.[7], is a method to evaluate subjective feeling, FS is the illustrations of a person from a smile (scale 1) to a tearful face (scale 20) as shown in Fig.2. The subject has only to answer with the number of FS expressing his current feeling.

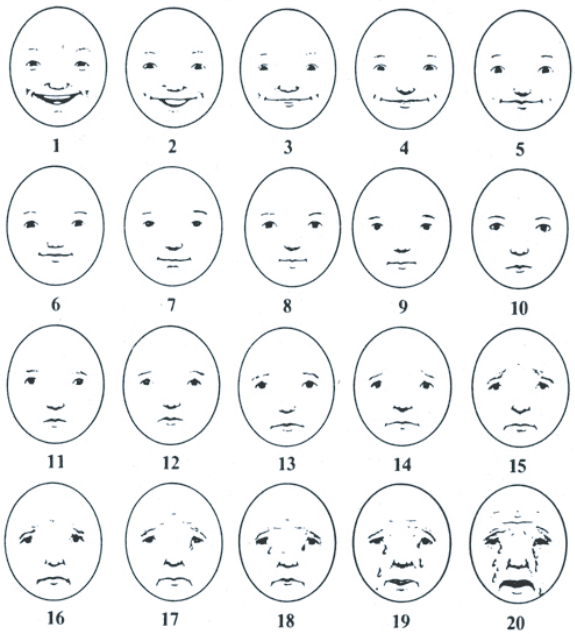

Fig. 2. Face Scale

There is a advantage to be able to perform the experiments in a short time. FS was also adopted as a method to evaluate a result of the treatment subjectively in the clinical medical field, and the effectiveness was reported[7]. This paper adopts FS to evaluate human subjective feeling, and attempts to find out a relationship between FS and $\mathrm{TPA_f}$.

III. EXPERIMENTS

We present our experimental method and the environment. We considered that it was important to measure FS and $\mathrm{TPA_f}$ at same time in order to investigate the relationship between them. Furthermore we considered that it was valid and proper to evaluate the human subjects who are in either normal mental state or stress state. Our experiment gave the subjects an artificial stressor such as mental arithmetic. The experiment evaluated the subjects in the three states that are pre-stress state, stress state and post-stress state.

A. Experimental Method

The experimental procedure is shown in Fig.3. Our experiment consists of three phases, the whole time was 15 min. In the first 5 min, human subjects closed their eyes. In the next 5 min, the subjects did mental arithmetics. While their constraining the mental arithmetic, they might have been directly under mental stress. Then they finished it and in the final 5 min, they closed their eyes or viewed the video. In the final 5 min they were not directly under mental stress, but its influences must have remained. Here we call the first 5 min, next 5 min and final 5 min 'pre-stress state', 'stress state' and 'post-stress state' respectively. After the end of each state, the human subjects chose FS number which was suitable to their own feeling at that time. In our experiment we prepared 'eyes closed' and 5 kinds of video image, each of which has

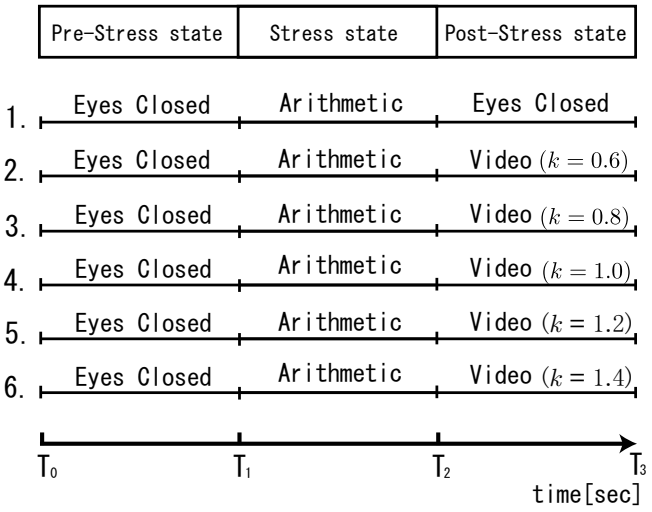

Fig. 3. Experimental Procedure

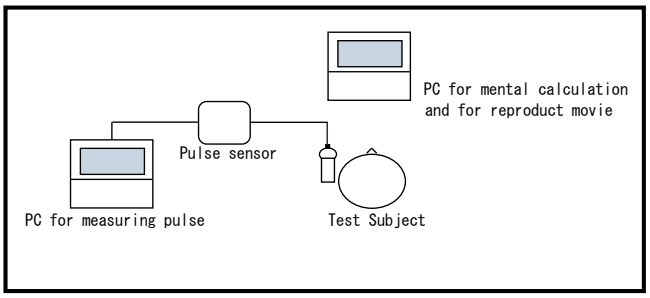

Fig. 4. Experimental Environment

different motion speed, for 'post-stress state' as shown in Fig. 3. The 'eyes closed' and the video were used for relaxation of the subjects [6]. The subjects performed all the experiments (1-6) in a different random order for each. Mental arithmetic was used as mental workload in the experiment. The details of mental arithmetic and the video images are mentioned later.

The experiment measured FS at T_1,T_2 and T_3. The time series of $TPA_f(t)$ were measured during all the time from T_0 to T_3. Here we define $TPA_f(t)$ which indicates a value of TPA_f at the time t.

The subjects were 9 males and 1 female in their 20s. Every subject didn't have the abnormal vision and were able to visually confirm the motions of the video. The experiment was conducted in the environment illustrated in Fig.4. The experiment environment was dark quiet room. The subjects kept sitting on the chair during the experiment. The computer displayed the questions of the mental arithmetic to enhance the subjects' mental workload, and the subjects answered them. The finger plethysmogram of the subjects were measured by the pulse sensor and the computer for measuring pulse wave.

B. Mental Workload

In the experiment, the mental arithmetic was used as mental workload [3]. The experiment required the subjects to repeat solving the mathematical questions: "Subtract 13 from a four-digit figure X". The first figure X_0 is given at random and you answer $X_1 = X_0 - 13$. Next you answer $X_1 - 13$. Thus the i-th question will be $X_{i+1} - 13$. When the subjects made a mistake in the arithmetic, it restarted over from the beginning: $X_i = X_0$ illustrated in Fig.5. The subjects answered questions of the mental arithmetic on the computer monitor (Fig.6).

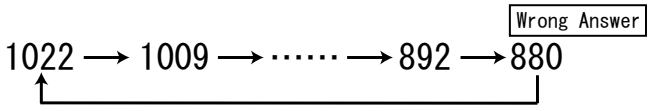

Fig. 5. Example of Mental Arithmetic the Human Subject Answered

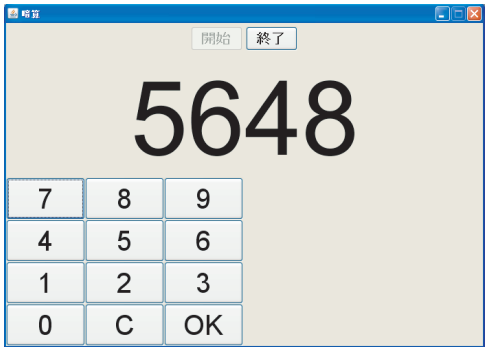

Fig. 6. Mental Arithmetic Application

Fig. 7. Capture Image of CG Video

C. Video Image

We adopt 'ripples appearing on the water surface' as a video that the subjects view in the post-stress state for their relaxation [6]. The ripples, which we use a CG technique for generating, are displayed on the monitor. Ripples appear from the center of the image and disappear outside of the image. A capture image of the video is shown in Fig.7. In the experiment 5 kinds of the video with different motion speed parameter k $(= 0.6, 0.8, 1.0, 1.2, 1.4)$.

IV. EXPERIMENTAL RESULTS AND ANALYSIS

A. Relationship between TPA_f and FS

$TPA_f(t)$ is changeable and it isn't easy to find out the relationship between $TPA_f(t)$ itself and FS at the time t. It is

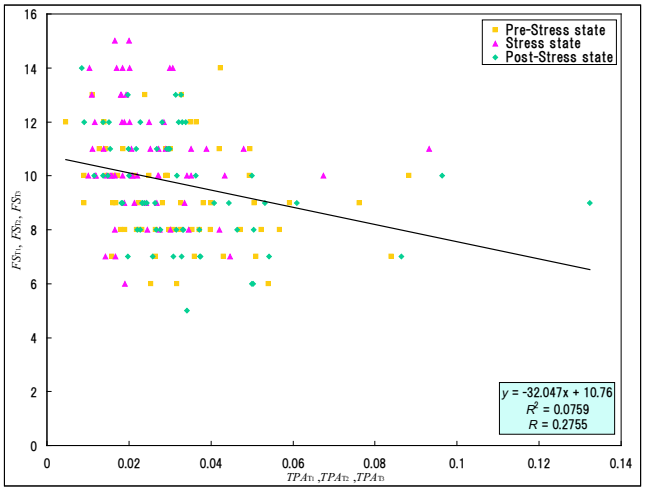

Fig. 8. Scatter plot of $\mathrm{TPA_f}$ and FS

said to be useful way to calculate the average value of 20-30 points of $TPA_f(t)$ [5].

Therefore we calculate $TPA_{\mathrm{T_i}}$ which is the average value of $TPA_f(t)$ for x seconds just before $\mathrm{T_i}$ as follows:

$$TPA_{\mathrm{T_1}} = \frac{1}{x}\int_{(\mathrm{T_1}-x)}^{\mathrm{T_1}} TPA_f(t)dt \quad (1)$$

$$TPA_{\mathrm{T_2}} = \frac{1}{x}\int_{(\mathrm{T_2}-x)}^{\mathrm{T_2}} TPA_f(t)dt \quad (2)$$

$$TPA_{\mathrm{T_3}} = \frac{1}{x}\int_{(\mathrm{T_3}-x)}^{\mathrm{T_3}} TPA_f(t)dt \quad (3)$$

In the each equation $\mathrm{T_0} = 0\mathrm{sec}$, $\mathrm{T_1} = 300\mathrm{sec}(5\mathrm{min})$, $\mathrm{T_2} = 600\mathrm{sec}(10\mathrm{min})$, and $\mathrm{T_3} = 900\mathrm{sec}(15\mathrm{min})$. x is 30 seconds in this experiment.

We use $TPA_{\mathrm{T_1}}$, $TPA_{\mathrm{T_2}}$ and $TPA_{\mathrm{T_3}}$ to evaluate pre-stress state, stress state and post-stress state respectively. As previous mentioned, each FS is also measured at $\mathrm{T_1}$, $\mathrm{T_2}$ and $\mathrm{T_3}$.

Fig.8 indicates the scatter plot of pre-stress state:($TPA_{\mathrm{T_1}}$, $FS_{\mathrm{T_1}}$), stress state: ($TPA_{\mathrm{T_2}}$, $FS_{\mathrm{T_2}}$) and post-stress state: ($TPA_{\mathrm{T_3}}$, $FS_{\mathrm{T_3}}$) of all the experiments to investigate the relationship between $\mathrm{TPA_f}$ and FS. The straight line represents the regression line in Fig.8. There is a small negative correlation (-0.2755) between $\mathrm{TPA_f}$ and FS, and Fig.8 indicates that it isn't easy to estimate the degree of FS with $\mathrm{TPA_f}$ itself.

We performed multiple comparison to confirm whether each state is different from each other or not. The multiple comparison that we apply is Kruskal Wallis test.

There is a significant difference at the 1% level between the pre-stress state and the stress state in Fig.9. What is more, there is also a significant difference at the 5% level between them in Fig.10. There are significant differences at the 5% level between the stress state and the post-stress state in Fig.9 and Fig.10. In addition, there are no significant differences between the pre-stress state and post-stress state in Fig.9 and Fig.10. In light of the results there is a possibility that $\mathrm{TPA_f}$

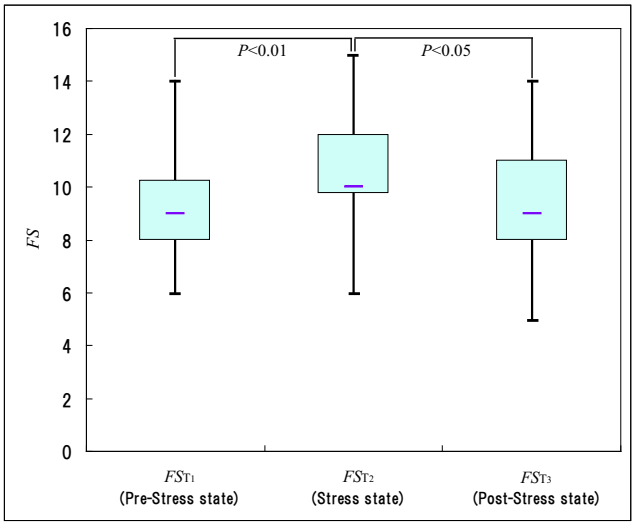

Fig. 9. Box plot of FS. Kruskal Wallis test is applied to the three states. There are significant differences at the 1% level among all of the states

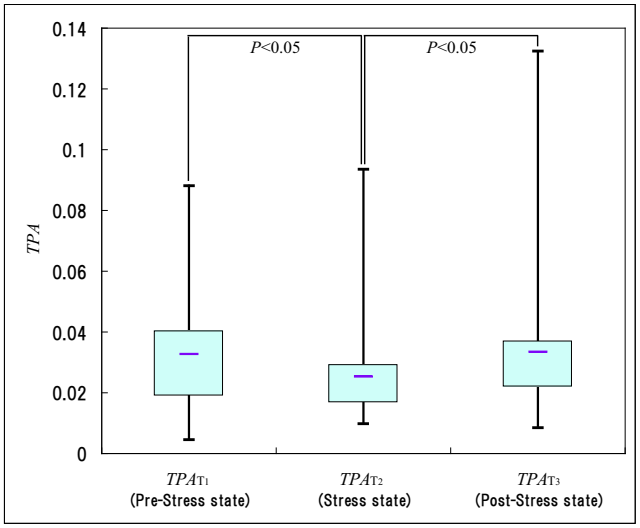

Fig. 10. Box plot of $\mathrm{TPA_f}$. Kruskal Wallis test is applied to the three states. There are significant differences at the 1% level among all of the states

can distinguish between the state under the direct stress (stress state) and the stress-free state after the stress released (pre-stress state and post-stress state). There could be a certain relationship between $\mathrm{TPA_f}$ and FS.

B. Relationship between ΔTPA and ΔFS

We focus on the amount of change of $\mathrm{TPA_f}$ and FS to discuss the relationship between them. The pre-stress state is prepared to lead the subjects to be in neutral mental state. Nonetheless, you can see and confirm $FS_{\mathrm{T_1}}$ and $TPA_{\mathrm{T_1}}$ have a large variance in Fig.9 and Fig.10 respectively. Therefore we define and adopt the amount of change of both $\mathrm{TPA_f}$ and FS from the pre-stress state(from the time $\mathrm{T_1}$). We introduced $\Delta TPA_{\mathrm{T_2T_1}}$ and $\Delta TPA_{\mathrm{T_3T_1}}$, which are defined and calculated with Eq.4 and 5. $\Delta FS_{\mathrm{T_2T_1}}$ and $\Delta FS_{\mathrm{T_3T_1}}$ are

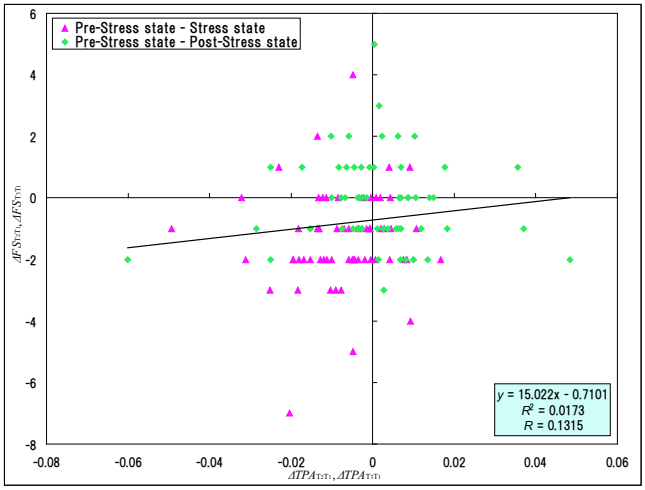

Fig. 11. Scatter plot of ($\Delta TPA_{\mathrm{T_2T_1}}$, $\Delta FS_{\mathrm{T_2T_1}}$) and ($\Delta TPA_{\mathrm{T_3T_1}}$, $\Delta FS_{\mathrm{T_3T_1}}$)

also defined as shown in Eq.6 and 7.

$$\Delta TPA_{\mathrm{T_2T_1}} = TPA_{\mathrm{T_2}} - TPA_{\mathrm{T_1}} \quad (4)$$
$$\Delta TPA_{\mathrm{T_3T_1}} = TPA_{\mathrm{T_3}} - TPA_{\mathrm{T_1}} \quad (5)$$

$$\Delta FS_{\mathrm{T_2T_1}} = FS_{\mathrm{T_1}} - FS_{\mathrm{T_2}} \quad (6)$$
$$\Delta FS_{\mathrm{T_3T_1}} = FS_{\mathrm{T_1}} - FS_{\mathrm{T_3}} \quad (7)$$

Note that Eq.4 and 5 are the subtraction from post-stress state, and Eq.6 and 7 are the subtraction from stress state.

Fig.11 shows the scatter plot of ($\Delta TPA_{\mathrm{T_2T_1}}$, $\Delta FS_{\mathrm{T_2T_1}}$) and ($\Delta TPA_{\mathrm{T_3T_1}}$, $\Delta FS_{\mathrm{T_3T_1}}$). The straight line represents the regression line in Fig.11. There might be little correlation between ΔTPA and ΔFS. Fig.11 also indicates that it is difficult to estimate the degree of FS with ΔTPA. We apply Wilcoxon test and paired t-test. Fig.12 and Fig.13 show more clearer significant differences (p&lt.; 0.01) than Fig.9 and Fig.10.

We adopt the other criteria to clarify the relationship between stress state and post-stress state. $\Delta TPA_{\mathrm{T_3T_2}}$ and $\Delta FS_{\mathrm{T_3T_2}}$ are defined and calculated with Eq.8 and 9.

$$\Delta TPA_{\mathrm{T_3T_2}} = TPA_{\mathrm{T_3}} - TPA_{\mathrm{T_2}} \quad (8)$$
$$\Delta FS_{\mathrm{T_3T_2}} = FS_{\mathrm{T_2}} - FS_{\mathrm{T_3}} \quad (9)$$

The equations represent the difference from stress state to post-stress state. In order to compare them with the difference from pre-stress state to stress state as defined in Eq.4 and 6. Fig.14 shows the scatter plot of ($\Delta TPA_{\mathrm{T_2T_1}}$, $\Delta FS_{\mathrm{T_2T_1}}$) and ($\Delta TPA_{\mathrm{T_3T_2}}$, $\Delta FS_{\mathrm{T_3T_2}}$). It is confirmed that the most of ($\Delta TPA_{\mathrm{T_2T_1}}$, $\Delta FS_{\mathrm{T_2T_1}}$) are plotted on the left low quadrant and the most of ($\Delta TPA_{\mathrm{T_3T_2}}$, $\Delta FS_{\mathrm{T_3T_2}}$) are plotted on the right upper quadrant. $\Delta TPA_{\mathrm{T_2T_1}}$ tends to take minus(-) when $\Delta FS_{\mathrm{T_2T_1}}$ is minus(-). Otherwise $\Delta TPA_{\mathrm{T_3T_2}}$ tends to take

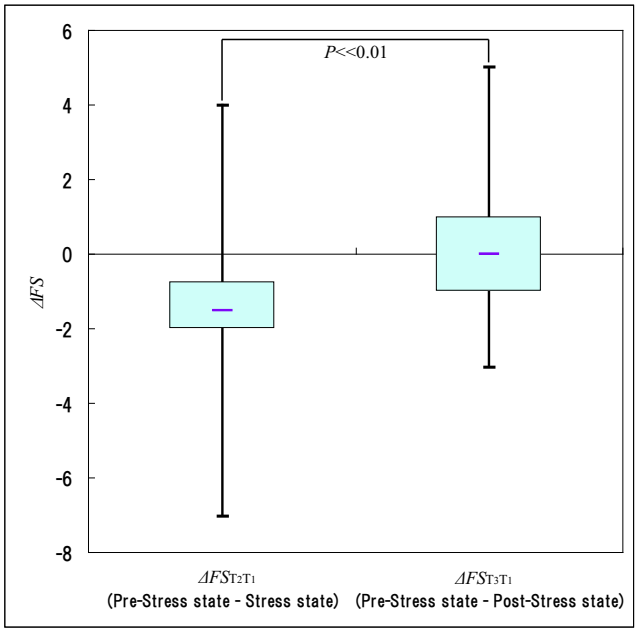

Fig. 12. Box plot of ΔFS. Wilcoxon test shows a significant differences at the 1% level between $\Delta FS_{\mathrm{T_2T_1}}$ and $\Delta FS_{\mathrm{T_3T_1}}$

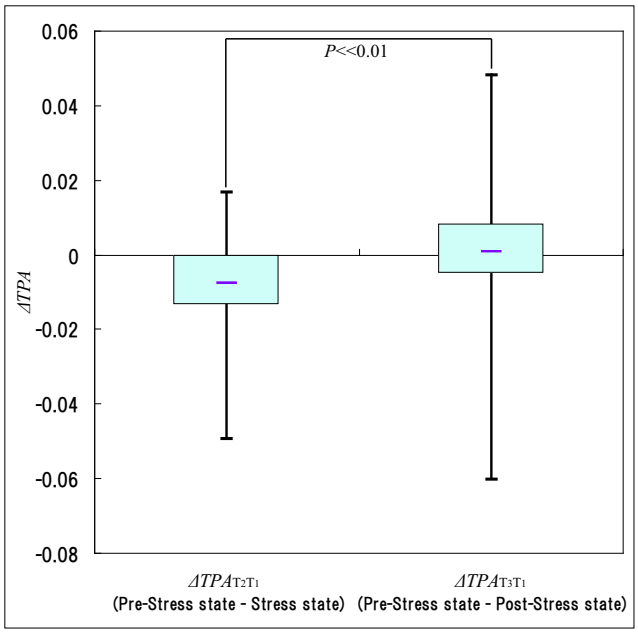

Fig. 13. Box plot of ΔTPA. Paired t-test shows a significant differences at the 1% level between $\Delta TPA_{\mathrm{T_2T_1}}$ and $\Delta TPA_{\mathrm{T_3T_1}}$

(+) when $\Delta FS_{\mathrm{T_3T_2}}$ is plus(+). Thus the change of plus-minus sign of ΔTPA could correspond to the change of the sign of ΔFS. The result of Fig.14 indicates that it might be possible that the difference of $\mathrm{TPA_f}$, which is observed objectively and quantitatively, can estimate the increase and the decrease of subjective stress.

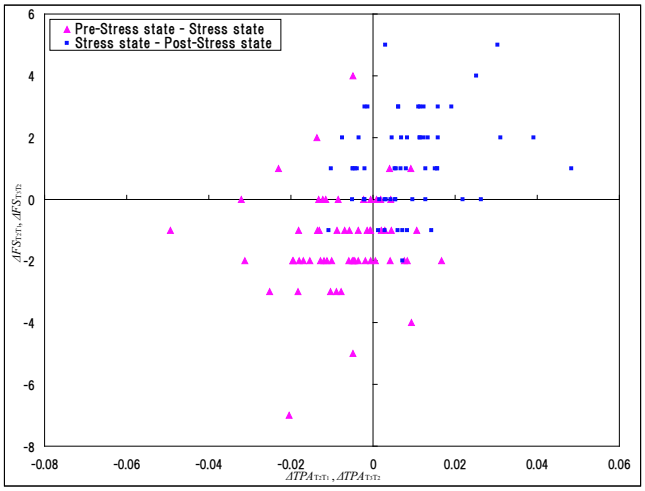

Fig. 14. Scatter plot of ($\Delta TPA_{\mathrm{T_2T_1}}$, $\Delta FS_{\mathrm{T_2T_1}}$) and ($\Delta TPA_{\mathrm{T_3T_2}}$, $\Delta FS_{\mathrm{T_3T_2}}$)

V. CONCLUSION

This study investigated the relationship between FS and $\mathrm{TPA_f}$ via finger plethysmogram. This paper shows that $\mathrm{TPA_f}$ could roughly estimate the change of human stress. We adopted a simple sensor and a simple method to measure and calculate $\mathrm{TPA_f}$. Furthermore $\mathrm{TPA_f}$ can be measured in near realtime. Therefore it couldn't be difficult to implement our method to robots. However we have some remaining problems to realize the robots that can estimate human stress or comfortableness. As first we must improve the accuracy to estimate human stress. Additon to that we might consider to combine $\mathrm{TPA_f}$ and other stress measures. The second is to conduct more experiments to collect the data from several environments and situations. The experiments woulld need to consider not only $\mathrm{TPA_f}$ but also other stress measures e.g. the amount of amylase in saliva and blood test. Addition to that, some researchers say that an effect of human stress is observed after a few seconds delay from finisning mental workload. In light of this we might consider to redesign the experiments The third is to develop a small sensor to measure finger plethysmogram like a wedding ring. We are planning to solve the problems in near future.

REFERENCES

[1] S. Tsujita and K. Morimoto, *Secretory IgA in saliva can be a useful stress marker*, Environmental Health and Preventive Medicine, Vol.4, pp.1-8, 1999.

[2] H.B. Valdimarsdottir and A.A. Stone, *Psychosocial factors and secretory immunoglobulin A*, Critical Reviews in Oral Biology and Medicine, Vol.8, No.4, pp.461-474, 1997.

[3] C. Kirschbaum and D.H. Hellhammer, *Salivary cortisol in psychoneuroendocrine research: Recemt developments and applications*, Psychoneuroendocrinology, Vol.19, No.4, pp.313-333, 1994.

[4] M. Pagani, F. Lombardi, S. Guzzetti, O. Rimoldi, R. Furlan, P. Pizzinelli, G. Sandrone, G. Malfatto, S. D. Orto, E. Piccaluga, M. Turiel, G. Basseli, S. Cerutti and A. Malliani, *Power spectral analysis of heart rate and arterial pressure variabilities as a marker of sympatho-vagal interaction in man and conscious dog*, Circulation Research, 59-2, pp.178-193, 1986.

[5] K. Yokoyama, N. Kamiya, *Simplified method for estimating high-frequency component of heart rate variability based on local characteristics in time series*, ERGONOMICS, Vol.40, No.6, pp.302-308, 2004.

[6] T. Sugiura, Y. Okudaira, Y. Kobashi, T. Nakamura, H. Itoh, *Relaxation effects of object speed in video images: Evaluation by heart rate variability analysis*, Kansei Engineering and Emotion Research, in CD-ROM, 2009.

[7] C.D. Lorish, R. Maisiak, *The face scale:a brief, nonverbal method for assessing patient mood*, Arthritis Rheum, Vol.29, pp.906-909, 1986.

[8] K. Wada, T. Shibata, *Living With Seal Robots. Its Sociopsychological and Physiological Influences on the Elderly at a Care House*, IEEE Transactions on Robotics, Vol.23, No.5, pp.972-980, 2007.

[9] T. Ando, M. Kanoh, *A Self-sufficiency Model Using Urge System*, IEEE World Congress on Computational Intelligence(WCCI 2010), pp.429-434, 2010.

2011 IEEE International Conference on Fuzzy Systems
June 27-30, 2011, Taipei, Taiwan

Human Preference Learning by Robot Partners Based on Multi-objective Behavior Coordination

Naoyuki Kubota
Graduate School of System Design,
Tokyo Metropolitan University
6-6 Asahigaoka, Hino-shi, Tokyo,
191-0065, Japan
kubota@tmu.ac.jp

Aiko Yaguchi
Graduate School of System Design,
Tokyo Metropolitan University
6-6 Asahigaoka, Hino-shi, Tokyo,
191-0065, Japan
yaguchi-aiko@sd.tmu.ac.jp

Utaki Ishikawa
Graduate School of System Design,
Tokyo Metropolitan University
6-6 Asahigaoka, Hino-shi, Tokyo,
191-0065, Japan
ishikawa-utaki@sd.tmu.ac.jp

***Abstract*—This paper discusses human preference learning by robot partners through interaction with a person. We use a robot music player; miuro, and we focus on the music selection for providing the person with comfortable sound field. First, we propose a control architecture of miuro based on autonomous behavior mode, interactive behavior mode, and human control mode. Next, we propose a learning method of the relationship between human position and its corresponding music selection based on Q-learning. Furthermore, we proposed a similarity matrix to reduce the learning time of Q-learning. The experimental results show that the proposed method can learn the relationship between human position and its corresponding human preferable music.**

Keywords- Robot Partners; Sound Field; Q-Learning; Boltzmann Selection; Fuzzy Control; Multi-Objective Behavior Coordination

I. INTRODUCTION

Recently, various types of human-friendly robots such as amusement robots, robot pets, and robot partners have been developed until now [1-6]. The advantage of robots is to realize human- or animal-like interaction and communication with people. A robot partner will be a concierge in the information service through interaction and communication. We can have three different types of robot partners from the interactive point of view (Fig.1) [7]. One is a physical robot partner. We can interact with the physical robot partner by using multi-modal communication like a human. The next one is a virtual robot partner. The virtual robot partner is in the virtual space built in the computer, but we can interact with it through the virtual person or robot in the virtual space. The last one is a pocket robot partner, and this is considered as the overlapping subcategory of physical and virtual robot partners. The pocket robot partner has a physical body but no mobile mechanism. We can easily bring it everywhere and can interact with the robot partner by touch and physical interface. The interaction style of these three robots is different, but they share the same personal database and interaction logs, and can interact with the person based on the same interaction rules independent from the style of interfaces. The person can accept the information service ubiquitously from a change of the style of robot partners according to the situation.

In general, the basic behaviors for robots are designed beforehand, but robot partners should perform social learning through interaction and communication with people. Various types of human-friendly robots have been developed, but the aim of most previous works is in the interaction between a robot and person, not the behavioral learning. Such a robot is used for direct interaction and communication with a person, but the mood and comfort by co-existing with the robot have not been discussed so much. Therefore, we discuss the mood and comfort for a human by co-existing with a robot partner. Sound field is one of the most important roles in constructing comfortable space. We proposed the learning method of human preferable music selection based on Boltzmann selection, and showed the experimental results of the relationship learning through continuous interaction [8]. Furthermore, we showed that the learning results by the pocket robot partner could be seamlessly reflected to the interaction rules of the physical robot partner. However, we do not discuss the location- or situation-dependent learning in the learning to extract human preference. Therefore, we propose a Q-learning algorithm for acquiring the relationship between human position in a room and its corresponding preferable music selection to construct a comfortable space by a robot partner. Furthermore, we should consider the regulation of the learning speed through continuous interaction in order to reduce the human load and the times of human interactions. Therefore, we propose a learning method based on similarity matrix used for evaluating human preference according to the similarity among songs.

This paper is organized as follows. Section 2 explains the concept of informationally structured space [8,9] used for the control and information processing of robot partners through wireless network. Next, we explain the hardware of robot partners used in this study, and the control architecture of the robot partners. Section 3 proposes decision making and learning method of robot partners based on computational intelligence. Section 4 shows several experimental results of the proposed method. Section 5 discusses the effectiveness of the proposed method, and concludes this paper.

978-1-4244-7316-8/11/$26.00 ©2011 IEEE

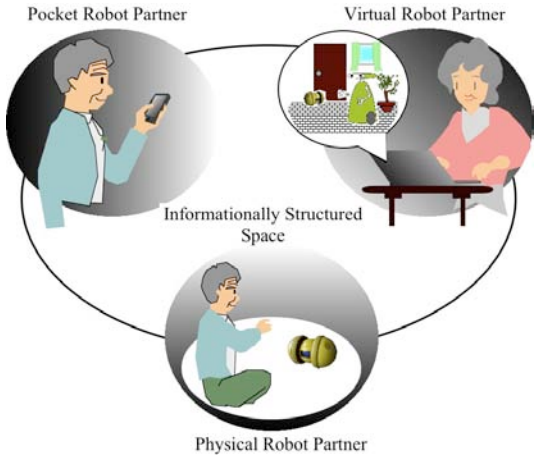

Fig.1. Interaction with robot partners.

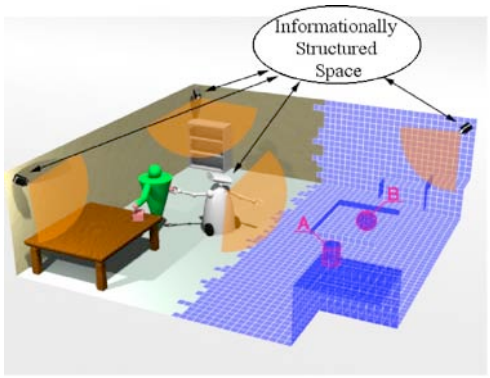

Fig.2. The concept of informationally structured space.

II. INFORMATIONALLY STRUCTURED SPACE FOR ROBOT PARTNERS

A. Informationally structured space and information service

Basically, information service to a person is used to find the required information from huge size of data, and provide them to the person in the suitable form. Robot partners are used as a concierge of daily information service, and require the emerging synthesis of information technology (IT), network technology (NT), and robot technology (RT). NT can provide the robot with computational capabilities based on various types of information outside of robots. Actually the robot directly receives the environmental information through a local area network without the measurement by the robot itself [10]. Wireless sensor networks realize to gather the huge data on environments [11]. However, it is very difficult to store all of huge data in real time. Furthermore, some features should be extracted from the gathered data to obtain the required information. Therefore, the environment surrounding people and robots should have a structured platform for gathering, storing, transforming, and providing information. Such an environment is called informationally structured space (Fig.2).

Basically, information is defined as meaningful or valuable data from the viewpoint of information science. On the other hand, sensory information includes visual information, audio information, tactile information, and olfactory information, from psychology [12-14]. This means we can perceive the meaning or value from such sensory information to perceive the environment. In this study, we try to realize information service by music, sound and voice. Especially, we discuss the method of providing a person with the comfortable mood by the sound field using music suitable to the situation.

B. A robot partner miuro

We use a robot music player called miuro as a physical robot partner developed by ZMP Inc. in Japan [4]. This robot can act in autonomous motion with the big size of wheels attached with both sides (Fig.3). The robot has many sensors such as a camera, 10 infrared distance sensors, touch sensors, and accelerometer. Furthermore, miuro can be controlled by infrared remote controller. The user can play music contents registered beforehand in miuro by the remote controller, and iPod can be connected and built within the body of miuro. The robot also can play music contents in a PC server and programs of Net Radio connected through wireless LAN (802.11b/g) by its high quality speakers.

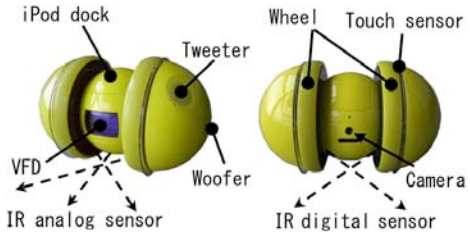

(a)back (b)front

Fig.3. Robot partner; miuro.

Figure 4 shows the roles of miuro in information service. The most important advantage of miuro is in the high quality of music play with autonomous sensing and moving capability. Therefore, miuro can provide a person with the sound field according to the situation extracted as a result of sensing. The second advantage of miuro is in wireless communication with PC server and Internet. The extracted information on preference and custom is stored in the PC server and referred from the PC server. Furthermore, miuro can download music contents from web sites according to the extracted preference of the person, and play them. However, the downloaded music contents might be different from the preference, but sometimes this can be a new finding of music for the person. This means the person does not perform the search of music contents, but miuro can be a concierge of information service.

The roles of music plays can be divided into music appreciation and background music. A person directly enjoys listening music in the music appreciation, while the person enjoys other tasks with listening music in the mode of background music. In the latter, the background music plays the important role in entraining the person into the target task. Based on the portability and mobility of miuro, we focus on the music selection as the background music.

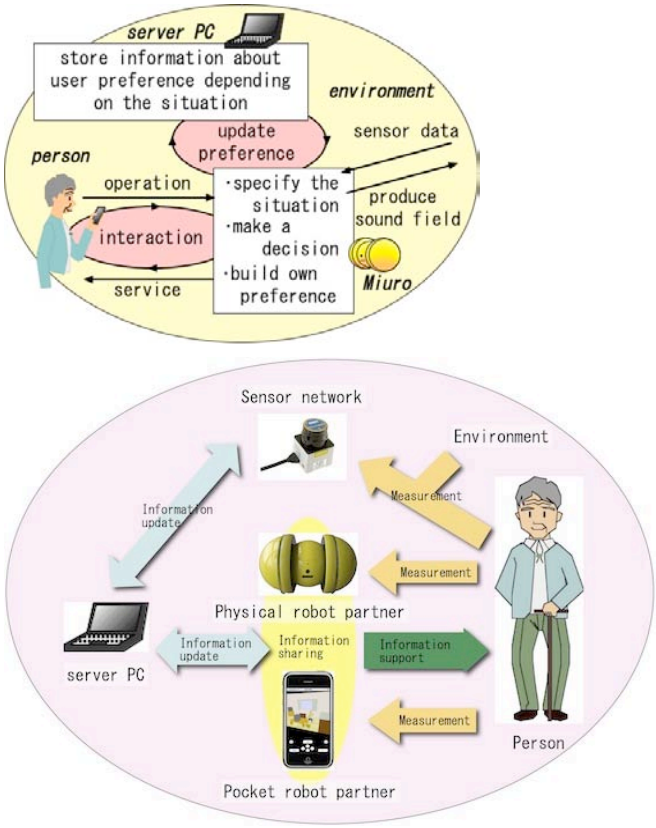

Fig.4. The roles of Miuro in information service.

C. Control architecture of Miuro

Basically, miuro has three behavior modes; human control mode, autonomous behavior mode, and interactive behavior mode. These modes are changed according to the remote controller or human interaction. In the human control mode, the user can directly control miuro, choose the predefined behaviors, and play the music contents by the remote controller. The autonomous behavior mode is composed of random walk, target tracing, information gathering, and map building. The action output of miuro is decided by the multi-objective behavior coordination according to the internal state and local sensing information from external environments. The interactive behavior mode is composed of music play, human tracking, and amusing play.

Figure 5 shows the detail of decision making of miuro. After the sensing, the behavior mode is transited to the human control mode if the remote controller is activated (Fig.5 (1)). In this mode, miuro is directly controlled and used as a music player. On the other hand, if the human interaction is extracted or recognized, the behavior mode is transited to the interactive behavior mode (Fig.5 (3)). In this mode, miuro also aggressively tries to contact and interact with the person, to collect and extract personal information such as preference and custom, and to provide various types of information suitable to the situation.

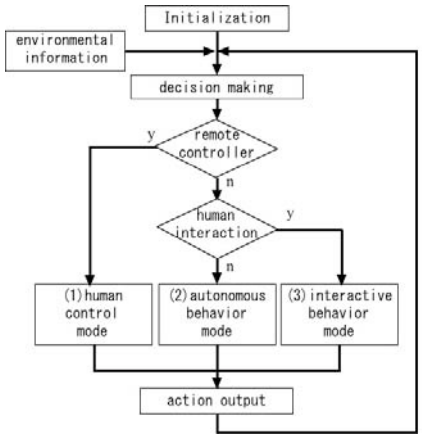

Fig.5. The total procedure of decision making of Miuro.

III. Computational Intelligence for Decision Making of Robot Partners

A. Autonomous behavior mode

Various intelligent methods for autonomous behavior control have been proposed such as production rules, Bayesian networks, neural networks, fuzzy inference systems, and classifier systems [15-20]. We have applied fuzzy inference systems to represent behavior rules of robots [10,21], because the behavioral rules can be designed easily and intuitively by human behavioral representations. We apply simplified fuzzy inference to the motion control of miuro. In general, a fuzzy if-then rule is described as follows,

If x_1 is $A_{i,1}$ and ... and x_M is $A_{i,M}$
Then y_1 is $w_{i,1}$ and ... and y_N is $w_{i,N}$

where $A_{i,j}$ and $w_{i,k}$ are the Gaussian membership function for the jth input and the singleton for the kth output of the ith rule; M and N are the numbers of inputs and outputs, respectively. Fuzzy inference is performed by,

$$\mu_{A_{i,j}}(x_j) = \exp\left(-\frac{(x_j - a_{i,j})^2}{b_{i,j}^2}\right) \tag{1}$$

$$\mu_i = \prod_{j=1}^{M} \mu_{A_{i,j}}(x_j) \tag{2}$$

$$y_k = \frac{\sum_{i=1}^{R} \mu_i w_{i,k}}{\sum_{i=1}^{R} \mu_i} \tag{3}$$

where $a_{i,j}$ and $b_{i,j}$ are the central value and the width of the membership function $A_{i,j}$; R is the number of rules. Moreover, the kth output y_k is motor output. In general, a mobile robot has a set of behaviors for achieving various objectives, and must integrate these behaviors according to the environmental conditions. Therefore, we proposed the method for multi-objective behavior coordination [22]. The multi-objective

behavior coordination can integrate outputs of several behaviors according to the time-series of perceptual information. A behavior weight is assigned to each behavior. Miuro can achieve a smooth behavior by dynamic update of the behavior weights along perceptual information. According to the behavior weights, the final output is calculated by,

$$y_k = \frac{\sum_{j=1}^{K} wgt_j(t) \cdot y_{j,k}}{\sum_{j=1}^{K} wgt_j(t)} \tag{4}$$

where K is the number of behaviors; $wgt_j(t)$ is a behavior weight of the jth behavior over the discrete trials t, and output $y_{j,k}$ is the calculation result from simplified fuzzy inference used for the jth behavior. The update amount of each behavior weight is calculated as follows,

$$\begin{bmatrix} \Delta wgt_1 \\ \Delta wgt_2 \\ \vdots \\ \Delta wgt_K \end{bmatrix} = \begin{bmatrix} dw_{1,1} & dw_{1,2} & \cdots & dw_{1,L} \\ dw_{2,1} & & & \\ \vdots & & \ddots & \vdots \\ dw_{K,1} & & \cdots & dw_{K,L} \end{bmatrix} \begin{bmatrix} ci_1 \\ ci_2 \\ \vdots \\ ci_L \end{bmatrix} \tag{5}$$

where ci_i is the parameter on the perceptual information; L is the number of perceptual inputs.

First, the multi-objective behavior coordination can integrate collision avoidance and target tracing behaviors. The inputs to the fuzzy controller for collision avoidance are the measured distance to the obstacle by infrared distance sensors equipped in front of the robot (Mc=3). The inputs to the fuzzy controller for target tracing are the estimated distance to the target point and the relative angle to the target point from the moving direction (Mt=2). Outputs are the moving velocity and the steering angle. Final outputs are calculated by the weighted average of outputs form these two behaviors based on the multi-objective behavior coordination according to the degree of danger. The degree of danger is calculated utilizing the minimum value of distances to obstacles by measurement as follows,

$$d = \left(S - \min_j x_j \right) / S \tag{6}$$

where S is the sensing range of infrared distance sensors.

B. Interactive behavior mode

The interactive behavior mode is composed of human tracking, music play, and amusing play. As mentioned before, miuro is designed as a music player, and this paper focuses on the method of providing a person with the comfortable mood by the sound field using music suitable to the situation. The individual preferable sound field corresponding to situations such as cooking, reading, studying, and sleeping is different among people. The robot music player, miuro, should provide the individual person with the comfortable mood, but it is difficult to design the relationship between a situation and its corresponding sound field. Furthermore, such relationship should be extracted and learned through communication and interaction with the person. In this paper, we assume a specific situation is corresponding to a specific human interaction.

We propose a learning method of the relationship between the human position and its corresponding music play through the interaction with the person. The robot selects human preferable music according to human position. Therefore, the learning results of the robot can reflect human preferences. Based on this assumption, we use Q-learning to obtain the relationship between the human interaction and its corresponding reaction of the robot.

C. Q-Learning for human preference extraction

Reinforcement learning methods build agents that maximize their expected utility only using reward or punishment from the environment [23]. Accordingly, the reinforcement learning does not use explicit teaching signals, but uses evaluative feedback obtained through the interaction with the environment. The tasks to be dealt with in the reinforcement learning are sequential decision problems based on four elements of a policy, a reward function, a value function, and optionally, a model of environment. In this paper, we must consider the continuity of environmental space and the discreteness of songs.

Q-learning is considered as an off-policy TD control method. Watkins proposed a simple method for assigning values to state-action pairs, and called the method incremental dynamic programming. The robot music player of the one-step Q-learning, which is the simplest method, learns the following action-value function,

$$\begin{aligned} Q(s_t, a_t) \leftarrow & (1-\alpha) \cdot Q(s_t, a_t) \\ & + \alpha \cdot \left[R_{t+1} + \eta \cdot \max_{a \in A} Q(s_{t+1}, a) \right] \end{aligned} \tag{7}$$

where R_{t+1} is a reward value, α is a learning rate ($0<a<1.0$); η is a temporal discounting rate ($0 \le \eta < 1.0$); and A is a set of songs (u_1, u_2, ..., u_S) corresponding to possible actions; S is the number of songs. It is very difficult to design the reward function for R in this application, because the reward value should be extracted through the interaction with the robot partner. In this paper, we assume a person keeps listening a favorite song. This means the human preference depends on the listening time of each song. If the person changes to another song soon, the preference is not suitable to the state s_t. Therefore, we use the following reward function,

$$R_t \leftarrow \tau(t_p) \cdot R_O \tag{8}$$

where $\tau(t_p)$ is a Sigmoid function; t_p is playing time of song a_t; R_O is a base value for the reward. Therefore, R_t is high as the playing time is long. Although the update rule is very simple, the action-value function approximates the optimal action-value function if all state-action pairs are updated repeatedly. However, the aim of this paper is not to obtain the optimal action-value function, but to obtain the feasible action-value function to extract human preference. Furthermore, as the difference from previous Q-learning, the state is not directly changed as a result of the selection by a_t. The state is updated

by the human movement in a room. This means we might not need to use Q-learning in this paper, but the advantage of Q-learning is the update of value functions in the multi-stage decision making. In this way, we apply Q-learning because we assume the selection of songs depends on the continuous space in a room.

We apply the softmax action selection (Boltzmann selection), and the ith action a_i is selected with the following probability,

$$p_t(a_i) = \frac{\exp(Q(s_t, a_i)/T)}{\sum_j \exp(Q(s_t, a_j)/T)} \tag{9}$$

where T is the temperature ($T_{\min} \le T \le T_{\max}$).When the temperature is high, the robot randomly selects a reaction. As the temperature decreases, the robot deterministically selects the reaction with the high selection strength even if the difference among selection strengths is very small. Generally, T is gradually reduced according to t, but we propose an updating method of the temperature according to the temporally changing pattern of human interactions.

$$T = \begin{cases} T \cdot \lambda & if\ x(t) = x(t-1) \\ T / \lambda & otherwise \end{cases} \tag{10}$$

where λ is the update rate ($0<\lambda<1.0$). In this paper, we use music play as reaction of the robot. Therefore, we prepare different types of songs as reaction candidates of the robot.

D. Q-Learning based on Similarity Matrix

There are two important problems in human preference extraction. As the first problem, it is very difficult to evaluate the quality of the extracted human preference. The problem of evaluation has a problem of the mutual nesting. A person can evaluate the preference of music from the candidates of music, while the candidate of music must be selected according to the human preference. This means the quality of the extracted human preference depends on the quality of the selection of music candidates. The second problem is the stability of human preference. This means the human preference can change according to the daily life. In this way, the robot music player should play various types of music, and extract human preference. However, if the robot music player prepares many songs, it takes much time to extract human preference by Q-learning because the state space is large. Therefore, we propose a Q-learning algorithm based on similarity matrix to enhance the learning of Q-learning. The similarity among songs in this paper is not only the objective similarity such as rhythm and tone, but also the subjective similarity like preference among songs.

In the above definition, $Q(v_t, a_t)$ is discretized where v_t is the state, and a_t is the song to be played. In previous works, fuzzy Q-learning was proposed to deal with continuous states and actions. In case of fuzz Q-learning, we can deal with the continuity of state and action by the shape of membership functions based on the distance space. However, it is very difficult to represent the distance based on the degree of similarity among songs by using membership functions. Therefore, we use the similarity matrix in the following;

$$\boldsymbol{M} = \begin{pmatrix} 1 & \cdots & m_{1N} \\ \vdots & \ddots & \vdots \\ m_{N1} & \cdots & 1 \end{pmatrix} \tag{11}$$

where the number of songs is N, and diagonal elements is set at 1; m_{ij} is the degree of similarity between two songs ($0 \leqq m_{ij} \leqq 1$, $m_{ij}=m_{ji}$). In the proposed method, when the kth song is selected ($a_t=u_k$), Q values are updated as follows;

$$\begin{aligned} Q(s_t, a_j) \leftarrow & (1-\alpha \cdot \mu_{k,j}) \cdot Q(s_t, a_j) \\ & + \alpha \cdot \mu_{k,j} \left[R_{t+1} + \eta \cdot \max_a Q(s_{t+1}, a) \right] \\ & \left(if\ \mu_{k,j} > 0 \right) \end{aligned} \tag{12}$$

where R_{t+1} is a reward value, α is a learning rate ($0<a<1.0$); η is a temporal discounting rate; $\mu_{k,j}$ is a similarity value between the kth and jth songs ($0<\eta<1.0$); the $\mu_{k,j}$ is calculated in the following;

$$\boldsymbol{\mu}_k = \begin{pmatrix} \mu_{k,1} \\ \vdots \\ \mu_{k,N} \end{pmatrix} = \boldsymbol{M}\boldsymbol{l} = \begin{pmatrix} 1 & \cdots & m_{1N} \\ \vdots & \ddots & \vdots \\ m_{N1} & \cdots & 1 \end{pmatrix} \begin{pmatrix} l_1 \\ \vdots \\ l_N \end{pmatrix} \tag{13}$$

$$\boldsymbol{l} = \begin{pmatrix} l_1, & \cdots, & l_N \end{pmatrix}^T, \quad l_i = \begin{cases} 1 & if\ a_t = u_k \\ 0 & otherwise \end{cases} \tag{14}$$

In the original Q-learning, the Q value of the selected action a_t at the current state s_t is only updated, but the proposed method updates the Q values of other actions not selected at the current state s_t according to the similarity matrix. In this way, the learning time of Q values is reduced.

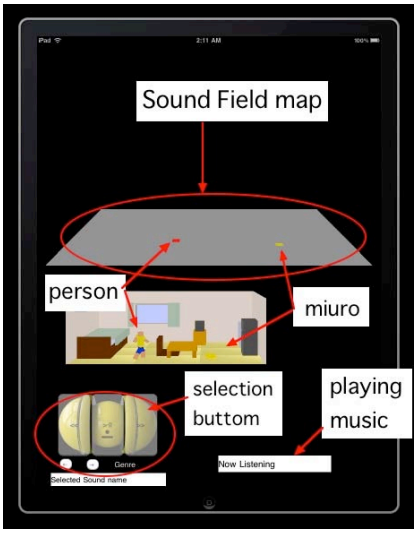

Fig.6. A simulator using iPad

IV. EXPERIMENTAL RESULTS

This section shows several experimental results of the proposed method. In order to realize the efficient and quick learning, we use iPad as the pocket robot partner. The touch interface provides a user with simple and repeatable interaction on the touch screen. After the learning on the pocket robot partner, we can transfer the learning result to the physical robot partner. The human interaction is done with Miuro on the simulator of iPad by the touch interface (Fig.6). The simulator is composed of sound preference map, environmental map simulating to a real room (Fig.7 (a)), and the control buttons of music plays. The human position is estimated by using the measured distance data of two laser range finders (Fig.7 (b)). Figure 8 shows the snapshot of autonomous behavior mode and interactive behavior mode in the pocket robot partner. The robot takes random walk in the autonomous behavior mode in Fig.8 (b), and the robot takes the human tracking behavior in the interactive behavior mode.

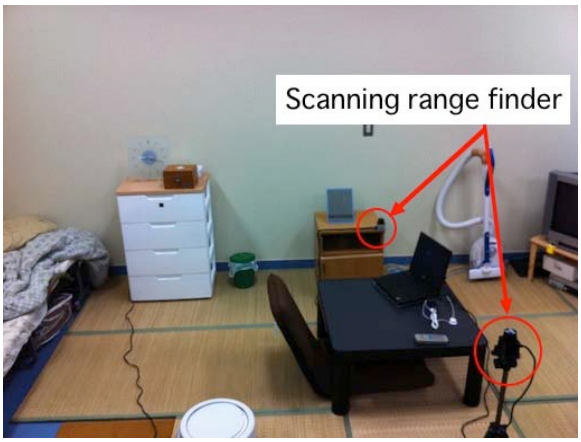

(a) One room used for experiments

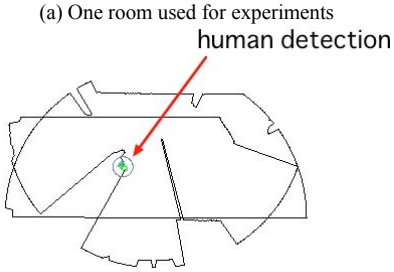

(b) Human detection by two laser range finders

Fig.7. Experimental environment and human detection with laser range finders.

(a) Autonomous behavior mode (b) Interactive behavior mode

Fig.8. Behavior modes in the pocket robot partner.

We conduct experiments on the learning of the relationship between human location and its corresponding preferable music selection as the generation of comfortable sound field.

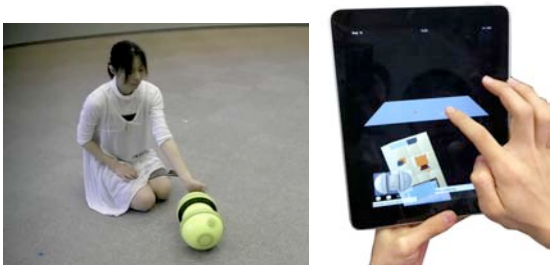

(a) with a physical robot partner (b) with a pocket robot partner

Fig.9. Human interaction used in the experiments.

The size of environment corresponding to states is 5×10. The number of songs is 10 (S=10), and the songs are categorized into three different types of classic, rock, and jazz. The current learning states based on the played songs are visualized by using color distribution where classic, rock, and jazz are depicted in red, green, and blue colors. Table 1 shows the values of parameters used in experiments. The values of similarity matrix are designed subjectively. The human position in the simulator is updated according to the estimated position by two laser range finders.

TABLE I. ARAMETERS USED FOR THE LEARNING IN EXPERIMENTS.

Learning rate α	Discount rate η	Standard value of Reward R_O	Number of songs
0.2	0.8	0.5	Classic : 3
			Rock : 3
			Jazz : 4

We conduct an experiment for 30 minutes, and the person selects songs according to the human position in the simulator. The person moves among four points of a bed, chair, cabinet, and sink unit. Figure 10 shows the preference learning in experimental results. Figure 10 (a) shows a result of preference learning at 17 seconds after the start. In this stage, the color distribution is still dark because the learning is not done much. The red color indicates classic songs are played in the sound field map. As time passes, the color of cells is updated gradually. In the final state, the sound preference map is in tinge of red. This means the person listened classic in the bedside, and both classic and jazz in the chair. The learning result is similar with the human preference obtained by the interview after the experiment. In the initial stage of learning, songs are selected almost randomly, but the similar songs based on current learning states are gradually selected by the effect of Q-learning based on similarity matrix. In this way, the proposed method can reduce the learning time while extracting human preference dependent on the human position.

(a) t=52; 00m:17s (b) t=452; 02m:30s

(c) t=2116; 11m:45s (d) t=5364; 29m:48s

Fig.10. Preference learning in experimental results

V. SUMMARY

This paper proposed a learning method of human preference based on a Q-learning algorithm, Boltzmann selection with temperature control, and similarity matrix. Furthermore, we used a robot music player named miuro as a robot partner. The experimental results show that the proposed method can learn the relationship between human position and its corresponding played songs. Furthermore, the proposed method can provide the person with the preferable song as the comfortable sound field. The essence of the proposed method in this paper is flexibility and adaptability in the update of parameters according to the change of situation and human position. Furthermore, the similarity matrix can reduce the learning time, but the similarity matrix is designed beforehand in this paper. The similarity matrix should be also updated through the interaction with a robot partner.

As future works, we intend to develop the perceptual system of robot partners for specifying the situation sharing with people, and to improve the performance of recognition methods of human gestures and interactions. Furthermore, we will propose a method of replacing song candidates according to human selection results.

REFERENCES

[1] R. C. Arkin, M. Fujita, T. Takagi and R. Hasegawa, An Ethological and Emotional Basis for Human-Robot Interaction, *Robot. Autonom. Syst.* **42** 2003, pp.191–201.

[2] T. Kanda, H. Ishiguro, T. Ono, M. Imai and R. Nakatsu, Development and Evaluation of an Interactive Humanoid Robot Robovie, in *Proc. of IEEE Int. Conf. Robot. Autom.*, Washington, D.C., 2002, pp.1848–1855.

[3] E. Sato, T. Yamaguchi and F. Harashima, Natural Interface Using Pointing Behavior for Human-Robot Gestural Interaction, *IEEE Trans. Ind. Electron.* **54**, 2007, pp.1105–1112.

[4] ZMP Inc. & C., Miuro, The Robot that Play Your Favorite Music at Your Favorite Place (in Japanese), *Journal of Robotics Society of Japan* **26**, 2008, pp.34–35.

[5] N. Kubota, D. Hisajima, F. Kojima and T. Fukuda, Fuzzy and Neural Computing for Communication of A Partner Robot, *Journal of Multiple-Valued Logic and Soft-Computing* **9**, 2003, pp.221–239.

[6] N. Kubota and K. Nishida, Perceptual Control Based on Prediction for Natural Communication of A Partner Robot, *IEEE Trans. Ind. Electron.* **54**, 2007, pp.866–877.

[7] N. Kubota and A. Yorita, Topological Environment Reconstruction in Informationally Structured Space for Pocket Robot Partners, in *Proc. of 2009 IEEE Int. Symp. on Computational Intelligence in Robotics and Automation*, Korea, 2009, pp.165–170.

[8] A. Yaguchi and N. Kubota, The Style of Information Service by Robot Partners, in *Proc. of The 2010 Int. Conf. on Intelligent Robotics and Applications*, 2010.

[9] N. Kubota, T. Obo and B. H. Lee, Localization of Human in Informationally Structured Space Based on Sensor Networks, in *Proc. of IEEE World Congress on Computational Intelligence 2010*, Barcelona, 2010, pp.2215–2221.

[10] N. Kubota and K. Nishida, Cooperative Perceptual Systems for Partner Robots Based on Sensor Network, *Int. J. Comput. Netw. Secur.* **6**, 2006, pp.19–28.

[11] I. Khemapech, I. Duncan and A. Miller, A Survey of Wireless Sensor Networks Technology, in *Proc. the 6th Annual PostGraduate Symposium on the Convergence of Telecommunications, Networking and Broadcasting*, Liverpool, 2005, pp.1–6.

[12] R. L. Gregory, *The Oxford Companion to The Mind*, Oxford University Press, New York, 1998.

[13] M. W. Eysenck, *Psychology: an Integrated Approach*, Prentice-Hall, Addison Wesley Longman Ltd. , Pearson Education, Ltd. , Edinburgh Gate, Harlow, 1998.

[14] K. J. Gergen and M. M. Gergen, *Social Psychology Second Edition*, Springer-Verlag New York, Inc. , New York, 1986.

[15] J. -S. R. Jang, C. -T. Sun and E. Mizutani, *Neuro-Fuzzy and Soft Computing*, Prentice-Hall, Inc. , Upper Saddle River, NJ, 1997.

[16] L. A. Zadeh, eds. G. J. Klir and B. Yuan, *Fuzzy Sets, Fuzzy Logic, and Fuzzy Systems*, World Scientific Publishing Co., Inc. , River Edge, NJ, 1996.

[17] J. A. Anderson and E. Rosenfeld, *Neurocomputing*, The MIT Press, Cambridge, MA, 1988.

[18] S. V. Kartalopoulos, *Understanding Neural Networks and Fuzzy Logic*, The IEEE Press, New York, 1996.

[19] S. J. Russell and P. Norvig, *Artificial Intelligence*, Prentice-Hall, Inc. , Englewood Cliffs, NJ, 1995.

[20] H. Liu, A Fuzzy Qualitative Framework for Connecting Robot Qualitative and Quantitative Representations, *IEEE Trans. Fuzzy Syst.* **16**, 2008, pp.1522–1530.

[21] N. Kubota, Multi-Objective Design of Neuro-Fuzzy Controllers for Robot Behavior Coordination, in *Multi-Objective Machine Learning, Studies in Computational Intelligence* **16**, ed. Y. Jin, Springer-Verlag New York, Inc. , Secaucus, NJ, 2006, pp.557–584.

[22] N. Kubota and N. Aizawa, Self-Adaptation in Intelligent Formation Behaviors of Multiple Robots based on Fuzzy Control, in *2009 IEEE International Conference on Fuzzy Systems*, Jeju Island, 2009, pp.900–905.

[23] S.Sutton, G Barto, *Reinforcement Learning*, A Bradford Book, 1998.

2011 IEEE International Conference on Fuzzy Systems
June 27-30, 2011, Taipei, Taiwan

A Report The Difference Features Of A Multi-agent Using An Overlay Knowledge In The Fire Panic Problem

Yukinobu HOSHINO
School of Systems Engineering
Kochi University of Technology
Kochi, Japan
hoshino.yukinobu@kochi-tech.ac.jp

***Abstract*—This report of this paper shows a performance of the heterogeneous multi-agent system using the overlay knowledge technique. The overlay knowledge is one kind of layered rule-based system. Basic idea is the tile-coding rule on reinforcement learning. But In the tile-coding rule, all reinforced rules are spread any categorical states of rule table. Proposal style of overlay knowledge is from a tile-coding. We examined the features of the learning principle about the heterogeneous multi-agent. It was proved that the overlay knowledge was useful sufficiently for the heterogeneous multi-agent. The robust characteristic was the cause which outputs absolute behavior. By changing of the robust levels, behaviors of the agent expected a change into the flexible movement.**

Keywords-component; multi-agent system ; overlay knowledge ; reinforce learn; fire panic

I. INTRODUCTION

The report on this paper shows a performance of the heterogeneous multi-agent, which have the overlay knowledge. The overlay knowledge is one kind of the layer type rule-based system. Our basic idea is the tile-coding rule of the reinforcement learning. In the tile-coding, all reinforced rules are tiled some categorical states of the rule table. Recently, there are the shaping style rules by using other training method. So we believe the robustness and applicability phenomenon between behavior and rule's amount. Especially, rule style of the overlay knowledge easy to find that phenomenon. We would like to show that in this paper and discuss the learning theorem in Multi-agent system.

II. LEARNING THEORY OF MULTI-AGENT SYSTEM

Learning system and intelligence are related to each other. Learning always has to do about the self-improvement of future behavior based on past experiment, which agent has gone. Leaning of the multi-agent system have two principal categories. One is centralized leaning or isolated learning. Another is decentralized leaning or interactive learning. In the multi-agent system, several centralized learning would like to try to obtain same activate at same time by same goal. There are several groups of agents that involved by different decentralized learning on each agent's. Especially, the heterogeneous multi-agent system has some group agents which have different behavior. Interactive learning process is feature quality. That two learning categories are a general nature and a broad variety forms of learning. Generally, the multi-agent system has six type difference features [9].

① The degree of decentralization :
The decentralization of a learning process concerns its distribution and parallelism. One normal case is that a single agent carries out all learning behavior. Other case is that the learning system is distribute and parallelism through all agents of a group.

② Interaction-specific features :
There is a number of features that can be applied to classifying the interactions request for realizing a decentralized learning process. Examples are the level interaction, the frequency interaction, pattern interaction, the variable interaction and so on.

③ Involvement-specific features :
That feature can be used for characterizing the involvement and role played during involvement. Learning processes of agent are the relevance of involvement and role played during involvement.

④ Goal-specific features :
Learning goal of multi-agent are the type of improvement that is tried to be achieved by learning and the compatibility of the learning goals traced by the agents.

⑤ The learning method :
The following learning methods or strategies used by an agent are usually distinguished. There are rote learning, learning from instruction and advice taking. Otherwise, learning from examples, practice leaning, analogy learning, learning by discovery and so on.

⑥ The learning feedback.

978-1-4244-7316-8/11/$26.00 ©2011 IEEE

The learning feedback indicates the performance level behavior. This is leading factor to follow classification, success, and goal by some feedbacks, are supervised learning and unsupervised learning. Reinforcement learning is a kind of unsupervised learning but the feedback is only specific signal of the utility, which depends on the actual behavior of learner. And the objective is to maximize for targets.

In the heterogeneous multi-agent system, leaning system has to follow those features. Interaction's reference is key-point and the research point of using the overlay knowledge.

III. Q-LEARNING

Q-learning is a type of unsupervised learning system. The evaluation about selected behaviors and policies, make renew/reinforce by a reward/penalty. The agent selects behaviors according to the observed state. The selected behaviors become the best behavior, because Selective Unit select them according to rules reinforced by $Q(s,a)$ where a is a behavior and s is the observed state.

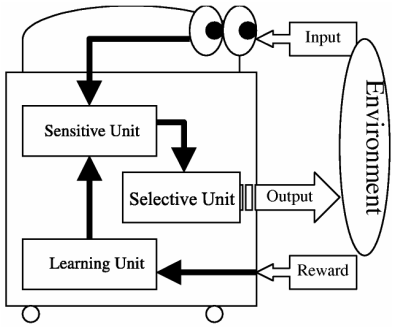

Fig.1 Framework of Q-learning

If there are no fitting rules, a new rule is created on the rule database; also rule base. Q-learning is able to learn from uncertain information. The learning systems are composed three units, including a sensitive unit, a learning unit, and a selection unit, as shown in Fig.1. If agents have received a positive reward, Q-value is renewed a positive direction. So, using rewards and penalties, the learning unit is able to change Q-value with the rules used. The renewal function f_t is given in Eq.(1) . $Q(s_t,a_t)$ is an evaluation to make renewal, shown in Eq.(2). In these cases, γ is the discount rate of $Q_{\max}$, d is the discount rate of a reward and α is the learning rate. s_t is observed state at the current time t. a_t is the selectable action at the current time t. Those parameters are in the range [0,1]. T is whole time of one episode. t is current time in one episode time T. Also, $Q_{\max}$ is the max evaluation of the best policy at the next state $S_{(t+1)}$. r is +1 as a reward or -1 as a penalty. Eq.(2) explains that Q-value is renewed by the reward.

$$f_t = \gamma Q_{\max} - Q(s_t, a_t) + d^{T-t} r \tag{1}$$

$$Q(s_t, a_t) \leftarrow Q(s_t, a_t) + \alpha f_t \tag{2}$$

An agent selects one behavior based on the view it has of the surrounding environment. The selection unit always uses probability based on Boltzman Distribution, as given Eq. (3). $Q(s,a)$ is Q-value about a target state s and a candidate action a. T is "Temperatures parameter" and p is probability to select a candidate action a.

$$p(a \mid s) = \frac{\exp(\frac{Q(s,a)}{T})}{\sum_{b \in action} \exp(\frac{Q(s,a)}{T})} \tag{3}$$

IV. THE FIRE PANIC PROBLEM

We show the fire panic problem on fig.2. In this problem, a fire exists in a field and it spreads throughout the space. The purpose of the agent is to reach an established goal without touching the fire that is in the environment. In order for the agents to avoid the fire spreading in the environment, they must acquire behaviors that allow them to reach a goal before the fire reaches them. The fire heats during three steps. After this three steps, the fire jumps to the randomly one direction (up, down, left or right) at one step. In the fire panic problem, all agents have to follow features①～④ about using the overlay knowledge. Please check a section II. LEARNING THEORY OF MULTI-AGENT SYSTEM

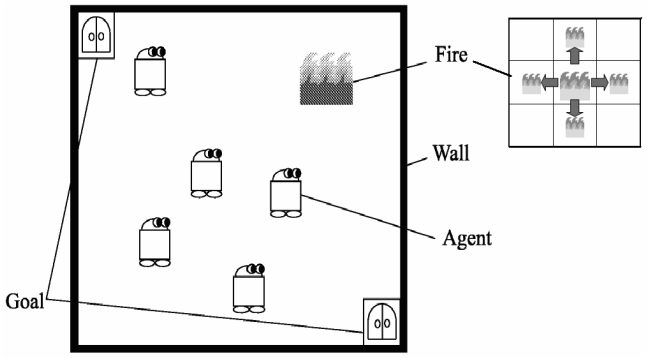

Fig.2 The fire panic problem

In this problem, we use two types of agents, A1 and A2. These agents are heterogeneous multi-agents with differing areas of view. The view area of A1 is 3x3. The view area of A2 is 5x5. Also, all agents can recognize all of these objects in the space: Fire, Wall, Agent, and Goal. All agents can select from these behaviors: Up, Down, Left, Right and Stop.

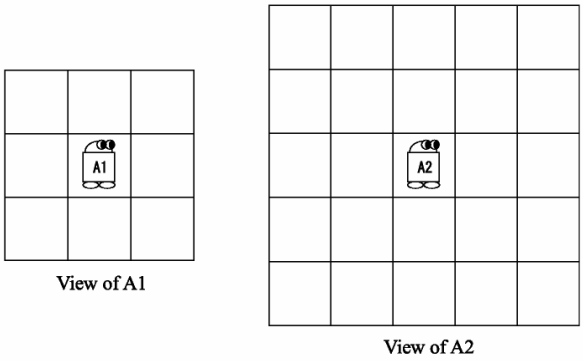

Fig. 3 Fields of view in agents A1 and A2

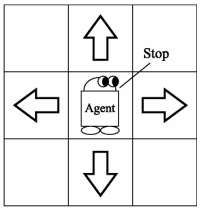

Fig. 4 Behavior of Agents

Agent is not able to enter any spaces that already contain Wall or Agent. In the fire panic problem, each action is one step. Each trial have 100 steps, all agents are able to move during 100 steps in a field. Agents learn behaviors using Q-learning or the our overlay knowledge system.

- If the agent reached a goal during the trial, the agent receives the reward r=+1.
- When a trial finished, agents on the field that are not touched by fire receive no-reword r=0.

If the agent touches the fire during the trial, the agent dies and receive the penalty r=–1.

V. APPLING Q-LEARNING

At first, we implemented Q-learning system for A2 agents in 30,000 trials. Then, after these trials, we introduce A1 agents, with smaller fields of view, into the space and we conducted 30,000 further trials in which A1 and A2 agents learn together in the same environment. Fig.5 shows the environments of the first and second trials. Fig.6 and Fig.7 show the number of times an agent reached a goal for every 1,000 trials.

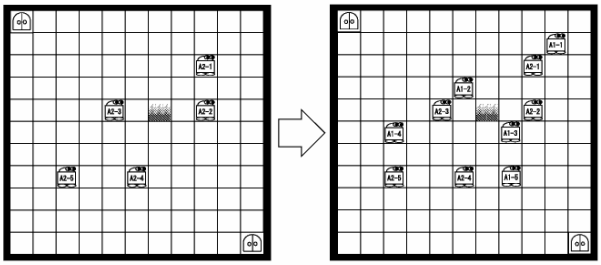

Fig. 5 First and second trials on the experiments

We could observe that A1 got the best behavior to reach a goal, show Fig.6. Then the number of goal on A2 has decreased at Fig.7. Those are results of using normal Q-Learning. About those curves, a vertical axis is a number of goal arrivals for every 1,000 trial. A horizontal axis is a number of trials. The number of goal has never increased again about A2 agents, given as Fig.7. We have kept experiment 60,000 trials, but the number of goal has maintained a low level. See Fig.8 (A), the best action of A2 is selecting a left move. During first term, A2 agents have never seen A1 type agents and finished a leaning to take the best action. But rule base is recorded view and Q-value with all action. See Fig.8 (B), if A2 agent has sensed A1 at first time, then A1 agent is not able to find an applicable rule. Because the rule base system seek a completely fitting rule. Basically, if there is not fitting rule in the rule base, then whole agents has no choice the best action. Thus, A2 agents cannot help choosing the random action, like a confusing behavior. Finally, A2 should learn same action on those views as a different situation.

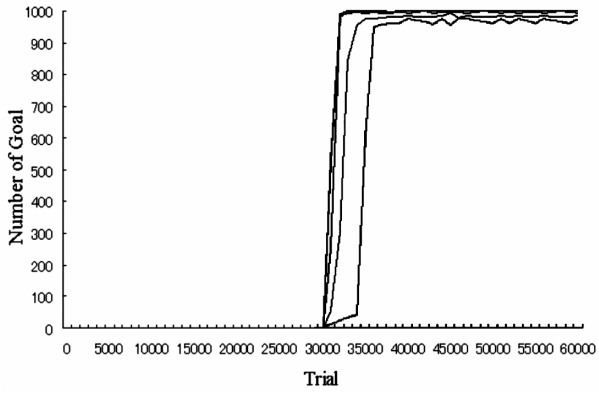

Fig. 6 Number of goal arrivals for A1 agents on Exp.1

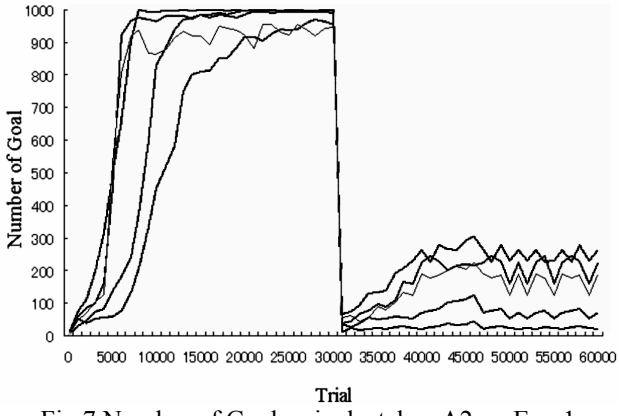

Fig.7 Number of Goal arrivals, taken A2 on Exp.1

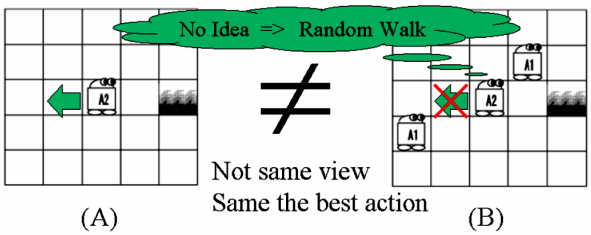

Fig.8 Process of the confusing the best action

VI. Reinforcement Learning Using The Overlay Knowledge

An applicable behavior is selected from a probability with the Boltzman distribution with Q-value. Proposal method is introduced in A2, in which the field of view is 5x5, and learning is determined in accordance with Q-learning. The proposed concept for our method used is shown in Fig. 9. The system renews Q-value with the learning layer. So this system was easy system.

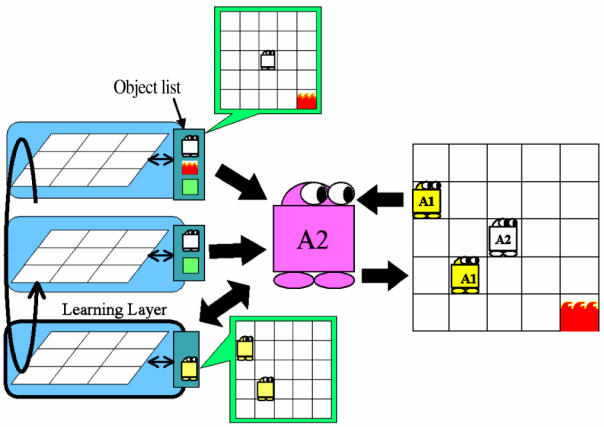

Fig.9 Framework of the overlay knowledge Method

In our learning system, we built the object list to switch layers. About an input status, the system searches object list of a current layer. Some objects are registered to the object list, if a target agent experienced objects in past times. In this fire panic problem, all agents have a possible to find A1 agent, A2 agent, fire, and wall as an object. If designer selected any items for target problem, then it is easy to add/record the object list, which would support any cases on the target problem. When the system learns by a reward, the system renews Q-value $q_{j(x,y)}$ on a current learning layer j. However before that process, the system check that observed objects exists in the object list of the learning layer j. During starting trials in the experiment, agents found new objects at all time, so adding object to the object list is anytime and quickly. When this system had some layers, the system was not able to follow the switching layers quickly. Because the system needs some layer know ledges for overlay Q-values. Then the system keep switch layers quickly, an approximating is impossible.

If new observed objects, which do not exist on the object list of the learning layer, then the system switch a current layer and create a new object list from new observed objects.

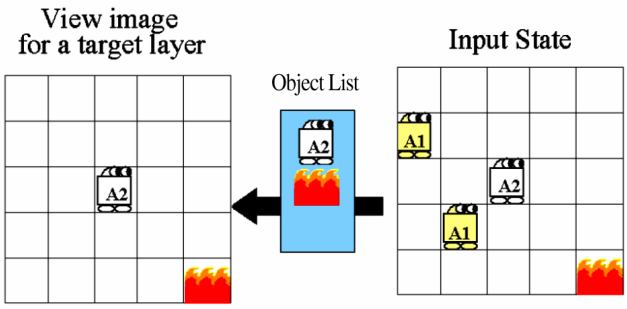

Fig.10 Object list and the masked view

The learning system adds the new rule and renews Q-value on the new learning layer. If a current layer is a last layer, then a current layer is switched to a first layer by the system; turn over to a first layer. This learning system can support several objects by the rule base on other layers. Proposal system has five layers with an object list. The input system masks out the unnecessary objects by checking the object list. And the system applies some Q-value from other masked layers, if the learning layer has no applicable rule. See Fig.10. Those preexisting Q-values on layers are possible to support an action about new situation, which the agent did not experience in past times. Additionally, proposal system has weight parameter w_i for each layer i. In a proposal system, the evaluation value $Q(s,a)$ is calculated by $q_i(s,a)$, as given Eq.(4). $q_i(s,a)$ is a output Q-value from a layer i. In this case, all q_i has evenly reach to $Q(s,a)$. The learning system searches a fitting $q_i(s,a)$ from all recorded q values with each layer i. The observed state keep changing dynamically, so the best policy will change by those situations. Weights show a possibility the applicable behavior for $q_i(s,a)$. We have tried some simulation experiment about weight parameters.

$$Q(s,a) = \sum_{i=1}^{m} w_i \times q_i(s,a) \qquad (4)$$

VII. Multi Lyaerd QL Method For Fire Panic With A1 And A2

Proposal system make Q (s,a) for select behavior by Eq.(3)(4). And we implement our overlay knowledge system for A2 agents, has **three layers**. A1 agents have normal Q-learning system. When an agent finished one trial, Q-value of used rules are renewed by the reinforce function as Eq.1 and Eq.2. And Q_{max} value is selected from a Q-value record in an experiment. Thus, this learn processes are executed when an agent finish one episode. See Fig.11. A current layer has 50.0% weight and a second layer and a last layer have 25.0% and 25.0%.

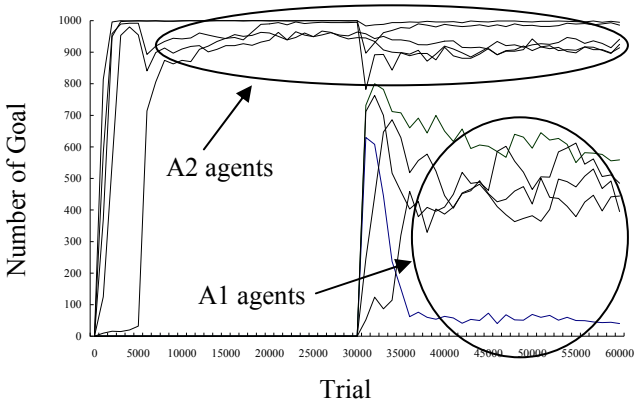

Fig.11 The curve of three layers and Result of weights are 50.0% 25.0% 25.0%

In this case, we took a good result normally, a goal number of A2 agent is decrease little bit when A1 agents came in. And the number of goal came back and kept high values. In this case, preexisting rules could work and support for new states with A1 agents coming. As a result A2 agents did not confuse about coming A1 agents in those views. Here, agent 2 supports a new condition without being confused by the show in the robust-ness of the overlaid knowledge. In this way, the overlaid knowledge is acting on the valid product. However, we can not judge applicability about behavior of the agent. Therefore, we discuss the possibility to realize applicable behavior by the weight parameter change and the algorithm change. Therefore, we change a parameter.

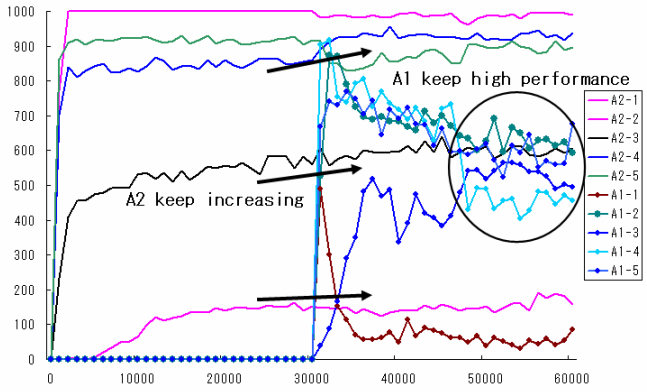

Fig.12 The curve of five layers and Result of weights are 92%, 2%, 2%, 2%, 2%

This system uses the Q value of the all layers. But layer weights, which except current layer, made low and even weight for experiment. On those weights, learning can make robust-ness to the overlay knowledge. So, a flexible action is led from the overlay. The learning uses the overlay knowledge of **five layers**. The weight of a current layer is 92%. The weights of other 2nd-5th layers are 2%. In fig.12, phenomena of curve show the flexible behavior successfully.

VIII. Conclusion

We examined the characteristic of overlay knowledge from the experiment from applying a fire panic problem. All agents have to follow features ①～④ in the fire panic. We examined the nature of the featuring learning principle about the heterogeneous multi-agent which followed features ⑤～⑥. About features ①～⑥, see. II. LEARNING THEORY OF MULTI-AGENT SYSTEM. As a result, it was proved that the overlay knowledge was useful sufficiently for the heterogeneous multi-agent. Also, we have showed the robust characteristic which depends on layer in overlay knowledge. Then, the robust characteristic was the cause which outputs absolute behavior. By the change of the robust levels, behavior of the agent expected a change into the flexible movement. The behavior which is passive about the reward is output. However, the overlay knowledge which was taken by the experimental result and we must analyze it for the rote. This is future work.

References

[1] C.J.C.H. Watkins, P. Dayan : "Technical Note: Q-Learning", Machine Learning, Vol.8, No.3, pp.279-292(1992)

[2] R.S. Sutton : Integrated architectures for learning, planing, and reacting based on approximate dynamic programming: Proceedings of the 7th International Conference on Machine Learning , pp.216-224 (1990)

[3] R.S. Sutton and A.G. Barto : Reinforcement Learning: The MIT Press (1998)

[4] Y. Hoshino and K. Kamei:A proposal of Reinforcement Learning System to Use Knowledge effectively: Proceedings of SICE Annual Conference 2003 in Fukui, Fukui University, Fukui, Japan, CD-ROM Version No.0538 TAI-14-2(4 Pages) (2003)

[5] Y. Hoshino, A. Sakakura , and K. Kamei: Research of Foresight Knowledge by CMAC based Q-learning in Heterogeneous Multi-Agent System : *Proceedings of* 4thInternational Symposium on Advanced Intelligent System, pp.280-283 (2003)

[6] Yukinobu HOSHINO, Akira SAKAKURA and Katsuari KAMEI: A proposal of CMAC with Foresight Knowledge Layer For Heterogeneous Multi-agent, *Proceedings of* International Conference on Fuzzy Systems 2004, Budapest, Hungary, CD-ROM Version 0047-1382.pdf, pp.449-452 (2004)

[7] J.S. Albus. A new approach to manipulator control: The cerebellar model articulation controller (cmac). Transactions of the ASME, Journal of Dynamics Systems Measurement and Control, Vol. 97, pp.220-227, 1975.

[8] Albus, J.S.,Mechanisms of planning and problem solving in the brain (1979) Mathematical Biosciences, 45 (3-4), pp. 247-293.

[9] Gerhard Weiss : Multi agent Systems, The MIT Press

[10] Yukinobu HOSHINO , Akira SAKAKURA and Katsuari KAMEI: A proposal of the learning system using the recordable multi-layer type rule base and its application for the Fire panic problem, *Proceedings of* the Joint International Conference on Cyber Games and Interactive Entertainment 2006 (CGIE2006), pp.137-140

[11] E. Uchibe, and K. Doya.: Competitive-Cooperative-Concurrent Reinforcement Learning with Importance Sampling, In *Proc. of* International Conference on Simulation of Adaptive Behavior: From Animals and Animats, pages 287-296, 2004

2011 IEEE International Conference on Fuzzy Systems
June 27-30, 2011, Taipei, Taiwan

Group Pressure Generation of Multi-Agents on Cross-cultural Simulation Game

Daisuke Katagami
Dept. of Applied Computer Science,
Faculty of Engineering
Tokyo Polytechnic University
1583 Iiyama, Atsugi, Kanagawa, Japan
katagami@cs.t-kougei.ac.jp

Tam Huynh van
Dept. of Applied Computer Science,
Faculty of Engineering
Tokyo Polytechnic University
1583 Iiyama, Atsugi, Kanagawa, Japan

***Abstract*—In this paper, we pay attention to strong atmosphere of a group momentarily constructed by a place because the agent who expresses gesture and face expression gathers plurals. We called the atmosphere socially constructed as group pressure of agents. The purpose of the paper is to develop a group pressure and investigate the influence to human. We verify if the group pressure made by multiple life-like agents exert an influence on the judgment of player by using the cross-cultural simulation game we developed before.**

Keywords- group pressure; cross-cultural simulation game; human-agent interaction; barnga

I. INTRODUCTION

In the world of human coexistence, social adaptability should be regarded as significant in order for machines to realize flexible communication with humans. However, no essential approach for social adaptability has been shown by the current research regarding Human-Agent Interaction (HAI). Conversely, this issue about social adaptability can be expected to become an important technology to develop a robot that can communicate well with a variety of people as well as to develop such characteristic robots.

There is a cross-cultural simulation game *BARNGA* [1] which is available to experience rules on group society as based on non-verbal interaction. *BARNGA* is an easy-to-use cards game for education. This game has been adopted in a training course of company, the field of education and so on all over the world. The authors have been developed *online BARNGA* [2, 3] which can provide not only human-to-human but also human-agent cross-cultural communication on online environment based on original *BARNGA*. We have been studied and learnt many findings in the adaptability of group on the human-agent cross-cultural environment. For example, we investigated action sequential data, electroencephalography (EEG) of human by fNIRS, impression evaluation by questionnaire by using *online BARNGA* [3]. However, it has never been figured out how construct a social pressure which subjects feel subjectively in the society group on the human-agent cross-cultural environment.

In this paper, we pay attention to strong atmosphere of a group momentarily constructed by a place because the agent who expresses gesture and face expression gathers plurals. We called the atmosphere socially constructed as group pressure of agents. The purpose of the paper is to develop a group pressure and investigate the influence to human. We verify if the group pressure made by multiple life-like agents exert an influence on the judgment of player by using the cross-cultural simulation game we developed before.

II. GROUP PRESSURE GENERATION BASED ON LIFE LIKE AGENTS

A. Communication with Life Like Agents

Realization of human-artifact communication is closely-related to the recognition of human intent and the function of expression. Development of life-like artifact have been performed by using the elements like line of sight, language, gesture, posture, appearance, tactile sense, sound and motion. Generally, the communication of meaning is performed by language as typified by utterance between humans communication. Meanwhile, the importance of non-verbal information like facial expression, line of sight, gesture [4]. Moreover, Mehrabian et. al. reported that language information like contents of utterances gives 7%, hearing sense like tone or speed of talk gives 38% and visual sense like appearance gives 55% influence to a conversational partner, in the experiment of normal reaction of the partner when an utterer talks a conflicted message to emotion and attitude.

This experiment indicates that the taker of the message tends to focus non-verbal information like tone of talk and body language than contents of utterance [5]. Ito et. al. proposed the way to adjust non-verbal information like line of sight and facial expression to realize the atmosphere the user specified by using life-like agent [6]. These researches indicate the designing non-verbal interaction nicely in order to realize smooth communication between human and artifact.

However, above experiments were conducted with pair of human and a life-like agent or human and human or two life-like agents. This paper will treat plural agents to communicate with a society.

978-1-4244-7316-8/11/$26.00 ©2011 IEEE

B. Group Pressure

Generally, a person becomes a member of a group with newcomer in the real social life. There is already in being a unique basis of the group at the times like this. The members keep the basis as if it were common sense. If the opinions or perspectives of the newcomer disagree with the basis, the person will get confused. In this case, the person have to judge between following behaviors [7].

1) The person accepts and agrees with the basis.
2) The person ignores the basis and behaves absolutely.
3) The person promotes the change of the basis.
4) The person leaves the group.

When a newcomer noticed that all members have same perspective without oneself in a group, the person feels a stress and pressure. This triggers a change of the opinion. We call this stress or pressure as a "group pressure". Following this pressure is the psychology of conformity.

Ash [8] investigated what condition will generate the conformity in the group in the creative experimental way.

C. Design of Group Pressure Genaration

We develop a simulation system of a group pressure by using plural life-like agents and realize various group pressures. And then, we validate the constructed atmosphere by the evaluation experiment. Life-like agent as a CG character represented human body is used as an interface which can be reduced human's cognitive load on the various tasks. So far, Galatea and TVML [9] are proposed as tools which can be develop a life-like agent relatively-easy. We use TVML for the construction of a group pressure of multiple agents. Figure 1 shows the developed agents. We prepared 4 agents, and set up the environment with interaction between 5 characters including one human person (Figure 2).

III. ONLINE BARNGA WITH GROUP PRESSURE

A. Cross-Cultural Simulation Game BARNGA

The authors have been developed *online BARNGA* which can provide not only human-to-human but also human-agent cross-cultural communication on online environment based on original *BARNGA*.

We used *online BARNGA* in this research in order to investigate an influence of the group pressure made by multiple life-like agents. In the following sections, we first explain about a trick-taking game conducted in *BARNGA* and then that is followed by an explanation about *BARNGA* itself. Afterward, *online BARNGA* is explained.

A trick-taking game is a card game. In general card games, the mark of each card, Spade, Heart, Club, and Diamond, is called a suite. The figures of each of face cards, Jack, Queen, King, and Ace, are called ranks. In this game, each player receives the same number of cards and the game is continued repeatedly until each person has used on the cards in their hand. In a trick, the dealer leads and other players do the same in order one by one. After all the players have played a card, the player who led the strongest card in that round wins the trick. Then the winner takes all the cards played in that trick. This is referred to as taking the trick and this is repeated until all the cards have been played and all the tricks taken. The player who obtains the largest number of cards becomes the winner of the trick-taking game.

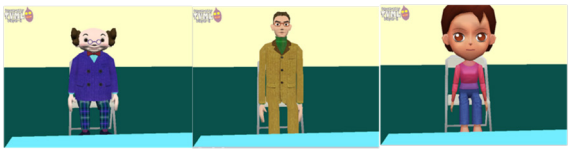

Agent A Male animation agent | Agent B Male real agent | Agent C Female animation agent

Figure 1. Life-like Agents based on TVML

Figure 2. Group Pressure based on Life-like Agents

The ranking of cards in trick-taking games varies depending on the game variation. Some trick-taking games contain trumps. A trump is a special suit of card set in advance, which is stronger than any other suits.

BARNGA is a simulation game, aiming at realizing a virtual cross-cultural experience. In this game, the rules of a card game are used to resemble a culture, and players can be surprised when they notice the differences in rules so as to experience culture shock.

The rules of *BARNGA* are simple and small in size compared to general social norms, and they are inadequate for recreating a society. However, this game contains coping problem in group society on which this research puts its focus. For this reason, we adopted this game since the acquisition of adaptability of group by players can be adequately observed.

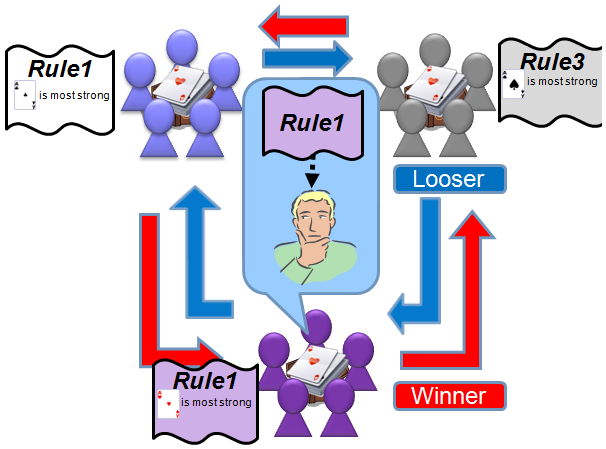

Figure 3. How a trade is done

The following explains the game content. During the game, players cannot converse. Therefore, players need to use nonverbal information such as physical gestures in order to convey their thoughts. Multiple tables are set in this game with four or five players at each table. An information sheet that contains the rules of this card game (initial rules) is distributed to each player when all the players have been seated. What is important in this game is that the game rules distributed to the players at this point vary slightly depending on each table. The differences in rules are simple regarding the types of trumps and rankings of strong cards. However, the players do not know that the rules vary slightly depending on each table. When all the players have finished reading the rules, the rule sheets are collected before the game is started. This means that the players cannot refer to the rules during the game. In this research, these small differences of the rules shows tacit rule. The players should acquire these rules actively. On the other hand, the common rules show regulations. All players acquired these rules passively in advance.

The game is played by the players on the same table. When the game advances to a certain degree, the game is stopped and those players winning and losing the most are moved to other tables by trading (Figure 3). After players have been traded, the game is restarted at each table. At this time, the traded players should experience discomfort because at the new tables, the game advances based on the different rules from the tables where they were previously seated. Similarly, those players that are not traded also feel something strange toward behavior of the new players that join in their table. *BARNGA* prohibits any conversations among players during the game. To ease this feeling of strangeness, the players need to observe the behavior and movements of the other players around them and use nonverbal information such as gestures in order to advance the game. In *BARNGA*, this feeling of strangeness is regarded as a cross-cultural experience.

The tacit rules we defined before [2] in *BARNGA* can be considered to be differences in rules. Given that, observing behavior of the players in this game serves to monitor the acquisition of tacit rules. *BARNGA* has also been utilized for agent research of group adaptability. However, interactions between players in this game are ambiguous, which makes it difficult for us to obtain and secure behavioral data from players during the game.

For this reason, we have developed *online BARNGA* in order to record behavioral data of players and clarify the interactions between players.

B. *Online BARNGA*

Going online with *BARNGA* has introduced the determination methods of winners and the scoring system into *BARNGA*, in order to realize clear interactions between players and to record the behavioral data of players. This adjustment for scoring can generate not only tacit rules as regulations, but also tacit rules as morality. In *online BARNGA*, each player joins in the game by connecting their individual computers to the server online. The gaming interface as shown in Figure 4 is displayed on each individual computer, and each player participates in the game on this interface. On the server side, the state of each player (hand, stock, and ranking) and player behavior (card led, and winner determination) are recorded as log data. Moreover, the introduction of clear determination methods for winners can offer social behavior of players as data. To realize this function, a scoring system has been introduced. The procedures of determining the winners and the flow of scoring transitions are shown as follows:

1) The dealer is selected from the table.
2) The dealer leads and the other players also play in order.
3) The dealer determines the winner.
4) The winner can get the Winner Point.
5) Non-dealers decide if they follow the decision or make complaints against the decision.
6) A non-dealer that made a complaint is given a deduction of Expense Points as a complaint cost.
7) The dealer and the winner are given a deduction in their Penalty Points on which the percentage of complaints is weighed.
8) A player that makes a complaint is given an increase in Bonus Points on which the percentage of complaints is weighed.

In *online BARNGA*, the parameters design in which the value of each score can be changed allows game designers to create group conditions. In the experiment we conducted, three kinds of group conditions were configured.

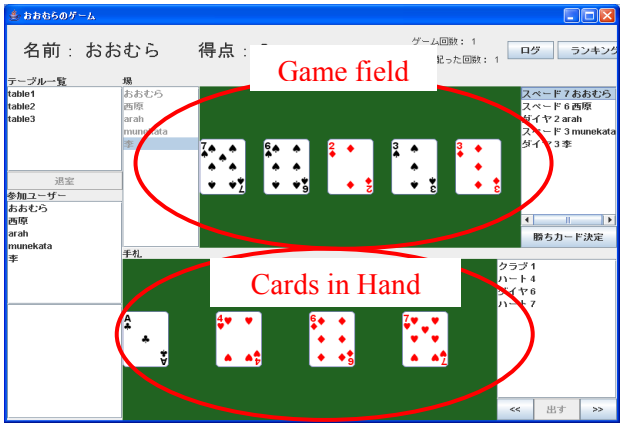

Figure 4. *Online BARNGA* Interface

C. Setting of Social Group Situation on Game

As to group conditions in the game, the following three settings which previous research [10] adopted were prepared. Standing on the viewpoint of group adaptability, we were able to examine the differences in player behavior under these conditions.

(1) Ordered condition:

This is a usual game condition before trades are conducted. Players can earn their scores by accumulating their Winner Points if they obediently follow the initial rules when leading by drawing a card necessary for winning the game. No penalty is charged by the group, there is no need to make complaints. The players almost never need to worry during the game.

(2) Cross-cultural condition:

Under this condition, only one player joins in the table traded from another table. The remaining four players on this table follow the same rules, so that there should be a variance due to the differences in initial rules. Observing behavior of other players, the traded player needs to learn the differences in the rules quickly, as well as to understand the rules commonly followed among other players at this table. The traded player needs to be free from the initial rules and take actions to learn the new rules. This should be the key to increase his score. The game result significantly varies depending on the level of player's group adaptability.

(3) Chaotic condition:

Under this condition, including the player, two other players also move in to a new table because of being traded. Three initial rules are now mixed together at this table, and high penalties also exist. At the same time, it is very hard to obtain Winners Points in a strategic sense. On the other hand, making complaints becomes a tacit rule since many complaints come to be made by players in this condition. It makes it possible for players to earn better scores by accumulating Bonus Points; however, this tacit rule is regarded as a new group rule.

D. Making Profiles based on Behavioral Logs

Behavioral logs of players obtained in *online BARNGA* consist of complaint rate, initial rule dependency rate, and acquired points. These logs can be recorded according to each social group condition. Examining these logs allow us to measure the group adaptability of players.

(1) Complaint rate (CR):

This rate indicates the probability of whether to make a complaint or not where the winner determination made by other players differs from the player's own win-loss standard. The greater this rate becomes, the more complaints the players make.

(2) Initial rule dependency rate (IR):

This rate indicates the probability of whether the complaint made by a player is dependent on the initial rules that the player follows. In the ordered condition, the greater this rate becomes, the more likely the player's behavior follows the initial rules. In the cross-cultural condition or the chaotic condition, however, the greater this rate becomes, the more the player is bound by the initial rules. This means that the player does not deal with social changes in a flexible way and continues to have headstrong attitudes.

(3) Thinking time (TT):

This is a time spent by a player in deciding whether to make a complaint or not. In the ordered condition, this time shows the discretion of individuals in thinking, that is how carefully one makes a usual decision. However, in the cross-cultural or the chaotic conditions, the longer this time is taken, the more the player thinks of dealing with a new condition in some way, thus learning the differences in the rules. This time is categorized into Total Thinking Time (TTT) and Total Thinking of Complaints (TTC).

(4) Acquired point (AP):

This indicates the points acquired by a player during the game. In the ordered condition, the player can acquire points by obediently following the rules. However, in the cross-cultural condition, the player is able to come to acquire points if he learns the differences in the rules, by demonstrating behavior that follows the new rules under the new situation and stops making complaints. On the other hand, in the chaotic condition, since there are three initial rules existing, it is difficult to learn and follow the new rules under the new situation. This is because all the players seating at the same table need to understand their initial tables (before trades are conducted twice) at the onset of the game, learning that the rules vary depending on each table. For this reason, strategic acquisition of Winner Points is difficult. However, the number of complaints made by other players naturally increases. If players can notice that Bonus Points for complaints are given every time, they can learn the tacit rule to make complaints. As a result, they can increase their scores.

IV. EXPERIMENTS

The purpose of the experiments is to investigate an influence of the group pressure made by multiple life-like agents by using *online BARNGA*.

A. Setting of Experiments

The procedures of the experiment are as follows. Three tables were prepared with 5 players at each table, a total of 15 players were allocated. Of the 15 players, one player was the test subject. The four life-like agents based on TVML works on the table with a subject and express gestures according to behavior of the player.

In the experiments, we compare between the results with group pressure by life-like agents (experimental group) and without group pressure (control group). The expressed gesture is anger face to subject when an agent player claims to judgment of dealer. If four life-like agents claimed to a player then the agents glare at the player with scary eyes.

During one turn, each player had a hand of five cards and did the trick-taking game for five sessions. Each test subject followed the following procedures to participate in the game.

1) The player does the game two sessions in the ordered condition.
2) Trades are made, and three members including the test player moves to other tables.
3) The player does the game two sessions in the cross-cultural condition.
4) Trades are made, and nine members including the test player move to other tables.
5) The player does the game two sessions in the chaotic condition.

The test subjects were 10 graduate students. TABLE I and TABLE II show the scoring settings and initial rules, respectively. All the test subjects answer questionnaires after the game has finished. Figure 5 shows the appearances of the experiments.

TABLE I. SCORING SETTINGS

Point	Description	Score
Winner Points	Winner's point	300
Penalty Points for the Winner	Penalty point against the dealer	100
Penalty Points for the Dealer	Penalty point against the winner	50
Bonus Points	Bonus point obtained in accordance with complaints	160
Expense Points	Point consumed every time a complaint is made	20

TABLE II. DIFFERENCES IN THE INITIAL RULES

	Trump	Ranking
Table 1	Heart	7>6>5>4>3>2>A
Table 2	Spade	A>7>6>5>4>3>2
Table 3	Club	2>A>7>6>5>4>3

B. Hypothesis

In the experiments, we validate following hypothesis.

1) Experimental group tends to group adaptation.

2) Experimental group tends to behave carefully with time and care compared with control group.

3) Experimental group tends to aqcuire game points compared with control group.

C. Experimental Results

Figure 6, 7, 8 and 9 show the experimental results. In the Figure 6, total thinking time (TTT) and thiking time of the claim (TTC) are not significantly different between groups. However, experimental group in both of time shows less 30 seconds on an average.

In Figure 7, experimental group in Game 1 (*Ordered condition*) shows less 50 seconds in TTT. Game 1 is significantly different between groups. In Figure 8, Game 1 shows more 5 seconds, Game 2 (*Cross-cultural condition*) and Game 3 (*Chaotic condition*) shows less 22 seconds and less 17 seconds respectively in TTC. In Figure 9, experimental group aqcuired 275 AP.

As a result, hypothesis 1) and 3) are supported and hypothesis 2) is not supported. In considersation of the results of hypothesis 2), we prospected experimental group spend much time in order to recognize emotional information of the agent players tuitively. In reverse the group can be available to cope with judgement of behavior with less time, because the group can observe and acquire the atmosphere as emotional information of a group.

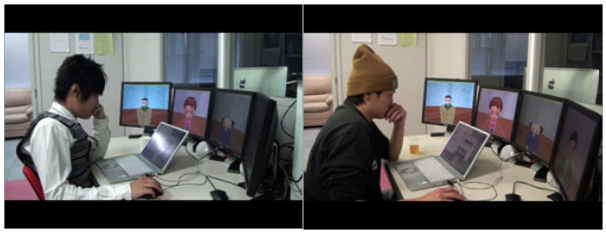

Figure 5. Appearances of The Experiments

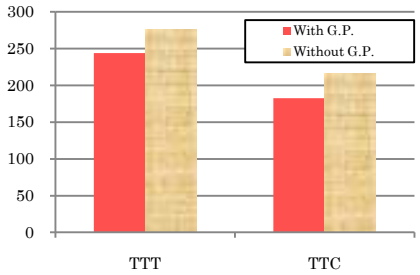

Figure 6. Thinking Time (TT) [sec]

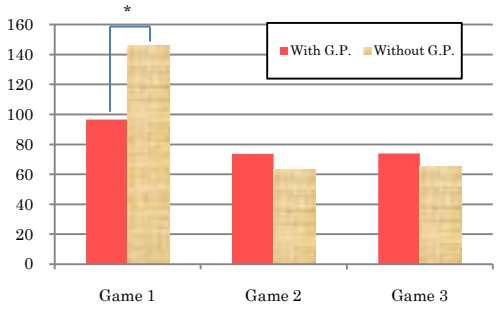

Figure 7. Total Thinking Time (TTT) [sec]

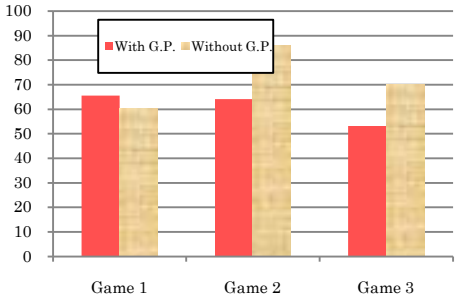

Figure 8. Thinking Time of Claim (TTC) [sec]

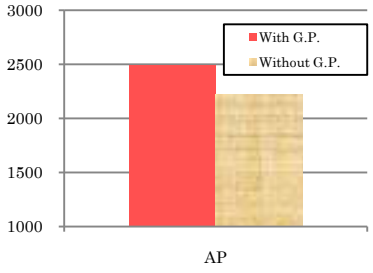

Figure 9. Acquired Points (AP)

V. CONCLUSION

We developed a virtual group pressure by using multiple life-like agents and investigate the influence to human. We verify if the group pressure made by multiple life-like agents exert an influence on the judgment of player by using the cross-cultural simulation game we developed before.

In near future, we will create a model of the mechanism of the group pressure constructed by the combination of the expressions of life-like agents.

REFERENCES

[1] S. Thiagarajan, "BARNGA: A Simulation Game on Cultural Clashes," *Intercultural Press Inc.*, 2006.

[2] H. Ohmura, D. Katagami, and K. Nitta, "Development of Social Adaptive Agents in Simulation Game of Cross-cultural Experience," *FUZZ-IEEE*, pp.981-986, 2009.

[3] D. Katagami, H. Ohmura, and K. Nitta, "Investigation of Social Adaptive Skills by Cross-cultural Simulation Game and KiSS-18," *Human-Agent Interaction Symposium 2009*, 2009. *(Japanese)*

[4] B. A. Kendon, "Do Gestures Communicate?," *A Review Research in Language and Social Interaction*, vol.27, no.3, pp.175-200, 1994.

[5] A. Mehrabian, "Silent messages," Wadsworth, 1971.

[6] A. Ito, K. Kakusho, and T. Minoh, "Control of Atmosphere Based on the Intimacy Equilibrium Model During the Dialogue Between Computer Graphics Animated Characters," *Technical report of IEICE.*, HIP2002-69, pp.37-42, 2003. *(Japanese)*

[7] I. Saito, "Phychology on Human Relationships", *seishinshobo*, 2007. *(Japanese)*

[8] S. E. Ash, "Effects of group pressure upon the modification and distortion of judgements", *In D. Cartwright & A. Zander (eds.)*, Group dynamics, Harper. 1953.

[9] TVML: http://www.nhk.or.jp/strl/tvml/

[10] D. Katagami, and T. Huynhvan, "Group Pressure Generation of Multi-Agents on Cross-cultural Simulation Game," *Human-Agent Interaction Symposium 2010*, 2010 *(Japanese)*

2011 IEEE International Conference on Fuzzy Systems
June 27-30, 2011, Taipei, Taiwan

H_2 Guaranteed Cost of Uncertain Continuous T-S Fuzzy Systems by Multiple Lyapunov Function Approach

Wen-Ren Horng, Chun-Hsiung Fang, Ching-Hsiang Lee and Jyh-Horng Chou*
*Department of Electric Engineering,
National Kaohsiung Univ. of Applied Sciences,
415 Chien-Kung Road, Kaohsiung 807,
Taiwan, R.O.C
Email: choujh@cc.kuas.edu.tw

***Abstract*—In this paper, the H_2 guaranteed cost control problem of uncertain continuous T-S fuzzy systems is investigated. We approach this problem by considering the multiple Lyapunov function and utilizing the non-PDC controller. Sufficient conditions for ensuring certain H_2 cost as well as asymptotical stability are derived and expressed in terms of LMIs. Unlike existing approaches, the assumption of known upper bounds on the time derivative of membership functions, which is quite unrealistic, is not required anymore in the present one. Numerical examples are also given to demonstrate our approach has lower H_2 guaranteed cost as well as control force in comparison with the existing ones.**

***Index Terms*—linear matrix inequality, T-S fuzzy model, H_2 guaranteed cost control.**

I. Introduction

In general, control of nonlinear systems can be a challenge task. The mathematic structure of non-linear systems makes the analysis and controller design very difficult. For the past decades, T-S fuzzy model [10] of non-linear systems has been demonstrated to be the powerful approach in non-linear system analysis and controller design. The T-S fuzzy is described fuzzy IF-THEN rules, which represent the linear input-output relations of nonlinear control systems. The main advantage of T-S fuzzy model is to express of the local dynamics of each fuzzy rule by linear system modeling to reduce the complexity of non-linear system analysis and controller design.

Stability and performance are most important issues in control systems. Once the the non-linear systems are expressed by T-S fuzzy model, stability analysis and performance design can be expressed by *linear Matrix Inequalities* (LMIs) [11], [1] and then can solved by available software. For example, the authors in [7], [5] studied the stabilization of T-S fuzzy systems. there also has been numerous results reported for design controller to ensure system performance such as mixed H_2/H_∞ [12], H_∞ [7], [8], [13], [22] and H_2 [19], [21]. On the other hand, the precise modeling of nonlinear system is sometimes impossible or difficult to achieve. The parametric uncertainties are always accompanied the system. The parametric uncertainties may degrade the system performance or even destabilize the system. Therefore, there are many researchers focusing on the issues such as robust stabilization, robust H_∞ and guaranteed cost of H_2 [19] to ensure the system stability with adequate performance level subjecting uncertainties. Comparing to the rich results in robust stabilization and robust H_∞ control for T-S fuzzy system, there are few results [19], [25] regarding to H_2 guaranteed cost control for continuous-time T-S fuzzy systems. Furthermore, although [19], [25] proposed solutions to deal with H_2 guaranteed cost control of T-S fuzzy systems, there are still some open issues to be addressed. The most results are derived based on a quadratic Lyapunov function or so-called "common" Lyapunov function(CLF) or single Lyapunov function (SLF); that is to search single P matrix in Lyapunov function to satisfy all LMI conditions. This is too conservative for some cases, especially higher number of fuzzy rules, due to less degree of freedom on P matrix. To overcome this, a nonquadratic Lyapunov function [15] or multiple Lyapunov function (MLF) [18] (or fuzzy Lyapunov function), in which the membership functions are contained , is proposed to deal with discrete-time T-S fuzzy systems . In addition, in [18], a multiple Lyapunov function is also applied to study stability of T-S fuzzy systems. From the numerical examples shown in the report [18], this type of Lyapnov function further relaxes the conservatism of stability and improve the system performance. The drawback of the approach in [18] is the upper bounds of time derivative on membership functions $|\dot{h}_i(f(t))|$ must be known as prior to derive the stability conditions. In [24], [27], [26], the information of time derivative on membership functions must be evaluated in advance as well. Finding information of time derivative on membership functions is difficult or unrealistic in some cases. Thus in [21], a line integral of multiple Lyapunov function is employed which leads to the derivative of membership functions vanishing. However, the P_i matrices in Lyapunov function must have a special structure and the conditions for controller design are in terms of BMIs. Therefore, no efficiency software exists to solve them.

Unlike the previous approaches, we introduce a slack matrix and employ the property $\sum_{i=1}^{r}(h_i(t) \pm \dot{h}_i(t)) = 1$ to deal with time derivative of membership functions. The multiple Lyapunov function and nonparallel distributed compensation

978-1-4244-7316-8/11/$26.00 ©2011 IEEE

(non-PDC) controller [18], [15] are proposed to derive H_2 guaranteed cost of uncertain T-S fuzzy system and to ensure closed-loop system asymptotically stable for all admissible parametric uncertainty. The conditions to ensure upper bound of H_2 cost and globally asymptotically stable are all in terms of LMI form. Thus, the guaranteed minimum H_2 cost can be reformulated as minimizing the upper bound of cost subjecting to LMI constraints and becomes a generalized eigenvalue problems (GEVP), which can be solved by efficiency tools such as MATLAB LMI toolbox.

The rest of paper is organized as follows. In section 2, the problem statement is made. Section 3 is the main results of this paper. The main theorem of guaranteed H_2 cost is presented in this section. Then numerical examples to demonstrate our result are given in section 4. Finally, conclusion are made in section 5.

The notation used in this paper is quite standard. $(X+\bigstar) = X + X^T$. $X > 0$ (or $X \geq 0$) means X is positive definite (or positive semidefinite). Likewise, $X < 0$ (or $X \leq 0$) means X is negative definite (or negative semidefinite). For shorthand, $h(x(t))$ is denoted by h; " $*$ " is denoted to be the symmetric term in the symmetric matrix.

II. Problem Formulation and Preliminary

We begin with considering a class of uncertain continuous non-linear systems which can be governed by following IF-THEN rule based T-S fuzzy system,
Plant Rule i: IF $f_1(x(t))$ is M_1^i and $\ldots$ and $f_s(x(t))$ is M_s^i THEN

$$\begin{array}{rcl} \dot{x}(t) & = & (A_i + \Delta A_i)x(t) + (B_{ui} + \Delta B_{ui})u(t), \\ z(t) & = & (C_{zi} + \Delta C_{zi})x(t) + (D_{zui} + \Delta D_{zui})u(t), \end{array} \quad (1)$$

where $x(t) \in \mathbb{R}^{n\times n}$ is state vector with $x(0) = x_0$, $u(t) \in \mathbb{R}^m$ is the input vector, $z(t) \in \mathbb{R}^p$ is the controlled output vector, $A_i \in \mathbb{R}^{n\times n}$, $B_{ui} \in \mathbb{R}^{n\times m}$, $C_{zi} \in \mathbb{R}^{n\times p}$, and $D_{zui} \in \mathbb{R}^{p\times m}$ are known system matrices, M_j^i denotes an j-based fuzzy set used for the ith fuzzy rule, θ_i is $i$the premise variable, $i = 1, \ldots, r$ and r is the total number of fuzzy rules. Assume ΔA_i, ΔB_{ui}, ΔC_{zi} and ΔD_{zui} represent unknown time-varying parametric uncertainty with following structure

$$\begin{bmatrix} \Delta A_i & \Delta B_{ui} \\ \Delta C_{zui} & \Delta D_{zui} \end{bmatrix} = \begin{bmatrix} H_{xi}F_\Delta \begin{pmatrix} E_{xi} & E_{ui} \end{pmatrix} \\ H_{zi}F_\Delta \begin{pmatrix} E_{zi} & E_{zui} \end{pmatrix} \end{bmatrix}, \quad (2)$$

where H_{xi}, E_{xi}, E_{ui}, E_{zi} and E_{zui} are known matrices with appropriate dimension. F_Δ is unknown matrices with satisfying property

$$F_\Delta \in \Omega_F := \{F^T(t)F(t) < I\}$$

and the elements of $F(t)$ are Lebesgue measurable.

Given a pair of $x(t)$, $u(t)$, the final outputs of fuzzy system can be inferred as:

$$\dot{x}(t) = \sum_{i=1}^{r} h_i((A_i + \Delta A_i)x(t) + (B_{ui} + \Delta B_{ui}))u(t) \quad (3)$$

$$z(t) = \sum_{i=1}^{r} h_i((C_{zi} + \Delta C_{zi})x(t) + (D_{zui} + \Delta D_{zui}))u(t), \quad (4)$$

with $x(0) = x_0$ and $i = 1, \ldots, r$ in which $f(x(t)) = \left[f_1(x(t)),\ f_2(x(t)),\ \ldots,\ f_s(x(t))\right]$ $\mu_i(f(x(t)) = \prod_{j=1}^{s} M_i^j(f_j(x(t))), h_i(x(t)) = \mu_i(f(x(t)))/\sum_{i=1}^{r}\mu_i(f(x(t)))$. In this paper, we will assume $\mu_i(f(x(t))) \geq 0$ for all t. Then we have following properties

$$h_i(x(t)) \geq 0, i = 1, \ldots, r, \text{ and } \quad \sum_{i=1}^{r} h_i(x(t)) = 1$$

for all t.

Next we define H_2 performance index function

$$J(H_2) = \int_0^\infty z^T(t)z(t)dt. \quad (5)$$

The goal is to design a feedback controller to the system described by (3) such that the closed-loop system is asymptotically stable and the upper bound of $J(H_2)$ is as small as possible for all admissible uncertainty described by (2).

Before we start to state our main results, two lemmas, which are repeatedly used through the derivation of main results, are given.

Lemma 1. *Schur Complement: Given matrices $Q(x) = Q^T(x)$, $R(x) = R^T(x)$, and $S(x)$ with appropriate dimensions*

$$\begin{bmatrix} Q(x) & S^T(x) \\ S(x) & R(x) \end{bmatrix} < 0$$
$$\iff \quad R(x) < 0 \quad \textit{and} \quad Q(x) - S^T(x)R^{-1}(x)S(x) < 0.$$

Lemma 2. *Given matrices S, H and E with proper dimensions and symmetric matrix S. Following inequality holds*

$$S + HFE + E^TF^TH^T < 0$$

for F satisfying $F^TF \leq R$ if and only if there exists $\varepsilon > 0$ such that

$$S + \begin{bmatrix} \varepsilon^{-1}E^T & \varepsilon H \end{bmatrix} \begin{bmatrix} R & 0 \\ 0 & I \end{bmatrix} \begin{bmatrix} \varepsilon^{-1}E \\ \varepsilon H^T \end{bmatrix} < 0.$$

III. Non-PDC Nonlinear Controller Synthesis

The nonlinear controller for the nonlinear uncertain systems is type of Non-PDC controller [17] described by (3)is proposed as

$$u(t) = \sum_{i=1}^{r} h_i F_i P^{-1}(x(t))x(t), \quad (6)$$

and consider a multiple Lyapunov function

$$V(x(t)) = x^T(t)P^{-1}(x(t))x(t) \quad (7)$$

where $F_i \in \mathbb{R}^{m\times n}$ is state feedback gain and $P(x(t)) = \sum_{j=1}^{r} h_j(x(t))P_j$, $P_j = P_j^T \in \mathbb{R}^{n\times n} > 0$, $j = 1,\ldots,r$. Note that here F_i and P_i are some matrices to be determined.

Remark 3. *According to $P_j > 0, j = 1,\ldots,r$ and the property of h_i, the invertibility and the positive definiteness of P are ensured, i.e P^{-1} exists. In addition, by the property of $h_i(x(t)) \geq 0$ and $\sum_{i=1}^{r} h_i(x(t)) = 1$, we have $V(x) > 0$ $\forall x(t) \neq 0$ as well.*

Remark 4. *If let $P_1 = P_2,\ldots,= P_r = \bar{P}$, one has $P = \bar{P}$. With this assumption, multiple Lyapunov function $V(x(t))$ is reduced to common Lyapunov function and Non-PDC control law $u(t)$ is reduced to PDC one. Thus multiple Lyapunov function is more general than common Lyaupunov function.*

The following theorem gives sufficient conditions to ensure T-S fuzzy system represented by (3)) is globally asymptotically stable and H_2 cost is bounded by a prescribed level β.

Theorem 5. *Assume the membership functions, h_i, $i = 1,\ldots,r$, are differentiable. The system described by (3) is stable and $J(H_2) < \beta$ if there exist $\varepsilon_{xii} > 0$, $\varepsilon_{xij} > 0$, $\varepsilon_{zij} > 0$, $P_i > 0, F_i, i = 1,\ldots,r; Q > 0; S > 0, X_{ii}, i = 1,\ldots,r; X_{ij} = X_{ji}^T, i < j, i, j = 1,\ldots,r$; $X_{(r+i)j} = X_{j(r+i)}^T, i = 1,\ldots,r; X_{(r+i)(r+i)}, i = 1,\ldots,r; X_{(r+i)(r+j)} = X_{(r+j)(r+i)}^T, i < j, i, j = 1,\ldots,r$ and satisfy*

$$\begin{bmatrix} \Psi_{ii} + \varepsilon_{xii}H_{xi}H_{xi}^T & * \\ E_{xi}P_i + E_{ui}F_i & -\varepsilon_{xii} \end{bmatrix} < 0,\ i = 1,\ldots,r, \tag{8}$$

$$\begin{bmatrix} \Psi_{ij} + \varepsilon_{xij}H_{xi}H_{xi}^T + \varepsilon_{xji}H_{xj}H_{xj}^T & * & * \\ E_{xi}P_j + E_{ui}F_j & -\varepsilon_{xij}I & 0 \\ E_{xj}P_i + E_{uj}F_i & 0 & -\varepsilon_{xji}I \end{bmatrix} < 0,$$
$$i, j = 1,\ldots,r, i < j, \tag{9}$$

$$-P_i < X_{(r+i)j} + X_{(r+i)j}^T,\ i, j = 1,\ldots,r, i < j, \tag{10}$$

$$-S < X_{(r+i)(r+i)},\ i = 1,\ldots,r, \tag{11}$$

$$-2S < X_{(r+i)(r+j)} + X_{(r+i)(r+j)}^T,\ i, j = 1,\ldots,r, i < j, \tag{12}$$

$$\begin{bmatrix} -Q & * & * \\ C_{zi}P_j + D_{zui}F_j & -I + \varepsilon_{zij}H_{zi}H_{zi}^T & 0 \\ E_{zi}P_j + E_{zui}F_j & 0 & -\varepsilon_{zij}I \end{bmatrix} < 0,$$
$$i, j = 1,\ldots,r, \tag{14}$$

$$\begin{bmatrix} \beta & x(0)^T \\ x(0) & \sum_i h_i(x(0))P_i \end{bmatrix} > 0. \tag{15}$$

where

$$\Psi_{ii} = ((A_iP_i + B_{ui}F_i) + \bigstar) + Q + S - X_{ii}$$
$$\Psi_{ij} = ((A_iP_j + B_{ui}F_j + A_jP_i + B_{uj}F_i) + \bigstar) + 2Q + 2S - X_{ij} - X_{ij}^T$$

Proof: For simplicity, define

$$\begin{bmatrix} A_i + \Delta A_i & B_{ui} + \Delta B_{ui} \\ C_{zi} + \Delta C_{zi} & D_{zui} + \Delta D_{zui} \end{bmatrix} = \begin{bmatrix} \bar{A}_i & \bar{B}_{ui} \\ \bar{C}_{zi} & \bar{D}_{zui} \end{bmatrix}$$

With the feedback control law (6), the closed loop becomes

$$\dot{x}(t) = \sum_{i=1}^{r}\sum_{j=1}^{r} h_ih_j(\bar{A}_i + \bar{B}_{ui}F_jP^{-1})x(t)$$
$$z(t) = \sum_{i=1}^{r}\sum_{j=1}^{r} h_ih_j(\bar{C}_{zi} + \bar{D}_{zui}F_jP^{-1})x(t).$$

Next define a function $H(x)$

$$H(x) \triangleq \dot{V}(x) + z^T(t)z(t). \tag{16}$$

By taking derivative on $V(x)$, we obtain

$$\begin{aligned} &\dot{V}(x) + z^T(t)z(t) \\ &= \sum_{i}^{r}\sum_{j}^{r} h_ih_j(x^T(t)(\bar{A}_i + \bar{B}_{ui}F_jP^{-1})^TP^{-1}x(t) \\ &+ x^T(t)P^{-1}(A_i + B_{ui}F_jP^{-1})x(t) - x^T(t)P^{-1}\dot{P}P^{-1}x(t) \\ &+ x^T(t)(\bar{C}_{zi} + \bar{D}_{zui}F_jP^{-1})^T(\bar{C}_{zi} + \bar{D}_{zui}F_jP^{-1})x(t)) \end{aligned} \tag{17}$$

Let $y(t) = P^{-1}x(t)$. Thus, (17) can be rewritten as

$$\begin{aligned} H(x) = &\sum_{i=1}^{r}\sum_{j=1}^{r} h_ih_jy^T(t)((\bar{A}_iP_j + \bar{B}_{ui}F_j) + (\bigstar))y(t) \\ &- \sum_{i=1}^{r}\sum_{j=1}^{r} \dot{h}_ih_jy^T(t)P_iy(t) \\ &+ y^T(t)\left(\sum_{i=1}^{r}\sum_{j=1}^{r} h_ih_j(\bar{C}_{zi}P_j + \bar{D}_{zui}F_j)^T\right. \\ &\left.\cdot \sum_{i=1}^{r}\sum_{j=1}^{r} h_ih_j(\bar{C}_{zi}P_j + \bar{D}_{zui}F_j)\right)y(t). \end{aligned} \tag{18}$$

Since $\sum_{i=1}^{r} \dot{h}_i = 0$, we have the properties $\sum_{i=1}^{r}(h_i + \dot{h}_i) = \sum_{j=1}^{r}(h_j - \dot{h}_j) = 1$. By introducing slack variable $S > 0$, and

$$\begin{bmatrix} X_{11} & \cdots & * & * & \cdots & * \\ \vdots & \ddots & \vdots & \vdots & \ddots & \vdots \\ X_{r1} & \cdots & X_{rr} & * & \cdots & * \\ X_{(r+1)1} & \cdots & X_{(r+1)r} & X_{(r+1)(r+1)} & \cdots & * \\ \vdots & \ddots & \vdots & \vdots & \ddots & \vdots \\ X_{(r+1)r} & \cdots & X_{(r+r)r} & X_{(r+r)(r+1)} & \cdots & X_{(r+r)(r+r)} \end{bmatrix} < 0, \tag{13}$$

adding $\sum_{i=1}^{r}\sum_{j=1}^{r}(h_i+\dot{h}_i)(h_j-\dot{h_j})S>0$ to (18), one has

$$\begin{aligned} H(x) < & \sum_{i=1}^{r}\sum_{j=1}^{r} h_i h_j y^T(t)((\bar{A}_i P_j + \bar{B}_{ui}F_j) + (\bigstar) \\ & + Q + S)y(t) - \sum_{i=1}^{r}\sum_{j=1}^{r}\dot{h}_i h_j y^T(t)(P_i + S - S)y(t) \\ & - \sum_{i=1}^{r}\sum_{j=1}^{r}\dot{h}_i\dot{h}_j y^T(t)Sy(t) - y^T(t)Qy(t) \\ & + \sum_{i=1}^{r}\sum_{j=1}^{r} y^T(t)h_i h_j(\bar{C}_{zi}P_j + \bar{D}_{zui}F_j)^T \\ & \cdot \sum_{i=1}^{r}\sum_{j=1}^{r} h_i h_j(\bar{C}_{zi}P_j + \bar{D}_{zui}F_j)y(t) \\ & = \sum_{i=1}^{r} h_i^2 y^T(t)((\bar{A}_i P_i + \bar{B}_{ui}F_i) + (\bigstar) + Q + S)y(t) \\ & + \sum_{i=1}^{r}\sum_{i<j}^{r} h_i h_j y^T(t)((\bar{A}_i P_j + \bar{B}_{ui}F_j) + (\bar{A}_j P_i + \bar{B}_{uj}F_i)) \\ & + \bigstar) + 2Q + 2S)y(t) - \sum_{i=1}^{r}\sum_{j=1}^{r}\dot{h}_i h_j y^T(t)(P_i)y(t) \\ & - \sum_{i=1}^{r}\dot{h}_i^2 y^T(t)Sy - \sum_{i=1}^{r}\sum_{i<j}^{r}\dot{h}_{i=1}^{r}\dot{h}_j y^T(t)2Sy(t) \\ & - y^T(t)Qy + \sum_{i=1}^{r}\sum_{j=1}^{r} y^T(t)h_i h_j(\bar{C}_{zi}P_j + \bar{D}_{zui}F_j)^T \\ & \cdot \sum_{i=1}^{r}\sum_{j=1}^{r} h_i h_j(\bar{C}_{zi}P_j + \bar{D}_{zui}F_j)y(t). \end{aligned}$$

On the other hand, if (8) is satisfied, by Schur Complement, we have

$$\begin{aligned} & \Psi_{ii} + \varepsilon_{xii}H_{xi}H_{xi}^T + (1/\varepsilon_{xii})(E_{xi}P_i + E_{ui}F_i)^T \\ & \quad \cdot (E_{xi}P_i + E_{ui}F_i) < 0, \end{aligned} \tag{19}$$

which is further equivalent to

$$\begin{aligned} & (A_i P_i + B_{ui}F_i + H_{xi}F_\Delta(E_{xi}P_i + E_{ui}F_i) + (\bigstar)) \\ & \quad + Q + S < X_{ii} \end{aligned} \tag{20}$$

for all $F_\Delta(t) \in \Omega$ by Lemma 2.

Furthermore, following the same manner, (9) is equivalent to

$$\begin{aligned} & \Psi_{ij} + \varepsilon_{xij}H_{xi}H_{xi}^T + (1/\varepsilon_{xij})(E_{xi}P_j + E_{ui}F_j)^T \\ & \cdot (E_{xi}P_j + E_{ui}F_j) + \varepsilon_{xji}H_{xj}H_{xj}^T \\ & + (1/\varepsilon_{xji})E_{xj}P_i + E_{uj}F_i)^T(E_{xj}P_i + E_{uj}F_i) < 0, \\ & \qquad i,j = 1,\ldots,r, i<j. \end{aligned} \tag{21}$$

By Lemma 2, (21) is equivalent to

$$\begin{aligned} & ((A_i + H_{xi}F_\Delta E_{xi})P_i + (B_{ui} + H_{xi}F_\Delta E_{ui})F_j + \\ & \quad (A_j + H_{xj}F_\Delta E_{xj})P_i + (B_{uj} + H_{xj}F_\Delta E_{uj})F_i) \\ & \quad + (\bigstar) + 2Q + 2S < X_{ij} + X_{ij}^T, \quad i,j = \ldots,r, i<j \end{aligned} \tag{22}$$

for all allowable F_Δ.

By (22) together with (10)-(13), one can readily obtain (23) as shown in the top of next page. Thus if (13) is held, we have $V(x) < 0\ \forall x(t) \neq 0$. This leads to imply the closed-loop system is asymptotically stable for all allowable F_Δ.

Next we consider the H_2 performance. By Lemma 1 Schur Complement, (14) can rewritten as

$$\begin{aligned} & \begin{bmatrix} -Q & * \\ C_{zi}P_j + D_{zui}F_j & -I \end{bmatrix} + \varepsilon_{zij}\begin{bmatrix} 0 \\ H_{zi} \end{bmatrix}\begin{bmatrix} 0 & H_{zi}^T \end{bmatrix} \\ & \qquad + (1/\varepsilon_{zij})\begin{bmatrix} (E_{zi}P_j + E_{zui}F_j)^T \\ 0 \end{bmatrix} \\ & \qquad \cdot \begin{bmatrix} E_{zi}P_j + E_{zui}F_j & 0 \end{bmatrix} < 0. \end{aligned} \tag{24}$$

Then, by Lemma 2, (24) is equivalent to

$$\begin{aligned} & \begin{bmatrix} -Q & * \\ C_{zi}P_j + D_{zui}F_j & -I \end{bmatrix} + (\begin{bmatrix} 0 \\ H_{zi} \end{bmatrix} F_\Delta \\ & \qquad \cdot \begin{bmatrix} E_{zi}P_j + E_{zui}F_j & 0 \end{bmatrix}) + (\bigstar) < 0. \end{aligned} \tag{25}$$

for all $F_\Delta \in \Omega$. Again (25) is equivalent to

$$-Q + (\bar{C}_{zi}P_j + \bar{D}_{zui}F_j)^T(\bar{C}_{zi}P_j + \bar{D}_{zui}F_j) < 0$$

by Schur Complement. Hence we have

$$\begin{aligned} & -y^T(t)Qy + \sum_{i=1}^{r}\sum_{j=1}^{r} y^T(t)h_i h_j(\bar{C}_{zi}P_j + \bar{D}_{zui}F_j)^T \\ & \qquad \cdot \sum_{i=1}^{r}\sum_{j=1}^{r} h_i h_j(\bar{C}_{zi}P_j + \bar{D}_{zui}F_j)y(t) < 0. \end{aligned}$$

Combining all together, we can obtain

$$\dot{V}(x(t)) + z^T(t)z(t) < 0 \tag{26}$$

$$V(x) < \begin{bmatrix} h_1 y \\ \vdots \\ h_r y \\ \dot{h}_1 y \\ \vdots \\ \dot{h}_r y \end{bmatrix}^T \begin{bmatrix} X_{11} & \cdots & * & * & \cdots & * \\ \vdots & \ddots & \vdots & \vdots & \ddots & \vdots \\ X_{r1} & \cdots & X_{rr} & * & \cdots & * \\ X_{(r+1)1} & \cdots & X_{(r+1)r} & X_{(r+1)(r+1)} & \cdots & * \\ \vdots & \ddots & \vdots & \vdots & \ddots & \vdots \\ X_{(r+1)r} & \cdots & X_{(r+r)r} & X_{(r+r)(r+1)} & \cdots & X_{(r+r)(r+r)} \end{bmatrix} \begin{bmatrix} h_1 y \\ \vdots \\ h_r y \\ \dot{h}_1 y \\ \vdots \\ \dot{h}_r y \end{bmatrix}. \quad (23)$$

Integrating both sides of (26) from 0 to ∞, we readily obtain

$$\int_0^\infty z^T(t)z(t)dt < V(x(0)) - V(\infty) < V(x(0)) = x(0)^T(\sum_{i=1}^r h_i(x(0))P_i)^{-1}x(0).$$

Therefore, if (15) is satisfied, we have $\int_0^\infty z^T(t)z(t) < \beta$. □
From theorem 5, to minimize H_2 cost (5) of system (3), we can reformulate the problem as

$$\min_{P_i, X_{ij}, Q, S, \varepsilon_{xij}, \varepsilon_{xji}, \varepsilon_{zij}} \beta \quad \text{subject to} \quad (8)-(15). \quad (27)$$

Remark 6. *[19] If the system is stochastic system, the cost function can be written as*

$$J(H_2) = \mathbb{E}\{z^T(t)z(t)\}, \quad (28)$$

where $\mathbb{E}$ is denoted as expectation operator. Furthermore if $x(0)$ is zero mean random variables and satisfies $\mathbb{E}\{x(0)x^T(0)\} = I$, the upper bound of cost can be expressed by

$$J(H_2) < \mathbb{E}\left\{x^T(0)(\sum_{i=1}^r h_i(x(0))P_i)^{-1}x(0)\right\} = \mathit{Trace}\{\bar{P}^{-1}\}. \quad (29)$$

Moreover, by introducing an auxiliary variable $U > 0$, $\min$ $\mathit{Trace}\{\bar{P}^{-1}\}$ subject to (8)-(15) can be equivalent to

$$\min_{P_i, X_{ij}, Q, S, U, \varepsilon_{xij}, \varepsilon_{xji}, \varepsilon_{zij}} \mathit{Trace}(U) \quad \mathit{subject\ to} \quad (8)-(15) \quad \mathit{and} \quad \begin{bmatrix} U & * \\ I & \bar{P} \end{bmatrix} > 0, \quad (30)$$

where $\bar{P} = \sum_{i=1}^r h_i(x(0))P_i$.

Theorem 5 can be specialized to conditions of systems without uncertainties by simply setting all uncertain matrices to 0. Thus following corollary is made.

Corollary 7. *For the systems without uncertainties, the (8), (9) and (14) are reduced to*

$$((A_iP_i + B_{ui}F_i) + \bigstar) + Q + S - X_{ii} < 0, \quad i = 1, \ldots, r, \quad (31)$$

$$((A_iP_j + B_{ui}F_j + A_jP_i + B_{uj}F_i) + \bigstar) + 2Q + 2S - X_{ij} - X_{ij}^T < 0, \ , i, j = 1, \ldots, r, i < j, \quad (32)$$

$$\begin{bmatrix} -Q & * \\ C_{zi}P_j + D_{zui}F_j & -I \end{bmatrix} < 0, \ , i, j = 1, \ldots, r. \quad (33)$$

IV. Illustrative Examples

To show the performance of our proposed T-S fuzzy controllers, two examples are given.One is for nominal systems. the other one is for the system with uncertainties.

A. Example 1

The example one is cart-pole-typed inverted pendulum problem [9]. In this example, we consider uncertain-free model. Its dynamic equation is given by

$$\ddot{\theta} = \frac{g\sin(\theta(t)) - aml\dot{\theta}^2(t)sin(2\theta(t))/2 - a\cos(\theta(t))u(t)}{4l/3 - aml\cos^2(\theta(t))}$$

where θ is angle of displacement in radians, M is the mass of cart, m is the mass of pendulum, g is the acceleration due to gravity, l is half length of pendulum, and $a = 1/(M+m)$. Here we chose $M = 8Kg$, $m = 2Kg$, $g = 9.8m/sec^2$, $l = 0.5m$. Its nonlinear model can be exactly represented by following T-S fuzzy rules,

Plant Rule1:
If $f_1(x(t))$ is M_1^1 and $f_2(x(t))$ is M_2^1 THEN

$$\dot{x}(t) = A_1x(t) + B_{u1}u(t)$$
$$z(t) = C_{z1}x(t) + D_{u1}u(t),$$

Plant Rule2:
If $f_1(x(t))$ is M_1^1 and $f_2(x(t))$ is M_2^2 THEN

$$\dot{x}(t) = A_2x(t) + B_{u2}u(t)$$
$$z(t) = C_{z2}x(t) + D_{u2}u(t),$$

Plant Rule3:
If $f_1(x(t))$ is M_1^2 and $f_2(x(t))$ is M_2^1 THEN

$$\dot{x}(t) = A_3x(t) + B_{u3}u(t)$$
$$z(t) = C_{z3}x(t) + D_{u3}u(t),$$

Plant Rule4:
If $f_1(x(t))$ is M_1^2 and $f_2(x(t))$ is M_2^2 THEN

$$\dot{x}(t) = A_4x(t) + B_{u4}u(t)$$
$$z(t) = C_{z4}x(t) + D_{u4}u(t),$$

in which $x(t) = \begin{bmatrix} x_1(t) & x_2(t) \end{bmatrix}^T = \begin{bmatrix} \theta & \dot{\theta} \end{bmatrix}^T$,

$$f_1(x(t)) = \frac{g - aml x_2^2(t)\cos(x_1(t))}{4l/3 - aml\cos^2(\theta(t))}\left(\frac{\sin(x_1(t))}{x_1(t)}\right),$$
$$f_2(x(t)) = \frac{-aml\cos(x_1(t))}{4l/3 - aml\cos^2(x_1(t))},$$
$$M_1^1(f_1(x(t))) = \frac{-f_1(x(t)) + 18}{9},$$
$$M_1^2(f_1(x(t))) = \frac{-f_1(x(t)) - 9}{9},$$
$$M_2^1(f_2(x(t))) = \frac{-f_2(x(t)) - 0.0052}{9},$$
$$M_2^2(f_2 x(t))) = \frac{-f_2(x(t)) + 0.1765}{0.1713},$$
$$A_1 = A_2 = \begin{bmatrix} 0 & 1 \\ 9 & 0 \end{bmatrix}, \quad A_3 = A_4 = \begin{bmatrix} 0 & 1 \\ 18 & 0 \end{bmatrix},$$

$B_{u1} = B_{u3} = \begin{bmatrix} 0 & -0.1765 \end{bmatrix}^T, B_{u2} = B_{u4} = \begin{bmatrix} 0 & -0.0052 \end{bmatrix}^T C_{z1} = C_{z2} = C_{z3} = C_{z4} = \begin{bmatrix} 1 & 0 \end{bmatrix}$, and $D_{zu1} = D_{zu2} = D_{zu3} = D_{zu4} = 0.001$.

After using proposed approach, LMI toolbox gives the minimized upper bound $\beta = 0.4938$, P_i matrices, and feedback gain F_i matrices,

$$P_1 = \begin{bmatrix} 11.0330 & -93.0483 \\ -93.0483 & 863.8462 \end{bmatrix}, \quad P_2 = \begin{bmatrix} 10.9363 & -44.8631 \\ -44.8631 & 184.0445 \end{bmatrix}$$
$$P_3 = 10^3 \begin{bmatrix} 0.0133 & -0.1136 \\ -0.1136 & 1.0096 \end{bmatrix}, \quad P_4 = \begin{bmatrix} 13.7524 & -66.7003 \\ -66.7003 & 323.5029 \end{bmatrix}$$
$$F_1 = 10^4 \begin{bmatrix} -0.4276 & 6.9868 \end{bmatrix}, \quad F_2 = 10^4 \begin{bmatrix} -0.4175 & 2.1680 \end{bmatrix}$$
$$F_3 = 10^4 \begin{bmatrix} -0.6545 & 9.0572 \end{bmatrix}, \quad F_4 = 10^4 \begin{bmatrix} -0.6992 & 4.3518 \end{bmatrix}$$

with initial condition $x(0) = \begin{bmatrix} \frac{22\pi}{50} & -3.3 \end{bmatrix}$. The time response is shown in Figure 1. With the proposed controller, we obtain $J(H_2) \approx 0.3811$. Thus $J(H_2) < \beta = 0.4938$.

Furthermore, the Table I shown below is the comparison of performance by our proposed approach and the approach in [19]. The comparison results show our approach obtains smaller upper bound and save more control energy.

Comparison	Theorem 5	SLF [19]
upper bond β	0.4938	4.0689
$\int_0^\infty u^T(t)u(t)dt$	$\approx 1.2454 \times 10^4$	$\approx 1.3951 \times 10^6$

TABLE I
PERFORMANCE COMPARISON OF CONTROL OF INVERTED PENDULUM

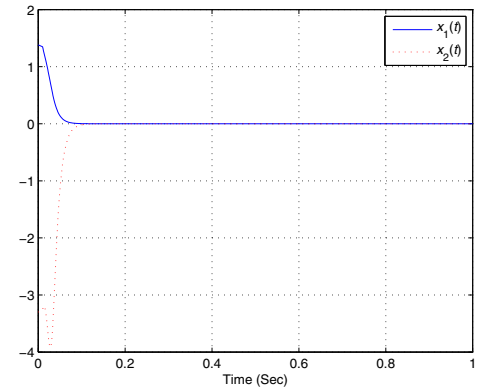

(a) Time response of $x_1(t) = \theta(t)$ and $x_2(t) = \dot{\theta}(t)$

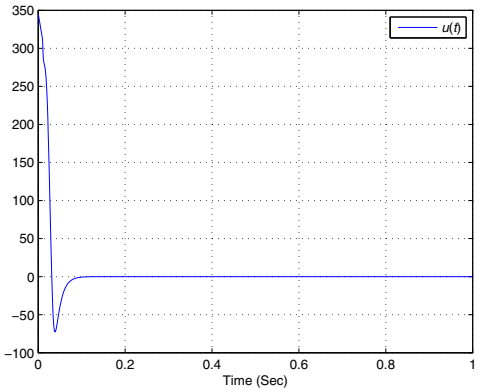

(b) Control action $u(t)$

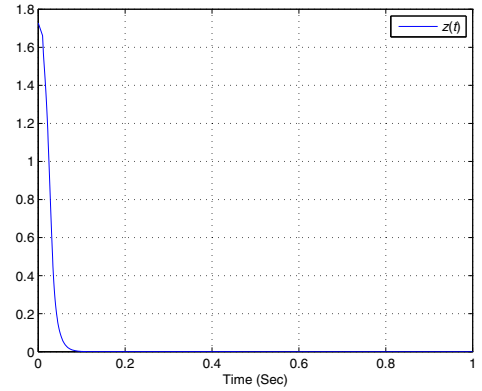

(c) Controlled output $z(t)$

Fig. 1. Time response of $\theta(t), \dot{\theta}(t), u(t)$, and $z(t)$

B. Example 2

In this example, an uncertain mass-spring-damped mechanic system is to be controlled to verify our proposed fuzzy controller. Its dynamic equation is depicted by

$$\ddot{x}(t) = c(t)\dot{x}(t) - 0.02x(t) - 0.67x^3(t) + u(t)$$

The system can be modeled by T-S fuzzy system,

Plant Rule1:

If $x(t)$ is M_1 THEN

$$\dot{\tilde{x}}(t) = (A_1 + \Delta A_1)\tilde{x}(t) + (B_{u1} + \Delta B_{u1})u(t)$$
$$z(t) = C_{z1}x(t) + D_{u1}u(t)$$

Plant Rule2:

If $x(t)$ is M_2 THEN

$$\dot{\tilde{x}}(t) = (A_2 + \Delta A_2)\tilde{x}(t) + (B_{u2} + \Delta B_{u2})u(t)$$
$$z(t) = C_{z2}\tilde{x}(t) + D_{u2}u(t)$$

where $\dot{\tilde{x}}(t) = \begin{bmatrix}\dot{x}(t)\\ x(t)\end{bmatrix}, A_1 = \begin{bmatrix}-0.1125 & -0.02\\ 1 & 0\end{bmatrix}, A_2 = \begin{bmatrix}-0.1125 & -1.527\\ 1 & 0\end{bmatrix}, B_{u1} = B_{u2} = \begin{bmatrix}1\\ 0\end{bmatrix}$
$C_{z1} = C_{z2} = \begin{bmatrix}0 & 1\\ 0 & 0\end{bmatrix}, D_{u1} = D_{u2} = \begin{bmatrix}0\\ 1\end{bmatrix}, H_{x1} = H_{x2} = \begin{bmatrix}-0.1125\\ 0\end{bmatrix}, E_{x1} = E_{x2} = \begin{bmatrix}0 & 1\end{bmatrix},$
$E_{u1} = E_{u2} = 0.$

By our derived theorem, the P_i matrices and feedback gains F_i are obtained as

$$P_1 = \begin{bmatrix}0.5191 & -0.3431\\ -0.3431 & 0.7620\end{bmatrix} \quad P_2 = \begin{bmatrix}1.3949 & -0.2965\\ -0.2965 & 0.7639\end{bmatrix}$$
$$F_1 = \begin{bmatrix}-0.9690 & -0.0325\end{bmatrix} \quad F_2 = \begin{bmatrix}-1.0026 & 0.0097\end{bmatrix}.$$

Given the initial condition $\tilde{x}(0) = \begin{bmatrix}-1 & -1.3\end{bmatrix}^T$, we obtain the optimal minimum bound $\beta = 4.4223$ and $J(H_2) \approx 3.4316$. Hence we see $J(H_2) < \beta$. The response of $\tilde{x}(t)$ and $u(t)$ is shown in figure 2.

The comparison of minimized upper bound obtained by our approach and common Lyapunov function approach is shown in Table II. Therefore, as our expectation, the guaranteed

Comparison	Theorem 5	SLF [19]
upper bond β	4.4223	9.4417
Trace(P^{-1})	2.4147	4.7176

TABLE II
PERFORMANCE COMPARISON OF MASS-SPRING DAMPED MECHANIC SYSTEMS

H_2 cost obtained by our proposed approach is lower than the previous common-Lyapunov function approach.

V. CONCLUSION

In this paper, we solve H_2 guaranteed cost of uncertain T-S fuzzy systems by multiple Lyapunov function. By our proposed approach, the priori information of derivative of membership functions can be completely removed. Thus, the controller is easy to implement and system is easy to analyze. Moreover, the guaranteed cost can be reformulated as minimizing an upper bound of cost function, which is a linear function, with some LMI constraints. Hence it can be efficiently solved by available software. From the numerical examples, it is also shown that the performance of designed system by our approach is better than the previous single Lyapunov function approach.

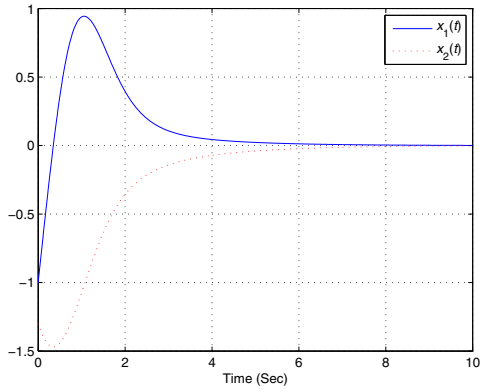

(a) Time response of $x_1(t) = x(t)$ and $x_2(t) = \dot{x}(t)$

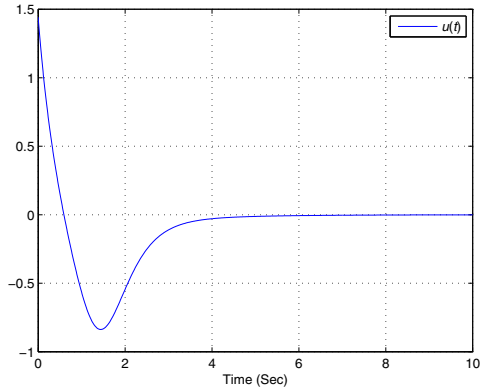

(b) Time response of $u(t)$

Fig. 2. Time response of state $\tilde{x}(t)$ and $u(t)$

REFERENCES

[1] S. Boyd, L. El Ghaoui, E. Feron, and V. Balakrishnan, *Linear Matrix Inequalities in Systems and Control Theory*, SIAM Press, Philadelphia, 1994.

[2] S. G. Cao, N. W. Rees, and G. Feng,"Analysis and design of a class of continuous time fuzzy control systems," *Int. J. Control,* vol. 64, pp. 1069-1087, 1996.

[3] S. G. Cao, N. W. Rees, and G. Feng, "Analysis and design for a class of complex control systems, Part II: Fuzzy controller design," *Automatica,* vol. 33, no. 6, pp. 1029-1039, 1997.

[4] B. C. Ding, H. X. Sun, and P. Yang, "Further studies on LMI-based stabilization conditions for nonlinear systems in Takagi-Sugeno's form," *Automatica,* vol. 42, no. 4, pp. 503-508, 2006.

[5] C. H. Fang, Y. S. Liu, S. W. Kau, L. Hong, and C. H. Lee, "A New LMI-Based Approach to Relaxed Quadratic Stabilization of T-S Fuzzy Control Systems," *IEEE Trans. Fuzzy Systems,* vol. 14, no. 3, pp. 386-397, Jun. 2006.

[6] T. M. Guerra and L. Vermeiren, "LMI-based relaxed nonquadratic stabilization conditions for nonlinear systems in the Takagi-Sugeno's form," *Automatica* vol. 40, pp. 823-829, 2003.

[7] E. Kim and H. Lee, "New approaches to relaxed quadratic stability condition of fuzzy control systems," *IEEE Trans. Fuzzy Systems,* vol. 8, no. 5, pp. 523-534, Oct. 2000.

[8] K. R. Lee, E. T. Jeung, and H. B. Park, "Robust fuzzy H_∞ control for uncertain nonlinear systems via state feedback: an LMI approach," *Fuzzy Sets and Systems,* vol. 120, no. 1, pp. 123-134, May 2001.

[9] H. K. Lam, F. H. Leung, and P. K. S. Tam, "Design and stability analysis of fuzzy model-based nonlinear controller for nonlinear systems using genetic algorithm," *IEEE Trans. Syst., Man, Cybern.,* vol. 33, no. 2, pp. 250-257, Apr. 2003.

[10] T. Takagi and M. Sugeno, "Fuzzy identification of systems and its application to modeling and control," *IEEE Trans. Syst., Man, Cybern.*, vol. SMC-15, no. 1,pp. 116-132, Jan. 1985.

[11] K. Tanaka and H.O Wang, "*Fuzzy Control Systems Design and Analysis:*

A Linear Matrix Inequality Approach," John Wiley & Sons Inc. New York, 2001.

[12] B.-S. Chen, C.-S. Tseng, and H.-J. Uang, "Mixed H_2/H_∞ fuzzy output feedback control design for nonlinear dynamic systems: an LMI approach," *IEEE Trans. Fuzzy Systems,* vol. 8, no. 3, pp. 249-265, Jun. 2000.

[13] X. Liu and Q. Zhang, "New Approaches to H_∞ controller design based on fuzzy observers for T-S fuzzy systems via LMI," *Automatic*, vol. 39, no 9, pp1571-1582, Sep. 2003.

[14] Sing Kiong Nguang, "H_∞ fuzzy output feedback control design for nonlinear system: an LMI approach," *IEEE Transactions on Fuzzy Systems,"* vol. 11, no. 3, pp331-340, Jun 2003.

[15] T. M. Guerra and L. Vermeiren, "LMI-based relaxed nonquadratic stabilization conditions for nonlinear systems in the Takagi-Sugeno's form," *Automatica,* vol. 40, pp. 823-829, 2003.

[16] H. K. Lam and L. D. Seneviratne, "LMI-based stability design of fuzzy controller for nonlinear systems," *IET Control Theory Appl.,* vol. 1, no. 1, pp. 393-401, Jan. 2007.

[17] K. Tanaka, H. Ohtake and H. O. Wang, "A Descriptor System Approach to Fuzzy Control System Design via Fuzzy Lyapunov Functions," *IEEE Trans. Fuzzy Systems,* vol. 15, no. 3, pp.333-341, Feb. 2007.

[18] K. Tanaka, T. Hori and H. O. Wang, "A multiple Lyapunov function approach to stabilization of fuzzy control systems, *"IEEE Trans. Fuzzy Systems,* vol. 11, no. 4, pp. 582-589, 2003.

[19] H.-N. Wu and K.-Y. Cai, "H_2 guarnateed cost fuzzy control for uncertain nonlinear systems via linear matrix inequalities," *Fuzzy Sets and Systems,* vol. 148, no. 1, pp. 411-429, 2004.

[20] S. Tong, and H.-H. Li, "Observer-based robust fuzzy control of nonlinear systems with parametric uncertainties," *Fuzzy Sets and Systems,* vol. 131, no. 2, pp.165-184, Oct. 2002.

[21] B. J. Rhee and S. Won, "A new fuzzy Lyapunov function approach for a Takagi-Sugeno fuzzy control system design," *Fuzzy Sets and Systems,* vol. 157, pp.1211-1228, Jan. 2006.

[22] M. L. Lin and J. C. Lo, "Static nonlinear output feedback H_2 control for T-S fuzzy models", *The IEEE International Conference on Fuzzy Systems*, pp.1380-1383, 2003.

[23] M. L. Lin and J. C. Lo, "Robust H_∞ nonlinear control via fuzzy static output feedback," *IEEE Trans. on Circuits and Systems*, vol 50, no. 11, pp1464-1502, Nov, 2003.

[24] H. K. Lam and F. H. F. Leung, "LMI-based stability and performance conditions for continuous-time nonlinear systems in Takagi-Sugeno's form", *IEEE Trans. Syst., Man, Cybern., PartB: Cybernetics,* vol. 37, no. 5, pp. 1396-1406, Oct, 2007.

[25] Ali Jadbabaie, Mohammad Jamshidi and Andre Titli, "Guaranteed-Cost Design of Continuous-Time Takagi-Sugeno Fuzzy Controllers via Linear Matrix Inequalities," *Proc IEEE World Congress Comput. Intell.,* pp268-273, May 1998.

[26] H. K. Lam, M. Narimani, J. C. Y. Lai, Leung, and F.H.F. Leung, Stability analysis of T-S fuzzy-model-based control systems using fuzzy Lyapunov function, *IEEE Conf. Fuzzy Systems*, pp. 931-938, June, 2008.

[27] H. K. Lam and L. D. Seneviratne " Stability anlysis of fuzzy-model-based control systems using fuzzy Lyapunov function", Manuscript report.

2011 IEEE International Conference on Fuzzy Systems
June 27-30, 2011, Taipei, Taiwan

Higher Order Sliding Fuzzy Type-2 Interval Control for SISO Uncertain Nonlinear Systems

Malik Manceur, Najib Essounbouli and Abdelaziz Hamzaoui
CReSTIC, University of Champagne-Ardenne, 9 Rue de Quebec B.P. 396- 10026 Troyes Cedex- France
Email: malik.manceur,najib.essounbouli,abdelaziz.hamzaoui@univ-reims.fr

***Abstract*—A higher order sliding fuzzy type-2 controller scheme for nonlinear uncertain perturbed systems is proposed in the paper. To overcome the constraint on the knowledge of the system model, local models related to some operating points were used to synthesize a nominal fuzzy type-2 global model. The controller uses integral sliding mode concept and contains two parts. The first one leads to achieve finite time stabilization of the higher order input output dynamics without uncertainties. The second part has the object to reject bounded uncertainties throughout the entire response of the system. Two adaptive fuzzy type-2 systems have been introduced to generate the two Super Twisting signals to avoid both the chattering and the constraint on the knowledge of upper bounds of both disturbances and uncertainties. These fuzzy type-2 systems are adjusted on-line by adaptation laws deduced from the stability analysis in Lyapunov sens. The advantages of the method are that its implementation is easy, the convergence time is chosen in advance and the robustness is ensured. A robot arm actuated by a DC motor is used as illustrative example. The obtained results show the good tracking performances and the applicability of the method.**

***Index Terms*—Higher order sliding mode control, fuzzy type-2 sets, T-S fuzzy systems, integral sliding mode control.**

I. Introduction

The sliding mode control (SMC) is a powerful method to control high-order nonlinear dynamic systems operating under uncertainty conditions [1],[2],[3]. The technique consists of two stages. First, a sliding surface, to which the controlled system trajectories must belong, is designed according to some performance criterion. Then, a discontinuous control is designed to force the system state to reach the sliding surface such that a sliding mode occurs on this manifold. When sliding mode is realized, the system exhibits robustness properties with respect to parameter perturbations and external matched disturbances [2]. In spite of claimed robustness properties, high frequency oscillations of the state trajectories around the sliding manifold known as chattering phenomenon [2],[3] are the major obstacles for the implementation of SMC in a wide range of applications. A number of methods have been proposed to reliably prevent chattering: among them, the boundary layer solution [4], [2], [5],[6], tangent hyperbolic [7] and observer-based solution [3]. This methods can eliminate chattering effect but a finite steady state error will exist [8] and requires a compromise between the level of tracking performance and a start-up control [9]. In [8], [9],[10] the modified switching signal (with saturation) is substituted by an adaptive fuzzy system. However, the convergence of the corresponding adaptive algorithm depends directly on the choice of the initial values of the adaptive fuzzy system. The state of the art of classical sliding mode control with soft computing has been examined in [11].

The "higher order SMC" approach has been recently proposed and developed as a generalization of the classical first order sliding mode theory [12],[13],[14],[15]. The current papers result is based on this latter approach and its main idea can be described as follows. Let $s(x,t)$ ($x \in \mathrm{R}^n$ is the state variable, $t \in \mathrm{R}^+$ the time variable) be the sliding variable and $r \in \mathrm{N}$ the sliding order. The control forces to zero in finite time s and its $(r-1)$ first higher time derivatives by acting discontinuously on the rth time derivative of s. Keeping the main advantages of standard SMC, the chattering effect is eliminated and higher order precision is provided. In the case of "real" SMC [12], if τ is the sampling time, the error is $o(\tau)$ in the case of standard SMC [16] whereas it is $o(\tau^r)$ in the rth order SMC [12].
In the case of second order SMC ($r = 2$), many works have given solutions. Several second order sliding mode algorithms are proposed in [14], [13] and [12]. Arbitrary-order sliding controllers for single-input single-output systems (SISO) with finite time convergence have been recently proposed in [15],[17],[18],[19]. In [20], the so-called terminal sliding modes control proposes a solution for arbitrary order finite time convergence sliding mode. A major drawback of this approach is that all trajectories have to start from a prescribed sector of state space in order to have finite control, which is restrictive in particular for practical applications. Many results concerning the high order SMC have been proposed for single Input single output in [13], [21] and [22]. However, the common drawback of this approach is the calculation of sliding gains used in the control law. Indeed, they are chosen to satisfy the finite time convergence condition, which required the well-knowledge of the system parameters.
The aim of this paper is to present an arbitrary-order sliding mode controller for uncertain SISO nonlinear systems. The main objective of this new approach is to propose a controller for which the implementation is easy, the convergence time is finite and well-known in advance and the computation of the gains control of the discontinuous part will be simplified. The design uses the integral sliding mode concept [23]. Actually, the problem of the higher order SMC of SISO minimum-phase uncertain systems is formulated in inputoutput terms only (as in [18]) through the differentiation of the sliding variable s, and is equivalent to the finite time stabilization of an rth order inputoutput linear dynamics with bounded uncertainties.

978-1-4244-7316-8/11/$26.00 ©2011 IEEE

The control strategy presented in the sequel, whose basic idea has been introduced in [19], contains two parts: a part is discontinuous, forces the establishment of a sliding mode on the integral sliding manifold, and ensures the robustness with respect to bounded uncertainties, throughout the entire response of the system. The other part, which is obtained through optimal feedback control over finite time interval with fixed final states [24], is used to stabilize to zero in finite time the rth order inputoutput dynamics without uncertainties. In [22], this part is based an close-loop control and has two dynamics, at $t \in [0, t_f]$ will be associated a forcing term δ and after $t > t_f$ will be removed. The computation of the control gains will be simplified by introducing two adaptive fuzzy type-2 systems in the second SMC. Their updates are performed using two adaptation laws derived from the study of stability in the sense of Lyapunov. Since the considered system is nonlinear and uncertain, we propose to use Takagi-Sugeno fuzzy system to construct a nominal model of the system. For this, we define some local models around some operating points, which will be used as conclusion of this Takagi-Sugeno system.

The paper is organized as follows. Section II gives an overview of the theory of the type-2 fuzzy systems. The problem formulation is presented in section III. The design procedure of higher SMC based an integral sliding mode and it's stability is discussed in section IV. The proposed sliding mode fuzzy type-2 interval controller is given in section V. Simulation example to demonstrate the performance of the proposed method is provided in section VI. Section VII gives the conclusions of this paper.

II. Type-2 Fuzzy Logic Systems

The main property that distinguishes fuzzy logic is its capacity of representing and modeling imprecision and uncertainty by giving each point in fuzzy set a value belonging to the interval $[0; 1]$. However, the imprecision in such classical fuzzy system, which is called some times Type-1 fuzzy logic system (T1FLS) is not fully exploited and can deliver a non-satisfactory performance. Practically, three ways of uncertainty can be observed in the fuzzy logic system (FLS): (1) the used words in antecedents and consequents of rules can mean different things to different people; (2) consequents obtained by polling a group of experts will often be different for the same rule and (3) both of training data and measurements used to activate the FLS are noisy [25],[26].

In the last few years, a markable attention has been given to another type of fuzzy system called Type-2 fuzzy logic system (T2FLS). In T2FLS, the uncertainty is represented using a function, which is it self a Type-1 fuzzy number and that is why T2FLS is referred to that fuzzy system. The membership functions of T2 fuzzy sets are three dimensional and include a foot print of uncertainty (FOU) with a new third dimension of Type-2 fuzzy sets. FOU provides additional degrees of freedom that make it possible to directly model and handle uncertainties and consequently, T2FLS has the potential to out perform T1FLS [27],[28] in such cases. Such advantage is quite important if we know that modeling of linguistic information and decision making represents the main application of FLS.

Figure 1 depicts the structure of a T2FLS [29],[30]; it is quite similar to a T1FLS, the only difference being that the antecedent and/or consequent sets in a T2FLS are type-2, so that each rule output set is a type-2. There are five principal parts in a T2FLS: fuzzifier, rule base, inference engine, type-reducer and defuzzifier.

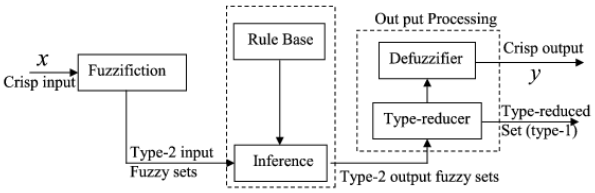

Fig. 1. The structure of T2FLS with its two out puts.

The type-reducer performs a type-reduction operation which is an extended version of T1 defuzzification. Type reduction yield a T1 set from the T2 rule output sets. The resulting T1 set is called type-reduced set. The type-reduced set can then be defuzzified to obtain a crisp output. We call the combination of type reduction and defuzzification output processing. The type reduced set of a T2FLS shows the possible variation in the crisp output of the FLS due to uncertain natures of the antecedents and/or consequents. The fuzzifier maps a crisp input vector with n inputs $x = (x_1, ..., x_n)^T \in X_1 \times X_2 \times ... \times X_n = X$ into input fuzzy sets which are T2 fuzzy input sets. However, we will use singleton fuzzification as it is fast to compute and thus suitable for real time applications. The T2 fuzzy rule base consists of a collection of IF-THEN rules in the following form [31]:

$R^i : IF\ x_1$ is $\tilde{F}_1^i$ and ...and x_n is $\tilde{F}_n^i$ THEN y is $\tilde{G}^i$

Where $\tilde{F}_j^i$s are antecedent T2 sets $(j = 1, 2, ..., n)$, $y \in Y$is the output, $\tilde{G}^i s$ are consequent type-2 sets and $i = 1, 2, ..., M$, where M is the total number of T2 fuzzy IF-THEN rules in the rule base.

The rule represents a T2 fuzzy relation between the input space $X_1 \times X_2 \times ... \times X_n$ and the output space Y of the FLS. The fuzzy inference engine is decision making logic, which employs fuzzy rules from the fuzzy rule base to determine the mapping from X to Y. A T2FLS is a mapping $f : \mathbb{R}^n \longrightarrow \mathbb{R}$. After fuzzification, fuzzy inference, type reduction and defuzzification, we obtain a crisp output. For an interval T2FLS, this crisp output is the center of type reduced set.

In interval T2FLS with meet under minimum or product t-norm, the firing interval $W^i = [\underline{w}^i, \overline{w}^i]$ of the i^{th} rule is an interval T1 set, which is determined by its left-most and right-most points $\underline{w}^i$ and $\overline{w}^i$ such that:

$$\begin{cases} \underline{w}^i = \left[\underline{\mu}_{\tilde{F}_1^i}(\underline{x}_1) \times ... \times \underline{\mu}_{\tilde{F}_n^i}(\underline{x}_n)\right] \\ \underline{w}^i = \left[\overline{\mu}_{\tilde{F}_1^i}(\underline{x}_1) \times ... \times \overline{\mu}_{\tilde{F}_n^i}(\underline{x}_n)\right] \end{cases} \quad (1)$$

Type reduction was proposed by Karnik and Mendel [32]. It is in extension of T1 defuzzification method and it is called type-reduction because this operation takes us from the T2 output sets of the FLS to a T1 set. This set may then be defuzzified to obtain a single crisp number. There exist many kinds of type-reduction [29],[33],[34]. In this paper, we will use the center of sets type reduction, which can be expressed in the case of interval T2 fuzzy sets as:

$$\begin{aligned} Y_{tr} &= \int_{y^1 \in [y_l^1, y_r^1]} \cdots \int_{y^M \in [y_l^M, y_r^M]} \int_{w^1 \in [\underline{w}^1, \overline{w}^1]} \\ &\cdots \int_{w^M \in [\underline{w}^M, \overline{w}^M]} 1 / \frac{\sum_i^M w^i y^i}{\sum_i^M w^i} \end{aligned} \tag{2}$$

$$Y_{tr} = [y_l, y_r]$$

where Y_{tr} is the interval set determined by two end points y_l and y_r, $y^i \in Y^i = \left[y_l^i, y_r^i\right]$, Y^i the centroid of the T2 interval consequent set $\tilde{G}^i$ and $w^i \in W^i = \left[\underline{w}^i, \overline{w}^i\right]$ the firing interval.

III. Problem Formulation

Consider the nth-order uncertain nonlinear system of the form:

$$\begin{cases} x^{(n)} = f(\underline{x}) + g(\underline{x}) \cdot u(t) + d \\ y = x \end{cases} \tag{3}$$

where $f(\underline{x})$ and $g(\underline{x})$ are two nonlinear continuous and uncertain bounded functions, $u \in \mathbb{R}$ and $y \in \mathbb{R}$ are the input and output of the system, respectively, d is an external unknown bounded disturbance. $\underline{x} = [x, \dot{x}, ..., x^{n-1}]^T \in \mathbb{R}^n$ is the measurable state vector and $s(\underline{x}, t)$ is the sliding variable. We assume that the two functions $f(\underline{x})$ and $g(\underline{x})$ can be written respectively as the sum of a nominal function and an unknown bounded uncertainty:

$$\begin{cases} f(\underline{x}) = f_0(\underline{x}) + \Delta f(\underline{x}); |\Delta f(\underline{x})| < \Delta_f \\ g(\underline{x}) = g_0(\underline{x}) + \Delta g(\underline{x}); |\Delta g(\underline{x})| < \Delta_g \end{cases} \tag{4}$$

where Δ_f and Δ_g are two positive constants. Replacing (4) into (3), we obtain:

$$\begin{cases} x^{(n)} = f_0(\underline{x}) + g_0(\underline{x}) \cdot u(t) + D \\ y = x \end{cases} \tag{5}$$

where

$$D = \Delta f(\underline{x}) + \Delta g(\underline{x}) u + d \tag{6}$$

The nominal model of the system can be obtained by identification or by approximation using a fuzzy system [35]. We consider the second case, because it allows us to exploit linguistic information from the expert human. The approximation can be made either using a Takagi-Sugeno classical fuzzy system or an adaptive one. This later can certainly get good results but requires a long computing time where we consider more than two inputs. Moreover, the linearisation techniques permit to transform the dynamics of the system into a local models around certain operating points. Thus, to calculate the nominal model, Takagi and Sugeno proposed in [36] a T1 fuzzy dynamic model formed by rules; where the conclusion part is a local model in the form :

$$x^{(n)} = A_i \underline{x} + B_i u \tag{7}$$

A_i and B_i are two matrix with appropriate dimension ($i = 1, 2, ..., r$). Then the corresponding IF-THEN fuzzy rule can be written as:

IF x is H_1^i and $\dot{x}$ is H_2^i and..... and $x^{(n-1)}$ is H_n^i THEN

$$x^{(n)} = A_i \underline{x}_i + B_i u \tag{8}$$

where $H_j^i, (j = 1, 2, ..., n)$ is the j^{th} fuzzy set of the i^{th} rule. However, as known in literature, the knowledge used to construct such rules are uncertain. This uncertainty leads to obtain rules whose premises or consequences uncertain, which can create uncertainty in the membership function. Since a T2 fuzzy system can take in account this uncertainties, we propose to extend the dynamic model given by (8), by introducing the concept of T2 fuzzy logic. Then, the nominal T2 fuzzy model related to the i^{th} rule will be given as follows [37]:

IF x is $\tilde{H}_1^i$ and $\dot{x}$ is $\tilde{H}_2^i$ and..... and $x^{(n-1)}$ is $\tilde{H}_n^i$ THEN

$$x^{(n)} = A_i \underline{x}_i + B_i u \tag{9}$$

Where $\tilde{H}_j^i, (j = 1, 2, ..., n)$ is the j^{th} interval T2 fuzzy set of the i^{th} rule. For a given pair $(\underline{x}, u)$, the fuzzy model resulting of the system appears as a weighted average of the local models used. If we use the product as an interference engine, the method of center set for the reduction type and center of gravity for defuzzification, the output fuzzy system will be giving by:

$$x^{(n)} = \frac{\sum_{i=1}^r w^i \left[A_i \underline{x} + B_i u\right]}{\sum_{i=1}^r w^i} = \frac{\sum_{i=1}^r w^i \left[A_i \underline{x}\right]}{\sum_{i=1}^r w^i} + \frac{\sum_{i=1}^r w^i \left[B_i u\right]}{\sum_{i=1}^r w^i} \tag{10}$$

If we denote by $f_0(\underline{x}) = \left[\frac{\sum_{i=1}^r w^i A_i \underline{x}}{\sum_{i=1}^r w_i}\right]$ and $g_0(\underline{x}) = \left[\frac{\sum_{i=1}^r w^i B_i}{\sum_{i=1}^r w^i}\right]$, the fuzzy nominal model will be giving by:

$$x^{(n)} = f_0(\underline{x}) + g_0(\underline{x}) u \tag{11}$$

where the variable w^i is the firing interval, which is determined by its most left and right points as given by (1). The reduction type algorithm given by karnik and Mendel [34] will be detailed in the third section .

The control objective is to fulfill the constraint of the sliding variable $s(\underline{x}, t) = 0$ in finite time and to keep it exactly by discontinuous feedback control, and to ensure that the system out-put y follows a reference trajectory y_d. The set:
$s^r = \{\underline{x} | s(\underline{x}, t) = \dot{s}(\underline{x}, t) = ... = s^{r-1}(\underline{x}, t) = 0\}$ called rth order sliding set, is non-empty and is locally an integral set in the Filippov sense [38], the motion on s^r is called rth order sliding mode with respect to the sliding variable s. The rth

order SMC approach allows the finite time stabilization to zero of the sliding variable s and its $r-1$ first time derivatives by defining a suitable discontinuous control function. s^r in function of the systems variables and the control variable u is given by [17]:

$$s^r = \phi(.) + \gamma(.)u \tag{12}$$

r means also the number of times to derive the sliding surface to appear explicitly the control variable.

In [22], [12], authors assume that: the functions $\phi(.)$ and $\gamma(.)$ are bounded uncertain functions, and, without loss of generality, let also the sign of the control gain $\gamma(.)$ be constant and strictly positive. Thus, there exist $K_m \in \mathrm{R}^{+*}$, $K_M \in \mathrm{R}^{+*}$, $C_0 \in \mathrm{R}^{+}$ such that $0 < K_m < \gamma < K_M$, $|\phi| \leq C_0$.
These assumption implies that this results are considered local. In the section V, we propose a method to avoid these restriction which makes the results global.
The rth order SMC with respect to the sliding variable s is equivalent to the finite time stabilization of [22]:

$$\begin{cases} \dot{z}_i = z_{i+1} \\ \dot{z}_r = \phi(.) + \gamma(.)u \end{cases} \tag{13}$$

with $1 \leq i \leq r-1$ and $z{=}[z_1\ z_2\ ...z_r]^T := [s\dot{s}...s^{(r-1)}]^T$.

IV. Control design

The control law is composed of two parts. The first one, named ideal control [23], is continuous and stabilizes in finite time (13) at the origin when there are no uncertainties. In fact, this control part is used in order to generate trajectories that the system is forced to track. The second part, named integral sliding mode control, provides the complete compensation of uncertainty for $t \geq 0$ and ensures that control objectives are reached.

A. Continuous Control Part Design

Consider system (13), according to some assumptions it can be trivially rewritten as [22]:

$$\begin{cases} \dot{z}_i = z_{i+1} \\ \dot{z}_r = \underbrace{\phi(.) + [\gamma(.) - 1]u}u + u \end{cases} \tag{14}$$

for $1 \leq i \leq r-1$, it yields

$$\begin{cases} \dot{z}_i = z_{i+1} \\ \dot{z}_r = \beta(.) + u \end{cases} \tag{15}$$

Let us define $u = u_0 + u_{dis}$, with u_0 being the ideal control, and u_{dis} being the integral sliding mode control. Consider now the particular case $\beta(.) = 0$. Then, as no control part u_{dis} is necessary in order to compensate the uncertainties, the control law u reads as $u = u_0$. One gets

$$\dot{z} = Az + Bu_0 \tag{16}$$

where A and B are defined by

$$A = \begin{bmatrix} 0 & 1 & \dots & 0 & \dots \\ \vdots & \ddots & \ddots & \ddots & \\ 0 & \ddots & \ddots & \dots & 1 \\ 0 & \ddots & \ddots & \ddots & 0 \end{bmatrix}_{r\times r}, \quad B = \begin{bmatrix} 0 \\ \vdots \\ 0 \\ 1 \end{bmatrix}_{r\times 1}.$$

The control objective is to drive the state of (16) to $z = 0$ at the fixed final time $t = t_f < +\infty$, with $z(0)$ being a bounded initial state vector. This objective can be done through the use of optimal control laws. The control law u_0 ensures the minimization of the following criterion:

$$J = \frac{1}{2}\int_0^{t_f} z^T Q z + u_0^2 dt \tag{17}$$

with $t_f < +\infty$, $|z(0)| < +\infty$ and Q a symmetric positive definite matrix under the fixed final state constraint $z(t_f) = 0$.

Theorem 1: [24] Consider linear system (16) with (A, B) reachable. A control law u_0 minimizing the criteria (17) and driving system (16) to $z(t) = 0$ at $t = t_f$ for an initial bounded condition $z(0)$ is given by (with $0 \leq t \leq t_f < +\infty$)

$$u_0 = -B^T M z(t) + B^T \delta(t) \tag{18}$$

with $\delta(t)$ and M are defined by

$$\begin{cases} \dot{\delta} = -(A^T - MBB^T)\delta \\ 0 = MA + A^T M - MBB^T M + Q \end{cases} \tag{19}$$

Initial condition $\delta(0)$ of $\delta(t)$ is selected in order to satisfy the terminal condition $z(t_f) = 0$.

The control law u_0 is defined in order to drive in finite time the system (16) to $z(t) = 0$ at $t = t_f$, then, the state variables of (16) converge exactly to the origin at $t = t_f$. The control law u_0 will maintain the required equilibrium state $z = 0$ even after the terminal time, i.e. $t > t_f$, provided that the forcing term $\delta(t)$ is removed at the terminal time, i.e. $u_0 = -B^T M z$ for $t > t_f$ [24]. Then, in order to reach in a finite time t_f the origin $z = 0$, and to maintain the system (16) at this point for $t > t_f$, a solution is [24]:

$$u_0 = \begin{cases} -B^T M z(t) + B^T \delta(t) \text{ for } 0 \leq t \leq t_f \\ -B^T M z(t) \text{ for } t > t_f \end{cases} \tag{20}$$

B. Integral Sliding Manifold

The basic idea consists in determining a sliding manifold such that the state trajectories start on this manifold at the initial time $t = 0$, which induces a sliding mode without reaching phase [2]. One has (for $1 \leq i \leq r-1$)

$$\begin{cases} \dot{z}_i = z_{i+1} \\ \dot{z}_r = \beta(.) + u_0 + u_{dis} \end{cases} \tag{21}$$

u_{dis} is a discontinuous function designed in order to exactly reject the perturbation $\beta(.)$ throughout the entire response of the system. In order to reach this objective, the integral sliding mode control is used [23],[3]. Let $\sigma \in \mathrm{R}$ the sliding manifold defined as

$$\sigma = \sigma_0 + \zeta \tag{22}$$

where σ_0 may be designed as the linear combination of the state variables of (21). The term $\zeta \in \mathrm{R}$ induces the integral term and will be determined below. In order to determine the motion equations on the sliding manifold, the equivalent control method is used [23]. The time derivative of σ reads as

$$\dot{\sigma} = \frac{\partial \sigma_0}{\partial z}(Az + Bu_0) + \frac{\partial \sigma_0}{\partial z_r}(u_{dis} + \beta(.)) + \dot{\zeta} \tag{23}$$

A sufficient condition ensuring $\dot{\sigma} = 0$ for $t \geq 0$ is that the equivalent control u_{eq} of u_{dis} reads as

$$u_{eq} = -\beta(.) \tag{24}$$

and $\dot{\zeta} = -\frac{\partial \sigma_0}{\partial z}(Az + Bu_0)$, $\zeta(0) = -\sigma_0(z(0))$, where $\zeta(0)$ is determined based on the requirement $\sigma(0) = 0$.
In this present work, to simplify the implementation of the method we consider the particle case

$$\sigma_0 = z_r \longrightarrow \dot{\sigma} = u + \beta(.) + \dot{\zeta} \tag{25}$$

In this case, condition (24) holds if

$$\dot{\zeta} = -u_0, \zeta(0) = -z_r(0) \tag{26}$$

C. Design of the Discontinuous Control u_{dis}

The control law u_{dis} is designed in order to ensure that the sliding motion on the sliding manifold is guaranteed for $t \geq 0$ in spite of uncertainties and disturbances. Due it's relative simplicity of implementation and their robustness, Super-Twisting algorithm is among the 2-sliding algorithms which are widely used, and reads [12]:

$$u_{dis} = -u_1 - u_2 \tag{27}$$

where $\dot{u}_1 = -\lambda_1 sign(\sigma) \longrightarrow u_1 = \int_0^t \lambda_1 sign(\sigma) dt$ and $u_2 = \lambda_2 |\sigma|^{\frac{1}{2}} sign(\sigma)$.$\lambda_1$ and λ_2 are a positive constants tuned such that the η-attractiveness condition is satisfied:

$$\sigma\dot{\sigma} \leq -\eta|\sigma|, \eta > 0 \tag{28}$$

The aim of our study is to determine a control law by employing 2-order sliding modes, so that the system output y follows a reference trajectory y_r and the tracking error $e = y - y_r$ converges to zero in the presence of uncertainties and disturbances. For this, we consider the following sliding surface [5]:

$$\begin{aligned} \sigma_0 &= \left(\frac{\partial}{\partial t} + \lambda\right)^{(n-1)} e \\ &= \sum_{k=0}^{n-1} \frac{(n-1)!}{k!\,(n-k-1)!} \left(\frac{\partial}{\partial t}\right)^{(n-k-1)} \lambda^k e \end{aligned} \tag{29}$$

$\lambda > 0$, the derivative of σ_0 can be expressed as:

$$\dot{\sigma_0} = \delta_{\sigma_0} - y_r^{(n)} + f_0(\underline{x}) + g_0(\underline{x})\, u + D \tag{30}$$

which has the same form as given by equation (12), with $r = 1$, $\phi(.) = \delta_{\sigma_0} - y_r^{(n)} + f_0(\underline{x}) + D$, $\gamma(.) = g_0(\underline{x})$ and $\delta_{\sigma_0} = \sum_{k=1}^{n} \frac{(n-1)!}{k!(n-k-1)!} \left(\frac{\partial}{\partial t}\right)^{(n-k-1)} \lambda^k \dot{e}$. Since the system is relative degree 1, the seconde derivative of σ_0 is given by:

$$\ddot{\sigma}_0 = \varphi + \varrho \dot{u} \tag{31}$$

with $\varphi = \dot{\delta}_{\sigma_0} - y_r^{(n+1)} + \dot{f}_0(\underline{x}) + \dot{D} + \dot{g_0}(\underline{x})\, u$ and $\varrho = g_0(\underline{x})$. In order to satisfy the constraint (28), Levant consider the system (31) without D and it's derivative and gave the following sufficient conditions [15]:

$$\begin{cases} \Delta > 0, |\varphi| \leq \Delta, 0 < \Gamma_m \leq \varrho \leq \Gamma_M \\ \lambda_1 > \frac{\Delta}{\Gamma_m},\ \lambda_2 \geq \frac{4\Delta}{\Gamma_m^2} \frac{\Gamma_M(\lambda_1 + \Delta)}{\Gamma_m(\lambda_1 - \Delta)} \end{cases} \tag{32}$$

In steady state, we will have $\sigma = 0$, choosing these sufficient conditions allow us easily to satisfy the condition (28) at startup. However, for optimal choice of λ_1 and λ_2 in the approaching phase, the knowledge of the D and $\dot{D}$'s upper bounds are required. Nevertheless even if the problem of determining these upper bounds is resolved, the presence of the function $sign(s(\sigma))$ causes a chattering phenomenon [37],[39],[40]. Even if it's order is less important than in the classical SMC, it's still residual. One way to eliminate the chattering phenomenon consists to define a transition band near the sliding surface. But in order to keep the same tracking performances, the introduction of this band induced an important initial solicitations. Thus, there is a tradeoff between the level of performances tracking (small time response and control without chattering) and a starting suitable control. The objective of the proposed approach in the next section, is to use the same control structure with smooth control signal without reducing the tracking performances.

V. Sliding Mode Type-2 Fuzzy Controller

In this section, we will replace the two switching signals u_1 and u_2 respectively, by two control signals from two adaptive T2 fuzzy systems in order to smooth the control signal. The adaptation laws of adjustable parameters of the fuzzy systems are deduced from the stability study of the closed-loop process in the sense of Lyapunov. This adaptation in addition to smooth the control signal will enable us to better anticipate disturbances by providing us in each instant the optimal value (λ_1^* and λ_2^*) of λ_1 and λ_2, which are hard to compute [41].

A. Proposed Type-2 Fuzzy Logic System

Both adaptive systems used to approximate the control gains, have the same structure as given by (2). The antecedent T2 Membership functions $\mu_{\tilde{F_i^j}}$ will be fixed as given in figure 3. The consequent sets which are the adjustable parameters will be fuzzy centroids T1.
The output fuzzy systems are given by:

$$\begin{aligned} Y_{tr} &= [y_l, y_r] \\ &= \int_{\theta^1} \ldots \int_{\theta^M} \int_{w^1} \ldots \int_{w^M} 1 \Big/ \frac{\sum_i^M w^i \theta^i}{\sum_i^M w^i} \end{aligned} \tag{33}$$

In the case of T2 fuzzy systems, the universal approximation property is retained with an additional phase of reduction type. Since each set on the right-hand side of (33) is an interval T1 set, hence Y_{tr} is an interval T1 set. So, to find the type-reduced set Y_{tr}, we just need to compute the two end points of these interval. The maximum value of y is y_r and it's minimum value is y_l,$\forall y \in Y_{tr}$, y can be represented as:

$$y = \frac{\sum_i^M w^i \theta^i}{\sum_i^M w^i} \tag{34}$$

The y_r points are associated solely with y_r^i, in same way y_l is associated solely with y_l^i. In the center of sets, Karnik and Mendel [32] have shown that the two end points of Y_{tr}, y_r and y_l depend only on a mixture $\underline{w}^i$ or $\overline{w}^i$ of values, since $w^i \in W^i = \left[\underline{w}^i, \overline{w}^i\right]$. In this case, each y_r and y_l can be represented as a vector of fuzzy basis functions (FBFs) expansion, that is:

$$y_l = \frac{\sum_{i=1}^{M} w_l^i \theta_l^i}{\sum_{i=1}^{M} w_l^i} = \sum_{i=1}^{M} \theta_l^i \xi_l^i \tag{35}$$

where w_l^i denotes the firing strength membership grade (either $\overline{w}^i$ or $\underline{w}^i$) of the i^{th} rule contributing to the left-most point y_l and $\xi_l^i = \frac{w_l^i}{\sum_{i=1}^{M} w_l^i}$ are the components of the first FBF vector ξ_l of y. Similarly:

$$y_r = \frac{\sum_{i=1}^{M} w_r^i \theta_r^i}{\sum_{i=1}^{M} w_r^i} = \sum_{i=1}^{M} \theta_r^i \xi_r^i \tag{36}$$

where w_r^i denotes the firing strength membership grade (either $\overline{w}^i$ or $\underline{w}^i$) contributing to the right-most point y_r and $\xi_r^i = \frac{w_r^i}{\sum_{i=1}^{M} w_r^i}$ are the components of the first FBF vector ξ_r of y.

Note that whereas a T1FLS is characterized by a single FBF expansion [42], an interval T2FLS is characterized by two FBF expansions. This difference is the consequence of the reduction type operation.

To obtain a crisp outputs from the T2FLS y, we must defuzzify the type-reduced set Y_{tr}. Since these type reduced set is interval set, therefore, the defuzzified output of y will be the average of y_l and y_r, that is:

$$y = \frac{y_l + y_r}{2} \tag{37}$$

Replacing (35) and (36) into (37), we obtain:

$$y = \frac{\underline{\theta}_l^T \underline{\xi}_l + \underline{\theta}_r^T \underline{\xi}_r}{2} = \underline{\theta}^T \left[\frac{\underline{\xi}_l + \underline{\xi}_r}{2}\right] = \underline{\theta}^T \underline{\xi} \tag{38}$$

Where $\underline{\xi} = \frac{\underline{\xi}_l + \underline{\xi}_r}{2}$ is the average FBF of y. In order to compute y_l and y_r Karnik and Mendel have developed a simple iterative algorithm. This algorithm is given as follows:

1 We assume that the parameters θ^i are arranged in ascending order, that is, $\theta^1 < \theta^2 < ... < \theta^M$.

2 Compute y_r in (37) by initially setting $w_r^i = \frac{\overline{w}^i + \underline{w}^i}{2}$, for $i = 1, ..., M$ and let $\grave{y}_r \equiv y_r$.

3 Find k $(1 \leq k \leq M-1)$ such that $y_r^k \leq \grave{y}_r \leq y_r^{k+1}$.

4 Compute $y_r = \frac{\sum_{i=1}^{M} w^i \theta^i}{\sum_{i=1}^{M} w^i}$ with $w_r^i = \begin{cases} \overline{w}^i, i \leq k \\ \underline{w}^i, i > k \end{cases}$, and let $\grave{\grave{y}}_r \equiv y_r$.

5 If $\grave{\grave{y}}_r \neq \grave{y}_r$, then go to setup 6. If $\grave{\grave{y}}_r = \grave{y}_r$, stop and put $\grave{\grave{y}}_r \equiv y_r$.

6 Set $\grave{y}_r = \grave{\grave{y}}_r$ and return to setup 3.

The procedure is similar to compute y_l, substituting y_r by y_l in setup 3, The calculation is done with

$w_l^i = \begin{cases} \overline{w}^i, i \leq k \\ \underline{w}^i, i > k \end{cases}$

Following the same reasoning the nominal model of the system given by equation (11) is calculated, and u_1 , u_2 are estimated.

B. Proposed Control Synthesis

In this subsection, we study the stability and the robustness of the closed loop system using two adaptive fuzzy systems to replace the functions $u_1 = \int_0^t \lambda_1 sign(\sigma) dt$ and $u_2 = \lambda_2 |\sigma|^{\left(\frac{1}{2}\right)} sign(\sigma)$. The terms of the high frequency component control will be given by: $\hat{u}_1(\sigma) = \underline{\theta}_1^T \underline{\xi} t_c$ and $\hat{u}_2(\sigma) = |\sigma|^{\frac{1}{2}} \underline{\theta}_2^T \underline{\xi}$. $\hat{u}_1(\sigma)$ and $\hat{u}_2(\sigma)$ are two fuzzy systems defined by (38), whose only input is the value of the sliding variable σ, and the outputs give the optimal values satisfying $\hat{u}_1^*(\sigma) = \lambda_1^* t_c$ and $\hat{u}_2^*(\sigma) = \lambda_2^* |\sigma|^{\frac{1}{2}}$ [37], t_c is the convergence time. In [37],[39] it is only estimated, in the present paper with the concept of integral sliding mode it's value is exactly determined in advance and chosen to be $t_c = t_f$.

So, the proposed control law is given by:

$$u = u_0 + u_{eq} - \hat{u}_1(\sigma) - \hat{u}_2(\sigma) \tag{39}$$

We consider the Lyapunov equation:

$$V = \frac{\sigma^2}{2} + \frac{1}{2\gamma_1} \tilde{\underline{\theta}}_1^T \tilde{\underline{\theta}}_1 + \frac{1}{2\gamma_2} \tilde{\underline{\theta}}_2^T \tilde{\underline{\theta}}_2 \tag{40}$$

with: $\tilde{\underline{\theta}} = \underline{\theta} - \underline{\theta}^*$, $\underline{\theta}^*$ is the optimal value of $\underline{\theta}$, γ_1 and γ_2 are two positive training constants.

The time derivative of V is :

$$\dot{V} = \dot{\sigma}\sigma + \frac{1}{\gamma_1} \tilde{\underline{\theta}}_1^T \dot{\underline{\theta}}_1 + \frac{1}{\gamma_2} \tilde{\underline{\theta}}_2^T \dot{\underline{\theta}}_2 \tag{41}$$

By replacing the proposed control into the derivative of the sliding variable, we obtain

$$\begin{aligned} \dot{\sigma} &= -\hat{u}_1(\sigma) - \hat{u}_2(\sigma) + D \\ &= -\hat{u}_1(\sigma) - \hat{u}_1^*(\sigma) + \hat{u}_1^*(\sigma) - \hat{u}_2(\sigma) - \hat{u}_2^*(\sigma) + \\ &\quad \hat{u}_2^*(\sigma) + D \end{aligned} \tag{42}$$

where $\hat{u}_2^*(\sigma) = |\sigma|^{\left(\frac{1}{2}\right)} \underline{\theta}_2^{*T} \underline{\xi}(\sigma)$ and $\hat{u}_1^*(\sigma) = \underline{\theta}_1^{*T} \underline{\xi}(\sigma) t_c$, then the derivative on the sliding surface can be given by:

$$\begin{aligned} \dot{\sigma} &= -\left(\underline{\theta}_1 - \underline{\theta}_1^*\right)^T \underline{\xi}(\sigma) t_c - \left(\underline{\theta}_2 - \underline{\theta}_2^*\right)^T |\sigma|^{\left(\frac{1}{2}\right)} \underline{\xi}(\sigma) \\ &\quad -\hat{u}_2^*(\sigma) - \hat{u}_1^*(\sigma) + D \end{aligned} \tag{43}$$

Substituting (43) into (41), we obtain:

$$\begin{aligned} \dot{V} &= -\sigma\left(\hat{u}_2^*(\sigma) + \hat{u}_1^*(\sigma)\right) + \frac{1}{\gamma_1} \tilde{\underline{\theta}}_1^T \left(\dot{\underline{\theta}}_1 - \gamma_1 \sigma \underline{\xi}(\sigma) t_c\right) \\ &\quad + \frac{1}{\gamma_2} \tilde{\underline{\theta}}_2^T \left(\dot{\underline{\theta}}_2 - \gamma_2 \sigma |\sigma|^{\left(\frac{1}{2}\right)} \underline{\xi}(\sigma)\right) + D\sigma \end{aligned} \tag{44}$$

If we choose the following adaptation laws:

$$\dot{\underline{\theta}}_1 = \gamma_1 \sigma \underline{\xi}(\sigma) t_c \tag{45}$$

$$\dot{\underline{\theta}}_2 = \gamma_2 \sigma |\sigma|^{\left(\frac{1}{2}\right)} \underline{\xi}(\sigma) \tag{46}$$

we obtain

$$\dot{V} = |\sigma|D - \left(\lambda_1^* t_c + \lambda_2^* |\sigma|^{\left(\frac{1}{2}\right)}\right)|\sigma| \leq 0 \tag{47}$$

Thus, the proposed control law guaranties both robustness and stability of the closed loop system. Moreover its simplicity allows an implementation for a real-time control.

VI. Illustrative Example

In this section, the proposed control is used to control an arm robot with single joint, of mass m and languor l. This arm is actuated by a DC motor as shown in figure 2.

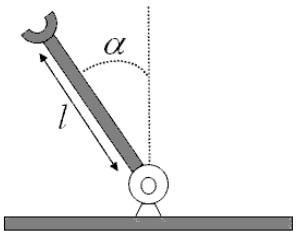

Fig. 2. Arm robot actuated by a DC motor

α means the angle rotation of the arm relative to the vertical. The dynamic of the robot is given by the $3rd$ order equation:

$$\alpha^{(3)} = f_0(\alpha, \dot{\alpha}) + g_0(\alpha, \dot{\alpha})u + D \tag{48}$$

$$\begin{cases} f_0(\alpha, \dot{\alpha}) = -\frac{R}{L}\ddot{\theta} - \left(\frac{K_b N^2 K_t}{ml^2 L} + \frac{g}{l} cos\alpha\right)\dot{\alpha} - \frac{Rg}{lL} sin\alpha \\ g_0(\alpha, \dot{\alpha}) = \dfrac{K_t N}{ml^2 L} \end{cases}$$

where $\alpha^{(3)}$, $\ddot{\alpha}$ and $\dot{\alpha}$ are the time derivatives of the angle α. g, L, R, N, K_b and K_t are respectively the gravity and the motor parameters whose signification is given in Table (1). $D = d + \Delta f + \Delta g$ means the sum of unknown external disturbances and model uncertainties.

TABLE I
Model parameters

Parameter	Notation	Value
Arm mass	m	2 Kg
Gravity	g	9.81 m/s
Arm languor	l	0.5 m
Resistance	R	1.5 Ω
Inductance	L	0.05 H
Constant EFM	K_b	0.2
Constant torque motor	K_t	0.3
Reduction ratio	N	60

As in [43],[37] the nominal fuzzy model is obtained using 2 rules describing the system dynamics around the operating points 0 and $\pm\frac{\pi}{2}$.

Rule*1*: IF $x_1(t)$ is close to 0
THEN

$$\begin{cases} \dot{x}(t) = A_1 x(t) + B_1 u(t) \\ y(t) = Cx(t) \end{cases} \tag{49}$$

Rule*2*: IF $x_1(t)$ is close to $\pm\pi/2$
THEN

$$\begin{cases} \dot{x}(t) = A_2 x(t) + B_2 u(t) \\ y(t) = Cx(t) \end{cases} \tag{50}$$

where:

$$A_1 = \begin{bmatrix} 0 & 1 & 0 \\ 0 & 0 & 1 \\ \frac{-Rg}{lL} & -\frac{g}{l} - \frac{K_b N^2 K_t}{ml^2 L} & \frac{R}{L} \end{bmatrix}, B_1 = \begin{bmatrix} 0 \\ 0 \\ \frac{K_t N}{ml^2 L} \end{bmatrix}$$

$$A_2 = \begin{bmatrix} 0 & 1 & 0 \\ 0 & 0 & 1 \\ \frac{-Rg}{lL} & -\frac{K_b N^2 K_t}{ml^2 L} & \frac{R}{L} \end{bmatrix}, B_2 = \begin{bmatrix} 0 \\ 0 \\ \frac{K_t N}{ml^2 L} \end{bmatrix}$$

$C = \begin{bmatrix} 1 & 1 & 0 \end{bmatrix}^T$ and $x(t) = \begin{bmatrix} \alpha & \dot{\alpha} & \ddot{\alpha} \end{bmatrix}^T$. The control objective is to control the state $x_1(t)$ of the system to track the reference trajectory $y_r(t) = sin(2t)$. Suppose that structural uncertainty, which represent the variation in the mass in this example, is in the form $dm = 0.02m(sin(2t)+sin(3t))$ while the external perturbation is assumed to be $d = sin(3t)$. According to the sliding surface given by Slotine [5] and since the system is of order $(n = 3)$, the sliding surface is given by $s = \ddot{e} + 2\lambda\dot{e} + \lambda^2 e$. e is the tracking error position $(e = x_1 - y_r)$, $\dot{e}$ is the tracking error velocity $(\dot{e} = x_2 - \dot{y}_r)$. To construct the nominal model as given by (10), we define three T2 fuzzy interval sets depending on the variable $x_1(t)$. Similarly to generate the two adaptive fuzzy systems allows us to approximate u_1 and u_2, we consider five interval fuzzy T2 sets: Negative, Small Negative, Zero, Small Positive and Positive, according to the variable s. In sliding regime, the transition between the approaching phase and the sliding phase occurs when the value of this one is zero. Therefore, in [9], it is showed that more the membership function corresponding to the fuzzy set zero is small, better are the tracking performances. The membership functions involved in building the model are given by the following equations:

$$\mu_{\tilde{H}_1^i} = 1/\left(1 + exp\left(1,8\left(x_1(t) + (0,61 + c_1)\right)/\left(\frac{\pi}{16}\right)\right)\right)$$
$$\mu_{\tilde{H}_2^i} = exp\left(-\left(x_1(t)/\left(\frac{\pi}{4.5+c_2}\right)^2\right)\right)$$
$$\mu_{\tilde{H}_3^i} = 1/\left(1 + exp\left(-1.8(x_1(t) + (0,61 + c_1))/\left(\frac{\pi}{16}\right)\right)\right)$$

where c_1 and c_2 designate an area of uncertainty, in the case of our application $c_1 \in [0, 0.2]$ and $c_2 \in [0, 1]$. Similarly the antecedent sets of the two adaptive systems are obtained by adding an area of uncertainty. Figure 3 (a and b) shows the shape fuzzy sets of the nominal model and the adaptive systems.

The time derivative of s reads as $\dot{s} = \phi(.) + \gamma(.)u$ with $\phi(.) = -y_r^{(3)} + f_0(x) + 2\lambda\ddot{e} + \lambda^2 e$ and $\gamma(.) = g_0(x)$. Let $z = s$, $A = [0]$ and $B = [1]$. Then as shown in section IV, the 2-order SMC is equivalent to the finite time stabilization of

$$\dot{z} = Az + Bu + [\phi(.) + (\gamma(.) - 1)u] \tag{51}$$

Let $t_f = 0.5s$. The state is initialized at $x(0) = \begin{bmatrix} 1 & 0 & 0 \end{bmatrix}$ (the others constant are:$\lambda = 20, \gamma_1 = 80$ and $\gamma_2 = 40$), which implies that $z(0) = -320$. As mentioned in [24], the initial condition of δ are computed in order that the sliding variable

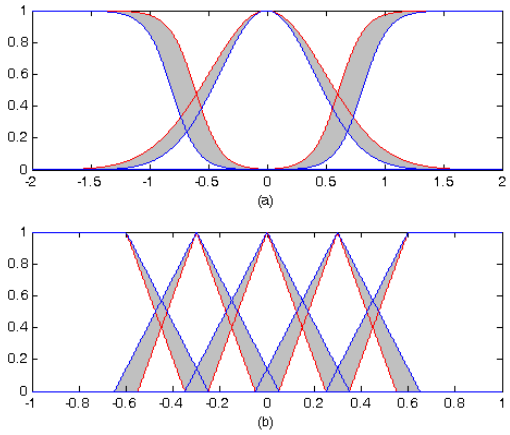

Fig. 3. (a) Interval type-2 antecedent membership functions of $x_1(t)$ defined for the interval nominal model; (b) Interval type-2 antecedent membership functions of s defined for the interval adaptive fuzzy systems.

s equal 0 at exactly $t = t_f = 0.5s$.
The first step consists in solving Riccatis equation (second line of (19) for a matrix Q which is symmetric positive definite. The solution of this equation, M, is a symmetric positive definite matrix. Q is stated as $Q = [10]$, then one gets $M = 3.1623$.
The second step consists in determining $\delta(0)$ such that $z(t_f) = 0$, knowing that only initial bounded condition $z(0)$ is known. From first line of (19), one gets

$$\delta(t) = e^{A_m t}\delta(0) \tag{52}$$

with $A_m = -[A^T - MBB^T]$. Then, by supposing that $t \leq t_f$, and from (16) and (20), one gets

$$\dot{z} = -A_m^T + BB^T e^{A_m t}\delta(0) \tag{53}$$

By multiplying both sides of previous equation by $e^{A_m^T t}$, one gets
$e^{A_m^T t}\dot{z} + e^{A_m^T t}A_m^T z = e^{A_m^T t}BB^T e^{A_m^T t}\delta(0)$
$\Rightarrow [[e^{A_m^T t}]^T z(t)] = e^{A_m^T t}BB^T e^{A_m^T t}\delta(0)$
By integrating this last equation from $t = 0$ to $t = t_f$, with $z(t_f) = 0$, one gets

$$z(0) = \left[-\int_0^{t_f} e^{A_m^T t}BB^T e^{A_m t}dt\right]\delta(0) \tag{54}$$

$H = [\int_0^{t_f} e^{A_m^T t}BB^T e^{A_m t}dt]$ is the partial reachability gramian. Then, the initial condition $\delta(0)$ ensuring that $z(t_f) = 0$ can be derived from $\delta(0) = -H^{-1}z(0)$. H is evaluated using an algorithm from [44], its Matlab code being available in [45] as grampar function. We get $\delta(0) = 89.4549$. Figure 4 and figure 5(a) display the convergence of s, $\dot{s}$ and the quadratic error e to $zero$ in exactly $0.5s$. Figure 5(b) displays the control signal which is smooth and free from chattering and abrupt variations. Figure 6 shows a good tracking of position and velocity trajectories. The state $(x_1(t), x_2(t))$ converge quickly to their references $(y_r, \dot{y}_r)$.

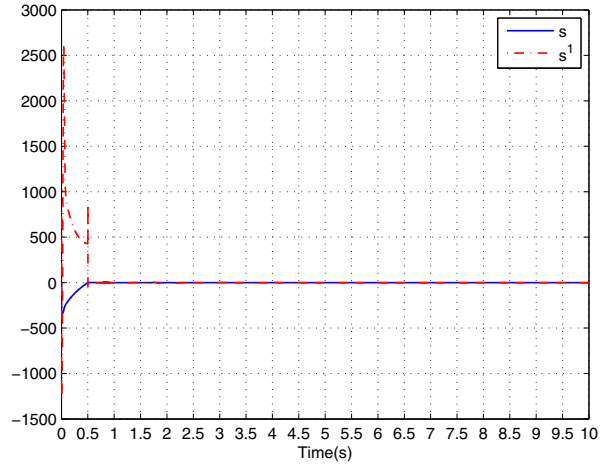

Fig. 4. s and $\dot{s}$ versus time(s)

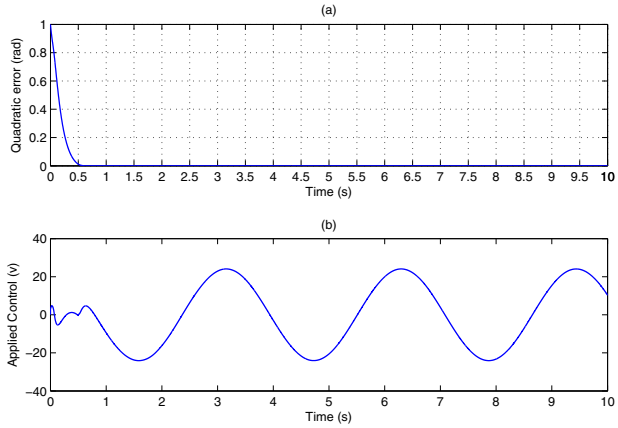

Fig. 5. (a) Trajectory of the quadratic tracking error position; (b) Control input u (v)

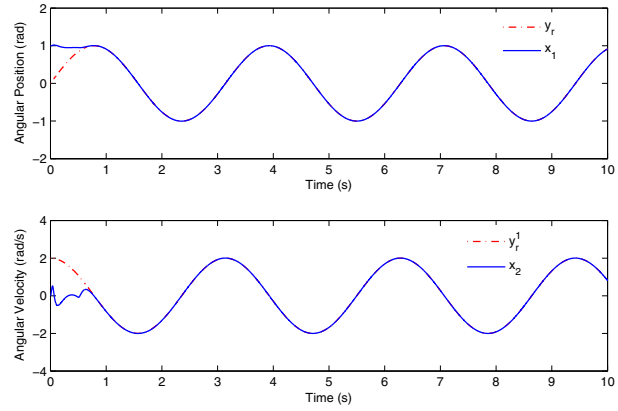

Fig. 6. (a) The state $x_1(t)$ (solid line) and it's reference y_r (dashed line);(b) The state $x_2(t)$ (solid line) and it's reference $\dot{y}_r$ (dashed line)

VII. Conclusion

In this paper, we have presented a type-2 fuzzy sliding modes controller for a perturbed uncertain nonlinear system. The control is generated from a nominal fuzzy type-2 model, who exploits the linear local models of the system. These local models are obtained by linearisation around some operating points. Two adaptive interval type-2 fuzzy systems are introduced to calculate the two switching control terms in order to overcome some restrictive constraints and to eliminate efficiency the chattering phenomenon. The stability and robustness of the closed loop system are proved analytically. The update of adjustable parameters of the two type-2 fuzzy systems are ensured by the adaptation laws derived using Lyapunov theory. The design uses the integral sliding mode concept. The controller is able to steer to zero in finite time the sliding surface and it's derivatives; the convergence time can be fixed in advance. A simulation example has been presented to illustrate the effectiveness and the robustness of the proposed approach. Currently we are working on the generalization of this approach to multi-input multi-output system with real-time implementation.

Acknowledgment

This work is developed for the project CPER-MOSYP and supported by both the Champagne-Adrdenne Region and the European found FEDER.

References

[1] V. I. Utkin. Variable structure systems with sliding modes. *IEEE Transactions on Automatic Control*, vol. 22, pp. 212–222, 1977.

[2] V. I. Utkin. *Sliding mode in control and optimization*. Berlin: Springer, 1992.

[3] V. I. Utkin, J. Gulder and J. Shi. Sliding mode in control in electromechanical systems. *London: Taylor & Francis*, 1999.

[4] J. J. Slotine. Sliding mode controller design for non-linear systems. *International Journal of Control*, pp. 421–434, 1984.

[5] J. J. Slotine and L. Weiping. *Applied Nonlinear Control,*. Printice Hall, 1991.

[6] J.Y. Humg, W.Gao and J.C. Hung. Variable structure control: a survey. *IEEE Transaction, Industrial Electronics*, vol. 40, no. 1, pp. 2–22, 1993.

[7] G. Song, L. Cai, Y. Wang and R.W. Longman. A sliding-mode based smooth adaptive robust controller for friction compensation. *International Journal of Robust and Nonlinear Control*, vol. 8, no. 8, pp. 725–739, 1998.

[8] H.F. Ho, Y.K. Wong and A.B. Rad. Adaptive fuzzy sliding mode control with chattering elimination for nonlinear SISO systems. *Simulation Modelling Practice and Theory*, vol. 17, no. 7, pp. 1199–1210, 2009.

[9] A. Hamzaoui, N.Essounbouli and J. Zaytoon. Commande par Mode glissant Flou d'un Systme Non linaire Incertain. *Electronique des Sciences et Technologies de l'Automatique, e-STA, SEE*, 2003.

[10] N. Noroozi, M. Roopaei and M.Z. Jahromi. Adaptive fuzzy sliding mode control scheme for uncertain systems. *Commun Nonlinear Sci Numer Simulat*, vol. 14, no. 11, pp. 3978–3992, 2009.

[11] X. Yu, O. Kaynak. Sliding-mode control with soft computing: a survey. *IEEE Transactions On Industrial Electronics*, vol. 56, no. 9, pp. 3275–3285, 2009.

[12] A. Levant. Sliding order and sliding accuracy in sliding mode control. *International Journal of Control*, vol. 58, no. 6, pp. 1247-1263, 1993.

[13] S. Emelyanov, S. Korovin and A. Levant. High-order sliding modes in control systems. *Computational Mathematics and Modeling*, vol. 7, no. 3, pp. 294-318, 1996.

[14] G. Bartolini, A. Ferrara and E. Ussai. Output tracking control of uncertain nonlinear second-order systems. *Automatica*, vol. 33, no. 12, pp. 2203-2212, 1997.

[15] A. Levant. Higher-order sliding modes, differentiation and outputfeedback control. *International Jornal of Control, Special issue on Sliding-Mode Control*, vol. 76, no. 9, pp. 924-941, 2003.

[16] K. Furuta. Sliding mode control of discrete system. *Systems & Control Letters*, vol. 14, no. 2, pp. 145-152, 1990.

[17] A. Levant. Homogeneity approach to high-order sliding mode design. *Automatica*, vol. 45, no. 5, pp. 823-830, 2005.

[18] A. Levant. Universal siso sliding-mode controllers with finite-time convergence. *IEEE Transactions on Automatic Control*, vol. 46, no. 9, pp. 1447-1451. 2001.

[19] S. Laghrouche, F. Plestan and A. Glumineau. *Higher order sliding mode control based on optimal linear quadratic control and integral sliding mode*. IFAC symposium on nonlinear control systems NOLCOS'04. Stuttgart, Germany. 2004.

[20] Y. Wu, X, Yu and Z. Man. Terminal sliding mode control design for uncertain dynamic systems. *Systems & Control Letters*, vol. 35, no. 5, pp. 281-2872, 1998.

[21] G. Bartolini, A. Ferrara, A. Levant and E. Ussai. *On second order sliding mode controllers*. in Variable Structure systems, Sliding Mode and Nonlinear Control, Springer Berlin / Heidelberg, 1999.

[22] S. Laghrouch, F. Plestan and A. Glumineau. Higher order sliding mode control based on integral sliding mode. *Automatica*, vol. 43, no. 3, pp. 531-537, 2007.

[23] V.I. Utkin and J. shi. *Integral sliding mode in systems operating under uncertainty*. Proceedings of the IEEE conference on decision and Control CDC96. Kobe, Japan, 1996.

[24] Z. V. Rekasius. An alternate approach to the fixed terminal point regulator problem. *IEEE Transactions on Automatic Control*, vol. 9, no. 3, pp. 290-292, 1964.

[25] K Chafaa, L Saidi, M Ghanai and K Benmahammed, "Indirect adaptive interval Type-2 fuzzy control for nonlinear systems," *International Journal of Modelling, Identification and Control*, vol. 2, no. 2, pp. 106–119. 2007.

[26] K Chafaa, L Saidi, M Ghanai and K Benmahammed, "Direct adaptive Type-2 fuzzy control for nonlinear systems," *International Journal of Computational Intelligence and Applications*, vol. 6, no. 3, pp. 389–411 . 2006.

[27] H.A. Hagras, "A hierarchical Type-2 fuzzy logic control architecture for autonomous mobile robots," *IEEE Transactions on Fuzzy systems*, vol. 12, no. 4, pp. 524-539. 2004.

[28] A. Mencattini, M. Salmeri and R. Lojacono, "Type-2 fuzzy sets for modeling uncertainty in measurement," *Proceedings of IEEE International Workshop on Advanced Methods for Uncertainty Estimation in Measurement*, pp. 8–13 . 20-21 April, Sardagna, Italia, 2006.

[29] N.N. Karnik, J.M. Mendel and Q. Liang. Type-2 fuzzy logic systems. *IEEE Transactions on Fuzzy Systems*, vol. 7, no. 6, pp. 643-658, 1999.

[30] J. Mendel. Uncertainty, fuzzy logic and signal processing. *Signal Processing*, vol. 8, no. 6, pp. 913–933, 2000.

[31] J. Mendel. Fuzzy logic systems for engineering: a tutorial. *IEEE Processings*, vol. 83, no. 3, pp 345–377, 1995.

[32] J. Mendel. *An introduction to type-2 fuzzy logic systems*. Univ Southern California, Los Angelos,CA.[Online].http://sip.usc.edu mendel/report. 1998.

[33] J. Mendel. Computing derivatives in interval type-2 fuzzy logic systems. *IEEE Transactions on Fuzzy Systems*, vol. 12, no. 1, pp. 84–98, 2004.

[34] D. Wu and J. Mendel. Enhanced Karnik-Mendel Algorithms. *IEEE Transactions on Fuzzy Systems*, vol. 17, no. 4, pp. 923–934, 2009.

[35] A. Hamzaoui, N. Essounbouli, K. Benmahammed and J. Zaytoon. State observer based robust adaptive fuzzy controller for nonlinear uncertain and perturbed systems. *IEEE Transactions on Systems Man, and Cybernetics*, vol. 34, no. 2, pp. 942-950, 2004.

[36] T. Takagi and M. Sugeno. Fuzzy identification of systems and its applications to modeling and control. *IEEE Transactions on Systems Man, and Cybernetics*, vol. 15, no. 1, pp. 116-132, 1985.

[37] M. Manceur, N. Essounbouli and A. Hamzaoui. *Robust Smooth Sliding Type-2 Interval Fuzzy Control For Uncertain System*. IEEE International Conference on Fuzzy Systems (FUZZ-IEEE 2010), Barcelone, Spain, July 18-23, pp. 2713–2720, 2010.

[38] A. F. Filippov. *Differential equations with discontinuous right-hand side*. Dordrecht: Kluwer Academic Publishers, 1988.

[39] M. Manceur, N. Essounbouli, and A. Hamzaoui. *MIMO Second Order Sliding Mode Fuzzy Type-2 Control*. IEEE International Conference on Systems, Man and Cybernetics, Istumbul, Turkey, October 10–13, pp. 1812–1820, 2010.

[40] Y. B. Shtessel, I. A. Shkolnikov and A. Levant. Smooth second-order sliding modes: Missile guidance application. *Automatica*, vol. 43, no. 8, pp. 1470–1476, 2007.

[41] L. Fridman and A. Levant. Higher-order Sliding Modes. In Handbook of Intelligent Control, W. Perruquetti and J. P. Barbot, *Neural, Fuzzy, and Adaptive Approaches*. Marcel Dekker, New York, 2002.

[42] L. X. Wang. *Adaptive Fuzzy Systems and Control: Design and Stability Analysis*. New Jersey: Printice Hall, 1994.

[43] B.K. Yoo and W. Chul Hum. Adaptative Control of Robot Manipulator Using Fuzzy Compensator. *IEEE Transactions on Fuzzy Systems*, vol. 8, no. 2, pp. 186–199, 2000.

[44] C. F. VanLoan. Computing Integrals Involving the Matrix Exponential. *IEEE Transactions on Automatic Control*, vol. 23, no. 3, pp. 395–404, 1978.

[45] P. de Larminat. *Contrle d'tat standart*. Herms. Paris, 2000.

2011 IEEE International Conference on Fuzzy Systems
June 27-30, 2011, Taipei, Taiwan

Output Regulation Using Integral Fuzzy Predictive Control with Piecewise Lyapunov Functions

Chien-Hung Liu
Department of Avionics
China University of Science and Technology
Hsinchu 31241, Taiwan
Telephone: 886-3-5935707-305
Fax: 886-3-5936591
E-mail: lch@cc.cust.edu.tw

Kuang-Yow Lian
Department of Electrical Engineering
National Taipei University of Technology
Taipei 10608, Taiwan
Telephone: 886-2-27712171-217
Fax: 886-2-27317187
E-mail: kylian@ntut.edu.tw

***Abstract*—This study proposes an LMI-based integral fuzzy model predictive control (MPC) for output regulation via piecewise Lyapunov function. In order to eliminate the system's bias and guarantee the zero-offset output regulation performance, firstly we take coordinate translation on equilibrium point and introduce an added integral state of output regulation error for the nonlinear plant, and then convert the resulting augmented system into a Takagi-Sugeno fuzzy model. Under the input constraint, an integrator based state feedback control law is computed by solving a convex optimization problem based on the infinite horizon predictive control scheme. Moreover, the proposed control design has following merits: i) reducing the conservatism by using piecewise Lyapunov function; ii) improving the transient performance by adding a decay rate condition; and iii) ensuring asymptotic stability for output regulation in the presence of time varying parameter. Finally, a numerical example is presented to demonstrate the effectiveness of the proposed integral fuzzy predictive controller.**

Keywords- Integral fuzzy model predictive control; linear matrix inequalities (LMIs); output regulation; Takagi-Sugeno fuzzy model; piecewise Lyapunov function

I. INTRODUCTION

Model predictive control (MPC) has developed considerably over the last two decades [1]. The strategy of MPC is to use the knowledge of the plant to predict how the system behaves and take an appropriate control action. Compared with other control techniques, the key advantage of MPC is that its control law is obtained from an optimization procedure at each sampling time, whose objective function is related to control efforts and the prediction of future states. In addition, it can handle input/output constraints directly. Recently, MPC has been applied widely to many systems, such as nonlinear complex systems, hybrid systems and piecewise affine systems [1]. In practice, most physical plants are nonlinear and contain uncertainties. For a highly nonlinear system, a linear MPC algorithm may not satisfy dynamic performance. Recently, several researchers have developed nonlinear model predictive control (NMPC) algorithms to deal with highly nonlinear industrial processes. In fact, NMPC generally requires an accurate model and then computes an optimal or suboptimal solution for a nonlinear nonconvex optimization problem at each sampling time. The increase of the prediction horizon further intensifies the time-consuming online computation load [2]. On the other hand, in order to handle the control of uncertain systems and reduce the computational burden, Kothare *et al*. [3] proposed an efficient procedure for robust constrained MPC by using linear matrix inequalities, which is suitable for online predictive controller's implementation. Since then, many LMI-based MPC approaches emerge, such as [4],[5]. More recently, the T-S fuzzy model approach has been incorporated into LMI-based MPC strategy to overcome previous drawbacks of NMPC because of its ability to accurately approximate complex nonlinear systems by a set of linear subsystems with associated membership functions [6],[7]. In stability analysis, it has been known that a common Lyapunov function might not exist for many fuzzy systems, especially for highly nonlinear complex systems. Instead, many authors [8]-[10] have presented a stability result of fuzzy systems using a piecewise Lyapunov function because of which can able to deal with a larger class of fuzzy dynamic systems in controller design.

The study of output regulation problems for nonlinear systems keeps attracting considerable attention due to demands from practical dynamical processes in mechanics, economics and biology. Based on this observation, many LMI-based fuzzy controller designs have been developed to solve output regulation control problems for nonlinear systems [11],[12]. In recently year, several well-developed approaches are proposed to design LMI-based NMPC algorithms for the purpose of regulating the system output at constant values [13],[14]. In this work, we combine coordinate translation, integral control technique, and fuzzy MPC scheme; meanwhile, a piecewise Lyapunov function is defined and utilized to synthesize the controller, to deal with the output regulation problem for nonlinear systems. As the result, at each time instant k, the fuzzy MPC controller with the input constraint is computed by solving a convex optimization problem over the infinite horizon objective function. Sufficient conditions are derived for asymptotic stabilizing the closed-loop predictive control system in linear matrix inequalities (LMIs). In addition, a decay rate conditions are also derived to improve the transient

This work was supported by the National Science Council, R.O.C, under Grant NSC 98-2221-E-027-116-MY3.

978-1-4244-7316-8/11/$26.00 ©2011 IEEE

control performance. Moreover, the piecewise Lyapunov function has been used to reduce the conservatism of the existing predictive controller. In order to reveal the validity of the proposed controller design, a nonlinear chaotic system with time varying parameter is considered to demonstrate the output regulation control task.

The contents of this paper are organized as follows. In Section II, problem formulation: coordinate translation and integral control are introduced. In Section III, Output regulation using integral fuzzy MPC based on piecewise Lyapunov functions is presented. The theorem result also includes the input constraint and decay rate conditions. Numerical simulation is carried out for the chaotic system to verify the proposed controller in Section IV. Finally, some conclusions are given in Section V.

II. Problem Formulation

A. Coordinate Translation and Integral Control

Consider a general discrete-time nonlinear system as follows:

$$\begin{aligned} x_p(k+1) &= f(x_p(k)) + g(x_p(k))u(k) + \eta \\ y(k) &= h(x_p(k)) \end{aligned} \tag{1}$$

where $x(k) \in R^{n_x}$ denotes the state variables; $y(k) \in R^{n_y}$ is the output vector; $u(k) \in R^{n_u}$ is input vector; $f(x)$, $g(x)$ and $h(x)$ are nonlinear function vectors with appropriate dimensions and η is system bias term. Note that if the system is controllable and subject to a constant bias term, it may have $f(x_p(k)) = 0$ at $x_p(k) = 0$, $g(x_p(k)) \neq 0 \ \forall \ x_p(k)$ and output function may have an offset such that $h(x_p(k)) \neq 0$ at $x_p(k) = 0$. Let $y_d \in R^{n_y}$ be a constant reference. In order to ensure zero offset output regulation performance in the presence of plant parameter variations, we want to design an integrator based controller such that $y(k) \to y_d$ as $k \to \infty$. Its principle is based on the procedure of introducing an integral action in the forward channel of tracking system to guarantee tracking property. To this end, we introduce an new state variable to account the resulting integrated tracking error, denoted by $x_e(k)$, is computed as

$$x_e(k+1) = x_e(k) + y_d - y(k) \tag{2}$$

Combining (1) with (2), we obtain the augmented dynamics as follows

$$\begin{aligned} x_p(k+1) &= f(x_p(k)) + g(x_p(k))u(k) + \eta \\ x_e(k+1) &= x_e(k) + y_d - h(x_p(k)) \end{aligned} \tag{3}$$

Let us define the regulation error as $e(k) = y_d - y(k)$. Without loss of generality, there always exists some equilibrium point for constant output reference y_d in practical industrial process control, denoted by the steady state $\bar{x}_p \in R^{n_x}$ and the corresponding input $\bar{u} \in R^{n_u}$. Then, the objective of output regulation for biased nonlinear system will be achieved by stabilizing the system at an equilibrium state which produces $e(k) = 0$. For this purpose, it follows that

$$\begin{aligned} \bar{x}_p - f(\bar{x}_p) - g(\bar{x}_p)\bar{u} - \eta &= 0 \\ y_d - h(\bar{x}_p) &= 0. \end{aligned} \tag{4}$$

Here (4) is assumed to have a unique solution $(\bar{x}_p, \bar{u})$. To eliminate the constant bias term η from the dynamics (3), we consider the coordinate translation: let $\tilde{x}_p(k) = x_p(k) - \bar{x}_p$ and $\tilde{u}(k) = u(k) - \bar{u}$. By using the property of (4), the dynamics of the system (3) can be written as follows:

$$\begin{aligned} \tilde{x}_p(k+1) &= f_s(\tilde{x}_p(k)) + g_s(\tilde{x}_p(k))\tilde{u}(k) \\ x_e(k+1) &= x_e(k) + h_s(\tilde{x}_p(k)) \end{aligned} \tag{5}$$

where $f_s(\tilde{x}_p(k)) = f(\tilde{x}_p(k) + \bar{x}_p) - f(\bar{x}_p) + [g(\tilde{x}_p(k) + \bar{x}_p) - g(\bar{x}_p)]\bar{u}$; $g_s(\tilde{x}_p(k)) = g(\tilde{x}_p(k) + \bar{x}_p)$; and $h_s(\tilde{x}_p(k)) = h(\bar{x}_p) - h(\tilde{x}_p(k) + \bar{x}_p)$. Clearly, $f_s(\tilde{x}_p(k)) = 0$, $h_s(\tilde{x}_p(k)) = 0$, $g_s(\tilde{x}_p(k)) \neq 0$, once $\tilde{x}_p(k) = 0$.

B. T-S Fuzzy Modeling

From (5), the transformed augmented system can be expressed as a state-space form with no bias terms and free-offset error signal $e(k)$:

$$\begin{aligned} \tilde{x}_p(k+1) &= A(\tilde{x}_p(k))\tilde{x}_p(k) + B(\tilde{x}_p(k))\tilde{u}(k) \\ x_e(k+1) &= x_e(k) + C(\tilde{x}_p(k))\tilde{x}_p(k) \end{aligned} \tag{6}$$

where A, B and C are the system matrix, the input matrix and the output matrix, respectively. Next, we employ the T-S fuzzy dynamic model proposed in [15] to represent the system (6) with fuzzy inference rules and local analytic linear models as follows:

Model Rule s :
IF $\tilde{z}_1(k)$ is F_{1s} and $\cdots$ and $\tilde{z}_g(k)$ is F_{gs}
THEN $\tilde{x}_p(k+1) = A_s\tilde{x}_p(k) + B_s\tilde{u}(k)$
$x_e(k+1) = x_e(k) + C_s\tilde{x}_p(k)$, $1 \leq s \leq r$

where $\tilde{z}(k) = [\tilde{z}_1(k)\, \tilde{z}_2(k) \cdots \tilde{z}_g(k)]$ are known premise variables that may be functions of the state variables; $F_{js}(j = 1, 2, \ldots, g)$ is the fuzzy set and r is the number of model rules; A_s, B_s and C_s are system matrices of appropriate dimensions. Using singleton fuzzifier, product inference and weighted average defuzzifier, the fuzzy system is inferred as follows:

$$\begin{aligned} \tilde{x}_p(k+1) &= \sum_{s=1}^{r} \mu_s(\tilde{z}(k))\{A_s\tilde{x}_p(k) + B_s\tilde{u}(k)\} \\ x_e(k+1) &= x_e(k) + \sum_{s=1}^{r} \mu_s(\tilde{z}(k))C_s\tilde{x}_p(k) \end{aligned} \tag{7}$$

where $\mu_s(\tilde{z}(k)) = w_s(\tilde{z}(k)) / \sum_{s=1}^{r} w_s(\tilde{z}(k))$ with $w_s(\tilde{z}(k)) = \prod_{j=1}^{g} F_{js}(\tilde{z}_j(k))$ for all k and $F_{js}(\tilde{z}_j(k))$ is the grade of membership of $\tilde{z}_j(k)$ in F_{js}. Note that $\sum_{s=1}^{r} \mu_s(\tilde{z}(k)) = 1$ for all k and $\mu_s(\tilde{z}(k)) \geq 0$, for $s = 1, 2, ..., r$, are regarded as grade function. Denoting the augmented state vector as $x_a(k) = \left[\tilde{x}_p(k)^T \ x_e(k)^T\right]^T$, the augmented system (7) becomes as

$$x_a(k+1) = \sum_{s=1}^{r} \mu_i(\tilde{z}(k))\{\tilde{A}_s x_a(k) + \tilde{B}_s u_a(k)\} \tag{8}$$

where

$$\tilde{A}_s = \begin{bmatrix} A_s & 0 \\ C_s & I \end{bmatrix}, \quad \tilde{B}_s = \begin{bmatrix} B_s \\ 0 \end{bmatrix}.$$

Then the resulting integral state feedback controller via the PDC

$$\begin{aligned} u_a(k) &= -\sum_{j=1}^{r} \mu_j(\tilde{z}(k)) K_j x_a(k) \\ &= -\sum_{j=1}^{r} \mu_j(\tilde{z}(k)) [K_{pt} \ K_{et}] \cdot \begin{bmatrix} \tilde{x}_p(k) \\ x_e(k) \end{bmatrix} \end{aligned} \tag{9}$$

where K_{pt} denotes the feedback gain for $\tilde{x}_p(k)$ and K_{et} is the gain associated with $x_e(k)$.

III. Output Regulation Using IFMPC Based on Piecewise Lyapunov Functions

A. Stability for Piecewise Lyapunov Functions

According to [9], the state space of the premise variable can be partitioned into a number of closed polyhedral regions, denoted as $\{\Im_m\}_{m\in N} \subseteq R^{n_x}$, where N is the index set of regions. For subsequent use, a set Γ that represents all possible transitions from one region to any region at the instant k is defined as

$$\Gamma := \{n, m | x_a(k) \in \Im_n, x_a(k+1) \in \Im_m\}. \tag{10}$$

A piecewise Lyapunov function for current region is defined as follows:

$$V(k) = x_a(k)^T P_n x_a(k), \quad x_a(k) \in \Im_n \tag{11}$$

Then we have

$$\begin{aligned} \Delta V(k) &= V(k+1) - V(k) \\ &= x_a(k+1)^T P_m x_a(k+1) - x_a(k)^T P_n x_a(k) \end{aligned} \tag{12}$$

If the Lyapunov function (12) satisfies that $\Delta V < 0$ for all time, the system can be guaranteed to be stable in the sense of Lyapunov.

B. Integral Fuzzy MPC with Input Constraint

In general, the MPC problem is formulated as solving optimal control problem subject to system dynamics and constraints involving states and controls. In this paper, we introduce a integral T-S fuzzy infinite horizon MPC scheme (IFMPC) to predict the future state of the plant (8) and state feedback control law (9) as follows:

$$\begin{aligned} x_a(k+i+1|k) = \sum_{s=1}^{r} \mu_s(\tilde{z}(k+i|k)) \{ &\tilde{A}_s x_a(k+i|k) \\ &+ \tilde{B}_s u_a(k+i|k) \} \end{aligned} \tag{13}$$

$$u_a(k+i|k) = -\sum_{j=1}^{r} \mu_j(\tilde{z}(k+i|k)) K_j(k) x_a(k+i|k). \tag{14}$$

where $x_a(k+i|k)$ denotes the system state at time $k+i$, predicted based on the measurements at time k and belongs to some region $x_a(k+i|k) \in \Im_n$; $u_a(k+i|k)$ denote the control input at time $k+i$, computed by the optimization problem at time k. The objective of the integral fuzzy predictive controller is to compute an optimal control sequence with respect to the following infinite horizon objective function [3], [4] at each time instant k.

$$\min_{u_a(k+i|k)=K_j(k)x_a(k+i|k),\ k,i\geq 0,\ 1\leq j\leq r} J_0^{\infty}(k) \tag{15}$$

subject to

$$\| u_a(k+i|k) \|_2 \leq u_{max}, \quad k, i \geq 0 \tag{16}$$

where

$$\begin{aligned} J_0^{\infty}(k) &= \sum_{i=0}^{\infty} (x_a(k+i|k)^T Q x_a(k+i|k) \\ &\quad + u_a(k+i|k)^T R u_a(k+i|k)) \\ &= x_a(k|k)^T Q x_a(k|k) + u_a(k|k)^T R u_a(k|k) \\ &\quad + J_1^{\infty}(k) \end{aligned} \tag{17}$$

with $Q \geq 0$ and $R > 0$ are weighted symmetric matrices. We introduce the following Lemmas which are needed for the proof of theorem.

Lemma 1 : Let μ_{1s}, μ_{2j} and h_r be the normalized membership functions. Then,

$$\sum_{s=1}^{p} \sum_{j=1}^{q} \mu_{1s} \mu_{2j} = \sum_{r=1}^{pq} h_r$$

with $h_r = \mu_{1\cdot s(r)} \mu_{2\cdot j(r)}$, where $s(r) = 1 + \lfloor \frac{r-1}{q} \rfloor$; $j(r) = r - \lfloor \frac{r-1}{q} \rfloor q$; and $\lfloor \cdot \rfloor$ denotes the floor function.

Lemma 2 : Let M_s be a matrix and h_s be the normalized membership function. Then,

$$\sum_{s=1}^{r} \sum_{j=1}^{r} h_s h_j M_s^T M_j \leq \sum_{s=1}^{r} h_s M_s^2$$

C. Output Regulation Using IFMPC Based on Piecewise Lyapunov Functions

Without loss of generality, suppose that the state will transit from one region $\Im_n$ to any possible region $\Im_m$ after instant k with $n, m \in \Gamma$. The piecewise Lyapunov function for predictive system at any time instant k can be defined by

$$\begin{aligned} V(i,k) &= x_a(k+i|k)^T P_n(k) x_a(k+i|k), \\ V(i+1,k) &= x_a(k+i+1|k)^T P_m(k) x_a(k+i+1|k), \\ &n, m \in \Gamma, P_n(k) > 0, P_m(k) > 0, \quad k, i \geq 0 \end{aligned} \tag{18}$$

where $P_n(k)$ denote the common positive definite matrix at time k and belong to region n. Let us suppose temporarily, that for any instant k and $i \geq 0$, the following inequality is satisfied:

$$\begin{aligned} \triangle V(i,k) \leq -((&x_a(k+i|k)^T Q x_a(k+i|k) \\ &+ u_a(k+i|k)^T R u_a(k+i|k)) \end{aligned} \tag{19}$$

Inspired by (19) and applying Lemma 1, Lemma 2 and rule reduction method in [15], we can lead to the following sufficient condition of stability:

$$\begin{aligned} G_{ss}^T P_m(k) G_{ss} - P_n(k) + Q + K_s(k)^T R K_s(k) < 0, \\ 1 \leq s \leq r \end{aligned} \tag{20}$$

$$\begin{aligned} (\frac{G_{sj} + G_{js}}{2})^T P_m(k) (\frac{G_{sj} + G_{js}}{2}) - P_n(k) + Q \leq 0, \\ 1 \leq s < j \leq r \end{aligned} \tag{21}$$

where $G_{sj} = \tilde{A}_s - \tilde{B}_s K_j(k)$. Further, summing (19) from $i = 1$ up to $i = \infty$ with $x_a(\infty|k) = 0$ and $V(\infty, k) = 0$, the following condition is obtained:

$$J_1^{\infty}(k) \leq V(1,k) = x_a(k+1|k)^T P_m(k) x_a(k+1|k) \tag{22}$$

Combining (17) and (22), we obtain the upper bound for $J_0^{\infty}(k)$ as follows

$$\begin{aligned} J_0^{\infty}(k) \leq\ & x_a(k|k)^T Q x_a(k|k) + u_a(k|k)^T R u_a(k|k) \\ & + x_a(k+1|k)^T P_m(k) x_a(k+1|k) \end{aligned} \tag{23}$$

In this paper, the output regulation problem under consideration is equivalent to design an integral fuzzy feedback controller (14) such that the resulting closed-loop fuzzy system (13) is asymptotically stable and the performance constraint (19) is fulfilled. Therefore the minimization problem (15) can be considered as $J_0^{\infty}(k) < \gamma < \infty$. Obviously, minimizing $J_0^{\infty}(k)$ with $P_t(k) > 0$ is equivalent to

$$\min_{\gamma, u_a(k|k), \bar{P}_t(k), M_t(k),\ t \in N} \gamma \tag{24}$$

subject to

$$\begin{aligned} & x_a(k|k)^T Q x_a(k|k) + u_a(k|k)^T R u_a(k|k) \\ & \quad + (\tilde{A} x_a(k|k) + \tilde{B} u_a(k|k))^T P_t(k) \\ & \quad \times (\tilde{A} x_a(k|k) + \tilde{B} u_a(k|k)) \leq \gamma \end{aligned} \tag{25}$$

where $\tilde{A} = \sum_{s=1}^{r} \mu_i(\tilde{z}(k|k)\tilde{A}_s$ and $\tilde{B} = \sum_{s=1}^{r} \mu_s(\tilde{z}(k|k)\tilde{B}_s$.

Summarizing the above arguments, the output regulation control gain via integral fuzzy MPC scheme can be obtained under the following theorem.

Theorem 1: Given $x_a(k|k)$, u_{max}, and weighting matrices Q and R for the system (1), the state feedback control law (14) will satisfy the performance constraint (19) and the minimized objective function (15) with input constraint (16) at each time instant k if there exist $u_a(k|k)$, a positive scalar γ, symmetric positive definite matrices $\bar{P}_n(k)$ and $\bar{P}_m(k)$, matrices $M_{ns}(k)$ such that the following convex objective minimization problem is feasible:

$$\min_{\gamma, u_a(k|k), \bar{P}_n(k), \bar{P}_m(k), M_{ns}(k)} \gamma$$

subject to

$$\begin{bmatrix} \bar{P}_n(k) & * \\ M_{ns}(k) & u_{max}^2 I \end{bmatrix} \geq 0, \qquad 1 \leq s \leq r \tag{26}$$

$$\begin{bmatrix} 1 & * & * & * \\ (\tilde{A} x_a(k|k) + \tilde{B} u_a(k|k)) & \bar{P}_m(k) & * & * \\ Q^{1/2} x_a(k|k) & 0 & \gamma I & * \\ R^{1/2} u_a(k|k) & 0 & 0 & \gamma I \end{bmatrix} \geq 0,$$

$$1 \leq s \leq r \tag{27}$$

$$\begin{bmatrix} \bar{P}_n(k) & * & * & * \\ \tilde{A}_s \bar{P}_n(k) - \tilde{B}_s M_{ns}(k) & \bar{P}_m(k) & * & * \\ Q^{1/2} \bar{P}_n(k) & 0 & \gamma I & * \\ R^{1/2} M_{ns}(k) & 0 & 0 & \gamma I \end{bmatrix} > 0,$$

$$n, m \in \Gamma,\ 1 \leq s \leq r \tag{28}$$

$$\begin{bmatrix} 4\bar{P}_n(k) & * & * \\ \Xi & \bar{P}_m(k) & * \\ 2Q^{1/2} \bar{P}_n(k) & 0 & \gamma I \end{bmatrix} \geq 0, \quad 1 \leq s < j \leq r \tag{29}$$

where the symbol $*$ induces a symmetric structure, $\Xi = \tilde{A}_s \bar{P}_n(k) - \tilde{B}_s M_{nj}(k) + \tilde{A}_j \bar{P}_n(k) - \tilde{B}_j M_{ns}(k)$, $\bar{P}_m(k) = \gamma P_m(k)^{-1}$, $\bar{P}_n(k) = \gamma P_n(k)^{-1}$, $M_{ns}(k) = K_s(k)\bar{P}_n(k)$. Moreover, the closed-loop regulation control system (13) is asymptotically stable.

In addition, the speed of the closed-loop system response can be influenced by specifying a desired decay rate on the piecewise Lyapunov function as follows [16]:

$$\Delta V(i,k)) \leq (\alpha - 1) V(i,k) \tag{30}$$

The requirement (30) denotes the *Decay Rate* condition which will significantly improve the transient response of the closed-loop system by carefully choosing $0 < \alpha < 1$. Hence, it can be shown that (30) becomes the LMIs as follows:

$$\begin{bmatrix} \alpha \bar{P}_n(k) & * \\ \tilde{A}_s \bar{P}_n(k) - \tilde{B}_s M_{ns}(k) & \bar{P}_m(k) \end{bmatrix} > 0, \quad 1 \leq s \leq r \tag{31}$$

$$\begin{bmatrix} 4\alpha \bar{P}_n(k) & * \\ \Pi & \bar{P}_m(k) \end{bmatrix} \geq 0, \qquad 1 \leq s < j \leq r \tag{32}$$

where $\Pi = \tilde{A}_s \bar{P}_n(k) - \tilde{B}_s M_{nj}(k) + \tilde{A}_j \bar{P}_n(k) - \tilde{B}_j M_{ns}(k)$.

Remark 1 : In above theorem 1, the controller design is called integral fuzzy MPC using piecewise Lyapunov function (IFMPC-PLF) which can directly extend to the integral fuzzy MPC with decay rate condition using piecewise Lyapunov function (IFMPC-PLFDR) by including LMIs (31) and (32).

Remark 2 : In fact, the common Lyapunov function can be considered as the special case of the more general piecewise Lyapunov function [14]. So, the integral fuzzy MPC with decay rate using common Lyapunov function method (IFMPC-CLFDR) can be obtained by replacing $\bar{P}_n(k)$ and $\bar{P}_m(k)$ with $\bar{P}(k)$, from (26) to (29) and (31) to (32).

IV. Numerical Example

The aim of this numerical section is to verify the validity of the proposed integral fuzzy MPC regulation controller for the nonlinear chaotic system with time-varying parameter. For comparing control laws, three integral fuzzy MPC approaches based on common Lyapunov function with decay rate, piecewise Lyapunov function and piecewise Lyapunov function with decay rate are investigated respectively.

A. Plant Description

Consider the Hénon map chaotic system [15], [17] given as follows:

$$\begin{aligned} x_1(k+1) &= -x_1^2(k) + \beta \cdot x_2(k) + 1.4 + u(k) \\ x_2(k+1) &= x_1(k) \\ \beta &= 0.3 \end{aligned} \tag{33}$$

For the integral output regulation control purpose, we define output equation:

$$y(k) = x_2(k) + 1 \tag{34}$$

and assume that $y(k) \to y_d$ as $k \to \infty$.

From the model (33), let the desired output $y_d = \lambda$, we can obtain the equilibrium points of the state and control input $\bar{x}_1 = \lambda - 1$, $\bar{x}_2 = \lambda - 1$ and $\bar{u} = \lambda^2 - (1+\beta)\lambda + \beta - 1.4$. Then the transformed augmented error dynamics (6) of the chaotic system is of the following form:

$$x_a(k+1) = \tilde{A}(x_p(k))x_a(k) + \tilde{B}u_a(k) \tag{35}$$

where $x_a(k) = [\tilde{x}_1(k)\ \tilde{x}_2(k)\ x_e(k)]^T$, $\tilde{B} = [1\ 0\ 0]^T$ and

$$\tilde{A}(x_p(k)) = \begin{bmatrix} -\tilde{x}_1(k) - 2\bar{x}_1(k) & \beta & 0 \\ 1 & 0 & 0 \\ 0 & -1 & 1 \end{bmatrix}$$

In the simulation, we assume the parameter β is time-varying and has ± 0.1 deviation on its nominal value. i.e., $\beta(k) = 0.1 * \sin(2\pi \cdot k/5) + \beta_0$, and $\beta_0 = 0.3$ is the nominal value. From (35), two premise variables can be defined as $\tilde{z}_1(k) = \tilde{x}_1(k)$ and $\tilde{z}_2(k) = \beta(k)$. Since having two variables in $\tilde{A}$, only four fuzzy rules are needed. Then, the dynamical equation (35) can be exactly presented as the following four-rules T-S fuzzy model:

Model Rule r :
IF $\tilde{z}_1(k)$ is $F_{1s(r)}$ and $\tilde{z}_2(k)$ is $F_{2j(r)}$
Then $x_a(k+1) = \tilde{A}_r x_a(k) + \tilde{B}_r u_a(k)$
$r = 1,2,3,4$

Let $\mu_{1s(r)}$ and $\mu_{2j(r)}$ be the normalized membership functions for $F_{1s(r)}$ and $F_{2j(r)}$ respectively, i.e., $\Sigma_{s=1}^{2}\mu_{1s} = \Sigma_{j=1}^{2}\mu_{2j} = 1$ and $0 \le \mu_{1s(r)} \cdot \mu_{2j(r)} \le 1$ for each $s(r)$ and $j(r)$. The system is inferred as follows:

$$x_a(k+1) = \sum_{r=1}^{4} h_r(\tilde{z}(k))\{\tilde{A}_r x_a(k) + \tilde{B}_r u_a(k)\} \tag{36}$$

where $h_r(\tilde{z}(k)) = \mu_{1s(r)}(\tilde{z}(k)) \cdot \mu_{2j(r)}(\tilde{z}(k))$ for $r = 1,2,3,4$. Due to the $\beta(k)$ is time-varying, the regions of the nonlinear terms are assumed with $\tilde{x}_1(k) \in [-d, d]$ and $\beta(k) \in [d_1, D_1]$, where $d = 3$, $d_1 = \beta_0 - 0.1$, $D_1 = \beta_0 + 0.1$, $\tilde{x}_1(k) = \mu_{11}d + \mu_{12}(-d)$ and $\beta(k) = \mu_{21}D_1 + \mu_{22}d_1$. According to [17], we can define the normalized membership functions as

$$\mu_{11} = \frac{1}{2} + \frac{\tilde{x}_1(k)}{2d},\ \mu_{12} = \frac{1}{2} - \frac{\tilde{x}_1(k)}{2d}$$
$$\mu_{21} = \frac{\beta(k) - d_1}{D_1 - d_1},\ \mu_{22} = \frac{D_1 - \beta(k)}{D_1 - d_1}$$

From Lemma 1, we obtain $s(r)$ and $j(r)$ and then $\tilde{A}_r$, $\tilde{B}_r$ and h_r, which are summarized in Table I. As a result, the system matrices in the consequent part are:

$$\tilde{A}_1 = \begin{bmatrix} d - 2\bar{x}_1 & d_1 & 0 \\ 1 & 0 & 0 \\ 0 & -1 & 1 \end{bmatrix},$$

$$\tilde{A}_2 = \begin{bmatrix} d - 2\bar{x}_1 & D_1 & 0 \\ 1 & 0 & 0 \\ 0 & -1 & 1 \end{bmatrix},$$

$$\tilde{A}_3 = \begin{bmatrix} -d - 2\bar{x}_1 & d_1 & 0 \\ 1 & 0 & 0 \\ 0 & -1 & 1 \end{bmatrix},$$

$$\tilde{A}_4 = \begin{bmatrix} -d - 2\bar{x}_1 & D_1 & 0 \\ 1 & 0 & 0 \\ 0 & -1 & 1 \end{bmatrix},$$

and $\tilde{B}_r = [1\ \ 0\ \ 0]^T,\ r = 1,2,3,4$.

TABLE I
System Matrices and Membership Functions of The Model

r	$s(r)$	$j(r)$	$\tilde{A}_r$	$\tilde{B}_r$	h_r
1	1	1	$\tilde{A}_1$	$\tilde{B}_1$	$h_1 = \mu_{11}\mu_{21}$
2	1	2	$\tilde{A}_2$	$\tilde{B}_2$	$h_2 = \mu_{11}\mu_{22}$
3	2	1	$\tilde{A}_3$	$\tilde{B}_3$	$h_3 = \mu_{12}\mu_{21}$
4	2	2	$\tilde{A}_4$	$\tilde{B}_4$	$h_4 = \mu_{12}\mu_{22}$

Consequently, the resulting fuzzy model can exactly represent the chaotic system, while the time varying parameter is put into the membership functions.

B. Simulation with IFMPC-CLFDR, IFMPC-PLF and IFMPC-PLFDR

To proceed on the simulation, we apply IFMPC-CLFDR, IFMPC-PLF, and IFMPC-PLFDR approaches to output regulation control the chaotic system with the same initial values and parameters for comparison as follows: $x_a(0) = [0.5\ -0.5\ 0.1]^T$, $\tilde{u}(0) = 1$, $u_{max} = 5$ and the desired output reference $y_d = 2$. Moreover, we choose $Q = 0.001 \times \mathrm{diag}\{10, 10, 5\}$, $R = 0.01$, $\gamma = 2$, and $\alpha = 0.5$ by try and error method. For the regulation control problem, there is feasible solution for IFMPC-CLFDR, and the other two methods not only lead to feasible solutions but also obtain good performance for regulation purpose even though exist the parameter variation. For IFMPC-CLFDR, the corresponding common positive definite matrix and integral fuzzy MPC state feedback gains are given as follows:

$$P = \begin{bmatrix} 5.8632 & 2.0437 & -2.2263 \\ 2.0437 & 1.3425 & -1.2982 \\ -2.2263 & -1.2982 & 1.3313 \end{bmatrix},$$

and

$$K_1 = \begin{bmatrix} 1.2522 & 0.5664 & -0.3620 \end{bmatrix},$$
$$K_2 = \begin{bmatrix} 1.2516 & 0.7654 & -0.3618 \end{bmatrix},$$
$$K_3 = \begin{bmatrix} -4.2460 & 0.6587 & -0.4702 \end{bmatrix},$$
$$K_4 = \begin{bmatrix} -4.2619 & 0.8382 & -0.4646 \end{bmatrix}.$$

For both IFMPC-PLF and IFMPC-PLFDR, the state space of premise variable is partitioned into two regions. The corresponding two different positive definite matrices and the integral fuzzy MPC state feedback gains are given, respectively,

$$P1 = \begin{bmatrix} 1.0557 & -0.0347 & -0.0006 \\ -0.0347 & 0.4289 & -0.0966 \\ -0.0006 & -0.0966 & 0.4188 \end{bmatrix},$$

$$P2 = \begin{bmatrix} 0.1028 & 0.0180 & 0.0016 \\ 0.0180 & 0.1291 & 0.0010 \\ 0.0016 & 0.0010 & 0.0954 \end{bmatrix},$$

and

$$K_1 = \begin{bmatrix} 0.5268 & 0.1651 & 0.0075 \end{bmatrix},$$
$$K_2 = \begin{bmatrix} 0.5255 & 0.3054 & -0.0008 \end{bmatrix},$$
$$K_3 = \begin{bmatrix} -2.7093 & 0.1090 & 0.0077 \end{bmatrix},$$
$$K_4 = \begin{bmatrix} -2.7068 & 0.2177 & -0.0056 \end{bmatrix},$$

for IFMPC-PLF. Similarly,

$$P1 = \begin{bmatrix} 1.4149 & -0.0431 & 0.0001 \\ -0.0431 & 0.6706 & -0.2723 \\ 0.0001 & -0.2723 & 0.6641 \end{bmatrix},$$
$$P2 = \begin{bmatrix} 0.1927 & 0.0172 & 0.0011 \\ 0.0172 & 0.1690 & 0.0011 \\ 0.0011 & 0.0011 & 0.1225 \end{bmatrix},$$

and

$$K_1 = \begin{bmatrix} 0.7880 & 0.2005 & 0.0054 \end{bmatrix},$$
$$K_2 = \begin{bmatrix} 0.7866 & 0.3856 & 0.0028 \end{bmatrix},$$
$$K_3 = \begin{bmatrix} -3.8631 & 0.1533 & 0.0023 \end{bmatrix},$$
$$K_4 = \begin{bmatrix} -3.8564 & 0.3041 & -0.0092 \end{bmatrix},$$

for IFMPC-PLFDR. The open-loop response for chaotic system is shown in Fig. 1. The closed-loop control results are shown in Figs. 2 to 5. It is shown that the proposed IFMPC-PLFDR obtains much better transient control performance than IFMPC-CLFDR and IFMPC-PLF under the same turning parameters and input constraints. Notice that three integral fuzzy MPC control methods have steered the chaotic system to regulate $y_d = 2$ trajectoy successfully. From the simulation results, we conclude that the integral fuzzy MPC scheme based on piecewise Lyapunov function with a decay rate is a powerful design. It can regularly control Hénon map system, achieving asymptotically stable, shorter transient time, lower overshot and rejecting the parameter variation.

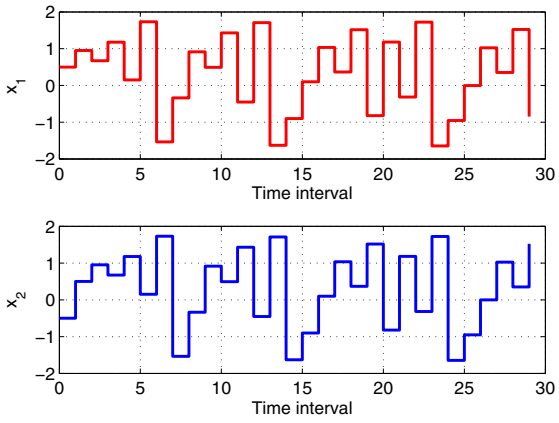

Fig. 1. Open-loop response for (a)state x_1 and (b)state x_2.

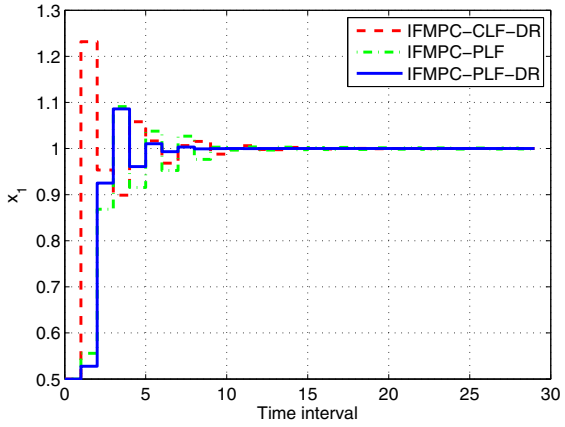

Fig. 2. Close-loop response for state x_1 controlled by three different IFMPC methods.

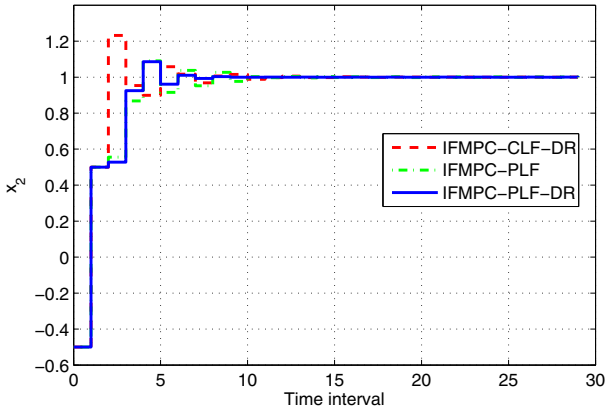

Fig. 3. Close-loop response for state x_2 controlled by three different IFMPC methods.

V. Conclusion

In this paper, an integral fuzzy MPC design for a nonlinear system using piecewise Lyapunov functions has been proposed to achieve output regulation. To this end, the nonlinear system is expressed by Takagi-Sugeno (T-S) fuzzy model via integral control and coordinate translation procedure. Then, the integral fuzzy regulation controller with input constraint is designed by infinite horizon MPC strategy and is formulated in terms of the LMIs. Finally, the numerical simulations for a chaotic system have shown the effectiveness of the proposed methods. It has been demonstrated that the IFMPC-PLFDR are less conservatism, but with short transient response, and zero-offset regulation performance when compared to IFMPC-CLF method.

References

[1] E. F. Camacho and C. Bordons, *Model Predictive Control*, Springer, 2003.
[2] D. Q. Mayne, J. B. Rawlings, C. V. Rao, and P. O. M. Scokaert, "Constrained model predictive control: Stability and optimality," *Automatica*, vol. 36, pp. 789-814, Jun. 2000.

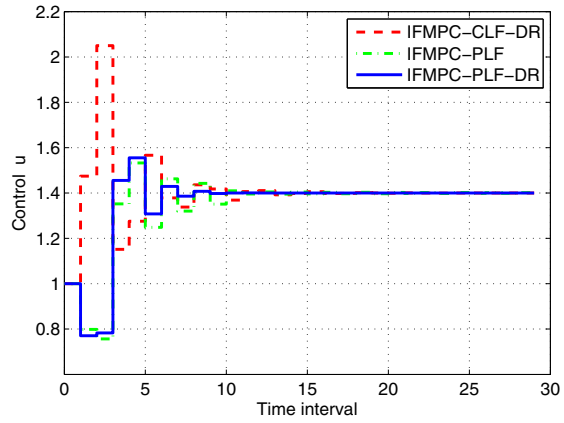

Fig. 4. Control input controlled by three different IFMPC methods.

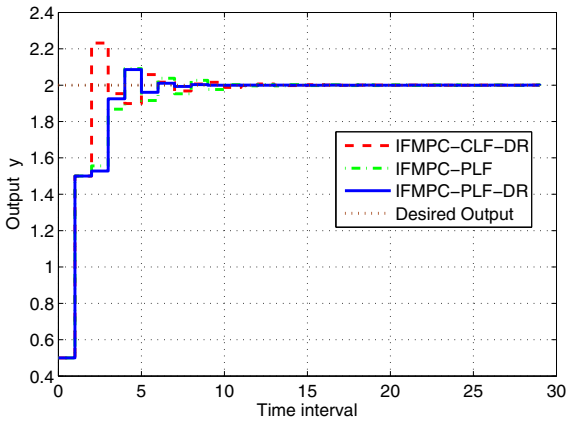

Fig. 5. Output regulation trajectory controlled by three different IFMPC methods.

[3] M. V. Kothare, V. Balakrishnan, M. Morari, "Robust constrained model predictive control using linear matrix inequalities," *Automatica*, vol. 32, no. 10, pp. 1361-1379, 1996.

[4] E. Granado, W. Colmenares, J.Bernussou and G. Garcia, "Linear matrix inequalities based model predictive controller," *IEE Proc.-Control Theory Appl.*, vol. 150, pp. 528-533, 2003.

[5] F. A, Cuzzola, J. C. Geromel, and M. Morari, "An improved approach for constrained robust model predictive control," *Automatica*, vol. 38, pp. 1183-1189, 2002.

[6] S. Mollov, R. Babuška, J. Abonyi, and H. B. Verbruggen, "Effective optimization for fuzzy model predictive control," *IEEE Trans. Fuzzy Syst.*, vol. 12, no. 5, pp. 661-675, 2004.

[7] Y. L. Huang, H. H. Lou, J. P. Gong, and T. F. Edgar, "Fuzzy model predictive control," *IEEE Trans. Fuzzy Syst.*, vol. 8, No. 6, pp.665-678, 2000.

[8] N. Wada, K. Saito and M. Saeki, "Model predictive control for linear parameter varying system using parameter dependent Lyapunov function," *IEEE Trans. Circuits and System*, vol. 53, no. 12, pp. 1446-1450, Dec. 2006.

[9] T. Zhang, G. Feng and J. Lu, "Fuzzy constrained minmax model predictive control based on piecewise Lyapunov functions.," *IEEE Trans. Fuzzy Syst.*, vol. 15, no. 4, pp. 686-698, Aug. 2007.

[10] M. Johansson, A. Rantzer, and K. Arzen, "Piecewise quadratic stability of fuzzy systems," *IEEE Trans. Fuzzy Syst.*, vol. 7, pp. 713-722, Dec. 1999.

[11] X. J. Ma and Z. Q. Sun,"Output tracking and regulation of nonlinear system based on Takagi-Sugeno fuzzy model," *IEEE Trans. Syst., Man, Cybern. B*, Vol. 30, no. 1, pp. 47-59, Feb. 2000.

[12] J. A. Meda-Campana and B. Castillo-Toledo,"On the output regulation for TS fuzzy model using sliding models," *2005 American Control Conference*, pp. 4062-4067, Jun. 8-10, 2005. Portland, OR, USA.

[13] H. Peng, Z. -J. Yang, W. Gui, M. Wu, H. Shioya, and K. Nakano,"Nonlinear system modeling and robust predictive control based on RBF-ARX model," *Engineer Applications of Artificial Intelligence*, vol. 20, pp. 1-9, 2007.

[14] T. Zhang, and G. Feng, "Rapid load following of an SOFC power system via stable fuzzy predictive tracking controller," *IEEE Trans. Fuzzy Syst.*, vol. 17, no. 2, pp. 357-371, 2009.

[15] K. Tanaka and C. S WANG, *Fuzzy Control Systems Analysis and Design: A Linear Matrix Inequality Approach*, New York: Wiley, 2001.

[16] J. Li, H. O. Wang, L. Bushnell, and Y. Hong, "A fuzzy logic approach to optimal control of nonlinear system," *Int. J. Fuzzy Systems*, vol. 2, no. 3, pp. 153-161, 2000.

[17] Lian K.-Y., Chiang T.-S., Chiu C.-S., and Liu P., "Synthesis of fuzzy model-based designs to synchronization and secure communications for chaotic systems," *IEEE Trans. Syst., Man, Cybern. B*, vol. 31, no. 1, pp. 66-83, 2001.

2011 IEEE International Conference on Fuzzy Systems
June 27-30, 2011, Taipei, Taiwan

Power Management of a Variable Speed Wind Turbine for Stand-Alone System using Fuzzy Logic

Huynh Quang Minh
Laboratory CReSTIC
IUT de Troyes
9 rue du Québec
10026 TROYES Cedex
FRANCE
minh.huynh-quang@etudiant.univ-reims.fr

Nollet Frédéric
Laboratory CReSTIC
IUT de Troyes
9 rue du Québec
10026 TROYES Cedex
FRANCE
frederic.nollet@univ-reims.fr

Essounbouli Najib
Laboratory CReSTIC
IUT de Troyes
9 rue du Québec
10026 TROYES Cedex
FRANCE
najib.essounbouli@univ-reims.fr

Hamzaoui Abdelaziz
Laboratory CReSTIC
IUT de Troyes
9 rue du Québec
10026 TROYES Cedex
FRANCE
abdelaziz.hamzaoui@univ-reims.fr

***Abstract*—In this paper, a wind energy conversion system (WECS) using a variable speed synchronous generator and a battery to store extra wind energy is proposed. A fuzzy logic supervisor is developed to manage both the energy production and its storage to obtain an optimal behaviour of the system and to ensure the load requirement. Many simulation results are presented to show that the proposed method gives good performance for its application in autonomous wind energy systems and can extend battery life.**

***Keywords*—Variable speed wind turbine, synchronous generator, fuzzy logic controller, stand-alone system.**

I. INTRODUCTION

Wind power generation is more and more growing all over the world. Wind energy is called to play a crucial role in the future energy supply of the European Union and of the world. There are now thousands of wind turbines operating, with a total capacity of 121,188 MW of which wind power in Europe accounts for 55% in 2008 [1].

Wind power also offers a feasible solution to distributed power generation for isolated communities where utility grids are not available. In such cases, stand-alone wind energy systems can be considered as an effective way to provide continuous power to electrical loads. For isolated settlements located far from a utility grid, one practical approach to self-sufficient power generation involves using a wind turbine with battery storage to create a stand-alone system. If wind conditions are favourable, these stand-alone wind energy systems can provide communities with electricity at the lowest cost. Stand-alone wind energy systems often include batteries, because available wind does not always produce the required quantities of power. If wind power exceeds the load demand, the surplus can be stored in the batteries [2,3].

Synchronous generator has the capability of direct connection to wind turbines, with no gearbox. This advantage is favourable with respect to lifetime and maintenance. Synchronous machines can use either electrically excited or permanent magnet rotor [4,5].

A comparison between the variable speed wind turbine and the constant speed wind turbine shows that variable speed reduces mechanical stresses: gusts of wind can be absorbed, dynamically compensate for torque and power pulsations caused by back pressure of the tower. This backpressure causes noticeable torque pulsations at a rate equal to the turbine rotor speed times the number of rotor blades. Variable speed use is good for extracting more prime mover power as in wind turbine or for providing optimum efficiency for the prime mover by increasing its speed with power. It also allows for a more flexible generator system [6].

In ancient autonomous systems, electrical power supplied by the turbine is transmitted to a battery and then the battery transfer energy for the load [7,8]. In modern structure, wind energy is primarily provided directly to the load and the battery is in second priority [9,10]. As a result, the number of charging and discharging of the battery is greatly reduced thereby extending battery life.

Intelligent controller based on fuzzy logic capable to ensure to the networks with distributed renewable energy generation. An increasing value of the energy available to users of the power system is expected as results of the implementation of the proposed intelligent load device [11].

Fuzzy logic provides a formal methodology for representing, manipulating, and implementing human's knowledge. We do not need the accurate model of the complex system. Fuzzy logic controller is also suitable for real time applications [12]. A fuzzy logic control for the photovoltaic systems with battery has designed in [13]. It controls the rate of current injection into the battery for energy storage or increases or decreases the load in priority order to match the optimal requirement.

In this paper, we propose a fuzzy power management for a WECS including a variable speed synchronous generator and a battery bank. This controller manages power production and power storage according to wind condition and load demand. Load is provided mainly by wind power, and when this power is not enough, the battery will be switched on to discharge. A resistance is switched on to waste the surplus if needed. By controlling duty cycle of the boost converter, we can manage battery charging process according to the available power and also can provide a suitable voltage for the inverter.

978-1-4244-7316-8/11/$26.00 ©2011 IEEE

II. System Description

Consider a stand-alone system with a 5.5kW pump, a 7.5kW induction motor and a 10kW water heater, powered by a 30kVA synchronous generator wind turbine and a battery storage.

In this variable speed wind turbine, a diode rectifier will rectify the AC power, then a boost converter will increase the DC voltage obtained to be suitable for both battery charging process and PWM inverter's operation.

If wind conditions are favorable, the wind turbine will be the main provider for load. If available wind does not produce the required quantities of power and battery's capacity is enough, the battery will be switched on to give power to load. If wind power exceeds load demand, the surplus can be stored in the battery and if the battery is full, the surplus will be discharged into a dumb resistance. Thus, the battery is not the main provider to load, so the charge-discharge cycle is reduced, battery life is extended.

We proposed a fuzzy controller to achieve these purposes. To do this, our controller needs two informations: the battery state-of-charge (SOC) and the error between wind power and load demand (DeltaP). Then our controller will decide the duty cycle of the boost converter (D), the moment to switch on and off the battery (S_1) and the moment to discharge the surplus into dumb resistance (S_2) (Fig. 1).

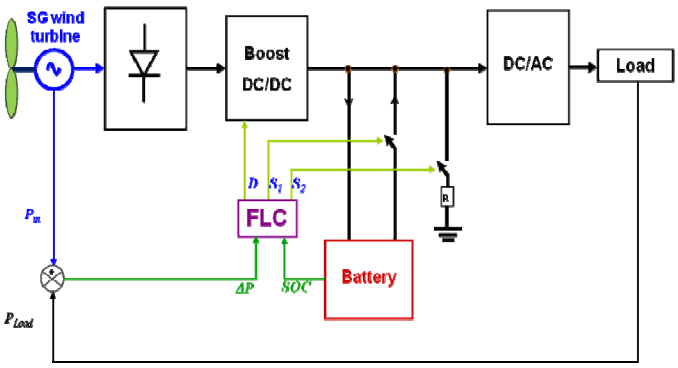

Figure 1. Proposed system with fuzzy controller.

III. Model Of Wind Turbine

The static characteristic of wind turbine can be described by the relation between total power in the wind and mechanical power of wind turbine as in (1). It presents a basic model for wind turbine in electric power system.

$$P_w = \frac{1}{2}\rho\pi R_{turbine}^2 v_{wind}^3 . \quad (1)$$

In wind power equation (1), ρ is air density (1.225 kg/m^3), $R_{turbine}$ is the turbine radius in meters, v_{wind} is the wind speed in m/s. It is not possible to extract all kinetic energy of wind, thus it is extracted a fraction of power in wind as given in (2) and it is called power coefficient C_p of the wind turbine.

$$P_m = \frac{1}{2}C_p\rho\pi R_{turbine}^2 v_{wind}^3 . \quad (2)$$

P_m is the mechanical power of wind turbine. The maximum power coefficient is given as C_p=*0.59*. This coefficient is also known as Betz's limit. It can be expressed as a function of tip speed ratio-λ and pitch angle-θ.

The tip speed ratio λ is defined as (3):

$$\lambda = \frac{\omega_{turbine} R_{turbine}}{v_{wind}} . \quad (3)$$

Assuming constant wind speed v_{wind}, the tips speed ratio λ will vary proportionally to the rotational speed of wind turbine rotor [14]. The highest value of C_p is typically obtained for λ values in the range of 8 to 9 (when the tip of the blades moves 8 to 9 times faster than incoming wind). On modern wind turbines, it is possible to adjust the pitch angle of the entire blade through servo mechanism [15]. If C_p - λ curve is known for specific wind turbine with a turbine rotor radius $R_{turbine}$, it is easy to construct the curve of C_p against rotational speed for any wind speed.

In this paper, we use a simple wind turbine model, where inputs are wind speed and rotor speed, output is the mechanical power.

IV. Power Electronic Device

A. Diode rectifier

Output voltage of the three phase diode bridge rectifier [16]:

$$V_{rec} = V_{RMS}\sqrt{2}\frac{\sin(\pi/6)}{\pi/6} = 1.35V_{RMS} . \quad (4)$$

where V_{RMS} is root-mean-square value of input line voltage.

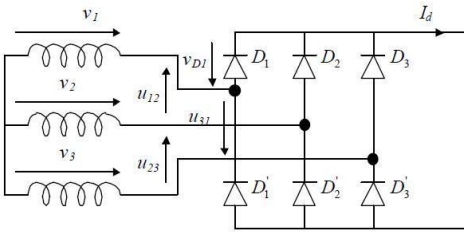

Figure 2. Three phase bridge rectifier.

B. DC-DC boost converter

Output voltage of the boost converter [17]:

$$V_{DC} = V_{rec}\cdot\frac{1}{1-D} . \quad (5)$$

where the switching frequency f_s of switch S equal to the inverse of the switching period T_s generally lies in the range of 1 kHz to 1 MHz, depending on the switching speed of the semiconductor devices. The duty ratio D is the fraction of time that the switch spends in position 1, and is a number between zero and one. Our fuzzy controller will decide the duty cycle D for this boost converter to have an output voltage suitable for the PWM inverter's functioning and battery charging process.

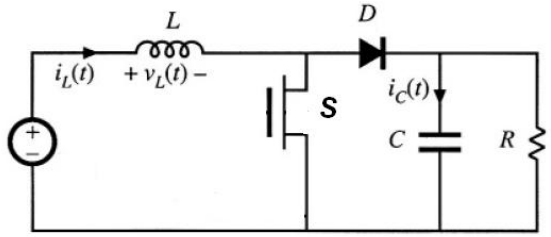

Figure 3. Boost converter.

Value of inductor L is chosen to minimize the ripple in current Δi:

$$L = \frac{V_{rec}}{2\Delta i} DT_s \cdot \tag{6}$$

Select the capacitor value C to obtain a given output voltage ripple peak magnitude Δv:

$$C = \frac{V_{DC}}{2R\Delta v} DT_s \cdot \tag{7}$$

Here we choose L=4mH, C=5000μF to have an acceptable ripple in voltage and current.

C. *Voltage source PWM inverter*

The modulation ratio is defined using reference and triangular voltage amplitudes [11]:

$$m = \frac{u_{ref}}{u_{tri}} \cdot \tag{8}$$

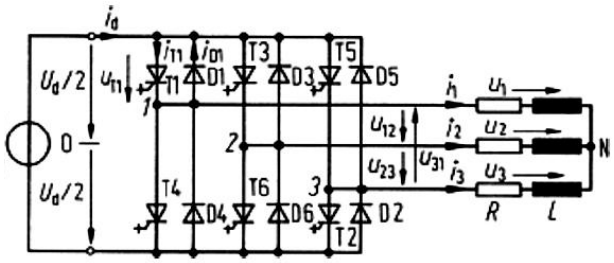

Figure 4. Voltage source PWM inverter.

In the region $m \bullet 1$ the fundamental output line-to-line voltage is a linear function of m:

$$U_{ab} = \frac{\sqrt{3}}{2\sqrt{2}} m.U_{DC} \cdot \tag{9}$$

Here we use the low-pass filter:

$$f_c = \frac{1}{2\pi\sqrt{LC}} \cdot \tag{10}$$

Choose L=8mH, C=100μF to pass the 1st and 3rd harmonic of the output voltage (f_c=177 Hz), assure the smooth sinusoidal output voltage for the load.

V. FUZZY CONTROLLER

Fuzzy controllers belong to the class of knowledge based systems. Their main goal is to implement human know-how or heuristic rules in the form of a computer program, so to provide a mathematical formalism for this goal. Fuzzy controllers make human experience in the form of linguistic if-then rules; a fuzzy inference engine computes the control actions for each given situation [12,18].

A. *Fuzzification*

The FLC controller input variables are the battery state-of-charge (SOC) and the power error DeltaP (difference between wind turbine power and load demand). The output is the duty cycle D applied to the boost converter in order to charge the battery (ensuring a safe and efficiency functioning) and to guarantee the voltage's input sufficient for the voltage-source PWM inverter.

The linguistic term sets used for:

- Error of power DeltaP [N(Negative); SP(Small Positive); P(Positive); VP(Very Positive)].
- Battery state-of-charge SOC [Empty, Average, Full], varying from 0% to 100%, SOC is smaller than 20% means the battery is empty.
- Duty cycle D [Small, Average, Big, VeryBig], varying from 22% to 34% because of the input voltage's limit of the PWM inverter and the charging voltage for the battery.
- Switch S_1 and S_2 [Open, Close].

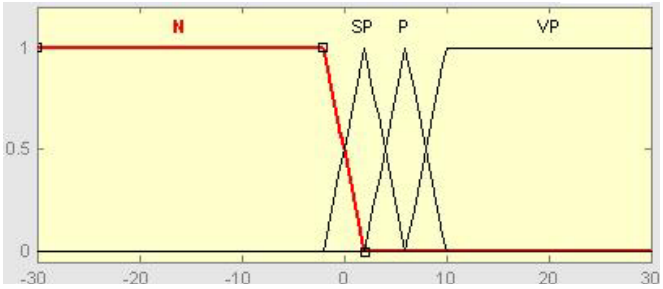

Figure 5. Five terms of error power DeltaP.

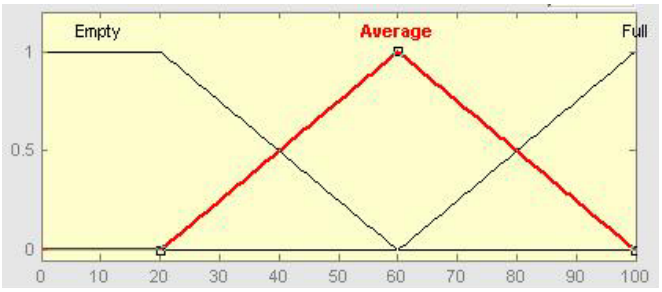

Figure 6. Three terms of battery state-of-charge SOC.

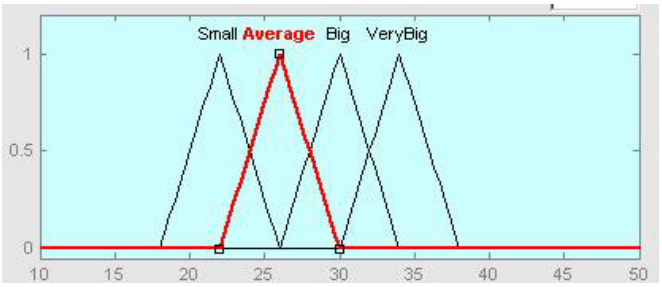

Figure 7. Five terms of duty cycle D.

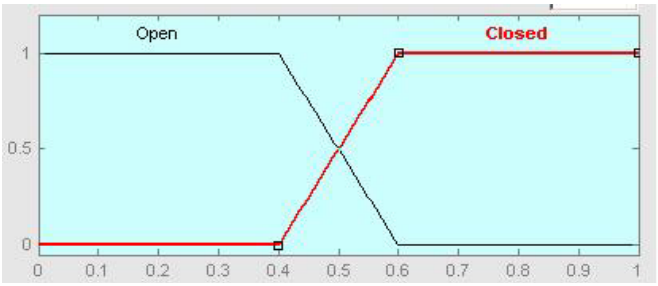

Figure 8. Two terms of state of switch S_1 and S_2.

As inference method for the rules describing FLC dynamic is used the method of inference min-max. This type of method implies a simple treatment of data and generates linear characteristics (for two or several sizes of inputs) with marked discontinuities.

$$\mu_{A\cap B}(x) = \min(\mu_A(x), \mu_B(x)) . \quad (11)$$

$$\mu_{A\cup B}(x) = \max(\mu_A(x), \mu_B(x)) . \quad (12)$$

B. *Fuzzy rules*

The design of the rules was based on Mamdani fuzzy rules [19]. Example, "If the error between wind power and load demand is VeryPositive and the battery state of charge is Full, then the duty cycle should be VeryBig, switch 1 should be Opened and switch 2 should be Closed ".

The inference mechanism and the twelve IF-THEN rules defined in relation with the considerations, generates the approximation of the FLC output represented in tables 1, 2, 3.

TABLE I. RULES OF D

D		***SOC***		
		Full	***Average***	***Empty***
DeltaP	***N***	Big	Big	Small
	SP	VeryBig	Big	Small
	P	VeryBig	VeryBig	Average
	VP	VeryBig	VeryBig	Average

TABLE II. RULES OF S_1

S_1		***SOC***		
		Full	***Average***	***Empty***
DeltaP	***N***	Close	Close	Open
	SP	Open	Open	Open
	P	Open	Open	Open
	VP	Open	Open	Open

TABLE III. RULES OF S_2

S_2		***SOC***		
		Full	***Average***	***Empty***
DeltaP	***N***	Open	Open	Open
	SP	Open	Open	Open
	P	Open	Open	Open
	VP	Close	Open	Open

C. *Defuzzification*

The overall fuzzy subset representing output control variable is defuzzified using centre of gravity method:

$$\mu_C = \frac{\sum_i \mu_C(x_i).x_i}{\sum_i \mu_C(x_i)} . \quad (12)$$

Where x_i is a point in the universe U of the conclusion (i = 1, 2…), and $\mu_c(x_i)$ its membership of the resulting conclusion set.

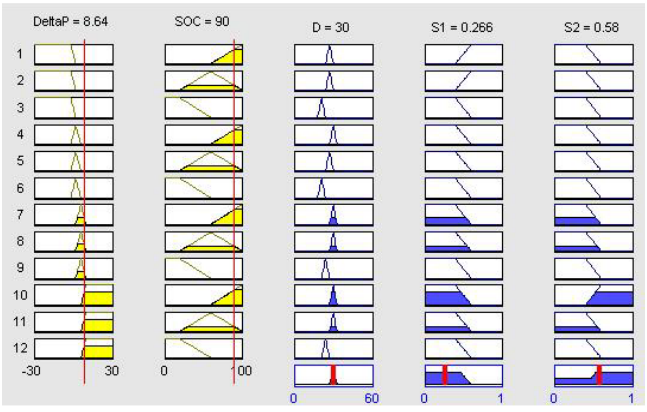

Figure 9. Defuzzification when DeltaP=8.64kW and SOC=90%.

VI. SIMULATION AND RESULTS

A. Initial condition

The system described in Section 2 is implemented in Matlab Simulink and the designed fuzzy logic controller is defined using the Fuzzy Logic Toolbox (Fig. 10).

The simulation is tested in 100 seconds, because of computer memory's limit. The water heater is supposed to work all the time, the pump and the induction motor will be switched on and off to vary load demand. Battery state-of-charge is supposed to be 95% (Full). In this case, we can verify the dissipation of surplus power to prevent the battery from gassing (operation of switch S_2). If wind power is not enough, switch S_1 will close to discharge the battery.

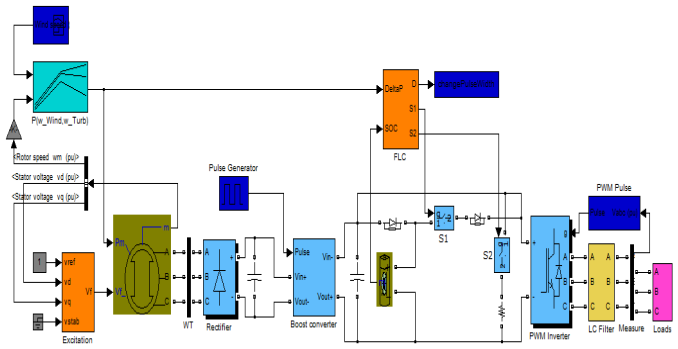

Figure 10. Implementation in Simulink.

The wind turbine output power according to wind speed and rotor speed is defined in (Fig. 11).

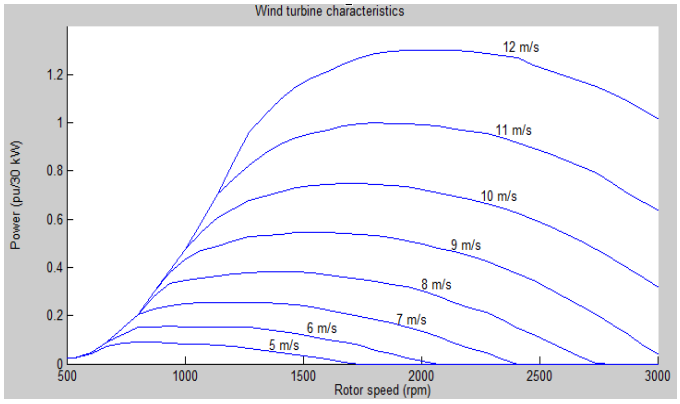

Figure 11. Wind turbine characteristics.

Supposed that at first the water heater and the pump are working (total load demand 15.5 kW). After 40 seconds, the pump is stopped (total 10 kW) and 40 seconds later, the induction motor is plugged in (total 17.5 kW). Wind speed changes from 9 m/s to 10 m/s and then slow down to 8 m/s (Fig. 12).

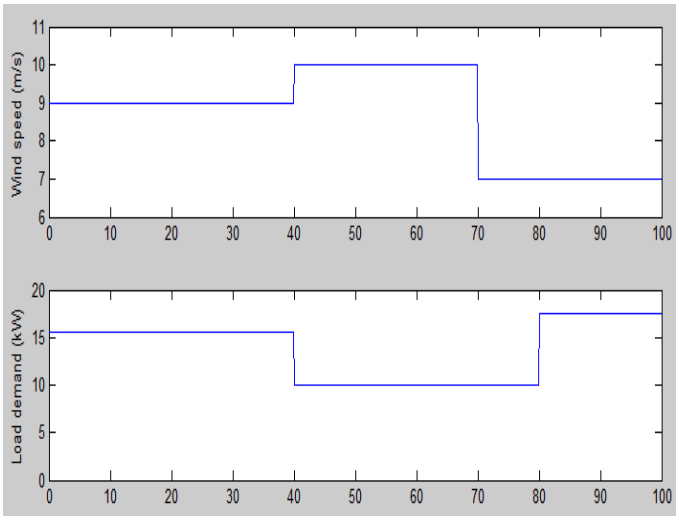

Figure 12. Wind speed and load demand

B. Results

In the first 40 seconds, the water heater and the pump are working (total 15.5 kW) while wind speed is 9 m/s, gives power output of wind turbine 16.6 kW (Fig. 13). The positive surplus (about 0.5kW) makes S_1 opened, but it's too small to charge the battery or to discharge through the dumb resistance, so S_2 is opened too. Duty cycle D is 29% (Fig. 14) makes a $715V_{DC}$ at boost converter's output, it is smaller than V_{bat} (738V) so the battery is not charged.

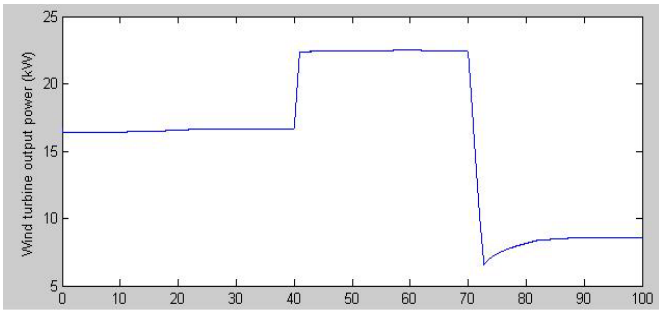

Figure 13. Wind turbine output power.

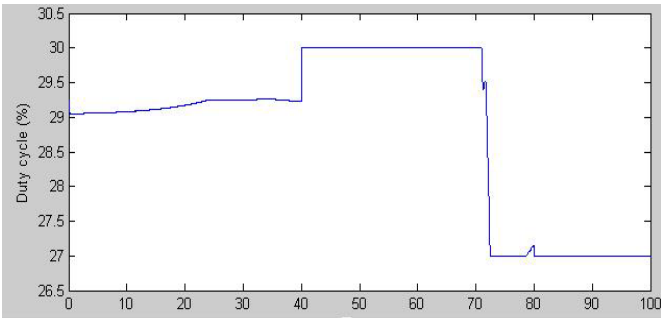

Figure 14. Duty cycle of the boost converter.

In the next 30 seconds, wind speed increases to 10 m/s while the pump is disconnected. The wind turbine output power is 22 kW while load demand is 10 kW.

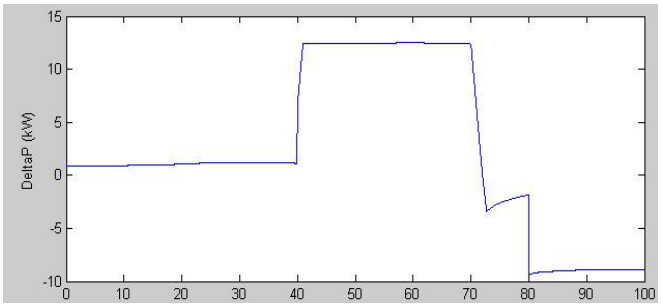

Figure 15. Error of power DeltaP.

So from now DeltaP is 12 kW (VeryPositive) (Fig. 15) while SOC is still 95% (Full), this surplus is so high for battery charging process, which may cause gassing the battery, so S_2 is closed to waste the rest into a dumb resistance (Fig. 16). Duty cycle D increases to 30%, but the battery is not charged because the voltage applied to battery's end is still smaller than 738V.

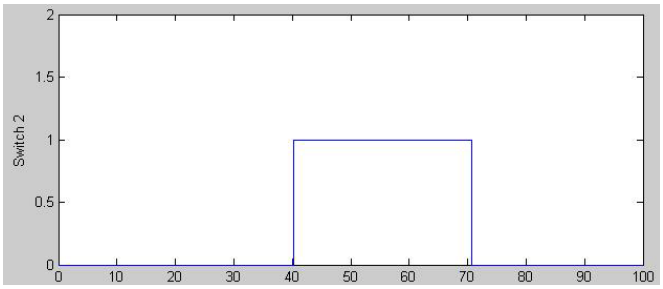

Figure 16. State of switch 2.

After 30 seconds, wind speed decreases to 8 m/s while load is still 10 kW. The wind turbine available power now is just 8 kW, we don't need to discharge no more then S_2 opened. The battery is used (S_1 closed) to provide power to load (Fig. 17), which leads to decrease SOC (Fig. 18). The duty cycle also decreases to 27% to keep the charging voltage below the battery voltage.

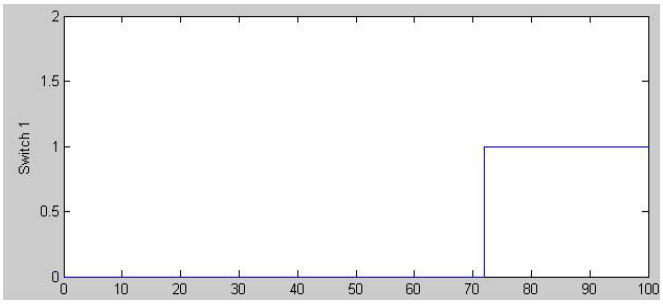

Figure 17. State of switch 1.

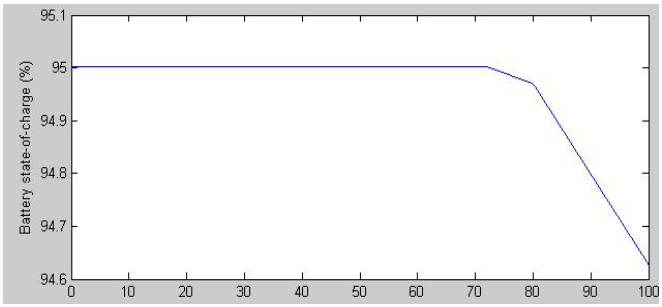

Figure 18. Battery state-of-charge.

In the last 20 seconds, the induction motor is on (load demand increases from 10 kW to 17.5 kW) while wind turbine output power now is still 8 kW, so the battery gives more power to meet load demand (Fig. 19).

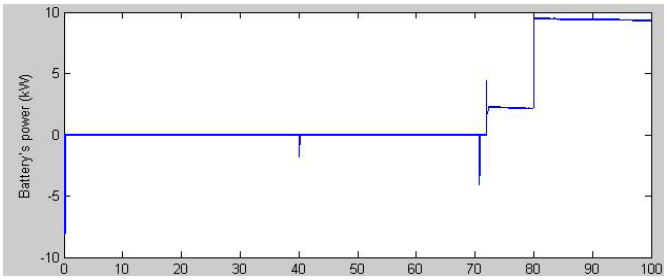

Figure 19. Battery power.

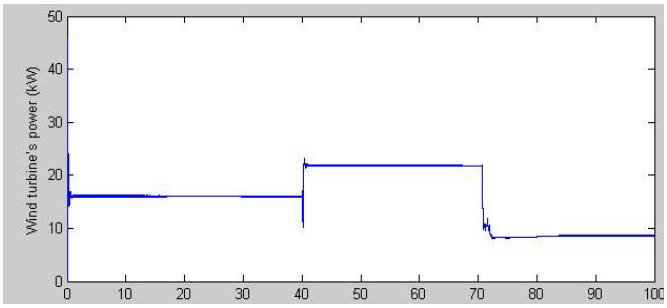

Figure 20. Wind turbine power.

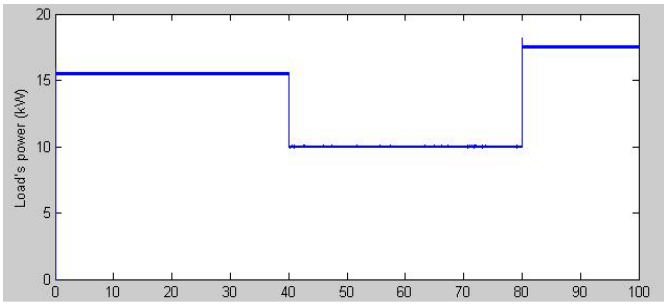

Figure 21. Load power.

Wind turbine available power is provided all before using the battery as supplement (Fig.20). Load demand is always respected despite wind speed conditions (Fig. 21).

In the load side, the DC voltage input for PWM inverter is kept in suitable value, so the load voltage quality is kept in good condition (Fig. 22). A 380V, 50 Hz voltage is always provided to load in any wind condition (Fig. 23, 24).

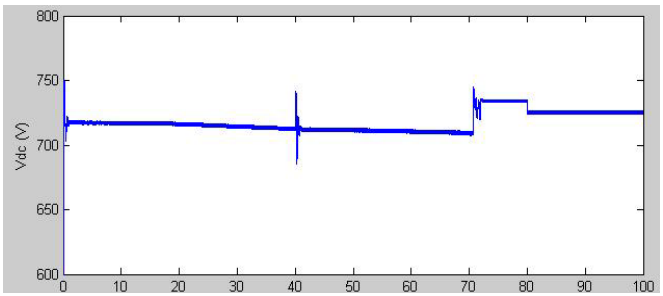

Figure 22. Output voltage of the boost converter.

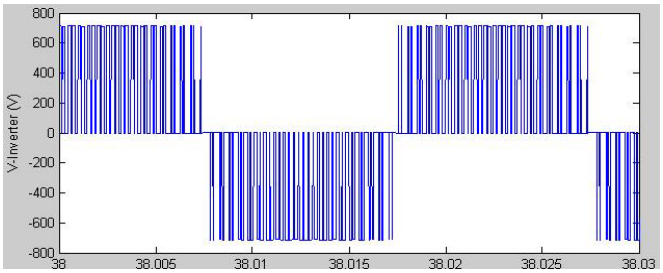

Figure 23. Output voltage of the PWM inverter.

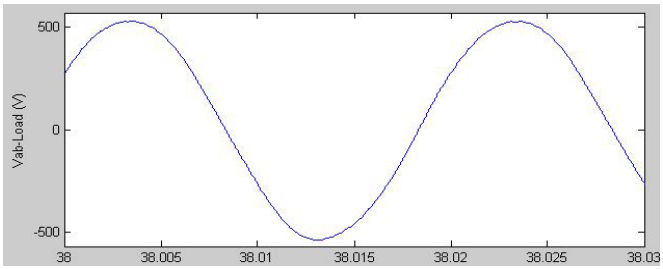

Figure 24. Load voltage.

These results show that our controller worked well. It assured the load demand despite wind condition with a good power quality and regulated battery charging process to prevent the battery from gassing and sulfating.

VII. CONCLUSIONS

This paper presents a fuzzy power management for electricity distribution for stand-alone system. With information about load and battery state-of-charge, control signals were generated to manage well the power production for any wind conditions in respecting load demand. The simulation results show a good behaviour of our controller.

Moreover, this performance has encouraged us to, in the future, develop our system by connecting with another source (photovoltaic, hydro...) and optimize the energy extraction for isolated systems. Then we'll verify it by experimental work.

REFERENCES

[1] A. Ucar and F. Balo, "Assessment of wind power potential for turbine installation in coastal areas of Turkey", Renewable and Sustainable Energy Reviews, vol. 14, issue 7, pp. 1901-1912, September 2010.

[2] H. Erich, Wind turbines: Fundamentals, Technologies, Application, Economics - 2nd Edition, Springer, 2005.

[3] J.F. Manwell, J.G. McGowan and A.L. Rogers, Wind energy explained : Theory, Design and Application, Wiley, 2002.

[4] R. Balduino, H. Wilfried, T. Martin and B. Andreas, "Voltage Regulator for Reactive Power Control on Synchronous Generators in Wind Energy Power Plants", NORPIE 2004 Trondheim, Norway, 2004.

[5] L. Freris and D. Infield, Renewable energy in power systems, Wiley, 2008.

[6] R. Wernher and H. Geoff, "Synchronous and Synchronised Wind Power Generation", New Zealand Wind Energy Association, 2004.

[7] S. Belakehal, H. Balena and A. Bentounsi, "Power maximization control of small wind system using permanent magnet synchronous generator", Revue des Energies Renouvelables, Vol. 12 N°2, pp. 307-319, 2009.

[8] M. Stiebler, Wind Energy Systems for Electric Power Generation, Springer, 2008.

[9] M. Kalantar, S.M. Mousavi G., "Dynamic behavior of a stand-alone hybrid power generation system of wind turbine, microturbine, solar array and battery storage", Applied Energy 87, pp. 3051–3064, 2010.

[10] J.K. Kaldellis, K.A. Kavadias, P.S. Koronakis, "Comparing wind and photovoltaic stand-alone power systems used for the electrification of remote consumers", Renewable and Sustainable Energy Reviews 11, pp. 57–77, 2007.

[11] F. Dragomir, "Fuzzy Control Techniques Used in Load Process of Pb Batteries Connected to a Photovoltaic System", 18th Mediterranean Conference on Control and Automation, 2010.

[12] K.M. Passino and S. Yurkovich, Fuzzy Control, Addison Wesley Longman, Inc, 1998.

[13] J.A. Momoh and A.R. Ofoli, "Load management and control of the photovoltaic system using fuzzy logic", Large Engineering Systems Conference on Power Engineering, 2001.

[14] J. Tande, "Applying Power Quality Characteristics of Wind Turbines for Assessing Impact on Voltage Quality", Wind Energy, pp. 37-52, 2002.

[15] P. Jorgensen, J.O. Tande, A. Vikkelso, P. Norgand, J.S. Christensen, P. Sorensen, J.D. Kledal and L. Sondergard, "Power Quality and Grid Connection of Wind Turbines", IEEE Conference Publication, pp. 438, 1997.

[16] M.H. Rashid, Power electronics handbook, Academic Press, 2001.

[17] R.W. Erickson, Fundamentals of Power Electronics Second Edition, Kluwer Academic Publishers, 2004.

[18] D. Driankov, H. Hellendoorn, M. Reinfrank, An introduction to fuzzy control second edition, Springer, 1995.

[19] H. Ying, Fuzzy Control and Modeling : Analytical Foundations and Applications, IEEE Press, 2000.

2011 IEEE International Conference on Fuzzy Systems
June 27-30, 2011, Taipei, Taiwan

Robust Stabilization For Continuous Fuzzy Systems With Time Varying Delay

Chedia Latrach, Mourad Kchaou and Ahmed Toumi
University of Sfax
National School of Engineers of Sfax
SFAX Tunisia
Email: chedia.latrach@yahoo.fr
Email: mouradkchaou@gmail.com

Ahmed El Hajjaji
University of Picardie Jules Verne
MIS Lab, 7 rue du Moulin Neuf Amiens France
Email: hajjaji@u-picardie.fr

***Abstract*—This paper focuses on the problem of robust control for Takagi-Sugeno (T-S) fuzzy systems with time-delay. The less conservative conditions are developed by considering a parameter dependent Lyapunov-Krasovskii functional and slack matrix variables. The design conditions are formulated as an LMI (linear matrix inequality) feasibility problem, that can be efficiently solved using convex optimization numerical techniques. Numerical examples are presented to illustrate the effectiveness of the proposed approach with the comparisons to other conditions from the literature.**

***Index Terms*—Takagi-Sugeno (T-S), Stability, Stabilization, Linear Matrix Inequalities (LMIs), Fuzzy Lyapunov-Krasovskii function(LKF)**

I. Introduction

In the last two decades, the stability analysis and control design of nonlinear systems described by Takagi-Sugeno (T-S) fuzzy model with time delay have been extensively studied (see [2], [4], [5], [7], [8], [12], [13], [14], [16], [18]) and references therein. Two main reasons are contributed to this fact : 1) Ability of T-S fuzzy models [17] to approximate large class of nonlinear systems; 2) The existence of delays in many industrial processes such as transportation systems, communication systems, chemical processing systems, environmental systems and power systems ... and its consequences on the stability and the performance degradation propagation/transportation of material, information, or energy [15].

Stability analysis and control design for T-S systems have been widely and systematically handled in the literature via Linear Matrix Inequalities (LMIs) approach (see [3], [9]). In this framework, several strategies have been used to overcome mathematical and numerical difficulties, promoting less-conservative conditions. The standard quadratic Lyapunov approach is the most popular one with the use of slack matrix variables into the LMI formulation [9], [10]. As an interesting alternative type of Lyapunov function, the fuzzy weighting-dependent Lyapunov function (FWLF) has been addressed for continuous-time fuzzy systems in [11].

In the context of stabilization problem of delayed systems, a very effective strategy consists on the use of the multiple Lyapunov-Krasovskii functional approach based on bounding techniques. It is well known that some weighted cross products may arise in the analysis of the delay-dependent stabilization problem. Thus, getting better bounds of them will play a key role in reduction conservatism.

Therefore, in this paper, new less-conservative conditions for stabilization of TS fuzzy systems subject to uncertainties and time delay are proposed.

This paper is organized as follows: system and some preliminaries are presented in Section 2. Section 3 contains the main result where a new delay dependent stabilization conditions are established. In Section 4, two numerical examples are given to demonstrate the effectiveness and the benefits of the proposed method. Some conclusions are drawn in Section 5.

Notations: $W+W^T$ is denoted as $Sym(W)$ for simplicity.

II. System description and preliminaries

Consider a nonlinear system with state-delay which could be represented by a (TS) fuzzy time-delay model described by Plant Rule i

IF $\theta_1(t)$ is N_{i1} and... $\theta_p(t)$ is N_{ip} THEN

$$\begin{aligned}\dot{x}(t) &= (A_i + \Delta A_i)x(t) + (A_{1i} + \Delta A_{1i})x(t-\sigma(t)) \\ &\quad + (B_i + \Delta B_i)u(t), \quad i = 1, \cdots, r\end{aligned} \tag{1}$$

Where $\theta_j(t)$ and $N_{ij}(i = 1, ..., r, j = 1, ..., p)$ are, respectively, the premise variables and the fuzzy sets ; $x(t) \in R^n$ is the state ; $u(t) \in R^m$ is the control input ; r is the number of IF-THEN rules; the time-delay, $\sigma(t)$, is a time -varying continuous function that satisfies

$$0 \leq \sigma(t) \leq \bar{\sigma}, \qquad \dot{\sigma}(t) \leq \beta \tag{2}$$

The parametric uncertainties ΔA_i, ΔA_{1i}, ΔB_i are time-varying matrices that are defined as follows: $\Delta A_i = D_A F_i(t) E_{Ai}$, $\Delta A_{1i} = D_{A1} F_i(t) E_{A1i}$, $\Delta B_i = D_B F_i(t) E_{Bi}$. Let $\bar{A}_i = A_i + \Delta A_i$; $\bar{A}_{1i} = A_{1i} + \Delta A_{1i}$; $\bar{B}_i = B_i + \Delta B_i$. Where A_i, A_{1i}, B_i, D_A, D_{A1}, D_B, E_{Ai}, E_{A1i}, E_{Bi} are constant known matrices and $F_i(t)$ is unknown and possibly time-varying matrix satisfying $F_i^T(t)F_i(t) \leqslant I$ for any given t. It is assumed the element of $F_i(t)$ are Lebesgue measurable. By using the commonly used center-average defuzzifier, product inference and singleton fuzzifier, the T-S fuzzy systems

978-1-4244-7316-8/11/$26.00 ©2011 IEEE

can be inferred as

$$\dot{x}(t) = \sum_{i=1}^{r} h_i(\theta(t))\Big\{ \bar{A}_i x(t) + \bar{A}_{1i} x(t-\sigma(t)) + \bar{B}_i u(t) \Big\} \tag{3}$$

where $\theta(t) = [\theta_1(t), \cdots, \theta_p(t)]$ and $\upsilon_i(\theta(t)) = \prod_{j=1}^{p} N_{ij}(\theta_j(t))$ are the membership functions of the system with respect to ith plan rule. Denote

$$h_i(\theta(t)) = \upsilon_i(\theta(t)) / \sum_{i=1}^{r} \upsilon_i(\theta(t)). \tag{4}$$

$h_i(\theta(t))$ is the averaging weight for each rule, representing the normalized grade of membership, and satisfies

$$h_i(\theta(t)) \geq 0, \quad \text{and} \quad \sum_{i=1}^{r} h_i(\theta(t)) = 1, (i = 1, 2, ..., r) \tag{5}$$

In order to obtain the main results in this paper, the following lemma is needed:

Lemma *2.1:* [5] Given matrices $D, E, F(t)$ with compatible dimensions and F(t) satisfying $F(t)^T F(t) \leq I$. Then, the following inequality holds for any $\epsilon > 0$:
$DF(t)E + E^T F(t)^T D^T \leq \epsilon DD^T + \epsilon^{-1} E^T E$

III. Main Results

A. Time delay dependent stabilization conditions

We consider the problem of delay-dependent stabilization of system (3). Based on the Parallel Distributed Compensation (PDC), the following fuzzy control law is employed to deal with the problem of stabilization via state feedback.
Controller Rule i:
IF $\theta_1(t)$ is N_{i1} and... $\theta_p(t)$ is N_{ip} THEN

$$u(t) = K_i x(t), i = 1, 2, \cdots, r. \tag{6}$$

Hence, the overall fuzzy control law is represented by

$$u(t) = \sum_{i=1}^{r} h_i(\theta(t)) K_i x(t), \tag{7}$$

where $K_i (i = 1, 2, \cdots, r)$ are the local control gain matrices. In the sequel, for brevity we use h_i to denote $h_i(\theta(t))$.
Consider system (3) associated with the control law (7), then the resulting closed-loop system can be expressed as follows:

$$\dot{x}(t) = \sum_{i=1}^{r} \sum_{j=1}^{r} h_i h_j \Big\{ \hat{A}_{ij} x(t) + \bar{A}_{1i} x(t-\sigma(t)) \Big\} \tag{8}$$

Where $\hat{A}_{ij} = \bar{A}_i + \bar{B}_i K_j$.

Theorem *3.1:* Case of nominal System:
System (8) is asymptotically stable, if there exist some matrices $\bar{P}_i > 0$, $\bar{H} > 0$, $\bar{S} > 0$ and $\bar{T} > 0$, any matrices Θ_i, Y_i, U, $\bar{P}_{\Phi,i}$, $\bar{L}$, $\bar{W}$,μ_1, μ_2 and μ_3 are positive scalars satisfying the following set of LMIs:

$$P_l + \Theta_i > 0 \tag{9}$$

$$\Lambda_{ii} < 0, \quad (i = 1, \cdots, r) \tag{10}$$

$$\Lambda_{ij} + \Lambda_{ji} < 0, \quad i < j \tag{11}$$

where

$$\Lambda_{ij} = \begin{bmatrix} \Gamma_{1ij} & * & * & * & * & * \\ \Gamma_{2ij} & \Gamma_{3i} & * & * & * & * \\ \Gamma_{4ij} & \Gamma_{5i} & \Gamma_6 & * & * & * \\ -\bar{W}_1 & -\bar{W}_2^T & 0 & -\bar{T} & * & * \\ \bar{L}_1^T & \bar{L}_2^T & 0 & 0 & -\bar{\sigma}^{-1}\bar{H} & * \\ \bar{W}_1^T & \bar{W}_2^T & 0 & 0 & 0 & -\bar{\sigma}^{-1}\bar{H} \end{bmatrix} \tag{12}$$

$$P_{\Phi,i} = \sum_{l=1}^{r} \Phi_l (P_l + \Theta_i) \tag{13}$$

where

$$\begin{aligned} \Gamma_{1ij} &= Sym(A_i U + B_i Y_j + \bar{L}_1) + \bar{P}_{\Phi,i} + \bar{S} + \bar{T} \\ \Gamma_{2ij} &= \mu_1 (A_i U + B_i Y_j) + U^T A_{1i}^T + \bar{L}_2 - \bar{L}_1^T + \bar{W}_1^T \\ \Gamma_{3i} &= \mu_1 Sym(A_{1i} U - \bar{L}_2 + \bar{W}_2) - (1-\beta)\bar{S} \\ \Gamma_{4ij} &= \mu_2 (A_i U + B_i Y_j) - U^T + \bar{P}_i^T \\ \Gamma_{5i} &= \mu_2 (A_{1i} U) - \mu_1 U^T \\ \Gamma_6 &= -\mu_2 Sym(U) + \bar{\sigma}\bar{H} \end{aligned}$$

Proof: For simplicity, we set $x_\sigma = x(t-\sigma(t))$, $x_{\bar{\sigma}} = x(t-\bar{\sigma})$, $L = \begin{bmatrix} L_1 \\ L_2 \\ 0 \\ 0 \end{bmatrix}$, $W = \begin{bmatrix} W_1 \\ W_2 \\ 0 \\ 0 \end{bmatrix}$, $M = \begin{bmatrix} M_1 \\ M_2 \\ M_3 \\ 0 \end{bmatrix}$ and $\Psi(t) = \begin{bmatrix} x(t) \\ x_\sigma \\ \dot{x}(t) \\ x_{\bar{\sigma}} \end{bmatrix}$
In this part we consider that ΔA_i , ΔB_i and $\Delta A_{1i} = 0$.
Let us choose a candidate Lyapunov-Krasovskii function as follows:

$$\begin{aligned} V &= V_1(t) + V_2(t) + V_3(t) \\ V_1(t) &= x^T(t) P(t) x(t) \\ V_2(t) &= \int_{t-\sigma(t)}^{t} x^T(s) S x(s)\, \mathrm{d}s + \int_{t-\bar{\sigma}}^{t} x^T(s) T x(s)\, \mathrm{d}s \\ V_3(t) &= \int_{-\bar{\sigma}}^{0} \int_{t+\alpha}^{t} \dot{x}^T(s) H \dot{x}(s)\, \mathrm{d}s \mathrm{d}\alpha \end{aligned} \tag{14}$$

where $P(t)$ is a fuzzy weighting-dependent Lyapunov function

$$P(t) = \sum_{i=1}^{r} h_i P_i \qquad (i = 1, 2, \cdots, r) \tag{15}$$

Taking the derivative of V_i, $1, \cdots, 3$ along the trajectory of system (8) yields

$$\dot{V}_1(x(t)) = 2\dot{x}^T(t) P(t) x(t) + x^T(t) \dot{P}(t) x(t)$$

The derivative of (15) provides information about time derivative of membership functions.Then, we assume that

$$|\dot{h_l}(\theta(t))| \leq \Phi_l \tag{16}$$

where $\Phi_l \geq 0$ $(l = 1, 2, \cdots, r)$
Considering the properties in (5) we have

$$\begin{aligned}\dot{P}(t) &= \sum_{l=1}^{r} \dot{h}_l(t) P_l = \sum_{i=1}^{r} (h_i(t)) \sum_{l=1}^{r} \dot{h}_l(t) P_l \\ &= \sum_{i=1}^{r}\sum_{l=1}^{r} h_i(t)\dot{h}_l(t) P_l \end{aligned} \tag{17}$$

Once again considering (5) the following equation holds:

$$\sum_{i=1}^{r}\sum_{l=1}^{r} h_i \dot{h}_l x^T(t)\Theta_i x(t) = 0 \tag{18}$$

where $\Theta_i > 0$ are slack matrices with appropriate dimensions. Assuming that the assumption (9) and (16) hold, it is easy to have

$$\dot{P}(t) \leq \sum_{i=1}^{r}\sum_{l=1}^{r} h_i(t)\Phi_l(P_l + \Theta_i) \tag{19}$$

On the other hand, from the defintion of (8) the following equation holds

$$\begin{aligned} 2\Big[x^T(t)M_1 + x_\sigma^T M_2 + \dot{x}(t)^T M_3\Big]\Big[-\dot{x}(t) \\ + \sum_{i=1}^{r}\sum_{j=1}^{r} h_i h_j(\hat{A}_{ij}x(t) + \bar{A}_{1i}x_\sigma)\Big] = 0 \end{aligned} \tag{20}$$

Adding the null terms (20) and (18), we obtain

$$\begin{aligned}\dot{V}_1(x(t)) \leq \sum_{i=1}^{r} h_i \Big\{ & 2x^T(t)P_i\dot{x}(t) \\ & + \sum_{l=1}^{r} \Phi_l x^T(t)(P_l + \Theta_i)x(t)\Big\} \end{aligned} \tag{21}$$

$$\begin{aligned} & + 2\Big[x^T(t)M_1 + x_\sigma^T(t)M_2 + \dot{x}(t)^T M_3\Big] \\ & \times \Big[-\dot{x}(t) + \sum_{i=1}^{r}\sum_{j=1}^{r} h_i h_j \hat{A}_{ij}x(t) + \bar{A}_{1i}x_\sigma\Big] \end{aligned} \tag{22}$$

$$\begin{aligned} & \leq \sum_{i=1}^{r} h_i\Big\{2x^T(t)P_i\dot{x}(t) + x^T(t)P_{\Phi,i}x(t)\Big\} \\ & + 2\sum_{i=1}^{r}\sum_{j=1}^{r} h_i h_j \Psi^T(t) M \begin{bmatrix}\hat{A}_{ij} & \bar{A}1i & -I & 0\end{bmatrix}\Psi(t) \end{aligned}$$

$$\begin{aligned}\dot{V}_2(x(t)) &= x^T(t)Sx(t) - (1-\dot{\sigma}(t))x_\sigma^T S x_\sigma \\ &\quad + x^T(t)Tx(t) - x_{\bar{\sigma}}^T T x_{\bar{\sigma}} \end{aligned} \tag{23}$$

$$\begin{aligned}\dot{V}_3(x(t)) &= \bar{\sigma}\dot{x}^T(t)H\dot{x}(t) \\ &\quad - \int_{-\bar{\sigma}}^{0} \dot{x}^T(t+\alpha)H\dot{x}(t+\alpha)\,\mathrm{d}\alpha \end{aligned} \tag{24}$$

$$\begin{aligned} & - \int_{-\bar{\sigma}}^{0} \dot{x}^T(t+\alpha)H\dot{x}(t+\alpha)\,\mathrm{d}\alpha = -\int_{t-\bar{\sigma}}^{t} \dot{x}^T(\alpha)H\dot{x}(\alpha)\,\mathrm{d}\alpha \\ & = -\int_{t-\bar{\sigma}}^{t-\sigma(t)} \dot{x}^T(\alpha)H\dot{x}(\alpha)\,\mathrm{d}\alpha - \int_{t-\sigma(t)}^{t} \dot{x}^T(\alpha)H\dot{x}(\alpha)\,\mathrm{d}\alpha \\ & \leq \bar{\sigma}\Psi^T(t)LH^{-1}L^T\Psi(t) + 2\Psi^T(t)L\int_{t-\sigma(t)}^{t}\dot{x}(\alpha)\,\mathrm{d}\alpha \\ & + \bar{\sigma}\Psi^T(t)WH^{-1}W^T\Psi(t) + 2\Psi^T(t)W\int_{t-\bar{\sigma}}^{t-\sigma(t)}\dot{x}(\alpha)\,\mathrm{d}\alpha \end{aligned}$$

The desired results are obtained by using the upper bound of the following terms (25) and (26) :

$$\begin{aligned} -2\Psi^T(t)L\int_{t-\sigma(t)}^{t}\dot{x}(\alpha)\,\mathrm{d}\alpha &\leq \sigma(t)\Psi^T(t)LH^{-1}L^T\Psi(t) \\ &\quad + \int_{t-\sigma(t)}^{t}\dot{x}^T(\alpha)H\dot{x}(\alpha)\,\mathrm{d}\alpha \\ &\leq \bar{\sigma}\Psi^T(t)LH^{-1}L^T\Psi(t) + \int_{t-\sigma(t)}^{t}\dot{x}^T(\alpha)H\dot{x}(\alpha)\,\mathrm{d}\alpha \end{aligned} \tag{25}$$

$$\begin{aligned} -2\Psi^T(t)W\int_{t-\bar{\sigma}}^{t-\sigma(t)}\dot{x}(\alpha)\,\mathrm{d}\alpha &\leq (\bar{\sigma}-\sigma(t))\Psi^T(t)WH^{-1}W^T\Psi(t) \\ &\quad + \int_{t-\bar{\sigma}}^{t-\sigma(t)}\dot{x}^T(\alpha)H\dot{x}(\alpha)\,\mathrm{d}\alpha \\ &\leq \bar{\sigma}\Psi^T(t)WH^{-1}W^T\Psi(t) + \int_{t-\bar{\sigma}}^{t-\sigma(t)}\dot{x}^T(\alpha)H\dot{x}(\alpha)\,\mathrm{d}\alpha \end{aligned} \tag{26}$$

where the well-known inequality $-2x^Ty \leq x^TH^{-1}x + y^THy$ with $H > 0$ is used to get the last inequalities. Then, we obtain

$$\begin{aligned}\dot{V}_3(x(t)) \leq\ & \bar{\sigma}\dot{x}^T(t)H\dot{x}(t) + \bar{\sigma}\Psi^T(t)LH^{-1}L^T\Psi(t) \\ & + \bar{\sigma}\Psi^T(t)WH^{-1}W^T\Psi(t) \\ & + 2\Psi^T(t)L\begin{bmatrix}I & -I & 0 & 0\end{bmatrix}\Psi(t) \\ & + 2\Psi^T(t)W\begin{bmatrix}0 & I & 0 & -I\end{bmatrix}\Psi(t) \end{aligned} \tag{27}$$

By letting, $M_1 = G^T$, $M_2 = \mu_1 G^T$ and $M_3 = \mu_2 G^T$, with μ_1, μ_2, μ_3 being positive scalars, the derivative of (14) along the trajectory of the closed-loop system (8) can be written as

$$\begin{aligned}\dot{V}(x(t)) &\leq \sum_{i=1}^{r}\sum_{j=1}^{r} h_i h_j \Psi^T(t)\bar{\Phi}_{ij}\Psi(t) \\ &= \sum_{i=1}^{r} h_i^2 \Psi(t)^T\bar{\Phi}_{ii}\Psi(t) \\ &\quad + 2\sum_{i=1}^{r}\sum_{j>i}^{r} h_i h_j \Psi(t)^T(\bar{\Phi}_{ij} + \bar{\Phi}_{ji})\Psi(t) \end{aligned} \tag{28}$$

where $\bar{\Phi}_{ij} = \bar{\lambda}_{ij} + \bar{\sigma}LH^{-1}L^T + \bar{\sigma}WH^{-1}W^T$

$$\bar{\lambda}_{ij} = \begin{bmatrix}\Omega_{1ij} & * & * & * \\ \Omega_{2ij} & \Omega_{3i} & * & * \\ \Omega_{4ij} & \Omega_{5i} & \Omega_6 & * \\ -W_1^T & -W_2^T & 0 & -T\end{bmatrix} \tag{29}$$

with
$\Omega_{1ij} = Sym(G^T\hat{A}_{ij} + L_1) + P_{\Phi,i} + S + T$,
$\Omega_{2ij} = \mu_1(G^T\hat{A}_{ij}) + \bar{A}_{1i}^T G + L_2 - L_1^T + W_1^T$,
$\Omega_{3i} = \mu_1 Sym(G^T\bar{A}_{1i} - L_2 + W_2) - (1-\beta)S$,
$\Omega_{4ij} = \mu_2(G^T\hat{A}_{ij}) - G + P_i^T$,
$\Omega_{5i} = \mu_2 G^T\bar{A}_{1i} - \mu_1 G$
$\Omega_6 = -\mu_2 Sym(G) + \bar{\sigma}H$

From (11) we have $\Gamma_6 < 0$, this imply $0 < \bar{\sigma}H < \mu_2 Sym(U)$, this indicate that U is non singular when $\mu_2 > 0$. Define $G = U^{-1}$ and $\Upsilon = diag(G, G, G, G)$. Let $\bar{L_1} = U^T L_1 U$, $\bar{S} = U^T S U$, $\bar{T} = U^T T U$, $\bar{P}_i = U^T P_i U$, $\bar{H} = U^T H U$, $\bar{L_2} = U^T L_2 U$, $\bar{W_1} = U^T W_1 U$, $\bar{W_2} = U^T W_2 U$, and $Y_i = K_i U$.

Pre-and post multiplying (11) by Υ^T and Υ, respectively, and applying the Schur complement, we obtain $\bar{\Phi}_{ij} + \bar{\Phi}_{ji} < 0$.

By following the similar way it is easy to obtain from (10) that $\bar{\Phi}_{ii} < 0$, then we have $\dot{V}(x(t)) < 0$ when $h_i \geq 0$, therefore, the system (8) is asymptotically stable. ■

Remark *3.1:* In some existing literature, for example [6], the term $\int_{t-\bar{\sigma}}^{t} \dot{x}^T(\alpha)H\dot{x}(\alpha)\,\mathrm{d}\alpha$ in the derivative of V(t) was often estimated as $\int_{t-\sigma(t)}^{t} \dot{x}^T(\alpha)H\dot{x}(\alpha)\,\mathrm{d}\alpha$ and the term $\int_{t-\bar{\sigma}}^{t-\sigma(t)} \dot{x}^T(\alpha)H\dot{x}(\alpha)\,\mathrm{d}\alpha$ was ignored .
This may bring conservativeness. In Theorem 3.1, all these terms are reserved, which can reduce conservativeness.

Corollary 3.2:
System (8) is asymptotically stable, if there exist some matrices $\bar{P}_i > 0$, $\bar{H} > 0$ and $\bar{S} > 0$, any matrices Θ_i, Y_i, U, $\bar{P}_{\Phi,i}$, $\bar{L}$, μ_1, μ_2 and μ_3 are positive scalars satisfying the following set of LMIs:

$$P_l + \Theta_i > 0 \tag{30}$$
$$\Lambda'_{ii} < 0 (i = 1, 2, \cdots, r) \tag{31}$$
$$\Lambda'_{ij} + \Lambda'_{ji} < 0, \quad i < j \tag{32}$$

where

$$\Lambda'_{ij} = \begin{bmatrix} \Gamma'_{1ij} & * & * & * \\ \Gamma'_{2ij} & \Gamma'_{3i} & * & * \\ \Gamma'_{4ij} & \mu_2(A_{1i}U) - \mu_1 U^T & \Gamma'_5 & 0 \\ \bar{\sigma}\bar{L}_1^T & \bar{\sigma}\bar{L}_2^T & 0 & -\bar{H} \end{bmatrix}$$

where $\Gamma'_{1ij} = Sym(A_iU + B_iY_j + \bar{L}_1) + \bar{P}_{\Phi,i} + \bar{S}$
$\Gamma'_{2ij} = \mu_1(A_iU + B_iY_j) + U^T A_{1i}^T + \bar{L}_2 - \bar{L}_1^T$
$\Gamma'_{3i} = \mu_1 Sym(A_{1i}U - \bar{L}_2) - (1-\beta)\bar{S}$
$\Gamma'_{4ij} = \mu_2(A_iU + B_iY_j) - U^T + \bar{P}_i^T$
$\Gamma'_5 = -\mu_2 Sym(U) + \bar{\sigma}\bar{H}$.

Theorem *3.2:* : Case of uncertain System:
System (8) is asymptotically stable, if there exist some matrices $\bar{P}_i > 0$, $\bar{H} > 0$, $\bar{S}$ and $\bar{T} > 0$, any matrices Θ_i, Y_i, U, $\bar{P}_{\Phi,i}$, $\bar{L}$, $\bar{W}$, ϵ_i, μ_1, μ_2 and μ_3 are positive scalars satisfying the following set of LMIs:

$$P_l + \Theta_i > 0 \tag{33}$$
$$\Lambda_{ii} < 0 (i = 1, 2, \cdots, r) \tag{34}$$
$$\Lambda_{ij} + \Lambda_{ji} < 0 (i < j = 1, 2, \cdots, r) \tag{35}$$

where

$$\Lambda_{ij} = \begin{bmatrix} \Gamma_{1ij} & * & * \\ \Gamma_{2ij} & \Gamma_{3i} & * \\ \Gamma_{4ij} & \mu_2(A_{1i}U) - \mu_1 U^T & \Gamma_5 \\ -\bar{W}_1^T & \bar{W}_2^T & 0 \\ \bar{L}_1^T & \bar{L}_2^T & 0 \\ \bar{W}_1^T & \bar{W}_2^T & 0 \\ E_{Ai}U & 0 & 0 \\ E_{Bi}Y_j & 0 & 0 \\ 0 & E_{A1i}U & 0 \end{bmatrix}$$
$$\begin{bmatrix} * & * & * & * & * & * \\ * & * & * & * & * & * \\ * & * & * & * & * & * \\ \Gamma_6 & * & * & * & * & * \\ 0 & -\bar{\sigma}^{-1}\bar{H} & 0 & * & * & * \\ 0 & 0 & -\bar{\sigma}^{-1}\bar{H} & * & * & * \\ 0 & 0 & 0 & -\epsilon_i I & * & * \\ 0 & 0 & 0 & 0 & -\epsilon_i I & * \\ 0 & 0 & 0 & 0 & 0 & -\epsilon_i I \end{bmatrix} \tag{36}$$

where $\Gamma_{1ij} = Sym(A_iU + B_iY_j + \bar{L}_1) + \bar{P}_{\Phi,i} + \bar{S} + \bar{T} + \epsilon_i D_A D_A^T + \epsilon_i D_B D_B^T + \epsilon_i D_{A1} D_{A1}^T$
$\Gamma_{2ij} = \mu_1(A_iU + B_iY_j) + U^T A_{1i}^T + \bar{L}_2 - \bar{L}_1^T + \bar{W}_1^T$
$\Gamma_{3i} = \mu_1 Sym(A_{1i}U - \bar{L}_2 + \bar{W}_2) - (1-\beta)\bar{S} + \mu_1^2\epsilon_i D_A D_A^T + \mu_1^2\epsilon_i D_B D_B^T + \mu_1^2\epsilon_i D_{A1} D_{A1}^T$
$\Gamma_{4ij} = \mu_2(A_iU + B_iY_j) - U^T + \bar{P}_i^T$
$\Gamma_5 = -\mu_2 Sym(U) + \bar{\sigma}\bar{H} + \mu_2^2\epsilon_i D_A D_A^T + \mu_2^2\epsilon_i D_B D_B^T + \mu_2^2\epsilon_i D_{A1} D_{A1}^T$
$\Gamma_6 = -\bar{T}$

Proof:

In this part we consider that ΔA_i , ΔBi and $\Delta A1i$ are $\neq 0$. By using Lemma 2.1 and the Schur complement, we obtain Theorem 3.2. Where the uncertain part is represented as : $\Delta\bar{\Phi}_{ij}$=$Sym(\check{D}\check{F}(t)\check{E}) \leq \epsilon_i\check{D}\check{D}^T + \epsilon_i^{-1}\check{E}^T\check{E}$ With

$$\check{D} = \begin{bmatrix} D_A & D_B & D_{A1} & 0 & 0 & 0 \\ \mu_1 D_A & \mu_1 D_B & \mu_1 D_{A1} & 0 & 0 & 0 \\ \mu_2 D_A & \mu_2 D_B & \mu_2 D_{A1} & 0 & 0 & 0 \\ 0 & 0 & 0 & 0 & 0 & 0 \\ 0 & 0 & 0 & 0 & 0 & 0 \\ 0 & 0 & 0 & 0 & 0 & 0 \end{bmatrix} \tag{37}$$

$$\check{F}(t) = \begin{bmatrix} F(t) & 0 & 0 & 0 & 0 & 0 \\ 0 & F(t) & 0 & 0 & 0 & 0 \\ 0 & 0 & F(t) & 0 & 0 & 0 \\ 0 & 0 & 0 & F(t) & 0 & 0 \\ 0 & 0 & 0 & 0 & F(t) & 0 \\ 0 & 0 & 0 & 0 & 0 & F(t) \end{bmatrix} \tag{38}$$

$$\check{E} = \begin{bmatrix} E_{Ai}U & 0 & 0 & 0 & 0 & 0 \\ E_{Bi}Y_j & 0 & 0 & 0 & 0 & 0 \\ 0 & E_{A1i}U & 0 & 0 & 0 & 0 \\ 0 & 0 & 0 & 0 & 0 & 0 \\ 0 & 0 & 0 & 0 & 0 & 0 \\ 0 & 0 & 0 & 0 & 0 & 0 \end{bmatrix} \quad (39)$$

■

IV. Numerical Examples

To illustrate the designed controller law for the T-S fuzzy model with time-varying delay, we consider the following examples.

Example 1. For fuzzy rules as $h_1 = 1-((x_2^2)/2.25)$ *and* $h_2 = x_2^2/2.25$, the following fuzzy T-S model is presented:

$$\dot{x}(t) = \sum_{i=1}^{r}\sum_{j=1}^{r} h_i h_j \Big\{ [(A_i + \Delta A_i) + B_i K_j]x(t) + (A_{1i} + \Delta A_{1i})x(t-\sigma(t)) \Big\} \quad (40)$$

where

$$A_1 = \begin{bmatrix} 0 & 0.6 \\ 0 & 1 \end{bmatrix}, A_2 = \begin{bmatrix} 1 & 0 \\ 1 & 0 \end{bmatrix}, A_{11} = \begin{bmatrix} 0.5 & -0.9 \\ 0 & 2 \end{bmatrix},$$
$$A_{12} = \begin{bmatrix} 0.9 & 0 \\ 1 & 1.6 \end{bmatrix}, B_1 = B_2 = \begin{bmatrix} 1 \\ 1 \end{bmatrix},$$

$$\Delta A_i = D_A F_i(t) E_{Ai}, \Delta A_{1i} = D_{A1} F_i(t) E_{A1i}, \quad (41)$$

$$D_A = D_B = D_{A1} = \begin{bmatrix} -0.03 & 0 \\ 0 & 1.6 \end{bmatrix}$$

$$E_{A1} = \begin{bmatrix} -0.15 & 0.2 \\ 0 & 0.04 \end{bmatrix}, \ E_{A2} = \begin{bmatrix} -0.15 & 0.2 \\ 0 & 0.04 \end{bmatrix},$$
$$E_{A11} = \begin{bmatrix} -0.05 & -0.35 \\ 0.08 & -0.45 \end{bmatrix}, \ E_{A12} = \begin{bmatrix} -0.05 & -0.35 \\ 0.08 & -0.45 \end{bmatrix},$$
$$E_{B1} = \begin{bmatrix} 0 & 0 \\ 0 & 0 \end{bmatrix}, E_{B2} = \begin{bmatrix} 0 & 0 \\ 0 & 0 \end{bmatrix}$$

The operating domain of the nonlinear plant are assumed to be $x_1(t) \in [-3, 3]$ and $x_2(t) \in [-1, 1]$. Thus, based on the derivative of the membership function, we assume that Φ_l= $\{3.5,3.5\}$.

It appears from Table 1 that our result improves the existing ones in the case of uncertain T-S fuzzy model with varying time-delay.

In fact, by solving the LMIs in Theorem 3 in [7], in Theorem 1 in [1] , in Corollary 3.2 and Theorem 3.2 , the maximum value of the time delay $\bar{\sigma}$ is found in theorem 3.2. Table 1 summarizes the results. By using theorem 3.2 with the choice of $\beta = 0.15$ and $\sigma(t)$=0.379+0.15 sin(t)($\bar{\sigma} = 0.529, \mu_1 = \mu_2 = 0.1$) we can obtain the following state-feedback gain matrices:

$$K_1 = 10^3.\begin{bmatrix} 0.9352 & -3.4038 \end{bmatrix} \quad (42)$$
$$K_2 = 10^3.\begin{bmatrix} 1.7298 & -6.2924 \end{bmatrix} \quad (43)$$

The simulation was tested under the initial conditions $x(t) = [2 \quad 0]^T, t \in [-0.529 \quad 0]$ and uncertainty function

$$F_i(t) = \begin{bmatrix} sin(t) & 0 \\ 0 & cos(t) \end{bmatrix} \quad (44)$$

From the simulation results in Figure 1, it can be clearly seen that our method allows to stabilize nonlinear systems represented by uncertain T-S fuzzy model with time -varying delay for the maximum value of delay which can be attain 0.529 s. Despite the presence of uncertainties, the system states converge asymptotically to zero.

TABLE I
Comparison among varying delay-dependent stabilization methods with uncertainties

Methods	Maximum allowed τ
theorem 1 of [1]	0.1498 s
theorem 3 of [7]	0.4770 s
Corollary 3.2	0.525 s
theorem 3.2	0.529 s

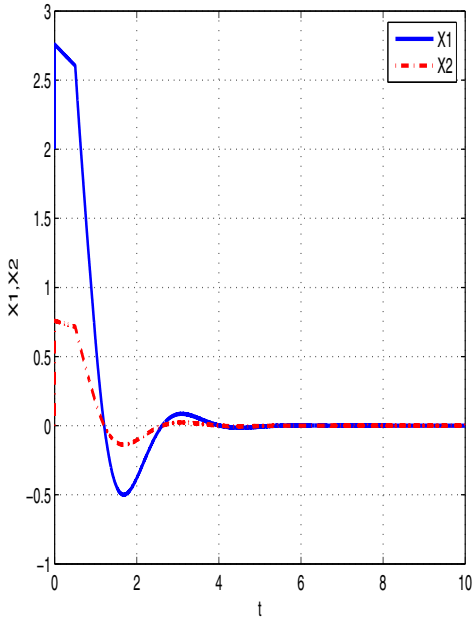

Fig. 1. Control results for system (45) with uncertainties

Example 2. To illustrate the designed controller laws for the T-S fuzzy model with time-varying delay,we consider the following example.

Example . For fuzzy rules as h_1=$1/2(1 + (c - x_1(t)/\gamma))$ and $h_2 = 1/2(1 - (c - /x_1(t)/\gamma)$

Where $\gamma = 6.3$, $a = 0.5$, $b_1 = b_2 = 0.2$, $c = 5.7$, the following fuzzy T-S model is presented:

$$\dot{x}(t) = \sum_{i=1}^{r}\sum_{j=1}^{r} h_i h_j \Big\{ [(A_i + \Delta A_i) + B_i K_j]x(t) + (A_{1i} + \Delta A_{1i})x(t-\sigma(t)) \Big\} \quad (45)$$

where

$$A_1 = \begin{bmatrix} 0 & -1 & -1 \\ 1 & b_1 & 0 \\ 0 & 0 & -\gamma \end{bmatrix}, \qquad A_2 = \begin{bmatrix} 0 & -1 & -1 \\ 1 & b_1 & 0 \\ 0 & 0 & \gamma \end{bmatrix},$$

$$A_{11} = A_{12} = \begin{bmatrix} a & 0 & 0 \\ 0 & 0 & 0 \\ 0 & 0 & 0 \end{bmatrix}, \qquad B_1 = B_2 = \begin{bmatrix} 0 \\ 0 \\ 1 \end{bmatrix},$$

The operating domain of the nonlinear plant are assumed to be $x_1(t) \in [-10, 12]$, $x_2(t) \in [-12, 8]$ and $x_3(t) \in [0, 25]$. Thus, based on the derivative of the membership functions, we choose Φ_l= {2.15,2.15}.

The free weighting approach gives the best result in the case of uncertain T-S fuzzy model with varying time-delay.

In fact, by solving the LMIs in Theorem 3.1 , and in Corollary 3.2 , the maximum value of the time delay $\bar{\sigma}$ is found in theorem 3.1. By using theorem 3.1 with the choice of $\beta = 0.15$ and $\sigma(t)$=2.274+0.15 sin(t)($\bar{\sigma} = 2.424, \mu_1 = \mu_2 = 1$) we can obtain the following state-feedback gain matrices:

$$K_1 = \begin{bmatrix} 14.9314 & 0.8607 & -2.4751 \end{bmatrix} \tag{46}$$

$$K_2 = \begin{bmatrix} 14.9314 & 0.8607 & -15.0751 \end{bmatrix} \tag{47}$$

The simulation was tested under the initial conditions $x(t) = [1.4 \quad 0.3 \quad -2.4]^T, t \in [-2.424 \quad 0]$. From the simulation results in Figure 2, it can be clearly seen that the free weighting matrix approach allows to stabilize nonlinear systems represented by uncertain T-S fuzzy model with time -varying delay for the maximum value of delay which can be attain 2.424 s.

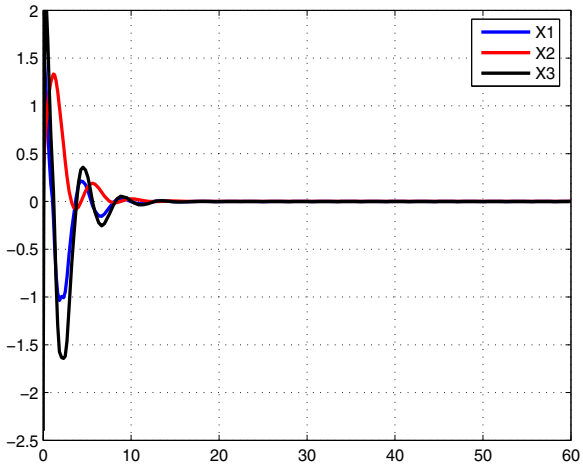

Fig. 2. Control results for system (45) without uncertainties $\bar{\sigma} = 2.424$

V. Conclusion

In this paper, we have presented new conditions for robust stabilization for uncertain fuzzy systems with time varying delay. The less conservatism sufficient conditions formulated in LMI terms are established based on the fuzzy weighting-dependent Lyapunov-Krasovskii functional method combined with the introduction of free weighting matrices. The merits and less conservatism of our method have been illustrated in comparison with existing works.

References

[1] B.Chen and X.Liu. Delay-dependent stability analysis and control synthesis of fuzzy dynamic systems with time delay. *Fuzzy sets and systems*, 157:2224–2240, 2006.

[2] Miguel Bernal and Thierry Marie Guerra. Generalized non-quadratic stability of continuous-time takagi-sugeno models. *TFS-2009-0321*, .:., 2009.

[3] C.Lin, Q-G.Wang, T.H .Lee, and Y.He. Lmi approach to analysis and control of takagi-sugeno fuzzy systems with time delay. *Newyork/Berlin,Heidelberg,Germany:Springer-Verlag*, 15:482–493, 2007.

[4] H. Gassara, A. EL Hajjaji, and M. Chaabane. Delay-dependant H_∞ exponential stabilization of T-S fuzzy systems with interval time-varying delay. *49th IEEE Conference on Decision and Control, IEEE-CDC, December 15-17, Atlanta-Georgia, USA*, .:4281–4286, 2010.

[5] H. Gassara, A. El Hajjaji, and M. Chaabane. Robust H_∞ control for T-S fuzzy systems with time varying delay. *International Journal of Systems Science*, 41:1481–1491, 2010.

[6] Wang H, Xue A, Lu R Wang, and J.. Delay-dependent robust stability and stabilization for uncertain singular system with time-varying delay. *American Control Conference, Westin Seattle Hotel, Seattle, Washington, USA,*, .:36263631, 2008.

[7] H.Gassara, A. El Hajjaji, and M. Chaabane. Robust control of T-S fuzzy systems with time-varying delay using new approach. *International Journal of Robust and Nonlinear Control*, 20:1566–1578, 2009.

[8] M. Kchaou and A. Toumi. Delay-dependent h1 resilient output fuzzy control for nonlinear discrete-time systems with time-delay. *International Journal of Uncertainty, Fuzziness and Knowledge-Based Systems*, 19:229250, 2011.

[9] K.Tanaka and H.O.Wang. Fuzzy control systems design and analysis: A linear matrix inequality approach. *New York: Wiley*, .:324–332, 2001.

[10] L.A.Mozelli, C.D.Campos, R.M.Pahares, L.A.B.Torres, and E.M.A.M.Mendes. Chaotic synchronization and information transmission experiments:a fuzzy relaxed H_∞ control approach. *Circ.Syst.Signal Process*, 26:427–449, 2007.

[11] L.A.Mozelli and R.M.Palhares. A systematic approach to improve multiple lyapunov function stability and stabilization conditions for fuzzy systems. *Informations Sciences*, 179:1149–1162, 2008.

[12] Li Li and Xiaodong Liu. New approach on robust stability for uncertain ts fuzzy systems with state and input delays. *Research Center of Information and Control, Dalian University of Technology,*, 40:23292339, 2007.

[13] C.H. Lien, K.W. Yu, W.D. Chen, Z.L. Wan, and Y.J. Chung. Stability criteria for uncertain takagisugeno fuzzy systems with interval time-varying delay. *The Institution of Engineering and Technology*, .:764769, 2007.

[14] JI-Qing Qiu, Zhi-Feng Gao, Ju-Fang Wang, and Yan-Jun Wang. Delay-dependent robust asymptotic stability for uncertain fuzzy systems with time delays. *Proceedings of the Sixth International Conference on Machine Learning and Cybernetics, Hong Kong*, .:19–22, August 2007.

[15] R.MPalhares, C.D.Capmos, P.Y Ekel M.C.R Lesles, and M.F.S. V .D'Angelo. Delay-dependent robust H_∞ control of uncertain linear systems with time-varying delays. *.Comp.Math.Appl*, 50:13–32, 2005.

[16] Fernando O. Souza, Leonardo A. Mozelli, and Reinaldo M. Palhares. On stability and stabilization of TS fuzzy time-delayed systems. *IEEE Transactions On Fuzzy Systems*, 17:1450–1455, 2009.

[17] T.Takagi and M.Sugeno. Fuzzy identification of system and its applications to modeling and control. *IEEE Trans ,Sys.,Man,Cybern*, 15:116–132, 1985.

[18] Zhong Yang and Yu-Pu Yang. New delay-dependent stability analysis and synthesis of ts fuzzy systems with time-varying delay. *International Journal Of Robust And Nonlinear Control*, .:., 2009.

2011 IEEE International Conference on Fuzzy Systems
June 27-30, 2011, Taipei, Taiwan

Splitting K-means Generated Neural Fuzzy System with Support Vector Regression

Cheng-Da Hsieh
Department of Electrical Engineering,
Hsiuping Institute of Technology
Taichung, Taiwan, R.O.C
Chengda.hsieh@msa.hinet.net

Chia-Feng Juang
Department of Electrical Engineering,
National Chung-Hsing University
Taichung, Taiwan, R.O.C
cfjuang@dragon.nchu.edu.tw

***Abstract*—This paper proposes a Splitting K-means generated Neural Fuzzy System with Support Vector Regression (SKNFS-SVR). The consequent layer in SKNFS-SVR is a Takagi-Sugeno-Kang (TSK)-type consequent. For structure learning, a splitting K-means algorithm clusters the input training data and determines the rule number. For parameter learning, a linear support vector regression (SVR) algorithm is proposed to tune free parameters in the consequent part. The motivation for using SVR for parameter learning is to improve the SKNFS-SVR generalization ability. This paper demonstrates the capabilities of SKNFS-SVR by conducting simulations in clean and noisy function approximations. This paper also compares simulation results from the SKNFS-SVR with Gaussian kernel-based SVR.**

Keywords-Fuzzy modeling, splitting K-means, support vector regression, support vectors, function approximation, fuzzy neural network.

I. INTRODUCTION

Fuzzy systems (FSs) and support vector regressions (SVRs) have been applied to solve the regression estimation and signal prediction problems in these years. FS is a well-known as a powerful tool for modeling nonlinear functions. SVR learning formulation [1, 2] is based on the principle of structural risk minimization and attempts to minimize a bound on the generalization error. The SVR learning approach also exhibits desirable properties such as generalization and over-fitting prevention capabilities.

Researchers have proposed several different neural learning techniques for constructing FSs [3]-[8], such as the self-constructing neural fuzzy inference network (SONFIN) [3] and the self-organizing fuzzy neural network (SOFNN) [7], and the Fuzzified Takagi-Sugeno-Kang (TSK)-type Neural Fuzzy Inference Network (FTNFIN) [8]. However, these neural fuzzy systems (NFS) are based on the minimization of training error (or empirical risk), they do not possess high generalization ability. For noisy regression problems, training error minimization may overtrain the noise into the learning model, leading to an unsatisfied test result. To address this problem, combination of fuzzy set theory and SVR has been proposed for regression problems [9]-[11]. In [9], the authors applied FCM clustering algorithm to obtain fuzzy rule that transforms input data to feature space. Then using SVR solves the weighting parameters. The authors in [10] introduced fuzzy SVM approach to seek a fuzzy linear function that model weights and bias term are fuzzy sets. The authors in [11] proposed a TSK FS-based SVR (TSFS-SVR) that combines the idea of TSK-type fuzzy system and SVR. The function of TSFS-SVR is a linear combination of TS-type kernel functions, where kernel and weight parameters are learned by clustering and SVR. However, there is only one free consequent parameter in each rule of the TS-kernel-based FS due to the constraint of a TS-kernel. This paper proposes an SVR-FS, whose rules are also TSK type. Different from the study in [11], all of the free consequent parameters in each TSK-type fuzzy rule are tunable.

This paper proposes a Splitting K-means generated Neural Fuzzy System with Support Vector Regression (SKNFS-SVR). The main purpose of the SKNFS-SVR is to introduce a new regression model utilizing FS and SVR. The SKNFS-SVR introduces a splitting K-means algorithm to cluster the input training data and determine the number of rules. We applied SVR to tune the consequent parameters in order to obtain a global regression model with good test performance. Representative simulation results show that the approach achieves better performance over the Gaussian kernel based SVR.

This paper is organized as follows. Section II introduces the SKNFS-SVR structure. Section III introduces splitting K-means algorithm and SKNFS-SVR structure learning. Section IV briefly reviews the basic theory of SVR and introduces SKNFS-SVR parameter learning using a linear SVR learning approach. Section V shows some representative simulations of function approximation. Section VI draws conclusions.

II. SKNFN-SVR STRUCTURE

This section introduces the structure of the SKNFS-SVR. SKNFS-SVR has a TSK-type consequent. The output is a linear combination of network inputs, i.e., $\sum_{j=1}^{n} a_{ij}x^j + a_{i0}$, where $a_{ij}s'$ are the consequent part parameters of rule i. For input variable x^j, the following Gaussian membership function is used

$$M_{ij}(x^j) = \exp\left\{-\left(\frac{(x^j - m_{ij})^2}{\sigma_{ij}^2}\right)\right\},\ i = 1,\ldots,r \text{ and } j = 1,\ldots,n \quad (1)$$

where m_{ij} and σ_{ij} denote the center and width of the Gaussian membership function, respectively, and r is the number of

rules. Using an algebraic product operation to obtain a spatial firing strength $u^i(\vec{x})$ that is determined by

$$u^i(\vec{x}) = \prod_{j=1}^{n} M_{ij}(\vec{x}^j) = \exp\left\{ -\frac{\left\| \vec{x} - \vec{m}_i \right\|^2}{\sigma_{ij}^2} \right\}. \quad (2)$$

Based on the simple weighted sum, the system output can be written as

$$y = \sum_{i=1}^{r} [u^i(\vec{x}) \cdot (\sum_{j=1}^{n} a_{ij} x^i + a_{i0})] + b \quad (3)$$

where b is a bias to account for the learning of a linear SVR (see (11)).

III. SKNFS-SVR STRUCTURE LEARNING

The primary task of SKNFS-SVR structure learning is determining the fuzzy rule number r. To generate a suitable number of clusters, a self-splitting K -means algorithm is proposed. In this algorithm, we first calculate the mean of all samples then the variance $\overline{\sigma}^2$ of a cluster is used as the criterion to decide whether or not a cluster should be split into two. The variance of a cluster i is defined as

$$\overline{\sigma}_i^2 = \sum_{j=1}^{n} \sigma_{ij}^2 \quad (4)$$

where σ_{ij} is the variance of the cluster in the j th input dimension, i.e.,

$$\sigma_{ij}^2 = \frac{1}{N_i} \sum_{\vec{x} \in C_i} (x^j - m_{ij})^2 \quad (5)$$

where $\vec{x} \in C_i$ denotes the samples belonging to cluster i 、 m_{ij} is the mean of samples and N_i is the number of samples in the cluster. For the existing r clusters, the algorithm finds

$$I = \arg\max_{1 \le i \le k} \sigma_i^2 \quad (6)$$

where σ_i^2 is the variance of clusters i . If σ_I^2 is larger than a predefined threshold V_{th} , then cluster I is split into two clusters, resulting in a total of $r+1$ clusters. Centers of the two new clusters are initially set as $\vec{m}_I + \vec{\varepsilon}$ and $\vec{m}_I - \vec{\varepsilon}$, where $\vec{m}_I = (m_1^I, \cdots, m_n^I)$ is the center I and $\vec{\varepsilon}$ is a small value. Then, new centers of these $r+1$ clusters are recomputed by splitting K-means algorithm. The whole process recurs until the maximum variance is less than V_{th} . The whole algorithm is summarized as follows:

Begin Algorithm

- ***Initialization***. *Set cluster number* r *=1. Find* $\vec{m}_1$.
- ***Step 1***. *Calculate (5) and (6).*
- ***Step 2.*** *If* $(\sigma_I^2 < V_{th})$
  {Stop}
  Else
  { Split cluster I *into two new clusters with centers* $\vec{m}_I + \vec{\varepsilon}$ *and* $\vec{m}_I - \vec{\varepsilon}$ *, Set* $r \leftarrow r+1$ *}*
- ***Step 3.*** *Find centers of these* r *clusters by K-means clustering*
  Go to Step 1.

End Algorithm

IV. SKNFS-SVR PARAMETER LEARNING

A. Basic SVR Concepts

This section briefly reviews the theory of SVR [12]. Suppose there is a labeled training set

$$S = \{(\vec{x}_1, y_1), (\vec{x}_2, y_2), \cdots, (\vec{x}_N, y_N)\} \quad (7)$$

where $\vec{x}_k \in \mathbb{R}^n$ and $y_k \in \mathbb{R}$, $k = 1, \ldots, N$. The main goal of ε -SVR regression is to find a function $f(\vec{x})$ that has no more than ε deviation from the actually obtained targets y_k for all the training data, and is as close as possible at the same time. First, consider the case of linear function $y'(\vec{x})$, taking the form

$$y'(\vec{x}) = \vec{w}^T \vec{x} + b \quad (8)$$

where $\vec{w} \in \mathbb{R}^n$ is a high dimensional weight vector and the bias $b \in \mathbb{R}$ is a scalar.

The convex optimization problem is feasible when a function $y'(\vec{x})$ exists that approximates all pairs $(\vec{x}_k, y_k)$ with ε precision in the above constraint. If the problem is infeasible or some errors are allowed, then the problem can be defined as

$$\begin{aligned} \text{Min}_{\vec{w}, \xi_k, \hat{\xi}_k} \quad & \frac{1}{2} \vec{w}^T \vec{w} + C \sum_{k=1}^{N} (\xi_k + \hat{\xi}_k) \\ \text{Subject to} \quad & y_k - (\vec{w}^T \vec{x}_k + b) \le \varepsilon + \hat{\xi}_k \\ & \vec{w}^T \vec{x}_k + b - y_k \le \varepsilon + \xi_k \\ & \hat{\xi}_k, \xi_k \ge 0, k = 1, 2, \cdots, N \end{aligned} \quad (9)$$

This formulation introduces two slack variables, $\hat{\xi}$ and ξ : one for exceeding the target value by more than ε , and the other for being more than ε below the target. The constant $C > 0$ is a user regulated positive parameter that controls the trade-off between the error and margin.

By applying the Karush-Kuhn-Tucker theorem, the constrained optimization problem above can be solved by defining a Lagrangian L [8]:

$$L(\vec{w},b,\xi_k,\hat{\xi}_k,\alpha_k,\hat{\alpha}_k)=\frac{1}{2}\vec{w}^T\vec{w}+C\sum_{k=1}^{N}(\xi_k+\hat{\xi}_k)-\sum_{k=1}^{N}(\eta_k\xi_k+\hat{\eta}_k\hat{\xi}_k) \\ -\sum_{k=1}^{N}\alpha_k(\varepsilon+\xi_k-y_k+\vec{w}^T\vec{x}_k+b) \\ -\sum_{k=1}^{N}\hat{\alpha}_k(\varepsilon+\hat{\xi}_k+y_k-\vec{w}^T\vec{x}_k-b) \tag{10}$$

where $\eta_k,\hat{\eta}_k,\alpha_k$ and $\hat{\alpha}_k$ are Lagrange multipliers. Minimizing $L(\vec{w},b,\xi_k,\hat{\xi}_k,\alpha_k,\hat{\alpha}_k)$ requires that the gradient of $L(\vec{w},b,\xi_k,\hat{\xi}_k,\alpha_k,\hat{\alpha}_k)$ with respect to $\vec{w}$, b, ξ_k and $\hat{\xi}_k$ must vanish, i.e.,

$$\frac{\partial L(\vec{w},b,\xi_k,\hat{\xi}_k,\alpha_k,\hat{\alpha}_k)}{\partial\vec{w}}=\vec{w}-\sum_{k=1}^{N}(\alpha_k-\hat{\alpha}_k)\vec{x}_k=0 \\ \Rightarrow \vec{w}=\sum_{k=1}^{N}(\alpha_k-\hat{\alpha}_k)\vec{x}_k \tag{11}$$

$$\frac{\partial L(\vec{w},b,\xi_k,\hat{\xi}_k,\alpha_k,\hat{\alpha}_k)}{\partial b}=\sum_{k=1}^{N}(\hat{\alpha}_k-\alpha_k)=0 \tag{12}$$

$$\frac{\partial L(\vec{w},b,\xi_k,\hat{\xi}_k,\alpha_k,\hat{\alpha}_k)}{\partial\xi_k}=C-\alpha_k-\eta_k=0\Rightarrow\eta_k=C-\alpha_k \tag{13}$$

$$\frac{\partial L(\vec{w},b,\xi_k,\hat{\xi}_k,\alpha_k,\hat{\alpha}_k)}{\partial\hat{\xi}_k}=C-\hat{\alpha}_k-\hat{\eta}_k=0\Rightarrow\hat{\eta}_k=C-\hat{\alpha}_k \tag{14}$$

Thus, the primal problem (9) can be converted into the following equivalent dual problem,

$$\text{Max}_{\alpha_k}L(\alpha_k)=-\frac{1}{2}\sum_{k,j=1}^{N}(\alpha_k-\hat{\alpha}_k)(\alpha_j-\hat{\alpha}_j)\vec{x}_k\cdot\vec{x}_j \\ -\varepsilon\sum_{k=1}^{N}(\alpha_k+\hat{\alpha}_k)+\sum_{k=1}^{N}y_k(\alpha_k-\hat{\alpha}_k) \tag{15}$$

$$\text{Subject to}\ \sum_{k=1}^{N}(\alpha_k-\hat{\alpha}_k)=0\ ,\ \alpha_k,\hat{\alpha}_k\in[0,C]$$

In dual problem (15), the dual variables η_k and $\hat{\eta}_k$ are eliminated through conditions (13) and (14). By substituting (11) into (8), one has

$$y'(\vec{x})=\sum_{k=1}^{N}(\alpha_k-\hat{\alpha}_k)\vec{x}_k\cdot\vec{x}+b \tag{16}$$

where the training samples for which $(\alpha_k-\hat{\alpha}_k)\neq 0$ are called support vectors (SVs).

The above linear SVR is employed to learn free parameters in a SKNFS-SVR. The advantage of using SVR instead of neural learning is that SVR is based on structural risk minimization (or minimizing the test error), so it can improve the SKNFS-SVR generalization ability.

B. SKNFS-SVR Parameter Learning

The objective of parameter learning is to tune the parameter a_{ij} of the constructed SKNFS-SVR to an optimal extent. Learning of parameter a_{ij} using a linear SVR algorithm is introduced as follows.

The output function of SKNFS-SVR in (3) can be written as follows

$$y=\sum_{i=1}^{r}u^i\cdot(\sum_{j=0}^{n}a_{ij}x^j)+b=\sum_{i=1}^{r}\sum_{j=0}^{n}a_{ij}u^ix^j+b \tag{17}$$

where $x_0(k)\triangleq 1$. Eq. (17) shows that the output y is a linear function of u^ix^j with weights a_{ij}. Therefore, linear SVR can be employed to learn parameters a_{ij}. After structure learning, the number of rules r and rule antecedent part parameters are determined. Each input data $\vec{x}_k$ at time step k is transformed to the following vector

$$\vec{\phi}(\vec{x}_k)=[u_k^1x^0,\ldots,u_k^1x^n,u_k^2x^0,\ldots,u_k^2x^n, \\ \ldots,u_k^rx^0,\ldots,u_k^rx^n]\in\mathbb{R}^{r(n+1)}. \tag{18}$$

The vector $\vec{\phi}$ is fed as input to a liner SVR, and the training data pairs in (8) are represented by

$$S=\{(\vec{\phi}(\vec{x}_1),y_1),(\vec{\phi}(\vec{x}_2),y_2),\cdots,(\vec{\phi}(\vec{x}_N),y_N)\} \tag{19}$$

According to (17), the optimal linear regression function is

$$y(\vec{x})=\sum_{k=1}^{N}(\alpha_k-\hat{\alpha}_k)<\vec{\phi}(\vec{x}),\vec{\phi}(\vec{x}_k)>+b \tag{20}$$

where α_k and $\hat{\alpha}_k$ are solved by the linear SVR in Subsection IV-A. Eq. (20) can be represented as follows

$$y(\vec{x})=\sum_{k=1}^{N}(\alpha_k-\hat{\alpha}_k)\sum_{m=1}^{r(n+1)}\phi^m(\vec{x})\phi^m(\vec{x}_k)+b \\ =\sum_{m=1}^{r(n+1)}[\sum_{k=1}^{N}(\alpha_k-\hat{\alpha}_k)\phi^m(\vec{x}_k)]\phi^m(\vec{x})+b \\ =\sum_{i=1}^{r}\sum_{j=1}^{n}[\sum_{k=1}^{N}(\alpha_k-\hat{\alpha}_k)u_k^ix_k^j]u_k^ix_k^j+b \\ =\sum_{i=1}^{r}\sum_{j=0}^{n}a_{ij}u_k^ix^j+b \tag{21}$$

where

$$a_{ij}=\sum_{k=1}^{N}(\alpha_k-\hat{\alpha}_k)u_k^ix_k^j\ ,\ i=1,\ldots,r\ \text{ and }\ j=0,\ldots,n \tag{22}$$

Eq. (21) is equivalent to the SKNFS-SVR output function in Eq. (16). That is, Equation (22) solves parameters a_{ij} in a SKNFS-SVR.

V. Simulation Results

This section uses computer simulations to illustrate the performance and capabilities of the proposed SKNFS-SVR in a function approximation problem. First, training data without noise was used to examine SKNFS-SVR performance. Training data with noise was then used to evaluate the robustness of the SKNFS-SVR. To determine the cost parameter C in a Gaussian kernel-based SVR and a linear SVR, different values ($C = 10^{-3}$, 10^{-2} , …, 10^{3}) were simulated, and only the ones that achieved relatively good performance were shown in the example.

Example 1. The approximated function is defined as follows:

$$f(x_1, x_2) = \frac{(5 - x_2)^2}{3(5 - x_1)^2 + (5 - x_2)^2}, x_1, x_2 \in [0,10] \qquad (23)$$

A clean training set containing 200 samples was randomly generated from the input domain. The testing set had 200 points randomly generated by the same way. For SKNFS-SVR training, the parameters in the clustering algorithm were set to V_{th}=0.024, and 9 clusters were generated. For the linear SVR for weight training, different insensitive values (ε=0.07, and 0.02) and cost parameters C were studied to determine their influence on performance. Table 1 shows the performance of SKNFS-SVR for the sets of parameters that achieve relatively good performance. The results show that with the same SKNFS-SVR structure, a smaller ε value generates smaller test error. The parameter set (ε, C)=(0.02, 10) achieves the minimum RMSE of 0.0641724.

A Gaussian kernel-based SVR was designed using the same set of training data. For Gaussian kernel-based SVR, different insensitive values (ε =0.07, and 0.02), cost parameters, C , and kernel width parameters, g , were studied. Table 1 shows the sets of parameters that achieve relatively good performance. The results indicate the parameter set (ε, g , C) =(0.02, 20, 10) achieves the minimum test RMSE of 0.0774.

Example 2. To compare robustness, a noisy training set was generated by adding white Gaussian noise with mean zero and standard deviation 0.05 to the output of the clean training set. The original clean test set was also used for testing. The SKNFS-SVR contains 9 clusters when V_{th}=0.024 as same as using the training data. Table 2 shows the test RMSE, and the total number of parameters in SKNFS-SVR with different ε and ε values, where it can be found that a minimum test RMSE of 0.0605 is achieved when (ε, C)=(0.02, 100). The test error may increase as ε decreases. This phenomenon is the opposite of training with clean data. The reason is that as ε decreases, more support vectors are generated and the SVR learns more noise information. This example demonstrates that SKNFS-SVR is more robust to noise than the Gaussian kernel-based SVR.

VI. CONCLUSION

This paper proposes a SKNFS-SVR for regression problems. The overall model size can be reduced because the size of SKNFS-SVR depends on the number of clusters instead of support vectors. Consequent parameters in the SKNFS-SVR are learned by a linear SVR, aiming to minimize structural risk instead of empirical risk. Such novel design provides the SKNFS-SVR with high generalization ability and noise resistance ability. Current simulation results show that the SKNFS-SVR achieves better performance over the Gaussian kernel based SVR for both noiseless and noisy data. Moreover, the SKNFS-SVR model size is relatively much smaller. In the future, comparisons with other types of regression models in different regression problems will be studied to verify the performance of the SKNFS-SVR.

Table 1. Test Results of Different Methods Using Clean Training Data .

	Gaussian SVR		SKNFS-SVR	
ε	0.07	0.02	0.07	0.02
C	10	10	10	10
g	20	20	--	--
Structure	54 SVs	97 SVs	9 rules	9 rules
Parameter number	163	293	55	55
Test RMSE	0.0752	0.0774	0.06653	0.06417

Table 2. Test Results of Different Methods Using Noisy Training Data..

	Gaussian SVR		SKNFS-SVR	
ε	0.07	0.02	0.07	0.02
C	100	100	100	100
g	50	40	--	--
Structure	75 SVs	158 SVs	9 rules	9 rules
Parameter number	277	476	55	55
Test RMSE	0.0719	0.0762	0.0557	0.0605

References

[1] V. Vapnik, The Nature of Statistical Learning Theory. New York : Springer - Verlag, 1995.

[2] C. Cortes, V. Vapnik. Support vector networks. Machine Learning Journal, vol. 20, no. 3, pp. 1-25, 1995.

[3] C. F. Juang and C. T. Lin, "An on-line self-constructing neural fuzzy inference network and its applications," *IEEE Trans. Fuzzy Systems*, vol. 6. no. 1, pp. 12-32, Feb. 1998.

[4] N. Kasabov, "Evolving fuzzy neural networks for supervised/unsupervised online knowledge-based learning," *IEEE Trans. Syst., Man and Cyber., Part B: Cyber.*, vol. 31, no. 6, pp. 902-918, Dec. 2001.

[5] N. K. Kasabov and Q. Song, "DENFIS: Dynamic evolving neural-fuzzy inference system and its application for time-series prediction," *IEEE Trans. Fuzzy Systems*, vol. 10, no. 2, pp. 144 -154, April 2002.

[6] P.P. Angelov and D. Filev, "An approach to online identification of Takagi-Sugeno fuzzy models," *IEEE Trans. Syst., Man and Cyber., Part B: Cyber.*, vol. 34, no. 1, pp. 484-498, Feb. 2004.

[7] G. Leng, T. M. McGinnity, G. Prasad, "An approach for on-line extraction of fuzzy rules using a self-organizing fuzzy neural network," *Fuzzy Sets and Systems*, vol. 150, no. 2, pp. 211-243, 2005.

[8] C. F. Juang and C. I. Lee, "A fuzzified neural fuzzy inference network for handling both linguistic and numerical information simultaneously," *Neurocomputing*, vol. 71, no. 1-3, pp. 342-352, Dec. 2007.

[9] A. Celikyilmaz and I. B. Turksen, "Fuzzy function with support vector machines," *Information Sciences*, vol. 177, pp. 5163-5177, 2007.

[10] P. Y. Hao and J. H. Chiang, "Fuzzy regression analysis by support vector Learning Approach," *IEEE Trans. Fuzzy Systems*, vol. 16, no. 2, pp. 428-441, 2008.

[11] C. F. Juang and C. D. Hsieh, "TS-fuzzy system based support vector regression," *Fuzzy Sets and Systems*, vol. 160, no. 17, pp. 2486-2504, Sep. 2009.

[12] N. Cristianini and J. S.-Taylor, *An Introduction to Support Vector Machines And Other Kernel-based Learning Methods*, Cambridge University Press, 2000.

[13] A. J. Smola and B. Scholkopf, "A tutorial on support vector regression," *Statistics and Computing,* vol.14, no. 3, pp. 199-222, 2004.

2011 IEEE International Conference on Fuzzy Systems
June 27-30, 2011, Taipei, Taiwan

Fuzzy Reinforcement Learning Control for Decentralized Partially Observable Markov Decision Processes

Rajneesh Sharma
Instrumentation and Control Division
Netaji Subhas Institute of Technology
New Delhi, India
rajneesh496@rediffmail.com

Matthijs T. J. Spaan
Institute for Systems and Robotics
Instituto Superior Tecnico
Lisbon, Portugal
mtjspaan@isr.ist.utl.pt

***Abstract*—Decentralized Partially Observable Markov Decision Processes (Dec-POMDPs) offer a powerful platform for optimizing sequential decision making in partially observable stochastic environments. However, finding optimal solutions for Dec-POMDPs is known to be intractable, necessitating approximate/suboptimal approaches. To address this problem, this work proposes a novel fuzzy reinforcement learning (RL) based game theoretic controller for Dec-POMDPs. The proposed controller implements fuzzy RL on Dec-POMDPs, which are modeled as a sequence of Bayesian games (BG). The main contributions of the work are the introduction of a game based RL paradigm in a Dec-POMDP settings, and the use of fuzzy inference systems to effectively generalize the underlying belief space. We apply the proposed technique on two benchmark problems and compare results against state-of-the-art Dec-POMDP control approach. The results validate the feasibility and effectiveness of using game theoretic RL based fuzzy control for addressing intractability of Dec-POMDPs, thus opening up a new research direction.**

Keywords- Reinforcement learning, Fuzzy systems, Cooperative multiagent systems, Decentralized POMDPs

I. INTRODUCTION

Finding optimal strategies for multiple agents operating in an uncertain environment is an active field of research in Artificial Intelligence. Sequential decision making in fully observable stochastic environments has been tackled effectively via the well known Markov decision process (MDP) framework [1]. Sensor uncertainty can be addressed through partially observable Markov decision process (POMDP) framework [2] that extends the MDP model by incorporating observations and their probability of occurrence conditional on the state of the environment. Our focus herein is on learning planning and control for multiple agents in uncertain environments in a cooperative setting. This is formalized by the Decentralized POMDP (Dec-POMDP) model [3] which essentially generalizes a POMDP to multiple agents and can be used to model a team of cooperative agents. In a Dec-POMDP, agents have to cope with uncertainty regarding other agents in addition to imperfect information about the underlying state, making the task computationally intractable (NEXP-complete for the finite horizon case) [3, 4].

Reinforcement learning (RL) has now established itself as a major technique for direct adaptive optimal control of uncertain systems [5]. In the RL paradigm, agents learn to behave optimally by repeated trial and error interactions with the environment. A recent review of multiagent RL can be found in [6] with comprehensive details of such techniques for fully cooperative, fully competitive and mixed tasks. However, these methods typically assume full state observability and/or knowledge of the complete joint action at each time step [7]. In contrast, we propose and study one of the first RL approaches to Decentralized POMDPs.

Our motivation for the proposed approach is inspired by a recently proposed Q value function for Dec-POMDPs Q_{BG}, based on joint action-observation histories [8]. This Q value formulation allows us to extend RL based approximation to Dec-POMDPs akin to the MDPs for which Q learning [9] has been successfully applied for a variety of systems and processes [10]. Various approximate Q value formulations for Dec-POMDPs have been analyzed [8], which are significantly easier to compute than the optimal Q value function Q^*. These approximate Q value functions typically employ a joint belief over the state space of the underlying POMDP, which can be computed assuming agents share observations, but not in the decentralized setting.

In the proposed approach each agent g maintains tunable q^g values over a continuous global belief space of the underlying POMDP. We use fuzzy functions as a generic function approximator, which are capable of approximating any real function to an arbitrary accuracy [11]. Fuzzy systems offer an elegant way of representing Dec-POMDP policies in a compact form, i.e., with a finite amount of memory. While convergence guarantees exist for tabular Q-learning [9], the same guarantees do not hold when function approximation is introduced [10]. As has been the case with other approaches that have used function approximation for Q-learning [10, 12] or the Markov game based learning [13], theoretical convergence of the learning process with function approximation cannot be guaranteed.

To the best of our knowledge this work is the first study of applying fuzzy RL for generating a learning controller for

978-1-4244-7316-8/11/$26.00 ©2011 IEEE

Dec-POMDPs in a game theoretic setting. Major contributions of our work being (i) Casting Dec-POMDPs as a game theoretic RL task (ii) Introducing Fuzzy Inference System (FIS) based generalization to Dec-POMDPs (pointed out by Seuken and Zilberstein [14] as a major need to improve scalability of Dec-POMDP solution techniques). We use RL to learn and progressively improve solution to the Dec-POMDP using FIS to effectively generalize over a continuous global belief space.

We empirically evaluate the proposed fuzzy Dec-POMDP control on the benchmark recycling robot [15] and the multi access broadcast channel [16] tasks and compare its performance against other state of the art infinite horizon Dec-POMDP control approach [15, 16, 17]. Results validate the feasibility of using a game theoretic RL controller for Dec-POMDPs, opening up a promising future research direction to improve scalability and tackle computational intractability being faced by majority of the current Dec-POMDP solution techniques.

The rest of the paper is organized as follows: Section II briefly sheds some light on background and related work, Section III describes the proposed fuzzy Dec-POMDP controller, Section IV presents empirical results on the recycling robot and multi access broadcast channel tasks, and Section V concludes the paper with a discussion on the future scope of the proposed approach.

II. BACKGROUND AND RELATED WORK

We assume prior reader familiarity with the basic concepts underlying Reinforcement Learning [5], POMDPs [2] and Fuzzy Systems [18] giving only a brief overview of the concepts that form the backbone of our work.

A. Dec-POMDPs

Multiagent sequential decision making problems under partial observability wherein agents cooperate to optimize joint performance are formalized in the Dec-POMDP model [3]. A Dec-POMDP models a number of agents that interact with their environment (system) at discrete time steps $t = 1, 2, \ldots$. At each time step t every agent takes an action and the combination of these actions (joint action) makes the system transit to the next state. At the next time step, each agent receives a local observation of the environment. State transition and observation probabilities model the dynamics of the environment while global reward specifies desired behavior or the goodness of taking joint action in a particular state. The agents optimize a form of joint long term reward. The framework is decentralized as no agent can control the whole process and none of the agent has access to the global state. Further, agents know only their own actions and observations and there is no communication between the agents.

In this paper, we define a Dec-POMDP as the following tuple $< N_a, S, \{U_g\}, P, \{\Omega_g\}, O, R, T >$ where S is the finite set of states, N_a is the number of agents, U_g is the finite set of actions available to agent g and $\bar{U} = \times_{g \in N_a} U_g$ is the set of joint actions with $\bar{u} = < u_1, \ldots, u_{N_a} >$ being joint action. P is the state transition function with $p(s' \mid s, \bar{u})$ being the probability of landing in state s' when joint action $\bar{u}$ is taken at state s. Ω_g is the finite set of observations available to the agent g and $\bar{\Omega} = \times_{g \in N_a} \Omega_g$ is the set of joint observations with $\bar{o} = < o_1, \ldots, o_{N_a} >$ being joint observation. $O : \bar{U} \times X \to P(\bar{\Omega})$ is an observation function with $O(\bar{o} \mid \bar{u}, s')$ being the probability of observing joint observation $\bar{o}$ given that joint action $\bar{u}$ was taken and led to state s'. $R : \bar{U} \times S \to \Re$ is the reward function. T is the horizon. In the infinite horizon case, we do not have the parameter T but instead a discount factor $0 \le \gamma < 1$ which limits the infinite horizon sum $\sum_{t=0}^{\infty} \gamma^t r_t$ (with r_t being the reward received at time step t) , which is what the agents optimize.

B. Dec-POMDPs as a sequence of Identical Payoff Bayesian games

A Bayesian game (BG) is an augmented normal form game in which players have some private information [19]. This private information defines the type of agent, i.e., a particular type $\theta_g \in \Theta$ of an agent g corresponds to that agent knowing some particular information. A BG is defined by the tuple $< N_a, \bar{U}, \Theta, P(\Theta), \{r^1, \ldots, r^{N_a}\} >$ where N_a is the number of agents, $\bar{U}$ is the set of joint actions, $\Theta = \times_{g \in N_a} \theta_g$ is the set of joint types over which a probability $P(\Theta)$ is defined, and $R : \Theta \times \bar{U} \to \Re$ is the payoff function.

In a BG, agents can condition their action on the private information they have. A joint policy in a BG is represented by $\beta = < \beta_1, \ldots, \beta_{N_a} >$ where individual policies are mappings from types to actions, i.e., $\beta_g : \theta_g \to U_g$ (U_g being the action set of agent g). The solution of a BG for identical payoffs is given by [19]:

$$\beta^* = \arg\max_{\beta} \sum_{\theta \in \Theta} p(\theta) r(\theta, \beta(\theta)) \qquad (1)$$

where $\beta(\theta) = < \beta_1(\theta), \ldots, \beta_{N_a}(\theta) >$ is the joint action specified by β, $p(\theta)$ is the probability associated with joint type θ and $r(\theta, \beta(\theta))$ is the payoff received.

In modeling Dec-POMDPs as a sequence of BGs [20] the payoff function of BG (one stage) for an agent g is $Q_{BG}^g(\bar{\theta}^t, \bar{u})$ where $\bar{\theta}^t = (\bar{o}^0, \bar{u}^0, \bar{o}^1 \ldots, \bar{o}^{t-1}, \bar{u}^{t-1}, \bar{o}^t)$ is the joint action-observation history up to time t, where initial joint observation $\bar{o}^0$ is assumed to be an empty observation: $\bar{o}^0 = \bar{o}_\varnothing = < o_{1,\varnothing}, o_{2,\varnothing}, \ldots, o_{N_a,\varnothing} >$. Oliehoek et. al. [8], define a new approximate Q-value function called Q_{BG} wherein BG have types that correspond to single observations instead of

complete action-observation histories leading to smaller and more tractable BGs.

C. Overview of Dec-POMDP methods

As this work concerns designing controllers for infinite horizon Dec-POMDPs, we limit this brief overview to infinite horizon Dec-POMDPs. For finite horizon counterpart we refer the interested reader to [14]. For tackling infinite horizon Dec-POMDPs most prominent and by far most successful approach envisages Dec-POMDP policy representation as a finite state controller [15]. Finite state controllers offer an elegant way of representing a Dec-POMDP policy using finite amount of memory. Finite state controllers do not store whole observation histories, instead they encapsulate key pieces of information concerning observation history with a fixed number of nodes.

The first approach by Szer and Charpillet [16] requires high memory and running time and is limited as it searches for optimal deterministic controllers. The second one proposed by Bernstein et. al. called Bounded Policy Iteration for Dec-POMDPs (Dec-BPI) [17] is a multiagent extension of the BPI algorithm [21]. Dec-BPI uses linear programming for iterating through the nodes of each agents controller and attempts to find an improvement. The methodology is promising as it offers scalability. The last one, a recent approach by Amato et al. [15] formulates fixed size controller solution as a nonlinear program (NLP) and exploits nonlinear optimization techniques to solve the problem. They also use a certain 'correlation device' which is a shared source of randomness to improve the solution quality.

Yagan and Tham [22] propose an RL solution to approximate the joint optimal policies for Dec-POMDPs by exploiting locality of interaction among agents. Effectiveness of the proposed algorithm is shown on multiagent wireless multihop networks and for cooperative retransmission in wireless networks [23]. However, the algorithm is not applicable to general Dec-POMDPs as it assumes that neighboring agents can interact and exploits the broadcast nature of wireless medium for effective retransmission of a failed packet (a domain specific feature). Recently, Wu et al. [24] propose a novel decentralized rollout sampling policy iteration algorithm for Dec-POMDPs based on a RL technique called Monte Carlo methods. The algorithm samples a set of reachable belief states based on some heuristic policies and computes a joint policy for each belief state based on rollout estimations. Algorithm claims linear time complexity over no. of agents, bounded memory usage and good solution quality.

D. FIS based Reinforcement Learning

Fuzzy logic is a mathematical approach to emulate human way of thinking and learning. In MDPs fuzzy systems have been used as function approximators to facilitate generalization in state space and for generating continuous actions. In [12], Jouffe introduced fuzzy Q learning wherein a collection of fuzzy rules is considered as an agent. The approach produces an action by triggering some rules and cooperating. Following on this idea Sharma and Gopal [13] introduced fuzzy Markov games where FIS is used to introduce generalization in Markov games. Fuzzy RL has also been used for multiagent systems, e.g., Duman et. al. [25] use fuzzy RL on a multiagent continuous pursuit domain. Tehrani et. al. [26] implement fuzzy RL on robotic soccer agents to enable them to coordinate their behavior locally and socially while learning from experience. To the best of our knowledge, until now there have been very few attempts at using fuzzy RL for effective learning in POMDPs and none for Dec-POMDPs.

III. Fuzzy Reinforcement Learning for Dec-POMDPs

In this paper, we propose a novel reinforcement learning approach for Dec-POMDPs. Given the overwhelming complexity of solving Dec-POMDPs, we propose to use a fuzzy RL based approach to learn controllers. Fuzzy membership functions are laid over the global belief space for each agent to generate what may be termed as a 'Fuzzy Dec-POMDP'. Each agent maintains its tunable parameters or the fuzzy q^g values (agent g). The use of Fuzzy Inference System (FIS) for mapping the continuous belief space of the underlying Dec-POMDP allows us to define and tune the q^g values. The Dec-POMDP is modeled as a two stage Bayesian game [19], the matrix entries for each stage being the fuzzy Q^g_{BG} values [8] obtained from the fuzzy Dec-POMDP rule base.

A. Acting in two-stage BGs

As our proposed approach uses a fuzzy RL framework, we define Q^g_{BG} at stage t as in [8] for a two stage BG corresponding to agent g. Crucially, in such a BG, (joint) types correspond to one (joint) actions and following by a (joint) observation. We define the Q function at stage t to be constructed from fuzzy q^g parameters (for agent g) defined at stage (t+1): $q^g(i,\vec{u}^t,\vec{o}^{t+1},\beta(\vec{o}^{t+1}))$ where i is an index specifying the fuzzy

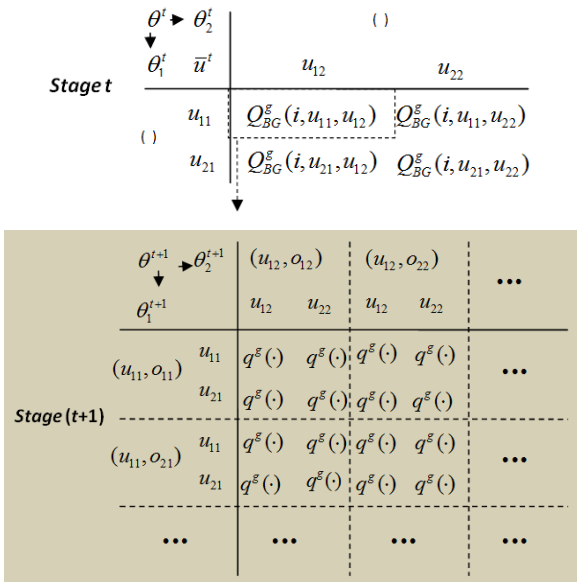

Figure 1 Fuzzy Dec-POMDP: Two stage Bayesian Game, where $q^g(\cdot) = q^g(i,\vec{u}^t,\vec{o}^{t+1},\beta(\vec{o}^{t+1}))$

rule Y_i, $\overline{u}^t$ is the joint action at stage t, $\overline{o}^{t+1}$ is the joint observation at stage (t+1), and $\beta(\overline{o}^{t+1})$ is the joint BG policy corresponding to $\overline{o}^{t+1}$ at stage (t+1). This conforms to the modeling of Dec-POMDPs as a series of BGs as introduced in [8].

Figure 1 shows the BG for time steps t and (t+1) for a fictitious Dec-POMDP with two agents each with two actions and two observations. $Q^g_{BG}(i,u_{m1},...,u_{mN_a}) \coloneqq Q^g_{BG}(i,\overline{u}^t)$ is the solution of BG defined for agent g at the next stage (t+1) corresponding to the tuple $< i,u_{m1},...,u_{mN_a} >$. It is calculated as the maximizing sum of the entries of next time step BG weighted by their respective type probabilities, i.e.,

$$Q^g_{BG}(i,\overline{u}^t) = \max_{\beta} \sum_{\overline{o}^{t+1}\in O} p(\overline{o}^{t+1} \mid \theta^t,\overline{u}^t) q^g(i,\overline{u}^t,\overline{o}^{t+1},\beta(\overline{o}^{t+1})) \tag{2}$$

The maximizing BG policy at next stage (t+1) is given by

$$\beta^*_g = \arg\max_{\beta} \sum_{\overline{o}^{t+1}\in O} p(\overline{o}^{t+1} \mid \theta^t,\overline{u}^t) q^g(i,\overline{u}^t,\overline{o}^{t+1},\beta(\overline{o}^{t+1})) \tag{3}$$

Thus, in order to code control policies, we maintain a parameter vector q^g defined as $q^g(i,\overline{u}^t,\overline{o}^{t+1},\beta(\overline{o}^{t+1}))$. These q^g values form the entries of the next step BG matrix for agent g, i.e., at time step (t+1). Type probability $p(\overline{o}^{t+1} \mid \theta^t,\overline{u}^t)\ \forall \theta^{t+1} \in \Theta$ is calculated as:

$$p(\overline{o}^{t+1} \mid \theta^t,\overline{u}^t) = \sum_{s^{t+1}\in S} \sum_{s^t\in S} O(\overline{o}^{t+1} \mid \overline{u}^t, s^{t+1}) p(s^{t+1} \mid \overline{u}^t, s^t) p(\theta^t) \tag{4}$$

It is to be noted that for updating type probability (4) the agent must have access to $\overline{o}^{t+1}$ and $\overline{u}^t$ (the joint observation and joint action, respectively) which are not available in standard Dec-POMDP setup. An agent g has access only to its own action (u^t_g) and observation (o^{t+1}_g) and the global reward signal (r_t) provided by the environment.

We propose to overcome this bottleneck by a judicious use of the information contained in the reward signal. Agent g samples action of other agents using the reward signal to get approximate $\overline{u}^t_{\neq g} \cong \hat{u}^t_{\neq g}$ ($\overline{u}^t_{\neq g}$ is the joint action of all agents except agent g). The sampled $\hat{u}^t_{\neq g}$ is combined with u^t_g to yield $\overline{u}^t = < \hat{u}^t_{\neq g}, u^t_g >$. We then update type probabilities for all $o^{t+1} \in O$ using (4). In contrast to [8], for instance, the proposed approach is an adaptive learning one based on the reinforcement learning technique. All RL techniques use the reinforcement signal (reward here) as the primary means to judge the goodness of taking a particular action. This enables the agent to discriminate amongst different actions and choose the one that produces a higher expected discounted reward [5].

Summarizing, we adapt a Dec-POMDP modeled as a sequence of BGs to fuzzy RL by using Q learning update for updating the q^g values at (t+1) stage BG matrix (Fig. 1). At each stage, we compute optimal $Q^g_{BG}(\cdot)$ value (2) and optimal joint policy β^*_g (3) corresponding to each fuzzy rule using a procedure referred to as the *forward sweep policy computation* [3].

B. *Fuzzy Dec-POMDPs*

In a POMDP an agent cannot observe state but it maintains a probability distribution over the state space called belief [2]. In a Dec-POMDP, a belief can typically not be computed as each agent only observes its own part of the joint observation. In the proposed fuzzy Dec-POMDP approach, we match an agent's perception of the global belief b^t_g (global belief state at time t) to fuzzy sets laid over the global belief space or in other words generate a fuzzy belief. We define fuzzy inference system for fuzzy Dec-POMDPs as consisting of a set of N rules (one set of rules for each agent) of the following form:

$$\begin{aligned} Y_i: \quad & \text{If } b^t_{g1} \text{ is } L^i_1 \text{ and } ... \text{ and } b^t_{gn} \text{ is } L^i_n \\ & \text{then } u_1 = u_{11} \text{ and } ... \text{ and } u_{N_a} = u_{1N_a} \text{ with } Q^g_{BG}(i,u_{11},...,u_{1N_a}) \\ & \text{or } \quad u_1 = u_{21} \text{ and } ... \text{ and } u_{N_a} = u_{1N_a} \text{ with } Q^g_{BG}(i,u_{21},...,u_{1N_a}) \\ & ..... \\ & \text{or } \quad u_1 = u_{m1} \text{ and } ... \text{ and } u_{N_a} = u_{mN_a} \text{ with } Q^g_{BG}(i,u_{m1},...,u_{mN_a}) \end{aligned} \tag{5}$$

where i is the index specifying rule Y_i, $m = \mid U_g \mid \forall g \in N_a$, i.e., action set of all agents is assumed to have same cardinality m. u_{kg} is the kth action in U_g or kth action of agent g, $b^t_g = [b^t_{g1},...,b^t_{gs},...,b^t_{gn}]$ is the global belief vector as perceived by agent g at time t, b^t_{gs} being the belief of agent g for state variable $s \in n$ (n being the number of state variables) at time t, L^i_s is the linguistic term (fuzzy label) of input variable b^t_{gs} in rule Y_i and its membership function denoted by $\mu_{L^i_s}$ corresponding to the state variable s. This matching leads to computation of rule firing strength ($\alpha^i(b^t_g)\ \forall i \in N$) as:

$$\alpha^i(b^t_g) = T(\mu_{L^i_1}(b^t_{g1}),...,\mu_{L^i_n}(b^t_{gn})) \tag{6}$$

where the T-norm is implemented by the product

$$\alpha^i(b^t_g) = \prod_{j=1}^{n} \mu_{L^i_j}(b^t_{gj}) \tag{7}$$

For each rule Y_i, we solve the BG at the next time step (t+1) as per (2) to get $Q^g_{BG}(i,\overline{u}^t)$ values that form the entries of the BG matrix at stage t (Fig. 1). Optimal one-step target value for rule Y_i, i.e., $V^i_{BG}(b^t_g)$ is the maximal value of the BG matrix at

stage t corresponding to agent g and rule Y_i and is computed as:

$$V_{BG}^{i}(b_g^t) = \max_{\bar{u}^t \in \bar{U}} Q_{BG}^{g}(i, \bar{u}^t) \tag{8}$$

and optimal one-step joint action $\bar{u}_g^*(i); i \in N$ is given by

$$\bar{u}_g^*(i) = \arg\max_{\bar{u}^t \in \bar{U}} Q_{BG}^{g}(i, \bar{u}^t) \tag{9}$$

optimal one-step policy for agent g at stage t is thus

$$\pi_g^* = [\bar{u}_g^*(1), ..., \bar{u}_g^*(i), ..., \bar{u}_g^*(N)] \tag{10}$$

index i corresponds to rule Y_i.

C. Fuzzy RL for Dec-POMDPs

In order to explore set of possible actions and to acquire experience through RL, we use pseudo stochastic exploration/exploitation (EEP) policy [10]. In the EEP strategy, we gradually reduce the exploration parameter ε according to some schedule, e.g., halve the ε value every 50 iterations (in our case). We use an ε-BG policy (ε-greedy in Q learning) meaning that we choose a random action with probability ε:

$$\bar{u}_g^{\dagger}(i) = \varepsilon\text{-BG } \bar{u}_g^*(i) = \begin{cases} \bar{u}^{rd}(i) \text{ with probability } \varepsilon \\ \bar{u}_g^*(i) \text{ with probability } (1-\varepsilon) \end{cases} \tag{11}$$

$\bar{u}^{rd}$ is a random action, i.e., $\bar{u}^{rd} = [u_1^{rd}, ..., u_{N_a}^{rd}]$ where each u_g^{rd} is an action chosen uniformly at random from the action set of the agent g: U_g, and the ε-BG policy is

$$\pi_g^{\dagger} = [\bar{u}_g^{\dagger}(1), ..., \bar{u}_g^{\dagger}(i), ..., \bar{u}_g^{\dagger}(N)] \tag{12}$$

Next, we generate global ε-BG action (agent g), $u_g^{\dagger}$ by summing the membership strength of each action in the action set of agent g under each rule and choosing the action that has the highest combined strength, i.e., one having maximum $\sum_{i \in N} \alpha^i(b_g^t)$ value. This procedure of computing $u_g^{\dagger}$ is repeated for each agent $g \in N_a$. The global ε-BG joint action is then given by $\bar{u}^{\dagger} = [u_1^{\dagger}, u_2^{\dagger}, ..., u_{N_a}^{\dagger}]$.

The computed joint action is then executed in a decentralized manner, i.e., each agent executes his component of $\bar{u}^{\dagger}$ or executes $u_g^{\dagger}$. Under this ε-BG joint action $\bar{u}^{\dagger}$ the environment transitions to the next state s^{t+1}. Each agent receives a local observation from the system, a global reward r_t and updates its perception of global belief state b_g^{t+1} using the standard Bayesian update [2] which has been adapted herein to cope with nonavailability of joint observation ($\bar{o}^t$). In particular, we loop over all possible joint observation sets given the local observation of agent g (o_g^t), by defining the joint observation as $\bar{o}^t = < o_g^t, \bar{o}_{\neq g}^t >$:

$$b_g^{t+1}(s^{t+1}) = \frac{\sum_{\bar{o}_{\neq g} \in O_{\neq g}} O(\bar{o}^t \mid \bar{u}^t, s^{t+1}) \sum_{s^t \in S} p(s^{t+1} \mid s^t, \bar{u}^t) b_g^t(s^t)}{\sum_{s^{t+1} \in S} \sum_{\bar{o}_{\neq g} \in O_{\neq g}} O(\bar{o}^t \mid \bar{u}^t, s^{t+1}) \sum_{s^t \in S} p(s^{t+1} \mid s^t, \bar{u}^t) b_g^t(s^t)} \tag{13}$$

where $\bar{o}_{\neq g}^t$ is the joint observation of all agents except agent g and $O_{\neq g}$ being observation functions of respective agents barring agent g. Each agent uses this updated belief in conjunction with the fuzzy rule base for computing rule strength values $\alpha^i(b_g^{t+1})$. The current q^g parameter estimates are used to compute global fuzzy BG target value (as in FQL [12]) as per:

$$V_{BG}^{*}(b_g^{t+1}) = \frac{\sum_{i=1}^{N} V_{BG}^{i}(b_g^{t+1}) \alpha^i(b_g^{t+1})}{\sum_{i=1}^{N} \alpha^i(b_g^{t+1})} \tag{14}$$

Global Q_{BG}^{g*} value

For each rule Y_i, one of the $Q_{BG}^{g}(i, \bar{u}^t)$ values is selected to compute global Q_{BG}^{g*} value as per the ε-BG policy (11) under each rule Y_i: $Q_{BG}^{g*}(i) = Q_{BG}^{g}(i, \bar{u}_g^{\dagger}(i))$. Global Q_{BG}^{g*} value is the weighted sum of these ε-BG (rule) values weighted by the rule firing strengths, i.e.,

$$Q_{BG}^{g*}(b_g^t) = \frac{\sum_{i=1}^{N} Q_{BG}^{g*}(i) \alpha^i(b_g^t)}{\sum_{i=1}^{N} \alpha^i(b_g^t)} \tag{15}$$

q^g update

We calculate TD(0) error [10] for tuning q^g parameter values as:

$$\Delta Q^g = r_t + \gamma V_{BG}^{*}(b_g^{t+1}) - Q_{BG}^{g*}(b_g^t) \tag{16}$$

where r_t is the global reward at stage t. Finally, q^g parameter values are updated for all rules $i \in N$ as per:

$$q^g(i, \bar{u}^t, \theta^{t+1}, \beta^*(\theta^{t+1})) \leftarrow q^g(i, \bar{u}^t, \theta^{t+1}, \beta^*(\theta^{t+1})) + \eta \Delta Q^g \frac{\alpha^i(b_g^t)}{\sum_{i=1}^{N} \alpha^i(b_g^t)}; \forall \theta^{t+1} \in \Theta \tag{17}$$

where $0 < \eta \leq 1$ is the learning rate parameter. Every agent uses (17) to independently update its q^g parameter values at

the end of each iteration.

IV. Empirical Results

This section describes the realization of the fuzzy Dec-POMDP controller and results of evaluating the approach on the recycling robot [15] and multiagent broadcast channel domains [16], which are two benchmark problems typically employed for comparing infinite-horizon Dec-POMDP methods. The first one involves robots that have the task of picking up cans in an office building, and has 4 states, 3 actions, and 2 observations. Each robot has three actions (i) search for a small can, (ii) search for a large can, or (iii) recharge the battery. The larger can be picked up only if both agents cooperate to pick it up at the same time. The robots have battery status of high and low, with an increased likelihood of transitioning to the low state or exhausting the battery after attempting to pick up the larger can.

The second problem considers two agents which need to share a communication channel, the Multiagent Broadcast Channel Access (MABC) problem. Each agent has a message buffer and it has to decide whether to send or not send the message through the channel. Only one message can go through the channel at one time, simultaneous sending results in a collision with the messages remaining in the buffers. We simulate the two agent case [16] with 4 states, 2 actions and 2 observations. New messages arrive with a rate of $p_1 = 0.9$ for agent 1 and $p_2 = 0.1$ for agent 2.

A. Recycling Robot

For the recycling robot problem, local state of either agent is battery low (BL) or battery high (BH). Global states being (BL,BL), (BL,BH),(BH,BL) and (BH,BH) or 4 states. We partition the belief corresponding to each state variable into three fuzzy subsets thereby generating $3^4 = 81$ fuzzy rules that map the global belief space to a fuzzy belief space. Linguistic terms for these fuzzy sets are Low(L), Medium(M), and High(H). The membership function for each fuzzy belief state variable (b_1, b_2, b_3, b_4) that correspond to belief over the state variables (s_1, s_2, s_3, s_4) are standard Gaussian membership functions defined by:

$$\mu_l(b_j) = e^{\frac{-(b_j - b_j^l)^2}{2(\sigma_j^l)^2}}; l = 1,2,3; \quad j = 1,2,3,4 \qquad (18)$$

where l are fuzzy labels for each variable $b_j (b_j = p(s_j))$ being the belief variable for the state variable s_j, $p_j(s_l)$ is the probability distribution over s_j. Fuzzy label centers are defined as $b_j^l = c_j + d_j(l-1)$ with $c_{1,\ldots,4} = 0, d_{1,\ldots,4} = 0.5$ and widths defined by $\sigma_j^1 = \sigma_j^3 = 0.15, \sigma_j^2 = 0.2$. The RL parameters being, discount factor $\gamma = 0.9$, learning rate $\eta = 0.9$. Exploration parameter ε is initialized from 0.9 and halved every 50 iterations. We refer to the time instant when one or both agents independently or jointly pick up a can generating a successful if the agents cooperate to lift the bigger can or pick

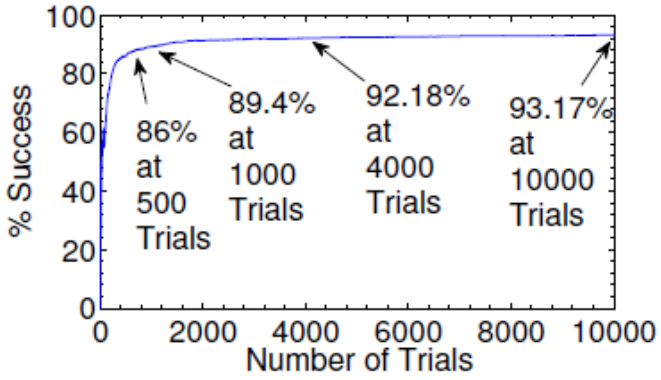

Figure 2 Fuzzy Dec-POMDP learning performance: Recycling Robot

global reward r_t as end of a trial. We consider the trial to be up smaller cans independently generating large reward. In all other cases the trial is considered a failure.

The figures 2 and 4 depict learning performance of the RL controller or how the performance improves as the controller attempts to discover the optimal policy by observing failures and rewards (while exploring). However, the figures 3 and 5 are about the performance of the learned policy, i.e., we use the final policy obtained at the end of 10000 trials and use it to find the cumulative reward (figure of merit) which is an indication of the quality of discovered policy. Episode means a set of trials; e.g., 100 trials (Fig. 2) and results have been averaged over 1000 such episodes. Figure 2 shows learning performance of the fuzzy Dec-POMDP controller, i.e., shows % success as a function of number of trials. We have averaged results over 100 episodes each of 10, 000 trials. The controller achieved a significant level of performance (86% success) in just about 500 trials. The performance reached 92.18% at 4000 trials and peaked to 93.18% success rate at the end of 10, 000 trials.

We also plot infinite horizon discounted reward achieved by the fuzzy Dec-POMDP approach (Figure 3). This value is a figure of merit for the quality of the learned policy, i.e., how much reward agents accumulate while following the discovered policy. We have averaged the results over 1000 episodes of 100 trials each. As can be seen, the value achieved is 22.80 in 20 trials and the final expected discounted infinite horizon value obtained is 26.07.

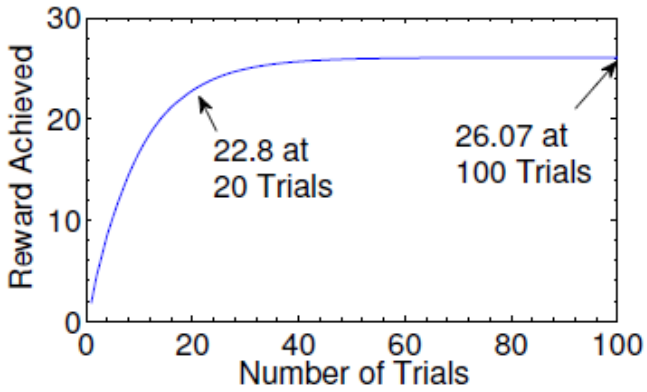

Figure 3 Quality of learned policy: Recycling robot

We compare performance of fuzzy Dec-POMDP against (i) Dec-BPI [17] which reaches a discounted reward of 26 to 27, and (ii) Finite state controller [15] which obtains 30 to 31 (read from figure). Our approach compares favorably against the Dec-BPI approach but is inferior in comparison to the fixed size controller. Fixed size controller's superior performance could be because the approach solves all the agent controllers centrally (in personal communication with the author of [15]) while in fuzzy Dec-POMDP control even the agent controllers are decentralized (solved independently). Furthermore, the performance of fixed size control approach is highly dependent on the controller size which is not the case with fuzzy Dec-POMDP control. Unlike Dec-BPI, performance of fuzzy Dec-POMDP approach does not depend on the finding appropriate fixed points on the belief space, instead it operates on the entire belief space. Even then our approach is able to find a comparable solution quality to the Dec-BPI.

B. Multiagent Broadcast Channel Access

In the MABC problem, each agent has two local buffer states (Empty, Full) resulting in 4 global states (cross product of the local buffer states). Here also we partition each belief variable into three fuzzy partitions leading to $3^4 = 81$ fuzzy rules that map the global belief space to a fuzzy belief space. Type of membership functions (18), their centers and widths are kept same as in the recycle robot task as also the RL parameters.

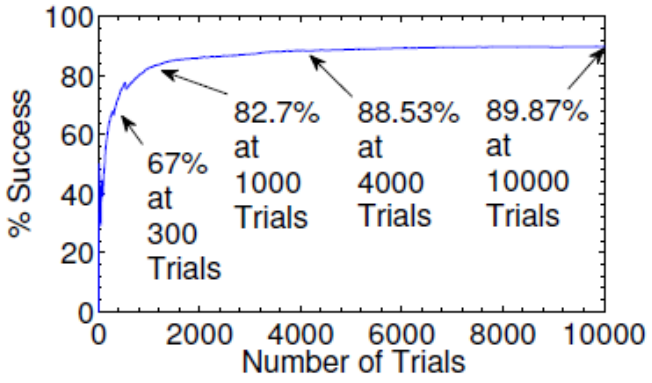

Figure 4 Fuzzy Dec-POMDP learning performance: Multiagent broadcast channel

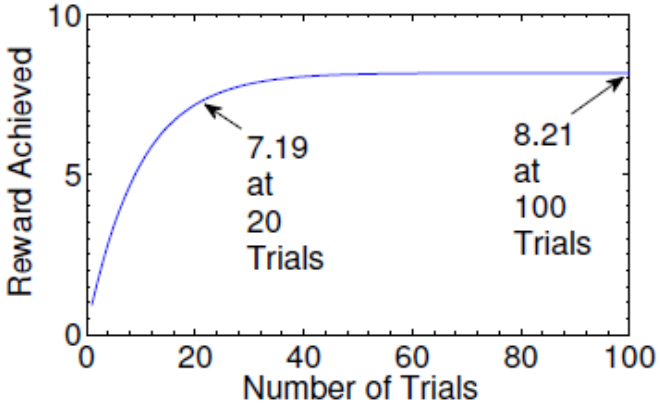

Figure 5 Quality of learned policy: Multiagent broadcast channel

Herein we consider a trial to be successful if the message (by either of the agents) gets transmitted through the channel successfully (without collision) generating a global reward of +1 or else the trial is a failure. Figure 4 shows learning performance of the fuzzy Dec-POMDP controller for the MABC task. We have averaged results over 100 episodes each of 10, 000 trials. The controller achieved a performance level of 67% success in just about 300 trials. The performance rose to 88.53% at 4000 trials and became 89.87% at the end of 10, 000 trials.

We also plot infinite horizon discounted reward achieved (Figure 5). Here also the results have been averaged over 1000 episodes of 100 trials each. As can be seen, the value achieved is 7.19 in 20 trials and the final expected discounted infinite horizon value obtained is 8.21. It is to be noted that the maximum value that can be achieved for this task with a discount factor $\gamma = 0.9$ is 9.0 [16]. The value of the proposed approach is superior to the one obtained by Szer and Charpillet [16], 8.0.

V. CONCLUSIONS

This paper presents a novel fuzzy reinforcement learning control scheme for Dec-POMDPs in a game-theoretic setting. We show how FIS based function approximation can be used as a principled means to effectively combat the time and space complexity of Dec-POMDPs. To the best of our knowledge, this work represents a first attempt in applying game theoretic learning to an FIS based Dec-POMDP setup. We elucidate feasibility of the proposed approach with empirical results on the benchmark recycling robot and multiagent broadcast channel problems. Proposed fuzzy Dec-POMDP controller successfully discovers a high quality optimal policy solution in a reasonable number of trials. Further, a comparison of the expected discounted reward value achieved against other recent state-of-the-art Dec-POMDP solution approaches [15, 16, 17] brings out the effectiveness of the proposed approach. In future work we plan to relax some of assumptions on knowledge of the system models, as well as identifying for which types of domains our approach is appropriate. Furthermore, the use of a fuzzy rule base opens the potential for generalization over continuous state spaces.

ACKNOWLEDGMENTS

This work was partially funded by Netaji Subhas Institute of Technology, New Delhi, India. This work was partially funded by Fundação para a Ciência e a Tecnologia (ISR/IST pluriannual funding) through the PIDDAC Program funds and was supported by project PTDC/EEA-ACR/73266/2006.

REFERENCES

[1] M. L. Puterman. *Markov Decision Processes—Discrete Stochastic Dynamic Programming*. John Wiley & Sons, Inc., New York, NY, 1994.

[2] L. P. Kaelbling, M. L. Littman, and A. R. Cassandra, "Planning and acting in partially observable stochastic domains", *Artificial Intelligence*, vol. 101, pp. 99–134, 1998.

[3] D. S. Bernstein, R. Givan, N. Immerman, and S. Zilberstein, "The complexity of decentralized control of Markov decision processes",

Mathematics of Operations Research, vol. 27, issue 4, pp. 819–840, 2002.

[4] C. Boutilier, "Planning, learning and coordination in multiagent decision processes", In *Theoretical Aspects of Rationality and Knowledge*, 1996.

[5] R. S. Sutton and A. G. Barto. *Reinforcement Learning: An Introduction*. MIT Press, 1998.

[6] L. Busoniu, R. Babuska, and B. De Schutter, "A comprehensive survey of multiagent reinforcement learning", *IEEE Transactions on Systems, Man and Cybernetics — Part C: Applications and Reviews*, vol. 38, issue 2, pp. 156–172, 2008.

[7] J. R. Kok and N. Vlassis, "Collaborative multiagent reinforcement learning by payoff propagation", *Journal of Machine Learning Research*, vol. 7, pp. 1789–1828, Sep. 2006.

[8] F. A. Oliehoek, M. T. J. Spaan and N. Vlassis., "Optimal and approximate Q-value functions for decentralized POMDPs", *Journal of Artificial Intelligence Research*, vol. 32, pp. 289–353, 2008.

[9] C. J. C. H. Watkins and P. Dayan, "Technical note: Q-learning", *Machine Learning*, vol. 8, issue 3, pp. 279–292, 1992.

[10] J. Si, A. G. Barto, W. B. Powell and D. Wunsch. *Handbook of Learning and Approximate Dynamic Programming*. Wiley-IEEE Press, 2004.

[11] L. X. Wang and J. M. Mendel, "Fuzzy basis functions, universal approximation, and orthogonal least-squares learning", *IEEE Transactions on Neural Networks*, vol. 3, pp. 807–814, 1992.

[12] L. Jouffe, "Fuzzy inference system learning by reinforcement methods", *IEEE Transactions on Systems, Man, and Cybernetics — Part C: Applications and Reviews*, vol. 28, issue 3, pp. 338–355, 1998.

[13] R. Sharma and M. Gopal., "A Markov game adaptive fuzzy controller for robot manipulators", *IEEE Transactions on Fuzzy Systems*, vol. 16, issue 1, pp. 171–186, 2008.

[14] S. Seuken and S. Zilberstein, "Formal models and algorithms for decentralized decision making under uncertainty", *Autonomous Agents and Multiagent Systems*, Feb. 2008.

[15] C. Amato, D. S. Bernstein, and S. Zilberstein, "Optimizing fixed-size stochastic controllers for POMDPs and decentralized POMDPs", *Autonomous Agents and Multiagent Systems*, 2009.

[16] D. Szer and F. Charpillet, " An optimal best-first search algorithm for solving infinite horizon DEC-POMDPs", In *European Conference on Machine Learning*, 2005.

[17] D. S. Bernstein, E. A. Hansen, and S. Zilberstein, " Bounded policy iteration for decentralized POMDPs", In *Proc. Int. Joint Conf. on Artificial Intelligence*, 2005.

[18] T. J. Ross. *Fuzzy Logic with Engineering Applications*. Wiley & Sons Inc., 2nd edition, 2004.

[19] G. Owen. *Game Theory*. Academic Press, Orlando, FL, 2nd edition, 1982.

[20] R. Emery-Montemerlo, G. Gordon, J. Schneider and S. Thrun, "Approximate solutions for partially observable stochastic games with common payoffs", In *Proc. of Int. Conference on Autonomous Agents and Multiagent Systems*, 2004.

[21] P. Poupart and C. Boutilier, "Bounded finite state controllers", In *Advances in Neural Information Processing Systems 16*. MIT Press, 2004.

[22] D. Yagan and C.-K. Tham, "Coordinated reinforcement learning for decentralized optimal control", In *IEEE Int. Symp. on Approximate Dynamic Programming and Reinforcement Learning*, 2007.

[23] G. N. Shirazi, P.-Y. Kong, and C.-K. Tham, "A cooperative retransmission scheme in wireless networks with imperfect channel state information", In *Proc. of the 2009 IEEE conf. on Wireless Communications & Networking Conference*, 2009.

[24] F. Wu, S. Zilberstein, and X. Chen, "Rollout sampling policy iteration for decentralized POMDPs", In *Proc. of Uncertainty in Artificial Intelligence*, 2010.

[25] E. Duman, M. Kaya, and E. Akin, "A multiagent fuzzy reinforcement learning method for continuous domains", In *Multi-Agent Systems and Applications IV*, LNCS, pp. 306–315. Springer, 2005.

[26] A. M. Tehrani, M. S. Kamel, and A. M. Khamis, " Fuzzy reinforcement learning for embedded soccer agents in a multiagent context", *International Journal of Robotics and Automation*, vol. 21, issue 2, pp. 110–119, 2006.

2011 IEEE International Conference on Fuzzy Systems
June 27-30, 2011, Taipei, Taiwan

A Challenge to Biometrics by Sole Pressure while Walking

Takahiro Takeda, Kei Kuramoto, Syoji Kobashi, Yutaka Hata
Graduate School of Engineering
University of Hyogo
Hyogo, JAPAN
eu11l002@steng.u-hyogo

***Abstract*—This paper describes a personal verification method based on fuzzy logic using dynamic sole pressure distribution while walking. The method employs a pair id sole pressure distribution change, and it is acquired by a mat type load distribution sensor. As a preliminary experiment for shoes, we take sole pressure data by bare foot and two kind of slippered foot. We extract thirty nine gait features from each sole pressure distribution change. We calculate a fuzzy degree of a feature from two fuzzy if-then rules and them fuzzy membership functions for a feature. These fuzzy membership functions are statistically determined by learning data. The fuzzy degree of acquisition sole pressure data is calculated by total of fuzzy degree of all features. The method verifies the walking person by using the fuzzy degree of the acquisition sole pressure data. When the fuzzy degree of acquisition data higher than a threshold, we verify the walking person as the target person. In our experiments, we employed 11 volunteers and took sole pressure data six times for each volunteer and foot situation. When the learning data included same kind of test data, we obtained low equal error rate. We obtained low false acceptance rate.**

Keywords-biometrics; personal verificaiton; walking; sole pressure; load distribution sensor

I. INTRODUCTION

Recently, personalized services are widely used for many situations. For example, we are use personal computer, e-mail services and several health monitoring services. However, these services frequently demand private and important information. Thus, personal authentication is more important technique for these personalized services. Password and PIN are major verification method, but these methods has disadvantage that we may forget these knowledge and other person can masquerade as us. To solve these problems, biometrics [1]-[3] is widely used in security field, and it has high accuracy and high user friendliness. Biometrics verifies person by physical features or behavioral features. The physical features such as fingerprint [4], [5], iris authenticate person with high accuracy. The behavioral features such as signature [6], voice [7] and walking [8]-[13] has high user friendliness. Personalized services are used in everyday lives. Thus, personal verification system required high user friendliness. By using walking, we are able to verify person passing a door or approaching a device of the service. In addition, the feature never force person to particular act such as speaking or writing. For these reasons, walking has the most high user friendliness.

In this paper, we describe a biometric personal verification method. We acquire walking data as dynamics of sole pressure. We have proposed a biometric personal authentication method using sole pressure while walking [13]. In this method, we employ a pair of right and left sole pressure distribution while walking. In past work, we have authenticated person with bare foot. However, we usually wear shoes at our everyday lives. In our goal, we aim to authenticate walking person wearing shoes. In this paper, we authenticate slippered person wearing slippers as a preliminary experiment for shoes. In this experiment, we take sole pressure data of bare foot and slippered foot, and authenticate them. We employ thinner type and thicker type slippers, and we use these data for learning data and test data. Firstly, we acquire sole pressure distribution while walking by mat type load distribution sensor. The load distribution sensor used here is good enough to obtain the walking data because it requires no special device carrying, no resistance like camera usage and easy tractable for users. Secondly, we extract thrifty nine gait features from each sole pressure data. Twelve features are based on footprint and twenty seven features are based on weight movement. Thirdly, we describe fuzzy if-then rules and fuzzy membership functions. The fuzzy membership functions are statistically determined by using learning data. Fourthly, we verify subjects by using fuzzy degree for acquisition sole pressure data. Fifthly, we show experimental result on 11 volunteers. In experiment, we took sole pressure data by three situations. Finally, we conclude the technical results.

II. PRELIMINARIES

A. Load Distribution Sensor

We acquire sole pressure data while walking by a mat type load distribution sensor (Arrow Industry Co., Ltd. AS-64X256-7PM) to authenticate person. Fig. 1 shows the load distribution sensor and our data acquisition system. This sensor is one of pressure sensors. Our experimental system consists of the load distribution sensor, a control device (Arrow Industry Co., Ltd. AS-64X256) and a personal computer. Effective sensing area of the load distribution sensor is 33 cm × 178 cm. The sensor has 64 vertical electrode sheets and 256 transverse electrode sheets. Distance between the nearest electrode sheets is 5.0 mm in a vertical direction (x-axis) and 7.0 mm (y-axis). In every intersection of vertical and transverse sheets, a resistive element is sandwiched in tow electrode sheets and this intersection point is a sensing point. The load distribution sensor has 64 × 256 sensing points. When we put pressure to

978-1-4244-7316-8/11/$26.00 ©2011 IEEE

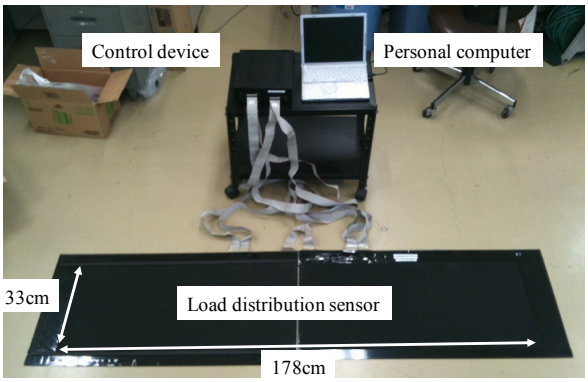

Figure 1. Composition of data acquisition system.

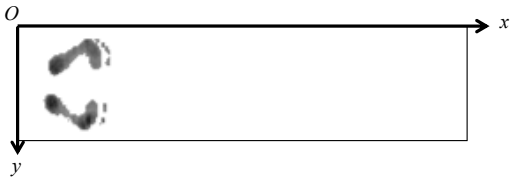

Figure 2. An example of load distribution data of one sampling time.

Slipper 1 *Slipper 2*

(a) Top view

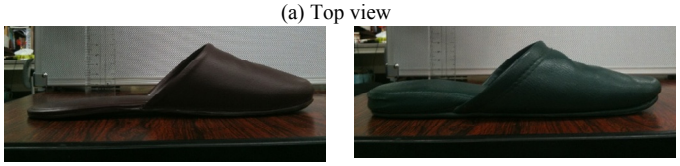

Slipper 1 *Slipper 2*

(a) Side view

Figure 3. View of sillipers.

the sensing points, the corresponding resistive elements decrease electric resistance. The control device converts the electric resistances of the sensing points into 8-bit (256 level) digital signal, and provides the digital signal for all pressure values to a personal computer. The personal computer stores the pressure value at the sampling interval. In our experiment, sampling interval is 100 ms. Fig. 2 shows an example of load distribution data of one sampling time.

B. Subjects and Data Acuisition Method

In our experiment, we employ 11 volunteers shown in Table I. To acquire sole pressure data, we ask volunteers to walk on the load distribution sensor. We acquire sole pressure data the load distribution change while walking as the sole pressure data. In our experiment, the volunteer walked along *x*-axis of the sensor by bare foot and two type slippers as shown in Fig. 3. In this figure, *Slippers 1* is thinner type slippers and the thickness is 0.6 cm. On the other hand, *Slippers 2* is thicker one and the thickness is 2.5cm in heel area and 1.5cm in toe area. We acquire sole pressure data six times for each type slippers and bare foot. Fig. 4 shows examples of the right sole pressure change by bare foot.

TABLE I. SUBJECTS INFORMATION

#	*Age [year]*	*Gender*	*Body height [cm]*	*Body weight [kg]*
1	24	Male	165	58
2	23	Male	172	63
3	22	Male	173	60
4	23	Male	170	81
5	24	Male	160	44
6	22	Male	171	62
7	22	Male	169	62
8	24	Male	175	62
9	23	Male	172	70
10	23	Male	162	48
11	23	Male	173	63

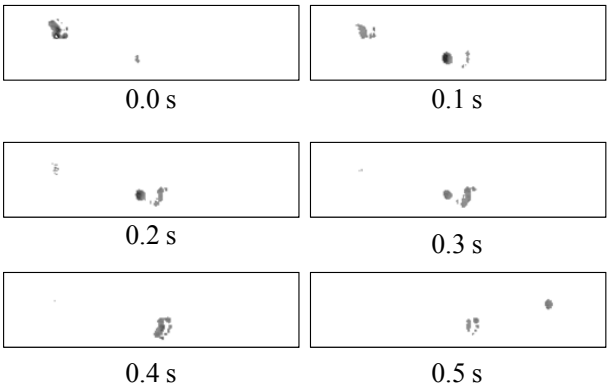

Figure 4. An example of sole pressure distribution chagne of one sole.

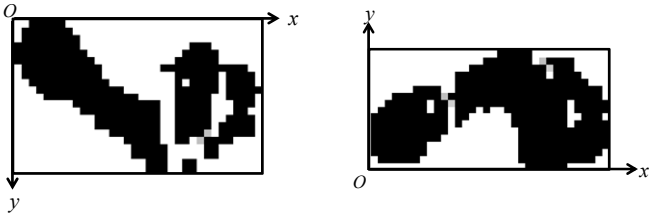

(a) Right sole coordinate system (b) Left sole pressure data

Figure 5. Right and left sole coordinate system.

For personal verification, we extract a right sole pressure data, X_R^S, and left sole pressure data, X_L^S, from the acquisition data, X^S. The notation X^S denotes an acquisition data when person "*S*" is walking. We define the right and left sole coordinate system in Fig. 5. We set the *x*-origin at heel side of a circumscribed rectangle, and we set *y*-origin at thumb side of the circumscribed rectangle.

Identify applicable sponsor/s here. *(sponsors)*

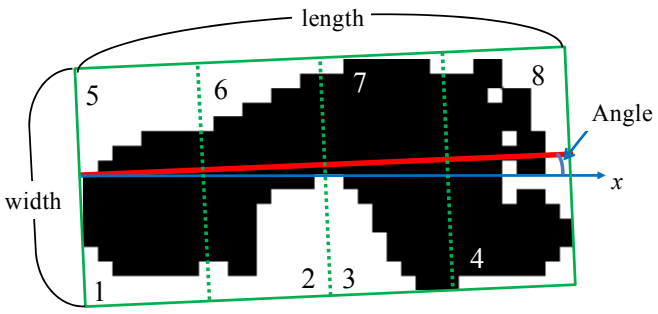

Figure 6. Examples of footprint and its features.

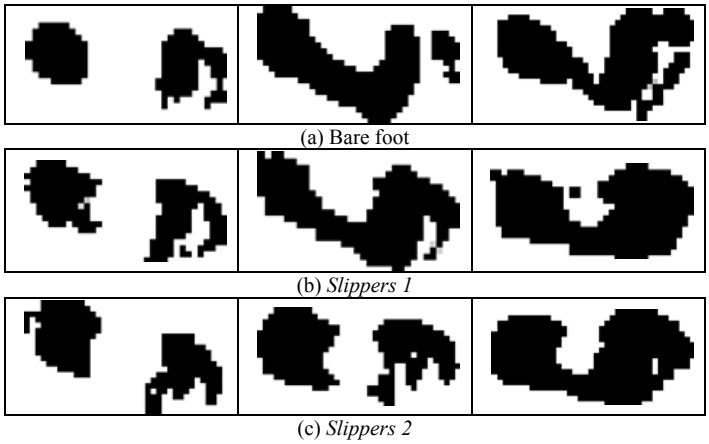

(a) Bare foot

(b) *Slippers 1*

(c) *Slippers 2*

Figure 7. Examples of footprint of three persons.

III. Personal Verification Method

The proposed method verifies person by using fuzzy logic. We extract features based on footprint and weight movement from each sole pressure data. We calculate fuzzy degree, μ^r_{Sole}, for the target person "r". If the fuzzy degree is higher than a threshed parameter, we verify the walking person as the target person.

A. Features of Sole Pressure Chagne

We extract features from sole pressure data X_k^S, where k denotes the index of right sole ($k = R$) or left sole ($k = L$). Twelve features are based on a footprint, and twenty seven features based on weight movement. In this paper, the notation $f_i(X_k^S)$ denotes a feature with respect to a sole pressure data X_k^S where i denotes the index of each feature.

The footprint is made by combining binarized image of sole pressure distribution for all frames. Fig. 6 shows an example of footprint and its features. In this figure, the black area shows sole area, the red straight line is obtained by least squares method for footprint, and green rectangle is the circumscribed quadrangle of the footprint. The length of footprint, $f_1(X_k^S)$, is calculated by the length of long side of the green circumscribed quadrangle. The width of footprint, $f_2(X_k^S)$, is calculated by the length of short side of the green circumscribed quadrangle. The area of footprint, $f_3(X_k^S)$, is calculated by the number of pixels including the sole area. The angle of footprint, $f_4(X_k^S)$, is calculated by the angle between the red straight line and x-axis of the sensor. The distribution of footprint, $f_5(X_k^S)$,..., $f_{12}(X_k^S)$ are calculated by numbers of sole pixels in the 1-8 small areas

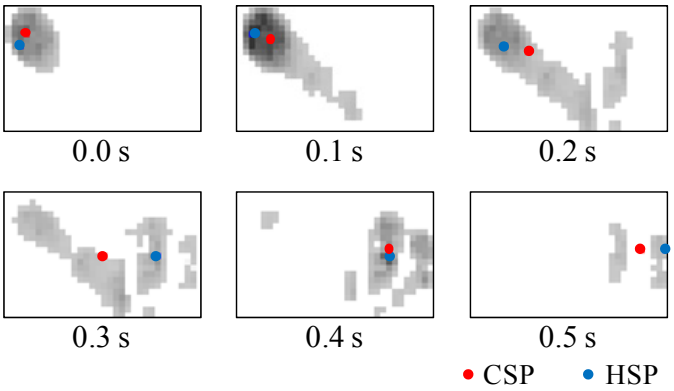

Figure 8. Examples of features from sole presure of each frame.

shown in Fig. 6. The Green dotted line quarter the circumscribed quadrangle. These features depend on the posture of walk and shape of foot. Several differences appear in the arch of a foot, the part of fingers and direction of footprint while walking. Even if persons wear same shoes, these features are different between persons. Fig. 7 shows examples of footprint of three persons.

We extract features from every frame of sole pressure data. We calculate the center of sole pressure (CSP), the highest sole pressure (HSP) and the area of footprint from each frame. The areas are calculated by the number of sole pixels from each frame. Fig. 8 shows the examples of CSPs and HSPs. There are several valuations among the sole pressure, and the numbers of frames are often different between two sole pressure data. Thus, we normalize these features to nine frames. We consider that the dynamic changes of each feature are similar in one step. We therefore interpolate nine points lining up in a polygonal line by liner interpolation and employ these points as features. The nine CSPs, $f_{13}(X_k^S)$,..., $f_{21}(X_k^S)$ and nine HSPs, $f_{22}(X_k^S)$,..., $f_{30}(X_k^S)$ are extracted from these trajectory. The nine areas, $f_{31}(X_k^S)$,..., $f_{39}(X_k^S)$ are extracted from the polygonal lines.

B. Fuzzy Degree Determination

In this method, we verify walking person by fuzzy degree, μ^r_{Sole}, of the acquisition data, X^S, for the target person, r. The fuzzy degree, μ^r_{Sole}, is calculated from fuzzy degrees of every feature. Firstly, we consider Knowledge 1: features of same person are similar, and Knowledge 2: the feature with higher classification score in learning pressure data is more primary for personal verification. From these knowledge, the following fuzzy if-then rules are derived.

Rule 1: IF feature, $f_i(X_k^S)$, is *CLOSE* to $\alpha^r_{k,i}$ of the registered person y_r, THEN the degree of a feature, $P^r_{k,i}$,is high.

Rule 2: IF classification score, $\beta^r_{k,i}$, of learning sole pressure data is *HIGH*, THEN the degree of a feature, $W^r_{k,i}$, is high.

These fuzzy membership functions *CLOSE* and *HIGH* are defined by Fig. 9. These fuzzy membership functions have statistically determined parameters, $\alpha^r_{k,i}$, $t^r_{k,i}$, $u^r_{k,i}$, $\beta^r_{k,i}$, and sum^r_k, and these are determined by learning process.

Here, we explain the method to determine $\alpha^r_{k,i}$, $t^r_{k,i}$, $u^r_{k,i}$ and $\beta^r_{k,i}$ in Fig. 10 for any k and i. In our learning process, every

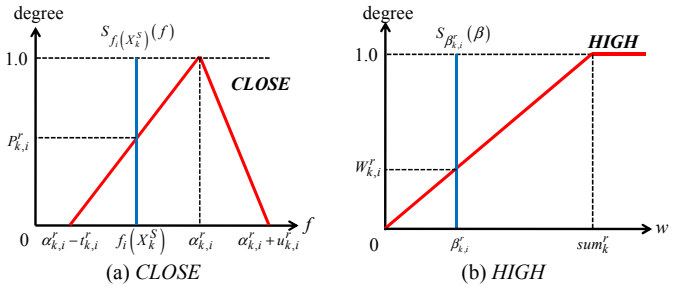

(a) *CLOSE* (b) *HIGH*

Figure 9. Fuzzy membership functions.

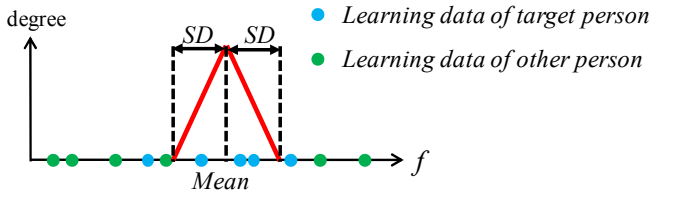

(a) Example of initialized fuzzy membership function *CLOSE*

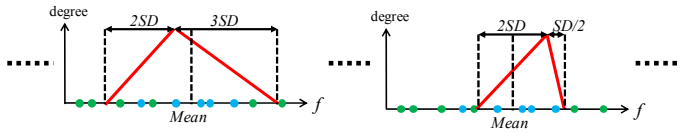

(b) Example of deformed fuzzy membership function *CLOSE*

Figure 10. Examples of fuzzy membership functon deformation.

registered subject has N learning data. Firstly, we calculate the mean value $Mean^r_{k,i}$, and the standard deviation, $SD^r_{k,i}$, of learning data for k and i of the target person. Secondly, we initialize $\alpha^r_{k,i} \leftarrow Mean^r_{k,i}$, $t^r_{k,i} \leftarrow SD^r_{k,i}$ and $u^r_{k,i} \leftarrow SD^r_{k,i}$. Here, the membership function, *CLOSE*, is deformed as shown in Fig. 10(a), and we calculate the fuzzy degree, $P^r_{k,i}$, of a feature $f_i(X^S_k)$ for the target person by (1).

$$P^r_{k,i}(X) = \min\left(CLOSE, S_{f_i(X)}(f)\right) \tag{1}$$

Here, we define fuzzy singleton function $S_a(x)$ by (2).

$$S_a(x) = \begin{cases} 1 & if\ x = a \\ 0 & otherwise \end{cases} \tag{2}$$

We calculate the fuzzy degree, $P^r_{k,i}$, from every learning pressure data. From these fuzzy degree, the classification score, $\beta^r_{k,i}$, is calculated by the difference between an average fuzzy degree $P^r_{k,i}$ for other person and an average fuzzy degree $P^r_{k,i}$ for the target person. Thirdly, we repeat the calculation of $\beta^r_{k,i}$ for all domains of $Mean^r_{k,i} - SD^r_{k,i} \le \alpha^r_{k,i} \le Mean^r_{k,i} + SD^r_{k,i}$, $0 \le t^r_{k,i} \le 4\,SD^r_{k,i}$ and $0 \le u^r_{k,i} \le 4\,SD^r_{k,i}$ at the interval of $SD^r_{k,i} / 10$. Fig. 10(b) shows examples of the deformed membership function, *CLOSE*. We obtain the classification score, $\beta^r_{k,i}$, from all domains. We employ the parameters $\alpha^r_{k,i}$, $t^r_{k,i}$ and $u^r_{k,i}$ with the highest $\beta^r_{k,i}$ among all domains for a feature. Fourthly, we repeat the determination process for all k and i. The parameter, sum^r_k, of membership function, *HIGH*, is the total of classification score, $\beta^r_{k,i}$, of the one sole pressure data, X^S_k, and it is calculated by (3).

$$sum^r_k = \sum_{i=1}^{39} \beta^r_{k,i} \tag{3}$$

The fuzzy degree, $Q^r_{k,i}$, of a feature is defined by (4).

$$Q^r_{k,i}\left(X^S_k\right) = P^r_{k,i}\left(X^S_k\right) \times W^r_{k,i}\left(\beta^r_{k,i}\right) \tag{4}$$

Here, the fuzzy degree, $W^r_{k,i}$, is defined by (5), and it means the effectiveness of the feature for the target person.

$$W^r_{k,i}(\beta) = \min\left(HIGH, S_\beta(w)\right) \tag{5}$$

Finally, we calculate the fuzzy degree, $Q^r_{k,i}$, for all k and i. The fuzzy degree, $\mu^r{}_{Sole}$, of the acquisition data is calculated by (6).

$$\mu^r_{Sole}\left(X^S\right) = \frac{1}{2}\left(\sum_{i=1}^{39} Q^r_{R,i}\left(X^S_R\right)\right) + \frac{1}{2}\left(\sum_{i=1}^{39} Q^r_{L,i}\left(X^S_L\right)\right) \tag{6}$$

C. Personal verification by fuzzy degree

The proposed method verifies walking person by the fuzzy degree, $\mu^r{}_{Sole}$, of the acquisition data, X^S. For personal verification, we acquire a pair of right and left sole pressure data, and extract features from the acquisition data. We calculate the fuzzy degree, $\mu^r{}_{Sole}$, for the target person. If the fuzzy degree is higher than a threshold parameter, the proposed method verifies walking person as the target person. On the other hand, if the fuzzy degree is lower than the threshold parameter, we verify the walking person is not the target person.

IV. Experimental Results

In our experiment, we employed 11 volunteers. We took the sole pressure data 18 times for a volunteer with bare foot (6 times), *Slipper 1* (6 times) and *Slipper 2* (6 times). In this experiment, we call these data set that *BARE*, *SL1* and *SL2*, respectively. We employ equal error rate (EER) for performance test. EER is the error rate at that false rejection rate (FRR) equals to false acceptance rate (FAR). Here, FRR is concerned with the number of instance defined as an authorized individual being falsely rejected by the system. FAR is concerned with the number of instances defined as an unauthorized individual being falsely accepted by the system.

We verified these volunteers by the proposed method. First, we tested our proposed method by learning data of each data set. Table II shows the verification results of each learning data and test data and Fig. 11 shows FRR and FAR with threshold parameter change. The proposed method obtained low EER for the test data of same type data as the learning data. However, we obtained high EER for the other test data. Second, we tested the proposed method by employing two or three type learning data for a volunteer. Table III shows the verification result of employing two or three type learning data for each volunteer. We obtained low EER when the learning data included the

TABLE II. VERIFICATION RESULTS BY ONE LEARNING DATA

Learning data	*EER for each test data [%]*			*Mean ± SD*
	BEAR	*SL1*	*SL2*	
BARE	1.29	23.79	26.7	17.24 ± 13.90
SL1	27.12	1.15	21.14	16.47 ± 13.60
SL2	25.68	12.65	0.15	12.82 ± 12.77

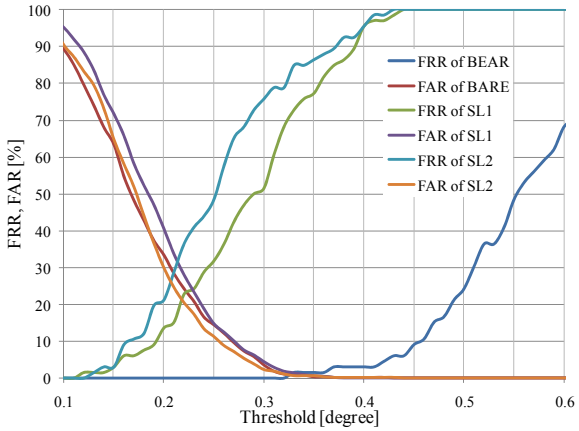

(a) FRR and FAR of lerning data, *BARE*.

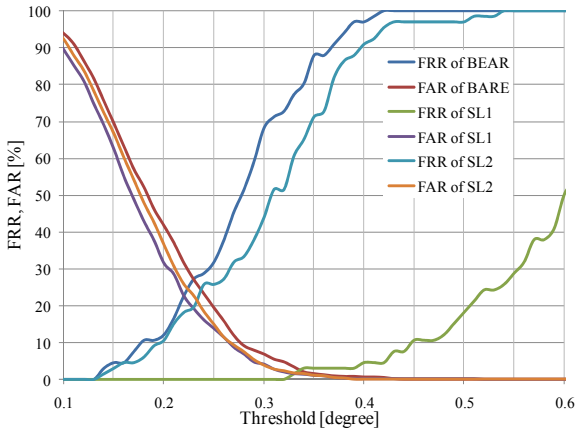

(b) FRR and FAR of lerning data, *SL1*

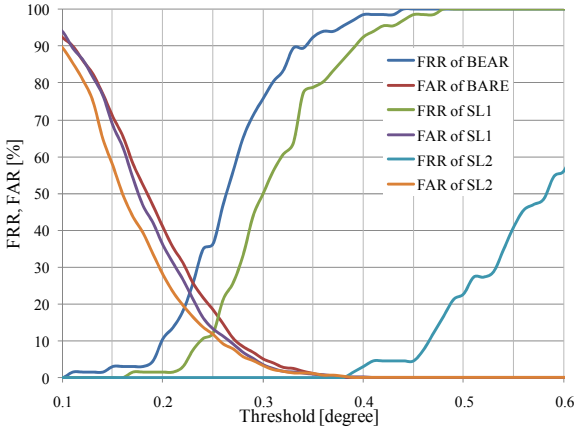

(c) FRR and FAR of lerning data, *SL2*

Figure 11. FRR and FARchange with threshold parameter change.

TABLE III. VERIFICATION RESULTS BY TWO OR THREE LEARNING DATA

Learning data	*EER for each test data [%]*			*Mean ± SD*
	BEAR	*SL1*	*SL2*	
BEAR and SL1	4.39	2.26	16.97	8.21 ± 7.61
BEAR and SL2	2.88	12.58	2.27	5.91 ± 5.78
SL1 and SL2	19.84	0.83	2.12	7.60 ± 10.62
BEAR, SL1 and SL2	6.44	3.33	2.87	4.22 ± 1.94

TABLE IV. FAR IN THRESHOLD PARAMETER WAS 0.35

Learning data	*EER for each test data [%]*			*Mean ± SD*
	BEAR	*SL1*	*SL2*	
BARE	0.12	0.00	0.15	0.09 ± 0.08
SL1	0.61	0.15	0.00	0.25 ± 0.32
SL2	0.00	0.15	0.00	0.05 ± 0.09
BEAR and SL1	1.97	1.06	1.06	1.36 ± 0.53
BEAR and SL2	1.21	1.36	0.91	1.16 ± 0.22
SL1 and SL2	2.42	0.91	0.91	1.41 ± 0.87
BEAR, SL1 and SL2	4.09	2.58	1.97	2.88 ± 1.09

same type data. In addition, we obtained lower EER for the other test than that of employing one test dat. Table IV shows the FAR of threshold parameter was 0.40. From these result, the proposed method was able to reject unauthorized individual being.

V. CONCLUSION

In this paper, we have proposed a biometric personal verification system based on fuzzy logic. We employed sole pressure distribution change while walking. The sole pressure data was acquired by mat type load distribution sensor. The proposed method verified the waking person by fuzzy degree of sole pressure data. We extracted features from right and left sole pressure change, and made fuzzy if-then rules with statistically determined membership functions by learning data. The fuzzy degree of sole pressure data was calculated from total of all fuzzy degree of each feature. In the experiments, we took sole pressure data three situations; volunteers walked with bare foot, they walked with thin slipper and they walked with thick slipper. We employed 11 volunteers, and we tested the proposed method. We obtained low EER when the learning data included the same type data. However, we obtained high EER for the other test data. The verification system had low FAR in threshold parameter was 0.40 for any learning data and test data. From these result, the proposed method was able to verify sole pressure data that was acquired same situation. From these results, we think that to verify walking person wearing shoes, the system needs to employ learning data of various situation.

In the feature, we will employ newly features of sole pressure for verification. We will try to authenticate person wearing shoes. We will add other biometric feature to the method.

REFERENCES

[1] S. Liu and M. Silverman, "A practical guide to biometric security technology," IEEE IT Proc., 2001, pp. 27-32.

[2] A.K. Jain, A. Ross, and S. Prabhakar, "An introduction to biometric recognition," IEEE Trans. on circuits and systems for video technology, vol. 14, no. 1, pp. 4-20, 2004.

[3] Biometrics security consortium. "Biometric security technology handbook", Biometrics security consortium, Ed., 1st Edn., Ohmhsa, Tokyo, Japan (2006). (in Japanese)

[4] K. Ito, H. Nakajima, K. Kobayashi, T. Aoki, and T. Higuchi, "A fingerprint matching algorithm using phase-only correlation," IEICE Trans. Fundamentals, vol.E87-A, no.3, pp.682-691, Mar, 2004.

[5] X. Chen, J. Tian, and X. Yang, "A new algorithm for distorted finger prints matching based on normalized fuzzy similarity measure," IEEE Trans. on Image processing, vol. 15, no. 3, pp. 767-776, 2006.

[6] A. Kholmatov and B. Yanikoglu, "Identity authentication using improved online signature verification method," Patten Recognition Letters, vol. 26, issue 15 pp. 2400-2408, 2005.

[7] D.A. Reynolds and R.C. Rose, "Robust text independent speaker identification using Gaussian mixture speaker models," IEEE Trans. on Speech and audio processing, vol, 3, no. 1, PP. 72-83, 1995.

[8] D.K. Wagg and M.S. Nizon, "On automated model-based extraction and analysis of gait," Proc. of the 6th IEEE Int. Conf. on Automatic Face and Gesture Recognition, pp. 11-16, May 2004.

[9] J. Mantyjarvi, M. Lindholm, E. Vildjiounaite, S.-M. Makela, and H. A. Ailisto, "Identifying users o portable devices from gait pattern with accelerometers," IEEE, ICASSP'05, vol. 2, pp. ii/973-ii/976, 2005.

[10] J. W. Jung, Z. Bien, and T. Sato, "Person recognition method using sequential walking footprints via overlapped foot shape and center-of-pressure trajectory," IEICE Trans. Fundamentals, vol.E87-A, no. 6, pp. 1393-1399, 2004.

[11] G. Qian, J. Zhang, and A. Kidane, "People identidication using gait via floor pressure sensing and analysis," Proc. of the 3rd European Conf. on Smart sensing and Context, pp. 83-98, 2008.

[12] T. Yamakawa, K. Taniguchi, T. Momen, S. Kobashi, K. Kondo, and Y. Hata, "Biometric personal identification based on foot pressure change," Int. Conf. on Soft Computing and Human Sciences, pp. 83-86, 2007.

[13] T. Takeda, K. Taniguchi, K. Asari, K. Kuramoto, S. Kobashi, and Y. Hata, "Biometric personal identification by dinamics of sole pressure at walking," Proc. of 2010 World Automation Cong., 2010.

2011 IEEE International Conference on Fuzzy Systems
June 27-30, 2011, Taipei, Taiwan

Six Degree of Freedom Calculation Based on Principal Component Analysis for the Knee Joint in MDCT Image

Yosuke Uozumi, Kouki Nagamune
Graduate School of Engineering, University of Fukui
Fukui, JAPAN
uozumi@me.his.u-fukui.ac.jp
Daisuke Araki, Tomoyuki Matsumoto,

Takehiko Matsushita, Seiji Kubo,
Ryosuke Kuroda, Masahiro Kurosaka
Kobe University Graduate School of Medicine
Kobe, JAPAN

***Abstract*—The anterior cruciate ligament (ACL) injury can cause a reason of instability along anterior - posterior translation at extension. Thus, it is important to examine the knee joint quantitatively for understanding clinical outcome. However, an quantitative calculation method of the knee joint has not been reported. Therefore, we have developed six degree of freedom (6 DOF) calculation based on principal component analysis (PCA) for the knee joint in multi-detecter row computer tomography (MDCT) image. The proposal method was applied to six ACL injured knees obtained at two periods. As a result, the proposed methods could calculated 6 DOF of the knee joint quantitatively.**

Keywords- Six Degrees-of-freedom; ACL Reconstruction; MDCT Image; Image Analysis

I. INTRODUCTION

The ACL injury can be a reason of instability along anterior-posterior direction at extension. It might result in working and daily life faced to obstacles. As examination methods of the ACL injury, manual tests have been proposed, however, it is difficult to calculate an attitude of the knee joint by using a general commercial device quantitatively. Therefore, this study sets a goal to calculate 6 DOF of the knee joint from MDCT image. In the experiment, the accuracy of the proposed method was examined for 6 DOF of the knee joint.

II. PRELIMINARY

A. MDCT(Multidetector - row CT) Device

An MDCT device is a CT (Computed Tomography) device with the multi-row detector. The MDCT device has thinner thickness and higher resolution than the CT. The MDCT image was obtained for patients peformed with ACL reconstruction. One slice consists of 512 × 512 (X × Y) voxels (TABLE I). The number of slices (Z) differ from patient to patient. The range of image was 5 cm proximal from the femur epicondyle and 5 cm distal from the tibial tubercle (Fig. 1).

TABLE I. ACQUISITION PARAMETERS

Resolution [pixel]	512 × 512
Color Depth [bits]	16
Slice Thickness [mm]	1.0
The Number of Slice	201~202
Pixel Spacing [mm]	0.5

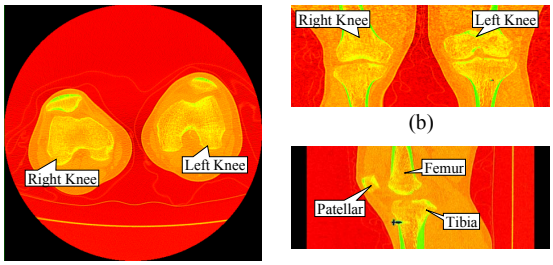

Figure 1. An Example of MDCT Image: (a) Axial (X-Y plane), (b) Coronal (X-Z plane), and (c) Sagittal (Y-Z plane).

B. ACL Injury

The ACL is a ligament which connects the femur and tibia, and plays a role of preventing an excessive anterior translation of the knee during knee rotation [1]. The ACL injury happens with high frequency among sports trautic injuries, and can cause a reason of increase of instability along anterior - posterior translation at extension [2]. When no treatment is applied to the ACL injury, it can result in secondary injuries (i.e., meniscus injury, articular cartilage lesion, etc.). Also, because a self-reparation of the ACL is rare due to its low healing ability, operative treatment is preferred rather than conservative treatment when instability of daily life is high for an active young person or a person with multiple ligament injuries [3-4].

978-1-4244-7316-8/11/$26.00 ©2011 IEEE

C. ACL Reconstruction

The ACL reconstruction has two techniques, that are single bundle technique and double bundle technique. The single and double are performed with one and two grafts, respectively [5]. In both of techniques, a bone tunnel(s) is/are required so that the graft is passing through it. Especially, two bone tunnels in double bundle technique are called as anteromedial (AM), and posterolateral (PL) as shown in Fig. 2.

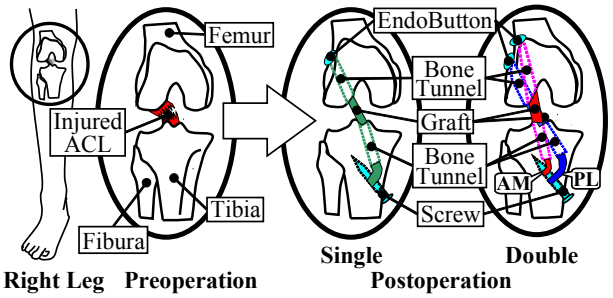

Figure 2. ACL Reconstruction.

D. Definition of Coordinate Systems

Coordinate systems are necessary to a quantitative evaluation by three dimensional attitude of the knee joint (Fig. 3). The coordinate systems consist of an anterior axis, lateral axis, distal axis, and origin point [6-8]. The coordinate systems are determined based on anatomical points and axes [9].

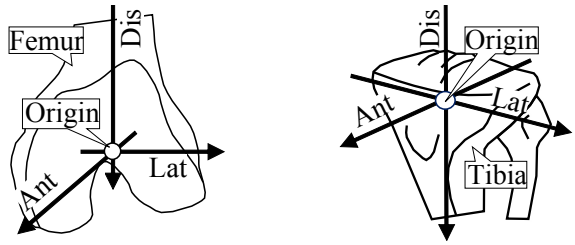

Figure 3. The coordinate systems. (a) The femur coordinate system. (b) The tibia coordinate system.

E. Six Degrees of Freedom

In the three dimensionnal space, total degree of freedom is six for summation of three translational DOF and three rotational DOF. This study calculates 6 DOF of the femur and tibia in MDCT image for analysis of attitude of the knee joint (Fig. 4).

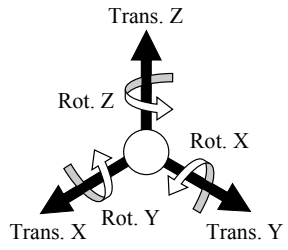

Figure 4. 6 DOF.

III. Proposed Method

The proposed method consists of three steps as shown in Fig. 5. The first step is determination of the coordinate systems in the femur and tibia. The second step is registration of the images in the femur and tibia. The third step is validation of the registration accuracy. The last step is evaluation of the 6 DOF for the coordinate systems.

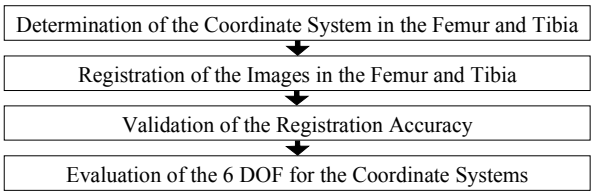

Figure 5. Procedure of proposal method.

A. Determination of the Coordinate Systems in the Femur and Tibia

The coordinate systems of the femur and of the tibia are determined from the information obtained by the following procedure.

1) The femur coordinate system

The femur coordinate system consists of five steps as shown in Fig. 6. The first step is determination of the distal axis. The second step is determination of the anterior direction in axial image. The third step is determination of the lateral axis. The fourth step is determination of the anterior axis. The last step is determination of the origin point.

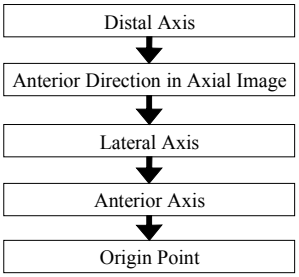

Figure 6. Procedure of the femur coordinate system.

a) Distal axis: The femur is depicted as comparatively circle in proximal slice. The gravity points of the proximal femur are detected, and are used as two points making the distal axis (Fig. 7).

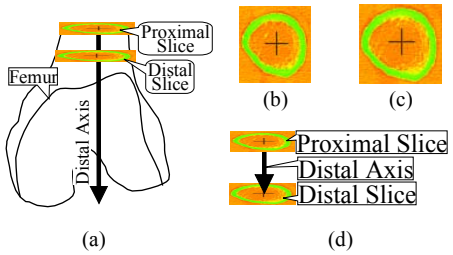

Figure 7. Distal axis: (a) the distal axis of the femur, (b) the proximal slice of the femur image, (c) the distal slice of the femur image, and (d) the calculated distal axis.

b) The anterior direction in axial Image: The epicondyles, which are necessary for determining the lateral axis and the anterior direction, are determined. Therefore, we determine the anterior direction in axial image.

Top(t), bottom(b), right(r), and left(l) points in each slice of the femur are detected (Fig. 8 (a)). Then, $t(i)$, $b(i)$, $l(i)$, and $r(i)$ that coordinate values of the s-th slice of the femur are calculated from

$$\begin{cases} 0 \le l(s) \le r(s) \le X \\ 0 \le t(s) \le b(s) \le Y \end{cases}, \quad (1)$$

where s is the slice number of the image, X and Y are the maximum coordinate values of the image, respectively.

The area of the rectangle based on these four points are calculated. Then, difference $dif_y(s)$ of t and b, and difference $dif_x(s)$ of l and r are calculated from

$$\begin{cases} dif_x(s) = |r(s) - l(s)| \\ dif_y(s) = |t(s) - b(s)| \end{cases}. \quad (2)$$

The slice with the maximum area is searched, then used as a target slice for the following process (Fig. 8 (b)). Then, an area $A(s)$ is calculated for each slice from

$$A(s) = dif_x(s) \cdot dif_y(s). \quad (3)$$

Then, the slice with the maximum area $slice_{max}$ is calculated from

$$slice_{\max} = \arg \max_{s \in [0, S-1]} (A(s)), \quad (4)$$

where S is the number of slices of the image.

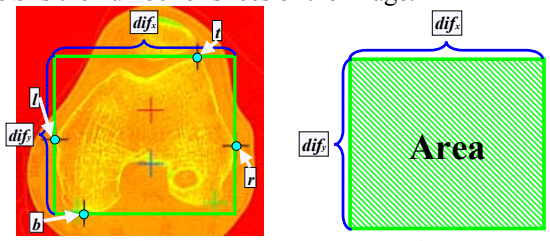

(a) (b)

Figure 8. The slice with the femur maximum area: (a) the feature points (t, b, l, r) of the femur image on the slice, and (b) the rectangle area of the femur image on the slice.

The intersection point of the target slice and the distal axis is regarded as the center point. Two points are searched so that the distances between the center point and two points are longest among the contour of the bone. Then the two points are determined as two postepicondyle points for analyzing a notch position. The bisector line is calculated from two epicondyle points and the center point. Then, the maximum evaluation function R is calculated from

$$R = \arg \max_{i \in [0, 2\pi - 1]} (A(i) \cdot B(i)), \quad (5)$$

where A and B are the differences of the center point of distal axis and postepicondyles on the slice. The notch position is determined by the bisector line and the contour of the femur (Fig. 9).

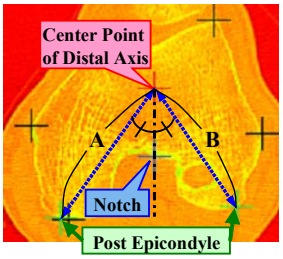

Figure 9. The notch on the slice of the maximum rectangle area.

The anterior direction of the femur is determined by connecting the notch and center point (Fig. 10).

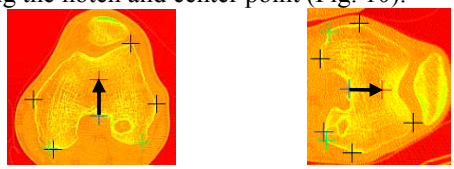

(a) (b)

Figure 10. Anterior direction in axial image: (a) the upward position of the knee image, and (b) the rightward position of the knee image.

c) Lateral axis: Vertical vectors that indicate contour points from anterior axis are calculated (Fig. 11 (a)). The longest vecter is regarded as the epicondyle. The longest vector of the medial and lateral are determined as the medial and lateral epicondyles, respectively (Fig. 11 (b)). The lateral axis is determined by connecting the medial and lateral epicondyles (Fig. 12).

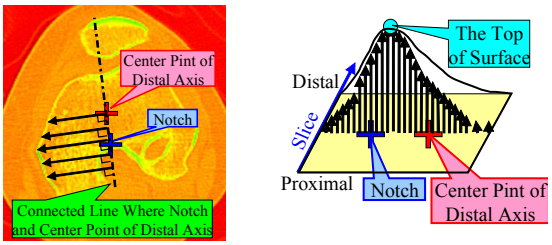

(a) (b)

Figure 11. The calculation of the top on the epicondyles: (a) the top on contour side in a slice, and (b) the three dimensional top of surface of the epicondyle .

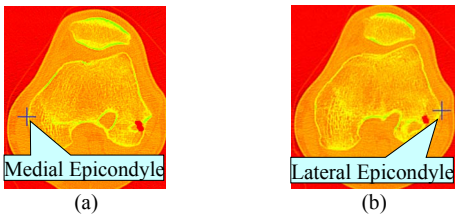

(a) (b)

Figure 12. The determinated epicondyles: (a) the medial epicondyle, and (b) the lateral epicondyle.

d) Anterior axis: The anterior axis is an outer product of the distal axis and the lateral axis.

e) Origin point: The middle point of the segment that connects the epicondyles is determined as the origin point of the coordinate system (Fig. 13). Then, the origin point $\vec{o}(o_1, o_2, o_3)$ is calculated from

$$\vec{o} = \left(\frac{m_1 + l_1}{2}, \quad \frac{m_2 + l_2}{2}, \quad \frac{m_3 + l_3}{2} \right), \tag{6}$$

where $\vec{m}(m_1, m_2, m_3)$ and $\vec{l}(l_1, l_2, l_3)$ are the medial and lateral epicondyles.

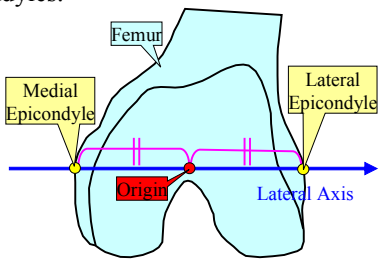

Figure 13. The origin point.

2) The tibia coordinate system

The tibia coordinate system consists of three steps as shown in Fig. 14. The first step is determination of the distal axis. The second step is determination of the anterior axis and lateral axis. The last step is determination of the origin point.

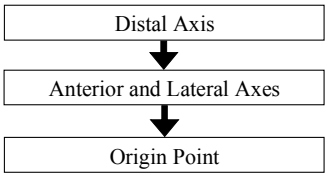

Figure 14. Procedure of the tibia coordinate system.

a) Distal axis: The tibia is depicted as comparatively circle in distal slice. The gravity points of the distal region of the tibia are detected, and are used for making the distal axis based on principal component analysis (Fig. 15).

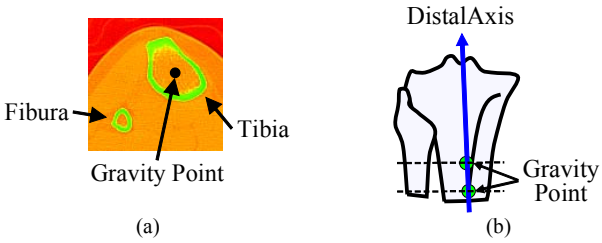

Figure 15. Determining the distal axis: (a) the gravity point on the axial image, (b) the distal axis.

b) Anterior and lateral axes: The plane which has the maximum area and is perpendicular to the calculated bone axis, is searched. Anterior axis and lateral axis are derived from the maximum area on the plane. At first, the gravity point of the bone profile is calculated. Here, two orthogonal lines are assumed so that the intersection point is located as the gravity point. The intersection points of the lines and the bone profile are regarded as points *A*, *B*, *C*, and *D*, respectively. These four distances (*a*, *b*, *c*, and *d*) from the gravity points to the four points are inserted by the following evaluation function *R*,

$$R_{\max} = \arg \max_{i \in [0, 2\pi - 1]} \frac{a(i) \cdot b(i) \cdot c(i)}{d(i)}, \tag{7}$$

The orthogonal lines are rotated based on the gravity point so that the evaluation function *R* is the maximum value. In the situation, the lines AB and CD are defined as the lateral and anterior axes, respectively.

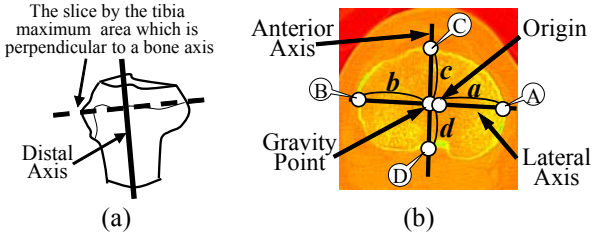

Figure 16. The tibia coordinate system: (a) The slice by the tibia maximum area which is perpendicular to a bone axis, (b) the anterior axis, the lateral axis and the origin point.

c) Origin point: The origin of a coordinate system is determined as a middle point of the line AB (Fig. 16). Then, the origin point $\vec{o}(o_1, o_2, o_3)$ is calculated from

$$\vec{o} = \left(\frac{a_1 + b_1}{2}, \quad \frac{a_2 + b_2}{2}, \quad \frac{a_3 + b_3}{2} \right), \tag{8}$$

where $\vec{a}(a_1, a_2, a_3)$ and $\vec{b}(b_1, b_2, b_3)$ are the medial and lateral epicondyles.

B. Registration of the Images in the Femur and Tibia

The 6 DOF is quantitatively evaluated in comparing to preoperative and postoperative data. In general, different acquired period data have tendency to make a little bit different coordinate system each other. To reduce the error, the data are unified by registration, and is evaluated in same coordinate system. The coordinate system are unified by registration of preoperative data and postoperative data.

Evaluation of registration is performed by using matching rate. The matching rate is calculated in each three planes (i.e., axial plane, coronal plane, and sagittal plane). The target data are projected to each planes by using maximum intensity projection (MIP) method (Fig. 17). The projected data are transformed to binary data by thresholding. These processing are applied for preoperative and postoperative data. A matching rate *R* is a value calculated by the following equation,

$$R = \frac{1}{2} \cdot \frac{S_1 + S_2}{S_1 \times S_2} S_R, \tag{9}$$

where S_R is an area of number of overlapped pixels of preoperative and postoperative data, S_1 and S_2 are areas of preoperative data and postoperative data, respectively.

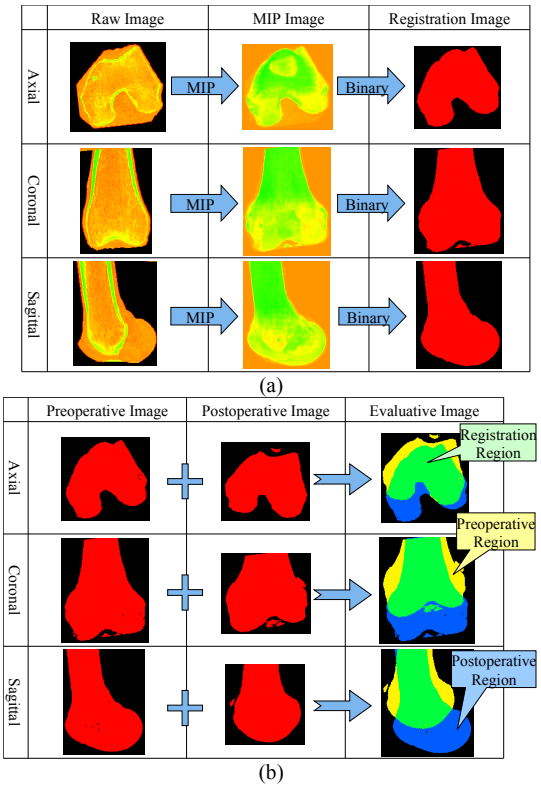

Figure 17. The evaluation of the registration: (a) Maximum Intensity Projection, and (b) the registration image.

The precise registration is performed so that the femur region of postoperative data are mostly overlapped to preoperative data (Fig. 18). After registration, the coordinate system determined from preoperative data are also used for postoperative data. It results that both of preoperative and postoperative data are evaluated on the same coordinate system.

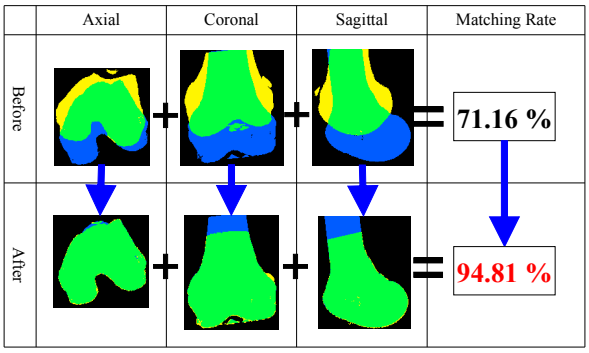

Figure 18. The precise registration.

C. Accuracy Validation of the Registration

An accuracy validation of the registration is used by the position of the screw. The intensity of screw is higher than a peripheral bone and an organization of the muscle etc. (Fig. 19 (a)). Only screw is extracted from the MDCT image (Fig. 19 (b)) by binarization with high thresholding value. The gravity point of the extracted object voxel is regarded as a barycentric position of the screw (Fig. 19 (c)).

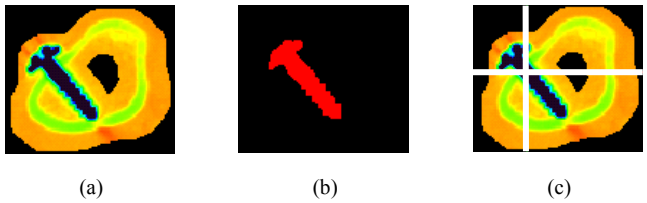

Figure 19. Evaluation of the knee joint pose.

The screw position was calculated by using the bone coordinate system of the tibia (Fig. 20). The validation of the registration accuracy is used by the position of the screw.

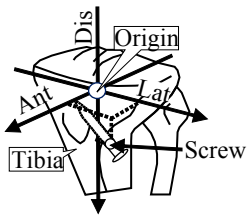

Figure 20. Evaluation of the screw.

D. Evaluation of the 6 DOF for the Coordinate Systems

Based on the femur and 6 DOF of the tibial coordinate system that we pursued, we evaluate attitude of the knee [10-11]. In general, range of motion is calculated by using this 6 DOF.

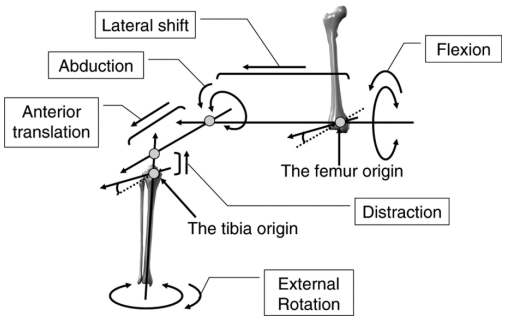

Figure 21. Evaluation of the knee joint pose.

IV. EXPERIMENTS

The subjects was fewer, because this study is a pilot study. The proposed method was applied for four subjects with single bundle that has informed consent. The sex was two males and one females. The age was 36.67 ± 13.50 (23-50). The injured knee was one right knee and two left knees (TABLE II). The one preoperative and one postoperative MDCT images were evaluated for each subjects. Quantitative comparison with the injured knee and the intact knee was performed.

TABLE II. SUBJECTS DATA

Subject	Sex	Age	Bundle	Injured Knee
1	F	37	S	L
2	M	23	S	R
3	M	50	S	L

V. RESULTS

The time-depend displacements of the screw was shown in TABLE III. The time-depend displacements of the screw were -0.28 ± 0.44 mm (anterior), 0.09 ± 0.25 mm (lateral), -0.07 ± 0.37 mm (distal), and 0.56 ± 0.24 mm (3D). "3D" was the three-dimensional time-depend displacement.

TABLE III. THE TIME-DEPEND DISPLACEMENTS OF THE SCREW.

Subject	Anterior	Lateral	Distal	3D
1	-0.79	0.24	-0.16	0.84
2	-0.02	0.23	0.34	0.41
3	-0.03	-0.20	-0.39	0.44

The results of evaluations were shown in TABLES IV - VI. In the tables, the 6 DOF (anterior, lateral, distal, flexion, rotation, and valgus) were evaluated at pre-time and post-time. The changes between the pre-time and post-time were tabulated. The difference was calculated by subtracting the injured knee from the intact knee.

TABLE IV. THE EVALUATION OF THE INJURED KNEE.

		Injured Knee (A)					
		Anterior	Lateral	Distal	Flexion	Rotation	Valgus
1	Pre-time	25.09	11.66	128.83	17.64	11.74	3.58
	Post-time	14.24	3.01	92.16	16.64	28.27	2.54
	Change	-10.85	-8.65	-36.67	-1.00	16.53	-1.04
2	Pre-time	14.46	30.56	146.52	2.52	13.90	16.56
	Post-time	10.00	17.45	126.72	5.00	9.74	11.88
	Change	-4.46	-13.11	-19.80	2.48	-4.16	-4.67
3	Pre-time	20.73	19.37	105.62	12.49	9.56	0.85
	Post-time	20.80	11.48	121.90	3.87	30.77	0.13
	Change	0.07	-7.88	16.28	-8.61	21.20	-0.72

(Anterior, Lateral, Distal: (mm), Flexion, Rotation, Valgus: (degree))

TABLE V. THE EVALUATION OF THE INTACT KNEE.

		Intact Knee (B)					
		Anterior	Lateral	Distal	Flexion	Rotation	Valgus
1	Pre-time	16.99	0.80	95.92	8.73	8.94	5.06
	Post-time	11.13	0.74	77.49	16.57	10.84	4.48
	Change	-5.86	-0.05	-18.42	7.84	1.91	-0.58
2	Pre-time	24.13	21.63	142.45	19.01	16.28	12.68
	Post-time	15.52	10.20	124.01	14.78	7.22	14.61
	Change	-8.60	-11.43	-18.44	-4.23	-9.06	1.93
3	Pre-time	21.20	6.45	97.63	6.89	17.70	4.50
	Post-time	17.66	14.22	105.23	14.01	17.80	5.79
	Change	-3.54	7.77	7.60	7.12	0.10	1.28

(Anterior, Lateral, Distal: (mm), Flexion, Rotation, Valgus: (degree))

TABLE VI. THE EVALUATION OF THE DIFFERENCE.

		Difference (B-A)					
		Anterior	Lateral	Distal	Flexion	Rotation	Valgus
1	Pre-time	-8.10	-10.86	-32.91	-8.91	-2.81	1.48
	Post-time	-3.11	-2.27	-14.67	-0.07	-17.43	1.94
2	Pre-time	9.67	-8.93	-4.06	16.49	2.38	-3.88
	Post-time	5.52	-7.25	-2.71	9.78	-2.52	2.73
3	Pre-time	0.46	-12.92	-7.98	-5.60	8.14	3.65
	Post-time	-3.14	2.74	-16.67	10.14	-12.96	5.66

(Anterior, Lateral, Distal: (mm), Flexion, Rotation, Valgus: (degree))

VI. DISCUSSION

The time-depend displacement (0.56 mm) of the screw was as small as the resolution (0.50 mm) of the image. The determination was no tendency in a direction of the displacement. This accuracy error was very small.

The changes of the injured knee were larger than the intact. It implys that the 6 DOF of the injured knee is effected by operation. The difference of post-time was close to zero more than pre-time. It might be that the 6 DOF of the injured knee was modified as the 6 DOF of the intact knee by the operation.

VII. CONCLUSION

We have proposed an analysis method of 6 DOF in the knee joint. The proposed method was applied for three patients of single bundle technique. The subjects was fewer, because this study is a pilot study. As a result, the proposed method could calculate the 6 DOF in the knee joint. This accuracy error was very small. It might be that the 6 DOF of the injured knee was modified as the 6 DOF of the intact knee by operation. We can apply the 6 DOF to the clinical examinations. This future work is to apply this method for many subjects.

REFERENCES

[1] G. Li, L. E. DeFrate, H. E. Rubash, T. J. Gill, "In Vivo Kinemetics of the ACL during Weight-bearing Knee Flexion," Journal of Orthopaedic Research, Vol. 23, pp.340-344, 2005.

[2] K. L. Markolf, J. S. Mensch, H. C. Amstutz, "Stiffness and laxity of the knee--the contributions of the supporting structures. A quantitative in vitro study," Vol. 58, pp.583-594, 1976.

[3] B. Beynnon , R. Johnson, J. Abate, B. Fleming, C. Nichols , "Treatment of anterior cruciate ligament injuries, Part I," The American Journal of Sports Medicine, Vol. 33, pp.1579-1602, 2005.

[4] B. Beynnon , R. Johnson, J. Abate, B. Fleming, C. Nichols , "Treatment of anterior cruciate ligament injuries, Part 2," The American Journal of Sports Medicine, Vol. 33, pp.1751-1767, 2005.

[5] J. A. Baumfeld, D. R. Diduch, L. J. Rubino, J. A. Hart, M. D. Miller, M. S. Barr, J. M. Hart, "Tunnel widegning following anterior cruciate reconstruction using hamstring autograft: a comparison between double cross-pin and suspencsory graft fixation," The Jounal of Kne Surg. Sports Traumatol. Arthrosc., Vol. 16, pp. 1108-1113, 2008.

[6] K. Nagamune, D. Araki, K. Nishimot, Y. Hoshino, S. Kubo, R. Kuroda, M. Kurosaka, "An Evaluation Method of EndoButton Position in MDCT Image After Anterior Cruciate Ligament Reconstruction," Proceedings of System, Man and Cybernetics, San Antonio, USA, (CD-ROM), 2009.

[7] Y. Uozumi, K. Nagamune, D. Araki, S. Kubo, R. Kuroda, M. Kurosaka, "An Analysis Method of direction of Bone tunnel Enlargement in MDCT Image After Anterior Cruciate Ligament Reconstruction," WAC 2010 Conference, Kobe, Japan, (CD-ROM), 2010.

[8] Y. Uozumi, K. Nagamune, D. Araki, S. Kubo, R. Kuroda, M. Kurosaka, "An Analysis Method of EndoButton Position with Registration in MDCT Images After Anterior Cruciate Ligament Reconstruction," WAC 2010 Conference, Kobe, Japan, (CD-ROM), 2010.

[9] M. Young, "The Technical Writer's Handbook," Mill Valley, CA: University Science, 1989.

[10] E. S. Grood, W. J. Suntay, "A Joint Coordinate System for the Clinical Description of Three-Dimensional Motions," Journal of Biomechanical Engineering, Vol. 105, pp.136-144, 1983.

[11] Yuichi Hoshino, Hirotsugu Muratsu, Kouki Nagamune, Masayoshi Yagi, Kiyonoryi Mizuno, Ryosuke Kuroda, Motoi Yamaguchi, Shinichi Yoshiya, Masahiro Kurosaka, "In Vivo Measurement of the Pivot Shift Test in the Anterior Cruciate Ligament Deficient Knee Using an Electromagnetic Device," American Journal of Sports Medicine, vol. 35, no. 7, pp. 1098-1104, Jul., 2007.

2011 IEEE International Conference on Fuzzy Systems
June 27-30, 2011, Taipei, Taiwan

Nursing-care Text Classification using Additional Term Information from Web

Manabu Nii*§, Takafumi Yamaguchi*, Yusuke Mori†, Yutaka Takahashi*,
Atsuko Uchinuno‡, and Reiko Sakashita‡
*Graduate School of Engineering, University of Hyogo, Himeji, Hyogo, Japan
Email: nii@eng.u-hyogo.ac.jp
†School of Engineering, University of Hyogo, Himeji, Hyogo, Japan
‡College of Nursing Art & Science, University of Hyogo, Akashi, Hyogo, Japan
§WPI Immunology Frontier Research Center, Osaka University, Suita, Osaka, Japan

***Abstract*—In this paper, for improving performance of the nursing-care text classification, we introduce a mechanism of retrieving terms from Web. Every year, the nursing-care texts are collected by using Web application to improve nursing-care quality in Japan. The collected nursing-care texts are decomposed into morphemes (i.e., terms), and then terms are stored as a term list. Each text is represented as a feature vector by using the term list and classified using a SVM based classification system. The training data sets for constructing SVM based classification system are different from the evaluation data sets. That is, there are differences between the term lists of the nursing-care texts because the nursing-care texts are collected and evaluated every year. To cover this difference, we introduce a mechanism of retrieving terms from Web. A new term which appeared in the evaluation data sets is used as a query of a search engine. The terms in the term list are also used as queries. Terms are represented by the search results, and then are compared with each other. We use the most similar term in the term list as an alternative of the new term. From experimental results, we show effectiveness of our proposed method.**

***Keywords*—nursing-care; text classification; SVM; fuzzy**

I. Introduction

In order to improve nursing-care quality, the data which consists of numerical data and freestyle texts are stored into our database. The numerical data is used for statistical analysis about the structure of hospitals. The text data is used for evaluating each nurse. In evaluating the text data, the experts need to read carefully and evaluate each nursing-care data because those data include freestyle Japanese texts which are written about actual nursing-care by nurses. For evaluating such texts automatically, we have developed several nursing-care text classification systems, such as using fuzzy classification systems [1], neural networks [2], and support vector machines (SVM) [3], [4]. In order to improve the classification performance of the SVM based classification system, we have proposed a GA-based term selection [5]–[8].

In the above mentioned classification systems, the collected nursing-care texts are decomposed into morphemes (i.e., terms), and then terms are stored as a term list. Each text is represented as a feature vector by using the term list and classified using a classification system. The training data sets for constructing classification system (e.g., SVM based classification system) are different from the evaluation data sets. That is, there are differences between the term lists of the nursing-care texts because the nursing-care texts are collected and evaluated every year. Therefore, the corresponding feature in the newer data set may not exist in the training data set because every year's term list has differences with each other. Such a feature which appears only in the new data set does not affect classification. The nursing-care texts which have such features may not be classified correctly.

In order to decrease such no-effect feature, we introduce a mechanism of retrieving terms from Web. A new term which appeared in the evaluation data sets is used as a query of a search engine. The terms in the term list are also used as queries. Terms are represented by the search results, and then are compared with each other. We use the most similar term in the term list as an alternative of the new term. Therefore, the no-effect feature can be expressed in the known feature approximately.

This paper is organized as follows. The overviews of nursing-care texts and preprocessing for classification using the morphological analysis software "MeCab" [9] are described in Section 2. In Section 3, the overview of nursing-care classification system and, in Section 4 our proposed method are explained. Then, simulation results are shown in Section 5.

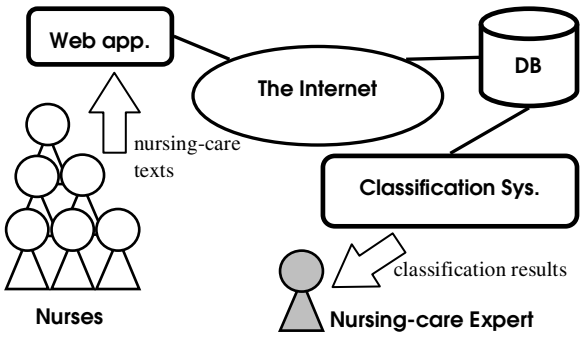

Fig. 1. Overview of our nursing-care data collection and classification

II. Nursing-care text

The nursing-care text data set consists of many freestyle Japanese texts. They are collected by using an Internet application and stored into our database. The overview of nursing-care data collection and classification is shown in Fig.1.

The nursing-care texts contain answers for a wide variety of questions from nurses about their subjects, technicality, etc. Some sample texts are shown in Fig.2. Usually long texts are good texts which explained good nursing-care. On the other hand, usually short texts are poor and lacking the appropriate technical information. Some nursing-care experts read those texts in detail, then evaluate the nursing practices of the nurses providing the information, and classify them into classes 1 (bad) to 4 (very good).

In our nursing-care text classification system, already classified nursing-care texts by experts are used as a training data set for a SVM. In preprocessing, a text set is converted from original texts to a "term-document matrix" by decomposing it into morphemes. We use "MeCab" as one of the morphological analysis software. All nouns and verbs (shown in shaded, see Fig.2) in decomposed morphemes are stored into a term list. We iterate the preprocessing until all texts are processed.

III. Nursing-care text classification system

A. Making feature vectors

A term list which stored terms collected in a certain year is represented by TL_{year}. For example, a term list of 2008 is TL_{08}. Each nursing-care text is converted into a feature vector by assigning '1' to that feature when a term in the nursing-care text existed in TL_{year}. Specifically, a nursing-care text is converted into a feature vector as the following manner.

Step 1 A nursing-care text is decomposed into morphemes.

Step 2 Nouns and verbs are selected from morphemes.

Step 3 If a selected term (i.e., a noun or verb) is appeared in the TL_{year}, then '1' is assigned to that feature. Otherwise '0' is assigned. That is, a feature vector is expressed as follows:

$$(x_1, \cdots, x_i, \cdots, x_{N_{TL_{year}}}), \tag{1}$$

$$x_i = \begin{cases} 1 & \text{if the term is appeared in } TL_{year}, \\ 0 & \text{otherwise,} \end{cases} \tag{2}$$

where $N_{TL_{year}}$ is the number of terms in the term list TL_{year}.

Step 4 Till all texts are converted, repeat Step 1 to 3.

A SVM based classification system is constructed by using the feature vectors as a training data set.

B. Discussion

In this subsection, we show some experimental results and problems for the unseen nursing-care text classification. The nursing-care classification system has been developed to classify the nursing-care text automatically. That is, in actual use, the classification system is constructed by using the last year's data set. The constructed classification system classifies the current year's data. We constructed the SVM based classification system by using 2008 nursing-care data (15 kinds of data sets). Table I shows the classification results when the 10-fold cross validation (10CV) was used on the training data set. We can see that we have good results even when the 10CV was used. This means that the SVM based classification system has good classification performance on the testing data set.

TABLE I
Classification results on the 2008 data (10CV)

Data Index	# of correctly classified patterns
P123	329/569 (57.8%)
P131	361/519 (69.6%)
P132	175/400 (43.8%)
P212	322/481 (66.9%)
P213	281/509 (55.2%)
P221	341/512 (66.6%)
P222	382/483 (79.1%)
P322	246/407 (60.4%)
P411	334/374 (89.3%)
P423	346/420 (82.4%)
P425	261/442 (59.0%)
P431	375/431 (87.0%)
P611	267/355 (75.2%)
P613	248/429 (57.8%)
P621	361/432 (83.6%)

TABLE II
Classification results on the 2009 data

Data Index	# of correctly classified patterns
P123	484/806 (60.0%)
P131	470/754 (62.3%)
P132	272/626 (43.5%)
P212	478/700 (68.3%)
P213	341/720 (47.4%)
P221	539/755 (71.4%)
P222	565/691 (81.8%)
P322	369/593 (62.2%)
P411	504/561 (89.8%)
P423	599/672 (89.1%)
P425	329/680 (48.4%)
P431	574/652 (88.0%)
P611	406/567 (71.6%)
P613	395/662 (59.7%)
P621	545/652 (83.6%)

On the other hand, Table II shows the classification results on the completely unseen data set (i.e., 2009 nursing-care data). From this table, we can see that there is classification performance deterioration on some data sets. Especially, P131, P213 and P425 have performance deterioration over 7%. We consider that this difference between the results on 2008 and 2009 data is caused by the following reasons.

1) There are some differences between TL_{08} and TL_{09}.
2) Expert's decision may be wavering every year.

Question P425
JPN: ＊＊さんの痛みの治療について医師にどのように働きかけていますか？＊＊さんにそのような状況がない場合は、違う事例や他の身体的苦痛に置き換えて考え、具体的にお答えください。
ENG: How did you work on the doctor about the medical treatment of your patient's pain? When your patient does not have such a situation, please transpose to different example and other physical pain, think, and answer concretely.

Class 4 (very good answers)
A1. JPN 牽引施行にて神経症状が悪化し疼痛も出現しているため、牽引の評価・中止を医師に提案・依頼。
ENG Since neurological symptoms got worse by traction enforcement and sharp pain has also appeared, I made a proposal and a request to my doctor, about evaluation and a stop of traction.
Morphological analysis 牽引/施行/にて/神経症/状/が/悪化/し/疼痛/も/出現/し/て/いる/ため/、/牽引/の/評価/・/中止/を/医師/に/提案/・/依頼/。
Feature vector JPN (牽引,施行,神経症,状,悪化,し,疼痛,出現,いる,評価,中止,医師,提案,依頼)
Feature vector ENG (Traction, enforcement, neurosis, state, getting worse, do, sharp pain, appear, is, evaluation, stop, doctor, proposal, request)

Class 3 (good answers)
A2. JPN: 現在の内服では疼痛は軽減しない。症状が憎悪しているのではないか。薬剤の増量か、薬剤の変更を医師に依頼する。
ENG: Sharp pain is not reduced in the present internal use. Is not the condition getting worse? I request my doctor to increase in quantity of a medicine or change a medicine.

Class 2 (almost good answers)
A3. JPN: 現在の鎮痛剤では、解熱せずに苦痛が軽減できていない。
ENG: In the present painkiller, fever is not alleviated and pain cannot be reduced.

Class 1 (bad answers)
A4. JPN: 今の鎮静剤でコントロールできているため医師に働きかけたことはない。
ENG: I have not worked on a doctor, since it is controllable with the present sedative.

A5. JPN: 特に行っていない。
ENG: I have not worked on a doctor.

Fig. 2. Examples of nursing-care texts and morphological analysis

TABLE III
DIFFERENCE BETWEEN TL_{08} AND TL_{09}

Data Index	# of terms appeared in both TL_{08} & TL_{09}	# of terms appeared in only TL_{09}
P131	489	405
P213	817	622
P425	583	599

We know the second reason is a very important problem which should be tackled. However let us assume that there is no wavering on expert's decision. In this paper, we consider only the first reason described above. We aim to reduce the differences between TL_{08} and TL_{09}, as much as possible.

Table III shows statistical information on the differences between TL_{08} and TL_{09} on P131, P213 and P425. From this table, we can see that almost 500 to 800 terms appeared in both TL. 400 to 600 terms appeared only in the TL_{09}. The features corresponding to these 400 to 600 terms in the 2009 nursing-care texts have no influence on classification, because such features were not used for training SVM based classification system.

Fig.3 shows classification results for the number of unknown terms which nursing-care texts contain. From this figure, it is shown that there is performance deterioration when the texts have two or more unknown terms. In Fig.3, classification performance of the case which has no unknown term is deteriorated from results of 10CV on the training data set. This means that the nursing-care text data set has some nature such as wavering on expert's decision.

IV. USING ADDITIONAL TERM INFORMATION FROM WEB

A simple technique is to use known terms in the term list which are most similar to the unknown terms. In order to consider that the unknown terms in the new data set (i.e., the evaluation data set which is different from the training data set) are approximately the same as the known terms, information from Web is used. We also have been considering using conceptual sets of terms. In this paper, we describe a technique of using information from Web.

A. Unknown terms

Here we define again the unknown terms as (3)-(5). The "unknown terms" are not stored terms in the term list.

$$KT_{last} = \{kt_i | kt_i \in TL_{last}, i = 1, 2, \cdots, N_{kt}\}, \quad (3)$$

$$UT_{current} = \{ut_j | ut_j \notin TL_{last}, ut_j \in TL_{current}, j = 1, 2, \cdots, N_{ut}\}, \quad (4)$$

$$TL_{current} = KT_{last} + UT_{current}, \quad (5)$$

where kt_i is a known term, ut_j is an unknown term, KT_{last} is a known term set at the last year, and $UT_{current}$ is an unknown term set at the current year.

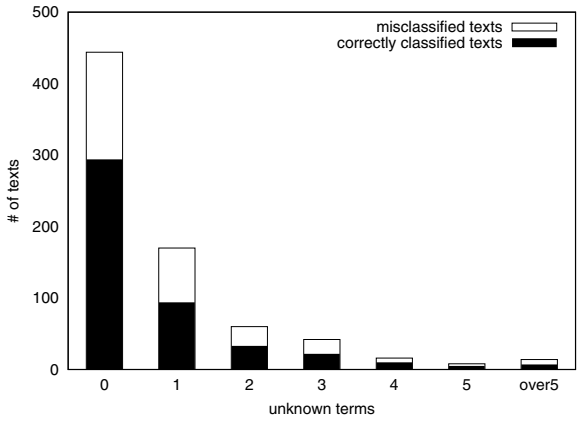

(a) P131

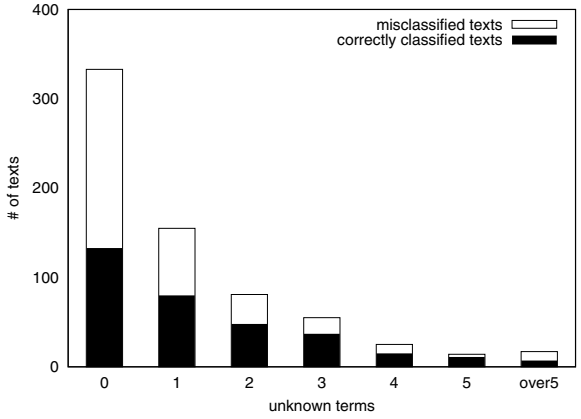

(b) P213

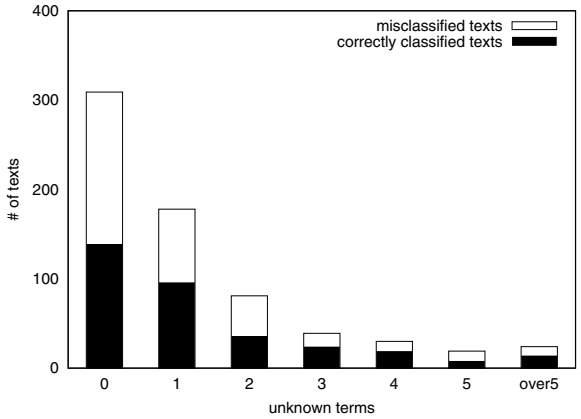

(c) P425

Fig. 3. Classification results for the number of unknown terms

B. Retrieving information from Web

When we use these unknown terms for classification the nursing-care texts, the information of similarity between unknown terms and known terms is needed. However, because there are only the nursing-care text sets of the last and current year, we have no additional information on the terms. In order to obtain information on the unknown terms, we try to retrieve information from the Internet. That is, each unknown term ut_j is used as a query to a search engine.

P best results (i.e., P pages of the search results) are used. The morphological analysis is applied to the texts in the <body> tag of the top P results. We extract nouns from the results of the morphological analysis. A set of nouns NS_{ut_j} for the unknown term ut_j is defined as,

$$NS_{ut_j} = \{noun_k | noun_k \in SR, k = 1, 2, \cdots, N_{\text{noun}}\}, \quad (6)$$

where SR is a noun set which is extracted from the set of search results. For selecting terms related to the unknown term ut_j, we consider the following three types of methods.

1) Frequency of terms: Then we count frequency of each noun in the search results. N_{FT} best nouns which are frequent terms are selected as the related terms.

$$FT_{ut_j} = \text{nbest}_n(\text{argmax}_{noun_k \in NS_{ut_j}} \ freq(noun_k)), \quad (7)$$

where $\text{nbest}_n()$ is a function which returns a subset of n-best solutions. In this paper, we use $n = 50$. On the known terms in the TL_{last}, we also apply the above mentioned procedure.

2) Weighted frequency by pages: When a $noun_k$ appeared several times in a single result, we consider the $noun_k$ is used in the specific situation. On the other hand, when a $noun_k$ appeared in some results, we consider the $noun_k$ has much relevance to the unknown term ut_j. (7) is modified by using the number of pages S in which the $noun_k$ appeared, as follows:

$$FT_{ut_j} = \text{nbest}_n(\text{argmax}_{noun_k \in NS_{ut_j}} \ freq(noun_k) \cdot S/N_{SP}), \quad (8)$$

where N_{SP} is the number of selected pages from search results. In this paper, we use $N_{SP} = 10$.

3) Weighted frequency by the distance: When a $noun_k$ appeared near the unknown term ut_j, we consider the $noun_k$ has some importance to represent the ut_j. Therefore, using the inverse of the distance between the ut_j and the $noun_k$, we modify (7) as follows:

$$dfreq(noun_k) = \sum_{p=1}^{P} \sum_{noun_k \in p} 1/D(ut_j, noun_k), \quad (9)$$

$$FT_{ut_j} = \text{nbest}_n(\text{argmax}_{noun_k \in NS_{ut_j}} \ dfreq(noun_k)), \quad (10)$$

where $D(ut_j, noun_k)$ is the distance between the ut_j and the $noun_k$, P is the number of pages of search results.

C. Selecting the similar term

Similarity between an unknown term and the known terms is measured using the cosine similarity $sim()$.

$$st_{ut_j} = \text{argmax}_{kt_l} \ sim(FT_{ut_j}, FT_{kt_l}). \quad (11)$$

A known term which has the highest similarity value to the unknown term is selected as the similar term of the unknown term.

TABLE IV
CLASSIFICATION RESULTS ON THE 2009 DATA BY USING PROPOSED THREE WEIGHTING SCHEMES

Data Index	Frequency	Weighted Frequency by pages	Weighted Frequency by the distance
P123	485/806 (60.2%)	484/806 (60.0%)	484/806 (60.0%)
P131	474/754 (62.9%)	483/754 (64.1%)	473/754 (62.7%)
P132	272/626 (43.5%)	268/626 (42.8%)	278/626 (44.4%)
P212	474/700 (67.7%)	478/700 (68.3%)	477/700 (68.1%)
P213	341/720 (47.4%)	348/720 (48.3%)	344/720 (47.8%)
P221	538/755 (71.3%)	539/755 (71.4%)	538/755 (71.3%)
P222	563/691 (81.5%)	564/691 (81.6%)	564/691 (81.6%)
P322	369/593 (62.2%)	373/593 (62.9%)	364/593 (61.4%)
P411	502/561 (89.5%)	503/561 (89.7%)	504/561 (89.8%)
P423	599/672 (89.1%)	599/672 (89.1%)	599/672 (89.1%)
P425	330/680 (48.5%)	332/680 (48.8%)	339/680 (49.9%)
P431	574/652 (88.0%)	574/652 (88.0%)	574/652 (88.0%)
P611	408/567 (72.0%)	408/567 (72.0%)	408/567 (72.0%)
P613	383/662 (57.9%)	384/662 (58.0%)	389/662 (58.8%)
P621	545/652 (83.6%)	545/652 (83.6%)	545/652 (83.6%)

V. EXPERIMENTAL RESULTS

In this section, computational experiments are described. 15 kinds of text sets collected in 2008 and 2009 were used for computer simulations. The 2008 nursing-care text sets were used for training. And the 2009 nursing-care text sets were used for testing. In the experiments, when a similar term selected by our proposed method has a similarity below the predefined arbitrary threshold value, we discarded it. It is because we consider that the terms with small similarity are not similar to the known terms.

Table IV shows the classification results on completely unseen data sets (i.e., 2009 nursing-care texts) when unknown terms are replaced by our proposed method. From experimental results, the classification performance was improved a little by our proposed method. Especially, the weighting schemes were effective over almost all data sets used in the experiments. However, since we have a slight performance improvement of classification, we have to advance our research.

VI. CONCLUSION

In this paper, to improve performance of the nursing-care text classification, a mechanism of retrieving terms from Web was proposed. The training data sets for constructing SVM based classification system are different from the evaluation data sets. That is, there are differences between the term lists of the nursing-care texts because the nursing-care texts are collected and evaluated every year. To cover the difference between the term lists of the nursing-care texts, a new term which appeared only in the evaluation data sets was used as a query of a search engine. The terms in the term list were also used as queries. Terms are represented by the search results from Web, and then are compared with each other. We used the most similar term in the term list as an alternative of the new term. From experimental results, the effectiveness of our proposed method was shown.

REFERENCES

[1] T. Sakaguchi, M. Nii, Y. Takahashi, A. Uchinuno, R. Sakashita, "Nursing-care Data Classification using Fuzzy Systems", Proc. of SCIS & ISIS 2006, Tokyo, Japan, pp. 2017–2022, 2006.

[2] M. Nii, Y. Takahashi, A. Uchinuno, R. Sakashita, "Nursing-care Data Classification Using Neural Networks", Proc. of 2007 IEEE ICME International Conference on Complex Medical Engineering, Beijing, China, pp. 431–436, 2007.

[3] M. Nii, S. Ando, Y. Takahashi, A. Uchinuno, R. Sakashita, "Nursing-care Freestyle Texts Classification using Support Vector Machines", 2007 IEEE International Conference on Granular Computing, CA, pp. 665–668, 2007.

[4] M. Nii, S. Ando, Y. Takahashi, A. Uchinuno, R. Sakashita, "Feature extraction from nursing-care texts for classification", Proc. of 6th International Forum on Multimedia and Image Processing, in CDROM (6pages), 2008.

[5] M. Nii, S. Ando, Y. Takahashi A. Uchinuno, and R. Sakashita, "GA based Feature Selection for Nursing-Care Freestyle Text Classification", Proc. of Joint 4th International Conference on Soft Computing and Intelligent Systems and 9th International Symposium on advanced Intelligent Systems, pp. 756–761, 2008.

[6] M. Nii, T. Yamaguchi, Y. Takahashi, R. Sakashita and A. Uchinuno, "Analysis of Nursing-care Freestyle Japanese Text Classification Using GA-based Term Selection", Proc. of World Automation Congress 2010, Kobe, Japan, IFMIP495 (CD-ROM, 6 pages), 2010.

[7] M. Nii, T. Yamaguchi, Y. Mori, Y. Takahashi, R. Sakashita, and A. Uchinuno, "Classification of Nursing-care Data using Additional Term Information", Proc. of SCIS & ISIS 2010, Okayama, Japan, pp. 1469–1474, 2010.

[8] M. Nii, T. Yamaguchi, Y. Takahashi, A. Uchinuno, R. Sakashita, "Improving Classification Performance of Nursing-Care Text Classification System by Using GA-based Term Selection", Journal of Advanced Computational Intelligence and Intelligent Information, Vol. 14, No. 2, pp. 142–149, 2010.

[9] MeCab, Yet Another Part-of-Speech and Morphological Analyzer, http://mecab.sourceforge.jp/.

2011 IEEE International Conference on Fuzzy Systems
June 27-30, 2011, Taipei, Taiwan

A Development of Navigation System for Mosaic Plasty using Electromagnetic Sensor

Takayasu Toyoshima, Kouki Nagamune
Graduate School of Engineering, University of Fukui
Fukui, Japan
toyoshima@me.his.u-fukui.ac.jp

Daisuke Araki, Tomoyuki Matsumoto, Seiji Kubo,
Takehiko Matsushita, Ryosuke Kuroda,
Masahiro Kurosaka
Graduate School of Medicine, Kobe University
Kobe, Japan

***Abstract*—Mosaic plasty is a surgery that transplant osteochondral grafts for osteochondritis dissecans. In mosaic plasty, cylindrical osteochondral grafts are harvested from normal area, and transplanted to injured area. The one of the most important thing of this surgery is that the graft should be perpendicular to the surface of the cartilage. The navigation system that aims improvement of precision is already studied, however cannot be applied to use an endoscope. In addition, it is a problem to have bad precision of the transplant in the freehand. Therefore, we thought that the system would widely used if we develop the mosaic plasty navigation system under an endoscope. This study proposes a navigation system to determine a proper position and pose for harvesting. In the experiments, a femoral imitation bone is used as a profile of the femoral joint surface. The experiment consists of the following three procedures: Trace and display of the femoral joint surface profile and a harvester. Display of a normal vector for the femoral joint surface. Measurement of the deviation of the normal vector. In the results, the developed system could display the femoral joint surface and the normal vector for the femoral joint surface virtually. Also, the deviation of the normal vector was an average of 7.27 degrees. As future works, there are to decrease the deviation of the normal vector by improving the precision to acquire the femoral joint surface profile, and to visualize the normal vector for the generated surface.**

Keywords-component; mosaic plasty; electromagnetic sensor; 3D image processing; navigation system

I. INTRODUCTION

One of the treatment of the cartilage damages of the knee is mosaic plasty. The self cartilage transplantation method such as mosaic plasty requires precision in 3D. The navigation system that aims improvement of precision is already studied, however cannot be applied to use an endoscope. In addition, it is a problem to have bad precision of the transplant in the freehand. Therefore, we thought that the system would widely used if we develop the mosaic plasty navigation system under an endoscope. We propose a system to navigate a perpendicular transplantation with a three-dimensional electromagnetic sensor under an endoscope. The system requires to navigate with precision same as freehand. The matter evaluated with precision is the angle which a normal for the joint surface and the axis of articular cartilage which is harvested and a transplanted. In the precedent study, freehand was 10.7 degrees[1].

A. ARTICULAR CARTILAGE

The articular cartilage is covering joint surfaces, and has a role to smooth the joint move. When this articular cartilage suffers the damage, a pain occurs to the joint. For a cure for articular cartilage, drillings for the subchondral bone had been performed in 1957 by Pridie. However, that drilling restores not the hyaline cartilage but the fibro cartilage. Then, Matsue et al. [2] and Brittberg et al. [3] reported a reproduction of the articular cartilage with the hyaline cartilage.

B. MOSAIC PLASTY

A method of transplantation grafts to the femoral condyles in autologous osteochondral transplantation is named as "mosaic plasty" by Dr. Hangony, and an original surgical instrument was developed and spread out rapidly[4]. It is a transplantation surgery that a graft is harvested from a non-load part of the bone surface, and inserted to the cartilage defect as shown in Fig. 1.

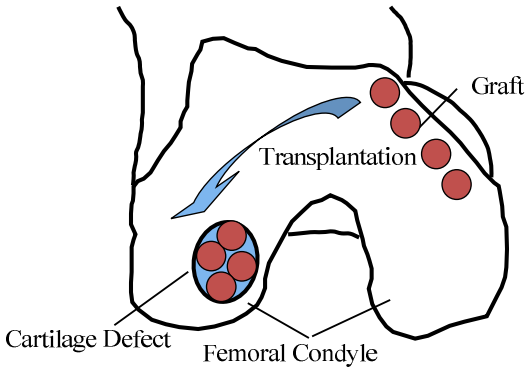

Figure 1. MOSAIC PLASTY

978-1-4244-7316-8/11/$26.00 ©2011 IEEE

C. SURGERY PROCEDURE

For the procedure of this surgery, It consist of the four following procedures as shown in Fig. 2.

- Loose body of the cartilage defect is removed.
- The place of the cartilage defect is drilled to making a hole.
- A cartilage graft is harvested with a harvester.
- The harvested graft is inserted to the defect.

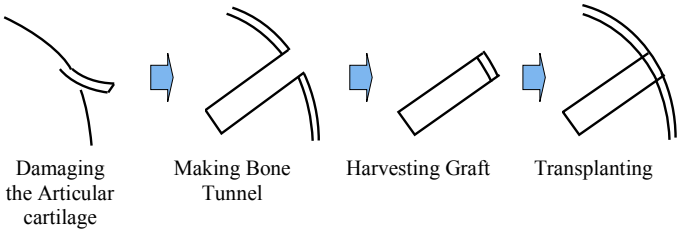

Figure 2. Surgery Procedure

D. THE PROBLEMS OF THE SURGERY

When a discontinuous surface is made after transplantation, there is a problem that it is easy to separate an articular cartilage from the bone surface. With a movement of the knee joint. It results in regenerating the cartilage defect. Therefore, it is important to harvest and transplant the cartilage graft vertically to the joint surface, so that the surface should be continuously.

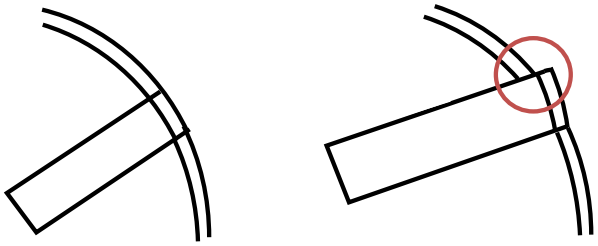

Figure 3. A proper and improper example of the transplant

II. MATERIALS AND METHODS

A. Electromagnetic Sensor

In this study, we perform the three-dimensional position and pose that we used electromagnetic sensor (Polhemus Inc., PATRIOT) as shown in Fig. 4 [5]. An electromagnetic sensor enables us to acquire data without being influenced by a physical obstacle. It is six degree of freedom measurements device consists of one transmitter, two receivers and a control unit. The precision of this device is 1.52 mm about the position 0.4 degree about the pose. This precision is guaranteed in 30 inches between a transmitter and receiver.

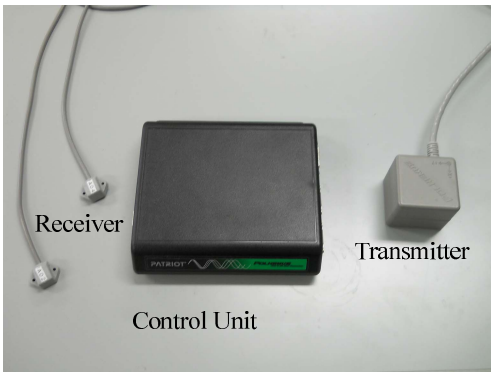

Figure 4. Electromagnetic sensor (PATRIOT)

B. Proposal Method

In this study, we use an electromagnetic sensor and propose a method to navigate the harvester which is perpendicular to the knee joint surface. The proposal method consists of three steps. The steps are A) Acquisition of the joint surface profile, B) Display of the joint surface profile and the harvester. C) Navigation of harvester.

1) Acquisition of the joint surface profile

A tracer whose tip has a force sensor is used to acquire a profit of the femoral joint surface. The receiver is attached to the tracer to obtain three-dimensional information. The joint surface is obtained by tracing the profile of the joint surface as shown in Fig. 5.

Here, to obtain information of the tip of the tracer , it is necessary to calibrate the position and pose of the sensor. Information of L_1 and L_2, that is relative position from the sensor to the tip of the tracer is known beforehand as shown in Fig. 6. In addition, Fig. 7 shows a relationship between the center of the sensor and the tip of the tracer which is determined by pose parameters of Ψ, Θ, and Φ. And positional informations of the sensor in it self are x, y, z.

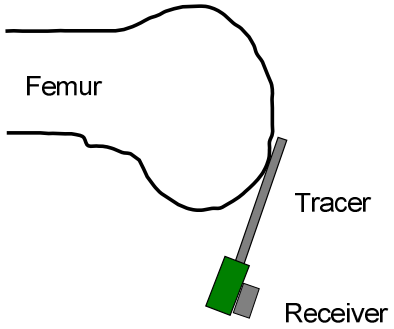

Figure 5. Tracer

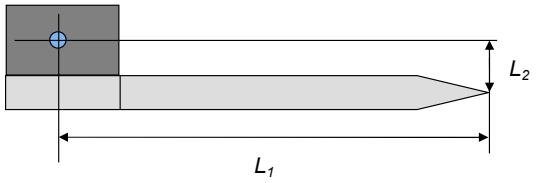

Figure 6. The distance between center of the sensor to the tip of the tracer

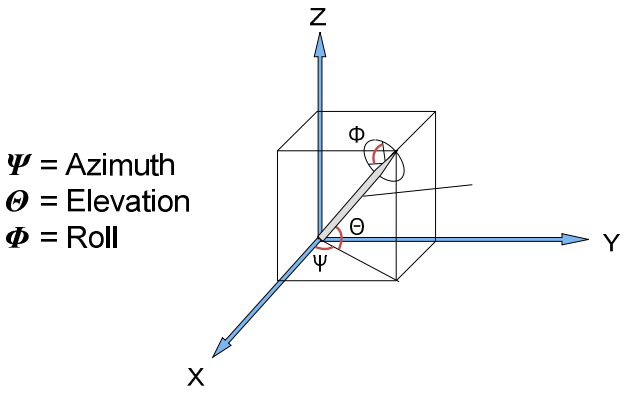

Figure 7. The pose between the center of the sensor to the tip of the tracer

The calibration is performed with the following equation,

$$x = L_1 \cos\psi\cos\theta + L_2(\sin\psi\sin\phi + \cos\phi\sin\theta\cos\phi)$$

$$y = L_1 \sin\psi\cos\theta + L_2(-\cos\psi\sin\phi + \sin\phi\sin\theta\cos\phi)$$

$$z = -L_1 \sin\theta + L_2 \cos\theta\cos\psi$$

2) Display of joint surface profile and harvester

The electromagnetic sensor is attached to the harvester which is a surgical instrument during the graft harvesting. The profile of the acquired femoral joint surface and the developed harvester are virtually visualized in a three-dimensional space on the computer.

a) Creation of virtual a joint surface profile

The information acquired using the tracer is displayed as points.Therefore a joint surface profile should be virtually created from the points.The reasons to create surface are the following things. It is easy to understand the femur profile rather than points. It shows a proper position and pose which is perpendicular to the knee joint surface. In this study, the marching cube method[6] was used to create the joint surface from the points. In the method, a data set should be three-dimensional volume data. Therefore, the collected points are approximated to the nearest points as vertexes of cube lattice of a size set beforehand as shown in Fig. 8. Vertexes *i*, *j*, *k* are set on axes *x*, *y*, *z* respectively. When a point is less than the midpoint of a distance between two vertexes, the point is set to be *i*, *j*, or *k*. In otherwise, the point is set to be *i*+1, *j*+1 or *k*+1 as shown in Fig. 9. In that process, when a point exists, it is set to be one. When no point exists, it is set to be zero. This time, to be used Marching cube method[6] as a way to create surface from point.

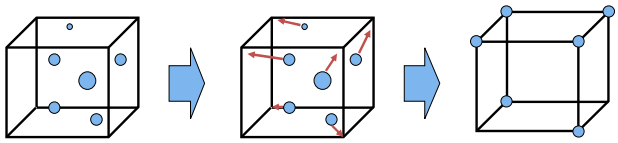

Figure 8. Similar to the vertex of the cube lattice

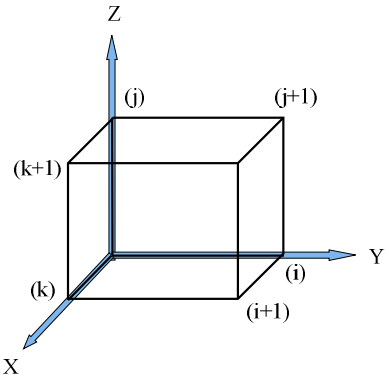

Figure 9. Approximate method to the vertex of the cube lattice

3) Navigation of harvester

The computer navigates a surgeon to hold the harvester at a proper position and pose in real-time the harvester is perpendicular to the bone surface as shown in Fig. 10.

The algorithm to display the normal vector devises the following. On real femoral joint surface, pointing the place that wants to let you display the normal vector in harvester. Existing points on a spherical surface of a radius of 10 mm around the tip of the tracer are selected as shown in Fig. 11 and Fig. 12. A spherical surface is shown as a brown line. Then points on the surface are shown as red points. Next, three points are extracted from the red points so that the three points close to be a equilateral triangle as shown in Fig. 13. Last, a normal vector could be calculated from the extracted three points, and the normal vector and the femoral joint surface are displayed simultaneously.

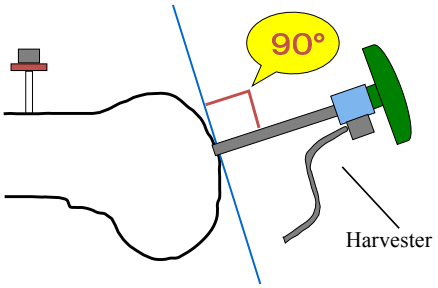

Figure 10. Navigation of harvester

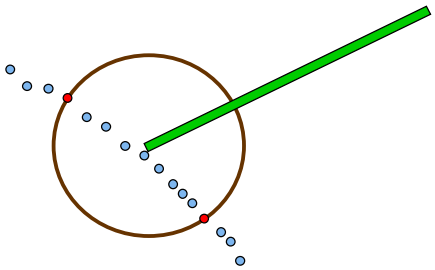

Figure 11. Normal vector indication algorithm (lateral viewpoint)

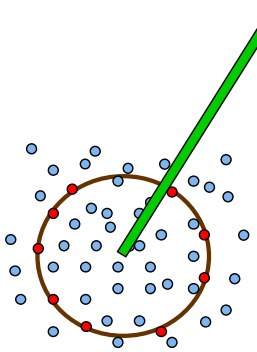

Figure 12. Normal vector indication algorithm (anterioris viewpoint)

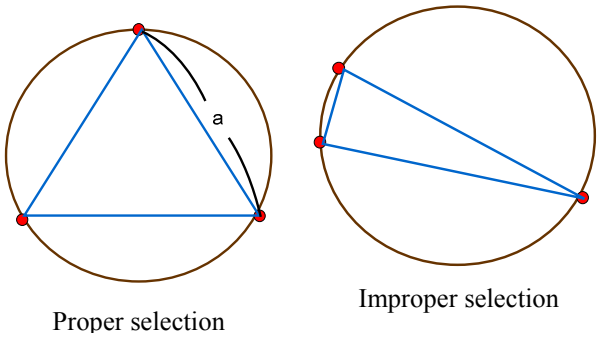

Figure 13. Three points of how to get to choose among the point

C. EXPERIMENTS

1) Display of the joint surface profile

In this experiment, the femoral sawbone is used as the shape of joint surface as shown in Fig. 14. As position and pose information is also required for sawbone, the titanium pins are inserted to the femoral sawbone approximately 80 mm in the proximal from the knee joint line, then the sensor is fixed to the pins with an attachment. Actual measurement scene is shown in Fig. 15.

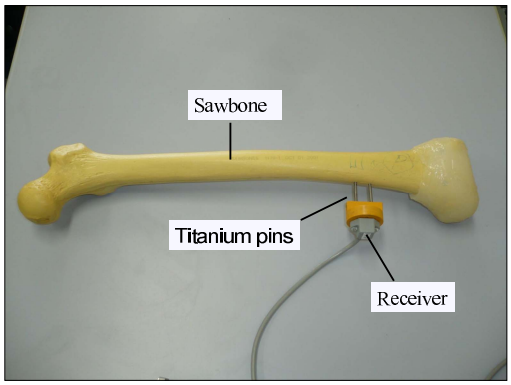

Figure 14. Femoral sawbone

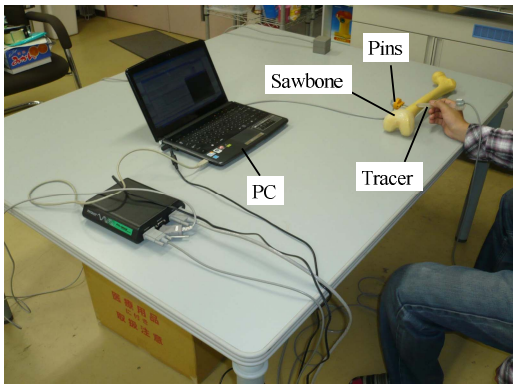

Figure 15. Measurement scene

2) Display of the normal vector for the knee surface

A place where the tip of the tracer is indicated is calculated on the computer. A normal vector which is located at the calculated position, and is perpendicular to the bone surface is analysed. The normal vector is displayed on the three-dimensional space as shown in Fig.16.

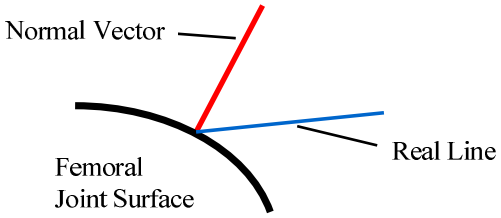

Figure 16. Normal vector

3) Measurement of deviation of the normal vector

In this experiment, we measure deviation of the normal vector. The deviation is calculated as the maximum angle between two poses of the normal vector when we keep pointing for 5 seconds to arbitrary point on the joint surface in same pose as shown in Fig. 17. The number of the measurement places is ten points at arbitrary position on the joint surface in same pose. To investigate the cause of the normal vector swing, we examine the position error of the tip of the tracer at the same time.

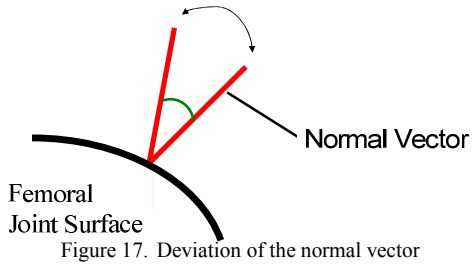

Figure 17. Deviation of the normal vector

III. RESULTS

A. Display of the joint surface profile

The obtained profile of joint surface is shown in Fig. 18. The figure is a result in the viewpoint from the frontal of the femur. Virtual display was realized by the proposal method.

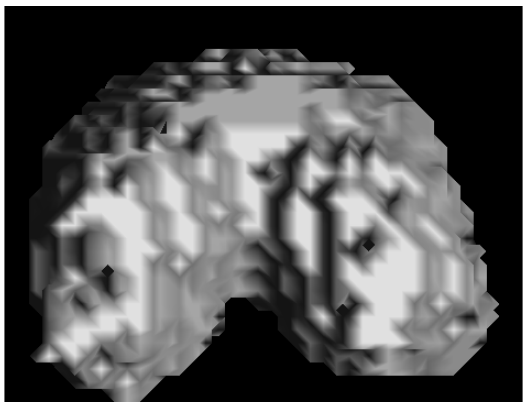

Figure 18. The acquisition of the joint surface profile

B. Display of the normal vector for the knee surface

A result of display of the normal vector is shown in Fig. 19. The figure is a viewpoint from the outside of the femur. In this figure, two lines show the normal vector for the joint surface and the real harvester. The harvester could be navigated as perpendicular to the bone surface by adjusting the pose of the harvester so that they overlap these two lines as shown in Fig. 20.

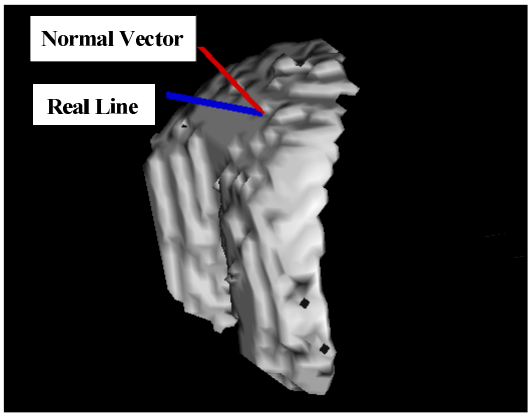

Figure 19. Display of the normal vector and the harvester

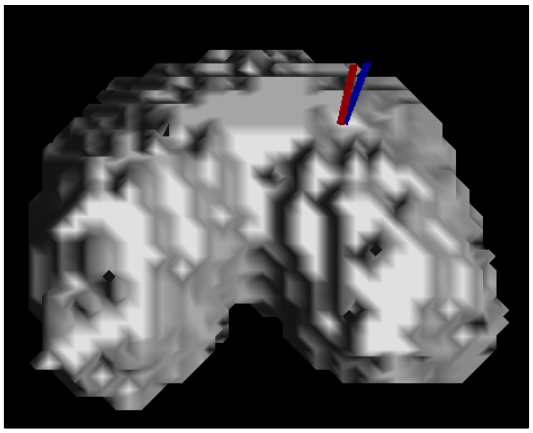

Figure 20. An example of overlap

C. Measurement of deviation of the normal vector

The result of deviation measurement of the normal vector is shown in TABLE I. From the results, the average of pose deviation of the normal vector was 7.27 degrees. The standard deviation was 3.29 degrees. The average of the position error was 0.0031 mm, the standard error was 0.001 mm. From the above, they have no association to deviation measurement of the normal vector and measurement of the position error.

TABLE I. MEASUREMENT OF THE POSITION ERROR AND MEASUREMENT POSE DEVIATION OF THE NORMAL VECTOR.

Place	*Position (mm)*	*Pose (degree)*
1	**0.00305**	**1.7819**
2	**0.00247**	**8.269**
3	**0.00352**	**12.9373**
4	**0.00531**	**10.8232**
5	**0.00236**	**6.0446**
6	**0.00328**	**4.4925**
7	**0.00234**	**4.7907**
8	**0.00211**	**6.1175**
9	**0.00216**	**9.38**
10	**0.00425**	**8.0687**
mean	**0.0031**	**7.27**

IV. DISCUSSION

Firstly, we developed the mosaic plasty navigation. In the experiment, we installed a sensor to a tracer and a femoral sawbone. We were able to display the normal vector in this time, it was developed that there was some deviation on the normal vector. It might be influence of the position error to make a deviation. However it is difficult to be decrease the error of the position, because the current value 0.0031 mm is too small to improve. However, the pose error is too large, then it showed be improved before applying a clinical situation.

In this study, the problem of this proposal method is that the extracted three points are affected by the position error of a sensor. To solve this problem, we should examine the changing algorithm to calculate a normal vector. One of the solution is to calculate the normal vector from the surface of the profile. By doing so, we reduce the deviation of the position and pose error.

V. CONCLUSION

In this study, we developed the mosaic plasty navigation system that we used an electromagnetic sensor. We traced the femoral sawbone and tried the acquisition of the femoral joint surface and the display of the normal vector. As a result, we were able to display the femoral sawbone joint surface and the normal vector, and the deviation of the normal vector was an average of 7.27 degrees.

Future works are to depress the deviation of the normal vector, to enable automatic acquisition of the femoral joint surface by the tracer with a force sensor, and to improve the position and pose precisions of the system.

REFERENCES

[1] Drimitrios K., et al., "Comparative Study of Navigation Versus Freehand Osteochondral Graft Transplantation of the Knee," Am. J. Sports Med., vol. 37, no. 4, pp.803-807, Feb., 2009.

[2] Matusue Y, et al., "Arthroscopic multiple osteochondral transplantation to the chondral defect in the knee associated with anterior cruciate ligament disruption," Arthroscopy, vol. 9, pp.318-321, 1993.

[3] Brittberg M, et al., "Treatment of deep cartilage defect in the knee with autologous chondrocyte transplantation," N. Eng. J. Med, vol. 331, pp.889-895, 1994.

[4] Hangony L, et al., "Osteochondral plugs: Autogenous osteochondral mosaicplasty for the treatment of focal chondral and osteochondral articular defects," Op. Tech. In Orthopaedics, vol. 7, pp.312-322, 1997.

[5] PATRIOT 6 Degree-Of-Freedom tracking system
-http://www.polhemus.com/?page=Motion_Patriot

[6] William E. Lorensen, Harvey E. Chine, "Marching Cubes:A High Resolution 3D Surface Construction Algorithm," Computer Graphics, vol. 21, no. 4, 1987.

2011 IEEE International Conference on Fuzzy Systems
June 27-30, 2011, Taipei, Taiwan

A Quantitative Measurement System of Endpoint during Lachman test with Force Sensor

Shogo Kawaguchi, Kouki Nagamune
Graduate School of Engineering, University of Fukui
Fukui, Japan
kawaguchi@me.his.u-fukui.ac.jp

Daisuke Araki, Tomoyuki Matsumoto, Seiji Kubo,
Takehiko Matsushita, Ryosuke Kuroda,
Masahiro Kurosaka
Graduate School of Medicine, Kobe University
Kobe, Japan

***Abstract*—Lachman test is one of manual tests for examining the anterior cruciate ligament (ACL). An examiner discreminates an injured degree of the ACL by feeling finger stress. Some measurement devices for Lachman test have been developed. However, these devices aim to analyze not the stress but a motion of the knee joint. Therefore, we set the goal of this study to develop a measurement system for the finger stress with force sensor during Lachman test. In the experiment, the developed system was applied to twelve healthy knees of six subjects by a beginner, and one injured and one healthy knee of two subjects by an expert. In the results, the maximum force of "endpoint" during Lachman test was analyzed. The variation of inter-subjects was larger than intra-subjects. Future works are to improve the finger force sensors, and to apply more subjects, so that the system could classify an examiner into a skill level.**

Keywords-Lachman test, Force Sensor, Anterior Cruciate Ligament, Manual test

I. INTRODUCTION

Lachman test is a manual test used for examining the Anterior Cruciate Ligament (ACL) of the knee for patients where there is a suspicion of a torn ACL. The Lachman test is recognized by most authorities as the most reliable and sensitive clinical test for the determination of ACL integrity, superior to the Anterior Drawer test commonly used in the past. To do this, lay the patient supine on an examination table. Put the patient's knee in about 20-30 degrees flexion, also according to Bates' Guide to Physical Examination the leg should be externally rotated [1]. The examiner should place one hand behind the tibia and the other on the patient's thigh. It is important that the examiner's thumb be on the tibial tuberosity. On pulling anteriorly on the tibia, an intact ACL should prevent forward translational movement of the tibia on the femur ("firm endpoint") as shown in Fig. 1. Anterior translation of the tibia associated with a soft or a mushy endpoint indicates a positive test. More than about 2 mm of anterior translation compared to the uninvolved knee suggests a torn ACL ("soft endpoint"), as does 10 mm of total anterior translation. An instrument called a "KT-1000" can be used to determine the magnitude of movement in mm [2-4]. "KT-1000" was not to be used as a device to measure the injured ACL [5]. This test can be done in an on the field evaluation in an acute injury setting, or in a clinical setting when a patient presents with knee pain. In either situation, ruling out fracture is important in the evaluation process. Also when evaluating the integrity of the ACL, it is important to test the integrity of the Medial Collateral Ligament (MCL), because this is a common ligament torn in an ACL injury as well. Some studies have reported the stress during Lachman test [6], however, they could not obtain the force data dynamically.

In previous studies, quantitative measurement of Pivot Shift test by three-dimensional electromagnetic sensors have been made [7, 8]. A quantitative force measurement of fingers of examiner during Lachman test has not been developed. This study set the goal to develop a quantitative measurement system of Lachman test with force sensors. The system could enable us to analyze a mechanism of the "endpoint" that indicates an injured degree of the ACL. This study explains mainly the principle of the measurement system. In the experiment, the developed system was applied to twelve healthy knees of six subjects. In the results, the maximum force of "endpoint" during Lachman test was analyzed. The variation of inter-subjects was larger than intra-subjects.

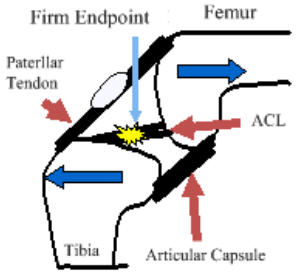

(a) Firm Endpoint

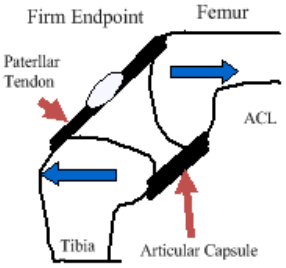

(b) Soft Endpoint

Figure 1. Endpoint

II. METHOD

A. Force Sensor

A force sensor is made by using conductive rubber (sili-us Fuso Gomu Co. Ltd.). Thickness of this rubber is 0.05mm. The rubber is cut as dimensions of 6.0 (mm) x 7.0 (mm) x 0.05 (mm). Then, a set of pattern for the sensor is made by using an extension board (ICB-075 san-hayato Co. Ltd.) which has cupper foils over the entire surface. This process is made use of thermal transfer printing method.

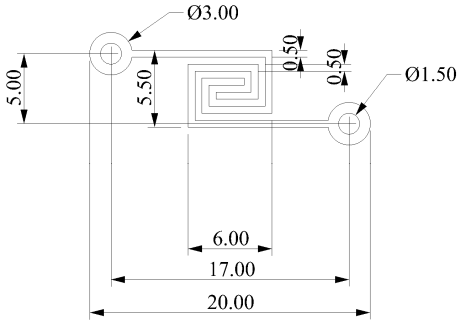

Figure 2. Design

Next, the rubber and copper foils are fixed by a laminating machine (LPD3213, Fujipura Co. Ltd.). Then, a profile of this sensor is modified as a bending shape by using a thermal heating device (EH-NW80-K, Panasonic Co. Ltd.) as shown in Fig. 3.

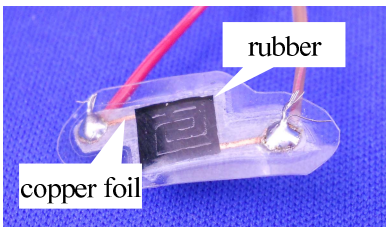

Figure 3. Real Sensor

A finger brace (Sawamura prosthetics and orthotics service Co. Ltd.) is used for fixing the force sensors to fingers. Then, the force sensor is pasted double-sided tape (NW-10S, Nichiban Co. Ltd.) on the surface of the board. Two sensors are attached to one finger brace. The finger brace is molded by using thermoplastic (JJ-210, Daicel Finechem Co. Ltd.). In this study, the attached sensor is called as "Finger Force Sensor" as shown in Fig. 4.

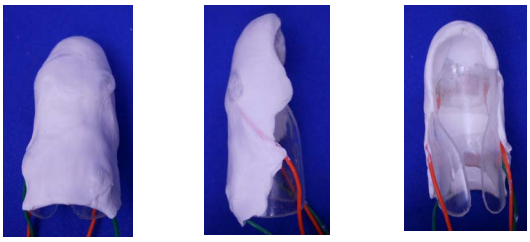

(a) Front (b) Left (c) Rear

Figure 4. Finger Force Sensor

This measurement system has ten finger force sensors. All the finger force sensors are attached to all fingers tightly. The channels number of thumb of right hand are Ch 0 and Ch 1. A channel number is allocated to sensors of right hand from thumb in order. The sensors of the little finger of the left hand are numbered as Ch 10 and Ch 11. Next channels are allocated to left thumb in order as shown in Fig. 5.

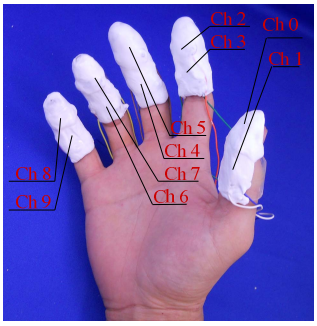

(a) Right hand

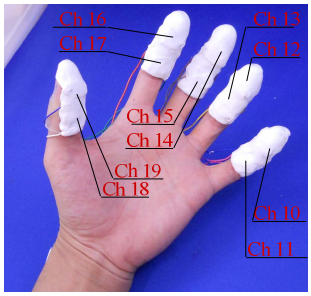

(b) Left hand

Figure 5. Finger Force Sensors

B. Measurement Circuit

1) Two Gauges Method

Sensor making use of a variable resistance as this force sensor is energy control type. Sensor of energy control type is easily affected by temperature. In this study, for guarantee of temperature two gauges method was used. This method used two sensors for one measurement as shown in Fig. 6. One of the sensors was for measurement, the another one was dummy. A measurement system measures a difference of a

measurement sensor and a dummy sensor. The measurement sensor and the dummy sensor are placed as same temperature, so that influence of temperature is same as both sensors. Thus, this system could measure without influence of any temperature.

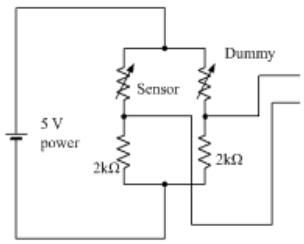

Figure 6. Two Gauges Method

2) Differential Amplifier Circuit

A differential value of the measurement sensor and the dummy sensor is small. A change of the differential value is more small. It is difficult to measure the real value due to a noise. Therefore, the differential value should be amplified. This measurement circuit has a differential amplifier circuits used by an operational amplifier (Fig. 7).

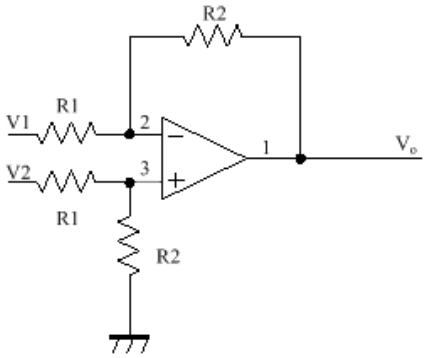

Figure 7. Differential Amplifier

The output value of this differential amplifier is

$$V_o = \frac{R_2}{R_1}(V_2 - V_1). \quad (1)$$

In this measurement circuit,

$$R_1 = 1.0 \times 10^3. \quad (2)$$

The R_2 is a variable resistance. A resistance of sensors is deviated for each sensors. Then, the resistance is adjusted so that the deviation should be controlled. In this study, a deviation of differential voltage is controled by using a factor R_2 which is a variable resistance. However, two resistances of R_2 are necessary for one measurement sensor. To control for two normal variable resistances is difficult, because values of two variable resistances must be same. In this study, control of deviation of differential voltage is used double volume resistance (RV16A01F-10-20S-B100KΩ, Aicoh electronics Co. Ltd.) as shown in Fig. 8.

Figure 8. Double Volume Resistance

C. Measurement System

A measurement system consists of a personal computer, an analog / digital (AD) converter, and finger force sensors. The A/D converter is AIO-16320FX-USB (CONTEC Co. Ltd.)(Fig. 9). This converter could connect by using USB. The data sampling is 1 [kHz]. The input range is from -10 to 10 V. The resolution is 16 bits (Table I).

Figure 9. A/D converter

TABLE I. SPECIFICATION OF A/D CONVERTER

Communication Bus	USB
Faculty	Input , output
Input ch num	Single end 32 ch（differential 16 ch）
Input range	±10 V， ±5 V， ±2.5 V， 0～10 V， 0～5 V， 0～2.5 V
Output ch num	2 ch
Output range	±10 V， ±5 V， ±2.5 V， ±1.25 V， 0～10 V， 0～5 V， 0～2.5 V
resolution	16 bit
A/D convert speed	2 μsec/ch(max.)
D/A convert speed	10 μsec(max.)

This measurement circuit is in aluminium case. In this circuit, there are a power supply, a circuit of power supply, a circuit for sensors, a circuit for differential amplifier (for right hand) and a circuit for differential amplifier (for left hand) as shown in Fig. 10. In this circuit of power supply, there are 5 [V] power supply for sensor and -15 [V] and 15 [V] power supply for operational amplifier. First, an analog amplified signal is converted to a digital signal by the A/D converter, the

digital signal is sent to personal computer by the universal serial bus. Finally, the voltage data is converted to load data by a program.

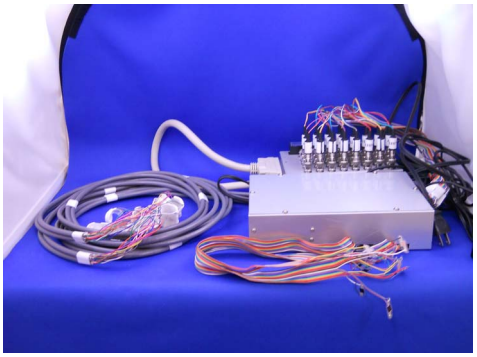

Figure 10. Measurement System

III. EXPERIMENT

A. Calibration Experiment

This system should calibrate before measuring the load data. A mechanical testing device is developed by using an electroactuation (PWA II Cyllinder, Orientalmotor Co., Ltd.), a load cell (Thin type load cell (multi-force sensor), Kyowa Electronic Instruments Co., Ltd) as shown in Fig. 11. Specification of the electroactuation is tabulated in Table II.

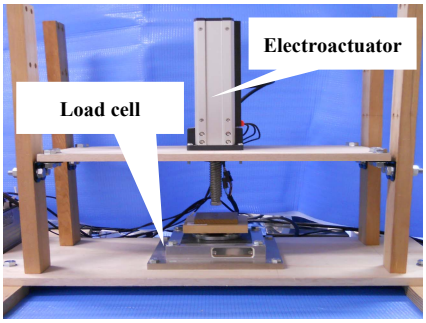

Figure 11. Mechanical testing Device

TABLE II. SPECIFICATION OF ELECTROACTUATION

Stroke (mm)	Maximum Load (N)	Resolution (mm)
100	1000	0.01

Calibration is performed for the force sensors beforehand (Fig. 12.) A plastic lump is inserted to each finger force sensor as shown in Fig. 12. Because the finger brace will be bent so that the calibration value is not measured well, if the calibration is performed without the plastic lump. These finger force sensors are calibrated at loads of 20 N, 40 N, 60N, 80 N, 100 N, 120 N, 140 N, 160 N, 180 N and 200 N. The load is vertically applied for surface of the finger force sensor. The tip of the stick of this electroactuator set to be placed the center of the conductive rubber of the sensor. On characteristic of the conductive rubber, the voltage values are measured at a few seconds later when the load had be steady condition. In this experiment, steady values are used for the calibration data .

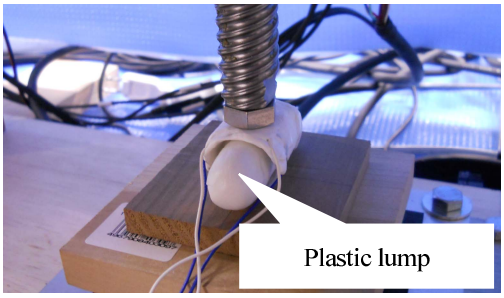

Figure 12. Calibration Scene

B. Manual test Experiment

1) Measurement by a beginner

Twelve knees joint of a subject (Table III) are observed by using the developed system. #2 and #6 in subjects had a injured knee except for the ACL. Lachman test is applied for the knee five times as usual manner. This Lachman test is expected as the finger of the right second finger, the right third finger and the left thumb are loaded. Other fingers are supported. Then, force distribution of the finger force sensors are analyzed when the maximum and minimum forces are detected. Data of 5 times of Lachman test in right and left knees of one subject are evaluated at student t-test (significance,$P \leq 0.01$).

Figure 13. Manual test Scene

TABLE III. SUBJECT INFORMATION BY A BEGINNER

Num	Sex	Height [cm]	Weight [kg]	Knee	Condition	History
#1	Male	174	66	Left	Intact	No
				Right	Intact	No
#2	Male	175	73	Left	Intact	Yes
				Right	Intact	No
#3	Male	170	78	Left	Intact	No
				Right	Intact	No
#4	Male	175	63	Left	Intact	No
				Right	Intact	No
#5	Male	163	70	Left	Intact	No
				Right	Intact	No
#6	Male	167	66	Left	Intact	Yes
				Right	Intact	No

2) Measurement by an expert

Two knees joint of a subject (TABLE IV) were observed by using the developed system. This measurement was observed by an expert who was an orthopedic surgeon in familier with Lachman test. One knee of observed knees was the injured ACL. These observed data were compared.

TABLE IV. SUBJECT INFORMATION BY A EXPERT

Num	Sex	Height [cm]	Weight [kg]	Knee	Condition	History
#1	Female			Right	Injured	No
#2	Male	168	70	Right	Intact	No

IV. RESULTS

A. Calibration Experiment

In this measurement circuit, the voltage is increased with loading, because the relationship of the voltage and the resistance has an inverse proportion. In Fig. 14, all the sensor show the relationship of the voltage and the load. This result is used for calculation of the force applied to the finger force sensors in the following experiment.

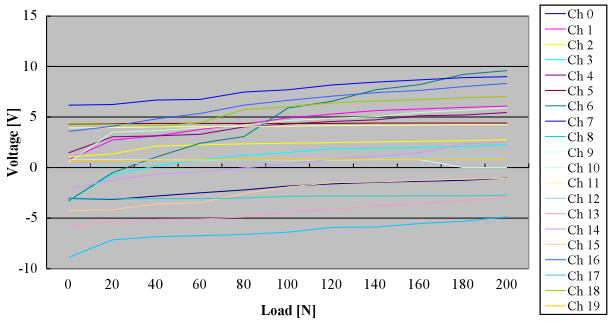

Figure 14. Result of Calibration

B. Manual test Experiment

1) Measurement of the beginner

A force changes of time course measured in the experiment is shown in Fig. 15. In this figure, only specific Chs are shown so that it is easy to understand the change. This change is dipicted as one time anterior motion of the knee. In the end period, comparatively higher force was observed. It is considered as "endpoint." The maximum force is analyzed among each trial. In the Lachman test, five endpoints were observed in one trial, because five anterior drawer motions were performed in one trial.

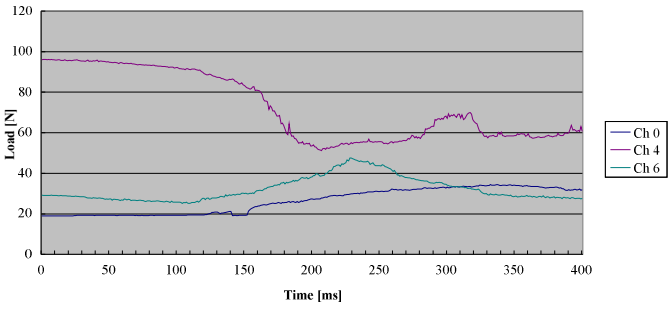

Figure 15. Result of Lachman test

The maximum forces of endpoints are shown in Fig. 16. In this figure, average and standard deviation are calculated in one trial. Then, the last column means averages of five trials. In this figure, The variation of inter-subjects was larger than intra-subjects. In the result of t-test, both knees of #2 and #6 had significant differences.

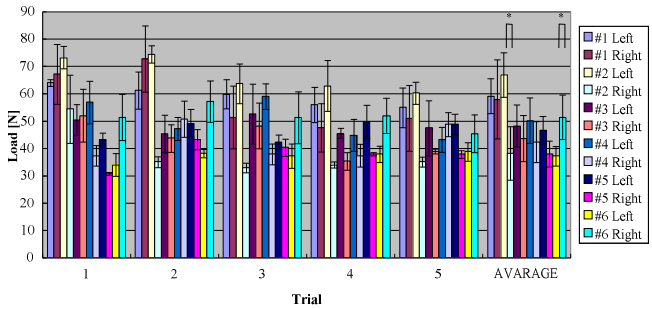

Figure 16. Result of Measured Force during Lachman test

2) Measurement of an expert

Two force changes of time course measured in the experiment are shown in Fig. 17 and Fig. 18. In this Fig.s, distinctive Chs (Ch4 and Ch5 are channels of the second finger of right hand, Ch 18 and Ch 19 are channels of the thumb of left hand) are picked up. In Fig. 17, the result of firm endpoint is shown. In this Fig., peak of Ch 5 is about 145[N]. In Fig. 18, the result of soft endpoint is shown. In this Fig., peak of Ch 5 is about 70[N]. During Lachman test, even if the ACL is injured or intact, a characteristic of left hand motion should be almost same. In fact, Ch 18 and Ch 19 of both of Fig. 17 and Fig. 18 are almost same. Thus, the result of Fig. 18 is regerded as a result of Soft endpoint.

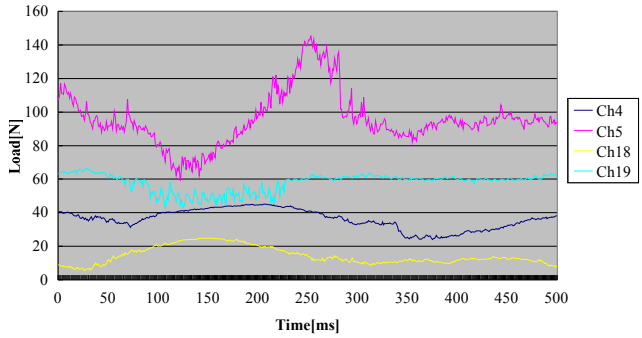

Figure 17. Result of Firm Endpoint

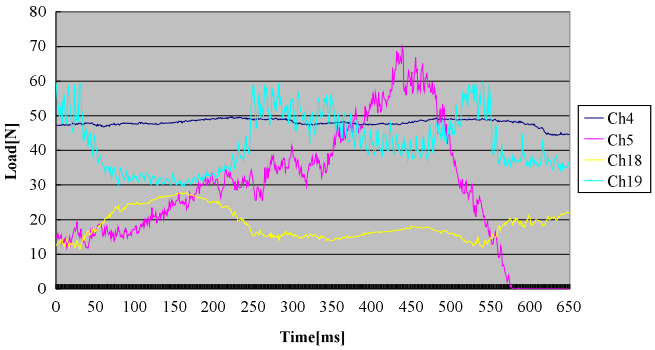

Figure 18. Result of Soft Endpoint

V. DISCUSSION

In the result of measured force during Lachman test by the beginner, both knees of #2 and #6 had significant differences. The difference was related to the injured knee except for the ACL. Both the injured knees of #2 and #6 were left knee. However the distinctive differential values were observed in in these knees. We thought a value of the injured knee was lower than the normal knee. The value of the injured knee of #6 was lower than the another knee. However #2 and #6 have a different tendency. In case of #2, subject was thought that he made his injured knee strong tension during Lachman test due to fear for the movement.

In the result of measured force during Lachman test by the expert, the difference was shown in the knee of the ACL injured knee. Because a knee in comparison with a injured knee was a normal knee of another person, a difference was seen in results. However although both of Ch 18 and Ch 19 were almost same, the largest load of Ch 5 became that the normal knee indicated twice loading of the injured knee. The difference was considered to be the difference of "soft endpoint" and "firm endpoint."

VI. CONCLUSION

This study aimed to develop a quantitative measurement system of endpoint during Lachman test using force sensor. The finger force sensor was made by attaching force sensors to finger braces. In the experiments, the developed system was applied to twelve healthy knees of six subjects. Forces of endpoints during Lachman test were analyzed. The variation of inter-subjects was larger than intra-subjects. Usually, the ACL injured knee had soft endpoint. In this experiment, the developed system showed both of firm and soft endpoint. Future works are to improve the finger force sensors, and to apply more subjects, so that the system could classify an examiner into a skill level.

ACKNOWLEDGMENT

This work was supported (in part) by the Support Program for Improving Graduate School Education from the Ministry of Education, Culture, Sports, Science and Technology of Japan.

REFERENCES

[1] D. C. Fitzpatrick, M. B. Sommers, B. C. C. Kam, J. L. Marsh, M. Bottlang, "Knee Stability After Articulated External Fixation," American Journal of Sports Medicine, vol. 33, pp. 1735-1741, 2005.

[2] A. J. Schuster, M. J. McNicholas, S. W. Wachtl, D. W. McGurty R. P. Jakob, "A New Mechnical testing Device for Measuring Anteroposterior Knee Laxity," the American Journal of Sports Medicine, vol. 32, pp. 1731-1735, 2004.

[3] K. Sun, S. Tian, J. Zhang, C. Xia, C. Zhang, T. Yu, "Anterior Cruciate Ligament Reconstruction with BPTB Autograft Irradiated Versus Non-Irradiated Allograft: a Prospective Randomized Clinical Study," Journal of Knee Surgery Sports Traumatology Arthroscopy, vol. 17, pp. 464-474, 2009.

[4] F. Gebhard, M. Authenrieth, W. Strecker, L. Kinzl, G. Hehl, "Ultrasound Evaluation of Gravity Induced Anterior Drawer Following Anterior Cruciate Ligament Lesion," Knee Surgery Sports Traumatology Arthroscopy, vol. 7, pp. 166-172, 1999.

[5] S.H. Wiertsema, H.J.A. van Hooff, L.A.A. Migchelsen, M.P.M. Steultjens, "Reliability of the KT1000 arthrometer and the Lachman test in patients with an ACL rupture," The Knee, no. 15, pp. 107-110, 2008.

[6] A. M. Rijke, C. J. Tegtmeyer, D. J. Weiland, F. C. McCue III, "Stress Examinaion of the Cruciate Ligaments: A Radiologic Lachman test," Radiology, vol. 165, no. 3, pp. 867-869, 1987.

[7] Yuichi Hoshino, Ryosuke Kuroda, Kouki Nagamune, Masayoshi Yagi, Kiyonori Mizuno, Motoi Yamaguchi, Hirotsugu Muratsu, Shinichi Yoshiya,and Masahiro Kurosaka, "In Vivo Measurement of the Pivot-Shift test in the Anterior Cruciate Ligament–Deficient Knee Using an Electromagnetic Device," American Journal of Sports Medicine, vol. 35, pp. 1098-1104, 2007.

[8] Ryosuke Kuroda, Yuichi Hoshino, Kouki Nagamune, Seiji Kubo, Koji Nishimoto, Daisuke Araki, Motoi Yamaguchi, Shinichi Yoshiya and Masahiro Kurosaka, "Intraoperative Measurement of Pivot Shift by Electromagnetic Sensors," Operative Techniques in Orthopaedics, vol. 18, pp. 190-195, 2008.

2011 IEEE International Conference on Fuzzy Systems
June 27-30, 2011, Taipei, Taiwan

Human Motion Tracking for Cognitive Rehabilitation in Informationally Structured Space Based on Sensor Networks

Yuichiro Toda
Tokyo Metropolitan University
Tokyo, Japan
toda-yuuichirou@sd.tmu.ac.jp

Yuki Kodai
Tokyo Metropolitan University
Tokyo, Japan
yuuki-kodai@sd.tmu.ac.jp

Eriko Hiwada
Tokyo Metropolitan University
Tokyo, Japan
hiwada-eriko@sd.tmu.ac.jp

Naoyuki Kubota
Tokyo Metropolitan University
Tokyo, Japan
kubota@tmu.ac.jp

***Abstract*—This paper discusses measurement methods of human behaviors based on sensor network and human interaction of rehabilitation using robot partners. First, we explain robot partners and sensor networks for rehabilitation. Next, we apply a steady-state genetic algorithm to extract human motions from 3D distance image. Finally, we discuss the effectiveness of the proposed methods through several experimental results.**

Keywords-component; Rehabilitation, Human Motion Tracking, Sensor Networks, Robot Partners, Evolutionary Computation

I. INTRODUCTION

Recently, as the increase of number of elderly people, much more caregivers are required for the support for them. The mental and physical care is very important in order to avoid the progress of dementia of elderly people living alone in home, but such people have little chances to talk with other people and to perform daily exercise. On the other hand, the number of patients of brain damage is also increasing. The cognitive therapeutic exercise is useful in the rehabilitation after brain damage [1]. In the cognitive rehabilitation, before the actual motions, a patient pays attention to the cognitive cycle of the pre-planning of actual motions and the prediction of sensing in the actual motion in order to recover the cognitive ability from perception to action. It takes much time and load for a therapist to observe and navigate the behaviors of a patient in the rehabilitation program. In the above discussion, the motion measurement, natural communication, and human-friendly interaction are very important and necessary for both elderly people and patients. Of course, it is really ideal that these roles should be done by human caregivers and therapists, but the number of caregivers and therapists is not enough in the current situation. The introduction of robot partners instead of people is one of possible solutions. Such a robot partner should understand human behaviors for natural communication with elderly people. However, it is also difficult for a robot partner to observe the human behaviors. Therefore, sensor network and portable sensing devices can be applied for observing and understanding human behaviors [2,3].

The emerging synthesis of information technology (IT), network technology (NT), and robot technology (RT) is one of the most promising approaches to realize a safe, secure, and comfortable society for the next generation [4]. NT can provide the robot with computational capabilities based on various types of information outside of robots. Actually the robot directly receives the environmental information through a local area network without the measurement by the robot itself [5,6]. Wireless sensor networks [7-9] realize to gather the huge data on environments. However, it is very difficult to store all of huge data in real time. Furthermore, some features should be extracted from the gathered data to obtain the required information. Therefore, intelligent technology is required in wireless sensor networks.

Intelligence technology and information technology have been discussed from various points of view. Information resources and the accessibility within an environment are essential for both people and robots. Therefore, the environment surrounding people and robots should have a structured platform for gathering, storing, transforming, and providing information. Such an environment is called informationally structured space [10,11] (Fig.1). The intelligent technology for the design and usage of the informationally structured space should be discussed from various points of view such as information gathering of real environment and cyber space, structuralization, visualization and display of the gathered information. The structuralization of informationally structured space realizes the quick update and access of valuable and useful information for people. It is very useful for both robots and people to easily access the information on real environments. The information is transformed into the useful form suitable to the features of robot partners and people. Furthermore, if the robot can share the environmental information with people, the communication with people might become very smooth and natural.

In this paper, we discuss the measurement method of human

978-1-4244-7316-8/11/$26.00 ©2011 IEEE

motions in the informationally structured space including robot partners and sensing devices. First, we apply a steady-state genetic algorithm (SSGA) [12,13] to perform human hand motion tracking by using the time series of 3D distance image based on differential extraction. SSGA is one of evolutionary optimization methods using selection, mutation, and crossover operators [14]. The shape and size of a template is updated by SSGA in this study. Next, we show experimental results, and discuss the effectiveness of the proposed method.

This paper is organized as follows. Section 2 explains the robot partners, and discusses how to use robot partners for rehabilitation. Section 3 proposes methods of human detection and human hand motion extraction. Section 4 shows experimental results of the proposed method, and Section 5 summarizes the paper, and discusses the future vision of robot partners for rehabilitation.

II. INFORMATIONALLY STRUCTURED SPACE

A. Robot Partners

We can use three different types of robot partners from the interactive point of view (Fig.2). One is a physical robot partner. We can interact with the physical robot partner by using multi-modal communication like a human [15]. The next one is a pocket robot partner. The pocket robot partner has no mobile mechanism, but we can easily bring it everywhere and can interact with the robot partner by touch and physical interface. The last one is a virtual robot partner. The virtual robot partner is in the virtual space in the computer, but we can immerse into the virtual space, and interact with it through the virtual person or robot. The interaction style of these three types of robot partners is different, but they share the same personal database and interaction logs, and can interact with the person based on the same interaction rules independent from the style of interfaces.

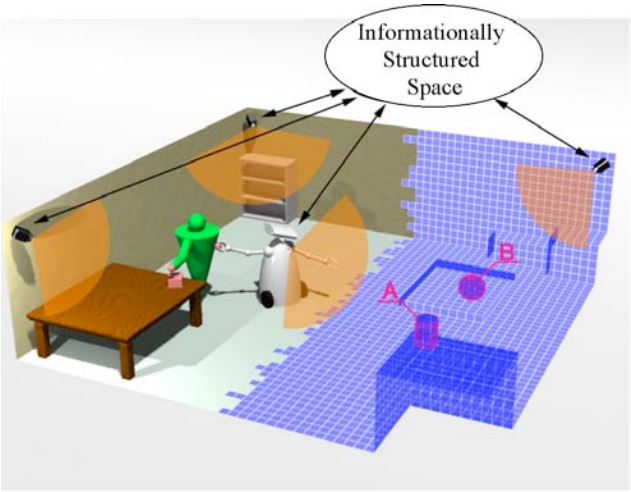

Figure 1. The concept of informationally structured space

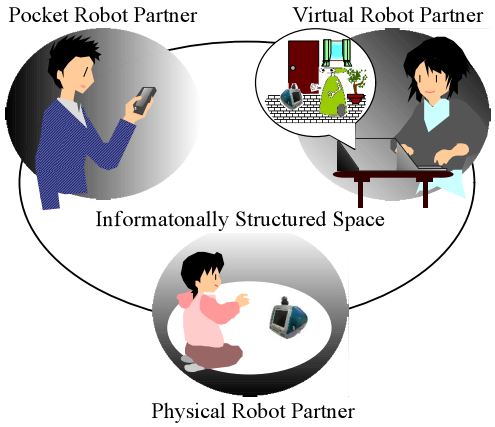

Figure 2. Interaction with robot partners

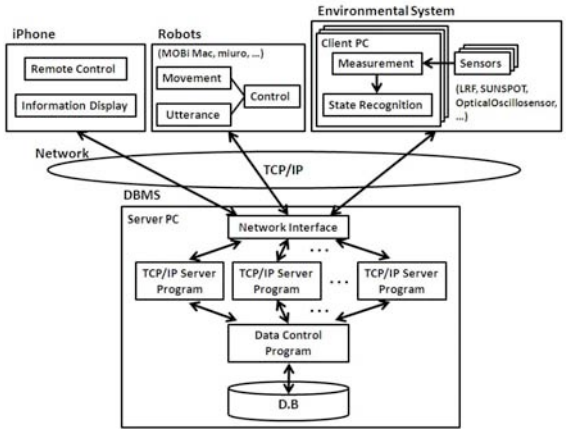

Figure 3. Data flow in informationally structured space

B. Data Flow in Informationally Structured Space

Figure 3 shows the data flow in the developed system based on informationally structured space. The developed system is divided into four components; (1) database management server, (2) robot systems, (3) environmental systems, and (4) human interface systems. The environmental system is based on a ubiquitous wireless sensor network composed of sensors equipped with wall, floor, ceiling, furniture, and home appliances. These sensors measure the environmental data and human motions. The measured data are transmitted to the database server, and then feature extraction is performed. Each robot can receive the environmental information from the database server, and serve as a partner to the person. Furthermore, the user interface device is used for the person to access the environmental information.

C. Rehabilitation Support in Informationally Structured Space

Figure 4 shows an example of rehabilitation support by a physical robot partner. A patient can perform the rehabilitation program through interaction with the robot. The robot can repeatedly show the behaviors demonstrated for the rehabilitation programs, and can observe behaviors of the

patience. The observed data can be useful and important information for the therapist to understand the state of rehabilitation, and to update the rehabilitation program. Furthermore, such a physical robot partner can avoid the progress of dementia of elderly people and urge daily routine exercises of the elderly people to make them maintain the physical and mental health.

Figure 4. A conceptual figure of rehabilitation by a robot partner

(a) Wireless accelerometer (b) Sensing direction

Figure 5. Wireless accelerometer developed by ZMP, Inc.

Figure 6. Wireless accelerometer built in a building block

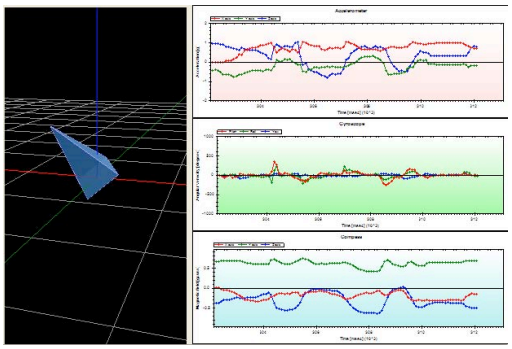

Figure 7. A measurement result of human hand motion

Next, we explain the sensor network devices. We use 3-axis accelerometer to measure the human hand posture of grasping blocks. Figure 5 shows the appearance of 3-axis accelerometer named IMU-Z developed by ZMP, Inc. [16]. The size of this device is 42[mm] x 52.5[mm] x 20.5[mm], but this device includes accelerometer, Jyro, electrical compass. The sampling interval is 10 [msec]. Furthermore, this device can be connected with PC through Bluetooth wireless communication. This device is built in a building block used for rehabilitation (Fig.6). Figure 7 shows a measurement result of posture of human grasping behavior of the block including the wireless sensor device. The experiment result shows the time-series of angle of X, Y, and Z axes. This shows the change of the posture according to the grasping behavior.

Figure 8. 3D distance image sensor of M Kinect sensor

TABLE I. SPECIFICATION OF KINECT SENSOR

Horizontal Field of View	57 degrees
Vertical Field of View	43 degrees
Physical Tilt Range	±27 degrees
Depth Sensor Range	1.2M – 3.5M
Number of Pixels	640 × 480

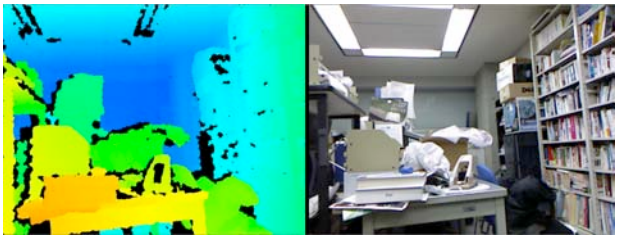

Figure 9. 3D distance image and color image

3D distance image sensor can measure the distance from the device like a camera in realtime. We use a Kinect sensor developed by Microsoft [17]. This device includes 3D distance image sensor, microphones, RGB camera, accelerometer, and tilting-up mechanism. This device can be connected with PC through USB. Table 1 shows the main specification of 3D distance image sensor. Figure 9 shows an example of the distance and color image measured by Kinect sensor.

Figure 10 shows an example of robot partner with Kinect sensor. The robot has three behavior modes of normal mode, interaction mode, and rehabilitation mode. In the normal mode, the behavior mode is transited to the interaction mode. Figure 11 shows an example of human interaction. In the normal mode, the kinect sensor is in the normal position (θ =0º) shown in Fig.11 (a). When a person approaches to a chair, the Kinect sensor is tilted up toward the human face (θ =27º) shown in Fig.11 (b). If the person tries to touch iPad built with the robot,

the robot supports the edges of iPad (Fig.11 (c). Finally, the behavior mode is transited to the normal mode after the person leaves the chair. In this way, the robot changes the behavior mode according to the human interaction.

Figure 10. A rehabilitation support system using a robot partner

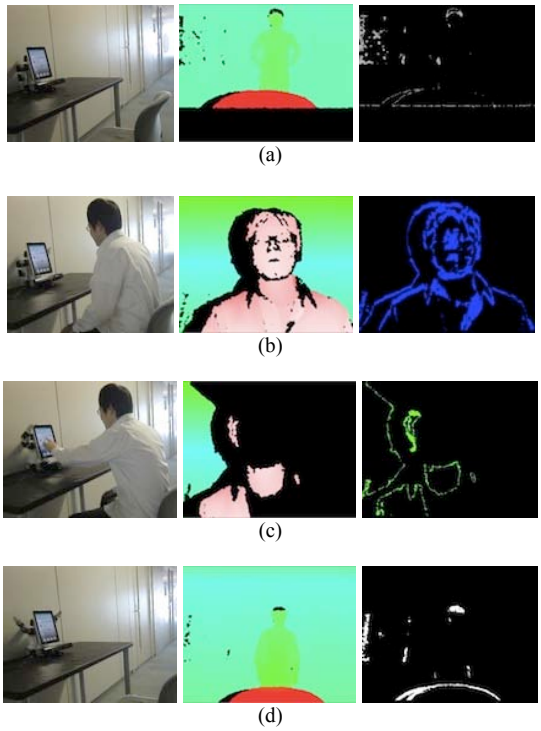

Figure 11. Interaction mode of the robot partner

III. HUMAN HAND MOTION TRACKING

A. Measurement by 3D Distance Image Sensor

We have proposed the concept of evolutionary robot vision based on the active vision and evolutionary search [15]. The time series of evolutionary search in dynamic environment is the most important in evolutionary robot vision. The structure of environmental changes is applied to the next visual search. We use a reliability space for human localization. The reliability space is built according to the temporal difference based on distance image. Figures 12 and 13 show the procedure of human hand motion extraction and an example of image processing, respectively. In the initialization, the long-term memory images of illumination and distance; $a^L_{i,j}$ is generated using the current images of distance, $a^C_{i,j}$ where i=$X_{\min}$, ..., $X_{\max}$ and j=$Y_{\min}$, ..., $Y_{\max}$. Furthermore, each value of the reliability space $b_{i,j}$ $\left(0 \le b_{i,j} \le 1\right)$ is initialized at 1. Next, the new images of illumination and distance are taken from the 3D distance image sensor. Figure 13 (a), (b), and (c) show the original images of distance, the result of edge detection, and the long-term memory images of distance, respectively. When a person enters into the view angle of the camera, we obtain the temporal difference images $d_{i,j}$ by the differential extraction between the current images and the long-term memory images in the following;

$$d_{i,j} = \left| a^C_{i,j} - a^L_{i,j} \right| \tag{1}$$

Next, the reliability space is updated in the following;

$$b_{i,j} \leftarrow \begin{cases} b_{i,j} - \alpha^B_1 & if\ d_{i,j} > \theta^B \\ b_{i,j} + \alpha^B_2 & otherwise \end{cases} \tag{2}$$

where $0 < \alpha^B_2 < \alpha^B_1 < 1$ and $\theta^B_k > 0$. The reliability of a pixel (i,j) decreases, as the temporal difference is large.

$$a^L_{i,j} \leftarrow \begin{cases} \left(1-\alpha^L_1\right) a^L_{i,j} + \alpha^L_1 \cdot a^C_{i,j} & if\ b_{i,j} > \theta^L \\ \left(1-\alpha^L_2\right) a^L_{i,j} + \alpha^L_2 \cdot a^C_{i,j} & otherwise \end{cases} \tag{3}$$

where $0 < \alpha^L_2 < \alpha^L_1 < 1$ and $0 < \theta^L < 1$. If the amount of the update of the long-term memory is large as the reliability is high. Next, we construct the search space, $c_{i,j}$ ($0 \le c_{i,j} \le 1$) by combining the temporal images of illumination and distance in the following weighted sum;

$$c_{i,j} = \alpha^S_1 \cdot d_{1,i,j} + \alpha^S_2 \cdot d_{2,i,j} \tag{4}$$

where $0 < \alpha^S_2, \alpha^S_1 < 1$.

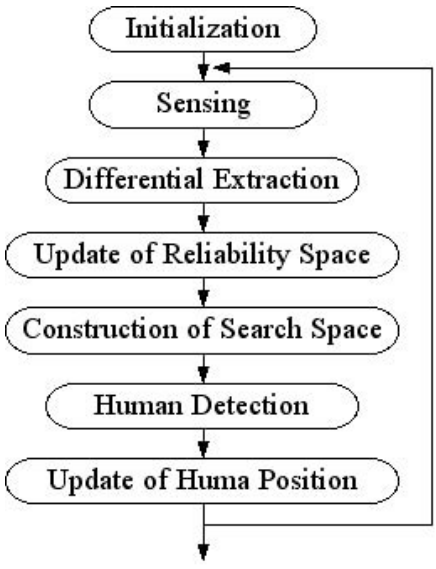

Figure 12. Procedure of human localization

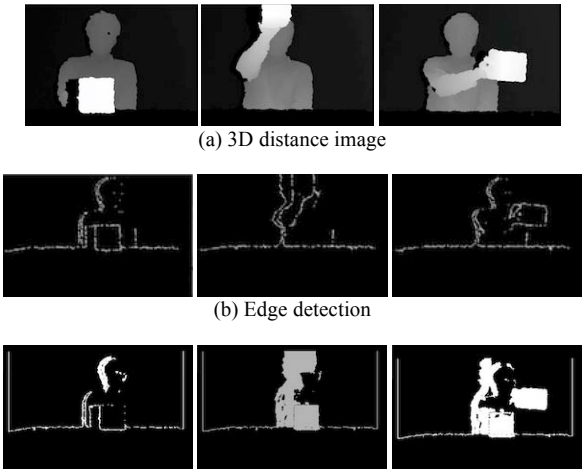

(a) 3D distance image

(b) Edge detection

(c) Differential Extraction with long term background image

Figure 13. Image processing based on distance data

B. Human Detection and Tracking

We use a steady-state genetic algorithm (SSGA) [12] based on template matching for extracting a human shape from the background image [12,13,18,19]. We assume that a person is moving in the image. Therefore, we use the search space constructed by the temporal difference. The shape of a candidate template is generated by the SSGA. We used an octagonal template. Figure 14 shows a candidate template used for detecting a target where the jth point $g_{i,j}^{O}$ of the ith template is represented by $(g_{i,1}^{O}+g_{i,j}^{O}\cos(g_{i,j+m}^{O}),\ g_{i,2}^{O}+g_{i,j}^{O}\sin(g_{i,j+m}^{O}))$, i=1, 2, ... , G^O, j=3, 4, ... , 2×m+2; O_i (=$(g_{i,1}^{O}, g_{i,2}^{O})$) is the center of a candidate template on the image; n and m are the number of candidate templates and the searching points used in a template (m=8), respectively. Therefore, a candidate template is composed of numerical parameters of $(g_{i,1}^{O}, g_{i,2}^{O},\ldots , g_{i,2m+2}^{O})$.

In SSGA, only few existing solutions are replaced with the candidate generated by genetic operators in each generation. In this paper, the worst candidate solution is eliminated ("Delete least fitness" selection), and it is replaced with the candidate solution generated by the crossover and mutation. The fitness value of kth is calculated by the following equation;

$$fit_i = \alpha_1 f_1 + \alpha_2 f_2 + \alpha_3 f_3 + \alpha_4 f_4 \qquad (5)$$

where f_1 indicates the number of pixels; f_2 indicates the evaluation value based on differential extraction; f_3 indicates the evaluation value on the degree of surface of the target building block; f_4 indicates the evaluation value of the movement of human hand; α_1 α_2 α_3 and α_4 are coefficients.

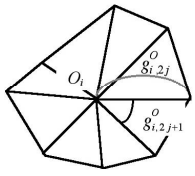

Figure 14. A template used for human detection in SSGA

We use an elitist crossover and an adaptive mutation. The elitist crossover randomly selects one individual and generates an individual by combining genetic information from the randomly selected individual and the best individual. If the crossover probability is satisfied, the elitist crossover is performed. Otherwise, a simple crossover is performed between two randomly selected individuals. Next, the following adaptive mutation is performed to the generated individual,

$$g_{i,j} \leftarrow g_{i,j} + \left(\beta_{1,j} \cdot \frac{f_{\max} - f_i}{f_{\max} - f_{\min}} + \beta_{2,j} \right) \cdot N(0,1) \qquad (6)$$

where f_i is the fitness value of the ith individual, f_{max} and f_{min} are the maximum and minimum of fitness values in the population; $N(0,1)$ indicates a normal random variable with a mean of zero and a variance of one; $\beta_{1,j}$ ($\beta_{1,j}$>0) and $\beta_{2,j}$ ($\beta_{2,j}$>0) are the coefficients and offset, respectively. In the adaptive mutation, the variance of the normal random number is relatively changed according to the fitness values of the population in case of maximization problems. Furthermore, we use k-means clustering algorithm to detect people, not a single person. The k-means is used for the clustering according to the distribution of the candidate solutions [18]. The genetic operators of selection and crossover are restricted within the subpopulation corresponding to the cluster as the result of the clustering. The candidate solutions are inherited and used in the next image. According to the evaluation based on the fitness function, some of candidate solutions are replaced with the randomly generated candidate solutions. In this way, the evolutionary search is performed to time series of 3D distance images.

The human hand motion tracking is performed according to the position of the mth candidate solution obtained by SSGA. The position of the hth human candidate in the human tracking, $(X_{h,1}^{H}, X_{h,2}^{H})$, is updated by the nearest human hand candidate position within the tracking range. The update is performed as follows (k=1, 2);

$$X_{h,k}^{H} \leftarrow (1-\alpha^{H}) X_{h,k}^{H} + \alpha^{H} \cdot \hat{x}_{m,k} \qquad (7)$$

where α^H is the update rate. The distance information $a_{i,j}^{C}$ of each pixel (i,j) is transformed into the position (x,y,z) = ($x_{1,i,j}$, $x_{2,i,j}$, $x_{3,i,j}$) in the Cartesian space. Therefore, the update amount $\hat{x}_{m,k}$ is obtained by the average of the position information of ($x_{1,i,j}$, $x_{2,i,j}$) of pixel (i,j) in the template of the mth candidate solution.

IV. Experimental Results

This section shows experimental results of the proposed method. The population size of SSGA is 100, and the number of iterations in the search is 200 per 3D distance image. The sampling interval of Kinect sensor is approximately 30 ms.

First of all, we show experimental results of human hand extraction and tracking of the triangular gesture of. Figure 15 shows the examples of the search result of the object

corresponding to human hand by SSGA. Figure 15 (a) shows the 3D distance image where the degree of gray depth indicates the distance from the 3D distance image sensor; (b) shows the result of differential extraction; and (c) hand detection and tracking results (t=10, 20, 30). The experimental results show that the proposed method can extract human hand position according to the size of the template and the distance from the distance image sensor.

t=10 t =20 t=30

(a) Distance image

(b) Differential extraction

(c) Hand detection and tracking result

Figure 15. A trajectory of human hand motion by human hand tracking (triangular gesture)

Figures 16 show the tracking results of human hand motions of a horizontal circular gesture. Figure 16 (a) shows the result of differential extraction; (c) hand detection and tracking results; and (c) the 3D distance image where the degree of gray depth indicates the distance from the 3D distance image sensor but the viewpoint is changed to the bird view from the person (t=10, 20, 30). Basically, it is very difficult to extract this gesture only by image processing, but the proposed method based on the distance image sensor can extract this complicated gesture. Furthermore, the transformed image of viewpoint from the person is very useful for a therapist to understand the hand motion of a patient.

V. SUMMARY

This paper developed a measurement system of human hand motion based on sensor network and robot partners for rehabilitation. First, we proposed the interaction system for a robot partner. Next, we applied a steady-state genetic algorithm to extract human hand motions from the 3D distance image. Experimental results show the effectiveness of the proposed methods. The obtained results are available for understanding and analysis of human hand motions.

As a future work, we intend to combine the voice recognition and visual perception to realize natural interaction of robot partners for rehabilitation. Furthermore, we use iPhone and iPod touch for cognitive rehabilitation therapy.

t=10 t =20 t=30

(a) Differential extraction

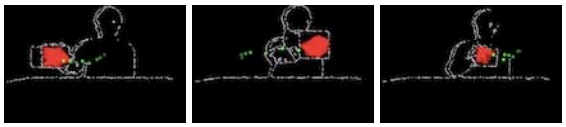

(b) Hand detection and tracking result

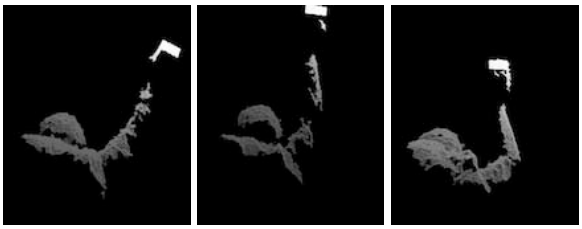

(c) Distance image

Figure 16. A trajectory of human hand motion extracted by SSGA (a horizontal circular gesture)

ACKNOWLEDGMENT

This research was partially supported by Grant-in-Aid for Scientific Research (B) No.22300082 from the Ministry of Education, Culture, Sports, Science and Technology of Japan.

REFERENCES

[1] S.F.Szekeres, M.Ylvisaker, S.B.Cohen, A Framework for Cognitive Rehabilitation Therapy, Community Re-entry for Head Injured Adults (edited by M.Ylvisaker, E.M.R.Gobble), Butterworth-Heinemann, pp.87-136, 1987.

[2] S.Attygalle, M.Duff, T.Rikakis, Jiping.H, Low-cost, at-home assessment system with Wii Remote based motion capture, In Proceedings of the Conference on Virtual Rehabilitation, pp.168-174, 2008.

[3] M.Duff, S.Attygalle, Jiping.H, T.Rikakis, A Portable, Low-cost Assessment Device for Reaching Times, Engineering in Medicine and Biology Conference (EMBC2008), pp.4150-4153, 2008.

[4] C. Corderio, D. Agrawal, Ad Hoc & Sensor Networks, World Scientific, 2006.

[5] I. Khemapech, I. Duncan and A. Miller, "A Survey of Wireless Sensor Networks Technology," Proc. of The 6th Annual PostGraduate Symposium on The Convergence of Telecommunications, Networking and Broadcasting, 2005.

[6] J-H. Kim, Y-D. Kim, and K-H. Lee, "The Third Generation of Robotics: Ubiquitous Robot," Proc. of 2nd International Conference on Autonomous Robots and Agents, 2004, pp.1-12.

[7] N.Kubota, Y.Shimomura, Human-Friendly Networked Partner Robots toward Sophisticated Services for A Community, Proc. of SICE-ICCAS 2006, pp. 4861-4866, 2006.

[8] N.Kubota, K.Nishida, Perceptual Control Based on Prediction for Natural Communication of A Partner Robot, IEEE Transactions on Industrial Electronics, Vol.54, No.2, pp.866-877, April, 2007.

[9] N.Kubota, T.Obo, T.Fukuda, An Intelligent Monitoring System based on Emotional Model in Sensor Networks, The 18th IEEE International

Symposium on Robot and Human Interactive Communication, pp.346-351, 2009.

[10] N.Kubota, H.Sotobayashi, T.Obo, Human Interaction and Behavior Understanding Based on Sensor Network with iPhone for Rehabilitation**,** Proc. of International Workshop on Advanced Computational Intelligence and Intelligent Informatics, 2009.

[11] N.Kubota, A.Yorita, Topological Environment Reconstruction in Informationally Structured Space for Pocket Robot Partners, 2009 IEEE International Symposium on Computational Intelligence in Robotics and Automation (CIRA 2009), pp.165-170 Daejeon, Korea, December 15-18, 2009.

[12] G.Syswerda, A Study of Reproduction in Generational and Steady-State Genetic Algorithms, In Foundations of Genetic Algorithms, Morgan Kaufmann Publishers, Inc., 1991.

[13] N.Kubota, K.Nishida, Cooperative Perceptual Systems for Partner Robots Based on Sensor Network, International Journal of Computer Science and Network Security, Vol.6, No.11, pp.19-28, 2006.

[14] D.B.Fogel, **"***Evolutionary Computation***"**, IEEE Press , 1995.

[15] N.Kubota, T.Shimizu, M.Abe, Joint Attention Between a Human Being and a Partner Robot Based on Computational Intelligence, Journal of Advanced Computational Intelligence and Intelligent Informatics, Vol.11, No.10, pp. 1275-1281, 2007.

[16] Z.Lin, M.Zecca, S.Sessa, H.Ishii, A.Takanishi, Ultra-Miniaturized Inertial Measurement Unit WB-3 for Jaw Movement Analysis during Free Chewing, Proc. of 2010 International Symposium on Robotics and Intelligent Sensors, 2010.

[17] http://www.xbox.com

[18] N.Kubota, Computational Intelligence for Structured Learning of A Partner Robot Based on Imitation, Information Sciences, No.171, pp.403-429, 2005.5.

[19] N.Kubota, K.Tomoda, Behavior Coordination of A Partner Robot based on Imitation, Proc. of 2nd International Conference on Autonomous Robots and Agents, pp.164-169, 2004.

2011 IEEE International Conference on Fuzzy Systems
June 27-30, 2011, Taipei, Taiwan

A Pervasive Multi-sensor Data Fusion for Smart Home Healthcare Monitoring

Hamid Medjahed
Dan Istrate
ESIGETEL, LRIT
Avon-Fontainebleau, France
Email: {hamid.medjahed,dan.istrate}@esigetel.fr

Jerome Boudy
Jean-Louis Baldinger
Bernadette Dorizzi
Telecom SudParis, EPH, Evry, France
Email: {jerome.boudy,jean-louis.baldinger}@it-sudparis.eu

***Abstract*—Today elderly people are the fastest growing segment of the population in developed countries, and they desire to live as independently as possible. But independent lifestyles come with risks and challenges. Medical in-home telemonitoring (and, more generally, telemedicine) is a solution to deal with these challenges and to ensure that elderly people can live safely and independently in their own homes for as long as possible. In this context we propose an automatic in-home healthcare monitoring system for several uses and to meet the needs identified above. The proposed telemonitoring system is a multimodal platform with several sensors that can be installed at home and enables us to have a full and tightly controlled universe of data sets. It integrates elderly physiological and behavioral data, the acoustical environment of the elderly, environmental conditions and medical knowledge. Each modality is processed and analyzed by specific algorithms. A data fusion approach based on fuzzy logic with a set of rules directed by medical recommendations, is used to fuse the various subsystem outputs. This multimodal fusion increases the reliability of the whole system by detecting several distress situations. In fact this fusion approach takes into account temporary sensor malfunction and increases the system reliability and the robustness in the case of environmental disturbances or material limits (Battery, RF range, etc.). The Fuzzy logic fusion methods brings high flexibility to the telemonitoring platform especially in combining modalities or adding other sensors. The proposed telemonitoring system will ensure pervasive in-home health monitoring for elderly people.**

Keywords: fuzzy logic, fuzzy control, multimodal data fusion, telemedicine, healthcare telemonitoring.

I. Introduction

France's population continues to age significantly and a recent study carried out by the French national institute of statistic and economic studies (INSEE) shows a new distribution of age classes in France. In fact, almost one in three people will be over 60 years in 2050, against one in five in 2005, and France will have over 10 million of people over 75 years and over 4 million of people over 85 years. Therefore, the aging population and the increase in life expectancy have led to new models of aging where technology can play a role in monitoring the quality of life, by detecting or even predicting adverse events and hence supporting independence. Automatic in-home telemonitoring of distress situations has been a common focus in Gerontechnology [1] because medical telemonitoring at home, is an interesting solution compared to health facility institutions for the elderly, since it offers medical surveillance in a familiar atmosphere for the patient.

To address these issues, researchers are developing technologies to enhance a resident's safety and monitor health conditions using sensors and other devices. Numerous projects are carried out in the world especially in Europe, Asia and North America, on the home healthcare telemonitoring topic. They aim for example to define a generic architecture for such telemonitoring systems [2], to conduct experiment of a remote monitoring system on a specific category of patients [3] (Insufficient cardiac heart, asthma, diabets, patients with Alzheimer's disease, or cognitive impairement, etc.), or to build smart apartments [4], sensors and alarm systems adapted to the healthcare telemonitoring requirements [5].

However, little research exists to motivate and guide such technology. For example, most monitoring systems use some form of learning method to discriminate between different types of normal and abnormal events. These algorithms require large amounts of training data that can be dificult to obtain, especially data describing abnormal events that are by definition scarce occurrences. The most crucial issue for all these systems is the lack of experimental data and information representing many situations and several person profiles. Most of these systems also take into account only one modality, like medical sensors (Blood pressure, pulse, oxymeter) or localization sensors (Infrared or contacts) to survey patient. But among established medical remote systems, there are few commercial solutions and business models.

In this paper we present the use of the multimodal system called EMUTEM (Environnement Multimodal pour la Télévigilance Médicale) [6] for distress situations detection. The proposed system was evaluated on two data bases: one recorded by our self and another one recorded in an experimental house by elderly people. The platform developed within this framework research manages a system consisting of:

- A set of microphones placed in all rooms of the elderly's house, that allow remote monitoring of the acoustical environment of the elderly (Anason [7]).
- A wearable device called RFpat [8] that can measure physiological data like ambulatory pulse heart rate, detect posture (standing/ sitting and laying), fall of the equipped person and his activity rate.

978-1-4244-7316-8/11/$26.00 ©2011 IEEE

- A set of infrared sensors that detect the person's presence in a portion of a given home part, his posture and also his movement (Gardien [8]). Plus a set of domotic sensors like contact sensors, temperature sensors and several other domotic sensors for environment conditions monitoring.

Subsystem data streams have been separately processed with suitable algorithms for abnormal situations detection. In order to maximize correct classification performance between normal and distress situations, data fusion over the different sensors types is studied.

The originality of this research is the combination of various modalities in the home, about its inhabitant and their surroundings. The new multimodal data fusion approach based on fuzzy logic allows high flexibility for the EMUTEM platform especially in combining modalities or adding other sensors. It constitutes an interesting benefit and impact for the elderly person sufering from loneliness. This work complements the stationary smart home environment in bringing to bear its capability for integrative continuous observation and detection of critical situations.

II. The Telemonitoring System

We define a smart environment as one with the ability to adapt the environment to the inhabitants and meet the goals of comfort and efficiency. In order to achieve these goals, our first aim was focused on providing such as environment. We consider our system as an intelligent agent, which perceives the state of the environment by using sensors and acts consequently with device controllers.

A. Environment Sensing and Data Collection

The experimental area is a surface of $20m^2$ in our laboratory which is arranged in two rooms with a technical area in order to evaluate and to supervise experiments. The hardware framework is reported in Figure 1. It integrates smart sensors (Infrared, change state sensors, audio, physiological,) linked to a PC. Microphones for audio monitoring are linked to the PC through an external sound card (in order to allow good signal to noise ratio independent from the PC), and can be interpreted

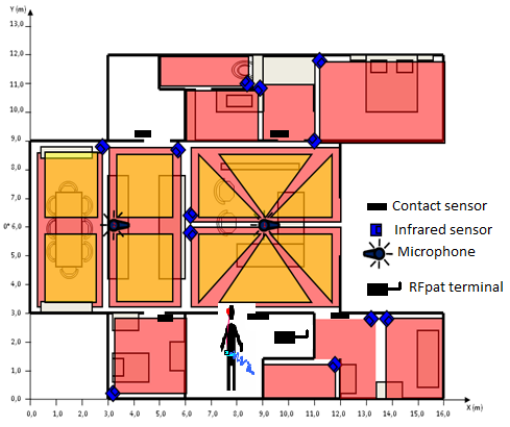

Fig. 1. In-home sensor disposal.

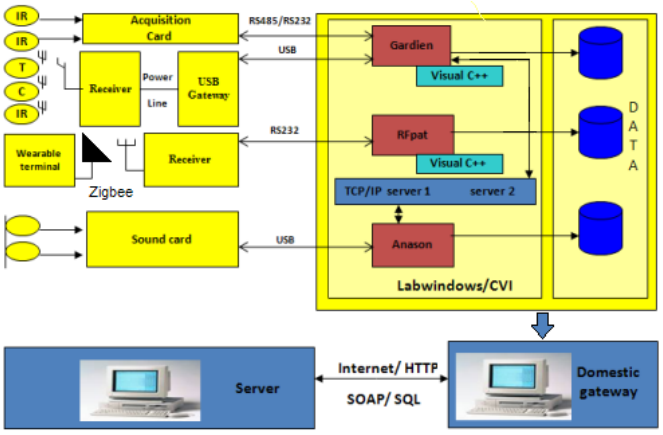

Fig. 2. EMUTEM software architecture.

as a single smart audio sensor achieved by Anason software. Infrared sensors are fixed on specific places of the house in walls and ceiling. They are in permanent communication via radio frequency communication, with one receiver, which is connected to the USB port of the PC. Change state sensors transmit also information to this receiver through radio frequency communication. The powerline is used to get back data from the receiver for software processing. The weareble device RFpat is caried by the elderly and continuously monitors his physiological data and emergency calls. It transmits these data to an indoor reception base station via ZigBee.

Figure 2 shows the software architecture of the multimodal platform EMUTEM. It provides a general user interface which encapsulates the Anason subsystem. It is implemented under LabWindows/CVI software and communicates with RFpat and Gardien sub-systems by a client-server model using TCP/IP and appropriate application protocols. Gardien is implemented in C++ and recovers data every 500 ms. RFpat is also implemented in C++ and receives data from a receiver every 30 s. The use of the inter-module communication through TCP/IP sockets allows each module (subsystem) to be run on a different computer, and to synchronize each telemonitoring modality channel.

The user can interact with the system via internet navigator and supervises the different applications. This feedback provides a significant help to the system manipulation and the system flexibility obtained through TCP/IP sockets communication allows adding other potential sensors such as a heart monitoring sensors (ECG). Data acquired from sensors are stored in the local computer directly as text files assigned to each modality. Data also could be exchanged using http or ftp protocol via web services technologies SOAP, and saved in a dedicated server.

III. Distress Situation Detection

Detecting and gathering data about the elderly person and his environment is the first step and one of the most fundamental tasks in building intelligent telemonitoring systems. With the increasing intelligence expectation, using multiple sensors

is the only way to obtain the required breadth of information, and fusing the outputs from these multiple sensors is often the only way to obtain the required depth of information when a single sensing modality is inadequate [9]. However, in our telemonitoring context different sensors use different physical principles, cover different information space, and generating data in different formats at different sampling rates. The obtained data have different resolution, accuracy, and reliability properties.

Based on those effects, the key to produce the required detection is to use the right method that properly fuses the provided data from various sources. This is what multimodal data fusion stands for. Therefore, typical multisensors data fusion methods are analyzed in this section, in seeking for a most generalizable and adaptable method.

A. Adapted Approaches for Multi-sensors Data Fusion

To select a suitable method for EMUTEM's multimodal data fusion module, we have probabilistic approaches whose performance can be reconsidered in our application for many reasons. The classical inference method quantitatively compares the probability that an observation can be attributed to a given assumed hypothesis. But it has the following major disadvantages [10], (1) difficulty in obtaining the density functions that describe observations used to classify the object, (2) complexities that arise when multivariate data are encountered, (3) its capability to assess only two hypotheses at a time, and (4) its inability to take direct advantage of a priori likelihood probabilities.

The Bayesian inference method [11] also has some weaknesses that prevent it from being used in our multimodal data fusion module. The key limits are: (1) difficulty in defining a priori probabilities, (2) complexities when there are multiple potential hypotheses and multiple conditionally dependent events, (3) mutual exclusivity required for competing hypotheses, and (4) inability to account for general uncertainty and to represent imprecision.

Even if Dempster-Shafer methods [12] use a general level of uncertainty, they cannot be the main data fusion method for two reasons: the difficulty to estimate mass function and their restrict domain of application.

The neural networks method [13] is not very well adapted to EMUTEM's Data fusion module because of drawbacks. First, the mapping mechanism is not well understood even if the network can provide the desired behavior. Second, the neural network method is, generally speaking, not suitable to work in a dynamic sensor configuration environment, because each sensor needs a unique input node and each possible sensor-set configuration needs to be specifically trained. Third, the complex architecture of neural networks prevents experts adding their knowledge easily.

SVM methods [14], despite their transit in the characteristics space which is disconnected from any physical reality, could fulfill the requirement of intelligibility because only support vectors are important in identifying margins between classes. However, it is necessary that boundaries between classes are rendered intelligible by a graphical way in the space of inputs. This vision must take into account an input space of any size even if greater than 3. In this case, the SVM identifies a large majority of learning examples as support examples. It means that an analyst should remember too many relevant individuals for the construction of boundaries between classes and this is impossible.

The fuzzy logic method [15] is the proposed way to meet these challenges of this multimodal data fusion application. According to the nature of data to process in EMUTEM platform, fuzzy logic is the well adapted approach for the telemonitoring decision. It deals with inaccuracy and uncertainty. It allows a great flexibility to combine several sensors.

IV. Implementation

A. Fuzzy Classifier

The main advantages of using fuzzy logic system are the simplicity of the approach and the capacity of dealing with the complex data acquired from the subsystems discribed previously in the second section. Fuzzy set theory offers a convenient way to do all possible combinations with these data. Fuzzy set theory is used in this system to determine the most likely distress situations that might occur for elderly persons in their home. The data fusion is carried out at three different levels: for sound/speech environement at the decision level, for smart home sensors system at the input data level and for the wearable physiological sensor at the representation level.

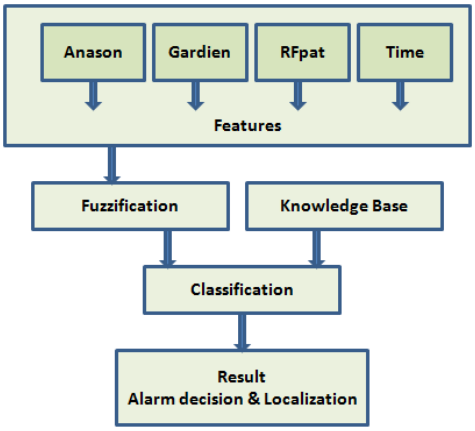

Fig. 3. Structure of the fuzzy classifier.

B. Input and Output fuzzification

The first step for implementing the fuzzy logic multimodal data fusion approach is the fuzzification of outputs and inputs of the fuzzy inference system (FIS) obtained from each subsystem.

From Anason subsystem three inputs are built. The first one is the sound environment classification. Sound classes are labeled on a numerical scale according to their alarm level. Four membership functions are set up in this numerical scale according to the following fuzzy levels: no signal, normal, possible alarm and alarm as it is shown in figure 4. The

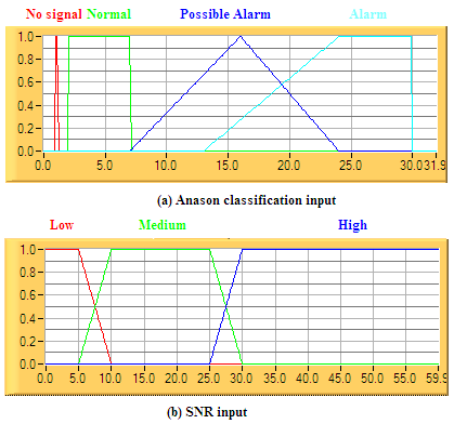

Fig. 4. Fuzzy sets defined for sound environment inputs.

second input is associated with the SNR (Signal-to-noise ratio) calculated on each microphone (two microphones are used in the current application), and this input is split into three fuzzy levels: low, medium and high.

RFpat provides physiological data to EMUTEM platform. RFpat produce five inputs:

- Heart rate is fuzzified with three fuzzy levels: normal, possible alarm and alarm.
- Activity has four fuzzy sets: immobile, rest, normal and agitation. The trapezoid function displays all these linguistic variables.
- Posture is represented by two membership functions standing up / seating down and lying.
- Fall and call have also two fuzzy levels: Fall/Call and No Fall/Call and a singleton function is associated to these linguistic variable.

Parameters of membership functions associated to the heart rate and the activity, are adjustable according to the monitored elderly person. An automatic procedure to adapt these intervals based on 30 minutes recording was proposed.

For each infrared sensor a counter of motion detection with

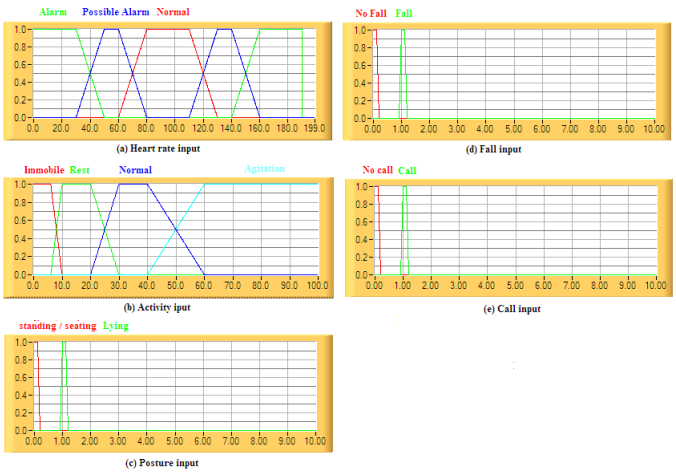

Fig. 5. Fuzzy sets defined for Vital data inputs.

three fuzzy levels (low, medium, high) is associated. It is reset every 5 seconds. A global counter for all infrared sensors with three fuzzy membership functions (low, medium, high) is also used and is reset every 60 seconds. A trapezoid membership function is chosen to characterize these fuzzy sets.

A singleton membership function is assigned to each change state sensor with two linguistic variables: On and Off.

The last input which is the time. It has two membership functions: day and night. These two membership functions are also adaptable to each patient habits. Trapezoid functions are used to divide the time input.

In order to reach the objective of the EMUTEM platform which is the identification of distress situations of an elderly person at home, two outputs are associated to the fuzzy inference engine of EMUTEM platform.

The first one is called Alarm with two linguistic variables normal and alarm.

To refine the decision of the EMUTEM platform a second output is added to its fuzzy inference system component. This second output is named Localization. It is a very important information for the diagnostic. The identification of the position of the monitored person during a distress situation is helpful knowledge for medical diagnosis.

Two membership function models are selected: Gaussian functions are chosen for the alarm outputs; Trapezoid functions for the localization output where the classical areas of a house are its fuzzy levels or linguistic variables.

C. Fuzzy Rules Aggregation and Defuzzification

The EMUTEM fuzzy inference engine is formulated by two groups of fuzzy IF-THEN rules. One group controls the output variable localization according to values of the input variables issued from infrared sensors and the SNR of each microphone. The other group controls the output linguistic variable alarm according to all inputs. These fuzzy rules are decided through experimentation and according to some expert knowledge.

A confidence factor is assigned for each rule. Outputs used in a rule are multiplied by the confidential factor issued from each subsystem. Thus the rule's output value depends on the reliability of each subsystem and the sureness of rules. To aggregate these rules we have chosen the Mamdani model [16] instead of the Takagi Sugeno. These two models are available under the EMUTEM fuzzy logic component. Mamdani model offers us a good way of modeling the normal and distress situations, because these two classes don't form a clean partition but a fuzzy one.

After rules aggregation the defuzzification is performed by the smallest value of maximum method for the alarm output in order to obtain also a confidence level of each alarm's decision, and the centroid of area for the localization output.

Each subsystem specifies the situation of the elderly person and the degree of anxiety. When a decision is very complicated, that is, there are many decisions; the fuzzy method is especially useful. It is also easy to check, modify, and add/delete every fuzzy variable for better automated analysis. To summarize the proposed data fusion method, the proposed fuzzy destress

situation classifier is comprised of two major function blocks, decisions of each subsystems and fuzzy classifier as shown in Figure 3. Decisions of subsystems are utilized as inputs for the classification using the fuzzy classifier. The derived parameters will be exported to the latter for the classification. The Mamdani fuzzy method is used. Fuzzy logic if-then rules are formed by applying fuzzy operations to these membership functions for given inputs and outputs. The resulting output membership functions are added together using desired weights yielding a sort of probability function. The resulting output areas can then be used to estimate the expected value of the output variable by using the specified defuzzification method. In general, any fuzzy classifier has to undergo iterative adjustment in terms of fuzzy variables, including the choice of membership functions, and the definition of rules in the knowledge base.

D. Software Architecture

Figure 6 provides a synoptic block-diagram scheme of the software architecture of the EMUTEM system; it is implemented under Labwindows CVI and C++ software. It is developed in a form of a design component.

We can distinguish three main components, the acquisition module, the synchronization module and the fuzzy inference component. It can run off-line by reading data from a data base or online by processing in real time data acquired via the acquisition module.

To avoid the loss of data, a real time module with two multithreading tasks is integrated in the synchronization component. The EMUTEM system is now synchronized on the smart home sensors (Gardien) subsystem because it has the lowest sampling rate (2 Hz) and periodicity. The data from others modalities are memorized and used several time in order to have the same sampling rate (RFPAT data is used 60 times).

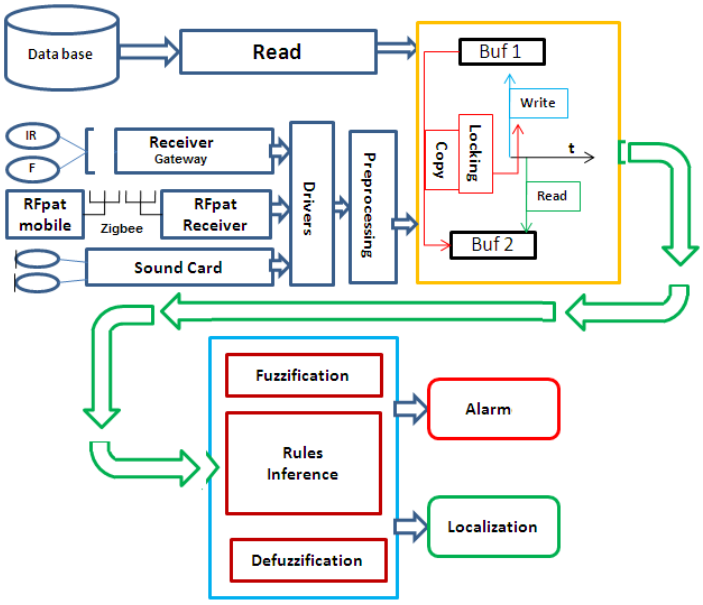

Fig. 6. EMUTEM software components design .

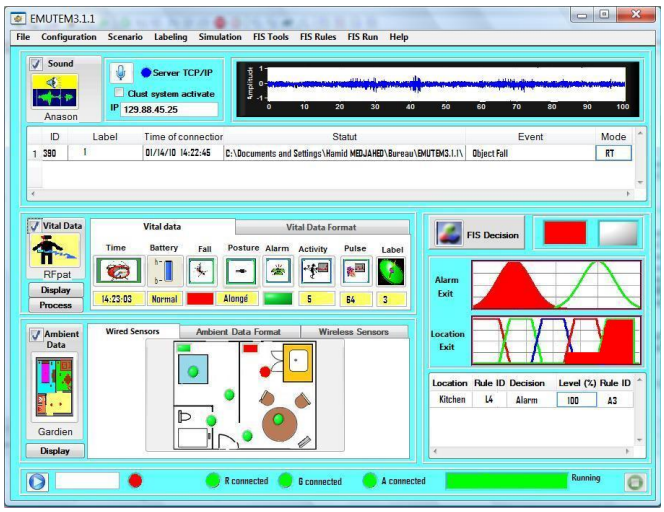

Fig. 7. Graphical Interfaces for Intelligibility.

This multithreading technique allows a maximum delay for an asynchronous data (Sound or alarm from RFPAT) of 0.5 s.

We have developed Fuzzy tools for the data fusion step. These tools allow the easy configuration of input/output intervals of Fuzzification, the writing of fuzzy rules and the configuration of the defuzzification method. It is also possible to add others modalities to this fuzzy inference system which make the EMUTEM platform flexible. Two outputs are associated to the fuzzy inference system, Alarm for distress situation detection and Localization for elderly person position detection.

E. Graphical Interfaces for Intelligibility

To offer enhanced intelligibility for the EMUTEM platform, a graphical user interface (GUI) was developed for this task. It facilitates the various configurations required for the functioning of the platform. It is very useful for users.

Figure 7 shows this general graphical interface. It is possible to build up membership functions of inputs and outputs and displaying them under this graphical interface.

We could also write rules via this graphical interface. It is also possible to write rules to text file by using a specific language, that we have developed, understandable by our system.

These Graphical interfaces provide EMUTEM with a useful simplicity for users and with a flexibility that allows adding other modalities. They allow experts to add their knowledge in a user friendly way.

V. The In Home Monitoring Database

In order to test and to validate the EMUTEM platform, an environment for acquiring and recording a multimodal database (HOMECAD [8]) is integrated under this platform. To record this multimodal database, users can interpret elderly activities by following a reference scenario which summarizes the everyday life of elderly persons. These scenarios are divided into two categories: either a critical scenario with one

or more distress events, or a normal one without any distress event. To define these scenarios a study is performed and they were instigated under CompanionAble European project. In this project, some elderly living alone were followed up by a co-worker team, in order to summarize and to describe their daily routine. The recorded multimodal database gathers physiological data, environment sounds and others different information gathered by ubiquitous sensors associated to Gardien subsystem.

First recordings were performed in our laboratory. Participants in this study were 10 adult volunteers who were recruited from the university and from the community. Participants ranged in age from 25 to 50 years. Participants were asked to perform several activities according to the used reference scenario. As each scenario lasts 10 minutes, this task corresponds to 200 minutes of recorded data.

The second stage of recording occurred in Broca Hospital in Paris under the framework of CompanionAble project. Ten adult volunteers from the community were enrolled to participate in this recording stage. The participants profile varied, ranged in age from 65 to 75 years, and the sample was 60% female and 40% male. The last stage of recording was also performed under the CompanionAble project and was performed in SmartHomes at Eindhoven. Fifteen adult volunteers were involved in this recording. For both stages of recording, a scenario lasts 15 minutes and each participant performs three different scenarios.

An additional process of simulation is also integrated in our platform as a way to overcome the lack of experimental data and the difficulty of recording some medical data such as the cardiac frequency during distress situations.

Taking into account the multimodality character of the data, a multidimensional indexing process is used in order to obtain a full description of data sets. In order to index our multimodal database, we have retained the SAM standard indexing file [17] generally used for speech database description. It indicates information about the file and describes it by delimiting the useful part for further analyzing and processing.

VI. Experimental Results and Validation

The realization of an experimental process requires the use of appropriate metrics for evaluating the performance of the platform by comparing the system's results to expected results. It is useful to describe some parameters or metrics that allows an objective evaluation of the results. To perform this experimental process we have selected the following metrics:

- *Sensitivity (Se)*: Identify patterns of real abnormal situations as distress ones.
- *Specificity (Sp)*: Don't identify normal situations as distress situations.
- *Error rate (Err)*: It is the ratio between the number of the misclassified samples and the total number of the samples.
- *Perfect classification(Pc)*: It is the ratio between the number of the correct classified samples and the total number of the samples.

		EMUTEM Classification	
		Distress sequence	Normal sequence
Simulated sequences	Distress sequence	68	2
	Normal sequence	1	29

TABLE I
Classification results for Alarm output with simulated data by using 10 rules

Indices of sensitivity (Se), specificity (Sp), error rate (Err) and perfect classification (Pc) are calculated from rates of true/false positive/negative, marked respectively with these symbols TP, FP, TN, and FN.

$$Se(\%) = \frac{TP}{TP+FN} \times 100 \quad (1)$$

$$Sp(\%) = \frac{TN}{TN+FP} \times 100 \quad (2)$$

$$Err(\%) = \frac{FN+FP}{TN+FN+FP+TP} \times 100 \quad (3)$$

$$Pc(\%) = \frac{TN+TP}{TN+FN+FP+TP} \times 100 \quad (4)$$

The just exposed metrics of the statistic data are very important to estimate the classification accuracy.

In order to demonstrate the effectiveness of this software, firstly we started by using simulated data in order to validate each rule. This first step of simulation gave very promising results for the alarm generation and localization without any false decision for each rule.

After that 100 sequences of simulation are used to test EMUTEM, where 70 sequences represent distress situation and 30 sequences represente normal situation, because we wanted especially to test the distress part that is more difficult to record in a real situation.

In order to evaluate the classification accuracy the confusion matrix has been calculated for this simulation. Table I displays the obtained results with 10 rules.

Sensitivity Se	97%
Specificity Sp	96%
Error rate Err	3%
Perfect classification Pc	97%

TABLE II
Performance indices for Alarm output obtained with simulated data by using 10 rules

From table I we can deduce some indices of performance which are displayed in table II. The obtained results of EMUTEM's performance are good and they demonstrate the reliability of the EMUTEM platform. Even if we have 3% of misclassified sequences, this error rate could be overcome by adding to the fuzzy inference system the right rules that take into account the misclassified situations, and also by associating to each rules the right weight.

For the localization output, also we have obtained about 98% of good localization.

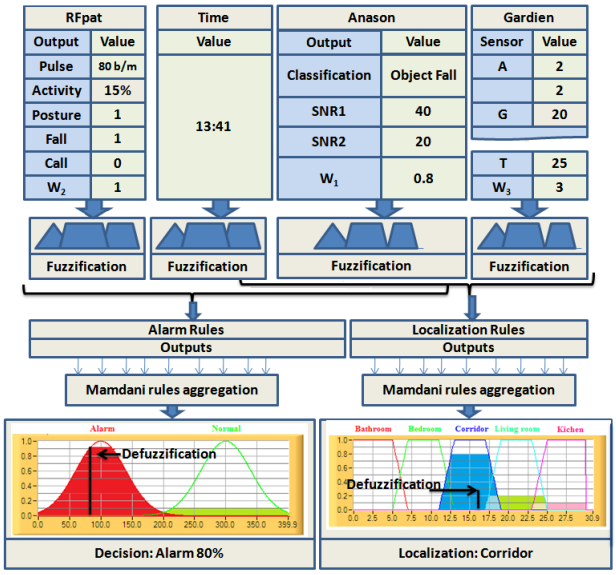

Fig. 8. Results for a stream of data

Figure 8 shows results for a steam of data and summarizes the process of the fuzzy inference system. The first step of this process is to determine the output of each membership function assigned to each input. Then the outputs of the rules are calculated by applying the fuzzy operators (AND and OR) in the antecedent part of all rules, using the T-norm and T-conform operators respectively and the implication from the antecedent to the consequent, using T-norm operator. After that the aggregation of the consequents across the rules of each output is performed by using the Mamdani model, it is the unification process of the all rule outputs. Finally the process of defuzzification is done by extracting out one crisp value as the output, the smallest value of maximum method is chosen for the alarm output and the centroid of area for the localization output.

The EMUTEM platform was tested with the HOMECAD database described in the previous section. This first study is devoted to the evaluation of the system by taking into account rules used in this fuzzy inference system. The strategy consisted in realizing several tests with different combination rules, and based on the obtained results, one rule is added to the selected set of rules, or removed from this selected set of rules in order to get the missed detection. Based on the obtained results some weights of rules are also changed. With this strategy good results are reached for the alarm output with 10 rules and 16 rules for the localization outputs. The data fusion classification using the fuzzy logic approach has given better performance results when compared to analytical method and using artificial neural networks (ANN) for classification (Table III). More over problems associated with conventional neural network architectures such as learning rate limitation and difficulty in selecting the optimal number of hidden units are eliminated.

With this strategy good results are reached for the alarm output with 10 rules and 16 rules for the localization outputs,

	Fuzzy classifier (10 rules)	ANN (3 hidden layers)
Se	95%	87%
Sp	93%	85%
Err	5%	12%
Pc	95%	88%

TABLE III
PERFORMANCE INDICES FOR ALARM OUTPUT OBTAINED WITH FUZZY CLASSIFIER AND ANN METHOD

about 95% of good Alarm detection and 97% for good Localization. The rate of misclassification for the alarm output corresponds to situation that are not detectible by the sensors used by EMUTEM and also the difficulty to find the right rule to overcome these situations. For the localization output the error rate could be justified by the fact that we use an area where an apartment is simulated thus the calibration of infrared sensors is very hard.

These first results encourage us to perform further tests in real time in order to have an effective evaluation of the EMUTEM platform.

VII. Conclusion

In this work, we focused on the area of automatic home healthcare telemonitoring, in which health information is automatically collected with the help of sensors and processed by special algorithms and fused in order to make good decisions about elderly persons living alone at home. The proposed multimodal data fusion method based on fuzzy logic represents a fast and easy tool for the interpretation of the fuzzy decision process even for very high dimensional input spaces and allows fast detection of errors. The impact of the input features plays an important role on the final decision process. The algorithm supports the implementation of the expert's knowledge and optimized the system easily. It is possible to increase the performance further by adding more related input variables and with more data to enrich the knowledge in the rules.

The EMUTEM platform which encloses this architecture is implemented and validated by simulation and by using real data. The experimental results were accurate and robust. The main advantage of the presented method consists of the low-computational expenses inherited from the characteristics of fuzzy systems. This approach allows the easiest combination between data and adding other sensors.

The fuzzy logic decision module reinforces the secure detection of older person distress events and his localization. This constitutes a great asset for the EMUTEM system, by offering the possibility in the near future, to implement a very intelligent remote monitoring system in care receiver houses, thus to build very reliable smart houses.

Acknowledgment

The authors would like to thank the contribution of European Community's Seventh Framework Programme (FP7/2007-2011), CompanionAble Project (grant agreement n.216487).

REFERENCES

[1] H. Bouma, *Gerontechnology: A framework on technology and aging, In H. Bouma and J. Graafmans, editors, Gerontechnology*, ISO Press. pages 1-6, Amsterdam, 1993.

[2] D. Doermann and D. Mihalcik, *A system approach to achieving carernet, an integrated and intelligent telecare system*, IEEE Trans Biomed Eng, 2:1-9, 1998.

[3] N. Noury, P. Barralon, G. Virone, P. Boissy, M. Hamel, and P. Rumeau, *A smart sensor based on rules and its evaluation in daily routines*, in Proc of the IEEE-EMBC, pages 3286-3289, Cancun, Mexico, september 2003.

[4] G. Elger and B. Furugren, *"smartbo",an ICT an computer-based demonstration home for disabled people*, in Proc. of the 3rd TIDE Congress : Technology for Inclusive Design and Equality Improving the Quality of Life for the European Citizen, Helsinki, Finland, 1998.

[5] G.A.W. West, S. Greenhill and S. Venkatesh, *A probabilistic approach to the anxious home for activity monitoring*, in Proc. 29th Annual International Computer Software and Applications Conference: COMPSAC, pages 335-340, Edinburgh, Scotland 2005.

[6] H. Medjahed, D. Istrate, J. Boudy and B. Dorizzi, *Human Activities of Daily Living Recognition Using Fuzzy Logic For Elderly Home Monitoring*, IEEE Fuzzy Systems (FUZ-IEEE) 2009, 20-24 Aout 2009, Jeju Island, Korea, pp.2001-2006.

[7] J.E. Rougui, D. Istrate, W. Souidene, *Audio Sound Event Identification for distress situations and context awareness*, EMBC2009, September 2-6, Minneapolis, USA, 2009, pp. 3501-3504.

[8] H. Medjahed, D. Istrate, J. Boudy, F. Steenkeste, J.L. Baldinger, I. Belfeki, V. Martins and B. Dorizzi, *A Multimodal Platform for Database Recording and Elderly People Monitoring*, BIOSIGNALS 2008, 28-31 janvier 2008, Funchal-Madeira, Portugal, pp.385-392.

[9] S. Stillman and I. Essa. *Toward reliable multimodal sensing in aware environments*, Perceptual User Interfaces (PUI 2001) Workshop (held in conjunction with ACM UIST 2001 Conference), Orlando, Florida, November 15-16, 2001.

[10] Lawrence A. Klein. *Fuzzy set theory in medical diagnosis*, IEEE Tr. On Syst.,Man, and Cybernetics, pages 260-265, March/April 1986.

[11] S.J Russell and P. Norvig, *Probabilistic reasoning in artificial intelligence: a modern approach*, Upper Saddle River 2nd, pages 492-494, N.J Prentice Hall, 2003.

[12] G. Shafer, *A mathematical theory of evidence*. Princeton University Press, Princeton, NJ, 1976.

[13] C. Bishop. *Neural networks for pattern recognition*, Oxford, 1995.

[14] C.J.C. Burges. *A tutorial on SVM for pattern recognition*, Data Mining and Knowledge Discovery, Volume 2, pages 121-167, 1998.

[15] L. Zadeh, *Fuzzy sets. in Fuzzy Models for Pattern Recognition: Methods That Search for Structures in Data*, edited by J. Bezdek and S. Pal, IEEE Press, pages 35-45, New York 1992.

[16] J.S.R. Jang, C.T Sun and E. Mizutani, *Neuro-Fuzzy and Soft Computing : A Computational Approach to Learning and Machine Intelligence*, Prentice Hall Upper Saddle River, NJ 1997.

[17] D. Well, J. Barry, W. Grice, M. Fourcin, and A. Gibbon, *Esprit project 2589-multilingual speech input/output assessmen, methodology and standardization, In final report*, Technical Report SAM-UCLG004, University College London, 2004.

2011 IEEE International Conference on Fuzzy Systems
June 27-30, 2011, Taipei, Taiwan

Value Driver Derivations for Embedded Memories by Fuzzy DEMATEL based Hybrid MCDM Methods

Chi-Yo Huang
Department of Industrial Education
National Taiwan Normal University
Taipei, Taiwan
cyhuang66@ntnu.edu.tw

Gwo-Hshiung Tzeng
Institute of Project Management
Kainan University
Luchu, Taiwan
ghtzeng@mail.knu.edu.tw

Abstract — **The embedded memories have already played a very important role in the modern system on a chip (SoC) designs from the aspects of performance enhancement, power reduction, form factor optimization, etc. Meanwhile, embedded memories usually occupied for the major portion of an SoC layout. Thus, how an embedded memory IP (intellectual property) provider can differentiate the product to maximize the value of that IP has already become a key factor for profit maximization. However, very few scholars tried to resolve such problems. The product and service differentiation problem of memory IPs is in nature a multiple attribute decision making (MADM) problem. Moreover, the differentiators of an embedded memory IP usually interact with each other. Furthermore, evaluations of customers' needs and wants, which are vague, are often required for such a product marketing strategy definition problem. Thus, a fuzzy DEMATEL based multiple criteria decision making (MCDM) framework will be proposed for maximizing the value of an embedded memory IP. The value driver for differentiating an embedded memory IP will first be derived by literature review. The most influential value drivers will be selected. Then, strategies will be proposed for maximizing the value through the most influential value drivers. An empirical study based on an embedded memory IP being provided by an SOC design service provider will be used for verifying the feasibility of the framework. Based on the empirical study results, both power consumption as well as the area of the embedded memory core are the most important value drivers. The proposed product marketing strategies can also be used for maximizing the value of the embedded IP.**

Keywords – Embedded memory; system on a chip (SOC); differentiation; Fuzzy DEMATEL; Fuzzy MCDM (Multiple Criteria Decision Making, MCDM).

I. INTRODUCTION

Memory plays a critical role in achieving the performance, power or cost goals of an electronic system [1]. For an SoC (System on a Chip), the memory and processors are implemented on the same chip while in this particular case, the memory is called the embedded memory [2]. Nowadays, over 50 % of the area in an SoC is occupied by the embedded memory [3]. As the integrated circuit migrates to the SoC era, the embedded memory technique is playing a daily important role. Furthermore, provisions of embedded memory intellectual properties (IP) and design services have become novel business models which emerged in the past decade.

Embedded memory may be more expensive to fabricate than separate memory chips, since the fabrication processes for memories and processors must be compatible [2]. Nevertheless, a large percentage of the total chip area maybe consumed by the memory [2]. Thus, the selection of an embedded memory IP and supplier is critical to the success of the design and the ramp to volume [3]. When designed correctly, an SoC incorporating embedded memory can offer higher speeds or lower power consumption and maintain the same or lower cost than a system designed with stand-alone memory [4].

Differentiation in the embedded memory IP can occur in the four mutually interacted dimensions, including the function, the speed, the area and the power consumption; albeit some RAMs offer functional differentiation, the key areas in which differentiation can exist are the trade-offs between the remaining three dimensions [5]. Further, from the SOC design service view, differentiation can happen in the time to market capability, SIP integration service capability, SIP verification capability, as well as the close relationship with foundries.

The embedded memories are usually provided by IP providers, design service providers or professional silicon foundries. However, providing a "me too" embedded memory product cannot assist a provider help customer maximize their value. Thus, how a design service provider can differentiate their products and maximize the value of their services has become a critical issue.

A company can differentiate its market offering through product, services, etc. [6]. The essence of differentiation advantage, to increase the perceived value of the offering to the customer either more effectively or at lower cost than do competitors, requires that the firm match the requirements and preferences of customers with its own capacity for creating uniqueness [7]. Products, services and technologies should be seen as vehicles for value creation [8]. Product managers are expected to set prices that capture the value offered by their products and that also maximize profits [9]. In order to build effective marketing strategy companies must first understand the factors that drive customer perceptions of value [10], or namely, value drivers, which can be defined as (1) customer needs upon which our product or service could have an impact [9] or (2) the decision-related attributes that are perceived by the customer to be the most important to the choice process [11].

978-1-4244-7316-8/11/$26.00 ©2011 IEEE

Apparently, how the value of a product can be maximized is a multiple attribute decision making problem (MADM) in nature. Further, due to the uncertainness of human beings' evaluations of needs, wants and intentions in their mindsets, applications of the fuzzy theory into the MADM framework(s) are very straightforward. Therefore, this research intends to define a fuzzy DEMATEL based multiple criteria decision making (MCDM) based framework for selecting product differentiation strategies for a company providing embedded memory products. At first, literature regarding to differentiating value drivers will be reviewed. The literature will serve as a basis for the MCDM framework development as well as possible alternatives for suitable fuel cell battery technologies. Then, the GRA will be used for deriving the relationships between the possible courses as well as the competences to be expanded. The courses with the highest Grey grades will be selected as the suitable courses of the curriculum.

An empirical study on maximizing the embedded memory IP belonging to an SoC design service firm will be provided for maximizing the value of the embedded memory IPs. The empirical study results can serve as a basis for the design service firm's value maximization of its IPs.

This research is organized as follows. The related literature regarding to differentiation and value drivers will be reviewed in Section II. The theory which is based on MCDM framework and using the GRA method will be introduced in Section III. An introduction to the embedded memory technologies will be given in Section IV. An empirical study on maximizing developing the product marketing strategies will be demonstrated in Section V for demonstrating the feasibility of this framework. Implications as well as discussion will be presented in Section VI. Finally, the whole article will be concluded in Section VII.

II. Product Differentiation and Profit Maximization

An early study by Dickson and Ginter [12] summarized definitions of product differentiation from marketing textbooks as an alternative to market segmentation or a complement or means of implementing market segmentation. The potential for differentiation in any business is vast while differentiation extends beyond technology, design, and marketing to include all aspects of a firm's interactions with its customers [7].

Six factors affecting customer purchase decisions include relative advantage, compatibility, complexity, trialability, ability to communicate product benefits and observability [8]. A company can differentiate its market offering through product, services, personnel, channel, and image while the decision variables belonging to the obvious means of product and services include form, features, conformance, durability, reliability, style, design, quality, ordering ease, delivery, installation, customer training, customer consulting, maintenance and repair, etc. [6]. Some physical products can be highly differentiated [13] through (1) form, (2) features, (3) performance quality, and (4) conformance quality [6]. Further, according to Kotler and Keller, Products, services and technologies should be seen as vehicles for value creation [8]. The essence of differentiation advantage, to increase the perceived value of the offering to the customer either more effectively or at lower cost than do competitors, requires that the firm match the requirements and preferences of customers with its own capacity for creating uniqueness [7]. A product's total economic value, then, is the price of the customer's best alternative (the reference value) plus the economic value of whatever differentiates the offering from the alternative (the differentiation value) [9]. Value appropriation means investing in strategies that allow the firm to differentiate its existing offerings in order extract profits in the market [8]. Even for high technology markets, the investors reacts more favorably when a firm increases its emphasis on value appropriation relative to value creation, constantly innovating and investing in R&D [8].

Only the part of economic value being associated with differentiation, or the differentiation value, can potentially be captured in the price; differentiation value comes in two forms: monetary and psychological, both of which may be instrumental in shaping a customer's choice but require very different approaches to estimate them [9]. In order to create the foundation for setting prices, it is critical to understand what the customer's value drivers are and how the purchase decision can be influenced [14]. The customers' value drivers need to be reflected in the design requirements of the software if the value is to be subsequently captured by the pricing mechanism on the product's launch [14].

In order to build effective marketing strategy companies must first understand the factors that drive customer perceptions of value [10], or namely, value drivers, which can be defined as the decision-related attributes that are perceived by the customer to be the most important to the choice process [11]. The value at the heart of pricing strategy is not use value, but is what economists call exchange value or economic value, which depends on the alternatives customers have available to satisfy the same need [9].

Value hypothesis development usually begins with a list of your offering's potential value drivers including superior performance, greater reliability, additional features, reduced maintenance costs, smaller startup costs, faster service, etc. [9]. Harmon and Laird [10] summarized the value drivers to be economic-value driver, performance/functional value, buyer's perceptions about the supplier, buyer's motivations and goals, and the buying situation.

Finally, the three steps for economic value include: study customer economics, quantify value drivers and finally, estimate differentiation value [9].

III. Analytic Framework For Maximizing Profits Through Product Differentiation

The analytical process for designing a capabilities-driven curriculum is initiated by collecting the capabilities and possible fuel cell courses being required to develop the national fuel cell industry by using the Delphi method. Then, the relations between the capabilities and the possible courses will be derived by using the Grey Relation Analysis.

A. Fuzzy DEMATEL Method

The Fuzzy DEMATEL can deal with the DEMATEL problem by introducing Fuzzy linguistic variables and matrices. According to the definition of Fuzzy DEMATEL, the linguistic matrices present the relationships between criteria. In the matrices, the numeral value depicts the influence versus each

criterion. Therefore, the Fuzzy DEMATEL method can transform the causes and effects relationship into a perspicuous structural model. The Fuzzy DEMATEL method has been studied and applied in many areas these years [15,16]. According to the advantages of Fuzzy DEMATEL, this research attempts to evaluate the preferences of lead users by using Fuzzy DEMATEL based on the definitions by Prof. Tzeng, Gwo-Hshiung [17]. The calculation process is demonstrated as below:

Step 1: Establishing the fuzzy linguistic scale

Establishing the linguistic sets of criteria is an essential procedure for Fuzzy DEMATEL. The major advantage of Fuzzy DEMATEL method is that it's effective to obtain the structural mode and divide the criteria into cause and effect groups, which consist of many complex aspects. To deal with the ambiguities of human feeling and evaluations, Li [18] introduces the fuzzy linguistic scale into the DEMATEL evaluation process. The strength of influence are divided into five linguistic levels as "Strong", "High", "Low", "No" and the linguistic levels will correspond to the triangular fuzzy numbers.

Step 2: Establishing the directed relation matrix

To measure the relationship versus each criterion $C=\{c_1,c_2,\ldots,c_n\}$, p lead users made evaluations in terms of linguistic terms toward the criteria. Thus, p fuzzy matrices $\tilde{\boldsymbol{Z}}^1,\tilde{\boldsymbol{Z}}^2,...,\tilde{\boldsymbol{Z}}^P$ each corresponds to a lead user. The Fuzzy matrix is called the initial direct relation fuzzy matrix. For simplicity, denote $\tilde{\boldsymbol{Z}}$ as $c_1,c_2...c_n$, or

$$\tilde{\boldsymbol{Z}}=\begin{matrix}c_1\\c_2\\\vdots\\c_n\end{matrix}\begin{bmatrix}0&\tilde{z}_{12}&\cdots&\tilde{z}_{1n}\\\tilde{z}_{21}&0&\cdots&\tilde{z}_{2n}\\\vdots&\vdots&\ddots&\vdots\\\tilde{z}_{n1}&\tilde{z}_{n2}&\cdots&0\end{bmatrix},$$

where $\tilde{z}_{ij}=\left(l_{ij},m_{ij},u_{ij}\right)$ are triangular fuzzy numbers, elements $\tilde{z}_{ii}=0,i=1,2...n$.

Step3: Establishing the structural model

In order to transform the criteria scales into comparable scales, the linguistic scale will be transformed into a normalization formula.

Let $\tilde{a}_{ij}=\sum_{j=1}^{n}\tilde{z}_{ij}=\left(\sum_{j=1}^{n}l_{ij},\sum_{j=1}^{n}m_{ij},\sum_{j=1}^{n}u_{ij}\right)$ and $u=\max_{1\le i\le n}\left(\sum_{j=1}^{n}u_{ij}\right)$.

Then, the normalized direct relation fuzzy matrix, denoted by $\tilde{\boldsymbol{X}}$, equals $\tilde{x}=u^{-1}\otimes\tilde{z}$. Or

$$\tilde{\boldsymbol{X}}=\begin{bmatrix}\tilde{x}_{11}&\tilde{x}_{12}&\cdots&\tilde{x}_{1n}\\\tilde{x}_{21}&\tilde{x}_{22}&\cdots&\tilde{x}_{2n}\\\vdots&\vdots&\ddots&\vdots\\\tilde{x}_{m1}&\tilde{x}_{m2}&\cdots&\tilde{x}_{mn}\end{bmatrix},$$

where $\tilde{x}_{ij}=\frac{\tilde{z}_{ij}}{u}=\left(\frac{l_{ij}}{u},\frac{m_{ij}}{u},\frac{r_{ij}}{u}\right)$. (1)

Fuzzy DEMATEL also assume that $\sum_{j=1}^{n}u_{ij}<u$ and $\lim_{k\to\infty}\tilde{x}=[0]_{0\times0}$.

Step 4: Deriving the total relation matrix

After calculating the normalized direct relation fuzzy matrix, the total relation matrix $\tilde{T}$ can be derived by the equation below:

$$\tilde{\boldsymbol{T}}=\tilde{\boldsymbol{X}}+\tilde{\boldsymbol{X}}^2+\cdots+\tilde{\boldsymbol{X}}^n=\tilde{\boldsymbol{X}}(\boldsymbol{I}-\tilde{\boldsymbol{X}})^{-1},$$

When $\lim_{k\to\infty}\tilde{X}=[0]_{n\times n}$

$$\tilde{\boldsymbol{T}}=\begin{bmatrix}\tilde{t}_{11}&\tilde{t}_{12}&\cdots&\tilde{t}_{1n}\\\tilde{t}_{21}&\tilde{t}_{22}&\cdots&\tilde{t}_{2n}\\\vdots&\vdots&\ddots&\vdots\\\tilde{t}_{m1}&\tilde{t}_{m2}&\cdots&\tilde{t}_{mn}\end{bmatrix};\tilde{t}_{ij}=\left(l_{ij}^{"},m_{ij}^{"},r_{ij}^{"}\right)$$

$$\left[l_{ij}^{"}\right]=\boldsymbol{X}_l-\left(\boldsymbol{I}-\boldsymbol{X}_l\right)^{-1},\ \left[m_{ij}^{"}\right]=\boldsymbol{X}_m-\left(\boldsymbol{I}-\boldsymbol{X}_m\right)^{-1},$$
$$\left[r_{ij}^{"}\right]=\boldsymbol{X}_r-\left(\boldsymbol{I}-\boldsymbol{X}_r\right)^{-1}$$

Step 5: Analyzing the sum of rows and columns

The row and column sums are individually indicated the sum of rows and columns of the total relation matrix $\boldsymbol{T}$ by using following equations (2), (3), and (4),

$$\tilde{\boldsymbol{T}}=[\tilde{t}_{ij}],\quad i,j\in\{1,2,...,n\} \tag{2}$$

$$\tilde{\boldsymbol{r}}=[\tilde{r}_i]_{n\times1}=\left[\sum_{j=1}^{n}\tilde{t}_{ij}\right]_{n\times1} \tag{3}$$

$$\tilde{\boldsymbol{c}}=[\tilde{c}_j]_{1\times n}=\left[\sum_{i=1}^{n}\tilde{t}_{ij}\right]_{1\times n} \tag{4}$$

where the $\boldsymbol{r}$ and $\boldsymbol{c}$ represent the sums of the rows and columns.

Step 6: Analyzing the results from $\boldsymbol{r}$ and $\boldsymbol{c}$

According to the sum of rows and columns, $(\tilde{r}_i+\tilde{c}_i)$ depicts the strength of the influence. If $(\tilde{r}_i-\tilde{c}_i)$ is positive, then criteria i is dispatching influence on other factors. On the other hand, if $(\tilde{r}_i-\tilde{c}_i)$ is negative, factor i is receiving influence from other criteria [15,19,20].

B. Analytic Network Process (ANP)

The ANP method, a multi criteria theory of measurement developed by Saaty [21], provides a general framework to deal with decisions without making assumptions about the independence of higher-level elements from lower level elements and about the independence of the elements within a level as in a hierarchy [21]. In this section, concepts of the ANP are summarized based on Saaty's earlier works [21, 22].

A component of a decision network which was derived by the DEMATEL method in Section 3.1 will be denoted by $\boldsymbol{C}_h$, $h=1,2,\cdots,m$, and assume that it has n_h elements, which we denote by e_{h1}, e_{h2}, $\cdots$, e_{hm}. The influences of a given set of

elements in a component on any element in the decision system are represented by a ratio scale priority vector derived from paired comparisons of the comparative importance of one criterion and another criterion with respect to the interests or preferences of the decision makers. This relative importance value can be determined using a scale of 1–9 to represent equal importance to extreme importance [21]. The influence of elements in the network on other elements in that network can be represented in the supermatrix as $\boldsymbol{W}_{ij} = [w_{ij}],\ i \in \{1,2,...,m\}$, $j \in \{1,2,...,m\}$. A typical entry $\boldsymbol{W}_{ij} = [w_{i_{nx} j_{ny}}],\ nx \in \{1,2,...,n_i\}$, $ny \in \{1,2,...,n_j\}$ in the supermatrix, is called a block of the supermatrix in the following form where each column of $\boldsymbol{W}_{ij}$ is a principal eigenvector of the influence of the elements (objective) in the ith component of the network on an element (objective) in the j^{th} component. Some of its entries may be zero corresponding to those elements (objective) that have no influence.

After forming the supermatrix, the weighted supermatrix is derived by transforming all columns sum to unity exactly. This step is very much similar to the concept of the Markov chain in terms of ensuring that the sum of these probabilities of all states equals 1. Next, the weighted supermatrix is raised to limiting powers, such as $\lim_{\theta \to \infty} \boldsymbol{W}^{\theta}$ to get the global priority vector or called weights [23].

In addition, if the supermatrix has the effect of cyclicity, the limiting supermatrix is not the only one. There are two or more limiting supermatrices in this situation, and the Cesaro sum would need to be calculated to get the priority.

IV. An Empirical Study of an Embedded Memory Value Maximization Strategies Definitions

As embedded memories are playing a daily critical role in modern SoC designs, novel techniques emerged. Further, embedded memory vendors, SoC design service providers, and professional foundry vendors are dedicated in providing novel services so as to fulfill customers' needs of one stop shopping, time to market, and thus, time to money.

Based on literature review and an expert's (with experiences in SoC design service and semiconductor memory sales and marketing for more than 10 years) opinions regarding to the value drivers of the embedded memory intellectual properties, the value drivers can be divided into two aspects, technology and service. From the technology aspect, the functionality (f_1), speed (f_2), area (f_3), and power consumption (f_4) of the memory IPs can be defined as the value drivers for an embedded memory IP. Further, from the service aspect, the time to market capability (f_5), the provision of the one stop shopping environment (f_6), the SIP design capability (f_7), the SIP integration service capability (f_8), the SIP verification capability (f_9) as well as the supply chain management capability (f_{10}) can be defined as the value drivers for an embedded memory IP.

At first, according the expert's opinion, the linguistic variables can be defined as Figure 1(a) while the initial direct relation fuzzy matrix $\tilde{\boldsymbol{Z}}$ can be defined as Figure 1(b).

Then, by introducing the Fuzzy DEMATEL ANP process being introduced in Section 3, the weights being associated with each work barrier can be derived (see Table II).

According to the empirical study results, the power consumption as well as the area is the most important value drivers for differentiating the embedded memory from both aspects of technology and services.

V. Discussion

In this research, embedded memory value drivers for product differentiation were derived from both aspects of technology and services. Following, managerial implications and future research possibilities will be presented.

At first, the embedded memory design and selection is in nature an MCDM problem by considering interdependences between criteria. Very limited scholars tried to address this issue by introducing the MCDM framework though the integrated circuit industry is migrating into the SoC era which embedded memories are playing a significant role from the aspects of area and its influences in SoC speed, power consumption, cost, etc. Thus, this research advanced the research in the related fields.

Variable	Upper	Medium	Lower
VL	0	30	60
L	50	60	70
M	60	68	75
H	70	78	85
VH	75	85	100

(a)

	f_1	f_2	f_3	f_4	f_5	f_6	f_7	f_8	f_9	f_{10}
f_1	0	VH	VH	VH	VH	VL	VL	VL	VL	VL
f_2	L	0	M	VH	VL	VL	VL	VL	VL	VL
f_3	VL	M	0	M	VL	VL	VL	VL	VL	VL
f_4	VL	VL	VL	0	VL	VL	VL	VL	VL	VL
f_5	VL	VL	VL	VL	0	VL	VL	VL	VL	H
f_6	VL	VL	VL	VL	VH	0	VL	VH	VL	VH
f_7	VH	VH	VH	VH	VH	VL	0	VH	VH	VH
f_8	VL	VL	VL	VL	VH	H	L	0	L	VH
f_9	VL	VL	VL	VL	VH	H	VL	VH	0	VH
f_{10}	VL	VL	VL	VL	VH	H	M	VH	M	0

(b)

Figure 1. (a) Linguistic variables and (b) the fuzzy matrix $\tilde{\boldsymbol{Z}}$

Table II. The weights versus criteria

Driver	f_1	f_2	f_3	f_4	f_5
Weight	0.068	0.068	0.114	0.341	0.068
Driver	f_6	f_7	f_8	f_9	f_{10}
Weight	0.068	0.068	0.068	0.068	0.068

Further, very few scholars tried to analyze how an embedded memory IP can analyzed from both aspects of technology and services. In this research, the authors adopted literature from both technology side and the business side and analyzed the casual relationships between two aspects. Further, the most important value drivers which can influence other criteria were also derived.

For the empirical study results, the functionality factor was weighted lower than the power consumption factor. Such tradeoff is common for SOC(s) being designed for portable devices. The empirical study results will be changed if the target applications are changed.

Finally, in this research, a conceptual framework was developed based on the opinions of sole expert. In the future,

empirical studies based on industry experts from both the management and technology departments can be very helpful for developing the embedded memory business. Further, how the innovation strategies can be introduced for differentiating the value drivers will also be beneficiary for the marketers in the future.

VI. CONCLUSIONS

Embedded memory has played a daily important role in SoC designs. However, how to differentiate an embedded memory and maximize the profits from both aspects of technology and business were seldom addressed. Due to the interdependence nature of the embedded memory technology and business models, the authors adopted a Fuzzy DEMATEL based MCDM framework for deriving the most important value drivers. In the future, the concepts and frameworks being derived in this research can further be adopted as the basis for differentiation and product marketing strategy definitions.

ACKNOWLEDGMENT

The authors gratefully acknowledge the support of Taiwan National Science Council through grant number NSC 97-2511-S- 003-039-MY2 and NSC 98-2511-S-003-068-MY2.

REFERENCES

[1] A. Shubat, "Perspectives: Moving the market to embedded memory," *Design & Test of Computers, IEEE,* vol. 18, pp. 5-6, 2001.

[2] P. Marwedel, *Embedded System Design: Embedded Systems Foundations of Cyber-Physical Systems*: Springer, 2010.

[3] V. Ratford, "Make your SOC design a winner: select the right memory IP," in *Design, Automation and Test in Europe Conference and Exhibition, 2002. Proceedings*, 2002, p. 15.

[4] A. Shubat, "Perspectives: Moving the market to embedded memory," *Design & Test of Computers, IEEE,* vol. 18, pp. 5-6, 2001.

[5] M. E. Jones, "Not All Memory IP Is Created Equal," *Electronic News,* vol. 45, 1999.

[6] P. Kotler and K. L. Keller, *A Framework for Marketing Management*. Upper Saddle River, N.J.: Pearson Prentice Hall, 2009.

[7] R. M. Grant, *Contemporary strategy analysis*: Blackwell Pub., 2005.

[8] J. J. Mohr, S. Sengupta and S.F. Slater, *Marketing of High-Technology Products and Innovations*: Prentice Hall, 2009.

[9] T. T. Nagle, J.E. Hogan and J. Zale, *The Strategy and Tactics of Pricing: A Guide to Growing More Profitably*, 5th ed.: Prentice Hall, 2010.

[10] R. R. Harmon and G. Laird, "Linking marketing strategy to customer value: implications for technology marketers," in *Innovation in Technology Management - The Key to Global Leadership. PICMET '97: Portland International Conference on Management and Technology*, 1997, pp. 896-900.

[11] J. C. Mowen, *Consumer Behavior*. New York: MacMillan Publishing Company, 1987.

[12] P. R. Dickson and J. L. Ginter, "Market segmentation, product differentiation, and marketing strategy," *The Journal of Marketing,* vol. 51, pp. 1-10, 1987.

[13] P. Kotler and K. Keller, *Marketing Management*, 13th. ed. Upper Saddle River, N.J.: Pearson Prentice Hall, 2009.

[14] R. Harmon, D. Raffo, S. Faulk, "Value-Based Pricing for New Software Products: Strategy Insights for Developers," in *Portland Intl. Conf. on the Management of Eng. and Tech.*, 2004.

[15] M. Tamura, H. Nagata and K. Akazawa, "Extraction and systems analysis of factors that prevent safety and security by structural models," in *Proceedings of the 41st SICE Annual Conference*, Osaka, Japan, 2002, pp. 1752-1759.

[16] M. Yamazaki, K. Ishibe and S. Yamashita, "An analysis of obstructive factors to welfare service using DEMATEL method," *Reports of the Faculty of Engineering*, vol. 48, pp. 25-30, 1997.

[17] C.-Y. Hsu, K.T. Chen and G.H. Tzeng,, "FMCDM with Fuzzy DEMATEL Approach for Customers' Choice Behavior Model," *International Journal of Fuzzy Systems*, vol. 9, pp. 236-246, 2007.

[18] R.J. Li, "Fuzzy method in group decision making," *Computers and Mathematics with Applications*, vol. 38, pp. 91-101, 1999.

[19] Y.-J. Chiu, H.C. Chen, J.Z. Shyu and G.H. Tzeng, "Marketing strategy based on customer behaviour for the LCD-TV," *International Journal of Management and Decision Making*, vol. 7, pp. 143-165, 2006.

[20] C. Y. Huang, J.Z. Shyu and G.H. Tzeng, "Reconfiguring the Innovation Policy Portfolios for Taiwan 's SIP Mall Industry," *Technovation*, vol. 27, pp. 744-765, 2007.

[21] T. L. Saaty, *Decision Making with Dependence and Feedback: The Analytic Network Process*. Pittsburgh: RWS Publication, 1996.

[22] T. L. Saaty, *Theory and Applications of the Analytic Network Process - Decision Making with Benefits, Opportunities, Costs, and Risks*. Pittsburg, PA: RWS Publications, 2005.

[23] J.-J. Huang, G.H. Tzeng and C.S. Ong, "Multidimensional data in multidimensional scaling using the analytic network process," *Pattern Recognition Letters,* vol. 26, pp. 755-767, 2005.

2011 IEEE International Conference on Fuzzy Systems
June 27-30, 2011, Taipei, Taiwan

Fuzzy Multiple Attribute Decision Making Theory With The Balanced Scorecard Application In Mobile Industry

Chiu-Hung Su
Department of Electrical Engineering
Hwa-Shia Institute of Technology,
Taipei 235,Taiwan
ritasu@cc.hwh.edu.tw

Ying-Hsun Hung
Department of Information
Management, Hwa-Shia Institute of
Technology, Taipei 235,Taiwan
horninch@gmail.com

Gwo-Hshiung Tzeng
Institute of Management of
Management, National Chiao Tung
University, Hsinchu 300, Taiwan
ghtzeng@cc.nctu.edu.tw

***Abstract*—this study is the use of fuzzy multi-attribute decision making as a business management application in the balanced scorecard performance assessment. The study expected to help enterprises to establish effective expression of those feelings with subjective indicators of weight value. In order to increase the accuracy of weight and practice, so that more perfect performance of the Balanced Scorecard in the business. The use of the Balanced Scorecard to evaluate the importance of screening criteria in Taiwan mobile industry operators and fuzzy multi attribute decision making through the match with the comparison with the fuzzy multiple criteria decision making, to establish Taiwan's mobile industry business model assessment. Fuzzy multi-attribute decision making can be vague, uncertain or unstructured problems trying to provide a solution to this. Finally, this study found results, the implementation of the model created to operate as a decision-making in Taiwan mobile industry reference, and can understand the fuzzy multiple attribute decision making not only in dealing with the definition of ambiguous or unclear information, as an effective Methods, but in the real world where a lot of created process can easily be used, it will also help assess the performance of the Balanced Scorecard.**

Keywords-component; Balanced Scorecard; Multi-attribute decision making; MADM; Fuzzy Linguistic Variables

I. INTRODUCTION

Taiwan's communications industry and the simultaneous development of global industry trends in the case of wireless communications equipment industry accounted for the proportion of the overall communications industry, forecast to 50.7 % from the year 2001 to 2010 grew 79.6 % to 9, 064 million NT Production value, mainly due to smart phones and wireless local area network products, such as the two major types of products.

Recently, wireless communications, the global communications industry and the market has gradually focused on the mobile Internet, in addition to continued improvement related products, Smart mobile phone wireless communication contains (Smartphone) , the new models iPhone, notebook and mini-notebook (Netbook) , TV, Blu-ray players, set-top boxes, Bluetooth, Zigbee low cost and low power , RFID and other video-related consumer electronics products. We can know the future of wireless communication industry is the star, intense competition and survival, in order to enhance the overall efficiency and effectiveness of operations, in order to pin down opponents in the market in order to grasp the opportunity to ensure their long term competitive advantage. How to give real assistance from the academic point of view as to the task of balance scorecard and fuzzy multi-attribute decision theory to solve performance management and enhancing competitiveness of the push is urgent. The communication devices also show the booming trend. Taiwan's communications industry and the simultaneous development of global industry trends in the case of wireless communications equipment industry accounted for the proportion of the overall communications industry, forecast to 50.7 % from the year 2001 to 2010 grew 79.6 % to 9, 064 million NT Production value, mainly due to smart phones and wireless local area network products, such as the two major types of products.

Based on the above reason, this study was to understand the following issues:

First, explore the use of Balanced Scorecard-based applications in the Mobile Enterprise applicability.

Second, the implementation of the case company Fuzzy multiple attribute decision making problems.

Third, set for enterprise performance management strategy for Mobile program.

Mobile SMEs in an attempt to enterprise applications into the Balanced Scorecard, Balanced Scorecard of the four dimensions with the financial side, customer, internal business process perspective and learning and growth surface indicators to develop a corporate cause and effect Diagram, and to assist with the fuzzy multiple attribute decision making in the case company's balanced scorecard results further explore the issue in depth in order to understand the management decision-making reference for efficiency.

II. RELATED RESEARCH

A. Balanced Scorecard

"Balanced Scorecard" (Balanced Scorecard, referred to as BSC) from the 1990 U.S. Professor David Norton and Robert

S. Kaplan of Harvard University study "Organization of future performance evaluation system ", it is a performance measurement model, which is a strategy; remuneration means a combination of strategic management tool. Emphasis on performance measurement should be achieved: (1) to measure the balance between internal and external: internal measure of emphasis on internal business process implementation and staff learning and growth surface, and an external measure of the emphasis on the financial side and customer side. (2) The results of surface measurement surface to measure the balance and the future: the results of surface Through the Balanced Scorecard applied to SMEs. We learned that the scorecard for small and medium enterprises also is

Eastern Media International Corporation has been building a strategic performance measurement system, and the concept of the Balanced Scorecard into the case company. The company has taken the traditional way of performance evaluation system and flexibility of management by objectives, which, strategy and incentive system has a high degree of association with low correlation of performance evaluation system. Among them, the import of this approach, top managers will need the support and full participation (Yuksel, 2010).

B. Multi-attribute decision making

In general, the term commonly used in decision making, Zeleny (1982) consider multiple criteria (multiple criteria) includes a number of attributes (multiple attributes) and multi-objective (multiple objectives); generally used to describe the four elements of MADM, (1) the alternatives (Alternatives), (2) set of attributes (Attributes), (3) goal set (Objectives) and (4) preference / weight set (Preferences / Weights).

Multi-attribute evaluation criteria is when policy-makers face multiple, even conflicting objectives, the assessment criteria must be choice, and multiple criteria decision making (MCDM) is the number of evaluation criteria used to assess the merits of different alternatives and their implementation the order of the systematic scientific methods. Therefore, the generalized multiple criteria decision making methods can be divided into multiple attribute, multi-objective decision making, covering multiple attribute decision making (Multi-Attribute Decision Making; called MADM), multi-objective decision analysis (Multi-Object Decision Making; referred MODM) generalized deal with the problem.

Multi-attribute decision making is the decision-makers may also consider the number of Conflicts, in a viable alternative, the decision to choose their preferred method (Yoon & Hwang, 1995) . To be addressed include the following four basic elements (Yu, 1995) .

(1) A fixed set of alternatives (Finite Set of Alternative)

(2) The set of assessment criteria (Set of Criteria)

(3) Each program performance value (Performance Rating)

(4)Decision makers preference structure (Preference Structure of Decision Maker)

The decision makers must decide from a group of action , the trade-offs by considering a variety of property relationship, try to choose the most appropriate programs to achieve goals in the process, that is, multiple attribute decision making (Multiple Attribute Decision Making, MADM) . Bellman and Zedeh (1970) that the real environmental issues among decision-making occurred, most of the objectives, limitations, and possible options for the results are inaccurate, they are also the first to MADM fuzzy set theory is applied to the field. Therefore, the fuzzy multiple attribute decision making (Fuzzy MADM, FMADM) it will be extended to the fuzzy MADM environment, refers to the attributes in the decision-making process, weights, targets and the nature of restrictions may be vague, fuzzy sets must be said that Or property may be fuzzy linguistic variables.

C. The DEMATEL Method

The original DEMATEL (DEcision-MAking Trial and Evaluation Laboratory) method studied the disjointed and antagonistic phenomena of world and investigated integrated solutions. In 1973, the Battelle Memorial Institute conducted the DEMATEL project through its Geneva Research Centre. In recent years, this method has become very popular in Japan.

It is especially practical and useful for visualizing the structure of complicated causal relationships with matrices or digraphs, which portray the contextual relations between the elements of a system, where a numeral represents the strength of influence. Therefore, the DEMATEL method can convert the relationship between the causes and effects of criteria into an intelligible structural model of the system.

The DEMATEL method has been successfully applied in many fields. For example, Tamura et al. (2002) try to decrease anxiety of people by extracting and analyzing various uneasy factors in order to create future safe, secure and reliable (SSR) society. More recently, Chiu et al. (2005) adopted the method to study marketing strategy based on customer behavior related to LCD-TVs. Also Hori and Shimizu (1999) employed it to design and evaluate the software of a display-screen structure for analyzing a supervisory control system.

D. The Fuzzy Number and Linguistic Variables

Since fuzzy set theory was initially proposed by Zadeh, and Bellman and Zadeh (1970) subsequently described the decision-making methods in fuzzy environments, an increasing number of studies have dealt with uncertain fuzzy problems by applying fuzzy set theory. Similarly, this study adopts fuzzy decision-making theory by considering possible fuzzy subjective judgments during the evaluation process of strategic planning for the Balanced Scorecard in mobile industry.

It is very difficult for traditional quantification methods to reasonably express situations that are overtly complex or hard to define; therefore, the notion of linguistic variables is a useful tool in such situations. The theory of linguistic variables is used to represent the imprecision of spatial data and human cognition in terms of the criteria used for the evaluation

process. A linguistic variable is a variable whose values are words or sentences in a natural or artificial language. We use this approach to evaluate criteria represented by linguistic variables in a fuzzy environment as “Very high influence”, “High influence”, “Low influence”, and “No influence” on a four-level fuzzy scale.

The use of linguistic variables is widespread and, in this study, the linguistic values of alternatives are primarily used to assess the linguistic ratings given by decision-makers. Furthermore, linguistic variables are used to measure the performance value of alternatives for each criterion as “no influence”, “low influence”, “high influence”, and “very high influence”. We use triangular fuzzy numbers to express the fuzzy scale, as shown in Step 1 of the evaluation process.

E. The ANP for Calculating Weights of Criteria Based on the NRM

The analytic hierarchy process (AHP) supposes independence among criteria, which is not reasonable in the real world. Saaty (1996) thus extended AHP to ANP to resolve problems with dependence or feedback between criteria, which primarily divides problems into numerous different clusters and every cluster includes multiple criteria. Moreover, there is outer dependence among clusters and inner dependence within the criteria of clusters as illustrated in Fig. 18. In addition, we figured the relative weights of criteria of respective matrices by pair-wise comparison and modifying the weights as eigenvectors. Then we integrated multiple matrices into a super matrix, because the capacity to examine the inner and outer dependence of clusters is the largest benefit of a super matrix.

There are three steps for the decision process of ANP. First, the decision problem and the structure of problem were built to offer an evident depiction of the problem and separate it into a relation network structure as shown in Fig. 1. Second, not only is pair-wise comparison matrix established, but also eigenvalue and eigenvector were figured. Pair-wise comparison is composed of clusters and criteria. Furthermore, the pair-wise comparison of clusters was separated into comparison of criteria within and between clusters. We utilize ratio scale (1 ~ 9) to determine the level of importance of the comparison. In addition, the data deriving from the survey of ANP were combined and transferred into pair-wise comparison matrix by geometric average. After building the matrix, we received the eigenvector $\boldsymbol{W}_{ii}$ through an equation: $\boldsymbol{Aw} = \lambda_{\max}\boldsymbol{w}$, where A is pair-wise comparison matrix, $\boldsymbol{w}=\left(w_1,\ldots,w_i,\ldots,w_n\right)'$ is the eigenvector, wi is the eigenvalue, then

$$\lambda_{\max} = \frac{1}{n}\sum_{i=1}^{n}\frac{(\boldsymbol{Aw})_i}{w_i}$$

where $(\boldsymbol{Aw})_i = \sum_{j=1}^{n} a_{ij}w_j$ and n equals the number of comparative criteria. Third, the super-matrix, tagged $\boldsymbol{W}$ (as shown in Equation 6), was formed. It was constructed by the dependence table obtained from the interrelations among criteria, and the eigenvectors received from the pair-wise comparison matrix served as the weights of it. No inner dependence among criteria or clusters was shown by a blank or zero. By Wu and Lee (2007), the usage of power matrix by $\boldsymbol{W}^h$ (multiplication) and $\lim_{h\to\infty}\boldsymbol{W}^h$ is a fixed convergence value; therefore, we can acquire weights in every criterion.

III. RESEARCH METHOD

A. Case study

This study adopts a case study (Case Study Research) manner, the main purpose of the concept of Balanced Scorecard framework, supplemented by the method of fuzzy multi-attribute performance evaluation. Therefore, this chapter will be the basic concept of case study method, including its definition, types, design, procedures and applicable time, and case studies to illustrate the causes and processes. Case studies often conducted in a single case, focusing on the depth of discussion and analysis, to programs such as case studies in Table II of the program (Yin, R. K., 1989).

Scholars Yin (1989) that the conditions for case study three:

(1) When the type of research question is “ How” and “ Why”

(2) The researchers studied no significant control over the event, or no control.

(3) The focus of the present rather than past events.

Therefore, when the case study focuses on contemporary issues and problems of control is small, the use of case study research is a better strategy. In early studies, the administration should be carefully considered for the problem through the "how" and "why " of deep thinking, and determine the reach of a valid target. Scholars Yin (1994) has decided that the research methods to be used, Ke Yi in the form of research questions, study the need for behavioral control, the focus of research is focused on current events upper three dimensions, as the choice of reference.

This study investigated the balanced scorecard and fuzzy multiple attribute decision making using of the Mobile industry. The relevant departments of the operation of field observations case, the case company looking to read all relevant information, interviews, related departments, etc., the case company's strategy, processes, performance evaluation, balanced scorecard to understand, to the line of the contents into a follow-up questions Explore the implementation problems encountered and possible improvements made under the direction of the results in order to enhance the case competition in IT services. This chapter will explore the case study approach, the use of case study of the theory and process of this study.

B. Balanced Scorecard

This study investigated the balanced scorecard and fuzzy multiple attribute decision making using of the Mobile industry. From the second half of 2010, gradually forming. The relevant departments of the operation of field observations case, the case company looking to read all relevant information, interviews, related departments, etc., the case company's strategy, processes, performance evaluation, balanced scorecard to understand, to the line of the contents into a follow-up questions Explore the implementation problems encountered and possible improvements made under the direction of the results in order to enhance the case competition in IT services. This chapter will explore the case study A case in order to understand the reason of the company began promoting promote the balanced scorecard, the researchers before the interview in advance cases to understand the company's corporate mission, vision and help the goal of:

Detailed planning steps are as follows:

- Stage one, the case company executives to Balanced Scorecard Introduction
- Phase II, the case company to collect the significant information to determine the executive structure to implement the Balanced Scorecard
- Stage III, the company announced the Balanced Scorecard to determine
- Phase IV, the case company teams at all levels About the Balanced Scorecard
- Stage five, the real implementation group set up developing develop with the four factors of corporate structure chart
- Phase VI, the first interview
- Phase VII, the first discussion
- Stage eight, the second interview
- Stage nine, the second talk
- Stage ten, received fuzzy multiple attribute decision making to establish meters for the case company helping help , the use of case study of the system and process of this study.

Avoid combining SI and CGS units, such as current in amperes and magnetic field in oersteds. This often leads to confusion because equations do not balance dimensionally. If you must use mixed units, clearly state the units for each quantity that you use in an equation.

TABLE I. BSC AND THE CASE COMPANY AND ITS MEASURE OF CORPORATE STRATEGY TABLE

Dimensions	***Policy Topics***	***Measure***
Customer Perspective	Customer Loyalty	1. Loyalty 2. Satisfaction 3. partner satisfaction
Financial Perspective	Stable earnings growth	1. Orders 2. renewal rate 3. revenue 4. Gross profit / profit / profit contribution
Process dimension	Reduce operating costs Continuous improvement process Internal employee satisfaction	1. operating cost control 2. time and commitment to customers 3. whether to solve the problem on the spot
Learning and growth perspective	Understanding of a shared vision Improving the Quality of Human Performance Evaluation and Rewards	1.employees aware of their responsibilities 2. formal staff turnover rate

C. Multi-attribute decision making

Step one: to define the various sectors of the property assessment indicators

The company implemented the Balanced Scorecard will be the case in four dimensions will be the key indicators of performance evaluation

It can be easily and clearly by a clear definition into two categories, one for the clear definition of a clear assessment can be the key performance index assessment, two values for the oral assessment can be the key performance indicators, the relationship these two categories.

Step Two: Setting fuzzy linguistic variables and fuzzy numbers

Step three: assess the performance of various departments

Step Four: Collect "key performance index of the weight "

D. The Fuzzy DEMATEL Method Procedure

A unique characteristic of this method is that it shows the relationships between Balanced Scorecard items with certain scores by using matrix operations. The relationship is that of “cause and effect”. Another important characteristic is that it grasps both the direct effects, and the indirect effects of competing components.

We use triangular fuzzy numbers (TFN) with fuzzy DEMATEL to establish fuzzy weights for the Balanced Scorecard components and to determine the relative importance of the criteria. Then, the performance value of each criterion can be derived by the decision-makers. After the synthetic utility values are derived, we rank the alternatives based on the best non-fuzzy performances (BNP). The procedures of the DEMATEL method and the evaluation methods can be summarized as follows:

Step 1: Producing the direct-relation matrix

Comparison scale of the DEMATEL method

Numeral	Definition
0	No influence
1	Low influence

2	High influence
3	Very high influence

Step 2: Normalizing the direct-relation matrix

On the basis of the direct-relation matrix $\boldsymbol{A}$, the normalized direct-relation matrix $\boldsymbol{X}$ can be obtained through formulas (2) and (3):

$$\boldsymbol{X} = k \cdot \boldsymbol{A} \quad (2)$$

$$k = \frac{1}{\max\limits_{1 \le i \le n} \sum\limits_{j=1}^{n} a_{ij}}, \quad i, j = 1, 2, ..., n. \quad (3)$$

Step 3: obtaining the total-relation matrix

Once the normalized direct-relation matrix $\boldsymbol{X}$ has been obtained, the total-relation matrix $\boldsymbol{T}$ can be derived by using formula (4), in which the $\boldsymbol{I}$ denotes the identity matrix.

$$\boldsymbol{T} = \boldsymbol{X} + \boldsymbol{X}^2 + \boldsymbol{X}^3 + ...$$

$$\boldsymbol{T} = \boldsymbol{X} + \boldsymbol{X}^2 + \boldsymbol{X}^3 + ... = \boldsymbol{X}(\boldsymbol{I} + \boldsymbol{X} + \boldsymbol{X}^2 + ...)$$

$$= \boldsymbol{X}\left(\frac{\boldsymbol{I} - \boldsymbol{X}^n}{\boldsymbol{I} - \boldsymbol{X}}\right)$$

$$= \boldsymbol{X}(\boldsymbol{I} - \boldsymbol{X})^{-1}, \text{ when } n \to \infty,\ \boldsymbol{X}^n = 0$$

$$\boldsymbol{T} = \boldsymbol{X}(\boldsymbol{I} - \boldsymbol{X})^{-1} \quad (4)$$

Step 4: Analyzing the results

In this step, the sum of rows and the sum of columns are used to derive vector $\boldsymbol{s}$ and vector $\boldsymbol{r}$ respectively, as shown in formulas (5), (6), and (7). Then, the horizontal axis vector ($\boldsymbol{s} + \boldsymbol{r}$), called "Prominence", is formed by adding $\boldsymbol{s}$ to $\boldsymbol{r}$, which indicates the level of importance of the criterion. Similarly, the vertical axis ($\boldsymbol{s} - \boldsymbol{r}$) called "Relation", is formed by subtracting $\boldsymbol{s}$ from $\boldsymbol{r}$, which may divide criteria into a cause group and an effect group. When ($\boldsymbol{s} - \boldsymbol{r}$) is positive, the criterion belongs to the cause group; otherwise, it belongs to the effect group. Therefore, the causal diagram can be derived by mapping the dataset of $(\boldsymbol{s} + \boldsymbol{r},\ \boldsymbol{s} - \boldsymbol{r})$, which provides valuable insights for making decisions.

$$\boldsymbol{T} = [t_{ij}]_{n \times n}, \quad i, j = 1, 2, ..., n \quad (5)$$

$$\boldsymbol{s} = \left[\sum_{j=1}^{n} t_{ij}\right]_{n \times 1} = [t_{i\cdot}]_{n \times 1} \quad (6)$$

$$\boldsymbol{r} = \left[\sum_{i=1}^{n} t_{ij}\right]_{1 \times n}^{t} = [t_{\cdot j}]_{n \times 1}, \quad (7)$$

where vector $\boldsymbol{s}$ and vector $\boldsymbol{r}$ respectively denote the sum of rows and the sum of columns from the total-relation matrix $\boldsymbol{T} = [t_{ij}]_{n \times n}$.

IV. Conclusion and Findings

We have proposed an approach for Balanced Scorecard evaluation in mobile industry based on effective group decision-making from the perspective of fuzzy multi-attribute decision making. The fuzzy DEMATEL method is used to establish fuzzy weights for Balanced Scorecard evaluation components.

The contribution of our approach is that it overcomes the limitations of traditional methods used to evaluate performance of mobile industry by Balanced Scorecard perspectives, as it does not have to accurately estimate the considered criteria in terms of numerical values for the anticipated alternatives. Applying fuzziness and the DEMATEL method for Balanced Scorecard evaluation allows practitioners to select components according to their organizations' priorities, and gather meaningful knowledge that captures the causal relationships between criteria.

The development of performance evaluation management system: the assessment of the case company does not have too many management systems, is not quantitative assessment of the project and assess the data. The purpose of daily operations, risk factors, such as timeliness and independent evaluation of the program flow is not related to each other. Data can not be automatically collected, the data obtained did not plan, can not understand the true value of the information, no relevant department or person responsible for data collection, resulting in missing data timeliness.

Structural organization of interdepartmental communication and consensus: The case company can provide the same services many companies are all competitors, the department of civil servants between the prevailing mindset, can not actively create the company with the best chance of combining customer service, real cause for concern.

Will promote the implementation of company strategy into the details: a positive vision combined with staff training / education, coupled with effective processes, customer satisfaction goals, and create a win-win target company shareholders and employees.

When we understand the theory and the four Balanced Scorecard dimensions, the dimensions will have to quantify these indicators, we must first determine through internal discussion and consensus on which indicators must be considered, and these indicators may be due to industry Different or change the company's vision, not necessarily take into account each company will have the same index.

In terms of strategic planning for the company, whether long or short, shall be convened by the company executives in charge of all a consensus on a common resolution. According to Company the specific action plan launched by the various

units in the company's goal to complete the year. The planning process of the balanced scorecard and corporate strategy, the company's specific action plan must take into account top-down driven; the results of the implementation level, is the bottom-up implementation, the company must develop a pragmatic Dimension in the four short-term goals can achieve. Therefore, measure of all sectors of the setting is very important because it is a business process assessment standard.

For important work, that is as soon as possible to assess the use of quantitative indicators. But the focus, it is not too much. For non-focused work, it can take fuzzy judgments, qualitative or quantitative management approach to determine. So the work can be focused, but also the employees ignore the non-priority work. Based on this concept, seven departments of the key indicators of performance evaluation, divided into two, one for the quantitative indicators, indicators of non-fuzzy, two non-quantitative indicators, and the fuzzy index, and the theory of multiple fuzzy attribute decision making Sector performance evaluation, in order to understand the applicability of the model, and the advantages and disadvantages of the operation in practice. Based on this concept, seven departments of the key indicators of performance evaluation, divided into two, one for the quantitative indicators, indicators of non-fuzzy, two non-quantitative indicators, and the fuzzy index, and the theory of multiple fuzzy attribute decision making Sector performance evaluation, in order to understand the applicability of the model, and the advantages and disadvantages of the operation in practice.

REFERENCES

[1] Kiran Jude Fernandes, Vinesh Raja, Andrew Whalley, "Lessons from implementing the balanced scorecard in a small and medium size manufacturing organization," *Technovation*, vol.26, no.5, 2006, pp. 623-634

[2] Kaplan, R. S. & D. P. Norton, The Balanced Scorecard: Translating Strategic Into Action. Boston, *Harvard Business School Press*. ,1996

[3] Robert S. Kaplan and David P. Norton, "The balanced scorecard : Measures that drive performance, " *Harvard Business Review*, Jan − Feb. ,1992, pp.71-79.

[4] Yin, R. K.,Case Study Research: Design and Methods , Sage Publications,1989, pp.17.

[5] Zairi, M. ,"Synchronisation of TQM. The TQM Magazine,2002, pp5-6.

[6] Ihsan Yuksel, Metin Dagdeviren, Using the fuzzy analytic network process (ANP) for Balanced Scorecard (BSC): A case study for a manufacturing firm," *Expert Systems with Applications*, vol.37, no.2, 2010, pp. 1270-1278

[7] Zeleny, M., "Multiple Criteria Decision-making," McGraw-Hill, New York, 1982.

[8] Hwang & Yoon , Multiple Decision Making : Method and Applications, 1981.

[9] Mobile Industry Report. Taipei: Market Intelligence & Consulting Institute, 2009, MIC.

[10] Bellman, R. E., and Zadeh, L. A., "Decision-making in a fuzzy environment," *Management Science*, vol 17, 1970, pp. 141-164.

[11] Chiu, Y. J., Chen, H. C., Tzeng. G. H., and Shyu, J. Z., "Marketing strategy based on customer behaviour for the LCD-TV," *International Journal of Management and Decision Making, vol.* 7, no.2, 2006, pp. 143-165.

[12] Hori,S., Shimizu, Y., "Designing methods of human interface for supervisory control systems," *Control Engineering Practice* vol. 7, 1999, pp. 1413-1419.

[13] Tsai, W. H., and Chou, W. C. "Selecting management systems for sustainable development in SMEs: A novel hybrid model based on DEMATEL, ANP, and ZOGP," *Expert Systems with Applications*, vol.36, no.2, 2009, pp. 1444-1458.

[14] Tzeng, G. H., Chiang, C. H., and Li, C. W. "Evaluating intertwined effects in e-learning programs: a novel hybrid MCDM model based on factor analysis and DEMATEL," *Expert Systems with Applications*, vol.32, no.4, 2007, pp. 1028-1044.

[15] Ou Yang, Y. P., Shieh, H. M., Leu, J. D., and Tzeng, G. H. "A novel hybrid MCDM model combined with DEMATEL and ANP with applications," *International Journal of Operations Research*, vol.5 no.3, 2008, pp.160-168.

[16] Y.-C. Chen, H.-P. Lien, G.-H. Tzeng, "Measures and evaluation for environment watershed plans using a novel hybrid MCDM model," *Expert systems with applications vol.*37, no.2, 2010, pp.926-938.

[17] J.-J. Huang, G.-H. Tzeng, C.-S. Ong, "Multidimensional data in multidimensional scaling using the analytic network process," *Pattern Recognition Letters* vol.26, no. 6, 2005, pp.755-767.

[18] J. Jones, D. Hunter, "Qualitative research: consensus methods for medical and health services research," *British Medical Journal,* vol.311,no. 7001, 1995, pp. 376-380.

[19] C.-L. Lin, G.-H. Tzeng, "A value-created system of science (technology) park by using DEMATEL," *Expert Systems with Applications,* vol.36, no.6, 2009, pp.9683-9697.

[20] J.-H. Liou, G.-H. Tzeng, H.-C. Chang, "Airline safety measurement using a hybrid model," *Journal of Air Transport Management,* vol.13, no.4, 2007, pp. 243-249.

[21] Y.-P. Ou-Yang, J.-D. Leu, G.-H. Tzeng, "A VIKOR-Based Multiple Criteria Decision Method for Improving Information Security Risk," *International Journal of Information Technology and Decision Making* vol.l8, no.2, 2009, pp.1-21.

[22] S. Opricovic, "Multicriteria Optimization of Civil Engineering Systems," Faculty of Civil Engineering, Belgrade, 1998.

[23] S. Opricovic, G.-H. Tzeng, "Compromise solution by MCDM methods: A comparative analysis of VIKOR and TOPSIS," *European Journal of Operational Research,* vol.156, no.2, 2004, pp. 445-455.

[24] T.L. Saaty, Decision making with dependence and feedback: The analytic network process. Pittsburgh: RWS Publications, 1996.

[25] T.L. Saaty, Fundamentals of the analytic network process. Japan: University of Pittsburgh, ISAHP, 1999. pp. 1-14.

[26] T.L. Saaty, "Rank from comparisons and from ratings in the analytic hierarchy/network processes," *European Journal of Operational Research* vol.168, no.2, 2006, pp. 557-570.

[27] G.-H. Tzeng, C.-H. Chiang, C.-W. Li, "Evaluating intertwined effects in e-learning programs: A novel hybrid MCDM model based on factor analysis and DEMATEL," *Expert Systems with Applications* vol.32, no.4, 2007, pp.1028-1044.

[28] G.-H. Tzeng, S.-H. Tsaur, Y.-D. Laiw, S. Opricovic, "Multicriteria Analysis of Environmental Quality in Taipei : Public Preferences and Improvement Strategies," *Journal of Environmental Management* vol.65,no.2, 2002, pp.109-120.

[29] P.-L. Wei, J.-H. Huang, G.-H. Tzeng, S.-I. Wu, "Causal modeling of web-advertising effects by improving SEM based on DEMATEL technique," *International Journal of Information Technology and Decision Making,* vol.9,no.5, 2010, pp.799-829.

[30] W.-W. Wu, "Choosing knowledge management strategies by using a combined ANP and DEMATEL approach," *Expert Systems with Applications,* vol.35,no.3, 2008, pp.828-835.

[31] C. Yang, G.-L.Fu, G.-H. Tzeng, "Multicriteria Analysis of the Strategies to Open Taiwan's Mobile Virtual Network Operators Services," *International Journal of Information Technology and Decision Making, vol.*6, no.1, 2007, pp.85-112.

2011 IEEE International Conference on Fuzzy Systems
June 27-30, 2011, Taipei, Taiwan

Fuzzy MCDM Application for Strategy Evaluation

Mei-Chen Lo
Department of Business Management
National United University
Miaoli, Taiwan
meichen_lo@nuu.edu.tw

Gwo-Hshiung Tzeng
Institute of Project Management
Kainan University
Taoyuan, Taiwan
ghtzeng@mail.knu.edu.tw

***Abstract*—The essence of strategy formulation is coping with competition. Therefore, the nature and degree of competition in an industry hinge on four basic forces: Production, Technology, Marketing and R&D are defined. To establish a strategic agenda for dealing with these contending currents and to grow despite them, a company must understand how they work in its industry and how they affect the company in its particular situation. This study adopt Fuzzy MCDM methods and details how these forces operate and suggests ways of adjusting to them, and, where possible of evaluation, of taking advantage of them. Knowledge of these underlying sources of competitive pressure provides the groundwork for a strategic agenda of action. The result highlights the critical strategies distance of the company, animate the positioning of the company in its industry, clarify the areas where strategic changes may yield the greatest payoff, and highlight the places where industry trends promise to hold the greatest significance as either opportunities or threats.**

Keywords-fuzzy multiple criteria decision making (FMCDM); fuzzy analytic network process (FANP); DEMATEL; strategy evaluation

I. INTRODUCTION

Every industry has an underlying structure, or a set of fundamental economic and technical characteristics, that gives rise to these competitive forces. Decision maker, wanting to position his company to cope best with its industry environment or to influence that environment in the company's favor, must learn what makes the environment tick. The essence of strategy formulation is coping with competition. Yet it is easy to view competition too narrowly and too pessimistically. Awareness of these forces can help a company stake out a position in its industry that is less vulnerable to attack.

The nature and degree of competition in an industry hinge on four forces: Production, Technology, Marketing and R&D [1]. To establish a strategic agenda for dealing with these contending currents and to grow despite them, a company must understand how they work in its industry and how they affect the company in its particular situation. This study details how these forces operate and suggests ways of adjusting to them, and, where possible, of taking advantage of them. Knowledge of these underlying sources of competitive pressure provides the groundwork for a strategic agenda of action [2]. They highlight the critical strengths and weaknesses of the company, animate the positioning of the company in its industry, clarify the areas where strategic changes may yield the greatest payoff, and highlight the places where industry trends promise to hold the greatest significance as either opportunities or threats. Understanding these sources also proves to be of help in considering areas for diversification.

The remainder of this paper is organized as follows. In Section 2, about strategy forces for business development is reviewed and the framework of dynamic strategy forces for efficiency business is built. In Section 3, the methodology of fuzzy hybrid MCDM model based on dynamic strategy is proposed for applying strategy forces. An empirical case and result are illustrated in Section 4. Discussions and implications are presented in Section 5. Finically conclusion is offered in Section 6.

II. ABOUT STRATEGY FORCES TO EVALUATION

The essence of strategy formulation is coping with competition. For a company in the fight for market share, competition is not manifested only in the other players. Rather, a competitive strategy in an industry is rooted in its underlying economics, and competitive forces exist not only from internal considerations but also that go well beyond the established combatants in the high-tech industry. The forces sources may gestate from customers, suppliers, potential entrants, and substitute products which are all competitors that may be more or less prominent or active depending on a particular industry.

The nature and degree of competition in the companies within the high-tech industry hinge on strategy forces [1][3], such as Production Capability (PC), Technology Competence (TC), R&D (RD), Marketing & Service (MS).

- Production Capability (PC)
- Technology Competence (TC)
- R&D (RD)
- Marketing & Service (MS)

Strategy-Forces based on answers to four generic questions about the strategy to be pursued by the organization which also assume the financial support and organizational deployment is available for high-tech competition game. Therefore, as Figure 1 these four questions, one about production, one about marketing, one about Technology, and one about R&D evolved quickly into a standard set of

"perspectives". The weaker the forces is to be collectively, however, the greater the opportunity can be for superior performance. Whatever their collective strength, the corporate strategist's goal is to find a position between company and industry where can best defend itself against these forces or can influence them in its favor [4].

Understanding these sources also proves to be of help in considering areas for diversification. A strategy map is a diagram that is used to document the primary strategic goals being pursued by an organization or management team and to help managers focus their attention more closely on the interventions necessary to ensure the strategy is effectively and efficiently executed. By providing managers with the direct feedback on whether the required actions are being carried out, and whether they are working. A performance management system is deciding what activities and outcomes to monitor. By providing a simple visual representation of the strategic objectives to be focused on, along with additional visual cues in the form of the perspectives and causal arrows, the strategy map has been found useful in enabling discussion within a management team about what objectives to choose, and subsequently to support discussion of the actual performance achieved.

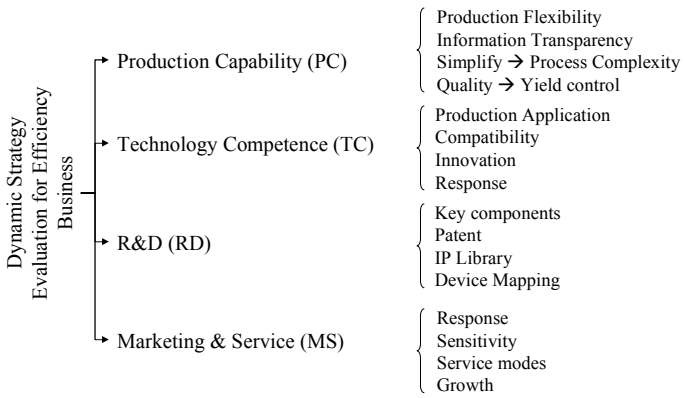

Figure 1. The Hierarchy Structure

III. MEASURING THE FORCES

This section is based on what factors the past scholars in the study of strategy forces considerations indicated and to further discuss the result of the study; hence, identify the flow of facts. This study uses the four main factors indicated by four-factor model as PC, TC, RD and MS factors to implement the strategies can be evaluated in dynamical considerations in time; identify the sub-factors that would affect the main factors, thus firmly develop evaluating criteria and its dynamic track of mapping.

A. Methodologies

The field of fuzzy multiple criteria decision making (FMCDM) concerns the problems that how decision makers should ideally do when facing multiple conflicting criteria. Group decision-making solve problems through a group of experts form their specific knowledge domain and help on business strategies decision-making [5][6]. There are considerable methods and models have been proposed for various FMCDM problems (as Figure 2) with respect to different perspectives and theories.

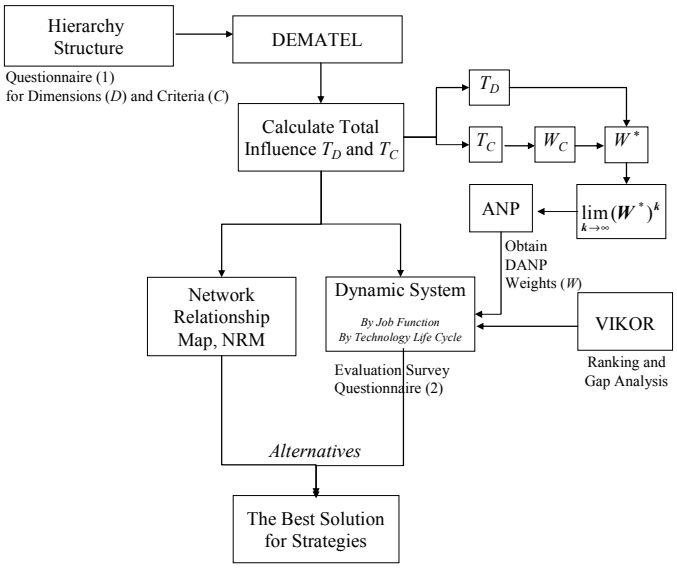

Figure 2. Framework of Hybrid Methodologies Application

B. Fuzzy Theory with AHP and ANP

Because of the subjective of the attributes used in the evaluation, AHP [7][8][9][10][11][12] is the most appropriate method for this problem. However, since the experts prefer natural language expressions rather than sharp numerical values in their assessments, the classical AHP may not yield with a satisfactory result. Expressions such as "not very clear", "probably so", and "very likely", are used often in daily life, and more or less represent some degree of uncertainty of human thought. The fuzzy set theory proposed by Zadeh [13], an important concept applied in the scientific environment, has been available to other fields as well. Consequently, the fuzzy theory has become a useful tool for automating human activities with uncertainty-based information. This study proposes a fuzzy AHP framework to weigh the talent selection implementation factors. This study model helps organizations identify the differences between the desired and current situations, and then identify the improvement areas and develop the strategies for the talent selection implementation.

In addition, the company can also use the assessment results as a benchmark with competitors and other "best-in-class" organizations. To manage talent selection successfully, its measurement indicators must be defined and prioritized. Because of the subjective of the attributes used in the evaluation, AHP [10][12] is the most appropriate method for this problem. However, since the experts prefer natural language expressions rather than sharp numerical values in their assessments, the classical AHP may not yield with a

satisfactory result. This study proposes a fuzzy AHP framework to weigh the talent selection implementation factors.

C. Fuzzy Decision-making

When people encounter uncertain or vague decision-making problems in the real world, they often express their thinking and subjective perception in words instead of probability and statistics. But the problem with words is that their meanings are often vague. Furthermore, even when people use the same words, individual judgment of events is invariably subjective and may differ. Moreover, even if the meaning of a word is well defined (e.g., the linguistic comparison labels in the standard AHP questionnaire responses), when we use the word to define a set, the boundary that separates whether an object does or does not belong to the set is often fuzzy or vague. This is why fuzzy numbers and fuzzy sets have been introduced to characterize linguistic variables. The preferences in AHP are essentially human judgments based on one's perception (this is especially true for intangibles), and we believe the fuzzy approach allows for a more accurate description of the decision making process.

FANP approach has been presented to prioritize strategy implementation factors for a manufacturing business to implement one of its most critical parts used in management decision process and under multiple criteria's decision-making in the fuzzy environment [11][14]. The main criteria and attributes have been decided which are based on the current business scenario and experience of the experts in the respective fields. The large number of criteria and attributes demonstrated the complexities being involved in the strategy implementation factors. Each factor affecting [15] as strategy forces and implementation has been analyzed and discussed. This paper has made a significant contribution to identify the important criteria and paves the way to consider these practically relevant and interesting issues of strategy forces factors in the fuzzy environment.

We emphasize that the contribution of this study which build up and apply the theoretical model of strategy implementation priority. This study takes a step in the direction of setting priorities of clarifying, guiding and integrating terms and concepts relevant to strategy implementation and management aspects in the firm process.

D. Mapping tools

A network connects the components of a decision system. According to size, there will be a system that is made up of subsystems, with each subsystem made up of components, and each component made up of elements. The elements in each component interact or have an influence on some or all of the elements of another component with respect to a property governing the interactions of the entire system.

DEMATEL

The DEMATEL method is based upon graph theory, enabling us to plan and solve problems visually, so that we may divide multiple criteria into a relationship of cause and effect group, in order to better understand causal relationships. Directed graphs (also called digraphs) are more useful than directionless graphs, because digraphs will demonstrate the directed relationships of sub-systems. A digraph typically represents a communication network, or a domination relationship between individuals, etc. The DEMATEL method can convert the relationship between the causes and effects of criteria into an intelligible structural model of the system [16][17].

A component of a decision network which was derived by the DEMATEL method is denoted by $\boldsymbol{C}_h, h = 1, \cdots, m,$ and assume that it has n_h elements (determinants), which we denote by $e_{h1}, e_{h2}, \cdots, e_{hm}$. The influences of a given set of elements (determinants) in a component on any element in the decision system are represented by a ratio scale priority vector derived from paired comparisons of the comparative importance of one criterion and another criterion with respect to the interests or preferences of the decision makers. This relative importance value can be determined using a scale of 1–9 to represent equal importance to extreme importance.

Dynamical system

A dynamical system (DS) is a concept in mathematics where a fixed rule describes the time dependence of a point in a geometrical space [18]. DS is a manifold *M* called the phase (or state) space endowed with a family of smooth evolution functions Φ^t that for any element of $t \in T$, the time, map a point of the phase space back into the phase space. The notion of smoothness changes with applications and the type of manifold. There are several choices for the set *T*. When *T* is taken to be the reals, the dynamical system is called a *flow*; and if *T* is restricted to the non-negative reals, then the dynamical system is a *semi-flow*. When *T* is taken to be the integers, it is a *cascade* or a *map*; and the restriction to the non-negative integers is a *semi-cascade*. DS is a means of describing how one state develops into another state over the course of time [19]. Technically, a DS is a smooth action of the reals or the integers on another object (usually a manifold). When the reals are acting, the system is called a continuous dynamical system, and when the integers are acting, the system is called a discrete dynamical system.

E. VIKOR method

The compromise-ranking method (VIKOR method) determines the compromise solution [20][21][22]; the obtained compromise solution is acceptable to the decision-makers because it provides a maximum group utility of the majority (represented by min *S*), and a minimum individual maximal regret of the opponent (represented by min *Q*). The model uses the DEMATEL and ANP procedures to obtain the weights of criteria with dependence and feedback and uses the VIKOR method to obtain the compromise solution.

IV. Empirical Case and Results

The example of High-Tech electronic company is illustrated to show the proposed method. Empirical findings these four factors have the relationship of mutually interactive and self-feedback. Therefore, this study provides set of patterns, and take major player of high-tech company, explained that manufacturer of using the way of business strategies in a dynamic industry nature. The result presents a comprehensive framework for making judgments to move forward about business strategies development is essential. The function is refers to completes this position or duty group of important abilities, therefore the application function examines whether matches is a very good concept.

Empirical case of high-tech company as the example is illustrated to show the proposed method. As for the numerical raw data was collected in fuzzy considerations and turned into the calculation in crisp numbers directly for further evaluation processes. The findings of these four factors have the relationship to mutually interactive and its self-feedback (as Table 1 and Table 2).

TABLE 1 The Distance of Influences by Aspects

Aspect		R	S	R+S	R-S	Rank
A	PC	4.239	4.068	8.306	0.171	3
B	TC	4.339	3.846	8.184	0.493	2
C	RD	3.571	4.908	8.479	-1.337	4
D	MS	4.485	3.813	8.298	0.673	1

Table 1 states "Market & Service" will be more important to fit the change of outside environment and close to real requirement and get the real necessity of customer needs. Besides, it shows the "Technology Competence" can be a potential to challenge and to complete rivals in a speedy growth industry nature.

TABLE 2 The Distance of Influences by Criteria

		Criteria	R	S	R+S	R-S	Rank
A	a1	Production Flexibility	5.556	4.518	10.074	1.038	1
	a2	Information Transparency	4.811	5.663	10.474	-0.852	14
	a3	Simplify operation -- Process Complexity	4.499	6.029	10.528	-1.53	16
	a4	Quality -- Yield control	5.445	4.584	10.029	0.861	3
B	b1	Production Application	4.676	5.469	10.145	-0.793	13
	b2	Compatibility	5.43	4.622	10.052	0.808	5
	b3	Innovation	5.429	4.591	10.02	0.838	4
	b4	Response	5.553	4.515	10.068	1.038	2
C	c1	Key components	4.995	5.032	10.027	-0.037	10
	c2	Patent	5.104	4.972	10.076	0.132	7
	c3	IP Library	4.925	5.054	9.979	-0.129	11
	c4	Device Mapping	4.507	5.733	10.24	-1.226	15
D	d1	Response	4.822	5.24	10.062	-0.418	12
	d2	Sensitivity	5.033	4.996	10.029	0.037	8
	d3	Service modes	5.08	5.105	10.185	-0.025	9
	d4	Growth	5.13	4.872	10.002	0.258	6

As the rank result (Table 2), "a1" and "b4" both locate higher position. Instantly, for pure foundry business, the "Production Flexibility" tasks have been always discussed by high-tech work environment. Due to the sensitivity of market and economic change, the globalized change may lead the change of corporate business strategies to fit the requirement of market (users) needs. Therefore, a continuous and monitored "Response" is required for deployment of internal resources and providing a well mechanism to feedback to end-users in time.

The essential alternatives are provides for the problems solving. According to Table 3, "R7: Financial support/ incentive program" and "R6: Competitiveness Evaluation System" are the most favor and satisfied issues while the performance evaluation to be measured. Not surprising that "R1: Innovation/Intelligent Property" reveals lowest credit which shows the importance of knowledge sharing and accumulation can possibly create a new hope of ideas generator toward a new challenge on the next business strategic move. As for the definition of those alternatives are showing as follows:

R1. Innovation/Intelligent property: build an innovative environment for continuously technology development achievement.

R2. Knowledge platform: provide a knowledge platform for knowledge accumulation, problem solving, lesson learned and information sharing.

R3. Response system: external environmental change to cause Market/Operation strategies to be adjusted.

R4. Communication system: a wide channel for customer services in viewing the progress of the on-line production and 24-hour on line service.

R5. Efficiency evaluation system: Internal and external factors to move the operation work in effectively.

R6. Competitiveness evaluation system: evaluate the way of technology adoption and shorten the time of technology development into production phase.

R7. Financial support/ incentive program: budget plan and financial support.

This research involves several objects from Taiwan High-Tech manufacturing related leaders, experts from different function which includes top management, senior R&D, the senior administrative personnel and marketing functions. The questionnaire of evaluation mainly was composed of two parts: questions for evaluating the relative importance of criteria and company's performance corresponding to each criterion.

The performance scores and gap (by VIKOR) are shown in Table 3. Using the performance values, relative results are obtained. We use the global weight in ANP to compare the performances of R1, R2, R3, R4, R5, R6, and R7 as the ANP provides significant feedback. The gap identified related needs-recognition and strategic behavior in sequence.

By integrating and calculating the investigated data, we determine the overall performance to guide the improvement of that R7 $\succ$ R6 $\succ$ R4 $\succ$ R5 $\succ$ R2 $\succ$ R3 $\succ$ R1. The overall performance value of R7 (28.613) and R6 (28.406) are close, whereas the range distance with R1 has the largest gap. Thus, R7, R6, R4, R5, R2, R3, and R1 have its sequence on enhancement of their business strategies or redefinition of management stages.

TABLE 3 Performance Evaluation by VIKOR

	Criteria \ Alternatives	Local weight	Global weight (ANP)	Aspired Level	R1	R2	R3	R4	R5	R6	R7
A.	Production capability (PC)	0.257			7.267	7.504	8.006	6.996	6.743	7.496	8.251
a1	Production Flexibility	0.251	0.064	10	8	7	9	8	7	8	9
a2	Information Transparency	0.253	0.065	10	9	8	8	5	4	7	8
a3	Simplify à Process Complexity	0.245	0.063	10	5	7	7	7	7	8	8
a4	Quality à Yield control	0.251	0.064	10	7	8	8	8	9	7	8
B.	Technology competence (TC)	0.257			4.765	5.214	5.509	5.692	5.481	5.959	6.226
b1	Production Application	0.239	0.061	10	5	6	6	8	7	9	8
b2	Compatibility	0.255	0.065	10	6	8	8	9	9	8	7
b3	Innovation	0.239	0.061	10	6	8	7	8	7	7	8
b4	Response	0.267	0.069	10	8	7	9	7	8	8	9
C.	R&D (RD)	0.257			5.852	5.756	5.726	8.000	7.364	7.480	7.852
c1	Key components	0.209	0.054	10	4	6	7	8	6	8	6
c2	Patent	0.271	0.069	10	7	6	5	8	9	8	9
c3	IP Library	0.276	0.071	10	6	6	7	8	8	7	8
c4	Device Mapping	0.244	0.063	10	6	5	4	8	6	7	8
D.	Marketing & service (MS)	0.257			7.202	7.735	6.786	6.743	6.980	7.471	6.284
d1	Response	0.265	0.068	10	7	7	8	7	7	6	7
d2	Sensitivity	0.276	0.071	10	6	8	7	6	7	8	6
d3	Service modes	0.239	0.061	10	9	8	5	8	6	8	7
d4	Growth	0.220	0.056	10	7	8	7	6	8	8	5
	TOTAL	5.027	1.027	10	25.086	26.210	26.028	27.431	26.568	28.406	28.613
	Performance Ranking for Alternative (Priority)				7	5	6	3	4	2	1

V. Discussions and Implications

There are most evidence of improvements in team performance attributed to management development, these typically related to process issues such as innovative activities, cost control, knowledge management, quality of service, better focus on customer needs, and improved customer relations etc. Managers in some organizations cited evidence of more strategic behavior and identified better procedures and monitoring of actions. Technology improvement from Cost reductions, efficiency gains and more effective quality control were also reported. To face external change and to fit the requirement of business opportunities, appropriate dynamical strategies give a challenged team performance arising from strategy.

Major difficulties of measurement of strategy forces and of attributing improvements to strategy in management development were encountered, especially where the same measures were used for function and business performance, or where the performance was regarded as a function of a manager's performance. Equally, business performance was difficult to separate from organizational performance and was affected by extraneous factors.

The alternatives which were ranked highest in terms of organizational performance improvements displayed quantified, written and corroborated evidence and respondents were unequivocal that strategic management development had contributed to all prime measures of business efficiency. The framework appears to be intuitive to managers and applicants who quickly adopt the terminology of the strategy forces. It offers a means of guiding easily recognized environmental components and provides a framework for combining these components to describe possible scenarios. In addition, it clearly distinguishes between the perspectives of different industry nature and increases the likelihood that decision makers will incorporate these perspectives into their decisions.

The decision-making and influence processes operating in decision events are likely to be advanced through a closer alignment with the problem solving and decision-making in the real world.

VI. Conclusion

The conclusions and learning points to be drawn from the research outlined above relate both to the substantive findings, which contribute to the debate on the role of business in improving performance, and the procedural aspects of the methodology developed to undertake the study.

A case-study approach was necessary in order to capture qualitative information, including such 'soft' measures as perceptions of individuals, as well as exploring the relevant development and performance processes within organizations at different functions. In adopting such a methodology, however, there was a risk of marginalizing the findings because policy makers invariably seek 'hard' measures, with quantitative data that can be subject more easily to statistical tests. The challenge, therefore, was to devise a methodology that could permit hard conclusions from soft data.

The strategy force describes the structure of business systems and the industry nature of the influence mechanisms that determine outcomes. The strategy evaluation reliance on business decisions rather than operation activities as the key structural component of the framework provides a flexible and generalizable framework around which existing strategy force research can be arrayed. It also provides a means of aligning technology research with the problem solving and decision-making literatures. More work remains to be done to fully identify and understand influence mechanisms in strategy

evaluation systems. The dynamic strategy evaluation in considering the strategic forces can assist these efforts by offering a simple and easily recognizable structure for organizing research and practice in a complex field where a great deal is yet to be learned.

ACKNOWLEDGEMENT

This study is granted by National Science Council (NSC 099-2811-H-424-001) with 3-year Post Doctoral Research Program.

REFERENCES

[1] M. C. Lo, J. Michnik and A. L.P. Cheng, "Technology Assessment as A Guidance to Business Management of New Technologies*", the 2007 IEEE International Conference on Industrial Engineering and Engineering Management (IEEM '07*), December 2-5, 2007, Singapore.

[2] M. E. Porter, "Competitive Strategy," *Measuring Business Excellence*, vol. 1, no. 2, pp. 12-17, 1993.

[3] A. Velosa, "Semiconductor Manufacturing: Boom Busts, and Globalization," *The Bridge*, vol. 35, no. 1, 2005.

[4] M. E. Porter, "Towards a dynamic theory of strategy," *Strategic Management Journal*, vol. 12, no. S2, pp. 95-117, 1991.

[5] P. L. Yu, "A class of solutions for group decision problems," *Management Science*, vol. 19, no. 8, pp. 936–946, 1973.

[6] M. Freimer and P. L. Yu, "Some new results on compromise solutions for group decision problems," *Management Science*, vol. 22, no. 6, pp. 688–693, 1976.

[7] T. L. Saaty, "Axiomatic foundations of the analytic hierarchy process," *Management Science*, vol. 32, pp. 841–855, 1986.

[8] T. L. Saaty, "Rank generation, preservation and reversal in the analytic hierarchy decision process," *Decision Sciences*, vol. 18, pp. 157–177, 1987.

[9] T. L. Saaty, The Analytic Hierarchy Process, The University of Pittsburgh, Pittsburgh, PA, revised edition, 1988.

[10] T. L. Saaty, Decision Making with Dependence and Feedback: The Analytic Network Process. Pittsburgh: RWS Publication, 1996.

[11] T. L. Saaty, "Fundamentals of the analytic network process - dependence and feedback in decision-making with a single network," *Journal of Systems Science and Systems Engineering*, vol. 13, no. 2, pp. 71-91, 2004.

[12] T. L. Saaty, Theory and Applications of the Analytic Network Process - Decision Making with Benefits, Opportunities, Costs, and Risks. Pittsburg, P.A.: RWS Publications, 2005.

[13] L. Zadeh, "Fuzzy sets," *Information and Control*, vol. 8, no. 3, pp. 338–353, 1965.

[14] T. L. Saaty, "Fundamentals of the Analytic Network Process," in Proceedings of *International Symposium on Analytical Hierarchy Process*, Japan, Kobe: 1999.

[15] R. W. Saaty, The Analytic Hierarchy Process (AHP) for Decision Making and The Analytic Network Process (ANP) for Decision Making with Dependence and Feedback. Pittsburgh, PA: Creative Decisions Foundation, 2003.

[16] G. H. Tzeng, W. H. Chen, R. Yu, and M. L. Shih, "Fuzzy Decision Maps - A Generalization of the DEMATEL Methods," Soft Computing, vol. 14, no. 11, pp. 1141-1150, 2010.

[17] G. H. Tzeng, C. H. Chiang and C. W. Li, "Evaluating intertwined effects in e-learning programs: a novel hybrid MCDM model based on factor analysis and DEMATEL," *Expert Systems with Applications*, vol. 32, no. 4, pp. 1028–1044, 2007.

[18] H. Ye, Michel, A. N. and L. Hou, "Stability theory for hybrid dynamical systems," *IEEE Transactions on Automatic control*, vol. 43, no. 4, pp. 461-474, 1998.

[19] K. Funahashi and Y. Nakamura, "Approximation of dynamical systems by continuous time recurrent neural networks," *Neural Networks*, vol. 6, no. 6, pp. 801-806, 1993.

[20] S. Opricovic and G.H. Tzeng, "Multicriteria planning of post-earthquake sustainable reconstruction," *Computer-Aided Civil and Infrastructure Engineering*, vol. 17, no. 3, pp. 211–220, 2002.

[21] S. Opricovic and G. H. Tzeng, "Compromise solution by MCDM methods: A comparative analysis of VIKOR and TOPSIS," *European Journal of Operational Research*, vol. 156, no. 2, pp. 445–455, 2004.

[22] S. Opricovic and G.H. Tzeng, "Extended VIKOR method in comparison with outranking methods," *European Journal of Operational Research*, vol. 178, no. 2, pp. 514–529, 2007.

2011 IEEE International Conference on Fuzzy Systems
June 27-30, 2011, Taipei, Taiwan

Exploring the SPM System Structure Model by Using Fuzzy DEMATEL for NPD

Yu-Yun Chang
Kainan University
Graduate Institute of Project Management
Taoyuan, Taiwan
m09924002@ms.knu.edu.tw

Meng-Jong Kuan
Kainan University,
Graduate Institute of Project Management
Taoyuan, Taiwan
mjkuan@mail.knu.edu.tw

Yen-Ching Chuang
Kainan University
Graduate Institute of Project Management
Taoyuan, Taiwan
m09824001@ms.knu.edu.tw

Gwo-Hshiung Tzeng
Graduate Institute of Project Management,
Kainan University, Taiwan
Institute of Management of Technology, National Chiao Tung University, Taiwan
ghtzeng@mail.knu.edu.tw;
ghtzeng@cc.nctu.edu.tw

***Abstract*—Standardized project management (SPM) is regarded as a well-structured system for improving the success of new product development projects. SPM can be defined as a standardized set of project management practices. It helps achieve the company's strategic goal through the effective use of project-driven approach. This paper used a Decision Making Trial and Evaluation Laboratory (DEMATEL) method to help companies to create a critical Standardized Project Management system and identify the influence of dimensions and criteria in the SPM system. First of all the dimensions and criteria of the SPM system are determined. DEMATEL approach is then applied to construct the SPM system structure model with Fuzzy number influence interrelationship among dimensions and associated criteria. An empirical case from industry is used to explore the effectiveness of the proposal approach.**

Keywords-fuzzy number; DEMATEL; Standardized project management (SPM); FDEMATEL.

I. INTRODUCTION

According to multiple empirical studies, a company's effectiveness partly depends on the success of its projects. (Kerzner and Cooper, 2000). And some companies in high-velocity industries have recognized a standardized project management (SPM) as a strategy for managing development projects (Milosevic and Patanakul, 2005).

In constructing a SPM system, the interrelationship among the dimensions and criteria is very critical for an effective SPM system. For this reason, we have adopted an integrated decision framework based on Decision Making Trial and Evaluation Laboratory (DEMATEL) and the triangular fuzzy number for constructing the most appropriate SPM system structure model.

DEMATEL method is usually applied in gathering group knowledge for forming a system structural model, as well as visualizing the causal relationship of sub-systems through a causal diagram. Here, DEMATEL is used to detect complex relationships and build relation structure among criteria for constructing SPM system. Additionally, set priorities among sub-system and criteria, and to determine the most appropriate SPM evaluation system structure.

We live in a global economy in which the turnaround of structural and technological change is rapid and sometimes unpredictable. Business processes are changing even as we speak, and traditional jobs and work settings are becoming virtual, e-driven, and mobile. This atmosphere of change creates the need to build the organization so that (1) people can create new products before they are anticipated by the customer, marketplace, or competition, and (2) the company can design, develop, and produce new products better, faster, and cheaper, and get them to market. Development life cycles have gone from years to months to days. (Barkley, 2008)

II. STANDARDIZED PROJECT MANAGEMENT SYSTEM

Some companies in high-velocity industries have recognized that a well-constructed standardized project management (SPM) is a critical success strategy for managing new product development projects. In their study, Milosevic and Patanakul (2005) have illustrated that SPM may increase new product development projects success which is approved. The Organizational Project Management Maturity Model (OPM3), a standard issued by Project Management Institute (PMI), also suggests SPM as a major strategy for projects success. These references suggest that SPM may have a significant place in many companies' approach to PM, especially to new product development (NPD) projects.

PMBOK has defined the PM life cycle which is divided into five phases: initial, planning, executing, control and closing. A company has to start to develop one NPD project in a fixed time before it has a full "strategy" to make sure achieve the goal. In the second phase, a cautious project management plan (PMP) is necessarily developed for PM. A good PMP is critical issue in the "process" planning which is required to show how to use the methodologies planning project and external environment interaction of PM. Those are the impact planning of the project processes. In the third phase, a project is executed by "people". People in the positive culture, to be independent finish missions and have a strong back-office team

978-1-4244-7316-8/11/$26.00 ©2011 IEEE

of project in company, they are making decision correctly in a project. In the fourth phase, a project must have right tools to control processes, people and technology. Finally, the study is has constructed a standardized project management system for new product development. All of above through the expert questionnaires select the critical factors of SPM. Besides, according to the literature review the "resource" also is the main success factor of projects. The integration of project planning with resource planning ensures that the company does not take one more than it can handle, and can avoid the kind of resource constraints or bottlenecks characterized in the critical chain concept (Barkley, 2008). Because of a project is usually under limited in resource so that the SPM performance evaluation system is divided into five dimensions of seventeen criteria in this study, the result is shown in TABLE I. .

TABLE I. FACTORS AFFECTING THE CONSTRUCTION OF SPM SYSTEM

Dimensions	Factors(Criteria)
A Strategy	a_1, The project management strategy a_2, Fit with long-term strategy a_3, Fit with new strategic intent
B People	b_1, Project organization b_2, Project culture b_3, Project leadership
C Tool	c_1, PM tools / template c_2, Technology dependency c_3, Information management system c_4, Project management measure index
D Process	d_1, Project environment d_2, Project management methodologies d_3, Project management process d_4, Project management metrics
E Resource	e_1, Cost / expenses e_2, Support of facility e_3, Support of employees

III. DEVELOPING SPM EVALUATION MODEL

This study will through the expert questionnaires to select the critical success factors of SPM system. Then, DEMATEL is applied to confirm the influence on each factor and to explore the relevance of the SPM's multiple criteria. This section includes three parts: the first part is application the triangular fuzzy number; the second part is developing network relationship with the DEMATEL; the last part is according to empirical analysis result to construct the SPM system for the new product development.

A. FUZZY NUMBER

B. Buckley (1985) proposed geometric mean method to calculate the final fuzzy weights for each fuzzy matrix. Given an m × m positive reciprocal matrix $A=\lfloor a_{ij}\rceil$ is derived by pairwise comparison from m participating evaluators, then $r_i\left(\prod_{j=1}^{m} a_{ij}\right)^{1/m}$ represents the geometric mean of each raw. According to Saaty's definition, $\lambda_{\max}$ be the largest eigen value of A and the weights, w_1 as the components of the normalized eigenvector corresponding to $\lambda_{\max}$,where $w_i = r_i/(r_1+\cdots+r_m)$.

Buckley (1985) further considered a fuzzy positive reciprocal matrix $\tilde{A}=[\tilde{a}_{ij}]$,extending the geometric mean method to the fuzzy geometric mean method and exploited which to find the final fuzzy weights of each criterion as follows:

$\tilde{r}_i = (\tilde{a}_{i1}\otimes\tilde{a}_{i2}\otimes\cdots\otimes\tilde{a}_{im})^{1/m}$ and $\tilde{w}_l = \tilde{r}_l\otimes(\tilde{r}_1\oplus\tilde{r}_l\oplus\cdots\oplus\tilde{r}_m)^{-1}$

where $\oplus$ and $\otimes$ called additive and multiplicative operators of two fuzzy number, respectively. These arithmetic operations will describe in next paragraph.

The evaluators choose a performance score for each participating company based on their subjective judgments. This way of estimating the achievement level of each criterion on each strategy can use the methods of fuzzy theory for treating the fuzzy environment. In evaluating process, after well define the criteria and their relationship, we have to determine the weights or measure of these criteria, and obtain then performance score of each alternative with respect to evaluated criteria. Furthermore, choose an suitable aggregating operator to derive the synthetic value of these alternatives respectively, the final step is to assign the preferred order for all alternatives based on their synthetic values.

In general case, we can employ triangular fuzzy number to express the aggregated fuzzy weights of *j*-th criterion as follows:

$$\tilde{w}_i = (l_i, m_i, u_i) \tag{1}$$

where $\tilde{w}_i$,is derived by Eq.(1)

It can be assumed that evaluation expert *k* has his fuzzy performance score of $\tilde{E}_{ij}^{k}$ for the criteria *j* under alternative *i*, and all the items to be evaluated is defined in feasible set *S*.

$$\tilde{E}_{ij}^{k} = \left(LE_{ij}^{k}, ME_{ij}^{k}, UE_{ij}^{k}\right),\quad j\in S \tag{2}$$

Each expert may has his different academic and business careers, so as his objective understanding on the linguistic variables. This study utilizes the average number to integrate the fuzzy judgment values given by *m* experts. That is, $\tilde{E}_{ij}$ express the average fuzzy judgment given by the participated evaluators. Its triangular fuzzy number is shown below:

$$\tilde{E}_{ij} = \left(LE_{ij}, ME_{ij}, UE_{ij}\right),\quad j\in S \tag{3}$$

where

$$\tilde{E}_{ij} = \left(1/m\right)\otimes\left(\tilde{E}_{ij}\oplus\cdots\oplus\tilde{E}_{ij}^{m}\right) \tag{4}$$

Specifically, $\tilde{E}_{ij}$ can be calculated by Buckley (1985a):

$$LE_{ij} = \left(1/m\right)\times\left(\sum_{k=1}^{m} LE_{ij}^{k}\right);\ ME_{ij} = \left(1/m\right)\times\left(\sum_{k=1}^{m} ME_{ij}^{k}\right);\ UE_{ij} = \left(1/m\right)\times\left(\sum_{k=1}^{m} UE_{ij}^{k}\right) \tag{5}$$

Moreover, the fuzzy synthetic matrix *R* can then be developed from both fuzzy weighting vector and fuzzy performance matrix as following:

$$\overline{\mathrm{R}} = \overline{\mathrm{w}} \Leftrightarrow \overline{\mathrm{E}} \tag{6}$$

where

$$\widetilde{w} = (\widetilde{w}_1, \cdots, \widetilde{w}_j, \cdots, \widetilde{w}_n)^t ;\ \widetilde{E} = [\widetilde{E}_{ij}] \tag{7}$$

"$\Leftrightarrow$"in Eq.(6)indicates the aggregating operator of fuzzy weighting vector and fuzzy performance matrix.

How to assess the measure of evaluated criteria is the critical process. In traditional evaluation methods such as Analytic Hierarchy Process, ELECTRE, PROMETHEE, TOPSIS, VIKOR and Grey Relation Analysis, assume definitely mutually independent between each pair criteria, and the simple additive weighted (SAW) method is appropriately to aggregate the synthetic value from criteria weights with performance scores. However, in most of MCDM problems, dependence or feedback may exist in evaluating structure. This independent relationship can not satisfy the nature of real situations. We can not employ SAW to derive the synthetic values if the relationship among these criteria are not independent, then the other aggregating tools is more suitable. For instance, fuzzy integral will provide appropriate estimate of synthetic values while in dependent situation; Analytic Network Process (ANP) can be applied to estimate the synthetic values while in the situation of feedback exists in considered dimension with its lower level of hierarch system.

Finally, the final fuzzy synthetic judgment of individual alternative for j evaluated criteria can be illustrated as follows:

$$\widetilde{R}_i = (LR_i, MR_i, UR_i) \quad \forall i \tag{8}$$

where

$$LR_i = \sum_{j=1}^{n} l_j \cdot LE_{ij};\ MR_i = \sum_{j=1}^{n} m_j \cdot ME_{ij};\ UR_i = \sum_{j=1}^{n} u_j \cdot UE_{ij} \tag{9}$$

According to Dubois and Prade (1978), a fuzzy number $\widetilde{A}$ is a fuzzy subset of a real number, and its membership function is $\mu_{\widetilde{A}}(x): R \to [0,1]$, where x represents the criteria, and is described by enshrined with the following characteristics:

(1) $\mu_{\widetilde{A}}(x)$ is a continuous mapping from R to the closed interval [0,1]

(2) $\mu_{\widetilde{A}}(x)$ is a convex fuzzy subset.

(3) $\mu_{\widetilde{A}}(x)$ is the normalization of a fuzzy subset, which means that there exists a number such that $\mu_{\widetilde{A}}(x_0) = 1$.

It cane be called fuzzy number if all the conditions above are satisfied. The triangular fuzzy number $\mu_{\widetilde{A}}(x) = (L, M, U)$ can be defined as Eq.(10) and Figure 1. :

$$\mu_{\widetilde{A}}(x) \begin{cases} (x-L)/(M-L) & L \le M \le M \\ (U-x)/(U-M) & M \le x \le U \\ 0 & \text{otherwise} \end{cases} \tag{10}$$

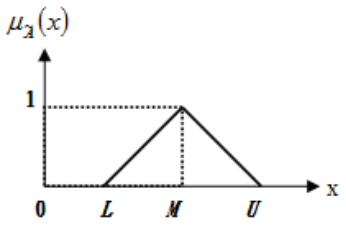

Figure 1. The triangular fuzzy number.

B. DEMATEL to develop network relationship

DEMATEL is an analytical method of structural model. It is mainly used to solve all kinds of complex problems to clarify the essential of the problem. Using matrix and related math theories to calculate the cause and effect on each element and the degree. This method widely used to solve various types of complex studies that can effectively understand the complex structure and provide viable options of problem solving (Tzeng, 2007).

DEMATEL divided into five steps. The first step is to confirm the system elements and develop the evaluating scale. To confirm the system has an elements and denoted by $E_1, E_2, \ldots, E_n$. Then, using pair of dimensions to compare and using evaluating scale ranging from 0, 1, 2, 3, and 4 which in turn represents: no influence"0", low influence"1", medium influence"2", high influence"3", and extremely high influence"4" as measuring standard. The second step is to calculate the direct relation average matrix. Using pair of degree of interaction to obtain directly influence matrix $\boldsymbol{K} = [k_{ij}]_{m \times m}$, k_{ij} represents the degree of effect on *i* factor effects *j* factor.

$$\boldsymbol{K} = \begin{bmatrix} k_{11} & k_{12} & \cdots & k_{1m} \\ k_{21} & k_{22} & \cdots & k_{2m} \\ \vdots & \vdots & \ddots & \vdots \\ k_{m1} & k_{m2} & \cdots & k_{mm} \end{bmatrix} \tag{11}$$

When the elements of *i* have a direct effect on the elements of *j*, then $k_{ij} \neq 0$, opposite $k_{ij} = 0$. The third step is to normalize the matrix. It can be obtained from formula (12) and (13). Its diagonal is 0, and maximum sum of row and column is 1.

$$\boldsymbol{X} = \frac{\boldsymbol{K}}{s} \tag{12}$$

$$s = \max\left(\max_{1 \le i \le n} \sum_{j=1}^{n} a_{ij}, \max_{1 \le j \le n} \sum_{i=1}^{n} a_{ij} \right) \tag{13}$$

The forth step is to obtain the total effect matrix $\boldsymbol{T}$.

When $\lim_{l \to \infty} \boldsymbol{X}^l = [0]_{n \times n}$,

Its can be obtained by $\boldsymbol{T} = \boldsymbol{X} + \boldsymbol{X}^1 + \boldsymbol{X}^2 + \boldsymbol{X}^3 + \cdots + \boldsymbol{X}^m = \boldsymbol{X}(\boldsymbol{I} - \boldsymbol{X})^{-1}$.

Where $\boldsymbol{I}$ represents the unit matrix. The fifth step is to obtain prominence and relation. To sum of each row and column of the total effect matrix $\boldsymbol{T}=[t_{ij}]$. Its will obtain the sum of all rows d and the sum of all columns r. If d_i represents the sum of all rows of the total effect matrix $\boldsymbol{T}$, meaning directly or indirectly affects degree; r_j represents the sum of all columns of the total effect matrix $\boldsymbol{T}$, meaning affected by other criteria. d_i represents the factor which will affect other factors, r_j represents the factor that is affected by other factors. According to the definition, $d_i + r_j$ presents the degree of relationship between factors, meaning "prominence"; $d_i - r_j$ presents the degree of effect and effected for the facto, meaning "relation" (Tamura et al., 2002; Tzeng et al., 2007).

IV. Application of The Proposed Framewor

The standardized project management system model aims to optimize the interface and standardization. It will survey research projects in the EU funded 6'h Framework Programmed (FP6) for standards related output, and serve as a platform to those projects seeking a cost-effective interface with standards bodies. In doing so, it will help projects upgrading their output and speed up market adoption of research results. Also, COPRAS will produce generic guidelines, supporting future research projects to build an interface to standardizations into their proposals, already at an early stage. In doing so, it will bring research and standardization closer together (Brusse & Wenning, 2005).

In this study will be exploring the quality assessment for SPM system within the case study of company X. We will consider standardized project management system model on purpose to constructing the mutual maneuverability and duplication in different projects.

A. DEMATEL to develop network relationship

The template is designed so that author affiliations are not repeated each time for multiple authors of the same affiliation. Please keep your affiliations as succinct as possible (for example, do not differentiate among departments of the same organization). This template was designed for two affiliations.

In this paper, we have confirmed FUZZY DEMATEL decision-making structure, and also analyzed five dimensions with seventeen criteria of the SPM system. According to the expert questionnaires, we obtain the total effect matrix T of SPM system's dimensions and criteria as shown in TABLE II. to TABLE III. We can find the cognition and opinion of experts in five dimensions and the relationship among the extents of the impact can be found which is compared to other dimensions as show in TABLE II. .

According to the prominence (r + d), the dimension B (people) is the highest impact of the strength of relation which means the most important influencing factors; in addition, the dimension E (resource) are all the factors that affect the least degree of other factors.

According to the relation (r – d), we also can find the dimensions A (strategy) and B (people) both are the highest degree of impact relationship that affect other factors directly. They also have the interact characteristics. Otherwise, dimension C (tool) is the most vulnerable to impact that compare with other dimensions.

According to TABLE III. We can obtain all the criteria of the impact of relations with each factor. Furthermore, we also find in TABLE III. Which illustrates the criterion a_1 (project management strategy) is the highest degree of impact relationship in all the criteria. Otherwise, the criterion b_2 (project culture) is the most vulnerable to impact of criteria that compare with other criteria.

B. Identify the Headings

They show the relationship of each dimension and criterion. According to Fuzzy DEMATEL model that it indicates the dimension A (strategy) is the main influence of all dimensions. A project must give a clear definition of its goals in strategy. This step is constructing the SPM of the first importance. In the other hand, the tool in the SPM model is influenced by other dimensions. It is shows that through a complete strategy can use the right people in the right position. And then, the project usually constrained by lack of resource so a good strategy can allocate well of limed resource.

Consequently, the allocation not only influences the project process but also tool in a project. And then, people need training by company strategy to operation tools. To sum up, the company's strategy is the critical factor of constructing SPM system structure model. See following Figure 2, Tables II and III.

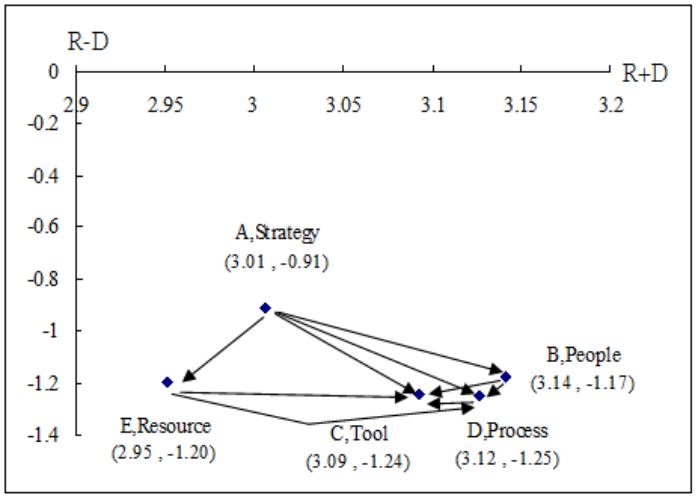

Figure 2. Influence map of total relationship of a standardized project management system model.

TABLE II. THE TOTAL EFFECT MATRIX OF T AND SUM OF EFFECTS ON DIMENSIONS

Dimensions	*A*	*B*	*C*	*D*	*E*	*r*	*d*	*r+d*	*r-d*
A	0.29	0.33	0.33	0.33	0.31	1.59	1.41	3.01	0.18
B	0.29	0.31	0.32	0.33	0.31	1.57	1.57	3.14	0.00
C	0.28	0.31	0.30	0.32	0.30	1.52	1.58	3.09	-0.06
D	0.29	0.32	0.32	0.31	0.30	1.53	1.59	3.13	-0.06
E	0.27	0.30	0.30	0.31	0.28	1.45	1.50	2.95	-0.05

TABLE III. THE FUZZY WITH DEMATEL MATRIX FOR CRITERIA

Criterias	a_1	a_2	a_3	b_1	b_2	b_3	c_1	c_2	c_3	c_4	d_1	d_2	d_3	d_4	e_1	e_2	e_3
a_1	0.28	0.32	0.31	0.33	0.37	0.33	0.35	0.33	0.36	0.36	0.35	0.35	0.36	0.36	0.32	0.30	0.35
a_2	0.30	0.25	0.29	0.31	0.34	0.31	0.32	0.30	0.32	0.33	0.32	0.32	0.33	0.34	0.30	0.29	0.33
a_3	0.30	0.29	0.24	0.31	0.34	0.31	0.33	0.30	0.32	0.33	0.33	0.32	0.32	0.33	0.29	0.30	0.33
b_1	0.32	0.31	0.28	0.28	0.36	0.32	0.33	0.32	0.35	0.35	0.35	0.33	0.35	0.34	0.31	0.30	0.35
b_2	0.29	0.29	0.28	0.31	0.29	0.31	0.32	0.29	0.33	0.32	0.33	0.32	0.33	0.33	0.29	0.29	0.33
b_3	0.30	0.30	0.28	0.32	0.34	0.27	0.32	0.30	0.33	0.33	0.32	0.32	0.32	0.33	0.30	0.29	0.34
c_1	0.29	0.28	0.26	0.30	0.32	0.29	0.27	0.28	0.32	0.31	0.30	0.29	0.31	0.31	0.28	0.27	0.31
c_2	0.27	0.27	0.26	0.29	0.31	0.30	0.31	0.25	0.31	0.30	0.30	0.30	0.31	0.30	0.28	0.28	0.31
c_3	0.30	0.30	0.29	0.32	0.35	0.32	0.33	0.32	0.29	0.33	0.33	0.32	0.34	0.33	0.31	0.30	0.34
c_4	0.30	0.29	0.28	0.32	0.34	0.31	0.33	0.30	0.32	0.29	0.33	0.32	0.33	0.34	0.30	0.29	0.34
d_1	0.29	0.28	0.27	0.31	0.33	0.31	0.31	0.29	0.32	0.32	0.27	0.31	0.32	0.33	0.27	0.29	0.33
d_2	0.31	0.30	0.28	0.33	0.35	0.32	0.33	0.32	0.34	0.33	0.32	0.28	0.34	0.34	0.30	0.29	0.34
d_3	0.30	0.29	0.28	0.30	0.34	0.31	0.32	0.30	0.33	0.32	0.32	0.31	0.28	0.31	0.29	0.29	0.32
d_4	0.29	0.28	0.26	0.30	0.33	0.30	0.32	0.30	0.32	0.31	0.31	0.30	0.31	0.27	0.28	0.28	0.32
e_1	0.27	0.26	0.25	0.28	0.30	0.29	0.30	0.27	0.32	0.30	0.31	0.29	0.29	0.30	0.24	0.27	0.31
e_2	0.26	0.25	0.25	0.28	0.29	0.26	0.28	0.27	0.30	0.29	0.30	0.28	0.28	0.29	0.27	0.23	0.30
e_3	0.30	0.29	0.29	0.32	0.34	0.31	0.32	0.31	0.33	0.33	0.33	0.33	0.34	0.34	0.30	0.28	0.29

C. Inluence map of each dimension

In the strategy dimension, the criterion a_1 (project management strategy) is the most critical influence of the Figure 3.

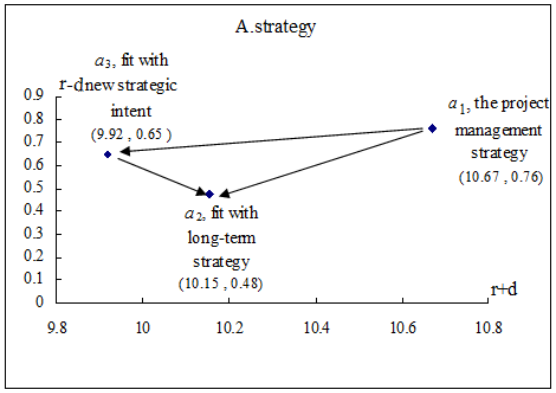

Figure 3. Influence map of strategy relationship.

In the people dimension, the criterion b_1 (project organization) is the most critical influencing factor. In a project which it has an excellent team-work to finishing the goal as soon as possible. Furthermore, the b_2 (project culture) and b_3 (project leadership) are influenced by the b_1 (project organization).

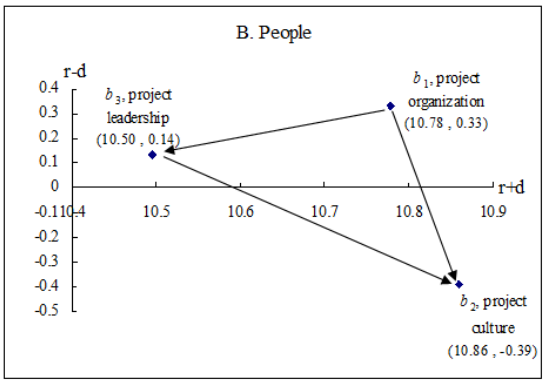

Figure 4. Influence map of people relationship.

The factor c_4 (information management system) is the infulence of the tool dimesion. In this study, we obtain that a project need a good communicate system with each team number to makesure their schedule every week.

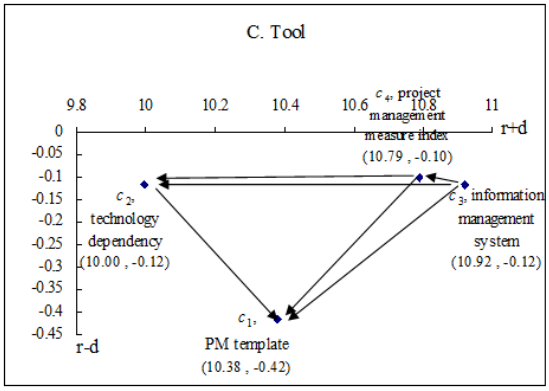

Figure 5. Influence map of tool relationship.

The factor d_2 (project methodologies) is the main influence in the dimension D "process". In this study, we obtain that a methodology made a great impact on the project process.

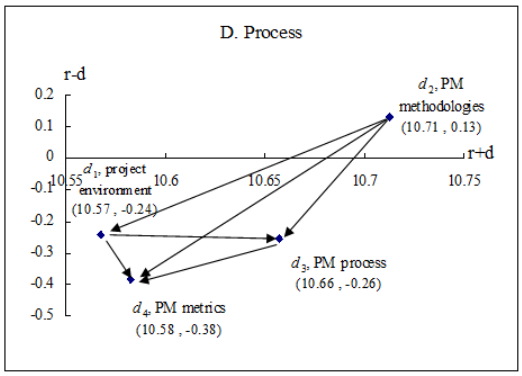

Figure 6. Influence map of process relationship.

Finally, a company always supplies a limted cost to development a project in practice. In the resource dimention, we also obtain the critical fator cost/expenses (e_1). Consequently, it is more or less of a company's budget which impactes the projcet with support of facility (e_2) and support of employee (e_3).

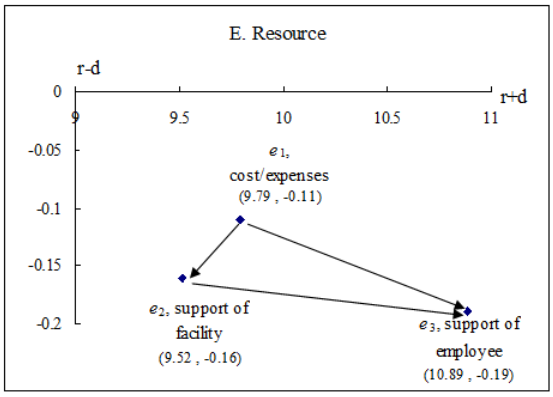

Figure 7. Influence map of resource relationship.

V. Results and Discussions

In this paper, we use FUZZY DEMATEL to develop network relationship. According to the results of empirical analysis and the literature review to the past research, the study illustrates that shows dimension A (Strategy) is the critical and dimension C (Tool) is ultimate influenced dimension in the standardized project management system, hence we can start improvement company total performance from company's strategy. Because of that the "Process" and "Tools" will be promoted to high level. And then, the Tools not only easy to using by people but also the resource are allocated efficiently. In order to achieving company's target it need change and improve all of dimensions from top to bottom.

In this paper, we find that dimensions of "Strategy", "People" and "Resource" are the critical factors for total performance evaluate of constructing standardized project management system. According to the empirical analysis, we have used DEMATEL to construct the standardized project management model especially for new product development projects. We also obtains that the dimension A "Strategy" is the main index in constructing the SPM system. The results from this study provide a project management team a guidance to satisfy the company's purpose and create the value of sustainable business.

The company must state that new product development and opportunity generation are the business. Not only remove barriers to the generation of new ideas and provide a system of information and feedback on current products and services but also create a positive, perhaps virtual place for new ideas to incubate. To generate a flexible process of filtering, evaluating and transitioning new ideas into a portfolio and new product development process and manage and control new product development and marketing. Then, real success stories are created to demonstrate that new ideas can produce products that grow the business.

ACKNOWLEDGEMENTS: NSC 99-2632-H-424-001-MY3

References

[1] U.S. Bititci, Suwignjo P., and Carrie A.S., Strategy management through quantitativemodeling of performance measurement systems, International Journal of Production Economics vol. 69, pp: 15-22, 2001.

[2] Dragan Milosevic, Peerasit Patanakul, "Standardized project management may increase development projects success," International Journal of Project Management vol. 23, pp. 181–192, 2005.

[3] Lin, C. L. and Tzeng, G. H., A value-created system of science (technology) park by using DEMATEL, Expert Systems with Applications, vol. 36(6), pp. 9683-9697, 2009.

[4] J. J. Huang, G. H. Tzeng, and C. S. Ong, Multidimensional data in multidimensional scaling using the analytic network process, Pattern Recognition Letters, vol. 26, pp: 755-767, 2005.

[5] International Journal of IT Standards and Standardization Research. vol. 3, no. 1, pp. 75-81. Jan.-June 2005.

[6] S. Opricovic, G. H. Tzeng, Compromise solution by MCDM methods: a comparative analysis of VIKOR and TOPSIS. European Journal of Operational Research, vol. 156, pp. 445e455, 2004.

[7] J. Poolton and I. Barclay, New product development from past research to future application, Industrial Marketing Management, vol. 27(3), pp. 197-212, 1998.

[8] Project Management Institute, "A Guide to The Project Management Body of Knowledge (PMBOK guide)", 2008 edition, PMI Standard Committee, USA.

[9] T. L. Saaty, Decision Making with Dependence and Feedback: The Analytic Network Process, RWS Publications, Pittsburgh, PA, 1996.

[10] G. H. Tzeng, C. H. Chiang and C. W. Li, Evaluating Intertwined Effects in E-learning Programs :A Novel Hybrid MCDM Model Based on Factor Analysis and DEMATEL. Expert Systems With Applications, vol 32(4), pp. 1028-1044, 2007.

[11] T. Bruce Barkley, Project Management in New Product Development, McGraw-Hill Companies, Inc., 2008.

2011 IEEE International Conference on Fuzzy Systems
June 27-30, 2011, Taipei, Taiwan

Interdependent Multiple Objective Programming- A Monte Carlo Method

Jih-Jeng Huang
Department of Computer Science & Information Management
Soochow University
Taipei, Taiwan
jjhuang@scu.edu.tw

Chin-Yi Chen
Department of Business Administration
Chung Yuan Chirstian University
Chungli, Taiwan
iris@cycu.edu.tw

***Abstract*—Although multiple objective programming (MOP) skills have been extensively studied in various issues, the problem of MOP with interdependence has received little attention. In this paper, we overcome the problem of Carlsson and Fullĕr's method and propose a novel index to measure the interdependence grade between objectives by using Monte Carlo simulation and regression analysis. Then, an interdependent multiple objective programming (IMOP) model is proposed. In addition, we give three numerical examples to demonstrate the proposed method. From the numerical results, we can conclude that the proposed method can rationally deal with the problem of MOP with interdependence.**

Keywords- Multiple objective programming (MOP); interdependence; interdependent multiple objective programming (IMOP).

I. INTRODUCTION

Since Kuhn and Tucker [1] proposed the concepts of vector optimization, and Koopmans [2] applied the efficient vector method to derive necessary conditions of efficient solution, more and more researchers engaged in studies about multiple objective programming (MOP) problems. The common characteristics of MOP can be described as: (1) a set of quantifiable objectives; (2) a set of well-defined constraints; (3) a process of obtaining some trade-off information, implicit or explicit, between the stated quantifiable objectives and also between stated or unstated non-quantifiable objectives [3]. The general form of MOP can be represented as solving the following mathematical programming problem:

$$\max_{x \in X} / \min \quad \{f_1(\boldsymbol{x}), f_2(\boldsymbol{x}), \cdots, f_n(\boldsymbol{x})\}, \tag{1}$$

$$s.t. \quad \boldsymbol{x} = \{\boldsymbol{x} \in \boldsymbol{R}^n \mid g_k(\boldsymbol{x}) \geq 0, \quad k = 1, \cdots, m\}.$$

Although MOP have been widely extended for many issues, such as global optimization [4, 5], multistage [6], and multilevel [7,8,9,10,11], the assumption of independent objectives should be released. That is, supportive and conflicting objectives usually happen in realistic multiple criteria decision making (MCDM) problems, and we should not ignore the problem of MOP with interdependence between objectives under the viewpoint of optimization.

Carlsson and Fullĕr [12-14] first proposed two methods to consider the problem of MOP with interdependence by estimating the interdependent grade between objectives. Thereafter, several issues have been proposed to consider further situations, such as uncertainty environment [13,14] and temporal interdependence [15]. However, several shortcomings of their methods should be modified so that we can employ interdependent multiple objective programming (IMOP) in practice. Firstly, their first method [12] does not precisely measure the supportive or conflicting grade between objectives and can only deal with the one-dimensional decision problem. In contrast, their second method [14] can only be suitable for symmetric linear interdependent multiple objective programming (SLIMOP). However, it can be seen that since real-life problems are usually complex and intricate, a general method should be given to handle all kinds of IMOP problems.

In this paper, Monte Carlo simulation and regression analysis are used to measure the grade of interdependence between objectives. The proposed method is suitable not only for the one-dimensional decision problem but also for the high-dimensional decision problem. In addition, the proposed index can also be suitable for asymmetric nonlinear interdependent multiple objective programming (ANIMOP). Three numerical examples are used to demonstrate the proposed method. The results are compared with the conventional MOP and Carlsson and Fullĕr's model. On the basis of the numerical results, we can conclude that the proposed method can deal with the IMOP problems and overcome the problem in [12-15].

The remainder of this paper is organized as follows. The problem of MOP is discussed in Section 2. The method to solve IMOP is proposed in Section 3. In Section 4, three numerical examples are used to demonstrate the proposed method and compared with the conventional MOP and

978-1-4244-7316-8/11/$26.00 ©2011 IEEE

Carlsson and Fullẽr's method. Discussions are presented in Section 5 and the conclusion is in the last section.

II. THE PROBLEM OF IMOP

The main problem of conventional MOP models is the unrealistic assumption of independence between objectives. In order to show the impact, we can transform the MOP model into the single-objective programming (SOP) model by using the following compromise programming [16]:

$$\begin{aligned} &\min \quad r(\boldsymbol{y}; p) = \| \boldsymbol{y} - \boldsymbol{y}^* \|_p \\ &s.t. \quad \boldsymbol{x} = \{\boldsymbol{x} \in \boldsymbol{R}^n \mid g_k(\boldsymbol{x}) \le 0, \quad k = 1, \cdots, m\}, \end{aligned} \tag{2}$$

where $r(\boldsymbol{y}; p)$ is a measurement of regret from $\boldsymbol{y}$ to $\boldsymbol{y}^*$ according to the l_p-norm, $\boldsymbol{y}$ denotes the objective vector, and $\boldsymbol{y}^*$ denotes the ideal-point vector.

Assume a biobjective problem and let $p = \infty$. Assume a biobjective problem and let $p = \infty$. Consider a case depicted in Figure 1. Then the optimal solution should be $\boldsymbol{y}^\infty$ if and only if $f_1(\boldsymbol{x})$ is independent of $f_2(\boldsymbol{x})$. However, if $f_1(\boldsymbol{x})$ supports $\hat{f}_2(\boldsymbol{x})$, the optimal solution should transfer from $\boldsymbol{y}^\infty$ to $\hat{\boldsymbol{y}}_\infty$.

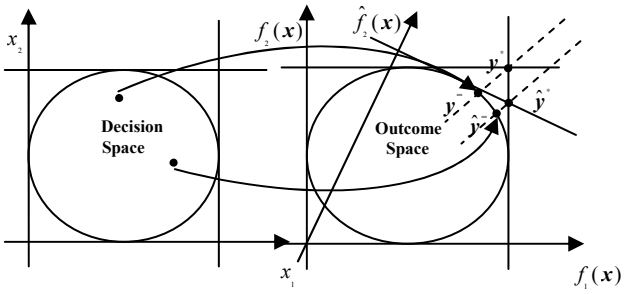

Figure 1. The optimal solution between independent and interdependent objectives

Therefore, if we want to extend MOP to IMOP, we should consider the interdependence between objectives as shown in Figure 2.

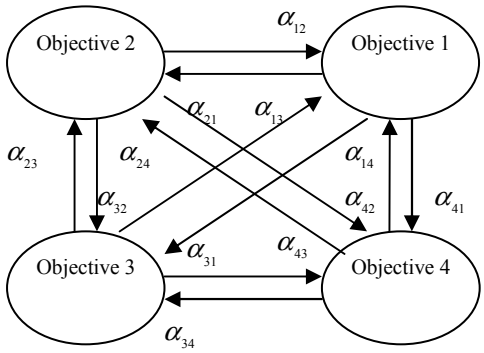

Figure 2. The interdependence with multiple objectives

From Figure 2, it can be seen that the objectives in MOP should be modified [12-14] as:

$$\hat{f}_i(\boldsymbol{x}) = f_i(\boldsymbol{x}) + \sum_{j=1, j \ne i}^{n} \alpha_{ij} f_j(\boldsymbol{x}), \quad \forall \quad 1 \le i, j \le n \tag{3}$$

where α_{ij} denotes the estimated grade of interdependence from the *j*th objective to the *i*th objective. Note that from Eq. (3), it can be seen that MOP is a special case while $\alpha_{ij} = 0$ in IMOP.

Therefore, the MOP problem should be reformulated as:

$$\begin{aligned} &\max/\min_{x \in X} \quad \{\hat{f}_1(\boldsymbol{x}), \hat{f}_2(\boldsymbol{x}), \cdots, \hat{f}_n(\boldsymbol{x})\} \\ &s.t. \quad \boldsymbol{x} = \{\boldsymbol{x} \in R^n \mid g_k(\boldsymbol{x}) \le 0, \quad k = 1, \cdots, m\}. \end{aligned} \tag{4}$$

In order to solve the IMOP problem above, the grade of interdependence should be derived first. In [12-14], they defined the grade of interdependence of the *i*th objective using the following equation:

$$\Delta(f_i) = \sum_{j=1, j \ne i}^{n} \text{sign}(\alpha_{ji}) \tag{5}$$

where $\Delta(f_i)$ is the number of objectives supported by the *i*th objective minus the number of objectives hindered by the *i*th objective.

Although using Eq. (5), we can reformulate conventional MOP to IMOP, two main shortcomings should be overcome so that we can solve IMOP problems more precisely. Firstly, it can be seen that Eq. (5) does not precisely reflect the supportive or conflicting grade between objectives because of using the sign operation. Furthermore, their method can only deal with the one-dimensional decision problem. To overcome the above problem, [4] proposed another index to measure the

grade of interdependence between objectives in the high-dimensional decision space as follows.

Assume two linear objectives, $f_i(\boldsymbol{x}) = <\boldsymbol{c}_i, \boldsymbol{x}>$ and $f_j(\boldsymbol{x}) = <\boldsymbol{c}_j, \boldsymbol{x}>$ where $\| \boldsymbol{c}_i \|$, $\| \boldsymbol{c}_j \| = 1$, then the grade of interdependence between $f_i(\boldsymbol{x})$ and $f_j(\boldsymbol{x})$ can be defined by:

$$k(f_i(\boldsymbol{x}), f_j(\boldsymbol{x})) = k(f_j(\boldsymbol{x}), f_i(\boldsymbol{x})) = \frac{1 - <\boldsymbol{c}_i, \boldsymbol{c}_j>}{2}, \quad (6)$$

where $<>$ denotes the dot product, $\| \cdot \|$ denotes the length of the specific vector, and $\alpha_{ij} = -2 \times k(f_i(\boldsymbol{x}), f_j(\boldsymbol{x})) + 1$.

According to Eq. (6), however, it can be seen the above index can only deal with the linear case. In addition, it is clear that α_{ij} is not always equal to α_{ji} in the realistic problems. In order to overcome the above problems, in this paper, we propose a novel index to measure the interdependent grade between objectives by using Monte Carlo simulation and regression analysis.

III. Interdependent Multiple Objective Programming

As mentioned above, the crucial point of dealing with IMOP is to obtain the grade of interdependence between objectives so that we can reformulate the conventional MOP model. To overcome the problem of interdependence in MOP, we first define the notations as follows.

Let $f_i(\boldsymbol{x})$ and $f_j(\boldsymbol{x})$ be two objectives. We say that

(i) $f_i(\boldsymbol{x})$ supports $f_j(\boldsymbol{x})$ on $\boldsymbol{X}$ (denoted by $f_i(\boldsymbol{x}) \uparrow f_j(\boldsymbol{x})$) if $f_i(\boldsymbol{x}') \geq f_j(\boldsymbol{x})$ entails $f_j(\boldsymbol{x}') \geq f_i(\boldsymbol{x})$, for all $\boldsymbol{x}', \boldsymbol{x} \in \boldsymbol{X}$; $\partial f_j(\boldsymbol{x}) / \partial f_i(\boldsymbol{x}) > 0, \forall \boldsymbol{x} \in \boldsymbol{R}^n$;

(ii) $f_i(\boldsymbol{x})$ is in conflict with $f_j(\boldsymbol{x})$ on $\boldsymbol{X}$ (denoted by $f_i(\boldsymbol{x}) \downarrow f_j(\boldsymbol{x})$) if $f_i(\boldsymbol{x}') \geq f_j(\boldsymbol{x})$ entails $f_j(\boldsymbol{x}') \leq f_i(\boldsymbol{x})$, for all $\boldsymbol{x}', \boldsymbol{x} \in \boldsymbol{X}$; $\partial f_j(\boldsymbol{x}) / \partial f_i(\boldsymbol{x}) < 0, \forall \boldsymbol{x} \in \boldsymbol{R}^n$;

(iii) $f_i(\boldsymbol{x})$ is independent with $f_j(\boldsymbol{x})$ on $\boldsymbol{X}$ (denoted by $f_i(\boldsymbol{x}) \perp f_j(\boldsymbol{x})$), otherwise.

If $\boldsymbol{X} \in \boldsymbol{R}^n$ then we say that $f_i(\boldsymbol{x})$ supports (or is in conflict with) $f_j(\boldsymbol{x})$ globally.

If the objective functions are differentiable on $\boldsymbol{X}$, we may define

(i) $f_i(\boldsymbol{x}) \uparrow f_j(\boldsymbol{x})$ on $\boldsymbol{X}$ $\Leftrightarrow$ $\partial_{\boldsymbol{e}} f_i(\boldsymbol{x}) / \partial_{\boldsymbol{e}} f_j(\boldsymbol{x}) \geq 0, \forall \boldsymbol{e} \in \boldsymbol{R}^n, \boldsymbol{x} \in \boldsymbol{X}$,

(ii) $f_i(\boldsymbol{x}) \downarrow f_j(\boldsymbol{x})$ on $\boldsymbol{X}$ $\Leftrightarrow$ $\partial_{\boldsymbol{e}} f_i(\boldsymbol{x}) / \partial_{\boldsymbol{e}} f_j(\boldsymbol{x}) \leq 0, \forall \boldsymbol{e} \in \boldsymbol{R}^n, \boldsymbol{x} \in \boldsymbol{X}$,

where $\partial_{\boldsymbol{e}} f_i(\boldsymbol{x})$ denotes the derivative of $f_i(\boldsymbol{x})$ with respect to the direction $\boldsymbol{e} \in \boldsymbol{R}^n$ at $\boldsymbol{x} \in \boldsymbol{R}^n$. If for a given direction $\boldsymbol{e} \in \boldsymbol{R}^n$, $\partial_{\boldsymbol{e}} f_i(\boldsymbol{x}) \partial_{\boldsymbol{e}} f_j(\boldsymbol{x}) \geq 0$ holds for all $\boldsymbol{x} \in \boldsymbol{X}$ then we say that $f_i(\boldsymbol{x})$ supports $f_j(\boldsymbol{x})$ with respect to the direction $\boldsymbol{e}$ on $\boldsymbol{X}$.

It is clear that the information of $\partial f_j(\boldsymbol{x}) / \partial f_i(\boldsymbol{x})$ is hard to obtain because it may vary with respect to different decision points. Therefore, the compromise is to find a constant estimated value of $\partial f_j(\boldsymbol{x}) / \partial f_i(\boldsymbol{x})$ by α_{ji}. Now, we depict Figure 3 to describe the concept of calculating α_{ji}. First, we transform objective value to satisfaction level $\lambda(\cdot)$. From Figure 3, it can be seen that $\partial f_j(\boldsymbol{x}) / \partial f_i(\boldsymbol{x})$ is negative because when the satisfaction level of $f_i(\boldsymbol{x})$ increases, the satisfaction level of $f_j(\boldsymbol{x})$ decreases, and vice versa. Due to the problem of obtaining the value of $\partial f_j(\boldsymbol{x}) / \partial f_i(\boldsymbol{x})$, we can calculate the estimated value of $\partial f_j(\boldsymbol{x}) / \partial f_i(\boldsymbol{x})$, i.e., α_{ji}, by using regression analysis to estimate the best fitted line and obtain the regression coefficient as α_{ji}. Note that except for linear regression analysis, we can also use spline regression analysis to calculate the piece wise situation.

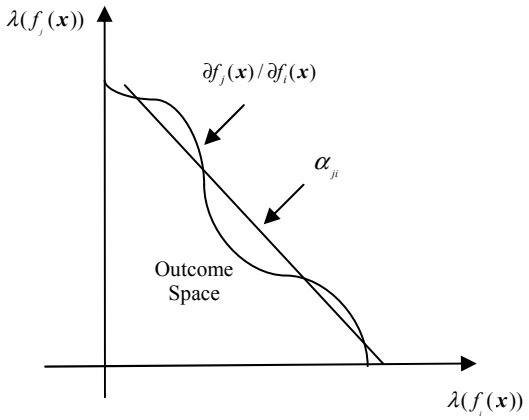

Figure 3. The concept of α_{ji}

According to the above concepts, the procedure of calculating the grade of interdependence between objectives can be developed as follows. First, we employ Monte Carlo simulation to calculate the value of each objective and the

corresponding satisfaction level ($\lambda_i(\boldsymbol{x})$) which is subject to the specific constraints, as shown in TABLE I.

TABLE I. Monte Carlo Sampling to Calculate Objective and Satisfaction Values.

Monte Carlo Simulation	*Calculate*						*Subject to*
	$f_1(\boldsymbol{x})$	⋯	$f_n(\boldsymbol{x})$	$\lambda_1(\boldsymbol{x})$	⋯	$\lambda_n(\boldsymbol{x})$	
1	f_{11}	⋯	f_{n1}	λ_{11}	⋯	λ_{n1}	$g_1(\boldsymbol{x}) \le 0$,
2	f_{12}	⋯	f_{n2}	λ_{12}	⋯	λ_{n2}	⋮
⋮	⋮	⋮	⋮	⋮	⋮	⋮	$g_m(\boldsymbol{x}) \le 0$.
N	f_{1N}	⋯	f_{nN}	λ_{1N}	⋯	λ_{nN}	

Note that the satisfaction of each objective can be represented as:

$$\lambda_i(\boldsymbol{x}) = \begin{cases} 1 & \text{if} \quad f_i(\boldsymbol{x}) \ge M_i, \\ 1 - \dfrac{M_i - f_i(\boldsymbol{x})}{M_i - m_i} & \text{if} \quad m_i < f_i(\boldsymbol{x}) < M_i, \\ 0 & \text{if} \quad f_i(\boldsymbol{x}) \le m_i, \end{cases} \qquad (9)$$

where $m_i = \min\{f_{ir}\}, \forall r = 1, \ldots, N$ and $M_i = \max\{f_{ir}\}, \forall r = 1, \ldots, N$. Next, we give two simple cases to describe the concepts of the proposed method.

Case 1. Consider the following biobjective mathematical programming:

$$\max\{f_1(\boldsymbol{x}), f_2(\boldsymbol{x})\},$$
$$\text{where } f_1(\boldsymbol{x}) = 2x_1^2 - 3x_2^2 \text{ and } f_2(\boldsymbol{x}) = -3x_1 + x_2^2.$$
$$s.t. \quad x_1 + x_2 \le 20,$$
$$x_1, x_2 \ge 0.$$

Next, we use Monte Carlo simulation with the uniform distribution and generate 5,000 samples to derive the feasible solutions of the above problem, as shown in Figure 4. It can be seen that Objective 1 and Objective 2 are in conflict with each other and the block line of the feasible solutions indicates the efficient set which represents the grade of interdependence between the objectives. Since the interdependent grade with respect to different point is a non-linear curve, we can estimate the approximate interdependent grade between the objectives by a straight line, as the dash line shown in Figure 4.

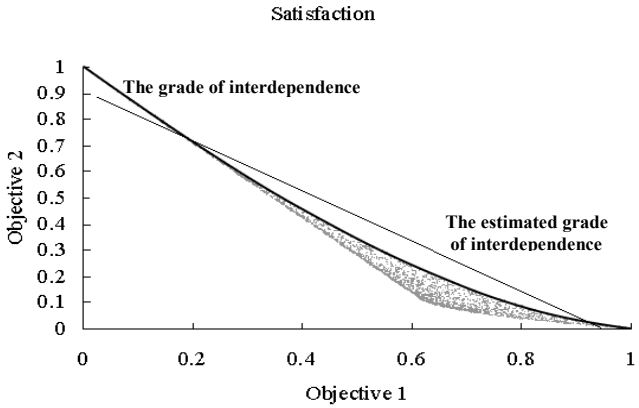

Figure 4. The conflicting case between the objectives.

Case 2. Consider the following biobjective mathematical programming:

$$\max\{f_1(\boldsymbol{x}), f_2(\boldsymbol{x})\},$$
$$\text{where } f_1(\boldsymbol{x}) = x_1^2 + 3x_2^2 \text{ and } f_2(\boldsymbol{x}) = 2x_1 + 3x_1x_2.$$
$$s.t. \quad 0 \le x_1, x_2 \le 2.$$

With the same procedures in **Case 1**, we can depict Figure 5 to represent the interdependent relationship between Objective 1 and Objective 2. From Figure 5, it can be seen that Objective 1 and Objective 2 are supportive to each other.

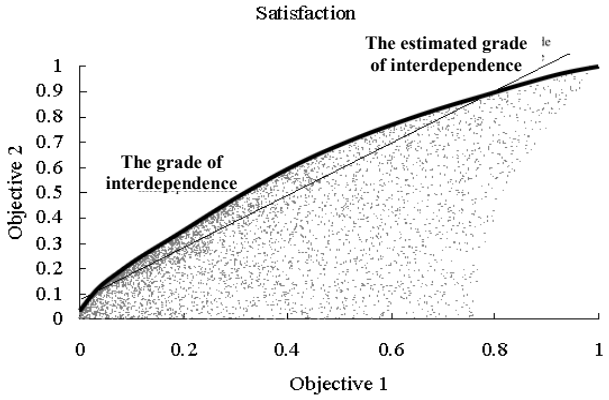

Figure 5. The supportive case between the objectives.

Then, we can calculate the estimated grade of interdependence between the objectives using the following regression equation:

$$\lambda_i(x) = \mu + \alpha_{ij} \times \lambda_j(x) + \varepsilon_{ij},$$

where μ denotes the intercept term, α_{ij} is the regression coefficient, and $\varepsilon_{ij} \sim N(0, \sigma^2)$ denotes the error term.

Now, we can incorporate the information about the grade of interdependence between objectives to developing IMOP

by adopting the ideas of Carlsson and Fullẽr [2-4] to reshape the satisfaction level. The grade of interdependence of the *i*th objective can be defined as $\Delta(f_i) = \sum_{j=1, j\neq i}^{n} \alpha_{ji}$. Then, the satisfaction level of the *i*th objective can be reformulated as:

For $\Delta(f_i) \geq 0$,

$$H_i(\boldsymbol{x}, \Delta(f_i)) = \begin{cases} 1 & if \quad f_i(\boldsymbol{x}) \geq M_i \\ \left(1 - \dfrac{M_i - f_i(\boldsymbol{x})}{M_i - m_i}\right)^{1/(\Delta(f_i)+1)} & if \quad m_i < f_i(\boldsymbol{x}) < M_i \\ 0 & if \quad f_i(\boldsymbol{x}) \leq m_i \end{cases}$$

. (12)

For $\Delta(f_i) < 0$,

$$H_i(\boldsymbol{x}, \Delta(f_i)) = \begin{cases} 1 & if \quad f_i(\boldsymbol{x}) \geq M_i \\ \left(1 - \dfrac{M_i - f_i(\boldsymbol{x})}{M_i - m_i}\right)^{|\Delta(f_i)|+1} & if \quad m_i < f_i(\boldsymbol{x}) < M_i \\ 0 & if \quad f_i(\boldsymbol{x}) \leq m_i \end{cases}$$

. (13)

The above concepts for reshaping the grade of satisfaction can be depicted by Figure 6:

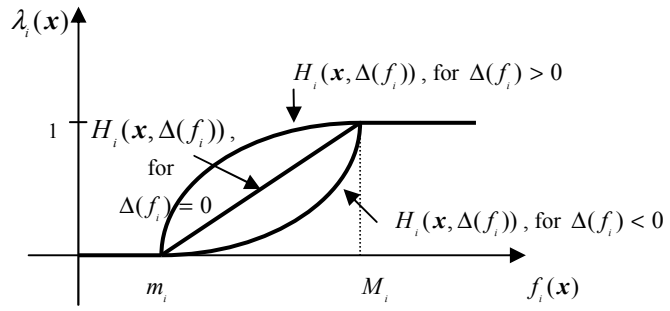

Figure 6. The reshaping grade of satisfaction

Finally, assume the optimal solution of a decision can be represented with "the average, the better." We can derive the optimal solution and reformulate the conventional MOP model to the following IMOP model:

$$\max \quad T(H_1(\boldsymbol{x}, \Delta(f_1)), \ldots, H_n(\boldsymbol{x}, \Delta(f_n)),) \quad , \quad (1 \qquad 5)$$
$$s.t. \quad \boldsymbol{x} = \{\boldsymbol{x} \in \boldsymbol{R}^n \mid g_j(\boldsymbol{x}) \geq 0, \quad j = 1, \cdots, m\},$$

where $T(\cdot)$ denotes the *t*-norm operation and indicates the preference structure of a decision maker in this paper. Note that other operations can also be used in the similar way to represent the specific preference structure of a decision maker.

IV. NUMERICAL EXAMPLES

In this section, three numerical examples are used to demonstrate the proposed method for dealing with IMOP problem. In addition, we also employ the conventional MOP model and Carlsson and Fullẽr's method to compare the results with the proposed method.

Example 1. This example contains five-objective and one-dimensional decision problem and is from Carlsson and Fullẽr [4].

$$\max\{f_1(x), f_2(x), f_3(x), f_4(x), f_5(x)\},$$
where, $f_1(x) = x$, $f_2(x) = (x+1)^2 - 1$, $f_3(x) = 2x + 1$,
$f_4(x) = x^4 - 1$, and $f_5(x) = -3x + 1$,
$s.t. \quad 0 \leq x \leq 2$.

It is easy to identify the interdependent grade between the objectives using Carlsson and Fullẽr's method as $\Delta(f_1) = \Delta(f_2) = \Delta(f_3) = \Delta(f_4) = 3 - 1 = 2$, $\Delta(f_5) = 0 - 4 = -4$. On the other hand, we can also use Monte Carlo simulation to calculate the interdependent grade between the objectives, as shown in TABLE II.

TABLE II. The Comparison of Various Methods

α_{21}	α_{31}	α_{41}	α_{51}	α_{12}
0.997	**1.000**	**0.790**	**-1.000**	**0.986**
α_{32}	α_{42}	α_{52}	α_{13}	α_{23}
0.986	**0.836**	**-0.986**	**1.000**	**0.997**
α_{43}	α_{53}	α_{14}	α_{24}	α_{34}
0.790	**-1.000**	**0.943**	**1.000**	**0.943**
α_{54}	α_{15}	α_{25}	α_{35}	α_{45}
-0.943	**-1.000**	**-0.997**	**-1.000**	**-0.790**

Next, we use MOP, Carlsson and Fullẽr's method (CF), and the proposed model (i.e., Eq. (11)) to derive the optimal solutions, as shown in TABLE III.

TABLE III. The Comparison of Various Methods

	x	$f_1(x)$	$f_2(x)$	$f_3(x)$	$f_4(x)$	$f_5(x)$
MOP	1.76	1.76	6.62	4.52	8.60	-4.28
CF	0.65	0.65	1.72	2.30	-0.73	-0.95
IMOP	0.69	0.69	1.86	2.38	-0.67	-1.07

From TABLE 3, it can be seen that the results of Carlsson and Fullẽr 's method are approximate to the proposed model, because of the similar interdependent grade between the objectives. In addition, compared to MOP, two IMOP models

suggest that we should decrease x to achieve the optimal solution.

Example 2. Consider the following three-objective and three-dimensional linear programming problem:

$$\max\{f_1(\boldsymbol{x}), f_2(\boldsymbol{x}), f_3(\boldsymbol{x})\},$$
$$\text{where } f_1(\boldsymbol{x}) = 4x_1 + 2x_2 - 3x_3,$$
$$f_2(\boldsymbol{x}) = 4x_1 + 3x_2 + 2x_3,$$
$$f_3(\boldsymbol{x}) = -7x_1 - 4x_2 + 6x_3.$$
$$s.t. \quad 0 \le x_1, x_2, x_3 \le 10.$$

To calculate the interdependent grade between the objectives, we can use Carlsson and Fullĕr 's method (i.e., Eq.(6)) and Monte Carlo simulation, respectively, as shown in TABLE IV.

TABLE IV. The interdependence grade between objectives of Example 2

	α_{21}	α_{31}	α_{12}	α_{32}	α_{13}	α_{23}
CF	0.552	-0.998	0.552	-0.517	-0.998	-0.517
IMOP	0.543	-0.988	0.544	-0.503	-1.000	-0.513

By incorporating the information of the interdependent grade between the objectives, we can derive the optimal solutions of **Example 2** using MOP, Carlsson and Fullĕr 's method, and the proposed method, respectively, as shown in TABLE V.

TABLE V. The Comparison of MOP and IMOPs in Example 2

	x_1	x_2	x_3	$f_1(\boldsymbol{x})$	$f_2(\boldsymbol{x})$	$f_3(\boldsymbol{x})$
MOP	2.8571	10.0000	10.0000	1.4286	61.4286	0.0000
CF	7.1987	2.0374	10.0000	2.8694	54.9068	1.4598
IMOP	7.3354	1.7810	10.0000	2.9036	54.6846	1.5282

Similar to Example 1, the proposed method and Carlsson and Fullĕr 's method have the approximate results. Both results show that we should decrease x_2 and increase x_1 to obtain the optimal solution.

Example 3. Consider the following three-objective and three-dimensional nonlinear programming problem:

$$\max\{f_1(\boldsymbol{x}), f_2(\boldsymbol{x}), f_3(\boldsymbol{x})\},$$
$$\text{where } f_1(\boldsymbol{x}) = 3x_1^2 + 6x_1x_2 + 2x_2x_3,$$
$$f_2(\boldsymbol{x}) = 4x_1 + 2x_2 + 3x_1x_3,$$
$$f_3(\boldsymbol{x}) = 2x_1x_3 + 3x_2 + 4x_3.$$
$$s.t. \quad 0 \le x_1 + x_2 + x_3 \le 10.$$

Note that since Carlsson and Fullĕr 's method cannot handle this nonlinear problem, only MOP is compared with the proposed model. Next, using Monte Carlo simulation and regression analysis, we can calculate the interdependent grade between the objectives, as shown in Table VI.

TABLE VI. The Interdependence Grade between Objectives of Example 3

α_{21}	α_{31}	α_{12}	α_{32}	α_{13}	α_{23}
-0.5535	-0.2577	-0.4843	0.4915	0.1738	0.5576

Next, we can solve the above problem by using MOP and IMOP to obtain the optimal solution, as shown in TABLE VII.

TABLE VII. The Comparison of MOP and IMOPs in Example 3

	x_1	x_2	x_3	$f_1(\boldsymbol{x})$	$f_2(\boldsymbol{x})$	$f_3(\boldsymbol{x})$
MOP	3.4257	2.2860	4.2883	101.7993	62.34609	53.39206
IMOP	2.7086	3.4074	3.8840	103.8525	49.20918	46.79829

Compared to the results with the conventional MOP, IMOP suggests that we should decrease both x_1 and x_3 and increase to x_2 achieve the optimal solution. Next, we give discussions in Section 5 according to the findings of our examples.

V. DISCUSSIONS

MOP has been widely applied in various areas to deal with MCDM problems. However, the problem of interdependence between objectives seems to be ignored in MOP for dealing well with the realistic decision problems. It can be seen that if we ignore the problem of interdependence between objectives, the result may be huge differences with the optimal solution.

Although Carlsson and Fullĕr have proposed several papers to deal with the IMOP problems, their method can only deal with the simple IMOP problems and cannot measure the grade of interdependence between the objectives precisely. In this paper, we propose another index by using Monte Carlo simulation and regression analysis to overcome the above problems simultaneously.

From the results of numerical examples, it can be seen that the interdependent grade of the proposed method and Carlsson and Fullĕr's method have the similar results. Therefore, it enhances the justification of the proposed method. On the other hand, it also shows that the proposed method should be more flexible and useful than Carlsson and Fullĕr's method because the proposed method can be used in the high-dimensional decision space, linear and nonlinear problems, and asymmetric interdependent grade situations. In addition, all kinds of interdependent grade between objectives can be solved using the standard operating procedures.

VI. CONCLUSIONS

In this paper, the problem of MOP with interdependence between objectives is considered. A novel index is proposed to measure the grade of interdependence between objectives by using Monte Carlo simulation and regression analysis. An IMOP model is developed to solve the IMOP problems. From the numerical results, we can conclude that the proposed method can provide a satisfactory solution to deal with the IMOP problems.

REFERENCES

[1] Kuhn, H. W. and Tucker, A. W., "Nonlinear Programming", Proceedings of the second Berkeley Symposium on Mathematical Statistics and Probability, *Berkeley: University of California Press*, 481-492 (1951).

[2] Koopmans, T., Activity Analysis of Production and Allocation, *New York: John Wiley and Sons*, 1951.

[3] Hwang, C. L. and Yoon, K., Multiple Attribute Decision Making: Methods and Applications, *NY: Springer-Verlag*, 1981.

[4] Coello Coello, C. A., David, A. V. V. and Gary, B. L., Evolutionary Algorithms for Solving Multi-Ojbective Proglems, *New York: Kluwer Academic/Plenum*, 2002.

[5] Deb, K., Multi-Objective Optimization Using Evolutionary Algorithms, *New York: John Wiley & Sons*, 2001.

[6] Yu, P. L. and Seiford, L., Multistage Decision Problems with Multicriteria, Multicriteria Analysis: Practical Methods, edited by NijKamp P. and Spronk, J. London, *Britain: Gower Press*, 1981.

[7] Bialas, W. F. and Karwan, M. H., "Two-Level Linear Programming", *Management Science* 30 (8), 1004-1020 (1983).

[8] Falk, J. E., "A Linear Max-Min Problem", *Mathematical Programming* 5 (1), 169-188 (1973).

[9] Fortuny-Amat, J. and McCarl, B., "A Representation and Economic Interpretation of a Two-Level Programming Problem", *Journal of Operational Research Society* 32 (9), 783-792 (1981).

[10] Hejazi, S. R., Memariani, A., Jahanshahloo, G. and Sepehri, M. M., "Linear Bilevel Programming Solution by Genetic Algorithm", *Computers & Operations Research* 29 (13), 1913-1925 (2002).

[11] Sinha, S., "Fuzzy Mathematical Programming Applied to Multi-Level Programming Problems", *Computers & Operations Research* 30 (9), 1259-1268 (2003).

[12] Carlsson, C. and Fullẽr, R., "Multiple Criteria Decision Making: the Case for Interdependence", *Computers & Operations Research* 22 (3), 251-260 (1995).

[13] Carlsson, C. and Fullẽr, R., "Interdependence in fuzzy multiple objective programming", *Fuzzy Sets and Systems* 65 (1), 19-29 (1994).

[14] Carlsson, C. and Fullẽr, R., Fuzzy Reasoning in Decision Making and Optimization, *Heidelberg: Physica-Verlag*, 2002.

[15] Östermark, R., "Temporal Interdependence in Fuzzy MCDM Problems", *Fuzzy Sets and Systems* 88 (1), 19-29 (1997).

[16] Yu, P. L., Multiple-Criteria Decision Making, *New York: Plenum Press*, 1985.

2011 IEEE International Conference on Fuzzy Systems
June 27-30, 2011, Taipei, Taiwan

Handling Fuzzy Decision Making Problem based on Linguistic Information and Intersection Concept

Chen-Tung Chen
Department of Information Management, National United University, Miao-Li, Taiwan
ctchen@nuu.edu.tw

Ping-Feng Pai
Department of Information Management, National Chi Nan University, Nan-Tou, Taiwan
paipf@ncnu.edu.tw

Wei-Zhan Hung
Department of International Business Studies, National Chi Nan University, Nan-Tou, Taiwan
steady_2006@hotmail.com

***Abstract*—Multi-criteria decision-making (MCDM) is one of the most widely used decision methodologies. Because every kind of MCDM approach has its strong point and weakness, it is hard to make sure that what kind of MCDM approach is suitable to a specific problem. Therefore, a new decision making method is proposed in this paper based on linguistic information and intersection concept which is called linguistic intersection method (LIM). The linguistic variables are used to express the opinion of each decision-maker. There are four MCDM methods such as TOPSIS, ELECTRE, PROMETHEE, and VIKOR are included in the linguistic intersection method. First, each MCDM approach is used to determine the ranking order of all alternatives in accordance with the linguistic evaluations by decision-makers. And then, the intersection set is determined for the better alternatives of all methods. Third, the final ranking order of alternatives in the intersection set can be determined by the proposed method. This study presented an example to implement and compare the proposed method with individual linguistic MCDM method. Finally, some conclusions and future research will be discussed at the end of this paper.**

Keywords- MCDM; Linguistic variables; linguistic intersection method.

I. INTRODUCTION

Decision-Making is the procedure to find the best action among a set of feasible actions [1]. Multi-criteria decision-making (MCDM) is one of the most widely used decision methodologies in the sciences, business, government and engineering worlds. MCDM methods can help to improve the quality of decisions by making the decision-making process more explicit, rational, and efficient [2].

Technique for order performance by similarity to ideal solution (TOPSIS) is first developed by Hwang and Yoon (1981) for solving a MCDM problem [3]. The concept of TOPSIS is choosing the best alternative according to the relative position [the shortest distance from the positive ideal solution (PIS) and the farthest from the negative ideal solution (NIS)] in all of the alternatives. Using TOPSIS method can make an efficacious and total ranking order of alternatives. But the drawback of TOPSIS is that it can not make a pairwise comparison and judge the degree of difference among all alternatives.

ELECTRE method is a highly developed multi-criteria analysis model which takes into account the uncertainty and vagueness in the decision process [4]. It is based on the axiom of partial comparability which is suitable for alternative selection. But the drawback of ELECTRE is that it is not easy to obtain the total ranking order of alternatives.

PROMETHEE (Preference Ranking Organization Method for Enrichment Evaluation) is a multi-criteria decision making method [5]. It is well adapted to problems where a finite number of alternative actions are to be ranked by considering several, sometimes conflicting, criteria [6]. There are six basic types of preference function in PROMETHEE method, so decision makers can establish flexible standard according to the requirement of particular decision making problem with respect to each criterion by PROMETHEE method.

VIKOR (VlseKriterijumska Optimizacija I Kompromisno Resenje in Serbian, means Multicriteria Optimization and Compromise Solution) is a multi criteria decision making method developed by Opricovic [6]. VIKOR determines a compromise solution that provides the maximum group utility for the majority and a minimum of individual regret for the opponent [7]. So, VIKOR can find a compromise priority ranking order of alternatives according to the selected criteria [8, 9]. According to the VIKOR method, the compromise ranking order could be performed by comparing the measure of closeness to the ideal alternative through the process of ranking and selecting a set of alternatives in the presence of conflicting criteria [7].

The information for choosing best alternative is including quantitative information and qualitative information. Quantitative information is easy to describe by crisp value. A more realistic approach may be to use linguistic assessments instead of crisp values [10]. The 2-tuple linguistic representation model is based on the concept of symbolic translation [11, 12]. It is an effective method to reduce the mistakes of information translation and avoid information loss by computing with words [13].

Because every kind of MCDM approach has its strong point and weakness, it is hard to make sure that what kind of MCDM approach is suitable to a specific problem. However, choosing the wrong MCDM approach to make decision will reduce the effectiveness and quality of decision-making. In order to avoid this problem, this study presented a linguistic intersection method (LIM) to handle the multi- criteria decision making problem in a fuzzy environment.

II. EVALUATION INFORMATION

The quantitative and qualitative information will be considered in the process of decision making problem.

978-1-4244-7316-8/11/$26.00 ©2011 IEEE

Qualitative information can be expressed by 2-tuple linguistic variable. The membership function of 2-tuple linguistic variable can be expressed as triangle fuzzy number [14]. There are two types of 2-tuple linguistic variable are applied in this study (shown as Table 1 and Figures 1-2).

TABLE 1. DIFFERENT TYPES OF LINGUISTIC VARIABLES

Linguistic variable	
Type I:	Extremely Poor (s_0^5) , Poor (s_1^5) , Fair (s_2^5) , Good (s_3^5) , Extremely Good (s_4^5)
Type II:	Extremely Poor (s_0^7) ,Poor (s_1^7) , Medium Poor (s_2^7) , Fair (s_3^7) , Medium Good (s_4^7) , Good (s_5^7) , Extremely Good (s_6^7)

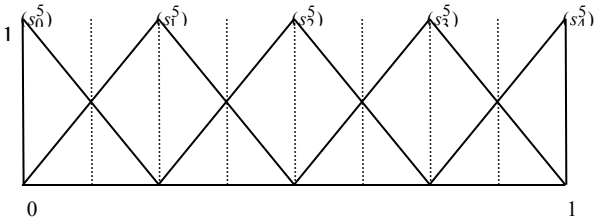

Figure. 1. Membership functions of linguistic variables at type 1 (t=1)

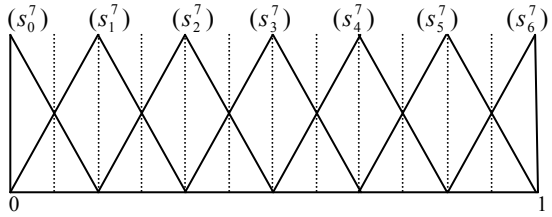

Figure. 2. Membership functions of linguistic variables at type 2 (t=2)

Let $S=\{s_0, s_1, s_2, ..., s_g\}$ be a finite and totally ordered linguistic term set. A 2-tuple linguistic variable can be expressed as $(s_i,\ \alpha_i)$, where s_i is the central value of i-th linguistic term in S and α_i is a numerical value representing the difference between calculated linguistic term and the closest index label in the initial linguistic term set. The symbolic translation function Δ is presented to translate β into a 2-tuple linguistic variable [14]. Then, the symbolic translation process is applied to translate β (β∈ [0, 1]) into a 2-tuple linguistic variable as [15]

$$\Delta(\beta)=(s_i,\alpha_i) \tag{1}$$

where $i=round(\beta\times g)$, $\alpha_i=\beta-\frac{i}{g}$ and $\alpha_i\in[-\frac{1}{2g},\frac{1}{2g})$.

A reverse function Δ^{-1} is defined to return an equivalent numerical value β from 2-tuple linguistic information $(s_i,\ \alpha_i)$. It can be represented as follows [15].

$$\Delta^{-1}(s_i,\alpha_i)=(\mathrm{i/g})+\alpha_i=\beta \tag{2}$$

Let $\mathrm{x}=\{(\mathrm{r}_1,\alpha_1),(\mathrm{r}_2,\alpha_2),...,(\mathrm{r}_\mathrm{n},\alpha_\mathrm{n})\}$ be a 2-tuple linguistic variable set and $\mathrm{W}=\{(\mathrm{w}_1,\alpha_{\mathrm{w}1}),(\mathrm{w}_2,\alpha_{\mathrm{w}2}),...,(\mathrm{w}_\mathrm{n},\alpha_{\mathrm{wn}})\}$ be the set of linguistic weight of each linguistic variable. The linguistic arithmetic mean $\bar{X}$ is computed as [16]

$$\bar{X}=\Delta\left(\frac{1}{n}\sum_{i=1}^{n}\Delta^{-1}(r_i,\alpha_i)\right)=(s_m,\alpha_m) \tag{3}$$

The linguistic weighted arithmetic mean is computed as [16]

$$\bar{X}^{\mathrm{w}}=\Delta\left(\frac{\frac{1}{n}\sum_{i=1}^{n}\left(\Delta^{-1}(r_i,\alpha_i)*\Delta^{-1}(\mathrm{w}_i,\alpha_{\mathrm{w}i})\right)}{\sum_{i=1}^{n}\Delta^{-1}(\mathrm{w}_i,\alpha_{\mathrm{w}i})}\right)=(s_{\mathrm{m}}^{\mathrm{w}},\alpha_{\mathrm{m}}^{\mathrm{w}}) \tag{4}$$

In general, decision makers would use different kind of 2-tuple linguistic variables based on their knowledge or experiences to express their opinions [17]. A transformation function is needed to transfer these 2-tuple linguistic variables from different kind of linguistic sets to a standard linguistic set at unique domain. In the method of Herrera and Martinez [18], the domain of the linguistic variables will increase as the number of linguistic variable is increased. To overcome this drawback, a translation function is applied here to transfer a crisp number or 2-tuple linguistic variable to a standard linguistic term at the unique domain [15]. Suppose that the interval [0, 1] is the unique domain. The linguistic variable sets with different semantics (or types) will be defined by partitioning the interval [0, 1]. Transforming a crisp number β (β∈ [0, 1]) into i-th linguistic term $(s_i^{n(t)},\alpha_i^{n(t)})$ of type t as

$$\Delta_t(\beta)=(s_i^{n(t)},\alpha_i^{n(t)}) \tag{5}$$

where $i=round(\beta\times g_t)$, $\alpha_i^{n(t)}=\beta-\frac{i}{g_t}$ $g_t=n(t)-1$ and n (t) is the number of linguistic variable of type t. Transforming i-th linguistic term of type t into a crisp number β as

$$\Delta_t^{-1}(s_i^{n(t)},\alpha_i^{n(t)})=\frac{i}{g_t}+\alpha_i^{n(t)}=\beta \tag{6}$$

where $g_t=n(t)-1$ and $\alpha_i^{n(t)}\in[-\frac{1}{2g_t},\frac{1}{2g_t})$.

Therefore, the transformation from i-th linguistic term $(s_i^{n(t)},\alpha_i^{n(t)})$ of type t to k-th linguistic term $(s_k^{n(t+1)},\alpha_k^{n(t+1)})$ of type t+1 can be expressed as

$$\Delta_{t+1}(\Delta_t^{-1}(s_i^{n(t)},\alpha_i^{n(t)}))=(s_k^{n(t+1)},\alpha_k^{n(t+1)}) \tag{7}$$

where $g_{t+1}=n(t+1)-1$ and $\alpha_k^{n(t+1)}\in[-\frac{1}{2g_{t+1}},\frac{1}{2g_{t+1}})$.

III. PROPOSED METHOD

In general, the content of decision making can include:

(1) A set of alternatives is called $A=\{A_1, A_2, ..., A_m\}$

(2) A set of criteria is called $C=\{C_1, C_2, ..., C_n\}$, there are n criteria which we will use. The quantitative criteria are from C_1 to C_Z. The qualitative criteria are from C_{Z+1} to C_n.

(3) A set of decision makers is called $D=\{E_1, E_2, ..., E_k\}$.

(4) $\widetilde{\mathrm{W}}=[\widetilde{w}_\mathrm{j}]_n, j=1,2,...,n$, $\widetilde{w}_j$ can be represented as the linguistic weight of j-th criterion.

(5) $\mathrm{D}=[\mathrm{x}_{\mathrm{ij}}]_{m\times n}, i=1,2,...,m, j=1,2,...,n$ is multi criteria decision making matrix. It can be represented as

$$D=\left[x_{ij}\right]_{mn}=\begin{array}{c} \\ A_1 \\ A_2 \\ \cdots \\ A_m \end{array}\begin{array}{c} \begin{array}{cccccc} C_1 & \cdots & C_z & C_{z+1} & \cdots & C_n \end{array} \\ \begin{bmatrix} x_{11} & \cdots & x_{1z} & \tilde{x}_{1z+1} & \cdots & \tilde{x}_{1n} \\ x_{21} & \cdots & x_{2z} & \tilde{x}_{2z+1} & \cdots & \tilde{x}_{2n} \\ \cdots & \cdots & \cdots & \cdots & \cdots & \cdots \\ x_{m1} & \cdots & x_{mz} & \tilde{x}_{mz+1} & \cdots & \tilde{x}_{mn} \end{bmatrix} \end{array} \tag{9}$$

In quantitative criteria, x_{ij} represents the performance of i-th alternative with respect to j-th criterion. We use crisp value CV_{ij} to represent x_{ij} . In qualitative criteria, $\tilde{x}_{ij}$ represents the linguistic performance of i-th alternative with respect to j-th criterion. Decision makers can use 2-tuple linguistic variable to express their opinions about linguistic performance. Let $F_j^k(A_i)=(S_{ij}^k,\alpha_{ij}^k)$ represent the linguistic performance of i-th alternative respect to j-th criterion which is expressed by k-th decision maker.

The formula of transfer crisp value CV_{ij} to a 2 tuple linguistic variable is as follows:

$$F_j(A_i)=\Delta^{-1}\left(\left(CV_{ij}-\min_i\left(CV_{ij}\right)\right)/\left(\max_i\left(CV_{ij}\right)-\min_i\left(CV_{ij}\right)\right)\right) \tag{10}$$

The formula of aggregating all of the opinions about the linguistic performance of i-th alternative with respect to j-th criterion is as follows:

$$F_j(A_i)=\Delta\ \left(\frac{1}{K}\sum_{k=1}^{K}\Delta^{-1}(S_{ij}^k,\alpha_{ij}^k)\right)=(S_{ij},\alpha_{ij}) \tag{11}$$

The formula of aggregating all of the opinions about the linguistic weight of j-th criterion is as follows:

$$\tilde{\mathrm{W}}_j=\Delta\ \left(\frac{1}{K}\sum_{k=1}^{K}\Delta^{-1}(S_{jk}^w,\alpha_{jk}^w)\right)=(S_j^w,\alpha_j^w) \tag{12}$$

A. Linguistic TOPSIS

The formula of linguistic weighted matrix is as follows:

$$\tilde{\mathrm{V}}=[\tilde{v}_{\mathrm{ij}}]_{m\times n}, i=1,2,...,m, j=1,2,...,n \tag{13}$$

where $\tilde{V}_{ij}=\Delta\left(\Delta^{-1}\left(\tilde{x}_{ij}\right)*\Delta^{-1}\left(\tilde{w}_j\right)\right)$.

The formula of positive ideal solution and negative ideal solution is as $\tilde{\mathrm{A}}^*=(\tilde{v}_1^*,\tilde{v}_2^*,...,\tilde{v}_n^*)$ and $\tilde{\mathrm{A}}^-=(\tilde{v}_1^-,\tilde{v}_2^-,...,\tilde{v}_n^-)$, where $\tilde{\mathrm{v}}_{\mathrm{j}}^*=\Delta\left(\max_i\left(\Delta^{-1}\left(\tilde{v}_{ij}\right)\right)\right)$ and $\tilde{\mathrm{v}}_{\mathrm{j}}^-=\Delta\left(\min_i\left(\Delta^{-1}\left(\tilde{v}_{ij}\right)\right)\right)$.

The formula of calculating the distance between the positive ideal solution and negative ideal solution is as follows:

$$d_i^*=d(\tilde{\mathrm{A}}_i,\tilde{\mathrm{A}}^*)=\sqrt{\sum_{j=1}^{n}\left(\max_i\left(\Delta^{-1}\left(\tilde{v}_{ij}\right)\right)-\Delta^{-1}\left(\tilde{v}_{ij}\right)\right)^2} \tag{14}$$

$$d_i^-=d(\tilde{\mathrm{A}}_i,\tilde{\mathrm{A}}^-)=\sqrt{\sum_{j=1}^{n}\left(\min_i\left(\Delta^{-1}\left(\tilde{v}_{ij}\right)\right)-\Delta^{-1}\left(\tilde{v}_{ij}\right)\right)^2} \tag{15}$$

The closeness coefficient can be computed as

$$CC_i=d_i^-/\left(d_i^*+d_i^-\right),\quad i=1,2,...,m \tag{16}$$

The ranking order of alternatives can be determined in accordance with the closeness coefficient. If $CC_i>CC_j$, then alternative A_i is better than A_j

B. Linguistic ELECTRE

According to the ELECTRE, the threshold of criteria which is including preference threshold p_j, indifference threshold q_j and veto threshold v_j .The concordance index $C_j(A_i,A_l)$ represents the degree of alternative A_i is better than A_l with respect to j-th criterion. It can be computed as

$$C_j(A_i,A_l)=\begin{cases} 1 & ,\Delta^{-1}\left(\tilde{x}_{ij}\right)\geq\Delta^{-1}\left(\tilde{x}_{lj}\right)-q_j \\ \dfrac{\Delta^{-1}\left(\tilde{x}_{ij}\right)-\Delta^{-1}\left(\tilde{x}_{lj}\right)+p_j}{p_j-q_j} & ,\Delta^{-1}\left(\tilde{x}_{lj}\right)-q_j\geq\Delta^{-1}\left(\tilde{x}_{ij}\right)\geq\Delta^{-1}\left(\tilde{x}_{lj}\right)-p_j \\ 0 & ,\Delta^{-1}\left(\tilde{x}_{ij}\right)\leq\Delta^{-1}\left(\tilde{x}_{lj}\right)-p_j \end{cases} \tag{17}$$

The overall concordance index $C(A_i,A_l)$ can be computed as

$$C(A_i,A_l)=\sum_{j=1}^{n}\left(\Delta^{-1}\left(\tilde{\mathrm{w}}_{\mathrm{j}}\right)/\sum_{\mathrm{k}=1}^{\mathrm{n}}\Delta^{-1}\left(\tilde{\mathrm{w}}_{\mathrm{k}}\right)\right)C_j(A_i,A_l) \tag{18}$$

The discordance index $D_j(A_i,A_l)$ represents the degree of alternative A_i is not better than A_l with respect to j-th criterion. It can be computed as

$$D_j(A_i,A_l)=\begin{cases} 1 & ,\Delta^{-1}\left(\tilde{x}_{ij}\right)\leq\Delta^{-1}\left(\tilde{x}_{lj}\right)-v_j \\ \dfrac{\Delta^{-1}\left(\tilde{x}_{lj}\right)-p_j-\Delta^{-1}\left(\tilde{x}_{ij}\right)}{v_j-p_j} & ,\Delta^{-1}\left(\tilde{x}_{lj}\right)-p_j\geq\Delta^{-1}\left(\tilde{x}_{ij}\right)\geq\Delta^{-1}\left(\tilde{x}_{lj}\right)-v_j \\ 0 & ,\Delta^{-1}\left(\tilde{x}_{ij}\right)\geq\Delta^{-1}\left(\tilde{x}_{lj}\right)-p_j \end{cases} \tag{19}$$

The credibility matrix $S(A_i,A_l)$ can be computed as

$$S(A_i,A_l)=\begin{cases} C(A_i,A_l),\ \ if\ \ D_j(A_i,A_l)\leq C(A_i,A_l)\ \ \forall j \\ C(A_i,A_l)\prod_{j\in J(A_i,A_l)}\dfrac{1-D_j(A_i,A_l)}{1-C(A_i,A_l)},\ \ otherwise \end{cases} \tag{20}$$

where $J(A_i,A_l)$ represents the set of criteria which satisfy the discordance index of the criteria is larger than the overall concordance index

The degree value of alternative A_i is better than all of the other alternatives can be computed as

$$\phi_{\mathrm{e}}^+(A_i)=\sum_{Al\in A}S(A_i,A_l) \tag{21}$$

The degree value of all of the other alternatives is better than alternative A_i can be computed as

$$\phi_{\mathrm{e}}^-(A_i)=\sum_{Al\in A}S(A_l,A_i) \tag{22}$$

Calculate the net flow of alternative A_i as

$$\phi_{\mathrm{e}}(A_i)=\phi_{\mathrm{e}}^+(A_i)-\phi_{\mathrm{e}}^-(A_i) \tag{23}$$

Normalized the net flow of alternatives as

$$OTI_e(A_i)=((\phi_{\mathrm{e}}(A_i)/\mathrm{m})+1)/2 \tag{24}$$

According to the OTI_e, we can determine the ranking order of all alternatives.

C. Linguistic PROMETHEE

Determine the preference functions and thresholds of all criteria, and calculate the individual preference value of alternative A_r is better than alternative A_s with respect to each criterion. In this paper, we use two kinds of preference function.

Level criterion with linear preference is

$$H(\tilde{x}_{rj},\tilde{x}_{sj})=\begin{cases}1, \Delta^{-1}(\tilde{x}_{rj})-\Delta^{-1}(\tilde{x}_{sj})>p\\ \frac{1}{2}, q\le\Delta^{-1}(\tilde{x}_{rj})-\Delta^{-1}(\tilde{x}_{sj})\le p\\ 0, q\le\Delta^{-1}(\tilde{x}_{rj})-\Delta^{-1}(\tilde{x}_{sj})\end{cases} \quad (25)$$

Criterion with linear preference and indifference area is

$$H(\tilde{x}_{rj},\tilde{x}_{sj})=\begin{cases}1 \quad , p<\Delta^{-1}(\tilde{x}_{rj})-\Delta^{-1}(\tilde{x}_{sj})\\ \frac{\Delta^{-1}(\tilde{x}_{rj})-q}{p-q}, q\le\Delta^{-1}(\tilde{x}_{rj})-\Delta^{-1}(\tilde{x}_{sj})\le p\\ 0 \quad , \Delta^{-1}(\tilde{x}_{rj})-\Delta^{-1}(\tilde{x}_{sj})<q\end{cases} \quad (26)$$

Calculate the overall preference value to represent alternative A_r is better than A_s as

$$\pi(A_r,A_s)=\sum_{j=1}^{n}\left(\Delta^{-1}(\tilde{w}_j)/\sum_{k=1}^{n}\Delta^{-1}(\tilde{w}_k)\right)*H_j(\tilde{x}_{rj},\tilde{x}_{sj}) \quad (27)$$

The degree about alternative A_r is better than all of the other alternatives as

$$\phi_p^+(A_r)=\sum_{b\in A}\pi(A_r,b) \quad (28)$$

The degree about all of the other alternatives is better than alternative A_r as

$$\phi_p^-(A_r)=\sum_{b\in A}\pi(b,A_r) \quad (29)$$

Calculate the net flow of alternative A_r as

$$\phi_p(A_r)=\phi_p^+(A_r)-\phi_p^-(A_r) \quad (30)$$

And then, normalized the net flow of alternative A_r as

$$OTI_p(A_r)=((\phi_p(A_r)/m)+1)/2 \quad (31)$$

According to the OTI_p, we can determine the ranking order of all alternatives can rank all of the alternatives.

D. Linguistic VIKOR

The linguistic positive-ideal solution (F_j^*) of each general criterion can be calculated as

$$F_j^*=\Delta\left(\underset{i}{Max}\ \Delta^{-1}(F_j(A_i))\right), \forall A_i\in A \quad (32)$$

The linguistic negative-ideal solution (F_j^-) of each general criterion can be calculated as

$$F_j^-=\Delta\left(\underset{i}{Min}\ \Delta^{-1}(F_j(A_i))\right), \forall A_i\in A \quad (33)$$

The group utility for the majority (S_i) of each alternative can be calculated as

$$S_i=\sum_{j=1}^{n}\Delta^{-1}(\tilde{w}_j)*\frac{\Delta^{-1}(F_j^*)-\Delta^{-1}(F_j(A_i))}{\Delta^{-1}(F_j^*)-\Delta^{-1}(F_j^-)} \quad \forall i \quad (34)$$

The individual regret rating for the opponent R_i of each alternative can be calculated as

$$R_i=\underset{j}{Max}\left(\Delta^{-1}(\tilde{w}_j)*\frac{\Delta^{-1}(F_j^*)-\Delta^{-1}(F_j(A_i))}{\Delta^{-1}(F_j^*)-\Delta^{-1}(F_j^-)}\right) \quad \forall i \quad (35)$$

R_i represents as the maximum regret by choosing i-th alternative as solution according to choose the worst performance in general criteria.

The value (Q_i) of each alternative can be calculated as

$$Q_i=v*\frac{S_i-S^*}{S^--S^*}+(1-v)*\frac{R_i-R^*}{R^--R^*} \quad \forall i \quad (36)$$

$$S^*=\underset{i}{Min}\ S_i, S^-=\underset{i}{Max}\ S_i, R^*=\underset{i}{Max}\ R_i, R^-=\underset{i}{Min}\ R_i$$

v represents the decision making coefficient, v is between 0 and 1. According to the Q_i, we can determine the ranking order of all alternatives.

E. Linguistic Intersection Method (LIM)

We can consider linguistic TOPSIS, linguistic ELECTRE, linguistic PROMETHEE and linguistic VIKOR methods as four experts who provide information of each alternative, respectively. Smart manager will make a decision by considering the suggestions of experts simultaneously. Let $\Omega_t=\{A_i \mid \mathrm{Rank}(CC_i)\le SN\}$, $\Omega_e=\{A_i \mid \mathrm{Rank}(OTI_e(A_i))\le SN\}$, $\Omega_p=\{A_i \mid \mathrm{Rank}(OTI_p(A_i))\le SN\}$ and $\Omega_v=\{A_i \mid \mathrm{Rank}(Q_i)\le SN\}$. Ω_t, Ω_e, Ω_p and Ω_v represents the best alternative set of linguistic TOPSIS, ELECTRE, PROMETHEE and VIKOR method. The $\mathrm{Rank}(CC_i)$, $\mathrm{Rank}(OTI_e(A_i))$, $\mathrm{Rank}(OTI_p(A_i))$ and $\mathrm{Rank}(Q_i)$ represent the alternative ranking order of each MCDM approach. SN represents the number of alternatives which manager considers the maximum volume of alternatives where alternative is better exists in each MCDM approach. We execute the intersection from four kinds of set as $\Omega_{can}=\Omega_t\cap\Omega_e\cap\Omega_p\cap\Omega_v$. The Ω_{can} represents the common set which is agreeable by four experts (MCDM methods) and can be defined as consensus alternative set.

According to the consensus alternative set, normalized the closeness coefficient value as

$$P_t(A_i)=\begin{cases}\frac{CC_i}{\sum_{A_i\in\Omega_{can}}CC_i}, A_i\in\Omega_{can}\\ 0, \quad A_i\notin\Omega_{can}\end{cases} \quad (37)$$

Normalized the OTI_e as

$$P_e(A_i)=\begin{cases}\frac{OTI_e(A_i)}{\sum_{A_i\in\Omega_{can}}OTI_e(A_i)}, A_i\in\Omega_{can}\\ 0, \quad A_i\notin\Omega_{can}\end{cases} \quad (38)$$

Normalized the OTI_p as

$$P_p(A_i)=\begin{cases}\frac{OTI_p(A_i)}{\sum_{A_i\in\Omega_{can}}OTI_p(A_i)}, A_i\in\Omega_{can}\\ 0, \quad A_i\notin\Omega_{can}\end{cases} \quad (39)$$

Normalized the Q_i, as

$$P_{\mathrm{v}}(A_i)=\begin{cases}\dfrac{(1-\mathrm{Q_i})}{\sum_{A_i\in\Omega_{can}}(1-\mathrm{Q_i})}, & A_i\in\Omega_{can}\\ 0, & A_i\notin\Omega_{can}\end{cases} \tag{40}$$

Let $P_{imp}(A_i)$ be the comprehensive performance of each alternative in the consensus alternative set. It can be integrated from four kinds of MCDM methods as

$$P_{imp}(A_i)=v_t * P_t(A_i)+v_e * P_e(A_i)+v_p * P_p(A_i)+v_{\mathrm{v}} * P_{\mathrm{v}}(A_i) \tag{41}$$

where $v_t+v_e+v_p+v_{\mathrm{v}}=1$ .The v_t , v_e , v_p and v_{v} represent the importance of four methods from the viewpoint of manager.

IV. NUMERICAL EXAMPLE

Suppose a notable gift manufacturer wants to sell famous gift. The manufacturer wants to entry the market of China, so they have to choose a sales channel company for outsourcing retail business. There are seven criteria are considered such as the market share rate of the sales channel company ($\mathrm{C_1}$), gross profit margin ($\mathrm{C_2}$), inventory turnover ratio ($\mathrm{C_3}$), current ratio ($\mathrm{C_4}$), brand image ($\mathrm{C_5}$), retail place ($\mathrm{C_6}$) and enterprise culture ($\mathrm{C_7}$). Brand image, retail place and enterprise culture are qualitative criteria. Gift manufacturer employs four enterprise consultants to evaluate twelve sales channel companies. The process of linguistic intersection method is shown as follows.

Step1. Collect quantitative information of twelve sales channel companies as Table 2.

TABLE 2. THE QUANTITATIVE INFORMATION

	$\mathrm{A_1}$	$\mathrm{A_2}$	$\mathrm{A_3}$	$\mathrm{A_4}$	$\mathrm{A_5}$	$\mathrm{A_6}$
C_1	4%	0.7%	3%	2.7%	1.6%	2.1%
C_2	10.2%	9.8%	7%	6.6%	12%	8%
C_3	7	6.8	8	4.2	7.5	6
C_4	1.5	1.2	1.4	1.8	2	1.5
	$\mathrm{A_7}$	$\mathrm{A_8}$	$\mathrm{A_9}$	$\mathrm{A_{10}}$	$\mathrm{A_{11}}$	$\mathrm{A_{12}}$
C_1	4.2%	1.2%	4%	1.6%	3%	0.5%
C_2	7.2%	6.4%	11.2%	5.6%	8%	7.5%
C_3	4.3	6.5	7	4.5	8	5.6
C_4	1.4	1.3	2	2.1	2.2	1.8

Step2. Transform quantitative information of twelve sales channel companies into 5 scale linguistic variable.

Step3. Four enterprise consultants choose linguistic variable flexibly to express their opinions about performance of each sales channel company with respect to each qualitative criterion as Table 3 and the weight of each criterion as Table 4. Enterprise consultants $\mathrm{E_1}$ and $\mathrm{E_2}$ choose 5 scale linguistic variable to express their opinions. Enterprise consultants $\mathrm{E_3}$ and $\mathrm{E_4}$ use 7 scale linguistic variable to express their opinions.

TABLE 3. THE WEIGHT LINGUISTIC VARIABLES

	C_1	C_2	C_3	C_4	C_5	C_6	C_7
$\mathrm{E_1}$	$(s_3^7,0)$	$(s_5^7,0)$	$(s_4^7,0)$	$(s_6^7,0)$	$(s_6^7,0)$	$(s_5^7,0)$	$(s_6^7,0)$
$\mathrm{E_2}$	$(s_6^7,0)$	$(s_4^7,0)$	$(s_6^7,0)$	$(s_6^7,0)$	$(s_3^7,0)$	$(s_6^7,0)$	$(s_4^7,0)$
$\mathrm{E_3}$	$(s_2^5,0)$	$(s_2^5,0)$	$(s_3^5,0)$	$(s_4^5,0)$	$(s_1^5,0)$	$(s_4^5,0)$	$(s_2^5,0)$
$\mathrm{E_4}$	$(s_1^5,0)$	$(s_3^5,0)$	$(s_2^5,0)$	$(s_2^5,0)$	$(s_2^5,0)$	$(s_1^5,0)$	$(s_3^5,0)$

TABLE 4. THE RATING LINGUISTIC VARIABLES

Criteria		$\mathrm{E_1}$	$\mathrm{E_2}$	$\mathrm{E_3}$	$\mathrm{E_4}$		$\mathrm{E_1}$	$\mathrm{E_2}$	$\mathrm{E_3}$	$\mathrm{E_4}$
C_5	$\mathrm{A_1}$	$(s_4^5,0)$	$(s_1^5,0)$	$(s_5^7,0)$	$(s_6^7,0)$	$\mathrm{A_7}$	$(s_1^5,0)$	$(s_3^5,0)$	$(s_6^7,0)$	$(s_5^7,0)$
	$\mathrm{A_2}$	$(s_1^5,0)$	$(s_4^5,0)$	$(s_3^7,0)$	$(s_3^7,0)$	$\mathrm{A_8}$	$(s_4^5,0)$	$(s_4^5,0)$	$(s_3^7,0)$	$(s_3^7,0)$
	$\mathrm{A_3}$	$(s_3^5,0)$	$(s_1^5,0)$	$(s_2^7,0)$	$(s_2^7,0)$	$\mathrm{A_9}$	$(s_3^5,0)$	$(s_0^5,0)$	$(s_5^7,0)$	$(s_6^7,0)$
	$\mathrm{A_4}$	$(s_4^5,0)$	$(s_3^5,0)$	$(s_3^7,0)$	$(s_6^7,0)$	$\mathrm{A_{10}}$	$(s_3^5,0)$	$(s_3^5,0)$	$(s_3^7,0)$	$(s_3^7,0)$
	$\mathrm{A_5}$	$(s_0^5,0)$	$(s_3^5,0)$	$(s_3^7,0)$	$(s_3^7,0)$	$\mathrm{A_{11}}$	$(s_2^5,0)$	$(s_2^5,0)$	$(s_3^7,0)$	$(s_5^7,0)$
	$\mathrm{A_6}$	$(s_2^5,0)$	$(s_0^5,0)$	$(s_6^7,0)$	$(s_5^7,0)$	$\mathrm{A_{12}}$	$(s_4^5,0)$	$(s_0^5,0)$	$(s_6^7,0)$	$(s_6^7,0)$
C_6	$\mathrm{A_1}$	$(s_2^5,0)$	$(s_1^5,0)$	$(s_3^7,0)$	$(s_4^7,0)$	$\mathrm{A_7}$	$(s_3^5,0)$	$(s_2^5,0)$	$(s_2^7,0)$	$(s_6^7,0)$
	$\mathrm{A_2}$	$(s_2^5,0)$	$(s_3^5,0)$	$(s_5^7,0)$	$(s_3^7,0)$	$\mathrm{A_8}$	$(s_4^5,0)$	$(s_4^5,0)$	$(s_4^7,0)$	$(s_3^7,0)$
	$\mathrm{A_3}$	$(s_0^5,0)$	$(s_0^5,0)$	$(s_5^7,0)$	$(s_6^7,0)$	$\mathrm{A_9}$	$(s_1^5,0)$	$(s_0^5,0)$	$(s_3^7,0)$	$(s_5^7,0)$
	$\mathrm{A_4}$	$(s_4^5,0)$	$(s_4^5,0)$	$(s_5^7,0)$	$(s_2^7,0)$	$\mathrm{A_{10}}$	$(s_0^5,0)$	$(s_1^5,0)$	$(s_4^7,0)$	$(s_3^7,0)$
	$\mathrm{A_5}$	$(s_3^5,0)$	$(s_0^5,0)$	$(s_6^7,0)$	$(s_4^7,0)$	$\mathrm{A_{11}}$	$(s_4^5,0)$	$(s_0^5,0)$	$(s_4^7,0)$	$(s_4^7,0)$
	$\mathrm{A_6}$	$(s_1^5,0)$	$(s_3^5,0)$	$(s_4^7,0)$	$(s_3^7,0)$	$\mathrm{A_{12}}$	$(s_0^5,0)$	$(s_0^5,0)$	$(s_6^7,0)$	$(s_6^7,0)$
C_7	$\mathrm{A_1}$	$(s_4^5,0)$	$(s_0^5,0)$	$(s_3^7,0)$	$(s_4^7,0)$	$\mathrm{A_7}$	$(s_2^5,0)$	$(s_0^5,0)$	$(s_5^7,0)$	$(s_2^7,0)$
	$\mathrm{A_2}$	$(s_3^5,0)$	$(s_2^5,0)$	$(s_3^7,0)$	$(s_6^7,0)$	$\mathrm{A_8}$	$(s_0^5,0)$	$(s_4^5,0)$	$(s_4^7,0)$	$(s_2^7,0)$
	$\mathrm{A_3}$	$(s_3^5,0)$	$(s_2^5,0)$	$(s_6^7,0)$	$(s_5^7,0)$	$\mathrm{A_9}$	$(s_2^5,0)$	$(s_0^5,0)$	$(s_3^7,0)$	$(s_3^7,0)$
	$\mathrm{A_4}$	$(s_0^5,0)$	$(s_4^5,0)$	$(s_3^7,0)$	$(s_5^7,0)$	$\mathrm{A_{10}}$	$(s_1^5,0)$	$(s_2^5,0)$	$(s_3^7,0)$	$(s_6^7,0)$
	$\mathrm{A_5}$	$(s_0^5,0)$	$(s_4^5,0)$	$(s_6^7,0)$	$(s_5^7,0)$	$\mathrm{A_{11}}$	$(s_0^5,0)$	$(s_3^5,0)$	$(s_6^7,0)$	$(s_3^7,0)$
	$\mathrm{A_6}$	$(s_3^5,0)$	$(s_2^5,0)$	$(s_4^7,0)$	$(s_2^7,0)$	$\mathrm{A_{12}}$	$(s_1^5,0)$	$(s_0^5,0)$	$(s_3^7,0)$	$(s_4^7,0)$

Step4. Manager determines the number of better alternatives (SN) in each MCDM approach. By the purpose of fairness, we set the number of better alternatives (SN) in each MCDM is the same and equal to six (fifty percent of number of alternatives). And then, the selected alternative set by TOPSIS is $\Omega_t=\{A_1,A_2,A_9,A_{11},A_5,\mathrm{A_3}\}$, the selected alternative set by ELECTRE is $\Omega_{\mathrm{e}}=\{A_5,A_{11},A_4,A_1,A_9,\mathrm{A_8}\}$, the selected alternative set by PROMETHEE method is $\Omega_{\mathrm{p}}=\{A_5,A_{11},A_1,A_4,A_9,\mathrm{A_8}\}$ and the selected alternative set by VIKOR is $\Omega_{\mathrm{v}}=\{A_{11},A_5,A_9,A_1,A_4,\mathrm{A_6}\}$. Final, we calculate the intersection set as $\Omega_{can}=\Omega_t\cap\Omega_e\cap\Omega_p\cap\Omega_{\mathrm{v}}=\{A_1,A_5,A_9,A_{11}\}$.

Step5. Manager determines the relative importance of TOPSIS $v_t=1/4$, ELECTRE $v_e=1/4$, PROMETHEE $v_{\mathrm{p}}=1/4$ and VIKOR $v_{\mathrm{v}}=1/4$. And calculate the relative evaluation value of TOPSIS(P_t), ELECTRE(P_e),PROMETHEE(P_p) and VIKOR(P_{v}). And then, calculate the overall performance of each alternative P_{imp} (see Table 11). Finally, the ranking order of alternatives is $A_{11}>\mathrm{A_5}>\mathrm{A_1}>\mathrm{A_9}$.

V. MCDM METHOD COMPARISON

In order to justify the effectiveness of proposed method, this paper compares the ranking result of the LIM with original linguistic TOPSIS, linguistic ELECTRE, linguistic PROMETHEE and linguistic VIKOR. It finds that alternative A_1, A_5, A_9 and A_{11} which are in intersection set are relatively stable and stand on the top 5 positions, no matter what kind of MCDM approach we use. On the other hand, the alternatives which are not in intersection set don't have a relatively consistent rank in every kind of linguistic MCDM method. If we consider that the sum ranking order of each alternative in each linguistic MCDM method, the final ranking order of alternatives is the same as LIM method (see Table 5).

TABLE 5 THE RANKING ORDER INFORMATION

Alternative	Rank of TOPSIS	Rank of ELECTRE	Rank of PROMETHEE	Rank of VIKOR	Sum of Rank	Overall Rank
A_{11}	4	2	2	1	9	1
A_5	5	1	1	2	9	1
A_1	1	4	3	4	12	3
A_9	3	5	5	3	16	4
A_4	10	3	4	5	22	5
A_2	2	7	7	11	27	6
A_3	6	8	8	8	30	7
A_8	12	6	6	9	33	8
A_6	11	10	10	6	37	9
A_7	9	9	9	10	37	9
A_{12}	8	12	11	7	38	11
A_{10}	7	11	10	12	40	12

VI. CONCLUSION AND FUTURE RESEARCH

In this paper, a linguistic intersection method (LIM) is presented to handle the MCDM problems in the fuzzy environment. The advantage of linguistic intersection method is illustrated as follows.

1. The picked alternative which is executed by LIM in accordance with the agreement of each MCDM approach. It can promote effectiveness of decision making.
2. Although LIM is a little complexity in executing decision making process, but all of the process is easy to calculate and can be done by computer program.
3. Linguistic TOPSIS, linguistic ELECTRE, linguistic PROMETHEE and linguistic VIKOR are used to determine the performance of each alternative in this study. In reality, LIM is an extendable method which can extend by adding new developed MCDM approach by empowering new developed MCDM approach.
4. The LIM can effective deal with MCDM problems based on quantitative and qualitative information simultaneously.

In the future, an interactive program will be developed to handle the fuzzy MCDM problems based on linguistic intersection method (LIM).

REFERENCES

[1] J. Figueira, S. Greco and M. Ehrgott, "Multiple Criteria decision Analysis: State of the art surveys", Springer. 2005.

[2] X. Wanga and E. Triantaphylloub,"Ranking irregularities when evaluating alternatives by using some ELECTRE methods", Omega, pp. 45-63, 2008.

[3] C. L. Hwang and K. Yoon, "Multiple Attributes Decision Making Methods and Applications", Springer, Berlin Heidelberg, 1981.

[4] A. Papadopoulos and A. Karagiannidis, "Application of the multicriteria analysis method Electre III for the optimisation of decentralised energy systems", Omega, vol. 36, pp. 766-776, 2008.

[5] M. Goumas and V. Lygerou, "An extension of the PROMETHEE method for decision making in fuzzy environment: Ranking of alternative energy exploitation projects", European Journal of Operational Research, vol. 123, pp. 606-613, 2000.

[6] S. Opricovic, "Multicriteria Optimization of Civil Engineering Systems", Faculty of Civil Engineering, Belgrade, 1998.

[7] L. Y. Chen and T. C. Wang, "Optimizing partners' choice in IS/IT outsourcing projects: The strategic decision of fuzzy VIKOR". International Journal of Production Economics, pp. 233-242, 2009.

[8] S. Opricovic, G. H. Tzeng, "Fuzzy multicriteria model for post-earthquake land-use planning". Natural Hazards Review, pp. 59-64, 2003.

[9] S. Opricovic, G. H. Tzeng, "Multicriteria planning of post-earthquake sustainable reconstruction", Computer-Aided Civil and Infrastructure Engineering, vol. 17, pp. 211-220, 2002.

[10] F. Herrera and E. Herrera-Viedma, "Linguistic decision analysis steps for solving decision problems under linguistic information", Fuzzy Sets and Systems, vol. 115, pp. 67-82, 2000.

[11] F. Herrera and L. Martinez, "A 2-tuple fuzzy linguistic representation model for computing with words", IEEE Transactions on Fuzzy Systems, vol. 8, pp. 746–752, 2000.

[12] Z. S. Xu, "Deviation measures of linguistic preference relations in group decision making", Omega, vol. 33, pp. 249-254, 2005.

[13] E. Herrera-Viedma, O. Cordón, M. Luque, A. G. Lopez and A. M. Muñoz, "A model of fuzzy linguistic IRS based on multigranular linguistic information", International Journal of Approximate Reasoning, vol. 34, Issue. 2-3, pp. 221-239, 2003.

[14] F. Herrera and L. Martinez, "A model based on linguistic 2-tuples for dealing with multigranular hierarchical linguistic contexts in multi-expert decision-making", IEEE Transactions on Systems, Man, and Cybernetics Part B: Cybernetics, vol. 31, pp.227-234, 2001.

[15] W. S. Tai and C. T. Chen, "A new evaluation model for intellectual capital based on computing with linguistic variable", Expert Systems with Applications, vol. 36, pp. 3483-3488, 2009.

[16] E. Herrera-Viedma, F. Herrera, L. Martínez, J. C. Herrera and A. G. López, "Incorporating filtering techniques in a fuzzy linguistic multi-agent model for information gathering on the web", Fuzzy Sets and Systems, vol. 148, pp. 61-83, 2004.

[17] F. Herrera, L. Martinez and P. J. Sanchez, "Managing non-homogeneous information in group decision making", European Journal of Operational Research, vol. 166, pp.115-132, 2005.

[18] M. Goumas and V. Lygerou, "An extension of the PROMETHEE method for decision making in fuzzy environment: Ranking of alternative energy exploitation projects", European Journal of Operational Research, vol. 123, pp. 606-613, 2000.

2011 IEEE International Conference on Fuzzy Systems
June 27-30, 2011, Taipei, Taiwan

Evaluate and Identify Optimal Weapon Systems Using Fuzzy Multiple Criteria Decision Making

Ying Bai
Dept. of Computer Science and Engineering
Johnson C. Smith University, Charlotte, NC, USA
ybai@jcsu.edu

Dali Wang
Dept. of Physical, Computer Science and Engineering
Christopher Newport University, Newport News, VA, USA, dwang@pcs.cnu.edu

***Abstract*— The weapon identification and selection issue is an important and strategic component and has a significant impact on the efficiency of defense system in US. The main purpose of this research is to develop a universal model and system to effectively assess, evaluate and identify the optimal weapons from a large collection of available weapon systems that have multiple criteria based on a fuzzy multiple criteria decision making (FMCDM) model. A simple but effective weight estimation method is adopted in this paper to make this selection more objective and reliable. There are some different weight estimation methods reported by researchers, however, most methods need a lot of mathematical operations and make the process very time consuming and even more complicated. In this paper, we utilized a weight estimation method based on the paired comparison matrix to simplify this estimation process. The evaluation and selection process can be significantly simplified and improved by using this method.**

Keywords- Optimal weapon systems; fuzzy multi-criteria decision making; similarity measure; decision matrix

I. INTRODUCTION

One of the most important and critical issues related to the national defense is to correctly evaluate and assess the optimal weapons or weapon systems from a large collection of weapons to improve and enhance the overall performance and productivity of the national defense system. This evaluation and assessing issue becomes more important after September 11, 2001 since some enemy countries have defined US as their target and began to attack the US territory in an offensive way. In order to effectively protect our country from being attacked by any foreign country who has offensive weapons and effectively attack back those enemy countries, developing and building efficient models and systems to correctly evaluate and assess the optimal weapons or weapon systems is a prerequisite task to the US defense system. In this research, we will develop and build a fuzzy multiple criteria decision making model (FMCDM) to perform this evaluation and assessing task in a more efficient and reliable way. The FMCDM technique is based on multiple criteria decision making (MCDM) technique.

The MCDM technique can be divided into two major categories: crisp or classical and fuzzy MCDMs. In recent years, many researchers have attempted to use fuzzy MCDM methods for optimal equipment selection problems. Such as Lin and Yang using the AHP method to build a machine selection model [1], Tabucanon et al. developed a decision support framework for selecting the most appropriate machines in flexible manufacturing systems (FMS) [2], Atmani and Lashkari developed a model for machine tool selection and operation allocation in FMS [3], Wang et al. presented a fuzzy multiple attribute decision making model to select the appropriate machines for FMS [4], Arslan et al. presented a multi-criteria weighted average (MCWA) method for machine tool selection [5]. Yurdakul proposed a model linking machine alternatives to manufacturing strategy for machine tool selection [6]. Ayag and Ozdemir used the fuzzy AHP technique to weight the machine tool alternatives under eight main and nineteen sub-criteria and then carried out benefit/cost ratio analysis by using both the fuzzy AHP score and procurement cost, of each alternative [7].

Some other researchers reported different methods to perform the optimal evaluations and estimations for various machine tools and equipments [8-13]. Although weapon evaluation and selection play an important role in the design of an effective defense system, however, the publications and researches on this subject are very limited [14-20].

Basically, correct evaluating and assessing of the optimal weapon systems can be defined as a decision making process. In recent years, different conventional decision making methods and models have been developed and adopted, such as the optimal estimation, linear programming and Karman filter. However, the fuzzy decision making model is a good candidate among those methods. As we know, one of the most useful aspects of fuzzy set theory is its ability to represent mathematically a class of decision problems called multiple objective decisions (MODs). This class of problems often involves many vague and ambiguous (and thus fuzzy) goals and constraint factors. The object of the fuzzy decision methodology is to obtain a decision, optimum in the sense that some set of goals is attained while observing (i.e. not violating) a simultaneous set of constraint factors.

The paper is organized as follows. The scope and objectives of this paper, combined with a technique review to FMCDM, are provided in section 1. The detailed description of the FMCDM model is described in section 2. The adopted method used to estimate the weight to the associated criteria or objectives is discussed in section 3. A case study with an example of evaluating and assessing the optimal weapon

978-1-4244-7316-8/11/$26.00 ©2011 IEEE

system (missiles) is given in section 4. Section 5 provides the conclusion for the paper.

II. FUZZY MCDM MODEL

Normally, a triangular fuzzy number A can be defined by a triplet *(a, b, c)* shown in Fig.1a. An example of a fuzzy member of an equipment cost is shown in Fig.1b. The membership function is defined as (1).

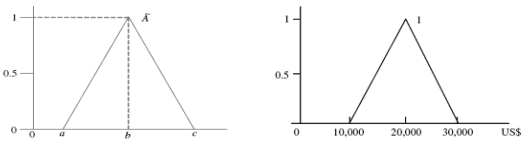

(a) (b)

Figure 1. A representation of a triangular fuzzy member

$$\mu_A(x)=\begin{cases}0, & x<a,\\ \dfrac{x-a}{b-a}, & a\le x\le b,\\ \dfrac{c-x}{c-b}, & b\le x\le c,\\ 0, & x>c.\end{cases} \tag{1}$$

The general multi-attribute decision making (MADM) model can be described as follows [11]:

- Let $X = \{X_i | i = 1, \ldots, m\}$ denote a finite discrete set of m *(≥2)* possible alternatives (courses of action, candidates);
- Let $A = \{A_j \mid j = 1, \ldots, n\}$ denote a finite set of n *(≥2)* criteria according to which the desirability of an alternative is to be judged,
- Let $\omega = (\omega_1, \omega_2, \ldots, \omega_n)^T$ be the vector of weights, where $\sum_{j=1}^{n} \omega_j = 1$, $\omega_j \ge 0$, $j = 1, \ldots, n$, and ω_j denotes the weight of criterion A_j,
- Let $R = (r_{ij})_{m\times n}$ denote the $m \times n$ decision matrix, where r_{ij} *(≥0)* is the performance rating of alternative X_i with respect to criterion A_j.

In this section, we will introduce in details the algorithm based on the theory of fuzzy MCDM, which includes the following steps [11].

A. Representation of Fuzzy Requirements

When evaluating and assessing the optimal weapon system from a number of similar alternatives, a decision maker normally develops in his/her mind some sort of ambiguity. Representation of fuzzy requirements has been introduced in the beginning of this section.

B. Similarity Measure

In step A, the requirements of selecting optimal weapon systems have been described as the triangular fuzzy number with respect to different criteria. In this step, we will take the requirement vector as the ideal weapon system, with the purpose to measure the similarity degree with the existing candidate weapon vectors, in which the specification values are known and determinate. As we know, a fuzzy number cannot be compared with a crisp one directly unless a non-fuzzy number has to be transformed into the form of fuzzy number firstly. For example, for a crisp number b, the form of its triangular fuzzy can be written as (2).

$$b = (b^L, b^M, b^U) \tag{2}$$

where $b^L = b^M = b^U$, and Similarity measure between two triangular fuzzy numbers can be calculated with (3) [21].

$$s(a,b)=\frac{a^L b^L + a^M b^M + a^U b^U}{\max[(a^L)^2+(a^M)^2+(a^U)^2,\,(b^L)^2+(b^M)^2+(b^U)^2]} \tag{3}$$

where two triangular fuzzy numbers are $a = (a^L, a^M, a^U)$ that represents the ideal number and $b = (b^L, b^M, b^U)$ that represents the real number, respectively.

Because there are various types of criteria for different weapon systems, in which some criteria, such as the missile launching distance, warhead and speed, are not suitable to be represented as a fuzzy number. Therefore these numbers can be expressed as crisp numbers.

C. Construction of Decision Matrix

Calculation result of the similarity measure between alternate weapon systems and the ideal weapon system can be concisely expressed in a matrix format, which is called decision matrix in MCDM problems, and in which columns indicate weapon criteria and rows alternate weapons. Thus, an element s_{ij} in the in Eq. (4) denotes the similarity degree to the ideal weapon of the ith weapon with respect to the jth criterion.

$$DM=\begin{bmatrix} s_{11}\ s_{12}\ s_{13}\ \ldots\ldots\ldots s_{1n}\\ s_{21}\ s_{22}\ s_{23}\ \ldots\ldots\ldots s_{2n}\\ \ldots\ldots\ldots\ldots\ldots\ldots\ldots\\ s_{m1}\ s_{m2}\ s_{m3}\ \ldots\ldots\ldots s_{mn}\end{bmatrix} \tag{4}$$

D. Normalization

In order to eliminate the difference of dimension among different criteria, the operation of normalization is needed to transform various criteria dimensions into the non-dimensional criteria. Generally, the criteria of alternative weapons can be divided into two categories: the 'benefit' type attributes (the larger the better) and the 'cost' type attributes (the smaller the better). For example, the cost and weight belong to the 'cost' attributes, and the range and speed are 'benefit' attributes. In order to normalize those 'cost' attribute values to make them equivalent to the 'benefit' attributes (the larger the better), we developed a converting equation similar to [11] for those attribute values. The 'cost' attribute is calculated as (5):

$$x_{cj} = \frac{x_{j\max} - x_j}{x_{j\max}} \quad j = 1, 2, 3, \ldots\ldots m \tag{5}$$

For instance, the converted weapons' cost values are: $c_{cj} = (c_{jmax} - c_j)/c_{jmax}$, ($j$=1, 2,…18), and c_{jmax}= 1200k in this study. Similar processing is performed for the weapons' weight attributes $w_{cj} = (w_{jmax} - w_j)/w_{jmax}$, where w_{jmax}= 3700 in this research.

Equations (6) and (7) are utilized to perform the normalization for the fuzzy attributes or criteria [11].

$$r_i = \left(\frac{a_i}{c_i^{\max}}, \frac{b_i}{b_i^{\max}}, \frac{c_i}{a_i^{\max}} \wedge 1 \right) \quad \text{for benefit criteria} \tag{6}$$

$$r_i = \left(\frac{a_i^{\min}}{c_i}, \frac{b_i^{\min}}{b_i}, \frac{c_i^{\min}}{a_i} \wedge 1 \right) \quad \text{for cost criteria} \tag{7}$$

where $(\bullet)^{\max}{}_i = \max\{(\bullet)_i\}$ and $(\bullet)^{\min}{}_i = \min\{(\bullet)_i\}$.

E. Rank of Alternate Weapons

The element s_{ij} in the decision matrix reflects the closeness degree of the ideal weapon with the ith alternate weapon with respect to the jth criterion. In this step, we can use the simple additive weighting (SAW) method, which is widely used in MCDM, to calculate the relative importance value with respect to all criteria, with which the ranking order of alternate weapons according to the relative importance value can be obtained. And we can consider the weapon with the highest relative importance value as the closest one to that of the decision maker requires. The relative importance value of ith alternate weapon can be calculated with (8).

$$U_i = \sum_{j=1}^{n} x_{ij}\omega_j \quad i = 1, 2, \ldots, m \tag{8}$$

And the maximum of relative importance value can be written as (9).

$$U_{max} = \max_i \sum_{j=1}^{n} x_{ij}\omega_j \quad i = 1, 2, \ldots, m \tag{9}$$

III. ALGORITHM OF THE WEIGHT ASSIGNMENT

Compared with most MCDM methods, the FMCDM model reported by Bin Zhu et al. is one of the simplest and most effective methods [11]. A similarity measure method is utilized to build the decision matrix. However, one problem of this method is that the weight associated with each alternative is estimated or determined by the decision maker or an evaluation team based on their experience. Generally, this kind of weight estimation is acceptable for a small set of alternatives, such as 5 or less than 10. However, for a large set of alternatives, which is a popular situation, this weight estimation is not accurate and correct based only on the decision make's experience.

A simple but effective weight estimation method is adopted in this paper to make this evaluation process more objective and reliable. There are some different weight estimation methods reported by researchers, such as Saaty who developed a paired comparison matrix and then an eigenvector that is equivalent to the weight for an associated alternative can be calculated based on that paired comparison matrix [22]. Yager multiplied the normalized eigenvector by the order of the system to obtain exponents for weighting the fuzzy criteria in a decision problem [23]. However, both methods need a lot of mathematical operations and therefore make the process very complicated and time consuming.

In this paper, we adopted a weight estimation method based on the paired comparison matrix to simplify this estimation process. The operational procedure is completed by the following steps:

1. List the degree of importance or importance level of each criterion relative to another criterion based on Table I [24].
2. Construct a paired comparison matrix W based on the importance levels in step 1. Each element w_{ij} in the matrix W is a ratio of the importance level of the *ith* criterion over to the *jth* criterion.
3. Add each row $\omega_i = \sum_{j=1}^{n} \omega_{ij}$; where i = 1 ~ n and n is the total number of criteria.
4. Calculate the normalized weight factor for each criterion using $\omega_{ni} = \frac{\omega_i}{\omega_n}$; where $\omega_n = \sum_{i=1}^{n} \omega_i$.
5. These weight factors can be used to build the decision matrix based on the similarity measure method.

TABLE I. WEIGHT ASSIGNMENT TO A PAIRED COMPARISON CRITERIA

Importance Value	Definition
1	Equal Importance
3	Weak importance of one over the other.
5	Strong importance of one over the other.
7	Demonstrated importance of one over the other.
9	Absolute domination of one over the other.
2, 4, 6, 8	Intermediate values between the two adjacent judgements..

In the following section, we will use an example to illustrate this weight estimation method.

IV. CASE STUDY

In this section, we use a group of weapon information [25-30], which is collected by Federation of American Scientists (FAS) and contains the updated missiles, as an example to illustrate the weight estimation method we adopted in this paper with the Fuzzy MCDM model we discussed in section 2 to evaluate and assess the optimal weapon systems (missiles) currently used in the U.S. defense system.

Based on the different target locations and launching methods, all missiles can be divided into four categories: Air-launched, Ground-launched, Ship-launched and Submarine-launched. In this study, we concentrate on the Air-launched guided missiles with the ground targets because this is a kind of popular missiles and widely utilized in the U.S. defense system. First let us create a specification table for those missile alternatives based on twelve (12) criteria, which is shown in Table II. The 'cost' type criteria such as weapon's cost and weight have been converted to the 'benefit' type criteria in columns c3 and c7, respectively.

It can be found from Table II that some criteria contain vague and ambiguous (and thus fuzzy) definitiions, such as Guidance, Propulsion, Platform and Fuse system. The reason for that is because those criteria cannot be determined or described by crisp variables, and some human-being-language related terminologies must be applied to define them. For instance, a guidance system of a missile can be evaluated as a *low* if only manual guidance system is adopted for that missile, and a *mid* can be used to describe a guidance system that contains passive radar homing system, and a *high* can be used for a guidance system that uses an Inertial Navigation System (INS) and Global Position System (GPS).

TABLE II. AIR-LAUNCHED GUIDED MISSILE ALTERNATIVES

Missile	c1	c2	c3	c4	c5	c6	c7	c8	c9	c10	c11	c12
AGM-12	L	10	0.518	1.8	W	P	0.988	L	970	13.6	18.0	48
AGM-45	M	28	0.895	2.0	M	G	0.973	L	145	10.0	8.0	36
AGM-62	L	16	0.696	2.5	W	M	0.984	L	825	11.3	12.5	45
AGM-65	M	12	0.875	0.9	M	M	0.986	M	125	8.2	12.0	28
AGM-78	M	65	0.635	2.0	M	G	0.750	M	223	15.0	13.5	39
AGM-84	H	60	0.603	0.7	S	G	0.604	M	488	15.0	13.5	36
AGM-86	H	600	0.122	0.7	M	P	0.500	M	1500	20.0	24.5	36
AGM-88	M	26	0.784	1.8	S	M	0.763	H	143	13.7	10.0	44
AGM-114	H	4	0.973	1.3	M	G	0.979	M	18	5.3	7.0	13
AGM-122	M	9	0.947	2.3	M	G	0.917	M	25	9.4	5.0	25
AGM-123	M	13	0.654	0.9	S	M	0.921	M	991	14.1	19.7	63
AGM-129	H	1620	0.000	0.9	M	P	0.000	H	290	20.8	27.8	122
AGM-130	H	35	0.212	0.8	M	M	0.625	H	2000	12.9	15.0	59
AGM-136	M	43	0.884	0.7	S	G	0.833	H	40	8.3	27.0	62
AGM-137	H	100	0.460	0.6	S	G	0.393	H	1000	14.0	30.0	100
AGM-142	H	43	0.189	1.2	M	M	0.150	H	750	15.8	21.0	68
AGM-154	H	60	0.595	0.7	M	G	0.765	H	500	14	13.0	106
AGM-158	H	200	0.392	0.9	S	G	0.417	H	1000	14	18.0	95

- c1: Guidance (L-low, M-mid, H-high)
- c2: Range (nautical miles)
- c3: Weight (pounds)
- c4: Speed (Mach)
- c5: Propulsion (W-weak, M-mid, S-strong)
- c6: Platforms (P-poor, M-mid, G-good)
- c7: Cost (US$ thousands dollars - k)
- c8: Fuse system (L-low, M-mid, H-high)
- c9: Warhead (pounds)
- c10: Length (feet)
- c11: Diameter (inches)
- c12: Wingspan (inches)

The mapping relationships between some non-crisp parameters and fuzzy definitions for each missile should be indicated clearly. Table III shows an example of this kind of mapping for the Platform parameter.

TABLE III. MAPPING BETWEEN PLATFORM AND FUZZY DEFINITIONS

Missile	Platform Description	Fuzzy Definitiion
AGM-12	F-4, F-105	poor
AGM-45	F-4, F-16, F-105, A-4, A-6, A-7, B-2	good
AGM-62	F-18, F-4, A-4, A-7	mid
AGM-65	A-10, F-15E, F-16	mid
AGM-78	F-16C, EA-6B, EF-18G, F/A-18, F-4G, F-105G	good
AGM-84	A-6, F/A-18, S-3, P-3, B-52H, Ships	good
AGM-86	B-52H	poor
AGM-88	F-4, F-16C, F/A-18, EA-6B	mid
AGM-114	AH-1G, AH-64, MD-530, OH-58D, SH-60, HH-60 UH-60A, S-70 RAH-66, SA-342, F-4, F-5E, F-16 F/A-18, OV-10D	good
AGM-122	F-8, F-14, F-15, F/A-18, AH-1, AV-8B, OV-10 Fighters/Bombers	good
AGM-123	A-6E, A-7, F/A-18	mid
AGM-129	B-52H	poor
AGM-130	F-4E, F-15E, F-111	mid
AGM-136	B-52H, All Fighters and Bombers	good
AGM-137	All Fighters and Bombers	good
AGM-142	F-4, F-15, F-111, B-52H	mid
AGM-154	F-14, F-15, F-16, F-117, B-1B, F/A-18, AV-8B B-52H, All Other Fighter and Bombers	good
AGM-158	All Fighters and Bombers	good

Next we need to build the relative important levels for all criteria. This level is represented by a ratio between two or a paired of criteria. The ratio between the same criteria is 1 and a number represented in the intersection of a row and a column represnets the importance ratio between that row and that column. For example, the number in the intersection cell of row c5 and column c4 is 2, which means that the criterion c5 (Propulsion of a missile) is 2 times more important than that of criterion c4 (Speed of the missile). A completed importance level of this example is shown in Table IV.

TABLE IV. RELATIVE IMPORTANT LEVEL OF ALL CRITERIA

	c1	c2	c3	c4	c5	c6	c7	c8	c9	c10	c11	c12
c1	1	2	3	5	2	5	6	6	4	8	8	8
c2	1/2	1	3	2	1	3	3	5	2	7	7	7
c3	1/3	1/3	1	1/2	1	2	3	5	1	5	5	5
c4	1/5	1/2	2	1	1	3	3	5	1/2	3	3	3
c5	1/2	1	1	1	1	3	4	3	1/2	3	3	3
c6	1/5	1/3	1/2	1/3	1/3	1	3	3	1/2	3	3	3
c7	1/6	1/3	1/3	1/3	1/4	1/3	1	3	1/2	3	3	3
c8	1/6	1/5	1/5	1/5	1/3	1/3	1/3	1	1/5	2	2	2
c9	1/4	1/2	1	2	2	2	2	5	1	5	5	5
c10	1/8	1/7	1/5	1/3	1/3	1/3	1/3	1/2	1/5	1	1	1
c11	1/8	1/7	1/5	1/3	1/3	1/3	1/3	1/2	1/5	1	1	1
c12	1/8	1/7	1/5	1/3	1/3	1/3	1/3	1/2	1/5	1	1	1

Table IV is exactly a paired comparison matrix **W** and the diagonal weight element $\omega_{ji} = 1/\omega_{ij}$.

Now let's calculate the overall weight for each row by adding each row $\omega_i = \sum_{j=1}^{n} \omega_{ij}$; where i = 1 ~ n and n=12 is the total number of the criteria. The result of this calculation is shown in Table V.

TABLE V. THE OVERALL WEIGHT FOR EACH CRITERION

	c1	c2	c3	c4	c5	c6
ω_i	58.00	41.50	29.17	25.20	24.00	18.20
	c7	**c8**	**c9**	**c10**	**c11**	**c12**
ω_i	15.25	8.97	29.75	5.50	5.50	5.50

The total weight is obtained by adding all weights of criteria together, which is 266.54. The normalized weight for each criterion is shown in Table VI.

TABLE VI. THE NORMALIZED WEIGHT FOR EACH CRITERION

	c1	c2	c3	c4	c5	c6
$\hat{\omega}_i$	0.218	0.156	0.109	0.095	0.090	0.068
	c7	**c8**	**c9**	**c10**	**c11**	**c12**
$\hat{\omega}_i$	0.057	0.034	0.112	0.021	0.021	0.021

Now we can perform step 4 in section II to add these normalized weight for each criterion with all criteria to construct the ideal and criteria weight table, which is shown in Table VII.

TABLE VII. THE IDEAL MISSILE AND CRITERIA WEIGHT

Criterion	Ideal	Lower	Upper	Normalized Weight
c1	4	1	8	0.218
c2	600	4	1620	0.156
c3	0.9	0.0	1.5	0.109
c4	2.0	0.5	2.5	0.095
c5	4	1	8	0.090
c6	4	1	8	0.068
c7	0.9	0.0	1.5	0.057
c8	4	1	8	0.034
c9	1500	18	2200	0.112
c10	15.0	5.0	21.0	0.021
c11	15.0	5.0	30.0	0.021
c12	60	12	125	0.021

The vector of the ideal missile can be represented as the following form of the triangualr fuzzy number (Table VII):

T = [(1 4 8), (4 600 1620), (0.0 0.9 1.5), (0.5 2.0 2.5), (1 4 8), (1 4 8), (0.0 0.9 1.5), (1 4 8), (18 1500 2200), (5.0 15.0 21.0), (5.0 15.0 30.0), (12 60 125)]

The corresponding vector of the criteria weight can be expressed as:

ω = (0.218, 0.156, 0.109, 0.095, 0.090, 0.068, 0.057, 0.034, 0.112, 0.021, 0.021, 0.021)

The decision matrix, which can be calculated based on the similarity degree with respect to each criterion between the ideal missile and the alternatives, is shown in Table VIII by using (3) – (7). The relative importance value of *ith* alternate missile with respect to all criteria can be computed by (8), and the final calculating results are shown in Table IX.

TABLE VIII. DECISION MATRIX

Missile	c1	c2	c3	c4	c5	c6	c7	c8	c9	c10	c11	c12
AGM-12	0.1605	0.0075	0.4060	0.8571	0.1605	0.1605	0.7745	0.1605	0.5086	0.8069	0.7826	0.4882
AGM-45	0.3210	0.0209	0.7016	0.8333	0.3210	0.6420	0.7634	0.1605	0.0760	0.5933	0.3478	0.3662
AGM-62	0.1605	0.0119	0.5458	0.6667	0.1605	0.3210	0.7719	0.1605	0.4326	0.6705	0.5435	0.4577
AGM-65	0.3210	0.0089	0.6864	0.4286	0.3210	0.3210	0.7732	0.3210	0.0655	0.4865	0.5217	0.2848
AGM-78	0.3210	0.0484	0.4981	0.8333	0.3210	0.6420	0.5882	0.3210	0.1169	0.8900	0.5870	0.3967
AGM-84	0.6420	0.0447	0.4727	0.3333	0.6420	0.6420	0.4739	0.3210	0.2559	0.8900	0.5870	0.3662
AGM-86	0.6420	0.4471	0.0954	0.3333	0.3210	0.1605	0.3922	0.3210	0.7866	0.6833	0.6803	0.3662
AGM-88	0.3210	0.0194	0.6147	0.8571	0.6420	0.3210	0.5987	0.6420	0.0750	0.8129	0.4348	0.4475
AGM-114	0.6420	0.0030	0.7631	0.6190	0.3210	0.6420	0.7680	0.3210	0.0094	0.3145	0.3043	0.1322
AGM-122	0.3210	0.0067	0.7430	0.7246	0.3210	0.6420	0.7190	0.3210	0.0131	0.5577	0.2174	0.2543
AGM-123	0.3210	0.0097	0.5125	0.4286	0.6420	0.3210	0.7222	0.3210	0.5197	0.8366	0.8460	0.6408
AGM-129	0.6420	0.4576	0.0000	0.4286	0.3210	0.1605	0.0000	0.6420	0.1521	0.6571	0.5995	0.5383
AGM-130	0.6420	0.0261	0.1660	0.3810	0.3210	0.3210	0.4902	0.6420	0.6197	0.7654	0.6522	0.6001
AGM-136	0.3210	0.0320	0.6932	0.3333	0.6420	0.6420	0.6536	0.6420	0.0210	0.4925	0.6173	0.6306
AGM-137	0.6420	0.0745	0.3602	0.2857	0.6420	0.6420	0.3085	0.6420	0.5244	0.8307	0.5556	0.6567
AGM-142	0.6420	0.0320	0.1484	0.5714	0.3210	0.3210	0.1176	0.6420	0.3933	0.8650	0.7937	0.6916
AGM-154	0.6420	0.0447	0.4664	0.3333	0.3210	0.6420	0.6000	0.6420	0.2622	0.8307	0.5652	0.6195
AGM-158	0.6420	0.1490	0.3074	0.4286	0.6420	0.6420	0.3268	0.6420	0.5244	0.8307	0.7826	0.6912

TABLE IX. THE FINAL RESULT

AGM-12	AGM-45	AGM-62	AGM-65	AGM-78	AGM-84
0.3374	0.3864	0.3290	0.3271	0.3804	0.4368
AGM-86	**AGM-88**	**AGM-114**	**AGM-122**	**AGM-123**	**AGM-129**
0.4493	0.4010	0.4265	0.3684	0.4068	0.3684
AGM-130	**AGM-136**	**AGM-137**	**AGM-142**	**AGM-154**	**AGM-158**
0.4106	0.3816	0.4605	0.3881	0.4297	0.4864

The relative importance level of *ith* alternate missile can be calculated with Eq. (8) as:

$$U_i = \sum_{j=1}^{n} s_{ij}\omega_j \qquad i = 1, 2, \ldots \text{m} \ \ (\text{m} = 12)$$

The maximum important level of missiles can be obtained as:

$$U_{\max} = \max_i \sum_{j=1}^{n} s_{ij}\omega_j \qquad i = 1, 2, \ldots \text{m} \ \ (\text{m} = 12)$$

The missile that has the maximum important level can be found from Table IX, which is the **AGM-158** with a most important level of **0.4864**. The order that shows the top-10 closeness degree to the missiles that have the more important levels is:

AGM-158 >AGM-137 >AGM-86 >AGM-84 >AGM-154 > AGM-114 >AGM-130 >AGM-123 >AGM-88 >AGM-142

This is the optimal missile sequence estimated and evaluated based on the FMCDM system we developed in this paper. This evaluation and estimation is based on multiple

criteria and missile properties given by some references listed on our reference list.

One point to be noted from this assessing result is that the data we collected and used for this FMCDM system come from different reports issued by different agencies since 1993. Since the defense situation is always changing, therefore this result may not make very sense to today's situation. We just use these data as an example to illustrate the effectiveness and avalibility of our proposed method. The real and actual assessing result is dependant on the updated data.

V. CONCLUSION

Decision making is one of the most important and popular research and application topics in the national defense and security. To assess and evaluate the optimal weapon system such as missiles from a large group of alternatives that contain multiple criteria is a challenging, sometimes may be a headach task to decision makers in the defense system. A correct or optimal model and the associated algorithm are critical tools to complete this task. In this paper, a fuzzy multi-criteria decision making model is developed to help decision makers to correctly estimate weight factors for all criteria to make this process simplier and easier. To correctly pridict and effectively protect our nationa's safety, accurately evaluate and correctly assess the optimal weapon system is a prerequsite and critical task. In this paper, we used a collection of weapon information reported by different agencies in recent years with a target example to illustrate how to use FMDCM model to simplify this assessing process. The actual and more updated assessing result depends on the updated information reported by different sources in the future.

ACKNOWLEDGMENT

Some missiles data used in this paper are originally published in the page: http://www.fas.org/man/dod-101/sys/smart/index.html by Federation of American Scientists (FAS), USA.

REFERENCES

[1] Lin, Z. C., & Yang, C. B., "Evaluation of machine selection by the AHP method", Journal of Materials Processing Technology, 1994, 57, pp. 253–258.

[2] Tabucanon, M. T., Batanov, D. N., & Verma, D. K., "Intelligent Decision Support System (DSS) for the selection process of alternative machines for Flexible Manufacturing Systems (FMS)", *Computers in Industry,* 1994, *25*, pp. 131–143.

[3] Atmani,A.,&Lashkari,R. S., "A model of machine tool selection and operation Allocation in flexible manufacturing systems", *International Journal of Production Research,* 1998, *36*, pp. 1339–1349.

[4] Wang, T. Y., Shaw, C. F., & Chen, Y. L., "Machine selection in flexible manufacturing cell: A fuzzy multiple attribute decision-making approach", *International Journal of Production Research,*2000, *38*, pp. 2079–2097.

[5] Arslan,M.C., Catay, B.,&Budak, E., "A decision support system for machine tool selection", Journal of Manufacturing Technology Management, 2004, 15, pp. 101–109.

[6] Yurdakul,M., "AHP as a strategic decision-making tool to justify machine tool selection", Journal of Materials Processing Technology,2004, 146, pp. 365–376.

[7] Ayag, Z., & Ozdemir, R. G., "A fuzzy AHP approach to evaluating machine tool alternatives", Journal of Intelligent Manufacturing, 2006, 17, pp. 179–190.

[8] Ayag, Z., " A hybrid approach to machine tool selection through AHP and simulation", International Journal of Production Research, 2007, 45(9), pp. 2029–2050.

[9] Mishra, S., Prakash, Tiwari, M. K., & Lashkari, R. S., "A fuzzy goal-programming model of machine tool selection and operation allocation problem in FMS: A quick converging simulated annealing-based approach", *International Journal of Production* Research, 2006, 44(1), pp. 43–76.

[10] Chan, F.T. S.,& Swarnkar, R., "Ant colony optimization approach to a fuzzy goal programming model for a machine tool selection and operation allocation problem in an FMS. Robotics and Computer-Integrated Manufacturing, 2006, 22, pp. 353–362.

[11] Bin Zhu, Zhan Wang, Haicheng Yang, Rong Mo and Yanwei Zhao, "Applying fuzzy multiple attributes decision making for product configuration", *Journal of Intelligent* Manufacturing, 2008, 19, pp. 591-598.

[12] http://www.emedicine.com/emerg/TOPIC924.HTM

[13] Dena M. Bravata, Vandana Sundaram, Kathryn M. McDonald, Wendy M. Smith, Herbert Szeto, Mark D. Schleinitz, and Douglas K. Owens, Emerging Infectious Diseases. www.cdc.gov/eid, Vol. 10, No. 1, January 2004

[14] Cheng, C.H., & Mon, M.L., " Evaluating weapon system by analytic hierarchy process based on fuzzy scales", *Fuzzy Sets and Systems,* 1994, 63, pp. 1-10.

[15] Cheng, C.H., " Evaluating naval tactical missile systems by fuzzy AHP based on the grade value of membership function.", *European Journal of Operational Research*, 1996, 96, pp. 343-350.

[16] Cheng, C.H., "Evaluating weapon systems using ranking fuzzy numbers", *Fuzzy Sets and Systems*, 1999, 107, pp. 25-35.

[17] Cheng, C.H., Yang, K.L. & Hwang, C.L., "Evaluating attack helicopters by AHP based on linguistic variable weights", *European Journal of Operational Research*, 1999, 116, pp. 423-435.

[18] Cheng, C.H., & Lin, Y., "Evaluating the best main battle tank using fuzzy decision theory with linguistic criteria evaluation", *European Journal of Operational Research*, 2002, 142, pp. 174-186.

[19] Mon, D.L., Cheng, C.H., & Lin, J.C., "Evaluating weapon system using fuzzy analytic hierarchy process based on entropy weight", *Fuzzy Sets and Systems*, 1994, 62, pp. 127-134.

[20] Wang, T.C., & Chang, T.H., "Application of TOPSIS in evaluating initial training aircraft under a fuzzy environment", *Expert Systems with Applications*, 2007, 33, pp. 870–880.

[21] Xu, Z. S., "Study on method for triangular fuzzy number based multi attribute decision making with preference information on alternatives", *Systems Engineering and Electronics,* 2002, *124* (18), pp. 9–12.

[22] Saaty, T.L., "A Scaling Method for Priorities in Hierarchical Structures", *J. Math.*Psychology, 1977, 15, pp. 234-281.

[23] Yager, R.R., "Multiple Objective Decision-Making Using Fuzzy Sets", *Intl. J. Man-Machine Studies*, 1977, 9, pp. 375-382.

[24] Metin Dagdeviren, "Decision making in equipment selection: an integrated approach with AHP and PROMETHEE", *Journal of Intelligent Manufacturing*, 2008, 19: pp. 397-406.

[25] http://www.fas.org/man/dod-101/sys/missile/

[26] http://www.fas.org/man/dod-101/sys/smart/index.html

[27] http://www.fas.org/programs/ssp/man/miltutorials/missile-dumb-smart_bomb.html.

[28] Hajime Ozu: "Missile 2000 - Reference Guide to World Missile Systems", Shinkigensha, 2000.

[29] "Vision... Presence... Power, A Program Guide to The U.S. Navy", 2002 Edition.

[30] "Gallery of USAF Weapons", 2008 Almanac, *Air Force Magazine*, May 2008, pp. 155.

2011 IEEE International Conference on Fuzzy Systems
June 27-30, 2011, Taipei, Taiwan

Fuzzy-rough Classifier Ensemble Selection

Ren Diao and Qiang Shen
Department of Computer Science
Aberystwyth University
Aberystwyth, SY23 3DB, UK
Email: {rrd09, qqs}@aber.ac.uk

***Abstract*—Classifier ensembles constitute one of the main research directions in machine learning and data mining. Ensembles allow higher accuracy to be achieved which is otherwise often not achievable with a single classifier. A number of approaches have been adopted for constructing classifier ensembles and aggregate ensemble decisions. In most cases, these constructed ensembles contain redundant members that, if removed, may further increase ensemble diversity and produce better results. Smaller ensembles also relax the memory and storage requirements of an ensemble system, reducing its run-time overhead while improving overall efficiency. In this paper, a new approach to classifier ensemble selection based on fuzzy-rough feature selection and harmony search is proposed. By transforming the ensemble predictions into training samples, classifiers are treated as features. Harmony search is then used to select a minimal subset of such artificial features that maximises the fuzzy-rough dependency measure. The resulting technique is compared against the original ensemble and ensembles formed using random selection, under both single algorithm and mixed classifier ensemble environments.**

Keywords: Classifier Ensemble Selection; Feature Selection; Harmony Search; Fuzzy-rough Sets

I. Introduction

The main purpose of a classifier ensemble is to improve the performance of single classifier systems. Different classifiers usually make different predictions on certain samples, caused by their diverse internal models. Combining such classifiers became the natural way of trying to increase classification accuracy, by exploiting their uncorrelated errors. Also, each ensemble member can potentially be trained using a subset of training samples, which may reduce the computational complexity issue which arises when a single classification algorithm is applied to very large datasets. Additionally, an ensemble can operate in a distributed environment, where datasets are physically separated and are cost ineffective or technically difficult to combine into one database, in order to train a single classifier. A typical approach to building classifier ensembles involves building a group of classifiers with diverse training backgrounds, before aggregating their decisions together to produce the final prediction.

The target of Classifier Ensemble Selection (CES) [21] is to select a subset from a pre-constructed pool of base classifiers, in order to form a reduced group that is still capable in producing good classification results. This is an intermediate stage between the ensemble building and aggregation. Efficiency is one of the obvious gains from CES. Having a reduced number of classifiers can eliminate a portion of run-time overheads, making the ensemble processing quicker; having fewer models also means relaxed memory and storage requirements. Removing redundant ensemble members can also lead to improved diversity within the group, further increase potential ensemble prediction performance. A number of existing techniques use clustering [9] to discover groups of models that share similar predictions, and subsequently prune each cluster separately. Alternative selection methods [22] focus on selecting potentially optimal subsets to maximise a pre-defined diversity measures.

Feature selection [4] (FS) aims to determine a minimal feature subset from a problem domain while retaining a suitably high accuracy in representing the original features. In dealing with real-world problems FS is usually necessary due to the abundance of noisy, irrelevant, redundant or misleading features [13]. For instance, by removing these factors, learning from data techniques such as text processing and web content classification can benefit greatly. Given a feature set size n, the task of FS can be seen as a search for an "optimal" feature subset through the competing 2^n candidate subsets. The definition of an optimal subset may vary, depending on the problem at hand. A data reduction approach for fuzzy-rough feature selection (FRFS), based on fuzzy-rough sets [7], has been developed [14]. Fuzzy-rough sets encapsulate the related but distinct concepts of vagueness (for fuzzy sets) and indiscernibility (for rough sets [19]),both of which occur as a result of uncertainty in knowledge. The fuzzy-rough set-based techniques consider the extent to which fuzzified values are similar. By employing fuzzy-rough sets, it is possible to perform better feature selection. An unsupervised FRFS method was also proposed [17].

Many existing FS algorithms employ heuristic search strategies in an attempt to avoid the prohibitive complexity of exhaustive method. For instance, FRFS uses an incremental hill-climbing algorithm to discover the best feature subset. However, this often led to the discovery of non-optimal feature subsets, both in terms of the resulting subset quality and the subset size. Other search mechanisms may help, harmony search (HS) [8] in particular, is a meta-heuristic algorithm that mimics the improvisation process of music players. It imposes only limited mathematical requirements and is insensitive to initial value settings. Due to its simplistic structure and powerful performance, HS algorithm has been very successful in a wide variety of optimisation problems [8], presenting several advantages with respect to traditional optimisation techniques. The basic HS algorithm has been improved by

978-1-4244-7316-8/11/$26.00 ©2011 IEEE

introducing methods to tune parameters dynamically [6] and also successfully applied to solve FS problems [5].

In this paper, a new CES approach based on FRFS is proposed. Inspired by the analogies in between CES and FS, fuzzy-rough CES aims to tackle CES problems from a different angle: by transforming the classifier predictions, each classifier is treated as an artificial feature in the transformed dataset, and classifier predictions as feature values. FS algorithms can then be used to remove redundant features (classifiers) in the present context, in order to select a minimal classifier subset while maintaining original ensemble diversity, and preserving ensemble prediction accuracy.

The rest of this paper is structured as follows. Section II describes the theory behind FRFS, and a most recently proposed unsupervised FRFS method which will be utilised in this work. Section III explains the basic structure of HS, and how it is applied to FRFS. Section IV introduces the key concepts of fuzzy-rough CES, demonstrates how CES can be modelled as an FS problem, and details the approaches developed to tackle the problem. Section V presents the experimentation results along with discussions. Section VI concludes the paper and proposes further work in the area.

II. Fuzzy-Rough Feature Selection

Rough set theory (RST) has been successfully used as an attribute selection tool to discover data dependencies and reduce the number of attributes contained in a dataset by purely structural means [20]. Given a dataset with discretised attribute values, RST can find a subset (termed *reduct*) of the original attributes that are the most informative; all other attributes can be removed from the dataset with minimal information loss. However, it is most often the case that the values of attributes may be both crisp and real-valued, and this is where traditional rough set theory encounters a problem. It is not possible in the theory to say whether two different attribute values are similar and to what extent they are the same. For example, two close values may only differ as a result of noise, but in the standard RST-based approach they are considered to be as different as two values of a different order of magnitude. Dataset discretisation must therefore take place before reduction methods based on crisp rough sets can be applied. This is often still inadequate, however, as the degrees of membership of values to discretised values are not considered and thus can result in information loss. In order to combat this, extensions of rough sets based on fuzzy-rough sets [7] have been developed. A fuzzy-rough set is defined by two fuzzy sets, fuzzy lower and upper approximations, obtained by extending the corresponding crisp rough set notions. In the crisp case, elements either belong to the lower approximationwith absolute certainty or not. In the fuzzy-rough case, elements may have a membership in the range [0,1], allowing greater flexibility in handling uncertainty.

A. Supervised Fuzzy-rough Feature Selection

Fuzzy-rough feature selection [14] (FRFS) is concerned with the reduction of information or decision systems through the use of fuzzy-rough sets. Let $I = (\mathbb{U}, \mathbb{A})$ be an information system, where $\mathbb{U}$ is a non-empty set of finite objects (the universe) and $\mathbb{A}$ is a non-empty finite set of attributes such that $a : \mathbb{U} \rightarrow V_a$ for every $a \in \mathbb{A}$. V_a is the set of values that attribute a may take. For decision systems, $\mathbb{A} = \{\mathbb{C} \cup \mathbb{D}\}$ where $\mathbb{C}$ is the set of input features and $\mathbb{D}$ is the set of decision features.

$$\mu_{\underline{R_P}X}(x) = \inf_{y \in \mathbb{U}} I(\mu_{R_P}(x,y), \mu_X(y)) \tag{1}$$

$$\mu_{\overline{R_P}X}(x) = \sup_{y \in \mathbb{U}} T(\mu_{R_P}(x,y), \mu_X(y)) \tag{2}$$

Here, I is a fuzzy implicator and T is a t-norm. R_P is the fuzzy similarity relation induced by the subset of features P,

$$\mu_{R_P}(x,y) = T_{a \in P}\{\mu_{R_a}(x,y)\} \tag{3}$$

where $\mu_{R_a}(x,y)$ is the degree to which objects x and y are similar for feature a.

FRQuickReduct($\mathbb{C}$,$\mathbb{D}$).
$\mathbb{C}$, the set of all conditional features;
$\mathbb{D}$, the set of decision features.

(1) $R \leftarrow \{\}$, $\gamma'_{best} \leftarrow 0$, $\gamma'_{prev} \leftarrow 0$
(2) **do**
(3) $T \leftarrow R$
(4) $\gamma'_{prev} \leftarrow \gamma'_{best}$
(5) $\forall x \in (\mathbb{C} - R)$
(6) **if** $\gamma'_{R \cup \{x\}}(\mathbb{D}) > \gamma'_T(\mathbb{D})$
(7) $T \leftarrow R \cup \{x\}$
(8) $\gamma'_{best} \leftarrow \gamma'_T(\mathbb{D})$
(9) $R \leftarrow T$
(10) **until** $\gamma'_{best} == \gamma'_{prev}$
(11) **return** R

Fig. 1. The fuzzy-rough QuickReduct algorithm

A fuzzy-rough QuickReduct algorithm, based on the crisp version [20], has been developed as given in Fig. 1. It employs a quality measure termed the fuzzy-rough dependency function γ' to choose which features to add to the current reduct candidate, which is defined by:

$$\gamma'_{P(Q)} = \frac{\sum_{x \in \mathbb{U}} \mu_{POS_{R_P}(Q)}(x)}{\|\mathbb{U}\|} \tag{4}$$

where the fuzzy positive region is defined as:

$$\mu_{POS_{R_P}(Q)}(x) = \sup_{q \in \mathbb{Q}} \mu_{\underline{R_P}Q}(x) \tag{5}$$

The algorithm terminates when the addition of any remaining feature does not increase the dependency. As with the original algorithm, for a dimensionality of n, the worst case dataset will result in $(n^2 + n)/2$ evaluations of the dependency function. However, as fuzzy-rough set based feature selection is used for dimensionality reduction prior to any involvement of a given

application which will exploit those features belonging to the resultant reduct, this operation has no negative impact upon the run-time efficiency of the system.

B. Unsupervised Fuzzy-rough Feature Selection

The central idea behind unsupervised FRFS (U-FRFS) [17] is that, as with the supervised FRFS, the fuzzy dependency measure can also be used to discover the inter-dependency of features. This can be achieved by simply substituting the decision feature(s) $\mathbb{D}$ of the supervised approach for any given feature or group of features Q. In this case, the fuzzy positive region defined in Eq 5 becomes:

$$\mu_{POS_{R_P}(Q)}(x) = \sup_{z \in \mathbb{U}} \mu_{\underline{R_P} R_Q z}(x) \tag{6}$$

where $R_Q z$ indicates the fuzzy tolerance class (or fuzzy equivalence class) for object z, and the lower approximation now becomes:

$$\mu_{\underline{R_P} R_Q z}(x) = \inf_{y \in \mathbb{U}} I(\mu_{R_P}(x, y), \mu_{R_Q}(y, z)) \tag{7}$$

III. Harmony Search for Fuzzy-rough Feature Selection

Harmony Search (HS) [8] mimics the improvisation process of musicians, during which, each musician plays a note for finding a best harmony all together. The basic concepts of HS and application of such concepts in performing optimisation are outlined below, together with an introduction to the dynamic parameter control involved in HS.

A. Key Concepts

The key concepts of HS are musicians, notes, harmonies and harmony memory. In most optimisation problems solvable by HS, the musicians are the decision variables of a certain function being optimised. The notes played by the musicians are the values each decision variable can take. The harmony contains the notes played by all musicians, or an emerging solution vector containing the values for each decision attribute. The harmony memory contains harmonies played by the musicians, or a storage place for potential solution vectors. A more concrete representation of harmony memory is a two dimensional matrix, where the rows contain harmonies (solution vectors) with the number of rows being predefined and bounded by the harmony memory size. Each column is dedicated to one musician, and the entire column stores all the notes played by the musician in all saved harmonies, referred to as the working note domain for each musician in this paper.

Harmony Search for Feature Selection (HSFS) [5] treats musicians as independent experts, and each musician can vote for one feature to be included in the feature subset when improvising a new harmony. The harmony is then the combined vote from all musicians, indicating which features are being nominated. The entire pool of original features forms the range of notes available to the musicians. Multiple musicians are allowed to choose the same attribute, and they may opt to choose no attribute at all. For example, the harmony {A,-,B,B,C,-} will translate into feature subset {A,B,C}, − here represents a null note.

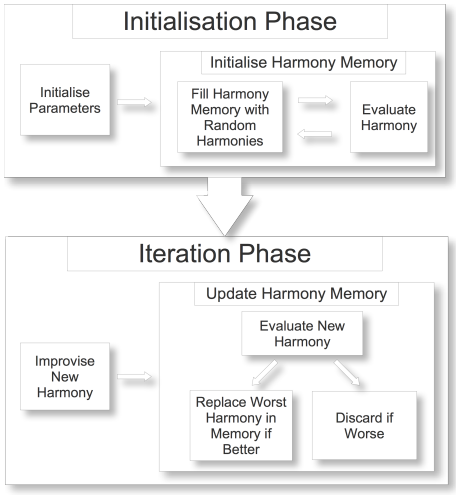

Fig. 2. Illustration of Harmony Search

B. Iteration Steps

HS can be divided into two core phases, initialisation and iteration, as illustrated in Fig 2.

a) Initialise Problem Domain: The parameters of HS are assigned according to the problem, including: size of harmony memory, number of musicians, max iteration, and the harmony memory considering rate (HMCR). The harmony memory of size m is initialised by random generation. This provides each musician a working note domain of m values, which may include identical notes, and nulls. A new harmony is produced by each musician randomly choosing one attribute from their note domain. The new harmony is then evaluated using the given cost function. It is used to replace the worst harmony in the harmony memory if a better score is achieved, or discarded otherwise.

b) Improvise New Harmony: A new value is chosen randomly by each musician out of their note domain, and together forms a new harmony. There are two factors which affect the note choice of a musician, HMCR and PAR. HMCR, ranging from 0 to 1, is the rate of choosing one value from the historical notes stored in the harmony memory, with $(1 - HMCR)$ set to be the rate of randomly selecting one value from the range of all possible notes of the corresponding variable. If HMCR is set low, the musicians will constantly explore other areas of the solution space, and a higher HMCR will restrict the musicians to historical choices.

The PAR parameter causes the musicians to select a neighbouring value based on the following formula $a + (random * bw)$, where bw is an arbitrary distance bandwidth, with $(1 - PAR)$ set to be the probability of using the chosen value without further alteration. The pitch adjustment is applied after a note is chosen by the musician, either from the HM or from the domain of all possible values. For FS problems that are dealt with in this paper, the PAR parameter is not used. This is because the underlying assumption of using PAR is that values that are very close by may provide more optimal solutions. However, when such values represent feature

indices, each index, and its neighbouring features, have no such general dependency in between.

c) Update Harmony Memory: If the new harmony is better than the worst harmony in the harmony memory, judged by the objective function, the new harmony is then included in harmony memory and the existing worst harmony is removed. The algorithm continues to iterate until the maximum number of iterations has been reached.

C. Parameter Control

TABLE I
PARAMETER SETTINGS IN DIFFERENT SEARCH STAGES

	Initialisation	Intermediate	Termination
HMCR	Small	Medium	Large
MS	Small	Medium	Large
Effect	High diversity. Deep Exploration	Steady improvement in harmonies	Fine tuning. Fast convergence

To improve HS and eliminate the drawbacks lying with the use of fixed parameter values, a dynamic parameter adjustment scheme [6] was proposed to modify parameter values at run time. Parameters are dynamically changed, and different settings are provided for different search stages. Table I shows the parameters relevant to FS. These parameters then gradually change through the initial solution space exploration, intermediate solution refinement, and fine tune optimal solution towards termination.

IV. FUZZY-ROUGH CLASSIFIER ENSEMBLE SELECTION

The overall approach developed in this work can be summarised in Fig 3, with each of the four key components described below.

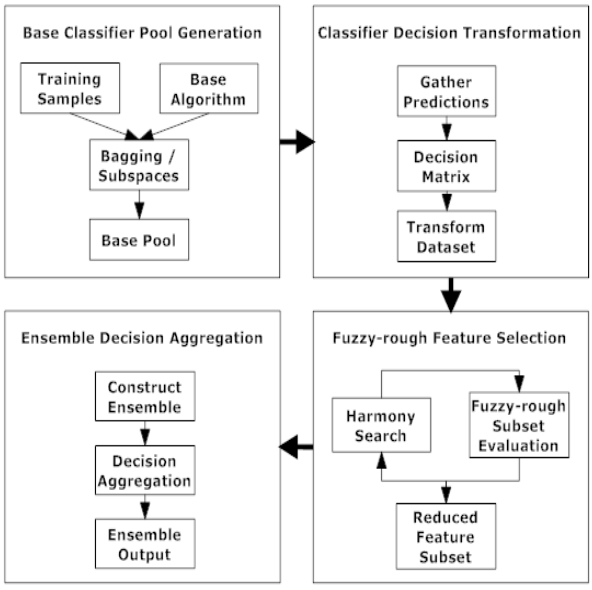

Fig. 3. Fuzzy-rough CES Flow Chart

A. Base Classifier Pool Generation

Forming a diverse base classifier pool (BCP) is the first step in producing a good classifier ensemble. Any preferred methods can be used to build the base classifiers, *Bagging* [2] and *Random Subspaces* [11] methods are adapted here. BCP can be created using a single classification algorithm as well as a mixed classifier scheme. *Bagging* randomly selects different subsets of training samples in order to build diverse classifiers. Differences in the training data present extra or missing information for different classifiers, resulting in different models. The *Random Subspaces* method randomly generates different subsets of domain attributes and builds various classifiers on top of each of such subsets. The differences between the subsets creates different view points of the same problem [3], typically resulting in different borders for classification. For a single base classification algorithm, these two methods both provide good diversities. In addition, a mixed classifier scheme is implemented in the presented work. By selecting classifiers from different schools of classification algorithms, the diversity is naturally achieved through the various foundations of the algorithms themselves.

B. Classifier Decision Transformation

TABLE II
DECISION MATRIX

	C_1	C_2	$\cdots$	C_i	$\cdots$	C_{N_C}
I_1	D_{1j}	D_{21}	$\cdots$	D_{1j}	$\cdots$	D_{N_C1}
I_2	D_{12}	D_{22}	$\cdots$	D_{2j}	$\cdots$	D_{N_C2}
$\vdots$	$\vdots$	$\vdots$		$\vdots$		$\vdots$
I_j	D_{1j}	D_{2j}	$\cdots$	D_{ij}	$\cdots$	D_{N_Cj}
$\vdots$	$\vdots$	$\vdots$		$\vdots$		$\vdots$
I_{N_I}	D_{1N_I}	D_{2N_I}	$\cdots$	D_{iN_I}	$\cdots$	$D_{N_CN_I}$

Once the base classifiers are built, their decisions on the training instances are also gathered. For base classifiers $C_i, i = 1, 2, \ldots, N_C$, and training instances $I_j, j = 1, 2, \ldots, N_I$, where N_C is the total number of base classifiers, and N_I is the total number of training instances, a decision matrix as shown in Table II can be constructed. The value D_{ij} represents the ith classifier's decision on the jth instance. For supervised FS, a class label is required for each training sample, the same class attribute is taken from the original dataset, and assigned to each of the instances. Note that both the total number of instances and the relations between instances and their class labels remain unchanged. Although all attributes and values are completely replaced by transformed classifier predictions, the original class labels remain the same. A new dataset is therefore constructed, each column represents an artificially generated feature, each row corresponds to a training instance, the cell then stores the transformed feature value.

C. Feature Selection on the Transformed Dataset

FRFS is then performed on the transformed dataset, evaluating each artificial feature subset using the fuzzy-rough dependency measure. HS optimises the quality of

discovered subsets, while trying to reduce subset sizes. A detailed explanation is already given in Section III. When HS terminates, its best harmony is translated into a feature subset and returned as the FS result. The features then indicate their corresponding classifiers which should be included in the learnt classifier ensemble. For example, if the best harmony given by HS is $\{-, C_9, C_3, C_{23}, C_3, C_5, C_{17}, -\}$, the translated artificial feature subset is then $\{C_3, C_5, C_9, C_{17}, C_{23}\}$. Thus, the 3rd, 5th, 9th, 17th and 23rd classifiers will be chosen from the BCP to construct the classifier ensemble. Note that the application of unsupervised FRFS is the same as above and hence is omitted to avoid repetition.

D. Ensemble Decision Aggregation

Once the classifier ensemble is constructed, new objects are classified by the ensemble members, and their results are aggregated to form the final ensemble decision output. The *Average of Probability* aggregation method is used in the paper. Given ensemble members $E_i, i = 1, 2, \ldots, N_E$, and decision classes $D_j, j = 1, 2, \ldots, N_D$, where$N_D$ is the ensemble size and N_D is the number of decision classes, classifier decisions can be viewed as a matrix of probability distributions $\{P_{ij}\}$. Here, P_{ij} indicates prediction from classifier C_i for decision class D_j. The final aggregated decision is the winning classifier that has the highest averaged prediction across all classifiers: $\{\sum_{i=1}^{N_E} P_{i1}/N_E, \sum_{i=1}^{N_E} P_{i2}/N_E, \ldots, \sum_{i=1}^{N_E} P_{iN_D}/N_E\}$. Note that this is effective because redundant classifiers are now removed. As such, the usual alternative aggregation method: *Majority Vote* is no longer favourable since the "majority" has been significantly reduced.

V. Experimentation and Discussion

To demonstrate the capability of fuzzy-rough CES, a number of experimentations have been carried out. These experiments are divided into three groups, based on the main methods adapted to generate the BCP: *Bagging*, *Random Subspaces*, and the mixed classifier scheme. For single base algorithm experiments, the facilitate comparative studies, the state of the art fuzzy-rough nearest neighbour (FRNN) [12] classifier is used. Both ordinary FRFS and unsupervised FRFS methods are examined. Classification accuracies are collected under stratified 10 fold cross validation, and each set of experiments is run 10 times with results averaged. Ten 10-fold cross validations are used as random factors are involved in creating the *Bagging* and *Random Subspaces* BCPs, as well as in the artificial feature selection process using HS. For comparison, the accuracy of the base algorithm, when trained using the original dataset without alteration is included, the averaged accuracy of the full BCP is also included. A total of 9 real-valued UCI datasets [18] are used in the experiments. Parameters used in the experiments and dataset information are summarised in Table III.

TABLE III
HS Parameter Settings and Dataset Information

Harmony Memory Size	# Musicians	HMCR	Max Iteration
10-20	$\frac{2}{3}$ # features	0.5-1	500
Dataset	**Objects**	**Attributes**	**# Classes**
cleveland	297	14	5
ecoli	336	8	8
glass	214	9	6
heart	270	13	2
ionosphere	230	35	2
sonar	208	60	2
water 3	390	38	3
water 2	390	38	2
wine	178	14	3

A. Bagging

In this set of experiments, the BCP is built using *Bagging* with FRNN being the base algorithm. Table IV shows the results of applying fuzzy-rough CES and unsupervised fuzzy-rough CES, as compared against the results of using: (1) the base algorithm, (2) the full base classifier pool, and (3) randomly formed ensembles. Entries annotated with *v* indicates that the selected ensemble performance is statistically significant when compared against random pick, using paired t test with two-tailed P threshold = 0.005.

TABLE IV
Fuzzy-rough Nearest Neighbour using Bagging

Dataset	Base	Full	FRFS	U-FRFS	Random
cleveland	53.20	57.91	57.21 (11.8) *v*	56.30 (8.9)	56.03
ecoli	81.85	86.01	85.97 (11.9)	85.52 (7.9)	85.52
glass	72.43	73.36	73.18 (11.3) *v*	73.04 (8.1)	73.04
heart	76.30	81.19	79.78 (8.0) *v*	79.22 (8.2)	78.69
ionosphere	90.43	88.43	88.70 (7.4) *v*	88.83 (7.5) *v*	87.85
sonar	85.10	85.72	85.96 (8.0)	85.91 (7.9)	85.32
water 3	80.26	81.51	81.38 (8.8)	81.62 (7.9) *v*	80.94
water 2	84.62	85.23	85.05 (7.9) *v*	84.69 (7.8)	84.35
wine	97.19	96.91	96.46 (7.6)	96.63 (7.8) *v*	96.35

The results show that the *Bagging* method improved over the base classifier. Column *Full* displays aggregated predictions from the entire base classifier pool of size 50. For 7 out of 9 datasets, greater classification accuracies have been achieved using the ensemble approach. The CES+FRFS method successfully selected classifier ensembles with reduced size, as shown in column *FRFS* with the numbers in the brackets indicating the selected ensemble sizes. Because ten fold cross validation is used, different classifiers are constructed and selected for each individual fold, hence performed in general differently, but the reported sizes are an average of 100 ensembles. Despite the reduced ensemble size, classification accuracies are further improved for the *sonar* and *ionosphere* datasets. For the other datasets, the accuracies are reduced very marginally, with less than 0.2% in 5 of the 7 total cases, and the greatest reduction being 0.7% (*cleveland*).

When compared against the use of supervised FRFS, CES equipped with unsupervised FRFS finds more compact ensembles with an averaged size of 8. This is possibly due to the fact that the class label is no longer considered in the dependency calculation, and therefore less consistency constraints are placed upon the construction of ensembles

(artificial feature subsets). The reduced ensembles still maintain reasonable classification accuracies, in comparison to the use of supervised FRFS, and the base pool. Both approaches generally deliver better results than randomly picked ensembles, except for *ecoli* and *glass* datasets, the unsupervised method seems to have an equal performance as random picking. One possible explanation is that the number of classes for a given training dataset has direct impact upon unsupervised FRFS performance. The more classes there are, the more various the classifier predictions become, thereby providing more available values for the artificial features. The transformed dataset is therefore more complex than ones originated from the training datasets with 2 or 3 classes. For such datasets like *cleveland* (5), *ecoli* (8), and *glass* (6), the extra consistency constraint from the class label itself must have aided the supervised method in selecting better artificial feature subsets, with the sacrifice of having larger ensembles.

B. Random Subspaces

TABLE V
FUZZY-ROUGH NEAREST NEIGHBOUR USING RANDOM SUBSPACES

Dataset	Base	Full	FRFS	U-FRFS	Random
cleveland	53.20	58.25	57.00 (8.1)	57.78 (7.4) *v*	56.37
ecoli	81.85	80.33	81.85 (9.8) *v*	78.63 (7.8)	77.98
glass	72.43	76.96	76.78 (7.6) *v*	76.87 (7.6) *v*	75.05
heart	76.30	82.59	80.89 (7.7)	79.96 (7.6)	80.28
ionosphere	90.43	89.87	89.87 (7.8) *v*	89.83 (7.7) *v*	89.48
sonar	85.10	88.89	88.22 (7.1) *v*	87.88 (7.4) *v*	87.24
water 3	80.26	80.97	81.90 (7.7) *v*	81.59 (7.8) *v*	80.63
water 2	84.62	85.46	85.15 (7.6) *v*	85.00 (7.6)	84.83
wine	97.19	97.81	97.02 (7.5) *v*	97.02 (7.8)	96.41

Table V shows the use of *Random Subspaces* builds slightly better quality base classifiers. In comparison with the base algorithm, the pool gains better accuracy in 8 out of 9 cases, except for dataset *ionoshpere*; and in 7 out of 9 cases, the averaged accuracies are higher than pools using *Bagging*. The FRFS method successfully reduced ensembles, and the ensemble sizes are smaller than previous discoveries for all datasets. A likely indication from these results is that the classifiers created using *Random Subspaces* contain more redundancy. Although the overall accuracies of the reduced ensembles are higher than those obtained by their counterpart via using the *Bagging* method, greater accuracy decrease is observed when compared with the base pools.

Unsupervised FRFS also finds smaller ensembles, with comparable accuracies except for *ecoli*, the reduced ensembles suffered more than 3% loss of accuracy when compared against the case when supervised FRFS is used. Both selection methods however entail better results than random selection.

C. Mixed Classifier Scheme

A total of 10 different base algorithms are selected for this experiment, one or two distinctive classifiers from each representative classifier groups, including fuzzy-based FuzzyNN [16], FuzzyRoughNN [12], VQNN [12], lazy-based IBk [1], tree-based J48 [23], REPTree [23], rule-based JRip [23], PART [23], NaiveBayes [15] and MultilayerPerceptron [10]. Given only 10 base algorithms, more variations are needed to produce as pool of size 50, *Bagging* and *Random Subspaces* are again used to create differentiation between classifiers. Tables VI and VII show the experimental results, using these two methods respectively.

For mixed classifiers created using *Bagging*, the FRFS method finds ensembles with much greater size variation and overall, considerably larger ensembles than previous experiments. For the *ecoli* dataset in particular, the averaged ensemble size is 15.98. Even with such a large ensemble, the underlying artificial feature subset still did not achieve 1 for the fuzzy-rough dependency measure. However, the results indicate that many distinctive features (i.e. classifiers) are present, therefore a larger subset is necessary to maintain consistency. For classifier ensembles, this means good diversity and many distinctive classifiers co-exist in the base pool, and thus less redundancy exists. This particular ensemble also results in the highest accuracy for *ecoli* compared against other approaches, with 87.67% BCP accuracy, and 86.66% ensemble accuracy. Although most ensembles can achieve comparable performance, large performance decreases are also noticed for the *sonar* and *heart* datasets. Interestingly, the use of the unsupervised method achieves better overall performance than its supervised counterpart, with smaller selected ensemble sizes. Reasons for such performance is unknown yet, but further investigation into this aspect is currently ongoing.

TABLE VI
MIXED CLASSIFIERS USING BAGGING

Dataset	Full	FRFS	U-FRFS
cleveland	54.94	52.92 (11.2)	54.27 (9.32)
ecoli	87.67	86.66 (15.98)	85.77 (8.7)
glass	71.12	69.62 (12.2)	69.62 (9.2)
heart	82.07	75.40 (8.76)	77.62 (8.42)
ionosphere	87.73	88.17 (8.36)	88.17 (8.56)
sonar	80.96	73.55 (8.5)	80.76 (8.68)
water 3	78.15	78.71 (9.26)	78.20 (8.72)
water 2	80.61	81.58 (8.72)	82.10 (8.84)
wine	98.31	97.52 (7.74)	97.40 (7.46)

TABLE VII
MIXED CLASSIFIERS USING RANDOM SUBSPACES

Dataset	Full	FRFS	U-FRFS
cleveland	56.57	57.85 (11.82)	57.10 (9.08)
ecoli	79.17	84.64 (12.16)	84.40 (7.8)
glass	75.61	71.50 (11.28)	73.08 (8.18)
heart	82.44	80.89 (7.96)	80.44 (8.16)
ionosphere	89.30	87.39 (8.1)	88.00 (7.58)
sonar	82.69	86.06 (7.86)	83.17 (7.88)
water 3	80.26	80.41 (9.16)	80.92 (8.04)
water 2	83.18	85.85 (7.86)	85.74 (7.92)
wine	98.09	97.53 (7.82)	97.75 (7.46)

The *Random Subspaces* based mixed classifier scheme produces better base pools in 7 out of 9 cases. Both FRFS and U-FRFS find smaller ensembles on average than the case where *Bagging* is used. Neither method suffers from extreme performance decreases following reduction unlike the results obtained when single base algorithm is employed. Despite having a BCP that under performs for the *ecoli* dataset, both methods manage to achieve an increase of 5% in accuracy.

However, the general quality of the mixed classifier group is lower than that of the FRNN based single algorithm approach. This is largely caused by the employment of non-optimised base classifiers. It can be expected that the results achievable after optimisation would be even better. Note that certain ensemble methods are less desirable for some datasets. For example, using the mixed classifier scheme can achieve an accuracy of 86.66% for *ecoli*, but using partition based approach only leads to an accuracy of 81.85%. Yet, the partition based approach results in 88.22% for *sonar*, while the mixed classifier scheme obtains a result as low as 73.55%. Further experimental investigation revealed that *ecoli* involves the least number (8) of attributes. Therefore *Random Subspaces*, which creates attribute subsets randomly, can easily remove an essential attribute, making it less suitable for ensemble generation. The massive performance gain for *sonar* dataset can be explained in a similar way: *Random Subspaces* can construct diverse classifiers reasonably well with 60 attributes.

VI. Conclusion

This paper has presented a new approach to classifier ensemble selection. It works by applying fuzzy-rough feature selection technique to minimise redundancy in an artificial dataset generated via transforming a given classifier pool's decision matrix. The aim is to further reduce the size of a classifier ensemble, while maintaining and improving classification accuracy, making the ensemble more efficient. Experimental comparative studies show that both supervised and unsupervised FRFS approaches can entail good solutions. Reduced ensembles are found with comparable classification accuracies as the base pools, and in most cases provide good improvements over the performance achievable by the base algorithms. In particular, the use of the unsupervised FRFS method can help create smaller ensembles, especially when complex mixed classifiers are used.

Although promising, much can be done to further improve the potential of the presented work. In particular, an alternative classifier decision matrix transformation procedure may be formulated. Some classifiers first produce a distribution of the likelihood that a particular instance may belong to the available classes, and the class with highest probability is then taken as the final prediction. These probability distributions may contain more information and are potentially more suitable to be used as the artificial feature values. In addition, other statistical information from the classifiers such as variance, may also be good candidates for use as part of the artificially generated features, in order to create a more comprehensive dataset for feature selection. Experimental evaluation of these ideas remains as active research, as well as the aforementioned investigation into the underlying reasons why the use of unsupervised FRFS helps more significantly overall, in simplifying the complexity of the leant ensembles.

Finally, it is worth noting that, instead of fully relying on FRFS and HS methods, the proposed approach can be generalised to work with other feature selection techniques and heuristic search strategies, making it a generic CES framework for future extensions. Fuzzy-rough CES can also be used in conjunction with other CES methods, in particular those that maximise a certain diversity measure, in order to further reduce ensemble size, whilst preserving ensemble performance.

References

[1] D. Aha and D. Kibler, Instance-based learning algorithms, Machine Learning, vol. 6, no. 1, pp. 37–66, 1991.

[2] L. Breiman, Bagging predictors, Machine Learning, vol. 24, no. 2, pp. 123–140, 1996.

[3] C. Christoudias, R. Urtasun, and T. Darrell, Multi-view learning in the presence of view disagreement, Proceedings of UAI 2008, 2008.

[4] M. Dash and H. Liu, Feature Selection for Classification, Intelligent Data Analysis, vol. 1, no. 3, pp. 131–156, 1997

[5] R. Diao and Q. Shen, Two New Approaches to Feature Selection with Harmony Search, Proceedings of the 19th International Conference on Fuzzy Systems, pp. 3161–3167, 2010.

[6] R. Diao and Q. Shen, Deterministic Parameter Control in Harmony Search, Proceedings of the 2010 UK Workshop on Computational Intelligence, 2010.

[7] D. Dubois and H. Prade, Putting rough sets and fuzzy sets together, Intelligent Decision Support, Kluwer Academic Publishers, Dordrecht, 1992.

[8] Z.W. Geem, J.H. Kim and G.V. Loganathan, A New Heuristic Optimization Algorithm: Harmony Search, Simulation, vol. 76, no. 2, pp. 60–68, 2001.

[9] G. Giacinto, F. Roli, and G. Fumera, Design of effective multiple classifier systems by clustering of classifiers, 15th International Conference on Pattern Recognition, ICPR 2000, pp. 160–163, 2000.

[10] S. Haykin, Neural Networks: A Comprehensive Foundation, Second Edition, Prentice Hall, 1998.

[11] T.K. Ho, The random subspace method for constructing decision forests, IEEE Transactions on Pattern Analysis and Machine Intelligence, vol. 20, no. 8, pp. 832–844, 2002.

[12] R. Jensen and C. Cornelis, A New Approach to Fuzzy-Rough Nearest Neighbour Classification, Transactions on Rough Sets XIII, LNCS 6499, pp. 56-72, 2011.

[13] R. Jensen and Q. Shen, Computational Intelligence and Feature Selection: Rough and Fuzzy Approaches, IEEE Press and Wiley & Sons, 2008.

[14] R. Jensen and Q. Shen, New Approaches to Fuzzy-Rough Feature Selection, IEEE Transactions on Fuzzy Systems, vol. 17, no. 4, pp. 824–838, 2009.

[15] G.H. John and P. Langley, Estimating Continuous Distributions in Bayesian Classifiers, Proceedings of the Eleventh Conference on Uncertainty in Artificial Intelligence, pp. 338–345, 1995.

[16] J. Keller, M. Gray, and J. Givens, A fuzzy k-nearest neighbor algorithm, IEEE Transactions on Systems, Man, And Cybernetics, vol. 15, no. 2, pp. 580–588, 1985.

[17] N. Mac Parthalain and R. Jensen, Measures for unsupervised fuzzy-rough feature selection. International Journal of Hybrid Intelligent Systems, vol. 7, pp. 1C11, 2010.

[18] D.J. Newman, S. Hettich, C.L. Blake, and C.J. Merz, UCI Repository of machine learning databases http://www.ics.uci.edu/~mlearn/MLRepository.html. Irvine, CA: University of California, Department of Information and Computer Science, 1998.

[19] Z. Pawlak, Rough Sets: Theoretical Aspects of Reasoning About Data, Kluwer Academic Publishing, Dordrecht, 1991.

[20] Q. Shen and A. Chouchoulas, A rough-fuzzy approach for generating classification rules, Pattern Recognition, vol. 35, no. 2, pp. 2425–2438, 2002.

[21] G. Tsoumakas, I. Partalas, and I. Vlahavas, A Taxonomy and Short Review of Ensemble Selection, ECAI 2008, Workshop on Supervised and Unsupervised Ensemble Methods and Their Applications, 2008.

[22] A. Tsymbal, M. Pechenizky, and P. Cunningham, Diversity in search strategies for ensemble feature selection, Information Fusion, vol. 6, pp. 83–98, 2005.

[23] I.H. Witten and E. Frank, Data Mining: Practical Machine Learning Tools and Techniques, Morgan Kaufmann, San Francisco, 2005.

2011 IEEE International Conference on Fuzzy Systems
June 27-30, 2011, Taipei, Taiwan

Kernel-Based Fuzzy-Rough Nearest Neighbour Classification

Yanpeng Qu, Changjing Shang,
Qiang Shen, Neil Mac Parthaláin
Dept. of Computer Science
Aberystwyth University
Aberystwyth, Ceredigion, Wales. UK
Email: {yyq09, cns, qqs, ncm}@aber.ac.uk

Wei Wu
School of Mathematical Sciences
Dalian University ofTechnology
Dalian, 116024, China
Email: wuweiw@dlut.edu.cn

***Abstract*—Fuzzy-rough sets play an important role in dealing with imprecision and uncertainty for discrete and real-valued or noisy data. However, there are some problems associated with the approach from both theoretical and practical viewpoints. These problems have motivated the hybridisation of fuzzy-rough sets with kernel methods. Existing work which hybridises fuzzy-rough sets and kernel methods employs a constraint that enforces the transitivity of the fuzzy T-norm operation. In this paper, such a constraint is relaxed and a new kernel-based fuzzy-rough set approach is introduced. Based on this, novel kernel-based fuzzy-rough nearest-neighbour algorithms are proposed. The work is supported by experimental evaluation, which shows that the new kernel-based methods offer improvements over the existing fuzzy-rough nearest neighbour classifiers. The abstract goes here.**

***Keywords*—Fuzzy-rough sets; Fuzzy tolerance relation; Kernel theory; Nearest neighbour classification**

I. Introduction

Fuzzy-rough set theory [1] is a hybridisation of rough sets [2] and fuzzy sets [3], which is capable of dealing with imprecision and uncertainty in data. As a hybridisation of fuzzy set theory and rough sets, fuzzy-rough sets not only inherit the domain independence of rough sets, but also address the inability of rough sets in handling real-valued data. That is, fuzzy-rough sets provide a means to deal with discrete or real-valued noisy data (or a mixture of both) without the need for user-supplied thresholding or domain information. As such, this technique can be applied to regression as well as classification tasks. The only additional information required is in the form of fuzzy partitions for each feature which can be automatically derived from the data [4].

Kernel methods [5] have the ability to deal with non-linear models by mapping a given problem from the (low dimensional) input space onto a new (higher-dimensional) space via a non-linear transformation. The resulting structure of the classification task is then linearly separable. From another perspective, the kernel defines a similarity measure between two data objects and thus allows the utilisation of prior knowledge of the problem domain. More importantly, the kernel provides all of the information about the relative positions of the inputs in the feature space so that the associated learning algorithm is based only on the kernel function. Classification can be carried out without explicit use of the feature space.

The initial work on hybridising fuzzy-rough sets and kernel methods is presented in [6]. This work exploited the approach as described in [7], which explored the relationship between kernels and T-transitivity. In particular, kernel methods are integrated into fuzzy-rough sets (and more recently gaussian kernels [8]). In the work of [6], the concept of *kernelised fuzzy-rough sets* was proposed, in which kernel functions are employed to compute the fuzzy similarity relations between samples. One of the shortcomings of this approach however, is the fact that the fuzzy relations are limited only to T_{cos} equivalence relations [7] in an attempt to guarantee T-transitivity. However, as argued in [9], T-transitivity does not necessarily need to be enforced for fuzzy-rough sets [10], as the use of fuzzy tolerance relations [11] may be sufficient [12].

In this paper, an improved approach to using kernel methods with fuzzy-rough sets is presented. The reason why the proposed method is termed *kernel-based fuzzy-rough sets* rather than *kernelised fuzzy-rough sets*, is that in such a combination, kernels are employed as a special means to construct fuzzy tolerance relations. The framework of fuzzy-rough sets is preserved, whilst a statistical perspective is used in order to investigate the properties of kernels which may be suitable for integration into fuzzy-rough sets. To demonstrate the utility of the new kernel-based fuzzy-rough sets approach, a new form of nearest-neighbour classifier is proposed. This type of classifier also employs a vaguely-quantified rough set measure [13], which is robust in the presence of noisy data.

The remainder of this paper is structured as follows. The theoretical background is presented in Section 2 with a short review of existing methods. The proposed kernel-based fuzzy-rough set approach and the associated nearest neighbour algorithms are described in Section 3. The new kernel-based classifier is compared to others, with experimental results shown in Section 4. Finally, section 5 concludes the paper with a short discussion of future work.

II. Theoretical Background

A. Hybridisation of Rough Sets and Fuzzy Sets

The work on rough set theory (RST)[2] provides a methodology that can be employed to extract knowledge from a

978-1-4244-7316-8/11/$26.00 ©2011 IEEE

domain in a concise way: It is able to minimise information loss whilst reducing the amount of knowledge involved. Central to rough set theory is the concept of indiscernibility. Let $I = (\mathbb{U}, \mathbb{A})$ be an information system, where $\mathbb{U}$ is a non-empty set of finite objects (the universe) and $\mathbb{A}$ is a non-empty finite set of attributes so that $a : \mathbb{U} \longrightarrow V_a$ for every $a \in \mathbb{A}$. V_a is the set of values that attribute a may take. For any $P \subseteq \mathbb{A}$, there exists an associated equivalence relation $IND(P)$:

$$IND(P) = \{(x, y) \in \mathbb{U}^2 \mid \forall a \in P, a(x) = a(y)\}. \quad (1)$$

The partition generated by $IND(p)$ is denoted $\mathbb{U}/IND(P)$ or abbreviated to $\mathbb{U}/P$ and is calculated as follows:

$$\mathbb{U}/IND(P) = \otimes\{a \in P : \mathbb{U}/IND(\{a\})\} \quad (2)$$

where,

$$\mathbb{U}/IND(\{a\}) = \{\{x \mid a(x) = b,\ x \in \mathbb{U}\} \mid b \in V_a\} \quad (3)$$

and,

$$A \otimes B = \{X \cap Y \mid \forall X \in A, \forall Y \in B, X \cap Y \neq \emptyset\}. \quad (4)$$

If $(x, y) \in IND(P)$, then x and y are indiscernible by attributes from P. The equivalence classes of the P-indiscernibility relation are denoted $[x]_P$. Let $X \subseteq \mathbb{U}$. X can be approximated using only the information contained in P by constructing the P-*lower* and P-*upper* approximations of X:

$$\underline{P}X = \{x \mid [x]_P \subseteq X\} \quad (5)$$

$$\overline{P}X = \{x \mid [x]_P \cap X \neq \emptyset\}. \quad (6)$$

The tuple $\langle \underline{P}X, \overline{P}X \rangle$ is called a rough set.

The process described above although useful can only operate effectively on datasets containing discrete values. As most datasets contain real-valued attributes, a subjective judgement or threshold must therefore be employed in order for RST to operate on such data. The imposition of such a subjective threshold is however, contrary to the concept of domain independence of RST. An appropriate way of handling the problem of real-valued data is the use of fuzzy-rough sets (FRS) [1]. FRS offers a high degree of flexibility in enabling the vagueness and imprecision present in real-valued data to be modelled effectively.

Definitions for the fuzzy lower and upper approximations can be found in [10], [14], where a T-transitive fuzzy similarity relation is used to approximate a fuzzy concept X:

$$\mu_{\underline{R_P}X}(x) = \inf_{y \in \mathbb{U}} I(\mu_{R_P}(x, y), \mu_X(y)) \quad (7)$$

$$\mu_{\overline{R_P}X}(x) = \sup_{y \in \mathbb{U}} T(\mu_{R_P}(x, y), \mu_X(y)). \quad (8)$$

Here, I is a fuzzy implicator and T is a T-norm. R_P is the fuzzy similarity relation induced by the subset of features P:

$$\mu_{R_P}(x, y) = T_{a \in P}\{\mu_{R_a}(x, y)\}. \quad (9)$$

$\mu_{R_a}(x, y)$ is the degree to which objects x and y are similar for feature a, and may be defined in many ways, for example:

$$\mu_{R_a}(x, y) = 1 - \frac{|a(x) - a(y)|}{|a_{max} - a_{min}|} \quad (10)$$

$$\mu_{R_a}(x, y) = \max\left(\min\left(\frac{(a(y) - (a(x) - \sigma_a))}{(a(x) - (a(x) - \sigma_a))}, \frac{((a(x) + \sigma_a) - a(y))}{((a(x) + \sigma_a) - a(x))}\right), 0\right) \quad (11)$$

where ${\sigma_a}^2$ is the variance of feature a. As these relations do not necessarily display T-transitivity, fuzzy transitive closure must be computed for each feature [9]. In other words, T-transitivity is not required for fuzzy-rough sets. Instead, fuzzy tolerance relations [11] can be employed to construct fuzzy-rough sets [12]. This technique is adopted in this paper also.

Note that formulas (7) and (8) are quite sensitive to noisy values, just like their crisp counterparts. Thus, the concept of vaguely-quantified rough set (VQRS) has been introduced in [13]. Following this approach, given a pair of fuzzy quantifiers (Q_u, Q_l), which are an increasing $[0, 1] \to [0, 1]$ mapping, the lower and upper approximation of X by R are defined by

$$\mu_{\underline{R_P}X}^{Q_u}(x) = Q_u\left(\frac{|R_P(x, y) \cap X|}{|R_P(x, y)|}\right) = Q_u\left(\frac{\sum_{y \in \mathbb{U}} \min(\mu_{R_P}(x, y), \mu_X(y))}{\sum_{y \in \mathbb{U}} \mu_{R_P}(x, y)}\right) \quad (12)$$

$$\mu_{\overline{R_P}X}^{Q_l}(x) = Q_l\left(\frac{|R_P(x, y) \cap X|}{|R_P(x, y)|}\right) = Q_l\left(\frac{\sum_{y \in \mathbb{U}} \min(\mu_{R_P}(x, y), \mu_X(y))}{\sum_{y \in \mathbb{U}} \mu_{R_P}(x, y)}\right), \quad (13)$$

The fuzzy set intersection is defined by the T-norm *min* and the fuzzy set cardinality by the sigma-count operation. As an important difference to (7) and (8), the VQRS approximations do not extend the classical rough set approximations, in a sense that when X and R are crisp, (12) and (13) may still be fuzzy.

B. Fuzzy-rough Nearest Neighbour Algorithm

A number of techniques have been developed for building fuzzy-rough nearest neighbour (FRNN) classifiers [15], [16]. Based upon such techniques, an approach which utilises the fuzzy upper and lower approximations to determine class membership is proposed in [17].

FRNN works by examining each of the decision classes in the training data in-turn. It computes the membership of a test object to the fuzzy lower and upper approximations of each class. These values are then compared with the highest existing values: $\mu_1(y)$ and $\mu_2(y)$. If the approximation membership

values for the currently considered class are higher, then both $\mu_1(y)$ and $\mu_2(y)$ are assigned these values and the class label is assigned to this test object. If not, the algorithm continues to iterate through all remaining decision classes. Classification accuracy is calculated by comparing the output with the actual class labels of the test objects.

An extension of FRNN is vaguely quantified rough nearest neighbour (FRNN-VQRS) [13] which employs (12) and (13), to determine class membership of test objects. The underlying learning mechanism is very similar to that of FRNN.

C. Classes of Kernels in Statistics

In a kernel algorithm, a mapping ϕ from the original space to a possibly high-dimensional space is employed to change the distribution of the data from nonlinear problem to linearly separable problem. By replacing the inner product with an appropriate kernel function, one can implicitly perform a nonlinear mapping to a high dimensional feature space without increasing the number of parameters. Consider the case of mapping an n-dimensional feature space to an m-dimensional feature space:

$$\phi : \mathbf{x} \to \phi(\mathbf{x}), \quad \mathbf{x} \in \mathbb{R}^n,\ \phi(\mathbf{x}) \in \mathbb{R}^m \tag{14}$$

A kernel denotes a function K such that for all $\mathbf{x}, \mathbf{y} \in \mathbb{R}^n$:

$$K(\mathbf{x}, \mathbf{y}) = \phi(\mathbf{x}) \cdot \phi(\mathbf{y}). \tag{15}$$

In statistics, symmetric positive definite functions are called covariances. Hence, kernels are covariance-based in essence. From a statistics perspective, generally, two important classes of kernels are: stationary kernels and non-stationary kernels [18]. The work in this paper focuses on stationary kernels.

Stationary kernels $K(\mathbf{x}, \mathbf{y}) = K_S(\mathbf{x} - \mathbf{y})$ do not depend on the data object values themselves, but only on the lag vector separating the two objects $\mathbf{x}$ and $\mathbf{y}$. Isotropic stationary kernels, which depend only on the norm of the lag vector, are most commonly used. For isotropic stationary kernels, the covariance form is:

$$K_{cov}(\mathbf{x}, \mathbf{y}) = K_I(\|\mathbf{x} - \mathbf{y}\|), \tag{16}$$

and the correlation form is

$$K_{cor}(\mathbf{x}, \mathbf{y}) = K_I(\|\mathbf{x} - \mathbf{y}\|)/K_I(0). \tag{17}$$

A *non-stationary* kernel $K(\mathbf{x}, \mathbf{y})$ is one which depends explicitly on the two data objects $\mathbf{x}$ and $\mathbf{y}$. Note that a special kind of non-stationary kernel, called a *reducible kernel*, can be reduced to a stationary kernel.

III. Kernel-based Fuzzy-rough Nearest Neighbour Classification

A. Kernel-based Fuzzy-rough Sets

The relationship between T-transitivity and kernels has been explored [7]. It has been shown that any kernel $K : X \times X \to [0, 1]$, $K(x, x) = 1\ \forall x \in X$, is T_{cos}-transitive, where $T_{cos}(a, b) = max(ab - \sqrt{1 - a^2}\sqrt{1 - b^2}, 0)$. As an initial attempt, kernelised fuzzy-rough sets, which combine kernel methods with concepts from fuzzy-rough set theory, have been presented in [6], [8]. In this approach, kernels $K(x, y)$ are constrained such that they impose: a) reflexivity, b) symmetry, and c) T_{cos}-transitivity. Such kernels are employed to calculate the degree to which objects x and y are similar for every feature. The fuzzy lower and upper approximations in kernelised fuzzy-rough sets are defined by:

$$\mu_{\underline{K_P}X}(x) = \inf_{y \in \mathbb{U}} I_{cos}(K_P(x, y), \mu_X(y)) \tag{18}$$

$$\mu_{\overline{K_P}X}(x) = \sup_{y \in \mathbb{U}} T_{cos}(K_P(x, y), \mu_X(y)), \tag{19}$$

where, the implicator

$$I_{cos} = \begin{cases} 1, & a \le b \\ ab + \sqrt{(1 - a^2)(1 - b^2)}, & a > b \end{cases}.$$

However, as shown previously, in fuzzy-rough sets, T-transitivity is not necessarily displayed, and fuzzy tolerance relations may be sufficient [12]. Moreover, as (9), the fuzzy similarity relation induced by the subset of features P should be a combination by T-norm. Specifically, for kernelised fuzzy-rough sets, it is:

$$K_P(x, y) = T_{a \in P}\{\mu_{R_a}(x, y)\}. \tag{20}$$

In this case, the choice of a kernel function becomes limited. This is due to the fact that not many kernel functions can be denoted by a T-norm-based combination of reflexive functions. For instance, the Gaussian kernel employed in [8] and [6] is workable, because for: $\mathbf{x} = (x_1, x_2, \ldots, x_n) \in \mathbb{R}^n$, $\mathbf{y} = (y_1, y_2, \ldots, y_n) \in \mathbb{R}^n$

$$\exp\left(-\frac{\|\mathbf{x} - \mathbf{y}\|^2}{\theta}\right) = \prod_{i=1}^{n} \exp\left(-\frac{(x_i - y_i)^2}{\theta}\right) \tag{21}$$

and because its product is still a T-norm. However, for most kernels, such as the rational quadratic kernel and the wave kernel (see below), this property may not hold. In order to address these problems, kernel-based fuzzy-rough sets are proposed in this paper.

In geometry, the inner product of two vectors is the projection of one onto another. Actually, the square of the norm distance in Hilbert space can be expressed by the inner product. In this case, the inner product can measure the similarity between the images of two features by mapping into a Hilbert space. Therefore, given a non-empty set $\mathbb{U}$ and a kernel function K being reflexive, (that is $K(x, x) = 1$), for an arbitrary fuzzy concept X, the lower and upper approximations of a kernel-based fuzzy-rough set can be defined as:

$$\mu_{\underline{R_P^K}X}(x) = \inf_{y \in \mathbb{U}} I(\mu_{K_P}(x, y), \mu_X(y)) \tag{22}$$

$$\mu_{\overline{R_P^K}X}(x) = \sup_{y \in \mathbb{U}} T(\mu_{K_P}(x, y), \mu_X(y)). \tag{23}$$

It is important to note that the framework of fuzzy-rough sets remains intact using the definition described in this paper. In other words, the kernel methods play a special role in calculating the fuzzy tolerance relations. It is because of this

fact that the term *kernel-based fuzzy-rough sets* (KFRS) is employed here rather than *kernelised fuzzy-rough sets*.

As well as fuzzy-rough sets, the corresponding the lower and upper approximations of the kernel-based vaguely quantified rough set (KVQRS) can be also be defined:

$$\mu_{\underline{R_P^K}X}^{Q_u}(x) = Q_u\left(\frac{|R_P^K(x,y)\cap X|}{|R_P^K(x,y)|}\right) = Q_u\left(\frac{\sum\limits_{y\in\mathbb{U}}\min(\mu_{K_P}(x,y),\mu_X(y))}{\sum\limits_{y\in\mathbb{U}}\mu_{K_P}(x,y)}\right) \quad (24)$$

$$\mu_{\overline{R_P^K}X}^{Q_l}(x) = Q_l\left(\frac{|R_P^K(x,y)\cap X|}{|R_P^K(x,y)|}\right) = Q_l\left(\frac{\sum\limits_{y\in\mathbb{U}}\min(\mu_{K_P}(x,y),\mu_X(y))}{\sum\limits_{y\in\mathbb{U}}\mu_{K_P}(x,y)}\right), \quad (25)$$

where, $\mu_{K_P}(x,y)$ is induced by the subset of features P and kernel function K:

$$\mu_{K_P}(x,y) = T_{a\in P}\{\phi(a(x))\cdot\phi(a(y))\} = T_{a\in P}\{K(a(x),a(y))\} = T_{a\in P}\{K_a(x,y)\}. \quad (26)$$

As established previously, all isotropic stationary kernels in correlation form (17) are suitable for being integrated into KFRS. A collection of certain commonly used isotropic stationary kernels in correlation form are listed as follows:

- Gaussian kernel: $K(\mathbf{x},\mathbf{y}) = \exp\left(-\frac{\|\mathbf{x}-\mathbf{y}\|^2}{\theta}\right)$
- Exponential kernel: $K(\mathbf{x},\mathbf{y}) = \exp\left(-\frac{\|\mathbf{x}-\mathbf{y}\|}{\theta}\right)$
- Rational quadratic kernel: $K(\mathbf{x},\mathbf{y}) = 1 - \frac{\|\mathbf{x}-\mathbf{y}\|^2}{\|\mathbf{x}-\mathbf{y}\|^2+\theta}$
- Wave kernel: $K(\mathbf{x},\mathbf{y}) = \frac{\theta}{\|\mathbf{x}-\mathbf{y}\|}\sin(\frac{\|\mathbf{x}-\mathbf{y}\|}{\theta})$.

It is worth noting that for specific non-stationary kernels, the reflexivity holds also. For instance, the non-stationary kernel [18],

$$K(\mathbf{x},\mathbf{y}) = \frac{\|\mathbf{x}\| + \|\mathbf{y}\| - \|\mathbf{x}-\mathbf{y}\|}{2\sqrt{\|\mathbf{x}\|\|\mathbf{y}\|}}, \quad (27)$$

is reflexive. This kernel is also reducible.

B. Kernel-based Fuzzy-rough Nearest Neighbour Classification

The present work initially aims to investigate the combination of kernel methods with conventional fuzzy-rough nearest neighbour approaches (FRNN and FRNN-VQRS) [17]. The resulting combined learning algorithm is outlined in Figure 1. As with FRNN, the rationale behind this algorithm is that the the lower and the upper approximations of each decision class (calculated by means of the nearest neighbours of a test object y) will provide helpful clues to predict the membership of a test object to any given class. The complexity of this algorithm is: $O(|\mathcal{C}|\cdot 2|\mathbb{U}|)$.

KFRNN($\mathbb{U}$,$\mathcal{C}$,y)
$\mathbb{U}$, the training set; $\mathcal{C}$, the set of decision classes;
y, the object to be classified.

(1) $N \leftarrow$ get Nearest Neighbour(y,k)
(2) $\mu_1(y) \leftarrow 0, \mu_2(y) \leftarrow 0, Class \leftarrow \emptyset$
(3) $\forall X \in \mathcal{C}$
(4) **if**$(\mu_{\underline{R_P^K}X}(y) \geq \mu_1(y) \&\& \mu_{\overline{R_P^K}X}(y) \geq \mu_2(y))$
(5) $\overline{Class} \leftarrow X$
(6) $\mu_1(y) \leftarrow \mu_{\underline{R_P^K}X}(y), \mu_2(y) \leftarrow \mu_{\overline{R_P^K}X}(y)$
(7) **output** $Class$

Fig. 1. The kernel-based fuzzy-rough nearest neighbour algorithm

The algorithm in Figure 1 can be further adapted to perform kernel-based vaguely quantified rough nearest neighbour (KFRNN-VQRS) classification, by replacing: $\mu_{\underline{R_P^K}X}(y)$ and $\mu_{\overline{R_P^K}X}(y)$ with $\mu_{\underline{R_P^K}X}^{Q_u}(y)$ and $\mu_{\overline{R_P^K}X}^{Q_l}(y)$, respectively.

In statistics, the stationary property is often mathematically assumed to describe the ability of ensuring that a random process maintains the same probabilistic characteristics such as mean, variance and autocorrelation. Typically, non-stationary and bifurcated regimes are always observed in the case of datasets with class imbalance [19]. Class imbalance occurs when one or more classes are over or under represented as a total number of objects of the whole dataset. Thus, for datasets which suffer from class imbalance, the distribution of and the similarity between the objects may be non-stationary. From this point of view, if a dataset is extremely imbalanced, the use of non-stationary kernels would be more appropriate. Further investigation would help to confirm this - see conclusion section for further discussion.

IV. Experimental Results

This section presents an experimental evaluation of the proposed algorithms (KFRNN-FRS and KFRNN-VQRS) using two different kernels: 1) an isotropic stationary kernel, and 2) a non-stationary kernel. Nine benchmark datasets obtained from[20] are employed. These datasets are small-to-medium in size, containing between 178 and 683 objects with feature numbers ranging from 6 to 279.

TABLE I
Evaluation Datasets

Dataset	Objects	Attributes
Arrhythmia	452	279
Glass	214	9
Heart	270	13
Liver	345	6
Sonar	208	60
Water 2	390	38
Water 3	390	38
Wine	178	14
Wisconsin	683	9

For the evaluation described here, k is set at an initial value of 10 for FRNN-VQRS and KFRNN-VQRS. For FRNN

the relation given in equation (10) is used. For the kernel-based methods, an exponential kernel (used as the isotropic stationary kernel), and the non-stationary kernel of (27) are employed. In the FRNN and KFRNN approaches, the Kleene-Dienes T-norm is used to implement the implicator, which is defined by $I(x,y) = \max(1-x,y)$. The FRNN-VQRS and KFRNN-VQRS approaches are implemented with $Q_l = Q_{(0.1,0.6)}$ and $Q_u = Q_{(0.2,1.0)}$, according to the general formula

$$Q_{(\alpha,\beta)}(x) = \begin{cases} 0, & x \leq \alpha \\ \frac{2(x-\alpha)^2}{(\beta-\alpha)^2}, & \alpha \leq x \leq \frac{\alpha+\beta}{2} \\ 1 - \frac{2(x-\beta)^2}{(\beta-\alpha)^2}, & \frac{\alpha+\beta}{2} \leq x \leq \beta \\ 1, & \beta \leq x \end{cases} . \quad (28)$$

Stratified 10 $\times$ 10-fold cross-validation (10-FCV) is employed for result validation. In 10-FCV, the original dataset is partitioned into 10 subsets. Of these 10 subsets, a single subset is retained as the testing data for the model, and the remaining 9 subsets are used for training. The cross-validation process is then repeated 10 times (the number of folds). The 10 sets of results are then aggregated via averaging to produce a single model estimation. The advantage of 10-FCV over random sub-sampling is that all objects are used for both training and testing, and each object is used for testing only once per fold. The stratification of the data prior to its division into folds ensures that each class label (as far as possible) has equal representation in all folds, thus helping to alleviate bias/variance problems. In order to investigate the level of 'fit' of these models, the root mean squared error (RMSE) measure is used. The RMSE is the squared root of the variance of the residuals. It indicates the absolute fit of a model to the data and how close the observed data objects are to the model predicted values. Note that, RMSE is an absolute measure. As the squared root of a variance, RMSE can be viewed as the standard deviation of the unexplained variance. Lower values of RMSE indicate better fit. RMSE is a good measure of how accurately the model predicts the response, and is a generally accepted criterion for assessing fit, if the purpose of the resulting model is for prediction. In addition, conventional classification accuracy is also used to assess the performance of learnt classifiers.

A. Performance Evaluation

A comparison of the kernel-based and FRFS-based nearest-neighbour techniques is shown in Tables II and III, where sKFRNN and nonsKFRNN stand for stationary kernel-based fuzzy-rough nearest neighbour and non-stationary kernel-based fuzzy-rough nearest neighbour methods, respectively. Correspondingly, stationary kernel-based vaguely quantified rough nearest neighbour and non-stationary kernel-based vaguely quantified rough nearest neighbour approaches are denoted by sKFRNN-VQRS and nonsKFRNN-VQRS, respectively.

Note that the *Water2* and *Water3* datasets, both suffer from class imbalance. In particular, the ratios of data between different classes are: 312 objects to 78 objects for classes 1 and 2 for *water2*, and 378 objects for class 1 and 12 objects for class 2 for *water3*. It can be seen from the experimental results that the non-stationary kernel based approaches, nonsKFRNN and nonsKFRNN-VQRS, consistently achieved the highest classification accuracy and smallest RMSE over all other methods for these datasets. However, for the rest datasets which are not highly imbalanced, the differences between the performance of two new approaches and existing techniques are not that significant. In fact, for *Liver* and *Glass*, both of sKFRNN and sKFRNN-VQRS reached the highest classification accuracy and smallest RMSE values. For *Heart*, *Sonar*, *Wine* and *Wisconsin*, the competitiveness of the kernel-based fuzzy-rough nearest neighbour classifiers are obvious. Putting these results together, it is clear that the present work helps to improve the quality of fuzzy-rough nearest neighbour classifiers.

B. Statistical Analysis

To further evaluate the kernel-based fuzzy-rough techniques, a paired t-test with significance level of 0.05 has been carried out. The baseline references for the tests are the results obtainable from FRNN and FRNN-VQRS classification, respectively. This is done in order to ensure that the aforementioned results are not discovered by chance. The statistical significance results are shown in Table IV and V, where the symbols 'v', '*' and '-' indicate that the results are statistically better, worse, or have no statical significance.

The results once again demonstrate that the kernel-based approaches achieve best performances overall for *Water2*, *Water3*, *Heart* and *Arrythmia*, etc. In particular, compared to FRNN, the non-stationary kernel-based methods are shown to be statistically better than the other methods for these datasets. Note however that no statistical differences are found amongst all tested algorithms for the *Glass*, *Liver*, *Wine* and *Wisconsin* datasets. Only a single dataset (*sonar*), do the proposed techniques occasionally return a result which is statistically worse than that attainable using FRNN. This may well be due to the use of the fuzzy quantifiers in FRNN-VQRS, though further experimental evaluation is required in order to verify this. For FRNN-VQRS, the kernel-based modification leads to a statistically similar performance generally. sKFRNN and nonsKFRNN are better than FRNN-VQRS statistically for the *Glass* and *Sonar* datasets, although worse for the *Arrythmia* and *Heart* datasets. This may possibly be caused by the existence of noisy data in *Arrythmia* and *Heart*.

V. Conclusion

This paper has presented a new technique for the hybridisation of fuzzy-rough sets and kernel methods, called kernel-based fuzzy-rough sets (KFRS). In contrast to previous work, the T_{cos}-transitivity constraint is relaxed. The only remaining constraint which the proposed approach imposes is reflexivity.

Whilst attempting to identify suitable kernels, the properties are analysed from statistics perspective. It has been demonstrated that all isotropic stationary kernels in the correlation form of (17) are suitable for use with the KFRS

TABLE II
COMPARISON BETWEEN FRNN, SKFRNN, NONSKFRNN

Dataset	FRNN		sKFRNN		nonsKFRNN	
	Accy.	RMSE	Accy.	RMSE	Accy.	RMSE
Arrhythmia	54.67	0.21	52.33	0.22	55.43	0.21
Glass	73.54	0.29	76.24	0.28	73.21	0.29
Heart	76.63	0.43	76.59	0.42	73.00	0.43
Liver	62.81	0.50	63.70	0.49	61.06	0.49
Sonar	85.25	0.43	84.69	0.43	85.95	0.43
Water 2	75.41	0.46	73.95	0.46	83.00	0.39
Water 3	67.87	0.40	65.79	0.39	75.77	0.34
Wine	97.47	0.20	98.15	0.21	96.12	0.21
Wisconsin	96.38	0.19	96.65	0.20	96.65	0.20

TABLE III
COMPARISON BETWEEN FRNN-VQRS, SKFRNN-VQRS, NONSKFRNN-VQRS

Dataset	FRNN-VQRS		sKFRNN-VQRS		nonsKFRNN-VQRS	
	Accy.	RMSE	Accy.	RMSE	Accy.	RMSE
Arrhythmia	60.40	0.21	59.42	0.21	62.13	0.20
Glass	68.95	0.27	74.08	0.26	66.57	0.29
Heart	82.19	0.35	82.41	0.35	75.81	0.43
Liver	66.26	0.48	67.19	0.48	67.72	0.48
Sonar	79.38	0.37	80.83	0.36	75.98	0.41
Water 2	79.59	0.39	80.49	0.40	84.92	0.33
Water 3	73.18	0.37	72.67	0.38	80.26	0.31
Wine	97.14	0.10	96.97	0.12	94.22	0.15
Wisconsin	96.69	0.16	96.16	0.17	96.81	0.15

TABLE IV
STATISTICAL SIGNIFICANCE USING PAIRED T-TEST FOR FRNN

Dataset	FRNN	sKFRNN	nonsKFRNN	sKFRNN-VQRS	nonsKFRNN-VQRS
Arrythmia	-	-	-	v	v
Glass	-	-	-	-	-
Heart	-	-	-	v	-
Liver	-	-	-	-	-
Sonar	-	-	-	-	*
Water2	-	-	v	v	v
Water3	-	-	v	-	v
Wine	-	-	-	-	-
Wisconsin	-	-	-	-	-

TABLE V
STATISTICAL SIGNIFICANCE USING PAIRED T-TEST FOR FRNN-VQRS

Dataset	FRNN-VQRS	sKFRNN	nonsKFRNN	sKFRNN-VQRS	nonsKFRNN-VQRS
Arrythmia	-	*	*	-	-
Glass	-	v	-	-	-
Heart	-	*	-	-	-
Liver	-	-	-	-	-
Sonar	-	-	v	-	-
Water2	-	-	-	-	-
Water3	-	-	-	-	-
Wine	-	-	-	-	-
Wisconsin	-	-	-	-	-

approach. Two kernel-based fuzzy-rough set classifiers: kernel-based fuzzy-rough nearest neighbour (KFRNN) and kernel-based vaguely quantified rough nearest neighbour (KFRNN-VQRS) have been introduced. The experimental results over 9 datasets, show that the new methods are effective, and that they generally outperform the original techniques.

Topics for further investigation include the impact of the choice of kernel, connectives and quantifiers on performance. Also, (and as mentioned previously), the relationship between the class imbalance of datasets and the statistical property of kernels is a worthwhile avenue of exploration. Considering hierarchical classification, another further extension to this

work would be to examine how KFRS performs for the task of feature selection [4].

REFERENCES

[1] D. Dubois and H. Prade, "Putting rough sets and fuzzy sets together," *Intelligent Decision Support*, pp. 203–232, 1992.

[2] Z. Pawlak, *Rough Sets: Theoretical Aspects of Reasoning About Data*. Kluwer Academic Publishing, 1991.

[3] L. Zadeh, "Fuzzy sets," *Information and Control*, vol. 8, pp. 338–353, 1965.

[4] R. Jensen and Q. Shen, *Computational Intelligence and Feature Selection: Rough and Fuzzy Approaches*. IEEE Press and Wiley & Sons, 2008.

[5] J. Shawe-Taylor and N. Christianini, *Kernel method for pattern analysis*. Cambridge: Cambridg University Press, 2004.

[6] Q. Hu, D. Chen, D. Yu, and W. Pedrycz, "Kernelised fuzzy rough sets," in *4th International Conference, Rough Sets and Knowledge Technology*, 2009, pp. 304–311.

[7] B. Moser, "On the T-transitivity of kernels," *Fuzzy Sets and Systems*, vol. 157, pp. 1787–1796, 2006.

[8] Q. Hu, L. Zhang, D. Chen, W. Pedrycz, and D. Yu, "Gaussian kernel based fuzzy rough sets: Model, uncertainty measures and applications," *International Journal of Approximate Reasoning*, vol. 51, no. 4, pp. 453–471, 2010.

[9] M. D. Cock, C. Cornelis, and E. Kerre, "Fuzzy rough sets: The forgotten step," *IEEE Transactions on Fuzzy Systems*, vol. 15, no. 1, pp. 121–130, 2007.

[10] A. Radzikowska and E. Kerre, "A comparative study of fuzzy rough sets," *Fuzzy Sets and Systems*, vol. 126, no. 2, pp. 137–155, 2002.

[11] M. Das, M. Chakraborty, and T. Ghoshal, "Fuzzy tolerance relation, fuzzy tolerance space and basis," *Fuzzy Sets and Systems*, vol. 97, pp. 361–369, 1998.

[12] R. Jensen and C. Cornelis, "Fuzzy-rough instance selection," in *Proceedings of the 19th International Conference on Fuzzy Systems*, 2010, pp. 1776–1782.

[13] C. Cornelis, M. D. Cock, and A. Radzikowska, "Vaguely quantified rough sets," *Lecture Notes in Artificial Intelligence*, vol. 4482, pp. 87–94, 2007.

[14] R. Jensen and Q. Shen, "New approaches to fuzzy-rough feature selection," *IEEE Transactions on Fuzzy Systems*, vol. 17, no. 4, pp. 824–838, 2009.

[15] H. Bian and L. Mazlack, "Fuzzy-rough nearest-neighbor classification approach," in *Proceeding of the 22nd International Conference of the North American Fuzzy Information Processing Society*, 2003, pp. 500–505.

[16] M. Sarkar, "Fuzzy-rough nearest neighbors algorithm," *Fuzzy Sets and Systems*, vol. 158, pp. 2123–2152, 2007.

[17] R. Jensen and C. Cornelis, "A new approach to fuzzy-rough nearest neighbour classification," in *Proceedings of the 6th International Conference on Rough Sets and Current Trends in Computing*, 2008, pp. 310–319.

[18] M. Genton, "Classes of kernels for machine learning: a statistics perspective," *Journal of Machine Learning Research*, vol. 2, pp. 299–312, 2001.

[19] C. Drioli and F. Avanzini, "Non-modal voice synthesis by low-dimensional physical models," in *Proceeding of the 3rd International Workshop on Models and Analysis of Vocal Emissions for Biomedical Applications*, 2003.

[20] C. Blake and C. Merz, "UCI repository of machine learning databases," 1998, university of California, Irvine, School of Information and Computer Sciences.

2011 IEEE International Conference on Fuzzy Systems
June 27-30, 2011, Taipei, Taiwan

FAPOP: Feature Analysis Enhanced Pseudo Outer-Product Fuzzy Rule Identification System

Sau Wai Tung and Chai Quek
Centre for Computational Intelligence
School of Computer Engineering
Nanyang Technological University
Singapore 639798
Email: swtung@pmail.ntu.edu.sg; ashcquek@ntu.edu.sg

Cuntai Guan
Institute for Infocomm Research
Agency for Science, Technology
and Research (A*Star)
Singapore 138632
Email: ctguan@i2r.a-star.edu.sg

***Abstract*—Most existing neural fuzzy systems either overlook the importance of feature analysis; or it is performed as a separate phase prior to the design stage of the systems. This paper proposes a novel neural fuzzy system, named *Feature Analysis Enhanced Pseudo Outer-Product Fuzzy Rule Identification System* (FAPOP), which integrates its design with feature analysis. The objective is two-folds; namely, (1) to improve the interpretability of the system by identifying features relevant to its computational structure; and (2) to improve the accuracy of the system by identifying features relevant to the application problem. The proposed FAPOP model is subsequently employed in a series of benchmark simulations to demonstrate its efficiency as a neural fuzzy modeling system, and excellent performances have been achieved.**

***Index Terms*—Feature analysis, Pseudo-outer product (POP), Categorical Learning Induced Partitioning (CLIP), Nakanishi dataset, Mackey-Glass prediction.**

I. Introduction

Existing neural fuzzy systems can be broadly classified into two classes; namely, linguistic fuzzy models [1] [2], which are focused on delivering a good level of interpretability to the structures of the models, and precise fuzzy models [3] [4], which are focused on achieving high accuracies in the modeling tasks. While Mamdani models [5] form the main focus in the former class; the latter class comprises mainly of the Takagi-Sugeno-Kang models [6] [7]. In general, having a good fuzzy rulebase interpretability and a high modeling accuracy are two contradictory requirements in the design of a neural fuzzy system [8].

With its success in data-mining applications, feature analysis techniques [9] are often performed either implicitly or explicitly as a *pre-processing* phase prior to the design stage of a neural fuzzy system. The main advantage is an improvement to the modeling accuracy through the removal of redundant/derrogative features and the identification of relevant features for the underlying application problem. Nevertheless, the decoupled stages do not consider the close relationship between feature analysis and system design [10], i.e., to identify features that are important for the application problem *and* are relevant to the output of the neural fuzzy system.

This paper presents the *Feature Analysis Enhanced Pseudo-Outer Product Fuzzy Rule Identification System* (FAPOP), a novel neural fuzzy system which integrates its design with feature analysis. An initial fuzzy rulebase is obtained via Quek and Zhou's pseudo-outer product (POP) rule identification algorithm [11]. Knowledge are then extracted simultaneously from the initial rulebase and a single-pass of the training data to incrementally update a relevance weight for each input feature. All input features are relevant by default; while irrelevant/redundant input features are marked by decreasing relevance weights. Since knowledge from both the initial rulebase and the training data are utilized to determine the relevance weights, this allows FAPOP to identify features that are important for both the system and the application. The objective is to provide a regulated balance between the two contradictory requirements; namely, (1) to improve the interpretability of the system by identifying features relevant to its computational structure; and (2) to improve the accuracy of the system by identifying features relevant to the application problem. Following that, irrelevant input features, together with contradictory and/or identical rules, are removed to maintain a compact structure in FAPOP.

The rest of the paper is organized as follows. The computational structure and the reasoning process of the FAPOP model are described in Section II. The proposed rule identification and feature selection methodologies are introduced in Section III. Section IV evaluates the learning and generalization abilities of FAPOP through a series of benchmark experimental simulations. Lastly, Section V concludes the paper.

II. FAPOP: Architecture and Reasoning Process

The proposed FAPOP model is a five layers neural fuzzy system as shown in Fig. 1. Layer 1 is the input variable nodes IV_i; layer 2 is the antecedent nodes A_{i,j_i}; layer 3 is the rule nodes R_k; layer 4 is the consequent nodes $C_{l_m,m}$; and layer 5 is the output variable nodes OV_m. In the FAPOP model, the input vector is denoted as $x = [x_1, \ldots, x_I]^T$ with corresponding desired output vector denoted as $d = [d_1, \ldots, d_M]^T$; while the computed output vector is denoted as $y = [y_1, \ldots, y_M]^T$. Each input variable node consists of J_i number of antecedent fuzzy labels; while each output variable node consists of L_m number of consequent fuzzy labels. Layer 3 of FAPOP represents the K fuzzy rules in the system such that each node encodes a

978-1-4244-7316-8/11/$26.00 ©2011 IEEE

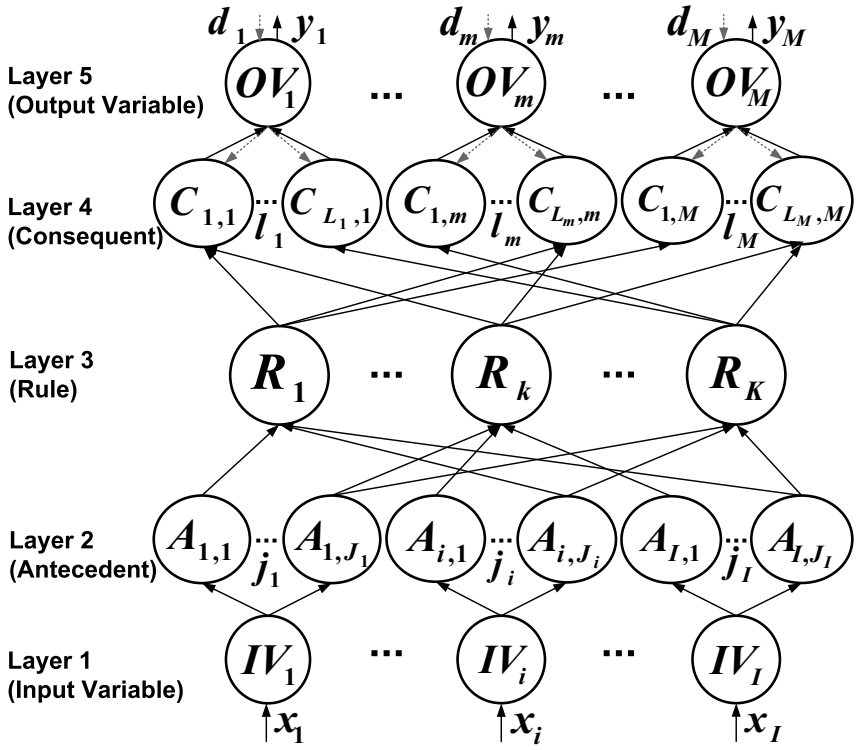

Fig. 1. Architecture of FAPOP.

fuzzy rule of the form given as in (1):

$$R_k : \text{IF } x_1 \text{ is } A^{(k)}_{1,j_1} \text{ and } \ldots \text{ and } x_I \text{ is } A^{(k)}_{I,j_I} \quad \text{THEN } y_1 \text{ is } C^{(k)}_{l_1,1} \text{ and } \ldots \text{ and } y_M \text{ is } C^{(k)}_{l_M,M} \tag{1}$$

where $A^{(k)}_{i,j_i}$ (resp. $C^{(k)}_{l_m,m}$) is the j_i-th antecedent (resp. l_m-th consequent) node associated with the i-th input (resp. m-th output) variable that is connected to the rule node R_k. The tunable parameters of FAPOP are the centres and widths of the fuzzy labels embedded in the antecedent and consequent nodes, where each node defines a gaussian membership function described as in (2):

$$\mu(c,\sigma;x) = e^{-((x-c)^2/\sigma^2)} \tag{2}$$

such that c and σ are the centre and width of the function respectively. Adaptation of the parameters is performed using backpropagation [12].

The reasoning process of FAPOP is represented by the forward solid arrows in Fig. 1 where the input vector x is presented to the system at layer 1. The proposed system then performs inference based on the input vector by propagating the information through layers 2 to 4. Consequently, the system produces a computed output vector y at layer 5. Each corresponding output for an arbitrary node is denoted as fo such that the reasoning process of FAPOP is discussed below:

Layer 1: The input node IV_i directly passes on the input value to the next layer such that its neural operation is described as in (3):

$$fo_i = x_i \ . \tag{3}$$

Layer 2: The antecedent node A_{i,j_i} performs similarity matching of the input value with the corresponding fuzzy label such that its neural operation can be described as in (4):

$$fo_{i,j_i} = \mu_{i,j_i}(c_{i,j_i}, \sigma_{i,j_i}; fo_i) \tag{4}$$

where $\mu_{i,j_i}(c_{i,j_i}, \sigma_{i,j_i}; x)$ refers to the gaussian membership function embedded in A_{i,j_i}.

Layer 3: Each rule node R_k computes the overall degree of similarity between the input vector and the antecedent part of the k-th fuzzy rule such that its firing rate is computed as in (5):

$$fo_k = \min_{i \in \{1 \ldots I\}} fo^{(k)}_{i,j_i} \ . \tag{5}$$

Layer 4: The consequent node $C_{l_m,m}$ performs consequent derivation for the fuzzy rules based on the information from the input vector. Since $C_{l_m,m}$ may serve as output to more than one fuzzy rule, its cumulative neural operation can be described as in (6):

$$fo_{l_m,m} = \max_{k \in \{1 \ldots K_{l_m,m}\}} fo^{(l_m,m)}_k \tag{6}$$

where $K_{l_m,m}$ is the total number of fuzzy rules in FAPOP that shares the same consequent node $C_{l_m,m}$ and $fo^{(l_m,m)}_k$ is the output of the k-th rule that shares $C_{l_m,m}$.

Layer 5: The output node OV_m performs defuzzification via the center of averaging method [13] to obtain a crisp output value such that its neural operation can be described as in (7):

$$y_m = fo_m = \frac{\sum_{l_m \in \{1 \ldots L_m\}} fo_{l_m,m} c_{l_m,m} \sigma_{l_m,m}}{\sum_{l_m \in \{1 \ldots L_m\}} fo_{l_m,m} \sigma_{l_m,m}} \tag{7}$$

where $c_{l_m,m}$ and $\sigma_{l_m,m}$ are the centre and width of the gaussian function embedded in $C_{l_m,m}$ respectively.

III. Learning Mechanisms of FAPOP

In the proposed FAPOP model, an initial fuzzy rulebase is obtained via Quek and Zhou's POP rule identification algorithm [11]. A relevance weight for each input feature is then incrementally determined using knowledge extracted from both the initial fuzzy system and a single-pass of the training data. The relevance weight of an input feature reflects its role in describing the underlying application problem and the output of the system. As stated before, all input features are assumed relevant at the beginning. Input features with consistently high relevance weights are selected; while input features with decreasing relevance weights are regarded as redundant and discarded. Subsequently, irrelevant input features, together with contradictory and/or identical rules, are removed to maintain a compact structure in the FAPOP model.

The learning mechanisms of FAPOP are discussed here as follows. Details of the neural computations in the proposed system are described in Section III.A.; Section III.B. reviews the POP algorithm; Section III.C. introduces the feature analysis technique in FAPOP; and Section III.D. illustrates the ideas discussed using a case study.

A. Neural Computations in FAPOP

Neural computations in the proposed FAPOP model are bi-directional, in the forward and backward sense as described below:

1. Forward Operation: The forward operation of FAPOP coincides with its reasoning path as described in Section II.
2. Backward Operation: The backward operation of FAPOP is represented by dotted arrows in Fig. 1, which is a mirrored computation of the forward operation. Each corresponding output for an arbitrary node is denoted as bo.

   Layer 5: The output node OV_m directly passes on the output value to the next layer such that its neural operation is described as in (8):

$$bo_m = d_m \ . \tag{8}$$

   Layer 4: The consequent node $C_{l_m,m}$ performs similarity matching of the output value with the corresponding fuzzy label such that its neural operation can be described as in (9):

$$bo_{l_m,m} = \mu_{l_m,m}(c_{l_m,m}, \sigma_{l_m,m}; bo_m) \tag{9}$$

   where $\mu_{l_m,m}(c_{l_m,m}, \sigma_{l_m,m}; x)$ refers to the gaussian membership function embedded in $C_{l_m,m}$.

B. POP algorithm

The POP algorithm consists of two phases in its learning process; namely, fuzzy partitioning and rule identification. In this paper, fuzzy partitioning is performed using the Categorical Learning Induced Partitioning (CLIP) [14]; while a description of the rule identification follows.

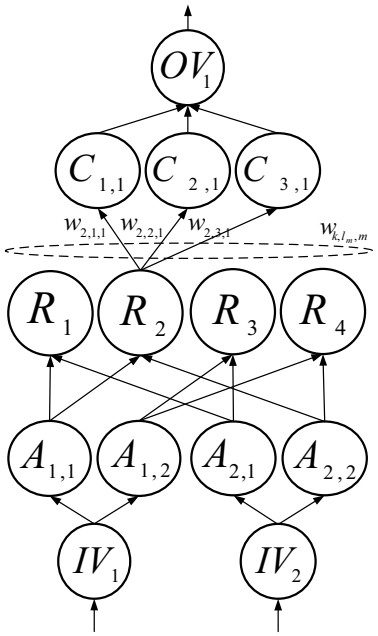

Fig. 2. Illustration for POP rule identification algorithm.

For simplicity, assume an application problem with 2 inputs-1 output as shown in Fig 2. Two fuzzy labels are determined by the CLIP algorithm for each input space; while three fuzzy labels are determined for the output space. The POP algorithm considers all possible rules, such that four fuzzy rules are initialized. The system is fully connected from the rule layer to the consequent layer with weights $w_{k,l_m,m}$, $k = 1 \ldots 4,\ l_m = 1 \ldots 3,\ m = 1$. Fig 2 illustrates the rule identification process for the rule node R_2:

1. Initialization: Set $w_{k,l_m,m} = 0$.
2. Weight Update: Through a single-pass of the training data, update the weights as follows:

$$w_{k,l_m,m} = \sum_N fo_k \cdot bo_{l_m,m}$$

   where N is the size of the training data.
3. Rule Formulation: Select the m-th consequent node for R_k as one with the maximum weight given as follows:

$$C^{(k)}_{l_m,m} = C_{l^\star_m,m}$$

   where $w_{k,l^\star_m,m} = \max_{l_m} w_{k,l_m,m}$.

C. Feature Analysis in FAPOP

The forward-and-backward neural computations (as described in Section III.A.) are defined to compute the instantaneous relevance weight of an input feature i when a data pair $[x, d]$ is presented to FAPOP. The instantaneous relevance weight $\widehat{\omega_i}$ is computed as in (10):

$$\widehat{\omega_i} = \max_{j_i} \left[\min_k \left(fo^{(k)}_{i,j_i}, bo^{(k)}_{l_m,m} \right) \right] \tag{10}$$

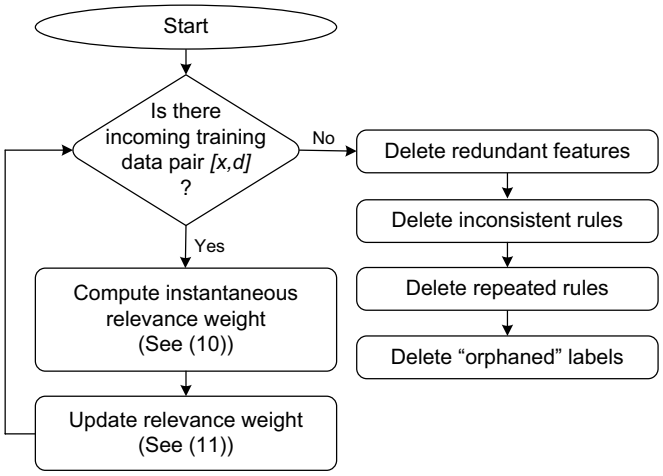

Fig. 3. Flowchart of the feature analysis process employed in FAPOP.

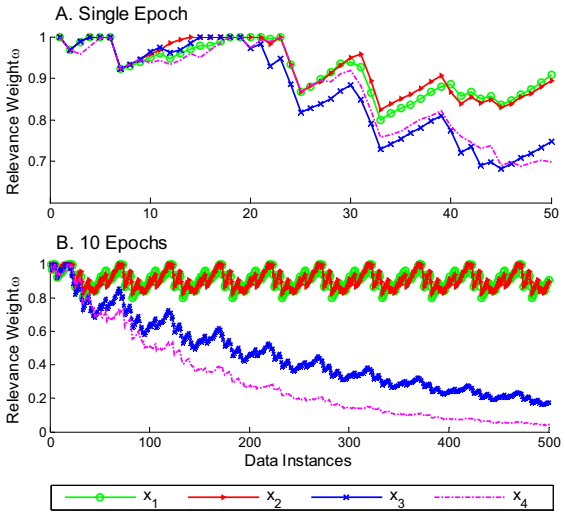

Fig. 4. Updates of the relevance weights for input features x_1–x_4 in the case study: A. For a single-pass of the training data; and B. For 10 passes of the training data.

where $fo_{i,j_i}^{(k)}$ (resp. $bo_{l_m,m}^{(k)}$) is the computed output of the antecedent node A_{i,j_i} (resp. consequent node $C_{l_m,m}$) that is connected to the rule node R_k. Knowledge is extracted from the structure of each rule node R_k, consisting of its antecedent and consequent parts, for the computation of the instantaneous relevance weight $\widehat{\omega}_i$. Subsequently, $\widehat{\omega}_i$ is given by the maximum activations of its respective fuzzy labels. That is, the instantaneous relevance weight $\widehat{\omega}_i$ of an input feature i represents the activation level of feature i by the current data pair based on the knowledge encoded in FAPOP.

Feature analysis in FAPOP proceeds with incrementally updating a relevance weight for each input feature. The relevance weight ω_i for an input feature i is computed as in (11):

$$\begin{aligned} \omega_i\,(0) &= 1\;; \\ \omega_i\,(t+1) &= \min\left[1,\ \omega_i\,(t) - \omega_i\,(t)\cdot(\eta_d - 1)\cdot(\widehat{\omega}_i\,(t) - h)\right] \end{aligned} \tag{11}$$

where $\eta_d < 1$ is a natural decaying constant and h is the harsh factor. The relevance weight of an input feature i is initialized to unity, assuming a high level of relevance since $0 < \omega_i \leq 1$. Harsh factor h, $0 \leq h \leq 1$, determines the level of stringency in the feature selection process, i.e., for a large value of h, only highly relevant features are selected; while for a lower value of h, some redundant features might be included in the selection. This is because when $\widehat{\omega}_i\,(t) < h$, we have $\omega_i(t+1) < \omega_i(t)$. Hence when h is a large value and most instants of $\widehat{\omega}_i$ fall below h, the resultant relevance weight of input feature i will be decreasing over time. On the other hand, when $\widehat{\omega}_i\,(t) > h$, we have $\omega_i(t+1) > \omega_i(t)$. Hence when h is a small value and most instants of $\widehat{\omega}_i$ are greater than h, the resultant relevance weight of input feature i will be increasing over time. Nevertheless, ω_i will be cap at unity.

Fig. 3 shows a flowchart of the feature analysis process employed in the proposed FAPOP model. With each incoming training data pair $[x, d]$, the instantaneous relevance weight $\widehat{\omega}_i$ of an input feature i is computed as the activation of the input feature by this current data pair based on the knowledge encoded in the system. FAPOP then proceeds with updating the relevance weight ω_i of an input feature i using (11). After a single-pass of the training data, redundant features in the proposed model are identified and removed from the system. Redundant features are recognized by their decreasing relevance weights. Subsequently, contradictory/inconsistent rules with lower weightages are removed. An inconsistent rulebase occurs when there exists two rules such that the antecedent conditions are similar but the resultant consequences differ; while the weightage of a fuzzy rule is defined as $\sum_m w_{k,l_m^\star,m}$. Following that, the system deletes repeated rules, i.e. , rules with similar antecedent and consequent segments. Finally, some of the fuzzy labels might be "orphaned" when all fuzzy rules associated with them have been deleted. The orphaned fuzzy labels are also removed to ensure that the resultant structure of FAPOP is compact.

D. Case Study

This section illustrates the proposed learning mechanisms in the FAPOP model with a case study. The dataset is generated by a nonlinear equation as described in (12):

$$y = \left(1 + x_1^{-2} + x_2^{-1.5}\right)^2 \tag{12}$$

where x_1 and x_2 are the two inputs in the system; while y is the output. Following the problem described in [15], a total of 50 data pairs are generated for $0 \leq x_1, x_2 \leq 5$. Two random variables x_3 and x_4, in the range of $[0, 5]$, are subsequently added as dummy inputs. Hence, the application problem is a 4 inputs-1 output system, such that input features x_3 and x_4 are expected to be indifferent to the output.

A total of 5, 4, 7 and 5 fuzzy labels are identified by the CLIP algorithm for the four input spaces respectively; and 3 fuzzy labels are determined for the output space. That means, 700 fuzzy rules have been initialized by the POP algorithm such that the initial structure of FAPOP is given

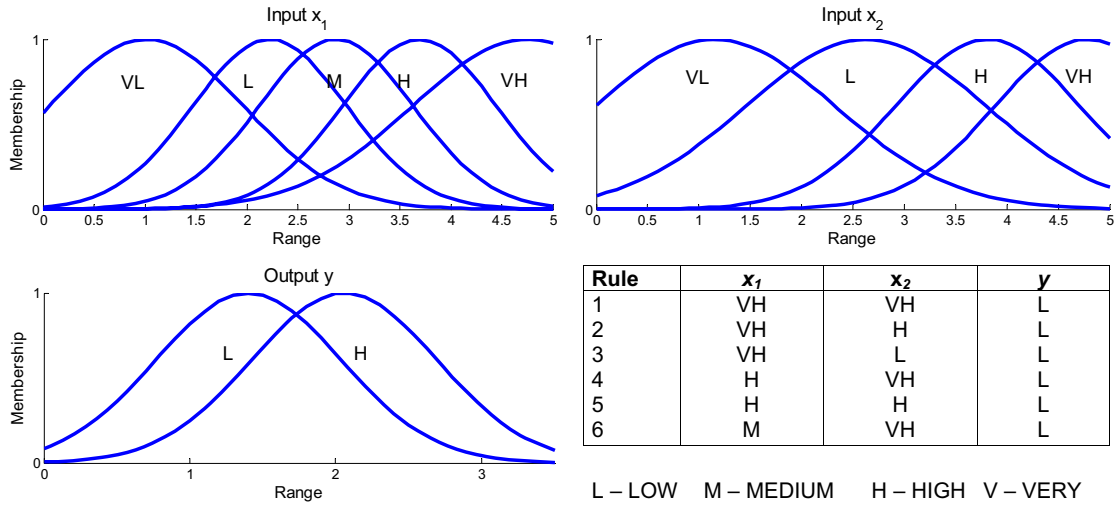

Rule	x_1	x_2	y
1	VH	VH	L
2	VH	H	L
3	VH	L	L
4	H	VH	L
5	H	H	L
6	M	VH	L

L – LOW M – MEDIUM H – HIGH V – VERY

Fig. 5. Fuzzy clusters identified for inputs x_1–x_2 and output y in the case study; and part of the identified rulebase in FAPOP.

by the configuration 4-21-700-3-1. Following that, FAPOP proceeds with the feature analysis process to identify relevant input features to the system and the application. Fig. 4 shows the updates for the relevance weights for the four inputs. After a single-pass of the training data (see Fig. 4.A.), the decline in the relevance weights for input features x_3 and x_4 are much faster compared to those for x_1 and x_2, indicating that they might be irrelevant. To emphasize the disparity in the relevance weights between the relevant and irrelevant features, the training data are cycled for ten epochs in this experiment as shown in Fig. 4.B. From the figure, the relevance weights of the redundant input features x_3 and x_4 approach zero with the increase in the number of running epochs, while that of the relevant input features x_1 and x_2 are maintained consistently at a high level. In general, irrelevant/redundant input features are marked by decreasing relevance weights, where the decline can be emphasize with an increase in the number of running epochs. Nevertheless, it should be noted that a large training dataset will lead to an increase in the time complexity with an increase in the number of running epochs. In this paper, the number of running epochs for the experiments is capped at 10.

After the redundant features (x_3 and x_4) have been identified, they are removed from the FAPOP model. Inconsistent rules of lower weightages, as well as identical rules, are also removed to maintain a compact structure in FAPOP. Finally, orphaned fuzzy labels are deleted from the system. The final structure of FAPOP is given by the configuration 4-9-20-2-1, i.e., there are 20 identified rules in the proposed model and one orphaned fuzzy label in the output space is also deleted. As seen, there is a significant reduction of 97% in the the number of identified rules.

Fig. 5 illustrates the identified fuzzy clusters in FAPOP for the input spaces x_1 and x_2, and that for the output space y. Since the fuzzy clusters are highly ordered, clear semantic meanings can be attached to the fuzzy clusters. A total of 20 fuzzy rules are identified by the FAPOP model, with six rules corresponding to a low output value, and fourteen rules corresponding to a high output value. Subsequently, the six rules are listed in Fig. 5. One can easily verify that the derived rulebase is consistent, with the identified fuzzy rules reflecting the relationship between the inputs and the output of the system, i.e., based on (12), for relatively high values of inputs x_1 and x_2, the resultant output y of the system is low. The reverse is also true for a high output value y.

IV. Experimental Results

This section illustrates the effectiveness of the proposed FAPOP model as a neural fuzzy modeling system by employing it in two benchmarking simulations; namely, (1) the three sets of experiments in Nakanishi's dataset [16] [17]; and (2) the prediction of Mackey-Glass chaotic system [18].

A. Nakanishi Dataset

The learning and modeling abilities of the proposed FAPOP model are evaluated using three sets of experiments; namely, (a) a nonlinear system; (b) the human operation of a chemical plant; and (c) the daily pricing of a stock in a stock market. The datasets are extracted from published papers in [16] and [17]. Each of the three datasets is split into three groups A, B, and C where A and B form the training dataset and C is the testing data. The benchmark for comparisons are the accuracies on the testing data (calculated as the mean squared error MSE) and the correspondence between the computed output with the testing data (calculated as the Pearson correlation coefficient R). The experimental results of FAPOP are subsequently benchmarked against the following models; namely, Hebb-R-R [2]; POPFNN [19]; RSPOP [8]; five of the six reasoning methods in [16] (Sugeno P&P-G, Sugeno P, Sugeno P-G, Mamdani, and Turksen IVCRI); ANFIS [3]; EFuNN [20]; DENFIS [4]; and FITSK [21].

1) A Nonlinear System: The objective of this experiment is to identify and model the underlying principles of a nonlinear system. In the original dataset, there were four inputs x_1–x_4 and one output y. Before the feature analysis process,

TABLE II
CONSOLIDATED EXPERIMENTAL RESULTS FOR THE NAKANISHI DATASET.

	Nonlinear System		Chemical Plant		Stock Prediction		
Model	MSE (Rank)	R (Rank)	MSE (Rank)	R (Rank)	MSE (Rank)	R (Rank)	Average Rank
Hebb-R-R	0.185 (1)	0.911 (2)	2.423×10^{4} (2)	0.998 (2)	15.14 (1)	0.947 (1)	1.5
POPFNN	0.270 (3)	0.877 (3)	5.630×10^{5} (8)	0.946 (9)	76.22 (10)	0.733 (10)	7.2
RSPOP	0.383 (7)	0.856 (4)	2.124×10^{5} (5)	0.983 (7)	24.86 (2)	0.922 (2)	4.5
Sugeno P&P-G	0.345 (6)	0.828 (7)	2.897×10^{5} (7)	0.973 (8)	94.58 (12)	0.706 (11)	8.5
Sugeno P	0.776 (12)	0.558 (12)	6.372×10^{5} (9)	0.933 (12)	35.47 (4)	0.883 (4)	8.8
Sugeno P-G	0.467 (9)	0.845 (6)	1.931×10^{6} (12)	0.990 (6)	168.9 (13)	0.700 (12)	9.7
Mamdani	0.862 (13)	0.490 (13)	6.580×10^{5} (10)	0.937 (11)	40.84 (7)	0.865 (7)	10.2
Turksen IVCRI	0.706 (11)	0.609 (11)	2.581×10^{5} (6)	0.993 (4)	93.02 (11)	0.661 (13)	9.3
ANFIS	0.286 (4)	0.853 (5)	2.968×10^{6} (13)	0.780 (13)	38.06 (5)	0.875 (6)	7.7
EFuNN	0.566 (10)	0.720 (10)	7.247×10^{5} (11)	0.946 (9)	72.54 (9)	0.756 (9)	9.7
DENFIS	0.411 (8)	0.805 (9)	5.240×10^{4} (4)	0.995 (3)	69.82 (8)	0.810 (8)	6.7
FITSK	0.336 (5)	0.828 (7)	3.862×10^{4} (3)	0.993 (4)	33.78 (3)	0.883 (4)	4.3
FAPOP	0.186 (2)	0.951 (1)	1.440×10^{4} (1)	0.999 (1)	38.47 (6)	0.898 (3)	2.3

TABLE I
EXPERIMENTAL RESULTS OF FAPOP FOR THE NAKANISHI DATASET.

	Nonlinear System	Chemical Plant	Stock Prediction
# Rules before feature analysis	108	81	17496
# Rules after feature analysis	12	12	6
Rule reduction %	89	85	99
MSE	0.186	1.440×10^{4}	38.47
R	0.951	0.999	0.898

108 fuzzy rules are initialized in FAPOP; while FAPOP identifies input feature x_3 as redundant after feature analysis. Subsequently, the application problem becomes a 3 inputs-1 output system. A total of twelve fuzzy rules are then identified by FAPOP for this experiment (see Table I). Consolidated experimental results on the benchmarking measures are given in Table II.

2) Human Operation of a Chemical Plant: The proposed FAPOP model is employed to model the human operation of a chemical plant in this experiment. Although there were five inputs x_1–x_5 and one output y in the original dataset, only selected relevant input features, x_1–x_3 and x_5, are used in defining the rules. Subsequently, a total of twelve fuzzy rules are extracted from the FAPOP model as shown in Table I. Consolidated experimental results on the benchmarking measures are given in Table II.

3) Daily Pricing of a Stock in a Stock Market: Using various statistics concerning a stock collected from a stock market, the proposed FAPOP model is employed to perform stock price prediction. Out of the original ten input features x_1–x_{10}, two features, x_7 and x_9, are redundant and discarded from the FAPOP model. A total of six fuzzy rules are then identified by FAPOP, indicating a remarkable reduction of 99% in the number of identified rules (see Table I). For comparison, the consolidated experimental results on the benchmarking measures are given in Table II.

4) Discussion: Table I shows the experimental results for the proposed FAPOP model in the Nakanishi dataset. There are significant reductions in the number of identified rules in all the three experiments. By keeping the number of identified rules low, this helps to improve the overall interpretability of the system.

Table II shows the consolidated experimental results for the Nakanishi dataset between FAPOP and the benchmarking models. FAPOP outperforms all the benchmarking models in the first two tasks by consistently ranking first in terms of MSE and R. In the task of modeling a nonlinear system, FAPOP achieves a MSE value of 0.186, similar to Hebb-R-R. In addition, there is a slight improvement of 4.39% in the R value compared to second place Hebb-R-R. For the second task of modeling a chemical plant, the proposed FAPOP model delivers an outstanding performance by achieving a reduction of 40.6% in terms of calculated MSE and a slight improvement of 0.001 in terms of correlation R compared to the second position Hebb-R-R. For the final task of stock prediction, the performance of FAPOP is comparable with FITSK, Sugeno P and ANFIS. It should also be noted that Hebb-R-R uses 20 fuzzy rules; while RSPOP uses 29 fuzzy rules [2]. Comparatively, FAPOP uses only six rules in the prediction task. This explains the slight compromise in the MSE and R values achieved. On average, the proposed FAPOP model achieves a ranking of 2.3 for all the three tasks, putting it at second position. This is a significant improvement compared to respective members in the family of pseudo outer-product-based neural fuzzy systems, i.e., POPFNN with an average ranking of 7.2, and RSPOP with an average ranking of 4.5. As a further comparison, the training time of the three members in the POP neural fuzzy systems are listed in Table III. As seen, the time complexity of the proposed FAPOP model is comparable with the first generation POPFNN model. This is a direct consequence of the POP rule identification algorithm,

TABLE III
TRAINING TIME(MS) OF MEMBERS OF THE POP NEURAL FUZZY SYSTEMS.

Model	Nonlinear System	Chemical Plant	Stock Prediction
POPFNN	46	485	1,082,866
RSPOP	188	202	184
FAPOP	62	468	1,012,500

where all possible combination of rules is considered, and hence the size of the initial rulebase increases exponentially with an increase in the number of input dimensions. This can be seen in the stock prediction experiment where the initial number of rules is 17496 in FAPOP (see Table II). As a result, it is time consuming and memory dependent at the beginning of the learning. On the other hand, RSPOP proposes a new rule identification algorithm, where the initial identified rulebase consists of only 50 rules prior to rule reduction [8]. This, subsequently, results in a significant saving in the time complexity. In conclusion, one can reduce the time complexity of the proposed FAPOP model by adopting alternative rule identification algorithms [22] [14] which are tailored to the numerical training data.

B. Prediction of Mackey-Glass Chaotic System

The learning and generalization abilities of the proposed FAPOP model is evaluated by employing it in a benchmark comparison involving the prediction of a chaotic system. The chaotic system is generated by a delay differential equation as described in (13):

$$\frac{\partial x(t)}{\partial t} = \frac{0.2x(t-\tau)}{1+x^{10}(t-\tau)} - 0.1x(t) \tag{13}$$

which was first investigated by Mackey and Glass [18]. A fourth-order Runge-Kutta method was applied to compute the numerical approximation of the series with conditions as follows: $\tau = 17$ and initial condition $x(0) = 1.2$. Four past values are used to predict the present value, where

$$\begin{aligned} \text{input vector} &= [x(t-24), x(t-18), x(t-12), x(t-6)] \ ; \\ \text{output vector} &= [x(t)] \ . \end{aligned}$$

A total of 1000 data pairs are extracted from the interval $t \in [118, 1117]$. The first 500 pairs are then used as training set; while the remaining 500 pairs are used for testing. The benchmark for comparisons are the accuracies on the testing data (given as the root mean squared error RMSE) and the interpretability of the systems (given as the number of identified fuzzy rules). The experimental results of FAPOP are subsequently benchmarked against the following models; namely, FALCON-ART [1]; FITSK [21]; and EFuNN [20].

Table IV shows the performance comparison for the Mackey-Glass chaotic system between the proposed FAPOP model and the benchmarking models. FAPOP achieves a RMSE value of 0.017, falling behind only the EFuNN model in terms of accuracy achieved on the testing data. Nevertheless, EFuNN uses 330% more rules compared to FAPOP (a jump from 20 to 86) in this prediction task, greatly decreasing the interpretability of the system. On the average, the proposed FAPOP is able to maintain a good balance between the two contradictory requirements, i.e., delivering a good fuzzy rulebase interpretability by identifying 20 fuzzy rules, and achieving a high modeling accuracy of 0.017.

TABLE IV
CONSOLIDATED EXPERIMENTAL RESULTS FOR THE MACKEY-GLASS SYSTEM.

Model	RMSE	# Rules
FALCON-ART	0.040	30
FITSK	0.034	16
EFuNN	0.010	86
FAPOP	0.017	20

V. CONCLUSION

This paper presents a novel neural fuzzy system named *Feature Analysis Enhanced Pseudo-Outer Product Fuzzy Rule Identification System* (FAPOP). A key strength of FAPOP is its feature analysis integrative design such that a regulated balance is achieved between the two contradictory interpretability-accuracy requirements in the design of a neural fuzzy system. This is done via two channels; namely, (1) improve the interpretability of the system by identifying features relevant to its computational structure; and (2) improve the accuracy of the system by identifying features relevant to the application problem. Subsequently, the learning mechanisms in the proposed FAPOP model are showcased through a case study where the system is able to identify a compact and highly interpretable rulebase by identifying relevant features to the system and application. Finally, FAPOP is employed in a series of benchmarking simulations to demonstrate its effectiveness as a neural fuzzy modeling system, and excellent performances have been achieved.

REFERENCES

[1] C. J. Lin and C. T. Lin, "An ART-based fuzzy adaptive learning control network," *IEEE Transactions on Fuzzy Systems*, vol.5, no.4, pp.477–496, Nov. 1997.

[2] F. Liu, C. Quek and G. S. Ng, "A novel generic hebbian ordering-based fuzzy rule base reduction approach to Mamdani neuro-fuzzy system," *Neural Computations*, vol.19, no.6, pp.1656–1680, Jun. 2007.

[3] J. S. R. Jang, "ANFIS: Adaptive-network-based fuzzy inference systems," *IEEE Transactions on Systems, Man and Cybernetics*, vol.23, no. 3, pp.665–685, May 1993.

[4] N. Kasabov and Q. Song, "DENFIS: Dynamic evolving neural-fuzzy inference system and its application for time-series prediction," *IEEE Transactions on Fuzzy Systems*, vol.10, no.2, pp.144–154, Apr. 2002.

[5] E. H. Mamdani, "Application of fuzzy logic to approximate reasoning using linguistic systems," *IEEE Transactions on Computers*, vol.26, no.12, pp.1182–1191, Dec. 1977.

[6] T. Takagi and M. Sugeno, "Fuzzy identification of systems and its applications to modeling and control," *IEEE Transactions on Systems, Man and Cybernetics*, vol.15, no.1, pp.116–132, 1985.

[7] M. Sugeno and G. T. Kang, "Structure identification of fuzzy model," *Fuzzy Sets and Systems*, vol.28, no.1, pp.15–33, Oct. 1988.

[8] K. K. Ang and C. Quek, "RSPOP: Rough set-based pseudo outer-product fuzzy rule identification algorithm," *Neural Computations*, vol.17, no.1, pp.205–243, Jan. 2005.

[9] I. Guyon and A. Elisseeff, "An introduction to variable and feature selection," *Journal of Machine Learning Research*, vol.3, pp.1157–1182, Jan. 2003.
[10] N. R. Pal, "Soft computing for feature analysis," *Fuzzy Sets and Systems*, vol.103, no.2, pp.201–221, Apr. 1999.
[11] C. Quek and R. W. Zhou, "The POP learning algorithms: Reducing work in identifying fuzzy rules," *Neural Networks*, vol.14, no. 10, pp.1431–1445, Dec. 2001.
[12] S. Haykin, *Neural networks: A comprehensive foundation.* Prentice Hall, 1998.
[13] C. T. Lin and C. S. G. Lee, *Neural fuzzy systems: A neuro-fuzzy synergism to intelligent systems.* Prentice Hall, 1996.
[14] S.W. Tung, C. Quek and C. Guan, "SaFIN: A self-adaptive fuzzy inference network," In preparation.
[15] D. Chakraborty and N. R. Pal, "Integrated feature analysis and fuzzy rule-based system identification in a neuro-fuzzy paradigm," *IEEE Transactions on Systems, Man and Cybernetics–Part B*, vol.31, no.3, pp. 391–400, Jun. 2001.
[16] H. Nakanishi, I. Turksen and M. Sugeno, "A review and comparison of six reasoning methods," *Fuzzy Sets and Systems*, vol.57, no.3, pp.257–294, Aug. 1993.
[17] M. Sugeno and T. Yasukawa, "A fuzzy-logic-based approach to qualitative modeling," *IEEE Transactions on Fuzzy Systems*, vol.1, no.1, pp.7–31, Feb. 1993.
[18] M. Mackey and L. Glass, "Oscillation and chaos in physiological control systems," *Science*, vol.197, no. 4300, pp.287–289, Jul. 1977.
[19] C. Quek and R. W. Zhou, "POPFNN: A pseudo outer-product based fuzzy neural network," *Neural Networks*, vol.9, no.9, pp.1569–1581, Dec. 1996.
[20] N. Kasabov, "Evolving fuzzy neural networks for supervised/ unsupervised online knowledge-based learning," *IEEE Transactions on Systems, Man and Cybernetics–Part B*, vol.31, no.6, pp.902–918, Dec. 2001.
[21] K. H. Quah and C. Quek, "FITSK: Online local learning with generic fuzzy input Takagi-Sugeno-Kang fuzzy framework for nonlinear system estimation," *IEEE Transactions on Systems, Man and Cybernetics–Part B*, vol.36, no.1, pp.166–178, Feb. 2006.
[22] W. L. Tung and C. Quek, "GenSoFNN: A generic self-organizing fuzzy neural network," *IEEE Transactions on Neural Networks*, vol.13, no.5, pp. 1075–1086, Sep. 2002.

2011 IEEE International Conference on Fuzzy Systems
June 27-30, 2011, Taipei, Taiwan

Tracking Control of Surface Vessels via Adaptive Type-2 Fuzzy Logic Control

Xue Tao Chen
Department of Electrical and Computer Engineering
National University of Singapore
Singapore 117576
Email: g0800483@nus.edu.sg

Woei Wan Tan
Department of Electrical and Computer Engineering
National University of Singapore
Singapore 117576
Email: wwtan@nus.edu.sg

***Abstract*—This paper presents an indirect adaptive type-2 fuzzy logic controller (FLC) as well as a direct adaptive type-2 FLC for tracking control of surface vessels under time-varying hydrodynamic disturbances. The combination of approximation-based adaptive control technique and type-2 fuzzy logic system (FLS) allows us to handle time-varying disturbances without exact information on them. The stability of the design is proved through Lyapunov analysis where globally asymptotical convergence of the tracking errors is guaranteed. Although designed from different points of view, both indirect and direct adaptive type-2 FLC yield same and passive closed-loop systems. Comparative simulations with their adaptive type-1 counterparts are carried out. The proposed techniques are found to be effective, robust, and reduce tracking errors.**

***Index Terms*—Adaptive control, type-2 fuzzy logic system, marine vehicle control, function approximation, tracking.**

I. Introduction

Essential to any controller design process is knowledge of the dynamic characteristics of the plant or physical system to be controlled. Accurate modeling of the plant can increase the probability that a satisfactory controller, designed based on mathematical plant model, achieves similar performance in reality. For this reason, more and more realistic dynamic models for surface vessels have been proposed [1]. One of the latest vessel models was presented in [2], [3]. Due to the time-varying hydrodynamic disturbances in this model, few controllers are designed for it. In [4], an indirect adaptive type-2 fuzzy logic controller (FLC) is proposed for regulation control of the vessels. As a complementary work to [4], this paper considers the tracking control of the vessels. In marine vessels tracking and guidance applications, the weakness of traditional model-based adaptive control is the requirement that uncertainties are parametric, time-invariant, and linear in the parameters [5]. Hence, approximation-based adaptive control technique [6], [7], which do not require parametric or functional certainty, is adopted to compensate for functional uncertainties and disturbances from environment. Such approximators normally have a standard regressor function whose configuration is independent of the dynamic characteristics of the vessel model.

It has been proved in [8]–[11] that type-1 fuzzy logic system (FLS) are universal approximators, i.e., for any given continuous nonlinear function, there exists a type-1 FLS such that it can uniformly approximate the function to any desired accuracy. As a extension of type-1 FLS, type-2 FLS has been proposed and drawn much attention [12]–[15]. The main differences between type-1 and type-2 FLS lie in for type-2 FLS at least one of the antecedent or consequent fuzzy sets is a type-2 fuzzy set, whose membership value is a type-1 fuzzy set. Thus a type-reducer is needed to convert the type-2 fuzzy output sets into type-1 sets so that they can be processed by the defuzzifier to produce a crisp output. The type-2 FLS has already found its applications to several engineering problems [16]–[19]. This paper serves as another engineering application to investigate the approximation property of type-2 FLS.

By combining approximation-based adaptive control technique and type-2 FLS, an indirect as well as a direct adaptive type-2 FLC are proposed for tracking control of newly developed vessel model [2], [3]. It is proved that the tracking errors under these two controller globally asymptotically converge to zero and the resultant closed-loop systems are passive.

The rest of the paper is organized as follows. Section II describes the singleton interval type-2 (IT2) FLS and constructs it in the linear in the parameters form. Next, the modeling of marine vessels is introduced in Section III. Then the design and stability analysis of the two adaptive type-2 FLCs is delineated in Section IV. After that, Section V describes the simulation results of the closed-loop system. Comparisons with their type-1 counterparts are also shown in this section. Finally, conclusions are drawn in Section VI.

II. Description of Singleton IT2 FLS

In this paper, a singleton IT2 FLS whose general configuration is depicted in Fig. 1 is considered. It contains five components which are fuzzifier, rule base, fuzzy inference engine, type-reducer, and defuzzifier. Here, a multi-input, single-out fuzzy system is described, as a multi-output system can generally be separated into several single-output systems.

1) Fuzzification: The fuzzifier maps a crisp point $\mathbf{x} = (x_1, \ldots, x_n) \in \mathbf{U} \subset R^n$ into a IT2 fuzzy set $\tilde{A}_{\mathbf{x}}$ in $\mathbf{U}$. In the singleton fuzzification, the input fuzzy set $\tilde{A}_{\mathbf{x}}$ has only a single point of nonzero membership as follows.

$$\mu_{\tilde{A}_{\mathbf{x}}}(\mathbf{x}) = \begin{cases} 1; & \mathbf{x} = \mathbf{x}' \\ 0; & \mathbf{x} \neq \mathbf{x}' \end{cases} \tag{1}$$

978-1-4244-7316-8/11/$26.00 ©2011 IEEE

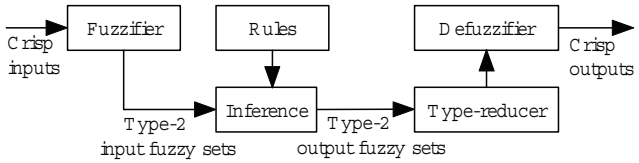

Fig. 1. A singleton interval type-2 FLS.

2) Rule Base: The fuzzy rule base consists of a group of fuzzy **IF-THEN** rules, which can be extracted from numerical data or provided by experts. Consider a IT2 FLS having n inputs and one output, then the lth rule in the rule base can be written as

$$R^l: \text{IF } x_1 \text{ is } \tilde{F}_1^l \text{ and } \cdots \text{and } x_n \text{ is } \tilde{F}_n^l \text{ THEN } y \text{ is } \tilde{G}^l \quad (2)$$

where $l = 1, 2, \ldots, M$, x_i $(i = 1, 2, \ldots, n)$ and y are the inputs and output to the IT2 FLS respectively, $\tilde{F}_i^l$ and $\tilde{G}^l$ are labels of antecedent and consequent fuzzy sets in $\mathbf{U}_i$ and R, respectively. This rule represents a type-2 relation between the input space $\mathbf{U}$ and output space R.

3) Fuzzy Inference Engine: The fuzzy inference engine combines fuzzy **IF-THEN** rules and provides a mapping from input IT2 fuzzy sets in $\mathbf{U}$ to output IT2 fuzzy set in R. Each rule is interpreted as a fuzzy implication. For the singleton IT2 FLS, using the extended sup-star compositional rule of inference, the output consequent set corresponding to rule R^l can be expressed as

$$\mu_{\tilde{B}^l}(y) = \mu_{\tilde{G}^l}(y) \sqcap \left[\sqcap_{i=1}^n \mu_{\tilde{F}_i^l}(x_i')\right]. \quad (3)$$

where the firing set $\sqcap_{i=1}^n \mu_{\tilde{F}_i^l}(x_i') \equiv F^l(\boldsymbol{x}')$ is an interval type-1 fuzzy set, i.e.,

$$F^l(\boldsymbol{x}') = \left[\underline{f}^l(\boldsymbol{x}'), \overline{f}^l(\boldsymbol{x}')\right] \quad (4)$$

$$\underline{f}^l(\boldsymbol{x}') = \underline{\mu}_{\tilde{F}_1^l}(x_1') \bigstar \cdots \bigstar \underline{\mu}_{\tilde{F}_1^n}(x_n') \quad (5)$$

$$\overline{f}^l(\boldsymbol{x}') = \overline{\mu}_{\tilde{F}_1^l}(x_1') \bigstar \cdots \bigstar \overline{\mu}_{\tilde{F}_1^n}(x_n'). \quad (6)$$

Here $\underline{\mu}_{\tilde{F}_i^l}(x_i')$ and $\overline{\mu}_{\tilde{F}_i^l}(x_i')$ are the lower and upper membership grade of IT2 fuzzy set $\tilde{F}_i^l$, respectively, symbol $\bigstar$ denotes the t-norm corresponding to the conjunction "and" in (2). The fired output consequent set $\mu_{\tilde{B}^l}(y)$ for the lth rule can be written as

$$\mu_{\tilde{B}^l}(y) = \int_{b^l \in \left[\underline{f}^l \bigstar \underline{\mu}_{\tilde{G}^l}(y), \overline{f}^l \bigstar \overline{\mu}_{\tilde{G}^l}(y)\right]} 1/b^l \quad (7)$$

where $\underline{\mu}_{\tilde{G}^l}$ and $\overline{\mu}_{\tilde{G}^l}$ are the lower and upper membership grades of consequent fuzzy set, $\tilde{G}^l$.

4) Type-Reduction and Defuzzification: By Passing through the type-reduction operator, the IT2 fuzzy sets, which are outputs of the inference engine, are type-reduced into a type-1 fuzzy set. This type-1 fuzzy set is then defuzzified to obtain crisp output. So far, there are many kinds of type-reduction method available, such as centroid, center of sums, height and center of sets type-reduction. In this paper, center of sets type-reduction is used, as it has reasonable computational complexity. Assume maximum t-conorm, product t-norm, and product implication are used. Then in the type-reduction, the type-reduced set is an interval type-1 fuzzy set $[y_l', y_r']$, whose left end point y_l' and right end point y_r' can be computed using the Karnik-Mendel iterative procedure [13]. In this procedure, assume singleton consequent sets are used, the consequent parameters have to be reordered in ascending order first. Let $\mathbf{y} = (y^1, \ldots, y^M)^{\mathrm{T}}$ represent the original rule-ordered consequent values, and let $\hat{\mathbf{y}} = (\hat{y}^1, \ldots, \hat{y}^M)^{\mathrm{T}}$ denote the reordered sequences, where $\hat{y}^1 \leq \hat{y}^2 \leq \ldots \leq \hat{y}^M$. The formula illustrating relationship between $\mathbf{y}$ and $\hat{\mathbf{y}}$ is

$$\hat{\mathbf{y}} = \mathbf{Q}\mathbf{y} \quad (8)$$

where $\mathbf{Q}$ is $M \times M$ permutation matrix with elementary vectors as columns, and these vectors are permuted to move elements in $\mathbf{y}$ to new reordered locations in ascending order in the transformed vector $\hat{\mathbf{y}}$. The original rule firing strength $\underline{\mathbf{f}} = (\underline{f}^1, \underline{f}^2, \ldots, \underline{f}^M)^{\mathrm{T}}$ and $\overline{\mathbf{f}} = (\overline{f}^1, \overline{f}^2, \ldots, \overline{f}^M)^{\mathrm{T}}$ are accordingly reordered. To compute the end points, the new orders for $\underline{\mathbf{f}}$ and $\overline{\mathbf{f}}$ are $\mathbf{Q}\underline{\mathbf{f}}$ and $\mathbf{Q}\overline{\mathbf{f}}$ respectively. According to [20], [21], the left end point y_l' can be computed as

$$\begin{aligned} y_l' &= \frac{\sum_{i=1}^L (\mathbf{Q}\overline{\mathbf{f}})_i \hat{y}^i + \sum_{i=L+1}^M (\mathbf{Q}\underline{\mathbf{f}})_i \hat{y}^i}{\sum_{i=1}^L (\mathbf{Q}\overline{\mathbf{f}})_i + \sum_{i=L+1}^M (\mathbf{Q}\underline{\mathbf{f}})_i} \\ &= \frac{\overline{\mathbf{f}}^{\mathrm{T}}\mathbf{Q}^{\mathrm{T}}\mathbf{E}_1^{\mathrm{T}}\mathbf{E}_1\mathbf{Q}\mathbf{y} + \underline{\mathbf{f}}^{\mathrm{T}}\mathbf{Q}^{\mathrm{T}}\mathbf{E}_2^{\mathrm{T}}\mathbf{E}_2\mathbf{Q}\mathbf{y}}{\mathbf{p}_l^{\mathrm{T}}\mathbf{Q}\overline{\mathbf{f}} + \mathbf{g}_l^{\mathrm{T}}\mathbf{Q}\underline{\mathbf{f}}} \end{aligned} \quad (9)$$

where L denotes the left crossover point,

$$\begin{aligned} \mathbf{p}_l &= (\underbrace{1, 1, \ldots, 1}_{L}, 0, \ldots, 0)^{\mathrm{T}} \in R^{M\times 1} \\ \mathbf{g}_l &= (0, \ldots, 0, \underbrace{1, 1, \ldots, 1}_{M-L})^{\mathrm{T}} \in R^{M\times 1} \\ \mathbf{E}_1 &= (\mathbf{e}_1, \mathbf{e}_2, \ldots, \mathbf{e}_L, \mathbf{0}, \ldots, \mathbf{0})^{\mathrm{T}} \in R^{L\times M} \\ \mathbf{E}_2 &= (\mathbf{0}, \ldots, \mathbf{0}, \boldsymbol{\varepsilon}_1, \boldsymbol{\varepsilon}_2, \ldots, \boldsymbol{\varepsilon}_{M-L})^{\mathrm{T}} \in R^{(M-L)\times M} \end{aligned}$$

and where $\mathbf{e}_i \in R^L$ and $\boldsymbol{\varepsilon}_i \in R^{M-L}$ are elementary vectors. Similarly, the output y_r' can be expressed as

$$\begin{aligned} y_r' &= \frac{\sum_{i=1}^R (\mathbf{Q}\underline{\mathbf{f}})_i \hat{y}^i + \sum_{i=R+1}^M (\mathbf{Q}\overline{\mathbf{f}})_i \hat{y}^i}{\sum_{i=1}^R (\mathbf{Q}\underline{\mathbf{f}})_i + \sum_{i=R+1}^M (\mathbf{Q}\overline{\mathbf{f}})_i} \\ &= \frac{\underline{\mathbf{f}}^{\mathrm{T}}\mathbf{Q}^{\mathrm{T}}\mathbf{E}_3^{\mathrm{T}}\mathbf{E}_3\mathbf{Q}\mathbf{y} + \overline{\mathbf{f}}^{\mathrm{T}}\mathbf{Q}^{\mathrm{T}}\mathbf{E}_4^{\mathrm{T}}\mathbf{E}_4\mathbf{Q}\mathbf{y}}{\mathbf{p}_r^{\mathrm{T}}\mathbf{Q}\underline{\mathbf{f}} + \mathbf{g}_r^{\mathrm{T}}\mathbf{Q}\overline{\mathbf{f}}} \end{aligned} \quad (10)$$

where R denotes the right crossover point,

$$\begin{aligned} \mathbf{p}_r &= (\underbrace{1, 1, \ldots, 1}_{R}, 0, \ldots, 0)^{\mathrm{T}} \in R^{M\times 1} \\ \mathbf{g}_r &= (0, \ldots, 0, \underbrace{1, 1, \ldots, 1}_{M-R})^{\mathrm{T}} \in R^{M\times 1} \\ \mathbf{E}_3 &= (\mathbf{e}_1, \mathbf{e}_2, \ldots, \mathbf{e}_R, \mathbf{0}, \ldots, \mathbf{0})^{\mathrm{T}} \in R^{R\times M} \\ \mathbf{E}_4 &= (\mathbf{0}, \ldots, \mathbf{0}, \boldsymbol{\varepsilon}_1, \boldsymbol{\varepsilon}_2, \ldots, \boldsymbol{\varepsilon}_{M-R})^{\mathrm{T}} \in R^{(M-R)\times M} \end{aligned}$$

and where $\mathbf{e}_i \in R^R$ and $\boldsymbol{\varepsilon}_i \in R^{M-R}$ are elementary vectors. Finally, the interval type-1 fuzzy set is defuzzified to generate

the system output by means of computing the average of y'_l and y'_r. Hence the defuzzified output is

$$y' = \frac{y'_l + y'_r}{2}. \tag{11}$$

View the consequent parameters $\boldsymbol{\theta} = \mathbf{y} = (y^1, \ldots, y^M)^{\mathrm{T}}$ as adjustable parameters, then (11) can be written as

$$y' = \boldsymbol{\phi}^{\mathrm{T}} \boldsymbol{\theta} \tag{12}$$

where

$$\begin{aligned} \boldsymbol{\phi}^{\mathrm{T}} = & \frac{\overline{\mathbf{f}}^{\mathrm{T}} \mathbf{Q}^{\mathrm{T}} \mathbf{E}_1^{\mathrm{T}} \mathbf{E}_1 \mathbf{Q} + \underline{\mathbf{f}}^{\mathrm{T}} \mathbf{Q}^{\mathrm{T}} \mathbf{E}_2^{\mathrm{T}} \mathbf{E}_2 \mathbf{Q}}{2(\mathbf{p}_l^{\mathrm{T}} \mathbf{Q} \overline{\mathbf{f}} + \mathbf{g}_l^{\mathrm{T}} \mathbf{Q} \underline{\mathbf{f}})} \\ & + \frac{\underline{\mathbf{f}}^{\mathrm{T}} \mathbf{Q}^{\mathrm{T}} \mathbf{E}_3^{\mathrm{T}} \mathbf{E}_3 \mathbf{Q} + \overline{\mathbf{f}}^{\mathrm{T}} \mathbf{Q}^{\mathrm{T}} \mathbf{E}_4^{\mathrm{T}} \mathbf{E}_4 \mathbf{Q}}{2(\mathbf{p}_r^{\mathrm{T}} \mathbf{Q} \underline{\mathbf{f}} + \mathbf{g}_r^{\mathrm{T}} \mathbf{Q} \overline{\mathbf{f}})} \end{aligned} \tag{13}$$

is a regressive vector. Now as illustrated in (12), the singleton IT2 FLS using maximum t-conorm, product t-norm, product implication, and center of sets type-reduction can be expressed as linear in the parameters.

III. Modeling of Marine Vessels

The model of surface vessels may be classified into two categories [22], namely process plant model and control plant model. The process plant model, which simulates the real plant dynamics as closely as possible including process disturbance, sensor outputs and control inputs, is used for numerical analysis and simulation of the performance and stability of the closed-loop system. The control plant model, which is a simplified form of the complicated process plant model, is used for controller design and theoretical stability analysis (e.g., in the sense of Lyapunov).

A. Process Plant Model

1) Kinematics: The motions and state variables of the surface vessels are conventionally defined and measured with respect to two coordinate frames as shown in Fig. 2, namely earth-fixed frame and body-fixed frame. The earth-fixed frame,

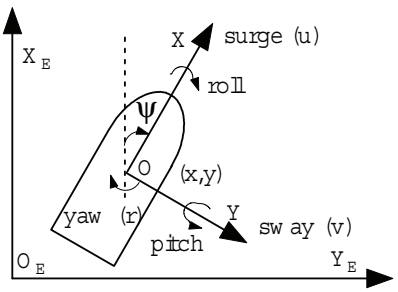

Fig. 2. 2D earth-fixed and body-fixed coordinate frames.

denoted as $\mathrm{X_E Y_E Z_E}$, is assumed fixed on the earth surface with X_E axis pointing north, the Y_E axis pointing east, and the Z_E axis down of the earth tangent plane. It is mainly used for global guidance and navigation. The body-fixed frame, denoted as XYZ, is fixed to the hull of the vessel, with X axis positive toward the bow, the Y axis positive towards starboard, and the Z axis positive downward. The origin of this frame is normally located at the vessel's center of gravity. The motion of a surface vessel has 6 degrees of freedom (DOF), which are surge, sway, heave, roll, pitch, and yaw. Let $\boldsymbol{\eta}' = [x, y, z, \phi, \theta, \psi]^{\mathrm{T}}$ be the vector representing the position and orientation of the vessel with respect to an earth-fixed frame, and let $\boldsymbol{\nu}' = [u, v, w, p, q, r]^{\mathrm{T}}$ denote the translation and rotation velocities of the vessel decomposed in the body-fixed frame. Then, the transformation between the earth-fixed and body-fixed velocity vectors is

$$\dot{\boldsymbol{\eta}}' = \mathbf{J}'(\boldsymbol{\eta}')\boldsymbol{\nu}'. \tag{14}$$

where $\mathbf{J}'(\boldsymbol{\eta}')$ is a state dependent transformation matrix, whose detailed definition can be found in [1].

2) Dynamics: The 6 DOF model formulation introduced here is based on [2], [3]. The equation of motion, which is in body-fixed frame, for a surface vessel whose speed is not low, is given by

$$\mathbf{M}'\dot{\boldsymbol{\nu}}' + \mathbf{C}'_{RB}\boldsymbol{\nu}' + \mathbf{C}'_A\boldsymbol{\nu}'_r + \bar{\mathbf{B}}'\boldsymbol{\nu}'_r + \mathbf{G}'\boldsymbol{\eta}' + \boldsymbol{\mu}' = \boldsymbol{\tau}' + \boldsymbol{\tau}'_{\mathrm{h}} \tag{15}$$

where $\mathbf{M}' = \mathbf{M}'_{RB} + \bar{\mathbf{A}}' \in R^{6\times 6}$ is the sum of the system inertia matrix and added mass matrix, $\mathbf{C}'_{RB} \in R^{6\times 6}$ is the Coriolis-Centripetal matrix, $\mathbf{C}'_A \in R^{6\times 6}$ is the constant infinite frequency added mass matrix, $\bar{\mathbf{B}}' \in R^{6\times 6}$ is the constant infinite frequency potential damping matrix, $\mathbf{G}' \in R^{6\times 6}$ is the restoring matrix, $\boldsymbol{\mu}' \in R^6$ is computed using a state space model to represent the fluid memory effect,

$$\dot{\boldsymbol{\chi}} = \mathbf{A}_r\boldsymbol{\chi} + \mathbf{B}_r\boldsymbol{\nu}'_r \tag{16}$$

$$\boldsymbol{\mu}' = \mathbf{C}_r\boldsymbol{\chi} + \mathbf{D}_r\boldsymbol{\nu}'_r \tag{17}$$

and where $(\mathbf{A}_r, \mathbf{B}_r, \mathbf{C}_r, \mathbf{D}_r)$ are constant matrices of appropriate dimensions. $\boldsymbol{\tau}' \in R^6$ is control force vector produced by thruster system, $\boldsymbol{\tau}'_{\mathrm{h}} = \boldsymbol{\tau}'_{\mathrm{CFD}} + \boldsymbol{\tau}'_{\mathrm{wave}} \in R^6$ is the sum of the cross-flow drag and surge resistance vector and wave load vector, which is computed according to Response Amplitude Operator tables, and $\boldsymbol{\nu}'_r = \boldsymbol{\nu}' - \boldsymbol{\nu}'_c \in R^6$ is the relative velocity vector between vessel velocity vector $\boldsymbol{\nu}'$ and sea current velocity vector $\boldsymbol{\nu}'_c$. All the detailed definition and computation of the above matrices and vectors can be found in [1], [2] and references therein.

B. Control Plant Model

The process plant model described in previous subsection is simplified on the basis of the following assumptions to facilitate the controller design and analytical stability analysis.

Assumption 1: The motions along heave, roll, and pitch directions are ignored for surface vessels. As a conventional vessel is metacentric stable, which means that there are restoring force and moments along those directions, this assumption is appropriate. As an application of this assumption, the dimension of the restoring matrix $\mathbf{G}' \in R^{6\times 6}$ in (15) is reduced to generate $\mathbf{G} \in R^{3\times 3} = \mathbf{0}$.

Assumption 2: The state variables of the vessel, i.e. displacements and velocities along surge, sway, and yaw, are measured by its own on-board devices such as gyro system, GPS, and accelerometers. Due to the development of modern

integration system of inertial sensors and satellite navigation system, this assumption is also appropriate.

Assumption 3: The influence of sea current is ignored. This assumption is mainly for the convenience of theoretical analysis.

Assumption 4: The time-varying hydrodynamic disturbances, i.e. $\boldsymbol{\mu}'$ and $\boldsymbol{\tau}'_{\rm h}$ in (15), could be estimated by singleton IT2 FLSs in the form of

$$\begin{aligned} \boldsymbol{\tau}'_d &= -\Phi'(\boldsymbol{\nu}')\Theta'. \\ &= \boldsymbol{\tau}'_{\rm h} - \boldsymbol{\mu}' \end{aligned} \tag{18}$$

where

$$\Theta' = (\boldsymbol{\theta}'^{\rm T}_1, \boldsymbol{\theta}'^{\rm T}_2, \ldots, \boldsymbol{\theta}'^{\rm T}_6)^{\rm T} \in R^{6M\times 1} \tag{19}$$

is a weighting vector and

$$\Phi'(\boldsymbol{\nu}') = {\rm diag}[\boldsymbol{\phi}'^{\rm T}_1, \boldsymbol{\phi}'^{\rm T}_2, \ldots, \boldsymbol{\phi}'^{\rm T}_6] \in R^{6\times 6M} \tag{20}$$

is a regressive matrix, M is the total number of rules for each sub-FLS. Thus far, this assumption has not been well established, for there is still a lack of rigorous proof showing singleton IT2 FLS could be universal approximator, but the propriety of this assumption will be checked by subsequent simulations.

1) Control Plant Model for Indirect Adaptive Control: Applying Assumptions 1-4 to (14) and (15), the following control plant model for indirect adaptive type-2 FLC design is obtained.

$$\dot{\boldsymbol{\eta}} = \mathbf{J}(\boldsymbol{\eta})\boldsymbol{\nu} \tag{21}$$

$$\mathbf{M}\dot{\boldsymbol{\nu}} + \mathbf{D}\boldsymbol{\nu} = \boldsymbol{\tau} - \Phi(\boldsymbol{\nu})\Theta \tag{22}$$

where $\boldsymbol{\eta} = [x, y, \psi]^{\rm T}$ is the displacement vector along surge, sway, and yaw, whereas $\boldsymbol{\nu} = [u, v, r]^{\rm T}$ is velocity vector, $\mathbf{J}(\boldsymbol{\eta}) \in R^{3\times 3}$ is the rotation matrix, note that $\mathbf{J}\mathbf{J}^{\rm T} = \mathbf{I}$ ($\mathbf{I}$ is the identity matrix), $\mathbf{M} \in R^{3\times 3}$ is the system inertia matrix including added mass, $\mathbf{D} = \mathbf{C}_{RB} + \mathbf{C}_A + \bar{\mathbf{B}} \in R^{3\times 3}$ is the damping matrix, and where $\mathbf{C}_{RB} \in R^{3\times 3}$, $\mathbf{C}_A \in R^{3\times 3}$, and $\bar{\mathbf{B}} \in R^{3\times 3}$ are three dimensional version of their corresponding matrices.

$$\Theta = (\boldsymbol{\theta}^{\rm T}_1, \boldsymbol{\theta}^{\rm T}_2, \boldsymbol{\theta}^{\rm T}_3)^{\rm T} \in R^{3M\times 1} \tag{23}$$

is the weighting vector and

$$\Phi(\boldsymbol{\nu}) = {\rm diag}[\boldsymbol{\phi}^{\rm T}_1(\boldsymbol{\nu}), \boldsymbol{\phi}^{\rm T}_2(\boldsymbol{\nu}), \boldsymbol{\phi}^{\rm T}_3(\boldsymbol{\nu})] \in R^{3\times 3M} \tag{24}$$

is the regressive matrix. Thus, here three sub-FLSs are used to approximate the hydrodynamic disturbances.

2) Control Plant Model for Direct Adaptive Control: Application of Assumptions 1-3 to (14) and (15) yields the following control plant model for direct adaptive type-2 FLC design.

$$\dot{\boldsymbol{\eta}} = \mathbf{J}(\boldsymbol{\eta})\boldsymbol{\nu} \tag{25}$$

$$\mathbf{M}\dot{\boldsymbol{\nu}} + \mathbf{D}\boldsymbol{\nu} + \boldsymbol{\mu} = \boldsymbol{\tau} + \boldsymbol{\tau}_{\rm h} \tag{26}$$

where $\boldsymbol{\mu} \in R^3$ and $\boldsymbol{\tau}_{\rm h} \in R^3$ are three dimensional version of $\boldsymbol{\mu}'$ and $\boldsymbol{\tau}'_{\rm h}$ respectively.

IV. Adaptive Fuzzy Logic Controller Design

The control objective in this paper is to manipulate a surface vessel to track the desired trajectory $\boldsymbol{\eta}_d = [x_d, y_d, \psi_d]^{\rm T}$, whose second derivative is continuous, as close as possible. In this section, both indirect and direct adaptive fuzzy logic controller are proposed for this control objective. However, the closed-loop systems under these two control schemes turn out to be same. The tracking error under these two control techniques is proved to globally asymptotically converge to zero. Rigorous analysis shows the closed-loop system is passive.

A. Indirect Adaptive Fuzzy Control

In indirect adaptive fuzzy control, the disturbances of the plant model are estimated by singleton IT2 FLSs as illustrated in (18) and the controller is designed assuming that the estimated disturbances represent the true time-varying disturbances. The control and adaptive law of the indirect adaptive type-2 FLC for plant (21), (22) are as follows.

$$\boldsymbol{\tau} = \mathbf{M}\dot{\boldsymbol{\nu}}_t + \mathbf{D}\boldsymbol{\nu}_t - \lambda_1\mathbf{s} + \Phi(\boldsymbol{\nu})\hat{\Theta} \tag{27}$$

$$\dot{\hat{\Theta}} = \lambda_2\Phi^{\rm T}(\boldsymbol{\nu})\mathbf{s} \tag{28}$$

where $\boldsymbol{\nu}_t = \boldsymbol{\nu}_d - \lambda_3\mathbf{J}^{\rm T}(\boldsymbol{\eta})\boldsymbol{e} = \mathbf{J}^{\rm T}(\boldsymbol{\eta})\dot{\boldsymbol{\eta}}_d - \lambda_3\mathbf{J}^{\rm T}(\boldsymbol{\eta})\boldsymbol{e} = \mathbf{J}^{\rm T}(\boldsymbol{\eta})(\dot{\boldsymbol{\eta}}_d - \lambda_3\boldsymbol{e})$, $\tilde{\Theta} = \Theta - \hat{\Theta} \in R^{3M}$ is the error vector between true Θ in (22) and adapted $\hat{\Theta}$, λ_i $(i = 1, 2, 3)$ are positive constant, and $\mathbf{s} = \boldsymbol{\nu} - \boldsymbol{\nu}_t = \mathbf{e}_\nu + \lambda_3\mathbf{J}^{\rm T}(\boldsymbol{\eta})\boldsymbol{e} = \mathbf{J}^{\rm T}(\boldsymbol{\eta})\dot{\boldsymbol{e}} + \lambda_3\mathbf{J}^{\rm T}(\boldsymbol{\eta})\boldsymbol{e} = \mathbf{J}^{\rm T}(\boldsymbol{\eta})(\dot{\boldsymbol{e}} + \lambda_3\boldsymbol{e})$, and where $\boldsymbol{e} = \boldsymbol{\eta} - \boldsymbol{\eta}_d \in R^3$ is the tracking error vector of vessel displacement, whereas $\boldsymbol{e}_\nu = \boldsymbol{\nu} - \boldsymbol{\nu}_d \in R^3$ is the tracking error vector of vessel velocity.

B. Direct Adaptive Fuzzy Control

In direct adaptive fuzzy control, the parameters of the controller are directly adjusted to reduce the tracking error. The direct adaptive type-2 FLC is designed based on the following assumption.

Assumption 5: The function of $\mathbf{M}\dot{\boldsymbol{\nu}}_t + \mathbf{D}\boldsymbol{\nu}_t - \boldsymbol{\tau}_{\rm h} + \boldsymbol{\mu} - \lambda_1\mathbf{s}$ could be estimated by singleton IT2 FLSs, i.e.,

$$\mathbf{M}\dot{\boldsymbol{\nu}}_t + \mathbf{D}\boldsymbol{\nu}_t - \boldsymbol{\tau}_{\rm h} + \boldsymbol{\mu} - \lambda_1\mathbf{s} = \Phi(\boldsymbol{\nu})\Theta. \tag{29}$$

The control and adaptive law of the indirect adaptive type-2 FLC for plant (25), (26) are as follows.

$$\begin{aligned} \boldsymbol{\tau} &= \Phi(\boldsymbol{\nu})\hat{\Theta} \\ &= \mathbf{M}\dot{\boldsymbol{\nu}}_t + \mathbf{D}\boldsymbol{\nu}_t - \boldsymbol{\tau}_{\rm h} + \boldsymbol{\mu} - \lambda_1\mathbf{s} - \Phi(\boldsymbol{\nu})\tilde{\Theta} \end{aligned} \tag{30}$$

$$\dot{\hat{\Theta}} = \lambda_2\Phi^{\rm T}(\boldsymbol{\nu})\mathbf{s} \tag{31}$$

C. Stability Analysis

Application of indirect and direct adaptive control and adaptive law (27), (28) and (30), (31) respectively to the plant (21), (22) and (25), (26) yields the same closed-loop system

$$\mathbf{M}\dot{\boldsymbol{s}} + \mathbf{D}\boldsymbol{s} = -\lambda_1\boldsymbol{s} - \Phi(\boldsymbol{\nu})\tilde{\Theta} \tag{32}$$

$$\dot{\tilde{\Theta}} = \lambda_2\Phi^{\rm T}(\boldsymbol{\nu})\boldsymbol{s} \tag{33}$$

$$\dot{\boldsymbol{e}} = -\lambda_3\boldsymbol{e} + \mathbf{J}(\boldsymbol{\eta})\boldsymbol{s}. \tag{34}$$

Theorem 1: The states $(\boldsymbol{s}, \boldsymbol{e})$ of the closed-loop system (32)-(34) globally asymptotically converge to $(\mathbf{0}, \mathbf{0})$.

Proof: Consider the following Lyapunov function candidate, which is positive definite.

$$V = \frac{1}{2}\boldsymbol{s}^{\mathrm{T}}\mathbf{M}\boldsymbol{s} + \lambda_1\lambda_3\boldsymbol{e}^{\mathrm{T}}\boldsymbol{e} + \frac{1}{2\lambda_2}\tilde{\Theta}^{\mathrm{T}}\tilde{\Theta} \tag{35}$$

Differentiation of V along the trajectory of the closed-loop system (32)-(34) yields

$$\begin{aligned}\dot{V} =& \boldsymbol{s}^{\mathrm{T}}(-\mathbf{D}\boldsymbol{s} - \lambda_1\boldsymbol{s} - \Phi(\boldsymbol{\nu})\tilde{\Theta}) + \tilde{\Theta}^{\mathrm{T}}\Phi^{\mathrm{T}}(\boldsymbol{\nu})\boldsymbol{s} \\ &+ 2\lambda_1\lambda_3\boldsymbol{e}^{\mathrm{T}}(-\lambda_3\boldsymbol{e} + \mathbf{J}(\boldsymbol{\eta})\boldsymbol{s}) \\ =& -\frac{1}{2}\boldsymbol{s}^{\mathrm{T}}(\mathbf{D} + \mathbf{D}^{\mathrm{T}})\boldsymbol{s} - \lambda_1\dot{\boldsymbol{e}}^{\mathrm{T}}\dot{\boldsymbol{e}} - \lambda_1\lambda_3^2\boldsymbol{e}^{\mathrm{T}}\boldsymbol{e} \\ \leq& 0\end{aligned}$$

which means the derivative of the Lyapunov function candidate is semi-negative definite. Moreover, the largest invariant set contained in the set $\dot{V} \equiv 0$ is contained in the set $(\boldsymbol{s}, \boldsymbol{e}) = (\mathbf{0}, \mathbf{0})$.

Now, according to Krasovskii-La Salle Invariant Set Theorem, we may conclude the point $(\boldsymbol{s}, \boldsymbol{e})$ globally asymptotically converges to $(\mathbf{0}, \mathbf{0})$ as time tends to infinite, and $\dot{\tilde{\Theta}} = 0$, which means $\hat{\Theta}$ is bounded. ■

Remark 1: Here, the theorem is developed for the case where the gains λ_i $(i = 1, 2, 3)$ are scalar, the case where the gains are matrices can be extended to in a similar approach.

D. Passivity Interpretation

According to energy-related considerations, by means of an input-output description passivity theory provides a framework for the design and analysis of control systems. And the input-output description further allows for a modular method of control systems design and analysis [23]. As shown in Fig. 3, the closed-loop system (32)-(34) can be interpreted as the negative feedback interconnection of three subsystems with respective inputs u_1, u_2, u_3 and outputs y_1, y_2, and y_3, with $y_1 = u_2 = u_3$ and $u_1 = -y_2 - y_3$, and the three subsystems as follows.

Subsystem 1:

$$\begin{cases}\mathbf{M}\dot{\boldsymbol{s}} + \mathbf{D}\boldsymbol{s} = u_1 \\ y_1 = \boldsymbol{s}\end{cases} \tag{36}$$

Subsystem 2:

$$\begin{cases}\dot{\tilde{\Theta}} = \lambda_2\Phi^{\mathrm{T}}(\boldsymbol{\nu})u_2 \\ y_2 = \Phi(\boldsymbol{\nu})\tilde{\Theta}\end{cases} \tag{37}$$

Subsystem 3:

$$\begin{cases}\dot{\boldsymbol{e}} = -\lambda_3\boldsymbol{e} + \mathbf{J}(\boldsymbol{\eta})u_3 \\ y_3 = \lambda_1 u_3\end{cases} \tag{38}$$

Theorem 2: The closed-loop system (32)-(34) is passive.

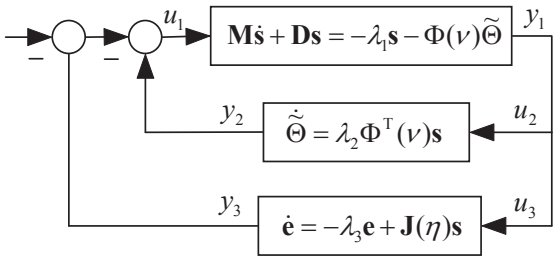

Fig. 3. Closed-loop equivalent representation.

Proof: For subsystem 1, its supply rate is

$$\begin{aligned}&\int_0^t u_1^{\mathrm{T}} y_1 dr \\ =& \int_0^t (\mathbf{M}\dot{\boldsymbol{s}} + \mathbf{D}\boldsymbol{s})^{\mathrm{T}}\boldsymbol{s} dr \\ =& \int_0^t \boldsymbol{s}^{\mathrm{T}}\mathbf{M}\dot{\boldsymbol{s}} dr + \int_0^t \boldsymbol{s}^{\mathrm{T}}\mathbf{D}\boldsymbol{s} dr \\ =& \frac{1}{2}\boldsymbol{s}^{\mathrm{T}}(t)\mathbf{M}\boldsymbol{s}(t) - \frac{1}{2}\boldsymbol{s}^{\mathrm{T}}(0)\mathbf{M}\boldsymbol{s}(0) + \int_0^t \boldsymbol{s}^{\mathrm{T}}\mathbf{D}\boldsymbol{s} dr\end{aligned}$$

Thus, the subsystem 1 is output strictly passive with supply rate $\int_0^t u_1^{\mathrm{T}} y_1 dr$ and storage function $\frac{1}{2}\boldsymbol{s}^{\mathrm{T}}\mathbf{M}\boldsymbol{s}$.

For subsystem 2 its supply rate is

$$\begin{aligned}\int_0^t u_2^{\mathrm{T}} y_2 dr =& \int_0^t \tilde{\Theta}^{\mathrm{T}}\Phi^{\mathrm{T}}(\boldsymbol{\nu})u_2 dr \\ =& \int_0^t \tilde{\Theta}^{\mathrm{T}}\frac{1}{\lambda_2}\dot{\tilde{\Theta}} dr \\ =& \frac{1}{2\lambda_2}\tilde{\Theta}^{\mathrm{T}}(t)\tilde{\Theta}(t) - \frac{1}{2\lambda_2}\tilde{\Theta}^{\mathrm{T}}(0)\tilde{\Theta}(0)\end{aligned}$$

which means the subsystem 2 is passive with supply rate $\int_0^t u_2^{\mathrm{T}} y_2 dr$ and storage function $\frac{1}{2\lambda_2}\tilde{\Theta}^{\mathrm{T}}\tilde{\Theta}$.

For subsystem 3, its supply rate is

$$\begin{aligned}\int_0^t u_3^{\mathrm{T}} y_3 dr =& \int_0^t u_3^{\mathrm{T}}\lambda_1 u_3 dr \\ =& \int_0^t \frac{1}{\lambda_1} y_3^{\mathrm{T}} y_3 dr \\ =& \frac{\lambda_1}{2}\int_0^t u_3^{\mathrm{T}} u_3 dr + \int_0^t \frac{1}{2\lambda_1} y_3^{\mathrm{T}} y_3 dr\end{aligned}$$

which means the subsystem 3 is very strictly passive with supply rate $\int_0^t u_3^{\mathrm{T}} y_3 dr$.

According to the fact that the negative feedback interconnection of two passive systems is passive, the closed-loop system (32)-(34), which can be interpreted as negative feedback interconnection of subsystem 1 and subsystem 2, then together with subsystem 3, is passive. ■

V. Simulation Studies

Marine System Simulator, which is developed in Norwegian University of Science and Technology [24], is employed as the platform for the simulation studies. The International Towing

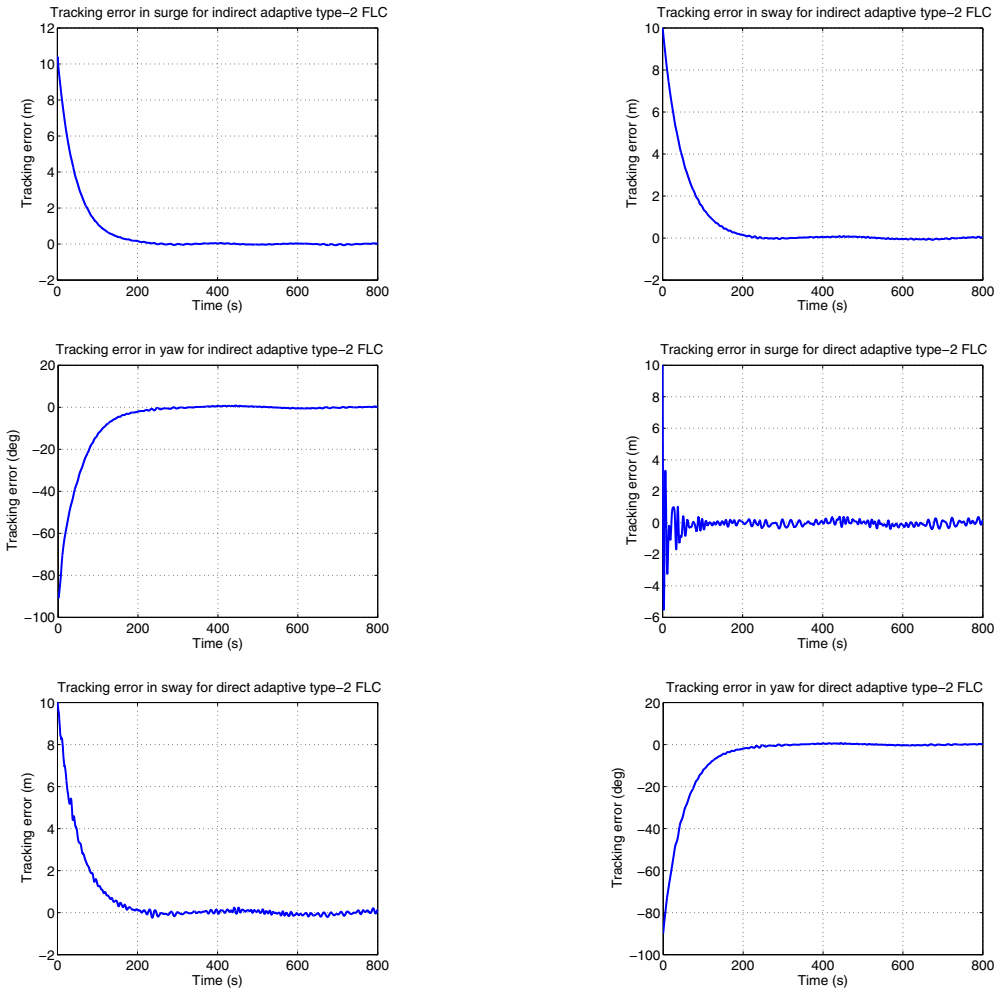

Fig. 4. Plots 1-3 show the tracking errors for indirect adaptive type-2 FLC. Plots 4-6 show the tracking errors for direct adaptive type-2 FLC.

Tank Conference (ITTC) wave spectrum with significant wave height $H_s = 3$ m and peak frequency $\omega_0 = 0.56$ rad/s is used to imitate rough sea with large waves. Sea current with speed $V_c = 0.2$ m/s and direction $\beta_c = 30^\circ$ is also included in the simulations, although ignored during the controller design. A container ship named as S-175 is used as case study. The control objective is to control the vessel to track the desired trajectory $\boldsymbol{\eta}_d = [x_d, y_d, \psi_d]^{\mathrm{T}}$, where $x_d = 8t$, $y_d = 200\cos(0.005\pi t)$, and $\psi_d = \arctan(y_d/x_d)$. The initial states are set as $[\boldsymbol{\eta}_0^{\mathrm{T}}, \boldsymbol{\nu}_0^{\mathrm{T}}] = [10, 210, 0, 0, 0, 0]$. All the IT2 FLSs in indirect adaptive fuzzy controller (27), (28) and direct adaptive fuzzy controller (30), (31) are configured as follows. As there are three degrees of freedom considered for the motion of the vessel, three singleton IT2 sub-FLSs are employed for each controller, which is demonstrated in (23) and (24). For each sub-system, three fuzzy membership functions labeled as **N**, **Z**, and **P** are employed to partition each of the input domain. As there are three inputs, there are totally 27 rules and 27 adjustable consequent parameters. Gaussian function with uncertain standard deviation is chosen to be the primary membership functions of the antecedent IT2 fuzzy sets and in the following form.

$$\mu_{\tilde{F}_i^j}(x_j) = \exp[-\frac{1}{2}(\frac{x_j - m_i}{\sigma})^2] \quad \sigma \in [\underline{\sigma}, \overline{\sigma}] \tag{39}$$

where $j = 1, 2, 3$ is the index of three inputs and $i = 1, 2, 3$ is the index of three fuzzy membership functions for jth input. For each input, the means of the Gaussian functions are $m_1 = -1$, $m_2 = 0$, and $m_3 = 1$, the standard deviations of the lower membership functions are $\underline{\sigma} = 0.6$, and the standard deviations of the upper membership functions are $\overline{\sigma} = 0.8$.

A. Closed-loop Performance

Although the indirect and direct adaptive fuzzy controllers (27), (28) and (30), (31) are designed based on the control plant models (21), (22) and (25), (26) respectively, they are tested with the process plant model (14), (15) in the simulations.

1) Indirect Adaptive Control: Set $\lambda_1 = 4.3 \times 10^8$, $\lambda_2 = 1 \times 10^8$, and $\lambda_3 = 0.02$ in (27) and (28). The tracking errors of the vessel to the desired trajectory under the indirect adaptive fuzzy controller are shown in plot 1-3 of Fig. 4, from which it can be observed that the tracking errors asymptotically

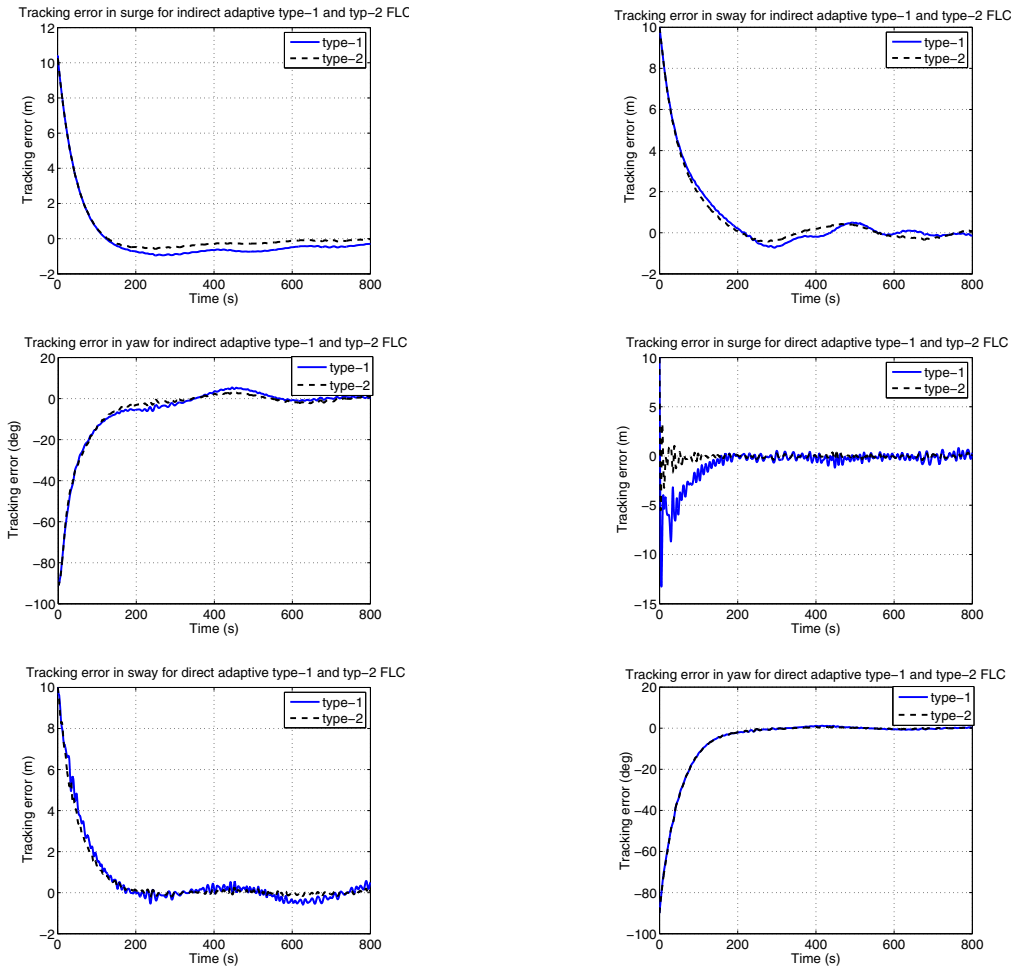

Fig. 5. Plots 1-3 show the tracking errors for indirect type-1 and type-2 FLC. Plots 4-6 show the tracking errors for direct type-1 and type-2 FLC.

converge to zero despite the time-varying hydrodynamic disturbances and the sub-FLSs effectively approximate the complex disturbances.

2) Direct Adaptive Control: Set $\lambda_2 = 1 \times 10^8$ and $\lambda_3 = 0.02$ in (30) and (31). The tracking errors under the direct adaptive fuzzy controller are shown in plot 4-6 of Fig. 4. The tracking performance is satisfactory in the presence of the time-varying disturbances, and the sub-FLSs effectively generate the control forces and moment. Fluctuations in the tracking errors are observed, that is because the inputs to the sub-FLSs are insufficient to make the sub-FLSs accurately approximate the complex function (29).

The control performance under indirect adaptive fuzzy control is noted to be better than that under direct adaptive fuzzy control. One may conclude without hesitation that the indirect adaptive fuzzy controller is better than the direct one, however, the direct adaptive fuzzy controller has an advantage over the indirect one, i.e., the direct adaptive fuzzy controller does not need the knowledge of inertial matrix $\mathbf{M}$ and damping matrix $\mathbf{D}$, thus can be used under the situation where such knowledge is not available.

B. Comparison with Adaptive Type-1 Fuzzy Controllers

Replace the components in (24) and correspondingly in indirect adaptive controller (27), (28) and direct adaptive controller (30), (31) with fuzzy basis function vector [7], [8],

$$\boldsymbol{\phi}^{\mathrm{T}} = (\phi^1(\mathbf{x}), \ldots, \phi^M(\mathbf{x})) \tag{40}$$

where fuzzy basis function is defined as

$$\phi^l(\mathbf{x}) = \frac{\Pi_{i=1}^n \mu_{F_i^l}(x_i)}{\Sigma_{l=1}^M (\Pi_{i=1}^n \mu_{F_i^l}(x_i))}, \tag{41}$$

the controllers (27), (28) and (30), (31) become adaptive type-1 FLCs. In this subsection, the adaptive type-2 FLCs are compared with their type-1 counterparts. For each sub-FLS in the type-1 cases, five fuzzy membership functions labeled as **NL**, **NS**, **Z**, **PS**, and **PL** are employed to partition each of the input domain. As there are three inputs, there are 125 rules and 125 adjustable consequent parameters in contrast to 27 rules and parameters for type-2 cases. Gaussian functions are chosen to be the membership functions of the antecedent sets for each input, they can be written as

$$\mu_{F_i^j}(x_j) = \exp[-\frac{1}{2}(\frac{x_j - m_i}{\sigma})^2], \tag{42}$$

where $j = 1, 2, 3$ is the index of three inputs and $i = 1, \ldots, 5$ is the index of five fuzzy membership functions for jth input. The means are fixed as $(m_1, \ldots, m_5) = (-1, -0.5, 0, 0.5, 1)$, whereas the standard deviations for all the Gaussian functions are set as $\sigma = 0.4$.

1) Indirect Adaptive Control: Set $\lambda_1 = 4.3 \times 10^8$, $\lambda_2 = 1 \times 10^7$, and $\lambda_3 = 0.02$ in (27) and (28) for both indirect adaptive type-1 and type-2 FLCs, the tracking errors are shown in plot 1-3 of Fig. 5.

2) Direct Adaptive Control: Set $\lambda_2 = 1 \times 10^8$ and $\lambda_3 = 0.02$ in (30) and (31) for both direct adaptive type-1 and type-2 FLCs, the tracking errors are depicted in plot 4-6 of Fig. 5.

It can be observed from Fig. 5 that the adaptive type-2 FLCs perform comparably with, if not better than, their type-1 counterparts, even though type-1 cases use more than four times the number of the rules. In order to quantify the performance differences between adaptive type-1 and type-2 FLCs, the integral of time-weighted absolute errors (ITAE) for all the above four cases in the following form are calculated.

$$P_x = \int_0^T t|e_x|dt \tag{43}$$

$$P_y = \int_0^T t|e_y|dt \tag{44}$$

$$P_\psi = \int_0^T t|e_\psi|dt \tag{45}$$

where T is the total simulation time and e_x, e_y, and e_ψ are three components of tracking error vector $\boldsymbol{e}$. According to the results shown in Table I, the values of the ITAE for the adaptive type-2 FLCs are smaller than those for type-1 cases along all the three degrees of freedom. As regards the computational burden, type-reductions for type-2 cases do take some time, but the time is very little as only a few rules are fired at the same time and Karnik-Mendel algorithm has been proved to be super-exponentially convergent [25]. Furthermore, it has been reported the type-2 FLS can be implemented in real-time applications [26]. Thus, type-reduction should not be an issue and will not cause any stability problem. In conclusion, It seems that the type-2 FLS has better approximation property with less rules than its type-1 counterpart in this application.

TABLE I
ITAE FOR ADAPTIVE TYPE-1 AND TYPE-2 FLCS

Cases	Indirect T1	Indirect T2	Direct T1	Direct T2
P_x	192746	81796	162892	53917
P_y	85064	66428	78648	43013
P_ψ	14154	9592	5680	4660

VI. CONCLUSIONS

In this paper, indirect and direct adaptive type-2 FLCs have been designed for tracking control of surface vessels in the presence of time-varying hydrodynamic disturbances. It has been proved the tracking errors under both of the proposed controls globally asymptotically converge to zero. Although designed through different approaches, the closed-loop systems for both indirect and direct type-2 FLCs are same and passive. Simulation results have demonstrated that the two controllers are effective and robust. Comparison with their type-1 counterparts suggests the type-2 FLS has comparable approximation property.

REFERENCES

[1] T. I. Fossen, *Marine Control Systems: Guidance Navigation and Control of Ships Rigs and Underwater Vehicles*. Trondheim, Norway: Marine Cybernetics, 2002.

[2] ——, "Nonliear time-domain strip theory formulation for low speed manoeuving and station-keeping," *Modelling, Id. Control*, vol. 25, no. 4, pp. 201–221, 2004.

[3] T. Perez and T. I. Fossen, "Kinematic models for manoeuvring and seakeeping of marine vessels," *Modelling, Id. Control*, vol. 28, no. 1, pp. 19–30, 2007.

[4] X. T. Chen and W. W. Tan, "An adaptive type-2 fuzzy logic controller for dynamic positioning," submitted to 2011 IEEE Int. Conf. on Fuzzy Syst.

[5] K. S. Narendra and A. M. Annaswamy, *Stable Adaptive Systems*. Englewood Cliffs, NJ: Prentice-Hall, 1989.

[6] S. S. Ge, C. C. Hang, T. H. Lee, and T. Zhang, *Stable Adaptive Neural Network Control*. Boston, MA: Kluwer, 2001.

[7] L. X. Wang, "Stable adaptive fuzzy control of nonlinear systems," *IEEE Trans. Fuzzy Syst.*, vol. 1, no. 2, pp. 146–155, May 1993.

[8] L. X. Wang and J. M. Mendel, "Fuzzy basis functions, universal approximation, and orthogonal least-squares learning," *IEEE Trans. Neural Netw.*, vol. 3, no. 5, pp. 807–814, Sep. 1992.

[9] J. L. Castro, "Fuzzy logic controllers are universal approximators," *IEEE Trans. Syst., Man, Cybern.*, vol. 25, no. 4, pp. 629–635, Apr. 1995.

[10] X. J. Zeng and M. G. Singh, "Approximation accuracy analysis of fuzzy systems as function approximators," *IEEE Trans. Fuzzy Syst.*, vol. 4, no. 1, pp. 44–63, Jan. 1996.

[11] H. Ying, *Fuzzy Control and Modeling: Analytical Foundations and Applications*. New York: IEEE Press, 2000.

[12] N. N. Karnik, J. M. Mendel, and Q. Liang, "Type-2 fuzzy logic systems," *IEEE Trans. Fuzzy Syst.*, vol. 7, no. 6, pp. 643–658, Dec. 1999.

[13] J. M. Mendel, *Uncertain Rule-Based Fuzzy Logic System: Introduction and New Directions*. Upper Saddle River, NJ: Prentice-Hall, 2001.

[14] J. M. Mendel and R. I. John, "Type-2 fuzzy sets made simple," *IEEE Trans. Fuzzy Syst.*, vol. 10, no. 2, pp. 117–127, Apr. 2002.

[15] R. John and S. Coupland, "Type-2 fuzzy logic: A historical view," *IEEE Comput. Intell. Mag.*, vol. 2, no. 1, pp. 57–62, Feb. 2007.

[16] H. Hagras, "A hierarchical type-2 fuzzy logic control architecture for autonomous mobile robots," *IEEE Trans. Fuzzy Syst.*, vol. 12, no. 4, pp. 524–539, Aug. 2004.

[17] D. R. Wu and W. W. Tan, "A type-2 fuzzy logic controller for the liquid-level process," in *Proc. IEEE Int. Conf. on Fuzzy Syst.*, Budapest, 2004, pp. 953–958.

[18] C. Wagner and H. Hagras, "Slices based general type-2 flc for the control of autonomous mobile robots in real world environments," in *Proc. IEEE Int. Conf. on Fuzzy Syst.*, Jeju Island, Korea, 2009, pp. 718–725.

[19] X. T. Chen and W. W. Tan, "A type-2 fuzzy logic controller for dynamic positioning systems," in *Proc. IEEE Int. Conf. on Control and Automation*, Xiamen, China, 2010, pp. 1013–1018.

[20] J. M. Mendel, "Computing derivatives in interval type-2 fuzzy logic system," *IEEE Trans. Fuzzy Syst.*, vol. 12, no. 1, pp. 84–98, Feb. 2004.

[21] C. F. Juang, R. B. Huang, and Y. Y. Lin, "A recurrent self-evolving interval type-2 fuzzy neural network for dynamic system processing," *IEEE Trans. Fuzzy Syst.*, vol. 17, no. 5, pp. 1092–1105, Oct. 2009.

[22] A. J. Sørensen, *Marine Cybernetics: Modelling and Control*, 5th ed. Trondheim, Norway: Dept. Marine Technology, NTNU, 2005.

[23] B. Brogliato, R. Lozano, B. Maschke, and O. Egeland, *Dissipative Systems Analysis and Control: Theory and Applications*, 2nd ed. London: Springer Verlag, 2007.

[24] MSS. (2010, Aug.) Marine Systems Simulator (2010). [Online]. Available: http://www.marinecontrol.org/

[25] J. Mendel and F. Liu, "Super-exponential convergence of the Karnik-Mendel algorithms for computing the centroid of an interval type-2 fuzzy set," *IEEE Trans. Fuzzy Syst.*, vol. 15, no. 2, pp. 309–320, Apr. 2007.

[26] C. Lynch and H. Hagras, "Developing embedded type-2 fuzzy logic controllers for handling the uncertainties in marine diesel engine speed control," *International Journal of Computational Intelligence Research*, vol. 4, no. 4, pp. 402–420, Oct. 2008.

2011 IEEE International Conference on Fuzzy Systems
June 27-30, 2011, Taipei, Taiwan

Relaxed Fuzzy Lyapunov Approach for Dynamic Local Model Networks

Christian H. Mayr*, Christoph Hametner†, Martin Kozek‡ and Stefan Jakubek§
Christian Doppler Laboratory for Model Based Calibration Methodologies
at the Institute of Mechanics and Mechatronics
Vienna University of Technology
Wiedner Hauptstrasse 8-10/325/A5, 1040 Vienna, Austria
*christian.mayr@tuwien.ac.at
†christoph.hametner@tuwien.ac.at
‡martin.kozek@tuwien.ac.at
§stefan.jakubek@tuwien.ac.at

***Abstract*—This paper deals with the problem of stability analysis of dynamic local model networks. Established methods in this context are mainly based on Lyapunov stability theory and are targeted to be as little conservative as possible. In this respect it is essential to take into account the transitions between the different local models. For that purpose this paper presents and discusses a method to determine possible model transitions of such dynamic local model networks utilizing identification or simulation data. The effectiveness of the proposed method is shown by a simulation example in connection with the fuzzy Lyapunov approach as a stability criterion. The example demonstrates how identification data can be used to reduce the conservatism compared to standard approaches.**

***Keywords*—local model networks, fuzzy Lyapunov function, stability, system identification**

I. Introduction

Local model networks (LMN) are a versatile architecture for the representation of a large class of nonlinear systems. The approximation is based on a partitioning of the nonlinearities into subdomains which can be accurately represented by simpler submodels, for example linear models [1]. The architecture of LMN offers good interpretability which is an important advantage for the design of controllers or observers. LMN are usually generated from measured input and output data of the process to be approximated.

When the structure of LMN is applied to nonlinear dynamic systems a main challenge is to provide stability criteria. A major difficulty lies in the fact that a dynamic LMN can become unstable in the large even when all local linear models are stable, [2].

Stability proofs of local model networks are mainly based on Lyapunov's direct method which results in linear matrix inequalities (LMIs) as stability criterion. Lyapunov stability criteria provide *sufficient* rather than a necessary conditions for stability. In this context the issue of *conservatism* is inherently linked to these methods: Depending on the type and structure of the chosen Lyapunov function a stability proof may fail even though the investigated system is stable.

The basic criterion is the so-called common quadratic Lyapunov approach, [2]. The main drawback of this approach is its conservatism since it aims to find one common Lyapunov function for all local linear models in an LMN. The reason lies in the fact that the LMI solver has to find a single positive definite matrix and must simultaneously fulfill as many LMIs as the number of local models. Thus, by increasing the number of local models, and increasing the accuracy of the LMN, it will be more difficult to find a common Lyapunov function.

In recent years advanced methods, based on the less conservative fuzzy Lyapunov approach have been developed, [3], [4], [5], [6], [7]. Basically this approach aims to find a Lyapunov function for each local model which are connected by so-called model transitions. A model transition occurs when the system state transits from one local model to another. The conservatism of the stability criterion is directly increased with the number of model transitions. Thus, in order to prove stability using the fuzzy Lyapunov approach without any additional structural information of the LMN it is mandatory to take into account how state trajectories can progress through different local models. This helps to reduce the conservatism because impossible transitions need not be considered. Due to the nature of local model networks only a limited number of model transitions actually take place or are theoretically feasible. Note, that the number of theoretically possible model transitions is increased with the number of local models.

For simple and low dimensional partitioning strategies (e.g. two dimensional trapezoid validity functions) it is possible to determine the model transition using the phase portrait of the considered local model network or the method presented in [4]. For high dimensional partition spaces and complex partitioning strategies such as [8], [9], [10], [11] and [12] the method of [4] is no longer feasible.

In this paper a systematic approach is introduced to determine all occurring model transitions in a dynamic LMN. The basic idea is to capture the model transitions by means of simulation data. Therefore an optimally designed input data sequence

This work was supported by Christian Doppler Research Association and AVL List GmbH

978-1-4244-7316-8/11/$26.00 ©2011 IEEE

regarding design of experiment (DoE) is required which must be *extensive* and *tight*, see [13]. For local model networks generated from a real physical process the identification data sequence can be used because it must fulfill the same requirements to capture the dynamics of the considered system within the operating area. For artificial local model networks the input data sequence has to be generated. Thus, all occurring model transition can be determined using simulation data generated by an optimally designed input data sequence. It must be noted, however, that the characteristics of the simulation data significantly contribute to the effectiveness of the proposed method. This is not a severe disadvantage, because the range of the excitation signal is either given (identification data) or user defined and can be chosen to the area of interest (e.g. operating area) for the stability criterion.

With the proposed method the conservatism of the fuzzy Lyapunov approach is reduced significantly making it a feasible method to prove stability of LMN. The main advantages of the transition determination of dynamic local model networks by utilizing the identification data sequence or an optimally designed excitation data sequence are:

- The conservatism does not grow automatically with the number of local models.
- It is independent regarding the dimensions of the partition space and the type of the validity function.
- It is applicable to arbitrary partitioning strategies, such as: equidistant grid [4]; recursive, axis orthogonal [8], [9], [14]; axis oblique [10], [15]; arbitrary functions [12]; hinging hyperplanes [11].

This paper is organized as follows: The architecture of local model networks is briefly described in section II. Section III generally addresses stability, the common quadratic Lyapunov approach, and the fuzzy Lyapunov approach for discrete-time LMN. Section IV describes the proposed procedure to determine all occurring model transitions utilize a DoE optimal excitation signal. In section V on the one hand the transition determination is described and on the other hand the improvement of finding a fuzzy Lyapunov function to prove stability using the proposed concept is demonstrated by means of illustrative examples. The paper is concluded by some remarks in section VI.

II. Local Model Networks

The architecture of dynamic local model networks is illustrated in Fig. 1.

First, an ordered set for the indices of the local models is defined as:

$$\mathcal{I} = (i \in \mathbb{N} | 1 \leq i \leq I) \tag{1}$$

where I denotes the number of local models. Local model networks with external dynamics have an input vector $\boldsymbol{z}(k)$ with past inputs and outputs according to Fig. 1:

$$\boldsymbol{z}(k) = [\boldsymbol{u}_{\mathcal{J}}(k - \mathcal{M})\ \hat{\boldsymbol{y}}(k - \mathcal{N})],\ \boldsymbol{z}(k) \in \mathbb{R}^O \tag{2}$$

where the ordered sets for the number of the input channels $\mathcal{J}$, the orders of the inputs $\mathcal{M}$, the orders of the feedback output

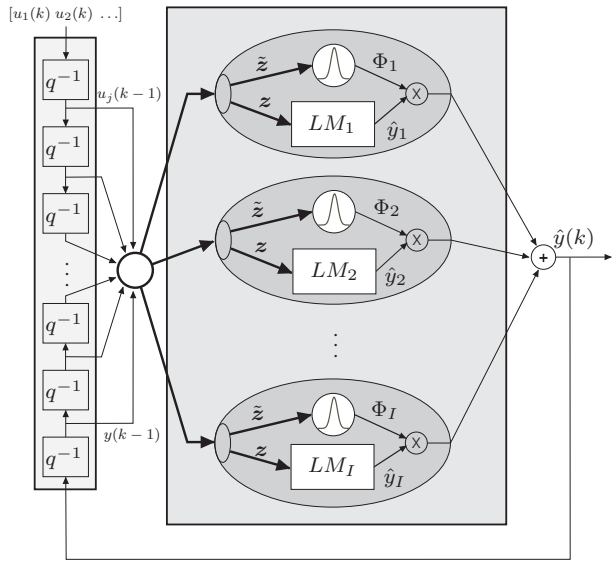

Fig. 1. Architecture of a local model network with external dynamics [15]

(=system order) $\mathcal{N}$ and the index $\mathcal{O}$ are as follows:

$$\mathcal{J}(j) = (j \in \mathbb{N} | 1 \leq j \leq J) \tag{3}$$

$$\mathcal{M}(m) = (m \in \mathbb{N} | 1 \leq m \leq M) \tag{4}$$

$$\mathcal{N}(n) = (n \in \mathbb{N} | 1 \leq n \leq N) \tag{5}$$

$$\mathcal{O}(o) = (o \in \mathbb{N} | 1 \leq o \leq O). \tag{6}$$

where J denotes the number of inputs, M denotes the order of the inputs, N denotes the system order and O denotes the dimension of the input vector. From Fig. 1 it becomes obvious that the input vector for the validity functions $\Phi_{\mathcal{I}}(\tilde{\boldsymbol{z}}(k))$ can be chosen differently to the input vector for the local model:

$$\tilde{\boldsymbol{z}}(k) = [\boldsymbol{u}_{\tilde{\mathcal{J}}}(k - \tilde{\mathcal{M}})\ \hat{\boldsymbol{y}}(k - \tilde{\mathcal{N}})] \subseteq \boldsymbol{z}(k),\ \tilde{\boldsymbol{z}}(k) \in \mathbb{R}^{\tilde{O}} \tag{7}$$

where the ordered sets $\tilde{\mathcal{J}}, \tilde{\mathcal{M}}, \tilde{\mathcal{N}}, \tilde{\mathcal{O}}$ are subsets of their corresponding sets as follows:

$$\tilde{\mathcal{J}}(\tilde{j}) \subseteq \mathcal{J}(j) \tag{8}$$

$$\tilde{\mathcal{M}}(\tilde{m}) \subseteq \mathcal{M}(m) \tag{9}$$

$$\tilde{\mathcal{N}}(\tilde{n}) \subseteq \mathcal{N}(n) \tag{10}$$

$$\tilde{\mathcal{O}}(\tilde{o}) \subseteq \mathcal{O}(o) \tag{11}$$

All local model outputs

$$\hat{y}_i(k) = \boldsymbol{z}(k)\boldsymbol{\theta}_i, \tag{12}$$

with the local parameter vector $\boldsymbol{\theta}_i$ are used subsequently to form the global model output $\hat{y}(k)$ by weighted aggregation, see Fig. 1:

$$\hat{y}(k) = \sum_{\mathcal{I}} \Phi_i(k)\hat{y}_i(k) \tag{13}$$

where the validity functions are constrained:

$$\sum_{\mathcal{I}} \Phi_i = 1 \tag{14}$$

$$0 \leq \Phi_i \leq 1,\ \forall i \in \mathcal{I}. \tag{15}$$

For stability analysis using Lyapunov approaches the local dynamics must be defined in state space notation. Thus, the discrete-time state space notation of local model networks can be generally defined using (1):

$$\begin{aligned} \boldsymbol{x}(k+1) &= \sum_{\mathcal{I}} \Phi_i(\tilde{\boldsymbol{z}}(k))(\boldsymbol{A}_i\boldsymbol{x}(k) + \boldsymbol{B}_i\boldsymbol{u}(k)) \\ \hat{y}(k) &= \boldsymbol{c}^T\boldsymbol{x}(k). \end{aligned} \tag{16}$$

III. Stability Concepts for Local Model Networks

In this section stability for discrete-time systems in general, the common quadratic Lyapunov approach and the fuzzy Lyapunov approach are described.

A. General

An autonomous dynamic system in discrete-time is represented by a set of difference equations in the form

$$\boldsymbol{x}(k+1) = \boldsymbol{f}(\boldsymbol{x}(k)), \;\; \boldsymbol{f} \in \mathbb{R}^{n\times 1} \tag{17}$$

where $\boldsymbol{f}$ is a nonlinear vector function, $\boldsymbol{x}$ is the $n \times 1$ state vector, and k denotes the sampling instant.
Nonlinear systems can have much more complex behavior than linear systems. A number of refined stability concepts, such as marginal stability and asymptotic stability, are needed, [16]:

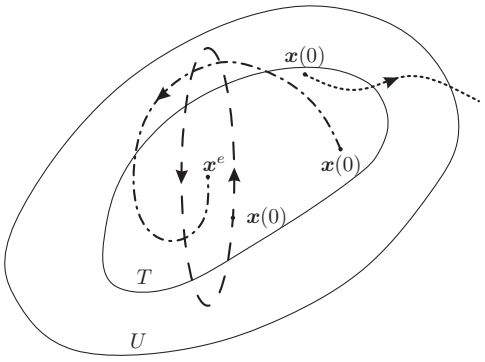

Fig. 2. Stability definitions

Definition 3.1: An equilibrium state $\boldsymbol{x}^e$ is *marginally stable* (Fig. 2, dashed line) if for every neighborhood $U > 0$ of $\boldsymbol{x}^e$ there is a neighborhood $T > 0,\ T \subseteq U$ of $\boldsymbol{x}^e$ such that every solution $\boldsymbol{x}(k)$ starting within $T(\boldsymbol{x}(0) \in T)$ remains within U for all $k > 0$. Otherwise the equilibrium point $\boldsymbol{x}^e$ is *unstable* (Fig. 2, dotted line).
Note that $\boldsymbol{x}(k)$ need not approach $\boldsymbol{x}^e$.

Definition 3.2: An equilibrium state $\boldsymbol{x}^e$ is *asymptotically stable* (Fig. 2, dash-dotted line) if it is marginal stable and additionally T can be chosen so that $\|\boldsymbol{x}(k) - \boldsymbol{x}^e\| \to 0$ as $k \to \infty$ for all $\boldsymbol{x}(0) \in T$.

B. Lyapunov Stability for Discrete-Time Local Model Networks

The stability of LMN can be proved by Lyapunov's direct method. This general approach is based on a state space formulation of the system, such as (16), and one has to find a suitable Lyapunov function, [9]. Since this is generally difficult it is common to restrict the search to the class of quadratic Lyapunov functions

$$V(k) = \boldsymbol{x}^T(k)\boldsymbol{P}\boldsymbol{x}(k) > 0, \quad \boldsymbol{P} \succ 0 \tag{18}$$

where $\boldsymbol{P}$ is a positive definite matrix and $\boldsymbol{x}(k)$ is the state of the model according to (16). For asymptotic stability, the Lyapunov function must be strictly monotonically decreasing over time k:

$$V(k+1) - V(k) < 0, \quad \forall k. \tag{19}$$

C. Common Quadratic Lyapunov Approach for Discrete-Time Systems

The common quadratic Lyapunov approach was the first stability criterion to be proposed for local model networks, [2]. It aims to find one common quadratic Lyapunov function for all local models. Using (16), (18) and (19) the common quadratic Lyapunov approach can be formulated as:

Theorem 1: A dynamic local model network is globally asymptotically stable if there exists *a common positive definite matrix* $\boldsymbol{P}$ for all local models:

$$\boldsymbol{P} \succ 0 \tag{20}$$

such that the following condition is satisfied:

$$\boldsymbol{A}_i^T\boldsymbol{P}\boldsymbol{A}_i - \boldsymbol{P} \prec 0, \quad \forall i \in \mathcal{I} \tag{21}$$

with $\boldsymbol{A}_i$ taken from (16), [2].
The proof of Theorem 1 is given in [2].

The stability condition (21) constitutes a set of *linear matrix inequalities* (LMIs) which is usually solved by numerical optimization.
In (21) a *common* matrix $\boldsymbol{P}$ must be found for *all* local system matrices $\boldsymbol{A}_i$. This is a much stronger condition than the individual stability of the local linear models, for which only $\boldsymbol{A}_i^T\boldsymbol{P}_i\boldsymbol{A}_i - \boldsymbol{P}_i \prec 0$ with individual $\boldsymbol{P}_i$ would be required, [9]. Note that it may not be possible to find a $\boldsymbol{P}$ that fulfills (21), although the global model may be stable. The condition (21) is therefore sufficient but not necessary.

D. Fuzzy Lyapunov Approach for Discrete-Time Systems

As the common quadratic Lyapunov approach tends to be conservative, it is desirable to have less conservative stability methods available. The fuzzy Lyapunov approach [3], [4], [5], [6], [7], [17] is one of the options for this purpose.
This approach aims to find a non-quadratic Lyapunov function for the global model

$$V(k) = \boldsymbol{x}^T(k)\Big(\sum_{\mathcal{I}} \Phi_i(\tilde{\boldsymbol{x}}(k))\boldsymbol{P}_i\Big)\boldsymbol{x}(k) > 0, \tag{22}$$

where each local model independently fulfills (18) (there is an individual $\boldsymbol{P}_i$ matrix associated to each local model).

Remark 1: The validity functions of the $\boldsymbol{P}_i$ matrices in (22) are equivalent to the validity functions of the local models in (16).

To fulfill (19) all local models must be stable as a prerequisite. Second, every possible trajectory must also satisfy (19). This

shows, that the occurring model transitions are of high interest when using the fuzzy Lyapunov approach:

Theorem 2: The dynamic local model network is asymptotically stable in the region U if there exists a *set of positive definite matrices* $\boldsymbol{P}_i$:

$$\boldsymbol{P}_i \succ 0, \quad \forall i \in \mathcal{I} \tag{23}$$

such that the following condition is satisfied:

$$\boldsymbol{A}_i^T \boldsymbol{P}_j \boldsymbol{A}_i - \boldsymbol{P}_i \prec 0, \quad \forall i \in \mathcal{I}, j \in \Omega_i \tag{24}$$

where the set Ω_i defines all possible model transitions of model i within region U, [4]. Defining the dominant region of a local model, according to [18], as

$$S_i = \{\tilde{\boldsymbol{x}} | \Phi_i(\tilde{\boldsymbol{x}}) > \Phi_l(\tilde{\boldsymbol{x}}),\ l \in \mathcal{I}, l \neq i\}, i \in \mathcal{I} \tag{25}$$

the possible transitions can be defined, as

$$\Omega_i = \{j | (\tilde{\boldsymbol{x}}(k) \in S_i \wedge \tilde{\boldsymbol{x}}(k+1) \in S_j) \vee (\tilde{\boldsymbol{x}}(k) \in S_j \wedge \tilde{\boldsymbol{x}}(k+1) \in S_i),\ j \in \mathcal{I}\},\ \forall i \in \mathcal{I}. \tag{26}$$

This includes the case $i = j$ which requires that every local model must have stable dynamics as a necessary condition. The proof of Theorem 2 is given in [4].

IV. Transition Determination

To reduce the conservatism of the fuzzy Lyapunov approach it is essential to determine all occurring model transition Ω_i. If no information about the model transitions is available, then transitions to all other models must be taken into account:

$$\Omega_i = \mathcal{I}, \quad \forall i \in \mathcal{I}. \tag{27}$$

Due to (26) each model transition results in two additional LMIs. Thus, the difficulty of finding a suitable Lyapunov function for the considered system is increased when additional model transitions are taken into account. Therefore, a proper determination of the occurring model transitions will help to reduce conservatism on the one hand, and often even makes a stability check on complex LMNs possible at all. Thus, in this section a method for the determination of all occurring model transitions is presented. One important point is the independency regarding the partitioning strategy of the considered local model network. Fig. 3 illustrates four common partitioning strategies of local model networks.

Obviously the determination of the model transitions by using the information of the partitioning can become difficult or impossible particularly for high order partition spaces and complex partitioning strategies as [10], [12] and [14]. Further, different types of validity functions are commonly used, see Fig. 4.

Thus, a method for the determination of the occurring model transitions, which is independent regarding the partitioning strategy and the type of validity function, is essential for the application of the fuzzy Lyapunov approach to local model networks.

The methodology proposed in this paper determines the possible transitions in a local model network by utilizing a simulation

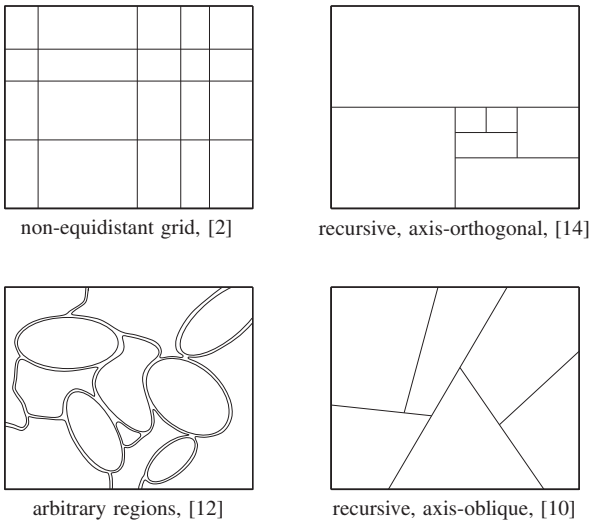

Fig. 3. Common partitioning strategies of local model networks

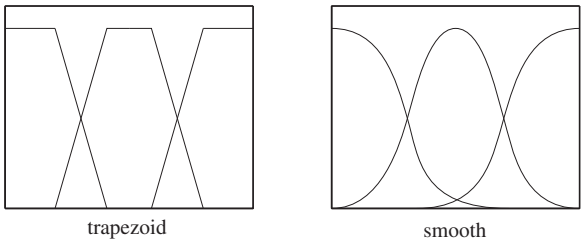

Fig. 4. Common validity functions of local model networks

result with an optimally designed excitation data sequence and is independent regarding the partitioning strategy and the used validity function. As a consequence the stability region U (Fig. 2) in the present paper is aimed to be identical to the convex hull of the used data sequence. In contrast, most available stability criteria for LMN aim to show *unbounded* global stability which can become too expensive when only a certain part of the LMN describes the actual dynamic operating range of the process. On the other hand, when using the approach of this paper all detected model transitions take place within the convex hull U of the identification data sequence. It can not be ruled out that outside of this hull unnoticed transitions could occur. Especially for the design of controllers or observers stability close to or beyond that boundary is of only limited interest.

Note that stable local dynamics are a prerequisite of the fuzzy Lyapunov approach. Thus, for unstable local dynamics, which could lead to an improper data sequence for the determination of the model transitions, the fuzzy Lyapunov approach will fail anyway, independent to the investigated model transitions.

The information about the model transitions for the local model network under consideration will be represented by a so-called *transition matrix* $\boldsymbol{\Xi}$. It is based on the simulation result with an excitation data sequence and the method to generate it will be described in the following.

The excitation signals $\boldsymbol{u}_{\mathcal{J}}(\mathcal{K})$, which are generated by a proper DoE [13] and the model output $\hat{\boldsymbol{y}}(\mathcal{K})$, which is generated by simulating the process using the considered LMN with the

excitation signal, are merged to a matrix

$$\boldsymbol{L}(k) = [\boldsymbol{u}_{\mathcal{J}}(k-\mathcal{M})\ \hat{\boldsymbol{y}}(k-\mathcal{N})],\ \forall k \in \mathcal{K},\ \boldsymbol{L} \in \mathbb{R}^{K \times O} \quad (28)$$

which rows correspond to the input vector $\boldsymbol{z}(k)$. The ordered set for the samples of the data sequence is given by

$$\mathcal{K} = (k \in \mathbb{N} | 1 \leq k \leq K) \quad (29)$$

where K is the number of samples. Those signals which are used as input arguments to the validity function form a subset of the data sequence. The choice of such a particular subset is strongly dependent on the system's nonlinearities and is thus usually done by the user. The input arguments to the validity function are denoted by $\tilde{\boldsymbol{L}}$ indicating that it is a sub-matrix of $\boldsymbol{L}$:

$$\tilde{\boldsymbol{L}} = \boldsymbol{L}(\mathcal{K}, \tilde{\mathcal{O}}),\ \tilde{\boldsymbol{L}} \in \mathbb{R}^{K \times \tilde{O}} \quad (30)$$

which rows correspond to $\tilde{\boldsymbol{z}}(k)$. Consequently the output of a validity function $\boldsymbol{C}$ can be formulated as

$$\boldsymbol{C}(\mathcal{K}, \mathcal{I}) = \Phi_{\mathcal{I}}(\tilde{\boldsymbol{L}}(\mathcal{K})),\ \boldsymbol{C} \in \mathbb{R}^{K \times I}. \quad (31)$$

When the state trajectory evolves over time and transits through different local models a matrix of indices of the two most dominant local models $\boldsymbol{D}$ (= local models with maximum Φ) can be generated in a similar way as $\boldsymbol{L}$ by using $\boldsymbol{C}$:

$$\begin{aligned}\boldsymbol{D}(k) = [&\{i_1 | \boldsymbol{C}(k, i_1) = \max(\boldsymbol{C}(k, \mathcal{I}))\} \\ &\{i_2 | \boldsymbol{C}(k, i_2) = \max(\boldsymbol{C}(k, \mathcal{I} \setminus i_1))\}], \\ &\forall k \in \mathcal{K},\ \boldsymbol{D} \in \mathbb{N}^{K \times 2}. \quad (32)\end{aligned}$$

The matrices $\boldsymbol{C}$ and $\boldsymbol{D}$ inherently contains the relevant information required to determine the actual model transitions. They are used to generate the *transition matrix* $\boldsymbol{\Xi}$ which compactly describes possible local model transits for the local model network under consideration. $\boldsymbol{\Xi}$ is a square matrix with boolean entries and has the following properties:

$$\dim \boldsymbol{\Xi} = I \times I \quad (33)$$

$$\boldsymbol{\Xi}(\xi_r, \xi_c) \in \{0, 1\},\ \forall \xi_r, \xi_c \in \mathcal{I} \quad (34)$$

The elements of $\boldsymbol{\Xi}$ can be interpreted as follows:

$\boldsymbol{\Xi}(\xi_r, \xi_c) =$1 if there is a transition from model ξ_r to ξ_c
and zero otherwise

Note that $\boldsymbol{\Xi}$ is generally *symmetric*, because the fuzzy Lyapunov approach requires that (24) is fulfilled for both interacting models.

To generate the transition matrix $\boldsymbol{\Xi}$ two steps are necessary:

① *Initialize $\boldsymbol{\Xi}$ as identity matrix*

$$\boldsymbol{\Xi} = \boldsymbol{I}_I \quad (35)$$

The main diagonal entries which formally refer to an interaction of a local model with itself must be set to one since the fuzzy Lyapunov approach requires stable local models.

② *Set the occurring model transitions*
From (32) the two most dominant local models are determined for each sample. A valid transition is detected whenever the dominant models change or when the validity functions do not change:

$$\begin{aligned}\boldsymbol{D}(k,1) = \boldsymbol{D}(k-1,2) \wedge \boldsymbol{D}(k,2) = \boldsymbol{D}(k-1,1) \vee \\ \boldsymbol{C}(k,\mathcal{I}) = \boldsymbol{C}(k-1,\mathcal{I}) \wedge \boldsymbol{D}(k,\mathcal{I}) = \boldsymbol{D}(k-1,\mathcal{I}), \\ \forall k \in \mathcal{K} \quad (36)\end{aligned}$$

Condition (36) is examined for all rows of $\boldsymbol{C}$ and $\boldsymbol{D}$, respectively. The detected transition directly follows when (36) is true for a k and the respective entry is set in the transition matrix:

$$\begin{aligned}\boldsymbol{\Xi}(\boldsymbol{D}(k-1,1), \boldsymbol{D}(k,1)) = \\ = \boldsymbol{\Xi}(\boldsymbol{D}(k,1), \boldsymbol{D}(k-1,1)) = 1 \quad (37)\end{aligned}$$

Using $\boldsymbol{\Xi}$ for the fuzzy Lyapunov approach (24) the set Ω_i corresponds to the i-th row of $\boldsymbol{\Xi}$:

$$\Omega_i = \{j | \boldsymbol{\Xi}(i,j) = 1,\ \forall j \in \mathcal{I}\},\ \forall i \in \mathcal{I} \quad (38)$$

V. Examples

In section V-A a simple example exemplarily shows a single transition from one model to another. The effectiveness of the fuzzy Lyapunov approach in conjunction with the proposed method is demonstrated by means of an illustrative nonlinear process in section V-B.

A. Single Transition

Fig. 5 illustrates an exemplary trajectory of an identification data sequence with constant input $u(k)$ and the 50% contour lines of the validity functions of the local models. The timestep from $k = 2$ to $k = 3$ is considered in detail.

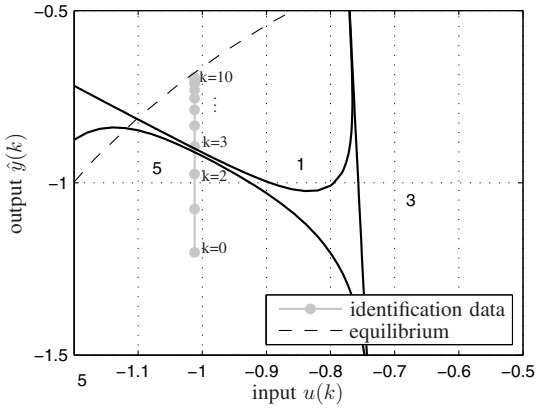

Fig. 5. Trajectory within partition space

The analysis of the trajectory by the method proposed in this paper is illustrated in Fig. 6.

The upper plot of Fig. 6 shows the system output over time, the middle one shows how the validity function outputs of local models 1 and 5, and the bottom one illustrates how the two most dominant models were determined by (37).

At $k = 2$ local model 5 is most dominant $(D(2,1) = 5)$ and

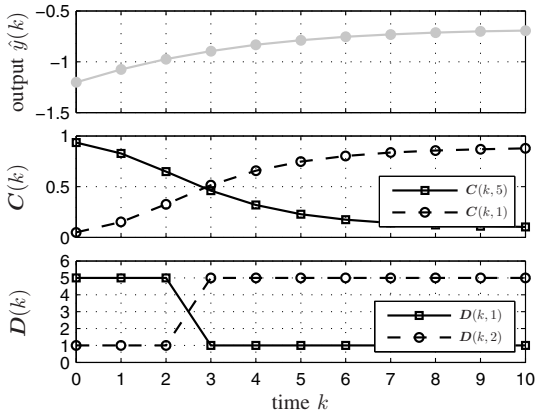

Fig. 6. Validity sequence

at $k = 3$ $(D(3,1) = 1)$ which indicates that model 1 is now dominating:

$$\boldsymbol{D}(2,1) = 5,\ \boldsymbol{D}(2,2) = 1,\ \boldsymbol{D}(3,1) = 1,\ \boldsymbol{D}(3,2) = 5 \quad (39)$$

Thus, according to (36) a valid transition is detected and the corresponding entry is set in the transition matrix according to (37):

$$\boldsymbol{\Xi}(5,1) = \boldsymbol{\Xi}(1,5) = 1$$

B. Nonlinear Dynamic Process

For illustrative purposes a nonlinear dynamic process is considered, which possesses strongly operating point dependent dynamics. This process is adopted from [9], [19] and can be described by the following difference equation:

$$\begin{aligned} y(k) &= 0.133u(k-1) - 0.0677u(k-2) + 1.5y(k-1) \\ &\quad - 0.7y(k-2) + u(k)[0.1y(k-1) - 0.2y(k-2)] \end{aligned} \quad (40)$$

In this example the input $u(k)$ is bounded to the interval $[-1.5\ 0.5]$.

Fig. 7 demonstrates that the system has weakly damped oscillatory behavior for large inputs whereas for small inputs strongly damped aperiodic behavior is present. For system

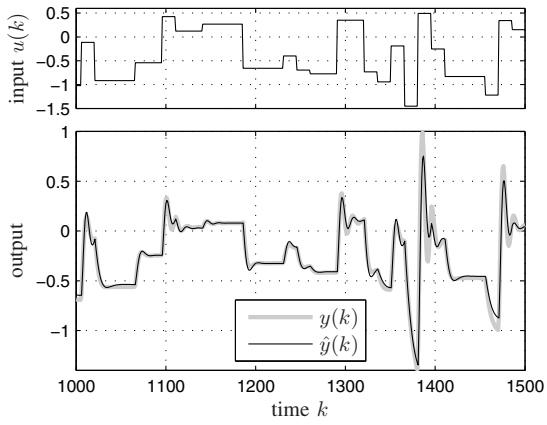

Fig. 7. In- and output of the system and the LMN

identification an excitation signal was generated to capture both the nonlinear dynamic and static behavior, [13].

From these data a local model network comprising six local models was generated by the algorithm presented in [10], where the local models are defined by an axis oblique decomposition of the partition space. Fig. 8 shows the partition space

$$\tilde{\boldsymbol{x}}(k) = [u(k-1)\ \hat{y}(k-1)] \quad (41)$$

as well as the identification data. The partitioning strategy of [10] uses statistical methods to avoid overfitting by local models generated with only few points.

The comparison of the system output and the output of the LMN in Fig. 7 shows that the LMN is accurately approximating the system within the whole operating range. The following system

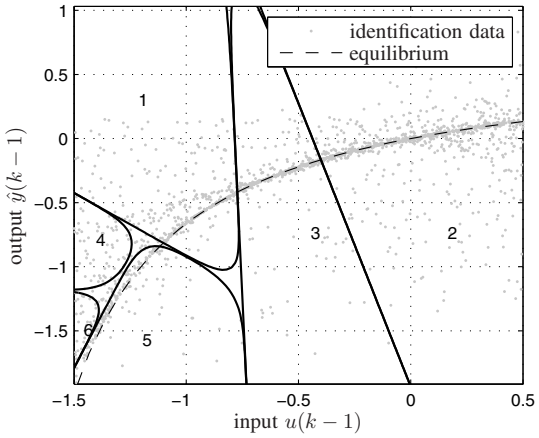

Fig. 8. Partition space and identification data sequence

matrices are obtained from the LMN when the discrete-time transfer functions of the local linear dynamics are represented in controllability canonical form:

$$\begin{aligned} \boldsymbol{A}_1 &= \begin{bmatrix} 0 & 1 \\ -0.71 & 1.668 \end{bmatrix},\ \boldsymbol{A}_2 = \begin{bmatrix} 0 & 1 \\ -0.736 & 1.525 \end{bmatrix} \\ \boldsymbol{A}_3 &= \begin{bmatrix} 0 & 1 \\ -0.622 & 1.488 \end{bmatrix},\ \boldsymbol{A}_4 = \begin{bmatrix} 0 & 1 \\ -0.844 & 1.832 \end{bmatrix} \\ \boldsymbol{A}_5 &= \begin{bmatrix} 0 & 1 \\ -0.767 & 1.74 \end{bmatrix},\ \boldsymbol{A}_6 = \begin{bmatrix} 0 & 1 \\ -0.733 & 1.702 \end{bmatrix} \end{aligned} \quad (42)$$

The local models have very different damping ratios, Fig. 9 shows their eigenvalues for illustration.

Fuzzy Lyapunov Approach with Transition Determination

The following transition matrix is generated using the proposed method of section IV):

$$\boldsymbol{\Xi} = \begin{bmatrix} 1 & 0 & 1 & 1 & 1 & 0 \\ 0 & 1 & 1 & 0 & 0 & 0 \\ 1 & 1 & 1 & 0 & 1 & 0 \\ 1 & 0 & 0 & 1 & 1 & 1 \\ 1 & 0 & 1 & 1 & 1 & 1 \\ 0 & 0 & 0 & 1 & 1 & 1 \end{bmatrix} \quad (43)$$

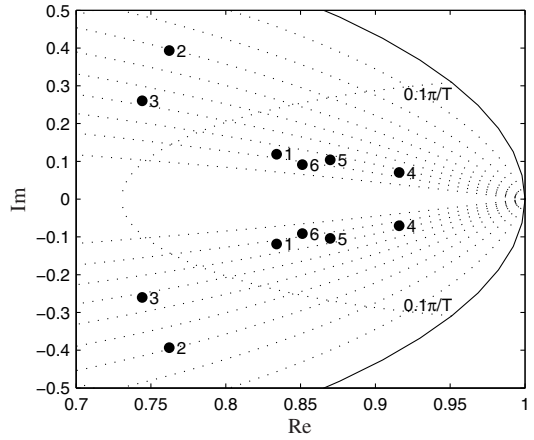

Fig. 9. Eigenvalues of the local models

Defining the model transitions Ω_i, according to (38) with (43):

$$\begin{aligned}&\Omega_1 = \{1,\ 3,\ 4,\ 5\},\ \Omega_2 = \{2,\ 3\},\\ &\Omega_3 = \{1,\ 2,\ 3,\ 5\},\ \Omega_4 = \{1,\ 4,\ 5,\ 6\},\\ &\Omega_5 = \{1,\ 3,\ 4,\ 5,\ 6\},\ \Omega_6 = \{4,\ 5,\ 6\}\end{aligned} \tag{44}$$

for the fuzzy Lyapunov approach, according to Theorem 2 and using the MATLAB LMI Toolbox® the following positive definite $\boldsymbol{P}_i$ matrices are determined:

$$\boldsymbol{P}_1 = \begin{bmatrix} 0.14 & -0.152 \\ -0.152 & 0.175 \end{bmatrix},\ \boldsymbol{P}_2 = \begin{bmatrix} 0.715 & -0.726 \\ -0.726 & 0.856 \end{bmatrix}$$
$$\boldsymbol{P}_3 = \begin{bmatrix} 0.082 & -0.086 \\ -0.086 & 0.1 \end{bmatrix},\ \boldsymbol{P}_4 = \begin{bmatrix} 0.191 & -0.209 \\ -0.209 & 0.237 \end{bmatrix}$$
$$\boldsymbol{P}_5 = \begin{bmatrix} 0.148 & -0.162 \\ -0.162 & 0.188 \end{bmatrix},\ \boldsymbol{P}_6 = \begin{bmatrix} 0.139 & -0.153 \\ -0.153 & 0.177 \end{bmatrix}$$

which satisfy (23) and (24). Thus it is guaranteed, that the considered LMN is asymptotically stable within U.

Common Quadratic- and Fuzzy Lyapunov Approach without Transition Determination

In this section it is assumed that no information about the model transitions is available for the fuzzy Lyapunov approach. Consequently all entries of $\boldsymbol{\Xi}$ are set to one. This leads to a more conservative result, because of additional LMIs. Thus, the classic fuzzy Lyapunov approach fails to prove stability of the considered LMN with six local models.
Using the common quadratic Lyapunov approach

$$\boldsymbol{A}_i^T \boldsymbol{P} \boldsymbol{A}_i - \boldsymbol{P} \prec 0 \tag{45}$$

for all $\boldsymbol{A}_i$ of (42) it is not possible to prove stability of the nonlinear dynamic process neither because of the different dynamic behavior. This is independent of the number of local models.

Influence of the number of local models

For the considered local model network with six local models it is only possible to prove stability using the proposed concept. Using the common quadratic Lyapunov approach or the fuzzy Lyapunov approach without the proposed concept increasing the number of local models result in an increased complexity of the stability criterion because of additional LMIs. Thus, in this section the influence of the number of local models and the number of the considered transitions on the stability criteria will be shown. For that purpose four different local model networks, comprising tree to six local models, are compared in the following. These local model networks are generated utilizing the same identification data sequence. Fig. 10 illustrated that the complexity of the local model network is generally increased by the number of local models.

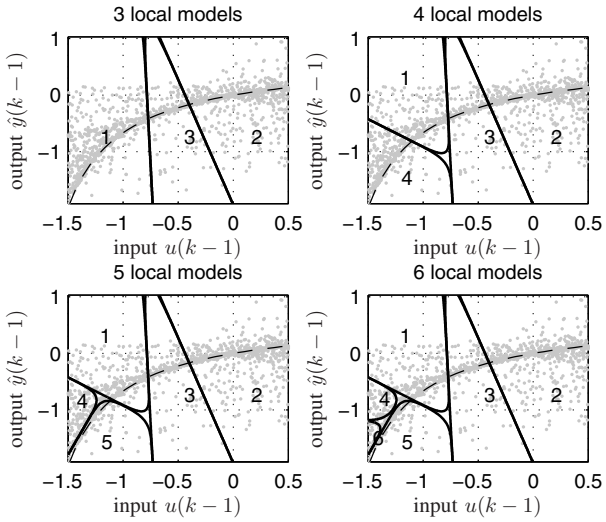

Fig. 10. Partition Space of local model networks with different number of local models

Fig. 11 shows that the complexity of the fuzzy Lyapunov approach can be significantly reduced by using the proposed method, particularly for local model networks with an high number of local models.

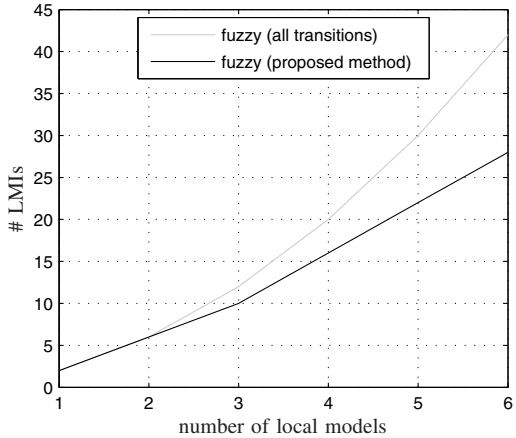

Fig. 11. Number of LMIs for different stability criterions and different number of local models

Table I shows an overview of the common quadratic Lyapunov approach, the fuzzy Lyapunov approach with all transitions and the fuzzy Lyapunov approach using the proposed method. Further, the influence of the number of local models on the stability criteria is presented utilizing the considered nonlinear dynamic process.

TABLE I
NONLINEAR DYNAMIC PROCESS: STABILITY CRITERIA

Method	# LMI variables	# LMIs	stable
6 local models			
common quadratic	1	7	
fuzzy (all transitions)	6	42	
fuzzy (proposed method)	6	28	✓
5 local models			
common quadratic	1	6	
fuzzy (all transitions)	5	30	✓
fuzzy (proposed method)	5	22	✓
4 local models			
common quadratic	1	5	
fuzzy (all transitions)	4	20	✓
fuzzy (proposed method)	4	16	✓
3 local models			
common quadratic	1	3	
fuzzy (all transitions)	3	12	
fuzzy (proposed method)	3	10	✓

The analysis of Table I shows that the conservatism of the Lyapunov approach can be generally reduced by using the proposed method because the number of LMIs is reduced in all cases. Further, it is even possible, that the conservatism decreases when the number of local models is increased. Using the common quadratic Lyapunov approach no stability proof is possible.

VI. CONCLUSION

This article addresses the problem of stability analysis of dynamic local model networks. In order to reduce the conservatism of established Lyapunov approaches a new method for the determination of the local model transitions in a dynamic local model network is proposed. The concept can be used for arbitrary partitioning strategies and high dimensional partition spaces and uses identification data to determine feasible model transitions. For artificial local model networks, which are not generated from identification data, the concept is also applicable using a proper excitation signal.

The effectiveness of the proposed method is shown by a simulation example with the fuzzy Lyapunov approach as a stability criterion. It is demonstrated how the information inherently contained in a proper simulation data sequence can be utilized to reduce conservatism and thus to extend the applicability of established stability criteria to more sophisticated dynamic local model networks.

REFERENCES

[1] R. Murray-Smith and T. A. Johansen, "Multiple Model Approaches to Modelling and Control," *Taylor & Francis, London*, Jan 1997.

[2] K. Tanaka and M. Sugeno, "Stability Analysis and Design of Fuzzy Control Systems," *Fuzzy Sets and Systems*, vol. 45, no. 2, pp. 135–156, 1992.

[3] K. Tanaka, T. Hori, and H. Wang, "A Multiple Lyapunov Function Approach to Stabilization of Fuzzy Control Systems," *IEEE Transactions on Fuzzy Systems*, vol. 11, no. 4, pp. 582–589, 2003.

[4] W. Wang and C. Sun, "A Relaxed Stability Criterion for T–S Fuzzy Discrete Systems," *IEEE Transactions on Systems*, Jan 2004.

[5] Y. Wang, Z. Sun, and F. Sun, "Stability Analysis and Control of Discrete-time Fuzzy Systems: A Fuzzy Lyapunov Function Approach," *Proceedings of the 5th Asian Control Conference*, Jan 2004.

[6] S. Zhou, G. Feng, J. Lam, and S. Xu, "Robust H_∞ Control for Discrete-time Fuzzy Systems via Basis-dependent Lyapunov Functions," *Information Sciences*, Jan 2005.

[7] C. Sun, Y. Su, and C. Chuang, "Relaxed Stabilization Criterion for TS Fuzzy Discrete System," 2009.

[8] O. Nelles and R. Isermann, "Basis Function Networks for Interpolation of Local Linear Models," *Proceedings of the 35th Conference on Decision and Control*, vol. 1, pp. 470 – 475 vol.1, 1996.

[9] O. Nelles, *Nonlinear System Identification: From Classical Approaches to Neural Networks and Fuzzy Models*, 2001.

[10] C. Hametner and S. Jakubek, "Neuro-Fuzzy Modelling Using a Logistic Discriminant Tree," *Proceedings of the 2007 American Control Conference*, pp. 864–869, Jul 2007.

[11] Breiman, "Hinging Hyperplanes for Regression, Classification, and Function Approximation," *IEEE Transactions on Information Theory*, vol. 39, no. 3, pp. 999 – 1013, 1993.

[12] S. Jakubek and N. Keuth, "A Local Neuro-Fuzzy Network for High-Dimensional Models and Optimization," *Engineering Applications of Artificial Intelligence*, Jan 2006.

[13] G. C. Goodwin and R. L. Payne, "Dynamic System Identification: Experiment Design and Data Analysis," p. 291, Jan 1977.

[14] O. Nelles, "Local Linear Model Trees for On-Line Identification of Time-Variant Nonlinear Dynamic Systems," *Artificial Neural Networks—ICANN 96*, Jan 1996.

[15] C. Hametner and S. Jakubek, "New Concepts for the Identification of Dynamic Takagi-Sugeno Fuzzy Models," *IEEE Conference on Cybernetics and Intelligent Systems*, pp. 1–6, Jun 2006.

[16] J.-J. E. Slotine and W. Li, *Applied Nonlinear Control*, 1991.

[17] G. Feng, "A Survey on Analysis and Design of Model-based Fuzzy Control Systems," *IEEE Transactions on Fuzzy systems*, vol. 14, no. 5, pp. 676–697, 2006.

[18] ——, "Stability Analysis of Discrete-Time Fuzzy Dynamic Systems Based on Piecewise Lyapunov Functions," *IEEE Transactions on Fuzzy Systems*, vol. 12, no. 1, pp. 22–28, 2004.

[19] I. Leontaritis and S. Billings, "Input-Output Parametric Models for Non-linear Systems Part I: Deterministic Non-linear Systems," *International Journal of Control*, Jan 1985.

2011 IEEE International Conference on Fuzzy Systems
June 27-30, 2011, Taipei, Taiwan

Vehicle Warning System for Land Departure and Collision Avoidance: Using Fuzzy Decision Making

Chih-Li Huo, Yu-Hsiang Yu, Jhih-Cheng Syu, Tsung-Ying Sun, *Member*, *IEEE,*
Department of Electrical Engineering
National Dong Hwa University
No. 1, Sec. 2, Da-Sh Rd., Shou-Feng, 97401, Hualien, Taiwan, R.O.C.
{d9823004, d9823010, m9823011}@ems.ndhu.edu.tw, sunty@mail.ndhu.edu.tw,

***Abstract*—This paper focuses on vehicle warning system based on fuzzy decision making for lane departure and forward collision avoidance for dealing with driver assistant system. The proposed system is composed of vision-based preprocessing and a fuzzy decision making. The objective of vision-based preprocessing part is lane tracking and forward vehicle detection, and provides the necessary information for fuzzy decision making to trigger the warning device. The fuzzy decision making unit can adjust the fuzzy decision rule base follow the driving behavior to increase the warning strength for lane departure and/ or forward collision.**

Keywords: lane departure, forward collision avoidance, vehicle warning system, fuzzy decision making.

I. INTRODUCTION

Traffic accident happens throughout the world in nearly every single second, the issue should be considered with high priority to deal with. A traffic environment is complicated and most sudden situations are hardly predicted. Driver-assistance systems that monitor driver intent, warn drivers of lane departures, or assist in vehicle guidance are all being actively considered [1]. Although lane position determination is an important component in driver-assistance systems, it is noticed that either lane departure assist or dynamic control assist alone is inadequate to construct a reliable driving assistant system. For drowsy or unawareness drivers, it is hazardous for both himself and other road users as the host vehicle may not be on the track of lane and keeping safety distance with the forwarding vehicles to avoid collision accident[2].

In this paper, we combine the two into a combo driving-assistant system. The concept is to create a fuzzy decision making for driver warning based on lane departure detection and forward vehicle collision detection. Therefore, this paper focuses on vehicle warning system based on fuzzy decision making for lane departure and forward collision avoidance for dealing with driver assistant system. The proposed system is composed of vision-based preprocessing and fuzzy decision making. The objective of vision-based preprocessing part is lane tracking and forward vehicle detection, and provides the necessary information for fuzzy decision making to trigger the warning device, while the increasing possibility for lane departure and/ or forward collision. The proposed system always supervises the vehicle driver on track in safe and stable velocity incorporated with collision avoidance to aid vehicle to keep safety distance apart.

In this paper, the vision-based preprocessing is composed of lane-marking tracking and vehicle detection. In the preliminary studies, we have proposed a new detection and tracking algorithm by means of Kalman Filter for lane detection [3], [4] and implemented the algorithm in a Multi-core DSP embedded system [5]. The proposed lane tracking system can reduce the operations of image data and increase the operating speed. Following the result of lane-making tracking, the region of interest (ROI) for detection forward vehicle and lane departure information can be obtained. Based on the preliminary study on collision-avoidance [6], an effective method for detecting forward vehicle was proposed in this paper.

This paper contains six sections. Section I is the Introduction. Section II describes the overview architecture of the proposed system. Section III introduces the two parts of preprocessing unit algorithm based on a moving object trajectory tracking. Section IV describes the proposed fuzzy decision making unit. The experimental results describe in Section V and conclusions in section VI.

II. SYSTEM ARCHITECTURE OVERVIEW

The proposed system, which architecture depicted as Fig. 1, consists of preprocessing unit and fuzzy making unit. The preprocessing unit is composed of lane-marking tracking (LMT) part and forward vehicle detection (FVD) part. It receives the image frames from the video camera to obtain the lane-marking area (LMA) in the image plane and lane-departure degree (LDD) follow the result of LMT. The LMA is regards as the region of interest (ROI) for FVD part to detect and compute information of the forwarding vehicle effectively. The output of FVD is velocity (V) of host vehicle, and relative distance between (D) the forward and host vehicle can be derived if a forward vehicle is detected in the ROI.

Fuzzy decision making (FDM) unit receives the outputs of preprocessing unit to identify the situations for warning decision of land-departure and/ or forward vehicle collision. When a forward vehicle is detected, the collision inference part receives V and D from FVD. Then, a predefined safety distance (SD) infers the measured D with current V to estimate time-to-collision (TTC) using a fuzzy inference. TTC is a measure for evaluating the emergent collision situation. The warning decision generates different types of alarm message based on the situations of the TTC and LDD. The proposed AFDM consists of collision inference and warning decision.

978-1-4244-7316-8/11/$26.00 ©2011 IEEE

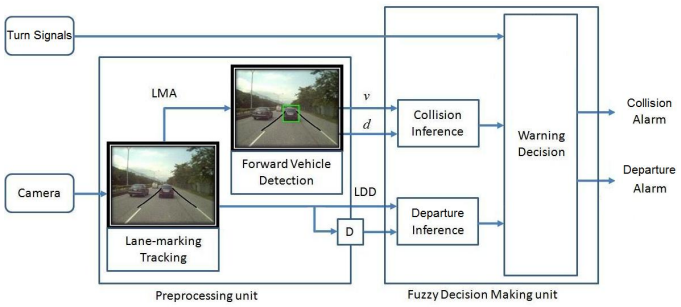

Fig. 1. Architecture of the proposed system

III. PREPROCESSING UNIT

The vision-based preprocessing unit is composed of lane-marking tracking (LMT) and forward vehicle detection (FVD).

A. Lane-marking Traking

This subsection describes the lane-marking Tracking (LMT) in detail. As shown in Fig. 2, the proposed algorithm consists of four steps.

Step 1. to convert input frame to a grayscale "R+G-B". This special intensity information can enhance the character of the lane-marking.

Step 2. to decide that an initial point is found out by lane-marking detection for initialization or updated by Nearest Neighbor Peak (NNP).

Step 3. to track the lane-marking trend. Kalman filter and NNP is used to track the trend of lane-markings in each frame. The flowchart is shown as Fig. 3. First, the tracking system is set the initial $x(0)$ which is found out from the Step 2. The predicting part is used to predict the next row of lane-marking location by NNP. If the successful measure is obtained, the predicted value will be updated by the predicting part and to next iteration. However, if the lane-marking is not a continuous type, the measure could not be found out. Therefore, Kalman filter uses the predicted location to present the trend of lane. Finally, if the iteration number k is to meet conditions which is tracking length. Then the tracking step will be stopped.

Step 4. to utilize the result of current tracking initiation to predict the tracking initiation of the next frame.

The proposed LMT algorithm needs only partial region to detect lane-marking location in each frame. The tracking results of LMT are lane-marking area (LMA) in the image plane shown as Fig. 4. The results show that it can reduce the complexity of vision data processing and meet the real-time requirements.

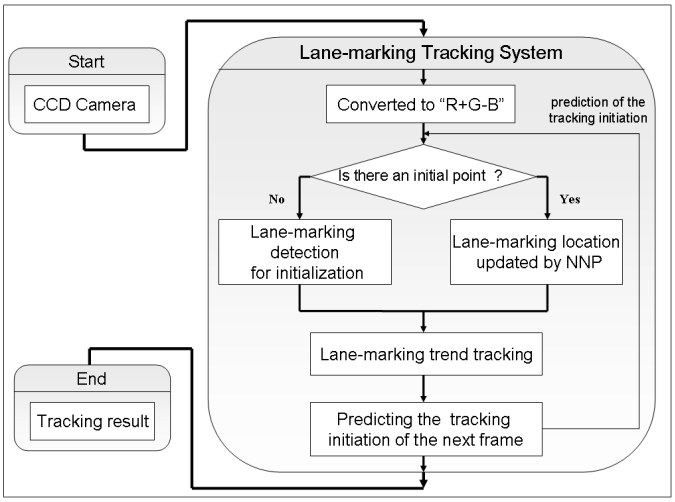

Fig. 2 Flowchart of Lane-marking tracking (LMT)

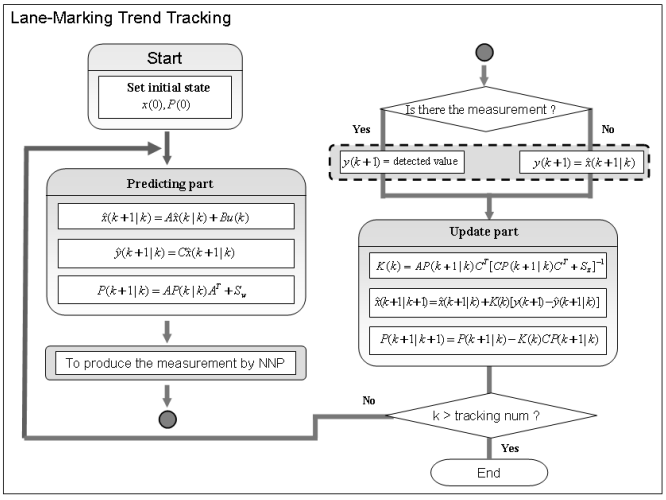

Fig. 3 Flowchart of Lane-marking trend tracking (LMTT)

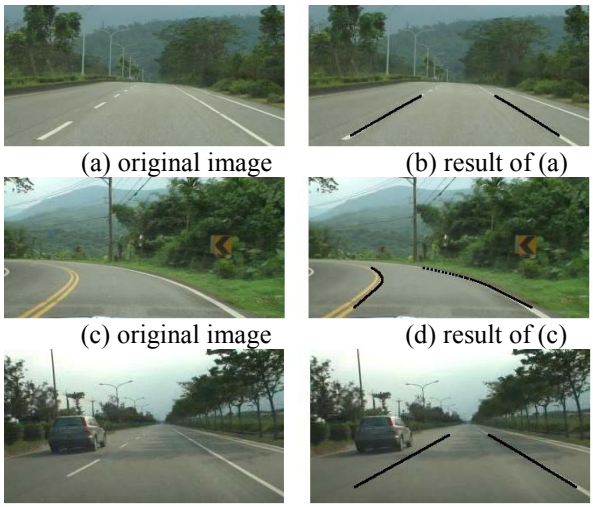

(a) original image (b) result of (a)

(c) original image (d) result of (c)

(e) original image (f) result of (e)

Fig. 4 LMA Results of LMT

B. *Forward Vehicle Detection*

This subsection describes the forward vehicle detection (FVD) in detail. As shown in Fig. 5, the proposed algorithm consists of four steps. The LMA, the tracking result from LMT, is the ROI for detecting forward vehicle in each image frames. There are three objectives of FVD. The first one is to derive the velocity of host vehicle (V) from global positioning system (GPS) module and the temporal-spatial measure between image frames. The second one is to detect the forward vehicle and calculate the relative distance (D) between forward and host vehicles. The third objective is to measure the lane-departure degree (LDD) of host vehicle for the triggering condition of the warning system.

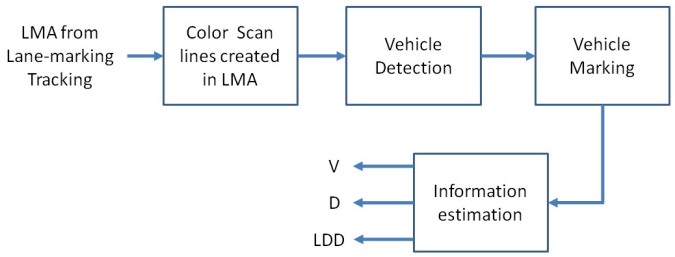

Fig. 5 Flowchart of Forward Vehicle Detection (FVD)

A set of color scan lines are created follow the obtained LMA, and convert into YCbCr color model. A threshold, L, could be decided using (1), where N denotes the total amount of scan line pixels. The set of shadowed pixels of the forward vehicle, E, is derived from (2). Following (3), the forward vehicle could be detected as V_p at the last pixel. The demonstrated examples are shown as Fig. 6. The red line is scan line. The row of detected V_p is sketched by yellow line.

$$L = \frac{\sum_{k=1}^{N} Y(k)}{N} \times \frac{3}{4} \quad (1)$$

$$E = \{e_i = e(k) \mid i = 1,2,...,n \text{ and } e(k) = k, \forall Y(k) < L\} \quad (2)$$

$$V_p = e(\text{end}),\ \text{end}: \text{the last pixel} \quad (3)$$

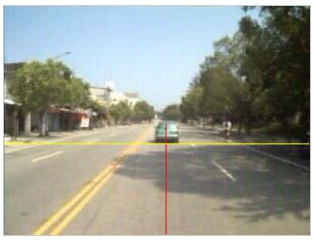

(a) shadowed road

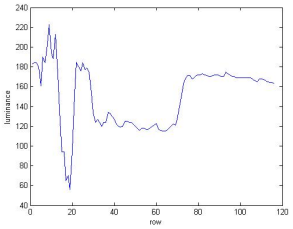

(b) Y values of scan line

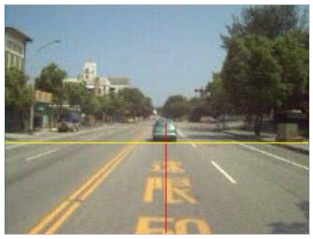

(c) marking in road

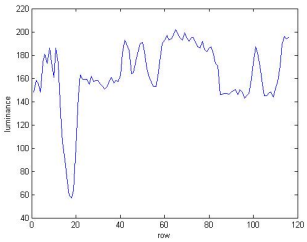

(d) Y values of scan line

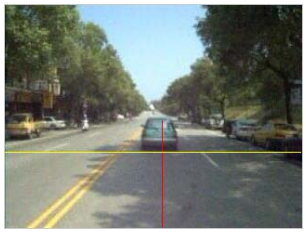

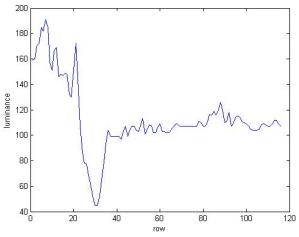

(e) vehicle in shadowed road (f) Y values of scan line

Fig. 6 Vehicle detection under different road conditions

When V_p is detected, coordinate mapping relationship (CMR) performs the distance measurement. CMR is the transformation between 2-D and 3-D coordinates systems [4]. If the information of one of coordinates is given, the other is obtained by mapping procedure. The proposed CMR not only derive the distance between image frame and forward vehicle but also the height and width of forward vehicle could be measured.

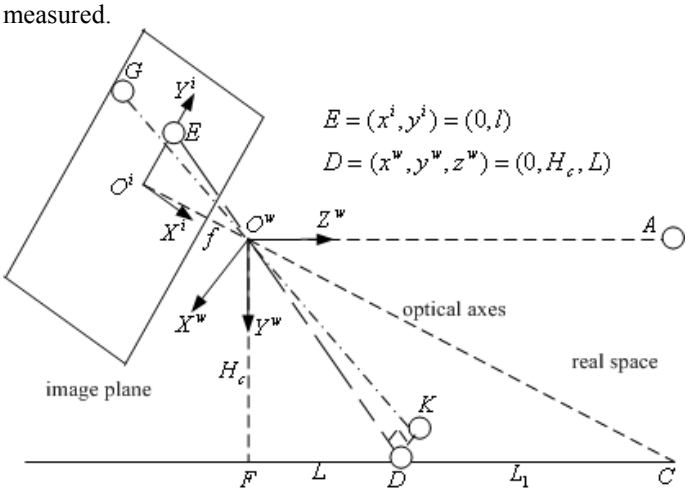

Fig 7. The geometric relationship

The geometric relationship between 2-D image plane and 3-D real-world illustrated as Fig.7. (X^i, Y^i) and (X^w, Y^w, Z^w) present the coordinate of image plane and real world respectively. O^i and O^w denote the geometric center of image plane and CCD lens respectively. H_c denote the height from O^w to ground. The focal length of CCD lens denote as f. Line $\overrightarrow{O^iO^w}$ is the focal axis of CCD and intersects to ground at point C. D and F present the shadow location of the bottom of forward vehicle and the location of CCD lens installed at host vehicle respectively. Therefore, point D is mapping to point E in image plane. Let L denotes the distance between D and F. If H_c and f are fixed, then L can be calculated by (4). In (4), $\theta_1 = \angle AO^wC$ is the depression angle of CCD which is calibrated by (5). c is half of vertical resolution of image plane (example for c=120 when image plane is 320*240). y_1 denote the location of image plane which is mapping the vanish point of road. $\triangle p_l$ is according to the resolution specification of image plane. It can be calculated by (6), where S is the diagonal length of CCD. In (4), $\theta_2 = \angle cO^wD$ is derived by (7),

where $l = \overline{O^i E}$ presents the distance in image plane which is calculated by (8).

$$L = \frac{H_c}{\tan(\theta_1 + \theta_2)} \tag{4}$$

$$\theta_1 = \tan^{-1}\left(\frac{H_c}{L_1}\right) = \tan^{-1}\left(\frac{\Delta p_l \times (c - y_1)}{f}\right) \tag{5}$$

$$\Delta p_l = S \times \frac{p_y}{\sqrt{p_x + p_y}} \times \frac{1}{p_y} \tag{6}$$

$$\theta_2 = \tan^{-1}\left(\frac{l}{f}\right) \tag{7}$$

$$l = p_l \times \Delta p_l \tag{8}$$

In Fig. 8, the size of the length of detection window l_{dw} could be calculated via (9) while the distance of the detected forward vehicle L is obtained by (4). In (9), c is half of vertical resolution of image plane (example for c=120 when image plane is 320*240), m is the vertical coordinate value of image plane which presents the bottom location of the detected forward vehicle. p_l' can be obtained from (10), where H_v and H_c denote the height and width of vehicle respectively. In (10), L_p denote the depth of 3-D space mapped to m, different L_p could derive different l_{dw}. Therefore, we require (11) to obtain L_p under different m, where θ_1 is the depression angle of CCD.

$$l_{dw} = C + p_l' - m \tag{9}$$

$$p_l' = \begin{cases} \frac{f}{\Delta p_l} \times \tan(\theta_1 - \tan^{-1}\left(\frac{H_C - H_V}{L_p}\right)) & \text{,if } H_V \le H_C \\ \frac{f}{\Delta p_l} \times \tan(\theta_1 + \tan^{-1}\left(\frac{H_V - H_C}{L_p}\right)) & \text{,if } H_V > H_C \end{cases} \tag{10}$$

$$L_p = \begin{cases} \frac{H_C}{\tan(\theta_1 + \theta_2)} & \text{,if } m \in [1, c] \\ \frac{H_C}{\tan(\theta_1 - \theta_2)} & \text{,if } m \in [c^+, 240] \end{cases} \tag{11}$$

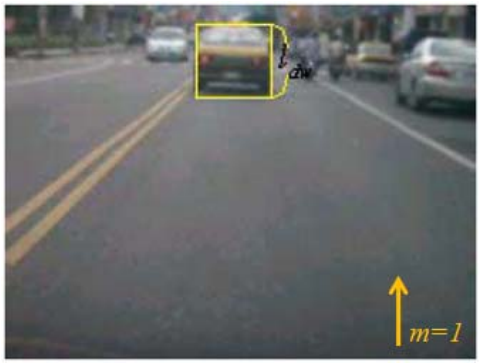

Fig. 8. The detection window of forward vehicle

Following the two stages of preprocessing unit, Fig. 9(a) presents original situation of a red scan line created by LMT part. In Fig. 9(b), a forward vehicle can be detected by FVD part and completely marked by a precise green box. The distance between the forward and host vehicles measured by CMR is 18.14 m.

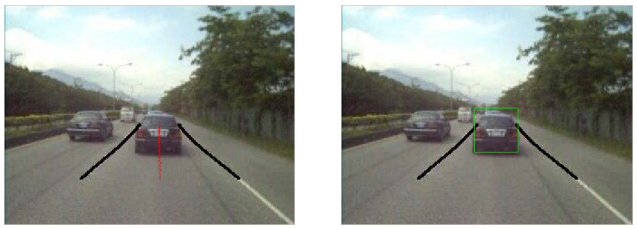

(a) original situation by L (b) detected result by FVD

Fig. 9 The result of preprocessing unit.

IV. Fuzzy Decision Making

FDM unit receives the outcomes of preprocessing unit. The objective is to identify different triggering situations under different conditions for warning decision of land-departure and/ or forward vehicle collision. When there are no detected forward vehicles, the LDD is calculated by FVD to check the departure situation of the host vehicle for lane-departure warning. When there are any forward vehicles detected by FVD, the collision inference part receives V and D from FVD. Then, a predefined safety distance (SD) infers the measured D with related V_r which is difference between V and velocity of forward vehicle, to estimate TTC for evaluating the emergent collision situation using a fuzzy inference; the departure index (DI) is estimated by departure inference simultaneously. Therefore, the warning decision generates different types of alarm message based on the situations of the TTC and LDD.

Collision inference is used to estimate dangerous level with forward vehicle, and departure inference is used to estimate host vehicle is inside the area of departure lane or not. Then, the warning decision is consider the dangerous level and alert driver. For collision inference, first, related velocity Vr between host vehicle and forward vehicle is calculated by FVD. Then, two input, D and V_r are considered to infer TTC, as Fig. 10. The domain of collision inference is defined by SD and V. It should note that boundary of domain is varied because SD and V are re-calculated in each sampling. The rule of collision inference is described as TABLE I. If D is less than SD and V_r is negative, then the TTC become small (C^+ become larger) that it represents host vehicle is near the forward vehicle. The smaller value the TTC is, the more dangerous vehicle will be.

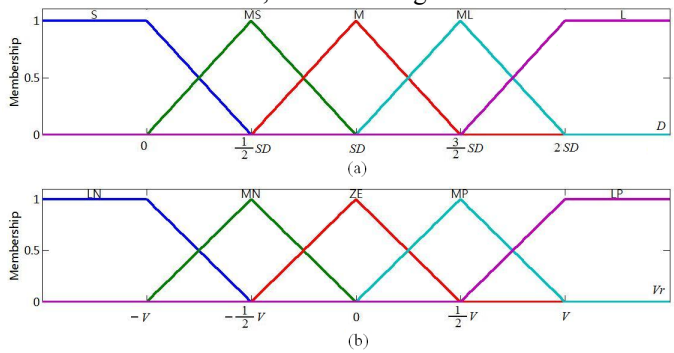

Fig. 10. The membership function of collision inference: (a) distance and (b) velocity membership function.

TABLE I. RULE TABLE FOR COLLISION INFERENCE

V_r \ D	S	MS	M	ML	L
LM	C^+	C^+	C	C^-	N
MN	C^+	C	C^-	N	S^-
ZE	C	C^-	N	S^-	S
MP	C^-	N	S-	S	S^+
LP	N	S^-	S	S^+	S^+

*C is collision index, N is normal index and S is safe index.

For departure inference, first, lane vanish point is set in center of video camera that it is ensure the vehicle locating the center of lane at initial setup. In other word, if the lane center is the center column of video frame C_{im}. Then, the right lane y_r and left lane y_l can be gotten by LMT, the lane center C_L is calculated as follows:

$$C_L = \frac{y_l + y_r}{2} \tag{12}$$

and the departure pixel P_{offset} is calculated as follows:

$$P_{offset} = C_L - C_{im} \tag{13}$$

The P_{offset} and ΔP_{offset} are consider to be input in departure inference and their membership function are designed as Fig 11. Values of both membership domains represent the departure pixel in video frame. By experiment result, it is normal driver with departure pixel form 30 to 40 on the way, and the larger ΔP_{offset} *is*, the more unusual driver is. The rule of departure inference is described as TABLE II, if P_{offset} is large negative and the ΔP_{offset} is negative, then the LDD left alarm is large; if if P_{offset} is large negative and the ΔP_{offset} is positive, then the LDD alarm is zero. Right alarm is similar to left rules.

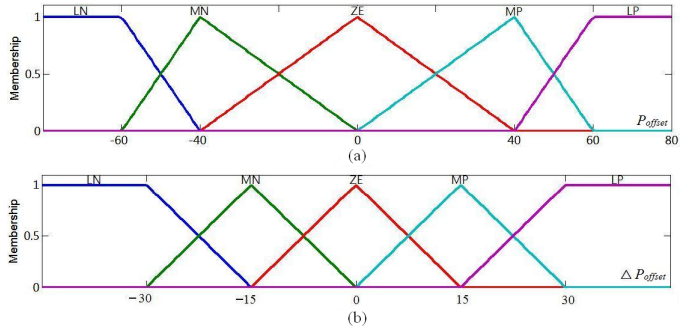

Fig. 11. The membership function of departure inference: (a) distance and (b) velocity membership function.

TABLE II. RULE TABLE FOR DEPARTURE INFERENCE

V_r \ D	LM	MN	ZE	MP	LP
LM	L^+	L	L^-	N	N
MN	L^+	L	L^-	N	N
ZE	L^-	L^-	N	R^-	R^-
MP	N	N	R^-	R	R
LP	N	N	R^-	R	R^+

*L is left departure index, N is normal index and R is right departure index.

The warning decision is used to warn the dangerous situation. When the TTC and *DI* are estimated by collision inference and departure inference, the warning decision is active to alarm that it is alert driver that this situation will be dangerous. For FVD, if the collision index is larger than safe index, the collision alarm is alerted which has several alarm level; if the departure index are larger than normal index, the departure alarm is alerted.

V. EXPERIMENTAL RESULTS

Now, it is consider the real driver behavior in the road. Experiment has two parts to show the performance of proposed system: *A*. Lane marking and forward vehicle detection, then the FVD is estimated. *B*. Lane marking, then LDD is estimated. the frame rate is 30 frame/sec in all of experiments.

A. FVD experiment

In this experiment, host vehicle accelerated to close the forward vehicle during 50 sec, the situation is shown as Fig. 12. The LMT and LDD results are shown in right column.

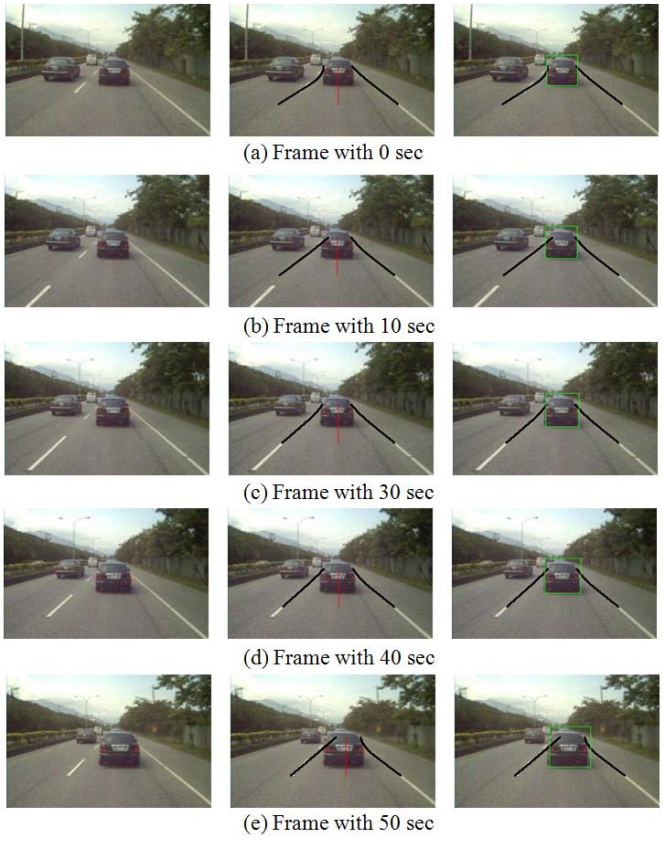

Fig. 12. Lane marking and FVD results

The result of collision inference is shown in Fig. 13, the host vehicle is safe at 20 sec ago. At 30 sec, the host vehicle approaches safety distance, however, it is alarm at 20 sec because the host vehicle accelerated to close the forward vehicle and forward vehicle braked at the same time. After 30 sec, the host vehicle accelerated still to close the forward vehicle lead alarm to be critical by the collision inference.

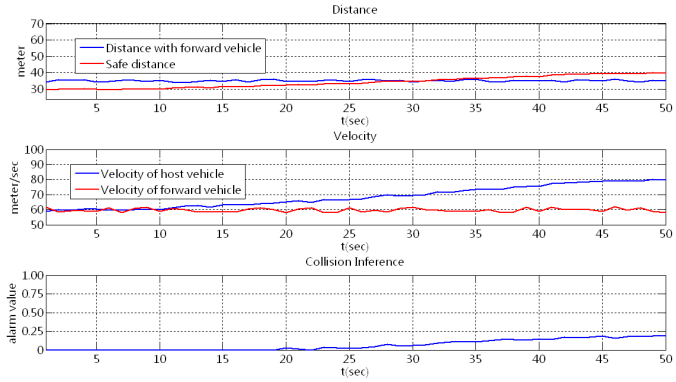

Fig. 13. The distance, velocity, and collision alarm value

B. *LDD experiment*

In this experiment, vehicle change from left lane to right lane, as Fig. 14. During total of 120 frames with 4 second, the host vehicle changes from left lane to right lane in frame 60 to 75, as Fig. 14 (g) to (h). In departure inference, the negative and positive alarm indicates that the host vehicle is departed to right side and left side respectively. In frame 68, the vehicle just enters the right lane lead inference value has a peak to indicate the left side departure from the lane center.

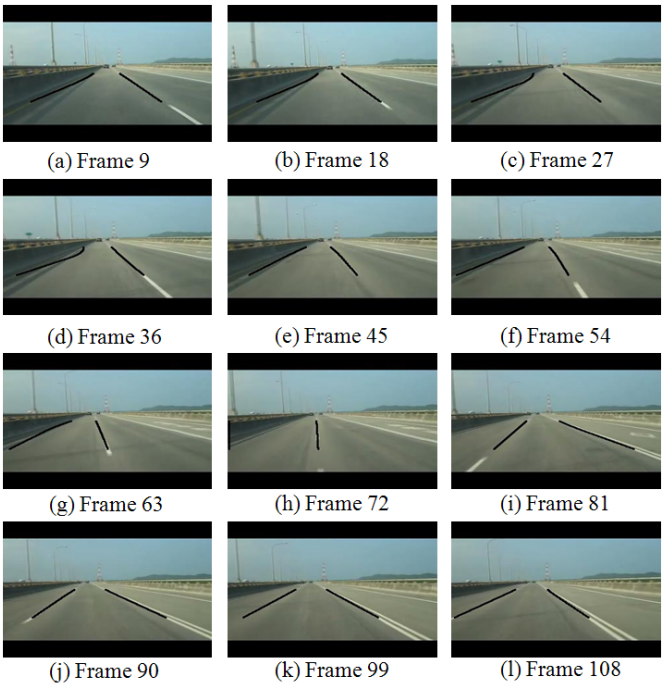

Fig. 14. Situation of change lane during 120 frames

In fact, vehicle always has departure values because video detection error and the behavioral of human driver. So the alarm has a threshold to restrain small departure value. By experiment, the threshold is set ±0.3.

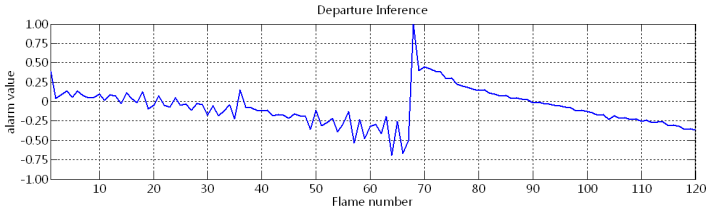

Fig. 15. The departure alarm value in departure inference

VI. CONCLUSION

This paper presents a fast lane-marking tracking, forward vehicle detection, and fuzzy inference to complete a driver assistance system for warning the situations of lane departure and the forward vehicle detection. Following the experiment results, the LMT has better preference and accuracy. Although the detection precision is influenced by the detection area and accuracy of LMT, the FVD also presents high grade. The designed fuzzy inferences are reliable to alert driver no matter departure lane or close the forward vehicle.

REFERENCES

[1] Joel C. McCall and Mohan M. Trivedi, "Video-Based Lane Estimation and Tracking for Driver Assistance: Survey, System, and Evaluation," *IEEE Transactions on Intelligent Transportation Systems*, vol. 7. No. 1, pp. 20- 37, Mar. 2006.

[2] Raphael Labayrade, Cyril Royere, and Didier Aubert, "Experimental Assessment of the RESCUE Collision-Mitigation System," *IEEE Transactions on Vehicular Technology*, vol. 56, no. 1, pp. 89-102, Jan. 2007.

[3] T. Y. Sun, S. J. Tsai and V. Chan, "HSI Color Model Based Lane Marking Detection," in *Proc. IEEE Int. Conf. Intelligent Transportation Systems*, pp. 1168-1172, Sep., 2006.

[4] T. Y. Sun, W. C. Huang and S. J. Tsai, "Robust Lane-markings Tracking Algorithm Based on Boundary Detection and Kalman Filter" in *Proc. Int. Symp. on Advanced Vehicle Control*, Vol. 1, pp. 164-167, Oct., 2008.

[5] T. Y. Sun and W. C. Huang, "Embedded vehicle lane-marking tracking system" in *Proc. IEEE Int. Symp. on Consumer Electronics*, pp. 627-631, May 2009.

[6] T. Y. Sun, S. J. Tsai, J. Y. Tseng and Y. C. Tseng "The Study on Intelligent Vehicle Collision-Avoidance System with Vision Perception and Fuzzy Decision Making," in *Proc. IEEE Intel. Vehicles Symp.*, pp. 112-117, June 2005.

2011 IEEE International Conference on Fuzzy Systems
June 27-30, 2011, Taipei, Taiwan

Centroid Density of Interval Type-2 Fuzzy Sets: Comparing Stochastic and Deterministic Defuzzification

Ondrej Linda, Milos Manic
University of Idaho
Idaho Falls, ID, USA
olinda@uidaho.edu, misko@ieee.org

Abstract— **Recently, Type-2 (T2) Fuzzy Logic Systems (FLSs) gained increased attention due to their capability to better describe, model and cope with the ubiquitous dynamic uncertainties in many engineering applications. By far the most widely used type of T2 FLSs are the Interval T2 (IT2) FLSs. This paper provides a comparative analysis of two fundamentally different approaches to defuzzification of IT2 Fuzzy Sets (FSs) - the deterministic Karnik-Mendel Iterative Procedure (KMIP) and the stochastic sampling defuzzifier. As previously demonstrated by other researchers, these defuzzification algorithms do not always compute identical output values. In the presented work, the concept of centroid density of an IT2 FS is introduced in order to explain such discrepancies. It was demonstrated that the stochastic sampling defuzzification method converges towards the center of gravity of the proposed centroid density function. On the other hand, the KMIP method calculates the midpoint of the interval centroid obtained according to the extension principle. Since the information about the centroid density is removed via application of the extension principle, the two methods produce inevitably different results. As further demonstrated, this difference significantly increases in case of non-symmetric IT2 FSs.**

Keywords-Interval Type-2 Fuzzy Sets; Defuzzification; Centroid; Karnik-Mendel Algorithms; Sampling Defuzzifier

I. INTRODUCTION

Type-2 Fuzzy Logic Systems (T2 FLSs), originally proposed by Zadeh [1], constitute powerful tool for dealing with dynamic uncertainty. The T2 Fuzzy Sets (FSs) introduce additional design dimension for modeling and describing the uncertainty in the specific problem domain [2]. Unlike the Type-1 (T1) FSs with fixed membership functions, the T2 fuzzy membership functions are defined using the Footprint-of-Uncertainty (FOU) offering more design degrees of freedom [3]. The defuzzification of T2 FSs contains a type-reduction phase, which acts as a mapping between the original T2 FS and the type-reduced T1 FS, also called the centroid of the T2 FS [2], [3]. Despite some new recently introduced representations of general T2 FSs such as geometric T2 fuzzy sets [4], *zSlices* [5], α - planes [6], [7] or α - cuts [8], the Interval T2 (IT2) FSs are still most commonly used [9]. IT2 FLSs have been successfully applied in a wide range of applications [10]-[15].

This paper provides a comparative analysis of two fundamentally different approaches to defuzzification of IT2 FSs [9], the Karnik-Mendel Iterative Procedure (KMIP) [16] and the sampling defuzzification method [17]. The KMIP is a deterministic approach, which concentrates on bounding the type-reduced centroid of the IT2 FS by its left-most and right-most points [18]. The sampling defuzzification method, proposed by Greenfield et al., uses stochastic sampling method to sample the set of all embedded fuzzy sets and provide an estimate of the true defuzzified value [19]. The sampling defuzzification method was developed as a cut-down version of the original exhaustive defuzzification method, which enumerates and defuzzifies all available embedded fuzzy sets [20]. Other available methods for defuzzification of IT2 FSs are the direct defuzzifier [21], the Nie-Tan method [22], or the collapsing method [23].

As demonstrated by other researchers, the KMIP method and the sampling defuzzification method do not always compute identical solutions [24]. In this paper, the concept of centroid density of an IT2 FS is introduced to provide an experimental explanation for such discrepancies. The concept of centroid density describes the histogram of defuzzified embedded fuzzy sets within the boundaries of the type-reduced centroid. It is shown through experimental study that the stochastic sampling defuzzification method converges towards the center of gravity of the proposed centroid density function. On the other hand, the KMIP method computes the midpoint of the interval centroid obtained according to Zadeh's extension principle. Because the information about the centroid density is removed via application of the extension principle, the two methods produce inevitably different results. This difference becomes especially significant in case of non-symmetric IT2 FSs.

The rest of the paper is organized as follows. Section II provides an overview of IT2 FSs together with a review of the considered defuzzification techniques. Section III introduced the concept of centroid density for an IT2 FS. The comparative analysis is presented in Section IV and the paper is concluded in Section V.

978-1-4244-7316-8/11/$26.00 ©2011 IEEE

II. INTERVAL TYPE-2 FUZZY SETS

This section reviews fundamentals about the IT2 fuzzy sets together with a brief description of the defuzzification techniques considered in this work.

A. Interval Type-2 Fuzzy Sets

The IT2 FSs were introduced as a simplification to the general T2 FSs, which have been rarely applied to engineering problems due to their immense computational complexity. An IT2 FS $\widetilde{A}$ can be described as:

$$\widetilde{A} = \int_{x \in X} \int_{u \in J_x} 1/(x,u) \qquad J_x \subseteq [0,1] \tag{1}$$

Here, x and u constitute the primary and the secondary variables and J_x is the primary membership of variable x. The secondary grades of IT2 FS are all limited to 1. Hence, the IT2 FS can be completely described by its Footprint of Uncertainty (FOU), which is the area of non-zero secondary grade.

The vertical slice of an IT2 fuzzy set defines the secondary membership function. It can be obtained by instantiating the primary variable x into a specific value x':

$$\mu_{\widetilde{A}}(x = x', u) \equiv \mu_{\widetilde{A}}(x') = \int_{u \in J_{x'}} 1/u \quad J_{x'} \subseteq [0,1] \tag{2}$$

Using the concept of vertical slices the FOU can be expressed as follows:

$$FOU(\widetilde{A}) = \bigcup_{x \in X} J_x \tag{3}$$

According the Mendel-John representation theorem [25], the IT2 FS can be also seen as a collection of all its embedded fuzzy sets. An embedded fuzzy $\widetilde{A}_e$ can be described as:

$$\widetilde{A}_e = \sum_{i=1}^{N} [1/\theta_i]/x_i \qquad \theta_i \in J_{x_i} \subseteq U \in [0,1] \tag{4}$$

Using this concept the IT2 FS $\widetilde{A}$ can be also expressed as:

$$\widetilde{A} = \bigcup_{j=1}^{n} \widetilde{A}_e^j \tag{5}$$

Alternatively, the FOU of an IT2 fuzzy set $\widetilde{A}$ can be conveniently and completely described by its upper and lower membership functions $\underline{\mu}(x)$ and $\overline{\mu}(x)$:

$$FOU(\widetilde{A}) = \bigcup_{\forall x \in X} (\underline{\mu}_{\widetilde{A}}(x),\ \overline{\mu}_{\widetilde{A}}(x)) \tag{6}$$

During the output processing stage the output IT2 FS $\widetilde{B}$ must be first type-reduced, which results in the centroid of the IT2 FS $C(\widetilde{B})$ [20]:

$$C(\widetilde{B}) = \int_{\theta_1 \in J_{x_1}} \cdots \int_{\theta_N \in J_{x_N}} 1 \Big/ \frac{\sum_{i=1}^{N} x_i \theta_i}{\sum_{i=1}^{N} \theta_i} \tag{7}$$

This formula was derived using Zadeh's extension principle [28]. In the special case of IT2 FSs the centroid $C(\widetilde{B})$ is an interval T1 FS, which can be described by its left and right boundary points y_L and y_R. Finally, this interval centroid can be defuzzified to obtain the final output value.

B. Exhaustive Defuzzification

The definition of the generalized centroid of the IT2 FS presented in (7), describes the centroid as a composition of individual centroids of all of its embedded fuzzy sets. The exhaustive defuzzification method constructs this interval centroid by enumerating all the embedded fuzzy sets and calculating their respective centroids. This exhaustive algorithm for defuzzification of general T2 FSs can be adapted for the case of IT2 FSs as follows [20]:

Step 1: Enumerate all possible interval type-2 embedded fuzzy sets. The are $n = \prod_{i=1}^{N} M_i$ embedded fuzzy sets, where N is the resolution of the primary domain and M_i is the resolution of the secondary domain at the i^{th} slice.

Step 2: For each embedded fuzzy set find the minimum secondary grade. This is trivial as all secondary membership grades equal to 1.

Step 3: For each embedded fuzzy set calculate the domain value of the centroid of the type-2 embedded fuzzy set.

Step 4: Pair the computed domain value from **Step 3** with the secondary grade of 1.

Step 5: For each unique domain value, the maximum secondary grade is selected. In case of IT2 FSs, this means that only a single record about a defuzzified embedded FS is kept for each unique domain value.

The set of ordered pairs defines the centroid. The crisp output can then be calculated as the average of all calculated centroid coordinates. The average will be uniformly weighted, as the secondary grade of each defuzzified embedded FS equals to 1. Note that if the primary domain is considered to be continuous as opposed to the discretized one, the centroid becomes a continuous interval T1 FS.

C. Karnik-Mendel Iterative Procedure (KMIP)

The centroid of the IT2 FS is an interval T1 FS. According to Karnik and Mendel, it can be completely described by its left and right end points y_L and y_R. As derived by Karnik and Mendel, these boundary points can be expressed as in [20]:

$$y_L = \frac{\sum_{i=1}^{L} x_i \overline{\mu}_{\widetilde{B}}(x_i) + \sum_{i=L+1}^{N} x_i \underline{\mu}_{\widetilde{B}}(x_i)}{\sum_{i=1}^{L} \overline{\mu}_{\widetilde{B}}(x_i) + \sum_{i=L+1}^{N} \underline{\mu}_{\widetilde{B}}(x_i)} \quad (8)$$

$$y_R = \frac{\sum_{i=1}^{R} x_i \underline{\mu}_{\widetilde{B}}(x_i) + \sum_{i=R+1}^{N} x_i \overline{\mu}_{\widetilde{B}}(x_i)}{\sum_{i=1}^{R} \underline{\mu}_{\widetilde{B}}(x_i) + \sum_{i=R+1}^{N} \overline{\mu}_{\widetilde{B}}(x_i)} \quad (9)$$

Points L and R are important switching points computed by the KMIP algorithm. Using the boundary values of the type-reduced centroid $C(\widetilde{B})$ the final crisp defuzzified value y can be computed as the mean of the centroid interval:

$$y = \frac{(y_L + y_R)}{2} \quad (10)$$

The KMIP algorithm calculates the switching points L and R in (8) and (9) and the boundaries y_L and y_R of the centroid of the respective IT2 FS. The description of the KMIP algorithm given below was adopted from [20]. The algorithm consists of two phases, which independently compute the values of y_L and y_R. The algorithm for computing the left boundary y_L can be described in several steps as follows:

Step 1: Initialize a vector of weights w_i as follows:

$$w_i = \frac{1}{2}\left[\overline{\mu}_{\widetilde{B}}(x_i) + \underline{\mu}_{\widetilde{B}}(x_i)\right] \qquad i = 1,..N \quad (11)$$

And compute the value of y:

$$y = \frac{\sum_{i=1}^{N} x_i w_i}{\sum_{i=1}^{N} w_i} \quad (12)$$

Step 2: Find switching point k ($1 \le k \le N-1$) such that

$$x_{k+1} \le y \le x_{k+1} \quad (13)$$

Step 3: Set

$$w_i = \begin{cases} \overline{\mu}_{\widetilde{B}}(x_i) & i \le k \\ \underline{\mu}_{\widetilde{B}}(x_i) & i \ge k+1 \end{cases} \quad (14)$$

And compute the value of y' as:

$$y' = \frac{\sum_{i=1}^{N} x_i w_i}{\sum_{i=1}^{N} w_i} \quad (15)$$

Step 4: If $y' = y$, stop and set $y_L = y$ and $L = k$. Otherwise, go to **Step 5**.

Step 5: Set $y = y'$ and go to **Step 2**.

The procedure for computing the value of y_R is identical to computing y_L except that in **Step 3** different update of weights w_i is used as follows:

$$w_i = \begin{cases} \underline{\mu}_{\widetilde{B}}(x_i) & i \le k \\ \overline{\mu}_{\widetilde{B}}(x_i) & i \ge k+1 \end{cases} \quad (16)$$

The final output value is assigned to y_R and $R=k$.

In [16], the Enhanced KMIP algorithm was presented. However, the proposed enhancements only improved the convergence of the algorithm. As both approaches produce numerically identical results, only the original KMIP algorithm is considered in the rest of this paper.

D. Sampling Defuzzification

The sampling defuzzification method for T2 FS was presented and analyzed in [17], [19], [24] and [27]. This method follows the steps of the exhaustive defuzzification method. The major difference is that only a subset of randomly sampled embedded fuzzy set is considered during the calculation. According to the description in [24] the sampling defuzzification for IT2 FS can be described in several steps as follows:

Step 1: Select the required number of embedded fuzzy sets to be sampled.

Step 2: Repeat for each sample:

Step 2.1: Select an embedded fuzzy set at random.

Step 2.2: Find the domain value by defuzzifying the sampled embedded fuzzy set.

Step 2.3: Find the minimum secondary grade. In case of IT2 FSs this is trivial as the secondary grade equals to 1.

Step 2.4: Add the paired defuzzified value with its secondary grade to the list of pairs constituting the type-reduced centroid.

Step 3: Defuzzify the type-reduced centroid.

The method was experimentally tested, showing a fast convergence towards the expected defuzzification value [17]. The convergence speed was dependent on the cardinality of the sampled set. Extension to the sampling defuzzification method via using the importance sampling technique was proposed in [28]. It was demonstrated that this modification resulted in reduced statistical variance of the computed defuzzified value.

III. CENTROID DENSITY OF IT2 FUZZY SETS

The exhaustive defuzzification method defuzzifies all embedded fuzzy sets and then constructs the interval centroid

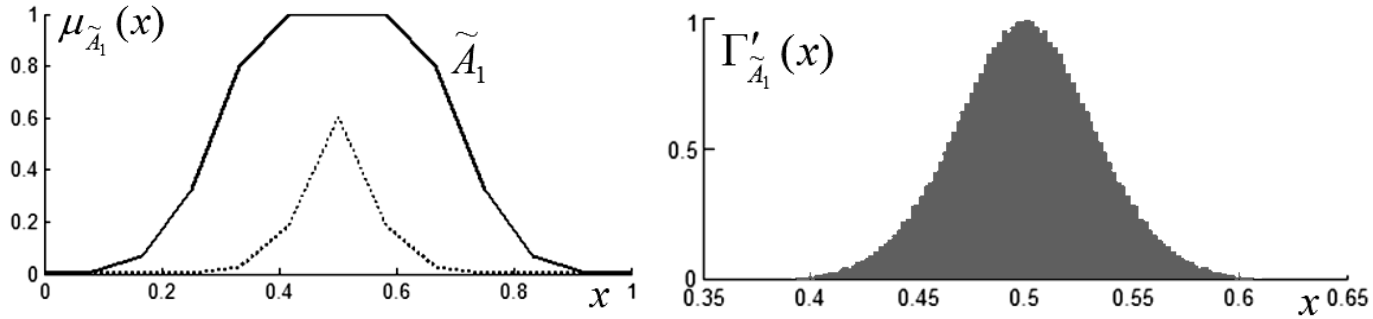

(a) (b)

Fig. 1 Interval Type-2 Gaussian fuzzy set with uncertain mean (a) and its corresponding discrete centroid density (b).

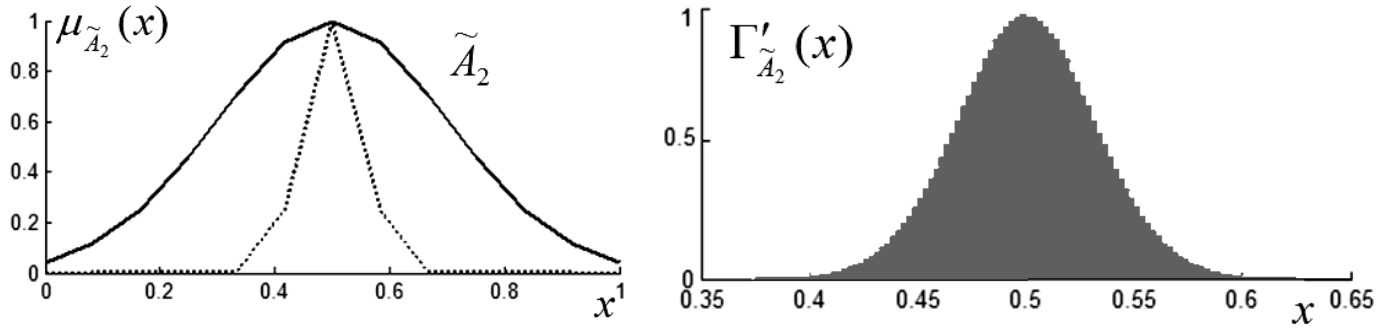

(a) (b)

Fig. 2 IT2 Gaussian fuzzy sets with uncertain standard deviation (a) and its corresponding discrete centroid density distribution (b).

as a composition of the calculated domain values. However, in **Step 5** of the exhaustive defuzzification method as described in Section II.B the set of defuzzified embedded fuzzy sets is considerably reduced. This is achieved via application of Zadeh's extension principle, which maps the IT2 FS back to its interval centroid. Here, only a single centroid of the embedded fuzzy sets per each unique domain value remains in the solution and have an impact on the geometrical properties of the final interval centroid. Hence, from the perspective of the type-reduction algorithm, all embedded fuzzy sets, which are defuzzified to an identical domain value form an equivalence class. The members of each such class are here termed *redundant* embedded fuzzy sets.

Definition 1: Two embedded fuzzy sets A_1 and A_2 are redundant if they both defuzzify into an identical domain value as $C(A_1) = C(A_2)$.

As an example, consider a group of embedded fuzzy sets that are vertically shifted in the domain of the secondary variable *u*. In **Step 5** of the exhaustive defuzzification method, those embedded fuzzy sets are treated as redundant and only a single representative one remains after the type-reduction process.

This redundancy pruning significantly simplifies the complex inner structure of the centroid. This inner structure is similar to the stratified structure of the type-reduced set presented in [19]. This paper further demonstrates that the distribution of redundant embedded fuzzy sets provides an insight into the discrepancies in the convergent behavior of the KMIP algorithm and the sampling defuzzification method [1].

Next, assume that apart from applying the extension principle, also the number of redundant embedded fuzzy sets for each unique domain value is being recorded during the exhaustive defuzzification process. The distribution function $\Gamma_{\tilde{A}}(x)$ of this quantity is denoted here as the centroid density function of the IT2 FS $\tilde{A}$.

Definition 2: The centroid density $\Gamma_{\tilde{A}}(x)$ for domain value *x* denotes the normalized number of redundant embedded fuzzy sets that are defuzzified to the identical domain value *x*:

$$\Gamma_{\tilde{A}}(x) = \alpha \sum_{i=1}^{N} f(A_i), \quad f(A_i) = \begin{cases} 0 & C(A_i) \neq x \\ 1 & C(A_i) = x \end{cases} \tag{17}$$

Here, *N* is the number of all embedded fuzzy sets, A_i is the embedded fuzzy set and α is the normalization factor, which denotes the maximum number of redundant embedded fuzzy sets for any value of the domain variable *x*, scaling it into the interval between 0 and 1.

Property 1: The value of the centroid density is zero outside the boundaries of the interval centroid:

$$\Gamma_{\tilde{A}}(x) = 0 \quad \forall\, x \notin [y_L, y_R] \tag{18}$$

Proof: By the definition of the KMIP method, bound y_L constitutes the left most location of any centroid of the available embedded fuzzy sets. Similarly, bound y_R is the right most location of any centroid of all available embedded fuzzy sets. Hence, the centroids of all embedded fuzzy sets are

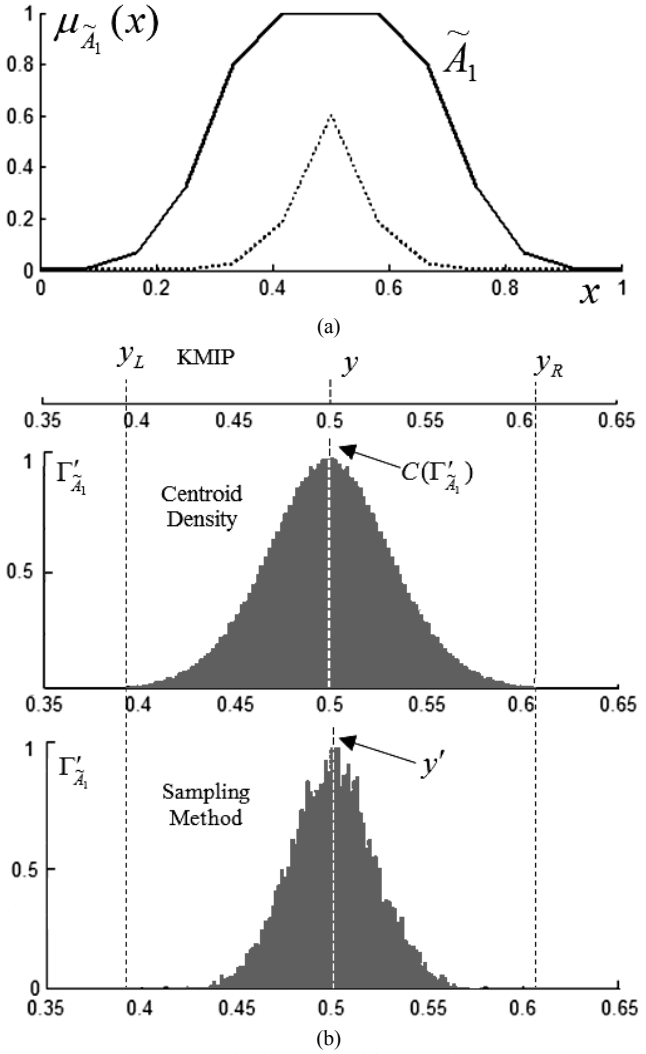

Fig. 3 Symmetric IT2 Gaussian fuzzy set with uncertain mean (a), its centroid density and the defuzzified values (b), y – center of gravity of the centroid density distribution, y ' – sampling defuzzifier.

located in this interval and the centroid density is thus zero outside this interval.

From the computational perspective, the discrete centroid density $\Gamma'_{\tilde{A}}(x)$ is more practical, since the primary domain must be discretized for practical implementations.

Definition 3: Assume that the primary domain is discretized into N samples $x_1, x_2, \ldots, x_N$ with an ε distance between two consecutive samples Then the discrete centroid density $\Gamma'_{\tilde{A}}(x_i)$ for value x_i denotes the normalized number of redundant embedded fuzzy sets that are defuzzified into the discretized interval around x_i:

$$\Gamma'_{\tilde{A}}(x_i) = \alpha \sum_{i=1}^{N} f(A_i), \quad f(A_i) = \begin{cases} 0 & C(A_i) \notin [x_i \pm \frac{\varepsilon}{2}] \\ 1 & C(A_i) \in [x_i \pm \frac{\varepsilon}{2}] \end{cases} \tag{19}$$

Again, the normalization factor α is the maximum number of redundant embedded fuzzy set for any discrete interval in the primary domain, scaling it to the interval between 0 and 1.

Finally, consider the center of gravity of function $\Gamma'_{\tilde{A}}(x)$, which can be denoted as $C(\Gamma'_{\tilde{A}})$ and computed as follows:

$$C(\Gamma'_{\tilde{A}}) = \frac{\sum_{i=1}^{N} \Gamma'_{\tilde{A}}(x_i) x_i}{\sum_{i=1}^{N} \Gamma'_{\tilde{A}}(x_i)} \tag{20}$$

An example of centroid density for two different IT2 FSs is presented in Fig. 1 and Fig. 2. The figures show symmetric Gaussian interval type-2 fuzzy set with uncertain mean and uncertain standard deviation, respectively. In both cases, variable x was discretized into 13 samples and each secondary membership function was sampled using 3 samples, leading to a total of 1,594,323 embedded fuzzy sets.

The centroid density function provides valuable insight into the inner structure of the interval centroid. The only available method for computing the centroid density function is the exhaustive defuzzification method that accounts for all available embedded fuzzy sets. However, the applicability of this approach is hindered by the vast amount of embedded fuzzy sets, which makes this method computationally intractable even for modest discretization levels.

The KMIP method offers an opposite approach. This algorithm only considers two special embedded fuzzy sets and only computes the two boundary points y_L and y_R of the interval centroid. In the final step of the KMIP defuzzification approach, the center of gravity of this interval centroid is computed as the mid-point between the boundary values y_L and y_R. One of the greatest advantages of the KMIP approach is its computational speed.

The sampling defuzzifier can be seen as a middle way between the KMIP method and the exhaustive defuzzification approach. This method approximates the final result by considering only a subset of the available embedded fuzzy sets.

IV. Experimental Results

In this section the convergent behavior of the sampling defuzzifier is experimentaly compared to the deterministic result produced with the KMIP. It is shown that unlike the KMIP approach, the sampling algorithm converges towards the center of gravity of the respective centroid density distrubution function. Two types of IT2 FS are considered in the study, symmetric and non-symmetric.

A. Symmetric IT2 fuzzy sets

Consider a symmetric IT2 fuzzy set $\tilde{A}$ the FOU of which is symmetrical about its mean m:

$$\overline{\mu}_{\tilde{A}}(m+x) = \overline{\mu}_{\tilde{A}}(m-x) \tag{21}$$

$$\underline{\mu}_{\tilde{A}}(m+x) = \underline{\mu}_{\tilde{A}}(m-x) \tag{22}$$

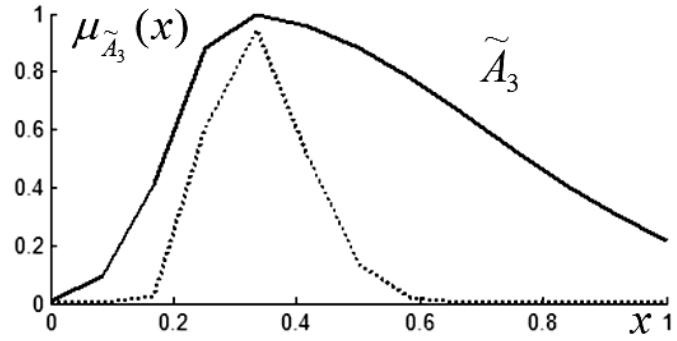

(a)

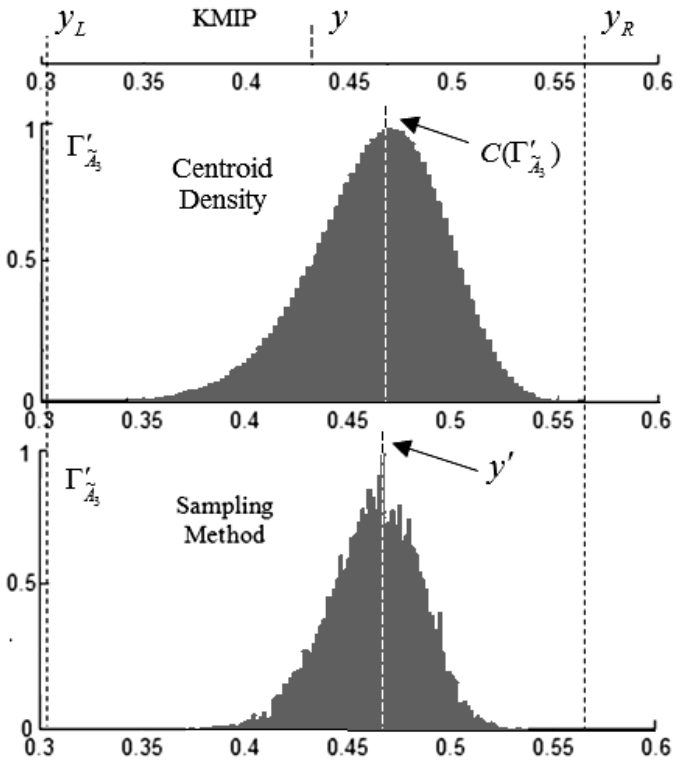

(b)

Fig. 4 Non-symmetric Interval Type-2 Gaussian fuzzy set (a), its centroid density distribution and the defuzzified values (b)), y – center of gravity of the centroid density distribution, y' – sampling defuzzifier.

TABLE I
COMPARISON OF THE DEFUZZIFIED OUTPUT VALUES

Fuzzy Set	Centroid Density	KMIP Method			Sampling Method
	$C(\Gamma'_{\tilde{A}})$	y	y_L	y_R	y'
Symmetric	0.5	0.5	0.3940	0.3001	0.5004 ± 0.0005
Non-Symmetric	0.4624	0.4311	0.6060	0.5621	0.4625 ± 0.0003

A symmetrical Gaussian IT2 FS $\tilde{A}_1$ with uncertain mean is denoted in Fig. 3(a). The domain of FS $\tilde{A}_1$ was again discretized into 13 samples in the x domain and 3 samples for each secondary membership function yielding a total of

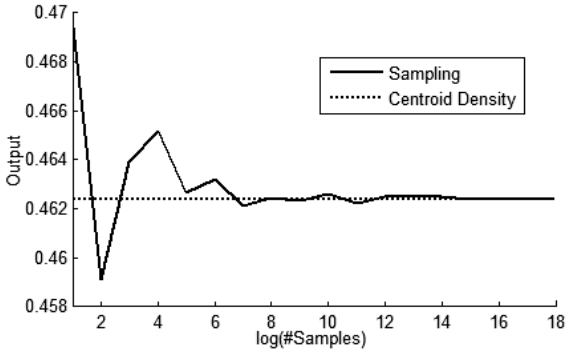

(a)

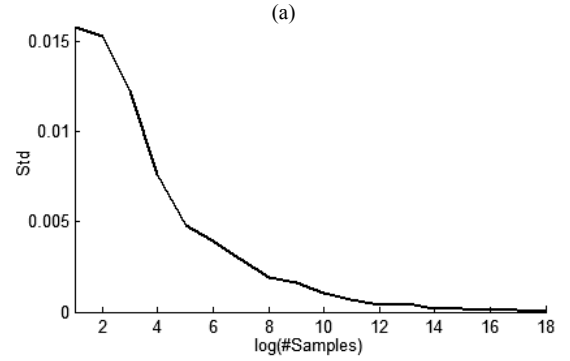

(b)

Fig. 5 The convergence of the mean (a) and the standard deviation (b) of the output value produced by the sampling defuzzifier with increasing number of samples.

1,594,323 available embedded fuzzy sets. This FS was first defuzzified using the KMIP algorithm. Next, the centroid density function was computed using the exhaustive defuzzification method evaluating all 1,594,323 embedded fuzzy sets. Finally, the IT2 FS $\tilde{A}_1$ was also defuzzified using the sampling defuzzifier randomly selecting only 10,000 embedded fuzzy sets. The comparison of the defuzzified values and a graphical view of the discrete centroid density function $\Gamma'_{\tilde{A}_1}(x)$ are presented in Table I and Fig. 3(b).

It can be observed, that the centroid density distribution $\Gamma'_{\tilde{A}_1}(x)$ follows approximately a symmetric Gaussian normal distribution. As demonstrated in Table I, the defuzzified values produced by the KMIP algorithm and the center of gravity of the centroid density function are in agreement. The defuzzified value produced by the sampling defuzzifier is shown to be converging towards the correct value. In order to obtain an accurate picture, the average of 20 defuzzification cycles is reported in Table I for the sampling defuzzifier, together with the standard deviation of the result.

B. Non-Symmetric IT2 Fuzzy Sets

Next, a non-symmetric IT2 FS $\tilde{A}_3$ with uncertain standard deviation was considered with its FOU as depicted in Fig. 4(a). All defuzzification methods have been applied with the same parameters as in the previous experiment.

The defuzzified values and the discrete centroid density function $\Gamma'_{\tilde{A}_3}(x)$ are reported in Table I and in Fig. 4(b). It could be observed that despite the centroid density function

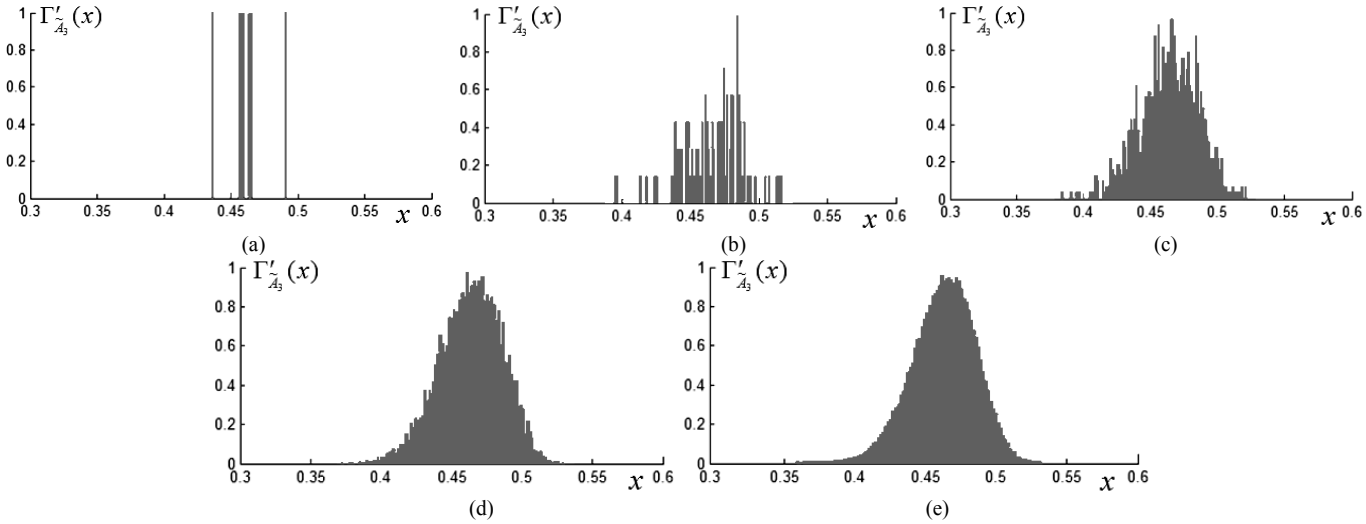

Fig. 6 The sampled centroid density distribution for the sampling defuzzifier using 10, 100, 1.000, 10.000, 100.000 (a)-(e) sampled embedded fuzzy sets.

$\Gamma'_{\tilde{A}_3}(x)$ having the nature of a Gaussian distribution, it is far from being symmetric. This observation can be attributed to the non-symmetric distribution of the width of the FOU of the original IT2 FS. This non-symmetric nature is also reflected in the centroid density function produced by the sampling defuzzification method. Both functions are shifted away from the mid-point of the centroid interval computed by the KMIP algorithm. The actual defuzzified values can be compared in Table I.

As it can be seen from the shown examples, given a non-symmetric IT2 FS, which is a typical case for the output fuzzy sets of IT2 FLSs, a significant difference between the defuzzified values produced by the KMIP algorithm and the sampling defuzzifier can be expected. The interpretation of these discrepancies is an open issue.

Recently, novel representations for general T2 fuzzy sets using α -planes [7] and *zSlices* [5] have been introduced. In [24] the results of defuzzification of α -plane based general T2 FS using the KMIP algorithm, sampling defuzzification and exhaustive defuzzification have been reported. It was demonstrated that for increasing number of α -planes the KMIP and the sampling method did not converge to identical values. The authors believe that the introduced concept of centroid density can provide further insight and explanations into such discrepancies.

C. Convergence of the Sampling Defuzzification

An additional set of experiments have been carried out in order to verify the convergence of the sampling defuzzifier towards the center-of-gravity of the centroid density function, which was computed using the exhaustive defuzzification technique. The sampling defuzzifier was applied to the non-symmetric IT2 FS $\tilde{A}_3$ depicted in Fig. 4(a). The number of sampled embedded fuzzy sets ranged from 2^2 to 2^{18}. Each experiment was repeated 20 times. The mean and the standard deviation of the defuzzified values are reported in Fig. 5. In addition, Fig. 6(a)-(e) visually demonstrates the convergence of the sampled centroid density function. From the presented results it can be noted that the sampling defuzzification method provides a steady convergence towards the center of gravity of the centroid density function.

Hence, it can be concluded that the sampling defuzzifier converges to the output value obtained by applying the weighted average to the centroid density function. On the other hand, the KMIP method computes the mid-point of the interval centroid calculated with accordance to the extension principle. The interval centroid does not maintain information about the centroid density function, since it was removed during the application of Zadeh's extension principle.

V. Conclusion

This paper presented a comparative analysis of the performance of two fundamentally different defuzzification techniques for IT2 FSs. The stochastic sampling defuzzification method and the deterministic KMIP method were considered in this work. The concepts of redundant embedded fuzzy sets and the notion of centroid density function of an IT2 FS were introduced. These novel concepts provided explanation for some of the discrepancies between the results produced by the KMIP method and the sampling defuzzifier.

It was shown that the sampling defuzzification approach converges towards the center of gravity of the centroid density function, which can be computed using the exhaustive defuzzification method. On the other hand, the KMIP algorithm calculates the results as the mid-point of the interval centroid computed with accordance to the extension principle. Since the application of the extension principle during the type-reduction removes the information about the centroid density, the KMIP and the sampling defuzzification techniques inevitable converge towards different results. This difference becomes especially significant for non-symmetric IT2 FS.

References

[1] L. A. Zadeh, "The Concept of a Linguistic Variable and its Approximate Reasoning - II," in *Information Sciences*, No. 8, pp. 301-357, 1975.

[2] J. M. Mendel, *Uncertain Rule-Based Fuzzy Logic Systems: Introduction and New Directions*, Prentice-Hall, Upper Saddle River, NJ, 2001.

[3] N. N. Karnik, J. M. Mendel, "Type-2 Fuzzy Logic Systems," in *IEEE Trans. on Fuzzy Systems*, vol. 7, no. 6, pp. 643-658, December 1999.

[4] S. Coupland, R. John, "Geometric Type-1 and Type-2 Fuzzy Logic Systems," in *IEEE Trans. on Fuzzy Systems*, vol. 15, no. 1, pp. 3-15, February 2007.

[5] Ch. Wagner, H. Hagras, "Toward General Type-2 Fuzzy Logic Systems Based on zSlices," in *IEEE Transaction of Fuzzy Systems*, vol. 18, no. 4, pp. 637-660, August, 2010.

[6] F. Liu, "An efficient centroid type-reduction strategy for general type-2 fuzzy logic system," in *Information Sciences*, vol. 178, issue: 9, pp 2224-2236, May 2008.

[7] J. M. Mendel, F. Liu, D. Zhai, "α -Plane Representation for Type-2 Fuzzy Sets: Theory and Applications," in *IEEE Trans. on Fuzzy Systems*, vol. 17, no. 5, pp. 1189-1207, October 2009.

[8] H. Hamrawi, S. Coupland, R. John, "A Novel Alpha-cut Representation for Type-2 Fuzzy Sets," in *Proc. of IEEE World Congress on Computational Intelligence*, Barcelona, Spain, pp. 351-358, June 2010.

[9] J. M. Mendel, R. John, F. Liu, "Interval Type-2 Fuzzy Logic Systems Made Simple," in *IEEE Trans. on Fuzzy Systems*, vol. 14, no. 6, pp. 808-821, December 2006.

[10] O. Linda, M. Manic, "Interval Type-2 Fuzzy Voter Design for Fault Tolerant Systems," in *Information Sciences*, 2011, in press.

[11] H. A. Hagras, "A Hierarchical Type-2 Fuzzy Logic Control Architecture for Autonomous Mobile Robots," in *IEEE Trans. Fuzzy Systems*, vol. 12, no. 4, pp. 524-539, August 2004.

[12] J. Figueroa, J. Posada, J. Soriano, M. Melgarejo, and S. Roj, "A type-2 fuzzy logic controller for tracking mobile objects in the context of robotic soccer games," *Proceeding of the 2005 IEEE International Conference on Fuzzy Systems*, Reno, USA, pp. 359–364, May 2005.

[13] Q. Liang and J. Mendel, "MPEG VBR video traffic modeling and classification using fuzzy techniques," in *IEEE Transactions on Fuzzy Systems*, vol. 9, issue: 1, pp. 183–193, February 2001.

[14] D. Wu and W. Tan, "Type-2 fuzzy logic controller for the liquid-level process," in *Proc. of the 2004 IEEE International Conference on Fuzzy Systems*, Budapest, Hungary, pp. 248–253, July 2004.

[15] R. Martinez, O. Castillo, L.T. Aguilar, "Optimization of interval type-2 fuzzy logic controllers for a perturbed autonomous wheeled mobile robot using genetic algorithms", in *Information Sciences,* vol. 179, issue: 13, pp. 2158–2174, June 2009.

[16] D. Wu, J. M. Mendel, "Enhanced Karnik-Mendel Algorithms", in *IEEE Transaction on Fuzzy Systems*, vol. 17, No. 4, pp. 923-934, August, 2009.

[17] S. Greenfield, R John, S. Coupland, "A Novel Sampling Method for Type-2 Defuzzification," in *Proc. UKCI 06*, pp. 120-127, 2005.

[18] H. Wu, J. M. Mendel, "Uncertainty Bounds and Their Use in the Design of Interval Type-2 Fuzzy Logic Systems, " in *IEEE Transaction of Fuzzy Systems*, vol. 10, no. 5, pp. 622-639, October, 2002.

[19] S. Greenfield, R. John, "Stratification in the Type-Reduced Set and the Generalized Karnik-Mendel Iterative Procedure," in *Proc. of IMPU*, pp. 1282-1289, June 2008.

[20] N. N. Karnik, J. M. Mendel, "Centroid of a type-2 fuzzy set," in *Information Sciences*, vo. 132, issues: 1-4, pp. 195-220, February 2001.

[21] S. Coupland, R. John, "An Investigation into Alternative Methods for the Defuzzification of an Interval Type-2 Fuzzy Set," in *Proc. IEEE International Conference on Fuzzy Systems*, Vancouver, Canada, pp. 1425-1432, July 2006.

[22] M. Nie, W. W. Tan, "Towards and efficient type-reduction method for interval type-2 fuzzy logic system," in *Proc. of FUZZ-IEEE*, Hong Kong, pp. 1425-1432, June 2008.

[23] S. Greenfield, F. Chiclana, S. Coupland, R. John, "The collapsing method of defuzzification for discretised interval type-2 fuzzy sets," in *Information Sciences*, vol. 179, issue: 13, pp. 2055-2069, June 2009.

[24] S. Greenfield, F. Chiclana, S. Coupland, R. John, "Type-2 Defuzzification: Two Contrasting Approaches." in *Proc. of IEEE World Congress on Computational Intelligence*, Barcelona, Spain, pp. 3183-3189, June 2010.

[25] J. M. Mendel, R. I. John, "A Fundamental Decomposition of Type-2 Fuzzy Sets," in *Proc. of Joint 9th IFSA World Congress and 20th NAFIPS Int'l. Conf.*, Vancouver, Canada, pp. 1896-1901, July 2001.

[26] S. Coupland, R. John, "An Investigation into Alternative Methods for the Defuzzification of an Interval Type-2 Fuzzy Set," in *Proc. IEEE Intl' Conf. on Fuzzy Systems*, Vancouver, Canada, pp. 1425-1432, September 2006.

[27] O. Linda, M. Manic, "Importance Sampling Based Defuzzification for General Type-2 Fuzzy Sets," in Proc. *2010 IEEE World Congress On Computational Intelligence, WCCI 2010 - FUZZ-IEEE 2010*, Barcelona Spain, pp. 1-7, July 2010.

[28] G. Klir, B. Yuan, *Fuzzy Sets and Fuzzy Logic: Theory and Applications*, Prentice Hall, Upper Saddle River, NJ, 1995.

2011 IEEE International Conference on Fuzzy Systems
June 27-30, 2011, Taipei, Taiwan

Statistical Scheme via AIC for Evaluating the Optimal Cut Off Level in Fuzzy Clustering

Shuya Kanagawa[1]
dept. Industrial & Management Systems
Tokyo City University
Tokyo, JAPAN
kanagaw@tcu.ac.jp

Kimiaki Shinkai
dept. Modern Human Economics
Tokyo Kasei Gakuin University
Tokyo, JAPAN

Hsunhsun Chung
dept. Mathematics
Waseda University
Tokyo, JAPAN

Kenichi Nagashima
dept. Mathematics
Waseda University
Tokyo, JAPAN

***Abstract*—In this paper we show a new statistical scheme to find the optimal cut off level in fuzzy clustering which is an improvement of Uesu and Shinkai et. al [4]~[7]. Deterministic algorithms which seek a certain equilibrium cluster level have essential disadvantage in principle. We focus in it and propose a statistical scheme via AIC.**

Keywords-component; fuzzy clustering; AIC; cut off level; partition tree

I. INTRODUCTION

When we analyze ambiguous information such as human behavior, mental process, social structure and so on, a fuzzy graph of the information is very useful in these problems (see e.g. Romsburg [3]). Since the fuzzy graph is constructed with clusters of some levels, the clustering level analysis of fuzzy graph is required for the above applications.

Let Fig.3 is a preference relationship between 26 students {1,2,…,26} of a high school. Fig.1 is a partition tree constructed from Fig.3 with 17 clustering cut off levels {**R**0.00, **R**0.08, **R**0.15, **R**0.28, **R**0.35, **R**0.38, **R**0.44, **R**0.45, **R**0.48, **R**0.54, **R**0.57, **R**0.65, **R**0.67, **R**0.71, **R**0.79, **R**0.83, **R**1.00} and there are 17 sets of clusters according to these clustering levels each other. For example the level **R**0.08 means that the set of ten points {1,2,…,26} is divided by 5 clusters {15,17}, {2,18,7,4,13,11,8,20,19,12}, {14,24,3,22,1, 26,16,5,9}, {21,25}, {6}, {10}, {23}. As for the selection of the optimal level in a partition tree in Fig.1 the gradient method in the multivariate analysis has been used very often.

On the other hand, in 1994 Tsuda and Yamashita [5] suggested a new method to estimate the optimal level to find a unique equilibrium point for the cluster number and the cluster size. It means to know a kind of stable classification of clusters for {1,2,…,26}. Their method fits in well with actual examples. Moreover Uesu and Shinkai et. al [4], [6]~[8] proposed a rational method to decide the optimal level of fuzzy clustering with a partition tree. However we have also had two questions about an objective validity of these deterministic algorithms which seek a certain equilibrium cluster level.

The first problem is that the above deterministic algorithms cannot easily make effective use of all the information of the partition tree. Especially, in principle, the gradient method uses only local information of the partition tree. From the view point we define a configuration of points {1,2,…,26} on the interval [0,16] measuring the distance between each adjoining two points in the partition tree (see Fig.3). For example, the clustering cut off level **R**0.83 implies that the distance between {2} and {18} is 0.17=1-0.83. Furthermore the distance between {14} and {27} is 0.21=1-0.79 from **R**0.79, and so on. Then we can construct a configuration of {1,2,…,26} on the interval [0,16] in Fig.3. Next we consider a distribution of the configuration. Every clustering cut off level corresponds to a histogram of the configuration, respectively. Therefore we can choose the optimal cut off level by comparing AIC of each histogram.

Figure 1. Partition tree *P*.

Another problem is "Does the true cluster level always mean an equilibrium or well balanced state?". From the point of a statistical view, we would reconsider the clustering level analysis in the past and propose a new scheme by applying the AIC method and obtain a statistically equilibrium optimal level of fuzzy clustering. Although we have proposed such statistical scheme in [2], we improve the scheme and show its

[1] The research of the first author was supported, in part, by Grant-in-Aid Scientific Research, No. 20540140, Ministry of Education, Science and Culture, Japan.

advantage to the deterministic algorithms since [2] can not apply to small sample size data.

II. UESU'S METHOD

Next, according to Uesu [7], we introduce Uesu's method to estimate the optimal clustering level for the partition tree P in Fig.1. His method shows that the optimal cut level is **R**0.38 from Fig. 2 by the following method.

Definition 1 *Crisp Node Fuzzy Graph*

A crisp node fuzzy graph G is defined by

$$G=(V,F):V=\{v_i\},F=(f_{ij}),0\le f_{ij}\le 1,$$

where V is the set of the nodes and F is an $n\times n$ matrix whose (i, j) component f_{ij} is a fuzziness of the arc from the node v_i to the node v_j.

Definition 2 *Fuzzy Node Fuzzy Graph*

A fuzzy node fuzzy graph G is defined by

$$G=(V,F):V=\{v_i/u_i\},Y=(y_{ij}),0\le u_i\le 1,\ 0\le y_{ij}\le 1,$$

where V is the set of the nodes and the fuzziness u_i is a fuzziness of the node v_i. Y is an $n\times n$ matrix whose (i, j) component y_{ij} is a fuzziness of the arc from the node v_i to the node v_j.

Definition 3 *Transformation from Fuzzy Node Fuzzy Graph to Crisp Node Fuzzy Graph*

A fuzzy node fuzzy graph $G=(V, Y)$ can be transformed to a crisp node fuzzy graph $G=(V,F)$ by the following method: Let

$$G=(V,F):V=\{v_i\},F=(f_{ij}),f_{ij}=T(u_i,y_{ij}),$$

where the fuzziness f_{ij} of the arc from the node v_i to the node v_j could be defined by applying T-norms. A fuzzy graph G is defined by

$$G=(V,Y),\ V=\{v_i\},\ F=(f_{ij}),\ 0\le f_{ij}\le 1,\ f_{ii}=1,1\le i\le n$$

where f_{ij} is a fuzziness of the arc from the node v_i to the node v_j . A symmetric relation matrix S is defined by

$$S=(s_{ij}),\quad \frac{2}{s_{ij}}=\frac{1}{f_{ij}}+\frac{1}{f_{ji}}$$

where $s_{ij}=0$ if $f_{ij}\cdot f_{ji}=0$.

Let $x(c)$ and $y(c)$ be the branching number and maximum cluster size of each Rc, respectively. The more the level Rc increases, the more the branching number $x(c)$ increases. On the other hand, the more the level Rc increases, the more the maximum cluster size $y(c)$ decreases. Since there is an inevitable trade off between the branching number $x(c)$ and the maximum cluster size $y(c)$ in this situation, we would decide the optimal cut level c_0.

Based on $x(c)$ and $y(c)$, we could define the cluster branch function $p(c)$ and the cluster size function $q(c)$ as follows:

Definition 4 The cluster branch function $p(c)$ and cluster size function $q(c)$ are defined by

$$p(c)=\frac{x(c)-1}{x(1)-1},\ q(c)=\frac{y(c)-1}{y(0)-1},$$

respectively.

Definition 5 Decision of Optimal Cut Level c_0

$$r(c)=p(c)\wedge q(c)$$

and

$$c_0=\max\{c:r(c)=\max r(x)\}. \qquad (1)$$

Then, by using these notions, an optimal cut level c_0 of the partition tree Fig.1 is decided as follows.

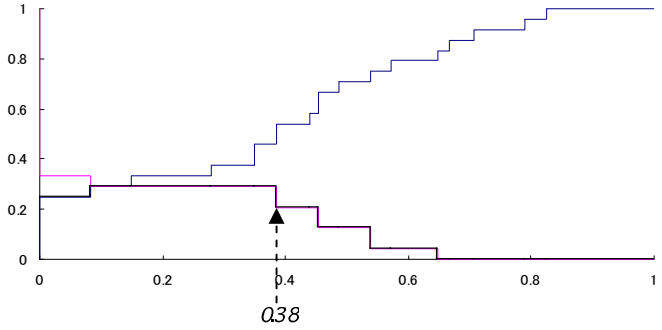

Figure 2. Fuzzy decision $r(c)$.

Applying the fuzzy decision, we obtain that the optimal cut off level is **R**0.38 as shown in Fig.2.

III. AIC

We shall define AIC as followings. Let $X_1, X_2, \ldots, X_n$ be independent and identically distributed random variables with the probability density function $f(x;\theta^*)$, where $\theta^*=(\theta_1^*,\theta_2^*,\cdots,\theta_K^*)$ is an unknown parameter of the distribution. Furthermore, for n random sample points $(x_1,x_2,\cdots,x_n)$,

$$\ell(\theta)=\sum_{i=1}^{n}\log f(x;\theta_i)$$

is the log likelihood and $\hat{\theta}_K$ is the maximal likelihood estimator for $\theta^*=(\theta_1^*,\theta_2^*,\cdots,\theta_K^*)$ defined by

$$\hat{\theta}_K=\max_{\theta\in\Theta_K}\ell(\theta),$$

where Θ_K is the space of all candidates $\theta=(\theta_1,\theta_2,\cdots,\theta_K)$ for the real parameter θ^* . The Kullback-Leibler information number $KLI(\theta^*,\theta)$ for the samples $(x_1,x_2,\cdots,x_n)$ is defined by

$$KLI(\theta^*,\theta)=\sum_{i=1}^{n}f(x;\theta^*)\log f(x;\theta^*)-\sum_{i=1}^{n}f(x;\theta^*)\log f(x;\theta),$$

which metrizes the distance between $f(x;\theta^*)$ and $f(x;\theta_i)$ using entropy. It is easy to see that $\hat{\theta}_K$ minimize the Kullback-Leibler information number $KLI(\theta^*,\theta)$ such that

$$KLI(\theta^*,\hat{\theta}_K) = \min_{\theta\in\Theta_K} KLI(\theta^*,\theta).$$

Now we define AIC (Akaike's information criterion) by

$$AIC(K) = -2\ell(\hat{\theta}_K) + 2K. \quad (2)$$

For comparing several models of $\theta^* = (\theta_1^*,\theta_2^*,\cdots,\theta_K^*)$ for known *K,* we can find the optimal $\theta = (\theta_1,\theta_2,\cdots,\theta_K)$ in Θ_K with large probability when it attains the smallest $AIC(K)$ for $(x_1,x_2,\cdots,x_n)$. In general, when *K* is unknown, $-2\ell(\hat{\theta}_K)$ decreases as the number of parameters *K* increases. Therefore $AIC(K)$ also gives the optimal *K* from the definition. By its sensitivity the AIC method is applied to various types of the model selection in many fields.

Let $\mathbf{q} = (q_1,q_2,\cdots,q_m)$ be a discrete distribution for integers $\{1,2,\cdots,m\}$. Put $\{x_1,x_2,\cdots,x_n\}$ be samples from a proportion of $\{1,2,\cdots,m\}$. Let n_i be a number of samples of each integer $i\in\{1,2,\cdots,m\}$ satisfying $n_1+n_2+\cdots+n_m = n$. From $K = m-1$ for the distribution $\mathbf{q}$, AIC of $\mathbf{q}$ is defined by

$$AIC(\mathbf{q}) = -2\sum_{i=1}^{m} n_i \log q_i + 2(m-1). \quad (3)$$

IV. Statistical Scheme via AIC

Step 1. *Find the configuration of {1,2,...,26} on the interval [0,16]. See Fig.3.*

Step 2. *Divide the interval [0,16] into 16 subintervals [i,i+1] for i=0,1,...,15.*

Step 3. *Make histograms and calculate AIC for each histogram.*

Make histogram for {1,2,…,26} according to each fuzzy clustering level. We can find which histogram (cluster level) is the best by comparing AIC's of each histogram. For example, Fig.4 and Fig.5 correspond to clustering levels $\mathbf{R}_{0.35}$ and $\mathbf{R}_{0.15}$, respectively. From (3) we have

AIC($\mathbf{R}_{0.45}$)= -2{2log[3/26] +log[3/26] + 10log[1/26] + log[2/26] + 4log[7/104]}+ 28= 132.837

AIC($\mathbf{R}_{0.44}$)= -2{3log[2/26] + log[3/26] + 8log[1/26] + 4log[7/104]} + 26= 119.426

AIC($\mathbf{R}_{0.38}$)= -2{2log[2/26] + log[3/26] + 2log[3/52] + 7log[1/26] + 5log[9/130]}+ 22= 120.306

AIC($\mathbf{R}_{0.35}$)= -2{2log[2/26] + log[3/26] + 3log[5/78] + 2log[1/26]+5log[9/130]+log[2/26]+3log[1/26]}+18= 101.83

AIC($\mathbf{R}_{0.28}$)= -2{6log[2/26] + 5log[1/26] + 5log[9/130]} + 16= 106.063

AIC($\mathbf{R}_{0.15}$)= -2{2log[2/26] + 4log[1/26] + 10log[9/130]} + 14= 92.6404

AIC($\mathbf{R}_{0.08}$)= -2{2log[2/26] + 6log[10/156] + 5log[9/130] + 3log[1/26]}+ 12= 101.479

Step 4. *Conclusion*

Since AIC($\mathbf{R}_{0.15}$) is smaller than other clustering cut off levels, we can evaluate that $\mathbf{R}_{0.15}$ is optimal.

V. Conclution

From the above statistical scheme we conclude that the optimal clustering cut off level is $\mathbf{R}_{0.15}$ which is different from Uesu's method ($\mathbf{R}_{0.38}$). Although it is difficult to discuss which level is better, we could evaluate with greater accuracy as we have a lot of criteria for judgment. Furthermore an example in [2] shows that the statistical scheme has an advantage over deterministic methods when $\mathbf{R}_{0.00}$ is the optimal cut off level. From the point of view we would like to propose the scheme in addition to deterministic methods.

Acknowledgment

The authors kindly thank three anonymous referees for their useful comments. They also would like to express their thanks to Professors H. Yamashita and T. Takizawa of Waseda University for useful discussions.

References

[1] H. Akaike, "Information theory and an extension of the maximum likelihood principle", 2nd Inter. Symp. on Information Theory, Akademiai Kiado, pp. 265-281, 1973.

[2] S. Kanagawa and K. Shinkai, "Fuzzy Clustering Level Analysis via Statistical Scheme Applying Akaike's Information Criterion", International Journal of Innovative Computing, Information and Control, Vol.4, pp.2523-2531, 2008.

[3] H. Romesburg, Cluster Analysis for Researchers, Lifetime Learning Publication, 1984.

[4] K. Shinkai and H. Yamashita, "Level Analysis of Fuzzy Partition Tree and its Application", *Int'l Workshop on Soft Computing Applications*, 2005.

[5] E. Tsuda and H. Yamashita, "Sociometry analysis using fuzzy graphs", *Journal of Japan SOFT*, vol. 6 , No.3, 1994 (in Japanese).

[6] H. Uesu, "Sociometry Analysis Applying Fuzzy Node Fuzzy Graph", Journal of Japan Society for Fuzzy Theory and Systems, Vol.14, No.3, 2002 (in Japanese).

[7] H. Uesu, "Structure Analysis of Fuzzy Node Fuzzy Graph and its Application to Sociometry Analysis", KES 2008, Part III, LNAI 5179, pp. 84–91, 2008, Springer-Verlag Berlin Heidelberg.

[8] H. Uesu and K. Shinkai, "Learning Structure Analysis System Applying Fuzzy Theory", Int'l Conference on Advanced Learning Technologies, 2004.

	1	2	3	4	5	6	7	8	9	10	11	12	13	14	15	16	17	18	19	20	21	22	23	24	25	26
1																6						9		3		12
2							6	1			1		10					11	1							
3													7	2		7						9		5		
4		1						4			10		5			3							3	2		
5	5					4							3	8		1						4				5
6	12	6	4	2																						
7		11						2					6					10	1							
8		6		2			2				1		5		4			7		3						
9						12								3		6						9				
10	4		3		4	5								4								3		2		
11		3		3				10					4		2		1		1	3						
12		2		1			3	3			7		6				4		1							
13		2		7			1							6				7				6		1		
14		2			2				1													3		9		3
15																	12									
16	8					4			5					3								4				5
17															12											
18		9																								
19		8								4	3	1	3	1		2		2					3			
20		4					9	9			7								1							
21											5				12		8		1						4	
22			8											9		5										6
23								2		4	5		3	4			2	3			3					
24			2								1			10									4			3
25															4						8					
26	6		4		6									3								7				

Figure 3. Preference relationship between {1,2,…,26}.

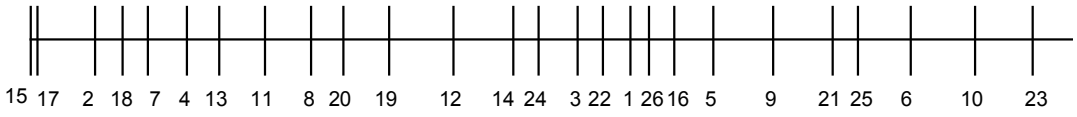

Figure 4. Configuration of {1,2,…,26}.

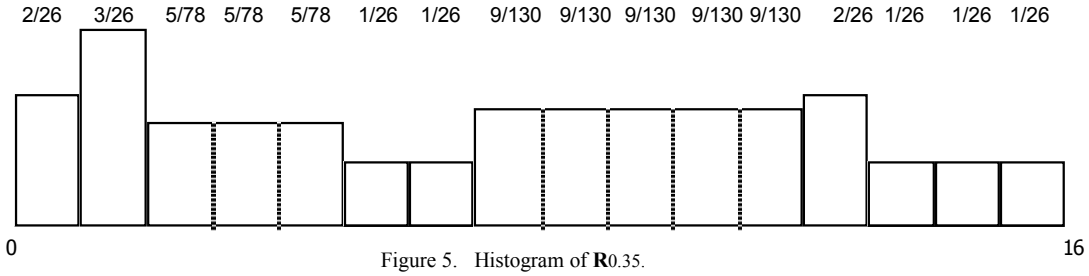

Figure 5. Histogram of **R**0.35.

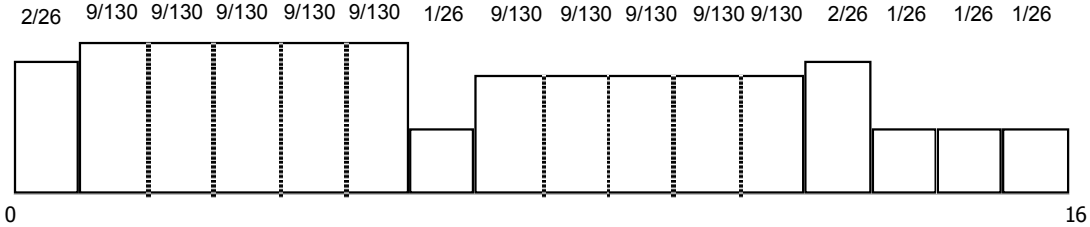

Figure 6. Histogram of **R**0.15.

2011 IEEE International Conference on Fuzzy Systems
June 27-30, 2011, Taipei, Taiwan

Genetic Algorithm Based Fully Automated and Adaptive Fuzzy Logic Controller

Pintu Chandra Shill†, Kishore Kumar Pal‡, Md. Faijul Amin†, Kazuyuki Murase†
† Department of System Design Engineering, University of Fukui, 3-9-1 Bunkyo, Fukui-910-8507, Japan
‡ Khulna University, Khulna, Bangladesh
{pintu,amin,murase}@ synapse.his.u-fukui.ac.jp, kkcseku@yahoo.com

***Abstract*—In this paper, an integration of fuzzy logic controller (FLC) and genetic algorithm (GA) is developed with a view to make the design process fully automatic, without requiring any human expert knowledge. Here, GA is used in two stages simultaneously: the first stage involves selection and definition of fuzzy rules, while the second stage performs an optimal selection of membership function types associated to the fuzzy rules. It is argued that the performance of an FLC greatly depends on the fuzzy rules as well as the types of membership functions associated to the fuzzy sets. Thus, the aforementioned two-stage GA is a viable solution for designing an efficient FLC system. In order to evaluate performance, the proposed approach is applied to a well-known benchmarking controller design task, "backing up a truck reversing system". The simulation result exhibits superior performance and thereby validates the proposed integrated GA and FLC system.**

Index Terms- Fuzzy Logic Controller; Fuzzy Rule Base; Genetic Algorithm; Optimization; Backing up a truck reversing problem

I. INTRODUCTION

Fuzzy logic controllers (FLCs) have numerous practical applications in control [1], [2], prediction [3] and inference [4]. Specifically, they have been used for designing a robust controller that can yield satisfactory performance and deal with uncertainty and imprecision. However, the vast majority of FLCs developed to date are based on the expert knowledge base derived from imprecise heuristic knowledge of experienced control engineers. Such manual approach is very time-consuming as it requires trial and error method to generate fuzzy rules and membership functions (MFs). Moreover, manual design does not guarantee generating optimal or near optimal fuzzy rules and MFs [5], [6]. Clearly, there is a need for developing an automatic FLC design procedure that would not involve any expert knowledge base derived from heuristic knowledge of experienced control operators/engineers.

The main issue in the FLC design includes deciding membership functions' parameters and types, and generating fuzzy rules. Even though all of these are subject to optimization for a better design, many efforts has been directed to the partial optimization, not the entire system. For example, some works optimize the parameters of MFs, while others optimize the fuzzy rules. The parameters of MFs are either decided on the basis of control operator's/person's experience or are generated automatically. Some methods, such as genetic algorithm (GA), tabu search (TS), particle swarm optimization (PSO) and self-organizing feature map (SOFM) can be used to improve the behavior of this parameter optimization problem [5]-[8], [9], [10].

GA was used by Arslan and Kaya [9] in the determination of membership functions. They applied GA to design a fuzzy logic control system having a single input and output. Bagis [6] proposed a method based on TS algorithm for the determination of membership functions. Bai and Chen [7] proposed an automatic method for students' evaluation task. Its purpose was to automatically construct the grade membership functions of lenient-type grades, strick-type grades, and normal-type grades of fuzzy rules, respectively. The system performs fuzzy reasoning to infer the scores of students based on the constructed grade-membership functions. Meredith et al. [11] presented an approach based on GA to the tuning of membership functions in a FLC for a helicopter. Wong et al. [8] applies PSO to determine appropriate membership functions of the fuzzy system (FS) automatically and presented a motion control structure with a distance fuzzy controller and an angle fuzzy controller for the two-wheeled mobile robot. Yang and Bose [10] presented a method for generating fuzzy membership functions with unsupervised learning using SOFM. The SOFM approach is a two-step procedure: firstly, generate the proper clusters and secondly, generate the fuzzy membership function according to the clusters in the first step. They applied this method to pattern recognition problems.

In this paper, an integrated architecture of FLC and GA has been developed for intelligent control of backing up a truck reversing problem. Here, GA is employed in two simultaneous stages; the first one, referred in this paper as module-1, for the selection and definition of fuzzy rules and the second one, module-2, for the selection of membership function type of each rule. The suggested method can deal with any type of membership functions (i.e., fuzzy sets). The method focuses on finding an optimum set of fuzzy rules and their respective types of membership functions. It is shown that the proposed innovative integrated architecture can generate comprehensible and reliable fuzzy rules and at the same time select the effective type of fuzzy sets (MFs) for each rule by a self-learning adaptive method.

978-1-4244-7316-8/11/$26.00 ©2011 IEEE

The organization of this paper is as follows: in Section II, we review the literature relevant to the FLCs. In Section III, we provide key ideas of integrated FLC and GA architecture and discuss how GAs can be used to generate a satisfactory fuzzy rule base and to select appropriate types of MFs simultaneously for FLCs. We also show how our proposed approach can be used to solve highly nonlinear complex problems such as backing up a truck control. In Section IV, we explain the problem of backing up a truck in a greater detail. In Section V we present our simulation results and finally section VI presents some concluding remarks based on the present study conclusions and some future directions.

II. FUZZY LOGIC CONTROLLER (FLC)

An FLC comprises four components, which are fuzzifier, knowledge base consisting of rule base (RB) and database (DB), fuzzy inference engine, and defuzzifier as depicted in Fig.1. The FLC works as follows, the crisp inputs are first fuzzified into, in general, input fuzzy sets (however, we will consider only non-singleton fuzzification) which then activate the inference engine and the knowledge base to produce output fuzzy sets. The defuzzifier can then defuzzify fuzzy outputs from the inference engine in order to produce crisp outputs. A brief description of each of the FLC components is given in the following subsections.

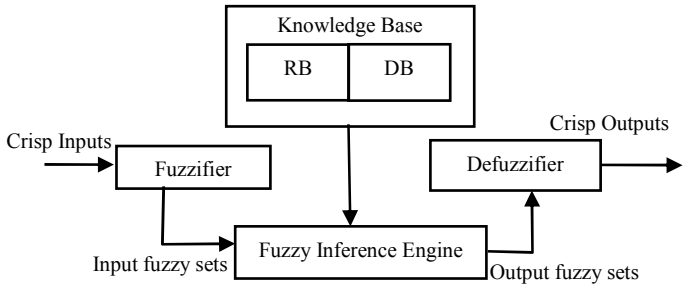

Figure 1. Fuzzy Logic Controller (FLC)

A. Membership functions

Triangular/Trapezoidal MF:

It has the function name *trimf* defined by three points delimiting a triangle.

$$f_{triangulae}(x)=\begin{cases}0, & \text{if } x<x_1\\ 2\dfrac{x-x_1}{x_2-x_1}, & \text{if } x_1\le x\le \dfrac{x_2+x_1}{2}\\ 2\dfrac{x_2-x}{x_2-x_1}, & \text{if } \dfrac{x_2+x_1}{2}<x\le x_2\\ 1, & \text{if } x>x_2\end{cases} \quad (1)$$

Gaussian MF:

Gaussian membership functions are built on the Gaussian distribution curve and are denoted by *gauss_mf*.

$$f_{Gaussian}(x)=e^{-0.5y^2} \quad \text{where } y=\frac{8(x-x_1)}{x_2-x_1}-4 \quad (2)$$

B. Fuzzifier

Since the input is in crisp normalized values, a fuzzification operator *fuzz* is used to fuzzify it in fuzzy form. The fuzzifier maps a crisp input vector with p inputs $x=(x_1,.....x_p)^T \in X_1\times X_2\times.....\times X_p\equiv X$ into input fuzzy set, A_x In Non-singleton fuzzifier: $\mu_A(x_i)$ realizes maximum value 1 at $x=x_i$ and decrease from 1 to 0 while moving away from $x=x_i$ [12]. The fuzzification of the input variable should be realistic. Experience and different procedures as well as different types of MFs should be followed while designing a large fuzzy system for the realistic and accurate output. The wrong fuzzification of the input variable(s) might cause instability and error in the system. Figure 2 shows how fuzzified inputs are calculated from its related different membership forms.

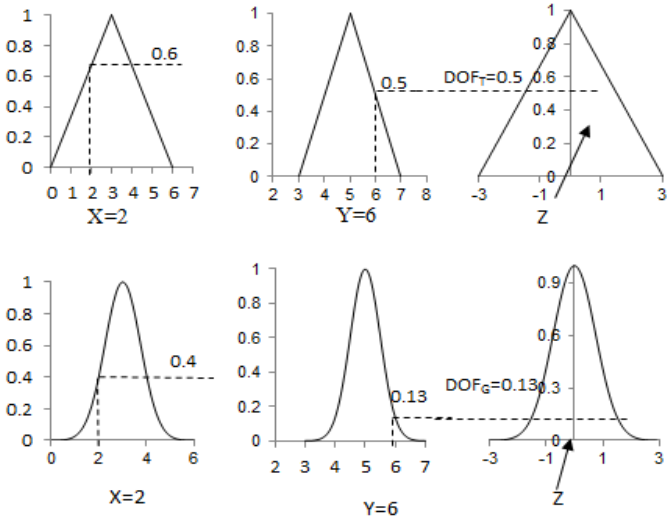

Figure 2. Two different kinds of fuzziness degrees (depends on type of MFs) for a crisp value X=2 and Y=6

C. Fuzzy Inference Engine

The fuzzy inference engine combines rules and gives a mapping from fuzzy sets in the input universe of discourse $U\in R^n$ to fuzzy sets in the output universe of discourse $V\in R$ based on the fuzzy logic principle. In the inference engine, multiple antecedents in the rules are connected using AND operation, and the degree of membership in the input set sets are combined using those in the output sets using sub-star composition, described in detail in [13]. Multiple rules are then combined by using a join operation.

D. Defuzzifier

The defuzzifier performs a mapping from the fuzzy sets in R to crisp points in R. It involves the selection, from the output fuzzy set, the numerical value v^* which can be considered as the best representative element of the fuzzy output set. Maximum defuzzifier produces a numerical value which exhibits the highest degree of membership. The most frequently used center of gravity (COG) defuzzifier takes output as the COG of the fuzzy output. The expression generally used for a discrete fuzzy set is as follows:

$$x_{n+1} = \frac{\int_{X \in U_{n+1}} X \mu_U(X) dX}{\int_{X \in U_{n+1}} \mu_U(X) dX} = \theta^{COG} = \frac{\sum_{j=1}^{p} \theta_j m_o(\theta_j)}{\sum_{j=1}^{p} m_o(\theta_j)}$$

where θ_j denotes the center of gravity (COG) of the consequent label C_j of the rule R_j, $m_o(\theta_j)$ is the firing strength of this rule, and p is the number of rules.

Consider a fuzzy controller with one output variable, and suppose that a given input datum excites two rules of the rule base. Now defuzzification process would yield an output value according to the membership function types associated to linguistic output labels of the two rules. In order to explicate this fact, we consider two cases; gaussian, and mixed MFs. Figure 3 shows that in each case results are different defuzzified value. However, it is easily conceivable that some value would be better than the others. Thus we need a way to define different member function types across the rule base. Some rule may prefer a particular type of MF than the others so as to make an optimal final decision.

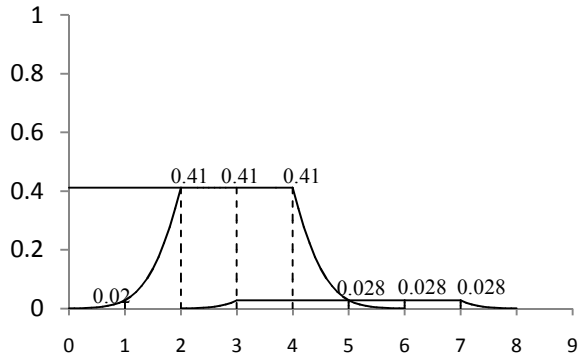

(a) Gaussian MFs for FLC

$$x_{n+1} = \frac{1*0.028 + 2*0.41 + 3*0.41 + 4*0.41 + 5*0.028 + 6*0.028 + 7*0.028}{0.028 + 0.41 + 0.41 + 0.41 + 0.028 + 0.028 + 0.028} = 3.14$$

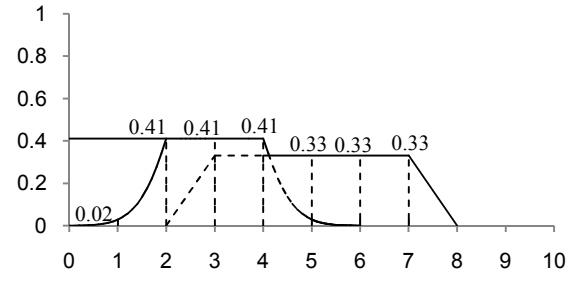

$$x_{n+1} = \frac{1*0.028 + 2*0.41 + 3*0.41 + 4*0.41 + 5*0.33 + 6*0.33 + 7*0.33}{0.028 + 0.41 + 0.41 + 0.41 + 0.33 + 0.33 + 0.33} = 4.31$$

(b) Mixed MFs (Gaussian and Triangular) for FLC

Figure 3. Effect of defuzzification process for selecting different types of MFs

The value of fuzzified and defuzzified may vary according to the type of MFs (Fig. 2 & 3). In this study, the effect of the type of the MF on fuzzification and defuzzification process to construct the fuzzy model is investigated along with the selection and definition of fuzzy rules.

E. Fuzzy Rule Base

The general form of a fuzzy rule used in most FLCs is as follows:

IF (*a* set of condition is satisfied)

THEN (a conclusions can be inferred)

Each fuzzy IF-THEN rule has a premise (or IF) part containing several preconditions and the conclusion (THEN) part describing the output action. The premise and conclusion parts are characterized by some fuzzy sets (or MFs). Suppose that we need to design a multiple-input-multiple-output (MIMO) FLC having p inputs $x_1 \in X_1, \ldots\ldots, x_p \in X_p$ and c outputs $y_1 \in Y_1, \ldots\ldots, y_c \in Y_c$ with i-th fuzzy rule of the form:

$$R^i_{MIMO}: \text{IF } x_1 \text{ is } F^i_1 \ldots\ldots \text{and } x_p \text{ is } F^i_p, \quad \text{THEN}$$

$$y_1 \text{ is } G^i_1 \ldots . y_c \text{ is } G^i_c, \quad i = 1, \ldots, M$$

where $F^i_1, \ldots\ldots, F^i_p$ and $G^i_1, \ldots\ldots, G^i_c$ are the antecedent and consequent MFs associated with the linguistic p input variables and c output variables, respectively; and M is the number of rules in the rule base.

III. Integration of FLCs and GA

The first step in designing an integrated FLCs and GA architecture, as depicted in Fig. 4, is to decide which parts of the knowledge base are subject to be optimized by the GA. Knowledge base of an FLC system is made up of two components: the parameters of the fuzzy rule base, constituted by the collection of fuzzy rules and MF types associated with the linguistic labels of each fuzzy rule. In this study, both of these two components of knowledge base are adapted using GA.

The integrated FLC and GA architecture consists of following basic steps:

Step1: Identify the variables (inputs, states, outputs) of the plant/problem.

Step 2: Partition the input and output universe of discourses or the interval spanned by each of the variables into a number of fuzzy regions (fuzzy sets) and assign a fuzzy MF i.e., linguistic label to each region.

Step 3: Encode fuzzy regions of the input and output spaces into bit-strings (0 or 1). Encode the MF types using bit-strings as follows: 00, 01, 10 and 11 for the triangular (T), left-triangular (LT), right-triangular (RT), and gaussian (G) respectively.

Step 4: Here, use GA in two stages, module-1 and module-2 (see Fig. 5), as self-learning adaptive methods to generate a set of fuzzy rules and select the MF types, respectively, for each rule.

Step 5: Decode the chromosome in both modules into fuzzy rules and their associative MFs type to determine the performance of a FLC and assign to a fitness value.

In order to clarify the basic ideas of our proposed approach, we have chosen backing up a truck reversing problem having

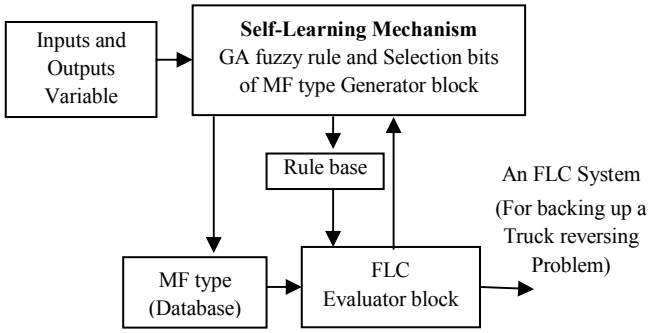

Figure 4. Integrated FLC and GAs Architecture

two inputs x, ϕ and one output θ. It is should be mentioned that there can be any number of input and output variables. In order to design an FLC, first divide the range of each variable, the inputs x and ϕ, and the output θ into fuzzy regions and assign a fuzzy MF to each region. We divide the domain regions for x into 5, ϕ into 7, and θ into 7 regions (The usual way to select an odd number between 3 and 9, which is usually same for all the variables). Consequently, there are 35 fuzzy rules (fuzzy rule base or FAM can be formed as a 5× (1×7) tables with rows to hold the corresponding actions (outputs).

After the division of input output spaces into fuzzy regions, each fuzzy rule can be represented as a bit string and the entire rule base as a table of strings as shown in Table I. Corresponding MFs selection bits are also included in each rule. Before the evolution process of GA the bit string is translated into fuzzy production rules like as Table IV.

To make calculations convenient, the consequent part of each rule and the associated type of MF is automatically set by two parallel GA modules, module-1 and module-2. The FLC generates a fitness value for each rule base according to the following fitness function:

$$Trajectory \quad \text{error/fitness} = \frac{\text{Length of Truck Trajectory}}{\text{Distance(Initail Position, Desired final Position)}}$$

We stop the simulation process and accept the fuzzy rules with respective type of fuzzy sets with fitness>Ω, where Ω defined as a specified number.

For the integrated architecture, the GA works in the following ways as shown in Fig.5 for graphical illustration:

Step1: Initialization: Some pairs of strings, each pair representing a potential solution, are generated by randomly chosen binary numbers (0 or 1). In each pair, the first string corresponds to a set of fuzzy rules of FLC (GA module-1) and the second string (GA module-2) denotes the types of MFs for corresponding fuzzy rules. Initialize P=1, N=65, g=1 and G=100 respectively (Fig. 5).

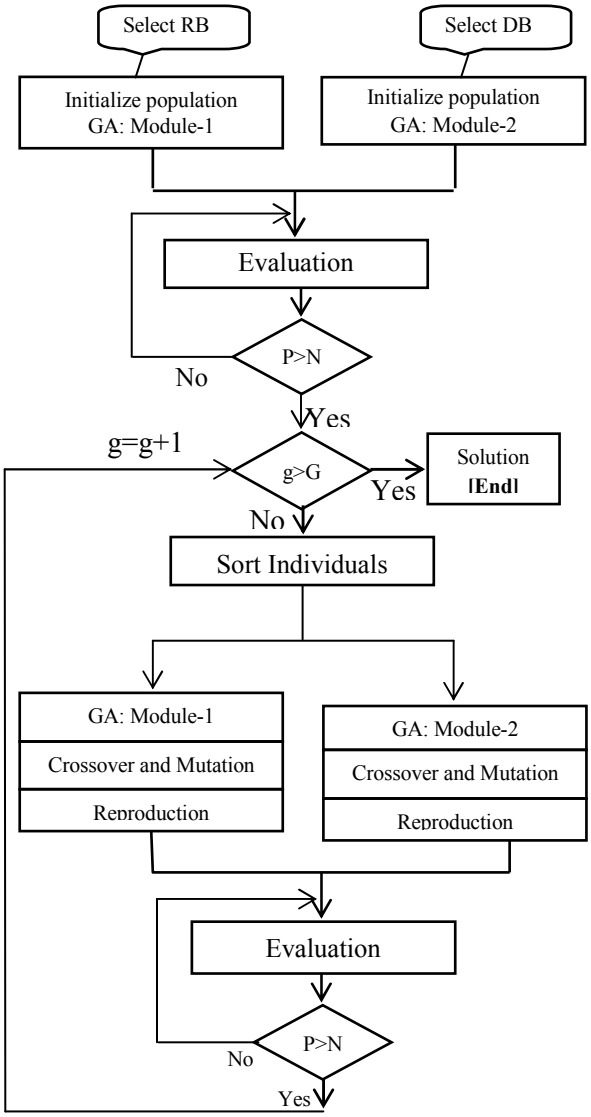

Figure 5. Flow chart for the design of FLC using GAs

Step2: Evaluation: Each potential solution is evaluated and assigned to a fitness value according to the solving performance of the problem. Sort the individuals according to their fitness value.

Step3: Recombination: Apply crossover and mutation operators to individuals of both modules and generate new individuals as well as new generation.

Step4: Evaluation: Evaluate the potential solution and check the termination condition.

Step5: Termination: If termination condition is satisfied then stop and return the best fitted chromosome (set of fuzzy rules of a FLC and membership function types) otherwise go to step3.

TABLE I. OPTIMAL CHROMOSOME OF GA

Input (x)					Input (ϕ)							Output (θ)							MF-Selection bits
LE	LC	CE	RC	RI	RB	RU	RV	VE	LV	LU	LB	NB	NM	NS	ZE	PS	PM	PB	
1	0	0	0	0	1	0	0	0	0	0	0	0	0	0	1	0	0	0	00 (Rule-1)
1	0	0	0	0	0	1	0	0	0	0	0	0	0	0	0	0	0	1	00 (Rule-2)
1	0	0	0	0	0	0	1	0	0	0	0	0	0	0	0	0	1	0	01 (Rule-3)
.	.	.	.	.	.	.	.	.	.	.	.	.	.	.	.	.	.	.	.
.	.	.	.	.	.	.	.	.	.	.	.	.	.	.	.	.	.	.	.
0	0	0	0	1	0	0	0	0	0	0	1	0	0	0	1	0	0	0	11 (Rule-35)

It is worth mentioning that the number of parameters such as the size of the population and the probability of applying the genetic operators (i.e., crossover and mutations) influence GAs.

IV. PROBLEM SPECIFICATION: BACKING UP A TRUCK CONTROL

Normal driving instincts can cheat us when attempting to back up a truck to a loading dock [14]. The task is such a difficult one that even for a highly skilled driver needs to go forward and backward numerous times in order to position the truck at the dock successfully. If the driver is not allowed to make forward movements, successful backing becomes improbable. So, the main challenge for the backing up a truck reversing control problem is to design a controller to successfully back up a truck to a loading dock from any initial position.

The problem, to back up a simulated truck to a loading dock in a planner parking lot is depicted in Fig. 6 with simulated geometry. The fuzzy logic control system must find incrementally a path to the loading dock independent of the initial position (x_0, y_0) of the truck. A state vector, consisting of the coordinates of the position of rear center of the truck (x, y) and the angle ϕ of the truck with the horizontal line define the actual position of the truck. The motion of the truck can be described by the following set of equations:

$$\begin{cases} x(t+1) = x(t) + b * \cos(\phi(t)) \\ y(t+1) = y(t) + b * \sin(\phi(t)) \\ \phi(t+1) = \phi(t) + \theta(t) \end{cases} \quad (3)$$

where θ is the steering angle. An FLC receives this state variable as input and calculates the appropriate steering angle $\theta = f(x,.\phi)$ that drives the truck toward the goal. The controller have to make the truck reach the loading dock at a right angle ($\phi = 90^0$) and to align the position (x, y) of the truck with the desired location (x_f, y_f). The truck should move backward for some fixed distance b at every stage. Assuming enough clearance between the truck and the loading dock we can ignore the y coordinate at the time of output (steering angle θ) calculation. There is no predefined path for each truck location and therefore the optimum steering angle is unknown. So, at every stage our proposed approach should calculate the steering angle $\theta = f(x, \phi)$ to back up the truck to a loading dock from any position and initial truck angle in the loading zone. The loading zone corresponds to the plane {0, 0} × {100, 100}.

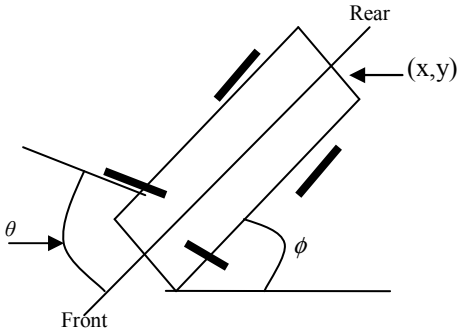

Figure 6. Diagram of Simulated Truck

This experiment is regarded as an example of highly nonlinear complex problems. The fuzzy logic controller must find the correct function that maps points from the three dimensional input-space to the appropriate output variable, continuously from the initial point until the loading dock, and for all combinations of the initial position.

The input and output variable domains are set to be as follows:

$$0 \le x \le 100$$
$$-90 \le \phi \le 270$$
$$-30 \le \theta \le 30$$

V. EXPERIMENTAL RESULTS AND COMPARATIVE ANALYSIS

To evaluate the accuracy of the proposed system, we have carried out a series of experiments in which the controller were evolved in our simulated arena. In this paper fuzzy control rules and MFs types associated to fuzzy control rules are adjusted based on GAs which enables the FLCs to backing up the truck with minimum trajectory error (fitness value).

A. Results

We have obtained the fuzzy control rules from the best chromosomes of GAs (module-1&2) after 100 generations. At the beginning of the simulation, the consequent part of each rule i.e., FAM (Fuzzy Associative Memories) cell is empty. To get the consequent part of each rule in terms of linguistic language form from the developed fuzzy rule generator block, let us start the simulation from thirty initial positions (x_0, y_0, ϕ_0): (25, 30, 60^0), (80, 30, 150^0), (30, 40, 90^0).. etc.

For all the given initial positions the GA converges to some sets of fuzzy control rules. During the simulation, we generate thirty sets of fuzzy rules (FAM) from thirty different initial positions. Then these rule bases are combined together to form the final FAM shown in table-II, using fuzzy amalgamation (FA) methodology [15, 16]. Table III shows the respective MFs type of fuzzy rules (FAM).

TABLE II. FAM-BANK MATRIX FOR THE FUZZY BACKING UP A TRUCK CONTROLLER

θ		ϕ						
		RB	*RU*	*RV*	*VE*	*LV*	*LU*	*LB*
x	*LE*	^{1}ZE	^{2}PB	^{3}PM	^{4}NM	^{5}NB	^{6}NB	^{7}NM
	LC	$^{8}\mathbf{PM}$	^{9}PS	^{10}NS	^{11}NM	^{12}NB	^{13}PB	^{14}NB
	CE	^{15}PS	^{16}PM	^{17}PM	^{18}ZE	^{19}NS	^{20}NM	^{21}NS
	RC	^{22}PB	^{23}PB	$^{24}\mathbf{NS}$	^{25}PM	^{26}ZE	^{27}NS	^{28}NM
	RI	^{29}PB	^{30}PB	^{31}PM	^{32}PB	^{33}PS	^{34}ZE	^{35}ZE

TABLE III. MEMBERSHIP FUNCTION TYPE OF FUZZY RULES(FAM)

θ		ϕ						
		RB	*RU*	*RV*	*VE*	*LV*	*LU*	*LB*
x	*LE*	^{1}T	^{2}T	^{3}LT	^{4}RT	^{5}G	^{6}T	^{7}G
	LC	$^{8}\mathbf{G}$	^{9}RT	^{10}G	^{11}T	^{12}LT	^{13}T	^{14}G
	CE	^{15}T	^{16}LT	^{17}G	^{18}LT	^{19}T	^{20}T	^{21}G
	RC	^{22}G	^{23}T	$^{24}\mathbf{T}$	^{25}G	^{26}T	^{27}T	^{28}G
	RI	^{29}G	^{30}T	^{31}T	^{32}G	^{33}T	^{34}T	^{35}G

TABLE IV. REPRESENTATION OF FUZZY IF-THEN CONTROL RULES

	GA (Best Chromosome)						
	Antecedents				***Consequents***		
		Input (X)	Operator	Input (ϕ)		Output (θ)	MFs Type
R-1	If	x=LE	and	ϕ=RB	Then	θ =ZE	Triangular
R-2	If	x=LE	and	ϕ=RU	Then	θ =PB	Triangular
R-3	If	x=LE	and	ϕ=RV	Then	θ =PB	L-Triangular
.	.	.	.	.	.	.	
R-35	If	x=RI	and	ϕ=LB	Then	θ =ZE	Gaussian

Figure 7 shows (example) the optimal fuzzy sets or membership function of the input and output terms. The MFs and the fuzzy rules specify a particular input-output mapping within a given range. In order to show the complete input-output relationship graphically, when the total number of input and output variables is no more than three, we can construct a control surface. The control surface is a convenient way to examine a two input/one-output control strategy and controller properties. It is obvious that using this useful feature one can more precisely fulfill a quality criterion in full operational range. Figure 8 shows the control surface defined with the *35* fuzzy control rules of Table II.

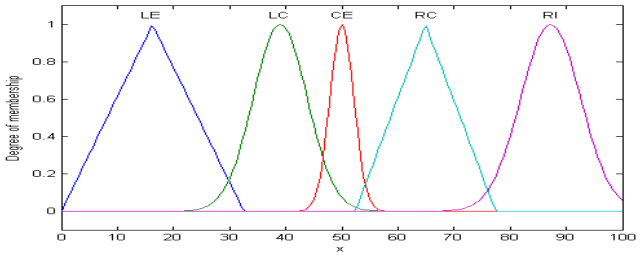

(a)

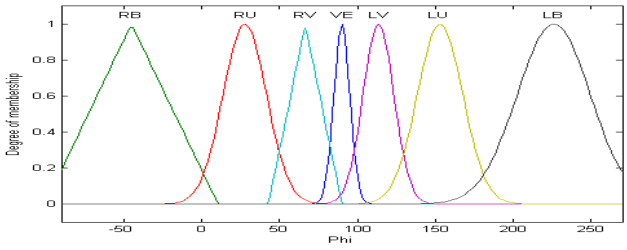

(b)

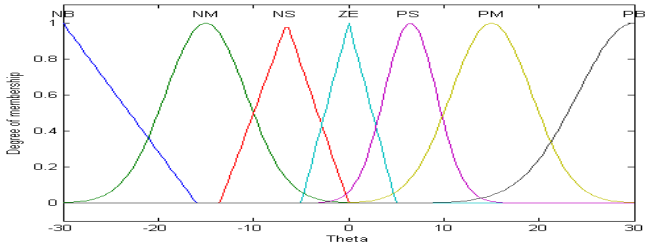

(c)

Figure 7. Variable domain and MFs for (a) x, (b) ϕ and (c) θ

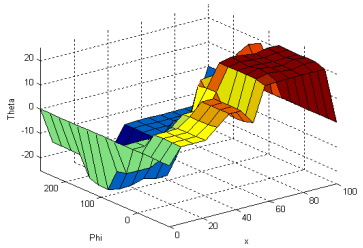

Figure 8. Surface generated by applied FLC

Figure 9 shows the example of two fuzzy control rules with two different types (gaussion and triangular) of MFs. After applying the FAM and their associated types of fuzzy sets (MFs), we obtain the trajectories with trajectory errors by the controller shown in Fig. 10 (a, b) for two different initial positions. The truck should hit the loading dock at a right angle, $\theta_f = 90°$, and the final position at (x_f, y_f)= (50, 100), for any initial state (x_0, y_o, ϕ_0) given to back up. The desired trajectory can be that the truck moves along the target line or coincides with the target line and then goes along y-axis to arrive at the goal.

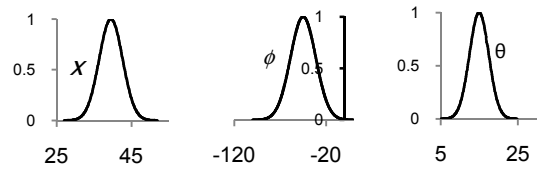

(a) RULE 8: IF x=LC ABD ϕ=RB THEN θ=PM

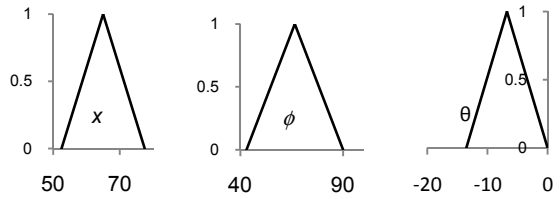

(b) RULE 24: IF x=RC AND ϕ=RV THEN θ=NS

Figure 9. Two different MFs form of fuzzy rule (a) Gaussian (b) Triangular

The minimized error after 100 generations for two positions (a, b) are 0.100996 and 0.104841. From Fig. 10 (a) it can be seen that for the initial position (25, 30, 60^0) the truck moves towards its goal with comparatively minimum trajectory error because the FLC can make the truck towards the goal position very quickly than that of other initial position, (80, 30, 150^0).

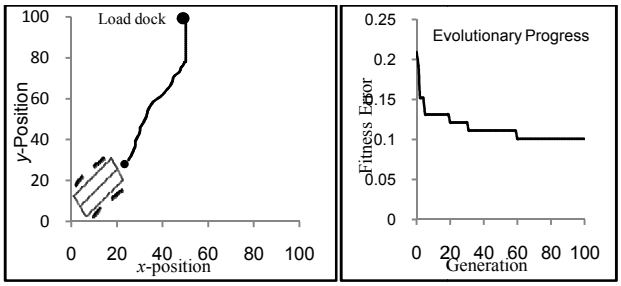

(a) Initial position (x_0, y_0, ϕ_0): (25, 30,60^0)

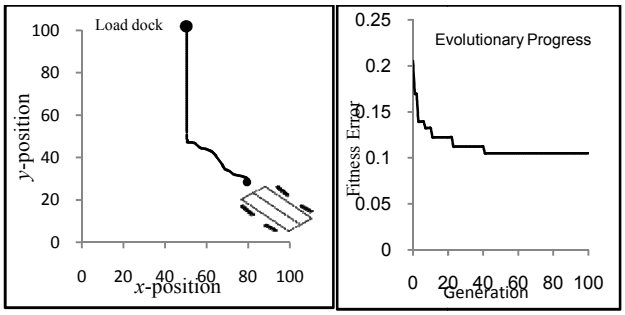

(b) Initial position (x_0, y_0, ϕ_0): (80, 30,150^0)

Figure 10. Trajectories and Fitness value of the backing up a truck controlled by the proposed approach.

B. Comparative Analysis:Effect for selecting different type of membership function

In this section, we investigate the FLC response with selection of different types of MFs and compared FLC response without section of MFs types. Here, we have used different types of MFs for fuzzy partitions to design an FLC called FLC-1 as shown in Fig. 7. The simple triangular, left-triangular, right-triangular or gaussian membership functions are often used, but they may not be the best choices. Using different MF types decreases the number of trajectory steps and improves the trajectories path that is found by applying only single type of MF. The following (Fig. 11) comparative analysis illustrates this fact.

The FLC-1 is generated by our proposed two-stage GA (module-1&2), while the standard FLC is based on the only single type of MF (triangular/Gaussian). The performance of each controller was observed for backing up a truck reversing problem. It can be seen from Fig. 11 that standard FLC need more time and iteration to converge (meets at $x=50$). On the other hand, FLC-1 reached faster in terms of iteration to converge.

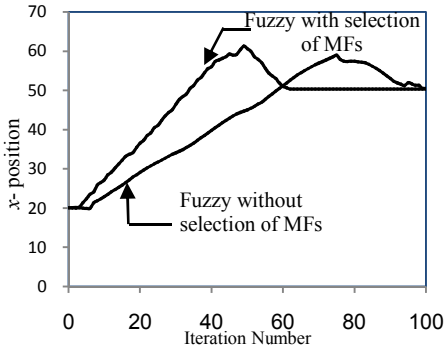

(a)

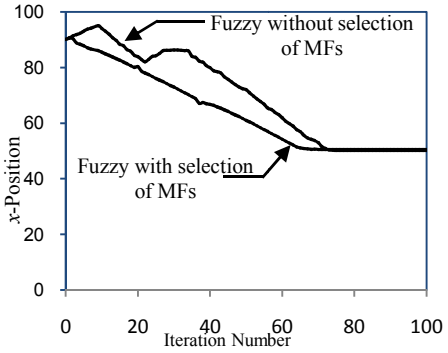

(b)

Figure 11. Comparison results between fuzzy with SMF and without SMF (a) Case-1: (20, 20, and 80^0) (b) Case-2: (90, 10, 110^0)

From the result given (Fig. 11), we can see standard FLC and FLC-1 have converged ($x=50$) at iteration 96 and 62, respectively for the case 1 (20, 20, and 80^0). FLC-1 also has achieved better precise value at position 50.2635 compare to 51.6439 for standard FLC. The second case (90, 10, 110^0) has achieved the same, FLC-1 achieve better convergence and closer to destination than standard FLC and get more precisely than standard FLC. The genetic progress is presented in Fig. 12 which demonstrations the performance of FLC with selection of different type of MFs is better than the response of FLC without selection of type of MFs.

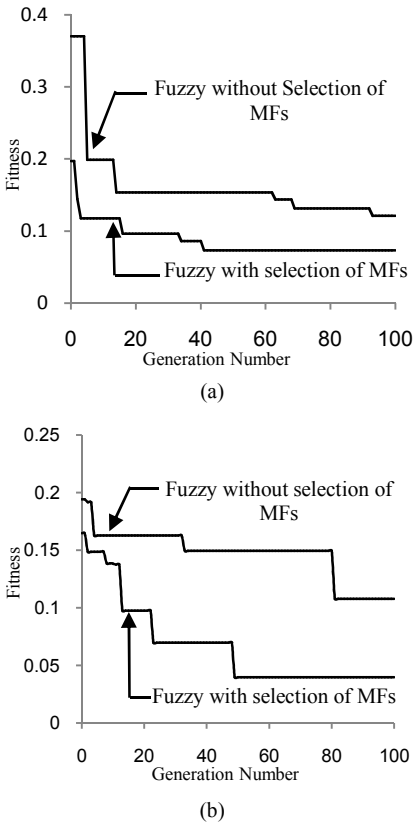

Figure 12. Fitness function value of the solution populations of the methods (a) Initial position (x_0, y_0, ϕ_0): (20, 20,80^0)) (b) Initial position (x_0, y_0, ϕ_0): (90, 10, 110^0)

Finally, we have shown that the shape and type of the MFs have a significant influence on the behavior of FLC response. Both the improvement and the deterioration of the systems' performance due to the changes in the MFs have been reported also.

VI. CONCLUSIONS

In this paper, we have found that the innovative integrated FLC and GA architecture is able to construct comprehensible and reliable fuzzy control rules by a self-learning adaptive technique. At the same time, we employed a two-stage GA to select the optimal type of MFs for FLC. The main features of the integrated FLCs and GAs architecture are given below.

The system is an automatic knowledge acquisition method and it is able to learn the fuzzy control rules without any prior knowledge. It also selects optimal types of MFs for FLC. In this way, GAs can build an effective controller relatively quickly. The comprehensive experimental studies also quantify a superb performance of the FLC with selection of different type of MFs when compared with the fuzzy controller without selection of type of MFs. This technique may lead to an increase in the use of FLCs as the previously time-consuming design procedure can be reduced dramatically. The architecture has a self-adaptive learning capability for constructing FLCs.

Suggestions for follow-up work that may come after this paper are as follows. This research work is to be extended for the intelligent control of a mobile robot, truck-trailer controller and control of a robotic arm in the presence of moving or fixed obstacle. This research work is also to be extended to the path planning problem for multiple mobile robots with more than one obstacles either moving or fixed in the workspace.

REFERENCES

[1] Y. F. Li and C. C. Lan," Development of fuzzy algorithms for servo systems," *IEEE Contr. Syst. Mag.,* vol. 9, no. 3, pp. 65-73,1989.

[2] W. Pedrycz, *Fuzzy Control and Fuzzy Systems*. New York: J. Wiley, 1989.

[3] C. H. Lee and C. C. Teng, "Identification and control of dynamic systems using recurrent fuzzy neural networks," *IEEE Trans. Fuzzy Syst.*, vol. 8, no. 4, pp. 349-366, Aug. 2000.

[4] T. Yamakawa and T. Koga,"Bio-inspired self-organizing relationship network as knowledge acquisition tool and fuzzy inference engine," *in Proc. IEEE world conf. Comput. Intell.,* 2008, pp. 159-180.

[5] A. Bagis, "Fuzzy and PD controller based intelligent control of spillway gates of dams," *J. Intell. Fuzzy Syst.,* vol. 14, no. 1, pp. 25–36, 2003.

[6] A. Bagis, "Determining fuzzy membership functions with tabu search-an application to control," *Fuzzy Sets and Syst*., vol. 139, pp. 209–25, Oct. 2003.

[7] S. Bai and S Chen, "Automatically constructing grade membership functions of fuzzy rules for students' evaluation," *Expert Syst. Appl.,* vol. 35, pp.1408–1414, Oct. 2008.

[8] C. C. Wong, H. Y. Wang and S.A. Li, "PSO-based motion fuzzy controller design for mobile robots," *Int. J. Fuzzy Syst.*, vol. 10, no. 1, pp. 24–32, Mar. 2008.

[9] A. Arslan and M. Kaya, "Determination of fuzzy logic membership functions using genetic algorithms," *Fuzzy Sets and Syst.*, vol. 118, pp. 297–306, Mar. 2001.

[10] C. C. Yang and N. K. Bose, "Generating fuzzy membership function with self-organizing feature map," *Pattern Recog. Letters*, vol. 27, no. 4, pp. 356–365, Apr. 2006.

[11] D. L. Meredith, C. L. Karr, and K. K. Kumar, "The use of genetic algorithms in the design of fuzzy logic controllers," *in Proc. third workshop on neural netw.,* vol. 1721, 1992, pp. 549-555.

[12] J. M. Mendel, *UNCERTAIN Rule-Based Fuzzy Logic Systems.* Engle-wood cliffs, NJ: Prentice-Hall PTR, Jan. 2001.

[13] L. X. Wang, *Adaptive Fuzzy Systems and Control – Design And Stability Analysis.* NJ: Prentice-Hall PTR, Feb. 1994.

[14] Li. Ying and Li. Yuanchun, "Neural-fuzzy control of truck backer-upper system using a clustering method," *Neurocomputing*, vol. 70, pp. 680-688, Jan. 2007.

[15] M. Mohammadian and R. J. Stonier, "Generating fuzzy rules by genetic algorithms," *in Proc. IEEE Int. Works. Robot and Human Comm.,* 1994, pp.362-367.

[16] R. J. Stonier, "Evolutionary learning of fuzzy logic controllers over a region of initial states," *in Proc. Congr. Evol. Comput.*, Jul. 1999.

[17] C. K. Chiang, H. Y. Chung, and Jin-Jye Lin, "A self-learning fuzzy logic controller using genetic algorithms with reinforcements," *IEEE Trans. Fuzzy Syst*., vol. 5, no.3, Aug. 1997.

[18] A. K. Nandi and D. K. Pratihar, "Automatic design of fuzzy logic controller using a genetic algorithm to predict power requirement and surface finish in grinding," *J. Materials Processing Tech.*, pp.288–300, 2004.

[19] D. H. Kim, K. B. Kim, and E.Y. Cha, "Fuzzy truck control scheme for obstacle avoidance," *J. of Neural Comput. and Appl.,* vol. 18, no. 7, pp. 801-811, Oct. 2009.

[20] F. Herrera and M. Lozano, "Adaptive genetic operators based on coevolution with fuzzy behaviors," *IEEE Trans. Evol. Comput.*, vol. 5, no. 2, pp. 149-165, Apr. 2001.

2011 IEEE International Conference on Fuzzy Systems
June 27-30, 2011, Taipei, Taiwan

A Comparison of Distance-based Semi-Supervised Fuzzy c-Means Clustering Algorithms

Daphne Teck Ching Lai and Jonathan M. Garibaldi
School of Computer Science, University of Nottingham
Email: dtl@cs.nott.ac.uk and jmg@cs.nott.ac.uk

***Abstract*—There are many issues to be considered in the design of distance-based fuzzy semi-supervised clustering (FSSC) algorithms. To identify these issues, we compare the performance of four such algorithms. We describe the properties of these algorithms, highlighting their key differences, and then experimentally compare their performance on common datasets. Several experimental conditions are investigated. Firstly, two forms of initialisation of the membership values of unlabelled patterns are used; $1/c$ and 0. Secondly, the algorithms are run with varying proportions of labelled patterns in the datasets, ranging from 2% to 40%. We find that no algorithm outperforms the others in all the datasets. We also observe that small modifications in similar objective functions can improve clustering, and that most of the algorithms perform slightly better with zero initialisation of unlabelled patterns. An interesting observation is that the increase in labelled patterns does not always improve clustering. From these results, we conclude that the number and scale of dimensions in the data set, initial partition matrix, distance metrics and objective functions, together, affect clustering results. In addition, we conclude that not all initially labelled patterns are good candidates for supervision.**

Keywords: **Fuzzy c-means, semi-supervised learning.**

I. Introduction

Clustering organises similar unlabelled patterns into clusters and is an unsupervised form of learning. In classification, however, labelled patterns are required to teach the algorithm the characteristics of classes, which is used to organise and tag unlabelled patterns. Thus, classification is supervised. Both techniques are widely applied in pattern recognition and data mining, often for investigation or decision-making. Good reviews of both techniques, particularly covering approaches and design issues, can be found in [1] and [2].

In fuzzy clustering [3], [4] and classification [5], membership values are assigned to patterns to indicate the degree of belongness each pattern has to clusters or classes respectively. These give a more realistic representation of patterns, as compared to a binary-valued approach.

In reality, labelled patterns are often scarce because they are difficult or expensive to record. To increase accuracy, clustering algorithms can take advantage of available labelled patterns as examples to learn from. These algorithms that make use of unlabelled data and available labelled patterns are termed *semi-supervised clustering* algorithms. There are three main types of fuzzy semi-supervised clustering (FSSC) algorithms; constraint-based [6], distance-based [7], [8], [9] and hybrids [10]. Distance-based FSSC algorithms are found to be popular and are approached using different techniques such as RBF mapping [11], evolutionary clustering [12] and adaptive metrics [13].

Different FSSC algorithms have previously been evaluated on different datasets using various ranges of labelled patterns, which makes fair comparison difficult. This motivated our study into a comparison of four distance-based semi-supervised Fuzzy c-Means (FCM) algorithms proposed by Pedrycz and Waletzky [14], Zhang et al. [15], Li et al. [16] and Endo et al. [17]. These were chosen because we found them to be simple in operation and they have been shown to produce good results. Our objectives are to (i) compare their performances with varying quantities of labelled patterns, and (ii) explore how issues that are common to fuzzy semi-supervised clustering, such as the number of dimensions, choice of datasets, initial membership values, objective functions, distance metrics and labelled patterns affect their clustering performance. Some of these issues have already been discussed in [18] in an investigation into different distance metrics of similar objective functions. We, however, compared algorithms with different objective functions that use three different distance metrics, and algorithms with similar objective functions that employed different forms of balance between supervised and unsupervised learning. In addition, we compared experimental results from two forms of initialisation for the cluster membership of unlabelled patterns; $1/c$ and 0.

One way of comparison is by using cluster validity indices, such as those discussed in [19] and particularly in FSSC algorithms [18]. In this preliminary work, however, we use classification rate to compare clustering performance among the algorithms, as was used in [14], [15], [16], [17]. We assume that algorithms that perform well are those that achieve a high percentage of correct classifications with a low percentage of labelled patterns.

II. Semi-Supervised FCM Clustering Algorithms

FCM was introduced by Dunn [20] and formalised by Bezdek [4]. Gustafson and Kessel [21] introduced fuzzy covariance to generalise the distance metric, which represents patterns in a more natural manner. Early semi-supervised fuzzy clustering algorithms [22], [23], [14] adopted these techniques and produced good clustering results. Today, many FSSC algorithms [24], [13], [10], [16], [17], [15], [8] exhibit new ways to exploit FCM. Further developments of FSSC clustering are found in [25], where Pedrycz discussed the

978-1-4244-7316-8/11/$26.00 ©2011 IEEE

TABLE I
PEDRYCZ-97 ALGORITHM

Objective Function	$J_k = \sum_{i=1}^{c}\sum_{k=1}^{N} u_{ik}^{p} d_{ik}^2 + \alpha \sum_{i=1}^{c}\sum_{k=1}^{N} (u_{ik} - f_{ik} b_k)^p d_{ik}^2$
Centroid	$v_i = \frac{\sum_{k=1}^{N} u_{ik}^2 \mathbf{x}_k}{\sum_{k=1}^{N} u_{ik}^2}$
Partition Matrix	$u_{ij} = \frac{1}{1+\alpha}\left\{ \frac{1+\alpha(1-b_j\sum_{l=1}^{c} f_{lj})}{\sum_{l=1}^{c}(\frac{d_{ij}}{d_{lj}})^2} + \alpha f_{ij} b_j \right\}$
Distance Metric	Mahalonobis

TABLE II
LI-08 ALGORITHM

Objective Function	$J_m = \sum_{i=1}^{c}\sum_{k=L+1}^{N} u_{ik}^m d_{ik}^2 + (1-a)\sum_{i=1}^{c}\sum_{k=1}^{L} u_{ik}^m d_{ik}^2 + a\sum_{i=1}^{c}\sum_{k=1}^{L}(u_{ik} - f_{ik})^m d_{ik}^2$
Centroid	$v_i^{(l)} = \frac{\sum_{k=1}^{N}(u_{ik}^{(l)})^2 \mathbf{x}_k}{\sum_{k=1}^{N}(u_{ik}^{(l)})^2}$
Partition Matrix	If unlabelled, $u_{ij} = \frac{1}{\sum_{l=1}^{c}(\frac{d_{ij}}{d_{lj}})^2} = u_{ij}^{FCM}$
	If labelled, $u_{ik} = (1-a)\left(\frac{1}{\sum_{l=1}^{c}(\frac{d_{ij}}{d_{lj}})^2}\right) + a f_{ik} = (1-a)u_{ik}^{FCM} + a f_{ik}$
Distance Metric	Mahalanobis

TABLE III
ZHANG-04 ALGORITHM

Objective Function	$J_m = 2\sum_{i=1}^{c}\sum_{k=1}^{N} u_{ik}^m (1 - K(x_k, v_i))$
Centroid	$v_i = \frac{\sum_{k=1}^{N_l}(u_{ik}^l)^m K(x_k^l, v_i) x_k^l + \sum_{k=1}^{N_u}(u_{ik}^u)^m K(x_k^u, v_i) x_k^u}{\sum_{k=1}^{N_l}(u_{ik}^l)^m K(x_k^l, v_i) + \sum_{k=1}^{N_u}(u_{ik}^u)^m K(x_k^u, v_i)}$
Partition Matrix	$u_{ik}^u = \frac{(1/(1-K(x_k^u, v_i)))^{1/(m-1)}}{\sum_{j=1}^{c}(1/(1-K(x_k^u, v_j)))^{1/(m-1)}}, 1 \le i \le c, 1 \le k \le N_u$
Distance Metric	Kernel-based distance

TABLE IV
ENDO-09 ALGORITHM

Objective Function	$J = \sum_{i=1}^{c}\sum_{k=1}^{N} u_{ik}\|\|x_k - v_i\|\|^2 + \lambda^{-1}\sum_{i+1}^{c}\sum_{k=1}^{N}(u_{ik} - \bar{u}_{ik}) log(u_{ik} - \bar{u}_{ik})$
Centroid	$v_i = \frac{\sum_{k=1}^{N} u_{ik} x_k}{\sum_{k=1}^{N} u_{ik}}$
Partition Matrix	$u_{ik} = \bar{u}_{ik} + \frac{e^{-\lambda d_{ik}}}{\sum_{j=1}^{c} e^{-\lambda d_{jk}}}\left(1 - \sum_{j=1}^{c}\bar{u}_{jk}\right)$
Distance Metric	Euclidean

idea of fuzzy semi-supervised clustering as a knowledge-based guidance mechanism to provide additional hints about data sets. Information can be represented in different levels of granularity, allowing it to represent heterogeneous data in both parametric and non-parametric models.

A. The Selected Algorithms

Tables I, II, III and IV illustrate the components in the semi-supervised FCM algorithms selected for study in this paper; Pedrycz-97 [14], Li-08 [16], Zhang-04 [15] and Endo-09 [17], respectively. The notation used is as follows: N, c, U and L denote the number of patterns, the number of clusters, the partition matrix and the number of labelled patterns, respectively. v_i, u_{ik}, f_{ik} (u_{ik}^l and $\bar{u}_{ik}$) and d_{ik} indicate, respectively, the prototype of cluster i, the membership value for pattern k in cluster i, the membership value of labelled pattern k in cluster i, and the distance between pattern k and prototype of cluster i. The equations for calculating the centroid and partition matrix are found in these tables. They are derived using a standard optimization technique called the Lagrange multipliers, the derivations are found in their respective papers and will not be discussed here. A semi-supervised FCM clustering algorithm iterates a series of steps to minimize the objective function until a termination criterion is satisfied. These steps are as follows:

1) Initialise c, U with known memberships and matrix F containing membership values of labelled patterns.
2) Calculate the centroids (prototypes of the clusters), v_i.
3) Calculate the similarities between clusters and patterns, d_{ik} using a chosen distance metric.
4) Update partition matrix U.
5) If $||U - U'|| < \epsilon$ (ϵ being a threshold value), stop. Else go to step 2.

B. Differences

Both Pedrycz-97 and Li-08 use Mahalonobis distance to update their partition matrix. In the objective function of Pedrycz-97, all patterns participate in unsupervised and supervised learning with parameter α to maintain a balance between the two types of learning. Li-08 is an improvement to avoid the redundant unsupervised learning of all labelled patterns in Pedrycz-97. Instead, it takes all unlabelled patterns and $1-a$ of

labelled patterns to participate in unsupervised learning, and a of labelled patterns to undergo supervised learning. Though presented separately for labelled and unlabelled patterns in Li-08, the equation to update the partition matrix is similar to Pedrycz-97 except for their balance parameters, a and α, respectively. Unlabelled patterns are not used in the calculation of Li-09's centroids, unlike the other algorithms. Like Pedrycz-97, the objective function of Endo-09 trains both labelled and unlabelled patterns in both unsupervised and supervised fashion, but using the Euclidean distance metric. The supervised training function, however, is entropy-regularised. Zhang et al. retained the objective function from the original FCM but replaced the Euclidean distance metric with a Gaussian kernel-based one. Unlike Pedrycz-97 and Li-08, in Zhang-04 only unlabelled patterns undergo supervised learning. This means that labelled patterns never gets updated or improved. As the unlabelled patterns do not contribute to the initial centroid, the labelled patterns act as seeds to form initial clusters, applied in FSSC learning [26] and non-fuzzy semi-supervised learning [27]. The trouble with using membership values of labelled patterns in both the calculation of centroids and the partition matrix, is that it makes the algorithm highly dependent on the initial membership values of labelled patterns, which can negatively impact the clustering results if they contain errors. This highlights the importance of balance parameters like α and a. In Endo-09's partition matrix equation, the membership values of labelled patterns themselves, denoted by $\bar{u}_{ik}$, are both learning components and balance parameters. In doing so, the reliance on initial membership values of labelled patterns is higher than the other three algorithms.

C. Summary

Three distance metrics are used by the four algorithms; Mahalanobis distance by Pedrycz-97 and Li-08, kernel-based distance by Zhang-04 and Euclidean distance by Endo-09. Pedrycz-97, Li-08 and Endo-09 algorithms use different approaches to incorporate the supervised learning element into the objective function of the original unsupervised FCM algorithm. We can observe this element in the second component of Pedrycz-97's and Endo-09's objective functions, and third component in Li-08's. The extended objective functions are then used to derive calculations of centroids and the partition matrix. Rather than using this extension in the objective function, Zhang-04 incorporated supervised learning during the calculation of the centroids. Thus, variations of both unsupervised and supervised learning components feature in these algorithms.

III. Experiments

Each algorithm, written in R, was run on ten datasets taken from non-linearly separable datasets Iris, Wine, XOR, Wisconsin Original Breast Cancer (WOBC), Pima Indians Diabetes (PID) and Wisconsin Diagnostic Breast Cancer (WDBC). Note that in Iris, the first class is linearly separable but the other two are not. The specifications of the datasets are shown in Table V. Apart from the XOR dataset which is manually built, all datasets are obtained from the UCI Machine Learning Repository [28]. For each dataset, experiments were repeated with different percentages of labelled patterns, 2%, 4%, 6%, 8%, 10%, 15%, 20%, 25%, 30% and 40%. Using the semi-supervised FCM algorithms, we can perform classification by having the labels replaced with numerals and the labelled patterns ordered such that the clusters and the numerically labelled classes will match. In this way, the unlabelled patterns after clustering can be matched with the numerically labelled classes from the datasets to verify correctness before counting the number of correctly matched patterns.

TABLE V
Datasets used in the experiments, where N, n and c are the number of patterns, features and clusters respectively.

dataset	N	n	c
Iris-2	150	2	3
Iris-4	150	4	3
Wine-2	178	2	3
Wine-13	178	13	3
XOR-2	200	2	4
WOBC-8	699	8	2
WOBC-2	699	2	2
PID-8	768	8	2
PID-2	768	2	2
WDBC-30	569	30	2

The following settings and modifications were made:

- Zhang et al. [15] used initial membership values of 1's and 0's to represent labelled and unlabelled patterns respectively. The assignment of initial membership values are not mentioned in the other algorithms. Like [18], however, we assume unlabelled patterns to hold equal initial memberships of all the clusters, having membership values of $1/c$ (where c is the number of clusters). The idea here is to improve learning using not only labelled patterns, but also unlabelled patterns.
- The membership value of each arbitrarily chosen labelled pattern belonging to a cluster is 0.9, with 0.1 membership divided among the other clusters. This is applied for the initial partition matrix of all datasets.
- From the Iris, Wine, WOBC and PID datasets, we created 2-dimensional datasets from these to observe the effects of number of attributes in datasets on clustering. We did not do this for WDBC because we felt that arbitrarily reducing a 30-dimensional image dataset to 2 dimensions was unlikely to improve clustering.
- Dimensions with missing values in the WOBC datasets were removed.
- The boolean matrix in Pedrycz-97 was removed since labelled and unlabelled patterns can be detected from the F matrix.
- We modified Endo-09 to compute prototypes from the initial partition matrix, like Pedrycz-97, rather than manually initialising them as the original algorithm did.
- Endo-09 ran into an infinity problem with datasets Wine-13, PID-8, PID-2 and WDBC-30. This will be discussed in the next section. We modified these datasets to Wine-10, PID-6, PID-2* and WDBC-23. The modified PID-2

contains two attributes that are different from the previous version.

- The stopping criterion used in all four algorithms is taken from Pedrycz-97 [14] as follows: $||U' - U|| = \sum_{i=1}^{c}\sum_{k=1}^{N}(u'_{ik} - u_{ik})^2$, where the threshold value is set to 0.01.
- In Pedrycz-97, α is calculated by N/L while a in Li-08 is calculated by $1-L/N$, where L is the number of labelled patterns and N is the total number of patterns.
- Following the original algorithms, p in Pedrycz-97 and m in Zhang-04 and Li-08 are set to 2 and λ in Endo-09 is set to 1.
- At least c labelled patterns, each an example of a different cluster, is required for the clustering to run properly (although semi-supervised algorithms for incomplete labelled patterns already exist [27]).
- Separate experiments were conducted on all algorithms and datasets with zero membership values for unlabelled patterns.
- Separate experiments with manual initialisation of Endo-09 prototypes were conducted.

IV. Results and Discussion

Table VI and Figure 1 show the percentage of correct classifications produced by each algorithm on different datasets. The symbol $*$ in this table indicates that the algorithm runs into an infinity problem. Overall, Li-08 performs better than the other algorithms, achieving more than 80% correct classifications in seven out of ten datasets with 4% of labelled patterns. With 4% of labelled patterns, it produces similar results to Pedrycz-97 in the Wine dataset and Zhang-04 in the WOBC dataset but, outperformed all in the XOR dataset. With 40% labelled data, it produces nearly 100% correct classification in six out of ten datasets. Pedrycz-97 achieves more than 80% correct classification in six out of ten datasets with 6% labelled patterns, while Zhang-04 achieves this with 15% labelled patterns and Endo-09 with 30% labelled patterns. We observe that Li-08 performs slightly better than Pedrycz-97 with its modified objective function.

The results of Pedrycz-97 and Li-08 are based on a Mahalanobis distance metric, which measures similarity using the sum of squared errors and the correlation with the membership values of the patterns. The presence of the inverse covariance matrix helps to normalise dimensions of different scales, preventing dominance from dimensions with greater scales. This may give a more realistic representation of the patterns. Zhang et al. replaced the Euclidean distance metric in FCM with a Gaussian kernel-induced distance metric. The Gaussian kernel measures similarity by $K(x,y) = exp(-||x-y||^2/\sigma^2)$, with the kernel width defined by the variance σ^2. This variance keeps the kernel value of patterns normalised. The idea behind kernel methods are their ability to solve non-linear problems by mapping the input space into higher dimensional space (the 'kernel trick' [29]), which is applied to distances [30]. We see this applied in Zhang-04 with prior information of data space computed in the variance. Both Mahalanobis and kernel-based distance metrics are competitive, each doing better than the other in different datasets with 2% of labelled patterns.

The 'curse of dimensionality' problem is apparent in the results produced by Endo-09. The Euclidean distance metric does not reflect scale differences among dimensions in high-dimensional datasets. Dimensions with smaller scales will have less influence on the distance in the presence of dimensions with larger scales. This results in biased distance values that decrease accuracy in classification. With increasing number of dimensions, distance increases exponentially. This makes Euclidean distance tricky to use in an exponential function, derived from the Endo-09 objective function. Large distance values yield a zero value in the exponential function of Endo-09 partition matrix update equation, which in turn returns infinity. Hence, the infinity problem arises in datasets with high dimensions, large scale differences in dimensions and/or large scales in dimensions such as Wine-13, PID-8, PID-6 and WDBC-30. When we removed three dimensions (those with higher scales) from the Wine dataset, the results improved drastically. Du and Urahama tackled this problem using a parameter δ, which is computed by the inverse sum of average distances with its nearest neighbours and average distances with its furthest neighbours [11].

The algorithms do not always produce better classifications using datasets that have more dimensions. For example, as can be seen in Figure 1, Pedrycz-97, Li-08 and Zhang-04 produce better results for WOBC-2 than for WOBC-8. This is because some features have higher discrimination power compared to others. Those that have low discrimination power add more computational cost and can deteriorate clustering results [2]. Through the selection of a subset of features, those that have high discrimination power can be retained while others discarded. Kong et al. [8] incorporated feature selection with fuzzy semi-supervised learning using a feature weight variable in its objective function.

All algorithms were able to cluster most of the non-linearly separable datasets, achieving more than 80% correct classifications with at most 30% labelled patterns. Zhang-04 and Endo-09 achieve less in the XOR dataset and none of the algorithms could achieve more than 80% classification with 40% labelled patterns in the PID datasets except Pedrycz-97. According to [31], the two classes in the PID dataset are not well separated, which makes it a challenge for the algorithms.

Interestingly and unexpectedly, increases in the number of labelled patterns do not always improve classification, indicated by the troughs in the graphs of Figure 1. This observation holds for all algorithms except Pedrycz-97 in Wine-2 dataset with 8% to 10% labelled patterns. Having said this, there is still a general trend of increasing correct classifications with increase in labelled patterns. This may suggest that not all labelled patterns are good candidates to guide clustering. The choice of suitable labelled patterns, prior to clustering, lies in their features, their initial membership values and the objective function of the algorithm. The presence of labelled patterns that do not strongly belong to one class but have high membership values will hinder the clustering process, reducing

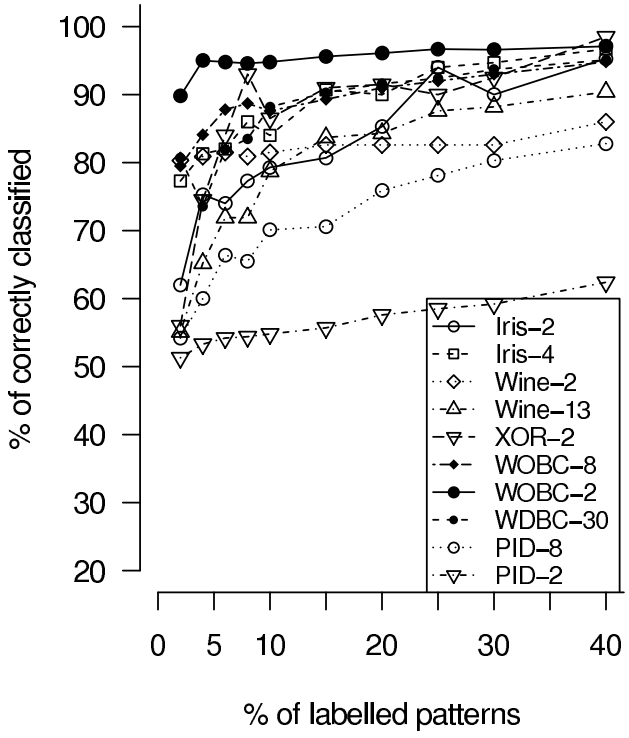

(a) Pedrycz-97

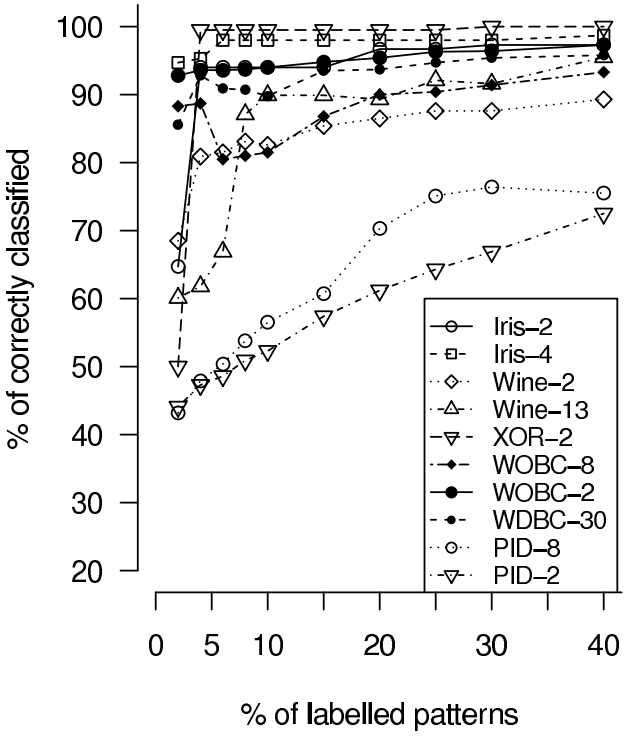

(b) Li-08

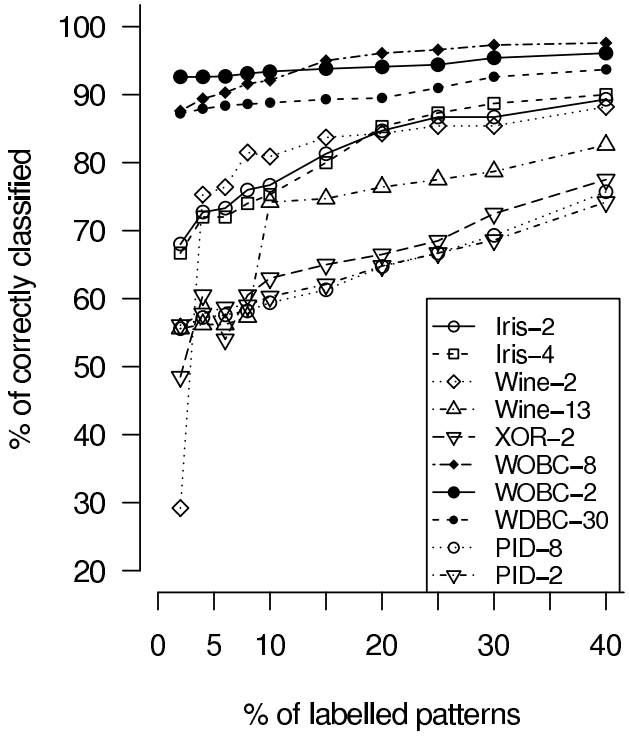

(c) Zhang-04

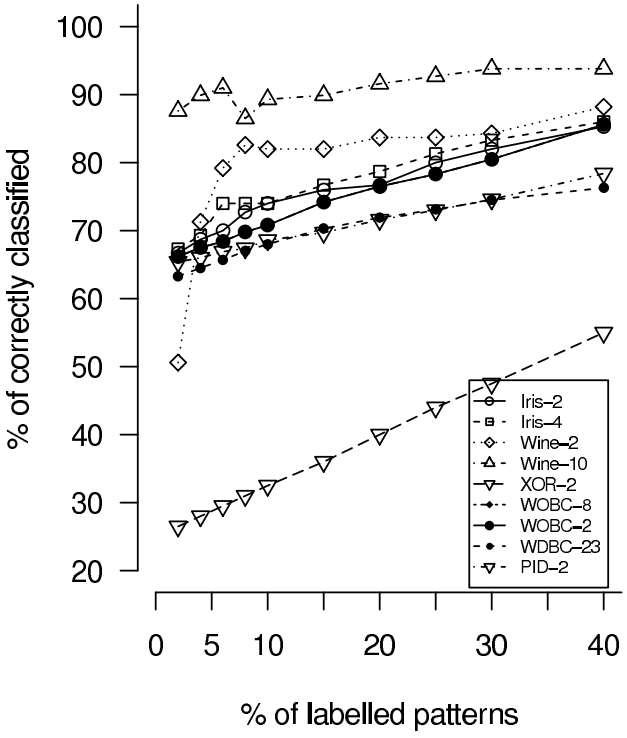

(d) Endo-09

Fig. 1. Graph of percentage of correct classification against proportion of labelled patterns with $1/c$ initialisation.

TABLE VI
TABLE SHOWING RESULTS FROM RUNNING THE ALGORITHMS USING $1/c$ AND ZERO INITIAL MEMBERSHIP VALUES FOR UNLABELLED PATTERNS.

	With initial membership of $1/c$						With initial membership of zero					
	% labelled											
dataset	2	4	6	8	10	20	2	4	6	8	10	20
Results produced by Pedrycz-97												
Iris-4	77.3	81.3	82.0	86.0	84.0	90.0	78.7	96.7	98.0	98.0	98.0	98.0
Iris-2	62.0	75.3	74.0	77.3	79.3	85.3	65.3	93.3	92.7	93.3	93.3	96.7
Wine-13	55.1	65.2	71.9	71.9	78.7	84.3	93.3	93.3	74.2	84.3	88.8	91.0
Wine-2	80.3	80.9	81.5	80.9	81.5	82.6	80.3	82.0	81.5	82.0	83.1	86.5
XOR-2	56.0	74.5	84.0	93.0	86.5	91.5	70.5	99.5	99.5	99.5	99.5	99.5
WOBC-8	79.5	84.1	87.8	88.7	87.6	91.0	79.3	80.3	80.5	81.1	81.7	89.7
WOBC-2	89.8	95.0	94.8	94.6	94.8	96.1	92.7	93.6	93.6	93.6	94.0	95.4
PID-8	54.2	60.0	66.4	65.5	70.1	75.9	44.3	59.1	50.8	54.4	56.6	73.7
PID-2	51.3	53.3	54.2	54.4	54.8	57.6	44.4	47.3	48.7	50.9	53.0	62.1
WDBC-30	80.7	73.6	81.9	83.5	88.2	91.6	*	85.4	88.8	87.0	89.3	90.9
Results produced by Li-08												
Iris-4	94.7	95.3	98.0	98.0	98.0	98.0	40.0	48.7	65.3	70.7	84.7	98.7
Iris-2	64.7	94.0	94.0	94.0	94.0	96.7	46.7	84.7	86.7	94.0	94.0	96.7
Wine-13	60.1	61.8	66.9	87.1	89.9	89.3	38.2	47.8	43.3	44.4	48.9	75.3
Wine-2	68.5	80.9	81.5	83.1	82.6	86.5	68.0	70.8	80.3	82.0	85.4	83.7
XOR-2	50.0	99.5	99.5	99.5	99.5	99.5	54.5	97.0	98.0	98.5	98.5	99.5
WOBC-8	88.3	88.7	80.5	81.0	81.5	90.0	67.1	87.4	92.4	90.8	91.6	92.7
WOBC-2	92.8	93.6	93.6	93.7	94.0	95.4	93.6	94.1	94.3	94.3	93.4	95.4
PID-8	43.2	47.9	50.4	53.8	56.5	70.3	46.2	62.8	66.4	70.2	73.6	75.9
PID-2	44.1	47.3	48.6	50.9	52.3	61.2	53.4	62.6	62.4	57.4	63.8	70.2
WDBC-30	85.6	92.8	90.9	90.7	89.8	93.7	*	92.8	93.1	93.3	93.1	93.7
Results produced by Zhang-04												
Iris-4	66.7	72.0	72.0	74.0	75.3	85.3	76.7	90.7	92.0	90.7	90.7	91.3
Iris-2	68.0	72.7	73.3	76.0	76.7	84.7	70.7	86.7	88.0	89.3	89.3	90.0
Wine-13	55.6	56.2	56.2	57.3	74.2	76.4	73.0	72.5	72.5	72.5	73.6	77.0
Wine-2	29.2	75.3	76.4	81.5	80.9	84.3	68.0	77.0	79.8	81.5	80.9	83.7
XOR-2	48.5	60.5	54.0	60.5	63.0	66.5	51.5	64.5	62.0	63.5	66.0	68.5
WOBC-8	87.6	89.4	90.3	91.6	92.1	96.1	96.7	63.4	96.9	95.9	96.6	97.1
WOBC-2	92.6	92.6	92.7	93.1	93.4	94.1	62.4	66.1	68.1	94.8	94.7	95.1
PID-8	55.6	57.2	57.6	58.2	59.4	64.7	54.4	52.0	56.0	56.6	57.7	62.5
PID-2	56.1	57.8	58.7	59.0	60.3	64.8	58.1	58.7	59.8	60.0	61.2	65.5
WDBC-30	87.2	87.9	88.4	88.6	88.8	89.5	81.4	83.8	91.4	91.7	91.0	91.7
Results produced by Endo-09												
Iris-4	67.3	69.3	74.0	74.0	74.0	78.7	90.0	90.7	90.7	92.7	94.0	96.7
Iris-2	66.7	68.7	70.0	72.7	74.0	76.7	88.0	88.7	88.7	88.7	89.3	92.0
Wine-10	87.6	89.9	91.0	86.5	89.3	91.6	87.1	87.1	87.1	87.6	87.1	90.4
Wine-2	50.6	71.3	79.2	82.6	82.0	83.7	40.4	80.3	80.3	80.3	80.3	83.1
XOR-2	26.5	28.0	29.5	31.0	32.5	40.0	49.5	57.5	56.5	57.5	60.5	67.5
WOBC-8	66.2	67.5	68.4	69.8	70.8	76.5	95.4	95.9	95.9	95.9	96.0	97.1
WOBC-2	66.2	67.5	68.4	69.8	70.8	76.5	93.0	93.8	94.0	94.1	94.6	96.4
PID-6	*						64.2	64.7	65.6	66.0	66.9	70.3
PID-2*	65.4	66.0	66.9	67.4	68.6	71.6	64.2	64.7	65.6	66.0	66.9	70.3
WDBC-23	63.3	64.5	65.7	67.0	68.0	71.9	51.7	52.5	53.3	54.7	55.5	60.5

accuracy. The objective function of the algorithm must have some corrective property to handle such patterns, such as in [24]. The authors extended the objective function to include the relationship between classes and clusters, and parameterised the confidence in the accuracy of data labels. The presence of labelled patterns with strong features of a cluster helps give a solid definition of a class. The idea of choosing unlabelled patterns to label before they are used to supervise clustering has been previously used in FSSC learning [6].

Two other separate experiments were conducted; one with zero membership values for unlabelled patterns and another on Endo-09 with manual initialisation of prototypes as performed in the original work. The results using zero membership values for unlabelled patterns are shown in the right half of Table VI. The key observations are as follows:

- In contrast to the previous experiment, Endo-09 achieves more than 80% correct classification in six out of nine datasets with 4% of labelled patterns. We observe that this algorithm is more sensitive to initial partition matrix for supervision than the other algorithms. Thus, unlabelled patterns with $1/c$ membership values may confuse prototypes and hinder good clustering results. This causes restricted learning and is not favourable in situations when there are weak labelled patterns. Pedrycz-97, Li-08 and Zhang-04 perform slightly better with zero initial membership values for unlabelled patterns in six, three and seven out of nine datasets, respectively.
- With manually initialised prototypes, the original Endo-09 produced final prototypes that are slightly different from those produced by the modified version, and so the results produced by these two versions are different. The dataset used in this experiment is provided in the original

paper [17], which is too small to deduce which of the two produced better results. Manually initialising prototypes of datasets with large dimensions will be impractical and can make the clustering highly inaccurate.

V. Conclusion

As preliminary work in fuzzy semi-supervised clustering, this study is aimed at investigating some existing distance-based semi-supervised fuzzy c-means algorithms running on popular datasets. We compared the clustering results of four such algorithms, testing them on two forms of initialisation of unlabelled patterns membership values; $1/c$ and zero. In most cases, results were more favourable when using zero membership for unlabelled patterns rather than using $1/c$. We observed that issues such as scale differences of dimensions in the data set, distance metrics, objective functions and quality of labelled patterns affect clustering results. From our experimental results, we observe that Mahalanobis distance provides slightly better performance than Gaussian kernel-based distance, and that the Euclidean distance metric performs least well, on the selected data sets.

We recognise that algorithms that can achieve very high percentage of correct classifications with few labelled patterns are desirable. Also, the percentage of correct classifications should increase with increasing percentage of labelled patterns since more examples are available to guide the clustering. However, some labelled patterns with poor discriminating power, when used in some algorithms, can negatively impact on clustering results. Research into algorithms that can filter out 'poorly' labelled patterns or identify 'good' unlabelled patterns to label prior to the clustering process is of interest to us. It would also be interesting to incorporate such features into existing dimensionality reduction algorithms and run comparative performance tests.

References

[1] A. K. Jain, M. N. Murty, and P. J. Flynn, "Data clustering: A review," *ACM Comput. Surv.*, vol. 31, pp. 264–323, September 1999.

[2] A. K. Jain, R. P. W. Duin, and J. Mao, "Statistical pattern recognition: A review," *IEEE Transaction on Pattern Analysis and Machine Intelligence*, vol. 22, no. 1, pp. 4–37, 2000.

[3] F. Hoppner, F. Klawonn, R. Kruse, and T. Runkler, *Fuzzy Cluster Analysis*. Wiley, 1999.

[4] J. C. Bezdek, *Pattern Recognition with Fuzzy Objective Function Algorithms*. Norwell, MA, USA: Kluwer Academic Publishers, 1981.

[5] L. I. Kuncheva, *Fuzzy Classifier Design (Studies in Fuzziness and Soft Computing)*. Heidelberg, Germany: Physica-Verlag HD, 2000, vol. 49.

[6] N. Grira, M. Crucianu, and N. Boujemaa, "Active semi-supervised fuzzy clustering," *Pattern Recognition.*, vol. 41, pp. 1851–1861, May 2008.

[7] J. Gao, P. ning Tan, and H. Cheng, "Semi-supervised clustering with partial background information," in *In Proceedings of the Sixth SIAM International Conference on Data Mining*, 2006.

[8] Y.-q. Kong and S.-t. Wang, "Feature selection and semisupervised fuzzy clustering," *Fuzzy Information and Engineering*, vol. 1, pp. 179–190, 2009.

[9] S. Miyamoto, M. Yamazaki, and W. Hashimoto, "Fuzzy semi-supervised clustering with target clusters using different additional terms," in *IEEE International Conference on Granular Computing*, 2009, pp. 444–449.

[10] N. Wang, X. Li, and X. Luo, "Semi-supervised kernel-based fuzzy c-means with pairwise constraints," in *IEEE International Joint Conference on Neural Networks (IEEE World Congress on Computational Intelligence)*, June 2008, pp. 1098–1102.

[11] W. Du and K. Urahama, "Semi-supervised pattern classification utilizing fuzzy clustering and nonlinear mapping of data," *Journal of Adv Comp Intelligence and Intelligent Informatics*, vol. 11, pp. 1159–1164, 2007.

[12] H. Liu and S.-T. Huang, "Evolutionary semi-supervised fuzzy clustering," *Pattern Recogn. Lett.*, vol. 24, pp. 3105–3113, December 2003.

[13] M. Ceccarelli and A. Maratea, "Semi-supervised fuzzy c-means clustering of biological data," *Fuzzy Logic and Applications*, vol. 3849, pp. 259–266, 2006.

[14] W. Pedrycz and J. Waletzky, "Fuzzy clustering with partial supervision," *IEEE Transactions on Systems, Man and Cybernetics*, vol. 27, no. 5, pp. 787–795, May 1997.

[15] D. Zhang, K. Tan, and S. Chen, "Semi-supervised kernel-based fuzzy c-means," *Lecture Notes in Computer Science: Neural Information Processing*, vol. 3316, pp. 1229–1234, July 2004.

[16] C. Li, L. Liu, and W. Jiang, "Objective function of semi-supervised fuzzy c-means clustering algorithm," in *IEEE International Conference on Industrial Informatics*, July 2008, pp. 737–742.

[17] Y. Endo, Y. Hamasuna, M. Yamashiro, and S. Miyamoto, "On semi-supervised fuzzy c-means clustering," *IEEE International Conference on Fuzzy Systems*, 2009.

[18] A. Bouchachia and W. Pedrycz, "Enhancement of fuzzy clustering by mechanisms of partial supervision," *Fuzzy Sets and Systems*, vol. 157, no. 13, pp. 1733–1759, 2006.

[19] N. Pal and J. Bezdek, "On cluster validity for the fuzzy c-means model," *IEEE Transactions on Fuzzy Systems*, vol. 3, no. 3, pp. 370–379, Aug 1995.

[20] J. C. Dunn, "A fuzzy relative of the isodata process and its use in detecting compact well-separated clusters," *Journal of Cybernetics*, vol. 3, no. 3, pp. 32–57, 1973.

[21] D. E. Gustafson and W. C. Kessel, "Fuzzy clustering with a fuzzy covariance matrix," in *IEEE Conference on Decision and Control including the 17th Symposium on Adaptive Processes*, vol. 17, January 1978, pp. 761–766.

[22] W. Pedrycz, "Algorithms of fuzzy clustering with partial supervision," *Pattern Recognition Letters*, vol. 3, no. 1, pp. 13–20, 1985.

[23] A. M. Bensaid, L. O. Hall, J. C. Bezdek, and L. P. Clarke, "Partially supervised clustering for image segmentation," *Pattern Recognition*, vol. 29, no. 5, pp. 859–871, 1996.

[24] A. Bouchachia and W. Pedrycz, "A semi-supervised clustering algorithm for data exploration," *Fuzzy Sets and Systems - IFSA 2003 (International Fuzzy Systems Association World Congress Istanbul, Turkey)*, vol. 2715, pp. 107–155, 2003.

[25] W. Pedrycz, *Knowledge-Based Clustering: From Data to Information Granules*. Wiley-Interscience, 2005.

[26] K. Li, Z. Cao, L. Cao, and R. Zhao, "A novel semi-supervised fuzzy c-means clustering method," in *Proceedings of Chinese Control and Decision Conference, CCDC '09.*, June 2009, pp. 3761 –3765.

[27] S. Basu, A. Banerjee, and R. J. Mooney, "Semi-supervised clustering by seeding," in *International Conference on Machine Learning*, ser. ICML '02. San Francisco, CA, USA: Morgan Kaufmann Publishers Inc., 2002, pp. 27–34.

[28] A. Asuncion and D. Newman, "UCI machine learning repository," 2007. [Online]. Available: http://www.ics.uci.edu/∼mlearn/MLRepository.html

[29] A. Aizerman, E. M. Braverman, and L. I. Rozoner, "Theoretical foundations of the potential function method in pattern recognition learning," *Automation and Remote Control*, vol. 25, pp. 821–837, 1964.

[30] B. Scholkopf, "The kernel trick for distances," in *Advances in Neural Information Processing Systems*, 2001, pp. 301–307.

[31] N. Päivinen, "Clustering with a minimum spanning tree of scale-free-like structure," *Pattern Recognition Letters.*, vol. 26, pp. 921–930, May 2005.

2011 IEEE International Conference on Fuzzy Systems
June 27-30, 2011, Taipei, Taiwan

Applying MDL in PSO for Learning Bayesian Networks

Shu-Ching Kuo
Department of Leisure and Information Management, Taiwan Shoufu University, Tainan, Taiwan

Hung-Jen Wang
Department of Computer Science and Multimedia Design, Taiwan Shoufu University, Tainan, Taiwan

Hsiao-Yi Wei
Institute of Information Management, National Cheng Kung University, Tainan, Taiwan

Chih-Chuan Chen
Department of Leisure and Information Management, Taiwan Shoufu University, Tainan, Taiwan.
Department of Industrial and Information Management, National Cheng Kung University, Tainan, Taiwan

Sheng-Tun Li*, *Member, IEEE*
Institute of Information Management, National Cheng Kung University, Tainan, Taiwan
Department of Industrial and Information Management, National Cheng Kung University, Tainan, Taiwan

***Abstract*—Since learning Bayesian networks from data is difficult, a new approach is proposed. The particle swarm optimization (PSO) and minimum description length (MDL) are combined to obtain a suitable Bayesian network. MDL is the fitness function in this learning algorithm to evaluate the goodness of the network. By adopting MDL, the balance between simplicity and accuracy is assured, which enables the optimal solution for complex models to be found in reasonable time. Base on the MDL principle, the PSO is used to enhance the structure learning in Bayesian networks. Moreover, conditional probabilities associated with the Bayesian networks are then statistically derived from these data. In the end, the Stroke data set is used for testing the efficiency and effectiveness of the stable network. Experimental results show that the proposed approach has a good accuracy than the comparative methods.**

Keywords- Bayesian networks; particle swarm optimization; minimum description length

I. INTRODUCTION

Bayesian networks provide an efficient method for representing conditional probabilities among a set of variables. A Bayesian network is a graphic representation that encodes probabilistic relationships among variables. Since it only depicts the known conditional dependencies among variables rather than consider all variables in the domain, it provides efficiency for acquiring and representing domain knowledge [1]. Because of the ability to properly express expert knowledge and to handle well for the uncertain-reasoning problems, Bayesian networks have increasingly gained popularity in the community of artificial intelligence in recent years [2].

Many approaches have been proposed to induce the structure of Bayesian Networks. Typically, a Bayesian network is constructed by eliciting knowledge from domain experts. It is however a labor intensive process and may generate some biases. To reduce these biases due to subjective judgments of experts and increase efficiency, learning a Bayesian network from collected data or past observations has become an active area of research. Several heuristic searching techniques have been used to create a Bayesian network. Among those heuristics, evolution computation has been intensively researched and proved to be effective in learning Bayesian networks [3-4].

Numerous evolution techniques such as ant colony optimization, genetic algorithm and evolutionary programming were developed for Bayesian network structure discovery from data. Compared with these algorithms, particle swarm optimization (PSO) has strong sociological activities that promote information sharing and, in addition, it stores the previously best explored areas of the search space among all particles. By well communicating with others, each particle thus shares the information and has more opportunities to trend to better places. Moreover, PSO converges rapidly and requires only primitive mathematical operators. It is easy to implement but has great capability to handle optimization problems with multiple local optima reasonably well with fairly high accuracy. PSO has been found being robust in solving nonlinear and high dimensional problems [5-6].

In this paper, PSO and minimum description length (MDL) are combined to obtain a well-defined Bayesian network to assist domain experts in making decisions. Since the experts may be uncertain about their diagnoses, the results predicted by Bayesian networks will be a direction to help them consider how to solve the uncertainty. Even if the experts can make their own decisions, a Bayesian network can be taken as a reference to make them assure the results and even inspire them to think about some implications behind the relations among random variables. Moreover, PSO algorithm is used to learn the structure of a Bayesian network and the MDL is applied as the fitness function of the algorithm so that the final network will be useful and having a good accuracy at the same time. Further, the less complicated structure allows the domain experts to easily understand and quickly catch the causes and effects between the variables.

The remainder structure of the research is organized as follows: Section II briefly addresses the concept of Bayesian networks, PSO algorithms and MDL metric. It also discusses how they work together in various different domains. The proposed scheme is shown in Section III. The experimental

*Corresponding author: stli@mail.ncku.edu.tw

978-1-4244-7316-8/11/$26.00 ©2011 IEEE

results are shown in Section IV. Finally, some conclusions are described in Section V.

II. RELATED WORKS

A. Particle Swarm Optimization

Particle swarm optimization (PSO) is a searching algorithm proposed by Kennedy and Eberhart [7]. Social behaviors of bird flocking motivated them to search and observe the effect of collaboration of species onto achieving their goals as a group. In PSO, a number of candidates, called particles, are placed in a *D*-dimensional search space looking for the optimal position to land. The particles will memorize the locations where they have their best locations and make this information available to its neighbors. Each particle adjusts its position by combining its own experience and the experience of other swarms as time passing. The next iteration takes place after all particles have been moved. In the end, the swarm is able to move close to an optimum of the fitness function.

Figure 1 shows the flow diagram of original PSO algorithm, and the corresponding Algorithm is given in Algorithm 1 [8]. In PSO, three parameters determine a particle's position including the current position $\vec{x_i}$, the previous best position $\vec{p_i}$, and the velocity $\vec{v_i}$. Each particle keeps track for the best solution called pbest. On the other hand, gbest is the best value tracked by the global version of the entire swarm. $U(0,\varphi_i)$ represents a vector of random numbers uniformly drawn on the interval (0, 1).

Algorithm 1. Original PSO algorithm.

Step 1. Initialize a population array of particles with random positions and velocities on *D* dimensions in the search space.
Step 2. Loop
Step 3. For each particle, evaluate the desired optimization fitness function in *D* variables.
Step 4. Compare particle *i*-th fitness evaluation with its pbesti . If current value is better than pbesti, then set pbesti equal to the current value, and $\vec{p_i}$ equal to the current location $\vec{x_i}$ in D-dimensional space.
Step 5. Compare particle *i*-th fitness evaluation with the population's overall previous best gbest. If current value is better than gbest, then reset gbest to the current particle's array index and value.
Step 6. Change the velocity and position of the particle according to the following equation:

$$\vec{v_i} \leftarrow \vec{v_i} + U(0,\varphi_1) \otimes \left(\vec{p_i} - \vec{x_i}\right) + U(0,\varphi_2) \otimes \left(\vec{p_g} - \vec{x_i}\right) \quad (1)$$

$$\vec{x_i} \leftarrow \vec{x_i} + \vec{v_i} \quad (2)$$

Step 7. If a criterion is met (usually a sufficiently good fitness or a maximum number of iterations), exit loop.
Step 8. End loop

The parameters φ_1 and φ_2 are often called acceleration coefficients which determine the weight of the random forces in the direction of personal best $\vec{p_i}$ and global best $\vec{p_g}$. φ_1 represents the attraction that a particle has toward its own success while φ_2 represents the attraction that a particle has toward the success of its neighbors. It is almost ubiquitously adopted to set $\varphi_1 = \varphi_2 = 2.0$, Each component of $\vec{v_i}$ is kept within the range $[-V_{\max}, +V_{\max}]$. The choice of the parameter $V_{\max}$ requires consideration since it appears to influence the balance between exploration and exploitation. If $V_{\max}$ is too high, particles may fly past the good positions. On the other hand, the particles could become trapped in local optima if $V_{\max}$ is too low.

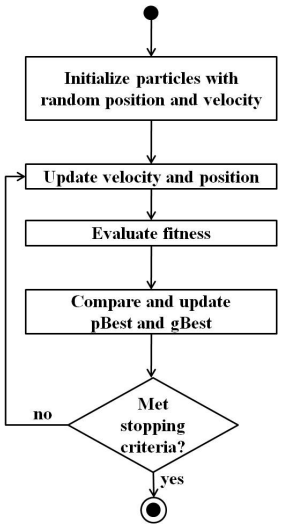

Figure 1. Particle Swarm Optimization flow diagram

B. Minimum Description Length

The minimum description length (MDL) principle proposed by Rissanen [9] is a learning criterion that selects the rule to find the best balance between the simplicity of a model and the goodness of fit to examples based on a data compression context. The fundamental insight behind the MDL Principle is that any regularity in a given set of data can be used to compress the data, that is, to describe it using fewer symbols than the number of symbols needed to describe the data literally [10]. Therefore, it embodies a form of Occam's Razor, a principle that claims the simpler one is the better when two competing theories that make exactly the same predictions. This idea can be applied to all sorts of inductive inference problems, and it turns out to be most fruitful in problems of model selection and, more generally, dealing with overfitting [11].

C. Bayesian networks

The Bayesian network which can also be referred to as a probabilistic network, belief network, Bayesian Belief Network and causal network was introduced for representing and reasoning with uncertainty [12]. In general, it consists of a graphical structure G which is a directed acyclic graph (DAG) and an associated probability distribution Pr. There are two parts to the Bayesian network. One is the qualitative relationships between the random domain variables, and the

other is the quantitative part, the probabilities over the variables.

Figure 2 shows a simple Bayesian network. Formally, let $N=[N_1,\cdots, N_n]$ be a set of nodes. Each node which is represented in the graph corresponds to a discrete random variable in the domain. The variables in a Bayesian network could be everything such as people, events and may be continuous or discrete. Each node has a number of states, that is, a set of probable values for each variable. There is a parent set, denoted by Π_p, for each node. For example, according to Figure 2, lung cancer may be caused by smoking or air pollution. Therefore, smoking and pollution together form the parent set of the node cancer.

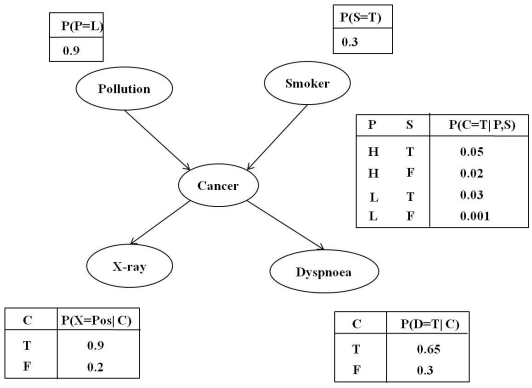

Figure 2. A simple Bayesian network representing the lung cancer problem

If a node has no parent nodes, its parent set would be empty and its probability table gives the marginal probabilities of the node. The directed arrows correspond to the dependence relationships between variable-pairs. It is usually called edge or arc. A node is taken to be dependent of its parents and children in the digraph, but is conditionally independent of any of its non-descendants given its parent.

In the Bayesian network, prior probabilities are assigned to source nodes (i.e., nodes without any incoming arcs), and conditional probabilities are associated with arcs. If a node X has only one parent Y, node X's probability table will contain the conditional probability $P(X|Y)$. Moreover, if X has multiple parents $(Y_1, Y_2,\cdots, Y_k)$, the table will contain the conditional probability $P(X|Y_1,Y_2,\cdots,Y_k)$.

This quantitative part encodes the joint probability distribution of these variables. The joint probability of any instantiation of all variables can be calculated as follows:

$$P(N_1,N_n)=\Pi_i p(N_i|Parents(N_i)) \tag{3}$$

where N_i represents the variables, and the value of the node is conditional only on the values of its parent nodes. Bayes' rule is used to update the conditional probabilities given evidence so the probabilities for all the nodes in the Bayesian network can be calculated. For example in Figure 2, the probability of the patient having cancer with smoking habit when the air pollution is high and the result of X-ray is true is $0.005-0.9/0.005-0.9+0.95-0.2=0.191$.

Building a Bayesian network involves three tasks. The first task is to identify the domain variables to be captured with the values they may adopt. Once the variables are decided, the causality relationships between these variables are identified and analyzed, and are expressed in a graphical structure. After creating the qualitative architecture, the next important task is to obtain the probabilities for each variable. The three tasks are typically iterated in a cyclic fashion since building the Bayesian network is flexible and creative.

D. Applying the MDL principle to Bayesian networks

MDL is first adopted for evaluating Bayesian networks by Lam and Bacchus [13]. The MDL principle suggests that the rule g that minimizes the description length given examples should be the output of the learning algorithm. As used in Bayesian belief network, each rule is views as a possible network structure and sequence given the rule g can be seen as the value of the *j*-th attribute. So in Bayesian belief network, the MDL principle is based on the idea that the desired model of a collection of data items is the model that minimizes the sum of the length of the encoding of the model and the length of the encoding of the data given the model. Even if the minimal network can't be found, structures with lower total description lengths are to be preferred. Such structures are superior to structures with longer total description lengths, in the precise sense that they are either more accurate, or are less complex, or are closer in structure to the original network. Hence, the total description length provides a metric by which alternate candidate structures can be compared [14].

The minimum description length metric can be expressed as:

$$D_t(B)=\sum_{N_i\in N} D_t(N_i,\Pi_{N_i})=\sum_{N_i\in N}\left(D_n(N_i,\Pi_{N_i})+D_d(N_i,\Pi_{N_i})\right) \tag{4}$$

where $D_t(B)$ is the total length of a network which is based on two components: the network description length D_n and the data description length D_d. The network description length (D_n) includes:

1. A list of the parents of each node.
   Suppose there are n nodes in the network, and each node has k different parents. For a node, $k\cdot\log_2(n)$ bits are needed to encode its parents.
2. The set of conditional probabilities associated with each node.
   To encode this part, it firstly needs to count the total number of conditional probabilities of each node. The number of bits required to store the numerical value of each conditional probability is also required. The encoding length will be the product of the number of bits and the number of conditional probabilities. Suppose a node takes on s_i values, F_i different parents each of which with distinct s_j values and d represents the number of bits required to store a numerical value. Thus for a node, $d(s_i-1)\Pi_{j\in F_i}s_j$ bits are needed.

Due to above two mentioned parts, the total description length for a particular network will be defined as

$$\sum_{i=1}^{n}\left[k_i \log_2(n) + d(s_i - 1)\Pi_{j \in F_i} s_j\right] \quad (5)$$

The data description length (D_d) is the length of the string encoding the database which can be expressed as

$$-N\sum_i p_i \log_2(q_i) \quad (6)$$

where N is the total number of records in the database, p_i is the true probability of an event and $-\log_2(q_i)$ is a codeword of length when run using this probability according to Huffman's algorithm. It is close to $-\log_2(p_i)$ since the probability q_i is determined by the network. Each event will have N_{pi} occurrences in the database.

III. Proposed Scheme

In this paper, construction of the Bayesian network is divided into two steps. The first step is network structure learning, and the second step is probability estimation. The whole process is represented in Figure 3. In the structure learning, a set of Bayesian networks are first randomly generated. Then, PSO is used to enhance these structures. After getting the best network, the probabilities associated with the networks are calculated according to the database. When the structure and probabilities are acquired, the final Bayesian network is obtained and can be used for prediction or classification.

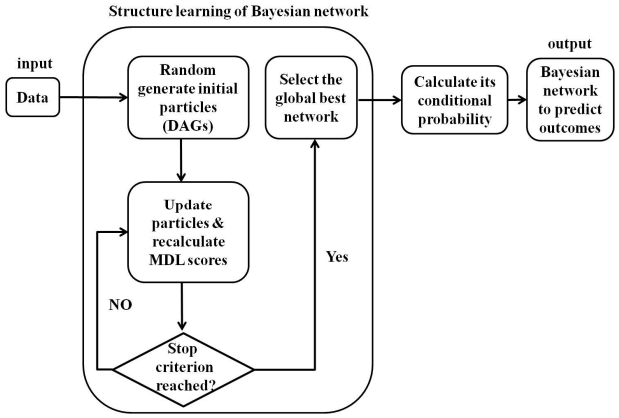

Figure 3. Bayesian Networks Learned by PSO

In structure learning, the PSO is adopted as a search algorithm which attempts to find an optimal Bayesian network. The search space of the networks is a DAG space, that is, every individual in the space is a directed acyclic graph (DAG). Before using PSO in a DAG space, several mathematical functions including (1) each particle's position, (2) each particle's velocity, (3) how to determine the new position of the particle, and (4) how to determine the new velocity of the particle should be defined.

In the research space, each particle represents a candidate Bayesian structure. The position of a particle is represented as an n x n adjacent matrix where n is the number of nodes in the problem. Elements in the matrix represent the dimension of the particle. The presence of zero in any element indicates that these two nodes have no linkage and one indicates that there is a connecting edge between the two nodes. An example of a matrix and its corresponding Bayesian Network structure is shown in Figure 4.

Velocity is used to determine the new position of a particle. It can measure the difference between two positions and thus move the particle. The velocity of a particle is also defined as an n x n matrix. The elements in the matrix are represented as discrete values {-1, 0, 1}. A velocity with -1 in an element means that the existing edge between two specified nodes in the DAG will be removed in the next generation, 0 means that the edge between two nodes remains unchanged, and 1 means that a new edge will be added between two specified nodes. In the velocity for each element indicates whether the edge represented by the element is to be removed, added or left unchanged.

$$\begin{bmatrix} & X_1 & X_2 & X_3 \\ X_1 & 0 & 1 & 1 \\ X_2 & 0 & 0 & 1 \\ X_3 & 0 & 0 & 0 \end{bmatrix}$$

(a)

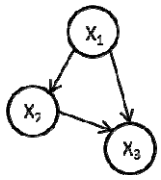

(b)

Figure 4. (a) Matrix of position. (b) Corresponding Bayesian network.

TABLE I. Velocity Update

Previous position	Current velocity	Current position	Action
0	0	0	Unchanged
0	-1	0	Unchanged
0	1	1	Add
1	0	1	Unchanged
1	1	1	Unchanged
1	-1	0	Remove

Since the constriction factor has a better performance than inertia weight [15], it is used to compute the new velocity of a particle, which is defined as Eq.(7).

$$\vec{v_i} \leftarrow \chi\left(\vec{v_i} + c_1 * rand(\,) * \left(\vec{p_i} - \vec{x_i}\right) + c_2 * rand(\,) * \left(\vec{p_g} - \vec{x_i}\right)\right) \quad (7)$$

$$\chi = \frac{2}{\varphi - 2 + \sqrt{\varphi^2 - 4\varphi}} \quad (8)$$

$$\varphi = c_1 + c_2 > 4 \quad (9)$$

In the initial generation, $\vec{v_1}$ is created randomly. Beginning from the second generation, it is updated by combining the current $\vec{v_1}$ and the cognitive and social influences respectively, working as the formula above. After updating the velocity, the value has to be translated into discrete values {-1, 0, 1}. To partition values of a continuous variable into a discrete variable, K equal lengths (equal intervals) is used since it is one of the most familiar methods to create partitions. K is chosen to provide a manageable number of discrete values, which gives a fair approximation of the continuous frequency distribution [16]. In this paper, K is set to 3.

In order to get the optimal network, a fitness function is necessary to evaluate the goodness of all candidate networks. In this paper, the Minimum description length (MDL) metric is applied to assess the models. In the MDL principle, the best model of a collection of data items is whose length is the minimum. The length is the sum of two parts: (1) the length of the encoding of the model, and (2) the length of the encoding of the data given the model. Both can be measured in bits. [13]

The structure learning of Bayesian network algorithm combines PSO and MDL, which includes two steps: create and update. The first step is the creation of a set of particles (DAGs) and initialization of the personal and global best positions. The second step is the calculation of velocities and update of the positions of the particles. The details of the algorithm are shown in Figure 5.

Let *N* be the set of all nodes.
Randomly generate *K* particles.
Set *round* to 0.
While *round* is smaller than the maximum number of generations,
  Each particle is evaluated with the fitness function. The best position of each individual and the best position of the global swarm are determined by the MDL scores.
  For each particle,
    Determine the next velocity and position of each particle using the velocity update equation.
    For each node,
      Run the *validation algorithm* of the structure to check whether it violates the Bayesian network standards. If cycles are not generated by inserting new edges into the DAG, then add the edges. If it creates cycles, then delete the edges or skip the generation.
  Perform the fitness function to assess the goodness of the DAG.
  Increase *round* by 1.
Let the DAG with the lowest fitness value found in any generation be the final best network.
Estimate the probabilities of the network.
Return this network as the result of the optimal Bayesian network.

Figure 5. Algorithm for PSO to learn Bayesian networks

After the validations, each particle is again evaluated by the MDL metric. This can ensure that the best particle of this generation will be stored to the next generation. After running a preset number of generations, an optimal particle is acquired. Probabilities of the nodes in the network are then calculated as described in the next section. There are two types of probabilities in a Bayesian network, which include prior probabilities and conditional probabilities. If a node has no parents, it is assigned to the prior probability. The prior probability is measured as the number of cases of this event divided by the total number of cases in the database, which is shown as:

$$P(N_i = c) = N_i / N \tag{10}$$

If a node has parents, it is assigned to the conditional probability. The conditional probability can be calculated as follows:

$$P\left(N_i = c \middle| \Pi_{N_i} = p\right) = \frac{N_{i,j,k} + 1}{N_{i,j} + r_i} \tag{11}$$

where r_i is the number of different values of variable N_i , $N_{i,j,k}$ is the number of cases in the database in which variable N_i has the value set c and Π_{N_i} has the value set p. $N_{i,j}$ is the sum of cases of different value that the variable Ni takes on in the database, which can be instantiated as

$$N_{i,j} = \sum_{k=1}^{r_i} N_{i,j,k} \tag{12}$$

After acquiring all prior and conditional probabilities, the Bayesian network can be used for probabilistic inference which refers to the process of computing the posterior probability of a query variable after obtaining observable variables [17], which can be defined as

$$P\left(N_i \middle| N_j\right) = \frac{P(N_i)P\left(N_j \middle| N_i\right)}{P(N_{i1})P\left(N_j \middle| N_{i1}\right) + P(N_{i2})P\left(N_j \middle| N_{i2}\right) + \cdots + P(N_{in})P\left(N_j \middle| N_{in}\right)} \tag{13}$$

where N_i is the query node, and N_j is the observable nodes. N_j is the child of N_i. $N_{i1}, \cdots, N_{in}$ are states of node N_i.

IV. EXPERIMENTAL RESULTS

In order to show that the proposed method has a good performance, the Stroke data set which is collected from a neurological clinic is used. There are 350 instances gathered from 2009 to 2010, in which 176 instances are with stroke and 174 instances without stroke. The details of the data set are presented in Table II. Each instance comprises 11 attributes, including age, gender, obesity, hypertension, diabetes mellitus, coronary artery disease, left ventricular hypertrophy, atrial fibrillation, smoking, cholesterol and high-density lipoprotein. The class is whether the patient suffers from stroke. All attributes are binary except for age which is trinary.

MDL is a measure to evaluate the learned Bayesian network. The lower the measure, the better the network is. In the first generation, the MDL score of the model is around 4320.55. Then the MDL metric of Bayesian network declines as the PSO algorithm learns better network models. The optimal network appeared at the 1050th generation, with a MDL score of 4122.54. Due to the fast learning rate to achieve optimal model, the proposed method is efficient. The trend of MDL scores is presented in Fig. 6.

The algorithm runs with particles set to 20, 50, 100, 150, and 200, respectively. Executing the algorithm over different particles can evaluate whether a better scoring Bayesian network can be generated by more explorations. 5000 iterations are executed. Other parameters such as constriction factor are set to 0.729, and the two learning factors are set to 2.05. Different values of particles of PSO are conducted to study its effect on the stroke problem. Structural difference is the measure to evaluate Bayesian network structure. It is defined as: $\sum_{i=1}^{n} \varphi_i$ where φ_i is the sum of the symmetric difference between the parent sets of node i in the learned network and the known network [3]. Ten trials of experiments are performed. The structural differences between the best Bayesian network structure found in each trial. There is no significant difference for various values of particles by using One-way analysis of variance (ANOVA) (F = 1.464, P = 0.228).

Accuracy of classification, sensitivity and specificity have been commonly used as indices to evaluate the quality of algorithms. Waikato Environment for Knowledge Analysis

(WEKA) system release no. 3.6.1 [18] thus is used as reference because it contains a large number of techniques divided into seven groups (Bayesian, based on functions, lazy, meta techniques, tree, rule and others). Support vector machine (SVM) and Bayes network are chosen to compare the classification performance with MDL-PSO. Parameters of each technique are the default values set in WEKA. The comparison results of Stroke breast cancer database are presented in Table III. The first row of Table III is the average accuracy of classification of each classifier. For the Stroke data set, MDL-PSO performs both better than SVM and BayesNet. The second and third rows are respectively sensitivity and specificity of the classifiers, which PSO-MDL got higher specificity than the other two classifiers. Sensitivity of PSO-MDL is lower than SVM but higher than BayesNet.

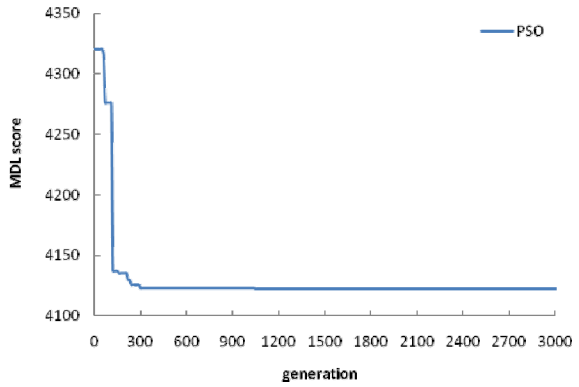

Figure 6. The MDL metric for Stroke data set

TABLE II. SUMMARY OF THE STROKE DATASET

Attribute	Data Type	Possible value
Age (<45, 45~65,>65)	Nominal	Young/Mid/Old
Gender	Nominal	Male/Female
Obesity (BMI>27)	Nominal	Yes/No
Hypertension	Nominal	Yes/No
Diabetes mellitus	Nominal	Yes/No
Coronary artery disease (>200)	Nominal	Yes/No
Left ventricular hypertrophy (<40)	Nominal	Yes/No
Atrial fibrillation	Nominal	Yes/No
Smoking	Nominal	Yes/No
Cholesterol(mg/dl)	Nominal	Normal/Abnormal
High-density lipoprotein(mg/dl)	Nominal	Normal/Abnormal
Class: Stroke or not	Nominal	Yes/No

V. CONCLUSION

PSO was adopted as the searching algorithm to learn the structure of Bayesian networks in this paper, and MDL was its fitness function. In addition, several constraints were used in order to keep the learning network from violating the standards of Bayesian networks. The learned Bayesian networks were also validated upon real data sets such as Stroke. The experimental results revealed that PSO-MDL was an efficient learning algorithm due to its fast learning rate. The accuracy is used to evaluate the effectiveness of PSO-MDL. As compared to SVM and BayesNet, the proposed method has a good accuracy.

TABLE III. THE COMPARISON RESULTS OF STROKE DATA SET

	MDL-PSO	SVM	BayesNet
Average accuracy	73.81%	68.86%	67.14 %
Sensitivity	70.5%	73.3%	65.3%
Specificity	65.5%	64.4%	63.2%

REFERENCES

[1] G. F. Cooper, "The computational complexity of probabilistic inference using Bayesian belief networks," *Artificial Intelligence*, vol. 42, pp. 393-405, 1992.

[2] J. Pearl, Probabilistic Reasoning in Intelligent Systems: Networks of Plausible Inference, San Francisco: Morgan Kaufmann, 1988.

[3] M. L. Wong, and K. S. Leung, "An Efficient Data Mining method for learning Bayesian networks using an evolutionary algorithm-based hybrid approach," *IEEE Transactions on Evolutionary Computation*, vol. 8, pp. 378-404, 2004.

[4] X. Li, S. Yuan, and X. He, "Learning Bayesian Networks Structures Based on Extending Evolutionary Programming," *Proceedings of the Third International Conference on Machine Learning and Cybernetics*, pp. 1594-1598, 2004.

[5] A. Salman, I. Ahmad, and S. Al-Madani, "Particle swarm optimization for task assignment problem," *Microprocessors and Microsystems*, vol. 26 (8), pp. 363-371, 2002.

[6] T. Du, S. S. Zhang, and Z. Wang, "Efficient Learning Bayesian Networks Using PSO," *International conference on Computational intelligence and security*, vol. 3801, pp. 151-156, 2005.

[7] J. Kennedy and R. Eberhart, "Particle swarm optimization," *Proceedings of the IEEE International Conference on Neural Networks*, pp. 1942-1948, 1995.

[8] R. Poli, J. Kennedy, and T. Blackwell, "Particle swarm optimization: An overview," *Swarm Intelligence*, vol. 1, 2007.

[9] J. Rissanen, "Modelling by the shortest data description," *Automatica*, vol. 14, pp. 465-471, 1978.

[10] J. Suzuki, "Learning Bayesian Belief Networks Based on the MDL Principle: An Efficient Algorithm Using the Branch and Bound Technique," *IEICE Trans. Inf. Sys.t*, vol. E82-D (2); pp.3 56-367, 1999.

[11] P. Graunwald, "A tutorial introduction to the minimum description length principle," In P. Graunwald, I. J. Myung, and M. Pitt, editors, Advances in Minimum Description Length: Theory and Applications. MIT press, 2005.

[12] M. J. Druzdzel and L. C. van der Gaag, "Building Probabilistic Networks: "Where Do the Numbers Come From?"," IEEE Transactions on Knowledge and Data Engineering, vol. 12(4), pp. 481-486, 2000.

[13] W. Lam and F. Bacchus, "Learning Bayesian Belief Networks: An Approach Based On The MDL Principle," *Compurafional Intelligenc*, vol. 10, 1994.

[14] W. Lam, "Bayesian Network Refinement Via Machine Learning Approach," *IEEE Transactions on Pattern Analysis and Machine Intelligence*, vol. 20(3), pp. 240 - 251, 1998.

[15] R. Eberhart and Y. Shi, "Comparing inertia weights and constriction factors in particle swarm optimization," *Proceedings of the 2000 congress on Evolutionary Computation*, pp. 84-88, 2000.

[16] E.J. Clarke and B.A. Barton, "Entropy and MDL Discretization of Continuous Variables for Bayesian Belief Networks," *International Journal of Intelligent Systems*, vol. 15, pp. 61-92, 2000.

[17] N. L. Zhang and D. Poole, "Exploiting causal independence in bayesian network inference," *Artificial Intelligenc*e, vol. 5, pp. 301-328, 1996.

[18] I. H. Witten and E. Frank, "Data Mining: Practical Machine Learning Tools and Techniques," San Francisco: Morgan Kaufmann, 2000.

2011 IEEE International Conference on Fuzzy Systems
June 27-30, 2011, Taipei, Taiwan

Relational Structure Analysis of Fuzzy Graph and its Application

For Analyzing Fuzzy Data of Human Relation

Hiroaki Uesu
Tokyo City University
Tokyo, Japan
uesu@suou.waseda.jp

Kenichi Nagashima
Waseda University
Tokyo, Japan

Hsunhsun Chung
Waseda University
Tokyo, Japan

Ei Tsuda
Kokugakuin S_R.High School
Tokyo, Japan

***Abstract*— Generally, we could efficiently analyze the inexact information and investigate the fuzzy relation by applying the fuzzy graph theory[1].**

We would extend the fuzzy graph theory, and propose a fuzzy node fuzzy graph. Since a fuzzy node fuzzy graph is complicated to analyze, we would transform it to a simple fuzzy graph by using T-norm family. In addition, to investigate the relations between nodes, we would define the fuzzy contingency table.

In this paper, we would discuss about five subjects, (1) new T-norm "Uesu product", (2) fuzzy node fuzzy graph, (3) fuzzy contingency table, (4) decision analysis of the optimal fuzzy graph G_{λ_0} in the fuzzy graph sequence $\{G_\lambda\}$ and (5) its application to sociometry analysis.

By using the fuzzy node fuzzy graph theory, the new T-norm and the fuzzy contingency table, we could clarify the relational structure of fuzzy information. According to the decision method in section 2, we could find the optimal fuzzy graph G_{λ_0} in the fuzzy graph sequence $\{G_\lambda\}$, and clarify the structural feature of the fuzzy node fuzzy graph .

Moreover, we would illustrate its practical effectiveness with the case study concerning sociometry analysis.

Keywords-component; fuzzy node fuzzy graph; optimal fuzzy graph; sociometry analysis; T-norm; contingency table

I. T-NORM, FUZZY NODE FUZZY GRAPH AND FUZZY CONTINGENCY TABLE

A. T-norm and its Family

T-norm (Triangular Norm) is a binary operation that is defined by the following:

Definition 1 T-norm is a binary operation

$p, q \in [0,1] \to T(p,q) \in [0,1]$

satisfying the following properties:

(1) Commutativity :

$T(p,q) = T(q,p)$

(2) Associativity :

$T(p,T(q,r)) = T(T(p,q),r)$

(3) Monotonicity :

$p \le q, \quad r \le s \Rightarrow T(p,r) \le T(q,s)$

(4) Boundary conditions :

$T(p,0) = 0, \quad T(p,1) = p$

The typical T-norms are the followings:

(1) Logical product :

$T_L(p,q) = p \wedge q$

(2) Algebraic product :

$T_A(p,q) = pq$

(3) Multi-valued product (Lukaszewicz product) :

$T_M(p,q) = (p+q-1) \vee 0$

(4) Drastic product :

$$T_D(p,q) = \begin{cases} 0 & , p \vee q < 1 \\ p \wedge q & , p \vee q = 1 \end{cases}$$

Here, " $a \wedge b$ " means " $\min(a,b)$ ", " $a \vee b$ " means " $\max(a,b)$ ".

Definition 2 Order of T-norms

For two T-norms T_α and T_β, if a relation

$$\mathsf{T}_\alpha(p,q) \le \mathsf{T}_\beta(p,q), \ (p,q) \in [0,1]^2$$

holds, we denote it by $\mathsf{T}_\alpha \le \mathsf{T}_\beta$.

For any T-norm T, a relation $\mathsf{T}_D \le \mathsf{T} \le \mathsf{T}_L$ always holds.

Definition 3 T-norm Family

For any $\lambda \in [a,b]$, when T_λ is T-norm, then we say that $\{T_\lambda\}$ is T-norm family that connects T_a with T_b.

The typical T-norm families are

(1) Dubois product :

$$T_\lambda(p,q) = \frac{pq}{p \vee q \vee \lambda}, \lambda \in [0,1]$$

(2) Weber product :

$T_\lambda(p,q) = 0 \vee \{(1+\lambda)(p+q-1) - \lambda pq\}, \lambda \ge -1$

(3) Schweizer product :

$T_\lambda(p,q)=\sqrt[\lambda]{0\vee(p^\lambda+q^\lambda-1)},\lambda>0$

(4) Uesu product :

$$T_\lambda(p,q)=\begin{cases}0 & ,p\vee q<1-\lambda\\ p\wedge q & ,p\vee q\geq 1-\lambda\end{cases},\lambda\in[0,1]$$

and so on.

The relation of typical T-norm families and Uesu product could be illustrated in Fig.1.

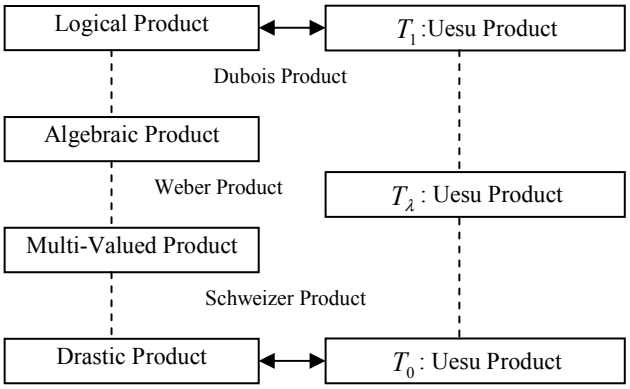

Figure 1. Relation of Typical T-norm Families

Here, in Fig.1, we could understand that Dubois product connects "logical product" with "algebraic product", Weber product does "algebraic product" with "multi-valued product", Schweizer product does "mulch-valued product" with "drastic product" and Uesu product does "logical product" with "drastic product".

B. *Fuzzy Node Fuzzy Graph*

Definition 4 Crisp Node Fuzzy Graph

A crisp node fuzzy graph G[6] is defined by

$$G=(V,F):V=\{v_i\},F=(f_{ij}),0\leq f_{ij}\leq 1$$

where V is the set of the nodes and F is an $n\times n$ matrix. (i, j) component f_{ij} of F is a fuzziness of the arc from the node v_i to the node v_j.

Definition 5 Fuzzy Node Fuzzy Graph

A fuzzy node fuzzy graph G[14] is defined by

$$G=(V,F):V=\{v_i/u_i\},Y=(y_{ij}),0\leq u_i\leq 1,\ 0\leq y_{ij}\leq 1$$

where V is the set of the nodes and the fuzziness u_i is a fuzziness of the node v_i. Y is a $n\times n$ matrix whose (i, j) component y_{ij} is a fuzziness of the arc from the node v_i to the node v_j.

A fuzzy node fuzzy graph is characterized by the fuzziness of the nodes and the fuzziness of the arcs. Therefore, the structure of a fuzzy node fuzzy graph is usually very complicated. Then, it should be interesting to transform a fuzzy node fuzzy graph to a crisp node fuzzy graph and we present a method to transform a fuzzy node fuzzy graph to a crisp node fuzzy graph.

Definition 6 Transformation from Fuzzy Node Fuzzy Graph to Crisp Node Fuzzy Graph

A fuzzy node fuzzy graph $G=(V, Y)$ can be transformed to a crisp node fuzzy graph $G=(V,F)$ by the following method: Let

$$G=(V,F):V=\{v_i\},F=(f_{ij}),f_{ij}=T(u_i,y_{ij})$$

where the fuzziness f_{ij} of the arc from the node v_i to the node v_j could be defined by applying T-norms.

This fuzzy node fuzzy graph analysis would be applied to the sociometry analysis, the instruction structure analysis and so on.

C. *Fuzzy Contingency Table*

Definition 7 Fuzzy Contingency Table

Let $\boldsymbol{x}$ and $\boldsymbol{y}$ be two vectors as follows:

$$x=(x_i),\ y=(y_i):0\leq x_i,y_i\leq 1,\ 1\leq i\leq n.$$

Then the fuzzy contingency table of $\boldsymbol{x}$ and $\boldsymbol{y}$ defined accordingly:

TABLE I. FUZZY CONTINGENCY TABLLE

$\boldsymbol{x}$ \ $\boldsymbol{y}$	1	0	Sum
1	a_{xy}	b_{xy}	$\sum_{k=1}^{n}x_k$
0	c_{xy}	d_{xy}	$n-\sum_{k=1}^{n}x_k$
Sum	$\sum_{k=1}^{n}y_k$	$n-\sum_{k=1}^{n}y_k$	n

$$a_{xy}=\sum_{k=1}^{n}T(x_k,y_k),\ b_{xy}=\sum_{k=1}^{n}x_k-a_{xy},$$

$$c_{xy}=\sum_{k=1}^{n}y_k-a_{xy},\ d_{xy}=n-\sum_{k=1}^{n}y_k-b_{xy}$$

From the fuzzy contingency table, we could computes any similarity coefficients. The typical similarity coefficients are

(1) Jaccard : $s_{xy}=\dfrac{a}{a+b+c}$

(2) Sorensen-Dice : $s_{xy}=\dfrac{2a}{2a+b+c}$

(3) Russell and Rao : $s_{xy}=\dfrac{a}{a+b+c+d}$

(4) Simple Matching : $s_{xy}=\dfrac{a+d}{a+b+c+d}$

(5) Rogers-Tanimoto : $s_{xy}=\dfrac{a+d}{a+2b+2c+d}$

(6) Simpson : $s_{xy}=\dfrac{a}{(a+b)\wedge(a+c)}$

(7) Ochiai : $s_{xy} = \dfrac{a}{\sqrt{(a+b)(a+c)}}$

(8) Phi : $s_{xy} = \dfrac{ad-bc}{\sqrt{(a+b)(a+c)(b+d)(c+d)}}$

(9) Yule : $s_{xy} = \dfrac{ad-bc}{ad+bc}$

and so on.

II. Fuzzy Graph and its Analysis

A. Cluster Analysis of Fuzzy Graph

A fuzzy graph G is defined by

$$G=(V,Y), V=\{v_i\}, F=(f_{ij}), 0\le f_{ij}\le 1, f_{ii}=1, 1\le i\le n$$

where f_{ij} is a fuzziness of the arc from the node v_i to the node v_j.

In order to analyze the similarity structure among nodes of a fuzzy graph, we use the symmetric relation matrix $S=(s_{ij})$. A symmetric relation matrix S could be defined by using the fuzzy contingency table and any similarity coefficients. Here, we define the symmetric relation matrix S by using the simple matching similarity coefficient.

In order to analyze the clustering structure among nodes, we have its max-min transitive closure $\hat{S}=(\hat{s}_{ij})$ which is computed by $\hat{S}=S^n$.

After that, we define the c-cut matrix S_c of $\hat{S}=(\hat{s}_{ij})$ as follows:

$$S_c=(s_{ij}^c),\quad s_{ij}^c=\begin{cases}1 & (\hat{s}_{ij}\ge c)\\ 0 & (\hat{s}_{ij}<c)\end{cases}, 0\le c\le 1$$

From the matrix S_c, we define the cluster $CL_{Sc}(i)$.

$$J_c(i)=\{j \mid s_{ij}^c=1, 1\le j\le n\}$$

$$CL_{Sc}(i)=\{v_j \mid j\in J_c(i)\}$$

The cluster $CL_{Sc(i)}$ gives an equivalence relation among nodes.

Thence, we can construct the partition tree by changing the level c of the c-cut matrix which represents the clustering situation of nodes in a fuzzy graph.

B. Decision Analysis of Optimal Value λ_0

Concerning the transformation from a fuzzy node fuzzy graph $G=(V,Y)$ to a fuzzy graph $G_\lambda=(V,F_\lambda)$, we could analyze a fuzzy node fuzzy graph by using Uesu product T_λ.

By changing the parameter λ, a sequence $\{G_\lambda\}$ of fuzzy graphs is composed.

Here, we would choose the optimal fuzzy graph G_{λ_0} from this fuzzy graph sequence $\{G_\lambda\}$.

Then, we would discuss the decision method of the optimal parameter λ_0.

In order to decide the optimal fuzzy graph G_{λ_0}, we would define two functions $d(\lambda)$ and $e(\lambda)$ as follows:

Definition 8 Distance Function $d(\lambda)$ and Connectivity Function $e(\lambda)$

$$d(\lambda)=d(F_\lambda,S_{c_0})=\frac{1}{n^2-n}\sum_{i=1}^{n}\sum_{j=1}^{n}\left|f_{ij}-s_{ij}^{c_0}\right|$$

$$e(\lambda)=e(F_\lambda)=\frac{\gamma(F_\lambda)}{n^2-n}$$

where, $\gamma(F_\lambda)=\#(\Gamma_\lambda), \Gamma_\lambda=\{f_{ij}^\lambda\in F_\lambda \mid f_{ij}^\lambda>0\}$.

And F_λ, S_{c_0} are given as follows:

$$F_\lambda=(f_{ij}^\lambda),$$

$$f_{ij}^\lambda=\begin{cases}0 & ,u_i\vee y_{ij}<1-\lambda\\ u_i\wedge y_{ij} & ,u_i\vee y_{ij}\ge 1-\lambda\end{cases}$$

$$S_{c_0}=(s_{ij}^{c_0}),\quad s_{ij}^{c_0}=\begin{cases}1 & (\hat{s}_{ij}\ge c_0)\\ 0 & (\hat{s}_{ij}<c_0)\end{cases}$$

Here, $d(\lambda)$ evaluates the feature between the fuzzy node fuzzy graph $G_\lambda=(V,F_\lambda)$ and the optimal clustering cut level c_0. If the value of $d(\lambda)$ is large, then G_λ reasonably shows the feature of the clustering level c_0.

On the other hand, $e(\lambda)$ evaluates the connectivity information of G_λ. If the value of $e(\lambda)$ is small, then G_λ reasonably shows the feature of the connectivity information.

Here, we would normalize the values of $d(\lambda)$ and $e(\lambda)$ respectively, and define $f_d(\lambda)$ and $f_e(\lambda)$ as follows:

Definition 9 Fuzzy Distance Function $f_d(\lambda)$ and Fuzzy Connectivity Function $f_e(\lambda)$

$$f_d(\lambda)=\frac{d_M-d(\lambda)}{d_M-d_m},\quad f_e(\lambda)=\frac{e(\lambda)-e_m}{e_M-e_m}$$

where,

$d_M=\bigvee_{\lambda\in[0,1]}\{d(\lambda)\}$, $d_m=\bigwedge_{\lambda\in[0,1]}\{d(\lambda)\}$, $e_M=\bigvee_{\lambda\in[0,1]}\{e(\lambda)\}$ and $e_m=\bigwedge_{\lambda\in[0,1]}\{e(\lambda)\}$.

By applying the maximal decision of the fuzzy decision, we could reasonably find the optimal value λ_0 concerning the sequence $\{G_\lambda\}$.

Definition 10 Decision of Optimal Value λ_0

$$f_m(\lambda)=f_d(\lambda)\wedge f_e(\lambda)$$

$$\lambda_0=\wedge\{\lambda : f_m(\lambda)=\bigvee_{x\in[0,1]} f_m(x)\}$$

III. Application to Sociogram Analysis

We would present a practical case study of the fuzzy sociogram analysis[5],[11] that has been experimented in high

school.

If we executed the questionnaires in Fig.2 to 10 students, we could obtain the response table *L*.

From the table *L*, we obtained the response matrix $K^{(1)}, K^{(2)}, K^{(3)}$ and the evaluation matrix *R*.

By analyzing the matrix *R*, we have the preferring matrix *Y*=(y_{ij}) in Fig.3 and the amicable matrix *S*=(s_{ij}) in Fig.4. From the amicable matrix *S*, we obtained the fuzziness u_i of member v_i. We illustrated the fuzzy node fuzzy graph *G*=(*V*, *Y*).

We could transform the fuzzy node fuzzy graph *G*=(*V*, *Y*) to the fuzzy graph *G*=(*V*, *F*) by applying Uesu product . By changing parameter λ, we obtained fuzzy graph sequence $\{G_\lambda\}$.

Next, we could obtain the partition tree *P* in Fig.5 if we execute the cluster analysis concerning the amicability matrix *S*.

Here, we could decide the optimal cut level c_0 =0.78.

By using c_0-cut matrix Sc_0 and the fuzzy graph sequence $\{G_\lambda\}$, we could decide the optimal fuzzy graph G_{λ_0}. Here, by calculating the distance function $d(\lambda)$ and the connectivity function $e(\lambda)$.

$$d(\lambda)=\frac{1}{90}\sum_{i=1}^{10}\sum_{j=1}^{10}\left|f_{ij}^{\lambda}-s_{ij}^{c_0}\right|$$

$$e(\lambda)=\frac{\gamma(F_\lambda)}{90}$$

where, $\gamma(F_\lambda)=\#(\Gamma_\lambda), \Gamma_\lambda=\{f_{ij}^{\lambda}\in F_\lambda \mid f_{ij}^{\lambda}>0\}$.

Then, we have normalized the value of $d(\lambda)$ and $e(\lambda)$, so we have calculated $f_d(\lambda)$ and $f_e(\lambda)$ as follows:

$$f_d(\lambda)=\frac{0.23-d(\lambda)}{0.23-0.15},\ f_e(\lambda)=\frac{e(\lambda)-0.21}{0.64-0.21}.$$

Select your friends and write them in order for each group activities.

Q_1 : Study in Group
Q_2 : Take Lunch Together
Q_3 : Do Sport Together

	1	2	3	4	…
Q_1					
Q_2					
Q_3					

Figure 2. Questionnaires

	1	2	3	4	5	6	7	8	9	10
1	1	0.50		0.42		0.58	1.00			
2	0.17	1	0.33	0.92			0.58	0.08	0.42	
3		0.92	1	0.58			0.58			0.33
4	1.00	0.33		1			0.33		0.75	
5		0.33	0.42	0.33	1		0.17	0.83	0.42	
6	0.08	0.75		0.33		1	0.67	0.08		
7	0.58	0.58				0.17	1		0.58	
8		0.33	0.08		1.00	0.08	0.42	1	0.42	0.17
9	0.58	0.42		0.83			0.33		1	
10	0.17	0.83					0.92		0.33	1

Figure 3. Preferring Matrix *Y*

	1	2	3	4	5	6	7	8	9	10
1	1	0.49	0.49	0.65	0.44	0.63	0.57	0.48	0.70	0.53
2	0.49	1	0.55	0.63	0.33	0.52	0.78	0.37	0.56	0.52
3	0.49	0.55	1	0.63	0.72	0.65	0.45	0.73	0.59	0.75
4	0.65	0.63	0.63	1	0.43	0.53	0.51	0.46	0.63	0.48
5	0.44	0.33	0.72	0.43	1	0.63	0.32	0.97	0.58	0.68
6	0.63	0.52	0.65	0.53	0.63	1	0.52	0.65	0.48	0.68
7	0.57	0.78	0.45	0.51	0.32	0.52	1	0.35	0.52	0.53
8	0.48	0.37	0.73	0.46	0.97	0.65	0.35	1	0.59	0.68
9	0.70	0.56	0.59	0.63	0.58	0.48	0.52	0.59	1	0.56
10	0.53	0.52	0.75	0.48	0.68	0.68	0.53	0.68	0.56	1

Figure 4. Amicable Matrix *S*

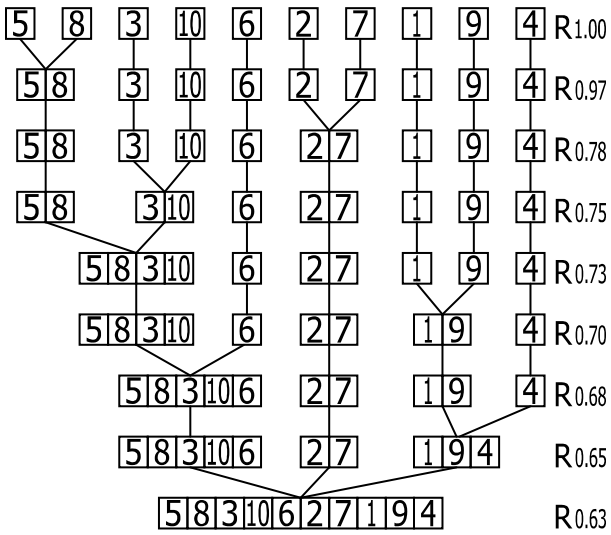

Figure 5. Partition Tree *P*

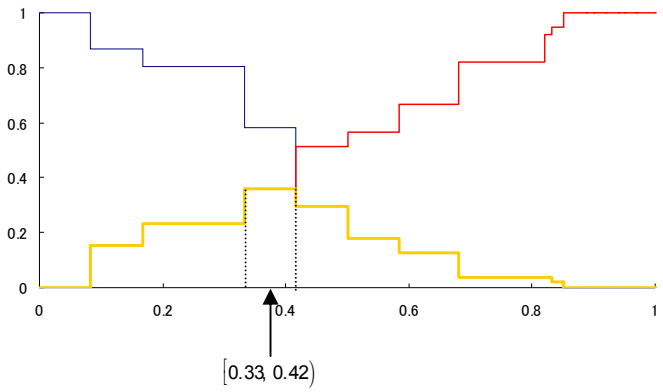

Figure 6. Fuzzy Decision $f_d(F) \wedge f_e(F)$

By applying the fuzzy decision, we could obtain the optimal value $\lambda_0 = 0.33$ as shown in Fig.6.

We would illustrate the fuzzy sociogram U^F, $z = c_0 = 0.58$ in Fig.7 which is based on the fuzzy graph $G_{\lambda_0} = (V, F_{\lambda_0})$, $\lambda_0 = 0.33$ in Fig.7. In this graph, we indicated the students in the same cluster at the optimal cut level $z = c_0 = 0.58$ with the same color and the opinion leaders are boldly marked.

This fuzzy sociogram U^F effectively represents the following results:

(1) The opinion leaders are 2 and 7 because these nodes is connected with many other nodes.
(2) The relatively isolated member is 10 because this node has not been connected with the others.
(3) The subgroups are {5, 8, 3, 10} and {2, 7}.

In this way, we could effectively analyze and clarify the interpersonal relation among members by applying the fuzzy node fuzzy graph and our analysis method.

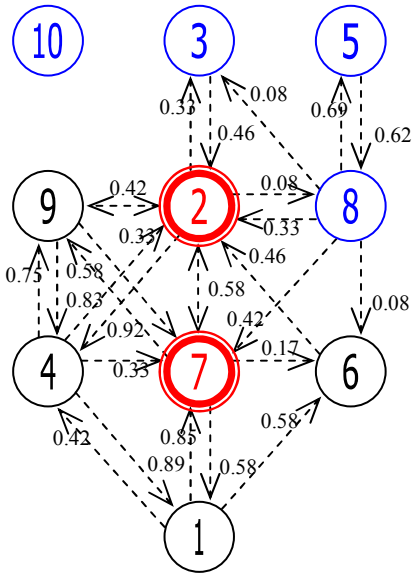

Figure 7. Fuzzy Sociogram U^F, $\lambda_0 = 0.33$, $z = 0.73$

IV. Conclusion

In this paper, we have mainly discussed the followings;

(1) fuzzy node fuzzy graph
(2) new T-norm "Uesu product"
(3) decision analysis of the optimal fuzzy graph G_{λ_0} in the fuzzy graph sequence $\{G_\lambda\}$
(4) fuzzy contingency table
(5) practical application and its effectiveness concerning the sociometry analysis

We have illustrated the practical effectiveness of the analysis method with the case study concerning the sociometry analysis. This method is also available for the instruction/ cognition analysis in education[10], the opinion poll in psychology and so on.

Finally, the author would be grateful to Prof. H.Yamashita of Waseda University for his helpful advices.

References

[1] L.Zadeh, "Fuzzy Sets", Information and Control VII, 1965 I, pp.338–353.

[2] A.Rosenfeld, "Fuzzy Graphs", Fuzzy Sets and Their Applications to Cognitive and Decision Processes, L.Zadeh edit, Academic Press, Inc, 1974, pp.77–95.

[3] A.Kaufmann, "Introduction to the Theory of Fuzzy Subsets", Academic Press, 1975.

[4] C.Negoita, "Application of Fuzzy Sets to System Analysis", Birkhauser Verlog, 1975.

[5] J.Moreno, "The Sociometry Readers", Free Press, 1960.

[6] T.Nishida, E.Takeda, "Fuzzy Sets and its Applications", Morikita Shuppan, 1978 (in Japanese).

[7] H.Romesburg, "Cluster Analysis for Researchers", Lifetime Learning Publications, 1984.

[8] Robert Aumann, "Lecture on Game Theory", Westview Press, 1989.

[9] H.Yamashita, H.Suda, "Approximate Expression of Fuzzy Graph and its Application", Int'l Fuzzy System Association VII, 1997, pp.435-438.

[10] H.Uesu, H.Yamahita, "Instruction and Cognition Analysis Applying Fuzzy Node Fuzzy Graph", 17th Fuzzy System Symposium 5E2-3, Japan Society for Fuzzy Theory and Systems, 2001, pp.221-222(in Japanese).

[11] H.Uesu, "Sociometry Analysis Applying Fuzzy Node Fuzzy Graph", Journal of Japan Society for Fuzzy Theory and Systems Vol.14, No.3, 2002, pp.299-309(in Japanese).

[12] H.Uesu, H.Yamashita, "Connectivity Properties of T-Norm Families and its Application", Int'l Conference on Computer, Communication and Control Technologies, 2003.

[13] H.Uesu, E.Tsuda, "Clustering Level Analysis Applying Fuzzy Theory and its Application", Conference of Japan Society for Educational Technology, 2003, pp.695-696(in Japanese).

[14] H.Uesu, "Fuzzy Node Fuzzy Graph, T-Norm and its Application", Journal of Japan Society for Fuzzy Theory and Intelligent Informatics Vol.16 No.1, 2004, pp.88-95 (in Japanese).

[15] K.Shinkai, "Level analysis of Fuzzy Partition Tree and its Application", IEEE International Workshop on Soft Computing Applications, 2005, pp.110-112.

[16] H.Uesu, "Optimal Fuzzy Graph Based on Fuzzy Node Fuzzy Graph Analysis", The 3rd International Conference on Soft Computing and Intelligent Systems, 2006, pp.1812-1817.

[17] H.Uesu, "Analysis of Fuzzy Node Fuzzy Graph and its Application", Int'l Conference on Soft Computing and Human Science, 2007, pp.27-32.

2011 IEEE International Conference on Fuzzy Systems
June 27-30, 2011, Taipei, Taiwan

On Another Approach to the Definition of an L-fuzzy Valued Integral

Vecislavs Ruza
University of Latvia
Department of Mathematics
Riga, Latvia LV
Email: vecislavs.ruza@ge.com

Svetlana Asmuss
University of Latvia
Department of Mathematics
Institute of Mathematics and Computer Science
Riga, Latvia
Email: svetlana.asmuss@lu.lv

***Abstract*—We continue to develop a construction of an L-fuzzy valued measure extending a crisp measure defined on a σ-algebra of crisp sets to an L-fuzzy valued measure defined on a T_M-tribe. We describe two equivalent approaches to define an L-fuzzy valued integral of non-negative measurable functions.**

***Index Terms*—L-set, L-fuzzy real number, L-fuzzy valued measure, L-fuzzy valued integral.**

I. Introduction

One can find a lot of works regarding fuzzy approach to measure and integral. The biggest scope on this subject can be found in [1], [2], [3]. Our interest is in developing a theory where not only sets are fuzzy, but also measure and integral take fuzzy real values. In the serious of our previous papers [4], [5], [6] the concepts of an L-fuzzy valued measure and integral were studied throughly. We continue to develop results obtained in the previous papers and show that L-fuzzy valued measure and integral preserve most of the properties of it's crisp analogues (see e.g. [7]).

Inspired by the fact from the classical measure theory stating that an integral of a given non-negative function can be considered as a measure we obtain two different approaches to define an L-fuzzy valued integral.

The idea of the first approach is to extend a crisp measure ν to the L-fuzzy valued measure μ by using the construction described in [5] and then defining the L-fuzzy valued integral

$$\mu_f(E) = \int_E f \, d\mu,$$

where f is an integrable real-valued function and E is a measurable L-set [6].

The second approach shows that an L-fuzzy valued integral can be obtained by considering the measure ν_f using a crisp measure ν as following:

$$\nu_f(M) = \int_M f \, d\nu,$$

where f is an integrable non-negative function and M is a measurable set. And then extending it to the L-fuzzy valued measure $\tilde{\mu}_f$ according to the construction described in [5].

Finally we show that both approaches give us equivalent ways to define the L-fuzzy valued integral, i.e. $\mu_f = \tilde{\mu}_f$. This result can be described by the following diagram:

$$\begin{array}{ccc} \nu & \longrightarrow & \mu \\ \downarrow & & \downarrow \\ \nu_f & \rightarrow & \mu_f \end{array}$$

The second approach to the definition gives us an opportunity to simplify calculations of the L-fuzzy valued integral.

Our investigations of the L-fuzzy valued integral are motivated by our intention to develop results on approximation from [8], [9]. For the problems that can be solved only approximately the notion of the error of a method of approximation plays the fundamental role. In order to estimate the quality of approximation on an L-fuzzy set, we need an appropriate L-fuzzy analogue of a norm. Our intention is to use the L-fuzzy valued integral to define an L-fuzzy valued norm for investigation of the error of approximation on an L-set.

II. Preliminaries

A. L-sets

Given a (crisp) universe X and a complete, completely distributive lattice $L(\wedge, \vee, 0_L, 1_L)$, an *L-subset* A of X (or, briefly, an L-set A) is a function $A : X \longrightarrow L$. The class of all L-subsets of X is denoted L^X. The operations for L-sets A, B are defined by using the minimum triangular norm T_M, its corresponding conorm S_M and decreasing involution N:

$$\begin{gathered}(A \wedge B)(x) = T_M(A(x), B(x)), \\ (A \vee B)(x) = S_M(A(x), B(x)), \\ A^c(x) = N(A(x)).\end{gathered}$$

A finite family of L-sets $A_1, A_2, \ldots, A_n$ is said to be *T_M-disjoint* (see e.g.[1]) iff for each $k \in \{1, \ldots, n\}$ we have

$$(\bigvee_{j=1, j\neq k}^{n} A_j) \wedge A_k = \emptyset.$$

A countable family of L-sets is said to be T_M-disjoint iff every finite subfamily of this family is T_M-disjoint.

We consider a class of L-sets called T_M-tribe (see e.g. [1]).

978-1-4244-7316-8/11/$26.00 ©2011 IEEE

Definition II.1. *A subclass $\Sigma \subset L^X$ is called a T_M-tribe on X if the following properties are satisfied:*

- $\emptyset \in \Sigma$;
- *for all* $A \in \Sigma$ *we have* $A^c \in \Sigma$;
- *for all sequences* $(A_n)_{n\in N} \subset \Sigma$ *we have* $\bigwedge_{n=1}^{\infty} A_n \in \Sigma$.

B. L-fuzzy real numbers

For our purposes we use the L-fuzzy real numbers as they were first defined by B. Hutton [10].

Definition II.2. *An L-fuzzy real number is a function $z : \mathbb{R} \to L$ such that*

- z *is non-increasing;*
- $\bigwedge_t z(t) = 0_L$, $\bigvee_t z(t) = 1_L$;
- z *is left semi-continuous, i.e. for all* $t_0 \in \mathbb{R}$ *we have* $\bigwedge_{t<t_0} z(t) = z(t_0)$.

In the original papers of this subject (see [10], [11], [12]) the L-fuzzy real numbers were defined not as order reversing functions, but as equivalence classes of such functions. However each class of equivalence has a unique left semi-continuous representative and therefore an L-fuzzy real number can be identified with this representative.

The set of all L-fuzzy real numbers is called *the L-fuzzy real line* and it is denoted by $\mathbb{R}(L)$. An L-fuzzy number z is called *non-negative* if $z(0) = 1_L$. We denote by $\mathbb{R}_+(L)$ the set of all non-negative L-fuzzy real numbers.

Operations with L-fuzzy real numbers such as addition $\oplus$ and multiplication by a real positive number are defined as following:

$$(z_1 \oplus z_2)(t) = \bigvee_{\tau} \{z_1(\tau) \wedge z_2(t-\tau)\},\ (zr)(t) = z(\frac{t}{r}).$$

The supremum and the infimum of a set of non-negative L-fuzzy numbers $F \subset \mathbb{R}_+(L)$ are defined by the formulas (see e.g. [8], [9]):

$$(Inf\ F)(t) = \bigwedge \{z(t) \mid z \in F\},\ t \in \mathbb{R},$$

$$Sup\ F = Inf\{z \mid z \in \mathbb{R}(L), z \geq z' \text{ for all } z' \in F\}.$$

Taking into account that F is bounded from below it is easy to see that $Inf\ F$ is an L-fuzzy real number. In case F is bounded from above (i.e. there exists $z_0 \in \mathbb{R}(L)$ such that $z \leq z_0$ for all $z \in F$), $Sup\ F$ is an L-fuzzy real number, otherwise the condition

$$\bigwedge_t SupF(t) = 0_L$$

does not necessarily hold.

Going forward we will need also the countable addition of non-negative fuzzy real numbers. Given a sequence of non-negative fuzzy real numbers $(z_n)_{n\in\mathbb{N}} \subset \mathbb{R}_+(L)$ we consider the countable sum

$$\bigoplus_{n=1}^{\infty} z_n = Sup\{z_1 \oplus z_2 \oplus \ldots \oplus z_n \mid n \in \mathbb{N}\}.$$

For $a \in \mathbb{R}_+$ and $\alpha \in L$ by $z(a,\alpha)$ we denote a special type of non-negative L-fuzzy real numbers

$$(z(a,\alpha))(t) = \begin{cases} 1, & t \leq 0, \\ \alpha, & 0 < t \leq a, \\ 0, & t > a, \end{cases}$$

that will play an important role in our work.

III. L-fuzzy valued measure

A. Definition of an L-fuzzy valued measure

We consider a measure that is defined on a T_M-tribe and takes values in $\mathbb{R}_+(L)$.

Definition III.1. *Let Σ be a T_M-tribe. A function $\mu : \Sigma \to \mathbb{R}_+(L)$ is called an L-fuzzy valued measure if it satisfies the following conditions:*

- $\mu(\emptyset) = z(0, 1_L)$;
- μ *is T_M-valuation, i.e. for all* $A, B \in \Sigma$ *it holds*

$$\mu(A \wedge B) \oplus \mu(A \vee B) = \mu(A) \oplus \mu(B);$$

- μ *is left T_M-continuous, i.e.*

$$Sup\{\mu(A_n) | n \in \mathbb{N}\} = \mu(A),$$

where $(A_n)_{n\in N} \subset \Sigma$, $\bigvee_{n\in\mathbb{N}} A_n = A \in \Sigma$.

B. Construction of an L-fuzzy valued measure

For a given σ-algebra of crisp sets $\Phi \subset 2^X$ and a finite measure $\nu : \Phi \to \mathbb{R}_+$ an L-fuzzy valued measure can be obtained by the following schema (see e.g. [4], [5]):

- For $M \in \Phi$, $\alpha \in L$ we define an L-fuzzy set

$$(A(M,\alpha))(x) = \begin{cases} \alpha, x \in M, \\ 0, x \notin M. \end{cases}$$

  All these L-sets form a class of L-sets that we denote by $\wp$.
- Next we define an L-fuzzy valued function $m : \wp \to \mathbb{R}_+(L)$ by

$$m(A(M,\alpha)) = z(\nu(M), \alpha),$$

  and we extend it to the L-fuzzy valued function $m^* : L^X \to \mathbb{R}_+(L)$ as following:

$$m^*(E) = Inf\ \{\bigoplus_{n=1}^{\infty} m(E_n) \mid (E_n)_{n\in\mathbb{N}} \subset \wp : E \leq \bigvee_{n=1}^{\infty} E_n\}.$$

- We denote by Σ the T_M-tribe of all so called m^*-measurable L-sets $E \in L^X$ such that for all $B \in L^X$ it holds

$$m^*(E) \oplus m^*(B) = m^*(E \wedge B) \oplus m^*(E \vee B),$$
$$m^*(E^c) \oplus m^*(B) = m^*(E^c \wedge B) \oplus m^*(E^c \vee B).$$

- Finally, we define μ as the restriction of m^* to Σ we can state that μ is an L-fuzzy valued measure and

$$\mu(E) = m^*(E),\ \text{for all } E \in \Sigma.$$

IV. An L-fuzzy valued integral

A. Definition of an L-fuzzy valued integral

In this section we define an L-fuzzy valued integral

$$\int_E f \, d\mu,$$

where $E \in \Sigma$ and $f : X \to \mathbb{R}$ is a non-negative measurable function with respect to σ-algebra Φ.

By analogy with the classical case ([7]) we define an L-fuzzy valued integral stepwise, first considering the case of simple non-negative measurable functions (for short SNMF):

$$\int_E (\sum_{i=1}^{n} c_i \chi_{C_i}) \, d\mu = \bigoplus_{i=1}^{n} (c_i \, \mu(C_i \wedge E)),$$

whenever

- $c_i \in \mathbb{R}_+, C_i \in \Phi$ for all $i = 1, ..., n$,
- χ_{C_i} is the characteristic function of C_i , $i = 1, ..., n$,
- $C_1, ..., C_n$ are pairwise disjoint sets.

Then considering the case for non-negative measurable function f (for short NMF):

$$\int_E f \, d\mu = Sup\{\int_E g \, d\mu \mid g \leq f \text{ and } g \text{ is SNMF}\}.$$

For $\mathbb{I}_f = \int_E f \, d\mu$ due to properties of the supremum of a set of L-fuzzy numbers, we have

- $\mathbb{I}_f$ is non-increasing,
- $\bigvee_t \mathbb{I}_f(t) = 1_L$,
- $\mathbb{I}_f$ is left semi-continuous, i.e. $\bigwedge_{t<t_0} \mathbb{I}_f(t) = \mathbb{I}_f(t_0)$.

Definition IV.1. *We say that a non-negative measurable function f is L-fuzzy integrable over L-set E iff*

$$\bigwedge_t \mathbb{I}_f(t) = 0_L.$$

Let us note that if f is non-negative integrable over X then it is also L-fuzzy integrable over every $E \in \Sigma$. Going forward we consider only such functions.

B. Properties of L-fuzzy valued integral

For L-fuzzy integrable non-negative functions $f, f_1, f_2, ..., f_n, ...$ and measurable L-sets $E, E_1, E_2, ..., E_n, ... \in \Sigma$ the following properties of L-fuzzy valued integral are true (see e.g. [6]).

($\mathbb{I}$1) $\int_E d\mu = \mu(E)$

($\mathbb{I}$2) $r \in \mathbb{R}_+ \Rightarrow \int_E r f d\mu = r \int_E f d\mu$

($\mathbb{I}$3) $f_1 \leq f_2 \Rightarrow \int_E f_1 d\mu \leq \int_E f_2 d\mu$

($\mathbb{I}$4) $E_1 \leq E_2 \Rightarrow \int_{E_1} f \, d\mu \leq \int_{E_2} f \, d\mu$

($\mathbb{I}$5) $\int_E (f_1 + f_2) d\mu = \int_E f_1 d\mu \oplus \int_E f_2 d\mu$

($\mathbb{I}$6) $E_1 \wedge E_2 = \emptyset \Rightarrow \int_{E_1 \vee E_2} f d\mu = \int_{E_1} f d\mu \oplus \int_{E_2} f d\mu$

($\mathbb{I}$7) $(E_n)_{n\in\mathbb{N}} : E_n \leq E_{n+1}$ and $\bigvee_{n\in\mathbb{N}} E_n = E \Rightarrow$
$\int_E f d\mu = Sup\{\int_{E_n} f d\mu \mid n \in \mathbb{N}\}$

($\mathbb{I}$8) $(f_n)_{n\in\mathbb{N}} : f_n \leq f_{n+1}$ and $\lim_{n\to\infty} f_n = f \Rightarrow$
$\int_E f \, d\mu = Sup\{\int_E f_n \, d\mu \mid n \in \mathbb{N}\}$

V. Two approaches to define L-fuzzy valued measure based on a function

A. The first approach

From the classical measure theory (see e.g [7]) it is known that having a measure ν and non-negative measurable function f we can get a new measure ν_f defined as following

$$\nu_f(M) = \int_M f \, d\nu.$$

By using the same logic in the fuzzy case we want to make sure that this statement will be preserved.
We define

$$\mu_f(E) = \int_E f \, d\mu,$$

where $\mu_f : \Sigma \to \mathbb{R}_+(L)$ and f is a real valued non-negative L-fuzzy integrable function.

Theorem V.1. *μ_f is an L-fuzzy valued measure.*

Proof: Due to integral property μ_f is left T_M-continuous. We need to prove that μ_f is T_M-valuation, i.e.

$\mu_f(E_1 \vee E_2) \oplus \mu_f(E_1 \wedge E_2) = \mu_f(E_1) \oplus \mu_f(E_1)$ for all $E_1, E_2 \in \Sigma$.

Considering $M_1 = \{x \in X \mid E_1(x) \geq E_2(x)\}$ and $M_1 = \{x \in X \mid E_1(x) < E_2(x)\}$ we can split L-sets E_1, E_2 into two T_M-disjoint L-sets as following:

$$E_1 = (E_1 \wedge M_1) \vee (E_1 \wedge M_2) \text{ and } E_2 = (E_2 \wedge M_1) \vee (E_2 \wedge M_2).$$

Obviously,

$$E_1 \vee E_2 = (E_1 \wedge M_1) \vee (E_2 \wedge M_2)$$

and

$$E_1 \wedge E_2 = (E_1 \wedge M_2) \vee (E_2 \wedge M_1).$$

Hence,

$$\int_{E_1} f \, d\mu \oplus \int_{E_2} f \, d\mu = \int_{(E_1\wedge M_1)\vee(E_1\wedge M_2)} f \, d\mu \oplus \int_{(E_2\wedge M_1)\vee(E_2\wedge M_2)} f \, d\mu =$$

$$= \int_{E_1\wedge M_1} f \, d\mu \oplus \int_{E_1\wedge M_2} f \, d\mu \oplus \int_{E_2\wedge M_1} f \, d\mu \oplus \int_{E_2\wedge M_2} f \, d\mu =$$

$$= \int_{E_1\vee E_2} f \, d\mu \oplus \int_{E_1\wedge E_2} f \, d\mu.$$

■

As we can see L-fuzzy valued measure μ_f was obtained by the following scheme:

- first extending crisp measure ν with construction described in section III-B;
- second defining a measure by using an integral with respect to L-fuzzy valued T_M-measure μ .

B. The second approach

Now if we change the order in scheme described above we get L-fuzzy valued measure $\tilde{\mu}_f$.

For a given σ-algebra $\Phi \subset 2^X$ and a finite measure $\nu : \Phi \to \mathbb{R}_+$ we define measure ν_f as following:

$$\nu_f(M) = \int_M f \, d\nu.$$

An L-fuzzy valued measure $\tilde{\mu}_f$ can be obtained by using the same scheme as in section III-B :

- We define an L-fuzzy valued function $m_f : \wp \to \mathbb{R}_+(L)$ by
$$m_f(A(M,\alpha)) = z(\nu_f(M),\alpha),$$
and we extend it to the L-fuzzy valued function $m_f^* : L^X \to \mathbb{R}_+(L)$ as following:
$$m_f^*(E) = Inf\ \{\bigoplus_{n=1}^{\infty} m_f(E_n) \mid (E_n)_{n\in\mathbb{N}} \subset \wp : E \le \bigvee_{n=1}^{\infty} E_n\}.$$
- We denote by Σ_f the class of all so called m_f^*-measurable L-sets $E \in L^X$ such that for all $B \in L^X$ it holds
$$m_f^*(B) \oplus m_f^*(E) = m_f^*(B \wedge E) \oplus m_f^*(B \vee E),$$
$$m_f^*(E^c) \oplus m_f^*(B) = m_f^*(E^c \wedge B) \oplus m_f^*(E^c \vee B).$$
- Finally, considering $\tilde{\mu}_f$ as restriction of m_f^* to Σ_f we obtain the L-fuzzy valued measure: $\tilde{\mu}_f = m_f^*(E)$.

VI. The equivalence of two definitions of an L-fuzzy valued integral

In this section we show that two approaches to define an L-fuzzy valued integral described in the previous section give us the equivalent result.

Theorem VI.1. *For all integrable non-negative functions f it holds:*

(T1) $\Sigma \subset \Sigma_f$,

(T2) *for all $E \in \Sigma$ we have $\mu_f = \tilde{\mu}_f$.*

To prove the Theorem VI.1 we use the following Lemma.

Lemma VI.2. *For all $E \in L^X$ it holds:*

(L1) *if f is SNMF (i.e. $f = \sum_{i=1}^{n} c_i \chi_{C_i}$), then*
$$m_f^*(E) = \bigoplus_{i=1}^{n} c_i \ m^*(E \wedge C_i);$$

(L2) *if $(f_n)_{n\in\mathbb{N}}$ is a sequence of SNMF such that $f_n \le f_{n+1}$ and $\lim_{n\to\infty} f_n = f$, then*
$$m_f^*(E) = Sup\{m_{f_n}^*(E) | n \in \mathbb{N}\}.$$

Proof: (L1) First we show that equality holds for L-set $E = A(M,\alpha) \in \wp$. Taking into account the properties of L-fuzzy real numbers we get:

$$m_f(A(M,\alpha)) = z(\nu_f(M),\alpha) = z(\int_M f \, d\nu, \alpha) =$$

$$= z(\int_M \sum_{i=1}^{n} c_i \ \chi_{C_i} \, d\nu, \alpha) = z(\sum_{i=1}^{n} c_i \ \nu(M \wedge C_i), \alpha) =$$

$$= \bigoplus_{i=1}^{n} c_i \ z(\nu(M \wedge C_i), \alpha) = \bigoplus_{i=1}^{n} c_i \ m(A(M,\alpha) \wedge C_i).$$

Now for the sequence of L-sets $(E_k)_{k\in\mathbb{N}} \subset \wp : E \le \bigvee_{k=1}^{\infty} E_k$ we obtain:

$$\bigoplus_{k=1}^{\infty} m_f(E_k) = \bigoplus_{k=1}^{\infty} \bigoplus_{i=1}^{n} c_i \ m(E_k \wedge C_i) = \bigoplus_{i=1}^{n} c_i \ \bigoplus_{k=1}^{\infty} m(E_k \wedge C_i).$$

Finally, recalling the definition of m_f^*:

$$m_f^* = Inf\ \{\bigoplus_{k=1}^{\infty} m_f(E_k) \mid (E_k)_{k\in\mathbb{N}} \subset \wp : E \le \bigvee_{k=1}^{\infty} E_k\} =$$

$$= \bigoplus_{i=1}^{n} c_i \ Inf\ \{\bigoplus_{k=1}^{\infty} \bigoplus_{k=1}^{\infty} m(E_k \wedge C_i) \mid (E_k)_{k\in\mathbb{N}} \subset \wp : E \le \bigvee_{k=1}^{\infty} E_k\} =$$

$$= \bigoplus_{i=1}^{n} c_i \ m^*(E \wedge C_i).$$

(L2) We start with an L-set $E = A(M,\alpha) \in \wp$. Using the properties of L-fuzzy real numbers we get:

$$Sup\{m_{f_n}(A(M,\alpha)) | n \in \mathbb{N}\} = Sup\{z(\nu_{f_n}(M),\alpha) | n \in \mathbb{N}\} =$$

$$= z(\sup_n(\nu_{f_n}(M)),\alpha) = z(\nu_f(M),\alpha) = m_f(A(M,\alpha)).$$

Now taking any $E \in L^X$ and the fact that L if completely distributive lattice we obtain:

$$Sup\ \{m_{f_n}^*(E) | n \in \mathbb{N}\} =$$

$$= Sup\{\ Inf\ \{\bigoplus_{k=1}^{\infty} m_{f_n}(E_k) \mid (E_k)_{k\in\mathbb{N}} \subset \wp : E \le \bigvee_{k=1}^{\infty} E_k\} | n \in \mathbb{N}\} =$$

$$= Inf\{\ Sup\ \{\bigoplus_{k=1}^{\infty} m_{f_n}(E_k) | n \in \mathbb{N}\} | (E_k)_{k\in\mathbb{N}} \subset \wp : E \le \bigvee_{k=1}^{\infty} E_k\} =$$

$$= Inf\{\bigoplus_{k=1}^{\infty} m_f(E_k) | (E_k)_{k\in\mathbb{N}} \subset \wp : E \le \bigvee_{k=1}^{\infty} E_k\} = m_f^*(E).$$

■

Coming back to theorem VI.1.

Proof: (T1) We consider $E \in \Sigma$ and start with the case when f - SNMF or $f = \sum_{i=1}^{n} c_i \chi_{C_i}$. For every $i \in \{1,...,n\}$ if $E \in \Sigma$ then $E \wedge C_i \in \Sigma$ and following for all $B \in L^X$ we have

$$m^*(E \wedge C_i) \oplus m^*(B \wedge C_i) =$$

$$= m^*(E \wedge B \wedge C_i) \oplus m^*((E \wedge C_i) \vee (B \wedge C_i)).$$

Now multiplying equality by c_i and summing up by i we obtain.

$$\sum_{i=1}^{\infty} c_i \ m^*(E \wedge C_i) \oplus \sum_{i=1}^{\infty} c_i \ \wedge m^*(B \wedge C_i) =$$

$$= \sum_{i=1}^{\infty} c_i \; m^*(E \wedge B \wedge C_i) \oplus \sum_{i=1}^{\infty} c_i \; m^*((E \wedge C_i) \vee (B \wedge C_i)).$$

And finally applying Lemma VI.2:

$$m_f^*(E) \oplus m_f^*(B) = m_f^*(E \wedge B) \oplus m_f^*(E \vee B).$$

By analogy we can prove the second equality

$$m_f^*(E^c) \oplus m_f^*(B) = m_f^*(E^c \wedge B) \oplus m_f^*(E^c \vee B).$$

In the case when f is NMF there exists a sequence of SNMF $(f_n)_{n\in\mathbb{N}}$ such that $f_n \leq f_{n+1}$ and $\lim_{n\to\infty} f_n = f$. For all f_n it holds

$$m_{f_n}^*(E) \oplus m_{f_n}^*(B) = m_{f_n}^*(E \wedge B) \oplus m_{f_n}^*(E \vee B).$$

Now taking *Sup* we obtain

$$Sup\{m_{f_n}^*(E) | n \in \mathbb{N}\} \oplus Sup\{m_{f_n}^*(B) | n \in \mathbb{N}\} =$$

$$= Sup\{m_{f_n}^*(E \wedge B) | n \in \mathbb{N}\} \oplus Sup\{m_{f_n}^*(E \vee B) | n \in \mathbb{N}\}.$$

And due to Lemma VI.2

$$m^*(E) \oplus m^*(B) = m^*(E \wedge B) \oplus m^*(E \vee B).$$

The same logic can be used to prove the second equality.

(T2) We start again with SNMF f. Using Lemma VI.2 we see that

$$\mu_f(E) = \int_E f \; d\mu = \bigoplus_{i=1}^{n} c_i \; \mu(E \wedge C_i) =$$

$$= \bigoplus_{i=1}^{n} c_i \; m^*(E \wedge C_i) = m_f^*(E) = \tilde{\mu}_f(E).$$

In the case when f is NMF we use a sequence $(f_n)_{n\in\mathbb{N}}$ such that $f_n \leq f_{n+1}$ and $\lim_{n\to\infty} f_n = f$. By using Lemma VI.2 and the fact that for the simple functions $\mu_{f_n} = \tilde{\mu}_{f_n}$ we get:

$$\mu_f(E) = \int_E f \; d\mu = Sup\{\int_E f_n \; d\mu \; | n \in \mathbb{N}\} = Sup\{\mu_{f_n}(E) \; | n \in \mathbb{N}\} =$$

$$= Sup\{\tilde{\mu}_{f_n}(E) \; | n \in \mathbb{N}\} = m_f^*(E) = \tilde{\mu}_f(E).$$

■

This result gives us an opportunity to define an L-fuzzy valued integral by applying the following formula:

$$\int_E f \; d\mu = \tilde{\mu}_f(E).$$

Summarizing, we want to mention that both ways of defining the L-fuzzy valued integral have their own motivation. The first approach (see V-A) has a theoretical foundation, while the second approach (see V-B) gives us an opportunity to simplify calculations of the L-fuzzy valued integral.

ACKNOWLEDGMENT

The paper was supported by ESF projects 2009/0138/1DP/1.1.2.1.2/09/IPIA/VIAA/004 and 2009/0223/1DP/1.1.1.2.0/09/APIA/VIAA/008.

REFERENCES

[1] E. Pap, Handbook of Measure Theory, Elsevier, Amsterdam, 2002.
[2] R. Mesiar, "Fuzzy measures and integrals", Fuzzy Sets and Systems, vol. 156, 2005, pp. 365–370.
[3] Z. Wang, G. J. Klir, Fuzzy measure theory, Plenum Press, New York, 1992.
[4] V. Ruzha, S. Asmuss, "A construction of a fuzzy valued measure based on minimum t-norm", In: New Dimensions in Fuzzy Logic and Related Technologies, Proceedings of the 5^{th} EUSFLAT Conference (EUSFLAT 2007), pp. 175–178, Ostrava (Czech Republic), 2007.
[5] V. Ruzha, S. Asmuss, "A construction of an L-fuzzy valued measure of L-fuzzy sets", Proceedings of the IFSA-EUSFLAT 2009 Conference (IFSA-EUSFLAT 2009), pp. 1735–1739, Lisbon (Portugal), 2009.
[6] V. Ruza, "On an L-fuzzy valued integral with respect to an L-fuzzy valued measure", Proceedings of the 10^{th} APLIMAT Conference (APLIMAT 2011), pp. 605–614, Bratislava (Slovakia), 2011.
[7] P. Halmos, Measure theory, IL, Moscow, 1953.
[8] S. Asmuss, A. Šostak, "Extremal problems of approximation theory in fuzzy context", Fuzzy Sets and Systems, vol. 105, 1999, pp. 249–257.
[9] S. Asmuss, A. Šostak, "On central algorithms of approximation under fuzzy information", Fuzzy Sets and Systems, vol. 155, 2005, pp. 150–163.
[10] B. Hutton, "Normality in fuzzy topological spaces", J.Math.Anal.Appl., vol. 50, 1975, pp. 74–79.
[11] R. Lowen, "On $(R(L), \oplus)$", Fuzzy Sets and Systems, vol. 10, 1983, pp. 203–209.
[12] S. E. Rodabaugh, "Fuzzy addition and the L-fuzzy real line", Fuzzy Sets and Systems, vol. 8, 1982, pp. 39–52.

2011 IEEE International Conference on Fuzzy Systems
June 27-30, 2011, Taipei, Taiwan

Evolving Fuzzy Image Segmentation

Ahmed A. Othman
Systems Design Engineering Department
University of Waterloo
Waterloo, Ontario, Canada
a4abdelr@uwaterloo.ca

Hamid R. Tizhoosh
Systems Design Engineering Department
University of Waterloo
Waterloo, Ontario, Canada
Tizhoosh@uwaterloo.ca

***Abstract*—Image segmentation is the process of assigning a label to every pixel in an image such that pixels with the same label are connected and meaningful, and share certain visual characteristics. Pixels in a region are similar with respect to some features or property, such as color, intensity, or texture. Adjacent regions may be significantly different with respect to the same characteristics. Therefore, it is difficult for a static (non-learning) segmentation technique to accurately segment different images with different characteristics. In this paper, an evolving fuzzy system is used to segment medical images. The system uses some training images to build an initial fuzzy system which then evolves online as new images are encountered. Each new image is segmented using the evolved fuzzy system and may contribute to updating the system. This process provides better segmentation results for new images compared to static paradigms. The average of segmentation accuracy for test images is calculated by comparing every segmented image with its gold standard image prepared manually by an expert.**

Keywords– Image segmentation, Evolving fuzzy systems, SIFT.

I. Introduction

Evolving fuzzy systems are a recent approach used in many applications to solve diverse problems through evolution of fuzzy rules. Evolving fuzzy systems, however, have not been used for image segmentation. Their dynamic capability could improve the segmentation accuracy of different images especially for real-world applications. In this paper, we propose a method that uses evolving fuzzy systems to segment digital images. The motivation for using evolving fuzzy systems is the higher degree of adaptability to the complex and dynamic nature of the segmentation problem. The experiments are performed on breast ultrasound images.

This paper is organized as follows: In section II, SIFT will be briefly described. In section III, the literature on fuzzy image segmentation techniques is briefly reviewed. In section IV, a review of the evolving fuzzy image segmentation is provided. Section V, the proposed evolving fuzzy image segmentation is described. In section VI, the results of applying the proposed system to a set of image data is presented and analysed. Section VII summarizes the paper.

II. Scale invariant feature transform (SIFT)

SIFT is an approach developed by Lowe [1] as a method for object recognition. It depends on detecting a set of key points in an object and calculates a set of descriptors (features) for these points. These features can be used to recognize one object from among different objects. The process of detecting key points and calculating descriptors consist of four stages:

1) Scale-space extrema detection: it uses a difference-of-Gaussian function in different scales and locations to calculate the potential of interest points that are invariant to scale and orientation.
2) Key point localization: for each candidate point, a measure of their stability is performed to discard points with low contrast or poorly located along the edges.
3) Orientation assignment: local image gradient directions are used to assign one or more orientations to each key point location, to make sure that the candidate points are invariant to orientation.
4) Key point descriptor: after selecting the candidate points, the local image gradients are measured in the region around each key point.

We use SIFT method to locate the key points inside the image that seems to be the most descriptive points. The features are extracted from a rectangle around each point.

III. Fuzzy image segmentation

Fuzzy approaches are relatively popular methods for image segmentation. Here we provide a brief review of fuzzy segmentation techniques that may be related to our work.

Fuzzy image segmentation has been used for processing color images. In an approach [2], the segment (separated by edges) within the image is treated as a fuzzy set and can grow using fuzzy criteria. Moreover, the edge detection and region growing algorithms are combined to find larger segments. In a different approach [3], fuzzy c-mean (FCM) and principle component analysis are combined to segment color images using eigen-based membership fuzzy function.

Karmakar et al. [4] propose a generic fuzzy rule-based segmentation technique that tries to solve the problem of manual selection of the parameters of the fuzzy membership in previous fuzzy segmentation techniques. This proposed technique is unlike the previous fuzzy segmentation as it is application-independent and incorporates spatial relationships between pixels.

Tao et al. [5] present a new algorithm for image segmentation by a three-level thresholding technique based on maximum fuzzy entropy and genetic algorithms. They divide the image into three parts and determine the width and attribute of the fuzzy region by maximizing fuzzy entropy. They use a genetic algorithm to find the optimal combination of all parameters.

978-1-4244-7316-8/11/$26.00 ©2011 IEEE

Cinque et al. [6] suggest a modification to the existing fuzzy approach for image segmentation adaptive reasoning theory (ART) model. They state that their proposed approach solves the problems of the existing ART model such as overfiting, complexity and inability to measure the extent of match between any two patterns.

Zhang et al. [7] suggest a new algorithm that uses a kernel-induced distance metric instead of the original Euclidean distance in the FCM and adding a spatial penalty on the membership functions to modify the objective function in the fuzzy C-means (FCM). They use their approach for segmentation of magnetic resonance imaging (MRI) data.

Cai et al. [8] propose a new fuzzy c-means clustering algorithm that combines spatial and gray-level information of the image for image segmentation. They called their algorithm fast generalized fuzzy c-means (FGFCM).

Fuzzy clustering is used for segmenting noisy images. That could be done by combining the spatial information which is the summation of the membership functions in the neighbourhood of each pixel under consideration of the image into the membership function for clustering [9]. In a different method, Fuzzy Tree Algorithm is used to represent the data (spatial) and the path compression which helps in reducing the CPU time [10]. In another approach, a modification of the existing fuzzy c-means is used to segment noisy images [11].

Zhuge et al. [12] present a fuzzy connected-based image segmentation to segment vectorial images. Their technique extends the previous work on scalar images to vectorial images. They apply their method on arbitrary dimensional vectorial medical MR images.

Dou et al. [13] propose a fuzzy fusion technique to segment brain tumours in MR images automatically. They suggest to build a separate fuzzy model for each type of MRI image that they may have some prior information about. The different fuzzy models are then fused into one model.

Ma et al. [14] present a modification to the fuzzy C-means image segmentation algorithm to be used with uneven illumination patterns. They insert biased illumination field estimation to the existing recursive FCM algorithm. Moreover, they used the intensity and average intensity of a pixel neighbourhood to define new clustering centre and fuzzy clustering functions and to dilate the initial segment to improve the segmentation process.

Han et al. [15] propose an improvement of the Ant Colony Algorithm (ACA) previously used in image segmentation but with high complexity. They suggest to improve the algorithm to reduce the computation time in image segmentation with a modified fuzzy clustering method.

Hata et al. [16] propose a fuzzy technique for the segmentation of the endorrhachis in magnetic resonance images. This algorithm checks the possibility of the endorrhachis regions in the image and gives the higher possibility a high fuzzy degree. Moreover, they describe a fuzzy maximum intensity projection (FMIP) technique that maps the higher fuzzy membership degrees to brighter values in the data set.

Fan et al. [17] propose a new remote sensing image segmentation approach that solves the problems of the clustering quality caused by the position of the initialization of the cluster centroids in the existing fuzzy C-means algorithm. They suggest to use a single point iterative procedure in the fuzzy C-means clustering to segment remote sensing images.

Foo et al. [18] propose a fuzzy rule-based image segmentation method to mark tumours in a three-dimensional CT data using initial selection of a region of interest (ROI) by the user.

Di Martino et al. [19] use fuzzy transform technique to compress images and then use the Fast Generalized Fuzzy C-Means clustering algorithm to segment the compressed images.

All previous fuzzy segmentation techniques used fuzzy rules and fuzzy clusters, or combined fuzzy rules with other techniques such as principle component analysis approach (PCA) to segment images. There is still need for a fuzzy method that can update the fuzzy rules during the segmentation process. Such dynamic approaches may help in improving the segmentation accuracy and reduce the time required for updating the rules manually.

IV. Evolving Fuzzy Systems

Evolving fuzzy systems are a rather recent development used for many applications. Fuzzy rules could evolve using different methods either by combining with neural networks or genetic algorithms or other techniques that update the fuzzy rules online. Evolving fuzzy rules have not been used for medical image segmentation. We provide here a review of evolving fuzzy systems and their applications.

Kasabov [20] proposed evolving fuzzy neural networks that can learn and perform reasoning, rule extraction and aggregation online. This network is applied to a bench-mark problem. The evolving fuzzy neural network system uses locally tuned elements to perform the process of incremental online learning. When there are more data, the network should be updated by pruning of the nodes, or aggregation of nodes. The network consists of five layers with nodes that are created and connected when data becomes available. The authors compare their algorithm with the fuzzy neural networks and the knowledge-based neural networks.

Futschik et al. [21] use evolving fuzzy neural networks to overcome the problem of transparency in the classification process of the existing statistical and machine learning methods. They used the evolving fuzzy neural networks to classify cancer tissue. They extract fuzzy rules associated with genes that are evidence of specific types of cancer.

Rivas et al. [22] propose a method to design fuzzy membership functions and fuzzy rules using evolutionary computation. They state that their design is simultaneous and its elements are mutually dependent. They also develop an algorithm that is applied directly to the data structure of the fuzzy logic system instead of a binary representation.

Angelov [23] proposed a fuzzy controller of Takagi-Sugeno type with evolving structure. He proposed a new technique for online identification of Takagi-Sugeno systems. He uses the data collected during the process of control to build up the Fuzzy rules of the structure of the controller. The fuzzy

controller is trained using the data collected during the process of control in a non-iterative, recursive way. He provides an example from air-conditioning systems to explain his method.

Chang et al. [24] propose a new hybrid model to forecast the future sales of a printed circuit board factory. They use Self Organization Maps (SOM) along with a Genetic Algorithm (GA) and Fuzzy Rule-Based system to build their hybrid model. They reduced the interaction between fuzzy rules by clustering the fuzzy rules into different clusters. They optimize the number of fuzzy terms of the input and output which turns the fuzzy rules into evolving fuzzy rules. Chang et al. [25] propose an approach that uses a weighted evolving fuzzy neural network system to forecast the future sales of printed circuit board.

Rong et al. [26] use the functional equivalence between a radial basis function network and a fuzzy inference system to develop a sequential adaptive fuzzy inference system. The proposed algorithm is an adaptive technique that depends on the input data to decide whether to add or remove a fuzzy rule from/to the fuzzy rule base.

Xydeas et al.[27] propose two new models to solve the problem of the classification of the brain signals (electroencephalogram (EEG)). They use dependant hidden Markov models to represent the inputs in their first method. In the second method, they use a recursive, online, and evolvable fuzzy rule base to classify the EEG signals.

Lin et al. [28] propose a self-adaptive neural fuzzy network with group-based symbiotic evolution to be used in prediction applications. Their approach contains a self-clustering algorithm (SCA) that addresses the internal structure in which the number of clusters (fuzzy rules) is equal to the true number of clusters in a given training data set. They use a group-based symbiotic evolution learning method that is used to get the desired output by adjusting the parameters.

Barros et al. [29] propose a model that makes an online identification of computationally undemanding evolving fuzzy models. They propose an approach that models non-linear dynamic systems using an online evolving fuzzy model. The rule base is built via incremental learning when accepting new input by adding new rule or deleting, updating existing rule base.

Linden et al. [30] use evolving fuzzy rules and genetic algorithm (in which the rules are represented as an expression in reverse Polish notation) to extract rules from micro array data. They apply their algorithm to problems arising in the construction of gene regulatory networks.

Angelov et al. [31] proposed an evolving fuzzy classifier using different model architectures. They suggest two different approaches for online evolving fuzzy classifiers that could work with different model architectures. Moreover, their first approach can have a multi-input-multi-output architecture. They apply their approach on handwriting recognition and, real-life problem of image classification.

Phan et al. [32] propose a direct self-structuring adaptive fuzzy control approach for affine nonlinear single-input-single output systems. This approach is a self-structuring approach that adds new membership functions and rules to adjust the system and reduce the number of rules by replacing the old membership functions by new ones.

Du et al. [33] study the application of evolving Takagi-Sugeno fuzzy model to non-linear system identification. The authors use genetic algorithm to propose a new encoding approach for learning the Takagi-Sugeno model. They suggest to represent the rules and the inputs and membership functions of the fuzzy system in one chromosome to be evolved.

Lai et al. [34] propose an evolving fuzzy decision tree for financial time series data forecasting for stocks in Taiwan Stock Exchange Corporation. They build a decision-making system by combining a clustering technique, a fuzzy decision tree, and genetic algorithms.

Lughofer [35] study the application on surface inspection using two different on-line evolving image classifiers. The first one is a supervised classification approach that uses conventional vector quantization and forming an incremental evolving variant around it.

Juang et al. [36] provide a dynamic system processing using recurrent self-evolving fuzzy neural network with local feedbacks. Their approach is an online approach that uses a learning process of the structures (generating the fuzzy rules online) and the parameters. A Kalman filter is used to learn the consequent parameters. As well, a gradient descent algorithm is used to learn the antecedent parameters.

V. Evolving Fuzzy Image Segmentation

The idea of evolving fuzzy image segmentation is straightforward: generate a rule-base for segmentation and then let the rules evolve to reach or maintain a high accuracy level.

We start with a set of training images randomly selected from the available set of test images along with their gold standard image. The algorithm should start with **extracting features**. For this purpose we use a set of points detected by the SIFT within a rectangle around the region of interest in these training images. We focus on the simplest form of segmentation, namely thresholding. A set of initial fuzzy rules can be built using the features of the training images as antecedent and their optimal threshold values as consequent. The remaining images in our test set are segmented using the initial fuzzy rules. Based on the quality of the result for any new image, the initial fuzzy rules are evolved. This process is repeated multiple times as long as new images coming, rules are updated. This should increase the segmentation accuracy of the coming new images. The results of segmentation of new images are recorded by calculating the average accuracies by comparing it with its gold standard image prepared manually by an expert.

A. Detection Algorithm

Since features would make more sense if they are calculated for the "region of interest", all images are first processed by a detection algorithm which finds the position of the first seed point inside the region of interest and create a rectangle R around this point. The algorithm performed as follow:

- The seed point P is calculated by tracing a 10×10 mask over the image I and calculating the sum and the standard deviation of every mask and the correlation between the mask and its neighbour. Based on empirical knowledge about our test images, the region of interest has low gray-level intensities and generally a low standard deviation. The mask that has minimum sum and minimum standard deviation is considered the mask contains the seed point. The correlation coefficients between the mask and its preceding mask are used to select the mask containing the seed point if the minimum sum and minimum standard deviation are in two different masks. Hence, for every 10×10 part of the image the minimum sum, standard deviation and correlation are considered to mark the position of a seed point inside the region of interest.
- The algorithm proceeds by constructing a rectangle around the region of interest using the point P as the center of the rectangle. Based on the empirical knowledge, the algorithm starts by finding a region around P as a $n \times n$ window (e.g. 100×100) and incrementally enlarges the window (e.g. with 10×10). This process stops when the standard deviation of one window becomes greater than or less than the standard deviation of the previous region by a certain limit ϵ (e.g. 3%); the last window is considered the region of interest R. These images are stored to be used for extracting feature in the training and testing phases. In most images, the detection algorithm detects a correct point inside the region of interest. For other images, it failed to detect a correct point but we proceed with the rectangle generated by the algorithm.

B. Training Phase

In this phase, we start with the process of feature extraction then the initial fuzzy system will be built (Fig. 1).

1) Feature Extraction: The proposed technique starts with extracting a set of features from training images and uses these features to assign best thresholds to different images using a fuzzy system consisting of fuzzy rules. The process of extracting features is performed as follow:

- The algorithm randomly selects 5 of 20 medical images (breast ultrasound scans) as a training set and the remaining 15 images are used for testing.
- For each training image, the rectangle R around the region of interest created by the detection algorithm is used.
- The rectangle around the region of interest R is provided to the SIFT algorithm which then returns a set of key points $p_1, p_2, \cdots, p_n$ within the rectangle R.
- For each key point assigned by SIFT a 40×40 rectangle is constructed around the point and a set of features are extracted.
- For each image, the optimal threshold is calculated in order to be used for rule generation.

We use simple features that can be calculated fast:

- The mean gray-level μ_S for each 40×40 rectangle S around each key point generated by SIFT: The average gray-level of a sub-image is an indication of its darkness/brightness.
- The standard deviation σ_S for each 40×40 rectangle S around each key point generated by SIFT: The intensity variation captured by the standard deviation quantifies our confidence in darkness/brightness of the sub-image.
- The distance $d_S = \max S - \min S$ between the maximum and the minimum of each 40×40 rectangle S around each key point generated by SIFT: This distance provides additional information to distinguish between different variation levels captured by standard deviation.

Using the SIFT guarantees that the features are extracted in regions with invariant significant characteristics.

2) Building the Initial Fuzzy System: The initial fuzzy system is built from a set of images randomly selected from the set of available images. The input to the fuzzy system consists of the three features calculated around each key point generated by SIFT:

- The mean gray-level μ_S
- The standard deviation σ_S
- The distance $d_S = \max S - \min S$ between the maximum and the minimum of each 40×40 rectangle S .

For each training image, SIFT assign n points inside the region of interest. The features are extracted and calculated from every training image from the rectangles around the n points assigned by SIFT. All features are recorded in a matrix called *Input* matrix. The Input matrix consists of three columns describing the three features and number of rows is equal the number of SIFT points in each image multiplied by the number of training images. In our case, we use five images for training, and the SIFT technique detects ten key points in every image. So the Input matrix has $5 \times 10 = 50$ rows.

The Output (optimal threshold) is a matrix consisting of the optimal thresholds for every training image.

We used the Matlab function "genfis" to generate the rules from the data. The *genfis* function takes two parameters, namely the Input and the Output matrix. A general example for the rules generated is as follows:
IF (μ IS μ_1) AND (σ IS σ_1) AND (d IS d_1)
THEN (Threshold IS th1)

C. Testing phase

After building the initial fuzzy system using randomly selected images, the remaining set of test images can be segmented using the evolving fuzzy system (Fig. 1) which can be described as follows:

1) For each image, the rectangle R around the region of interest created by the detection algorithm is used.
2) The rectangle R is fed into SIFT which returns a set N of key points inside R.
3) The set of features are now calculated from a 40×40 rectangle around each point in N.
4) For every coming new image,
   - The extracted features from every point are used to run the initial fuzzy system which assigns the image a threshold for each point in N.

- The extracted features are stored to be added to the Input matrix later.
- The threshold T^* for segmenting the image is calculate by taking the average of all thresholds for each point $n_i \in N_1$: $T^* = \frac{1}{|N_1|}\sum_{i=1}^{|N_1|} T_i$
- For each Image, the assigned threshold is used to segment the image I.
- The thresholded image is preseneted to an expert to judge its quality. The expert's evaluation may be:
  a) The threshold is too high (threshold adjustment set to $\Delta = -25$), *OR*
  b) The threshold is high (threshold adjustment set to $\Delta = -15$), *OR*
  c) The threshold is low (threshold adjustment set to $\Delta = +15$), *OR*
  d) The threshold is too low (threshold adjustment set to $\Delta = +25$).
- The adjusted threshods along the newly extracted features are inserted to the Output and Input matrices, respectively.
- The new Input and Output matrices are used in the Matlab function "genfis" to evolve the initial fuzzy rules.
- The next new image is segmented using the newly generated rules and the process repeated.

5) After finishing all test images, the average of segmentation accuracy and other statistics are now calculated.

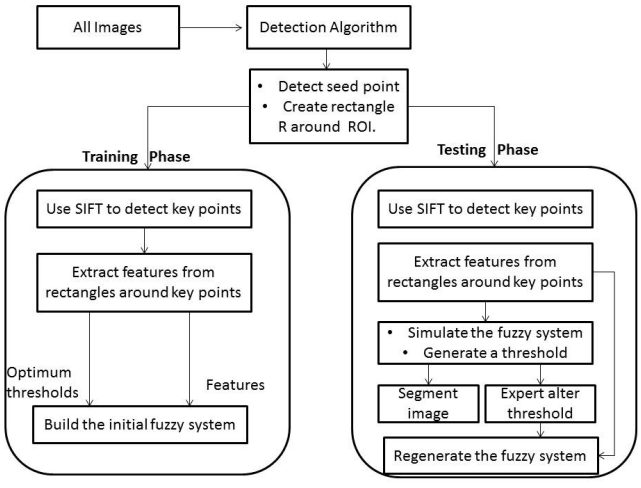

Fig. 1. The evolving fuzzy segmentation

VI. Experiment and Results

The proposed approach randomly selects 5 of 20 medical images as a training set and the remaining 15 images are used for testing. All results of 10 different training sets are calculated and recorded in the Table I.

The following metrics have been employed to verify the performance of the proposed approach (A and B are two segments, one of them being the gold standard):

1) The Dice coefficient D of segmentation accuracy,
$$D(A,B) = \frac{2 * |A \cap B|}{|A| + |B|} \quad (1)$$
2) The standard deviation σ_D of the Dice coefficient.
3) The average of segmentation accuracy J is calculated using the area overlap (also called Jaccard Index)
$$J(A,B) = \frac{|A \cap B|}{|A \cup B|} \quad (2)$$
4) The standard deviation σ_J of the Jaccard index.
5) The confidence interval (CI) of Jaccard index CI_J.
6) The null hypothesis (T-test) between the fuzzy results and the evolving fuzzy results helps to ensure that they are really different.

Sample results of the proposed algorithm are shown in Figure 2. In all images, there is a high improvement in the segmentation accuracy when applying the evolving fuzzy proposed algorithm compared with the ordinary fuzzy rule-based segmentation.

Generally, it is obvious from the Table I that the proposed algorithm performs segmentation more accurately than the conventional fuzzy algorithm. The proposed algorithm has the highest segmentation accuracy and the lowest standard deviation in all training sets. For example, in the fourth training set, the segmentation accuracy increases from 64% in the fuzzy segmentation to 74% in the proposed evolving fuzzy segmentation, and the standard deviation decreased from 25% to 18%. On the other hand, the dice value increased from 75% to 84% and its standard deviation decreased from 22% to 14%. Moreover, the 95% confidence interval of the Jaccard index increased from 50%-78% to 64% - 84%. As well, the 95% confidence interval of the dice value increased from 63%-88% to 76% - 92% which means that the proposed system is more consistent. The validation of the null hypothesis indicates that in the half of the training sets the segmentation accuracy improved.

VII. Conclusions

An evolving fuzzy system was used to segment images by updating the fuzzy rules. Initial fuzzy rules were generated and then updated online. Initial fuzzy rules were created from a number of images randomly selected from the available image set of medical images. The remaining set of images was segmented using the initial fuzzy rules. New images were segmented using the evolving fuzzy rule base. Based on expert's evaluation, the new rules were calculated for every new image and used to evolve the existing fuzzy rules to segment the following images more accurately. Results show clear improvements in segmentation accuracy.

References

[1] D. Lowe, "Distinctive image features from scale-invariant keypoints," *International journal of computer vision*, vol. 60, no. 2, pp. 91–110, 2004.
[2] A. Moghaddamzadeh and N. Bourbakis, "A fuzzy region growing approach for segmentation of color images," *Pattern recognition*, vol. 30, no. 6, pp. 867–881, 1997.

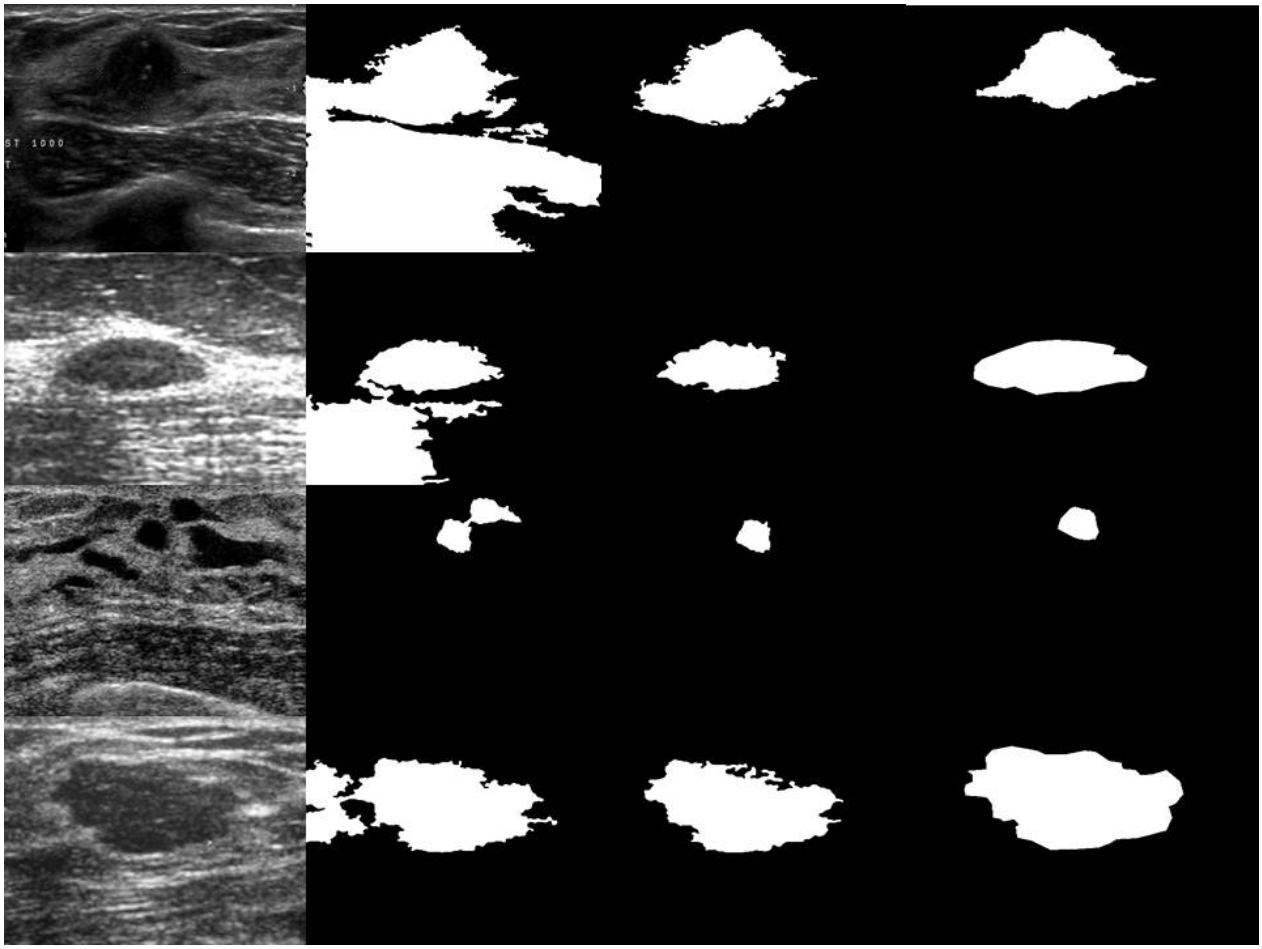

Fig. 2. Sample results (from left to right): original image, fuzzy results, evolving fuzzy results, and corresponding gold standard images.

[3] J. Yang, S. Hao, and P. Chung, "Color image segmentation using fuzzy C-means and eigenspace projections," *Signal Processing*, vol. 82, no. 3, pp. 461–472, 2002.

[4] G. Karmakar and L. Dooley, "A generic fuzzy rule based image segmentation algorithm," *Pattern Recognition Letters*, vol. 23, no. 10, pp. 1215–1227, 2002.

[5] W. Tao, J. Tian, and J. Liu, "Image segmentation by three-level thresholding based on maximum fuzzy entropy and genetic algorithm," *Pattern Recognition Letters*, vol. 24, no. 16, pp. 3069–3078, 2003.

[6] L. Cinque, G. Foresti, and L. Lombardi, "A clustering fuzzy approach for image segmentation," *Pattern Recognition*, vol. 37, no. 9, pp. 1797–1807, 2004.

[7] D. Zhang and S. Chen, "A novel kernelized fuzzy c-means algorithm with application in medical image segmentation," *Artificial Intelligence in Medicine*, vol. 32, no. 1, pp. 37–50, 2004.

[8] W. Cai, S. Chen, and D. Zhang, "Fast and robust fuzzy c-means clustering algorithms incorporating local information for image segmentation," *Pattern Recognition*, vol. 40, no. 3, pp. 825–838, 2007.

[9] K. Chuang, H. Tzeng, S. Chen, J. Wu, and T. Chen, "Fuzzy c-means clustering with spatial information for image segmentation," *Computerized Medical Imaging and Graphics*, vol. 30, no. 1, pp. 9–15, 2006.

[10] A. Doncescu, J. Aguilar-Martin, and J. Atine, "Image color segmentation using the fuzzy tree algorithm T-LAMDA," *Fuzzy sets and systems*, vol. 158, no. 3, pp. 230–238, 2007.

[11] Z. Yang, F. Chung, and W. Shitong, "Robust fuzzy clustering-based image segmentation," *Applied Soft Computing*, vol. 9, no. 1, pp. 80–84, 2009.

[12] Y. Zhuge, J. Udupa, and P. Saha, "Vectorial scale-based fuzzy-connected image segmentation," *Computer Vision and Image Understanding*, vol. 101, no. 3, pp. 177–193, 2006.

[13] W. Dou, S. Ruan, Y. Chen, D. Bloyet, and J. Constans, "A framework of fuzzy information fusion for the segmentation of brain tumor tissues on MR images," *Image and Vision Computing*, vol. 25, no. 2, pp. 164–171, 2007.

[14] L. Ma and R. Staunton, "A modified fuzzy C-means image segmentation algorithm for use with uneven illumination patterns," *Pattern recognition*, vol. 40, no. 11, pp. 3005–3011, 2007.

[15] Y. Han and P. Shi, "An improved ant colony algorithm for fuzzy clustering in image segmentation," *Neurocomputing*, vol. 70, no. 4-6, pp. 665–671, 2007.

[16] Y. Hata and S. Kobashi, "Fuzzy segmentation of endorrhachis in magnetic resonance images and its fuzzy maximum intensity projection," *Applied Soft Computing*, vol. 9, no. 3, pp. 1156–1169, 2009.

[17] J. Fan, M. Han, and J. Wang, "Single point iterative weighted fuzzy C-means clustering algorithm for remote sensing image segmentation," *Pattern Recognition*, vol. 42, no. 11, pp. 2527–2540, 2009.

[18] J. Foo, G. Miyano, T. Lobe, and E. Winer, "Three-dimensional segmentation of tumors from CT image data using an adaptive fuzzy system," *Computers in biology and medicine*, vol. 39, no. 10, pp. 869–878, 2009.

[19] F. Di Martino, V. Loia, and S. Sessa, "A segmentation method for images compressed by fuzzy transforms," *Fuzzy Sets and Systems*, vol. 161, no. 1, pp. 56–74, 2010.

[20] K. Kasabov, "On-line learning, reasoning, rule extraction and aggregation in locally optimized evolving fuzzy neural networks," *Neurocomputing*, vol. 41, no. 1-4, pp. 25–45, 2001.

[21] M. Futschik, A. Reeve, and N. Kasabov, "Evolving connectionist systems for knowledge discovery from gene expression data of cancer tissue," *Artificial Intelligence in Medicine*, vol. 28, no. 2, pp. 165–189, 2003.

[22] V. Rivas, J. Merelo, I. Rojas, G. Romero, P. Castillo, and J. Carpio, "Evolving two-dimensional fuzzy systems," *Fuzzy sets and systems*, vol. 138, no. 2, pp. 381–398, 2003.

TABLE I

SUMMARY OF THE RESULTS FUZZY SEGMENTATION (FS) AND EVOLVING FUZZY SEGMENTATION (EFS): JACCARD INDEX J (ACCURACY), ITS STANDARD DEVIATION σ_J AND 95%-CONFIDENCE INTERVAL CI_J, THE DICE COEFFICIENT D (ACCURACY), ITS STANDARD DEVIATION σ_D AND 95%-CONFIDENCE INTERVAL CI_D.

Training Set	Method	J	σ_J	CI_J	D	σ_D	CI_D	$NullHypo.$
First Training set	FS	70%	24%	57%-84%	80%	20%	69%-92%	
	EFS	70%	24%	57%-84%	80%	20%	69%-92%	0
Second Training set	FS	58%	27%	43%-74%	70%	25%	56%-84%	
	EFS	73%	19%	62%-84%	83%	16%	73%-92%	1
Third Training set	FS	61%	24%	48%-75%	73%	21%	61%-85%	
	EFS	67%	25%	53%-81%	77%	22%	65%-90%	0
Fourth Training set	FS	64%	25%	50%-78%	75%	22%	63%-88%	
	EFS	74%	18%	64%-84%	84%	14%	76%-92%	1
Fifth Training set	FS	61%	24%	47%-74%	72%	21%	60%-84%	
	EFS	71%	23%	58%-84%	81%	20%	69%-92%	1
Sixth Training set	FS	73%	20%	62%-85%	83%	18%	73%-93%	
	EFS	77%	18%	67%-87%	86%	16%	77%-95%	0
Seventh Training set	FS	72%	23%	59%-85%	81%	20%	70%-93%	
	EFS	73%	23%	60%-85%	82%	20%	70%-93%	0
Eighth Training set	FS	55%	29%	39%-71%	66%	26%	52%-81%	
	EFS	71%	23%	58%-84%	81%	20%	69%-92%	1
Nineth Training set	FS	51%	28%	36%-67%	63%	26%	49%-78%	
	EFS	64%	23%	51%-77%	75%	20%	64%-87%	1
Tenth Training set	FS	63%	27%	48%-79%	74%	25%	60%-88%	
	EFS	72%	24%	59%-86%	81%	20%	70%-93%	0

[23] P. Angelov, "A fuzzy controller with evolving structure," *Information Sciences*, vol. 161, no. 1-2, pp. 21–35, 2004.

[24] P. Chang, C. Liu, and Y. Wang, "A hybrid model by clustering and evolving fuzzy rules for sales decision supports in printed circuit board industry," *Decision Support Systems*, vol. 42, no. 3, pp. 1254–1269, 2006.

[25] P. Chang, Y. Wang, and C. Liu, "The development of a weighted evolving fuzzy neural network for PCB sales forecasting," *Expert Systems with Applications*, vol. 32, no. 1, pp. 86–96, 2007.

[26] H. Rong, N. Sundararajan, G. Huang, and P. Saratchandran, "Sequential Adaptive Fuzzy Inference System (SAFIS) for nonlinear system identification and prediction," *Fuzzy sets and systems*, vol. 157, no. 9, pp. 1260–1275, 2006.

[27] C. Xydeas, P. Angelov, S. Chiao, and M. Reoullas, "Advances in classification of EEG signals via evolving fuzzy classifiers and dependant multiple HMMs," *Computers in biology and medicine*, vol. 36, no. 10, pp. 1064–1083, 2006.

[28] C. Lin and Y. Xu, "A self-adaptive neural fuzzy network with group-based symbiotic evolution and its prediction applications," *Fuzzy Sets and Systems*, vol. 157, no. 8, pp. 1036–1056, 2006.

[29] J. de Barros and A. Dexter, "On-line identification of computationally undemanding evolving fuzzy models," *Fuzzy sets and systems*, vol. 158, no. 18, pp. 1997–2012, 2007.

[30] R. Linden and A. Bhaya, "Evolving fuzzy rules to model gene expression," *Biosystems*, vol. 88, no. 1-2, pp. 76–91, 2007.

[31] P. Angelov, E. Lughofer, and X. Zhou, "Evolving fuzzy classifiers using different model architectures," *Fuzzy Sets and Systems*, vol. 159, no. 23, pp. 3160–3182, 2008.

[32] P. Phan and T. Gale, "Direct adaptive fuzzy control with a self-structuring algorithm," *Fuzzy Sets and Systems*, vol. 159, no. 8, pp. 871–899, 2008.

[33] H. Du and N. Zhang, "Application of evolving Takagi-Sugeno fuzzy model to nonlinear system identification," *Applied Soft Computing*, vol. 8, no. 1, pp. 676–686, 2008.

[34] R. Lai, C. Fan, W. Huang, and P. Chang, "Evolving and clustering fuzzy decision tree for financial time series data forecasting," *Expert Systems with Applications*, vol. 36, no. 2, pp. 3761–3773, 2009.

[35] E. Lughofer, "On-line evolving image classifiers and their application to surface inspection," *Image and Vision Computing*, vol. 28, no. 7, pp. 1065–1079, 2010.

[36] C. Juang, Y. Lin, and C. Tu, "A recurrent self-evolving fuzzy neural network with local feedbacks and its application to dynamic system processing," *Fuzzy Sets and Systems*, vol. 161, no. 19, pp. 2552–2568, 2010.

2011 IEEE International Conference on Fuzzy Systems
June 27-30, 2011, Taipei, Taiwan

On Spline Methods of Approximation under L-fuzzy Information

Svetlana Asmuss
University of Latvia
Department of Mathematics
Institute of Mathematics and Computer Science
Riga, Latvia
Email: svetlana.asmuss@lu.lv

Alexander Šostak
University of Latvia
Department of Mathematics
Institute of Mathematics and Computer Science
Riga, Latvia
Email: sostaks@lanet.lv

***Abstract*—This work is closely related to our previous papers on algorithms of approximation under *L*-fuzzy information. In the classical theory of approximation central algorithms were worked out on the basis of usual, that is crisp splines. We describe central methods for solution of linear problems with balanced *L*-fuzzy information and develop the concept of *L*-fuzzy splines.**

***Index Terms*—Error of approximation, central algorithm of approximation, spline, *L*-fuzzy real number, *L*-fuzzy information, *L*-fuzzy spline.**

I. Introduction

In the literature one can find two different approaches to the approximation problem when the conditions which must be satisfied under the process of approximation are not strictly defined. One of them, we call it *the statistical approach*, is applicable in cases when the approximation relies on information given with some error and is based on the use of distribution functions. The second, so called *interval method* considers approximation when imprecision of the used information is implied by inevitable interval estimation. As different from these two approaches we propose here an alternative approach to approximation problem which could be helpful in cases when the imprecision of information used in the approximation process has fuzzy, or vague nature.

We consider the problem of approximation of an operator B defined on a set X and taking values in a normed space Y. To find an approximation of the exact value Bx, we must know something about the problem element $x \in X$. We denote the information of x by Ax and suppose that this information is given by an information vector z. Usually the information is imprecise, thus there may exist many different information vectors z, corresponding to one problem element $x \in X$. Under such interpretation it seems natural to consider information Ax as a fuzzy, rather than as a crisp one, i.e. to realize it as an L-fuzzy set Ax by using a lattice L.

In order to estimate the "quality" of *approximation under fuzzy data*, we need an appropriate L-fuzzy analogue of a real number. Notice that the error of a method of approximation in this case is characterized by the supremum of the corresponding L-fuzzy set of real numbers. The principal aim of our work (see also [1], [2], [3]) is to generalize for the case of L-fuzzy information the idea of an *optimal error method* of approximation (the method whose error is the infimum of the errors of all methods for a given problem using the same information) and the concept of a *central algorithm*, which is always an optimal error algorithm and in the crisp case is useful in practice as well as in the general theory (see e.g. [4]).

In the classical approximation theory central methods for solution of linear problems with balanced information usually are based on splines. In the crisp case (see e.g. [5], [6], [7], [8]) one can distinguish three types of splines used in the study of approximation problems: they are respectively *the interpolation splines, the smoothing splines* and, the most general, *splines on the basis of convex sets*. Generalizing the last type of crisp splines, here we introduce the concept of *an L-fuzzy spline* on the basis of L-fuzzy sets and with the help of such splines initiate to develop an approach to study of the approximation problem in case when L-fuzzy information is taken as the basis for this approximation.

We suppose that $L = (L, \leq, \wedge, \vee)$ is a complete, completely distributive lattice, and denote its bottom and top elements by 0 and 1 respectively.

II. Preliminaries

A. L-fuzzy real numbers

In the literature on fuzzy mathematics one can find several different schemes for defining fuzzy real numbers. For our purposes the most appropriate is the approach originating in B. Hutton's paper [9] and further developed by several authors (see e.g. [10], [11], [12], [13], [14], [15]). However, we had to modify it a little.

Definition II.1. *An L-fuzzy real number is a function $z : \mathbb{R} \to L$ such that*

- *z is non-increasing;*
- *$\bigwedge_t z(t) = 0$;*
- *z is left semi-continuous, i.e. for all $t_0 \in \mathbb{R}$ we have $\bigwedge_{t<t_0} z(t) = z(t_0)$.*

Thus we omit the condition $\bigvee_t z(t) = 1$, which is requested by B.Hutton and his followers.

978-1-4244-7316-8/11/$26.00 ©2011 IEEE

In the original papers on this subject L-fuzzy real numbers were defined not as order reversing functions, but as equivalence classes of such functions. However, as noticed in [13], each class of equivalence has a unique left semi-continuous representative and therefore an L-fuzzy real number can be identified with this representative.

The set $\mathbb{R}(L)$ of all L-fuzzy real numbers is called *the L-fuzzy real line*.

Given $z_1, z_2 \in \mathbb{R}(L)$ let

$$(z_1 \oplus z_2)(t) = \bigvee_{\tau} \big(z_1(\tau) \wedge z_2(t-\tau)\big).$$

The operation of fuzzy addition $\oplus$ is a jointly continuous extension of addition $+$ from the real line $\mathbb{R}$ to the fuzzy real line $\mathbb{R}(L)$.

The operation $\oplus$ can be naturally extended to the case of L-fuzzy subsets M, N of a linear space X (that is mappings $M, N : X \to L$) as follows:

$$M \oplus N : X \to L : \quad (M \oplus N)(x) := \bigvee_{y \in X} (M(y) \wedge N(x-y)).$$

The definition of the product $\odot$ of L-fuzzy numbers is more complicated if compared with the definition of their sum. However, for our purposes we need only to multiply an L-fuzzy number by a real number $\gamma \in \mathbb{R}$. In this case we define the multiplication by the following simple formula:

$$(\gamma \odot z)(t) = z\left(\frac{t}{\gamma}\right) \text{ if } \gamma \neq 0,$$

and

$$(0 \odot z)(t) = \begin{cases} \bigvee\limits_{\tau \in \mathbb{R}} z(\tau) & \text{for } t \leq 0, \\ 0 & \text{for } t > 0. \end{cases}$$

In case $\gamma > 0$ this definition is equivalent to the standard one (see e.g. [11]). The operation of product is in accordance with the addition and is jointly continuous.

The operation $\odot$ can be naturally extended to the case of an L-fuzzy subset M of a linear space X as follows:

$$(\gamma \odot M)(x) = M\left(\frac{x}{\gamma}\right), \ x \in X, \text{ for any real number } \gamma \neq 0.$$

B. Infimum and supremum

Here we recall some concepts and results from [1], [2].

Definition II.2. *The infimum and the supremum of a set of L-fuzzy numbers $F \subset \mathbb{R}(L)$ are defined by the formulas :*

$$(Inf\ F)(t) = \bigwedge \{z(t) \mid z \in F\}, \ t \in \mathbb{R},$$

$$Sup\ F = Inf\{z \mid z \in \mathbb{R}(L), z \geq z' \text{ for all } z' \in F\}.$$

It is easy to see that $Inf\ F$ is an L-fuzzy real number. In case F is bounded from above (i.e. there exists $z_0 \in \mathbb{R}(L)$ such that $z \leq z_0$ for all $z \in F$), $Sup\ F$ is an L-fuzzy real number, otherwise the condition

$$\bigwedge_t SupF(t) = 0$$

does not necessarily hold.

Definition II.3. *By the supremum of a bounded L-fuzzy set $M : \mathbb{R} \to L$ we call the L-fuzzy real number*

$$\mathcal{S}up(M) : \mathbb{R} \to L$$

defined by the equality

$$\mathcal{S}up(M)(t) = \bigwedge_{u<t} \big(\bigvee_{\tau>u} M(\tau)\big).$$

One can prove that $\mathcal{S}up(M)$ is an L-fuzzy real number. Let us note that we define the supremum only for the case of a bounded L-fuzzy set. Recall that in case X is metric, an L-fuzzy set $M : X \to L$ is called *bounded* if $M^{-1}[\alpha, 1]$ is a bounded subset of X for any $\alpha \neq 0$. Similarly the supremum for an unbounded L-fuzzy set could be defined, however in this case it woudn't be a fuzzy number: the condition $\bigwedge\limits_t z(t) = 0$ will be violated.

Obviously, in case when M is crisp, this definition reduces to the classical definition of the supremum.

In case $M = \varphi(\mathcal{V})$, where $\mathcal{V} : X \to L$ and $\varphi : X \to \mathbb{R}$, we write

$$\mathcal{S}up_{x \tilde{\in} \mathcal{V}} \varphi(x) \quad \text{or} \quad \mathcal{S}up\{\varphi(x) : x \tilde{\in} \mathcal{V}\}$$

instead of

$$\mathcal{S}up(\varphi(\mathcal{V})).$$

Recall that the image $\varphi(\mathcal{V})$ of a fuzzy set $\mathcal{V} \in L^X$ under a mapping $\varphi : X \to \mathbb{R}$ is defined by the equality

$$\varphi(\mathcal{V})(x) = \bigvee \{\mathcal{V}(y) : \varphi(y) = x\}.$$

Given an L-fuzzy set $M : X \to L$, where X is a normed space, we define its L-valued norm as an L-fuzzy number

$$\|M\|^L : \mathbb{R} \to L$$

given by the equality

$$\|M\|^L(t) = Sup\{M(x) \mid \|x\|_X = t\}.$$

One can prove that

$$\|\gamma \odot M\|^L = |\gamma| \odot \|M\|^L$$

and

$$\|M \oplus N\|^L \leq \|M\|^L \oplus \|N\|^L$$

for any L-fuzzy sets $M, N : X \to L$, and hence

$$\| \ \|^L : L^X \to L^{\mathbb{R}}$$

inherits the standard properties of a norm.

C. Radius, diameter and centre of an L-fuzzy set

Here we recall some concepts and results from [3]. Given an L-fuzzy set $V : X \to L$, where X is a normed space.

Definition II.4. *The radius and the diameter of a bounded L-fuzzy set V are defined, respectively by*

$$rad(V) = Inf_{x\tilde{\in}X} Sup_{y\tilde{\in}V} \|x-y\|_X$$

and

$$diam(V) = Sup_{x,y\tilde{\in}V} \|x-y\|_X.$$

Definition II.5. *If for a bounded L-fuzzy set V there exists $c \in X$ such that*

$$rad(V) = Sup_{x\tilde{\in}V} \|c-x\|_X$$

then c is called a centre of V and it is denoted by $c(V)$.

Note that $c(V)$ can be an element "outside" V and need not be unique.

We say that an L-fuzzy set V is symmetric with respect to an element $x_0 \in X$, if for any element $x \in X$ it holds

$$V(x_0+x) = V(x_0-x).$$

We call an L-fuzzy set symmetric in case it is symmetric with respect to some element.

Proposition II.6. *If a bounded L-fuzzy set V is symmetric with respect to an element $c \in Y$, then c is the centre of V.*

III. On methods of approximation under L-fuzzy information

A. Approximation under L-fuzzy information

In this section, following [2], [3] we generalize the well known notions of "classic" or "crisp" approximation theory (see, e.g. [4]) to the L-fuzzy case. We consider the problem (A,B) of approximation of an operator $B : X \to Y$ defined in a set X and taking values in a normed space Y under information given by an operator $A : X \to L^{\mathbb{R}^n}$.

By a method (an algorithm) of solution of the problem (A,B) we mean any operator $\varphi : \mathbb{R}^n \to Y$. For an information vector $z \in \mathbb{R}^n$ the value $\varphi(z)$ must approximate the exact value of solution Bx for the problem element x corresponding to the information vector z:

$$x \in X \Longrightarrow z\tilde{\in}Ax \in L^{\mathbb{R}^n} \Longrightarrow \varphi(z) \approx Bx \in Y.$$

For most problems the information operator is not one-to-one and a given information vector z does not determine the problem element x (the solution element Bx) in the unique way. Thus there may exist many different problem elements (solution elements) with the same information. Such problems also cannot be solved exactly. For problems which can be solved only approximately the notion of the error of a method of approximation plays the fundamental role.

B. Error of a method of approximation under L-fuzzy information

We investigate the error of approximation on a non-empty subset X_0 of the set X. Let $\varphi : \mathbb{R}^n \to Y$ be a method for solving the problem (A,B). Our aim is to define the error of the method for an element $x \in X_0$. There may exist many different elements $u \in X_0$ corresponding to the same information Ax. Since each of them has the correspondness degree characterized by the value $Ax(z)$, such elements form an L-fuzzy subset of X_0. Let us denote it by U_z:

$$U_z(x) = Ax(z) \quad \text{for all} \quad x \in X_0; \quad U_z(x) = 0 \quad \text{for all} \quad x \notin X_0.$$

Thus knowing only z it is impossible to recognize which problem element $x\tilde{\in}U_z$ is being actually approximated and we consider all of them.

Definition III.1. *The error of approximation an element $x \in X_0$ by a method φ is given by the value*

$$e(\varphi,z) = Sup_{x\tilde{\in}U_z} \|Bx - \varphi(z)\|_Y.$$

It is easy to see that the radius of the L-fuzzy set $V_z = B(U_z)$ plays the essential role for the value $e(\varphi,z)$.

Proposition III.2. $rad(V_z) \le e(\varphi,z)$.

Definition III.3. *The error of approximation by a method φ is given by the value*

$$e(\varphi) = Sup_{z\in\mathbb{R}^n} e(\varphi,z).$$

Definition III.4. *A method φ^o is called an optimal error method iff*

$$e(\varphi^o) = Inf_{\varphi} e(\varphi).$$

C. Central methods of approximation under L-fuzzy information

In [2] it is proved that for any method φ

$$e(\varphi) = Sup_{x\in X_0} Sup_{z\tilde{\in}Ax} \|Bx - \varphi(z)\|_Y$$

and

$$r(A,B) \le e(\varphi),$$

where $r(A,B)$ is the radius of information for a problem (A,B) defined by

$$r(A,B) = Sup_z \ rad(V_z).$$

In the sequel we assume that the radius $r(A,B)$ of information is finite.

Definition III.5. *A method φ^c is called a central method on $\mathbb{R}^n$ iff*

$$\varphi^c(z)) = c(V_z) \quad \textit{for all} \quad z \in \mathbb{R}^n.$$

Proposition III.6. *For any central algorithm φ^c*

$$e(\varphi^c) = r(A,B).$$

This proposition implies that:

1) any central algorithm φ^c is an optimal error algorithm;

2) if for problem (A,B) there exists a central algorithm, then

$$r(A,B) = e(\varphi^o).$$

IV. Spline methods for solving linear problems of approximation

A. Linear problems with balanced information

In this work we consider algorithms of approximation of a linear operator under balanced L-fuzzy information, i.e. we investigate approximation methods under assumptions that

$$A : X \to L^{\mathbb{R}^n}$$

is a linear operator defined on a vector space X, i.e.

$$A(\gamma_1 x_1 + \gamma_2 x_2) = \gamma_1 A x_1 \oplus \gamma_2 A x_2 \text{ for all } x_1, x_2 \in X,\ \gamma_1, \gamma_2 \in \mathbb{R},$$

and an information A is balanced in the following sense: for any $x \in X$ the set $Ax \in L^{\mathbb{R}^n}$ is symmetric, i.e. there exists an element $z_x \in \mathbb{R}^n$ such that

$$Ax(z_x + z) = Ax(z_x - z) \quad \text{for all} \quad z \in \mathbb{R}^n$$

and

$$\bigvee_{z \in \mathbb{R}^n} Ax(z) \quad = \quad Ax(z_x).$$

Under these assumptions (A,B) is called a linear problem with balanced information.

We assume also that the set X_0 is given by a linear operator T defined on X and taking values in a Hilbert space W as follows

$$X_0 = \{x \in X : \quad \|Tx\|_W \le 1\}.$$

Note that central methods for solution of linear problems with balanced information worked out on the basis of *usual*, that is *crisp* splines. To define them we use the defuzzyfication

$$a : X \to \mathbb{R}^n$$

of an operator A:

$$a(x) = z_x \quad \text{for all} \quad x \in X.$$

B. Spline methods

In the sequel assume that $T(Ker(a))$ is closed and $a(X) = \mathbb{R}^n$. Under this assumption for any $z \in \mathbb{R}^n$ there exists an element $s_z \in X$ such as

$$\|Ts_z\|_W = \inf_{x \in X, z_x = z} \|Tx\|_W,$$

called *a spline interpolating z*. The space of all interpolating splines $S(T,a)$ is described by the formula

$$S(T,a) = \{s \in X : \quad < Ts, Tx >_W = 0 \quad \text{for all} \quad x \in Ker(a)\},$$

where $Ker(a)$ is the kernel of an operator a.

For the notions and results on splines see e.g. [5], [6], [7], [8].

The spline algorithm may be derived as follows. Let

$$e^i = (0,0,...,0,1,0,...,0) \in \mathbb{R}^n$$

denote the i-th unit vector, $i = 1,2,...,n$. Find a spline s_i interpolating e^i. The spline algorithm φ^s is of the form:

$$\varphi^s(z) = Bs(z), \quad \text{where} \quad s(z) = \sum_{i=1}^{n} z_i s_i \quad \text{for all} \quad z \in \mathbb{R}^n.$$

Proposition IV.1. *The method φ^s is a central method.*

This proposition implies that:
1) the spline algorithm φ^s is an optimal error algorithm;
2) for linear problems (A,B) with balanced information:

$$r(A,B) = e(\varphi^s).$$

C. L-fuzzy splines

In this section we generalize the concept of a spline. For a given vector $z \in \mathbb{R}^n$ we consider the following problem of minimization

$$\|TS_z\|^L = Inf_{x \in A^{-1}(z)} \|Tx\|_W,$$

where S_z is an L-fuzzy set in X. A solution of this problem $S_z : X \to L$ is called *an L-fuzzy spline interpolating z*. We denote by $S(T,A,L)$ the set of all L-fuzzy splines.

Proposition IV.2. *If an information operator $A : X \to L^{\mathbb{R}^n}$ is given by a usual operator $a : X \to \mathbb{R}^n$ as follows*

$$Ax(z) = \begin{cases} 1, \text{ if } z = a(x), \\ 0, \text{ if } z \neq a(x), \end{cases}$$

then for any vector $z \in \mathbb{R}^n$ an interpolating L-fuzzy spline $S_z \in S(T,A,L)$ is the crisp set of all splines $s_z \in S(T,a)$ interpolating z, i.e.

$$S_z(X) = \{0,1\}, \quad \text{and} \quad S_z(s_z) = 1$$

iff

$$\|Ts_z\|_W = \inf_{x \in X, a(x) = z} \|Tx\|_W.$$

Proposition IV.3. *If an information operator $A : X \to L^{\mathbb{R}^n}$ is given by a usual operator $a : X \to \mathbb{R}^n$ and a positive number ε as follows*

$$Ax(z) = \begin{cases} 1, \text{ if } \|a(x) - z\| \le \varepsilon, \\ 0, \text{ if } \|a(x) - z\| > \varepsilon, \end{cases}$$

then for any vector $z \in \mathbb{R}^n$ an interpolating L-fuzzy spline $S_z \in S(T,A,L)$ is the crisp set of all splines $s_z \in S(T,a)$ smoothing z with parameter ε, i.e.

$$S_z(X) = \{0,1\}, \quad \text{and} \quad S_z(s_z) = 1$$

iff

$$\|Ts_z\|_W = \inf_{x \in X, \|a(x) - z\| \le \varepsilon} \|Tx\|_W.$$

V. Conclusion

Central algorithms play fundamental role in classical approximation theory. In our previous work [3] we have introduced the generalized concept of a central algorithm of approximation of an operator under L-fuzzy information. The central methods for solution of linear problems with balanced information relay on splines. In [3] we studied central algorithm of approximation of an operator under L-fuzzy information which is based on usual, that is crisp splines. As different from that research the aim of this work is to start further development of the approximation theory in the context of fuzzy information which would be based on the use of L-fuzzy splines - the concept introduced and studied here. The research developed here embraces the case when an L-fuzzy spline $S_z \in S(T,A,L)$ interpolating vector z, is the crisp set of all splines $s_z \in S(T,a)$ interpolating or smoothing it. The general case of an L-fuzzy interpolating spline will be the subject of a forthcoming research.

Acknowledgement

The paper was partly supported by the ESF project 2009/0223/1DP/1.1.1.2.0/09/APIA/VIAA/008 and by the grant 09.1570 of the Latvian Council of Science.

References

[1] S. Asmuss, A. Šostak, "Extremal problems of approximation of fuzzy sets", Acta Univ. Latviensis, (Ser. Math.), vol. 606, 1997, pp.9–18.

[2] S. Asmuss, A. Šostak, "Extremal problems of approximation theory in fuzzy context", Fuzzy Sets and Systems, vol. 105, 1999, pp. 249–257.

[3] S. Asmuss, A. Šostak, "On central algorithms of approximation under fuzzy information", Fuzzy Sets and Systems, vol. 155, 2005, pp.150–163.

[4] J.F. Traub, H. Wozniakowski, A general theory of optimal algorithms. Academic Press, New York, 1980.

[5] P.-J. Laurent, Approximation et optimisation. Hermann. Paris, 1972.

[6] A.Yu. Bezhaev, V.A. Vasilenko, Variational theory of splines. Kluwer Academic Plenum Publishers, New York, 2001.

[7] L. Schumaker, Spline functions: basic theory. Cambridge University Press, 2007.

[8] P. Massopust, Interpolation and approximation with splines and fractals. Oxford University Press, 2010.

[9] B. Hutton, "Normality in fuzzy topological spaces", J. Math. Anal. Appl., vol. 50, 1975, pp. 74–79.

[10] T.E. Gantner, R.C. Steinlage, R.H. Warren, "Compactness in fuzzy topological spaces", J. Math. Anal. Appl., vol. 62, 1978, pp. 547–562.

[11] S.E. Rodabaugh, "Fuzzy addition and the fuzzy real lines", Fuzzy Sets and Systems, vol. 8, 1982, pp. 39–52.

[12] R. Lowen, "On $(R(L),\oplus)$", Fuzzy Sets and Systems, vol. 10, 1983, pp. 203–209.

[13] T. Kubiak, "Extending continuous L-real functions", Math. Japonica, vol. 31, 1986, pp. 875–887.

[14] U. Höhle, "Fuzzy real numbers as Dedekind cuts with respect to multiple-valued logic", Fuzzy Sets and Systems, vol. 24, 1987, pp. 263–278.

[15] S.E. Rodabaugh, "Fuzzy real lines and dual lines for poslat topological, uniform and metric ordered semirings with unity", Chapter 10, in Mathematics of fuzzy sets: logic, topology and measure theory, U. Höhle and S.E. Rodabaugh, Eds. Handbook Series, vol. 3, Kluwer Academic Plenum Publishers, 1999, pp. 607–632.

2011 IEEE International Conference on Fuzzy Systems
June 27-30, 2011, Taipei, Taiwan

Local Non-Quadratic H-Infinity Control For Continuous-Time Takagi-Sugeno Models

Miguel Bernal, Adolfo Soto-Cota, Joaquín Cortez
Dept. of Electric and Electronics Engineering,
Sonora Institute of Technology
Ciudad Obregón, Sonora, Mexico
email: miguel.bernal@itson.edu.mx

José Luis Pitarch
DISA, Universidad Politécnica de Valencia
Valencia, Spain

Abdelhafidh Jaadari
LAMIH, University of Valenciennes and H.C.
Valenciennes, France

***Abstract* — This paper extends to H_∞ performance design a recent local approach for non-quadratic stabilization of continuous-time Takagi-Sugeno (TS) models based on the fuzzy Lyapunov function (FLF). The main obstacle for using FLFs altogether with TS models consists in handling the time-derivatives of the membership functions (MFs). By reducing global stability goals via local considerations, the aforementioned impediment has been removed leading to stabilization domains where H_∞ disturbance rejection is guaranteed. Conditions are expressed as linear matrix inequalities (LMIs), thus enabling systematic and efficient solutions which are solved by convex optimization techniques.**

***Keywords* — Fuzzy Lyapunov Function (FLF), Linear Matrix Inequality (LMI), Local Stabilization, H_∞ disturbance rejection, Takagi-Sugeno (TS) models.**

I. Introduction

SINCE its appearance, Takagi-Sugeno models (TS) [1] have attracted the interest of researchers in control because of their systematic construction methodology which leads to exact convex representations of nonlinear models in a compact set of the state variables [2]. These convex representations facilitate system analysis and control design [3], [4] via the direct Lyapunov method with quadratic Lyapunov functions [5]. Parallel distributed compensation (PDC) is widely used among quadratic schemes because it naturally fits with the structure of TS models providing a fuzzy controller that allows performance design via linear matrix inequalities (LMIs) [6].

Despite its success, there are several sources of pessimism for stabilization of TS models: model construction is not unique [7], membership functions (MFs) can only be partially taken into account through different and not necessarily compatible approaches [8], [9], [10], [11], quadratic Lyapunov functions are a subclass of more complex and powerful choices that may not be easy to implement. This work extends the existing results in the latter direction since it uses a fuzzy Lyapunov function which includes the quadratic case. Nevertheless, an important feature of the proposed approach lies on its local nature which exploits the fact that TS models are only valid in a compact set of the state space. Global stabilization results as those available in the quadratic case prove to be more restrictive than local results in a non-quadratic framework.

Otherwise than the quadratic framework, piecewise [12], [13], integral [14], and fuzzy Lyapunov functions [15] have been proposed. Among the latter, continuous-time results have not been as powerful as those for the discrete-time case [16], [17], [18]. This unevenness is caused by the presence of time-derivatives of the MFs in the analysis, which destroys the convex structure leading to LMIs. Most of the palliative solutions to this problem assume the knowledge of bounds for the time-derivatives of the MFs, which is an unrealistic assumption especially concerning algebraic loops in control design [19]. Other solutions lead to bilinear matrix inequalities, which cannot be guaranteed to be optimally solved [14].

The approach first appeared in [20] and further extended in [21] for local stability analysis of continuous-time TS models is formulated in LMIs and does not require more than a-priori-known bounds from the TS model construction. Based on these works, a paper proposing a control law for local stabilization has been proposed in [22]. This paper extends the former results for local stabilization of a TS model with H_∞ disturbance rejection.

The paper is organized as follows: section II introduces notation, the considered TS model, the Lyapunov function candidate, and the proposed control law; section III extends to H_∞ disturbance rejection the results in [22]; in section IV some illustrative examples are shown; finally section V closes the paper providing some conclusions and perspectives.

II. Preliminaries

Consider the following nonlinear affine-in-control model:

The present paper has been supported by the National Council of Science and Technology of Mexico (CONACYT-SNI), the French National Center for Scientific Research (CNRS), and the PROMETEO project from the Comunitát Valenciana (Spain). The authors gratefully acknowledge the support of these institutions.

$$\begin{aligned}\dot{x}(t) &= f_1(z)x(t)+f_2(z)u(t)+f_3(z)\omega(t)\\ y(t) &= f_4(z)x(t)+f_5(z)u(t)+f_6(z)\omega(t)\end{aligned} \quad (1)$$

with input vector $u(t)\in\mathbb{R}^m$, disturbance vector $\omega(t)\in\mathbb{R}^q$, $\|\omega(t)\|_2 \le \bar{\omega}$, state vector $x(t)\in\mathbb{R}^n$, premise vector $z(x(t))\in\mathbb{R}^p$ bounded in a compact region $\Delta \supset \mathbf{0}$, output vector $y(t)\in\mathbb{R}^o$, and $f_1(\cdot),\ldots,f_6(\cdot)$ nonlinear functions depending on $z(x(t))$. Let $nl_j(\cdot)\in\left[\underline{nl_j},\overline{nl_j}\right]$, $j\in\{1,\cdots,p\}$ be the bounded nonlinearities of (1) in the compact region Δ. By sector nonlinearity approach [3] the following weighting functions are defined to capture nonlinearities in (1):

$$w_0^j(\cdot)=\frac{\overline{nl_j}-nl_j(\cdot)}{\overline{nl_j}(\cdot)-\underline{nl_j}},\quad w_1^j(\cdot)=1-w_0^j(\cdot),\ j\in\{1,\cdots,p\} \quad (2)$$

from which membership functions (MFs)

$$h_i = h_{1+i_1+i_2\times 2+\cdots+i_p\times 2^{p-1}} = \prod_{j=1}^{p} w_{i_j}^j(z_j), \quad (3)$$

$i\in\{1,\cdots,2^p\}$, $i_j\in\{0,1\}$, are defined satisfying the convex-sum property $\sum_{i=1}^{r} h_i(\cdot)=1$, $h_i(\cdot)\ge 0$ in Δ.

Notation: Arguments are omitted where convenient. An asterisk $(*)$ inside a block matrix represents the transpose of the symmetric element. Sums $\Upsilon_z=\sum_{i=1}^{r}h_i\Upsilon_i$, $\Upsilon_z^{-1}=\left(\sum_{i=1}^{r}h_i\Upsilon_i\right)^{-1}$ will be used to simplify expressions. Thus, an exact representation of nonlinear model (1) in Δ can be written as the following TS model:

$$\begin{aligned}\dot{x}(t) &= \sum_{i=1}^{r} h_i(z(t))\left(A_i x(t)+B_i u(t)+E_i\omega(t)\right)\\ &= A_z x(t)+B_z u(t)+E_z\omega(t)\\ y(t) &= \sum_{i=1}^{r} h_i(z(t))\left(C_i x(t)+D_i u(t)+F_i\omega(t)\right)\\ &= C_z x(t)+D_z u(t)+F_z\omega(t)\end{aligned} \quad (4)$$

where A_i, B_i, C_i, D_i, E_i, F_i, $i=1,\ldots,r$ are matrices of the proper size and $r=2^p\in\mathbb{N}$ is the number of rules (linear models) of the fuzzy interpretation of (4).

Double convex sums involving MFs will appear in the sequel. In order to obtain LMI conditions these MFs must be removed. The following result will be applied to perform this task since it combines simplicity and a good solutions' quality:

Relaxation Lemma [8]: Let Υ_{ij}, $i,j\in\{1,\cdots,r\}$ be matrices of certain dimension. Condition

$$\sum_{i=1}^{r}\sum_{j=1}^{r} h_i(z(t))h_j(z(t))\Upsilon_{ij}<0 \quad (5)$$

is verified if:

$$\begin{aligned}&\Upsilon_{ii}<0,\quad \forall i\in\{1,\cdots,r\}\\ &\frac{2}{r-1}\Upsilon_{ii}+\Upsilon_{ij}+\Upsilon_{ji}<0,\quad \forall(i,j)\in\{1,\cdots,r\}^2,\ i\ne j.\end{aligned} \quad (6)$$

A non-quadratic control law taken from [16] will be used:

$$u(t)=G_z P_z^{-1}x(t)=\left(\sum_{i=1}^{r}h_i(z)G_i\right)\left(\sum_{i=1}^{r}h_i(z)P_i\right)^{-1}x(t) \quad (7)$$

where $G_i\in\mathbb{R}^{m\times n}$ are gains and $P_i\in\mathbb{R}^{n\times n}$, $P_i=P_i^T>0$ are matrices associated with a fuzzy Lyapunov function. Thus, the closed-loop TS model is:

$$\begin{aligned}\dot{x}(t) &= \left(A_z+B_zG_zP_z^{-1}\right)x(t)+E_z\omega(t)\\ y(t) &= \left(C_z+D_zG_zP_z^{-1}\right)x(t)+F_z\omega(t)\end{aligned} \quad (8)$$

The following candidate fuzzy Lyapunov function will be adopted [15]:

$$V(x(t))=x^T(t)P_z^{-1}x(t)=x^T(t)\left(\sum_{i=1}^{r}h_i(z(t))P_i\right)^{-1}x(t). \quad (9)$$

III. H_∞ CONTROL

The nonlinear model (1), or its equivalent TS model (4), satisfy the H_∞ attenuation criterion in Δ if disturbances $\omega(t)$ are bounded at the output by:

$$\sup_{\|\omega(t)\|_2\ne 0}\frac{\|y(t)\|_2}{\|\omega(t)\|_2}\le\gamma \quad (10)$$

where $\|\bullet\|_2$ stands for the L_2-norm.

As shown in [3], condition (10) is satisfied if:

$$\dot{V}(x(t))+y^T(t)y(t)-\gamma^2\omega^T(t)\omega(t)\le 0. \quad (11)$$

Taking into account (4) and (9), (11) can be rewritten by developing the time-derivative of $V(x(t))$ along the trajectories of (8):

$$\begin{aligned}&\dot{V}(x(t))+y^T(t)y(t)-\gamma^2\omega^T(t)\omega(t)\\ &=x^T(t)P_z^{-1}\dot{x}(t)+\dot{x}^T(t)P_z^{-1}x(t)+x^T(t)\left(\dot{P}_z^{-1}\right)x(t)-\gamma^2\omega^T(t)\omega(t)\\ &+\left(\left(C_z+D_zG_zP_z^{-1}\right)x(t)+F_z\omega(t)\right)^T\left(\left(C_z+D_zG_zP_z^{-1}\right)x(t)+F_z\omega(t)\right)\\ &=x^T\left(P_z^{-1}\left(A_z+B_zG_zP_z^{-1}\right)+\left(A_z+B_zG_zP_z^{-1}\right)^TP_z^{-1}+\dot{P}_z^{-1}\right.\\ &\left.+\left(C_z+D_zG_zP_z^{-1}\right)^T\left(C_z+D_zG_zP_z^{-1}\right)\right)x+\omega^T\left(F_z^TF_z-\gamma^2I\right)\omega\\ &+x^T\left(\left(C_z+D_zG_zP_z^{-1}\right)^TF_z+P_z^{-1}E_z\right)\omega+\omega^T\left(F_z\left(C_z+D_zG_zP_z^{-1}\right)+E_z^TP_z^{-1}\right)x\\ &=\begin{bmatrix}x\\ \omega\end{bmatrix}^T\begin{bmatrix}\Gamma_1 & (*)\\ F_z^T\left(C_z+D_zG_zP_z^{-1}\right)+E_z^TP_z^{-1} & F_z^TF_z-\gamma^2I\end{bmatrix}\begin{bmatrix}x\\ \omega\end{bmatrix}\le 0\end{aligned} \quad (12)$$

with $\Gamma_1=P_z^{-1}\left(A_z+B_zG_zP_z^{-1}\right)+\left(A_z+B_zG_zP_z^{-1}\right)^TP_z^{-1}+\dot{P}_z^{-1}+\left(C_z+D_zG_zP_z^{-1}\right)^T\left(C_z+D_zG_zP_z^{-1}\right)$.

Obviously, (12) is satisfied if the block-matrix therein is not positive-definite. Pre- and post-multiplying the referred matrix in (12) by full-rank matrix $\begin{bmatrix}P_z & 0\\ 0 & I\end{bmatrix}$ as well as using the property $P_z\dot{P}_z^{-1}P_z=-\dot{P}_z$, it is possible to guarantee (12) if

$$\begin{bmatrix}\Gamma_2 & P_zC_z^TF_z+G_z^TD_z^TF_z+E_z\\ F_z^TC_zP_z+F_z^TD_zG_z+E_z^T & F_z^TF_z-\gamma^2I\end{bmatrix}\le 0 \quad (13)$$

with $\Gamma_2 = A_z P_z + B_z G_z + P_z A_z^T + G_z^T B_z^T - \dot{P}_z + P_z C_z^T C_z P_z + P_z C_z^T D_z G_z + G_z^T D_z^T C_z P_z + G_z^T D_z^T D_z G_z = A_z P_z + B_z G_z + P_z A_z^T + G_z^T B_z^T - \dot{P}_z + \left(P_z C_z^T + G_z^T D_z^T\right)\left(C_z P_z + D_z G_z\right)$.

Applying Schur complement to expression (13) gives

$$\begin{bmatrix} A_z P_z + B_z G_z + P_z A_z^T + G_z^T B_z^T - \dot{P}_z & (*) & (*) \\ C_z P_z + D_z G_z & -I & \mathbf{0} \\ F_z^T C_z P_z + F_z^T D_z G_z + E_z^T & \mathbf{0} & F_z^T F_z - \gamma^2 I \end{bmatrix} \le 0 . \quad (14)$$

Any term in inequality (14) is an LMI except for the term $\dot{P}_z = \sum_{i=1}^{r} \dot{h}_i\left(z(t)\right) P_i$ which includes the time-derivatives of the MFs. To deal with this problem, most of the published works on the subject propose a bound of the form $\left\|\dot{P}_z\right\| < \phi_z$ [23], [24]. Nevertheless, these bounds cannot be established a priori and can create algebraic loops when applied to stabilization problems. The approach here employed overcomes the aforementioned problem by focusing on local stabilization.

In [20] it has been shown that

$$\begin{aligned} \dot{P}_z &= \sum_{k=1}^{p} \frac{\partial w_0^k}{\partial z_k}\left(P_{g_1(z,k)} - P_{g_2(z,k)}\right)\dot{z}_k \\ &= \sum_{j=1}^{r}\sum_{k=1}^{p} h_j \frac{\partial w_0^k}{\partial z_k}\left(P_{g_1(j,k)} - P_{g_2(j,k)}\right)\dot{z}_k \end{aligned} \quad (15)$$

with

$$\begin{aligned} g_1(j,k) &= \left\lfloor (j-1)/2^{p+1-k} \right\rfloor \times 2^{p+1-k} + 1 + (j-1) \bmod 2^{p-k} \\ g_2(j,k) &= g_1(j,k) + 2^{p-k} \end{aligned} \quad (16)$$

and $\lfloor \cdot \rfloor$ standing for the floor function. Note that

$$\dot{z}_k = \left(\frac{\partial z_k(t)}{\partial x(t)}\right)^T \dot{x}(t) = \left(\frac{\partial z_k(t)}{\partial x(t)}\right)^T \left(A_z x(t) + B_z u(t) + E_z \omega(t)\right), \quad (17)$$

so expression (15) can be rewritten as:

$$\begin{aligned} \dot{P}_z &= \sum_{k=1}^{p} \frac{\partial w_0^k}{\partial z_k}\left(P_{g_1(z,k)} - P_{g_2(z,k)}\right)\left(\frac{\partial z_k(t)}{\partial x(t)}\right)^T \left(A_z x(t) + B_z u(t) + E_z \omega(t)\right) \\ &= \sum_{k=1}^{p}\sum_{v=1}^{n}\sum_{s=1}^{n} \frac{\partial w_0^k}{\partial x_v} x_s \left(A_z\right)_{vs}\left(P_{g_1(z,k)} - P_{g_2(z,k)}\right) \\ &\quad + \sum_{k=1}^{p}\sum_{v=1}^{n}\sum_{e=1}^{m} \frac{\partial w_0^k}{\partial x_v} u_e \left(B_z\right)_{ve}\left(P_{g_1(z,k)} - P_{g_2(z,k)}\right) \\ &\quad + \sum_{k=1}^{p}\sum_{v=1}^{n}\sum_{d=1}^{q} \frac{\partial w_0^k}{\partial x_v} \omega_d \left(E_z\right)_{vd}\left(P_{g_1(z,k)} - P_{g_2(z,k)}\right). \end{aligned} \quad (18)$$

The terms $\left|\frac{\partial w_0^k}{\partial x_v} x_u\right|$, $\left|\frac{\partial w_0^k}{\partial x_v} u_e\right|$, and $\left|\frac{\partial w_0^k}{\partial x_v} \omega_d\right|$ can now be bounded since their components are known *a priori* or can be designed to be bounded.

In order to bund the input $\|u\|_2 < \mu$, consider $|x(0)| < c$ and $P_z \ge c^2 I$ (or $P_z^{-1} \le c^{-2} I$); this provided, since the Lyapunov function is a monotonous decreasing function, it can be shown that $V\left(x(t)\right) \le x^T(t) P_z^{-1} x(t) \le x^T(0) P_z^{-1} x(0) \le 1$, from which $\|u\|_2 < \mu$ if $\frac{1}{\mu^2}\|u\|_2^2 \le x^T(t) P_z^{-1} x(t) \le 1$, i.e.:

$$\frac{1}{\mu^2} x^T(t) P_z^{-1} G_z^T G_z P_z^{-1} x(t) \le x^T(t) P_z^{-1} x(t) \quad (19)$$

which by Schur complement can be written as:

$$\begin{bmatrix} P_z & G_z^T \\ G_z & \mu^2 I_m \end{bmatrix} > 0 \quad (20)$$

Then, the aforementioned bounds can be written as:

$$\left|\frac{\partial w_0^k}{\partial x_v} x_s\right| \le \lambda_{kvs}, \left|\frac{\partial w_0^k}{\partial x_v} u_e\right| \le \mu \eta_{kv}, \left|\frac{\partial w_0^k}{\partial x_v} \omega_d\right| \le \bar{\omega} \eta_{kv} \quad (21)$$

In order to use (21) taking into account (18) as to obtain LMI conditions implying (14), expression

$$W + \left(\frac{\partial w_0^k}{\partial x_v} x_s\right) X + \left(\frac{\partial w_0^k}{\partial x_v} u_e\right) Y + \left(\frac{\partial w_0^k}{\partial x_v} \omega_d\right) Z \le 0 \quad (22)$$

is going to be guaranteed by

$$W \pm \lambda_{ksv} \times X \pm \eta_{kv} \times \mu Y \pm \eta_{kv} \times \bar{\omega} Z \le 0, \quad (23)$$

which represents all the possible sign combinations for every bounded term.

Theorem: If there are matrices of proper size $P_i = P_i^T > c_i^2 I$, G_i, satisfying the following LMI conditions for $i, j, k \in \{1, \cdots, r\}$, $\alpha \in \left\{1, \cdots, 2^{p \times n \times (n+m+q)}\right\}$:

$$\begin{bmatrix} P_j & G_j^T \\ G_j & \mu^2 I \end{bmatrix} > 0 \quad (24)$$

$$\frac{2}{r-1} \Upsilon_{iik}^{\alpha} + \Upsilon_{ijk}^{\alpha} + \Upsilon_{jik}^{\alpha} < 0, \quad (25)$$

with $\Upsilon_{ijk}^{\alpha} = \begin{bmatrix} A_i P_j + B_i G_j + P_j A_i^T + G_j^T B_i^T - \bar{P}_{ij}^{\alpha} & (*) & (*) \\ C_i P_j + D_i G_j & -I & \mathbf{0} \\ F_k^T C_i P_j + F_k^T D_i G_j + E_i^T & \mathbf{0} & F_i^T F_j - \gamma^2 I \end{bmatrix}$,

$$\begin{aligned} \bar{P}_{ij}^{\alpha} &= \sum_{k=1}^{p}\sum_{v=1}^{n}\sum_{s=1}^{n} (-1)^{b_{kv(s+m+q)}^{\alpha}} \lambda_{kvs} \left(A_i\right)_{vs}\left(P_{g_1(j,k)} - P_{g_2(j,k)}\right) \\ &\quad + \sum_{k=1}^{p}\sum_{v=1}^{n}\sum_{e=1}^{m} (-1)^{b_{kv(e+q)}^{\alpha}} \eta_{kv} \mu \left(B_i\right)_{ve}\left(P_{g_1(j,k)} - P_{g_2(j,k)}\right) \\ &\quad + \sum_{k=1}^{p}\sum_{v=1}^{n}\sum_{d=1}^{q} (-1)^{b_{kvd}^{\alpha}} \eta_{kv} \bar{\omega} \left(E_i\right)_{vd}\left(P_{g_1(j,k)} - P_{g_2(j,k)}\right), \end{aligned}$$

b_{kvl}^{α} defined from the binary representation of $\alpha - 1 = b_{pn(n+m+q)}^{\alpha} + b_{pn(n+m+q-1)}^{\alpha} \times 2 + \cdots + b_{111}^{\alpha} \times 2^{pn(n+m+q)-1}$, and $g_1(j,k)$, $g_2(j,k)$ defined as in (16), then $x(t)$ in (8) is locally asymptotically stable for every initial condition $x(0)$, $|x(0)| < c$, inside the biggest equipotential R_o contained in $R = \bigcap_{e,k,s,v} \left\{x : \left|\frac{\partial w_0^k}{\partial x_v} x_s\right| \le \lambda_{kvs}, \left|\frac{\partial w_0^k}{\partial x_v} u_e\right| \le \mu \eta_{kv}\right\}$; moreover, the model output $y(t)$ satisfies the H_∞ criterion in (10) for disturbances holding the property $\left\|\omega(t)\right\|_2 \le \bar{\omega}$.

Proof: By relaxation lemma in (6), LMI (25) implies:

$$\Upsilon_{zz}^{\alpha}=\begin{bmatrix} A_zP_z+B_zG_z+P_zA_z^T+G_z^TB_z^T-\bar{P}_{ij}^{\alpha} & (*) & (*) \\ C_zP_z+D_zG_z & -I & \mathbf{0} \\ F_z^TC_zP_z+F_z^TD_zG_z+E_z^T & \mathbf{0} & F_z^TF_z-\gamma^2 I \end{bmatrix}\le 0 \quad (26)$$

Since all the possible sign combinations in $\bar{P}_{ij}^{\alpha}$ are taken into account and inequalities in (21) bound the time-derivative $\dot{P}_z$, it follows that (26) is a simple extension of property (22); in other words, (26) implies (14), which guarantees the H_∞ criterion in (10) to be satisfied.

Note that bounds in (21) are essential to guarantee implication (26) $\Rightarrow$ (14); these bounds stem from a) the fact that $x(t)$ belongs to a compact set Δ in which the TS model is defined, b) the bounds on the input which are designed via LMIs (24), and c) from the disturbances bound $\bar{\omega}$.

Remark 1: Writing $\dot{P}_z$ in the form described in (18) plays a fundamental role in the proposed local approach. The interested reader is referred to [20] for more details.

Remark 2: Besides the region on which the TS model has been defined, other design parameters intervene in the control law: the bound on the input, the bound on the initial conditions, and the attenuation factor $\gamma>0$. Bounding the disturbance vector is also a reasonable requirement in this kind of problems.

Remark 3: The theorem above guarantees H_∞ performance in the region $R_o \subseteq R$. Should the biggest region R_o be of interest, a simple algorithm can be implemented by linear programming to find it [20]: a) initialize η_{kv}, λ_{kvs} to any initial feasible bounds η_{kv}^0, λ_{kvs}^0; b) search the biggest value $\varepsilon>0$ such that conditions in the theorem above are satisfied with $\eta_{kv}=\varepsilon\eta_{kv}^0$ and $\lambda_{kvs}=\varepsilon\lambda_{kvs}^0$. Consider $R_o \subseteq R$ defined from the last values thus found.

Remark 4: The previous algorithm is compatible with the minimization of the attenuation factor γ. Once ε is established, the minimum attenuation factor γ guaranteeing H_∞ performance design in the region thus defined can be searched as an LMI problem.

IV. Examples

Two examples are shown in this section to illustrate the advantages of the proposed methodology. The first one is stabilized in the absence of disturbances to show the influence of certain design parameters; the second one shows the effectiveness of the H_∞ control design for different regions and parameters.

Example 1 : Consider the following TS model:

$$\dot{x}(t)=\sum_{i=1}^{2} h_i\left(z(t)\right)\left(A_i x(t)+B_i u(t)\right) \quad (27)$$

with system matrices

$$A_1=\begin{bmatrix} 2 & -10 \\ 2 & 0 \end{bmatrix},\ A_2=\begin{bmatrix} -20 & -5 \\ 1 & 2 \end{bmatrix},\ B_1=\begin{bmatrix} 0.1 \\ 1 \end{bmatrix},\ B_2=\begin{bmatrix} 0.3 \\ 0.2 \end{bmatrix},$$

and MFs

$$h_1(x_1)=\frac{1-\sin(x_1)}{2},\ h_2(x_1)=\frac{1+\sin(x_1)}{2},$$

defined in $\Delta=\left\{x\in\mathbb{R}^2, |x_i|<\frac{\pi}{2}\right\}$.

When no perturbations are considered, the proposed approach depends upon the parameter μ (bound on the input $|u|<\mu$) and parameter c (bound on the initial conditions $|x(0)|<c$). In practice, these bounds are directly derived from the model, so LMI conditions in the theorem above are fully determined.

Fig. 1 shows the influence of parameter μ for the model (27) with $|x(0)|<c=\sqrt{2}\pi/2$. As expected, the bigger the values of μ, the bigger the stabilization region R_0. To determine the biggest stabilization region, the algorithm in Remark 3 has been used. Four state trajectories are shown to illustrate the effectiveness of the stabilization method with $|u|<\mu=40$ (solid trajectories with arrows pointing towards the origin).

In Fig. 2 the effects of changing the modelling region of the TS model (27) for $\Delta=\left\{x\in\mathbb{R}^2, |x_i|<\pi/4\right\}$ are studied. In both regions, bounds $|x(0)|<c=\pi/2$ and $|u|<\mu=30$ are assumed. Dotted lines show the borders of R for the original case.

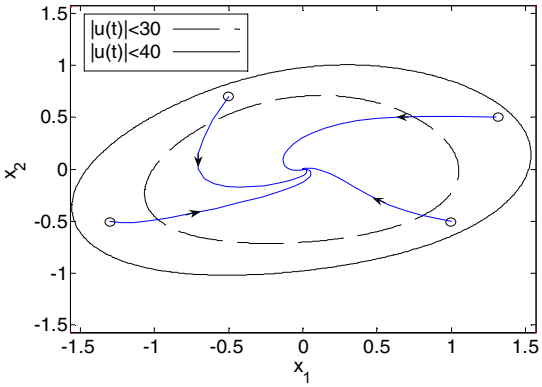

Figure 1: Effects of the input bound μ.

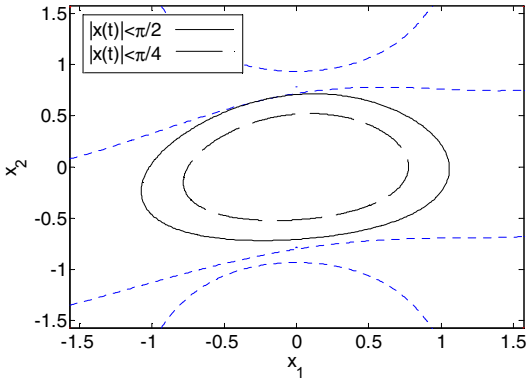

Figure 2: Effects of the region Δ.

It is important to notice that augmenting the modelling region of the TS model do not necessarily mean that a bigger stabilization region will be found. Bigger modelling regions imply that the initial conditions can be further from the origin, thus reducing feasibility of LMIs in (24) since $P_i = P_i^T > c_i^2 I$, $|x(0)| < c$.

Example 2: Consider the following TS model subject to scalar perturbations $\omega(t) = e^{-t}\cos(t)$, $|\omega(t)| \le 1$:

$$\dot{x}(t) = \sum_{i=1}^{2} h_i(z(t))\left(A_i x(t) + B_i u(t) + E_i \omega(t)\right)$$
$$y(t) = \sum_{i=1}^{r} h_i(z(t)) C_i x(t) \qquad (28)$$

with system matrices

$$A_1 = \begin{bmatrix} -5 & -4 \\ -1 & -2 \end{bmatrix}, \quad A_2 = \begin{bmatrix} -2 & -4 \\ 20 & -2 \end{bmatrix}, \quad B_1 = \begin{bmatrix} 0 \\ 10 \end{bmatrix}, \quad B_2 = \begin{bmatrix} 0 \\ 3 \end{bmatrix},$$

$$C_1 = C_2 = \begin{bmatrix} 1 \\ 0 \end{bmatrix}^T, \; E_1 = E_2 = \begin{bmatrix} 1 \\ 1 \end{bmatrix},$$

and MFs $h_1(x_1) = \dfrac{1-\sin(x_1)}{2}$, $h_2(x_1) = \dfrac{1+\sin(x_1)}{2}$ defined in $\Delta = \left\{ x \in \mathbb{R}^2, |x_i| < \dfrac{\pi}{2} \right\}$.

As mentioned in Remark 4, given a specific region $R = \bigcap_{e,k,s,v} \left\{ x : \left| \dfrac{\partial w_0^k}{\partial x_v} x_s \right| \le \lambda_{kvs}, \left| \dfrac{\partial w_0^k}{\partial x_v} u_e \right| \le \mu \eta_{kv} \right\}$, the theorem above can be used to minimize the attenuation H_∞ factor $\gamma > 0$.

Since for TS model (28) in Δ the following bounds hold $\left| \dfrac{\partial w_0^k}{\partial x_1} x_s \right| \le \left| \dfrac{\cos(x_1)}{2} \cdot \dfrac{\pi}{2} \right| \le \dfrac{\pi}{4}$, and $\left| \dfrac{\partial w_0^k}{\partial x_2} x_s \right| = 0$, let's define $R_{l,\mu} = \bigcap_{e,k,s,v} \left\{ x : \left| \dfrac{\partial w_0^k}{\partial x_v} x_s \right| \le \dfrac{\pi}{4} l, \left| \dfrac{\partial w_0^k}{\partial x_v} u_e \right| \le \dfrac{\pi}{2} \mu l \right\}$ in order to check the behaviour of the minimum γ found with the aforementioned algorithm under the testing values $(l, \mu) = ((11-i)/10, 1)$ (different sizes of R) and $(l, \mu) = (1, 10^{i-1})$ (different bounds for μ), $i = 1, \ldots, 9$.

Fig. 3 shows the behaviour of the minimum γ found via the proposed theorem when parameter l varies, thus changing the modelling region of the TS model. As expected, since this is a local approach, the smaller the modelling region, the smaller minimum attenuation factor γ. In other words, restricting the state space it is easier to satisfy the constraints for H_∞ disturbance rejection.

Fig. 4 shows the behaviour of the minimum attenuation factor γ found through the theorem above when the input bound μ varies. Logically, bigger values of μ allow smaller values of γ, since bigger control gains provide higher flexibility in (7).

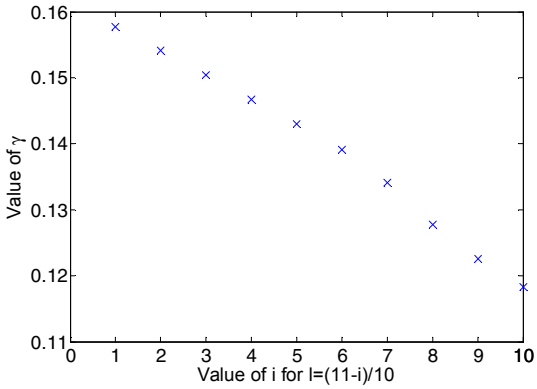

Figure 3: Attenuation factor with different regions (parameter l) and fixed input bound $\mu = 1$.

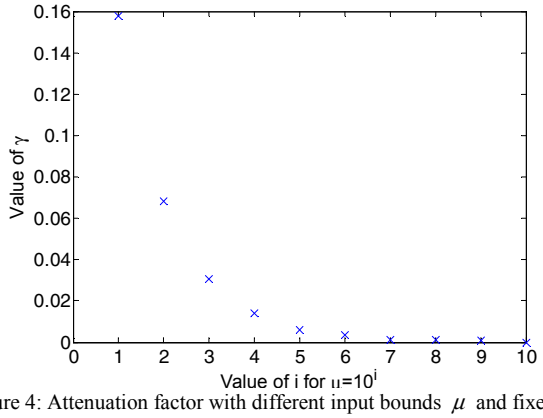

Figure 4: Attenuation factor with different input bounds μ and fixed region size $l = 1$.

V. Conclusions and Perspectives

This paper presented a novel non-quadratic approach for stabilization of continuous-time TS models with H_∞ disturbance rejection. Based on a recently appeared local approach that solves the problem of handling time-derivatives of the MFs, fuzzy Lyapunov functions have been used to design a non-quadratic control law which stabilizes and performs H_∞ disturbance rejection for nonlinear models locally exactly represented via TS models. Two examples are included to illustrate the effectiveness of the approach and to show the effect of the different design parameters.

References

[1] T. Takagi and M. Sugeno, "Fuzzy identification of systems and its application to modelling and control", IEEE Trans. on System Man and Cybernetics, vol.15 (1), 1985, pp. 116-132.

[2] T. Taniguchi, K. Tanaka, and H.O. Wang, "Model construction, rule reduction and robust compensation for generalized form of Takagi-Sugeno fuzzy systems", IEEE Trans. on Fuzzy Systems, vol.9 (4), 2001, pp. 525-537.

[3] K. Tanaka and H.O. Wang, Fuzzy control systems design and analysis. A linear matrix inequality approach. John Wiley and Sons, New York, 2001.

[4] A. Sala, T.M. Guerra, and R. Babuska, “Perspectives of fuzzy systems and control”, Fuzzy Sets & Systems, vol. 156, 2005, pp. 432-444.

[5] G. Feng, “A survey on analysis and design of model-based fuzzy control systems”, IEEE Trans. on Fuzzy Systems, vol. 14 (5), 2006, pp. 676–697.

[6] H.O. Wang, K. Tanaka, and M. Griffin, “An approach to fuzzy control of nonlinear systems: Stability and Design Issues”, IEEE Trans. on Fuzzy Systems, vol. 4 (1), 1996, pp. 14-23.

[7] K. Ohtake, K. Tanaka, and H.O. Wang, “Switching Fuzzy model construction based an optimal dividing plane”, Proc. of the Fuzz’ IEEE Conference, Jeju Island South Korea, 2009.

[8] H.D. Tuan, P. Apkarian, T. Narikiyo, and Y. Yamamoto, “Parameterized linear matrix inequality techniques in fuzzy control system design”, IEEE Trans. on Fuzzy Systems, vol. 9 (2), 2001, pp. 324–332.

[9] A. Sala and C. Ariño, “Asymptotically necessary and sufficient conditions for stability and performance in fuzzy control: Applications of Polya's theorem”, Fuzzy Sets & Systems, vol. 158 (24), 2007, pp. 2671-2686.

[10] A. Sala and C. Ariño, “Relaxed stability and performance conditions for Takagi-Sugeno fuzzy systems with knowledge on membership-function overlap”. IEEE Trans. on System, Man and Cybernetics-B, vol. 37 (3), 2007, pp. 727–732.

[11] M. Bernal, T.M. Guerra, and A. Kruszewski, “A membership-function-dependent approach for stability analysis and controller synthesis of Takagi-Sugeno models”, Fuzzy Sets & Systems. vol. 160 (19), 2009, pp. 2776-2795.

[12] M. Johansson, A. Rantzer, and K. Arzen, “Piecewise quadratic stability of fuzzy systems”, IEEE Trans. on Fuzzy Systems, vol.7, 1999, pp. 713-722.

[13] G. Feng, C.L. Chen, D. Soun, and Yan Zhu, “Hinf controller synthesis of fuzzy dynamic systems based on piecewise Lyapunov functions and bilinear matrix inequalities”, IEEE Trans. on Fuzzy Systems, vol. 13 (1), 2005, pp. 94–103.

[14] B.J. Rhee and S. Won, “A new fuzzy Lyapunov function approach for a Takagi–Sugeno fuzzy control system design”, Fuzzy Sets & Systems, vol. 157 (9), 2006, pp. 1211-1228.

[15] Y. Blanco, W. Perruquetti, and P.Borne, “Stability and stabilization of nonlinear systems and Tanaka-Sugeno fuzzy models”, Proc. of the European Control Conference, Lisbon, Portugal, 2001.

[16] T.M. Guerra and L. Vermeiren, “LMI-based relaxed non-quadratic stabilization conditions for nonlinear systems in Takagi-Sugeno's form”, Automatica, vol. 40 (5), 2004, pp. 823-829.

[17] B.C. Ding, H.X. Sun, and P. Yang, “Further studies on LMI-based relaxed stabilization conditions for nonlinear systems in Takagi-Sugeno’s form”, Automatica, vol. 42, 2006, pp. 503-508.

[18] A. Kruszewski, R. Wang, and T.M. Guerra, “Non-quadratic stabilization conditions for a class of uncertain non linear discrete-time T-S fuzzy models: a new approach”, IEEE Trans. on Automatic Control, vol. 53 (2), 2008, pp. 606-611.

[19] K. Tanaka, T. Hori, and H.O. Wang, “A multiple Lyapunov function approach to stabilization of fuzzy control systems”, IEEE Trans. on Fuzzy Systems, vol. 11 (4), 2003, pp. 582-589.

[20] T.M. Guerra and M. Bernal. “A way to escape from the quadratic framework”. Proc. of the Fuzz’IEEE Conference, Jeju, Korea, 2009.

[21] M. Bernal and T.M. Guerra, “Generalized non-quadratic stability of continuous-time Takagi-Sugeno models”, IEEE Trans. on Fuzzy Systems, vol. 18 (4), 2010, pp 815-822.

[22] M. Bernal, T.M. Guerra, and A. Jaadari, “Non-quadratic stabilization of Takagi-Sugeno models: a local point of view”; Proc. of FUZZ-IEEE Conference, Barcelona, Spain, 2010, pp. 2375-2380.

[23] K. Guelton, T. Bouarar, and N. Manamanni, “Robust dynamic output feedback fuzzy Lyapunov stabilization of Takagi–Sugeno systems—A descriptor redundancy approach”, Fuzzy Sets & Systems, vol. 160 (19), 2009, pp. 2796-2811.

[24] L.A. Mozelli, R.M. Palhares, F.O. Souza, and E.M.A.M. Mendes, “Reducing conservativeness in recent stability conditions of TS fuzzy systems”, Automatica, vol. 45 (6), 2009, pp. 1580-1583.

2011 IEEE International Conference on Fuzzy Systems
June 27-30, 2011, Taipei, Taiwan

Fuzzy Active Contour Models

Cesar Lima Pereira, Carlos A.C.M. Bastos, Tsang Ing Ren and George D.C. Cavalcanti
Center of Informatics, Federal University of Pernambuco
Recife, PE, Brazil - www.cin.ufpe.br/~viisar
{clp,cacmb,tir,gdcc}@cin.ufpe.br

***Abstract*—This paper presents a Fuzzy Active Contour Model for image segmentation using three variations. The proposed models are based on the Fuzzy Energy-Based Active Contour model introduced by Krinidis and Chatzis. First, an update criteria that changes only localized membership values at each iteration is introduced. Second, the model is extended to a type-2 fuzzy logic. And finally, a multiple object segmentation schema is applied to the original model. We present some experimental results, showing the performance for each modification and some of its advantages.**

***Keywords*—Image segmentation, active contour models, fuzzy logic**

I. Introduction

In problems related to image processing and computer vision, image segmentation is an important task that can be critical for the success of any image related procedure. Image segmentation is defined as the process to localize or isolate regions or object of interest in a particular image. Several different procedures for image segmentation have been proposed [1]. However, the segmentation procedure is still considered an essential and a difficult process, specially due to the complexity presented by several images.

Active contour models (ACM) are a well known technique used in image segmentation. Due to its capabilities, ACM are successfully applied in object detection and motion tracking [2], [3]. The idea behind active contour models (or snakes) is a curve that evolves subject to restrictions imposed by characteristics of the images and the curve itself. This evolution is guided by a minimization of an energy function.

The classical active contour models use energy functions based on edge information. Therefore they can only detect objects defined by explicit edges. Objects with smooth or discontinuous edges may not be properly detected. Many authors developed different techniques to overcome this limitation [3], [4], [5]. Chan and Vese proposed a well-known model called Active Contours Without Edges. This model uses an energy function based on the Mumford-Shah segmentation technique and is able to detect contour both with or without gradient information [3].

In Fuzzy Energy-Based Active Contour model [6], proposed by Krinidis and Chatzis, the clustering capabilities presented by fuzzy systems are combined with active contour methodology. It uses fuzzy logic to define the membership of each pixel in the image to the object. So, the fuzzified energy is able to reject local minima, which is a characteristic of fuzzy models. Krinidis and Chatzis used a pseudo level-set formulation that allows the minimization not to be computed using the Euler-Lagrange equations. This procedure decreases the computational time compared with other techniques that use Euler-Lagrange approach. The model is also able to detect objects with discontinuous or smooth edges.

The Fuzzy Energy-Based Active Contour model achieves good segmentation results when applied to two phase images, but it is not appropriate when gradual tonality variations appears in the image. Since it fails to find the object contour, it considers as object other elements of the scene. We propose to modify the Fuzzy Energy-Based Active Contour model so that it is able to deal with more complex images. Besides that, we also extend the model to type-2 fuzzy, in which each primary membership value has a correspondent secondary membership. Increasing the fuzziness of the model means increase the ability to handle inexact information [7]. Last but not least, we present a generalization on the base model that allows it to segment images in more than two areas.

This paper is organized as follows. The base model is described in Section 2. In Section 3, we describe the proposed modifications to the base model: the Morphological Fuzzy Active Contour, Morphological Type-2 Fuzzy Active Contour and Fuzzy Multi Active Contour models. Section 4 describes the experimental results and Section 5 presents the conclusions.

II. Fuzzy Energy-Based Active Contour model (FEB-AC)

The Fuzzy Energy-Based Active Contour model consists in an algorithm that aims to segment regions of interest in a two phase image. First, it is provided to the algorithm an initial partition of the image, i.e., an initial contour. This partition defines the curve that will iteratively evolve by a minimization process. This curve defines the boundaries of the segmented region.

Considering C a curve that is able to evolve in the image domain Ω and I an image composed by two regions, the energy function to be minimized is defined by [6]:

$$\begin{aligned} F(C, c_1, c_2, u) = \mu \cdot Length(C) \\ +\lambda_1 \int_{\Omega} [u(x,y)]^m |I(x,y) - c_1|^2 dxdy \\ +\lambda_2 \int_{\Omega} [1 - u(x,y)]^m |I(x,y) - c_2|^2 dxdy, \quad (1) \end{aligned}$$

This work was partially supported by CAPES.

where u is the membership function, m is a weighting exponent to the fuzzy membership, $\mu \geq 0$ and λ_1, $\lambda_2 > 0$, are fixed values. c_1 and c_2 are the average intensity of the inside and outside areas of the object, respectively, both taking into account their correspondent membership values. c_1 and c_2 are defined by:

$$c_1 = \frac{\int_\Omega [u(x,y)]^m I(x,y) dxdy}{\int_\Omega [u(x,y)]^m dxdy}, \tag{2}$$

$$c_2 = \frac{\int_\Omega [1-u(x,y)]^m I(x,y) dxdy}{\int_\Omega [1-u(x,y)]^m dxdy}. \tag{3}$$

Keeping the values of c_1 and c_2 fixed, the membership of each pixel, $u(x,y)$, is then computed using:

$$u(x,y) = \frac{1}{1 + \left(\frac{\lambda_1 (I(x,y)-c_1)^2}{\lambda_2 (I(x,y)-c_2)^2} \right)^{\frac{1}{m-1}}}. \tag{4}$$

In (1), the length term is approximated by:

$$Length(C) = \sum_{i,j} \sqrt{(Q_{i+1,j} - Q_{i,j})^2 + (Q_{i,j+1} - Q_{i,j})^2}, \tag{5}$$

where $Q_{i,j} = H(u(i,j) - 0.5)$, and $H(\cdot)$ is the Heaviside function [6].

Instead of using a Lipschitz function ϕ, Krinidis and Chatizis used a pseudo level-set formulation, based on the membership function u, to represent different areas of the image, i.e., the curve and the inner and outer regions. The pseudo level-set formulation is defined as:

$$\begin{cases} C & = & \{(x,y) \in I \,|\, u(x,y) = 0.5\} \\ inside(C) & = & \{(x,y) \in I \,|\, u(x,y) > 0.5\} \\ outside(C) & = & \{(x,y) \in I \,|\, u(x,y) < 0.5\}. \end{cases}$$

The algorithm that minimizes the fuzzy energy function $F(C, c_1, c_2, u)$ is described as follows [6]:

1) Assign an initial partition to the image. For the inner part use $u > 0.5$, for the outer part use $u < 0.5$;
2) Compute c_1 and c_2 using equations (2) and (3), respectively;
3) Update the membership value u_o of the pixel I_o with u_n, following equation (4), only if the total energy decreases. That is, $\Delta F < 0$, where this variation is defined by:

$$\Delta F = \lambda_1 s_1 \frac{[u_n^m - u_0^m](I_o - c_1)^2}{s1 + u_n^m - u_0^m} + \lambda_2 s_2 \frac{[(1-u_n)^m - (1-u_0)^m](I_o - c_2)^2}{s2 + (1-u_n)^m - (1-u_0)^m}, \tag{6}$$

   where $s_1 = \sum_{i,j} [u(i,j)]^m$ and $s_2 = \sum_{i,j} [1-u(i,j)]^m$;
4) Repeat Step 3 for each pixel of the image;
5) Repeat Steps 2 to 4 while the total energy keeps changing.

This model achieves good results detecting objects with boundaries that are not defined by gradient and also in the presence of noise. However, it has some drawbacks when dealing with images that present strong pixel intensity variation in its background. The proposed method tries to overcome this limitation by applying an evolving curve procedure similar to other active contour techniques.

III. Proposed Modifications

Active contour models that possess a geometric formulation, as in level-sets, use a high order function ϕ to define the curve boundaries and to control its evolution. This kind of model evolves the contour in regions near to the boundaries.

Due to the pseudo level-set formulation used in Fuzzy Energy-Based Active Contour model, the membership of all pixels in the image may be updated in a single iteration. Consequently, the curve can evolve not only in regions near to its boundaries. In this situation the contour is not continuous, leading to incorrect segmentation results.

A. Morphological Fuzzy Active Contour Model (MF-AC)

In this work we propose a modification of the model introduced by Krinidis and Chatizis that enables the contour to evolve gradually. The main idea is to limit the update area in each iteration to those close to the current contour boundaries. Thus, as the membership function is updated, the border moves, therefore, enabling new areas to be updated. To limit the update area it is necessary to modify the membership values update equation (4) to:

$$u'(x,y) = \frac{\delta\left(u'(x,y) - 0.5\right)}{1 + \left(\frac{\lambda_1 (I(x,y)-c_1)^2}{\lambda_2 (I(x,y)-c_2)^2} \right)^{\frac{1}{m-1}}}, \tag{7}$$

where $\delta(\cdot)$ is the δ Dirac function. Thus, δ act as a weighting coefficient to control the update of the membership values. In this way only the pixels at the boundaries are allowed to update their membership values. However, due to the expression in the denominator of (7), it is not easy to accurately find the boundaries of the contour using this function.

Figure 1 shows this situation: (a) shows the original histogram of an image and (b) shows the histogram of the membership values after the first iteration. The fuzzy energy pushes the membership values towards the centers c_1 and c_2, creating a region with low pixel density close to the value 0.5. Due to this behavior, it is hard to define the boundaries using the δ function. To overcome this problem, we applied mathematical morphology to obtain this desired behavior. Therefore, the new update rule is stated as follows:

$$u'(x,y) = \frac{\beta(H\left(u'(x,y) - 0.5\right)) \oplus R}{1 + \left(\frac{\lambda_1 (I(x,y)-c_1)^2}{\lambda_2 (I(x,y)-c_2)^2} \right)^{\frac{1}{m-1}}}, \tag{8}$$

where $\beta(A) = A - (A \ominus B)$ is a morphological boundary extraction operation from image A using suitable structuring element B to cause an erosion and R is another structuring element used to expand the boundaries to neighbor areas. We used the structuring elements B and R, respectively, as a 3x3 square and a circle with radius 5.

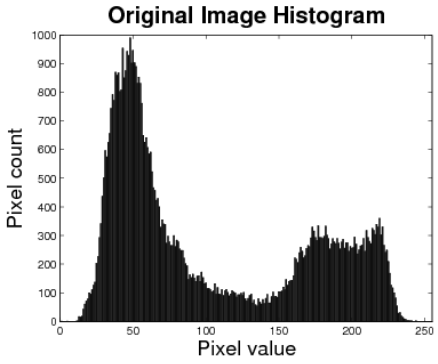

(a)

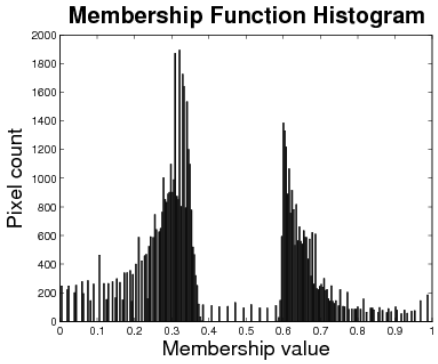

(b)

Figure 1: Histogram comparison. (a) Histogram of the original image. (b) Histogram of the membership function after the first iteration.

B. Morphological Type-2 Fuzzy Active Contour Model (MT2F-AC)

Type-2 fuzzy sets are a generalization of common type-1 fuzzy sets. In type-2, the membership value itself is a fuzzy set. In that way, with type-2 fuzzy is possible to model uncertainties because their membership functions are fuzzy themselves. This does not happen with type-1 fuzzy, in which membership functions are totally crisp [8].

In this model we used interval type-2 fuzzy set, that are also called first-order uncertainty fuzzy models. In this case, secondary memberships are either zero or one, reducing the complexity compared when dealing with general type-2 fuzzy [7]. To do so, we extend the type-1 membership values u, calculated using (4), to the type-2 $\tilde{u}$ by assigning a membership function to each membership value of type-1. We have tried four different functions (graphically shown in Figure 2):

- Triangular (Figure 2a):

$$\tilde{u}(x,y) = u(x,y) - \frac{1-u(x,y)}{2} \tag{9}$$

- Exponential (Figure 2b):

$$\tilde{u}(x,y) = e^{u(x,y)^2} - 1 \tag{10}$$

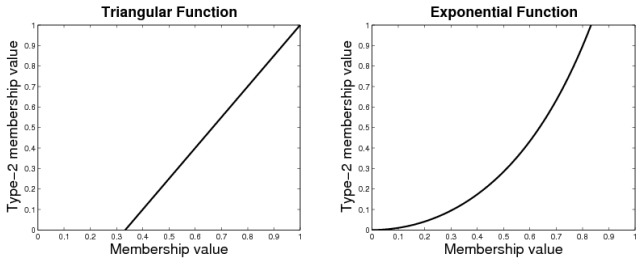

(a) Triangular. (b) Exponential.

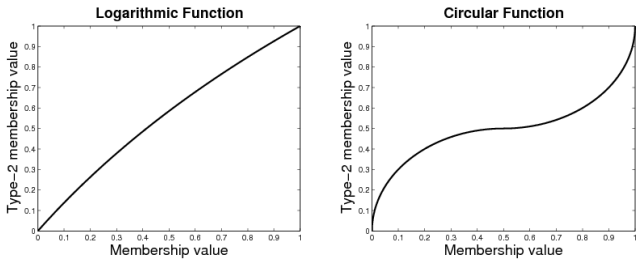

(c) Logarithmic. (d) Circular.

Figure 2: Type-2 membership functions.

- Logarithmic (Figure 2c):

$$\tilde{u}(x,y) = \log_2(u(x,y)+1) \tag{11}$$

- Circular (Figure 2d):

$$\tilde{u}(x,y) = \begin{cases} \sqrt{u(x,y) - u(x,y)^2}, & \text{if u(x,y) } <0.5 \\ 1 - \sqrt{u(x,y) - u(x,y)^2}, & \text{else} \end{cases} \tag{12}$$

Then, instead of using u, which is type-1, we applied the type-2 values $\tilde{u}$ in equations (2) and (3), represented now by $\tilde{c_1}$ and $\tilde{c_2}$, respectively. So, the total energy is given by:

$$\begin{aligned} F(C, \tilde{c_1}, \tilde{c_2}, \tilde{u}) &= \mu \cdot Length(C) \\ &+\lambda_1 \int_\Omega [\tilde{u}(x,y)]^m |I(x,y) - \tilde{c_1}|^2 dxdy \\ &+\lambda_2 \int_\Omega [1-\tilde{u}(x,y)]^m |I(x,y) - \tilde{c_2}|^2 dxdy, \end{aligned} \tag{13}$$

Similarly, the length term (5) and the partial energy variation (6) are computed applying new type-2 membership values.

C. Fuzzy Multi Active Contour Model (FM-AC)

The method described in this section extends the Morphological Fuzzy Active Contour Model to use multiple centers, allowing multiple regions be segmented at once. The main difference from the FEB-AC model relies on the pseudo level-set formulation. Instead of using a (similar) distance function to define inner and outer areas (because only two regions are assumed) the new formulation use group indexes to define regions. In this case, the contour is extracted finding the boundaries between groups.

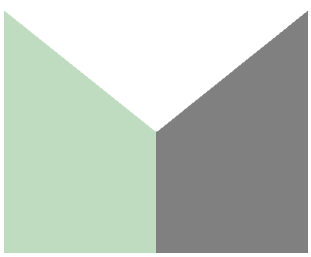

(a) Three groups.

(b) Computed distance for group one.

(c) Computed distance for group two.

(d) Computed distance for group three.

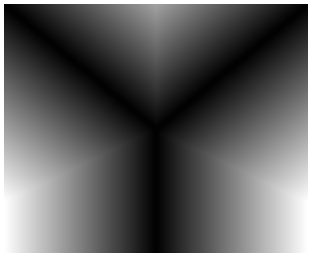

(e) Combined distances.

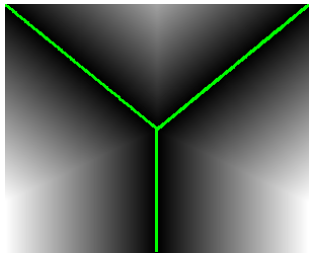

(f) Combined distances with contour extracted.

Figure 3: The process used to identify the contour between different groups. The most distant pixels to any other group are displayed in white.

In this proposed modification, the membership function u is used to assign pixels to each of the K disjoint groups ($K > 2$). This process is represented by:

$$I(x,y) \in k \mid u_k = \max\left(u_j\right),\ j = 1,\ 2,\ \ldots,\ K.$$

Then, the contour is extracted, finding the borders between regions. To perform this operation we first find all pixels that belongs to a disjoint group k, then we compute the distance d_k from these pixels to the nearest pixel that belongs to any other group. In each group, pixels that are neighbor with other group will have a distance value equals to 1, and the pixels in other groups will have the value equals to zero. This process is repeated for every group and the distances $d_k(x,y)$ are combined (summed). Finally, the contour C is extracted by finding the positions (x,y) with minimal distance (in this case the minimum value is one):

$$C = \left\{ (x,y) \in I \mid \sum_{k=1}^{K} d_k(x,y) = 1 \right\}. \tag{14}$$

Figure 3 shows an example on how to obtain the contour: (a) a general partition with three groups; (b, c and d) the computed distances d_k for each group; (e) the combined distances; and (f) the combined distances with the contour highlighted.

To allow the use of multiple centers, the fuzzy energy (1) is modified to:

$$F(C) = \mu \cdot Length(C) + \sum_{k=1}^{K} \lambda_k \int_{\Omega} [u_k(x,y)]^m |I(x,y) - c_k|^2 dxdy, \tag{15}$$

where $Length(C)$ is just the number of pixels in the C set.

The centers c_k are now computed using:

$$c_k = \frac{\int_{\Omega} [u_k(x,y)]^m I(x,y) dxdy}{\int_{\Omega} [u_k(x,y)]^m dxdy}, \tag{16}$$

and the membership update rule follows:

$$u_k(x,y) = \frac{1}{\sum_{j=1}^{K} \left(\frac{\lambda_k (I(x,y) - c_k)^2}{\lambda_j (I(x,y) - c_j)^2} \right)^{\frac{1}{m-1}}}. \tag{17}$$

The algorithm is stated as:

1) Provide an initial partition with K disjoint groups and compute the initial membership values. We used:
$$u_k(x,y) = \begin{cases} 0.5 & , if\ (x,y) \in k \\ 0.5/(K-1) & , elsewhere \end{cases} \tag{18}$$
2) Compute the centers c_k using (16);
3) Update the membership values using (17) where $(x,y) \in I \mid \sum_{k=1}^{K} d_k(x,y) \leq \alpha$; α defines the thickness around the contour;
4) Compute the total energy of the model using (15);
5) Repeat Steps 2 to 4 while the total energy keeps changing.

IV. Experimental Results

The experimental results are presented by applying the proposed models to both natural and artificial images. First, we compare the results using the FEB-AC and the MF-AC models. Then, we applied the type-2 fuzzy model (MT2F-AC). Finally, a FM-AC segmentation experiment is also presented. In all experiments we used $\lambda_1 = \lambda_2 = \lambda_k = 1$, and $m = 2$. The initial membership value to the inner region of the contour was set to $u = 0.8$, except for the FM-AC model which follows (18). Finally, the value of μ showed minor changes to the final contour and its value was set empirically to zero.

We present in Figure 4 a comparison of some intermediary steps between FEB-AC and MF-AC models. Note that the original model converges to a wrong configuration that is close to the final solution in early steps of the procedure. On the other hand, with the proposed modifications the contour evolves gradually, correcting the initial partition and approaching to the desired solution. In the FEB-AC model the update of the membership values can occurs on the whole image. In the MF-AC model, only the pixels in a narrow band

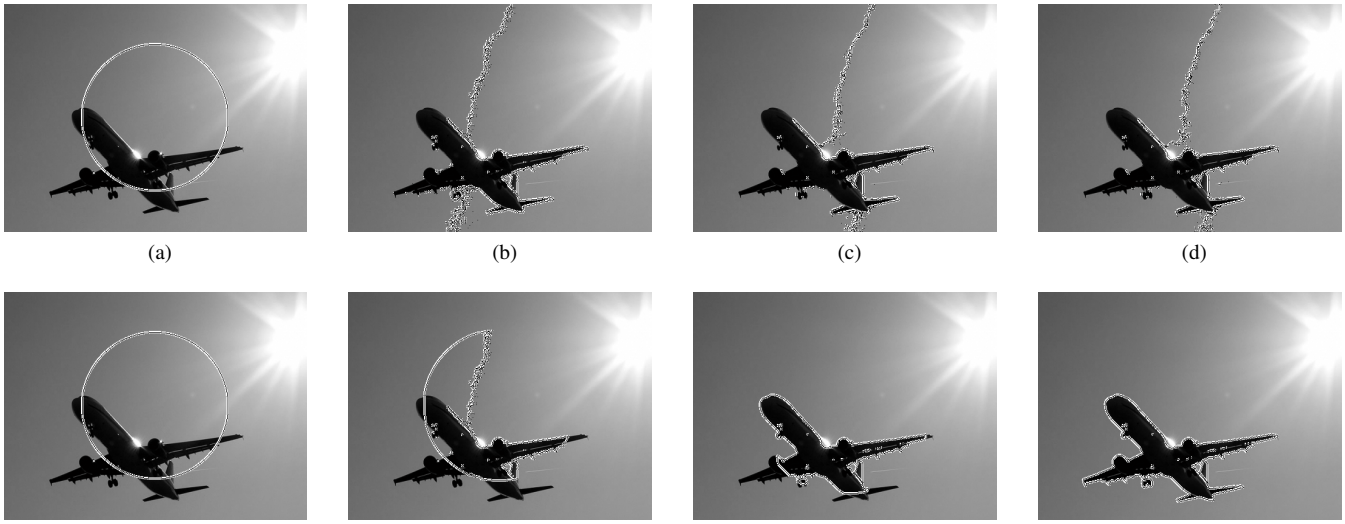

(a) (b) (c) (d)

(e) (f) (g) (h)

Figure 4: Comparison between the results of the segmentation procedures applying in an image of containing an airplane (including some intermediary steps): (a) to (d) using the FEB-AC model, and (e) to (h) using the MF-AC model.

near the boundaries are able to have their membership updated. In this case there is a localized energy decrease.

Figure 5 shows the segmentation results for FEB-AC and MF-AC models, using a flower image. This image has a distinct and well defined foreground and background and both models have similar results, except in the area near the center of the flower. The FEB-AC model correctly find the borders between the flower and the background but the interior, which is darker then the petals, is excluded from the object. The MF-AC model in addition to correctly detect the borders, was also able to include the interior of the flower. This behavior results from the localized membership update.

(a) Original.

(b) Initial Contour.

(c) Final segmentation using FEB-AC model.

(d) Final segmentation using MF-AC model.

Figure 5: A flower image and the segmentation results using the FEB-AC and MF-AC models.

Figure 6 shows a comparison between the segmentation results between FEB-AC and MF-AC models. Note that the background in the space shuttle image presents high variation. As the FEB-AC model allows all pixels to have their membership updated at once, this variation in the background interfere in the computation of c_1 and c_2 constants and in the membership u itself. Due to this fact, the model was unable to correctly segment the contour of the desired object. In this image, the MF-AC model was able to extract the desired object because of the restriction on membership update.

(a) Original.

(b) Initial Contour.

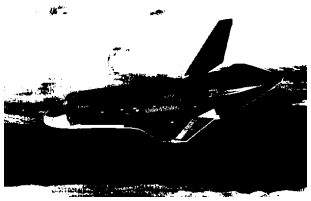

(c) Final segmentation using FEB-AC model.

(d) Final segmentation using MF-AC model.

Figure 6: A Space shuttle image and the segmentation results using the FEB-AC and MF-AC models.

(a) Original image.

(b) Initial contour.

(c) FEB-AC.

(d) MF-AC.

(e) Triangular.

(f) Exponential.

(g) Logarithmic.

(h) Circular.

Figure 7: Segmentation results using: (c) FEB-AC; (d) MF-AC; (e, f, g, and h) MFT2-AC with different type-2 functions. The comparison shows that type-2 models are able to detect the airplane under high background variation.

In Figure 7 experimental results using another airplane image are presented. In this case the MFT2-AC model was used. This image presents a strong spot of light that contributes to a high illumination variation in the background of the scene, causing the FEB-AC and MF-AC models to loose the contour of the central object. This effect does not happen with any of the versions of the proposed MFT2-AC model. The introduced type-2 mapping functions contribute to the algorithm to find the correct contour of the object.

The use of triangular, exponential, and logarithmic type-2 functions spreads the membership values between inner and outter regions. The circular type-2 function, however, narrows membership values to a small range near the value of the contour ($u = 0.5$). Besides that, in this image, the circular function was also able to segment the airplane.

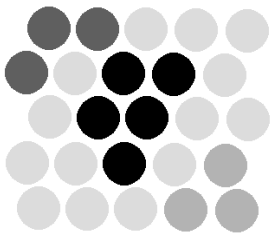

(a) Original.

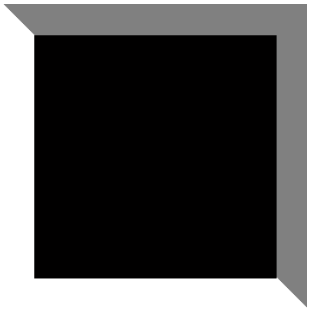

(b) Initial partition (three groups).

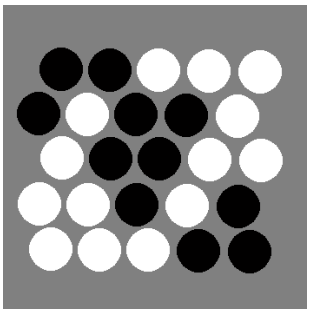

(c) Final segmentation.

Figure 8: An artificial grayscale image, segmented using FM-AC model.

The use of fuzzy mutiple centers model (FM-AC) is showed in Figure 8. In this experiment, an artificial image composed by dots of different grayscale intensities was used. The image, originally with five different intensities was segmented in three groups using pixel intensity similarity to join the groups.

These experiments give an overview of the capabilities of proposed models: by applying an evolution scheme in the base model, the algorithm is capable to handle the segmentation more efficiently. Type-2 fuzzy sets can deal with some scenes that the MF-AC is not able to correctly segment. The change in the membership function may, for instance, give more importance to a higher membership values and decreases even more the memberships that are already small. This adjustment, depending on the image, contribute to the separation process between the object and the background, by adding a new level of uncertainty. The multiple centers model generalizes the base model so that its is able to identify an arbitrary number of groups in a given image. It is useful when one needs to separate multiple objects.

V. Conclusions

In this paper, we proposed a time step evolution to the Fuzzy Energy-Based Active Contour model. In order to achieve this behavior, morphological operators are used to limit the fuzzy membership updates at each iteration. We also extended

this new model to use type-2 fuzzy sets, assigning to each membership value a secondary membership, that adds a new level of uncertainty to the membership. We also generalized the original algorithm to allow the division of the image in an arbitrary number of groups. The experiments showed that each proposed modification improves the power of the model to segment correctly certain types of images.

REFERENCES

[1] R. C. Gonzalez and R. E. Woods, *Digital image processing*, 2nd ed. Prentice-Hall, 2002.

[2] M. Kass, A. Witkin, and D. Terzopoulos, "Snakes: Active contour models," *Intl. Journal of Computer Vision*, vol. 1, no. 4, pp. 321–331, 1988.

[3] T. F. Chan and L. A. Vese, "Active contours without edges," *IEEE Trans. on Image Processing*, vol. 10, no. 2, pp. 266–77, 2001.

[4] A. Tsai, A. Yezzi, and A. Willsky, "Curve evolution implementation of the mumford-shah functional for image segmentation, denoising, interpolation, and magnification." *IEEE Trans. on Image Processing*, vol. 10, no. 8, pp. 1169–1186, 2001.

[5] A. Yezzi, A. Tsai, and A. Willsky, "A fully global approach to image segmentation via coupled curve evolution equations," *Journal of Visual Communication and Image Representation*, vol. 13, pp. 195–216, 2002.

[6] S. Krinidis and V. Chatzis, "Fuzzy energy-based active contours," *Trans. on Image Processing*, vol. 18, pp. 2747–2755, 2009.

[7] Q. Liang and J. Mendel, "Interval type-2 fuzzy logic systems: theory and design," *IEEE Transactions on Fuzzy Systems*, vol. 8, no. 5, pp. 535–550, 2000.

[8] J. Mendel and R. John, "Type-2 fuzzy sets made simple," *IEEE Transactions on Fuzzy Systems*, vol. 10, no. 2, pp. 117–127, 2002.

2011 IEEE International Conference on Fuzzy Systems
June 27-30, 2011, Taipei, Taiwan

Discretization of Fuzzy Transitive Relations.

D. Boixader, J. Recasens
E.T.S. d'Arquitectura del Vallès
Universitat Politècnica de Catalunya
Sant Cugat del Vallès, Catalonia, Spain, EU
dionis.boixader@upcedu

***Abstract*—Fuzzy transitivity is a key property for many fuzzy relational structures, such as Fuzzy Preorders and Equivalences. Theoretical models for practical problems which are based on fuzzy relations make use of continuous scales, mostly the unit interval [0,1]. Practical implementation of these models though, involves their discretization into finite scales, which generally results in some loss of transitivity. In this paper we study if there are any transitivity preserving discretization strategies. Also, we evaluate the loss of transitivity in some commonly used discretization approaches**

Keywords - fuzzy relation; fuzzy equivalence; T-transitivity; indistinguishability operator

I. INTRODUCTION

Fuzzy relational structures play an important role in fuzzy modelling. Fuzzy transitivity is probably the most important property among those involved in the definition of the more complex relational structures, such as *Fuzzy Preorders* and *Fuzzy Equivalence Relations* [1,2].

Generally speaking, theoretical models of continuous problems make use of continuous scales. In the case of fuzzy modelling, the paradigm of such scales is the real unit interval [0,1]. For computing purposes though, discretization has to be inevitably introduced at some stage, resulting in a distortion of the original modelling structure.

The discrete, finitely-valued operations on the unit interval, such as t-norms, t-conorms and OWA operators, have been widely studied by G.Mayor et al. See [3] for an excellent survey. On the other hand, the topic of fuzzy relational structures based on finitely-valued operations has been developed by J. Recasens et al. [4]. A comprehensive and readable introduction can be found in [2].

The present paper is about the fuzzy relations which are obtained from continuously valued fuzzy relations through a process of discretization. Those relations are not necessarily *finitely valued* preorders or equivalences in the sense of [3,4] owing to two reasons: the involved continuous t-norm is not required to become a finitely valued one, and fuzzy transitivity is not always preserved through discretization.

Let us recall some basic definitions the present work relies upon.

Definition 1.1: An operation T on the unit interval [0,1] is called a *t-norm* if it is associative, commutative and it satisfies the boundary conditions $T(x,0) = T(0,x) = 0$ and $T(x,1) = T(1,x) = x$ for all x in [0,1].

Definition 1.2: A fuzzy relation R on a universe X, i.e. a mapping $R : X \times X \to [0,1]$, is:

Reflexive, if $R(x,x) = 1$ for every x in X.

Symmetric, if $R(x,y) = R(y,x)$ for every x and y in X.

Transitive with respect to a given t-norm T, or *T-transitive*, if $T(R(x,y),R(y,z)) \le R(x,z)$ for every x, y and z in X.

Definition 1.3: A *Fuzzy Proximity* is a reflexive and symmetrical fuzzy relation.

Definition 1.4: A *Fuzzy Preorder* is a reflexive and *T*-transitive fuzzy relation.

Definition 1.5: A *Fuzzy Equivalence Relation*, or *Indistinguishability Operator* is a reflexive, symmetrical and *T*-transitive fuzzy relation.

There are other names in use such us Zadeh's original *Similarity Relations* [5] or *T-Indistinguishability Operators* [6].

The concept of t-norm has become a standard in fuzzy logic. The reader is referred to [7] for an excellent state of the art on the subject. Throughout this paper, we will assume t-norms to be continuous, which in practice means only T=MIN (the *minimum* t-norm), T=LUK (the *Lukasiewicz* t-norm) and T=PROD (the *standard product* t-norm) are considered. Any other continuous t-norm is either isomorphic to one of these, or is isomorphic to an ordinal sum of many of these.

Fuzzy transitivity introduced via a t-norm, or *T-transitivity* for short, is closely related to the *triangle inequality* for distances, $d(x,z) \le d(x,y) + d(y,z)$, where the standard sum of real numbers play a similar role to that of the t-norm T. The standard order is though reversed, so that equivalence degrees near 1 correspond to distances near 0. Thus, points linked by high degrees of equivalence become close points. Consequently, the results we present in this paper also apply to the discretization of metric spaces.

Let us state precisely what is to be understood by discretization in the context of this paper.

This work was supported in part by the Spanish DGI research project TIN2009-07235

Definition 1.6: A discrete scale $L_N = \{a_N \ldots a_0\}$, a_i in [0,1], is a finite ordered subset such that:

1. $a_0 = 1$ and $a_N \geq 0$
2. $a_j < a_k$ if $j > k$.

Definition 1.7: A *discretization function* is a mapping $\Delta : [0,1] \to L_N$ such that:

1. $\Delta(a) \leq \Delta(b)$ if $a \leq b$, for all a, b in [0,1].
2. $\Delta(\Delta(a)) = \Delta(a)$ for all a in [0,1].
3. $\Delta(1) = 1$

A discretization of a fuzzy relation E is simply the fuzzy relation $\Delta(E)$, that is, the image of E through a discretization function.

Note that no specific assumptions are made on E, and consequently no specific requirements can be stated regarding t-norms, not being any involved at this stage.

Having fuzzy transitivity in mind makes it very tempting to tie the previous definitions to a t-norm by asking, for example, that $T(a_i, a_j) \in L_N$ for all a_i, a_j in L_N (definition 1.6), or that for $T(\Delta(a), \Delta(b)) \in L_N$ for all a and b in [0,1] (definition 1.7). Although for practical reasons this becomes very often the case, such an assumption would confine our research to the topics of finitely valued t-norms and finitely valued fuzzy preorders and equivalences, which is too restrictive a setting. Our only concern here has to do with assessing the regularity of the distorted relation $\Delta(E)$ with respect to its continuously valued original model E and therefore, the originally involved continuous t-norm.

This section ends with a simple yet fundamental example showing that T-transitivity is not necessarily preserved through discretization.

Example 1.8 Let X be the unit interval [0,1], T=T_{LUK} the Lukasiewicz t-norm, i.e. $T_{LUK}(a,b) = \max\{a + b - 1, 0\}$, the discrete scale $L_1 = \{a_0\ a_1\} = \{0, 1\}$ and the discretization function $\Delta : [0,1] \to L_1$ defined by $\Delta(a) = 1$ if $a \geq 0.5$ and $\Delta(a) = 0$ otherwise, where a,b are in [0,1].

The fuzzy relation considered will be $E(x,y) = 1 - |x - y|$ for all x,y in X=[0,1]. E is called the *residuated biimplication*, or *natural equivalence relation*, associated with the t-norm T_{LUK} so it is a fundamental example [2].

Consider any three real numbers such that $0 \leq x_1 \leq x_2 \leq x_3 \leq 1$, $x_2 - x_1 \leq 0.5$ and $x_3 - x_2 \leq 0.5$, but $x_3 - x_1 > 0.5$. Then $\Delta(E(x_1, x_2)) = 1$ and $\Delta(E(x_2, x_3)) = 1$, but $\Delta(E(x_1, x_3)) = 0$, so that

$1 = T(\Delta(E(x_1, x_2), \Delta(E(x_2, x_3)) > \Delta(E(x_1, x_3)) = 0$

and thus the breach of transitivity. ■

II. Proximity relations and min-transitive relations

Let us start with two kinds of fuzzy relations which behave in a way of their own with respect to discretization: proximity relations (definition 1.3) where transitivity is not involved, and those which are transitive with respect to the minimum t-norm, with Zadeh's *Similarity Relations* standing as their most prominent example [5].

Proposition 2.1 Let E be a proximity relation on a universe X. Then $\Delta(E)$ is also a proximity relation.

The result is an obvious one. More interesting is the case of *MIN*-transitive relations.

Proposition 2.2 Let E be a *MIN*-transitive relation on a set X. Then $\Delta(E)$ is also *MIN*-transitive.

Proof: We need to prove *MIN*-transitivity for $\Delta(E)$, that is, $MIN(\Delta(E(x,y)), \Delta(E(y,z))) \leq \Delta(E(x,z))$

Since $MIN(E(x,y), E(y,z)) \leq E(x,z)$ we apply 1.7.1 to obtain $\Delta(MIN(E(x,y), E(y,z))) \leq \Delta(E(x,z))$

Also, since [0,1] is a totally ordered set $MIN(E(x,y), E(y,z))$ equals either $E(x,y)$ or $E(y,z)$, or both. Without loss of generality we may assume it is $MIN(E(x,y), E(y,z)) = E(x,y)$. Then $E(x,y) \leq E(y,z)$, $\Delta(E(x,y)) \leq \Delta(E(y,z))$ (1.7.1), and

$\Delta(MIN(E(x,y), E(y,z))) = MIN(\Delta(E(x,y), \Delta(E(y,z))$.

As a consequence, $MIN(\Delta(E(x,y)), \Delta(E(y,z))) =$

$\Delta(MIN(E(x,y), E(y,z))) \leq \Delta(E(x,z))$ ■

Next is a corollary of propositions 2.1 and 2.2.

Corollary 2.3 Let E be a similarity relation on a set X. Then $\Delta(E)$ is also a similarity relation.

Corollary 2.4 Let E be a *MIN*-transitive relation on a set X. Then $\Delta(E)$ is T-transitive for any continuous t-norm T.

Corollary 2.4 follows from the fact that $MIN \geq T$ for any t-norm T (a well known fact. See, for example, [3]).

III. The case of transitivity with respect to Archimedean t-norms

Continuous Archimedean t-norms are either strict or non-strict. Strict Archimedean t-norms are isomorphic to the product t-norm, i.e. $T_{PROD}(a,b) = a \cdot b$ for all a,b in [0,1], while the non-strict ones are isomorphic to the Lukasiewicz t-norm (introduced above). Archimedean t-norms can be obtained from decreassing mappings $f : [0,1] \to [0, f(0)] \subseteq [0, +\infty]$ called additive generators by $T(a,b) = f^{[-1]}(f(a) + f(b))$. The symbol $f^{[-1]}$ stands for the pseudo-inverse of f, that is, the mapping $f^{[-1]} : [-\infty, +\infty] \to [0,1]$ defined by $f^{[-1]}(a) = f^{-1}(a)$

if $a \in [0, f(0)]$, $f^{[-1]}(a) = 1$ if $a < 0$ and $f^{[-1]}(a) = 0$ if $a \geq f(0)$. Strict Archimedean t-norms are those with $f(0) = \infty$, in which case $f^{[-1]} = f^{-1}$ and they are isomorphic to the sum of positive real numbers, while the non-strict ones are those with $f(0) < \infty$ and their behaviour is that of a bounded sum of positive real numbers.

The following theorem characterizes those discretization functions that preserve *T*-transitivity, provided that *T* is Archimedean.

Theorem 3.1 Let *T* be an Archimedean t-norm, $L_N = \{a_N \ ... \ a_0\}$ a discrete scale and Δ a discretization function. Then, $\Delta(E)$ is *T*-transitive for any *T*-transitive fuzzy relation *E* on some universe *X* if, and only if, $T(\Delta(a), \Delta(b)) \leq \Delta(T(a,b))$ for all *a*, *b* in [0,1].

Proof. [$\Rightarrow$] Given *a* and *b* in [0,1] let *E* be the *T*-transitive relation defined on *X*=[0,1] by $E(x,y) = f^{[-1]}(f(x) - f(y))$ where *f* is an additive generator of *T*. *E* is *T*-transitive because

$T(E(x,y), E(y,z)) =$

$f^{[-1]}(f(f^{[-1]}(f(x) - f(y))) + f(f^{[-1]}(f(y) - f(z)))) \leq$

$f^{[-1]}(f(x) - f(y) + f(y) - f(z)) =$

$f^{[-1]}(f(x) - f(z)) = E(x,z)$

and, under the hypothesis, so is $\Delta(E)$. We may then consider $x = 1$, $y = a$, $z = T(a,b)$ so that $E(x,y) = a$, $E(y,z) \geq b$ and $E(x,z) = T(a,b)$. Since $\Delta(E)$ is T-transitive we have that

$T(\Delta(a), \Delta(b)) \leq T(\Delta(E(x,y)), \Delta(E(y,z)) \leq$

$\Delta(E(x,z)) = \Delta(T(a,b))$

[$\Leftarrow$] Let us suppose now that $T(\Delta(a), \Delta(b)) \leq \Delta(T(a,b))$ for all *a*, *b* in [0,1]. If *E* is a T-transitive fuzzy relation on a set *X*, then $T(E(x,y), E(y,z)) \leq E(x,z)$ for all *x*, *y*, *z* in *X*. By taking $a = E(x,y)$ and $b = E(y,z)$ we obtain:

$T(\Delta(E(x,y)), \Delta(E(y,z)) = T(\Delta(a), \Delta(b)) \leq$

$\Delta(T(a,b)) = \Delta(T(E(x,y), E(y,z))) \leq \Delta(E(x,z))$

thus proving the T-transitivity of $\Delta(E)$ ■

An important consequence of theorem 3.1 is that arbitrarily chosen discretization functions and scales do not necessarily preserve transitivity with respect to Archimedean t-norms. We will focus on *homogeneous* (or *equidistant*) finite scales, where lower truncation is (almost) the only discretisation strategy that may be applied to the unit interval as a whole.

Definition 3.2 Let *T* be an Archimedean *t*-norm, and $L_N = \{a_N \ ... \ a_0\}$, a_i in [0,1], a finite scale such that $a_N > 0$ if *T* is strict. In this situation, L_N is homogeneous or equidistant with respect to the t-norm *T* if $f^{[-1]}(f(a_i) - f(a_{i+1})) = f^{[-1]}(f(a_{i-1}) - f(a_i))$, *i* = 1 ... *N*-1 for some additive generator *f* of *T*.

NOTES: 1. Either all the additive generators of *T* satisfy the condition or all of them fail to satisfy it (see [3]).

2. $a_N > 0$ in the strict Archimedean case because $f(0) = \infty$, which makes equidistance impossible.

Example 3.3 Consider $L_N = \{a_N \ ... \ a_0\}$ with $a_i = \frac{N-i}{N}$, *i* = 0 ... *N*. L_N is a homogeneous finite scale with respect to the Lukasiewicz t-norm T_{LUK} but it is not homogeneous with respect to the product t-norm T_{PROD}.

This is a consequence of the different behaviour of the two t-norms' additive generators with respect to L_N. Taking $f(a) = f_{LUK}(a) = 1 - a$ and $g(a) = f_{PROD}(a) = -\ln(a)$ as generators, while $g^{[-1]}(g(a_{i+1}) - g(a_i)) = \frac{N-i}{N-i+1}$ depends on *i*, $f^{[-1]}(f(a_{i+1}) - f(a_i)) = \frac{N-1}{N}$ remains constant. ■

Example 3.4 Consider $L_N = \{a_N \ ... \ a_0\}$ with $a_i = p^i$ for a fixed *p*, $0 < p < 1$, *i* = 0 ... *N*. L_N is a homogeneous finite scale with respect to the product t-norm T_{PROD} but it is not homogeneous with respect to the Lukasiewicz t-norm T_{LUK}.

In the present case $g^{[-1]}(g(a_{i+1}) - g(a_i)) = p$ does not depend on *i*, while $f^{[-1]}(f(a_{i+1}) - f(a_i)) = 1 - |\, p^{i+1} - p^i \,|$ obviously does. Also, note that $a_N > 0$ no matter how big the chosen *N* for the particular scale, which makes the cardinality of the scale as big as required. ■

Within any fixed interval $[a_{i+1}, a_i]$ there are only three possible discretization functions: lower truncation, upper truncation and rounding.

Upper truncation is defined by $\Delta_U(a) = \overline{a} = a_i$ if $a_{i+1} < a \leq a_i$. Lower truncation by $\Delta_L(a) = \underline{a} = a_{i+1}$ if $a_{i+1} \leq a < a_i$. In order to precisely define rounding, an additional b_{i+1} between a_i and a_{i+1} is to be considered. Then $\Delta_R(a) = \widehat{a} = a_{i+1}$ if $a_{i+1} \leq a < b_i$, or $\Delta_R(a) = \widehat{a} = a_i$ if $b_i \leq a \leq a_i$. The fact that no more discretization functions are possible inside $[a_{i+1}, a_i]$ is a simple consequence of 1.7.1 and 1.7.2.

When it is the whole unit interval that is taken into account, things become a bit more complicated. Roughly speaking, only lower truncation keeps *T*-transitivity in a general sense, although some especial situations may occur when slightly different discretization functions may perform as well.

Lemma 3.5 Let *T* be an Archimedean *t*-norm, and $L_N = \{a_N \ ... \ a_0\} \subseteq [0,1]$ a homogeneous finite scale. If $i + j \leq N$ then $T(a_i, a_j) = a_{i+j}$

Proposition 3.6 (*strict case*) Let $L_N = \{a_N \ldots a_0\}$ be a homogeneous finite scale w.r.t. a strict Archimedean t-norm T. Then the discretization function

$$\Delta(a) = \begin{cases} \overline{a} & \text{if } 0 \le a < a_N \\ \underline{a} & \text{if } a_N \le a \le a_0 \end{cases}$$

preserves *T*-transitivity.

Proof: For any *a*, *b* in [0,1] we need to prove that $T(\Delta(a),\Delta(b)) \le \Delta(T(a,b))$. There are two different situations, depending on the value of $T(a,b)$.

Case 1. If $T(a,b) \le a_N$ then $\Delta(T(a,b)) = \overline{T(a,b)} = a_N$. Now, if $a \le a_N$ or $b \le a_N$ then $\Delta(a) = a_N$ or $\Delta(b) = a_N$ so that $T(\Delta(a),\Delta(b)) \le a_N$ and therefore $T(\Delta(a),\Delta(b)) \le \Delta(T(a,b))$ On the other hand, if $a > a_N$ and $b > a_N$ then $\Delta(a) = \underline{a} \le a$ and $\Delta(b) = \underline{b} \le b$ so that $T(\Delta(a),\Delta(b)) \le T(a,b) \le a_N$ and we also conclude $T(\Delta(a),\Delta(b)) \le \Delta(T(a,b))$.

Case 2. If $T(a,b) > a_N$ then let *i* and *j* be such that $a_{i+1} \le a < a_i$ and $a_{j+1} \le b < a_j$. Then, by Lemma 3.5 we have $a_{i+j+2} = T(a_{i+1}, a_{j+1}) \le T(a,b) < T(a_i, a_j) = a_{i+j}$ so that $\Delta(T(a,b)) \ge \underline{T(a,b)} \ge a_{i+j+2}$. On the other hand, since

$$\Delta(a) = \underline{a} = a_{i+1} \text{ and } \Delta(b) = \underline{b} = a_{j+1}$$

then $T(\Delta(a),\Delta(b)) = T(a_{i+1}, a_{j+1}) = a_{i+j+2}$ follows (Lemma 3.5), and again $T(\Delta(a),\Delta(b)) \le \Delta(T(a,b))$. ■

Proposition 3.7 (*non-strict case*) Let $L_N = \{a_N \ldots a_0\}$, a_i in [0,1], be a homogeneous finite scale w.r.t. a non-strict Archimedean t-norm T. Then the discretization function $\Delta(a) = \underline{a}$ preserves *T*-transitivity.

Proof: Similar to proposition 3.6, the only difference being $a_N = 0$ which hardly matters. ■

Now we will show that both upper truncation and rounding fail to preserve *T*-transitivity at some point.

Lemma 3.8 Let $L_N = \{a_N \ldots a_0\}$ be a finite scale and Δ a discretization function such that $\Delta(\alpha) = a_0 = 1$ for some $a_1 < \alpha < a_0$. Then Δ does not preserve *T*-transitivity with respect to any Archimedean t-norm.

Proof: Consider $x_1 = \alpha < x_2 < \ldots < x_{k-1} \le a_1 < x_k$ where $x_2 = T(\alpha,\alpha) = \alpha^2$, ... $x_k = T(\alpha, \alpha^{k-1}) = \alpha^k$. Such a chain exists for *T* is Archimedean. Then $\Delta(E(x_1, x_k)) \le a_1$ while $T(\ldots(T(\Delta(E(x_1,x_2)),\Delta(E(x_2,x_3))))\ldots) = T(\ldots(T(1,1))\ldots) = 1$ which is against the *T*-transitivity of $\Delta(E)$. ■

As a consequence the next two propositions naturally follow.

Proposition 3.9 Upper truncation discretization does not preserve *T*-transitivity with respect to any Archimedean t-norm.

Proposition 3.10 Rounding discretization does not preserve *T*-transitivity with respect to any Archimedean t-norm.

Propositions 3.9 and 3.10 exclude upper truncation and rounding as global discretization strategies when the whole unit interval is considered. However, they say nothing of their suitability to handle *T*-transitivity when mixed with lower truncation at specific, on-purpose chosen intervals $[a_i, a_{i+1}]$. A such 'custom-made' discretization is shown in the next example.

Example 3.11 Let L_4 be the finite scale $\{a_4 = 0,\ a_3 = 0.25,\ a_2 = 0.5,\ a_1 = 0.75,\ a_0 = 1\}$ which is homogeneous with respect to T_{LUK}, the Lukasiewicz t-norm. The discretization function $\Delta(a) = \begin{cases} \underline{a} & \text{if } a_4 \le a < a_2 \\ \overline{a} & \text{if } a_2 \le a \le a_0 \end{cases}$ preserves T_{LUK}-transitivity.

IV. TRANSITIVITY LOSS IN UPPER TRUNCATION AND ROUNDING

Fuzzy transitivity is not a crisp notion [8,9,10]. Even when a fuzzy relation *E* fails to be strictly *T*-transitive with respect to a given *t*-norm *T*, some degree of transitivity can still be assigned to it depending on how strongly the relation fails to comply with that property, or how far it falls from any truly *T*-transitive relation of reference.

Since we know that both upper truncation and rounding fail to preserve *T*-transitivity for Archimedean *t*-norms, it makes sense to ask ourselves about the extent of the transitivity loss through these two discretization functions.

Transitivity with respect to a t-norm can be turned into a gradual concept in mostly two different ways. The first way assigns a transitivity degree to any fuzzy relation on a triplet by triplet basis:

Definition 4.1: A fuzzy relation *R* on a universe *X* is *a-Transitive* with respect to a given t-norm *T*, or *a-T-transitive*, if $T(a, T(R(x,y), R(y,z))) \le R(x,z)$ for a given *a* in [0,1], and for every *x*, *y* and *z* in *X*.

The second way takes an overall criteria in order to assign a degree of transitivity, which is called the *strong T-transitivity* degree. Strong T-transitivity is based on the closeness between the actual fuzzy relation *E* and its transitive closure $\overline{E}$ [11]. The *transitive closure* $\overline{E}$ of an arbitrary fuzzy relation *E* is the lowest *T*-transitive relation which is above *E* with respect to the pointwise order ($E \le_X \overline{E}$). The closer *E* is to $\overline{E}$, the higher its degree of transitivity. Closeness in that context is measured through the *natural indistinguishability operator*, defined as follows.

Definition 4.2: Let T be an Archimedean t-norm, and f one of its additive generators. The fuzzy relation

$E_T(x,y) = f^{[-1]}(|f(x)-f(y)|)$ for all x and y in [0,1] is called the natural indistinguishability associated with T.

NOTE: E_T does not depend on the particular f chosen.

Definition 4.3: The natural indistinguishability between two fuzzy relations E and F defined on a set X is $\mathcal{E}_T(R,S) = \inf_{x,y\in X} E_T(R(x,y),S(x,y))$

Definition 4.4: A fuzzy relation E on a universe X is *strong a-Transitive* with respect to a given t-norm T, or *a-T-strong transitive*, if $\mathcal{E}_T(E,\overline{E}) \geq a$ for a given a in [0,1].

The general idea is that both upper truncation and rounding behave quite similarly, showing a loss of transitivity degree (in the sense of definition 4.1) which is in accordance with the coarseness of the finite scale in use.

Proposition 4.5: Let E be a fuzzy T-transitive relation, f an additive generator of the t-norm T, and $L_N = \{a_N \ldots a_0\}$ a homogeneous finite scale of [0,1]. Then:

4.5.1 The fuzzy relation $\Delta_U(E)$ (upper truncation of E) is δ-T-transitive with $\delta \geq f^{[-1]}(f(a_i)-f(a_{i+1}))$

4.5.2 The fuzzy relation $\Delta_R(E)$ (rounding) is δ-T-transitive with $\delta \geq f^{[-1]}(f(a_i)-f(a_{i+1}))$

NOTE: The expression $\delta \geq f^{[-1]}(f(a_i)-f(a_{i+1}))$ includes the case when $\delta = 1$, i.e. E is fully T-transitive. This situation occurs, for example, when the fuzzy relation E is *MIN* transitive (Corollary 2.4).

Proof: 4.5.1 For a given tern x, y and z in X let i and j be such that $a_{i+1} < E(x,y) \leq a_i$ and $a_{j+1} < E(y,z) \leq a_j$. Then $\Delta_U(E(x,y)) = a_i$, $\Delta_U(E(y,z)) = a_j$ and

$T(\Delta_U(E(y,z)),\Delta_U(E(y,z))) = a_{i+j}$

On the other hand $a_{i+j+2} < T(E(x,y),E(y,z) \leq a_{i+j}$. Since $T(E(x,y),E(y,z) \leq E(x,z)$ (E is T-transitive), the inequality $a_{i+j+2} < E(x,z)$ also holds, and thus $a_{i+j+1} \leq \Delta_U(E(x,z))$.

Finally, $T(T(\Delta_U(E(y,z)),\Delta_U(E(y,z))),\delta_0) =$

$T(a_{i+j},\delta_0) = a_{i+j+1} \leq \Delta_U(E(x,z))$

where $\delta_0 = f^{[-1]}(f(a_i)-f(a_{i+1}))$.

The proof of 4.5.2 involves a tedious case by case study of four different possible situations. We will skip that, as the ideas involved in there have already been shown in 4.5.1 ■

Proposition 4.5 provides an easy criterion to decide whether a finitely valued fuzzy relation can be obtained from a continuously valued T-transitive one. Finitely valued relations with a breach of transitivity heavier than the step of the mesh $\delta = f^{[-1]}(f(a_i)-f(a_{i+1}))$ are automatically discarded. The question of whether this criterion is actually a characterization remains open, though.

However, when the strong transitivity degree is considered (definition 4.2), both upper truncation and rounding may end up in heavy loss of transitivity, even if precise, very fine scales are used. The problem is illustrated by the following example.

Example 4.6 (Upper truncation) Let us consider X=[0,1], T=T_{LUK} the Lukasiewicz t-norm, E the fuzzy relation on X defined by $E(x,y) = 1-|x-y|$, $L_N = \{a_N \ldots a_0\}$ with $a_i = \frac{N-i}{N}$ and upper rounding, i.e. $\Delta(a) = \Delta_U(a) = a_i$ for all a in $(a_{i+1}, a_i]$, as the chosen discretization function. Then the transitive closure of $\Delta(E)$ is the relation $F = \overline{\Delta(E)} = 1$, and the strong transitivity degree is then 0.

Proof. The strong transitivity degree is (definition 4.2)

$\mathcal{E}_T(\Delta(E),F) = \inf_{x,y\in X} E_T(\Delta(E(x,y)),F(x,y)) =$

$\inf_{x,y\in X} E_T(\Delta(E(x,y)),1) = 0$

which accounts for the last part of the example.

To prove that $F = 1$ is the transitive closure of $\Delta(E)$, notice that for any pair x, y such that $E(x,y) > a_{N-1} = \frac{N-1}{N}$ its discretized value is $\Delta(E(x,y)) = a_N = 1$ and therefore $F(x,y) = 1$.

Now, if x and y are such that $E(x,y) \leq a_{N-1} = \frac{N-1}{N}$ with $x < y$, we may consider

$x_0 = x,\ x_1 = x+\varepsilon,\ x_2 = x+2\varepsilon \ldots x_M = x+M\varepsilon$

such that $E(x_i,x_{i+1}) = 1-|x_i - x_{i+1}| = 1-\varepsilon$, where $\frac{1}{N} > \varepsilon > 0$ with $y < x_M = x+M\varepsilon$. Since F is T-transitive,

$F(x,y) \geq T(\ldots T(T(F(x,x_1),F(x_1,x_2)))\ldots F(x_{M-1},y)) =$

$T(\ldots T(T(1,1))\ldots 1) = 1$ and thus $F(x,y) = 1$ for all x, y in X.

■

The previous example can be easily adapted to the case of rounding by choosing an ε which is small enough in relation to the finite scale L_N.

More generally, the situation illustrated by the previous example occurs in all those situations where the elements of X may be linked to each other by chains of closely enough laid elements.

Theorem 4.7 Let T be an Archimedean t-norm, E a T-transitive relation on a set X and $L_N = \{a_N \ldots a_0\} \subseteq [0,1]$ an homogeneous finite scale. If for all x and y in X there is a chain $x = x_0, x_1, x_2 \ldots x_M = y$ with $E(x_i,x_{i+1}) > \delta$ for all i, then $\overline{\Delta(E)} = 1$ ■

In that case, the strong transitivity degree may fall to 0.

V. CONCLUSIONS

Fuzzy transitive relations with respect to a continuous t-norm are a prominent class of fuzzy relations. They include fuzzy preorders and fuzzy equivalence relations, which are widely used in a variety of soft-computing areas ranging from approximate reasoning to clustering or pattern recognition.

From any practical purpose, discretization of the continuously valued models remains crucial. However, discretized *T*-transitivity fuzzy relations when *T* is an Archimedean t-norm do not always behave as expected. Only lower truncation discretization succeeds at preserving *T*-transitivity.

At the other end, *MIN*-transitivity is always preserved regardless the discretization strategy adopted, a fact that boosts the theoretical soundness of Similarity Relations, a class of fuzzy relations which is the choice of reference in many applied domains.

REFERENCES

[1] D. Boixader, J. Jacas and J. Recasens, "*Fuzzy equivalence relations: advanced material*" in Fundamentals of Fuzzy Sets, D. Dubois and H. Prade eds, Kluwer 2000, pp.261-290.

[2] Recasens, J. Indistinguishability Operators. Modelling Fuzzy Equalities and Fuzzy Equivalence Relations Series: Studies in Fuzziness and Soft Computing, Vol. 260. 2011. Springer Verlag. ISBN 978-3-642-16221-3.

[3] Mayor, G., Torrens, J.: Triangular norms on discrete settings. In: Klement, E.P., Mesiar, R. (eds.) Logical, Algebraic, Analytic, and Probabilistic Aspects of Triangular Norms, pp. 189-230. Elsevier BV. (2005)

[4] Mayor, G, Recasens, J. Finitely valued indsitinguishability operators IPMU2010. Dortmund. (2010). LNAI 6178. 39-48.

[5] L. A. Zadeh, "Similarity relations and fuzzy orderings," *Information Sciences*, 3, 1971, pp. 177–200.

[6] Trillas, E.: Assaig sobre les relacions d'indistingibilitat. Proc. Primer Congrés Català de Lògica Matemàtica, Barcelona, 51-59 (1982) (In Catalan)

[7] Klement, E.P., Mesiar, R., Pap E.: Triangular norms. Kluwer Academic Pub lishers, Dordrecht (2000)

[8] S. Gottwald, "Fuzzified fuzzy relations. *Proc. of the 4th IFSA congress,* vol. Mathematics, Brussels 1991, pp.82-86.

[9] L. Behounek, Bodenhofer and Cintula "Relations in Fuzzy Class Theory - initial steps" FSS 159 (2008) pp.1729-1772.

[10] D. Boixader and J. Recasens, "Approximate Fuzzy Preorders and Equivalences" *Proc. FuzzIEEE 2009*, Korea.

[11] Boixader, D., Recasens, J. "Approximating fuzzy preorders and equivalences. A similarity based approach" *WCCI-FUZZ'IEEE2010*. Barcelona.

2011 IEEE International Conference on Fuzzy Systems
June 27-30, 2011, Taipei, Taiwan

Tridimensional Fuzzy Pain Assessment

Ernesto Araujo
Hospital Municipal Dr. José de Carvalho Florence (HMJCF)
São José dos Campos, SP, Brazil, 12243-000

Health Informatics Department (DIS)
Universidade Federal de São Paulo (UNIFESP)
São Paulo, SP, Brazil, 04023-062

Assoc. Paulista para o Desenvolvimento da Medicina (SPDM)
São Paulo, SP, Brazil, 04024-002

Email: ernesto.araujo.br@gmail.com, ernesto.araujo@unifesp.br

Susana A. Miyahira
Anesthesiology Dpt.
Hospital Municipal Dr. José de Carvalho Florence (HMJCF)
São José dos Campos, SP, Brazil, 04023-062
Email: susana_miyahira@uol.com.br

***Abstract*—A tridimensional fuzzy pain assessment for representing professional, social, and sexual aspects concerned to the fifth vital sign of medical condition is proposed in this paper. According to the 3D fuzzy pain assessment herein, pain is not only caused by activity in nociceptive information in the brain. The proposed approach embodies such sensorial information simultaneously that contextualize it within cultural aspects that permeate the human life. This paper extends both previous unidimensional fuzzy pain intensity scale and the accepted professional-social–sexual pain assessment to fuzzy inference systems. The fuzzy professional–social–sexual pain assessment is able to represent the inherent physiological, psychological characteristics by taking into account the emotional, complex perceptual, subjective, and personal phenomenon involving all domains of an individual meanwhile can deal with cultural mechanisms within individual life experience. According to the proposed approach, not only fuzzy set theory but fuzzy systems can also direct and immediately improve medicine and healthcare in general, and pain assessment, in particular, in a subjective and multi–dimensional model.**

***Index Terms*—Pain Assessment, Classification, Decision Support System, Fuzzy Logic, Artificial Intelligence, Computational Intelligence, Professional–Social–Sexual Disabilities**

I. Introduction

Pain afflicts postoperative patients, patients with advanced cancer, residents in long-term care facilities, recipients of end–of–life care, for one side, and the elderly, the young, and minorities, on other side [1]. Further, there is no distinction between economical-social-sexual-racial characteristics; all individuals are subject to this vital signal in medicine and healthcare. Understood as the signal for diagnosing medical conditions related to the presence of disease or abnormality [2], [3], pain assessment is still a challenge for medical and healthcare professionals.

Many are the sources of difficulties for medical and healthcare professionals. The foremost challenge is, mostly, concerned to the patient's self-report intensity during physical examinations; the preferable indicator of pain. Pain is, primary, determined by sensorial information. Stimulus in free endings of thin myelinated and nonmyelinated fibers sends nociceptive information to pain receptors (Nociceptors) in the brain that detect noxious agents [4]. Related to genetic composition, there is a huge variability in the pain perception and pain expression for the same painful stimuli [5].

Intensity is, however, not the only aspect employed to define pain. Due to its nature, it is not only physiological but psychological, as well. Being a perception, pain is considered an emotional, complex perceptual, subjective, and personal phenomenon involving all domains of individual life experiences [5]. The challenge in pain assessment for representing basic bodily functions and health quality of life also encompass pain-related disability, pain duration, pain affect etc. [6]. Cultural mechanisms and derived social aspects such as individual life experience, learned behavior, daily life activities, only to mention few, affect patient's pain perception [7], [8]. Pain is, thus, understood as a multi-faceted subjective response related to a biopsychosocial experience.

All these characteristics encompass a variety of clinical scenarios and make pain assessment and management a complex task for therapeutic decisions. To improve pain assessment and management, fuzzy set theory is employed in [5] to address the subjectivity of the pain intensity reported by patients. The most common, international standards (systematic mechanisms) related to unidimensional intensity rating assessment are modified by using fuzzy set theory yielding fuzzy visual analog scale (FVAS), fuzzy numerical rating scale (FNRS), fuzzy qualitative pain scale (FQPS), and fuzzy face pain scale (FFPS). Therein, possibility distribution functions are used to best represent the inherent imprecision, uncertainty and vagueness related to the fifth vital sign of medical condition, present in the pain report and assessment. Such an approach is used as an alternative to build up a fuzzy pain assessment system [9].

Unidimensional fuzzy pain intensity scale was first chosen due to its immediate and general applications, for one side, and the reinforcement of the Joint Commission on Accreditation of Healthcare Organizations (JCAHO) for using easier tools as the key element for successful pain assessment and treatment [10], on the other side. Nevertheless, unidimensional pain measurements fail in capturing other elements and aspects that

978-1-4244-7316-8/11/$26.00 ©2011 IEEE

can influence the perception of the patients.

Pain can be assessed by employing unidimensional or multidimensional mechanisms according to the objective and interests to be achieved during diagnosis. This paper addresses the use of fuzzy set theory and fuzzy logic to represent multi-faceted, tridimensional pain assessment encompassing pain-related disability, i.e., pain-related interference with activities. Along with this real-world, ordinary life activities are professional, social, and sexual (PSS) features as examples of cultural mechanisms that compose such a behavior pain assessment. This paper extends both previous unidimensional fuzzy pain intensity scale and the international professional–social–sexual pain assessment to synthesis a fuzzy inference system able to gather the inherent physiological, psychological, and cultural mechanisms within individual life experiences.

II. Tridimensional Fuzzy Pain Assessment

For each of the different aspects concerning pain, different assessment instruments should exist. Measurement of pain intensity does not capture sensory, affective, behavioral, social, and attitudinal factors. Along with pain intensity, pain-related interference with activities is seen as a major indicator for the severity of a pain condition [6], [11].

A. 3–D Professional–Social–Sexual Pain Assessment

Behavioral and social limitations are important elements for pain measurement. For instance, dressing, walking, family life, sexual relationship, professional performance etc. are examples from simple to complex activities affected by pain. Unfortunately, this list extends so far.

Several pain assessment approaches have been developed to assess the pain-related disability. These approaches assess the limitations in different activities of daily living. A list of multi-faceted, multi-items, multidimensional pain measures is detailed in [11].

The literature points out professional, social, and sexual limitations as three great groups for classifying pain-related disabilities. Tridimensional Fuzzy Professional–Social-Sexual (FPSS) Pain Assessment is, thus, proposed in this paper.

B. 3–D Fuzzy Professional–Social–Sexual Pain Assessment

Taking into account the inherent imperfection (uncertainty, imprecision, vagueness) present in this natural phenomenon, fuzzy set theory is a primary approach for representing pain [5]. While a unidimensional fuzzy set, M_i, can immediately be employed to represent unidimensional pain intensity, n-dimensional fuzzy sets:

$$M_{(1,\ldots,i,\ldots n)} = M_1 \ \cap \ldots \cap \ M_i \ \cap \ldots \cap \ M_n \qquad (1)$$

can be an alternative for describing multidimensional pain conditions. N-dimensional fuzzy sets advantage of gathering distinct characteristics associated to an object under analysis, each one represented, respectively, by distinct universes of discourse, X_i. The fuzzy sets can be represented by simple fuzzy propositions, $P_i = \langle x_i \text{ is } M_i \rangle$, in a natural or synthetic

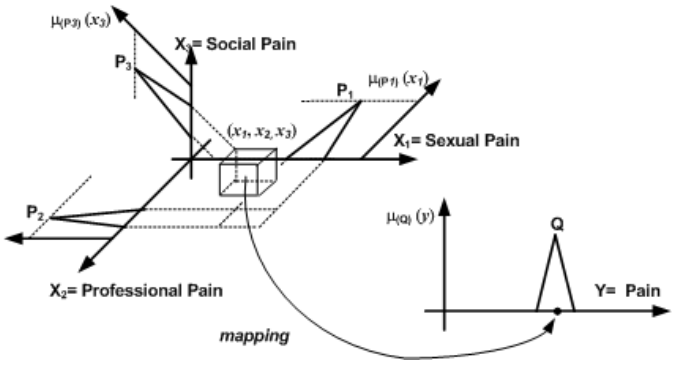

Fig. 1. Tridimensional Fuzzy Pain Measurement

language. In general, simple fuzzy propositions when put together allow building compound fuzzy propositions:

$$P_1 \text{ AND} \ldots \text{AND } P_i \text{ AND} \ldots \text{AND } P_n \qquad (2)$$

such that, the intersection set operation, $\cap$, in (1) corresponds to the linguistic expression, AND in (2). Further, the resulting value can yet be related to fuzzy classes by employing a fuzzy inference mechanism also denominated *fuzzy conditional proposition* as given as:

$$\text{IF } P_1 \text{ AND} \ldots \text{AND } P_i \text{ AND} \ldots \text{AND } P_n \text{ THEN } P_{n+1} \ , \qquad (3)$$

Due to its equivalence to linguistic expressions in the form of arguments to represent rules of inference it is associated to human approximate reasoning.

In this paper, professional–social–sexual pain-related disabilities are simultaneously represented in a tridimensional premise space, as depicted in Fig. 1, and mapped into an output associated to pain assessment, in the general form:

$$\begin{aligned} \mathrm{R}_i : \text{IF } & \left\langle \textit{professional pain} \text{ is } M_{ij_{professional}}^{professional} \right\rangle \text{ AND } \ldots \\ & \left\langle \textit{social pain} \text{ is } M_{ij_{social}}^{social} \right\rangle \text{ AND } \ldots \\ & \left\langle \textit{sexual pain} \text{ is } M_{ij_{sexual}}^{sexual} \right\rangle \\ \text{THEN } & \left\langle \textit{disability pain} \text{ is } N_{ij_{disability-pain}}^{disability-pain} \right\rangle \ , \end{aligned} \qquad (4)$$

where the elements $M_{ij(\cdot)}^{(\cdot)}$ and $N_{ij(\cdot)}^{(\cdot)}$ are fuzzy sets (also named *linguistic terms*) partitioning the respective universes of discourse, X_k and Y. The amount of partitions is given by $j(\cdot) = 1, \ldots, m_{(\cdot)}$ such that $M_{j(\cdot)}^{(\cdot)}(x_k) \subset X_k \ \forall k = 1, \ldots, n$ and $N^{disability-pain} \subset Y$. The number of rules is given by $i = 1, \ldots, N_r$. The input vector of the premise is given by $x = [x_1, x_2, x_3]^T$, while the output is associated to y. The input variables are *professional pain* $\in X_1$, *social pain* $\in X_2$, *sexual pain* $\in X_3$ while the output variable is *disability pain* $\in Y$. As proposed, $n = 3$ in this paper determines the number of input universes of discourse and represents the tridimensionality of the premises.

The universes of discourse of the proposed 3–D fuzzy pain measurement is equivalent in structure to Fuzzy Qualitative Pain Scale (Fig. 1). The FQPS consists of a verbal rating

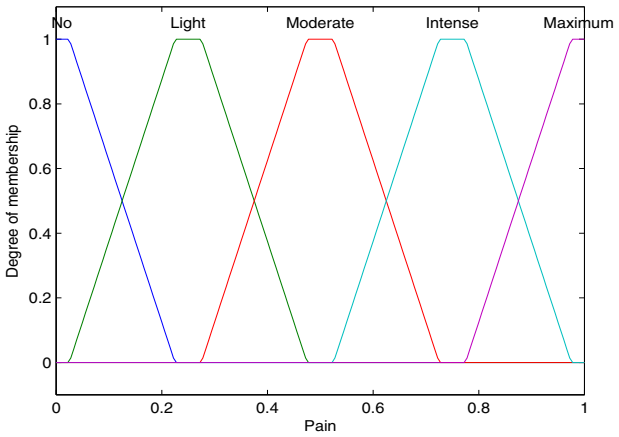

Fig. 2. Equivalent structure of Unidimensional Fuzzy Quality Pain Scale (FQPS) to input and output universes of discourse for Fuzzy Professional–Social–Sexual (FPSS) pain assessment

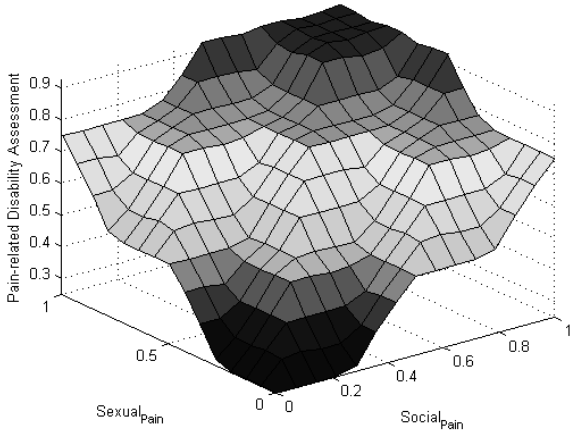

Fig. 4. Sexual and Social input relationship to pain–related disability degree of severity.

scale in which categories are labeled with words. Each of the input and output universes of discourse can, thus, adopt the same linguistic terms and number of partitions. In the FQPS, the patient is asked to classify the pain intensity according to linguistic expressions (adjectives) from a list of (1) *no pain*, (2) *light pain*, (3) *moderate pain*, (4) *intense pain*, (5) *maximum pain*. The linguistic expressions for representing pain may be directly represented by fuzzy sets as depicted in Fig. 2 [5]. In so doing, the linguistic terms $M^{professional}_{j_{professional}}$, $M^{social}_{j_{social}}$, and $M^{sexual}_{j_{sexual}}$, respectively, with $j_{professional} = j_{social} = j_{sexual} = 1, \ldots, 5$, yield a set of 125 fuzzy regions in the tridimensional input space, as illustrated in Fig. 1.

The 3D Fuzzy PSS pain assessment is, thus, represented as

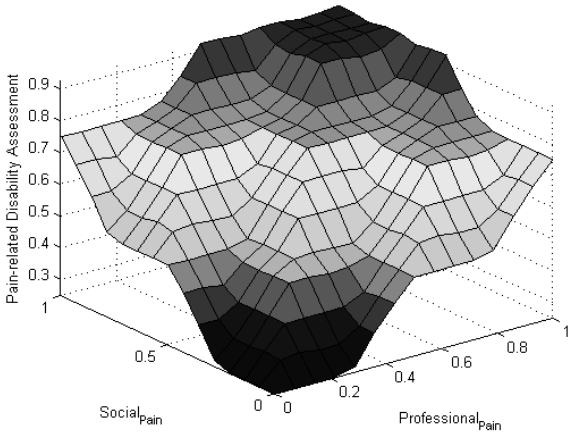

Fig. 3. Social and professional input relationship to pain–related disability degree of severity.

IF-THEN *fuzzy rules* in the form:

$$
\begin{aligned}
\mathrm{R}_1 : \text{IF } &\langle \textit{professional}_{pain} \text{ is } \mathrm{No}_{professional} \rangle \text{ AND } \ldots \\
&\langle \textit{social}_{pain} \text{ is } \mathrm{No}_{social} \rangle \text{ AND } \ldots \\
&\langle \textit{sexual}_{pain} \text{ is } \mathrm{No}_{sexual} \rangle \\
\text{THEN } &\langle \textit{disability pain} \text{ is } \mathrm{No}_{disability} \rangle \ , \\
\mathrm{R}_2 : \text{IF } &\langle \textit{professional}_{pain} \text{ is } \mathrm{No}_{professional} \rangle \text{ AND } \ldots \\
&\langle \textit{social}_{pain} \text{ is } \mathrm{No}_{social} \rangle \text{ AND } \ldots \\
&\langle \textit{sexual}_{pain} \text{ is } \mathrm{Light}_{sexual} \rangle \\
\text{THEN } &\langle \textit{disability pain} \text{ is } \mathrm{Light}_{disability} \rangle \ , \\
&\ldots \\
\mathrm{R}_{124} : \text{IF } &\langle \textit{professional}_{pain} \text{ is } \mathrm{Maximum}_{professional} \rangle \text{ AND } \ldots \\
&\langle \textit{social}_{pain} \text{ is } \mathrm{Maximum}_{social} \rangle \text{ AND } \ldots \\
&\langle \textit{sexual}_{pain} \text{ is } \mathrm{Intense}_{sexual} \rangle \\
\text{THEN } &\langle \textit{disability pain} \text{ is } \mathrm{Maximum}_{disability} \rangle \ , \\
\mathrm{R}_{125} : \text{IF } &\langle \textit{professional}_{pain} \text{ is } \mathrm{Maximum}_{professional} \rangle \text{ AND } \ldots \\
&\langle \textit{social}_{pain} \text{ is } \mathrm{Maximum}_{social} \rangle \text{ AND } \ldots \\
&\langle \textit{sexual}_{pain} \text{ is } \mathrm{Maximum}_{sexual} \rangle \\
\text{THEN } &\langle \textit{disability pain} \text{ is } \mathrm{Maximum}_{disability} \rangle \ .
\end{aligned}
\tag{5}
$$

The fuzzy IF-THEN rules in (5) are denominated *fuzzy model*, as well. In this way, the proposed 3D Fuzzy PSS pain assessment is, actually, a fuzzy model for pain assessment when behavior and disability aspects are taken into account.

The proposed fuzzy professional–social–sexual pain assessment may be employed with any shape of fuzzy sets available in literature. Here, trapezoidal membership functions are utilized to illustrate the proposed approach. The resulting fuzzy pain-related disability assessment when concerning social–professional input variables, sexual–social input variables, and

professional–sexual input variables are, respectively, depicted in Fig. 3, Fig. 4, and 5.

C. Singleton Pain and Fuzzy Pain Measurements in Fuzzy PSS Pain Assessment

The fuzzy model for PSS pain assessment works as an alternative when interested in reporting behavior and disability aspects. The fuzzy professional–social–sexual pain assessment advantages in being able to deal with both singleton and fuzzy pain measurement for any of the input dimension (Fig. 6).

Singleton pain measurement can be obtained by employing, for instance, but not limited to, visual analog scale, numeric rating scale, verbal rating scale, change in back pain intensity, increased pain during or after exercise, low back pain rating scale, pain frequency, pressure pain threshold, 5-point categorical, 6-point categorical, 11-point intensity. They can immediately be used to supply singleton inputs for the fuzzy PSS assessment system, as depicted in Fig. 6(a).

Nevertheless, emotional states and in doubt individuals when reporting their pain perception are related to the absence of crisp boundaries and singleton values. An international standard proposed for pain assessment based on fuzzy sets and fuzzy numbers for representing inaccuracy, flexibility, doubt, and emotionality in pain intensity measurement is described in [5]. Likewise occurs with singleton pain measurement scales, fuzzy visual analog scale (FVAS) and fuzzy numerical rating scale (FNRS) are alternatives for supplying fuzzy inputs for the fuzzy PSS assessment system, as depicted in Fig. 6(b).

Visual comparative analysis among classic Visual Analog Scale (VAS) and Numerical Rating Scale (NRS) and FVAS, FNRS are, respectively, depicted in Figs. 7 and 8. When using the fuzzy visual analog scale, the value of pain intensity is obtained by the distance from the beginning of a 10 cm single line assigned in one border labeled *no pain* and in the other extremity *maximum pain* to the patient's marks. This distance is directly measured in centimeters by employing a ruler or by using a computational system [9]. While the classic visual

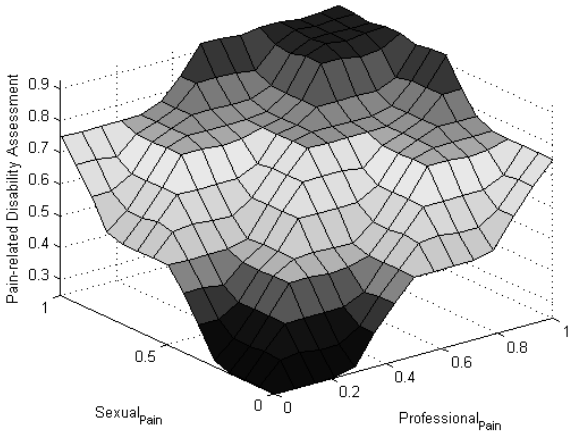

Fig. 5. Professional and sexual input relationship to pain–related disability degree of severity.

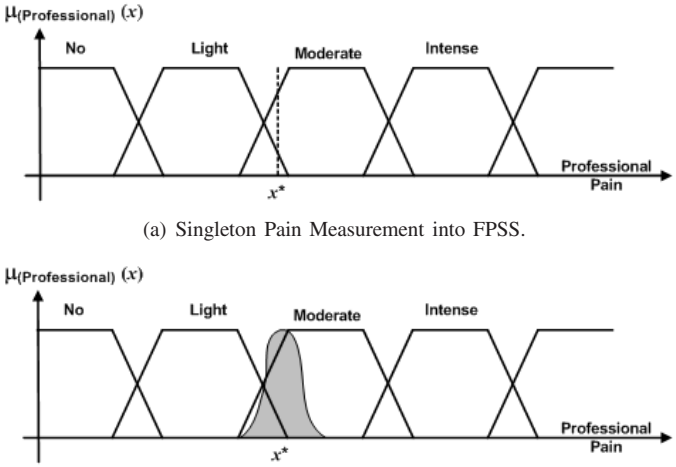

(a) Singleton Pain Measurement into FPSS.

(b) Fuzzy Pain Measurement into FPSS.

Fig. 6. Both types of singleton and fuzzy pain measurement supplied to FPSS pain assessment, for instance, into professional pain dimension.

analog scale is represented as a singleton value, the fuzzy visual analog scale is able to represent the inaccuracy in the pain indication (Fig. 7(b)) by using fuzzy sets [5].

Similarly, fuzzy numerical rating scale consists of a graded line scale identified by eleven numbers from 0 to 10 (Fig. 8(a)). The patient marks this scale with the pain intensity that better represents the assumed physical discomfort. The value of pain intensity is obtained by the distance from the beginning of the graded line to the patient's marks. This distance is directly measured in centimeters by employing a ruler or by using a computational system [9]. While the classic numerical rating scale is represented as a singleton value, the fuzzy numerical rating scale uses a fuzzy set to represent the subjectivity, vagueness in indication of the pain (Fig. 8(b)) [5].

It is worth mentioning that nothing prevents the use of mixed singleton and fuzzy pain measurements for representing behavior and disability pain condition.

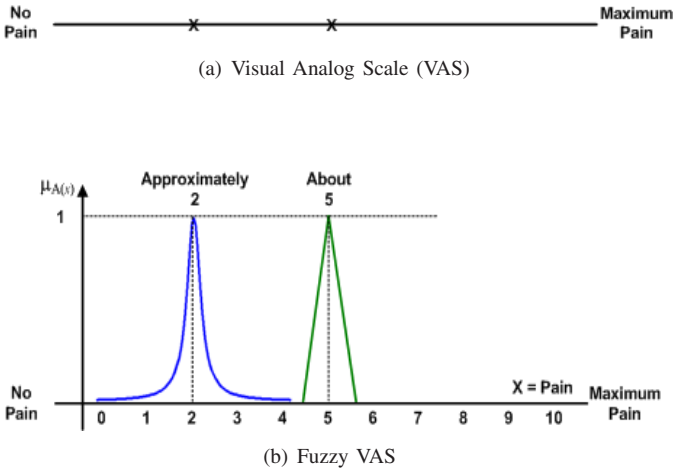

(a) Visual Analog Scale (VAS)

(b) Fuzzy VAS

Fig. 7. Unidimensional Fuzzy Visual Analog Scale (FVAS).

D. Exemplifying Patient's Self-Report Fuzzy Behavioral and Disability Pain Modeling

Consider a patient who reports social and professional difficulties due to the presence of a back pain during medical diagnosis. The patient declares the interest in not getting out due to the pain. Working in security, the back pain assumes a more important role because the patient carries a revolver. Further, the afflicted pain does not limit the sexual experience but a patient's self-report pain measurement indicates a small discomfort.

Simple, unidimensional pain scales can, at first, be used to identify the pain intensity, be it a singleton or fuzzy measure. Nevertheless, being able to capture presence and intensity, they do not determine the real significance of the pain. The preferable indicator of pain must capture the importance of not being able to adequately handle a revolver. The intensity pain scale does not measure the impact and social frustration upon patient's family due to the limitation imposed by the patient's pain. Neither, the sexual discomfort is taken into account.

The tridimensional pain-related disability model presented in (4) is a feasible alternative for comprehensively representing the inherent complexity, subjectivity comprising this sort of pain. In this illustrative example, it is considered the simplest condition. A singleton pain scale is furnished to the patient who, in turn, marks three distinct amplitudes for professional, social, and sexual pain according to the well established NRS. It was required first to the patient to mark the intensity of pain, i.e., marking a unidimensional pain scale. Second, it is asked to the patient to include not only intensity of pain but limitations and other aspects concerning each one of the input premises for completely describing the suffering. These marks are presented in Fig. 9. Distinct values among the four pain measurements based on real–world data (patients)

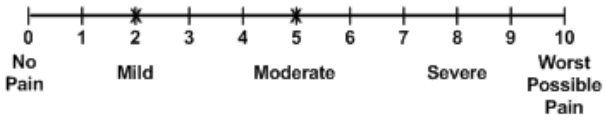

(a) Numerical Rating Scale (NRS)

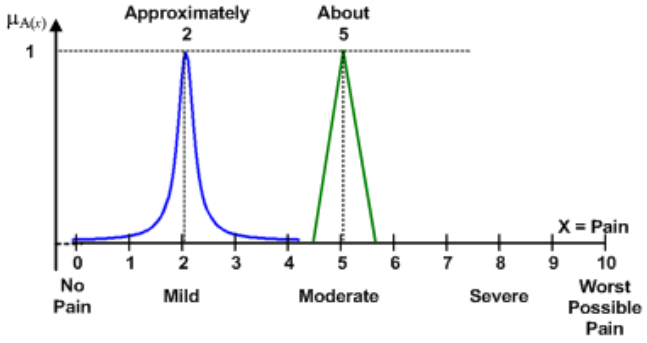

(b) Fuzzy NRS (FNRS)

Fig. 8. Unidimensional Fuzzy Numerical Rating Scale (FNRS)

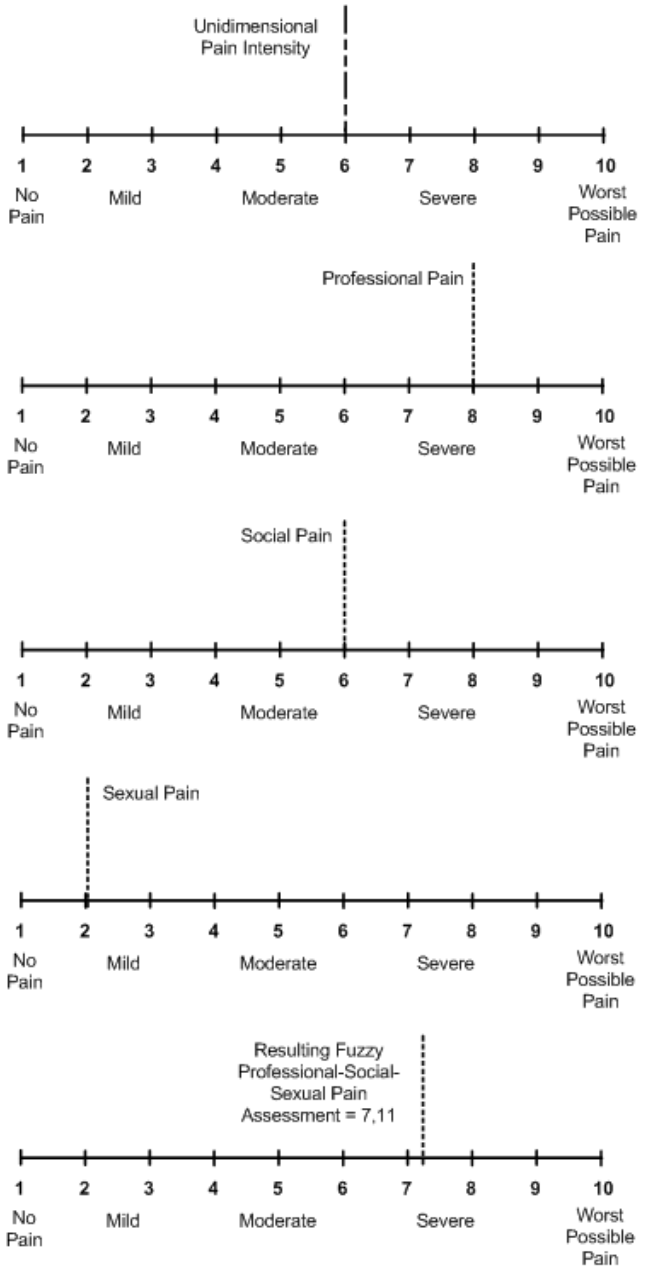

Fig. 9. Trade–off between Fuzzy Professional–Social–Sexual Pain Assessment and Classic Unidimensional Pain Intensity Measurement.

are: (a) simple intensity of pain, (b) professional pain, (c) social pain, and (d) sexual pain. Notice yet the (e) resulting fuzzy professional–social–sexual pain value computed by a 3D Fuzzy PSS pain assessment system.

III. Conclusion

In this paper a novel, feasible approach for modeling pain-related behavioral and disability assessment based on fuzzy set theory and fuzzy logic is presented. Professional pain, social pain, and sexual pain are three great groups for classifying pain-related disabilities used for generating a tridimensional fuzzy pain modeling. The proposed approach advantages of

being able to deal with both with singleton and fuzzy pain input measurements. Each input dimension can assume singleton pain values, or fuzzy pain values, or yet a mixed singleton and fuzzy pain values. The proposed fuzzy professional–social–sexual pain assessment is able not only of capturing sensory, affective, behavioral, social, and attitudinal factors concerning presence and intensity of afflicted pain but determine the real significance of the pain according to the inherent complexity, subjectivity comprising behavioral and disability aspects. The 3–D FPSS is a comprehensively manner to describe the physiological, psychological, and cultural present in mankind pain condition.

REFERENCES

[1] C. M. Mar, C. Chabal, R. A. Anderson, and A. E. Vore, "An interactive computer tutorial to teach pain assessment," *Journal of Health Psychology*, vol. 8, no. 1, pp. 161–173, 2003.

[2] M. McCaffery and C. L. Pasero, "Pain ratings: The fifth vital sign," *American Jornal of Nursery*, vol. 97, no. 2, pp. 15–16, 1997.

[3] M. K. Merboth and S. Barnason, "Managing pain: The fifth vital sign," *Nurs. Clin. Nor. Amer.*, vol. 35, no. 2, pp. 375–383, 2000.

[4] R. A. Meiss, "Sensory physiology," in *Medical Physiology*, R. A. Rhoades and G. A. Tanner, Eds., ch. 4, pp. 63–89, 739 p.

[5] E. Araujo and S. A. Miyahira, "Unidimensional fuzzy pain scale," in *Intern. Conference on Fuzzy Systems*. IEEE, 2009, pp. 185–190.

[6] M. Haefeli and A. Elfering, "Pain assessment," *European Spine Journal*, vol. 15, pp. S17–S24, 2006.

[7] T. D. Walsh, "Practical problems in pain measurements," *Pain*, vol. 19, pp. 96–98, 1984.

[8] R. Ohrbach and S. F. Dworkin, "Five-year outcomes in tmd: Relationship of changes in pain to changes in physical and psychological variables," *Pain*, vol. 74, pp. 315–326, 1998.

[9] E. S. Bocato, E. Araujo, and S. Miyahira, "Fuzzy system for pain assessment by using api swing and java computational tools," in *Brazilian Congress of Health Informatics*. SBIS, 2010, in Portuguese.

[10] *Pain as the 5-th vital sign Toolkit*, Joint Commission on Accreditation on Healthcare Organizations (JCAHO), Illinois, Jan. 2000, cited 2006 Abr 27. [Online]. Available: http://www.vachronicpain.org/Downloads/pain5thvitalsignv2.PDF

[11] L. Litcher-Kelly, S. A. Martino, J. E. Broderick, and A. A. Stone, "A systematic review of measures used to assess chronic musculoskeletal pain in clinical and randomized controlled clinical trials," *The Journal of Pain*, vol. 8, no. 12, pp. 906–913, 2007.

2011 IEEE International Conference on Fuzzy Systems
June 27-30, 2011, Taipei, Taiwan

Integrate Variable Precision Rough Sets and Modified PBMF Index Function for Partitioning and Classifying Complex Datasets

Kuang Yu Huang
Department of Information Management
Ling Tung University
#1 Ling Tung Road, Taichung City 408, Taiwan
kyhuang@mail.ltu.edu.tw

*Yu-Hsin Cheng
Department of Information Networking and System Administration, Ling Tung University
#1 Ling Tung Road, Taichung City 408, Taiwan
hsin@teamail.ltu.edu.tw

***Abstract*—This study proposes a method for partitioning and classifying complex datasets using a hybrid method based on Fuzzy C-Means (FCM) method, Variable Precision Rough Set (VPRS) theory and a modified form of the PBMF index function (a cluster validity index function). The proposed VPRS index method partitions the attributes within the dataset rather than the data and achieves both the optimal number of clusters and the optimal classification accuracy. The validity of the proposed approach is confirmed by comparing the clustering results obtained from the VPRS method for a hypothetical function and a typical stock market system with those obtained from the conventional RS and PBMF methods, respectively. Overall, the results show that the VPRS index method not only has a better clustering performance than the PBMF method, but also achieves greater classification accuracy, and therefore provides a more reliable basis for the extraction of decision-making rules.**

Keywords-Fuzzy C-Means; Variable Precision Rough Set; VPRS index method; PBMF-index method; Classification; Cluster

I. INTRODUCTION

Classification, which is a task of grouping data with multiple attributes into relevant categories, has become the most valuable process to learn the implicit knowledge among dataset. However, difficulties have been found in many classification approaches, and one of the major problems is related to clustering－partition the real-value attributes into discrete groups. In order to conduct a dataset classification, attribute clustering must be performed in prior, and accurate clustering is the premise to meaningful classifications.

In general, the problem of evaluating the optimality of the clustering results obtained for a particular dataset is referred to as the cluster validity problem [1]. Many methods have been proposed for assessing the validity of the clustering results obtained using fuzzy clustering schemes [2]. Amongst these methods, early indices such as the partition coefficient [3, 4] and classification entropy [5, 6] are based simply on the membership values of the instances within the dataset and are therefore computationally straightforward. In general, existing clustering methods cluster the dataset in accordance with the norms of the instances rather than the values of the individual attributes. The results obtained using traditional clustering methods fail to take sufficient account of the complex interrelationships amongst the various attributes of the dataset. Therefore, in constructing data partitioning and classification algorithms, it is preferable to apply some form of classification-defining knowledge to the attribute values of the dataset such that the complex interrelationships amongst the various attributes can be taken more properly into account.

The literature contains many algorithms for automatic classification purposes, including decision-tree algorithms such as ID3 [7], rule-based algorithms such as CN2 [8], back-propagation networks [9], support vector machines [10], conformal predictors [11], Bayesian classifiers [12], and so forth. Whilst such algorithms have found widespread use in a diverse range of applications, including weather prediction, manufacturing process planning, medical diagnosis, and so on, they can not deal effectively with systems characterized by uncertain or missing information. Furthermore, to the best of the current authors' knowledge, only few attempts [13] have so far been made to integrate these classification algorithms with any form of cluster validity index in order to evaluate the optimality of the clustering results.

Rough Set (RS) theory was first introduced more than twenty years ago [14] and has emerged as a powerful technique for the automatic classification of instances [15]. However, performing a classification operation with a controlled degree of uncertainty or misclassification error is beyond the ability of the RS approach [16]. In an attempt to extend RS theory to such classification applications, Ziarko proposed a Variable Precision Rough Set (VPRS) methodology in which the instances within the dataset were analyzed and classified in terms of their statistical tendencies rather than their functional patterns [16, 17]. In VPRS theory, the uncertain nature of the information within the system of interest is handled using the concept of β-lower and β-upper approximate sets. However, as with the RS method, the classification performance of VPRS models is constrained by the quality of the original clustering results. Therefore, in meeting the needs of decision-makers for

* Corresponding author

sophisticated methods capable of extracting reliable decision rules from complex information systems, it is necessary to integrate the VPRS method with some form of optimized clustering scheme.

Accordingly, this study proposes a hybrid scheme for the partitioning and classification of complex datasets based upon the FCM clustering method and a VPRS model in which the optimal threshold parameter β is determined using the method presented by Huang [18]. In the proposed approach, the dataset is partitioned in terms of the attribute values of the instances rather than the norms of the instances in order to capture the complex interactions amongst the various instances.

The remainder of this paper is organized as follows. Section II presents the fundamental principles of the FCM method, VPRS theory and the conventional PBMF clustering validity index, respectively. Section III describes the integration of these concepts to create the proposed VPRS partitioning and classification scheme. Section IV compares the performance of the proposed scheme with that of the conventional RS index function method and the PBMF (FCM-based) clustering method, respectively. Finally, Section V presents some brief concluding remarks and indicates the intended direction of future research.

II. Review of Related Methodologies

A. Index function $I_{\max}$

Assume that each instance x_i in the dataset has has m conditional attributes and the l -th attribute a_l can be partitioned into p_l clusters, then $C_{a_l}(x_i)$ gives the index of the cluster to which the l -th attribute a_l of instance x_i belongs. Here $C_{a_l}(x_i)$ is given by $C_l(x_i) = I_{\max}(\mu_j(x_i(a_l))) = \text{Index}(\max(\mu_j(x_i(a_l))))$ for $1 \le l \le m, 1 \le i \le n$, where $I_{\max}(\mu_j(x_i(a_l)))$ returns the index of the cluster corresponding to the maximum value amongst all the membership functions of the l -th attribute of x_i.

B. Fundamental principles of VPRS theory

VPRS operates on what may be described as a knowledge-representation system, or information system [16]. The basic principles and notations of information systems (S) and the application of VPRS theory to the processing of such systems are described in the sections below.

1) β -lower and β -upper approximate sets: For a given dataset, any instances which are indistinguishable from one another when evaluated using a particular subset of all the attributes define an equivalence or indiscernibility relationship. In RS theory, this indiscernibility concept is handled using approximate sets. A typical information system has the form $S = (U, A, V_q, f_q)$, where U is a non-empty finite set of instances, A is a non-empty finite set of attributes describing these instances and $X \subseteq U$ and $R \subseteq A$. Generally speaking, the attributes in set A can be partitioned into a set of conditional attributes $C \neq \{\}$ and a set of decision attributes $d \neq \{\}$, i.e. $A = C \cup d$ and $C \cap d = \{\}$. For each attribute, $q \in A$, V_q represents the domain of q, i.e. $V = \cup V_q$. Finally, $f_q : U \times A \to V$ is an information function defined such that $f(x,q) \in V_q$ for $\forall q \in A$ and $\forall x \in U$. The VPRS method proposed in this study utilizes the systematic method presented by the current author in [18] to determine an appropriate value of the threshold parameter β, i.e., the value of β at which a certain proportion of the instances in a particular conditional class are classified into the same decision class. When processing an information system using a VPRS model with $0.5 < \beta \le 1$, the objective is to identify the β -lower and β -upper approximate sets associated with each cluster of the decision attribute. In general, the β -lower approximation of sets $X \subseteq U$ and $P \subseteq C$ can be expressed as

$$\underline{R}_P^{\beta}(X) = \{x \in U : P(X/[x]_P) \ge \beta\} = \cup\{[x]_P : P(X/[x]_P) \ge \beta\}$$

Similarly, the β -upper approximation of sets $X \subseteq U$ and $P \subseteq C$ is given by

$$\overline{R}_P^{\beta}(X) = \{x \in U : P(X/[x]_P) > 1-\beta\} = \cup\{[x]_P : P(X/[x]_P) > 1-\beta\}$$

Note that $P(X/Y) = \dfrac{|X \cap Y|}{|Y|}$ if $|Y| > 0$, and $P(X/Y) = 1$ otherwise. Note also that $|X|$ denotes the cardinality of set X.

In the particular case of $\beta = 1$, $\underline{R}_P^{\beta}(X)$ and $\overline{R}_P^{\beta}(X)$ are equivalent to the lower and upper approximate sets in RS theory. In other words, the VPRS model reverts to the traditional RS model.

2) Accuracy of VPRS classification results: The accuracy of the VPRS classification results can be quantified as follows:

$$\alpha_c^{\beta} = \left|\underline{R}_P^{\beta}(d \mid C_d(x) = c)\right| \Big/ \left|\overline{R}_P^{\beta}(d \mid C_d(x) = c)\right|,$$

where $\left|\underline{R}_P^{\beta}(d \mid C_d(x) = c)\right|$ and $\left|\overline{R}_P^{\beta}(d \mid C_d(x) = c)\right|$ are the cardinalities of the β -lower and β -upper approximate sets obtained when ranking the elements (x) in terms of the c -th cluster of the decision attribute d.

C. PBMF index function

The PBMF cluster validity index function [19] ensures the formation of a small number of compact clusters within the dataset and maximizes the separation distance between at least two of these clusters. The PBMF index function is formulated as $PBMF(K) = \left(\frac{1}{K} \times \frac{\overline{E_1}}{J_{m'}} \times D_K\right)$, where K is the number of clusters, $J_{m'} = \sum_{k=1}^{K}\sum_{j=1}^{n} \mu_{kj}^{m'} \left\| x_j - z_k \right\|$, $\overline{E_1}$ is constant for a given dataset and is used to prevent the value of the second term from approaching zero, and $D_K = \max_{i,j=1}^{K} \left\| z_i - z_j \right\|$. In addition, n is the total number of instances in the dataset, $U(X) = \lfloor \mu_{kj} \rfloor_{K \times n}$

is the matrix used to partition the data, m' is the fuzzification parameter, and z_k is the centroid of the k-th cluster. In utilizing the PBMF index function for data clustering purposes, the objective is to find the value of K (i.e. the number of clusters) which maximizes the index value.

III. VPRS INDEX METHOD

This study proposes a hybrid scheme comprising a Variable Precision Rough Set (VPRS) model and a modified form of the PBMF index function for optimizing both the number of clusters within the dataset and the corresponding classification accuracy. Assuming that U is the domain of discourse and R is the set of equivalences of U, the VPRS classification problem can be formulated as

$$X \subseteq U \text{ is : } (\underline{R}_P^{\beta}(X), \overline{R}_P^{\beta}(X)), BND_P^{\beta}(X),$$

where X is the set of instances; U/I_P is the quotient set of U; I_P is the indiscernibility of R; {} is the empty set; R is the attribute set of X and includes both the conditional attribute set（C） and the decision attribute set (d), $P \subseteq C$; $\underline{R}_P^{\beta}(X)$ is the β-lower approximate set of X; $\overline{R}_P^{\beta}(X)$ is the β-upper approximate set of X; and $BND_P^{\beta}(X)$ is the boundary set of X.

Significantly, the VPRS index method proposed in this study clusters the attribute values of the instances within the dataset rather than the norms of the instances. Thus, in contrast to the PBMF index function method, the proposed approach takes better account of the intrinsic interrelationships amongst the various independent parameters of the dataset. The detailed parameters of the VPRS index function are discussed in the following section.

A. Parameters of VPRS index function

The VPRS index function proposed in this study has the form

$$VPRS(N, \alpha_c^{\beta}) = \left(\frac{1}{N} \times \frac{\overline{E_1}}{F'_N} \times D'_N \right)$$

where N is the number of clusters assigned to the conditional and decision attributes and α_c^{β} is the classification accuracy when evaluated in terms of the c-th cluster of the decision attribute. In addition, F'_N is obtained by aggregating the value of E'_c for each cluster of the decision attribute (d), where E'_c is given by $E'_c = \sum_{j=1}^{n} \overline{\mu}_{cj}^{m'}(x_j(d)) \left\| x_j - z'_c \right\| \Big/ \alpha_c^{\beta}$, in which $\overline{\mu}_{cj}(x_j(d))$ is the membership function of instance x_j in the c-th cluster of the decision attribute d and z'_c is the multi-dimensional centroid of the β-lower approximate sets associated with the c-th cluster of the decision attribute d and is obtained by computing the mean values of the conditional and decision attributes of each instance within the corresponding sets. Furthermore, m' is the fuzzification parameter and n is the total number of instances in the dataset. Finally, the value of D'_N is equal to the maximum separation distance amongst the centroids of all the β-lower approximate sets associated with the different clusters of the decision attribute, i.e. $D'_N = \max_{i,j=1}^{N} \left\| z'_i - z'_j \right\|$. Note that the value of $D_N{}'$ is upper bounded by the maximum separation distance amongst all possible pairs of data points in the dataset.

Note that parameter F'_N in the VPRS index function differs slightly from parameter $J_{m'}$ in the PBMF index function in that its value depends on E'_c and therefore takes the classification accuracy into account.

B. Tendencies of terms within VPRS index function

As discussed in Section III.A, the VPRS index function has the form $VPRS(N, \alpha_c^{\beta}) = \left(\frac{1}{N} \times \frac{\overline{E_1}}{F'_N} \times D'_N \right)$. In other words, the index function comprises three terms, namely, $1/C$, $\overline{E_1}/F'_N$ and $D_N{}'$. Clearly, the value of the first term decreases as the number of clusters assigned to the conditional and decision attributes, N, increases. In other words, the value of the index function decreases with an increasing value of N. Regarding the second term in the index function, the value of $\overline{E_1}$ is constant for a given dataset and is equal to $\overline{E_1}$ in the conventional PBMF index function. Meanwhile, as discussed in the previous section, F'_N is equal to the sum of all $E_c{}'$, where each $E_c{}'$ includes the classification accuracy α_c^{β} associated with the c-th cluster of the decision attribute d. Hence, the VPRS index function increases as $E_c{}'$ decreases. The third term, $D_N{}'$, measures the maximum distance between the centroids of the β-lower approximate sets associated with the different clusters of the decision attribute, and increases as N increases. Thus, the contribution of $D_N{}'$ to the value of the VPRS index function increases as the number of decision attribute clusters increases.

C. Detailed processing steps in proposed VPRS index function method

The details of each processing step are summarized in the following paragraphs.

Step 1: Specify number of clusters per attribute in interval [2, N_{max}]

As described in Section I, the proposed VPRS index method utilizes an iterative procedure to optimize the number of clusters assigned to each conditional and decision attribute

within the system of interest. (Note that the number of conditional attributes to be considered in the optimization process is specified in advance by the user and the number of decision attributes is set by default to one.) As described in Section III, the conditional and decision attributes are partitioned into an equal number of clusters, N, where N is bounded by the interval $[2, \mathrm{N}_{\max}]$, in which 2 represents the minimal number of clusters per attribute (and is the default setting) and $\mathrm{N}_{\max}$ represents the maximum permissible number of clusters per attribute and is set on a case-by-case basis in such a way as to achieve a satisfactory trade-off between the classification performance and the computational complexity of the solution procedure.

Step 2: Fuzzify attributes of information system using FCM method.

In general, a continuous-value information system can only be converted into an equivalent fuzzy information system once a classified fuzzy set has been obtained. In the FCM clustering procedure performed in the VPRS index function method, the interval values $[\alpha, \beta]$ of all the conditional and decision attributes are assigned to p_l fuzzy clusters. The continuous-value information system (U, A, V_q, f_q) is then converted into the fuzzy information system $(U, \widetilde{A}, \Phi, d)$, where $\Phi = \{\widetilde{A}_{lj} \mid l \le m, j \le p_l\}$, in which $\widetilde{A}_{lj} = \mu_j(x_i(a_l))$ and indicates the values of the membership functions associated with the l-th conditional attribute a_l of the i-th instance.

Step 3: Assign each instance attribute to appropriate conditional or decision attribute cluster.

Utilizing the index function $C_{a_l}(x_i) = I_{\max}(\mu_j(x_i(a_l))) = Index(\max(\mu_j(x_i)))$ for $1 \le l \le m, 1 \le i \le n$, the membership functions of each attribute of each instance are processed in order to determine the cluster to which the attribute value belongs.

Step 4: Identify VPRS sets and compute corresponding classification accuracy.

Having mapped the attribute values of all the instances to the appropriate conditional or decision attribute clusters, the procedure described in [18] is applied to determine an appropriate value of the threshold parameter β in the VPRS model. The β-lower approximate sets and boundary sets associated with each cluster c of the decision attribute d are then extracted in accordance with the definitions presented in Section II.C. Finally, the classification accuracy associated with each cluster of the decision attribute is evaluated by computing the cardinality ratio of the corresponding β-lower approximate sets to the β-upper approximate sets.

Step 5: Calculate centroids of β-lower approximate sets associated with each cluster of decision attribute.

The multi-dimensional centroids of the β-lower approximate sets associated with each cluster of the decision attribute d are obtained by calculating the mean values of the conditional and decision attributes of all the instances within the corresponding sets.

Step 6: Determine the value of the VPRS cluster validity index.

Having determined the classification accuracy and centroids of the β-lower approximate sets, the optimality of the clustering solution is evaluated using the VPRS cluster validity index given in Section III.A.

Step 7: Check termination criterion.

Having computed the value of the index function for the current number of clusters per attribute N, a check is made to see whether or not N is equal to the upper bound value ($N = \mathrm{N}_{\max}$). In the event that N is not equal to $\mathrm{N}_{\max}$, the value of N is incremented by 1, and the FCM, VPRS and cluster validity index computation procedures are repeated. Once the termination criterion is satisfied, the iteration procedure ceases and the computational process moves to the final step.

Step 8: Identify value of VPRS cluster validity index.

Once the termination criterion has been satisfied, the values of the VPRS index function obtained for $N = 2 \sim \mathrm{N}_{\max}$ are compared. The maximum value of the index function amongst all $2 \sim \mathrm{N}_{\max}$ solutions is taken as the VPRS cluster validity index and corresponds to the clustering solution which optimizes both the number of clusters per attribute and the overall classification accuracy of the dataset.

IV. Performance Evaluation of VPRS Index Method

In this section, the validity and effectiveness of the proposed VPRS index method is evaluated by considering three illustrative examples, namely one example relating to a dataset in which the conditional and decision attributes are related via a hypothetical function and two examples relating to electronic stock data extracted from the financial database maintained by the Taiwan Economic Journal (TEJ) [18]. In performing the evaluations, the effectiveness of the proposed method is explored by comparing the partitioning and classification results obtained for the three illustrative examples with those obtained from a Rough Set (RS) method and the conventional PBMF index (FCM-based) method, respectively. The PBMF index method clusters the norms of the instances within the dataset, whereas the VPRS and RS index methods cluster the attribute values. Note that the RS index method [13] is a particular case of the VPRS index method in which the cluster indices obtained from the FCM procedure are processed using a RS model rather than the VPRS model.

A. An illustrative example

The performance of the VPRS index method in partitioning and classifying real-world complex datasets was evaluated using electronic stock data extracted from the financial database maintained by the Taiwan Economic Journal (TEJ) [18] for the first quarter of 2008. The database maintains a total

of 53 financial indices for each company. However, for simplicity, the performance evaluations considered just one decision attribute, i.e. EPSNet Income, and 12 conditional attributes, i.e. (i) Business Profit Rate, (ii) PreTax Income %, (iii) Net Nonop.Inc./Rev, (iv) PSPre_Tax Income, (v) Oper.Income/Capital, (vi) PreTax Income/Capital, (vii) DaysA/R Turnover, (viii) DaysInventory Turn, (ix) DaysA/P Turnover, (x) Net Operating Cycle, (xi) PSOperating Income, and (xii) D/E Ratio. Having deleted the records for which one or more fields were incomplete, a total of 327 records were obtained (see Table 1 for representative values of each index for a selected subset of these 327 records).This illustrative example considers the performance improvement obtained in the VPRS method when increasing both the number of attributes considered within the clustering process and the number of clusters assigned to each attribute. Accordingly, the stock market data was processed repeatedly by the FCM clustering process with the number of conditional attributes specified in the range $[2,12]$, respectively, and the number of clusters specified in the range $[2,39]$.

The results presented in Table 2 show that the cardinality of the β-lower approximate sets obtained in the VPRS index method is larger than or equal to that of the lower approximate sets obtained in the RS index method. In other words, the VRPS β-lower approximate sets contain a greater number of instances than the RS lower approximate sets. For the case in which the clustering process is based on a small number of conditional attributes, i.e. {2, 3, 4, 5}, the approximate sets obtained using the RS index method contain a very small number of instances, while those obtained using the VPRS index method contain virtually all of the instances within the dataset. However, some of the instances within the VPRS approximate sets are subject to uncertainty. For example, when the number of conditional attributes and the number of clusters are both specified as 2, the RS index method yields only 3 instances, whereas the VPRS index method clusters all 327 instances. In other words, neither method accurately captures the relationship between the conditional attributes and the decision attribute. Thus, when classifying complex datasets using either method, a greater number of conditional attributes should be considered in the clustering process in order to ensure the completeness and reliability of the clustering results.

V. CONCLUSIONS

This paper has presented a cluster validity index method based on a Variable Precision Rough Set (VPRS) model and a modified form of the PBMF index function for the partitioning and classification of complex, real-world datasets. In the proposed approach, designated as the VPRS index method, the dataset is partitioned in accordance with the specified number of attributes and attribute clusters by the Fuzzy C-Means (FCM) clustering method and the resulting cluster indices are then processed by a VPRS model in order to identify the β-lower approximate sets associated with each cluster of the decision attribute and to evaluate the corresponding classification accuracy. Finally, the quality of the clustering solution is evaluated using a modified form of the PBMF index function. The effectiveness of the proposed approach has been confirmed by comparing the results obtained for the partitioning and classification of a real-world database containing stock market information with the corresponding results obtained using the RS index method. The evaluation results support the following major conclusions:

(1) In the PBMF index method, the optimality of the clustering results is evaluated in accordance with (a) the distance between each instance and the cluster centroids, and (b) the maximum separation distance between the cluster centroids. By contrast, in the VPRS index method, the quality of the clustering solution is evaluated in terms of (a) the distance between the instances and the centroids of the β-lower approximate sets associated with each cluster of the decision attribute, (b) the maximum distance between the centroids of the β-lower approximate sets associated with the different clusters of the decision attribute, and (c) the classification accuracy of the clustering results as evaluated by the cardinality ratio of the β-lower approximate sets to the β-upper approximate sets for each cluster of the decision attribute. In other words, in contrast to the conventional PBMF index method which only determines the optimal clustering of the data within the dataset given a specified number of clusters, the VPRS index method determines both the optimal number of attribute clusters within the dataset and the optimal classification accuracy.

(2) The PBMF index method clusters the norms of the instances within the dataset, whereas the VPRS and RS index methods cluster the attribute values. As a result, the VPRS and RS index methods take better account of the intrinsic interrelationships amongst the various conditional and decision attributes in the dataset when partitioning the instances and prevent the clustering results from being dominated by the attribute(s) with a higher order of magnitude.

(3) When using the RS and VPRS index methods to classify complex datasets based on a limited number of attributes, the cardinality of the β-lower approximate sets obtained in the VPRS index method is larger than or equal to that of the lower approximate sets obtained in the RS index method. As the number of attributes considered in the clustering process is increased, the difference between the cardinality of the β-lower approximate sets and that of the lower approximate sets classified by the two methods reduces. However, the number of instances classified by the VPRS method is still greater than that classified by the RS method.

(4) Although the VPRS index method classifies a far larger subset of the instances than the RS method when used to cluster complex datasets on the basis of a limited number of attributes, some of the

instances are characterized by uncertainty. In other words, the VPRS model fails to capture the true relationship between the conditional attributes and the decision attribute. Therefore, a greater number of conditional attributes are required in order to accurately model the interdependencies between the conditional attributes and decision attribute of the dataset.

Overall, the results presented in this study have confirmed that the proposed VPRS index method provides an effective tool for optimizing both the number of attribute clusters and the classification accuracy when applied to the partitioning and classification of complex, real-world datasets. However, the quality of the clustering results is degraded as the number of attributes considered in the clustering process is reduced. Therefore, reducing the number of uncertain instances in the β -lower approximate sets of the dataset is essential in improving the performance of the proposed method. Thus, a future study will explore the feasibility of improving the performance of the proposed VPRS classification method by processing (simplifying) the dataset utilizing a β -reducts method when applying the FCM, VPRS and cluster validity index function computation procedures.

REFERENCES

[1] J.C. Bezdek, "Cluster validity with fuzzy sets," J. Cybernet., vol. 3, pp. 58-74, 1974.

[2] W. Wang, and Y. Zhang, "On fuzzy cluster validity indices," Fuzzy Sets and Systems, vol. 158, pp. 2095-2117, 2007.

[3] E. Trauwaert, "On the meaning of Dunn's partition coefficient for fuzzy clusters," Fuzzy Sets and Systems, vol. 25, pp. 217-242, 1988.

[4] J. C. Bezdek, Pattern Recognition with Fuzzy Objective Function Algorithms, Plenum Press, New York, 1981.

[5] J. C. Bezdek, "Cluster validity with fuzzy sets," J. Cybernet., vol. 3, pp. 58-73, 1974.

[6] J. C. Bezdek, "Numerical taxonomy with fuzzy sets," J. Math. Biol., vol. 1, pp. 57-71, 1974.

[7] J. Ross Quinlan, Induction of decision trees. Machine Learning, Kluwer Academic Publishers, vol.1, 1986, pp. 85-106.

[8] P. Clark, and T. Niblett, The CN2 induction algorithm. Machine Learning, Kluwer Academic Publishers, vol. 3(4), 1989, pp. 261-283.

[9] D.E. Rumelhart, G.E. Hinton, and R.J. Williams, "Learning internal representations by error propagation," In: Rumelhart DE, McClelland JL, editors. Parallel distributed processing: explorations in the microstructure of cognition. Cambridge: MIT Press, pp. 318-363, 1986.

[10] V.N. Vapnik, The nature of statistical learning theory, New York: Springer, 2000.

[11] V. Vovk, A. Gammerman, and G. Shafer, Algorithmic learning in a random world, New York: Springer, 2005.

[12] N. Friedman, D. Geiger, and M. Goldsmidt, Bayesian network classifiers. Machine Learning, vol. 29(2), 1997, pp. 131-163.

[13] K. Y. Huang, "Applications of an Enhanced Cluster Validity Index method based on the Fuzzy C-means and Rough Set Theories to Partition and Classification," Expert Systems With Applications, vol. 37, pp. 8757-8769, 2010.

[14] Z. Pawlak, "Rough sets," International Journal of Information and Computer Sciences, vol. 11(5), pp. 341-356, 1982.

[15] K. Y. Huang, and C. J. Jane, "A Hybrid Model for Stock Market Forecasting and Portfolio Selection Based on ARX, Grey System and RS Theories," Expert Systems With Applications, vol. 36, pp. 5387-5392, 2009.

[16] W. Ziarko, "Variable precision rough set model," Journal of Computer and System Sciences, vol. 46, pp. 39-59, 1993.

[17] W. Ziarko, "Probabilistic decision tables in the variable precision rough set model," Computational Intelligence, vol. 17, pp. 593-603, 2001.

[18] K. Y. Huang, "Application of VPRS model with enhanced threshold parameter selection mechanism to automatic stock market forecasting and portfolio selection," Expert Systems With Applications, vol. 36, pp. 11652-11661, 2009.

[19] M. K. Pakhira, S. Bandyopadhyay, and U. Maulik, "A study of some fuzzy cluster validity indices, genetic clustering and application to pixel classification," Fuzzy Sets and Systems, vol. 155, pp. 191-214, 2005.

Table1 Illustrative financial data records extracted from TEJ database for first quarter in 2008

Company codes	(a)	(b)	(c)	(d)	(e)	(f)	(g)	(h)	(i)	(j)	(k)	(l)	(m)
1	-2.17	-3.78	-1.61	-0.01	-0.04	-0.07	96.85	252.7	6.8	342.7	0	97.51	0.16
2	-1.58	0.34	1.92	0.01	-0.38	0.08	90.42	56.26	38.85	107.8	-0.04	37.07	0.73
3	-1.58	82.01	80.67	2.42	0.38	23.33	60.36	91.89	38.72	113.5	0.04	141.5	-0.07
4	37.16	31.04	-6.12	2.6	31.07	25.69	85.92	84.46	57.44	112.9	3.11	55.07	9.16
…	…	…	…	…	…	…	…	…	…	…	…	…	…
324	8.17	9.37	1.2	1.35	11.68	13.4	102.0	26.22	44.16	84.02	1.21	53.21	6.18
325	7.38	7.37	-0.01	1.05	10.56	10.54	43.8	21.31	29.23	35.87	1.06	20.97	3.73
326	0.08	-0.97	-1.05	-0.07	0.06	-0.69	102.0	15.24	88.44	28.77	0.01	33.46	3.13
327	1.99	3.41	1.42	0.32	1.84	3.16	46.88	129.5	63.08	113.3	0.18	192.8	2.24

Column headings: (a) Business Profit Rate (b) Pre-Tax Income % (c) Net Non-op.Inc./Rev. (d) PS-Pre_Tax Income (e) Oper.Income/Capital (f) Pre Tax Income/Capital (g) Days-A/R Turnover (h) Days-Inventory Turn. (i) Days-A/P Turnover (j) Net Operating Cycle (k) PS-Operating Income (l) D/E Ratio (m) EPS-Net Income

Table 2 Cardinalities of VPRS β-lower approximate sets and RS lower approximate sets for financial data extracted from TEJ database as function of number of clusters per attribute and number of conditional attributes. (Note that entries in parentheses indicate the cardinality of the RS lower approximate sets.)

No. of clusters	No. of conditional attributes										
	2	3	4	5	6	7	8	9	10	11	12
2	327(3)	327(62)	327(62)	303(77)	303(131)	325(164)	327(176)	325(188)	325(191)	325(191)	325(191)
3	306(3)	325(35)	325(38)	315(46)	315(49)	319(91)	317(128)	304(200)	304(223)	304(223)	312(215)
4	255(12)	242(16)	288(40)	314(74)	312(80)	319(134)	304(212)	309(269)	303(281)	303(281)	313(304)
5	288(12)	187(12)	318(37)	315(53)	306(80)	303(150)	305(238)	301(268)	305(305)	307(291)	311(307)
6	61(11)	102(19)	288(45)	287(76)	276(73)	275(174)	283(240)	303(294)	315(305)	317(315)	323(321)
7	81(12)	129(14)	299(71)	292(105)	295(98)	274(210)	315(294)	321(315)	321(318)	323(320)	325(325)
8	105(15)	97(28)	255(85)	253(126)	233(134)	273(239)	313(313)	319(319)	319(319)	321(319)	327(327)
9	60(16)	80(38)	185(105)	251(148)	262(191)	280(271)	317(317)	321(323)	325(323)	325(325)	327(327)
10	35(17)	85(37)	215(111)	214(168)	227(177)	290(278)	315(310)	325(325)	323(323)	325(325)	327(327)
11	47(27)	88(43)	203(128)	220(171)	228(194)	307(291)	325(320)	327(327)	327(327)	327(327)	327(327)
12	58(34)	82(53)	227(174)	234(210)	258(231)	307(303)	323(321)	325(325)	325(325)	327(325)	327(327)
13	58(28)	107(71)	198(164)	230(219)	261(230)	305(303)	323(323)	327(327)	327(327)	327(327)	327(327)
14	73(29)	118(79)	240(194)	272(240)	270(244)	320(314)	325(325)	327(327)	327(327)	327(325)	327(327)
15	67(35)	112(74)	221(200)	269(255)	275(256)	319(319)	327(327)	327(327)	327(327)	327(327)	327(327)
16	57(39)	135(84)	246(219)	288(275)	281(264)	321(321)	327(325)	327(327)	327(327)	327(327)	327(327)
17	84(39)	132(100)	258(246)	293(292)	286(282)	327(327)	327(327)	327(327)	327(327)	327(327)	327(327)
18	67(55)	154(119)	256(245)	296(294)	304(297)	327(327)	327(327)	327(327)	327(327)	327(327)	327(327)
19	70(60)	165(134)	265(268)	298(293)	300(293)	325(325)	327(327)	327(327)	327(327)	327(327)	327(327)
20	88(52)	185(155)	288(269)	305(305)	312(302)	325(325)	327(327)	327(327)	327(327)	327(327)	327(327)
21	97(74)	182(158)	287(275)	311(305)	315(310)	325(325)	327(327)	327(327)	327(327)	327(327)	327(327)
22	92(75)	169(168)	288(294)	316(303)	312(306)	327(327)	327(327)	327(327)	327(327)	327(327)	327(327)
23	83(78)	193(182)	292(295)	316(312)	317(316)	327(327)	327(327)	327(327)	327(327)	327(327)	327(327)
24	99(89)	200(177)	309(304)	312(309)	320(317)	327(327)	327(327)	327(327)	327(327)	327(327)	327(327)
25	99(92)	196(191)	310(306)	320(320)	320(318)	327(327)	327(327)	327(327)	327(327)	327(327)	327(327)
26	126(106)	208(212)	308(303)	321(321)	321(321)	327(327)	327(327)	327(327)	327(327)	327(327)	327(327)
27	134(113)	214(225)	313(311)	323(319)	323(321)	327(327)	327(327)	327(327)	327(327)	327(327)	327(327)
28	120(113)	232(231)	315(315)	325(323)	323(323)	327(327)	327(327)	327(327)	327(327)	327(327)	327(327)
29	130(127)	238(226)	307(319)	327(321)	323(323)	327(327)	327(327)	327(327)	327(327)	327(327)	327(327)
30	128(134)	234(240)	321(317)	325(325)	325(323)	327(327)	327(327)	327(327)	327(327)	327(327)	327(327)
31	146(144)	232(248)	319(313)	323(323)	325(325)	327(327)	327(327)	327(327)	327(327)	327(327)	327(327)
32	150(145)	253(250)	319(317)	325(325)	325(325)	327(327)	327(327)	327(327)	327(327)	327(327)	327(327)
33	156(155)	242(253)	319(319)	327(327)	325(321)	327(327)	327(327)	327(327)	327(327)	327(327)	327(327)
34	154(146)	249(252)	321(321)	323(323)	323(325)	327(327)	327(327)	327(327)	327(327)	327(327)	327(327)
35	176(160)	248(253)	319(317)	325(325)	325(323)	327(327)	327(327)	327(327)	327(327)	327(327)	327(327)
36	167(160)	256(251)	325(321)	325(323)	325(323)	327(327)	327(327)	327(327)	327(327)	327(327)	327(327)
37	178(157)	265(261)	319(323)	325(325)	325(323)	327(327)	327(327)	327(327)	327(327)	327(327)	327(327)
38	183(170)	263(273)	321(321)	325(319)	323(323)	327(327)	327(327)	327(327)	327(327)	327(327)	327(327)
39	184(176)	267(261)	325(323)	327(325)	323(325)	327(327)	327(327)	327(327)	327(327)	327(327)	327(327)

2011 IEEE International Conference on Fuzzy Systems
June 27-30, 2011, Taipei, Taiwan

Anti-Swing Control of A New Container Crane With Fuzzy Uncertainties Compensation

Weimin Xu, Wei Gu, Aidi Shen, Janxin Chu, Wangqiang Niu
Key Laboratory of Marine Technology and Control Engineering
Shanghai Maritime University
Shanghai, China

Abstrac —**A class of new container cranes with eight-link lifting mechanics which can reduce sway efficiently as a result of improved lifting structure have been put to use recently, and both modeling and swing control of such a crane system attracts a lot attention in the field of control technology development. In this paper, dynamics model of the new container crane is investigated, an anti-swing control scheme with fuzzy uncertainty compensation is proposed to ensure the positioning control as well as overall closed-loop system stability. None of the system parameters is required for the controller design in a priori. In the proposed control laws, the position error can be driven to a bounded area while the swing angle can also be rapidly damped so as to achieve minimal sway of the crane system. Stability analysis of the controller is also given. Finally, simulation results show the performance successfully.**

Keywords-container crane; eight-link lifting; anti-swing control; fuzzy uncertainty compensation; positioning control

I. INTRODUCTION

Container crane systems are widely used throughout the world in thousands of harbors, warehouses, and etc. for loading and transporting heavy cargos. Crane systems are desired to be able to move to the required position as fast and as accurate as possible while placing the payload at the appropriate position, meanwhile, the payload swing angle should be kept as small as possible. However, these crane structures are highly flexible in nature, apart from their underactuated dynamics property in control, some external disturbances, such as wind, hit or motion of the crane support unit can cause the payload to oscillate, as a result, this oscillation may bring damage to surrounding equipment and the payload itself, also, swing of the payload or hook makes precision positioning time consuming and inefficient for transporting operation.

Generally, difficulties in using a container crane lies in three aspects: motion-induced oscillation, disturbance-induced oscillation, and positioning capability. Many works have been done to improve the structure of container cranes practically, e.g. enhance the stiffness of lifting-link mechanism, and develop swing-free equipments, as well as investigate new control methods for crane system.

Many solutions [1]-[14] have been extensively studied in recent years for the simultaneous control of payload swing and of crane trajectory tracking, and some of them have led to industrial applications. Generally speaking, the dynamic equations of a crane are coupling, nonlinear and time-varying differential equations. The control schemes developed in the literature may be broadly grouped into three categories [11]: optimal control and linearized control [1], [4], and [5], command shaping control [6], [8], and nonlinear control [2], [9]. The implementation of these various control methods still presents several challenges. A common difficulty is the nonlinear behavior of drives and motors that actuate crane motion. Nonlinear behaviors such as friction, variables coupling of overhead crane system have been difficult to evaluate with traditional analysis techniques, and are, therefore, often neglected in controller design.

Resort to linearized theorem and optimal control approaches, many work has been done to design controller according to linearized crane model. A problem related to linearized control is its inability to be implemented in real-time, owing to the necessity of precomputation of system trajectories. Moreover, these linearized methods (such as time-optimal control etc.) cannot provide the sufficient accuracy of information about position error and load swing. Besides, the uncertain nonlinear factors such as the wind, the hit, and the friction of track will also reduce the performance of linearized crane control systems [12]. Command shaping is a reference signal modification technique that is implementable in real time [7]. Input shaping techniques have proven effective at significantly reducing motion-induced cable sway during crane motion. However, approaches on input shaping control which is naturally of open-loop control focused on the suppression of load swing but not solve the problem of position error during crane motion. Besides, the time period between the impulses of the input shaping method was also hard to obtain [11]. Nonlinear control is the most common strategy used in research efforts to mitigate positioning and cable sway errors, and some wonderful solutions for crane control have been derived by this means. However, these methods unavoidably need the prior knowledge of the crane dynamics which is actually hardly acquired, moreover, it is not easy for an engineer to design an industrial crane controller based on the mathematic model of the crane. For many years, the intelligent control (such as fuzzy-based methods and neural network-based methods) [13], [14] has been considered as a none-model based solution to nonlinear systems. It is well known that intelligent control derived from the desire of linguistic description or approximation of the whole nonlinearity for complex system, and it can be utilized to

978-1-4244-7316-8/11/$26.00 ©2011 IEEE

formulate and imitate the human intelligence to construct control strategies, as well as approximate arbitrarily nonlinear dynamics.

In this paper, dynamics model of a new container crane system is investigated, then, an anti-swing tracking control law for this container crane system with fuzzy uncertainties compensation is presented to ensure the positioning control as well as overall closed-loop system stability. None of the crane dynamics parameters are needed for the controller design in a priori. In the developed control laws, the position error will be driven to zero while the sway angle being also rapidly damped so as to achieve minimal swing of the payload. Stability analysis of the proposed control law is given. Finally, simulation results show the performance successfully.

This paper is organized as follows. The modeling of the new container crane system and trajectory tracking problem is presented in Section II. The proposed adaptive anti-swing control law is illustrated in Section IV. In Section V, simulation results are given. This paper concludes with a summary in Section VI.

II. PROBLEM FORMULATION

A. Container Crane Dynamics

The schematic drawing in figure 1 presents a structure of a new container crane system with eight-link lifting mechanism which has been put in use recent years.

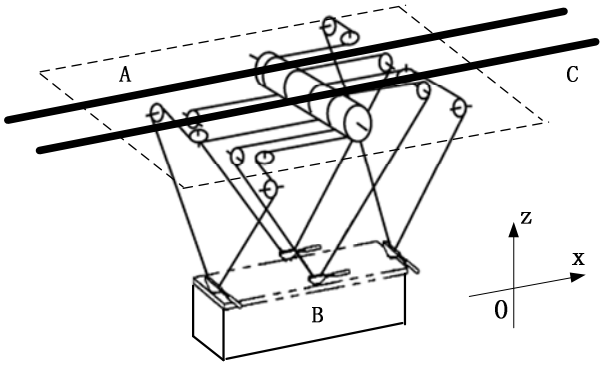

Figure 1. a new container crane system with eight-link lifting mechanism.

A – trolley system B – payload C – track

To facilitate modeling the new container crane system, it is assumed that the crane system possesses the following characteristics:

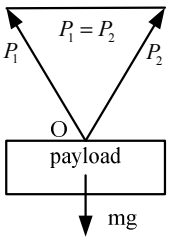

Figure 2. inverted-triangle and payload with $P_1 = P_2$.

- The payload mass B and crane trolley A are assumed to be connected by eight massless, rigid links
- The payload mass B is assumed to be concentrated at a point and the value of this payload mass and the overall trolley mass are known exactly.
- The pulley wheels in A and hinged joints, where the payload links connect to crane trolley are assumed to be frictionless.

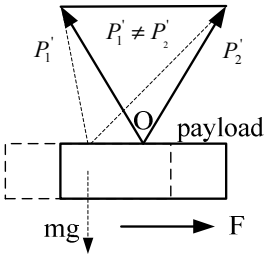

Figure 3. inverted-triangle link and payload with $P_1 \neq P_2$.

- The control input to the system is the mechanical force applied directly to the trolley.

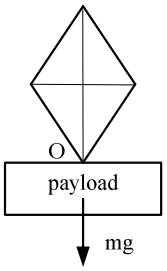

Figure 4. equivalent parallelogram mechanism for an inverted-triangle link system.

- To simplify the analysis, only trolley moving along x-axis direction will be considered.

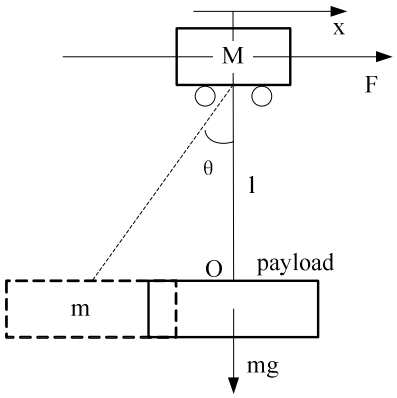

Figure 5. swing of the payload in x-z plane.

In figure 1, when the trolley moves at a constant speed, the inverted-triangle link mechanism endures a balanced force $P_1 = P_2$ as shown in figure 2, and the payload moves accompanying with crane trolley at the same velocity. When the trolley starts up or brakes down, an inertial force coming from payload drives the inverted-triangle link frame

distorted, then $P_1^{'} < P_2^{'}$ as shown in figure 3, while the projection force F of $P_1^{'}$ and $P_2^{'}$ on x-axis given by the distorted inverted-triangle system tries to reject this distortion and draw back the payload mass to its 'origin' O, as a result, swing of payload along x-axis shrinks. Furthermore, when the inverted-triangle link frame is forced to distort due to starting up or braking down, the link system is therefore equivalently stretched along x-axis. This effect of interplay force given by link system can be described using a parallelogram mechanism as shown in figure 4 [15]. The complex force F of the parallelogram system eventually has the payload move along horizontal direction rather than arc of a pendulum as shown in figure 5. Then, this kind of linear motion of payload under effect of parallelogram mechanism can be modeled as a spring oscillator system, the new container crane finally can be present as figure 6, where M, m are mass of the trolley and payload respectively, x position of the trolley, l the equivalent length of link, θ payload angle with respect to the vertical.

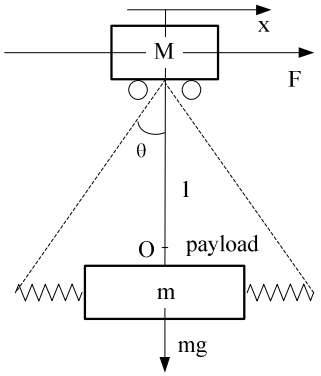

Figure 6. equivalent model for the container crane system

The purpose of this paper is to control the motion of the container crane in figure 6 to achieve the desired position of its payload along a given trajectory.

To derive dynamic equation of the above crane system, the total energy associated with the crane system needs to be computed using the Lagrangian approach. The kinetic energy of the above crane can be divided into two parts: $K = K_{trolley} + K_{payload}$, where $K_{trolley} = \frac{1}{2} M \dot{x}^2$ denotes trolley kinetic energy and $K_{payload} = \frac{1}{2} m(\dot{x} + l\dot{tg}\theta)^{'2}$ is payload kinetic energy. Finally, we have

$$K = \frac{1}{2}(M+m)\dot{x}^2 + ml\sec^2\theta \cdot \dot{\theta} \cdot \dot{x} + \frac{1}{2} ml^2 \sec^4\theta \cdot \dot{\theta}^2 \quad (1)$$

The potential energy of the payload shifting from its origin can be express using spring oscillator system, i.e.

$$P = -\frac{1}{2} k_s (ltg\theta)^2 = -\frac{1}{2} k_s l^2 tg^2\theta \quad (2)$$

where k_s is an equivalent spring coefficient which relates to the structure of reverted-triangle system and its links.

The Lagrange equations of motion are formed as

$$\frac{d}{dt}\left[\frac{\partial L}{\partial \dot{x}}\right] - \frac{\partial L}{\partial x} = u$$
$$\frac{d}{dt}\left[\frac{\partial L}{\partial \dot{\theta}}\right] - \frac{\partial L}{\partial \theta} = 0 \quad (3)$$

where u represents control force acting on the trolley.

After calculation about above equations, the dynamics of the new container crane depicted in figure 6 may be expressed in the Lagrange form as

$$M(q)\ddot{q} + C(q,\dot{q})\dot{q} + G(q) + \tau_d = U \quad (4)$$

where $q(t) = [x(t), \theta(t)]^T$ is position and swing angle variable vector, $M(q)$ is the inertia matrix, $C(q,\dot{q})$ is the coriolis/centripetal matrix, $G(q)$ is the gravity vector, τ_d denotes bounded unknown disturbance (including e.g. unstructured unmodeled dynamics), and $U = [u(t), 0]^T$ is the control input torque. For the 2D container crane shown in Figure 6, we have the followings,

$$M(q) = \begin{bmatrix} M_{pp} & M_{p\theta} \\ M_{p\theta} & M_{\theta\theta} \end{bmatrix}, \quad C(q,\dot{q}) = \begin{bmatrix} C_{pp} & C_{p\theta} \\ C_{p\theta} & C_{\theta\theta} \end{bmatrix},$$
$$G(q) = \begin{bmatrix} G_p \\ G_\theta \end{bmatrix}, \quad \tau_d = \begin{bmatrix} \tau_p \\ \tau_\theta \end{bmatrix}, \quad U = \begin{bmatrix} u \\ 0 \end{bmatrix} \quad (5)$$

The following properties are easily be demonstrated for the container crane [16]:

Property 1: $M(q)$ is a positive definite symmetric matrix bounded by $\alpha_1 I \le M(q) \le \alpha_2 I$ with $\alpha_{1,2}$ positive constant.

Property 2: $C(q,\dot{q})$ is bounded by $c_b(q)\left\|\dot{q}\right\|$ with $c_b(q) \in R$.

Property 3: The matrix $\dot{M} - 2C$ is skew-symmetric.

B. Trajectory Tracking Problem

Given a desired trajectory within a compact set, i.e. $q_d(t) \in R^{2\times 1}$, the tracking error is $e(t) = q_d(t) - q(t)$ and the filtered tracking error may be defined as

$$s(t) = [s_x(t), s_\theta(t)]^T = \dot{e}(t) - \lambda e(t) \quad (6)$$

where $\lambda = \lambda^T > 0$ is a design parameter matrix, usually selected diagonal. A controller will be designed to keep the filtered tracking error $s(t)$ bounded.

Since the linear time-invariant system (6) is exponentially stable from the input $s(t)$ to output $e(t)$, the boundedness of the $s(t)$ implies the boundedness of the output tracking error $e(t)$. In fact, these ultimate bounds can be related as

$$\|e\|_2 \le \frac{\|s\|_2}{\sigma_{\min}(\lambda)}, \quad \left\|\dot{e}\right\|_2 \le \|s\|_2 \tag{7}$$

where $\sigma_{\min}(\lambda)$ is the minimum singular value of λ.

Differentiate $s(t)$ and using (6), the crane dynamics (4) may be written in terms of the filtered tracking error as

$$M\dot{s} = -Cs + f + \tau_d - U \tag{8}$$

where the nonlinear function $f(X)$ is

$$f(X) = \left[f_x, f_\theta\right]^T = M(q)(\ddot{q}_d + \lambda\dot{e}) + C(q,\dot{q})(\dot{q}_d + \lambda e) + G(q) \tag{9}$$

The generalized input vector $X \in R^{N\times 2}$ may be selected as $X = \left[q^T, \dot{q}^T, q_d^T, \dot{q}_d^T \ddot{q}_d^T\right]^T$.

Let's define a computed-torque like input in terms of a feedback linearization estimate plus PD control law as

$$U_0 = \hat{f} + K_v s \tag{10}$$

where $\hat{f}(X)$ is any estimate of $f(X)$ and $K_v = K_v^T > 0$ is a gain matrix. The closed-loop error system then becomes

$$M\dot{s} = -(K_v + C)s + \tilde{f} + \tau_d \tag{11}$$

where the functioned estimate error is $\tilde{f} = f - \hat{f}$.

Therefore, (11) is an error system wherein the filtered tracking error $s(t)$ is driven by the functional error $e(t)$ and the disturbances. Define a lumped system uncertainty $\zeta = \tilde{f} + \tau_d$, then (11) can be rewritten as

$$M\dot{s} = -(K_v + C)s + \zeta \tag{12}$$

Lemma 1: The system (12) with input ζ and output $s(t)$ is BIBS stable.

Proof: Let the Lyapunov function be

$$L = \frac{1}{2}s^T M s \tag{13}$$

Differentiation L along (12) obtains

$$\dot{L} = -s^T K_v s + \frac{1}{2}s^T\left(\dot{M} - 2C\right)s + s^T\zeta \tag{14}$$

Using property 3 results in

$$\dot{L} = -s^T K_v s + s^T\zeta \le -\|s\|^T\left(K_{v\min}\|s\| - \|\zeta\|\right) \tag{15}$$

Let $\zeta \in L_\infty$ be bounded by b_ζ. Then $\dot{L}$ is decreasing when

$$\|s\| > b_\zeta / K_{v\min} \tag{16}$$

As inside the bounded region defined by (16) about the origin, $s(t)$ is bounded, and outside of it, $s(t)$ is a non-increasing function, i.e. there exist some constant $\gamma_1, \gamma_2 > 0$ such that $\|s(t)\| < \gamma_1 b_\zeta + \gamma_2$, thus, $s(t) \in L_\infty$. This shows that bounded input results in bounded states. □

III. Adaptive Anti-Swing Controller Design

A. Fuzzy Uncertain Compensator

In this paper, a fuzzy uncertainty observer (FUO) $\hat{f}(X)$ is applied to estimate the nonlinear dynamics $f(X)$, moreover, a parameter adaptive law is also provided so that the estimate is guaranteed to monitor and represent well the whole uncertain dynamics existing in the container crane, as well as the asymptotic stability is preserved.

The basic configuration of a fuzzy system consists of fuzzifier, fuzzy rule base, fuzzy inference engine, and defuzzifier. The fuzzy inference engine maps from input vector $X = \left(x_1, x_2 \cdots, x_n\right)^T \in R^n$ to an output variable $Y \in R$ for single output case, which is based on the fuzzy IF-THEN rules. The *ith* IF-THEN rule of k fuzzy rules defining fuzzy implication can be written as

$Rule^i$: If x_1 is A_1^i and $\cdots$ and x_n is A_n^i,
then y is y^i

where A_j^i and y^i denote a fuzzy variable for premise part and a singleton for consequent part respectively. Then, the output of the fuzzy system with center average defuzzifier, product inference engine and singleton fuzzifier can be obtained as

$$y(x) = \frac{\sum_{i=1}^{k} y^i\left(\prod_{j=1}^{n}\mu_{A_j^i}\left(x_j\right)\right)}{\sum_{i=1}^{k}\left(\prod_{j=1}^{n}\mu_{A_j^i}\left(x_j\right)\right)} = \hat{\phi}^T\xi(x) \tag{17}$$

with $\xi^T = \left(\xi^1, \xi^2, \cdots \xi^k\right)$, where ξ^i is fuzzy basis function, expressed as

$$\xi^i = \frac{\prod_{j=1}^{n}\mu_{A_j^i}\left(x_j\right)}{\sum_{i=1}^{k}\left(\prod_{j=1}^{n}\mu_{A_j^i}\left(x_j\right)\right)} \tag{18}$$

and $\hat{\phi}^T = \left(y^1, y^2, \cdots, y^k\right)$ is an adjustable parameter vector, $\mu_{A_j^i}(\cdot)$ is the membership function of fuzzy variable A_j^i.

In this paper, the universal approximation capability of above fuzzy system will be implemented as a fuzzy uncertain observer (FUO) [18].

To construct a FUO for estimating $\hat{f}(X)$ in (9), we have the following assumption:

Assumption 1: Let the input vector X for the fuzzy logic system (17) belong to a compact set M_X, the optimal parameter vector ϕ of (17) is defined as

$$\phi^* = \arg\min_{\phi\in M_\phi}\left(\sup_{X\in M_X}\left|f(X) - \hat{f}(X\,|\,\hat{\phi})\right|\right) \tag{19}$$

which exists in a convex region $M_\phi = \{\phi \| \phi \| \le m_\phi\}$, where m_φ is a design parameter. Then, the fuzzy logic system (17), which is a zero-order TS fuzzy system, is employed as a FUO for the estimate of the uncertain f as follows:

$$\hat{f} \triangleq \hat{\phi}^T \xi(X) \tag{20}$$

Remark 1: to avoid algebraic loop in the implementation of FUO [18], $X = \left[q^T, \dot{q}^T, q_d^T, \dot{q}_d^T \ddot{q}_d^T \right]^T$ is used instead of control input U, Since the control input is a function of the state q and reference trajectory q_d, Then, the following observation dynamics is applied [18],

$$\dot{\mu}_i = -\sigma \mu_i + p_i(i, \dot{i}, \hat{\phi}) \tag{21}$$

where $p(i, \dot{i}, \hat{\phi}) \triangleq \hat{f}(X \mid \hat{\phi}) + F + GU + \sigma_i \dot{i}$, $\sigma_i > 0$ is an observer design parameter, and an observer error variable is defined as $\varsigma_i = \dot{i} - \mu_i$, moreover, observation error dynamics can be obtained as

$$\dot{\varsigma}_i = -\sigma \varsigma_i + f(X) - \hat{f}(X \mid \hat{\phi}) \tag{22}$$

By assumption 1 and the universal approximation capability of the FUO in (20), the nonlinear dynamics $f(X)$ can be described as

$$f(X) = \hat{f}(X \mid \phi^*) + \varepsilon(X) \tag{23}$$

where $\varepsilon(X)$ denotes an uncertain estimation error satisfying $|\varepsilon(X)| \le \bar{\varepsilon}$, and its upper bound $\bar{\varepsilon}$ can be arbitrarily shrunk by increasing the number of the fuzzy rules.

Then (22) becomes

$$\dot{\varsigma}_i = -\sigma \varsigma_i + \hat{f}(X \mid \hat{\phi}^*) - \hat{f}(X \mid \hat{\phi}) + \varepsilon(X) \tag{24}$$

Remark 2: if the bounded and adjustable parameter vector $\hat{\phi}$ is updated by adaptive law

$$\dot{\hat{\phi}} = \rho \varsigma \xi(X) \tag{25}$$

where $\rho > 0$ is an observer design parameter, then the uncertainty observation error is uniformly ultimately bounded within a region of which size can be kept arbitrarily small (see Theorem 1 in [18]). Therefore, if the observation error ς converges to zero, $\hat{f}(X)$ converges to the close neighborhood of the actual nonlinear $f(X)$.

B. Controller Design

A FUO is employed as uncertainty compensator for the container crane dynamics in above section. The nonlinear crane function $f(X)$ in (9) can be uniformly approximated by the FUO in (23) for some optimal parameter ϕ^*, where the estimate error $\varepsilon(X)$ is bounded by a known $\bar{\varepsilon}$ constant. Note that ε becomes smaller as the number of the fuzzy rules increases.

Assumption 2: The desired trajectory is bounded, i.e. $\left\| q_d^T, \dot{q}_d^T, \ddot{q}^T \right\| \le Q_d$ with Q_d known constant.

Assumption 3: The unknown disturbance τ_d in (4) is bounded, i.e. $\|\tau_d\| \le b_{\tau_d}$ with b_{τ_d} known.

Assumption 4: The fuzzy logic input X is bounded above by $\|X\| \le c_1 + c_2 \|s\|$ with c_1, c_2 known computable constants.

Define now a control input torque as

$$U_c = U_0 - V = \hat{f} + K_v s - V \tag{26}$$

with an addition $V(t)$ to enhance robustness of the system is given as

$$V = K_z \left(\left\| \hat{\varphi} \right\| + m_\phi \right) s \tag{27}$$

where m_ϕ is a design parameter which satisfies $\|\phi\| \le m_\phi$, and $K_z = K_z^T > 0$ a design parameter. Observer that $V(t)$ vanishes when $s(t) \to 0$.

Substituting the control (26) into (8) results in

$$M \dot{s} = -(K_v + C) s - V + \begin{bmatrix} f_p - \hat{f}_p \\ f_\theta - \hat{f}_\theta \end{bmatrix} + \tau_d \tag{28}$$

Let $f = \left[f_p, f_\theta \right]^T$, and $s = \left[s_p, s_\theta \right]^T$, the functional approximation error $\tilde{f}$ is

$$\tilde{f} = f - \hat{f} = \hat{f}\left(X \mid \hat{\phi}^* \right) - \hat{f}\left(X \mid \hat{\phi} \right) + \varepsilon(X) \tag{29}$$

Then, substitute (29) into (28) yields the final form of the closed-loop error system dynamics as

$$\begin{aligned} M \dot{s} = & -(K_v + C) s \\ & + \begin{bmatrix} \hat{f}_x\left(x \mid \hat{\phi}_x^* \right) - \hat{f}_x\left(x \mid \hat{\phi}_x \right) + \varepsilon(x) \\ \hat{f}_\theta\left(\theta \mid \hat{\phi}_\theta^* \right) - \hat{f}_\theta\left(\theta \mid \hat{\phi}_\theta \right) + \varepsilon(\theta) \end{bmatrix} - V + \tau_d \end{aligned} \tag{30}$$

Rewriting (30), we have closed-loop error dynamics as

$$M \ddot{e} + (\lambda M + K_v + C) \dot{e} + (K_v + C) \lambda e = \tilde{f} + \tau_d - V \tag{31}$$

Moreover, by define $\mathrm{E} = \left(e, \dot{e}, \varsigma \right)^T$ and using (24) and (31), the augmented closed-loop trajectory tracking error dynamics becomes

$$\dot{\mathrm{E}} = \Pi \mathrm{E} + \Gamma \phi^T \xi(X) + \Gamma_1 V + \Gamma \tau_d \tag{32}$$

with $\Pi = \begin{bmatrix} A & B^T \\ B & D \end{bmatrix}$ is a stable matrix, $\Gamma = \begin{bmatrix} H \\ I \end{bmatrix}$, $\Gamma_1 = -\begin{bmatrix} H \\ O \end{bmatrix}$, where $A = \begin{bmatrix} O & I \\ -k_1 & -k_2 \end{bmatrix}$, $D = \begin{bmatrix} -\sigma_x & 0 \\ 0 & -\sigma_\theta \end{bmatrix}$, $H = \begin{bmatrix} O \\ I \end{bmatrix}$, and $B \in R^{2\times 4}$, $I \in R^{2\times 2}$, $O \in R^{2\times 2}$ denote identity and null matrices, respectively, k_1, k_2 are known matrices relate to M, C, K_v, and λ.

Remark 3: there exists a positive definite matrix P such that

$$\Pi^T P + P\mathrm{E} = -R \tag{33}$$

for an arbitrary positive definite matrix R [20].

Theorem: Consider the 2D container crane with uncertainties in (4), let assumption 1~4 hold, the control input torque (26) with $K_z > c_2$ is given as (26) and (28), the filtered trajectory tracking error dynamics $s(t)$ is asymptotically stable, and FUO estimate is uniformly ultimately bounded with the specific bounds. Moreover, the tracking error may be kept arbitrarily small by increasing the gain K_v.

Proof: Let the Lyapunov function candidate be

$$L = \frac{1}{2}\mathrm{E}^T P \mathrm{E} + \frac{1}{2}\tilde{\phi}^T \tilde{\phi} \tag{34}$$

which is a positive definite function since assumption 4 holds.

Differentiate (34) with respect to time along the solution of the error dynamics (31) yields,

$$\begin{aligned} \dot{L} &= \mathrm{E}^T P \Pi \mathrm{E} + \mathrm{E}^T P \Gamma \phi^T \xi + \mathrm{E}^T P \Gamma \tau_d + \mathrm{E}^T P \Gamma_1 V + \tilde{\phi}^T \dot{\tilde{\phi}} \\ &= \mathrm{E}^T P \Pi \mathrm{E} + \mathrm{E}^T P \Gamma \tau_d + \mathrm{E}^T P \Gamma_1 V + \tilde{\phi}^T \left(\mathrm{E}^T P \Gamma \xi + \dot{\tilde{\phi}} \right) \end{aligned} \tag{35}$$

By choosing fuzzy rule tuning methods as

$$\dot{\tilde{\phi}} = -\mathrm{E}^T P \Gamma \xi \ , \ (\dot{\hat{\phi}} = -\mathrm{E}^T P \Gamma \xi) \tag{36}$$

and using $\Lambda = \Gamma \varepsilon + \Gamma_0 V$, then we have

$$\dot{L} \le -\frac{1}{2}\mathrm{E}^T Q \mathrm{E} + \mathrm{E}^T P \Lambda \tag{37}$$

By completing the square, after adding and subtracting $\frac{\alpha}{4}\mathrm{E}^T P \mathrm{E} + \frac{1}{\alpha}\Lambda^T P \Lambda$, (37) becomes

$$\begin{aligned} \dot{L} &\le -\frac{1}{2}\mathrm{E}^T Q \mathrm{E} + \frac{\alpha}{4}\mathrm{E}^T P \mathrm{E} + \frac{1}{\alpha}\Lambda^T P \Lambda \\ &\le -\frac{1}{4}\lambda_{\min}(Q)\|\mathrm{E}\|^2 + \frac{\lambda_{\max}(P)^2}{\lambda_{\min}(Q)}\|\Lambda\|^2 \\ &\le -\frac{1}{4}\lambda_{\min}(Q)\|\mathrm{E}\|^2 + \frac{\lambda_{\max}(P)^2}{\lambda_{\min}(Q)}\left(2\|\tau_d\|^2 + \|V\|^2\right) \end{aligned} \tag{38}$$

where $\alpha = \lambda_{\min}(Q)/\lambda_{\max}(P)^2$, $\lambda_{\max}(\cdot)$ and $\lambda_{\min}(\cdot)$ denote maximum and minimum eigenvalues respectively.

Thus, $\dot{L}$ is negative outside a compact set and the augmented error E is uniformly ultimately bounded. Moreover, using Barbalat's Lemma [19], $\|\mathrm{E}(t)\| \to 0$ as $t \to 0$.

IV. Simulation Results

The proposed controller performance is tested under two different payload conditions, first set is selected to mimic a light weight application condition where $M = 10kg$, $m = 5kg$, $l = 1m$ and $k_s = 50$, then, change the crane payload with $M = 10kg$, $m = 50kg$, and $l = 1m$ to simulate a heavy load application, and test the performance of the proposed controller without incorporating any additional information about the system. Normal parameters employed in simulation are given as gain $K_v = [12,5]^T$, and $\lambda = (1.2,1.2)^T$. For the premise parts of the FUO in (20), seven Gaussian functions and two sigmoid functions are used as in [18]. Both simulation results are compared with performance of PID controller for container crane, given in [21], where parameters of PID controller are $(20, 0.1, 40)$.

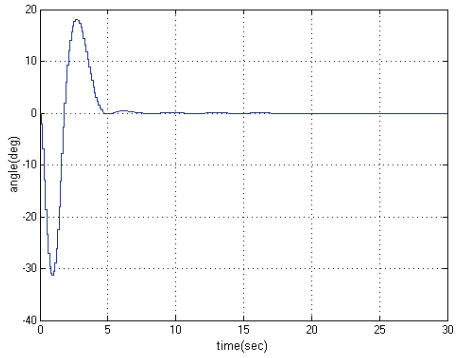

(a) swing angle of the payload

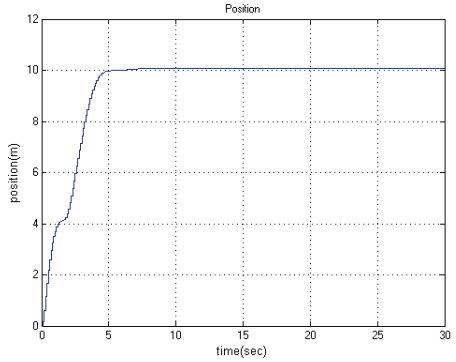

(b) position of the trolley

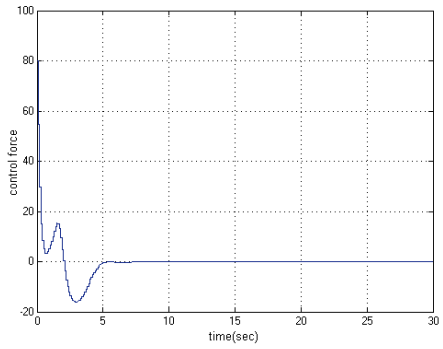

(c) control input U_c

Figure 7. performance of proposed controller with light payload

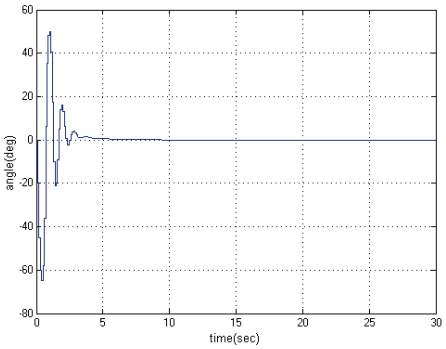

(a) swing angle of the payload

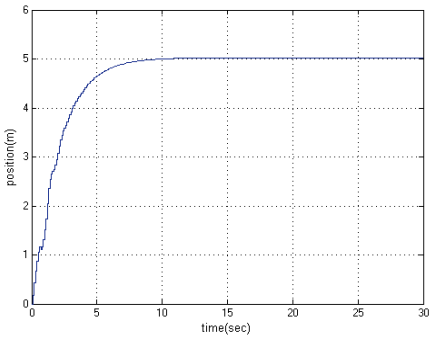

(b) position of the trolley

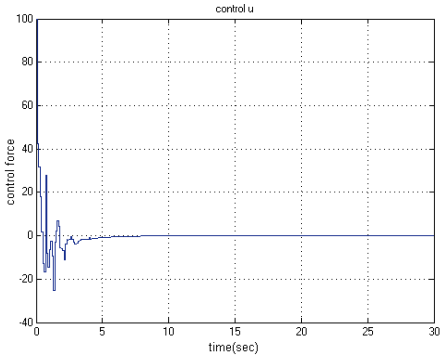

(c) control force

Figure 8 performance of PID controller with light payload

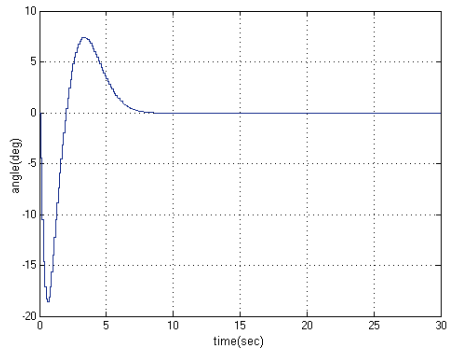

(a) swing angle of the payload

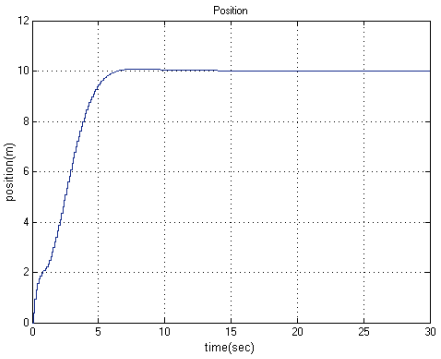

(b) position of the trolley

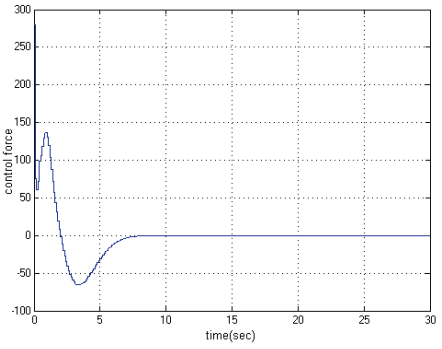

(c) control input U_c

Figure 9 performance of proposed controller with heavy payload

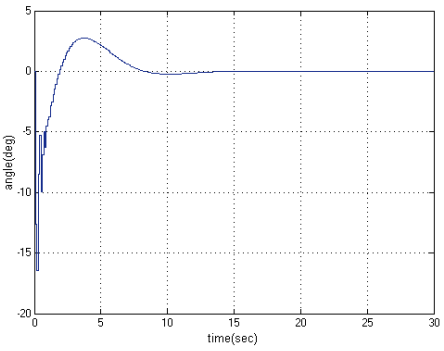

(a) swing angle of the payload

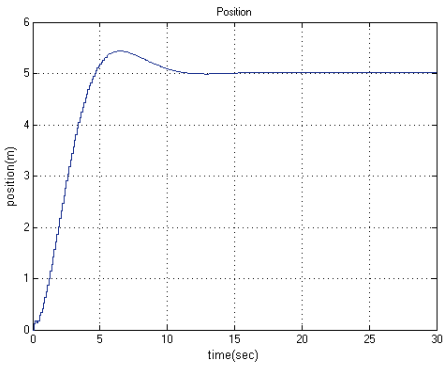

(b) position of the trolley

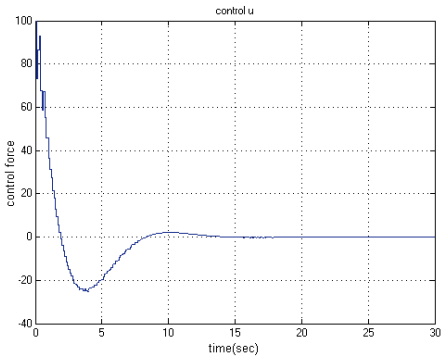

(c) control force

Figure 10 performance of PID controller with heavy payload

From figure 7 to figure 10, it is shown that the proposed controller guarantees robust performance against payload variations and system parameters changing, and shows good transient response performance compared with PID controller.

V. CONCLUSION

Dynamics model of a new container crane system is investigated. A FUO based controller law is proposed for the container crane with underactuated dynamics problem. Multi-loop controller compromising an inner loop consisting of fuzzy uncertain observer with online adaptive update law and robustness terms making the whole system to remain bounded, hence keeping the internal signals in a compact region. Controller design does not rely on any prior knowledge of crane nonlinear system dynamics. The developed controller has been applied to two different crane applications for simulation study, and the simulation results have shown performance of the controller successfully.

VI. ACKNOWLEDGMENT

This work was supported by the National High-Tech Research and Development Program of China (2009AA043000), the Innovation Program of Shanghai (10110502600), Shanghai Leading Academic Discipline Project (S30602), and the Fund of Shanghai Maritime University (20100083).

REFERENCES

[1] Andreas Johansson, "A Sufficient Condition for Invalidation of Linear State-Space Systems With Uncertain Time-Varying Parameters", IEEE Trans. on Automatic Control, Vol. 54(12), pp. 2915-2910, Dec., 2009.

[2] Dongkyoung Chwa,. "Nonlinear Tracking Control of 3-D Overhead Cranes Against the Initial Swing Angle and the Variation of Payload Weight." IEEE Trans. on control systems technology, vol. 17(4), pp. 876-883, July 2009.

[3] Kim, Y. -S., Hong, K. -S., & Sul, S. -K. "Anti-sway control of container cranes: Inclinometer, observer, and state feedback". International Journal of Control, Automation, and Systems, (2), pp. 435–449, 2004.

[4] T. J. J. van den Boom, J. B. Klaassens and R. Meiland, "Real-time-optimal control for a nonlinear container crane using a neural network", Informatics in Control, Automation and Robotics II, pp. 79–84, 2007.

[5] Carlos Vazquez and Joaquin Collado, "Optimal delayed control for an overhead crane," 6th International Conference on Electrical Engineering, Computing Science and Automatic Control, pp. 1-6, 2009.

[6] William Singhose "Command Shaping for Flexible Systems- A Review of the First 50 Years". International journal of precision engineering and manufacturing, Vol. 10(4), pp. 153-168, 2009.

[7] M.A. Ahmad and Z. Mohamed, "Hybrid Fuzzy Logic Control with Input Shaping for Input Tracking and Sway Suppression of a Gantry Crane System" American J. of Engineering and Applied Sciences, vol. 2(1), pp. 241-251, 2009.

[8] Khalid, A., Singhose, W., Huey, J., & Lawrence, J., "Study of operator behavior, learning, and performance using an input-shaped bridge crane". In Proceedings of the conference on control applications, Taipei, Taiwan, 2004.

[9] Nader A. Nayfeh ·William T. Baumann, "Nonlinear analysis of time-delay position feedback control of container cranes", Nonlinear Dyn. Vol. 53, pp. 75–88, 2008.

[10] G. J. Klir and B. Yuan, Fuzzy Sets and Fuzzy Logic, Theory and Applications. Engle wood Cliffs, NJ: Prentice-Hall, 1995.

[11] K. L. Sorensen, W. Singhose, S. Dickerson. "A controller enabling precise positioning and sway reduction in bridge and gantry cranes". Control Engineering Practice, vol. 15, pp. 825–837, 2007.

[12] Cheng-Yuan Chang. "Adaptive Fuzzy Controller of the Overhead Cranes With Nonlinear Disturbance". IEEE trans. on industrial informatics, Vol.3, No. 2, MAY 2007.

[13] Cheng-Yuan Chang and Kuo-Hung Chiang, "Intelligent fuzzy accelerated method for the nonlinear 3-D crane control", Expert Systems with Applications, vol. 36, pp. 5750–5752, 2009.

[14] A. Yesildirek, "Intelligent Control of Overhead Gantry Cranes", 6th International Symposium on Mechatronics and its Applications, pp: 1-6, Mar. 2009.

[15] Tang, Yuan-yang, et al, "Simulation of the anti-sway system of container crane based on MATLAB", Chinese journal of Mechanical and Electrical Equipment, vol. 25(3), pp. 52-55, 2008.

[16] Yang, Jung Hua, etc., "Adaptive Control for 3-D Overhead Crane Systems", Proceedings of the American Control Conference Minneapolis, Minnesota, USA, pp. 1832-1837, June, 2006.

[17] L. Wang, A Course in Fuzzy Systems and Control, Prentice Hall, International Edition, 1997.

[18] E. Kim, "A Fuzzy Disturbance Observer and Its Application to Control," IEEE Trans., Fuzzy, Syst., Vol. 10(1), pp. 77-84, 2002.

[19] J. E. Slotine, et al., Applied Nonlinear Control, Prentice Hall, 1991.

[20] M. -S Park, D. Chwa, and S. -K. Hong, "Adaptive Fuzzy Nonlinear Anti-Sway Trajectory Tracking Control of Uncertain Overhead Cranes with High-Speed Load Hoisting Motion", International Conference on Control, Automation and Systems, in COEX, Seoul, Korea, Oct., 2007.

[21] W. Sridokbuap, S. Nundrakwang,etc, "I-PD and PD Controllers Designed by CRA for Overhead Crane System", International Conference on Control, Automation and Systems, pp. 326-330, in COEX, Seoul, Korea Oct. 2007.

2011 IEEE International Conference on Fuzzy Systems
June 27-30, 2011, Taipei, Taiwan

A Robust Method for Image Segmentation of Noisy Digital Images

Prabhjot Kaur
Reader, Deptt. of Information Tech.
MSIT, Affiliated to GGSIP University
New Delhi, INDIA.
E-mail: thisisprabhjot@gmail.com

Dr. I. M. S. Lamba
Professor, Deptt. of Computer Sci.,
SET, Sharda University,
Greater Noida, Uttar Pradesh, INDIA
E-mail: lambaims@yahoo.com

Dr. Anjana Gosain
Associate Professor,
USIT, GGSIP University,
New Delhi, INDIA
E-mail: anjana_gosain@hotmail.com

***Abstract*— A robust image segmentation algorithm called Extended Fuzzy C means (EFCM) is presented in this paper which preprocesses the image to reduce the noise effect and then apply FCM algorithm for image segmentation. Preprocessing of image is influenced by the direct eight neighborhood pixels of study pixel of an image under consideration. The advantages of the propose algorithm is: (1) Least execution time compared to other techniques. (2) It yields regions more homogeneous than those of other techniques. (3) It removes noisy spots and is less sensitive to noise. The propose technique is a powerful method for noisy image segmentation with least computation time and convergence rate compared to other image segmentation techniques.**

Keywords—Fuzzy Clustering, Fuzzy C-Means, Robust Image Segmentation

I. INTRODUCTION

A. Image segmentation

Image segmentation plays an important role in image analysis and computer vision. The goal of image segmentation is partitioning of an image into a set of disjoint regions with uniform and homogeneous attributes such as intensity, color, tone etc. The image segmentation approaches can be divided into four categories; thresholding, clustering, edge detection, and region extraction. In image processing, two terms are usually seen very close to each other: clustering and segmentation. When analyzing the color information of the image, e.g. trying to separate regions or ranges of color components having same characteristics, the process is called color clustering. Mapping the clusters onto the spatial domain and physically separated regions in the image is called segmentation. In color images, the boundaries between objects are blurred and distorted due to the imaging acquisition process. Furthermore, object definitions are not always crisp and knowledge about the objects in a scene may be vague. Fuzzy set theory and Fuzzy logic are ideally suited to deal with such uncertainties. Fuzzy clustering models have proved a particularly promising solution to the color clustering problem. Such unsupervised models can be analysis, clustering, and classifier designs in fields such as astronomy, geology, medical imaging, target recognition, used with any number of features and clusters. The Fuzzy C means (FCM) [1] algorithm, proposed by Bezdek (1981), is the most widely used algorithm in image segmentation because it has robust characteristics for ambiguity and can retain much more information than hard segmentation methods. FCM has been successfully applied to feature and image segmentation. An image can be represented in various feature spaces and the FCM algorithm classifies the image by grouping similar data points in the feature space into clusters. In case the image is noisy or distorted then FCM technique wrongly classify noisy pixels because of its abnormal feature data. Various approaches are proposed by researchers to compensate this drawback of FCM.

B. FCM Related Extensions

Tolias and Panas post-processed the membership function to smooth the noise effect [2]. Acton and Mukherjee incorporated multiscale information to enforce spatial constraints [3]. The most popular approach for increasing the robustness of FCM is to modify the objective function directly. Dave proposed the idea of a noise cluster to deal with noisy data using the technique, known as Noise Clustering [4]. He separated the noise into one cluster but this technique is not suitable for image segmentation, since we cannot separate pixels from the image. Noisy pixels can be processed and assigned to most appropriate cluster. Another similar technique, PCM, proposed by Krishnapuran and Keller [5] interprets clustering as a possibilistic partition. However, it caused clustering being struck in one or two clusters. Ahmed et al. [6] modified the objective function of FCM by introducing a term that allowed the labeling of a pixel to be influenced by the labels in its immediate neighborhood. Zhang Yang, Fu-lai Chuang et al. [7] developed a robust clustering technique by deriving a novel objective function for FCM. Jiayin Kang et al. [8] proposed another technique which modified FCM objective function by incorporating the spatial neighborhood information into the standard FCM algorithm. Y. Yang et al. [9] proposed a noval penelized FCM (PFCM) for image segmentation where penalty term acts as a regulizer in the algorithm which is inspired by neighborhood maximization (NEM) algorithm [10] and is modified in order to satisfy the criterion of FCM algorithm. S. Shen, W. Sandham et al. [11] presented an algorithm called Improved FCM (IFCM) which changed the distance function used in FCM i.e. the distance between pixel intensity and cluster intensities and applied neural network

978-1-4244-7316-8/11/$26.00 ©2011 IEEE

optimization technique to adjust parameters in the modified distance function. Keh-Shih Chuang, Hong-Long Tzeng et al. [12] presented a FCM algorithm that incorporated spatial information into the membership function of clustering. The membership weighting of each cluster is altered after the cluster distribution in the neighbourhood is considered. Rhee and Hwang [13] proposed Type 2 fuzzy clustering. Type 2 fuzzy set is the fuzziness in a fuzzy set. In this algorithm, the membership value of each pattern in the image is extended as Type 2 fuzzy membership by assigning membership grades (triangular membership function) to Type 1 fuzzy membership. The membership values for the Type 2 membership are obtained as:

$$a_{ik} = u_{ik} - \frac{1 - u_{ik}}{2}$$

where a_{ik} and u_{ik} are the Type 2 and Type 1 fuzzy membership respectively. The cluster centers are updated accordingly using conventional FCM taking into account the new Type 2 fuzzy membership.

Problem with all these methods is that they increase the complexity of the algorithms by introducing new equations into the standard equations of FCM algorithm which inevitably introduced computation issues. By changing the objective function and membership function of standard FCM algorithms, we are losing the continuity from FCM, which is well-realized function in many types of software, such as MATLAB. In this paper, a new extension to FCM is proposed, which consists of image enhancement and segmentation. We are pre-processing the image before segmentation to reduce the noisy pixels which is influenced by the direct eight neighborhood pixels of noisy pixels. Strength of the propose algorithm is its least execution time and convergence rate compare to other robust image segmentation techniques.

The organization of the paper is as follows: Section II, briefly review Fuzzy C-Means (FCM) [1], Spatial FCM (sFCM) [12], and cluster validity functions for the evaluation of segmentation performance. Section III describes the proposed algorithm, Extended Fuzzy C Means (EFCM). Section IV evaluates the performance of the proposed EFCM algorithm and compares it with sFCM, FCM type-II, and conventional FCM algorithm followed by concluding remarks in Section V.

II. Background Information

This section briefly discusses the Fuzzy C-Means (FCM) and Intuitionistic Fuzzy C means (IFCM) algorithms. In this paper, the data-set is denoted by 'X', where $X=\{x_1, x_2, x_3, \ldots\ldots x_n\}$ specifying an image with 'n' pixels in M-dimensional space to be partitioned into 'c' clusters. Centroids of clusters are denoted by v_i and d_{ik} is the distance between x_k and v_i.

A. The Fuzzy C-Means Algorithm

FCM [1] is the most popular fuzzy clustering algorithm. It assumes that number of clusters 'c' is known in priori and minimizes the objective function (J_{FCM}) as:

$$J_{FCM} = \sum_{i=1}^{c}\sum_{k=1}^{n} u_{ik}^{m} d_{ik}^{2} \tag{1}$$

Where $d_{ik} = \|x_k - v_i\|$, and u_{ik} is the membership of pixel 'x_k' in cluster 'i', which satisfies the following relationship:

$$\sum_{i=1}^{c} u_{ik} = 1; \;\; i = 1,2,\ldots\ldots n \tag{2}$$

Here 'm' is a constant, known as the fuzzifier (or fuzziness index), which controls the fuzziness of the resulting partition. m=2 is used in this paper. Any norm $\|\bullet\|$ can be used for calculating d_{ik}. Minimization of J_{FCM} is performed by a fixed point iteration scheme known as the alternating optimization technique. The conditions for local extreme for (1) and (2) are derived using Lagrangian multipliers:

$$u_{ik} = \frac{1}{\sum_{j=1}^{c}\left(\frac{d_{ik}}{d_{jk}}\right)^{\frac{2}{m-1}}} \quad \forall \; k, i \tag{3}$$

where $1 \le i \le c; \;\; 1 \le k \le n$
and

$$v_i = \frac{\sum_{k=1}^{n}(u_{ik}^{m} x_k)}{\sum_{k=1}^{n}(u_{ik}^{m})} \;\; \forall \; i \tag{4}$$

The FCM algorithm iteratively optimizes $J_{FCM}(U,V)$ with the continuous update of U and V, until $|U^{(l+1)} - U^{(l)}| <= \varepsilon$, where 'l' is the number of iterations. FCM works fine for the images which are not corrupted with noise but if the image is noisy or distorted then it wrongly classifies noisy pixels because of its abnormal feature data which is pixel intensity in the case of images, and results in an incorrect membership and improper segmentation.

B. Spatial Fuzzy C Means (sFCM)

Spatial Fuzzy C means [12] algorithm modifies FCM membership function by introducing spatial information into it. sFCM defines spatial function as:

$$h_{ij} = \sum_{k \in NB(x_j)} u_{ik} \tag{5}$$

where $NB(x_j)$ represents a square window centered on pixel x_j in the spatial domain. sFCM considered 5x5 window. Just like the membership function, the spatial function 'h_{ij}' represents the probability that pixel x_j belongs to i^{th} cluster. Spatial function is incorporated into membership function as:

$$u'_{ij} = \frac{u_{ij}^p h_{ij}^q}{\sum_{k=1}^{c} u_{ij}^p h_{ij}^q} \quad (6)$$

where 'p' & 'q' are parameters which control the relative importance of both functions. For a noisy pixel, this formula reduces the weighting of a noisy cluster by the labels of its neighboring pixels. Disadvantage of this algorithm is that it is a two-pass process for every pass of FCM algorithm. In the first pass, conventional FCM algorithm is used to calculate membership function and in the second pass, the membership information of each pixel is mapped to the spatial domain, and the spatial function is calculated from that. The FCM iteration proceeds with the new membership that is incorporated with the spatial function. Hence, the complexity of this algorithm is very high compared to FCM technique, which introduces computational issues.

C. Cluster Validity Functions

To evaluate the performance of segmentation quantitatively, two types of cluster validity functions are generally used: the fuzzy partition and the feature structure. The representative functions for the fuzzy partition are partition coefficient [14] and partition entropy [15]. They are defined as:

$$V_{pc}(U) = \sum_{i=1}^{n}\sum_{k=1}^{c} u_{ki}^2 \quad (7)$$

$$V_{pe}(U) = -\frac{1}{n}\left\{\sum_{i=1}^{n}\sum_{k=1}^{c}[u_{ki} log u_{ki}]\right\} \quad (8)$$

Best clustering results can be achieved when the value V_{pc} is maximal or V_{pe} is minimal. Disadvantage of V_{pc} and V_{pe} are that they measure only the fuzzy partition and do not specify featuring property. To solve this problem, other validity functions based on the feature structures are used [16], [17]. They are defined as:

$$V_{fs}(U,V;X) = \sum_{k=1}^{c}\sum_{i=1}^{n} u_{ik}^m(\|x_i - v_k\|^2 - \|v_k - \bar{v}\|^2) \quad (9)$$

Where $\bar{v} = \frac{1}{c}\sum_{k=1}^{c} v_k$

$$V_{xb}(U) = -\frac{\sum_{k=1}^{c}\sum_{i=1}^{n} u_{ki}^2\|x_i - v_k\|^2}{n * \left(\min_{k\neq j}\left\{\|v_k - v_j\|^2\right\}\right)} \quad (10)$$

Where V_{fs} is a Fukuyama-Sugeno function and V_{xb} is Xie-Beni function. When either V_{fs} or V_{xb} is minimal, a better clustering result is achieved [16], [17].

III. The Proposed Technique, Extended Fuzzy C Means (EFCM)

Earlier, we proposed a robust clustering algorithm, called Density Oriented Fuzzy C-Means (DOFCM) [18] for numerical data. The concept of DOFCM was to identify noise points, based upon the number of other points in its neighborhood, before clustering and separate it into one cluster. In case of image segmentation that algorithm is not appropriate as we cannot separate noisy pixels from the image. But noisy pixels can be processed and assign to the appropriate cluster. Here, in the propose technique, we are using the same concept i.e. processing image before segmentation and modifies DOFCM algorithm for image segmentation.

FCM is a good segmentation technique if there is no noise in the image. Keeping this in view, we are proposing a very simple and effective method, which preprocess noisy pixels in the image and then apply conventional FCM algorithm for segmentation.

The pixels in an image are highly correlated i.e. the pixels in the immediate neighborhood possess nearly the same feature data. In the propose technique, we are trying to regenerate the value of noisy pixels by processing every pixel of an image based upon its immediate neighborhood pixels. Neighborhood structure considered in the propose technique is shown in Fig. 1. Value of every pixel is influenced by its eight direct neighborhood pixels. We are considering an image in RGB format. Let size of an image is R*C*K, where R is the number of rows, C is the number of columns, and K is 3 (for color image). So every pixel will be processed using equation:

$$pixel(l,m,k) = \sum_{k=1}^{3}\frac{1}{N}\left(\left(\sum_{i=l-1}^{l+1}\sum_{j=m-1}^{m+1} pixel(i,j,k)\right) - pixel(l,m,k)\right) \quad (11)$$

Where N = 8, denoting 8 neighborhood points of a study pixel

pixel (i, j, k) = intensity value of pixel at i,j,k location

pixel (l, m, k)= intensity value of study pixel

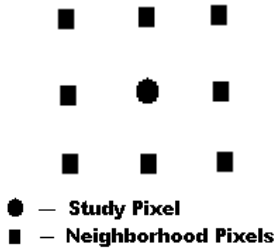

Figure 1. Neighborhood structure for study pixel

In the homogeneous region, this function simply fortifies the same characteristics and the clustering result remains unchanged. However, for a noisy pixel, this formula tries to regenerate the value of original pixel. As a result, misclassified pixels from noisy regions can easily be corrected. After processing the noisy pixels, FCM is used to do segmentation. Here, we are processing the image only once before segmentation, which does not increase the complexity of the program compare to Spatial FCM and other robust clustering algorithms for image segmentation. Other methods mostly changed the standard FCM equations and introduced new functions which are calculated for every pass of the FCM algorithm i.e. they are extremely computationally intensive so the strength of the proposed technique is its least execution time, which is approximately equal to the conventional FCM method. Also, it does not modify FCM algorithm so does not lose the continuity of FCM function which is given in many softwares like MATLAB. Various steps involved in the proposed technique used for image segmentation are shown in Fig. 2.

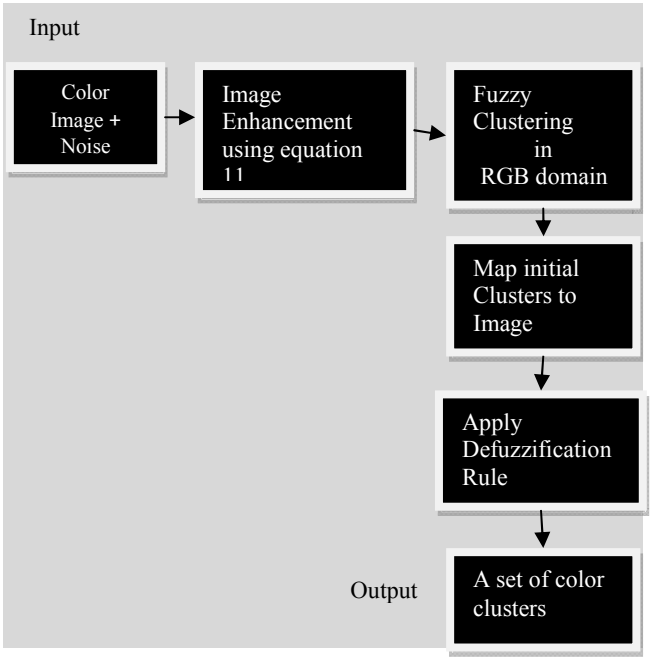

Figure 2. Block diagram of the steps used for image segmentation using proposed method along with input and output.

IV. RESULTS

In this section, experimental results are presented to compare the segmentation performance of EFCM with FCM, FCM Type II, and sFCM. Two types of images are used: (1) Synthetic images (2) Real world image. For all data-sets, we are assuming the following computational protocols: $\varepsilon = 0.00001$, Total number of iterations = 100. We chose m=2, which is a common choice for fuzzy clustering. Experiments are implemented and simulated using MATLAB Version 7.0.

A. Circle Image

A grayscale circle image (256x256 pixels) representing two intensity levels is used. It is corrupted with gaussian noise. The intensity levels of two classes are 0 and 255. Fig. 3(a) & 3(b) show original and noisy version of circle image. Fig. 3(c)-(f) shows the segmentation result of FCM, sFCM, EFCM, and Fuzzy Type-II respectively. Although FCM, Fuzzy Type-II, and sFCM successfully segmented the image into the desired regions but did not totally recover it from the noise whereas, EFCM totally recovered the image from noise.

In addition to the analyses of the qualitative evaluation presented above, a quantitative evaluation using several cluster validity functions is necessary. As described in part II.C, the better performance of clustering is achieved if the partition coefficient V_{pc} is maximal and/or the partition entropy value V_{pe}, the Fukuyama-Sugeno function V_{fs}, and the Xie-Beni function V_{xb} are minimal. Table I shows performance comparison of FCM, Fuzzy type-II, sFCM, and our proposed EFCM in terms of cluster validity functions.

B. Square Image

A synthetic square image (160 x 170 x 3 pixels) consisting of 9 squares is generated. It contains gaussian noise to create noisy version of original image (Fig. 4a) as shown in Fig. 4(b). The image represents three intensity levels with the values 255, 128 and 0. Fig. 4(c)-(f) shows segmentation results of FCM, sFCM, EFCM, and Fuzzy Type-II. FCM, Fuzzy type-II, and sFCM did not completely remove the noise where as EFCM totally removed noise in the same intensity region but noise effect can be seen at the boundaries where the intensity level is changing. TABLE-I shows performance comparison of these algorithms in terms of cluster validity functions.

C. Bacteria Image

A real bacteria image (126 x 140 x 3 pixels) consisting of two classes is considered and it is corrupted with gaussian noise to show the performance of purpose technique. The bacteria are separated from its background using all the three methods. Fig. 5(a)-(b) show original image and its noisy version respectively. Fig. 5(c)-(f) shows segmentation result and 5(g)-(j) shows clustering result of FCM, sFCM, EFCM, and Fuzzy type-II respectively. It is observed that EFCM is able to retain the boundary of bacteria more effectively as compared to other methods. TABLE-I shows

performance of these algorithms quantitatively using cluster validity functions.

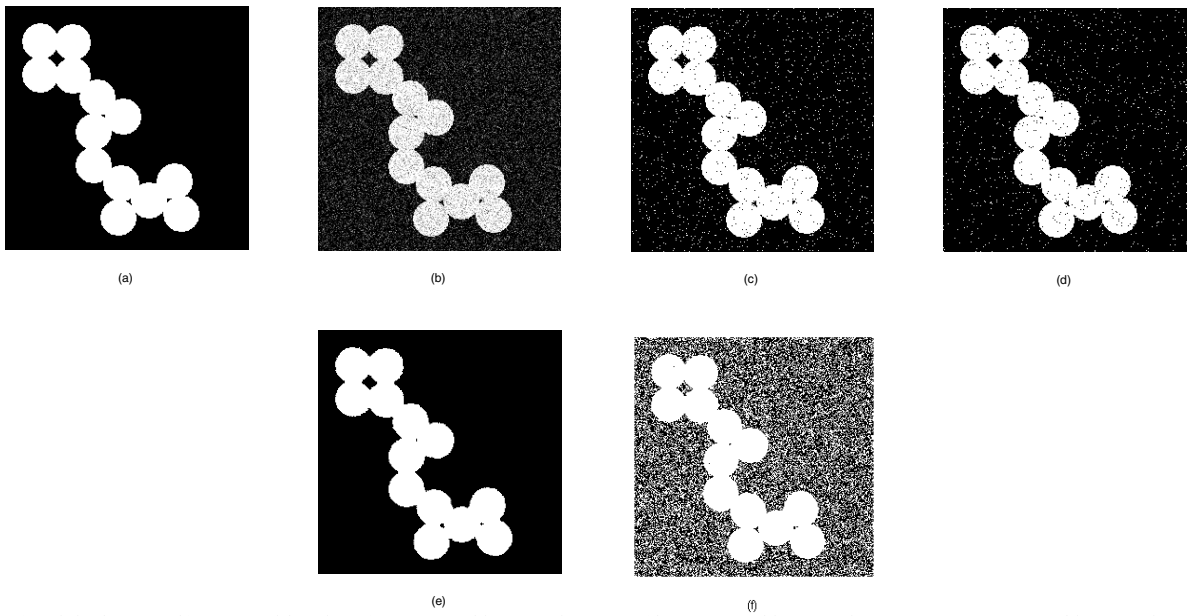

Figure 3. (a) Original Image (b) Image with noise (c) Segmented image using FCM (d) Segmented image using sFCM (e) Segmented image using EFCM (f) Segmented image using FCM Type-II

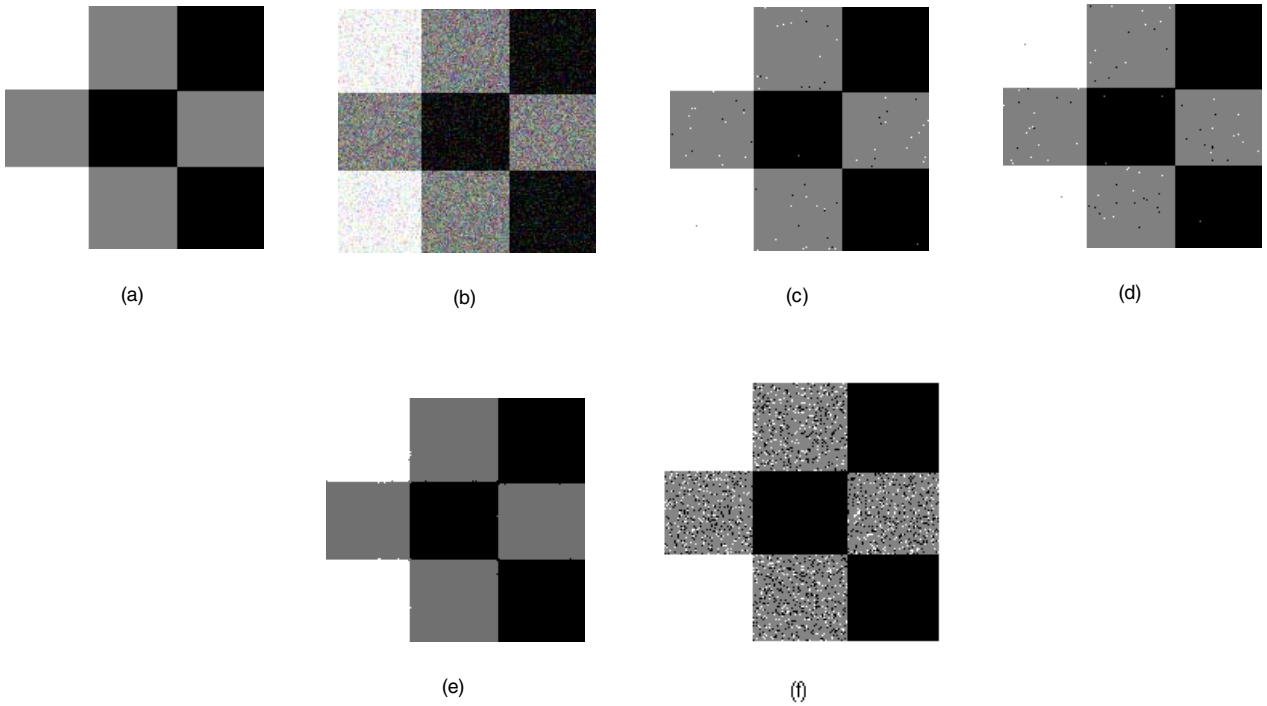

Figure 4. (a) Original Image (b) Image with noise (c) Segmented image using FCM (d) Segmented image using sFCM (e) Segmented image using EFCM (f) Segmented image using FCM Type-II

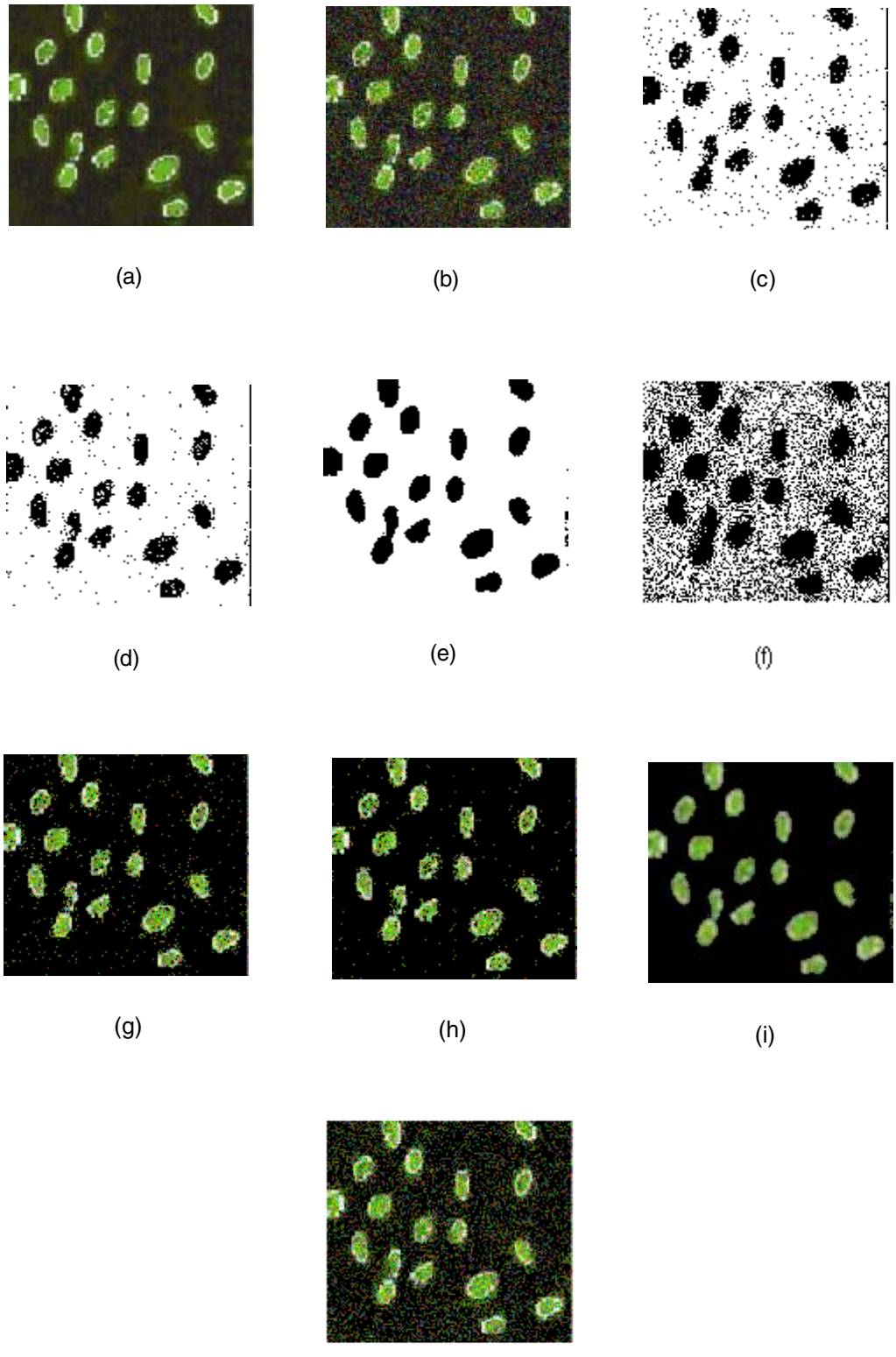

Figure 5. (a) Original Image (b) Image with noise (c)-(f) Segmented image using FCM, sFCM, EFCM, and FCM Type-II respectively (g)-(j) Objects shown in one cluster using FCM, sFCM, EFCM, and FCM Type-II respectively

Performance of algorithms based upon execution time

Fig. 6 shows bar chart of the execution time of FCM, Fuzzy type-II, sFCM, and EFCM for the above three images. TABLE-II lists execution time and number of iterations of the algorithms. Advantage of the propose technique is that it has least execution time compared to other color image segmentation techniques. From TABLE-II, it is observed that almost in all cases, proposed technique converges even before FCM algorithm because it is preprocessing the image before applying FCM technique which increases the convergence rate. Its execution time is almost close to FCM technique.

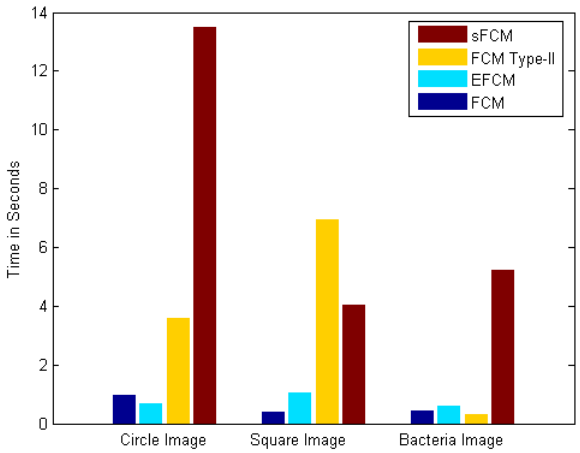

Figure 6. Performance of algorithms based upon execution time

TABLE-I
PERFORMANCE COMPARISON OF FCM, SFCM, FCM TYPE-II, AND EFCM IN TERMS OF CLUSTER VALIDITY FUNCTIONS

Image Name	Number of Clusters	Technique	The value of Validity Functions			
			V_{pc}	V_{pe}	V_{xb}	V_{fs}
Circle	2	FCM	0.93720	0.11520	0.020900	$-613x10^{6}$
		sFCM	0.94270	0.10630	0.020941	$-622x10^{6}$
		FCM TYPE-II	0.8361	-0.0794	3.8448	$1.017x10^{8}$
		EFCM	0.98120	0.04000	0.006880	$-628x10^{6}$
Square	3	FCM	0.84075	0.31734	0.052073	-24228
		sFCM	0.80990	0.36713	0.055247	-22762
		FCM TYPE-II	1.281	0.5018	1.6823	69705
		EFCM	0.95311	0.10662	0.012342	-29338
Bacteria	2	FCM	0.77803	0.36518	0.151760	4540
		sFCM	0.81035	0.32098	0.129740	4106.1
		EFCM	0.91911	0.15477	0.038946	3773.8
		FCM TYPE-II	0.4329	-0.3115	0.9543	1112.6

TABLE-II
PERFORMANCE COMPARISON OF FCM, SFCM, FCM TYPE-II AND EFCM IN TERMS OF EXECUTION TIME & CONVERGENCE RATE

Image Name	Technique	Execution Time in Seconds	Number of Iterations (Convergence Rate)
Circle	FCM	0.953	21
	sFCM	13.48	40
	FCM TYPE-II	3.594	52
	EFCM	0.65	13
Square	FCM	0.406	14
	sFCM	4.04	21
	FCM TYPE-II	6.93	200
	EFCM	1.03	12
Bacteria	FCM	0.43	32
	sFCM	5.235	62
	FCM TYPE-II	0.312	23
	EFCM	0.578	15

V. CONCLUSION

Digital images generally contain unknown noise and considerable uncertainty. Traditionally, FCM is a popular segmentation method for digital images. However, it is an intensity-based clustering algorithm which is not robust against noisy images. The pixels in an image are highly co-related and this spatial information is an important characteristic for color image segmentation which is not utilized in FCM. Although, many extended algorithms based upon FCM have been developed to overcome this shortcoming by incorporating spatial information either in the objective function or in the membership function of FCM algorithm. But they all have increased the complexity of the standard algorithm by introducing new equations for spatial membership that are calculated for every pass of FCM algorithm.

In this paper, we proposed an extended FCM (EFCM) algorithm which preprocesses the image before segmentation. Preprocessing of image is influenced by the direct eight neighborhood pixels of every pixel of an image under consideration. Its strength is its least execution time and fast convergence rate compared to other image segmentation techniques. It is tested on noisy synthetic images and real images and evaluated quantitatively with four different cluster validity functions. Results showed that the performance of proposed technique is best over FCM, Fuzzy Type-II, and sFCM.

REFERENCES

[1] J.C. Bezdek (1981), "Pattern Recognition with Fuzzy Objective Function Algorithm", Plenum, NY.

[2] Y.A. Tolias and S.M. Panas (1998), "On applying Spatial Fuzzy Image Clustering using a Fuzzy Rule based System", IEEE Signal Processing Letters 5, 245.247 (1998).

[3] S. T. Acton and D. P. Mukherjee (2000), "Scale Space Classification using Area Morphology," *IEEE Trans. Image Process.*, vol. 9, no. 4, pp. 623–635, Apr. 2000.

[4] R.N. Dave and R. Krishnapuram (1997), "Robust Clustering Methods: A Unified View", IEEE Transactions on Fuzzy Systems, May, Vol 5, No. 2.

[5] R. Krishnapuram and J. Keller (1993), "A Possibilistic Approach to Clustering", IEEE Trans. on Fuzzy Systems, vol .1. No. 2, pp.98-1 10.

[6] M. N. Ahmed, S. M. Yamany, N. Mohamed, A. A. Farag, and T. Moriarty(2002), "A Modified Fuzzy c-means algorithm for bias field Estimation and Segmentation of MRI data," *IEEE Trans. Med. Imag.*, vol. 21, no. 3, pp. 193–199, Mar. 2002.

[7] Yang Zhang, Chung Fu-Lai, et al,(2009), "Robust Fuzzy Clustering-based Image Segmentation, *Applied Soft Computing*, vol(9), no. 1, Jan (2009), pp. 80-84.

[8] Kang Jiayin, Min Lequan et al. (2009), "Novel modified fuzzy c-means algorithm with applications", *Digital Signal Processing*. March (2009),vol 19, no. 2, pp. 309-319.

[9] Yang Y., Zheng Ch., and Lin P. Fuzzy c-means clustering algorithm with a novel penalty term for image segmentation. *Opto-electronic review*, Vol.13, Issue 4, 2005, pp. 309-315.

[10] C. Ambroise and G. Govaert,(1998), "Convergence of an EM-type algorithm for spatial clustering.", Pattern Recognition Letters 19, 919.927(1998).

[11] Shen Shan, Sandham W., and Sterr A.(2005), "MRI Fuzzy Segmentation of Brain Tissue using Neighbourhood Attraction with Neural Network Optimization", *IEEE transactions on information technology in biomedicine*,Vol. 9, issue 3, September 2005, pp. 459-467.

[12] Chuang Keh-Shih, Tzeng Hong-Long, Chen Sharon et al.(2006),"Fuzzy C-means clustering with Spatial Information for Image Segmentation,", *Computeried Medical Imaging and graphics,* 30(2006) 9-15.

[13] F.C.H. Rhee, C. Hwang, "A Type-2 fuzzy c means clustering algorithm", in: Proc. in Joint 9th IFSA World Congress and 20th NAFIPS International Conference 4, 2001, pp. 1926–1929.

[14] Bezdek JC.(1974), "Cluster validity with fuzzy sets", J Cybern 1974; 3:58–73.

[15] Bezdek JC.(1975), "Mathematical models for systematic and taxonomy", In: proceedings of eigth international conference on numerical taxonomy, San Francisco; 1975, p. 143–66.

[16] Fukuyama Y, Sugeno M. (1989), "A new method of choosing the number of clusters for the fuzzy c-means method", In: proceedings of fifth fuzzy system symposium; 1989, p. 247–50.

[17] Xie XL, Beni GA. (1991), "Validity measure for fuzzy clustering", IEEE Trans Pattern Anal Mach Intell 1991;3:841–6

[18] Prabhjot Kaur and Anjana Gosain (2010), "Density Oriented Approach to identify Outliers and get Noiseless clusters in Fuzzy C Means", 2010 IEEE Conference of Fuzzy Sets and Systems, Barcelona, Spain, July 18-23, pp. 1-8.

2011 IEEE International Conference on Fuzzy Systems
June 27-30, 2011, Taipei, Taiwan

The Fuzzy DEMATEL based Job Accommodation Strategy Definitions for Operators with Hearing Impairments

Chi-Yo Huang
Dept. of Industrial Education
Nat. Taiwan Normal
University, No. 162, Ho-Ping
East Road I, Taipei, Taiwan
cyhuang66@ntnu.edu.tw

Gwo-Hshiung Tzeng
Inst. of Project Management
Kainan University
No. 1, Kainan Road,
Luchu, Taiwan
ghtzeng@mail.knu.edu.tw

Abstract — **The job accommodation, the redesign of a job or the creation of new vacancies for optimizing the utilization of manpower through job analysis, has become an important concept during the past decades. Effective job accommodation strategies can assist the people with disabilities in general, and hearing impaired people, who accounted for a majority of the disabilities in the labor market, in special, to expand their capability set and maximize their work performance. However, very few researches have been developed on how the job accommodation strategies can be defined. Furthermore, most available job accommodation strategies as well as assistive technologies were based on researches being developed one decade ago, which are not feasible and should be updated for modern industries. Thus, a fuzzy DEMATEL based MCDM framework will be introduced for deriving suitable accommodation strategies. An empirical study based on the operators from the electronic industry advanced and verified both available job accommodation strategies as well as job accommodation research methods. In the future, the proposed strategies as well as the research framework can be used to enhance the welfare of the disabilities.**

Keywords – Job accomodation strategy; Fuzzy DEMATEL; Fuzzy MCDM (Multiple Criteria Decision Making, MCDM).

I. INTRODUCTION

People with disabilities work in a variety of environments including management, administration, technology, design, and industry settings [1]. The potential for and importance of job accommodations, the redesign of a job or the creation of new vacancies for optimizing the utilization of manpower through job analysis, for qualified individuals with disabilities is clear in light of developments in human rights, technological innovations, and changing perceptions of the environmental barriers and facilitators for inclusion in work and in society at large [2]. Effective workplace accommodations are essential for the economic independence and self-determination of people with disabilities, and to maintain a productive workforce [2]. However, a large portion of adults with disabilities had no jobs though these people are willing to work. Recent studies reveal a paucity of workplace accommodations to compensate for loss of hearing [3]. Thus, researches on how job accommodation strategies and use of assistive technology resources and services can be defined can help to level the playing field for persons with disabilities so that they can compete on an equal basis in finding and maintaining employment [4].

Severity of a disability impacts an individual's ability to work [1]. People with physical and sensory limitations are more likely to have lost work days than the general population [1]. As summarized by Zolna et al. [5], reviews and reports of general accommodation strategies, specific interventions, vocational rehabilitation methods, etc. have all addressed the use of specialized designs and assistive technologies (AT) as workplace accommodations for people with disabilities. However, some accommodations have been successful, whereas others have not [5].

The existing knowledge base of accommodations contains a wealth of information about the needs, functional abilities, and criteria for successful intervention. While aggregated, these data can be crucial in informing [5]. Employers and persons with disabilities are likely to enjoy successful employment outcomes through increased knowledge and information sharing [2]. Proactive policies that allow for matching between employees' needs and job skills and available resources may help to bridge the gap between current and state of the art accommodations [2].

The total, civilian, non-institutionalized hearing-impaired population is estimated at 9.4% while the world population percentage is expected to be similar [6]. Further, recent statistics demonstrate that the people with hearing impairments has accounted for about 40% of the labor market. Apparently, employees with hearing impairments can be classified as one of the major groups of employees with disabilities to be focused. Further, in some electronic industries of the developed East Asian countries like Taiwan, the hearing impaired operators have already accounted for a significant percentage to the total employees with disabilities. Job accommodation strategy definitions for the hearing impaired operators are worth further study.

Albeit important, very limited study has empirically evaluated the importance of on-the-job accommodations for persons who are hard of hearing while accommodation practices were found to be a significant factor in employment success for persons who were deaf [7]. Allaire et al. also mentioned that relatively little is known about the kinds of work barriers experienced by employed persons with arthritis and other rheumatic diseases and to what extent these individuals utilize job accommodations. Further, the job accommodation is by nature an MCDM problem. According to the job accommodation procedure being proposed by Schneider [8], the major steps include determine alternatives and outline strategies for modifying the specific job task in question, review the alternatives/strategies with the employer and finally, agree on the appropriate modification or

978-1-4244-7316-8/11/$26.00 ©2011 IEEE

adaptation. The availability of accommodations, therefore, is likely to be related to attributes of employees and employers but limited attention has been paid to identifying covariates of either the availability of, or the need for, accommodations for people who are deaf or hard-of-hearing [3].

Therefore, this research intends to define a fuzzy DEMATEL based multiple criteria decision making (MCDM) based framework for selecting defining job accommodation strategies for operators with hearing impairments. At first, literature regarding to job accommodation strategies for disabilities and the selection criteria will be reviewed. The literature will serve as a basis for the MCDM framework development as well as possible alternative derivations for suitable job accommodation strategies. Then, the fuzzy DEMATEL will be used for constructing the structure of the decision problem. The weights being versus the criteria will be derived by using the ANP then. Finally, the GRA will be used for deriving the relationships between the possible job accommodation strategies as well as the criteria. The job accommodation strategies with the highest Grey grades will be selected as the suitable ones.

This research is organized as follows. The related literature regarding to capability set expansions and the job accommodation strategies will be reviewed in Section II. The theory which is based on MCDM framework and using the fuzzy DEMATEL based MCDM method will be introduced in Section III. An empirical study on expanding the capabilities of hearing impaired people will be used for demonstrating the feasibility of the proposed fuzzy MCDM framework in Section IV. Implications as well as discussion will be presented in Section V. Finally, the whole article will be concluded in Section VI.

II. Capability Set Expansions and Accomodation Strategies

An adoption of the accommodation strategies for the people with disabilities is a typical example for capability set expansion problem. By introducing the accommodation strategies, persons with disabilities can be assisted to expand their capability set and then level the playing field for persons with disabilities so that they can compete on an equal basis in finding and maintaining employment [4]. Following, past researches and concepts regarding to the capability, the capability set, people with disabilities as well as accommodation strategies with a focus on accommodation strategies for people with hearing impairments will be reviewed as a basis for the decision making framework.

Capability is an integration of knowledge, skills, personal qualities and understanding used appropriately and effectively - not just in familiar and highly focused specialist contexts but in response to new and changing circumstances while competence is primarily about the ability to perform effectively, concerned largely with the here and now [9]. Stephenson argued that narrowly defined competencies were only part of human capability [10]. Fraser and Greenhalgh [11] mentioned that capability is more than competence since competence is what individuals know or are able to do in terms of knowledge, skills, attitude while the capability is the extent to which individuals can adapt to change, generate new knowledge, and continue to improve their performance. Doncaster and Lester [12] further argued that capability is not restricted to being "almost synonymous with competence, but with less of a normative connotation" [13], but also implies a capacity to develop additional competence and to move beyond competence to being able to work effectively in unpredictable and changing contexts [12].

According to Yu [14-16], for each decision problem (e.g. job selection, corporate strategic definition, conflict resolution, etc.), a competence set consisting of ideas, knowledge, information and skills for its satisfactory solution exists. However, since competencies were only part of human capability, the concept of the competence set can further be expanded to the capability set. According to the definition by Srinivasan [17], the capability set is the set of vectors of functions the states of being and doings such as being healthy and avoiding premature mortality, available to a person.

People with disabilities work in a variety of environments and accommodations in these environments enable them to enter and remain in the workplace while the rate of employment is dependent on the educational level of the person as well as the physical and cognitive capacities of the person [1]. However, workplace environments are not optimally suited for people with disabilities even when people with disabilities are more likely to remain employed if their employer provides necessary accommodations [1].

Workplace accommodations, by their very nature, are solutions that are either individualized for specific employees or for groups of employees (e.g., wheelchair users or aging workers) [5]. The most frequently mentioned direct benefits from implementing workplace accommodations were retained a qualified employee, increased worker productivity, eliminated the cost of training a new employee, etc. [18]. As a result, specialized accommodations, such as those for people with mobility and dexterity impairments are not typically considered to be usable by all people, to the greatest extent possible [5].

According to the summarization in the work by Zolna et al. [5], the most commonly seen barriers to work include functional limitations due to the design of furnishings and workstations, computer-related difficulties, macro environmental barriers included transportation problems (e.g. parking and commuting) as well as and access to specific spaces required for activities of daily living (e.g. bathrooms), functional limitations including fatigue, pain, physical weakness, inability to stand for long periods, changes in physical sensation which become barriers to work. Scherich [19] further identified the six difficult workplace situations being identified by workers with hearing impairments: receiving instructions/supervision, department/staff meetings, in-service or training activities, performance evaluations, socializing with co-workers, and work-related social functions.

According to Schneider [8], it is possible to minimize the effect of a functional impairment by working in two different areas: the functional level of the individual and the environment. Butterfield and Ramseur [1] further summarized that types of accommodations include workplace provisions for computer technologies, environmental access such as ramps, elevators, parking and new workstations as well as structural changes to the physical workplace to promote participation in work activities including provisions for general access accommodation, floor surface changes, environmental control, signage, and evacuation routes, tool operation including telecommunication aids and assistive technology devices, workstation modifications and adaptive strategies, and seating and positioning such as equipment modifications. Zolna et al. [5] also summarized that type of accommodations include assistive technology, physical work environment, job requirements and personal assistance and training.

Finally, for accommodation strategies being suitable for workers with hearing impairments, Scherich [19] summarized devices as well as equipment, support personnel (ex:

interpreters, job coaches), job restructuring, etc. are accommodation strategies to be suitable for workers with hearing impairments. Geyer and Schroedel further identified sixteen feasible strategies, including TDD or TTY, phone amplifier, flashing lights for fire alarm, flashing lights on machines for safety, assistive listening device for meetings, pager device or beeper, e-mail, note-taking assistances by computers, sign class for co-workers who hear, co-worker takes notes for you at meetings, summary of meeting notes, interpreters, improved lighting in your work area, moved things around so you can see other people better, hearing people answer the phone, changed job duties for working better.

The extent of a functional impairment can be defined as the difference or gap between the level of function for the individual, and what the environment demands of him or her [8]. Apparently, appropriate accommodation strategies can be introduced so as to expand the capabilities, or capability set, of people with disabilities to close the gap. In the following Section, a fuzzy DEMATEL based MCDM framework will be proposed for correlating difficulties being faced by persons with hearing impairments

III. Analytic Framework For Defining Accomodation Strategies

The analytical process for deriving the job accommodation strategy is initiated by deriving the possible strategies and criteria being required to evaluating the strategies based on literature review. Then, the relations between the criteria will be derived by using the DEMAETL. The weights versus the criteria will be derived by using the ANP then. Finally, possible strategies will be derived by using the Grey Relation Analysis.

A. Fuzzy DEMATEL Method

The Fuzzy DEMATEL can deal with the DEMATEL problem by introducing Fuzzy linguistic variables and matrices. According to the definition of Fuzzy DEMATEL, the linguistic matrices present the relationships between criteria. In the matrices, the numeral value depicts the influence versus each criterion. Therefore, the Fuzzy DEMATEL method can transform the causes and effects relationship into a perspicuous structural model. The Fuzzy DEMATEL method has been studied and applied in many areas these years [20,21]. According to the advantages of Fuzzy DEMATEL, this research attempts to evaluate the preferences of lead users by using Fuzzy DEMATEL based on the definitions by Prof. Tzeng, Gwo-Hshiung [22]. The calculation process is demonstrated as below:

Step 1: Establishing the fuzzy linguistic scale

Establishing the linguistic sets of criteria is an essential procedure for Fuzzy DEMATEL. The major advantage of Fuzzy DEMATEL method is that it's effective to obtain the structural mode and divide the criteria into cause and effect groups, which consist of many complex aspects. To deal with the ambiguities of human feeling and evaluations, Li [23] introduces the fuzzy linguistic scale into the DEMATEL evaluation process. The strength of influence are divided into five linguistic levels as "Strong", "High", "Low", "No" and the linguistic levels will correspond to the triangular fuzzy numbers.

Step 2: Establishing the directed relation matrix

To measure the relationship versus each criterion $C = \{c_1, c_2, \ldots, c_n\}$, p lead users made evaluations in terms of linguistic terms toward the criteria. Thus, p fuzzy matrices $\tilde{\boldsymbol{Z}}^1, \tilde{\boldsymbol{Z}}^2, ..., \tilde{\boldsymbol{Z}}^P$ each corresponds to a lead user. The Fuzzy matrix is called the initial direct relation fuzzy matrix. For simplicity, denote $\tilde{\boldsymbol{Z}}$ as $c_1, c_2 ... c_n$, or

$$\tilde{\boldsymbol{Z}} = \begin{matrix} c_1 \\ c_2 \\ \vdots \\ c_n \end{matrix} \begin{bmatrix} 0 & \tilde{z}_{12} & \cdots & \tilde{z}_{1n} \\ \tilde{z}_{21} & 0 & \cdots & \tilde{z}_{2n} \\ \vdots & \vdots & \ddots & \vdots \\ \tilde{z}_{n1} & \tilde{z}_{n2} & \cdots & 0 \end{bmatrix},$$

where $\tilde{z}_{ij} = \left(l_{ij}, m_{ij}, u_{ij}\right)$ are triangular fuzzy numbers, elements $\tilde{z}_{ii} = 0, i = 1, 2 ... n$.

Step3: Establishing the structural model

In order to transform the criteria scales into comparable scales, the linguistic scale will be transformed into a normalization formula.

Let $\tilde{a}_{ij} = \sum_{j=1}^{n} \tilde{z}_{ij} = \left(\sum_{j=1}^{n} l_{ij}, \sum_{j=1}^{n} m_{ij}, \sum_{j=1}^{n} u_{ij} \right)$ and $u = \max_{1 \le i \le n} \left(\sum_{j=1}^{n} u_{ij} \right)$.

Then, the normalized direct relation fuzzy matrix, denoted by $\tilde{\boldsymbol{X}}$, equals $\tilde{x} = u^{-1} \otimes \tilde{z}$. Or

$$\tilde{\boldsymbol{X}} = \begin{bmatrix} \tilde{x}_{11} & \tilde{x}_{12} & \cdots & \tilde{x}_{1n} \\ \tilde{x}_{21} & \tilde{x}_{22} & \cdots & \tilde{x}_{2n} \\ \vdots & \vdots & \ddots & \vdots \\ \tilde{x}_{m1} & \tilde{x}_{m2} & \cdots & \tilde{x}_{mn} \end{bmatrix},$$

where $\tilde{x}_{ij} = \frac{\tilde{z}_{ij}}{u} = \left(\frac{l_{ij}}{u}, \frac{m_{ij}}{u}, \frac{r_{ij}}{u} \right)$. (1)

Fuzzy DEMATEL also assume that $\sum_{j=1}^{n} u_{ij} < u$ and $\lim_{k \to \infty} \tilde{x} = [0]_{0 \times 0}$.

Step 4: Deriving the total relation matrix

After calculating the normalized direct relation fuzzy matrix, the total relation matrix $\tilde{\boldsymbol{T}}$ can be derived by the equation below:

$$\tilde{\boldsymbol{T}} = \tilde{\boldsymbol{X}} + \tilde{\boldsymbol{X}}^2 + \cdots + \tilde{\boldsymbol{X}}^n = \tilde{\boldsymbol{X}}(\boldsymbol{I} - \tilde{\boldsymbol{X}})^{-1},$$

When $\lim_{k \to \infty} \tilde{X} = [0]_{n \times n}$

$$\tilde{\boldsymbol{T}} = \begin{bmatrix} \tilde{t}_{11} & \tilde{t}_{12} & \cdots & \tilde{t}_{1n} \\ \tilde{t}_{21} & \tilde{t}_{22} & \cdots & \tilde{t}_{2n} \\ \vdots & \vdots & \ddots & \vdots \\ \tilde{t}_{m1} & \tilde{t}_{m2} & \cdots & \tilde{t}_{mn} \end{bmatrix}; \tilde{t}_{ij} = \left(l_{ij}^{"}, m_{ij}^{"}, r_{ij}^{"} \right)$$

$$\left[l_{ij}^{''}\right]=\boldsymbol{X}_l-\left(\boldsymbol{I}-\boldsymbol{X}_l\right)^{-1},\ \left[m_{ij}^{''}\right]=\boldsymbol{X}_m-\left(\boldsymbol{I}-\boldsymbol{X}_m\right)^{-1},$$
$$\left[r_{ij}^{''}\right]=\boldsymbol{X}_r-\left(\boldsymbol{I}-\boldsymbol{X}_r\right)^{-1}$$

Step 5: Analyzing the sum of rows and columns

The row and column sums are individually indicated the sum of rows and columns of the total relation matrix $\boldsymbol{T}$ by using following equations (2), (3), and (4),

$$\tilde{\boldsymbol{T}}=[\tilde{t}_{ij}],\ \ i,j\in\{1,2,...,n\} \quad (2)$$

$$\tilde{\boldsymbol{r}}=[\tilde{r}_i]_{n\times 1}=\left[\sum_{j=1}^{n}\tilde{t}_{ij}\right]_{n\times 1} \quad (3)$$

$$\tilde{\boldsymbol{c}}=[\tilde{c}_j]_{1\times n}=\left[\sum_{i=1}^{n}\tilde{t}_{ij}\right]_{1\times n} \quad (4)$$

where the $\boldsymbol{r}$ and $\boldsymbol{c}$ represent the sums of the rows and columns.

Step 6: Analyzing the results from $\boldsymbol{r}$ and $\boldsymbol{c}$

According to the sum of rows and columns, $(\tilde{r}_i+\tilde{c}_i)$ depicts the strength of the influence. If $(\tilde{r}_i-\tilde{c}_i)$ is positive, then criteria i is dispatching influence on other factors. On the other hand, if $(\tilde{r}_i-\tilde{c}_i)$ is negative, factor i is receiving influence from other criteria [20, 24, 25].

B. Analytic Network Process (ANP)

The ANP method, a multi criteria theory of measurement developed by Saaty [26], provides a general framework to deal with decisions without making assumptions about the independence of higher-level elements from lower level elements and about the independence of the elements within a level as in a hierarchy [26]. In this section, concepts of the ANP are summarized based on Saaty's earlier works [26, 27].

A component of a decision network which was derived by the DEMATEL method in Section 3.1 will be denoted by $\boldsymbol{C}_h,\ h=1,2,\cdots,m,$ and assume that it has n_h elements, which we denote by $e_{h1}, e_{h2},\cdots, e_{hm}$. The influences of a given set of elements in a component on any element in the decision system are represented by a ratio scale priority vector derived from paired comparisons of the comparative importance of one criterion and another criterion with respect to the interests or preferences of the decision makers. This relative importance value can be determined using a scale of 1–9 to represent equal importance to extreme importance [26]. The influence of elements in the network on other elements in that network can be represented in the supermatrix as $\boldsymbol{W}_{ij}=[w_{ij}],\ i\in\{1,2,...,m\}$, $j\in\{1,2,...,m\}$. A typical entry $\boldsymbol{W}_{ij}=[w_{i_{nx}j_{ny}}]$, $nx\in\{1,2,...,n_i\}$, $ny\in\{1,2,...,n_j\}$ in the supermatrix, is called a block of the supermatrix in the following form where each column of $\boldsymbol{W}_{ij}$ is a principal eigenvector of the influence of the elements (objective) in the ith component of the network on an element (objective) in the j^{th} component. Some of its entries may be zero corresponding to those elements (objective) that have no influence.

After forming the supermatrix, the weighted supermatrix is derived by transforming all columns sum to unity exactly. This step is very much similar to the concept of the Markov chain in terms of ensuring that the sum of these probabilities of all states equals 1. Next, the weighted supermatrix is raised to limiting powers, such as $\lim_{\theta\to\infty}\boldsymbol{W}^{\theta}$ to get the global priority vector or called weights [28].

In addition, if the supermatrix has the effect of cyclicity, the limiting supermatrix is not the only one. There are two or more limiting supermatrices in this situation, and the Cesaro sum would need to be calculated to get the priority.

The weights of the k^{th} criteria being derived by using the above ANP processes, namely $\omega_k,\ k\in\{1,2,...,n\}$, will be used as the weight for the k^{th} criteria in the following Section 3.3.

C. GRA

GRA is used to determine the relationship between two sequences of stochastic data in a Grey system. The procedure bears some similarity to pattern recognition technology. One sequence of data is called the 'reference pattern' or 'reference sequence,' and the correlation between the other sequence and the reference sequence is to be identified [29-32]. To apply the GRA, definitions were cited from the early works by Tzeng and Huang [25, 33].

According to Deng, the mathematical equation for deriving the grey relation coefficient is:

$$\gamma(x_0(k),x_i(k))=$$
$$(\min_{\forall i}\min_{\forall k}\left|(x_0(k)-x_i(k))\right|+\zeta\max_{\forall i}\max_{\forall k}\left|(x_0(k)-x_i(k))\right|)\times$$
$$(\left|(x_0(k)-x_i(k))\right|+\zeta\max_{\forall i}\max_{\forall k}\left|(x_0(k)-x_i(k))\right|)^{-1}$$

where ζ is the distinguished coefficient ($\zeta\in[0,1]$). Generally, we pick ζ =0.5. When the grey relational coefficient is conducted with respect to the courses, we then can derive the grade of the grey relation $\gamma(\boldsymbol{x}_0,\boldsymbol{x}_i)$ between the reference alternative $\gamma(\boldsymbol{x}_0,\boldsymbol{x}_i)=\sum_{k=1}^{n}n^{-1}\gamma(x_0(k),x_i(k))$, where k is the number of capabilities while the weight being associated to the criterion is assumed to be equal. $\gamma(\boldsymbol{x}_0,\boldsymbol{x}_i)$ represents the grade of grey relation in x_i (the k^{th} strategy) correspondence to x_0. In this study, we make the order of the strategies following the grade of grey relation.

IV. ACCOMODATION STRATEGY DEFINITIONS FOR OPERATORS WORKING IN THE ELECTRONIC INDUSTRY

The electronic industry of the developed East Asian countries, including Japan, South Korea and Taiwan have already been well developed and contributed to a significant percentage of the GDPs of the countries. In Taiwan, the electronic industry has also become the major source of job vacancies for workers with disabilities. In the electronic factories, operators accounted for significant share of the total employers. To maximize the capability of operators with disabilities in general and the hearing impaired operators in

special, an empirical study based on interviews of the Taiwanese hearing impaired operators as well as an industry expert was introduced for verifying and demonstrating the feasibility of the proposed Fuzzy DEMATEL based MCDM framework for job accommodation strategy definitions.

Based on the interview results from seven operators who have been working in Taiwanese high technology firms, including the semiconductor testing houses as well as liquid crystal display panel vendors, following work barriers were summarized: colleagues' low/no intention to communicate by pen (p_1), managers' terrible attitude (p_2), noisy work environment (p_3), no hearing aid or requirements for better hearing aid (p_4), lip reading difficulties (p_5), no idea regarding to how capabilities can be enhanced (p_6), requirements in word processing software training (p_7), and no idea(s) regarding to possibilities of career development (p_8).

Since the former accommodation strategies being proposed by Geyer and Schroedel [3] cannot fulfill the needs of the electronic industry, seven novel accommodation strategies are proposed. The strategies include the electronic white board (a_1), digital electronic hearing aid (a_2), summary meeting notes (a_3), interpreters (a_4), on-job training of computer software (a_5), career planning courses (a_6) as well as assistances by hearing co-worker(s) (a_7).

At first, according the expert's opinion, the linguistic variables can be defined as Figure 1(a) while the initial direct relation fuzzy matrix $\tilde{Z}$ can be defined as Figure 1(b).

Variable	Upper	Medium	Lower
VL	0	30	50
L	40	50	60
M	60	70	80
H	75	85	95
VH	85	95	100

(a)

$$\begin{bmatrix} 0 & H & VL & H & H & VL & L & VL \\ M & 0 & VL & VL & VL & VL & M & VL \\ M & L & 0 & H & VL & VL & VL & VL \\ VL & M & VL & 0 & VL & VL & VL & VL \\ H & H & VL & H & 0 & VL & VL & VL \\ VL & VL & VL & VL & VL & 0 & VL & VL \\ VL & M & VL & VL & VL & VL & 0 & VL \\ VL & VL & VL & VL & VL & VH & VL & 0 \end{bmatrix}$$

(b)

Figure 1. (a) Linguistic variables and (b) the fuzzy matrix $\tilde{Z}$

Then, by introducing the Fuzzy DEMATEL ANP process being introduced in Section 3, the weights being associated with each work barrier can be derived (see Table I).

Table I. The weights versus criteria

Barrier	p_1	p_2	p_3	p_4	p_5	p_6	p_7	p_8	Sum
Weight	0.133	0.133	0.167	0.167	0.133	0.100	0.067	0.100	1.000

Finally, by introducing the GRA being introduced in Section 3.3, the Grey grades versus each accommodation strategy can be derived (see Table II). Based on the derivation results, the electronic white board (a_1), digital electronic hearing aid (a_2), interpreters (a_4), and assistances by hearing co-worker(s) (a_7) are the most helpful strategies.

Table II. The Grey Coefficients and Grey Grades

Strategy \ Barrier	p_1	p_2	p_3	p_4	p_5	p_6	p_7	p_8	Grey Grades
a_1	0.133	0.067	0.167	0.056	0.089	0.033	0.022	0.033	0.511
a_2	0.133	0.133	0.111	0.167	0.133	0.033	0.022	0.033	0.678
a_3	0.089	0.089	0.056	0.056	0.089	0.033	0.022	0.033	0.378
a_4	0.133	0.089	0.167	0.056	0.133	0.033	0.022	0.033	0.578
a_5	0.044	0.089	0.056	0.056	0.044	0.033	0.067	0.033	0.289
a_6	0.044	0.053	0.056	0.056	0.044	0.100	0.033	0.100	0.253
a_7	0.133	0.133	0.167	0.167	0.133	0.050	0.044	0.050	0.733

V. DISCUSSION

In this research, accommodation strategies for hearing impaired operators were derived by introducing the Fuzzy DEMATEL based MCDM approach. Following, the managerial implications as well as advances in research methods of job accommodation strategy definitions will be discussed.

For the accommodation strategies being suitable for the electronic industry, the past researches or assistive technologies are very limited. The accommodation strategies being developed one decade ago cannot fulfill modern requirements. Further, modern electronic technologies have already advanced the assistive technologies. Apparently, updates of both work barriers in the modern industry as well as available accommodation strategies are very helpful. The research results being demonstrated in this paper advanced both aspects of the job accommodation strategies as well as work barriers in the electronic industry.

For the research results, the electronic white board, digital electronic hearing aid, interpreters, and assistances by hearing co-worker(s) are the most helpful accommodation strategies. However, these results were derived based on one expert's opinion by summarizing interview results of the hearing impaired operators. How the accommodation strategies can be derived based on the viewpoints of the business managers will also be very helpful and make the accommodation strategies really feasible. Thus, further researches by introducing the opinions from the industry managers, experts from the academic or social welfare institutes as well as the hearing impaired operators will be very helpful.

For the advances in incorporating the idea of MCDM into researches of accommodation strategy definitions, the perfect match between the MCDM methods as well as the job accommodation strategy definition process being proposed by the job accommodation procedure being proposed by Schneider [8] have already been addressed in the first Section. Further, the empirical study based on the case studies on the hearing impaired operators from the electronic industry has verified the effectiveness of the proposed MCDM framework. In the future, the MCDM framework can be applied in the job accommodation strategy definition problems for other disabilities. Meanwhile, the effectiveness of the strategies can further be compared with the job accommodation strategies being derived by other research methods.

VI. CONCLUSIONS

Job accommodation strategies have become daily important for the people with disabilities in general and hearing impaired people in special. However, very few researches have been developed on how the job accommodation strategies can be defined. Meanwhile, job accommodation strategy definitions based on research results being developed one decade ago are not feasible for modern

industries. In this paper, the fuzzy DEMATEL based MCDM framework was first introduced into the job accommodation strategy definition problem due to the nature match between the job accommodation strategy definition process as well as the MCDM framework. An empirical study based on the operators from the electronic industry advanced and verified both available job accommodation strategies as well as job accommodation research methods. In the future, the proposed strategies as well as the research framework can be used to enhance the welfare of the disabilities.

ACKNOWLEDGMENT

The authors gratefully acknowledge the support of National Taiwan Normal University through grant number NTNU 98T0513-1 and NTNU 98T0513-3.

REFERENCES

[1] T. M. Butterfield and J. H. Ramseur, "Research and case study findings in the area of workplace accommodations including provisions for assistive technology: A literature review," *Technology & Disability,* vol. 16, pp. 201-210, 2004.

[2] N. Schreuer, W. N. Myhill, T. Aratan-Bergman, D. Samant, P. Blanck, "Workplace accommodations: Occupational therapists as mediators in the interactive process," *Work: A Journal of Prevention, Assessment and Rehabilitation,* vol. 34, pp. 149-160, 2009.

[3] P. D. Geyer and J. G. Schroedel, "Conditions Influencing the Availability of Accommodations for Workers Who Are Deaf or Hard-of-Hearing.," *Journal of Rehabilitation,* vol. 65, pp. 42-50, 1999.

[4] A. J. Langton and H. Ramseur, "Enhancing employment outcomes through job accommodation and assistive technology resources and services," *Journal of Vocational Rehabilitation,* vol. 16, pp. 27-38, 2001.

[5] J. S. Zolna, J. Sanford, D. Sabata, J. Goldthwaite, "Review of accommodation strategies in the workplace for persons with mobility and dexterity impairments: Application to criteria for universal design," *Technology and Disability,* vol. 19, p. 189, 2007.

[6] H. Hosford-Dunn, R.J. Roeser, M. Valente, *Audiology practice management*, 2nd. ed. New York, N.Y.: Thieme Medical Publishers, Inc., 2008.

[7] D. L. Scherich, "Accommodating Specific Job Functions for People with Hearing Impairments.," *The Journal of Rehabilitation,* vol. 62, pp. 28-35, 1996.

[8] M. Schneider, "Achieving greater independence through assistive technology, job accommodation and supported employment," *Journal of Vocational Rehabilitation,* vol. 12, pp. 159-164, 1999.

[9] J. Stephenson and M. Yorke, *Capability and quality in higher education*: Kogan Page, 1998.

[10] J. Stephenson, "Capability and competence: are they the same and does it matter?," *Capability,* vol. 1, pp. 3-5, 1994.

[11] S. W. Fraser and T. Greenhalgh, "Coping with complexity: educating for capability," *British Medical Journal,* vol. 323, pp. 799-803, 2001.

[12] K. Doncaster and S. Lester, "Capability and its development: experiences from a workbased doctorate," *Studies in Higher Education,* vol. 27, pp. 91-101, 2002.

[13] M. Eraut, *Professional knowledge and competence*. Brighton: Falmer Press, 1994.

[14] P. L. Yu, *Habitual Domains and Forming Winning Strategies*. Hsinchu, Taiwan: NCTU Press, 2002.

[15] P. L. Yu and D. Zhang, "Competence set analysis for effective decision making," *Control Theory and Advanced Technology,* vol. 5, pp. 523-547, 1989.

[16] P. L. Yu and D. Zhang, "Marginal analysis for competence set expansion," *Journal of Optimization Theory and Applications,* vol. 76, pp. 87-109, 1993.

[17] T. N. Srinivasan, "Human Development: A New Paradigm or Reinvention of the Wheel?," *The American Economic Review,* vol. 84, pp. 238-243, 1994.

[18] T. I. Solovieva*, et al.*, "Employer benefits from making workplace accommodations," *Disability and Health Journal,* vol. 4, pp. 39-45, 2011.

[19] D. L. Scherich, "Job Accommodations in the Workplace for Persons who are Deaf or Hard of Hearing: Current Practices and Recommendations," The Journal of Rehabilitation, vol. 62, pp. 27-35, 1996.

[20] M. Tamura, H. Nagata and K. Akazawa, "Extraction and systems analysis of factors that prevent safety and security by structural models," in *Proceedings of the 41st SICE Annual Conference*, Osaka, Japan, 2002, pp. 1752-1759.

[21] M. Yamazaki, K. Ishibe and S. Yamashita, "An analysis of obstructive factors to welfare service using DEMATEL method," *Reports of the Faculty of Engineering*, vol. 48, pp. 25-30, 1997.

[22] C.-Y. Hsu, K.T. Chen and G.H. Tzeng, "FMCDM with Fuzzy DEMATEL Approach for Customers' Choice Behavior Model," *International Journal of Fuzzy Systems*, vol. 9, pp. 236-246, 2007.

[23] R.J. Li, "Fuzzy method in group decision making," *Computers and Mathematics with Applications*, vol. 38, pp. 91-101, 1999.

[24] Y.-J. Chiu, H.C. Chen, J.Z. Shyu and G.H. Tzeng, "Marketing strategy based on customer behaviour for the LCD-TV," *International Journal of Management and Decision Making*, vol. 7, pp. 143-165, 2006.

[25] C. Y. Huang, J.Z. Shyu and G.H. Tzeng, "Reconfiguring the Innovation Policy Portfolios for Taiwan 's SIP Mall Industry," *Technovation*, vol. 27, pp. 744-765, 2007.

[26] T. L. Saaty, *Decision Making with Dependence and Feedback: The Analytic Network Process*. Pittsburgh: RWS Publication, 1996.

[27] T. L. Saaty, *Theory and Applications of the Analytic Network Process - Decision Making with Benefits, Opportunities, Costs, and Risks*. Pittsburg, PA: RWS Publications, 2005.

[28] J.-J. Huang, G.H. Tzeng and C.S. Ong, "Multidimensional data in multidimensional scaling using the analytic network process," *Pattern Recognition Letters,* vol. 26, pp. 755-767, 2005.

[29] J. L. Deng, *Grey Forecasting and Decision*. Wuhan, China: Huazhong University of Science and Technology Press, 1986.

[30] G. H. Tzeng and S. H. Tasur, "The multiple criteria evaluation of Grey relation model," *The Journal of Grey System,* vol. 6, pp. 87-108, 1994.

[31] D. L. Mon, G. H. Tzeng and H. C. Lu, "Grey decision making in weapon system evaluation," *Journal of Chung Chen Institute of Technology,* vol. 24, pp. 73-84, 1995.

[32] H. S. Wu, J. L. Deng, and K. L. Wen, *Introduction of Grey Analysis*. Taipei, Taiwan: Gau-Li Publication Inc., 1996.

[32] G. H. Tzeng and C. Y. Huang,"Combined DEMATEL technique with a Novel MCDM Method for Creating the Aspired Intelligent Global Manufacturing & Logistics Systems," *Annals of Operations Research* (Forthcoming), 2011.

2011 IEEE International Conference on Fuzzy Systems
June 27-30, 2011, Taipei, Taiwan

Expert Decision Making Method Based On Uncertain Linguistic Variables

Tzung-Nan Chuang
Dept. of Business and Management
National University of Tainan, Taiwan
chua@mail.nutn.edu.tw

Jung-Yuan Kung
Dept. of Information Management
Naval Academy
Kaohsiung, Taiwan
jykung@cna.edu.tw

Yin-Fang Lin
Dept. of Business and Management
National University of Tainan, Taiwan
smallj624@gmail.com

Hsiang-Chun Ku
Dept. of Business and Management
National University of Tainan, Taiwan
rmprmpr@hotmail.com

***Abstract*- In this paper, we propose an expert decision making method, UL-TOPSIS. Through giving experts the flexibility of evaluation, they can choose two items of linguistic variables by the multiple-choice method, with an interval range of uncertain linguistic variables to express their real thinking. The method is also used to resolve the problem of too wide range of an individual expert opinion or too large differences between experts opinions. We hope that the new method can capture the opinions of experts better, integrate the opinions of all experts appropriately, and make more accurate decisions for decision makers.**

Keywords-expert decision making; fuzzy sets theory; uncertain linguistic variable; TOPSIS

I. INTRODUCTION

It is well-known that the quality of decision-making affects the organizational operation and performance deeply. In the process of decision-making, how to capture the opinion of decision makers exactly is extremely important. In tradition, MADM methods often solve the problems involving the crisp ratings of alternatives under attributes with crisp weights. However, in real cases the available data used in decision-making problems are often imprecise and vague. For example, the linguistic statement is very often used to evaluate alternatives and/or to indicate the importance of attributes. Linguistic variables are variables whose values (interpretation) are not numbers but words or sentences in a natural or artificial language [1]. The concept of linguistic variable is very useful to treat situations that are too ill-defined or too complicated to be appropriately described in traditional quantitative expressions. Xu(2004) presented that it is unavoidable that experts can only provide uncertain linguistic information due to time pressure and/or lack of sufficient information. Therefore it derived to use linguistic variables to show expression of opinions and preferences [3]. For giving decision-makers the flexibility of evaluation, they can choose two items of linguistic variables by the multiple-choice way with an interval range of uncertain linguistic variables to express their real thinking. For instance, if one decision-maker wants to give the evaluation that is between "fair" and "satisfied", then the decision-maker is able to evaluate with such uncertain linguistic variable [fair, satisfied]. Nevertheless, we find it also brings another problem which may produce too large interval range. It includes two kinds of situations. One is too wide range of evaluation from a decision-maker, and the other is too large differences between these evaluations from decision-makers. Therefore, for decision quality, it is necessary to overcome these problems when using such uncertain linguistic variable in evaluation.

Therefore, in this study we develop the UL-TOPSIS (Uncertain Linguistic Technique for Order Preference by Similarity to Ideal Solution), which is used uncertain linguistic variable as input value and applied the theory and spirit of TOPSIS to lead to develop a new operational process. We call the method as Uncertain Linguistic Technique for Order Preference by Similarity to Ideal Solution, UL-TOPSIS, hope to use it to capture the opinions of exports better and make more accurate

II. LITERATURE REVIEW

A. Linguistic Variable

In order to be able to transform the description of natural language into logical description by logic speculation, linguistic variable in fuzzy sets is used to describe the natural language under the domain of specification,. The linguistic variable is based on word or sentence as a variable rather than a number [1]. According to Zadeh (1975) description of linguistic variables, the linguistic terms is referred to the adjective phrase that is used by describing their own feelings of external things in human daily life [1]. For example, the linguistic variable "satisfaction", which can be used in linguistic terms "very dissatisfied ", "not satisfied" and " fair", "satisfied", "very satisfied" and other words to express.

B. Likert Scale

About the questionnaire design of expert opinions for the

978-1-4244-7316-8/11/$26.00 ©2011 IEEE

criteria, the quantitative method of traditional rating scale is based on using a single value that corresponding to the opinion. That is Likert Scale which is generally familiar with. It is shown in Table I [4].

TABLE I. LIKERT SCALE

Linguistic variable	Very dissatisfied	dissatisfied	general	satisfied	Very satisfied
Corresponding function value	1	2	3	4	5

Likert Scale is used the value of equal difference to converse the answer that is chosen from all options by experts. That is conversed through the correlation between function, as shown in Table I. For different linguistic variables "very satisfied, satisfied, general, satisfactory, very satisfactory " to give the value "1,2,3,4,5," and then to quantify the linguistic variables and proceed follow-up calculation and decision-making.

C. Nine-point Scale

In the decision making methods AHP and ANP that Saaty proposed, it must be evaluate the importance of criteria before decision-making. It is divided into nine levels of importance for experts based on the questionnaire format Saaty designed. Levels of importance are separated into "Equal Importance", "Moderate Importance ", "Strong Importance", "Demonstrated Importance ", "Extreme Importance ", and take intermediate value between each level [6]. So we can let the experts proceed evaluating between two levels .The measure scale is shown in Table II as follow:

TABLE II. MEASURE SCALE

measure scale	Intensity of Definition Importance	Description
1	Equal Importance	Two activities contribute equally to the objective
3	Moderate Importance	Experience and judgment slightly favor one activity over another
5	Strong Importance	Experience and judgment strongly favor one activity over another
7	Demonstrated Importance	An activity is favored very strongly over another; its dominance demonstrated in practice
9	Extreme Importance	The evidence favoring one activity over another is of the highest possible order of affirmation
2, 4, 6, 8	Intermediate Value between two level	Between above of description

source：Saaty, 2006

D. Uncertain Linguistic Variable

In real life, when the experts or policy makers in the assessment criteria, the individual's thinking and cognitive differences have in determining the degree of differentiation, and implied uncertainty. In order to reflect model of human thinking more closely, we can let the experts use uncertain linguistic directly for expression. The uncertain linguistic representation is an "interval range" of linguistic variables. It is used an "interval range" to replace the option of single linguistic variables, and hoping to more fully express a personal thought and cognition by giving experts flexibility of evaluation, in order to facilitate more effective decision-making activities.

By using the example Xu(2004) mentioned in his study to illustrate that when evaluating criteria, linguistic variable is distinguished between nine terms. S represents a set which include nine linguistic variables:

$$S=\{s_1 = \text{extremly dissatisfied}, s_2 = \text{very dissatisfied}, s_3 = \text{dissatisfied}, s_4 = \text{slightly dissatisfied}, s_5 = \text{fair}, s_6 = \text{slightly satisfied}, s_7 = \text{satisfied}, s_8 = \text{very satisfied}, s_9 = \text{extremly satisfied}\}$$

where s_i represents a possible value for a linguistic variable [3].

However today expert A wants to give the evaluated value which has no clear boundary. He considers that it is fall between "fair" and "satisfaction." Therefore expert A could use [s4, s6] such a uncertain linguistic for expression. According to expert B's thinking, the evaluated value he given is between "very dissatisfied" and "slightly satisfied", so he can represent it with [s0, s3].

E. TOPSIS

TOPSIS (Technique for Order Preference by Similarity to Ideal Solution) is a multi-attributed evaluation method that have developed by Hwang and Yoon (1981) [7]. It is applied widely in decision-making problems. Followed developing by Yoon (1987) and Hwang and others, the theory have been more complete.

The basic concept of TOPSIS is that the decision-maker based on all evaluated criteria of alternatives to find out the Positive Ideal Solution which is composed of the greatest value of those criteria and the Negative Ideal Solution which is composed of the worst value of those criteria for comparison. The so-called positive ideal solution is to enable the alternatives to be increased to the greatest of effectiveness attribute and reduced to the smallest of cost attribute; The negative ideal solution is to enable the alternatives to be dropped to the smallest effectiveness attribute and to be increased to the greatest of cost attributes.

III. UNCERTAIN LINGUISTIC TECHNIQUE FOR ORDER PREFERENCE BY SIMILARITY TO IDEAL SOLUTION

Uncertain Linguistic Technique for Order Preference by Similarity to Ideal Solution, UL-TOPSIS, which is used uncertain linguistic variable as input value and applied the theory and spirit of TOPSIS. Moreover, it can extend to deal with too much difference of expert opinions, and led to develop a new operational process.

UL-TOPSIS that developed in this study is the assessment of experts in order semantic uncertainty expressed, one expert expressed by the interval range of input values, applied to make expert decisions TOPSIS methods, procedures and contents are described below:

UL-TOPSIS developed in this study is expressed the opinion of experts by the uncertain linguistic, and used the interval range of expert expression as the input value for applying TOPSIS method to make expert decision. The steps and description as follow:

Step1. Establish a multi-criteria decision-making matrix

$$D_e = \begin{array}{c} \\ A_1 \\ A_2 \\ \vdots \\ A_m \end{array} \begin{array}{c} \begin{array}{cccc} C_1 & C_2 & \dots & C_n \end{array} \\ \begin{bmatrix} x_{11}^e & x_{12}^e & \dots & x_{1n}^e \\ x_{21}^e & x_{22}^e & \dots & x_{2n}^e \\ \dots & \dots & \dots & \dots \\ x_{m1}^e & x_{m2}^e & \dots & x_{mn}^e \end{bmatrix} \end{array}, e = 1,2,\dots,h \qquad (1)$$

$$W_j = [w_1, w_2, \dots, w_n].$$

D_e is the multi-criteria decision-making matrix of the eth expert, e=1, 2, …, h, A_i indicate the ith alternative, i=1, 2, …, m ; C_j indicate the jth *criteria*, j = 1, 2, …, n ; x_{ij}^e indicate the value that expert e give the jth criteria for ith alternative, x_{ij}^e = [a_{ij}^e , b_{ij}^e] ; and w_j indicate the importance relative to criteria C_j, $j = 1,2,\dots,n$。

Let $b_j - a_j$ be the difference between expert opinions. If $b_j - a_j \geqq 5$, we define this as the difference between expert opinions too much.

Step2. To integrate the opinions of each expert who give the same criteria under the same alternative.

$$X_{ij} = \left[\min_{e=1}^{h} a_{ij}^e, \max_{e=1}^{h} b_{ij}^e \right] = [a_{ij}, b_{ij}] \qquad (2)$$

Step3. To use the method when the differences between expert opinions are too much

if $b_j - a_j \geqq 5$, then do the following steps:

1. Under the same alternative, for the same criteria (j), to calculate the distance of each S_{ij}

$$d(x_{ij}^e, x_{ij}^k) = \sqrt{(b_{ij}^k - b_{ij}^e)^2 + (a_{ij}^k - a_{ij}^e)^2} \qquad (3)$$

$e \neq k$, e=1, 2, …, m-1

k=e+1, e+2, …, h , for each i, j

2. To compare the distance $d(S_{ij}, S_{kj})$ and eliminate the outlier

   Finding the maximum $d(S_{ij}, S_{kj})$ and eliminate it. We will not to consider the score which the expert given.
3. Then come back to Step 2.

Step4. To normalized the evaluated values of each alternative for the criteria.

$$r_{ij} = \frac{x_{ij}}{9}, \quad i = 1, 2, \dots, m \quad ; \quad j = 1, 2, \dots, n \qquad (4)$$

The normalized decision-making matrix could be displayed with $R = [r_{ij}]_{m \times n}$

$$R = \begin{array}{c} \\ A_1 \\ A_2 \\ \vdots \\ A_m \end{array} \begin{array}{c} \begin{array}{cccc} C_1 & C_2 & \dots & C_n \end{array} \\ \begin{bmatrix} r_{11} & r_{12} & \dots & r_{1n} \\ r_{21} & r_{22} & \dots & r_{2n} \\ \dots & \dots & \dots & \dots \\ r_{m1} & r_{m2} & \dots & r_{mn} \end{bmatrix} \end{array}, \qquad (5)$$

$$W_j = [w_1, w_2, \dots, w_n].$$

Step5. To make the relative weight of each criteria multiply into the standard matrix to create a normalized weighted matrix

$$V_{ij} = w_j r_{ij}, \quad i = 1,2,\dots,m \quad ; \quad j = 1,2,\dots,n \qquad (6)$$

where w_j is the weight of C_j

Step6. To determine the positive ideal solution and negative ideal solution

let [9,9] and [1,1] separately be the positive ideal solution and negative ideal solution of single criteria that not yet be added the weight and normalized.

After normalizing, $r^* = \left[\frac{9}{9}, \frac{9}{9}\right]$ $r^- = \left[\frac{1}{9}, \frac{1}{9}\right]$

After multiplying the weight value,

$$V^* = w_j r^* \quad ; \quad V^- = w_j r^- \qquad (7)$$

Then the positive ideal solution A^* of each criteria could be showed as follow:

$$A^* = [V_1^*, V_2^*, \dots, V_j^*, \dots, V_n^*] \qquad (8)$$

And the negative ideal solution A^- of each criteria could be showed as follow:

$$A^- = [V_1^-, V_2^-, \dots, V_j^-, \dots, V_n^-] \qquad (9)$$

Step7. To calculate the Separation measure

The distance between each alternative and the positive

ideal solution, represents as Separation measure Si*:

$$S_i^* = \left\{ \sum_{j=1}^{n} \left(V_{ij} - V_j^* \right)^2 \right\}^{1/2}, i = 1,2,\ldots,m \qquad (10)$$

The distance between each alternative and the negative ideal solution, represents as Separation measure Si—:

$$S_i^* = \left\{ \sum_{j=1}^{n} \left(V_{ij} - V_j^* \right)^2 \right\}^{1/2}, i = 1,2,\ldots,m \qquad (11)$$

Step8. To calculate the relative similarity to the positive ideal solution and negative ideal solution of the compared alternatives, RC_i^* is obtained:

$$RC_i^* = \frac{S_i^-}{S_i^* + S_i^-}, \; i = 1,2,\ldots, m, \; 0 \le RC_i^* \le 1 \qquad (12)$$

Step9. By the relative similarity RC_i^* to the positive ideal solution and negative ideal solution of the compared alternatives, we can know the relative position of compared alternatives to the positive and negative ideal solution, to rank the order of all alternatives. When the value RC_i^* is getting more close to 1, it means the alternative is getting more near the positive ideal solution, and more away from negative ideal solution. Which alternative is the better one. Otherwise, When the value RC_i^* is getting more close to 0, it means that the alternative is getting more near the negative ideal solution, and more away from positive ideal solution. Which alternative is the worse one. Therefore, the greater value RC_i^* of alternative is the priority.

IV. CONCLUSION

The purpose of this study is to provide a practical reference through proposing a new expert decision-making method and applying it to deal with the decision-making problems that practical business management often faced. So we develop the UL-TOPSIS which is used uncertain linguistic variable as input value and applied the theory and spirit of TOPSIS. Moreover, it can extend to deal with too much difference of expert opinions, and led to develop a new operational process. We could use it to capture the opinions of exports better, integrate the opinions of all experts appropriately, and make more accurate decisions for decision makers.

However, there are many multi-criteria decision-making methods, for example: AHP, ANP, etc. In the future, the researchers that interested in it can also use the uncertain linguistic variables and the concepts of dealing with too large differences in this study to apply in the multiple-criteria decision making method. And use it to develop the more diversified approach of decision-making and operational processes to provide a reference that could handle the more complex problems of management decision-making in practice.

REFERENCES

[1] L. A. Zadeh, "The concept of a linguistic variable and its application to approximate reasoning I, II, III," Information Science, 8, 199-251, 301-357, 9 , pp. 43-80, 1975.

[2] R. E. Bellman and L. A. Zadeh, "Decision-making in a fuzzy environment," Management Science, 17(4), pp. 141-146, 1970.

[3] Z. Xu, "Uncertain linguistic aggregation operators based approach to multiple attribute group decision making under uncertain linguistic environment," Information Sciences, 168, pp. 171-184, 2004.

[4] R. Likert, "A Technique for the Measurement of Attitudes, " Archives of Psychology, 140, pp. 1-55, 1932.

[5] T. L. Saaty, "The analytic hierarchy process," McGraw-Hill, New York, 1980.

[6] T. L. Saaty and L. G. Vargas, "Decision Making With the Analytic Network Process: Economic, Political, Social And Technological Applications With Benefits, Opportunities, Costs and Risks," Springer Verlag, 2006.

[7] Hwang, C.L., & Yoon, K.,. "Multiple Attributes Decision Making Methods and Applications," Springer, Berlin Heidelberg, 1981.

2011 IEEE International Conference on Fuzzy Systems
June 27-30, 2011, Taipei, Taiwan

Apply Fuzzy Vector Quantization to Improve The Observation-Based Discrete Hidden Markov Model --An example on electroencephalogram (EEG) signal recognition

Shing-Tai Pan
Department of Computer Science and Information Engineering
National University of Kaohsiung
Kaohsiung, Taiwan R.O.C.
stpan@nuk.edu.tw

Sheng-Fu Liang
Department of Computer Science and Information Engineering
National Cheng Kung University
Tainan, Taiwan R.O.C.
sfliang@mail.ncku.edu.tw

Tzung-Pei Hong
Computer Science and Information Engineering
National University of Kaohsiung
Kaohsiung, Taiwan R.O.C.
tphong@nuk.edu.tw

Jian-Hong Zeng
Computer Science and Information Engineering
National University of Kaohsiung
Kaohsiung, Taiwan R.O.C.
mafiajerry@msn.com

Abstract—**This paper applies fuzzy vector quantization (FVQ) to the modeling of observation-based Discrete Hidden Markov Model (DHMM) and then to improve the speech recognition rate for the Mandarin speech. Vector quantization based on a codebook is a fundamental process to recognize the speech signal by DHMM. A codebook will be first trained by K-means algorithms using Mandarin training speech. Then, based on the trained codebook, the speech features are quantized by the fuzzy sets defined on each vectors of the codebook. Subsequently, the quantized speech features are statistically applied to train the model of DHMM for the speech recognition. All the speech features to be recognized should go through the FVQ based on the fuzzy codebook before being fed into the DHMM model for recognition. Experimental results in this paper shows that the speech recognition rate can be improved by using FVQ algorithm to train the model of DHMM.**

Keywords- Fuzzy Vector Quantization, EEG signal, Discrete Hidden Markov Model

I. INTRODUCTION

Recently, the Hidden Markov Model (HMM) is applied in many applications for prediction duo to its statistic properties [1]. It is especially successful on the automatic speech recognition (ASR). According to the type of the probability distributions used in HMMs, HMMs can be categorized as Continuous Hidden Markov Model (CHMM) and Discrete Hidden Markov Model (DHMM). The DHMM provides more stable recognition results and faster training with the recognition accuracy that is no less than CHMM. Therefore, the DHMM is adopted in this paper. The codebook for the feature quantization of the target signal will be recognized plays an important role on the training of DHMM model. A well-trained codebook will enhance the total performance of the recognition systems. In the past, the features are quantized by a codebook trained by K-means algorithm. This winner-take-all algorithm can not perform well on vector quantization, since multiple level of an element in some vectors exists in many applications. Consequently, the fuzzy vector quantization is used improve the performance of the vector quantization. Many research shows that the fuzzy vector quantization outperform VQ [2]. Besides, the relative works of fuzzy vector quantization, e.g. the fuzzy clustering [3-4] and fuzzy data retrieval systems [5] also demonstrate the benefit of fuzzy quantization method.

Besides, sleep is very importance to human's health. Humans spend averagely about 7 to 8 hours a day on sleep, which is equivalent to one third of our lifetime. At night, an 8-hour sleep contains about 4 to 5 sleep cycles and each cycle lasts about 90 minutes with different stages including light sleep (Stages 1 & 2), deep sleep (Slow Wave Sleep) and rapid eye movement (REM). The deep sleep stages become shorter as sleep cycle progresses. In human physiology, a good deep sleep (SWS) stage can help with physical recovery; as well, a good rapid eye movement (REM) stage can improve one's learning abilities and memories. Sleep diseases, such as insomnia and obstructive sleep apnea, seriously affect patients' quality of life. Without restrictive criteria, the prevalence of insomnia symptoms is approximately 33% in the general population. Obstructive sleep apnea affects over 2% of adult women and 4% of adult men [6]. These sleep issues may cause daytime sleepiness, irritability, depression, anxiety or even death.

For the diagnosis of sleep issues, all night polysomnographic (PSG) recordings, including electroencephalogram (EEG), electrooculogram (EOG) and electromyogram (EMG), are usually taken from the patients and the recordings are scored by a well-trained expert

978-1-4244-7316-8/11/$26.00 ©2011 IEEE

according to the Rechtschaffen & Kales (R&K) rules presented in 1968. According to the R&K rules, each epoch (i.e., 30 s of data) is classified into one of the sleep stages, including wakefulness (Wake), non-rapid eye movement (stages 1-4, from light to deep sleep) and non-rapid eye movement (NREM).

Consequently, in this paper, the recognition of the sleep stage form EEG signal is used as an example to demonstrate the improvement of DHMM by FVQ.

II. FVQ AND DHMM

This paper introduces the proposed fuzzy vector quantization for the features used to train DHMM through a well trained codebook.

A. Fuzzy Vector Quantization

In order to train the DHMM model, a codebook should be set up first. In the codebook, feature vector must be classed as by vector quantization [1]. The *K*-means algorithm is adopted to train the codebook at head. Then, combing the fuzzy set, the codebook is arranged as a fuzzy codebook and all the features in training phase and in testing phase will be fuzzy vector quantized through the fuzzy codebook. Suppose a set of real numbers are expressed as $\{v_1, v_2, \cdots, v_n\}$ in which $v_i \in R$ and the corresponding fuzzy set is expressed as $\{u_i(x) \mid i = 1, 2, \cdots n\}$, where $\sum_1^n u_i(x) = 1, \forall x \in R.$ The triangular fuzzy set is depicted in Fig. 1. It is noted that since the elements of the codebook are not uniformly distributed in the domain of the speech signal after the training by *K*-means algorithm, the triangular fuzzy set is not symmetric in this application. The membership function in Fig. 2 is described as [2]:

$$u_i(x) = \begin{cases} \dfrac{x - v_{i-1}}{v_i - v_{i-1}}, & \forall x \in [v_{i-1}, v_i], \\ \dfrac{x - v_{i+1}}{v_i - v_{i+1}}, & \forall x \in [v_i, v_{i+1}]. \end{cases}$$

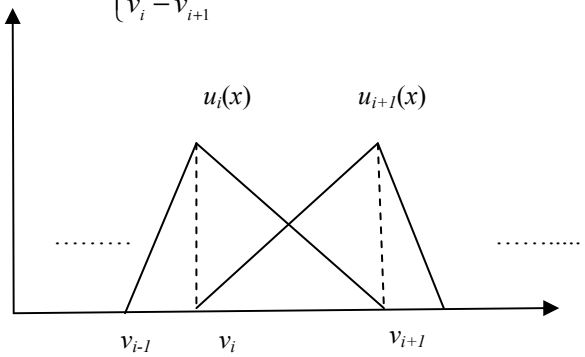

Fig. 1 Fuzzy set corresponding to each element of codebook

B. Discrete Hidden Markov Model (DHMM)

The DHMM is a double layers random process. The transfer of hidden states will correspond to the transfer of observations. Each model of DHMM can describe a specific signal to be recognized. The features of a signal are the observations used to estimate the hidden states. The target signal can be recognized by calculating the probability of the DHMM model. The model with highest probability in all DHMM models represents the most possibility of the recognized signal corresponding to the model [1].

In this section, the DHMM model is denoted as

$$\lambda = \{A, B, \pi, S, V\} \tag{1}$$

in which

$S = \{s_1, s_2, \cdots, s_N\}$ is the hidden state;

$V = \{v_1, v_2, \cdots, v_M\}$ is the output set of the DHMM model;

$A = \{a_{ij}\}, a_{ij} = P(q_t = s_j \mid q_{t-1} = s_i)$ is the probability matrix of state transfer;

$B = \{b_j(k)\}, b_j(k) = P(o_t = v_k \mid q_t = s_j)$ is the probability matrix of transfer out from each states;

$\pi = \{\pi_i\}, \pi_i = P(q_1 = s_i), 1 \le i \le N$ is the initial state probability;

$O = \{o_1, o_2, \cdots, o_T\}$ is the observation sequence;

$Q = \{q_1, q_2, \cdots, q_T\}$ is the state sequence.

As for the training of the DHMM model, the matrices *A*, *B*, and π are randomly generated initially. Then, the matrices are updated by the following algorithm.

$$state_t = \arg \max_{0 \le i \le 6} \alpha_t(i) \tag{2}$$

in which $state_t$ is the best estimated hidden state at time *t*; $\alpha_t(i)$ is the probability for *i*th guessed state at time *t* according to *A*, *B*, and π. Moreover, the matrices *A* and *B* are trained as follows.

The trained parameter $\overline{a}_{ij}$ of a_{ij} and $\overline{b}_j(k)$ of $b_j(k)$ is described as

$$\overline{a}_{ij} = \frac{n(u_{ij})}{n(u_{i\bullet})} \tag{3}$$

$$\overline{b}_j(k) = \frac{n(u_{\bullet j}, o = v_k)}{n(u_{\bullet j})} \tag{4}$$

in which

u_{ij} is the event that the state s_i transfer to s_j;

$u_{i\bullet}$ is the event that the state s_i transfer to other states;

$u_{\bullet j}$ is the event that enter the state s_j;

$n(u_{ij})$ is the number of times that s_i transfer to s_j;

$n(u_{i\bullet})$ is the number of times s_i transfer to other states;

$n(u_{\bullet j})$ is the number of times that enter the state s_j;

$n(u_{\bullet j}, o = v_k)$ is the number of times that the observation v_k occur when enter the state s_j.

The number $n(u_{\bullet j}, o = v_k)$ is obtained through the fuzzy codebook as follows. Suppose that the features are classified into *n* classes by *K*-means algorithm, i.e., the trained codebook is expressed as $CB_{n\times m} = \{FK_1, FK_n, \cdots, FK_n\}^T$ where $FK_i \in R^m$ is the center vector of *i*th class. The fuzzy degree contribute to the number $n(u_{\bullet j}, o = v_k)$ for each feature $f \in R^m$ is computed as $u_i(v_i + \|FK_i - f\|)$ for $n(u_{\bullet j}, o = v_i)$ and $u_i(v_{i+1} - \|FK_{i+1} - f\|)$ for $n(u_{\bullet j}, o = v_{i+1})$. This tactic is not only used for the training phase of the DHMM model but also for the testing phase of the speech recognition. In this paper, the strategy of using DHMM to recognize the signal is that we train first DHMM model λ for each corresponding signal by fuzzy codebook. Then, in testing phase, the tested signal features which is viewed as a sequence of observation *O* are fed into each DHMM model. The highest probabilities are found from computing the probability for all models by using the following equation:

$$P(O|\lambda) = \sum_{allQ} P(O,Q|\lambda) = \sum_{q1,q2,\ldots,qT} \pi_{q1} \cdot b_{q1}(o_1) \cdot a_{q1q2} \cdot b_{q2}(o_2) \cdot a_{q2q3} \cdots a_{qT-1qT} \cdot b_{qT}(o_T). \quad (5)$$

Figure 2 shows the processes for the training of the fuzzy codebook and DHMM model. Besides, the speech recognition process also can be found in the figure.

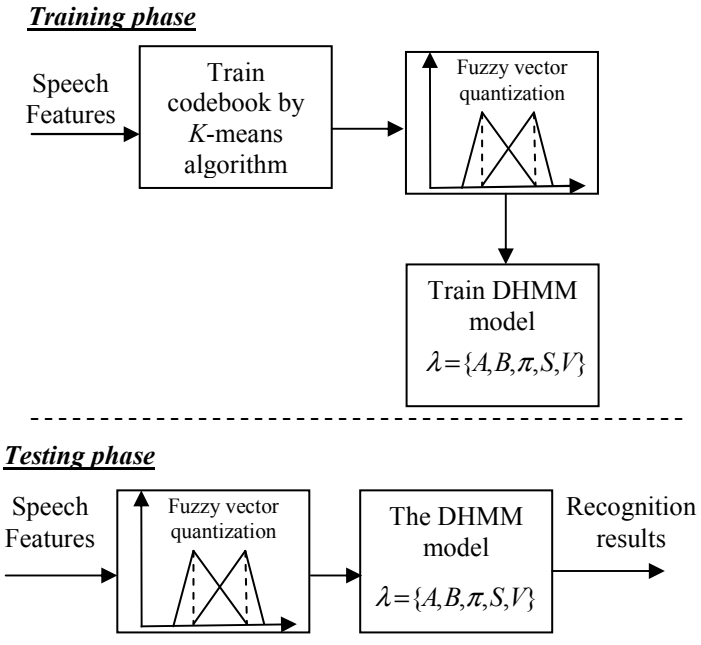

Fig. 2 Strategy of the proposed FVQ on speech recognition by DHMM

III. SLEEP STAGE AND EEG

The main purpose of this section is to enable the understanding of the basic elements of sleep stages. First, we introduce polysomnography, which includes electroencephalogram (EEG), electrooculogram (EOG), electromyogram (EMG) [7]. Then, we introduce the classification of sleep stages used in the R&K rules, and explain why we adopte the new sleep staging classification.

Polysomnography (PSG) is a multi-parametric test used in the study of sleep, as well, it is used as a diagnostic tool in sleep clinical trials. The test result is called a polysomnogram. Polysomnography is a comprehensive recording of the biophysiological changes that occur during sleep. The PSG monitors many body functions including brain activities (Electroencephalogram), eye movements (Electrooculogram), muscle activity or skeletal muscle activation (Electromyogram) and heart rhythm (Electrocardiogram) during sleep [8].

Electroencephalography (EEG) is the recording of electrical activity along the scalp produced by the firing of neurons within the brain. The sleep analysis, the EEG, is based on the characteristics of brain activities, and it can be divided into several different frequency bandwidths. The main EEG frequency bandwidths are given below in Table 1 [9]:

Table 1 Various signals in EEG [9]

Type	Frequency (Hz)	Waveform
Delta	0 – 4 Hz	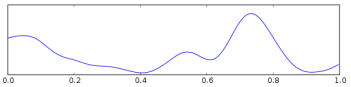
Theta	4 – 8 Hz	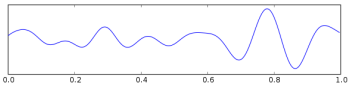
Alpha	8 – 13 Hz	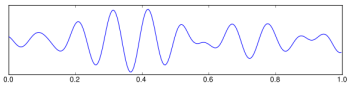
Beta	13 – 30 Hz	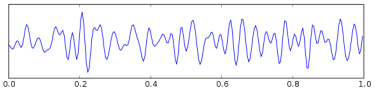

Electrooculogram (EOG) is the resulting signal of a technique for measuring the resting potential of the retina. Eye movements are usually measured by placing pairs of electrodes either above and below, or to the left and right of the eye [10]. If the eye is moved from the center position towards one electrode, this electrode realizes the positive side of the retina, and the opposite electrode realizes the negative side of the retina. Consequently, a potential difference occurs between the electrodes. Assuming that the resting potential is constant, the recorded potential is a measurement for the eye

position [11]. In this paper, we use one EOG feature to recognize mainly the REM stage.

Electromyogram (EMG) is a technique for evaluating and recording the electrical activities produced by skeletal muscles. In sleep analysis, the electrodes are typically placed on the chin of the subject. The impulse (action potential) for muscle activation begins from the central nervous system, and it reaches the muscle via the spinal cord and the motor neuron. The action potential can be measured as EMG signals [12]. From the EMG signal, we will be able to tell whether the subject has entered deep sleep, and whether his muscles are in a relaxed state. In this paper, we will use three EMG features to recognize mainly the Wake stage.

3.1 Sleep Stages

In this subsection, we introduce the manual sleep staging rules by R&K rules and new sleep stage by AASM. Furthermore, the Mov stage which is used in previous research is included in this study and will be explained later.

2.2.1 Manual Staging Rules

The standard of manual sleep staging is R&K rules, which is proposed by Rechtschaffen and Kales in 1968 [13]. According to R&K rules, the stages are scored epoch-by-epoch in 20-30 second intervals. Then, the sleep is divided into six stages: stage wake(Wake), stage 1(S1), stage 2(S2), stage 3(S3), stage 4(S4), and stage rapid eye movement (REM). The details of each stage in R&K rules are described as follows [14].

Stage wake (Wake):

There is a low voltage (10−30μV) and mixed frequency (2-7 Hz) EEG during wakefulness. Possible features are alpha (8-13 Hz) activity in EEG and relatively high tonic EMG, about > 50% of the epoch.

Stage 1 (S1):

S1 is characterized by low voltage, mixed frequency EEG with the highest amplitude in the 2-7 Hz range. The vertex sharp waves may occur, and their amplitude can reach the value of about 200 μV. The alpha activity is less than 50% of an epoch.

Stage 2 (S2):

S2 is characterized by wave-pattern sleep spindles (12–15 Hz), K-complexes (sharp negative waves) and the absence of slow waves. The duration of these patterns should be a minimum of 0.5 second. If the time duration between two succeeding occurrences of sleep spindles or K-complexes is less than 3 minutes, this epoch is scored as S2, otherwise it is scored as S1.

Stage 3 (S3):

S3 is characterized by the presence of a minimum of 20-50% delta waves ranging from 0.5-2 Hz EEG and having a peak-to-peak amplitude > 75 μV. Sleep spindles and K-complexes may occur during S3.

Stage 4 (S4):

S4 has the same attributes as S3, 0.5-2 Hz EEG and amplitude > 75 μV. The only difference is the delta waves are more than 50% of an epoch.

Stage REM (REM):

REM shows low voltage and mixed (2-7 Hz) frequency of EEG similar to S1. Sawtooth wave patterns in EEG is often present. Moreover, EMG reaches the lowest level in this stage. In 2007, the American Academy of Sleep Medicine (AASM) group decided the new stage name terminology as follow: Stage W (Wakefulness), Stage N1 (NREM 1 sleep), Stage N2 (NREM 2 sleep), Stage N3 (NREM 3 sleep), Stage R (REM sleep). It is noted that NREM is non-REM stage, which consists of three stages N1, N2 and N3 [15]. The stages N1 and N2 are equivalent to S1 and S2 in the R&K rules respectively, and are light sleep. The stage N3 is equivalent to the stage that combined S3 and S4 in the R&K rules. Because the characteristics of the two stages S3 and S4 are much similar, in order to facilitate simplicity and accuracy of sleep staging, AASM group hence decided to combine stages S3 and S4 as N3. Stage N3 is also called deep sleep, or slow wave sleep (SWS) stage. The term SWS is used for revealing the physical meaning of this stage, therefore, in this paper, we adopt the five stages classification: Wake, S1, S2, SWS, and REM.

IV. Sleep Stage by Observation-Based DHMM

In observation-based DHMM, the DHMM are modeled for each sleep stage. Therefore, there are five DHMM models corresponding to each sleep stage. The transition for each DHMM model is illustrated in Fig. 3. The hidden states are arbitrarily defined in this strategy. The features become the observation codes via vector quantization. For the DHMM $\lambda = (A, B, \pi)$, A is the probability matrix of the transference from one hidden state to another hidden state. The matrix B is the probability matrix of the observation of a hidden state. The matrix π is the probability of the hidden state at the beginning. In this strategy, we focus on the probability of the five DHMM models, corresponding to the five sleep stages for a feature vector (observation). The DHMM model with maximum probability among all models is distinguished, and the corresponding sleep stage is the estimated stage for the feature vector. This strategy is shown in Fig. 4. In the Fig. 4, P_{Wake}, P_{S1}, P_{S2}, P_{SWS} and P_{REM} are the probability of the five DHMM models for feature vectors calculated from a 30-second sample of a sleep stage, corresponding to the five sleep stages Wake, S1, S2, SWS and REM, respectively.

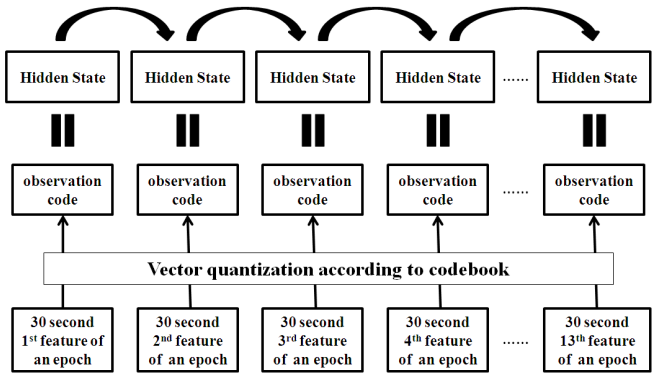

Fig. 3 DHMM for sleep staging.

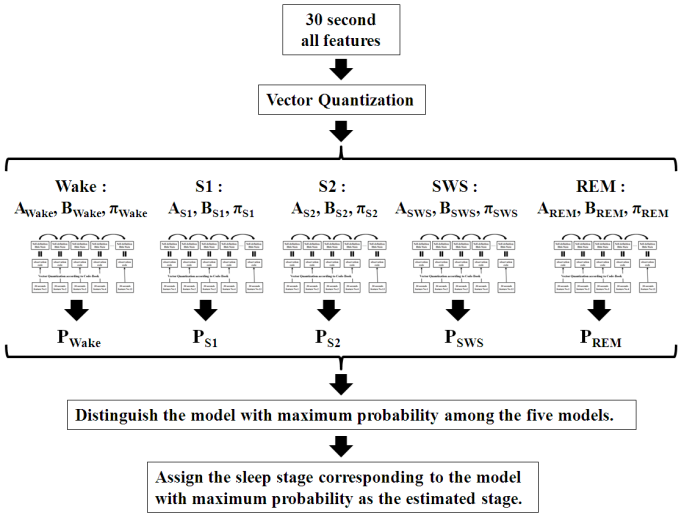

Fig. 4 Strategy of observation-based DHMM sleep staging.

Based on the above discussion, the sleep staging procedure by observation-based DHMM is then summarized as follows.

Procedure of observation-based DHMM sleep staging

Step 1. Train codebook by K -mean method.

Step 2. Generate five DHMM models by finding (A,B,π) of the corresponding sleep stages.

Step 3. Generate the observation codes by quantizing the feature vectors based on the codebook.

Step 4. Calculate the probability of all sleep models using the corresponding (A,B,π).

Step 5. Choose the model with the highest probability among all of the sleep models for the feature vector and assign the corresponding sleep stage as the estimated sleep stage.

Step 6. Repeat Steps 3 to 5 until all the feature vectors of the epochs are completed.

V. SLEEP STAGE BY OBSERVATION-BASED DHMM

In our experiment, we use the signals measured from three EEG channels (C3, F3, and P3), EMG and EOG to generate the features for training and testing. The sleep data used in the experiments are collected from twenty subjects and are numbered from No. 1 to No. 20 for convenience. The 158 hours of sleep data are recorded, and then used to train seventeen subjects and test three subjects. There are three different combinations of the training and testing set, named Set 1, Set 2 and Set 3, are used in this experiment and are listed in Table 2.

Table 2 Former class with three testing subjects.

Combination sets	Training subjects	Testing subjects
Set 1	{No. 1 ~ No. 20}/{Testing subjects}	No. 10, No. 14, No. 17
Set 2	{No. 1 ~ No. 20}/{Testing subjects}	No. 3, No. 9, No. 20
Set 3	{No. 1 ~ No. 20}/{Testing subjects}	No. 5, No. 12, No. 19

Table 3 shows the recognition rates of the proposed various tactics which are designed based on the DHMM without FVQ while Table 4 is those with FVQ. A more detail comparison on the recognition rate of each sleep stage and means for the three sets Set 1, Set 2 and Set 3 are depicted in Fig. 5 – Fig. 8. These figures reveal that the DHMM with FVQ performs much better than DHMM without FVQ. This verify that the proposed FVQ on DHMM is efficient.

Table 3(a) Recognition rate for *Set 1* by DHMM without FVQ

DHMM without FVQ (Set 1)						
R&K		Wake	S1	S2	SWS	REM
	Wake (%)	**79.17**	8.33	6.25	6.25	0
mean: 78.35%	S1 (%)	5.44	**12.72**	48.44	4.17	29.22
	S2 (%)	0.43	2.89	**81.05**	11.57	4.06
	SWS (%)	0.33	0.56	7.35	**91.75**	0
	REM (%)	0.53	9	27.74	0.47	**62.26**

Table 3(b) Recognition rate for *Set 2* by DHMM without FVQ

DHMM without FVQ (Set 2)						
R&K		Wake	S1	S2	SWS	REM
	Wake (%)	**74.22**	8.69	2.56	9.54	4.99
mean: 76.75%	S1 (%)	5.67	**7.04**	36.77	1.42	49.09
	S2 (%)	0.28	2.34	**82.36**	5.68	9.33
	SWS (%)	1.95	0.57	18.02	**78.19**	1.27
	REM (%)	0.40	5.26	19.37	0.21	**74.77**

Table 3(c) Recognition rate for *Set 3* by DHMM without FVQ

DHMM without FVQ (Set 3)						
R&K		Wake	S1	S2	SWS	REM
	Wake (%)	**62.15**	6.42	10.76	1.91	18.75
mean: 79.11%	S1 (%)	4.44	**5.93**	43.43	3.70	42.49
	S2 (%)	0.37	1.72	**82.03**	8.72	7.17
	SWS (%)	0.61	0.66	8.06	**90.35**	0.31
	REM (%)	0	4.63	19.30	0.89	**75.22**

Table 4(a) Recognition rate for *Set 1* by DHMM with FVQ

DHMM with FVQ (Set 1)

R&K		Wake	S1	S2	SWS	REM
mean: 86.64%	Wake (%)	**97.92**	0	2.08	0	0
	S1 (%)	14.72	**10.45**	39.39	0	35.44
	S2 (%)	0.35	0.21	**88.56**	8.47	2.41
	SWS (%)	0.65	0	5.01	**94.34**	0
	REM (%)	0.75	3.79	14.47	0.47	**80.52**

Table 4(b) Recognition rate for *Set 2* by DHMM with FVQ

DHMM with FVQ (Set 2)

R&K		Wake	S1	S2	SWS	REM
mean: 81.96%	Wake (%)	**94.66**	0.92	3.49	0	0.93
	S1 (%)	18.03	**5.65**	31.15	0	45.17
	S2 (%)	0.21	0.36	**87.57**	3.80	8.06
	SWS (%)	1.73	0.86	12.66	**84.75**	0
	REM (%)	0.34	3.14	17.17	0.13	**79.22**

Table 4(c) Recognition rate for *Set 3* by DHMM with FVQ

DHMM with FVQ (Set 3)

R&K		Wake	S1	S2	SWS	REM
mean: 84.36%	Wake (%)	**65.97**	17.19	10.42	2.78	3.64
	S1 (%)	7.17	**7.29**	43.55	0	41.99
	S2 (%)	0	0.22	**87.86**	9.77	2.15
	SWS (%)	0.20	0.16	5.57	**94.07**	0
	REM (%)	0	1.16	16.04	0.47	**82.33**

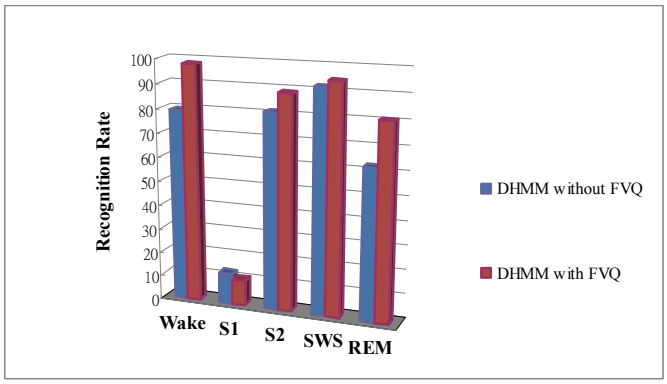

Fig. 5 Recognition rate on each sleep stage for Set 1

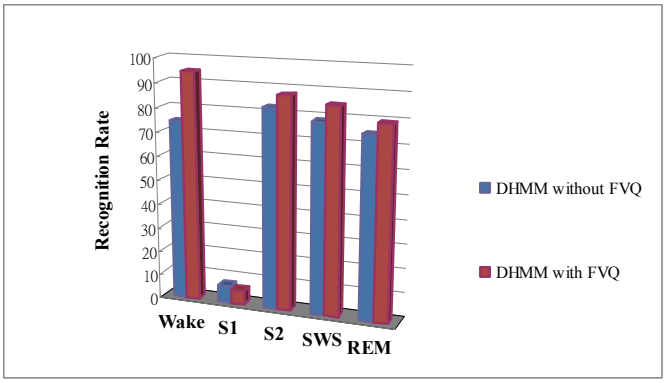

Fig. 6 Recognition rate on each sleep stage for Set 2

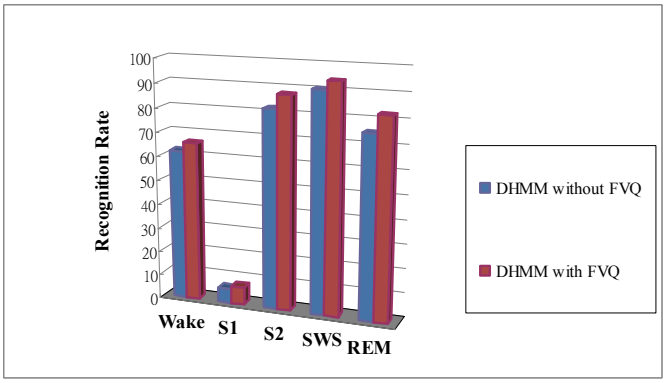

Fig. 7 Recognition rate on each sleep stage for Set 3

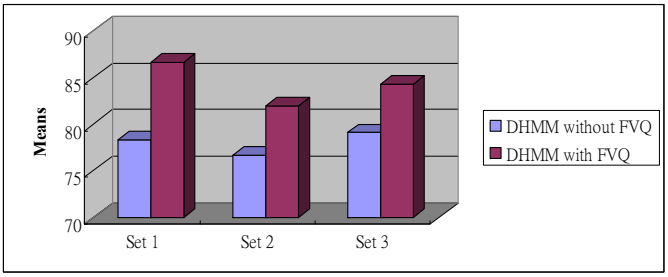

Fig. 8 Means of recognition rate for Set 1, Set 2 and Set 3

VI. CONCLUSIONS

The fuzzy vector quantization (FVQ) had been used on the modeling of Discrete Hidden Markov Model (DHMM) to improves the recognition rate for the sleep stages based on EEG, EOG and EMG signals. First, a codebook was trained by *K*-means algorithms. Based on the trained codebook, the features are quantized by the fuzzy sets defined on the trained codebook. Subsequently, the quantized features are used to the modeling of DHMM for the sleep stage recognition. All the features should go through the FVQ based on the fuzzy code book before being fed into the DHMM model for recognition. Experimental results reveal that the speech recognition rate can be improved by using FVQ algorithm to train the model of DHMM.

ACKNOWLEDGMENT

This research work was supported by the National Science Council of the Republic of China under contract NSC 99-2221-E-390-027.

REFERENCES

[1] X. Huang, A. Acero, and H. Wuenon, *Spoken Language Processing A Guide to Theory, Algorithm and System Developmen*. Pearson, 2005.

[2] W. Pedrycz and K. Hirota, " Fuzzy Vector Quantization with The Particle Swarm Optimization: A Study in Fuzzy Granulation-Degranulation Information Processing," *Signal Processing*, Vol. 87, pp. 2061-2074, 2007.

[3] V. Kapoor, S. S. Tak, and V. Sharma, " Location Selection – A Fuzzy Clustering Approach," *International Journal of Fuzzy Systems*, Vol. 10, No. 2, pp. 123-128, June 2008

[4] C. H. Li, W. C. Huang, B. C. Kuo, and C. C. Hung, *"* A Novel Fuzzy Weighted C-Means Method for Image Classification," *International Journal of Fuzzy Systems*, Vol. 10, No. 3, pp. 168-173, June 2008

[5] A. Lakdashti, M. S. Moin, and K. Badie, "Reducing the Semantic Gap of the MRI Image Retrieval Systems Using a Fuzzy Rule Based Technique," *International Journal of Fuzzy Systems,* Vol. 11, No. 4, pp. 232-249, December 2009.

[6] C. Iber, S. Ancoli-Israel, A. L. Chesson and S. F. Quan, *The AASM manual for the Scoring of Sleep and Associated Events*, American Academy of Sleep Medicine, 2007.

[7] K. Šušmáková, "Human Sleep and Sleep EEG," *Measurement Science Review*, Vol. 4, pp. 59-74, 2004.

[8] R. Agarwal and J. Gotman, "Computer-Assisted Sleep Staging," *IEEE Transactions on Biomedical Engineering*, Vol. 48, No. 12, pp. 1412-1423, December 2001.

[9] M. Teplan, "Fundamentals of EEG measurement," *Measurement Science Review*, Vol. 2, Section 2, pp. 1–11, 2002.

[10] M. Fejtova and J. Fejt, "Eye as a new computer periphery," *Lékař a technika*, Vol. 36, No. 1, pp. 45-50, 2006.

[11] M. Brown, M. Marmor, Vaegan, E. Zrenneer, M. Brigell and M. Bach, "ISCEV Standard for Clinical Electro-oculography(EOG) 2006," *Doc Ophthalmol*, Vol. 113, pp. 205-212, 2006.

[12] M. B. I. Raez, M. S. Hussain and Y. F. Mohd-Yasin, "Techniques of EMG signal analysis: detection, processing, classification and applications," *Biological Procedures Online*, Vol. 8, No. 1, pp. 11-35, March 2006.

[13] A. Rechtschaffen and A. Kales, *A Manual of Standardized Terminology, Techniques and Scoring System for Sleep stages of Human Subjects*, Brain Inform Service/Brain Res. Inst., Univ. California, Los Angeles, 1968.

[14] Y. S. Cheng, *A rule-based automatic sleep staging method*, Department of Computer Science and Information Engineering, National Cheng Kung University, Master Paper, 2009.

[15] M. H. Silber, S. Ancoli-Israel, M. H. Bonnet, et al, "The visual scoring of sleep in adults," *Journal of Clinical Sleep Medicine*, Vol. 3, No. 2, pp. 121-131, 2007.

2011 IEEE International Conference on Fuzzy Systems
June 27-30, 2011, Taipei, Taiwan

Design of Interval Type-2 Fuzzy Logic Systems Using Prior Knowledge via Optimization Algorithms

Tiechao Wang and Jianqiang Yi , *Senior Member, IEEE*
Institute of Automation
Chinese Academy of Sciences
Beijing 100190, China
Email: {tiechao.wang & jianqiang.yi}@ia.ac.cn

Tiechao Wang
College of Electrical Engineering
Liaoning University of Technology
Jinzhou 121001, China
Email: tiechao.wang@gmail.com

***Abstract*—The paper presents the methods of integrating prior knowledge with a first-order Single-Input Single-Output (SISO) Interval Type-2 Takagi-Sugeno-Kang (TSK) Fuzzy Logic System (IT2FLS) for function approximation under noisy circumstances. Firstly, sufficient conditions on the antecedent and the consequent parameters of the IT2FLS are given to ensure that three kinds of prior knowledge – monotonicity, symmetry and special points, can be embedded into the IT2FLS. And then, we use three optimization algorithms – constrained least squares algorithm, active-set algorithm and hybrid learning algorithm to design the IT2FLS, respectively. The effectiveness of the three algorithms and the comparisons of their performance are demonstrated by simulation examples.**

Keywords* – *interval type-2 fuzzy logic system; optimization algorithm; prior knowledge

I. Introduction

Prior knowledge is a kind of important information sources and can play a significant role in many real problems, especially when input-output data are not informative enough or corrupted by noise. For a grey-box identification problem, it is not necessary to estimate what we already know, but instead we should take advantage of the prior knowledge of plants or systems. In the past several years, some work was done to incorporate some prior knowledge with neural network systems [1] or fuzzy logic systems [2] – [4]. In [1], Joerding studied methods for incorporating the monotonicity into feedforward networks. Lindskog [2] proposed a fuzzy model structure to ensure monotonic gain characteristics in identified models. Li [3, 4] integrated the prior knowledge of bounded range, symmetry and monotonicity into a zeroth-order IT2FLS and designed the fuzzy system by constrained least squares algorithm.

Type-2 Fuzzy Logic Systems (T2FLSs) can better handle different sources of uncertainties and debilitate noisy disturbance than traditional or type-1 fuzzy logic systems (T1FLSs) [5, 6]. A lot of excellent work focused on how to design T1FLSs and T2FLSs. Jang [7] presented the ANFIS architecture which is a type-1 fuzzy inference system implemented in the framework of adaptive network, and by using hybrid learning procedure, the ANFIS can yield remarkable results. In [8], Castro proposed an efficient mechanism for modeling by combined hybrid learning algorithm with an interval type-2 fuzzy neural network. Méndez [9] presented a novel hybrid learning method to construct an interval type-2 TSK fuzzy model capable of approximating the behavior of steel strip temperature based on orthogonal least squares and back propagation methods. At present, to the authors' knowledge, there is no literatures about designing first-order SISO IT2FLSs with prior knowledge description via constrained hybrid method. In this paper, we first give the sufficient conditions which ensure the above-mentioned three kinds of prior knowledge can be combined with the IT2FLS. And then, we design the first-order SISO IT2FLS via constrained least squares algorithm, active-set algorithm and hybrid learning algorithm, respectively.

II. IT2FLSs and Parameter Conditions for Prior Knowledge

In this section, the basic concepts about first-order SISO IT2FLSs are introduced. And then, we give the sufficient conditions on the parameters of the IT2FLS which ensure that the prior knowledge of monotonicity, symmetry and special points can be integrated into the IT2FLS.

A. First-order SISO IT2FLSs

Consider a first-order SISO IT2FLS whose fuzzy rule base consists of M fuzzy rules. The ith rule R^i is denoted as

$$R^i: \text{ IF } x \text{ is } \widetilde{A}^i, \text{ THEN } y^i = w_0^i + w_1^i x,$$

where $i = 1, 2, \ldots, M$; x is the input variable, $\widetilde{A}^i$s are triangular IT2FSs which can be completely depicted by the lower and the upper membership functions – $\underline{\mu}_{\widetilde{A}^i}(x)$ and $\overline{\mu}_{\widetilde{A}^i}(x)$ which are expressed by (1) and (2), as illustrated in Fig. 1.

$$\underline{\mu}_{\widetilde{A}^i}(x) = \begin{cases} 0, & x < \underline{a}^i; \\ \frac{\underline{h}^i(x-\underline{a}^i)}{b^i-\underline{a}^i}, & \underline{a}^i \le x < b^i; \\ \frac{\underline{h}^i(\underline{c}^i-x)}{\underline{c}^i-b^i}, & b^i \le x < \underline{c}^i; \\ 0, & x \ge \underline{c}^i. \end{cases} \tag{1}$$

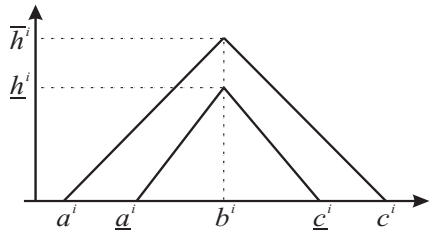

Fig. 1. Interval type-2 triangular membership function.

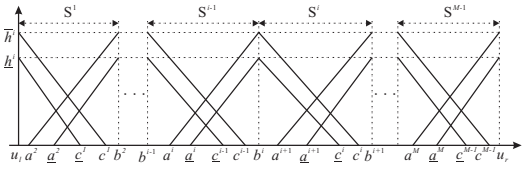

Fig. 2. Interval type-2 fuzzy partition.

$$\overline{\mu}_{\widetilde{A}^i}(x) = \begin{cases} 0, & x < a^i; \\ \frac{\overline{h}^i(x-a^i)}{b^i-a^i}, & a^i \le x < b^i; \\ \frac{\overline{h}^i(c^i-x)}{c^i-b^i}, & b^i \le x < c^i; \\ 0, & x \ge c^i. \end{cases} \tag{2}$$

where $a^i \le \underline{a}^i \le b^i \le \underline{c}^i \le c^i$.

The firing set F^i of rule R^i is an interval type-1 set, i.e., $F^i = [\underline{\mu}_{\widetilde{A}^i}(x), \overline{\mu}_{\widetilde{A}^i}(x)]$. w_0^i and w_1^i are real constants of the consequent part, so the consequent output y^i of each rule is a crisp value.

Then, using the center-of-sets (COS) type-reducer and the center average defuzzifier [5], the defuzzification output $\widehat{y}(x)$ of the IT2FLS is inferred as

$$\widehat{y}(x) = \frac{1}{2}\big(y_l(x) + y_r(x)\big). \tag{3}$$

where $y_l(x)$ and $y_r(x)$ are the left and the right end points of a type-reduced interval set and can be expressed as

$$y_l(x) = \frac{\sum_{i=1}^{L} \overline{\mu}_{\widetilde{A}^i}(x) y^i + \sum_{i=L+1}^{M} \underline{\mu}_{\widetilde{A}^i}(x) y^i}{\sum_{i=1}^{L} \overline{\mu}_{\widetilde{A}^i}(x) + \sum_{i=L+1}^{M} \underline{\mu}_{\widetilde{A}^i}(x)}, \tag{4}$$

$$y_r(x) = \frac{\sum_{i=1}^{R} \underline{\mu}_{\widetilde{A}^i}(x) y^i + \sum_{i=R+1}^{M} \overline{\mu}_{\widetilde{A}^i}(x) y^i}{\sum_{i=1}^{R} \underline{\mu}_{\widetilde{A}^i}(x) + \sum_{i=R+1}^{M} \overline{\mu}_{\widetilde{A}^i}(x)}, \tag{5}$$

in which L and R can be computed by the iterative Karnik-Mendel algorithm [5].

B. Prior Knowledge of Monotonicity

We shall study the prior knowledge of monotonicity which includes the monotonically increasing and the monotonically decreasing properties. Here, for conciseness, we give the sufficient conditions to ensure that IT2FLSs monotonic properties without proof.

Theorem 2.1: Assume that an IT2FLS is single-input single-output, and that the input domain of the IT2FLS is $U = [u_l, u_r]$. The IT2FLS increases monotonically with respect to x, if the following conditions are satisfied:

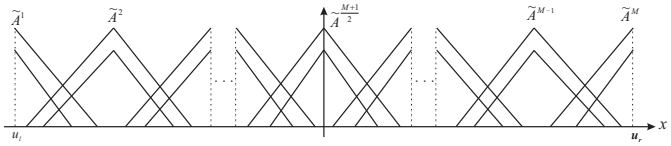

Fig. 3. Interval type-2 fuzzy symmetric partition with M triangular membership function.

1) The input domain U is partitioned by IT2FSs $\widetilde{A}^1, \widetilde{A}^2, \ldots, \widetilde{A}^M$ shown in Fig. 2, that is, $a^1 = b^1 = \underline{a}^1 = \underline{b}^1 = u_l$, $b^M = c^M = \underline{b}^M = \underline{c}^M = u_r$, $a^{i+1} \ge b^i$, $b^{i+1} \ge c^i$, $\underline{c}^i \ge \underline{a}^{i+1}$, for $i = 1, 2, \ldots, M-1$;
2) $w_1^i \ge 0$, for $i = 1, 2, \ldots, M$;
3) $w_0^{i+1} + w_1^{i+1} x \ge w_0^i + w_1^i x$, for all $x \in S^i$, and $i = 1, 2, \ldots, M-1$.

Theorem 2.2: Assume that an IT2FLS is single-input single-output, and that the input domain of the IT2FLS is $U = [u_l, u_r]$. The IT2FLS decreases monotonically with respect to x, if the following conditions are satisfied:

1) The input domain U is partitioned by M IT2FSs $\widetilde{A}^1, \widetilde{A}^2, \ldots, \widetilde{A}^M$ shown in Fig. 2, that is, $a^1 = b^1 = \underline{a}^1 = \underline{b}^1 = u_l$, $b^M = c^M = \underline{b}^M = \underline{c}^M = u_r$, $a^{i+1} \ge b^i$, $b^{i+1} \ge c^i$, $\underline{c}^i \ge \underline{a}^{i+1}$, for $i = 1, 2, \ldots, M-1$;
2) $w_1^i \le 0$, for $i = 1, 2, \ldots, M$;
3) $w_0^{i+1} + w_1^{i+1} x \le w_0^i + w_1^i x$, if $u_l \ge 0$ or $u_r \le 0$ for all $x \in S^i$ and $i = 1, 2, \ldots, M-1$; if $U \in \mathbb{R}$ for all $x \in U$ and $i = 1, 2, \ldots, M-1$.

C. Prior Knowledge of Symmetry

In this subsection, we give the sufficient conditions about the prior knowledge of symmetry which includes even symmetry and odd symmetry without proof.

Theorem 2.3: An IT2FLS is even symmetric, that is, $\widehat{y}(x) = \widehat{y}(-x)$, if the following conditions are satisfied:

1) The input domain of x is partitioned symmetrically around 0 by triangular IT2FSs $\widetilde{A}^1, \widetilde{A}^2, \ldots, \widetilde{A}^M$ shown in Fig. 3, where M is an odd number.
2) The consequent parameters of the rules R^i and R^{M-i+1} satisfy that $w_0^i = w_0^{M-i+1}$, $w_1^i = -w_1^{M-i+1}$ $(i \ne \frac{M+1}{2})$, and $w_1^{\frac{M+1}{2}} = 0$.

Theorem 2.4: An IT2FLS is odd symmetric, that is, $\widehat{y}(x) = -\widehat{y}(-x)$, if the following conditions are satisfied:

1) The input domain of x is partitioned symmetrically around 0 by triangular IT2FSs $\widetilde{A}^1, \widetilde{A}^2, \ldots, \widetilde{A}^M$ shown in Fig. 3, where M is an odd number.
2) The consequent parameters of the rules R^i and R^{M-i+1} satisfy that $w_0^i = -w_0^{M-i+1} (i \ne \frac{M+1}{2})$, $w_0^{\frac{M+1}{2}} = 0$ and $w_1^i = w_1^{M-i+1}$

D. Prior Knowledge of Special Points

In many practical systems the initial status is usually zero, and a lot of function curves pass through some special points such as origin. Hence, the prior knowledge of special points is widespread and important.

From a purely mathematic viewpoint, we formulate the prior knowledge of special points as follows

$$\widehat{y}(x)\big|_{x=x_0} = y(x_0), \tag{6}$$

where $\widehat{y}(x)$ is the output of the above-mentioned SISO IT2FLS. $y(x_0)$ is the known special point.

For example, when $\widehat{y}(x)\big|_{x=0} = 0$ for the first-order SISO IT2FLS in Theorem 2.1, from (4) and (5) we have $y_l(x) = y_r(x) = w_0^{\frac{M+1}{2}}$. Then, it follows from (3) that $\widehat{y}(x) = w_0^{\frac{M+1}{2}}$. Therefore, we can derive the constraint condition of the prior knowledge, i.e., $w_0^{\frac{M+1}{2}} = 0$.

III. Design of IT2FLSs via optimization algorithms

Suppose there exist r input-output data pairs (x_1, y_1), $\ldots, (x_r, y_r)$. And our objective is that the parameters of the IT2FLS can be optimized subject to the following training criteria (7) such that the overall error measure E is minimal.

$$\min_{\boldsymbol{\theta}} E = \min_{\boldsymbol{\theta}} \sum_{k=1}^{r} \big(\widehat{y}(x_k) - y_k\big)^2, \tag{7}$$

where $\boldsymbol{\theta}$ is all the parameters which need to be optimized, and $k = 1, 2, \ldots, r$. Next, according to this objective, we design the IT2FLS based on prior knowledge and sample data via constrained least squares algorithm, active-set algorithm and hybrid learning algorithm, respectively.

A. Design of IT2FLSs via Least Squares Algorithm

In this subsection, we design the IT2FLS via constrained least squares algorithm. Firstly, we should determine whether the output of the IT2FLS is linear with its consequent parameters.

Since no more than two fuzzy rules are fired, Equations (4) and (5) can be rewritten as

$$y_l(x) = \frac{\sum_{i=1}^{M} \mu_{\widetilde{A}_l^i}(x) w_0^i}{\sum_{i=1}^{M} \mu_{\widetilde{A}_l^i}(x)} + \frac{\sum_{i=1}^{M} \mu_{\widetilde{A}_l^i}(x) x w_1^i}{\sum_{i=1}^{M} \mu_{\widetilde{A}_l^i}(x)}, \tag{8}$$

$$y_r(x) = \frac{\sum_{i=1}^{M} \mu_{\widetilde{A}_r^i}(x) w_0^i}{\sum_{i=1}^{M} \mu_{\widetilde{A}_r^i}(x)} + \frac{\sum_{i=1}^{M} \mu_{\widetilde{A}_r^i}(x) x w_1^i}{\sum_{i=1}^{M} \mu_{\widetilde{A}_r^i}(x)}. \tag{9}$$

where

$$\mu_{\widetilde{A}_l^i}(x) = \begin{cases} \underline{\mu}_{\widetilde{A}^i}(x), & x \in S^{i-1}, \quad y^{i-1} \le y^i; \\ \overline{\mu}_{\widetilde{A}^i}(x), & x \in S^{i-1}, \quad y^{i-1} > y^i; \\ \overline{\mu}_{\widetilde{A}^i}(x), & x \in S^{i}, \quad y^{i} \le y^{i+1}; \\ \underline{\mu}_{\widetilde{A}^i}(x), & x \in S^{i}, \quad y^{i} > y^{i+1}. \end{cases}$$

$$\mu_{\widetilde{A}_r^i}(x) = \begin{cases} \overline{\mu}_{\widetilde{A}^i}(x), & x \in S^{i-1}, \quad y^{i-1} \le y^i; \\ \underline{\mu}_{\widetilde{A}^i}(x), & x \in S^{i-1}, \quad y^{i-1} > y^i; \\ \underline{\mu}_{\widetilde{A}^i}(x), & x \in S^{i}, \quad y^{i} \le y^{i+1}; \\ \overline{\mu}_{\widetilde{A}^i}(x), & x \in S^{i}, \quad y^{i} > y^{i+1}. \end{cases}$$

in which $y^i = w_0^i + w_1^i x$.
Then, it follows from (3), (8) and (9) that

$$\widehat{y}(x) = \boldsymbol{\phi}^{\mathrm{T}}(x)\boldsymbol{\omega}, \tag{10}$$

where

$$\boldsymbol{\omega} = [w_0^1, w_0^2, \ldots, w_0^M, w_1^1, w_1^2, \ldots, w_1^M]^{\mathrm{T}},$$
$$\boldsymbol{\phi}(x) = [\phi_0^1(x), \phi_0^2(x), \ldots, \phi_0^M(x), \phi_1^1(x), \phi_1^2(x), \ldots, \phi_1^M(x)]^{\mathrm{T}},$$

in which

$$\phi_0^i(x) = \frac{1}{2}\Big(\frac{\mu_{\widetilde{A}_l^i}(x)}{\sum_{i=1}^{M} \mu_{\widetilde{A}_l^i}(x)} + \frac{\mu_{\widetilde{A}_r^i}(x)}{\sum_{i=1}^{M} \mu_{\widetilde{A}_r^i}(x)}\Big),$$
$$\phi_1^i(x) = \frac{1}{2}\Big(\frac{\mu_{\widetilde{A}_l^i}(x)x}{\sum_{i=1}^{M} \mu_{\widetilde{A}_l^i}(x)} + \frac{\mu_{\widetilde{A}_r^i}(x)x}{\sum_{i=1}^{M} \mu_{\widetilde{A}_r^i}(x)}\Big).$$

From (10), we can conclude that the output of the IT2FLS is linear with its consequent parameters. Furthermore, the training criteria (7) can be rewritten as:

$$\min_{\boldsymbol{w}} E = \min_{\boldsymbol{w}} (\Phi\boldsymbol{w} - \boldsymbol{y})^{\mathrm{T}}(\Phi\boldsymbol{w} - \boldsymbol{y}), \tag{11}$$

where

$$\boldsymbol{y} = [y_1, y_2, \ldots, y_r]^{\mathrm{T}},$$
$$\Phi = \big[\boldsymbol{\phi}^{\mathrm{T}}(x_1), \boldsymbol{\phi}^{\mathrm{T}}(x_2), \ldots, \boldsymbol{\phi}^{\mathrm{T}}(x_r)\big]^{\mathrm{T}} \in \mathbb{R}^{r \times 2M}.$$

If the partitions of the IT2FLS are determined beforehand according to the conditions in the above theorems, we can use the sample data to train the consequent parameters of the IT2FLS via constrained least squares algorithm. Note that the given sample data (x_k, y_k) $(k = 1, 2, \ldots, r)$ should conform to the above-mentioned some or all prior knowledge. Also, in Theorems 2.1 – 2.4, if antecedent parameters are determined, the conditions on the consequent parameters can be expressed as linear inequalities and/or linear equalities with respect to the parameters. Then, the minimization problem (11) can be abstractly formulated as the following constrained least squares optimization problem,

$$\begin{cases} \min\limits_{\boldsymbol{w}} (\Phi\boldsymbol{w} - \boldsymbol{y})^{\mathrm{T}}(\Phi\boldsymbol{w} - \boldsymbol{y}) \\ \text{subject to} \quad C\boldsymbol{w} \le 0 \ \text{ and/or } \ C_{eq}\boldsymbol{w} = 0 \end{cases} \tag{12}$$

where both C and C_{eq} are linear constraint matrixes.

Next, we deduce the definite form of $C\boldsymbol{w} \le 0$ or $C_{eq}\boldsymbol{w} = 0$ according to the different prior knowledge.

1) Monotonically increasing property: The constraints on the consequent parameters of the IT2FLS in Conditions 2) and 3) of Theorem 2.1 can be expressed as

$$-w_1^i \le 0, \ \text{for } \ i = 1, 2, \ldots, M,$$
$$w_0^i - w_0^{i+1} + w_1^i x_k - w_1^{i+1} x_k \le 0,$$
$$\text{for } \ x_k \in S^i, \ i = 1, 2, \ldots, M-1.$$

Here, assume there are n_i data pairs on interval S^i. Hence, there exist $M + \sum_{i=1}^{M-1} n_i$ linear inequality constraints for these consequent parameters, and the constraints can be written as the following matrix form.

$$\begin{bmatrix} V_0 \\ V_1 \\ \vdots \\ V_{M-1} \end{bmatrix} \boldsymbol{w} \le \mathbf{0}_{(M+\sum_{i=1}^{M-1} n_i)\times 1}, \tag{13}$$

where

$$V_0 = \begin{bmatrix} \mathbf{0}_M & -I_M \end{bmatrix},$$

$$V_i = \begin{array}{c} \\ \\ \\ \\ \\ \\ \end{array} \begin{array}{c} \begin{array}{cccccccc} & & & i & i+1 & & & \end{array} \\ \begin{bmatrix} 0 & \dots & 0 & 1 & -1 & 0 & \dots & 0 \\ \vdots & \dots & \vdots & \vdots & \vdots & \vdots & \dots & \vdots \\ 0 & \dots & 0 & 1 & -1 & 0 & \dots & 0 \end{bmatrix} \\ \begin{array}{cccccccc} & & & M+i & M+i+1 & & & \end{array} \\ \begin{bmatrix} 0 & \dots & 0 & x_{i,1} & -x_{i,1} & 0 & \dots & 0 \\ \vdots & \dots & \vdots & \vdots & \vdots & \vdots & \dots & \vdots \\ 0 & \dots & 0 & x_{i,n_i} & -x_{i,n_i} & 0 & \dots & 0 \end{bmatrix} \end{array},$$

in which x_{i,n_i} denotes the n_ith datum on interval S^i. $\mathbf{0}_M$ is M by M zero matrix, I_M is M by M identify matrix, $V_0 \in \mathbb{R}^{M\times M}$, and $V_i \in \mathbb{R}^{(M-1)\times 2M}$.

Remarks: Especially, when $U \in [0, +\infty]$, inequalities

$$w_1^i \geq 0, \text{ for } i = 1, 2, \dots, M,$$
$$w_0^i \leq w_0^{i+1},\ w_1^i \leq w_1^{i+1} \text{ for } i = 1, 2, \dots, M-1,$$

can ensure that Conditions 2) and 3) hold, and can be expressed as the following matrix form.

$$\begin{bmatrix} \mathbf{0}_M & -I_M \\ \Lambda_M & \mathbf{0}_{(M-1)\times M} \\ \mathbf{0}_{(M-1)\times M} & \Lambda_M \end{bmatrix} \boldsymbol{w} \leq \mathbf{0}_{(3M-2)\times 1}, \tag{14}$$

where

$$\Lambda_M = \begin{bmatrix} 1 & -1 & 0 & \dots & 0 & 0 \\ 0 & 1 & -1 & \dots & 0 & 0 \\ \vdots & \vdots & \vdots & \ddots & \vdots & \vdots \\ 0 & 0 & 0 & \dots & 1 & -1 \end{bmatrix} \in R^{(M-1)\times M}.$$

2) Monotonically decreasing property: If $U \in [0, +\infty]$ or $U \in [-\infty, 0]$, the constraints on the consequent parameters of the IT2FLS in Conditions 2) and 3) of Theorem 2.2 can be expressed as $M + \sum_{i=1}^{M-1} n_i$ linear inequalities, and can be transformed into the following matrix form.

$$\begin{bmatrix} -V_0 \\ -V_1 \\ \vdots \\ -V_{M-1} \end{bmatrix} \boldsymbol{w} \leq \mathbf{0}_{(M+\sum_{i=1}^{M-1} n_i)\times 1} \tag{15}$$

Remarks: Especially, when $U \in [-\infty, 0]$, inequalities

$$w_1^i \leq 0, \text{ for } i = 1, 2, \dots, M,$$
$$w_0^i \geq w_0^{i+1},\ w_1^i \leq w_1^{i+1}, \text{ for } i = 1, 2, \dots, M-1,$$

can ensure that Conditions 2) and 3) hold, and can be expressed as the following matrix form.

$$\begin{bmatrix} \mathbf{0}_M & I_M \\ -\Lambda_M & \mathbf{0}_{(M-1)\times M} \\ \mathbf{0}_{(M-1)\times M} & \Lambda_M \end{bmatrix} \boldsymbol{w} \leq \mathbf{0}_{(3M-2)\times 1} \tag{16}$$

3) Even symmetry: The constraints on the consequent parameters of the IT2FLS in Condition 2) of Theorem 2.3 can be expressed as

$$w_0^i - w_0^{M-i+1} = 0,$$
$$w_1^i + w_1^{M-i+1} = 0,$$
$$w_1^{\frac{M+1}{2}} = 0, \text{ for } i = 1, 2, \dots, \frac{M-1}{2}.$$

Furthermore, the M inequalities can be written as the following matrix form.

$$\begin{bmatrix} I_{\frac{M-1}{2}} & \mathbf{0}_{\frac{M-1}{2}\times 1} & -I^R_{\frac{M-1}{2}} & \mathbf{0}_{\frac{M-1}{2}\times M} \\ \mathbf{0}_{\frac{M-1}{2}\times M} & I_{\frac{M-1}{2}} & \mathbf{0}_{\frac{M-1}{2}\times 1} & I^R_{\frac{M-1}{2}} \\ \mathbf{0}_{1\times M} & \mathbf{0}_{1\times \frac{M-1}{2}} & 1 & \mathbf{0}_{1\times \frac{M-1}{2}} \end{bmatrix} \times \boldsymbol{w} = \mathbf{0}_{M\times 1} \tag{17}$$

where I^R_M is the $M \times M$ matrix which is obtained by rotating I_M 90 degrees clockwise.

4) Odd symmetry: The constraints on the consequent parameters of the IT2FLS in Conditions 2) of Theorem 2.4 can be expressed as M linear inequalities, and can be transformed into the following matrix form.

$$\begin{bmatrix} I_{\frac{M-1}{2}} & \mathbf{0}_{\frac{M-1}{2}\times 1} & I^R_{\frac{M-1}{2}} & \mathbf{0}_{\frac{M-1}{2}\times M} \\ \mathbf{0}_{1\times \frac{M-1}{2}} & 1 & \mathbf{0}_{1\times \frac{M-1}{2}} & \mathbf{0}_{1\times M} \\ \mathbf{0}_{\frac{M-1}{2}\times M} & I_{\frac{M-1}{2}} & \mathbf{0}_{\frac{M-1}{2}\times 1} & -I^R_{\frac{M-1}{2}} \end{bmatrix} \times \boldsymbol{w} = \mathbf{0}_{M\times 1} \tag{18}$$

In conclusion, we make use of the following steps to construct the IT2FLS:

step 1) Determine the membership functions of IT2FSs $\widetilde{A}^1$, $\widetilde{A}^2$, $\dots$, $\widetilde{A}^M$ according to condition 1) in the Theorems 2.1 – 2.4 and the corresponding prior knowledge.

step 2) Let $C\boldsymbol{w} \leq 0$ in (12) be (13) for monotonically increasing property; (15) for monotonically decreasing property. Let $C_{eq}\boldsymbol{w} = 0$ be (17) for even symmetry; (18) for odd symmetry. Solve the constrained least squares optimization problem (12). Obtain the consequent parameter vector $\boldsymbol{w}$.

B. Design of IT2FLSs via Active-set Algorithm

In this subsection, we use active-set algorithm [10] to optimize all the parameters of the IT2FLS subject to (7).

Let us define $\boldsymbol{v}_i = [a^{i+1}, \underline{a}^{i+1}, \underline{c}^i, c^i, b^{i+1}]^{\mathrm{T}} (i \neq M-1)$ and $\boldsymbol{v}_{M-1} = [a^M, \underline{a}^M, \underline{c}^{M-1}, c^{M-1}]$, where M is the number of IT2FSs. Furthermore the antecedent parameters can be defined as $\boldsymbol{v} = [\boldsymbol{v}_1, \boldsymbol{v}_2, \dots, \boldsymbol{v}_{M-1}]^{\mathrm{T}} \in \mathbb{R}^{5M-6}$. Then, we can use the active-set algorithm to determine all the antecedent parameters $\boldsymbol{v}$ and the consequent parameters $\boldsymbol{w}$ according to different prior knowledge.

1) Monotonically increasing property: According to Condition 1) in Theorems 2.1, the constraints on the antecedent parameters can be expressed as

$$a^{i+1} \leq \underline{a}^{i+1} \leq \underline{c}^i \leq c^i, \text{ for } i = 1, 2, \dots, M-1;$$
$$c^i \leq b^{i+1}, \text{ for } i = 1, 2, \dots, M-2;$$

Furthermore, the $5M-7$ inequalities can be written as the following matrix form.

$$\Lambda_{5M-6}\boldsymbol{v} \le \mathbf{0}_{(5M-7)\times 1}, \tag{19}$$

Since b^i $(i=2,\ldots,M-1)$ is optimization parameters, in Condition 3) $x \in S^i$ should be changed into $x \in U$. Hence, V_i can be written as

$$V_i = \begin{array}{c} \\ \\ \\ \\ \\ \end{array} \begin{array}{c} \begin{array}{cccccccc} & & & & i & i+1 & & \end{array} \\ \begin{bmatrix} 0 & \ldots & 0 & 1 & -1 & 0 & \ldots & 0 \\ \vdots & \ldots & \vdots & \vdots & \vdots & \vdots & \ldots & \vdots \\ 0 & \ldots & 0 & 1 & -1 & 0 & \ldots & 0 \end{bmatrix} \\ \begin{array}{cccccccc} & & & & M+i & M+i+1 & & \end{array} \\ \begin{bmatrix} 0 & \ldots & 0 & x_1 & -x_1 & 0 & \ldots & 0 \\ \vdots & \ldots & \vdots & \vdots & \vdots & \vdots & \ldots & \vdots \\ 0 & \ldots & 0 & x_k & -x_k & 0 & \ldots & 0 \end{bmatrix}, \end{array}$$

According to Condition 3), since $b^i, b^{i+1} \in S^i$ and w^i are unknown variables, if we want to determine all the antecedent and the consequent parameters, there exist $2M-4$ nonlinear inequality constraints as follows:

$$\begin{aligned} w_0^{i+1} - w_0^i + \left(w_1^{i+1} - w_1^i\right)b^i \ge 0, \text{ for } i = 2,\ldots,M-1 \\ w_0^{i+1} - w_0^i + \left(w_1^{i+1} - w_1^i\right)b^{i+1} \ge 0, \text{ for } i = 1,\ldots,M-2 \end{aligned} \tag{20}$$

Hence, the minimization problem (7) can be abstractly formulated as the following constrained optimization problem:

$$\begin{cases} \min\limits_{\boldsymbol{v},\boldsymbol{w}} \sum\limits_{k=1}^{r} \left(\widehat{y}(x_k) - y_k\right)^2 \\ \text{subject to} \quad (13),\ (19) \text{ and } (20). \end{cases} \tag{21}$$

2) Monotonically decreasing property: Similarly, when $u_l \ge 0$ and $u_r \le 0$, according to the conditions in Theorems 2.2, the minimization problem (7) can be abstractly formulated as the following constrained optimization problem:

$$\begin{cases} \min\limits_{\boldsymbol{v},\boldsymbol{w}} \sum\limits_{k=1}^{r} \left(\widehat{y}(x_k) - y_k\right)^2 \\ \text{subject to} \quad (15),\ (19) \text{ and} \end{cases} \tag{22}$$

$$\begin{aligned} w_0^{i+1} - w_0^i + \left(w_1^{i+1} - w_1^i\right)b^i \le 0 \text{ for } i = 2,\ldots,M-1, \\ w_0^{i+1} - w_0^i + \left(w_1^{i+1} - w_1^i\right)b^{i+1} \le 0 \text{ for } i = 1,\ldots,M-2. \end{aligned}$$

3) Even Symmetry: According to Condition 1) in Theorems 2.3, the constraints on the antecedent parameters can be expressed as

$$\begin{aligned} &a^{i+1} \le \underline{a}^{i+1} \le \underline{c}^i \le c^i, \text{ for } i = 1,2,\ldots,\tfrac{M-1}{2}; \\ &c^i \le b^{i+1}, \text{ for } i = 1,2,\ldots,\tfrac{M-3}{2}; \\ &a^i = c^{M-i+1},\ \underline{a}^i = \underline{c}^{M-i+1}, \text{ for } i = 2,\ldots,M; \\ &b^{\frac{M+1}{2}} = 0,\ b^i = b^{M-i+1}, \text{ for } i = 2,\ldots,M-1,\ i \ne \tfrac{M-1}{2}; \end{aligned}$$

Furthermore, the $\frac{5M-9}{2}$ inequalities and the $\frac{5(M-1)}{2}$ equalities can be written as the following matrix form.

$$\begin{bmatrix} W & \mathbf{0}_{\frac{5M-7}{2}\times\frac{5M-7}{2}} \end{bmatrix}\boldsymbol{v} \le \mathbf{0}_{\frac{5M-7}{2}\times 1}, \tag{23}$$

$$\begin{bmatrix} I_{\frac{5M-7}{2}} & \mathbf{0}_{\frac{5M-7}{2}\times 1} & I^R_{\frac{5M-7}{2}} \\ \mathbf{0}_{1\times\frac{5M-7}{2}} & 1 & \mathbf{0}_{1\times\frac{5M-7}{2}} \end{bmatrix}\boldsymbol{v} = \mathbf{0}_{\frac{5(M-1)}{2}\times 1}. \tag{24}$$

where

$$W = \begin{bmatrix} 1 & -1 & 0 & \ldots & 0 & 0 \\ 0 & 1 & -1 & \ldots & 0 & 0 \\ \vdots & \vdots & \vdots & \ddots & \vdots & \vdots \\ 0 & 0 & 0 & \ldots & 1 & -1 \end{bmatrix} \in R^{\frac{5M-7}{2}\times\frac{5M-5}{2}}$$

Hence, the minimization problem (7) can be abstractly formulated as the following constrained optimization problem:

$$\begin{cases} \min\limits_{\boldsymbol{v},\boldsymbol{w}} \sum\limits_{k=1}^{r} \left(\widehat{y}(x_k) - y_k\right)^2 \\ \text{subject to} \quad (17),\ (23) \text{ and } (24). \end{cases} \tag{25}$$

4) Odd Symmetry: Similarly, according to Condition 1) in Theorems 2.4, the minimization problem (7) can be abstractly formulated as the following constrained optimization problem:

$$\begin{cases} \min\limits_{\boldsymbol{v},\boldsymbol{w}} \sum\limits_{k=1}^{r} \left(\widehat{y}(x_k) - y_k\right)^2 \\ \text{subject to} \quad (18),\ (23) \text{ and } (24). \end{cases} \tag{26}$$

In conclusion, we utilize the following steps to construct the IT2FLS via the active-set algorithm:

step 1) Determine the initial value of the antecedent and the consequent parameters of the IT2FLS according to the conditions in Theorems 2.1 – 2.4 and the corresponding prior knowledge.

step 2) Solve (21) for monotonically increasing property; (22) for monotonically decreasing property. Solve (25) for even symmetry; (26) for odd symmetry. And then obtain the antecedent and the consequent parameters of the IT2FLS.

C. Design of IT2FLSs via Hybrid Learning Algorithm

The fuzzy rules of IT2FLSs consist of the antecedent part and the consequent part. We use constrained least squares algorithm to determine the consequent parameters, and then use active-set algorithm to determine the antecedent parameters. The procedure is repeated on the specified demand. Next, we give the design steps of monotonic IT2FLSs and symmetric IT2FLSs, respectively.

1) Design steps of monotonic IT2FLSs:

Step 1) Determine the number of the fuzzy system rules and the initial antecedent and consequent parameters of the IT2FLS, and then solve the following optimization problems to obtain the consequent parameters via constrained least squares algorithm. If a target function monotonically increases, then (27) should be solved.

Else if the target function monotonically decreases, then (28) should be solved.

$$\begin{cases} \min\limits_{\boldsymbol{w}} (\Phi \boldsymbol{w} - \boldsymbol{y})^{\mathrm{T}} (\Phi \boldsymbol{w} - \boldsymbol{y}) \\ \text{subject to} \quad (13). \end{cases} \tag{27}$$

$$\begin{cases} \min\limits_{\boldsymbol{w}} (\Phi \boldsymbol{w} - \boldsymbol{y})^{\mathrm{T}} (\Phi \boldsymbol{w} - \boldsymbol{y}) \\ \text{subject to} \quad (15). \end{cases} \tag{28}$$

Step 2) The consequent parameters are fixed, and only the antecedent parameters are adjusted by solving the following constraint optimization problem via the active-set algorithm.

$$\begin{cases} \min\limits_{\boldsymbol{v}} \sum\limits_{k=1}^{r} \left(\widehat{y}(x_k) - y_k \right)^2 \\ \text{subject to} \quad (19). \end{cases} \tag{29}$$

Step 3) If the overall error measure E is less than a desired level or the number of the iterative steps reaches a specified value, then stop. Otherwise return to Step 1.

2) Design steps of symmetric IT2FLSs:

Step 1) Determine the number of the fuzzy system rules and the initial antecedent and consequent parameters of the IT2FLS, and then solve the following optimization problems to obtain the consequent parameters via constrained least squares algorithm. If a target function is even symmetry, then (30) should be solved. Else if the target function is odd symmetry, then (31) should be solved.

$$\begin{cases} \min\limits_{\boldsymbol{w}} (\Phi \boldsymbol{w} - \boldsymbol{y})^{\mathrm{T}} (\Phi \boldsymbol{w} - \boldsymbol{y}) \\ \text{subject to} \quad (17). \end{cases} \tag{30}$$

$$\begin{cases} \min\limits_{\boldsymbol{w}} (\Phi \boldsymbol{w} - \boldsymbol{y})^{\mathrm{T}} (\Phi \boldsymbol{w} - \boldsymbol{y}) \\ \text{subject to} \quad (18). \end{cases} \tag{31}$$

Step 2) The consequent parameters are fixed, and only the antecedent parameters are adjusted by solving the following constraint optimization problem via the active-set algorithm.

$$\begin{cases} \min\limits_{\boldsymbol{v}} \sum\limits_{k=1}^{r} \left(\widehat{y}(x_k) - y_k \right)^2 \\ \text{subject to} \quad (23) \text{ and } (24). \end{cases} \tag{32}$$

Step 3) If the overall error measure E is less than a desired level or the number of the iterative steps reaches a specified value, then stop. Otherwise return to Step 1.

IV. Simulation

In this section, we will give a simulation to show the usefulness of the prior knowledge and compare constrained least squares algorithm, active-set algorithm and hybrid learning algorithm when the output of a target function is corrupted by white noise.

Consider the following nonlinear function:

$$y = \left(\frac{x}{3} \right)^2 \tanh(|x|), \tag{33}$$

where $x \in U = [-3, 3]$. It is obvious that the curve of Function (33) passes through origin, is even symmetric, monotonically increases when $x \geq 0$, and monotonically decreases when $x \leq 0$.

In order to demonstrate the superiority of IT2FLSs, the output of the target function is corrupted by $Noise$ which is the uniformly distributed noise on interval $[-n_b, n_b]$ $(n_b = 0.2)$. From $\widetilde{y} = y + Noise$, we can create 500-sample-data set $\mathfrak{D}$ whose elements are $(x_i, \widetilde{y}_i)$ $(i = 1, \ldots, 500)$, in which r_k training data were randomly chosen as the elements of training data subset $\mathfrak{D}_k$. From (33), we can create 500-sample-data set $\mathfrak{E}$ whose elements are (x_i, y_i) $(i = 1, \ldots, 500)$, in which r_k sample data were randomly chosen as the elements of test data subset $\mathfrak{E}_k$. In this simulation, five cases are considered, that is, r_k equals 12, 25, 45, 70, 90, where $k = 1, \ldots, 5$.

Firstly, we design a first-order SISO IT2FLS via the above-mentioned three optimization algorithms with and without Prior Knowledge description (PK), and then evaluate the approximation performance and the generalization performance of the IT2FLS, which are measured by Root Mean Square Error (RMSE) of the training data and the test data, and the two performance indices are formulated as follows:

$$ap_k = \left(\frac{1}{r_k} \sum_{i=1}^{r_k} \left(\widehat{y}(x_i) - \widetilde{y}_i \right)^2 \right)^{\frac{1}{2}}, \tag{34}$$

$$gp_k = \left(\frac{1}{r_k} \sum_{i=1}^{r_k} \left(\widehat{y}(x_i) - y_i \right)^2 \right)^{\frac{1}{2}}, \tag{35}$$

where r_k is the size of the training data subset $\mathfrak{D}_k$ and the test data set $\mathfrak{E}_k$ in case k; ap_k can reflect the approximation ability of the IT2FLS for the training data; gp_k can reflect the generalization ability of the IT2FLS for test data. For the two indices, the less the values are, the better the performances are. Also, the statistical indices, ap_{sk} and gp_{sk}, which are the arithmetic mean of the corresponding indices obtained by the random training-test-data-selection process from 30 runs, are shown in Fig. 4 in semilogarithmic coordinates. For the sake of clarity, we plot the performance curves of the three algorithm with PK in cartesian coordinates once again shown in Fig. 5.

From Fig. 4, we observe that, generally, for generalization performance the algorithms with PK perform better than the ones without PK, and for approximation performance the algorithms without PK outperform the ones with PK except for the active-set algorithm. Furthermore, from Fig. 4 and Fig. 8, using the algorithms with PK can obtain better the overall performance, especially when the element number of a data subset is few.

From Fig.5, among the three optimization algorithms with PK, we can observe that the approximation performance and the generalization performance of the IT2FLS are the worst via the active-set algorithm. The IT2FLS achieves the best approximation performance via hybrid learning algorithm, and achieves the best generalization performance via constrained least squares algorithm. The least squares algorithm can overcome overfitting, and can obtain good results for generalization performance. For each iteration, the consequent parameters

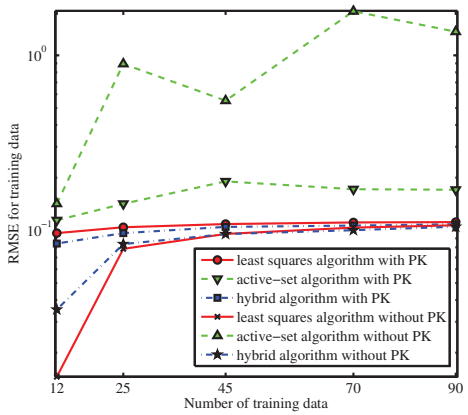

(a)

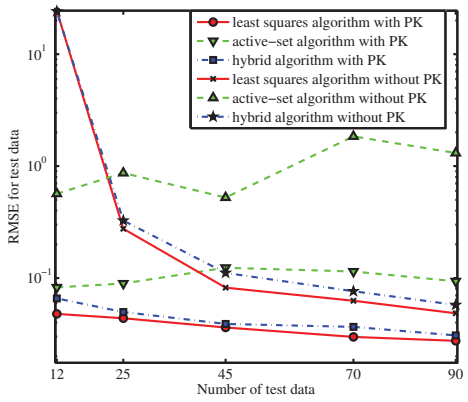

(b)

Fig. 4. The performance curves of the three algorithms with and without prior knowledge description in semilogarithmic coordinates when $r_k \in \{12, 25, 45, 70, 90\}\,(k = 1, \ldots, 5)$ and $n_b = 20\%$: (a) approximation performance (b) generalization performance.

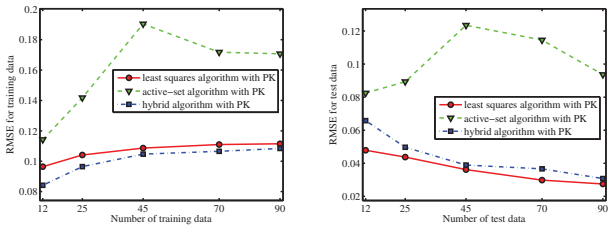

(a) (b)

Fig. 5. The performance curves of the three algorithms with prior knowledge description when $r_k \in \{12, 25, 45, 70, 90\}\,(k = 1, \ldots, 5)$ and $n_b = 20\%$: (a) approximation performance (b) generalization performance.

are updated via the constrained least squares estimator of the hybrid learning algorithm, and then the antecedent parameters are adjusted via the active-set algorithm part of the hybrid learning algorithm. In this case, by adjusting the antecedent parameters the overall error measure E is reduced further, but the algorithm needs iterative computation to achieve the smaller

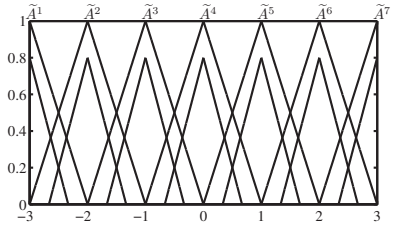

Fig. 6. Type-2 initial fuzzy partition of the IT2FLS.

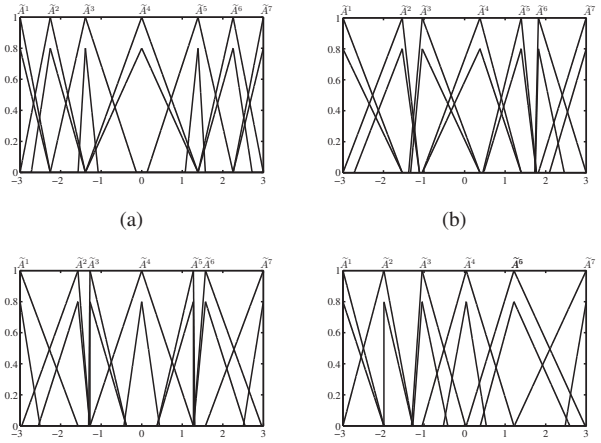

(a) (b) (c) (d)

Fig. 7. Type-2 fuzzy partitions of the IT2FLS via different optimization algorithms: (a) active-set algorithm with PK (b) active-set algorithm without PK (c) hybrid learning algorithm with PK (d) hybrid learning algorithm without PK.

E. Hence the hybrid learning algorithm can better improve the approximation and the generalization performance than the active-set algorithm, but it consumes more computation time and more computer resources.

We use 7 fuzzy rules to describe the first-order SISO IT2FLS. For each optimization algorithm, the initial fuzzy partitions are shown in Fig. 6. After optimization computation with PK via active-set algorithm and hybrid learning algorithm, the fuzzy partitions of the IT2FLS are shown in Fig. 7(a) and 7(c), and the fuzzy partitions via the algorithms without PK are shown in Fig. 7(b) and 7(d). The consequent parameters of the IT2FLS via the three algorithms with and without PK are listed in Table I and Table II. Note that the fuzzy partitions in Fig. 7(a) and 7(c) and the consequent parameters satisfy the conditions in Theorem 2.1 – 2.3. Fig. 8 is one of identification results of the target function (33). From the figures, we can observe that the identification results are consistent with Fig. 4 and Fig. 5 on the whole.

In conclusion, from the standpoint of the approximation performance, generally speaking, the hybrid learning algorithm is the best among the three optimization algorithm. From the standpoint of the generalization performance and computational complexity, the constrained least squares algorithm is the best among the three optimization algorithm.

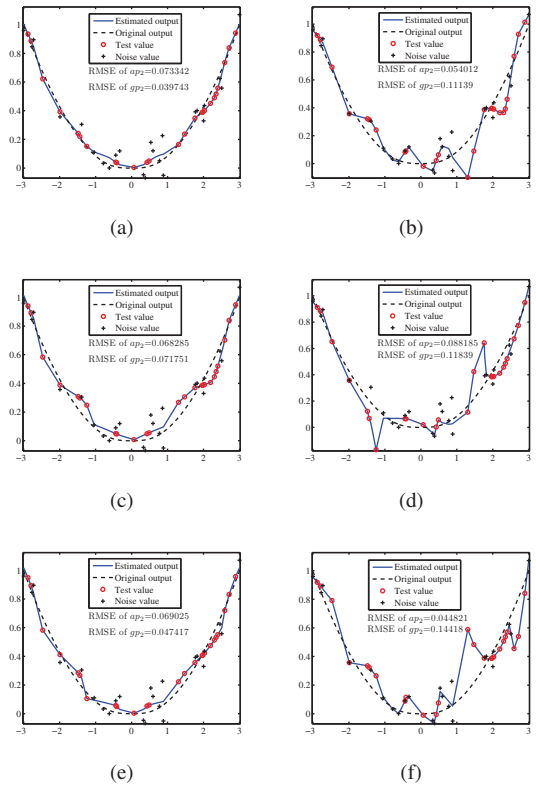

Fig. 8. One of identification results when the $r_2 = 25$ and $n_b = 20\%$: (a) constrained least squares algorithm with PK (b) constrained least squares algorithm without PK (c) active-set algorithm with PK (d) active-set algorithm without PK (e) hybrid learning algorithm with PK (f) hybrid learning algorithm without PK.

TABLE I
FUZZY RULES OF THE IT2FLS WITH PRIOR KNOWLEDGE

Antecedent part x	Consequent part y^i least squares	active-set	hybrid learning
$\widetilde{A}^1$	$0.39 - 0.20x$	$0.56 - 0.15x$	$0.32 - 0.23x$
$\widetilde{A}^2$	0.39	$0.37 - 0.017x$	0.32
$\widetilde{A}^3$	0.10	$0.27 - 0.017x$	0.11
$\widetilde{A}^4$	0	0	0
$\widetilde{A}^5$	0.10	$0.27 + 0.017x$	0.11
$\widetilde{A}^6$	0.39	$0.37 + 0.017x$	0.32
$\widetilde{A}^7$	$0.39 + 0.20x$	$0.56 + 0.15x$	$0.32 + 0.23x$

V. CONCLUSION

We have presented three efficient methods to design a first-order SISO IT2FLS for function approximation under noisy circumstances. The three kinds of prior knowledge – symmetry, monotonicity and special points are combined with the IT2FLS to solve the grey-box identification problem via constrained least squares algorithm, active-set algorithm and hybrid learning algorithm. From the simulation results and comparisons, we can conclude that the three kinds of prior knowledge can improve the generalization performance of the IT2FLS, and that the hybrid learning algorithm with PK performs best among the three optimization algorithms for approximation capability, and constrained least squares algorithm performs best for the generalization capability and computational complexity.

TABLE II
FUZZY RULES OF THE IT2FLS WITHOUT PRIOR KNOWLEDGE

Antecedent part x	Consequent part y^i least squares	active-set	hybrid learning
$\widetilde{A}^1$	$0.57 - 0.13x$	$2.04 + 0.36x$	$0.94 - 0.005x$
$\widetilde{A}^2$	$-0.37 - 0.37x$	$1.25 + 0.68x$	$-0.0065 - 0.16x$
$\widetilde{A}^3$	$-0.69 - 0.78x$	$3.85 + 3.62x$	$-0.86 - 0.93x$
$\widetilde{A}^4$	$-0.013 - 0.88x$	$-1.37 + 3.46x$	$0.042 - 1.005x$
$\widetilde{A}^5$	$1.22 - 1.26x$	$-5 + 3.68x$	$1.10 - 0.95x$
$\widetilde{A}^6$	$2.49 - 1.05x$	$0.38 + 0.0084x$	$0.013 + 0.53x$
$\widetilde{A}^7$	$2.83 - 0.59x$	$-1.26 + 0.77x$	$-6.22 + 2.43x$

ACKNOWLEDGMENT

This work was supported by the National Natural Science Foundation of China under Grant No. 60975060.

REFERENCES

[1] Wayne H. Joerding, and Jack L. Meador, "Encoding a priori information in feedback networks," *Neural Networks*, vol. 4, pp. 847–856, 1991.
[2] Peter Lindskog and Lennart Ljung, "Ensuring monotonic gain characteristic in estimated models by fuzzy model structures," *Automatica*, vol. 36, pp. 311–317, Jun. 2000.
[3] Chengdong Li, Jianqiang Yi and Dongbin Zhao, "Analysis and design of monotonic type-2 fuzzy inference system," *2009 IEEE International Conference on Fuzzy Systems*, Jeju Island, Korea, Aug. 2009, pp. 1193–1198.
[4] Chengdong Li, Jianqiang Yi and Dongbin Zhao, "Design of interval type-2 fuzzy logic system using sampled data and prior knowledge," *ICIC Express Letters*, vol. 3, pp. 695–700 , Sep. 2009.
[5] J. M. Mendel, *Uncertain Rule-Based Fuzzy Logic Systems: Introduction and New Directions*, New Jersey : Prentice-Hall, 2001.
[6] J. M. Mendel, "Advances in type-2 fuzzy sets and systems," *Information Sciences*, vol. 177, pp. 84–110, Jan. 2007.
[7] J. S. Jang, "ANFIS: Adaptive-Network-Based Fuzzy Inference System," *IEEE transaction on systems, man, and cybernetics*, vol. 23, pp. 665 – 685, 1993.
[8] J. R. Csatro, O. Castillo, P. Melin, R. Antonio "A Hybrid Learning Algorithm for a Class of Interval Type-2 Fuzzy Neural Networks," *Information Sciences*, vol. 179, pp. 2175 – 2193, 2009.
[9] G. M. Méndez, M. A. Hernandez "Hybrid Learning for Interval Type-2 Fuzzy Logic Systems Based on orthogonal least-squares and back-propagation methods," *Information Sciences*, vol. 179, pp. 2146 – 2157, 2009.
[10] Fletcher, R. and M.J.D. Powell, "A Rapidly Convergent Descent Method for Minimization," *Computer Journal*, Vol. 6, pp. 163-168, 1963.

2011 IEEE International Conference on Fuzzy Systems
June 27-30, 2011, Taipei, Taiwan

Fuzzy Reinforcement Learning for System of Systems (SOS)

Hamid Berenji, IEEE Fellow
IIS Corp
MS: 566-108, NASA Research Park
Moffett Field, CA 94035

Mo Jamshidi, IEEE Fellow
University of Texas at San Antonio
ACE Center, ECEC Dept.
San Antonio, TX 78249

***Abstract*— The System of Systems (SOS) technology is an advanced technology for Intelligent Systems that is developed with multiple intelligent systems. Recently, there has been a growing interest in a class of complex systems (robotic swarm as an example) whose constituents are themselves complex. Performance optimization, robustness and reliability among an emerging group of heterogeneous systems in order to realize a common goal have become the focus of various applications including military, security, aerospace, space, manufacturing, service industry, environmental systems, and disaster management, to name a few. In this paper, we discuss how Fuzzy Reinforcement Learning (FRL) can be used in SOS.**

Keywords- System of Systems (SOS); Fuzzy Reinforcement Learning (FRL); robots; cooperation; Unmanned Ground Vehicles (UGVs)

I. INTRODUCTION

This paper proposes SOS-Robotics, a software-hardware environment for planning and simulating a group of complex subsystems for management all within a System of Systems (SoS) environment. SOS-Robotics uses DEVS-Java for mathematically simulating the performance of a group of Unmanned Automated Systems (UAS) and assures the correctness of the group performance. The SOS-Robotics will be in demand by many of NASA and DOD organizations that have to manage the performance of groups of highly complex air, land, and undersea robots. SOS-Robotics generates plans for achieving a goal assigned by an operator and can quickly re-plan due to some unexpected events such as weather changes. It will also find many applications in group operations such as response to threats and robotic searches.

A. System of Autonomous Rovers

The system of autonomous rovers, at the IIS Corp-ACE Center, the University of Texas, San Antonio, comprises four components: Base Rover, Swarm Robots, Sensors and a Threat. The sensors represent a standalone system able to sense a Threat and ability to communicate with the Base Rover. The Thereat is spatially dynamic and it is assumed that it is detectable by the chosen sensors. Fig. 1 shows a system of two rovers working outdoor to coordinate Thereat detection collectively. The navigation of this system of rovers was done using GPS along with other sensors. In order to facilitate reasonable outdoor navigation, a task-relevant augmentation of the track rover (Fig. 1), with various sensory and control systems has been realized ([14]). The rover's onboard sensors include a GPS for absolute positioning in outdoor environments, wireless video for a view of the remote environment, ultrasonic range-finding for obstacle detection, 3-axis gyro for orientation, 3-axis accelerometer for motion capture and encoders for monitoring the vehicles velocity. The rover's computation is achieved through an on-board Windows-based PC.

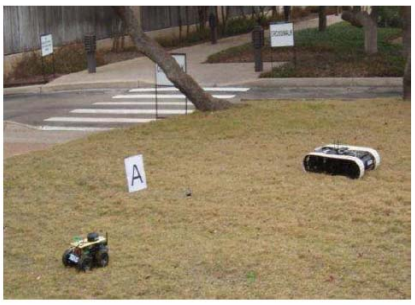

Figure 1. A system of two rovers performing a joint task on a field (Courtesy, ACE Center, University of Texas, San Antonio)

B. Navigation and Task Distribution for a System of Rovers

It is a state-of-the art approach for the coordination of a large number of robots. Fig. 2 shows such a scenario where ground robots are working together with a UAV. The UAV can survey a particular zone of interest. If it finds an object of interest (or a potential threat) in this zone then it can communicate to the ground robots and instruct them to further check it out. The ground robots can also communicate and coordinate among themselves to accomplish the task properly. They can also send the status report of their individual tasks back to the UAV or to a manned supervisory station for further instructions. To achieve such coordination capabilities, swarm robotics have many underlying issues that need to be addressed in order to create a practically applicable system. Robot communication, path planning, tracking, workload distribution, choice of sensors, system reliability, is just some of the most basic issues that need to be addressed. This work addresses the path planning, tracking and navigation so that mobile robots can reach to the object of interest effectively. In order to interact and distribute the task among the members, it is needed to create a communication system with a common protocol.

978-1-4244-7316-8/11/$26.00 ©2011 IEEE

The communication protocol needs to be dynamically expandable where additional robots can be added easily during a real-time application. Exact requirements of data types in the communication protocol can vary depending upon the swarm mission. On the ground domain, two wheeled robots, one track-robot and four small scout robots work together (two Pioneer P2-AT8 slip-drive robots from ActivMedia Mobile Robotics and one custom built track-robot). To coordinate commands within the ground swarm, one robot acts as the master. These are equipped with GPS receivers and radio modems for proper navigation and communication. The aerial domain consists of one fixed-wing aircraft (KADET, LT-40) with radio modem, GPS and a camera for proper communication, navigation and surveillance. Utilizing the GPS, camera and the processing suite on-board the aircraft, an estimated location of an object of interest is identified. This estimated GPS location can be sent to the master on the ground in order to investigate the object of interest. Once the master of the ground swarm evaluates the transmitted commands to investigate GPS coordinates, it directs the slave robots to search the surrounding areas of the object of interest. When the slave robots reach their destination, the mission task can be performed as directed by the ground master. Fig. 3 shows the real time GPS based navigation of Pioneer II P2AT-8 robot.

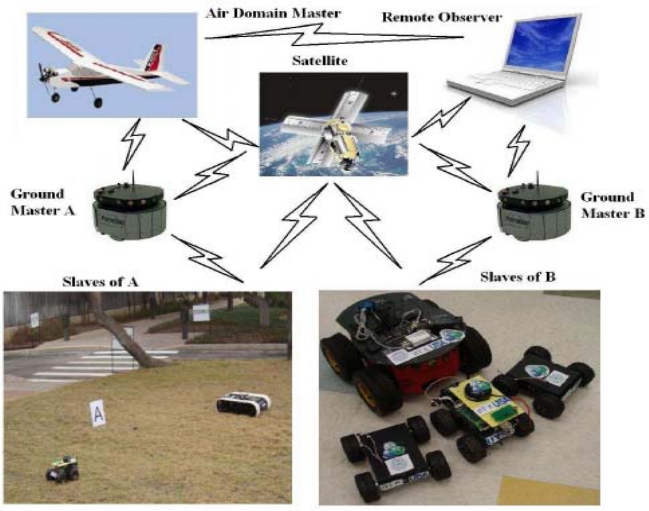

Figure 2. Hierarchy of multi-domain system of systems (Courtesy, ACE Center, University of Texas, San Antonio)

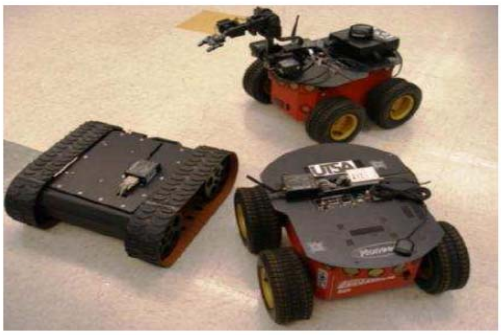

Figure 3. Pioneer II P2AT-8 Detector-Robot, Loader-Robot, Carrier-Robot and custom built robots at ACE Lab. (Courtesy, ACE Center, University of Texas, San Antonio)

In this approach, the environment and the Robotic agents will be simulated including real Robots in the environment. Without a real UAS in the field, a simulation of UAST specific scenarios cannot generate realistic test and evaluation parameters and results. Thus, in the proposed approach, the environment and UAS agents need be modeled accurately such that the simulation environment can have real UAS agents as well as virtual agents. This is extremely critical if the emergent or social behaviors of a team of UAS are being evaluated. For example, a UAS agent can be evaluated in a swarm of UAS agents by creating virtual swarms in the simulation environment and assigning a task to the swarm. The same approach can be used when a multi-modal decision making capabilities of a team of UAS is being evaluated.

II. TECHNICAL APPROACH

The problem of threat detection in an environment is considered. Three systems, comprising of robots and sensors, are proposed to form a system of systems to find a solution to this problem. In the land part of the proposed work, three wheel robots and a track robot comprise a system of rovers. The small wheel robots are in charge of detecting spots which are considered as threatening spots and they communicate with the big track robot to report the fire to the master robot (the track robot) and send and receive data through the designed communication scheme in order to do the desired tasks as a part of a system of systems.

A set of independent robots managed by System of Systems (SoS) architecture and programmed in DEVSJAVA [15-16] is proposed to serve as long term. The IIS Corp- University of Texas at San Antonio's Autonomous Control Engineering (ACE) lab has the objective to build and deploy Land, Air and Sea autonomous robotic vehicles that can independently operate toward a common pre-programmed objective.

In real world systems, the problem is addressed in a higher level where the systems send and receive data from other systems in the SoS and make a decision that leads the SoS to its global goals. Let's take the military surveillance example where different units of the Army collect data through sensors to locate a threat or to determine the identity of a target. In this type of situations, army command center receives data from these heterogeneous sensor systems such as AWACS, ground RADARS, and submarines. These systems are the parts of the SoS that make the decision; say the command and control station. However, they may be developed with different technologies. This will create a huge barrier in data aggregation and data fusion using the data received from these systems because they would not be able to interact successfully without hardware and/or software compatible [14]. In addition, the data coming from these systems are not unified which will add to the barrier in data aggregation and cooperation among the SoS components.

One solution to the problem is to modify the communication medium among the SoS components. Two possible ways of accomplishing this task are:

A. *Create a Software Model of Each System*

In this approach, each component in the SoS talks to a software module embedded in itself. The software module collects data from the system and through the software model generates outputs and sends to the other SoS components. If these software modules are written with a common architecture and a common language, then the SoS components can communicate effectively regardless of their internal hardware and/or software architectures [14].

Create a common language to describe data, where each system can express its data in this common language so that other SoS components can parse the data successfully.

The overhead that needs to be generated to have software models of each system on a SoS could be enormous and must be redone for new member of the SoS. In addition, this requires the complete knowledge of the state-space model of each SoS components, which is often not possible.

Consequently, recent research on SoS concepts focus on the study of coming up with a common language to describe the data of each system in a SoS in order to create an effective communication medium in the SoS. There are some research activities on using a language based on Extensible Markup Language (XML) in order to wrap data coming from different sources in a common way [13-14]. In these research activities, the XML is used to describe each component of the SoS and their data in a unifying way. If XML based data architecture is used in a SoS, only requirement for the SoS components is to understand/parse XML file received from the components of the SoS [13-14].

B. *Integration*

Integration is extremely important for both SoS and robotic swarms since both needs to expand and shrink with ease during the operation. In a SoS, it is critical to have the ability to bring a system into the SoS without any major problem such as redesign, restart, and/or reprogram the system. Integration in a SoS has two main components. The first one is to have adaptive communication schemes which allow the inclusion of a new system member. The second one is to have a common language which any new system can send its data to other systems in the SoS without any difficulty or major effort. The common language such as XML is a critical necessity for a SoS. The architecture for such as language can be incorporated with a discrete event simulation tool so that the SoS concepts can be simulated before they are applied to real problems. Consequently, the integration characteristics of a SoS require effective and adaptive communication among the systems. When the systems in a SoS are heterogeneous in hardware and software, the XML like common language becomes very essential. However, since all the members in a swarm have either identical or very similar hardware and software components, necessity of a common language is not so critical. Thus, in a robotic swarm, the design need not have an XML like common language. Instead, a common protocol or a common format will suffice.

The communication scheme needs to have ability to adapt itself for the population changes in the swarm. In order to achieve this goal, processes for accepting new members to the swarm and removing a member from a swarm need to be implemented as part of the communication scheme.

III. FUZZY REINFORCEMENT LEARNING (FRL) IN SOS

In this section, we discuss how fuzzy control can be used for an unmanned Air Vehicle. This is based on the works of Gomez and Jamshidi [8]. There are a total of six output variables that need to be fuzzified and they are: roll, pitch, airspeed, airspeed error, heading error and altitude error. The ranges of these variables are given in Table I.

TABLE I. VARIABLE RANGES

Variable	Actual Range		Range Used	
Altitude Error	-1 km	1 km	-0.5 m	0.5 m
Heading Error	-360°	360°	-1°	1°
Pitch	-180°	180°	-10°	10°
Roll	-180°	180°	5°	5°
Airspeed Error & Heading Control	-100 m/s	100 m/s	-100 m/s	100 m/s
Altitude & Throttle Control	-0.1	0	-0.01	0

It is possible to create a fuzzy controller that will encase the whole range of values for each variable, but it will take a large number of rules making the calculation of the control much slower. The range used to decide the placement of the membership functions was decided by the fact that we want to reduce the number of rules. By taking a small range and scaling the different variables allows for a smaller number of rules, and the precision will not be lost.

The following figures represent the membership functions of the linguistic variables used for the creation of the different controls. The higher the precision the better the fuzzy controller will function, but it also means more memory needed to store those values. The same can be said about the number of membership functions, a bigger number usually means a smoother control output. Thus, the increase in membership functions leads to an increase in the number of rules

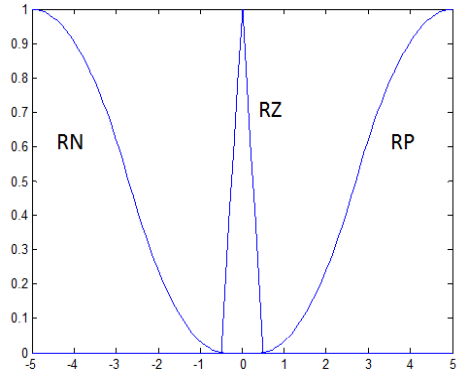

Figure 4. Roll membership functions

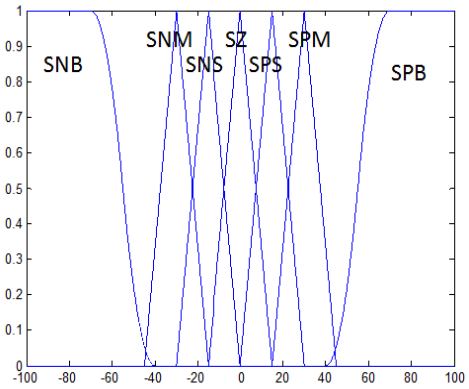

Figure 5. Control output membership functions

If Heading Error is HP and Roll is RP
then Heading Control is SNB
⋮
If Heading Error is HN and Roll is RN
then Heading Control is SPB

The relationship between the altitude error and the pitch angle create the control surface. The higher the precision the better the fuzzy controller will function, but it also means more memory needed to store those values. The same can be said about the number of membership functions, a bigger number usually means a smoother control output. Thus, the increase in membership functions leads to an increase in the number of rules

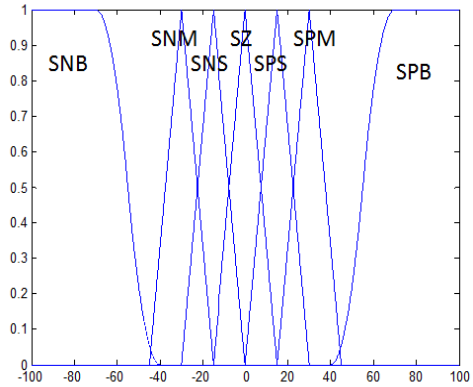

Figure 6. Control output membership functions

If Heading Error is HP and Roll is RP
then Heading Control is SNB
⋮
If Heading Error is HN and Roll is RN
then Heading Control is SPB

If Heading Error is HP and Roll is RP
then Heading Control is SNB
⋮
If Heading Error is HN and Roll is RN
then Heading Control is SPB

A simple graphical example of how the different rules give us the control output is shown in the figure below.

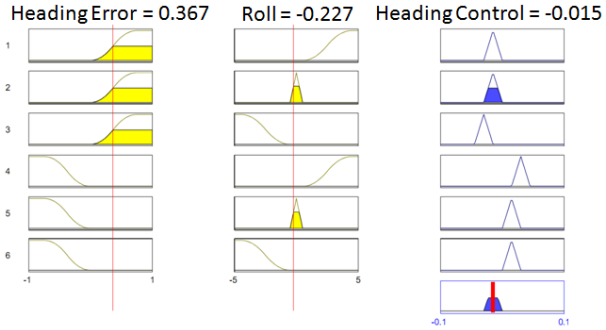

Figure 7. Visual representation of the altitude control rules

The same procedure was followed to create the heading control, six rules relating the heading error and the roll, and an extra rule to maintain the airplane from over rolling.

FRL can be applied for formation control of UGVs according to [3]. For navigation of UGVs, Fuzzy rules can be written according to the above and their parameters can be updated based on GARIC-Q [5,6] and MULTI-GARIC-Q [6]. The use of FRL is not limited to UGVs only and any system of our SOS can use FRL for updating its parameters. For example, [1] focuses on using the FRL for UAVs.

IV. SYSTEM OF SYSTEMS SIMULATION

In a System of Systems, systems and/or subsystems often interact with each other because of interoperability and over all integration of the SoS. These interactions can be achieved by efficient communication among the systems using either peer-to-peer communication or through central coordinator in a given SoS. Since the systems within a SoS are operationally independent, interactions between systems are generally asynchronous in nature. A simple yet robust solution to handle such asynchronous interactions (specifically, receiving messages) is to throw an event at the receiving end to capture the messages from single or multiple systems. Such system interactions can be represented effectively as discrete-event models [15]. In discrete-event modeling, events are generated at variable time intervals as opposed to some pre-determined time interval seen commonly in discrete-time systems. More specifically, the state change of a discrete-event system happens only upon arrival (or generation) of an event, not necessarily at equally spaced time intervals. To this end, a discrete-event model is a feasible approach in simulating the proposed SoS framework and its interaction [15]. Several discrete-event simulation engines [13-16] are available that can be used in simulating interaction in a heterogeneous mixture of

independent systems. We consider one such simulation framework – Discrete Event System Specification (DEVS) because of the available effective mathematical representation and its support to distributed simulation using DoD's High Level Architecture (HLA).

A. DEVS Modeling and Simulation

Discrete Event System Specification (DEVS) [13-16] is a formalism, which provides a means of specifying the components of a system in a discrete event simulation. In DEVS formalism, one must specify *Basic Models* and how these models are connected together. These basic models are called *Atomic* models and larger models which are obtained by connecting these atomic blocks in meaningful fashion are called *Coupled* models. Each of these atomic models has *inports* (to receive external events), *outports* (to send events), a set of *state variables*, *internal transition*, *external transition*, and *time advance functions*.

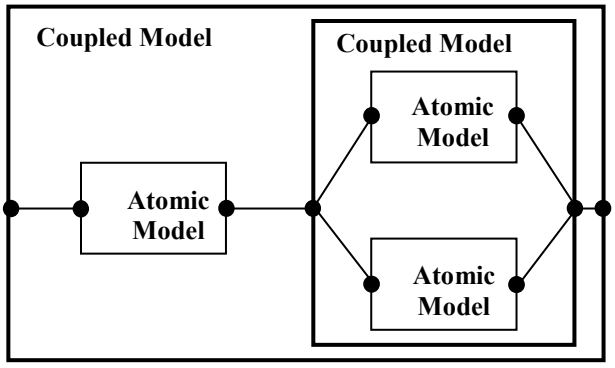

Figure 8. DEVS models for system and sub-systems

Next we present a simulation example using the DEVS simulation environment [13-16]. This is a scenario where a target is being tracked by a group of sensors deployed in the region of interest. The sensors are grouped to form clusters, with each cluster having a cluster-head that can send and receive information to a command center (base-station). The entire simulation can be performed by "coupling" all the DEVS atomic models together with meaningful interconnections. In order to test our SoS architecture in the DEVS environment, our XML based data representation needs to be embedded in to the simulation environment.

B. XML and DEVS

In DEVS, messages can be passed from one system (coupled or atomic model) to another using either predefined or user-defined message formats. Since the systems within a SoS maybe different in hardware and/or software, there is a need for a unifying language for message passing. Each system need not necessarily have the knowledge (operation, implementation, timing, data issues, and so on) of another system in a SoS. Therefore, one has to work at a high-level (information or data level) in order to understand the present working condition of the system. Fig. 9 describes conceptually a SoS simulation example to show the use of XML in the DEVS formalism.

C. SOS Simulation Framework

Based on the system of systems architecture, we have simulated robust threat detection data aggregation Scenario) where there is a base robot, two swarm robots, five sensors, and a threat. The sensors are stationed such that they represent a sensor network covering an area. The threat is moving in the area and is detected by sensors when the threat is sufficiently close to a sensor node. All sensors communicate with a base robot which itself does not actively seek threat. Instead, the base robot processes the information using sensor data and data sent by swarm robots. A command center can collect processed data (aggregated data) from the base robot without interacting with other components of the SoS such as sensors and swarm robots. Robust threat detection works as follows. When a sensor detects the threat, they notify the Base Robot. Then, the Base Robot sends the Swarm Robots the location of the threat based on the information sent by the sensors. This is crucial in order to get rid of false detections as they can cause inefficient usage of system components.

D. XML Format

As mentioned before, the hardware and/or software architectures of these systems will not be the same in reality. Thus, they may not able to talk to each other successfully even though they can operate independently. We have implemented XML based SoS, message architecture in DEVSJAVA software [15]. In this XML based message architecture, each system has an XML-like message consisting of their name and a data vector. The name of each system represents an XML tag. The data vectors are used to hold the data of the systems. The length of the data vectors in each system can be different based on the amount of data each system contains.

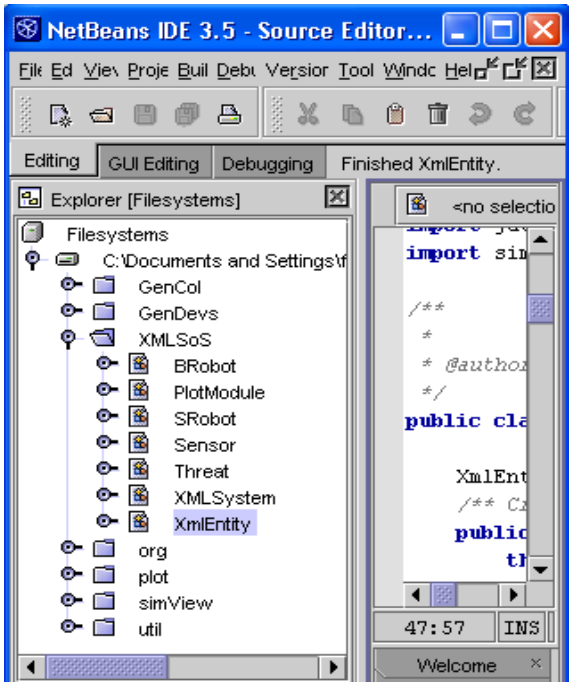

Figure 9. Atomic models and DEVSJAVA components

REFERENCES

[1] Berenji, H. R. and D. Vengerov and J. Ametha , “Perception based Reinforcement Learning for Sensor Allocation in Unmanned Aerial Vehicles”, the 12th IEEE International Conference on Fuzzy Systems, 2003.

[2] Berenji, H. R. and D. Vengerov, “Advantages of Cooperation Between Reinforcement Learning Agents in Difficult Stochastic Problems”. In proceedings of the 9th IEEE International Conference on Fuzzy Systems, 2000.

[3] Berenji, H.R. and D. Vengerov, “Convergent Actor Critic-based Fuzzy Reinforcement Learning Apparatus and Method”, US patent 6,917,925 B2, Filed Dec. 21, 2001.

[4] Berenji, H.R “Collaborative fuzzy reinforcement learning agents”, International Fuzzy Systems Association World Congress, 1997.

[5] Berenji, H.R. and D. Vengerov, “Cooperation and Coordination between teams of Fuzzy Reinforcement Agents”, FUZZ-IEEE, Seoul, Korea, FUZZ-IEEE, Seoul, Korea, 1999.

[6] Berenji, H.R. and S. Saraf, “Competition and Collaboration among Fuzzy Reinforcement Learning Agents”, Seventh IEEE International conference on Fuzzy Systems, Anchorage, Alaska, May 1998.

[7] Crossley, W.A., "System of Systems: An Introduction” of Purdue University Schools of Engineering's Signature Area."

[8] Gomez, J. F and M. Jamshidi,”Fuzzy Logic Control of a Fixed Wing Unmanned Aerial Vehicle”, WAC 2010, Kobe, Japan.

[9] Jamshidi, M., “Theme of the IEEE SMC 2005”, Waikoloa, Hawaii, USA”.

[10] Luskasik, S.J., "Systems, “Systems of Systems, and the Education of Engineers”, Artificial Intelligence for Engineering Design, Analysis, and Manufacturing, Vol. 12, No. 1, pp. 11-60, 1998.

[11] Meilich, A., “System of Systems (SoS) Engineering & Architecture Challenges in a Net Centric Environment,” Proc. of IEEE International Conference on System of Systems Engineering, Los Angeles, April 2006.

[12] Sage, A. P. and C. D. Cuppan, "On the Systems Engineering and Management of Systems of Systems and Federations of Systems," Information, Knowledge, Systems Management, Vol. 2, No. 4, pp. 325-34, 2001.

[13] Sahin, F. and P. Sridhar and B. Horan and V. Raghavan and Mo Jamshidi, “System of Systems Approach to Threat Detection and Integration of Heterogeneous Independently Operable Systems”, “ IEEE Conference on Systems, Man and Cybernetics, Montreal, Canada, October 2007.

[14] Sahin, F. and M. Jamshidi, and P. Sridhar, “A Discrete Event XML based Simulation Framework for System of Systems Architectures,”IEEE International Conference on System of Systems, April 2007.

[15] Ziegler, B.P. and H. Sarjoughian, “Introduction to DEVS Modeling and Simulation with JAVA A Simplified Approach to HLA-Compliant Distributed Simulations,” ACIMS, httw://www.acims.arizona.edu

[16] Ziegler, B. P. and H. Praehofer. and T.G., Kim, “Theory of Modeling and Simulation”, Second edition, Academic Press, Boston, 2000

2011 IEEE International Conference on Fuzzy Systems
June 27-30, 2011, Taipei, Taiwan

Partially Exclusive Condition for Sequential Fuzzy Co-cluster Extraction

Katsuhiro Honda, Akira Notsu, Hidetomo Ichihashi
Department of Computer Science and Intelligent Systems
Osaka Prefecture University
1-1 Gakuen-cho, Nakaku, Sakai, Osaka 599-8531, Japan
Email: {honda, notsu, ichi}@cs.osakafu-u.ac.jp

***Abstract*—Sequential fuzzy co-cluster extraction has been proven to be useful for collaborative filtering tasks by extracting user-item co-clusters, in which promising items are connected to the corresponding users in each co-cluster. Since some popular items can be shared by multiple clusters in collaborative filtering problems, exclusive conditions, which force objects to belong to only one cluster, were used only for users. In this paper, it is demonstrated that such user-only exclusive conditions may cause poor clustering results, and partially exclusive conditions, in which part of items are also forced to be exclusive, are introduced. In addition, connections with neural approaches for co-clustering are discussed, in which co-clustering problems are identified using a modified model of principal component analysis.**

***Keywords*—co-clustering, collaborative filtering, principal component analysis.**

I. Introduction

Collaborative filtering is a promising approach for achieving personalized recommendation in network communities [1]. Many collaborative filtering algorithms are based on the concept of connecting promising items to users by considering mutual similarities among users (and/or items) [2], [3]. Co-clustering is a direct approach for extracting user-item clusters, in which not only similar users but also their associated items are gathered into a cluster. Once we estimate co-cluster structures buried in user-item relational data matrices, items that are supposed to be closely related are recommended to their corresponding users [4], [5].

Honda *et al.* [6], [7] proposed a sequential approach for the fuzzy co-clustering model, which is a combination of the structural balancing model in social science [9] and sequential fuzzy cluster extraction [10]. In collaborative filtering tasks, the co-clustering model plays a role for simultaneously partitioning users and items into several clusters by calculating the principal eigenvector of a modified adjacency matrix. In order to disjoint clusters, penalty weights are added to the diagonal elements of the adjacency matrix. Besides the fully exclusive condition where all users and items can belong to only a single cluster, the user-only exclusive condition can also be applied in such a case where some popular items are shared by multiple clusters. In a collaborative filtering problem, it was demonstrated that the sequential co-clustering model obtained using the user-only exclusive condition has a high recommendation ability with a low memory requirement. In addition, a modified calculation algorithm for reducing computational costs in cluster structure estimation was proposed, which makes it possible to easily apply the co-cluster structural information to new users [8].

In collaborative filtering tasks, it is also possible that some typical items can be used to distinguish a small community having a special preference. Such typical items should be assigned to only a single cluster, while popular items can be shared by multiple clusters. In this paper, a partially exclusive condition is introduced, in which some items are forced to be exclusive, while other popular items can be shared.

Recently, Oja [11] discussed co-clustering problems (bi-clustering problems) in the context of a modified principal component analysis (PCA) approach. This paper also discusses some connections with such neural approaches.

The remainder of this paper is organized as follows: Section II briefly reviews the sequential approach for fuzzy co-cluster extraction. Section III introduces the partially exclusive condition for items and presents a discussion of the relationship with other co-clustering models. Section IV presents several experimental results in order to demonstrate the characteristic features of the proposed approach. Section V summarizes the conclusions of this paper.

II. Brief Review of Sequential Approach for Fuzzy Co-cluster Extraction

A. Structural Balance and Sequential Fuzzy Cluster Extraction

Assume that we have a graph G defined by an adjacency matrix $A(G) = [a_{ij}]$, the elements of which are

$$a_{ij} = \begin{cases} 1 & : \text{if } i \text{ and } j \text{ have positive relation,} \\ -1 & : \text{if } i \text{ and } j \text{ have negative relation,} \\ 0 & : \text{if the relation of } i \text{ and } j \text{ does not exist.} \end{cases} \quad (1)$$

The structure theorem proposed by Cartwright and Harary [9] revealed that the set of vertices (notions) can be partitioned into two subsets (one of which may be empty), the elements of which have positive relations with members of the same subset and negative relations with members of different subsets in a balanced system.

Katai and Iwai [12] discussed how to derive an approximately optimum two-cluster structure and proposed a tech-

This work was funded in part by the Ministry of Internal Affairs and Communications, Japan, under the Strategic Information and Communications R&D Promotion Programme (SCOPE) and in part by the Ministry of Education, Culture, Sports, Science and Technology, Japan, through a Grant-in-Aid for Scientific Research (20700214).

978-1-4244-7316-8/11/$26.00 ©2011 IEEE

nique for calculating a cluster indicator using the eigenvector of $A(G)$ corresponding to the maximum eigenvalue.

The calculation procedure in the eigenvalue problem has some connections with sequential fuzzy clustering models although they use different types of similarity matrices. Fuzzy clustering, most of the algorithms of which are motivated by fuzzy c-Means (FCM) [13], is an unsupervised classification method that can deal with ambiguous boundaries among clusters or overlapping clusters using fuzzy memberships. In addition to FCM-like batch algorithms, sequential clustering models extract clusters having high degrees of aggregation one by one.

Sequential fuzzy cluster extraction (SFCE) [10] estimates cluster memberships by calculating the eigenvector of a modified similarity matrix. Let e_{ij} be the similarity between samples i and j ($e_{ij} = e_{ji}$, $e_{ij} \geq 0$). Here, the goal is to extract a fuzzy cluster having the maximum degree of aggregation. The criterion function to be maximized is formulated as:

$$L_{sfce} = \sum_{i=1}^{n} \sum_{\substack{j=1 \\ j \neq i}}^{n} e_{ij} w_{1i} w_{1j}, \tag{2}$$

where $\boldsymbol{w}_1 = (w_{11}, \ldots, w_{1n})^\top$ is an n-dimensional membership indicator vector satisfying the following constraints:

$$0 \leq w_{1i} \leq 1, \quad i = 1, \ldots, n, \tag{3}$$

$$||\boldsymbol{w}_1||^2 = \sum_{i=1}^{n} w_{1i}^2 = 1. \tag{4}$$

The optimal cluster indicator for the first cluster $\boldsymbol{w}_1$ is derived as the eigenvector corresponding to the largest eigenvalue of the modified similarity matrix $S = \{s_{ij}\}$ [10]:

$$s_{ij} = \begin{cases} e_{ij} & ; i \neq j \\ 0 & ; i = j \end{cases}$$

In order to obtain K disjoint clusters one by one, the optimization problem must be solved repeatedly under the additional constraint that $\boldsymbol{w}_k^\top \boldsymbol{w}_{k-1} = \cdots = \boldsymbol{w}_k^\top \boldsymbol{w}_1 = 0$.

Tsuda et al. [10] introduced a penalty term to the aggregation criterion in order to avoid duplication, as follows:

$$L_{sfce} = \sum_{i=1}^{n} \sum_{\substack{j=1 \\ j \neq i}}^{n} e_{ij} w_{ki} w_{kj} - \frac{1}{k-1} \sum_{t=1}^{k-1} \beta_t \mathrm{dup}(\boldsymbol{w}_k, \boldsymbol{w}_t), \tag{5}$$

where the penalty term $\mathrm{dup}(\boldsymbol{w}_k, \boldsymbol{w}_t)$ is the duplication measure to be minimized, and β_t is the weight for the penalty to be set by users. In [10], β_t was determined by the degree of cluster aggregation, as follows:

$$\beta_t = \eta \sum_{i=1}^{n} \sum_{\substack{j=1 \\ j \neq i}}^{n} e_{ij} w_{ti} w_{tj}. \tag{6}$$

The weight η is tuned so that the additional penalty term is sufficiently larger than the aggregation criterion.

The optimal solution for $\boldsymbol{w}_k$ is then given as the eigenvector corresponding to the largest eigenvalue of the modified similarity matrix $S_k = \{s_{kij}\}$:

$$s_{kij} = \begin{cases} e_{ij} & ; i \neq j \\ -\dfrac{1}{k-1} \displaystyle\sum_{t=1}^{k-1} \beta_t w_{ti}^2 & ; i = j \end{cases}$$

B. Sequential Fuzzy Co-cluster Extraction

In order to apply the SFCE clustering model to rectangular relational matrices given in collaborative filtering problems, Honda *et al.* [6], [7] combined the concepts of the structural balancing approach. Davis [14] implied that a signed graph having two clusters is further clusterable if each positive line joins two nodes in the same subset but is not clusterable for different subsets. Taking Davis's suggestion into account, Honda et al. introduced a modified relational data matrix, in which only positive relations in the rectangular relational matrix were considered in order to extract subsets.

Assume that there are n users and m items and that we have an $n \times m$ partial adjacency matrix $Z = [z_{ij}]$, where z_{ij} is given by:

$$z_{ij} = \begin{cases} 1 & \text{if } x_{ij} \geq \epsilon \text{ (positive relation)}, \\ -1 & \text{if } x_{ij} < \epsilon \text{ (negative relation)}, \\ 0 & \text{if } i \text{ did not evaluate } j, \end{cases} \tag{7}$$

where x_{ij} is the evaluation value for item j by user i and ϵ is a pre-defined threshold.

This type of relational matrix is called "a rectangular relational" matrix and most relational clustering models can be applied only after reconstruction of the full-square relational matrix. For example, Bezdek *et al.* [15] performed visual assessment of the cluster tendency by imputing missing relations (user-user relations and item-item relations) based on a concept similar to the Expectation-Maximization (EM) algorithm [16]. The goal of collaborative filtering, however, is the estimation of missing relations, and such preprocessing as imputation is not applicable.

In [6], the influences of missing relations (user-user relations and item-item relations) were ignored based on the concept of the structural balancing approach, and the diagonal block matrices corresponding to user-user relations and item-item relations were given by zero-matrices. In addition, all elements of the relational data matrix must be non-negative elements if we want to apply SFCE to the square relational matrices. Taking Davis's suggestion into account, in [6], only positive relations in the rectangular relational matrix are considered to extract subsets, such that each positive line joins users and items in the same subset, and the partial adjacency matrix $Z = [z_{ij}]$ is generated by ignoring not only negative relations but also unknown relations, as follows:

$$z_{ij} = \begin{cases} 1 & \text{if } x_{ij} \geq \epsilon \text{ (positive relation)}, \\ 0 & \text{if } x_{ij} < \epsilon \text{ (negative relation)}, \\ 0 & \text{if } i \text{ did not evaluate } j. \end{cases} \tag{8}$$

For example, this type of relational data is common in purchase history data, in which the zero-relation of 'not yet bought'

includes both 'negative feelings toward an item' and 'not yet but might buy'.

Then, the modified similarity matrix $S = \{s_{ij}\}$ is given as the following $(n+m) \times (n+m)$ block matrix:

$$S = \begin{pmatrix} O & Z \\ Z^\top & O \end{pmatrix}. \tag{9}$$

If all users and items are disjoint, then the constraint for indicator vectors $\boldsymbol{w}_1, \ldots, \boldsymbol{w}_k$ is given by $\boldsymbol{w}_k^\top \boldsymbol{w}_{k-1} = \cdots = \boldsymbol{w}_k^\top \boldsymbol{w}_1 = 0$. On the other hand, if all users are disjoint, but some items can be shared, then the exclusive condition is forced only on users. Let $\boldsymbol{w}_t = (\boldsymbol{w}_t^{u\top}, \boldsymbol{w}_t^{i\top})^\top$, where $\boldsymbol{w}_t^u = (w_{t1}, \ldots, w_{tn})^\top$ and $\boldsymbol{w}_t^i = (w_{t(n+1)}, \ldots, w_{t(n+m)})^\top$. The user-only exclusive constraint is given as $\boldsymbol{w}_k^{u\top} \boldsymbol{w}_{k-1}^u = \cdots = \boldsymbol{w}_k^{u\top} \boldsymbol{w}_1^u = 0$, and the diagonal elements of the modified similarity matrix s_{ii} for k-th cluster are re-formulated as

$$s_{ii} = \begin{cases} -\frac{1}{k-1} \sum_{t=1}^{k-1} \beta_t w_{ti}^2 & ; i \leq n \\ 0 & ; i > n \end{cases} \tag{10}$$

In order to reduce the computational cost of eigenvalue problems, an improved procedure was proposed [8], in which two membership vectors of $\boldsymbol{w}_1^u$ for users and $\boldsymbol{w}_1^i$ for items are calculated separately. In the improved procedure, either of $\boldsymbol{w}_1^u$ or $\boldsymbol{w}_1^i$ is first calculated by solving an eigenvalue problem of a smaller relational matrix (the size of the relational matrix is reduced by 75% or more) and the remaining membership indicator is calculated by a simple calculation process. Divided calculation processes are also useful for handling new users or items without re-calculating the eigenvalues.

III. Partially Exclusive Condition and Connection With Other Models

A. Partially Exclusive Condition for Sequential Fuzzy Co-cluster Extraction

In collaborative filtering tasks, it is often the case that some popular items may be preferred by many people having various preference characteristics. Therefore, such popular items should be shared by multiple clusters and the user-only exclusive condition appears to be reasonable for finding items to be recommended to users classified into disjoint clusters. It is also possible that some typical items can be used to distinguish a small community having special preferences. Such typical items should be assigned to only a single cluster in order to be assigned to users having such special preferences for the single cluster while popular items can be shared by multiple clusters. In this paper, a partially exclusive condition is introduced, in which certain items are forced to be exclusive while other popular items can be shared.

Without loss of generality, assume that the first p among m items are to be assigned only to a single cluster and the others can be shared by multiple clusters. The exclusive condition, which forces an item to have a large membership value only in a single cluster, is used only for certain items.

$$w_{k(n+j)} \cdot w_{(k-1)(n+j)} = \cdots = w_{k(n+j)} \cdot w_{1(n+j)} = 0, \quad j = 1, \ldots, p. \tag{11}$$

Here, all users are forced to be exclusive as $\boldsymbol{w}_k^{u\top} \boldsymbol{w}_{k-1}^u = \cdots = \boldsymbol{w}_k^{u\top} \boldsymbol{w}_1^u = 0$.

Then, in order to achieve the partially exclusive condition, the diagonal elements of the modified similarity matrix s_{ii} for the k-th cluster are re-defined as

$$s_{ii} = \begin{cases} -\frac{1}{k-1} \sum_{t=1}^{k-1} \beta_t w_{ti}^2 & ; i \leq n+p \\ 0 & ; i > n+p \end{cases} \tag{12}$$

The clustering algorithm is equivalent to the conventional clustering algorithm without the penalty weights.

B. Connection With Other Models

Fuzzy clustering for categorical multivariate (FCCM) data [17] and fuzzy co-clustering of documents and keywords (Fuzzy CoDoK) [18] are FCM-type co-clustering models, in which the relational fuzzy c-Means (RFCM) [19] for square relational matrices is extended for rectangular matrices using two different types of memberships. The first type of membership is the conventional fuzzy membership for objects, which are forced to be exclusive, and the second type of membership is the additional membership for items, which represents the relative typicalities of items in each cluster. In this clustering model, the item memberships are used not for partitioning items, but rather for finding representative items in each cluster. Therefore, certain items can be shared by multiple clusters, and the clustering model has similar features to sequential fuzzy co-cluster extraction under the user-only exclusive condition although FCM-type models are easily influenced by model parameters and missing elements [7]. In addition, FCM-type models cannot consider the partially exclusive condition for items.

Recently, Oja [11] discussed co-clustering problems (bi-clustering problems) in the context of a modified principal component analysis (PCA) approach. When we have an $n \times m$ data matrix X and the m columns are considered to be data vectors, the approximation $X \approx WW^\top X$ performs sparse feature extraction. On the other hand, if n rows are considered to be data vectors, an approximation $X \approx XWW^\top$ performs clustering of the rows. If all of the elements of the data matrix X are non-negative, as in the case of the modified adjacency matrix given by Eq.(9) for sequential fuzzy co-cluster extraction, the matrix factorization process can be reduced to the estimation of an almost orthogonal non-negative matrix W [20]. Then, a biclustering model is constructed based on the approximation $X \approx LL^\top XRR^\top$, in which L and R are the cluster indicators for row and column objects, respectively. The multiplicative rules for neural learning have been reported in [11]. In addition, as suggested in [21], non-negative learning tends to yield high orthogonality. Therefore, the biclustering model essentially forces the exclusive condition to both row and column objects and has features similar to sequential fuzzy co-cluster extraction under the fully exclusive condition. In order to achieve the partially exclusive condition in the neural approach, some modifications are necessary in the approximation part.

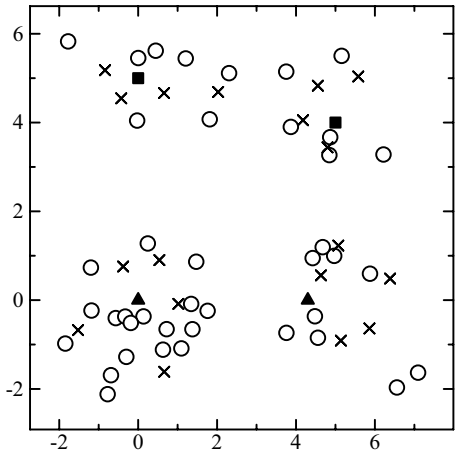

Fig. 1. Artificial data set (○: user, ×: item)

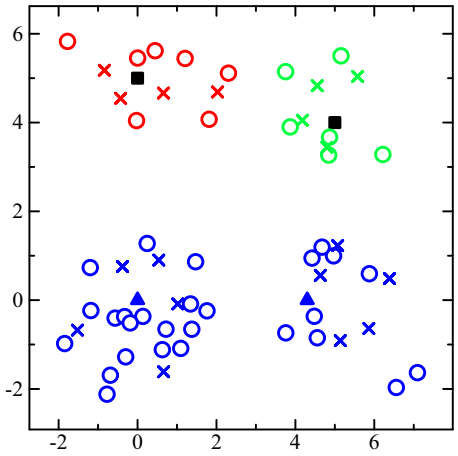

Fig. 2. Cluster partition obtained under fully exclusive condition

IV. Numerical Experiments

In this section, experimental results are presented in order to demonstrate the characteristic features of the proposed approach.

A. Artificial Data Set

Figure 1 shows the artificially generated data set used in this experiment, in which ○ and × denote users and items, respectively. The data set, which was composed of 40 users and 20 items, formed four loose clusters in a 2-D space, and the lower two masses are larger than the upper two masses. Black triangles and squares are shared items that should belong to two clusters, e.g., the item shown in the black triangle is shared by the lower two clusters. Then, a 40×20 relational data matrix $Z = [z_{ij}]$, the elements of which are given by an alternative process, was constructed by calculating mutual Euclidean distances d_{ij} among users and items. Here, d_{ij} for the shared items (black triangle and square) is given by the distance to the nearest mark. The element z_{ij} was given by

$$z_{ij} = \begin{cases} 1 & \text{if } d_{ij}^2 \leq 10, \\ 0 & \text{if } d_{ij}^2 > 10, \end{cases} \tag{13}$$

which is calculated by Eq.(8) with $\epsilon = 10$. The modified similarity matrix $S = \{s_{ij}\}$ was calculated using Eq.(9). The cluster number k and the penalty weight η were set as $k = 3$ and $\eta = 10$, respectively.

First, the data set was partitioned by sequential fuzzy co-cluster extraction under the fully exclusive condition. The maximum membership partition is shown in Fig. 2. The item indicated by the black square had very small membership degrees in all clusters. Because of the strong influence of the most popular item (blue triangle), the lower two masses (larger data masses) were merged into a dominant single cluster. The exclusive condition forcing all items to belong to only one cluster tends to generate a far more dominant cluster and may fail to find useful structural information.

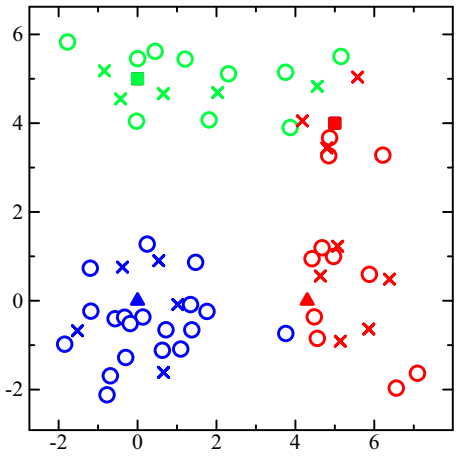

Fig. 3. Cluster partition obtained under user-only exclusive condition

Second, the data set was partitioned under the user-only exclusive condition. Figure 3 shows the derived cluster partition. Since the most popular item (filled triangle) is shared by two clusters (blue and red clusters), the lower two data masses were successfully partitioned. However, the items denoted by the filled squares were also illegally shared by the green and red clusters because these items were weakly shared by many users. Then, the upper right cluster was divided into two clusters. The results imply that the user-only exclusive condition may destroy the cluster structure of small data masses.

Third, the data set was partitioned with the proposed partially exclusive condition and the cluster partition shown in Fig. 4 was derived. Here, only the item indicated by the black square was forced to be exclusive. Using a partially exclusive condition, the intrinsic co-cluster structure was clarified.

In this way, the proposed approach, in which only some of the items are forced to be exclusive, is useful for decreasing the inappropriate influences of popular items and weakly shared items.

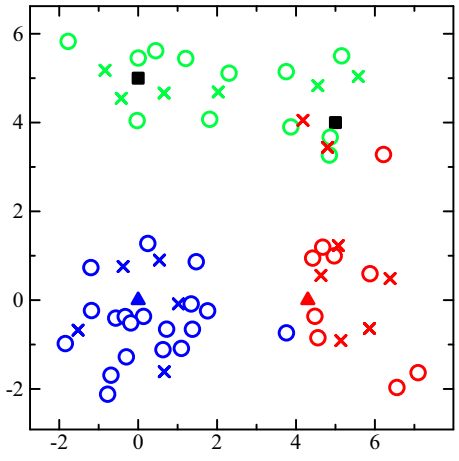

Fig. 4. Cluster partition obtained under partially exclusive condition

B. Purchase History Data

Next, a purchase history data set collected by Nikkei Inc. in 2000 is used in a collaborative filtering task. The data set used in [7] includes the purchase history of 996 users ($n = 996$) on 18 items ($m = 18$). The elements z_{ij} of 996×18 relational data matrix $Z = [z_{ij}]$ is 1 if user i has item j while otherwise 0. In this experiment, Piano (the 2nd item), VD (the 8th item) and Oven (the 14th item), which relatively fewer users have, are selected for items to be predicted, and the goal is to predict the applicability of the items for the second half of 996 users whose corresponding element z_{ij} were all withheld so as to be '$z_{ij} = 0$'.

First, the users and items were partitioned into 10 co-clusters under the constraint of $\boldsymbol{w}_k^{u\top}\boldsymbol{w}_{k-1}^{u} = \cdots = \boldsymbol{w}_k^{u\top}\boldsymbol{w}_1^{u} = 0$, where all items can be shared by multiple clusters. Then, the applicability of the target items for each user was predicted by considering the fuzzy membership degrees of the items to the cluster, in which the user have the maximum membership. If the membership degree of the target item to the cluster is higher than a threshold, the item is recommended to the user.

Second, 10 co-clusters were extracted by forcing the 15th item (Coffee Maker) to be exclusive. The 15th item was selected because its average membership degree was the smallest in the first co-cluster extraction, i.e., it might be only weakly shared by all clusters without belonging to a certain cluster. So, in this second co-cluster extraction, the 15th item was assigned only to a single cluster under exclusive condition without belonging to all clusters.

Table I compares the recommendation abilities of the two co-cluster partitions. The recommendation ability is assessed by ROC sensitivity [22]. The ROC curve is a true positive rate vs. false positive rate plots drawn by changing the threshold of the applicability level in recommendation, and the lower are of the curve becomes large as the recommendation ability is higher. The table implies that the proposed model with the partially exclusive condition has higher recommendation ability than the conventional model.

TABLE I
COMPARISON OF RECOMMENDATION ABILITIES: AREA OF LOWER PART OF ROC CURVES

item	conventional	partial exclusive
Piano	0.644	0.651
VD	0.547	0.578
Oven	0.575	0.598

V. CONCLUSION

In this paper, a modified condition for fuzzy co-clustering was considered. It was demonstrated that the partially exclusive condition is useful for clarifying intrinsic co-cluster structures when some items are very popular with or are weakly shared by many users. In a comparative discussion, it was revealed that the sequential fuzzy co-clustering model can derive similar partitions to both FCM-type co-clustering models and neuro-learning-based biclustering models using different exclusive conditions while the partially exclusive condition yields another type of cluster partition.

In a collaborative filtering task, an item that was weakly shared by all clusters was forced to be exclusive so that it assigned to a single cluster without evenly belonging to all clusters. Then, the recommendation ability for items that relatively fewer users have could be improved by considering the partially exclusive condition.

A potential future work is to develop a technique for evaluating the degree of responsibility of items in order to automatically select items to be made exclusive.

REFERENCES

[1] J. A. Konstan, B. N. Miller, D. Maltz, J. L. Herlocker, L. R. Gardon and J. Riedl, "Grouplens: applying collaborative filtering to usenet news," *Communications of the ACM*, vol.40, no.3, pp.77-87, 1997.

[2] J. L. Herlocker, J. A. Konstan, A. Borchers and J. Riedl, "An algorithmic framework for performing collaborative filtering," *Proc. of Conference on Research and Development in Information Retrieval*, 1999.

[3] G. Linden, B. Smith and J. York, "Amazon.com recommendations: item-to-item collaborative filtering," *IEEE Internet Computing*, Jan-Feb, pp.76-80, 2003.

[4] L. Ungar and D. Foster, "Clustering methods for collaborative filtering," *Proc. of Workshop on Recommendation Systems*, 1998.

[5] R. Jin, L. Si and C. X. Zhai, "A study of mixture models for collaborative filtering," *Information Retrieval*, vol.9, no.3, pp.357-382, 2006.

[6] K. Honda, A. Notsu and H. Ichihashi, "Collaborative filtering by sequential extraction of user-item clusters based on structural balancing approach," *Proc. of 2009 IEEE International Conference on Fuzzy Systems*, pp.1540-1545, 2009.

[7] K. Honda, A. Notsu and H. Ichihashi, "Collaborative filtering by sequential user-item Co-cluster extraction from rectangular relational Data," *International Journal of Knowledge Engineering and Soft Data Paradigms*, vol.2, no.4, pp.312-327, 2010.

[8] K. Honda, A. Notsu and H. Ichihashi, "An efficient algorithm for collaborative filtering based on sequential user-item co-cluster extraction," *Proc. of Joint 5th International Conference on Soft Computing and Intelligent Systems and 11th International Symposium on Advanced Intelligent Systems*, pp.4-8, 2010.

[9] D. Cartwright and F. Harary, "Structural balance, a generalization of Heider's theory," *Psychological Review*, vol. 63, pp. 167-293, 1956.

[10] K. Tsuda, M. Minoh and K. Ikeda, "Extracting straight lines by sequential fuzzy clustering," *Pattern Recognition Letters*, vol. 17, pp. 643-649, 1996.

[11] E. Oja, A. Ilin, J. Luttinen and Z. Yang, "Linear expansions with nonlinear cost functions: modeling, representation, and partitioning," *2010 IEEE World Congress on Computational Intelligence, Plenary and Invited Lectures*, pp.105-123, 2010.
[12] O. Katai and S. Iwai, "On the characterization of balancing processes of social systems and the derivation of the minimal balancing processes," *IEEE Trans. Systems, Man, and Cybernetics*, vol. SMC-8, no. 5, pp. 337-348, 1978.
[13] J. C. Bezdek, *Pattern Recognition with Fuzzy Objective Function Algorithms*, Plenum Press, 1981.
[14] J. A. Davis: Clustering and structural balance in graph; *Human Relation*, Vol. 20, pp. 181-187 (1967)
[15] J. C. Bezdek, R. J. Hathaway and J. M. Huband, "Visual assessment of clustering tendency for rectangular dissimilarity matrices," *IEEE Trans. Fuzzy Systems*, vol. 15, no. 5, pp. 890-903, 2007.
[16] A. P. Dempster, N.M. Laird, and D.B. Rubin, "Maximum likelihood from incomplete data via the EM algorithm," *J. of the Royal Statistical Society*, Series B, vol. 39, pp. 1–38, 1977.
[17] C.-H. Oh, K. Honda and H. Ichihashi, "Fuzzy clustering for categorical multivariate data," *Proc. of Joint 9th IFSA World Congress and 20th NAFIPS International Conference*, pp. 2154-2159, 2001.
[18] K. Kummamuru, A. Dhawale and R. Krishnapuram, "Fuzzy co-clustering of documents and keywords," *Proc. of 12th IEEE international conference on fuzzy systems*, pp. 772-777, 2003.
[19] R. J. Hathaway, J. W. Davenport and J. C. Bezdek, "Relational duals of the *c*-means clustering algorithms," *Pattern Recognition*, vol. 22, no. 2, pp. 205-212, 1989.
[20] Z. Yang and E. Oja, "Linear and nonlinear projective nonnegative matrix factorization," *IEEE Transactions on Neural Networks*, vol.21, no.5, pp.734-749, 2010.
[21] Z. Yang and J. Laaksonen, "Multiplicative updates for nonnegative projections," *Neurocomputing*, vol.71, no.13, pp.363-373, 2007.
[22] J. A. Swets, "Measuring the accuracy of diagnostic systems," *Science*, vol.240, no.4857, pp.1285-1289, 1988.

2011 IEEE International Conference on Fuzzy Systems
June 27-30, 2011, Taipei, Taiwan

DEA based Hierarchical Structure Evaluation and Visualization Method

Kazushige Inoue
Department of Computer Science and Intelligent Systems
Osaka Prefecture University
Osaka, Japan
inoue@mis.fcs.osakafu-u.ac.jp

Takeo Ichinotsubo
Department of Computer Science and Intelligent Systems
Osaka Prefecture University
Osaka, Japan
ichinotsubo@mis.cs.osakafu-u.ac.jp

Shingo Aoki
Department of Computer Science and Intelligent Systems
Osaka Prefecture University
Osaka, Japan
aoki@cs.osakafu-u.ac.jp

Abstract— **Data Envelopment Analysis (DEA) is a method for evaluating the management efficiency of Decision Making Units (DMUs) relatively. However, when the number of inputs and outputs items is increased, the results of evaluation value are similar regretfully. In order to evaluate Japanese universities which have various activities, this study proposed the hierarchical structure DEA model which is divided into some activities (finance, achievement, attractiveness, research, and education). Hierarchical structure has constructed by some layers based on the theory that the efficiencies of lower layer can not exceed the ones of upper layer. In addition, this paper proposed the visualization method that the analyst can visually understand which field is strong or weak. Using proposed DEA model and visualizing method, the numerical study showed us to be able to understand the feature of each university.**

Keywords-Decision Support System; Data Envelopment Analysis; Vissualizaiion Method;

I. INTRODUCTION

Data Envelopment Analysis (DEA) is a nonparametric method for evaluating relative efficiency of Decision Making Unit (DMU) [1]. DEA assumes DMU's activity that multiple inputs to yield multiple outputs, and estimates this converting process as one evaluation value, so called "efficiency score". DEA has been applied to a variety of managerial and economic problem situations in both public and private sectors [2, 3, 4, 5, 6].

However, there are some problems in applying DEA to data set that consists of a lot of activities such as university [7]. In order to express a lot of activities, it is necessary to prepare a lot of inputs and outputs data. A use of larger data set causes following DEA problems: (1) evaluation does not make sense because the values of efficiency scores for each DMU may be similar, (2) understanding the strong points or weak points of DMU are difficult for analyst because complex relations among a lot of inputs and outputs data is expressed by tablet type result.

To deal with upper DEA problem, DEA analyst uses tacit knowledge that the number of DMUs should be satisfied with restriction of n > max {m*s, 3*(m+s)}. Where, n indicates the number of DMUs, and m, s indicate the number of inputs and outputs [2]. Therefore, if analyst can not collect an enough number of DMUs (n), analyst should decrease the number of inputs and outputs data (m, n). A difficult problem of extracting effective data set for a larger data set still remains.

To deal with lower DEA problem, traditional studies make an attempt to develop the visualization method [8, 9, 10]. These techniques help to understand the shape of efficiency frontier which is used as evaluation criteria. Using these methods, analyst can visually capture the existence of his competitors. However, these methods can not support to know the reason why specific DMU is his competitor.

In order to overcome above two DEA problems, this paper proposes the hierarchical structure DEA model which is divided into some activities and proposes the visualization method that analyst can understand which field is strong or weak.

II. DATA ENVELOPMENT ANALYSIS

A. Overview

DEA is a nonparametric method for identifying efficient production frontiers and evaluating the relative efficiency of DMUs, each of which is a company responsible for converting multiple inputs into multiple outputs. DEA assumes DMUs activity that uses multiple inputs to yield multiple outputs, and defines the process which changes multiple inputs into multiple outputs as efficiency. By comparison with Pareto optimal solution so called "efficient frontier", performance of DMUs is measured relatively.

B. Evaluation Value

In order to describe the mathematical structure of the evaluation value, this paper assumes that there are n DMUs ($DMU_1, DMU_2, \cdots, DMU_k, \cdots, DMU_n$), where each DMU is characterized by m inputs ($x_{1k}, x_{2k}, \cdots, x_{ik}, \cdots x_{mk}$) and s outputs ($y_{1k}, y_{2k}, \cdots, y_{rk}, y_{sk}$). Evaluation value of DMU_k is mathematically formulated by

$$\text{Evaluation value of DMU}_k = \frac{u_1 y_{1k} + u_2 y_{2k} + \cdots + u_s y_{sk}}{v_1 x_{1k} + v_2 x_{2k} + \cdots + v_m x_{mk}} \qquad (1)$$

Here u_r is multiplier weight given to the r^{th} output, and v_i is multiplier weight given to the i^{th} input. In DEA, the optimal weights may vary from on DMU to another DMU. Each DMU is assigned a best set of weights with values. There are some calculation algorisms [2, 11] of input/output weights in formula (1). This paper uses the BCC model which is one of basic model. The optimal weights u_r and v_i are measured by following linear programming:

$$\begin{aligned} \text{Maximize} \quad & \sum_{r=1}^{s} u_r y_{rk} + \delta \\ \text{subject to} \quad & -\sum_{i=1}^{m} v_i x_{ij} + \sum_{r=1}^{s} u_r y_{rj} + \delta \le 0 \\ & (j = 1,2,\ldots,n) \qquad (2) \\ & \sum_{i=1}^{m} v_i x_{ik} = 1 \\ & v_i \ge 0, u_r \ge 0, \delta : \text{free} \end{aligned}$$

Here, first restriction represents the condition that the productivity of all DMU becomes 100% or less. And the objective function represents the maximization of the virtual outputs of DMU_k, setting that the virtual inputs of DMU_k is equal to one which represented second restriction. Therefore, the optimal weights represent the convenient weight for DMU_k. Using these optimal weights, the evaluation value of DMU_k is called "efficiency score" in the manner that $\theta_k = 1 (100\%)$ means the state of efficiency, while $\theta_k < 1$ means the state of inefficiency.

III. PROPOSED METHOD

A. Overview

This paper proposes the hierarchical structure DEA model and visualization method in order to overcome following two problem: (1) there are similar evaluation values among competitors due to a use of larger data set, (2) understanding the strong points or weak points of DMU are difficult.

B. Hierarchical structure DEA model

Hierarchical structure DEA model makes layered structure based on evaluation perspective and assigns input and output elements to each node that is perspective. Then input and output of upper layer include those of lower layer. It is possible to evaluate based on each perspective by calculating efficiency value of each node.

There are n evaluated DMUs. And they have m input elements and s output elements. Here input elements are $X = (X_1, \ldots, X_m)$ and expressed as $X_i = (x_{i1}, \ldots, x_{in})$. So X_i indicates i input group of all DMUs. Equally, $Y = (Y_1, \ldots, Y_s)$, $Y_r = (y_{r1}, \ldots, y_{rn})$ are defined. The efficiency value of DMU_k shown as θ_K is calculated by formula (2). Moreover, efficiency value is calculated based on possible production set S formed by input and output.

Next it is necessary to consider the case that specific input and output are utilized for analysis. New input and output groups are selected and they are denoted as $X' = \{X' \in X, X' \neq \phi\}$, $Y' = \{Y' \in Y, Y' \neq \phi\}$. Then the efficiency value of DMU_k shown as θ'_K based on this data set (X', Y') is calculated by formula (2). It means this efficiency value is calculated based on possible production set S'. Thus $S' \in S$ is satisfied and two different efficiency values θ_K, θ'_K are followed inequality $\theta_K \ge \theta'_K$. The efficiency value of selected data is less than that of original data.

The proposed method hierarchizes by resolving the evaluation perspective and assigns input and output elements to each node. In this time, input and output of upper layer have to include those of lower layer. Then analysis is carried out in each node. Thanks to the proposition in previous section, the efficiency value of lower layer never exceeds that of upper layer. Therefore, it is possible to treat the efficiency value of each node evenly since efficiency signifies the state of each DMU by unified way. Thus inefficient DMU as a whole never be the state of efficient in some node. And the reason for decline about efficiency is revealed. For example, which parts of node affect to the efficiency badly or how degree the specific DMU influences the efficiency. It is possible to analyze these kinds of knowledge from all perspective analyst prepares.

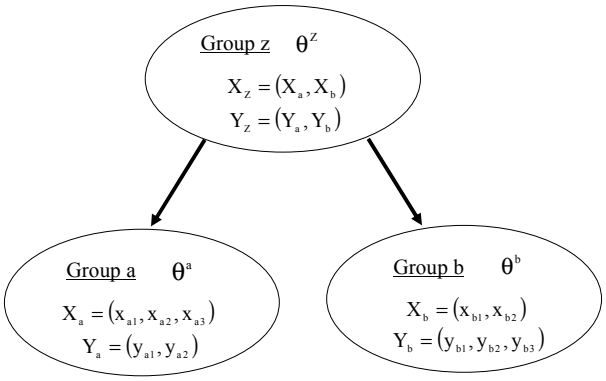

Figure 1. The example of hierarchical structure

Fig 1 shows the example of hierarchical structure. There are two layers (Group z and Group a plus Group b). Group z is divined into two another group (Group a, Group b). Lower nodes use a part of input and output elements in upper layer (Group z). So, proposed structure utilizes the DEA sensitivity analysis technique [2]. Therefore, the efficiency value of the lower nodes (θ^a, θ^b) cannot be exceed the one's of upper node (θ^z).

Using this mathematical character, this paper overcomes first problem that there are similar evaluation values among

competitors due to a use of larger data set. So, this example assumed that Group z has a larger data set. If there is no difference of the efficiency value θ^z among competitors, the analyst can make a search for own character by digging down the layer.

C. Visualizaiton Method

This paper proposed the visualization method in order to overcome the problem that understanding the strong points or weak points of DMU is difficult.

This study puts the each node in 2D map. Coordinate is sets the efficiency value of each node to vertical axis, and sets the difference with average of each efficiency value to horizon axis.

Fig 2 shows the example of visualization. The node of Group z is set at high-middle position. This means that a similar evaluation among the competitors occurs because Group z has a larger data set. So, this evaluation criterion in Group z does not make a sense. However, second layer shows the difference with Group z. The node of Group a is set at high-right position. This mean that DMU has the strong points in the evaluation criterion Group a because a high efficiency value is maintained compared with competitors. Oppositely, the node of Group b is set at low-left position and analyst can understand the weak point in the evaluation criteria Group b.

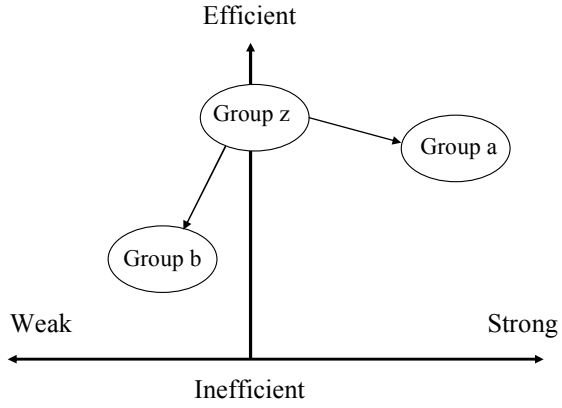

Figure 2. Example of visualization method

IV. NUMERICAL STUDY

A. Data Set

This paper carried out the numerical study using data of Japanese thirty-one universities [7]. There are following six input and eight output data:

Input:

x_1 : number of faculty,

x_2 : number of worker,

x_3 : education and research expense,

x_4 : grant-in aid for management,

x_5 : general and administrative expenses,

x_6 : profit of donation,

Output:

y_1 : maximum T-score,

y_2 : number of paper,

y_3 : number of graduate student,

y_4 : number of undergraduate student,

y_5 : number of books,

y_6 : grant-in-aid for scientific research,

y_7 : contract research funds,

y_8 : profit of business.

B. Hierarchical Structure

These data set is not satisfied the following tacit knowledge that the number of DMUs should be satisfied with restriction of $n > \max\{m*s, 3*(m+s)\}$. Where, n indicates the number of DMUs, and m, s indicate the number of inputs and outputs.

Then, this paper divided this data set into three layers which has eight nodes (University, Management, Research and Education, Finance, Achievement, Attractiveness, Research, and Education). Each layer and node has following input and output data.

<Third layer>

"Finance" uses three input and one output data (x_4, x_5, x_6, y_8). This efficiency value signifies how much university can get profit with possible funds that are input.

"Achievement" uses four input and one output data $(x_2, x_4, x_5, x_6, y_1)$. This efficiency value signifies how high university has T-score with possible funds and human resources.

"Attractiveness" uses four input and two output data $(x_2, x_4, x_5, x_6, y_3, y_4)$. This efficiency value signifies how many university gather students with possible funds and human resources.

"Research" uses two input and two output data (x_1, x_3, y_3, y_4). This efficiency value signifies how many university get external funds or accomplishments of research.

"Education" uses two input and three output data $(x_1, x_3, y_2, y_6, y_7)$. This efficiency value signifies how much university invests funds and human resources to education for students.

<Second layer>

"Management" is combined by three lower nodes "Finance", "Achievement", and "Attractiveness". Therefore, this node uses four input and four output data $(x_2, x_4, x_5, x_6, y_1, y_3, y_4, y_8)$.

"Research and Education" is combined by two lower nodes "Research" and "Education". This node uses two input and five output data $(x_1, x_3, y_2, y_3, y_4, y_6, y_7)$.

<First layer>

"University" uses all input and output data ($x_1 \sim x_6, y_1 \sim y_8$). This node estimates the total efficiency of university.

C. *Result of Hierarchical Sturcture*

Figure 3 shows the result of hierarchical structure in one university. Score in box shows the each efficiency values. And the box also includes the following information: Range, Average, and Variance.

In the node "University", we confirm that the high efficiency value "Score" is caused by a large data set. So, we can not estimate the character of DMU with only this node. However, we can make a search for DMU's character by dipping down the layer. This DMU has a strong point in the evaluation criteria "Management", "Achievement", and "Attractiveness". This means that proposed hierarchical structure overcome the following problem: (1) there are similar evaluation values among competitors due to a use of larger data set, (2) understanding the strong points or weak points of DMU are difficult.

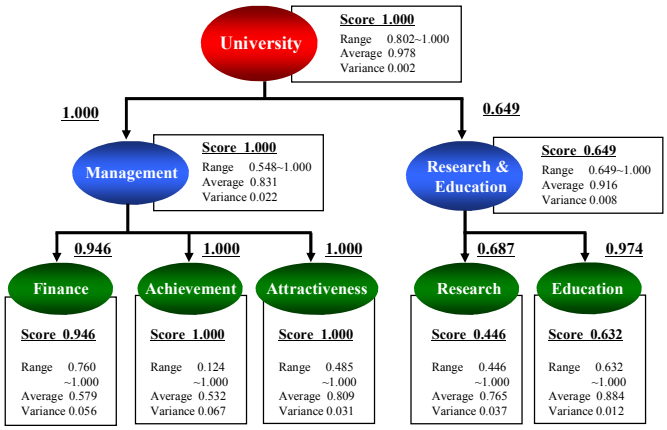

Figure 3. The result of hierarchical structure

D. *Visualizaiton Method*

Figure 4 shows the result of the visualization method in one university (University A). This figure has same volume of information as Figure 3. This method can intuitively understand the feature of DMU by seeing whether to be located right or left without seeing the numerical data of the score and average.

V. CONCLUSION

In order to evaluate Japanese universities which have various activities, this study proposed the hierarchical structure DEA model which is divided into some activities. Hierarchical structure has constructed by some layers based on the theory that the efficiencies of lower layer can not exceed the ones of upper layer. In addition, this paper proposed the visualization method that the analyst can visually understand which field is strong or weak. Using proposed DEA model and visualizing method, the numerical study showed us to be able to understand the feature of university.

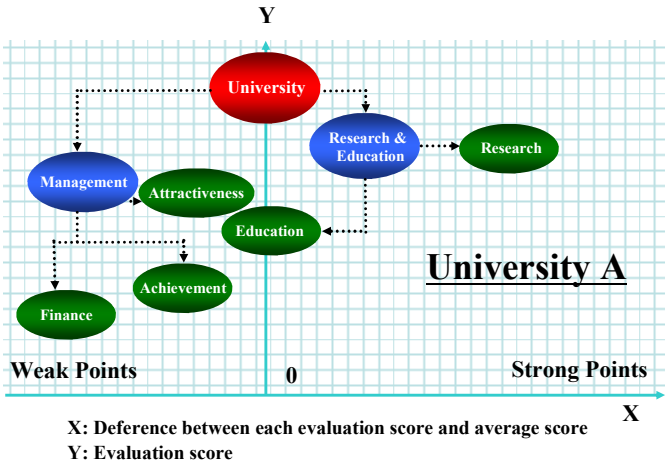

Figure 4. The result of visualization method

REFERENCES

[1] A.Charnes, W.W.Cooper and E.Rhodes, "Measuring the efficiency of decision making units", European Journal of Operational Research, Vol.2, pp429-444 (1978)

[2] W.W.Cooper, L.M.Seiford and K.Tone, "Data Envelopment Analysis: A comprehensive text with models, applications, references and DEA-Solver software", Kluwer Academic Publishers (2000)

[3] S. Aoki, K. Mishima and H. Tsuji, "Two-Staged DEA model with Malmquist Index for Brand Value Estimation", The 8th World Multiconference on Systemics, Cybernetics and Informatics, Vol. 10, pp.1-6 (2004)

[4] E. W. N. Bernroider and V. Stix , "The Evaluation of ERP Systems Using Data Envelopment Analysis", Information Technology and Organizations, Idea Group Pub, USA, pp.283-286 (2003)

[5] Y. Zhou and Y. Chen, "DEA-based Performance Predictive Design of Complex Dynamic System Business Process Improvement", Proceeding of Systems, Man and Cybernetics, IEEE International Conference, pp.3008-3013 (2003)

[6] T. Sueyoshi, K. Onishi and Y. Kinase, "A Bench Mark Approach for Baseball Evaluation", European Journal of Operational Research, Vol. 115, pp.429-438 (1999)

[7] S. Aoki, K. Inoue and R. Gejima, "Data Envelopment Analysis for Evaluating Japanese Universities", Journal of Artificial Life and Robotics, Vol. 15, No. 2, pp.165-170 (2010)

[8] K. Honda, A. Notsu, H. Ichihashi, "PCA-guided k-Means with Variable Weighting and Its Application to Document Clustering," Modeling Decisions for Artificial Intelligence (MDAI) 2009, Lecture Notes in Artificial Intelligence 5861, Springer, pp.282-292 (2009)

[9] S. Aoki, K. Toyozumi, and H. Tsuji, "Visualizing Method for Data Envelopment Analysis," Proc. of 2007 IEEE International Conference on Systems, Man and Cybernetics, pp. 474-479 (2007)

[10] K. Honda, H. Ichihashi, F. Masulli, S. Rovetta, "Linear Fuzzy Clustering With Selection of Variables Using Graded Possibilistic Approach," IEEE Transactions on Fuzzy Systems, Vol. 15, No. 5, pp.878-889 (2007)

[11] H. Nakayama, M. Arakawa, Y. B. Yun, "Data Envelopment Analysis in Multicriteria Decision Making",M. Ehrgott and X. Gandibleux (eds.) Multiple Criteria Optimization: State of the Art Annotated Bibliographic Surveys, Kluwer Acadmic Publishiers (2007)

2011 IEEE International Conference on Fuzzy Systems
June 27-30, 2011, Taipei, Taiwan

Group Decision Focusing on Outliers

Tomoe Entani
Department of Economics and Social Sciences
Kochi University
2-5-1 Akebono Kochi 780-8520
Email: entani@kochi-u.ac.jp

***Abstract*—This paper investigates a group decision problem focusing on outliers in a group. The group decision in this paper is considered as approximation of all individual opinions, which are given normalized crisp or interval values. The difference of an individual opinion from the group opinion represents his/her compromise in order to reach a consensus so that it should be minimized. The first step is to detect outliers in a group and assign outlier degree to individual. The outlier degree is distance of an individual from the group of others and defined as the reduction of compromise by excluding him/her from the group. The outlier degree of a unique individual is more than those of other general individuals. Similarly to outlier degree, inlier degree is closeness of others to an individual and defined as the compromise of the group without him/her. The second step is to approximate individual opinions so as to be a group opinion. The weighted sum of compromises of all individuals is minimized introducing the outlier degrees as the weights of individuals. In this model, outliers are considered positively into account for a group opinion. Therefore, based on compromises of individuals, the models to define outlier degree and to obtain group opinion by approximating individual opinions are proposed in this paper.**

***Index Terms*—Group decision making, Outlier, Compromise**

I. Introduction

A group decision is often believed to be better than individual decision simply because of cumulating all members' knowledge, being able to check errors carefully and so on. Although it is mentioned that a group performs better than "average" individual but worse than "best" individual [1], the developed techniques of integrating and combining individual judgments are effective in part. Aside from the issues on managements of decision makers and their characters, the technique in group decision making can be applied not only when decision makers give their judgments but when various evaluations from different viewpoints, such as time series, are given. One of the advantages of group decision making over individual one is that it facilitates creativity and develops new ideas by inspiring each other [1]. It often happens that when the discussion is stable and static, a unique opinion stimulate it and it becomes active again. Individuals may realize that relatively extreme individual holds opinion closer to the group's most admired position and this comparison may act to move moderate individuals toward a more extreme position [2]. In this sense, a unique opinion might be worth being paid attention. In case of the group consisting of various stakeholders, powerful or major opinion sometimes breaks down the other small or minor opinions, even if they are important. Such a situation as depending on majority too much might be controlled by including unique opinion positively in the decision. In this way, outlier helps to induce a fresh and fair decision. This paper emphasizes group opinions in which a unique opinion is positively reflected. While, for instance, the decision problem to determine next year's plan from past years' results, it is reasonable to consider an average and general year more than unique years. In the case where it is not necessary to pay attention to a unique individual and/or generality is important, inlier degree is considered, instead of outlier degree.

The situation that a group reaches a consensus is explained in various ways; such that all individuals are unanimous for the decision, they agree to support or practice the decision, or the decision meets their interests [3]. It is also assumed that the compromises of all individuals are limited to be as less as possible [4], [5]. So, the group opinion in this study is obtained, in other words, by approximating individual opinions so as to minimize the errors of estimated value from the observed value. The concept is similar to regression analysis, except that it assumes a linear or other regression model beforehand.

This paper consists as follows. In Section II, when individual opinions are given as crisp or interval, individual compromise in order to reach a consensus is measured as difference between individual and group evaluations. In Section III, from the viewpoint of compromises, outlier degree representing distance of an individual from the group of others is defined, and inlier degree as well. Then, in Section IV, the model to obtain a group opinion as the approximation of individual opinions is shown. The compromises of all individuals are weighted by their outlier degrees and minimized so as to reach a consensus. Finally, in Section V, the proposed compromise-weighted model is tested with two numerical examples on budget.

II. Compromises of individuals

At first, both the individual and group opinions are assumed as crisp evaluations of alternatives as in Table I. Individual i gives his/her opinion as evaluation of alternative j, w_{ij}, and for all alternatives they are normalized as $\sum_j w_{ij} = 1$. A group opinion in this problem setting is an approximation of individual opinions so that they are normalized as:

$$\sum_j w_j = 1.$$

The group opinion w_j can be smaller or greater than the

978-1-4244-7316-8/11/$26.00 ©2011 IEEE

TABLE I
GIVEN INDIVIDUAL EVALUATIONS AND OBTAINED GROUP EVALUATIONS

Individual	Alternative 1	$\cdots$	j	$\cdots$	n	Sum
1	w_{11}	$\cdots$	w_{1j}	$\cdots$	w_{1n}	1
$\vdots$	$\vdots$	$\ddots$	$\vdots$	$\ddots$	$\vdots$	$\vdots$
i	w_{i1}	$\cdots$	w_{ij}	$\cdots$	w_{in}	1
$\vdots$	$\vdots$	$\ddots$	$\vdots$	$\ddots$	$\vdots$	$\vdots$
m	w_{m1}	$\cdots$	w_{mj}	$\cdots$	w_{mn}	1
Group	w_1	$\cdots$	w_j	$\cdots$	w_n	1

corresponding individual opinion w_{ij};

$$\begin{array}{rlll} & w_j \leq w_{ij} & \text{or} & w_j > w_{ij} \\ \Leftrightarrow & w_j = w_{ij} - \underline{d}_{ij} & \text{or} & w_j = w_{ij} + \overline{d}_{ij}. \end{array}$$

The positive and negative deviations from a group opinion, $\overline{d}_{ij}$ and $\underline{d}_{ij}$, represent compromise of individual i in order to reach a consensus on alternative j. In other words, his/her compromised opinion is denoted as interval $[w_{ij} - \underline{d}_{ij}, w_{ij} + \overline{d}_{ij}]$ and should include the obtained group opinion as;

$$w_{ij} - \underline{d}_{ij} \leq w_j \leq w_{ij} + \overline{d}_{ij}.$$

In interval regression analysis, errors between observed values and estimated intervals by the regression model are minimized [6] and their relations are also considered in [7]. Here, no regression models are assumed so that the simple sum of errors between all the given individual opinions and the obtained group opinions should be minimized as:

$$\min \textstyle\sum_i (\overline{d}_{ij} + \underline{d}_{ij}),$$

which is, in other words, the compromise of all individuals to reach the group decision.

Following these conditions, total compromise of the group is obtained as follows:

$$\begin{array}{rl} c = & \min \sum_{i,j} (\overline{d}_{ij} + \underline{d}_{ij}), \\ \text{s.t.} & w_{ij} - \underline{d}_{ij} \leq w_j \ \forall i, j, \\ & w_j \leq w_{ij} + \overline{d}_{ij} \ \forall i, j, \\ & \sum_j w_j = 1 \ \forall j, \\ & w_j, \underline{d}_{ij}, \overline{d}_{ij} \geq 0 \ \forall i, j, \end{array} \tag{1}$$

where the variables are group evaluations, w_j, and positive and negative compromises, $\overline{d}_{ij}$ and $\underline{d}_{ij}$. It is apparent that positive and/or negative compromise is 0, since both group and individual evaluations, $w_{ij}$and w_j, in the first two constraints are crisp. By approximating observed values; individual evaluations, so as to minimize errors of estimated values, group evaluations; total compromise of the group is obtained as sum of errors.

Next, both the individual and group opinions are extended into interval evaluations of alternatives as $W_{ij} = [\underline{w}_{ij}, \overline{w}_{ij}]$ and $W_j = [\underline{w}_j, \overline{w}_j]$, respectively. In order to normalize intervals, definition of interval probability, originally proposed in [8] and also used in [9], [10], is used.

Definition of Interval Probability The set of intervals denoted as $\{W_1, ..., W_n\}$ where $W_i = [\underline{w}_i, \overline{w}_i]$ are called interval probabilities if and only if

$$\begin{array}{ll} 1) & 0 \leq \underline{w}_i \leq \overline{w}_i, \ \forall i, \\ 2) & \sum_{i \neq j} \overline{w}_i + \underline{w}_j \geq 1, \ \forall j, \\ 3) & \sum_{i \neq j} \underline{w}_i + \overline{w}_j \leq 1, \ \forall j. \end{array} \tag{2}$$

From (2), the following two inequalities hold:

$$\textstyle\sum_i \underline{w}_i \leq 1 \text{ and } \sum_i \overline{w}_i \geq 1.$$

Then, (2) is regarded as the normality condition of intervals corresponding to the conventional one; $\sum_i w_i = 1$. It is noted that in interval probabilities there are many combinations of crisp values whose sum is one. The conventional probabilities, such as $\underline{w}_i = \overline{w}_i = w_i \geq 0 \ \forall i$, also satisfy the requirements in (2) as follows: 1) is apparent and 2) and 3) are verified as

$$\textstyle\sum_{i \neq j} w_i + w_j = \sum_i w_i = 1.$$

Therefore, the interval probability is an extension of the conventional probability.

As an extension of crisp evaluation, the compromised opinion with interval evaluation is denoted as interval $[\underline{w}_{ij} - \underline{d}_{ij}, \overline{w}_{ij} + \overline{d}_{ij}]$ which should include group opinion as:

$$\underline{w}_{ij} - \underline{d}_{ij} \leq \underline{w}_j \ \text{ and } \overline{w}_j \leq \overline{w}_{ij} + \overline{d}_{ij}.$$

Similarly to (1) with crisp evaluations, the total compromise is obtained as the optimal objective function value of the following problem:

$$\begin{array}{rl} c = & \min \sum_{i,j} (\overline{d}_{ij} + \underline{d}_{ij}), \\ \text{s.t.} & \underline{w}_{ij} - \underline{d}_{ij} \leq \underline{w}_j \ \forall i, j, \\ & \overline{w}_j \leq \overline{w}_{ij} + \overline{d}_{ij} \ \forall i, j, \\ & \sum_{j \neq k} \overline{w}_j + \underline{w}_k \geq 1 \ \forall k, \\ & \sum_{j \neq k} \underline{w}_j + \overline{w}_k \leq 1 \ \forall k, \\ & \underline{d}_{ij}, \overline{d}_{ij} \geq 0 \ \forall i, j, \\ & 0 \leq \underline{w}_j \leq \overline{w}_j \ \forall j. \end{array} \tag{3}$$

Focusing on the first two constraints, when the following relation is satisfied, i.e.,:

$$\max_i \underline{w}_{ij} < \min_i \overline{w}_{ij}, \tag{4}$$

the solutions of (3), $\underline{w}_j$ and $\overline{w}_j$, may be interval included in interval $[\max_i \underline{w}_{ij}, \min_i \overline{w}_{ij}]$ and the positive and negative compromises are 0; $\underline{d}_{ij} = \overline{d}_{ij} = 0 \ \forall i$. However, since interval evaluation reflects fluctuations of judgments on alternatives, relation (4), where the upper bound of interval evaluation given by any individual should be more than the lower bound given by anyone, is strict. It often happens that relation (4) is not satisfied, i.e.,:

$$\max_i \underline{w}_{ij} \geq \min_i \overline{w}_{ij}.$$

In such a case, solutions of (3) are $\underline{w}_j = \overline{w}_j$ so as to satisfy the first two constraints and minimize the sum of positive and negative compromises. Then, when even individual opinions are given as interval evaluations, the group evaluations are

often obtained as crisp, much less when they are given as crisp. In case of crisp individual evaluations, the interval group evaluations are never obtained because two constraints contradict to be interval as follows.

$$\begin{cases} \underline{w}_j = \max_i w_{ij} \\ \overline{w}_j = \min_i w_{ij} \end{cases} \not\Rightarrow \quad \underline{w}_j \le \overline{w}_j.$$

Only in case that the given individual evaluations are similar enough to satisfy relation (4), the group evaluation is obtained as interval. In other cases, by assuming group evaluation as crisp, it is also rewritten as (1).

III. Detection of outliers based on compromises

The first step of this paper is to detect outliers in a group and determine their outlier degrees based on individual compromises. The outlier degree represents distance of an individual from the group of others and is measured as the difference between the compromises of groups with and without the individual. Therefore, the outlier degree of a unique individual is more than those of other general individuals. In this section, we assumed that crisp individual evaluations are given so that group opinions are also obtained as crisp. The total compromise of the group without individual k, is obtained as the optimal objective function value by the following problem based on (1).

$$\begin{array}{rl} c_k = & \min \sum_{i \neq k, j} (\overline{d}_{ij} + \underline{d}_{ij}), \\ \text{s.t.} & w_{ij} - \underline{d}_{ij} \le w_j \ \forall i \neq k, j, \\ & w_j \le w_{ij} + \overline{d}_{ij} \ \forall i \neq k, j, \\ & \sum_j w_j = 1, \\ & w_j, \underline{d}_{ij}, \overline{d}_{ij} \ge 0 \ \forall i \neq k, j, \end{array} \tag{5}$$

where the optimal solutions satisfying the optimal objective function value are not unique because of LP problem, but they are not used in the following. For interval group evaluations, constraints are transformed as in (3).

The optimal objective function value c_k, which is smaller than that of (1), denotes the compromise remained in the group by excluding individual k. It is explained from two viewpoints and illustrated conceptually in Fig. 1, where large and small circles denote total compromises without and with individual k, respectively. From the viewpoints of individuals except k, compromise increases more from c_k to c as k is farther from them. While, from the viewpoint of individual k, compromises decreases more from c to c_k as other individuals are closer to him/her. The former viewpoint leads to outlier degree and the latter one leads to inlier degree, respectively.

As for outlier degree, the distance of individual k from the group of others is measured as reduction of total compromise by excluding him/her; $c - c_k$. Based on such a difference of total compromises with and without an individual in the group, outlier degree is defined as follows:

$$p_k = \frac{c - c_k}{\sum_i (c - c_i)} \ \forall k, \tag{6}$$

where distances for all individuals are normalized so are individual and group evaluations. The outlier degree of a unique individual is more than those of general ones.

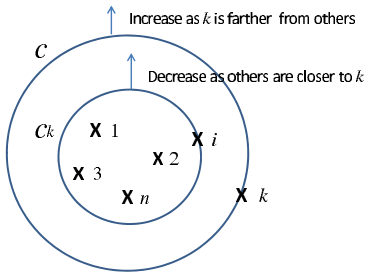

Fig. 1. Total compromises with and without an individual

Similarly to outlier degree, inlier degree is measured as the closeness of other individuals to individual k, which is the total compromise without k. Based on such a remained compromise by normalizing for all individuals, inlier degree is defined as follows.

$$q_k = \frac{c_k}{\sum_i c_i} \ \forall k, \tag{7}$$

where a general individual has more inner degree than unique ones do.

IV. Group opinions considering outlier degrees

The second step of this paper is to approximate individual opinions so as to be a group opinion. Group decision making is discussed in many literatures. For instance, in the well-known method, AHP (Analytic Hierarchy Process), by adding a decision makers' hierarchy to the top of the problem structure, the priority weights of alternatives are summed up reflecting the decision makers' weights obtained at the hierarchy [11], [12], [13]. Such a weighted summation technique is useful to take all decision makers' judgments into account. In order to determine the decision makers' weights, the corresponding pairwise comparison matrix should be given in AHP or they might be given directly. Here, the proposed outlier degree by (6) are introduced as the weight of an individual in the group so that no one needs to give the corresponding judgments. Then, the group evaluation is obtained as:

$$w_j = \sum_i p_i w_{ij} \ \forall j, \tag{8}$$

where the weights of individuals are directly multiplied to their evaluations.

It is also practical to measure fairness of consensus by individual compromises. From individual viewpoint, his/her difference from a group decision is one of concerns since it is recognized just by comparing two values. Considering such a difference, in other words, an individual compromise, the other model to obtain group opinion is formulated as follows:

$$\begin{array}{rl} & \min \sum_{i,j} p_i (\overline{d}_{ij} + \underline{d}_{ij}), \\ \text{s.t.} & \text{constraints in (1)}, \end{array} \tag{9}$$

where the objective function in (1) is transformed into outlier degree based weighted compromises so that (9) is called compromise-weighted model. In the sense of focusing on

TABLE II
RATIONS OF SIX EXPENSES OF FIVE TOWNS IN 2004, THEIR GROUP DECISION, AND THE MERGED CITY IN 2005

Year	Town	Budget size billion	Ratio Expense 1	Expense 2	Expense 3	Expense 4	Expense 5	Expense 6
2004	A	2.4	0.232	0.267	0.046	0.253	0.092	0.109
2004	B	2.6	0.297	0.245	0.049	0.132	0.135	0.142
2004	C	4.8	0.237	0.203	0.083	0.222	0.129	0.126
2004	D	1.9	0.294	0.242	0.052	0.097	0.169	0.145
2004	E	1.7	0.236	0.438	0.042	0.100	0.097	0.087
	Group decision by (9)		0.237	0.267	0.049	0.192	0.129	0.126
	Group decision by (8)		0.254	0.298	0.053	0.160	0.120	0.116
2005	City	15.2	0.244	0.219	0.064	0.254	0.128	0.090

the difference between given individual and obtained group evaluations, individuals in a group can easily understand the procedure and accept the results. This model is based on the idea that outliers are taken positively into account for a group opinion.

Since outlier degree represents the distance of an individual from the group, the unique opinion is reflected in group opinion positively in (8) and (9). While, such a decision problem that unique opinion is not welcomed to the group one, inlier degrees are introduced as weights of individuals. The models are formulated by replacing outlier degrees p_i in (8) and (9) into inlier degrees q_i.

V. NUMERICAL EXAMPLES

From the viewpoint of a group decision making, two examples on planning budgets of local governments are tested. One is the case of new city consisting of several towns and its budget is estimated from the member towns' results [14]. In order not to neglect smaller or unique town's status, outlier degrees are used. The other is the case of prefecture running stable for recent years and its budget is estimated from its past years' results [15]. In order not to be affected by transient situation, inlier degrees are used. Although all the given ratios are crisp in both examples, in case of interval ratios, the similar procedure can be applied.

A. Group decision with outlier degrees

Table II shows ratios on six expenses, such as 1-personnel 2-public loan, 3-aid, 4-investment, 5-nonpersonnel and 6-subsidy, of five small towns in 2004 and their budget sizes. They were merged into a city in 2005 so that at that time the new city is forced to plan new budget referring to the results of five towns in 2004. This decision problem is used in this section. As show in Table II, the size of Town E is almost one third of the largest one, Town C, and Expense 2 of Town E is apparently different from other towns. Though, since small towns often have some difficulties to adapt a new situation, the status of Town E is also or more carefully considered. First, by (5) total compromise without each town is obtained and by (6) the outlier degrees are obtained as shown in Table III. The smallest budget Town E has the greatest outlier degree. Then, introducing outlier degrees as weights of towns, the approximations of five towns' ratios as a group decision are obtained by compromise-weighted model (9) and shown at the third bottom line of Table II. The obtained ratios equal to the medians of the corresponding five given ratios, except expense 4, whose obtained ratio is around the median so as to normalize for all expenses. To comparison, those by (8), where given ratio is weighted directly, and the results of the city in 2005 are shown at the bottom two lines of Table II. The budget size was enlarged by merging but the ratios by (9) are more similar to the real ratios than those by (8). The compromise, which is the difference of each town's ratio from the group ratio by both models are shown in Table III. The total compromise of Town E, which might be an outlier so that its weight is the largest among five towns, by (8) is restrained to be 0.281, less than 0.342 by (9). In details, Town E compromises on six expenses by (8) as 0.281=0.017+0.140+0.011+0.060+0.023+0.030 and by (9) as 0.342=0.000+0.171+0.008+0.092+0.032+0.039. As for Expense 2, on which Town E is different from other towns, its compromise by (8) is less than that by (9). These facts might refer that when individual towns' ratios are weighted directly as in (8), group ratio might be overfitted to Town E. By weighting individual towns' compromises as in (9), the compromise of Town E is fairly and properly reflected in the obtained group ratio.

TABLE III
OUTLIER DEGREES AND COMPROMISES OF TOWNS

Town	Outlier degree	Compromise By (8)		By (9)
A	0.217	0.187	$>$	0.123
B	0.124	0.169	$>$	0.165
C	0.187	0.223	$>$	0.128
D	0.180	0.238	$<$	0.239
E	0.292	0.281	$<$	0.342
Sum of compromises		1.098	$>$	0.996

B. Group decision with inlier degrees

Table IV shows ratios of four cost divisions, such as 1-personnel related cost 2-nonpersonnel related cost, 3-investment related cost, 4-other cost of the prefecture from 2004 to 2008 and their budget sizes. The decision problem for the prefecture is to plan its next fiscal year's budget referring to its past five years' results. As shown in Table IV, the differences of ratios between years are smaller comparing to Table II. It may not be necessary to pay attention to a unique year because of similar results; moreover, it may not be reasonable to be affected by transient year. Therefore, inlier

TABLE IV
RATIOS OF FOUR COST DIVISIONS FOR FIVE YEARS AND THEIR GROUP APPROXIMATION

Year	Budget size billion	Ratio Division 1	Division 2	Division 3	Division 4	Sum of deviations
2008	372	0.382	0.289	0.272	0.057	
2007	354	0.379	0.278	0.287	0.056	
2006	388	0.361	0.304	0.271	0.064	
2005	376	0.370	0.264	0.275	0.091	
2004	413	0.345	0.298	0.288	0.070	
Group approximation by (9)		0.372	0.289	0.275	0.064	0.029
Group approximation by (8)		0.368	0.287	0.278	0.067	0.031
2009	352	0.374	0.281	0.287	0.057	

TABLE V
INLIER DEGREES AND DIFFERENCES FROM PAST RESULTS

Year	Inlier degree	Compromise By (8)		By (9)
2008	0.222	0.031	$>$	0.020
2007	0.197	0.041	$>$	0.039
2006	0.213	0.034	$>$	0.030
2005	0.183	0.052	$<$	0.054
2004	0.184	0.045	$<$	0.053
Sum of compromises		0.204	$>$	0.196

degree of each year is obtained by (7) from total compromise without a year by (5) and shown in Table V. Although the inlier degrees of all years are around 0.2, it could be said that those of 2004 and 2005 are less than those of 2006, 2007 and 2008, the more recent three years. This might be because the budget has been changed gradually for years and reflecting the recent years' results in a plan is practical. Then, introducing inlier degrees as weights of years, the approximations of five years results as a group decision are obtained by compromise-weighted model (9) and to comparison by (8). They are shown at the second and third bottom lines of Table IV and differences from past years' result is shown in Table V. Those of 2008, 2007 and 2006 by (9) are smaller than those by (8). The obtained ratios by compromise-weighted model (9) are more similar to the more recent three years. Comparing the deviations between the ratios by (8) and (9) to real ratios of 2009 shown at the right row of Table IV, those by (9) are slightly smaller than those by (8).

VI. CONCLUSION

Focusing on outliers, group decision is obtained as the approximation of the given individual opinions. The models to define outlier degree and to obtain group opinion are proposed from the viewpoint of compromise. Since one of the major concerns of an individual in the group decision making is the difference of the obtained group opinion from his/her opinion, the compromise represented as such a difference is focused on in this paper. The outlier degree is used as an individual weight based on the idea that a unique opinion is sometimes worth being paid attention. It is measured as the distance of an individual from the group of others and defined as the reduction of total compromise by excluding the individual from the group. Similarly, inlier degree is used, when general opinions seem to be paid more attention. Then, the group opinion is obtained by minimizing weighted compromises so as to reach a consensus. The easily recognized compromise for group members is a useful and reasonable measurement and the proposed models based on it are practical in real problems.

REFERENCES

[1] S. French, J. Maule and N. Papamichail. *Decision Behaviour, Analysis and Support*, New York: Cambridge University Press, 2009.

[2] J. S. Valacich, S. Sarker, J. Pratt and M. Groomer. Understanding risk-taking behavior of groups: A "decision analysis" perspective, *Decision Support Systems*, Vol. 46, pp.902-912, 2009.

[3] D. Straus. *How to Make Collaboration Work: Powerful Ways to Build Consensus, Solve Problems, and Make Decisions*, San Fransisco: Berrett-Koehler Publishers, 2002.

[4] T. Entani. Interval AHP for a group of decision makers, *Proc. of IFSA/EUSFLAT 2009*, pp.155-160, 2009.

[5] T. Entani and M. Inuiguchi. Group decisions in Interval AHP based on interval regression analysis, *Proc. of International Symposium on Integrated Uncertainty Management and Applications*, pp.269-280, 2010.

[6] H. Tanaka and P. Guo. *Possibilistic Data Analysis for Operations Research*, Heidelberg, New York: Physica-Verlag, A Springer-Verlag Company, 1999.

[7] M. Inuiguchi and T. Tanino. Interval linear regression methods based on minkowski difference - a bridge between traditional and interval linear regression models, *Kybernetika*, Vol. 42, pp.423-440, 2006.

[8] L. M. de Campos, J. F. Huete and S. Moral. Probability intervals: a tool for uncertain reasoning, *International Journal of Uncertainty*, Vol.2, pp.167-196, 1994.

[9] H. Tanaka, K. Sugihara and Y. Maeda. Non-additive measures by interval probability functions, *Information Sciences*, Vol.164, pp.209-227, 2004.

[10] H. Tanaka and T. Entani Properties of evidences based on interval probabilities obtained by pairwise comparisons in AHP, *Proc. of Taiwan-Japan Symposium on Fuzzy Systems and Innovation Computing*, pp.35-40, 2006.

[11] T. L. Saaty. *The Analytic Hierarchy Process*, New York: McGraw-Hill, 1980.

[12] R. F. Dyer and E. H. Forman. Group decision support with the Analytic Hierarchy Process, *Decision Support Systems*, Vol.8, pp.94–124, 1992.

[13] T. L. Saaty. Group decision making and the AHP, B. L. Golden et.al., Editors, *The Analytic Hierarchy Process: Applications and Studies*, pp.59-67 New York: McGraw-Hill, 1989.

[14] Financial reports of Akaoka, Kagami, Noichi, Yasu and Yoshikawa in 2004 and Kami city in 2005, http://www.soumu.go.jp/iken/kessan_jokyo_2.html.

[15] Financial reports of Kochi prefecture from 2004 to 2008, http://www.pref.kochi.lg.jp/~zaisei/kessan/index.html.

2011 IEEE International Conference on Fuzzy Systems
June 27-30, 2011, Taipei, Taiwan

PCA-guided k-Means Clustering With Incomplete Data

Katsuhiro Honda, Ryoichi Nonoguchi, Akira Notsu, Hidetomo Ichihashi
Department of Computer Science and Intelligent Systems
Osaka Prefecture University
1-1 Gakuen-cho, Nakaku, Sakai, Osaka 599-8531, Japan
Email: {honda, notsu, ichi}@cs.osakafu-u.ac.jp

***Abstract*—This paper considers k-Means clustering of incomplete data sets including missing values. Although the main purpose of k-Means clustering is to partition samples into several homogeneous clusters by minimizing within-cluster errors, it has been shown that a relaxed solution of k-Means can be recovered in a PCA-guided manner. In this paper, the PCA-guided k-Means procedure is extended to a situation in which some observations are missing. Principal component scores, which can be identified with a rotated solution of cluster indicators of k-Means clustering, are estimated in an iterative process without imputation. Besides solving the eigenvalue problem of covariance matrices, k-Means-like partitions are derived through lower rank approximation of the data matrix ignoring missing elements. Several experimental results demonstrate that the PCA-guided process is more robust to initialization problems even though it is based on iterative optimization, just as the k-Means procedure is.**

***Keywords*—k-means clustering, missing value, principal component analysis.**

I. Introduction

k-Means clustering [1] is a fundamental technique for revealing intrinsic cluster structures of multivariate data sets. Although the k-Means process has been demonstrated to be very useful for extracting spherical clusters based on iterative optimization, it often suffers from initialization problems such that bad initializations lead to convergence to the wrong local minima. Recently, Ding and He [2] discussed a close relation between k-Means solutions and principal component scores, and proposed the principal component analysis (PCA)-guided k-Means procedure based on a deterministic method for finding the optimal (unique) k-Means partition. In the clustering model, a relaxed k-Means cluster indicator is identified with a rotated principal component score matrix, although the rotation matrix cannot be explicitly estimated and an approach such as visualization by ordering of samples in connectivity matrices [3] has to be used in order to visually access the cluster structures.

In [4], a noise rejection mechanism was introduced on the basis of noise fuzzy clustering [5]. In the fuzzy PCA-guided robust k-Means (FPR k-Means) procedure, both the responsibility weight of each sample with respect to the k-Means process and a rotated-cluster indicator are estimated by an iterative procedure. Removing the noise samples, a robust cluster indicator is estimated in a deterministic manner.

In addition to noisy data, incomplete data are common in real applications where some observations are missing. In order to apply k-Means-like clustering algorithms to incomplete data sets without a priori imputation, Hathaway and Bezdek [6] introduced four strategies in the Fuzzy c-Means (FCM) clustering algorithm [7]. Although the simple whole data strategy (WDS) eliminating all incomplete samples can be adopted if there are have only a few missing elements, it is useless in many real applications. In the partial distance strategy (PDS), clustering criteria of distances between samples and prototypes are calculated using observed coordinates only. In [6], it was also shown that some iterative completion strategies such as the optimal completion strategy (OCS) and nearest prototype strategy (NPS) also work well, although they require more computational effort.

In the application of PCA to incomplete data sets, several methods that extract principal components without any preprocessing of data have been proposed. Ruhe [8], Wiberg [9], and Shibayama [10] proposed PCA-like methods for capturing the structure of incomplete multivariate data without any imputations or statistical assumptions. Especially, Shibayama's approach made it possible to calculate principal components by a computationally efficient algorithm. Shum *et al.* [11] applied such techniques to object modeling. These methods are based on the lower rank approximation of the data matrix, which accomplishes the minimization of the least square criterion, and the methods extract principal components of the covariance matrix of the sample data set. Honda *et al.* [12] extended the PCA model to a linear fuzzy clustering algorithm by considering the close connection between PCA and linear fuzzy clustering algorithms such as Fuzzy c-Varieties (FCV) and Fuzzy c-Elliptotypes (FCE) [13].

In this paper, Shibayama's PCA-like method is applied to the k-Means problem with incomplete data in order to estimate a relaxed solution. Several experimental results demonstrate that the PCA-guided process is more robust to initialization problems, even though it is also based on iterative optimization, the same as the k-Means procedure.

The remainder of this paper is organized as follows: Section II briefly reviews k-Means and PCA-guided k-Means. Section III introduces Shibayama's PCA-like method for incom-

This work was funded in part by the Ministry of Internal Affairs and Communications, Japan, under the Strategic Information and Communications R&D Promotion Programme (SCOPE) and in part by the Ministry of Education, Culture, Sports, Science and Technology, Japan, through a Grant-in-Aid for Scientific Research (20700214).

978-1-4244-7316-8/11/$26.00 ©2011 IEEE

plete data, which is then applied to k-Means tasks. Section IV presents several experimental results to demonstrate the characteristic features of the proposed approach. Section V summarizes the conclusions of this paper.

II. Brief Review of k-Means and PCA-guided k-Means

A. k-Means Clustering and Partial Distance Strategy

Assume that we have n samples with m-dimensional observation $\boldsymbol{x}_i$, $i = 1, \ldots, n$, and the goal is to partition the samples into several clusters where samples belonging to the same cluster are similar while samples belonging to different clusters are dissimilar.

k-Means [1] is a non-hierarchical prototype-based clustering in which prototypes (centroids) are used for representing clusters and the objective function is defined as the sum of within-cluster errors:

$$\begin{aligned} L_{km} &= \sum_{k=1}^{K} \sum_{i \in G_k} d_{ki} \\ &= \sum_{k=1}^{K} \sum_{i \in G_k} ||\boldsymbol{x}_i - \boldsymbol{b}_k||^2, \end{aligned} \tag{1}$$

where K is the pre-defined number of clusters and $\boldsymbol{b}_k$ is the representative prototype (centroid) of cluster G_k.

The k-Means process is composed of two phases: prototype estimation and sample assignment. The two phases are iterated until the solution is trapped at a local minimum. Because of the greedy nature of the updating algorithm, the k-Means procedure often suffers from the initialization problem that the process converges to a different local optimum for a different initialization.

When some observations are missing, we need a modified clustering criterion d_{ki} that can be reconstructed using only the remaining observations. PDS is a simple but useful approach in which squared distances are calculated considering the observed coordinates only.

$$d_{ki} = \sum_{j=1}^{m} z_{ij} (x_{ij} - b_{kj})^2, \tag{2}$$

where z_{ij} is a bivariate variable as follows:

$$z_{ij} = \begin{cases} 1 & ; \text{if } x_{ij} \text{ is observed.} \\ 0 & ; \text{if } x_{ij} \text{ is missing.} \end{cases} \tag{3}$$

B. PCA-guided k-Means

Ding and He [2] revealed a close relation between PCA and k-Means clustering. The k-Means objective function of Eq.(1) can be re-defined by a centroid-less formulation as follows:

$$L_{km} = \sum_{i=1}^{n} ||\boldsymbol{x}_i||^2 - \sum_{k=1}^{K} \frac{1}{n_k} \sum_{i,j \in G_k} \boldsymbol{x}_i^\top \boldsymbol{x}_j, \tag{4}$$

where n_k is the number of samples belonging to cluster G_k. Because the first term is a constant, the optimal k-Means partition is derived by minimizing the second term, which is the sum of within-cluster (inner product) similarities. In this contex, the (hard) k-Means cluster partition is represented by K non-negative bivariate indicator vectors $H_K = (\boldsymbol{h}_1, \ldots, \boldsymbol{h}_K)$,

$$h_{ki} = \begin{cases} \frac{1}{n_k^{1/2}} & ; \text{if sample } i \text{ belongs to cluster } G_k. \\ 0 & ; \text{otherwise.} \end{cases}$$

In order to relax the k-Means problem, Ding and He introduced a rotated solution Q_K by considering $K \times K$ orthogonal transformation $T = \{t_{ij}\}$,

$$Q_K = (\boldsymbol{q}_1, \ldots, \boldsymbol{q}_K) = H_K T, \tag{5}$$

where, avoiding redundancies, the last column of T is set as:

$$\boldsymbol{t}_n = (\sqrt{n_1/n}, \ldots, \sqrt{n_K/n})^\top, \tag{6}$$

which brings $\boldsymbol{q}_K = (\sqrt{1/n}, \ldots, \sqrt{1/n})^\top$. Considering the mutual orthogonality of $\boldsymbol{h}_k$, we have the following conditions:

$$Q_{K-1}^\top Q_{K-1} = I_{K-1}, \tag{7}$$

$$\sum_{i=1}^{n} q_{ki} = 0, \qquad k = 1, \ldots, K-1, \tag{8}$$

where $Q_{K-1} = (\boldsymbol{q}_1, \ldots, \boldsymbol{q}_{K-1})$ and $\boldsymbol{q}_k = (q_{k1}, \ldots, q_{kn})^\top$. Then, the k-Means objective function can be written as

$$L_{km} = \sum_{i=1}^{n} ||\boldsymbol{x}_i||^2 - \frac{1}{n} \boldsymbol{e}^\top X^\top X \boldsymbol{e} - \mathrm{Tr}(Q_{K-1}^\top X^\top X Q_{K-1}), \tag{9}$$

where $X = (\boldsymbol{x}_1, \ldots, \boldsymbol{x}_n)$, and $\boldsymbol{e}$ is the n-dimensional vector whose elements are all 1.

Here, we can see that the k-Means problem is free from the influences of parallel transformation and that the original data $\boldsymbol{x}_i$ can be replaced with the centered data $\boldsymbol{y}_i$ without loss of generality. Then, the objective function can be written as:

$$L_{km} = \sum_{i=1}^{n} ||\boldsymbol{y}_i||^2 - \mathrm{Tr}(Q_{K-1}^\top Y^\top Y Q_{K-1}), \tag{10}$$

where $Y = (\boldsymbol{y}_1, \ldots, \boldsymbol{y}_n)$ and $Y\boldsymbol{e} = \boldsymbol{0}$.

The optimal solutions for the transformed discrete membership indicator vectors Q_{K-1} are derived by maximizing $\mathrm{Tr}(Q_{K-1}^\top Y^\top Y Q_{K-1})$, and continuous (relaxed) solutions are the eigenvectors corresponding to the $K-1$ largest eigenvalues of $Y^\top Y$. Therefore, the optimal Q_{K-1} can be identified with the principal component scores in PCA, and a continuous solution for k-Means clustering is derived in a PCA-guided manner.

If we want to know the cluster structure from the (continuous) solution for Q_{K-1}, we need to compute the optimal transformation T, although this is not easy in many case. In [2], cluster connectivity analysis is performed by calculating the following connectivity matrix C:

$$C = \frac{1}{n} \boldsymbol{e}\boldsymbol{e}^\top + \sum_{k=1}^{K-1} \boldsymbol{q}_k \boldsymbol{q}_k^\top, \tag{11}$$

and a probability for the connectivity between samples i and j is given as:

$$p_{ij} = \frac{c_{ij}}{\sqrt{c_{ii}c_{jj}}}. \tag{12}$$

Cluster structure is shown in the diagonal block structure using the spectral ordering [3].

III. Principal Components Estimation from Incomplete Data and Its Application to k-Means Cluster Indicator Estimation

A. PCA-like Method for Incomplete Data

Assume that a data set is represented by the $m \times n$ data matrix $X = (\boldsymbol{x}_1, \ldots, \boldsymbol{x}_n)$ and the goal is to extract a p ($p < m$)-dimensional principal component score for each sample. The PCA process is achieved by estimating the lower rank approximation of X as follows:

$$X \approx AF + \boldsymbol{v}\boldsymbol{e}^\top, \tag{13}$$

where A is the $m \times p$ principal component matrix $A = (\boldsymbol{a}_1, \ldots, \boldsymbol{a}_p)$, and F is the $p \times n$ principal component score matrix $F = (\boldsymbol{f}_1, \ldots, \boldsymbol{f}_n)$. $\boldsymbol{v}$ is the centering vector.

In order to estimate principal components from incomplete data, Shibayama [10] considered minimization of the following least square criterion:

$$\begin{aligned} L &= \mathrm{Tr}\big(Z \odot (X - AF + \boldsymbol{v}\boldsymbol{e}^\top)\big)^\top \big(Z \odot (X - AF + \boldsymbol{v}\boldsymbol{e}^\top)\big) \\ &= \sum_{i=1}^{n}\sum_{j=1}^{m} z_{ij}\left(x_{ij} - \sum_{k=1}^{p} f_{ik}a_{kj} - v_j\right)^2, \end{aligned} \tag{14}$$

where $Z = \{z_{ij}\}$ is given by Eq.(3) and $\odot$ denotes the Hadamard product.

This model is based on a concept similar to PDS in k-Means clustering, namely that the partial errors calculated only by the observed elements are minimized.

If the data matrix X does not include any missing elements, the PCA model is equivalent to the standard formulation in which the centering vector $\boldsymbol{v}$ is given by the mean vector and the principal component vectors $\boldsymbol{a}_k$, $k = 1, \ldots, p$ are derived as the eigenvectors corresponding to the principal eigenvalues of the scatter matrix. However, if the data matrix includes missing elements, the PCA process cannot be reduced to an eigen problem.

In the Shibayama's PCA-like method [10], principal components are estimated on the basis of an iterative optimization scheme. Under the constraints $F\boldsymbol{e} = \boldsymbol{0}$ and $FF^\top = I$, the updating rule for each step is derived as follows:

$$\tilde{\boldsymbol{a}}_j = (F\tilde{Z}_j F^\top)^{-1} F\tilde{Z}_j(\tilde{\boldsymbol{x}}_j - v_j\boldsymbol{e}), \tag{15}$$

$$v_j = (\boldsymbol{e}^\top \tilde{Z}_j \boldsymbol{e})^{-1}\boldsymbol{e}^\top \tilde{Z}_j(\tilde{\boldsymbol{x}}_j - F^\top \tilde{\boldsymbol{a}}_j), \tag{16}$$

$$\boldsymbol{f}_i = (A^\top Z_i A)^{-1} A^\top Z_i(\boldsymbol{x}_i - \boldsymbol{v}), \tag{17}$$

where $A = (\tilde{\boldsymbol{a}}_1, \ldots \tilde{\boldsymbol{a}}_m)^\top$, $X = (\tilde{\boldsymbol{x}}_1, \ldots, \tilde{\boldsymbol{x}}_m)^\top$ and $Z_i = \mathrm{diag}(z_{i1}, \ldots, z_{im})$, $\tilde{Z}_j = \mathrm{diag}(z_{1j}, \ldots, z_{nj})$.

Beside random initialization, initial values for A, F and $\boldsymbol{v}$ can be estimated by WDS in which the standard PCA model is applied after removing all samples including missing elements. The iterative procedure of updating A, F, and $\boldsymbol{v}$ is continued until convergence while normalizing F in each iteration.

B. k-Means Cluster Indicator for Incomplete Data

Although the iterative optimization process of the PCA-like method with bad initialization may become trapped at local minima, we can expect that a plausible estimator of principal component scores can be obtained using the multi-starting strategy even when data matrices include missing elements. Therefore, the derived principal component scores F are promising candidates for the relaxed cluster indicator in the PCA-guided k-Means procedure.

The procedure for deriving the relaxed cluster indicator matrix Q_K in the K cluster case can be summarized as follows:

Step.1 Set the dimension of principal components as $p = K - 1$ and initialize A, F, and $\boldsymbol{v}$.
Step.2 Repeat the PCA-like process until convergence.
Step.3 Substitute F into Q_{K-1}.
Step.4 Set $\boldsymbol{q}_K$ as $\boldsymbol{q}_K = (\sqrt{1/n}, \ldots, \sqrt{1/n})^\top$.

Once the relaxed cluster indicator Q_K is estimated, cluster structures can be captured by a technique such as cluster connectivity analysis.

IV. Numerical Experiments

In this section, several experimental results are shown in order to demonstrate the characteristic features of the proposed approach.

A. Iris Data Set

The first experiment was performed with the Iris data set that is available from the UCI Machine Learning Repository [14]. In this experiment, 150 instances ($n = 150$) with four-dimensional observation ($m = 4$) drawn from three classes were partitioned into three clusters without using the class label. The data set does not include any missing elements. It is well known that the k-Means model can capture the three dense masses of the three labeled classes in many trials using the multi-starting strategy, although whereas one class is well separated from others, the remaining two classes somewhat overlap.

In this experiment, the frequencies of good results in the proposed approach using the multi-starting strategy are compared with that in the k-Means using PDS. Here, a "good" result does not necessarily mean that all instances are correctly classified into the three classes without using class labels, but rather it means that the three cluster centers were located near the center of each class.

Table I compares the clustering performances of the proposed approach and the k-Means procedure using PDS with incomplete data. Various incomplete data sets were generated by withholding one observation (attribute) from randomly selected instances. The table shows the average frequencies of good results in 100 different data sets with 100 trials

TABLE I
AVERAGE FREQUENCIES (%) OF "GOOD" RESULTS IN 10000 TRIALS WITH INCOMPLETE DATA SET (IRIS DATA SET)

# missing elements	PCA-guided	k-Means (PDS)
0	100.00	79.01
50	100.00	85.01
60	95.84	82.46
70	92.23	79.04
80	90.37	78.58
90	84.19	75.49
100	82.46	73.20
110	82.34	69.57
120	79.34	67.47
130	74.84	65.15
140	71.91	63.42
150	70.14	60.21

with random initialization. The result of the no missing value situation for the PCA-guided approach is the same as that given by the conventional PCA-guided k-Means procedure and is free from random initialization based on the deterministic procedure. Note that the k-Means procedure may become trapped at a local minimum even when the data set includes no missing values.

The table demonstrates that the proposed PCA-guided approach is still robust to initialization when the number of missing values is not too large, e.g., 50 missing elements, although the PCA process is based on an iterative optimization scheme. As the number of missing elements increase, the frequency of good results decrease. However, the proposed PCA-guided approach is always more robust than the k-Means procedure using PDS. This result implies that the PCA-guided approach is more reliable than the conventional k-Means procedure even when data sets includes missing elements.

B. Document Clustering

Next, the characteristic feature of the proposed approach is demonstrated in a document clustering task using the Japanese novel *Kokoro* by Soseki Natsume, which can be downloaded from Aozora Bunko (http://www.aozora.gr.jp). The novel is composed of three chapters ("Sensei and I", "My Parents and I", "Sensei and His Testament") and the chapters include 36, 18, and 56 sections, respectively. In this experiment, the sections are regarded as individual text documents (number of samples is $n = 110$) and the documents are partitioned into three clusters ($K = 3$) without using the chapter information. This data set forms roughly three clusters in the 83-dimensional data space [16], as shown in Fig. 1-(a). Thus, the goal of the experiment is to reconstruct the intrinsic chapter information from a word analysis. The text documents were preprocessed using a morphological analysis system software "Chasen" (http://chasen.naist.jp/hiki/ChaSen/), which segments Japanese text strings into morphemes and tags these morphemes with their parts of speech and pronunciations. The 83 most frequently used substantives and verbs (they were used more than 50 times in the novel) were used as attributes to be analyzed with their tf-idf weights [15].

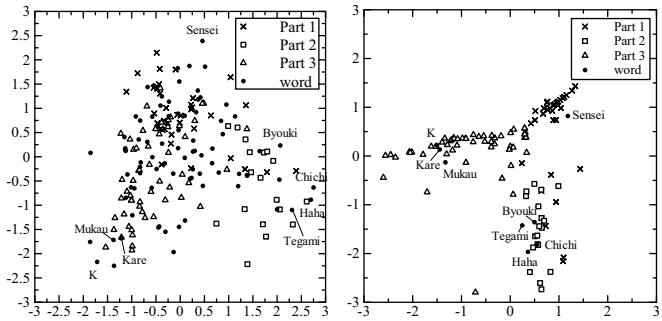

(a) 83 words (b) 8 words

Fig. 1. 2-D biplots of Japanese novel *Kokoro* [16]: (a) 83 words, (b) 8 words

TABLE II
AVERAGE FREQUENCIES (%) OF "GOOD" RESULTS USING AN INCOMPLETE DATA SET (JAPANESE NOVEL *Kokoro* WITH 83 WORDS (ATTRIBUTES))

# missing elements	PCA-guided	k-Means (PDS)
0	100.00	100.00
10	100.00	88.12
20	99.30	76.24
30	99.40	72.28
40	98.73	59.45
50	98.68	48.56
60	98.69	43.61
70	98.50	38.64
80	95.51	26.81
90	96.20	18.87
100	94.91	7.98
110	93.39	1.10

A comparison of the frequencies of good results is shown in Table II. Various incomplete data sets were generated in a similar manner as in the previous experiment. The proposed PCA-guided approach is much more robust than the k-Means procedure using PDS when data sets include many incomplete instances. This is because very ambiguous cluster boundaries easily trap the k-Means procedure using PDS at local minima whereas the PCA-guided approach is seldom influenced by a slight loss of information (in only 1 of 83 attributes).

Second, the same experiment was repeated, but using fewer words (attributes). In [16], it was shown that the three-cluster structure is clarified by using eight significant words. Therefore, only wight words (eight attributes) were used for this experiment. Table III shows a comparison of the results. The performance of the proposed PCA-guided approach is inferior to that shown in Table II because information loss became relatively large (in 1 of 83 attributes). On the other hand, the performance of the k-Means procedure using PDS is almost equivalent to that shown in Table II, although in this case as well, it is inferior to the PCA-guided approach.

These experimental results imply that the PCA-guided procedure for k-Means is also useful for incomplete data sets.

TABLE III
AVERAGE FREQUENCIES (%) OF "GOOD" RESULTS USING AN INCOMPLETE DATA SET (JAPANESE NOVEL *Kokoro* WITH 8 WORDS (ATTRIBUTES))

# missing elements	PCA-guided	k-Means (PDS)
0	100.00	100.00
10	98.62	88.12
20	96.81	76.25
30	93.32	72.29
40	91.86	59.47
50	90.05	48.57
60	88.92	43.61
70	77.59	38.61
80	67.05	26.80
90	65.84	18.93
100	54.35	8.00
110	54.64	1.07

V. CONCLUSION

In this paper, a PCA-guided procedure for k-Means clustering of incomplete data sets is proposed. Although the PCA-like method is not a deterministic procedure but rather is based on an iterative optimization scheme, the PCA-guided approach is still more robust to initialization problems than the k-Means procedure using PDS.

Comparison with other techniques for handling missing values, such as OCS, remains for future work. Other potential future work involves component-wise robust PCA [17], [18], in which component-wise noise is ignored by means of an M-estimation scheme [19].

REFERENCES

[1] J. B. MacQueen, "Some methods of classification and analysis of multivariate observations," *Proc. of 5th Berkeley Symposium on Math. Stat. and Prob.*, pp. 281-297, 1967.

[2] C. Ding and X. He, "K-means clustering via principal component analysis," *Proc. of Int'l Conf. Machine Learning (ICML 2004)*, pp. 225-232, 2004.

[3] C. Ding and X. He, "Linearized cluster assignment via spectral ordering," *Proc. of Int'l Conf. Machine Learning (ICML 2004)*, pp. 233-240, 2004.

[4] K. Honda, A. Notsu and H. Ichihashi, "Fuzzy PCA-guided robust k-means clustering," *IEEE Transactions on Fuzzy Systems*, vol. 18, no. 1, pp. 67-79, 2010.

[5] R. N. Davé, "Characterization and detection of noise in clustering," *Pattern Recognition Letters*, vol. 12, no. 11, pp. 657-664, 1991.

[6] R. J. Hathaway, and J. C. Bezdek, "Fuzzy c-means clustering of incomplete data," *IEEE Trans. Syst., Man, Cybern.*, vol.B31, pp. 735-744, 2001.

[7] J. C. Bezdek, *Pattern Recognition with Fuzzy Objective Function Algorithms*, Plenum Press, 1981.

[8] A. Ruhe, "Numerical computation of principal components when several observations are missing," Tech. Rep. UMINF-48-74, Dept. Information Processing, Umea Univ., 1974.

[9] T. Wiberg, "Computation of principal components when data are missing," in *Proc. 2nd Symposium on Computational Statistics*, pp. 229-236, 1976.

[10] T. Shibayama, "A PCA-like method for multivariate data with missing values," *Japanese Journal of Educational Psychology*, vol.40, pp. 257-265, 1992. (in Japanese)

[11] H. Shum, K. Ikeuchi, and R. Reddy, "Principal component analysis with missing data and its application to polyhedral object modeling," *IEEE Trans. Pattern Analysis and Machine Intelligence*, vol.17, pp. 854-867, 1995.

[12] K. Honda and H. Ichihashi, "Linear fuzzy clustering techniques with missing values and their application to local principal component analysis," *IEEE Trans. Fuzzy Systems*, vol. 12, no. 2, pp. 183-193, 2004.

[13] J. C. Bezdek, C. Coray, R. Gunderson and J. Watson, "Detection and characterization of cluster substructure 2. Fuzzy c-varieties and convex combinations thereof," *SIAM J. Appl. Math.*, vol.40, pp. 358-372, 1981.

[14] A. Asuncion and D.J. Newman, UCI Machine Learning Repository [http://www.ics.uci.edu/ mlearn/MLRepository.html], Irvine, CA: University of California, School of Information and Computer Science, (2007).

[15] G. Salton and C. Buckley: Term-weighting approaches in automatic text retrieval, *Information Processing and Management*, vol.24, issue 5, pp.513-523, 1988.

[16] K. Honda, H. Wada, H. Ichihashi and A. Notsu: An intuitive text mining method based on variable selection in principal component analysis, *Proc. of 8th International Symposium on Advanced Intelligent Systems*, pp.334-337, 2007.

[17] F. de la Torre and M. J. Black: A framework for robust subspace learning; *International Journal of Computer Vision*, vol. 54, pp. 117-142 (2003)

[18] K. Honda and H. Ichihashi, "Component-wise robust linear fuzzy clustering for collaborative filtering," *International Journal of Approximate Reasoning*, vol. 37, no. 2, pp. 127-144, 2004.

[19] P. W. Holland and R. E. Welsch, "Robust regression using iteratively reweighted least-squares," *Communications in Statistics*, vol. A6, no. 9, pp. 813-827 (1977)

2011 IEEE International Conference on Fuzzy Systems
June 27-30, 2011, Taipei, Taiwan

Proposed Particle-Filtering Method for Reinforcement Learning

Akira Notsu, Katsuhiro Honda and Hidetomo Ichihashi
Osaka Prefecture University
1-1 Gakuencho, Nakaku, Sakai, Osaka 599-8531, JAPAN
Email: {notsu, honda, ichi}@cs.osakafu-u.ac.jp

***Abstract*—We propose a novel action-search particle-filtering algorithm for reinforcement learning processes. This algorithm is designed to perform search domain reduction and heuristic space segmentation. In this method, each action space is divided into several new segments using particles. Appropriate search domain reduction can minimize learning time and enable the recognition of the evolutionary process of learning. In a numerical experiment, the proposed filtering method is applied to a single-pendulum simulation in order to demonstrate the adaptability of this simulation model.**

***Index Terms*—reinforcement learning, particle-filter, space segmentation.**

I. Introduction

This paper proposes a novel particle-filtering algorithm for reinforcement learning that periodically divides the agent environment and action search space during the learning process. The standard reinforcement learning algorithm [1], [2] requires well-suited segmentation before learning. In the proposed method, each state is searched by several particles, and distances between states are fixed according to the importance of each state. Herein, human-like space segmentation in actor-critic learning, which we investigated previously [3], [4], is further refined.

In post-supervised design, clustering, which is done after many trial and error iterations, is a probabilistic method. A genetic algorithm representative of these schemes is called a learning classifier system [5], [6]. In this system, inputted data are encoded as binary rules that a genetic algorithm alters before selecting from them the best rules. However, inputted data can be encoded during the learning, as in the previously investigated method. Our proposed algorithm is applicable not only to reinforcement learning but also to social simulation, which requires each agent to behave rationally during the trial and error iterations. Such an approach provides clues for understanding culture and language.

II. Reinforcement learning

Reinforcement learning assumes that agents can visit only a finite number of states, and that when visiting a state, they will collect a numerical reward (which can be interpreted as a punishment in the case of a negative reward [7]). Each state has a different value associated with it. Given an initial state, subsequent states are reached according to actions. The value of a given state is defined as the average reward that can be collected by selecting actions available in that state.

A. Particle in state and action space

A high-performance agent usually needs appropriately segmented state set S and action set A because of agent state-space explosion. Generally, a genetic algorithm is used to search for appropriate segmentation in such individual double-loop learning. In particular, we use a particle swarm, which is a classification system in which a minimization of (2) under the following condition takes place:

$$\sum_{i=1}^{c} u_{ki} = 1, \tag{1}$$

where c is the number of clusters and u_{ki} is called a membership function.

$$L = \sum_{i=1}^{c} \sum_{k=1}^{N} u_{ki} D\left(x_k, v_i\right), \tag{2}$$

where N is the amount of data, c is the number of clusters, and $D\left(x_k, v_i\right)$ denotes the distance between data vector x_k and cluster center v_i: the difference between expected utility V and observed utility V' in the learning process.

B. Actor-critic

The actor-critic method includes the critic, which maintains the state value estimate V, and the actor, which is responsible for choosing the appropriate actions at each state (Fig. 1).

Value function approaches attempt to find a policy that maximizes the return by maintaining a set of estimates of expected rewards based on a policy π. In this method, an agent attempts to estimate the expected reward $V(s)$:

$$V(s) = E\left[R|s_t, \pi\right] = r_t + \gamma E\left[R|s_{t+1}, \pi\right] \tag{3}$$

for an agent following π and taking an action in state s.

step 1 Agent observes state s and actor selects action a according to its stochastic policy π.

step 2 Critic receives reward and calculates the following TD-error.

$$\text{TD-error} = r_t + \gamma V(s_{t+1}) - V(s_t), \tag{4}$$

where γ is discount factor.

step 3 Actor updates its stochastic policy π according to the TD-error.

(TD-error)> 0 Selected action a is favorable, so increase action a selection probability.

978-1-4244-7316-8/11/$26.00 ©2011 IEEE

(TD-error)<0 Selected action a is not favorable, so decrease action a selection probability.

step 4 Update value function (Fig. 2).

$$V(s_t) \leftarrow V(s_t) + \alpha \text{TD-error}, \tag{5}$$

where α is the learning rate.

step 5 Go to **step 1**.

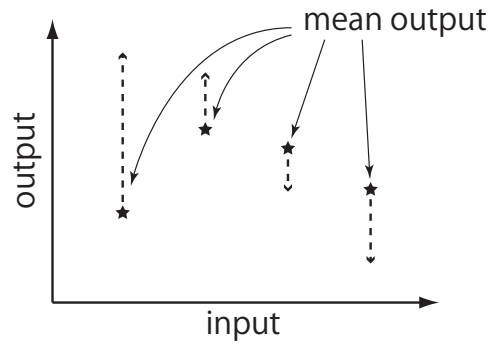

Fig. 1. Actor-critic

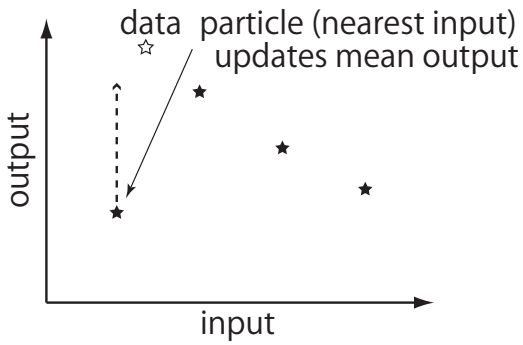

Fig. 2. Actor-critic

In this paper, we use a normal distribution as stochastic policy π (Fig. 3). Updating the stochastic policy is carried out by adjusting the particle's mean $\boldsymbol{a}$ and variance v of output (which is an agent's action).

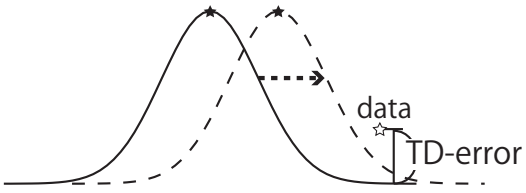

Fig. 3. Updating stochastic policy π

If (TD-error)>0,

$$\boldsymbol{a} \leftarrow (1-\alpha_a)\boldsymbol{a} + \alpha_a \text{vector[output]} \tag{6}$$

$$v \leftarrow (1-\beta_1)v. \tag{7}$$

Else if (TD-error)<0,

$$\boldsymbol{a} \leftarrow (1+\alpha_a)\boldsymbol{a} - \alpha_a \text{vector[output]} \tag{8}$$

$$v \leftarrow (1-\beta_2)v. \tag{9}$$

Here, α_a, β_1, and β_2 are parameters.

C. Particle filter

The particle-filtering method is a model estimation technique based on Bayesian models in which the latent variables are connected in a Markov chain. A particle filter estimates the sequence of hidden parameters on the basis of only on the observed data.

The method assumes that x_k and the observations y_k can be modeled in the following form:

$x_0, x_1, \ldots$ is a first-order Markov process such that

$$x_k|x_{k-1} \sim p_{x_k|x_{k-1}}(x|x_{k-1}), \tag{10}$$

where the initial distribution $p(x_0)$ is given.

Although each particle filter yields only a rough approximation, with enough particles, the estimate can be quite accurate.

The particle-filtering method generates a set of samples that approximate the filtering distribution $p(x_k|y_0,\ldots,y_k)$. With P samples, expectations with respect to the filtering distribution are approximated by

$$\int f(x_k)p(x_k|y_0,\ldots,y_k)dx_k \approx \frac{1}{P}\sum_{L=1}^{P} f(x_k^{(L)}), \tag{11}$$

and $f(\cdot)$ can provide all the moments of the distribution up to some degree of approximation.

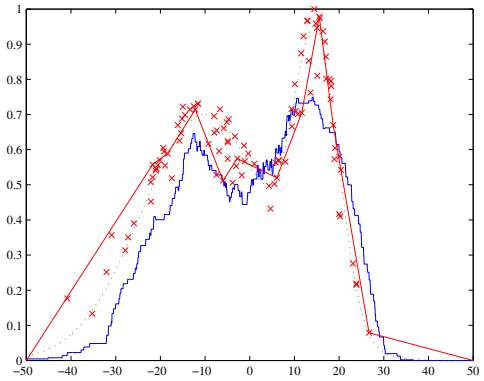

Fig. 4. Example of a particle filter

III. Particles in each action space

We propose particles in the action space. The proposed method using particles can search for the global solution (best output) and a local solution, which has the potential of being the global solution.

In each state, several particles have expected rewards according to expected utility V. If inputted data have a positive TD-error, the nearer particle is updated (shown in Fig. 5). This method decreases the probability of the local solution.

In addition, because an evenly segmented state is not always good for learning, we also propose adjusting the distance

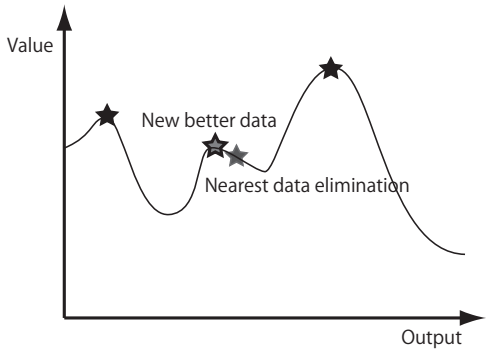

Fig. 5. Updating the output according TD-error

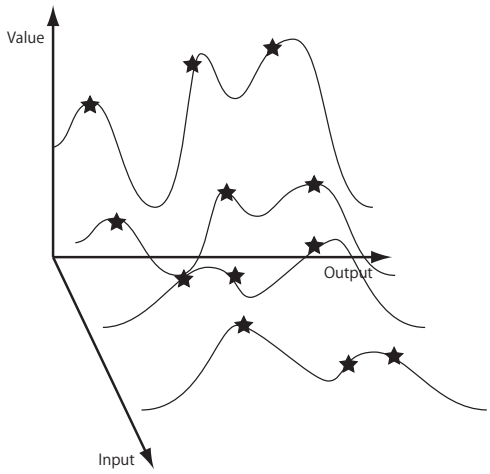

Fig. 6. Particles in the space

between state prototypes by setting the distance between successive best particles in the output-input space (in fig. 7). This is based on the fact that if the best output is quite different, near states should be searched closely, and otherwise do not need to be. In the process, the updated particle entrains the state particle.

Therefore, our proposed method requires that the input and output spaces be normalized.

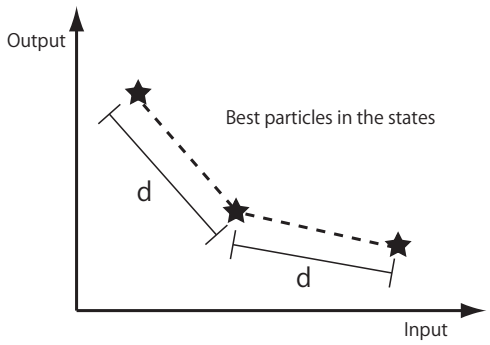

Fig. 7. Updating the input space distribution by distance

IV. Single-pendulum simulation

We simulated the single-pendulum standing task (fig. 8). This physical calculation is performed by a Runge–Kutta method.

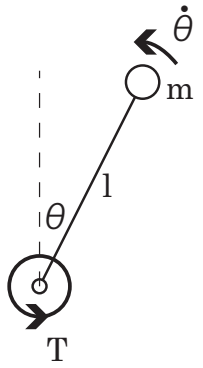

Fig. 8. Single pendulum

The following motion equation is simulated in increments of 0.05 seconds:

$$m\ddot{\theta} = -mgl\sin(\pi - \theta) + T + (-k\dot{\theta}) \tag{12}$$

where the parameters and variables are define as

- $m = 1$ (kg)
- $l = 1$(m)
- $k = 0$
- $g = 9.8(m/s^2)$
- $-\pi < \theta \leq \pi$
- $-3\pi < \dot{\theta} \leq 3\pi$
- $-20 < \ddot{\theta} \leq 20$
- 1 episode = 5 seconds
- 1 learning cycle = 0.2 seconds
- $\theta = \pi, \dot{\theta} = \ddot{\theta} = 0$, in the initial state
- $R = (\pi - |\theta|)/\pi - T/40$
- $\alpha = 0.1$
- $\gamma = 0.9$
- variance $V_0 = \pi/2, V_{1000} = V_0 \cdot \beta^{1000} = 0.0001 \cdot V_0$ for constant β.

Figs. 9 to 11 show the results of several simulations. The vertical axes in these figures show the reward and the horizontal axes show episode times. In each figure, the left panel shows the 100-trial mean of the reward and the right panel shows the best reward. The shown results are for the normal method (blue), our proposed method in which couple particles are applied (green), and our proposed method along with adjusting the distance between state prototypes (red). The agent has 100 states in the learning process. In the simulations shown in Fig. 9, each state is segmented evenly. As shown, the proposed method is not always good for learning; however, it does not inhibit the learning process.

In Figs. 10 (over-segmented position space) and 11 (over-segmented velocity space), the state is not segmented appropriately. As shown, the proposed method leads to a better reward history in terms of speed and value.

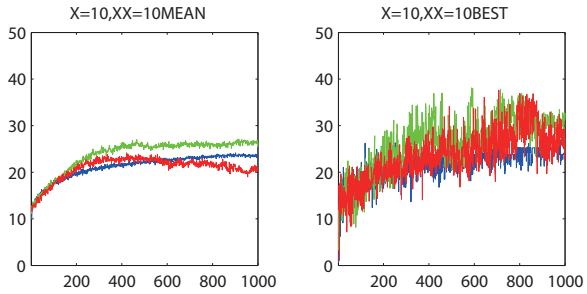

Fig. 9. Results in better segmentation by the particles

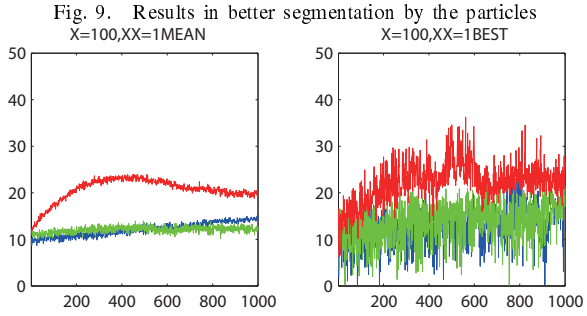

Fig. 10. Results in worse segmentation by the particles

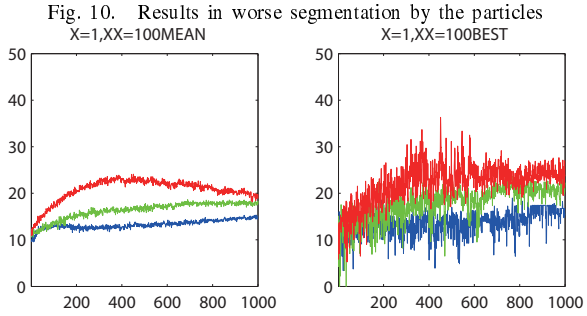

Fig. 11. Results in worse segmentation by the particles

Our simple segmentation method, especially in the state space, worked very well. Further adjustments in the parameters of the proposed method have the potential of further improving the results.

V. Conclusion

We proposed a novel particle-filtering approach to create a novel reinforcement learning algorithm that segments the agent's environment and action. The proposed filtering method is applied to a single-pendulum simulation in order to demonstrate the adaptation ability of the model.

Acknowledgment

This work was supported in part by the Ministry of Education, Culture, Science and Technology, Japan under Grant-in-Aid for Scientific Research No. 21700242 and funded by the Ministry of Internal Affairs and Communications, Strategic Information and Communications R&D Promotion Programme.

References

[1] T. Jaakkola, M. Jordan, and S. P. Singh, On the Convergence of Stochastic Iterative Dynamic Programming Algorithms, Neural Computation, vol. 6, pp. 341–362, 1992.

[2] C. J. C. H. Watkins and P. Dayan, Technical Note: Q-Learning, Machine Learning, vol. 8, pp. 56–68, 1992.

[3] A. Notsu, H. Ichihashi, K. Honda, State and Action Space Segmentation Algorithm in Q-learning, Proc. of 2008 International Joint Conference on Neural Networks, pp. 2385–2390, 2008.

[4] A. Notsu, H. Wada, K. Honda, and H. Ichihashi, Cell Division Approach for Search Space in Reinforcement Learning, International Journal of Computer Science and Network Security, vol. 8, 6, pp. 18–21, 2008.

[5] J. H. Holland and J. Reitman, Cognitive Systems Based on Adaptive Algorithms, in D. A. Waterman and F. Hayes-Roth (Eds.), Pattern Directed Inference Systems, Academic Press, 1978.

[6] J. H. Holland, K. J. Holyoak, R. E. Nisbett, and P. R. Thagard, Induction, The MIT Press, 1986.

[7] R. S. Sutton, Learning to Predict by Method of Temporal Differences, Machine Learning, vol. 3, 1, pp. 9–44, 1988.

2011 IEEE International Conference on Fuzzy Systems
June 27-30, 2011, Taipei, Taiwan

Formalizing Object Membership in Fuzzy Ontology with Property Importance and Property Priority

Yi Cai
School of Software Engineering
South China University of Technology
Guangzhou 510006, China
Email: caiyi1023@hotmail.com

Ho-fung Leung
Department of Computer Science and Engineering
The Chinese University of Hong Kong
Hong Kong, China
Email: lhf@cuhk.edu.hk

***Abstract*—In this paper, we formalize the object membership in fuzzy ontology with property importance and property priority, while previous models lack building blocks to handle the importance and priority of properties. A formal mechanism used to measure object memberships in concepts is proposed. Such a mechanism can measure object memberships in concepts defined by properties with importance or priority well. We show that our model is more reasonable in measuring object memberships in concepts than previous models by examples and experiments.**

***Index Terms*—Fuzzy ontology, Property importance, Property priority**

I. Introduction

Traditional ontology is represented as a crisp set of objects [1] and objects are considered either to belong to or not to belong to a concept. However, there are many fuzzy concepts (e.g., 'hot water' and 'yellow car') in reality, and traditional ontology cannot handle these fuzzy concepts. Fuzzy ontologies are proposed to extend the representation ability of ontologies to handle fuzzy concepts such as [2] [3] [4]. Object membership is an important measurement of objects in fuzzy concepts and it refers to the degree of an object belonging to a concept. However, object memberships are given by users manually or obtained by fuzzy functions defined by users in these fuzzy ontologies. While concepts, objects and properties are building blocks of ontologies, these fuzzy ontologies lacks of a formal mechanism to determine memberships of objects in concepts automatically based on the defining properties of concepts and properties which objects possess.

Au Yeung and Leung [5] formalize object memberships in concepts based on theories in cognitive psychology and present a mechanism to measuring object memberships based on properties of concepts and objects automatically. Their work is extended by Cai and Leung [6]. Besides, all these works consider that properties used to define a concept are equivalent. In other words, all properties have the same importance or the same priority, and we name them as **equivalent properties**. However, some properties are more important than other properties in many situations. We name the properties with different importance in concepts as **weighted properties**. For example, when some one wants to rent a house, he may consider price of the house is more important than the location of the house. In addition, some properties are priori to other properties in measuring object memberships. We name the properties with different priorities in concepts as **prioritized properties**. For example, when measuring how great an athlete is in the Olympic Games, the number of goal medals the athlete obtained is priori to the number of silver medals the athlete obtained. The effect of an athlete obtaining one goal medal cannot be substituted by that of no matter how many silver medals the athlete obtained. Although different properties having different importance or priorities are prevalent, previous works cannot handle object memberships in concepts defined by weighted properties or prioritized properties well. For the rifeness of property importance and priority, we consider that it is necessary to model them in ontology.

In this paper, we formalize the object membership in fuzzy ontology with property importance and property priority. The formal mechanism we proposed for measuring object memberships in concepts can handle not only concepts defined by equivalent properties, but also concepts defined by weighted properties or prioritized properties well, which cannot be handled well in previous models. Besides, we formally model property importance and property priority in fuzzy ontology, and point out and discuss the differences between property importance and property priority. Experiments are conducted to validate the proposed model. To the best of our knowledge, it is the first work of modeling object memberships in fuzzy ontology with weighted properties and prioritized properties.

II. Background and Related Work

A. Classical View of Concept Representation

In cognitive psychology, it is generally accepted that concepts are characterized by properties [7]. One important model of concept representation based on properties is classical view. The classical view [8] [9] of concepts posits that each concept is defined by a set of properties which are individually necessary and collectively sufficient. Properties are atomic units which are the basic building blocks of concepts. In classical view, there are clear-cut boundaries between members and non-members of the category. As a result, the classical view cannot handle the vague concepts.

B. Fuzzy Ontology and Object Membership

Currently, most ontologies are based on DLs (description logics) [10] and concepts are represented as crisp sets of ob-

978-1-4244-7316-8/11/$26.00 ©2011 IEEE

jects (e.g., ontologies written in OWL DL) [11]. These ontologies cannot represent the fuzzy concepts. Several fuzzy DLs are proposed to handle the fuzzy concepts by combining fuzzy set theory [12] and description logics. For example, Straccia proposes a fuzzy $\mathcal{ALC}$ in [2] and a fuzzy $\mathcal{SHOIN}(\mathcal{D})$ in [3]. Stoilos et al. present a fuzzy $\mathcal{SHIN}$ in [4]. These fuzzy DLs vary in possessing different expressive power, complexity and reasoning capabilities. Some fuzzy ontologies are constructed based on fuzzy DLs or fuzzy logic [13]. Besides, some works apply fuzzy ontologies for some applications. For instance, Cross and Voss [14] explore the potential that fuzzy mathematics and ontologies have for improving performance in multilingual document exploitation. These works lack a formal mechanism to obtain the membership degrees of objects in concepts automatically, and they do not take how people representing concepts in their mind into consideration.

Recently, Au Yeung and Leung [5] propose a formal model for fuzzy ontology based on the idea of classical view. They have formalized the membership degrees of objects in concepts by constructing several vectors in ontologies. To overcome previous models' limitations, Cai and Leung [6] propose a novel formal model of fuzzy ontology with property hierarchy and object membership. However, all these works cannot handle the concepts defined by properties which have different importance degrees or priorities. They lack formal mechanisms for measuring object memberships in concepts defined by weighted properties and prioritized properties. Besides, Bobillo and Straccia explore an expressive fuzzy description logic reasoner [15], which include the weighted sum constructor.

III. Limitations of Previous Models

We use some motivating examples to illustrate the limitations of previous models and make our motivation more clear in this section.

Example 1. Suppose that Bob wants to rent a room for 10 months from a real estate agent when he visits the Chinese University of Hong Kong. The rent of such a room would be the best if it is less than or equal to 2800 HKD each month, and he cannot offer too much more for the rent. He would like the room with a short walk distance to the university and there are some living facilities such as a bed, internet, TV, refrigerator and so on. He takes these requirements into consideration synthetically and defines the concept 'The suitable room to rent' (denoted as S_r) by some properties which are 'Price', 'Rental period', 'Time cost of walk' and 'Facilities'. In his consideration, some properties are more important than other properties. He concentrates more on the 'Price' and less on 'Rental period', 'Time cost of walk' and 'Facilities' for the reason that he has limited budget for rent. The importance weights of these properties are given in table I. The concept S_r is defined as following:

$$S_r : [A]_{0.95}, [B]_{0.9}, [C]_{0.85}, [D]_{0.8}$$

where the subscript of each property is the minimal requirement of the property. Objects (e.g., all candidate rooms) satisfying all minimal requirements of defining properties of S_r (e.g., 'The suitable room to rent') belong to S_r to a degree 1 [5] [6]. Suppose there are two candidate rooms denoted by O_1 and O_2 as following (properties of O_1 and O_2 are shown in table II).

TABLE I
Importance weights of properties of the concept Sr.

	A	B	C	D
	Price	Rental period	Time cost of walk	Facilities
weight	0.4	0.3	0.2	0.1

TABLE II
Properties of the Objects O_1 and O_2.

	Price	Rental period	Time cost of walk	Facilities
O_1	2600 HKD	10 months	11 minutes	basic
O_2	3500 HKD	12 months	8 minutes	convenience

$$O_1 : [A]_1, [B]_1, [C]_{0.9}, [D]_{0.4}; O_2 : [A]_{0.6}, [B]_{0.8}, [C]_1, [D]_1$$

The subscript of each property is the degree of an object possessing the property. We want to calculate object memberships for two rooms O_1 and O_2 in concept S_r.

We use equations in AuYeung-Leung model [5] to measure the memberships of O_1 and O_2 and obtain the following results:

$$\mu_{S_r}(O_1) = 0.52, \mu_{S_r}(O_2) = 0.604$$

Besides, we also calculate the memberships of O_1 and O_2 in S_r according to the axioms and equations in Cai-Leung model [6] and get the results as following:

$$\mu_{S_r}(O_1) = 0.5, \mu_{S_r}(O_2) = 0.6136$$

We can find that the results calculated by previous models are not intuitive. The room O_1 satisfies properties A and B to high degrees and these properties are considered as top two important properties for Bob. Although O_2 possesses properties C and D to high degrees, it possesses the more important (more considerable) properties A and B to lower degrees. What is more, the rent of O_2 also are too much more than the budget of rent that Bob can offer, and it requires Bob to rent the room for at least 12 months which is longer than the visiting period of Bob. Thus, it is clearly that O_1 should be a better candidate than O_2 for Bob to rent and should be given a higher object membership in S_r. Previous models take all properties into account equivalently and cannot reflect the importance of properties, thus the object memberships in concepts defined by properties with different importance are not intuitive and reasonable.

Example 2. Suppose in an IT company, a secretary need to find a suitable time slot to arrange a meeting for discussing a project. The CTO of the company, the project team leader, project coordinator and the team members must attend the meeting. To which a time slot is a suitable one for the meeting depends on preference degrees (PDs) of the people who attend the meeting. Besides, from the point of view of the secretary, the priorities of preferences of these people are different. The preference of the CTO is prior to that of others. The

TABLE III
DEFINING PROPERTIES AND THEIR PRIORITIES IN CONCEPT S_t

A	PDs of CTO	first priority
B	PDs of team leader	second priority
C	PDs of project coordinator	second priority
D	PDs of team member	third priority

preference of the team leader is as the same as that of the project coordinator, and is priori to the team members. Thus, for the concept 'suitable time slot for the meeting' denoted by S_t, it is defined by four properties with priorities shown in table III.

We consider that the concept S_t is defined as following:

$$S_t : [A]_1, [B]_{0.95}, [C]_{0.9}, [D]_{0.8}$$

where the subscript of each property is the minimal requirement of the property. For three time slots denoted by O_{t1}, O_{t2}, O_{t3} as following, we want to calculate object memberships for them in concept S_t.

$$O_{t1} : [A]_1, [B]_{0.9}, [C]_{0.65}, [D]_{0.5}$$

$$O_{t2} : [A]_{0.9}, [B]_{0.72}, [C]_{0.65}, [D]_1$$

$$O_{t3} : [A]_{0.9}, [B]_{0.85}, [C]_{0.75}, [D]_{0.6}$$

The subscript of each property is the degree of an object possessing the property. We use equations in AuYeung-Leung model [5] to measure the memberships of O_{t1}, O_{t2} and O_{t3} and obtain the following results:

$$\mu_{S_t}(O_{t1}) = 0.6, \mu_{S_t}(O_{t2}) = 0.685, \mu_{S_t}(O_{t3}) = 0.68$$

Similarly, we calculate the memberships of O_{t1}, O_{t2} and O_{t3} in S_t according to the axioms and equations in the [6] and get the results as following:

$$\mu_{S_t}(O_{t1}) = 0.6667, \mu_{S_t}(O_{t2}) = 0.8667, \mu_{S_t}(O_{t3}) = 0.8$$

We can find that the results calculated by previous models are not intuitive. The CTO and the team leader prefer time slot O_{t1} to a higher degree than other time slots, while the project coordinator prefer O_{t3} and other team members prefer O_{t2}. O_{t1} should be a more suitable time slot for the meeting than O_{t2} and O_{t3} for the reason that the CTO has the highest priority. Similarly, O_{t3} should have higher membership in S_t than O_{t2} for the similar reason.

According to the above examples, we can find that previous models cannot handle the cases of which defining properties of concepts have different importance degrees or priority degrees.

IV. A FORMAL MODEL OF ONTOLOGY WITH PROPERTY IMPORTANCE AND PROPERTY PRIORITY

In this section, we propose a novel formal model of fuzzy ontology with property importance and property priority.

A. A Conceptual Model of Fuzzy Ontology

Following the works in [6], we consider a fuzzy ontology O in a particular domain Δ consisting of a set of fuzzy concepts, a set of fuzzy properties and a set of objects.[1]

An object in an ontology is represented by a set of properties named **object property vector**. An object property vector $\overrightarrow{P}_a$ of an object a is a vector of $property^{value}$ pairs as following:

$$\overrightarrow{P}_a = (p_{a,1}^{v_{a,1}}, p_{a,2}^{v_{a,2}}, ..., p_{a,n}^{v_{a,n}}), 1 \leq i \leq n$$

where $p_{a,i}$ is a property a possessing, $v_{a,i}$ is the degree to which a possesses property $p_{a,i}$. The relation among properties in the object property vector is conjunction.

We combine the classical view and fuzzy set theory so that our model can handle vague concepts. We consider that all members of a concept should possess all defining properties of the concept to some degrees. A concept can be defined by a set of properties. Besides, there is a minimal requirement for each defining property of concepts. If an object possesses all defining properties of a concept to higher degrees, then it means that the object satisfies the minimal requirements of defining properties to higher degrees. Thus the object is given a higher membership degree in the concept.

Based on classical view and fuzzy set theory, the generation of representation of a concept C is as following [6]:

$$\overrightarrow{C} = (\overrightarrow{S}_1, \overrightarrow{S}_2, ..., \overrightarrow{S}_m), 1 \leq i \leq m$$

and

$$\overrightarrow{S}_i = (p_{i,1}^{w_{i,1}}, p_{i,2}^{w_{i,2}}, ..., p_{i,n_i}^{w_{i,n_i}}), 1 \leq j \leq n_i$$

where n_i is the number of properties in $\overrightarrow{S}_i$. A $\overrightarrow{S}_i$ is named a **characteristic vector** of C which consists of a set of defining properties. The relation among characteristic vectors is union, and the relation among defining properties in a $\overrightarrow{S}_i$ is conjunction. $p_{i,j}$ is a defining property in a $\overrightarrow{S}_i$. $w_{i,j}$ is considered as a minimal requirement of property $p_{i,j}$ and $w_{i,j} \in (0, 1]$. Thus, a concept can be defined by some characteristic vectors, and such a representation of a concept can handle conjunction concepts, disjunction concepts and combination concepts [6].

B. Modeling Property Importance

The membership of an object in a concept is affected by the satisfaction degrees of the object satisfying minimal requirements of all defining properties of the concept. Among all defining properties, some properties have more affection on the object membership measurement than others and we consider that such properties are more important than other properties for object membership calculation. For different concepts, their defining properties are different and the importance of those defining properties are different also. The effect caused by decreasing of the degree of an object possessing a property with a higher importance may be compensated by (be substituted by) increasing more degrees of the object possessing other properties with relative lower priority in a

[1]In the rest of this paper, all concepts, and properties are referred to fuzzy concepts and fuzzy properties respectively unless otherwise specified.

concept. For example, although the location of a house is worse than that of another one, if its rent is much more cheaper than that of the other one then it still is a better candidate to rent.

According to some main dictionaries, importance means a quality or aspect having great worth or significance, and it implies a value judgment of the superior worth or influence of something or someone. What is more, weight implies a judgment of the immediate relative importance of something. Thus, we can consider that there is a weight distribution among all defining properties, and such weights are corresponding to the importance of the corresponding defining properties, the sum of all weights is 1.

The importance of properties in a concept are represented by a **property importance vector** in which values are used to indicate effect of corresponding defining properties on object membership measurement in the concept.

Definition 1. A **property importance vector** of a concept c, denoted by $\overrightarrow{t}^c$, is a vector of $property^{value}$ pairs as following:

$$\overrightarrow{t}^c = (p_1^{r_1}, p_2^{r_2}, \cdots, p_n^{r_n}), 1 \leq i \leq n, r_i \in (0, 1]$$

where n is the number of properties in the domain, r_i is the importance value of property p_i.

If a property p_i is more important than another property p_j in a concept definition, i.e., p_i has more affection on object membership than p_j, then importance value r_i of p_i is greater than that (i.e., r_j) of p_j in $\overrightarrow{t}^c$. If $r_i = 1$ and $\sum_{i=1}^{n} r_i = 1$ means that there is only one defining property for the concept, and this single defining property is absolutely important. $\sum_{i=1}^{n} r_i = 1$ means that measuring memberships of objects in a concept is based on all defining properties of the concept. In different application domains, users have different perspective for concepts. Thus, such a property importance vector is given by users.

C. Modeling Property Priority

According to main English dictionaries, priority is used to measure the relative precedence among things in a group. The higher the priority of one thing, the earlier the thing should be handled or the more preferred is the thing.

According to people's intuition and the explanation of main English dictionaries, the essential meaning of priority is that, the effect of a property with higher priority on object membership is in a higher level than that of property with lower priority. In other words, the effect caused by any decreasing of the degree of an object possessing a property with a higher priority cannot be compensated by increasing no matter to what degrees the object possessing other properties with lower priority in a concept. If one wants to raise the object membership of an object in a concept, a defining property with a relatively higher priority must be sufficiently satisfied prior to a defining property with a relatively lower priority.

We consider that priorities of properties in a concept are represented by a property priority vector of the concept, in which are used to indicate preference order of satisfying properties on measuring object memberships.

Definition 2. A **property priority vector** of a concept c is a vector of $property^{value}$ pairs as following:

$$\overrightarrow{\rho}^c = (p_1^{u_1}, p_2^{u_2}, \cdots, p_n^{u_n}), 1 \leq i \leq n, u_i \in \Omega$$

where n is the number of properties in the domain, u_i is the priority value of property p_i and Ω is a total order set.

Such a property priority vector is given by users for the reason that different users have different consideration on property priorities. In the property priority vector, u_i is the priority value of corresponding property p_i, and it is used to indicate the priority (preference order) of p_i. Furthermore, we present two propositions for priority ordering.

Proposition 1. If a property p_i **is prior to** (more preference than) property p_j in concept c, then u_i is succeeded by u_j in Ω, denoted by $u_i \succ_c u_j$.

Proposition 2. If a property p_i **is prior to or have the same priority with** property p_j in a concept c, then u_i is succeeded by u_j or u_i is equal to u_j, denoted by $u_i \succeq_c u_j$.

V. Formalizing Object Memberships

As mentioned above, the membership of an object in a concept depends on aggregating satisfaction degrees of the object satisfying the minimal requirements of all defining properties of the concept.

A. Local Satisfaction Degrees

Definition 3. The **local satisfaction degree** (LSD) of an object a for a properties p_i in a characteristic vector $\overrightarrow{S}_x$ is the degree of object a satisfying the minimal requirement of p_i in $\overrightarrow{S}_x$.

The local satisfaction degree (LSD) of object a for property p_i in a characteristic vector $\overrightarrow{S}_x$ is a degree in the range of [0,1] and it is given by a local satisfaction function ℓ.

$$\ell : Q \times O \rightarrow [0, 1]$$

where Q is the set of defining properties, O is the set of object property vector. If $\ell(p_i, \overrightarrow{P}_a) = 1$, it means that object a definitely satisfies the minimal requirement of property p_i. If $\ell(p_i, \overrightarrow{P}_a) = 0$, it means that object a does not satisfy the minimal requirement of property p_i at all. We present some axioms for the local satisfaction function ℓ to observe.

Axiom 1. For an object a, a defining property $p_{S,i}$ in characteristic vector $\overrightarrow{S}$, if a possesses property $p_{S,i}$ to a degree greater than the minimal requirement of $p_{S,i}$, i.e., $v^a_{S,i} \geq w_{S,i}$, then $\ell(p_{S,i}, \overrightarrow{P}_a) = 1$.

Axiom 2. For an object a, a defining property $p_{S,i}$ in characteristic vector $\overrightarrow{S}$, if a possesses property $p_{S,i}$ to a degree 0, i.e., $p^a_{S,i} = 0$, then $\ell(p_{S,i}, \overrightarrow{P}_a) = 0$.

Axiom 3. For an object a, two defining properties $p_{S,i}$ and $p_{S,j}$ in characteristic vector $\overrightarrow{S}$, $v^a_{S,i} < w_{S,i}$ and $v^a_{S,j} < w_{S,j}$, and $v^a_{S,i} = v^a_{S,j}$, $w_{S,i} \geq w_{S,j}$, then $\ell(p_{S,i}, \overrightarrow{P}_a) \leq \ell(p_{S,j}, \overrightarrow{P}_a)$

Axiom 4. For an object a, two defining properties $p_{S,i}$ and $p_{S,j}$ in characteristic vector $\overrightarrow{S}$, $v^a_{S,i} < w_{S,i}$, $v^a_{S,j} < w_{S,j}$ and $v^a_{S,i} \geq v^a_{S,j}$, if $w_{S,i} = w_{S,j}$, then $\ell(p_{S,i}, \overrightarrow{P}_a) \geq \ell(p_{S,j}, \overrightarrow{P}_a)$

Axiom 5. For two objects a and b, a defining property $p_{S,i}$ in characteristic vector $\overrightarrow{S}$, $v^b_{S,i} \leq v^a_{S,i} < w_{S,i}$, then $\ell(p_{S,i}, \overrightarrow{P}_a) \geq \ell(p_{S,i}, \overrightarrow{P}_b)$

Theorem 1. For an object a, two defining properties $p_{S,i}$ and $p_{S,j}$ in characteristic vector $\overrightarrow{S}$, $v^a_{S,i} < w_{S,i}$, $v^a_{S,j} < w_{S,j}$ and $v^a_{S,i} \geq v^a_{S,j}$, if $w_{S,i} \leq w_{S,j}$, then $\ell(p_{S,i}, \overrightarrow{P}_a) \geq \ell(p_{S,j}, \overrightarrow{P}_a)$

Axioms 1 and 2 specify the boundary cases of local satisfaction degrees of objects for properties. Axioms 3 specifies the influence of minimal requirements of properties, and it means that the higher minimal requirement of a property is the stricter requirement of the property, thus the less LSDs for an object for the property. Axioms 4 and 5 specify the influence of degrees of objects possessing properties, and they show the monotonic increase of the LSDs of objects for properties as the increase of degrees of objects possessing properties.[2]

We propose a possible function which satisfies the Axioms 1 to 5.

$$\ell(p_{S,i}, \overrightarrow{P}_a) = \begin{cases} v_{S,i} + (1 - w_{S,i}) & v^a_{S,i} < w_{S,i} \\ 1 & v^a_{S,i} \geq w_{S,i} \end{cases} \quad (1)$$

B. Global Satisfaction Degrees with Weighted Properties

After obtaining all local satisfaction degrees of an object for all defining properties in a characteristic vector, we need to aggregate all of them and the aggregation degree is named as **Global Satisfaction Degree** (GSD). There are two kinds of Global Satisfaction Degree. One is corresponding to characteristic vectors defined with weighted properties and another is corresponding to characteristic vector defined with prioritized properties.

Definition 4. The global satisfaction degree (GSD) of an object a for a characteristic vector $\overrightarrow{S}$ defined with weighted properties is an aggregation degree of aggregating all local satisfaction degrees of a for properties in $\overrightarrow{S}$, which is in the range of [0,1].

While a concept is defined by a set of weighted properties, the global satisfaction degree of an object for a characteristic vector depends on aggregating not only all local satisfaction degrees, but also the importance of the corresponding properties. The higher degree of an object satisfying an property and the more importance of the property are, the higher object membership.

We consider that the global satisfaction degree of an object for a characteristic vector consisting of weighted properties is given by a function:

$$g^t : (T \times L)^n \rightarrow [0, 1]$$

where T is the set of property importance vectors, L is the set of LSDs of objects for properties and n is the set of numbers of defining properties in characteristic vectors.

We also can represent such a function as the following:

$$g^t_{S,a} = \oplus^n_{i=1}\{(r_{S,i}, \ell(p_{S,i}, \overrightarrow{P}_a)) | p_{S,i} \in \overrightarrow{S}\}$$

[2]We do not show the verification of all axioms and the proof of all theorems in the paper for the limitation of space.

where $p_{S,i}$ is a defining property of a characteristic vector $\overrightarrow{S}$, $r_{S,i}$ is the importance value of property p_i in a concept C where $\overrightarrow{S} \in \overrightarrow{C}$ and $\oplus$ is an aggregation function.

Properties with higher importance have more effects on the global satisfaction degrees than other properties with lower importance while aggregating all local satisfaction degrees. It means that an object can possess a higher GSD if it satisfies properties which are more important to higher degrees. This is in line with the intuition of people and the essence of the importance.

The function $g^t_{S,a}$ should observe the following axioms:

Axiom 6. For an object a and a characteristic vector $\overrightarrow{S}$, if $\exists i$ where $p_{S,i} \in \overrightarrow{S}$, $\ell(p_{S,i}, \overrightarrow{p}_a) = 0$, then $g^t_{S,a} = 0$

Axiom 7. For an object a and a characteristic vector $\overrightarrow{S}$, if $\forall i$ where $p_{S,i} \in \overrightarrow{S}$, $\ell(p_{S,i}, \overrightarrow{p}_a) = 1$, then $g^t_{S,a} = 1$

Axiom 8. For two objects a and b, a characteristic vector $\overrightarrow{S}$, if for some properties $p_{S,i} \in \overrightarrow{S}$, $\ell(p_{S,i}, \overrightarrow{p}_a) \geq \ell(p_{S,i}, \overrightarrow{p}_b)$, and $\forall x$ where $x \neq i, p_{S,x} \in \overrightarrow{S}$ and $\ell(p_{S,x}, \overrightarrow{p}_a) = \ell(p_{S,x}, \overrightarrow{p}_b)$, then $g^t_{S,a} \geq g^t_{S,b}$

Axiom 9. For an object a, two characteristic vectors $\overrightarrow{S}$ and $\overrightarrow{K}$, if for property $p_{S,i} \in \overrightarrow{S}$ and property $p_{K,j} \in \overrightarrow{K}$, $i \neq j, r_{S,i} = r_{K,j}$, $\ell(p_{S,i}, \overrightarrow{p}_a) \geq \ell(p_{K,j}, \overrightarrow{p}_a)$, and for all other properties x in $\overrightarrow{S}$ are also shared by $\overrightarrow{K}$, $x \neq i \neq j, \ell(p_{S,x}, \overrightarrow{p}_a) = \ell(p_{K,x}, \overrightarrow{p}_a)$, then $g^t_{S,a} \geq g^t_{K,a}$

Axiom 10. For two objects a and b, two defining properties $p_{S,i}$ and $p_{S,j}$ in a characteristic vector $\overrightarrow{S}$, $r_{S,i} > r_{S,j}$, if $r_{S,i} - r_{S,j} = \gamma, \gamma > 0$, $\ell(p_{S,i}, \overrightarrow{P}_a) - \ell(p_{S,i}, \overrightarrow{P}_b) = \delta, \delta \geq 0$ and $\ell(p_{S,j}, \overrightarrow{P}_b) - \ell(p_{S,j}, \overrightarrow{P}_a) = \delta', \delta' \geq 0$, and $\forall x$ where $x \neq i \neq j, \ell(p_{S,x}, \overrightarrow{P}_a) = \ell(p_{S,x}, \overrightarrow{P}_b)$, and $\exists \epsilon \geq 0, \delta' - \delta = \epsilon$, then $g^t_{S,b} \leq g^t_{S,a}$.

Axioms 6 and 7 specify the boundary cases of global satisfaction degrees of objects for characteristic vectors. Axioms 8 and 9 specify the influence of the LSDs of objects for properties on GSDs of objects for characteristics vectors consisting of weighted properties. They show the monotonicity of the aggregation, i.e., the global satisfaction degree of an object for a characteristic vector should increase when the local satisfaction degrees of the objects for defining properties in the characteristic vector increase.

Axiom 10 shows the essential of importance of properties. The effect of a more important property on GSDs of objects for a characteristic vector is greater than that of less importance properties. Besides, the effects reduced by decreasing the importance of properties can be compensated by increasing LSDs of objects for other properties.

We present a possible function which satisfies Axiom 6 to 10 as following:

$$g^t_{S,a} = \begin{cases} \sum^n_{i=1} r_{S,i} \times \ell(p_{S,i}, \overrightarrow{p}_a) & others \\ 0 & \exists i, \ell(p_{S,i}, \overrightarrow{p}_a) = 0 \end{cases} \quad (2)$$

If all properties in a characteristic vector have the same importance (i.e., the same weight), it is a special case of characteristic vector with weighted properties. In such a special case, all properties in a characteristic vector are equivalent properties and the function $g^t_{S,a}$ does not need to satisfy Axiom

10 (only need to observe Axioms 6 to 9) for the reason that all property importance are the same. In this special case, the GSD of an object for a characteristic vector defined by equivalent properties is given by a function denoted by $g^l_{S,a}$:

$$g^l_{S,a} = \Phi^n_{i=1}\{\ell(p_{S,i}, \overrightarrow{P}_a)|p_{S,i} \in \overrightarrow{S}\}$$

where Φ is an aggregation function only satisfying Axioms 6-9. We present a possible function for $g^l_{S,a}$ as following:

$$g^l_{S,a} = \begin{cases} \frac{\sum_{i=1}^{n} \ell(p_{S,i}, \overrightarrow{p}_a)}{n} & others \\ 0 & \exists i, \ell(p_{S,i}, \overrightarrow{p}_a) = 0 \end{cases} \quad (3)$$

Equation 3 observes Axioms 6 to 9 and does not observe Axiom 10, and it is also a special case of Equation 2. In such a special case, for Equation 2, the weight of each property in characteristic vector $\overrightarrow{S}$ is $\frac{1}{n}$, i.e., $\forall i, r_{S,i} = \frac{1}{n}$.

C. Global Satisfaction Degrees with Prioritized Properties

Property priority is different from property importance. The affections of properties with different priority on object membership are in different level. Each priority value in Ω is corresponding to a priority level. The effect of increase of LSDs of an object for lower priority properties cannot be cumulated so as to compensate that of decrease of LSDs of the object for higher priority properties. In other words, if the local satisfaction degree of an object O_a for the highest priority property in a concept C is greater than that of another object O_b, then the object membership of O_a in C is greater than that of O_b no matter to what degrees the LSDs of these two objects for other properties with lower priorities are. For example, the vetoes of permanent member of the UN Security Council (i.e., USA, UK, France, Russia and China) have higher priority than that of other members, and if a proposal is not approved by any one of the permanent members, then the proposal cannot be passed even if all non-permanent members agree to it. Thus, we cannot combine the LSDs of objects for higher priority properties with that of the LSDs of objects for lower priority properties by simply aggregation as introduced in Section 5.2.

To reflect the characteristics of priority of properties, we consider that there is a corresponding global satisfaction degree for each priority level.

Definition 5. The **ith-level global satisfaction degree** of object a for a characteristic vector $\overrightarrow{S}$ denoted by $g^{\rho,i}_{s,a}$ is an aggregation degree of aggregating all local satisfaction degrees of the object for properties with a priority i ($i \in \Omega$) in $\overrightarrow{S}$, which is in the range of [0,1].

There may be some properties which have the same priority. In other words, there are some properties in ith priority level, and these properties are considered as equivalent properties in ith priority level. We consider that ith-level global satisfaction degree of an object a for a characteristic vector $\overrightarrow{S}$ is determined as following:

$$g^{\rho,i}_{S,a} = \Phi^n_{x=1}\{\ell(p_{S,x}, \overrightarrow{P}_a)|p_{S,x} \in \overrightarrow{S}, u_{S,x} = i\} \quad (4)$$

where $\ell(p_{S,x}, \overrightarrow{P}_a)$ is the local satisfaction degree of object a for property $p_{S,x}$, $u_{S,x}$ is the priority of $p_{S,x}$ and Φ is an aggregation function as introduced in Section 5.2.

Definition 6. The global satisfaction degree of object a for a characteristic vector $\overrightarrow{S}$ with prioritized properties is a tuple consists of all ith-level GSDs, i.e.,

$$g^{\rho}_{S,a} = (g^{\rho,1}_{S,a}, g^{\rho,2}_{S,a}, ..., g^{\rho,n}_{S,a})$$

where n is the number of priority levels of properties in $\overrightarrow{S}$.

For the reason that global satisfaction degrees of objects for a characteristic vectors with prioritized properties are tuples, we present some axioms for comparing them.

Axiom 11. For two objects a and b, a characteristic vector $\overrightarrow{S}$ with prioritized properties, if for a priority level i, $g^{\rho,i}_{S,a} > g^{\rho,i}_{S,b}$, and for those priority levels x where $u_{S,x} \succeq u_{S,i}$ we have $g^{\rho,x}_{S,a} = g^{\rho,x}_{S,b}$, then $g^{\rho}_{S,a} > g^{\rho}_{S,b}$.

Axiom 12. For two objects a and b, a characteristic vector $\overrightarrow{S}$ with prioritized properties, if for all priority levels i where $g^{\rho,i}_{S,a} = g^{\rho,i}_{S,b}$, then $g^{\rho}_{S,a} = g^{\rho}_{S,b}$.

Theorem 2. For two objects a and b, a characteristic vector $\overrightarrow{S}$ with prioritized properties, if for all priority levels i, $g^{\rho,i}_{S,a} \geq g^{\rho,i}_{S,b}$, then $g^{\rho}_{S,a} \geq g^{\rho}_{S,b}$.

Axiom 11 shows the essential of priorities of properties. If the LSD of an object a for a property with a priority (i.e., priority level i) is greater than that of another object b, and the LSDs of a and b for properties with higher priorities are the same (i.e., priority level x), then the GSD of a will greater than that of b no matter to which degree of object a and b satisfy other properties with lower priority than i. Axiom 12 specifies the case that when two objects' GSDs are the same. If all LSDs of the two objects for all defining properties in a characteristic vector are the same, then the GSDs of them for the characteristic vector are the same.

If all properties in a characteristic vector have the same priority, it is a special case of characteristic vector with prioritized properties. In such a special case, there is only one priority level (i.e., 1st-level), and all properties in a characteristic vector are equivalent properties in the same priority level. Thus, the GSD of an object a for a characteristic vector $\overrightarrow{S}$ is equal to the 1st-level GSD (a tuple consisting only the 1st-level global satisfaction degree), i.e.,

$$g^{\rho}_{S,a} = g^{\rho,1}_{S,a} = \Phi^n_{i=1}\{\ell(p_{S,i}, \overrightarrow{P}_a)|p_{S,i} \in \overrightarrow{S}, u_{S,i} = 1\}$$

D. Measuring Object Membership

We consider the fuzzy membership of an object a in fuzzy concept C depends on the following equation:

$$\mu_C(a) = max(g'_{S_1,a}, g'_{S_2,a}, ..., g'_{S_m,a}) \quad (5)$$

where m is the number of characteristic vectors in concept C and $g'_{S_i,a}$ is the global satisfaction degree of object a for characteristic $\overrightarrow{S}_i$ in concept C. If the properties in $\overrightarrow{S}_i$ are weighted properties, then $g'_{S_i,a} = g^t_{S_i,a}$, which is a numerical value defined in Section 5.2; if the properties in $\overrightarrow{S}_i$ are prioritized properties, then $g'_{S_i,a} = g^{\rho}_{S_i,a}$, which is a tuple defined in Section 5.3.

An object may satisfy all the property minimal requirements of more than one characteristic vectors. We use the maximal value of $g'_{S_i,a}$ as the membership of a in C because that the relation among $\overrightarrow{S}_i$ is disjunction.

TABLE IV
LSDs OF O_1 AND O_2 IN THE CONCEPT S_r

	$p_{S_r,A}$	$p_{S_r,B}$	$p_{S_r,C}$	$p_{S_r,D}$
O_1	1	1	1	0.65
O_2	0.65	0.9	1	1

TABLE V
LSDs OF O_1, O_2 AND O_3 IN S_t

	$p_{S_t,A}$	$p_{S_t,B}$	$p_{S_t,C}$	$p_{S_t,D}$
O_1	1	0.95	0.75	0.7
O_2	0.9	0.77	0.75	1
O_3	0.9	0.9	0.85	0.8

VI. ILLUSTRATING EXAMPLES

Let us revisit the Example 1 in Section 3. For our model, the property importance vector of S_r is given as following:

$$\overrightarrow{t}^{S_r} = (A^{0.4}, B^{0.3}, C^{0.2}, D^{0.1})$$

Based on Equation 1, we obtain the local satisfaction degrees of O_1 and O_2 for properties in S_r shown in table IV.

We use Equations 2 and 5 to calculate the object memberships for O_1 and O_2 and get the following results:

$$\mu_{S_r}(O_1) = 0.96, \mu_{S_r}(O_2) = 0.83$$

Such a result is more intuitive than previous models. Based on our model, the room O_1 satisfies the top two importance properties A and B to higher degrees than O_2 even though it possesses properties C and D to lower degrees than O_2, thus the global satisfaction degree of O_1 for concept S_r is greater than that of O_2. Previous models do not take property importance into consideration and cannot handle objects memberships in concepts with weighted properties.

For the Example 2 in Section 3, in our model, the property importance vector of S_t is given as following:

$$\overrightarrow{\rho}^{S_t} = (A^{first}, B^{second}, C^{third}, D^{fourth})$$

Based on Equation 1, we obtain the local satisfaction degrees of O_{t1}, O_{t2} and O_{t3} for properties in the concept S_t shown in table V.

We use Equation 3, 4 and 5 to obtain the global satisfaction degree of object O_{t1}, O_{t2} and O_{t3} as following:

$$\mu_{S_t}(O_{t1}) = (1, 0.85, 0.7), \mu S_t(O_{t2}) = (0.9, 0.76, 1)$$

$$\mu S_t(O_{t3}) = (0.9, 0.875, 0.8)$$

Based on Axioms 11 and 12, the object membership comparison result of O_{t1}, O_{t2} and O_{t3} is as following:

$$\mu_{S_t}(O_{t1}) > \mu_{S_t}(O_{t3}) > \mu_{S_t}(O_{t2})$$

Such a result is more reasonable than previous models.

In the above two examples, both concepts S_r and S_t have only one characteristic vector (i.e., in Equation 5, $m = 1$), and the object memberships of objects in these two concepts depend on the object property vectors, the unique characteristic vector for each concept and property importance vector (or property priority vector).

VII. EXPERIMENT

A. Evaluation on Concepts with Property Importance

We collect the information of 200 rental houses in Hong Kong. We want to measure the membership degrees of these 200 houses for the concept of 'suitable houses to rent' for users. There are four properties for each house, which are 'Price', 'Rental period', 'Time cost of walk' and 'Facilities'. We let each user input his personal importance degrees of properties for measurement. Different users may give different importance weights for properties.

In our experiment, the standard result is a ranking of object memberships given by users through questionnaires. It is not suitable to ask people to rank too many objects based on memberships because people may be confused with too many objects in a questionnaire, so we randomly select 10 houses from those 200 houses for questionnaires of users. For each user, the randomly selected 10 houses may be different. We evaluate the calculation results of our model on the 10 houses by comparing them with the standard results given by users.

We propose a measure function $Precision$ for evaluating the calculation results based on the questionnaire.

$$Precision = 1 - \frac{\sum_{i=1}^{n} |CRank_i - QRank_i|}{m}$$

where n is the number of objects, m is the possible maximal difference between the calculation ranking of objects and questionnaire ranking of objects, $CRank_i$ is the rank number of the ith object obtained by calculation, $QRank_i$ is the rank number of the ith object given by the user. The $Precision$ function is a decreasing function of average of distances between corresponding objects' memberships rankings in calculation and questionnaire. There are 10 objects and thus m (the denominator in the equation) is 50. The precision comparison of our model and the model in [6] on concepts with property importance are shown in Fig. 1.

According to Fig. 1, our method is more accurate than previous method without property importance. The reason is that our method takes the property importance into consideration and this is in line with users. Previous method just treats all properties equivalently, thus the results of membership ranking are the same for all users, i.e., it does not distinguish different users' requirements on property importance.

B. Evaluation on Concepts with Property Priority

To evaluate our method on handling the cases with property priority, we collect the medal information of 87 countries that have medals in 2008 Olympic Games. We want to measure the membership degrees of these countries for the concept of 'Outstanding Country in 2008 Olympic Games'. There are three properties for each country, which are 'Number of Gold Medals', 'Number of Silver Medals', and 'Number of Bronze Medals'. In our method, we give the first priority to 'Number of Gold Medals', the second priority to 'Number of Silver Medals' and third priority to 'Number of Bronze Medals'. We also use the precision metric and the standard answer is obtained from the 'medal table' in 2008 Olympic Games

Fig. 1. Comparison of precision with concepts with property importance

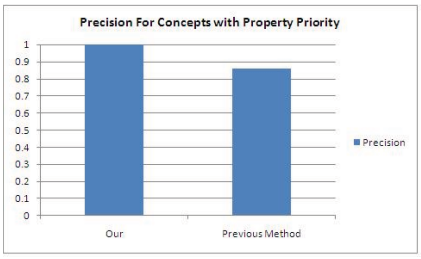

Fig. 2. Comparison of precision with concepts with property priority

website.[3] The precision comparison of our method and the method in [6] on concepts with property importance are shown in Fig. 2. According to Fig. 2, similar to Fig. 2, our method is more accurate (the same ranking as the standard answer) than previous method without property priority.

VIII. Discussions

Importance and priority are two different subjective judgements of people on properties.

Property importance is used to indicate the influence effects of corresponding properties on a cognitive task (e.g., measuring object membership in this paper). One interesting characteristic of weighted property is that the effect of a weighted property on object membership measurement can be substituted (compensated) by effects of other weighted properties. For a concept defined by weighted properties, the membership of an object in the concept is the combination degree of the object satisfying all defining properties. Properties having different importance in a characteristic vector can form a weight distribution among properties, the more important the more weight of a property. All the weighted properties can affect the object membership measurement simultaneously instead of a sequence comparison of defining properties. For instance, in Example 1, the membership of a candidate room in concept S_r depends on aggregating the local satisfaction degrees of the house for all defining properties of S_r simultaneously.

Property priority is used to indicate the preference order of satisfying defining properties for increasing object memberships. For a concept defined by prioritized properties, object membership of an object in the concept is a tuple of degrees instead of a number in the range of [0,1], and the object membership comparison depends on a sequence comparison from properties with higher priority to properties with lower priority. For a prioritized property with higher priority, the effect of it on object membership measurement cannot be substituted by effects of other prioritized properties with lower priority values. Thus, it is more reasonable to model the membership of an object in a concept defined by prioritized properties as a tuple consisting of different level GSDs instead of a number and compare the memberships of two objects level-by-level (from higher to lower priority) as a sequence comparison. For instance, in Example 2, the choose of a suitable time slot for the meeting depends on comparing the different level GSDs from high to low priority level.

[3]http://match.2008.sina.com.cn/bj2008/all_medal.php

IX. Conclusion

In this paper, we formalize object membership in fuzzy ontology with property importance and property priority. We also show that our model is more reasonable and intuitive in measuring object memberships in concepts with property importance or property priority than previous models by examples. Our formal mechanism used to measure object memberships in concepts can handle not only concepts defined by equivalent properties, but also concepts defined by weighted properties or prioritized properties well, which cannot be handled well in previous models.

Acknowledgment

The work presented in this paper is partially supported by a CUHK Research Committee Funding (Direct Grant) (Project Code EE10513).

References

[1] S. Staab and R. Studer, *Handbook on Ontologies*. Springer, 2004.
[2] U. Straccia, "A fuzzy description logic," in *AAAI '98/IAAI '98*, 1998, pp. 594–599.
[3] U. Straccia, "Towards a fuzzy description logic for the semantic web," in *ESWC 2005*, 2005, pp. 167–181. [Online]. Available: citeseer.ist.psu.edu/straccia05towards.html
[4] G. Stoilos, G. Stamou, V. Tzouvaras, J. Z. Pan, and I. Horrocks, "The Fuzzy Description Logic f-SHIN," in *Proc. of the International Workshop on Uncertainty Reasoning for the Semantic Web*, 2005.
[5] C. M. Au Yeung and H. F. Leung, "Ontology with likeliness and typicality of objects in concepts," in *ER 2006*, vol. 4215, 2006, pp. 98–111.
[6] Y. Cai and H. F. Leung, "A formal model of fuzzy ontology with property hierarchy and object membership," in *ER 2008*, 2008, pp. 69–82.
[7] E. E. Smith and D. L. Medin, *Categories and Concepts*. Harvard University Press, 1981.
[8] G. L. Murphy, *The big book of concepts*. MIT Press, 2002.
[9] K. M. Galotti, *Cognitive Psychology In and Out of the Laboratory*. Belmont, CA: Wadsworth, third edition, 2004.
[10] F. Baader, D. Calvanese, D. L. McGuinness, D. Nardi, and P. F. Patel-Schneider, Eds., *The Description Logic Handbook: Theory, Implementation, and Applications*. Cambridge University Press, 2003.
[11] G. Antoniou and F. van Harmelen, *A Semantic Web Prime: Cooperative Information Systems*. Cambridge , Mass MIT Press, 2004.
[12] L. A. Zadeh, "Fuzzy sets," *Information and Control*, vol. 8, pp. 338–353, 1965.
[13] G. J. Klir and B. Yuan, *Fuzzy sets and fuzzy logic:theory and applications*. Prentice hall PTR, 1995.
[14] V. Cross and C. R. Voss, "Fuzzy ontologies for multilingual document exploitation," in *Proceedings of the 1999 conference of NAFIPS*, 1999, pp. 392–397.
[15] F. Bobillo and U. Straccia, "fuzzyDL: An expressive fuzzy description logic reasoner," in *FUZZ-IEEE 2008*, 2008, pp. 923–930.

2011 IEEE International Conference on Fuzzy Systems
June 27-30, 2011, Taipei, Taiwan

Aggregation Operators and Fuzzy OWL 2

Fernando Bobillo
Dpt. of Computer Science and Systems Engineering
University of Zaragoza, Spain
fbobillo@unizar.es

Umberto Straccia
ISTI - CNR
Pisa, Italy
straccia@isti.cnr.it

***Abstract*—Fuzzy Description Logics (Fuzzy DLs) are logics that allow to deal with structured knowledge affected by fuzziness. Fuzzy DLs are at the heart of Fuzzy OWL 2, a fuzzy version of the standard ontology language OWL 2. Although a relatively important amount of work has been carried out in the last years, fuzzy DLs are open to be extended with several features worked out in other fields. In particular, the integration of aggregation operators (AOs) in fuzzy DLs has received little attention so far.**

In this work, we show how to support aggregation operators in fuzzy DLs. We provide syntax and semantics of a fuzzy DL extended with AOs, and provide a calculus for a family of AOs (weighted sum, OWA and quantifier-guided OWA). We also show how to encode them into our proposal for Fuzzy OWL 2.

***Keywords*—Fuzzy ontologies, Fuzzy Description Logics, Fuzzy OWL 2, Aggregation operators, OWA operators**

I. Introduction

Description Logics (DLs) [1] play a key role in the design of *Ontologies*. An Ontology consists of a hierarchical description of important concepts in a particular domain, along with the description of the properties (of the instances) of each concept. In this context, DLs are important as they are essentially the theoretical counterpart of the *Web Ontology Language OWL 2* [2], the standard language to represent ontologies.

It is well-known that "classical" ontology languages are not appropriate to deal with *vague knowledge*, which is inherent to several real world domains [3], [4]. *Fuzzy ontologies* emerge as useful in several applications, such as (multimedia) information retrieval, image interpretation, ontology mapping, matchmaking, multi-criteria decision making [5] and the Semantic Web [6]. So far, several fuzzy extensions of DLs can be found in the literature (see the survey in [6]).

A representation of fuzzy ontologies using OWL 2 annotation properties has been recently proposed (in this paper, we will call it *Fuzzy OWL 2*) [7]. The use of annotation properties makes it possible to use current OWL 2 editors for fuzzy ontology representation, such as Protégé. This approach has reached a sufficient level of maturity and there exists a Protégé plug-in to edit fuzzy ontologies, as well as some parsers that translate fuzzy ontologies represented using this approach into the languages supported by some fuzzy DL reasoners.

Aggregation Operators (AOs) are mathematical functions that are used to combine information [8]. The arithmetic mean, the weighted sum, the median and, more generally Ordered Weighted Averaging (OWA) [9] are the most well-known AOs. AOs have been widely used in computational intelligence because of their ability to fuse linguistically expressed pieces of information.

The integration of AOs and fuzzy ontologies is of great interest, in order to combine the advantages of both formalisms. In this work, we show *how to support AOs in fuzzy ontologies*. In particular, we provide syntax and semantics of a fuzzy DL extended with AOs, provide a calculus for a family of aggregation operators, such as weighted sum, OWA and quantifier-guided OWA, and show how to represent them using our previous proposal for Fuzzy OWL 2 [7].

There is little related work combining AOs and fuzzy DLs. [10] presents a fuzzy DL with AOs, but the expressivity is very limited. Also, weighted sum concepts have been proposed in the literature (see e.g., [11]). Our contributions consists of a more expressive fuzzy DL, independent of the fuzzy operators considered, together with a reasoning algorithm and a representation using OWL 2, for a family of AOs.

In the following, we proceed as follows. Section II recalls basic notions on mathematical fuzzy logic and aggregation operators. Then, Section III introduces fuzzy DLs that support aggregation operators. We provide the syntax, semantics, and reasoning algorithms for a family of AOs. Then, Section IV shows how to support them within fuzzy OWL 2 [7]. Finally, Section V sets out some conclusions and discusses future work.

II. Preliminaries

A. Mathematical Fuzzy Logic

In *Mathematical Fuzzy Logic* [12], the convention prescribing that a statement is either true or false is changed and is a matter of degree measured on an ordered scale that is no longer $\{0,1\}$, but the $[0,1]$. This degree is called *degree of truth* of the statement ϕ in the interpretation $\mathcal{I}$. In this section, *fuzzy statements* have the form $\phi \geqslant r$ or $\phi \leqslant r$, where $r \in [0,1]$ (see, e.g. [12], [13]) and ϕ is a statement, which encode that the degree of truth of ϕ is *at least* r (resp. *at most* r).

A *fuzzy interpretation* $\mathcal{I}$ maps each basic statement p_i into $[0,1]$ and is then extended inductively to all statements: $\mathcal{I}(\phi \wedge \psi) = \mathcal{I}(\phi) \otimes \mathcal{I}(\psi)$, $\mathcal{I}(\phi \vee \psi) = \mathcal{I}(\phi) \oplus \mathcal{I}(\psi)$, $\mathcal{I}(\phi \rightarrow \psi) = \mathcal{I}(\phi) \Rightarrow \mathcal{I}(\psi)$, $\mathcal{I}(\neg\phi) = \ominus\mathcal{I}(\phi)$, $\mathcal{I}(\exists x.\phi(x)) = \sup_{a\in\Delta^{\mathcal{I}}} \mathcal{I}(\phi(a))$, $\mathcal{I}(\forall x.\phi(x)) = \inf_{a\in\Delta^{\mathcal{I}}} \mathcal{I}(\phi(a))$, where $\Delta^{\mathcal{I}}$ is the domain of $\mathcal{I}$, and $\otimes$, $\oplus$, $\Rightarrow$, and $\ominus$ are *t-norms*, *t-conorms*, *implication functions*, and *negation functions*, respectively, which extend the Boolean conjunction, disjunction, implication, and negation, respectively, to the fuzzy case.

One usually distinguishes three different logics, namely Łukasiewicz, Gödel, and Product logics [12]. Zadeh logic,

978-1-4244-7316-8/11/$26.00 ©2011 IEEE

	Łukasiewicz logic	Gödel logic	Product logic
$a \otimes b$	$\max(a+b-1,0)$	$\min(a,b)$	$a \cdot b$
$a \oplus b$	$\min(a+b,1)$	$\max(a,b)$	$a+b-a \cdot b$
$a \Rightarrow b$	$\min(1-a+b,1)$	$\begin{cases} 1 & \text{if } a \leq b \\ b & \text{otherwise} \end{cases}$	$\min(1,b/a)$
$\ominus a$	$1-a$	$\begin{cases} 1 & \text{if } a=0 \\ 0 & \text{otherwise} \end{cases}$	$\begin{cases} 1 & \text{if } a=0 \\ 0 & \text{otherwise} \end{cases}$

namely $a \otimes b = \min(a,b)$, $a \oplus b = \max(a,b)$, $\ominus a = 1-a$ and $a \Rightarrow b = \max(1-a,b)$, is entailed by Łukasiewicz logic.

A *fuzzy set* R over a countable crisp set X is a function $R\colon X \to [0,1]$. The trapezoidal (Fig. 1 (a)), the triangular (Fig. 1 (b)), the L-function (left-shoulder function, Fig. 1 (c)), and the R-function (right-shoulder function, Fig. 1 (d)) are frequently used to specify membership degrees.

The notions of satisfiability and logical consequence are defined in the standard way. A fuzzy interpretation $\mathcal{I}$ *satisfies* a fuzzy statement $\phi \geqslant r$ (resp., $\phi \leqslant r$) or $\mathcal{I}$ is a *model* of $\phi \geqslant r$ (resp., $\phi \leqslant r$), denoted $\mathcal{I} \models \phi \geqslant r$ (resp., $\mathcal{I} \models \phi \leqslant r$), iff $\mathcal{I}(\phi) \geqslant r$ (resp., $\mathcal{I}(\phi) \leqslant r$).

B. Aggregation Operators

Aggregation Operators (AOs) (see, e.g. [8]) are mathematical functions that are used to combine information. There exist a large number of different AOs that differ on the assumptions on the data (data types) and about the type of information that we can incorporate in the model. To what concerns us, an AO of dimension n is a mapping $@ : \mathbb{R}^n \to \mathbb{R}$ that satisfies:

1) $@(a) = a$ (idempotent if unary)
2) $@(0,\ldots,0) = 0$ and $@(1,\ldots,1) = 1$ (boundary conditions)
3) $@(a_1,\ldots,a_n) \leq @(b_1,\ldots,b_n)$ if $\forall i, a_i \leq b_i$ (monotone)

Note that we always have that

$$\min(a_1,\ldots,a_n) \leq @(a_1,\ldots,a_n) \leq \max(a_1,\ldots,a_n) \ .$$

Often, an AO $@$ is parameterised with a vector of n weights $W = [w_1,\ldots,w_n]$ such that $w_i \in [0,1]$ and $\sum_i w_i = 1$. In that case we will denote the AO as $@_W$.

Examples of AOs are the *arithmetic mean*,

$$@^{\text{avg}}(a_1,\ldots,a_n) = \frac{1}{n}\sum_i a_i \tag{1}$$

the *weighted sum*

$$@^{\text{ws}}_W(a_1,\ldots,a_n) = \sum_i w_i a_i \ , \tag{2}$$

and the *Ordered Weighted Averaging* (OWA) operators and the quantifier-guided OWAs that we shall present next.

The OWA operators [9], [14], [15] provide a parameterised class of mean type AOs. Formally, an OWA operator of dimension n is an AO such that

$$@^{\text{owa}}_W(a_1,\ldots,a_n) = \sum_j w_j b_j \ , \tag{3}$$

where b_j is the j-th largest of the a_i.

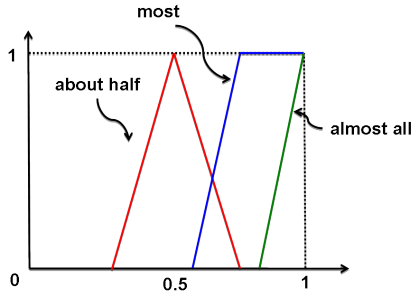

Fig. 2. Some examples of fuzzy quantifiers.

A fundamental aspect of these operators is the reordering step. In particular, a weight w_i is not associated with a specific argument but with an ordered position of the aggregate. By choosing different W we can implement different AOs. The OWA operator is a non-linear operator as a result of the process of determining the b_j. An OWA operator $@$ is a mean operator and is also symmetric and idempotent:

$$\begin{aligned} &\textit{Symmetric} : @(a_1,\ldots,a_n) = @(a_{\pi(1)},\ldots,a_{\pi(n)}) \\ &\textit{Idempotent} : @(a,\ldots,a) = a \end{aligned}$$

where π is a permutation. Notable OWA operators are:

$$\begin{aligned} f(a_1,\ldots,a_n) &= \max(a_1,\ldots,a_n) \text{ for } W = [1,0,\ldots,0] \\ f(a_1,\ldots,a_n) &= \min(a_1,\ldots,a_n) \text{ for } W = [0.\ldots,0,1] \\ f(a_1,\ldots,a_n) &= \text{avg}(a_1,\ldots,a_n) \text{ for } W = [1/n,1/n,\ldots,1/n] \\ f(a_1,\ldots,a_n) &= \text{med}(a_1,\ldots,a_n) \text{ for } w_i = 0, \\ &\qquad n \text{ odd and } w_{(n+1)/2} = 1, \text{ or} \\ &\qquad n \text{ even and } w_{n/2} = 0.5 = w_{n/2+1} \end{aligned}$$

In the equations above, avg and med are the average and median value of the a_i, respectively.

As next we recap *quantifier aggregations* [14], [16], [17], [18]. Classical logic has two quantifiers, the universal $\forall$ and the existential $\exists$ quantifier. These are extremal ones among several other linguistic quantifiers such as *most, few, about half, some, many*, etc. Quantifiers can be seen as absolute of proportional (see, e.g. [18]). To what concerns us, we consider the proportional ones. In this case, a proportional type quantifier, such as *most*, can be represented as a fuzzy subset $Q : [0,1] \to [0,1]$ such that for each $r \in [0,1]$, the membership grade $Q(r)$ indicates the degree to which the proportion r satisfies the linguistic quantifier that Q represents. See Figure 2 for examples of fuzzy quantifiers.

An important class of quantifiers are the *monotone quantifiers* that satisfy the following conditions:

1) $Q(0) = 0$,
2) $Q(1) = 1$,
3) $Q(r_1) \leq Q(r_2)$ if $r_1 \leq r_2$.

Essentially, these quantifiers are characterised by the idea that as the proportion increases, the degree of satisfaction does not decrease. For two quantifiers Q_1, Q_2, we write $Q_1 \leq Q_2$ if for all r, $Q_1(r) \leq Q_2(r)$. We recall that the two classical quantifiers $\exists, \forall$ may be defined as the monotone quantifiers $Q_\exists(r) = 0$ if $r \neq 1$ and $Q_\forall(r) = 1$ if $r \neq 0$, respectively. Note that for any monotone quantifier Q, we have that

$$Q_\forall \leq Q \leq Q_\exists \tag{4}$$

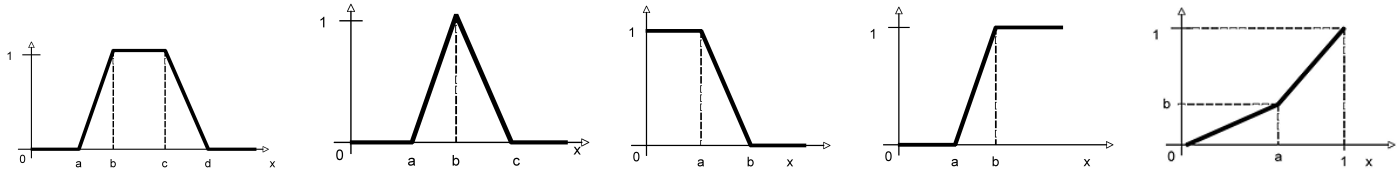

(a) (b) (c) (d) (e)

Fig. 1. (a) Trapezoidal function; (b) Triangular function; (c) L-function; (d) R-function; (e) Linear function .

dictating that $\forall$ and $\exists$ are indeed the lower and upper bounds of monotone quantifiers.

To introduce quantifier-guided aggregation, we consider first the evaluation of quantified propositions. So, let Y be a (crisp) set of objects and B some fuzzy subset of Y. A quantified proposition is a statement of the form

$$QY\text{'s are } B \quad .$$

An example of such a statement is "most students are young". Yager [16] suggested an approach to evaluate the truth of such quantified propositions using OWA. In the following we will assume that Q is a monotone quantifier. The first step consists in associating to Q an OWA weighting vector W_Q of dimension $n = |Y|$, where $|S|$ is the cardinality of a denumerable set S. The weights are obtained as

$$w_j = Q(\frac{j}{n}) - Q(\frac{j-1}{n}) \ . \tag{5}$$

Note that for Q monotone, $w_j \in [0,1]$ and $\sum_j w_j = 1$. Now, we can obtain the truth t of the statement "QY's are B" as

$$t = @^{\text{owa}}_{W_Q}(a_1, \ldots, a_n) \tag{6}$$

where $a_i = B(y_i)$, $y_i \in Y$ and $@^{\text{owa}}_{W_Q}$ is the OWA operator obtained using the weights W_Q found from Q as above.

We turn now to the issue of quantifier-guided aggregation, that have been shown to be useful for evaluating multi-criteria decision problems [19]. So, assume X to be a set of alternatives and we have a collection of n criteria A_i that are of concern in a given problem. For $x \in X$, with $A_i(x)$ we indicate the degree to which the i-th criterion is satisfied by alternative x. It is easily verified that the degree to which *all* criteria are satisfied by x can be determined by $D(x) = \min(A_1(x), \ldots, A_n(x))$ while the degree to which *some* criteria is satisfied by x can be determined by $D(x) = \max(A_1(x), \ldots, A_n(x))$. In general, for a monotone quantifier Q, the degree to which

$$Q \text{ of the criteria are satisfied by } x$$

can be formalised as

$$D(x) = @^{\text{owa}}_{W_Q}(A_1(x), \ldots, A_n(x)) \ , \tag{7}$$

where $@^{\text{owa}}_{W_Q}$ is the OWA operator obtained using the weights W_Q found from Q.

Thus, by selecting an appropriate weighting vector W, we are essentially implementing a kind of quantifier-guided aggregation.

III. Aggregation Operators and Fuzzy DLs

The aim of this section is to show how current fuzzy DLs can be extended to support AOs. For illustrative purposes and for reasons of space, we will just consider a minimal fuzzy DL (see, e.g. [11] for a more expressive fuzzy DL). For the sake of our purpose, we will consider $\mathcal{ALCF}(\mathbf{D})$ [20], which is the basic DL $\mathcal{ALC}$ extended with functional roles (letter $\mathcal{F}$) and fuzzy concrete domains (letter $\mathbf{D}$).

A. The Fuzzy DL $\mathcal{ALCF}(\mathbf{D})$ with Aggregation Operators

In general, a *fuzzy concrete domain* (or simply *fuzzy domain*) is a pair $\langle \Delta_{\mathbf{D}}, \Phi_{\mathbf{D}} \rangle$, where $\Delta_{\mathbf{D}}$ is an interpretation domain and $\Phi_{\mathbf{D}}$ is the set of *fuzzy domain predicates* $\mathbf{d}$ with a predefined arity n and an interpretation $\mathbf{d}^{\mathbf{D}} \colon \Delta^n_{\mathbf{D}} \to [0,1]$, which is a n-ary fuzzy relation over $\Delta_{\mathbf{D}}$ [20]. In our specific fuzzy DL, we assume that predicates are unary and $\Delta_{\mathbf{D}}$ are non-negative real numbers.

Now, consider pair wise disjoint alphabets of *concepts names* (denoted A), *abstract roles names* (denoted R) and *concrete roles names* (denoted T). Within the alphabet of abstract and concrete roles, we have distinguished subsets of *abstract functional roles names* (denoted f) and *concrete functional roles names* (denoted t), respectively. Functional roles are also called *features*.

Concepts (denoted C or D) of the language can be built inductively from atomic concepts (A), top concept $\top$, bottom concept $\bot$, abstract roles (R), concrete roles (T) as follows. The syntax of fuzzy concepts is as follows [11]:

$$\begin{array}{rcl} C, D & \to & \top \mid \bot \mid A \mid C \sqcap D \mid C \sqcup D \mid \neg C \mid \\ & & \forall R.C \mid \exists R.C \mid \forall T.\mathbf{d} \mid \exists T.\mathbf{d} \\ \mathbf{d} & \to & ls(a,b) \mid rs(a,b) \mid tri(a,b,c) \mid trz(a,b,c,d) \end{array}$$

where ls, rs, tri, trz stand for left-shoulder, right-shoulder, triangular and trapezoidal membership functions. These are our concrete domain predicates. So, for instance the expression $Human \sqcap \exists hasChild.Lovely$ is a concept (unary predicate), which will denote the fuzzy set of humans that have a lovely child, while $Human \sqcap \forall hasChild.Lovely$ will denote the fuzzy set of humans that have only lovely children. Also, the expression $Human \sqcap \exists hasAge.ls(10,30)$ will denote the set of young humans (their age is $ls(10,30)$).

We next extend fuzzy DLs to support AOs. Consider a family of AOs $(@_n)$, $n \in \mathbb{N}$, each of arity $a(n)$. Then, similarly to [10], the following are concept expressions

$$C \quad \to \quad C \mid @_n(C_1, \ldots, C_{a(n)}) \ .$$

Example 1: The following concept expressions denote the fuzzy set of hotels that are cheap, close to the venue and comfortable, in which the degree is computed respectively as the weighted sum, the OWA aggregation and the quantifier-guided aggregation.

$$Hotel \sqcap @^{\text{ws}}_{W}(Cheap, CloseToVenue, Comfortable)$$
$$Hotel \sqcap @^{\text{owa}}_{W}(Cheap, CloseToVenue, Comfortable)$$
$$Hotel \sqcap @^{\text{owa}}_{W_Q}(Cheap, CloseToVenue, Comfortable)$$

It is interesting to note that a weighted sum concept $@^{\text{ws}}_{W}(C_1, \ldots, C_n)$ cannot be represented using an OWA operator $@^{\text{owa}}_{W}(C_1, \ldots, C_n)$, because in a weighted sum concept every weight is assigned to a specific concept, whereas in OWA operators every weight is associated to the concept that corresponds to a specific position after a reordering step.

A *Fuzzy Knowledge Base* (or *fuzzy Ontology*) comprises a fuzzy ABox $\mathcal{A}$ and a fuzzy TBox $\mathcal{T}$. A *fuzzy ABox* consists of a finite set of *fuzzy assertions* of one of the following types: a fuzzy *concept assertion* of the form $\langle a{:}C, r\rangle$ (with informal meaning, individual a is an instance of concept C with degree at least r), or a fuzzy *role assertion* of the form $\langle (a,b){:}R, r\rangle$ (the pair of individuals (a,b) is an instance of role R with degree at least r), with $r \in [0,1]$. In FOL, $\langle a{:}C, r\rangle$ may be seen as a fuzzy statement of the form $C(a) \geqslant r$, while $\langle (a,b){:}R, r\rangle$ may be seen as a fuzzy statement of the form $R(a,b) \geqslant r$.

A *fuzzy TBox* consists of a finite set of *fuzzy General Concept Inclusions (fuzzy GCIs)*, which are expressions of the form $\langle C \sqsubseteq D, r\rangle$ (with informal meaning, the degree of subsumption between concept C and D is not less than r). $C \equiv D$ is a shorthand for both $\langle C \sqsubseteq D, 1\rangle$ and $\langle D \sqsubseteq C, 1\rangle$.

From a semantics point of view, a *fuzzy interpretation* $\mathcal{I} = (\Delta^{\mathcal{I}}, \cdot^{\mathcal{I}})$ relative to the fuzzy concrete domain $\langle \Delta_{\mathbf{D}}, \Phi_{\mathbf{D}}\rangle$, consists of a nonempty set $\Delta^{\mathcal{I}}$ (the *domain*), disjoint from $\Delta_{\mathbf{D}}$, and of a *fuzzy interpretation function* $\cdot^{\mathcal{I}}$ that coincides with $\cdot_{\mathbf{D}}$ on every fuzzy concrete predicate, and it assigns: (i) to each abstract concept C a function $C^{\mathcal{I}}\colon \Delta^{\mathcal{I}} \to [0,1]$; (ii) to each abstract role R a function $R^{\mathcal{I}}\colon \Delta^{\mathcal{I}} \times \Delta^{\mathcal{I}} \to [0,1]$; (iii) to each abstract feature f a partial function $f^{\mathcal{I}}\colon \Delta^{\mathcal{I}} \times \Delta^{\mathcal{I}} \to \{0,1\}$ such that for all $u \in \Delta^{\mathcal{I}}$ there is an unique $w \in \Delta^{\mathcal{I}}$ on which $f^{\mathcal{I}}(u,w)$ is defined; (iv) to each concrete role T a function $T^{\mathcal{I}}\colon \Delta^{\mathcal{I}} \times \Delta_{\mathbf{D}} \to [0,1]$; (v) to each concrete feature t a partial function $t^{\mathcal{I}}\colon \Delta^{\mathcal{I}} \times \Delta_{\mathbf{D}} \to \{0,1\}$ such that for all $u \in \Delta^{\mathcal{I}}$ there is an unique $v \in \Delta_{\mathbf{D}}$ on which $t^{\mathcal{I}}(u,v)$ is defined.

Given arbitrary t-norm $\otimes$, t-conorm $\oplus$, negation function $\ominus$ and implication function $\Rightarrow$, the fuzzy interpretation function is extended to *complex concepts* and *fuzzy axioms* as in Figure 3, where @ is an AO[1].

Now, we will define some common reasoning tasks [3]. Let $\alpha \in \{a{:}C, (a,b){:}R, C \sqsubseteq D\}$ and $\tau = \langle \alpha, r\rangle$. A fuzzy interpretation $\mathcal{I}$ *satisfies* (is a *model* of) a fuzzy axiom τ iff $\alpha^{\mathcal{I}} \geq r$. A fuzzy KB $\mathcal{K}$ is *satisfiable* iff there is a model $\mathcal{I}$ which satisfies each of the fuzzy axioms in $\mathcal{K}$. A fuzzy axiom τ is a *logical consequence* of a fuzzy KB $\mathcal{K}$ iff, for every model $\mathcal{I}$ of $\mathcal{K}$, $\mathcal{I} \models \tau$. The *Best Entailment Degree* (BED) of an axiom α w.r.t. a fuzzy KB $\mathcal{K}$ is defined as $bed(\mathcal{K}, \alpha) = \sup\{r \mid \mathcal{K} \models \langle \alpha, r\rangle\}$. The *Best Satisfiability Degree* (BSD) of a concept C w.r.t. a fuzzy KB $\mathcal{K}$ as $bsd(\mathcal{K}, C) = \sup_{\mathcal{I} \models \mathcal{K}} \sup_{x \in \Delta^{\mathcal{I}}} C^{\mathcal{I}}(x)$ [11].

Example 2: Suppose we have some data about hotels, as shown in the following table:

$hotel$	$price$	$distance$	$star$
h_1	150	300	4
h_2	100	500	2

Assume that we are looking for a cheap, close to the venue and comfortable hotel. To this end, we may encode the problem using a fuzzy KB $\mathcal{K}$ with the following ABox $\mathcal{A}$:

$$Hotel(h_1), Hotel(h_2), price(h_1, 150), price(h_2, 100),$$
$$distance(h_1, 300), distance(h_2, 500), star(h_1, 4), star(h_2, 2)$$

where $price, distance$ and $star$ are concrete features.

The TBox $\mathcal{T}$ holds some definitions for cheap, close and comfortable hotels and contains the following axioms:

$$\begin{aligned} Cheap &= Hotel \sqcap \exists price.ls(60, 120) \\ CloseToVenue &= Hotel \sqcap \exists distance.ls(200, 400) \\ Comfortable &= Hotel \sqcap \exists star.ls(3, 5)\ . \end{aligned}$$

Note that, e.g., we have that $\mathcal{K} \models \langle h_2{:}Cheap, 0.33\rangle$, i.e., h_2 is a cheap hotel to degree no less than 0.33 (it is easily verified that this degree is also tight). Now, for some suitable AO @, we may compute the degree n_i to which hotel h_i satisfies our request as

$$n_i = bed(\mathcal{K}, h_i{:}@(Cheap, CloseToVenue, Comfortable))$$

B. A Reasoning Algorithm

We next provide a reasoning procedure that supports a family of AOs for fuzzy DLs. To simplify our exposition, we will make the following assumptions. We restrict the fuzzy DL to the case of Lukasiewicz fuzzy logic (and, thus, support "Zadeh logic" as well). Other fuzzy logics could be dealt with similarly as in [20], [21]. Furthermore, we will restrict KBs to be *unfoldable* [22], which is defined as follows.

A fuzzy TBox $\mathcal{T}$ is *unfoldable* iff it verifies the following three constraints: (i) every axiom in $\mathcal{T}$ is either of the form $\langle A \sqsubseteq C, 1\rangle$ or $A \equiv C$, where A is an atomic concept [2]; (ii) there is no concept A such that it appears more than once on the left hand side of some axiom in $\mathcal{T}$; and (iii) no cyclic definitions are present in $\mathcal{T}$. We will say that A *directly uses* primitive concept B in $\mathcal{T}$, if there is some axiom $\tau \in \mathcal{T}$ such that A is on the left hand side of τ and B occurs in the right hand side of τ. Let *uses* be the transitive closure of the relation *directly uses* in $\mathcal{T}$. $\mathcal{T}$ is *cyclic* iff there is A such that A uses A in $\mathcal{T}$. Analogously, a fuzzy KB is said to be *unfoldable* when its TBox is unfoldable.

Unfoldable TBoxes can be eliminated through an *expansion process* [23].Essentially, each axiom $A \sqsubseteq C \in \mathcal{T}$ can be replaced with $A = C \sqcap A^*$, where A^* is a new concept name.

[1]For ease of presentation, we identify the interpretation of ls, rs, tri, trz and @ with the functions themselves.

[2]In particular this forbids concept $\top$ on the left hand side of axioms.

Concept		Semantics
$(\top)^{\mathcal{I}}(x)$	=	1
$(\bot)^{\mathcal{I}}(x)$	=	0
$(A)^{\mathcal{I}}(x)$	=	$A^{\mathcal{I}}(x)$
$(C \sqcap D)^{\mathcal{I}}(x)$	=	$C^{\mathcal{I}}(x) \otimes D^{\mathcal{I}}(x)$
$(C \sqcup D)^{\mathcal{I}}(x)$	=	$C^{\mathcal{I}}(x) \oplus D^{\mathcal{I}}(x)$
$(\neg C)^{\mathcal{I}}(x)$	=	$\ominus C^{\mathcal{I}}(x)$
$(@(C_1, \ldots, C_n))^{\mathcal{I}}(x)$	=	$@({C_1}^{\mathcal{I}}(x), \ldots, {C_n}^{\mathcal{I}}(x))$

Concept		Semantics
$(\forall R.C)^{\mathcal{I}}(x)$	=	$\inf_{y \in \Delta^{\mathcal{I}}} \{R^{\mathcal{I}}(x,y) \Rightarrow C^{\mathcal{I}}(y)\}$
$(\exists R.C)^{\mathcal{I}}(x)$	=	$\sup_{y \in \Delta^{\mathcal{I}}} \{R^{\mathcal{I}}(x,y) \otimes C^{\mathcal{I}}(y)\}$
$(\forall T.\mathbf{d})^{\mathcal{I}}(x)$	=	$\inf_{v \in \Delta_{\mathbf{D}}} \{T^{\mathcal{I}}(x,v) \Rightarrow \mathbf{d}^{\mathbf{D}}(v)\}$
$(\exists T.\mathbf{d})^{\mathcal{I}}(x)$	=	$\sup_{v \in \Delta_{\mathbf{D}}} \{T^{\mathcal{I}}(x,v) \otimes \mathbf{d}^{\mathbf{D}}(v)\}$
$(a{:}C)^{\mathcal{I}}$	=	$C^{\mathcal{I}}(a^{\mathcal{I}})$
$((a,b){:}R)^{\mathcal{I}}$	=	$R^{\mathcal{I}}(a^{\mathcal{I}}, b^{\mathcal{I}})$
$(C \sqsubseteq D)^{\mathcal{I}}$	=	$\inf_{x \in \Delta^{\mathcal{I}}} \{C^{\mathcal{I}}(x) \Rightarrow D^{\mathcal{I}}(x)\}$

Fig. 3. Semantics of fuzzy concepts and axioms.

Let $\mathcal{K}'$ the obtained knowledge base. $\mathcal{K}'$ can be *expanded* by substituting every concept name A occurring in $\mathcal{K}$, which is defined in $\mathcal{T}$, with its defining term in $\mathcal{T}$.

Note that reasoning with fuzzy GCIs requires so-called blocking conditions [1] and are known to work properly for Zadeh logic only [24]. See [22] for problems risen by GCIs within Lukasiewicz logic. These problems do not appear here due to our, by purpose, simplified assumptions.

The basic idea of the reasoning algorithm is as follows and is common to most fuzzy DLs algorithms (see, e.g. [21]). Consider $\mathcal{K} = \langle \mathcal{T}, \mathcal{A} \rangle$, where $\mathcal{T}$ is unfoldable. In order to solve the BED problem, we combine appropriate DL tableaux rules with methods developed in the context of *many-valued logics* (MVLs) [13]. In order to determine e.g., $bed(\mathcal{K}, a{:}C)$, we consider an expression of the form $\langle a{:}\neg C, 1 - x \rangle$ (informally, $\langle a{:}C \leq x \rangle$), where x is a $[0,1]$-valued variable. Then we construct a tableaux for $\mathcal{K} = \langle \mathcal{T}, \mathcal{A} \cup \{\langle a{:}\neg C, 1 - x \rangle\} \rangle$ in which the application of satisfiability preserving rules generates new fuzzy assertion axioms together with *inequations* over $[0,1]$-valued variables. These inequations have to hold in order to respect the semantics of the DL constructors. Hence, we *minimise* the original variable x such that all constraints are satisfied[3].

Similarly, for $C \sqsubseteq D$, we can compute $bed(\mathcal{K}, C \sqsubseteq D)$ as the minimal value of x such that $\mathcal{K} = \langle \mathcal{T}, \mathcal{A} \cup \{\langle a : C, x_1 \rangle\} \cup \{\langle a : D, x_2 \rangle\} \rangle$ is satisfiable under the constraints expressing that $x_1 \Rightarrow x_2 \leq x, x_1 \in [0,1]$ and $x_2 \in [0,1]$, where a is new abstract individual.

Finally, $bed(\mathcal{K}, (a,b){:}R)$ is equivalent to $bed(\mathcal{K} \cup \{\langle b : B, 1 \rangle\}, a{:}\exists R.B)$, where B is a new concept (which does not appear in $\mathcal{K}$).

Therefore, the BED problem can be reduced to minimal satisfiability problem of a KB. Finally, concerning the best satisfiability bound problem, $bsd(\mathcal{K}, C)$ is determined by the maximal value of x such that $\langle \mathcal{T}, \mathcal{A} \cup \{\langle a{:}C, x \rangle\} \rangle$ is satisfiable.

In general, depending on the semantics of the DL constructors and fuzzy domain predicates we may end up with a general, bounded *Mixed Integer Non Linear Programming* (MINLP) optimization problem. In this paper, however, due to our restrictions above and those we will impose to AOs, we will end up with a *Mixed Integer Linear Program* (MILP) optimization problem [25]. Interestingly, as for the MVL case, the tableaux we are generating contains *one* branch only and, thus, just *one* MILP problem has to be solved.

We recall that a general MILP problem consists in minimizing a linear function with respect to a set of constraints that are linear inequations in which rational and integer variables can occur. More precisely, let $x = \langle x_1, \ldots, x_k \rangle$ and $y = \langle y_1, \ldots, y_m \rangle$ be variables over $\mathbb{Q}$ and $\mathbb{Z}$ respectively, over the integers and let A, B be integer matrices and h an integer vector. The variables in y are called *control variables*. Let $f(x,y)$ be an $k+m$-ary linear function. Then the general MILP problem is to find $\bar{x} \in \mathbb{Q}^k, \bar{y} \in \mathbb{Z}^m$ such that $f(\bar{x}, \bar{y}) = \min\{f(x,y) \mid Ax + By \geq h\}$. Furthermore, we say that $M \subseteq [0,1]^k$ is MILP-representable iff there is a MILP (A, B, h) with k real and m $0-1$ variables such that $M = \{x : \exists y \in \{0,1\}^m$ such that $Ax + By \geq h\}$. In general, we require that a constructor f is MILP representable. In particular, the sets $g(f) = \{\langle x_1, \ldots, x_k, x \rangle \colon f(x_1, \ldots, x_k) \geq x\}$ and $\bar{g}(f) = \{\langle x_1, \ldots, x_k, x \rangle \colon f(x_1, \ldots, x_k) \leq x\}$ should be MILP-representable.

For instance, under Łukasiewicz t-norm, $x_1 \otimes x_2 \geq l$ can be written as $\{l \leq y, x_1 + x_2 - 1 \leq l, x_1 + x_2 - y \geq l, y \in \{0,1\}\}$. Therefore, $g(\otimes)$ is MILP representable.

To guarantee that our reasoning process ends up to solve a MILP problem, we require that every constructor is MILP representable. For instance, classical logic, Zadehs fuzzy logic, and Lukasiewicz connectives, are MILP-representable. It is not difficult to see that indeed the functions ls, rs, tri and trz are MILP representable as well (see, e.g. [20], [21]).

To guarantee that also a concept expression of the form $@(C_1, \ldots, C_n)$, involving an AO $@$, can be handled appropriately by our reasoning method, we have further to impose that $@$ is indeed MILP representable. For instance, it is easy to see that this is the case of the weighted sum, $@^{\text{ws}}_W$, while more difficult is the notably case of the OWAs, $@^{\text{owa}}_W$, for which we provide the encoding in the Appendix. Therefore, this covers also the case of quantifier based OWAs. Note that in this latter case, no particular restriction is due on the quantifier except of being monotone and computable in finite time. Furthermore, we may support also so-called OWA approximations such as those proposed in [26], [27], that are less demanding from a computational point of view.

Like most of the tableaux algorithms, our algorithm works on *completion-forests*. Let $\mathcal{K} = \langle \mathcal{T}, \mathcal{A} \rangle$ be a fuzzy KB. A completion-forest $\mathcal{F}$ for $\mathcal{K}$ is a collection of trees whose

[3]Informally, suppose the minimal value is $\bar{n}$. We will know then that for any interpretation $\mathcal{I}$ satisfying the knowledge base such that $(a{:}C)^{\mathcal{I}} < \bar{n}$, the starting set is unsatisfiable and, thus, $(a{:}C)^{\mathcal{I}} \geq \bar{n}$ has to hold. Which means that $bed(\mathcal{K}, a{:}C) = \bar{n}$

distinguished roots are arbitrarily connected by edges. Each node v is labelled with a set $\mathcal{L}(v)$ of expressions of the form $\langle C, l\rangle$, where $C \in sub(\mathcal{K})$ ($sub(\mathcal{K})$ is the set of named concepts appearing in $\mathcal{K}$), and l is either a rational, a variable x, or a negated variable, i.e., of the form $1 - x$, where x is a variable. The intuition is that v is an instance of C to degree equal or greater than the evaluation of l.

Each edge $\langle v, w\rangle$ is labelled with a set $\mathcal{L}(\langle v, w\rangle)$ of expressions of the form $\langle R, l\rangle$, where $R \in \mathcal{R}_\mathcal{K}$ ($\mathcal{R}_\mathcal{K}$ is the set of roles in $\mathcal{K}$). The intuition here is that $\langle v, w\rangle$ is an instance of R to degree greater or equal than the evaluation of l.

The forest has associated a set $\mathcal{C}_\mathcal{F}$ of constraints of the form $l \leq l'$, $l = l'$, $x_i \in [0, 1], y_i \in \{0, 1\}$, where l, l' are arithmetic expressions, on the variables occurring in the node labels and edge labels.

The algorithm initializes a forest $\mathcal{F}$ to contain *(i)* a root node v_0^i, for each individual a_i occurring in $\mathcal{A}$, labelled with $\mathcal{L}(v_0^i)$ such that $\mathcal{L}(v_0^i)$ contains $\langle C_i, r\rangle$ for each fuzzy assertion $\langle a_i{:}C_i, r\rangle \in \mathcal{A}$, and *(ii)* an edge $\langle v_0^i, v_0^j\rangle$, for each fuzzy assertion $\langle (a_i, a_j){:}R_i, r\rangle \in \mathcal{A}$, labelled with $\mathcal{L}(\langle v_0^i, v_0^j\rangle)$ such that $\mathcal{L}(\langle v_0^i, v_0^j\rangle)$ contains $\langle R_i, r\rangle$. $\mathcal{F}$ is then expanded by repeatedly applying the completion rules described below. The completion-forest is complete when none of the completion rules are applicable. Then, the MILP problem on the set of constraints $\mathcal{C}_\mathcal{F}$ is solved.

With x_α we denote the variable associated to the *assertion* α of the form $a{:}C$ or $(a, b){:}R$. x_α will take the truth value associated to α. With x_c we will denote the variable associated to the concrete individual c.

Let us discuss now how to deal with feature roles. Let $\mathcal{F}$ be a forest, p an abstract or concrete feature such that we have two edges $\langle v, w_1\rangle$ and $\langle v, w_1\rangle$ such that $\langle p, l_1\rangle$ and $\langle p, l_2\rangle$ occur in $\mathcal{L}(\langle v, w_1\rangle)$ and $\mathcal{L}(\langle v, w_2\rangle)$, respectively (informally, $\mathcal{F}$ contains $\langle (v, w_1){:}p, l_1\rangle$ and $\langle (v, w_2){:}p, l_2\rangle$). Then we call such a pair a *fork*. As p is a partial function, such a fork means that w_1 and w_2 have to be interpreted as the same individual. Such a fork can be deleted by adding both $\mathcal{L}(\langle v, w_2\rangle)$ to $\mathcal{L}(\langle v, w_1\rangle)$ and $\mathcal{L}(w_2)$ to $\mathcal{L}(w_1)$, and then deleting node w_2. At the beginning, we remove the forks from the initial forest. We assume that forks are eliminated as soon as they appear (as part of a rule application) with the proviso that newly generated nodes are replaced by older ones and not vice-versa.

Now we are ready to present the inference rules. Recall that $\mathbf{d} \in \{ls, rs, tri, trz\}$, while $@ \in \{@^{\text{avg}}, @_W^{\text{ws}}, @_W^{\text{owa}}\}$:

($\bot$). If $\langle \bot, l\rangle \in \mathcal{L}(v)$ then $\mathcal{C}_\mathcal{F} = \mathcal{C}_\mathcal{F} \cup \{l = 0\}$.

(R). If $\langle R, l\rangle \in \mathcal{L}(\langle v, w\rangle)$ then $\mathcal{C}_\mathcal{F} = \mathcal{C}_\mathcal{F} \cup \{x_{(v,w):R} \geq l\} \cup \{x_{(v,w):R} \in [0, 1]\}$. The case for concrete roles T is similar.

(f). If $\langle f, l\rangle \in \mathcal{L}(\langle v, w\rangle)$ then $\mathcal{C}_\mathcal{F} = \mathcal{C}_\mathcal{F} \cup \{x_{(v,w):f} \geq l\} \cup \{x_{(v,w):f} \in \{0, 1\}\}$. The case for concrete features t is similar.

(C). If $\langle C, l\rangle \in \mathcal{L}(v)$ then $\mathcal{C}_\mathcal{F} = \mathcal{C}_\mathcal{F} \cup \{x_{v:C} \geq l\} \cup \{x_{v:C} \in [0, 1]\}$.

($\sqcap$). If $\langle C \sqcap D, l\rangle \in \mathcal{L}(v)$ then *(i)* append $\langle C, x_{v:C}\rangle$, and $\langle D, x_{v:D}\rangle$ to $\mathcal{L}(v)$, and *(ii)* $\mathcal{C}_\mathcal{F} = \mathcal{C}_\mathcal{F} \cup \{x_{v:C} \otimes x_{v:D} \geq l\}$.

($\sqcup$). If $\langle C \sqcup D, l\rangle \in \mathcal{L}(v)$ then *(i)* append $\langle C, x_{v:C}\rangle$ and $\langle D, x_{v:D}\rangle$ to $\mathcal{L}(v)$, and *(ii)* $\mathcal{C}_\mathcal{F} = \mathcal{C}_\mathcal{F} \cup \{x_{v:C} \oplus x_{v:D} \geq l\}$.

($\neg$). If $\langle \neg C, l\rangle \in \mathcal{L}(v)$ then *(i)* append $\langle C, x_{v:C}\rangle$ to $\mathcal{L}(v)$, and *(ii)* $\mathcal{C}_\mathcal{F} = \mathcal{C}_\mathcal{F} \cup \{x_{v:\neg C} = 1 - x_{v:C}\}$.

($\forall$). If *(i)* $\langle \forall R.C, l_1\rangle \in \mathcal{L}(v)$, $\langle R, l_2\rangle \in \mathcal{L}(\langle v, w\rangle$, and *(ii)* the rule has not been already applied to this pair then *(i)* append $\langle C, x_{w:C}\rangle$ to $\mathcal{L}(w)$, and *(ii)* $\mathcal{C}_\mathcal{F} = \mathcal{C}_\mathcal{F} \cup \{x_{w:C} \geq l_1 \otimes l_2\}$.

($\exists$). If $\langle \exists R.C, l\rangle \in \mathcal{L}(v)$ then *(i)* create a new node w, and *(ii)* append $\langle R, x_{(v,w):R}\rangle$ to $\mathcal{L}(\langle v, w\rangle)$, and *(iii)* append $\langle C, x_{w:C}\rangle$ to $\mathcal{L}(w)$, and *(iv)* $\mathcal{C}_\mathcal{F} = \mathcal{C}_\mathcal{F} \cup \{x_{w:C} \otimes x_{(v,w):R} \geq l\}$.

($\forall_\mathbf{D}$). If $\langle \forall T.\mathbf{d}, l\rangle \in \mathcal{L}(v)$, the case is similar as in rule ($\forall$).

($\exists_\mathbf{D}$). If $\langle \exists T.\mathbf{d}, l\rangle \in \mathcal{L}(v)$, the case is similar as in rule ($\exists$).

($\mathbf{d}$). If $\langle d, l\rangle \in \mathcal{L}(v)$ then $\mathcal{C}_\mathcal{F} = \mathcal{C}_\mathcal{F} \cup \{\gamma(v{:}\mathbf{d}, l)\}$, where the set $\gamma(v{:}\mathbf{d}, l)$ is obtained from the MILP representation of $g(\mathbf{d})$ by replacing all occurrences of x with l and x_1 with x_v.

($\bar{\mathbf{d}}$). The case $\langle \neg\mathbf{d}, l\rangle \in \mathcal{L}(v)$ is similar as in rule ($\mathbf{d}$), where we use the MILP representation of $\bar{g}(\mathbf{d})$ in place of $g(\mathbf{d})$.

(@). If $\langle @(C_1, \ldots, C_n), l\rangle \in \mathcal{L}(v)$ then *(i)* append all $\langle C_i, x_{v:C_i}\rangle$ to $\mathcal{L}(v)$, and *(ii)* $\mathcal{C}_\mathcal{F} = \mathcal{C}_\mathcal{F} \cup \{\gamma(x_{v:C_1}, \ldots, x_{v:C_n}, l)\}$, where the set $\gamma(x_{v:C_1}, \ldots, x_{v:C_n}, l)$ is obtained from the MILP representation of $g(@)$ by replacing all occurrences of x with l and x_i with $x_{v:C_i}$.

Now, the following proposition can be shown.

Proposition 1 (Termination, Soundness, Completeness): For a given a KB $\mathcal{K}$ (i) the tableau algorithm terminates; (ii) if the expansion rules can be applied to $\mathcal{K}$ such that they yield a complete completion-forest $\mathcal{F}$ such that $\mathcal{C}_\mathcal{F}$ has a solution, then $\mathcal{K}$ has a model; and (iii) if $\mathcal{K}$ has a model, then the expansion rules can be applied in such a way that the tableaux algorithm yields a complete completion-forest for $\mathcal{K}$ such that $\mathcal{C}_\mathcal{F}$ has a solution. □

IV. Representation of some AOs in Fuzzy OWL 2

In this section, we will consider the representation of fuzzy ontologies using a fuzzy extension of OWL 2[4]. In particular, we will show how to represent weighted concepts, OWA operators, and quantifier-guided AOs.

The idea of this methodology for fuzzy ontology representation is to use an OWL 2 ontology and to extend their elements with annotations representing the features of the fuzzy ontology that OWL 2 cannot directly encode. In order to separate the annotations including fuzzy information from other annotations, we use a new annotation property called `fuzzyLabel`, and every annotation is identified by the tag `fuzzyOwl2`, with an attribute `fuzzyType` that specifies the type of element that is being annotated. For full details, we refer the reader to [7].

Now we are ready to show how to represent some cases of AOs, namely weighted concepts, OWA operators, and quantifier-guided AOs. For each of these concepts, we create a new concept and add an annotation property to it (describing the type of the constructor and the value of their parameters).

[4]http://www.straccia.info/software/FuzzyOWL/

Hence, the domain of the annotation is an OWL 2 concept declaration, and the value of the attribute `fuzzyType` is `concept`.

Then, we use a tag `Concept`, with an attribute `type`, describing the type of fuzzy concept that is represented, and other attributes that depend on the concept constructor. In the case of the concept constructors that we consider in this section, such attributes will be used to represent the weights, the concepts to be aggregated, and (possibly) the quantifier. Let us consider each case in detail.

A. Weighted sum concepts

The value of the attribute `type` is `weightedSum`. There are also several additional tags, each of them represented by a pair formed by a weight and a concept. Such pairs are usually called weighted concepts in the fuzzy DL literature and can be considered as fuzzy concepts themselves. For coherence, the syntax of a weighted concept use another tag `Concept`, with the `type` being `weighted`, and attributes `value` and `base` for the weight and the name of the base concept, respectively. Formally, the syntax for the annotation of weighted sum concepts is the following:

```
<fuzzyOwl2 fuzzyType="concept">
  <Concept type="weightedSum">
    (<WEIGHTED>)+
  </Concept>
</fuzzyOwl2>

<WEIGHTED> := <Concept type="weighted" value="<DOUBLE>"
              base="<STRING>" />
```

B. OWA aggregation concepts

Now, the value of the attribute `type` is `owa`. Due to the reordering step, it is not necessary to associate every weight to a particular concept, so we use two separate list of weights and concept names. The formal syntax is the following:

```
<fuzzyOwl2 fuzzyType="concept">
  <Concept type="owa">
    <Weights>
        ( <Weight><DOUBLE></Weight> )+
    </Weights>
    <Names>
        ( <Name><STRING></Name> )+
    </Names>
  </Concept>
</fuzzyOwl2>
```

Example 3: Assume that we want to represent the concept $@^{\text{owa}}_{W}(Cheap, CloseToVenue, Comfortable)$, where $W = (0.1, 0.3, 0.6)$. So, we create a new atomic concept A and annotate it as follows: (the example uses OWL/XML syntax [28]):

```
<AnnotationAssertion>
  <AnnotationProperty IRI='#fuzzyLabel'/>
  <IRI>#A</IRI>
  <Literal datatypeIRI='&rdf;PlainLiteral'>
    <fuzzyOwl2 fuzzyType="concept">
      <Concept type="owa">
        <Weights>
            <Weight>0.1</Weight>
            <Weight>0.3</Weight>
            <Weight>0.6</Weight>
        </Weights>
        <Names>
            <Name>Cheap</Name>
            <Name>CloseToVenue</Name>
            <Name>Comfortable</Name>
        </Names>
      </Concept>
    </fuzzyOwl2>
  </Literal>
</AnnotationAssertion>
```

C. Quantified-guided OWA aggregation concepts

This case is similar to the previous one, with the difference that we must also represent the quantifier. As possible quantifiers, we propose to use left-shoulder functions (Fig. 1 (b)) and linear functions (Fig. 1 (e))[5] restricted to the interval $[0, 1]$. These functions produce monotone quantifiers and have already being considered in Fuzzy OWL 2 [7].

So, the first step is to create a new datatype representing the quantifier, and add an annotation to it, specifying the `fuzzyType` as `datatype`, and including a tag `Datatype` with some attributes encoding the type of the function (`rightshoulder` or `linear`), and the parameters `a` and `b`. Formally, the syntax is the following[6]:

```
<fuzzyOwl2 fuzzyType="datatype">
  <DATATYPE>
</fuzzyOwl2>

<DATATYPE> :=
  <Datatype type="leftshoulder" a="<DOUBLE>" b="<DOUBLE>" /> |
  <Datatype type="linear" a="<DOUBLE>" b="<DOUBLE>" />
```

Now, the differences with the previous case is that the value of the attribute `type` is `qowa`, that there is an additional attribute `quantifier` relating the concept with the previously defined quantifier, and that the quantifiers do not need to be represented, as they are implicitly determined by the quantifier. Formally, the syntax is:

```
<fuzzyOwl2 fuzzyType="concept">
  <Concept type="qowa" quantifier="<STRING>" >
    <Names>
        ( <Name><STRING></Name> )+
    </Names>
  </Concept>
</fuzzyOwl2>
```

Example 4: Let $Q = linear(0.6, 0.4)$. We want to represent $@^{\text{owa}}_{W_Q}(Cheap, CloseToVenue, Comfortable)$. Note that $w_1 = Q(1/3) - Q(0) = 0.22$, $w_2 = Q(2/3) - Q(1/3) = 0.49 - 0.22 = 0.27$, and $w_3 = Q(1) - Q(2/3) = 1 - 0.49 = 0.51$. Now, we create a new datatype called Q and annotate it as follows:

```
<AnnotationAssertion>
   <AnnotationProperty IRI='#fuzzyLabel'/>
   <IRI>#Q</IRI>
   <Literal datatypeIRI='&rdf;PlainLiteral'>
   <fuzzyOwl2 fuzzyType="datatype">
     <Datatype type="linear" a="0.6" b="0.4" />
  </fuzzyOwl2>
  </Literal>
</AnnotationAssertion>
```

Then, we create a new atomic concept A and annotate it as:

```
<AnnotationAssertion>
  <AnnotationProperty IRI='#fuzzyLabel'/>
  <IRI>#A</IRI>
  <Literal datatypeIRI='&rdf;PlainLiteral'>
```

[5]Linear functions are determined by a parameter c that makes it possible to define $a = c/(c+1), b = 1/(c+1)$.

[6]Note that other functions (e.g. ls, tri, trz) can be used as fuzzy datatypes, but they are not covered here because they cannot be used as quantifiers.

```
    <fuzzyOwl2 fuzzyType="concept">
      <Concept type="qowa" quantifier="Q" >
        <Names>
            <Name>Cheap</Name>
            <Name>CloseToVenue</Name>
            <Name>Comfortable</Name>
        </Names>
      </Concept>
    </fuzzyOwl2>
  </Literal>
</AnnotationAssertion>
```

V. Conclusion

In this work we have shown how to include aggregation operators within fuzzy DLs. Our contribution consist of: (i) definition of syntax and semantics for fuzzy DLs supporting AOs; (ii) a reasoning algorithm for a wide class of AOs that are MILP representable, that includes average, weighted sum and notably OWA and quantifier-based OWA operators; and (iii) a mechanism to support these AOs in Fuzzy OWL 2, a fuzzy version of the standard ontology language OWL 2. Our approach is implemented in the plug-in Fuzzy OWL 2 and in the fuzzyDL reasoner [11].

Concerning future work, we note that the realm of AOs is quite large (see, e.g. [8]). It remains to see which of them and especially *how* they can be encoded within our reasoning algorithm framework based on (especially) MILP or, more generally, on MINLP optimisation tools.

Appendix

We succinctly show that OWA operators are MILP representable. Yager [17] has shown that the *maximisation* of $@^{\text{owa}}_W(x_1, \ldots, x_n)$ can indeed be encoded as a MILP problem. However, this encoding does not work in our setting as we are not maximising $@^{\text{owa}}_W(x_1, \ldots, x_n)$, but rather need to show that the set $g(@^{\text{owa}}_W) = \{\langle x_1, \ldots, x_k, x\rangle \colon @^{\text{owa}}_W(x_1, \ldots, x_k) \geq x\}$ is MILP representable. To this end, we need a different encoding. So, let $N = \{1, \ldots, n\}$. Similarly to [17], we introduce new $[0, 1]$-valued variables y_i ($i \in N$) and impose

$$y_1 \geq y_2 \geq \ldots \geq y_n \ . \tag{8}$$

The intuition is that y_i will take the value of the i-th largest of the x_j. Hence, by definition of OWA, y_i has weight w_i and therefore, we add also the constraint

$$\textstyle\sum_i w_i y_i \geq x \ . \tag{9}$$

The remaining of the encoding concerns now to establish which one among $x_1, \ldots, x_n$ are the y_i. Consider the following set of equations: for $i, j \in N$, $k = 2$, new binary variables z_{ij}

$$\begin{array}{lll} y_i \leq x_j + k z_{ij} & & x_j \leq y_i + k z_{ij} \\ \textstyle\sum_j z_{ij} = n - 1 & \textstyle\sum_i z_{ij} = n - 1 & z_{ij} \in \{0, 1\} \ . \end{array} \tag{10}$$

It can be verified that (i) if $z_{ij} = 0$ then $y_i = x_j$ is imposed; (ii) for any y_i, there is only one x_j imposed to be equal to y_i; and (iii) for any x_j, there is only one y_i imposed to be equal to x_j. That is, there is a bijection among the y_j and the x_i, which together with Eq. (8) guarantees that the equations Eq. (8) - (10) correctly encode $@^{\text{owa}}_W(x_1, \ldots, x_k) \geq x$.

References

[1] F. Baader, D. Calvanese, D. McGuinness, D. Nardi, and P. F. Patel-Schneider, Eds., The Description Logic Handbook: Theory, Implementation, and Applications. Cambridge University Press, 2003.

[2] B. Cuenca-Grau, I. Horrocks, B. Motik, B. Parsia, P. F. Patel-Schneider, and U. Sattler, "OWL 2: The next step for OWL", Journal of Web Semantics, vol. 6:4, pp. 309–322, 2008.

[3] U. Straccia, "Reasoning within fuzzy Description Logics", Journal of Artificial Intelligence Research, vol. 14, pp. 137–166, 2001.

[4] U. Straccia, "A fuzzy Description Logic for the semantic web", in Fuzzy Logic and the Semantic Web, E. Sanchez, Ed. Elsevier, 2006, pp. 73–90.

[5] U. Straccia, "Multi-criteria decision making in fuzzy Description Logics: a first step", in Proceedings of the 13th International Conference on Knowledge-Based & Intelligent Information & Engineering Systems (KES 2009), ser. LNAI, no. 5711. Springer, 2009, pp. 79–87.

[6] T. Lukasiewicz and U. Straccia, "Managing uncertainty and vagueness in Description Logics for the semantic web", Journal of Web Semantics, vol. 6, pp. 291–308, 2008.

[7] F. Bobillo and U. Straccia. "Representing fuzzy ontologies in OWL 2", in Proceedings of the 19th IEEE International Conference on Fuzzy Systems (FUZZ-IEEE 2010). IEEE Press, 2010, pp. 2695–2700.

[8] V. Torra, Y. Narukawa, Modeling Decisions - Information Fusion and Aggregation Operators. Springer Verlag, 2007.

[9] R. R. Yager, "On ordered weighted averaging aggregation operators in multicriteria decision making", IEEE Transactions on Systems, Man and Cybernetics, vol. 18, pp. 183–190, 1988.

[10] P. Vojtáš, "A fuzzy $\mathcal{EL}$ Description Logic with crisp roles and fuzzy aggregation for web consulting", in Proceedings of the 11th International Conference on Information Processing and Management of Uncertainty in Knowledge-Based Systems (IPMU 2006), 2006, pp. 1834–1841.

[11] F. Bobillo and U. Straccia, "fuzzyDL: an expressive fuzzy Description Logic reasoner", in 2008 International Conference on Fuzzy Systems (FUZZ-IEEE 2008). IEEE Computer Society, 2008, pp. 923–930.

[12] P. Hájek, Metamathematics of fuzzy logic. Kluwer, 1998.

[13] R. Hähnle, "Advanced many-valued logics", in Handbook of Philosophical Logic, 2nd Edition, D. M. Gabbay and F. Guenthner, Eds. Kluwer, 2001.

[14] R. R. Yager, "Families of OWA operators", Fuzzy Sets and Systems, vol. 59, pp. 125–148, 1993.

[15] R. R. Yager, J. Kacprzyk, Eds., The ordered weighted averaging operators: theory and applications. Kluwer Academic Publishers, 1997.

[16] R. R. Yager, "Connectives and quantifiers in fuzzy sets", Fuzzy Sets and Systems, vol. 40, pp. 39–75, 1991.

[17] R. R. Yager, "Constrained OWA aggregation", Fuzzy Sets and Systems, vol. 81, pp. 89–101, 1996.

[18] G. J. Klir and B. Yuan, Fuzzy Sets and Fuzzy Logic: Theory and Applications." Prentice-Hall, Inc., 1995.

[19] R. Bellmann and L. Zadeh, "Decision-making in a fuzzy environment", Management Sciences, vol. 17, pp. 141–164, 1970.

[20] U. Straccia, "Description logics with fuzzy concrete domains", in Proceedings of the 21st Conference on Uncertainty in Artificial Intelligence (UAI 2005). AUAI Press, 2005, pp. 559–567.

[21] F. Bobillo and U. Straccia, "Fuzzy Description Logics with general t-norms and datatypes", Fuzzy Sets Systems, vol. 160(23), pp. 3382—3402, 2009.

[22] F. Bobillo, F. Bou, and U. Straccia, "On the failure of the finite model property in some fuzzy Description Logics", Fuzzy Sets and Systems, vol. 172(1), pp. 1-12, 2011.

[23] B. Nebel, "Terminological reasoning is inherently intractable, Artificial Intelligence", vol. 43, pp. 235–249, 1990.

[24] G. Stoilos, U. Straccia, G. Stamou, and J. Pan, "General concept inclusions in fuzzy Description Logics", in Proceedings of the 17th Eureopean Conference on Artificial Intelligence (ECAI 2006). IOS Press, 2006, pp. 457–461.

[25] H. Salkin and M. Kamlesh, Foundations of Integer Programming. North-Holland, 1988.

[26] M. Grabisch, "Alternative representations of OWA operators", in The ordered weighted averaging operators. Kluwer Academic Publishers, 1997, pp. 73–85.

[27] J. L. Marichal, Aggregation Operators for Multicriteria Decision Aid. Ph.D. dissertation, Universite de Liege, Belgium, 1999.

[28] B. Motik, B. Parsia, and P. F. Patel-Schneider, Eds., OWL 2 Web Ontology Language XML serialization, http://www.w3.org/TR/owl2-xml-serialization, 2009.

2011 IEEE International Conference on Fuzzy Systems
June 27-30, 2011, Taipei, Taiwan

Are Fuzzy Description Logics with General Concept Inclusion Axioms Decidable?

Franz Baader and Rafael Peñaloza
Theoretical Computer Science, TU Dresden
Email: {baader, penaloza}@tcs.inf.tu-dresden.de

***Abstract*—This paper concentrates on a fuzzy Description Logic with product t-norm and involutive negation. It does not answer the question posed in its title for this logic, but it gives strong indications that the answer might in fact be "no." On the one hand, it shows that an algorithm that was claimed to answer the question affirmatively for this logic is actually incorrect. On the other hand, it proves undecidability of a variant of this logic.**

***Index Terms*—Fuzzy Description Logics, Undecidability, Reasoning**

I. Introduction

Description logics (DLs) [1] are a well-investigated family of logic-based knowledge representation formalisms, which can be used to model a given application domain using terminological axioms and assertional axioms. On the terminological side, modern DL systems provide their users with so-called concept inclusion axioms. The availability of these axioms increases the complexity of reasoning, both from a complexity theoretic and a practical point of view. For example, for the standard DL $\mathcal{ALC}$, the complexity rises from PSpace to ExpTime if these axioms are added. In addition, the tableau-based reasoning procedure used by most DL systems run into a termination problem: one has to add so-called blocking conditions in order to ensure their termination [2].

Fuzzy variants of DLs were introduced in order to deal with applications where precise definitions are not possible [3]. Decidability of fuzzy DLs is often shown by adapting the tableau-based algorithms for the corresponding crisp DL to the fuzzy case. This was first done for the case of DLs without concept inclusion axioms [4], [5] or with only *crisp* concept inclusion axioms [6], [7], but then also extended to DLs with concept inclusion axioms [8], [9]. In particular, Bobillo and Straccia [10], [11] have developed such an algorithm for a DL with product t-norm and involutive negation. Whereas [11] focuses only on so-called acyclic TBoxes, the algorithm from [10] allows for general concept inclusion axioms. More precisely, this algorithm is supposed to check whether an ontology expressed in this DL has a so-called witnessed model. Actually, the proof of correctness of this algorithm implies that, whenever such an ontology has a witnessed model, then it has a finite model. However, it was recently shown in [12] that this is not the case in the presence of general concept inclusion axioms, i.e., there is an ontology written in this logic that has a witnessed model, but does not have a finite model. Of course, this does not automatically imply that the algorithm itself is wrong. In fact, if one applies the algorithm from [10] to the ontology used in [12] to demonstrate the failure of the finite model property, then one obtains the correct answer.

In this paper, we will first show that the algorithm is indeed incorrect by exhibiting an example ontology on which it gives an incorrect answer. This shows that the question of whether (witnessed) consistency of this logic is decidable or not is an open question. The second result shown in this paper gives an indication that the answer could in fact be "no." We prove undecidability for a slightly modified problem where (i) we allow not only $\geq$ but also $>$ in our fuzzy concept inclusion axioms, and (ii) consider a somewhat weaker notion of witnessed model.

II. Preliminaries

We introduce the logic *fuzzy $\mathcal{ALC}$ with product t-norm and involutive negation* and the tableau-based algorithm for this logic presented in [10], and then give an example that shows that this algorithm is not correct.

A. Fuzzy $\mathcal{ALC}$ with Product t-norm and involutive negation

The syntax of fuzzy $\mathcal{ALC}$ concepts is the same as for crisp $\mathcal{ALC}$. From two disjoint sets $\mathcal{N}_\mathcal{C}$ and $\mathcal{N}_\mathcal{R}$ of *concept-* and *role-names*, respectively, fuzzy $\mathcal{ALC}$ concepts are built using the syntax rule:

$$C ::= \top \mid \bot \mid A \mid C_1 \sqcap C_2 \mid C_1 \sqcup C_2 \mid \neg C \mid \exists r.C \mid \forall r.C,$$

where $A \in \mathcal{N}_\mathcal{C}$ and $r \in \mathcal{N}_\mathcal{R}$.

The syntax of the axioms in this logic is slightly different from the crisp case since they need to state a degree of truth with which they hold. A *fuzzy $\mathcal{ALC}$ ABox* is a finite set of *concept assertion axioms* of the form $\langle a : C \geq q\rangle$ and *role assertion axioms* $\langle (a,b) : r \geq q\rangle$, where C is a fuzzy $\mathcal{ALC}$ concept, $r \in \mathcal{N}_\mathcal{R}$, q is a rational number in $[0,1]$, and $a, b \in \mathcal{N}_\mathcal{I}$, with $\mathcal{N}_\mathcal{I}$ the set of *individual names*. A *fuzzy $\mathcal{ALC}$ TBox* is a finite set of *concept inclusion axioms* of the form $\langle C \sqsubseteq D \geq q\rangle$, where C, D are $\mathcal{ALC}$ concepts and q is a rational number in $[0,1]$. A *fuzzy ontology* $\mathcal{O} = (\mathcal{A}, \mathcal{T})$ consists of a fuzzy ABox $\mathcal{A}$ together with a fuzzy TBox $\mathcal{T}$.

The semantics of this logic extends the classical semantics of $\mathcal{ALC}$ by interpreting concepts and roles as fuzzy sets over an interpretation domain. Given a non-empty set Δ (the domain), a *fuzzy set* over Δ is a function $F : \Delta \to [0,1]$, with the intuition that an element $\delta \in \Delta$ belongs to F with *degree* $F(\delta)$. The semantics of the different concept constructors depends on the class of fuzzy operators chosen to interpret them. In this

978-1-4244-7316-8/11/$26.00 ©2011 IEEE

paper, we use the binary operators *product t-norm* $\otimes$, *product t-conorm* $\oplus$, and *residuum* $\rightarrow$, and the unary operator *involutive negation* $\ominus$ over the interval $[0,1]$. These operators are defined as follows, for every $\alpha, \beta \in [0,1]$:

$$\begin{aligned} \alpha \otimes \beta &:= \alpha \cdot \beta, \\ \alpha \oplus \beta &:= \alpha + \beta - \alpha \cdot \beta, \\ \alpha \rightarrow \beta &:= \begin{cases} 1 & \text{if } \alpha \leq \beta \\ \beta/\alpha & \text{otherwise,} \end{cases} \\ \ominus\alpha &:= 1 - \alpha. \end{aligned}$$

It is useful to notice that, for every $\alpha, \beta, q \in [0,1]$, we have $\alpha \rightarrow \beta \geq q$ iff $\beta \geq q \cdot \alpha$. In particular, this means that (i) $\alpha \rightarrow \beta \geq 1$ iff $\beta \geq \alpha$ and (ii) $1 \rightarrow \beta = \beta$. We will often make use of these properties in the rest of this paper.

The semantics of fuzzy $\mathcal{ALC}$ is based on the notion of an *interpretation*, which is a tuple $\mathcal{I} = (\Delta^{\mathcal{I}}, \cdot^{\mathcal{I}})$ where $\Delta^{\mathcal{I}}$ is a non-empty set, called the *domain*, and the function $\cdot^{\mathcal{I}}$ maps each individual name a to an element of $\Delta^{\mathcal{I}}$, each concept name A to a function $A^{\mathcal{I}} : \Delta^{\mathcal{I}} \rightarrow [0,1]$ and each role name r to a function $r^{\mathcal{I}} : \Delta^{\mathcal{I}} \times \Delta^{\mathcal{I}} \rightarrow [0,1]$. The interpretation function is extended to arbitrary fuzzy $\mathcal{ALC}$ concepts as follows. For every $\delta \in \Delta^{\mathcal{I}}$,

$$\begin{aligned} \top^{\mathcal{I}}(\delta) &= 1 \\ \bot^{\mathcal{I}}(\delta) &= 0 \\ (C_1 \sqcap C_2)^{\mathcal{I}}(\delta) &= C_1^{\mathcal{I}}(\delta) \cdot C_2^{\mathcal{I}}(\delta) \\ (C_1 \sqcup C_2)^{\mathcal{I}}(\delta) &= C_1^{\mathcal{I}}(\delta) + C_2^{\mathcal{I}}(\delta) - C_1^{\mathcal{I}}(\delta) \cdot C_2^{\mathcal{I}}(\delta) \\ (\neg C)^{\mathcal{I}}(\delta) &= 1 - C^{\mathcal{I}}(\delta) \\ (\exists r.C)^{\mathcal{I}}(\delta) &= \sup_{\gamma \in \Delta^{\mathcal{I}}} (r^{\mathcal{I}}(\delta,\gamma) \cdot C^{\mathcal{I}}(\gamma)) \\ (\forall r.C)^{\mathcal{I}}(\delta) &= \inf_{\gamma \in \Delta^{\mathcal{I}}} (r^{\mathcal{I}}(\delta,\gamma) \rightarrow C^{\mathcal{I}}(\gamma)). \end{aligned}$$

The interpretation $\mathcal{I} = (\Delta^{\mathcal{I}}, \cdot^{\mathcal{I}})$ satisfies the concept assertion $\langle a : C \geq q \rangle$ iff $C^{\mathcal{I}}(a^{\mathcal{I}}) \geq q$, it satisfies the role assertion $\langle (a,b) : r \geq q \rangle$ iff $r^{\mathcal{I}}(a^{\mathcal{I}}, b^{\mathcal{I}}) \geq q$, and it satisfies the concept inclusion $\langle C \sqsubseteq D \geq q \rangle$ iff $\inf_{\delta \in \Delta^{\mathcal{I}}} (C^{\mathcal{I}}(\delta) \rightarrow D^{\mathcal{I}}(\delta)) \geq q$. This interpretation is called a *model* of the ontology $\mathcal{O}$ if it satisfies all the axioms in $\mathcal{O}$.

An important notion in fuzzy DLs is that of witnessed models [13], [14]. A model is called *witnessed* if for every $\delta \in \Delta^{\mathcal{I}}$, role r and concepts C, D there exist $\gamma, \gamma' \in \Delta^{\mathcal{I}}$ such that

- $(\exists r.C)^{\mathcal{I}}(\delta) = r^{\mathcal{I}}(\delta,\gamma) \cdot C^{\mathcal{I}}(\gamma)$ and
- $(\forall r.C)^{\mathcal{I}}(\delta) = r^{\mathcal{I}}(\delta,\gamma') \rightarrow C^{\mathcal{I}}(\gamma')$.

Notice that, in the literature (e.g. [11], [12], [15]), witnessed models are usually required to satisfy additionally that, for every two concepts C, D, there is a γ such that

$$\inf_{\eta \in \Delta^{\mathcal{I}}} (C^{\mathcal{I}}(\eta) \rightarrow D^{\mathcal{I}}(\eta)) = C^{\mathcal{I}}(\gamma) \rightarrow D^{\mathcal{I}}(\gamma).$$

We call those witnessed models that satisfy this additional restriction *strongly witnessed* models.

The reason why we do not include this condition is that, in our opinion, it does not capture the spirit of fuzzy concept inclusions: the axiom $\langle C \sqsubseteq D \geq q \rangle$ is meant to constrain the interpretation of concepts and roles such that, for each individual $\delta \in \Delta$, we have $C^{\mathcal{I}}(\delta) \rightarrow D^{\mathcal{I}}(\delta) \geq q$. With this point of view, it is not really necessary that the infimum of the values for the residuum is indeed reached. In contrast, for the value restriction, this infimum is really the degree of this restriction, and thus it makes sense to require that this degree is witnessed by a role successor.

We say that an ontology $\mathcal{O}$ is *consistent* if it has a model, it is *witnessed consistent* if it has a witnessed model, and it is *strongly witnessed consistent* if it has a strongly witnessed model.

As it has been shown in [11], consistency does not imply witnessed consistency in fuzzy $\mathcal{ALC}$. However, it is standard in fuzzy DL to restrict reasoning to witnessed models only (see for instance [10], [11]).

Notation. *We will often use the expression $\langle C = q \rangle$ to abbreviate the two axioms $\langle \top \sqsubseteq C \geq q \rangle, \langle \top \sqsubseteq \neg C \geq 1 - q \rangle$, and the expression $\langle C \equiv D \rangle$ to abbreviate $\langle C \sqsubseteq D \geq 1 \rangle$, $\langle D \sqsubseteq C \geq 1 \rangle$. Likewise, $\langle a : C = q \rangle$ is an abbreviation for $\langle a : C \geq q \rangle, \langle a : \neg C \geq 1 - q \rangle$.*

Intuitively, the expressions $\langle C = q \rangle, \langle C \equiv D \rangle$, and $\langle a : C = q \rangle$ restrict every model $\mathcal{I}$ to be such that, for all $\delta \in \Delta^{\mathcal{I}}$, we have $C^{\mathcal{I}}(\delta) = q, C^{\mathcal{I}}(\delta) = D^{\mathcal{I}}(\delta)$, and $C^{\mathcal{I}}(a^{\mathcal{I}}) = q$, respectively.

B. The Original Algorithm of [10]

A tableau-based algorithm for deciding strongly witnessed consistency of a fuzzy $\mathcal{ALCF}(D)$ ontology was presented in [10].[1] However, as we will show, this algorithm is incorrect, even if restricted to fuzzy $\mathcal{ALC}$. We now briefly introduce the algorithm, leaving aside all the steps corresponding to expressivity beyond that of fuzzy $\mathcal{ALC}$. In the following, x (possibly with sub- or superindices) denotes a *continuous variable* taking values from $[0,1]$, q denotes a *constant* in $[0,1]$, l denotes a *literal*, that is, a continuous variable x, a *negated variable* $1 - x$ or a constant, and y denotes a *Boolean variable* taking values from $\{0,1\}$.

The algorithm constructs a completion forest; that is, a collection of trees whose roots may be arbitrarily interconnected by edges. Every node v in this forest is labeled by a set $\mathcal{L}(v)$ of labeled concepts of the form $\langle C, l \rangle$ and a set $\mathcal{C}(v)$ of inequalities. Intuitively, $\langle C, l \rangle \in \mathcal{L}(v)$ means that v belongs to C with degree at least l and the inequalities in $\mathcal{C}(v)$ constrain the valuations of the different variables used. Additionally, every edge (v_1, v_2) is labeled with a set $\mathcal{L}(v_1, v_2)$ of labeled role names $\langle r, l \rangle$ with the meaning that (v_1, v_2) are in an r-relation with degree at least l.

The algorithm initializes the completion forest to contain one *root node* v_i for each individual name a_i appearing in the ABox $\mathcal{A}$ with $\mathcal{L}(v_i) = \{\langle C, l \rangle \mid \langle a_i : C \geq l \rangle \in \mathcal{A}\}$ and $\mathcal{L}(v_i, v_j) = \{\langle r, l \rangle \mid \langle (a_i, a_j) : r \geq l \rangle \in \mathcal{A}\}$. The sets $\mathcal{C}(v_i)$ are all initialized as empty. This completion forest is extended

[1] Fuzzy $\mathcal{ALCF}(D)$ is fuzzy $\mathcal{ALC}$ extended with additonal constructors that are not relevant for this paper.

(A) if $\langle A, l\rangle \in \mathcal{L}(v)$ then add $x_{v:A} \geq l$ to $\mathcal{C}(v)$

$(\overline{A})$ if $\langle \neg A, l\rangle \in \mathcal{L}(v)$ then add $x_{v:A} \leq 1 - l$ to $\mathcal{C}(v)$

(r) if $\langle r, l\rangle \in \mathcal{L}(v, w)$ then add $x_{(v,w):r} \geq l$ to $\mathcal{C}(w)$

$(\top)$ if $\langle \top, l\rangle \in \mathcal{L}(v)$ or $\langle \neg\bot, l\rangle \in \mathcal{L}(v)$ then add $l = 1$ to $\mathcal{C}(v)$

$(\bot)$ if $\langle \bot, l\rangle \in \mathcal{L}(v)$ or $\langle \neg\top, l\rangle \in \mathcal{L}(v)$ then add $l = 0$ to $\mathcal{C}(v)$

$(\neg\neg)$ if $\langle \neg\neg C, l\rangle \in \mathcal{L}(v)$ then add $\langle C, l\rangle$ to $\mathcal{L}(v)$

$(\sqcap)$ if $\langle C \sqcap D, l\rangle \in \mathcal{L}(v)$ then add $\langle C, x_1\rangle, \langle D, x_2\rangle$ to $\mathcal{L}(v)$ and $x_1 \cdot x_2 \geq l$ to $\mathcal{C}(v)$

$(\overline{\sqcap})$ if $\langle \neg(C \sqcap D), l\rangle \in \mathcal{L}(v)$ then add $\langle \neg C \sqcup \neg D, l\rangle$ to $\mathcal{L}(v)$

$(\sqcup)$ if $\langle C \sqcup D, l\rangle \in \mathcal{L}(v)$ then add $\langle C, x_1\rangle, \langle D, x_2\rangle$ to $\mathcal{L}(v)$ and $x_1 + x_2 - x_1 \cdot x_2 \geq l$ to $\mathcal{C}(v)$

$(\overline{\sqcup})$ if $\langle \neg(C \sqcup D), l\rangle \in \mathcal{L}(v)$ then add $\langle \neg C \sqcap \neg D, l\rangle$ to $\mathcal{L}(v)$

$(\forall)$ if $\langle \forall r.C, l_1\rangle \in \mathcal{L}(v)$ and $\langle r, l_2\rangle \in \mathcal{L}(v, w)$ then add $\langle C, x\rangle$ to $\mathcal{L}(w)$ and $x \geq l_1 \cdot l_2$ to $\mathcal{C}(w)$

$(\overline{\exists})$ if $\langle \neg\exists r.C, l_1\rangle \in \mathcal{L}(v)$ and $\langle r, l_2\rangle \in \mathcal{L}(v, w)$ then add $\langle \neg C, 1 - x_1\rangle$ to $\mathcal{L}(w)$ and $x_{(v,w):r} \leq x_2, x_1 \cdot x_2 = 1 - l_1$ to $\mathcal{C}(w)$

$(\overline{\forall})$ if $\langle \neg\forall r.C, l\rangle \in \mathcal{L}(v)$ then create a new node w and add $\langle r, x_1\rangle$ to $\mathcal{L}(v, w)$, $\langle C, x_2\rangle$ to $\mathcal{L}(w)$ and $y \cdot x_1 + (1 - y) \cdot x_2 \geq y \cdot x_2 + (1 - y) \cdot x_1, l \leq y, y \cdot x_2 \leq x_1 - l \cdot x_1$ to $\mathcal{C}(w)$

$(\exists)$ if $\langle \exists r.C, l\rangle \in \mathcal{L}(v)$ then create a new node w and add $\langle r, x_1\rangle$ to $\mathcal{L}(v, w)$, $\langle C, x_2\rangle$ to $\mathcal{L}(w)$ and $x_1 \cdot x_2 \geq l$ to $\mathcal{C}(w)$

$(\sqsubseteq)$ if $\langle C \sqsubseteq D \geq q\rangle \in \mathcal{T}$ and v is a node in the forest, then add $\langle \neg C, 1 - x_1\rangle, \langle D, x_2\rangle$ to $\mathcal{L}(v)$ and $x_2 \geq x_1 \cdot q$ to $\mathcal{C}(v)$.

TABLE I
COMPLETION RULES FOR FUZZY $\mathcal{ALC}$ CONSISTENCY.
x, x_1, x_2, y ARE ALWAYS NEW VARIABLES

by application of the completion rules from Table I. As is standard with tableau-based algorithms, these rules are only applied as long as something new is added to the completion forest.

The main idea of these rules is that they decompose complex concepts into their subconcepts, while preserving the fuzzy semantics through the restrictions in $\mathcal{C}$. Assume for the moment that the algorithm has terminated (i.e., no more completion rules are applicable) and that the constraint system $\mathcal{C} := \bigcup_v \mathcal{C}(v)$ generated by the algorithm has a solution in $[0, 1]$. The claim is then that the completion forest obtained by the algorithm describes a model of the ontology, where the membership degree of a node v to a concept name A corresponds to the value of the variable $x_{v:A}$, and accordingly for roles. Conversely, from any model of the ontology it is possible to build a satisfying valuation of the variables in $\mathcal{C}$.

However, as it is also the case for crisp $\mathcal{ALC}$, this completion forest construction may not terminate, due to the fact that concept inclusions can express cyclic relationships between concepts, which may enforce an infinite generation of new individuals. In order to ensure termination, a blocking condition is used, which disallows the application of "generating" rules; i.e., the $(\exists)$ and $(\overline{\forall})$ rules cannot be applied in any node that is considered to be blocked.

Definition 1 (blocking [10]). *Two non-root nodes v, w are called* equivalent*, denoted as $\mathcal{L}(v) \approx \mathcal{L}(w)$, if $\mathcal{L}(v) = \{\langle C_1, l_1\rangle, \ldots, \langle C_k, l_k\rangle\}, \mathcal{L}(v) = \{\langle C_1, l'_1\rangle, \ldots, \langle C_k, l'_k\rangle\}$ and for every $1 \leq i \leq k$, l_i, l'_i are either both variables, or are both negated variables, or are both the same constant.*

A node v is directly blocked *iff it is not a root node and it has an ancestor w such that $\mathcal{L}(v) \approx \mathcal{L}(w)$; in this case we say that w is the* blocking *node of v. A node is* blocked *if it is directly blocked or its predecessor is blocked.*

With this blocking condition, it is not hard to show that the algorithm always terminates. It then answers that the input ontology $\mathcal{O}$ is strongly witnessed consistent iff the system of inequalities $\mathcal{C}$ generated by this terminating run on input $\mathcal{O}$ has a solution.

The idea behind the proof of correctness of this algorithm, as presented in [10], is that the variables appearing in blocking and blocked nodes can be evaluated to the same numerical value in a solution of $\mathcal{C}$. If correct, this proof would show that an ontology that has a strongly witnessed model always has a finite model. Indeed, the interpretation constructed from the completion forest generated by a terminating run of the algorithm is finite. Unfortunately, as we will see below, it need not be a model. The first blow to the claimed correctness of the algorithm came when it was shown in [12] that the logic does not have the finite model property. More precisely, in [12] the authors present a simple ontology that is strongly witnessed consistent, but does not have a finite model. Thus, the approach through which the algorithm tries to build a (finite) model is wrong. However, this does not automatically imply that the algorithm itself is wrong. In fact, if one applies the algorithm to the ontology used in [12], then one obtains the correct answer, namely that the ontology is strongly witnessed consistent. The authors conjecture in [12] that the algorithm is still correct.[2]

Note that the algorithm tries to construct a finite portion of a model. If the input ontology is indeed consistent, and thus has a (possibly infinite) model, then it is easy to see that this construction will always succeed (i.e., the constraint system generated by the algorithm is satisfiable). This means that the algorithm is complete.

Remark 2. *The algorithm from [10] is complete for strongly witnessed consistency; that is, it yields the right answer whenever the input ontology is strongly witnessed consistent.*

Unfortunately, as the following example shows, it is not sound since it fails to correctly identify inconsistency.

Example 3. *Consider the ontology with the following axioms:*

$ax_1 : \langle a : A \geq 0.1\rangle$
$ax_2 : \langle A \sqsubseteq (\forall r.A) \sqcap B \geq 1\rangle$
$ax_3 : \langle \top \sqsubseteq \neg B \geq 0.5\rangle$
$ax_4 : \langle \top \sqsubseteq \exists r.\top \geq 1\rangle$.

We will prove first that this ontology is inconsistent, and thus also not (strongly) witnessed consistent. We then show that the algorithm described above yields the wrong answer, i.e., it claims that the ontology is strongly witnessed consistent.

[2]Independently from us, a counterexample to the correctness of the algorithm in [10] has now also been found by the authors of [12]. This counterexample, which is presented in [16], is different from the one we give here. The paper [16], which is an improved version of [12], was available online only after we had submitted the present paper.

Suppose that there is a model (not necessarily witnessed) $\mathcal{I} = (\Delta^{\mathcal{I}}, \cdot^{\mathcal{I}})$ of this ontology, and let $v_0 \in \Delta^{\mathcal{I}}$ be any element of the domain. From axiom ax_4, we obtain that

$$1 = (\exists r.\top)^{\mathcal{I}}(v_0) = \sup_{\delta \in \Delta^{\mathcal{I}}} r^{\mathcal{I}}(v_0, \delta).$$

This means that there must exist $v_1 \in \Delta^{\mathcal{I}}$ such that $r^{\mathcal{I}}(v_0, v_1) > 0.99$.[3] From ax_3 it follows that $(\neg B)^{\mathcal{I}}(v_0) \geq 0.5$; i.e., $B^{\mathcal{I}}(v_0) \leq 0.5$; additionally, from ax_2 we know

$$A^{\mathcal{I}}(v_0) \leq (\forall r.A)^{\mathcal{I}}(v_0) \cdot B^{\mathcal{I}}(v_0) \leq (\forall r.A)^{\mathcal{I}}(v_0) \cdot 0.5,$$

or equivalently,

$$\begin{aligned} 2 \cdot A^{\mathcal{I}}(v_0) \leq (\forall r.A)^{\mathcal{I}}(v_0) &= \inf_{\delta \in \Delta^{\mathcal{I}}} r^{\mathcal{I}}(v_0, \delta) \to A^{\mathcal{I}}(\delta) \\ &\leq r^{\mathcal{I}}(v_0, v_1) \to A^{\mathcal{I}}(v_1) \\ &\leq 0.99 \to A^{\mathcal{I}}(v_1). \end{aligned} \quad (1)$$

Additionally, it holds that $0.99 \to A^{\mathcal{I}}(v_1) \leq 1$, and so $A^{\mathcal{I}}(v_0) \leq 0.5$. Recall that v_0 was an arbitrary element of the domain, and thus the previous holds also for v_1; in particular we have that $A^{\mathcal{I}}(v_1) \leq 0.5$ and $0.99 \to A^{\mathcal{I}}(v_1) = c \cdot A^{\mathcal{I}}(v_1)$, where $c = 100/99$. Since $2/c > 1$, it follows from the inequality (1) that

$$A^{\mathcal{I}}(v_0) < (2/c) \cdot A^{\mathcal{I}}(v_0) \leq A^{\mathcal{I}}(v_1) \leq 0.5.$$

Once again, since all the previous is true for any element of the domain, it follows that there must exist infinitely many elements $v_2, v_3, \ldots$ such that for every $n \geq 0$ it holds

$$(2/c)^n \cdot A^{\mathcal{I}}(v_0) \leq A^{\mathcal{I}}(v_n) \leq 0.5$$

But since $2/c > 1$, it then follows that $A^{\mathcal{I}}(v_0) = 0$. In particular, this is true for $v_0 = a^{\mathcal{I}} \in \Delta^{\mathcal{I}}$. But this is a contradiction to the assumption that $\mathcal{I}$ is a model of the axiom ax_1. Thus, the ontology is inconsistent.

Let us now analyse the execution of the algorithm on this input. The algorithm starts with a single root node v_0 with $\mathcal{L}(v_0) = \{\langle A, 0.1\rangle\}$ and $\mathcal{C}(v_0) = \emptyset$. Application of the rule $(\sqsubseteq)$ with axioms ax_2, ax_3 and ax_4 will add

$$\langle \neg A, 1 - x_1\rangle, \langle (\forall r.A) \sqcap B, x_2\rangle, \langle \neg\top, 1 - x_3\rangle, \langle \neg B, x_4\rangle, \langle \neg\top, 1 - x_5\rangle, \langle \exists r.\top, x_6\rangle$$

to $\mathcal{L}(v_0)$ and $x_1 \leq x_2, 0.5 \cdot x_3 \leq x_4, x_5 \leq x_6$ to $\mathcal{C}(v_0)$. The rule $(\sqcap)$ then adds $\langle \forall r.A, x_7\rangle, \langle B, x_8\rangle$ to $\mathcal{L}(v_0)$ and $x_2 = x_7 \cdot x_8$ to $\mathcal{C}(v_0)$. The rules $(A), (\overline{A})$, and $(\bot)$ then yield

$$0.1 \leq x_{v_0:A} \leq x_1,\ x_8 \leq x_{v_0:B} \leq 1 - x_4,\quad 1 - x_3 = 0,\ 1 - x_5 = 0.$$

Finally, an application of the rule $(\exists)$ produces a new node v_1 with labels $\mathcal{L}(v_1) = \{\langle \top, x_9\rangle\}$, $\mathcal{L}(v_0, v_1) = \{\langle r, x_{10}\rangle\}$, and $\mathcal{C}(v_1) = \{x_9 \cdot x_{10} = x_6\}$. The rule $(\forall)$ then adds $\langle A, x_{11}\rangle$ to $\mathcal{L}(v_1)$ and $x_{11} \geq x_7 \cdot x_{10}$ to $\mathcal{C}(v_1)$.

Notice that all the concepts and constraints added to the labels of v_0, except $\langle A, 0.1\rangle$, were caused by the axioms ax_2 to ax_4, and thus they will also be added to v_1. The result of the rule applications to this node is then

$$\begin{aligned} \mathcal{L}(v_1) = \{ &\langle A, x_{11}\rangle, \langle \neg A, 1 - x_1'\rangle, \langle (\forall r.A) \sqcap B, x_2'\rangle, \\ &\langle \neg\top, 1 - x_3'\rangle, \langle \neg B, x_4'\rangle, \\ &\langle \neg\top, 1 - x_5'\rangle, \langle \exists r.\top, x_6'\rangle, \langle \forall r.A, x_7'\rangle, \langle B, x_8'\rangle\}, \\ \mathcal{C}(v_1) = \{ &x_9 \cdot x_{10} = x_6, x_{11} \geq x_7 \cdot x_{10}, x_1' \leq x_2', \\ &0.5 \cdot x_3' \leq x_4', x_5' \leq x_6', x_2' = x_7' \cdot x_8', \\ &x_{11} \leq x_{v_1:A} \leq x_1', x_8' \leq x_{v_1:B} \leq 1 - x_4', \\ &1 - x_3' = 0, 1 - x_5' = 0\}. \end{aligned}$$

Once again we can apply the $(\exists)$ rule to obtain a new individual v_2. From the $(\forall)$ rule and again the application of $(\sqsubseteq)$ rule with axioms ax_2 to ax_4 we obtain

$$\begin{aligned} \mathcal{L}(v_2) = \{ &\langle A, x_{11}'\rangle, \langle \neg A, 1 - x_1''\rangle, \langle (\forall r.A) \sqcap B, x_2''\rangle, \\ &\langle \neg\top, 1 - x_3''\rangle, \langle \neg B, x_4''\rangle, \\ &\langle \neg\top, 1 - x_5''\rangle, \langle \exists r.\top, x_6''\rangle, \langle \forall r.A, x_7''\rangle, \langle B, x_8''\rangle\}, \\ \mathcal{C}(v_2) = \{ &x_9' \cdot x_{10}' = x_6', x_{11}' \geq x_7' \cdot x_{10}', x_1'' \leq x_2'', \\ &0.5 \cdot x_3'' \leq x_4'', x_5'' \leq x_6'', x_2'' = x_7'' \cdot x_8'', \\ &x_{11}' \leq x_{v_2:A}' \leq x_1'', x_8'' \leq x_{v_2:B} \leq 1 - x_4'', \\ &1 - x_3'' = 0, 1 - x_5'' = 0\}. \end{aligned}$$

At this point $\mathcal{L}(v_1) \approx \mathcal{L}(v_2)$, and hence node v_2 is blocked and the algorithm terminates.

It is easy to verify that the valuation that sets

$$\begin{aligned} 0.1 &= x_1 = x_2 = x_{v_0:A}, \\ 0.2 &= x_7 = x_{11} = x_1' = x_2' = x_{v_1:A}, \\ 0.4 &= x_7' = x_{11}' = x_1'' = x_2'' = x_{v_2:A}, \\ 0.5 &= x_4 = x_4' = x_4'' = x_8 = x_8' = x_8'' \\ &= x_{v_0:B} = x_{v_1:B} = x_{v_2:B}, \\ 0.8 &= x_7'' \end{aligned}$$

and all other variables to 1 satisfies all the constraints in $\mathcal{C}$. Thus the algorithm returns "strongly witnessed consistent" as an answer, which we have shown to be incorrect.

Notice that the arguments used to show inconsistency in this example do not depend on the exact value of the constant 0.1 in ax_1. In order to make the ontology inconsistent, any constant κ greater than 0 can be used. However, the algorithm multiplies this value with 2 three times before stopping (see the valuation of x_7'' above). To ensure that the algorithm finishes with a satisfiable system of constraints, the constant chosen has to be small enough to ensure that $8 \cdot \kappa \leq 1$.

We emphasize that the ontology from the previous example has no model at all, which means that the algorithm is incorrect even if we do not restrict to only strongly witnessed models. Thus, at this moment there is no known algorithm for deciding consistency, witnessed consistency, or strongly witnessed consistency of fuzzy $\mathcal{ALC}$ ontologies under the product t-norm and involutive negation. In fact, it is not even clear whether this is a decidable problem. In [13] it was shown that, in the absense of concept inclusion axioms,

[3] Notice that the choice of 0.99 is an arbitrary one; the same arguments can be used with any constant $\kappa > 0.5$.

consistency of fuzzy $\mathcal{ALC}$ with product t-norm and residual negation w.r.t. witnessed models is decidable; this result was extended to so-called quasi-witnessed models (but still without concept inclusion axioms) in [17]. However, there is so far no result regarding the use of involutive negation or concept inclusion axioms. In the following section, we show that for a small extension of this logic, witnessed consistency becomes undecidable.

III. An Undecidability Result

We now consider the logic fuzzy $\mathcal{ALC}^+$, which extends fuzzy $\mathcal{ALC}$ by *strict concept inclusions*.

Definition 4 (strict concept inclusion)**.** *A* strict concept inclusion axiom *is an expression of the form* $\langle C \sqsubseteq D > q \rangle$ *where* C, D *are fuzzy* $\mathcal{ALC}$ *concepts and* $q \in [0, 1)$*. An interpretation* $\mathcal{I}$ *satisfies this axiom if for every* $\delta \in \Delta^{\mathcal{I}}$ *it holds that*

$$C^{\mathcal{I}}(\delta) \to D^{\mathcal{I}}(\delta) > q.$$

For models that are not strongly witnessed, the semantics for strict axioms introduced above may differ from the one given by

$$\inf_{\delta \in \Delta^{\mathcal{I}}} (C^{\mathcal{I}}(\delta) \to D^{\mathcal{I}}(\delta)) > q$$

since the infimum may be q although there is no witness δ actually yielding the value q. In contrast, for the case of non-strict axioms, saying that the infimum is $\geq q$ is the same as saying that the values for all individuals are $\geq q$, i.e., $C^{\mathcal{I}}(\delta) \to D^{\mathcal{I}}(\delta) \geq q$ for all $\delta \in \Delta$. As argued before, we think that the essence of a concept inclusion axiom is to enforce the inequality for the value of all individuals, and not to say something about the infimum of these values. This explains why we do not use the infimum in our definition of the semantics for strict concept inclusions.

We will show that witnessed consistency of fuzzy $\mathcal{ALC}^+$ ontologies is undecidable, by a reduction from the Post correspondence problem, which is well-known to be undecidable [18].

Definition 5 (PCP)**.** *Let* $v_1, \ldots, v_m$ *and* $w_1, \ldots, w_m$ *be two finite lists of words over an alphabet* $\Sigma = \{1, \ldots, s\}, s > 1$*. The* Post correspondence problem *(PCP) asks whether there is a non-empty sequence* $i_1, i_2, \ldots, i_k$*,* $1 \leq i_j \leq m$ *such that* $v_{i_1} v_{i_2} \cdots v_{i_k} = w_{i_1} w_{i_2} \cdots w_{i_k}$*. If such a sequence exists, it is called a* solution *of the problem.*

We assume w.l.o.g. that $v_i \neq w_i$ for every $i, 1 \leq i \leq m$ since otherwise the problem has a trivial solution. Note that we assume the alphabet Σ to consist of the first s positive integers. We can thus view every word in Σ^* as a number in base $s+1$ representation in which 0 never occurs. Using this intuition, we will represent the empty word as the number 0.

Before describing the reduction in detail, we introduce a useful abbreviation.

Notation. *Let* C, D *be two concepts and* r *a role name. We use the expression* $\left\langle D \overset{r}{\rightsquigarrow} C \right\rangle$ *to abbreviate the two axioms* $\langle D \sqsubseteq \forall r.C \geq 1 \rangle, \langle \neg D \sqsubseteq \forall r.\neg C \geq 1 \rangle$.

To understand this abbreviation, consider an interpretation $\mathcal{I}$ satisfying $\left\langle D \overset{r}{\rightsquigarrow} C \right\rangle$ and let $\delta, \gamma \in \Delta^{\mathcal{I}}$ with $r^{\mathcal{I}}(\delta, \gamma) = 1$. From the first axiom it follows that

$$\begin{aligned} D^{\mathcal{I}}(\delta) \leq (\forall r.C)^{\mathcal{I}}(\delta) &= \inf_{\eta \in \Delta^{\mathcal{I}}} r^{\mathcal{I}}(\delta, \eta) \to C^{\mathcal{I}}(\eta) \\ &\leq r^{\mathcal{I}}(\delta, \gamma) \to C^{\mathcal{I}}(\gamma) = 1 \to C^{\mathcal{I}}(\gamma) \\ &= C^{\mathcal{I}}(\gamma). \end{aligned}$$

Analogously, from the second axiom we can deduce that

$$1 - D^{\mathcal{I}}(\delta) \leq 1 - C^{\mathcal{I}}(\gamma),$$

and hence $D^{\mathcal{I}}(\delta) = C^{\mathcal{I}}(\gamma)$. Thus, $\left\langle D \overset{r}{\rightsquigarrow} C \right\rangle$ expresses that the value of $D^{\mathcal{I}}(\delta)$ is propagated to the valuation of the concept C on all r successors with degree 1 of δ.

Let now C, D be two concepts and $\mathcal{T}$ the TBox

$$\begin{aligned} \text{ax}_1 &: \langle C \sqcup Y_1 \equiv X_1 \rangle \\ \text{ax}_2 &: \langle X_1 \equiv S \sqcap \neg Y_1 \rangle \\ \text{ax}_3 &: \langle \neg Y_1 \sqcap D \equiv Y_1 \rangle \end{aligned}$$

For every model $\mathcal{I}$ of $\mathcal{T}$ and $\delta \in \Delta^{\mathcal{I}}$ it holds that

$$C^{\mathcal{I}}(\delta)(1 - Y_1^{\mathcal{I}}(\delta)) + Y_1^{\mathcal{I}}(\delta) = X_1^{\mathcal{I}}(\delta), \tag{2}$$

$$X_1^{\mathcal{I}}(\delta) = S^{\mathcal{I}}(\delta)(1 - Y_1^{\mathcal{I}}(\delta)), \tag{3}$$

$$D^{\mathcal{I}}(\delta)(1 - Y_1^{\mathcal{I}}(\delta)) = Y_1^{\mathcal{I}}(\delta), \tag{4}$$

where equalities (2), (3), and (4) follow from axioms ax_1, ax_2, and ax_3, respectively. Additionally, ax_3 implies that $Y_1^{\mathcal{I}}(\delta) \neq 1$ since otherwise $Y_1^{\mathcal{I}}(\delta)$ must also be 0. It then holds that

$$C^{\mathcal{I}}(\delta) + D^{\mathcal{I}}(\delta) = S^{\mathcal{I}}(\delta).$$

We can thus introduce the concept constructor $\boxplus$ to denote this addition without extending the expressivity of the logic. Notice however that the TBox having the axioms ax_1 to ax_3 is only satisfiable by models where $C^{\mathcal{I}}(\delta) + D^{\mathcal{I}}(\delta) \leq 1$ for all $\delta \in \Delta^{\mathcal{I}}$. One must keep this in mind when using this constructor to avoid making the ontology inconsistent. Given $C^{\mathcal{I}}(\delta)$ and $D^{\mathcal{I}}(\delta)$, there is exactly one value for $X_1^{\mathcal{I}}(\delta)$ and $Y_1^{\mathcal{I}}(\delta)$ that will satisfy the three axioms above. Then, describing the valuation of the concepts C and D suffices for knowing also the valuation of the auxiliar concepts X_1, Y_1.

Notation. *Let* C, D *be two concepts, then* $C \boxplus D$ *is also a concept, with the semantics* $(C \boxplus D)^{\mathcal{I}}(\delta) = C^{\mathcal{I}}(\delta) + D^{\mathcal{I}}(\delta)$.

Let $\mathcal{P} = (v_1, \ldots, v_m, w_1, \ldots, w_m)$ be an instance of the PCP. We will construct an ontology $\mathcal{O}_{\mathcal{P}}$ whose models represent a search tree for a solution for $\mathcal{P}$. More precisely, every model of $\mathcal{O}_{\mathcal{P}}$ will contain one node δ for each possible sequence of indices $i_1, \ldots, i_k$, such that the interpretations of two concept names A and B in δ encode the words $v_{i_1} \cdots v_{i_k}$ and $w_{i_1} \cdots w_{i_k}$, respectively. Then $\mathcal{P}$ has a solution iff for every model $\mathcal{I}$ of $\mathcal{O}_{\mathcal{P}}$ there is a δ such that $A^{\mathcal{I}}(\delta)$ and $B^{\mathcal{I}}(\delta)$ encode the same word.

Let $\Sigma = \{1, \ldots, s\}$ be the alphabet over which $\mathcal{P}$ is defined. We will encode words in Σ^* using numbers from the interval $[0, 1]$ in base $s+1$. For technical reasons that will become

clear later, the concepts A and B will encode words in a slightly different way. For every sequence of indices $i_1, \dots, i_k$, there will be a node δ such that $A^{\mathcal{I}}(\delta) = 0.1v_{i_1} \cdots v_{i_k}$ and $B^{\mathcal{I}}(\delta) = 0.0w_{i_1} \cdots w_{i_k}$ (see Figure 1).

If there is a node δ encoding the words v and w, then we want to ensure the existence of a node γ that encodes their concatenation with the i-th pair; i.e., vv_i and ww_i. To do this, we define, for every $i, 1 \leq i \leq m$, the TBox $\mathcal{T}^i_{\mathcal{P}}$ as follows:

$$\begin{aligned}\mathcal{T}^i_{\mathcal{P}} :=& \{\langle \exists r_i.\top = 1\rangle, \langle V_i = 0.0v_i\rangle, \langle W_i = 0.0w_i\rangle, \\ & \left\langle L_{v_i} = (s+1)^{-|v_i|}\right\rangle, \left\langle L_{w_i} = (s+1)^{-|w_i|}\right\rangle, \\ & \left\langle A \boxplus (V_i \sqcap L_A) \overset{r_i}{\rightsquigarrow} A\right\rangle, \left\langle L_A \sqcap L_{v_i} \overset{r_i}{\rightsquigarrow} L_A\right\rangle, \qquad (5) \\ & \left\langle B \boxplus (W_i \sqcap L_B) \overset{r_i}{\rightsquigarrow} B\right\rangle, \left\langle L_B \sqcap L_{w_i} \overset{r_i}{\rightsquigarrow} L_B\right\rangle\}. \qquad (6)\end{aligned}$$

Let $\mathcal{I}$ be a witnessed model of $\mathcal{T}^i_{\mathcal{P}}$ and $\delta \in \Delta^{\mathcal{I}}$ such that $A^{\mathcal{I}}(\delta) = 0.1v$ and $B^{\mathcal{I}}(\delta) = 0.0w$ for some words $v, w \in \Sigma^*$. Assume additionally that $L^{\mathcal{I}}_A(\delta) = (s+1)^{-|v|}$ and $L^{\mathcal{I}}_B(\delta) = (s+1)^{-|w|}$; that is, L_A, L_B yield information about the length of the words encoded by A and B in δ. From the first axiom we know that $(\exists r_i.\top)^{\mathcal{I}}(\delta) = 1$, and since $\mathcal{I}$ is witnessed, there must exist $\gamma \in \Delta^{\mathcal{I}}$ such that $r^{\mathcal{I}}_i(\delta, \gamma) = 1$. The axioms in line (5) ensure that

$$\begin{aligned}A^{\mathcal{I}}(\gamma) &= (A \boxplus (V_i \sqcap L_A))^{\mathcal{I}}(\delta) \\ &= A^{\mathcal{I}}(\delta) + (V_i^{\mathcal{I}}(\delta) \cdot L^{\mathcal{I}}_A(\delta)) \\ &= 0.1v + (0.0v_i \cdot (s+1)^{-|v|}) = 0.1vv_i \\ L^{\mathcal{I}}_A(\gamma) &= (L_A \sqcap L_{v_i})^{\mathcal{I}}(\delta) \\ &= (s+1)^{-|v|} \cdot (s+1)^{-|v_i|} = (s+1)^{-|vv_i|}\end{aligned}$$

and the axioms in (6) analogously entail

$$\begin{aligned}B^{\mathcal{I}}(\gamma) &= 0.0ww_i \\ L^{\mathcal{I}}_B(\gamma) &= (s+1)^{-|ww_i|}.\end{aligned}$$

Thus, the interpretation of A, B at node γ encodes the words vv_i, ww_i, and the concepts L_A, L_B yield information on the lengths of these words.

As we have seen, we can use the TBox $\mathcal{T}^i_{\mathcal{P}}$ to ensure that the concatenation of some words with the i-th pair of $\mathcal{P}$ will be encoded in every model. The following ABox $\mathcal{A}_{\mathcal{P}}$ introduces the root of the search tree, where A and B both encode the empty word, which obviously has lenght 0.

$$\begin{aligned}\mathcal{A}_{\mathcal{P}} := \{ &\langle a : A = 0.1\rangle, \langle a : B = 0\rangle, \\ &\langle a : L_A = 1\rangle, \langle a : L_B = 1\rangle\}\end{aligned}$$

Notice that every finite sequence of indices $i_1, \dots, i_k$, with $1 \leq i_j \leq m$ can be seen as a word $\nu \in \{1, \dots, m\}^*$. For a word $\nu = i_1 i_2 \cdots i_k \in \{1, \dots, m\}^*$, let v_ν and w_ν represent the words $v_{i_1} \cdots v_{i_k}, w_{i_1} \cdots w_{i_k} \in \{1, \dots, s\}^*$, respectively. We define the tree-like interpretation $\mathcal{I}_{\mathcal{P}} := (\Delta^{\mathcal{I}_{\mathcal{P}}}, \cdot^{\mathcal{I}_{\mathcal{P}}})$, where

- $\Delta^{\mathcal{I}_{\mathcal{P}}} = \{1, \dots, m\}^*$,
- $a^{\mathcal{I}_{\mathcal{P}}} = \varepsilon$,
- $A^{\mathcal{I}_{\mathcal{P}}}(\nu) = 0.1v_\nu$, $B^{\mathcal{I}_{\mathcal{P}}}(\nu) = 0.0w_\nu$,
- $L^{\mathcal{I}_{\mathcal{P}}}_A(\nu) = (s+1)^{-|v_\nu|}$, $L^{\mathcal{I}_{\mathcal{P}}}_B(\nu) = (s+1)^{-|w_\nu|}$, and

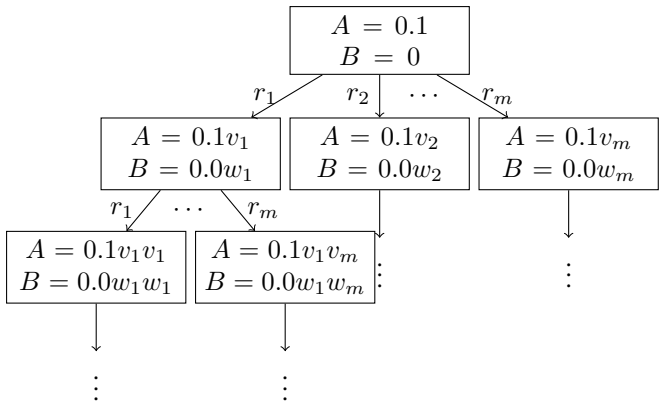

Fig. 1. The tree-shaped interpretation $\mathcal{I}_{\mathcal{P}}$.

for all $i, 1 \leq i \leq m$

- $r^{\mathcal{I}_{\mathcal{P}}}_i(\nu, \nu i) = 1$ and $r^{\mathcal{I}_{\mathcal{P}}}_i(\nu, \nu') = 0$ if $\nu' \neq \nu i$,
- $V^{\mathcal{I}_{\mathcal{P}}}_i(\nu) = 0.0v_i$, $W^{\mathcal{I}_{\mathcal{P}}}_i(\nu) = 0.0w_i$, $L^{\mathcal{I}_{\mathcal{P}}}_{v_i}(\nu) = (s+1)^{-|v_i|}$, and $L^{\mathcal{I}_{\mathcal{P}}}_{w_i}(\nu) = (s+1)^{-|w_i|}$.

The main idea underlying this interpretation is depicted in Figure 1. It is easy to see that this interpretation is a model of the ontology $\mathcal{O}_{\mathcal{P}} := (\mathcal{A}_{\mathcal{P}}, \bigcup_{i=1}^n \mathcal{T}^i_{\mathcal{P}})$.

Lemma 6. *$\mathcal{I}_{\mathcal{P}}$ is a model of $\mathcal{O}_{\mathcal{P}}$.*

More interesting, however, is that every witnessed model of $\mathcal{O}_{\mathcal{P}}$ must "include" $\mathcal{I}_{\mathcal{P}}$, as stated by the following lemma.

Lemma 7. *Let $\mathcal{I}$ be a witnessed model of $\mathcal{O}_{\mathcal{P}}$. Then there exists a function $f : \Delta^{\mathcal{I}_{\mathcal{P}}} \to \Delta^{\mathcal{I}}$ such that $C^{\mathcal{I}_{\mathcal{P}}}(\nu) = C^{\mathcal{I}}(f(\nu))$ holds for every concept name C occurring in $\mathcal{O}_{\mathcal{P}}$ and every $\nu \in \Delta^{\mathcal{I}_{\mathcal{P}}}$.*

Proof: We first remark that every model of $\mathcal{O}_{\mathcal{P}}$ must interpret the concept names V_i, W_i, L_{v_i}, and L_{w_i} with the same constant function defined by the TBox; e.g. $V^{\mathcal{I}}_i(\delta) = 0.0v_i$ for every model $\mathcal{I}$ and $\delta \in \Delta^{\mathcal{I}}$. Thus, the interpretation function of any model is fully determined by the interpretation of the concept names A, B, L_A, L_B.

We build the function f inductively on the length of ν. First, since $\mathcal{I}$ is a model of $\mathcal{A}_{\mathcal{P}}$, there must be a $\delta \in \Delta^{\mathcal{I}}$ such that $a^{\mathcal{I}} = \delta$. We fix $f(\varepsilon) := \delta$, and verify that

$$\begin{aligned}A^{\mathcal{I}}(\delta) = 0.1 &= A^{\mathcal{I}_{\mathcal{P}}}(\varepsilon) \\ B^{\mathcal{I}}(\delta) = 0 &= B^{\mathcal{I}_{\mathcal{P}}}(\varepsilon) \\ L^{\mathcal{I}}_A(\delta) = L^{\mathcal{I}}_B(\delta) = 1 &= L^{\mathcal{I}_{\mathcal{P}}}_A(\varepsilon) = L^{\mathcal{I}_{\mathcal{P}}}_B(\varepsilon).\end{aligned}$$

Let now ν be such that $f(\nu)$ has been defined. Then by induction we assume $A^{\mathcal{I}}(f(\nu)) = 0.1v_\nu$, $B^{\mathcal{I}}(f(\nu)) = 0.0w_\nu$, and L_A, L_B represent the lengths of these words. Since $\mathcal{I}$ is a witnessed model, for every $i, 1 \leq i \leq m$ there must exist a $\gamma \in \Delta^{\mathcal{I}}$ with $r^{\mathcal{I}}_i(f(\nu), \gamma) = 1$, $A^{\mathcal{I}}(\gamma) = 0.1v_\nu v_i$, $B^{\mathcal{I}}(\gamma) = 0.0w_\nu w_i$, and L_A, L_B encode the respective lengths. We set $f(\nu i) := \gamma$, which as we have seen satisfies the required property. ∎

From this lemma it follows that, if the PCP $\mathcal{P}$ has a solution

ν for some $\nu \in \{1,\dots,m\}^+$, then every witnessed model $\mathcal{I}$ must contain a node $\delta = f(\nu)$ such that $A^{\mathcal{I}}(\delta) = 0.1 + B^{\mathcal{I}}(\delta)$; that is, where A and B encode the same word. Thus, to decide whether $\mathcal{P}$ has a solution, we will search for a node δ such that $((\neg A) \boxplus B)^{\mathcal{I}}(\delta) = 1 - 0.1 = s/(s+1)$. Conversely, if every witnessed model contains such a node, then in particular $\mathcal{I}_{\mathcal{P}}$ has such a node, and thus $\mathcal{P}$ has a solution.

We now show how to detect whether a node where A and B encode the same non-empty word exists in every interpretation $\mathcal{I}$. To do this, we will introduce *flag* concepts that are interpreted as 1 whenever a given condition is satisfied. Let C, D be two concepts and $q \in [0,1]$. The axiom

$$\langle \neg F \sqsubseteq \neg F \sqcap \neg F \geq 1 - q \rangle$$

restricts every model $\mathcal{I}$ to satisfy, for every $\delta \in \Delta^{\mathcal{I}}$

$$((\neg F)^{\mathcal{I}}(\delta))^2 \geq (\neg F)^{\mathcal{I}}(\delta) \cdot (1-q);$$

that is, for every $\delta \in \Delta^{\mathcal{I}}$, it holds that either $(\neg F)^{\mathcal{I}}(\delta) = 0$ or $(\neg F)^{\mathcal{I}}(\delta) \geq 1 - q$. If we add the axiom $\langle C \sqsubseteq F \geq 1 \rangle$, then it follows that $C^{\mathcal{I}}(\delta) \leq F^{\mathcal{I}}(\delta)$, and hence, $F^{\mathcal{I}}(\delta) = 1$ if $C^{\mathcal{I}}(\delta) > q$. We will denote this concept F as $\mathbb{F}_{[C>q]}$. In addition, if we have the axioms

$$\langle \neg F \sqsubseteq \neg F \sqcap \neg F > q \rangle, \langle \neg F \sqsubseteq C \geq 1 \rangle$$

then it follows that for every $\delta \in \Delta^{\mathcal{I}}$, $F^{\mathcal{I}}(\delta) < 1 - q$ or $F^{\mathcal{I}}(\delta) = 1$, and that $1 - C^{\mathcal{I}}(\delta) \leq F^{\mathcal{I}}(\delta)$, and hence $F^{\mathcal{I}}(\delta) = 1$ if $C^{\mathcal{I}}(\delta) \leq q$. Such concept F will be denoted as $\mathbb{F}_{[C\leq q]}$.[4] In a similar way, we can define flags $\mathbb{F}_{[C<q]}$ and $\mathbb{F}_{[C\geq q]}$. Finally, the flag $\mathbb{F}_{[C=q]}$ is defined by $\langle \mathbb{F}_{[C=q]} \equiv \mathbb{F}_{[C\leq q]} \sqcap \mathbb{F}_{[C\geq q]} \rangle$.

Notation. *For a concept C and $q \in [0,1]$, the expression $\mathbb{F}_{[C\bowtie q]}$, where $\bowtie$ is one of $>, <, \geq, \leq, =$, denotes a concept such that for every model $\mathcal{I}$ and $\delta \in \Delta^{\mathcal{I}}$, $\mathbb{F}^{\mathcal{I}}_{[C\bowtie q]}(\delta) = 1$ if $C^{\mathcal{I}}(\delta) \bowtie q$.*

Using these flags, we can detect whether A and B encode the same word, that is $((\neg A) \boxplus B)^{\mathcal{I}}(\delta) = s/(s+1)$, by checking whether the flag $\mathbb{F}_{[(\neg A)\boxplus B = s/(s+1)]}$ is interpreted as 1, and test that this word is not the empty word using the flag $\mathbb{F}_{[A\sqcup B>0.1]}$. Notice, additionally, that $A^{\mathcal{I}_{\mathcal{P}}}(\delta) \geq B^{\mathcal{I}_{\mathcal{P}}}(\delta)$ for all δ, and thus the concept $(\neg A) \boxplus B$ is well-defined; that is, the axioms that are used to encode it are satisfied by $\mathcal{I}_{\mathcal{P}}$.

Thus, for a node δ, if $A^{\mathcal{I}}(\delta)$ and $B^{\mathcal{I}}(\delta)$ encode the same non-empty word, then

$$(\mathbb{F}_{[(\neg A)\boxplus B = s/(s+1)]} \sqcap \mathbb{F}_{[A\sqcup B>0.1]})^{\mathcal{I}}(\delta) = 1.$$

We now define the ontology $\mathcal{O}'_{\mathcal{P}} := (\mathcal{A}_{\mathcal{P}}, \mathcal{T}_{\mathcal{P}})$ where

$$\mathcal{T}_{\mathcal{P}} := \bigcup_{i=1}^{m} \mathcal{T}^i_{\mathcal{P}} \ \cup \ \{\top \sqsubseteq \neg(\mathbb{F}_{[(\neg A)\boxplus B = s/(s+1)]} \sqcap \mathbb{F}_{[A\sqcup B>0.1]}) > 0\}.$$

Theorem 8. *The instance $\mathcal{P}$ of the PCP has a solution iff the ontology $\mathcal{O}'_{\mathcal{P}}$ is not witnessed consistent.*

[4]Notice that this is the first instance of a strict axiom used in our construction so far.

Proof: Assume first that $\mathcal{P}$ has a solution $i_1, \dots, i_k$ and let $\nu = i_1 i_2 \cdots i_k \in \{1,\dots,m\}^*$ and $u = v_\nu = w_\nu$. Suppose there is a witnessed model $\mathcal{I}$ of $\mathcal{O}'_{\mathcal{P}}$. Since $\mathcal{O}_{\mathcal{P}} \subseteq \mathcal{O}'_{\mathcal{P}}$, $\mathcal{I}$ must also be a model of $\mathcal{O}_{\mathcal{P}}$. From Lemma 7 it follows that there is a node $\delta \in \Delta^{\mathcal{I}}$ such that

$$A^{\mathcal{I}}(\delta) = A^{\mathcal{I}_{\mathcal{P}}}(\nu) = 0.1u,$$
$$B^{\mathcal{I}}(\delta) = B^{\mathcal{I}_{\mathcal{P}}}(\nu) = 0.0u,$$

We thus have $((\neg A) \boxplus B)^{\mathcal{I}}(\delta) = s/(s+1)$ and hence $\mathbb{F}_{[(\neg A)\boxplus B = s/(s+1)]} = 1$. Additionally, since u is not the empty word, it follows that $(A \sqcup B)^{\mathcal{I}}(\delta) > 0.1$ and thus $\mathbb{F}_{[A\sqcup B>0.1]} = 1$. But this violates the last axiom in $\mathcal{T}_{\mathcal{P}}$, and hence $\mathcal{I}$ cannot be a model of $\mathcal{O}'_{\mathcal{P}}$.

To show the converse, we will extend $\mathcal{I}_{\mathcal{P}}$ to interpret the three flag concepts $\mathbb{F}_{[(\neg A)\boxplus B\geq s/(s+1)]}$, $\mathbb{F}_{[(\neg A)\boxplus B\leq s/(s+1)]}$, and $\mathbb{F}_{[A\sqcup B>0.1]}$ as follows for every $\delta \in \Delta^{\mathcal{I}_{\mathcal{P}}}$:

$$\mathbb{F}^{\mathcal{I}_{\mathcal{P}}}_{[C\bowtie q]}(\delta) = \begin{cases} 1 & \text{if } C^{\mathcal{I}_{\mathcal{P}}}(\delta) \bowtie q \\ C^{\mathcal{I}_{\mathcal{P}}}(\delta) & \text{otherwise} \end{cases}$$

if $\bowtie$ is either $\geq$ or $>$, and

$$\mathbb{F}^{\mathcal{I}_{\mathcal{P}}}_{[C\leq q]}(\delta) = \begin{cases} 1 & \text{if } C^{\mathcal{I}_{\mathcal{P}}}(\delta) \leq q \\ 1 - C^{\mathcal{I}_{\mathcal{P}}}(\delta) & \text{otherwise.} \end{cases}$$

It is easy to see that this valuation satisfies the two axioms that define each flag concept.

Additionally, every element $\nu \in \Delta^{\mathcal{I}_{\mathcal{P}}}$ has exactly one r_i-sucessor for every $i, 1 \leq i \leq m$, i.e. there is exactly one element $\nu' \in \Delta^{\mathcal{I}_{\mathcal{P}}}$ such that $r_i^{\mathcal{I}_{\mathcal{P}}}(\nu, \nu') > 0$. Thus, the interpretation $\mathcal{I}_{\mathcal{P}}$ trivially satisfies the two conditions of witnessed models.

Suppose now that $\mathcal{O}'_{\mathcal{P}}$ is not witnessed consistent. Then $\mathcal{I}_{\mathcal{P}}$ is not a model of $\mathcal{O}'_{\mathcal{P}}$. Since it is a model of $\mathcal{O}_{\mathcal{P}}$ and satisfies the axioms defining each of the three flag concepts, it must violate the last axiom added to $\mathcal{T}_{\mathcal{P}}$. Thus, there is a node $\nu \in \Delta^{\mathcal{I}_{\mathcal{P}}}$ such that $\mathbb{F}^{\mathcal{I}_{\mathcal{P}}}_{[(\neg A)\boxplus B = s/(s+1)]}(\nu) = 1$ and $\mathbb{F}^{\mathcal{I}_{\mathcal{P}}}_{[A\sqcup B>0.1]}(\nu) = 1$. By our interpretation of these flag concepts, it then follows that $1 - A^{\mathcal{I}_{\mathcal{P}}}(\nu) + B^{\mathcal{I}_{\mathcal{P}}}(\nu) = s/(s+1)$, or equivalently, $A^{\mathcal{I}_{\mathcal{P}}}(\nu) = 0.1 + B^{\mathcal{I}_{\mathcal{P}}}(\nu)$ which means that $A^{\mathcal{I}_{\mathcal{P}}}(\nu)$ and $B^{\mathcal{I}_{\mathcal{P}}}(\nu)$ encode the same word. From the second flag, it follows that they both encode a non-empty word. But then, this same ν must be a solution of $\mathcal{P}$, which finishes the proof. ∎

IV. Conclusions

We have shown that the algorithm from [10] is incorrect, and given an undecidability result for a small extension of fuzzy $\mathcal{ALC}$ with product t-norm and involutive negation. Our results do not show that the logic used in [10] is undecidable since we (i) added expressivity by means of the strict axioms, and (ii) used a weaker notion of witnessed models, which we believe to be more closely related to the idea of concept inclusions in DL. As future work, we will analyse the decidability status of consistency (witnessed consistency, strongly witnessed consistency) for the logic considered in [10], [11] with general concept inclusions. On the one hand, this involves

trying to correct the algorithm from [10] by introducing a more sophisticated blocking condition. On the other hand, we will also try to modify our undecidability proof such that it does not use strict inclusion axioms, or such that it can also deal with pure consistency or strongly witnessed consistency.

Another area for future work includes studying the impact of concept inclusion axioms when reasoning w.r.t. other t-norm based semantics, in particular with the Łukasiewicz t-norm. We will also analyse the applicability of other reasoning techniques to fuzzy DLs. It is important to notice that under the product t-norm semantics, the models of an ontology may, in general, require infinitely many different interpretation values. Hence, the methods for transforming fuzzy DL ontologies into crisp DL ontologies [19], [20], [21] cannot be applied in this setting.

REFERENCES

[1] F. Baader, D. Calvanese, D. McGuinness, D. Nardi, and P. F. Patel-Schneider, Eds., *The Description Logic Handbook: Theory, Implementation, and Applications*. Cambridge University Press, 2003.

[2] F. Baader and U. Sattler, "An overview of tableau algorithms for description logics," *Studia Logica*, vol. 69, pp. 5–40, 2001.

[3] T. Lukasiewicz and U. Straccia, "Managing uncertainty and vagueness in description logics for the semantic web," *Journal of Web Semantics*, vol. 6, no. 4, pp. 291–308, 2008.

[4] U. Straccia, "Description logics with fuzzy concrete domains," in *Proceedings of the 21st Conference in Uncertainty in Artificial Intelligence (UAI'05)*. AUAI Press, 2005, pp. 559–567.

[5] G. Stoilos, G. B. Stamou, V. Tzouvaras, J. Z. Pan, and I. Horrocks, "The fuzzy description logic f-SHIN," in *Proceedings of Uncertainty Reasoning for the Semantic Web (URSW'05)*, 2005, pp. 67–76.

[6] U. Straccia, "Reasoning within fuzzy description logics," *Journal of Artificial Intelligence Research (JAIR)*, vol. 14, pp. 137–166, 2001.

[7] G. Stoilos, U. Straccia, G. B. Stamou, and J. Z. Pan, "General concept inclusions in fuzzy description logics," in *Proceedings of the 17th European Conference on Artificial Intelligence (ECAI'06)*, ser. Frontiers in Artificial Intelligence and Applications, vol. 141. IOS Press, 2006, pp. 457–461.

[8] U. Straccia and F. Bobillo, "Mixed integer programming, general concept inclusions and fuzzy description logics," in *Proceedings of the 5th EUSFLAT Conference*. Universitas Ostraviensis, 2007, pp. 213–220.

[9] F. Bobillo and U. Straccia, "On qualified cardinality restrictions in fuzzy description logics under lukasiewicz semantics," in *Proceedings of the 12th International Conference on Information Processing and Managment of Uncertainty in Knowledge-Based Systems, (IPMU-08)*, 2008, pp. 1008–1015.

[10] ——, "A fuzzy description logic with product t-norm," in *Proceedings of the IEEE International Conference on Fuzzy Systems (FUZZ-IEEE 2007)*. IEEE Press, 2007, pp. 1–6.

[11] ——, "Fuzzy description logics with general t-norms and datatypes," *Fuzzy Sets and Systems*, vol. 160, no. 23, pp. 3382–3402, 2009.

[12] F. Bobillo, F. Bou, and U. Straccia, "On the failure of the finite model property in some fuzzy description logics," *CoRR*, vol. abs/1003.1588, 2010.

[13] P. Hájek, "Making fuzzy description logic more general," *Fuzzy Sets and Systems*, vol. 154, no. 1, pp. 1–15, 2005.

[14] ——, "On witnessed models in fuzzy logic," *Mathematical Logic Quarterly*, vol. 53, no. 1, pp. 66–77, 2007. [Online]. Available: http://dx.doi.org/10.1002/malq.200610027

[15] A. García-Cerdaña, E. Armengol, and F. Esteva, "Fuzzy description logics and t-norm based fuzzy logics," *International Journal of Approximate reasoning*, vol. 51, pp. 632 – 655, July/2010 2010.

[16] F. Bobillo, F. Bou, and U. Straccia, "On the failure of the finite model property in some fuzzy description logics," *Fuzzy Sets and Systems*, vol. 172, no. 1, pp. 1–12, 2011.

[17] M. Cerami, F. Esteva, and F. Bou, "Decidability of a description logic over infinite-valued product logic," in *Proceedings of the 12th International Conference on the Principles of Knowledge Representation and Reasoning (KR 2010)*. AAAI Press, 2010, pp. 203–213.

[18] E. Post, "A variant of a recursively unsolvable problem," *Bulletin of the American Mathematical Society*, vol. 52, pp. 264–268, 1946.

[19] U. Straccia, "Transforming fuzzy description logics into classical description logics," in *Proceedings of the 9th European Conference on Logics in Artificial Intelligence (JELIA-04)*, ser. Lecture Notes in Computer Science, no. 3229. Lisbon, Portugal: Springer Verlag, 2004, pp. 385–399.

[20] F. Bobillo, M. Delgado, J. Gómez-Romero, and U. Straccia, "Fuzzy description logics under Gödel semantics," *International Journal of Approximate Reasoning*, vol. 50, no. 3, pp. 494–514, 2009.

[21] F. Bobillo and U. Straccia, "Reasoning with the finitely many-valued łukasiewicz fuzzy description logic $\mathcal{SROIQ}$," *Information Sciences*, vol. 181, pp. 758–778, 2011.

2011 IEEE International Conference on Fuzzy Systems
June 27-30, 2011, Taipei, Taiwan

Fuzzy Concept Lattice Construction

A Basis for Building Fuzzy Ontologies

Valerie Cross
Computer Science and Software Engineering
Miami University
Oxford, OH USA
crossv@muohio.edu

Meenakshi Kandasamy
Information Technology Services
Miami University
Oxford, OH USA
kandasm@muohio.edu

***Abstract*— Fuzzy concept lattices are being used as the basis for creating fuzzy ontologies. Fuzzy formal contexts serve as the starting point for which a variety of proposed methods have been used to create fuzzy concept lattices from them. This paper reviews two of these methods: the one-sided threshold approach and the fuzzy closure operator approach and presents the first comparison between these two approaches. Some simple examples are used and then bioinformatics data, specifically several gene annotation data files. The results show that the fuzzy closure approach produces huge numbers of concepts as compared to the threshold approach, and the extents produced by the threshold approach are a subset of the extents produced by the fuzzy closure approach.**

Keywords-Fuzzy concept lattices; threshold method; fuzzy closure method; fuzzy ontologies; fuzzy formal concept analysis

I. INTRODUCTION

Ontologies have become accepted as the main knowledge representation method for making domain knowledge available on the web. Ontologies typically are specified in a machine-readable format and represent domain knowledge by defining concepts, attributes of the concepts and relationships between the concepts with the taxonomic is-a relationship creating the ontology structure. More formal ontology languages such as OWL [1] also allow axioms to be specified in the definition of the ontology. Ontologies facilitate the use of web resources and knowledge sharing by web applications.

One of the bottlenecks in the use of ontologies, however, is the time and effort to create them. Much research has been undertaken to automate as much as possible the building of ontologies [2]. More recently formal concept analysis (FCA) is being used to aid in constructing ontologies [3][4]. FCA was developed in the early 1980's [5] and has grown into a widely used tool for knowledge discovery [6]. FCA is an unsupervised learning method to cluster data to create concepts where a formal concept has two components, the instance objects which are its extent, and the attributes describing the objects, which are its intent.

Since real-world knowledge can be vague or uncertain, researchers have focused on integrating fuzzy logic into the modeling of domain knowledge and the result is the definition of fuzzy ontologies [7]. A natural extension to the use of FCA for creating ontologies is the use of fuzzy formal concept analysis (FFCA) to build fuzzy ontologies. In crisp FCA, the association of an attribute with an object is either complete or not at all. In FFCA an attribute may only be partially associated with an object, i.e., an attribute has a degree of association or membership when used to describe the object. The fuzzy formal context is typically specified by a matrix with a set of objects for its rows and a set of attributes or properties for its columns as shown in Fig. 1. It is basically a formal context where the relation R between the objects and the attributes is a fuzzy binary relation; that is, instead of a crisp 0 or 1 degree, the degree is taken from the interval [0, 1] and indicates that the object x_i possesses the attribute y_j to the specified degree.

	y_1	y_2	y_3	y_4	y_5
x_1	1	0.5	0.5	1	1
x_2	1	1	1	1	0.5
x_3	0	0	0.5	0.5	1

Fig. 1. A fuzzy formal context [11].

Numerous researchers have developed approaches for creating fuzzy concept lattices that are then used to develop fuzzy ontologies [8] [9] [10]. These approaches use an α-cut on the fuzzy formal context to first convert to a crisp formal context and then use standard FCA to both create the formal concepts and the structure of the concept lattice. The fuzziness is introduced back into concept lattice using several fuzzy operators on the fuzzy formal context. This method is referred to as the one-sided α-cut thresholding approach to fuzzy concept lattice creation. Recently a new approach to creating a fuzzy concept lattice that works directly on the fuzzy formal context has been introduced [11]. It is uses a fuzzy closure operator to calculate all fixpoints in a finite set over a finite chain of truth degrees. These fixpoints are the fuzzy formal concepts. The partial order on the set of all fixpoints is also determined to create the structure of the fuzzy concept lattice.

This paper extends the work in [12] and presents a more detailed comparison of these two approaches. Both algorithms have been implemented in Java and various test cases have been used to compare their results, first using a simple example and then using a gene annotation data set with three different protein families. Currently, these two different approaches have not been directly compared. For the most part, the fuzzy

978-1-4244-7316-8/11/$26.00 ©2011 IEEE

closure approach has simply been used on experimentally generated fuzzy formal contexts with a focus on its practical performance [11]. The threshold approach has been experimented with to examine its usefulness for creating fuzzy concept lattices as a foundation for developing fuzzy ontologies [10]. The focus in this present paper is examining the differences in the interpretation of the two approaches and actually applying them to the same real world fuzzy formal context based on gene annotation data which plays an important role in bioinformatics research. Section 2 describes the one-sided α-cut threshold approach to fuzzy concept lattice creation. Section 3 describes the fuzzy closure approach. Both of these sections use the simple fuzzy formal context shown in Fig. 1 to illustrate the two different approaches. Section 4 outlines the experimental data used to compare the two approaches. The results of these experiments are analyzed in section 5. Section 6 summarizes the research and outlines plans to further experiment with these two approaches.

II. ONE-SIDED THRESHOLD APPROACH

A fuzzy formal context is basically a formal context where the relation between the objects and the attributes is a fuzzy binary relation R between a set of objects X and a set of attributes Y as illustrated in Fig. 1. For example, object x_1 possesses attribute y_3 to degree 0.5, i.e., $R(x_1,y_3)= 0.5$. The fuzzy formal context is viewed as a set of fuzzy sets where each fuzzy set describes either an object or an attribute, i.e., the side that is selected or given preference. If the object is given preference, then an object $x_i \in X$ in a fuzzy formal context K with attribute set Y is represented by a fuzzy set $\Phi(x_i)$ as $\{ R(x_i,y_1)/y_1, R(x_i,y_2)/y_2, ..., R(x_i,y_n)/y_n \}$ where $R(x_i,y_j)$ is the degree to which object x_i possesses attribute y_j. For example, the row for object x_3 specifies its fuzzy set description over the attributes, $\{0.5/y_3, 0.5/y_4, 1.0/y_5\}$. An attribute can also be represented as a fuzzy set over the objects, i.e., the column for attribute y_3 specifies its fuzzy set description over the objects, $\{0.5/x_1, 0.5/x_2, 1.0/x_3\}$. With this view, algorithms for creating the fuzzy formal concepts that include the extent and intent, the concept lattice structure, and the strength of the links from a parent concept to its children concepts have been developed.

In [10], the threshold approach is used to generate fuzzy ontologies from fuzzy formal context by taking α-cuts on the fuzzy formal context where the object is given preference. Then a fuzzy formal concept is defined by specifying an α value, also referred to as a confidence threshold. For $A \subseteq X$, then the crisp definition simply is modified to require $R(x,y) \geq \alpha$ instead of $R(x,y) = 1$ as given:

$$A' = \{y \in Y \mid \forall x \in A, R(x,y) \geq \alpha\} \quad (1)$$

and similarly, $B \subseteq Y$

$$B' = \{x \in X \mid \forall y \in B, R(x,y) \geq \alpha\} \quad (2)$$

The threshold α restricts the fuzzy concept lattice generation since it eliminates from the original fuzzy formal context all (x, y) pairs whose degree is less than the threshold and basically converts the fuzzy formal context into a crisp context for all those remaining pairs. This method then simply uses standard FCA to create the concepts and the concept lattice structure, but no fuzziness exists in the extent or intent at that point. The crisp formal concept must be transformed into a fuzzy formal concept.

The fuzzy formal concept of a fuzzy formal context K with a confidence threshold α is a pair (A_f, B), where $A'=B$ and $B'=A$ and each $x \in A$ has a membership degree defined as

$$A_f(x) = \min_{y \in B} R(x,y). \quad (3)$$

If B is the empty set, then $A_f(x) = 1$ for every x. A is the extent and B is the intent of the fuzzy formal concept. If attributes are given preference then the formula becomes

$$B_f(x) = \min_{x \in A} R(x,y). \quad (4)$$

The term fuzzy concept is used in the remainder of the paper as an abbreviation for fuzzy formal concept. Note that when the object is given preference, the extent of the fuzzy concept is a fuzzy set. The membership degree belonging to the object in the fuzzy extent is interpreted as the degree to which the object belongs to the fuzzy concept and specifies the minimum degree to which the object possesses all the attributes in the intent. The partial ordering of fuzzy concepts ≤ is defined such that $(A1_f, B1) \leq (A2_f, B2)$ if and only if $A1_f \subseteq A2_f$ and equivalently $B2 \subseteq B1$. This approach creates a set of fuzzy concepts and a fuzzy concept lattice based on the ≤ ordering.

Although the fuzzy concept lattice can be created from the fuzzy concepts and the ordering, the subsumption or ordering relation does not provide a degree of similarity or strength between the parent fuzzy concept and the child fuzzy concept. Thus a measure of fuzzy concept similarity between concepts $c1 = (A1, B1)$ and $c2 = (A2, B2)$ is defined using the Jaccard fuzzy set similarity measure between two fuzzy sets as

$$E(c1,c2) = \frac{|A1_f \cap A2_f|}{|A1_f \cup A2_f|}. \quad (5)$$

This approach has been used in recent papers focusing on fuzzy ontology generation [8]-[10]. If the attribute set is given preference, then the intents are fuzzy sets and the A sets would be replaced with corresponding B sets in (5).

For the fuzzy formal context in Fig. 1 and selecting the object side with a threshold of the minimum degree in the fuzzy formal context, i.e., 0.5, produces the following two concepts labeled 0 and 1 followed by the intent set and the extent set of each one:

0: $[0.5/x_1, 0.5/x_2, 0.5/x_3]$; $[y_3, y_4, y_5]$
1: $[0.5/x_1, 0.5/x_2]$; $[y_1, y_2, y_3, y_4, y_5]$

Since the minimum membership degree in the fuzzy formal context is selected as the threshold, any nonzero membership degree indicates that the object possess the attribute. The top concept 0 shows all objects in X possess attributes y_3, y_4 and y_5 to some degree, but the minimum degree of possession over all attributes in the intent of concept 0 is 0.5 for each of the objects. The bottom concept 1 shows that all attributes are possessed by both objects x_1 and x_2.

Again, the minimum degree of possession over all attributes in the intent of concept 1 is 0.5 for both x_1 and x_2. Concept 0 has concept 1 as its child with a link strength of 0.667 between them.

Using a threshold of 1.0 greatly changes the results. Only pairs of objects and attributes which have a 1.0 membership degree in the fuzzy formal context are considered. The following concepts are produced:

0: [1.0/ x_1, 1.0/x_2, 1.0/x_3]; []
1: [1.0/ x_1, 1.0/ x_2]; [y_1, y_4]
2: [1.0/ x_2]; [y_1, y_2, y_3, y_4]
3: [1.0/x_1, /1.0/x_3]; [y_5]
4: [1.0/ x_1]; [y_1, y_4, y_5]
5: []; [y_1, y_2, y_3, y_4, y_5]

The top concept 0 in the lattice shows that not a single attribute is possessed by all objects at the 1.0 degree. Concept 5, the bottom concept of the lattice, shows that not a single object possesses all attributes to degree 1.0. Concept 1 which is a child of concept 0 with a link strength of 0.667 shows that object x_1 and x_2 possess both attributes y_1 and y_4. Concept 3 which is also a child of concept 0 with a link strength of 0.667 shows that objects x_1 and x_3 possess attribute y_5. Concept 2 which is a child of concept 1 with a link strength of 0.5 shows that object x_2 possesses the attributes y_1, y_2, y_3, and y_4. Finally concept 4 which is a child of concept 1 with a link strength of 0.5 and a child of concept 3 with a link strength of 0.5 shows object x_1 possesses attributes y_1, y_4, and y_5. Concept 5 as the bottom concept is a child of both concepts 2 and 4 but with a link strength of 0.0 since its extent is empty and the intersection of it with the extents of concepts 2 and 4 is empty.

III. FUZZY CLOSURE APPROACH

The threshold approach can give preference to either the objects or the attributes. In its fuzzy concepts, a fuzzy extent exists if the objects are given preference, or a fuzzy intent exists if the attributes are given preference. In the fuzzy closure approach, however, the fuzzy concepts contain both fuzzy extents and fuzzy intents since it looks at the complete fuzzy formal context without giving preference to either objects or attributes. It also differs from the threshold approach in that it does not convert the fuzzy formal context into a crisp formal context in order to create the initial formal concepts and concept lattice structure. It also does not propose a link strength between fuzzy concepts although the fuzzy similarity measure given in (5) could be used between the intent fuzzy sets, the extent fuzzy sets or both to determine a link strength between a parent and child concept. A detailed description of the fuzzy closure approach and its algorithm can be found in [11] and an explanation and insights into the workings of the algorithm are provided in [12]. Here a summary and discussion of the important points of this approach are presented.

The fuzzy closure approach requires that the $R(x,y)$ values in the fuzzy formal context be taken from a complete residuated lattice L in the real unit interval [0,1], well-known in fuzzy logic [13]. L is assumed to be finite and linearly ordered. The lattice structure requires the two operations of fuzzy conjunction $\otimes$ and a residuum $\rightarrow$, a special kind of fuzzy implication operator defined as

$$a \rightarrow b = max\{c \text{ in } L \mid a \otimes c \leq b\}.$$

A residuum satisfies an adjointness condition: $a \otimes b \leq c$ iff $a \leq b \rightarrow c$. With the operations $\otimes$ and $\rightarrow$, L forms a complete residuated lattice. In [11], the example uses the Lukasiewiz operators

$$\begin{aligned} a \otimes b &= \max(0, a + b - 1) \\ a \rightarrow b &= \min(1 - a + b, 1) \end{aligned} \quad . \tag{5}$$

The set of all fuzzy sets using L in a universe X is denoted by L^X where a fuzzy set A means a mapping $A: X \rightarrow L$ assigning to any $x \in X$ a truth degree $A(x) \in L$ to which x belongs to A. Given the fuzzy formal context $<X, Y, R>$ where X is the set of objects, Y is the set of attributes, and R is the fuzzy binary relation, for fuzzy sets $A \in L^X$ and $B \in L^Y$, , fuzzy sets $A\uparrow \in L^Y$ and $B\downarrow \in L^X$ are defined as

$$\begin{aligned} A\uparrow &= min_{x \in X} (A(x) \rightarrow R(x,y)) \\ B\downarrow &= min_{y \in Y} (B(y) \rightarrow R(x,y)) \end{aligned} \tag{6}$$

The interpretation of $A\uparrow(y)$ based on fuzzy logic is that the membership degree of y in $A\uparrow$ specifies the truth degree that the attribute y is possessed by all objects in the fuzzy set A. Similarly, the membership degree of x in $B\downarrow$ specifies the truth degree that the object x possesses all attributes in the fuzzy set B. $<A, B>$ is a fuzzy formal concept in the fuzzy concept lattice if $A\uparrow = B$ and $B\downarrow = A$. Denote $\mathbf{B}$ <X, Y, R> = $\{<A, B> \mid A\uparrow = B, B\downarrow = A\}$ as the set of all fuzzy concepts for the fuzzy formal context $<X, Y, R>$.

The conceptual hierarchy is modeled by the relation $\leq$ defined on $\boldsymbol{B}$ $<X, Y, R>$ by $<A_1, B_1> \leq <A_2, B_2>$ if and only if $A_1 \subseteq A_2$ (or, equivalently $B_1 \supseteq B_2$). The set $\boldsymbol{B}$<X, Y, R> under the relation $\leq$ is a fuzzy concept lattice. Since fuzzy concepts are simply the fixpoints of a particular fuzzy closure operator [14], computing all fuzzy concepts reduces to computing all fixpoints of a fuzzy closure operator.

A fuzzy closure operator C on a universe X is a mapping $C: L^X \rightarrow L^X$ such that the following three conditions are satisfied: $A \subseteq C(A)$ (extensivity), $A \subseteq B$ implies $C(A) \subseteq C(B)$ (monotony), and $C(A) = C(C(A))$ (idempotency). If $A=C(A)$, then A is called a fixpoint of C. The set of all fixed points of C is denoted by $fix(C)$, such that $fix(C) = \{A \in L^X \mid A=C(A)\}$. Given a formal context $<X, Y, I>$, the compound mapping $\uparrow\downarrow: L^X \rightarrow L^X$ is a fuzzy closure operator in X and $\downarrow\uparrow: L^Y \rightarrow L^Y$ is a fuzzy closure operator in Y. The fixpoints of $\uparrow\downarrow$ and the fixpoints of $\downarrow\uparrow$ are just the extents and intents respectively of the fuzzy formal concepts of $<X, Y, I>$.

A brute-force method to determine all the fixpoints would be to simply generate all $A \in L^X$ and then output those where $A = C(A)$. This method has exponential time complexity and, therefore, is of no use. The research in [11] presents an algorithm to compute a fuzzy concept lattice, i.e., all the fixpoints of a fuzzy closure operator as well as the structure of the fuzzy concept lattice. It is based on extending the NEXTNEIGHBOR algorithm [15] which computes crisp concept lattices.

This recursive algorithm begins by calculating the fuzzy closure ↓↑ on the empty attribute set to produce the first intent B_0 of the fuzzy concept lattice. B_0 is the intent of the top concept $(B_0\downarrow, B_0)$ in the fuzzy concept lattice. The algorithm proceeds by generating from B_0 (GenerateFrom procedure) the intents of its set of upper neighbors (Neighbors procedure), i.e., the intents of the fuzzy concepts that are subconcepts of the fuzzy concept $(B_0\downarrow, B_0)$. A neighbor generated for fuzzy concept $(B_0\downarrow, B_0)$ has an intent that is a superset of B_0 and an extent that is a subset of the extent of $B_0\downarrow$, where the standard definition of inclusion on fuzzy sets is used, i.e., $F_1 \subseteq F_2$ if $\forall x \in X, \mu_{F_1}(x) \leq \mu_{F_2}(x)$. Each of these neighbors is then linked to $(B_0\downarrow, B_0)$. The generated intents of the neighbors not already in the set of intents for $\boldsymbol{B}$<X, Y, R> are then added to the set. Each intent added to the set of intents is then input to the GenerateFrom procedure to generate its neighbors. This process repeats recursively up to the intent consisting of *Y*, the complete attribute set, which is the greatest fixpoint of *C*.

The challenging part is finding the upper neighbor intents for a given input intent *B*. The *upper neighbor* $D \in fix(C)$ w.r.t *C*, written as $B \prec^C D$, is established if $B \in fix(C)$ such that *i)* $B \subset D$ *ii)* there is no $D' \in fix(C)$ such that $B \subset D' \subset D$. The Neighbors procedure relies on several lemmas and theorems proven in [11] that show each upper neighbor intent is in fact produced by some $y \in Y$. Two orderings are required by the Neighbors procedure: the ordered membership degrees in $L = \{a_1, a_2, \ldots a_k\}$ such that $0 = a_1 < a_2 < \ldots < a_k = 1$ and a fixed ordering of attributes from $Y = \{y_1, y_2, \ldots y_n\}$ and $y_i < y_j$ if $i < j$. The Neighbors procedure systematically proceeds through this fixed ordering checking each y_i that does not already have a membership degree of 1.0 in *B* as a possible generator of an upper neighbor of *B*. It does this by first modifying *B* to produce *B'*. Assume $B(y_i) = a_j$, then *B'* becomes $B \cup \{a_{j+1}/y_i\}$, that is, the membership degree of y_i in *B'* becomes the next membership degree in the ordering that is greater than the membership of y_i in *B*. Then the potential upper neighbor *D* which must be a fixpoint of *C* is calculated as $D = C(B')$. The problem, however, is that there might exist $D' \in fix(C)$ such that $B \subset D' \subset D$. The algorithm uses the fixed ordering of the attributes *Y* to make sure that the calculated *D* is selected as an upper neighbor of *B* only if no other *D'* exists.

The fuzzy formal context in Fig. 1 with $L = \{0, 0.5, 1.0\}$ and the implication operator → given in (5) was used to verify our implementation of the fuzzy closure operator approach to creating fuzzy concept lattices. The results produced are identical to those provided in [11]

0: [1.0/x1, 1.0/x2, 1.0/x3]; [0.5/y3, 0.5/y4, 0.5/y5]
1: [1.0/x1, 1.0/x2, 0.5/x3]; [0.5/y1, 0.5/y2, 0.5/y3, 1.0/y4, 0.5/y5]
2: [1.0/x1, 0.5/x2, 1.0/x3]; [0.5/y3, 0.5/y4, 1.0/y5]
3: [1.0/x1, 1.0/x2]; [1.0/y1, 0.5/y2, 0.5/y3, 1.0/y4, 0.5/y5]
4: [0.5/x1, 1.0/x2, 0.5/x3]; [0.5/y1, 0.5/y2, 1.0/y3, 1.0/y4, 0.5/y5]
5: [1.0/x1, 0.5/x2, 0.5/x3]; [0.5/y1, 0.5/y2, 0.5/y3, 1.0/y4, 1.0/y5]
6: [0.5/x1, 1.0/x2]; [1.0/y1, 1.0/y2, 1.0/y3, 1.0/y4, 0.5/y5]
7: [1.0/x1, 0.5/x2]; [1.0/y1, 0.5/y2, 0.5/y3, 1.0/y4, 1.0/y5]
8: [0.5/x1, 0.5/x2]; [1.0/y1, 1.0/y2, 1.0/y3, 1.0/y4, 1.0/y5]
9: [0.5/x1, 0.5/x2, 0.5/x3]; [0.5/y1, 0.5/y2, 1.0/y3, 1.0/y4, 1.0/y5]

The concept lattice hierarchy produced by our implementation shows the first the concept number followed by concept numbers of its children and agrees with that given in [11]:

0: 1; 2;
1: 3; 4; 5;
2: 5;
3: 6; 7;
4: 6; 9;
5: 7; 9;
6: 8;
7: 8;
8:
9: 8;

The results from the threshold approach for 0.5 threshold with object preference produced two very simple fuzzy concepts; whereas the fuzzy closure approach produces a more complex concept lattice with 10 fuzzy concepts where both the extents and intents are fuzzy sets. Notice that (3) used to produce the fuzzy extent in the threshold approach is basically using $B\downarrow$ given in (6); however, since the threshold approach assumes a membership degree of 1 for all attributes in the intents, $B\downarrow$ in (6) simply becomes $(1\text{-}1+ R(x,y))$ or simply $R(x,y)$ with the → operation given in (5). Notice that the results of the threshold approach with a 0.5 value produce a top concept 0 that is similar to the top concept 0 of the fuzzy closure approach. Both have the same objects in the extent and the same attributes in the intent. A major difference is that in threshold approach with object preference, an object is described as a fuzzy set over attributes; therefore, an object's membership degree in the extent of the fuzzy concept indicates the minimum degree to which the object possesses all of the attributes in the intent. For the fuzzy closure approach the top concept 0 has an extent where each object fully belongs. Here performing ↑ on this extent produces the corresponding fuzzy intent. Each attribute's membership degree indicates the truth degree that the attribute is shared by all objects in the extent. This truth degree is affected by how strongly the objects themselves belong to the fuzzy extent.

Similarly, the bottom concept 1 for the threshold approach agrees with the bottom concept 8 for the fuzzy closure approach with respect to the objects in the extent and the attributes in the intent. However, in this case the membership degrees also match. As pointed out in the fuzzy closure algorithm the greatest fixpoint of *C* is the set *Y* which is the intent of the bottom concept. All membership degrees are 1.0 so that performing $B\downarrow$ on this intent of Y simply reduces to using (3) with the Lukasiewicz implication operator in (5).

Notice that when the threshold is 1.0, the results for the top and bottom concepts are quite different from that of the fuzzy closure approach. This difference is to be expected since the threshold approach ignores all entries in the fuzzy formal context that do not meet the threshold value while the fuzzy closure approach uses all the non-zero entries.

IV. EXPERIMENTAL TEST CASES

In [11], the experiments that were run using the fuzzy closure approach focused on its practical performance in terms of the algorithm's running time as influenced by characteristics of the formal context such as the size and distribution of the truth degrees. The formal contexts used in these performance experiments were not real world data but randomly generated. Another characteristic considered in the performance evaluation is the number of truth degrees in L. The performance of the fuzzy closure approach is compared to that of a fuzzy extension to the NEXTCLOSURE presented in [16]. The results of these experiments showed that the algorithm in [16] performs best when only the fuzzy concepts need to be computed. The fuzzy closure approach, however, performs considerably better when the structure of the fuzzy concept lattice is also needed.

In [10] the experiment using the threshold approach has as its objective to determine the usefulness of the fuzzy concept lattice as a foundation for developing a fuzzy ontology and how to represent the fuzzy ontology using OWL. There is no comparison of other algorithms for creating fuzzy concept lattices. The experiments described in this present paper differs from the previous ones done separately with these two approaches since the objective is to compare the resulting fuzzy concepts and fuzzy concept lattices produced by these two different approaches. The following discusses the various test cases used in the experiments.

A. Olympic Data

The first test case is the formal context developed using Olympic data for several athletes and is taken from [11]. It was selected since it could be used as another verification test case for the software implementation of the fuzzy closure approach algorithm and provides a smaller fuzzy formal context for comparing the two approaches. It also provides a more complex formal context than the x objects and y attributes formal context and a larger L set with L = {0.0, 0.25, 0.5, 0.75, 1.0}. Here the five objects represent athletes and the ten attributes are Olympic events. The fill ratio, the fraction of non-zero degrees in the fuzzy formal context, is 100%. The membership degree can be interpreted as an indication of how well the athlete performs in the event.

	100m	long Jump	shot Put	high Jump	400m	110m Hurdl	discus Throw	pole Vault	Javekin Throw	1500m
Sebrle	0.5	1	1	1	0.75	1	0.75	0.75	1	0.75
Clay	1	1	0.75	0.75	0.5	1	0.75	0.5	1	0.5
Karpov	1	1	0.75	0.75	1	1	1	0.25	0.25	0.75
Macey	0.5	0.5	0.75	1	0.75	0.5	0.75	0.25	0.5	1
Warners	0.75	0.75	0.5	0.5	0.75	1	0.25	0.5	0.25	0.75

Figure 2. Olympic data [11].

B. Gene Annotation Data

A gene can be annotated with concepts from the Gene Ontology (GO) [17]. An evidence code is provided with an annotation, for example, Traceable Author Statement (TAS). The evidence code is translated into a degree of evidence strength between a GO concept and a gene product. In the following, the evidence codes are translated into membership degrees as done in [18]. Traceable Author Statement (TAS) is 1.0. Inferred from Sequence Similarity (ISS) is 0.8. Inferred from Electronic Annotation (IEA) is 0.6. Non-traceable Author Statement (NAS) is 0.4. Not Documented (ND) and Not Recorded (NR) were modified from 0.1 to 0.2 since the fuzzy closure operator approach requires that the set of membership degrees in L must form a closed lattice, i.e., they must be closed on the implication operator so that L= {0, 0.2, 0.4. 0.6, 0.8, 1.0} for all the annotation data test cases.

A fuzzy formal context can be created from an annotation data file with the genes as the objects, the GO terms as the attributes. The numeric evidence codes are interpreted as the degree to which a gene is annotated by a GO concept. For the experiments, the gene annotation data file GPD 194 data set [18] is used. It contains 194 human gene products (proteins). Here genes are classified into three families: collagen, myotubularin, and receptor precursor.

For the collagen annotation data shown in Fig. 3, there are 13 genes annotated by 23 GO terms. The fill-ratio is 20%.

GO term / gene	5201	5581	8147	1501	5584	5198	7155	8544	7605	5585	7397	8015	5586	5587	3019 8	5194	8285	9405	7517	5588	0004	5578	5594
1A2	.6	.6	.2	1	.2																		
21A1						.6	.6																
24A1	.6	.6					.6																
27A1	.6	.6																					
2A1	.6	.6	.2	1	.2			1	.6	.2													
3A1	.6	.6									.2	1	1										
4A1	.6													.2									
4A2	1													1	.4								
4A3	.6						.6		1			1		1		.6	1	1					
4A6	.4						.6							.4	.4	.6							
5A3	.6	.6					.6				1								1	1			
9A1	.4						.6				1										.2	.6	1
9A2	.6			1																		.6	1

Figure 3. Fuzzy formal context for the Collagen Family.

Fig. 4 shows the fuzzy formal context for the myotubularin family that has 7 (genes) and 14 (GO terms) The fill ratio is 35% .

Go Term / gene	4722	4725	16787	6470	8372	4727	7517	8151	8138	5737	16020	4721	8270	6118
MTMR1	.8	.8	.6	.8	.2									
MTMR2	.4		.6	.4	.2	.6	1	1	.4					
MTMR3			.6	1		.6			1	1	1			
MTMR4				.6								.6	.6	
MTMR6	.4	.4	.6	.4	.2									
MTMR7		1	.6	1										.6
MTMR8			.6	.6								.6		

Figure 4. Fuzzy formal context for the Myotubularin Family.

For the receptor precursor annotation, there are 7 genes annotated by 35 GO terms with a fill-ratio of 33%. This data set is not shown due to space limitations. In the combined gene annotation data, all three families, collagen, myotubularin and receptor, are considered as a single test. It contains 27 (13+7+7) genes as objects and 63 GO terms

(23+14+35 – 9 common terms) as attributes with a fill ratio of 10%. Due to the large size of this combined fuzzy formal context, it is not provided here. The rows are simply the union of all three sets of genes in each of the families and its columns are simply the union of all GO terms in the above three previous tables.

V. Analysis of the Experimental Results

The fuzzy closure approach uses the complete fuzzy formal context; thus, the results for the threshold approach are only given using the minimum membership degree in each of the fuzzy formal contexts in section IV. Other threshold values instead of the minimum degreet alters the fuzzy formal context from the one used by the fuzzy closure approach so that an unbiased comparison is not possible.

A. Olympic Data

The membership degrees in L can be interpreted as 0.0 does not performs in the event, 0.25 performs but not very well, 0.5 performs average in this event, 0.75 performs well in the event, and 1.0 performs exceptionally well in the event.

Threshold Approach: With $\alpha \geq 0.25$, only one concept which is both the top and bottom concept is produced :

0: [0.5/Sebrle, 0.5/Clay, 0.25/Karpov, 0.25/Macey, 0.25/Warners];
[100m, longJump, shotPut, highJump, 400m, 110mHurdl, discusThrow, poleVault, javekinThrow, 1500m]

The extent of concept 0 indicates that for this fuzzy formal context all of the objects possess all of the attributes to at least a degree value of 0.25. This result is expected since the fill ratio is 100%. The membership degrees in the extent, however, indicate for each object (athlete) the minimum degree of possession across all the attributes (events) in the intent. For example, the athlete Sebrle performs at least fair in all the events (his minimum degree in any event is 0.5). An examination of the formal context for the Olympic data confirms that indeed the 100m event has 0.5 degree, i.e., his weakest Olympic event.

Fuzzy Closure Approach: The Lukasiewicz implication operator produces 128 concepts. Fig. 5 provides a summary of this result since providing the complete listing of the concepts and the concept hierarchy would requires too much space. The complete results on this data set were verified by requesting from the authors of [11] their fuzzy concept lattice results since these were not provided in their original paper. An exact match existed with their produced fuzzy concepts and fuzzy concept lattice hierarchy.

Notice that the results of the threshold approach with a 0.25 value produce a top concept 0 that is similar to the top concept 0 of the fuzzy closure approach as seen for the simple fuzzy formal context in Fig. 1. For the threshold approach, the membership degree of the object in the extent of the fuzzy concept indicates the minimum degree to which the athlete performs in all the events in the intent. For the fuzzy closure

Detail	Concept Id	Concepts
Top Concept	0	**0:** [1.0/Sebrle, 1.0/Clay, 1.0/Karpov, 1.0/Macey, 1.0/Warners]; [0.5/100m, 0.5/longJump, 0.5/shotPut, 0.5/highJump, 0.5/400m, 0.5/110mHurdl, 0.25/discusThrow, 0.25/poleVault, 0.25/javekinThrow, 0.5/1500m]
Children of top concept	1, 2, 3	**1:** [1.0/Sebrle, 1.0/Clay, 1.0/Karpov, 0.75/Macey, 1.0/Warners]; [0.5/100m, 0.75/longJump, 0.5/shotPut, 0.5/highJump, 0.5/400m, 0.75/110mHurdl, 0.25/discusThrow, 0.25/poleVault, 0.25/javekinThrow, 0.5/1500m] **2:** [1.0/Sebrle, 1.0/Clay, 1.0/Karpov, 1.0/Macey, 0.75/Warners]; [0.5/100m, 0.5/longJump, 0.75/shotPut, 0.75/highJump, 0.5/400m, 0.5/110mHurdl, 0.5/discusThrow, 0.25/poleVault, 0.25/javekinThrow, 0.5/1500m] **3:** [1.0/Sebrle, 0.75/Clay, 1.0/Karpov, 1.0/Macey, 1.0/Warners]; [0.5/100m, 0.5/longJump, 0.5/shotPut, 0.5/highJump, 0.75/400m, 0.5/110mHurdl, 0.25/discusThrow, 0.25/poleVault, 0.25/javekinThrow, 0.75/1500m]
Bottom concept	31	31: [0.5/Sebrle, 0.5/Clay, 0.25/Karpov, 0.25/Macey, 0.25/Warners]; [1.0/100m, 1.0/longJump, 1.0/shotPut, 1.0/highJump, 1.0/400m, 1.0/110mHurdl, 1.0/discusThrow, 1.0/poleVault, 1.0/javekinThrow, 1.0/1500m]
Parents of Bottom Concept	30, 35, 55	30: [0.5/Sebrle, 0.5/Clay, 0.25/Karpov, 0.5/Macey, 0.25/Warners]; [1.0/100m, 1.0/longJump, 1.0/shotPut, 1.0/highJump, 1.0/400m, 1.0/110mHurdl, 1.0/discusThrow, 0.75/poleVault, 1.0/javekinThrow, 1.0/1500m] 35: [0.5/Sebrle, 0.5/Clay, 0.25/Karpov, 0.25/Macey, 0.5/Warners]; [1.0/100m, 1.0/longJump, 1.0/shotPut, 1.0/highJump, 1.0/400m, 1.0/110mHurdl, 0.75/discusThrow, 1.0/poleVault, 0.75/javekinThrow, 1.0/1500m] 55: [0.75/Sebrle, 0.5/Clay, 0.25/Karpov, 0.25/Macey, 0.25/Warners]; [0.75/100m, 1.0/longJump, 1.0/shotPut, 1.0/highJump, 1.0/400m, 1.0/110mHurdl, 1.0/discusThrow, 1.0/poleVault, 1.0/javekinThrow, 1.0/1500m]

Figure 5. Olympic Data Summary for Fuzzy Closure Approach.

approach the top concept 0 has an extent where each athlete fully belongs to the extent. Here performing $\uparrow$ on this extent produces the corresponding fuzzy intent. Each event's membership degree in the intent indicates the truth degree that the event is shared by all athletes in the extent.

Similarly, the bottom concept 0 (also the same as the top) for the threshold approach agrees with the bottom concept 31 for the fuzzy closure approach with respect to the athletes in the extent and the events in the intent. However, in this case the membership degrees also match as seen for the simple fuzzy formal context given in Fig. 1. As pointed out in the fuzzy closure algorithm the greatest fixpoint of C is the set Y which is the intent of the bottom concept, i.e. all events. All membership degrees for the events are 1.0 so that performing $B\downarrow$ on this intent Y simply reduces to using (3) with the Lukasiewicz implication operator in (5).

Fig. 5 also shows the children fuzzy concepts of the top concept 0, that is fuzzy concepts 1, 2, and 3 and the parent fuzzy concepts of the bottom concept 31, that is, fuzzy concepts 30, 35, and 55. For the children of the top concept, notice that each child has one or more athletes in the extent whose memberships is decreased by 0.25 from the extent of

the top concept and one or more events in the intent that are increased by 0.25 from the intent of the top concept. For example, fuzzy concept 3 has Clay's membership decreased by 0.25 in the fuzzy extent and has the 400m and the 1500 memberships increased by 0.25 in the fuzzy intent. For the parents of the bottom concept, each parent has one or more athletes in the extent whose memberships is increased by 0.25 and one or more events in the intent that are decreased by 0.25. For example, fuzzy concept 30 has Macy's membership increased by 0.25 in the fuzzy extent and has the pole vault membership decreased by 0.25 in the fuzzy intent. From this example, one can see that the fuzzy closure operator approach generates a vast number of fuzzy concepts, many of which are very close or similar to already existing fuzzy concepts.

B. Gene Annotation Data

For all analysis, $\alpha \geq 0.2$ threshold is used. To illustrate and explain the similarities between the two approaches the collagen data set is selected. Fig. 6 shows the concepts produced for this data set. The concept lattice hierarchy is not shown due to space limitations but is described here. The top concept 0 has child concept 1 whose extent shows that almost all genes (one is missing) can be described by GO_0005201 with at least the minimum evidence code of 0.2. The extent of concept 7, the other child concept of the top concept 0, shows six genes can all be described by GO_0007155. The bottom concept 6 has several parent concepts 5, 10, 12, 16, 18, 22, 23, and 25, each having one gene described by a set of several GO terms. Concepts 10 and 12 have the largest intents with 12 GO terms; the single gene in their extents is described by the greatest number of GO terms at the minimum evidence code or better.

Since 1160 concepts are produced using the fuzzy closure approach, the results are not presented, but the similarities between the two approaches are discussed. For the collagen data set fuzzy closure top concept 0 has an empty intent and an extent with every gene having a 1.0 membership degree. Similarly, the bottom concept has an empty extent and an intent with every GO term having a 1.0 membership degree. No GO term is shared by all genes and no gene is shared by all GO terms. This result is similar to that of the threshold approach.

The two children of the top concept are concepts 1 and 2 and given below.

1: [1.0/COL1A2, 0.8/COL21A1, 1.0/COL24A1, 1.0/COL27A1, 1.0/COL2A1, 1.0/COL3A1, 1.0/COL4A1, 1.0/COL4A2, 1.0/COL4A3, 1.0/COL4A6, 1.0/COL5A3, 1.0/COL9A1, 1.0/COL9A2]; [0.2/GO_0005201]
2: [0.8/COL1A2, 1.0/COL21A1, 1.0/COL24A1, 0.8/COL27A1, 0.8/COL2A1, 0.8/COL3A1, 0.8/COL4A1, 0.8/COL4A2, 1.0/COL4A3, 1.0/COL4A6, 1.0/COL5A3, 1.0/COL9A1, 0.8/COL9A2]; [0.2/GO_0007155]

They have the same two GO terms found for the two children concepts of the top concept in the threshold approach, concepts 1 and 7; however, they disagree in the membership degrees with a 0.2 membership for both GO_0005201 and GO_0007155. This degree represents the truth degree that the specified GO term is possessed by all genes in its respective intent. The genes in the extents differ between the two approaches. For the threshold concept 1, the missing gene is COL21A1. In Fig. 3, one can see that this gene is not annotated by this GO term GO_0005201. Looking at concept 1 in the fuzzy closure approach, one sees that COL21A has a 0.8 membership degree. Similarly, for threshold concept 7, there are 7 missing genes in the extent that can be found with a 0.8 membership degree in the extent of concept 2 for the fuzzy closure approach. A similar analysis occurs for all the other gene data sets when comparing the threshold approach to the fuzzy closure approach. The top and bottom concepts agree with respect to the genes in the extent and the GO terms in the intent. They may have different membership degrees.

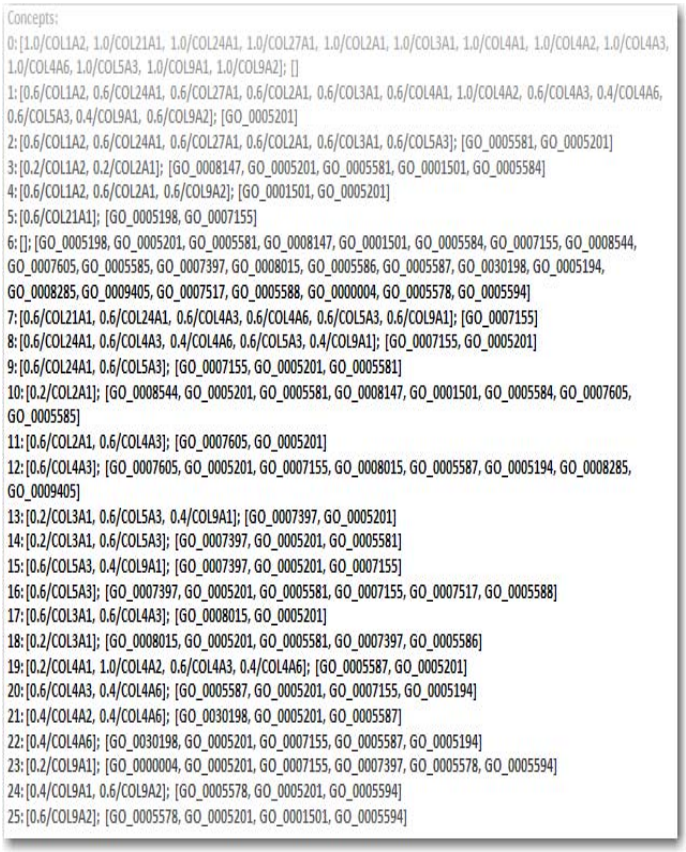
Concepts:
0: [1.0/COL1A2, 1.0/COL21A1, 1.0/COL24A1, 1.0/COL27A1, 1.0/COL2A1, 1.0/COL3A1, 1.0/COL4A1, 1.0/COL4A2, 1.0/COL4A3, 1.0/COL4A6, 1.0/COL5A3, 1.0/COL9A1, 1.0/COL9A2]; []
1: [0.6/COL1A2, 0.6/COL24A1, 0.6/COL27A1, 0.6/COL2A1, 0.6/COL3A1, 0.6/COL4A1, 1.0/COL4A2, 0.6/COL4A3, 0.4/COL4A6, 0.6/COL5A3, 0.4/COL9A1, 0.6/COL9A2]; [GO_0005201]
2: [0.6/COL1A2, 0.6/COL24A1, 0.6/COL27A1, 0.6/COL2A1, 0.6/COL3A1, 0.6/COL5A3]; [GO_0005581, GO_0005201]
3: [0.2/COL1A2, 0.2/COL2A1]; [GO_0008147, GO_0005201, GO_0005581, GO_0001501, GO_0005584]
4: [0.6/COL1A2, 0.6/COL2A1, 0.6/COL9A2]; [GO_0001501, GO_0005201]
5: [0.6/COL21A1]; [GO_0005198, GO_0007155]
6: []; [GO_0005198, GO_0005201, GO_0005581, GO_0008147, GO_0001501, GO_0005584, GO_0007155, GO_0008544, GO_0007605, GO_0005585, GO_0007397, GO_0008015, GO_0005586, GO_0005587, GO_0030198, GO_0005194, GO_0008285, GO_0009405, GO_0007517, GO_0005588, GO_0000004, GO_0005578, GO_0005594]
7: [0.6/COL21A1, 0.6/COL24A1, 0.6/COL4A3, 0.6/COL4A6, 0.6/COL5A3, 0.6/COL9A1]; [GO_0007155]
8: [0.6/COL24A1, 0.6/COL4A3, 0.4/COL4A6, 0.6/COL5A3, 0.4/COL9A1]; [GO_0007155, GO_0005201]
9: [0.6/COL24A1, 0.6/COL5A3]; [GO_0007155, GO_0005201, GO_0005581]
10: [0.2/COL2A1]; [GO_0008544, GO_0005201, GO_0005581, GO_0008147, GO_0001501, GO_0005584, GO_0007605, GO_0005585]
11: [0.6/COL2A1, 0.6/COL4A3]; [GO_0007605, GO_0005201]
12: [0.6/COL4A3]; [GO_0007605, GO_0005201, GO_0007155, GO_0008015, GO_0005587, GO_0005194, GO_0008285, GO_0009405]
13: [0.2/COL3A1, 0.6/COL5A3, 0.4/COL9A1]; [GO_0007397, GO_0005201]
14: [0.2/COL3A1, 0.6/COL5A3]; [GO_0007397, GO_0005201, GO_0005581]
15: [0.6/COL5A3, 0.4/COL9A1]; [GO_0007397, GO_0005201, GO_0007155]
16: [0.6/COL5A3]; [GO_0007397, GO_0005201, GO_0005581, GO_0007155, GO_0007517, GO_0005588]
17: [0.6/COL3A1, 0.6/COL4A3]; [GO_0008015, GO_0005201]
18: [0.2/COL3A1]; [GO_0008015, GO_0005201, GO_0005581, GO_0007397, GO_0005586]
19: [0.2/COL4A1, 1.0/COL4A2, 0.6/COL4A3, 0.4/COL4A6]; [GO_0005587, GO_0005201]
20: [0.6/COL4A3, 0.4/COL4A6]; [GO_0005587, GO_0005201, GO_0007155, GO_0005194]
21: [0.4/COL4A2, 0.4/COL4A6]; [GO_0030198, GO_0005201, GO_0005587]
22: [0.4/COL4A6]; [GO_0030198, GO_0005201, GO_0007155, GO_0005587, GO_0005194]
23: [0.2/COL9A1]; [GO_0000004, GO_0005201, GO_0007155, GO_0007397, GO_0005578, GO_0005594]
24: [0.4/COL9A1, 0.6/COL9A2]; [GO_0005578, GO_0005201, GO_0005594]
25: [0.6/COL9A2]; [GO_0005578, GO_0005201, GO_0001501, GO_0005594]

Figure 6. Collagen data threshold approach with $\alpha \geq 0.2$.

Fig. 7 compares the approaches. Column 1 gives the test data set. Columns 2 and 3 gives the number of concepts produced by the respective approaches. Column 4 gives the number of α-cut concepts exactly matching a fuzzy closure concept. For this column, the extent of the α-cut concept must agree with that of the fuzzy closure concept both with respect to the set of objects and their membership degrees. The intent of the α-cut concept, however, only has to agree with the set of attributes in the intent of the fuzzy closure concept since the α-cut intents assume degree of 1.0 for each attribute. Column 5 gives the number of concepts from the fuzzy closure approach that match an α-cut concept ignoring the membership degrees. Column 6 gives the number of concepts in the threshold approach having exactly the same extent including matching degrees. Column 7 gives the number of extents from the fuzzy closure approach that match to an α-cut extent, ignoring the membership degrees.

Column 8 gives the number of intents from the fuzzy closure approach that match to an α-cut intent, ignoring the membership degrees.

Test Cases	# concepts		#concepts exact matches	# concepts matches	# extent exact matches	# extent matches	# intent matches
	Alpha-cut	Fuzzy Closure					
x-object, y-attribute	2(0.5)	10	1	6	2	10	10
Olympic	1(0.25)	128	1	128	1	128	128
Collagen	26(0.2	1160	2	12	26	1160	1160
Myotubularin	13(0.2)	470	1	5	13	470	470
Receptor	17(0.2)	913	1	19	17	913	913
Combined gene	62(0.2)	3495	4	30	62	3495	3495

Figure 7. Summary comparing threshold to fuzzy closure approach.

Both column 3 and 7 have identical values. That is, each extent produced by threshold approach maps exactly to an extent in one of the concepts produced by the fuzzy closure approach. The conclusion is that extents produced by the threshold approach are a subset of the extents produced by the fuzzy closure approach. Secondly, the numbers in column 7 and column 8 are identical to that of column 3. Ignoring degrees, the extents produced by the closure approach result in the same set of extents produced by the threshold approach. A large number of extents produced by the closure approach are identical in the set of objects they contain. For example, for the 1160 extents of the collagen data, 26 sets of objects are unique and repeatedly used with varying membership degrees and similarly, for the intents of the collagen data. These test cases show that the fuzzy closure operator approach generates a vast number of fuzzy concepts, many of which are very close or similar to already existing fuzzy concepts within the lattice. Threshold approach using the smallest membership degree in the fuzzy formal context as the α-cut value is much simpler and produces all the extent sets and intent sets of the fuzzy closure approach ignoring membership degrees. The fuzzy closure approach provides additional information with respect to the intents membership degrees. Examining such large fuzzy concept lattices to uncover information hidden in the fuzzy formal context, would be very challenging.

VI. Conclusions and Future Work

The threshold approach and the fuzzy closure approach to creating fuzzy concept lattices from a fuzzy formal context have been implemented and verified using examples provided in [11]. GO annotation data files have also been used to experiment on larger fuzzy formal contexts. The two approaches have been compared using these data sets. The fuzzy closure approach produces an explosion in the number of fuzzy concepts compared to the threshold approach. The extents produced by the threshold approach are a subset of those produced by the fuzzy closure approach. Currently, the recommended factor analysis method [11] is being implemented to identify the significant fuzzy concepts from a fuzzy formal context. Different implication operators are currently being tested for the closure operator to compare the differences in the resulting lattices. Future plans are to apply this software to other real world application data to validate and enhance its usability.

References

[1] Web Ontology Language (OWL), http://www.w3.org/2004/OWL/.

[2] M. Cristani and R. Cuel, "A Survey of Ontology Creation Methodologies," International Journal on Semantic Web & Information Systems, vol. 1, no. 2, 2005, pp 49–69.

[3] S-H. Hwang, H-G. Kim, M-K, Kim, S-H. Chou, and H-S. Yang, "A Data-Driven Approach to Constructing an Ontological Concept Hierarchy Based on the Formal Concept Analysis," ICCSA 2006, Lecture Series in Computer Science, vol. 3983, Eds. M. Gavrilova, Heidelberg: Springer Berlin, 2006, pp. 937–946.

[4] Jian Wang and Keqing He, "Towards Representing FCA-based Ontologies in Semantic Web Rule Language," Sixth IEEE International Conference on Computer and Information Technology (CIT'06), 2006, pp. 41–41.

[5] R. Wille,"Restructuring lattice theory: An approach based on hierarchies of concepts," Ordered Sets, Ed. I. Rival, Dordrecht: Reidel, pp. 445–470, 1982.

[6] C. Carpineto and G. Romano, Concept Data Analysis: Theory and Applications, Wiley, 2004.

[7] S. Calegari and D. Ciucci, "Fuzzy Ontology, Fuzzy Description Logics and Fuzzy-OWL," Applications of Fuzzy Sets Theory, Lecture Series in Computer Science, vol. 4578, Eds. F. Masulli, S. Mitra, and G. Pasi, Heidelberg: Springer Berlin, 2007, pp. 118–126.

[8] Q.T. Tho, S.C. Hui, A.C.M Fong, and T. H. Cao, "Automatic Fuzzy Ontology Generation for the Semantic Web," IEEE Transactions on Knowledge and Data Engineering, vol. 18, no. 6, pp. 842–856, 2006.

[9] C. Wei, Q. Yang, L ,Zhu, and B. Wen, "Research on Automatic Fuzzy Ontology Generation from Fuzzy Context," Proceedings of the 2009 Second International Conference on Intelligent Computation Technology and Automation, Washington, D. C., pp. 764–767, 2009.

[10] C. De Maio, G. Fenza, V. Loia, and S. Senatore, "Towards Automatic Fuzzy Ontology Generations," Proceedings of the 2009 IEEE International Conference on Fuzzy Systems, Jeju Island, Korea, Aug 20-24, pp. 1044–1049, 2009.

[11] R. Belohlavek, B. De Baets, J. Outrata, and V. Vychodil, "Computing the Lattice of All Fixpoints of a Fuzzy Closure Operator," IEEE Trans. Fuzzy Systems, vol 18, no. 3, pp. 546–7557, June 2010.

[12] V. Cross, M. Kandasamy,and W. Yi, "Comparing Two Approaches to Creating Fuzzy Concept Lattices," Proc.of the North American Fuzzy Information Processing Society, El Paso, TX, March 18-19, 2011.

[13] U. Hohle,, "On the fundamentals of fuzzy set theory,". J. Math. Anal. Appl., vol. 201, 1996, pp. 786–826.

[14] R. Belohlavek, Fuzzy Relational Systems: Foundations and Principles. New York: Kluwer, Academic/Plenum Publishers, 2002.

[15] C. Lindig, "Fast concept analysis," in Working with Conceptual Structures – Contributions to ICCS 2000, Ed. G. Stumme. Aachen: Shaker Verlag, 2000, pp. 152–161.

[16] R. Belohlavek, "Algorithms for fuzzy concept lattices," Proc. Fourth Int. Conf. on Recent Advances in Soft Computing. Nottingham, United Kingdom, Dec 12–13, 2002, pp. 200–205.

[17] Gene Ontology Consortium, "Gene Ontology: Tool For the Unification of Biology," *Nature Genetics*, vol. 25, no. 1, pp. 25-29

[18] M. Popescu, J. Keller, and J. Mitchell, "Fuzzy Measures on the Gene Ontology for Gene Product Similarity," IEEE/ACM Transactions on Computational biology and bioinformatics, vol. 3, no. 3, pp. 263-274, July/Sept 2006.

2011 IEEE International Conference on Fuzzy Systems
June 27-30, 2011, Taipei, Taiwan

Fuzziness, OWA and Linguistic Quantifiers for Web Selection Processes

Ronald R. Yager
Machine Intelligence Institute
Iona Collage, New Rochelle, USA
yager@panix.com

Visiting Distinguished Scientist
King Saud University
Riyadh, Saudi Arabia

Marek Z. Reformat
Electical & Computer Eng.
University of Alberta
Edmonton, AB, Canada
Marek.Reformat@ualberta.ca

Giray Gumrah
Electrical & Computer Eng.
University of Alberta
Edmonton, AB, Canada
gumrah@ualberta.ca

***Abstract*—The Internet becomes an enormous source of information containing billions of documents. Users deal with an overwhelming number of alternatives, and continuously make decisions anytime they want to obtain meaningful information.**

The paper describes an approach for a simple yet effective selection of the most suitable information that fits user's needs. The novelty of the approach is twofold: the concept of lexicographical-like preferences used for a multi-criteria decision-making with elements of fuzziness and OWA operator; a simple fuzzy number based mechanism for estimating user's degrees of acceptance of criterion satisfaction. The lexicographic preferences allow for mimicking user's attitude that some criteria should be satisfied before other criteria are considered. The acceptance of criterion satisfaction levels are defined with a single threshold that represents a boundary value between acceptable and unacceptable values of attributes of alternatives.

The paper includes results of a simple case study preformed on a prototype of a web selection system built using the proposed approach.

Keywords-component; multi-criteria decision-making, fuzziness, lexicographic preferences, degrees of acceptance, satisfaction levels, OWA operator

I. INTRODUCTION

The Internet is a multi-user, multi-source information repository with billions of documents and millions of users. In order to transform the Web into a user-friendly environment where everyone can easily and precisely find suitable things there is a need for tools and systems that support users in coping with constant inflow of information and selection of the most suitable things they are looking for, e.g., books, hotels, or movies. In many cases, users' search is limited to a few or several alternatives – more extensive search leads to more time spent on browsing the web.

Up to date, a variety of systems – called recommender systems – supporting users in their selection activities have been proposed. The most popular ones apply the concept of collaboration filtering. This selection mechanism provides suggestions to the user based on selections made by users that are similar in their selecting/purchasing patterns with the user under consideration. These types of systems work pretty well for simple items. However, in more complex situations – more sophisticated requirements and more complicated items – these systems are not very effective. In order to address that issue, knowledge-based systems has been proposed. They use knowledge about a user. The suggestions they provide are derived using different decision making mechanisms based on users' direct input [1]. They build users' models and apply aggregation techniques, examples of some of them can be found in [2] and [3]. In many cases, these are complex and computationally intense approaches.

In this paper, we present a new approach of making suitable selection among all alternatives obtained from the web. The process takes into consideration multiple requirements that could be associated with different levels of importance. Additionally, the process of evaluating alternatives requires minimal input from the user representing user's estimation of usability of a given alternative.

The novelty of the proposed method is based on the application of a very simple yet effective method of ranking user's criteria. It uses the idea of a lexicographical (hierarchical) ordering. This ordering combined with a basic fuzzy operation is used for calculating values of weights required for an OWA-based aggregation of degrees of acceptance of criteria satisfaction levels. Our intention is to mimic the human method of making selections when some criteria dominate other criteria. In such case, levels of satisfaction of higher ranked criteria have influence on the ability of lower ranked criteria to contribute to the final decision. This influence is controlled by a t-norm operation.

As mentioned above, the presented approach for supporting selection processes relies on just a few pieces of information about the user. The user needs to identify her criteria of interest, provide ranking of those criteria, and give a basic information – in a form of single values – required for construction of fuzzy numbers representing user's levels of acceptance of criteria satisfaction levels.

This novel approach has been used to build a prototype system called *Personal Evaluation Tool* (*PET*).

II. SELECTION AND DECISION-MAKING PROCESS

A. Systems Supporting Human Activities on the Web

It is quite common to use the web for finding information, buying different items, making travel arrangements, and looking for different sorts of entertainment. A process of

finding suitable items translates into a process of identifying the best-fitted alternative among a set of responses the web provides as the result of user's request. In a nutshell, the purpose of systems performing such duties – called recommender systems – [4] is quite simple: they suppose to find an alternative – a product, a service, or a piece of information – that fits user's interests. Such systems can be applied in a variety of activities, from online shopping to service selection.

There are multiple ways how the most suitable item or service response can be recognized. It can be done based on 1) finding similarities between users based on ratings of different alternatives/items provided by them using so called collaborative filtering systems [5], or 2) identifying similarities between alternatives and products that users have already bought, used, or liked – content-based recommender systems [6]. Some of the most popular similarity measures used for recommendation purposes are cosine similarity, naive Bayesian (NB) classifier, and Pearson correlation. Research activities in the area of recommender systems have led to many different variations of both types of those systems.

A need for more tuned and personalized recommendations have resulted in a new set of selection techniques focusing on matching user's needs and preferences to a set of available alternatives [1]. Systems that consider user's information – such as their preferences and satisfaction levels, belong to the category of knowledge-based recommender systems [7]. Those systems can learn a profile of user's interests implicitly based on attributes of alternatives rated by a user in the past [6], or explicitly gaining this information from a user [8].

A successful selection of the most suitable alternative depends on modeling of user's preferences. The preferences represent user's expectations and requirements set against the most desirable alternative, i.e., the alternative that satisfies user's demands to the highest degree. In the case of constructing a user's model (preferences and needs) a number of techniques have been investigated: a causality-driven user's model representing more domain-relevant aspects of the selection process [3], incomplete preference relations [9], question-based dialogue [10], dialogue-wise techniques based on a finite state model [11], and cross recommender mediation [12] to name a few.

B. Multi-criteria Decision Making in Web Applications

The problem of identifying the most suitable alternative in the presence of user's needs is also addressed by algorithms and techniques originated in the domain of multi-criteria decision-making. The topic of finding a best alternative has already drawn a lot of attention for many years [13]. In a nutshell, a selection process of multi-criteria decision-making consists of evaluating each alternative based on multiple measures, comparing obtained evaluations, and selecting an alternative with the best (usually the highest) evaluation value.

Elicitation of preferences is not a trivial process and may cause problems in obtaining a true reflection of user's needs. In some decision-making approaches, a user provides preferences inspecting directly all possible alternatives. Other techniques, such as verbal decision analysis and its variations, have been proposed. Once user's preferences are known, a multi-criteria decision-making system has to induce a final selection. Many approaches identifying a final selection, such as the ones based on the concepts of Utility Theory, Analytic Hierarchy, and outranking approach, assume that a user provides preferences without any imprecision.

Another representation of user's needs is a set of criteria. Criteria represent principles by which a user would judge alternatives. A user specifies criteria as "constrains" imposed on the values of alternative attributes (an alternative is treated as a set of attributes. The values assigned to attributes constitute an "instance" of alternative). Based on comparison of a single criterion with an attribute value, a criterion evaluation value is generated. That value reflects how well a given criterion is satisfied by a given alternative. This process is performed for each criterion-attribute pair. A single alternative "generates" a number of criterion evaluation values (one for each criterion). These values have to be combined to obtain a final evaluation value of alternative. This step is called an aggregation of evaluation results. A number of possible aggregation operators can be applied here. Some of most popular ones are [2]:

- ordered weighted aggregation (OWA) operator [14];
- quasi-arithmetic means (different variations such as: quasi-linear means, weighted root-power mean, weighted harmonic mean, and weighted arithmetic mean);
- weighted median, and Sugeno interval.

Most of the above methods require weights. However, a process of identifying values of weights for aggregation calculations is not easy. Techniques dedicated to elicitation of weights involve asking a decision maker to answer simple questions about relative importance of criteria, analyzing these responses, and estimating 'true' weights. The weights used for OWA, and quasi-arithmetic means are calculated using criteria and regular non-decreasing quantifiers. For weighted median and Sugeno interval, weight values are obtained via a "try and error" approach process of satisfying user's criteria.

C. Lexicographical Rules

As mentioned above, once a given alternative is evaluated against each criterion, the results are aggregated and a single value representing goodness of this alternative is obtained. These processes are built based on diverse multi-criteria decision-making approaches suitable for aggregating multiple values [15]. The very captivating issue here is to perform such aggregation in a human-like way [16].

Mimicking a human decision-making process has been a subject of research activities for many years. One of the most popular techniques that fits a description of a human-like method and is applied for aggregation purposes are lexicographical rules [17, 18].

The lexicographical-based comparison of two alternatives is straightforward: it relays on a simple idea of comparing alternatives using one criterion at a time. The criteria are sorted based on their priorities, and a comparison sequence starts with a criterion of the highest priority. The choice between two alternatives A1 and A2 is made if the first criterion can identify a better alternative, if not, the second

criterion is used, and so on. If none criterion can do it, a random selection is applied. The method has been already applied in a number of different applications required simple, yet human-like decision making processes [19, 20].

The "popularity" of lexicographical decision-making rules has been also confirmed by studies in different application areas: for brand quality allocation, for estimating vales of rural landscape attributes, or for management decision-making in petroleum refinery industry for distribution of oil to the various depots in a form of lexicographic goal programming (LGP) model.

D. OWA and Linguistic Quantifiers

Aggregation of different pieces of information is a common aspect of any system that has to infer a single outcome from multiple facts. A very interesting class of aggression operators is called Ordered Weighted Averaging (OWA) [21]. In the simplest possible statement, this operator is a weighted sum over ordered pieces of information. In a formal representation, the operator, defined on the unit interval I and having dimension n, is a mapping $F_W : I^n \to I$ such that:

$$F_W(a_1,\ldots,a_n) = \sum_{j=1}^{n}(w_j \cdot b_j) \quad (1)$$

where b_j is the jth largest of all arguments $a_1, a_2, \ldots, a_n$, and w_j is a weight such that w_j is in [0,1] and $\sum_{j=1}^{n} w_j = 1$.

In the mid-nineties, Yager showed that a linguistic quantifier could be used to obtain weights associated with an OWA aggregation. He has introduced parameterized families of the Regular Increasing Monotone (RIM) quantifiers [22]. These quantifiers are able to guide aggregation procedures by verbally expressed concepts in a description independent dimension. A RIM quantifier is a fuzzy subset Q over $I=[0,1]$ in which for any proportion $r \in I$, $Q(r)$ indicates the degree to which r satisfies the concept indicated by the quantifier Q [22]. A fuzzy subset Q represents a RIM quantifier if: $Q(0)=0$, $Q(1)=1$, and *if* $r1 > r2$ *then* $Q(r1)>Q(r2)$.

Assuming a RIM quantifier, we can associate with Q an OWA weights such that for $j=1$ to n,

$$w_j = Q(\frac{j}{n}) - Q(\frac{j-1}{n}) \quad (2)$$

where n is a number of pieces of information to be aggregated. Using this expression the values of weights can be obtained directly from the expression representing the quantifier.

For example, let us take a look at the parameterized family $Q(r) = r^p$, where $p \in [0,\infty)$. Here if $p=0$, $w_1=1$ and $w_j=0$ for $j \neq 1$, we obtain the *existential (MAX)* quantifier, which makes the OWA operator F closer to an "or" operator; when $p \to \infty$, $w_n=1$ and $w_j=0$ for $j \neq n$, we have the quantifier *ALL (MIN)*, which makes the OWA operator F closer to an "and" operator; and when $p=1$ we have $Q(r)=r$, $w_j=1/n$ and we deal with the quantifier *SOME*.

The OWA aggregation has been used in multiple different applications including web-based information retrieval [23].

III. Fuzzy-based Selection Process: Human-Centric Aspects

There is a genuine need for tools and systems that are capable of supporting individual users in their unique way of exploring and utilizing information and services available on the Web. These systems should be able to mimic human selection processes in finding a single alternative that "fits" users' needs when multiple alternatives are available.

The most important challenges encountered by those systems are the abilities to perform multi-criteria decision-making that replicates user's selection behavior, and to elicit user's criterion satisfaction and acceptance levels in an easy and simple way.

In real life, selections performed by people can be quite complex. They can involve decisive factors influencing evaluation of each alternative. Alternatives can be evaluated using multiple criteria, and different strategies can be used to identify the most suitable alternatives. A truly human-friendly system has to deal with multi-criteria evaluation of alternatives, and be able to handle criteria with differing importance levels. We will look at features of such a human-friendly system from the following aspects: importance of criteria, acceptance of criterion satisfaction levels, and aggregation procedure.

A. Criteria Ranking

It is clear that utilization of multiple criteria does not mean that all criteria are equally important. Some of them can be critical, while some of them can represent requirements that are not essential – kind of 'good to have" requirements. As discussed in [14] user's behavior can be summarized in the following way: if the higher priority criteria are not satisfied it is irrelevant if lower priority criteria are satisfied or not. That attitude can be also observed in many other situations related to Internet activities. Thus a user needs a certain degree of satisfaction to their higher priority criteria before allowing some compensation by lower priority criteria.

Such approach for evaluating alternatives can be implemented when a user provides a ranking of his/her criteria. This ranking defines an ordering in which evaluations are aggregated, and how evaluation values of different criteria contribute to the evaluation value of a given alternative [14].

B. Acceptance (Process) Levels

A ranking list of available alternatives should reflect the user's degree of acceptance of these alternatives. An acceptance level for each alternative is estimated based on how well this alternative satisfies user's criteria, i.e., what is the acceptance level associated with each criterion, and how these levels can be aggregated. In order to evaluate an alternative based on a criterion, the user has to identify how different values of alternative's attribute related to this criterion satisfy his/her needs. In other words, the user has to provide some information allowing us to estimate up to what degree he/she is able to accept a particular value of an attribute. This information is applied to construct fuzzy numbers that are used for this estimation process.

An important objective of the proposed approach is to keep the process of elicitation of information required for determination of criterion acceptance levels as simple as possible. Since it is much easier for humans to provide values of directly observable attributes as opposed to introspective satisfaction levels of criteria, we have tried as much as possible to make use of values of attributes to determine the alternative's level of acceptance. The user provides only single threshold values for attributes associated with criteria. Once those thresholds are known, the system is able to generate acceptance levels directly from the values of attributes associated with given criteria.

In the approach proposed, the user is informed about minimum and maximum values of an attribute, and has to specify a threshold value within this range. It is explained to the user that the threshold is the attribute value at which he/she feels the full acceptance begins to deteriorate. More specifically, for a criterion whose acceptance level increases with bigger values of the attribute value its threshold can be described as "the smallest value of the attribute" which gives full acceptance (Fig. 1(a)). For those, such as cost, in which acceptance decreases with bigger values of the attribute value the threshold can be explained as "the biggest value of the attribute" which gives the full acceptance (Fig. 1(b)). In Fig. 1 we illustrate constructed fuzzy numbers used to transform attribute values into criterion acceptance levels. This figure represents two plots of criterion acceptance degrees – we will call them acceptance fuzzy numbers. As it can be seen, the acceptance levels below the threshold (Fig. 1(a)) are equal to *max_level* (usually 1.0), while the values above the threshold are monotonically decreasing. The decrease represents user's changes in criterion acceptance degree when the values of attribute become larger than the threshold. The maximum attribute value is associated with a small, non-zero value – *min_level*. Equivalently the same concept is applied when the desired attribute values should be larger – closer to the maximum (Fig. 1(b)). More sophisticated fuzzy numbers can be used if we are willing elicit more introspective information from a user.

C. Lexicographical-based Aggregation Method: Concept

The process of evaluating or scoring a single alternative based on a set of criteria depends on combining the following pieces of information:

- degrees of acceptance of individual criteria;
- weights reflecting priorities assigned to criteria.

One of the simplest ways of aggregating multiple pieces of information in order to obtain a single score representing the acceptance level of an alternative is a weighted sum. The formula is:

$$Score = \sum_{i=1}^{no_of_attributes} criterion_weight_i * acceptance(attribute_i) \quad (3)$$

Each component of the sum is a product of an acceptance level that is the result of application of an acceptance fuzzy number to an i-th $attribute_i$ and a weight associated with the equivalent criterion i – $criterion_weight_i$. The weights have to be determined for each criterion. They should denote user's preferences and his/her objectives regarding contribution of acceptance levels of individual criteria to the overall score.

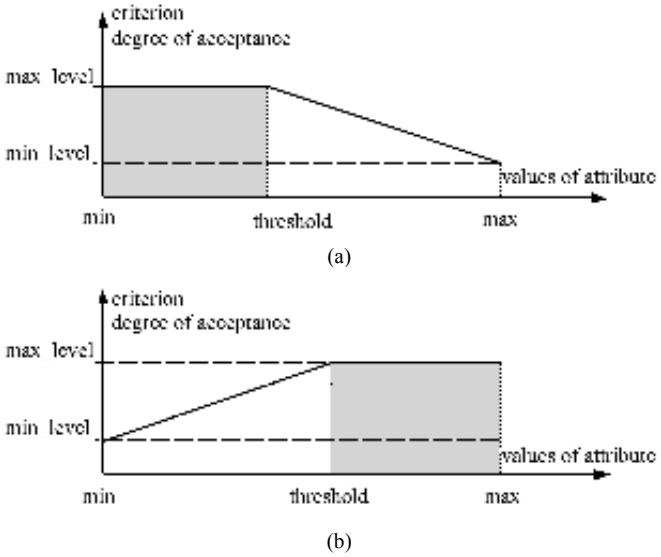

Fig. 1. Graphical representation of fuzzy numbers representing degree of acceptance for two scenarios: decreasing acceptance with increasing attribute value (a), and increasing acceptance with increasing attribute value (b).

The weights can be assigned in a universal way so they can be used in determining the scores for different alternatives. However, this universal assignment of weights independent of consideration of the alternative being evaluated is not always right. It is possible that if the highest criterion is not fully satisfied, high acceptance levels of low priority criteria can bring the *score* to the level that is higher then the *score* of another alternative satisfying the highest priority criterion but not satisfying low priority criteria. In such a case, a selection mechanism would indicate an alternative with low satisfaction of highest priority criteria as a winner.

Here we shall use a procedure, proposed in [14], for determining the criterion weights that avoids this problem. The weights are calculated via a unique combination of the criteria ranking and criterion acceptance levels. This leads to a schema that is very similar to lexicographic preferences. The criteria weights for a given alternative are calculated based on to the following formula where the term $acceptance(attribute_k)$ represents the level of acceptance of the *k-th* criteria for the alternative being scored

$$criterion_weight_i = \prod_{k=1}^{i-1} acceptance(attribute_k) \quad (4)$$

for $i=2, \ldots, n$, where n is a number of criteria, while **T** is a t-norm. It can be observed that the weight of i criterion depends on the acceptance levels obtained for all $i-1$ criteria that have a higher priority than i attribute (The indexing of criteria is equivalent to a hierarchy of criteria). For $i=1$ (the first criterion of the highest priority), its *criterion_weight* is equal to 1.0. Such approach prevents cases where lower priority

criteria can contribute to the overall evaluation value so much that this alternative is more "attractive" than an alternative with higher acceptance of high priority criteria but lower acceptance of low priority criteria.

The degree of contribution of the higher priority criteria on the weight of lower priority criteria is "controlled" by the type of applied t-norm (4). For the product t-norm, the weight of the attribute *i* is a product of acceptance levels of all criteria that have higher priority levels. It means that each criterion of lower priority has lower or the same weight comparing with the weights of criteria of higher priority. For the min t-norm, the weight value is equal to the smallest acceptance level among all i-1 criteria. It means that the weights of all criteria with priorities lower then the criterion with the lowest acceptance have the same weight and potentially the same contribution to the overall score.

Please note that the criteria weights in this approach will be different for each alternative as they have different acceptance levels for the criteria.

IV. Lexicographic-based Aggregation in Multi-Criteria Decision-Making

The proposed method for determining an alternative's aggregated score can be used in situation in which there are ties between criteria with respect to their level of importance. This induces a grouping of criteria. In this case, there are several groups of criteria, and each group has different priority, while all criteria from the same group have the same priority.

Let us assume that there are *g* different groups (levels) of criteria. The criteria C_{11}, C_{12}, ..., C_{1i}, ..., C_{1n_1} belong to the group of the most important criteria, C_{21}, C_{22}, ..., C_{2i}, ..., C_{2n_2} belong to the second most important group, and C_{g1}, C_{g2}, ..., C_{gi}, ..., C_{gn_g} to the least important group *g*. In total, there are $n=n_1+n_2+\ldots+n_g$ criteria. In this case, the attributes of an alternative x_k are indexed in the following way: $x_{k,(11)}$, $x_{k,(12)}$, ..., $x_{k,(1i)}$, ..., $x_{m,(1n1)}$, ..., $x_{k,(21)}$, $x_{k,(22)}$, ..., $x_{k,(2i)}$, ..., $x_{m,(2n2)}$, ..., $x_{k,(g1)}$, $x_{k,(g2)}$, ..., $x_{k,(gi)}$, ..., $x_{m,(gng)}$ (the indexes in the brackets represents indexes of attributes, and they are equal to the indexes of equivalent criteria).

Let $C_{ij}(x_{k,(ij)})$ represents a value of criteria C_{ij} for an attribute *j* in the group priority *i* of an alternative x_k. In the case of priority groups the aggregation process obeys the following formula:

$$Score(x_k) = \sum_{i=1}^{g} \sum_{j=1}^{n_i} w_{ij} C_{ij}(x_{k(ij)}) \tag{5}$$

The values of weights w_{ij} are obtained using the following procedure. Let S_i represents an acceptance value obtained for an alternative x_k based on the criteria from a priority group *i*. S_i can be calculated using the OWA operator. In such case:

$$S_i(x_k) = OWA\{C_{i1}(x_{k,(i1)}), C_{i2}(x_{k,(i2)}), \ldots, C_{in_i}(x_{k,(in_i)})\} \tag{6}$$

Different linguistic quantifiers can be combined with OWA (Section II.D). The quantifiers can represent different ways of user's needs imposed on the group criteria. One of them is *ALL* – all criteria in the group should be satisfied, and *SOME* – some criteria have to be satisfied in order to treat the criteria group as satisfied. Those quantifiers represent different "personalities" of users – *ALL* represents users more demanding and strict in their requirements, and *SOME* represents users who are willing to "forget" that all criteria in a group should be satisfied.

The values of S_i are calculated for each group and are directly used in calculations of pre-weights (7). The pre-weights for all criteria that belong to the same group are the same. In this case we talk about group pre-weights instead of individual criteria pre-weights.

$$\begin{aligned}
&u_{11} = u_{12} = u_{13} = \ldots = u_{1n_1} = 1 \\
&u_{21} = u_{22} = u_{23} = \ldots = u_{2n_2} = S_1(x_k) \\
&u_{31} = u_{32} = u_{33} = \ldots = u_{3n_3} = \prod_{i=1}^{2} S_i(x_k) \\
&\ldots \\
&u_{g1} = u_{g2} = u_{g3} = \ldots = u_{gn_g} = \prod_{p=1}^{g} S_p(x_k)
\end{aligned} \tag{7}$$

To ensure that an alternative with a full acceptance of all criteria obtains an overall score of 1.0, the values of the weights are obtained by dividing the pre-weights by the total number of criteria. Here, the total number of criteria is:

$$T = \sum_{i=1}^{g} n_i$$

and then

$$w_{ij} = \frac{u_{ij}}{T}. \tag{8}$$

Assuming that

$$\begin{aligned}
&w_{11} = w_{12} = w_{13} = \ldots = w_{1n_1} = w_1 \\
&w_{21} = w_{22} = w_{23} = \ldots = w_{2n_2} = w_2 \\
&w_{31} = w_{32} = w_{33} = \ldots = w_{3n_3} = w_3 \\
&\ldots \\
&w_{g1} = w_{g2} = w_{g3} = \ldots = w_{gn_g} = w_g
\end{aligned}$$

a new form of the equation (5) is:

$$Score(x_k) = \sum_{i=1}^{g} w_i \sum_{j=1}^{n_i} C_{ij}(x_{k(ij)}) \tag{9}$$

V. A Simple Web-based PET Architecture

The proposed lexicographical-based approach supporting user's selections process is a pivotal element of a *Personal Evaluation Tool* (*PET*). The *PET* is a simple web-based system that allows its users to input information about priorities of criteria and values of parameters needed for defining satisfaction level functions. As the result, the *PET* provides users with ranked – based on data entered by users – alternatives. The architecture of the *PET* is presented in Fig. 2. The *PET* consists of three execution components:

Web Interaction Unit: It is a simple unit that initiates a service processing activity based on a query provided by the user. Based on this query – received from the Browser-based User Interaction Unit – the unit performs a simple keyword-based web search. The result of that search – a set of responses matching the query keywords – is provided to the Selection Unit. Each response represents an alternative that is compared against users preferences and levels of acceptance.

Selection Unit: It is a "brain" of the *PET*. This is the place where each alternative is evaluated using acceptance fuzzy numbers. This process is a full implementation of the approach described in Section IV.

Browser-based User Interaction Unit: In order to utilize the presented priority-based approach, a web-based user interface has been developed. It allows a user to rank criteria, and enter her information about different criteria satisfaction levels.

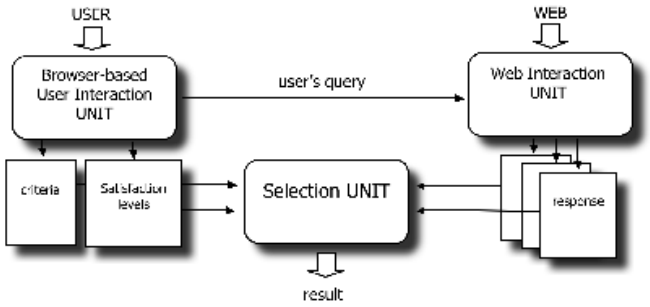

Fig. 2. Architecture of the Web-based *Personal Evaluation Tool* (*PET*)

The web-based interface has been developed for Hotel Reservation. The following criteria are identified:

- *room price*;
- *location* (here, we assume the distance from a hotel to the downtown);
- *access* (central reservation or not);
- *security* (personal safe, peephole, door chain);
- *services* (airport shuttle, room service, high speed internet, fax, photocopying, laundry/dry cleaning, lounge, bar);
- *tangibles* (family room, minibar, Jacuzzi, parking);
- *facilities* (printer, swimming pool).

The user has to provide information regarding ranking and satisfaction levels for all criteria. Once, the user selects the Hotel Reservation service, he/she ranks all criteria. We allow the user to identify more than one criterion at the same level of importance. Only relevance of positions is taken into consideration.

For acceptance levels, a user navigates to the page that allows for entering pieces of necessary information. For the criteria: *room price* and *location* – the user is provided with sliders that can be moved to positions representing the border (threshold) between a full acceptance and decreasing acceptance level. For example, for the *room price* – the user is satisfied with the price up to $140 (the level of acceptance for any price below the threshold of $140 is 1.0), any *room price* above that value means a decreased acceptance level. For location acceptance, a distance up to 2 km is okay for the user, any larger distance means lower level of acceptance – the value of acceptance reaches 0.1 for the distance of 5 km.

There are also few "radio button" entries that allow the user to select choices related to *access, security, services*, *tangibles* and *facilities*. Several sub-criteria are defined for each of them. The options provided to the user are "should have" and "don't care". In this case the values of acceptance are binary – it equals *one* if an alternative hotel has that feature, or *zero* if it does not.

VI. Case Study

A. Overview

The proposed lexicographical-based approach for effective selection of the most suitable alternative in the context of a web search process is validated, as well as compared with another method. The validation process is performed via comparison of the results obtained from the prototype *PET* with a realistic human selection process. The comparison of *PET*'s results with another method is focused on finding similarities and differences between *PET*'s selections and selections provided by a simple lexicographic-based approach "*Take-The-Best*" (*TTB*).

Take-the-Best

Our motivation for selecting another lexicographical-based method, called *Take-the-Best*, is based on a simple fact that it works surprisingly well when compared to statistical benchmarks [24]. The method uses a very strict and simple lexicographical rule. Once alternatives are evaluated against each criterion they are being pair-wise compared. The choice between two alternatives A and B is made if the first criterion can identify a better alternative, if not, the second criterion is used, and so on. If none criterion can do it, a random selection is applied. This means that once we have knowledge about priorities of criteria we sort them and perform comparison using sorted criteria on one at a time basis.

Normalized Distance-based Performance Measure (NDPM)

NDPM was proposed by Yao [24]. He developed *NDPM* theoretically, using an approach from decision and measurement theory. *NDPM* can be used to compare two different weakly ordered rankings.

$$NDPM = \frac{2P^c + P^o}{2P^t} \tag{10}$$

P^c is the number of contradictory preference relations between the system ranking and the user ranking. A contradictory preference relation happens when the system says that item A will be preferred to item B, and the user ranking says the opposite. P^o is the number of compatible preference relations, where the user rates item A higher than item B, but the system ranking has item A and item B at equal preference levels. P^t is the total number of "preferred" relationships in the user's ranking (i.e. pairs of items rated by the user for which one is rated higher than the other). This metric is comparable among different datasets (it is normalized), because the numerator represents the distance, and the denominator represents the worst possible distance.

Let us assume that we have a user's ranking of items: *Ia, Ib, Ic, Id, If*. For five items the value of P^t is ten – there are ten different pairs of items. The value of *NDPM* is 0.0 when the ranking is compared with another identical ranking. If both rankings differ in one pair the value of *NDPM* is equal to 0.1, two different pairs lead to 0.2. If there are ten differences – it means that the other ranking is totally different: *If, Id, Ic, Ib, Ia* – the value of *NDPM* is 1.0.

B. Hotel Reservation Service

The case study illustrates a Hotel Reservation service. The experiment involves eleven users. The selection process for the most suitable hotel takes into accounts six different criteria: *room price*, *location* (we assumed that the point of interest for each user is a downtown, therefore the location represents a distance from a given hotel to the downtown), *access*, *security services*, *tangibles*, and *facilities*. Such criteria as *security*, *additional services, tangibles,* and *leisure facilities*, contain multiple sub-criteria.

The case study is performed with five different hotels. The detailed information about each hotel is presented in Table 1. Each of users has identified his/her priorities, and provided information needed for construction of acceptance fuzzy numbers. Following that, each user has ranked all five hotels based on all features (Table 1).

TABLE 1. HOTEL RESERVATION SERVICE ALTERNATIVES

		H1	H2	H3	H4	H5
Price (single room)		$249	$199	$129	$99	$159
Location (distance from downtown)		0.5km	2.3km	1.9km	3.5km	1.0km
Access	Central reservation	x	x	-	-	-
Security	Personal safe in room	x	-	-	-	x
	Peephole, door chain	-	-	x	x	x
Additional Services	Airport shuttle	x	x	-	-	-
	Room service	x	x	x	-	x
	High speed internet	x	x	x	-	-
	Fax, photocopying	x	x	-	-	x
	Laundry/dry cleaning	x	-	-	-	x
	Lounge/bar	x	x	x	x	x
Tangibles	Family room	-	-	-	-	x
	Minibar	x	x	x	-	x
	Jacuzzi	x	x	-	-	-
	Parking	-	x	-	x	-
Leisure Facilities	Children's leisure	-	-	-	-	x
	Swimming pool	x	x	-	-	-
	Golf course	x	-	-	-	-

The selection process based on the proposed lexicographical-based approach has a number of variations. Such elements as a t-norm or OWA linguistic quantifier should be determined. In the case of a t-norm our choice is the min t-norm. The reason for that is the close resemblance of the proposed approach with the min t-norm to the lexicographical one. Additional experiments about suitability of different types of t-norm have been left for later. For the selection of a linguistic quantifier required for determining the value of S_i (6) we investigate two quantifiers *ALL* and *SOME*. The results of this work are shown below.

PET vs. *Users (NDPM)*

Firstly, the evaluation of *PET* results is performed using *NDPM*. As it has been indicated earlier, the ranking of five items leads to ten different preferences pairs. In this case the value of *NDPM* of 0.1 means that the rankings differ in one preference pair. The *NDPM* values calculated for a pair of rankings – one ranking given by the user, and the other offered by *PET* based on priorities and criteria entered by this user – for all eleven users and two linguistic quantifiers ALL and SOME are shown in Table 2. On average the value of *NDPM* is 0.3 meaning that on average the *PET's* rankings have three pairs of preferences different from the rankings provided by the users. The smallest difference between the *PET* and the user rankings is observed for the **user_#5** for *ALL* and the **user_#1** and **user_#3** for *SOME*. In the case of **user_#5** the contradictory pair has been observed for positions 3 and 4 – the user's rank of hotels is: **H5**, **H3**, **H4**, **H1**, **H2** (from the most to the least suitable), while the *PET's* ranking is: **H5**, **H3**, **H1**, **H4**, **H2**. The biggest difference is observed for the **user_#7** (for both *ALL* and *SOME*) – in this case, there are six contradictory preferences. The user's ranking is: **H5**, **H3**, **H2**, **H1**, **H4**, while *PET's* is: **H1**, **H2**, **H5**, **H3**, **H4**. A short discussion with the user has led to the conclusion that the user is not consistent – the preferences and criteria (s)he has entered to the *PET* system are different then those (s)he has used to make the selection. As we can observe, there is a small difference – on average – between results for quantifiers *ALL* and *SOME*.

TABLE 2. *NDPM* VALUES FOR RECOMMENDATIONS OBTAINED FROM *PET* WHEN COMPARED WITH RANKINGS PROVIDED BY THE USERS

	value of NDPM	
	OWA: ALL	OWA: SOME
user #1	0.25	**0.10**
user #2	**0.25**	0.30
user #3	0.15	**0.10**
user #4	0.20	0.20
user #5	**0.10**	0.20
user #6	0.30	0.30
user #7	0.60	0.60
user #8	0.30	0.30
user #9	0.55	**0.50**
user #10	**0.30**	0.50
user #11	0.25	**0.20**
average	**0.30**	**0.30**

PET vs. *TTB (1st recommendation)*

The *TTB* method (the simplest possible lexicographical-based selection technique) can only recommend a single hotel. Therefore, the analysis of results is done by comparison of the *PET's* 1st recommendation with the suggestion provided by *TTB*. The linguistic quantifier used here is *ALL* – this quantifier "is closer" to the original lexicographical approach. The results for *PET* and *TTB* are presented in Table 3. We can see that *TTB* is correct in four cases only. Looking at the first

position of the ranking provided by the *PET*, the *PET* is correct six times.

The *PET* prototype provides ranking of all hotel alternatives. Therefore, we also compare the top-2 and top-3 "suggestions" given by *PET* with the user's first choice. For the top-2, the *PET* finds the user's top choice for ten users (Table 3). For the top-3 recommended hotels, the *PET* system is able to identify the user's first choice for all eleven individuals.

TABLE 3. RESULTS FOR HOTEL RESERVATION SERVICE OBTAINED FROM *PET* AND *TTB* WHEN COMPARED TO THE USER'S FIRST CHOICE

	# of correct	# of incorrect
TTB – first recommendation	4	7
PET – first recommendation	6	5
PET – first two recommendations	10	1
PET – first three recommendations	11	0

VII. CONCLUSIONS

Increased popularity of the Internet triggered interest in development of methods and techniques supporting users' search for relevant information and services. One of the most challenging requirements is the ability to mimic human way of making selections and recommendations.

The paper proposes a novel technique for selecting the most suitable alternative based on multiple criteria. The technique combines information about ranking of criteria with criterion levels of satisfaction and acceptance. A new algorithm that calculates the evaluation value of each alternative has been proposed and described. The algorithm uses the principle of weighted aggregation – it dynamically calculates weights following the idea of lexicographic preferences combined with fuzzy operations – t-norms – and the OWA operator. The weights are recalculated for each alternative, and their values depend on location of a given criterion in criteria hierarchy and how well the satisfaction of criteria are acceptable for the user. The criteria acceptance levels are estimated using a newly proposed and simple process of constructing fuzzy numbers based on a single parameter representing a boundary value between acceptable and unacceptable values of criterion.

A simple system – called *PET* – has been developed based on the proposed technique. The case study has been preformed to assess usability of the proposed method. It indicated a good correlation of the rankings deduced by the *PET* prototype with the rankings provided by the users. An important conclusion of the performed comparison is a need for tracking changes in users' criteria – mismatches are the consequence of users' inconsistency in their preferences. More experiments are planed for investigations focused on different types of t-norms and linguistic quantifiers.

REFERENCES

[1] R. Burke, "Hybrid Recommender Systems: Survey and Experiments", User Modeling and User-Adapted Interact, vol. 12, pp. 331-370, 2002.

[2] R. Smolikova, and M.P. Wachowiak, M.P., "Aggregation operators for selection problems", Fuzzy Sets and Systems, vol. 131, pp. 23-34, 2002.

[3] B. Towle, and C. Quinn, "Knowledge Based Recommender Systems Using Explicit User Models", Knowledge-Based Electronic Markets, the AAAI Workshop, Menlo Park, CA: AAAI Press, pp. 74-77, 2000.

[4] P. Resnick, N. Iacovou, N. Suchak, P. Bergstrom, and J. Riedl, "GroupLens: an open architecture for collaborative filtering of netnews", Computer Supported Collaborative Work (CSCW), Chapel Hill, NC, USA, pp. 175-186, 1994.

[5] J.L. Herlocker, J.A. Konstan, L.G. Terveen, and J. T. Riedl, "Evaluating Collaborative Filtering Recommender Systems", ACM Transactions on Information Systems, vol. 22(1), pp. 5-53, 2004.

[6] M.J. Pazzani, "A Framework for Collaborative, Content-Based and Demographic Filtering", Artificial Intelligence Review, vol. 13(5/6), pp. 393-408, 1999.

[7] R. Burke, "Knowledge-based Recommender Systems", in A. Kent (ed.), Encyclopedia of Library and Information Systems, vol. 69, Supp. 32, New York: Marcel Dekker, 2000.

[8] M. Zanker, and M. Jessenitschnig, "Case-studies on exploiting explicit customer requirements in recommender systems", User Modeling and User-Adapted Interaction, vol. 19, pp. 133-166, 2009.

[9] L. Martinez, L.G. Perez, M.J. Barranco, and M. Espinilla, "A Knowledge Based Recommender System Based on Consistent Preference Relations", Studies in Computational Intelligence (SCI) 117, pp. 93-111, 2008.

[10] C. Thompson, M. Goker, and P. Langley, "A Personalized System for Conversational Recommendations", Journal of Artificial Intelligence Research, vol. 21, pp. 393-428, 2004.

[11] A. Felfernig, G. Friedrich, D. Jannach, and M. Zanker, "An Integrated Environment for the Development of Knowledge-Based Recommender Applications", Int. Journal of Electronic Commerce, vol. 11(2), pp. 11-34, 2006.

[12] F. Herrera, E. Herrera-Viedma, and F. Chiclana, "Multiperson decision-making based on multiplicative preference relations", European Journal of Operational Research, vol. 129, pp. 372-385, 2001.

[13] E. Triantaphyllou, Multi-Criteria Decision Making Methods: A comparative Study, Springer, 2000.

[14] R.R. Yager, "Prioritized aggregation operators", International Journal of Approximate Reasoning, vol. 48(1), pp. 263-274, 2008.

[15] G. Adomavicius, and Y.O. Kwon, "New Recommendation Techniques for Multicriteria Rating Systems", IEEE Intelligent Systems, vol. 22(3), pp. 48-55, 2007.

[16] G. Giegerenzer, and D.G. Goldstein, "Reasoning the Fast and Frugal Way: Models of bounded Rationality", Psychological Review, vol. 103(4), pp. 650-669, 1996.

[17] K. W. Church, "Approximate Lexicography and Web Search", International Journal of Lexicography, vol. 21(3), pp 325-336, 2008.

[18] R. H. Hogarth, and N. Karelaia, "Take-the-Best" and Other Simple Strategies: Why and When They Work "Well" with Binary Cues, Theory and Decision, vol. 61, pp. 205-249, 2006.

[19] M. Ehrgott, A characterization of lexicographic max-ordering solutions, in A. Göpfert, J. Seeländer, and C. Tammer, editors, Methods of Multicriteria Decision Theory, Proceedings of the 6th Workshop of the DGOR-Working Group Multicriteria Optimization and Decision Theory, pp. 193-202, 1997.

[20] K.-W. Jee, D. L. McShan, and B. A. Fraass, "Lexicographic ordering: intuitive multicriteria optimization for IMRT", Physics in Medicine and Biology, vol. 52, pp. 1845-1861, 2007.

[21] R.R. Yager, "On ordered weighted averaging aggregation operators in multi-criteria decision making", IEEE Transactions on Systems, Man and Cybernetics, vol. 18, pp. 83-190, 1988.

[22] R.R. Yager, "Families of OWA operators", Fuzzy Sets and Systems, vol. 59, pp. 125-148, 1993.

[23] H. Amiri, A. AleAhmad, F. Oroumchian, C. Lucas, M. Rahgozar, Using OWA Fuzzy Operator to Merge Retrieval System Results, 2nd Workshop on Computational Approaches to Arabic Script-based Languages, pp. 13-21, 2007.

[24] Y.Y. Yao, "Measuring Retrieval Effectiveness Based on User Preference of Documents", Journal of the American Society for Information Science, vol. 46, pp. 133-145, 1995.

2011 IEEE International Conference on Fuzzy Systems
June 27-30, 2011, Taipei, Taiwan

Visual Stability Improvement of SOM's Feature Map by Initial Value Assignment

MOMOI Shinji
Department of Media Informatics,
Graduate School of Science and Technology,
Ryukoku University
t11m090@mail.ryukoku.ac.jp

MIYOSHI Tsutomu
Department of Media Informatics,
Faculty of Science and Technology,
Ryukoku University
mijosxi@i.ryukoku.ac.jp

***Abstract*— In SOM learning, learning result depends on initial value of feature map and the location of the node or the distance between nodes on feature map is important factor to determine feature of individual data. For example, in data detection of hematopoietic tumors, given data is detected by location of the feature map. In this paper, we forcused on visual stability of SOM feature map, and we proposed new initialization method of SOM feature map. The purposes of proposed method are improvement of visual stability of SOM feature map, and utilization of generalization ability of SOM. By experiments, proposed method is visually stable than conventional method in the point of feature map location, and the computational complexity of proposed method is greatly reduced.**

Keywords-component; self-organizing map; feature maps; visual stability; improvement method;

I. INTRODUCTION

Kohonen's Self Organizing Map (SOM) involves neural networks, for which an algorithm learns the feature of input data through unsupervised, competitive neighborhood learning. The SOM is applied in many fields and has been widely studied [4-7]. Based on the conventional SOM learning algorithm, SOM learning is influenced by the sequence of learning data and the initial feature map. The location of the node or the distance between nodes on feature map is important factor to determine feature of individual data.

In conventional method, initial value of feature map has set at random, so a different mapping appears even by same input data. Consequently, it can be said that it lacks visual stability. For example, in data detection of hematopoietic tumors, given data is detected by location of the feature map. If given data are near to the area of physically unimpaired person then the data consider to normal, and if the data are near to the area of tumors then the data consider to abnormal. As well as this example, in many applications the judgment is made by a person depending on a location on the feature map.

If the learning results are visually unstable, maps must become different impressions in each learning, and maps of different impressions could be increased to the same data in different diagnosis.

To solve this visually unstable problem, there are steadies, that euclidean distance of learning data is pre-calculated and vector of feature map permute based on the result of pre-calclate. Because it is necessary to compare distance of all vectors, however, the computational complexity becomes very high, and a lot of time will be spent in analysis of learning data. As a result, generalization ability of SOM is not fully utilized. Moreover, the method focused on high speed leaning, so, there are not enough discussion about visual stability.

In this paper, we focused on visual stability of SOM feature map, and we proposed new initialization method.

II. SELF-ORGANIZING MAP

Kohonen's self-organizing map (SOM) [1] involves of neural networks, that learn the features of input data through unsupervised, competitive neighborhood learning. The SOM is mapping from high to low dimensional space, usually as a two-dimensional (2D) map. It provides a feature map that arranges similar classes nearer to one another to visualize high-dimensional information in a 2D feature map. Map representation makes it easier to understand relations between data. (Fig.1)

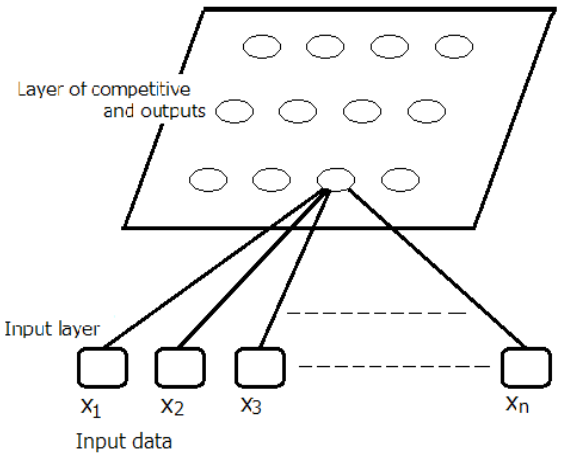

Figure 1. SOM overview

The SOM generally has two layers, an input layer and an output layer. Output layer nodes usually form a 2D grid and input layer nodes are fully connected with those at output layer nodes. Each connection has a connection weight, so all output layer nodes have patterns or vectors to be learned.

After learning, each node represents a group of individuals with similar features, the individual corresponding to the same node or to neighboring nodes. That is, the SOM configures output nodes into a topological representation of original data through a process called self-organization.

In learning process, when an input pattern or input vector is presented to the input layer as learning data, output layer nodes compete mutually for the right to be declared the winner. The winning node is the output layer node whose incoming connection weights are the closest to the input pattern in Euclidean distance. The connection weights of the winning node and its neighbor nodes are then adjusted, i.e., moved closer toward the input pattern.

As learning process progresses, the learning rate and the size of the neighbor area around the winning node decreases, so in an early stage of learning process, large numbers of output layer nodes are adjusted strongly and, in the final stage, the winning node alone is adjusted weakly.

III. Problem of Conventional Technology

A. Initial Value of Reference Vector

Vector of SOM's feature maps (reference vector) has been initializing by random number on conventional technology as described ahead. However, in learning process of SOM, simply initializing by random number has a big influence chiefly first learning. The example of possible problem in case of simply initializing it by random number is enumerated as follows.

First of all, there are large change of coordinates of winning node even if used same leaning data, because value of reference vector is selected by random number. In different learning, the location of winning node for the same leaning data is usually different, because initial vector is randomly set its values. The example is shown in figure 2.

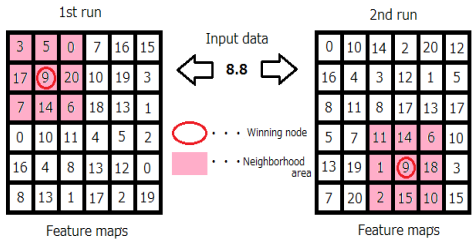

Figure 2. Difference of coordinates of winning node by random number

In the example, feature maps is 6×6, input data is 8.8, and neighborhood area is one surrounding space. Whenever winning node becomes completely random when value of reference vector is completely random like this. Vector surrounding winning node, i.e., vector in neighborhood area, also have random value, so, influence of learning is different in each leaning.

B. Data Pre-calculation Method

There are a method which initial value is calculated from input data. The method proposed by Mu-Chun Su [2] is enumerated as an example. (1) four vectors whose distance is the longest in input data are extracted. (2) it is allocated in the four corners of feature maps as weight. (3) data that is the furthest from both ends is allocated to opposite weight. (4) until all weights are assigned, this can be done clockwise repeatedly. As for the method of analyzing input data like this example and deciding initial value, the following problems are enumerated.

First of all, by this initialization method, learning data are analyzed their feature, so SOM leaning is used to miner adjustment. The purpose to use SOM is to analyze what kind of relations are exist in input data. The purpose might be lost by separately analyzing input data to decide initial value of reference vector.

Second, there is a problem that the computational complexity depends on the number of input data and number of dimensions. Therefore, a lot of procedures will be added before it learns by SOM.

Third, the method focused on high speed leaning, so, there are not enough discussion about visual stability.

C. Node Exchange Method

In the research of Miyoshi[3], they proposed initialization method that tried to utilize generalization ability of SOM. The method is to purpose at the speed-up study by improving the procedure of deciding initial value at random. This method relates input vector space to the position of feature maps in exchanging nodes of feature maps referring to learning data at initialization. The average moved distance of all nodes is shortened when this method is used, and the speed-up of the learning speed is confirmed.

In point of view that utilize generalization ability of SOM, this method has same purpose, however, the purpose to improve visual stability of output result is not discussed enough in the research.

IV. Proposed Method

The purposes of proposed method are (1) improvement of visual stability for output result, and (2) utilization of generalization ability of SOM. To achieve second purpose, renge of vector values are calculated from small number of learning data. And to achieve first pupose, reference vectors are sorted and allocated to give feature maps location tendency.

A. Range of Values

To reduce the complexity of learning, we try to limit the range of random values. To determine the range of values, randomly selected from a small number of learning data and approximate the maximum and minimum values for these data. Number of randomly selected data is determined by following formula:

$$n = \frac{N}{\left(\frac{E}{Z}\right)^2\left(\frac{N-1}{P(1-P)}\right)+1} \quad (1)$$

where, n is number of randomly selected data, N is a population, E is maximum error, Z is reliability coefficient, and P is population proportion. Using this formula, number of randomly selected data can be kept at a constant value.

Then the random numbers are provisionally allocated as initial value of reference vector. The advantage of this method is shown below. By this algorithm, it is possible to make the range of reference vector correspond to the range of learning data, and the calculation cost doesn't hang so much.

B. *Vector Sorting*

To give feature map location tendency, reference vector are sorted and allocated to feature map. First, the average of all dimentions value of each reference vector are calculated and, by using these averages as sorting key, reference vectors are sorted. Averages is caluclated by the following formula:

$$A = \left(m_{ij0} + m_{ij1} + m_{ij2} + \cdots + m_{ijk}\right)/k \quad (2)$$

where, A is average, m is reference vector, i is x axis of feature map, j is y axis of feature map, and k is value of dimention.

Then, vectors are allocated to feature map in sorting order. The image of sorting is shown in figure 3.

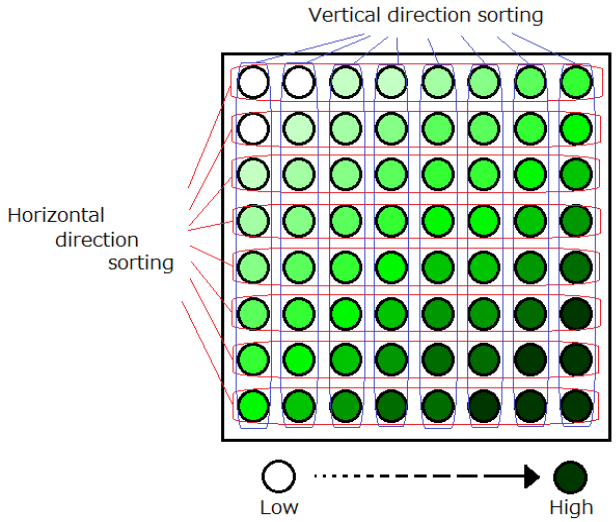

Figure 3. The image of sorting

As a result, the difference of winning node to same learning data is reduced. So, it is thought that output result is become steady.

C. *Algorithm of Feature Map Initialization*

Algorithm of Proposed Method is following.

- From the learning data, randomly select a value.
- From the selected value to determine the minimum and maximum values.
- random numbers are generated at the range of minimum and maximum values.
- Generated random number are temporarily assigned to the reference vector.
- To calculate the average value of the reference vectors.
- Based on the average, reference vector is done to quick sort in ascending order for the vertical direction feature map.
- Based on the average, reference vector is done to quick sort in ascending order for the horizontal direction feature map.
- Feature maps are made by this sorting, is initial value.

V. EXPERIMENTS FOR VISUAL STABILITY

To compare visual stability between conventional method and proposed method, we performed experiments. Conventional method is that of having initial value of reference vector by random numbers. The experiments are giving the same learning data to these two programs. In order to simplify the visual changes, bi-polarization data was used. The image of learning data is shown in figure 4.

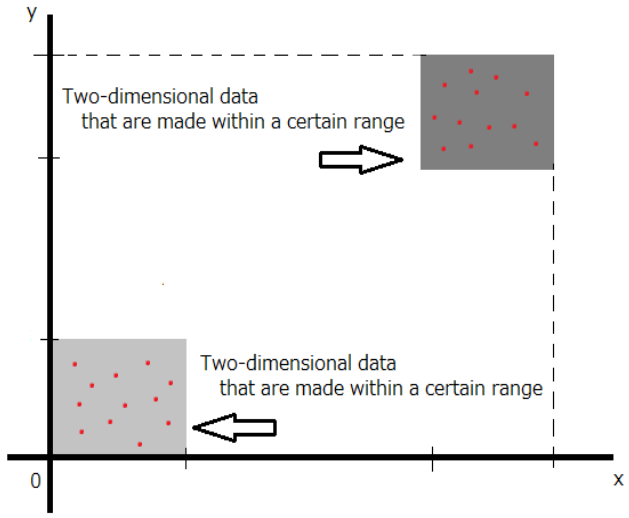

Figure 4. The image of learning data

Experiment parameters are followings. Learning data set is 3*200, feature maps size is 30*30 nodes, learning repetition is 4000 times, neighborhood area is 20 (it decreased from 20 to 1), and learning rate is 0.01*(neighborhood area size).

A. *Learning Results*

The experimental results is shown in figure 5. The left hand side are results of conventional method and, the right hand side are results of proposed method.

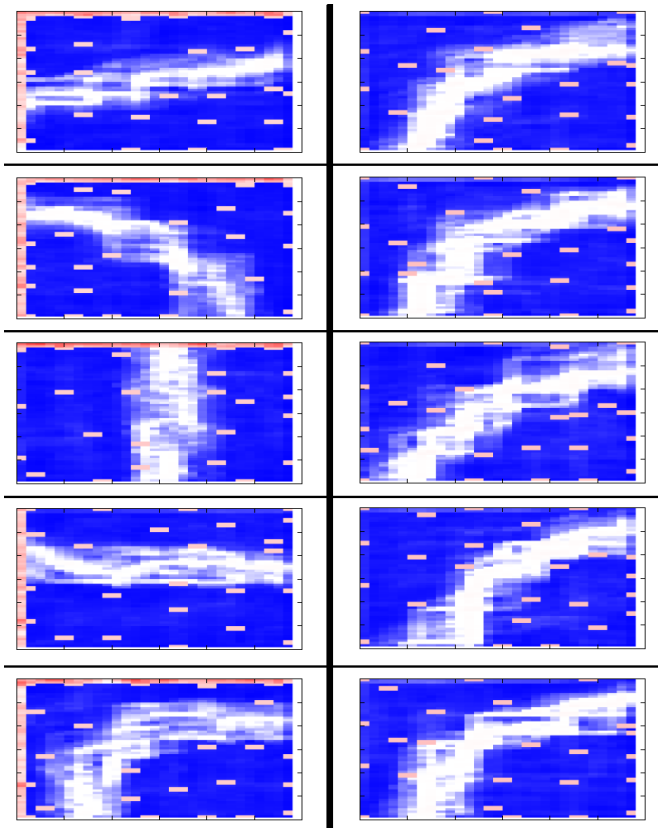

Figure 5. Output result of existing technology and proposal technique

According to the results of conventional method, visually different feature maps are generated at every single learning, even if leaning data is completely same. So, winning node of same input data is located in different part of each feature map. On the other hand, according to the results of proposed method, visually similar feature map are generated by same learning data. So, winning nodes of same input data are located in similar part of feature maps. The position of all input data showed similar tendency, typical winning nodes location are shows in figure 6.

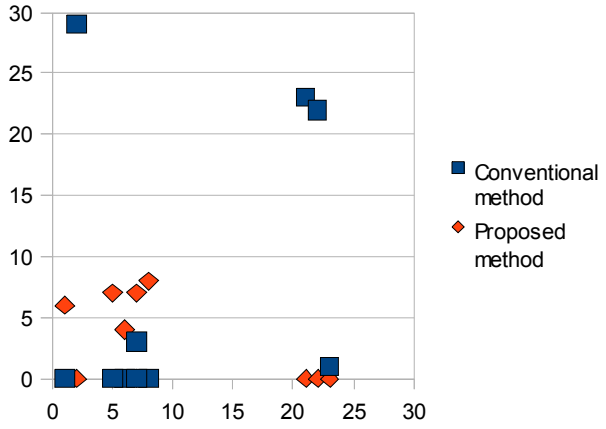

Figure 6. Feature map coordinates on a single input data

Figure 6 shows the location of winning nodes in five different feature maps for a single input data. X axis is x-coordinate and y axis is y-coordinate of feature map. According to Figure 6, winning node locations of conventional method are widely scattered even though input data is same. On the other hand, winning node locations of proposed method is almost unchanged corresponding to same input data.

The computational complexity of conventional method is estimated to $O(n!)$, and the one of proposed method is estimated to $O(n \log n)$. So, it can be said that the computational complexity of proposed method is greatly reduced.

VI. Conclusion

In this paper, we proposed new initialization method of SOM feature map. The purposes of proposed method are improvement of visual stability for output result, and utilization of generalization ability of SOM. The renge of reference vector values are calculated from maximum and minimum values approximated by randomly selected small number of learning data, and reference vectors are sorted and allocated to give location tendency in feature map.

By experiments, followings are revealed that, proposed method is visually stable than conventional method in the point of feature map location, the computational complexity of proposed method is greatly reduced.

As for further research, it is necessary to think about sorting method not related to number of dimensions. The average is sorting key in this time. However, sorting key to which stability of output result is kept even if the dimension increases is preferable. In addition, this study used a graph to show minutely the stability of the output information on input data. However, we need to think interface to output result more visually clear.

References

[1] Teuvo Kohonen, Self-Organizing Maps, Springer Verlag, 1995.

[2] Mu-Chun Su, Hsiao-Te Chang, "Fast Self-Organizing Feature Map Algorithm" IEEE Transactions on Neural Networks, Vol.11, No.3, 2000, pp.721-733.

[3] Tsutomu Miyoshi, "Relation Organization of SOM Initial Map by Improved Node Exchange," Journal of Computers (JCP), ISSN 1976-203X, Vol.3, No.9, 2008, pp.77-84.

[4] SHIEH Shu-Ling, LIAO I-En, "A New Clustering Validity Index for Cluster Analysis Based on a Two-Level SOM" IEICE transactions on information and systems, Vol.92, No.9, 2009, pp.1668-1674.

[5] SHIEH Shu-Ling, LIAO I-En, HWANG Kuo-Feng, CHEN Heng-Yu, "An Efficient Initialization Scheme for SOM Algorithm Based on Reference Point and Filters" IEICE transactions on information and systems, Vol.92, No.3, 2009, pp.422-432.

[6] KATO Satoru, HORIUCHI Tadashi, ITOH Yshio, "A Study on Clustering Method by Self-Organizing Map and Information Criteria" Journal of Japan Society for Fuzzy Theory and Intelligent Informatics, Vol.21, No.4, 2009, pp.452-460.

[7] Jun YoungPyo, Yoon Hyunsoo, Cho JungWan, "L^* Learning: A Fast Self-Organizing Feature Map Learning Algorithm Based on Incremental Ordering" IEICE transactions on information and systems, Vol.76, No.6, 1993, pp.698-706.

2011 IEEE International Conference on Fuzzy Systems
June 27-30, 2011, Taipei, Taiwan

Study of Morphogenesis of a Large-span Roof That Satisfies Its Form Design Requirements

Two-purpose Evaluation of Image and Mechanical Rationality

YUYA TAKEDA
College of Systems Engineering and Science
Shibaura Institute of Technology
Saitama city, Japan
Email:r07052@shibaura-it.ac.jp

KAZUTOSHI TSUTSUMI
College of Systems Engineering and Science
Shibaura Institute of Technology
Saitama city, Japan
Email: tutumi@shibaura-it.ac.jp

***Abstract*— We developed an idea support morphogenesis system that satisfies the designer's image and proposes the form with high mechanical rationality using a Genetic Algorithm. The image of an old system was input in two directions (X and Y). In the new system, the complex forms are created by the image input for three directions (X1, Y1, and Y2) or four directions (X1, X2, Y1, and Y2). The form is defined by control points of a spline curve. The form created by the image input is changed slightly by moving the control points. This system creates various forms by changing the moving quantities of control points and proposes Pareto solutions of "image" and "mechanical rationality." Based on the results, we analyze how the form is changed by differences in the moving quantities of control points.**

Keywords-component; Morphogenesis , Large-span roof , Evolutionary Computation , Designer's image

I. RESEARCH BACKGROUND

The performance of computers has been improving over time, and various system optimizations have been developed by evolutionary computing. [1].

In morphogenesis, there have been many studies of mechanical optimization for structural forms, but there have been few studies of morphogenesis taking into consideration the designer's esthetic sensibility and image. We developed an idea support morphogenesis system that satisfies the form design requirements and proposed the design with a high mechanical rationality using a genetic algorithm (GA). [2] [3].

However, the form design proposed by existing research is limited because of its symmetric form, and the proposed design does not provide a guarantee of satisfying the designer's form requirements.

To resolve these problems and to develop a more effective system, the following improvements were made in this study:

1) Enable the input of an asymmetric form design.
2) Propose Pareto solutions to a two-purpose optimization problem of "image satisfaction" and "equivalent stress," and develop a system by which the designer can specify the final form.
3) Obtain design knowledge related to morphological changes necessary to improve mechanical rationality.

II. OUTLINE OF THE EXISTING SYSTEM

The existing system is composed of an image input system and a rational valuation system.

In the image input system, the designer inputs his image by setting certain control points, and the system displays his image in 3D form.

In the rational valuation system, the control points input by the designer using the image input system are moved slightly, and mechanically excellent roof forms are generated using the GA. The GA can solve this optimization problem easily because genetic loci can easily express the amounts of change in the control points.

In particular, the control points of a spline curve expressing the form are moved slightly along the vertical direction using the 15 patterns listed in Table 1, thus, generating a new form. FEM analysis is performed for this new form, and the fitness of the GA is calculated as the mean value of the analyzed equivalent stresses for each element.

The GA is repeated until the specified generations by the designer and the form with minimum equivalent stress is proposed. The results of these analyses for a similar model of Ogunityoumin-taiikukan are shown in Fig. 1.

TABLE 1 Gene locus for changing pattern for the control points

0	0	0	0	−0.7 × α(m)	1	0	0	0	0.7 × α(m)
0	0	0	1	−0.6 × α(m)	1	0	0	1	0.6 × α(m)
0	0	1	0	−0.5 × α(m)	1	0	1	0	0.5 × α(m)
0	0	1	1	−0.4 × α(m)	1	0	1	1	0.4 × α(m)
0	1	0	0	−0.3 × α(m)	1	1	0	0	0.3 × α(m)
0	1	0	1	−0.2 × α(m)	1	1	0	1	0.2 × α(m)
0	1	1	0	−0.1 × α(m)	1	1	1	0	0.1 × α(m)
0	1	1	1	0m	1	1	1	1	0m

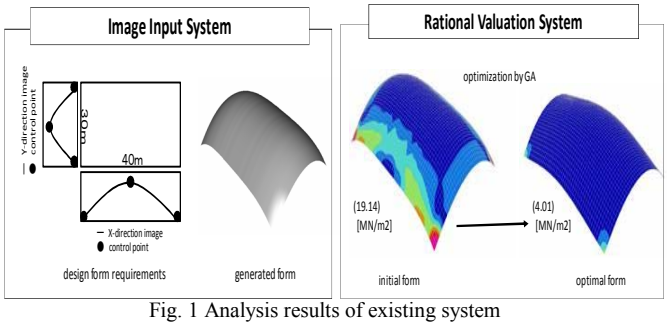

Fig. 1 Analysis results of existing system

III. OUTLINE OF THE NEW SYSTEM

In the existing system, the confronted two facades among the four outer facades are assumed to be the same facade. The designer inputs his image from two directions (X and Y). So, the existing system can create only symmetrical forms.

However, because the designer's proposed form may be asymmetric, the new system was improved to allow creation of asymmetric and complex forms by image input from three facades. The control point variation coefficient α is a variable that shows the amount of movement from the initial image.

In the existing system, the rational valuation system was implemented for the designated control point variation coefficient α by the designer. However, in this method, the obtained optimum solution is limited within that range. It is difficult to specify the control point variation coefficient α, and better optimum solutions may exist outside the designated α. Therefore, we developed a new system in which the rational valuation system was implemented using many control point variation coefficients without using the specified control point variation coefficient by the designer, and supposed the mechanically optimum form for each control point variation coefficient as the Pareto optimal solution of [Change of image] and [Equivalent stress].

The form that satisfies the requirements of both "image satisfaction" and "equivalent stress" is selected by the designer from all elite forms as the final form. The flow chart of the new system is shown in Fig. 2.

IV. APPLICATION EXAMPLE

To obtain design knowledge regarding the morphological changes in each control point variation coefficient, we created model-1, which has curvatures in one direction, and model-2, which has curvatures in two directions, using the image input system. The control points of these models were applied to the rational valuation system by 14 patterns of each control point variation coefficient α from 0.5 to 5.0, with an interval of 0.25. However, the control points of edges were not applied and were not moved. The planar shapes of both model-1 and model-2 are 40 m in the X direction and 30 m in the Y direction.

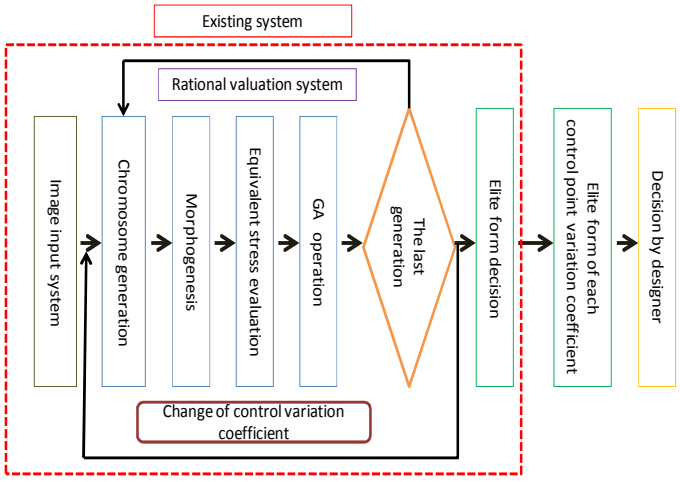

Fig. 2 Flow chart of new system

A. Outline of model-1

The characteristics of model-1 are as follows:

- Roof thickness of 0.15 m, load of 0.0036 MN/m^2 (only self-weight), modulus of elasticity of 20600 N/mm^2, and Poisson's ratio of 0.16.
- The parameters of the GA are as follows: The number of individuals is 40, the last generation is 50, the intersection method is a multi-point intersection method, the intersection rate is 100%, and the mutation rate is 5%.
- This model has three control points in the Y1 direction, three control points in the X direction, and five control points in the Y2 direction (Fig. 3).
- The edges are not moved because they are support points. The control points other than the edges are moved.
- This model has a single curvature in the X and Y1 directions, and multiple curvatures in the Y2 direction.
- The fitness of the GA is equal to the equivalent stress, which is calculated on the basis of the Mises yield criterion.

B. Execution results of model-1

Figure 4 shows the relationship between the control point variation coefficient α and the equivalent stress obtained from the analytical results. Figure 5 shows the elite forms of each control point variation coefficient. Figure 6 shows the relationship between the vertical coordinate values of the control points and the control point variation coefficient α.

The following points should be considered:

1) The equivalent stress converges when α exceeds 3.5 (Fig. 4), and the vertical coordinates of the control points (No. 8, 9, and 10 in the Y2 direction) with multiple curvatures become almost equal. This shows that mechanical rationality tends to increase when a curved surface with multiple curvatures is transformed to a curved surface with a single curvature.
2) Control point No. 2 in the Y1 direction and control point No. 5 in the X direction, each of which has a single curvature, tended to move in the direction in which the rise ratio increased.

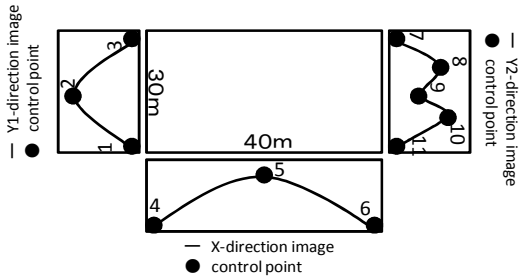

Fig. 3 Control points of model-1

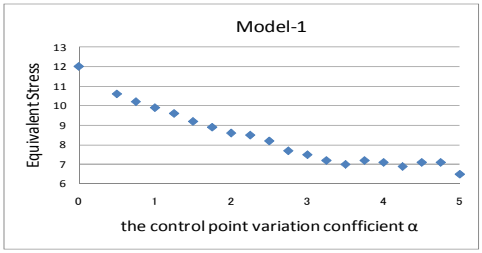

Fig. 4 Relation of equivalent stress and the control point variation coefficient α

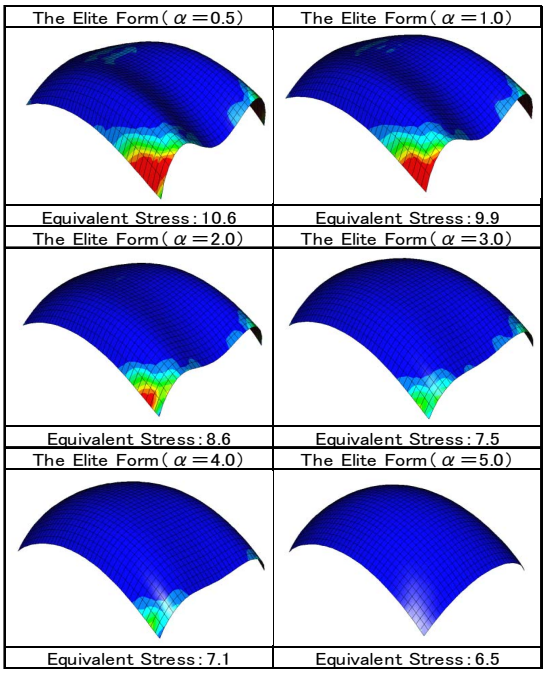

Fig. 5 Elite forms per the control point variation coefficient α

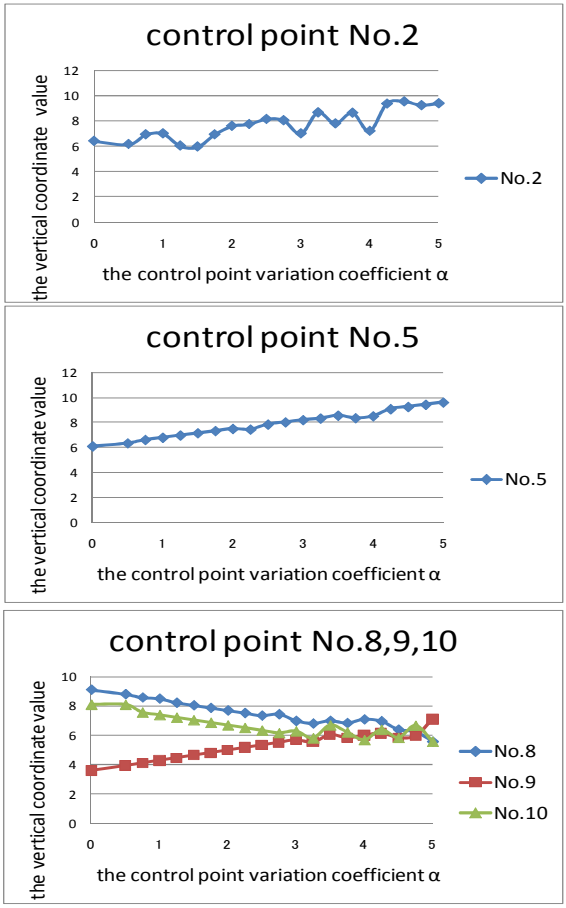

Fig. 6 Relation of the vertical coordinates of control points and the control point variation coefficient α

C. *Outline of model-2*

The characteristics of model-2 are as follows:

- Roof thickness of 0.15 m, load of 0.0036 MN/m^2 (only self-weight), modulus of elasticity of 20600 N/mm^2, and Poisson's ratio of 0.16.
- The parameters of the GA are as follows: The number of individuals is 40, the last generation is 50, the intersection method is a multi-point intersection method, the intersection rate is 100%, and the mutation rate is 5% (Fig. 7).
- This model has three control points in the Y1 direction, five control points in the X direction, and five control points in the Y2 direction.
- The edges are not moved because they are support points. The control points other than the edges are moved.
- This model has a single curvature in the X direction and multiple curvatures in the Y1 and Y2 directions.
- The fitness of the GA is equal to the equivalent stress, which is calculated on the basis of the Mises yield criterion.

D. *Execution results of model-2*

Figure 8 shows the relationship between the control point variation coefficient α and the equivalent stress obtained from the analytical results. Figure 9 shows the elite forms of each control point variation coefficient. Figure 10 shows the relationship between the vertical coordinate values of the control points and the control point variation coefficient α.

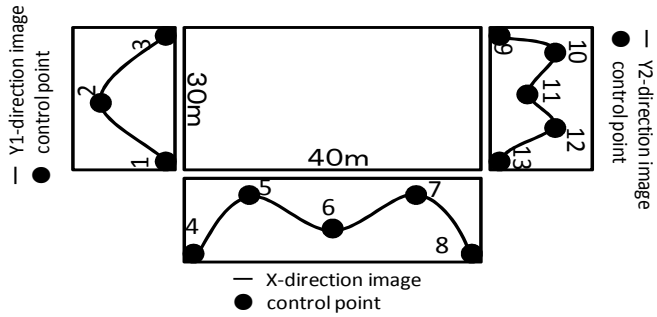

Fig. 7 Control points of model-2

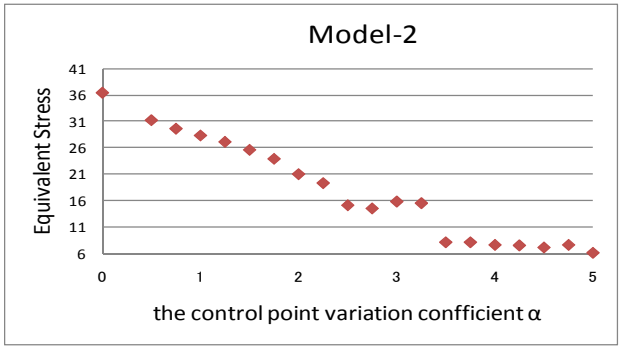

Fig. 8 Relation of equivalent stress and the control point variation coefficient α

1) In the case of model 2, the equivalent stress converges into two stages. The first convergence occurs when the control point variation coefficient α exceeds 2.5, and the vertical coordinates of the control points (No. 5, 6, and 7 in the X direction) with multiple curvatures become almost equal. That is, convergence occurs when a surface with multiple curvatures transforms to a surface with a single curvature.
2) The second convergence occurs when the control point variation coefficient α exceeds 3.5, and the vertical coordinates of the control points (No. 10, 11, and 12 in the Y2 direction) with multiple curvatures become almost equal. That is, convergence occurs when a surface with multiple curvatures transforms to a surface with a single curvature. Control point No. 2 in the Y1 direction, which has a single curvature, tends to move in the direction in which the rise ratio increases.

V. CONCLUSIONS

The following conclusions can be drawn from this study:

1) The equivalent stress decreases with an increase in the control point variation coefficient; however, the difference in the form image from the initial form increases. Thus, there is a trade-off between "image satisfaction" and "equivalent stress."
2) It becomes possible for the designer to select the form with both high image and mechanical rationality by proposing several elite forms for each control point variation coefficient.
3) From the execution results of model-1 and model-2, it is clear that mechanical rationality increases when a surface with multiple curvatures transforms to a surface with a single curvature.

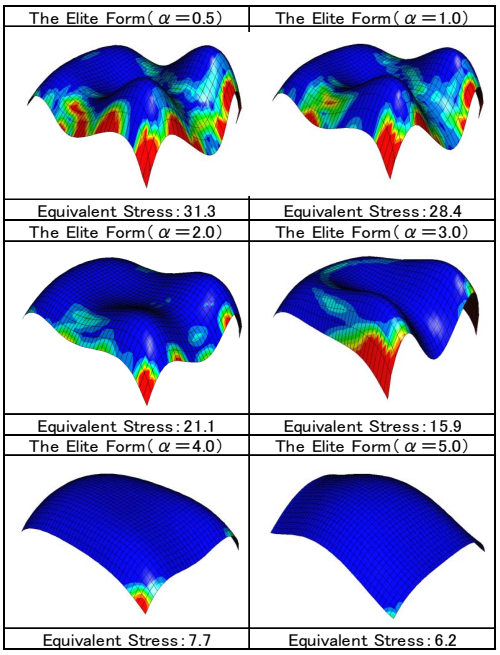

Fig. 9 Elite forms per the control point variation coefficient α

VI. FUTURE TASKS

We intend to improve the proposed design in the following manner:

1) Input the image from four directions
2) Diversify the planar shape
3) Diversify the fitness function

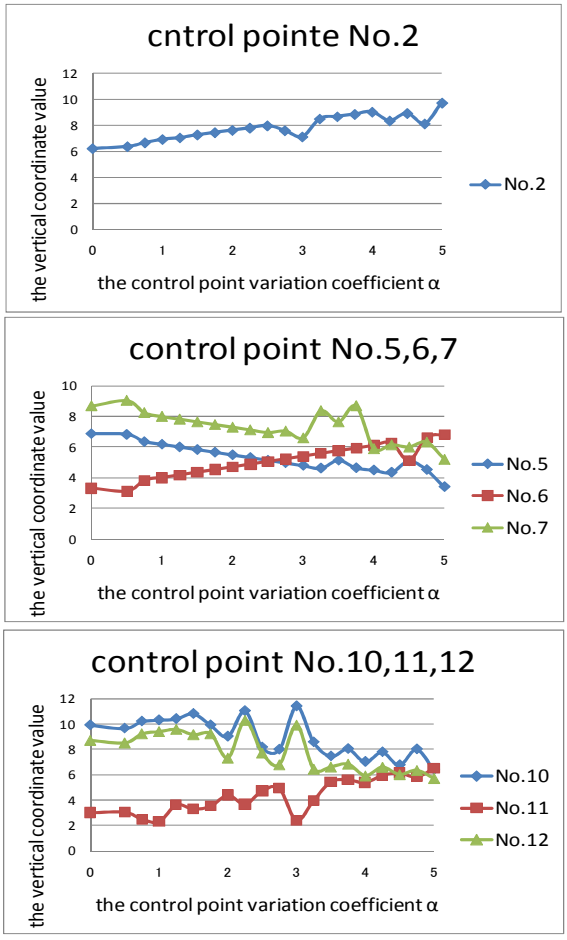

Fig. 10 Relation of the vertical coordinates of control points and the control point variation coefficient α

REFERENCES

[1] K.Mitsui,M. Ohsaki,H.Ohmori,H.Tagawa,T.Honma: Calculation engineering series 4 Structural form and system by heuristic optimization technique, CORONA PUBLISHING, 2004.7[in Japanese]

[2] K.Tsutsumi,E.Kumakawa: A study on the shape generation of large span roof with a window ~Analysis of stress changes and form changes for difference of window position~: *Sumaries of technical papers of annual meeting architectural institute of Japan 2009.8 (Tohoku),pp819-822 [in Japanese]*

[3] K.Tsutsumi,Y.Kitamura:A Study on Shorting Computation Time of Morphogenesis System by Evolutionary Computation (part1,part2), *Sumaries of technical papers of annual meeting architectural institute of Japan 2010.9 (Hokuriku),pp831-834 [in Japanese]*

[4] M.Hosaka:Modeling of curve curved surface in CAD/CAM , Tokyo Denki University publication,1996.1[in Japanese]

2011 IEEE International Conference on Fuzzy Systems
June 27-30, 2011, Taipei, Taiwan

Multiobjective Two-Level 0-1 Programming through Distributed Genetic Algorithms

Keiichi Niwa
Faculty of Economics
Hiroshima University of Economics
5-37-1, Asaminami-ku, Hiroshima,
731-0192, Japan
Email: ki-niwa@hue.ac.jp

Tomohiro Hayashida
Graduate School of Engineering
Hiroshima University
1-4-1, Kagamiyama, Higashi-Hiroshima,
739-8527, Japan
Email: hayashida@hiroshima-u.ac.jp

Masatoshi Sakawa
Graduate School of Engineering
Hiroshima University
1-4-1, Kagamiyama, Higashi-Hiroshima,
739-8527, Japan
Email: sakawa@hiroshima-u.ac.jp

***Abstract*—In this paper we focus on a multiobjective two-level 0-1 programming problem in which the decision maker at the upper level has an objective function and the decision maker at the lower level has multiple objective functions. We assume that there is not coordination between the decision maker at the upper level and the decision maker at the lower level. The decision maker at the upper level must take account of multiple rational responses of the decision maker at the lower level in the problem. We examine two kinds of situations based on anticipation of the decision maker at the upper level; an optimistic anticipation and a pessimistic anticipation. We show mathematical programming problems for obtaining the Stackelberg solutions based on two kinds of anticipation and propose computational methods using genetic algorithms for obtaining the Stackelberg solutions. In order to demonstrate feasibility and effectiveness of the proposed computational methods through genetic algorithms, we plan to conduct numerical experiments.**

I. Introduction

In this paper, we deal with a multiobjective two-level 0-1 programming problem in which there is not coordination between the decision maker at the upper level (leader) and the decision maker at the lower level (follower). Each decision maker knows completely the objective functions and constraints of the opponent and self. For traditional two-level programming problems, the leader first specifies a decision and then the follower specifies a decision so as to optimize the objective with full knowledge of the decision of the leader. According to the rule, the leader also specifies the decision so as to optimize the objective function. We call the solution defined as the above mentioned procedure the Stackelberg solution [37].

It is often assumed that a set of rational responses $R(\boldsymbol{x})$ of the follower is a singleton in conventional two-level 0-1 programming problems. In multiobjective environments, however, the assumption is not realistic and consequently the leader takes into consideration multiple responses or an infinite number of responses of the followers with respect to the decision specified by the leader. In this paper we provide a prescriptive approach to the multiobjective two-level 0-1 programming problem from a viewpoint of the leader. We assume that the leader has some subjective anticipation or belief. Such anticipation or belief can be considered in two cases: (i) the leader anticipates that the follower will take a decision desirable for the leader (optimistic anticipation); (ii) the leader anticipates that the follower will take a decision undesirable for the leader (pessimistic anticipation).

On the other hand, genetic algorithms (GAs) [19] have received a great deal of attention regarding their potential as optimization techniques for solving discrete optimization problems or other hard optimization problems. Although GAs were not much known at the beginning, after the publication of Goldberg's book [17], many researchers in various fields have recently attracted much attention to GAs as a methodology for optimization, adaptation and learning [21], [34].

In order to solve multiobjective optimization problems, various types of GAs are proposed by many researchers [20], [16], [43], [11], [42], [9], [13], [41]. As an early GA application, Shaffer [36] proposes vector evaluated genetic algorithms (VEGA). VEGA performs independent selection cycles according to each objective. Then the whole population is thoroughly shuffled to apply a crossover operator and a mutation operator. Afterward, multiobjective genetic algorithms (MOGAs) are proposed by C. M. Fonseca *et al.* [15] and a non-dominated sorting genetic algorithm (NSGA) based on the non-dominated sorting procedure [17] are proposed by Srinivas *et al.* [38]. Also, Tamaki *et al.* [39] propose to preserve solution non-dominated in the current population. Then, K. Deb *et al.* [10] propose a non-dominated sorting genetic algorithm II (NSGA-II) for solving some problems of NSGA and show the effectiveness of the proposed method by performing numerical experiments.

As an overview of research dealing with two-level programming problems that include discrete variables, Bard *et al.* develope algorithms based on the branch-and-bound techniques for obtaining Stackelberg solutions to two-level 0-1 programming problems [6] and two-level mixed integer programming problems [5]. Wen *et al.* [40] propose an exact computational method and a heuristic method for obtaining a Stackelberg solution to two-level mixed 0-1 programming problems with 0-1 decision variables of the leader and continuous decision variables of the follower. Anandalingam *et al.* [3] propose a computational method using GAs for deriving a Stackelberg solution for two-level linear programming problems. Niwa *et al.* [27], [28] propose computational methods through GAs

978-1-4244-7316-8/11/$26.00 ©2011 IEEE

with double string proposed by Sakawa *et al.* [34] so as to derive a Stackelberg solution for 0-1 programming problems related to two-level decentralized systems. Also, Niwa *et al.* propose computational methods that implement sharing [23] and cluster analysis [30] methods so as to improve the computational accuracy of the Stakelberg solution. Moreover, Niwa *et al.* propose a computational method through parallel genetic algorithms (single-population master-slave GAs) for obtaining a Stackelberg solution to two-level 0-1 programming problems [31] and develope computational methods using distributed genetic algorithms so as to solve two-level 0-1programming problems [26] and decentralized two-level 0-1 programming problems [25]. Specifically, in these computational methods, parallel genetic algorithms and distributed genetic algorithms are introduced with respect to the upper level GA, which handles decision variables for the upper level decision maker. Use of these methods allows for the derivation of approximate Stackelberg solutions with high precision and in a short time.

For the multiobjective two-level linear programming problems, Nishizaki *et al.* [22] propose solution concepts with the leader anticipation and develop computational methods based on the idea of the k th best method proposed by Bialas *et al.* [7] and a computational method by using branch-and-bound technique proposed by Bard *et al.* [4]. Niwa *et al.* develop computational methods through the vector evaluated genetic algorithms for obtaining Stackelberg solutions to multiobjective two-level 0-1 programming problems [29] and multiobjective two-level integer programming problems [24].

In this paper, therefore, we focus on a multiobjective two-level 0-1 programming problem and propose two types of computational methods for obtaining the Stackelberg solution. Specifically, in order to reduce computational time, we consider parallelization of a genetic algorithm handling the decision of the leader and adopt a distributed genetic algorithm as the genetic algorithm. Also, we consider parallelization of the genetic algorithm handling the decision of the follower. Moreover, a first type of proposed computational method adopts the vector evaluated genetic algorithms [36], [39] for deriving multiple rational responses of the follower. A second type of proposed computational method introduces NSGA-II [10] so as to derive multiple rational responses of the follower. In order to demonstrate the effectiveness and the feasibility of the proposed computational methods, we plan to conduct numerical experiments.

II. Multiobjective two-level 0-1 programming problem

In this paper, we consider a multiobjective two-level programming problem in which the leader has an objective function and the follower has multiple objective functions and decision variables of the leader and the follower are 0-1 variables. A multiobjective two-level 0-1 programming problem for obtaining a Stackelberg solution is represented as

$$\left.\begin{array}{ll} \underset{\boldsymbol{x}}{\text{minimize}} & \boldsymbol{z}_1(\boldsymbol{x},\boldsymbol{y}) = \boldsymbol{c}_1\boldsymbol{x} + \boldsymbol{d}_1\boldsymbol{y} \\ \text{where } \boldsymbol{y} \text{ solves} & \\ \underset{\boldsymbol{y}}{\text{minimize}} & \boldsymbol{z}_{21}(\boldsymbol{x},\boldsymbol{y}) = \boldsymbol{c}_{21}\boldsymbol{x} + \boldsymbol{d}_{21}\boldsymbol{y} \\ & \cdots \\ \underset{\boldsymbol{y}}{\text{minimize}} & \boldsymbol{z}_{2k_2}(\boldsymbol{x},\boldsymbol{y}) = \boldsymbol{c}_{2k_2}\boldsymbol{x} + \boldsymbol{d}_{2k_2}\boldsymbol{y} \\ \text{subject to} & A\boldsymbol{x} + B\boldsymbol{y} \leq \boldsymbol{b} \\ & x_i \in \{0,1\}, i = 1, ..., n_1 \\ & y_j \in \{0,1\}, j = 1, ..., n_2, \end{array}\right\} \quad (1)$$

where $\boldsymbol{c}_1$, $\boldsymbol{c}_{2k}, k = 1, \ldots, k_2$ are n_1-dimensional constant row vectors; $\boldsymbol{d}_1$, $\boldsymbol{d}_{2k}, k = 1, \ldots, k_2$ are n_2-dimensional constant row vectors, respectively. $\boldsymbol{b}$ is an m-dimensional constant column vector; A is an $m \times n_1$ constant matrix; B is an $m \times n_2$ constant matrix; these coefficients are assumed to be integer constants; $z_1(\boldsymbol{x},\boldsymbol{y})$ is the leader's objective function; $z_{2k}(\boldsymbol{x},\boldsymbol{y}), k = 1, \ldots, k_2$ are the follower's objective functions; $\boldsymbol{x}$ and $\boldsymbol{y}$ are the leader's and the follower's 0-1 decision variables, respectively.

For conventional two-level 0-1 programming problems, the leader first makes a decision and then the follower specifies a decision in order to optimize the objective function of the follower with full knowledge of the decision of the leader. According to the rule, the leader also determines a decision so as to optimize the objective function of self. We call the solution defined as the above mentioned procedure the Stackelberg solution. In this case, it is often assumed that the set of rational responses $R(\boldsymbol{x})$ for each of all the possible decisions $\boldsymbol{x}$ of the leader is a singleton. However, in multiobjective environment, the above assumption becomes meaningless and hence the leader takes into consideration multiple responses or an infinite number of responses of the follower with respect to the decision specified by the leader. It seems reasonable to suppose that at least the set of rational responses $R(\boldsymbol{x})$ is imposed is the Pareto optimality.

Therefore, we introduce the following set of Pareto optimal responses $P(\boldsymbol{x})$ as a substitute for the set of rational responses $R(\boldsymbol{x})$.

$$\begin{aligned} P(\boldsymbol{x})=\{\boldsymbol{y} \in S(\boldsymbol{x}) \mid & \text{ there does not exist another } \boldsymbol{y}' \in S(\boldsymbol{x}) \\ & \text{such that } z_{2k}(\boldsymbol{x},\boldsymbol{y}') \leq z_{2k}(\boldsymbol{x},\boldsymbol{y}), \forall k, k = 1, \ldots, k_2 \\ & \text{and } z_{2\ell}(\boldsymbol{x},\boldsymbol{y}') \neq z_{2\ell}(\boldsymbol{x},\boldsymbol{y}) \text{ for at least one } \ell.\}, \end{aligned} \quad (2)$$

where $S(\boldsymbol{x}) = \{\boldsymbol{y} \mid B\boldsymbol{y} \leq \boldsymbol{b} - A\boldsymbol{x},\ y_j \in \{0,1\}, j = 1, ..., n_2\}$.

For a decision $\boldsymbol{x}$ determined by the leader, the leader can presume only that a response $\boldsymbol{y}$ of the follower with respect to $\boldsymbol{x}$ belongs to the set of Pareto optimal responses $P(\boldsymbol{x})$.

As done in a conventional two-level 0-1 programming problem, the leader first has specified a decision $\boldsymbol{x}$ and then the follower takes a decision $\boldsymbol{y}$ which belongs to the set of Pareto optimal responses $P(\boldsymbol{x})$. However, the leader does not know which a response is chosen from the set of Pareto optimal responses by the follower. Then we can provide reasonable decisions of the leader in accordance with some subjective anticipation or belief if a prescriptive approach should be employed. Such anticipation or belief can be considered in two cases: i) a case where the leader anticipates that the follower

will take a decision desirable for the leader (the optimistic anticipation); ii) a case where the leader anticipates that the follower will take a decision undesirable for the leader (the pessimistic anticipation). When the leader does not know the preference of the follower, the leader would make a decision by consulting outcomes yielded from the optimistic anticipation and the pessimistic anticipation. We show multiobjective two-level 0-1 programming problems based on the optimistic anticipation and the pessimistic anticipation.

A. Optimistic Stackelberg solution

After the leader has chosen a decision $\hat{\boldsymbol{x}}$, the follower makes a decision $\boldsymbol{y}$ with full knowledge of the decision $\hat{\boldsymbol{x}}$ of the leader by solving the multiobjective 0-1 programming problem:

$$\left.\begin{array}{ll} \underset{\boldsymbol{y}}{\text{minimize}} & z_{21}(\hat{\boldsymbol{x}}, \boldsymbol{y}) = \boldsymbol{d}_{21}\boldsymbol{y} + \boldsymbol{c}_{21}\hat{\boldsymbol{x}} \\ & \cdots\cdots\cdots\cdots\cdots\cdots \\ \underset{\boldsymbol{y}}{\text{minimize}} & z_{2k_2}(\hat{\boldsymbol{x}}, \boldsymbol{y}) = \boldsymbol{d}_{2k_2}\boldsymbol{y} + \boldsymbol{c}_{2k_2}\hat{\boldsymbol{x}} \\ \text{subject to} & B\boldsymbol{y} \leq \boldsymbol{b} - A\hat{\boldsymbol{x}} \\ & y_j \in \{0,1\}, j = 1, ..., n_2. \end{array}\right\} \quad (3)$$

Let $P(\hat{\boldsymbol{x}})$ denote the set of Pareto optimal responses (solutions) of the multiobjective integer programming problem (3).

Hereafter, we call a Stackelberg solution based on the optimistic anticipation the optimistic Stackelberg solution simply. The optimistic Stackelberg solution is an optimal solution to the following problem (4).

$$\left.\begin{array}{ll} \min\limits_{\boldsymbol{x}} \min\limits_{\boldsymbol{y}} & \boldsymbol{z}_1(\boldsymbol{x}) = \boldsymbol{c}_1\boldsymbol{x} + \boldsymbol{d}_1\boldsymbol{y} \\ \text{subject to} & \boldsymbol{y} \in P(\boldsymbol{x}) \\ & A\boldsymbol{x} + B\boldsymbol{y} \leq \boldsymbol{b} \\ & x_i \in \{0,1\}, i = 1, ..., n_1 \end{array}\right\} \quad (4)$$

Problem (4) expresses a situation where the leader chooses a decision $\boldsymbol{x}$ so as to minimize the leader's objective function on the assumption that, for the given $\boldsymbol{x}$ of the leader, the follower takes a decision $\boldsymbol{y}$ in the set of Pareto optimal responses $P(\boldsymbol{x})$ such that the leader's objective function is minimized.

B. Pessimistic Stackelberg solution

Suppose that the leader makes a decision $\boldsymbol{x}$ and anticipates that the follower chooses a decision undesirable for the leader in the set of Pareto optimal responses $P(\boldsymbol{x})$. We call a Stackelberg solution based on the pessimistic anticipation the pessimistic Stackelberg solution. The pessimistic Stackelberg solution can be obtained by solving the problem

$$\left.\begin{array}{ll} \min\limits_{\boldsymbol{x}} \max\limits_{\boldsymbol{y}} & \boldsymbol{z}_1(\boldsymbol{x}) = \boldsymbol{c}_1\boldsymbol{x} + \boldsymbol{d}_1\boldsymbol{y} \\ \text{subject to} & \boldsymbol{y} \in P(\boldsymbol{x}) \\ & A\boldsymbol{x} + B\boldsymbol{y} \leq \boldsymbol{b} \\ & x_i \in \{0,1\}, i = 1, ..., n_1. \end{array}\right\} \quad (5)$$

This problem can be solved by an algorithm similar to the algorithm for the optimistic Stackelberg solutions.

III. Computational Methods through Genetic Algorithms

In this paper, we propose computational methods through genetic algorithms for obtaining Stackelberg solutions based on the optimistic anticipation and the pessimistic anticipation to multiobjective two-level 0-1 programming problems. The proposed computational methods are described as follows.

We propose two types of computational methods using GAs for obtaining Stackelberg solutions to the problem (4) and (5). The proposed computational methods use the double string [32] which composed of the substring corresponding to the decision of the leader, and the substring corresponding to the decision of the follower. In order to solve the problem (4) and (5), the decisions of the leader and the follower are handled by performing genetic operators on each substring. Specifically, in order to reduce computational time, we consider parallelization of a genetic algorithm handling the decision of the leader and adopt a destributed genetic algorithm as the genetic algorithm. Also, we consider parallelization of the genetic algorithm handling the decision of the follower. The above-mentioned parallelization approaches are improvements common to two types of the proposed computational methods. Moreover, a first type of the proposed computational method adopts VEGA [36], [39] for deriving multiple rational responses of the follower. Also, a second type of proposed computational method introduces NSGA-II [10] so as to derive multiple rational responses of the follower.

In the following sections III-A, III-B, III-C, III-D, we show common operators or procedures used for the proposed computational methods. In section III-E, we describe a reproduction operator used for each computational method in detail. Finally, we show algorithms used in the computational methods after improvement in section III-F.

A. Coding and decoding

For solving 0-1 programming problems using genetic algorithms, an individual is usually represented by a binary 0-1 string [18], [17], [21]. However, this representation may weaken the ability of genetic algorithms since an individual whose phenotype is feasible is scarcely generated under this representation.

For multidimensional 0-1 knapsack problems, Sakawa *et al.* [32] propose a double string representation and a decoding algorithm for eliminating infeasible solutions. In this paper, a double string which is composed of the substring corresponding to the decision of the leader, $\boldsymbol{x}$, and the substring corresponding to the decision of the follower, $\boldsymbol{y}$, as shown in Fig.1 is used so as to derive only feasible solutions.

The decisions of the leader and the follower are handled by applying genetic operators on each substring. We call the genetic algorithm operating to the decision $\boldsymbol{x}$ of the leader the upper level GA, and the genetic algorithm operating to the decision $\boldsymbol{y}$ of the follower the lower level GA.

$s_{i_x(m)} \in \{0,1\}, i_x(m) \in \{1, \ldots, n_1\}$, and for $m \neq m'$ it is assumed that $i_x(m) \neq i_x(m')$. Similarly, $s_{i_y(m)} \in \{0,1\}, i_y(m) \in \{1, \ldots, n_2\}$, and for $m \neq m'$ it is assumed

← Individual for $\boldsymbol{x}$ →			← Individual for $\boldsymbol{y}$ →		
$i_x(1)$	$\cdots$	$i_x(n_1)$	$i_y(1)$	$\cdots$	$i_y(n_2)$
$S_{i_x(1)}$	$\cdots$	$S_{i_x(n_1)}$	$S_{i_y(1)}$	$\cdots$	$S_{i_y(n_2)}$

Fig. 1. Double string

that $i_y(m) \neq i_y(m')$. Also, in the double string, $i_x(m)$, $i_y(m)$ and $s_{i_x(m)}$, $s_{i_y(m)}$ express indexes of the elements of each solution vector respectively, and their values.

Also, a decoding algorithm proposed by the Niwa *et al.* [27] is also applied to the upper level GA and the lower level GA so as to generate only feasible solutions.

B. Crossover and mutation

If a one-point or multi-point crossover operator is applied to individuals represented by double strings then there is a possibility that infeasible individuals may be generated because the indexes occurring in the offspring, $i_x(m)$, $i_x(m')$, $m \neq m'$ or $i_y(m)$, $i_y(m')$, $m \neq m'$, may have the same number. When solving the traveling salesman problem or the scheduling problem through GAs, this kind of violation occurs. One possible approach to circumvent such violation, a crossover method called partially matched crossover (PMX) is useful [18]. In this paper, a modified version of PMX is used in order to handle the double string proposed by Sakawa *et al.* [34]. Also, when determining whether or not to apply the crossover operator, the prespecified probability p_c is used. Its value is set in advance.

A mutation operator is thought to fulfill the role of local random search in genetic algorithms. In this paper, for the lower string of a double string, mutation of bit-reverse type is adopted. For the upper string of a double string, an inversion is used. When applying the mutation operator to individuals, it is first determined whether or not the mutation operator will be applied to an individual according to the prespecified probability p_m. In the case that mutation is applied, it is then determined whether to apply an inversion or mutation of bit-reverse type according to the prespecified probability M_{Pum}.

C. Application of parallel genetic algorithms

It is possible to divide the operations without a reproduction operator included in genetic algorithms, and to solve those operations simultaneously using multiple processors. However, in a reproduction operator, an evaluation value (ex. objective function value) for each individual is calculated, and fitness values for individuals are computed by using the evaluation values. Because it is necessary to divide this process in a reproduction operator, direct application of parallel processing is difficult. Research related to the parallelization of GAs started with improvements to such barriers to the implementation of parallelization, and a variety of types of models have been proposed and their effectiveness noted by numerous researchers. In general, parallel genetic algorithms are classified broadly into four types: 1) Single-population master-slave GAs, 2) Multiple-population GAs, 3) Fine-grained GAs, and 4) Hierarchical hybrids [8]. Single-population master-slave GAs have a single population. The master performs a selection operator a crossover operator and a mutation operator. Slaves only evaluate the fitness of the individuals. Multiple-population GAs or multiple-deme GAs consist of several subpopulations that exchange individuals every so often. This exchange of individuals is called migration. The subpopulations are assigned to multiple processors. A reproduction operator, a crossover operator and a mutation operator are performed on each subpopulation. These models are also known as distributed GAs or island parallel GAs. Fine-grained GAs consist of a single spatially-distributed population. Each processor has a very small number of individuals. Ideally, an individual is assigned to one processor and all individuals are evaluated simultaneously. Selection and mating are applied to a small neighborhood around each individual. The neighborhoods overlap, so that eventually the good characters of a superior individual can spread to the whole population. Hierarchical hybrids combine multiple-population GAs with single-population master-slave GAs or fine-grained GAs.

The single-population master-slave GAs executes parallel processing by not dividing the population, and using multiple processors only for the evaluation of individuals [1], [14]. This model may be used in a situation which spends too much time calculating the fitness of each individual. By adopting this model, calculated load may be able to distribute. Another characteristic is that it also implements a simpler algorithm than the other three models, and because there are no changes to the population due to parallelization, there will be no effects on the search for a solution.

A computational method proposed by Niwa *et al.* [31] adopts the single-population master-slave GAs as the upper level GA. In the computational method, a master only executes a reproduction operator and slaves evaluate the fitness of the individuals and performs a crossover operator and a mutation operator. Also, the computational method divides operations of the lower level GA and assigns them across multiple processors. By assigning calculations of fitness for individuals, a crossover operator and a mutation operator to multiple processors, calculation times are reduced. We call the computational method the computational method using master-slave GAs (MGA).

Moreover, Niwa *et al.* proposed computational methods through multiple-population GAs (distributed GAs) in order to solve a two-level 0-1 programming problem [26] and a decentralized two-level 0-1 programming problem [25]. We call these computational methods the computational methods using distributed GAs (DGA). In order to verify the effectiveness of DGA, numerical experiments are carried out. From the results, DGA is superior to MGA and the existing computational method through GAs [27], both from a standpoint of solution precision and required computational time.

In this paper, therefore, we employ computational methods thorough distributed GAs so as to reduce calculation times and obtain good approximate Stackelberg solutions.

D. Lower level GA avoidance procedures

We introduce a storage region shown in Fig. 2.

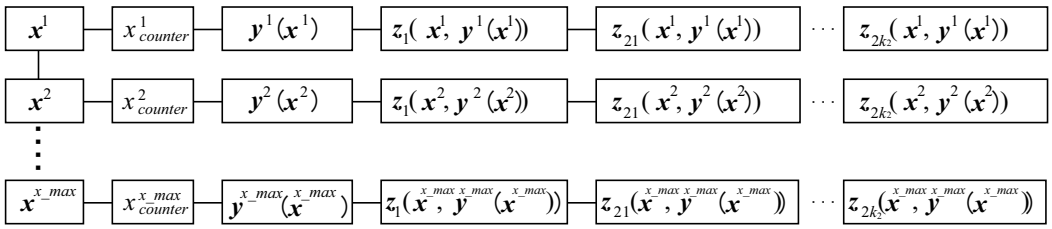

Fig. 2. Storage for saving $\boldsymbol{x}$ and $\boldsymbol{y}(\boldsymbol{x})$

Here, $\boldsymbol{x}^i, i = 1, \ldots, x_max$ indicate the values of $\boldsymbol{x}$ already handled as individuals by the upper level GA, and $\boldsymbol{y}^i(\boldsymbol{x}^i), i = 1, \ldots, x_max$ indicate the Pareto optimal responses associated with $\boldsymbol{x}^i$ obtained by the lower level GA. $x^i_{counter} \in \{1, 2, \ldots, y_max\}, i = 1, \ldots, x_max$ indicate the number of times that the lower level GA was used to find the Pareto optimal response $\boldsymbol{y}^i(\boldsymbol{x}^i)$ for $\boldsymbol{x}^i$. x_max indicates the maximum number of stored decisions $\boldsymbol{x}$, and y_max indicates the maximum number of times that the lower level GA can be repeatedly used to find the Pareto optimal response $\boldsymbol{y}^i(\boldsymbol{x}^i)$ for $\boldsymbol{x}^i$. $z_1(\boldsymbol{x}^i, \boldsymbol{y}^i(\boldsymbol{x}^i))$ is the value of the leader's objective function for $\boldsymbol{x}^i$ and $\boldsymbol{y}^i(\boldsymbol{x}^i)$. $z_{21}(\boldsymbol{x}^i, \boldsymbol{y}^i(\boldsymbol{x}^i))$, ..., $z_{2k_2}(\boldsymbol{x}^i, \boldsymbol{y}^i(\boldsymbol{x}^i))$ are the values of the follower's objective functions for $\boldsymbol{x}^i$ and $\boldsymbol{y}^i(\boldsymbol{x}^i)$. By using the following algorithm, the number of applications of the lower level GA is reduced, and unnecessary calculation times eliminated.

Storage of Pareto optimal response $y(x)$ and lower level GA avoidance procedures

Step 1 If an individual $\bar{\boldsymbol{x}}$ of the upper level GA exists in $\boldsymbol{x}^i$, proceed to Step 2. If such an individual does not exist, then check if the number of $\boldsymbol{x}^i$ has reached x_max, and if so continue on to Step 3. If not, proceed to Step 4.

Step 2 If $x^i_{counter}$ has reached y_max, then the saved $\boldsymbol{y}^i(\boldsymbol{x}^i)$ is returned to the upper level GA as the Pareto optimal response and the algorithm terminates. If not reached, proceed to Step 4.

Step 3 Select the worst value $z_1(\boldsymbol{x}^i, \boldsymbol{y}^i(\boldsymbol{x}^i))$ from the stored $\boldsymbol{x}^i$, and take that $\boldsymbol{x}^i$ value as $\boldsymbol{x}^k$. After applying the lower level GA and thus obtaining the Pareto optimal response $\boldsymbol{y}(\bar{\boldsymbol{x}})$ for $\bar{\boldsymbol{x}}$, if $z_1(\boldsymbol{x}^k, \boldsymbol{y}^k(\boldsymbol{x}^k)) \geq z_1(\bar{\boldsymbol{x}}, \boldsymbol{y}(\bar{\boldsymbol{x}}))$, save $\bar{\boldsymbol{x}}$, $\boldsymbol{y}(\bar{\boldsymbol{x}})$, $z_1(\bar{\boldsymbol{x}}, \boldsymbol{y}(\bar{\boldsymbol{x}}))$, $z_{21}(\bar{\boldsymbol{x}}, \boldsymbol{y}(\bar{\boldsymbol{x}})), \ldots, z_{2k_2}(\bar{\boldsymbol{x}}, \boldsymbol{y}(\bar{\boldsymbol{x}}))$ in the storage region $\boldsymbol{x}^k$, and terminate the algorithm.

Step 4 After obtaining the Pareto optimal response $\boldsymbol{y}(\bar{\boldsymbol{x}})$ for $\bar{\boldsymbol{x}}$ by applying the lower level GA, $\bar{\boldsymbol{x}}, \boldsymbol{y}(\bar{\boldsymbol{x}}), z_1(\bar{\boldsymbol{x}}, \boldsymbol{y}(\bar{\boldsymbol{x}})), z_{21}(\bar{\boldsymbol{x}}, \boldsymbol{y}(\bar{\boldsymbol{x}})), \ldots, z_{2k_2}(\bar{\boldsymbol{x}}, \boldsymbol{y}(\bar{\boldsymbol{x}}))$ are saved, and the algorithm is terminated.

E. Reproduction

We first describe the reproduction operator of the upper level GA. In the upper level GA, the value of $\boldsymbol{x}$ obtained by decoding individuals in the upper level GA and the follower's Pareto optimal responses $\boldsymbol{y}(\boldsymbol{x}) \in P(\boldsymbol{x})$ obtained by applying the lower level GA are substituted into the objective function of the leader $z_1(\boldsymbol{x}, \boldsymbol{y})$, and the value of the evaluation function for each individual is thus obtained. Next, the fitness value for each individual is calculated by applying linear scaling and adopting a clustering method. The individuals remaining in the next generation are determined by applying elitist expected value selection based on these fitness values.

Next, we describe the reproduction operator of the lower level GA. In the lower level GA, the value of $\boldsymbol{y}$ obtained by decoding individuals in the lower level GA, and the given values of the decision variables in the upper level GA, $\boldsymbol{x}$, are substituted into the follower's objective functions $z_{2k}(\boldsymbol{x}, \boldsymbol{y}), k = 1, \ldots, k_2$, and the value of the evaluation function for each individual is thus obtained. Then, in the first type of the proposed computational method, the reproduction operator of VEGA [36], [39] is adopted by using the value of the evaluation function for deriving multiple rational responses of the follower. Also, in the second type of the proposed computational method, the reproduction operator of NSGA-II [10]is applied by using the value of the evaluation function.

F. Algorithms for the proposed computational methods

Initially, an algorithm used in the first type of the proposed computational method after improvement can be summarized as follows. N_p denotes the number of processors.

Step 1 For each processor $q, q = 1, \ldots, N_p$, apply the upper level GA operations on Step1 through Step7. Generate N_u individuals at random to form the initial population. Set the generation index $t_{uq} := 0$ and determine the value of the maximal generation T_u.

Step 2 For each individual $\boldsymbol{x}$ in the upper level GA, determine whether or not to apply the operations of the lower level GA. If it is applied, then apply the lower level GA operations in Step 2-a through Step 2-c,

and obtain a Pareto optimal response $\boldsymbol{y}(\boldsymbol{x})$. If it is not applied, then a stored $\boldsymbol{y}(\boldsymbol{x})$ is taken as a Pareto optimal response, and proceed to Step 4.

Step a Randomly generate N_l lower level GA individuals $\boldsymbol{y}$, and take these as the initial population of the lower level GA. Set the generation index $t_l := 0$ and determine the value of the maximal generation T_l. Proceed to Step 2-b.

Step b By using $\boldsymbol{x}$ given as the upper level GA individual and $\boldsymbol{y}$ generated by the lower level GA, the follower's objective function values are calculated. As the reproduction operator, the parallel selection method is applied. Preserve non-dominated solutions in the population. Proceed to Step 2-c.

Step c If t_l has exceeded the maximal generation T_l, take the individual with the best fitness value as the optimal individual $\boldsymbol{y}(\boldsymbol{x})$, and proceed to Step 3. Otherwise, apply a crossover operator and a mutation operator to each lower level GA individual. Select individuals from the population at random, and exchange the individuals for the non-dominated solutions (individuals). Let $t_l = t_l + 1$, and proceed to Step 2-b.

Step 3 By using the follower's Pareto optimal response $\boldsymbol{y}(\boldsymbol{x})$ obtained by operation of the lower level GA and the individual $\boldsymbol{x}$ of the upper level GA, calculate objective function values for the leader and the follower. Perform the procedures required to save $\boldsymbol{x}$ and its Pareto optimal response $\boldsymbol{y}(\boldsymbol{x})$ to the storage region and proceed to Step 4.

Step 4 Calculate the leader's objective function value for each upper level GA individual $\boldsymbol{x}$, and after performing linear scaling, apply the clustering method to measure the level of convergence of the individuals. Depending upon the degree of convergence, calculate the fitness value of each individual. Proceed to Step 5.

Step 5 If t_{uq} has exceeded the maximal generation T_u, then terminate the algorithm. In that case, the individual obtained up to that generation with the best fitness value is taken as the optimal individual $(\boldsymbol{x}, \boldsymbol{y})$. Otherwise, proceed to Step 6.

Step 6 A reproduction operator is performed using the fitness values of each individual of the upper level GA. Apply a crossover operator and a mutation operator to each upper level GA individual, and proceed to Step7.

Step 7 If t_{uq} mod m_i (migration interval) = 0, after performing synchronization between the processors, apply migration. Return to Step 2 with $t_{uq} := t_{uq} + 1$.

Next, we show an algorithm used for the second type of the proposed computational method. Because the difference of two computational methods is only procedures to apply the lower level GA, an algorithm for the lower level GA is shown as follows.

Step a Set the generation index $t_l := 0$ and determine the value of the maximal generation T_l. Generate N_l lower level GA individuals $\boldsymbol{y}$ at random, and take these individuals as the initial population $P(t_l)$ of the lower level GA. Proceed to Step 2-b.

Step b If t_l has exceeded the maximal generation T_l, take the individual with the best fitness value as the optimal individual $\boldsymbol{y}(\boldsymbol{x})$, and proceed to Step 3. Otherwise, apply a crowded tournament selection operator, a crossover operator and a mutation operator to each lower level GA individual in $P(t_l)$ and form a population $Q(t_l)$ by use of these individuals.

Step c Let $R(t_l) = P(t_l) \cup Q(t_l)$. By using $\boldsymbol{x}$ given as an individual of the upper level GA and $\boldsymbol{y}$ given as an individual of the lower level GA in $R(t_l)$, the follower's objective function values are calculated. Based on these values, a non-dominated sorting is applied as a reproduction operator. Then, create the new population $P(t_l+1)$ of the next generation t_l+1. Let $t_l = t_l + 1$, and proceed to Step 2-b.

By using these coputational methods, it is possible to obtain the Stackelberg solutions to the problem (4) and (5).

IV. Conclusion

This paper has focused on a multiobjective two-level 0-1 programming problem in which there is not coordination between the decision maker at the upper level and the decision maker at the lower level. We have considered two kinds of situations based on anticipation of the decision maker at the upper level; an optimistic anticipation and a pessimistic anticipation. Mathematical programming problems for obtaining the Stackelberg solutions based on two kinds of anticipation have been shown and two types of computational methods for obtaining the Stackelberg solutions have been proposed. In order to demonstrate the effectiveness of the proposed methods, it is intended to conduct numerical experiments into both the solution precision and computation time, and thus compare the proposed computational methods with previous methods.

References

[1] D. Abramson and J. Abela, "A parallel genetic algorithm for solving the school timetabling problem," *Proceedings of the Fifteenth Australian Computer Science Conference,* Vol. 14, pp. 1–11, 1992.

[2] G. Anandalingam, "A mathematical programming model of decentralized multi-Level systems," *Journal of Operational Research Society,* Vol. 39, pp. 1021–1033, 1988.

[3] G. Anandalingam, R. Mathieu, C.L. Pittard and N. Sinha, "Artificial intelligence based approaches for solving hierarchical optimization problems," in: Sharda, Golden, Wasil, Balci and Stewart (eds.), *Impacts of Recent Computer Advances on Operations Research,* North-Holland, pp. 289–301, 1989.

[4] J. Bard and J. Moore, "A branch and bound algorithm for the bilevel programming problem," *SIAM Journal on Scientific and Statistical Computing,* Vol. 11, pp. 281–292, 1990.

[5] J. Bard and J. Moore, "The mixed integer linear bilevel programming problem," *Operations Research,* Vol. 38, pp. 911–921, 1990.

[6] J. Bard and J. Moore, "An algorithm for the discrete bilevel programming problem," *Naval Research Logistics,* Vol. 39, pp. 419–435, 1992.

[7] W.F. Bialas and M.H. Karwan, "Two-level linear programming," *Management Science,* Vol. 30, pp. 1004–1020, 1984.

[8] E. Cantú-Paz: *Efficient and Accurate Parallel Genetic Algorithms,* Kluwer Academic Publishers, Norwell, Massachusetts, 2000.

[9] N. Chaiyaratana, T. Piroonratana and N. Sangkawelert, "Effects of diversity control in single-objective and multi-objective genetic algorithms," *Journal of Heuristics,* Vol. 13, No. 1, pp. 1–34, 2007.

[10] K. Deb, A. Pratap, S. Agarwal and T. Meyarivan, "A fast and elitist multiobjective genetic algorithm: NSGA-II," *IEEE Transactions on Evolutionary Computation,* Vol. 6, No. 2, pp. 182–197, 2002.

[11] K. Deb and T. Goel, "Controlled elitist non-dominated sorting genetic algorithms for better convergence," *Lecture Notes in Computer Science,* Vol. 1993, pp. 67–81, 2001.

[12] K. Deb, A. Pratap, S. Agarwal and T. Meyarivan, "A fast and elitist multiobjective genetic algorithm: NSGA-II," *IEEE Transactions on Evolutionary Computation,* Vol. 6, No. 2, pp. 182–197, 2002.

[13] K. Deb, L. Thiele, L. Laumanns and E. Zitzler, "Scalable test problems for evolutionary multi-objective optimization," *Evolutionary Multiobjective Optimization,* pp. 105–145, 2005.

[14] T.C. Fogarty and R. Huang, "Implementing the genetic Algorithm on Transputer Based Parallel Processing Systems," *Proceedings of the First International Conference on Parallel Problem Solving from Nature,* pp.145-149, 1990.

[15] C. M. Fonseca and P. J. Fleming, "Genetic algorithms for multiobjective optimization: formulation, discussion and generalization," *Proceedings of the Fifth International Conference on Genetic Algorithms,* pp. 416–423, 1993.

[16] C. M. Fonseca and P. J. Fleming, "Multiobjective optimization and multiple constraint handling with evolutionary algorithms-Part 1: A united formulation," *IEEE Transactions on Systems, Man and Cybernetics, Part A: Systems and Humans,* Vol. 28, No. 1, pp. 26-37, 1998.

[17] D.E. Goldberg, *Genetic Algorithms in Search, Optimization, and Machine Learning,* Addison Wesley, Massachusetts, 1989.

[18] D.E. Goldberg and R. Lingle, "Alleles, loci, and the traveling salesman problem," *Proceedings of the First International Conference on Genetic Algorithms and Their Applications*, Lawrence Erlbaum Associates, Hillsdale, NJ, pp. 154–159, 1985.

[19] J.H. Holland, *Adaptation in Natural and Artificial Systems,* University of Michigan Press, 1975, MIT Press, Cambridge, 1992.

[20] J. Horn and N. Nafpliotis, and D. E. Goldberg, "A niched Pareto genetic algorithm for multiobjective optimization," *Proceedings of the First IEEE Conference on Evolutionary Computation,* pp. 82–87, 1994.

[21] Z. Michalewicz, *Genetic Algorithms + Data Structures = Evolution Programs,* Third, revised and extended edition, Springer-Verlag, 1996.

[22] I. Nishizaki and M. Sakawa, "Stackelberg solutions to multiobjective two-level linear programming problems," *Journal of Optimization Theory and Applications,* Vol. 103, pp. 161-182, 1999.

[23] K. Niwa, "Revised computational methods for using genetic algorithms for obtaining Stackelberg solutions to two-level 0-1 programming problems," *Essays and Studies in Commemoration of the 40th Anniversary of the Founding of Hiroshima University of Economics,* Hiroshima University Economics, pp. 771–794, 2007, (in Japanese).

[24] K. Niwa, T. Hayashida and M. Sakawa, "Multiobjective Two-Level Integer Programming through Genetic Algorithms," *Joint 5th International Conference on Soft Computing and Intelligent Systems and 11th International Symposium on Advanced Intelligent Systems Conference Proceedings,* pp. 1038–1043, 2010.

[25] K. Niwa, T. Hayashida, M. Sakawa and Y. Yang, "Decentralized Two-Level 0-1 Programming through Distributed Genetic Algorithms," *Lecture Notes in Engineering and Computer Science: Proceedings of The International MultiConference of Engineers and Computer Scientists 2010,* Vol. 3, pp. 2163–2168, 2010.

[26] K. Niwa, T. Hayashida and M. Sakawa, "Computational Methods for Two-Level 0-1 Programming Problems through Distributed Genetic Algorithms," *Journal of Telecommunications and Information Technology,* Vol. 2, pp. 78–87, 2010.

[27] K. Niwa, I. Nishizaki and M. Sakawa, "Decentralized two-level 0-1 programming through genetic algorithms with double strings," in: L.C. Jain and R.K. Jain (eds.), *In proceedings of Second International Conference on Knowledge-Based Intelligent Electronic Systems,* Vol. 2, pp. 278–283, 1998.

[28] K. Niwa, I. Nishizaki and M. Sakawa, "Computational methods for decentralized two-level zero-one programming problems through genetic algorithms," *Proceedings of the Eighth International Fuzzy Systems Association World Congress,* Vol. 2, pp. 986–990, 1999.

[29] K. Niwa, I. Nishizaki and M. Sakawa, "Multiobjective two-level zero-one programming problems through genetic algorithms," *Proceedings of the Second Asia-Pacific Conference on Industrial Engineering and Management Systems,* pp. 493–496, 1999.

[30] K. Niwa, I. Nishizaki and M. Sakawa, "Two-Level 0-1 Programming Using Genetic Algorithms and a Sharing Scheme Based on Cluster Analysis," *International MultiConference of Engineers and Computer Scientists 2008 Proceedings,* pp. 1931–1936, 2008.

[31] K. Niwa, I. Nishizaki and M. Sakawa, "Two-Level 0-1 Programming through Parallel Genetic Algorithms," *International MultiConference of Engineers and Computer Scientists 2009 Proceedings,* Vol. 2, pp. 2000–2005, 2009.

[32] M. Sakawa, K. Kato, H. Sunada and T. Shibano, "Fuzzy programming for multiobjective 0-1 programming problems through revised genetic algorithms," *European Journal of Operational Research,* Vol. 8, pp. 149–158, 1997.

[33] M. Sakawa and K. Kato, "Integer Programming through Genetic Algorithms with Double Strings Based on Reference Solution Updating," IECON-2000, pp. 2744-2749, 2000.

[34] M. Sakawa, M. Tanaka, *Genetic Algorithms*, Asakura Publishing, 1995, (in Japanese).

[35] K. Niwa, I. Nishizaki and M. Sakawa, "Multiobjective two-level zero-one programming problems through genetic algorithms," *Proceedings of the Second Asia-Pacific Conference on Industrial Engineering and Management Systems,* pp. 493–496, 1999.

[36] J.D. Schaffer, "Multiple objective optimization with vector evaluated genetic algorithms," *Proceedings of the Ist International Conference on Genetic Algorithms and Their Applications,* Lawrence Erlbaum Associates Publishers, New Jersey, pp. 93-100, 1985.

[37] M. Simaan and J.B. IR. Cruz, "On the Stackelberg strategy in nonzero-sum games," *Journal of Optimization Theory and Applications,* Vol. 11, pp. 533–555, 1973.

[38] N. Srinivas and K. Deb, "Multi-objective optimization using non-dominated sorting genetic algorithms," *Evolutionary Computation,* Vol.2, No.3, pp. 221–248, 1994.

[39] H. Tamaki, M. Mori and M. Araki, "Generation of a set of Pareto-optimal solutions by genetic algorithms," *Transactions of the Society of Instrument and Control Engineers,* Vol. 31, pp. 1185–1192, 1995 (in Japanese).

[40] W.P. Wen, and Y.H. Yang: "Algorithms for solving the mixed integer two-level linear programming problem," *Computers and Operations Research,* Vol. 17, pp. 133–142, 1990.

[41] E. Zitzler, K. Deb and L. Thiele, "Comparison of multiobjective evolutionary algorithms: Empirical Results," *Evolutionary Computation,* Vol. 8, No. 2, pp. 173–195, 2000.

[42] E. Zitzler, M. Laumanns and L. Thiele: SPEA2: "Improving the strength Pareto evolutionary algorithm for multiobjective optimization," *Evolutionary Methods for Design Optimization and Control,* pp. 95–100, 2002.

[43] E. Zitzler and L. Thiele, "Multiobjective evolutionary algorithms: A comparative case study and the strength Pareto approach," *IEEE Transactions on Evolutionary Computation,* Vol. 3, No. 4, pp. 257–271, 1999.

2011 IEEE International Conference on Fuzzy Systems
June 27-30, 2011, Taipei, Taiwan

Optimal Static Output Feedback Control of Fuzzy-Model-Based Control Systems

Wen-Hsien Ho
Department of Medical Information Management
Kaohsiung Medical University
Kaohsiung, Taiwan
whho@kmu.edu.tw

Shinn-Horng Chen
Department of Mechanical Engineering
National Kaohsiung University of Applied Sciences
Kaohsiung, Taiwan
shchen@cc.kuas.edu.tw

Jyh-Horng Chou and Chun-Chin Shu
Institute of System Information and Control
National Kaohsiung First University of Science and Technology
Kaohsiung, Taiwan
choujh@nkfust.edu.tw

***Abstract*—By integrating the stabilizability condition, the orthogonal-functions approach (OFA), and the hybrid Taguchi-genetic algorithm (HTGA), an integrative method is presented in this paper to design the stable and quadratic-optimal static output feedback parallel-distributed-compensation (PDC) controller such that (i) the Takagi-Sugeno (TS) fuzzy-model-based control system can be stabilized, and (ii) a quadratic integral performance index for the TS-fuzzy-model-based control system can be minimized. In this paper, the stabilizability condition is proposed in terms of linear matrix inequalities (LMIs). A design example of stable and quadratic-optimal static output feedback PDC controller for a nonlinear inverted pendulum system controlled by a separately excited direct-current (DC) motor is given to demonstrate the applicability of the proposed new integrative approach.**

Keywords-static output feedback PDC controller; Takagi-Sugeno fuzzy model; orthogonal-functions approach; hybrid Taguchi-genetic algorithm; linear matrix inequalities

I. INTRODUCTION

Recently, it has been shown that the fuzzy-model-based representation proposed by Takagi and Sugeno [1], known as the TS fuzzy model, is a successful approach for dealing with the nonlinear control systems, and there are many successful applications of the TS-fuzzy-model-based approach to the nonlinear control systems [2].

Despite the success of applying the TS-fuzzy-model-based approach to the nonlinear control systems, it has become evident that many research issues remain to be addressed. In fact, in many cases it is very difficult, if not impossible, to obtain a full order output feedback controller of a nonlinear control system. This is due to the unaccessible measurement or the expensive measure. Therefore, recently, some researches [3]-[5] have proposed the linear-matrix-inequality-based (LMI-based) approach to design the static output feedback parallel-distributed-compensation (PDC) controllers for the TS-fuzzy-model-based control systems. Therefore, summing up the above statements and reasons, we can see that it is worth while to present an efficiently numerical optimization approach accompanied with the stabilizability condition to design the stable and quadratic-optimal static output feedback PDC controllers for the TS-fuzzy-model-based control systems, where the performance index subject to the constraint of stabilizability is considered to be directly minimized.

The purpose of this paper is to propose a numerical optimization method accompanied with the stabilizability condition to design the stable and quadratic-optimal static output feedback PDC controllers for the optimal control problem of the TS-fuzzy-model-based control systems by integrating the OFA, the hybrid Taguchi-genetic algorithm (HTGA) and the LMI technique, where the LMI technique is used to derive the stabilizability condition for ensuring that the closed-loop TS-fuzzy-model-based control systems can be stabilized. An illustrative example is also given in this paper to demonstrate the applicability of the proposed new integrative method.

II. PROBLEM STATEMENT

The TS-fuzzy-model-based control system for the nonlinear control system can be obtained as the following form:

$$\widetilde{R}^i: \text{IF } z_1(t) \text{ is } M_{i1} \text{ and } \ldots \text{ and } z_g(t) \text{ is } M_{ig},$$
$$\text{THEN } \begin{cases} \dot{x}(t) = A_i x(t) + B_i u(t), \\ y(t) = C_i x(t), \end{cases} \tag{1}$$

with the initial state vector $x(0)$, where $\widetilde{R}^i \ \ (i = 1, 2, \ldots, N)$ denotes the i-th implication, N is the number of fuzzy rules, $x(t) = [x_1(t), x_2(t), \ldots, x_n(t)]^{\mathrm{T}}$ denotes the n-dimensional state vector, $y(t) = [y_1(t), y_2(t), \ldots, y_r(t)]^{\mathrm{T}}$ denotes the r-dimensional output vector, $u(t) = [u_1(t), u_2(t), \ldots, u_p(t)]^{\mathrm{T}}$ denotes the p-dimensional input vector, $z_i(t) \ \ (i = 1, 2, \ldots, g)$ are the premise variables, A_i, B_i and $C_i \ \ (i = 1, 2, \ldots, N)$ are, respectively, the $n \times n$, $n \times p$ and $r \times n$ consequent constant matrices, and M_{ij} $(i = 1, 2, \ldots, N$ and $j = 1, 2, \ldots, g)$ are the fuzzy sets.

The resulting TS-fuzzy-model-based dynamic system inferred from (1) is represented as

$$\dot{x}(t) = \sum_{i=1}^{N} h_i(z(t))(A_i x(t) + B_i u(t)), \tag{2a}$$

$$y(t)=\sum_{i=1}^{N}h_i(z(t))C_i x(t), \tag{2b}$$

in which $z(t)=[z_1(t), z_2(t),\ldots, z_g(t)]^{\mathrm{T}}$ denotes the g-dimensional premise vector, $h_i(z(t))=w_i(z(t))\Big/\sum_{i=1}^{N}w_i(z(t))$, $w_i(z(t))=\prod_{j=1}^{g}M_{ij}(z_j(t))$, and $M_{ij}(z_j(t))$ are the grades of membership of $z_j(t)$ in the fuzzy sets M_{ij} $(i=1, 2,\ldots, N$ and $j=1, 2,\ldots, g)$. It can be seen that, for all t, $h_i(z(t))\ge 0$ and $\sum_{i=1}^{N}h_i(z(t))=1$.

The given dynamic system can be stabilized by the following static output feedback PDC controller:

$$\begin{aligned}u(t)&=-\sum_{i=1}^{N}h_i(z(t))F_i y(t)\\&=-\sum_{i=1}^{N}\sum_{j=1}^{N}h_i(z(t))h_j(z(t))F_i C_j x(t),\end{aligned} \tag{3}$$

where F_i $(i=1, 2,\ldots, N)$ denote the $p\times r$ local static output feedback gain matrices.

By substituting (3) into (2a), we can get the closed-loop TS-fuzzy-model-based dynamic system as

$$\dot{x}(t)=\sum_{i=1}^{N}\sum_{j=1}^{N}\sum_{k=1}^{N}h_i(z(t))h_j(z(t))h_k(z(t))(A_i-B_iF_jC_k)x(t). \tag{4}$$

In what follows, we present an LMI-based stabilizability criterion to analyze whether the closed-loop TS-fuzzy-model-based dynamic system in (4) can be stabilized by the static output feedback PDC controller or not, where the local static output feedback gain matrices F_j have been specified in advance.

Theorem:

The closed-loop TS-fuzzy-model-based dynamic system in (4) is stable, if, for the specified local static output feedback gains matrices F_j $(j=1, 2,\ldots, N)$ in (3), there exist a symmetric positive definite matrix P and the symmetric positive semidefinite matrices Q_k $(k=1, 2,\ldots, N)$ such that the following LMIs are simultaneously satisfied:

$$G_{kii}^{\mathrm{T}}P+PG_{kii}+(\bar{s}-1)Q_k<0, \tag{5a}$$

and

$$\left(\frac{G_{kij}+G_{kji}}{2}\right)^{\mathrm{T}}P+P\left(\frac{G_{kij}+G_{kji}}{2}\right)-Q_k\le 0, \tag{5b}$$

where $G_{ijk}=A_i-B_iF_jC_k$, $i<j$, $\bar{s}>1$, and $i, j, k=1, 2,\ldots, N$.

Proof: Here we omit it due to space limitation.

The problem considered in this paper is how to specify the local static output feedback gain matrices F_i $(i=1, 2,\ldots, N)$ of the static output feedback PDC controller in (3) such that the constraint of LMI-based stabilizability condition in (5) for the closed-loop TS-fuzzy-model-based dynamic system in (4) can be satisfied, and such that the optimal control performance for the TS-fuzzy-model-based dynamic system in (2) can be achieved by minimizing the following quadratic integral performance index:

$$\begin{aligned}J&=\int_0^{qt_f}\left[y^{\mathrm{T}}(t)Qy(t)+u^{\mathrm{T}}(t)Ru(t)\right]dt\\&=\sum_{k=0}^{q-1}\int_{kt_f}^{(k+1)t_f}\left[y^{\mathrm{T}}(t)Qy(t)+u^{\mathrm{T}}(t)Ru(t)\right]dt,\end{aligned} \tag{6}$$

where t_f denotes a small time interval which is chosen for the independent variable t, q is a positive integer specified by the designer, Q is a symmetric positive-semidefinite matrix, and R is a symmetric positive-definite matrix.

III. Stable and Quadratic-Optimal Static Output Feedback PDC Controllers Design

Here, consider the time interval $kt_f\le t\le(k+1)t_f$, where t_f is chosen for the independent variable t, and let us define

$$t=kt_f+\eta, \tag{7}$$

and

$$x_k=x(kt_f), \tag{8}$$

in which $k=0, 1, 2,\ldots, q-1$, and $0\le\eta\le t_f$.

The state vector $x(t)$, within $kt_f\le t\le(k+1)t_f$, can be approximated by the truncated orthogonal-functions (OF) representation as

$$x(t)=\sum_{s=0}^{m-1}x_s^{(k)}T_s(t)=\tilde{x}^{(k)}T(t), \tag{9}$$

where m is the number of terms required for the OF, $T(t)=[T_0(t), T_1(t),\ldots, T_{m-1}(t)]^{\mathrm{T}}$ denotes the $m\times 1$ OF basis vector, $T_i(t)$ $(i=0, 1,\ldots, m-1)$ denote the OF, $x_s^{(k)}$ $(s=0, 1,\ldots, m-1)$ are the $n\times 1$ coefficient vector, and $\tilde{x}^{(k)}=[x_0^{(k)}, x_1^{(k)},\ldots, x_{m-1}^{(k)}]$ is the $n\times m$ coefficient matrix of $x(t)$.

Substituting (3) and the truncated OF representation of $x(t)$ in (9) into the quadratic integral performance index in (6), the quadratic integral performance index J becomes the following algebraic form:

$$\begin{aligned}J=\sum_{k=0}^{q-1}\mathrm{trace}\Bigg[&W(\tilde{x}^{(k)})^{\mathrm{T}}\Bigg(\sum_{i=1}^{N}\sum_{j=1}^{N}\sum_{l=1}^{N}\sum_{o=1}^{N}h_i(z_k)h_j(z_k)h_l(z_k)h_o(z_k)\\&C_i^{\mathrm{T}}(Q+F_j^{\mathrm{T}}RF_l)C_o(\tilde{x}^{(k)})\Bigg)\Bigg],\end{aligned} \tag{10}$$

where the constant matrix W is the product-integration-matrix of two OF basis vectors [6].

Since, before the consequent output can be inferred within the small time interval $kt_f\le t\le(k+1)t_f$, the degree of fulfillment of the antecedent must be computed in advance, so, as the works given by Ho and Chou [7], we can let the value of $h_i(z(t))$, within $kt_f\le t\le(k+1)t_f$, be $h_i(z(kt_f))$. Then, integrating (2a) from $t=kt_f$ to $t=t$ within $kt_f\le t\le(k+1)t_f$, we obtain

$$x(t)-x(kt_f)=\sum_{i=1}^{N}h_i(z_k)\left[A_i\int_{kt_f}^{t}x(t)dt+B_i\int_{kt_f}^{t}u(t)dt\right], \quad (11)$$

where $h_i(z_k)=h_i(z(kt_f))$ and $k=0,\ 1,\ 2,\ldots,\ q-1$.

Using the following integral property of the OF:

$$\int_{kt_f}^{t}T(t)dt=HT(t), \quad (12)$$

and applying (3), (8) and (9), equation (11) can be cast into the form

$$\begin{aligned}&\tilde{x}^{(k)}-[x_k,\ 0,\ 0,\ldots,\ 0]\\&=\sum_{i=1}^{N}\sum_{j=1}^{N}\sum_{l=1}^{N}h_i(z_k)h_j(z_k)h_l(z_k)(A_i-B_iF_jC_l)\tilde{x}^{(k)}H,\end{aligned} \quad (13)$$

in which H is the operational matrix of integration for the OF [7].

Equation (13) can be rewritten as

$$\tilde{x}^{(k)}-\sum_{i=1}^{N}\sum_{j=1}^{N}\sum_{l=1}^{N}h_i(z_k)h_j(z_k)h_l(z_k)(A_i-B_iF_jC_l)\tilde{x}^{(k)}H=\tilde{Q}^{(k)}, \quad (14)$$

where $\tilde{Q}^{(k)}=[x_k,\ 0,\ 0,\ldots,\ 0]$ is an $n\times m$ matrix.

Making use of the Kronecker product, the explicit form for the coefficient matrix $\tilde{x}^{(k)}$ comes directly from (14) as

$$\begin{aligned}\hat{x}^{(k)}=\Bigg[I_{mn}-\sum_{i=1}^{N}\sum_{j=1}^{N}\sum_{l=1}^{N}h_i(z_k)h_j(z_k)h_l(z_k)\\(H^{\mathrm{T}}\otimes(A_i-B_iF_jC_l))\Bigg]^{-1}\hat{Q}^{(k)},\end{aligned} \quad (15)$$

where I_{mn} denotes the $mn\times mn$ identity matrix, $\hat{x}^{(k)}=\left[x_0^{(k)\mathrm{T}},\ x_1^{(k)\mathrm{T}},\ldots,\ x_{m-1}^{(k)\mathrm{T}}\right]^{\mathrm{T}}$, $\hat{Q}^{(k)}=[x_k^{\mathrm{T}},\ 0^{\mathrm{T}},\ 0^{\mathrm{T}},\ldots,\ 0^{\mathrm{T}}]^{\mathrm{T}}$, and $\otimes$ denotes the Kronecker product [8]. This implies that $\tilde{x}^{(k)}$ can be obtained from (15).

The value of the performance index of algebraic form in (10) is actually dependent on the set of local static output feedback gain matrices $\{F_1, F_2,\ldots, F_N\}$, which means

$$J=G(f_{111},\ f_{112},\ldots,\ f_{Npr}), \quad (16)$$

where f_{ijk} $(i=1,2,\ldots,N,\quad j=1,2,\ldots,p$ and $k=1,2,\ldots,r)$ denote the elements of the local static output feedback gain matrices F_i. This is equivalent to the static constrained-optimization problem in the following:

$$\text{minimize } J=G(f_{111},\ f_{112},\ldots,\ f_{Npr}) \quad (17)$$

subject to $|f_{ijk}|\le C_{ijk}$, and subject to the constraint that there exist a symmetric positive definite matrix P and the symmetric positive semidefinite matrices Q_k $(k=1,2,\ldots,N)$ to make the LMIs in (5) hold, for $i=1,2,\ldots,N,\quad j=1,2,\ldots,p$ and $k=1,2,\ldots,r$, where C_{ijk} are the positive real numbers given from the practical consideration, respectively. Then, the HTGA [9] can be employed to search for the optimal solution of the static constrained-optimization problem in (17).

IV. Illustrative Example

A nonlinear inverted pendulum system controlled by a separately excited direct-current (DC) motor [10] is considered in this example as

$$\begin{bmatrix}\dot{x}_1(t)\\\dot{x}_2(t)\\\dot{x}_3(t)\end{bmatrix}=\begin{bmatrix}x_2(t)\\K_1\sin x_1(t)+K_2x_3(t)\\K_3x_2(t)+K_4x_3(t)\end{bmatrix}+\begin{bmatrix}0\\0\\K_5\end{bmatrix}u(t), \quad (18)$$

where $x_1(t)\in[-\pi,\pi]$ is the angle of the pendulum, $x_2(t)=\dot{x}_1(t)$ is the angular velocity, $x_3(t)$ is the current of the motor, $u(t)$ denotes the control input voltage, $K_1=9.8$ $(1/\sec^2)$, $K_2=1$ $(1/\mathrm{A}\cdot\sec^2)$, $K_3=-10$ $(\mathrm{V}\cdot\sec/\mathrm{rad}\cdot\mathrm{mH})$, $K_4=-10$ (Ω/mH), and $K_5=10$ $(1/\mathrm{mH})$. The TS-fuzzy-model-based dynamic system for (18) can be obtained as following:

$$\tilde{R}^1:\ \text{IF } z_1(t) \text{ is } M_{11},\ \text{THEN } \begin{cases}\dot{x}(t)=A_1x(t)+B_1u(t),\\y(t)=C_1x(t),\end{cases} \quad (19a)$$

$$\tilde{R}^2:\ \text{IF } z_1(t) \text{ is } M_{21},\ \text{THEN } \begin{cases}\dot{x}(t)=A_2x(t)+B_2u(t),\\y(t)=C_2x(t),\end{cases} \quad (19b)$$

where

$z_1(t)=\sin x_1(t)/x_1(t)$, $x(t)=[x_1(t),\ x_2(t),\ x_3(t)]^{\mathrm{T}}$,

$x(0)=[\pi/6,\ 0,\ 0]^{\mathrm{T}}$, $x_1(t)\in[-\pi,\pi]$, $A_1(t)=\begin{bmatrix}0&1&0\\9.8&0&1\\0&-10&-10\end{bmatrix}$,

$A_2(t)=\begin{bmatrix}0&1&0\\0&0&1\\0&-10&-10\end{bmatrix}$, $B_1(t)=B_2(t)=[0,\ 0,\ 10]^{\mathrm{T}}$,

$C_1=C_2=\begin{bmatrix}1&0&0\\0&1&0\end{bmatrix}$ denote the feedback of the angle and angular velocity of the pendulum, simultaneously, $M_{11}(z_1(t))=\begin{cases}z_1(t), & x_1(t)\ne 0,\\1, & \text{otherwise},\end{cases}$ and $M_{21}(z_1(t))=1-M_{11}(z_1(t))$.

The quadratic integral performance index is

$$\begin{aligned}J&=\int_0^5[y^{\mathrm{T}}(t)Qy(t)+u^{\mathrm{T}}(t)Ru(t)]dt\\&=\sum_{k=0}^{q-1}\int_{kt_f}^{(k+1)t_f}[y^{\mathrm{T}}(t)Qy(t)+u^{\mathrm{T}}(t)Ru(t)]dt,\end{aligned} \quad (20)$$

where $q=500$, $t_f=0.01$, $Q=\mathrm{diag}\{1,\ 1\}$ and $R=1$.

By using the proposed integrative approach and the LMI toolbox [11], we can obtain a symmetric positive definite matrix P and the symmetric positive semidefinite matrix Q_1 and Q_2, respectively, as

$$P=\begin{bmatrix}167.7466&7.3397&0.7956\\7.3397&6.4890&0.1333\\0.7956&0.1333&0.0294\end{bmatrix},$$

$$Q_1=\begin{bmatrix}6.6895&0.5061&0.5553\\0.5061&12.5640&0.2238\\0.5553&0.2238&0.0690\end{bmatrix}$$

and

$$Q_2 = \begin{bmatrix} 59.2127 & 18.7103 & 0.5746 \\ 18.7103 & 13.1713 & 0.0558 \\ 0.5746 & 0.0558 & 0.0463 \end{bmatrix}.$$

The responses of the angle of the pendulum $x_1(t)$, and the angular velocity $x_2(t)$ for a nonlinear inverted pendulum system controlled by a separately excited DC motor system with the designed stable and quadratic-optimal static output feedback PDC controller obtained by using the proposed integrative approach are, respectively, shown in Figures 1 and 2. It can be seen that the proposed approach can have the satisfactory control results.

V. CONCLUSIONS

Based on the OFA, an algorithm has been presented in this paper for solving the TS-fuzzy-model-based feedback dynamic equations. Then, the presented algebraic algorithm is integrated with the HTGA to design the stable and quadratic-optimal static output feedback PDC controllers of the TS-fuzzy-model-based control systems such that the control objective of directly minimizing a quadratic integral performance index subject to the constraint of LMI-based stabilizability condition can be achieved, where the quadratic integral performance index is also converted into the algebraic form by using the OFA. The illustrative example regarding the nonlinear inverted pendulum system controlled by a separately excited DC motor has shown that the proposed approach is effective for designing the stable and quadratic optimal static output feedback PDC controllers of the TS-fuzzy-model-based control systems.

ACKNOWLEDGMENT

This work was in part supported by the National Science Council, Taiwan, Republic of China, under grant numbers NSC 99-2221-E327-043-MY3 and NSC 98-2221-E-037-006.

REFERENCES

[1] T. Takagi, and M. Sugeno, "Fuzzy identification of systems and its applications to modeling and control," IEEE Trans. on Systems, Man and Cybernetics, vol. 15, pp. 116-132, 1985.

[2] K. Tanaka and H. O. Wang, Fuzzy Control Systems Design and Analysis: A Linear Matrix Inequality Approach. New York: John Wiley and Sons, 2001.

[3] C. H. Fang, Y. S. Liu, S. W. Kan, L. Hong, and C. H. Lee, "A new LMI-based approach to relaxed quadratic stabilization of T-S fuzzy control systems," IEEE Tran. on Fuzzy Systems, vol. 14, pp. 386-397, 2006.

[4] H. Y. Chung, S. M. Wu, F. M. Yu, and W. J. Chang, "Evolutionary design of static output feedback controller for Takagi-Sugeno fuzzy systems," IET Control Theory and Applications, vol. 1, pp. 1096-1103, 2007.

[5] D. Huang and S. K. Nguang, "Static output feedback controller design for fuzzy systems: an LMI approach," Information Sciences, vol. 177, pp. 3005-3015, 2007.

[6] W. H. Ho and J. H. Chou, "Design of optimal controller for Takagi-Sugeno fuzzy model based systems," IEEE Trans. on Systems, Man and Cybernetics, Part A, vol. 37, pp. 329-339, 2007.

[7] W. H. Ho and J. H. Chou, "Solutions of Takagi-Sugeno fuzzy-model-based dynamic equations via orthogonal functions," IEICE Trans. on Fundamentals of Electronics, Communications and Computer Sciences, vol. E87-A, pp. 3439-3442, 2004.

[8] S. Barnett, Matrix Methods for Engineers and Scientists. New York: McGraw-Hill, 1979.

[9] J. T. Tsai, T. K. Liu, and J. H. Chou, "Hybrid Taguchi-genetic algorithm for global numerical optimization," IEEE Trans. on Evolutionary Computation, vol. 8, pp.365-377, 2004.

[10] K. Tanaka, T. Ikeda, and H. O. Wang, "Fuzzy regulators and fuzzy observers: relaxed stability conditions and LMI-based designs," IEEE Trans. on Fuzzy Systems, vol. 6, pp. 250-265, 1998.

[11] P. Gahinet, A. Nemirovski, A. J. Laub, and M. Chilali, LMI Control Toolbox. Massachusetts: The Math Works Inc, 1995.

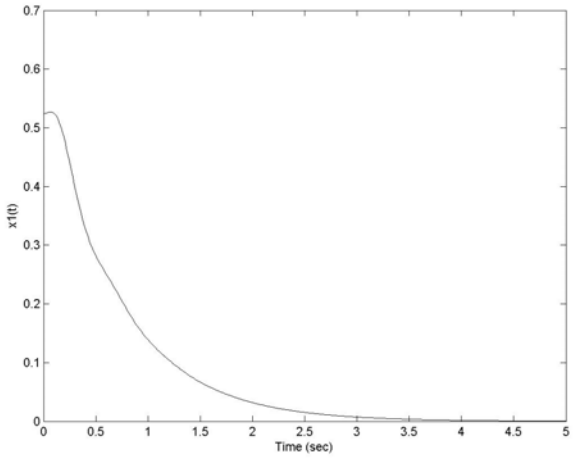

Figure 1. Response of the angle of the pendulum $x_1(t)$ for the nonlinear inverted pendulum system controlled by a separately excited DC motor.

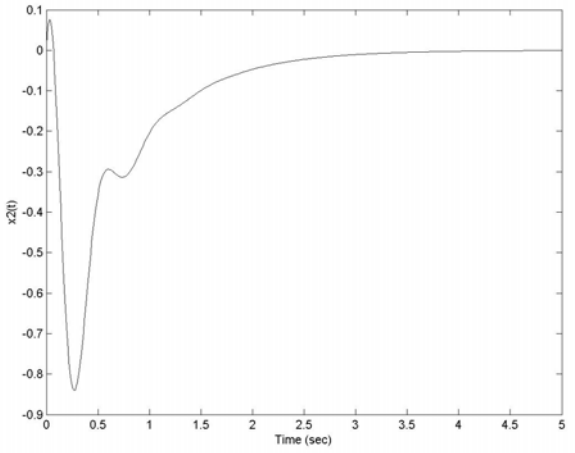

Figure 2. Response of the angular velocity $x_2(t)$ for the nonlinear inverted pendulum system controlled by a separately excited DC motor.

2011 IEEE International Conference on Fuzzy Systems
June 27-30, 2011, Taipei, Taiwan

An Interactive Satisficing Method for Multiobjective Random Fuzzy Programming Problems through the Possibility-Based Probability Model

Hideki Katagiri
Graduate School of Engineering
Hiroshima University
1-4-1 Kagamiyama, Higashi-Hiroshima, 739-8527 Japan
Email: katagiri-h@hiroshima-u.ac.jp

Masatoshi Sakawa
Graduate School of Engineering
Hiroshima University
1-4-1 Kagamiyama, Higashi-Hiroshima, 739-8527 Japan
Email: sakawa@hiroshima-u.ac.jp

Takeshi Matsui
Graduate School of Engineering
Hiroshima University
1-4-1 Kagamiyama, Higashi-Hiroshima, 739-8527 Japan
Email: tak-matsui@hiroshima-u.ac.jp

***Abstract*—This paper considers multiobjective linear programming problems where each coefficient of the objective functions is expressed by a random fuzzy variable. A new decision making model is proposed in order to maximize both of possibility and probability with respect to the objective function values. An interactive algorithm is constructed to obtain a satisficing solution for a decision maker from among a set of Pareto optimal solutions.**

***Index Terms*—random fuzzy variable; multiobjective programming; interactive algorithm; possibility measure; probability maximization**

I. Introduction

In the real-world, we are often faced with decision making problems under uncertainty. Recently, many researchers focus on mathematical programming problems including not only randomness but fuzziness. One of mathematical concepts dealing with both fuzziness and randomness is a *fuzzy random variable* [1], [2], and its applications are discussed [3], [4], [5], [6], [7], [8].

On the other hand, very recently, a random fuzzy variable [11] draws attention as a new tool for decision making under uncertainty. For example, parameters such as mean and variance of random variables may not be estimated as constants. In this case, random variables with fuzzy mean are expressed as random fuzzy variables.

Some studies focus on applications of random fuzzy variable [9], [10], [11], [12], [13]. These previous studies discussed a single objective case. However, when considering the real-world decision making situation that there are several conflicting objective functions, it needs to tackle a multiobjective case under random fuzzy environments. Therefore, this article develops a new multiobjective random fuzzy programming model which obtains a satisficing solution from among a Pareto optimal solution for a decision maker.

II. Random fuzzy variable

In the framework of stochastic programming [14], [15], [16], it is implicitly assumed that the uncertain parameter which well represents the stochastic factor of real systems can be definitely expressed as a single random variable. However, from the expert's experimental point of view, the experts may think of a collection of random variables to be appropriate to express stochastic factors rather than only a single random variables. In this case, reflecting the expert's conviction degree that each of random variables properly represents the stochastic factor, it would be quite reasonable to assign the different degrees of possibility to each of random variables. For handling such an uncertain parameter, a random fuzzy variable was defined by [11] as a function from a possibility space to a collection of random variables, which is considered to be an extended concept of fuzzy variable [17]. Considering that the fuzzy variables can be viewed as another way of dealing with the imprecision which was originally represented by fuzzy sets, the random fuzzy variable can be defined as an extension of fuzzy sets using the concept of membership function, instead of fuzzy variables. In this paper, we define the random fuzzy variables along the fusion line of membership functions and random variables.

Definition 1 (Random fuzzy variable) *Let Γ be a collection of random variables. Then, a random fuzzy variable $\tilde{\bar{C}}$ is defined by its membership function*

$$\mu_{\tilde{\bar{C}}} : \Gamma \to [0, 1]. \tag{1}$$

In Definition 1, the membership function $\mu_{\tilde{\bar{C}}}$ assigns each random variable $\bar{\gamma} \in \Gamma$ to a real number $\mu_{\tilde{\bar{C}}}(\bar{\gamma})$. It should be noted here that if Γ is defined as $\mathbb{R}$, then (1) becomes equivalent to the membership function of an ordinary fuzzy set. In this sense, a random fuzzy variable can be regarded as

978-1-4244-7316-8/11/$26.00 ©2011 IEEE

an extended concept of fuzzy sets. On the other hand, if Γ is defined as a singleton $\Gamma = \{\bar{\gamma}\}$ and $\mu_{\bar{\tilde{C}}}(\bar{\gamma}) = 1$, then the corresponding random fuzzy variable $\bar{\tilde{C}}$ can be viewed as an ordinary random variable.

When taking account of the imprecise nature of the realized values of random variables, it would be appropriate to employ the concept of fuzzy random variables. However, it should be emphasized here that if mean and/or variance of random variables are specified by the expert as a set of real values or fuzzy sets, such uncertain parameters can be represented by not fuzzy random variables but random fuzzy variables.

As a simple example of random fuzzy variables, we consider a Gaussian random variable whose mean value is not definitely specified as a constant. For example, when some random parameter $\bar{\gamma}$ is represented by the Gaussian random variable $N(s_i, 10^2)$ where the expert identifies a set $\{s_1, s_2, s_3\}$ of possible mean values as $(s_1, s_2, s_3) = (90, 100, 110)$, if the membership function $\mu_{\bar{\tilde{C}}}$ is defined by

$$\mu_{\bar{\tilde{C}}}(\bar{\gamma}) = \begin{cases} 0.5 & \text{if } \bar{\gamma} \sim N(90, 10^2) \\ 0.7 & \text{if } \bar{\gamma} \sim N(100, 10^2) \\ 0.3 & \text{if } \bar{\gamma} \sim N(110, 10^2) \\ 0 & \text{otherwise,} \end{cases}$$

then $\bar{\tilde{C}}$ is a random fuzzy variable. More generally, when the mean values are expressed as fuzzy sets or fuzzy numbers, the corresponding random variable with the fuzzy mean is represented by a random fuzzy variable, as will be discussed in the following sections.

III. Problem formulation

Most of the real-world decision making problems usually involve multiple, noncommensurable, and conflicting objectives which should be considered simultaneously. In this paper, we consider the following multiobjective programming problem in which random fuzzy variables are involved in the objective functions:

$$\left.\begin{array}{ll} \text{minimize} & \bar{\tilde{\boldsymbol{C}}}_1\boldsymbol{x} \\ & \cdots \\ \text{minimize} & \bar{\tilde{\boldsymbol{C}}}_k\boldsymbol{x} \\ \text{subject to} & A\boldsymbol{x} \le \boldsymbol{b},\ \boldsymbol{x} \ge \boldsymbol{0}, \end{array}\right\} \tag{2}$$

where $\boldsymbol{x}$ is an n-dimensional decision variable column vector, A is an $m \times n$ matrix, $\boldsymbol{b}$ is an $m \times 1$ constant column vector, and $\bar{\tilde{\boldsymbol{C}}}_l = (\bar{\tilde{C}}_{l1}, \ldots, \bar{\tilde{C}}_{ln})$ is a random fuzzy variable coefficient vector. Here, assume that $\bar{\tilde{C}}_{lj}$ is a Gaussian random variable whose mean value is a fuzzy number $\tilde{M}_{lj}$ characterized by the membership function

$$\mu_{\tilde{M}_{lj}}(\tau) = \begin{cases} L\left(\dfrac{m_{lj} - \tau}{\alpha_{lj}}\right) & \text{if } m_{lj} \ge \tau \\ R\left(\dfrac{\tau - m_{lj}}{\beta_{lj}}\right) & \text{if } m_{lj} < \tau, \end{cases} \tag{3}$$

where L and R are nonincreasing continuous functions from $[0, \infty)$ to $[0, 1]$.

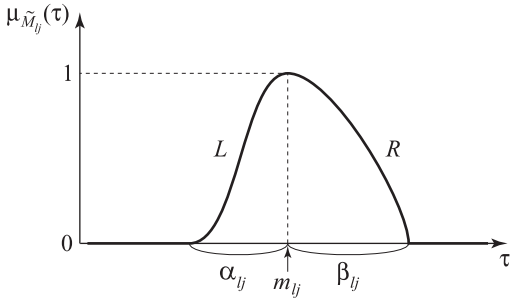

Fig. 1. Membership function $\mu_{\tilde{M}_{lj}}$.

Let Γ be a collection of all possible Gaussian random variables $N(s, \sigma^2)$ where $s \in (-\infty, \infty)$ and $\sigma^2 \in (0, \infty)$. Then, the membership function of $\bar{\tilde{C}}_{lj}$ is expressed as

$$\mu_{\bar{\tilde{C}}_{lj}}(\bar{\gamma}_{lj}) = \{\mu_{\tilde{M}_{lj}}(s_{lj}) | \bar{\gamma}_{lj} \sim N(s_{lj}, \sigma_{lj}^2)\},\ \forall \bar{\gamma}_{lj} \in \Gamma. \tag{4}$$

Using the Zadeh's extension principle, each objective function $\bar{\tilde{\boldsymbol{C}}}_l\boldsymbol{x}$ is expressed as a single random fuzzy variable characterized by the membership function

$$\mu_{\bar{\tilde{\boldsymbol{C}}}_l\boldsymbol{x}}(\bar{u}_l) \triangleq \sup_{\bar{\boldsymbol{\gamma}}_l} \left\{ \min_{1 \le j \le n} \mu_{\bar{\tilde{C}}_{lj}}(\bar{\gamma}_{lj}) \;\middle|\; \bar{u}_l = \sum_{j=1}^{n} \bar{\gamma}_{lj} x_j \right\},\ \forall \bar{u}_l \in \Gamma, \tag{5}$$

where $\bar{\boldsymbol{\gamma}}_l = (\bar{\gamma}_1, \ldots, \bar{\gamma}_n)$.

By substituting (4) into (5), the membership function of a random fuzzy variable corresponding to the objective function $\bar{\tilde{\boldsymbol{C}}}_l\boldsymbol{x}$ in (2) is rewritten as

$$\begin{aligned} & \mu_{\bar{\tilde{\boldsymbol{C}}}_l\boldsymbol{x}}(\bar{u}_l) \\ = & \sup_{\boldsymbol{s}_l} \left\{ \min_{1 \le j \le n} \mu_{\tilde{M}_{lj}}(s_{lj}) \;\middle|\; \bar{u}_l \sim N\Big(\sum_{j=1}^{n} s_{lj} x_j, \sum_{j=1}^{n} \sigma_{lj}^2 x_j^2 \Big) \right\}, \end{aligned} \tag{6}$$

where $\boldsymbol{s}_l = (s_{l1}, \ldots, s_{ln})$.

IV. Possibility-based probability model

Assuming that the DM concerns about the probability that each of the objective function values $\bar{\tilde{\boldsymbol{C}}}_l\boldsymbol{x}$ is smaller than or equal to a certain target values f_l, $l = 1, \ldots, k$, we introduce the probability $P\left(\omega \;\middle|\; \tilde{\boldsymbol{C}}_l(\omega)\boldsymbol{x} \le f_l\right)$ which is expressed as a fuzzy set $\tilde{P}_l$ with the membership function

$$\mu_{\tilde{P}_l}(p_l) = \sup_{\bar{u}_l} \left\{ \mu_{\bar{\tilde{\boldsymbol{C}}}_l\boldsymbol{x}}(\bar{u}_l) \;\middle|\; p_l = P\left(\omega \mid u_l(\omega) \le f_l\right) \right\}, \tag{7}$$

where f_l, $l = 1, \ldots, k$ are specified by the DM as constants. In order to consider the imprecise nature of the DM's judgments for the probability with respect to the lth objective function, we introduce the fuzzy goal $\tilde{G}_l$ with the nondecreasing continuous membership function $\mu_{\tilde{G}_l}$.

Recalling that the membership function $\mu_{\tilde{P}_l}(p_l)$ can be viewed as a possibility distribution on the basis of the concept of possibility measure [18], [19], the degree of possibility that

the fuzzy goal $\tilde{G}_l$ for the probability $\tilde{P}_l$ is satisfied is expressed by

$$\Pi_{\tilde{P}_l}(\tilde{G}_l) \triangleq \sup_{p_l} \min\{\mu_{\tilde{P}_l}(p_l),\ \mu_{\tilde{G}_l}(p_l)\}. \tag{8}$$

Then, we consider the possibility-based probability model for multiobjective random fuzzy programming problems formulated as

$$\left.\begin{array}{ll} \text{maximize} & \Pi_{\tilde{P}_1}(\tilde{G}_1) \\ & \cdots\cdots \\ \text{maximize} & \Pi_{\tilde{P}_k}(\tilde{G}_k) \\ \text{subject to} & A\boldsymbol{x} \le \boldsymbol{b},\ \boldsymbol{x} \ge \boldsymbol{0} \end{array}\right\} \tag{9}$$

or equivalently

$$\left.\begin{array}{ll} \text{maximize} & h_1 \\ & \vdots \\ \text{maximize} & h_k \\ \text{subject to} & \Pi_{\tilde{P}_l}(\tilde{G}_l) \ge h_l,\ 0 \le h_l \le 1,\ l = 1, \ldots, k \\ & A\boldsymbol{x} \le \boldsymbol{b},\ \boldsymbol{x} \ge \boldsymbol{0}. \end{array}\right\} \tag{10}$$

It should be noted here that (10) is regarded as a multiobjective decision making problem, and that there rarely exists a complete optimal solution that simultaneously optimizes all the objective functions. In this case, it is reasonable to find a Pareto optimal solution or a non-dominated solution.

V. Interactive satisficing method

By introducing an aggregation function $f_D(\boldsymbol{x}, \boldsymbol{h})$ for the k objective functions in (10), where $\boldsymbol{h} = (h_1, \ldots, h_k)$, the multiobjective programming problem (10) can be generally rewritten as

$$\left.\begin{array}{ll} \text{maximize} & f_D(\boldsymbol{x}, \boldsymbol{h}) \\ \text{subject to} & (\boldsymbol{x}, \boldsymbol{h}) \in X, \end{array}\right\} \tag{11}$$

where X is a feasible solution of (10).

The most crucial problem in (11) is probably the identification of an appropriate aggregation function which well represents the DM's preference. If $f_D(\boldsymbol{x}, \boldsymbol{h})$ can be explicitly identified, then (11) can be reduced to a standard mathematical programming problem, and the corresponding optimal solution is regarded as a Pareto optimal solution which is most desirable for the decision maker. However, the success in identifying such an aggregation function rarely happens, and then as an alternative way, it is recommended for the DM to examine multiple possible solutions in the set of Pareto optimal solutions through an interactive solution procedure to find a satisficing solution to (11).

In such an interactive satisficing method, to generate a candidate for a satisficing solution which is also Pareto optimal, the DM is asked to specify the aspiration levels of achievement for all the objective function values, called the reference levels.

For the DM's reference levels $\hat{h}_l$, $l = 1, \ldots, k$, the corresponding Pareto optimal solution, which is the nearest to the vector of the given reference levels in the minimax sense or better than it if the reference levels are attainable, is obtained by solving the minimax problem

$$\left.\begin{array}{ll} \text{minimize} & \max\limits_{l=1,\ldots,k} \left\{\hat{h}_l - h_l\right\} \\ \text{subject to} & \Pi_{\tilde{P}_l}(\tilde{G}_l) \ge h_l,\ l = 1, \ldots, k \\ & A\boldsymbol{x} \le \boldsymbol{b},\ \boldsymbol{x} \ge \boldsymbol{0}. \end{array}\right\} \tag{12}$$

Here, it should be stressed that if an optimal solution $(\boldsymbol{x}^*, \boldsymbol{h}^*)$ to (12) is not unique, then Pareto optimality of $\boldsymbol{x}^*$ is not guaranteed, and just weak Pareto optimality is assured. To obtain a Pareto optimal solution in a strict sense, we consider the augmented minimax problem

$$\left.\begin{array}{ll} \text{minimize} & \max\limits_{l=1,\ldots,k} \left\{\hat{h}_l - h_l + \rho \sum\limits_{l=1}^{k} (\hat{h}_l - h_l)\right\} \\ \text{subject to} & \Pi_{\tilde{P}_l}(\tilde{G}_l) \ge h_l,\ l = 1, \ldots, k \\ & A\boldsymbol{x} \le \boldsymbol{b},\ \boldsymbol{x} \ge \boldsymbol{0}, \end{array}\right\} \tag{13}$$

where ρ is a sufficiently small positive number.

From (8), the constraint $\Pi_{\tilde{P}_l}(\tilde{G}_l) \ge h_l$ in (13) is equivalently replaced by the condition that there exists a p_l such that $\mu_{\tilde{P}_l}(p_l) \ge h_l$ and $\mu_{\tilde{G}_l}(p_l) \ge h_l$, namely,

$$\sup_{\boldsymbol{s}_l} \min_{1 \le j \le n} \left\{ \mu_{\tilde{M}_{lj}}(s_{lj}) \;\middle|\; p_l = P\left(\omega \mid u_l(\omega) \le f_l\right), \right. \\ \left. \bar{u}_l \sim N\Big(\sum_{j=1}^{n} s_{lj} x_j, \sum_{j=1}^{n} \sigma_{lj}^2 x_j^2 \Big) \right\} \ge h_l \tag{14}$$

and $p_l \ge \mu^{\star}_{\tilde{G}_l}(h_l)$, where $\mu^{\star}_{\tilde{G}_l}(h_l)$ is a pseudo inverse function defined as $\mu^{\star}_{\tilde{G}_l}(h_l) = \sup\{p_l \mid \mu_{\tilde{G}_l}(p_l) \ge h_l\}$. This implies that there exists a vector $(p_l, \boldsymbol{s}_l, \bar{u}_l)$ such that

$$\min_{1 \le j \le n} \mu_{\tilde{M}_{lj}}(s_{lj}) \ge h_l,\ \bar{u}_l \sim N\left(\sum_{j=1}^{n} s_{lj} x_j, \sum_{j=1}^{n} \sigma_{lj}^2 x_j^2 \right), \\ p_l = P\left(\omega \mid u_l(\omega) \le f\right),\ p_l \ge \mu^{\star}_{\tilde{G}_l}(h_l),$$

which can be equivalently transformed into the condition that there exists a vector $(\boldsymbol{s}_l, \bar{u}_l)$ such that

$$\left.\begin{array}{l} \mu_{\tilde{M}_{lj}}(s_{lj}) \ge h_l,\ j = 1, \ldots, n, \\ \bar{u}_l \sim N\left(\sum\limits_{j=1}^{n} s_{lj} x_j, \sum\limits_{j=1}^{n} \sigma_{lj}^2 x_j^2 \right), \\ P\left(\omega \mid u_l(\omega) \le f_l\right) \ge \mu^{\star}_{\tilde{G}_l}(h_l). \end{array}\right\} \tag{15}$$

In view of (3), it follows that

$$\mu_{\tilde{M}_{lj}}(s_{lj}) \ge h_l \Leftrightarrow s_{lj} \in [m_{lj} - L^{\star}(h_l)\alpha_{lj},\ m_{lj} + R^{\star}(h_l)\beta_{lj}],$$

where $L^{\star}(h_l)$ and $R^{\star}(h_l)$ are pseudo inverse functions defined as $L^{\star}(h_l) = \sup\{t \mid L(t) \ge h_l\}$ and $R^{\star}(h_l) = \sup\{t \mid R(t) \ge h_l\}$. Hence, (15) is rewritten as the equivalent condition that there exists a $\bar{u}$ such that

$$P\left(\omega \mid u_l(\omega) \le f_l\right) \ge \mu^{\star}_{\tilde{G}}(h_l), \\ \bar{u}_l \sim N\left(\sum_{j=1}^{n} \{m_{lj} - L^{\star}(h_l)\alpha_{lj}\} x_j, \sum_{j=1}^{n} \sigma_{lj}^2 x_j^2 \right).$$

Since $P(\omega \mid u_l(\omega) \leq f_l)$ is transformed into

$$P\left(\omega \;\middle|\; \frac{u_l(\omega) - \sum_{j=1}^{n}\{m_{lj} - L^\star(h_l)\alpha_{lj}\}x_j}{\sqrt{\sum_{j=1}^{n}\sigma_{lj}^2 x_j^2}} \leq \frac{f_l - \sum_{j=1}^{n}\{m_{lj} - L^\star(h_l)\alpha_{lj}\}x_j}{\sqrt{\sum_{j=1}^{n}\sigma_{lj}^2 x_j^2}}\right),$$

in consideration of

$$\frac{\bar{u}_l - \sum_{j=1}^{n}\{m_{lj} - L^\star(h_l)\alpha_{lj}\}x_j}{\sqrt{\sum_{j=1}^{n}\sigma_{lj}^2 x_j^2}} \sim N(0,1),$$

(16) is equivalently transformed as

$$\Phi\left(\frac{f_l - \sum_{j=1}^{n}\{m_{lj} - L^\star(h_l)\alpha_{lj}\}x_j}{\sqrt{\sum_{j=1}^{n}\sigma_{lj}^2 x_j^2}}\right) \geq \mu_{\tilde{G}_l}^\star(h_l), \qquad (16)$$

where Φ is a probability distribution function of the standard Gaussian random variable $N(0,1)$.

From the monotone increasingness of Φ, (16) is rewritten as

$$\sum_{j=1}^{n}\{m_j - L^\star(h_l)\alpha_{lj}\}x_j + \Phi^{-1}(\mu_{\tilde{G}_l}^\star(h_l))\sqrt{\sum_{j=1}^{n}\sigma_{lj}^2 x_j^2} \leq f, \qquad (17)$$

where Φ^{-1} is the inverse function of Φ.

From (14)$-$(17), it holds that

$$\Pi_{\tilde{P}_l}(\tilde{G}_l) \geq h \Leftrightarrow \sum_{j=1}^{n}\{m_{lj} - L^\star(h_l)\alpha_{lj}\}x_j + \Phi^{-1}(\mu_{\tilde{G}_l}^\star(h_l))\sqrt{\sum_{j=1}^{n}\sigma_{lj}^2 x_j^2} \leq f. \qquad (18)$$

Consequently, (13) is rewritten as

$$\left.\begin{array}{ll} \text{minimize} & \max\limits_{l=1,\ldots,k}\left\{\hat{h}_l - h_l + \rho\sum\limits_{l=1}^{k}(\hat{h}_l - h_l)\right\} \\ \text{subject to} & \sum\limits_{j=1}^{n}\{m_{lj} - L^\star(h_l)\alpha_{lj}\}x_j \\ & \quad + \Phi^{-1}(\mu_{\tilde{G}_l}^\star(h_l))\sqrt{\sum\limits_{j=1}^{n}\sigma_{lj}^2 x_j^2} \leq f_l,\ l = 1,\ldots,k \\ & A\boldsymbol{x} \leq \boldsymbol{b},\ \boldsymbol{x} \geq \boldsymbol{0}. \end{array}\right\} \qquad (19)$$

Observing that (19) is a nonconvex nonlinear programming problem, we can employ genetic algorithms such as GENOCOPIII [20] or the revised GENOCOPIII [21] in order to obtain an approximate solution.

Now we are ready to construct an interactive algorithm for deriving the satisficing solution for the DM from among the Pareto optimal solution set.

Interactive satisficing method for the possibility-based probability model

Step 1: Ask the DM to specify the membership functions $\mu_{\tilde{G}_l}$ and the target values f_l, $l = 1,\ldots,k$.

Step 2: Set the initial reference possibility levels at 1s, which can be viewed as the ideal values, i.e., $\hat{h}_l = 1,\ l = 1,\ldots,k$.

Step 3: For the current reference possibility levels $\hat{h}_l$, $l = 1,\ldots,k$, solve the augmented minimax problem (19).

Step 4: The DM is supplied with the corresponding Pareto optimal solution $\boldsymbol{x}^*$. If the DM is satisfied with the current objective function values $h_l^*,\ l = 1,\ldots,k$, then stop. Otherwise, ask the DM to update the reference possibility levels $\hat{h}_l,\ l = 1,\ldots,k$ by considering the current values of objective functions $h_l,\ l = 1,\ldots,k$, and return to step 3.

It should be noted for the DM that any improvement of one objective function value can be achieved only at the expense of at least one of the other objective function values for the fixed target values $f_l,\ l = 1,\ldots,k$.

VI. Conclusions

In this paper, we have considered multiobjective programming problems in which the coefficients of the objective functions are random fuzzy variables. Incorporating the concept of possibility measure into the stochastic programming models, we have proposed a possibility-based probability model for random fuzzy programming problems. It has been shown that the formulated problem based on the proposed model can be transformed into deterministic nonlinear programming problem. In order to obtain a satisficing solution for a decision maker from among a Pareto optimal solution set, we have constructed an interactive satisficing algorithm.

In the future, we will consider more general problems in which random fuzzy variables are involved not only in the objective function but also in the constraints. Furthermore,

extensions of the proposed models to integer problems will be discussed elsewhere.

REFERENCES

[1] H. Kwakernaak, "Fuzzy random variable-1," Information Sciences, vol. 15, pp. 1–29, 1978.

[2] M.L. Puri and D.A. Ralescu, "Fuzzy random variables. "Journal of Mathematical Analysis and Applications" vol. 14, pp. 409–422, 1986.

[3] H. Katagiri, E.B. Mermri, M. Sakawa, K. Kato and I. Nishizaki, "A possibilistic and stochastic programming approach to fuzzy random MST problems" IEICE Transaction on Information and Systems, vol. E88-D, pp. 1912–1919, 2005.

[4] H. Katagiri and M. Sakawa, "An interactive fuzzy satisficing method for fuzzy random linear multiobjective 0-1 programming problems through the expectation optimization model," Mathematical and Computer Modelling, vol. 40, pp. 411–421, 2004.

[5] H. Katagiri, M. Sakawa, K. Kato and I. Nishizaki, "Interactive multiobjective fuzzy random programming: maximization of possibility and probability," European Journal of Operational Research, vol. 188, pp. 530–539, 2008.

[6] H. Katagiri and M. Sakawa, "Interactive multiobjective fuzzy random programming through the level set-based probability model," Information Sciences, vol. 181, pp. 1641–1650, 2011.

[7] B. Liu, "Fuzzy random chance-constrained programming," IEEE Transaction on Fuzzy Systems, vol. 9, pp. 713–720, 2001.

[8] M.K. Luhandjula, "Fuzzy stochastic linear programming: survey and future research directions," European Journal of Operational Research, vol. 174, pp. 1353–1367, 2006.

[9] X. Huang, "Optimal project selection with random fuzzy parameters," International Journal of Production Economics, vol. 106, pp. 513–522, 2007.

[10] X. Huang, "A new perspective for optimal portfolio selection with random fuzzy returns," Information Sciences, vol. 177, pp. 5404–5414, 2007.

[11] B. Liu, "Random fuzzy dependent-chance programming and its hybrid intelligent algorithm," Information Sciences, vol. 141, pp. 259–271, 2002.

[12] M. Wen and K. Iwamura, "Facility location-allocation problem in random fuzzy environment: Using (α, β)-cost minimization model under the Hurewicz criterion," Computers and Mathematics with Application, vol. 55, pp. 704–713, 2008.

[13] T. Hasuike, H. Katagiri and H. Ishii, "Portfolio selection problems with random fuzzy variable returns," Fuzzy Sets and Systems, vol. 18, pp. 2579–2596, 2009.

[14] I.M. Stancu-Minasian, "Overview of different approaches for solving stochastic programming problems with multiple objective functions," R. Slowinski and J. Teghem (eds.): Stochastic Versus Fuzzy Approaches to Multiobjective Mathematical Programming under Uncertainty, Kluwer Academic Publishers, Dordrecht/Boston/London, pp. 71–101, 1990.

[15] P. Kall and J. Mayer, Stochastic Linear Programming: Models, Theory, and Computation, 2nd Edition, Springer-Verlag, New York/Dordrecht/Heidelberg/London, 2010.

[16] G. Infanger, Stochastic Programming: The State of the Art in Honor of George B. Dantzig, Springer-Verlag, New York/Dordrecht/Heidelberg/London, 2010.

[17] S. Nahmias, "Fuzzy variables," Fuzzy Sets and Systems, vol. 1, pp. 97–110, 1978.

[18] D. Dubois and H. Prade, Fuzzy Sets and Systems. Academic Press, New York, 1980.

[19] L.A. Zadeh, "Fuzzy sets as a basis for a theory of possibility," Fuzzy Sets and Systems, vol. 1, pp. 3–28, 1978.

[20] Z. Michalewicz and G. Nazhiyath, "GenocopIII: a co-evolutionary algorithm for numerical optimization problems with nonlinear constraints," Proceedings of the Second IEEE International Conference on Evolutionary Computation, pp. 647–651, 1995.

[21] M. Sakawa, Genetic Algorithms and Fuzzy Multiobjective Optimization, Kluwer Academic Publishers, Boston, 2001.

2011 IEEE International Conference on Fuzzy Systems
June 27-30, 2011, Taipei, Taiwan

Improving Ontology Alignment through Memetic Algorithms

Giovanni Acampora*, Pasquale Avella†, Vincenzo Loia*, Saverio Salerno‡ and Autilia Vitiello*
*Dept. of Computer Science
University of Salerno, Fisciano, Italy 84084
Email: {gacampora, loia, avitiello}@unisa.it
†Dept. of Engineering
University of Sannio, Benevento, Italy 82100
Email: avella@unisannio.it
‡Dept. of Electronic Engineering and Information Engineering
University of Salerno, Fisciano, Italy 84084
Email: salerno@unisa.it

***Abstract*—Born primarily as means to model knowledge, ontologies have successfully been exploited to enable knowledge exchange among people, organizations and software agents. However, because of strong subjectivity of ontology modeling, a matching process is necessary in order to lead ontologies into mutual agreement and obtain the relative alignment, i.e., the set of correspondences among them. The aim of this paper is to propose a memetic algorithm to perform an automatic matching process capable of computing a suboptimal alignment between two ontologies. To achieve this aim, the ontology alignment problem has been formulated as a minimum optimization problem characterized by an objective function depending on a fuzzy similarity. As shown in the performed experiments, the memetic approach results more suitable for ontology alignment problem than other evolutionary techniques such as genetic algorithms.**

***Index Terms*—Memetic Algorithms, Ontology Alignment, Optimization.**

I. Introduction

Nowadays, ontologies are recognized to be the most appropriate means to support information sharing and reuse in all modern knowledge based systems. They have been successfully exploited in many research areas such as artificial intelligence (AI), information retrieval (IR), database theory, and most recently, World Wide Web (in particular for Semantic Web), e-Commerce and e-Learning. According to [1], an ontology is an explicit specification of a conceptualization, i.e., the objects, concepts, and other entities that are presumed to exist in some area of interest and the relationships that hold them[2]. Unfortunately, the variety of ways that a domain can be conceptualized (by considering different concepts, constraints and properties) results in the creation of different ontologies with contradicting or overlapping parts[3]. Therefore, a so called *mapping process* is necessary in order to reconcile heterogeneous ontologies and allow system interoperability. The recent researches about ontologies are heavily focused in the development of several automatic reconciliation processes to overcome this heterogeneity. One of the principal techniques is the so-called *matching process* which consists in detecting correspondences among existing ontologies in order to make them consistent. Different from other mapping methods such as *integration* and *merging* which return a single ontology, the matching process keeps separate the original ontologies and generates in output an *alignment*, i.e., the set of correspondences among them. In order to perform a matching process and to find an appropriate alignment between two ontologies, a lot of techniques[4][5][6] based on different theories have been exploited. The main aim of this paper is to propose an innovative method to perform an automatic matching process based on the so-called *memetic algorithms*, i.e, optimization hybrid methods which combine evolutionary algorithms with local search techniques [7]. In order to solve the ontology alignment problem through a memetic approach, a formulation of the alignment problem as a minimization problem has been provided by defining an appropriate objective function based on a fuzzy similarity measure able to quantify the matching level between ontologies entities.

In the experimental results section, our proposal is compared with genetic algorithms in order to show, in the ontology alignment problem context, the more suitability and efficiency of the memetic approach than other evolutionary techniques. The evaluation of the algorithms is executed through a statistical analysis, and precisely, by means of the well-known Wilcoxon's signed rank test[8]. The used benchmarks are provided by the Ontology Alignment Evaluation Initiative (OAEI) 2009 [9].

II. The Ontology Alignment Problem

In this section, a set of formal definitions concerning to matching process are given. According to [10], a matching process consists of generating an alignment (A') from a pair of ontologies (o and o') given in input. So, before formally defining the matching process, the conventional definitions of ontology and alignment are provided.

Definition 1 (Ontology): An ontology O is a triple

$$O = (C, P, I)$$

978-1-4244-7316-8/11/$26.00 ©2011 IEEE

where C is the set of *classes*, P the set of *properties* and I the set of *individuals*.

Definition 2 (Alignment): An alignment is a set of so-called *mapping elements*. A mapping element is a 5-uple: $\langle id, e, e', n, R\rangle$ where

- id is a unique identifier of the given mapping element;
- e and e' are the entities (e.g., tables, XML elements, properties, classes) of the first and the second ontology respectively;
- n is a confidence measure in some mathematical structure (typically in the [0,1] range) holding for the correspondence between the entities e and e';
- R is a relation (e.g., equivalence ($=$); more general ($\sqsupseteq$); disjointness ($\perp$); overlapping ($\sqcap$)) holding between the entities e and e'.

In order to compute a mapping element, a matching process uses a *similarity measure* which determines the closeness between the entities e and e' in the range $[0, 1]$ where 0 stands for complete inequality and 1 for complete equality. A lot of kinds of similarity measures exist in literature. In particular, there are techniques which rely on vector representations of ontologies and use distances measures between these vectors and other approaches which consider an ontology as a set of entities and so depend on the techniques used for establishing the distance among ontology entities. A comparison between similarity distances is provided in [11].

In order to perform a matching process two input ontologies o and o' are needed, but also other optional inputs can be specified: a partial alignment A which is to be completed by the process to obtain A'; some parameters such as weights and thresholds and some external resources such as lexicons and databases. Therefore, the matching or alignment process can be formally defined as follows:

Definition 3 (Matching process): The matching process can be seen as a function ϕ which, from a pair of ontologies o and o' to align, an input alignment A, a set of parameters p, a set oracles and resources r, returns a new alignment A' between these ontologies:

$$A' = \phi(o, o', A, p, r).$$

In order to evaluate the quality of the output alignment A' provided by a matching process, typically conformance measures derived from the information retrieval field [12] are exploited. These methods require the employment of a *reference alignment* R. The most commonly used conformance measures are *precision*, *recall* and *f-measure* which represents a combination of the first ones. Formally:

Definition 4 (Precision): Given a reference alignment R, the precision of an alignment A is given by

$$Pr(A, R) = \frac{|R \cap A|}{|A|}.$$

Definition 5 (Recall): Given a reference alignment R, the recall of an alignment A is given by

$$Rec(A, R) = \frac{|R \cap A|}{|R|}.$$

Definition 6 (F-measure): Given a reference alignment R and a number α between 0 and 1, the F-measure of an alignment A is given by

$$M_\alpha = \frac{Pr(A, R) \cdot Rec(A, R)}{(1 - \alpha) \cdot Pr(A, R) + \alpha \cdot Rec(A, R)}.$$

If $\alpha = 1$, then the F-measure is equal to precision and if $\alpha = 0$, the F-measure is equal to recall. In between, the higher α, the more importance is given to precision with regard to recall. Very often, the value $\alpha = 0.5$ is used, i.e.,

$$M = \frac{2 \times Pr(A, R) \times Rec(A, R)}{Pr(A, R) + Rec(A, R)},$$

the harmonic mean of precision and recall.

In order to perform a matching process and to find an appropriate alignment between two ontologies, a lot of techniques based on different theories have been exploited. All methods can be classified as *instance-based* and *schema-based*: in order to perform a matching process, the former use all entities of an ontology including the individuals, the latter use only entities as classes and properties. A furthermore classification based on the kinds of inputs is possible among schema-based methods obtaining the following three categories: *terminological*, *structure* and *semantics* methods. A complete discussion can be found in [13]. Only recently, also evolutive methods such as machine learning and genetic algorithms have been exploited to solve the alignment problem[14][15][16].

Taking a cue from these new researches, our work proposes to detect correspondences between two ontologies by means of a memetic algorithm which performs a schema-based matching process taking in input two ontologies (leaving out the other input parameters) and considering a string distance based similarity measure.

III. Ontology Alignment as Optimization Problem

In this section, a formal definition of the ontology alignment problem is given by reformulating it as a minimization problem based an objective function that uses a fuzzy similarity in order measure the correspondence between ontology entities.

Beside the general scheme presented in the section II, the alignment process can be opportunely restricted in order to deliver a particular kind of alignment useful for a particular kind of applications. In particular, in our approach, the ontology alignment problem is depending upon the following features:

- a simplified definition of mapping element, renamed *correspondence* (see definition 7), which implies the equality as the relation R;
- cardinality $n : 1$ (many-to-one), i.e., an entity of the first ontology can be associated with an only entity of the second one, whereas, an entity of the second ontology can be associated also with more entities of the first one.

Definition 7 (Correspondence): For two ontologies O_1 and O_2, a correspondence is defined as:

$$c = (e_i, e_j)$$

where e_i is the i^{th} entity of ontology O_1 whereas e_j is the j^{th} entity of ontology O_2 and the implied relation is the equality with a confidence measure in $[0, 1]$.

Basing on these features, the formal definition of the ontology alignment problem taken into account in this work can be provided.

Definition 8 (Alignment): An alignment A between two ontology O_1 and O_2 is the set:

$$A = \{c_k = (e_i, e_j) | e_i \in O_1 \text{ with } i = 0, \ldots, h_1 - 1, \\ e_j \in O_2 \text{ with } j \in \{0, \ldots, h_2 - 1\} \text{ and} \\ k = 1, 2, \ldots, h_1\}$$

where $h_1 = |O_1|$ and $h_2 = |O_2|$.

In order to formulate the considered alignment problem as optimization problem, it is necessary to introduce the concept of the *evaluation of a correspondence*. The evaluation is performed by a method whose aim is to determine the goodness of a correspondence to achieve an optimal alignment. In general, the evaluation method is a function $f : A \rightarrow \mathbb{R}$ which associates a real value to each correspondence in A. In our work, a *fuzzy similarity* between the name labels of the entities composing a correspondence is chosen to realize the evaluation method. Precisely, the goodness of a correspondence is evaluated through a fuzzy relation between entity names computed by means of the well-known *levenshtein string distance* [17]. Formally, by considering s_1 and s_2 the name labels of the entities involved in the correspondence $c \in A$, the exploited evaluation method is given by the formula:

$$f(c) = \mu(s_1, s_2)$$

where $\mu : S \times S \rightarrow [0, 1]$ (S is the set of all entities names) is a membership function defined as follows:

$$\mu(s_1, s_2) = \frac{lev(s_1, s_2)}{N}$$

where

- $lev(s_1, s_2)$ is the levenshtein distance between the two strings s_1 and s_2, i.e, the minimum number of edits needed to transform the string s_1 into s_2, with the allowable edit operations being insertion, deletion, or substitution of a single character;
- $N = max(N_1, N_2)$ with N_1 and N_2, respectively, the lengths of the strings s_1 and s_2.

Finally, the alignment problem can be formulated as an optimization problem.

Definition 9 (Alignment problem): The alignment problem can be defined as the tuple (O_1, O_2, A_{set}, F) where:

- O_1 and O_2 are the ontologies to align:
- A_{set} is the set of all possible alignments between O_1 and O_2;
- $F : A \rightarrow \mathbb{R}$ is the objective function defined in the following way:

$$F(A) = \sum_{i=1}^{|A|} f(c_i) \text{ with } c_i \in A \quad (1)$$

In other words, it is possible to calculate the evaluation value of a specific alignment A by considering the sum of fuzzy evaluations of its correspondences. Since the correspondence evaluation function f is a distance measure between the correspondence entity names, the lower are $F(A)$ values and the alignment A is nearer to optimal one, so our aim is to minimize $F(A)$ values. Therefore, the considered alignment problem is a minimum optimization problem.

IV. Our proposal for the alignment problem: Memetic Algorithms

This paper aims of presenting a novel technique to solve the ontology alignment problem by exploiting an emergent hybrid method named Memetic Algorithms (MAs). The MAs are population-based search methods which combine evolutionary algorithms with local search (LS) methods. The name is inspired by Richard Dawkins concept of a *meme*, which represents a unit of cultural evolution that can exhibit local refinement [18]. Indeed, the MAs have the capability of realizing local search processes within the successive generations characterizing global search methods in order to refine population individuals.

In this section, a memetic algorithm which extends a genetic algorithm with the Stochastic Hill Climbing search is presented. Initially, the two components (the genetic algorithm and the Hill Climbing search) to be combined to realize our proposal are separately described. Then, their merging to perform an automatic matching process is discussed.

A. The First Component: a Genetic Algorithm

Our proposal is to realize a memetic algorithm as extension of a precise category of evolutionary methods, the genetic algorithms. For this reason, in this section the fundamental evolutive concepts and the genetic algorithm which will be extended to solve the considered alignment problem are given.

The interest in genetic algorithms began as early as the 1970s when Holland [19] first proposed them as search methods inspired by the mechanisms of evolutionary processes in nature. In particular, genetic algorithms are based on Darwinian principle of the natural selection which leads to the survival of the only fittest individuals. More in detail, in nature, evolution manifests itself as a succession of changes in species' features determined by genetic reproduction. The individual features, represented by chromosomes (formed in turn by genes), determine the survival capacity of individuals. Indeed, only fittest individuals capable of adapting to the changing environment survive and reproduce. Therefore, the evolution process is derived from the joint action of natural selection and the recombination of genetic material that occurs during reproduction and that generates diversity in the *gene pool* [20].

Genetic algorithms try to solve an optimization (or search) problem by manipulating a *population* of potential solutions and by reproducing the natural evolution process. Specifically, they operate on encoded representations of the solutions, called *chromosomes*, that equivalent to the representations of individual features in nature. The algorithm evolution starts from

a population of randomly generated individuals and consists in successive *generations*. In each generation, as in nature, a *selection process* provides the mechanism for selecting better solutions to survive. Each solution is evaluated by means a *fitness function* that reflects how good it is, compared with other solutions in the population. The higher is the fitness value of an individual and higher are its chances of surviving. Recombination of genetic material in genetic algorithms is simulated through two operators: *crossover* that exchanges portions between two randomly selected chromosomes and *mutation* that causes random alteration of the chromosome genes. The algorithm evolution terminates when specified conditions such as the maximum number of generations are reached. The general genetic algorithm structure is shown in the figure IV-A.

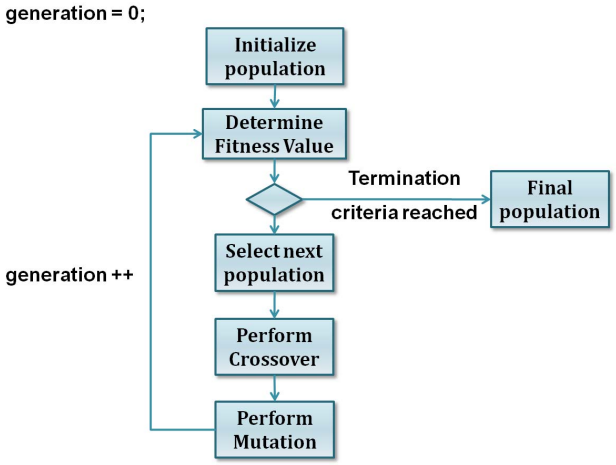

Fig. 1. The typical steps of a genetic algorithm.

In order to customize the building of the starting genetic algorithm for the considered alignment problem, it is necessary to define the chromosome structure in order to represent the solution of our problem, i.e, an alignment, and a fitness function which allows the evaluation of the considered solutions.

In particular, with regard to fitness function, simply it is to minimize the described function F (see eq.1), whereas, the proposed chromosome structure requires a more detailed description.

By remembering the definitions 7 and 8 and considering that each ontology entity is enumerated from 0 to $n+m+k-1$ where m, n, k are, respectively, the cardinalities of the sets C, P, I which compose an ontology, a chromosome representing an alignment A is a integer vector where each cell represents a correspondence between an entity of the first ontology and any entity of the second one. More in detail, by considering that the i^{th} vector cell contains the integer j, the cell represents the correspondence (e_i, e_j). The vector length is the same of the cardinality of alignment A, i.e., the number of the entities of the first ontology. Formally:

Definition 10 (Alignment Chromosome): A chromosome S representing an alignment A between two ontology O_1 and O_2 is the set:

$$S = \{(e_0, e_{j_0}), (e_1, e_{j_1}), (e_2, e_{j_2}), \ldots, (e_h, e_{j_h})\}$$

where $h = |O_1| - 1$ and $j_l \in \{0, 1, 2, \ldots, |O_2| - 1\}$ with $l = 0, 1, 2, \ldots, h$.

Therefore, the chromosome dimension depends on alignment problem instance.

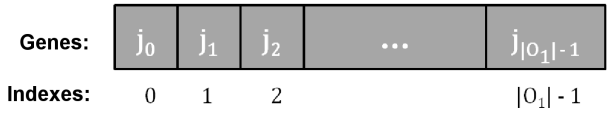

Fig. 2. The general structure of an alignment chromosome: each gene represents the correspondence (e_i, e_{j_i}) where $i = 0, 1, 2, \ldots, |O_1| - 1$ and $j_i \in 0, 1, 2, \ldots, |O_2| - 1$

In order to complete the initial genetic algorithm, the description of termination criteria has to be given. In details, our proposal is to consider a combined termination criterion which stops the genetic algorithm if the maximum number of iterations or the alignment f-measure value (definition 6) is achieved.

Once defined the alignment chromosome, the fitness function and the termination criteria, the genetic algorithm (shown in the table I) could be run in order to solve the described alignment problem.

B. The Second Component: the Hill Climbing Search

The local search strategies such as steepest-descent, conjugate-gradient and linear approximation methods perform iterative search for optimum solution in the *neighborhood* of a candidate. Starting from a single candidate solution, these methods use *local* information to decide which neighbor they should move to next [21]. In each iteration, typically, a mutation operator is applied in order to improve current candidate. The process ends when there are not changes which improve current solution or after a specific number of iterations.

In particular, the Hill Climbing algorithm is a local search iterative method which starts with an arbitrary solution to the problem at issue. During iterations, the algorithm attempts to find a better solution by incrementally changing a single component of the current one. If the change improves the current solution, then the new one becomes the current one. The search is repeated until no further improvements can be found or after a maximum number of iterations. There are several variants of Hill Climbing search depending on how the next solution is tried. For example, the *Simple Hill Climbing algorithm* chooses the first closer node to solution, whereas the *Steepest Ascent Hill Climbing search* compares all successors and then selects the closest.

Our proposal is to use the stochastic version of Hill Climbing search which represents a trade-off between the previous mentioned variants in terms of efficiency and efficacy. The Stochastic Hill Climbing algorithm, presented in the table II, selects a neighbor at random, and then decides whether to move to that neighbor or to examine another by considering the amount of improvement.

TABLE I
LISTING OF THE GENETIC ALGOTIRTHM.

Input: entity name string sets S_1 and S_2 of two ontologies O_1 and O_2 to align; the number of the entities n_1 and n_2 of the ontologies; parameters of GA (size of the population pop_size, crossover rate p_c, mutation rate p_m), temination criteria (maximum number of iterations max_iter and desidered f-measure value $f_{measure}$).

Output: the best optimized alignment (represented by the final best chromosome) between the ontologies O_1 and O_2.

$gen \leftarrow 0$;
$pop \leftarrow$ generatePopulation(pop_size); // Generate randomly an initial population pop of pop_size chromosomes
evaluateFitness(pop); // Evaluate fitness value for each chromosome
$best_chromosome \leftarrow$ getBestChromosome(pop); // Select the best chromosome of the current population
$quality \leftarrow$ evaluateAlignment($best_chromosome$); // $quality$ contains the f-measure value for the current best chromosome
while ($gen \leq max_iter$ AND $quality \leq f_{measure}$) **do**
  executeCrossover(pop, p_c); // Crossover chromosomes according to a crossover rate p_c to add new chromosomes to population pop
  executeMutation(pop, p_m); // Mutate chromosomes with a mutation probability p_m to add new chromosomes to population pop
  evaluateFitness(pop); // Evaluate fitness value for new chromosomes
  executeSelection(pop, pop_size); // Select pop_size chromosomes to generate next new population pop
  $best_chromosome \leftarrow$ getBestChromosome(pop); // Select the best chromosome of the current population
  preserveBestChromosome(pop, $best_chromosome$); // Preserve the best chromosome of the current population: Elitist Strategy
  $gen \leftarrow gen + 1$; // Increment number of iterations
  $quality \leftarrow$ evaluateAlignment($best_chromosome$); // $quality$ contains the f-measure value for the current best chromosome
end while
return $best_chromosome$;

TABLE II
LISTING OF THE STOCHASTIC HILL CLIMBING ALGORITHM.

Input: an alignment chromosome $align_solution$ representing the initial solution, the maximum number of iterations max_iter.

Output: the alignment chromosome sol which represents the solution optimized by means of local search.

$sol \leftarrow align_solution$;
$iter \leftarrow 0$;
while ($iter < max_iter$) **do**
  $new_sol \leftarrow$ getRandomNeighbor(sol);
  if (evaluate(new_sol) $<$ evaluate(sol)) **then**
    $sol \leftarrow new_sol$;
    $iter \leftarrow 0$;
  end if
end while
return sol;

C. Our Memetic Algorithm to Solve the Alignment Problem

In spite of their known efficiency, all local search approaches suffer from the same drawback: they tend to get stuck in local optima. Instead, thanks to their capability of exploring and exploiting promising regions of search space, the genetic algorithms have the strong benefit not to prone to stalling at local optima. However, they can take to relatively long time to locate the exact local optimum in a region of convergence (and may sometimes not to find the optimum with sufficient precision) [21]. For this reason, the idea to create an hybrid method that combines the genetic algorithms with the local search methods, i.e, the MAs.

The MAs, representing the marriage between global search and local improvement, have the complementary advantages of EAs (generality, robustness and global search efficiency) and local search methods (rapid convergence toward local minima). In the figure IV-C the typical structure of MAs which, in literature, are known also as hybrid EAs (e.g., [22]), genetic local searchers (e.g.,), Lamarckian GAs (e.g., [23]), Baldwinian GAs (e.g.,[24]), etc., is presented.

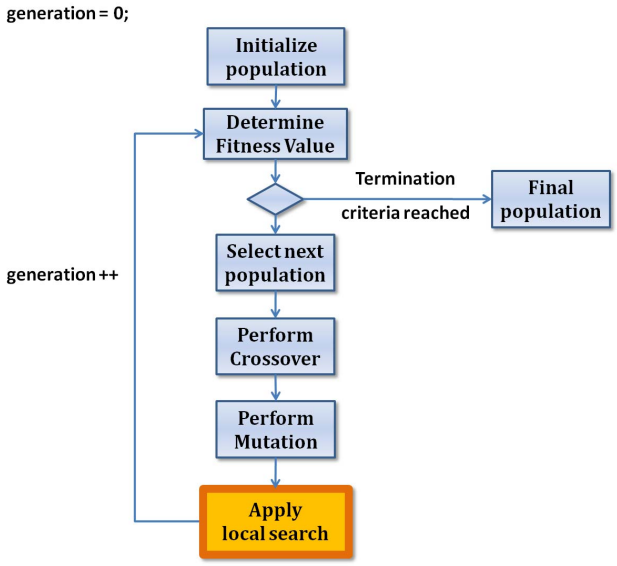

Fig. 3. The general structure of a memetic algorithm

In order to design a *competent* [25] MA a lot of issues must be addressed over the two principal components. Perhaps the foremost of these issues may be stated as [26]: *What is the best tradeoff between local search and the global search provided by evolution?*. This issue leads naturally to questions such as the following:

- *Local search frequency*: How often should local search be applied within the evolutionary cycle?
- *Order respect to genetic operators*: When should local search be applied?

- *Individual selection mechanism*: Which individuals in the population should be improved by local search?
- *Local search intensity*: How much computational effort should be allocated to each local search?

Therefore, in order to complete the design of a memetic algorithm for ontology alignment problem, the aforementioned issues must be considered. Our proposal is to build a memetic algorithm which has the following features:

- *Local search frequency = 1*, i.e., the local search is applied within each evolutionary cycle;
- *Order respect to genetic operators = after*, i.e., local refinement is executed after crossover and mutation operators;
- *Individual selection mechanism = only the best*, i.e., only the best chromosome of population is improved by the local search process;
- *Local search intensity = equal to n local search iterations*, i.e., each local search process ends after running n iterations.

Finally, the whole proposed memetic algorithm is presented in the table III.

V. Experimental results

In this section, an experimentation is led in order to investigate the performances of the proposed memetic algorithm and show the suitability of memetic approach in the ontology alignment context. To achieve this aim, the proposed algorithm is compared with the genetic algorithm shown in the table I.

In our experimentation, the matching process involves ontologies charactering the well-known benchmarks provided by the OAEI 2009. Table IV shows a brief description about the features of the used benchmarks.

TABLE IV
Benchmarks descriptions

Identifier	Description
101	Strictly identical ontologies
103	A regular ontology and other with a language generalization
104	A regular ontology and other with a language restriction
204	Ontologies with different naming conventions
221	A regular ontology and other with no specialisation
224	Identical ontologies without instances
225	Identical ontologies without restrictions

The evaluation of the algorithms is realized by means of a non-parametric statistical procedure for performing pairwise comparisons named Wilcoxon's signed rank test.

A. Characteristics of Experimentation

In this section, a description of the features of the performed experiments is reported.

In particular, the experiments are carried out as follows:

- The memetic and genetic algorithm are run 20 times for each selected benchmark;
- Each run stops when the computed alignment is characterized by a f-measure value equal to 0.8 or after executing 100000 iterations;
- The averages of number of fitness evaluations for each benchmark and for both algorithms are computed and shown in the table V.

The used parameters are the following ones:

- The GA parameters for both algorithms are:
  - population size = 20 chromosomes;
  - crossover rate = 0.8;
  - mutation rate = 0.02.
- The local search parameters are:
  - maximum number of iterations = 50.

Finally, the platform characteristics where the algorithms were run are:

- Processor: Intel Core 2 Duo;
- CPU Speed: 1.83 GHz;
- RAM Capacity: 2GB.

TABLE V
Samples for the Wilcoxon's test: the sigle AE stands for *average of the number of fitness evaluations over the executed 20 runs*

Identifier	Memetic AE	Genetic AE
101	12.120,70	36.287,45
103	11.524,00	33.735,70
104	12.234,85	35.798,70
204	28.558,50	97.602,90
221	11.652,15	34.569,15
224	13.202,50	35.168,30
225	11.532,40	35.167,05

B. Experimentation: Wilcoxon's test

As described in [27], the Wilcoxon's test is a non-parametric procedure employed in a hypothesis testing situation involving a design with two samples. It is a pairwise test used for answering this question: do two samples represent two different populations? Therefore, it can be employed to detect significant differences between the behavior of two algorithms and so it is suitable for our experimentation: showing that the memetic approach is better than genetic one for solving ontology alignment problem.

In order to compute the Wilcoxon's test, two samples related to the two compared algorithms have to be chosen. In our experimentation, the performance of algorithms depends on the executed number of fitness evaluations n_E: the smaller the value n_E and better is the algorithm at issue. For this reason, the two considered samples are represented by the data shown in the table V, i.e, the obtained averages of the number of fitness evaluations related to the two compared algorithms.

In general, a hypothesis testing as the Wilcoxon's test is a procedure in which sample data are employed to evaluate a hypothesis. In details, in order to evaluate the research hypothesis, i.e., the statement of what a researcher predicts,

TABLE III
LISTING OF THE MEMETIC ALGOTIRTHM.

Input: entity name string sets S_1 and S_2 of two ontologies O_1 and O_2 to align; the number of the entities n_1 and n_2 of the ontologies; GA parameters (size of the population pop_size, crossover rate p_c, mutation rate p_m), temination criteria (maximum number of iterations max_iter and desidered f-measure value $f_{measure}$); local search parameters (maximum number of iterations max_local_iter).

Output: the best optimized alignment (represented by the final best chromosome) between the ontologies O_1 and O_2.

$gen \leftarrow 0$;
$pop \leftarrow$ generatePopulation(pop_size); // Generate randomly an initial population pop of pop_size chromosomes
evaluateFitness(pop); // Evaluate fitness value for each chromosome
$best_chromosome \leftarrow$ getBestChromosome(pop); // Select the best chromosome of the current population
$quality \leftarrow$ evaluateAlignment($best_chromosome$); // $quality$ contains the f-measure value for the current best chromosome
while ($gen \leq max_iter$ AND $quality \leq f_{measure}$) **do**
  executeCrossover(pop, p_c); // Crossover chromosomes according to a crossover rate p_c to add new chromosomes to population pop
  executeMutation(pop, p_m); // Mutate chromosomes with a mutation probability p_m to add new chromosomes to population pop
  evaluateFitness(pop); // Evaluate fitness value for new chromosomes
  executeSelection(pop, pop_size); // Select pop_size chromosomes to generate next new population pop
  $best_chromosome \leftarrow$ getBestChromosome(pop); // Select the best chromosome of the current population
  preserveBestChromosome(pop, $best_chromosome$); // Preserve the best chromosome of the current population: Elitist Strategy
  $local_chr \leftarrow$ **executeHillClimbingSearch**($best_chromosome$, max_local_iter); // Execute the local search process on the best chromosome
  replaceWorstChromosome(pop, $local_chr$); // Select the worst chromosome and replace it with that obtained by the local search process
  $gen \leftarrow gen + 1$; // Increment number of iterations
  $quality \leftarrow$ evaluateAlignment($local_chr$); // $quality$ contains the f-measure value for the current best chromosome
end while
return $best_chromosome$;

two statistical hypotheses are needed: the so called *null hypothesis* (H_0) and the so called *alternative hypothesis* (H_1). In our experimentation, the null hypothesis states no difference between algorithms, i.e $H_0 : \theta_D = 0$, indicating that in the underlying populations represented by the two samples related to compared algorithms, the median of the difference scores equals zero. On the other side, a directional alternative hypothesis $H_1 : \theta_D < 0$ is chosen to indicate a difference between the memetic algorithm and the genetic one and specifically the superiority of the first one on the second one. Since the statement of our research hypothesis predicts the presence of a difference between algorithms which are being studied, and in particular, the superiority of memetic one, as result of our experimentation, the null hypothesis is expected to be rejected in favor of the alternative one.

The Wilcoxon's test is usually included in well-known statistical software packages such as SPSS, SAS and R. In particular, our experiment is performed by means of R tool by using the *wilcox* command in this way:

$$wilcox.text(x, y, \text{paired='TRUE', alternative='less'})$$

where x and y are two vectors which contain the averages of numbers of fitness evaluations, respectively, of the memetic and genetic algorithms.

However, before running the Wilcoxon's test, the used level of significance α for the performed experiment has to be decided. In particular, for our experimentation, a level of significance $\alpha = 0.05$ was chosen.

In the figure V-B, the R output for the executed Wilcoxon's test is shown. The computed p-value is 0.007813. Since the output of experimentation results in a p-value $< \alpha$, our experiment rejects the null hypothesis and affirms the superiority of memetic method over genetic approach in the context of the ontology alignment problem.

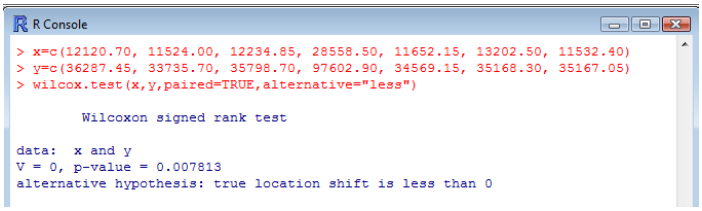

Fig. 4. The result of Wilcoxon's test

VI. CONCLUSIONS

The main aim of this paper is to apply the memetic approach to solve the ontology alignment problem. Memetic algorithms are an emergent optimization technique which combines evolutionary and local search methods. Therefore, in order to exploit a memetic algorithm capable of realizing a so-called matching process between two ontologies, it has been necessary to formulate the ontology alignment problem as a minimum optimization problem and to describe an appropriate objective function defined by means of a fuzzy similarity between the ontology entities. In order to prove the more suitability of the memetic proposal than other evolutionary techniques, an experimentation has been led by comparing the proposed memetic algorithm with the extended genetic one. The performed Wilcoxon's signed rank test shows the higher performances provided by the designed memetic approach.

REFERENCES

[1] Gruber, T. R., "A Translational Approach to Portable Ontology Specifications," *Knowledge Acquisition*, vol.5, pp. 199–220, 1993.
[2] M. R. Genesereth and N. J. Nilsson, "*Logical Foundations of Artificial Intelligence*," San Mateo, CA: Morgan Kaufmann Publishers, 1987.

[3] G. Stoilos, G. Stamou and S. Kollias, "A String Metric for Ontology Alignment," in *Proceedings of the ninth IEEE International Symposium on Wearable Computers*, pp.624–637, 2005.
[4] H. H. Do and E. Rahm, "COMA - a system for flexible combination of schema matching approaches," in *Proceedings of the Very Large Data Bases Conference (VLDB)*, pp. 610621, 2001.
[5] J. Madhavan, P. Bernstein, and E. Rahm. "Generic schema matching with Cupid," in *Proceedings of the Very Large Data Bases Conference (VLDB)*, pp. 4958, 2001.
[6] N. Noy and M. Musen. "Anchor-PROMPT: using non-local context for semantic matching," in *Proceedings of the workshop on Ontologies and Information Sharing at the International Joint Conference on Artificial Intelligence (IJCAI)*, pp. 6370, 2001.
[7] P. Moscato, "On evolution, search, optimization, GAs and martial arts: toward memetic algorithms," California Inst. Technol., Pasadena, CA, Tech. Rep. Caltech Concurrent Comput. Prog. Rep. 826, 1989.
[8] F. Wilcoxon, "Individual comparisons by ranking methods," *Biometrics*, vol.1, pp.8083, 1945.
[9] Ontology Alignment Evaluation Initiative (OAEI). http://oaei.ontologymatching.org/2009.
[10] P. Bouquet, J. Euzenat, E. Franconi, L. Serafini, G. Stamou, and S. Tessaris. D2.2.1: Specification of a common framework for characterizing alignment. Technical report, NoE Knowledge Web project delivable, 2004. http://knowledgeweb.semanticweb.org/.
[11] Jrme David and Jrme Euzenat. Comparison between ontology distances (preliminary results). In Proc. 7th conference on international semantic web conference (ISWC), Karlsruhe (DE), pages 245260, 2008.
[12] C. J. Van Rijsbergen, *Information Retrieval. 2nd edition*, London, Butterworths, 1979.
[13] Shvaiko, P., Euzenat, J., "A survey of schema-based matching approaches," *Journal on Data Semantics IV*, pp.146-171, 2005.
[14] J. Wang, Z. Ding, C. Jiang, "GAOM: Genetic Algorithm based Ontology Matching," in *Proceedings of IEEE Asia-Pacific Conference on Services Computing*, 2006.
[15] Martinez-Gil, J.; Alba, E.; and Montes, J. F. A. "Optimizing ontology alignments by using genetic algorithms," In Guret, C.; Hitzler, P.; and Schlobach, S., eds., *Nature inspired Reasoning for the Semantic Web (NatuReS2008), volume 419 of CEUR Workshop Proceedings*, 2008.
[16] Anhai Doan, Jayant Madhavan, Pedro Domingos, and Alon Halevy, "Ontology Matching: A Machine Learning Approach," in *Handbook on Ontologies in Information Systems*, pp. 397–416, 2003.
[17] Levenshtein VI, "Binary codes capable of correcting deletions, insertions, and reversals," *Soviet Physics Doklady*, vol.10, pp. 707710, 1966.
[18] R. Dawkins, *The Selfish Gene*. New York: Oxford Univ. Press, 1976.
[19] J.H. Holland, "*Adaptation in Natural and Artificial Systems*," Univ. of Michigan Press, Ann Arbor, Mich., 1975.
[20] M. Srinivas and L. M. Patnaik, "Genetic algorithms: A survey," *IEEE Comput.*, vol. 27, no. 6, pp 17-26, June 1994.
[21] Y. S. Ong, Q. H Nguyen, M. H. Lim and T. Jing, "A Development Platform for Memetic Algorithm Design," *Joint 3rd International Conference on Soft Computing and Intelligent Systems and 7th International Symposium on Advanced Intelligent Systems*, O-okayama Campus West Bldg. 9, Tokyo Institute of Technology, Japan, 20-24 September , 2006.
[22] L. He and N. Mort, "Hybrid genetic algorithms for telecommunications network back-up routing," *BT Technol. J.*, vol. 18, no. 4, pp. 4256, 2000.
[23] G. M. Morris, D. S. Goodsell, R. S. Halliday, R. Huey,W. E. Hart, R. K. Belew, and A. J. Olson, "Automated docking using a lamarkian genetic algorithm and an empirical binding free energy function," *J Comput. Chem.*, vol. 14, pp. 16391662, 1998.
[24] K. Ku and M. Mak, "Empirical analysis of the factors that affect the Baldwin effect," in *Lecture Notes in Computer Science*, 1998, Proc. Parallel Problem Solving From NaturePPSN-V, pp. 481490.
[25] D. Goldberg, *The Design of Innovation: Lessons From and for Competent Genetic Algorithms*. Norwell, MA: Kluwer, 2002.
[26] N. Krasnogor and J. Smith, "A Tutorial for Competent Memetic Algorithms: Model, Taxonomy, and Design Issues," in *IEEE Transactions On Evolutionary Computation*, vol. 9, no. 5, October 2005.
[27] S. Garca, D. Molina,M. Lozano, F. Herrera, "A study on the use of non-parametric tests for analyzing the evolutionary algorithms behaviour: a case study on the CEC2005 Special Session on Real Parameter Optimization," *J Heuristics*, vol.15, pp.617644, 2009.
[28] J.H. Zar, *Biostatistical Analysis*. Prentice Hall. 1999.

2011 IEEE International Conference on Fuzzy Systems
June 27-30, 2011, Taipei, Taiwan

Genetic Fuzzy Markup Language for Diet Application

Chang-Shing Lee
Mei-Hui Wang
Zhi-Wei Chen
National University of Tainan,
Tainan, Taiwan
leecs@mail.nutn.edu.tw

Chin-Yuan Hsu
Institute for Information Industry
Kaohsiung, Taiwan

Su-E Kuo
Hui-Ching Kuo
Hui-Hua Cheng
National Cheng Kung University Hospital
Tainan, Taiwan

Akio Naito
Osaka Prefecture University
Osaka, Japan

***Abstract*—In this paper, the genetic fuzzy markup language (GFML) is presented to describe the knowledge base and rule base of the diet domain, including ingredients and the contained servings of six food categories of some common food. The domain experts first define the nutrient facts of the common food to construct the fuzzy food ontology. Meanwhile, the involved Taiwanese students of National University of Tainan (NUTN) record their daily meals for a constant period of time. Then, based on the built fuzzy food ontology, a GFML-based learning mechanism combining the genetic learning mechanism with the fuzzy markup language (FML) is carried out to infer the possibility of dietary healthy level for one-day meals. From the experimental results, it is known that the proposed GFML-based learning mechanism is workable for the diet-domain healthcare applications.**

Keywords: Fuzzy Ontology; Fuzzy Markup Language; Genetic Learning; Dietary Healthy Level Assessment

I. INTRODUCTION

A balanced diet must contain correctly proportioned carbohydarte, protein, fat, vitamins, mineral salts, and fiber because each nutrient plays an important role in supporting humans' everyday physical activities. However, what is a balanced diet? According to [1], eating a balanced diet means choosing a wide variety of foods and drinks from all the food groups. It also means eating certain things in moderation. The goal of the balanced diet is to take in nutrients you need for health at the recommended levels. And, how to begin a balanced diet is also a difficult problem for most of the people. At the present day, the desirable eating habits cannot be obtained easily since our lifestyle is getting diversified. To meet this requirement, some approaches intergrating the fuzzy inference mechanism and ontology have been proposed to support the diet assessment for the past few years. For example, Lee *et al.* proposed a type-2 fuzzy ontology to apply to the personal diabetic-diet recommendation [2] and diet assessment [3], [4].

Ontolgoies have become ubiquitous in information systems. As ontology development becomes increasingly widespread and collaborative, developers are creating ontologies using different tools and languages [6]. For example, Zouaq and Nkambou [7] presented the knowledge puzzle onotlogy learning tool to extract concept maps from text and export them into a domain ontology. Hisham and Nguyen [8] proposed a new ontology-structure-based technique for measuring the semantic similarity in single ontology and across multiple ontolgoies in the biomedical domain within the frameswork of Unified Medical Language System (UMLS). Ontology also has been extensively studied in many research fields, including the news summariation, multi-agent systems, webservice, natural language processing, medical science, computer game, and e-commerce platforms. For instance, Lee *et al.* proposed a fuzzy ontology to apply to news summarization [9] and diabetes decision support [5]. Chou *et al.* [10] focused on developing an ontology structure of elements for Web-based disaster management systems to assist developers and evaluators of Web sites in such domains.A fuzzy markup language (FML) implementation is based on the employment of tags able to model different parts of the fuzzy controller in a taxonomic way. It can be not only considered a standalone language used to model the fuzzy controllers, but also can effectively describe the knowledge base and rule base of the fuzzy logic system; therefore, the previous studies employed it to incorporate with the fuzzy inference mechanism [3], [4], [11], [12]. There are many FML-based apptications, such as Acompra et al. [19] proposed an Interoperable and adaptive fuzzy services for ambient intelligence application Lee er al. [3] [4] applied FML to diet assessment.

The genetic algorithm (GA) has been applied to to various research topics[13]. For example, Lee *et al.* proposed a genetic-based fuzzy image filter and its application to image processing [14] and meeting scheduling decision support system [15]. Khoo and Suganthan [16] presented a GA-based optimization procedure for structural pattern recognition in a model-based recognition system. The GFML-based fuzzy learning mechanism combined GA with FML is proposed and applied to the diet domain in this paepr. Based on the proposed food ontology, the devolped approach is able to show the involved people the healthy level of the eaten food to make them not only enjoy the delicous food but also eat healthily.

The remainder of this paper is structured as follows. The Taiwanes and Japanese fuzzy food ontologies are introduced in Section II. The GFML and the GFML-based learning mechanism are presented in Section III. The GFML-based learning mechanism on the diet application is introduced in Section IV. Experimental results are shown in Section V. Finally, some conclusions are given in Section VI.

II. FUZZY FOOD ONTOLOGY

It has been widely pointed out that classical ontology is not

978-1-4244-7316-8/11/$26.00 ©2011 IEEE

sufficient to deal with imprecise and vague knowledge for some real-world applications [2]. On the other hand, fuzzy ontology can effectively help to handle and process uncertain data and knowledge [2], [17]. The fuzzy ontology is an extension of the domain ontology that is more suitable to describe the domain knowledge for solving the uncertainty reasoning problems [2]. In this paper, the Taiwanese fuzzy food ontology is constructed to describe the fuzzy concepts and fuzzy relations for some common Taiwanese food. The proposed *fuzzy ontology* is an extended version of our previous research works [2], [9].

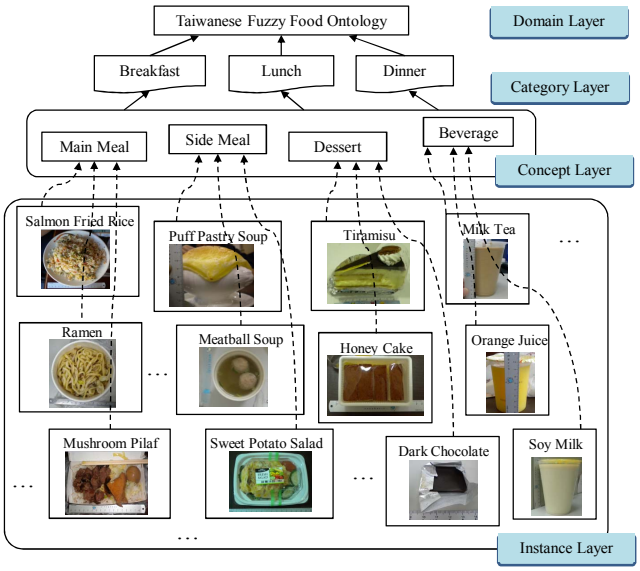

Fig. 1. Taiwanese fuzzy food ontology

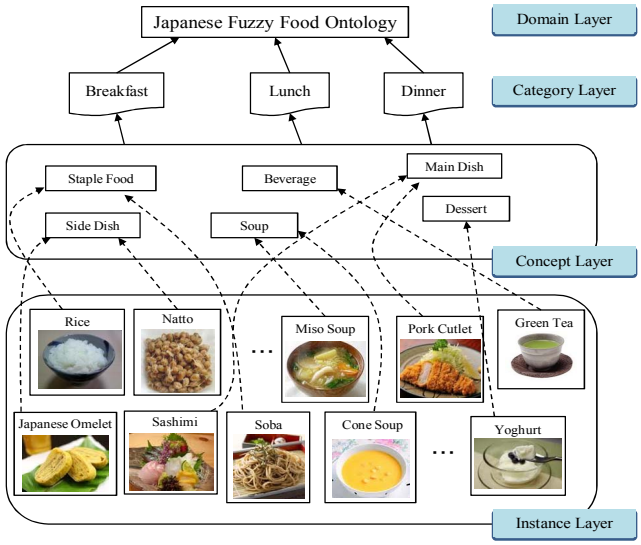

Fig. 2. Japanese fuzzy food ontology [18]

Figs. 1 and 2 show the four-layer fuzzy food ontology for Taiwanese food and Japanese food, respectively. The fuzzy food ontology is composed four layers, including (1) *Domain Layer*: This layer represents the domain name of the ontology. (2) *Category Layer*: In this layer, it comprises various categories defined by domain experts. In this paper, the category in Figs. 1 and 2 is divided into three meals, *Breakfast*, *Lunch*, and *Dinner* to simplify the ontology's structure. (3) *Concept layer*: This layer describes some components of the category layer. For Taiwanese fuzzy food ontology, there are concepts such as *Main Meal*, *Side Meal*, *Dessert*, and *Beverage*. On the other hand, for the Japanese food, some concepts like *Staple Food*, *Main Dish*, *Side Dish*, *Soup*, *Beverage*, and *Dessert* make up of this layer. (4) *Instance layer*: This layer consists of lots of instances of each concept in the *concept layer* [18].

There is a relationship between one concept and a lot of instances. For example, ramen is one kind of main meal for the Taiwanese food so Fig. 1 shows a relationship between Instance *Ramen* and concept *Main Meal*. Similarity, miso soup is one kind of soup for the Japanese food so there is a relationship between Instance *Miso Soup* and concept *Soup* in Fig. 2. In addition to showing the relationship among the food, the predefined fuzzy ontology also contains the nutritional information of each food, such as how many grams of carbohydrates, protein, and fat per portion and how many servings of six food groups per portion are contained. In this way, the proposed approach can evaluate how much healthy people's one-day meals are based on the fuzzy food ontology and people's basic personal profile such as height, weight, age, and everyday physical activity.

III. GENETIC FUZZY MARKUP LANGUAGE

In this paper, the genetic learning mechanism is embedded into the fuzzy markup language, and this novel approach is named the genetic fuzzy markup language learning mechanism. The details of the GFML-based learning mechanism like how to encode one GFML ontology into one chromosome and what is the mutation restriction will be introduced in this section.

A. Chromosome Representation of GFML

An example of how to encode the FML ontology into the chromosome is given in this sub-section. The FML ontology is encoded into one chromosome with a lot of genes. The genes on each chromosome are composed of three parts, including the rule-based part, knowledge-based part, and fuzzy-hedged part. The rule-based genes are a collection of the weight of the fuzzy rules. For example, there are four fuzzy rules listed in Table I. The genes of the chromosome about the rule-based part is {*1 0 0 1*}.

TABLE I. EXAMPLE ABOUT RULE-BASED GENES

```
<RuleBase type="mamdani" activationMethod="MIN" andMethod="MIN"
orMethod="MAX" name="RuleBase1">
    + <Rule connector="and" operator="MIN" weight="1" name="Rule1">
    + <Rule connector="and" operator="MIN" weight="0" name="Rule2">
    + <Rule connector="and" operator="MIN" weight="0" name="Rule3">
    + <Rule connector="and" operator="MIN" weight="1" name="Rule4">
</RuleBase>
```

The type about the knowledge-based genes is a hash table. The key and the value of this hash table are composed of the fuzzy variables' names and the objects with the fuzzy terms of their own fuzzy variables, respectively. The object could be a *TriangularShape*, *TrapezoidShape*, …, and so on. Take the Table II for an example. The genes about the knowledge-based part contain a dictionary entry, including the key is *CPURate*

and this key's value is {*<TriangularShape Param1="0" Param2="0" Param3="50" /><TriangularShape Param1="25" Param2="50" Param3="75" /><TriangularShape Param1="50" Param2="100" Param3="100" />*}. The fuzzy-hedged genes are also described as a hash table whose key is the fuzzy variable names, and the value of the key is represented by the fuzzy terms' hedge of the fuzzy variables. The value of the hedge (δ) is calculated by Eq. (1). For example, the key and the value of the fuzzy-hedged genes listed in Table III are *MemoryRate* and {*11111*}, respectively.

TABLE II. EXAMPLE ABOUT KNOWLEDGE-BASED GENES

```
<KnowledgeBase>
    <FuzzyVariable domainleft="0" domainright="100" name="CPURate"
    scale="%" type="input">
        <FuzzyTerm name="Low" hedge="Normal">
            <TriangularShape Param1="0" Param2="0" Param3="50" />
        </FuzzyTerm>
        <FuzzyTerm name="Medium" hedge="Normal">
            <TriangularShape Param1="25" Param2="50" Param3="75" />
        </FuzzyTerm>
        <FuzzyTerm name="High" hedge="Normal">
            <TriangularShape Param1="50" Param2="100" Param3="100" />
        </FuzzyTerm>
    </FuzzyVariable>
</KnowledgeBase>
```

$$\delta = \begin{cases} 1, \text{if linguistic hedge is normal} \\ 2, \text{if linguistic hedge is very} \\ 0.5, \text{if linguistic hedge is less or more} \end{cases} \quad (1)$$

TABLE III. EXAMPLE ABOUT FUZZY HEDGE GENES

```
<KnowledgeBase>
    <FuzzyVariable domainleft="0" domainright="100" name="MemoryRate"
    scale="%" type="input">
        <FuzzyTerm name="VeryLow" hedge="Normal">
            <TriangularShape Param1="0" Param2="0" Param3="20" />
        </FuzzyTerm>
        <FuzzyTerm name="Low" hedge="Normal">
            <TriangularShape Param1="0" Param2="20" Param3="40" />
        </FuzzyTerm>
        <FuzzyTerm name="Medium" hedge="Normal">
            <TriangularShape Param1="20" Param2="40" Param3="60" />
        </FuzzyTerm>
        <FuzzyTerm name="High" hedge="Normal">
            <TriangularShape Param1="40" Param2="60" Param3="80" />
        </FuzzyTerm>
        <FuzzyTerm name="VeryHigh" hedge="Normal">
            <TriangularShape Param1="60" Param2="100" Param3="100" />
        </FuzzyTerm>
    </FuzzyVariable>
</KnowledgeBase>
```

B. GFML-based Learning Mechanism

The flowchart of GFML-based learning mechanism, shown in Fig. 3, operates as follows.

- **Part 1: Parameter Initialization**
- Initialize all of the necessary parameters including (1) crossover probability $p_{crossover}$, (2) mutation probability $p_{mutation}$, (3) generation number $N_{generation}$, (4) maximum evaluation number $N_{generation_max}$, (5) minimum fitness value $fitness_{minimum}$, (6) size of population of chromosomes $S_{population}$, and (7) maximum size of population of chromosomes $S_{population_max}$.
- **Part 2: Genetic Population Initialization**
- Encode before-learned FML ontology into one chromosome, herein, the FML ontology stores all of the information of the knowledge base and rule base of the FML-based inference mechanism.
- Mutate the generated chromosome based on the mutation probability.
- Decode the after-mutated chromosome into the GFML ontology, herein, the GFML ontology stores all of the information of the knowledge base and rule base of the GFML-based inference mechanism.
- Input the training data to execute the GFML-based inference mechanism to obtain the inferred results.
- Input the desired output, and then execute the fitness function to calculate the fitness value of the after-mutated chromosome, that is, compute the sum of the difference value between the inferred results and desired output of the training data.
- Repeat Part 2 until the size of the population reaches the maximum size of the population.

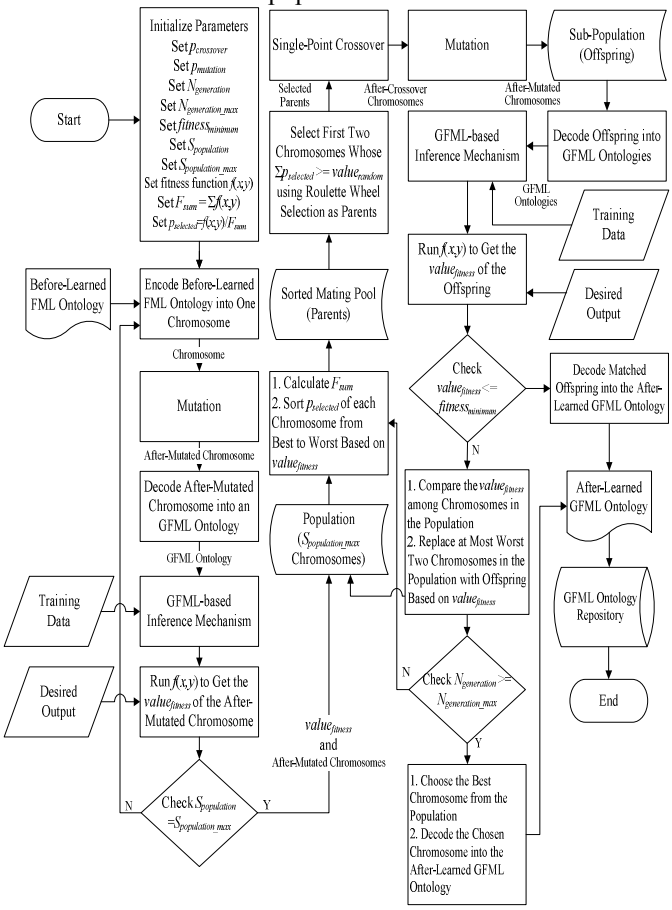

Fig. 3. GFML-based learning mechanism flowchart

- **Part 3: Genetic Evolution**
- Calculate the sum of the fitness value of all chromosomes in the population.
- Sort the selected probability of all chromosomes in the population from the best to the worst one based on each chromosome's fitness value.

- Based on the roulette wheel selection, choose the first two chromosomes whose sum of the selected probability is over the random created value as parents.
- Based on the crossover probability, make the single-crossover for the selected parents to generate the after-crossover chromosomes.
- Based on the mutation probability, mutate the after-crossover chromosomes to generate the offspring.
- Put the generated offspring into the sub-population.
- Decode the offspring into the GFML ontolgoies.
- Input the training data to execute the GFML-based inference mechanism to obtain the inferred results.
- Input the desired output, and then execute the fitness function to calculate the fitness value of the after-mutated chromosomes.
- Check if the fitness value of any one of offspring is less than the minimum fitness value.
- If it is positive, then decode the matched offspring into the after-learned GFML ontology, store it into the GFML ontology repository, and finally terminate the GFML-based learning mechanism.
- If it is negative, then compare the fitness value of all chromosomes in the population and replace at most worst two chromosomes in the population with the offspring.
- Check if the generation number is over the maximum generation number.
- If it is positive, then choose the best chromosome from the population, decode the chosen chromosome into the after-learned GFML ontology, store it into the GFML ontology repository, and eventually terminate the GFML-based learning mechanism.
- If it is negative, repeat Part 3 until the generation number reaches the maximum generation number or the minimum fitness value is matched.

C. *Mutation Restriction*

In this sub-section, the mutation restriction about the knowledge-based genes is introduced by Table IV. The membership functions of the fuzzy variables *Low* and *High* are depicted by Fig. 4.

TABLE IV. EXAMPLE ABOUT KNOWLEDGE-BSED GENES' MUTATION

```
<KnowledgeBase>
    <FuzzyVariable domainleft="Domain Left" domainright=" Domain Right"
    name="SampleFML " scale="%" type="input">
        <FuzzyTerm name="Low" hedge="Normal">
            <TriangularShape Param1="A" Param2="B" Param3="C" />
        </FuzzyTerm>
        <FuzzyTerm name="High" hedge="Normal">
            <TriangularShape Param1="A'" Param2="B'" Param3="C'" />
        </FuzzyTerm>
    </FuzzyVariable>
</KnowledgeBase>
```

The key of the knowledge-based genes is *SampleFML*, and the value of this key is {*<TriangularShape Param1="A" Param2="B" Param3="C" /><TriangularShape Param1=" A′ " Param2=" B′ " Param3=" C′ " />*}. The genes' mutation restriction of the knowledge-based part is to randomly select the values of parameters in order within a reasonable range. For example, the mutation value of *A* is a random value between *Domain Left* and *B*, and then the mutation value of *B* is a random value between the mutation-generated *A* and *A′*. Likely, the other parameters also are mutated in the same way as parameters *A* and *B*. After the mutation, the new genes about the knowledge-based part with the new parameters are obtained and correctly decoded it into the GFML ontology.

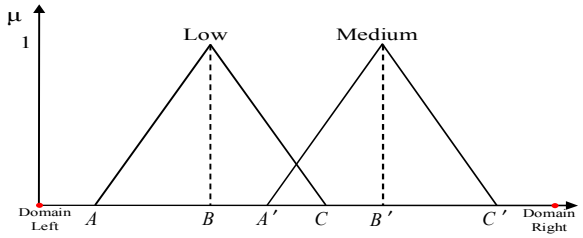

Fig. 4. Membership functions of the fuzzy variables Low and High

IV. GFML-BASED LEARNING MECHANISM ON DIET APPLICATION

A. *Structure*

The proposed diet healthy assessment system was introduced in previous work [3], [18]. Fig. 5 shows an overview of the GFML-based diet application and its procedures are as follows: (1) Nutrition facts of some popular food are gathered from the Internet, convenient stores, or fast food stores. (2) Domain experts, like dieticians, verify and define the detailed nutrient facts for each food item. (3) The fuzzy food ontology is constructed via the provided GFML editor. (4) The involved subjects record and input the daily eaten meals through the constructed platform. (5) The healthy-level evaluation of the eaten food is carried out by the GFML-based learning mechanism based on each subject's personal information and built fuzzy food ontology. Then, the output is stored into the dietary healthy level repository. (6) Finally, the involved subjects get the feedback and evaluated results from the domain experts via the provided interface.

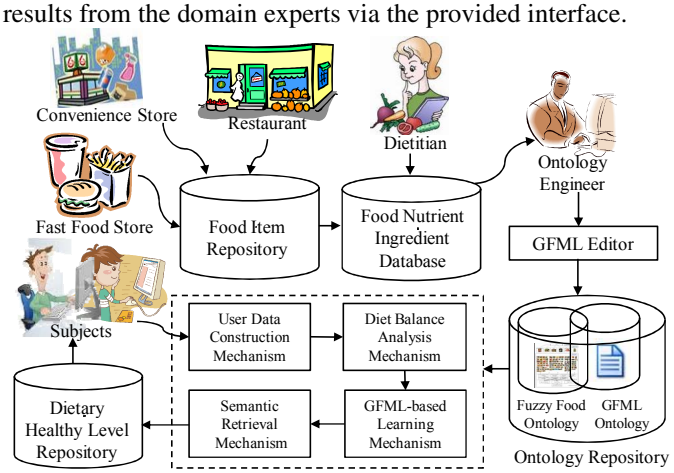

Fig. 5. Structure of the GFML-based diet application

B. *Considered Factors for Dietary Healthy Level*

Based on the collected meal records and the pre-defined fuzzy food ontology, everyday meals' Percentage of Calories from Carbohydrate (*PCC*), Percentage of Calories from Protein (*PCP*), Percentage of Calories from Fat (*PCF*), the Percentage of Caloric Ratio (*PCR*), and Food Group Balance (*FGB*) are acquired. The detailed information about these five fuzzy variables is described as followings.

In order to support one-day energy, it is necessary to consume the enough calories via the everyday diet. However, the main source of the calories is decided by the fact how many grams of the carbohydrate, protein, and fat that the food contains. As a result, to eat healthily, it is necessary for people to consider the balance of these three main nutrients, namely the carbohydrate, protein, and fat, when consuming your one-day meals. For this reason, this paper sets *PCC*, *PCP*, and *PCF* to represent the percentage of calories from carbohydrate, protein, and fat, respectively. According to [1], it indicates that (1) the suggested percentages of the daily intake for carbohydrate, protein, and fat are 55%~65%, 10%~20%, and 25%~35%, respectively, and (2) the contained calories for each gram of the carbohydrate, protein, and fat is 4kcal, 4kcal, and 9kcal, respectively. Based on the above-mentioned discussions, the *PCC*, *PCP*, and *PCF* are calculated by Eqs. (2), (3), and (4), respectively.

$$PCC(\%) = \frac{\text{Contained Grams of Carbohydrate} \times 4}{\text{Total Consumed Carloies}} \times 100\% \quad (2)$$

$$PCP(\%) = \frac{\text{Contained Grams of Protein} \times 4}{\text{Total Consumed Carloies}} \times 100\% \quad (3)$$

$$PCF(\%) = \frac{\text{Contained Grams of Fat} \times 9}{\text{Total Consumed Carloies}} \times 100\% \quad (4)$$

Besides considering the balance of the three main nutrients, the ratio of actual calories people consume to the planned caloric intake set by nutritionists is also an important factor to affect the healthy diet, especially for the fat and the slim. According to the involved domain experts' opinions, the one-day actually consuming calories for common people should be between 90% and 110% of the planned calories set by the dieticians. The domain experts set a planned goal for each person according to individual's height, weight, and daily physical activities. Based on the planned goal and the actual acquiring energies, the value of *PCR* is obtained by Eq. (5).

$$PCR(\%) = \frac{\text{Actual Consuming Calories}}{\text{Planned Consuming Calories}} \times 100\% \quad (5)$$

The balance of six food groups, including grains & starches, vegetables, fruits, milk, meats & proteins, and fats, is the most important factor to decide how much healthy level the eaten meals are. This is because the lack of some beneficial nutrients for our bodies such as fiber cannot be known if we only consider the balanced intake of carbohydrate, protein, and fat. So, in addition to planning the daily calories, the dieticians also plan one-day unique consuming servings of each food group for each person. Moreover, the contained quantity of sugar also affects the balance of intake-in food. Owing to the present-day living style, most people purchase the processed food as their usual meals from the shopping mall. However, unfortunately, the processed food frequently contains much more sugar than the natural food, and it is harmful for our bodies if too much sugar is eaten by people. The suggested percentage of daily sugar's intake is less than 10% of the planned caloric intake each day. The value of *FGB* is calculated by Eq. (6). With the retrieved information, including the values of *PCC*, *PCP*, *PCF*, *PCR*, and *FGB*, from the collected one-day meals, the dietary healthy level (*DHL*) is obtained after implementing the proposed approach.

$$FGB = BL_{Grains\&Starches} + BL_{Vegetables} + BL_{Fruits} + BL_{Milk} + BL_{Meats\&Proteins} + BL_{Fats} - CL_{Sugar} \quad (6)$$

where (1) $BL_{Grains\&Starches}$, $BL_{Vegetables}$, BL_{Fruits}, BL_{Milk}, $BL_{Meats\&Proteins}$, and BL_{Fats} represent the balanced level of the food groups grains & starches, vegetables, fruits, milk, meats & proteins, and fats, respectively. The higher the value is, the healthier the meals are; (2) CL_{Sugar} denotes the contained level of sugar for the meals. The lower the value is, the healthier the meals are; and (3) *FGB* value lies in the interval [0, 6].

C. GFML-based Inference Mechanism

In order to make the proposed system much more suitable to apply to the particular diet application, so the GFML is proposed in the paper. The GFML ontology is composed of the knowledge base and the rule base. Therefore, the GFML-based inference mechanism cannot be carried out until the GFML ontology is defined. Based on the above-discussed descriptions, the shapes and parameters of each factor's membership function are decided. Next is to design the rule base consisting of the 243 fuzzy rules. The involved dieticians regard that the *FGB* plays the most important role on the dietary healthy level. But, the *FCR* is as important as the *FGB* when people those who people are losing weight or gaining weight are neglected. As for *PCC*, *PCP*, and *PCF*, generally speaking, these three factors are equally important, but the dietary healthy level will be affected much when the *PCF* is not within the balanced range. Eventually, the fuzzy relation ratio of *PCC*:*PCP*:*PCF*:*PCR*:*FGB* (1:1:2:3:3) is determined by the involved domain experts.

Take one fuzzy rule for an example. Assume there is one fuzzy rule, and the if-part is "IF *PCC* is *Medium* AND *PCP* is *Medium* AND *PCF* is *Medium* AND *PCR* is *Medium* AND *FGB* is *Medium*." Computed by Eq. (7), this fuzzy rule's score (*S*) can be obtained according to Table V.

$$S = \frac{1\times 2 + 1\times 2 + 2\times 2 + 3\times 2 + 3\times 1}{1+1+2+3+3} = 1.7 \quad (7)$$

TABLE V. THE FUZZY RELATION OF EACH INPUT FUZZY VARIABLE

No	Fuzzy Variable	Fuzzy Relation	Fuzzy Term (Score)		
1	PCC	1	Low (1)	Medium (2)	High (1)
2	PCP	1	Low (1)	Medium (2)	High (1)
3	PCF	2	Low (1)	Medium (2)	High (0)
4	PCR	3	Low (1)	Medium (2)	High (1)
5	FGB	3	Low (0)	Medium (1)	High (2)

After the normalization, the normalized rule score (S_N) is acquired by Eq. (8), where the S_{min} and S_{max} are the minimum and maximum rule scores, respectively. Based on the normalized rule score, the then-part of the fuzzy rule could be determined by Table VI. Finally, the completed fuzzy rule is represented as "IF *PCC* is *Medium* AND *PCP* is *Medium* AND *PCF* is *Medium* AND *PCR* is *Medium* AND *FGB* is *Medium* THEN *DHL* is *VeryHigh*." The dietary healthy level is then inferred by carrying out the proposed method to indicate how much healthy, namely very high, high, medium, low, or very low, the eaten meals are. The before-learned membership functions of the fuzzy variables *PCC*, *PCP*, *PCF*, *PCR*, *FGB*, and *DHL* are illustrated in Fig. 6 and the partial before-learned fuzzy rules are shown in Table VII.

$$S_N = \frac{S - S_{min}}{S_{max} - S_{min}} = 0.83 \quad (8)$$

TABLE VI. S_N RANGE OF THE OUTPUT FUZZY VARIABLE

Fuzzy Term	VeryLow	Low	Medium	High	VeryHigh
S_N Range	[0, 0.2]	(0.2, 0.4]	(0.4, 0.6]	(0.6, 0.8]	(0.8, 1.0]

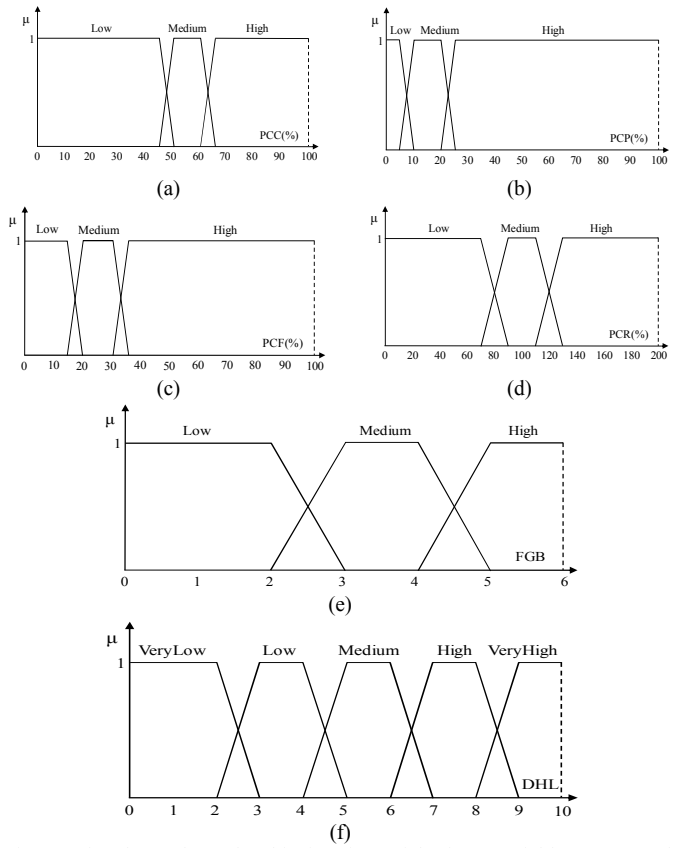

Fig 6. Before-learned membership functions of the fuzzy variables (a) *PCC*, (b) *PCP*, (c) *PCF*, (d) *PCR*, (e) *FGB*, and (f) *DHL*

TABLE VII. PARTIAL BEFORE-LEARNED FUZZY RULES

No	PCC	PCP	PCF	PCR	FGB	DHL
1	Low	Low	Low	Low	Low	VeryLow
2	Low	Low	Low	Low	Medium	Low
3	Low	Low	Low	Low	High	Medium
4	Low	Low	Low	Medium	Low	Low
5	Low	Low	Low	Medium	Medium	Medium
6	Low	Low	Low	Medium	High	High
7	Low	Low	Low	High	Low	VeryLow
8	Low	Low	Low	High	Medium	Low
9	Low	Low	Low	High	High	Medium
10	Low	Low	Medium	Low	Low	Low
11	Low	Low	Medium	Low	Medium	Medium
12	Low	Low	Medium	Low	High	High
13	Low	Low	Medium	Medium	Low	Medium
14	Low	Low	Medium	Medium	Medium	High
15	Low	Low	Medium	Medium	High	VeryHigh
16	Low	Low	Medium	High	Low	Low
17	Low	Low	Medium	High	Medium	Medium
18	Low	Low	Medium	High	High	High
19	Low	Low	High	Low	Low	VeryLow
20	Low	Low	High	Low	Medium	VeryLow
…						
224	High	High	Low	High	Medium	Low
225	High	High	Low	High	High	Medium
226	High	High	Medium	Low	Low	Low
227	High	High	Medium	Low	Medium	Medium
228	High	High	Medium	Low	High	High
229	High	High	Medium	Medium	Low	Medium
230	High	High	Medium	Medium	Medium	High
231	High	High	Medium	Medium	High	VeryHigh
232	High	High	Medium	High	Low	Low
233	High	High	Medium	High	Medium	Medium
234	High	High	Medium	High	High	High
235	High	High	High	Low	Low	VeryLow
236	High	High	High	Low	Medium	VeryLow
237	High	High	High	Low	High	Low
238	High	High	High	Medium	Low	VeryLow
239	High	High	High	Medium	Medium	Low
240	High	High	High	Medium	High	Medium
241	High	High	High	High	Low	VeryLow
242	High	High	High	High	Medium	VeryLow
243	High	High	High	High	High	Low

V. EXPERIMENTAL RESULTS

In this section, some experimental results are given. The proposed GFML-based learning mechanism is implemented with the C# programming language. The research performance presented in this paper is a research project involving with the National University of Tainan (NUTN) and National Cheng Kung Hospital in Taiwan. With the support of the involved domain experts, the proposed method is applied to the diet domain. There are seven students involved in this research project. The involved students of NUTN are responsible for routinely recording their meals and three involved domain experts evaluate the proposed method performance. For the involved students, the meal records are collected through Monday to Friday for one month so that the total collected records are 140. Table VIII shows the partial before-learned FML ontology for the diet application in this paper.

TABLE VIII. PARTIAL BEFORE-LEANRED FML ONTOLOGY

```
<?xml version="1.0"?>
<FuzzyController ip="localhost" name="">
  <KnowledgeBase>
    <FuzzyVariable domainleft="0" domainright="100" name="PCC"
scale="percentage" type="input">
      <FuzzyTerm name="Low" hedge="Normal">
        <TrapezoidShape Param1="0" Param2="0" Param3="45" Param4="50" />
      </FuzzyTerm>
      <FuzzyTerm name="Medium" hedge="Normal">
        <TrapezoidShape Param1="45" Param2="50" Param3="60" Param4="65" />
      </FuzzyTerm>
      <FuzzyTerm name="High" hedge="Normal">
        <TrapezoidShape Param1="60" Param2="65" Param3="100" Param4="100" />
      </FuzzyTerm>
    </FuzzyVariable>
…
</KnowledgeBase>
  <RuleBase activationMethod="MIN" andMethod="MIN" orMethod="MAX"
name="RuleBase1" type="mamdani">
    <Rule name="Rule1" connector="and" weight="1" operator="MIN">
      <Antecedent>
        <Clause>
          <Variable>PCC</Variable>
          <Term>Low</Term>
        </Clause>
        <Clause>
          <Variable>PCP</Variable>
          <Term>Low</Term>
        </Clause>
        <Clause>
          <Variable>PCF</Variable>
          <Term>Low</Term>
        </Clause>
        <Clause>
          <Variable>PCR</Variable>
          <Term>Low</Term>
        </Clause>
        <Clause>
          <Variable>FGB</Variable>
```

```
            <Term>Low</Term>
          </Clause>
        </Antecedent>
        <Consequent>
          <Clause>
            <Variable>DHL</Variable>
            <Term>VeryLow</Term>
          </Clause>
        </Consequent>
      </Rule>
…
</RuleBase>
</FuzzyController>
```

In order to implement the genetic learning mechanism based on GFML, one-student 20 records are used as the training data listed in Table IX, and the rest of six-student 120 records are the testing data. In Table IX, the columns DHL_{DO} and DHL_{GFML} represent the desired output from the dieticians and the inferred results from the proposed method, respectively. In this paper, the values of the $N_{generation_max}$, $p_{crossover}$, $p_{mutation}$, $fitness_{minimum}$, and $S_{population}$ are 1000, 0.9, 0.1, 0, and 100, respectively. Fig. 7 shows the after-learned membership functions for fuzzy variables *PCC*, *PCP*, *PCF*, *FCR*, *FGB*, and *DHL*.

TABLE IX. PARTIAL TRAINING DATA WITH DESIRED OUTPUT AND INFERRED RESULTS

Meal ID	*PCC* (%)	*PCP* (%)	*PCF* (%)	*FCR* (%)	*FGB*	DHL_{DO}	DHL_{GFML}
1	48.29	16.44	35.28	128.43	0.71	4	4.14
2	50.17	14.95	34.88	112.98	1.81	4.67	5.26
3	47.59	20.35	32.06	90.91	1	4	0
4	44.44	17.04	38.52	108.67	0.35	4.67	0
5	51.4	13.69	34.91	96.17	0.75	5	2.23
6	57.28	14.86	27.86	100.42	2.34	5	4.14
7	49.77	17.65	32.58	114.51	0.5	5	0
8	51.84	12.06	36.1	147.93	0	2.67	0
9	37.25	18.79	43.96	113.78	1	4.33	4.13
10	56.26	14.27	29.47	84.02	1.47	3.67	2.15
11	58.26	13.22	28.51	135.11	1	3.67	1.66
12	56.95	11.81	31.24	117.92	0.22	3.33	0
13	53.13	14.35	32.52	115.58	2.36	3.33	4.13
14	35.66	18.72	45.62	86.9	0.25	3.67	0
15	40.51	19.9	39.59	113.21	2.1	4.33	5.54
16	56.24	13.15	30.61	137.11	0	3.67	0
17	37.93	17.56	44.51	107.39	1	4	4.13
18	55.02	12.21	32.77	130.91	0.8	2.67	1.66
19	55.94	13.62	30.43	107.26	1	4	1.66
20	45.97	14.38	39.64	115.87	1	4.33	4.13

The mean square error (*MSE*) is utilized to evaluate the performance of the proposed method in this paper. The *MSE* is calculated by Eq. (9) and the lower *MSE* is, the better the performance is. Fig. 8 shows the distribution of the number when MSE_{GFML} is less than or equal to MSE_{GFML}, *Count* ($MSE_{GFML} \le MSE_{FML}$), and the number when MSE_{GFML} is bigger than MSE_{FML}, *Count* ($MSE_{GFML} > MSE_{FML}$), for the training data and the testing data. Fig. 8 indicates that the performance of the proposed approach is better than the FML-based inference mechanism for the training data. On the other hand, for the testing data, the FML-based inference mechanism is superior to the GFML-based inference mechanism. In addition, we also need to further use more number of training and testing subjects to demonstrate the performance of the proposed system in the future.

$$MSE = \frac{1}{n}\sum_{i=1}^{n} e_i^2, e_i = Y_i - \hat{Y}_i \tag{9}$$

where, Y_i represents the inferred results via the FML-based inference mechanism (DHL_{FML}) or the GFML-based learning mechanism (DHL_{GFML}), $\hat{Y}_i$ denotes the desired output recommended from the dieticians (DHL_{DO}), and n is the number of the meal records.

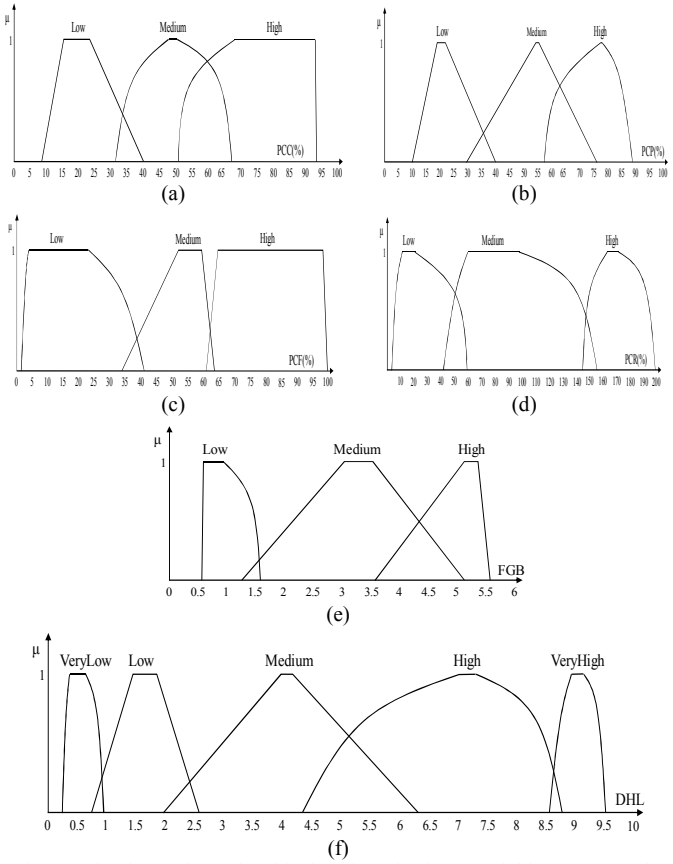

Fig. 7. After-learned membership functions for fuzzy variables (a) *PCC*, (b) *PCP*, (c) *PCF*, (d) *PCR*, (e) *FGB*, and (f) *DHL*

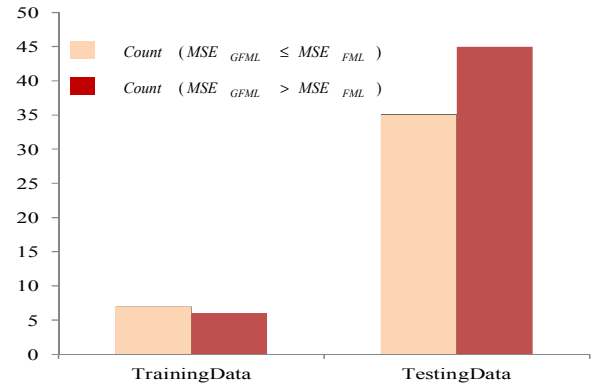

Fig. 8. Distribution for the training data and testing data

VI. CONCLUSIONS

The GFML-based learning mechanism combined the FML with the genetic learning mechanism is presented and applied

to the diet domain to infer the dietary healthy level of one-day eaten food. The effectiveness of the proposed method is verified by comparing with the results of dieticians' assessment. However, some noises such as the gray-marked records in Table IX are generated after executing the GFML-based learning mechanism; therefore, in the future, creating more training data and making some comparisons with other combinations of training and testing subjects are necessary to further improve the performance of the proposed method. Additionally, it is also feasible to introduce the proposed approach to other countries' diet in the future.

ACKNOWLEDGMENT

The authors would like to thank the National Science Council of Taiwan for financially supporting this international cooperation research project under the grant NSC98-2221-E-024-009-MY3, NSC 99-2622-E-024-003-CC3, and NSC 99-2911-I-024-004. The authors also would like to thank the involved students for their joining this research project.

REFERENCES

[1] D. L. Katz and H. Gonalez, "The way to eat: a six-step path to lifelong weight control," Sourcebooks Inc, Napervilee, Illinois, USA, 2004.

[2] C. S. Lee, M. H. Wang, and H. Hagras, "A type-2 fuzzy ontology and its application to personal diabetic-diet recommendation," *IEEE Transactions on Fuzzy Systems*, vol. 18, no. 2, pp. 374-395, Apr. 2010.

[3] M. H. Wang, C. S. Lee, K. L. Hsieh, C. Y. Hsu, G. Acampora, and C. C. Chang, "Ontology-based multi-agents for intelligent healthcare applications," *Journal of Ambient Intelligence and Humanized Computing*, vol. 1, no. 2, pp. 111-131, Jun. 2010.

[4] C. S. Lee, M. H. Wang, G. Acampora, C. Y. Hsu, and H. Hagras, "Diet assessment based on type-2 fuzzy ontology and fuzzy markup language," *International Journal of Intelligent System*, vol. 25, no. 12, pp. 1187-1216, Dec. 2010.

[5] C. S. Lee and M. H. Wang, "A fuzzy expert system for diabetes decision support application," *IEEE Transactions on Systems, Man, and Cybernetics Part B*: *Cybernetics*, vol. 41, no. 1, pp. 139-153, Feb. 2011.

[6] N. F. Noy and M. A. Musen, "Ontology versioning in an ontology management framework," *IEEE Intelligent Systems*, vol. 19, no. 4, pp. 6-13, Jul./Aug. 2004.

[7] A. Zouaq and R. Nkambou, "Evaluating the generation of domain ontologies in the knowledge puzzle project, " *IEEE Transactions on Knoweldge and Data Engineering*, vol. 21, no. 11, pp. 1559-1572, Nov. 2009.

[8] A. M. Hisham and H. A. Nguyen, "Measuring semantic similarity between biomdecial concepts within multiple ontologies," *IEEE Transactions on Systems, Man, and Cyernetics-Part C: Applications and Reviews*, vol. 39, no. 4, pp. 389-398, Jul. 2009.

[9] C. S. Lee, Z. W. Jian, and L. K. Huang, "A fuzzy ontology and its application to news summarization," *IEEE Transactions on Systems, Man, and Cybernetics, Part B*: *Cybernetics*, vol. 35, no. 5, pp. 859-880, Oct. 2005.

[10] C. H. Chou, F. M. Zahedi, and H. Zhao, "Ontology for developing web sites for natural disaster management: methodology and implementation," *IEEE Transactions on Systems, Man, and Cyernetics-Part A: Systems and Humans*, vol. 41, no. 1, pp. 50-62, Jan. 2011.

[11] G. Acampora and V. Loia, "Fuzzy control interoperability and scalability for adaptive domotic framework," *IEEE Transactions on Industrial Informatics*, vol. 1, no. 2, pp. 97-111, May 2005.

[12] G. Acampora and V. Loia, "Using FML and fuzzy technology in adaptive ambient intelligence environments," *International Journal of Computational Intelligence Research*, vol. 1, no. 2, pp. 171-182, 2005.

[13] K. F. Man, K. S. Tang, and S. Kwong, "Genetic Algorithms," Springer-Verlag, London, UK, 1999.

[14] C. S. Lee, S. M. Guo, and C. Y Hsu, "Genetic-based fuzzy image filter and its application to image processing," *IEEE Transactions on Systems, Man and Cybernetics Part B*: *Cybernetics*, vol. 35, no. 4, pp. 694-711, Aug. 2005.

[15] C. S. Lee and C. Y Pan, "An intelligent fuzzy agent for meeting scheduling decision support system," *Fuzzy Sets and Systems*, vol. 142, no. 3, pp. 467-488, Mar. 2004.

[16] K. G. Khoo and P. N. Suganthan "Structural pattern recognition using genetic algorithms with specialized operators," *IEEE Transactions on Systems, Man and Cybernetics Part B*: *Cybernetics*, vol. 33, no. 1, pp. 156-165, Feb. 2003.

[17] T. T. Quan, S. C. Hui, A. C. M. Fong, and T. H. Cao, "Automatic fuzzy ontology generation for semantic web," *IEEE Transactions on Knowledge and Data Engineering*, vol. 18, no. 6, pp. 842-856, Jun. 2006.

[18] M. H. Wang, A. Naito, Z. W. Chen, and C. S. Lee, "FML-based Japanese food ontology applications," *Japan-Cambodia Joint Symposium on Information Systems and Communication Technology* (*JCAICT 2011*), Phnom Penh, Cambodia, Jan. 6-8, 2011.

[19] G. Acampora, M. Gaeta, V. Loia, and A. V. Vasilakos, "Interoperable and adaptive fuzzy services for ambient intelligence applications," *ACM Transactions on Autonomousand Adaptive Systems*, vol. 5, no. 2, 2010.

2011 IEEE International Conference on Fuzzy Systems
June 27-30, 2011, Taipei, Taiwan

A Hierarchical Approach to Assess Keyword Dependencies in Fuzzy Keyword Ontologies

Christer Carlsson
IAMSR, Åbo Akademi University
Joukahaisenkatu 3-5A
FIN-20520 Åbo, Finland
Email: christer.carlsson@abo.fi

Robert Fullér
IAMSR, Åbo Akademi University
Joukahaisenkatu 3-5A
FIN-20520 Åbo, Finland
Email: rfuller@abo.fi

Mario Fedrizzi
DISA, Faculty of Economics
University of Trento
via Inama 5, 38122 Trento, Italy
Email: mario.fedrizzi@unitn.i

***Abstract*—The Knowledge Mobilization project (KNOWMOBILE) has been a joint effort by Institute for Advanced Management Systems Research, Åbo Akademi University and VTT Technical Research Centre of Finland. Its goal was to better "mobilize" knowledge stored in heterogeneous databases for users with various backgrounds, geographical locations and situations. The working hypothesis of the project was that fuzzy mathematics combined with domain-specific data models, in other words, fuzzy ontologies, would help manage the uncertainty in finding information that matches the users needs. In this way, KNOWMOBILE places itself in the domain of knowledge management. In this paper we describe an industrial demonstration of fuzzy ontologies in information retrieval in the paper industry where problem solving reports are annotated with keywords and then stored in a database for later use. Furthermore, using Bellmann-Zadeh's principle to fuzzy decision-making we will show a method for identifying keyword dependencies in the keyword taxonomic tree.**

***Keywords*—Fuzzy ontology; keyword ontology; fuzzy coverage**

I. Introduction

Fuzzy ontologies have been proposed as a solution for addressing semantic meaning in an uncertain and inconsistent world. Since many concepts that are needed for intelligent systems lack well defined boundaries, or precisely defined criteria of membership, we need fuzzy logic to deal with notions of vagueness and imprecision. As with fuzzy logic, reasoning is approximate rather than precise. The aim is to avoid the theoretic pitfalls of monolithic ontologies, facilitate interoperability between different and independent ontologies [1], and provide flexible information retrieval capabilities [2]–[5]. In the KNOWMOBILE project, we developed a concept of a tool for searching plant knowledge with a search engine based on a fuzzy ontology. The usage scenario for the tool was that a process expert, dealing with a problem in the process chemistry of a paper machine, wishes to find past problem solving cases of a similar setting in order to find possible solutions to a current issue. This setting is a universal one: pieces of knowledge, called "nuggets", are written and stored by companies on different domains in the form of incident reports.

In the KNOWMOBILE project we have focused on the chemistry of the "wet end" in order to limit the work effort needed to construct the domain ontology and concentrate on a subject on which domain expertise and actual data were available. Nuggets are documents than can contain all kinds of raw data or multimedia extracted from different information systems. An expert author annotates the nuggets with suitable keywords, and it is these keywords that the search is then based on. In addition to providing exact results to queries, the tool uses a fuzzy domain ontology to extend the query to related keywords (see Figure 1). As a result, the search results include nuggets that may not necessary deal with exactly the same process equipment, variable, function or chemical, but nuggets that may still provide valuable insight to solving the problem at hand. The terms defined in the ontology should be familiar to the users of the system, e.g. for plant operators, process developers and chemical suppliers. On the other hand, the terminology should be based on sound principles of conceptual modeling and ontology development. Furthermore, the goal should be to have common concepts and plant models with equipment manufacturers and engineering contractors that provide the initial information and often participate in modifications and upgrade projects. This creates a link to the ongoing development of engineering data models for various industrial areas. Fuzzy keyword ontologies should thus make use of relevant product and plant modeling standards and more general upper ontologies. The key research question of the KNOWMOBILE project is [6]: How to build fuzzy ontologies for the process industry domain to enhance knowledge retrieval?

II. Fuzzy ontology for process industry

Our demonstration works with both engineering and operational knowledge of an industrial plant and we used the following taxonomic system,

- Top layer: general concepts (based on international standards).
- Middle layer: vocabulary defined and shared by business partners to share knowledge of, e.g. the type and structure of process equipment. This layer extends the top layer with domain-specific keywords.
- Bottom layer: custom, company-specific concepts, e.g. specific products and component types, or even individual process plants.

The system of keywords represents concepts, properties, relationships, axioms, and reasoning schemes relevant for the

978-1-4244-7316-8/11/$26.00 ©2011 IEEE

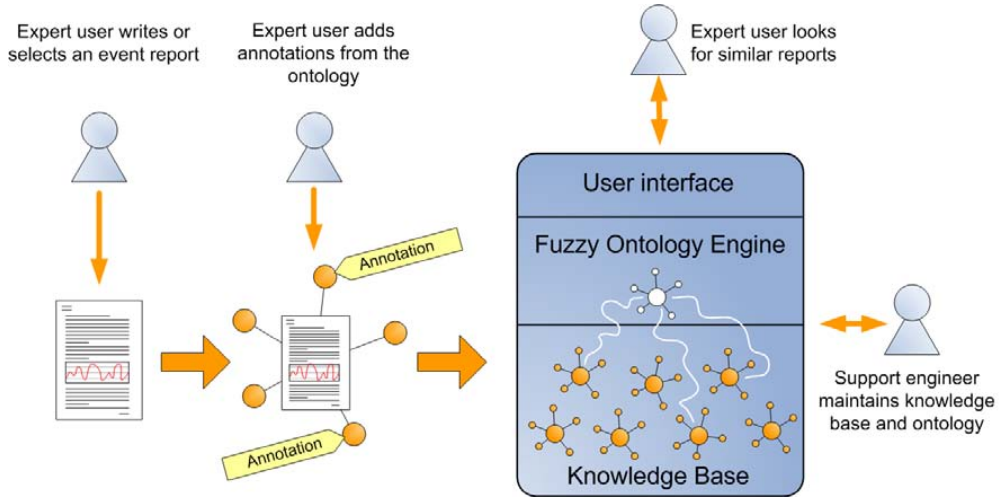

Fig. 1. System concept - a knowledge base of event reports [6].

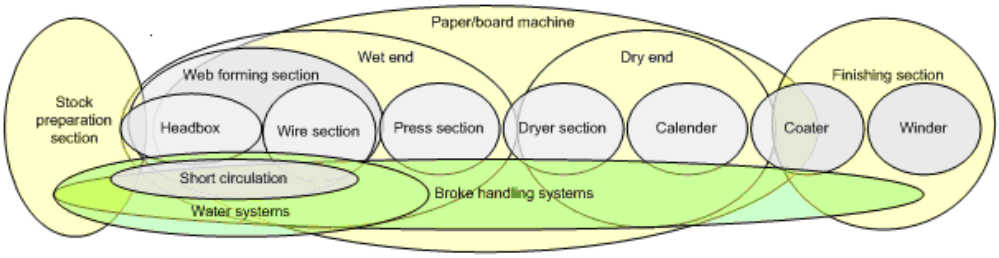

Fig. 2. System example - a fuzzy decomposition of a paper making line. [6].

application area. On the basis of various upper ontologies and industrial data models we identified that the following keyword categories are needed to characterize event reports:

- Systems: types of real-world components of a process plant, e.g. machines, buildings, software and people. (see Figure 2)
- Functions: phenomena and activities carried out at an industrial plant.
- Variables: properties and state variables of various entities, e.g. temperature.
- Events: types of interesting periods of plant life described in event reports, e.g. test runs or equipment failures.
- Materials: raw materials, products, consumables etc. handled in a process plant.

Our basic approach to conceptualize our application is shown in the informal Unified Modeling Language (UML) class diagram below (Figure 3).

Event reports describe events that are related to various entities of a process plant, e.g. to equipment, processing functions and materials. Nothing is assumed about the internal structure of event reports. Instead, they are characterized by an expert with keywords selected from a fuzzy ontology. The expert can select the keywords from five categories: event,

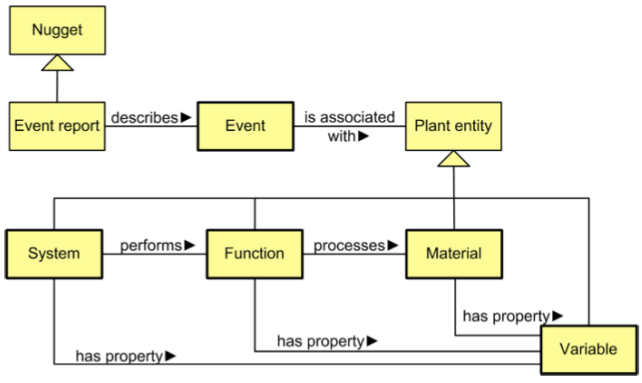

Fig. 3. Overall domain concepts [6].

system, function, material and variable. All keywords represent an entity type and can have subtypes and smaller parts. In the KNOWMOBILE demonstration tool keywords are used to characterize event reports and other nuggets stored in a database.

Classification (is-a) and decomposition (part-of) can be found in most ontologies and data models. They are important in the industrial context as well. So, the keywords in each cat-

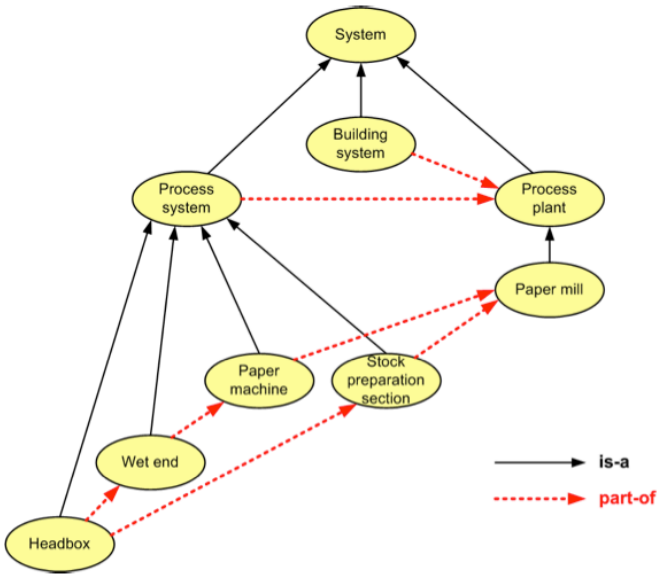

Fig. 4. Simplified event classification matrix [7].

egory are linked by is-a and part-of relationships as illustrated in Figure 4. Furthermore, the ontology should model functional and other kinds of dependencies between keywords in various keyword categories. As an example, systems can be or are used for some purposes, i.e. they play various roles in carrying out one or more functions. This creates a link between the keywords ”wire section (a part of paper machine)” and ”formation (a quality measure of the produced paper)”. Modeling classifications, decompositions and various dependencies leads to a situation where we have a taxonomy tree for each keyword category and a set of part-of relationships trees describing the decomposition to various domain entities (Figure 5). In addition, there are dependency relationships linking keywords to each other.

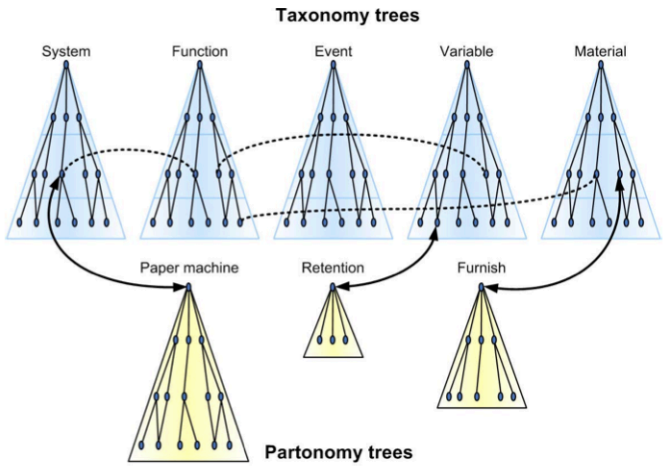

Fig. 5. The fuzzy ontology defines classification, decomposition and miscellaneous dependency relationships between keywords [7].

III. The keyword ontology

For developing a software tool the ontology should be expressed and stored in a more formal way. The basic approach for representing a fuzzy ontology is illustrated in Figure 6 with a combination of UML class and instance diagrams.

From all kinds of nuggets, the demonstration only looks at event reports that usually describe problematic situations. Each report, like the specific instance ”Report #1” in the diagram, is related to types of systems, plant functions, events, etc. Only the reference ”Report #1” to the keyword ”Holes” is shown in Figure 6 . As indicated by the ”instance of” associations, all keywords seen by the users are individuals, .i.e. instances of a subclass of ”Keyword category”. Fuzzy dependencies between keyword instances are described by a few fundamental relationship types like is-a (specialization), part-of and, as an option, instantiation. In the first version we focus on ”specializations”, i.e. fuzzy classification of keywords. The degree of overlapping (or inclusion) of the sets represented by the keywords is described by linguistic labels, i.e. natural language words like ”moderate” or ”significant”. So, the instance named ”Specialization #1” in Figure 6 tells us that ”Holes” is ”to a large extent” understood as a subclass of ”Quality problem but only represents a minor part of its scope”. In addition, the keyword ”Holes” may also specialize other problem types. In the KNOWMOBILE project we have modelled dependencies with one single dependency relationship. For simplicity it is symmetric and has a strength value between zero (independence) and one (full dependence).

IV. A Minimax Approach to Assess Keyword Dependencies

Now we show a method for approximating keyword dependencies in the keyword ontology. This method uses Bellman-Zadeh’s principle to fuzzy decision making [8]. An event type fuzzy taxonomy is shown in Figure 7. For example, consider the second column of event classification matrix ”Problem”. All ”Technical problems” are ”Problems” and they represent around 80% of all possible problems. That is ”Technical problem” covers ”Problem” with degree 0.8. Similarly, ”Human errors” are ”Problems ” and they represent around 30% of all possible problems. That is ”Human error” covers ”Problem” with degree 0.3. Following Bordogna and Pasi ([9], page 804) we will assume that if A and B are two keywords in the keyword taxonomic tree then

$$\text{coverage}(A, B) = \text{fuzzy inclusion}(A, B). \quad (1)$$

For example, ”System fault = {Device fault, Design flaw}” that is, ”System fault” is a union of these two events. Furthermore, ”Function failure = {Design flaw, Drift, Oscillation}” that is ”Function failure” is the union of these three events. ”Design flaw” covers ”System fault” with degree 0.6 and at the same time ”Design flaw” covers ”Function failure” with degree 0.4 (see Figure 7). Moreover, ”System fault” and ”Function failure” do not have any more component in common. We compute the degree of dependency between ”System fault”

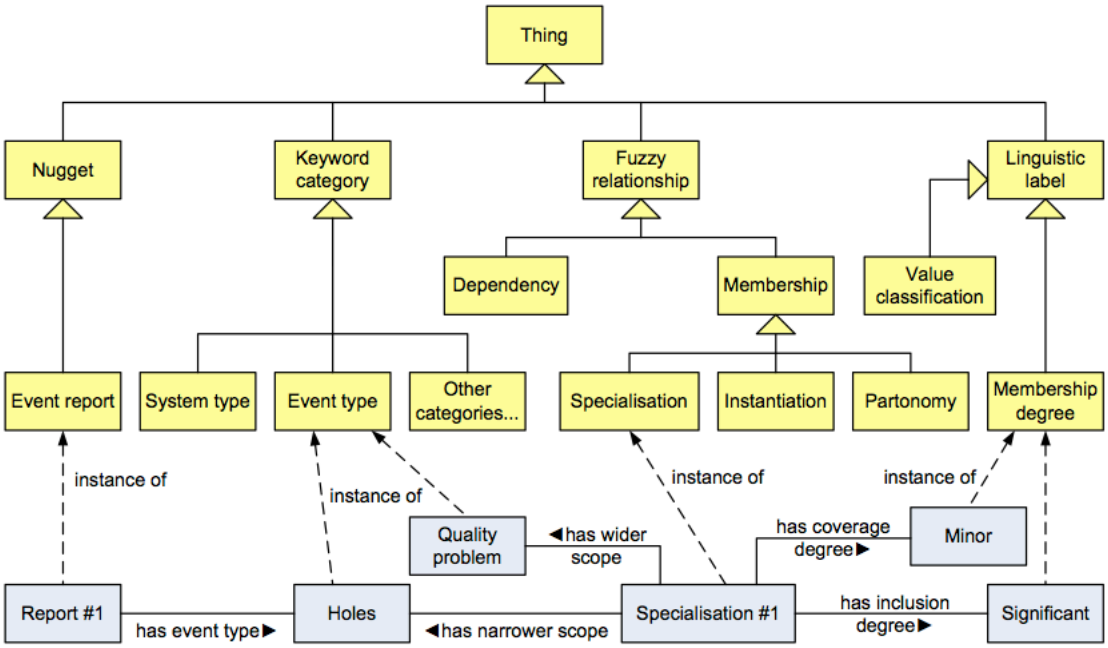

Fig. 6. Representing fuzzy keyword ontology with object classes and their instances [7].

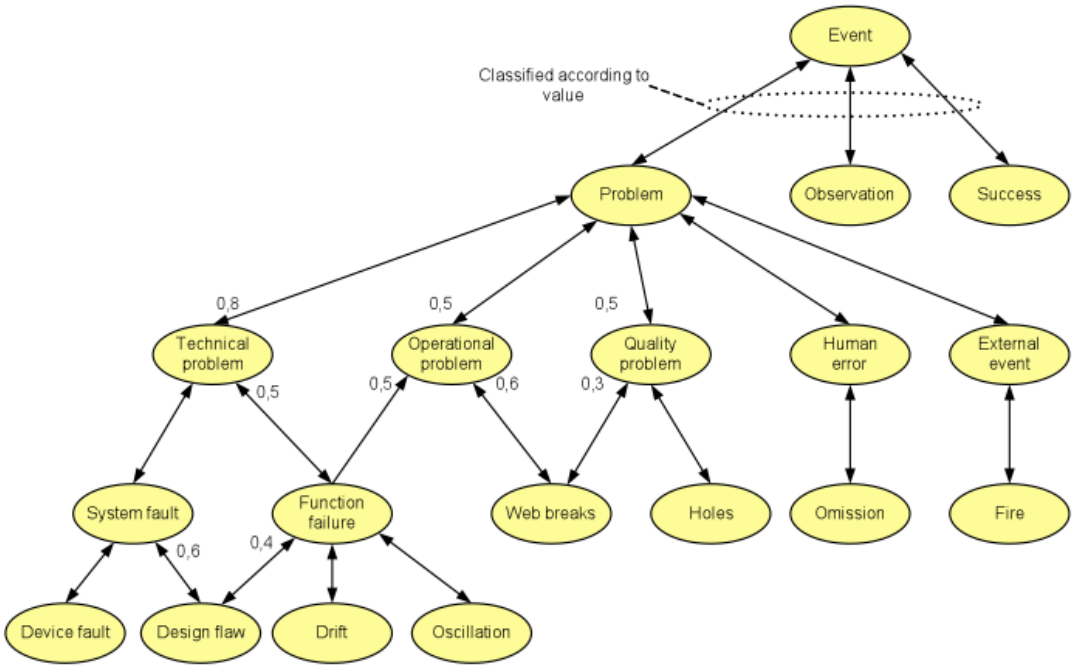

Fig. 7. A fragment of the event type fuzzy taxonomy [7].

(SF) and "Function failure" (FF) as their joint coverage by "Design flaw" (DF)

$$\text{dependency}(SF, FF) = \min\{\text{coverage}(DF, SF), \text{coverage}(DF, FF)\},$$

that is,

$$\text{dependency}(SF, FF) = \min\{0.6, 0.4\} = 0.4 \quad (2)$$

It is easy to see in Figure 7 that keywords "Function failure" and "Fire" are independent since they do not have any component in common. In this case we have,

$$\text{dependency}(\text{"Function failure"}, \text{"Fire"}) = 0. \quad (3)$$

Zero means independence, one means full dependence, and values between zero and one denote intermediate degrees of dependency between keywords. It can happen that two keywords have more than one joint component. Then we apply Bellman-Zadeh's principle (max-min approach) to fuzzy decision making to measure their dependency. For example, suppose that "System fault" and "Function failure" wrere to have two joint components, where the first one is "Design flaw" and the second one "Fluctuation" that has a coverage values 0.7 and 0.5, respectively. Then we measure the degree of dependency between "System fault" and "Function failure" according to Bellman-Zadeh's principle to fuzzy decision making as

$$\begin{aligned}\text{dependency}\{SF, FF\} &= \max\{\min\{0.6, 0.4\}, \min\{0.7, 0.5\}\} \\ &= \max\{0.4, 0.5\} = 0.5.\end{aligned}$$

Supposing that all the coverage degrees are given by experts. Then we can summarize our algorithm as follows: *Compute the degrees of dependency between keywords on the immediate upper level using the max-min approach. Then repeat this procedure until the top layer.* For example, consider keywords "Technical problem" (TP) and "Operational problem" (OP). Then we find (Figure 7),

$$\text{dependency}\{TP, OP\} = \min\{\text{coverage}(FF, TP), \text{coverage}(FF, OP)\} = 0.5.$$

One can further improve this model by introducing degrees of inclusion and coverage between concepts as suggested by Holi and Hyvönen [10], and Holi [11].

V. Demo architecture and implementation

The component-based demo architecture has been implemented by VTT Technical Research Centre of Finland, using the Protégé ontology editor to maintain the fuzzy ontology in OWL format (as shown in Figure 8). The GUI component (Graphical User Interface) guides the user in specifying the information query, and presents the results. Tools for browsing and evaluating the fuzzy reasoner component directly were also provided. A database adapter is used to access report data, which in this case was stored locally in XML files. Similarly, an ontology adapter is used to provide access to the fuzzy ontology, in this case stored in OWL files.

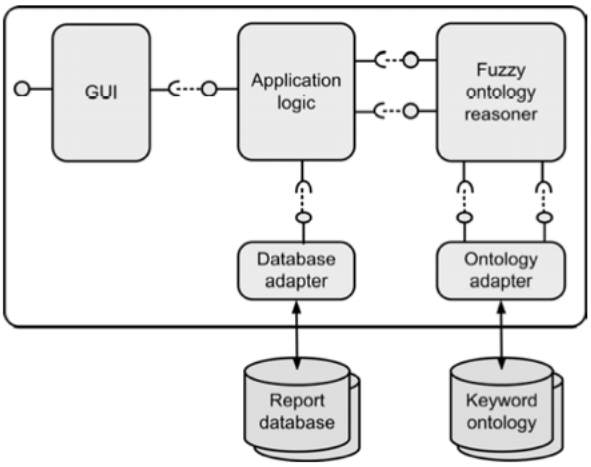

Fig. 8. Component-based demo application architecture [7].

The adapters help hide the different interfaces and protocols of different data sources (e.g. SQL, HTTP) and provide transparent access via an agreed interface. The fuzzy ontology reasoner component is used to process ontology-based information. Its main function in the demo is to extend a list of query keywords to a list of their closest neighbors in terms of fuzzy ontology relationships. For maintenance and evaluation purposes, the component interface also provides methods for directly accessing the ontology concepts and relationships. Finally, the application logic component binds all the functionality together by taking the query, using the reasoner component to extend it, passing the extended query to the report database and then combining and ordering the results for the GUI. The fuzzy ontology with fuzzy concepts, relations, and instances was defined using Protégé version 3.4. The developed ontology was exported for the reasoning software as a standard OWL file. Protégé is a widely used tool for developing ontologies. As such it provides some advantages, for example a forms-based interface for editing the basic classes and adding the individual keywords, reports, as well as their relationships. Protégé does not have a built-in support for modeling uncertainties, however in late 2010 Straccia [12] introduced new plug-in, called SoftFacts, which is an ontology mediated top-k information retrieval system over relational databases.

VI. Summary

We have examined the possible use of fuzzy ontologies in the retrieval of stored reports of industrial plant knowledge. Since no well-established definitions or mature tools exist, we have adopted a practical approach - defining those constructs that we deemed necessary in order to adequately capture domain semantics, and implementing a demonstration application in which to test those constructs against actual industrial data. The demo has been evaluated with the help of industry experts. Although the extended query tool seems to be promising, there has been a great deal of worry about the amount of

work needed for maintaining the fuzzy ontology relationship weights.

REFERENCES

[1] V. Cross, "Fuzzy semantic distance measures between ontological concepts," IEEE Annual Meeting of the North American Fuzzy Information Processing Society (NAFIPS 2004), Banff, AB, Canada, pp. 635-640, June, 2004.

[2] G. Acampora and V. Loia, "Fuzzy control interoperability and scalability for adaptive domotic framework," IEEE Trans. Ind. Inf., vol. 1, pp. 97-111, May 2005.

[3] G. Acampora, M. Gaeta, V. Loia, A.V. Vasilakos, "Interoperable and adaptive fuzzy services for ambient intelligence applications," ACM Trans. Auton. Adap. vol. 5, pp. 8:1-8:26, May 2010.

[4] C.-S. Lee, Z.-W. Jian and L.-K. Huang, "A fuzzy ontology and its application to news summarization," IEEE Trans. Syst. Man Cybern. Part B Cybern., vol. 35, pp. 859-880, October 2005

[5] C.-S. Lee, M.-H. Wang, G. Acampora, C.-Y. Hsu and H. Hagras, "Diet assessment based on type-2 fuzzy ontology and fuzzy markup language," Int. J. Intell. Syst., vol. 25, pp. 1187-1216, October 2010.

[6] J. Hirvonen, T. Tommila, A. Pakonen, C. Carlsson, M. Fedrizzi, R. Fullér, "Fuzzy keyword ontology for annotating and searching event reports," International Conference on Knowledge Engineering and Ontology Development (KEOD 2010), Valencia, Spain, October, 2010.

[7] T. Tommila, J. Hirvonen, A. Pakonen, "Fuzzy ontologies for retrieval of industrial knowledge - a case study," VTT Working Papers, no. 153, November 2010.

[8] R. E. Bellman and L. A. Zadeh, "Decision-making in a fuzzy environment," Manage. Sci., Ser. B, vol. 17, pp. 141-164, December 1970.

[9] G. Bordogna, G. Pasi "A flexible multi criteria information filtering model," Soft Comput., vol. 14, pp. 799-809, June 2010.

[10] M. Holi and E. Hyvönen, "Modeling degrees of overlap in semantic web ontologies," ISWC Workshop Uncertainty Reasoning for the Semantic Web, Galway, Ireland, Nov. 2005.

[11] M. Holi, Crisp, fuzzy and probabilistic faceted semantic search, Doctoral dissertation, Aalto University School of Science and Technology, Helsinki, Finland, 2010.

[12] U. Straccia, "SoftFacts: A top-k retrieval engine for ontology mediated access to relational databases," 2010 IEEE International Conference on Systems Man and Cybernetics, pp. 4115-4122, October 2010.

2011 IEEE International Conference on Fuzzy Systems
June 27-30, 2011, Taipei, Taiwan

Improving Disease Prediction Using ICD-9 Ontological Features

Mihail Popescu
Health Management and Informatics Department
University of Missouri
Columbia, MO 65211 USA
popescum@missouri.edu

Mohammad Khalilia
Computer Science Department
University of Missouri
Columbia, MO 65211 USA
mohammedsk@gmail.com

Abstract— **Disease prediction has become important in a variety of applications such as health insurance, tailored health communication and public health. Disease prediction is usually performed using publically available datasets such as HCUP, NHANES or MDS that were initially designed for health reporting or health cost evaluation but not for disease prediction. In these datasets, medical diagnoses are traditionally arranged in "diagnose-related groups" (DRGs). In this paper we compare the disease prediction based on crisp DRG features with the results obtained employing a new set of features that consist of the fuzzy membership of patient diagnoses in the DRG groups. The fuzzy membership features were computed using an ICD-9 ontological similarity approach. The prediction results obtained on a subset of 9,000 patients from the 2005 HCUP data representing three diseases (diabetes, atherosclerosis and hypertension) using two classifiers (random forest and SVM trained on 21,000 samples) show significant (about 10%) improvement as measured by the area under the ROC curve (AROC).**

Keywords-component; disease prediction; ICD-9 similarity measure; ontological features; random forest; SVM.

I. INTRODUCTION

Disease prediction is employed in different domains such as risk management, tailored health communication and public health. Risk management plays an important role in health insurance industry, mainly in the underwriting process. Health insurers use a process called underwriting in order to classify the applicant as standard or substandard, based on which they compute the policy rate and the premiums individuals have to pay [1].

Another domain where disease prediction may be applied is tailored health communication. For example, we can target specific medical educational materials and news to a subgroup within the general population that has a high predicted risk for a given disease. Cohen et al [2] discussed how tailored health communication for cancer patients can motivate cancer prevention and early detection. Disease risk prediction along with tailored health communication represents an effective preventive medicine method that may lead in the long-run to a reduction in the cost of medical care.

The reporting requirements of various US governmental agencies such as Center for Disease Control (CDC), Agency for Health Care Quality (AHRQ) and US Department of Health and Human Services Center for Medicare Services (CMS) have created huge public datasets that, we believe, are not utilized to their full potential. For example, CDC (www.cdc.gov) makes available National Health and Nutrition Examination Survey (NHANES) data. Using NHANES data, Yu et al. [3] predicts diabetes risk using an SVM classifier. CMS (www.cms.gov) uses the Medicare and Medicaid claims to create the minimum dataset (MDS). Herbert et al. [4] uses MDS data to identify people with diabetes. In this paper we use the National Inpatient Sample (NIS) data created by AHRQ (www.ahrq.gov) Healthcare Utilization Project (HCUP), to predict the risk for three diseases: diabetes, atherosclerosis and hypertension. To compute the disease risk we use a new set of ICD-9 features based on ontological similarity between the ICD-9 diagnoses contained in a DRG and the ICD-9 diagnoses of the patient. We compare this approach with the prediction of the same diseases described in [5].

The remainder of this article is structured thusly: in Section II we describe the ICD-9 medical taxonomy together with the similarity measure used in the feature extraction process. In Section III we describe the proposed ontological feature extraction algorithm together with a brief description of the classifiers employed, in Section IV we show some results obtained on a subset of 2005 HCUP patient dataset and in Section V we provide some conclusions and ideas for future research.

II. ICD-9 MEDICAL TAXONOMY AND SIMILARITY MEASURE

International classification of diseases-version 9 (ICD-9) is a diagnose coding system [6] used in hospitals for data retrieval and billing purposes. Every code represents a disease, condition, symptom, or cause of death. However, from our point of view ICD-9 represents an ontology, i.e. a controlled vocabulary overlaid with a "is-a" term hierarchy. The controlled vocabulary allows for detection of synonymy when two diagnoses are compared. The hierarchy (tree) structure allows for assessing the semantic similarity between diagnoses. A snippet of the ICD-9 tree is shown in Fig. 1.

This work has been supported in part by a UM Research Board grant.

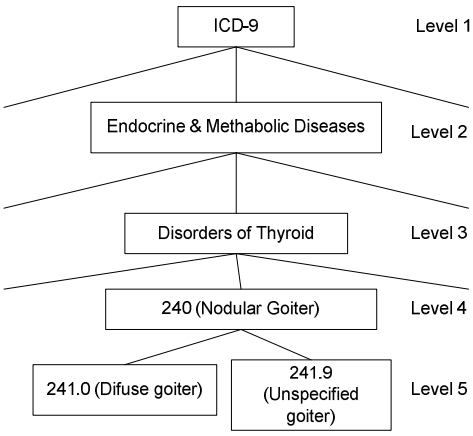

Figure 1. Partial view of the ICD-9 hierarchy

From Fig. 1 we see that diagnoses 241.0 and 241.9 are semantically related although they are syntactically (string-wise) different. Unfortunately, the ICD-9 hierarchy has only 5 levels. This will have an impact on the granularity of the term similarity as many pairs of terms will have the same similarity coefficient. However, even with this low granularity the impact on prediction performance is significant.

In our view, the hierarchical structure of the ICD-9 ontology represents the knowledge of the medical field as viewed by the domain experts (physicians). The key of our approach is to use the domain knowledge (hierarchy) in computing patient similarities. Given two patients described by a sequence of ICD-9 diagnoses, T_{ij}, we first consider the problem of computing the association (seen as fuzzy membership), $s(T_1, T_2)$, between two terms (diagnoses) T_1 and T_2.

There are many algorithms for defining term similarity in a taxonomy (see Chapter 2 in [7]). One way of computing term similarity is to assign each term T_i weights based on its importance, IMP, within the ontology. As a consequence, two patients are more similar if they both have the same rare (in the database) disease (say cystic fibrosis) than if they both have flu. The term importance can be computed (see Chapter 2 in [7]) using path-based, depth-based, density-based, information content-based approaches. In this work we use a depth-based approach. The importance IMP, of a term in the ICD-9 taxonomy is computed as IC=1-1/n where n = {1, 2, 3, 4, 5} is the level of the term within the hierarchy. For example, the IMP of diagnosis code 241 (Goiter, level 4) is IMP(241) = 1-1/n = 1-1/4 = 0.75. For consistency, we consider IMP(level 5) = 1. Now, returning to the problem from the beginning of this paragraph, the similarity of two diagnosis terms, $s(T_1, T_2)$, is defined as:

$$s(T_1, T_2)=IMP(NCA(T_1, T_2)). \quad (1)$$

where NCA="nearest common ancestor" of the two terms in the ontology.

In Fig. 1, the nearest common ancestor (NCA) of 241.0 and 241.9 is 241, and so, the similarity between the two diagnoses is s(241.0, 214.9)=IMP(241)=0.75. This is clearly the simplest approach and it is only used here for illustrative purposes.

For two sets of ICD-9 terms, $P_1 = \{T_{11}, \ldots, T_{1n}\}$ and $P_2=\{T_{21}, \ldots, T_{2m}\}$ we can define a variety of similarities (see Chapter 2 in [7] for details). In this paper we consider the following simple formula:

$$s(P_1, P_2)=\max_{ij}\{s(T_{1i}, T_{2j})\}. \quad (2)$$

III. STUDY METHODOLOGY

To better understand the feature extraction process we first describe the 2005 HCUP dataset used in this paper (denoted henceforth HCUP2005).

A. The HCUP2005 dataset

The Nationwide Inpatient Sample (NIS) is a database of hospital inpatient admissions that dates back to 1988 and it is used to identify, track, and analyze national trends in health care utilization, access, charges, quality, and outcomes. The NIS database is developed by the Healthcare Utilization Project (HCUP) and sponsored by the AHRQ. This database is publicly available and does not contain any patient identifiers. The database contains discharge level information on all inpatients from a 20% stratified sample of hospitals across the United States, representing approximately 90% of all US hospitals [8]. HCUP data from the year 2005, denoted as HCUP2005, will be used in this paper.

The data set contains 7,995,048 hospital stays and 126 clinical and nonclinical data elements for each hospital stay. Nonclinical elements include patient demographics, hospital identification, admission date, zip code, calendar year, total charges and length of stay. Clinical elements include procedures, procedure categories, diagnosis codes and diagnosis categories. Every record contains a vector of 15 ICD-9 diagnosis codes. In addition, every record contains a vector of 15 diagnosis category codes (DRGs). The diagnosis categorization is performed using the Clinical Classification Software (CCS) developed by HCUP. There are numerous ICD-9 codes, over 14,000, in HCUP; CCS collapsed these codes into a smaller number of clinically meaningful DRGs. There are 259 diagnosis categories in the HCUP2005 dataset, every category is denoted by a value in the range 1-259. Demographics such as age, race and sex are also included in our data set and used predicting the three medical conditions.

The prevalence in the HCUP2005 dataset of three diseases used in this paper (hypertension, diabetes mellitus and coronary atherosclerosis) is given in table I below. As we see from table I, some diseases like testis cancer might not have a sufficient number of samples for training a classifier even on such a large dataset.

TABLE I. THE PREVALENCE OF FOUR DISEASES IN THE HCUP2005 DATASET

Disease	Prevalence
Hypertension	29.1%
Diabetes mellitus, no complications	12%
Coronary Atherosclerosis	27.65%
Testis Cancer	0.046%

B. ICD-9 based Ontological Features

To predict a disease, we extract from HCUP2005 a random set of N patients, N/2 with the disease and N/2 without it. For each patient, P_i with i = {1, … , N}, we used from HCUP2005 the following variables: age, race, sex, 15 ICD-9 codes ($P_{i,ICD9}$) and 15 diagnosis categories ($P_{i,DRG}$). As mentioned before, there are 259 DRGs, DRG_j with j = {1, …, 259}, and every group contains a set of ICD-9 codes, DRG_j = {$ICD9_{j1}$, …, $ICD9_{jk}$}. In [5] we represented each patient P_i using a feature vector $\mathbf{x}_i^{crisp} \in R^P$, with P=262 dimensions. Features 1-259 (DRG related) were computed as:

$$x_{ip}^{crisp} = \begin{cases} 1 & P_{i,ICD9} \cap DRG_p \neq \varnothing \\ 0 & P_{i,ICD9} \cap DRG_p = \varnothing \end{cases} \quad (3)$$

Essentially, since the DRGs were computed for us, the feature vector had an 1 in position p if DRG_p was contained in the diagnoses set of patient i, $P_{i,DRG}$. As a result, each feature vector contained at most 15 ones (the number of DRGs stored per patient) which was a rather sparse representation. The last 3 features (index 260, 261, 262) were sex, age and race, respectively.

In this paper we propose to compute the 259 diagnose related features using a fuzzy membership in each DRG_j, i.e. a value between 0 and 1 that represents the similarity between a diagnose and DRG_j. The proposed features will be calculated as:

$$x_{ip} = s(P_{i,ICD9}, DRG_p), p \in \{1, \ldots, 259\}, \quad (4)$$

where the above similarity, s, is computed using formula (2). Features with index 260, 261 and 262 are similar to the ones we used in [5], i.e. age, race and sex.

Example 1

Consider a patient with the following set of diagnoses P={682.6, 486, 453.42, 493.92,41.11,250.00,782.3,278.01}. The crisp [5] and the fuzzy (ontological) features (index 1-259) related to this patient are shown in Fig. 2.

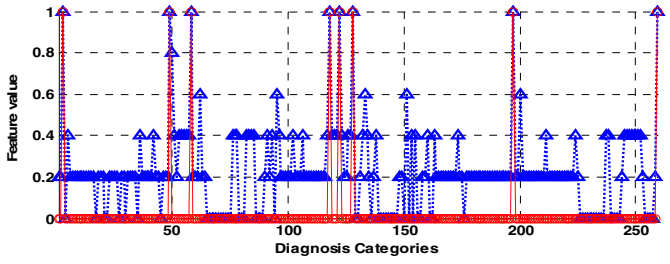

Figure 2. The crisp (red) and fuzzy ontological (blue) features for patient P from example 1.

We note that the ontological features coincide with the crisp ones for DRGs that contain one of the ICD-9 codes from the diagnoses set (in number of 8). An example is DRG index 49 ("diabetes mellitus without complications") that contains the ICD-9 code 250.00 ("Diabetes mellitus without complication type II or unspecified type not stated as uncontrolled"). However, there are other indices where the ontological features have a high value. Take for example DRG index 50 ("diabetes mellitus with complications") that contains among others the ICD-9 code 250.03 ("Diabetes mellitus without complication type I uncontrolled"). Since P does not contain code 250.0, $x_{50}^{crisp} = 0$. However, since s(250.00, 250.03) = 0.8, the related ontological feature is greater than zero, i.e. $x_{50} = 0.8$. Aside from the fact that by using the relations from the ICD-9 taxonomy we provide a better representation of the diagnoses set, we also account for the uncertainty of the coding process itself (known to be somewhat unreliable).

C. Classifiers used

In this paper we present experiments performed with two classifiers, random forests (RF) [9] and support vector machines (SVM) [10].

RF is an ensemble learner, a method that generates many classifiers and aggregates their results. RF adds a layer of randomness to bagging by building large collection of de-correlated trees. RF will create multiple CART-like trees, each trained on a bootstrap sample of the original training data and searches across a randomly selected subset of input variables to determine the split. Each tree in RF will cast a vote for some input x, then the output of the classifier is determined by majority voting of the trees. Since the focus of this paper is on features rather than on classifiers themselves, we refer the reader to [9] and [10] for more details on RF and SVM.

We performed the classification using R, which is an open source statistical software. We used R *randomForest* and *SVM* (e1071) packages. The parameters to the RF were as follows: number of trees (ntree) was set to 500. Overall, the number of trees didn't seem to influence the classification results. The number of variables randomly sampled as candidates at each split (mtry) is equal to the square root of the number of features. Since in our case we have 262 features, mtry was consequently set to 16.

For SVM we used a linear kernel, termination criterion (tolerance) was set to 0.001, epsilon for the insensitive-loss function was 0.1 and the regularization term (cost) was 1.

D. Experiments

We tested both classifiers, RF and SVM, with N=10,000 patients extracted from HCUP2005, N_d=5,000 that had the disease and N_n=5,000 that didn't. Out of the 10,000 samples, 7,000 were used for training and 3,000 for testing. Obviously, we excluded the target disease from the diagnosis set of the N_d patients that had it. We performed the same experiment for three diseases (first 3 lines in table I): hypertension, diabetes mellitus and arteriosclerosis. The results obtained are showed in the next section.

IV. Results

The classification results, area under the curve (AROC) and receiver operating characteristic (ROC) curve, for diabetes are shown in table II and Fig. 3.

TABLE II. AROC RESULTS FOR DIABETES PREDICTION

	Crisp Features	Fuzzy Features
RF	0.9524	0.9996
SVM	0.8567	0.981

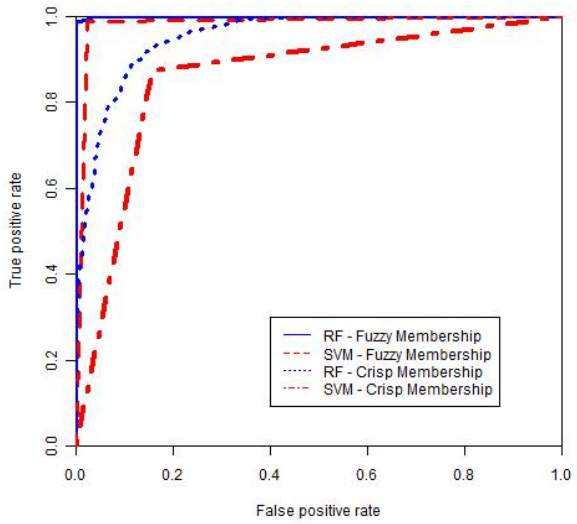

Figure 3. ROC curves for diabetes prediction obtained with random forest (blue) and SVM (red).

The AROC improvement was smaller for RF than for SVM, since RF had already a good prediction performance dues to its builtin feature selection property.

The results obtained for atheoriosclerosis prediction are shown in table III and Fig. 4.

TABLE III. AROC RESULTS FOR ARTHERIOSCLEROSIS PREDICTION

	Crisp Features	Fuzzy Features
RF	0.9647	0.9995
SVM	0.8833	0.9737

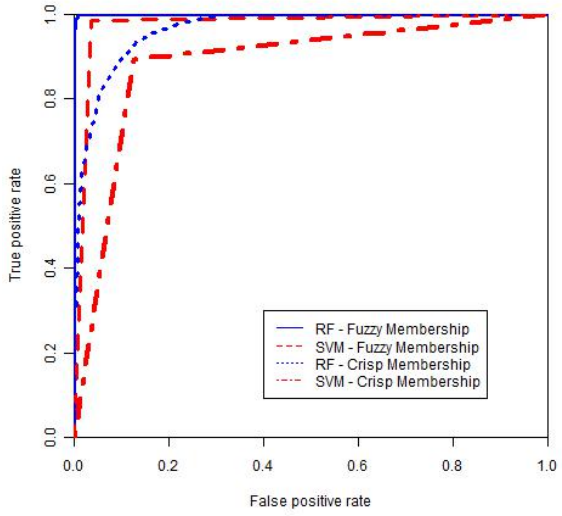

Figure 4. ROC curves for aterioscleroses prediction obtained using random forest (blue) and SVM (red)

For the atherioscelrosis prediction, too, we obtained a significant performance improvement (3-9%) when fuzzy features are used.

The results obtained for hypertension prediction are shown in table IV and Fig. 5. Again, a notable AROC improvement (5-13%) is obtained by using the fuzzy features instead of the crisp ones.

TABLE IV. AROC RESULTS FOR HYPERTENSION PREDICTION

	Crisp Features	Fuzzy Features
RF	0.9454	0.9991
SVM	0.8537	0.989

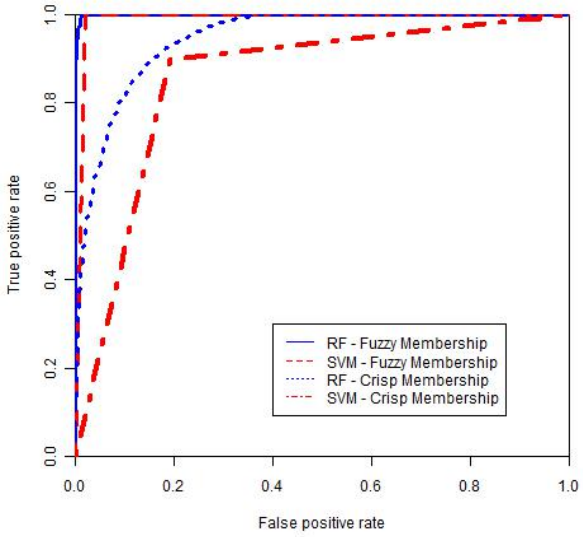

Figure 5. ROC curves for hypertension prediction obtained using random forest (blue) and SVM (red)

V. CONCLUSIONS

In this paper we presented a method for disease predicting using large public medical datasets. Disease prediction is important in a variety of applications such as health insurance, tailored health communication and public health. The presented method is based on employing ICD-9 diagnostic groups (DRGs) and demographics variables in conjunction with classification algorithms, such as SVM and RF. As opposed to using a crisp DRG membership for the ICD-9 codes, we introduced a novel fuzzy membership computed based on ICD-9 ontological similarity. The results presented on three different diseases and two classifiers show that the fuzzy features lead to an important improvement (between 3 and 13%) in prediction performance. The improvement is due to the fact that the fuzzy features capture the relationships between the DRG groups in the process of feature extraction.

In the near future, we plan to extend our approach to all 259 disease categories present in the HCUP dataset.

REFERENCES

[1] T. Yi, Z. Guo-Ji. The application of machine learning algorithm in underwriting process", Proceedings of the 4th International Conference on Machine Learning and Cybernetics, Guangzhou, China, Aug. 2005, p. 3524-3527.

[2] E. Cohen, C. A. Caburnay, D.A. Luke, S. Rodgers, G.T. Cameron, M.W. Kreuter, "Cancer coverage in general-audience and black newspapers", *Health Communication*, 2008. 23(5): p. 427-435.

[3] W. Yu, T. Liu, R. Valdez, M. Gwinn, M.J. Khoury, "Application of support vector machine modeling for prediction of common diseases: the case of diabetes and pre-diabetes", *BMC Medical Informatics and Decision Making*, 2010. 10(1): p. 16.

[4] P. Hebert, L. Geiss, E. Tierny, M. Engelgau, B. Yawn, A. McNeab, "Identifying persons with diabetes using Medicare claims data", *American Journal of Medical Quality*, 1999. 14(6): p. 270.

[5] M. Khalilia, M. Popescu, "Predicting disease risks from highly unbalanced data using random forest", submitted to BMC Medical Informatics and Decision Making, 2011.

[6] http://www.cms.hhs.gov/ICD9ProviderDiagnosticCodes

[7] M. Popescu, D. Xu, Eds., Data Mining in Biomedicine using ontologies, Artech House, Norwood, MA 2009.

[8] HCUP (2009), Overview of the Nationwide Inpatient Sample (NIS), www.ahrq.com.

[9] L. Breiman, "Random Forests", *Machine Learning*, 45 (1):5-32.

[10] C. Cortes and V. Vapnik, "Support-Vector Networks", *Machine Learning*, 20, 1995.

2011 IEEE International Conference on Fuzzy Systems
June 27-30, 2011, Taipei, Taiwan

Software Maintenance Scenarios Simulation with Fuzzy Cognitive Maps

Cristina Lopez
School of Engineering
University Pablo de Olavide
Seville, Spain
clopvar@upo.es

Jose L. Salmeron
School of Engineering
University Pablo de Olavide
Seville, Spain
salmeron@acm.org

Sebastian Lozano
School of Engineering
University of Seville
Seville, Spain
slozano@us.es

***Abstract*—Successful performance of software, and indeed Enterprise Resource Planning (ERP), depends on proper system maintenance. For this reason, firms should follow a maintenance process that drives the ERP system toward success. However, in general terms, ERP maintenance managers do not know what conditions they should target to successfully maintain their ERP systems. Moreover, numerous risks threaten ERP maintenance, but they are normally dealt trusting on experience. To address this requirement, we have built a FCM-based tool that helps ERP teams to simulate the impact of risks on ERP maintenance.**

Keywords: Simulation; Software maintenance; ERP; Fuzzy Cognitive Maps; Risks Simulation

I. INTRODUCTION

Enterprise Resource Planning (ERP) is one the most common and critical systems implemented by firms around the world. These systems allow the modeling, automation and integration of company business processes, grouping all data into a single database and providing relevant and updated information for decision-making and control.

Many firms have implemented ERP packages to fully integrate, standardize and coordinate their processes. These systems are more or less customized to fit them to the adopting company through the implementation process. But when the ERP is operative, practitioners undergo changes in the system. These modifications are carried out to correct or prevent failures, migrate the ERP to new releases and align the application regarding the specific business requirements or ERP users' expectations.

If the company does not properly maintain the ERP system, failures will arise, performance will decrease and the expected benefits will not be obtained [1]. This may even lead to early retirement of the ERP application. Hence, ERP maintenance becomes a key process in the post-implementation stage.

Given the significant risks inherent in ERP maintenance and the serious consequences that may follow, it is necessary to manage all risks properly. However, research on this particular issue remains inadequate. Previous studies neither indicate which conditions must be satisfied to support successful ERP maintenance, nor identify the risks that may threaten maintenance.

Accordingly, we assess the effects of risks on the success of ERP maintenance through a systematic approach similar to that proposed elsewhere. With this in mind, we identify risks to ERP maintenance success. Finally, we built a Fuzzy Cognitive Map to model risk effects on ERP maintenance success and simulate distinct scenarios.

Section 2 presents a literature review of theoretical background about ERP maintenance and risk. Section 3 presents the fundamentals of Fuzzy Cognitive Maps. Moreover, this section presents key aspects of the tool. Section 4 describes the process for building a Fuzzy Cognitive Map to model risk in ERP maintenance. Section 5 studies the results of the FCM simulation and the risks impacts on ERP maintenance. For this purpose, we define two scenarios and simulate them using the Fuzzy Cognitive Map. Finally, Section 6 offers the conclusions.

II. BACKGROUND

A. Enterprise Resource Planning

Enterprise Resource Planning (ERP) is one the most adopted enterprise systems. An ERP is a large commercial off-the-shelf configurable application that integrates the core enterprise business functions.

An ERP can be defined as a single software system to support the complete integration of information from all functional areas of a company by means of a single database that is accessible through a unified interface and channel of communication.

The ERP life cycle begins when top management decides to install the software. Following this decision, numerous tasks are carried out to implement the system. However, the ERP life cycle is not finished as soon as the application is operative and the ERP implementation stage has been concluded. At that moment, ERP enters into the post-implementation stage, which continues until its retirement.

B. ERP maintenance

ERP adopters have to perpetually maintain their ERPs until the end of its life span. However, frequent ERP modifications cause high risks and costs, which impact on software performance [2]. In such a case, the daily activity of the firm

Sponsors: Spanish Ministry of Science and Innovation and Andalusian Regional Government

978-1-4244-7316-8/11/$26.00 ©2011 IEEE

would be hindered. Hence, ERP maintenance is considered a critical process, which needs to be managed carefully.

ERP maintenance can be defined as the process addressed to identify and perform changes required for improving or maintaining system performance through the ERP post-implementation stage. The maintenance team implements each maintenance request by means of projects.

In the literature, various papers propose models to support ERP maintenance [3], [4]. Despite this, models aware of risk have not been developed. For this reason, the aim of our research was to develop a formal model for managing ERP maintenance risks.

C. Risks within ERP maintenance

ERP system maintenance is a large-scale, unstructured and highly complex undertaking [5]. In some cases, it even requires the use of unfamiliar technologies and tools. Hence many controllable and uncontrollable risks can affect its outcome.

A risk is an event characterized by uncertainty because it may or may not occur. If this risk turns into a real problem, it may cause dangerous failures. In such case, the project performance and the maintained ERP will be seriously damaged. Therefore, risk management becomes a crucial process to ensure ERP success.

A proper risks management helps practitioners to be aware of the real situation of the project, their problematic aspects and potential causes existing of ERP project failure. They will thus resolve more efficiently the threats' projects. Otherwise, improper risks management lead the carrying out of evitable error and the appearance of potential problems, which make the achievement ERP maintenance project outcomes difficult. Therefore, active risks management is key to reach ERP maintenance projects success.

In this way, the literature provides numerous methods, checklists, analytical frameworks, risk assessment tools and risk response strategies to help project managers to handle risk factors more effectively [6]. These studies mainly focus on classic software projects. However, different risks affect ERP project success, because classic software projects and ERP projects are not similar [3]. This has encouraged the appearance of ERP project risk studies in the literature. However, these studies focus on the implementation stage.

Various research efforts have identified risk in the context of ERP projects. Sumner [7] identified, described and categorized the risk factors associated with ERP implementation. Moreover, Sumner also marked which risks are unique in ERP projects. Huang et al. combined a multi-criteria methodology and the Delphi method to identify and prioritize risks [8]. By contrast, post-implementation stage risk research is scarce in the literature.

III. FUZZY COGNITIVE MAPS

FCMs describe a cognitive map model with two significant characteristics. First, causal relation-ships between nodes have different intensities represented by fuzzy numbers. A fuzzy number is a quantity whose value is uncertain, rather than exact. It can be thought of as a function whose domain is usually the interval between 0 and 1 (or -1 and 1), inclusive. Each numerical value in the interval represents the degree of membership in a fuzzy set, where 0 is non-membership and 1 represents full membership. The second characteristic is that the system is dynamic – it evolves with time. The system involves feedback, and a change in a concept node may affect other concept nodes, which in turn can impact the node initiating the change. Feedback plays a prominent role in FCMs by propagating causal influences along complicated pathways.

Moreover, FCMs provide an intuitive, yet precise, way of expressing concepts and reasoning about them at their natural level of abstraction. By transforming decision modeling into causal graphs, decision makers with no technical background can understand all of the components in a given situation. In addition, with an FCM, it is possible to identify and consider the most relevant factor that seems to affect the expected target variable. For these reasons, we think that FCMs are a worthy tool.

A. FCM fundamentals

A FCM is a digraph composed of nodes and edges. The nodes (x_i) are the most relevant dynamic variables or factors describing a target real-world dynamic system. These may represent concepts such as costs, diseases, medication, investment, or marketing strategy, to name a few. For any context, the nodes are a set of entities that are relevant to the domain of study.

Relationships between nodes are represented by directed edges. An edge linking two nodes can model the influence of the causal variable on the effect variable [9]. In addition, edges also indicate the type of connection, incorporating either a plus (+) or a minus (-) sign. A positive relationship between two factors indicates that an increase or decrease in a causal variable causes the effect variable(s) to change in the same direction. When the relationship is negative, the change in the effect variable is in the opposite direction (i.e., an increase in the cause variable causes a decrease in the effect variable).

Because FCMs are hybrid methods that mix fuzzy logic and neural networks [10], each cause is assessed by its intensity, $w_{ij} \in [-1,+1]$, where i is the pre-synaptic (causal) node and j is the post-synaptic (effect) node one.

FCMs are dynamic systems involving feedback whereby change in a node may affect other nodes, which in turn can affect the node initiating the change. The analysis begins with the design of the initial vector state (C^0), which represents the initial value of each variable or concept (node). The initial vector state with n nodes is denoted as:

$$C^0 = \begin{pmatrix} C_1^0 & C_2^0 & \cdots & C_n^0 \end{pmatrix} \quad (1)$$

The new values of the nodes are computed in an iterative vector-matrix multiplication process with an activation function, which is used to monotonically map the node value into a normalized range [0,1]. The sigmoid is the most common function [11] when the concept (node) value maps onto the range [0,1].

B. FCM dynamics

The vector state C_i^{t+1} at the instant $t+1$ would be computed as:

$$C_i^{t+1} = f\left(\sum_{\substack{i=1 \\ i\neq j}}^{n} C_i^t \cdot w_{ij}\right) \tag{2}$$

where $f(x)$ is the transformation function.

The state changes along the process. Usually, two kinds of transformation functions are used in FCM dynamics. The first one is the unipolar sigmoid:

$$f(x) = \frac{1}{1+e^{-\lambda \cdot x}} \tag{3}$$

The second is the hyperbolic tangent:

$$f(x) = \tanh(x) = \frac{e^{\lambda \cdot x} - e^{-\lambda \cdot x}}{e^{\lambda \cdot x} + e^{-\lambda \cdot x}} \tag{4}$$

Both functions use λ as a constant for function slope (degree of fuzzification). The FCM designer has to specify the lambda value. For large values of lambda (e.g., $\lambda \geq 10$) the sigmoid approximates a discrete function that maps its results to interval (0,1); for smaller values of lambda (e.g., $\lambda \leq 1$) the sigmoid approximates a linear function; while values of lambda closer to 5 provide a good degree of fuzzification in the [0,1] interval [11].

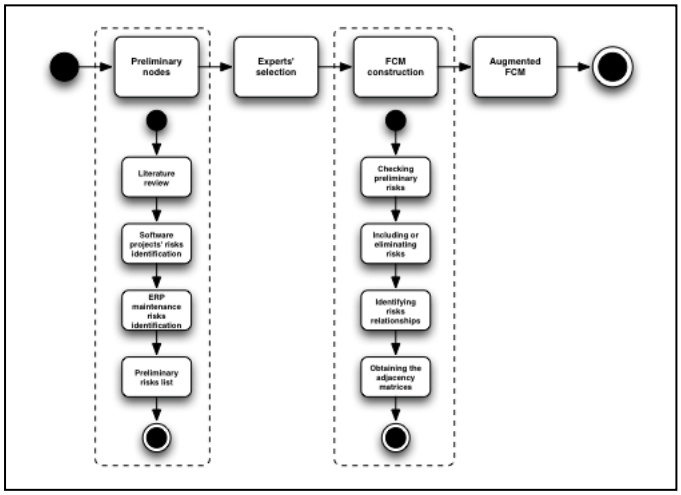

Figure 1. FCM construction process

The FCM inference process finishes when stability is reached. The final vector state shows the effect of the change in the value of each node on the FCM. After the inference process, the FCM reaches one of three states following a number of iterations. It settles down to a fixed pattern of node values, the so-called hidden pattern or fixed-point attractor.

Alternatively, the state can continue cycling between several fixed states, known as a limit cycle. With a continuous function, a third possibility is a chaotic attractor. This occurs when, instead of stabilizing, the FCM continues to produce different results (state vector values) for each cycle. In this case, the technique fails to offer a useful outcome for risk analysis.

IV. FCM CONSTRUCTION

The aim of this study was to create a FCM to simulate the risks' impact on ERP maintenance. We carried out the steps indicated in Figure 1 to build the FCM model. Firstly, we identified the preliminary nodes to help the experts create their FCMs. To do so, we performed a broader literature review on software projects risks and ERP projects. We thus achieved an initial large risks list. But, the initial list does not solely gather ERP maintenance risks.

So, we carefully analyzed the initial list to identify ERP maintenance risks. Subsequently, those risks affecting ERP maintenance were renamed, while the other risks were eliminated. In this way, we obtained the preliminary risks nodes of FCM.

The following activity consisted of selecting experts who were willing to participate in our research. In no case, did we select the experts because they were easily accessible. The main selection criterion considered was profound knowledge in the ERP maintenance and absence of conflicts of interest. A total of 10 leading experts decided to take part with us in this study. These experts belong to different professional scales. Moreover, they had participated or participate in the maintenance of ERP solutions supplied by different vendors. Therefore, we achieved the making up of a heterogeneous group of experts.

Thirdly, each expert individually built an FCM. To help them, we sent the list of preliminary risks nodes, which were only indicative. So, they checked them and eliminated those risks nodes, which do not affect ERP maintenance. Moreover, those experts, who concluded that we had not identified all ERP maintenance risks, added the non-identified risk(s) node(s) to the initial list. Subsequently, the experts state the relationship between the nodes. They also pointed out the risks impacts on ERP performance. We thus achieved one adjacency matrix for each expert.

We finally constructed the augmented matrix (A^*) adding the adjacency matrix of each one of them [10]. The elements' aggregation depend on if there are or are not common nodes. The experts' adjacency matrix had common nodes. So, the elements (w_{ij}^*) in the augmented matrix are computed by [12]:

$$w_{ij}^* = \frac{\Sigma_{k=1}^{n} A_k}{n} = \frac{\Sigma_{k=1}^{n} w_{ij}^k}{n} \tag{5}$$

n being the number of FCMs added, one per expert. The A^* obtained is the following:

$$A^* = \begin{bmatrix} 0 & .06 & 0 & 0 & .07 & 0 & 0 & 0 & .12 & .04 & 0 & 0 & -.05 \\ 0 & 0 & 0 & 0 & 0 & .03 & 0 & 0 & 0 & 0 & .01 & 0 & -.108 \\ 0 & 0 & 0 & .255 & .325 & .185 & .05 & 0 & 0 & 0 & 0 & 0 & 0 \\ 0 & 0 & .15 & 0 & .105 & 0 & 0 & 0 & 0 & 0 & 0 & 0 & 0 \\ 0 & 0 & 0 & .04 & 0 & .625 & 0 & .17 & 0 & 0 & 0 & 0 & -.018 \\ 0 & 0 & 0 & 0 & 0 & 0 & 0 & .06 & 0 & 0 & 0 & 0 & -.109 \\ 0 & 0 & 0 & 0 & 0 & .23 & 0 & .08 & 0 & 0 & 0 & 0 & -.038 \\ 0 & 0 & 0 & 0 & 0 & .11 & 0 & 0 & 0 & 0 & .08 & 0 & -.029 \\ 0 & 0 & 0 & 0 & 0 & 0 & 0 & 0 & 0 & 0 & 0 & 0 & 0 \\ 0 & 0 & 0 & 0 & 0 & 0 & 0 & 0 & 0 & 0 & 0 & 0 & -.025 \\ 0 & 0 & 0 & 0 & 0 & 0 & 0 & 0 & 0 & 0 & 0 & 0 & -.032 \\ 0 & .14 & 0 & 0 & 0 & .28 & .315 & .035 & 0 & .02 & .02 & 0 & -.134 \\ 0 & 0 & 0 & 0 & 0 & 0 & 0 & 0 & 0 & 0 & 0 & 0 & 0 \end{bmatrix} \quad (6)$$

Figure 2 shows the FCM obtained, representing how existing risks in the implementation of maintenance request impacted on ERP performance.

V. FCM SIMULATION

Firstly, we defined what-if scenarios at the instant $t=0$. In other words, the values of all variables of the FCM are represented in an $1\times n$ initial state vector C^0.

We formulate several questions as following: which risks will impact the strongest on ERP performance during the system maintenance: risks derived from external or internal agents or both at the same time? How will these impacts on the rest of the risks? To answer the previous questions, we created three Scenarios and simulated them:

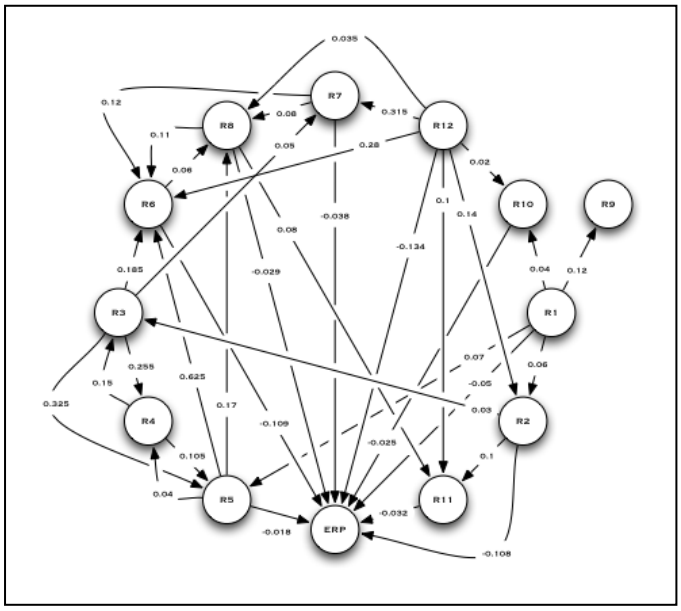

Figure 2. FCM-based ERP maintenance risks model

In Scenario 1 ($C^0_{S_1}$), we activated the risk derived from the external agents. In Scenario 2 ($C^0_{S_2}$), we activated risks derived from the internal agents.

$$C^0_{S1} = (0 \quad 0 \quad 0 \quad 0 \quad 0 \quad 0 \quad 0 \quad 0 \quad 0 \quad 0 \quad 0 \quad 1 \quad 0) \quad (7)$$

$$C^0_{S2} = (0 \quad 0 \quad 1 \quad 1 \quad 1 \quad 0 \quad 0 \quad 0 \quad 0 \quad 0 \quad 0 \quad 0 \quad 0) \quad (8)$$

Subsequently, we simulated these Scenarios computing A^* and $C^0_{S_i}$. Specifically, Scenarios were transformed using hyperbolic tangent function (4). We select this activation function (7) because the values of the nodes can fall within the range [-1, 1], 5 being the value assigned to λ.

The simulation finishes when the vector state reaches the stability (at a fixed point or limit cycle) or a chaotic behavior. In this research, both scenarios reached the stability. Table 1 presents the results obtained simulating each Scenario.

TABLE 1. Scenarios simulation results

Node	Description	Scenario 1	Scenario 2
R1	Continuous organizational changes	0	0
R2	Requirements incomplete and/or unclear	0.023556521	0
R3	Instability in maintenance team members	0	0.50123746
R4	Lack group spirit and attitude in maintenance team members	0	0.575731388
R5	Inadequate mix of team skills	0	0.637508649
R6	Quality of original programming	0.255256472	0.830216721
R7	Methodology and maintenance process are not defined	0.030705553	0.327804561
R8	Maintenance tasks are excessively hard	0.226292501	0.641248801
R9	Project milestones cannot be defined	0	0
R10	Use of inadequate technology for system testing	0.012737097	0
R11	Wrongly-fit system with pre-existing applications	0.229341662	0.442749349
R12	Lack active participation by external parties	0.005477003	0
ERP		**-0.308378881**	**-0.619552233**

The findings of Scenario 1 show that the impact of the unsuitable involvement of external agents in the project was positive and varied from null to low on the rest of the risks. The quality of the original programming (R6) and fit software with pre-existing applications (R11) were the ones highest affected by R12, both technical risks. The intensity of influence of R12 on ERP performance was higher than on the risks. This specifically was negative and slightly moderate. Therefore, R12 directly affected ERP performance instead of indirectly, that is, by means of other risks.

The results of the simulation of Scenario 2 show that the effect of risks derived from internal agents in the project was also positive. However, in this simulation, the effects on ERP maintenance risks were higher by far. In fact, the intensity of impacts was usually high. The intensities of impacts were from

2 to 6 times higher in Scenario 2 with respect to Scenario 1. Specifically, the influence of R3, R4 and R5 on other risks was from null to strong. As well as Scenario 1, R6 was the highest impacted risk. But the intensity of impact of risks activated in Scenario 2 was three times greater than the risk activated in Scenario 1.

The intensity of influence of risks activated in Scenario 2 on ERP performance was two times greater than the risk activated in Scenario 1. This was negative and slightly strong. R3, R4 and R5 impact directly less on ERP performance than on some other risks. Therefore, risks derived from internal agents directly and indirectly affect ERP performance.

VI. CONCLUSIONS

ERP maintenance is necessary to maintain or improve the usability and system performance. With this in mind, risky and complex maintenance projects follow one another continuously through the ERP life span.

However, numerous risks can arise during the implementation of maintenance requests. To prevent these risks negatively affecting system performance, practitioners have to manage them properly. But, in many cases, they deal these risks with intuitively and inefficiently.

In order to avoid this, this research aims at supporting practitioners work managing ERP maintenance risks. To do so, we decided to create an FCM. This identifies ERP maintenance risks as well as the existing connections between them. In addition, at any time the practitioner can easily modify the model, adding or eliminating further variables and/or relationships, to faithfully represent the phenomena.

The dynamic analysis of the FCM will help practitioners to take more efficient measures to minimize ERP maintenance risks. Static analysis specifically indicates which risks have more influence on other risks or impact stronger on ERP performance.

In contrast, the dynamic analysis of the FCM allows ERP practitioners to predict the effects of risks activated in the implementation of maintenance requests on ERP performance over time.

The result of dynamic analysis reveals that the risks derived from team maintenance have strongest impact on ERP performance. Hence, in order to achieve successful ERP maintenance, managers should create teams made up of highly qualified professionals in ERP technology, reduce the instability in maintenance team members, as well as improving the motivation and training of the members of maintenance teams.

Looking to the future, it is necessary to undertake further research on the existing risks in ERP maintenance. To manage such risks most effectively, managers should know which risks are most important to ERP maintenance success. Therefore, research that answers this question is required. The development of techniques to forecast the risks appearance within ERP maintenance projects is also very worthwhile.

ACKNOWLEDGMENT

The authors wish to thank the Spanish Ministry of Science and Innovation (MICINN-ECO2009.12853) and the Andalusian Regional Government (CICE-P07-SEJ-03080) for their financial support.

REFERENCES

[1] C.S.P. Ng, G. Gable and T. Chan, “A ERP client-benefits-oriented maintenance taxonomy”, Journal of Systems and Software, vol. 64, no. 2, pp. 87-109, 2002.

[2] D. Chand, G. Hachey, J. Hunton, V. Owhoso and S. Vasudevan, “A balanced scorecard based framework for assessing the strategic impacts of ERP systems”, Computers in Industry, vol. 56, no. 6, pp. 558-572, 2005.

[3] C.S.P. Ng, G.G. Gable and T. Chan, “An ERP maintenance model”, Proc. 36th Annual Hawaii International Conference on Sys-tem Science, pp. 1-10, 2003, doi:10.1109/HICSS.2003.1174609.

[4] O.B. Kwon and J.J. Lee, “A Multi-agent intelligent system for efficient ERP maintenance”, Expert System with Applications, vol. 21, no. 4, pp. 191-202, 2001.

[5] R. Mookerjee, “Maintaining enterprise software applications”, Communications of the ACM, vol. 48, no. 11, pp. 75-79, 2005.

[6] P.L. Bannerman, “Risk and risk management in software pro-jects: A reassessment”, Journal of Systems and Software, vol. 81, no. 12, pp. 2118-2133, 2008.

[7] M. Sumner, “Risk factors in enterprise-wide/ERP projects”, Journal of Information Technology, vol. 15, no. 4, pp. 317-327, 2000.

[8] Sh.-M. Huang, I-Ch. Chang, Sh.-H. Li and M.-T. Lin, “Assessing in ERP projects: identify and prioritize the factors”, Industrial management & data systems, vol. 8, no. 8, pp. 681-688, 2004.

[9] G. Xirogiannis and M. Glykas, “Fuzzy cognitive maps in business analysis and performance-driven change”, IEEE Transactions on Engineering Management, vol. 51, no. 3, pp. 334–351, 2004.

[10] B. Kosko, Fuzzy Engineering. Prentice Hall, 1996.

[11] S. Bueno and J.L. Salmeron, “Benchmarking main activation functions in fuzzy cognitive maps”, Expert Systems with Applications, vol. 36, no. 3, pp. 5221-5229, 2009.

[12] J.L. Salmeron, "Augmented fuzzy cognitive maps for modelling LMS critical success factors", Knowledge-Based Systems, vol. 22, no. 4, 2009, pp. 275–278.

2011 IEEE International Conference on Fuzzy Systems
June 27-30, 2011, Taipei, Taiwan

Train Fuzzy Cognitive Maps by Gradient Residual Algorithm

Huiliang Zhang[1], Zhiqi Shen[2], Chunyan Miao[1]
[1] School of Computer Engineering,
[2]School of Electrical and Electronic Engineering
Nanyang Technological University,
Singapore
{PG04043187, ZQShen, ASCYMiao}@ntu.edu.sg

***Abstract*—Fuzzy Cognitive Maps (FCM) is a popular technique for describing dynamic systems. A FCM for a dynamic system is a signed graph consisted of relevant concepts and causal relationships/weights between the concepts in the system. With suitable weights defined by experts in the related areas, the inference of the FCM can provide meaningful modeling of the system. Thus correctness of the weights is crucial to the success of a FCM system. Normally the weights are set by experts in the related areas. Considering the possible inefficiency and subjectivity of experts when judging the weights, it is an appealing idea to generate weights automatically according to the samples obtained through observation of the system. Some training algorithms were proposed. However, to our best knowledge, few learning algorithm has been reported to generate weight matrix based on sample sequences with continuous values. In this paper, we introduce a new learning algorithm to train the weights of FCM. In the proposed algorithm, the weights are updated by gradient descent on a squared Bellman residual, which is an accepted method in machine learning. The experiment results show that given sufficient training samples, the correct weights can be approximated by the algorithm. The algorithm proposes a new way for FCM research and applications.**

Keywords- Fuzzy cognitive maps

I. INTRODUCTION

Fuzzy Cognitive Maps (FCMs) was introduced [1] as an extension of cognitive maps proposed by political scientist Robert Axelrod [2]. A cognitive map is *signed digraph*, in which nodes are variable concepts and edges represent causal connections between the concepts. The positive or negative sign on a directed edge between two concepts indicates whether the change of the first concept causally increases or decreases the second concept. A matrix consisted of the signs of the edges is used to represent the cognitive map. In the matrix, a positive edge is shown as 1, a negative edge as -1 and 0 for unrelated concepts. Kosko proposed to apply fuzzy logic technique to represent the causal relationships between concepts. Fuzzy causal algebra was proposed to infer how a concept will influence another concept. Then Kosko proposed Bidirectional Associative Memories in neural networks [3]. This provides a theoretical base for simple FCM inference algorithm which is widely used in current FCM researches and applications. FCM inference is a qualitative approach for a dynamic system, where the gross behaviors of a system can be observed quickly and without the services of an operations research expert [4].

Since proposed, FCM has been researched and applied in many areas. The original application of FCM shown by Kosko was to predict political status changes [1]. Later the application of FCM was extended to simulation of virtual worlds. In [5], FCMs are designed for a virtual sea world. The behaviors of dolphin, fish and shark are predicted based on their behavior FCMs. For example, a FCM for the control of a dolphin consists of concepts such as 'Hunger', 'Food Search', 'Chase food' and so on. Through FCM inference, the status changes of the dolphin from an initial status can be observed. The status of the dolphin will finally reach a stable status or repeat for a cycle of limited statuses. The examples show that FCM output states can guide a cartoon of the virtual world. Besides the applications in virtual worlds, FCM technique is applied to solve real-world problems. For example, FCM applications are used in intelligent intrusion detection system [6], the system to control the valves based on the tank height and the gravity of the liquid in the tank [7], the brain tumor characterization system [8], the web surveillance system [9], and so on. FCM shows high efficiency and accuracy in these systems.

In these systems, it is very important to assign suitable weights to the causal relationships between concepts. In the early FCMs designed by Dickerson and Kosko [5], the weights take value as 1, -1 or 0. It is a rather easy job to assign weights by judging the positive, negative or neutral influences from one concept to another. However, in a real system where weights will take continuous values as suggested in [10], assignment of the weights is dependent on experts' personal knowledge and subjective judgments, which might not always be precise. So it is very appealing if the weights can be generated automatically. Some automatic algorithms have been proposed. We summarize them in the section of related work. No learning algorithm has been proposed to train FCM based on samples with continuous values. In this paper, we propose a gradient residual method to train the weights with some given sample sequences of a dynamic system. The algorithm updates the weights by gradients of squared

978-1-4244-7316-8/11/$26.00 ©2011 IEEE

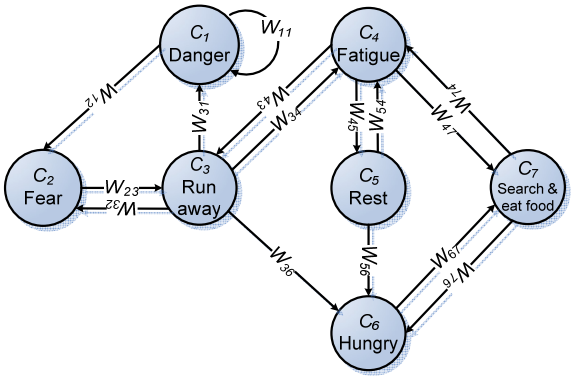

Figure 1. Example of a FCM.

Bellman residual. Experimental results show that the algorithm is very effective if sufficient sample sequences are given.

The rest of the paper is organized as following. We first give a brief illustration of FCM in Section II. Then the gradient algorithm to train FCM weights is explained in Section III and experimental results are shown in Section IV. Other FCM training methods are discussed in related work in Section V. Finally, a conclusion is given.

II. FUZZY COGNITIVE MAP

A. Definition

As introduced in last section, FCM is a directed graph which depicts a dynamic system. The nodes represent the concepts in the system. Weight on an edge between two nodes shows how much a concept will affect the next concept. The weight matrix can be shown as:

$$W = \begin{bmatrix} W_{11} & W_{12} & \dots & W_{1n} \\ W_{21} & W_{22} & \dots & W_{2n} \\ \dots & \dots & \dots & \dots \\ W_{n1} & W_{n2} & \dots & W_{nn} \end{bmatrix}$$

where, n is the number of concepts in the FCM.

An example FCM is shown in Figure 1. The FCM consists of seven concepts, which represent the status of a system to control an animal's behaviors. The possible relationships between the concepts are identified and shown in the figure.

In general, a weight W_{ij} takes values in the fuzzy causal interval [-1, 1]. A positive value means that the increase (decrease) of concept C_i will increase (decrease) the value of concept C_j. A negative value indicates the value of C_j will change in an opposite direction with C_i. A zero value means that C_i will not affect C_j. Only none-zero weights are shown in Figure 1. For example, we can say that the value of "Hungry" has no effect on "Rest". However, the value of "Hungry" will affect how the animal decides to "Search & eat food".

At a time t, the status vector of the FCM system is represented as $C^{(t)}=(C_1^{(t)}, C_2^{(t)}, \dots, C_n^{(t)})$. The initial status vector of FCM is shown as $C^{(0)}$. The status of a concept C_i in a time t can be calculated by summing the influences from last time. The equation is shown as:

$$C_i^{(t)} = f\left(\sum_{j=1}^{n} (C_j^{(t-1)} * W_{ji}) \right) \quad (1)$$

where, f is the threshold function.

Normally Sigmoid function is used as threshold function for FCM with continuous concept values. It is shown as:

$$f(x) = \left(1 + e^{-\lambda x}\right)^{-1} \quad (2)$$

where, λ is a parameter deciding the width of the sigmoid function. In this paper, λ takes default value 1.

The initial values of FCM concepts are obtained through measuring the concepts in the real system. Then the inference is performed by continuously calculating the status using the equations (1) and (2). The calculation does not stop until the model reaches a limit cycle or exhibits a chaotic change. The outputs of the FCM inference show how the system will change from the initial status.

Take the FCM example shown in Figure 1. A weight matrix W is decided by the experts in the domain of animal research and shown in Table I. Now we assume that the system starts from an initial status vector, $C^{(0)}$=(0.6, 0.3, 0.3, 0.6, 0.7, 0.7, 0.7). For example, the fuzzy value for concept "Fear" is 0.3, which means that the animal is in a status of being a little vigilant. The values of concepts at each step of FCM interaction can be calculated by using equation (1) and (2). The outputs are shown in Table II. It can be seen that the FCM

TABLE I. WEIGHT MATRIX W FOR FCM IN FIGURE 1.

	C_1	C_2	C_3	C_4	C_5	C_6	C_7
C_1	1	.89	0	0	0	0	0
C_2	0	0	.75	0	0	0	0
C_3	-.67	-.7	0	.9	0	.89	0
C_4	0	0	-.71	0	.94	0	.41
C_5	0	0	0	-.31	0	.07	0
C_6	0	0	0	0	0	0	.99
C_7	0	0	0	.52	0	-.81	0

TABLE II. THE VALUES OF CONCEPTS IN FCM INTERACTION.

t	C_1	C_2	C_3	C_4	C_5	C_6	C_7
0	.6	.3	.3	.6	.7	.7	.7
1	.598	.58	.45	.603	.637	.438	.719
2	.574	.554	.502	.641	.638	.466	.664
3	.559	.54	.49	.645	.646	.488	.674
4	.557	.539	.487	.644	.647	.484	.679
5	.557	.539	.487	.644	.647	.482	.678
6	.557	.539	.487	.643	.647	.482	.677
7	.557	.539	.487	.643	.647	.483	.677
8	.557	.539	.487	.643	.647	.483	.677

calculation converges at step 8. This means that without disturbs the animal will exhibit same behaviors after step 7.

B. *Generate FCM for a System*

A big question of FCM application is how to generate the weight matrix as shown in Table I. The normal method to construct a FCM relies heavily on a group of experts of the system. Each expert evaluates a causal relationship with a different fuzzy value depending on his personal experiences. Then the fuzzy rules are composited and de-composited to generate a fuzzy value which stands for the relationship [8]. It is obvious that the correctness of the weight matrix depends on the experts' personal experience and subjective judgments.

An alternative method is to automatically learn the weight matrix from the model of the dynamic system, which can be observed. Thus it is very attractive if the weight matrix could be generated from observed sample sequences as shown in Table II. Several learning algorithms have been introduced as summarized in Section V. In the next section, we will introduce our training algorithm to generate matrix from sample sequences.

III. GRADIENT FCM TRAINING ALGORITHM

A. *Problem Definition*

The training objective is to generate weight matrix of FCM based on sample sequences. An illustration of the training system is shown in Figure 2.

An initial weight matrix is input to the training algorithm as shown by arrow 1 in Figure 2. The original weights can be designed to show the basic positive or negative relationships between the concepts. However, there is no demand that the original weight W_{ij} must correctly indicate the causal positive or negative relationship from C_i to C_j. A value which is closer to the correct weight will save the training effort. 0 is assigned to W_{ij} if C_i has no influence to C_j. As we will show in the following algorithm, we must be very careful to set 0 as initial value for a weight because a weight with value 0 will not be updated by the training algorithm. If unsure, a random value other than 0 is suggested to be assigned to W_{ij}.

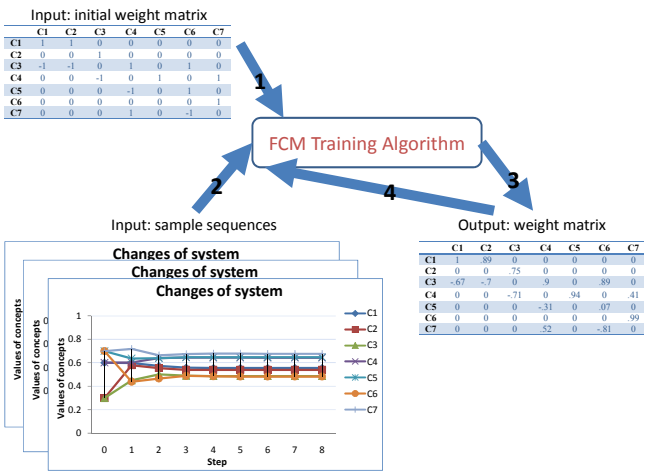

Figure 2. FCM training system.

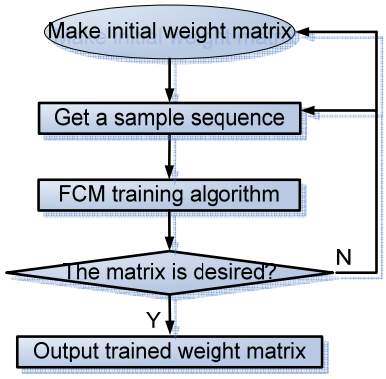

Figure 3. FCM training procedure.

Then some sample sequences are input as indicated by arrow 2 in Figure 2. The FCM training algorithm will train the initial matrix with the first sample sequence. After the training algorithm converges, a resulting weight matrix is output as shown by arrow 3 in Figure 2. The user needs to judge whether the output matrix meets the expectation. If not, the output matrix will be input into the training algorithm for next training as shown with arrow 4 in Figure 2. To be clear, an illustration about this procedure is shown in Figure 3.

Here it must be pointed out that human interference is still very important in the training system. System experts are needed to decide whether the output matrix is reasonable. As we will show later, the gradient training algorithm may be trapped in local minima or return a solution which is not desired. In these cases, a new initial weight matrix may be needed. However, it can be seen that in our training system the experts' jobs to observe system dynamics, make initial weight matrix, and judge whether the output matrix is desirable are easier, which are more objective than the jobs in traditional system to directly figure out the weight values [8]. In fact, as we will discuss in Section V, all other kinds of FCM learning algorithm also need human interference to judge whether their output weight matrix are suitable.

In the following, we will focus on the FCM training algorithm. Assume that a sample sequence is defined as: $\{S^{(0)}, S^{(1)}, \ldots, S^{(m)}\}$, where m is the number of steps in the sample sequence. Each status vector is defined as $S^{(t)}=(S_1^{(t)}, S_2^{(t)}, \ldots, S_n^{(t)})$, where n is the number of concepts. The training algorithm needs to update the initial weight matrix to get a new matrix such that with the output matrix, the FCM inference will be matching the sample sequence. We set $C^{(0)}$ as $S^{(0)}$. Thus the objective is to update each weight, which affects $C_i^{(t)}$, to decrease the difference between the calculated $C_i^{(t)}$ and the expected value $S_i^{(t)}$. The idea of residual algorithm used for function approximation system in machine learning can be exploited. We will first give a simple introduction about the residual algorithm. Then our gradient FCM training algorithm will be explained.

B. *Residual Algorithm*

Residual algorithm [11] is designed to modulate the weights of neural network which is used for approximating the expected values/rewards in machine learning. In a learning algorithm, Q is a value function to calculate the reward if an

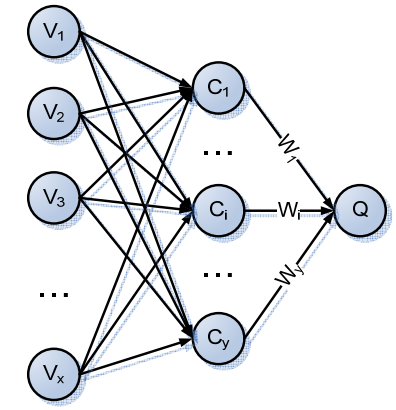

Figure 4. Function approximation system.

action is executed in a state. The objective of residual algorithm is to modulate the parameters in the Q function to make the function better approximate the expected reward.

The mean squared Bellman residual is defined as:

$$E = \frac{1}{|\Sigma|} * \Sigma (R + \gamma * v_{new} - Q)^2 \quad (3)$$

where, R is the immediate reward after an action is executed, γ represents the discount rate of future rewards, v_{new} is the value function for the successor state, Q is the current value function of the current state.

A simple illustration can be seen in Figure 4. Given an input vector $<V_1, V_2, \ldots, V_x>$, the neural network will output a value. In machine learning, the input variables represent the status and possible actions. The output represents the reward after executing the actions in the status. The residual algorithm will update the weights $<W_1, W_2, \ldots, W_y>$ to make the output value approximate to the expected value, correct reward. For this example, $E = (R - Q)^2$.

During training, the weights can be updated by performing gradient descent on the mean squared Bellman residual:

$$\Delta W_i = -\alpha * \frac{\partial E}{\partial W_i} \quad (4)$$

where, α is the learning rate.

The gradient residual algorithm guarantees to converge to a minimum, which is sometimes local. Although some mechanisms were proposed to avoid local minimum in gradient learning [12], no algorithm has been able to perfectly solve the problem. To solve this problem is not the intention of this paper. The algorithm proposed in this paper is just an application of the gradient method. In our training system, experts' judgment is needed to decide whether a final solution is suitable. If not, a new training will begin until an acceptable solution is found.

In the following, we will apply the idea of residual algorithm to the problem of FCM training.

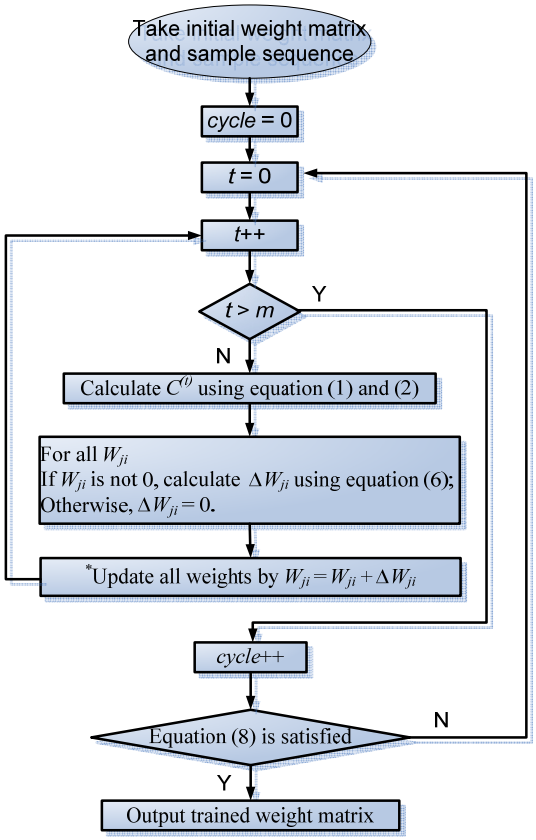

Figure 5. Residual training algorithm.

C. Gradient Algorithm for FCM Training

In FCM training, for each step t, the squared Bellman residual for a concept C_i is defined as:

$$E_i^{(t)} = \left(C_i^{(t)} - S_i^{(t)}\right)^2 \quad (5)$$

where, $C_i^{(t)}$ is the value of concept calculated by using equations (1) and (2) with the input value of $S^{(t-1)}$.

According to the residual algorithm, the update for W_{ji}, which affects $C_i^{(t)}$, is defined as:

$$\Delta W_{ji} = -\eta * \left[C_i^{(t)} - S_i^{(t)}\right] * \frac{\partial C_i^{(t)}}{\partial W_{ji}} \quad (6)$$

where, η is the learning rate.

With the equations (1) and (2), the gradient is calculated by:

$$\frac{\partial C_i^{(t)}}{\partial W_{ji}} = \frac{e^{-\lambda * \sum_{k=1}^{n} \left(W_{ki} * S_k^{(t-1)}\right)} * \lambda * S_j^{(t-1)}}{\left[1 + e^{-\lambda * \sum_{k=1}^{n} \left(W_{ki} * S_k^{(t-1)}\right)}\right]^2} \quad (7)$$

The weights will be updated at each step and the updated weight matrix will be used in next step.

The training algorithm is shown in Figure 5. Variable *cycle* is used to count how many cycles the FCM is trained. It is noticed that a standard is needed to judge whether the training converges. In this paper, a standard equation is designed as:

$$\sum_{i=1}^{n}\sum_{j=1}^{n}\left|\sum_{t=1}^{m}\Delta W_{ij}^{(t)}\right| < threshold \qquad (8)$$

where, the *threshold* value is used to decide whether the sum of changes of weights has been small enough.

It should be pointed out that if W_{ji} is updated to 0 from a non-zero value during the training, a very small value should be assigned to W_{ji}, instead of 0. This will ensure that W_{ji} is updated in future. This also means that if a user is not sure about a weight, a small value other than 0 should be used in the initial weight matrix.

Different training samples may produce different output matrices. However, all the output matrices should be able to satisfy the criteria in Equation (8) when being used to approximate the specific training samples. When more training samples are used to refine the output matrix, the final matrix to satisfy all the training samples will be produced.

We will show the experiment results of this algorithm in next section.

IV. EXPERIMENT

We realized the above training algorithm using Visual J#. The program is run on a desktop PC with Intel(R) Core(TM)2 Quad CPU Q9400 @ 2.66GHz, 3.37GB of RAM. The program is single thread and just one core of the CPU is utilized. To show the result of the training algorithm, the FCM system shown in Figure 1 is used as an example. We designed 3 experiments with different initial weight matrix.

TABLE III. INITIAL WEIGHT MATRIX *W* FOR TRAINING FCM.

	C_1	C_2	C_3	C_4	C_5	C_6	C_7
C_1	1	1	0	0	0	0	0
C_2	0	0	1	0	0	0	0
C_3	-1	-1	0	1	0	1	0
C_4	0	0	-1	0	1	0	1
C_5	0	0	0	-1	0	1	0
C_6	0	0	0	0	0	0	1
C_7	0	0	0	1	0	-1	0

TABLE IV. THE OUTPUT WEIGHT MATRIX *W*.

	C_1	C_2	C_3	C_4	C_5	C_6	C_7
C_1	.999	.881	0	0	0	0	0
C_2	0	0	.752	0	0	0	0
C_3	-.671	-.687	0	.859	0	.909	0
C_4	0	0	-.71	0	.94	0	.411
C_5	0	0	0	-.581	0	.311	0
C_6	0	0	0	0	0	0	.99
C_7	0	0	0	.806	0	-1.052	0

A. Experiment 1

In the first case, the initial weight matrix is made based on the causal relationships between the identified seven concepts. A positive relationship is assigned a weight, 1. A negative relationship is assigned a weight, -1. Otherwise, 0 is assigned. The initial weight matrix we created is shown in Table III. The sample values shown in Table II was used as the first training sample sequence.

Using parameters η as 0.1 and *threshold* as 0.00001, the training algorithm converges after 90,938 cycles in 2.39 seconds. The output matrix is shown in Table IV. We can see that the output matrix is quite close to the original matrix shown in Table I except the weights associated with C_4 and C_6. The matrix in Table IV is returned instead of the matrix in Table I because the training algorithm stops at a local minimum before the global optimal solution is found.

The values of concepts through FCM interaction are calculated using the output matrix in Table IV and shown in Table V. Although with the differences in the weights associated with C_4 and C_6, the calculated values are still very close to the original input sample sequence in Table II.

Compared to Table I, it is obvious that the output matrix in Table IV is not desired. Then we train the output matrix in Table IV with a new sample sequence as shown in Table VI. With the new training sample sequence, the learning algorithm converges in 7,289 cycles in 0.15625 seconds. The output matrix is shown in Table VII. This new output matrix is close to the matrix shown in Table I with negligible differences.

By this example, we can see that given sufficient training samples, the gradient learning algorithm is able to generate weight matrix for FCM system very precisely.

B. Experiment 2

In the second experiment, we will show how the initial input weight matrix will affect the learning. Like Experiment 1, the sequence in Table II is used as the first training sample. A new initial weight matrix is designed by setting all causal relationships in Table III as -1.

This time the learning algorithm converges in 54,787 cycles in 1.46875 seconds. The output matrix is shown in Table VIII. It is noticed that this output matrix is different from the matrix in Table IV.

The FCM inference results using this output weight matrix are very close to the original training sequence in Table II. Using this output weight matrix in Table VIII and the second training sample sequence in Table VI, the training algorithm converges after 7,333 cycles in 0.140625 seconds. The output weight matrix is shown in Table IX. The resultant output weight matrix is very close to the original weight matrix in Table I.

It is shown in Tables VII and IX the first weight of the output matrices is 1.001, which exceeds the range for weights, [-1, 1]. In these cases, the upper bound 1 is used to replace

TABLE V. THE VALUES OF CONCEPTS IN FCM INTERACTION.

	C_1	C_2	C_3	C_4	C_5	C_6	C_7
0	.6	.3	.3	.6	.7	.7	.7
1	.598	.58	.45	.602	.637	.439	.719
2	.573	.554	.502	.645	.638	.463	.664
3	.559	.54	.49	.645	.647	.489	.673
4	.557	.539	.487	.643	.647	.485	.679
5	.557	.539	.487	.643	.647	.482	.678
6	.557	.539	.487	.643	.647	.483	.677
7	.557	.539	.487	.643	.647	.483	.678
8	.557	.539	.487	.643	.647	.483	.678

TABLE VI. THE NEW TRAINING SAMPLE SEQUENCE.

	C_1	C_2	C_3	C_4	C_5	C_6	C_7
0	.3	.6	.3	.8	.2	.6	.7
1	.525	.514	.471	.639	.68	.429	.715
2	.552	.534	.483	.642	.646	.472	.665
3	.557	.538	.486	.641	.646	.484	.675
4	.558	.539	.487	.643	.646	.483	.677
5	.558	.539	.487	.643	.647	.483	.677
6	.558	.539	.487	.643	.647	.483	.677

TABLE VII. THE NEW OUTPUT WEIGHT MATRIX *W*.

	C_1	C_2	C_3	C_4	C_5	C_6	C_7
C_1	1.001	.881	0	0	0	0	0
C_2	0	0	.745	0	0	0	0
C_3	-.669	-.69	0	.887	0	.886	0
C_4	0	0	-.706	0	.941	0	.413
C_5	0	0	0	-.309	0	.076	0
C_6	0	0	0	0	0	0	.983
C_7	0	0	0	.527	0	-.811	0

TABLE VIII. THE OUTPUT WEIGHT MATRIX *W*.

	C_1	C_2	C_3	C_4	C_5	C_6	C_7
C_1	.999	.88	0	0	0	0	0
C_2	0	0	.751	0	0	0	0
C_3	-.671	-.686	0	.925	0	.844	0
C_4	0	0	-.71	0	.94	0	.409
C_5	0	0	0	-.053	0	-.235	0
C_6	0	0	0	0	0	0	.991
C_7	0	0	0	.257	0	-.488	0

TABLE IX. THE OUTPUT WEIGHT MATRIX *W*.

	C_1	C_2	C_3	C_4	C_5	C_6	C_7
C_1	1.001	.88	.0	.0	.0	.0	.0
C_2	.0	.0	.748	.0	.0	.0	.0
C_3	-.669	-.689	.0	.899	.0	.877	.0
C_4	.0	.0	-.708	.0	.941	.0	.407
C_5	.0	.0	.0	-.305	.0	.074	.0
C_6	.0	.0	.0	.0	.0	.0	.991
C_7	.0	.0	.0	.515	.0	-.804	.0

1.001 in the final matrix. The same method applies in other similar cases.

From this experiment, we can see that the output weight matrix will not be affected by initial weight matrix given sufficient training sample sequences. However, we still suggest adopting good initial weight matrix considering existence of local minima in the learning algorithm.

TABLE X. INITIAL WEIGHT MATRIX *W* FOR TRAINING FCM.

	C_1	C_2	C_3	C_4	C_5	C_6	C_7
C_1	.5	.1	0	0	0	0	0
C_2	0	0	.6	0	0	0	0
C_3	-.2	-.4	0	.7	0	.3	0
C_4	0	0	.2	0	-.5	0	.8
C_5	0	0	0	.1	0	.7	0
C_6	0	0	0	0	0	0	.3
C_7	0	0	0	1	0	-.2	0

TABLE XI. THE OUTPUT WEIGHT MATRIX *W*.

	C_1	C_2	C_3	C_4	C_5	C_6	C_7
C_1	.993	.875	.0	.0	.0	.0	.0
C_2	.0	.0	.748	.0	.0	.0	.0
C_3	-.664	-.68	.0	.887	.0	.88	.0
C_4	.0	.0	-.707	.0	.94	.0	.418
C_5	.0	.0	.0	-.332	.0	.075	.0
C_6	.0	.0	.0	.0	.0	.0	.98
C_7	.0	.0	.0	.549	.0	-.807	.0

C. *Experiment 3*

In this time, we assign random values to the initial weights. The initial weight matrix is shown in Table X.

We use the first sample sequence to train the weight matrix. The training algorithm converges after 26,730 cycles in 0.71875 seconds. The output matrix is shown in Table XI. We could see that this matrix is very close to the matrix shown in Table I.

More experiments with different initial weight matrixes which are randomly assigned are not shown. In these experiments, the gradient algorithm is also able to generate solution weight matrixes successfully.

V. RELATED WORKS

The idea to automatically generate weights matrix for FCM has been researched by many researchers. The proposed algorithms mostly fall into two groups, Hebbian learning algorithm and evolutionary algorithm.

Hebbian learning algorithm was first applied in training FCM by Kosko [13]. Before that, Kosko proposed a temporal associative memories (TAMs) algorithm [14]. TAMs can store only a few patterns. Then Kosko proposed to use the Differential Hebbian Law (DHL) to encode the usual binary changes in concepts. The experiment result in [5] shows that the algorithm was quite good at generating FCM weights to replicate the usual binary changes. Then an extension of DHL, Balanced Differential Learning (BDL) algorithm, was proposed in [15]. The new algorithm considered more factors while deciding how to update weights. Experiment results show that this algorithm is better to learn patterns. These two algorithms aim to learn the binary changes of concepts. Two more

extensions of DHL were also proposed to learn the weights of systems with continuous values [7], active hebbian learning (AHL) algorithm and nonlinear hebbian learning (NHL) algorithm. Different to other algorithms, the inputs of AHL and NHL are desirable regions of output concepts. These two algorithms need many user interferences to ensure that proper weights are trained. To the best of our knowledge, no learning algorithm which generates weight matrices based on sample sequences with continuous values has been reported.

Evolutionary algorithm is another frequently used algorithm when learning FCM weights matrix. The general idea is to search the weights matrix which can best replicate the training samples [16]. Red-coded genetic algorithms (RCGA) adds a floating-point extension to basic genetic algorithm, which makes genetic algorithm more effective for training weights with continuous values [17]. Another improvement of genetic algorithm can be seen in [18]. Tabu search method was applied to avoid local optima in genetic algorithms. The comparison results show that Tabu search is faster and can find solutions with better fitness than traditional genetic algorithms. Particle swarm optimization (PSO) is another kind of evolutionary algorithm which comes from swarm intelligence algorithms [19]. Besides these, simulated annealing method for training FCM is proposed recently [20]. Simulated annealing makes a serial of moves from an initial solution before it finds solution or is frozen in local optima. Evolutionary algorithm is an applicable way to find good weight matrix for FCM. However, like in our algorithm, human interference is needed to judge whether an output matrix meets the expectation.

VI. CONCLUSION

In this paper, we propose a gradient residual training algorithm for generating weights of FCM. The algorithm updates weights by trying to decrease the squared Bellman residual. The equations to update the weights and the training system are demonstrated. Then the experiments using the algorithm are shown. The results show that with sufficient training samples, the learning algorithm can generate output weight matrix which is very close to the desired matrix. It is an efficient algorithm for generating FCM weight matrix of a dynamic system given the change models of the system. The observations of system models are normally easier than to estimate the possible influences between the concepts. Thus the algorithm proposes a new direction for FCM research and applications. In future, more experiments will be performed in real applications to test the training system.

The example FCM in this paper contains seven concepts. The number of time steps is thus short (e.g. 8 steps). Some large FCMs with many concepts may generate infinite steps. The residual algorithm works quite well with such cases in our other experiments. In these experiments, the algorithm works well even for a FCM with 80 concepts. Due to the page limit, we cannot display many large matrices. Another point is that in the training, not all steps before convergence are required to train a weight matrix. The benefit of providing more steps is to generate matrix closer to the original matrix. More experiments and comparative analysis of residual algorithm and the GA algorithm by Stach [21] will be reported soon.

ACKNOWLEDGMENT

This research is financially supported by Singapore National Research Fund.

REFERENCES

[1] B. Kosko, "Fuzzy Cognitive Maps," *Int. J. Man-Machine Studies,* vol. 24, pp. 65-75, 1986.

[2] R. M. Axelrod, *Structure of Decision: The Cognitive Maps of Political Elites*: Princeton University Press, 1976.

[3] B. kosko, "bidirectional associative memories," *IEEE transactions Systems, Man, and Cybernetics,* vol. 18, pp. 49-60, 1988.

[4] J. Aguilar, "A survey about fuzzy cognitive maps papers," *International Journal of Computational Cognition,* vol. 3, no. 2, pp. 27-33, 2005.

[5] J. A. Dickerson, and B. Kosko, "Virtual worlds as fuzzy cognitive maps." pp. 471-477.

[6] C.-P. Mu, H.-K. Huang, and S.-F. Tian, "Fuzzy cognitive maps for decision support in an automatic intrusion response mechanism." pp. 1789-1794.

[7] E. I. Papageorgiou, C. Stylios, and P. P. Groumpos, "Unsupervised learning techniques for fine-tuning fuzzy cognitive map causal links," *International Journal of Human-Computer Studies,* vol. 64, no. 8, pp. 727-743, Aug, 2006.

[8] E. I. Papageorgiou, P. Spyridonos, D. Glotsos *et al.*, "Brain Tumor Characterization using the Soft Computing Technique of Fuzzy Cognitive Maps," *Applied Soft Computing,* vol. 8, pp. 820-828, 2008.

[9] G. Meghabghab, "Mining User's Web Searching Skills through Fuzzy Cognitive State Map vs. Markovian modeling," *International Journal of Computational Cognition,* vol. 1, no. 3, pp. 51-92, September, 2003.

[10] Y. Miao, Z.-Q. Liu, C. K. Siew *et al.*, "Dynamical cognitive network - an extension of fuzzy cognitive map," *IEEE Transactions on Fuzzy Systems,* vol. 9, no. 5, pp. 760-770, Oct, 2001.

[11] L. C. Baird III, "Reinforcement Learning Through Gradient Descent," School of Computer Science, Carnegie Mellon University, Pittsburgh, PA 15213, 1999.

[12] M. Gori, and A. Tesi, "On The Problem Of Local Minima In Backpropagation," *IEEE Transactions on Pattern Analysis and Machine Intelligence,* vol. 14, no. 1, pp. 76-86, January, 1992.

[13] B. Kosko, *Neural networks and fuzzy systems: a dynamical systems approach to machine intelligence*: Prentice Hall; Har/Dis edition, 1992.

[14] B. Kosko, "Hidden Patterns in Combined and Adaptive Knowledge Networks," *International Journal of Approximate Reasoning,* vol. 2, pp. 337-393, 1988.

[15] A. V. Huerga, "A balanced differential learning algorithm in fuzzy cognitive maps," *the 16th International Workshop on Qualitative Reasoning*, 2002.

[16] D. E. Koulouriotis, I. E. Diakoulakis, and D. M. Emiris, "Learning fuzzy cognitive maps using evolution strategies: a novelschema for modeling and simulating high-level behavior." pp. 364-371.

[17] W. Stach, L. Kurgan, and W. Pedrycz, "Parallel Learning of Large Fuzzy Cognitive Maps." pp. 1584-1589.

[18] S. Alizadeh, M. Ghazanfari, M. Jafari *et al.*, "Learning FCM by Tabu Search," *International Journal of Computer Science,* vol. 2, no. 2, pp. 142-149, 2007.

[19] E. I. Papageorgiou, K. E. Parsopoulos, P. P. G. C. D. Stylios *et al.*, "Fuzzy Cognitive Maps Learning Using Particle Swarm Optimization," *International Journal of Intelligent Information Systems,* vol. 25, no. 1, pp. 95-121, July, 2005.

[20] S. Alizadeh, and M. Ghazanfari, "Learning FCM by chaotic simulated annealing," *Chaos, Solitons & Fractals*, June 2008.

[21] W. Stach, L. Kurgan, W. Pedrycz *et al.*, "Learning Fuzzy Cognitive Maps with Required Precision Using Genetic Algorithm Approach," *Electronics Letters,* vol. 40, no. 24, pp. 1519-1520, 2004.

2011 IEEE International Conference on Fuzzy Systems
June 27-30, 2011, Taipei, Taiwan

Causal Modeling Approximations In The Medical Domain

Lawrence J. Mazlack
Applied Computational Intelligence Laboratory
University of Cincinnati
mazlack@uc.edu

***Abstract*---Studies in the health sciences often seek to discover cause-effect relationships among observed variables of interest, for example: treatments, exposures, preconditions, and outcomes. Consequently, causal modeling and causal discovery are central to medical science. In order to algorithmically consider causal relations, the relations must be placed into a representation that supports manipulation and discovery. Knowledge of at least some causal effects is inherently imprecise or approximate. The most widespread causal representation is directed acyclic graphs (DAGs). However, DAGs are limited in what they can represent. Another graph methodology, fuzzy cognitive maps (FCMs) hold promise as a model that overcomes some of the difficulties found in other approaches. This paper considers causality and suggests fuzzy cognitive maps as a useful causal representation methodology.**

Keywords-causal, modeling, cognitive map

I. Introduction

Causal knowledge makes up much of what we know and want to know in science [1]. Causal modeling and causal discovery are central to medical science as recognition of cause-effect can lead to robust treatments. Causality is a *relation,* relating *causes* to *effects* [2]. Experimental studies, such as randomized controlled trials, often provide the trust worthiest results for establishing causal relationships. However, human experimental studies, while potentially informative, may not be: safe, ethical, logistically feasible, or financially worthwhile. Alternatively, observational data is often available in the form of medical records; this data can be analyzed to attempt to recognize causal relationships. Sometimes, there is insufficient data to draw precise results; or, the available data is imprecise, incomplete, or contradictory; this leads to the need to accommodate imprecision in a casual model.

The target of many studies in the health sciences is the discovery of cause-effect relationships among recorded variables of interest, for example: treatments, exposures, preconditions, and outcomes [3]. Yet, until recently, the dominant methodology in health science research has been statistical analysis. Statistical analysis of recorded data can provide information about correlations (or associations), but not necessarily information about causal relationships. For example, the correlation between a patient's *coughing* and *fever* may be high. But, this does not necessarily indicate a causal relationship; i.e., someone's *cough* is *caused* by their *fever* (or the other way around). A high correlation does not indicate causality. All that a high correlation tells us is that, for some reason, certain items often occur at the same time.

Causal relationships can be described as having varying strengths; i.e., we can say that they are *always true, often, sometimes true, rarely true, etc*. Zadeh [4] calls approximating natural language terms: *linguistic variables*. Linguistic imprecision can be best manipulated and represented using *fuzzy arithmetic* which is based on *fuzzy sets* [5].

Statistical analysis of observational data can provide information about correlations, but not necessarily information about causal relationships. For example,

> In a grocery store, the correlation between customer purchases of bread and the purchases of milk may be high and may be a frequently occurring data pair (association).

This does not necessarily indicate a causal relationship; i.e.,

> Someone's purchase of bread is caused by their purchase of milk (or the other way around).

Sometimes, high medical attribute correlations have led to questionable causal statements. For example,

> A Prussian army physician, Hans Reiter, observed a syndrome (called Reiter's syndrome) that often occurred where the patient also had syphilis. He concluded that Reiter's syndrome was caused by syphilis.

This causal connection description has found its way into many medical textbooks. Unfortunately for this causal connection statement, the incidence of syphilis was high in most armies of that time and almost any disorder, including the common cold, could have been similarly causally connected (by a high correlation) to syphilis. (In the Prussian army, the incidence of Reiter's syndrome was lower than the incidence of either syphilis or common colds.)

Similarly, some years ago,

> Epidemiologists found that women taking hormone therapy replacement therapy (HRT) had fewer heart attacks [6]. However follow on controlled studies showed that HRT caused more heart attacks. It turned out that women taking HRT in the epidemiologic study were from higher socio-economic classes, so they ate and exercised better. Economic class caused both HRT and fewer heart attacks.

Networks (graphs) of causes and effects can be constructed; i.e.,

$$(\alpha \rightarrow \beta,\gamma), (\beta \rightarrow \delta), (\gamma \rightarrow \varphi), (\beta \cap \delta \rightarrow \lambda)$$

The question is: How to best represent a causal network if the following characteristics are to be part of it: direction, strength, imprecision, network (graph) structure?

978-1-4244-7316-8/11/$26.00 ©2011 IEEE

When trying to *precisely* reason about causality, complete knowledge of all of the relevant events and circumstances is needed. As complete knowledge may not be possible, imprecise causal reasoning is needed.

A. An Association Does Not, By Itself, Mean Causality

Associations or correlations do not *necessarily* describe causality. Sometimes, the association might be causal; for example, if

Someone eats salty peanuts, then drinks beer.

or

Someone drinks beer, then becomes inebriated.

there may be a degree of a causal relationship. On the other hand, if

A rooster grows, then the sun rises.

or

Someone wears a 'lucky' shirt, then wins a lottery.

there may not be a causal relationship. Recognizing true causal relationships greatly enhances the decision value of data analysis.

The naïve use of simple associations may lead to errors. Errors might occur; either if causality is recognized where there is no causality; or if the direction of the causal relationship is wrong [7] [8]. For example, if

A study of past customers shows that 94% are sick.

- Is it the following rule?

Our customers are sick, so they buy from us.

- Is it the following complementary rule?

If people use our products, they are likely to become sick.

When making a decision, it is not enough to know that

People both buy our products and are sick.

what is needed is knowledge of what causes what; and, to what degree is something a causal effect of another thing.

B. Granularity

Causality is often granular. This is true both with commonsense reasoning as well as for more formal mathematical and scientific approaches. At a very fine-grained level, the physical world itself may be granular [9]. Commonsense perceptions of causality are often large-grained while the underlying causal structures may be fine-grained.

Larger-grained causal objects are often more imprecise than some of the components that are collected into the larger-grained object. Some components of a larger-grained causal object may be precisely known, while others maybe be somewhat imprecise, and others unknown. The larger the grain, the greater is the likelihood that there might be missing or unknown components.

How to best evaluate the impreciseness of a larger-grained causal object when the impreciseness of the underlying cascade of components is not clear; perhaps, some form of Type-II fuzzy [10] manipulation might be helpful.

C. Reasoning

Commonsense understanding of the world tells us that we have to deal with imprecision, uncertainty and imperfect knowledge. This is also the case with scientific knowledge of the world. A difficulty is striking a good balance between precise formalism and commonsense imprecise reality.

Causal relationships exist in the commonsense world; for example:

When a glass is pushed off a table and breaks on the floor

it might be said that

Being pushed from the table *caused* the glass to break.

Although,

Being pushed from a table is not a ***certain*** *cause* of breakage; sometimes the glass bounces and no break occurs; or, someone catches the glass before it hits the floor.

Counterfactually, usually (but not always),

Not falling to the floor prevents breakage.

Sometimes,

A glass breaks when an errant object hits it, even though it does not fall from the table.

Positive causal relationships can be described as: *if* α *then* β (or, $\alpha \rightarrow \beta$). For example:

When an automobile driver fails to stop at a red light and there is an accident; it can be said that the failure to stop was the accident's *cause*.

However, negating the causal factor does not mean that the effect does not happen; sometimes effects can be *overdetermined.* For example:

An automobile that did not fail to stop at a red light can still be involved in an accident; another car can hit it because the other car swerved and hit it while the car was stopped.

Similarly, negating a causal description often does not work. This is often because an effect can be overdetermined. Also, negative statements are weaker than positive statements as the negative statements can become *overextended.* For example, it cannot be said that $\neg\alpha \rightarrow \neg\beta$, for example:

Failing to stop at a red light is not a ***certain*** *cause* of an accident occurring; sometimes no accident at all occurs. (There may be no other cars; the other cars brake in time; etc.)

Negative causal relationships are less sure as negative statements are easily overextended; but negative causal relationships are often stated; for example, it is often said that:

Not walking under a ladder prevents bad luck.

Or, usually (but not always), as before

Stopping for a red light avoids an accident.

Perhaps, complete knowledge of all possible factors might lead to a crisp understanding of whether an effect will occur. However, it is unlikely that all possible factors can be known for most situations, as the knowledge of at least some causal effects is imprecise for both positive and negative descriptions. Consequently, causal reasoning models must accommodate inherent ambiguity [13].

When trying to precisely reason about causality, complete knowledge of all of the relevant events and circumstances is needed. In commonsense, every day reasoning, approaches are used that do not require complete knowledge. Often, a *satisficing* [14] paradigm is acceptable.

II. Granularity And Complexes

When events happen, there are usually other related events. The entire collection of events can be called a complex. A "mechanism" [15] or a "causal complex" [16] [17] is a collection of events whose occurrence or non-occurrence results in a consequent event happening.

Each complex, taken as a whole, often can be reduced to a granule if the grain size is increased. Alternatively, larger complexes often can be decomposed into smaller complexes; going from large grained to small grained. For example, when describing starting an automobile, A large-grained to small-grained, nested causal view could start with

> When an automobile's ignition switch is turned on, this *causes* the engine to start.

But, it would not happen if a large system of other conditions were not in place.

> There has to be available fuel. The battery has to be good. The switch has to be connected to the battery so electricity can flow through it. The wiring has to connect the switch to the starter and ignition system (spark plugs, etc.). The engine has to be in good working order; and so forth.

Turning the ignition switch on is one action in a complex of conditions required to start the engine. One of the events might be used to represent the collection of equal grain sized events; or, a higher-level granule might be specified with the understanding that it will invoke a set of finer-grained events.

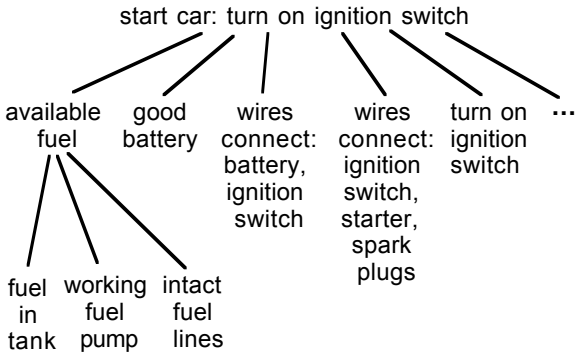

Figure 1. Nested causal complex.

In nested complex granules, the largest-grained event is the sole causal element: *Turn on the ignition switch*. The complex's other elements represent finer-grains. These elements in turn could be broken down into still finer-grains; for example: "available fuel" can be broken down into:

> fuel in tank, working fuel pump, intact fuel lines, ...

Sometimes, it is enough to know what happens at a large-grained level; at other times it is necessary to know the fined grained result. For example, if

> Bill believes that turning the ignition key of his automobile *causes* the automobile to start.

It is enough if

> Bill engages an automobile mechanic when his automobile does not start when he turns the key on.

However,

> The automobile mechanic needs to know a finer-grained view of an automobile's causal complex than does Robin.

Instead of being concerned with all of the fined grained detail, a better approach may be to incorporate granulation using rough sets [18] and/or fuzzy sets to soften the need for preciseness.

In causal reasoning, commonsense reasoning may recognize that a complex collection of elements can be involved causally in a particular effect, even if the precise elements of the complex are unknown. It may not be known what events are in the complex; or, what constraints and laws the complex is subject to. Sometimes, the details underlying an event are known, sometimes not. For example:

> A traffic jam might be observed in mid-town Manhattan. A reasonable supposition might be made that the jam was caused by a complex collection of elements. It might be possible to conjecture what were some of the causes; but, it is unlikely to be able to precisely know what were the complete set of actual causes.

Causal complexes may be described using nested granularity. A complex may have several larger-grained elements. In turn, each of the larger-grained elements may be made up of a complex of more fine-grained elements. Recursively, in turn, these elements may be made up still finer-grained elements. In general, people are more successful in applying commonsense reasoning to a few large-grain sized events than to many fine-grained elements.

When using large-grained commonsense reasoning, people do not always need to know the extent of the underling complexity.

> Somebody waiting for a dinner companion in mid-town Manhattan who observed a traffic jam might presume that they might be late because their taxi would most likely be delayed. Only the imprecise large-grained knowledge of the traffic jam would be needed; knowing the more precise finer-grained details of the jam are not be needed.

Not needing to know fine grained detail is also true for situations not involving commonsense reasoning; i.e.:

> When designing an electric circuit, designers are rarely concerned with the precise properties of the materials used; instead, they are concerned with the devices functional capabilities and take the device as a larger-grained object.

Hobbs [16] uses first order logic to describe his causal complexes. Pearl [19] develops probabilistic causal networks of directed graphs (DAGs). The causal complexes explicitly considered separately by Hobbs and Pearl have a required structure that may be overly restrictive for commonsense causal understanding:

- If *all* of the events in the causal complex appropriately happen, then the effect will occur
- There is nothing in the causal complex that is irrelevant to the effect

These requirements are probably too precise and extensive to be realized in a commonsense world. Sometimes, only some of the events need to happen. For example,

> Someone may be able to save more money:
> • If their taxes are lowered or
> • If they earn more money.

Either may lead to greater savings. However,

Neither may result in increased savings if they also have to pay a large divorce settlement.

If all of the events happen, the effect may happen. If some events happen, the effect may still happen. In the commonsense world, we rarely know whether all of the events are in a complex are necessary. For example,

A man may want to attract the attention of a woman. He may do a large number of things (e.g., hair, clothes, learn to dance, etc.). If he does attract the woman, he may never know which things were relevant and which were not

An example of restructuring a causal graph by increasing the grain size can be seen in Figures 2a,b. In Figure 2a, the idea is that solid, middle-sized, spherical things all roll are replaced with the concept class representation "ball" of Figure 2b. However, the price of collapsing the variables is a decrease in precision.

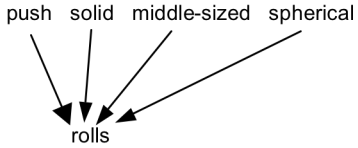

Figure 2a. Variables (solid, middle-sized, spherical) with common effect. [20]

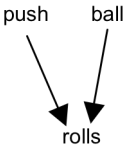

Figure 2b. Variables with a common effect (solid, middle-sized, spherical) collapsed into the concept "ball." [20]

An issue is how to distinguish between what is in a complex and what is not. Another issue is how to distinguish between the things that deserve to be called "causes" and those that do not. Hobbs [16] suggests that a consideration of causal complexes can be divided into:

- Distinguishing what events are in a causal complex from those outside of it. [21] [22] [15] [11] [19]
- Within a causal complex, recognizing the events that should be identified as causes from those that are not. [23] [24]

A major question concerning complexes is: To what extent can we increase the causal grain size and still have useful causal information? Conversely, can we start with a large-grained causal event and then derive the finer-grained structure? Can we measure and/or control the imprecision involved in changing grain size? If we start with a large-grained structure and resolve it, will our computational complexity burdens be reduced?

III. Directed Causal Graph Elements

The idea of "positive" causation ($\alpha \rightarrow \beta$) is at the commonsense causal reasoning core. Often, a positive causal relationship is represented as a network of nodes and branches with causal direction shown by an arrow.

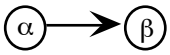

Figure 3. Diagram indicating that α is causally dependent on β.

A. Directed Acyclic Graphs (DAGs)

Various graph based Bayesian based methods have been suggested to describe causality. Probably the best known is the class of methods based on Directed Acyclic Graphs (DAGs). The most fully developed approach is Pearl [19]. Silverstein [25] [26] followed a similar approach. From the commonsense causal reasoning view, the various directed graph methods have similar liabilities, specifically:

A.1 *Liability:* Discrete or continuous data must be reduced to Boolean values. This is an early technique that was and is used in data mining when analyzing market basket data. However, it is essentially flawed. Quantities do matter; some data co-occurrences are conditioned on there being a sufficiency of a co-occurring attribute. Also, some relationships may be non-linear based on quantity [8].

A.2. *Liability:* There can be no missing data. This is at variance with day-to-day experience. There is often missing data of some sort. Data collection is rarely fully representative and complete. Incremental data is often acquired that is at variance with previously acquired data. A methodology that is not brittle in the face of incompleteness is needed.

A.3. *Liability:* Causal relationships are not cyclic, either directly or indirectly (through another attribute). This is at variance with our commonsense understanding of the world. Within cyclic dependencies, there are several variants.

A.3.1 Cycles with time lag: There are many commonsense examples where cycles with a time lag are needed.

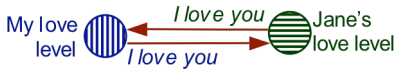

Figure 4. Positive feedback cycle: I tell Jane that I love her. Then, she tells me that she loves me. Then, I tell Jane that I love her more than before. Then, she … and so forth and so forth. Clearly, the cyclic reinforcement would be substantial.

Some cycles can be reasonably collapsed, some cannot be.

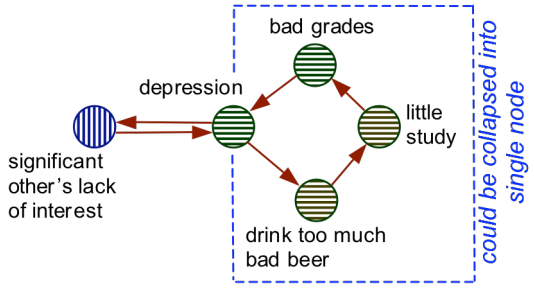

Figure 5. Cyclic relationship that can be collapsed while retaining meaning.

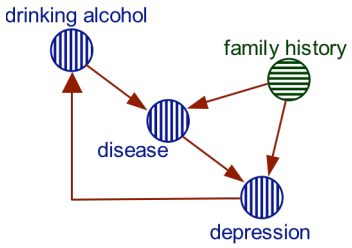

Figure 6. Cyclic relationship that cannot be easily collapsed while retaining meaning.

A.3.2 Concurrent cycles. Another form of a cycle is *joint mutual dependency.* It is possible that there might be mutual dependencies [13]; i.e., $\alpha \rightarrow \beta$ as well as $\beta \rightarrow a$. It seems to be possible that they do so with different strengths. They can be described as shown in the following figure where $S_{i,j}$ represents the strength of the causal relationship from i to j .

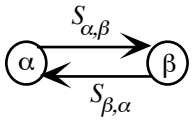

Figure 7. Cyclic relationship: Mutual unequal dependency. [13]

A.3.2.1 Different causal strengths for the same activity, occurring at the same time. Some argue that causality should be completely asymmetric and if it appears that items have mutual influences it is because there is another cause that causes both. A problem with this is that it can lead to eventual regression to a first cause. Whether this is true or not, it is not useful for commonsense understanding and representation. In contrast, Simon [15] and Shoham [27] identify cases where causality is simultaneous.

Mutual causal influences are also our commonsense experience. For example, in the preceding figure, α could be *short men* and β could be *tall women*. If $S_{\alpha,\beta}$ meant the strength of desire for a social meeting, it might be that $S_{\alpha,\beta} > S_{\beta,\alpha}$.

A.3.2.2 Different causal strengths for symmetric activities, occurring at different times. It would seem that if there were causal relationships in market basket data, there would often be imbalanced dependencies. For example, if

A customer first buys strawberries, there may be a reasonably good chance that they will then buy whipped cream.

Conversely, if

They first buys whipped cream, the subsequent purchase of strawberries may be less likely.

A.4 *Liability:* Markov Stationary Condition holds: Probabilities are time independent (DAG requirement). This does not correspond to our commonsense understanding of the world. When one event is dependent on two causal events, if one causal event happens much earlier (or later) than the other event, there may well be a different result. For example, if the goal is to have a successful dinner party, the catered food should be delivered before the guests arrive.

A.5 *Liability:* The Markov Memoryless Condition holds (DAG requirement). The *Markov Condition* is defined as: Let A be a node in a causal Bayesian network, and let B be any node that is not a descendant of A in the network. Then the Markov (Markoff) condition holds if A and B are independent, conditioned on the parents of A. The intuition of this condition is: If A and B are dependent, then B must either be (a possibly indirect) cause of A or (possibly indirectly) caused by A. In the second case, B is a descendant of A, while in the first B is an ancestor of A and has no effect on A once A's immediate parents are fixed. This makes sense in the example shown in the following figure.

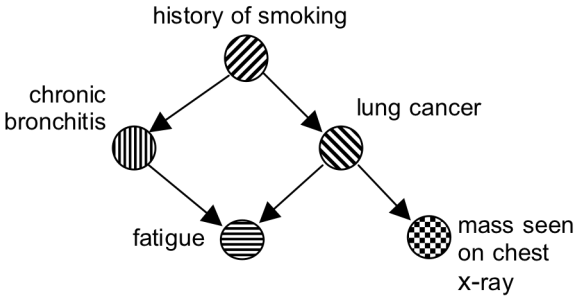

Figure 8. Memoryless Markov condition holds

However, not all commonsense perceptions of causality work this way. Often, we believe that history matters as in the example shown in the following figure.

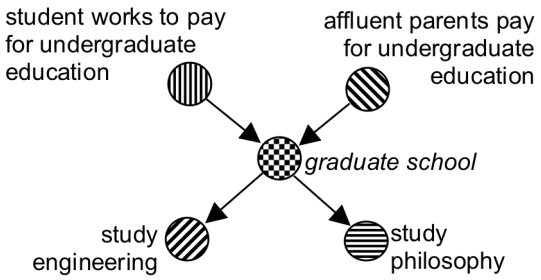

Figure 9. Causality where memory play a part. Memoryless Markov condition does not hold.

B. Markov Models

One possible way of describing the causal relationships is with first order Markov Models. They treat a system as a series of states with specific, constant rate transitions between them. At all times, the system is in exactly one state. (Transitions are considered to be instantaneous.) The only information available is the current state, the allowed transitions, and the probability of these transitions. This means that the system is totally characterized by its current state. None of the past states or transitions have any effect on the transitions out of the current state.

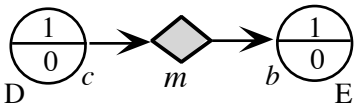

Figure 10. Random Markov model: c = P(D), m = the possibility/probability that when D is present, the causal mechanism brings about E, b = the probability that some other (unspecified) causal mechanism brings about E.

Describing the relationships between the nodes can be complex. One possibility is an extension of the random Markov model, shown in the following figure.

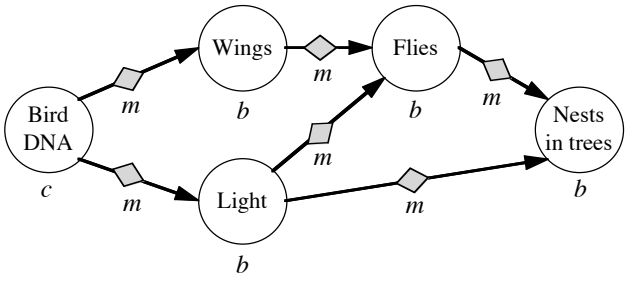

Figure 11. Markov model applied to a "bird" example [28]

Perhaps, fuzzy sets and fuzzy Markov algorithms in particular might be a good way of approaching causality represented by Markov models. Cheok [29] shows how the probabilities in the classic Markov model may be extended to fuzzy possibilities. The generalized hidden Markov Model can be defined with the same type of model parameters, but with a different mathematical basis than the classic one. Fuzzy logic replaces probability theory and this leads to a new definition of the model variables. The structure in terms of states and observations remains the same.

There has been a fair amount of work in fuzzy Markov models [30] [31] [32]. A fair amount of the work has a control theory or medical diagnostic orientation. Whether it can be extended to representing causality is to be seen. While Markov models are intuitively appealing, they have some of the cyclic representational problems as do DAGs. Consequently, they may not be a good solution.

IV. Fuzzy Cognitive Maps

A potentially useful form for representing causal structures that overcomes some of the deficiencies of directed acyclic graphs or similar representations is Fuzzy Cognitive Maps (FCMs). They bring their own liabilities in that how to autonomously form FCMs through data mining is unresolved.

Fuzzy Cognitive Maps are fuzzy structures that resemble neural networks. They have powerful and far-reaching consequences as a mathematical tool for modeling complex systems. At first, Axelord [33] used cognitive maps as a formal way of representing social scientific knowledge and modeling decision making in social and political systems [34]. Then, Kosko enhanced cognitive maps considering fuzzy values for them [35] [36] [37] [38].

Indeterminacy and unpredictability of life affect causal descriptions almost as much as the determined factors. It is a major handicap in mathematical modeling if we are only able to give precise values for known concepts and relationships between concepts, thereby presenting onto ourselves a skewed view. Fuzzy theory can offer more choices. Mendel [10] and Kandasamy [39] have introducing indeterminacy into Fuzzy theory; Mendel uses Type-2 Fuzzy Logic while Kandasamy uses Neutrosophic structures.

A FCM describes the behavior of a system in terms of concepts; each concept represents a state or a characteristic of the system. A FCM illustrates the system by a graph showing cause and effect between concepts. FCMs model the world as a collection of classes and causal relations between classes. FCMs are fuzzy signed directed graphs with feedback. The directed edge *Wij* from causal concept *Ci* to concept *Cj* measures how much *Ci* causes *Cj*. The time varying concept function *Ci(t)* measures the non-negative occurrence of some fuzzy event.

A Fuzzy Cognitive Map consists of nodes that represent concepts and arcs (edges) between concepts [40]. Each concept represents a characteristic of the system; in general it stands for events, actions, goals, values, trends of the system. A number Ai that represents its value characterizes each concept and it results from the transformation of the value of the system's variable, for which this concept stands, in the interval [-1,1]. The graph's edges are the casual influences between the concepts.

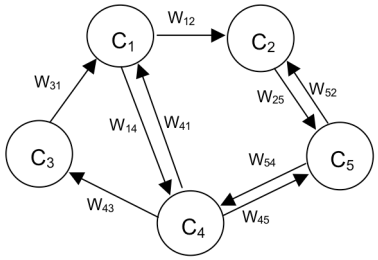

Figure 12. Example of a simple Fuzzy Cognitive Map

The edges *Wij* takes values in the fuzzy causal interval [–1, 1]. The weights of the arcs between concept *Ci* and concept *Cj* could be positive ($Wij > 0$) which means that an increase in the value of concept *Ci* leads to the increase of the value of concept *Cj* , and a decrease in the value of concept *Ci* leads to the decrease of the value of concept *Cj* . Or there is negative causality ($Wij < 0$) which means that an increase in the value of concept *Ci* leads to the decrease of the value of concept *Cj* and vice versa. $Wij = 0$ indicates no causality.

State vectors $\boldsymbol{C}$ are repeatedly passed through the FCM connection matrix $\boldsymbol{W}$, thresholding or non-linearly transforming the result after each pass. The limit cycle or fixed-point inference summarizes the joint effects of all the interacting fuzzy knowledge.

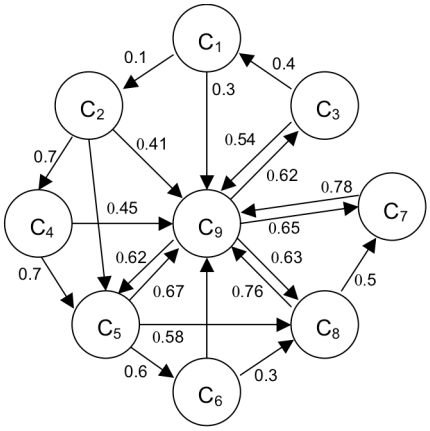

Figure 13. A urinary bladder tumor grading model [41]

The previous figure shows how a medical FCM application; where C_n, $n=1…8$ represent histological features using five positive linguistic variables depending on the characteristics of each particular concept. C_9 represents the target, tumor grade. The concepts are:

C_1: Cell distribution: Even, clustered
C_2: Cell size: Uniform, pleomorphic
C_3: Cell number: Numerous, variable
C_4: Cytoplasm: Homogeneous, variable
C_5: Nuclei: Uniform, irregular, very irregular, bizarre
C_6: Nucleoi: Inconspicuous, evident, prominent
C_7: Neocrosis: Inconspicuous, frequent
C_8: Mitoses: Absent-rate, occasional, numerous
C_9: Degree of tumor grade

The value of a node reflects the degree to which the concept is active in the system at a particular time. This value is a function of the sum of all incoming edges multiplied and the value of the originating concept at the immediately preceding state. The threshold function applied to the weighted sums can be fuzzy in nature. Concept values are expressed on a normalized range denoting a degree of activation rather than an exact quantitative value.

The mathematical model consists of $1 \times n$ state vector $\boldsymbol{A}$ that includes the values of the n concepts and a $n \times n$ weight matrix $\boldsymbol{W}$ that gathers the weights W_{ij} of the interconnections between the n concepts of the FCM. The matrix $\boldsymbol{W}$ has n rows and n columns where n equals the total number of distinct concepts of the FCM and the matrix diagonal is zero since it is assumed that no concept causes itself. The value of each concept is influenced by the values of the connected weighted concepts and by its previous value. The value A_i for each concept C_i is calculated by:

$$A_i f\left(\sum_{\substack{j=1 \\ j\neq 1}}^{n} A_j W_{ji}\right) + A_i^{old}$$

where Ai is the activation level of concept Ci at time t+1, Aj is the activation level of concept Cj at time t+1, Aj is the activation level of concept Ci at time t, and Wji is the weight of the interconnection between Cj and Ci, and f is a threshold function.

$$A_{new} = f\left(A_{old} \circ W\right) + A_{old}$$

The new state vector $\boldsymbol{A}_{new}$ is computed by multiplying the previous state vector $\boldsymbol{A}_{old}$ by the weight matrix $\boldsymbol{W}$. The new vector shows the effect of the change in the value of one concept in the entire Fuzzy Cognitive Map.

The simplest FCMs act as asymmetrical networks of threshold or continuous concepts and converge to an equilibrium point or limit cycles. FCMs have nonlinear structure of their concepts and differ in their global feedback dynamics [42] [38].

There are several unsupervised learning algorithms that might be used to reach convergence, or at least convergence within an acceptable tolerance [43] [44] [45] [46] [47] [48] [49]; the algorithms can be comparatively analyzed [50]; however, neither particular methods or a comparative analysis of the methods are within the scope of this paper. The FCM system model takes the initial values of the concepts from the real system and is free to interact. The interaction happens because of change in the value of one or more concepts [51]. The interaction continues until the model:

- Reaches equilibrium at a fixed point, with the output concept values stabilizing.
- Exhibits limit cycle behavior, with the concept values falling in a loop.
- Exhibits chaotic behavior in a non-deterministic way.

Causal feedback loops can occur in FCMs. FCM feedback allows causal adaptation. FCM feedback forces the abandonment of classic graph search, forward and backward chaining. Instead, the FCM is a dynamical system and take its equilibrium behavior as a forward-evolved inference. A FCM has the ability to specify a complex model, shows linear or non-linear relations and allows causal propagation [52].

The development of a FCM often occurs within a group context. Experts can pool or fuse their knowledge by adding the underlying FCM causal matrices [43]. The obvious advantage is that a causal relationship can be described in stages. If some form of data min-ing is discovering the causal relation-ships, it could be a highly desirable incremental method. Another claimed advantage [34] is that combining incomplete, conflicting opinions of different experts may cancel out the effect of oversight, ignorance and prejudice; although this would seem to require a fairly large number of overlapping relationships so a useful average relationship would be developed.

V. Epilogue

The target of many studies in the health sciences is the discovery of cause-effect relationships among observed variables of interest, for example: treatments, exposures, preconditions, and outcomes. Causal modeling and causal discovery are central to medical science. In order to algorithmically consider causal relations, the relationships must be placed into a representation that supports manipulation. An algorithmic way of handling causal imprecision is needed. There are several needs of a causal model. The needs are:

- Represent causal direction
- Represent degree of causal effect
- Represent causal imprecision
- Accommodate changes in grain size
- Describe complexes
- Support cycle models of all times
- Be time varying
- Not be restricted by Markov conditions

The most widespread causal representation is directed acyclic graphs (DAGs). However, DAGs are severely limited in what they can represent. This paper considered the needs of commonsense causality and suggested Fuzzy Cognitive Maps as an alternative to DAGs. Fuzzy Cognitive Maps appear to be a good approximation of complex casual complexes. They appear to be a comprehensive representation. Their primary difficulty lies with establishing their initial values.

References

[1] G. F. Cooper and C. You, "Causal Discovery From A Mixture Of Experimental And Observational Data," presented at UAI, 116-125, 1999.

[2] F. Heylighen, "Causality As Distinction Conversation: A Theory Of Predictability, Resersibility, And Time Order," *Cybernetics And Systems*, vol. 20, pp. 361-384, 1988.

[3] J. Pearl, "Causal Inference In The Health Sciences: A Conceptual Introduction," *Health Services And Outcomes Research Methodology*, vol. 2, pp. 189-220, 2001.

[4] L. A. Zadeh, "The Concept Of A Linguistic Variable And Its Application To Approximate Reasoning - I," *Information Sciences*, vol. 8, pp. 199-249, 1975.

[5] L. A. Zadeh, "Fuzzy Sets," *Information and Control*, vol. 8, 1965.

[6] M. Ridley, "When Scientists Confuse Cause And Effect," in *Wall Street Journal*, 2011, pp. C4.

[7] S. Brin, R. Motwani, and C. Silverstein, "Beyond Market Baskets: Generalizing Association Rules To Correlations," presented at ACM SIGMOD International Conference, SIGMOD'97, 265-276, SIGMOD Record, 1997.

[8] L. J. Mazlack, "Causality Recognition For Data Mining In An Inherently Ill Defined World," presented at 2003 BISC FLINT-CIBI International Joint Workshop On Soft Computing For Internet And Bioinformatics, Berkeley, California, 2003.

[9] L. Smolin, "Atoms of Space And Time," in *Scientific American*, 2004, pp. 66-75.

[10] J. Mendel, *Uncertain Rule-Based Fuzzy Logic Systems: Introduction and New Directions*. New Jersey: Prentice Hall, 2000.

[11] C. L. Ortiz, "A Commonsense Language For Reasoning About Causation And Rational Action," *Artificial Intelligence*, vol. 108, pp. 125-178, 1999.

[12] L. A. Zadeh, "From Computing With Numbers To Computing With Words - From Manipulation Of Measurements To Manipulation Of Perceptions," *IEEE Transactions on Circuits and Systems*, vol. 45, pp. 108-119, 1999.

[13] L. J. Mazlack, "Commonsense Causal Modeling In The Data Mining Context," presented at IEEE International Conference on Data Mining series (ICDM), Melbourne, Florida, 2003.

[14] H. A. Simon, "A Behavior Model Of Rational Choice," *Quarterly Journal of Economics*, vol. 59, pp. 99-118, 1955.

[15] H. A. Simon, "Nonmonotonic Reasoning and Causation: Comment," *Cognitive Science*, vol. 15, pp. 293-300, 1991.

[16] J. R. Hobbs, "Causality," presented at Common Sense 2001, Fifth Symposium on Logical Formalizations of Commonsense Reasoning, 145-155, New York University, New York, 2001.

[17] J. R. Hobbs, "Causality And Modality: The Case Of 'Would'," *Journal of Semantics*, 2003.

[18] Z. Pawlak, *Rough Sets: Theoretical Aspects of Reasoning About Data* . Dordrecht, Netherlands: Kluwer Academic Publishing, 1991.

[19] J. Pearl, *Causality*. New York, NY: Cambridge University Press, 2000.

[20] C. Glymour, *The Mind's Arrows, Bayes Nets and Graphical Causal Models in Psychology*. Cambridge, Massachusetts: MIT Press, 2001.

[21] D. Lewis, "Causation," in *Philosophical Papers II*: Oxford University Press, 1986, 159–213.

[22] H. A. Simon, "On The Definition Of The Causal Relation," *Journal of Philosophy*, vol. 49, pp. 517-528, 1952.

[23] J. Mackie, "Causes and Conditions," *American Philosophical Quarterly 2*, pp. 245-64, 1965.

[24] Y. Shoham, "Nonmonotonic Reasoning And Causation," *Cognitive Science*, vol. 14, pp. 213-252, 1990.

[25] C. Silverstein, S. Brin, and S. Mani, "Beyond Market Baskets: Generalizing Association Rules To Dependence Rules," *Data Mining And Knowledge Discovery*, vol. 2, pp. 39-68, 1998.

[26] C. Silverstein, S. Brin, R. Motwani, and J. Ullman, "Scalable Techniques For Mining Causal Structures," presented at International Conference on Very Large Databases, 594-605, New York, NY, 1998.

[27] Y. Shoham, "Remarks on Simon's Comments," *Cognitive Science*, vol. 15, pp. 301-303, 1991.

[28] B. Rehder, "A Causal-Model Theory of the Conceptual Representation of Categories," presented at FLAIRS 2002 Workshop on Causality, Pensacola, Florida, 2002.

[29] A. Cheok, S. Chevalier, M. Kaynak, K. Sengupta, and K. Chung, "Use of a Novel Generalized Fuzzy Hidden Markov Model for Speech Recognition," presented at IEEE International Conference on Fuzzy Systems, Melbourne, Australia, 2002.

[30] L. Jeanpierre and F. Charpillet, "Hidden Markov Models for Medical Diagnosis," presented at International Workshop on Enterprise Networking and Computing in Health Care Industry, HEALTHCOM'2002, Nancy, France, 2002.

[31] M. Leuschen, I. Walker, and J. Cavallaro, "Robot Reliability Through Fuzzy Markov Models," presented at IEEE Annual Reliability and Maintainability Symposium, 209-214, Anaheim, CA, 1998.

[32] L. A. Zadeh, "Maximizing Sets And Fuzzy Markov Algorithms," *IEEE Transactions on Systems, Man, and Cybernetics - Part C: Applications and Reviews*, vol. 28, pp. 9-15, 1998.

[33] R. Axelord, *Structure Of Decision: The Cognitive Maps Of Political Elites*. Princeton, New Jersey: Princeton University Press, 1976.

[34] J. Aguilar, "A Survey About Fuzzy Cognitive Maps Papers," *International Journal Of Computational Cognition*, vol. 3, pp. 27-33, 2005.

[35] B. Kosko, "Fuzzy Cognitive Maps," *Int. J. Man-Machine Studies*, vol. 24, pp. 65-75, 1986.

[36] B. Kosko, *Neural Nets And Fuzzy Systems, A Dynamic System Approach To Machine Intelligence*. New Jersey: Prentice Hall, 1992.

[37] B. Kosko and J. Dickerson, "Fuzzy Virtual Worlds," *AI Expert*, pp. 25-31, 1994.

[38] B. Kosko, *Fuzzy Engineering*. New Jersey: Prentice Hall, 1997.

[39] W. B. V. Kandasamy and F. Smardandache, *Fuzzy Cognitive Maps And Neutrosophic Cognitive Maps*. Phoenix: Xiquan, 2003.

[40] C. D. Stylios, V. Georgopoulos, and P. P. Groumpos, "The Use Of Fuzzy Cognitive Maps In Modeling Systems," presented at The 5th IEEE Mediterranean Conference on Control and Systems (MED5), paper 67 (CD-ROM), Paphos, Cyprus, 1997.

[41] E. I. Papageorgiou, P. Spyridonos, C. Stylios, P. Ravazoula, P. P. Groumpos, and G. Nikiforidis, "A Fuzzy Cognitive Map Model For Grading Urinary Bladder Tumors," presented at 5th Int. Conf. in Neural Networks & Experts Systems in Medicine & Healthcare 1st Int. Conf. in Computational Intelligence in Medicine & Healthcare, NNESMED/CIMED Conference, 6, 2003.

[42] B. Kosko, "Fuzzy Associative Memory Systems," in *Fuzzy Expert Systems*, A. Kandel, Ed. Boca Raton, Florida, 1992, 135-162.

[43] R. Taber, R. R. Yager, and C. M. Helgason, "Quantization Effects on the Equilibrium Behavior of Combined Fuzzy Cognitive Maps," *International Journal of Intelligent Systems*, vol. 22, pp. 181-202, 2007.

[44] E. I. Papageorgiou, C. Stylios, and P. P. Groumpos, "An Activation Hebbian Learning Algorithm To Train Fuzzy Cognitive Maps," *International Journal of Approximate Reasoning*, vol. 37, pp. 219-249, 2004.

[45] Y. Cai, C. Miao, A.-H. Tan, and Z. Shen, "Context Modeling With Evolutionary Fuzzy Cognitive Map In Interactive Storytelling," presented at Fuzz-IEEE, 2320-2325, Hong Kong, China, 2008.

[46] A. Konar and U. K. Chakraborty, "Reasoning And Unsupervised Learning In A Fuzzy Cognitive Map," *Information Sciences*, vol. 170, pp. 419-441, 2005.

[47] S.-J. Li and R.-M. Shen, "Fuzzy Cognitive Map Learning Based On Improved Nonlinear Hebbian Rule," presented at Proceedings Of International Conference On Machine Learning And Cybernetics 4, 2301-2306, 2004.

[48] E. I. Papageorgiou and P. P. Groumpos, "A Weight Adaptation Method For Fuzzy Cognitive Maps To A Process Control Problem," in *Lecture Notes In Computer Science*, vol. 3037. Berlin: Springer, 2004.

[49] W. Stach, L. Kurgan, W. Pedrycz, and M. Reformat, "Genetic Learning Of Fuzzy Cognitive Maps," *Fuzzy Sets And Systems*, vol. 143, pp. 371-401, 2005.

[50] A. K. Tsadiras, "Comparing The Inference Capabilities Of Binary, Trivalent And Sigmoid Fuzzy Cognitive Maps," *Information Sciences*, vol. 178, pp. 3880-3894, 2008.

[51] E. I. Papageorgiou, C. Stylios, and P. P. Groumpos, "Unsupervised Learning Techniques For Fine-Tuning Fuzzy Cognitive Map Causal Links," *Human-Computer Studies*, vol. 64, pp. 727-743, 2006.

[52] C. D. Stylios and P. P. Groumpos, "The Challenge Of Modeling Supervisory Systems Using Fuzzy Cognitive Maps," *Journal of Intelligent Manufacturing*, vol. 9, pp. 339-345, 1998.

2011 IEEE International Conference on Fuzzy Systems
June 27-30, 2011, Taipei, Taiwan

Interactive Fuzzy Programming through Possibility Measures and Probability Maximization for Two-Level Linear Programming Problems Involving Fuzzy Random Variable Coefficients

Masatoshi Sakawa
Faculty of Engineering
Hiroshima University
Hiroshima, JAPAN
Email: sakawa@hiroshima-u.ac.jp

Hideki Katagiri
Faculty of Engineering
Hiroshima University
Hiroshima, JAPAN
Email: katagiri-h@hiroshima-u.ac.jp

Takeshi Matsui
Faculty of Engineering
Hiroshima University
Hiroshima, JAPAN
Email: tak-matsui@hiroshima-u.ac.jp

***Abstract*—In this research, focusing on two-level linear programming problems involving fuzzy random variables, we propose a new decision making model through possibility measures. Taking into account vagueness of judgments of decision makers for each objective function, fuzzy goals are introduced. Noting that the degree of the possibility fluctuates stochastically, we propose a probability maximization model in stochastic programming. Through probability maximization, the transformed stochastic two-level programming problem can be reduced to a deterministic one. Interactive fuzzy programming to derive a satisfactory solution for the decision maker at the upper level in consideration of the cooperative relation between decision makers is presented.**

***Index Terms*—two-level programming; possibility; probability maximization; interactive fuzzy decision making**

I. Introduction

In the real world, the coefficients of objectives or constraints in problems are rather uncertain than constant. In order to deal with such uncertainty, stochastic programming [3] and fuzzy programming [21] were considered. They are useful tools for the decision making under a stochastic environment or a fuzzy environment, respectively. Most studies in respect to mathematical programming take account of either fuzziness or randomness. However, in practice, decision makers are faced with the situations where both fuzziness and randomness exist. In the case where some expert estimates coefficients of objective functions or constraints with uncertainty, they do not always represent the coefficients as random variables or fuzzy sets but as the values including both fuzziness and randomness. In such a case, it is important to realize that simultaneous considerations of both fuzziness and randomness would be required. A fuzzy random variable [7] is one of the mathematical concepts dealing with fuzziness and randomness simultaneously. Let us consider the situation that a profit per unit crop acreage is dependent on weathers, i. e., fine, cloudy, rain, etc., which are considered as scenarios that occur randomly. When a realized profit under each scenario is estimated as a fuzzy set or fuzzy number, it turns out that the profit is expressed by a fuzzy random variable. Studies on linear programming problems with fuzzy random variable coefficients, called fuzzy random linear programming problems, were initiated by Wang and Qiao [19], Qiao, Zhang and Wang [11] as seeking the probability distribution of the optimal solution and optimal value. A brief survey of major fuzzy stochastic programming models was found in the paper by Luhandjula [9].

Meanwhile, we often encounter situations where there are two or more decision makers in an organization with a hierarchical structure, and they make decisions in turn or at the same time so as to optimize their objective functions. In particular, consider a case where there are two decision makers; one of the decision makers first makes a decision, and then the other who knows the decision of the opponent makes a decision. Such a situation is formulated as a two-level programming problem [13]. In the context of two-level programming, the decision maker at the upper level first specifies a strategy, and then the decision maker at the lower level specifies a strategy so as to optimize the objective with full knowledge of the action of the decision maker at the upper level. In conventional multi-level mathematical programming models employing the solution concept of Stackelberg equilibrium, it is assumed that there is no communication among decision makers, or they do not make any binding agreement even if there exists such communication [1], [16], [17]. Compared with this, for decision making problems in such as decentralized large firms with divisional independence, it is quite natural to suppose that there exists communication and some cooperative relationship among the decision makers [13].

Assuming that the decision makers essentially cooperate with each other, Sakawa et al. [14], [15] have proposed interactive fuzzy programming for two-level or multi-level linear programming problems to obtain satisfactory solution for decision makers by eliminating the fuzzy goals for the decision variables.

Under these circumstances, in this research, assuming coop-

978-1-4244-7316-8/11/$26.00 ©2011 IEEE

erative behavior of the decision makers, we consider solution methods for decision making problems in hierarchical organizations under fuzzy random environments. To deal with the formulated two-level linear programming problems involving fuzzy random variables, possibility measures are introduced and a stochastic two-level linear programming problem is defined for guaranteeing the degree of realization of the problem. Taking into account vagueness of judgments of decision makers, fuzzy goals are introduced and the stochastic two-level linear programming problem is transformed into the problem to maximize the satisfaction degree for each fuzzy goal. Following probability maximization, the transformed stochastic two-level programming problem can be reduced to a deterministic one. Interactive fuzzy programming to obtain a satisfactory solution for the decision maker at the upper level in consideration of the cooperative relation between decision makers is presented. It is shown that all of the problems to be solved in the proposed interactive fuzzy programming can be easily solved by the simplex method or the combined use of the bisection method and the simplex method.

II. Fuzzy random two-level linear programming problem

Fuzzy random variables, first introduced by Kwakernaak [7], have been defined in various ways [7], [10], [6], [8]. For example, as a special case of fuzzy random variables given by Kwakernaak, Kruse and Meyer [6] defined a fuzzy random variable as follows.

Definition 1 (Fuzzy random variable): Let (Ω, B, P) be a probability space, $F(\mathcal{R})$ the set of fuzzy numbers with compact supports and X a measurable mapping $\Omega \to F(\mathcal{R})$. Then X is a fuzzy random variable if and only if given $\omega \in \Omega$, $X_\alpha(\omega)$ is a random interval for any $\alpha \in (0, 1]$, where $X_\alpha(\omega)$ is an α-level set of the fuzzy set $X(\omega)$.

Although there exist some minor differences in several definitions of fuzzy random variables, fuzzy random variables are considered to be random variables whose observed values are fuzzy sets.

In this paper, we deal with two-level linear programming problems involving fuzzy random variable coefficients in objective functions formulated as:

$$\left.\begin{array}{ll} \underset{\text{for DM1}}{\text{minimize}} & z_1(\boldsymbol{x}_1, \boldsymbol{x}_2) = \tilde{\tilde{\boldsymbol{C}}}_{11}\boldsymbol{x}_1 + \tilde{\tilde{\boldsymbol{C}}}_{12}\boldsymbol{x}_2 \\ \underset{\text{for DM2}}{\text{minimize}} & z_2(\boldsymbol{x}_1, \boldsymbol{x}_2) = \tilde{\tilde{\boldsymbol{C}}}_{21}\boldsymbol{x}_1 + \tilde{\tilde{\boldsymbol{C}}}_{22}\boldsymbol{x}_2 \\ \text{subject to} & A_1\boldsymbol{x}_1 + A_2\boldsymbol{x}_2 \le \boldsymbol{b} \\ & \boldsymbol{x}_1 \ge \boldsymbol{0},\ \boldsymbol{x}_2 \ge \boldsymbol{0} \end{array}\right\} \quad (1)$$

where $\boldsymbol{x}_1$ is an n_1 dimensional decision variable column vector for the DM at the upper level (DM1), $\boldsymbol{x}_2$ is an n_2 dimensional decision variable column vector for the DM at the lower level (DM2), $z_1(\boldsymbol{x}_1, \boldsymbol{x}_2)$ is the objective function for DM1 and $z_2(\boldsymbol{x}_1, \boldsymbol{x}_2)$ is the objective function for DM2.

It should be emphasized here that randomness and fuzziness of the coefficients are denoted by the "dash above" and "wave above" i.e., " ¯ " and " ˜ ", respectively. In this formulation, $\boldsymbol{x}_1$ is an n_1 dimensional decision variable column vector for the DM at the upper level (DM1), $\boldsymbol{x}_2$ is an n_2 dimensional decision variable column vector for the DM at the lower level (DM2), $z_1(\boldsymbol{x}_1, \boldsymbol{x}_2)$ is the objective function for DM1 and $z_2(\boldsymbol{x}_1, \boldsymbol{x}_2)$ is the objective function for DM2. In (1), $\tilde{\tilde{\boldsymbol{C}}}_{lj}$, $l = 1, 2$, $j = 1, 2$ are vectors whose elements $\tilde{\tilde{C}}_{ljk}$, $k = 1, 2, \ldots, n_j$ are fuzzy random variables characterized by the following membership function:

$$\mu_{\tilde{\tilde{C}}_{ljk}}(\tau) = \begin{cases} L\left(\dfrac{\bar{d}_{ljk} - \tau}{\beta_{ljk}}\right) & , \quad \text{if } \tau \le \bar{d}_{ljk} \\ R\left(\dfrac{\tau - \bar{d}_{ljk}}{\gamma_{ljk}}\right) & , \quad \text{otherwise} \end{cases}$$

where $L : [0, \infty) \to [0, 1]$ is a monotone decreasing function defined as $L(t) = \max\{0, \lambda(t)\}$ and $R : [0, \infty) \to [0, 1]$ is also a monotone decreasing function defined as $R(t) = \max\{0, \rho(t)\}$. Here, $\lambda(t)$ and $\rho(t)$ are monotone decreasing functions which satisfy $\lambda(0) = 1$ and $\rho(0) = 1$, respectively. Furthermore, parameters $\bar{d}_{ljk}$, β_{ljk} and γ_{ljk} represent a mean value, the left spread and the right spread of $\tilde{\tilde{C}}_{ljk}$, respectively. In this paper, parameters $\bar{d}_{ljk}$ are random variables defined as $\bar{d}_{ljk} = d^1_{ljk} + \bar{t}_l d^2_{ljk}$, using random variables $\bar{t}_l$ with mean M_l, $l = 1, 2$. This definition of random variables is one of the simplest randomization modeling of coefficients using dilation and translation of random variables, as discussed by Stancu-Minasian [18] and Katagiri et al. [5].

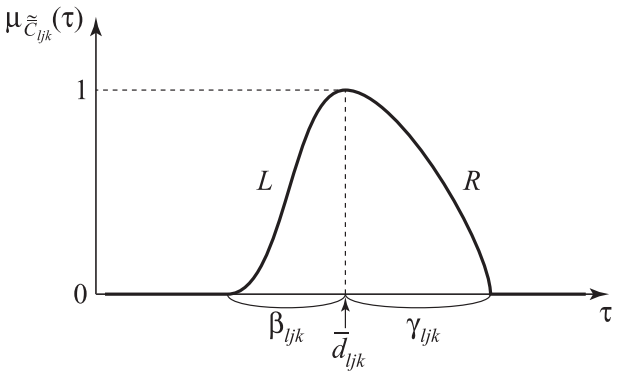

Fig. 1. An example of the membership function $\mu_{\tilde{\tilde{C}}_{ljk}}(\cdot)$ of a fuzzy random variable $\tilde{\tilde{C}}_{ljk}$.

Fig. 1 illustrates an example of the membership function of a fuzzy random variable $\tilde{\tilde{C}}_{ljk}$.

Fuzzy random two-level linear programming problems formulated as (1) are often seen in actual decision making situations. For example, consider a supply chain planning [12] where the distribution center (DM1) and the production part (DM2) hope to minimize the distribution cost and the production cost respectively. Since coefficients of these objective functions are often affected by the economic conditions varying at random, they can be regarded as random variables. In addition, since observed values of them are often ambiguous and estimated by fuzzy numbers, they are expressed by fuzzy random variables. Then, the supply chain planning problem

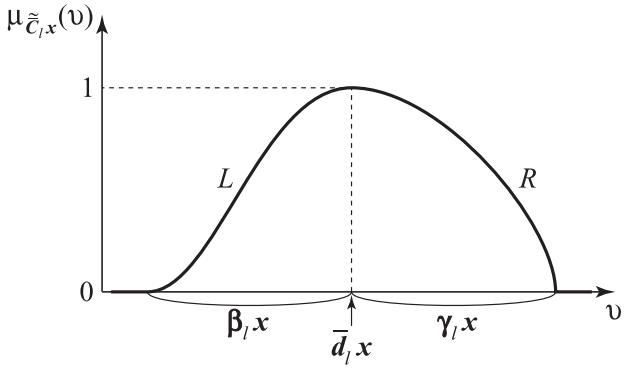

Fig. 2. An example of the membership function $\mu_{\tilde{\tilde{\boldsymbol{C}}}_l \boldsymbol{x}}(\cdot)$ of the objective function of DMl.

can be formulated as a two-level linear programming problem involving fuzzy random variable coefficients like (1).

Since each coefficient $\tilde{\tilde{C}}_{ljk}$ is a fuzzy random variable defined as a random variable whose observed values are L-R fuzzy numbers, each objective function $\tilde{\tilde{\boldsymbol{C}}}_l \boldsymbol{x} = \tilde{\tilde{\boldsymbol{C}}}_{l1} \boldsymbol{x}_1 + \tilde{\tilde{\boldsymbol{C}}}_{l2} \boldsymbol{x}_2$ is also a fuzzy random variable whose observed values are fuzzy numbers characterized by the following membership function.

$$\mu_{\tilde{\tilde{\boldsymbol{C}}}_l \boldsymbol{x}}(\upsilon) = \begin{cases} L\left(\dfrac{\bar{\boldsymbol{d}}_l \boldsymbol{x} - \upsilon}{\boldsymbol{\beta}_l \boldsymbol{x}}\right) & , \quad \text{if } \upsilon \leq \bar{\boldsymbol{d}}_l \boldsymbol{x} \\ R\left(\dfrac{\upsilon - \bar{\boldsymbol{d}}_l \boldsymbol{x}}{\boldsymbol{\gamma}_l \boldsymbol{x}}\right) & , \quad \text{otherwise} \end{cases}$$

An example of the membership function of the objective function of DMl is shown in Fig. 2.

III. Probability Maximization Model through Possibility Measures

Problem (1) is not a well-defined problem due to both fuzziness and randomness of the coefficients, and it cannot be minimized in the sense of deterministic mathematical programming. Therefore, it is necessary to interpret the problem from some point of view and to transform the problem into the deterministic equivalent one. Katagiri and Ishii [4] proposed a fuzzy random programming model using a possibility measure [20] for a linear programming problem where the right-hand side of a constraint is a fuzzy random variable. In this research, assuming that the decision makers are interested in the probability that each objective function attains a goal value rather than the expectation or variance of each membership function, we consider the case where the decision maker prefers to maximize the degree of possibility that the objective function value satisfies the fuzzy goal.

A. Fuzzy goal

A fuzzy goal for the objective is characterized by the following linear membership function:

$$\mu_{\tilde{G}_l}(y) = \begin{cases} 1 & (y < g_l^1) \\ g_l(y) & (g_l^1 \leq y \leq g_l^0) \\ 0 & (y > g_l^0) \end{cases}$$

where $g_l(y)$ is a monotone decreasing function.

B. Possibility and stochastic programming approach

Using the concept of a possibility measure, we define a degree of possibility that the objective function value $\tilde{\tilde{Y}}$ satisfies a fuzzy goal $\tilde{G}$ by

$$\Pi_{\tilde{\tilde{Y}}_l}(\tilde{G}_l) = \sup_y \min\{\mu_{\tilde{\tilde{Y}}_l}(y), \mu_{\tilde{G}_l}(y)\}$$

where Π denotes a possibility measure. Then, if the decision maker prefers to maximize the degree of possibility, problem (1) is reformulated as

$$\left.\begin{array}{ll} \underset{\text{for DM1}}{\text{maximize}} & \Pi_{\tilde{\tilde{\boldsymbol{C}}}_1 \boldsymbol{x}}(\tilde{G}_1) \\ \underset{\text{for DM2}}{\text{maximize}} & \Pi_{\tilde{\tilde{\boldsymbol{C}}}_2 \boldsymbol{x}}(\tilde{G}_2) \\ \text{subject to} & A_1 \boldsymbol{x}_1 + A_2 \boldsymbol{x}_2 \leq \boldsymbol{b} \\ & \boldsymbol{x}_1 \geq \boldsymbol{0},\ \boldsymbol{x}_2 \geq \boldsymbol{0} \end{array}\right\}. \tag{2}$$

The degree of possibility is expressed as the crossing point of two membership functions.

Since $\Pi_{\tilde{\tilde{\boldsymbol{C}}}_l \boldsymbol{x}}(\tilde{G}_l), l = 1, 2$ varies randomly due to the randomness of $\bar{c}_j$, problem (2) can be regarded as a stochastic linear programming problem. In stochastic programming, there are some major models [3]: an expectation optimization model, a variance minimization model and a probability maximization model.

In this research, we focus on the probability maximization model, which is to maximize the probability that the profit is greater than or equal to a certain permissible level and formulate the following problem:

$$\left.\begin{array}{ll} \underset{\text{for DM1}}{\text{maximize}} & \Pr[\Pi_{\tilde{\tilde{\boldsymbol{C}}}_1 \boldsymbol{x}}(\tilde{G}_1) \geq h_1] \\ \underset{\text{for DM2}}{\text{maximize}} & \Pr[\Pi_{\tilde{\tilde{\boldsymbol{C}}}_2 \boldsymbol{x}}(\tilde{G}_2) \geq h_2] \\ \text{subject to} & A_1 \boldsymbol{x}_1 + A_2 \boldsymbol{x}_2 \leq \boldsymbol{b} \\ & \boldsymbol{x}_1 \geq \boldsymbol{0},\ \boldsymbol{x}_2 \geq \boldsymbol{0} \end{array}\right\} \tag{3}$$

where $\Pr[\cdot]$ denotes probability and h_l is a goal value, called a permissible level, for the membership function $\mu_l(\cdot)$.

Since $\mu_l(\cdot), l = 1, 2$ are monotone decreasing, (3) can be rewritten as:

$$\left.\begin{array}{ll} \underset{\text{for DM1}}{\text{maximize}} & \Pr[\Pi_{\tilde{\tilde{\boldsymbol{C}}}_1 \boldsymbol{x}}(\tilde{G}_1) \leq \mu^*_{\tilde{G}_1}(h_1)] \\ \underset{\text{for DM2}}{\text{maximize}} & \Pr[\Pi_{\tilde{\tilde{\boldsymbol{C}}}_2 \boldsymbol{x}}(\tilde{G}_2) \leq \mu^*_{\tilde{G}_2}(h_2)] \\ \text{subject to} & A_1 \boldsymbol{x}_1 + A_2 \boldsymbol{x}_2 \leq \boldsymbol{b} \\ & \boldsymbol{x}_1 \geq \boldsymbol{0},\ \boldsymbol{x}_2 \geq \boldsymbol{0} \end{array}\right\} \tag{4}$$

where $\mu^*_{\tilde{G}_l}(\cdot)$ is a pseudo-inverse function of $\mu_{\tilde{G}_l}(\cdot)$ defined by $\mu^*_{\tilde{G}_l}(h_l) = \sup\{r | \mu_{\tilde{G}_l}(r) \geq h_l\}$ for $h_l \in (0, 1]$.

Let $L^*(\cdot)$ be a pseudo-inverse function of $L(\cdot)$ defined by $L^*(h_l) = \sup\{r | L(r) \geq h_l, r \geq 0\}$ Then the left side of the first and second constraint in (4) can be expressed as:

$$\Pr[\Pi_{\tilde{\tilde{\boldsymbol{C}}}_l \boldsymbol{x}}(\tilde{G}_l) \leq \mu^*_{\tilde{G}_l}(h_l)] = \Pr[\{\bar{\boldsymbol{d}}_l - L^*(h_l)\bar{\boldsymbol{\beta}}_l\}\boldsymbol{x} \leq \mu^*_{\tilde{G}_l}(h_l)].$$

From the assumption, $\bar{\boldsymbol{d}}_l$ is a random variable vector defined as $\bar{\boldsymbol{d}}_l = \boldsymbol{d}_l^1 + \bar{t}_l \cdot \boldsymbol{d}_l^2$ using a random variable $\bar{t}_l$ with mean M_l.

Provided that $\boldsymbol{d}_l^2\boldsymbol{x} > 0$, $l = 1, 2$,

$$
\begin{aligned}
&\Pr[\Pi_{\tilde{\boldsymbol{C}}_l\boldsymbol{x}}(\tilde{G}_l) \geq h_l] \\
&= \Pr[\{\bar{\boldsymbol{d}}_l - L^*(h_l)\bar{\boldsymbol{\beta}}_l\}\boldsymbol{x} \leq \mu^*_{\tilde{G}_l}(h_l)] \\
&= \Pr[\{(\boldsymbol{d}_l^1 + \bar{t}_l\boldsymbol{d}_l^2) - L^*(h_l)(\boldsymbol{\beta}_l^1 + \bar{t}_l\boldsymbol{\beta}_l^2)\}\boldsymbol{x} \leq \mu^*_{\tilde{G}_l}(h_l)] \\
&= \Pr\left[\bar{t}_l \leq \frac{\{L^*(h_l)\boldsymbol{\beta}_l^1 - \boldsymbol{d}_l^1\}\boldsymbol{x} + \mu^*_{\tilde{G}_l}(h_l)}{\{\boldsymbol{d}_l^2 - L^*(h_l)\boldsymbol{\beta}_l^2\}\boldsymbol{x}}\right] \\
&= T_l\left(\frac{\{L^*(h_l)\boldsymbol{\beta}_l^1 - \boldsymbol{d}_l^1\}\boldsymbol{x} + \mu^*_{\tilde{G}_l}(h_l)}{\{\boldsymbol{d}_l^2 - L^*(h_l)\boldsymbol{\beta}_l^2\}\boldsymbol{x}}\right) \\
&= T_l\left(\frac{\displaystyle\sum_{j=1}^{2}\sum_{k=1}^{n_j} L^*(h_l)\{\beta_{ljk}^1 - d_{ljk}^1\}x_{jk} + \mu^*_{\tilde{G}_l}(h_l)}{\displaystyle\sum_{j=1}^{2}\sum_{k=1}^{n_j}\{d_{ljk}^2 - L^*(h_l)\beta_{ljk}^2\}x_{jk}}\right)
\end{aligned}
$$

where $T_l(\cdot)$ is a probability distribution of $\bar{t}_l$ for DMl.

In this way, (4) can be transformed int the following problem:

$$
\left.
\begin{array}{ll}
\underset{\text{for DM1}}{\text{maximize}} & p_1(\boldsymbol{x}_1, \boldsymbol{x}_2) = \\
& T_1\left(\dfrac{\displaystyle\sum_{j=1}^{2}\sum_{k=1}^{n_j} L^*(h_1)\{\beta_{1jk}^1 - d_{1jk}^1\}x_{jk} + \mu^*_{\tilde{G}_1}(h_1)}{\displaystyle\sum_{j=1}^{2}\sum_{k=1}^{n_j}\{d_{1jk}^2 - L^*(h_1)\beta_{1jk}^2\}x_{jk}}\right) \\
\underset{\text{for DM2}}{\text{maximize}} & p_2(\boldsymbol{x}_1, \boldsymbol{x}_2) = \\
& T_2\left(\dfrac{\displaystyle\sum_{j=1}^{2}\sum_{k=1}^{n_j} L^*(h_2)\{\beta_{2jk}^1 - d_{2jk}^1\}x_{jk} + \mu^*_{\tilde{G}_2}(h_2)}{\displaystyle\sum_{j=1}^{2}\sum_{k=1}^{n_j}\{d_{2jk}^2 - L^*(h_2)\beta_{2jk}^2\}x_{jk}}\right) \\
\text{subject to} & A_1\boldsymbol{x}_1 + A_2\boldsymbol{x}_2 \leq \boldsymbol{b} \\
& \boldsymbol{x}_1 \geq \boldsymbol{0},\ \boldsymbol{x}_2 \geq \boldsymbol{0}
\end{array}
\right\}. \tag{5}
$$

IV. Interactive fuzzy programming

Observing the transformed problem (5) is a deterministic two-level programming problem, we can now construct the interactive algorithm to derive a satisfactory solution for the decision maker at the upper level in consideration of the cooperative relationships between DM1 and DM2.

Interactive fuzzy programming

Step 1: In order to calculate the individual minimum of $\mathrm{E}\{z_l(\boldsymbol{x}_1, \boldsymbol{x}_2)\}$, solve the following problems:

$$
\left.
\begin{array}{ll}
\text{minimize} & \mathrm{E}\{z_l(\boldsymbol{x}_1, \boldsymbol{x}_2)\} = \left(\boldsymbol{d}_l^1 + m_l \cdot \boldsymbol{d}_l^2\right)\boldsymbol{x} \\
\text{subject to} & A_1\boldsymbol{x}_1 + A_2\boldsymbol{x}_2 \leq \boldsymbol{b} \\
& \boldsymbol{x}_1 \geq \boldsymbol{0},\ \boldsymbol{x}_2 \geq \boldsymbol{0}
\end{array}
\right\}, \quad l = 1, 2. \tag{6}
$$

Let $\boldsymbol{x}^l_{\min}$ and $z^E_{l,\min}$ be optimal solutions to (6) and minimal objective function values to (6), respectively. Observing that (6) are linear programming problems, they can be easily solved by some linear programming technique like the simplex method.

Step 2: Ask DMs to specify the membership functions $\mu_l(\cdot)$, $l = 1, 2$ by considering the obtained values of $z^E_{l,\min}$, $l = 1, 2$.

Step 3: Ask DM1 to determine the permissible range $[\Delta_{\min}, \Delta_{\max}]$ and the initial value of permissible levels h_l, $l = 1, 2$.

Step 4: For the specified values of h_l, $l = 1, 2$, the following maximin problem is solved:

$$
\left.
\begin{array}{ll}
\underset{l\,=\,1,\,2}{\text{maximize}} & \min\left\{T_l\left(\dfrac{L^*(h_l)\{\boldsymbol{\beta}_l^1 - \boldsymbol{d}_l^1\}\boldsymbol{x} + \mu^*_{\tilde{G}_l}(h_l)}{\{\boldsymbol{d}_l^2 - L^*(h_l)\boldsymbol{\beta}_l^2\}\boldsymbol{x}}\right\}\right) \\
\text{subject to} & A_1\boldsymbol{x}_1 + A_2\boldsymbol{x}_2 \leq \boldsymbol{b} \\
& \boldsymbol{x}_1 \geq \boldsymbol{0},\ \boldsymbol{x}_2 \geq \boldsymbol{0}
\end{array}
\right\}. \tag{7}
$$

In view of (5), this problem is rewritten as:

$$
\left.
\begin{array}{ll}
& \text{maximize } v \\
& \text{subject to} \\
& T_1\left(\dfrac{(-\boldsymbol{d}_1^1 + L^*(h_1)\boldsymbol{\beta}_1)\boldsymbol{x} + \mu^*_{\tilde{G}_1}(h_1)}{(\boldsymbol{d}_1^2 - L^*(h_1)\beta_1^2)\boldsymbol{x}}\right) \geq \mu_1^*(v) \\
& T_2\left(\dfrac{(-\boldsymbol{d}_2^1 + L^*(h_2)\boldsymbol{\beta}_2)\boldsymbol{x} + \mu^*_{\tilde{G}_2}(h_2)}{(\boldsymbol{d}_2^2 - L^*(h_2)\beta_2^2)\boldsymbol{x}}\right) \geq \mu_2^*(v) \\
& A_1\boldsymbol{x}_1 + A_2\boldsymbol{x}_2 \leq \boldsymbol{b} \\
& \boldsymbol{x}_1 \geq \boldsymbol{0},\ \boldsymbol{x}_2 \geq \boldsymbol{0}
\end{array}
\right\} \tag{8}
$$

equivalently,

$$
\left.
\begin{array}{ll}
& \text{maximize } v \\
& \text{subject to} \\
& \dfrac{(-\boldsymbol{d}_1^1 + L^*(h_1)\boldsymbol{\beta}_1)\boldsymbol{x} + \mu_1^*(h_1)}{(\boldsymbol{d}_1^2 - L^*(h_1)\beta_1^2)\boldsymbol{x}} \geq T_1^*(\mu_1^*(v)) \\
& \dfrac{(-\boldsymbol{d}_2^1 + L^*(h_2)\boldsymbol{\beta}_2)\boldsymbol{x} + \mu_2^*(h_2)}{(\boldsymbol{d}_2^2 - L^*(h_2)\beta_2^2)\boldsymbol{x}} \geq T_2^*(\mu_2^*(v)) \\
& A_1\boldsymbol{x}_1 + A_2\boldsymbol{x}_2 \leq \boldsymbol{b} \\
& \boldsymbol{x}_1 \geq \boldsymbol{0},\ \boldsymbol{x}_2 \geq \boldsymbol{0}
\end{array}
\right\} \tag{9}
$$

where $T_l^*(\cdot)$ is a pseudo-inverse function of $T_l(\cdot)$. Obtaining the optimal value of v to this problem is equivalent to finding the maximum of v so that the set of feasible solutions to (9) is not empty. Although this problem is a nonlinear programming problem, we can easily find the maximum of v by the following algorithm based on the bisection method and the simplex method since the constraints of (9) are linear if v is fixed.

The combined use of the bisection method and the simplex method

4-1 Set $l := 0$ and $v := 0$. Test whether the set of feasible solutions to (9) for $v = 0$ is empty or not using the phase one of the simplex method. If it is empty, DMs must reassess

membership functions, α or h_l. Otherwise, let $v_{\text{feasible}} := v$ and go to 4-2

4-2 Set $v := 1$. Test whether the set of feasible solutions to (9) for $v = 1$ is empty or not using the phase one of the simplex method. If it is not empty, $v = 1$ is the optimal value v^* to (9) and the algorithm is terminated. Otherwise, the maximum of v so that the set of feasible solutions to (9) is not empty exists between 0 and 1. Let $v_{\text{infeasible}} := v$ and go to 4-3.

4-3 Set $v := (v_{\text{feasible}} + v_{\text{infeasible}})/2$, $l := l + 1$ and go to 4-4.

4-4 Test whether the set of feasible solutions to (9) for v determined in 4-3 is empty or not using the phase one of the simplex method. Observe that the sensitivity analysis technique can be applied for this test. If it is not empty and $(1/2)^l \leq \varepsilon$, the current value of v is regarded as the optimal value v^* to (9) and the algorithm is terminated. If it is not empty and $(1/2)^l > \varepsilon$, let $v_{\text{feasible}} := v$ and return to 4-3. On the other hand, if it is empty, let $v_{\text{infeasible}} := v$ and return to 4-3.

Then, for the obtained optimal value v^*, we can determine the corresponding optimal value $\boldsymbol{x}^*$ by solving the following linear fractional programming problem:

$$\left.\begin{array}{ll} \text{maximize} & p_1(\boldsymbol{x}_1, \boldsymbol{x}_2) \\ \text{subject to} & p_2(\boldsymbol{x}_1, \boldsymbol{x}_2) \geq \mu_2^*(v^*) \\ & A_1\boldsymbol{x}_1 + A_2\boldsymbol{x}_2 \leq \boldsymbol{b} \\ & \boldsymbol{x}_1 \geq \boldsymbol{0},\ \boldsymbol{x}_2 \geq \boldsymbol{0} \end{array}\right\} \tag{10}$$

It should be noted here that linear fractional programming problems can be reduced to equivalent linear programming problems through the variable transformation method by Charnes and Cooper [2]. Therefore, we can obtain an optimal solution to (10) by some linear programming technique.

Step 5: The DM1 is supplied with the current values of $\mu_1(p_1(\boldsymbol{x}_1^*, \boldsymbol{x}_2^*))$ and $\mu_2(p_2(\boldsymbol{x}_1^*, \boldsymbol{x}_2^*))$ for the optimal solution $\boldsymbol{x}^*$ calculated in step 4. If DM1 is satisfied with the current membership function values, the interaction process is terminated. If DM1 is not satisfied and desires to update h_l, $l = 1, 2$, ask DM1 to update h_l and return to step 4. Otherwise, ask DM1 to specify the minimal satisfactory level $\hat{\delta}$ for $\mu_1(p_1(\boldsymbol{x}_1, \boldsymbol{x}_2))$ and the permissible range $[\Delta_{\min}, \Delta_{\max}]$ of the ratio of membership functions $\Delta = \mu_2(p_2(\boldsymbol{x}_1, \boldsymbol{x}_2))/\mu_1(p_1(\boldsymbol{x}_1, \boldsymbol{x}_2))$.
Observe that the larger the minimal satisfactory level is assessed, the smaller the DM2's satisfactory degree becomes. Consequently, in order to take account of the overall satisfactory balance between both decision makers, DM1 needs to compromise with DM2 on DM1's own minimal satisfactory level. To do so, the permissible range of the ratio of the satisfactory degree of DM2 to that of DM1 is helpful.

Step 6: For the specified value of $\hat{\delta}$, solve the following problem to maximize the membership function $\mu_2(p_2(\boldsymbol{x}_1, \boldsymbol{x}_2))$ of DM2 considering the constraint that the membership function $\mu_1(p_1(\boldsymbol{x}_1, \boldsymbol{x}_2))$ of DM1 must be greater than or equal to $\hat{\delta}$.

$$\left.\begin{array}{ll} \text{maximize} & \mu_2(p_2(\boldsymbol{x}_1, \boldsymbol{x}_2)) \\ \text{subject to} & \mu_1(p_1(\boldsymbol{x}_1, \boldsymbol{x}_2)) \geq \hat{\delta} \\ & A_1\boldsymbol{x}_1 + A_2\boldsymbol{x}_2 \leq \boldsymbol{b} \\ & \boldsymbol{x}_1 \geq \boldsymbol{0},\ \boldsymbol{x}_2 \geq \boldsymbol{0} \end{array}\right\} \tag{11}$$

This problem can be rewritten as:

$$\left.\begin{array}{ll} \text{maximize} & p_2(\boldsymbol{x}_1, \boldsymbol{x}_2) \\ \text{subject to} & p_1(\boldsymbol{x}_1, \boldsymbol{x}_2) \geq \mu_1^*(\hat{\delta}) \\ & A_1\boldsymbol{x}_1 + A_2\boldsymbol{x}_2 \leq \boldsymbol{b} \\ & \boldsymbol{x}_1 \geq \boldsymbol{0},\ \boldsymbol{x}_2 \geq \boldsymbol{0} \end{array}\right\} \tag{12}$$

Observing that problem (12) is a linear fractional programming problem, it can be easily solved by some linear programming technique through the variable transformation method by Charnes and Cooper [2] like (10). For the optimal solution $\boldsymbol{x}^*$ to (11), calculate $p_1(\boldsymbol{x}_1^*, \boldsymbol{x}_2^*)$, $p_2(\boldsymbol{x}_1^*, \boldsymbol{x}_2^*)$ and Δ.

Step 7: DM1 is supplied with the current values of $p_1(\boldsymbol{x}_1^*, \boldsymbol{x}_2^*)$, $p_2(\boldsymbol{x}_1^*, \boldsymbol{x}_2^*)$ and Δ calculated in step 6. If $\Delta \in [\Delta_{\min}, \Delta_{\max}]$ and DM1 is satisfied with the current membership function values for the optimal solution $\boldsymbol{x}^*$, the interaction process is terminated. Otherwise, ask DM1 to update the permissible level h_l, $l = 1, 2$ or the minimal satisfactory level $\hat{\delta}$, and return to step 6.

In the proposed algorithm, $\Delta_{\min}$ and $\Delta_{\max}$ are usually set to be less than 1 since $p_1(\boldsymbol{x}_1^*, \boldsymbol{x}_2^*)$ should be greater than $p_2(\boldsymbol{x}_1^*, \boldsymbol{x}_2^*)$ because of the priority of DM1. In Step 6, if $\Delta < \Delta_{\min}$, i.e., $p_1(\boldsymbol{x}_1^*, \boldsymbol{x}_2^*)$ is much greater than $p_2(\boldsymbol{x}_1^*, \boldsymbol{x}_2^*)$, DM1 will decrease $\hat{\delta}$ to improve $p_2(\boldsymbol{x}_1^*, \boldsymbol{x}_2^*)$ and increase Δ. Conversely, if $\Delta_{\max} < \Delta$, i.e., $p_1(\boldsymbol{x}_1^*, \boldsymbol{x}_2^*)$ is slightly greater or less than $p_2(\boldsymbol{x}_1^*, \boldsymbol{x}_2^*)$, DM1 will increase $\hat{\delta}$ to improve $p_1(\boldsymbol{x}_1^*, \boldsymbol{x}_2^*)$ and decrease Δ. On the other hand, if DM1 decreases (increases) h_l, $l = 1, 2$, both $p_1(\boldsymbol{x}_1^*, \boldsymbol{x}_2^*)$ and $p_2(\boldsymbol{x}_1^*, \boldsymbol{x}_2^*)$ would increase (decrease). With this observation, it can be expected that desirable values of $p_1(\boldsymbol{x}_1^*, \boldsymbol{x}_2^*)$, $p_1(\boldsymbol{x}_1^*, \boldsymbol{x}_2^*)$ and Δ will be obtained through a series of update procedures of $\hat{\delta}$, h_l, $l = 1, 2$ with DM1.

V. Conclusion

In this research, assuming cooperative behavior of the decision makers, interactive decision making methods in hierarchical organizations under fuzzy random environments were considered. For the formulated fuzzy random two-level linear programming problems, possibility measures were introduced and a stochastic two-level linear programming problem was defined for guaranteeing the degree of realization of the problem. Considering the vague natures of decision makers' judgments, fuzzy goals were introduced and the stochastic

two-level linear programming problem was transformed into the problem to maximize the satisfaction degree for each fuzzy goal. Through the possibility maximization model, the transformed stochastic two-level programming problem was reduced to a deterministic one. Interactive fuzzy programming to obtain a satisfactory solution for the decision maker at the upper level in consideration of the cooperative relation between decision makers was presented. In near future, we will report the result of the application of the proposed method to a numerical example to derive a satisfactory solution.

REFERENCES

[1] W. F. Bialas and M. H. Karwan, "Two-level linear programming, " Management Sciences, 30(8): 1004–1020, 1984.

[2] A. Charnes and W. W. Cooper, "Programming with linear fractional functions, " Naval Research Logistics Quarterly, 9(3–4): 181–186, 1962.

[3] A. Charnes and W. W. Cooper, "Deterministic equivalents for optimizing and satisficing under chance constraints, " Operations Research, 11: 18–39, 1963.

[4] H. Katagiri and H. Ishii, "Linear programming problem with fuzzy random constraint, " Mathematica Japonica, 52(1): 123–129, 2000.

[5] H. Katagiri, M. Sakawa, K. Kato and I. Nishizaki, "Interactive multiobjective fuzzy random linear programming: maximization of possibility and probability, " European Journal of Operations Research, 188(2): 530–539, 2008.

[6] R. Kruse and K. D. Meyer, *Statistics with Vague Data*, Dordrecht, D. Riedel Publishing Company, 1987.

[7] H. Kwakernaak, "Fuzzy random variable-1, " Information Sciences, 15(1): 1–29, 1978.

[8] Y.-K. Liu and B. Liu, "Fuzzy random variables: a scalar expected value operator, " Fuzzy Optimization and Decision Making, 2(2): 143–160, 2003.

[9] M. K. Luhandjula, "Fuzzy stochastic linear programming: survey and future research directions, " European Journal of Operations Research, 174(3): 1353–1367, 2009.

[10] M. L. Puri and D. A. Ralescu, "Fuzzy random variables, " Journal of Mathematical Analysis and Applications, 114(2): 409–422, 1986.

[11] Z. Qiao, Y. Zhang and G.-Y. Wang, "On fuzzy random linear programming, " Fuzzy Sets and Systems, 65(1): 31–49, 1994.

[12] E. Roghanian, S. J. Sadjadi and M. B. Aryanezhad, "A probabilistic bi-level linear multi-objective programming problem to supply chain planning, " Applied Mathematics and Computation, 188(1): 786–800, 2007.

[13] M. Sakawa and I. Nishizaki, *Cooperative and Noncooperative Multi-Level Programming*, New York, Springer, 2009.

[14] M. Sakawa, I. Nishizaki and Y. Uemura, "Interactive fuzzy programming for multi-level linear programming problems, " Computers and Mathematics with Applications, 36(2): 71–86, 1998.

[15] M. Sakawa, I. Nishizaki and Y. Uemura, "Interactive fuzzy programming for two-level linear fractional programming problems with fuzzy parameters, " Fuzzy Sets and Systems, 115(1): 93–103, 2000.

[16] K. Shimizu, Y. Ishizuka and J. F. Bard, *Nondifferentiable and Two-Level Mathematical Programming*, Boston, Kluwer Academic Publishers, 1997.

[17] M. Simaan and J. B. Cruz Jr., "On the Stackelberg strategy in nonzero-sum games, " Journal of Optimization Theory and Applications, 11(5): 533–555, 1973.

[18] I. M. Stancu-Minasian, "Overview of different approaches for solving stochastic programming problems with multiple objective functions, " in *Stochastic Versus Fuzzy Approaches to Multiobjective Mathematical Programming under Uncertainty*, R. Slowinski and J. Teghem, Eds., Dordrecht/Boston/London, Kluwer Academic Publishers, pp. 71–101, 1990.

[19] G.-Y. Wang and Z. Qiao, "Linear programming with fuzzy random variable coefficients, " Fuzzy Sets and Systems, 57(3): 295–311, 1993.

[20] L. A. Zadeh, "Fuzzy sets as a basis for a theory of possibility, " Fuzzy Sets and Systems, 100(1): 9–34, 1999.

[21] H.-J. Zimmermann, "Fuzzy programming and linear programming with several objective functions, " Fuzzy Sets and Systems, 1(1): 45–55, 1978.

2011 IEEE International Conference on Fuzzy Systems
June 27-30, 2011, Taipei, Taiwan

Decentralized Fuzzy Fault Tolerant Control for Multiple Satellites Attitude Synchronization

Junquan Li*, K. D. Kumar†,
* † Department of Aerospace Engineering
Ryerson University
Toronto, Canada
Email: junquan.li@ryerson.ca, kdkumar@ryerson.ca

***Abstract*—This paper presents a decentralized adaptive approximation design to achieve attitude tracking control for decentralized formation flying in presence of control input saturation, model uncertainties, external disturbances and reaction wheel faults. A nonsingular fast terminal sliding mode control is designed for finite time distributed cooperative attitude synchronization. In the proposed control scheme, a fuzzy logic system (FLS) is introduced to approximate unknown individual satellite attitude dynamics on-line due to the actuators fault. In order to achieve the capability of fault management without the involvement of ground station operators, the proposed control laws do not requite an explicit fault detection and isolation mechanism. In the attitude control system of each satellite four reaction wheels are placed in a pyramid configuration, numerical simulation results including actuator dynamics and initial conditions' uncertainties show that the proposed strategy with FLS can compensate for the fault and the system continues to operate satisfactorily with wheel voltage or wheel speed faults and the closed loop distributed tracking control system is stochastically stable. Several simulation examples compared with the existing decentralized fault tolerant contoller are presented for illustrating the effectiveness of the proposed fault tolerant control methodology.**

Keywords: Fuzzy Logic System; Fast Terminal Sliding Mode Control; Decentralized Fault Tolerant Control

I. INTRODUCTION

Decentralized multi-agent cooperative control, including consensus, formation control and flocking has been studied extensively. The benefits such as scalability, robustness and easy maintenance can be obtained by embodying decentralized cooperative control [1]. The motivation of decentralized controller is to avoid the complete redesign of the control system when new subsystems are added and also guarantee the stability of the whole system. One limitation of those above approaches is that they did not provide finite-time control of a group of spacecraft, which could provide faster formation rearrangement capability during attitude coordination. In the reference [2], it is proved that nonsingular fast terminal sliding mode control can get rid of the singularity problem completely. Neural networks and fuzzy logic systems have been proposed as the tools to be capable of approximating any well defined functions over a compact set to arbitrary accuracy [3][4]. The fuzzy logic system is a very powerful technique in the discipline of systems with large uncertainties and strong nonlinearities. Therefore, a nonsingular terminal sliding mode control with fuzzy logic system is proposed in this paper as a fault-tolerant control strategy. Inspired by the work in [2] and [5], a nonsingular fast terminal fuzzy sliding mode control (NFFTSMC) is proposed for distributed cooperative attitude synchronization and precise 3-axis attitude tracking control of picosatellites in the presence of control input saturation, model uncertainties, and external disturbances. Also, the existing attitude synchronization or coordination literature addresses important issues relating to attitude control of multiple spacecraft, such as adapting the control system to modeling uncertainties, robust capability to attenuate external disturbances, communication delay, and actuator saturation constraint accommodation. Most traditional attitude fault-tolerant control reconfiguration techniques rely on failure detection and isolation. Reconfigurable attitude control system design for spacecraft based on FDI approaches and system redesign is fairly complex and depends strongly on the efficacy of the fault detection algorithm. Also, explicit failure identification and system redesign may require substantial on-board computational resources that works against the prevailing cost reduction measures undertaken by most commercial and military satellite markets. The problem of fault tolerance for attitude synchronization systems is still an open problem and there are a lot of theoretical challenges. An alternative approach to reconfigurable ACS design is based on adaptive or approximation control theory where the controller parameters are constantly updated based on adaptive or other estimates of the altered dynamics after failure. Neural network for adaptive approximation has been successfully applied to the design of nonlinear fault tolerant controllers [6]. In this paper, a fault-tolerant control strategy using adaptive nonsingular fast terminal fuzzy sliding mode control is proposed for multiple picosatellite attitude synchronization which is represented by quaternion. In order to achieving the capability of fault management without involvement of ground station operators, the proposed control laws do not require an explicit fault detection and isolation mechanism. Therefore, failure time instants, patterns, and values of actuator failures are unknown to the designer. When a reaction wheel failure or fault occurs, the control signals are autonomously redistributed to the remaining healthy wheels using an adaptive gain that is updated on-line based on the attitude tracking error. Each satellite with four reaction wheels is in a pyramid configuration. The numerical simulation results and a predicted theoretical

978-1-4244-7316-8/11/$26.00 ©2011 IEEE

framework show that the proposed strategy can compensate for faults, the system continues to operate satisfactorily with initial conditions' uncertainites or wheel speeds faults, and the closed loop distributed tracking control system is stochastically stable.

A. Satellite With Four Reaction Wheels Attitude Dynamics and Kinematics Model

The individual satellites in the formation are modeled as rigid bodies [7]. The proposed system consists of four *rigid body satellites* in a circular orbit around the Earth. An *Earth centered inertial* (ECI) frame, denoted by Ł$-_{X_I Y_I Z_I}$, has its origin located at the center of the Earth, with Z_I-axis passing through the celestial North pole, X_I-axis directed towards the vernal equinox, and Y_I-axis completes the right-handed triad. Next, we define a local vertical local horizontal (LVLH) orbital reference frame $\pounds-_{x_o y_o z_o}$ fixed at the center of the satellite with the x_o-axis along the direction of motion, the y_o-axis opposite to the direction of the angular velocity (normal to the orbit plane), and the z_o-axis pointing towards the Earth. The nodal line represents the reference line in orbit for the measurement of the true anomaly (eccentric orbit) or reference angle θ (circular orbit). The corresponding principal body-fixed coordinate axes of the satellite are denoted by $\jmath - xyz$ with its origin located at the center of mass of the satellite. The notation [8] used for representing the relative velocity vector, $\mathbf{v}$, of frame $\pounds$ relative to frame Ł, expressed in the coordinates of $\jmath$ is: $\mathbf{v}_{LI}^{B}$. The cross-product of vectors $a \times b$ is defined as $[a^{\times}]b$ where $[a^{\times}]$ is a skew-symmetric operator.

Consider the i'th rigid satellite with a 4-wheel cluster installed to provide internal torques. The attitude dynamics of a rigid satellite controlled by reaction wheels can in general be described the following nonlinear differential equation [9]:

$$J_i \dot{\omega}_{iBI}^{B} = -\omega_{iBI}^{B} \times (J_{si}\omega_{iBI}^{B} + A_i J_{wi}\Omega_i) + A_i \tau_{rwi} + \tau_{ie} \quad (1)$$

The torques generated by the reaction wheels τ_{rwi} are given by

$$\tau_{rwi} = J_{wi}(\dot{\Omega}_i + A_i^T \dot{\omega}_{iBI}^{B}) \quad (2)$$

where ω_{iBI}^{B} is the angular velocity of the satellite relative to the inertial frame Ł, expressed in the $\jmath$ frame, and $\tau_{ie} \in \mathbb{R}^{3\times 1}$ represents the external torque acting on the system. A_i is the 3×4 matrix whose columns represent the influence of each reaction wheel on the angular acceleration of the satellite. We define a matrix $J_i = J_{si} - A_i J_{wi} A_i^T$, where $J_{si} \in \mathbb{R}^{3\times 3}$ is the moment of inertia of the satellite, including the wheels, and $J_{wi} \in R^{4\times 4} = \mathrm{diag}([J_{wi1}, J_{wi2}, J_{wi3}, J_{wi4}])$ denotes the axial moment of inertia of the reaction wheels. $\Omega_i \in \mathbb{R}^{4\times 1}$ denotes the axial angular velocity of the reaction wheels.

The external torques (τ_{ie}) are assumed to include gravity gradient torque (τ_{gi}) acting on the satellite. The gravity gradient torque is given by [10]

$$\tau_{ie} = 3\omega_0^2 [\hat{c}_3^{\times}] J_{si} \hat{c}_3, \qquad \hat{c}_3 = C_{iL}^{B}[0\ 0\ 1]^T \quad (3)$$

In this paper, we adopt the unit quaternion[7] to describe the attitude of the satellite. The unit quaternion $\bar{q}_i$ is defined by

$$\bar{q}_i = \begin{bmatrix} \bar{e}\sin(\Phi/2) \\ \cos(\Phi/2) \end{bmatrix} = \begin{bmatrix} q_{vi} \\ q_{4i} \end{bmatrix} \quad (4)$$

where Φ denotes the principal angle, and $\bar{e} = [e_1, e_2, e_3]^T$ denotes the principal axis associated with Euler's Theorem ($e_1^2 + e_2^2 + e_3^2 = 1$). $q_{4i} \in R$ and $q_{vi} \in \mathbb{R}^{3\times 1} = [q_{i1}, q_{i2}, q_{i3}]^T$ denote the Euler parameters that represent the orientation of the satellite body frame, $\jmath$, with respect to the orbital frame, $\pounds$, and satisfy the constraint $q_{vi}^T q_{vi} + q_{4i} = 1$. The nonlinear differential equations governing the kinematics of the satellite in terms of Euler parameters can be expressed as

$$\begin{bmatrix} \dot{q}_{vi} \\ \dot{q}_{4i} \end{bmatrix} = \frac{1}{2} \begin{bmatrix} q_{4i} I + [q_{vi}^{\times}] \\ -q_{vi}^T \end{bmatrix} \omega_{iBL}^{B} \quad (5)$$

where $I \in R^{3\times 3}$ represents the identity matrix, and $[q_{vi}^{\times}]$ denotes a skew-symmetric matrix which is given by

$$[q_{vi}^{\times}] = \begin{bmatrix} 0 & -q_{i3} & q_{i2} \\ q_{i3} & 0 & -q_{i1} \\ -q_{i2} & q_{i1} & 0 \end{bmatrix} \quad (6)$$

The angular velocity of the body-fixed reference frame, $\jmath$, with respect to the inertial frame, Ł, can be expressed as

$$\omega_{iBI}^{B} = \omega_{iBL}^{B} + \omega_{iLI}^{B} \quad (7)$$

The direction cosine matrix C_{iL}^{B} that describes the orientation of the satellite body-fixed frame, $\jmath$, with respect to the LVLH reference frame, $\pounds$ defined in terms of Euler parameters is given by

$$C_{iL}^{B} = (q_{4i}^2 - q_{vi}^T q_{vi})I + 2q_{vi}q_{vi}^T - 2q_{4i}[q_{vi}^{\times}] \quad (8)$$

The orbital angular velocity expressed in the $\jmath$ frame, ω_{iLI}^{B}, can be obtained by rotating the angular velocity in $\pounds$ using the transformation matrix C_{iL}^{B} as follows:

$$\omega_{iLI}^{B} = C_{iL}^{B} \begin{bmatrix} 0 & -\omega_{i0} & 0 \end{bmatrix}^T \quad (9)$$

where $\omega_{i0} = \dot{\theta}$ is the magnitude of orbital angular velocity of the LVLH frame. For a circular orbit, $\dot{\theta} = \sqrt{\mu_e / R_c^3}$, where μ represents the gravitational parameter of the Earth, and R_c defines the distance of the spacecraft measured from the center of the Earth.

Reaction wheels are widely used to perform precise satellites attitude maneuvers because they allow continuous and smooth control. They are capable of changing its internal angular momentum vector as each wheel spins about a body-fixed axis with variable spin speed [10]. Torques are produced on the satellites by accelerating or decelerating the reaction wheels. Let the torque demanded by the satellite be denoted as τ_{rwi}. The input voltage required to control the actuator dynamics of the reaction wheel can be shown as

$$e_{ai} = K_{bi}\Omega_i - R_{bi}K_{ti}^{-1}(A_i' \tau_{rwi}) \quad (10)$$

where $K_{ti} \in \mathbb{R}^{4\times 4} = \mathrm{diag}([k_{t1}, k_{t2}, k_{t3}, k_{t4}])$ is the motor torque constant. $K_{bi} \in \mathbb{R}^{4\times 4} = \mathrm{diag}([k_{b1}, k_{b2}, k_{b3}, k_{b4}])$ is the back-EMF constant, $R_{bi} \in \mathbb{R}^{4\times 4} = \mathrm{diag}([r_{b1}, r_{b2}, r_{b3}, r_{b4}])$ is the armature resistance, and we ignore the friction in the reaction wheels.

B. Station Keeping Attitude Tracking and Formation Keeping Attitude Tracking

In the case of tracking a desired rotational motion, the target attitude of the i'th satellite in the desired reference frame $\jmath_o$ with respect to the LVLH frame $\pounds$ is described by the orientation $(q_{dvi},\, q_{d4i}) \in \mathbb{R}^3 \times \mathbb{R}$ that satisfies the constraint $q_{dvi}^T q_{dvi} + q_{d4i}^2 = 1$. Let $\omega_{di} \in \mathbb{R}^3$ denote the angular velocity of $\jmath_o$ with respect to $\pounds$, expressed in the frame $\jmath_o$. To address the station-keeping attitude tracking problem, we define the quaternion absolute tracking error $(q_{ie},\, q_{i4e}) \in \mathbb{R}^3 \times \mathbb{R}$ as the relative orientation between the body-fixed frame $\jmath$ and the desired reference frame $\jmath_o$, which is computed as

$$\begin{aligned} q_{ie} &= q_{d4i} q_{vi} - q_{4i} q_{dvi} + [q_{vi}^{\times}] q_{dvi} \\ q_{i4e} &= q_{d4i} q_{4i} + q_{dvi}^T q_{vi} \end{aligned} \tag{11}$$

where $q_{ie}^T q_{ie} + q_{i4e}^2 = 1$. The corresponding rotation matrix $C_{ie} = C_i(q_{ie},\, q_{i4e}) \in SO(3)$ is given by

$$C_{ie} = (q_{i4e}^2 - q_{ie}^T q_{ie}) I + 2 q_{ie} q_{ie}^T - 2 q_{i4e} [q_{ie}^{\times}] \tag{12}$$

where $C_{ie}^T C_{ie} = 1$, $\|C_{ie}\| = 1$, $\det(C_{ie}) = 1$, and $\dot{C}_{ie} = -[\omega_{ie}^{\times}] C_{ie}$. Next, we define the absolute angular velocity tracking error $\omega_{ie} \in \mathbb{R}^3$ of $\jmath$ with respect to $\pounds$ as follows:

$$\omega_{ie} = \omega_{iBL}^B - C_{ie} \omega_{id} \tag{13}$$

From Eqs. (5), (11), and (13), the equations that govern the absolute attitude (station-keeping) error dynamics and kinematics are given by

$$\dot{q}_{ie} = \frac{1}{2} (q_{i4e} I + [q_{ie}^{\times}]) \omega_{ie} \tag{14}$$

$$\dot{q}_{i4e} = -\frac{1}{2} q_{ie}^T \omega_{ie} \tag{15}$$

Assumption 1: We assume that there exists known, finite constant, $c_1 > 0$ such that $\|q_{di}\|^2 + \|\dot{q}_{di}\|^2 + \|\ddot{q}_{di}\|^2 \le c_1$ for all $t \ge 0$.

We choose $\bar{q}_{ij}$ and ω_{ij} to represent the quaternion mapping of the i'th satellite body-fixed coordinate with respect to the j'th satellite body-fixed coordinate and the angular velocity of the i'th satellite with respect to the j'th satellite [11]

$$\bar{q}_{ij} = \left[{q_{ij}}^T q_4 \right]^T = \bar{q}_i \otimes \bar{q}_j^{-1} \tag{16}$$

$$q_{v_{ij}} = q_{v_i} - C_{ij} q_{v_j} \tag{17}$$

$$\omega_{ij} = \omega_i - C_{ij} \omega_j \tag{18}$$

where C_{ij} is the rotation matrix from the i'th body reference frame to the j'th body reference frame, which is a proper orthogonal matrix. $q_{v_{ij}}$ is defined as the formation flying attitude error.

$$C_{ij} = C_{ij}(\bar{q}_i \otimes \bar{q}_i^{-1}) = C_i(\bar{q}_i) C_j(\bar{q}_j)^T \tag{19}$$

According to Eq. (8),

$$C_i(\bar{q}_i) = ({q_{4i}}^2 - {q_{v_i}}^T q_{v_i}) I + 2 q_{v_i} {q_{v_i}}^T - 2 q_{4i} [{q_{v_i}}^{\times}] \tag{20}$$

The quaternion $(q_{v_{ij}})$ differential equations are obtained by the reference.

$$\dot{q_{v_{ij}}} = \frac{1}{2} (q_{ij_4} \omega_{ij} - \omega_{ij} \otimes q_{ij}) \tag{21}$$

C. Consensus Tracking

A weighted graph $G = (V, E, \bar{A})$ consists of a node set v, an edge set E and a weighted adjacency matrix $\bar{A}$. It is natural to describe the topology of the information flow between satellites in the formation by a graph. The weighted adjacency matrix $A = a_{ij} \in \mathbb{R}^{n \times n}$ is the weighted adjacency matrix of graph G with nonnegative elements. Node v_i represents the i'th satellite, and an edge in G is denoted by an unordered pair (ij). $ij \in E \Leftrightarrow ji \in E$. The adjacency element a_{ij} denotes the communication quality between the i'th satellite and the j'th satellite. It is assumed that $a_{ij} = a_{ji}$ and $\bar{A}$ is a symmetric matrix.

Let $D = diag(d_1, d_2, ..., d_n)$ be the degree matrix of G. The Laplacian matrix of L of the weighted graph G is defined by

$$L = D - \bar{A} \tag{22}$$

It is assumed that the multi-satellites formation flying studied in this paper has a connected graph topology G. The theorem [12] gives the existing results of the Laplacian matrix and graph theory.

Theorem 1: If $G = (V, E, \bar{A})$ is an undirected connected graph, then the graph Laplacian matrix L is a symmetric matrix with n real eigenvalues in an ascending order as:

$$0 = \lambda_1, \lambda_2 \le \lambda_3 ... \le \lambda_n \le 2 d_M \tag{23}$$

where $d_M = max_{1 \le i \le n} \{d_i\}$ is the maximum degree of a graph, and λ_2 is called the algebraic connectivity of a graph.

Let $a_{i1} \in \mathbb{R}^3$ and $a_{i2} \in \mathbb{R}^3$ be the consensus attitude error including the station-keeping and formation-keeping errors of the i'th satellite in the formation, which are defined as:

$$a_{i1} = k_p \sum_{j=1, i \ne j}^{n} a_{ij} q_{v_{ij}} + k_i q_{ie} \tag{24}$$

$$a_{i2} = k_p \sum_{j=1, i \ne j}^{n} a_{ij} \dot{q_{v_{ij}}} + k_i \dot{q_{ie}} \tag{25}$$

where $i = 1, 2, ..., n$. a_{ij} is the element of the weighted adjacency matrix A. k_p and k_i are positive constants determined by the controller designer, respectively.

The consensus error is used to evaluate the motion synchronization performance. Eqs. (24), (25) have to be written as follows:

$$a_{i1} = k_p \sum_{j=1}^{n} l_{ij} q_{j_e} + k_i q_{ie} \tag{26}$$

$$a_{i2} = k_p \sum_{j=1}^{n} l_{ij} \dot{q_{j_e}} + k_i \dot{q_{ie}} \tag{27}$$

Define $A_1 = ({a_{11}}^T, {a_{21}}^T, ..., {a_{n1}}^T)$, $A_2 = ({a_{12}}^T, {a_{22}}^T, ..., {a_{n2}}^T)$, $E_1 = ({qe_{11}}^T, {qe_{21}}^T, ..., {qe_{n1}}^T)$, $E_2 = ({\dot{q}e_{11}}^T, {\dot{q}e_{21}}^T, ..., {\dot{q}e_{n1}}^T)$, and $K = diag(k_1, k_2, ..., k_n)$. The Eqs. (26), (27) can be expressed in terms of the aforementioned quantities as follows:

$$A_1 = (k_p L \otimes I_3 + K \otimes I_3)E_1 \tag{28}$$

$$A_2 = (k_p L \otimes I_3 + K \otimes I_3)E_2 \tag{29}$$

Lemma 1: The matrix $M_1 = (k_p L \otimes I_3 + K \otimes I_3)$ is symmetric and positive definite.

$$\lambda_m \|x\|^2 \leq x^T((k_p L \otimes I_3 + K \otimes I_3))x \leq \lambda_M \|x\|^2, \forall x \in \mathbb{R}^{mn} \tag{30}$$

where $\lambda_m = min_{1 \leq i \leq n}(k_i)$ and $\lambda_M = k_p \lambda_n + max_{1 \leq i \leq n}(k_i)$ are positive constants.

The objective of control design becomes to design appropriate control input that guarantees the convergence of both the station-keeping q_{ie} and formation-keeping q_{vij} tracking error and consensus synchronization error a_{i1} and a_{i2}, even in the presence of unknown constant parameters,periodic disturbances, and actuator faults. In short, one needs to achieve $q_{ie}, q_{vij} \to 0$ and $a_{i1} \to 0$ as $t \to \infty$.

D. Finite Time Stability

The finite time convergence means that the system will converge on the sliding surface. On the sliding surface, the system is totally determined by a reduced-order system determined by the designer. Without the finite time convergence, the system moves in a vicinity of the sliding surface, where the system may converge slowly or even may not converge, determined by the sliding surface, the whole system dynamics including disturbances and uncertainties. Besides, with the finite time convergence, the matched disturbances and/or uncertainties can be rejected completely.

Lemma 2: [13] Assume there is a continuous positive definite function $V(t)$ satisfying the following differential inequality:

$$\dot{V} \leq -\gamma_1 V^{\bar{\rho}} \quad \forall t \geq t_0, V(t_0) \geq 0, \tag{31}$$

where $\gamma_1 > 0$ and $0 < \bar{\rho} < 1$ are positive constants. Then, for any given t_0, $V(t)$ satisfies the following inequality:

$$V^{1-\bar{\rho}}(t) \leq V^{1-\bar{\rho}}(t_0) - \gamma_1(1-\bar{\rho})(t-t_0), t_0 \leq t \leq t_1 \tag{32}$$

and $V(t) \equiv 0, \forall t \geq t_1$ with $t_1 = t_0 + \frac{V^{1-\bar{\rho}}(t)}{\gamma_1(1-\bar{\rho})}$.

E. Fuzzy Logic System

Fuzzy logic system is a collection of IF-THEN fuzzy rules as:

$$R^k: \quad IF \quad x_1 \quad is \quad A_1^k, \quad and, \quad \cdots, \quad x_n \quad is \quad A_n^k, \quad THEN \quad y \quad is \quad B^k. \tag{33}$$

The output of the fuzzy system (using singleton fuzzification, product inference and center average defuzzification) can be written as

$$y_{out} = \frac{\sum_{l=1}^{P} \theta_F^l(X) \prod_{i=1}^{N} \mu_{Ai^l(x_i)}^l}{\sum_{l=1}^{P} \prod_{i=1}^{N} \mu_{Ai^l(x_i)}^l} = \theta^T \xi \tag{34}$$

where P is the total fuzzy rules number. The membership functions $\mu_{A1^l(x_1)}, ..., \mu_{An^N(x_n)}$ (N is the number of membership functions) are Gaussian functions, ξ is fuzzy basis function $\left(\xi^l(x) = \frac{\prod_{i=1}^{N} \mu_{Ai^l(x_i)}}{\sum_{l=1}^{P} \prod_{i=1}^{N} \mu_{Ai^l(x_i)}}\right)$. In this paper, $N = 7$. Therefore, the membership functions can be chosen as linguistic terms Negative Big (NB), Negative Medium (NM), Negative Small (NS), Zero (ZE), Positive Small (PS), Positive Medium (PM) and Positive Big (PB), that are assigned to the inputs (x_1 to x_n) and the output ($\hat{F}$).

Therefore, the continuous nonlinear function $F_i(x)$ of each satellite can be approximated by the fuzzy logic system [14].

$$\hat{F}_i(x) = {\theta_i}^T \xi_i(x) \tag{35}$$

where ξ_F is the vector of the fuzzy basis function and is supposed to be fixed, while the parameters $\theta_{F_i}^T$ are the variable which will be designed by adaptive laws. It is assumed that there exists an optimal fuzzy logic system to learn the nonlinear terms $F_i(x)$ such that

$$F_i(x) - \hat{F}_i^*(x) = \varepsilon \tag{36}$$

where ε is the approximation error and is bounded. Approximation errors can be reduced by increasing the number of fuzzy rules.

In order to decrease the fuzzy rules, we use the nonsingular fast terminal sliding surface S instead of the state x for the adaptive parameters. Then, the adaptive parameters θ_F are updated by the following adaptive laws:

$$\dot{\theta}_i = \alpha_i M_2 \sigma_2 p/q \dot{A}_1^{p/q-1} S \xi_i \tag{37}$$

$$\xi_i(s_i) = \frac{\prod_{i=1}^{N} \mu_{Ai^l(s_i)}}{\sum_{l=1}^{P} \prod_{i=1}^{N} \mu_{Ai^l(s_i)}} \tag{38}$$

where α_i is a positive constant.

In order to guarantee that the estimated Fuzzy Logic System parameters remain within some known bounded sets, the smooth projection is considered in this paper. Let θ_i be the estimation of the optimal weight matrix θ_i^*, and define a smooth projection of θ_i as:

$$\pi_i(\theta_i) = \theta_{i\pi} = \pi_{i,jk}(\theta_{i,jk}), j = 1, 2, ..., m, k = 1, 2, ..., N_1 \tag{39}$$

Each projection operator $\pi_{i,jk}$ is a real-value smooth nondecreasing function defined by

$$\pi_{i,jk}(\theta_{i,jk}) = \theta_{i,jk} \tag{40}$$

Define $\tilde{\theta}_i = {\theta_i}^* - \theta_i$, $\tilde{\theta}_{i\pi} = {\theta_i}^* - \theta_{i\pi}$, and

$$V_{\theta_i} = \frac{1}{\delta_i} \sum_{j=1}^{m} \sum_{k=1}^{N_1} \int_0^{\tilde{\theta}_i} ({\theta^*}_{i,jk} - \pi_{i,jk}({\theta^*}_{i,jk} - \omega_{i,jk}) d\omega_{i,jk} \tag{41}$$

where, V_{θ_i} is positive definite with respect to $\tilde{\theta}_{i,jk}$ for $\theta_{i,jk}^* \in [\theta_{imin}, \theta_{imax}]$. Furthermore,

$$\dot{V}_{\theta_i} = -\frac{1}{\delta_i} \sum_{j=1}^{m} \sum_{k=1}^{N_1} \tilde{\theta}_{i\pi,jk} \dot{\theta}_{i,jk}^*, i = 1, 2, ..., n \tag{42}$$

Assumption 2: ε is bounded such that $\|\varepsilon_i\| \leq \varepsilon_{Mi} (i = 1, 2, ..., n)$, where ε_{Mi} is a positive constant.

Assumption 3: The optimal weight matrix $\theta_i^*(i=1,2,...,n)$ lies in a known bounded set ϱ_{Wi} defined by

$$\theta_i^* \in \varrho_{Wi} = \left\{\theta_i^* : \theta_{imin}^* \leq \theta_{i,jk}^* \leq \theta_{imin}^*\right\} \tag{43}$$

where θ_{imin}^* and θ_{imax}^* are known constants, respectively.

F. Mathematical Model for Controller Design

To employ the proposed control design methodology described in this paper, we need to construct a model to represent the nonlinear equations Eq. (1).

Denoting $p = 2[q_{4i}I + (q_{vi}^{\times})]^{-1}$, after taking the time derivative of Eq. (5), we obtain the following expression of ω_{iBL}^{B}:

$$\dot{\omega_i}_{BL}^{B} = \dot{p}\dot{q}_{vi} + p\ddot{q}_{vi} \tag{44}$$

where $T = [q_{4i}I + (q_{vi})^{\times}]^{-1}$.

Making use of Eq. (5) and Eq. (44), the quaternion equation can be written as:

$$\ddot{q}_{vi} = 2(T^{-1})^{T}(\dot{\omega_i}_{BI}^{B} - \dot{\omega_i}_{LI}^{B}) - 4(T^{-1})^{T}(\dot{T}^{-1})\dot{q}_{vi} \tag{45}$$

Since T is a skew-symmetric matrix, we derive $\dot{T}^{-1} = -T^{-1}\dot{T}T^{-1}$.

Substituting the Eqs. (1) and (9) into the Eq. (45), we obtain:

$$\begin{aligned}\ddot{q}_{vi} = 2(T^{-1})^{T}[{J_i}^{-1}(-\omega_{iBI}^{B} \times (J_{si}\omega_{iBI}^{B} + A_i J_{wi}\Omega_i) \\ + A_i\tau_{rwi} + \tau_{ie}) - \dot{\omega_i}_{LI}^{B}] - 4(T^{-1})^{T}(\dot{T}^{-1})\dot{q}_{vi}\end{aligned} \tag{46}$$

Using $\dot{C_L^B} = -[{\omega_{BL}^{B}}^{\times}]C_L^B$, we have:

$$\dot{\omega_i}_{LI}^{B} = -\omega_{iLI}^{B} \times \omega_{iLI}^{B} \tag{47}$$

The dynamics equation with actuator fault can be written as:

$$\ddot{q}_{vi} = f_i(q_{ie}, \dot{q}_{ie}) + (\tau_i + \Delta\tau_i) + \nu_i \tag{48}$$

A dynamic model of the satellite's relative attitude tracking with multiplicative reaction wheel faults (e.g. reduced control torque) is represented by a diagonal matrix E.

$$\begin{aligned}f_i(q_{ie}, \dot{q}_{ie}) = 2(T^{-1})^{T}[{J_i}^{-1}(-\omega_{iBI}^{B} \times (J_{si}\omega_{iBI}^{B} + A_i J_{wi}\Omega_i)] \\ - 4(T^{-1})^{T}(\dot{T}^{-1})\dot{q}_{vi} + 2(T^{-1})^{T}{J_i}^{-1}\omega_{iLI}^{B} \times \omega_{iLI}^{B}\end{aligned} \tag{49}$$

$$\tau_i = E[2(T^{-1})^{T}{J_i}^{-1}A_i\tau_{rwi}] \tag{50}$$

$$\nu_i = 2(T^{-1})^{T}{J_i}^{-1}\tau_{ie} \tag{51}$$

Assumption 4: The disturbance ν_i is bounded such that $\|\nu_i\| \leq \nu_{Mi}(i=1,2,...,n)$, where ν_{Mi} is a positive constant.

Assumption 5: The fault $\Delta\tau_i$ is bounded such that $\|\Delta\tau_i\| \leq \Delta\tau_{iMi}(i=1,2,...,n)$, where τ_{iMi} is a positive constant.

II. Design of Nonsingular Fast Fuzzy Terminal Sliding Mode Control

In this section we present the theoretical basis for developing NFFTSMC control algorithms for the four rigid body satellites attitude consensus tracking. The controller is decentralized as each controller does not require the decision from the other controllers. For each satellite, the NFFTSMC control overall design can be divided into two main steps. Step 1 involves the construction of a sliding surface containing absolute attitude and relative attitude tracking errors to ensure that once the system is restricted to the sliding surface, the satellite can be expected to be in the desired trajectory. Step 2 entails the derivation of parameter adaptation laws and fuzzy logic feedback control gains that can drive the relative state trajectory to the sliding surface, and maintain it in the manifold.

A. Nonsingular Fast Terminal Sliding Mode

The nonsingular fast terminal sliding mode can be defined by the following nonlinear differential equation:

$$s = x + \sigma_1 sign(x) + \sigma_2 \dot{x}^{\frac{p}{q}} \tag{52}$$

where $x \in \mathbb{R}$ and σ_1, σ_2 are positive constants. The positive odd integers p, q are chosen such that $1 < q/p < 2$.

We define the fast terminal sliding mode $s_i \in \mathbb{R}^m$ for the i'th satellite in the formation as:

$$s_i = a_{i2} + \beta_i a_{i1} = \Lambda_i + \beta_i \tag{53}$$

$$\begin{aligned}\Lambda_i(a_{i1}) &= a_{i1} + \sigma_{i1} sign(a_{i1}) \\ \beta_i(a_{i2}) &= \sigma_{i2} a_{i2}^{\frac{p}{q}}\end{aligned} \tag{54}$$

where $i = 1,2,...,n$. $\Lambda_i(a_{i1})$ and $\beta_i(a_{i2}) \in \mathbb{R}^m$. σ_{i1} and σ_{i2} are positive constants for the designer.

Defining $\beta = ({\beta_1}^{T}, {\beta_2}^{T}, ..., {\beta_n}^{T})^{T}$ and $s = ({s_1}^{T}, {s_2}^{T}, ..., {s_n}^{T})^{T}$, we have

$$s = \Lambda + \beta \tag{55}$$

The time derivative of the sliding mode Eq. (55) is given by

$$\dot{s} = \bar{\Lambda} + \bar{\beta} \tag{56}$$

B. Nonsingular Fast Fuzzy Terminal Sliding Mode Controller Design

The controller design for the i'th satellite in the formation is now given by

$$\tau_{rwi} = \bar{\tau}_i = \ddot{q}_d - K_{i1}s_i - K_{i2}{s_i}^{\rho} - \frac{q}{p\sigma_2}a_{i2}^{2-p/q} - \theta_i^T\xi_i - \varphi_i \tag{57}$$

where K_{i1} and K_{i2} are designed parameters.

with φ_i defined by [15]

$$\varphi_i \equiv \kappa_i tanh(\frac{3K_u\kappa_i s_i}{\epsilon}) \tag{58}$$

The controller consists three components: the nonlinear compensator $\ddot{q}_d$ is applied to compensate for the desired satellite dynamics, motivated by the fact that the attitude of each satellite in the formation reaches the desired trajectory of the formation, then station-keeping errors and formation-keeping errors will be zero. The nonlinear feedback $K_{i1}s_i + K_{i2}{s_i}^{\rho} + \frac{q}{p\sigma_2}a_{i2}^{2-p/q}$ is used to drive the satellite attitude to the sliding surface in finite time. The robust term $\varphi_i + \theta_i^T\xi_i$ is used to counteract the external disturbance and unknown system uncertainties due to the actuator faults. κ_i is a positive constant

satisfying $\varphi_i \geq d_{Mi}$. ϵ is a positive scalar. K_{i1} and K_{i2} are positive definite, diagonal and constant matrices. ρ is p/q. The proposed controller can provide finite time stability in both the reaching phase and the sliding phase, which is guaranteed by the Lyapunov theory described in the next subsection.

C. Stability Analysis

Theorem 2: Consider the system Eq. (48) and Assumption $1 \sim 5$, the nonsingular fast fuzzy terminal sliding control laws defined by Eqs. (57-58), with adaptive control laws given by Eq. (37) guarantees the state of the system starting from any initial point will move toward the switching surface and reach the sliding surface $s = 0$ in a finite time. Furthermore, the aggregated attitude tracking errors $a_{i1,j}$ and $a_{i2,j}$ ($i = 1, 2, ..., n$,j=1,2,3) will converge to the regions in finite time, respectively, and the station-keeping attitude tracking errors will converge to the regions in finite time, respectively.

Proof of Theorem 2: The dynamics equations for the absolute errors of the i'th satellite can be written as:

$$q_{ie} = e_{1i} \quad \dot{q}_{ie} = e_{2i} \tag{59}$$

$$\dot{e}_{i1} = e_{i2} \quad \dot{e}_{i2} = -\ddot{x}_{id} + f_i(q_{ie}, \dot{q}_{ie}) + \tau_i + \Delta\tau_i + \nu_i \tag{60}$$

Define $E_1 = ({e_{11}}^T, {e_{21}}^T, ..., {e_{n1}}^T)$, $E_2 = ({e_{12}}^T, {e_{22}}^T, ..., {e_{n2}}^T)$, $Q_d = (\ddot{q}_1^T, \ddot{q}_2^T, ..., \ddot{q}_n^T)$, $F = ({f_1}^T, {f_2}^T, ..., {f_n}^T)$, $\bar{\tau} = (\bar{\tau}_1^T, \bar{\tau}_2^T, ..., \bar{\tau}_n^T)$, $\Delta\tau = ({\Delta\tau_{i1}}^T, {\Delta\tau_{i2}}^T, ..., {\Delta\tau_{in}}^T)$ and $\nu = (\bar{\nu}_1^T, \bar{\nu}_2^T, ..., \bar{\nu}_n^T)$. The Eqs. (59) can be expressed in terms of the aforementioned quantities as follows:

$$\begin{aligned} \dot{E}_1 &= E_2 \\ \dot{E}_2 &= -Q_d + F + \tau + \Delta\tau + \nu \end{aligned} \tag{61}$$

Denote $M_1 = (k_p L + K) \otimes I_3$. Eqs. (28) and (29) can be expressed in terms of the aforementioned quantities as follows:

$$\begin{aligned} A_1 &= M_1 E_1 \\ A_2 &= M_1 E_2 \end{aligned} \tag{62}$$

The dynamics equations for A_1 and A_2 are defined as:

$$\begin{aligned} \dot{A}_1 &= A_2 \\ M_2 \dot{A}_2 &= -Q_d + F + \tau + \Delta\tau + \nu \end{aligned} \tag{63}$$

respectively, where $M_2 = M_1^{-1}$.

Using Eqs. (56) and (63), we obtained

$$\begin{aligned} M_2 \dot{s} &= M_2 \bar{\Lambda} + M_2 \bar{\beta} = M_2 \dot{A}_1 \\ &+ M_2 \sigma_2 p/q \dot{A}_1^{p/q-1} (-Q_d + F + \tau + \Delta\tau + \nu) \end{aligned} \tag{64}$$

Using the approximation property of Fuzzy Logic Systems, the unknown function $f_i (i = 1, 2, ..., n)$ can be approximated over the compact set Ω_d by Eqs. (35) and (37). Substituting the control law Eq. (57) into the error dynamics Eq. (64) yields the following dynamic equation for sliding surface s.

$$\begin{aligned} M_2 \dot{s} &= M_2 \bar{\Lambda} + M_2 \bar{\beta} \\ &= M_2 \dot{A}_1 + M_2 \sigma_2 p/q \dot{A}_1^{p/q-1} (-Q_d + F - F_d + F_d \\ &- \theta^T \xi - K_1 s - K_2 s^\rho \frac{q}{p\sigma_2} \dot{A}_1^{2-p/q} - \varphi + \nu + \Delta\tau) \\ &= M_2 \sigma_2 p/q \dot{A}_1^{p/q-1} (\varsigma + \tilde{\theta}^T \xi - K_1 s - K_2 s^\rho \\ &- \varphi + \nu + \varepsilon + \Delta\tau) \end{aligned} \tag{65}$$

where $\varsigma = -Q_d + F - F_d$ and $K_1 = ({K_{11}}^T, {K_{21}}^T, ..., {K_{n1}}^T)$, $K_2 = ({K_{12}}^T, {K_{22}}^T, ..., {K_{n2}}^T)$, $\varphi = ({\varphi_1}^T, {\varphi_2}^T, ..., {\varphi_n}^T)$, $\varepsilon = ({\varepsilon_1}^T, {\varepsilon_2}^T, ..., {\varepsilon_n}^T)$, $\theta^* = diag({\theta_1^*}^T, {\theta_2^*}^T, ..., {\theta_n^*}^T))$, $\theta = diag({\theta_{1\pi}}^T, {\theta_{2\pi}}^T, ..., {\theta_{n\pi}}^T))$, $\theta_\pi^* = \theta^* - \theta_\pi$, and $\xi = ({\xi_1}^T, {\xi_2}^T, ..., {\xi_n}^T)$.

Consider the following Lyapunov function candidate

$$V = \frac{1}{2} s^T M_2 s + \sum_{i=1}^{n} V_{\theta_i} \tag{66}$$

Thus, the time derivative of V is obtained as

$$\dot{V} = s^T M_2 \dot{s} + \sum_{i=1}^{n} \dot{V}_{\theta_i} \tag{67}$$

Due to the fact that

$$s^T M_2 \sigma_2 p/q \dot{A}_1^{p/q-1} \tilde{\theta}^T \xi - \frac{1}{\delta_i} \sum_{j=1}^{m} \sum_{k=1}^{N_1} \tilde{\theta}_{F_{i\pi,jk}} \dot{\theta}_{i,jk}^* = 0 \tag{68}$$

Substituting the Eqs. (42) and (65) to the Eq. (67), we obtain:

$$\begin{aligned} \dot{V} &= M_2 \sigma_2 p/q \dot{A}_1^{p/q-1} (s^T \varsigma + s^T \tilde{\theta}^T \xi - s^T K_1 s - s^T K_2 s^\rho - s^T \varphi \\ &+ s^T (\nu + \varepsilon + \Delta\tau) - \frac{1}{\delta_i} \sum_{j=1}^{m} \sum_{k=1}^{N_1} \tilde{\theta}_{F_{i\pi,jk}} \dot{\theta}_{i,jk}^*) \\ &= M_2 \sigma_2 p/q \dot{A}_1^{p/q-1} (s^T \varsigma - s^T K_1 s - s^T K_2 s^\rho - s^T \varphi \\ &+ s^T (\nu + \varepsilon + \Delta\tau)) \end{aligned} \tag{69}$$

Using the following inequalities

$$0 \leq -s^T \varphi + s^T (\nu + \varepsilon + \Delta\tau) \leq n\epsilon \tag{70}$$

$$0 \leq s^T \varsigma \leq c_5 s^T s + \frac{{\varsigma^2}_M}{4c_5} \tag{71}$$

where c_5 is a positive constant satisfying $c_5 < \lambda_{min}(K_1)$ with $\lambda_{min}(K_1)$ being the minimum eigenvalue of the matrix K_1, Eq. (69) becomes

$$\begin{aligned} \dot{V} &\leq M_2 \sigma_2 p/q \dot{A}_1^{p/q-1} (-(\lambda_{min}(K_1) - c_5) s^T s + c_4 - s^T K_2 s^\rho) \\ &\leq -M_2 \sigma_2 p/q \dot{A}_1^{p/q-1} |s|^2 \end{aligned} \tag{72}$$

where $c_4 = n\epsilon + \frac{\varsigma_M^2}{4c_5}$ is a positive constant.

$$
\begin{aligned}
-s^T K_2 s^\rho &\le -\lambda_{min}(K_2) \sum_{i=1}^{n}\sum_{j=1}^{m} s_{ij}^{\rho+1} \\
&\le -\lambda_{min}(K_2) \left(\frac{2}{\lambda_{max}}\right)^{(\rho+1)/2} \left(\sum_{i=1}^{n}\sum_{j=1}^{m} \frac{\lambda_{max}}{2} s_{ij}^2\right)^{(\rho+1)/2} \\
&\le -\lambda_{min}(K_2) \left(\frac{2}{\lambda_{max}}\right)^{(\rho+1)/2} \left(0.5 s^T M_2 s\right)^{(\rho+1)/2} \\
&= -\gamma_2 V^{\rho+1}/2
\end{aligned} \tag{73}
$$

where $\gamma_2 = \lambda_{min}(K_2)(2/\lambda_{max}(M_2))^{(\rho+1)/2}$. The Eq. (72) can be expressed as:

$$
\dot{V} \le -\gamma_1 V - \gamma_2 V^{(\rho+1)/2} + c_4 \tag{74}
$$

where $\gamma_1 = 2(\lambda_{min}(K_1) - c_5)/\lambda_{max}(M_2)$.

Then Eq. (74) can be written as the following two forms:

$$
\dot{V} \le -\gamma_1 V - (\gamma_2 - \frac{c_4}{V^{(\rho+1)/2}}) V^{(\rho+1)/2} \tag{75}
$$

From Eq. (75), if $\gamma_1 - c_4/V > 0$, then the finite-time stability is still guaranteed. According to the reference [16], the sliding surface s will reach the region $\|s\| \le \Delta$ in finite time, which means $s_{ij} \le \Delta \quad i = 1, 2, .., n, j = 1, 2, ..., m, i.e..$ All signals in the closed-loop system are uniformly ultimately bounded.

III. Results and Discussion

To study the effectiveness and performance of the proposed controller, the detailed response is numerically simulated using the set of governing system equations of motion Eq. (48) in conjunction with the control laws Eqs. (57-58).

The information exchange among satellite is represented by a graph with the weighted adjacency matrix $\bar{A}$ defined by

$$
\bar{A} = \begin{bmatrix} 0 & 0.5 & 0 & 0 \\ 0.5 & 0 & 0.6 & 0 \\ 0 & 0.6 & 0 & 0.7 \\ 0 & 0 & 0.7 & 0 \end{bmatrix}
$$

Seven Gaussian membership functions are defined for each variable $\tilde{A}_i, i = 1, 2, \cdots, 7$ as:

$$
\begin{aligned}
\mu_{\tilde{A}_1}(s_i) &= \frac{1}{1 + \exp(5(s_i + 0.9 \times a))}, \\
\mu_{\tilde{A}_2}(s_i) &= \exp\left(-\left(\frac{s_i + 0.6 \times a}{b}\right)^2\right), \\
\mu_{\tilde{A}_3}(s_i) &= \exp\left(-\left(\frac{s_i + 0.3 \times a}{b}\right)^2\right), \\
\mu_{\tilde{A}_4}(s_i) &= \exp\left(-\left(\frac{s_i}{b}\right)^2\right), \\
\mu_{\tilde{A}_5}(s_i) &= \exp\left(-\left(\frac{s_i - 0.3 \times a}{b}\right)^2\right), \\
\mu_{\tilde{A}_6}(s_i) &= \exp\left(-\left(\frac{s_i - 0.6 \times a}{b}\right)^2\right), \\
\mu_{\tilde{A}_7}(s_i) &= \frac{1}{1 + \exp(5(s_i - 0.9 \times a))}
\end{aligned} \tag{76}
$$

where a and b are different constant numbers designed according to s_i. In this paper, $a = b = 1$.

In this section, we present the simulation results for the following case I: Desired Attitude Trajectory is $q_d = [0, 0.05cos(0.02t), 0.05sin(0.02t)]^T$. For reaction wheel pyramid configuration, with desired trajectory q_d, after $t = 50s$, the wheels of satellites $three$ and $four$ only supply 40% and 50% of the designed speed. After $t = 70s$ another fault of satellite one occurs: three wheels of satellite one only supply 70% of their design speed and the second wheel's input voltage is zero. There is no fault within satellite two.

To compare the control performances of the nonsingular fast fuzzy terminal sliding control laws defined by Eqs. (57-58), a nonsingular fast terminal sliding mode controller $\hat{\tau}_{rwi}$ is designed in Eq.77 as following:

$$
\hat{\tau}_{rwi} = \ddot{q}_d - K_{i1} s_i - K_{i2} s_i^\rho - \frac{q}{p\sigma_2} a_{i2}^{2-p/q} - \varphi_i \tag{77}
$$

Figs. 1 shows the station-keeping attitude tracking errors by using quaternion $e_i (i = 1, 2, 3, 4)$, respectively. The formation-keeping attitude error case is given in Fig. 2. It is found that the proposed controller can still drive the station-keeping attitude tracking errors and formation-keeping to the neighborhood around zero in finite time even when the faults happened. Therefore, the proposed controller can still provide finite-time control for a group of satellite under actuation faults as in the previous case. Without the Fuzzy Logic System, the station keeping and formation keeping tracking errors can not drive the system back to the neighborhood around zero in finite time.

IV. Conclusions

The primary contribution of this paper is the development and analysis of a decentralized, attitude-coordinated control law that provides finite-time stability and convergence of attitude synchronization. The simulation results clearly establish

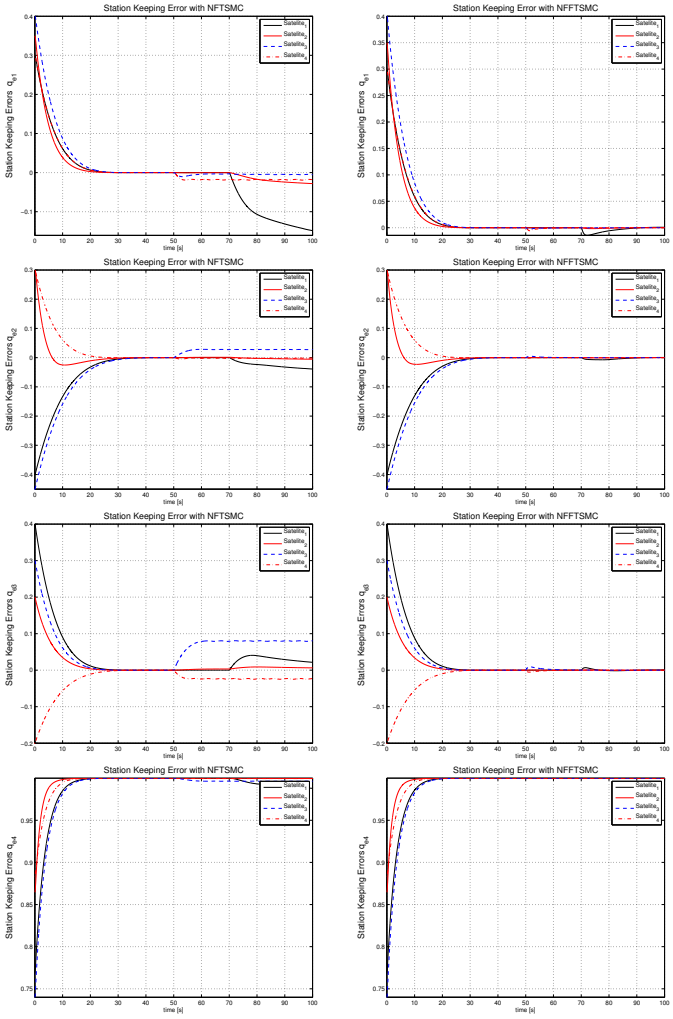

Fig. 1. Station-keeping Tracking Errors using Quaternion Simulation Result without Fuzzy Logic System and with Fuzzy Logic System

the robustness of the proposed adaptive control methodologies using nonsingular fast terminal sliding mode and fuzzy logic systems in tracking the attitude of formation flying satellites in the presence of actuator faults and time-varying disturbances.

REFERENCES

[1] Y. C. Cao, W. Ren, and Z. Y. Meng, "Decentralized finite-time sliding mode estimators and their applications on decentralized finite-time formation tracking," *Systems and Control Letters*, DOI:10.1016/j.sysconle.2010.06.002.

[2] L. Yang and J. Y. Yang, "Nonsingular fast terminal sliding mode control for nonlinear dynamical system," *International Journal of Robust and Nonlinear Control*, DOI:10.1002/RNC.1666, 2010.

[3] S. Yu, X. Yu, B. Shirnzadeg, and Z. Man, "Continuous finite time control for robotic manipulators with terminal sliding mode," *Automatica*, vol. 41, pp. 1957–1964, 2005.

[4] L. X. Wang and J. Mendel, "Fuzzy basis function, universal approximation, and orthogonal least-squares learning," *IEEE Transactions on Neural Networks*, vol. 3, no. 5, pp. 807–814, 1992.

[5] S. Y. Chen and F. J. Lin, "Robust nonsingular terminal sliding mode control for nonlinear magnetic bearing system," *IEEE Transactions on Control System Technology*, DOI 10.1109/TCST.2010.2050484.

[6] P. Panagi and M. M. Polycarpou, "Decentralized fault tolerant control of a class of interconnected nonlinear systems," *IEEE Transactions on Automatic Control*, vol. 56, no. 1, pp. 178–184, 2011.

[7] B. Wie, *Space Vehicle Dynamics and Control*. Reston, VA: AIAA Education Series, 1998.

[8] D. Fragopoulos and M. Innocenti, "Stability considerations in quaternion attitude control using discontinuous lyapunov functions," *IEE Proceedings-Control Theory and Applications*, vol. 151, no. 3, pp. 253–258, 2004.

[9] J. Jin, S. Ko, and C.-K. Ryoo, "Fault tolerant control for satellites with four reaction wheels," *Control Engineering Practice*, vol. 16, no. 10, pp. 1250–1258, 2008.

[10] H. Schaub and J. Junkins, *Analytical Mechanics of Space Systems*. Reston, VA: AIAA Education Series, 2003.

[11] I. Changa, S.-Y. Park, and K.-H. Choi, "Decentralized coordinated attitude control for satellite formation flying via the state-dependent riccati equation technique," *International Journal of Non-Linear Mechanics*, vol. 44, no. 8, pp. 891–904, 2009.

[12] C. Godsil and G. Royle, *Algebraic Graph Theory*. New York: Springer-Verlag, 2001.

[13] H. Wang, Z. Z. Han, Q. Y. Xie, and W. Zhang, "Finite-time chaos control via nonsingular terminal sliding mode control," *Commun Nonlinear Sci Numer Simulat*, vol. 14, pp. 2728–2733, 2009.

[14] L. X. Wang, *A Course in Fuzzy Systems and Control*. New York, NY: Prentice-Hall, 1997.

[15] Z.-G. Hou, A.-M. Zou, L. Cheng, and M. Tan, "Adaptive control of an electrically driven nonholonomic mobile robot via backstepping and fuzzy approach," *IEEE Transactions on Control System Technology*, vol. 17, no. 4, pp. 803–815, 2009.

[16] S. B. Li, K. Q. Li, J. Q. Wang, and F. Gao, "Nonsingular and fast terminal sliding mode control method," *Information and Control*, vol. 38, no. 1, 2009.

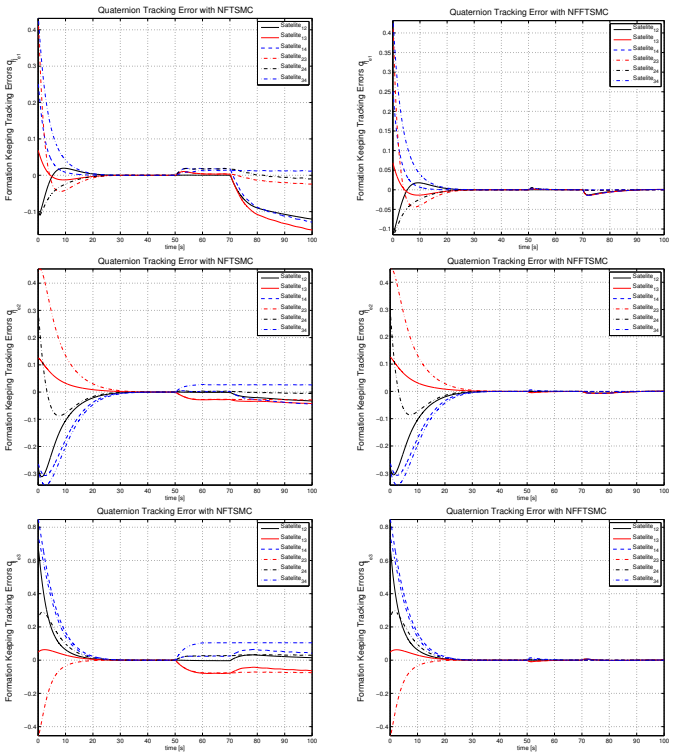

Fig. 2. Formation-keeping Tracking Errors Simulation Result without Fuzzy Logic System and with Fuzzy Logic System

2011 IEEE International Conference on Fuzzy Systems
June 27-30, 2011, Taipei, Taiwan

T-S Fuzzy Tracking and Synchronous Control in a Gantry Stage

Chin-Sheng Chen
Graduate Institute of Automation Technology
National Taipei University of Technology
Taipei, Taiwan
saint@ntut.edu.tw

Chao-Feng Lee
Graduate Institute of Automation Technology
National Taipei University of Technology
Taipei, Taiwan
t8618018@ntut.edu.tw

Po-Huan Chou
Department of Electrical Engineering
National Dong Hwa University
Hualien, Taiwan
d9623002@ems.ndhu.edu.tw

Faa-Jeng Lin
Department of Electrical Engineering
National Central University
Chungli, Taiwan
linfj@ee.ncu.edu.tw

Shun-Hung Tsai
Graduate Institute of Automation Technology
National Taipei University of Technology
Taipei, Taiwan
shtsai@ntut.edu.tw

***Abstract*—In this paper, we propose a T-S fuzzy model based controller for the H-type gantry stage. The synchronized error, which is caused by mismatch quality and friction, is an important control problem for the H-type gantry stage. Utilizing a Lagrangian equation, all states can be formulated as a state equation. Furthermore, the T-S fuzzy model based controller is designed to reduce velocity error, and the position error can also be obtained through internal transformation. Moreover, by utilizing additional transformations, the stabilization problem can be transformed into a linear matrix inequalities (LMIs) problem. Finally, numerical simulation and experimental results are illustrated to demonstrate that the control scheme can effectively reduce synchronized error and tracking error of a gantry stage.**

Keywords: gantry stage; T-S fuzzy model; Lagrangian equation; Linear Matrix Inequalities (LMIs);

I. INTRODUCTION

With the growth of industrial technology, motion systems with high speed and high precision have attracted increasing study and applications. As a coordinate system, the H-type gantry stage is widely applied in many fields, such as microelectronics, aerospace, solar cells, and flat panel manufacturing and inspection. Two motors of the stage are mounted on parallel slides that simultaneously push the third axis and motor, and a load can be installed on the third axis for applying in different systems. But motion of the load will affect behavior of the two parallel motors on the base, reducing precision and harming the machine's structure. Therefore, control of the synchronous error in the gantry configuration has become a challenge due to the increasing demands for high-speed and high-accuracy manufacturing and inspection.

Generally, the control problem of a gantry stage can be concluded as cascade control and parallel control. Cascade control contains two parallel axes, a master axis and a slave axis. For this control structure, control commands were sent to the master axis, and the response of master axis becomes a new command for slave axis. But the disadvantage of this structure is that it will cause state and input delays. For this reason, most studies adopt parallel control, which is a biaxial structure, can be independently designed, and can give same command simultaneously. Koren proposed cross-coupled biaxial computer control in 1980 [1], and variable-gain cross-coupling controller in 1991 [2]. Other studies utilize the optimum concept to decouple the structure [3-4]. In addition, other cross-coupled controllers have been investigated in parallel control structures [5]. However, these studies all discuss similar control structures. Teo first proposed a Lagrangian model to analyze the H-type gantry stage [6-7].

Fuzzy control technique has been widely used in many physical and engineering systems, especially for systems with incomplete plant information. In addition, fuzzy control has been widely applied to controller designs for nonlinear systems [8-14]. In most of these papers, a so-called Takagi-Sugeno (T-S) fuzzy model is adopted to approximate a nonlinear system, and then a fuzzy controller is designed via the parallel distributed compensation (PDC) scheme to stabilize the T-S fuzzy model. By examining, problems of stability and stabilization, LMI techniques have been adopted to find solutions for the T-S fuzzy model based control system.

In this paper, we propose a novel control scheme based on the Lagrangian model [6-7] and present a systematic design procedure to analyze this model. First we design a T-S fuzzy model based controller for velocity error. Secondly, through

978-1-4244-7316-8/11/$26.00 ©2011 IEEE

state internal transformations, we obtain the controller gains of the velocity error and position error. Furthermore, by utilizing the structure, controller gains can be obtained through the LMIs and the velocity error and position error can be reduced. The main contributions of this paper include: i) first use of a T-S fuzzy model based control scheme for the H-type gantry stage, ii) propose a transformation method to transform the velocity error gains into position error gains, and iii) formulation all of stability and stabilization conditions into an LMI form.

This paper is organized as follows. In Section II, we discuss the development of dynamic Lagrangian model of gantry stage. In section III, the T-S fuzzy model based scheme is designed for this physical model utilizing the Lyapunov direct method, and stability/stabilization conditions are proposed to guarantee the system is asymptotic stable. Numerical simulation and experimental results are illustrated in Section IV. Finally, conclusions are given in Section V.

II. DYNAMIC MODELING OF GANTRY SYSTEM

A. Description of a gantry stage

A typical gantry mechanism and the corresponding coordinates are shown in Fig. 1. It can be considered as a three-degree-of-freedom servo mechanism. Two servo motors in y axis, considered in this paper are PMLSMs, carry a gantry on which a slider in x axis holding the inspection tool is mounted. Two motors on the y axis yield displacement d_{y_1} and d_{y_2} respectively. These two displacements will be equal when the two servo motors move synchronously, that implies $d_{y_1} = d_{y2}$. But in practice, their movements will be different due to the different dynamics exhibited in the two servo motors and the time-varying loading presented by translation of the slider along the gantry. The central point C of the gantry is thus constrained to move along the central dashed line with one degree of freedom. Due to the deviation between d_{y_1} and d_{y_2}, the gantry may also rotate about the center C, and the rotated angle is indicated as θ.

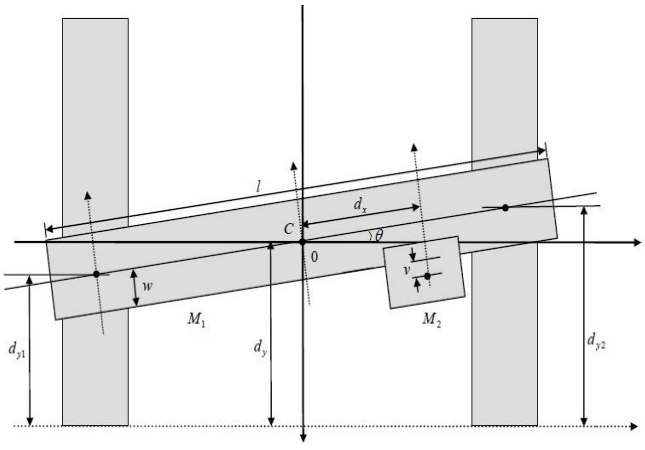

Figure 1. Three-degree-of-freedom scheme.

B. Lagrangian-based three-degree-of-freedom dynamic model

Let M_1 and M_2 denote the mass of the gantry and the slider, respectively; l and $2w$ denote the length and width of the gantry, respectively; and I_{M_1} and I_{M_2} denote the moment of inertia of the gantry and of the slider corresponding to the cntrer point C, respectively.

$$I_{M_1} = \frac{M_1}{12}\left(l^2 + (2w)^2\right) \tag{1}$$

$$I_{M_2} = M_2\left(d_x{}^2 + (w+v)^2\right) \tag{2}$$

Then the positions corresponding to the center of gravity of M_1 and M_2, $\mathbf{p}_{M_1}$ and $\mathbf{p}_{M_2}$ are represented as

$$\mathbf{p}_{M_1} = \begin{bmatrix} 0 \\ d_y \end{bmatrix} \tag{3}$$

$$\mathbf{p}_{M_2} = \begin{bmatrix} d_y - (w+v)\cos\theta + d_x \sin\theta \\ d_x \cos\theta + (w+v)\sin\theta \end{bmatrix} \tag{4}$$

where $d_y = d_{y1} + \left(d_{y2} - d_{y1}\right)/2$. The velocities corresponding, $\mathbf{v}_{M_1}$ and $\mathbf{v}_{M_2}$, to the center of gravity of M_1 and M_2 are represented as

$$\mathbf{v}_{M_1} = \begin{bmatrix} 0 \\ \dot{d}_y \end{bmatrix} \tag{5}$$

$$\mathbf{v}_{M_2} = \begin{bmatrix} \dot{d}_y + (w+v)\dot{\theta}\sin\theta + \dot{d}_x \sin\theta + d_x\dot{\theta}\cos\theta \\ \dot{d}_x \cos\theta - d_x\dot{\theta}\sin\theta + (w+v)\dot{\theta}\cos\theta \end{bmatrix} \tag{6}$$

Then the translational and rotational kinetic energy of the gantry and slider are shown as

$$K_{M_1} = \frac{1}{2}M_1 \mathbf{v}_{M_1}{}^T \mathbf{v}_{M_1} + \frac{1}{2}I_1\dot{\theta}^2 \tag{7}$$

$$K_{M_2} = \frac{1}{2}M_2 \mathbf{v}_{M_2}{}^T \mathbf{v}_{M_2} + \frac{1}{2}I_2\dot{\theta}^2 \tag{8}$$

Thus the total kinetic energy may be computed as

$$K = K_{M_1} + K_{M_2}$$

$$= \frac{1}{2}M_1 \mathbf{v}_{M_1}{}^T \mathbf{v}_{M_1} + \frac{1}{2}M_2 \mathbf{v}_{M_2}{}^T \mathbf{v}_{M_2} + \frac{1}{2}\left(I_1 + I_2\right)\dot{\theta}^2$$

$$= \frac{1}{2}\left(M_1 + M_2\right)\dot{d}_y{}^2 + \frac{1}{2}\left(I_1 + I_2 + M_2 d_x^2 + M_2(w+v)^2\right)\dot{\theta}^2$$

$$+\frac{1}{2}M_2\dot{d}_x^2+\dot{d}_y\dot{\theta}M_2\left[(w+v)\sin\theta+d_x\cos\theta\right]$$

$$+\dot{d}_y\dot{d}_xM_2\sin\theta+\dot{\theta}\dot{d}_xM_2(w+v) \tag{9}$$

which can be further written as

$$K=\frac{1}{2}\dot{\mathbf{X}}^T\mathbf{D}\dot{\mathbf{X}} \tag{10}$$

where $\mathbf{X}=\begin{bmatrix}d_y & \theta & d_x\end{bmatrix}^T$ and $\mathbf{D}$ is the inertia matrix given by

$$\mathbf{D}=\begin{bmatrix} M_1+M_2 & M_2(w+v)\sin\theta+M_2d_x\cos\theta & M_2\sin\theta \\ I_1+I_2+M_2d_x^2+M_2(w+v)^2 & M_2(w+v) & \\ M_2(w+v) & M_2 & \end{bmatrix} \tag{11}$$

The government equation of the gantry mechanism can be derived from the Lagrange equation

$$\frac{d}{dt}\left[\frac{\partial L}{\partial\dot{\mathbf{X}}}\right]-\frac{\partial L}{\partial\mathbf{X}}=\mathbf{F}+\mathbf{U} \tag{12}$$

where $L=K-V$, in which K is the summation of kinetic energy, V is potential energy and $\mathbf{U}$ is the driven force provided by motor and $\mathbf{F}$ is the friction force. Next, derive the elements of the Coriolis and centrifugal matrix $\mathbf{C}$ from

$$C_{ij}=\sum_{k=1}^{3}\left(c_{ijk}\dot{q}_k\right) \tag{13}$$

where d_{ij} represents the element in the i th row and j th column of the inertia matrix $\mathbf{D}$. Substituting the inertia equations I_1 and I_2 into (11) and computing (13), the matrix $\mathbf{C}$ can be obtained as

$$\mathbf{C}=M_2\begin{bmatrix} 0 & -d_x\dot{\theta}\sin\theta+d\dot{\theta}\cos\theta+\dot{d}_x\cos\theta & \dot{\theta}\cos\theta \\ \left(-d_x\sin\theta+d\cos\theta\right)\dot{d}_y+2d_x\dot{d}_x & 2d_x\dot{\theta}+\dot{d}_y\cos\theta & \\ 2d_x\dot{\theta}+\dot{d}_y\cos\theta & 0 & \end{bmatrix} \tag{14}$$

Finally, the dynamic model of the gantry position stage can be represtented as

$$\mathbf{D}\ddot{\mathbf{X}}+\mathbf{C}\dot{\mathbf{X}}=\mathbf{E}(\mathbf{U}-\mathbf{F}) \tag{15}$$

where

$$\mathbf{E}=\begin{bmatrix} 1 & 1 & 0 \\ l\cos\theta & -l\cos\theta & 0 \\ 0 & 0 & 1 \end{bmatrix} \tag{16}$$

$$\mathbf{F}=\begin{bmatrix}F_{y1}, & F_{y2}, & F_x\end{bmatrix}^T \tag{17}$$

$$\mathbf{U}=\begin{bmatrix}u_{y1}, & u_{y2}, & u_x\end{bmatrix}^T \tag{18}$$

F_{y1}, F_{y2} and F_x are the frictional forces, and u_{y1}, u_{y2} and u_x are the generated mechanical forces along d_{y1}, d_{y2} and d_x respectively. The frictional forces are described as LuGre Model

$$\frac{dz}{dt}=v-\sigma_0\frac{|v|}{g(v)}z \tag{19}$$

$$F_i=\sigma_0z+\sigma_1\frac{dz}{dt},\quad i=y1,y2,x \tag{20}$$

The LuGre model proposed by C. Canudas de Wit [15], can capture most of the known frictional behaviors and is suitable for control systems. Here z is the average bending displacement of virtual bristles between the interface of two bodies, $g(v)$ is a positive function of velocity, and where σ_0 and σ_1 are the stiffness and damping coefficients of average behavior of bristles.

III. T-S FUZZY MODEL BASED CONTROLLER DESIGN

In this study, a controller based on the T-S fuzzy model, used to enhance the approximate ability of nonlinear system, is proposed to control the gantry position stage. Further rewrite the state equation (15) as

$$\ddot{\mathbf{X}}(t)=\mathbf{A}\dot{\mathbf{X}}(t)+\mathbf{B}\mathbf{U}(t) \tag{21}$$

where $\mathbf{A}=-\mathbf{D}^{-1}\mathbf{C}$ and $\mathbf{B}=\mathbf{D}^{-1}\mathbf{E}$. We propose a novel control scheme based on the T-S fuzzy model, as shown in Fig. 2, to simultaneously achieve two control objectives: 1) position and velocity control of the gantry and slider, and 2) minimization of the synchronous position and velocity errors.

According to T-S fuzzy modeling method, the following equation can be obtained

$$\ddot{\mathbf{X}}(t)=\sum_{i=1}^{2}\sum_{j=1}^{2}\sum_{k=1}^{2}h_iw_jp_k(z(t))(\mathbf{A}_{ijk}\dot{\mathbf{X}}(t)+\mathbf{B}_{ijk}\mathbf{U}(t)) \tag{22}$$

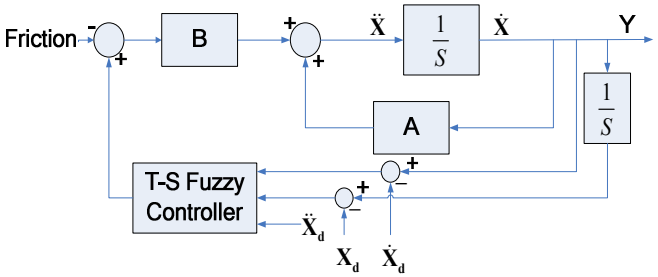

Figure 2. T-S fuzzy model based control scheme.

where $h_i w_j p_k(z(t)) = h_i(z(t)) w_j(z(t)) p_k(z(t))$. Two fuzzy rules of $\dot{d}_y(t)$, $\dot{\theta}(t)$ and $\dot{d}_x(t)$ are adopted in this study. The boundary of $\dot{d}_y(t)$ and $\dot{d}_x(t)$ are chosen as the maximum speed of servo motor which is about $\pm 0.5 m/s$, and the boundary of $\dot{\theta}(t)$ is chosen as $\pm 0.1 rad/s$, shown in Table. I and Fig. 3.

A. T-S fuzzy model based controller design

In general, the velocity tracking controller can be designed based on a T-S fuzzy model. That implies the objective is required to satisfy $[\dot{\mathbf{X}}(t) - \dot{\mathbf{X}}_\mathbf{d}(t)] \to 0$ as $t \to \infty$, where $\dot{\mathbf{X}}(t) = \begin{bmatrix} \dot{d}_y & \dot{\theta} & \dot{d}_x \end{bmatrix}^T$ and $\dot{\mathbf{X}}_\mathbf{d}(t)$ represent the velocity response and desired velocity command, respectively. Hence, the acceleration tracking error can be derived as

$$\begin{aligned}
\ddot{\tilde{\mathbf{X}}}(t) &= \ddot{\mathbf{X}}(t) - \ddot{\mathbf{X}}_\mathbf{d}(t) \\
&= \sum_{i=1}^{2}\sum_{j=1}^{2}\sum_{k=1}^{2} h_i w_j p_k(z(t))(\mathbf{A}_{ijk}\dot{\mathbf{X}}(t) + \mathbf{B}_{ijk}\mathbf{U}(t)) - \ddot{\mathbf{X}}_d(t) \\
&= \sum_{i=1}^{2}\sum_{j=1}^{2}\sum_{k=1}^{2} h_i w_j p_k(z(t))\mathbf{A}_{ijk}\dot{\mathbf{X}}(t) \\
&\quad - \sum_{i=1}^{2}\sum_{j=1}^{2}\sum_{k=1}^{2} h_i w_j p_k(z(t))\mathbf{A}_{ijk}\dot{\mathbf{X}}_\mathbf{d}(t) \\
&\quad + \sum_{i=1}^{2}\sum_{j=1}^{2}\sum_{k=1}^{2} h_i w_j p_k(z(t))\mathbf{B}_{ijk}\mathbf{U}(t) \\
&\quad + \sum_{i=1}^{2}\sum_{j=1}^{2}\sum_{k=1}^{2} h_i w_j p_k(z(t))\mathbf{A}_{ijk}\dot{\mathbf{X}}_\mathbf{d}(t) - \ddot{\mathbf{X}}_\mathbf{d}(t)
\end{aligned} \tag{23}$$

Furthermore, we design a reference control effort $\boldsymbol{\tau}(t)$ and it must be satisfied

$$\sum_{i=1}^{2}\sum_{j=1}^{2}\sum_{k=1}^{2} h_i w_j p_k(z(t))\mathbf{B}_{ijk}\boldsymbol{\tau}(t)$$

$$= \sum_{i=1}^{2}\sum_{j=1}^{2}\sum_{k=1}^{2} h_i w_j p_k(z(t))\mathbf{B}_{ijk}\mathbf{U}(t)$$

$$+ \sum_{i=1}^{2}\sum_{j=1}^{2}\sum_{k=1}^{2} h_i w_j p_k(z(t))\mathbf{A}_{ijk}\dot{\mathbf{X}}_\mathbf{d}(t) - \ddot{\mathbf{X}}_\mathbf{d}(t) \tag{24}$$

Substituting (24) into (23), the following equation can be obtained

$$\ddot{\tilde{\mathbf{X}}}(t) = \sum_{i=1}^{2}\sum_{j=1}^{2}\sum_{k=1}^{2} h_i w_j p_k(z(t))\mathbf{A}_{ijk}\dot{\tilde{\mathbf{X}}}(t)$$

$$+ \sum_{i=1}^{2}\sum_{j=1}^{2}\sum_{k=1}^{2} h_i w_j p_k(z(t))\mathbf{B}_{ijk}\boldsymbol{\tau}(t) \tag{25}$$

According to each rule of $h_i(z(t))$, $w_j(z(t))$ and $p_k(z(t))$, the new controller is designed as

$$\boldsymbol{\tau}(t) = -\mathbf{k}_{ijk}\dot{\tilde{\mathbf{X}}}(t) \tag{26}$$

Substituting (26) into (25), the closed loop form can be rewritten as

$$\ddot{\tilde{\mathbf{X}}}(t) = \sum_{i=1}^{2}\sum_{l=1}^{2}\sum_{j=1}^{2}\sum_{m=1}^{2}\sum_{k=1}^{2}\sum_{n=1}^{2} h_i w_j p_k(z(t)) h_l w_m p_n(z(t))(\mathbf{A}_{ijk} - \mathbf{B}_{ijk}\mathbf{k}_{lmn})\dot{\tilde{\mathbf{X}}}(t) \tag{27}$$

Let

$$\alpha(t) = \sum_{i=1}^{2}\sum_{j=1}^{2}\sum_{k=1}^{2} h_i w_j p_k(z(t))\mathbf{A}_{ijk}$$

$$\beta(t) = \sum_{i=1}^{2}\sum_{j=1}^{2}\sum_{k=1}^{2} h_i w_j p_k(z(t))\mathbf{B}_{ijk}$$

The relationship between actual and reference control efforts can be obtained from (24) as

$$\beta(t)(\mathbf{U}(t) - \boldsymbol{\tau}(t)) = -\alpha(t)\dot{\mathbf{X}}_\mathbf{d}(t) + \ddot{\mathbf{X}}_\mathbf{d}(t) \tag{28}$$

Then, substituting (28) into (25), the control effort $\mathbf{U}(t)$ in the controller can be obtained as

$$\mathbf{U}(t) = -\sum_{i=1}^{2}\sum_{j=1}^{2}\sum_{k=1}^{2} h_i w_j p_k(z(t))\mathbf{k}_{ijk}\dot{\tilde{\mathbf{X}}}(t)$$

$$+ \beta^{-1}(t)(\ddot{\mathbf{X}}_\mathbf{d}(t) - \alpha(t)\dot{\mathbf{X}}_\mathbf{d}(t)) \tag{29}$$

TABLE I. FUZZY IF-THEN RULE

Rule		If	Then
$\dot{d}_y(t)$	$i=1$	$\dot{d}_y(t) \approx 0.5$	$h_1(z(t))=1, h_2(z(t))=0$
	$i=2$	$\dot{d}_y(t) \approx -0.5$	$h_1(z(t))=0, h_2(z(t))=1$
$\dot{\theta}(t)$	$j=1$	$\dot{\theta}(t) \approx 0.1$	$w_1(z(t))=1, w_2(z(t))=0$
	$j=2$	$\dot{\theta}(t) \approx -0.1$	$w_1(z(t))=0, w_2(z(t))=1$
$\dot{d}_x(t)$	$k=1$	$\dot{d}_x(t) \approx 0.5$	$p_1(z(t))=1, p_2(z(t))=0$
	$k=2$	$\dot{d}_x(t) \approx -0.5$	$p_1(z(t))=0, p_2(z(t))=1$

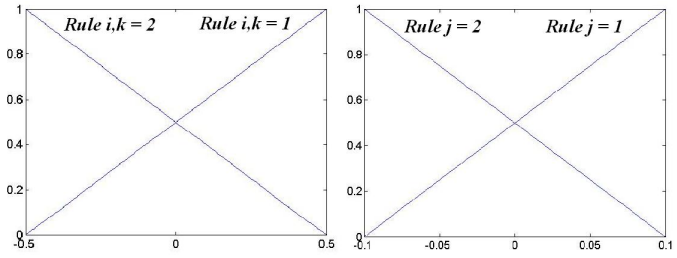

Figure 3. Membership function of rule i, j, k

B. T-S fuzzy model based controller with internal transformation

In the previous section, the controller is designed for velocity error, but real applications always demand high-precision position control. To design a new control gain of position error, first divide $\mathbf{k}_{ijk}$ into $\mathbf{k}_{ijk}^1$ and $\mathbf{k}_{ijk}^2$ as

$$\mathbf{k}_{ijk} = \mathbf{k}_{ijk}^1 + \mathbf{k}_{ijk}^2 \tag{30}$$

To obtain the information of $\tilde{\mathbf{X}}(t)$, design a new feedback controller $\mathbf{U}_{ijk}^2(t)$ to satisfy

$$\dot{\tilde{\mathbf{X}}}(t) = \mathbf{k}_{ijk}^{2\,-1}(\tilde{\mathbf{X}}(t) + \mathbf{U}_{ijk}^2(t)) \tag{31}$$

where $\mathbf{U}_{ijk}^2(t)$ is designed as (32), and the closed loop form can be obtained as (33)

$$\mathbf{U}_{ijk}^2(t) = -\mathbf{h}_{ijk}\tilde{\mathbf{X}}(t) \tag{32}$$

$$\dot{\tilde{\mathbf{X}}}(t) = \mathbf{k}_{ijk}^{2\,-1}(\mathbf{I} - \mathbf{h}_{ijk})\tilde{\mathbf{X}}(t) \tag{33}$$

Substituting (33) into (29), $\mathbf{U}(t)$ can be rewritten as

$$\mathbf{U}(t) = -\sum_{i=1}^{2}\sum_{j=1}^{2}\sum_{k=1}^{2} h_i w_j p_k(z(t))(\mathbf{k}_{ijk}^1 \dot{\tilde{\mathbf{X}}}(t) + (\mathbf{I} - \mathbf{h}_{ijk})\tilde{\mathbf{X}}(t))$$

$$+\beta^{-1}(t)(\ddot{\mathbf{X}}_{\mathbf{d}}(t) - \alpha(t)\dot{\mathbf{X}}_{\mathbf{d}}(t)) \tag{34}$$

The T-S fuzzy model based controller with our proposed internal transformation is shown in Fig. 4.

C. Lyapunov stability analysis

The augmented matrix of velocity and position tracking errors is given by

$$\mathbf{\Phi}^T(t) = [\dot{\tilde{\mathbf{X}}}^T(t) \quad \tilde{\mathbf{X}}^T(t)]^T \tag{35}$$

After internal transformation, the following equation will be satisfied.

$$\dot{\mathbf{\Phi}}(t) = \boldsymbol{\gamma}\mathbf{\Phi}(t) \tag{36}$$

where

$$\boldsymbol{\gamma} = \begin{bmatrix} \alpha(t) - \beta(t)\mathbf{k}_{ijk} & 0 \\ 0 & \sum_{i=1}^{2}\sum_{j=1}^{2}\sum_{k=1}^{2} h_i w_j p_k(z(t))(\mathbf{k}_{ijk}^{2\,-1}(\mathbf{I} - \mathbf{h}_{ijk})) \end{bmatrix} \tag{37}$$

The Lyapunov function can be represented as $V(\mathbf{\Phi}(t)) = \mathbf{\Phi}^T(t)\mathbf{P}\mathbf{\Phi}(t)$, where $\mathbf{P}$ is chosen a positive matrix, and the differential of the Lyapunov function can be represented as

$$\dot{V}(\mathbf{\Phi}(t)) = \dot{\mathbf{\Phi}}^T(t)\mathbf{P}\mathbf{\Phi}(t) + \mathbf{\Phi}^T(t)\mathbf{P}\dot{\mathbf{\Phi}}(t)$$

$$= \mathbf{\Phi}^T(t)\boldsymbol{\gamma}^T\mathbf{P}\mathbf{\Phi}(t) + \mathbf{\Phi}^T(t)\mathbf{P}\boldsymbol{\gamma}\mathbf{\Phi}(t)$$

$$= \mathbf{\Phi}^T(t)(\boldsymbol{\gamma}^T\mathbf{P} + \mathbf{P}\boldsymbol{\gamma})\mathbf{\Phi}(t) \tag{38}$$

From (37), $\mathbf{A} - \mathbf{B}\mathbf{k}_{ijk}$ and $\mathbf{k}_{ijk}^{2\,-1}(\mathbf{I} - \mathbf{h}_{ijk})$ can be separately designed by the separation theorem. In addition, the choice of $\mathbf{k}_{ijk}^2$ must guarantee that $\mathbf{k}_{ijk}^{2\,-1}$ exists. Then we can obtain positive definite matrix $\mathbf{P_1}, \mathbf{P_2}$ and feedback gains $\mathbf{k}_{ijk}, \mathbf{h}_{ijk}$ by using iteration method to solve linear matrix inequalities (LMIs). Therefore, the condition of $\dot{V}(\mathbf{\Phi}(t)) < 0$ can be obtained because $\boldsymbol{\gamma}$ is negative definite, which implies the system will be asymptotic stable.

IV. SIMULATION AND EXPERIMENTAL RESULTS

A. Simulation Results

To verify the effectiveness of the proposed T-S fuzzy model based controller, the PID control which using three PID controllers for each independent axis is proposed in this study to compare the control performance. For the PID controller, time-domain tuning design is used to find the parameters, and MATLAB simulation is used for two cases. The measurement parameters of gantry system are selected as follows: M_1 =2.88kg, M_2 =0.5kg, l =0.5m, w =0.0285m, and the LuGre friction parameters are $\sigma_0 = 230.087$,

$\sigma_1 = 35.835$, $F_c = 0.72$, $F_s = 2.15$, $v_s = 0.005$. The high speed sine command (position, velocity) is depicted in Fig. 5.

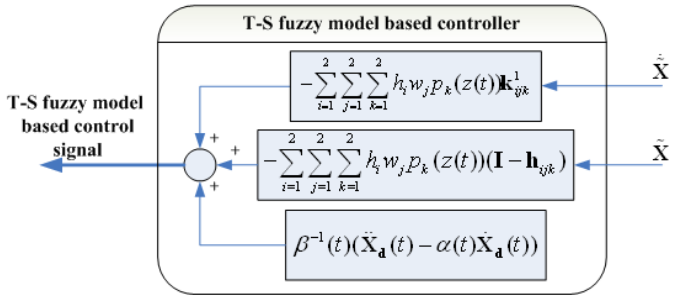

Figure 4. T-S fuzzy model based controller with control internal transformation.

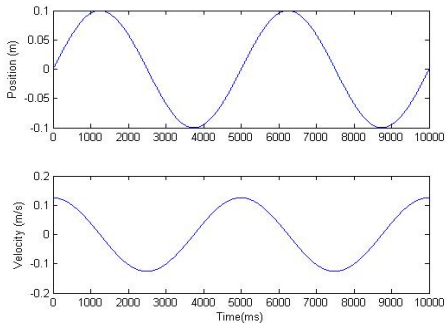

Figure 5. Desired high speed sine command.

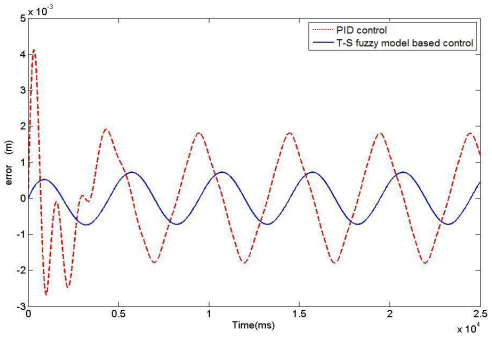

Figure 6. Tracking error of d_y (m).

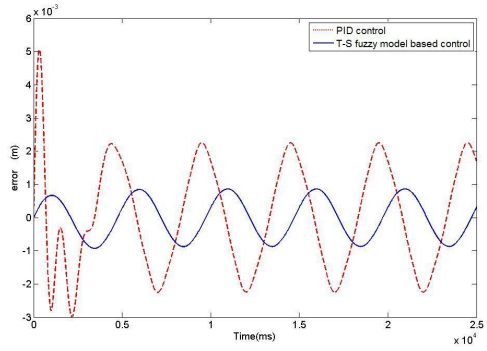

Figure 7. Tracking error of d_x (m).

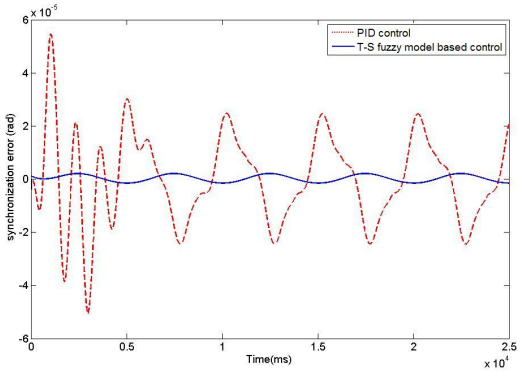

Figure 8. Synchronized error (rad).

TABLE II. SIMULATION RESULTS

Performance index \ Control system		PID control	T-S fuzzy model based control
Tracking error of d_y (m)	*Max*	0.0041	0.000742
	IAE	27.4033	11.1556
Tracking error of d_x (m)	*Max*	0.0051	0.000929
	IAE	35.3768	13.5032
synchronized error (rad)	*Max*	5.47×10^{-5}	3.79×10^{-6}
	IAE	0.3389	0.0282

The simulation results showing the error responses of d_y , d_x are depicted in Fig. 6 and Fig. 7, while the synchronized error(θ) is shown in Fig. 8. The high speed sine command initially rises fast, usually bringing with it a large error. From Fig. 6 and Fig. 7, the T-S fuzzy model based control outperforms the PID control, especially at the beginning. So when the velocity changes quickly, the proposed approach quickly yields significantly improved performance over PID control.

Fig. 8 shows that the proposed control algorithm provides cross-coupled control signal from state θ , which can dramatically reduce the synchronized error, better than PID independence control. Furthermore, the E_{Max} and E_{IAE} from the Table. II illustrate that the proposed control algorithm can minimize the tracking error and synchronized error.

B. Experimental Results

The block diagram of the DSP-based computer-controlled gantry position stage is shown in Fig. 9. A TMS320VC33 floating-point DSP is the core of the control computer. In addition, the control computer includes multi-channels of analog-to-digital converters (ADCs), digital-to-analog converters (DACs), parallel input/output (PIO) and encoder interface. The resolution of the linear scales for the PMLSM is $1\mu m$. Furthermore, the proposed control algorithms are

realized in the DSP using the "C" and "Assembly" languages. All the programs are developed under a Windows environment in a PC and then downloaded to the Flash ROM of the DSP.

The methodology proposed for the implementation of the real-time T-S fuzzy model based control system consists of a main program and one interrupt service routine (ISR). In the main program, parameters and input/output initialization are set first. Next, the interrupt interval for the ISR is set. After enabling the interrupt, the ISR with 1ms sampling rate is used for the encoder interface and DACs. The ISR first reads the positions of the three PMLSMs of the gantry position stage from the encoders and the velocities of the three PMLSMs of the gantry position stage are derived from the positions. Then the ISR calculates the tracking errors and generates the control Efforts $\mathbf{U}(t)$, according to the proposed control algorithms. Finally, the calculated commands are sent to the x-axis, $y1$-axis and $y2$-axis motor servo drives via three DACs. Photos of the experimental setup, including the gantry position stage, PMLSM drives and DSP-based control computer are shown in Fig. 10. Moreover, the field-oriented control mechanism is implemented in the PMLSM drives.

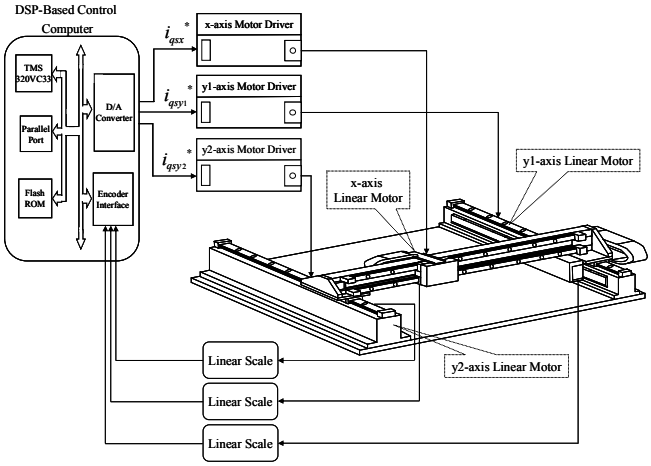

Figure 9. DSP-based computer-controlled gantry stage.

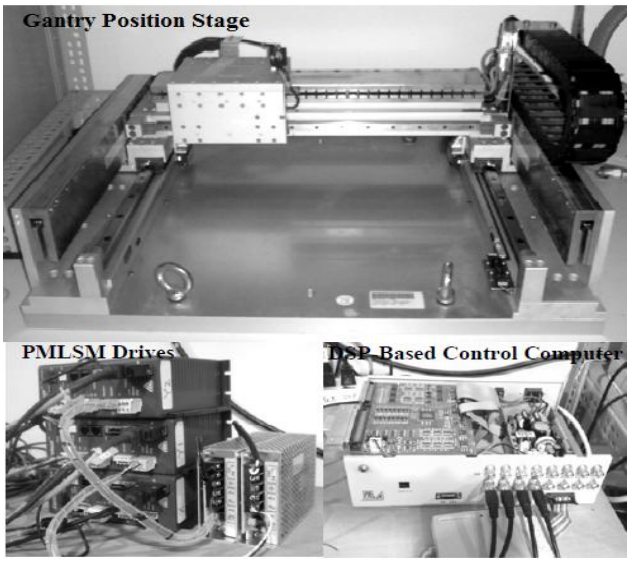

Figure 10. Experimental setup.

For PID-controlled implementation, where system identification is necessary, the closed velocity loop was excited by 1 volt step input as a test input and its output was recorded with a data acquisition system. From the experimental data, the approximate model parameters were obtained assuming the first order approximation as follows

$$G_i(s) = \frac{K_i}{\tau_i s + 1} (i = d_{y_1}, d_{y_2}, d_x) \tag{39}$$

The system Identification Toolbox in MATLAB can solve the parameters in (39), obtaining three transfer functions. Based on time-domain tuning design, the independent PID controllers are tuned as $K_{Py1} = 36.724$, $K_{Py2} = 35.883$, $K_{Px} = 33.671$, $K_{Iy1} = 1.386$, $K_{Iy2} = 1.353$, $K_{Ix} = 1$, $K_{Dy1} = 0.173$, $K_{Dy2} = 0.169$, $K_{Dx} = 0.125$.

Trajectory commands of the software simulation are used and the results are shown in Figs. 11–13. Fig. 11 and Fig. 12 are similar to the software simulations results, in steady state, performance of the T-S fuzzy model based controller is nearly the same as the PID controller, but it can effectively reduce the tracking error when the velocity is changing quickly. The E_{Max} and E_{IAE} from Table. III show that the T-S fuzzy model based controller is effective than the PID controller, especially in E_{Max}. In addition, Fig. 13 shows that the T-S fuzzy model based controller is able to minimize the synchronized error, whereas the PID controllers were only able to track individual trajectories independently. Table. III also shows the E_{Max} and E_{IAE} of synchronized error are reduced to 42.7% and 81.6 % respectively when using T-S fuzzy model based control.

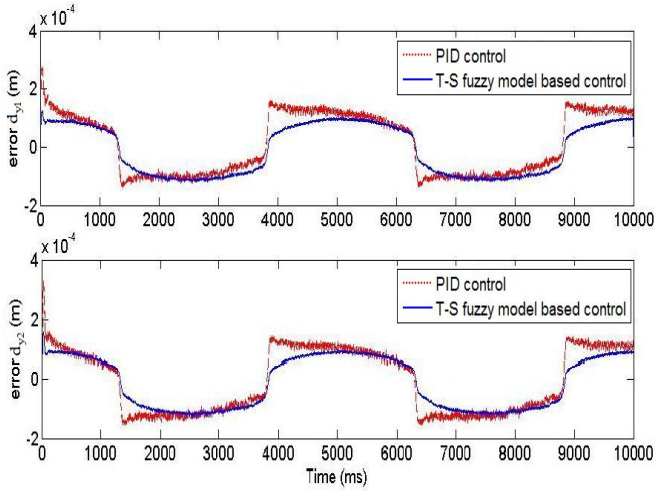

Figure 11. Tracking error of d_{y_1} , d_{y_2} respectively (m).

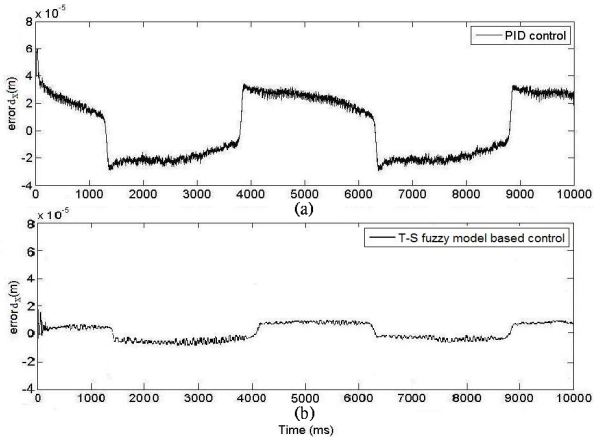

Figure 12. Tracking error of d_X using (a) PID control and (b)T-S fuzzy model based control.

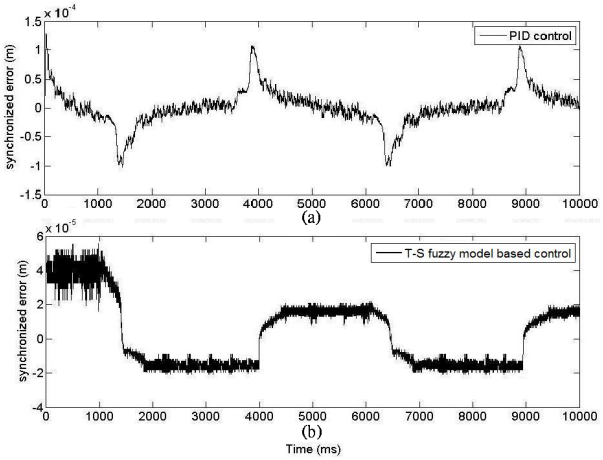

Figure 13. Synchronized error (m). Using (a) PID control, (b)T-S fuzzy model based control.

TABLE III. EXPERIMENTAL RESULTS

Performance index \ Control system		PID control	T-S fuzzy model based control
Tracking error of d_y (m)	***Max***	0.000269	0.000178
	IAE	1.1577	0.91583
Tracking error of d_x (m)	***Max***	5.94×10^{-5}	1.88×10^{-5}
	IAE	0.23153	0.12323
synchronized error (m)	***Max***	1.293×10^{-4}	5.525×10^{-5}
	IAE	0.21389	0.17366

V. CONCLUTION

In this paper, we propose a T-S fuzzy model based controller for a gantry stage. Utilizing the Lagrangian equation, all states can be formulated as a state equation. Then a novel T-S fuzzy model based control scheme is proposed to achieve two control objectives together: 1) position and velocity control of the gantry and slider, and 2) minimization of the synchronous position and velocity errors. The simulation and experimental results show that this control system can dramatically decrease both the tracking error and synchronized error.

References

[1] Y. Koren, "Cross-coupled biaxial computer control for manufacturing systems," Journal of Dynamic Systems, Measurement and Control, vol. 102, no. 4, pp. 265-272, December 1980.

[2] Y. Koren and C. C. Lo, "Variable-gain cross-coupling controller for contouring," CIRP Annals-Manufacturing Techology, vol. 40, no. 1, pp. 371-374, January 1991.

[3] P. K. Kulkarni and K. Srinivasan, "Optimal contouring control of multi-axial feed drive servomechanisms," Journal of Engineering for Industry, vol. 111, no. 2, pp. 140-148, 1989.

[4] K. Srinivasan and P. K. Kulkarni, "Cross-coupled control of biaxial feed drive servomechanisms," Journal of Dynamic Systems, Measurement and Control, vol. 112, no. 2, pp. 225-232, June 1990.

[5] Dongmei Yu, Qingding Guo, Qing Hu and Jiang Lili, "Position synchronized control of dual linear motors servo system using fuzzy logic," IEEE Intelligent Control and Automation, pp. 8041-8044, October 2006.

[6] C. S. Teo, K. K. Tan, S. Y. Lim, S. Huang and E. B. Tay, "Dynamic modeling and adaptive control of a H-type gantry stage," Mechatronics, vol. 17, no. 7, pp. 361–367, April 2007.

[7] C. S. Teo, K. K. Tan and S. Y. Lim, "Dynamic geometric compensation for gantry stage using iterative learning control," IEEE Transactions on Instrumentation and Measurement, vol. 57, no. 2, pp. 413-419, January 2008.

[8] S. Labiod and T. M. Guerra, "Adaptive fuzzy control of a class of SISO nonaffine nonlinear systems," Fuzzy Sets and Systems, vol. 158, no. 10, pp. 1126–1137, May 2007.

[9] G. Feng, "A survey on analysis and design of model-based fuzzy control systems," IEEE Transactions on Fuzzy Systems, vol. 14, no. 5, pp. 676–697, October 2006.

[10] K. Tanaka and H. O. Wang, Fuzzy Control Systems Design and Analysis: A Linear Matrix Inequality Approach., New York: Wiley, 2001.

[11] H. O. Wang, K. Tanaka, and M. Griffin, "An approach to fuzzy control of nonlinear systems: stability and design issues," IEEE Transactions on Fuzzy Systems, vol. 4, no. 1, pp. 14–23, February 1996.

[12] K. Y. Lian, and J. J. Liou, "Output tracking control for fuzzy systems via output feedback design," IEEE Transactions on Fuzzy Systems, vol. 14, no. 5, pp. 628-639, October 2006.

[13] T. H. S. Li, S. H. Tsai, and M. Y. Hsiao, "Robust H_∞ fuzzy control for a class of time-delay fuzzy bilinear systems with an additive disturbance," International Journal of Nonlinear Sciences and Numerical Simulation, vol. 10, no. 3, pp. 313-321, March 2009.

[14] S. H. Tsai, "Robust H_∞ control for Van de Vusse Reactor via T-S fuzzy bilinear scheme," Expert Systems with Applications, vol. 38, no. 5, pp. 4935-4944, May 2011.

[15] C. Canudas de Wit, H. Olsson, K. J. Astrom and P. Lischinsky, "A new model for control systems with friction," IEEE Transactions on Automatic Control, vol. 40, no. 3, pp. 419–425, March 1995.

2011 IEEE International Conference on Fuzzy Systems
June 27-30, 2011, Taipei, Taiwan

Observer-Based Adaptive FNN Control of Robot Manipulators: PSO-SA Self Adjust Membership Approach

Kai-Shiuan, Shih
Department of Electrical Engineering
National Cheng Kung University
Tainan, Taiwan 701, R.O.C.
N2894115@ccmail.ncku.edu.tw

Tzuu-Hseng S., Li
Department of Electrical Engineering
National Cheng Kung University
Tainan, Taiwan 701, R.O.C.
thsli@mail.ncku.edu.tw

Shun-Hung, Tsai
Graduate Institute of Automation Technology
National Taipei University of Technology
Taipei, Taiwan, R.O.C.
shtsai@ntut.edu.tw

***Abstract*—In this paper, a novel observer-based adaptive fuzzy-neural network (FNN) control scheme for robotic systems is proposed for tracking performance and to suppress the effects caused by uncertainties, and disturbances. A PSO-SA based adaptive FNN system is used to approximate an unknown system from the manipulation of the model following tracking errors. The proposed scheme uses an observer, which allows for identifying the state of an unknown state in the system, simultaneously. It is shown that the proposed control scheme can guarantee the better tracking performance and suppress internal uncertainties or external disturbance. Simulations are given to show the validity and confirm the performance of the proposed scheme.**

Keywords- *FNN, Robust, PSO-SA, MIMO*

I. INTRODUCTION

Recently, adaptive fuzzy control methods have been proposed to deal with nonlinear systems [1-5]. Based on the universal approximation theorem [1], adaptive fuzzy control schemes have been developed for a class of nonlinear uncertain systems [2]. In above schemes, the stability of the closed-loop system is established according to Lyapunov's theory. In order to process approximation errors and external disturbances, these adaptive fuzzy controllers are added by a robust compensator. However, in such schemes are based on the assumption that the states of the systems are measured directly.

Hence, the design of the observer for an uncertain nonlinear system is a very important issue. Direct and indirect adaptive fuzzy control schemes have been developed based on state or error observers [6-9]. In [8,10], the authors developed indirect and direct adaptive fuzzy controllers based on an observer for a class of single-input single-output (SISO) and multi-input multi-output (MIMO) nonlinear systems, respectively. In above schemes, the adaptive fuzzy control scheme can ensure the stability of the closed-loop system and achieve a prescribed tracking performance. However, most of adaptive fuzzy control scheme are usually operated based on human knowledge. Thus, they pose additional difficulties to the stabilization control design and, especially, the tracking control design. In order to overcome shortcomings in the design of a controller, various methods have been developed in the last decades. In this, a successful scheme is fuzzy logic control with tuning capability in neural weights. Recently, adaptive FNN control has attracted increasing attention, essentially because it can provide a powerful learning technique for complex unknown plants to perform complex tasks in highly nonlinear dynamical environments. Furthermore, it can make available information from repetitive adjustment of the system with better performance than those of adaptive fuzzy schemes with constant rules [11,12]. However, mathematical expressions of FNN must be derived for each network layer of a network topology, and it is very difficult to find the optimum solution. In order to overcome these drawbacks, the particle swarm optimization (PSO) based method is proposed.

Particle swarm optimization (PSO) is a relatively novel evolutionary algorithm that may be used to find optimal or near optimal solutions in multi-dimensional search spaces [13]. However, for the basic PSO algorithm, all particles are prone to be trapped in the local minimum of the later phase of convergence. The optimal value found is thus often a local minimum instead of a global minimum. To overcome the shortcomings of the basic PSO algorithm, we use a method which combines the PSO algorithm (PSO) with the simulated annealing (SA) algorithm.

The rest of this paper is organized as follows. In Section 2, the system description and the design of the FNN system are presented. The adaptive FNN controller based on PSO-SA and combined with observer is described in Section 3. Numerical simulations are given and the results show that the designed observers and controllers are feasible and valid in Section 4. Finally, conclusions are given in Section 5.

978-1-4244-7316-8/11/$26.00 ©2011 IEEE

II. Problem Statement and Preliminaries

Consider the dynamical equation of an n -link robotic manipulator with external disturbances .The class of uncertain nonlinear systems to be studied in this paper is described by the following set of time-varying differential equations:

$$\mathbf{M}(q)\ddot{q} + c(q,\dot{q}) + g(q) + \tau_d(q,\dot{q}) + \tau_c(q,\dot{q}) = u\,, \qquad (1)$$

where $\mathbf{M}(q) \in \mathbf{R}^{n\times n}$ is the bounded positive definite inertia matrix; $c(q,\dot{q}) \in \boldsymbol{R}^n$ is the vector expressing centrifugal and Coriolis effects; $g(q)$ is the vector representing gravitational torques; $\tau_c(q,\dot{q}) \in R^n$, $\tau_d(q,\dot{q}) \in R^n$ are the vectors which represent the dynamic effects as nonlinear frictions, and bounded torque disturbances.

$u \in R^n$ is the vector of joint torques; $q \in R^n$ the vector of joint positions; $\dot{q} \in R^n$ the vector of joint velocities; and $\ddot{q} \in R^n$ is the vector of joint accelerations. Here $\boldsymbol{x} = [x_1, \cdots, x_n]^T \in R^n$, is the state vector which is assumed to be unavailable for measurement, the robot model (1) can be rewritten as:

$$\dot{x} = Ax + B\left[F(q,\dot{q}) + G(q)u + \Delta d(q,\dot{q})\right]\,, \qquad (2)$$

where

$F(q,\dot{q}) = \left[f_1(q,\dot{q}), \cdots, f_n(q,\dot{q})\right]^T$, $G(q) = \left[G_1(q), \cdots, G_n(q)\right]$, $G_i(q) = \left[g_{1i}(q), \cdots, g_{ni}(q)\right]^T$, $A = diag\left[A_1, \cdots, A_n\right]$, $B = diag\left[B_1, \cdots, B_n\right]$, $\Delta d(q,\dot{q}) = \left[\Delta d_1(q,\dot{q}), \cdots, \Delta d_n(q,\dot{q})\right]^T$.

The following assumption is made for the controller design:

Assumption 2.1. [14] The matrix $G(q)$, as previously defined, is nonsingular, i.e., $G^{-1}(q)$ exists, and bounded for all $q \in U$, where $U \in R^n$ is a compact set.

Based on Assumption 2.1, if $F(q,\dot{q})$ and $G(q)$ are exact known, with $G^{-1}(q) \neq 0$ and based on the equivalent approach, then the control law can be represented as belows:

$$u = G^{-1}(q)[-F(q,\dot{q}) + y_d^{(n)} - K_c e(t) + u_a(t)]\,, \qquad (3)$$

where K_c is a control gain vector and u_a is designed for compensating the approximation errors and the eliminate disturbance.

Control Objectives:

The tracking control problem can be stated as: for given bounded reference trajectories, the control input torques such as the robot's states follow the reference trajectories, with all involved signals in the closed loop remaining bounded.

Let $y_{1d}, \cdots, y_{nd}$ be the given bounded desired output signal that contains finite derivatives up to the n th order. The tracking errors of the system are found at:

$$\begin{aligned}\dot{e}_{in_i}(t) &= y_i^{(n_i)}(t) - y_{id}^{(n_i)}(t) \\ &= f_i(q,\dot{q}) + \sum_{j=1}^{n} g_{ij}(q)u_j - y_{id}^{(n)}(t) + \Delta d_i(q,\dot{q})\,, \end{aligned} \qquad (4)$$

where $i = 1, \cdots, n$. After some simple manipulations, we can obtain the error equation:

$$\dot{e}(t) = Ae(t) + B\left[F(q,\dot{q}) + G(q)u - y_d^{(n)}(t) + \Delta D(q,\dot{q})\right], \quad (5)$$

where $e = \left[e_1, \cdots, e_p\right]^T$, $\Delta D = \left[\Delta d_1, \cdots, \Delta d_n\right]^T$.

A. Fuzzy-neural network structure

The fuzzy rule base consists of a collection of fuzzy IF-THEN rules:

$R^{(l)}$: If x_1 is F_1^l and x_2 is F_2^l ... and x_n is F_n^l , $l = 1, 2, ..., n$.

then y_s is G_s^l , $s = 1, 2, ..., p$, (6)

where $x = \left[x_1, \cdots, x_n\right]^T$ is the fuzzy system input; y is the fuzzy system output; and F_n^l and G_s^l are fuzzy sets. The output of the fuzzy logic system can then be expressed as:

$$y_s = \theta_s^T \xi(x)\,, \; s = 1, \cdots, p\,, \qquad (7)$$

where $\theta_s^T = \left[\theta_s^1, \cdots, \theta_s^N\right]$, with each variable θ_s^l being the point at which the fuzzy membership function of G_s^l achieves the maximum value; and $\xi(x) = \left[\xi_1(x), \cdots, \xi_n(x)\right]^T$ with each variable ξ_l being the fuzzy basis function defined as:

$$\xi_l(x) = \prod_{i=1}^{n} \mu_{F_i^l}(x_i) \Big/ \sum_{l=1}^{N} \left(\prod_{i=1}^{n} \mu_{F_i^l}(x_i)\right), \qquad (8)$$

where $\mu_{F_i^l}(x_i)$ is the membership function of the fuzzy set.

The inputs are then fed into the fuzzy-neural network (FNN) shown in Figure 1. The outputs (layer IV) of the fuzzy-neural system are expressed as in (9). The fuzzy system based on the neural networks can then be established [15]. The approximator has four layers. At layer I, input nodes represent vector $x^T = \left[x_1, \cdots, x_n\right]$, while at layer II, they represent the values of the membership function. Each node in layer II performs a membership function value. At layer III, nodes are the values of the fuzzy basis vector ξ , with each node performing a fuzzy rule. The links between layer III and layer IV are fully connected by the weighting factors, i.e., the adjusted parameters $\theta^T = \left[\theta_1^T, \cdots, \theta_p^T\right]$. At layer IV, the outputs represent the values of the output y .

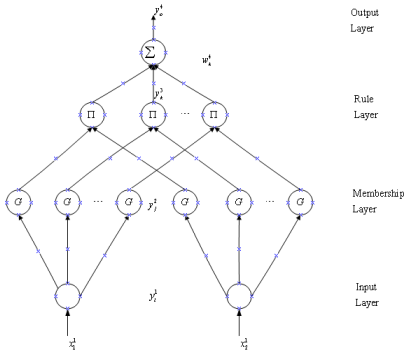

Figure 1. Structure is of a fuzzy-neural network.

Denote $\theta^T = diag\left[\theta_1^T, \cdots, \theta_p^T\right]$ and $\Phi(x) = diag\left[\xi(x), \cdots, \xi(x)\right]$. The FNN can be designed as:

$$y = \theta^T \Phi(x), \tag{9}$$

Let the nonlinear functions approximated by FNN be rewritten as:

$$\hat{F}((q,\dot{q})\big|\theta_f) = \theta_f^T \xi_f(x), \tag{10}$$

$$\hat{G}(q,\big|\theta_g) = \theta_g^T \xi_g(x). \tag{11}$$

III. Controller Design

In this section, we aim to design an observer-based adaptive fuzzy-neural network controller with PSO-SA for the robot system..

A. Basic PSO Algorithm

The concept of the PSO is the mathematical modeling and simulation of the food searching activities of a flock of birds. In multi-dimensional space, each particle moves toward the optimal point by changing its position according to a velocity. The cognitive component models the memory of the bird about its previous best position. The social component models the memory of the bird about the best position among the particles [16,17]. The mathematical model for PSO can be written ass:

$$\begin{aligned} V_i(k+1) &= V_i(k) + c_1 \cdot rand_1(\cdot) \times \left(Pbest_i - X_i(k)\right) \\ &\quad + c_2 \cdot rand_2(\cdot) \times \left(Gbest_n - X_i(k)\right) \\ X_i(k+1) &= X_i(k) + V_i(k+1),\ i = 1, \cdots, N_{swarm}, \end{aligned} \tag{12}$$

where V_i is the velocity of particle i; X_i represents the position of particle i; $Pbest_i$ and $Gbest_n$ are the best historical position of particle i and the best historical position of the neighbor of particle i, respectively; while $rand_1(\cdot)$ and $rand_2(\cdot)$ are random numbers between 0 and 1, constants c_1 and c_2 are the weighting factors of the stochastic acceleration terms, which pull each particle towards $Pbest_i$ and $Gbest_n$. Usually $Gbest_n$ is often replaced by $Gbest_g$, which is the global best position with an objective value. However, the method has the drawback of being easily trapped in the local minima; therefore, the following intelligence algorithm was proposed to overcome this shortcoming.

B. Simulated Annealing

The SA algorithm is introduced to prevent particles from becoming trapped in a local minimum and to increase the diversity of the particle swarm. Kirkpatrick [18] applied it to combinatorial optimization including the traveling salesman problem (TSP).

As mentioned before, in PSO, $Gbest_g$ is an element of the set of all $Pbest_i$, which can be regarded as a set of local optima. Thus, we modify the selection of $Gbest_g$ to overcome premature convergence. In particular, we employ the jumping mechanism of the SA for the selection of $Gbest_n$ instead of $Gbest_g$. $Pbest_i$ has better quality should have a larger probability of being selected. Borrowing the mechanism of the SA, all other $Pbest_i$ can be regarded as special solutions worse than $Gbest_g$. Meanwhile, we can set $e^{-(F_{F_i} - F_{F_g})/t}$ as the fitness value of each $Pbest_i$ to replace $Gbest_g$ at a certain temperature t. The largest fitness belongs to $Gbest_g$ and equals 1, with other fitness values within the interval $(0,1]$. Thus, the probability of selecting $Pbest_i$ as $Gbest_g$ can be calculated as follows:

$$\left(e^{-(F_{F_i} - F_{F_g})/t}\right) \Big/ \sum_{j=1}^{N_{swarm}} e^{-(F_{F_i} - F_{F_g})/t}, \tag{13}$$

Then, roulette wheel selection can be applied to randomly determine which $Pbest_i$ to select as $Gbest_g$.

C. Optimization of FNN with PSO-SA

For the FNN controller that has 3 membership functions (15 fuzzy sets) and 25 rules, there are a total of 60 parameters to be adjusted. Now the particles are manipulated as follows:

$$P_i = \left[{}^i\sigma_{11}\ {}^ic_{11}, \cdots, {}^i\sigma_{55}\ {}^ic_{55}\right],\ i = 1,2,3 \tag{14}$$

where parameters σ and c represent the center and deviation of the Gaussian membership functions, respectively.

The strategies of the PSO-SA are described as:

Step1: Let $k = 0$, and randomly initialize $X_i(0)$ and $V_i(0)$, $i = 1, \cdots, N_{swarm}$. Then, evaluate objective value F_i for all particles.

Step2: Initialize $Pbest_i$ with a copy of $X_i(0)$; initialize $Gbest_g$ with a copy of the best $Pbest_i$; and initialize the temperature $t(0) = t_0$.

Step3: Repeat until the stopping criterion is satisfied.

Calculate the fitness:

$$\text{Fitness}_i = \exp\left[-(F_{p_i} - F_{p_g})/t(k)\right], \quad (15)$$

$$\text{where} \quad F_p = \frac{1}{N_{swarm}} \sum_{i=1}^{N_{swarm}} \sqrt{e^2(i)} \ . \quad (16)$$

Step4: For every particle i, apply roulette wheel selection from the set of all $Pbest_i$, and then update V_i and X_i via the following equations.

$$V_i(k+1) = \chi \times \{V_i(k) + c_1 \cdot rand_1(\cdot) \times (Pbest_i - X_i(k)) + c_2 \cdot rand_2(\cdot) \times (Gbest_n - X_i(k))\}$$

$$X_i(k+1) = X_i(k) + V_i(k+1) \ , \quad (17)$$

where χ is called a constriction coefficient.

$$\chi = \frac{2}{\left|2 - C - \sqrt{C^2 - 4C}\right|} \ , C = c_1 + c_2 \ , \quad (18)$$

Step5: Evaluate the new objective value F_i for all particles, and then update $Pbest_i$ and $Gbest_g$ (including position values and objective values).

Step6: Set the annealing temperature to obtain $t(k+1)$, and let $k = k+1$.

Step7: The solution is then $Gbest_g$.

The biggest probability is selected as the fitness value of all $Pbest_i$ solutions as $Gbest_g$.

Remark 1. The initial temperature t_0 affects the performance of the PSO-SA. In these, the initial temperature can be written as:

$$t_0 = -F_{p_g} / \ln(0.8) \ . \quad (19)$$

D. Observer-Based Adaptive Fuzzy-Neural Robust Controller Design

Generally, an unknown numerical can be described as follows:

$$\hat{F}((q,\dot{q})|\theta_f) = \theta_f^T \xi_f(x) \ . \quad (20)$$

$$\hat{G}(q|\theta_g) = \theta_g^T \xi_g(x) \ . \quad (21)$$

$$\hat{g}_d((q,\dot{q})|\theta_{g_d}) = \theta_{g_d}^T \xi_{g_d}(x) \ . \quad (22)$$

The following technical assumption is necessary for the proof of the main statement.

Assumption 3.1: $\|\Delta D(x)\| \le g_d(x)$, (23)

where $g_d(x)$ is the unknown positive smooth continuous function.

In short, the control law (3) can be rewritten as:

$$u = \hat{G}^{-1}(q|\theta_g)[-\hat{F}((q,\dot{q})|\theta_f) + y_d^{(n)} - K_c e(t) + u_a(t)] \ , \quad (24)$$

where K_c is the control gain vector, and u_a is designed for compensating the approximation errors and the uncertainty.

Where

$$u_a = -\hat{w}_c - \frac{B_c^T P \tilde{e}_c}{\left\|\tilde{e}_c^T P_1 B_c\right\|}(\hat{g}_d(q,\dot{q})|\theta_{g_d}) - \frac{B_c^T P \tilde{e}_c}{\left\|\tilde{e}_c^T P_1 B_c\right\|^2}\left[\hat{e}^T P_2 K_o \tilde{e}_1\right]. \quad (25)$$

Furthermore, the parameter update laws are chosen as follows:

$$\dot{\theta}_f = \gamma_f \xi_f(\hat{x}) \tilde{e}_c^T P_1 B_c \ , \quad (26)$$

$$\dot{\theta}_g = \gamma_g \xi_g(\hat{x}) u \tilde{e}_c^T P_1 B_c \ , \quad (27)$$

$$\dot{\theta}_{g_d} = \gamma_{g_d} \left\|\tilde{e}_c^T P_1 B_c\right\| \xi_{g_d}(\hat{x}) \ , \quad (28)$$

$$\dot{\hat{w}}_c = \gamma_c \tilde{e}_c^T P_1 B_c \ , \quad (29)$$

where $\gamma_f > 0$, $\gamma_g > 0$, $\gamma_{g_d} > 0$, and $\gamma_c > 0$ are positive adaptive gains to be determined.

In order to constrain the parameters θ_f , θ_g , and θ_{gd} within the sets M_f , M_g , and M_{gd} , respectively, the proposed adaptive laws (26)-(28) can be modified as follows:

$$\dot{\theta}_f = \begin{cases} \gamma_f \xi_f(\hat{x}) \tilde{e}_c^T P_1 B_c, \ if \ \left(\|\theta_f\| \le M_f \right) \\ \qquad or \left(\begin{array}{l} \|\theta_f\| = M_f \\ and \ \tilde{e}_c^T P_1 B_c \theta_1^T \xi_f(\hat{x}) \le 0 \end{array} \right) \\ P\left\{\gamma_f \xi_f(\hat{x}) \tilde{e}_c^T P_1 B_c\right\}, if \ \left(\begin{array}{l} \|\theta_f\| = M_f \\ and \ \tilde{e}_c^T P_1 B_c \theta_1^T \xi_f(\hat{x}) > 0 \end{array} \right) \end{cases} , \quad (30)$$

where

$$P\left\{\gamma_f \xi_f(\hat{x}) \tilde{e}_c^T P_1 B_c\right\} = \gamma_f \xi_f(\hat{x}) \tilde{e}_c^T P_1 B_c - \gamma_f \frac{\theta_f \theta_f^T}{\|\theta_f\|} \xi_f(\hat{x}) \tilde{e}_c^T P_1 B_c \ .$$

$$\dot{\theta}_g = \begin{cases} \gamma_g \xi_g(\hat{x}) u \tilde{e}_c^T P_1 B_c, \ if \ \left(\|\theta_g\| \le M_g \right) \\ \qquad or \left(\begin{array}{l} \|\theta_g\| = M_g \\ and \ \tilde{e}_c^T P_1 B_c \theta_2^T \xi_g(\hat{x}) u \le 0 \end{array} \right) \\ P\left\{\gamma_g \xi_g(\hat{x}) u \tilde{e}_c^T P_1 B_c\right\}, if \ \left(\begin{array}{l} \|\theta_g\| = M_g \\ and \ \tilde{e}_c^T P_1 B_c \theta_g^T \xi_g(\hat{x}) u > 0 \end{array} \right) \end{cases} , \quad (31)$$

where

$$P\left\{\gamma_g \xi_g(\hat{x}) u \tilde{e}_c^T P_1 B_c\right\} = \gamma_g \xi_g(\hat{x}) u \tilde{e}_c^T P_1 B_c - \gamma_g \frac{\theta_g \theta_g^T}{\left\|\theta_g\right\|} \xi_g(\hat{x}) u \tilde{e}_c^T P_1 B_c$$

.

$$\dot{\theta}_{g_d} = \begin{cases} \gamma_{g_d} \left\|\tilde{e}_c^T P_1 B_c\right\| \xi_{g_d}(\hat{x}), \ if \ \left(\left\|\theta_{g_d}\right\| \le M_{\theta g_d}\right) \\ \qquad or \begin{pmatrix} \left\|\theta_{g_d}\right\| = M_{\theta_{g_d}} \\ and \ \left\|\tilde{e}_c^T P_1 B_c\right\| . \theta_{g_d}^T \xi_{g_d}(\hat{x}) \le 0 \end{pmatrix} \\ P\left\{\left\|\tilde{e}_c^T P_1 B_c\right\| \gamma_{g_d} \xi_{g_d}(\hat{x})\right\}, if \ \begin{pmatrix} \left\|\theta_{g_d}\right\| = M_{\theta_{g_d}} \\ and \ \left\|\tilde{e}_c^T P_1 B_c\right\| \theta_{g_d}^T \xi_{g_d}(\hat{x}) u > 0 \end{pmatrix} \end{cases}, \quad (32)$$

where

$$P\left\{\gamma_{g_d} \xi_{g_d}(\hat{x}) \tilde{e}_c^T P_1 B_c\right\} = \gamma_{g_d} \xi_{g_d}(\hat{x}) \left\|\tilde{e}_c^T P_1 B_c\right\| - \gamma_{g_d} \frac{\theta_{g_d} \theta_{g_d}^T}{\left\|\theta_{g_d}\right\|} \xi_{g_d}(\hat{x}) \left\|\tilde{e}_c^T P_1 B_c\right\| .$$

In this, the control input can be arranged as:

$$u = \hat{G}^{-1}(q|\theta_g)[-\hat{F}((q,\dot{q})|\theta_f) + y_d^{(n)} - K_c \hat{e}(t) + u_a(t)] . \quad (33)$$

By (6), (33) can be arranged:

$$\dot{e}(t) = Ae(t) - BK_c \hat{e}(t) + B\{F((q,\dot{q})) - \hat{F}((q,\dot{q})|\theta_f) + [G(q) - \hat{G}(q|\theta_g)]u(t) + u_a(t) + \Delta D((q,\dot{q}))\} . \quad (34)$$

The output tracking error vector is redefined as follows:

$$\dot{\hat{e}}(t) = (A - BK_c)\hat{e}(t) + K_o(e_q(t) - \hat{e}_q(t)) , \quad (35)$$

where K_o is the observer gain vector.

Define the observation error vector as:

$$\tilde{e}(t) = e(t) - \hat{e}(t) , \quad (36)$$

In short, one can obtain:

$$\dot{\tilde{e}} = (A - K_0 C)\tilde{e} + B\{[F(q,\dot{q}) - \hat{F}((q,\dot{q})|\theta_f)] + [G(q) - \hat{G}(q|\theta_g)]u(t) + u_a(t) + \Delta D((q,\dot{q}))]\} , \quad (37)$$

Define the optimal parameter vectors θ_f^*, θ_g^*, and $\theta_{g_d}^*$ as:

$$\theta_f^* = \arg \min_{\theta_f \in \Omega_f} \left\{ \sup_{x \in U_x, \hat{x} \in U_{\hat{x}}} \left| F(q,\dot{q}) - \hat{F}((q,\dot{q})|\theta_f) \right| \right\} , \quad (38)$$

$$\theta_g^* = \arg \min_{\theta_g \in \Omega_g} \left\{ \sup_{x \in U_x, \hat{x} \in U_{\hat{x}}} \left| G(q) - \hat{G}(q|\theta_g) \right| \right\} , \quad (39)$$

$$\theta_{g_d}^* = \arg \min_{\theta_{gd} \in \Omega_{g_d}} \left\{ \sup_{x \in U_x, \hat{x} \in U_{\hat{x}}} \left| g_d((q,\dot{q})) - \hat{g}_d((q,\dot{q})|\theta_{g_d}) \right| \right\} , \quad (40)$$

where $\tilde{\theta}_f = \theta_f^* - \theta_f$, $\tilde{\theta}_g = \theta_g^* - \theta_g$, and $\tilde{\theta}_{g_d} = \theta_{g_d}^* - \theta_{g_d}$ are parameter estimation errors.

The errors can be defined as:

$$w = F(q,\dot{q}) - \hat{F}((q,\dot{q})|\theta_f^*) + \left(G(q) - \hat{G}(q|\theta_g^*)\right)u + g_d(q,\dot{q}) - \hat{g}_d((q,\dot{q})|\theta_{g_d}^*) . \quad (41)$$

The linear transfer function $H(s)$ is realized using standard techniques by $H(s) = C\left(sI - \left(A - K_o C\right)\right)^{-1} B$, and it used SPR-Lyapunov design approach, and after some simple manipulations, we can obtain the equation:

$$\tilde{e}_q(t) = H(s)L(s)\left[L(s)^{-1}\tilde{\theta}_f^T \xi_f(\hat{x}) + L(s)^{-1}\tilde{\theta}_g^T \xi_g(\hat{x})u(t) + L(s)^{-1}\left(w + u_a(t) + \Delta D(q,\dot{q})\right)\right] , \quad (42)$$

where $L(s) = \left[L_1(s), \cdots, L_n(s)\right]$ and $L_i(s) = s^{m_i} + b_{i1}s^{m_i - 1} + \cdots + b_{im_i}$, $(m_i = n_i - 1)$, $i = 1, 2, \cdots, p$.

Hence, the state-space realization can be rewritten as follows:

$$\dot{\tilde{e}}_c = \left(A - K_0 C\right)\tilde{e}_c + B_c[\tilde{\theta}_f^T \xi_{cf}(\hat{x}) + \tilde{\theta}_g^T \xi_{cg}(\hat{x})u(t) + w_c + u_{ca}(t) + \Delta D_c(q,\dot{q})] , \quad (43)$$

where $B_c = diag\left[B_{c1}, \cdots, B_{cp}\right]$, $B_{ci} = diag\left[1, b_{i1}, \cdots, b_{im_i}\right]$, $\xi_{cf}(\hat{x}) = L(s)^{-1}\xi_f(\hat{x})$, $w_c = L(s)^{-1}w$, $\Delta D_c(q,\dot{q}) = L(s)^{-1}\Delta D(q,\dot{q})$, and $\xi_{cg}(\hat{x}) = L(s)^{-1}\xi_g(\hat{x})$.

Lemma 3.1 [14] Assuming that X and Y are vectors or matrices with corresponding dimensions, the following equation holds:

$$X^T X + Y^T Y \ge 2X^T Y . \quad (44)$$

Theorem 3.1: *For the given positive definite matrices $\boldsymbol{Q}_1$ and $\boldsymbol{Q}_2$, the augmented control system (2) containing the observer (35) is asymptotically stabilized via the controller (24) if there exist symmetric positive definite matrices $\boldsymbol{P}_1$ and $\boldsymbol{P}_2$ such that the following Lyapunov equations are satisfied.*

$$\left(A - K_o C\right)^T \boldsymbol{P}_1 + \boldsymbol{P}_1 \left(A - K_o C\right) \le -\boldsymbol{Q}_1 ,$$
$$\left(A - BK_c\right)^T \boldsymbol{P}_2 + \boldsymbol{P}_2 \left(A - BK_c\right) \le -\boldsymbol{Q}_2 . \quad (45)$$

Proof of Theorem 3.1

Consider the Lyapunov function as:

$$V = \frac{1}{2}\tilde{e}_c^T \boldsymbol{P}_1 \tilde{e}_c + \frac{1}{2}\hat{e}^T \boldsymbol{P}_2 \hat{e} + \frac{1}{2\gamma_f} tr\left(\tilde{\theta}_f^T \tilde{\theta}_f\right) + \frac{1}{2\gamma_g} tr(\tilde{\theta}_g^T \tilde{\theta}_g)$$

$$+ \frac{1}{2\gamma_c}(\tilde{w}^T \tilde{w}) + \frac{1}{2\gamma_{g_d}} tr(\tilde{\theta}_{g_d}^T \tilde{\theta}_{g_d}), \qquad (46)$$

Then, the time derivative of the Lyapunov (46) is:

$$\dot{V} = \frac{1}{2}\dot{\tilde{e}}^T \boldsymbol{P}_1 \tilde{e} + \frac{1}{2}\tilde{e}^T \boldsymbol{P}_1 \dot{\tilde{e}} + \frac{1}{2}\dot{\hat{e}}^T \boldsymbol{P}_2 \hat{e} + \frac{1}{2}\hat{e}^T \boldsymbol{P}_2 \dot{\hat{e}} - \frac{1}{\gamma_f} tr\left(\tilde{\theta}_f^T \dot{\hat{\theta}}_f\right)$$

$$- \frac{1}{\gamma_g} tr(\tilde{\theta}_g^T \dot{\hat{\theta}}_g) - \frac{1}{\gamma_{g_d}} tr(\tilde{\theta}_{g_d}^T \dot{\hat{\theta}}_{g_d}) - \frac{1}{\gamma_c}(\tilde{w}^T \dot{\hat{w}}). \quad (47)$$

After some simple manipulations, we can obtain as:

$$\dot{V} \le \frac{1}{2}\tilde{e}_c^T \left[(A - K_o C)^T \boldsymbol{P}_1 + \boldsymbol{P}_1 (A - K_o C)\right]\tilde{e}_c + \frac{1}{2}\hat{e}^T \left[(A - BK_c)^T \boldsymbol{P}_2 \right.$$
$$\left. + \boldsymbol{P}_2 (A - BK_c)\right]\hat{e} + \tilde{e}_c^T \boldsymbol{P}_1 B_c u_a + \tilde{e}_c^T \boldsymbol{P}_1 B_c \tilde{\theta}_f^T \xi_f(\hat{x})$$
$$+ \tilde{e}_c^T \boldsymbol{P}_1 B_c \tilde{\theta}_g^T \xi_g(\hat{x}) u + \tilde{e}_c^T \boldsymbol{P}_1 B_c (\tilde{w} + \hat{w}) + \left\|\tilde{e}_c^T \boldsymbol{P}_1 B_c\right\| \cdot \left\|\Delta D_f\right\|$$
$$+ \hat{e}^T \boldsymbol{P}_2 K_o \tilde{e}_1 - \frac{1}{\gamma_f} tr\left(\tilde{\theta}_f^T \dot{\theta}_f\right) - \frac{1}{\gamma_g} tr(\tilde{\theta}_g^T \dot{\theta}_g) - \frac{1}{\gamma_c}(\tilde{w}^T \dot{\hat{w}})$$
$$- \frac{1}{\gamma_{g_d}} tr(\tilde{\theta}_{g_d}^T \dot{\theta}_{g_d}). \qquad (48)$$

By using Lemma 3.1 and Assumption 2.1-3.1, we further have:

$$\dot{V} \le \frac{1}{2}\tilde{e}_c^T \left[(A - K_o C)^T \boldsymbol{P}_1 + \boldsymbol{P}_1 (A - K_o C)\right]\tilde{e}_c + \frac{1}{2}\hat{e}^T \left[(A - BK_c)^T \boldsymbol{P}_2 \right.$$
$$\left. + \boldsymbol{P}_2 (A - BK_c)\right]\hat{e} + \tilde{e}_c^T \boldsymbol{P}_1 B_c u_a + \tilde{e}_c^T \boldsymbol{P}_1 B_c \tilde{\theta}_f^T \xi_f(\hat{x})$$
$$+ \tilde{e}_c^T \boldsymbol{P}_1 B_c \tilde{\theta}_g^T \xi_g(\hat{x}) u + \tilde{e}_c^T P_1 B_c (\tilde{w} + \hat{w}) + \left\|\tilde{e}_c^T \boldsymbol{P}_1 B_c\right\|$$
$$\times \hat{g}_d((q, \dot{q})\big|\theta_{g_d}) + \left\|\tilde{e}_c^T \boldsymbol{P}_1 B_c\right\| \cdot \tilde{\theta}_{g_d}^T \xi_{g_d}(\hat{x}) + \hat{e}^T \boldsymbol{P}_2 K_o \tilde{e}_1$$
$$- \frac{1}{\gamma_f} tr\left(\tilde{\theta}_f^T \dot{\theta}_f\right) - \frac{1}{\gamma_g} tr(\tilde{\theta}_g^T \dot{\theta}_g) - \frac{1}{\gamma_c}(\tilde{w}^T \dot{\hat{w}})$$
$$- \frac{1}{\gamma_{g_d}} tr(\tilde{\theta}_{g_d}^T \dot{\theta}_{g_d}). \qquad (49)$$

Then, (49) can be written as:

$$\dot{V} \le \frac{1}{2}\tilde{e}_c^T \left[(A - K_o C)^T \boldsymbol{P}_1 + \boldsymbol{P}_1 (A - K_o C)\right]\tilde{e}_c + \frac{1}{2}\hat{e}^T \left[(A - BK_c)^T \boldsymbol{P}_2 \right.$$
$$\left. + \boldsymbol{P}_2 (A - BK_c)\right]\hat{e}. \qquad (50)$$

Finally:

$$\dot{V} \le -\frac{1}{2}\tilde{e}_c^T Q_1 \tilde{e}_c - \frac{1}{2}\hat{e}^T Q_2 \hat{e}.$$

Q.E.D

IV. SIMULATION

This section presents the simulation results of the proposed observer-based adaptive fuzzy-neural network robust controller with PSO-SA for robot systems to illustrate that the stability for the closed-loop system. In order to demonstrate the effectiveness of the proposed approach, we apply it to a two-link plane robot system.

Example*:*

$$\mathbf{M}(q)\ddot{q} + c(q, \dot{q})\dot{q} + g(q) + \tau_d(q, \dot{q}) + \tau_c(q, \dot{q}) = u, \qquad (51)$$

where

$$\mathbf{M} = \begin{bmatrix} (m_1 + m_2)l_1^2 & m_2 l_1 l_2 (s_1 s_2 + c_1 c_2) \\ m_2 l_1 l_2 (s_1 s_2 + c_1 c_2) & m_2 l_2^2 \end{bmatrix},$$

$$c = \begin{bmatrix} -m_2 l_1 l_2 (c_1 s_2 - s_1 c_2)\dot{q}_2^2 \\ -m_2 l_1 l_2 (c_1 s_2 - s_1 c_2)\dot{q}_1^2 \end{bmatrix},\ g = \begin{bmatrix} -g(m_1 + m_2)s_1 l_1 \\ -g m_2 l_2 s_2 \end{bmatrix}.$$

In the simulation, the parameters are chosen as:

$c_1 = \cos(q_1)$, $c_2 = \cos(q_2)$, $s_1 = \sin(q_1)$, and $s_2 = \sin(q_2)$ .The robot physical parameters are: $l_1 = l_2 = 1\text{m}$, $m_1 = m_2 = 1\text{kg}$, $g = 9.8\,\text{m}/s^2$.

$$\Delta d(q, \dot{q}) = \begin{bmatrix} \sin(2q_1) + 2sign(\dot{q}_1) \\ \sin(q_2) + sign(\dot{q}_2) \end{bmatrix}.$$

The design algorithm is as follows:

Step1: Let parameters for PSO-SA at $c_1 = 1$, $c_2 = 1$, and $N_{swarm} = 100$.

Step2: Specify a positive definite $\boldsymbol{Q}_1 = diag[1,1,1,1]$, and $\boldsymbol{Q}_2 = diag[1,1,1,1]$ $\gamma_f = \gamma_g = 0.1$, $\gamma_{g_d} = 0.1$, $r_c = 0.01$,

Step3: Specify the design parameters $K_c = \begin{bmatrix} 4 & 4 & 0 & 0 \\ 0 & 0 & 4 & 4 \end{bmatrix}$,

$$K_o = \begin{bmatrix} 90 & 185 & 0 & 0 \\ 0 & 0 & 90 & 185 \end{bmatrix}^T.$$

Step4: The membership functions of the fuzzy controller are given by:

$$\mu_{F_i^1}(x_i) = 1/1 + \exp(5 \times (x_i + 2)),$$

$$\mu_{F_i^2}(x_i) = \exp[-(x_i + 1)^2],$$

$$\mu_{F_i^3}(x_i) = \exp[-x_i^2],$$

$$\mu_{F_i^4}(x_i) = \exp[-(x_i - 1)^2],$$

$$\mu_{F_i^5}(x_i) = 1/1 + \exp(5 \times (x_i - 2)).$$

Step5: Obtain the control law.

The initial conditions are $\boldsymbol{x}(0)=[2,2,2,2]^T$, $\boldsymbol{\theta}_f(0)=0$, $\boldsymbol{\theta}_g(0)=0.2$, and $\boldsymbol{\theta}_{g_d}(0)=0$. The initial membership functions for u are depicted as Figure 2 and Figure 3. Then, Figure 4 and Figure 5 show membership functions of u after self-adjustment with PSO-SA for u_1 and u_2 . In order to compare the stabilization and tracking performance of the proposed controller with that of a conventional observer-based fuzzy adaptive robust controller, we consider the example [19]. Figures 6-9 show the response of the system under the traditional control law and the proposed method for the same initial conditions. It is clear that the proposed controllers can stabilize the nonlinear system and show faster tracking responses than traditional control law.

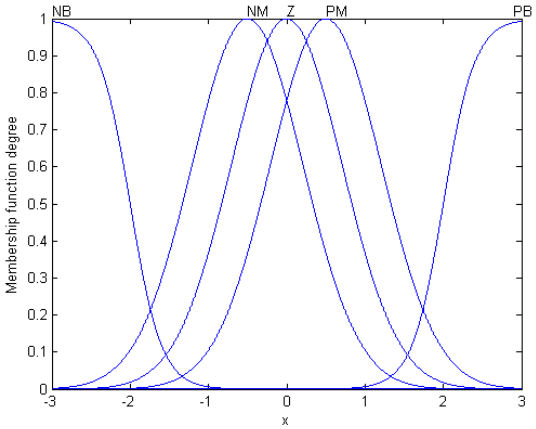

Figure 2. Membership functions of u_1 .

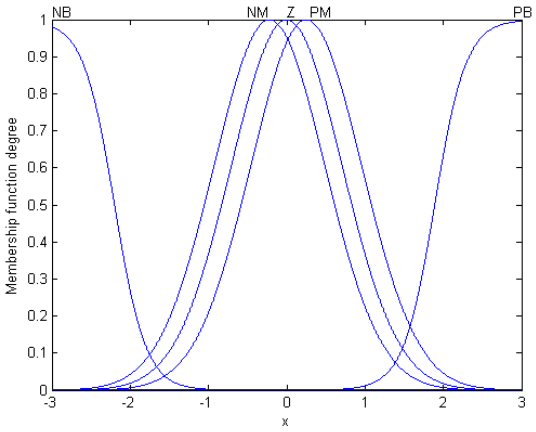

Figure 3. Membership functions of u_2 .

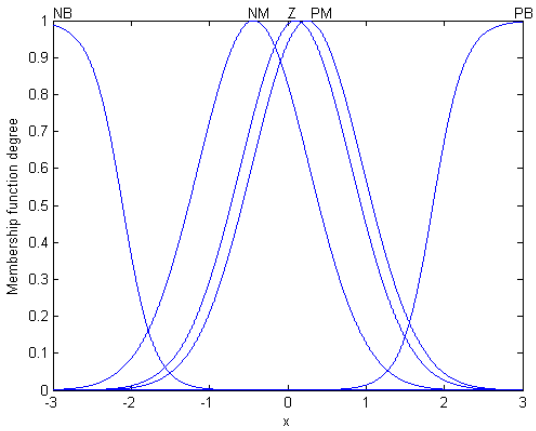

Figure 4. Membership functions after training of input variables for u_1 .

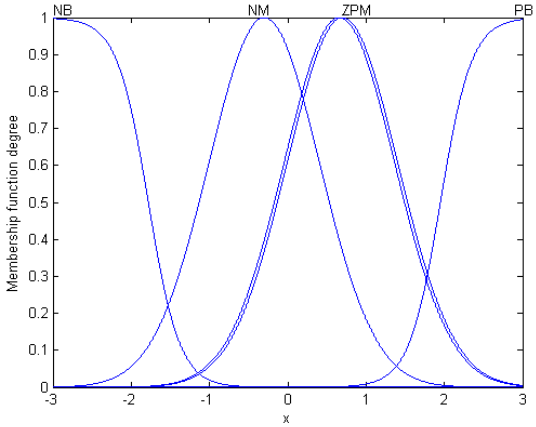

Figure 5. Membership functions after training of input variables for u_2 .

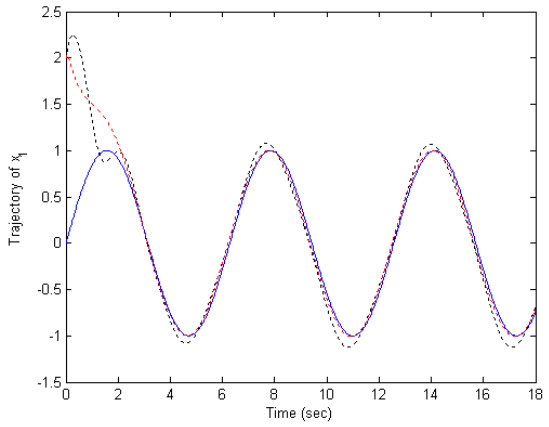

Figure 6. Trajectories of q_1 . (Red: Proposed controller; Black: Traditional control [19])

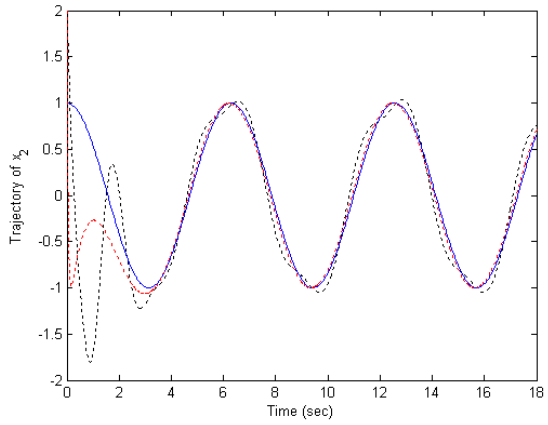

Figure 7. Trajectories of $\dot{q}_1$. (Red: Proposed controller; Black: Traditional control [19])

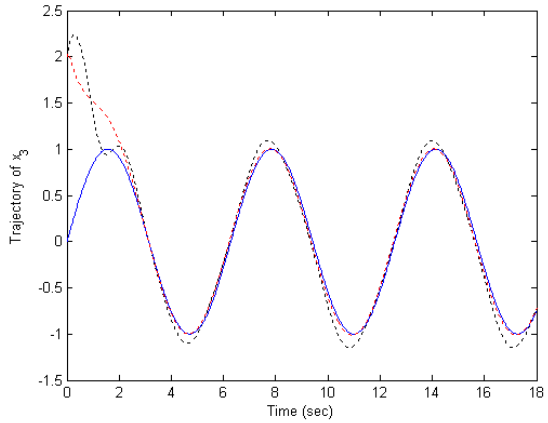

Figure 8. Trajectories of q_2. (Red: Proposed controller; Black: Traditional control [19])

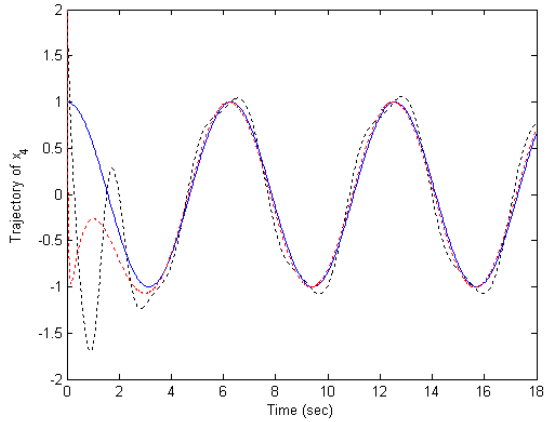

Figure 9. Trajectories of $\dot{q}_2$. (Red: Proposed controller; Black: Traditional control [19])

V. CONCLUSION

An observer-based adaptive FNN controller design was proposed for robot systems. The main contributions of this paper are as follows: Firstly, a robust term is introduced to eliminate disturbance and the controller doesn't require a priori knowledge of the sign of the control coefficient. Secondly, PSO-SA is used to self-adjust membership function for the sub-optimal solution. Thirdly, the PSO-SA based adaptive FNN controller can generate a reduction in the dependence on expert knowledge, while the stabilization condition of the closed-loop was proposed using the Lyapunov theorem. Finally, stability conditions can be efficiently checked using dedicated optimization software.

REFERENCES

[1] X. Wang, S. Li, and W. Cai, "Multi–model direct adaptive decoupling control with application to the wind tunnel system," ISA Transactions, vol. 44, pp. 131-143, 2005.

[2] S. Alavandar and M. J. Nigam, "New hybrid adaptive neuro–fuzzy algorithms for manipulator control with uncertainties–Comparative study," ISA Transactions, vol. 48, pp. 497-502, 2009.

[3] T. Bouarar, K. Guelton, and N. Manamanni, "Robust fuzzy Lyapunov stabilization for uncertain and disturbed Takagi–Sugeno descriptors," ISA Transactions, vol. 49, pp. 447-461, 2010.

[4] L. X. Wang, Adaptive Fuzzy Systems and Control: Design and Stability Analysis, NJ: Englewood Cliffs, 1994.

[5] J. Yoneyama, "Design of H∞ control for fuzzy time-delay systems," Fuzzy Sets and Systems, vol. 19, pp. 224-256, 2004.

[6] Y. Zhao, E. G. C. Jr, and D. A. Cartes, "Self–tuning adaptive control for an industrial weigh belt feeder," ISA Transactions, vol. 42, pp. 437-350, 2003.

[7] J. W. Macki, P. Nistri, and P. Zecca, "Mathematical models for hysteresis," SIAM Review, vol. 35, pp. 94-123, 1993.

[8] I. D. Mayergoyz, The Preisach Model for Hysteresis, Springer-Verlag. Berlin: Germany, 1991.

[9] N. J. Ahmad and F. Khorrami, "Adaptive control of systems with backlash hysteresis at the input," Proceedings of American Control Conference, vol. 1, pp. 3018-3022, 1999.

[10] J. Zhou, C. Zhang, and C. Wen, "Robust adaptive output control of uncertain nonlinear plants with unknown backlash nonlinearity," IEEE Transactions on Automatic Control, vol. 52, pp. 503-509, 2007.

[11] T. P. Zhang and S. S. Ge, "Adaptive neural control of MIMO nonlinear state time-varying delay systems with unknown dead-zones and gain signs," Automatica, vol. 43, pp. 1021-1033, 2007.

[12] Y. J. Liu and N. Zhou, "Observer–based adaptive fuzzy–neural control for a class of uncertain nonlinear systems with unknown dead–zone input," ISA Transactions, vol. 49, pp. 462-469, 2010.

[13] Kennedy and J., Eberhart, R. (1995), 'Particle swarm optimization', In: Proc. IEEE Internat. Conf. on Neural Networks, pp. 1942–1948.

[14] P. A. Ioannou, J. Sun, Robust Adaptive Control, Englewood Cliffs, NJ: 1996.

[15] M. J. Er and Y. Gao, "A fast approach for automatic generation of fuzzy rules by generalized dynamic fuzzy neural networks," IEEE Transactions on Fuzzy System, vol. 9, pp. 578-594, 2001.

[16] S. Naka, T. Genji, T. Yura, and Y. Fukuyama, "A hybrid particle swarm optimization for distribution state estimation," IEEE Trans. Power Systems, vol.18, pp.60-68, 2003.

[17] I. C. Trelea, "The particle swarm optimization algorithm: convergence analysis and parameter selection," Inform. Process. Lett, vol.85, pp.317-325, 2003.

[18] Kirkpatrick, C. D. Gelatt, and M. P. Vecchi, "Optimization by simulated annealing," Science, vol.220, pp.671-680, 1983.

[19] N. Gole´a, A. Gole´a, K. Barra, and T. Bouktir, "Observer-based adaptive control of robot manipulators: Fuzzy systems approach," Applied Soft Computing 8 778–787, 2008.

2011 IEEE International Conference on Fuzzy Systems
June 27-30, 2011, Taipei, Taiwan

Design of Digital Battery Charger System Based on PV-Module

Ta-Tau Chen
Department of Electrical Engineering
Kun Shan University
Tainan, Taiwan
e-mail:chen0221@mail.ksu.edu.tw

Ming-Ying Hsiao*
Department of Electrical Engineering, Fortune Institute of Technology, Kaohsiung, Taiwan
e-mail:myhsiao@gmail.tw

Shun-Hung Tsai
Graduate Institute of Automation Technology, National Taipei University of TechnologyTaipei, Taipei, Taiwan
e-mail:shtsai@ntut.edu.tw

Che-Nan Lin
Department of Electrical Engineering
Kun Shan University
Tainan, Taiwan
e-mail:Lin2357602@mail.ksu.edu.tw

***Abstract*—This paper aims at to realize the solar cell charged systems of 120W PV module with the dsPIC30F4011 control chip. All of the control schemes are written and accomplished with the C language. In the power converter, a single-ended primary inductance converter (SEPIC) is adopted which has the features including the buck-boost operating mode, no polarity inversion, low input current pulsation, and wide input voltage range, so, it is very suitable for the conversion of solar cell. In order to obtain the high efficient solar cell energy conversion, a fuzzy maximum power point tracking (MPPT) control is activated if the solarization is insufficient. The fuzzy controller is to maintain a charged current so as that the battery voltage can reach to desired value. The effectiveness of the proposed methods is demonstrated with the experimental results.**

Keywords-PV module; MPPT; SEPIC converter;

I. INTRODUCTION

Solar energy from the sun is fruitful without environmental pollution. It does not consume the earth's resources and cause global warming. A solar panel is a device comprised of a number of solar cells connected series/parallel units which are used to convert solar energy into electricity. Solar panels have been used more and more each day. As the solar panel has been constructed, the only need is sunlight to create energy. The economic value of the solar panel is a popular choice to battle the rising cost of electricity. The solar energy technology has been developed for many years, but it is utilized today more than ever. One main reason for its rising usage is its renewable capability. The sun will always provide the Earth with more energy continuously than human being can consume.

The output voltage, current, and power of the solar panel are highly nonlinear and closely related to effects, such as: the sunlight intensity, working temperature, aging of components, and types of optical materials. The solar panels have their own inherent unique working curve with a corresponding maximum power point only, namely, the optimal working point of solar panels, therefore, to fully utilize solar energy, we need to enable the design of appropriate control algorithms in a variety of different working environments to obtain the maximum power from solar panels. This control method is called the maximum power tracking method. Maximum power point tracking methods are discussed in many literatures with different tracking ways to obtain the overall efficiency; so, we need to select the appropriate maximum power tracking method according to the actual environmental conditions. To select the maximum power tracking methods, one must understand the characteristics of solar panels, such as, output power, temperature, sunlight intensity, and the relationship between the loads. It is almost impossible to utilize all the available solar energy in varying load and atmospheric conditions with an uncontrolled system; so, there are several maximum power point extraction solutions via different type DC–DC converters presented in the literature [1-9]. The perturbation and observation method is the most often used algorithm which is based on periodically changing the operating point and observing the resultant change in power. Although, it is well established algorithm, some confusions and instabilities may occur when the irradiation and/or load changes rapidly and randomly. In this paper a fuzzy method is adopted for MPPT, The fuzzy MPPT method is simple and easy to be implemented which is based on the relationship that exists between the PV panel current and voltage. The charged system is implemented with the single-ended primary inductance converter (SEPIC). The SEPIC converter is very effective to charge a battery by PV panel, because the battery voltage could be higher or lower than the PV module voltage, and also the buck boost feature of the SEPIC widens the applicable PV voltage and thus increases the adopted PV module flexibility. Single-ended primary-inductor converter (SEPIC) is a type of DC-DC converter that allows its output voltage to be greater than or less than its input voltage; the output of the SEPIC is controlled by the duty cycle of the control transistor. Figure 1 shows the circuit diagram of the SEPIC converter with two inductors.

There are several advantages by using SEPIC in the charging system of PV module. For instance, the buck-boost

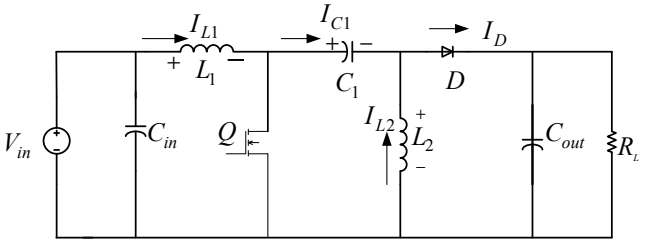

Figure 1. The SEPIC converter diagram

The authors would like to thank the National Science Council for financially supporting this research under contract N.O. 98-2622-E-168-013-CC3 and NSC-99-2221-E-027-101-.

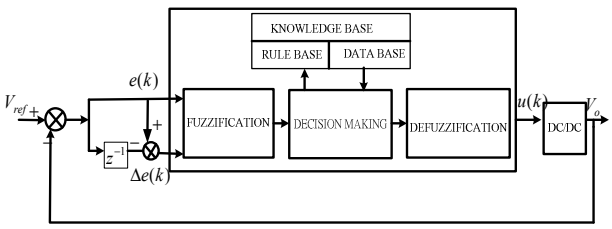

Figure 2. Block diagram of the FLC for DC–DC converters

converter operating voltage can be used to increasing the PV cells voltage range, and SEPIC converter output voltage does not reverse polarity problem. SEPIC converter inductively coupled inductor technology can be used to reduce the size of inductor. The input circuit has inductor can reduce the input current ripple and thus increase the precision of the maximum power point tracking [10, 11].

The fuzzy logic control (FLC) has been successfully applied to many control problems that the conventional one has difficulties to deal with when the controlled systems are complex, not well defined and/or model-free and can be controlled by a skilled human operator with the knowledge of their underlying dynamics. There are many papers pointed a way for an effective utilization of fuzzy control for both practical situations [14-23]. The block diagram of the FLC for DC–DC converters is shown in Figure 2. The fuzzy logic controller can be divided into four part: fuzzification is the input variable partition into suitable fuzzy sets; knowledge base includes fuzzy rule base and data base, they contain knowledge of the control rules and linguistic labels; decision making is inferring control action from rule base; defuzzification is the conversion from the inferred fuzzy value to real control crisp value [13].

The main work of this paper is to integrate fuzzy methodology and SEPIC DC-DC converter so as to realize a charged system of 120W PV module. The control chip is adopted dsPIC30F4011 in the circuit, and all of the control actions are written and completed with the software C program. In the DC-DC power converter, a single-ended primary inductance converter (SEPIC) is adopted. The SEPIC has the features of the buck-boost operating mode, no polarity inversion, low input current pulsation, and wide input voltage range, it is very suitable for the conversion of solar cell. In order to obtain the highest efficient solar cell energy, a fuzzy maximum power point tracking (MPPT) control is adopted, in the hope of reaching steady charging. Three stages of charging process are taken in this work. While the battery voltage is not full and the solarization is insufficient such that available power of the PV module is not enough to produce the charged current between 0.1C and 0.01C to battery, then fuzzy maximum power point tracking (MPPT) control is activated. As the battery voltage is not full, the solarization is sufficient, and the available peak power of the PV module is enough to produce 0.1C charged current to battery, then, 0.1C charged current is set as command and a fuzzy controller is taken to maintain 0.1C charged current of battery. No matter what the solarization is sufficient or not, once the battery voltage reaches a predefined value, the current command will be shifted to 0.01C, then, the fuzzy controller is activated to maintain a litter charged current so as the battery voltage can reach the desired value. The effectiveness of the proposed methods will be demonstrated by the experimental results.

TABLE I. SPECIFICATIONS AND PARAMETERS OF THE SEPIC.

Input voltage range	Charge voltage range	Input current range
5-40V	12V-14.4V	0.1-10A
Charge current range	Switching frequency	Output power range
0.1A-10A	100 kHZ	1W-120W
Coupled Inductor	Switch components	Coupling capacitor
63 mh	IRFP048NI	490uf/150V
Output diode	Duty cycle range	I/O filter capacitor
B20100 (20A/100V)	10%-70%	4700uF 53V

This paper is organized as follows. In Section II, the circuit characteristics of the SEPIC are described. The fuzzy maximum power point tracking and fuzzy control strategy is addressed in Section III. The experimental results are given in Section IV. Finally, the conclusions are drawn in Section V.

II. SEPIC CIRCUIT CHARACTERISTICS

Roberto *et al* [12] presented a simple method to properly choose the better DC-DC converter to be applied as MPPT in photovoltaic systems, as a function of the radiation, temperature operation range, and load connected at the photovoltaic module. The theory shows that buck and boost converters, although widely used on the literature, might not be the better option to work as MPPT, once they have tracking problems under different radiation and temperature combinations. Before to evaluate parameters of each component, there are some assumptions should be made first: (a) SEPIC operating in continuous conduction mode (CCM); (b) Circuit is at the steady state; (c) All semiconductor components are at ideal case; (d) The energy storage element is not considered. The parameters are listed in Table I.

Referring to the equivalent circuit of SEPIC converter at ON and OFF states as shown in Figure 3 and 4, respectively, when Q turns ON, the energy is stored in the inductor L1. At this time the inductor voltage equals to input voltage, and the energy stored in capacitor C1 will be transferred to inductor L2. The load is supplied by capacitor C2. Similarly, when Q turns OFF, the energy stored in inductor L1 is transferred to C1. The energy stored in L2 is transferred to C2 through D1 and supplying the energy to load. Figure 5 shows the corresponding switching waveforms of the SEPIC converter [23].

The relationship of SEPIC output and input voltage conversion in the static state can be expressed as

$$\frac{V_{in}}{V_{out}} = \frac{D}{1-D} \tag{1}$$

where V_{in} and V_{out} are the input and output voltage, respectively, and D is the duty cycle. Considering the diode forward bias voltage with the input maximum value, the maximum duty cycle $D_{\max}$ can be expressed as follow

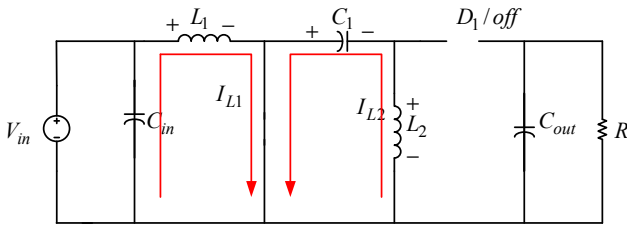

Figure 3. SW on

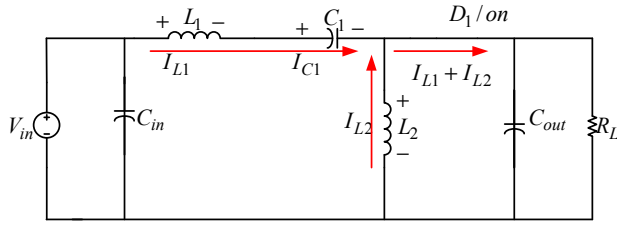

Figure 4. SW off

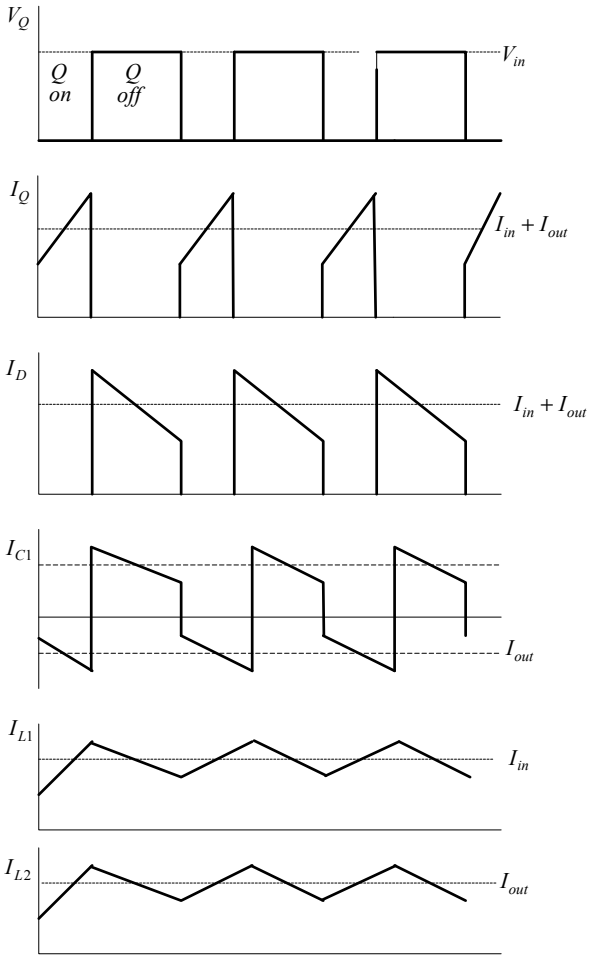

Figure 5. SEPIC Converter Switching Waveforms

$$D_{\max} = \frac{V_{out} + V_D}{V_{in(\max)} + V_{out} + V_D} \tag{2}$$

where V_D is the diode voltage. Because inductor L1 is in the input, the inductor peak to peak ripple current for the maximum input current of 40% is selected, so the L1 inductor ripple current is:

$$\Delta L_1 = I_{in} \times 40\% = \frac{I_{out}}{V_{in(\min)}} \times 40\% \tag{3}$$

Operating under the CCM, L1 must be equal to L2, the inductor value can be calculated as:

$$L_1 = L_2 \tag{4}$$

In order to ensure that the inductor saturation does not occur, the peak inductor current to be met is as follows

$$I_{L1(peak)} = \frac{V_{out} I_{out}}{V_{in(\min)}} \times (1 + \frac{40\%}{2}) \tag{5}$$

$$I_{L2(peak)} = I_{out} \times (1 + \frac{40\%}{2}) \tag{6}$$

where the inductor L1 and L2 are winded on the same core and the inductance value is half of L, then

$$L_1 = L_2 = \frac{L}{2} = D_{\max} \times \frac{V_{in(\min)}}{2 \times \Delta I_{L1} \times f_{SW}} \tag{7}$$

where f_{SW} is the switching frequency. According to the switching modes shown in Figure 3 and 4, the switch maximum voltage stress and the switch maximum current stress can be obtained, and then, the selected MOSFET switch specification will be as (8) and (9).

$$I_{SW} = I_{L1(peak)} + I_{L2(peak)} \tag{8}$$

$$V_{SW} = V_{out(\max)} + V_{in(\max)} \tag{9}$$

In the SEPIC converter circuit, the output diode D1 should withstand the reverse bias and peak output voltage.

$$V_{D(\max)} = V_{out(\max)} + V_{in(\max)} \tag{10}$$

At a fixed switching frequency and maximum duty cycle, the SEPIC coupling capacitor voltage must be greater than the maximum input voltage. The voltage ripple can be determined by the coupling capacitor, so the peak ripple voltage can approach to the input voltage as

$$\Delta V_C = \frac{I_{out} \times D_{\max}}{C_S \times f_{SW}} \times 40\% \tag{11}$$

where C is the battery capacitance. The battery capacity, adopted at the experiment, is 12V45AH with the maximum charging current limit set to 0.1C, When the battery voltage reaches to 14.4V, the minimum charge current command will be activated, and then the floating charge current command is shifted to 0.01C. Table I is SEPIC power converter implementation specifications and parameters list.

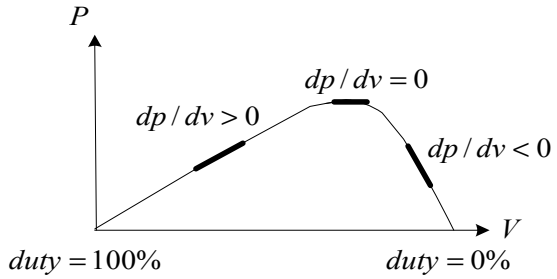

Figure 6. The PV panel power and voltage curve

III. FUZZY MAXIMUM POWER POINT TRACKING AND FUZZY CONTROL STRATEGY

In general, there are many different implementation methods for solar power systems to achieve maximum power point tracking control. One of the most popular methods used is P&O one which can be easy to be implemented, but, there are some disadvantages, for example: power will oscillates near the maximum point resulting to reduce energy efficiency of solar panels. Here, we use the fuzzy controller method for MPPT instead of the simple P&O one [1-3]. The fuzzy controller not only can reduce the time required to track the MPPT but also can reduce the fluctuation of power output. A simple fuzzy maximum power tracking control law is proposed here only with three fuzzy if-then control rules to complete the maximum power tracking work.

From PV panel power and voltage curve in Figure 6, one can see that the slope of PV curve can be partition into three parts, i.e. slope of $\Delta p/\Delta v > 0$, slope of $\Delta p/\Delta v = 0$, and slope of $\Delta p/\Delta v < 0$. Therefore; according to the slope of PV located in which part, the rate of increase of $\Delta u(k)$ is selected as one of the P, Z, or N, which denote positive, zero, and negative, respectively. The input of the proposed fuzzy logic controller is the slope $\Delta p/\Delta v$ and the output is rate change in duty ratio $\Delta u(k)$. The slope of $\Delta p/\Delta v$ is fuzzified into three partitions with triangular membership function labeled with P, Z, and N as shown in Figure 7(a). Similarly, the rate of increase of $\Delta u(k)$ is also fuzzified into three partitions with triangular membership function labeled with P, Z, and N as shown in Figure 7(b).

Thus; the fuzzy maximum power tracking control rules are given by

If $\Delta p/\Delta v$ is P Then Δu is N

If $\Delta p/\Delta v$ is Z Then Δu is Z

If $\Delta p/\Delta v$ is N Then Δu is P

The rate of increase of Δp and Δu are defined as follows:

$$\Delta p = p(k) - p(k-1) \tag{12}$$

$$\Delta v = v(k) - v(k-1) \tag{13}$$

The final control output is given by

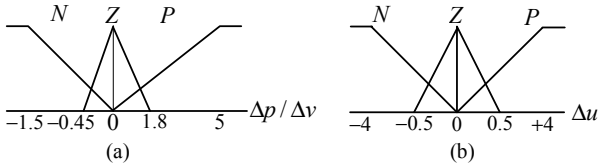

Figure 7. The membership functions of $\Delta p/\Delta v$ and Δu

$$u(k) = u(k-1) + \Delta u(k) \tag{14}$$

The actual control command $u(k)$ which is used to control the duty ratio of the switching pulse is calculated by the center weighted average defuzzification method, *i.e.*,

$$\Delta u = \frac{\sum_{i=1}^{3} w_i C_{R_i}}{\sum_{i=1}^{3} w_i} \tag{15}$$

where w_i is the antecedent part's membership function value of the *i*th-rule, C_{Ri} is the center of Consequent parts of the *i*th-rule.

When the charged current command is shifted to 0.1C or 0,01C, the fuzzy controller is activated to maintain the charged current reach to desired command value. In this situation, for precision control goal, the input variable $e(k)$, $\Delta e(k)$ and output variable $\Delta u(k)$ are fuzzified into seven fuzzy sets which are labeled as negative big (NB), negative medium (NM), negative small (NS), zero (ZE), positive small (PS), positive medium (PM), positive big (PB). The fuzzy sets used in input and output are triangular membership functions as shown in Figure 8 and Figure 9, respectively. The error e and difference of error Δe are defined as

$$e = I_{ref} - I_{BAT} \tag{16}$$

$$\Delta e(k) = e(k) - e(k-1) \tag{17}$$

where I_{ref} is the reference charged current of battery, which

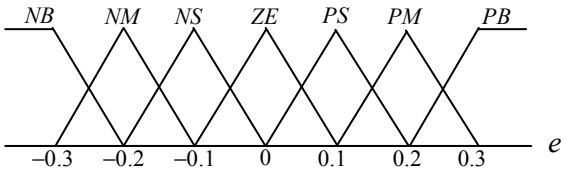

Figure 8. The the membership function of e

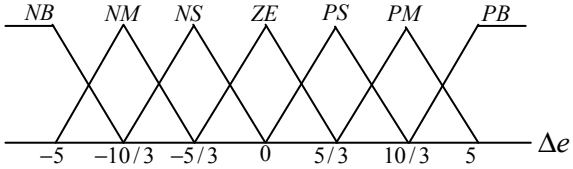

Figure 9. The the membership function of Δe

depended on how sufficiency is the solarization such that PV panel can provide either 0.1C or 0.01C current command. To simplify the design scheme of the fuzzy control, the discourse of universe of $e(k)$ is taken the same value for both 0.1C and 0.01C. and also as $\Delta e(k)$. The crisp output of the duty ratio of the switching pulse is calculated by the center weighted average defuzzification method that the same as (15). The output of the FLC is changed in duty ratio $\Delta u(k)$. The duty cycle $u(k)$ at the k*th* sampling time is defined as

$$u(k) = u(k-1) + \Delta u(k) \tag{18}$$

Then, it is sent through the PWM to DC–DC converter to generate desired switching action. The control rule must be designed in order that input variable $e(k)$ has to always be zero. The rule table of the FLC is listed in Table 2.

TABLE II. THE CONTROL RULE BASE

e\de	NB	NM	NS	ZE	PS	PM	PB
PB	ZE	NS	NM	NB	NB	NB	NB
PM	PS	ZE	NS	NM	NB	NB	NB
PS	PM	PS	ZE	NS	NM	NB	NB
ZE	PB	PM	PS	ZE	NS	NM	NB
NS	PB	PB	PM	PS	ZE	NS	NM
NM	PB	PB	PB	PM	PS	ZE	NS
NB	PB	PB	PB	PB	PM	PS	ZE

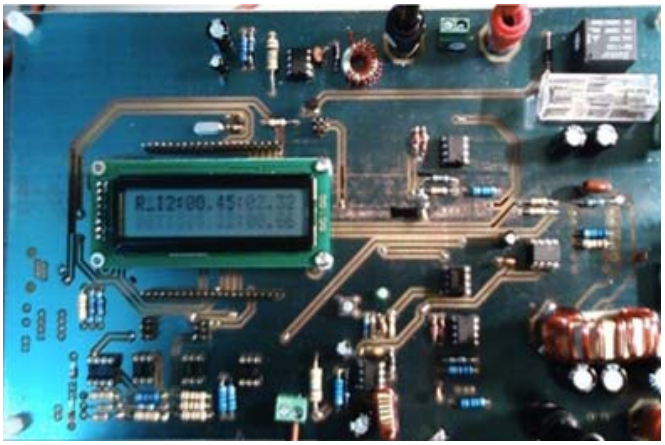

Figure 10. digital charged system circuit board.

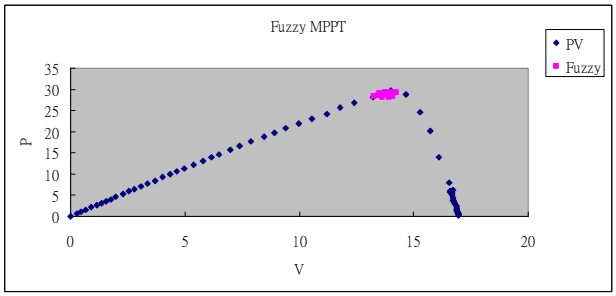

Figure 11. The fuzzy MPPT record curve and solar cell P-V curve

IV. EXPERIMENTS AND RESULTS

A. *Halogen irradiation experiments:*

The completed digital charged system circuit board is shown as Figure 10. Because of the sunlight is lack in winter, so that the experiment environment is emulated by using four 500W halogen lamps to irradiate the 120W solar cell instead. The wavelength between halogen lamp and sunlight is different, so the power generated by using halogen lamps is smaller than that from sunlight. In Figure 11, the red graph is the record for the fuzzy MPPT method, the blue curve graph is

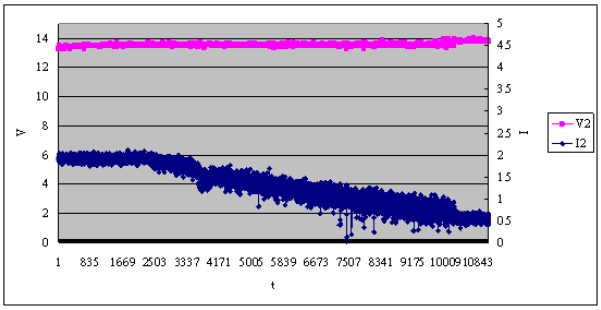

Figure 12. The battery charge voltage (red) and charge current (blue).

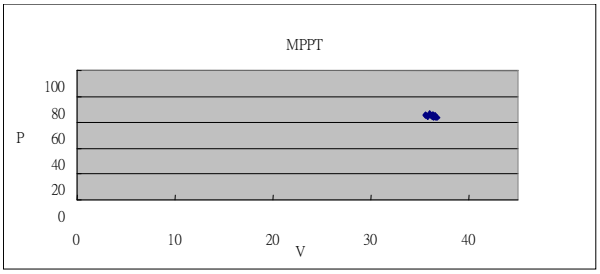

Figure 13. The maximum power graph.

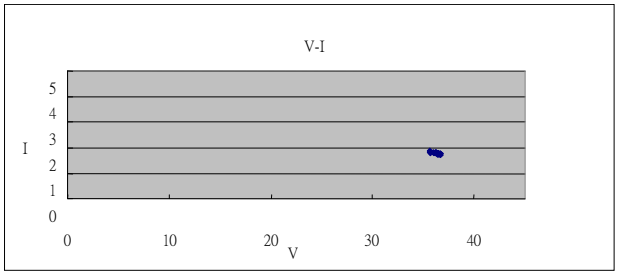

Figure 14. The solar cell VI curve

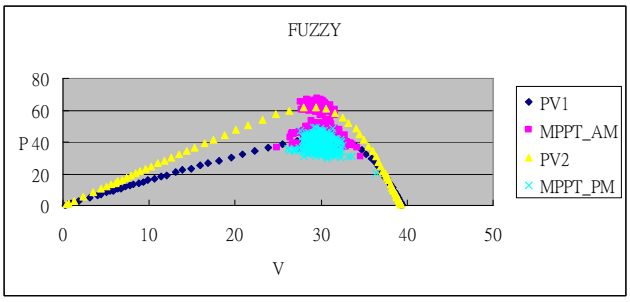

Figure 15. the Maximum power tracking graph in the insufficient light case in the morning and afternoon.

the record of solar cell power versus voltage data.

The battery charged voltage (red) and charge current (blue) are shown in Figure 12. When the battery voltage is close to the setpoint voltage 14.3V, then controller reduce the charge current command limit to 0.01C to float charge state to keep the battery maintain full voltage state, and ultimately battery voltage will maintain at the setpoint value 14.3V.

B. solar irradiation experiments: Cloudy 12:35

At this condition, the sun illumination is 714W/m2 and the solar cells temperature is 60 degrees, Figure 13 is the maximum power point tracking record graph. At this time, because the sun illumination not enough to make controller to set the charge current command limit to 0.1C, therefore; controller is set to MPPT charge mode, Figure 14 is the solar cell V-I curve.

Due to insufficient light in the morning and afternoon, he battery voltage is less than 14.3, the controller is set to MPPT charge mode automatically, and therefore maximum power tracking is activated. Figure 15 is the Maximum power tracking record plots in a long period of time.

V. CONCLUSIONS

This paper have completed SEPIC converter circuit board and implemented the fuzzy control strategy. In order to obtain the high efficient solar cell energy conversion, a FMPPT control is activated if the solarization is insufficient. The fuzzy controller has been successfully to maintain a charged current so as that the battery voltage can reach to desired value, 0.1C charged current command and 0.01C floating charged current command. Three cases of the experimental results show that the circuit design and the proposed charge strategy are effective and feasible.

ACKNOWLEDGMENT

The work is supported by the National Science Council, Taiwan, under grants NSC-99-2221-E-027-101 and NSC-98-2622-E-168-013-CC3.

REFERENCES

[1] C. C. Hua and C. M. Shen, "Control of DC/DC Converters for Solar Energy System with Maximum Power Tracking," *Industrial Electronics, Control and Instrumentation*, vol.3, pp. 1705–1710, 1996.

[2] L. Zhang, A. A. Amoudi and Y. F. Bai, "Real–Time Maximum Power Point Tracking for Grid–Connected Photovoltaic Systems," *Power Electronics and Variable Speed Drives*, No. 475, pp. 124–129, 2000.

[3] H. S. H. Chung, K. K. Tse, S. Y. R. Hui and C. M. Mok, "A Novel Maximum Power Point Tracker for PV Systems," *IEE proc. Gener. Transm. Distrib*, pp. 321–327, 2001.

[4] K. H. I. Husein, T. Hoshino, and M. Osakada, "Maximum Photovoltaic Power Tracking: An algorithm for Rapidly Changing Atmospheric Condition," *IEE Proceedings: Generation, Transmission and Distribution*, vol. 142, No. 1, pp. 59-64, 1995.

[5] H. Tarik Duru, "A maximum power tracking algorithm based on Impp =f(Pmax) function for matching passive and active loads to a photovoltaic generator," *Solar Energy*, vol. 80 pp.812–822, 2006.

[6] R. Ito, Y. Matsuzaski, T Tani,.and T. Yachi, "Evaluation of performance of MPPT equipment in photovoltaic system," *INTELEC 03*, pp. 256–260, 2003.

[7] H. S.-H. Chung, K. K. Tse, S. Y. R. Hui, C. M. Mok, and M. T. Ho,"A Novel Maximum Power Point Tracking Technique for Solar Panels Using a SEPIC or Cuk Converter," *IEEE Transaction on Power Electronics,* Vol. 18, No. 3, pp.717-724, 2003.

[8] C. C. Hua, C M. Shen, "Control of DC/DC Converters for Solar Energy System with Maximum PowerTracking,"*Industrial Electronics, Control and Instrumentation*, vol.3, pp. 1705–1710, 1996.

[9] H. S. H. Chung, K. K. Tse, S. Y. R. Hui and C. M. Mok, "A Novel Maximum Power Point Tracker for PV Systems," *IEE proc. Gener. Transm. Distrib*, pp. 321–327, 2001.

[10] D. Adar, G. Rahav, and S. Ben-Yaakov, "A unified Behavioral Average Model of SEPIC Converters with Coupled Inductors," *IEEE PESC,* pp.441-446,1997.

[11] S. J. Chiang, H. J. Shieh, and M. C. Chen, "Modeling and Control of PV Charger System with SEPIC Converter," *IEEE Transaction on Industrial Electronics*, Vol. 56, pp. 4344 – 4353,2009.

[12] R. F. Coelho, F. Concer, and D. C. Martins, "A study of the basic DC-DC converter applied in maximum power point tracking," *COBEP '09*, pp. 673 – 678, 2009.

[13] C. Elmas, O. Deperlioglu, and H. H. Sayan, "Adaptive fuzzy logic controller for DC–DC converters," *Expert Systems with Applications*, Vol. 36,pp. 1540–1548,2009.

[14] C.-C. LEE, "fuzzy logic in control sytems:part I," *IEEE Transactions on systems, Man, and Cybernetics ,* vol. 20, no.2, 1990.

[15] C. Elmas, O. Deperlioglu, and H. H. Sayan, "Adaptive fuzzy logic controller for DC–DC converters," *Expert Systems with Applications*, vol. 36 pp.1540–1548,2009.

[16] Y. M..Park, U. C. Moon, and Lee, K. Y., "A self-organizing a fuzzy logic controller for dynamic systems using a fuzzy auto-regressive average model," *IEEE Transactions on Fuzzy Systems*, vol.3, pp.75–82, 1995.

[17] L. X. Wang, "Stable adaptive fuzzy logic controller of nonlinear systems,". *IEEE Transactions on Fuzzy Systems*, 1(2), 146–155, 1993.

[18] G. C. Hwang and S. C. Lin, "A stability approach to fuzzy control design for nonlinear systems," *Fuzzy sets and Systems*, vol. 48, pp. 79-287, 1992.

[19] T. Furukawa, S. Kawamoto, and T. Taniguchi, "Sliding mode controller design based on fuzzy inference for nonlinear systems," *IEEE Trans. on Industrial Electronics,* vol. 40, pp. 64-70, 1993.

[20] J. Y. Chen, "Expert SMC-based fuzzy control with genetic algorithms," *Journal of the Franklin Institute,* vol. 336, pp. 589-610, 1999.

[21] C. C. Wong and S. M. Feng, "Switching-type fuzzy controller design by genetic algorithms," *Fuzzy Sets and Systems*, vol.74, pp. 174-185, 1995.

[22] S. C. Lin and Y. Y. Chen, "Design of self-learning fuzzy sliding mode controllers based on genetic algorithms," *Fuzzy Sets and Systems*, vol. 86, pp. 129-153, 1997.

[23]J. Falin, "Designing DC/DC Converter Based on SEPIC topology," Texas Instrunments Incorporated, Power Management, Senior Appliction Engineer,2008.

2011 IEEE International Conference on Fuzzy Systems
June 27-30, 2011, Taipei, Taiwan

Fuzzy Approaches for Multiobjective Stochastic Linear Programming Problems Considering Both Probability Maximization and Fractile Optimization

Hitoshi Yano
School of Humanities and Social Sciences, Nagoya City University
Yamanohata, Mizuho-cho, Mizuho-ku, Nagoya, 467-8501, Japan
Email: yano@hum.nagoya-cu.ac.jp

***Abstract*—In this paper, we propose two kinds of fuzzy approaches to obtain a satisfactory solution for multiobjective stochastic linear programming problems, in which the criteria of probability maximization and fractile optimization are considered simultaneously. In the first approach, a probability maximization model is applied to multiobjective stochastic linear programming problems, where the decision maker is required to specify not permissible objective levels but the corresponding membership functions which represent fuzzy goals for permissible objective levels. By adopting the fuzzy decision to integrate both the membership functions for permissible objective levels and the ones for the probability functions, a probability maximization model is transformed to the maxmin problem without permissible objective levels as parameters. Similarly, in the second approach, a fractile optimization model is applied to multiobjective stochastic linear programming problems, where the decision maker is required to specify not permissible probability levels but the corresponding membership functions which represent fuzzy goals for permissible probability levels. By adopting the fuzzy decision to integrate both the membership functions for permissible probability levels and the ones for the objective functions, a fractile optimization model is transformed to the maxmin problem without permissible probability levels as parameters. It is shown that such two fuzzy approaches are same.**

Keywords- multiobjective stochastic linear programming; probability maximization; fractile optimization; fuzzy decision

I. INTRODUCTION

In the real world decision making situations, we often have to make a decision under uncertainty. In order to deal with decision problems involving uncertainty, stochastic programming approaches and fuzzy programming approaches have been developed. In stochastic programming approaches, two stage problems [3] and chance constrained programming models [1] have been investigated in various ways, and they were extended to multiobjective stochastic programming problems [7],[10]. In fuzzy programming approaches, various types of fuzzy programming problems have been formulated and investigated [5],[6],[12]. As a natural extension, multiobjective fuzzy programming technique first proposed by Zimmermann [11], and many methods have been proposed [8],[12].

Recently, in order to deal with probabilistic uncertainty and fuzzy one simultaneously, the hybrid approaches of stochastic programming and fuzzy programming have been proposed [4]. Especially, Sakawa et al. [9] proposed an interactive fuzzy satisficing method for multiobjective linear programming problem with random variable coefficients. In their method, a probability maximization model was adopted to transform stochastic programming problems into well-defined mathematical programming ones. When adopting a probability maximization model, it is required in advance that the decision maker specifies permissible levels for objective functions (called permissible objective levels) in his/her subjective manner. However, it seems to be very difficult to specify such values in advance, because there exist conflicts among permissible objective levels and the corresponding distribution function values. This means that the less values of permissible objective levels for minimization problems results in the less values of the corresponding distribution function. On the other hand, when a fractile optimization model is adopted, it is required in advance that the decision maker specifies permissible levels for the probability levels (called permissible probability levels) in his/her subjective manner. Similar to a probability maximization model, there exist conflicts among permissible probability levels and the corresponding objective function values. This means that the larger values of permissible probability levels results in the larger values of the corresponding objective function for minimization problems.

In this paper, we propose two kinds of fuzzy approaches to obtain a satisfactory solution for multiobjective stochastic linear programming problems, in which the criteria of probability maximization and fractile optimization are considered simultaneously. In section II, in order to deal with a probability maximization model and a fractile optimization model for multiobjective stochastic linear programming problems, P-Pareto optimal solution concept and F-Pareto optimal solution concept are defined respectively. The relationships between them are investigated. In section III, a probability maximization model is applied to multiobjective stochastic linear programming problems, where the decision maker is required to specify the membership functions which represent fuzzy goals for permissible objective levels. By adopting the fuzzy decision [8],[12] to integrate both the membership functions for permissible objective levels and the ones for the probability functions, a probability maximization model is transformed

978-1-4244-7316-8/11/$26.00 ©2011 IEEE

to the maxmin problem without permissible objective levels as parameters. In section IV, a fractile optimization model is applied to multiobjective stochastic linear programming problems, where the decision maker is required to specify the membership functions which represent fuzzy goals for permissible probability levels. By adopting the fuzzy decision [8],[12] to integrate both the membership functions for permissible probability levels and the ones for the objective functions, a fractile optimization model is transformed to the maxmin problem without permissible probability levels as parameters. It is shown that two types of maxmin problems based on a probability maximization model and a fractile optimization model are same. In section V, an illustrative numerical example, which is formulated by Sakawa et al. [9], for multiobjective stochastic linear programming problems demonstrates the feasibility of the proposed approach.

II. Two Formulations for Multiobjective Stochastic Linear Programming Problems Through a Probability Maximization Model and a Fractile Optimization Model

In this section, we focus on multiobjective linear programming problem involving random variable coefficients in objective functions and the right-hand side of constraints, which is called multiobjective stochastic linear programming problem (MOSLP). MOSLP can be formally formulated as follows.

[MOSLP]

$$\min_{\boldsymbol{x}\geq\boldsymbol{0}} \boldsymbol{z}(\boldsymbol{x},\omega) = (z_1(\boldsymbol{x},\omega),\cdots,z_k(\boldsymbol{x},\omega)) \tag{1}$$

subject to

$$A\boldsymbol{x} \leq \boldsymbol{b}(\omega) \tag{2}$$

where $\boldsymbol{x} = (x_1, x_2, \cdots, x_n)^T$ is an n dimensional decision variable column vector,

$$z_i(\boldsymbol{x},\omega) = \boldsymbol{c}_i(\omega)\boldsymbol{x} + \alpha_i(\omega), i = 1,\cdots,k, \tag{3}$$

are multiobjective functions involving random variable coefficients, $\boldsymbol{c}_i(\omega)$ is a n dimensional random variable row vector expressed by $\boldsymbol{c}_i(\omega) = \boldsymbol{c}_i^1 + t_i(\omega)\boldsymbol{c}_i^2$ where $t_i(\omega)$ is a random variable and $\alpha_i(\omega)$ is a random variable row vector expressed by $\alpha_i(\omega) = \alpha_i^1 + t_i(\omega)\alpha_i^2$. A is an $(m\times n)$ coefficient matrix, $\boldsymbol{b}(\omega) = (b_1(\omega),\cdots,b_m(\omega))^T$ is an m dimensional column vector, whose elements $b_j(\omega), j = 1,\cdots,m$ are random variables independent each other. Let us denote distribution functions of random variables $t_i(\omega)$ and $b_j(\omega)$ as follows.

$$T_i(r) \stackrel{\text{def}}{=} \Pr(t_i(\omega) < r), i = 1,\cdots,k \tag{4}$$

$$F_j(r) \stackrel{\text{def}}{=} \Pr(b_j(\omega) < r), j = 1,\cdots,m \tag{5}$$

It is assumed that distribution functions $T_i(\cdot), i = 1,\cdots,k$ and $F_j(\cdot), j = 1,\cdots,m$ are strictly increasing and continuous.

Since MOSLP contains random variable coefficients in objective functions and the right-hand side of constraints, mathematical programming techniques can not be directly applied. In order to deal with MOSLP, we interpret the constraints (2) as chance constrained conditions [1], which mean that the j-th constraint of (2) is required to be satisfied with a certain probability β_j (called a constraint probability level) and over.

$$X(\boldsymbol{\beta}) = \{\boldsymbol{x} \geq \boldsymbol{0} \mid \Pr(\boldsymbol{a}_j\boldsymbol{x} \leq b_j(\omega)) \geq \beta_j, j = 1,\cdots,m\} \tag{6}$$

where $\boldsymbol{a}_j$ is the j-th row vector of A. Using a distribution function $F_j(r)$, the j-th constraint in (6) can be rewritten as follows.

$$\begin{aligned} & \Pr(\boldsymbol{a}_j\boldsymbol{x} \leq b_j(\omega)) \geq \beta_j, \\ \Leftrightarrow\ & 1 - F_j(\boldsymbol{a}_j\boldsymbol{x}) \geq \beta_j, \\ \Leftrightarrow\ & F_j(\boldsymbol{a}_j\boldsymbol{x}) \leq 1 - \beta_j, \\ \Leftrightarrow\ & \boldsymbol{a}_j\boldsymbol{x} \leq F_j^{-1}(1-\beta_j) \end{aligned}$$

where $F_j^{-1}(\cdot)$ means a pseudo-inverse function corresponding to $F_j(\cdot)$ defined by $F_j^{-1}(h) = \inf\{y \mid F_j(y) \geq h\}$.

Under the above chance constrained conditions (6), if we adopt a probability maximization model for the objective functions in MOSLP, we can substitute the minimization of the objective functions $z_i(\boldsymbol{x},\omega) = \boldsymbol{c}_i(\omega)\boldsymbol{x} + \alpha_i(\omega), i = 1,\cdots,k$ for the maximization of the probability that each objective functions $z_i(\boldsymbol{x},\omega)$ is less than or equal to a certain permissible level $\bar{f}_i$ (called a permissible objective level). Such a probability function can be defined as follows.

$$p_i(\boldsymbol{x},\bar{f}_i) \stackrel{\text{def}}{=} \Pr(z_i(\boldsymbol{x},\omega) \leq \bar{f}_i), i = 1,\cdots,k \tag{7}$$

where

$$\bar{\boldsymbol{f}} = (\bar{f}_1,\cdots,\bar{f}_k). \tag{8}$$

is a k-dimensional vector of permissible objective levels which are specified by the decision maker in his/her subjective manner. Then, MOSLP can be converted as the following form.

[MOP1($\bar{\boldsymbol{f}},\boldsymbol{\beta}$)]

$$\max_{\boldsymbol{x}\in X(\boldsymbol{\beta})} (p_1(\boldsymbol{x},\bar{f}_1),\cdots,p_k(\boldsymbol{x},\bar{f}_k)) \tag{9}$$

In MOP1($\bar{\boldsymbol{f}},\boldsymbol{\beta}$), assuming that $\boldsymbol{c}_i^2\boldsymbol{x} + \alpha_i^2 > 0, i = 1,\cdots,k$ for any $\boldsymbol{x} \in X(\boldsymbol{\beta})$, we can rewrite the objective function $p_i(\boldsymbol{x},\bar{f}_i)$ as follows.

$$\begin{aligned} p_i(\boldsymbol{x},\bar{f}_i) &= \Pr(z_i(\boldsymbol{x},\omega) \leq \bar{f}_i) \\ &= \Pr(\boldsymbol{c}_i(\omega)\boldsymbol{x} + \alpha_i(\omega) \leq \bar{f}_i) \\ &= \Pr((\boldsymbol{c}_{r\ell}^1 + t_{r\ell}(\omega)\boldsymbol{c}_{r\ell}^2)\boldsymbol{x} \\ &\quad +(\alpha_{r\ell}^1 + t_{r\ell}(\omega)\alpha_{r\ell}^2) \leq f_{r\ell}) \\ &= \Pr\left(t_i(\omega) \leq \frac{\bar{f}_i - (\boldsymbol{c}_i^1\boldsymbol{x} + \alpha_i^1)}{\boldsymbol{c}_i^2\boldsymbol{x} + \alpha_i^2}\right) \\ &= T_i\left(\frac{\bar{f}_i - (\boldsymbol{c}_i^1\boldsymbol{x} + \alpha_i^1)}{\boldsymbol{c}_i^2\boldsymbol{x} + \alpha_i^2}\right) \end{aligned}$$

In order to deal with MOP1($\bar{\boldsymbol{f}},\beta$), we introduce a P-Pareto optimal solution concept as follows.

Definition 1.

$\boldsymbol{x}^* \in X(\boldsymbol{\beta})$ is said to be a P-Pareto optimal solution to MOP1($\bar{\boldsymbol{f}},\boldsymbol{\beta}$), if and only if there does not exist another $\boldsymbol{x} \in X(\boldsymbol{\beta})$ such that $p_i(\boldsymbol{x},\bar{f}_i) \geq p_i(\boldsymbol{x}^*,\bar{f}_i)$, $i = 1,\cdots,k$, with strict inequality holding for at least one i.

On the other hand, if we adopt a fractile optimization model for the objective functions in MOSLP under the chance constrained conditions (6), we can convert MOSLP to the following multiobjective programming problem.

[MOP2($\bar{\boldsymbol{p}}, \boldsymbol{\beta}$)]

$$\min_{\boldsymbol{x} \in X(\boldsymbol{\beta}), \bar{f}_i, i=1,\cdots,k} (\bar{f}_1, \cdots, \bar{f}_k) \tag{10}$$

subject to

$$p_i(\boldsymbol{x}, \bar{f}_i) \geq \bar{p}_i, i = 1, \cdots, k \tag{11}$$

where

$$\bar{\boldsymbol{p}} = (\bar{p}_1, \cdots, \bar{p}_k) \tag{12}$$

is a k-dimensional vector of permissible probability levels which are specified by the decision maker in his/her subjective manner.

In MOP2($\bar{\boldsymbol{p}}, \beta$), since a distribution function $T_i(\cdot)$ is continuous and strictly increasing and continuous, the constraints (11) can be transformed to the following form.

$$\begin{aligned} \bar{p}_i &\leq p_i(\boldsymbol{x}, \bar{f}_i) = T_i\left(\frac{\bar{f}_i - (\boldsymbol{c}_i^1 \boldsymbol{x} + \alpha_i^1)}{\boldsymbol{c}_i^2 \boldsymbol{x} + \alpha_i^2}\right) \\ \Leftrightarrow \bar{f}_i &\geq T_i^{-1}(\bar{p}_i) \cdot (\boldsymbol{c}_i^2 \boldsymbol{x} + \alpha_i^2) + (\boldsymbol{c}_i^1 \boldsymbol{x} + \alpha_i^1) \end{aligned} \tag{13}$$

Let us define the right-hand side of the inequality (13) as follows.

$$f_i(\boldsymbol{x}, \bar{p}_i) \stackrel{\text{def}}{=} T_i^{-1}(\bar{p}_i) \cdot (\boldsymbol{c}_i^2 \boldsymbol{x} + \alpha_i^2) + (\boldsymbol{c}_i^1 \boldsymbol{x} + \alpha_i^1) \tag{14}$$

Then, MOP2($\bar{\boldsymbol{p}}, \boldsymbol{\beta}$) can be equivalently reduced to the following simple form, where $\bar{f}_i, i = 1, \cdots, k$ are disappeared.

[MOP3($\bar{\boldsymbol{p}}, \boldsymbol{\beta}$)]

$$\min_{\boldsymbol{x} \in X(\boldsymbol{\beta})} (f_1(\boldsymbol{x}, \bar{p}_1), \cdots, f_k(\boldsymbol{x}, \bar{p}_k)) \tag{15}$$

In order to deal with MOP3($\bar{\boldsymbol{p}}, \boldsymbol{\beta}$), we introduce an F-Pareto optimal solution concept as follows.

Definition 2.

$\boldsymbol{x}^* \in X(\boldsymbol{\beta})$ is said to be an F-Pareto optimal solution to MOP3($\bar{\boldsymbol{p}}, \boldsymbol{\beta}$), if and only if there does not exist another $\boldsymbol{x} \in X(\boldsymbol{\beta})$ such that $f_i(\boldsymbol{x}, \bar{p}_i) \leq f_i(\boldsymbol{x}^*, \bar{p}_i),\ i = 1, \cdots, k$, with strict inequality holding for at least one i.

The relationships between a P-Pareto optimal solution to MOP1($\bar{\boldsymbol{f}}, \boldsymbol{\beta}$) and an F-Pareto optimal solution to MOP3($\bar{\boldsymbol{p}}, \boldsymbol{\beta}$) can be characterized by the following theorem.

Theorem 1.

(1) If $\boldsymbol{x}^* \in X(\boldsymbol{\beta})$ is a P-Pareto optimal solution to MOP1($\bar{\boldsymbol{f}}, \boldsymbol{\beta}$) for some given permissible objective levels $\bar{\boldsymbol{f}}$, then, there exist some permissible probability levels $\bar{\boldsymbol{p}}$ such that $\boldsymbol{x}^* \in X(\boldsymbol{\beta})$ is an F-Pareto optimal solution to MOP3($\bar{\boldsymbol{p}}, \boldsymbol{\beta}$).

(2) If $\boldsymbol{x}^* \in X(\boldsymbol{\beta})$ is an F-Pareto optimal solution to MOP3($\bar{\boldsymbol{p}}, \boldsymbol{\beta}$) for some given permissible probability levels $\bar{\boldsymbol{p}}$, then, there exist some permissible objective levels $\bar{\boldsymbol{f}}$ such that $\boldsymbol{x}^* \in X(\boldsymbol{\beta})$ is a P-Pareto optimal solution to MOP1($\bar{\boldsymbol{f}}, \boldsymbol{\beta}$).

(Proof)

(1) Assume that $\boldsymbol{x}^* \in X(\boldsymbol{\beta})$ is a P-Pareto optimal solution to MOP1($\bar{\boldsymbol{f}}, \boldsymbol{\beta}$) for some given permissible objective levels $\bar{\boldsymbol{f}}$. Then, from Definition 1, there does not exist $\boldsymbol{x} \in X(\boldsymbol{\beta})$ such that

$$\begin{aligned} & p_i(\boldsymbol{x}, \bar{f}_i) \geq p_i(\boldsymbol{x}^*, \bar{f}_i) \\ \Leftrightarrow\ & T_i\left(\frac{\bar{f}_i - (\boldsymbol{c}_i^1 \boldsymbol{x} + \alpha_i^1)}{\boldsymbol{c}_i^2 \boldsymbol{x} + \alpha_i^2}\right) \geq T_i\left(\frac{\bar{f}_i - (\boldsymbol{c}_i^1 \boldsymbol{x}^* + \alpha_i^1)}{\boldsymbol{c}_i^2 \boldsymbol{x}^* + \alpha_i^2}\right) \\ & i = 1, \cdots, k \end{aligned} \tag{16}$$

with strict inequality holding for at least one i. For the left-hand side of the inequality (16), let us set as :

$$\bar{p}_i = T_i\left(\frac{\bar{f}_i - (\boldsymbol{c}_i^1 \boldsymbol{x}^* + \alpha_i^1)}{\boldsymbol{c}_i^2 \boldsymbol{x}^* + \alpha_i^2}\right). \tag{17}$$

Then, because of the definition (14) and $\boldsymbol{c}_i^2 \boldsymbol{x} + \alpha_i^2 > 0$, the inequality (16) can be transformed as follows.

$$\begin{aligned} & T_i\left(\frac{\bar{f}_i - (\boldsymbol{c}_i^1 \boldsymbol{x} + \alpha_i^1)}{\boldsymbol{c}_i^2 \boldsymbol{x} + \alpha_i^2}\right) \geq \bar{p}_i \\ \Leftrightarrow\ & \bar{f}_i - (\boldsymbol{c}_i^1 \boldsymbol{x} + \alpha_i^1) \geq T_i^{-1}(\bar{p}_i) \cdot (\boldsymbol{c}_i^2 \boldsymbol{x} + \alpha_i^2) \\ \Leftrightarrow\ & \bar{f}_i \geq f_i(\boldsymbol{x}, \bar{p}_i) \end{aligned} \tag{18}$$

On the other hand, from the relationship (17), it immediately holds that

$$\begin{aligned} \bar{f}_i &= T_i^{-1}(\bar{p}_i) \cdot (\boldsymbol{c}_i^2 \boldsymbol{x}^* + \alpha_i^2) + (\boldsymbol{c}_i^1 \boldsymbol{x}^* + \alpha_i^1) \\ &= f_i(\boldsymbol{x}^*, \bar{p}_i). \end{aligned}$$

This means that there does not exist $\boldsymbol{x} \in X(\boldsymbol{\beta})$ such that $f_i(\boldsymbol{x}, \bar{p}_i) \leq f_i(\boldsymbol{x}^*, \bar{p}_i),\ i = 1, \cdots, k$ with strict inequality holding for at least one i. Therefore, $\boldsymbol{x}^* \in X(\boldsymbol{\beta})$ is an F-Pareto optimal solution to MOP3($\bar{\boldsymbol{p}}, \boldsymbol{\beta}$).

(2) The proof is same to (1).

Sakawa et al.[9] formulated multiobjective linear programming problems with random variable coefficients in objective functions through a probability maximization model. In their approach, assuming that the decision maker has a fuzzy goal for each distribution function $p_i(\boldsymbol{x}, \bar{f}_i)$, the satisfactory solution is derived from among M-Pareto optimal solution set by updating the reference membership levels in membership space. However, in a probability maximization model, the permissible objective levels $\bar{f}_i, i = 1, \cdots, k$ for the original objective functions $z_i(\boldsymbol{x}, \omega), i = 1, \cdots, k$ must be specified in advance by the decision. The less values for the permissible objective levels $\bar{f}_i, i = 1, \cdots, k$ in MOP1($\bar{\boldsymbol{f}}, \boldsymbol{\beta}$) will give the less values for the corresponding distribution functions $p_i(\boldsymbol{x}, \bar{f}_i), i = 1, \cdots, k$. As a result, if the decision maker specifies the less values for the permissible objective levels $\bar{f}_i, i = 1, \cdots, k$, he/she may not be able to accept any candidate of the satisfactory solution, because the corresponding values of the distribution functions $p_i(\boldsymbol{x}, \bar{f}_i), i = 1, \cdots, k$ will become close to zero.

On the other hand, instead of a probability maximization model, let us consider the case where a fractile optimization model is adopted to formulate multiobjective linear programming problems with random variable coefficients in objective functions. In such a model, the permissible probability levels $\bar{p}_i, i = 1, \cdots, k$ must be specified by the decision maker in advance. The larger values for the permissible probability

levels $\bar{p}_i, i = 1, \cdots, k$ will give the larger values for the objective functions $f_i(\boldsymbol{x}, \bar{p}_i), i = 1, \cdots, k$ for minimization problems. As a result, similar to the case where a probability maximization model is adopted, if the decision maker specifies the larger values for the permissible probability levels $\bar{p}_i, i = 1, \cdots, k$, he/she may not be able to accept any candidate of the satisfactory solution, because the corresponding values of the objective functions $f_i(\boldsymbol{x}, \bar{p}_i), i = 1, \cdots, k$ will become the larger values.

In the next section, we assume that, the decision maker has fuzzy goals for not only each distribution function $p_i(\boldsymbol{x}, \bar{f}_i)$ but also each permissible objective levels $\bar{f}_i$ for MOSLP through a probability maximization model. After eliciting the membership functions for such fuzzy goals, we propose a fuzzy approach for MOSLP through a probability maximization model. to obtain the satisfactory solution.

III. A Fuzzy Approach for Multiobjective Stochastic Linear Programming Problems Through a Probability Maximization Model

In this section, we propose a fuzzy approach to MOP1($\bar{\boldsymbol{f}}, \boldsymbol{\beta}$) where MOSLP is formulated through a probability maximization model. In order to deal with MOP1($\bar{\boldsymbol{f}}, \boldsymbol{\beta}$), the decision maker must specify his/her permissible objective levels $\bar{\boldsymbol{f}}$ in advance. However, in general, the decision maker seems to prefer not only the larger value of the distribution function $p_i(\boldsymbol{x}, \bar{f}_i)$ but also the less value of permissible objective level $\bar{f}_i$. Since these values conflict with each other, the less values of permissible objective level $\bar{f}_i$ results in the less value of probability function $p_i(\boldsymbol{x}, \bar{f}_i)$. From such a point of view, we consider the following multiobjective programming problem which can be regarded as a natural extension of MOP1($\bar{\boldsymbol{f}}, \boldsymbol{\beta}$).

[MOP4($\boldsymbol{\beta}$)]

$$\max_{\boldsymbol{x} \in X(\boldsymbol{\beta}), \bar{f}_i, i=1,\cdots,k} \big(p_1(\boldsymbol{x}, \bar{f}_1), \cdots, p_k(\boldsymbol{x}, \bar{f}_k), -\bar{f}_1, \cdots, -\bar{f}_k\big) \tag{19}$$

It should be noted in MOP4($\boldsymbol{\beta}$) that the permissible objective levels $\bar{f}_i, i = 1, \cdots, k$ are not the fixed values but the decision variables.

Considering the imprecise nature of the decision maker's judgment, it is natural to assume that the decision maker have fuzzy goals for each objective function in MOP4($\boldsymbol{\beta}$). In this section, we assume that such fuzzy goals can be quantified by eliciting the corresponding membership functions. Let us denote a membership function of a probability function $p_i(\boldsymbol{x}, \bar{f}_i)$ as $\mu_{p_i}(p_i(\boldsymbol{x}, \bar{f}_i))$, and a membership function of a permissible objective level $\bar{f}_i$ as $\mu_{\bar{f}_i}(\bar{f}_i)$ respectively. Then, MOP4($\boldsymbol{\beta}$) can be transformed as the following multiobjective programming problem.

[MOP5($\boldsymbol{\beta}$)]

$$\max_{\boldsymbol{x} \in X(\boldsymbol{\beta}), \bar{f}_i, i=1,\cdots,k} \big(\mu_{p_1}(p_1(\boldsymbol{x}, \bar{f}_1)), \cdots, \mu_{p_k}(p_k(\boldsymbol{x}, \bar{f}_k)), \mu_{\bar{f}_1}(\bar{f}_1), \cdots, \mu_{\bar{f}_k}(\bar{f}_k)\big) \tag{20}$$

Throughout this section, we make the following assumptions.

Assumption 1.
$\mu_{\bar{f}_i}(\bar{f}_i), i = 1, \cdots, k$ are strictly decreasing and continuous with respect to $\bar{f}_i$.

Assumption 2.
$\mu_{p_i}(p_i(\boldsymbol{x}, \bar{f}_i)), i = 1, \cdots, k$ are strictly increasing and continuous with respect to $p_i(\boldsymbol{x}, \bar{f}_i)$.

For example, we can define the membership functions $\mu_{\bar{f}_i}(\bar{f}_i)$, $\mu_{p_i}(p_i(\boldsymbol{x}, \bar{f}_i)), i = 1, \cdots, k$ as follows. Considering the individual minimum and maximum of $E(z_i(\boldsymbol{x}, \omega))$:

$$\min_{\boldsymbol{x} \in X(\boldsymbol{\beta})} \; / \; \max_{\boldsymbol{x} \in X(\boldsymbol{\beta})} E(z_i(\boldsymbol{x}, \omega)), i = 1, \cdots, k,$$

the decision maker subjectively specifies a sufficiently satisfactory maximum value $f_{i\min}$ and an acceptable maximum value $f_{i\max}$. Then, the domain of $\mu_{\bar{f}_i}(\bar{f}_i)$ can be set as:

$$F_i = [f_{i\min}, f_{i\max}]. \tag{21}$$

According to Assumption 1, the decision maker can define his/her membership function $\mu_{\bar{f}_i}(\bar{f}_i)$ on the domain F_i. Corresponding to the domain F_i, let us denote the domain of $\mu_{p_i}(p_i(\boldsymbol{x}, f_i))$ as:

$$P_i(F_i) = [p_{i\min}, p_{i\max}]. \tag{22}$$

where $p_{i\min}$ is an acceptable minimum value and $p_{i\max}$ is a sufficiently satisfactory minimum value. $p_{i\max}$ can be obtained by solving the following problem.

$$p_{i\max} = \max_{\boldsymbol{x} \in X(\boldsymbol{\beta})} p_i(\boldsymbol{x}, f_{i\max}) \tag{23}$$

It should be noted here that the above problem is equivalent to the following linear fractional programming problem [2] because a distribution function $T_i(\cdot)$ is strictly increasing and continuous.

$$\max_{\boldsymbol{x} \in X(\boldsymbol{\beta})} \left(\frac{f_{i\max} - (\boldsymbol{c}_i^1 \boldsymbol{x} + \alpha_i^1)}{\boldsymbol{c}_i^2 \boldsymbol{x} + \alpha_i^2} \right) \tag{24}$$

On the other hand, in order to obtain $p_{i\min}$, we first solve $\max_{\boldsymbol{x} \in X(\boldsymbol{\beta})} p_i(\boldsymbol{x}, f_{i\min})$, and denote the corresponding optimal solution as $\boldsymbol{x}_i$. Using the optimal solutions $\boldsymbol{x}_i, i = 1, \cdots, k$, $p_{i\min}$ can be obtained as follows.

$$p_{i\min} = \min_{\ell=1,\cdots,k, \ell \neq i} p_i(\boldsymbol{x}_\ell, f_{i\min}) \tag{25}$$

According to Assumption 2, the decision maker can define his/her membership function $\mu_{p_i}(p_i(\boldsymbol{x}, \bar{f}_i))$ on the domain $P_i(F_i)$.

Then, if the decision maker adopts the fuzzy decision [8],[12] as an aggregation operator for MOP5($\boldsymbol{\beta}$), the satisfactory solution is obtained by solving the following maxmin problem.

[MAXMIN1]

$$\max_{\boldsymbol{x} \in X(\boldsymbol{\beta}), \bar{f}_i \in F_i, i=1,\cdots,k, \lambda \in [0,1]} \lambda \tag{26}$$

subject to

$$\mu_{p_i}(p_i(\boldsymbol{x}, \bar{f}_i)) \geq \lambda, i = 1, \cdots, k \tag{27}$$

$$\mu_{\bar{f}_i}(\bar{f}_i) \geq \lambda, i = 1, \cdots, k \tag{28}$$

Because of Assumption 2 and $\boldsymbol{c}_i^2\boldsymbol{x}+\alpha_i^2>0$, the constraints (27) can be transformed as:

$$\begin{aligned}
&\mu_{p_i}(p_i(\boldsymbol{x},\bar{f}_i))\geq\lambda,\\
\Leftrightarrow\quad & p_i(\boldsymbol{x},\bar{f}_i)\geq\mu_{p_i}^{-1}(\lambda),\\
\Leftrightarrow\quad & T_i\left(\frac{\bar{f}_i-(\boldsymbol{c}_i^1\boldsymbol{x}+\alpha_i^1)}{\boldsymbol{c}_i^2\boldsymbol{x}+\alpha_i^2}\right)\geq\mu_{p_i}^{-1}(\lambda),\\
\Leftrightarrow\quad & \bar{f}_i-(\boldsymbol{c}_i^1\boldsymbol{x}+\alpha_i^1)\geq T_i^{-1}(\mu_{p_i}^{-1}(\lambda))\cdot(\boldsymbol{c}_i^2\boldsymbol{x}+\alpha_i^2),
\end{aligned}\tag{29}$$

where $\mu_{p_i}^{-1}(\cdot)$ is a pseudo-inverse function. From the constraints (28) and Assumption 1, it holds that $\bar{f}_i\leq\mu_{\bar{f}_i}^{-1}(\lambda)$. Therefore, the constraint (29) can be reduced to the following inequality where a permissible objective level $\bar{f}_i$ is disappeared.

$$\mu_{\bar{f}_i}^{-1}(\lambda)-(\boldsymbol{c}_i^1\boldsymbol{x}+\alpha_i^1)\geq T_i^{-1}(\mu_{p_i}^{-1}(\lambda))\cdot(\boldsymbol{c}_i^2\boldsymbol{x}+\alpha_i^2)\tag{30}$$

Then, MAXMIN1 is equivalently transformed into the following problem.

[MAXMIN2]

$$\max_{\boldsymbol{x}\in X(\boldsymbol{\beta}),\lambda\in[0,1]}\ \lambda\tag{31}$$

subject to

$$\begin{aligned}
\mu_{\bar{f}_i}^{-1}(\lambda)-(\boldsymbol{c}_i^1\boldsymbol{x}+\alpha_i^1)\quad\geq\quad & T_i^{-1}(\mu_{p_i}^{-1}(\lambda))\cdot(\boldsymbol{c}_i^2\boldsymbol{x}+\alpha_i^2),\\
& i=1,\cdots,k
\end{aligned}\tag{32}$$

It should be noted here that the constraints (32) can be reduced to a set of linear inequalities for some fixed value $\lambda\in[0,1]$. This means that an optimal solution $(\boldsymbol{x}^*,\lambda^*)$ of MAXMIN2 is obtained by combined use of the bisection method with respect to λ and the first-phase of the two-phase simplex method of linear programming.

The relationships between the optimal solution $(\boldsymbol{x}^*,\lambda^*)$ of MAXMIN2, P-Pareto optimal solutions to MOP1$(\bar{\boldsymbol{f}},\boldsymbol{\beta})$, and F-Pareto optimal solutions to MOP3$(\bar{\boldsymbol{p}},\boldsymbol{\beta})$ can be characterized by the following theorem.

Theorem 2.

(1) If $(\boldsymbol{x}^*,\lambda^*)$ is a unique optimal solution of MAXMIN2, then $\boldsymbol{x}^*\in X(\boldsymbol{\beta})$ is a P-Pareto optimal solution to MOP1$(\bar{\boldsymbol{f}}^*,\boldsymbol{\beta})$, where $\bar{\boldsymbol{f}}^*=(\bar{f}_1^*,\cdots,\bar{f}_k^*)=(\mu_{\bar{f}_1}^{-1}(\lambda^*),\cdots,\mu_{\bar{f}_k}^{-1}(\lambda^*))$.

(2) If $(\boldsymbol{x}^*,\lambda^*)$ is a unique optimal solution of MAXMIN2, then $\boldsymbol{x}^*\in X(\boldsymbol{\beta})$ is an F-Pareto optimal solution to MOP3$(\bar{\boldsymbol{p}}^*,\boldsymbol{\beta})$, where $\bar{\boldsymbol{p}}^*=(\bar{p}_1^*,\cdots,\bar{p}_k^*)=(\mu_{p_1}^{-1}(\lambda^*),\cdots,\mu_{p_k}^{-1}(\lambda^*))$.

(Proof)

(1) Let $(\boldsymbol{x}^*,\lambda^*)$ be a unique optimal solution of MAXMIN2. Since an optimal solution $(\boldsymbol{x}^*,\lambda^*)$ satisfies the constraints (32), it holds that

$$\begin{aligned}
&\mu_{\bar{f}_i}^{-1}(\lambda^*)-(\boldsymbol{c}_i^1\boldsymbol{x}^*+\alpha_i^1)\\
&\geq T_i^{-1}(\mu_{p_i}^{-1}(\lambda^*))\cdot(\boldsymbol{c}_i^2\boldsymbol{x}^*+\alpha_i^2),\\
\Leftrightarrow\quad & T_i\left(\frac{\mu_{\bar{f}_i}^{-1}(\lambda^*)-(\boldsymbol{c}_i^1\boldsymbol{x}^*+\alpha_i^1)}{\boldsymbol{c}_i^2\boldsymbol{x}^*+\alpha_i^2}\right)=p_i(\boldsymbol{x}^*,\mu_{\bar{f}_i}^{-1}(\lambda^*))\\
&\geq\mu_{p_i}^{-1}(\lambda^*),i=1,\cdots,k.
\end{aligned}$$

Assume that $\boldsymbol{x}^*\in X(\beta)$ is not a P-Pareto optimal solution to MOP1$(\bar{\boldsymbol{f}}^*,\boldsymbol{\beta})$, where $\bar{\boldsymbol{f}}^*=(\mu_{\bar{f}_1}^{-1}(\lambda^*),\cdots,\mu_{\bar{f}_k}^{-1}(\lambda^*))$, then there exists $\boldsymbol{x}\in X(\boldsymbol{\beta})$ such that

$$\begin{aligned}
&p_i(\boldsymbol{x},\mu_{\bar{f}_i}^{-1}(\lambda^*))\geq p_i(\boldsymbol{x}^*,\mu_{\bar{f}_i}^{-1}(\lambda^*))\geq\mu_{p_i}^{-1}(\lambda^*),\\
&i=1,\cdots,k.
\end{aligned}$$

This means that there exists $\boldsymbol{x}\in X(\boldsymbol{\beta})$ such that

$$\begin{aligned}
\mu_{\bar{f}_i}^{-1}(\lambda^*)-(\boldsymbol{c}_i^1\boldsymbol{x}+\alpha_i^1)\quad\geq\quad & T_i^{-1}(\mu_{p_i}^{-1}(\lambda^*))\cdot(\boldsymbol{c}_i^2\boldsymbol{x}+\alpha_i^2),\\
& i=1,\cdots,k,
\end{aligned}$$

which contradicts the fact that $(\boldsymbol{x}^*,\lambda^*)$ is a unique optimal solution of MAXMIN2.

(2) Assume that $\boldsymbol{x}^*\in X(\boldsymbol{\beta})$ is not an F-Pareto optimal solution to MOP3$(\bar{\boldsymbol{p}}^*,\boldsymbol{\beta})$, where $\bar{p}_i^*=\mu_{p_i}^{-1}(\lambda^*),i=1,\cdots,k$. Then, because of (14), there exists $\boldsymbol{x}\in X(\boldsymbol{\beta})$ such that

$$\begin{aligned}
&f_i(\boldsymbol{x},\bar{p}_i^*)\leq f_i(\boldsymbol{x}^*,\bar{p}_i^*)\\
\Leftrightarrow\quad & T_i^{-1}(\bar{p}_i^*)\cdot(\boldsymbol{c}_i^2\boldsymbol{x}+\alpha_i^2)+(\boldsymbol{c}_i^1\boldsymbol{x}+\alpha_i^1)\\
\leq\quad & T_i^{-1}(\bar{p}_i^*)\cdot(\boldsymbol{c}_i^2\boldsymbol{x}^*+\alpha_i^2)+(\boldsymbol{c}_i^1\boldsymbol{x}^*+\alpha_i^1)\stackrel{\text{def}}{=}\bar{f}_i^*\\
\Leftrightarrow\quad & \bar{f}_i^*-(\boldsymbol{c}_i^1\boldsymbol{x}+\alpha_i^1)\geq T_i^{-1}(\bar{p}_i^*)\cdot(\boldsymbol{c}_i^2\boldsymbol{x}+\alpha_i^2)\\
\Leftrightarrow\quad & \bar{f}_i^*-(\boldsymbol{c}_i^1\boldsymbol{x}+\alpha_i^1)\geq T_i^{-1}(\mu_{p_i}^{-1}(\lambda^*))\cdot(\boldsymbol{c}_i^2\boldsymbol{x}+\alpha_i^2)
\end{aligned}$$

On the other hand, since $(\boldsymbol{x}^*,\lambda^*)$ is an optimal solution of MAXMIN2, from (32), it holds that

$$\mu_{\bar{f}_i}^{-1}(\lambda^*)-(\boldsymbol{c}_i^1\boldsymbol{x}^*+\alpha_i^1)\geq T_i^{-1}(\mu_{p_i}^{-1}(\lambda^*))\cdot(\boldsymbol{c}_i^2\boldsymbol{x}^*+\alpha_i^2).$$

This means that

$$\begin{aligned}
\mu_{\bar{f}_i}^{-1}(\lambda^*)\quad\geq\quad & (\boldsymbol{c}_i^1\boldsymbol{x}^*+\alpha_i^1)+T_i^{-1}(\mu_{p_i}^{-1}(\lambda^*))\cdot(\boldsymbol{c}_i^2\boldsymbol{x}^*+\alpha_i^2)\\
=\quad & \bar{f}_i^*.
\end{aligned}$$

Therefore, it holds that

$$\begin{aligned}
\mu_{\bar{f}_i}^{-1}(\lambda^*)-(\boldsymbol{c}_i^1\boldsymbol{x}+\alpha_i^1)\quad\geq\quad & T_i^{-1}(\mu_{p_i}^{-1}(\lambda^*))\cdot(\boldsymbol{c}_i^2\boldsymbol{x}+\alpha_i^2),\\
& i=1,\cdots,k,
\end{aligned}$$

which contradicts the fact that $(\boldsymbol{x}^*,\lambda^*)$ is a unique optimal solution of MAXMIN2.

IV. A Fuzzy Approach for Multiobjective Stochastic Linear Programming Problems Through a Fractile Optimization Model

In this section, we propose a fuzzy approach to MOP3$(\bar{\boldsymbol{p}},\boldsymbol{\beta})$ where MOSLP is formulated through a fractile optimization model, and show that the corresponding formulation is same to MAXMIN2. In order to deal with MOP3$(\bar{\boldsymbol{p}},\boldsymbol{\beta})$, the decision maker must specify permissible probability levels $\bar{\boldsymbol{p}}$ in advance. However, in general, the decision maker seems to prefer not only the less value of the objective function $f_i(\boldsymbol{x},\bar{p}_i)$ of MOP3$(\bar{\boldsymbol{p}},\boldsymbol{\beta})$ but also the larger value of the permissible probability level $\bar{p}_i$. Since these values conflict with each other, the larger value of the permissible probability level $\bar{p}_i$ results in the larger value of the objective function $f_i(\boldsymbol{x},\bar{p}_i)$ of MOP3$(\bar{\boldsymbol{p}},\boldsymbol{\beta})$. From such a point of view, we consider the following multiobjective programming problem which can be regarded as a natural extension of MOP3$(\bar{\boldsymbol{p}},\boldsymbol{\beta})$.

[MOP6($\boldsymbol{\beta}$)]

$$\min_{\boldsymbol{x}\in X(\boldsymbol{\beta}),\bar{p}_i,i=1,\cdots,k} (f_1(\boldsymbol{x},\bar{p}_1),\cdots,f_k(\boldsymbol{x},\bar{p}_k),-\bar{p}_1,\cdots,-\bar{p}_k) \tag{33}$$

It should be noted in MOP6($\boldsymbol{\beta}$) that permissible probability levels $\bar{p}_i, i=1,\cdots,k$ are not the fixed values but the decision variables.

Considering the imprecise nature of the decision maker's judgment, we assume that the decision maker has fuzzy goals for each objective function in MOP6($\boldsymbol{\beta}$). Such fuzzy goals can be quantified by eliciting the corresponding membership functions. Let us denote a membership function of an objective function $f_i(\boldsymbol{x},\bar{p}_i)$ as $\mu_{f_i}(f_i(\boldsymbol{x},\bar{p}_i))$, and a membership function of a permissible probability level $\bar{p}_i$ as $\mu_{\bar{p}_i}(\bar{p}_i)$ respectively. Then, MOP6($\boldsymbol{\beta}$) can be transformed as the following multiobjective programming problem.

[MOP7($\boldsymbol{\beta}$)]

$$\max_{\boldsymbol{x}\in X(\boldsymbol{\beta}),\bar{p}_i,i=1,\cdots,k} (\mu_{f_1}(f_1(\boldsymbol{x},\bar{p}_1)),\cdots,\mu_{f_k}(f_k(\boldsymbol{x},\bar{p}_k)), \mu_{\bar{p}_1}(\bar{p}_1),\cdots,\mu_{\bar{p}_k}(\bar{p}_k)) \tag{34}$$

Throughout this section, we make the following assumptions.

Assumption 3.

$\mu_{\bar{p}_i}(\bar{p}_i), i=1,\cdots,k$ are strictly increasing and continuous with respect to $\bar{p}_i$.

Assumption 4.

$\mu_{f_i}(f_i(\boldsymbol{x},\bar{p}_i)), i=1,\cdots,k$ are strictly decreasing and continuous with respect to $f_i(\boldsymbol{x},\bar{p}_i)$.

For example, we can define the membership functions $\mu_{\bar{p}_i}(\bar{p}_i)$, $\mu_{f_i}(f_i(\boldsymbol{x},\bar{p}_i))$ as follows. At first, the decision maker specifies permissible probability intervals in his/her subjective manner,

$$P_i = [p_{i\min}, p_{i\max}], i=1,\cdots,k, \tag{35}$$

where $p_{i\min}$ is an acceptable minimum value and $p_{i\max}$ is a sufficiently satisfactory minimum value. According to Assumption 3, the decision maker can define his/her membership function $\mu_{\bar{p}_i}(\bar{p}_i)$ on the domain P_i. Corresponding to the domain P_i, Let us denote the domain of $\mu_{f_i}(f_i(\boldsymbol{x},\bar{p}_i))$ as:

$$F_i(P_i) = [f_{i\min}, f_{i\max}], \tag{36}$$

where $f_{i\min}$ is a sufficiently satisfactory maximum value and $f_{i\max}$ is an acceptable maximum value. $f_{i\min}$ can be obtained by solving the following linear programming problem.

$$f_{i\min} = \min_{\boldsymbol{x}\in X(\boldsymbol{\beta})} f_i(\boldsymbol{x}, p_{i\min}) \tag{37}$$

In order to obtain $f_{i\max}$, we first solve the following k linear programming problems.

$$\min_{\boldsymbol{x}\in X(\boldsymbol{\beta})} f_i(\boldsymbol{x}, p_{i\max}), i=1,\cdots,k \tag{38}$$

Let $\boldsymbol{x}_i, i=1,\cdots,k$ be the above optimal solution. Using the optimal solutions $\boldsymbol{x}_i, i=1,\cdots,k$, $f_{i\max}$ can be obtained as follows.

$$f_{i\max} = \max_{\ell=1,\cdots,k,\ell\neq i} f_i(\boldsymbol{x}_\ell, p_{i\max}) \tag{39}$$

According to Assumption 4, the decision maker can define his/her membership function $\mu_{f_i}(f_i(\boldsymbol{x},\bar{p}_i))$ on the domain $F_i(P_i)$.

Then, if the decision maker adopts the fuzzy decision [8],[12] as an aggregation operator for MOP7($\boldsymbol{\beta}$), the satisfactory solution is obtained by solving the following maxmin problem.

[MAXMIN3]

$$\max_{\boldsymbol{x}\in X(\boldsymbol{\beta}),\bar{p}_i\in P_i,i=1,\cdots,k,\lambda\in[0,1]} \lambda \tag{40}$$

subject to

$$\mu_{f_i}(f_i(\boldsymbol{x},\bar{p}_i)) \geq \lambda, i=1,\cdots,k \tag{41}$$

$$\mu_{\bar{p}_i}(\bar{p}_i) \geq \lambda, i=1,\cdots,k \tag{42}$$

Because of Assumption 4 and $\boldsymbol{c}_i^2\boldsymbol{x}+\alpha_i^2 > 0$, the constraints (41) can be transformed as:

$$\begin{aligned} & \mu_{f_i}(f_i(\boldsymbol{x},\bar{p}_i)) \geq \lambda, \\ \Leftrightarrow\ & f_i(\boldsymbol{x},\bar{p}_i) \leq \mu_{f_i}^{-1}(\lambda), \\ \Leftrightarrow\ & T_i^{-1}(\bar{p}_i)\cdot(\boldsymbol{c}_i^2\boldsymbol{x}+\alpha_i^2)+(\boldsymbol{c}_i^1\boldsymbol{x}+\alpha_i^1) \leq \mu_{f_i}^{-1}(\lambda), \\ \Leftrightarrow\ & \bar{p}_i \leq T_i\left(\frac{\mu_{f_i}^{-1}(\lambda)-(\boldsymbol{c}_i^1\boldsymbol{x}+\alpha_i^1)}{\boldsymbol{c}_i^2\boldsymbol{x}+\alpha_i^2}\right) \end{aligned} \tag{43}$$

where $\mu_{f_i}^{-1}(\cdot)$ is a pseudo-inverse function. From the constraints (42) and Assumption 3, it holds that $\bar{p}_i \geq \mu_{\bar{p}_i}^{-1}(\lambda)$. Therefore, the constraint (43) can be reduced to the following inequality where a permissible probability level $\bar{p}_i$ is disappeared.

$$\begin{aligned} & \mu_{\bar{p}_i}^{-1}(\lambda) \leq T_i\left(\frac{\mu_{f_i}^{-1}(\lambda)-(\boldsymbol{c}_i^1\boldsymbol{x}+\alpha_i^1)}{\boldsymbol{c}_i^2\boldsymbol{x}+\alpha_i^2}\right) \\ \Leftrightarrow\ & \mu_{f_i}^{-1}(\lambda)-(\boldsymbol{c}_i^1\boldsymbol{x}+\alpha_i^1) \\ & \geq T_i^{-1}(\mu_{\bar{p}_i}^{-1}(\lambda))\cdot(\boldsymbol{c}_i^2\boldsymbol{x}+\alpha_i^2) \end{aligned} \tag{44}$$

Then, MAXMIN3 is equivalently transformed into the following problem.

[MAXMIN4]

$$\max_{\boldsymbol{x}\in X(\boldsymbol{\beta}),\lambda\in[0,1]} \lambda \tag{45}$$

subject to

$$\mu_{f_i}^{-1}(\lambda)-(\boldsymbol{c}_i^1\boldsymbol{x}+\alpha_i^1) \geq T_i^{-1}(\mu_{\bar{p}_i}^{-1}(\lambda))\cdot(\boldsymbol{c}_i^2\boldsymbol{x}+\alpha_i^2), \quad i=1,\cdots,k \tag{46}$$

It should be noted here that MAXMIN4 is equivalent to MAXMIN2, and the constraints (46) can be reduced to a set of linear inequalities for some fixed value $\lambda\in[0,1]$. This means that an optimal solution $(\boldsymbol{x}^*,\lambda^*)$ of MAXMIN4 is obtained by combined use of the bisection method with respect to λ and the first-phase of the two-phase simplex method of linear programming.

The relationship between the optimal solution $(\boldsymbol{x}^*,\lambda^*)$ of MAXMIN4, P-Pareto optimal solutions to MOP1($\bar{\boldsymbol{f}},\boldsymbol{\beta}$), and F-Pareto optimal solutions to MOP3($\bar{\boldsymbol{p}},\boldsymbol{\beta}$) can be characterized by the following theorem.

Theorem 3.
(1) If $(\boldsymbol{x}^*, \lambda^*)$ is a unique optimal solution of MAXMIN4, then $\boldsymbol{x}^* \in X(\boldsymbol{\beta})$ is a P-Pareto optimal solution to MOP1($\bar{\boldsymbol{f}}^*, \boldsymbol{\beta}$), where $\bar{\boldsymbol{f}}^* = (\bar{f}_1^*, \cdots, \bar{f}_k^*) = (\mu_{f_1}^{-1}(\lambda^*), \cdots, \mu_{f_k}^{-1}(\lambda^*))$.
(2) If $(\boldsymbol{x}^*, \lambda^*)$ is a unique optimal solution of MAXMIN4, then $\boldsymbol{x}^* \in X(\boldsymbol{\beta})$ is an F-Pareto optimal solution to MOP3($\bar{\boldsymbol{p}}^*, \boldsymbol{\beta}$), where $\bar{\boldsymbol{p}}^* = (\bar{p}_1^*, \cdots, \bar{p}_k^*)$ = $(\mu_{\bar{p}_1}^{-1}(\lambda^*), \cdots, \mu_{\bar{p}_k}^{-1}(\lambda^*))$.
(Proof)
(1) Let $(\boldsymbol{x}^*, \lambda^*)$ be a unique optimal solution of MAXMIN4. Since an optimal solution $(\boldsymbol{x}^*, \lambda^*)$ satisfies the constraints (46), it holds that

$$\begin{aligned} & \mu_{f_i}^{-1}(\lambda^*) - (\boldsymbol{c}_i^1 \boldsymbol{x}^* + \alpha_i^1) \\ & \geq T_i^{-1}(\mu_{\bar{p}_i}^{-1}(\lambda^*)) \cdot (\boldsymbol{c}_i^2 \boldsymbol{x}^* + \alpha_i^2), \\ \Leftrightarrow \quad & T_i\left(\frac{\mu_{f_i}^{-1}(\lambda^*) - (\boldsymbol{c}_i^1 \boldsymbol{x}^* + \alpha_i^1)}{\boldsymbol{c}_i^2 \boldsymbol{x}^* + \alpha_i^2}\right) = p_i(\boldsymbol{x}^*, \mu_{f_i}^{-1}(\lambda^*)) \\ & \geq \mu_{\bar{p}_i}^{-1}(\lambda^*), i = 1, \cdots, k. \end{aligned}$$

Assume that $\boldsymbol{x}^* \in X(\beta)$ is not a P-Pareto optimal solution to MOP1($\bar{\boldsymbol{f}}^*, \boldsymbol{\beta}$), where $\bar{\boldsymbol{f}}^* = (\mu_{f_1}^{-1}(\lambda^*), \cdots, \mu_{f_k}^{-1}(\lambda^*))$. Then there exists $\boldsymbol{x} \in X(\boldsymbol{\beta})$ such that

$$\begin{aligned} & p_i(\boldsymbol{x}, \mu_{f_i}^{-1}(\lambda^*)) \geq p_i(\boldsymbol{x}^*, \mu_{f_i}^{-1}(\lambda^*)) \geq \mu_{\bar{p}_i}^{-1}(\lambda^*), \\ & i = 1, \cdots, k. \end{aligned}$$

This means that there exists $\boldsymbol{x} \in X(\boldsymbol{\beta})$ such that

$$\begin{aligned} \mu_{f_i}^{-1}(\lambda^*) - (\boldsymbol{c}_i^1 \boldsymbol{x} + \alpha_i^1) \quad \geq \quad & T_i^{-1}(\mu_{\bar{p}_i}^{-1}(\lambda^*)) \cdot (\boldsymbol{c}_i^2 \boldsymbol{x} + \alpha_i^2), \\ & i = 1, \cdots, k, \end{aligned}$$

which contradicts the fact that $(\boldsymbol{x}^*, \lambda^*)$ is a unique optimal solution of MAXMIN4.
(2) Assume that $\boldsymbol{x}^* \in X(\boldsymbol{\beta})$ is not an F-Pareto optimal solution to MOP3($\bar{\boldsymbol{p}}^*, \boldsymbol{\beta}$), where $\bar{p}_i^* = \mu_{\bar{p}_i}^{-1}(\lambda^*), i = 1, \cdots, k$. Then, because of (14), there exists $\boldsymbol{x} \in X(\boldsymbol{\beta})$ such that

$$\begin{aligned} & f_i(\boldsymbol{x}, \bar{p}_i^*) \leq f_i(\boldsymbol{x}^*, \bar{p}_i^*) \\ \Leftrightarrow \quad & T_i^{-1}(\bar{p}_i^*) \cdot (\boldsymbol{c}_i^2 \boldsymbol{x} + \alpha_i^2) + (\boldsymbol{c}_i^1 \boldsymbol{x} + \alpha_i^1) \\ \leq \quad & T_i^{-1}(\bar{p}_i^*) \cdot (\boldsymbol{c}_i^2 \boldsymbol{x}^* + \alpha_i^2) + (\boldsymbol{c}_i^1 \boldsymbol{x}^* + \alpha_i^1) \stackrel{\text{def}}{=} \bar{f}_i^* \\ \Leftrightarrow \quad & \bar{f}_i^* - (\boldsymbol{c}_i^1 \boldsymbol{x} + \alpha_i^1) \geq T_i^{-1}(\bar{p}_i^*) \cdot (\boldsymbol{c}_i^2 \boldsymbol{x} + \alpha_i^2) \\ \Leftrightarrow \quad & \bar{f}_i^* - (\boldsymbol{c}_i^1 \boldsymbol{x} + \alpha_i^1) \geq T_i^{-1}(\mu_{\bar{p}_i}^{-1}(\lambda^*)) \cdot (\boldsymbol{c}_i^2 \boldsymbol{x} + \alpha_i^2) \end{aligned}$$

On the other hand, since $(\boldsymbol{x}^*, \lambda^*)$ is an optimal solution of MAXMIN4, from (46), it holds that

$$\mu_{f_i}^{-1}(\lambda^*) - (\boldsymbol{c}_i^1 \boldsymbol{x}^* + \alpha_i^1) \geq T_i^{-1}(\mu_{\bar{p}_i}^{-1}(\lambda^*)) \cdot (\boldsymbol{c}_i^2 \boldsymbol{x}^* + \alpha_i^2).$$

This means that

$$\begin{aligned} \mu_{f_i}^{-1}(\lambda^*) \quad \geq \quad & (\boldsymbol{c}_i^1 \boldsymbol{x}^* + \alpha_i^1) + T_i^{-1}(\mu_{\bar{p}_i}^{-1}(\lambda^*)) \cdot (\boldsymbol{c}_i^2 \boldsymbol{x}^* + \alpha_i^2) \\ = \quad & \bar{f}_i^*. \end{aligned}$$

Therefore, it holds that

$$\begin{aligned} \mu_{f_i}^{-1}(\lambda^*) - (\boldsymbol{c}_i^1 \boldsymbol{x} + \alpha_i^1) \quad \geq \quad & T_i^{-1}(\mu_{\bar{p}_i}^{-1}(\lambda^*)) \cdot (\boldsymbol{c}_i^2 \boldsymbol{x} + \alpha_i^2), \\ & i = 1, \cdots, k, \end{aligned}$$

which contradicts the fact that $(\boldsymbol{x}^*, \lambda^*)$ is a unique optimal solution of MAXMIN4.

TABLE I
CONSTANT COEFFICIENTS OF OBJECTIVE FUNCTIONS AND CONSTRAINTS

$\boldsymbol{x}$	x_1	x_2	x_3	x_4	x_5	x_6	x_7	x_8	x_9	x_{10}
$\boldsymbol{c}_1^1$	19	48	21	10	18	35	46	11	24	33
$\boldsymbol{c}_1^2$	3	2	2	1	4	3	1	2	4	2
$\boldsymbol{c}_2^1$	12	-46	-23	-38	-33	-48	12	8	19	20
$\boldsymbol{c}_2^2$	1	2	4	2	2	1	2	1	2	1
$\boldsymbol{c}_3^1$	-18	-26	-22	-28	-15	-29	-10	-19	-17	-28
$\boldsymbol{c}_3^2$	2	1	3	2	1	2	3	3	2	1
$\boldsymbol{a}_1$	12	-2	4	-7	13	-1	-6	6	11	-8
$\boldsymbol{a}_2$	-2	5	3	16	6	-12	12	4	-7	-10
$\boldsymbol{a}_3$	3	-16	-4	-8	-8	2	-12	-12	4	-3
$\boldsymbol{a}_4$	-11	6	-5	9	-1	8	-4	6	-9	6
$\boldsymbol{a}_5$	-4	7	-6	-5	13	6	-2	-5	14	-6
$\boldsymbol{a}_6$	5	-3	14	-3	-9	-7	4	-4	-5	9
$\boldsymbol{a}_7$	-3	-4	-6	9	6	18	11	-9	-4	7

V. A NUMERICAL EXAMPLE

We consider the following three-objective linear programming problems involving random variable coefficients, which is formulated by Sakawa et al. [9], to demonstrate the feasibility of our proposed fuzzy approach.
[MOSLP]

$$\min \ (\boldsymbol{c}_1^1 + t_1(\omega)\boldsymbol{c}_1^2)\boldsymbol{x} + (\alpha_1^1 + t_1(\omega)\alpha_1^2)$$

$$\min \ (\boldsymbol{c}_2^1 + t_2(\omega)\boldsymbol{c}_2^2)\boldsymbol{x} + (\alpha_2^1 + t_2(\omega)\alpha_2^2)$$

$$\min \ (\boldsymbol{c}_3^1 + t_3(\omega)\boldsymbol{c}_3^2)\boldsymbol{x} + (\alpha_3^1 + t_3(\omega)\alpha_3^2)$$

subject to $\boldsymbol{a}_i \boldsymbol{x} \leq b_i(\omega), i = 1, \cdots, 7, \boldsymbol{x} \geq \boldsymbol{0}$

where $\boldsymbol{x} = (x_1, x_2, \cdots, x_{10})^T$ is a ten-dimensional decision column vector, $\boldsymbol{a}_i, i = 1, \cdots, 7, c_1^1, c_1^2, c_2^1, c_2^2, c_3^1, c_3^2$ are ten-dimensional coefficient row vectors (Table 1), and $\alpha_1^1 = -18, \alpha_1^2 = 5, \alpha_2^1 = -27, \alpha_2^2 = 6, \alpha_3^1 = -10, \alpha_3^2 = 4$. $t_i(\omega), i = 1, \cdots, 3$, $b_j(\omega), j = 1, \cdots, 7$ are Gaussian random variables defined as follows.

$$\begin{aligned} & t_1(\omega) \sim \mathrm{N}(4, 2^2), && t_2(\omega) \sim \mathrm{N}(3, 3^2), \\ & t_3(\omega) \sim \mathrm{N}(3, 2^2), && b_1(\omega) \sim \mathrm{N}(164, 30^2), \\ & b_2(\omega) \sim \mathrm{N}(-190, 20^2), && b_3(\omega) \sim \mathrm{N}(-184, 15^2), \\ & b_4(\omega) \sim \mathrm{N}(99, 22^2), && b_5(\omega) \sim \mathrm{N}(-150, 17^2), \\ & b_6(\omega) \sim \mathrm{N}(154, 35^2), && b_7(\omega) \sim \mathrm{N}(142, 42^2). \end{aligned}$$

Let us assume that the hypothetical decision maker sets constraint probability levels as $\boldsymbol{\beta} = (\beta_1, \cdots, \beta_7) = (0.85, 0.95, 0.8, 0.9, 0.85, 0.8, 0.9)$ for the constraints in MOSLP, which are same values to the numerical example [9]. Since, in the numerical example [9], a probability maximization model is adopted to formulate MOSLP, we adopt MAXMIN2 for MOSLP in order to compare our proposed fuzzy approach with the results of Sakawa et al.[9].

Let us set the membership functions $\mu_{p_i}(p_i(\boldsymbol{x}, \bar{f}_i))$ for distribution functions $p_i(\boldsymbol{x}, \bar{f}_i)$, $i = 1, 2, 3$ as follows, which

are same to [9].

$$\mu_{p_1}(p_1(\boldsymbol{x}, \bar{f}_1)) = \frac{p_1(\boldsymbol{x}, \bar{f}_1) - 0.502}{(0.88 - 0.502)}$$
$$\mu_{p_2}(p_2(\boldsymbol{x}, \bar{f}_2)) = \frac{p_2(\boldsymbol{x}, \bar{f}_2) - 0.06}{(0.783 - 0.06)}$$
$$\mu_{p_3}(p_3(\boldsymbol{x}, \bar{f}_3)) = \frac{p_3(\boldsymbol{x}, \bar{f}_3) - 0.446}{(0.664 - 0.446)}$$

In the numerical example [9], as permissible objective levels for a probability maximization model, $\bar{\boldsymbol{f}} = (\bar{f}_1, \bar{f}_2, \bar{f}_3) = (2150, 450, -950)$ are adopted. Corresponding to these values, we assume that the hypothetical decision maker sets his/her membership functions $\mu_{\bar{f}_i}(\bar{f}_i)$ for permissible objective levels $\bar{f}_i$, $i = 1, 2, 3$ as follows.

$$\mu_{\bar{f}_1}(\bar{f}_1) = \frac{3000 - \bar{f}_1}{(3000 - 2150)}$$
$$\mu_{\bar{f}_2}(\bar{f}_2) = \frac{1000 - \bar{f}_2}{(1000 - 450)}$$
$$\mu_{\bar{f}_3}(\bar{f}_3) = \frac{-900 - \bar{f}_3}{((-900) - (-950))}$$

For these membership functions, MAXMIN2 is solved by combined use of the bisection method with respect to λ and the first-phase of the two-phase simplex method of linear programming. The optimal solution $(\boldsymbol{x}^*, \lambda^*)$ is obtained at $\lambda^* = 0.826714$. The corresponding membership function values are obtained as $\mu_{\bar{f}_i}(\bar{f}_i^*) = \mu_{p_i}(p_i(\boldsymbol{x}^*, \bar{f}_i^*)) = 0.826714, i = 1, 2, 3$, where

$$\bar{f}_i^* = (\boldsymbol{c}_i^1 \boldsymbol{x}^* + \alpha_i^1) + T_i^{-1}(\mu_{p_i}^{-1}(\lambda^*)) \cdot (\boldsymbol{c}_i^2 \boldsymbol{x}^* + \alpha_i^2),$$
$$p_i(\boldsymbol{x}^*, \bar{f}_i^*) = T_i \left(\frac{\bar{f}_i^* - (\boldsymbol{c}_i^1 \boldsymbol{x}^* + \alpha_i^1)}{\boldsymbol{c}_i^2 \boldsymbol{x}^* + \alpha_i^2} \right).$$

In Table 2, not only the optimal values $\bar{f}_i^*, p_i(\boldsymbol{x}^*, \bar{f}_i^*)$, $i = 1, 2, 3$ of MAXMIN2 but also the results of Sakawa et al. (especially, $p_i(\boldsymbol{x}^*, \bar{f}_i)$ for the fixed values of permissible objective levels $(\bar{f}_1, \bar{f}_2, \bar{f}_3) = (2150, 450, -950)$ at the first interaction of Table 3 [9]) are shown. From Table 2, it can be understood that, at the optimal solution of MAXMIN2, the distribution function $p_i(\boldsymbol{x}^*, \bar{f}_i^*)$ is improved at the expense of the permissible objective level in comparison with the results of Sakawa et al. [9]. From this result, it is expected that the proper balance between the distribution function $p_i(\boldsymbol{x}, \bar{f}_i)$ and the permissible objective level $\bar{f}_i$ in a probability maximization model will be attained at the optimal solution of MAXMIN2. Similarly, it is also expected that the proper balance between the objective function $f_i(\boldsymbol{x}, \bar{p}_i)$ and the permissible probability level $\bar{p}_i$ in a fractile optimization model will be attained at the optimal solution of MAXMIN4.

TABLE II
THE OPTIMAL SOLUTIONS OF MAXMIN2 AND THE FIRST INTERACTION IN TABLE 3 [9]

	MAXMIN2	The first interaction in Table 3 [9]
$\bar{f}_1^*$	2297.29	2150.0
$\bar{f}_2^*$	545.308	450.0
$\bar{f}_3^*$	-941.336	-950.0
$p_1(\boldsymbol{x}^*, \bar{f}_1^*)$	0.814498	0.719
$p_2(\boldsymbol{x}^*, \bar{f}_2^*)$	0.657714	0.474
$p_3(\boldsymbol{x}^*, \bar{f}_3^*)$	0.626224	0.571

VI. CONCLUSION

In this paper, two fuzzy approaches to multiobjective stochastic linear programming problems through a probability maximization model and a fractile optimization model are proposed. MAXMIN2 is formulated for multiobjective stochastic linear programming problems through a probability maximization model to obtain a satisfactory solution of the decision maker. Similarly, MAXMIN4 is formulated for multiobjective stochastic linear programming problems through a fractile optimization model to obtain a satisfactory solution of the decision maker. Both problems can be easily solved by linear programming technique and, at the optimal solution, it is expected that a proper balance between permissible objective levels and the corresponding distribution function values or permissible probability levels and the corresponding objective function values is attained. It has been also shown that such two problems are same. Although a probability maximization model or a fractile optimization model is one of the most efficient tool to transform stochastic programming problems into well-defined mathematical programming ones, appropriate permissible levels are not known for the decision maker in advance. In order to overcome such a difficulty, we have proposed fuzzy approaches for multiobjective stochastic linear programming problems.

REFERENCES

[1] A. Charnes and W. W. Cooper, "Chance Constrained Programming," Management Science, vol. 6, pp. 73-79, 1959.

[2] A. Charnes and W. W. Cooper, "Programming with Linear Fractional Functions," Naval Research Logistic Quarterly, vol. 9, pp. 181-186, 1962.

[3] G. B. Danzig, "Linear Programming under Uncertainty," Management Science, vol. 1, pp. 197-206, 1955.

[4] S. Hulsurkar, M. P. Biswal, and S. B. Shinha, "Fuzzy Programming Approach to Multi-Objective Stochastic Linear Programming Problems," Fuzzy Sets and Systems, vol. 88, pp. 173-181, 1997.

[5] Y. J. Lai and C. L. Hwang, Fuzzy Mathematical Programming, Springer, 1992.

[6] H. Rommelfanger, "Fuzzy Linear Programming and Applications," European Journal of Operational Research, vol. 92, pp. 512-527, 1997.

[7] I. M. Stancu-Minasian, "Overview of Different Approaches for Solving Stochastic Programming Problems with Multiple Objective Functions," in Stochastic Versus Fuzzy Approaches to Multiobjective Mathematical Programming under Uncertainty, R. Slowinski and J. Teghem Eds., Kluwer Academic Publishers, 1990, pp. 71-101.

[8] M. Sakawa, Fuzzy Sets and Interactive Multiobjective Optimization, Plenum Press, 1993.

[9] M. Sakawa, K. Kato, and H. Katagiri, "An Interactive Fuzzy Satisficing Method for Multiobjective Linear Programming Problems with Random Variable Coefficients Through a Probability Maximization Model," Fuzzy Sets and Systems, vol. 146, pp. 205-220, 2004.

[10] J. Teghem, D. Dufrane, and M. Thauvoye, "STRANGE: An Interactive Method for Multi-Objective Linear Programming Under Uncertainty," European Journal of Operational Research, vol. 26, pp. 65-82, 1986.

[11] H.-J. Zimmermann, "Fuzzy Programming and linear programming with several objective functions," Fuzzy Sets and Systems, vol. 1, pp. 45-55, 1978.

[12] H.-J. Zimmermann, Fuzzy Sets, Decision-Making and Expert Systems, Kluwer Academic Publishers, 1987.

2011 IEEE International Conference on Fuzzy Systems
June 27-30, 2011, Taipei, Taiwan

Performance Enhancement of Hierarchical Document Signature: A Comprehensive Study

Sukanya Manna
Research School of Computer Science
The Australian National University
Canberra ACT 0200
Email: sukanya.manna@anu.edu.au

Tom Gedeon
Research School of Computer Science
The Australian National University
Canberra ACT 0200
Email: tom.gedeon@anu.edu.au

***Abstract*—Hierarchical Document Signature (HDS) has been successfully applied in document computing to find similarity between different pieces of text [1], [2], [3]; for example sentence-sentence similarity, sentence-phrase similarity. HDS is application specific, it is dependent on different features at different levels. This paper hence presents a comprehensive study of enhancement of the performance of HDS to find semantic sentence similarity by tuning some of its significant features. The experimental results support this and show the optimal conditions at which HDS performs similarly to humans.**

***Keywords*- Fuzzy signature, Hierarchical Document Signature, sentence similarity, word similarity**

I. Introduction

It is important to abstract information available to form humanly accessible structures. The way people think and talk is hierarchical with limited information presented in any one sentence, and that information is always linked together to further information. As such, Hierarchical Document Signature (HDS) is a significant way to represent sentences when finding their similarity.

Sentences are considered to be the same if they share the same or similar meaning. There are different methods to find sentence similarities [4], [5], and [6], and HDS is one of them. Manna et al., have discussed two different HDS models in [1], [3]. In this paper we focus on the model described in [3] where similarities between sentence pairs are computed using semantic information from the source text.

The following sections briefly describe HDS, and different experiments at word and sentence level to show optimal parameters for the enhancement of performance of HDS for computing sentence similarity.

II. Brief Description of HDS

Hierarchical Document Signature (HDS) [1], [3] is a special form of Fuzzy Signature (FS) [7] meant for document analysis. In this case, the natural hierarchy of a document is maintained through the structure of HDS; document level to sentence level, sentence level to word level. HDS, like fuzzy signatures, can describe, compare and classify objects with complex structure and interdependent features. The hierarchical organization of HDS expresses the structural complexity of a problem. The local preference relations among the hierarchies and sub-branches of a document signature can be used to approximate the global preference relation of a decision problem.

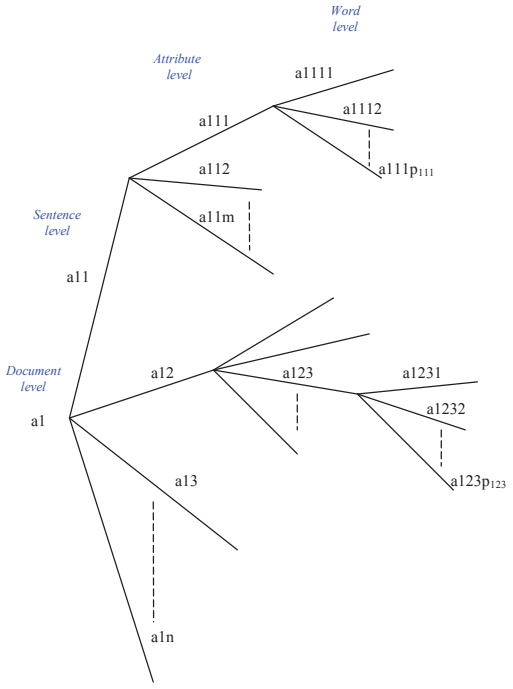

Fig. 1. Generic illustration of Hierarchical Document Signature

In fig.1, $a1$ represents a document at *document level*. A document is now segmented into n sentences, which we denote by $a11$ to $a1n$. This is the *sentence level* of the signature we developed. Next is the *attribute level*, which basically classifies the words of the sentences into their corresponding major *parts of speech*, namely *noun*, *verb*, *adjective* and *adverb*. So, for each sentence, we have m different attributes, which is fixed for each document signature. In general m is a integer, but it is constant with specific application for the ease of comparison. Now each attribute of each sentence has words, and this level is called *word level*. There can be any number of words in each attribute (POS). Here, p_{111} is the maximum number of words for attribute $a111$.

HDS can be used for computing semantic similarity of contexts. Its levels can vary depending on applications where it is used. In this case, parts of speech (POS) is a level

978-1-4244-7316-8/11/$26.00 ©2011 IEEE

which deals with the semantic information of the sentences of a document. The aggregations at different level contribute to the final similarity value. It uses Fuzzy Word Similarity (FWS) [8] at the word level to deal with the similarity or relatedness of a word pair; which then propagates to the next higher level using appropriate aggregations and continues till it reaches the document level. In this application, sentence-sentence similarity is computed.

III. Word level Scenario

The performance of HDS is mainly dependent on the word level. The similarity computed at this level is aggregated and propagated to the next higher level; thus it is essential to tune different features to achieve good performance. This word pair similarity used is known as Fuzzy Word Similarity (FWS) which was introduced in [8]. Choice of proper membership function, similarity threshold as well as the input similarity measures are different essential factors which can affect the results of FWS. So the following experiments will deal with each of these separately with proper illustrations.

a) Input Similarity Measures for FWS: As explained in [8], FWS requires two different types of similarity measures to compute PGMeasure; path based measures and gloss based measures. For path based, Lin's [9] as well as Jiang and Conrath's [10] are both experimented on. These effects can be seen in tables IV to XXVIII with different datasets in different conditions.

b) Impact of membership functions: Three sets of membership functions are shown in the table I. The membership functions are tuned based on repeated experiments and expert comments. In [8] it is seen that triangular membership functions performed better than trapezoidal at the output. But when it is further tuned, it is noticed that the trapezoidal membership functions can also be used at the output and it also gives reasonably good results. The corresponding results can be seen in tables IV to XXVIII.

TABLE I
Co-ordinates of different membership functions of fuzzy sets used here

Set I	INPUT Low_trapez	(0, 1)	(0.3, 1)	(0.4, 0)	-
	INPUT Medium_trapez	(0.3, 0)	(0.4, 1)	(0.6, 1)	(0.7, 0)
	INPUT High_trapez	(0.6, 0)	(0.8, 1)	(1, 1)	-
	OUTPUT Low_trapez	(0, 1)	(0.3, 1)	(0.4, 0)	-
	OUTPUT Medium_trapez	(0.3, 0)	(0.4, 1)	(0.6, 1)	(0.7, 0)
	OUTPUT High_trapez	(0.6, 0)	(0.8, 1)	(1, 1)	-
Set II	INPUT Low_trapez	(0, 1)	(0.3, 1)	(0.4, 0)	-
	INPUT Medium_trapez	(0.3, 0)	(0.4, 1)	(0.6, 1)	(0.7, 0)
	INPUT High_trapez	(0.6, 0)	(0.8, 1)	(1, 1)	-
	OUTPUT Low_tri	(0, 0)	(0.3, 1)	(0.6, 0)	-
	OUTPUT Medium_tri	(0.3, 0)	(0.55, 1)	(0.8, 0)	-
	OUTPUT High_tri	(0.6, 0)	(0.8, 1)	(1, 0)	-
Set III	INPUT Low_trapez	(0, 1)	(0.2, 1)	(0.3, 0)	-
	INPUT Medium_trapez	(0.2, 0)	(0.3, 1)	(0.4, 1)	(0.5, 0)
	INPUT High_trapez	(0.4, 0)	(0.5, 1)	(1, 1)	-
	OUTPUT Low_trapez	(0, 1)	(0.1, 1)	(0.3, 0)	-
	OUTPUT Medium_trapez	(0.1, 0)	(0.3, 1)	(0.5, 1)	(0.7, 0)
	OUTPUT High_trapez	(0.5, 0)	(0.7,1)	(1, 1)	-

c) Fuzzy rule-bases: In fuzzy system, there are different rule extraction methods as seen in [11] besides expert knowledge, where the rules are decided manually based on expert's understanding about the similarity measures. These rules have been used to compute FWS between a word pair.

Rule 1: If path is L AND gloss is L THEN output is L.
Rule 2: If path is L AND gloss is M THEN output is L.
Rule 3: If path is L AND gloss is H THEN output is M.
Rule 4: If path is M AND gloss is L THEN output is L.
Rule 5: If path is M AND gloss is M THEN output is M.
Rule 6: If path is M AND gloss is H THEN output is H.
Rule 7: If path is H AND gloss is L THEN output is M.
Rule 8: If path is H AND gloss is M THEN output is H.
Rule 9: If path is H AND gloss is H THEN output is H.

d) Impact of thresholds at word level: Similarity thresholds also affect the performance of HDS. Normally, for similarity computations, similarity value of 0.5 [12] is considered. But due to fuzzy approximations which initiate at word level, a new threshold of 0.4 is also experimented with and seen to be more suitable for this application.

IV. Experiments at Word Level

A. Evaluation metrics at word level

In this sub-section, evaluation of three different word similarity approaches (*path measure*, *gloss overlap* and *PGMeasure*) are presented. This has been taken directly from [8]. Unlike [12], the following metrics are defined at *word level* instead of sentence level. These are *Recall*, *Precision*, *F-measure*, *Rejection*, *Accuracy*, and *f1*. **Recall** is a proportion of correctly predicted similar word pairs compared to all similar word pairs. **Precision** is a proportion of correctly predicted similar word pairs compared to all predicted similar word pairs. **F-Measure (F1)** is a uniform harmonic mean of precision and recall. **Rejection** is a proportion of correctly predicted dissimilar word pairs compared to all dissimilar word pairs. **Accuracy** is a proportion of all correctly predicted word pairs compared to all word pairs. Lastly, **f1** is defined as a uniform harmonic mean of rejection and recall. In this work, *accuracy*, *rejection* and *f1* metrics are included in addition to the standard precision-recall based metrics as it presents another aspect of the performance based on the tradeoff between true positive and true negative judgments.

B. Evaluation process

Two words are considered to be similar if they reach certain threshold value. A scoring threshold for similar pairs is defined at 0.5 [12]. But in this case, threshold of 0.4 is also evaluated because of fuzzy approximations used in formulating PGMeasure (FWS). Thus for each kind of input and output fuzzy sets shown in table. I, results with both the thresholds are shown for each method; which will clearly explain why 0.4 has been preferred over 0.5 for word similarity computation using FWS.

C. Datasets

Results on two datasets are shown. One is data from Test of English as a Foreign Language (ESL) and the other from [13] which is called Rubenstein data in this paper. The dataset is prepared by human assessors and then experimented on.

1) ESL dataset: There is no standard benchmark dataset for computing word similarity. Generally people have evaluated their word similarities [14], [15] using some kind of multiple choice questions and their answers in TOEFL (Test of English as a Foreign Language) or ESL[1](English as a second language) or any other linguistic exams. Thus, for this work, a dataset is prepared from ESL mock exams. Like [16], the experiment is not restricted to verbs, rather all four main parts of speech are covered which have been encountered in the multiple choice questions (MCQ) in ESL. Each practice exams had several questions; with 4 choices. Out of these four, one gives you the exact match. Like Microsoft Research paraphrase corpus, [17] binary judgements are assigned to the word pair similarity instead of sentence similarity as mentioned in the dataset. For the correct choices, based on ESL answer set, 1 is assigned as relevancy score of the word pair similarity, for the rest of the incorrect answers, 0 is assigned. Antonyms are chosen deliberately for the incorrect choices (out of 3 incorrect choices) except for the questions which had some other options. Linguistically, it is difficult to determine any crisp boundary for word similarity. The binary scores are assigned as a benchmark. It is also found that for some words, which returned 'incorrect choice' in ESL test set, has some degree of similarity linguistically, might not be very relevant to the context of the question being asked. So, for these words, there are false negatives. Respective parts of speech are also assigned for the word pairs. Here, in table. II a snapshot of the dataset generated from ESL multiple choice questions is shown.

TABLE II
SNAPSHOT OF DATASET GENERATED FROM ESL MULTIPLE CHOICE QUESTIONS

Relevance	word_1	word_2	POS
1	balmy	warm	adjective
0	balmy	cold	adjective
1	pored	examined	verb
0	pored	memorized	verb
1	intersection	crossing	noun
0	intersection	ending	noun
1	repugnant	disgusting	adjective
0	repugnant	delightful	adjective
1	diligence	dedication	noun
0	diligence	ease	noun
0	widespread	limited	adjective
1	harsh	extreme	adjective
0	harsh	pleasant	adjective
1	touched	began	verb
...			

a) Comparison of different senses of word pairs using different methods: Table. III is a snapshot of the results obtained at word sense level. In some words, gloss overlap is 0, which signifies that semantically they do not share any information, but due to their taxonomical location in WordNet, they have some information in common. The PGMeasure combines these kinds of information which can be seen from this table. The tuning of membership functions can definitely provide more refined similarity values for the word pairs.

It is known that each word can have many synsets. So when similarity between two words are computed, similarity between all their combinations of synsets are computed using both gloss overlap and path measure. Maximum similarity between the synsets contribute to the word pairs' final similarity. This is used in the tables for comparison with PGMeasure.

TABLE III
WORD SIMILARITY RESULTS AT SENSE LEVEL: A SNAPSHOT OF RESULTS

(w_i#s_k,w_j#s_l)	P	G	PG
(enquiry#1,investigation#1)	0.05	0.25	0.30
(enquiry#1,investigation#2)	0.09	0.0	0.30
(enquiry#2,investigation#1)	0.48	0.0	0.30
....			
(enquiry#1,interview#1)	0.46	0.2	0.30
(enquiry#1,interview#2)	0.06	0.0	0.30
...			
(outlets#1,stores#2)	0.06	0.0	0.30
...			

b) ESL experiment results with similarity threshold = 0.5: Tables IV to XV show the comparisons of path, gloss and PGMeasure using ESL dataset with the membership functions shown in table. I at similarity threshold at 0.5 and 0.4 respectively. In this case, to measure *path measure* of two given words, maximum similarity score of the synset pairs are taken to represent the overall similarity of a word pair. Likewise for the other two measures. The effects of variation in performance due to different membership functions used, threshold, as well as different path based measures are also shown. Initially the experiments were done using Set I and Set II of table. I; where the combination of Lin's similarity score as path measure with triangular membership function for the output fuzzy set has given better performance in terms of the evaluation metrics. Inspite of 'Center Of Gravity' approximation of the trapezoidal membership functions, it is seen in that if the values of the membership functions are tuned further, then it gives very sensible results. Thus the experiments are redone using set III of table. I and the results are presented.

TABLE IV
COMPARISON OF DIFFERENT WORD SIMILARITY MEASURES USING JIANG AND CONRATH'S PATH MEASURE AS ONE OF THE INPUTS IN FIS WITH THE MEMBERSHIP FUNCTIONS OF SET I, THRESHOLD = 0.5, ESL DATASET

Methods	recall	precision	F1	accuracy	rejection	f1
Path	0.2	1.0	0.33	0.61	1.0	0.33
Gloss	0.36	1.0	0.53	0.69	1.0	0.53
PGMeasure	0.24	1.0	0.39	0.63	1.0	0.39

[1]https://www.esl.org/

TABLE V
COMPARISON OF DIFFERENT WORD SIMILARITY MEASURES USING LIN'S PATH MEASURE AS ONE OF THE INPUTS IN FIS WITH THE MEMBERSHIP FUNCTIONS OF SET I, THRESHOLD = 0.5, ESL DATASET

Methods	recall	precision	F1	accuracy	rejection	f1
Path	0.44	0.61	0.51	0.59	0.73	0.55
Gloss	0.36	1.0	0.53	0.69	1.0	0.53
PGMeasure	0.36	0.75	0.49	0.63	0.89	0.51

TABLE VI
COMPARISON OF DIFFERENT WORD SIMILARITY MEASURES USING JIANG AND CONRATH'S PATH MEASURE AS ONE OF THE INPUTS IN FIS WITH THE MEMBERSHIP FUNCTIONS OF SET II, THRESHOLD = 0.5, ESL DATASET

Methods	recall	precision	F1	accuracy	rejection	f1
Path	0.2	1.0	0.33	0.61	1.0	0.33
Gloss	0.36	1.0	0.53	0.69	1.0	0.53
PGMeasure	0.24	1.0	0.39	0.63	1.0	0.39

TABLE VII
COMPARISON OF DIFFERENT WORD SIMILARITY MEASURES USING LIN'S PATH MEASURE AS ONE OF THE INPUTS IN FIS WITH THE MEMBERSHIP FUNCTIONS OF SET II, THRESHOLD = 0.5, ESL DATASET

Methods	recall	precision	F1	accuracy	rejection	f1
Path	0.44	0.61	0.51	0.59	0.73	0.55
Gloss	0.36	1.0	0.53	0.69	1.0	0.53
PGMeasure	0.36	0.75	0.49	0.63	0.88	0.51

TABLE VIII
COMPARISON OF DIFFERENT WORD SIMILARITY MEASURES USING JIANG AND CONRATH'S PATH MEASURE AS ONE OF THE INPUTS IN FIS WITH THE MEMBERSHIP FUNCTIONS OF SET III, THRESHOLD = 0.5, ESL DATASET

Methods	recall	precision	F1	accuracy	rejection	f1
Path	0.2	1.0	0.33	0.61	1.0	0.33
Gloss	0.36	1.0	0.53	0.69	1.0	0.53
PGMeasure	0.2	1.0	0.33	0.61	1.0	0.33

TABLE IX
COMPARISON OF DIFFERENT WORD SIMILARITY MEASURES USING LIN'S PATH MEASURE AS ONE OF THE INPUTS IN FIS WITH THE MEMBERSHIP FUNCTIONS OF SET III, THRESHOLD = 0.5, ESL DATASET

Methods	recall	precision	F1	accuracy	rejection	f1
Path	0.44	0.61	0.51	0.59	0.73	0.55
Gloss	0.36	1.0	0.53	0.69	1.0	0.53
PGMeasure	0.28	0.78	0.41	0.61	0.92	0.43

Tables IV to IX illustrate the results with threshold = 0.5. For all cases, performance of PGMeasure is higher when Lin's measure is used as one of the inputs to FIS. At 0.5 threshold using Set I and II, PGMeasure performed as expected using Lin's method as a path measure. The recall is lowered but the precision and rejection has increased showing that the method could properly identify predicted similar and dissimilar word pairs using set III.

c) ESL experiment results with similarity threshold = 0.4: Tables X to XV illustrate the evaluation results with threshold of 0.4. Like the previous cases, here too using Lin's path measure as input to FIS has shown better performance than Jiang and Conrath's. With further tuning of membership functions in Set III of table. I, the recall score has improved to a greater extent. Now if the same methods are compared at threshold 0.4 and 0.5, as per expert's comments, the similarities at 0.4 level by PGMeasure are more accurate.

Using Jiang and Conrath's similarity measure as one of the inputs of FIS, the precision and rejection for all the three sets of membership functions are higher for PGMeasure than Lin's when used in FIS; but recall is lower. Recall and accuracy increased using set III of membership functions showing overall improvement with slight reduction in precision.

TABLE X
COMPARISON OF DIFFERENT WORD SIMILARITY MEASURES USING JIANG AND CONRATH'S PATH MEASURE AS ONE OF THE INPUTS IN FIS WITH THE MEMBERSHIP FUNCTIONS OF SET I, THRESHOLD = 0.4, ESL DATASET

Methods	recall	precision	F1	accuracy	rejection	f1
Path	0.28	0.88	0.42	0.63	0.96	0.43
Gloss	0.36	0.9	0.51	0.67	0.96	0.52
PGMeasure	0.24	1.0	0.39	0.63	1.0	0.39

TABLE XI
COMPARISON OF DIFFERENT WORD SIMILARITY MEASURES USING LIN'S PATH MEASURE AS ONE OF THE INPUTS IN FIS WITH THE MEMBERSHIP FUNCTIONS OF SET I, THRESHOLD = 0.4, ESL DATASET

Methods	recall	precision	F1	accuracy	rejection	f1
Path	0.48	0.55	0.51	0.55	0.62	0.54
Gloss	0.36	0.9	0.51	0.67	0.96	0.53
PGMeasure	0.36	0.69	0.47	0.61	0.85	0.51

TABLE XII
COMPARISON OF DIFFERENT WORD SIMILARITY MEASURES USING JIANG AND CONRATH'S PATH MEASURE AS ONE OF THE INPUTS IN FIS WITH THE MEMBERSHIP FUNCTIONS OF SET II, THRESHOLD = 0.4, ESL DATASET

Methods	recall	precision	F1	accuracy	rejection	f1
Path	0.28	0.875	0.42	0.63	0.96	0.43
Gloss	0.36	0.9	0.51	0.67	0.96	0.52
PGMeasure	0.28	1.0	0.44	0.65	1.0	0.44

2) Rubenstein dataset: Similar evaluation is done with data collected from Rubenstein's paper [13]. Words pairs are assigned a score rated by human assessors. If table. XVI is noticed, the relevance scores assigned by humans are unnormalized. But normalization is required for evaluation. So, the values are normalized by,

$$x_i^{norm} = \frac{x_i - min_X}{max_X - min_X},\ i \in [1, |X|] \tag{1}$$

where X is a set of word pairs.

TABLE XIII
COMPARISON OF DIFFERENT WORD SIMILARITY MEASURES USING LIN'S PATH MEASURE AS ONE OF THE INPUTS IN FIS WITH THE MEMBERSHIP FUNCTIONS OF SET II, THRESHOLD = 0.4, ESL DATASET

Methods	recall	precision	F1	accuracy	rejection	f1
Path	0.48	0.55	0.51	0.55	0.62	0.54
Gloss	0.36	0.9	0.51	0.67	0.96	0.52
PGMeasure	0.4	0.71	0.51	0.63	0.85	0.54

TABLE XIV
COMPARISON OF DIFFERENT WORD SIMILARITY MEASURES USING JIANG AND CONRATH'S PATH MEASURE AS ONE OF THE INPUTS IN FIS WITH THE MEMBERSHIP FUNCTIONS OF SET III, THRESHOLD = 0.4, ESL DATASET

Methods	recall	precision	F1	accuracy	rejection	f1
Path	0.28	0.88	0.42	0.63	0.96	0.43
Gloss	0.36	0.9	0.51	0.67	0.96	0.52
PGMeasure	0.4	1.0	0.57	0.71	1.0	0.57

TABLE XV
COMPARISON OF DIFFERENT WORD SIMILARITY MEASURES USING LIN'S PATH MEASURE AS ONE OF THE INPUTS IN FIS WITH THE MEMBERSHIP FUNCTIONS OF SET III, THRESHOLD = 0.4, ESL DATASET

Methods	recall	precision	F1	accuracy	rejection	f1
Path	0.48	0.55	0.51	0.55	0.62	0.54
Gloss	0.36	0.9	0.51	0.67	0.96	0.52
PGMeasure	0.64	0.70	0.67	0.69	0.73	0.68

TABLE XVI
SNAPSHOT OF RUBENSTEIN DATASET

word_1	word_2	Relevance
cord	smile	0.02
hill	woodland	1.48
rooster	voyage	0.04
car	journey	1.55
noon	string	0.04
cemetery	mound	1.69
fruit	furnace	0.05
glass	jewel	1.78
autograph	shore	0.06
magician	oracle	1.82
...		

a) Rubenstein experiment results with similarity threshold = 0.5: Now, tables XVII to XXII present evaluation result with Rubenstein's data at similarity threshold of 0.5. Like ESL's results, here too Lin's method gives better performance than Jiang and Conrath. But in this case Set III are not as good as Set I and II at this threshold.

Set I and II showed better evaluation metrics for set I and set II, but not for set III at this threshold for this dataset.

b) Rubenstein experiment results with similarity threshold = 0.4: Tables XXIII to XXVIII show performance of different similarity measures 0.4 threshold. Like the other cases illustrated so far, Lin's method for each of these sets perform better. But Set III's performance is best here and can be seen in table. XXVIII.

Now, at threshold of 0.4, using set I and set II of table. I, the evaluation metrics are little lower than 0.5. Set III has given better recall and more practical evaluation scores at 0.4 with this dataset like ESL.

TABLE XVII
COMPARISON OF DIFFERENT WORD SIMILARITY MEASURES USING JIANG AND CONRATH'S PATH MEASURE AS ONE OF THE INPUTS IN FIS WITH THE MEMBERSHIP FUNCTIONS OF SET I, THRESHOLD = 0.5, RUBENSTEIN DATA SET

Methods	recall	precision	F1	accuracy	rejection	f1
Path	0.54	1.0	0.70	0.8	1.0	0.70
Gloss	0.36	1.0	0.53	0.72	1.0	0.53
PGMeasure	0.46	1.0	0.63	0.77	1.0	0.63

TABLE XVIII
COMPARISON OF DIFFERENT WORD SIMILARITY MEASURES USING LIN'S PATH MEASURE AS ONE OF THE INPUTS IN FIS WITH THE MEMBERSHIP FUNCTIONS OF SET I, THRESHOLD = 0.5, RUBENSTEIN DATASET

Methods	recall	precision	F1	accuracy	rejection	f1
Path	0.82	0.89	0.85	0.88	0.92	0.87
Gloss	0.36	1.0	0.53	0.72	1.0	0.53
PGMeasure	0.79	1.0	0.88	0.91	1.0	0.88

TABLE XIX
COMPARISON OF DIFFERENT WORD SIMILARITY MEASURES USING JIANG AND CONRATH'S PATH MEASURE AS ONE OF THE INPUTS IN FIS WITH THE MEMBERSHIP FUNCTIONS OF SET II, THRESHOLD = 0.5, RUBENSTEIN DATA SET

Methods	recall	precision	F1	accuracy	rejection	f1
Path	0.54	1.0	0.70	0.8	1.0	0.70
Gloss	0.36	1.0	0.53	0.72	1.0	0.53
PGMeasure	0.5	1.0	0.67	0.78	1.0	0.67

TABLE XX
COMPARISON OF DIFFERENT WORD SIMILARITY MEASURES USING LIN'S PATH MEASURE AS ONE OF THE INPUTS IN FIS WITH THE MEMBERSHIP FUNCTIONS OF SET II, THRESHOLD = 0.5, RUBENSTEIN DATASET

Methods	recall	precision	F1	accuracy	rejection	f1
Path	0.82	0.89	0.85	0.88	0.92	0.87
Gloss	0.36	1.0	0.53	0.72	1.0	0.53
PGMeasure	0.79	1.0	0.88	0.91	1.0	0.88

TABLE XXI
COMPARISON OF DIFFERENT WORD SIMILARITY MEASURES USING JIANG AND CONRATH'S PATH MEASURE AS ONE OF THE INPUTS IN FIS WITH THE MEMBERSHIP FUNCTIONS OF SET III, THRESHOLD = 0.5, RUBENSTEIN DATASET

Methods	recall	precision	F1	accuracy	rejection	f1
Path	0.54	1.0	0.70	0.8	1.0	0.70
Gloss	0.36	1.0	0.53	0.72	1.0	0.53
PGMeasure	0.36	1.0	0.53	0.72	1.0	0.53

TABLE XXII
COMPARISON OF DIFFERENT WORD SIMILARITY MEASURES USING LIN'S PATH MEASURE AS ONE OF THE INPUTS IN FIS WITH THE MEMBERSHIP FUNCTIONS OF SET III, THRESHOLD = 0.5, RUBENSTEIN DATASET

Methods	recall	precision	F1	accuracy	rejection	f1
Path	0.82	0.89	0.85	0.88	0.92	0.87
Gloss	0.36	1.0	0.53	0.72	1.0	0.53
PGMeasure	0.36	1.0	0.53	0.72	1.0	0.53

TABLE XXIII
COMPARISON OF DIFFERENT WORD SIMILARITY MEASURES USING JIANG AND CONRATH'S PATH MEASURE AS ONE OF THE INPUTS IN FIS WITH THE MEMBERSHIP FUNCTIONS OF SET I, THRESHOLD = 0.4, RUBENSTEIN DATA SET

Methods	recall	precision	F1	accuracy	rejection	f1
Path	0.48	1.0	0.65	0.75	1.0	0.65
Gloss	0.32	1.0	0.49	0.68	1.0	0.49
PGMeasure	0.45	1.0	0.62	0.74	1.0	0.62

TABLE XXIV
COMPARISON OF DIFFERENT WORD SIMILARITY MEASURES USING LIN'S PATH MEASURE AS ONE OF THE INPUTS IN FIS WITH THE MEMBERSHIP FUNCTIONS OF SET I, THRESHOLD = 0.4, RUBENSTEIN DATASET

Methods	recall	precision	F1	accuracy	rejection	f1
Path	0.74	0.89	0.81	0.83	0.91	0.82
Gloss	0.32	1.0	0.49	0.68	1.0	0.49
PGMeasure	0.71	1.0	0.83	0.86	1.0	0.83

TABLE XXV
COMPARISON OF DIFFERENT WORD SIMILARITY MEASURES USING JIANG AND CONRATH'S PATH MEASURE AS ONE OF THE INPUTS IN FIS WITH THE MEMBERSHIP FUNCTIONS OF SET II, THRESHOLD = 0.4, RUBENSTEIN DATA SET

Methods	recall	precision	F1	accuracy	rejection	f1
Path	0.48	1.0	0.65	0.75	1.0	0.65
Gloss	0.32	1.0	0.49	0.68	1.0	0.49
PGMeasure	0.48	1.0	0.65	0.75	1.0	0.65

TABLE XXVI
COMPARISON OF DIFFERENT WORD SIMILARITY MEASURES USING LIN'S PATH MEASURE AS ONE OF THE INPUTS IN FIS WITH THE MEMBERSHIP FUNCTIONS OF SET II, THRESHOLD = 0.4, RUBENSTEIN DATASET

Methods	recall	precision	F1	accuracy	rejection	f1
Path	0.74	0.89	0.81	0.83	0.91	0.82
Gloss	0.32	1.0	0.49	0.68	1.0	0.49
PGMeasure	0.71	1.0	0.83	0.86	1.0	0.83

Thus from both the sets of data, it is seen that using Lin's path similarity for PGMeasure at threshold of 0.4 with Set III of table. I can give more accurate word similarity results which is more similar to human judgements.

TABLE XXVII
COMPARISON OF DIFFERENT WORD SIMILARITY MEASURES USING JIANG AND CONRATH'S PATH MEASURE AS ONE OF THE INPUTS IN FIS WITH THE MEMBERSHIP FUNCTIONS OF SET III, THRESHOLD = 0.4, RUBENSTEIN DATASET

Methods	recall	precision	F1	accuracy	rejection	f1
Path	0.48	1.0	0.65	0.75	1.0	0.65
Gloss	0.32	1.0	0.49	0.68	1.0	0.49
PGMeasure	0.52	1.0	0.68	0.77	1.0	0.68

TABLE XXVIII
COMPARISON OF DIFFERENT WORD SIMILARITY MEASURES USING LIN'S PATH MEASURE AS ONE OF THE INPUTS IN FIS WITH THE MEMBERSHIP FUNCTIONS OF SET III, THRESHOLD = 0.4, RUBENSTEIN DATASET

Methods	recall	precision	F1	accuracy	rejection	f1
Path	0.74	0.89	0.81	0.83	0.91	0.82
Gloss	0.32	1.0	0.49	0.68	1.0	0.49
PGMeasure	0.74	0.89	0.81	0.83	0.91	0.82

V. SIMILARITY COMPUTATION WITH HDS

A document is modularized into sentences, and then the words of the sentences are grouped based on their POS. Using fuzzy word similarity measure (PGMeasure) similarity between two words are calculated and assigned them as the similarity score for each word in a sentences with respective POS. Then aggregations are applied at each level to get final similarity between a sentence pair. The similarity value of 0 shows the sentences are not at all related and 1 means they are identical. But practically due to fuzzy approximations at word level, the value of 1 can not be reached even if all the words are identical.

This experimental setup is taken directly from [3] with variations in the features. So, in this paper, we only mention them.

A. Evaluation Metrics at Sentence Level

Similar evaluation settings are set here as in IV-A but at sentence level. The similarities computed are evaluated with respect to the benchmark similarities provided by humans in the dataset used. The same metrics are used here as used by [12] which are namely *recall*, *precision*, *F1*, *accuracy*, *rejection*, and *f1* respectively.

The definitions are re-defined at sentence level. **Recall** is a proportion of correctly predicted similar sentences compared to all similar sentences. **Precision** is a proportion of correctly predicted similar sentences compared to all predicted similar sentences. **F1** is a uniform harmonic mean of precision and recall. **Rejection** is a proportion of correctly predicted dissimilar sentences compared to all dissimilar sentences. **Accuracy** is a proportion of all correctly predicted sentences compared to all sentences. Lastly, we define **f1** as a uniform harmonic mean of rejection and recall. A scoring threshold for positive pairs is defined at 0.4 is used unlike [12], where it was 0.5.

This has to be done due to fuzzy membership tuning at the word level.

Other than HDS, *cosine similarity*[2] is used for comparison of results; it is basically a vector space model and works on only 'bag of words' concept.

With similar reasoning as word level, in this case the experiments are done at similarity threshold of 0.4. It is also shown that set II and III of the membership functions work better for this application than set I. So we focus on experiments with these two only.

B. Dataset - The Microsoft Paraphrase Corpus

In 2005, Microsoft researchers Dolan, Brocket, and Quirck [17] published the first paraphrase corpus containing 5801 pairs of sentences with 3900 tagged as "semantically equivalent" or true paraphrases. Sentences were obtained from massive parallel news sources and tagged by 3 human raters according to guidelines described in [17]. This corpus will be referred to below as the MSRPC.

At the word level computation of HDS, membership functions mentioned in Set II and III of table. I are used by FWS. As shown in the word similarity evaluations, similarity threshold of 0.4 is used for all the evaluation in this chapter as well. Tables XXIX and XXX are based on Set II membership functions.

TABLE XXIX
EVALUATION METRIC OF SENTENCE SIMILARITY WITH 500 SENTENCE PAIRS OF MSRPC TEST DATASET

Methods	recall	precision	F1	accuracy	rejection	f1
CosineSim	1	0.68	0.81	0.68	0	0
HDS	0.88	0.71	0.79	0.68	0.24	0.38

TABLE XXX
EVALUATION METRIC OF SENTENCE SIMILARITY WITH WHOLE MSRPC TEST DATASET

Methods	recall	precision	F1	accuracy	rejection	f1
CosineSim	1	0.66	0.80	0.66	0	0
HDS	0.87	0.69	0.77	0.65	0.24	0.37

In table. XXX, it is seen that HDS has higher precision than cosine similarity. But there is minor drop in performance due to wrongly tagged words by the parser used. This is detected when the tagging was checked manually. There is slight rejection of 0.1 in the similarity findings. In the dataset, the humans assigned either 1 or 0 for similar or dissimilar sentences. But this is not very appropriate because similarity measurements when done by humans, can have certain level of uncertainty, which can be captured using fuzzy methods. This is actually done by HDS and the snapshot is shown in table. XXXI.

[2]http://www10.org/cdrom/papers/519/node12.html

TABLE XXXI
SNAPSHOT OF RESULTS WITH MSRPC

Sent1ID	Sent2ID	HumanScore	CosineSim	HDS Sim
3354381	3354396	0	1.0	0.37
1390995	1391183	1	0.99	0.5
2201401	2201285	0	1.0	0.55
...	...	...	...	...

c) Effect of tuning membership functions at word level computation: The HDS structure explained here is dependent on the features of the word level. The semantic similarity between words are computed by PGMeasure as discussed in [8]. The similarity values depend on the tuning of membership functions at this word level. The better the membership functions chosen, the more the results will be similar to human approximations. Here a new set (Set III of table. I) of membership functions are used and the HDS is again run on MSRP corpus and the results are observed in tables XXXII and XXXIII.

TABLE XXXII
EVALUATION METRIC OF SENTENCE SIMILARITY WITH 500 SENTENCE PAIRS OF MSRPC TEST DATASET

Methods	recall	precision	F1	accuracy	rejection	f1
CosineSim	1.0	0.68	0.81	0.68	0	0
HDS	1.0	0.69	0.82	0.70	0.05	0.10

TABLE XXXIII
EVALUATION METRIC OF SENTENCE SIMILARITY WITH WHOLE MSRPC TEST DATASET

Methods	recall	precision	F1	accuracy	rejection	f1
CosineSim	1.0	0.66	0.80	0.66	0	0
HDS	0.99	0.67	0.80	0.67	0.03	0.06

From tables XXXII and XXXIII, it is clearly noticed that the recall and precision have improved over the previous cases.

C. Effect of different Parts of Speech on HDS performance

Similarity of words are determined based on context. It is rather difficult to say which words are similar without a context. But if they belong to same parts of speech then it can be assumed that the contextual appearance of the words will also be similar if not exactly the same. Since HDS uses the word level similarity to propagate to the sentence level, it is essential to identify these words based on their proper parts of speech; as it is known that the same word in different parts of speech may have different meaning. Thus it is necessary to formulate a method which disambiguates the interpretational uncertainties and delivers more contextually appropriate word similarity - taking into account different measures, such as - graph based measures and glosses of the contextual senses. Hierarchical Document Signature (HDS) is hence chosen. It organizes a sentence into a hierarchical structure that helps to compare two or more sentences based on their part-of-speech

(POS) using fuzzy aggregation. As such, its result is effected by the result of POS tagging directly.

Now another experiment is conducted to see the effect of different POS taggers on HDS. Normally, for the previous evaluations, Stanford POS tagger is used. But it is seen that there are many instances when Stanford POS tagger produces errors and lead to wrongly tagged words. As HDS is dependent on POS, so proper tagging is required. Here, four different taggers 'hunpos' [18], 'opennlp' [19], 'crftag' [20], and 'lingpipe' [21] are used and sentence similarity is recomputed with different taggers using 500 MSRP data and the results are shown in fig. 2. It reflects that the performance of HDS can be improved using a better tagging algorithm.

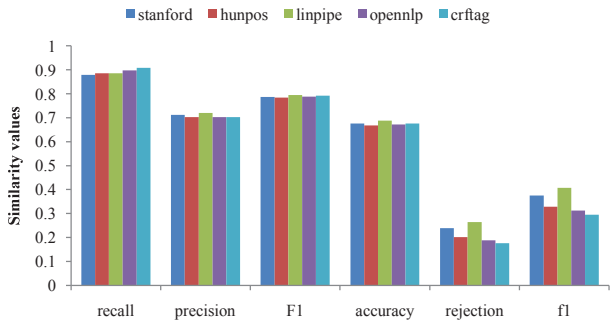

Fig. 2. Comparison of performance evaluation with varying POS taggers

VI. Conclusion

This paper discusses a detailed study of different features for improving the performance of the Hierarchical Document Signature. It is seen that proper tuning of features like fuzzy membership functions, similarity thresholds, input fuzzy sets and even a better choice of POS tagger improve HDS' performance. As future work, the main aim will be to tune the features automatically based on the nature of the dataset.

References

[1] S. Manna, B. Mendis, and T. Gedeon, "Hierarchical document signature: a specialized application of fuzzy signature for document computing," in *Fuzzy Systems, 2009. FUZZ-IEEE 2009. IEEE International Conference on*. IEEE, 2009, pp. 1083–1088.

[2] S. Manna, T. Gedeon, and B. Mendis, "Enhancement of subjective logic for semantic document analysis using hierarchical document signature," *Neural Information Processing. Theory and Algorithms*, pp. 298–306, 2010.

[3] S. Manna and T. Gedeon, "Semantic Hierarchical Document Signature for determining sentence similarity," in *Fuzzy Systems (FUZZ), 2010 IEEE International Conference on*. IEEE, pp. 1–8.

[4] M. Bilotti, P. Ogilvie, J. Callan, and E. Nyberg, "Structured retrieval for question answering," in *Proceedings of the 30th Annual International ACM SIGIR Conference on Research and Development in information retrieval*. ACM New York, NY, USA, 2007, pp. 351–358.

[5] S. Shehata, F. Karray, and M. Kamel, "A concept-based model for enhancing text categorization," in *Proceedings of the 13th ACM SIGKDD international conference on Knowledge discovery and data mining*. ACM New York, NY, USA, 2007, pp. 629–637.

[6] P. Achananuparp, X. Hu, and C. Yang, "Addressing the Variability of Natural Language Expression in Sentence Similarity with Semantic Structure of the Sentences," in *Proceedings of the 13th Pacific-Asia Conference on Advances in Knowledge Discovery and Data Mining*. Springer, 2009, p. 555.

[7] B. S. U. Mendis, "Fuzzy signatures: Hierarchical fuzzy systems and alpplications (phd thesis)," Ph.D. dissertation, College of Engineering and Computer Science, The Australian National University, Australia, 2008.

[8] S. Manna and B. Mendis, "Fuzzy word similarity: A semantic approach using WordNet," in *Fuzzy Systems (FUZZ), 2010 IEEE International Conference on*. IEEE, pp. 1–8.

[9] D. Lin, "Using syntactic dependency as local context to resolve word sense ambiguity," in *Annual Meeting-Association For Computational Linguistics*, vol. 35. Association For Computational Linguistics, 1997, pp. 64–71.

[10] J. Jiang and D. Conrath, "Semantic similarity based on corpus statistics and lexical taxonomy," *Arxiv preprint cmp-lg/9709008*, 1997.

[11] A. Chong, T. D. Gedeon, K. W. Wong, and L. T. Kóczy, "A histogram-based rule extraction technique for fuzzy systems," in *FUZZ-IEEE*, 2001, pp. 638–641.

[12] P. Achananuparp, X. Hu, and X. Shen, "The evaluation of sentence similarity measures," in *DaWaKD08: Proceedings of the 10th international conference on Data Warehousing and Knowledge Discovery*. Springer, pp. 305–316.

[13] H. Rubenstein and J. Goodenough, "Contextual correlates of synonymy," *Communications of the ACM*, vol. 8, no. 10, p. 633, 1965.

[14] T. Landauer and S. Dumais, "A solution to Plato's problem: The latent semantic analysis theory of acquisition, induction, and representation of knowledge," *Psychological review*, vol. 104, no. 2, pp. 211–240, 1997.

[15] D. Tatsuki, "Basic 2000 Words-Synonym Match 1," *Interactive JavaScript Quizzes for ESL Students, http://www. aitech. ac. jp/˜iteslj/quizzes/js/dt/mc-2000-01syn. html*, 1998.

[16] D. Yang and D. Powers, "Word similarity on the taxonomy of WordNet."

[17] B. Dolan, C. Quirk, and C. Brockett, "Unsupervised construction of large paraphrase corpora: Exploiting massively parallel news sources," in *Proceedings of the 20th international conference on Computational Linguistics*. Association for Computational Linguistics Morristown, NJ, USA, 2004.

[18] P. Halácsy, A. Kornai, and C. Oravecz, "HunPos: an open source trigram tagger," pp. 209–212, 2007.

[19] J. Baldridge, T. Morton, and G. Bierner, "The opennlp maximum entropy package," 2002.

[20] X. Phan, "Crftagger: Crf english pos tagger," 2006.

[21] B. Baldwin and B. Carpenter, "LingPipe."

2011 IEEE International Conference on Fuzzy Systems
June 27-30, 2011, Taipei, Taiwan

Sliding Adaptive Fuzzy Control for a Class of Time-Delayed Chaotic Systems

Negin Farzbod
Engineering Department
Imam Khomeini International University of Qazvin
Qazvin, Iran
negin.farzbod@ yahoo.com

Hassan Zarabadipour
Faculty of Electrical Engineering, Engineering Department
Imam Khomeini International University of Qazvin
Qazvin, Iran
H_zarabadi@ikiu.ac.ir

Mahdi Aliyari Shoorehdeli
Faculty of Electrical & Computer Engineering,
Mechatronics Department
K. N. Toosi University of Technology
Tehran, Iran
Aliyari@eetd.kntu.ac.ir

Faezeh Farivar
Faculty of Engineering, Mechatronics Department
Science and Research Branch, Islamic Azad University
Tehran, Iran
f.farivar@srbiau.ac.ir

***Abstract*— In this study, sliding adaptive fuzzy control (SAFC) is proposed to chaos control for a class of time-delayed chaotic systems. An adaptation law based on Gradient Descent (GD) method is utilized to determine the parameters of fuzzy controller. The first derivation of Lyapunov function is considered as the cost function which must be minimized, so the stability of proposed method is guaranteed with Lyapunov stability theory. Moreover, the changes of parameters and delay time are investigated. Simulation results show that the proposed method is appropriate to chaos control and it is robust with respect to changes of parameters. Also it is illustrated that the performance of proposed method is better than the performance of sliding mode controller.**

Keywords: Chaos control, Sliding mode control, Adaptive fuzzy Control , Time-delayed chaotic systems

I. INTRODUCTION

Chaos is the long and finite aperiodic behavior in deterministic systems which are extremely sensitive to initial conditions [1, 2]. This phenomenon has occurred in many fields such as physical, chemical, biological process and secure communications [3, 4]. Chaos is often undesirable or unwanted, so the chaos control is required to attain the system with the regular behavior. However, sometimes it is useful as in mixing and coding process [5, 6]. Since Ott, Grebogi and Yorke proposed the OGY method in 1990 [7], chaos control has been one of the interesting topics for researchers. Many various control methods have been studied to chaos control such as fuzzy [5, 6], sliding mode control (SMC) [8, 9], delayed feedback [10], and radial basis function (RBF) sliding mode controller [11].

Since Mackey and Glass observed the oscillation and chaos in physiological systems by first order differential delay equations in 1977 [12], time-delayed chaotic systems have attracted many interests. After that, many time-delayed chaotic systems were found with one state variable, such Ikeda model simplified the model of a laser with optical feedback. Logistic model is the other one which describes the model of population increasing in an unchangeable environment. One of the important researches studied the behavior of these systems is presented in [13]. In 2004, Ikeda model and bifurcation phenomenon are restudied in [14]. Logistic model is studied in [15]. The bifurcation phenomenon in Logistic model is investigated with considering the different delay in [16].

Time-delayed chaotic systems introduce infinite dimension, so chaos control in these systems is more complicated than in the chaotic systems with finite dimension. Many studies have been done on chaos control in these systems, for example, the occasional proportional feedback [17], and the delayed feedback controller (DFC) [18]. Hybrid control including SMC and delayed feedback controller is designed to stabilize unstable periodic orbits (UPO's) and unstable fixed points (UFP's) [19]. An observer-based approach to control of time-delay chaotic systems via Takagi – Sugeno fuzzy model is studied in [20].

In this study, an adaptive fuzzy controller is applied to stabilize UPO's and UFP's .The input of this controller is a sliding surface. The basic idea of this method is minimizing the first derivation of Lyapunov function, so that the stability is achieved. Notice that, to stabilize UPO's, sliding adaptive fuzzy control (SAFC) based delayed feedback is proposed in this paper. Also, the effect of model parameters and time delay are investigated with considering different values of them. The SAFC is implemented on Mackey-Glass and Logistic models.

This paper is organized as follows: in section 2, the model of time-delayed chaotic systems and its properties are described. The structure of proposed controller constitutes section 3. Stability analysis is studied in section 4. Simulation results and conclusion are given in section 5 and 6, respectively.

978-1-4244-7316-8/11/$26.00 ©2011 IEEE

II. MODEL OF SYSTEM

A class of time-delayed systems is considered as follows:

$$\dot{x}(t) = -ax(t) + f_b(x(t-\tau)) + u(t) \tag{1}$$

where, $x, u \in R$ are the state variable and control input, respectively. a, b, τ are the system parameters , $\tau \succ 0$. Time-delayed system in (1) can show chaotic behavior when the nonlinear function $f_b(.)$ satisfies the following conditions [21, 22]:

$(i) f_b(0) = 0;$

$(ii) \forall x \quad x f_b(x) \geq 0;$

$(iii) \exists x_{eq} \succ 0 \quad f_b(x_{eq}) = x_{eq};$

$(iiii) \exists r \in (0, x_{eq}) : \forall x \quad f_b(x) \leq f_b(r) = M \quad , M \succ 0.$

Some time-delayed chaotic systems satisfied above conditions are Mackey-Glass, Ikeda and Logistic models. These models are given as

Mackey-Glass Model [12, 21]

$$f_b(z) = \frac{bz}{1 + |z|^C} \quad (C \succ 1) \tag{2}$$

Ikeda model [13, 21, 23]

$$f_b(z) = \begin{cases} b\sin(z) & |z| \leq \pi \\ 0 & otherwise \end{cases} \tag{3}$$

Logistic model [22]

$$f_b(z) = \begin{cases} bz(1-z) & 0 \leq z \leq 1 \\ 0 & otherwise \end{cases} \tag{4}$$

In this paper, Mackey-Glass and Logistic models are studied.

III. DESIGN OF CONTROLLER

In this section, sliding adaptive fuzzy control is designed to chaos control in time-delayed chaotic systems. Gradient Descent (GD) is applied to train the parameters of fuzzy controller. In this method, minimizing the first derivation of Lyapunov function is considered, so that the stability is achieved. This derivation is applied as a cost function to determine unknown parameters to design of controller. Based on the Lyapunov theorem, the sliding surface reaching condition is $s\dot{s} \prec 0$.

Sliding surface is defined as follows:

$$s(t) = e(t) = \begin{cases} x(t) - x_{eq} & ; to\ stabilize\ UFP's \\ x(t) - \alpha x(t-T) & ; to\ stabilize\ UPO's \end{cases} \tag{5}$$

where $0 \prec \alpha \prec 1$. If $\alpha = 1$, then a stable periodic solution is obtained and if $\alpha \prec 1$, the origin will be stabilized. Notice that to stabilize UPO's, it is assumed that $x^*(t)$ is considered as the desired UPO with $x^*(t+T) = \alpha x^*(t)$ .The fuzzy system used in this study has product inference engine, singleton fuzzifier, center average defuzzifier, and Gaussian membership function. So, the fuzzy system is given as

$$u_1 = \frac{\sum_{l=1}^{E} y^l \left[\prod_{i=1}^{n} \exp(-(\frac{s - c_i^l}{\sigma})^2) \right]}{\sum_{l=1}^{E} \left[\prod_{i=1}^{n} \exp(-(\frac{s - c_i^l}{\sigma})^2) \right]} = \hat{Y}^T \phi \tag{6}$$

where $\hat{Y} = [y^1, ..., y^n]^T$, E is fixed, y^l , c_i^l and σ are free parameters. $s \in R^n$ is the input of the fuzzy system, and $u_1 \in R$ is the output of the fuzzy system. y^l is the center of fuzzy set. Parameters c_i^l and σ are centers and radius of basis function, respectively. In this paper, c_i^l and σ are chosen arbitrarily. Since this fuzzy system is considered with one input, n is equal to 1. To design the controller, the parameter y^l must be determined based on the reaching condition, $s\dot{s} < 0$. Thus, the GD method is applied to determine it as follows:

$$\dot{y}^l = -\gamma \frac{\partial s(t)\dot{s}(t)}{\partial y^l(t)} \tag{7}$$

Equation (7) can be rewritten as

$$\dot{y}^l = -\gamma \frac{\partial s(t)\dot{s}(t)}{\partial y^l(t)} = -\gamma \frac{\partial s(t)\dot{s}(t)}{\partial u(t)} \frac{\partial u(t)}{\partial y^l(t)} \tag{8}$$

Let us to define

$$u = u_1 + u_2 \tag{9}$$

where $u_2 = -f_b(x(t-\tau))$, so the non-linear term is cancelled. Then

$$\begin{aligned}\dot{y}^l &= -\gamma \frac{\partial s(t)\dot{s}(t)}{\partial y^l(t)} = -\gamma \frac{\partial s(t)\dot{s}(t)}{\partial u(t)} \frac{\partial u(t)}{\partial y^l(t)} \\ &= -\gamma \frac{\partial s(t)\dot{s}(t)}{\partial u_1(t)} \frac{\partial u_1(t)}{\partial y^l(t)} \\ &= -\gamma s(t) \frac{\exp(-(\frac{s-c^l}{\sigma})^2)}{\sum_{l=1}^{E} \exp(-(\frac{s-c^l}{\sigma})^2)} = -\gamma s(t)\phi_l(s)\end{aligned} \tag{10}$$

where γ is the learning rate parameter. Finally, y^l can be on-line adjusted as it was shown in (10). The SAFC will be compared with SMC described as

$$u(t) = -k_1 sat(\frac{x(t) - x_{eq}}{k_2}) \tag{11}$$

where x_{eq} is the desired fixed point and k_1, k_2 are the controller parameters. This controller has been used in [19]. Since (1) shows chaotic behavior, many unstable periodic orbits exist in its attractor. The SAFC based delayed feedback can be useful to stabilize UPO's with desired period. The SAFC based delayed feedback is described as

$$u(t) = \alpha u(t-T) + u_1 + u_2 \tag{12}$$

Notice that $x^*(t+T) = \alpha x^*(t)$, and $x^*(t)$ is considered as the desired UPO.

IV. STABILITY ANALYSIS

Lyapunov stability analysis is applied to prove the stability of UFP's and UPO's. From the theory of sliding mode control, a perfect control law is obtained as

$$u_{eq} = \begin{cases} \dot{x}(t) + ax(t) + \dot{s}(t) + \lambda s(t) & ; for\ UFP's \\ -\alpha u(t-T) + \dot{x}(t) & \\ \quad + ax(t) + \dot{s}(t) + \lambda s(t) & ; for\ UPO's \end{cases} \tag{13}$$

where s is presented in (5).
First, to analyze the stability, (9) is substituted in (1):

$$\dot{x}(t) = \begin{cases} -ax(t) + u_1(t) & ; for\ UFP's \\ -ax(t) + \alpha u(t-T) + u_1(t) & ; for\ UPO's \end{cases} \tag{14}$$

if u_1 is substituted with u_{eq} then $\dot{s}(t) + \lambda s(t) = 0$. Since λ is a positive constant parameter, the sliding surface variable s will converge to zero, gradually. So, e will converge to zero. From (13) and (14):

$$\dot{s}(t) = -\lambda s(t) + (u_{eq}(t) - u_1(t)) \tag{15}$$

Theorem ([24]). *Suppose that the input universe of discourse U is a compact set in R^n. Then, for any given real continuous function $g(z)$ on U and arbitrary $\xi \succ 0$, there exists a fuzzy system $F(z)$ in the form of (10) such that*

$$\sup_{z \in U} \left\| g(z) - F(z) \right\| \le \xi$$

That is, the fuzzy systems with product inference engine, singleton fuzzifier, center average defuzzifier, and Gaussian membership functions are universal approximators.

Therefore, the control law u_1 can be obtained via the optimal weighting vector $\overline{Y}$ of the fuzzy system. The designed control is applied to estimate the u_{eq}. This approximation can be achieved with the error which is smaller than ξ.

$$\max \left| \overline{u}(x, \overline{Y}) - u_{eq}(x) \right| \prec \xi$$

where $\overline{u}(x, \overline{Y}) = \sum_{l=1}^{E} \overline{y}^l \phi_l = \overline{Y}^T \phi$ and $u_{eq}(x) = \overline{Y}^T \phi + \xi$.

Define $\widetilde{Y} = \overline{Y} - \hat{Y}$ as the weighting error, and then (15) can be rewritten as

$$\dot{s}(t) = -\lambda s(t) + (\widetilde{Y}^T \phi + \xi) \tag{16}$$

Notice that $\overline{Y}$ and $\hat{Y}$ are the optimal and estimated values of Y, respectively.
Define the Lyapunov function as follows:

$$V(s, \widetilde{Y}) = \frac{1}{2} s^2 + \frac{1}{2\gamma} \widetilde{Y}^T \widetilde{Y} \tag{17}$$

The first derivation of (17) with respect to time is obtained as

$$\dot{V} = s\dot{s} + \frac{1}{\gamma} \widetilde{Y}^T \dot{\widetilde{Y}} \tag{18}$$

Substituting (10), (16) in to (18), then

$$\dot{V} = s(-\lambda s + \tilde{Y}^T \phi + \xi) + \frac{1}{\gamma}\tilde{Y}^T(-\gamma s \phi) = -\lambda s^2 + s\xi \quad (19)$$

Thus

$$\dot{V} \le |s|(-\lambda|s| + \xi) \quad (20)$$

So, if $|s| \ge \xi/\lambda$, then $\dot{V} \le 0$ which means that this Lyapunov function will decrease gradually. It can be concluded that the error of state variable will converge into a boundary layer ξ/λ around $e = s = 0$ in the phase plane. Hence, it can be resulted that the SAFC is stable and the error of state variable will converge into a small value.

V. SIMULATION RESULTS

A. Implementation with constant values of a, b, τ

In this section, the behavior of two considered models with $\tau = 10$, $a = 1$, $b = 2$ (for Mackey-Glass model), $b = 4$ (for Logistic model), $C = 10$ and $x(0) = 0.1$ is studied. For Mackey-Glass and Logistic models, UFP's other than the origin are $\pm 10\sqrt{\frac{b-a}{a}} = \pm 1$ and $\frac{b-a}{b} = 0.75$, respectively. Fig. 1 shows the phase plane of the uncontrolled system.

The SAFC and the SAFC based delayed feedback are applied to stabilize the UFP'S and UPO's, respectively. The parameters of SMC are $k_1 = 3, k_2 = 0.1$ and the reason of these choices has been described in [19]. System responses are shown in Fig. 2. As it is shown in Fig. 3 the control effort of SAFC is less than the control effort of SMC and the control signal of SAFC is smoother than the control signal of SMC. Notice that the speed of SAFC and SMC is controllable. The SAFC speed is improved with a proportional gain. Also, the speed of response with SMC becomes better if k_1 is chosen larger than 3 or k_2 is chosen smaller than 0.1. Notice that if k_1 is chosen larger than 3, the control signal will become larger. In this mode, system may be damaged, and if k_2 is chosen smaller than 0.1, the control effort will become more that it is not desired. Furthermore, it is assumed that $|s(t)| \le k_2$ is $s(t)$'s domain of attraction, so very small value of k_2 is not desired. In summary, with comparing the response speeds and control efforts of SAFC and SMC, it is obtained that the performance of SAFC is better than the performance of SMC. To show the effect of small value of k_2, its value is changed to 0.0001. Fig. 3 shows that in this case, the control effort becomes more, although the speed of response becomes better.

To stabilize UPO's, it is assumed that $\alpha = 1, T = 13$. The results obtained after using SAFC based delayed feedback at $t = 100$ are shown in Fig. 5. As it is shown in this figure, the period of the response is exactly the same as it has been desired.

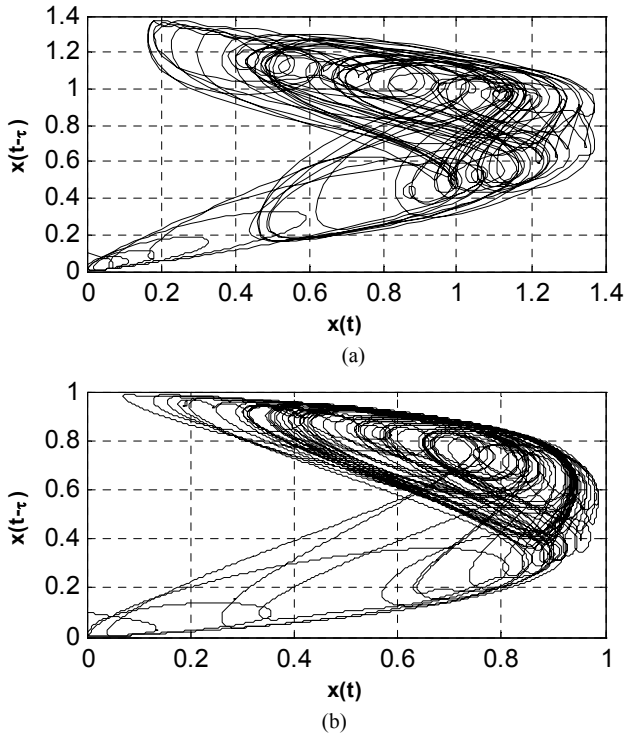

Figure 1. Phase plane of the uncontrolled systems, for (a) Mackey-Glass, (b) Logistic model.

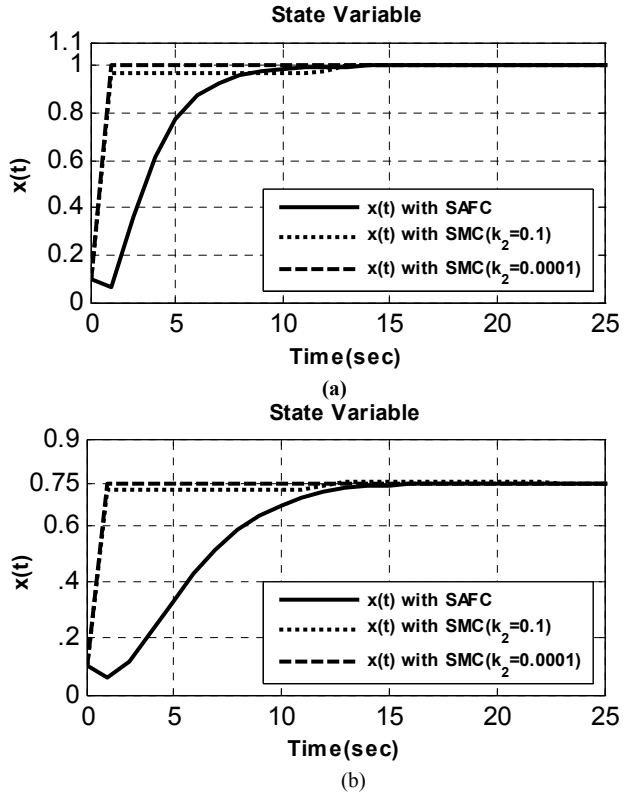

Figure 2. System response of (a) Mackey-Glass , (b) Logistic model to SAFC and SMC.

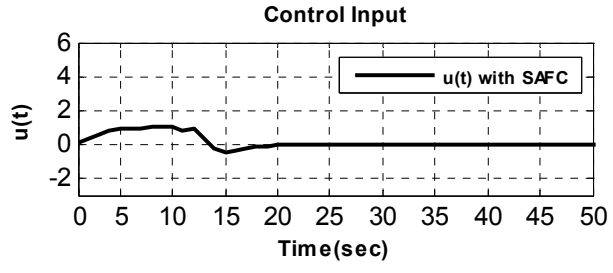

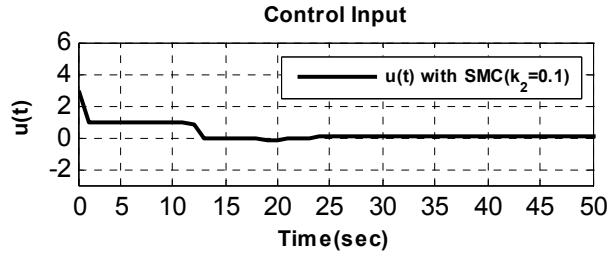

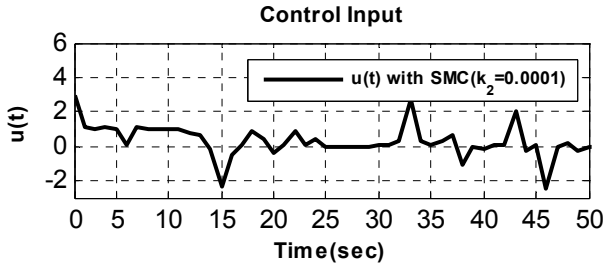

(a)

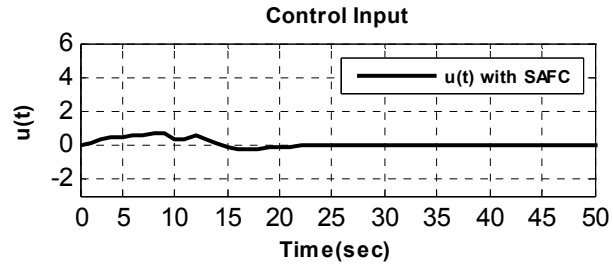

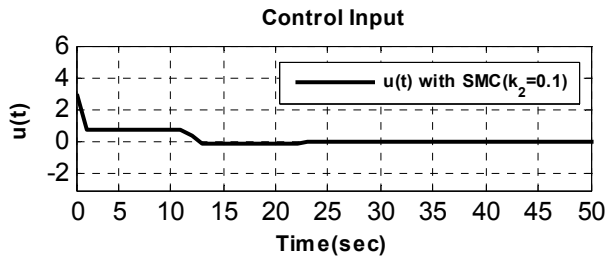

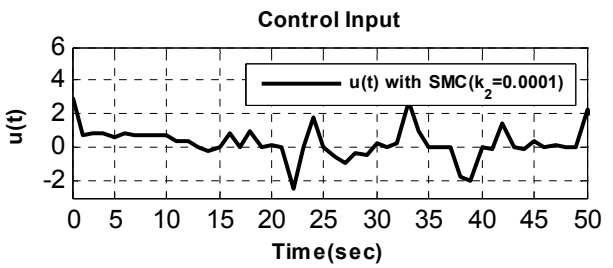

(b)

Figure 3. Control effort of (a) Mackey-Glass, (b) Logistic model in SAFC and SMC cases.

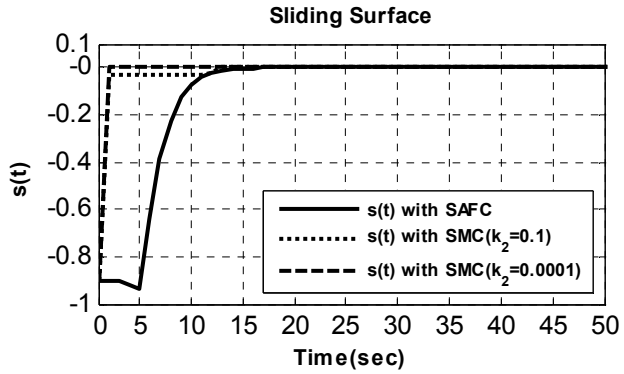

(a)

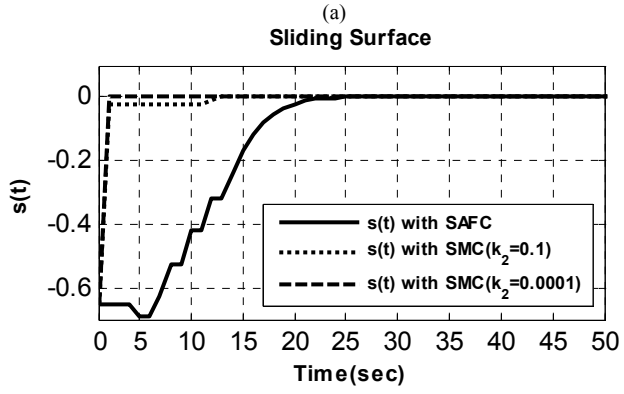

(b)

Figure 4. Sliding surface of (a) Mackey-Glass, (b) Logistic model in SAFC and SMC cases.

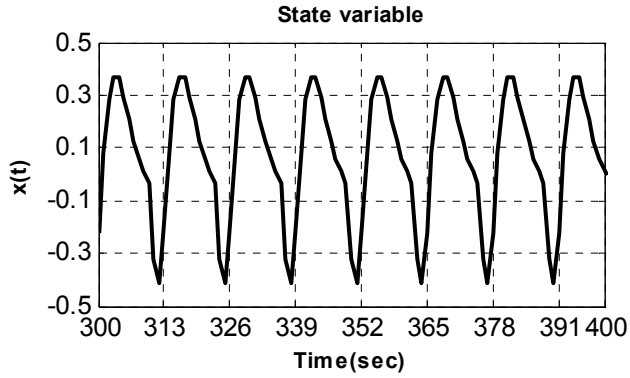

(a)

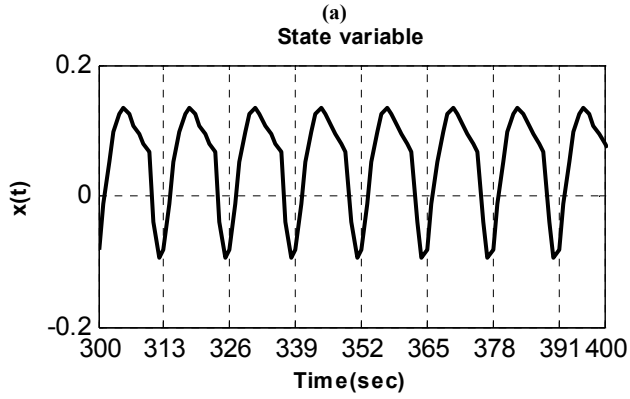

(b)

Figure 5. Response of (a) Mackey-Glass , (b) Logistic model to SAFC based delayed feedback with $T = 13, \alpha = 1$. The control force was applied at $t = 100$.

For better comparison, the performance of two considered controllers is compared with the following criteria:

1. Mean square error after 10τ (MSE).
2. Output error variance after 10τ (EV).
3. Output error settling time. It is the time at which $|e| < 0.1$ (EST).
4. Control signal variance after 10τ (CV).
5. Maximum of absolute value of control signal (MAC) after 0.1τ .

As we know, the less the MSE and EV, the better control is achieved. The less the EST, the sooner is the convergence. Moreover, less control effort (CV) and lower magnitude of the control signals (MAC) is desired in real-time control applications. The results of these comparisons for Mackey-Glass and Logistic models are given in Table 1, 2 respectively.

TABLE I. COMPARISONS BETWEEN DIFFERENT METHODS OF CHAOS CONTROL FOR MACKEY-GLASS MODEL

Criterion	Control Method		
	SAFC	***SMC*** ($k_2 = 0.1$)	***SMC*** ($k_2 = 1e-4$)
MSE	0	8.1690e-008	7.2888e-10
EV	0	7.9303e-008	7.3373e-10
EST(sec)	11	2	2
CV	0	7.1373e-005	0.6604
MAC	0.9784	0.9818	2.8349

TABLE II. COMPARISONS BETWEEN DIFFERENT METHODS OF CHAOS CONTROL FOR LOGISTIC MODEL

Criterion	Control Method		
	SAFC	***SMC*** ($k_2 = 0.1$)	***SMC*** ($k_2 = 1e-4$)
MSE	0	2.6254e-008	5.8916e-010
EV	0	2.4969e-008	5.7386e-010
EST(sec)	10	2	2
CV	4.415e-031	2.2472e-005	0.5165
MAC	0.6936	0.7350	2.7129

These results show that SAFC is better than SMC in all cases except EST.

B. Synchronization of two nonidentical systems with known parameter Implementation with differences in values of a, b, τ s

To study the effect of parameters changing, the parameters of Mackey-Glass and Logistic models are changed to $a = 6, b = 8$ at $t = 400$, so new UFP of Mackey-Glass and Logistic model are 0.89595 and 0.25, respectively and the time delay is changed to $\tau = 105$ at $t = 70$. Figs. 6, 7, 8 Show that the SAFC acts as well as when the parameters are not changed and SMC performance becomes worse when τ is changed to 105 at $t = 70$.

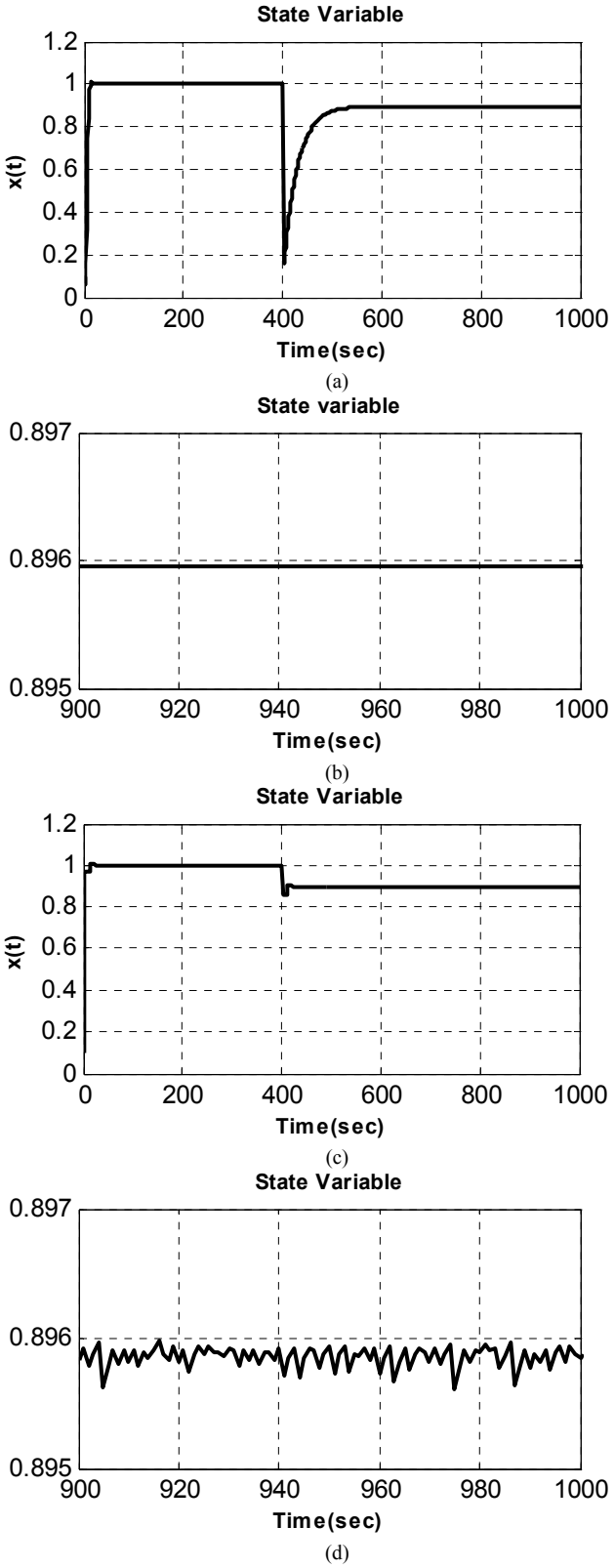

Figure 6. System response of Mackey-Glass model to (a, b) SAFC, (c, d) SMC when the parameters a, b are changed at $t = 400$.

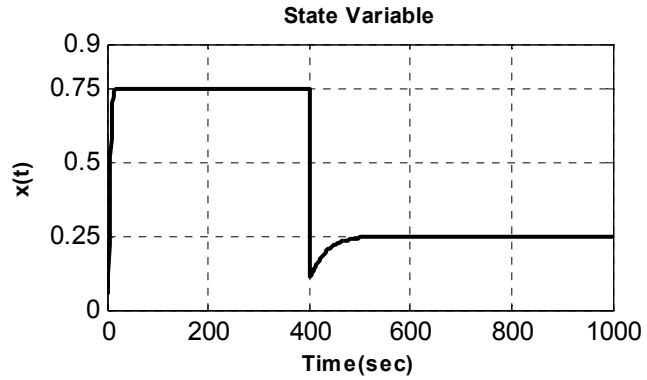

(a)

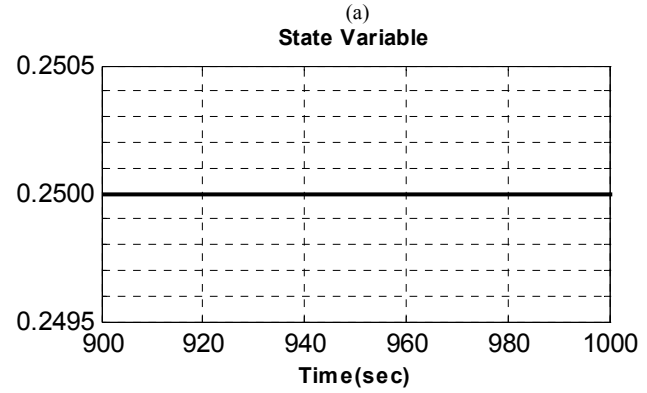

(b)

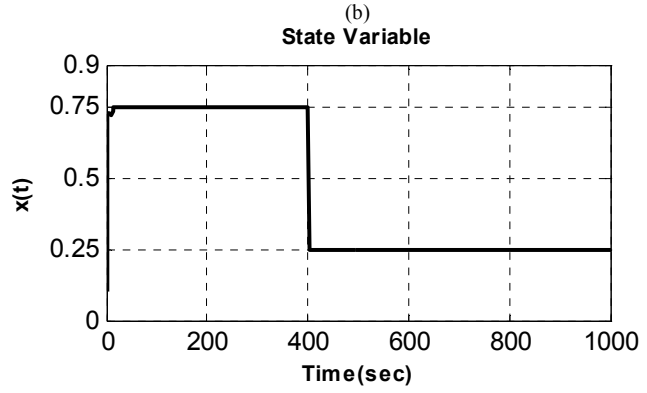

(c)

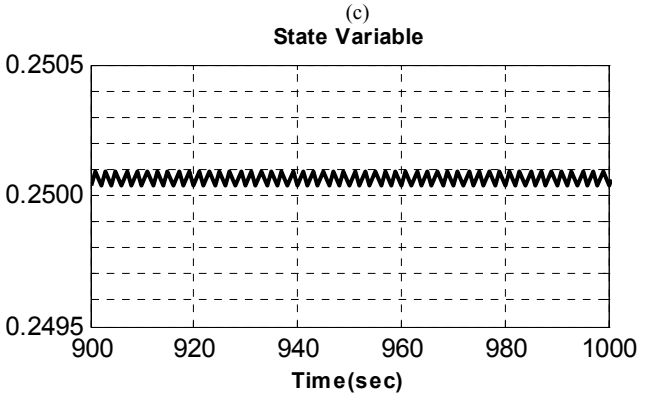

(d)

Figure 7. System response of Logistic model to (a, b) SAFC, (c, d) SMC when the parameters a, b are changed at $t = 400$.

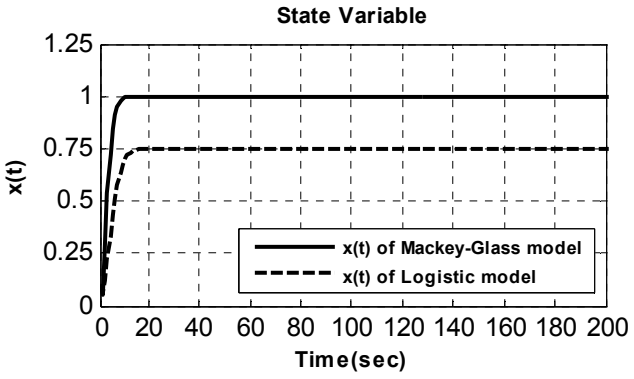

(a)

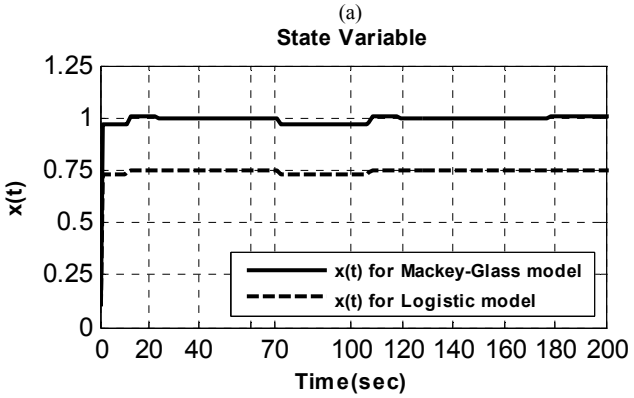

(b)

Figure 8. . System response of Mackey-Glass and Logistic model to (a) SAFC, (b) SMC when the parameter τ is changed at $t = 70$.

In summary, the SAFC performance is better than SMC performance in the cases considered in this section.

VI. CONCLUSION

In this paper, the behavior of two time-delayed chaotic systems is studied; Mackey-Glass and Logistic models. The sliding adaptive fuzzy controller and the sliding adaptive fuzzy controller based delayed feedback are applied to stabilize UFP's and UPO's respectively. Also, the SAFC has been compared with SMC applied to stabilize UFP's. The simulation results show that the SAFC is robust with respect to offline and online changes of parameters. Finally, it is concluded that SAFC is effective to chaos control in time-delayed chaotic systems and its performance is better than the SMC performance in many cases considered in this paper.

REFERENCES

[1] M. Young, The Technical Writer's Handbook. Mill Valley, CA: University Science, 1989.

[2] G. Chen, Controlling Chaos and Bifurcations in Engineering Systems. CRC Press LLC, 2000.

[3] E. Schöll, H. G. Schuster, Handbook of Chaos Control, 2nd ed. Wiley-VCH, Weinheim, 2008.

[4] G. Chen, X. Dong, From Chaos to Order, World Scientific, Singapore, 1998 .

[5] C. C. Hua, X. P. Guan, "Communication scheme via cascade chaotic systems," Chin Phys Lett, vol. 21, pp. 1441-1444, 2004.

[6] B. R. Andrievskii, A. L. Fradkov, "Control of Chaos. Methods and Applications. I. Methods," Automation and Remote Control, vol. 64, pp. 673-713, 2003.

[7] B. R. Andrievskii, A. L. Fradkov, "Control of Chaos. Methods and Applications. II. Applications," Automation and Remote Control, vol. 6, pp. 505-533, 2004.

[8] E. Ott, C. Grebogi, J. Yorke, "Controlling Chaos," Phys. Rev. Lett, vol 64, pp. 1196-1199, 1990.

[9] J. M. Nazzal, A. N. Natsheh, "Chaos control using sliding-mode theory," Chaos Solitons & Fractals, vol. 33, pp. 695-702, 2007.

[10] H.T. Yau, J. J. Yan, "Robust controlling hyperchaos of Rössler system subject to input nonlinearity by using sliding mode control," Chaos Solitons & Fractals, vol. 33, pp. 1767-76, 2007.

[11] K. Pyragas, "Continuous control of chaos by self-controlling feedback," Phys. Lett. A, vol. 170, pp. 421-428, 1992.

[12] H. Guo, S. Lin, J. Liu, "A radial basis function sliding mode controller for chaotic Lorenz system," Phys. Lett. A, vol.351, pp. 257-261, 2006.

[13] M. Mackey, L. Glass, "Oscillation and chaos in physiological control system," Science, vol. 197, pp.287-289, 1977.

[14] J. D. Farmer, "Chaotic attractors of an infinite-dimensional dynamical system," Physica D, vol. 4, pp. 366-393, 1982.

[15] T. Erneux, L. Larger, M. W. Lee, J. P. Goedgebuer, "Ikeda Hopf bifurcation revisited," Physica D, vol. 194, pp. 49–64, 2004.

[16] J. Arino, L. Wang, G. S. K. Wolkowicz, "An alternative formulation for a delayed logistic equation," Journal of Theoretical Biology, vol. 241, pp. 109–119, 2006.

[17] F. Giannakopoulos, A. Zapp, "Local and global Hopf bifurcation in a scalar delay differential equation," J. Math. Analys. Appl, vol. 237, pp. 425-450, 1999.

[18] L. R. Senesac, W. E. Blass, G. Chin, "Controlling chaotic systems with occasional proportional feedback," Rev Sci Instr, vol. 70, pp. 1719-1724, 1999.

[19] N. Vasegh, A. Khaki Sedigh, "Chaos control via TDFC in time-delayed systems: The harmonic balance approach," Phys. Lett. A, vol. 373,pp. 354-358, 2008.

[20] N. Vasegh, A. Khaki Sedigh, "Chaos control in delayed chaotic systems via sliding mode based delayed feedback,". Chaos Solitons & Fractals, vol. 40, pp. 159-165, 2009.

[21] S. T. Chen, "An observer-based approach to controlling time-delay chaotic systems via Takagi–Sugeno fuzzy model," Information Sciences, vol. 177,pp. 4314–4328, 2007.

[22] Y. C. Tian, F. Gao, "Simple delay systems with chaotic dynamics," IEEE CDC , St. Petersburg, Russia, pp. 319-20, 1997.

[23] Y. C. Tian, F. Gao, "Adaptive control of chaotic continuous-time systems with delay," Physica D, vol. 117, pp. 1-12, 1998.

[24] H. Lu, Z. He, "Chaotic behaviors in first order autonomous continuous time systems with delay," IEEE Trans CAS 1 , vol. 43, pp. 700-702, 1996.

[25] L. X. Wang , A Course in Fuzzy Systems and Control, Prentice-Hall International, Inc, p. 124, 1997.

2011 IEEE International Conference on Fuzzy Systems
June 27-30, 2011, Taipei, Taiwan

Estimating Missing Value in Microarray Gene Expression Data Using Fuzzy Similarity Measure

Amit Paul
Computer Science and Engineering Department
St. Thomas College of Engineering and Technology
khidirpore, India
Email:amitpaul83@gmail.com

Jaya Sil
Computer Science and Technology Department
Bengal Engineering and Science University
Shibpur, India
Email: js@cs.becs.ac.in

***Abstract*—Microarray experiments usually generate data sets with multiple missing value due to several reasons. In the paper a robust method has been proposed to estimate the missing value of microarray experimental data. Missing values are imputed using fuzzy similarity measure by identifying the genes having similar characteristics to that of the gene with missing values. In this approach, biological knowledge of the gene is extracted using fuzzy relation and based on that knowledge, missing value is predicted and optimized. The estimation accuracy of the proposed method is compared with the existing K-nearest neighbour (KNN) based missing value imputing method. The result demonstrates that the proposed method outperforms the KNN based method.**

***Index Terms*—Microarray gene expression, missing value, fuzzy similarity, biological knowledge**

I. Introduction

Microarray technology, a high throughput technology [1] evaluates the expression of thousands of genes simultaneously [2]. A microarray experiment typically assesses a large number of DNA sequences (genes, cDNA clones, or expressed sequence tags) under multiple conditions. These conditions may be a time series during a biological process or a collection of different tissue samples (e.g., normal versus cancerous tissues). Data obtained from a microarray experiment is represented by a real-valued gene expression matrix, where the rows form the expression patterns of genes, columns represent expression profiles of the samples and each cell is the measured expression level of gene samples.

Usually, data from microarray experiments contain missing value due to different reasons including dust or scratches on the slide, error in experiments, image corruption and insufficient resolution. Typically 1-50% of data are missing [3], affecting up to 95% of the genes. Missing value is a predominant problem for the analysis of microarray data, which needs attention in order to obtain accurate results from microarray data analysis [2], [4]. Therefore, as a preprocessing step missing value estimation is essential. Existing algorithms require a full dataset for statistical analysis of microarray data [4] because the underlying statistical methodology is based on balanced datasets. There are many approaches to deal with missing value, including:

a) Repeating the experiment [5]
b) Ignoring objects containing missing value [6]
c) Estimating the missing value

The first approach is expensive and time consuming while the second approach usually lost too much useful information and may bias the results if the remaining cases don't represent the entire sample properly. The third approach can be subdivided into two groups. The missing value estimation methods of the first group substitute the missing values by a global constant such as 'zero' [6] or by the average of the available gene expression values [7] resulting distortion in relationships among the variables. Correlation structure is considered in the second group in two steps. At first, genes similar to the gene with missing value(s) are identified and then the missing values are predicted with the help of the observed values of the identified genes. The widely used weighted *K*-nearest neighbor imputation (KNN impute) procedure [8] reconstructs the missing values using a weighted average of *K* most similar genes [9]. These methods have better performance though the estimation ability largely depends on the selection of *K* parameter. There is no theoretical way to determine the value of *K* appropriately but to specify by the user. In cluster-based algorithms [10], [11] determination of missing values have been proposed where number of cluster either predetermined or the user have to specify that. Moreover, since the accuracy of the clustering algorithms depends on number of clusters, its selection becomes very crucial. The limitation of the existing methods is due to the fact that the estimation is based solely on the gene expression data ignoring biological information, which is inherent in the gene dataset.

Fig. 1 shows three genes g_1, g_2, and g_3 on seventeen experimental conditions c_j for j = 1,..., 17 where the y-axis shows the expression level of a gene g_i on a particular condition c_j, plotted along x axis. Based on a distance function g_1 and g_2 are clustered together. However, from the biological viewpoint, it is more appropriate to cluster g_1 and g_3 because g_1 and g_3 exhibit similar tendency along a subset of conditions. It is therefore, concluded [12]-[14] that strong correlations may

978-1-4244-7316-8/11/$26.00 ©2011 IEEE

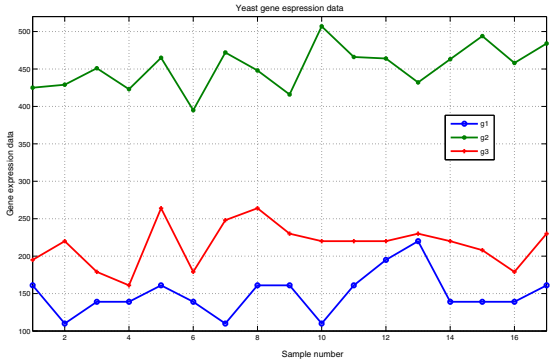

Fig. 1. Three genes with seventeen experimental conditions.

exist among a set of genes, even if their spatial localities are far apart from each other. Pattern-based and tendency-based biclustering algorithms were proposed [15] to overcome the conventional constraints of spatial proximity and able to discover clusters in all subspaces by pattern/tendency similarities. However, a pattern-based model is only capable of identifying positive correlated genes if and only if some linear transformation relationships such as shifting [14], [16], [17] and scaling [18] exist among their expression levels. The mechanism of gene regulation is complicated and becomes oversimplified if one assumes that only linear relationships exist in coregulated gene profiles [19]. Order Preserving Cluster (OP-CLUSTER) [12] and Tendency Preserving cluster (TP-CLUSTER) [13] are tendency based clustering algorithms adopt a model for efficient discovery of genes. Here, the gene expression levels synchronously rise and fall in a subspace while at the same time do not impose any particular magnitude transformation relationships among the genes. However, recent research work [19], [20] provides a greater diversity of correlations among coregulated genes such as genes with a negative pattern or inverted behavior, where existing pattern-based and tendency-based algorithms lost their significance.

In the paper, a robust method has been proposed to estimate the missing value of microarray experimental data by considering both positive and negative correlated genes. Missing values are imputed by identifying the genes which have similar characteristics to that of the gene with missing value, determined by soft class membership value using fuzzy similarity measure. The paper briefly addresses the approaches for finding related genes followed by the discussions of necessities for finding co-relational gene, with support from real examples.

The rest of the paper is organized as follows. The proposed method is described in section II. Experimental results are presented in section III. Concluding remarks and suggestions for future work are given in section IV.

II. Methodology

Clustering is an unsupervised learning technique that aims at partitioning a given set of objects into subgroups or clusters based on the similarity of objects. It has been observed that each gene may be involved in more than one biological activity, therefore, hard clustering which assign each gene to a single cluster fails to express the total characteristics of the genes [21]. In the paper, first gene expression dataset is normalized and then clustered using fuzzy c means clustering algorithm [22] that measures similarity between genes. The belongingness of a single gene into multiple clusters is determined with varied degree of membership value obtained using clustering analysis. The proposed method determines the functional similarity between the genes inherent in the sample values in order to acquire more biologically interpretable clusters.

A. Pattern Similarity Matching (PSM) Algorithm

Few terminologies are defined below for understanding the proposed PSM algorithm.

Normalized gene expression ($NGE_{(i,j)}$): Difference between the j^{th} sample value of each i^{th} gene_expression and mean of the sample values of the corresponding gene_mean represent zero mean normalize gene expression, defined in (1). The available sample values of genes are normalized and the gene expression matrix is reconstructed with the new gene expression data (*Normalized gene expression*). This represent zero mean relational activity level of that gene for the sample.

$$NGE_{(i,j)} = gene_expression_{(i,j)} - gene_mean_{(i,j)} \quad (1)$$

Activation level ($Al_{(i)}$): Distribution of gene expression data in two-dimension space reveals the fact that several genes are highly active compare to others. Initialize the activation level of each gene to zero. Increase the activation level of gene i by one when its present sample, say j having higher value than its previous sample, as defined in (2).

$$Al_{(i)} = Al_{(i)} + 1 \quad if \quad NGE_{(i,j)} > NGE_{(i,j-1)} \quad (2)$$

Depending on the activity of gene i, its class membership value $Mfl_{(i)}$ is evaluated using the concept of fuzzy similarity measure, defined in (3) that represent its degree of belongingness in a particular class.

$$Mfl_{(i)} = \frac{Al_{(i)}}{gs} \quad (3)$$

where gs is the number of samples in gene i without any missing value.

Missing gene list(*misg*): The list contains genes having one or more missing sample value.

Not A Number (*NaN*): Not a Number (*NaN*)[23] represents fractional sample value of a gene. *NaN*'s are represented by a bit pattern with an exponent of all 1s with non-zero fraction value.

Gene expression data represents the logarithmic value of gene's protein production under a particular time interval. Generally, each gene expression data is distinct, so normalization

is required to find out the similar active genes. The normalized value of a particular sample is basically information about the gene's protein production, typically the zero mean, depicted in (1). The PSM algorithm calculates similarity of the genes based on their class membership value(*M fl*) as given in equation (3). If a set of genes (i = 1 ... n) have similar activity level of protein production with a gene having missing value (l) then a particular sample position among the similar genes is selected using (4) to impute the missing value at k^{th} sample position of l^{th} gene.

$$Optv = min_{(\forall i, \forall j)}(|gene_expression(i,j) - gene_expression(i,k)|) \quad (4)$$

Optv is the difference between the sample value at missing position k with other sample positions of the respective gene belonging to the same cluster. Minimum difference occurs say, at sample position *s* of a particular gene. Now the sample value at position *s* of the missing gene (l) is used to impute the missing value at position *k*.

Missing gene expression value can be estimated from k^{th} sample position of missing gene *l*.

B. Procedure:

Input: Microarray gene expression data, with some genes' (object) sample (attribute) value missing.

Output: Microarray gene expression data, with some artificial data impute.

Step1: *mean_gene*:= mean*(gene_array)*

Step2: *misg*:=find_missing_gene(*gene*)

Step3: for all *i gene* in *gene_array* do

for all *j sample* of the *gene* do

$NGE_{(i,j)}$:= $gene_array_{(i,j)}$- $mean_gene_{(i)}$

if ($NGE_{(i,(j-1))} > NGE_{(i,j)}$) then

$Al_{(i)} := Al_{(i)}$ + 1

end if

end j^{th} loop

$Mfl_{(i)}$:=$\frac{Al_{(i)}}{gs}$

end i^{th} loop

Step4: for all *l gene* having missing value in *misg* do
$smi_Mfl_{(l)}$:= fuzzy similar gene ($Mfl_{(l)}$)

miss:= find missing sample*(gene_array(misg(l)))*

for i^{th} gene in $smi_Mfl_{(l)}$ do

for all *k* missing sample in *miss* do

for all *j* sample in $smi_Mfl_{(l,i)}$
without *NaN* gene expression for that sample in l^{th} and i^{th} both gene

$Optv := |gene_array_{(smi_Mfl_{((l,i),j))}} - gene_array_{(smi_Mfl_{((l,i),k))}}|$

if *Optv* is minimum then
selected_sample:=j^{th}

Step5:

$gene_array_{(misg(l),k)} := gene_array_{(misg(l),selected_sample)}$

The following example illustrates the above procedure and summarized in tables I, II, III, IV and V by considering twelve genes, each having six samples.

TABLE I
AFTER RANDOMLY DELETION OF DATA FROM ORIGINAL MICROARRAY GENE EXPRESSION MATRIX

Gene id	S_1	S_2	S_3	S_4	S_5	S_6
G_1	7.5	7.58	7.66	7.68	7.01	7.47
G_2	80.2	80.7	80.3	NaN	81	82
G_3	8	8.9	9	9.5	8	8.5
G_4	80	82	84	88	81	79
G_5	2.5	3	2.7	3.2	4	3.5
G_6	3	3	2.7	3.2	3.5	3.5
G_7	72.4	73	62	61	60	58
G_8	82.3	83	82.7	80.2	80	80.5
G_9	92.5	92	91.7	93.2	91	90.8
G_{10}	32	31.6	31.7	31.8	31	30
G_{11}	50	49	48	48.5	49	50
G_{12}	62	62.8	62.1	62.5	62.1	62

TABLE II
MEAN OF EACH GENE IN MICROARRAY GENE EXPRESSION MATRIX

Gene id	Mean
G_1	7.48
G_2	80.84
G_3	8.43
G_4	82.33
G_5	3.15
G_6	3.15
G_7	64.4
G_8	81.45
G_9	91.87
G_{10}	31.35
G_{11}	49.08
G_{12}	62.25

According to the PSM algorithm, *Optv* value (tableV) of all genes (tableI) that are similar to gene with missing value i.e. G_2 are calculated. The minimum value ($|G_1, S_4$ - $G_1, S_3|$ = 0.02) occurs at sample position 3. Now impute (G_2, S_4) using 80.3 from (G_2, S_3) to remove missing value in the original microarray gene expression matrix (table I) .

TABLE III
RECONSTRUCTION OF MICROARRAY GENE EXPRESSION MATRIX AFTER NORMALIZATION OF DATA

Gene id	S_1	S_2	S_3	S_4	S_5	S_6
G_1	0.02	0.10	0.18	0.20	-0.47	-0.01
G_2	-0.64	-0.14	-0.54	NaN	0.16	1.16
G_3	-0.43	0.47	0.57	1.07	-0.43	0.07
G_4	-2.33	-0.33	1.67	5.67	-1.33	3.33
G_5	-0.65	-0.15	-0.45	0.05	0.85	0.35
G_6	-0.15	-0.15	-0.45	0.05	0.35	0.35
G_7	8.00	8.60	-2.40	-3.40	-4.40	-6.40
G_8	0.85	1.55	1.25	-1.25	-1.45	-0.95
G_9	0.63	0.13	-0.167	1.33	-0.867	-1.067
G_{10}	0.65	0.25	0.35	0.45	-0.35	-1.35
G_{11}	0.92	-0.08	-1.08	-0.58	-0.08	0.92
G_{12}	-0.25	0.55	-0.15	0.25	-0.15	-0.25

TABLE IV
ACTIVITY LEVEL AND *Mfl* OF EACH GENE IN MICROARRAY GENE EXPRESSION MATRIX

Gene id	Activity level	*Mfl*
G_1	4	0.67
G_2	3	0.6
G_3	4	0.67
G_4	4	0.67
G_5	3	0.5
G_6	2	0.33
G_7	1	0.167
G_8	1	0.167
G_9	1	0.167
G_{10}	2	0.33
G_{11}	2	0.33
G_{12}	2	0.33

The following example illustrates the above procedure with multiple missing values and summarized in tables VI, VII, VIII, IX, X and XI by considering fourteen genes, each having six samples.

Using (4) *Optv* value (tableX) of all genes (tableVI) that are similar to gene with missing value i.e. G_1 are calculated. Minimum value ($|G_3, S_4$ - $G_3, S_3|$ = 0.5) occurs at sample position 3, as given in table X. Now impute (G_1, S_4), which had missing value in the original microarray gene expression matrix (table VI) using 7.77 from (G_1, S_3). Similarly (G_2, S_3) is imputed from (G_2, S_2) considering similar gene G_4. It has been observed that G_3 with multiple missing value is similar to G_1 and minimum *Optv* value is attained in (G_1, S_6) from table XI. But (G_3, S_6) is NaN, so search for next minimum *Optv* value, occurred at $(G_1, S_1)$and (G_3, S_5) is imputed using (G_3, S_1).

TABLE V
Optv FOR GENE G_1

Sample id	*Optv*
S_1	0.18
S_2	0.1
S_3	**0.02**
S_5	0.67
S_6	0.21

TABLE VI
AFTER RANDOMLY DELETION OF DATA FROM ORIGINAL MICROARRAY GENE EXPRESSION MATRIX

Gene id	S_1	S_2	S_3	S_4	S_5	S_6
G_1	7.38	7.45	7.77	NaN	7	7.2
G_2	40.65	40	NaN	41	41.20	41.80
G_3	34	35.7	35	35.2	NaN	NaN
G_4	34	34.8	34.2	34	33	34
G_5	8	8.9	9	9.5	8	8.5
G_6	80	82	84	88	81	79
G_7	2.5	3	2.7	3.2	4	3.5
G_8	3	3	2.7	3.2	3.5	3.5
G_9	72.4	73	62	61	60	58
G_{10}	82.3	83	82.7	80.2	80	80.5
G_{11}	92.5	92	91.7	93.2	91	90.8
G_{12}	32	31.6	31.7	31.8	31	30
G_{13}	50	49	48	48.5	49	50
G_{14}	62	62.8	62.1	62.5	62.1	62

III. RESULTS AND COMPARISONS

A. Data set

In this paper, the performance of each method is evaluated using [24]. RNA was obtained from histologically normal bronchial epithelium of smokers during time of clinical bronchoscopy from relatively accessible airway tissue. Gene expression data from smokers with lung cancer was compared with samples of smokers without lung cancer.

B. Measurements for performance

The gene expression matrix obtained from the microarray experiment is modified by replacing all the rows containing missing values with randomly generated artificial missing

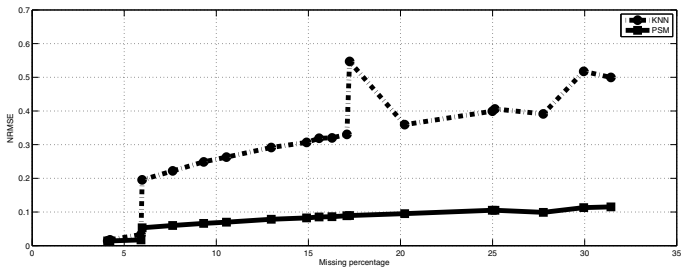

Fig. 2. Comparison of NRMSE value with PSM and KNN for GSE4115 data set

TABLE VII
MEAN OF EACH GENE IN MICROARRAY GENE EXPRESSION MATRIX

Gene id	Mean
G_1	7.36
G_2	40.93
G_3	34.975
G_4	34
G_5	8.43
G_6	82.33
G_7	3.15
G_8	3.15
G_9	64.4
G_{10}	81.45
G_{11}	91.87
G_{12}	31.35
G_{13}	49.08
G_{14}	62.25

TABLE VIII
RECONSTRUCTION OF MICROARRAY GENE EXPRESSION MATRIX AFTER NORMALIZATION OF DATA

Gene id	S_1	S_2	S_3	S_4	S_5	S_6
G_1	0.02	0.09	0.41	NaN	-0.36	-0.16
G_2	-0.28	-0.93	NaN	0.07	0.27	0.87
G_3	-0.975	0.725	0.025	0.225	NaN	NaN
G_4	0	0.8	0.2	0	-1	0
G_5	-0.43	0.47	0.57	1.07	-0.43	0.07
G_6	-2.33	-0.33	1.67	5.67	-1.33	3.33
G_7	-0.65	-0.15	-0.45	0.05	0.85	0.35
G_8	-0.15	-0.15	-0.45	0.05	0.35	0.35
G_9	8.00	8.60	-2.40	-3.40	-4.40	-6.40
G_{10}	0.85	1.55	1.25	-1.25	-1.45	-0.95
G_{11}	0.63	0.13	-0.167	1.33	-0.867	-1.067
G_{12}	0.65	0.25	0.35	0.45	-0.35	-1.35
G_{13}	0.92	-0.08	-1.08	-0.58	-0.08	0.92
G_{14}	-0.25	0.55	-0.15	0.25	-0.15	-0.25

values. The performance is measured by Normalise Root Mean Square Error (NRMSE) evaluated for error detection of Y_{guess}, where Y_{guess} is estimated by the proposed algorithm and Y_{answer} is the original microarray gene expression value.

$$NRMSE = \frac{\sqrt{(mean[(Y_{guess} - Y_{answer})^2])}}{Var(Y_{answer})} \quad (5)$$

Where *Var(x)* returns the variance of matrix *x* and *mean(y)* mean of the *y* matrix.

In Figure 2 and 3 comparison of NRMSE value for GSE4115 and GDS2771 series data are shown by applying PSM and KNN algorithms, respectively. Estimated sample value based on PSM impute method is closer to experimental data. KNN impute method estimates zero value if the sample value at the same position of *k* nearest neighbor genes is missing. On the other hand, if every gene consists missing

TABLE IX
ACTIVITY LEVEL AND *Mfl* OF EACH GENE IN MICROARRAY GENE EXPRESSION MATRIX

Gene id	Activity level	*Mfl*
G_1	3	0.6
G_2	2	0.4
G_3	2	0.5
G_4	2	0.33
G_5	4	0.67
G_6	4	0.67
G_7	3	0.5
G_8	2	0.33
G_9	1	0.167
G_{10}	1	0.167
G_{11}	1	0.167
G_{12}	2	0.33
G_{13}	2	0.33
G_{14}	2	0.33

TABLE X
Optv OF G_3 FOR GENE G_1

Sample id	*Optv*
S_1	1.7
S_2	0.7
S_3	**0.5**
S_5	NaN
S_6	NaN

value then KNN fails to impute any such missing value. However, the proposed PSM method able to impute 100% missing value in several passes varying with different rate of success. Keeping the missing percentage same with respect to microarray data, increase of number of missing value resulting rapid increase of NRMSE value in case of KNN while in case of PSM the rate is significantly less.

The PSM impute method shows comparable results with the previously developed methods in present research. The outstanding estimation ability of this impute method is partly due to the use of the most missing value information by incorporating fuzzy relation scheme. The results show that the estimating sample values obtained by the proposed PSM

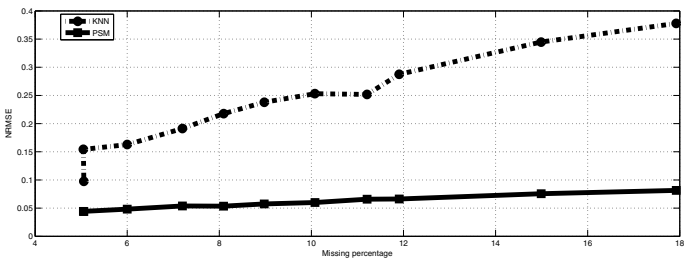

Fig. 3. Comparison of NRMSE value with PSM and KNN for GDS2771 data set

TABLE XI
Optv OF G_1 FOR GENE G_3

Sample id	*Optv*
S_1	0.38
S_2	0.45
S_3	0.77
S_5	NaN
S_6	0.2

impute method of gene expression data for different genes are less deviated with respect to the microarray data. KNN method depends on how far sample value of *K* number of genes are closed with the missing value ignoring the characteristic pattern of genes, which are might be different. But the PSM algorithm depends on the characteristic pattern, and here *K* varies depending on characteristics of genes. KNN impute method find out *K* nearest gene for each missing value from the remaining gene. Time complexity is high in KNN method due to large number of comparisons, whereas in PSM based impute method time complexity depends on number of unique active level. Therefore, application of PSM algorithm provides better result in less time than KNN impute method in microarray data set consisting of genes with sample values not very close to each other.

IV. Conclusion

The proposed PSM method demonstrates better results in comparisons with the existing method. Here biological knowledge has been exploited to determine similar genes for prediction of missing values unlike the previous works where distance measures were used for missing value prediction, ignoring the inherent knowledge of the genes.The missing value in a gene is predicted from the available value of the same gene, resulting least error in estimation of sample value. The optimized missing value thus provides near exact knowledge for important application. Moreover, time complexity of the PSM algorithm is much less compare to the KNN due to search of selective genes for imputing missing value.

References

[1] D.J. Lockhart and E. A. Winzeler, "Genomics, gene expression and DNA arrays," Nature, vol. 405, pp. 827-836, 2000.

[2] M. Ouyang, A.T. Garnett, T.M. Han, K. Hama, A. Lee, Y. Deng, N. Lee, H.Y. Liu, S.L. Amacher, S.A. Farber, and S.Y. Ho, "A web based resource characterizing the zebrafish developmental profile of over 16,000 transcripts," Gene Expr. Patterns, vol. 8(3), pp. 171-180, 2008.

[3] A.G. Brevern, S. Hazout and A. Malpertuy, "Influence of microarrays experiments missing values on the stability of gene groups by hierarchical clustering," BMC Bioinformatics, vol. 22(5), pp. 566-572, 2004.

[4] E. Wit and J. McClure, "Statistics for Microarrays Design, Analysis and Inference," John Wiley & Sons, 2004.

[5] A. J. Butte, and J. Ye, "Determining significant fold differences in gene expression analysis," Pac. Symp. Biocomput., vol. 6, pp. 6-17, 2001.

[6] A. A. Alizadeh, M. B. Eisen, R. E. Davis, C. Ma, I. S. Lossos, A. Rosenwald, J. C. Boldrick, H. Sabet, T. Tran, X. Yu, J. I. Powell, L. Yang, G. E. Marti, T. Moore, J. Hudson, L. Lu, D. B. Lewis, R. Tibshirani, G. Sherlock, W. C. Chan, T. C. Greiner, D. D. Weisenburger, J. O. Armitage, R. Warnke, R. Levy, W. Wilson, M. R. Grever, J. C. Byrd, D. Botstein, P. O. Brown and L. M.Staudt, "Distinct types of diffuse large B-cell lymphoma identified by gene expression profiling," Nature, vol. 403, pp. 503-511, 2000.

[7] J. L. Schafer and J. W. Graham, "Missing data: our view of the state of the art", Psychol. Methods, vol. 7, pp. 144-177, 2002.

[8] P. Meesad, K. Hengpraprohm, "Combination of KNN-Based Feature Selection and KNNBased Missing-Value Imputation of Microarray Data," Innovative Computing Information and Control, ICICIC apos, vol. 18(20), pp. 341-341, 2008.

[9] O. Troyanskaya, M. Cantor, G. Sherlock, P. Brown, T. Hastie, R. Tibshirani, D. Botstein and R. B. Altman, "Missing value estimation methods for DNA microarrays," BIOINFORMATICS, vol. 17, pp. 520-525, 2001.

[10] J. Luo, T. Yang and Y. Wang, "Missing Value Estimation For Microarray Data Based On Fuzzy C-means Clustering," The Eighth International Conference on High-Performance Computing in Asia-Pacific Region, 2005.

[11] S. Zhang, J. Zhang, X. Zhu, Y. Qin and C. Zhang, "Missing Value Imputation Based on Data Clustering," Transactions on Computational Science I, vol. 4750, pp. 128-138, Springer, Heidelberg, 2008.

[12] J. Liu and W. Wang, "Op-Cluster: Clustering by Tendency in High-Dimensional Space," Proc. Third IEEE Int'l Conf. Data Mining (ICDM '03), pp. 187-194, 2003.

[13] J. Liu, J. Yang and W. Wang, "Biclustering in Gene Expression Data by Tendency," Proc. Third IEEE Int'l Computational Systems Bioinformatics Conf. (CSB '04), pp. 182-193, 2004.

[14] H. Wang, W. Wang, J. Yang, and P.S. Yu, "Clustering by Pattern Similarity in Large Data Sets," Proc. ACM SIGMOD '02, pp. 394-405, 2002.

[15] S. Erdal, O. Ozturk, D. Armbruster, H. Ferhatosmanoglu, W.C. Ray, "A Time Series Analysis of Microarray Data," Proc. Fourth IEEE Int'l Symp. Bioinformatics and Bioeng. (BIBE '04), pp. 366-378, 2004.

[16] J. Pei, X. Zhang, M. Cho, H. Wang, P.S. Yu, "Maple: A Fast Algorithm for Maximal Pattern-Based Clustering," Proc. Third IEEE Int'l Conf. Data Mining (ICDM '03), pp. 259-266, 2003.

[17] H. Wang, F. Chu, W. Fan, P.S. Yu and J. Pei, "A Fast Algorithm for Subspace Clustering by Pattern Similarity," Proc. 16th Int'l Conf. Scientific and Statistical Database Management (SSDBM '04), pp. 51-62, 2004.

[18] L. Zhao and M.J. Zaki, "Tricluster: An Effective Algorithm for Mining Coherent Clusters in 3D Microarray Data," Proc. ACM SIGMOD '05, pp. 51-62, 2005.

[19] Y. Zhang, H. Zha and C.H. Chu, "A Time-Series Biclustering Algorithm for Revealing Co-Regulated Genes," Proc. IEEE Int'l Symp. Information Technology: Coding and Computing (ITCC '05), pp. 32-37, 2005.

[20] H. Yu, N.M. Luscombe, J. Qian and M. Gerstein, "Genomic Analysis of Gene Expression Relationships in Transcriptional Regulatory Networks," Trends Genet, vol. 19(8), pp. 422-427, 2003.

[21] http://biodata.mshri.on.ca/yeast_ grid/servlet/.

[22] D. Dembélé and P. Kastner, "Fuzzy c-means method for clustering microarray data," Bio-Informatics, vol. 19(8), PP 973-980, 2003.

[23] IEEE Computer Society : IEEE Standard for Binary Floating-Point Arithmetic,IEEE Std 754-2008, 2008.

[24] P.T. Spellman, G. Sherlock, M.Q. Zhang, V.R. Iyer, K. Amders, M.B. Eisen, P.O. Brown, D. Botstein, B. Futcher "Comprehensive identification of cell cycle-regulated genes of the yeast Saccharomyces cerevisiae by microarray hybridization," Mol Biol Cell, vol. 9, pp. 3273-3297, 1997.

2011 IEEE International Conference on Fuzzy Systems
June 27-30, 2011, Taipei, Taiwan

Interval Fuzzy Modeling Applied to Model Based Fault Detection of an Active Suspension System

T.S. Ghiasi
Engineering Department, Imam. Khomeini international university of ghazvin, Iran
(e-mail: tayebe.ghiasi@gmail.com)

H. zarabadipour
Engineering Department, Electrical Faculty, Imam. Khomeini international university of ghazvin, Iran
(e-mail:h_zarabadi@ikiu.ac.ir)

M. Aliyari Shoorehdeli
Electrical and computer Engineering Department, Mechatronics Faculty, K. N. Toosi University of TechnologyTehran, Iran
(e-mail: Aliyari@eetd.kntu.ac.ir)

Abstract: **This paper presented an investigation on fault detection of an active suspension system using interval fuzzy modeling. A well known nonlinear classical controller called back-stepping method is used to simulate dynamic response of a half-car suspension system. Confidence bands for the system input-outputs data is approximated using an interval fuzzy model. Then Fault detection has been done by the use of these confidence bands. Simulation results depict that the proposed fault detection is highly effective in evaluating the performance of an active suspension system.**

Keywords: Active Suspension System; Fault Detection; Interval Fuzzy modeling.

I. INTRODUCTION

The interval fuzzy model identification is a methodology for approximating the functions of a finite set of input and output measurements. This approach can also be used to compress information in the case of a nonlinear function family approximation to obtain the interval of parameters that results in a band containing the whole set of measurements [4-6]. Interval fuzzy model also has been used for detecting faults of nonlinear input-output systems with unstructured uncertainties or interval type parameters [7-9].

The residual signal formation and evaluating of it, is a very important part of a fault detection procedure. The major advantage of using interval fuzzy model is, easier generation of residual signal than other methods.

This study tries to use Interval fuzzy model for evaluating the performance of active suspension system. A suspension system is one of the important components of a vehicle which plays a crucial role in handling ride convenience and safety of a vehicle. There are three types of suspension: passive suspension, active suspension and semi-active suspension. An active suspension system is specified by employing some types of suspension force generation such as pneumatic, electromagnetic or hydraulic actuators. Interests are significantly growing on designing and controlling of active suspension systems for automotives in the past three decades. Most of the researches have been done till now, focused on designing a controller for a passive system to improve the driving characteristics of an automobile or simply changing passive systems to active ones. Just a few amounts of recent published papers have also chosen more complex models in order to more precise results, Such as the half-car model with four degree of freedom using various types of controllers as linear and fuzzy logic controllers and also the classical back stepping scheme. Complete modeling of active suspension systems using simulation tools and software has also been done. Identification of active suspension systems have been performed in many cases for specific purposes by the use of various approaches as a basis for controller design and for model based fault detection on a quarter-car model [2,6].

The paper is organized as follows. Firstly, the model of a half-car suspension system is introduced .Then a nonlinear back-stepping controller applied on it. Furthermore the interval fuzzy model of a half-car suspension system is presented after derivation of an interval fuzzy model. Finally residual formation with a fault-diagnostic scenario is described with some concluding remarks.

II. SUSPENSION MODEL, DYNAMICS AND SIMULATION

The model of a half-car suspension system is shown in Figure 1[6]. The model is excited by road surface bump.

The displacements of the sprung mass (car body) for front and rear bodies are given by

Front Body

$$Z_{sf} = Z - a\sin\theta \approx Z - a\theta \tag{1}$$

Rear Body

$$Z_{sr} = Z + b\sin\theta \approx Z + b\theta \tag{2}$$

where Z_{sf} is the front body displacement, Z_{sr} is the rear body displacement, a is the longitudinal distance between front axle and centre of gravity, b is the longitudinal distance between rear axle and centre of gravity, θ is the stroke angel and Z is the displacement of centre of gravity.

978-1-4244-7316-8/11/$26.00 ©2011 IEEE

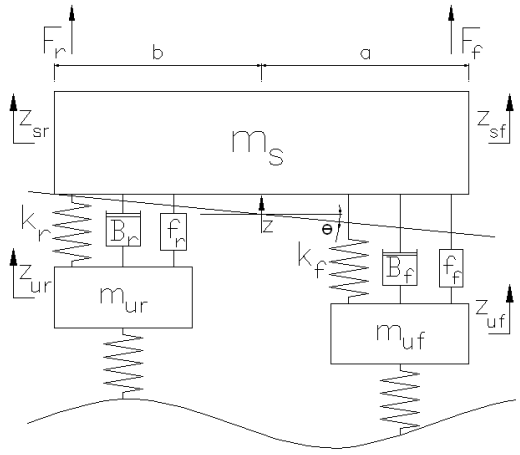

Figure 1: Half car active suspension system model

By applying Newton's second law, the equations of motion for front and rear bodies of the half-car suspension system model are as following

Front Body

$$m_s\ddot{Z}_{sf} = -K_f(Z_{sf} - Z_{uf}) - B_f(\dot{Z}_{sf} - \dot{Z}_{uf}) \\ -k_r(Z_{sr} - Z_{ur}) - B_r(\dot{Z}_{sr} - \dot{Z}_{ur}) + f_f + f_r - am_s\ddot{\theta} \quad (3)$$

Rear Body

$$m_s\ddot{Z}_{sr} = -K_f(Z_{sf} - Z_{uf}) - B_f(\dot{Z}_{sf} - \dot{Z}_{uf}) \\ -k_r(Z_{sr} - Z_{ur}) - B_r(\dot{Z}_{sr} - \dot{Z}_{ur}) + f_f + f_r + bm_s\ddot{\theta} \quad (4)$$

where f_f and f_r are the front and rear control input force, B_f and B_r are the front and rear damping coefficients, k_f and k_r are the front and rear spring coefficients and Z_{uf} and Z_{ur} are the front and rear wheel displacements, respectively.

Knowing that J_y is the centroidal moment of inertia of the car and using $J_y = m_s r^2_y$ where r_y is the radius of gyration and m_s is the mass of the car body, one can get the equation of motion for the angular stroke motion

$$\ddot{\theta} = \frac{1}{m_s r_y^2}\begin{bmatrix} aK_f(Z_{sf} - Z_{uf}) - bK_r(Z_{sr} - Z_{ur}) \\ + aB_f(\dot{Z}_{sf} - \dot{Z}_{uf}) - bB_r(\dot{Z}_{sr} - \dot{Z}_{ur}) \\ - af_f + bf \end{bmatrix} \quad (5)$$

The equations of motion for the front and rear unsprung masses (front and rear wheels) can be obtained again by applying Newton's second law as follows:

Front wheel

$$m_{uf}\ddot{Z}_{uf} = K_f(Z_{sf} - Z_{uf}) + B_f(\dot{Z}_{sf} - \dot{Z}_{uf}) \\ -K_{tf}(Z_{uf} - Z_{rf}) - f_f \quad (6)$$

Rear wheel

$$m_{ur}\ddot{Z}_{ur} = K_r(Z_{sr} - Z_{ur}) + B_r(\dot{Z}_{sr} - \dot{Z}_{ur}) \\ -K_{tr}(Z_{ur} - Z_{rr}) - f_r \quad (7)$$

The system state variables will be then set as $x_1 = Z_{sf}$ for the front sprung mass displacement, $x_2 = \dot{Z}_{sf}$ for the front sprung mass velocity, $x_3 = Z_{uf}$ for the front unsprung mass displacement, $x_4 = \dot{Z}_{uf}$ for the front unsprung mass velocity, $x_5 = Z_{sr}$ for the rear sprung mass displacement, $x_6 = \dot{Z}_{sr}$ for the rear sprung mass velocity, $x_7 = Z_{ur}$ for the rear unsprung mass displacement and $x_8 = \dot{Z}_{ur}$ for the rear unsprung mass velocity, respectively.

The state equations with these assigned state variables for the half-car suspension system are then given as follows

$$\dot{x}_1 = x_2$$

$$\dot{x}_2 = -\alpha K_f x_1 - \alpha B_f x_2 + \alpha K_f x_3 + \alpha B_f x_4 - \beta K_r x_5 - \beta B_r x_6 + \beta K_r x_7 + \beta B_r x_8 + \alpha f_f + \beta f_r$$

$$\dot{x}_3 = x_4$$

$$\dot{x}_4 = \frac{1}{m_{uf}}[K_f x_1 + B_f x_2 - (K_f + K_{tf})x_3 - B_f x_4 + K_{tf} z_{rf} - f_f]$$

$$\dot{x}_5 = x_6$$

$$\dot{x}_6 = -\beta K_f x_1 - \beta B_f x_2 + \beta K_f x_3 + \beta B_f x_4 - \gamma K_r x_5 - \gamma B_r x_6 + \gamma K_r x_7 + \gamma B_r x_8 + \beta f_f + \gamma f_r$$

$$\dot{x}_7 = x_8$$

$$\dot{x}_8 = \frac{1}{m_{ur}}[K_r x_5 + B_r x_6 - (K_r + K_{tr})x_7 - B_r x_8 + K_{tr} z_{rr} - f_r] \quad (8)$$

f_f And f_r are actuator inputs of the front and rear wheels which have been taken from an available back stepping control scheme [1].The equations for these two control laws have been given as

Front control law

$$f_f = \frac{1}{\alpha}[\beta k_r x_5 + \beta B_r x_6 - \beta k_r x_7 - \beta B_r x_8 \\ - z_1 - c_2 z_2 - \mu_2] + k_f x_1 + B_f x_2 - k_f x_3 - B_f x_4 \quad (9)$$

Rear control law

$$f_r = \frac{1}{\gamma}[\beta k_f x_1 + \beta B_f x_2 - \beta k_f x_3 - \beta B_f x_4 \\ - z_3 - c_4 z_4 - \mu_4] + k_r x_5 + B_r x_6 - k_r x_7 - B_r x_8 \quad (10)$$

where

$$\alpha=\frac{1}{m_s}+\frac{a^2}{J_y},\beta=\frac{1}{m_s}-\frac{ab}{J_y},\gamma=\frac{1}{m_s}+\frac{b^2}{J_y}$$

$z_1,z_2,z_3,z_4,\mu_2,\mu_4$ are nonlinear parameters and functions which are obtained through controller procedure design and certainly affect our simulations; But their equations have not been represented here again. Figure 2 illustrates the effect of controller on the front body mass displacement.

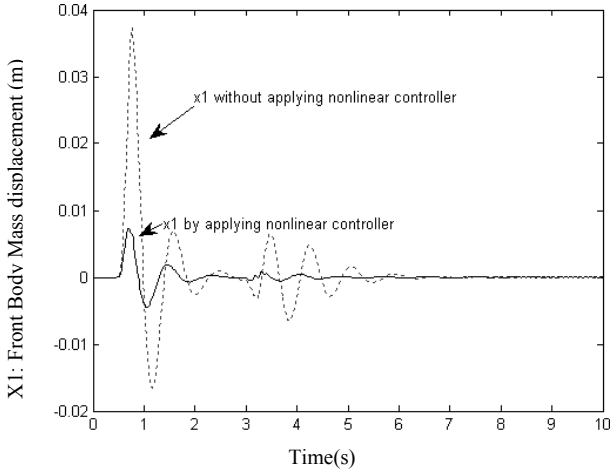

Figure 2: the effect of controller on the front body mass displacement

Z_{rf} And Z_{rr} are the road excitations that have been chosen as

$$z_{rf}(t)=\mu_r(1-rand(1)) \quad , 0.5\le t\le 0.75 \tag{11}$$

$$z_{rr}(t)=\mu_r(1-rand(1)) \quad , \quad 3\le t\le 3.25 \tag{12}$$

where μ_r is amplitude defining the bump height here set to $\mu_r=0.025$ for a bump height of 5cm. The parameters of the half-car model selected for this study are taken from [1].

III. MODELING AND FAULT DETECTION OF THE HALF-CAR MODEL WITH INTERVAL FUZZY MODEL

In this section after derivation of an interval fuzzy model interval fuzzy model of a half-car suspension system has been presented.

A. Derivation of an interval fuzzy model

A typical fuzzy TS-type model in affine form can be supposed as a set of rules.

$$R_j\text{: If } x_p=A_j \text{ , then y}=\theta_j^T x, \quad \text{j=1}\cdots\text{n} \tag{13}$$

The variable x_p=u is the model input and y is the model output and θ_j is a vector of fuzzy parameters, respectively. The consequent vector is denoted $x^T=[u,1]$. Unity is added to the vector for describing the output functions in affine form. Equation (13) can be rewritten as following.

$$y=\beta^T(x_p)\Theta x \tag{14}$$

$\beta^T(x_p)=[\beta_1(x_p),\beta_2(x_p),\cdots,\beta_m(x_p)]$ is a vector of normalized membership functions. Matrix of the coefficients for the whole set of rules is $\Theta^T=[\theta_1,\theta_2,\cdots,\theta_m]$.

Now, we want to find upper and lower boundary functions that satisfy following conditions for any arbitrary ε>0 and for each z=$[x_p\ x^T]^T$.

$$\bar{g}(\text{Z})\ge\text{Max g (z)}, \exists\, g\epsilon\mathcal{G}:\ \bar{g}(\text{z})<\text{g (z)}+\varepsilon \tag{15}$$

$$\underline{g}(\text{Z})\ge\text{Min g (z)}, \exists\, g\epsilon\mathcal{G}:\ \underline{g}(\text{z})>\text{g (z)}+\varepsilon \tag{16}$$

In the above equations, it has been let that C$\subset R^{n+2}$ is a compact set and $\mathcal{G}$= {g: C→R} is a class of nonlinear functions. Finding bounds in (15) and (16) requires masses data; therefore it is impossible to find exact bounds because only finite amount of data is available.

For solving this problem Stone-Weierstrass theorem has been used. This theorem says that, for any real continuous function g, on a compact set C$\subset R^d$ and arbitrary ε>0, there exist a fuzzy system f, such that [7-9]

$$sup|f(z_i)-g(z_i)|_{z_i\epsilon z}<\varepsilon \qquad \forall i \tag{17}$$

By Stone-Weierstrass extension theorem the following equations will be obtained.

$$0<\bar{f}(z_i)-g(z_i)<\varepsilon \quad \forall i \tag{18}$$

$$-\varepsilon<\underline{f}(z_i)-g(z_i)<0 \quad \forall i \tag{19}$$

The defined band should be as narrow as possible. The upper and the lower fuzzy functions can be found by solving the following optimization problems, respectively. Both problems can be known as linear programming problems.

$$min_{\underline{\Theta}}max_{z_i\epsilon z}\left|y_i-\underline{f}(z_i)\right| \ \ s.t \ \ y_i-\underline{f}(z_i)\ge 0 \tag{20}$$

$$min_{\overline{\Theta}}max_{z_i\epsilon z}\left|y_i-\overline{f}(z_i)\right| \ \ s.t \ \ y_i-\overline{f}(z_i)\ge 0 \tag{21}$$

$\underline{f}(z_i)=\beta^T(x_p)\underline{\Theta}x$ and $\overline{f}(z_i)=\beta^T(x_p)\overline{\Theta}x$ in (20), (21). Required data are obtained by sampling different functions from $\mathcal{G}$ with arbitrary values of z_i.

B. Interval fuzzy model of half-car suspension system

In this section interval fuzzy model has been used for identification and modeling of half car suspension system. As mentioned before, this method is used for functions of a finite set of input and output measurements or systems with interval parameters on the other hand there is a class of functions for description of one system.

It is assumed that parameters' uncertainty of the half-car suspension is 1%. On the other word it is assumed 1% perturbation of nominal value of parameters is acceptable. It's the key idea for using interval fuzzy model for identification of the purposed system. Therefore new model for active suspension system with uncertain parameter will be obtained.

This new model is used to produce the data set for identification of the interval fuzzy model. Responses of the system were studied by 80 different simulations. In each iteration the input signal remained fixed where as uncertain parameters' value changed. The input vector includes Z_{rf} and Z_{rr} . Training of the model has achieved by first 60 simulations and 20 iteration used for validation.

All of the eight state variables of the half-car suspension system have been identified with 8 multi input-Single output interval fuzzy models (INFUMO). Main system and its nonlinear controller consider as a single system. Thus the resultant system is nonlinear. The results of these identifications for two state variables are presented in figures 4 and 5.

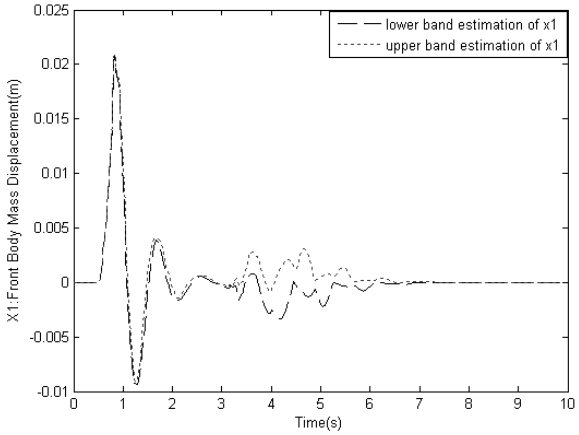

Figure 3: identification of the front body mass displacement with interval fuzzy model

Identified bounds have been used for fault detection of purposed system. Using resultant Interval fuzzy models residual signal could be obtained.

The benefit of this method is that confidence bands for output signals could be obtained easily, and these bands could be used for generating residual signal. The residual signal could be defined in the following way [7-9]:

$$if\ y_{out}<\hat{y}, re(y_{out}) = \frac{y_{out}-\hat{y}}{\underline{\hat{y}}-\hat{y}} \quad (22)$$

$$if\ y_{out}>\hat{y}, re(y_{out}) = \frac{y_{out}-\hat{y}}{\overline{\hat{y}}-\hat{y}} \quad (23)$$

$$\hat{y}=\frac{\overline{\hat{y}}+\underline{\hat{y}}}{2} \quad (24)$$

The residual signal in (22), (23) is zero when the output is equal to $\hat{y}$ and approaches the value 1 if the measurement output is close to one of the interval bounds.

C. Fault detection

Different fault detection methods have been applied to passive, semi-active, and active suspension systems till now. Fault detection of front and rear damper and springs were not possible in Karami et.al [6] model at all whereas it has been done in this research. As mentioned in the previous section, in this case study, it has been supposed that 1% perturbation of nominal parameters' values is acceptable.

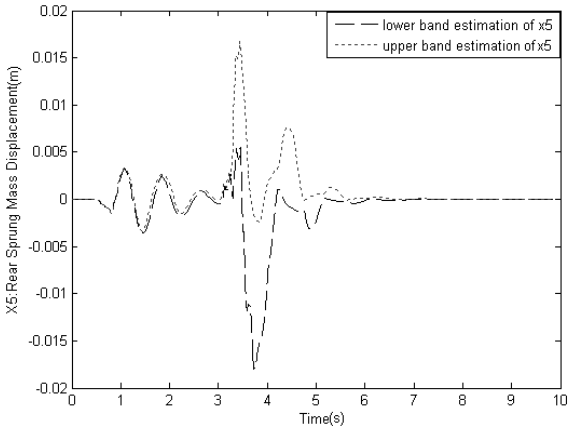

Figure 4: identification of the rear sprung mass displacement with interval fuzzy model

Figure 6 shows the fault detection scheme that has been used in this paper. Each of the state variables of the half-car suspension system assumed to be an output of the system.

In the previous section for each of the state variables an INFUMO has been found. Interval fuzzy models have been put in the parallel position with the main system.

It is possible to use only one INFUMO however eight INFUMOs are used for more accurate fault detection. Residual signals enter the alarm signal blocks, if the value of residual signals are more than unity output of the alarm signal blocks become one otherwise it will be zero.

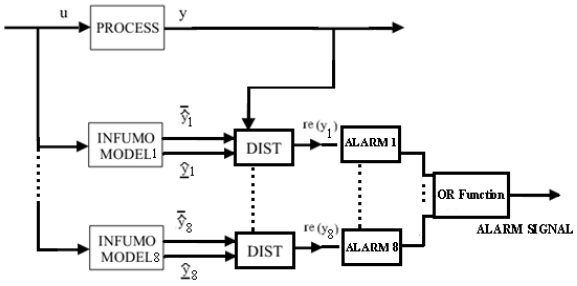

Figure 5: Fault detection using INFUMO model

The last alarm signal is logical OR of eight outputs of the alarm signal blocks. Therefore, if all outputs of system belong to the corresponding identified bounds the performance of the system is correct; otherwise a fault occurred in the system.

10% and 20% fault have been applied on different rear and front component of half-car suspension system. The time of simulation is ten seconds. Since faults have been applied on the system before starting simulation, the alarm signal value expected to be unity during whole time of simulation.

Results are shown in figs 6 to 11. Figure 6 shows an instance of residual signal and its corresponding alarm signal these signals are obtained when 20% fault occurred on the rear damper. Figs 7 to 11 are the main alarm signals that show the occurrence of fault in the different component of the half-car suspension system. Totally these figures reveal that

particularly for up to 20% applied fault, there is a good agreement with the expected result of the problem. Although for 20% fault better results have been obtained, this method can be used for detecting 10% fault that occurred on system's rear and front dampers and springs. The results have been briefly presented in the table 1.

Finally, 30% abrupt fault has been applied on sensor1 at t=4s. The result has been shown in fig11. This figure shows that by this method it is possible to detect the time of occurrence of fault.

TABLE I. RESULT OF FAULT DETECTION FOR DIFFERENT COMPONENT OF HALF-CAR SUSPENSION SYSTEM

Fault	B_r	B_f	K_r	K_f
20% fault	Well	Well	Well	Well
10% fault	Well	Well	Not bad	Not bad

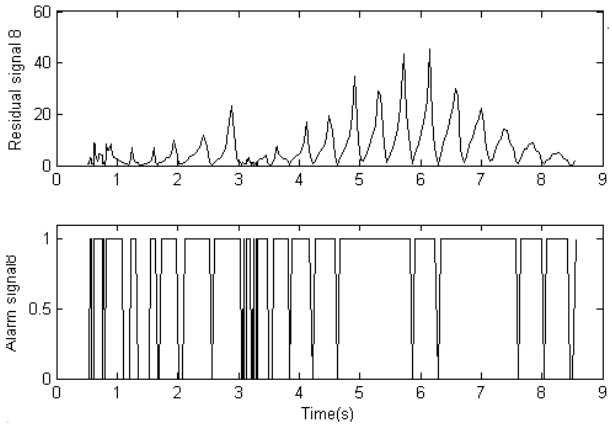

Figure 6: a. shows residual signal when 20% fault occurred on Br. b. shows alarm signal when 20% fault occurred on Br

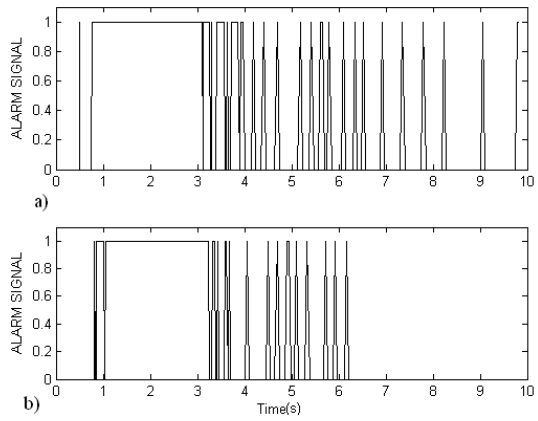

Figure 7: .a. shows alarm signal when 20% fault occurred on Kf. b. shows alarm signal when 10% fault occurred on Kf

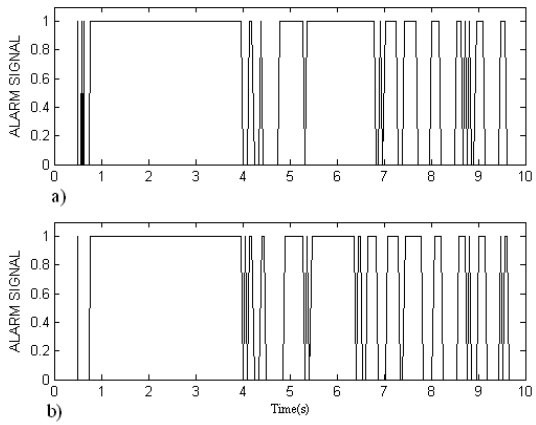

Figure 8: a. shows alarm signal when 20% fault occurred on Bf. b. shows alarm signal when 10% fault occurred on Bf

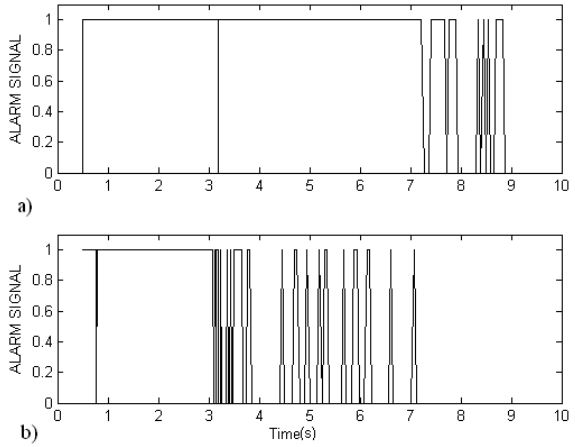

Figure 9: a. shows alarm signal when 20% fault occurred on Kr. b. shows alarm signal when 10% fault occurred on Kr

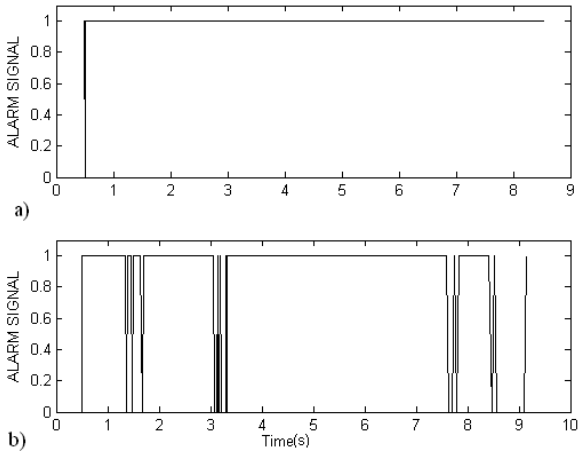

Figure 10: a. shows alarm signal when 20% fault occurred on Br. b: shows alarm signal when 10% fault occurred on Br

IV. CONCLUSION

An application of interval fuzzy model for fault detection of an active suspension system is introduced in this paper. Interval fuzzy model was applied for residual signal generation. Introduced approach has been employed in fault detection for a class of the processes with interval-type parameters or for a nonlinear system with uncertain parameters. In this paper uncertainty was added to the active suspension system. Therefore, the novelty of this paper is applying interval fuzzy model for fault detection of half-car suspension system that hasn't uncertain parameters.

Simulation results have shown that proposed method could be an effective tool for fault detection of active sustention system. This method was able to detect 20% fault very well and also it has good result for 10% fault. Furthermore this method can be used for on-line application too.

For more accurate fault detection, finding more narrow confidence bands for state variables is suggested. In this work it is assumed 1% uncertainty exists in the parameters value. If less uncertainty to be assumed for parameters value, more narrow bands can be obtained.

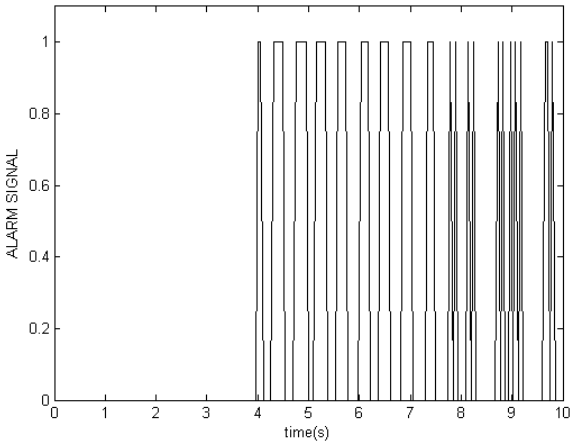

Figure 11: alarm signal when 30% fault occurred on sensor1 (output1) at t=4s

REFERENCES

[1] Chiou-Jye Huang, Jung-Shan Liu. "Nonlinear Active Suspension Control Design Applied to a Half-Car Model", IEEE International Conference on Networking, Sensing 8; Control. Taipei, Ttiaan,2004

[2] D. Fischer, E. Kaus and R. Isermann. "Fault Detection for an Active Vehicle Suspension", American Control Conference, vol. 5, pp. 4377 – 4382, 2003

[3] Igor Skrjanc, Saso Blazic, and Osvaldo, Enrique Agamennoni. " Interval Fuzzy Modeling Applied to Wiener Model with Uncertainties". IEEE transactions on systems, man, and cybernetics. Part B: cybernetics, vol.35, NO.5, October 2005

[4] Igor Skrjanc,SaSo Blazic ,and Osvaldo Agamennoni. " Interval Fuzzy Model Identification Using l_∞ -Norm". IEEE transactions on fuzzy systems. vol .13 ,no.5,October 2005

[5] Igor Skrjanc,SaSo Blazic ,and Osvaldo. " Identification of dynamical systems with a robust interval fuzzy model". Automatica 41, pp. 327–332, November 2005

[6] R.Karami, F. Najafi, and M. Aliyari Shoorehdeli. "Model Based Identification and Fault Detection of an Active Suspension System". IFAC 2007.

[7] Simon Oblak, Igor Skrjanc,SasoBlazic. "On applying interval fuzzy model to fault detection and isolation for nonlinear input- output systems with uncertain parameters" IEEE Conference on Control Applications. Toronto, Canada. August 2005

[8] Simon Oblak," Interval fuzzy modeling in fault detection for a class of processes with interval-type parameters". EUROCON 2005, Serbia & Montenegro Belgrade, November 2005

[9] Simon Oblak, Igor Skrjanc, SasoBlazic."Fault detection for nonlinear systems with uncertain parameters based on the interval fuzzy model". Engineering Applications of Artificial Intelligence, pp. 503–510,2007

2011 IEEE International Conference on Fuzzy Systems
June 27-30, 2011, Taipei, Taiwan

Uncertainty Management in Type-2 Fuzzy Face-Space for Emotion Recognition

Rajshree Mandal, Anisha Halder, Pavel Bhowmik, Amit Konar
ETCE Department, Jadavpur University, Kolkata-32. India
rajshree.mondal@gmail.com, halder.anisha@gmail.com, bpavel88@gmail.com, konaramit@yahoo.co.in

Aruna Chakraborty
Department of Computer Science and Engineering, St. Thomas' College of Engineering and Technology, Kolkata, India
aruna_stcet@rediffmail.com

Atulya K. Nagar
Department of Math and Computer Science, Liverpool Hope University, Liverpool, UK.
nagara@hope.ac.uk

***Abstract*—Manifestation of a given emotion on facial expression is not always unique, as the facial attributes in different instances of similar emotional experiences may vary widely. When a number of facial attributes are used to recognize the emotion of a subject, the variation of individual attributes together makes the problem more complicated. This variation is the main source of uncertainty in the emotion recognition problem, which has been addressed here in two steps using type-2 fuzzy sets. First a type-2 fuzzy face-space is constructed with the background knowledge of facial features of different subjects for different emotions. Second, the emotion of the unknown subject is determined based on the consensus of the measured facial features with the fuzzy face-space. The face-space comprises both primary and secondary membership distributions. The primary membership distributions here have been constructed based on the highest frequency of occurrence of the individual attributes. Naturally, the membership values of an attribute at all except the point of highest frequency of occurrence suffer from inaccuracy, which has been taken care of by secondary memberships. An algorithm for the evaluation of the secondary membership distribution from its type-2 primary counterpart has been proposed. The uncertainty management policy adopted using general type-2 fuzzy set has a classification accuracy of 96.67% in comparison to 88.67% obtained by interval type-2 counterpart only.**

Keywords-Emotion Recognition, Facial feature extraction , Type-2 primary membership, Type-2 secondary membership

I. INTRODUCTION

Emotion recognition is currently gaining importance for its increasing scope of applications in human-computer interactive systems. Several modalities of emotion recognition, including facial expression, voice, gesture and posture have been studied in the literature. However, irrespective of the modality, emotion recognition comprises two fundamental steps involving feature extraction and classification [1]. Feature extraction refers to determining a set of features/attributes, preferably independent, which together represents a given emotional expression. Classification aims at mapping emotional features into one of several emotion classes.

Both feature extraction and classification are equally important to determine the performance of an emotion recognition system. Sometimes, a good classification algorithm cannot yield high classification accuracy for poorly selected features. Naturally, selection of good features is a pre-requisite for high classification accuracy. Several methods of emotion recognition from facial expression have been developed over the last three decades. The study undertaken so far aimed at improving the performance of emotion classification by either selecting suitable features [2], [3], [4], [5], [6], [7], [8], [9], or by identifying the right classifier [10], [11], [12], [13], [14], [15], [6], [16], [17].

Emotional features, on many occasions are subjective. For example, facial expression of a representative emotion varies greatly from person to person. Further, facial expression of a given subject experiencing similar instances of a given emotion looks different. Naturally, it is difficult to have a unique set of features for a given emotion, free from both intra- and inter-personal level variations. In this paper, we thus attempted to consider emotion recognition as a problem of *uncertainty management* with an aim to minimize the effect of intra- and inter-personal level variations in features on emotion classification.

Type-2 fuzzy set has the potential to handle both intra- and inter-personal level uncertainty [18], which usually is modeled by the primary and secondary membership distributions of each measurement variable obtained from different sources. This characteristic of type-2 fuzzy sets motivated us to employ it for emotion classification of an unknown person. The principle of type-2 fuzzy emotion classification comprises two fundamental steps. First a type-2 fuzzy face-space, containing primary and secondary membership distributions of facial features for different subjects carrying distinct emotions, is created. Next to determine the emotion of an unknown person, selective facial features of the person are extracted and encoded using type-2 fuzzy sets, and finally an approximate matching algorithm is invoked to compare the fuzzy encoded features with those in the fuzzy face-space. The classification of the given facial expression to one of several emotion classes is determined by a simple but robust fuzzy decision making algorithm. It is indeed

978-1-4244-7316-8/11/$26.00 ©2011 IEEE

important to note here that the decision making process here considers taking support of individual emotion class to a given set of fuzzy measurements, and declaring the class with the *maximum support* as the winner.

Experiments reveal that the classification accuracy of emotion of an unknown person by the general type-2 fuzzy set based scheme is as high as 96%. When secondary memberships are ignored, and classification is performed with only interval type-2 fuzzy sets, the classification accuracy falls by a margin of 8%. The additional 8% classification accuracy obtained by general type-2 fuzzy set, however, has to pay a price for additional complexity of ($m \times n \times k$) multiplications, where m, n and k denote the number of features/subject, no. of subjects, and no. of emotion classes respectively.

The paper is divided into seven sections. In section II, we propose the principle of uncertainty management in fuzzy face-space for emotion recognition. Section III is concerned with the computation of fuzzy type-2 membership distributions. Section IV provides the main steps for emotion classification with a more emphasis on feature extraction. Experimental details are given in section V. Performance Analysis is given in section VI. Conclusions are listed in section VII.

II. Uncertainty Management In Fuzzy Face-Space For Emotion Recognition

This section provides a general overview of the proposed scheme for emotion recognition using type-2 fuzzy sets. Here, the emotion recognition problem is considered as uncertainty management in fuzzy space after encoding the measured facial attributes by type-2 fuzzy sets.

Let $F=\{f_1, f_2, \ldots, f_m\}$ be the set of m facial features. Let $\mu_A(f_i)$ be the primary membership in [0,1] of the feature f_i to be a member of set A, and $\mu(f_i, \mu_A(f_i))$ be the secondary membership of the measured variable f_i in [0,1]. If the measurement of a facial feature, f_i, is performed p times on the same subject experiencing the same emotion, and the measurements are quantized into q intervals of equal size, we can evaluate the frequency of occurrence of the measured variable f_i in q quantized intervals. The interval containing the highest frequency of occurrence then can be identified, and its centre, m_i, approximately represents the mode of the measurement variable f_i. The second moment, σ_i, around m_i is determined, and an exponential bell-shaped (Gaussian) membership function centered on m_i and with spread σ_i is used to represent the membership function of the random variable f_i. This function represents the membership of f_i to be CLOSE-TO the central value, m_i. It may be noted that a bell-shaped (Gaussian-like) membership curve would have a peak at the centre with a membership value one, indicating that membership at this point is the largest for an obvious reason of having the highest frequency of f_i at the centre.

On repetition of the above experiment for variable f_i on n subjects, each experiencing the same emotion, we obtain n such membership functions, each one for one individual subject. Naturally, the measurement variable f_i now has both intra- and inter-personal level uncertainty. The intra-personal level uncertainty occurs due to pre-assumption of the bell-shape (Gaussian distribution) of the membership function, and the inter-personal level uncertainty occurs due to multiplicity of the membership distribution for n subjects. Thus a new measurement for an unknown person can be encoded using all the n-membership curves, giving n possible membership values, thus giving rise to uncertainty in the fuzzy space.

The uncertainty involved in the present problem has been addressed here by two distinctive approaches, using: i) Interval Type-2 Fuzzy Set (IT2FS), and ii) General Type-2 Fuzzy Set (GT2FS). Naturally, the former approach is simple, but more error-prone as it ignores the intra-personal level uncertainty. The second approach is more robust, and is capable to take care of both the uncertainties. But it needs additional complexity as it involves more computation. Though both the approaches have many common steps, we briefly outline the first one for its simplicity, and then explain the latter without repeating the common steps further.

A. First Approach

Let $f_i^{/}$ be the measurement of the i-th feature for an unknown subject experiencing an emotion of class c. Now, by consulting the n known primary membership distributions for a given emotion, we obtain n primary membership values of the variable. Let they be $\mu^1_A(f_i^{/})$, $\mu^2_A(f_i^{/}),\ldots,$ $\mu^n_A(f_i^{/})$. Here, $\mu^k_A(f_i^{/})$ represents the degree of membership of a feature $f_i^{/}$ for the unknown subject in a fuzzy set A, interpreted using the known membership distribution of the same feature for the k-th subject.

We now determine the maximum and minimum of these n membership values, and thus obtain an interval $[\mu^{min}_A(f_i^{/}), \mu^{max}_A(f_i^{/})]$, representing the entire span of uncertainty of the measurement variable $f_i^{/}$ in the fuzzy space, induced by n subjects. If there exist m different facial features, then for each feature we would have such an interval, and consequently we obtain m such intervals given by

$$[\mu^{min}_A(f_1^{/}),\ \mu^{max}_A(f_1^{/})],\ [\mu^{min}_A(f_2^{/}),\ \mu^{max}_A(f_2^{/})],\ \ldots.,\ [\mu^{min}_A(f_m^{/}),\ \mu^{max}_A(f_m^{/})].$$

Since an emotion is characterized by all of these m features, to find the overall support of the m features (m measurements made for the unknown subject) to the emotion class c represented by the n primary memberships, we use the fuzzy meet operation to get the interval $S_{c\text{-}i} = [s_c^{min}, s_c^{max}]$, where

$$s_c^{min} = Min\{\mu^{min}_A(f_1^{/}), \mu^{min}_A(f_2^{/}), \ldots, \mu^{min}_A(f_m^{/})\},$$

and $$s_c^{max} = Min\{\mu^{max}_A(f_1^{/}), \mu^{max}_A(f_2^{/}), \ldots, \mu^{max}_A(f_m^{/})\}.$$

Thus we can say that the unknown subject is experiencing the emotion class c at least to the extent s_c^{min}, and at the most to the extent s_c^{max}.

To reduce the non-specificity associated with the interval $S_{c\text{-}i}$, different approaches can be taken. For example, the most conservative approach would be to use lower bound, while the most liberal view would to use the upper bound of the interval as the support for the class c. In absence of any additional information, a balanced approach would be to use center of the interval as the support for the class c by the n primary memberships to unknown subject. This idea is supported by Mendel [31] and Lee [32]. Thus, we compute the centre, S_c of the interval $S_{c\text{-}i}$,

$S_c = (s_c^{min} + s_c^{max})/2$.

Thus S_c is the degree of support that the unknown subject is in emotion class c.

Now to predict the emotion of a person from his facial expression, we determine S_c for each emotion class. Presuming that there exist k emotion classes, let us denote them by S_1, S_2,…., S_k for emotion class 1, 2,…, k, respectively. Since a given facial expression may convey different emotions with different degrees, we resolve the conflict by ranking the S_j for j = 1 to k, and thus determine the emotion class *l*, for which $S_l >= S_j$ for all j.

To make the algorithm robust, we consider association of fuzzy encoded measurements with emotion class by considering the weakest reliability of the joint occurrence of the fuzzy measurements, and identify the winning emotion class having this measure of reliability superseding the same of other emotion classes.

B. Second Approach

The second approach employs similar methodology like the first one to reduce inter-personal level uncertainty, but considers secondary memberships to reduce intra-personal level uncertainty as well. The main step in the second approach is to evaluate type-2 secondary membership values from the primary membership distributions. This, of course, is a difficult problem, and is discussed in detail in section III. The intra-personal level uncertainty in primary membership is reduced by correctly adjusting them with their secondary membership by the following transformation.

Let f_i' be the measurement of the i-th feature for an unknown subject. Now, by consulting the n primary membership functions for a given emotion, we obtain n primary membership values of the variable given by $\mu^1_A(f_i')$, $\mu^2_A(f_i')$,…, $\mu^n_A(f_i')$. Let the secondary membership values for each primary membership respectively be $\mu(f_i', \mu^1_A(f_i'))$, $\mu(f_i', \mu^2_A(f_i'))$,…, $\mu(f_i', \mu^n_A(f_i'))$. Since the secondary memberships denote the degree of accuracy of the primary memberships, the uncertainty in a primary membership distribution can be reduced by multiplying each primary membership value by its secondary membership. Thus the modified primary membership values are given by

$$^{mod}\mu^1_A(f_i') = \mu^1_A(f_i') \times \mu(f_i', \mu^1_A(f_i')),$$

$$^{mod}\mu^2_A(f_i') = \mu^2_A(f_i') \times \mu(f_i', \mu^2_A(f_i')), \ \ldots..,$$

$$^{mod}\mu^n_A(f_i') = \mu^n_A(f_i') \times \mu(f_i', \mu^n_A(f_i')),$$

where $^{mod}\mu^j_A(f_i')$ denotes the modified primary membership value for j-th subject. The rest of the procedure in approach 2 is similar to approach 1 with replacement of $\mu^j_A(f_i')$ by $^{mod}\mu^j_A(f_i')$ for all j = 1 to n.

III. FUZZY TYPE-2 MEMBERSHIP EVALUATION

This section provides an introduction to type-2 membership evaluation [20], [21], [22]. Classical fuzzy sets consider primary membership distribution $\mu_A(x)$ of a fuzzy linguistic variable *x*, in a fuzzy set A, where $x \in X$ and $A \subseteq X$. Usually $\mu_A(x)$ is defined by an expert in a specialized domain. However, it has been found that different experts assign different membership distribution for the variable *x*. Consider for example, a fuzzy linguistic variable age in universe AGE, where age belongs to 0 to 120 years. Let YOUNG be a fuzzy set in the universe AGE. Now, the membership distribution $\mu_{YOUNG}(age)$ can be assigned by different people in different forms. Considering a Gaussian type distribution, for $\mu_{YOUNG}(age)$, we note that the peak of the distribution may be fixed at 18, 20 or 22 years depending on the relative preference of the individual. Such membership distributions suffer from two distinct type of uncertainty. The first type of uncertainty, called the intra-personal level uncertainty, is due to approximate values of membership within a given distribution assigned by an expert. The inter-personal level uncertainty refers to relative variations among the membership distributions for a given value of age.

Although theoretically very sound, type-2 fuzzy set has limitedly been used over the last two decades because of the users' inadequate knowledge to correctly assign the secondary memberships. This paper, however, overcomes this problem by extracting type-2 membership distribution from its type-1 counterpart by an evolutionary algorithm. A brief outline to the construction of secondary membership distribution is given in this section.

Intuitively, when an expert assigns a grade of membership distribution, she is relatively more certain to determine the location of the peaks and the minima over the distribution, but may not have enough background to correctly assign the membership values in the rest. Presuming that the membership values at the peak and the minima are close to 1, we attempt to compute secondary memberships at the rest of the secondary distribution. The following assumptions are used to construct an objective function, which needs to be minimized to obtain the solution of the problem.

1. Let $x=x_p$ and $x=x_q$ be two successive optima (peak/minimum) on the primary membership distribution $\mu_A(x)$. Then at any point *x* lying between x_p and x_q, the secondary membership $\mu(x, \mu_A(x))$ will be smaller than both $\mu(x_p, \mu_A(x_p))$ and $\mu(x_q, \mu_A(x_q))$.

2. The fall-off in secondary membership at a point *x* away from a peak/minimum $\mu(x_p, \mu_A(x_p))$ is exponential, given by

$$\mu(x, \mu_A(x)) = \mu(x_p, \mu_A(x_p)).\ exp(-|(x- x_p|) \quad (1)$$

The secondary membership at any point *x* between two consecutive optima at $x=x_p$ and $x=x_q$ in the primary membership is selected from the range $[\alpha, \beta]$, where

$$\alpha = \mu(x_p, \mu_A(x_p)).\ exp(-|(x- x_p|) \quad (2)$$

$$\text{and } \beta = \mu(x_q, \mu_A(x_q)).\ exp(-|(x- x_q|) \quad (3)$$

3. The defuzzified signal obtained on averaging the primary membership distributions at all *x* from n sources, is equal to the defuzzified signal obtained from type-2 primary and secondary distributions. The logic behind this, though apparent, is briefly explained here. The inter-

personal level uncertainty involved in the averaged membership distribution is the minimum with respect to individual primary distribution, as the uncertainty is also averaged at a given value of x, and is thus reduced.

4. The secondary membership at two consecutive values of x separated by a small positive δ has a small difference. This is required to avoid sharp changes in the secondary grade.

Given the primary membership distributions from n sources be $\mu_{A1}(x)$, $\mu_{A2}(x)$,....., $\mu_{An}(x)$, then the average membership distribution which represents a special form of fuzzy aggregation is given by

$$\mu_A(x) = \frac{\sum_{i=1}^{n} \mu_{Ai}(x)}{n}, \forall x \tag{4}$$

i.e., at each position of $x=x_j$, the above membership aggregation is employed to evaluate a new composite membership profile $\mu_A(x)$.The defuzzified signal obtained by the centroidal method [23] from the averaged primary membership distribution is given by

$$\bar{\bar{x}} = \frac{\sum_{\forall x} x \mu_A(x)}{\sum_{\forall x} \mu_A(x)}. \tag{5}$$

Further, the type-2 centroidal defuzzified signal obtained from the i-th primary and secondary membership distributions is given by

$$\bar{x} = \frac{\sum_{\forall x} x \mu_{Ai}(x).\mu_{Ai}(x, \mu_{Ai}(x))}{\sum_{\forall x} \mu_{Ai}(x).\mu_{Ai}(x, \mu_{Ai}(x))} \tag{6}$$

Using assumptions 3 and 4, we construct a performance index J given by (7)

$$J = \left(\bar{x} - \bar{\bar{x}}\right)^2 + \sum_{x=x_1}^{x_{n-1}} \{\mu((x+\delta), \mu_A(x+\delta)) - \mu(x, \mu_A(x))\}^2 \tag{7}$$

The secondary membership evaluation problem, now, transforms to minimization of J by selecting $\mu(x, \mu_A(x))$ from a given range $[\alpha, \beta]$, where α and β are the secondary memberships at the two optima in secondary distribution around the point x. Expressions (2) and (3) are used to compute α and β for each x separately.

Any derivative-free optimization algorithm can be used to minimize J, and obtain $\mu(x, \mu_A(x))$ at each x except the optima on the secondary distribution. Differential Evolution (DE) is one such derivative-free optimization algorithm, which has fewer control parameters, and has outperformed the well-known binary coded Genetic Algorithm and Particle Swarm Optimization algorithms with respect to standard benchmark functions. Further, DE is simple and has only a few lines code, which motivated us to employ it for the above optimization problem. The details of DE are not given here for lack of space. Readers may have it from the standard literature [24]. The main steps of the secondary membership evaluation procedure are outlined below.

1. Obtain the averaged primary membership distribution $\mu_A(x)$ from the primary distributions $\mu_{Ai}(x)$ obtained from n sources, i.e., i=1 to n. Evaluate $\bar{\bar{x}}$, and also $\bar{x}$ for a selected primary membership distribution $\mu_{Ai}(x)$ using (5) and (6) respectively.

2. Find the optima on $\mu_{Aj}(x)$ for a given j. Let the set of x corresponding to the optima be S. Set the secondary membership $\mu(x, \mu_{Aj}(x))$ to 0.99(close to one) for all $x \in X$.

3. For each $x \in X$, where $x \notin S$, identify the optima closest around x from S. Let they be located at $x=x_p$ and $x=x_q$, where $x_p < x < x_q$. Determine α and β for each x, given by (2) and (3).

4. For each x, where $\mu(x, \mu_A(x))$ lies in $[\alpha,\beta]$, minimize J by DE.

5. Obtain $\mu(x, \mu_A(x))$ for all x after the DE converges.

6. Repeat step 2 onwards for all j.

An illustrative plot of secondary membership distribution for a given primary is given in Fig. 1

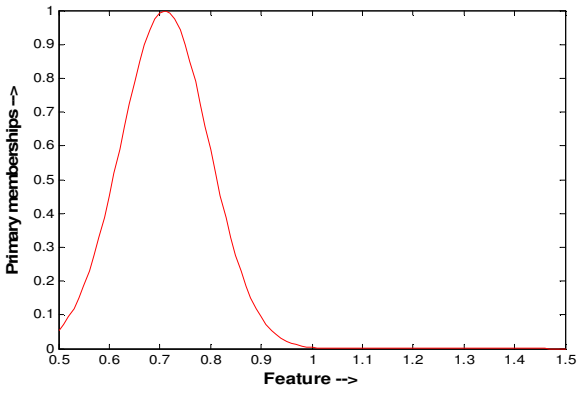

(a)

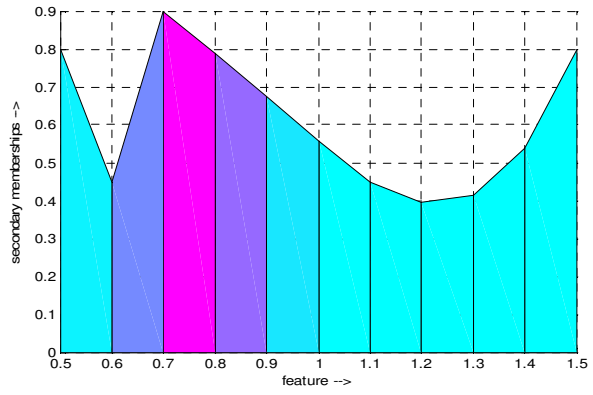

(b)

Fig. 1.(a) Primary distribution (b) Secondary distribution from the primary .

IV. METHODOLOGY

In this section, we present the methodology of emotion recognition using the principles introduced in section II and III. We here consider 5 emotion classes, (i.e., k=5) including anger, fear, disgust, happiness and relaxation. We consider n=10 subjects to characterize the type-2 membership distributions. To study the performance of the proposed scheme, we consider 30 facial expressions taken from 6 unknown persons. Five facial features, (i.e., m=5) have been used here to design the type-2 fuzzy face-space. The whole process of emotion recognition of an unknown person from his/her facial expression is divided into six main steps, as outlined below.

1. Facial feature extraction,
2. Type-2 primary membership evaluation from n-curves, one for each known subject,
3. Type-2 secondary membership evaluation corresponding to n primary membership values,
4. Reducing intra-personal level uncertainty by re-defining primary membership as the product of primary and secondary membership,
5. Evaluation of interval S^j and finally S_c^j for k competitive emotion classes using modified primary memberships,
6. Determining the winning emotion class l by selecting S_c^l, where S_c^l is the largest among S_c^j for emotion class j.

The explanation of all the steps except step 1 has already been outlined in section II. So, we now give an overview to step 1 only.

In order to extract the facial features from emotionally expressive facial images, it is essential to list down the most important features of the face. From earlier research results [19], [17], it is evident that the most important regions for recognizing the emotion of a person are the eyes and lips. This motivated us to select the following features: Left Eye Opening (EO_L), Right Eye Opening (EO_R), Distance between the Lower Eyelid to Eyebrow for Left Eye (LEE_L), Distance between the Lower Eyelid to Eyebrow for Right Eye (LEE_R), and Maximum Mouth opening (MO) including lower and upper lips. Fig. 2 explains the above facial features on a selected facial image.

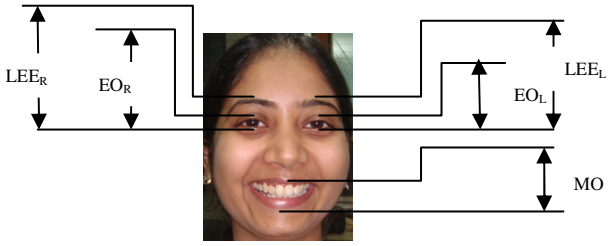

Fig. 2 Facial Features

For extraction of any of the features mentioned above, the first step that needs to be carried out is to separate out the skin and the non-skin regions of the image.

Estimation of Eye features (EO_L , LEE_L, EO_R and LEE_R): To estimate the eye features, we first localize the eye region as shown in Fig. 3 (a). A look at Fig. 3 reveals that there is a sharp change in color while moving from the forehead region to the eyebrow region. Thus to detect the location of the eyebrow, we take the average intensity (in three primary color planes) over each row of the image from the top, and identify the row with a maximum dip in all the three planes. This row indicates the top of the eyebrow region (Fig.3b). Similarly, we detect the lower eyelid by identifying the row with a sharp dip in intensity in all the three planes, while scanning the face up from the bottommost row. The location of the top eyelid region is identified by scanning the face up from the marked lower eyelid until a dip in the three color planes are noted together.

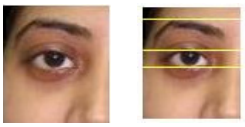

(a) (b)

Fig. 3. (a) Localized Eye search region , (b) Detection of eye features

Estimation of Mouth Opening (MO): In order to estimate the MO, we first localize the mouth region as shown in Fig. 4(a). Then a conversion from rgb to lab color space is undertaken. The k-means clustering algorithm is applied next on this image to get three clusters. The three clusters are: skin cluster, lip cluster and teeth cluster. We select the lip cluster (Fig. 4(b)) to determine the mouth opening. To obtain mouth-opening, we take the average intensity of three primary pixel colors, and plot the row-average of such value contributed by each pixel against the row number (Fig. 4c). It is observed that the width of the zero-crossing zone in Fig. 4c provides a measure of mouth-opening.

Fig. 4.a Fig. 4.b Fig. 4.c

Fig. 4.(a) Mouth search area (b) Lip cluster (c) Graph of average intensity over each row against the row position.

V. EXPERIMENTAL DETAILS

The experiment is conducted in Jadavpur University with two sets of subjects: a) the first set of 10 subjects (n=10) is considered for designing the fuzzy face-space and, b) the other set of 30 facial expressions taken from 6 unknown subjects is considered to validate the result of the proposed emotion classification scheme. The experiment thus consists of two distinct phases as indicated in the next two sub-sections.

A. Creating the type-2 fuzzy face-space

Type-2 fuzzy face-space contains both primary and secondary membership distributions for each facial feature. Since we have 5 facial features and the experiment includes 5 distinct emotions of 10 subjects, we obtain 10×5×5=250 primary membership curves. These 250 membership curves are grouped into 25 heads, each containing 10 membership curves of ten subjects for a specific feature representing a given emotion. Fig. 5 gives an illustration of one such group of 10

membership distributions for the feature EO $_L$ for the emotion: disgust.

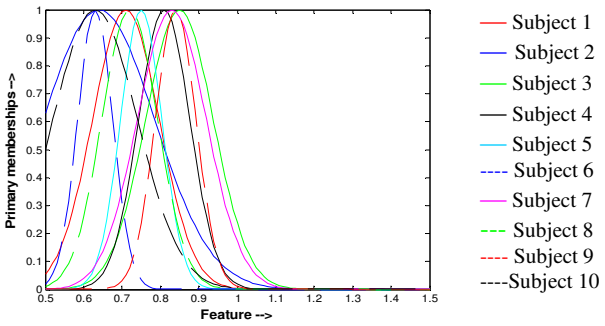

Fig. 5 Membership distributions for emotion disgust and feature EO_L

For each primary membership distribution, we have a corresponding secondary membership distribution. Thus we obtain 250 secondary membership distributions. Two illustrative type-2 secondary distributions for subject 1 and 2 for the feature EO_L for emotion disgust are given in Fig. 6. The axes in the figure represent feature (EO_L), primary and secondary membership values as indicated.

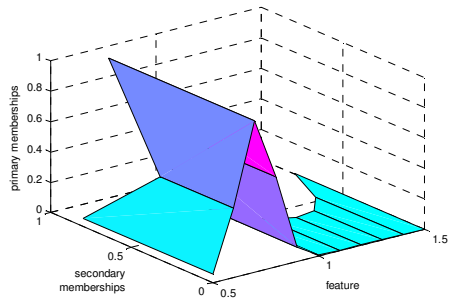

Fig. 6a Secondary Membership curve of Subject1

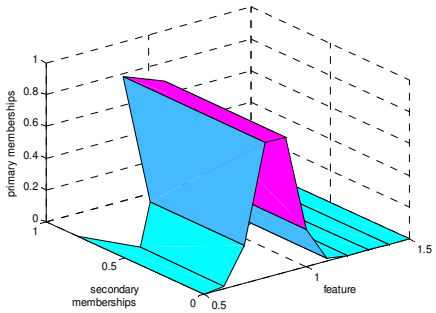

Fig. 6.b Secondary Membership curve of Subject2

B. *Emotion recognition of an unknown subject*

Suppose we want to recognize the correct emotion class of the facial image in fig. 7.

Fig. 7 Facial Image of an unknown subject

First, the facial features are extracted as mentioned in section IV. The extracted features are self-normalized by dividing individual feature obtained in a given emotional state by its value in the relaxed state. This nullifies the effect of the distance variation while image capturing. The extracted features for Fig.7 are enlisted in Table I.

TABLE I. EXTRACTED FEATURES OF FIG. 7

EO_L	EO_R	MO	LEE_L	LEE_R
0.636	0.6371	1.77	0.969	0.968

Now, for each facial feature, we consult 5 sets of 10 primary membership distributions as in Fig. 5, each corresponding to one distinct emotion of 10 subjects. Thus we obtain 10 primary membership values of that feature to fall in a given emotion class. Secondary memberships corresponding to a given feature and obtained primary membership are determined using curves like Fig. 6. Table II provides the summary of the primary and secondary memberships obtained for EO_L for the emotion disgust.

TABLE II. CALCULATED MEMBERSHIP VALUES FOR FEATURE :EO_L EMOTION: DISGUST

Feature	Primary Memberships (μ_{pri})	Secondary memberships (μ_{sec})	$\mu_{pri} \times \mu_{sec}$	Range after intersection
EO_L	0.1562	0.6371	0.0980	0.0056-0.8011
	0.6531	0.6039	0.3940	
	0.0983	0.5566	0.0545	
	0.9471	0.8460	0.8011	
	0.0983	0.5513	0.0540	
	0.2496	0.5961	0.1487	
	0.0100	0.5566	0.0056	
	0.9000	0.8513	0.7662	
	0.6241	0.8539	0.5290	
	0.5134	0.5724	0.2947	

In Table II, we computed the product of primary and secondary memberships, and then obtain the minimum and maximum of the product to determine its range, as indicated in the last column of Table II.

For each feature we obtain 5 Tables like Table II, each one for a given emotion. Thus for 5 features, we would have altogether 25 such tables. The range for each feature corresponding to individual emotions is given in Table III. Now, we obtain a new range with lower (upper) boundary equal to the intersection of the lower (upper) range boundaries for different features under a given emotion. This measure, enumerated in the last column of Table III, indicates an interval of fuzzy certainty about the joint occurrence of the features in a given facial expression representing a specific emotion class.

The center of the interval has minimum uncertainty, and so we compared them, and finally determine the winning emotion with the largest centre. It is clear from Table III that the centre value is maximum for emotion happiness. So, we regard the emotion portrayed in Fig. 7 as Happiness.

TABLE III. CALCULATED FEATURE RANGES AND CENTRE VALUE FOR EACH EMOTION

Emotion	Range of Features					Range S_c^j after Intersection (centre)
	EO_L	EO_R	MO	LEE_L	LEE_R	
Anger	0-0.199	0 - 0.239	0.439 -0.964	0.0034 - 0.8145	0.0027-0.7813	0-0.239 (0.1195)
Disgust	0.0056-0.8011	0.0021-0.798	0-0	0-0.39	0.0011-0.261	0-0 (0)
Fear	0 - .298	0-0.1751	0.004-0.912	0.024-0.673	0.077-0.715	0-0.1751 (0.0875)
Happiness	0 - 0.555	0.0011-0.604	0.673-0.975	0.1343-0.8151	0.3214-0.7213	0-0.555 (0.2775)
Relaxed	0 - 0.132	0-0.221	0-0	0.013-0.458	0.046-0.552	0-0 (0)

VI. PERFORMANCE ANALYSIS

We now analyze the performance of our method with 30 facial expressions, each representing a given emotion. The emotion conveyed in each image is analyzed, and the results are tabulated in the form of confusion matrix [14], [19], [25]. It may be noted that in section II, we introduced two methods for emotion recognition. The first method yields a confusion matrix given in Table IV, while the confusion matrix obtained by method 2 is given in Table V. It is clear from Table V that the relaxation and disgust emotion can be classified with 100 % high accuracy followed by happiness (96%). Fear and anger are often confusing, and thus classification accuracy is relatively low for both.

TABLE IV. CONFUSION MATRIX FOR TYPE-2 PRIMARY FUZZY FACE-SPACE WITH ENTRIES IN %

In/Out	Anger	Disgust	Happiness	Fear	Relaxed
Anger	83.33	0	10	16.66	0
Disgust	0	93.33	0	0	0
Happiness	3.33	3.33	86.66	3.33	0
Fear	13.33	0	3.33	80	0
Relaxed	0	3.33	0	0	100

TABLE V. CONFUSION MATRIX FOR TYPE-2 SECONDARY FUZZY FACE-SPACE WITH ENTRIES IN %

In/Out	Anger	Disgust	Happiness	Fear	Relaxed
Anger	93.33	0	3.33	6.66	0
Disgust	0	100	0	0	0
Happiness	0	0	96.66	0	0
Fear	6.66	0	0	93.33	0
Relaxed	0	0	0	0	100

A look at Table IV and V reveals that the percentage accuracy obtained in Table-V is better than the same in Table-IV. It may be recalled that Table-V employed both primary and secondary memberships (i.e., GT2FS), while Table-IV used only primary membership distributions for n-sources (i.e., IT2FS). This justifies the significance of GT2FS in emotion recognition. Average accuracy obtained by ranking the diagonal entries of Table IV and V are 88.66% and 96.67% respectively.

Table VI shows the comparison of our proposed emotion recognition scheme with other existing methods. It is clear from the Table that the proposed method has the highest classification accuracy with respect to the published results.

TABLE VI. COMPARISON OVER OTHER TECHNIQUES

Facial Emotion Recognition by	Success rate
Multi-Layer Perceptron(MLP) and Radial Basis Function Network (RBFN) [26][27]	73% for MLP, and 65% for RBFN
Fuzzy Neural Network and HMM [10]	Higher than 78%
Using Linear Support Vector Machine [17]	95%
(Type-1) Fuzzy Relational Approach [19]	88.2% for adult male and 92.2 for adult female
Bayesian classifier[28][29]	63% to 71%
Fuzzy Kernel Clustering and Support Vector Machines[30]	90%
Principal Component Analysis (PCA) [25]	Average classification accuracy is 100% on train data and 95.47% on cross validation data.
Our proposed method	**96.67%**

VII. CONCLUSION

The paper proposed a simple and time-efficient scheme for emotion recognition from a pre-constructed type-2 fuzzy face-space. Experiments reveal that the classification accuracy of emotion by considering GT2FS is as high as 96.67%. The accuracy falls off by 8% when the solution is obtained by using IT2FS formulation. The classical rule based method for emotion classification [19] depends largely on the relational matrix used to represent implication relations. In the present context, the emotion analysis is performed intentionally on the fuzzy encoded measurement space to make the system performance robust.

REFERENCES

[1] A. Konar and A. Chakraborty (Eds.), Advances in Emotion Recognition, Wiley-Blackwell, 2011 (to appear).

[2] M.Rizon, M. Karthigayan, S.Yaacob and R. Nagarajan, "Japanese face emotions classification using lip features," Universiti Malaysia Perlis, Jejawi, Perlis, Malaysia, Geometric Modelling and Imaging (GMAI'07), IEEE 2007.

[3] H. Kobayashi and F. Hara, "Measurement of the strength of six basic facial expressions by neural network," Trans. Jpn. Soc. Mech. Eng. (C), vol. 59, no. 567, pp. 177–183, 1993.

[4] H. Kobayashi and F. Hara, "Recognition of mixed facial expressions by neural network," Trans. Jpn. Soc. Mech. Eng. (C), vol. 59, no. 567, pp. 184–189, 1993.

[5] H. Kobayashi and F. Hara , "The recognition of basic facial expressions by neural network," Trans. Soc. Instrum. Contr. Eng, vol. 29, no. 1, pp. 112–118, 1993.

[6] H.Tsai, Y.Lai and Y.Zhang, "Using SVM to design facial expression recognition for shape and texture features," Proceedings of the Ninth International Conference on Machine Learning and Cybernetics, Qingdao, 11-14 July 2010, IEEE 2010

[7] P. Ekman and W. V. Friesen, "Unmasking the Face: A Guide to Recognizing Emotions From Facial Clues," Englewood Cliffs, NJ: Prentice-Hall, 1975.

[8] O. A. Uwechue and S. A. Pandya, "Human Face Recognition Using Third-Order Synthetic Neural Networks," Boston, MA: Kluwer, 1997.

[9] Marco Paleari & Ryad Chellali and B.Huet, "Features for Multimodal Emotion Recognition: An Extensive Study," Italian Institute of Technology, Genoa, Italy, IEEE 2010

[10] A.Bhavsar and H.M.Patel, "Facial Expression Recognition Using Neural Classifier and Fuzzy Mapping," IEEE Indicon 2005 Conference, Chennai, India.

[11] Yimo Guo, Huanping Gao, "Emotion Recognition System in Images Based On Fuzzy Neural Network and HMM," Proc. 5th IEEE Int. Conf. on Cognitive Informatics (ICCI'06), IEEE 2006

[12] H.Zhao, Z.Wang and J.Men, "Facial Complex Expression Recognition Based on Fuzzy Kernel Clustering and Support Vector Machines," Third International Conference on Natural Computation (ICNC 2007), IEEE 2007.

[13] Y.Lee, C.W.Han and J.Shim, "Fuzzy Neural Networks and Fuzzy Integral Approach to Curvature-based Component Range Facial Recognition," 2007 International Conference on Convergence Information Technology, IEEE 2007

[14] G. U. Kharat and S.V.Dudul, "Neural Network Classifier for Human Emotion Recognition from Facial Expressions Using Discrete Cosine Transform," First International Conference on Emerging Trends in Engineering and Technology, IEEE 2008

[15] J. M. Sun, X. S. Pei and S. S. Zhou, "Facial Emotion Recognition in modern distant system using SVM," Proceedings of the Seventh International Conference on Machine Learning and Cybernetics, Kunming, July 2008, IEEE 2008

[16] B. Biswas, A. K. Mukherjee, and A. Konar , "Matching of digital images using fuzzy logic," AMSE Publication, vol. 35, no. 2, pp. 7–11, 1995.

[17] S. Das, A. Halder, P. Bhowmik, A. Chakraborty, A. Konar, A. K. Nagar, "Voice and Facial Expression Based Classification of Emotion Using Linear Support Vector," 2009 Second International Conference on Developments in eSystems Engineering, IEEE 2009

[18] J. M. Mendel, "Fuzzy Sets for Words: A New Beginning," IEEE Int. Conf. on Fuzzy Systems, 2003.

[19] A.Chakraborty, A.Konar, U.K.Chakraborty and A.Chatterjee, "Emotion Recognition From Facial Expressions and Its Control Using Fuzzy Logic", IEEE Transactions on Systems, Man and Cybernetics, IEEE 2009

[20] J.M Mendel and H. Wu "Type-2 Fuzzistics for Symmetric Interval Type-2 Fuzzy Sets: Part 1, Forward Problems," IEEE Transactions on Fuzzy Systems, Vol. 14, No.6, Decmber,2006.

[21] J.M Mendel and D. Wu, Perceptual Computing, IEEE Press, Wiley Publications, 2010.

[22] J.M Mendel and R.I John, "Type-2 fuzzy sets made simple," IEEE Transactions on Fuzzy Systems, April 2002.

[23] H.J Zimmermann, Fuzzy Set Theory and its Applications, Springer, Netherlands, 2001.

[24] K. V. Price, R. M. Storn and J. A. Lampinen (Eds.), Differential Evolution: A Practical Approach, Springer, 2005.

[25] G.U. Kharat and S.V. Dudul , "Emotion Recognition from Facial Expression Using Neural Networks," Human-Computer Sys. Intera., AISC 60, pp. 207–219 Springer-Verlag Berlin Heidelberg 2009

[26] Dae-Jin Kim, Sang-Wan Lee and Zeungnam Bien, "Facial Emotional Expression Recognition with Soft Computing Techniques," 2005 IEEE International Conference on Fuzzy Systems

[27] M.Gargesha and P.Kuchi, "Facial expression recognition using a neural network," Artificail Neural Computation Systems, 2002.

[28] Y. Zhang, Q. J i. "Active and dynamic information fusion for facial expression understanding from image sequences", IEEE Transactions on Pattern Analysis and Machine Intelligence, 2005, 27 (5): 699-714.

[29] C. Liu and H.Wechsler, "Probablistic reasoning models for face recognition," Computer Vision and Pattern Recognition Conference Proceeding, pp. 827- 832, 1998.

[30] Hui Zhao Zhiliang Wang Jihui Men, "Facial Complex Expression Recognition Based on Fuzzy Kernel Clustering and Support Vector Machines," Third International Conference on Natural Computation (ICNC 2007), IEEE.

[31] J.M. Mendel, R. I. John, F. Liu, "Interval Type-2 Fuzzy Logic Systems Made Simple," IEEE Trans. on Fuzzy systems, vol. 14, no. 6, Dec. 2006.

[32] J. M. Mendel, "On the importance of interval sets in type-2 fuzzy logic systems," In Proc. Joint 9th IFSA World Congress 20th NAFIPS Int. Conf., Vancouver, BC Canada, July 25-28, 2001, pp. 1647-1652.

[33] Dae-Jin Kim, Sang-Wan Lee and Zeungnam Bien, "Facial Emotional Expression Recognition with Soft Computing Techniques," HWRS-ERC),Dept. of EECS, Korea, IEEE 2009.

[34] R. Cowie, E. Douglas-Cowie, J.G Taylor, S. Ioannou, M. Wallace, S. Kollias, "An Intelligent System for facial emotion recognition," Department of Psychology, Queen's University of Belfast, Northern Ireland, United Kingdom.IEEE 2005.

[35] M.H.Bindu, P.Gupta and U.S.Tiwary,, "Cognitive Model Based Emotion Recognition From Facial Expressions For Live Human Computer Interaction," Proceedings of the 2007 IEEE Symposium on Computational Intelligence in Image and Signal Processing (CIISP 2007), IEEE 2007

[36] N.Esau, E.Wetzel, L.Kleinjohann and B.Kleinjohann, "Real-Time Facial Expression Recognition Using a Fuzzy Emotion Model," University of Paderborn, Germany, IEEE 2007.

[37] A.Khanam, M.Z.Shafiq and M.U.Akram, "Fuzzy Based Facial Expression Recognition," 2008 Congress on Image and Signal Processing, IEEE 2008

[38] H. Zhao and Z. Wang, "Facial Action Units Recognition Based on Fuzzy Kernel Clustering," Fifth International Conference on Fuzzy Systems and Knowledge Discovery, IEEE 2008

[39] Y.Sun, Z.Li and C.Tang, "An Evolving Neural Network for Authentic Emotion Classification," 2009 Fifth International Conference on Natural Computation, IEEE 2009

[40] C.Chang,Y.Huang and C.Yang, "Personalized Facial Expression Recognition in Color Image," 2009 Fourth International Conference on Innovative Computing, Information and Control, IEEE 2009

[41] M.Fu, Y.Kuo and K. Lee, "Fusing Remote Control Usages and Facial Expression for Emotion Recognition," 2009 Fourth International Conference on Innovative Computing, Information and Control, IEEE 2009

[42] C.Huang and Y.Huang, "Facial Expression Recognition Using Model-Based Feature Extraction and Action Parameters Classification," Journal of visual communication and image representation

[43] K.Huang, S.Huang and Y.Kuo, "Emotion Recognition Based on a Novel Triangular Facial Feature Extraction Method," National Cheng Kung University, Tainan, Taiwan, IEEE 2010

[44] A. Konar and A. Chakraborty, Emotional Intelligence: A Cybernetic Approach , Springer, Heidelberg, 2009.

2011 IEEE International Conference on Fuzzy Systems
June 27-30, 2011, Taipei, Taiwan

Generation of Takagi-Sugeno Fuzzy Systems with Minimum Rules in Modeling and Identification

Feng Wan and Chenglin Hu

Department of Electrical and Electronics Engineering
Faculty of Science and Technology
University of Macau
E-mail: *fwan@umac.mo*, *ma76567@umac.mo*

***Abstract*— An improvement is presented for the tunnel algorithm introduced in [17] for determining the minimum number of rules required by a fuzzy system for modeling and identification in the SISO case. The original tunnel algorithm can deal with only Mamdani type fuzzy systems, while the Testing Point algorithm proposed in this paper, can be used to construct Takagi-Sugeno type fuzzy systems with consequent parts of any order and has the potential to be further extended to the MISO case. Numerical examples are given to illustrate the idea and improvement.**

Keywords-Fuzzy modeling and identification; Takagi-Sugeno fuzzy systems; Rule reduction

I. INTRODUCTION

How to construct fuzzy systems using as less as possible rules with guaranteed performance is a difficult but important problem, which has attracted much attention over the fuzzy society [1], [3]-[15], [17], [19]-[24]. Among them, a so-called tunnel algorithm (TA) was proposed by [17], which can partition the input domain in a non-uniform manner according to the sampling data distribution and the approximation error tolerance, when dealing with the following problem in fuzzy modeling and identification.

Given a limited number of input-output data pairs or say samples $\{x_k, g(x_k)\}$, $k=1,2,\cdots,N$, of a single-input-single-output (SISO) system with an unknown analytical representation $g(x)$, it is expected to construct a fuzzy system $f(x)$ using M rules to approximate the unknown function $g(x)$, where M should be the minimum, and the approximation errors at each data point are less than a predefined error tolerance ε. From mathematical point of view, the task can be formulated as the following optimization problem:

$$\begin{aligned} &\text{minimize: } M, \\ &\text{subject to: } \max_{k=1,2,\ldots,n} \left| g(x_k) - f(x_k) \right| \le \varepsilon. \end{aligned} \tag{1}$$

The rest of this section briefly reviews the tunnel algorithm proposed in [17]. Restricted by the error tolerance ε, each sampling point $p_k = \{x_k, g(x_k)\}$, $k=1,2,\cdots,N$, as shown in Fig. 1, has its upper limit $p_k^+ = \{x_k, g(x_k)+\varepsilon\}$ and lower limit $p_k^- = \{x_k, g(x_k)-\varepsilon\}$. Connecting all the points p_k, p_k^+ and p_k^- respectively by lines in order along axis x, forms three piecewise lines PL, PL_ε^+ and PL_ε^-. PL_ε^- and PL_ε^+ are called the lower and upper boundaries of PL, respectively. *Tunnel* $P(\varepsilon)$ is the polygon area encircled by PL_ε^+ and PL_ε^-. The line segments $e = \overline{p_1^+ p_1^-}$ and $e' = \overline{p_N^+ p_N^-}$ are called the *edges* of the tunnel $P(\varepsilon)$.

Owing to the nice property of the Mamdani type fuzzy systems, the design problem can be reduced to finding as less as possible continuous line segments with guaranteed approximation accuracy. The key idea is to convert the optimization problem in (1) into an *edge-visibility* problem using the concepts and techniques from computational geometry. More specifically, "*a* is *visible* from *b*" means there exists a straight-line path connecting *a* and *b*, where *a* and *b* can be points, edges, polygons or any combination of them. If the edge $\overline{p_N^+ p_N^-}$ is invisible from $e = \overline{p_1^+ p_1^-}$, then the whole polygon $P(\varepsilon)$ can be divided into two parts: the *visible polygon* and the *invisible polygon*. The intersection of the boundaries of the visible and invisible polygons is called the *window* from the edge e in the polygon P.

The Tunnel Algorithm (TA)

The tunnel algorithm goes through five steps as follows.

Step 1: Initialization. Form the upper and lower boundaries PL_ε^+ and PL_ε^- for the given data set $\{x_k, g(x_k)\}, k=1,2,...,N$. The initial tunnel is $P_1 = P(\varepsilon)$. Set the edge $e_1 = \overline{p_1^+ p_1^-}$ and $i=1$.

Step 2: Searching.

WHILE $\overline{p_N^+ p_N^-}$ is not visible from e_i in polygon P_i DO

e_{i+1} = window from e_i to $\overline{p_N^+ p_N^-}$ in polygon P_i;

This work is supported in part by the Macau Science and Technology Development Fund under Grant FDCT/017/2007/A and the University of Macau Research Committee under Grant RG076/07-08S/WF/FST.

P_{i+1} = invisible polygon of e_i containing $\overline{p_N^+ p_N^-}$ in polygon P_i;

q_i = point of intersection of the line containing e_{i+1} and the edge e_i;

$i = i+1$.

Step 3: Output the searching results. $m = i+1$; find a point q_{m-1} on the edge e_i and a point q_m on the edge $\overline{p_N^+ p_N^-}$ that are visible from each other within the polygon P_{m-1}.

Step 4: Use the data at the points $q_l, l = 1,2,\cdots,m$, to compute the parameters $\{a_l, b_l\}$ of the line segments $\overline{q_l q_{l+1}}$, for $l = 1,2,\cdots,m-1$.

Step 5: Determine the minimum rule number and compute the parameters for the Mamdani type fuzzy system. According to Theorem 1 in [17], the number of fuzzy rule M equals m+1. The centers of M fuzzy sets in the IF part can be expressed as $A_l = x(q_l), l = 1,2,\cdots,M$. The corresponding centers of M fuzzy sets in the THEN part is $y_l = y(q_l), l = 1,2,\cdots,M$. With $x(q_l)$ and $y(q_l)$ standing for the coordinate values of point q_l, the l-th rule can be expressed as

$$R_l: \text{IF}(x \text{ is } A_l), \text{THEN}(y \text{ is } y_l). \quad (2)$$

The number of the rules extracted by the tunnel algorithm has been proved to be the minimum in [17].

Remark 1: The original tunnel algorithm gives an optimal solution to the problem (1) restricted inside the tunnel; however, this solution can be further improved. According to the optimization problem (1), the built fuzzy system is constrained to the accuracy requirement on the N output values observed at the input values $x_k, k = 1,2,\cdots,N$, and no more information other than these discrete points is available, thus no further restriction is necessary. Therefore, except at these N discrete points $x_k, k = 1,2,\cdots,N$, the upper and lower boundaries of the tunnel, need not to be considered as constraints for accuracy. Next section begins with a modification aiming at breaking the tunnel and the consequent limitation aforementioned, to improve the original algorithm for a better result.

II. Testing Point Algorithm

In this section, two examples in [17] are first revisited, to show the above-mentioned restriction due to the tunnel, and the modification is proposed to break the restriction. Then, in order to extend the algorithm for the design of Takagi-Sugeno (TS) type fuzzy system, an algebraic approach is proposed which can be used to construct TS type fuzzy system with any-order consequences.

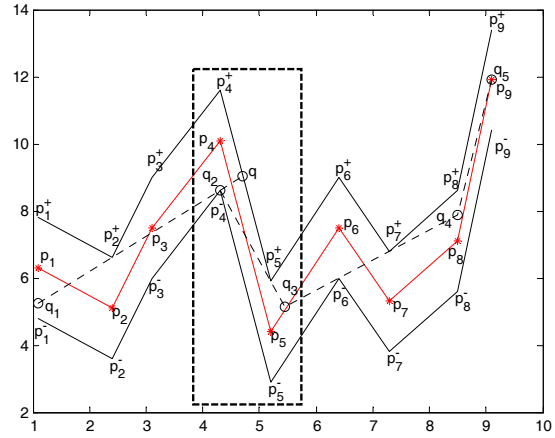

Fig. 1. Result of the tunnel algorithm. (red "*" : the available data points; dashed line: the output of the fuzzy system)

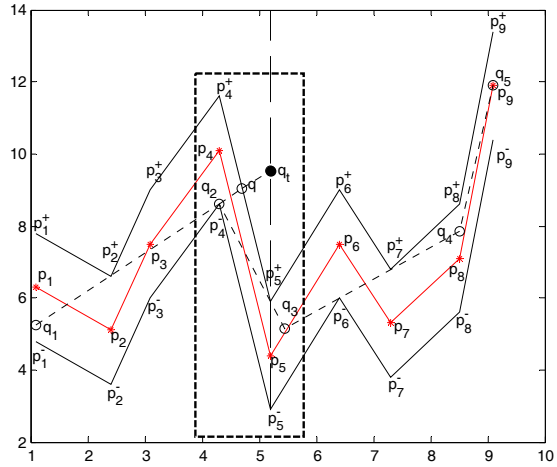

Fig. 2. Illustration of how to remove the restriction due to the tunnel.

Example 1 [17]: Construct a standard Mamdani type fuzzy system given the following nine pairs of input-output data:

$$\left\{\begin{matrix}(1.1,6.3),(2.4,5.1),(3.1,7.5),(4.3,10.1),(5.2,4.4)\\(6.4,7.5),(7.3,5.3),(8.5,7.1),(9.1,11.9)\end{matrix}\right\}.$$

The number of rules in the fuzzy system should be minimal, while the approximation error should be less than 1.5. The result of the tunnel algorithm is shown in Fig. 1.

The initial edge is the line segment $e = \overline{p_1^+ p_1^-}$. Because $\overline{p_N^+ p_N^-}$ is invisible, the whole polygon should be divided into two parts to form a window for the next search. Tunnel algorithm finds the line segment $\overline{p_4^- q}$ as the first window. Within the square area in Fig. 1, obviously the end point q of the window determined by the tunnel degrades the optimality. If the tunnel boundaries can be broken, the new constructed window will have a wider field of vision. This improved window begins with p_4^- and ends at the point intersected by $x = x_5$ (see Fig. 2 for details, where $\overline{p_4^- q_t}$ is the improved window). As stated in Remark 1, whether the output of the

fuzzy system goes through the line segments $\overline{p_4^+ p_4^-}$ and $\overline{p_5^+ p_5^-}$ is the only concern on accuracy, since what response in between the region (x_4, x_5) does not violate the accuracy tolerance. Example 1 shows the idea of the modification, its performance is to be elaborated through a comparison study in the next example.

Example 2 [17]: A standard Mamdani type fuzzy system is constructed to model an unknown plant described by the nonlinear function $g(x) = \cos\left(\left(e^x\right)^2\right)$. The modeling error tolerance is $\varepsilon = 0.05$. A set of input-output pairs of the plant are provided, in which the inputs x_k are evenly distributed in the interval $[0,2]$ with space 0.05. Fig. 3 shows the response of the final fuzzy system developed by the original tunnel algorithm while Fig. 4 shows the results from the improved tunnel algorithm. Red "*" represents the sampling data, boundaries of the tunnel are depicted by black lines, black circles are the *q's* with each of which one can conclude a fuzzy rule, and the output of the fuzzy system is drawn by dashed lines. The areas marked by blue dashed ellipses show the improvement owning to the proposed algorithm. In or near the marked areas, there may be a rule reduction due to the improvement through tunnel breaking. It is clear that in most of the areas the number of *q* points for rules in Fig. 4 is less than that in Fig. 3. In fact, the original tunnel algorithm extracts 25 fuzzy rules while the improved algorithm finally extracts only 19.

The above example shows a large improvement of the proposed algorithm in determining the minimum number of fuzzy rules. However, the algorithm is based on the computational geometry, which is not easy for further extension to high-order or high-dimension cases. In what follows, the strategy using visibility concepts from computational geometry will be reformulated and extended to the design of TS type fuzzy systems, which are much more widely used than Mamdani type fuzzy systems in real applications.

Compared with Mamdani type fuzzy systems, the major difference is that the consequent parts of a TS type fuzzy system are polynomial functions of its inputs. Consider the simplest case, where the *l-th* rule of a TS type fuzzy system is in the form of

$$R_l: \text{IF}\left(x \text{ is } A_l\right), \text{ THEN}\left(y = f_l(x)\right) \tag{3}$$

with linear consequent parts $f_l(x) = \beta_1^l x + \beta_2^l$, where β_1^l and β_2^l are constant coefficients.

Replacing the rule base (2) with (3) in the fuzzy system results in a first order TS type fuzzy system, which means the consequent part of each rule is a first order polynomial function of its inputs. If for simplicity the triangular membership functions are used, the mapping defined by this first order TS type fuzzy system becomes

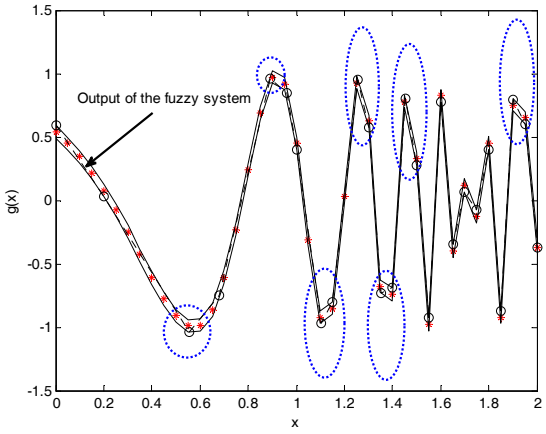

Fig. 3. Result by the tunnel algorithm in Example 2.

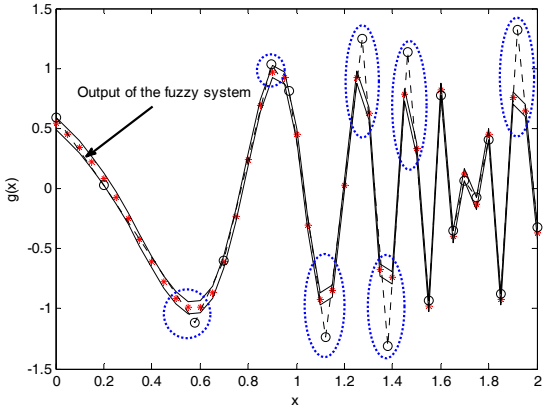

Fig. 4. Result by the improved tunnel algorithm in Example 2.

$$f(x) = \frac{\sum_{l=1}^{M}\left(f_l(x)\mu_{A_l}(x)\right)}{\sum_{l=1}^{M}\mu_{A_l}(x)}. \tag{4}$$

Theorem 1: The TS type fuzzy system in (4) draws piecewise parabolas, and the number of rules used in the fuzzy system is equal to the number of the segments plus one.

Proof: Because of the localization property of the triangular membership function, among all the membership values $\mu_{A_l}(x)$ for any x, at most two but at least one value will be nonzero while the others are zero. Therefore, the input domain can be decomposed as $D = D^1 \cup \cdots \cup D^{M-1}$, where $D = [x_{\min}, x_{\max}]$ and $D^l = [d_l, d_{l+1}], l = 1,2,\cdots,M-1$. For any $x \in D^l$, it is known that $\mu_{A_l}(x) + \mu_{A_{l+1}}(x) = 1$, so the fuzzy system (4) in D^l can be simplified as

$$\begin{aligned} f(x) &= \sum_{j=1}^{M} f_j(x)\mu_{A_j}(x) = \sum_{j=l}^{l+1} f_j(x)\mu_{A_j}(x) \\ &= \left(1 - \frac{x-d_l}{\Delta d_l}\right)\left(\beta_1^l x + \beta_2^l\right) + \frac{x-d_l}{\Delta d_l}\left(\beta_1^{l+1} x + \beta_2^{l+1}\right) \\ &= \frac{\beta_1^{l+1} - \beta_1^l}{\Delta d_l}x^2 + \frac{\beta_1^l d_{l+1} - \beta_1^{l+1} d_l + \beta_2^{l+1} - \beta_2^l}{\Delta d_l}x + \frac{\beta_2^l d_{l+1} - \beta_2^{l+1} d_l}{\Delta d_l} \end{aligned} \tag{5}$$

Therefore, the fuzzy system over the whole domain D consists of $M-1$ pieces of parabolas. This proves the theorem. □

The judging of visibility from geometry point of view for parabola curves is quite difficult. In the following, an algebraic approach is proposed to convert the edge-visibility problem into a Testing Point problem which can be easily extended to any order TS type fuzzy system. The following notations and theorems are necessary and straightforward.

Let the (n-1)-*th* order polynomial function be ($n \geq 2$)

$$p(x) = a_1 x^{n-1} + a_2 x^{n-2} + \cdots + a_{n-1} x + a_n , \quad (6)$$

where $a_i, i = 1, \cdots, n$, are the constant coefficients.

Theorem 2: To determine the coefficients of an (n-1) order ($n \geq 2$) polynomial curve characterized by $p(x)$, n distinct samples on this curve are required.

Proof: Substituting n distinct samples to the polynomial function gives n linear independent equations. Thus, the n coefficients $\{a_1, a_2, \cdots, a_n\}$ can be computed by solving the linear equations. This proves Theorem 2. □

Theorem 3: If a polynomial function $p(x)$ in (6) is specified by n distinct samples $(x_k, y_k'), k = 1, 2, \cdots, n$, then $y = p(x_{n+1})$ that $p(x)$ can generate at the point x_{n+1} can be written as a weighted linear combination of y_k', $k = 1, 2, \cdots, n$, i.e. $y = c_1 y_1^{'} + c_2 y_2^{'} + \cdots + c_n y_n^{'}$, where c_i, $i = 1, 2, \cdots, n$, are constants which are determined by the samples.

Proof: In view of linear dependency, the conclusion is apparent. The following deduces an exact expression of the linear combination. Substituting $(x_k, y_k'), k = 1, 2, \cdots, n$, to (6) results in n linear equations. Let $\mathbf{A} = [a_1, a_2, \cdots, a_n]^T$, $\mathbf{Y} = [y_1^{'}, y_2^{'}, \cdots, y_n^{'}]^T$ and $\mathbf{X} = \begin{bmatrix} x_1^{n-1} & x_1^{n-2} & \cdots & x_1 & 1 \\ x_2^{n-1} & x_2^{n-2} & \cdots & x_2 & 1 \\ \vdots & \vdots & \vdots & \vdots & \vdots \\ x_n^{n-1} & x_n^{n-2} & \cdots & x_n & 1 \end{bmatrix}$.

The linear equations can be written as

$$\mathbf{XA} = \mathbf{Y} , \quad (7)$$

and $\mathbf{X}$ can be treated as a Vandermonde matrix with $\det(\mathbf{X}) = \prod_{1 \leq i < j \leq n} (x_i - x_j)$.

Since the n samples are different, i.e. $x_i \neq x_j$ when $i \neq j$, $\det(\mathbf{X}) \neq 0$. Hence, $\mathbf{X}$ is invertible.

Denote $\mathbf{IX} = \mathbf{X}^{-1}$, then matrix $\mathbf{A}$ can be obtained from $\mathbf{A} = \mathbf{IX} * \mathbf{Y}$ and its *k-th* element ($k = 1, 2, \cdots, n$) can be expressed as

$$a_k = \mathbf{IX}(k,1) \cdot y_1' + \mathbf{IX}(k,2) \cdot y_2' + \cdots + \mathbf{IX}(k,n) \cdot y_n' . \quad (8)$$

Therefore,

$$y = p(x_{n+1}) = a_1 x_{n+1}^{n-1} + a_2 x_{n+1}^{n-2} + \cdots + a_{n-1} x_{n+1} + a_n . \quad (9)$$

Substituting (8) to (9) and performing simplification gives

$$y = c_1 y_1^{'} + c_2 y_2^{'} + \cdots + c_n y_n^{'} \quad (10)$$

where

$$c_k = \mathbf{IX}(1,k) \cdot x_{n+1}^{n-1} + \mathbf{IX}(2,k) \cdot x_{n+1}^{n-2} + \cdots + \mathbf{IX}(n-1,k) \cdot x_{n+1} + \mathbf{IX}(n,k), \quad k = 1, 2, \cdots, n$$

are constants. □

Following the edge-visibility strategy, notations (p and q) have the same meaning as the original tunnel algorithm, and the window e_k, $k \geq 2$ (e_1 is a line segment for initialization), which is a matrix consists with n different points, is the *k-th* polynomial curve found by the algorithm. Theorem 3 reveals the idea of the testing point algorithm. More specifically, equation (10) shows that the value $y = p(x_{n+1})$ at the point x_{n+1} is a weighted linear combination of y_k''s , $k = 1, 2, \cdots, n$, i.e. $y = c_1 y_1^{'} + c_2 y_2^{'} + \cdots + c_n y_n^{'}$ where $c_i, i = 1, 2, \cdots, n$ are constants already fixed by the n samples. When x_k is given and fixed, the only changeable values are the y_k''s which are constrained by the error bands as $y_k' \in [g(x_k) - \varepsilon, g(x_k) + \varepsilon]$. Each combination of the n y_k''s represents a normal polynomial curve, therefore all the combinations of y_k''s form a family of curves.

Definition 1: The data point $p_j = (x_j, g(x_j))$ is *reachable* by a curve family means that its range, in which this curve family and the line $x = x_j$ intersect, has a non-empty intersection with the tolerance band $[g(x_j) - \varepsilon, g(x_j) + \varepsilon]$.

The above range of the curve family can be derived directly from (10), as equation (10) is apparently continuous and its extreme points can be easily computed based on the signs of c_k's . For instance, if c_k's are all positive, the upper limit of the range $y_j^{\max}$ can be calculated when all the y_k''s are equal to their upper limits $g(x_k) + \varepsilon$ and the lower limit of the range $y_j^{\min}$ is calculated when all the y_k''s are equal to their lower limits $g(x_k) - \varepsilon$. Because of the continuity in (10), the range can be written as $[y_j^{\min}, y_j^{\max}]$ whose limits are determined by only the limits of its variables y_k''s . With the help of the above definitions, theorems and proofs, the following testing point algorithm is thus straightforward.

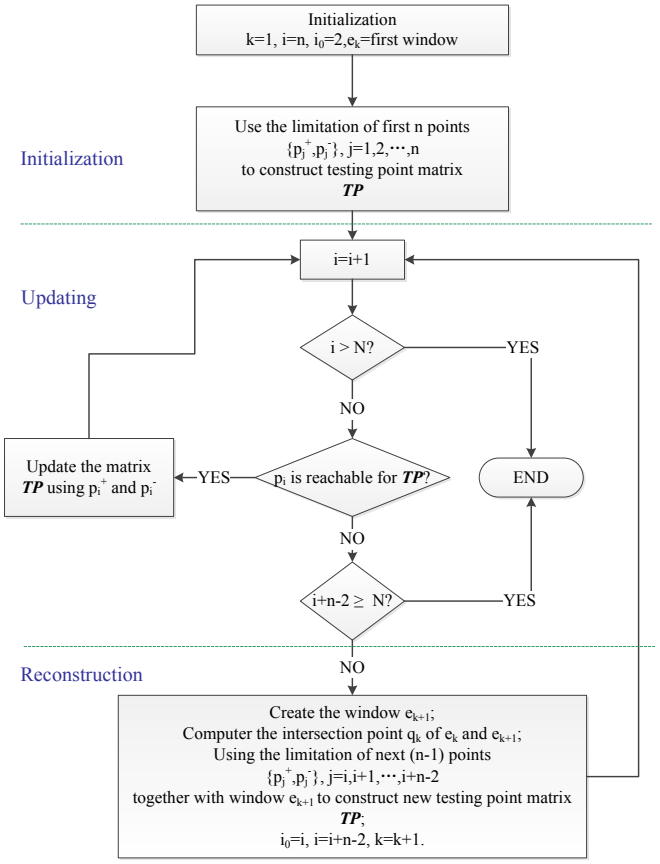

Fig. 5. Flowchart of the proposed testing point algorithm, where *TP*: the matrix stores the polynomials to be checked; *k*: the index of the created windows; *i*: the index of the sampling data; i_0: the index of the first sampling data to be checked from the current window; e_k: the *k-th* window.

The Testing Point Algorithm (TPA)

Step 1: Initialization. Set $k=1,\ i_0=2,\ i=n,\ e_k=\{p_1^+, p_1^-\}$, the array **isReachable** $=0^{N\times 1}$. Form the testing point matrix $\mathbf{TP}\in R^{2^n\times n}$ which consists with all the combinations of the upper and lower limits of the first *n* points shown below.

$$\mathbf{TP}=\begin{bmatrix} p_1^+ & p_2^+ & \cdots & p_n^+ \\ \vdots & \vdots & \vdots & \vdots \\ p_1^+ & p_2^- & \cdots & p_n^- \\ p_1^- & p_2^- & \cdots & p_n^- \end{bmatrix} \tag{11}$$

Step 2: Judging. $i=i+1$. If $i>N$, go to Step 5. Otherwise, determine whether the point p_i is reachable or not. If p_i is reachable, set **isReachable**$(i)=1$ and go to Step 3; otherwise, set **isReachable**$(i)=0$ and go to Step 4.

Step 3: Updating. Since p_i is reachable, use $\{p_i^-, p_i^+\}$ to update **TP** through the following procedure.

Replacing all the elements in a column in **TP** with p_i^+ creates a submatrix. Therfore, the replacement of the *n* columns leads to *n* submatrices. The same number of submatrix is obtained when using p_i^- for replacement. The updated $\mathbf{TP}_{updated}$ are constructed by combining all of the submatrices and the original **TP**. As several rows may be the same in the $\mathbf{TP}_{updated}$, it is necessary to remove the redundant rows from $\mathbf{TP}_{updated}$. Each row of $\mathbf{TP}_{updated}$ represents a normal polynomial curve, and all of the polynomial curves are checked one by one to see whether the points $p_{i_0}, p_{i_0+1},\cdots, p_i$ are all reachable from the selected polynomial curve. If not, the corresponding row in the $\mathbf{TP}_{updated}$ is removed. After this procedure, set $\mathbf{TP}=\mathbf{TP}_{updated}$ and finish the updating step.

Step 4: Reconstruction. This step handles the **TP** construction when the judging step finds immediately p_i not reachable. It needs (*n*-1) new points together with the window e_{k+1} to reconstruct the **TP** for testing on the next samples. If $i+n-2\geq N$ which means the remaining data points are just enough to form one polynomial function, go to Step 5 to finish. Otherwise, reconstruct the testing point matrix **TP**.

The reconstruction is very similar to Step 1. The difference is that the first point p_{fst} is the limit point from the area that the window e_{k+1} is able to cover, instead of the limit points of the line segment such as $\overline{p_1^- p_1^+}$.

Select the polynomial function e_{k+1} which is the closest one to the point p_i from **TP**. Theorem 3 shows that **TP** consists with several limit points. Pick the point p_{fst}^1 with the largest value in *x*-axis from e_{k+1}, then calculate the intersection point p_{fst}^{end} between e_{k+1} and the line $\overline{p_i^- p_i^+}$. The limit points of the reachable points **rP** from e_{k+1} in between the range $\left[p_{fst}^1, p_{fst}^{\text{end}}\right]$ are treated as the elements of p_{fst}. Then, the upper and lower limits of next (*n*-1) points together with p_{fst} are used to construct the new **TP** in the form of (11). There may be some illegal rows constructed from which the polynomial function violates the accuracy requirement. The **TP** is therefore checked, by testing whether the points in **rP** are all reachable from the polynomial under checking or e_{k+1}. If not reachable, the row is considered as illegal and thus removed. This constructs a new **TP** for the test on the next samples.

q_k can be calculated as the intersection between e_{k+1} and e_k. Set $i_0=i, i=i+n-2, k=k+1$.

Step 5: End. This is the ending process, where the last polynomial function e_{k+1} is found with its range $[q_k, q_{k+1}]$ for the fuzzy system.

If $i>N$ (jumped from Step 2), which means the last point p_N is reachable from the current **TP**, then find a representative one e_{k+1} from the **TP** which reaches p_N. A

typical choice is the one who is the closest to p_N. Then, calculate the q_k where e_k and e_{k+1} intersect. The final point q_{k+1} is the intersection between e_{k+1} and the line segment $\overline{p_N^- p_N^+}$.

If $i \le N$ (jumped from Step 4), which means the point p_i is not reachable but p_{i-1} is reachable from the current **TP** and the number of remaining un-judged sample points is equal or less than n, then we need to construct the e_{k+1} as $e_{k+1} = \{q_k, p_i, p_{i+1}, \cdots, p_N\}$ where q_k is the intersection between e_k and the line segment $\overline{p_{i-1}^- p_{i-1}^+}$. If the elements of e_{k+1} are not enough to determine a polynomial function, the designer can arbitrarily add some points into it (this will not affect the fuzzy rule number). A typical suggestion is to select the midpoints of line segments $\overline{p_{i+j} p_{i+j+1}}, j = 0,1,\cdots, N-i-1$.

Step 6: This step determines the minimum rule number and computes the parameters in the TS type fuzzy system. From the above five steps, q_j are used to store the partitions of the fuzzy sets and e_{j+1} to store the outputs in the range $x \in [q_j, q_{j+1}]$, $j = 1,2,\cdots,k$. For (n-1)-*th* order TS type fuzzy system, each e_{j+1} contains (n+1) points, while the response within this area is interacted by the two rules j and (j+1) each of which has n parameters. In total, there are 2n parameters to be computed. Obviously, when $2n > (n+1)$, i.e. $n \ge 2$, the solution is not unique. The reason is that the parameters $\{\beta_i^1\}, i = 1,2,\cdots,n$ of the first rule can be only evaluated through the first area $[q_1, q_2]$. Since the degree of freedom is more than the number of equations, the solution can only show a relationship between $\{\beta_*^1\}$ and $\{\beta_*^2\}$ (Subscript "*" represents an index in $[1,2,\cdots,n]$), the solution in $[q_2, q_3]$ gives a relationship between $\{\beta_*^2\}$ and $\{\beta_*^3\}$, and similarly in all areas $[q_j, q_{j+1}]$, $j = 1,2,\cdots,k$. The sets of parameters are nesty related: if one is specified, all of the rest can be determined uniquely. A suggested choice for simplicity is to let the first rule be

$$\text{IF}\left(x \text{ is } A_1\right), \text{ THEN}\left(y = y\left(q_1\right)\right), \tag{12}$$

and then all the parameters can be determined.

The flowchart of the proposed testing point algorithm for (n-1)-*th* order TS type fuzzy system is given in Fig. 5.

Remark 2: No matter what parameters of the final fuzzy system are determined through the above algorithm, the number of the rules can be guaranteed to be the minimum, which is of the most importance and the target of this research.

Remark 3: In most applications, TS type fuzzy systems with first order consequent parts are used, although less fuzzy rules may be needed if the order of the consequences is increased, because higher order interpolation may increase the computational complexity and cause the so-called Runge's phenomena (artificial oscillations with amplitude increasing with the degree of the interpolating polynomial) [17] which are not preferred. Nevertheless, in some special cases, to model highly nonlinear systems for instance, higher order TS type fuzzy system may be adopted, for which the solution to the design (based on maximal absolute error and minimum number of rules) is also provided by the proposed testing point algorithm.

III. Simulation Results

The testing point algorithm works for the (n-1)-*th* order TS type fuzzy system in modeling and identification. In the following, we just demonstrate the algorithm for modeling with the first order TS type fuzzy system, suggested by Remark 3.

Example 3 [17]: Consider the same problem in Example 2, the process to be modeled is characterized by $g(x) = \cos\left(\left(e^x\right)^2\right)$. Fig. 6 gives the final result and Fig. 7 shows the partitions of the input domain and the membership functions obtained from q_k's.

Eventually 12 fuzzy sets $\{A_1, A_2, \cdots, A_{12}\}$ are found centered at:

$$\begin{aligned}\{\alpha_1, \alpha_2, \cdots, \alpha_{12}\} = \{&0, 0.549, 0.876, 1.084, 1.237, 1.380,\\ &1.543, 1.650, 1.750, 1.850, 1.950, 2.000\}\end{aligned} \tag{13}$$

The l-th rule ($l = 1,2,\cdots,12$) of the first order TS type fuzzy system is in the form of

$$R_l\text{: IF}\left(x \text{ is } A_l\right), \text{THEN}\left(y \text{ is } \beta_1^l x + \beta_2^l\right), \tag{14}$$

where β_1^l and β_2^l are constants.

In the partitions $[\alpha_l, \alpha_{l+1}], l = 1,2,\cdots,k$, the output of the fuzzy system can be derived from (6), which can be re-written as

$$\begin{aligned} f_l(x) = &\frac{\beta_1^{l+1} - \beta_1^l}{\alpha_{l+1} - \alpha_l} x^2 \\ &+ \frac{\beta_1^l \alpha_{l+1} - \beta_1^{l+1} \alpha_l + \beta_2^{l+1} - \beta_2^l}{\alpha_{l+1} - \alpha_l} x + \frac{\beta_2^l \alpha_{l+1} - \beta_2^{l+1} \alpha_l}{\alpha_{l+1} - \alpha_l}. \end{aligned} \tag{15}$$

Substituting all the points stored in $e_{l+1}, l = 1,2,\cdots,11$ to (14) with corresponding l generates in total 12 linear equations. According to (12), let $\beta_1^1 = 0, \beta_2^1 = y\left(q_1\right)$. It is easy to solve the equations and finally obtain all the remaining parameters $\{\beta_1^l, \beta_2^l\}, l = 2,3,\cdots,12$. The 12 fuzzy rules can then be concluded as

$$R_1\text{: IF}\left(x \text{ is } A_1\right), \text{THEN}\left(y = 0 \cdot x + 0.5903\right)$$

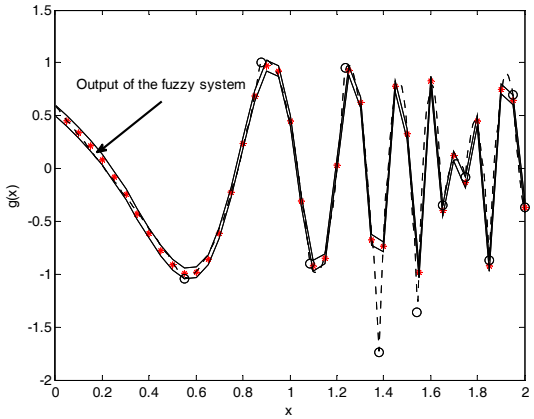

Fig. 6. First order TS type fuzzy system constructed in Example 3.

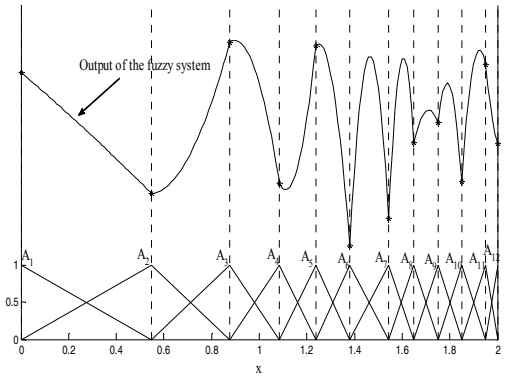

Fig. 7. The partitions of the input domain and the output of the fuzzy system in Example 3.

$$R_2\text{: IF}\left(x \text{ is } A_2\right), \text{THEN}\left(y = -0.2607x - 0.8981\right)$$

$$R_3\text{: IF}\left(x \text{ is } A_3\right), \text{THEN}\left(y = 5.5178x - 3.8344\right)$$

$$R_4\text{: IF}\left(x \text{ is } A_4\right), \text{THEN}\left(y = -5.8993x + 5.4988\right)$$

$$R_5\text{: IF}\left(x \text{ is } A_5\right), \text{THEN}\left(y = 12.7912x - 14.8718\right)$$

$$R_6\text{: IF}\left(x \text{ is } A_6\right), \text{THEN}\left(y = -10.0108x + 12.0781\right)$$

$$R_7\text{: IF}\left(x \text{ is } A_7\right), \text{THEN}\left(y = -67.8593x + 103.3699\right)$$

$$R_8\text{: IF}\left(x \text{ is } A_8\right), \text{THEN}\left(y = -128.1263x + 211.0606\right)$$

$$R_9\text{: IF}\left(x \text{ is } A_9\right), \text{THEN}\left(y = -139.3971x + 243.8665\right)$$

$$R_{10}\text{: IF}\left(x \text{ is } A_{10}\right), \text{THEN}\left(y = -174.5493x + 322.0426\right)$$

$$R_{11}\text{: IF}\left(x \text{ is } A_{11}\right), \text{THEN}\left(y = -206.1204x + 402.6349\right)$$

$$R_{12}\text{: IF}\left(x \text{ is } A_{12}\right), \text{THEN}\left(y = -195.4124x + 390.4542\right)$$

where $\{A_1, A_2, \cdots, A_{12}\}$ are shown in Fig. 7 with centers in (13). As shown in Fig. 6, for the training data, the maximal absolute error is less than $\varepsilon = 0.05$. Table 1 concludes the results from different algorithms for the same modeling problem and clearly shows the improvement of the proposed testing point algorithm.

Table 1: Numbers of Extracted Rules by Different Algorithms in Example 3

	Mamdani type Fuzzy System		TS type Fuzzy System
	Tunnel Algorithm	Testing Point Algorithm	Testing Point Algorithm
Number of Rules	25	19	12

IV. Concluding Remarks

An improved algorithm based on the geometric approach in [17] was proposed to build any order TS type fuzzy model with minimum number of rules and guaranteed approximation accuracy, from the input-output data of an unknown nonlinear system. Comparison study through numerical simulations demonstrates the effectiveness of the method.

This proposed testing point algorithm in its current format works only for SISO cases. Extension to higher dimension, i.e. MIMO (multiple-input-multiple-output) cases will greatly expand the applicability of the strategy and is a major concern for the future work.

References

[1] S. Aja-Fernandez and C. Alberola-Lopez, "Matrix modeling of hierarchical fuzzy systems," IEEE Transactions on Fuzzy Systems, vol. 16, no. 3, pp. 585-599, 2008.

[2] R. Babuška, Fuzzy Modeling for Control. Kluwer Academic Publishers, Boston, 1998.

[3] P. Baranyi, A. R. Varkonyi-Koczy, Y. Yam, and R. J. Patton, "Adaptation of TS fuzzy models without complexity expansion: HOSVD-based approach," IEEE Transactions on Instrumentation and Measurement, vol. 54, no. 1, pp. 52-60, 2005.

[4] P. Baranyi, Y. Yam, A. R. Varkonyi-Koczy, R. J. Patton, P. Michelberger, and M. Sugiyama, "SVD-based complexity reduction to TS fuzzy models," IEEE Transactions on Industrial Electronics, vol. 49, no. 2, pp. 433-443, 2002.

[5] Y. S. Ding, H. Ying, and S. H. Shao, "Necessary conditions on minimal system configuration for general MISO Mamdani fuzzy systems as universal approximators," IEEE Transactions on Systems, Man, and Cybernetics, Part B: Cybernetics, vol. 33, no. 6, pp. 857-864, 2000.

[6] K. Cpalka., "A new method for design and reduction of neuro-fuzzy classification systems," IEEE Transactions on Neural Networks, vol. 20, no. 4, pp. 701-714, 2009.

[7] A. Gegov, Complexity Management in Fuzzy Systems: a Rule Base Compression Approach, Springer, Berlin Heidel-berg, 2007.

[8] M. K. Güven and K. M. Passino, "Avoiding exponential parameter growth in fuzzy systems," IEEE Transactions on Fuzzy Systems, vol. 9, no. 1, pp. 194-199, 2001.

[9] H. Ishibuchi and T. Yamamoto, "Fuzzy rule selection by multi objective genetic local search algorithms and rule evaluation measures in data mining," Fuzzy Sets Systems, vol. 141, pp. 59-88, 2004.

[10] Y. C. Jin, "Fuzzy modeling of high-dimensional systems: Complexity reduction and interpretability improvement," IEEE Transactions on Fuzzy Systems, vol. 8, no. 2, pp. 212-221, 2000.

[11] M. G. Joo and T. Sudkamp, "A method of converting a fuzzy system to a two-layered hierarchical fuzzy system and its run-time efficiency," IEEE Transactions on Fuzzy Systems, vol. 17, no. 1, pp. 93-103, 2009.

[12] A. Riida and E. Rüsternb, "Identification of transparent, compact, accurate and reliable linguistic fuzzy models," Information Sciences, in press.

[13] M. Setnes, R. Babuška, U. Kaymak, and H. R. van Nauta Lemke, "Similarity measures in fuzzy rule base simplification," IEEE Transactions on System, Man, and Cybernetics B, vol. 28, no. 3, pp. 376-386, 1998.

[14] M. Setnes and R. Babuška, "Rule base reduction: some comments on the use of orthogonal transforms," IEEE Transactions on System, Man, and Cybernetics, Part C: Applications and Reviews, vol. 31, no. 2, pp. 199-206, 2001.

[15] T. Sudkamp, A. Knapp, and J. Knapp, "Model generation by domain refinement and rule reduction," IEEE Transactions on Systems, Man, and Cybernetics, Part B: Cybernetics, vol. 33, no. 1, pp. 45-55, 2003.

[16] T. Takagi and M. Sugeno, "Fuzzy identification of systems and its application to modeling and control," IEEE Transactions on Systems, Man, and Cybernetics, vol. 15, no. 1, pp. 116-132, 1985.

[17] F. Wan, H. L. Shang, L. X. Wang, and Y. X. Sun, "How to determine the minimum number of fuzzy rules to achieve given accuracy: a computational geometric approach to SISO case," Fuzzy Sets and Systems, vol. 150, no. 2, pp. 199-209, 2005.

[18] L. X. Wang, "Fuzzy systems are universal approximators," Proc. IEEE International Conf. on Fuzzy Systems, San Diego, pp. 1163-1170, 1992.

[19] L. X. Wang, "Analysis and design of hierarchical fuzzy systems," IEEE Transactions on Fuzzy Systems, vol. 7, no. 5, pp. 617-624, 1999.

[20] Y. Yam, P. Baranyi, and C. T. Yang, "Reduction of fuzzy rule base via singular value decomposition," IEEE Transactions on Fuzzy Systems, vol. 7, no. 2, pp. 120-132, 1999.

[21] J. Yen and L. Wang, "Simplifying fuzzy rule-based models using orthogonal transformation methods," IEEE Transactions on Systems, Man, and Cybernetics, Part B: Cybernetics, vol. 29, no. 1, pp. 13-24, 1999.

[22] J. Yen, L. Wang, and C. W. Gillespie, "Improving the interpretability of TSK fuzzy models by combining global learning and local learning," IEEE Transactions on Fuzzy Systems, vol. 6, no. 4, pp. 530-537, 1998.

[23] H. Ying, "Sufficient conditions on general fuzzy systems as function approximations," Automatica, vol. 30, no. 3, pp. 521-525, 1994.

[24] H. Ying, "Sufficient conditions on uniform approximation of multivariate functions by general Takagi-Sugeno fuzzy systems with linear rule consequent," IEEE Transactions on Systems, Man, and Cybernetics, Part A: Systems and Humans, vol. 28, no. 4, pp. 515-520, 1998.

[25] H. Ying, Fuzzy Control and Modeling: Analytical Foundations and Applications, IEEE Press, NewYork, 2000.

2011 IEEE International Conference on Fuzzy Systems
June 27-30, 2011, Taipei, Taiwan

Maximum Power Point Tracker for a PV Cell using a Fuzzy Agent adapted by the Fractional Open Circuit Voltage Technique

M. Adly
Information Engineering & Technology, GUC
Cairo, Egypt
moustafa.adly@guc.edu.eg

H. El-Sherif
Information Engineering & Technology, GUC
Cairo, Egypt
hisham.elsherif@guc.edu.eg

M. Ibrahim
Energy Management Dept.
Heilbronn University
Heilbronn, Germany
ibrahim@hs-heilbronn.de

***Abstract*— The Photovoltaic cells have P-V characteristics which indicate that there is only one point that produces a maximum output power. The point of the maximum power lies at the knee of the I-V curve. Tracking this point is a very important issue concerning the energy yield of the PV systems. One of the efficient tracking techniques is based on the Fuzzy agents which are able of fine tuning the cell operating voltage and current to keep the maximum possible output power. In this paper, a fuzzy agent with two input parameters enhanced by the fractional open circuit voltage technique will be used to track the MPP in a fast and accurate manner that is better than the traditional techniques. Assigning different weights for the two inputs of the fuzzy agent adapts the power response to achieve fast settling and accurate tracking of the cell maximum output power even under extreme variable atmospheric conditions in an efficient manner with better performance than conventional fuzzy MPPT technique.**

Keywords- Adaptive Fuzzy agent, Fractional Open circuit Voltage, Fuzzy Control, MPPT, Photovoltaic modules.

I. INTRODUCTION

Achieving the maximum possible output power from a PV module is an important aim in any PV system to compensate its initial cost. The task can be handled using a DC-DC converter with variable duty cycle D that is determined through a maximum power point tracker MPPT. The aim of the tracker is to vary the module operating current and voltage such that the maximum output power is achieved in a fast and accurate manner even under variable irradiance or temperature conditions. At the maximum power point, the power variation with respect to voltage variation or current variation is zero as will be seen. So, using this variation as an input signal to a fuzzy agent beside another input which is the variation of the first input helps the fuzzy agent to vary and fine tune the duty cycle of the DC-DC converter in a manner that keeps the maximum power transfer to the desired load even under large atmospheric variations. The usage of the fractional open circuit voltage is useful in reducing the searching and hence the settling times. The proposed technique has the advantage of fast settling and accurate tracking without steady state error.

II. MPPT TECHNIQUES

The I-V and P-V characteristics of the photovoltaic module under study are shown in fig. 1. The maximum power occurs at the knee of the I-V curve as shown in the same figure. The characteristics are for the module GUC09 of the commercial type *BP7185S-Saturn 7* series.

Many MPPT techniques were developed in the literature aiming at fast and accurate tracking. As in [1] and [2], some of them will be discussed.

A. Fractional Open-Circuit Voltage

This method uses the approximate ratio of the PV module maximum power point voltage V_{MPP} to the to its open circuit voltage V_{OC} which is nearly constant as a simple feed forward technique for tracking the maximum output power, as can be seen from (1).

$$V_{MPP} \approx K_1 \times V_{OC} \tag{1}$$

The factor K_1 has been reported to be between 0.71 and 0.78. Once the constant K_1 is calculated, V_{MPP} is computed by measuring V_{OC} periodically using pilot PV cells.

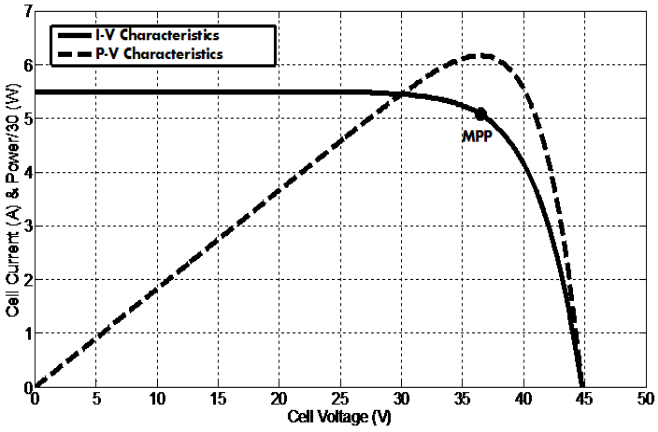

Fig. 1. I-V & P-V characteristics of a PV module

The problem is that the factor K_1 is temperature and irradiance dependent as was stated in [3] and hence the obtained results of such a technique are not accurate. Although the implementation of this method is simple and cheap, its tracking efficiency is relatively low due to the utilization of inaccurate values of the constant K_1 in the computation of V_{MPP}.

B. Fractional Short-Circuit Current

As in the fractional open circuit voltage, it was found also that the ratio between the maximum power point current and the short circuit current is also constant as in (2).

$$I_{MPP} = K_2 \times I_{SC} \tag{2}$$

Where I_{MPP} is the maximum power point current, I_{SC} is the short circuit current, and K_2 is the proportionality constant. According to [1], the constant K_2 ranges between 0.78 and 0.92 and depends on the PV module characteristics and the atmospheric conditions. The method depends on periodic measurements of the short circuit current as it is not fixed. The measurement of the short circuit current requires the usage of a pilot cell for periodic measurement. The method is then simple but needs a current sensor which is expensive and unreliable. The method can be either analog or digital. An atmospheric compensation for K_2 is proposed also in [4].

C. Perturb and Observe P&O

According to [5], the Perturb & Observe method operates by setting an initial operating voltage for the PV module and then a perturbation or voltage change is made and afterwards an observation for the power is made. If the perturbation (voltage change) is positive (increase) and a positive observation (power increase) is detected, the next perturbation will be positive and if a negative observation is detected, the next perturbation will be negative. While if the perturbation is negative (decrease) and a positive observation is detected, the next perturbation will be negative and if a negative observation is detected, the next perturbation will be positive. Of course this is done by sampling both the PV current and voltage. The tracker operates by periodically incrementing or decrementing the solar module voltage. Actually, the system oscillates about the MPP. Reducing the perturbation step size can minimize the oscillation. However, small step size slows down the MPPT. To solve this problem, a variable perturbation size that gets smaller towards the MPP should be used. However, the P&O method can fail under rapidly changing atmospheric conditions. Several research activities have been carried out to improve the traditional Hill-climbing and P&O methods.

D. Incremental Conductance

The method is based on the principle that the slope of the PV module power curve is zero at the maximum power point. In this method, the operating voltage is changed until dP/dV equals zero which occurs at the maximum power point as stated in [6]. Using fig.1, the ratio $\Delta P/\Delta V$ follows one of the cases described in (3). The incremental conductance method requires both voltage and current sensors in addition to a DSP or microcontroller. This method is a digital tracking method not an analog one and hence cost factor may be taken into consideration. The accuracy of this technique is good but it is usually better when combined with the P&O MPPT technique.

$$\begin{cases} \dfrac{\Delta P}{\Delta V} = 0, \textit{ at MPP} \\ \dfrac{\Delta P}{\Delta V} > 0, \textit{ left of MPP} \\ \dfrac{\Delta P}{\Delta V} < 0, \textit{ right of MPP} \end{cases} \tag{3}$$

III. PROPOSED MPPT TECHNIQUE

Using (3) and fig. 1, the parameter $\Delta P/\Delta V$ will be defined as the error signal E which should be equal to zero for best performance and it will be fed to a Fuzzy agent for the purpose of maximum power point tracking. At the maximum power point, the error signal equals zero and hence it is desired to keep the error signal at zero value in order to track the MPP. For fine tuning, the variation of the error signal ΔE is defined as a second input for the fuzzy agent. For simulation purposes, the PV model driven in [7] and [8] will be adapted to the available practical module and will be used. According to [1], the error E and its change ΔE can be defined by (4) and (5) respectively.

$$E(k) = \frac{P(k) - P(k-1)}{V(k) - V(k-1)} \tag{4}$$

$$\Delta E(k) = E(k) - E(k-1) \tag{5}$$

The fuzzy knowledge-base controller is one part of Fuzzy Logic Control which is composed of three main parts: fuzzification, inference engine, and defuzzification as in [9].

A. Fuzzification

Membership function values are assigned to the linguistic variables, using five fuzzy subsets: NB (negative big), NS (negative small), ZE (zero), PS (positive small), and PB (positive big). The partition of fuzzy subsets and the shape of membership functions, which can adapt shape up to appropriate system, are shown in fig. 2.

The choice of the member ship functions is based on the error signal variations with voltage as can be seen from fig. 3.

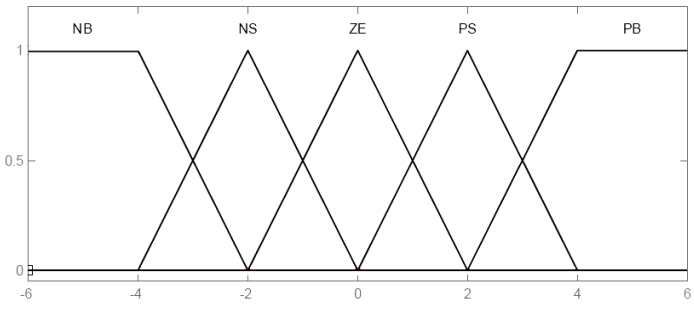

Fig. 2. Membership functions of E and ΔE

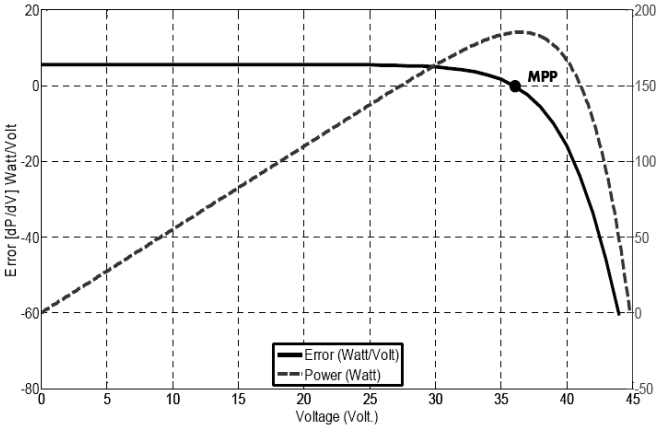

Fig. 3. Error Variations with the module voltage

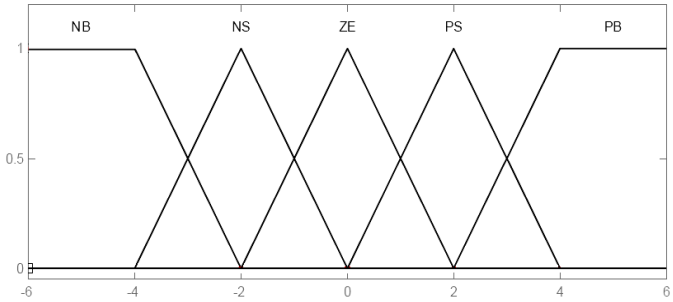

Fig. 4. Output Membership functions

The output (ΔV) membership functions are shown in fig. 4.

B. *Inference method*

As in [9], the composition operation is the method by which a control output is generated. Several composition methods such as Max–Min and Max-Dot have been proposed in the literature. The commonly used method, Max–Min, is used in this paper. The output membership function of each rule is given by the Min (minimum) operator and Max (maximum) operator. Table 1 shows the rule base of the FLC like some rules of [10]. The fuzzy rule base table depends basically on the error E variations with voltage change shown in fig. 3.
From fig. 3, it is clear that the error is positive constant till V=25 V and then it will be positive decaying till V=36 V (at MPP). After the MPP, the error is negative decaying. As long

TABLE I. FUZZY RULE TABLE

Error E	**Change of Error ΔE**				
	NB	***NS***	***ZE***	***PS***	***PB***
NB	NS	ZE	PB	PB	PB
NS	ZE	ZE	PS	PS	PS
ZE	PS	ZE	ZE	ZE	NS
PS	NS	NS	NS	ZE	ZE
PB	NB	NB	NB	ZE	PS

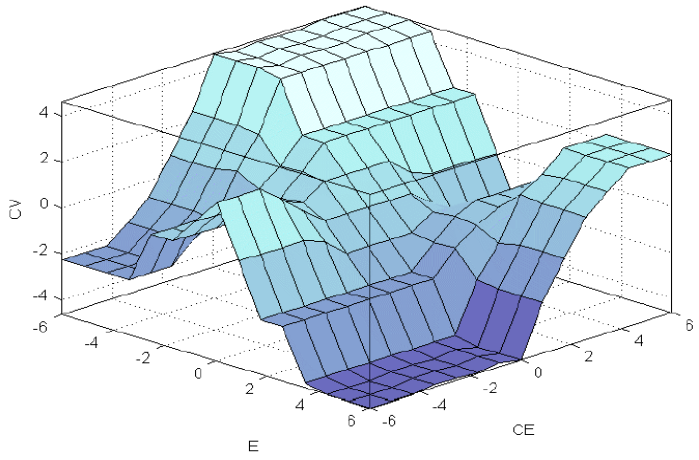

Fig. 5. Fuzzy Rule Surface

as the error is positive, the voltage should be increased and the rate of increase depends on the rate of change of the error signal ΔE which is used for fine tuning. When the error is negative, the voltage should be decreased and the rate of decrease depends on the fine tuning factor (ΔE).
The control rule surface is shown in fig. 5.

C. *Defuzzification*

The output of this fuzzy controller is a fuzzy subset of control. To get a non-fuzzy value of control, a defuzzfication stage is necessary. Defuzzification for this system can be performed by height method. The non fuzzy value of control output can be gained using a discrete time integrator simply and quickly because the output is the voltage change ΔV.

A simple block diagram representation of the whole PV and MPPT system is shown in fig. 6. The controller is a fuzzy agent adapted by the fractional open circuit voltage technique to reduce the settling or tracking time by giving an initial estimation for the operating voltage. The technique is applied to the BP7185S-Saturn 7 series with the electrical characteristics shown in Table 2 with 72 series PV cells.
If no fractional open circuit voltage is used as the traditional fuzzy techniques, the power response of the module will have a large settling time (62 m sec) as shown in fig. 7 and hence the use of the fractional open circuit voltage leads to a faster power response as shown in fig. 8. The time step in the graph is (m sec) and it may depend on the used data acquisition system.

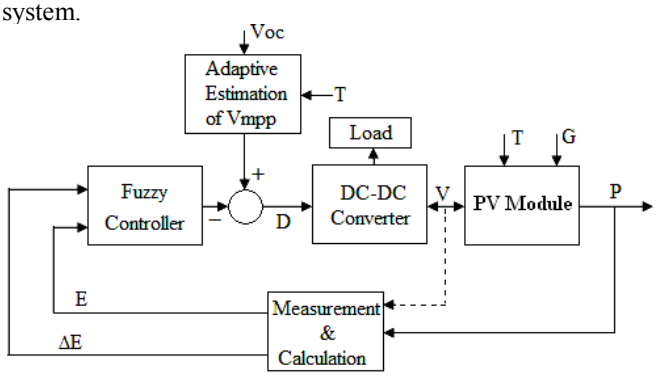

Fig. 6. PV MPPT System

TABLE II. ELECTRICAL CHARACTERISTICS OF BP7185S

Parameter	Value
Warranted minimum power	185 W
Voltage at MPP (V_{MPP})	36.5 V
Current at MPP (I_{MPP})	5.1 A
Open Circuit Voltage (V_{OC})	44.8 V
Short Circuit Current (I_{SC})	5.5 A
Temperature coefficient of V_{OC}	-(160±20)mV/K
Temperature coefficient of I_{SC}	(0.065±0.015)%/K
Temperature coefficient of P	-(0.5±0.05)%/K
NOCT (Air 20ºC; Sun 800W/m^2; wind 1m/s)	47±2 Cº
Maximum series fuse rating	15 A
Maximum System Voltage	1000 V (IEC 61215 rating)

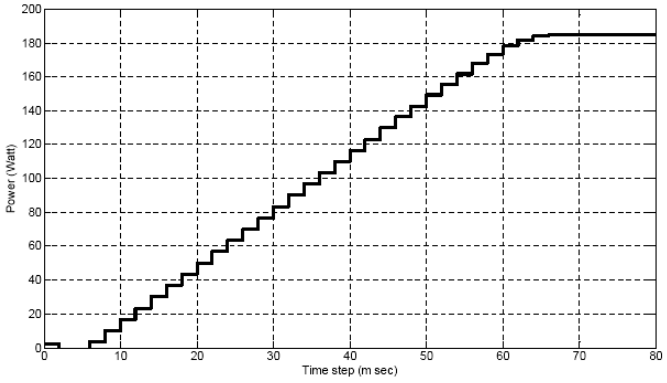

Fig. 7. Power response for no Fractional V_{OC}

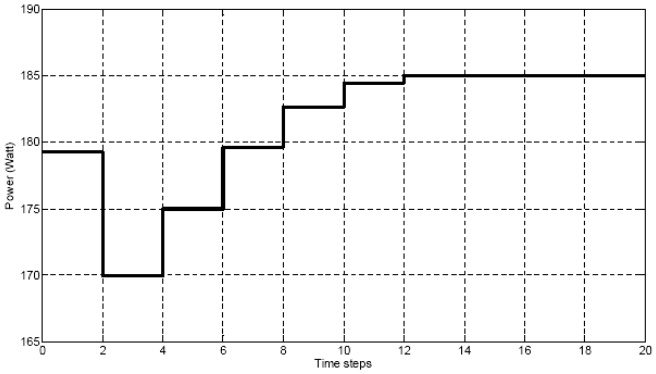

Fig. 8. Power response using Fractional V_{OC}

In fig. 8, there is no steady state error in the output power (which settles at 185 W) and the searching time is smaller than the traditional fuzzy method of fig. 7 by more than 50 m sec, which is a good improvement.

The fuzzy agent in turn controls the duty cycle of the DC-DC converter used for load matching in order to keep the operating point of the PV module at (V_{MPP}, I_{MPP}). For a load of 12 V DC as an example, the duty cycle will vary with time as shown in fig. 9 through a fuzzy agent adapted by fractional open circuit voltage.

Based on the adaptation idea developed in [11], another adaptation idea is to add different weights for the inputs of the fuzzy agent. The error signal should have the full weight while the fine tuning signal which is the change in the error signal

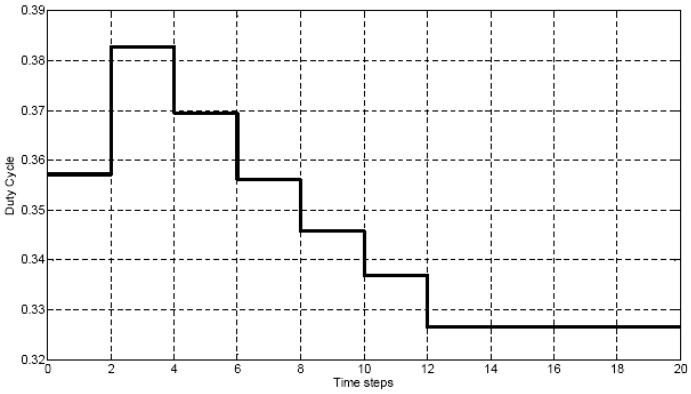

Fig. 9. Duty cycle variations using fractional V_{OC}

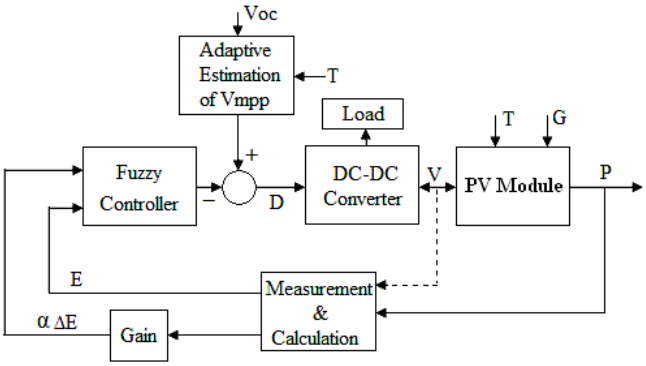

Fig. 10. Adaptive Fuzzy MPPT

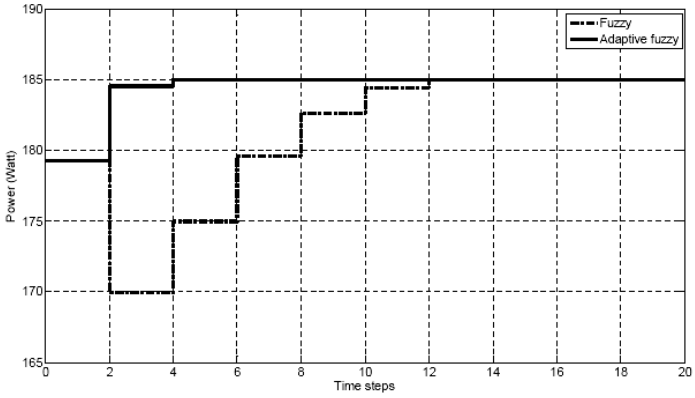

Fig. 11. Fuzzy vs. Adaptive fuzzy power response

may have a smaller weight compared to the error signal. The block diagram of the adaptive technique is shown in fig. 10.

The response of this case in comparison with the previous case is shown in fig. 11 knowing that both techniques use fractional open circuit voltage for initial estimation of V_{MPP}.

The proposed adaptive tracking technique shows a good response even under variable atmospheric conditions as can be seen in fig. 12.

Fig. 12 shows that the proposed technique is suitable for any atmospheric conditions such as variable module temperature or variable irradiance. The proposed technique has a better response under variable atmospheric conditions than the traditional MPPT technique driven in [12].

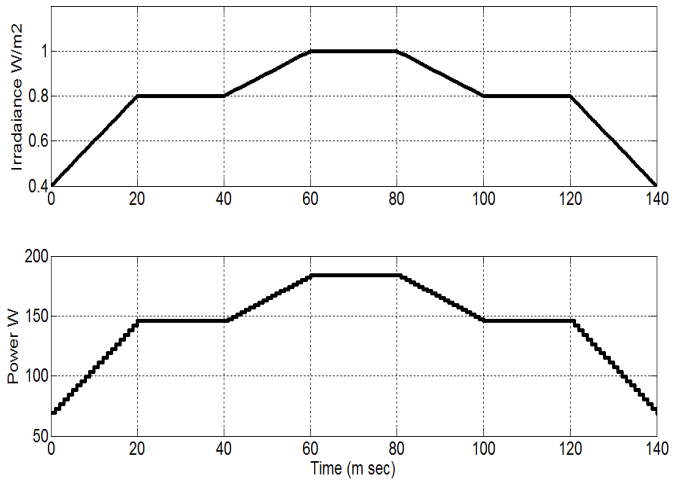

Fig. 12. Power response under variable irradiance

In the literature, the change in the converter duty cycle may be used as a third input for the fuzzy agent in order to improve the power response of the PV module but with more complexity. The tracking speed of the proposed technique is even better than the other traditional MPPT techniques like that in [2] which has a searching time of about 20 m sec.

A comparison between the traditional MPPT techniques and the newly adapted fuzzy technique based on [1] is given in table 3 where New fuzzy represents the developed technique.

TABLE III. COMPARISON BETWEEN MPPT TECHNIQUES

MPPT Technique	Module - dependent	True MPP	Tracking speed	Tracking accuracy	Atmospheric effect
Fractional V_{OC}	Yes	No	Medium	Low	High
Fractional I_{SC}	Yes	No	Medium	Low	High
P & O	No	Yes	Varies	Varies	High
Inc. Cond.	No	Yes	Varies	Varies	Low
Fuzzy	Yes	Yes	Fast	High	Low
New Fuzzy	Yes	Yes	Very Fast	Very High	Low

IV. CONCLUSION

The fuzzy agent with two input parameters, which are E= $\Delta P/\Delta V$ and its change ΔE, enhanced by an initial estimation for the MPP voltage V_{MPP} using the fractional open circuit voltage technique leads to a good power response. This technique achieves the maximum possible output power from the PV module (185 W) without any steady state error in a small searching time (10 m sec). The improvement achieved by the proposed technique compared to the traditional fuzzy technique appears in the small searching time of the MPP by reducing the searching time to 20% from its traditional value. The developed MPPT technique shows a good response even under variable atmospheric conditions depending on the temperature adaptation of the initial estimation of V_{MPP} and the closed loop advantage of the fuzzy control scheme. Adaptation of the fuzzy agent may be done by giving the fuzzy agent inputs different weights causing a smaller settling time (2 m sec) and high accuracy thus leading to a newly developed efficient technique. The proposed technique has the advantages of fast settling, accurate tracking, and simple implementation. Moreover, it is faster than the traditional MPPT techniques. Also, the technique is a closed loop control system which is able of avoiding aging effects of the PV module which is not available in feed forward MPPT systems.

REFERENCES

[1] Trishan Esram, Patrick L. Chapman, "Comparison of Photovoltaic Array Maximum Power Point Tracking Techniques", *IEEE Transactions on Energy Conversion,* Vol. 22, No. 2, June 2007, pp. 439-449.

[2] Mohamed Azab, "A New Maximum Power Point Tracking for Photovoltaic Systems", *International Journal of Electrical Power and Energy Systems Engineering,* Vol. 4, No. 44, August 2008, pp. 571-574.

[3] D. P. Hohm and M. E. Ropp, "Comparative Study of Maximum Power Point Tracking Algorithms", *IEEE Photovoltaic Specialists Conference*, 2000, pp. 1699-1702.

[4] T. Noguchi, S. Togashi, and R. Nakamoto, "Short-current pulse based adaptive maximum-power- point tracking for photovoltaic power generation system", *IEEE Transactions on Industrial Electronics,* Vol. 49, No. 1, 2002, pp. 217-223.

[5] L. Mac Isaac, A. Knox, "Improved Maximum Power Point Tracking Algorithm for Photovoltaic Systems", *International Conference on Renewable Energies and Power Quality (ICREPQ'10)*, Granada (Spain), March 2010, Paper ID 250.

[6] Hairul Nissah Zainudin, Saad Mekhilef, "Comparison Study of Maximum Power Point Tracker Techniques for PV Systems", *Proceedings of the 14th International Middle East Power Systems Conference (MEPCON'10)*, Cairo University, Egypt, December 2010, Paper ID 278.

[7] Huan-Liang Tsai, Ci-Siang Tu, and Yi-Jie Su, "Development of Generalized Photovoltaic Model Using MATLAB/SIMULINK", *Proceedings of the World Congress on Engineering and Computer Science 2008, WCECS 2008*, October 2008, San Francisco, USA.

[8] F.M. Gonzàlez-Longatt, "Model of Photovoltaic Module in Matlab", *II CIBELEC,* Puerto La Cruz, Venezuela, Dec. 2005.

[9] Nopporn Patcharaprakiti, Suttichai Premrudeepreechacharn, and Yosanai Sriuthaisiriwong, "Maximum power point tracking using adaptive fuzzy logic control for grid-connected photovoltaic system", *Renewable Energy International Journal,* Vol. 30, No. 11, September 2005, pp. 1771-1788.

[10] M.S. Aït Cheikh, C. Larbes, G.F. Tchoketch Kebir and A. Zerguerras, "Maximum power point tracking using a fuzzy logic control scheme", *Review of Renewable Energy,* Vol. 10, No.3, 2007, pp. 387 – 395.

[11] N. Tkouti, A. Moussi, "Optimisation of the Photovoltaic Grid Connected System Using Fuzzy Logic Control", *Courrier du Savoir,* No. 06, June 2005, pp.43-47.

[12] Guohui Zeng, Xiubin Zhang, Junhao Ying,Changan Ji, "A Novel Intelligent Fuzzy Controller for MPPT in Grid-connected Photovoltaic Systems", *Proc. of the 5th WSEAS/IASME Int. Conf. on Electric Power Systems, High Voltages, Electric Machines*, Tenerife, Spain, December 2005, pp. 515-519.

2011 IEEE International Conference on Fuzzy Systems
June 27-30, 2011, Taipei, Taiwan

Improvement of Digital Image Motion Compensation by Fuzzy Inference

Sheng-Che Hsu
Department of Electrical Engineering
Ta Hwa Institute of Technology
Qionglin Shiang, Hsinchu County
eehsu@et4.thit.edu.tw

Abstract— **In this paper, a fuzzy inference digital image stabilization method is proposed to adaptively determine better motion compensation method through the selection of two different motion compensation methods. The experimental results show the good performance. It solves the problem of lag and overshoot of motion trajectory.**

Keywords- fuzzy inference; DIS; motion compensaton;

I. INTRODUCTION

Digital image stabilization (DIS) system is generally composed of two processing units. One is the motion estimation unit and the other is the motion compensation unit. The purpose of motion estimation unit is to estimation the reliable camera global movement. The motion compensation unit generates the compensation motion vector to obtain a smoother image sequence [1]-[5].

In the motion compensation of DIS, accumulated motion vector estimation and frame position smoothing (FPS) are the two popular approaches [6]. The accumulated motion vector estimation needs to compromise stabilization and intentional panning (constant motion) preservation since the panning condition causes a steady-state lag in the motion trajectory. The FPS accomplished the smooth reconstruction of an actual long-term camera motion by filtering out jitter components based on the concept of designing the filter with appropriated cut-off frequency. The disadvantage of FPS is that it does not guarantee the availability of the determined compensating motion vector when the specified-bound is restricted to preserve the effective image area in the DIS applications [8].

Fig. 1 shows the motion compensation schematics. The window of frame(t-1) is the previous compensated image. The compensating motion vector v is generated by the DIS according to the global motion vector between two consecutive images. The window of frame(t) is the picking window according to the compensating motion vector v to minimize the shaking effect. Compensating motion vector should be less than window shifting allowance for preservation of the whole image presented in the frame. How to generate motion compensation vector to achieve the optimal stabilization of shaking images within a specified compensation range (window shifting allowance) is a state of the art.

This work was supported by the National Science Council of Taiwan under the Grant NSC 99-2632-E-233-001-MY3.

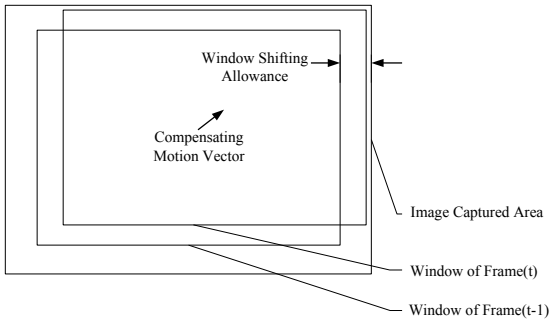

Fig. 1. Motion compensation schematics.

J. K. Paik proposed the accumulated motion vector method in 1992. The computation procedure is given by:[1]

$$CMV(t) = k(CMV(t-1)) + (\alpha GMV(t) + (1-\alpha)GMV(t-1)), \quad (1)$$

where t represents the frame number, $0 < k < 1$ and $0 \le \alpha \le 1$. The constant k is used for smooth panning. The constant α is used to filter out the unexpected noise effect. The increase in k causes the decrease in unwanted shaking effect but the increase in the value of CMV leads more allowance to compensate. It means that, in the definite allowance, it may not fully stabilize the image sequence by the CMV, especially in a high panning condition.

S. C. Hsu etc. proposed the CMV computation procedure to attack the drawback of tremendous lag during constant panning in 2005. This is presented by: [7]

$$\begin{aligned} CMV(t) &= \mathbf{k} \bullet CMV(t-1) + GMV(t) - \boldsymbol{\beta} \bullet CMV_I(t-1) \\ CMV_I(t) &= CMV_I(t-1) + CMV(t) \\ CMV(t) &= \frac{1}{2}\left(|CMV(t)+l| - |CMV(t)-l|\right) \end{aligned} \quad , \quad (2)$$

where $\begin{bmatrix} 0 \\ 0 \end{bmatrix} \le \mathbf{k}, \boldsymbol{\beta} \le \begin{bmatrix} 1 \\ 1 \end{bmatrix}$, $\bullet$ denotes array multiplication.

The objective of motion compensation is to achieve the optimal stabilization of shaking images within a specified compensation range (window shifting allowance). Eq. 1 can get a good result in a general case. But in the constant motion case, the undesired shaking effect cannot be eliminated by this method. The equation proposed in Eq. 2 can overcome this

drawback. The inner feedback-loop integrator was combined with a clipper function to reduce the steady-state lag for steady motion, as well as to keep the CMV operating in the appropriate range. Due to the characteristics of the integral, the overshoot will occur in certain back and forth low frequency image panning. Fig. 2 shows overshoot in low frequency back and forth image panning. The motion trajectory has obvious overshoot. This overshoot will reduce the effect of stabilization.

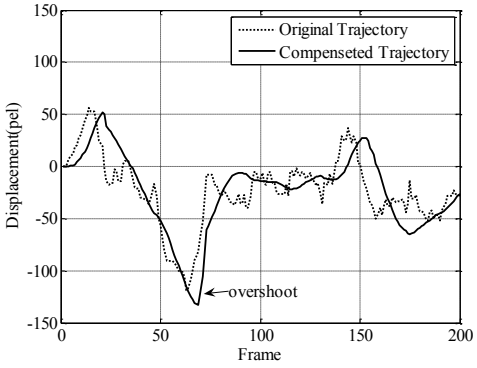

Fig. 2. Overshoot in low frequency back and forth image panning.

In this paper, two methods of motion compensation will combine through fuzzy inference to decide the optimal compensation method. In the next section, the architecture of fuzzy inference applied to DIS will be proposed. Section III shows the experimental results and section IV makes a discussion.

II. METHOD

A. Architecture of fuzzy inference

The typical architecture of a fuzzy logic decision system is comprised of four principal components: a fuzzifier, a fuzzy rule base, an inference engine, and a defuzzifier. The fuzzifier transforming crisp measured data into suitable linguistic values. The fuzzy rule base stores the empirical knowledge of the operation. The inference engine is the kernel of the decision system, and it has the capability of simulation human decision making by performing approximate reasoning to achieve a desired result based on the fuzzy rule base. The defuzzifier yields a nonfuzzy decision to perform the desired action [9][10].

In this paper, the design idea is to keep the merits of each motion compensation method, i.e. reduce compensated motion trajectory lag and overshoot, to improve the DIS in different conditions. Fig. 3. shows the architecture of fuzzy inference applied to digital image stabilization. The system architecture will focus on the motion compensation unit. The motion compensation unit includes two motion compensation methods, fuzzy inference system and motion compensation. Due to the differences of environments, conditions and shaking patterns of the captured images, the different motion compensation methods have individual merits separately. Fig. 4 shows the architecture of the fuzzy inference system. The pre-process block inputs global motion vector (GMV), compensating motion vector #1&#2 (CMV#1, CMV#2) are to transform into delta of short term smoothness index($\Delta SI(n)$) and delta of deviation(Δd) which are inputs of fuzzy inference. The fuzzy inference determines the weighted value to calculate the compensation vector. And then the block of image compensation uses the compensation vector to stabilize the image sequence.

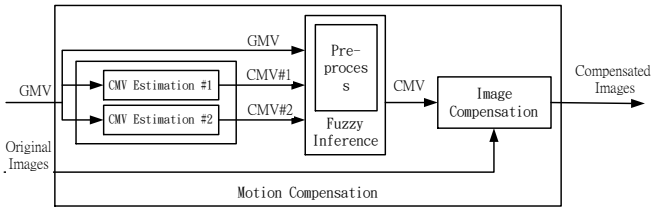

Fig. 3. The architecture of fuzzy inference applied to digital image stabilization

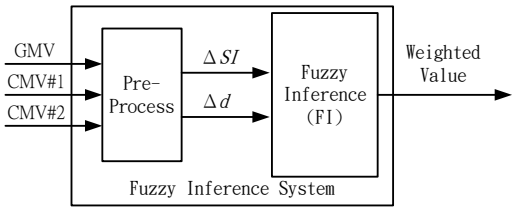

Fig. 4. The architecture of the fuzzy inference system

B. Pre-process

The main function of pre-process is to transform external signals into distinguished signals of fuzzy inference input. The major consideration is the smoothness index. To realize the effect of the compensation method in a short term period, the short term smoothness index $SI(n)$ is defined as

$$SI(n) = \frac{1}{p+1}\sum_{i=n-p}^{n}\Delta m(i) = \frac{1}{p+1}\sum_{i=n-p}^{n} m\times\left|GMV(i)-GMV(i-1)\right| \quad (3)$$

where n is the frame number, p is the short term frame amount. The delta of short term smoothness index($\Delta SI(n)$) can be expressed as

$$\Delta SI(n) = SI\#1(n) - SI\#2(n) \quad (4)$$

where $SI\#1(n)$ and $SI\#2(n)$ are short term smoothness indexes generated by Eq. 1 and 2 , respectively.

When $\Delta SI(n) < 0$, the motion trajectory compensated by CMV#1 is smoother than what was compensated by CMV#2 and vice versa. The secondary consideration is the deviation between the original and compensated motion trajectories. The deviation ($d(n)$) is defined as

$$d(n) = \left|MTraj_o(n) - MTraj_c(n)\right| \quad (5)$$

where $MTraj_o(n)$ is the original motion trajectory and $MTraj_c(n)$ is the compensated motion trajectory. The motion trajectories are define as

$$MTraj_o(t) = \sum_{i=1}^{t} GMV(i) \quad (6)$$

$$MTraj_o(t) = \sum_{i=1}^{t} GMV(i), \quad (7)$$

The large deviation between original and compensated motion trajectories will affect the image stabilization result. Therefore, the delta of deviation (Δd) is defined as a distinguished signal which is expressed as

$$\Delta d(n) = d\#1(n) - d\#2(n) \quad (8)$$

where $d\#1(n)$ and $d\#2(n)$ are deviations of motion trajectory compensated by CMV#1 and CMV#2. When $\Delta d(n) < 0$ means the deviations of motion trajectory compensated by CMV#1 is better than compensated by CMV#2 and vice versa.

C. Membership functions

Fig. 5 shows the Architecture of internal fuzzy inference. It contains a fuzzifier, a fuzzy rule base, an inference engine and a defuzzifier. The function of the fuzzifier is to transform crisp measured data $\Delta SI(n)$ and $\Delta d(n)$ into suitable linguistic values. The membership functions of these two signals are shown in Fig. 6. The linguistic descriptors are: large negative (FN), small negative (SN), zero (Z), small positive (SP), large positive (LP). Fuzzy rule base is characterized by a collection of fuzzy IF-THEN rules in which the preconditions and consequents involve linguistic variables. The collection of fuzzy inference rules characterizes the simple input-output relation of the system. The Eq. 9~19 are the statements of fuzzy rules:

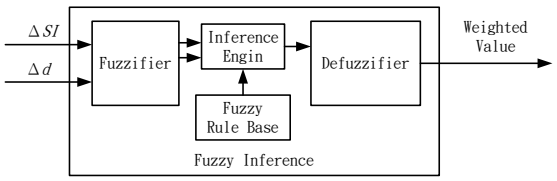

Fig. 5. Architecture of internal fuzzy inference.

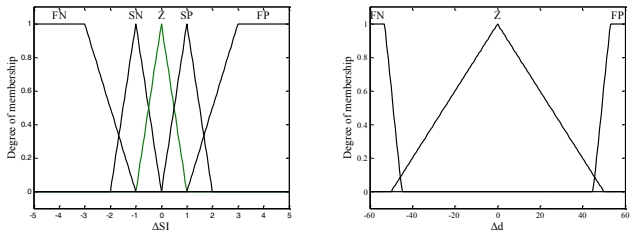

Fig. 6. Membership functions of inputs (a) $\Delta SI(n)$; (b) $\Delta d(n)$.

IF ΔSI is SN and Δd is FN THEN Output is L (9)
IF ΔSI is SN and Δd is Z THEN Output is L (10)
IF ΔSI is SN and Δd is FP THEN Output is M (11)
IF ΔSI is Z and Δd is FN THEN Output is L (12)
IF ΔSI is Z and Δd is Z THEN Output is M (13)
IF ΔSI is Z and Δd is FP THEN Output is S (14)
IF ΔSI is SP and Δd is FN THEN Output is M (15)
IF ΔSI is SP and Δd is Z THEN Output is S (16)
IF ΔSI is SP and Δd is FP THEN Output is S (17)
IF ΔSI is FN THEN Output is L (18)
IF ΔSI is FP THEN Output is S (19)

Mamdani's fuzzy implication method R_c , associated with the min operation, is used in the proposed inference system. The membership function of output signal is shown in Fig. 7. The linguistic descriptors are: large (L), Medium (M), small (S). The output represents the weighted value of motion compensation method#1. Because two methods are included in the system, the final motion compensation vector is calculated by:

$$\begin{aligned} CMV(n) = {} & k \times CMV(n-1) \\ & + y(n) \times (CMV\#1(n) - CMV\#1(n-1)) \\ & + (1 - y(n)) \times (CMV\#2(n) - CMV\#2(n-1)) \end{aligned} \quad (20)$$

where y(n) is the weighted value, $0 < k < 1$, $CMV\#1(n)$ and $CMV\#2(n)$ are the compensated vectors estimated by method #1 and #2.

Defuzzifier is a mapping from a space of fuzzy set defined over an output universe of discourse into a space of nonfuzzy set. The method of defuzzification used in the fuzzy inference system is the center of area (COA).

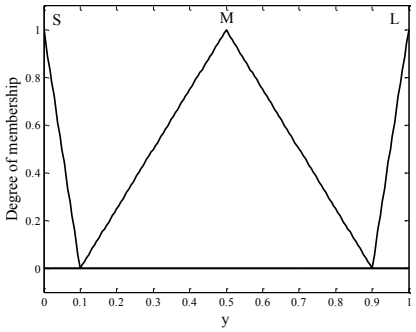

Fig. 7. Membership function of output.

III. EXPERIMENTAL RESULTS

In this section, the performance of proposed method in various conditions is demonstrated. To do this, GMVs estimated by three real video sequences that contain 200 frames are named GMV#1~3. To simplify the problem, one horizontal dimension is discussed and illustrated. The characteristics of GMVs are: GMV#1 contains constant speed movement and small fluctuation, GMV#2 contains constant speed movement and large fluctuation, GMV#3 contains only fluctuation without constant speed movement. The three sets of GMV observe the effects of image stabilization. The image size of the experiment is 640x480 pels. The clipper is bounded within ±53 pels. Parameters of MC#1 are set $k =$ and

$\alpha =$, MC#2 are set $k = 0.95$ and $\beta = 0.015$, the proposed method is set $k = 0.98$.

Fig. 8. shows the result of proposed method which uses a short term smoothness index to determine the better compensation method. The sequence n=1~200 corresponds to GMV#1, n=201~400 corresponds to GMV#2, and so on. In the first segment (n=1~200), the CMVs processed by MC#1 and MC#2 have almost the same $SI(n)$. Therefore, the fuzzy output is about 0.5. In the segment of n=250~400, the $SI(n)$ of MC#1 is higher; then the fuzzy output is close to 0. In other words, MC#2 has a better $SI(n)$ in this segment. In the segment of n=422~438, the $SI(n)$ of MC#2 has a spiked shape. Therefore, the fuzzy output approaches 1 and MC#1 is selected to compensate. Obviously, FIDIS is superior to MC#1, MC#2, respectively, for evaluating motion trajectory, the smoothness index or the short term smoothness index.

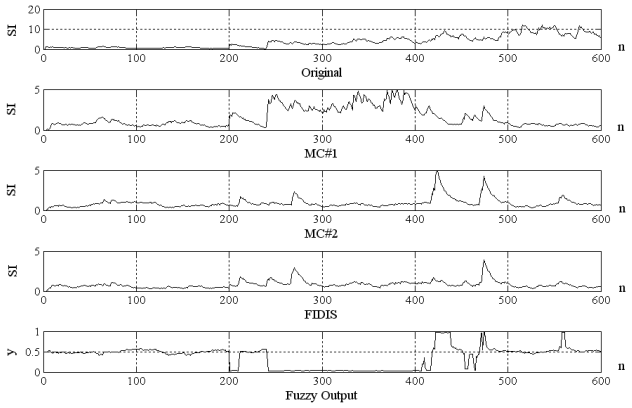

Fig. 8. Proposed method illustrated by short term smoothness $SI(n)$ and fuzzy output.

IV. DISCUSSION

The objective of motion compensation is to achieve the optimal stabilization of shaking images within a specified compensation range. The proposed method combines two motion compensation methods to adaptively determine a better method for motion compensation. It solves the problem of lag and overshoot of motion trajectory. The proposed method shows effective improvements in different conditions of image sequence through the evaluations of a smoothness index and motion trajectory.

ACKNOWLEDGMENT

The author would like to thank Chair Prof. C. T. Lin for providing the valuable opinions and part of resources to fulfill the whole research.

REFERENCES

[1] J. K. Paik, Y. C. Park, and D. W.. Kim, "An adaptive motion decision system for digital image stabilizer based on edge pattern matching," *IEEE Trans. on Consumer Electronics*, vol. 38, no. 3, pp. 607-616, Aug. 1992.

[2] S. J. Ko, S. H. Lee, and K. H. Lee, "Digital image stabilizing algorithms based on bit-plane matching," *IEEE Tran. on Consumer Electronics*, vol. 44, no. 3, pp. 617-622, Aug. 1998.

[3] K. Uomori, et al., "Automatic image stabilizing system by full-digital signal processing," *IEEE Trans. on Consumer Electronics*, vol. 36, no. 3, pp. 510-519, Aug. 1990.

[4] Y. Egusa, et al., "An application of fuzzy set theory for an electronic video camera image stabilizer," *IEEE Transactions on Fuzzy Systems*, vol. 3, no. 3, pp. 351-356, Aug. 1995.

[5] F. Vella, et al., "Digital image stabilization by adaptive block motion vectors filtering," *IEEE Trans. on Consumer Electronics*, vol. 48, no. 3, pp. 796-801, Aug. 2002.

[6] S. Erturk, "Image sequence stabilisation: motion vector integration (MVI) versus frame position smoothing (FPS)," Proc. of the 2nd International Symposium on Image and Signal Processing and Analysis, pp. 266-271, 2001.

[7] S. C. Hsu, S. F. Liang, C. T. Lin, "A robust digital image stabilization technique based on inverse triangle method and background detection," *IEEE Transactions on Consumer Electronics*, vol. 51, no. 2, pp. 335 - 345, May 2005.

[8] S. C. Hsu, S. F. Liang, K. W. Fan and C. T. Lin, "A Robust In-Car Digital Image Stabilization Technique," *IEEE Transactions on Systems, Man, and Cybernetics, Part C: Applications and Reviews*, vol. 37, no. 2, pp. 234-247, Mar. 2007.

[9] M. K. Gullu, S. Erturk, "Membership function adaptive fuzzy filter for image sequence stabilization," *IEEE Trans. on Consumer Electronics*, vol. 50, no. 1, pp. 1-7, Feb. 2004.

[10] Chin-Teng Lin, and S. George Lee C. *Neural fuzzy systems : a neuro-fuzzy synergism to intelligent systems*. Upper Saddle River, NJ: Prentice Hall PTR.

2011 IEEE International Conference on Fuzzy Systems
June 27-30, 2011, Taipei, Taiwan

A Semisupervised Feature Extraction Method Based on Fuzzy-type Linear Discriminant Analysis

Hui-Shan Chu
Graduate Institute of Educational Measurement and Statistics, National Taichung University of Education, Taichung, Taiwan, R.O.C.
Roxanne90@gmail.com

Cheng-Hsuan Li
Institute of Electrical Control Engineering, National Chiao Tung University, Hsinchu, Taiwan, R.O.C.
ChengHsuanLi@gmail.com

Bor-Chen Kuo
Graduate Institute of Educational Measurement and Statistics, National Taichung University of Education, Taichung, Taiwan, R.O.C.
kbc@mail.ntcu.edu.tw

Chin-Teng Lin
Institute of Electrical Control Engineering, National Chiao Tung University, Hsinchu, Taiwan, R.O.C.
ctlin@mail.nctu.edu.tw

***Abstract*—Linear discriminant analysis (LDA) is a commonly used feature extraction (FE) method to resolve the Hughes phenomenon for classification. The Hughes phenomenon (also called the curse of dimensionality) is often encountered in classification when the dimensionality of the space grows and the size of the training set is fixed, especially in the small sampling size problem. Recent studies show that the spatial information can greatly improve the classification performance. Hence, for hyperspectral image classification, it is not only necessary to use the available spectral information but also to exploit the spatial information. In this paper, a semisupervised feature extraction method which is based on the scatter matrices of the fuzzy-type LDA and uses the semi-information is proposed. The experimental results on two hyperspectral images, the Washington DC Mall and the Indian Pine Site, show that the proposed method can yield a better classification performance than LDA in the small sampling size problem.**

Keywords--feature extraction; linear discriminate analysis

I. INTRODUCTION

Linear discriminant analysis (LDA) [4] is a commonly used feature extraction (FE) method to resolve the Hughes phenomenon (also called the curse of dimensionality) which means that when the dimension of the space grows and the size of the training set is fixed, the classification accuracy reach a maximum for a given size, then it decreases for the hyperspectral image classification. Recently, a fuzzy-type LDA (FLDA), an unsupervised version of linear discriminant analysis (UFLDA), based on the membership values is proposed [3]. The membership values of the scatter matrices in FLDA are obtained from the cluster result of fuzzy linear discriminant clustering (FLDC). Then the generalized eigenvectors form the transformation matrix to transform the samples in the space with lower dimensionality.

Moreover, the spatial information by considering semi-labels can greatly improve the accuracy of the hyperspectral image classification [1]-[2]. Using the semi-labels of the unknown samples can not only increase the training samples but also decrease the imprecise estimation of samples, which have very similar spectral properties, and have difficulty distinguishing the unlabeled patterns [1]-[2].

Therefore, in this study, we want to integrate the scatter matrices of FLDA and semi-information to develop spatial scatter matrices. The membership values of the scatter matrices of FLDA are determined by the posteriors of every pixel in the image from the previous classification results. After obtaining the within- and between-cluster scatter matrices based on the spatial information, combine with the scatter matrices of LDA to form semi-scatter matrices. Therefore, in this paper, a LDA based on semi-information (SLDA) is proposed. The experimental results on the Washington DC Mall image and the Indian Pine Site image data sets show that the proposed method can yield a better classification performance than LDA when sampling size is small.

The study is organized as followed. The LDA and its unsupervised version will be introduced in section II. Section III describes our proposed method, SLDA, and the experimental results are shown in Section IV. Finally, some conclusions are addressed in Section V.

II. LINEAR DISCRIMINANT ANALYSIS AND ITS UNSUPERISED VERSION

A. Linear Discriminant Analysis (LDA)

LDA [4] uses the mean vector and covariance matrix of each class, to formulate within-class, between-class, and mixture-class scatter matrices. Based on the Fisher criterion, the LDA method finds features such that the ratio of the between-class scatter to the average within-class scatter is maximized, in a lower dimensional space. By applying the concept of class scattering to class separation, the Fisher criterion, takes the large values from samples when they are well clustered around their mean within each class, and the

978-1-4244-7316-8/11/$26.00 ©2011 IEEE

clusters of the different classes are well separated. The formula is stated as the following:

Suppose $H_i = \{x_1^{(i)},...,x_{N_i}^{(i)}\} \subset R^d$ were the set of samples in class i, N_i were the number of samples in class i, $i = 1,\ldots,L$, and $N = N_1 + \cdots + N_L$ were the number of all training samples. The between-class scatter matrix S_b^{LDA} and the within-class scatter matrix S_w^{LDA} would be defined as

$$S_b^{LDA} = \sum_{i=1}^{L} \frac{N_i}{N}(m_i - m)(m_i - m)^T \quad (1)$$

and

$$S_w^{LDA} = \sum_{i=1}^{L}\sum_{j=1}^{N_i} \frac{1}{N}\left(x_j^{(i)} - m_i\right)\left(x_j^{(i)} - m_i\right)^T \quad (2)$$

where m_i were the class mean defined by $m_i = \frac{1}{N_i}\sum_{j=1}^{N_i} x_j^{(i)}$ and $m = \frac{1}{N}\sum_{i=1}^{L}\sum_{j=1}^{N_i} x_j^{(i)}$ representing the total mean.

The optimal features are determined by optimizing the Fisher criterion given by $J_{LDA} = tr[(S_w^{LDA})^{-1} S_b^{LDA}]$. This is equivalent to solving the generalized eigenvalue problem, $S_b^{LDA} v_z = \lambda_z S_w^{LDA} v_z$, $z = 1,\ldots,d$ with $\lambda_1 \geq \lambda_2 \geq \cdots \geq \lambda_d$ where the extracted eigenvectors are used to form the transformation matrix of LDA, i.e., the transformation matrix from the original space to the reduced subspace is defined by: $A^{LDA} = [v_1, v_2, ..., v_p]$. The Fisher criterion J_{LDA} is able to detect the capacity of the separability for the transformed training samples.

B. Fuzzy-type Linear Discriminant Analysis (FLDA)

In the subsection, an unsupervised LDA, fuzzy-type LDA (FLDA), using the concept of membership values is described [3].Let X be a hyperspectral d-dimensional image of size $N \times z$ pixels, and $\{x_1,...,x_{N\times z}\} \subset R^d$ be all samples in the image. The between scatter matrix S_b^{FLDA} and the within scatter matrix S_w^{FLDA} as follows:

$$S_b^{FLDA} = \sum_{i=1}^{L} \frac{\sum_{t=1}^{N\times z} u_{it}}{N \times z}(m_i - m)(m_i - m)^T \quad (3)$$

and

$$S_w^{FLDA} = \sum_{i=1}^{L}\sum_{t=1}^{N\times z} \frac{u_{it}}{N \times z}(x_t - m_i)(x_t - m_i)^T \quad (4)$$

where u_{it} means the membership value of the sample x_t in class i,

$$m_i = \sum_{t=1}^{N\times z} \frac{u_{it}}{\sum_{k=1}^{N} u_{ik}} x_t$$

is the class mean, and $m = \frac{1}{N\times z}\sum_{t=1}^{N\times z} x_t$ represents the total mean.

The weight $\sum_{t=1}^{N\times z} u_{it}/(N\times z)$ indicates the influence of the samples in class i. If clustering results show that the number of samples in cluster i is larger than in cluster k, then

$$\sum_{t=1}^{N\times z} u_{it}/(N\times z) > \sum_{t=1}^{N\times z} u_{kj}/(N\times z),$$

i.e., the influence of m_i is larger than m_k in measuring the between separability. The weight $u_{it}/(N\times z)$ indicates the influence of the t-th sample in class i. If $u_{it}/(N\times z) > u_{kt}/(N\times z)$, then the k-th sample favors in class i. Hence, the corresponding weights in the within measure is larger.

Furthermore, it is easy to observe that the scatter matrices of LDA are special cases of the scatter matrices of FLDA [3], i.e., $u_{it} = 1$ and $u_{kt} = 0, k \neq i$ when x_t is the training sample in class i. In [3], the clustering performance of FLDA outperforms the clustering performance of principal component analysis (PCA) and independent component analysis (ICA).

III. A SPECTRAL AND SPATIAL FEATURE EXTRACTION METHOD

In this section, we propose a semi-information based LDA (SLDA) algorithm. The purpose of incorporating the semi-information in feature extraction is to increase the useable samples. In this study, the posteriori probabilities by applying the Gaussian classifier are used to form the weights in the scatter matrices of FLDA. Then the semi-information then can be both used to adjust the extracted direction, and the classification performance will be improved.

After applying the Gaussian classifier [4], the class-conditional probability density function of the unknown sample x_j is

$$p(x_j \mid i) = \frac{1}{(2\pi)^{d/2} \mid \Sigma_i \mid^{1/2}} \exp\left(-\frac{1}{2}(x_j - m_i)^T \Sigma_i^{-1}(x_j - m_i)\right)$$

where $m_i = \frac{1}{N_i}\sum_{\ell=1}^{N_i} x_\ell^{(i)}$ is the mean of class i,

$$\Sigma_i = \frac{1}{N_i}\sum_{\ell=1}^{N_i}(x_\ell^{(i)} - m_i)(x_\ell^{(i)} - m_i)^T$$

is the $d \times d$ covariance matrix, and $|\Sigma_i|$ denotes the determinant of Σ_i. Then x_j is distinguished to class i, if

$$p(x_j \mid i)p(i) \geq p(x_j \mid k)p(k)$$

for all $k \neq i$, where $p(i)$ is the priori probability of class i.

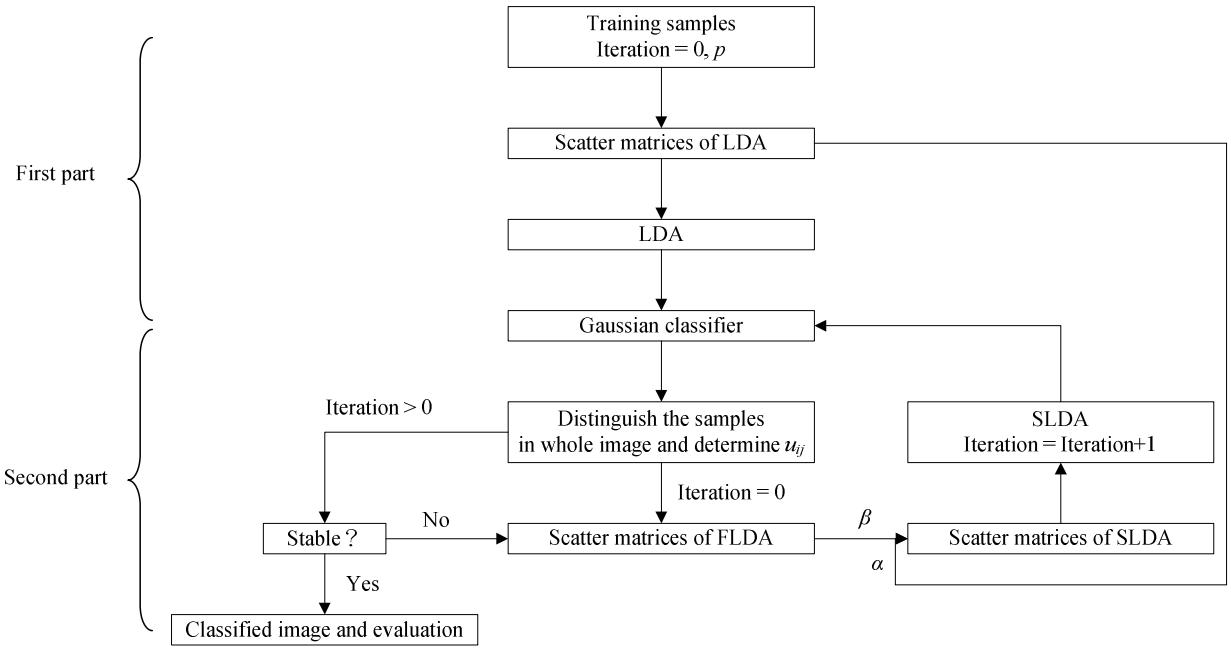

Figure 1. The framework of the proposed method, SLDA, which is based on semi-information.

In SLDA, the membership values of the semi-scatter matrices are defined as the posterior probabilities. According to the Bayes rule, the membership value u_{iq} of the unknown sample x_q, is defined as

$$u_{iq} = p(i \mid x_q) = \frac{p(x_q \mid i)p(i)}{\sum_{i=1}^{L} p(x_q \mid i)p(i)} .$$

for $i = 1, \ldots, L$, and $q = 1, \ldots, N \times z$.

The between scatter matrix S_b^{SLDA} and the within scatter matrix S_w^{SLDA} are defined as follows:

$$S_b^{SLDA} = \alpha S_b^{LDA} + \beta S_b^{FLDA} \tag{5}$$

and

$$S_w^{SLDA} = \alpha S_w^{LDA} + \beta S_w^{FLDA} \tag{6}$$

where α and β are two parameters to control the influences of the scatter matrices of LDA and semi-scatter matrices of FLDA. In this paper, the *k*-fold cross validation method is used to determined the proper parameters, α and β.

The features of SLDA can be obtained by solving the following generalized eigenvalue problem: $S_b^{SLDA} v_z = \lambda_z S_w^{SLDA} v$. The extracted eigenvectors form the transformation matrix of SLDA, i.e.,

$$A^{SLDA} = [v_1, v_2, ..., v_p].$$

One can find that if $\beta = 0$, then

$$A^{SLDA} = A^{LDA} .$$

TABLE I. THE ALGORITHM OF SLDA

Step 1:	Set the number of extracted features $p \le d$. Use the transformation A^{LDA} to project the samples in the image and obtain the semi-labels by the Gaussian classifier.
Step 2:	Compute u_{it} for every sample x_t in the whole image.
Step 3:	Compute S_b^{FLDA} and S_w^{FLDA}.
Step 4:	Compute S_b^{SLDA} and S_w^{SLDA} by multiplying the parameters α and β.
Step 5:	Solve the eignevalue problem $S_b^{SLDA} v_z = \lambda_z S_w^{SLDA} v_z$, $z = 1, \ldots, d$ with $\lambda_1 \ge \lambda_2 \ge \cdots \ge \lambda_d$.
Step 6:	The transformation function from the original space to the reduced subspace is defined by $A^{SLDA} = [v_1, v_2, \ldots, v_p]$.
Step 7:	Use the transformation A^{SLDA} to project the samples in the image and obtain the new semi-labels by the Gaussian classifier.
Step 8:	Repeat steps 2 and 7 until the iteration and the above iteration is below a certain tolerance value or it's no longer decreasing.

Fig. 1 is the framework of the proposed method, SLDA, which is based on semi-information. Given the training samples and determine the reduced dimensionality *p*. In the first part, the scatter matrices of LDA are computed and LDA is used for feature extraction. After applying the Gaussian classifier, the semi-labels and membership values can be obtained, and the scatter matrices of FLDA in the second part can be computed. By multiplying the parameters α and β, the scatter matrices of SLDA can be computed. After applying the SLDA and the Gaussian classifier, the new semi-labels and membership values can be obtained. If the change rate of semi-

labels is less than a threshold, then stop the iteration. Otherwise, continue the second part until the change rate of semi-labels is less than a threshold. The algorithm of SLDA is described in the Table I.

IV. Experimental Results

A. Experimental Data and Design

In this study, two real data sets are applied to evaluate the classification performances. They are the Indian Pine site (IPS): a mixed forest/agricultural site in Indiana [5] and the Washington, D.C. Mall hyperspectral image [5] as an urban site.

The IPS dataset was gathered by a sensor known as the Airborne Visible/Infrared Imaging Spectrometer (AVIRIS). This dataset was obtained from an aircraft flown at 65000ft. altitude and operated by the NASA/Jet Propulsion Laboratory, with a size of 145×145 pixels and has 220 spectral bands measuring approximately 20m across the ground. The grayscale IR image and ground truth of IPS are shown in Figs. 2 and 3, respectively. There are 9 different land-cover classes available in the original ground-truth. 9 categories, Corn – no till, Corn – min till, Grass / Pasture, Grass / Trees, Hay – windrowed, Soybean – no till, Soybean – min till, Soybean – clean till, Woods, would be used in our experiments.

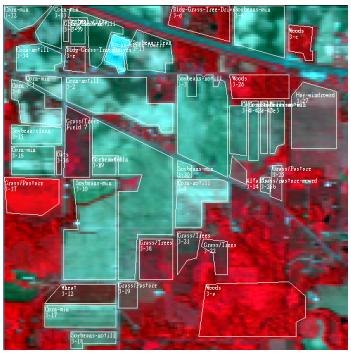

Figure 2. A portion of the Indian pine site image with a size of 145×145 pixels.

Figure 3. The ground truth of Indian pine site dataset.

The second data set, the Washington, D.C. Mall (DC) from an urban area, is a Hyperspectral Digital Imagery Collection Experiment (HYDICE) airborne hyperspectral data flightline over the Washington, DC Mall. Two hundred and ten bands were collected in the 0.4–2.4 μm region of the visible and infrared spectrum. Some water absorption channels are discarded, resulting in 191 channels. The dataset is available in the student CD-ROM of (Landgrebe, 2003). In our experiment, there are 7 classes, grass (class 1), tree (class 2), roof (class 3), water (class 4), road (class 5), trail (class 6), and shadow (class 7). The grayscale IR image of a portion of the image and the corresponding seven categories are shown in Fig. 4.

No.	Category
1	grass
2	tree
3	roof
4	water
5	road
6	trail
7	shadow

Figure 4. The false-color IR image of a portion of Washington, D.C. Mall image with a size of 205×307 pixels. There are seven categories, grass, tree, roof, water, road, trail, and shadow.

In the experiment, for investigating the influence of training sample size to the dimensionality, three distinct subsets, which N_i is the number of each class training samples, d is the number of dimension, and N is the number of total training samples. N_u=20 < N < d (case 1), N_u=40 < d < N (case 2), and d < N_u=300 < N (case 3), will be discussed in these two hyperspectral image data sets. For example, the Indian Pine site (IPS) dataset. In case 1, N_u = 20 < N =180 < d is a so called ill-posed classification situation, which means data dimensionality exceeds the total number of independent training samples in every class. In case 2, N_u = 40 < d < N is a so called poorly-posed classification situation, which means data dimensionality is greater than or comparable to the number of (independent) per-class representative training samples, but smaller than the total number of representative samples. In case 3, there are enough independent training samples. The MultiSpec [5] was used to select training and testing samples (100 testing samples per class) randomly in our experiments [6]-[8].

In the experiments, the classification performances by applying LDA and SLDA with the Gaussian classifier are compared. The grid search with k-fold cross validation is used to find the proper parameters α and β within a set $\{0, 0.1, 0.2, \ldots, 2\}$.

B. Results

In the experimental results, the classification accuracies in percentages for two different data sets are showed in Table II-IV. Because of LDA only can extract L–1 (number of classes minus one) features. For example, the Indian Pine site (IPS) dataset has 9 categories, so LDA only can extract 8 features. As result of `experiment we can know that the number of dimensionality with the classification accuracies has weak correlation. The classification performances by applying our proposed SLDA are higher than the classification performances by applying LDA in cases 1 and 2. However, in case 3 (Table IV), the accuracies by applying our proposed method are similar to that by applying LDA. Hence, in the small sample

size problem, the proposed method can yield a better classification performance than LDA.

Fig. 5-7 and 8-10 show the classification maps of the IPS and DC data sets by applying LDA and SLDA with the Gaussian classifier in three cases, respectively. From Fig. 5-6 and 8-9, i.e., case 1 and case 2, the proposed method SLDA can not only increase the classification performance but also decrease the imprecise estimation of samples, especially, "Woods," "Grass/trees," "Grass/pasture," "Soybeans-clean till," and "Hay-windowed" for IPS dataset, and all classes for DC dataset. Similarly, the classification maps are similar by applying LDA and SLDA for these two data sets except the "trail" in DC dataset. For this class ("trail"), SLDA outperforms LDA.

TABLE II. THE ACCURACY IN PERCENTAGES FOR TWO DIFFERENT DATA SETS IN CASE 1, N_U=20. THE NUMBER IN BRACKET IS THE REDUCED DIMENSIONALITY

FE	IPS	DC
LDA	55.89% (7)	47.71% (3)
SLDA	69.56% (8)	90.86% (4)

TABLE III. THE ACCURACY IN PERCENTAGES FOR TWO DIFFERENT DATA SETS IN CASE 2, N_U=40. THE NUMBER IN BRACKET IS THE REDUCED DIMENSIONALITY

FE	IPS	DC
LDA	69.00% (8)	86.29% (6)
SLDA	78.89% (8)	92.00% (4)

TABLE IV. THE ACCURACY IN PERCENTAGES FOR TWO DIFFERENT DATA SETS IN CASE 3, N_U=300. THE NUMBER IN BRACKET IS THE REDUCED DIMENSIONALITY

FE	IPS	DC
LDA	87.78% (8)	96.14% (5)
SLDA	87.56% (8)	94.71% (6)

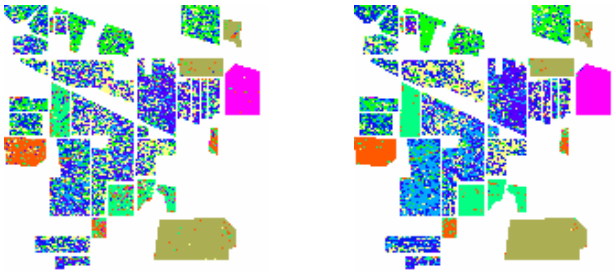

(a) LDA (b) SLDA

Figure 5. (a) and (b) are the classification maps of the IPS dataset by applying LDA and SLDA with the Gaussian classifier in case 1 (N_u=20), respectively.

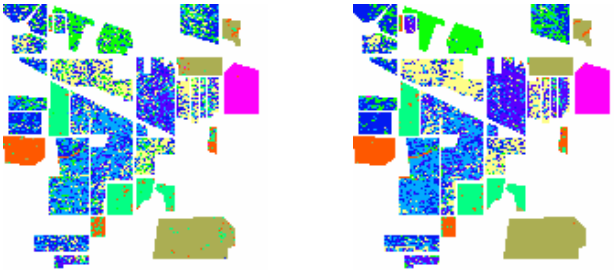

(a) LDA (b) SLDA

Figure 6. (a) and (b) are the classification maps of the IPS dataset by applying LDA and SLDA with the Gaussian classifier in case 2 (N_u=40), respectively.

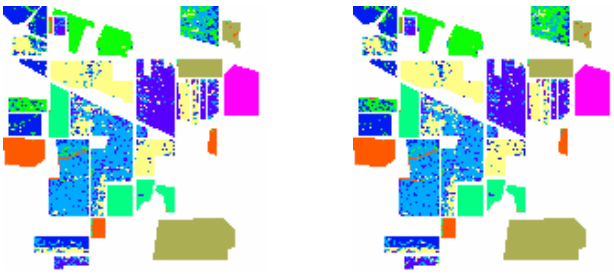

(a) LDA (b) SLDA

Figure 7. (a) and (b) are the classification maps of the IPS dataset by applying LDA and SLDA with the Gaussian classifier in case 3 (N_u=300), respectively.

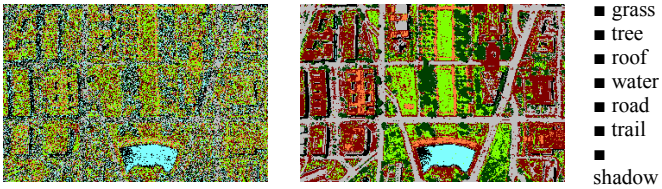

(a) LDA (b) SLDA

Figure 8. (a) and (b) are the classification maps of the DC dataset by applying LDA and SLDA with the Gaussian classifier in case 1 (N_u=20), respectively.

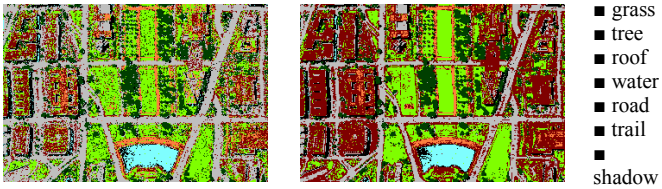

(a) LDA (b) SLDA

Figure 9. (a) and (b) are the classification maps of the DC dataset by applying LDA and SLDA with the Gaussian classifier in case 2 (N_u=40), respectively.

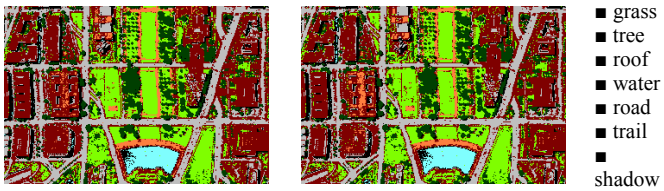

(a) LDA (b) SLDA

Figure 10. (a) and (b) are the classification maps of the DC dataset by applying LDA and SLDA with the Gaussian classifier in case 3 (N_u=300), respectively.

V. CONCLUSION

In this paper, a semi-information based LDA (SLDA) algorithm is proposed. The posteriors after applying the Gaussian classifier were used to determine the membership values of FLDA. Combining the scatter matrices of LDA and semi-scatter matrices of FLDA, the scatter matrices of SLDA are computed. According to the experiments on the Washington DC Mall image and the Indian Pine Site image data sets, SLDA can yield a better classification performance than LDA when sampling size is small.

ACKNOWLEDGMENT

The authors would like to thank Dr. Landgrebe for providing the Indian Pines site and The Washington DC Mall data sets. This work was supported in part by the National Science Council, Taiwan, under Grant NSC 98-2221-E-142-005.

REFERENCES

[1] K. Fukunaga, *Introduction to Statistical Pattern Recognition*, 2nd ed., San Diego, CA: Academic, 1990.

[2] C.-H. Li, B.-C. Kuo, and C.-T. Lin,“ LDA-based Clustering Algorithm and Its Application to an Unsupervised Feature Extraction,” *IEEE Transactions on Fuzzy Systems,* vol. 19, no. 1, pp.152-163, Feb. 2011.

[3] Q. Jackson and D.A. Landgrebe, “Adaptive Bayesian Contextual Classification Based on Markov Random Fields,” *IEEE Trans. Geosci. Remote Sens.*, vol. 40, no. 11, pp. 2454-2463, 2002.

[4] B.-C. Kuo, C.-H. Chuang, C.-S. Huang, and C.-C. Hung, “A nonparametric contextual classification based on Markov random fields,” in the *Proceedings First Workshop on Hyperspectral Image and Signal Processing: Evolution in Remote Sensing*, 2009. WHISPERS '09.

[5] D. A. Landgrebe, *Signal Theory Methods in Multispectral Remote Sensing*, John Wiley and Sons, Hoboken, NJ: Chichester, 2003.

[6] B.-C. Kuo, C.-H. Li, and J.-M. Yang, “Kernel Nonparametric Weighted Feature Extraction for Hyperspectral Image Classification,” *IEEE Trans. Geosci. Remote Sens.*, vol. 47, no. 4, pp.1139-1155, April 2009.

[7] J.-M. Yang, P.-T. Yu, and B.-C. Kuo, “A Nonparametric Feature Extraction and Its Application to Nearest Neighbor Classification for Hyperspectral Image Data,” *IEEE Trans. Geosci. Remote Sens.*, vol. 48, no. 3, pp.1279-1293, March 2010.

[8] J.-M. Yang, B.-C. Kuo, P.-T. Yu, and C.H. Chuang, “A Dynamic Subspace Method for Hyperspectral Image Classification,” *IEEE Trans. Geosci. Remote Sens.*, vol. 48, no. 7, pp.2840-2853, July 2010.

2011 IEEE International Conference on Fuzzy Systems
June 27-30, 2011, Taipei, Taiwan

The Emotion Recognition System with Heart Rate Variability and Facial Image Features

Pei-Yang Hsieh and Chiun-Li Chin
The Department of Applied Information Science
Chung Shan Medical University
Taichung, Taiwan
calvin147258@hotmail.com
ernestli@csmu.edu.tw

Abstract—**Amid the rapid advance of technologies in recent years, people live at fast paces and suffer invisible pressures in family, at workplace as well as in school. Emotional undulation tends easily to lead to melancholy. Statistically, the number of bipolar disorder sufferers in the last three years was 40 times that in the past 10 years. What should be more attended to is that 90 percent of suicide cases involved a history of "depression" or "bipolar disorder". Currently, to assess the mental pressure on an individual, questionnaires or interviews are applied and determination is made by physician's personal experiences. The development of a more viable quantitative method for assessing individual psychological pressure would facilitate self-management of health. This paper thus aims to CCD-capture human face, measure user's physiological data using BtECG and determine his/her emotional status by using the fuzzy theory based on the analysis of human face, eyes and Heart Rate Variability. The features of measurements and the determination are also fed to database, which can serve as reference for doctors in consulting related psychological disorders in future.**

Keywords-component: Bipolar Disorder, Fuzzy Inference, Heart Rate Variability, BtECG, Emotion State

I. INTRODUCTION

Living at fast paces and in a hectic society, people today suffer invisible pressures in family, at workplace as well as in school. They find themselves disoriented from motional undulation and, additionally, are liable to be in an ill cycle of melancholy due to complex interpersonal competitions which arise when mental adaption or external support is not complete. As a result, working efficiency drops, more frustration and setbacks follow with the ill cycle, causing not only psychological problems but also physiological disorders.

The object of this paper is to develop an emotion recognition system by combining the analysis of Heart Rate Variability (HRV) and the recognition of facial expressions. As psychological disorders are relatively difficult to detect in normal conditions, it is hope to determine, as early as possible, the presence of these disorders by measurement of HRV and recognition of facial expressions. Or, otherwise, the abnormal emotions due to illness are hoped to be diagnosed as early as possible, in order to prevent tragedies. With the development of the system, not only is it possible to measure user's emotional status, but also can the measurements be saved in the database as future reference for doctors in case medical aid is sought.

II. DOCUMENTARY REVIEW AND EXPLORATION

Sufferers of psychological disorders like depression and bipolar disorder increase in recent years. According to statistics, the number of bipolar disorder sufferers in the last three years was 40 times that in the past 10 years. More importantly, 90 percent of suicide cases involved a history of "depression" or "bipolar disorder". According to data from the Suicide Prevention Center of Department of Health, averagely one person commits suicide in every two hours and two minutes. Last year 1,472,000 Taiwan residents "thought of" ending their lives, with 416,000 people "did attempt to end their lives", of whom 130,000 "attempted more than once". Depression occurring on children or teenagers generally differs from that on adults: children tend not to talk about their own symptoms or describe their moods using the terms like melancholy; but they are more likely to express it through behaviors. In contrast, the depression in the elderly is obscure partly because it is traditionally believed that the elderly are losing their mobility and look less lively such that they are often thought to be simply getting old by their offspring, with the potential symptoms of depression being ignored. Hence the development of emotion recognition system becomes necessary.

Reference is first made to Heart Rate Variability, HRV. Heart Rate Variability means the beat-to-beat variation in time within a certain period of sinus rhythm, i.e., the analysis of the magnitude and regularity of the variation in heart rate [1]. Unlike mean heart rate variance which is expressed in minute, the HRV analysis examines the nuance time variance in each cycle of heartbeat and its regularity. Because heart rate is subject to many effects like breathing, blood pressure, endocrine and emotion, it can be used to observe the interaction between autonomic nerve and sino-atrial node. As well as a tool to analyze the conditions of cardiovascular diseases, it is a valuable index in predicting sudden cardiac death and cardiac arrhythmia.

The common methods of HRV analysis include Time Domain Methods and Frequency Domain Methods [1].

1. Time Domain Methods:

This can be divided in statistic and diagram approaches. Overall, time domain methods use indices that depict the shapes of standard deviation of all normal to normal R-R intervals (SDNN), and the root mean square of successive

978-1-4244-7316-8/11/$26.00 ©2011 IEEE

differences between adjacent normal cycles (RMSSD), quantitatively HRV RMSSD with broader shape indicates bigger HRV, and vice versa.

2. Frequency Domain Methods:

The common methods of transforming HRV curves into spectra include Fast Fourier Transform (FFT). Frequency domain methods make differences in the meaning of analytic results between long periods and short ones. With analyses of shorter periods (5min), it needs to control the well surrounding conditions so as to avoid that affecting autonomic nervous activities. With analyses of longer periods (24hr), as it is difficult to control the factors like smoking, drinking and emotional undulation, only the overall condition can be generally reflected. In their research, Akselrod discovered in 1981, that the power spectra of HRV features derived from ECG signals obtained by non-invasive measuring which have further been processed by Fourier transform can reflect the control of sympathetic and parasympathetic nervous systems on physiological mechanisms. By doing spectrum analysis on R-R interval, it is possible to observe three noticeable spectral peaks, which are high frequency (HF), low frequency (LF) and very-low frequency (VLF) and which are reflected in HRV. In 1996, the American Heart Association (AHA) set new criteria for the bandwidths of HRV, which are 0.15-0.4 Hz as HF bands, 0.04-0.15Hz as LF bands and 0.003-0.04Hz as VLF bands. The LF represents sympathetic nervous activity, HF for parasympathetic nervous activity and VLF for temperature regulation, Rennin-Agiotensin-Aldosterone System (RAA System) and part of parasympathetic nervous functions. HRV is controlled by autonomic nervous system (ANS), whereby to maintain the body balance, and the variance in heartbeat interval is affected by sympathetic and parasympathetic nervous systems; hence, the study of HRV can serve as an index for the autonomic nervous system [2].

HRV analysis, as a physiological index, began to catch doctors' attention in recent years. It has been used to monitor the regulation of human body by the autonomic nervous system, also served as a reference index in the death rate due to cardiovascular diseases. The commonly seen indices for death due to cardiovascular diseases are the LF rise of sympathetic and partly parasympathetic nervous regulations, and the HF decrease of parasympathetic nervous regulation. When the diagnosis is a likely coronary artery disease, it often further takes cardiac catheterization. Patients are often seen with emotions like anxiety and unease and become anxious or fearful for the dangers and side effects that may occur during the examination or the uncertainty of examination results, where they need appropriate caring guide to mitigate the anxiety. These emotions are potential pressures to patients of cardiovascular diseases. In anxiety, the rate of occurrence of sudden heart diseases also increases while the HRV is seen decreasing. Research showed that in patients of Myocardial Infarction, the emotions of anxiety and panic is associated with HRV decrease, and that both anxiety and melancholy decrease HRV and are related to the increase in risk of cardiovascular death in patients of coronary artery disease and irregular heartbeats. When Zen meditation is used to intervene in the measurement of characteristic anxiety scale and the changes of HRV analysis, the findings were that in sufferers of high-degree anxiety who underwent Zen meditation training and concentrated, the anxiety decreased the scores on the scale, the scores on characteristic anxiety scale were reversely related to slow alpha wave ($r=-0.482$, $p<0.05$)and positively related to HF index of HRV ($r=0.555$,$p<0.01$), but were not significantly related to LF and LF/HF ratio ($r=0.305$,$p<0.17$). It was reported that before cardiac catheterization, both contextual anxiety score and characteristic anxiety score in men were lower than in women, where the characteristic anxiety scale and HRV were significantly different in terms of gender ($t=-2.44$,$p<0.019$), while contextual anxiety scores were insignificant statistically. Also, in the gender differences in HRV analysis, it was seen that SDNN of HRV by time domain methods and HF and LF indices in women were all significantly greater than in men ($p<0.05$). Mental stress causes unstable emotions like negative one such as dysphoria, anger and discontentment, which affect the autonomic nervous system, stimulate the changes in sympathetic and parasympathetic nervous activities and are reflected in heart rate. In the research in short-period R-R interval and spectra analysis of cardiovascular systolic pressure, which explored the effects of psychological stress on autonomic nervous system and circulation system, the finding was that when concentrating, the subjects had higher-than-usual energy in the LF bands. That same study observed the correlations between skin temperature, vascular changes and sympathetic nervous activities using the indices of HRV, changes in skin temperature and vasomotor nervous activities of peripheral vessels, in the condition of mental stress and biofeedback. It was believed in that document that the degree of sympathetic nervous activities could serve as an index for durability to pressures. It was reported that under mental stress, HF energy dropped greatly and LF/HF noticeably rose and was significant statistically ($P<0.05$); when mental stress decreased, the LF/HF ratios lowered notably and was significant statistically ($P<0.05$). It is thus clear that when mental stress is strong, sympathetic nervous activities would increase by far, which can serve as an index for the assessment of the condition of mental stress, further to assist in clinic testing and diagnosis.

Now we talk about the recognition of facial emotions. Ekman and Friesen were the first to develop Facial Action Coding System (FACS), which defined 44 different Action Units (AU) by the principle that man pulls different facial muscles when making different expressions [3]. As Fig.1 shows, Fig.(a) is action units of upper face and some combinations of action units, and Fig.(b) action units of lower face. By combining certain action units, human facial expressions can be depicted. The FACS theory has been applied in most research to identify facial expressions. While applying it, a study made a difference in the capturing of facial features and the selection of recognition and sorting methods [4]. It divided the facial features in constant features and transient ones; the former were the changes in eyes and mouth and the latter were the wrinkle changes in between the

brows, cheeks and upper mouth edges. That study manually set the initial positions for these feature points, followed by tracking the changes of these points and then recognizing them with Artificial Neural Network [4]. Another study used Optical flow to track the movement of multiple feature points, which were set in a first image of a sequence of images. The characteristic vectors that were produced combining the feature point displacements in the first image and the last one were used to identify different action units and different facial expressions [5].

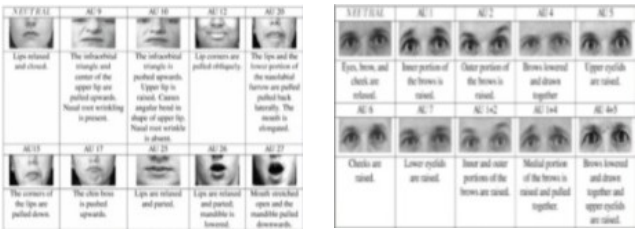

(a) (b)

Figure 1. Facial Action Units [5]

Feature capturing involves two aspects: the holistic approach and the local approach. The holistic approach is about first obtaining feature areas or feature points, whereby to detect deformation or movement, such as optical flow and characteristic tracking [6]. The local approach divides human face in several key blocks and then extracts characteristic information from them for determining the action [7].

This paper includes four chapters, first chapter is introduction, second is documentary review and exploration, the third is methodology and steps, we introduce hardware architecture and our methods, the fourth is experiment results, and the last is conclusions.

III. METHODOLOGY AND STEPS

Figure 2. Diagram of system framework

The development of emotion recognition system plays an important role in the research of psychological disorders and health care. This system will be discussed in separate sections: software and hardware. The hardware comprises an embedded system as the core, which works with Webcam to capture facial images and with Blue-tooth electrocardiograph (BtECG), to measure physiological signals. The software incorporates Webcam driver, Fuzzy Inference method, HRV analysis, facial detection and the techniques of eye and mouth state recognition.

In the system, the Webcam captures facial images; for reference values used to determine by the Fuzzy Inference method, thirteen features, as follows, are used: distance between eyeballs, number of changes in eyeball height, the extent to which the mouse opens, SDNN, Standard deviation of the averages of NN intervals in all 5-minute segments of the entire recording (SDANN), RMSSD, Number of pairs of adjacent NN intervals differing by more than 50 ms in the entire recording (NN50 count), NN50 count divided by the total number of all NN intervals (pNN50), Mean RR intervals (RRI-Mean), Standard deviation of differences between adjacent RR intervals (SDSD), Standard deviation of all normal to normal intervals index (SDNN index), VLF, LF, HF and analysis of LF/HF power. The job of embedded system is processing the measured HRV features and the imaged the Webcam sent, and detecting user's facial positions and identifying the state of the eyes and the mouth by facial detection and eye-and-mouth state identification. In this paper to combine the Fuzzy Inference method to distinguish the differences in degree of emotion based on the features of the eyes, the mouth and HRV. The system outputs the results of determination to a screen or informs relevant persons by texting. Elaboration will now be made on the software.

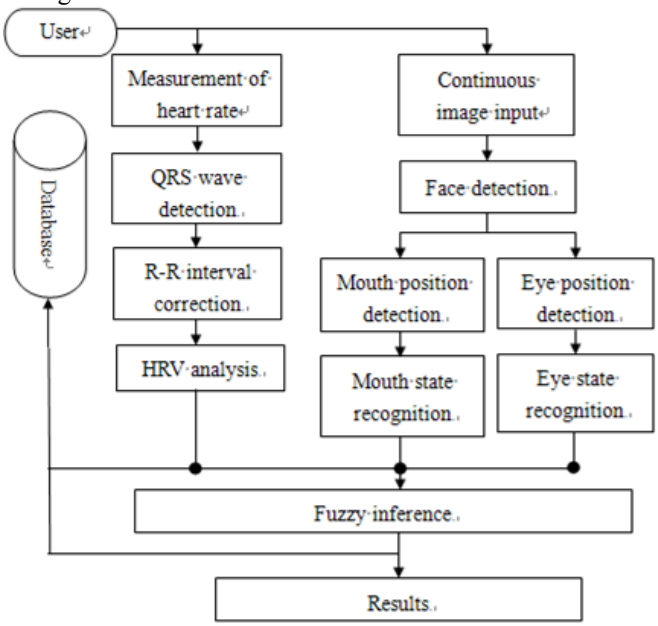

Figure 3. Flow chart for emotion recognition system

The flow chart of this paper is shown in Fig.3. To begin with, relevant data are downloaded to the embedded system via a USB device for use. That is followed by developing USB Webcam driver codes in the embedded system to enable the WINCE platform to drive Webcam to capture images, which will be saved in the embedded system. Again, this is followed by pre-process of the user's image, which aims to eliminate the influences of indoor light and noises in order to enhance the accuracy of capturing. A technique of graph identification is used to detect the state of the eyes and the mouth and then a BtECG is used to transmit physiological signals to the embedded system. The QRS-wave detection is employed to make correction to R-R interval before analyzing HRV by time domain methods and frequency domain methods with the features. When characteristic identification has been conducted, the fuzzy inference method is applied to combine the HRV features and the features on images, with their

degrees distinguished. Lastly, based on different degrees, the system analyzes and determines the user's emotional state.
In respect of above flow, the research method is divided in below steps:

A. Facial detection

(1) Preprocessing: the system employs an image pro-process, of which the object is to eliminate noise interference in the image and to adjust brightness as well as remove the noise.

(2) Skin region detection:

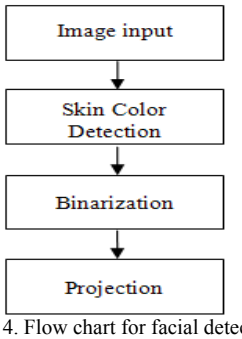

Figure 4. Flow chart for facial detection

Detection of facial and eye position is the first and important step of eye status recognition. There are many detection methods of facial position; but this paper employs facial complexion in detection. Also in this paper, the images having been processed by binarization are taken to locate the face after horizontal and vertical projection. The method of complexion detection uses the information on complexion to capture the face in an image, discerning it from the background. An image is transformed from the RGB space to the YC_bC_r space.

$$\begin{bmatrix} Y \\ C_b \\ C_r \end{bmatrix} = \begin{bmatrix} 0.299 & 0.587 & 0.114 \\ -0.1687 & -0.3312 & 0.5 \\ 0.5 & -0.4183 & 0.0816 \end{bmatrix} \begin{bmatrix} R \\ G \\ B \end{bmatrix} \quad (1)$$

$$60 < Y < 255 \quad (2)$$

$$25 < C_b < 0 \quad (3)$$

$$10 < C_r < 45 \quad (4)$$

As the complexion has a fixed zonal distribution in the YC_bC_r space, this paper sets the pixels that distribute in such zone as 1 and the values in this zone as 0. As the face occupies the largest one of a great number of blocks taken in the image by complexion, the method of projection is used to identify the complexion block of biggest area. The area is gradually closed by morphological operations algorithm, and the separate pixels are conjoined through expansion; further, the areas that are weakly connected are separated by erosion to obtain binary images.

B. The Detection of Feature Point Position

(1)Eye detection:

The length of human face is about 1.2 times of the width. According to the facial features proportion, when starting from the top of the face, the pupil will be at the 4/12 to 7/12 of the face length. Starting from the left of the face, the pupil will be at the 2/16 to 15/16 of the face width. We find the pupil in this area. Compared with the nearby area, the pupil is of darker color. Thus we use the dynamic method to find the critical value. First calculate the grayscale histogram of this area. Since the pixels of the pupil is within the 1% of the darkest area, we calculate from the grayscale of 0, accumulate to the 1% of the total pixels of this area and set the value of this pixel as the critical value. When the pixel value of the area is smaller than the critical value, set it as 1, otherwise set as 0, as shown in Fig. 5.

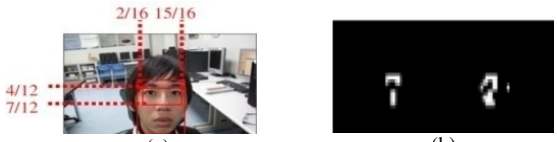

(a) (b)

Figure 5. (a)The approximate area of the eye (b)The result of the binarization of the dynamic critical value of the pupil area

Then we separate the eye area into right and left two sections. Raise the left pupil as an example, in the process of binarization of the pupil, it may also binarize the eyebrow and hair near the eye. This will affect our action of finding the position of the pupil. However, because the eyebrow and hair are above the pupil, our algorithm may search the first pixel of 1' in a bottom up way. And then use this pixel as starting point, which, together with two pixels on the left and right, and 5 pixels above will generate a 5*5 area. And then calculate the center of gravity of all the pixel value 1's pixels in this area. We find that this center of gravity is the position of the pupil. For the same reason, we can find the right pupil with the same method. And then use the distance(d) of the two pupils as in Fig. 6, follow the relationship of the human face features' proportion to generate the area of the eye. The eye area is at the place where the pupil is the center, go up and downwards 1/6 distance, left and rightwards 1/3 pupil distance area.

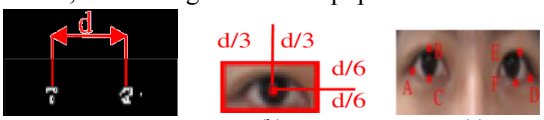

(a) (b) (c)

Figure 6. (a)Pupil distance d (b)the eye area detection result (c)the feature point of the outer corner of the eye.

After finding the eye area, we utilize the pixel center of gravity obtained by the above 5*5 area. As this pixel center of gravity is always inside the pupil area and the grayscale value is similar to that of the other pixels in the pupil, we use the Region Growing method to use the pixel center of gravity as seed to grow complete pupil area. In this way, we will know the coordinates of the uppermost pixel point and that of the bottommost pixel point.

When we find the top and bottom threshold of the pupil, we will find the outer corner of the eye to be the other feature point for identification. Use the top and bottom feature points as the upper and lower bounds along the y axis. Then use the pixel center of gravity as the starting point and seed along the

x axis. Similarly we use the Region Growing method along the outer corner of the eye orderly. When scanning the connecting zone of the pupil and the white of the eye, due to the fact that the white of the eye is not the pupil area, the grayscale may change greatly. Record this pixel point as the first point, then use the next pixel point, i.e. the pixel point inside the white of the eye as seed for processing. Similarly when scanning the connecting zone of the white of the eye and the skin; the grayscale may change greatly. Record this pixel point as the second point. Repeat these processing steps till the boundary of the eye area. Finally find the outermost point of the points we record. This is the feature point of the outer corner of the eye we need, as shown in Fig. 6(c).

(2) Mouth detection:

When acquiring the feature point of the mouth, we first use the facial features proportion to generate the approximate area of the mouth. The position of the mouth will be at the 7/10 to 9/10 face length and 2/6 to 5/6 face width area when starting from the top of the face, as shown in Fig. 7. As the color of the lip is redder than other skin, we use this information to obtain the feature point of the mouth. First convert the human face image from RGB color space to HSV color space. In this way we can separate the color and the brightness to avoid the influence from the outside light source. Then use (1) to transform the H (hue) value in the HSV color space. The equation is as follows:

$$f(h)=\begin{cases}1-\dfrac{(h-h_0)^2}{w^2}, & |h-h_0|\le w\\ 0 & |h-h_0|\ge w\end{cases} \qquad (5)$$

Where the h is the h value of the mouth area, h_0 is the offset value defined according to the hue. Here we set it as 1/3. The w is set as 0.60. This equation can be viewed as use the h_0 as center and use w to filter the area that can be accepted. Farther the distance between h value and h_0 of the mouth area, smaller the value will be. The value of f (h) is between 0 and 1. Then we amplify the f (h) value of the mouth area. Round off the f (h)*100 value into integer and amplify it 100 times to produce histogram as shown in Fig. 8. We found from the observation that when the value of f (h)*100 is between 50 and 100, there is a peak as the skin. There is a point on the left-hand side with a large slope. When the gradient is gentle, it is suitable to be the critical value to separate the mouth and the skin. Thus if the f (h)*100 value is smaller than this critical value, it is the mouth area. Set the pixel value as 1, otherwise set it as 0. Binarize the image as shown in Fig. 9.

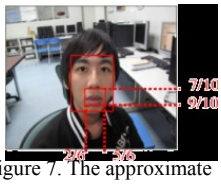

Figure 7. The approximate mouth area

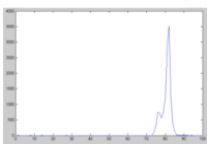
Figure 8. f (h)*100 histogram

Figure 9. Mouth area binarization result.

As the mouth has the horizontal edge direction tendency, we use the horizontal Sobel wave filter to generate the horizontal direction edge of the mouth area and do the binarization. Then search from left to right to find the point where the first mouth binarization and Sobel binarization pixel value both are 1. This is the feature point G. Search from right to left to find the point where the first mouth binarization and Sobel binarization pixel value both are 1. This is the feature point I. From the horizontal direction center point of the left and right feature points, 2 pixels on the right and left, there will be 5 horizontal pixels in total. Search top-down to find the point where the first in these five horizontal pixels, the mouth binarization and Sobel binarization pixel value both are 1. This is the feature point H. Search bottom- up to find the point where the first in these five horizontal pixels, the mouth binarization and Sobel binarization pixel value both are 1. This is the feature point J as shown in Fig. 11.

Figure 10. Mouth Sobel binarization result

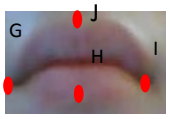

Figure 11. Mouth feature points

C. Heart Rate Variation Analysis

Regarding the studies of the periodicity of the heart beat, they mostly use the continuous R-R interval as the continuous period of the heart beat. The R wave of the electrocardiogram is the most commonly used in the heart rate variation analysis. By calculating the time interval between the RR, we get a series of numbers. The heart rate variation analysis usually excludes the Arrhythmia case. It focuses on the slight heart rate variation of the normal rhythm for study.

First, we stick the sticky thread on the user's left and right wrist, and then use the BtEEG to measure the physical signal of the user. The measuring time is 5 minutes. Transfer the physical signal to the mosaic system through the BtEEG. To reduce the interference of the heart rate variation result, we keep the environment quiet. In this paper we use the method proposed by Willis J. Tompkins to detect QRS wave. This method follows the frequency range of the signal to filter out the noise to get the QRS wave. We can find the position of the R wave through the QRS wave. Fig. 12 is the flow chart of using the Willis J. Tompkins' method detecting QRS wave.

- Band-pass integer filter: As the center frequency of QRS wave is about 17Hz, we use a low-pass filter (25Hz) and a high-pass filter (15Hz) to form a band-pass integer filter and keep the frequency between 15 and 25Hz. In this way, we can get a clearer QRS complex wave and reduce the T wave substantially.
- Differential: After the signal passes the band-pass integer filter, we can use differential to make features of QRS wave more high-lighted. After differential, we can easily distinguish the R wave.
- Square: In order to convert the signal into the positive and make high-frequency part of the QRS wave more obvious, we use square to make it stand out.
- The acquisition of R wave's position: We get the peak value of R wave by adjusting the threshold dynamically. However, someone's T wave is higher than his R wave or only slightly

lower than his R wave. We have to filter out T wave before catching R wave, and then search the peak value of R wave. In this way, we can find the next R wave and obtain the R-R interval.

However, R-R interval will change because of age or certain diseases of the user. Therefore, this program will use the above method to find the R-R interval, and modify it by using the methods proposed by [7]. The specific steps are as follows:

1. Expand the above R-R interval*0.6 to the left of R point and R-R interval * 0.3 to the right of R point. Repeat this step and select 20 heartbeats randomly.
2. Use the method of Signal averaging to make 20 heartbeats' electrocardiogram point at R point. After getting the cumulative average, we should calculate the related feature value for identification.

At present, there are two kinds of methods on analysis of heart rate variability, namely time domain analysis and frequency domain analysis. Time domain analysis is to record the statistical analysis result of R-R interval between two neighboring heart rates, while frequency domain analysis is to use the fast Fourier transform to convert the R-R interval from time domain into frequency domain for Power Spectral Density (PSD) analysis. This program will analyze time domain and frequency domain, and make time domain analysis through the following features

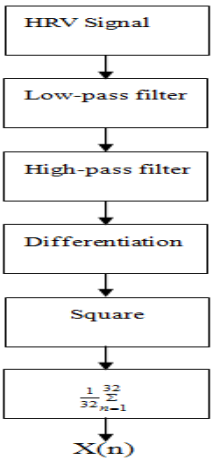

Figure 12. The flow chart of using Willis J. Tompkins' method to detect QRS wave[8].

1. SDNN: Standard deviation of Sinus rhythm, with the clinical significance to estimate the overall heart rate variability.
2. SDANN: Standard deviation of the interval average of all normal heartbeats every five minutes.
3. RMSSD: The square and the average square root of neighboring R-R interval difference.
4. NN50 count: The count of the time interval of each pair of neighboring normal heart rates that is more than 50 milliseconds.
5. pNN50: NN50 count divides all the normal heartbeat intervals in the ECG.
6. RRI-Mean: The average RR interval every 5 minutes.
7. SDSD: Standard deviation of differences between adjacent RR intervals.
8. SDNN index: Calculation of the standard deviation of normal heartbeat every 5 minutes and then get the average value.

This program adopts the above eight features to analyze time domain, and uses the Bluetooth ECG machine of Yang Yin Inc. to conduct a five-minute measurement of the user.

Frequency domain analysis:

We use the fast Fourier transform to convert the R-R interval from time domain into frequency domain and then display it in the way of Power Spectral Density (PSD). According to the size of the different frequency, Power Spectral is divided into total power, ultra-low frequency, low frequency, high frequency and low frequency vs. high frequency. This program will focus on analysis of ultra- low frequency, low frequency, high frequency and low frequency vs. high frequency.

D. Feature Identification

After getting the position of various features and the features of heart rate variability, we will make the feature acquisition calculation. This program touches upon the values of thirteen features, namely, the distance between eyeballs, the size of open mouth, times of eyeball height changes, SDNN, SDANN, RMSSD, NN50 count, pNN50, RRI-Mean, SDSD, SDNN index, ultra-low frequency, low frequency and high frequency vs. low frequency. As the above feature values will vary in different emotional states, the distance between eyeballs and times of eyeball height changes will vary with the emotion. We can analyze the distance between eyeballs through (2):

$$eyed = \frac{|B-C|}{d} \tag{6}$$

As is shown in Fig. 7 (c), $|B-C|$ is the vertical distance from B to C of the feature point in the right eye, while "d" is the distance between two pupils in Fig. 7(a). In different emotional states, two eyes do the same action, so we make judgment based on the right eye. We analyze the mouth openness through the Euler distance, which is the vertical distance from H to J in Fig. 11. Accordingly, there are also different conditions on heart rate variability, for example, when depressed, SDNN value will be lower than usual, and the high frequency energy will plummet. Low-frequency will increase remarkably when there is huge mental stress, and it will decrease significantly when the mental stress is decreased. This program will analyze four emotional states, normal, happy, sad and angry through Fuzzy Inference method. We will use the thirteen features to find out the attribution between the input and output variables. First, we will set up the semantic formula of fuzzy inference on input and output variables:

(1) The distance between eyeballs: If it is smaller than 0.125 cm , it is diagnosed as mild eye openness(S), from 0.1 to 0.15 cm as moderate eye openness (M), and higher than 0.125 cm as high eye openness (L), whose membership function is μ_{eyed}

(2)Times of the height change of eyeballs: If it is less than 10 times, it is small amount of change (S), 5 to 20 times is

moderate changes (M), and more than 10 times is large amount of change (L), whose membership function is μ_{eyeh} (3)The frequency: if it is higher than 0.15, it is called high frequency, from 0.05 to 0.15 is called low frequency, and lower than 0.05 is called ultra-low frequency, whose membership function is $\mu_{frequenct}$ (4)SDNN: the attribution function is μ_{SDNN} (5)SDANN: the attribution function is μ_{SDANN} (6)RMSSD: the attribution function is μ_{RMSSD} (7)NN50 count: the attribution function is $\mu_{NN50count}$ (8)pNN50:the attribution function is μ_{pnn50} (9)RRI-Mean: the attribution function is $\mu_{RRI-Mean}$ (10)SDSD: the attribution function i μ_{SDSD} (11)SDNN index: the attribution function is $\mu_{SDNNINDEX}$ (12)Low frequency vs. high frequency: the attribution function is $\mu_{LF/HF}$ (13)The mouth openness: If the distance from H to J is less than 1.48 cm, it is slight openness (S), from 1 to 2.21 cm, it is moderate openness (M), and larger than 1.48 cm is large openness (L), whose attribution function is μ_{mouth} .

In the following construction of fuzzy rules, we can use semantic fuzzy rules obtained by the doctor or through learning, and finally get the fuzzy sets. Then we use Center of Gravity Method for defuzzification. We can also distinguish the four emotions into three levels, that is slight(S), moderate(M) and large(L). Fig. 13 is the attribution function of the above features and each kind of emotion.

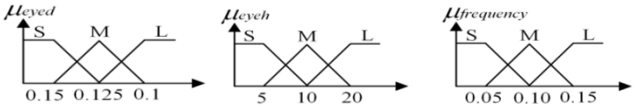

(a) (b) (c)

(a) The attribution function of the distance between eyeballs. (b)The attribution function of times change of eyeball height. (c)The attribution function of the heart rate feature of HRV.

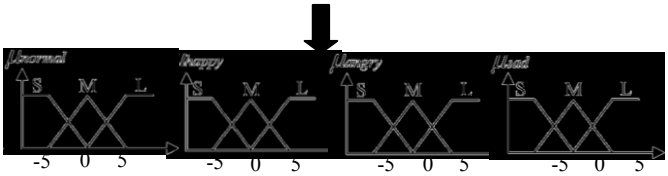

(d)Normal (e)Happy (f) Angry (g) Sad

Figure 13. The flow chart of emotional state inference.

E. The Output Result

Based on the input image and the features of heart rate variability, this program shows the emotional states of the current users by using inference results of Fuzzy Inference, that is, normal, happy, sad and angry. What's more, this program stores the image, features of heart rate variability and emotional states into the database, which can provide the reference for doctors in case of medical treatment in the future.

IV. EXPERIMENT RESULTS

The results of this paper, we propose an intelligent method to construct the emotion recognition system for testing and discussion its recognition rate. Herein, the CCD camera is QuickCam™ Pro 4000 of Logitech. The image resolution is 320×240, and the camera capture 30 images per second. Because the measured time is five minutes, we can capture 9000 images. Meanwhile, the paper uses embedded system for testing, and its operating system is Windows Embedded CE 6.0 R2, the RAM size is 1024MB. The distance from human face to CCD camera is 40cm~60cm, the speed of recognition spends about 0.4~0.6sec. In addition, the part of measuring heart rate, we use Bluetooth ECG device to do measurement, which is produced by yang yin co. The measuring environment is in the laboratory, and keeps quiet for five minutes measurement; we conducted heart rate and face test for 20persons.

Fig. 16 and 17 show the results of face detection; however, because of light and noises we still have mistakes in human face detection. Fig. 16 shows successful cases in human face detection and Fig. 17 shows failure detections. And the failure is resulted from skin's color range and lights.

Figure 14. Successful cases in human face detection

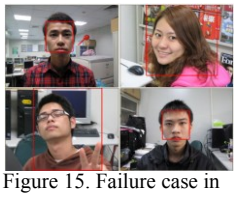

Figure 15. Failure case in human face detection

After detecting human face, we proceed to extract facial features. Fig. 18 shows the result of the extraction of feature points.

Figure 16 shows the result of the extraction of feature points.

Next, to extract the feature of heart rate, we extract 20 people's respectively extract 4 emotions electrocardiogram for each 20 persons, Fig. 19 show the electrocardiogram of (a)normal, (b)happy, (c) angry, (d) sad, respectively.

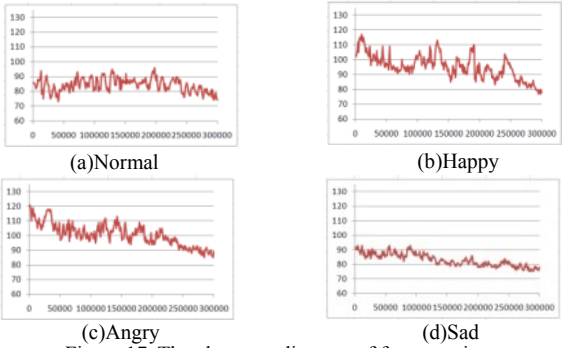

(a)Normal (b)Happy

(c)Angry (d)Sad

Figure 17. The electrocardiogram of four emotions

After obtaining above features, the paper use fuzzy inference method to judge emotion state. In fuzzy inference, we use 13 features, and divide them into three levels. They are slight(S), moderate (M) and large (L), respectively. The system is multi-input and single-output, and the emotion is divided into sad, angry, happy, normal, after deduction. We

also divided 4 emotions into three levels. Because there are 13 features in the system and infer a emotion state, total rules have 3^{14} rules, after reducing, the total rules remain 3^{10} rules. For instance:

R^1:if eyed is S, eyeh is S, frequency is M, SDNN is M, SDANN is S, RMSSD is S, NN50 count is S, pNN50 is S, RRI-Mean is S, SDSD is M, SDNN index is M, $\frac{LF}{HF}$ is S, mouth is S Then normal is S.

R^2:if eyed is M, eyeh is M, frequency is M, SDNN is M, SDANN is S, RMSSD is M, NN50 count is M, pNN50 is S, RRI-Mean is S, SDSD is M, SDNN index is M, $\frac{LF}{HF}$ is S, mouth is M Then happy is M.

R^3:if eyed is L, eyeh is L, frequency is L, SDNN is M, SDANN is L, RMSSD is M, NN50 count is L, pNN50 is L, RRI-Mean is S, SDSD is M, SDNN index is M, $\frac{LF}{HF}$ is M, mouth is M Then angry is M.

Table I shows the average successful rate of mouth and eyes detection is 82.03%.The success rate of our system is 84.31%.

Table I: the success rate of facial feature points detection

	The number of detection of eyes error	**The number of detection of mouth error**	**Success rate**
video 1	818	886	81.06%
video 2	952	1159	76.54%
video 3	1102	897	77.79%
video 4	1452	1220	70.31%
video 5	891	925	79.82%
video 6	751	862	82.07%
video 7	991	1123	76.51%
video 8	729	982	80.98%
video 9	902	1163	77.05%
video10	685	746	84.10%
video11	859	957	79.82%
video12	745	712	83.81%
video13	812	892	81.07%
video14	688	657	85.06%
video15	901	972	79.19%
video16	742	803	82.83%
video17	992	902	78.95%
video18	817	933	80.56%
video19	700	721	84.21%
video20	1102	801	79%
Average successful rate 82.03%			

V. CONCLUSIONS

We provide an emotion recognition system by using eye's close/open condition, mouth close/open condition, physiological signals, and the method of Fuzzy Inference and apply emotion recognition system in the embedded system. This system is light, so has less spatial constraint. However, there are still parts required improvements in this emotion recognition system. For example, we hope natural light can be used to replace external light, so they obtained eyeball images will not so easily be influenced by reflection points and image capturing will be more accurate. Another solution is to find a webcam that has higher resolution and can filter some external image noises. However, problems regarding how to reduce dynamic distribution but with clear captures on the eyes or how to emphasize pupil's features should be dealt with by designing other appropriate image processing rules. In addition, we want to improve QRS detection in heart rate detection. In facial detection, the average successful rate is 82.03%, and the success rate of our system is 84.31%.

In the future, we expect that in the parts of human face detection, features capture and heart rate detection, we can process with better algorithm (for example, the color space of light's images and capturing more featured areas), establish a database to collect more reference materials.

REFERENCES

[1] G. Zhou, Y. Zhan and J. Zhang, "Facial expression recognition based on selective feature extraction," *International Conf. on Intelligent Systems Design and Applications*, Vol. 2, pp. 412–417, 2006.

[2] T. Salonidis, P. Bhagwat, L.Tassiulas, R.LaMaire, "Distributed topology construction of Bluetooth personal area networks," *INFOCOM. Twentieth Annual Joint Conference of the IEEE Computer and Communications Societies. Proceedings. IEEE*, vol. 3, pp.1577 -1586, April 2001.

[3] P. Ekman and W.V. Friesen, "The facial action coding system: A Technique for The measurement of facial movement," *San Francisco, Consulting Psychologists Press*,1978.

[4] J. F. Cohn, A. J. Zlochower, J. J. Lien and T. Kanade, "Feature-Point tracking by optical flow discriminates subtle Differences in facial expression," *Third IEEE International Conference on Automatic Face and Gesture Recognition*, Nara,Japan, pp. 396-401, 1998.

[5] Ying-li Tian, T. Kanade and J.F. Cohn, "Recognizing action units for facial expression analysis," *IEEE Transaction on Pattern Analysis and Machine Intelligence*, vol. 23, no. 2, pp. 97-115, 2001.

[6] Jiapu Pan, and W. J. Tompkins, "A Real-time QRS Detection algorithm," *Trans. On Biomed. IEEE*, Vol. 32, No.3, pp.230-236, 1985.

[7] Fleet, R., Lavoie, K., & Beitman, B. D., "Is panic disorder associated with coronary artery disease? A critical review of the literature," *Journal of Psychosomatic Research,* Vol.48, pp.347-356, 2000.

[8] Murata, T., Takahashi, T., Hamada, T., Omori, M., Kosaka, H., Yoshida, H., "Individual trait anxiety levels characterizing the properties of zen meditation," *Neuropsy-chobiology,*Vol.50, pp.189-194, 2005.

2011 IEEE International Conference on Fuzzy Systems
June 27-30, 2011, Taipei, Taiwan

Fuzzy Control of a Bi-directional Inverter with Nonlinear Inductance for DC Microgrids

Gwo-Ruey Yu
Department of Electrical Engineering
National Chung Cheng University
Chia-Yi, Taiwan
E-mail: ieegwoyu@ccu.edu.tw

Jing-Siou Wei
Department of Electrical Engineering,
National Chung Cheng University
Chia-Yi, Taiwan

***Abstract*—This paper proposes the design of fuzzy control of a bi-directional converter with variable inductance for dc microgrids. The nonlinear inductance model is developed and taken into consideration in the controller design of the bi-directional inverter to promote the performance. A novel fuzzy control strategy is proposed to increase the magnetizing voltage such that the current distortion is reduced. Simulated results demonstrated the effectiveness of the design.**

Keywords- Bi-directional converter, fuzzy control, dc microgrids

I. INTRODUCTION

Energy crisis inevitably brings nearer for the depletion of fossil. The greenhouse effect becomes more serious by the increased requirements for electric power. In recent years, renewable energy has received great attention due to the advantages of clean, no pollution and huge reserves. Many distributed generations such as photovoltaic cells, wind turbines and fuel cells have been linked with the utility grids [1]. However, the power quality of utility grids will be decreased by distributed generations [2]. To reduce conversion losses and supply high quality power, the dc microgrid is proposed in this paper.

Power electronic converters are one of the most important devices among the components of the microgrid [3]. In this paper, a bi-directional converter is designed to regulate the dc bus voltage for different types of energy sources and energy storage. The functions of the bi-directional inverter include grid connection mode and rectification mode. Fig. 1 shows the schema of the microgrid system.

The inductance is usually assumed to be a constant in the design of the inverter controller [4]. However, the inductance is a highly nonlinear function varied with the current. It is important to take the inductance variation into account when the operational principle of the bi-directional inverter is designed. In this paper, the methodology of nonlinear least squares is applied to build the nonlinear inductance model such that the performance of the bi-directional inverter is improved. Besides, the magnetizing voltage will be too low to track the reference current if the inductor is magnetized only with line voltage in rectification mode. A current hollow will appear near the zone of zero crossing no matter how the control duty ratio is filled. Thus, a novel fuzzy control strategy is proposed to increase the magnetizing voltage such that the current distortion is reduced.

Fuzzy theory is introduced by Zadeh in 1965 [5]. In artificial intelligence, fuzzy sets could be applied to control the plant. Based on fuzzy logic, a fuzzy controller converts a linguistic control strategy into an automatic control strategy, and fuzzy rules are constructed by expert experience or knowledge. The main feature [6] of fuzzy control is that the controller design doesn't rely on a mathematical model of a plant. The fuzzy inference system employing fuzzy if-then rules can control a plant using the human knowledge. Fuzzy controller has been widely used in industry for its easy realization and good robustness. Accordingly, the fuzzy logic is employed to design the PWM gain of the bi-directional inverter for dc microgrid.

The rest of this paper is organized as follows. Section 2 describes the model of the bi-directional inverter. Section 3 proposes the design of fuzzy controller. Section 4 shows simulation results with the presented scheme. Section 5 gives the conclusion.

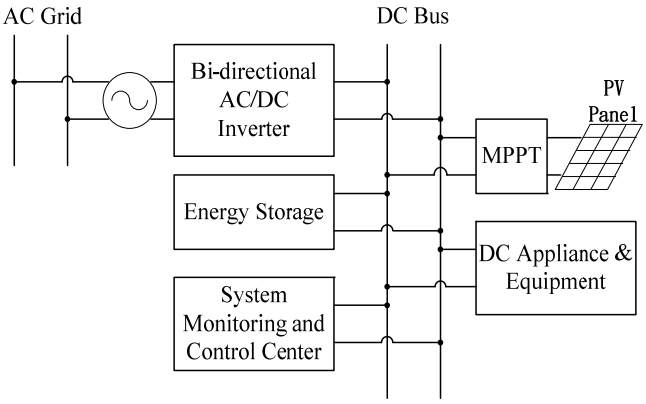

Fig. 1 The schema of the microgrid system

II. THE BI-DIRECTIONAL INVERTER

A. Circuit Configuration

Fig. 2 shows the proposed bi-directional inverter with a full-bridge configuration. The functions of the bi-directional

inverter include grid connection mode and rectification mode mode. The inverter senses inductor current i_L and uses the dc-link voltage v_{dc} and line voltage v_s in the single-chip microcontroller (dsPIC30F2023) to determine a control for operating the inverter stably.

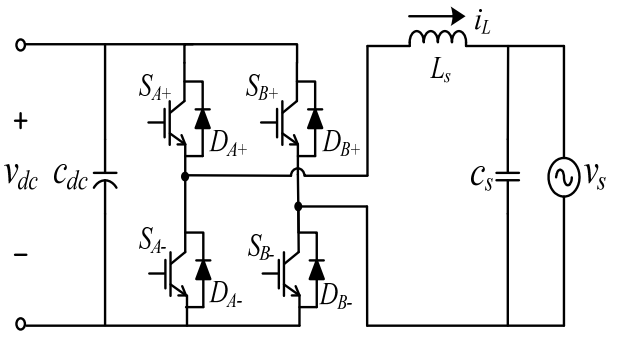

Fig. 2 The circuit configuration of the bi-directional inverter

B. Duty Ratio

In the grid connection mode, $\Delta i_L = \Delta i_{L(on)} + \Delta i_{L(off)}$

$$\Delta i_L = \frac{v_{dc} - |v_s|}{L} dT_s - \frac{|v_s|}{L}(1-d)T_s \tag{1}$$

where T_S is the period of the PWM. The duty ratio can be expressed as

$$d = \frac{\Delta i_L \cdot L}{v_{dc} \cdot T_s} + \frac{|v_s|}{v_{dc}} \tag{2}$$

In the rectification mode,

$$\Delta i_L = \frac{|v_s|}{L_s} dT_s - \frac{v_{dc} - |v_s|}{L_s}(1-d)T_s \tag{3}$$

The duty ratio can be expressed as

$$d = \frac{\Delta i_L \cdot L_s}{v_{dc} \cdot T_s} + \frac{v_{dc} - |v_s|}{v_{dc}} \tag{4}$$

C. Nonlinear Inductance Model

Let the nonlinear inductance model be

$$y = f(x) = ax^2 + bx + c \tag{5}$$

where y is the estimated value of inductance, x is the value of current. The sum of square error between the estimated and measured value of inductance will be

$$\sum \left[ax_i^2 + bx_i + c - y_i \right]^2 \tag{6}$$

where n is the total number of experimental date (x_i, y_i).

To minimize the sum of square error, taking the partial derivative to a, b and c, respectively gets

$$\begin{cases} \sum 2x_i^2 (ax_i^2 + bx_i + c - y_i) = 0 \\ \sum 2x_i (ax_i^2 + bx_i + c - y_i) = 0 \\ \sum 2(ax_i^2 + bx_i + c - y_i) = 0 \end{cases} \tag{7}$$

After substituting the experimental date (x_i, y_i) into the above equation, we can get a nonlinear inductance model to approximate the nonlinear mapping between the inductance and the current.

D. Refining Tracking Error

If the inductor L_s is magnetized by only turning on S_{A+} in the rectification mode, the magnetizing voltage v_s will be too low to track the reference current near the zero crossing. To refine the waveform of inductor current, a novel PWM strategy is developed as shown in Fig. 3. The magnetizing voltage should be increased to $v_L = v_{dc} + v_s$ by appropriately turning on S_{A+} and S_{B-}.

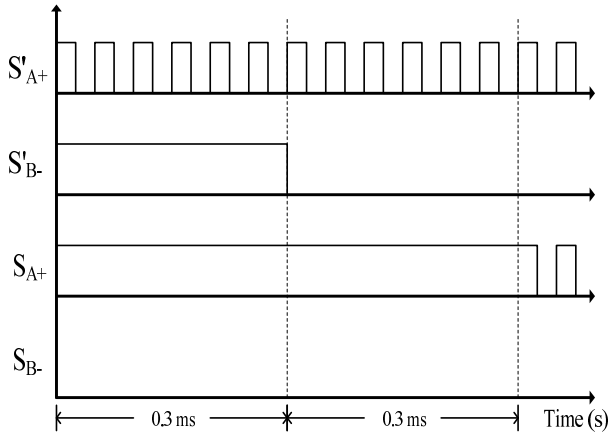

Fig. 3 Different switching sequence

III. Fuzzy Control

A. Fuzzification

The design procedure of fuzzy logic controller includes fuzzification, fuzzy rule base, fuzzy inference and defuzzification. In this paper, the linguistic variables are state error e, change in error Δe and fuzzy gain u. The Mamdani fuzzy inference system uses minimum and maximum for T-norm and T-conorm operators, respectively.

The fuzzy sets and the fuzzy rules are defined as follows. The linguistic variables of input e and Δe are defined as {N, Z, P}, where N means negative, Z means zero and P means positive. The linguistic variables of output u are defined as {SS, SM, SB, MS, MM, MB, BS, BM, BB}, where S means small, M means medium and B means big.

The universe of discourse of e is assigned to be [-1 1]. The universe of discourse of Δe is assigned to be [-1 1]. The membership functions of the fuzzy sets corresponding to variables e and Δe are shown in Fig. 4.

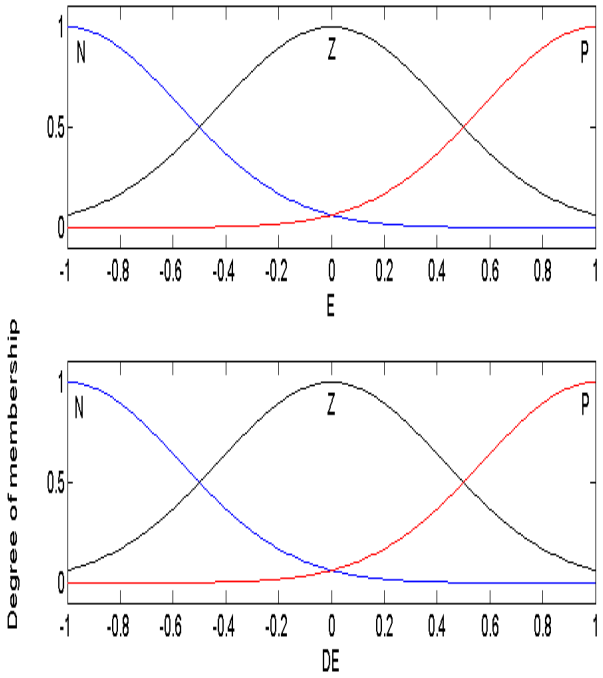

Fig. 4 Membership Functions

B. *Fuzzy Inference Engine*

The minimum inference engine is applied to design fuzzy inference mechanism in this study. With max-min composition, the consequence $\mu_{B'}(y)$ is

$$\mu_{B'}(y) = \max_{l=1}^{m}[\mu_{A_1^l}(x_1) \wedge \mu_{A_2^l}(x_2) \wedge \mu_{B^l}(y)] \tag{8}$$

where x_1, x_2 and y represent the fuzzy sets e, Δe and u, respectively; $\mu_{A_1^l}(x_1)$, $\mu_{A_2^l}(x_2)$ and $\mu_{B^l}(y)$ mean the membership functions of e, Δe and u, respectively; l is the index of membership functions for every fuzzy set; m is the number of triggered fuzzy rules.

C. *Fuzzy Rules*

According to the Mamdani inference method, fuzzy if-then rules are designed. By means of using three linguistic variables N, Z and P of each input variable, nine fuzzy rules are derived. These fuzzy inference rules are summarized in Table 1.

Table 1. Fuzzy inference rules

	e(t)			
		N	Z	P
Δe	N	BM	SM	MM
	Z	BS	SS	MB
	P	MS	SB	BB

D. *Defuzzification*

Defuzzification is used to extract a crisp value from a fuzzy set. There are a lot of methods for defuzzifying a fuzzy set. The center of gravity defuzzification is used in this paper

$$Y^* = \frac{\sum_{i=1}^{m} \mu_{B^i}(y_i) \cdot y_i}{\sum_{i=1}^{m} \mu_{B^i}(y_i)} \tag{9}$$

where Y^* is the crisp values of fuzzy gain u, i is the index of consequent rules.

IV. Simulation Results

Fig. 5(a) shows the shows the experimental data of measured inductance. After substituting these experimental date (x_i, y_i) into the equation (7), we can get the following nonlinear inductance model

$$L_S = 2.851 I_L^{\,2} - 244.6 I_L + 5604 \tag{10}$$

Fig. 5(b) shows the comparison between the nonlinear inductance model and the measured values. Obviously, the nonlinear model is very similar to the experimental data.

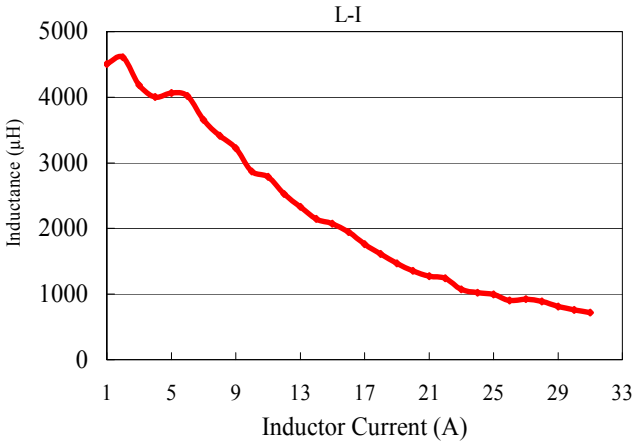

Fig. 5(a) Experimental data of inductance variation

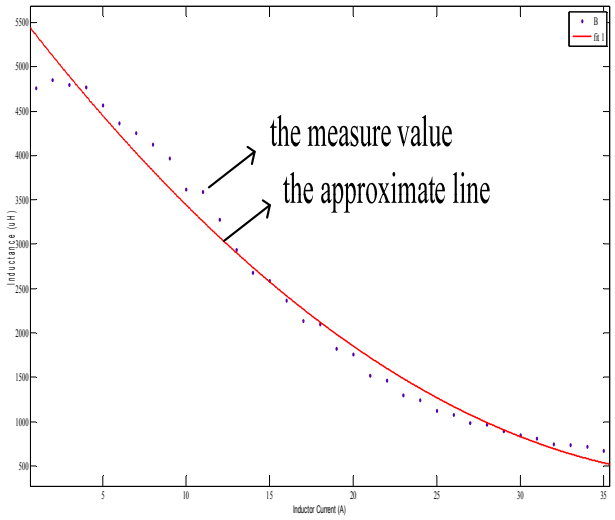

Fig. 5(b) The nonlinear model of inductance variation

Modeling and simulation are essential for developing controller programs. In this paper, the Matlab and Simulink software is utilized for modeling and simulating. Fig. 6(a) shows the simulation response without considering inductance variation in the grid connected mode. Fig. 6(b) shows the simulation response considering inductance variation in the grid connected mode. Apparently, the inductance current will have better waveform when the controller design takes the inductance variation into consideration. Fig. 7(a) shows the simulation response without considering inductance variation in the rectification mode. Fig. 7(b) shows the simulation response considering inductance variation in the rectification mode. Again, the inductance current will have more fluctuation if the controller design shorts of inductance variation consideration. Fig. 8(a) shows the simulation response of inductor current by turning on S_{A+} only. Fig. 8(b) shows the simulation response of inductor current by turning on S_{A+} and S_{B-}. The tracking error is significantly reduced between the reference current and the inductor current.

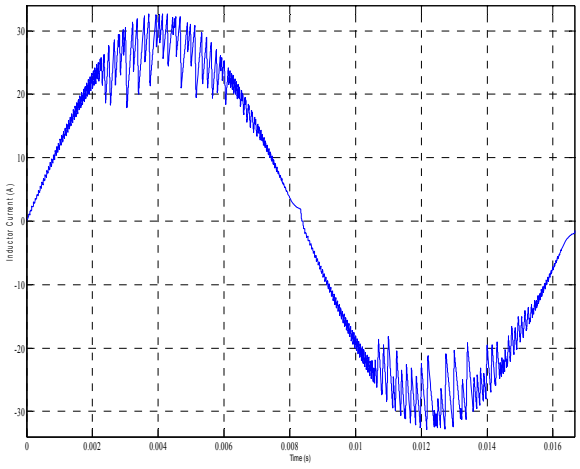

Fig. 6(a) Simulation response (GC mode) without inductance variation

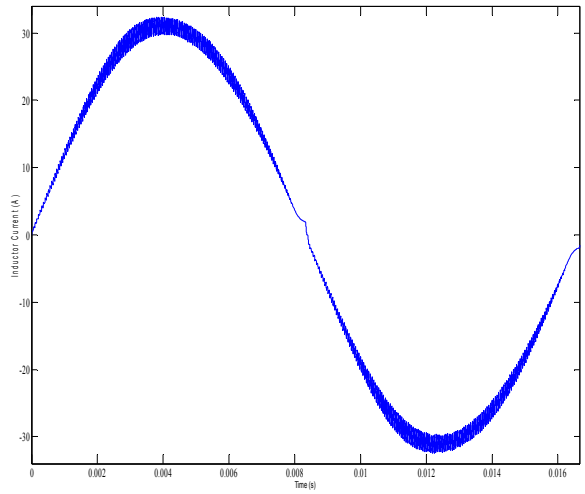

Fig. 6(b) Simulation response (GC mode) with inductance variation

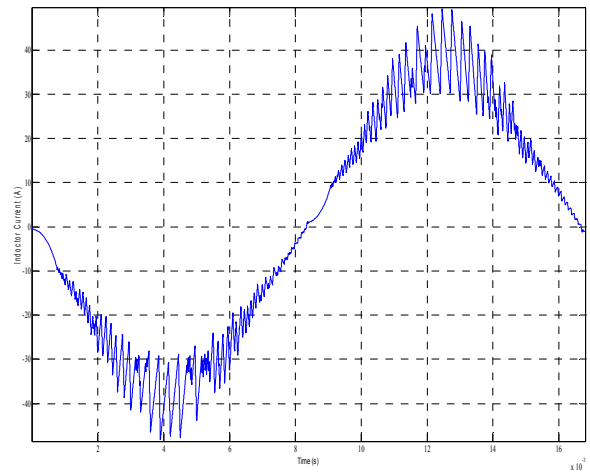

Fig. 7(a) Rectification mode without inductance variation

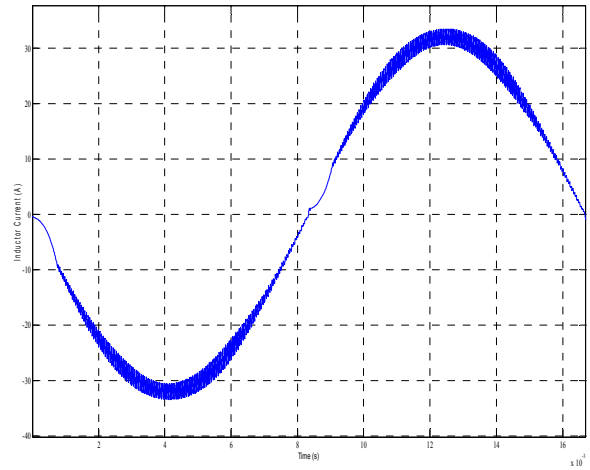

Fig. 7(b) Rectification mode with inductance variation

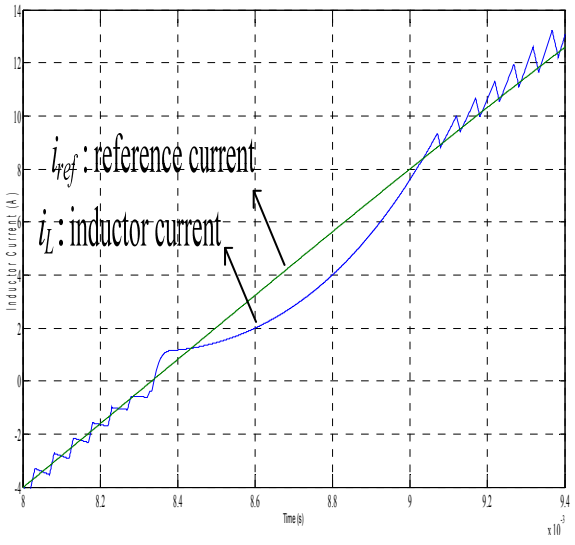

Fig. 8(a) Simulation response (S_{A+} on)

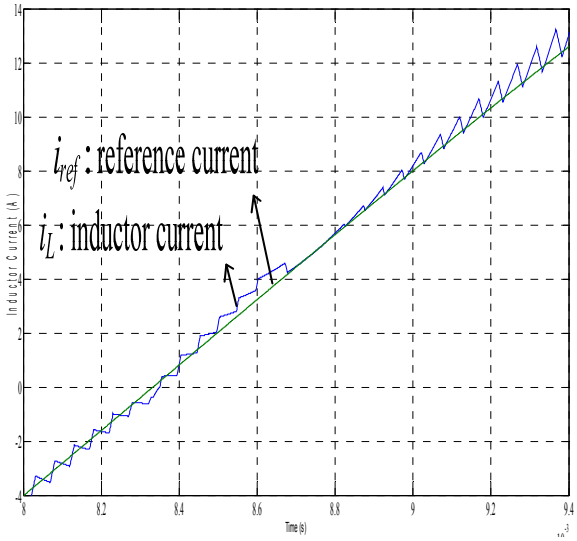

Fig. 8(b) Simulation response (S_{A+} and S_{B-} on)

V. Conclusion

We considered the dc bus voltage regulation problem of the bi-directional converter using fuzzy control strategy. Furthermore, to promote the regulation performance, a nonlinear inductance model between the current and the inductance mapping is established. Then, a novel fuzzy control strategy which takes account of inductance variation is proposed to increase the magnetizing voltage such that the current distortion is reduced. Last, the computer simulation shows that the fuzzy controller with inductance variation design is superior to the fuzzy controller without inductance variation design.

Acknowledgment

This research is sponsored by means of the National Science Council of the Republic of China, under Grant NSC 99-2221-E-197-022 and NSC 99-3113-P-194-001-.

References

[1] D. Salomonsson, L. Soder and A. Sannino, "An adaptive control system for a dc microgrid for data centers," *IEEE Trans. on Industry Applications*, vol. 44, Nov. 2008, pp. 1910-1917.

[2] E. Reutzel and S. Sanders, "A single-stage single-phase bi-directional grid interface circuit with digital lookup table based control" *Proceedings of the IEEE APEC 2010*, pp. 1430-1434.

[3] T.-F. Wu, S.-A. Wang, C.-L. Kuo and K.-Y. Lee, "Design and implementation of a push-pull phase-shifted bi-directional inverter with a dsPIC controller," *Proceedings of the IEEE PEDS 2009*, pp. 728-733.

[4] T.-F Wu, H.-S Nein, C.-L Shen and T.-M Chen, "A single-phase inverter system for PV power injection and active power filtering with nonlinear inductor consideration," *IEEE Trans. on Industry Applications*, Vol. 41, No. 4, pp. 1075-1083, July-August, 2005.

[5] Chin-Teng Lin and C.S. George Lee, *Neural Fuzzy Systems*, Prentice-Hall, New Jersey, 2005.

[6] Li-Xin Wang, *A course in fuzzy system and control*, Prentice-Hall, New Jersey, 2003.

2011 IEEE International Conference on Fuzzy Systems
June 27-30, 2011, Taipei, Taiwan

The Development of the Automatic Lane Following Navigation System for the Intelligent Robotic Wheelchair

Wen-Chang Cheng and Chia-Ching Chiang
Depart. of Computer Science and Information Engineering,
Chaoyang University of Technology,
168, Jifong E. Rd., Wufong Township Taichung County, 41349,
{wccheng, s9927623}@cyut.edu.tw

***Abstract*—In this paper, we constructed an intelligent robotic wheelchair equipped with automatic tracking function in barrier-free environment of campus; the system used video paint line detection as the basis of automatic tracking navigation; since the barrier-free environment of campus includes indoor and outdoor environment and the outdoor environment includes gentle slopes, sidewalk and etc, we proposed a paint line detection method, which showed color distribution and judgment of paint line using Gaussian mixture models; the input image completed paint line detection and parameters calculation with this method and then input them into the fuzzy logic controller of wheelchair and in this way, the tracking navigation control of wheelchair was performed; the system was actually tested on barrier-free paths in campus, including straight and curve barrier-free paths; the result showed that the system could make the wheelchair keep moving on the paint line correctly and the mean deviation was kept within ±10 cm, which proved the navigation of intelligent robotic wheelchair could be realized automatically and successfully on barrier-free paths in campus.**

Keywords-path lane following; gaussian mixture models; color spacec conversion; color segmentation; fuzzy control.

I. INTRODUCTION

In Taiwan, the percentage of population of the old aged above 65 to the total population increased from 10.4% in 2008 to 10.6% in 2009; it is estimated that the aging population will account for 20.04% of the total population in 2070[1, 2]; these figures show Taiwan has entered the aging society, therefore, there is an urgent need of the care for the aged. As more and more people are using wheel chairs in aging society, barrier-free space is built out in succession in many places; Chaoyang University of Technology has been always paying much attention to this issue, so a barrier-free space has been built in the campus; to apply the technology to the concept of holistic care [3], we introduced the intelligent robotic wheelchair in barrier-free environment in campus and created a intelligent robotic wheelchair equipped with automatic tracking navigation based on computer vision; the system captures images of barrier-free environment with a camera installed on the wheelchair and controls the automatic tracking navigation of robotic wheelchair in barrier-free environment in campus through real time detection of paint line and fuzzy control.

The automatic tracking navigation technology based on paint line detection of computer vision has been mentioned in many related researches [4-13]; generally, the common detection methods include comparison based on characteristics, colors, models, etc; to highlight positions, the distinct paint line was used as path guide in barrier-free environment, so we used color detection method in this paper. The simplest method for color detection is critical value method; range of critical value was set according to the distribution of color to be detected; when color fell into the range, it was deemed to be the color detected, otherwise it was not; furthermore, some scholars proposed the method using the single Gaussian function to show the distribution of specific color in space [14]; since the barrier-free environment of campus includes indoor and outdoor environment and there is shadow, tree shade and stain, etc in outdoors, which can not be shown by the single Gaussian function, we proposed to express the probability distribution of color of paint line with Gaussian mixture models which are composed of several Gaussian functions according to different weight values, thus it can show the probability distribution of color of paint line more correctly; the input image could complete the detection of color of paint line through Gaussian mixture models more accurately; moreover, color of paint line changed at any time with environment and external light source, so we updated Gaussian mixture models at real time with the updating algorithm of dynamic Gaussian mixture models to make the paint line detection of the system more stable and more suitable for various environments. After paint line detection, calculate the position and angle of paint line with Hough transform, input the result into the entry of fuzzy controller of wheelchair and control the difference between velocity of the right wheel and left wheel through fuzzy logic to control wheel chair direction and then complete the tracking navigation function of robotic wheelchair.

The other structures of the paper are described as below; Section II proposes system architecture; Section III introduces methods to detect paint line; Section IV introduces fuzzy system control of automatic lane following of robotic

978-1-4244-7316-8/11/$26.00 ©2011 IEEE

wheelchair; the simulated experiment and the actual experimental results are shown in Section V; the last section is conclusion and discussion.

II. SYSTEM ARCHITECTURE

Fig.1 shows the system architecture of intelligent robotic wheelchair proposed by us, which includes image capture and correction, paint line detection, parameter calculation, graphical operation interface, fuzzy controller, etc. Image capture and correction read images into the system through camera and capture card and converting camera into space coordinates; as camera coordinates are different from space coordinates, the input images should be converted to aerial view through coordinate conversion; paint line detection and parameter calculation detect color of paint line through images and calculate angular separation between paint line position and wheelchair direction through Hough transform.

Fuzzy logic controller is responsible for controlling tracking navigation of wheelchair; it has two entries, which are angular separation between straight line of paint line and wheelchair direction; while the output controls the difference between velocities of two wheels directly, getting an angular velocity through changes of the difference between velocities of two wheels to make wheelchair be able to make a turn to proceed towards the correct direction; the last part is graphical operation interface; the system operation can be simplified through graphical operation interface to make the mobility-handicapped or senior citizen be able to operate the system by clicking.

We will elaborate on technologies of every part in Fig.1 in the following chapters.

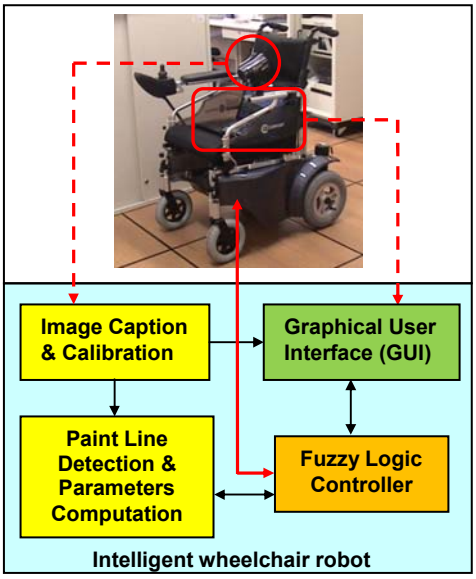

Figure 1. System architecture

III. PAINT LINE DETECTION

It was difficult to detect the position of paint line with color; since color of paint line was susceptible to light source, weather, stain, shadow and etc, we proposed a set of robust paint line detection method in this paper; this method learned the probability distribution of color of paint line using a Gaussian mixture model and the input image detected position of paint line of image through a Gaussian mixture model it had learnt before. Below is detailed description.

A. Color space conversion

To reduce the effect of light source on color detection, we used a and b in CIE-Lab color space as the basis of paint line detection; in this paper, we used BT-709 format conversion of ITU-R and employed D65 as reference white point; since RGB color space could not correspond to Lab color space directly, it must be converted to XYZ color space first and then converted to Lab color space; the conversion of RGB color space to XYZ color space can be expressed by the matrix operation equation (1) below:

$$\begin{bmatrix} X \\ Y \\ Z \end{bmatrix} = \begin{bmatrix} 0.4124 & 0.3576 & 0.1805 \\ 0.2126 & 0.7152 & 0.0722 \\ 0.0193 & 0.1192 & 0.9505 \end{bmatrix} \begin{bmatrix} R \\ G \\ B \end{bmatrix}, \tag{1}$$

while the conversion of XYZ color space to Lab color space can be defined as the equation (2):

$$\begin{aligned} L &= 116 f\left(\frac{Y}{Y_n}\right) - 16, \\ a &= 500\left[f\left(\frac{X}{X_n}\right) - f\left(\frac{Y}{Y_n}\right)\right], \\ b &= 200\left[f\left(\frac{Y}{Y_n}\right) - f\left(\frac{Z}{Z_n}\right)\right], \\ f(t) &= \begin{cases} t^{\frac{1}{3}}, & t > 0.008856 \\ 7.787t + \frac{16}{116}, & t \le 0.008856 \end{cases}, \end{aligned} \tag{2}$$

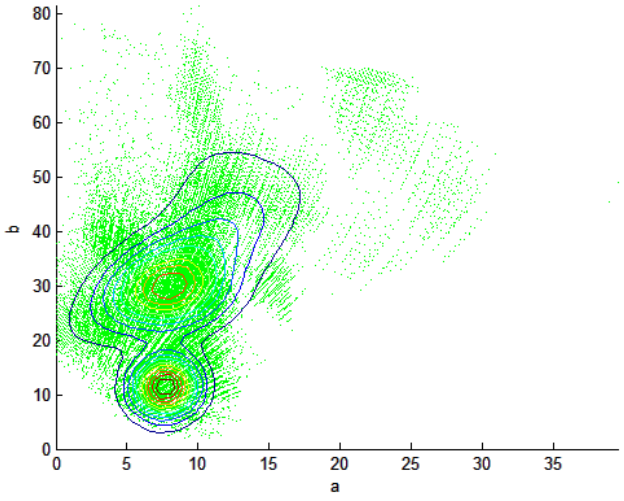

Figure 2. Distribution of a-b values of paint line color and the contour line of 5 Gaussian mixture models

where, $X_{n,}$=0.9504, Y_n=1 and Z_n=1.0883 are D65 reference white points. Fig.2 shows the distribution map of a-b values of paint line color, where every blue point represents the sampling value of every paint line color a-b. We collected a-b values of 1,250,000 paint line colors under many circumstances (indoors and outdoors; the latter includes rainy

days, sunny days, at dusk, daytime, etc); we can find from the figure that the distribution of *a-b* values of paint line color is irregular, so it can not be expressed by setting range of critical values or by the single Gaussian function and we used mixed model of Gaussian function to learn the probability distribution of *a-b* values of paint line color.

B. *The expression of paint line color by Gaussian mixture models*

Gaussian mixture model (GMM) refers to a mixed model composed of multiple Gaussian functions; because GMM can approach probability density distribution of any shape, it is very suitable for modeling the probability distribution of *a-b* values of paint line color; GMM can be represented by the weight sum of *K* Gaussian functions and the definition is shown as equation(3):

$$p(\mathbf{x}_i|\mathbf{\Theta}) = \sum_{k=1}^{K} p_k p(\mathbf{x}_i|\boldsymbol{\mu}_k, \boldsymbol{\Sigma}_k), k = 1, 2, ..., K, \quad (3)$$

where $\mathbf{x}_i \in R^2$, i = 1, 2, …, n, is input vector; n refers to number of samples input; $\mathbf{\Theta} = \{\boldsymbol{\mu}_1, \boldsymbol{\mu}_2, ..., \boldsymbol{\mu}_K | \boldsymbol{\Sigma}_1, \boldsymbol{\Sigma}_2, ..., \boldsymbol{\Sigma}_K\}$, where $\boldsymbol{\mu}_k$ and $\boldsymbol{\Sigma}_k$ refer to the mean value and covariance matrix of the kth Gaussian function separately; p_k, k = 1, 2, …, K, represents the weight value of component of every Gaussian function in Gaussian mixture models and every Gaussian function can be expressed as equation (4):

$$p(\mathbf{x}_i|\boldsymbol{\mu}_k, \boldsymbol{\Sigma}_k) = \frac{1}{\sqrt{(2\pi)^d |\boldsymbol{\Sigma}_k|}} \exp\left[-\frac{1}{2}(\mathbf{x}_i - \boldsymbol{\mu}_k)^T \boldsymbol{\Sigma}_k^{-1}(\mathbf{x}_i - \boldsymbol{\mu}_k)\right], \quad , k = 1, 2, ..., K, \quad (4)$$

where, $\boldsymbol{\mu}_k$ and $\boldsymbol{\Sigma}_k$ refer to the mean value and covariance matrix of the kth Gaussian function separately, therefore, there are K mean values and K covariance matrixes; $\mathbf{\Theta} = \{\boldsymbol{\mu}_1, \boldsymbol{\mu}_2, ..., \boldsymbol{\mu}_K | \boldsymbol{\Sigma}_1, \boldsymbol{\Sigma}_2, ..., \boldsymbol{\Sigma}_K\}$; the method used to train Gaussian mixture models is called EM algorithm which is a recursive algorithm including two procedures, namely, estimation procedure(*E*-procedure) and update procedure (*M*-procedure) separately; *E*-procedure refers to estimating the probability that every input sample belongs to individual Gaussian function based on the current parameters of Gaussian mixture models and its calculation is defined as:

$$\hat{p}(k|i) = p(y_i = k|\mathbf{x}_i, \boldsymbol{\theta}_k), \forall k, i, \quad (5)$$

where, k = 1, 2, …, K, K refers to the number of Gaussian functions used by GMM; i = 1, 2, …, n, n refers to the number of samples input, so $\hat{p}(k|i)$ stands for the probability that the input $\mathbf{x}_i$ *the kth* belongs to Gaussian function; $\boldsymbol{\theta}_k = \{\boldsymbol{\mu}_k, \boldsymbol{\Sigma}_k\}$, $\boldsymbol{\mu}_k$ and $\boldsymbol{\Sigma}_k$ refer to the mean value and covariance matrix of the kth Gaussian function separately; *M*-procedure updates all parameters with $\hat{p}(k|i)$ and its calculation is defined as below:

$$\hat{n}_k \leftarrow \sum_{i=1}^{n} \hat{p}(k|i), \forall k, \quad (6)$$

$$\hat{p}_k \leftarrow \frac{\hat{n}_k}{n}, \forall k, \quad (7)$$

$$\hat{\boldsymbol{\mu}}_k \leftarrow \frac{1}{\hat{n}_k} \sum_{i=1}^{n} \hat{p}(k|i)\mathbf{x}_i, \forall k, \quad (8)$$

$$\hat{\boldsymbol{\Sigma}}_k \leftarrow \frac{1}{\hat{n}_k} \sum_{i=1}^{n} \hat{p}(k|i)(\mathbf{x}_i - \hat{\boldsymbol{\mu}}_k)(\mathbf{x}_i - \hat{\boldsymbol{\mu}}_k)^T, \forall k, \quad (9)$$

Repeat *E*-procedure and *M*-procedure above until the convergence.

The contour line in Fig.2 shows Gaussian mixture model which uses 5 Gaussian functions to learn the result of probability distribution of *a-b* values of paint line color; it can be clearly seen from the figure that the probability distribution of two Gaussian functions is more distinct mainly because most *a-b* values of paint line color are converged in the range covered by the two Gaussian functions. After learning, Gaussian mixture models can be used to show the probability distribution of *a-b* values of paint line color, therefore, the *a-b* values of each pixel color of any input image can be substituted in Gaussian mixture models that has learnt in advance; after simple critical value judgment, the image result of paint line corresponding to input image can be obtained and its calculation definition is shown as below:

$$F(\mathbf{x}_i) = \begin{cases} 1, & p(\mathbf{x}_i|\mathbf{\Theta}) \geq Th1 \\ 0, & otherwise \end{cases}, \quad (10)$$

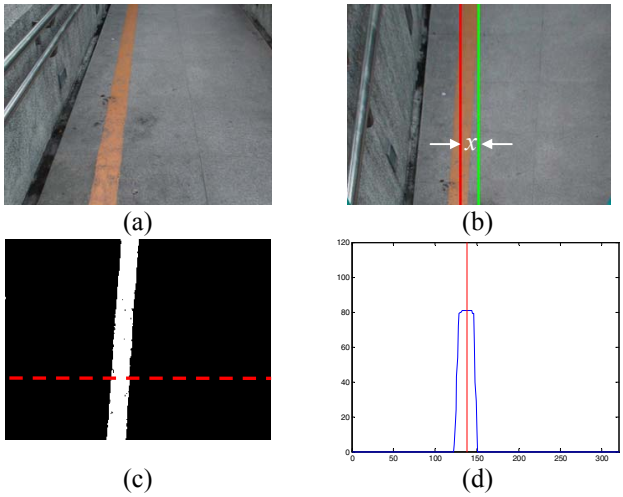

Figure 3. Example of paint line detection, (a) original input image, (b) aerial view of input image, (c) result of paint line detection, and (d) result of paint line position detection

where F represents the image result of paint line detection and $Th1$ is critical value 0.0005. Fig.3 is an example of paint line detection; Fig.3(a) is original input image; Fig.3(b) is the aerial view of input image after coordinate conversion; Fig.3(c) is result of paint line detection of the aerial view; the result shown in Fig.3(d) can be obtained by accumulating the 2/3

height of paint line image to its projection from the bottom to the horizontal axis; in Fig.3(d), we can find the mean value of the horizontal position corresponding to the maximum value, as shown by the red vertical full line in Fig.3(b) and (d), therefore, the width between the mean position to the imaging centre is defined as x(as pointed at by white arrow in Fig.3(b), where the green vertical line is the horizontal and center of image) and the variable quantity of x is defined as dx; these two values are used as two input parameters of fuzzy control system, which will be introduced in the following chapter.

IV. FUZZY CONTROL OF WHEELCHAIR

In this paper, we used fuzzy logic to control wheelchair for tracking navigation because the advantage of fuzzy control is that it can express the expert knowledge as system easily to make the system closer to human thinking and comply with the nonlinear system in real world better. Fig.4 shows the fuzzy control system architecture proposed by us; the architecture includes two input parameters x and dx, and one output parameter is angular acceleration of wheelchair; a_1 and a_2 in the figure stand for normalized coefficients of input parameters and normalize input parameters to values within [-1, 1]; a_3 represents the output value, which was changed from output parameter by [-1, 1] to corresponding motor control; Fig.5, 6 and 7 show triangular fuzzy membership function corresponding to input parameters x and dx, and angular acceleration of output, we use triangular membership functions, the main reason is simplify computation, and effective expression expert knowledge; each input parameter has 5 membership functions: {LE, LC, CE, RC, RI} and {LE', LC', CE', RC', RI'}, where LE means Left, LC means Left Center, CE means Center, RC means Right Center, RI means Right, each output parameter has 5 membership functions: {NM, NS, ZE, PS, PM}, where NM means Negative Medium, NS means Negative Small, ZE means Zero, PS means Positive Small, PM means Positive Medium, so there are 25 fuzzy rules in the rule base; table 1 lists membership functions of output corresponding to fuzzy rules; Fig.8 is the output fuzzy graph of fuzzy control system.

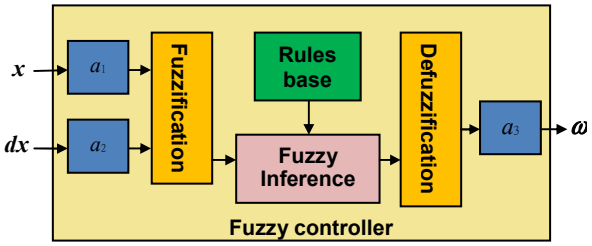

Figure 4. Fuzzy control system of wheelchair

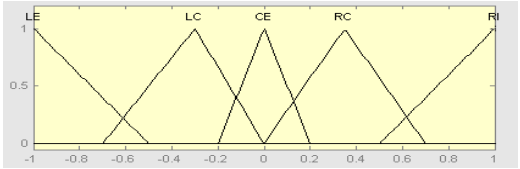

Figure 5. Membership function of input x

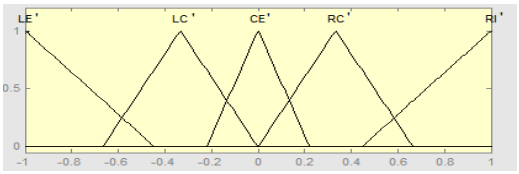

Figure 6. Membership function of input dx

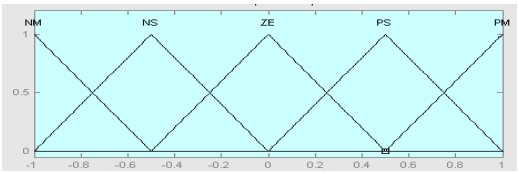

Figure 7. Output membership function

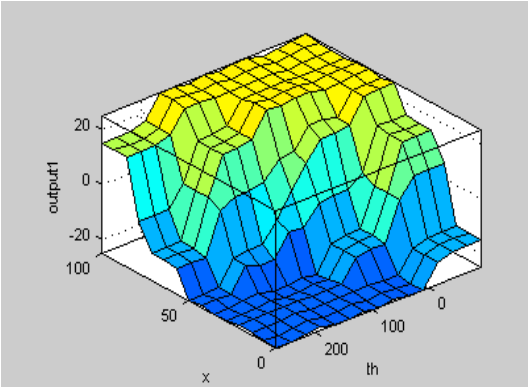

Figure 8. Output figure of fuzzy control system

TABLE 1. RULE BASE OF FUZZY CONTROL SYSTEM

x / dx	LE	LC	CE	RC	RI
LE'	NS	PS	PM	PM	PM
LC'	NM	NS	PS	PM	PM
CE'	NM	NM	ZE	PM	PM
RC'	NM	NM	NS	PS	PM
RI'	NM	NM	NM	NS	PS

V. EXPERIMENTAL RESULT

In this paper, to verify the method proposed by us can complete paint line detection and automatic tracking navigation effectively, we conducted a simulated experiment and an actual test, which will be described below respectively.

A. Simulation test of wheelchair motion equation

To verify that the fuzzy control system can be applied to wheelchair control, we first use the equation of wheelchair motion to simulate the tracking control performance of wheelchair; Fig.9 is a schematic diagram of a robotic wheelchair which is driven mainly by two rear wheels; the two front wheels are steering auxiliary wheels which can support 360-degree steering and are used to stabilize wheelchair besides direction control; v stands for velocity of wheelchair and ϕ for the included angle between wheelchair and paint line; assume the right and left wheel velocities are defined as ω_l and ω_r and tyro radius of driving wheel of wheelchair is r, and then the velocity of the right and left wheels can be defined as:

$$v_l = r\omega_l \quad \text{and} \quad v_r = r\omega_r. \tag{11}$$

Since wheelchair velocity can be expressed as $v = (v_r + v_l)/2$, substitute the equation (11) into it and we can get:

$$v = \frac{r}{2}(\omega_r + \omega_l). \tag{12}$$

Finally, we can get the equation of wheelchair motion:

$$\dot{y} = v\cos(\phi), \dot{x} = v\sin(\phi), \text{and } \dot{\phi} = \omega, \tag{13}$$

where $\dot{y}$ and $\dot{x}$ refer to the variable quantity in the direction of x and y, and $\dot{\phi}$, the variable quantity of angle, is the angular velocity of wheelchair. Simulate the motion of wheelchair with the equation of wheelchair motion and fuzzy control and the result is shown in Fig.10, where the red block stands for wheelchair and the green arrow stands for the moving direction and the blue curve for the position of paint line; in this example, assume the initial position of wheelchair is 20 cm from the right of paint line and the wheelchair moves in parallel with the paint line; it is found after simulation of fuzzy control that the wheelchair approaches the paint line slowly and moves forward along the paint line indeed. Fig.11 shows x, the distance between wheelchair and paint line; Fig.12 shows the angle between wheelchair and paint line.

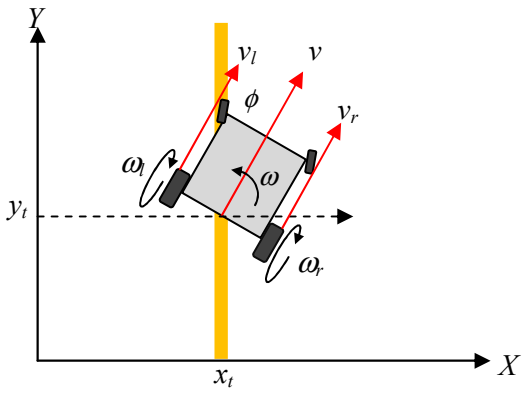

Figure 9. Motion model of wheelchair

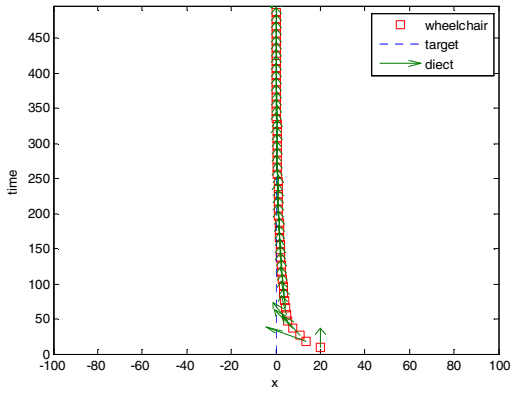

Figure 10. Lane following navigation simulation

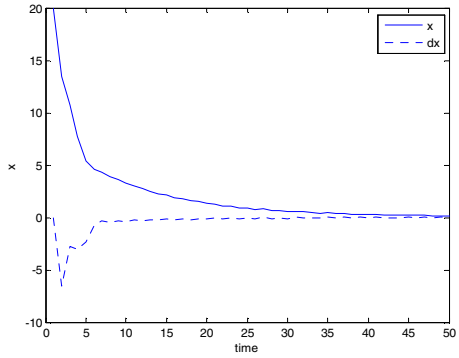

Figure 11. Result of navigation simulation at horizontal position

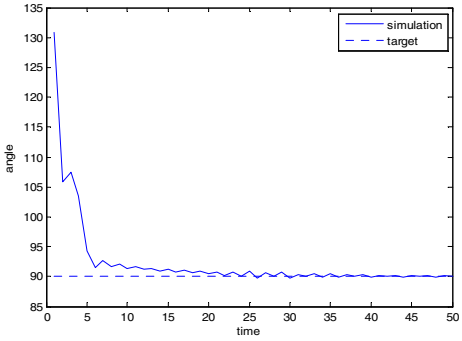

Figure 12. Result of navigation simulation at angle

B. *Field testing*

For this experiment, we divided it into two parts for description, namely, paint line detection and field test; for paint line detection, we performed it based on the effect of Gaussian functions of different numbers on Gaussian mixture models; we used GMM with best Gaussian function numbers to complete the field test. They will be discussed and described separately below:

First, perform test on paint line detection based on Gaussian functions of different numbers; we used images in different environment and under different light sources for tests; the results of paint line detection by GMMs with 1, 3, 5 and 10 Gaussian functions separately were used in the experiment(Fig. 15); it could be found from the experimental result that the result based on 1 Gaussian function was the worst; the result based on 3 Gaussian functions was much better than that of 1 Gaussian function; the result based on 5 and 10 Gaussian functions were improved, compared with that of 3 Gaussian functions under certain condition; there was little difference between detection results based on 5 and 10 Gaussian functions, therefore, we used GMM with 5 Gaussian functions for the subsequent tests.

Next test on environment of barrier-free path was performed; we experimented with a barrier-free space in campus, which included two paths which were a straight path of paint line as shown in Fig.13(a) and a quarter-turn curve path as shown in Fig.13(b) with the overall length of 40m; upon the start of the experiment, we pointed the camera on wheelchair at the position 20cm from the right of paint line and made it parallel to the paint line; the wheelchair advanced at about 5 km/h; because the camera was not completely against the pain line direction at first, it was obvious that the

wheelchair moved to the left after program execution in an attempt to make the camera pointing at the paint line; Fig.14 shows *x*, the distance between paint line and the horizontal center of image during experiment; it can be seen clearly from Fig.14(a) that the distance between paint line in image and the horizontal center of image was -20cm at first and it approached zero slowly, which took about 1second (10~15 frames/sec), and then the wheelchair moved forward along the paint line; Fig.14(b) shows the result of experiment in the quarter-turn curve path, from which we can find that the wheelchair entered the turn in 380 frame, when the distance between paint line in image and the median of image was significantly negative (as pointed by the first arrow in Fig.14(a)) and the wheelchair turned left; immediately the wheelchair approached paint line slowly(as pointed by the second arrow in Fig.14(b)); at last, *x*, the distance between paint line and the center of image, approached zero again and the wheelchair moved forward along the paint line continuously. Table 2 shows the performance of paint line detection and the *MSE* defines as following:

$$MSE = \frac{1}{N}\sum_{i=1}^{N} x_i^2, \tag{14}$$

where *N* is the number of frames.

(a) (b)

Figure 13. Actual testing environment (rainy day), (a) path of straight paint line, (b) path of curve paint line

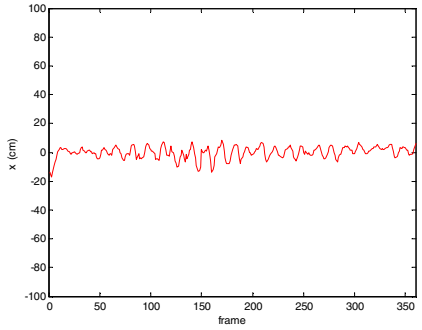

(a)

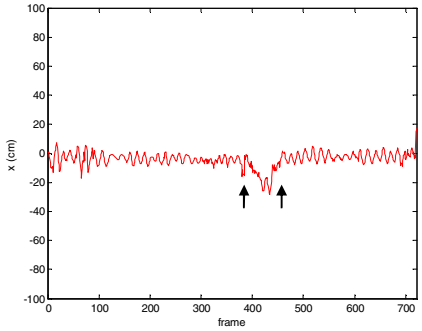

(b)

Figure 14. Result of navigation in real barrier-free route, (a) path of straight paint line, (b) path of curve paint line

TABLE 2. THE DETECTION ACCURACY AND THE CONTROLER MSE

Scene	Frames	Hit	Miss	Accuracy (%)	MSE(cm^2)
1	6,420	6,420	0	100.00	9.05
2	3,615	3,609	6	99.83	25.05
3	7,111	7,111	0	100.00	23.01
Average	5715.33	5713.33	2	99.94	19.04

VI. CONCLUSION AND FUTURE RESEARCH

In this paper, we constructed an intelligent robotic wheelchair equipped with automatic tracking navigation, which used video paint line detection and fuzzy logic control for automatic tracking navigation of wheelchair; for paint line color detection, we proposed a robust method to detect color of paint line, which is suitable for indoor and outdoor barrier-free path; in addition, for wheelchair control, we used fuzzy logic to complete the control system of robotic wheelchair and the system is actually tested in experiment of barrier-free path in campus, including straight and curve barrier-free paths; the result shows the system could make the wheelchair move along the paint line correctly and the mean deviation was kept within ±10cm. In future research, the robotic wheelchair will be equipped with ultrasonic range sensors all around to avoid colliding pedestrians or obstacles on barrier-free paths and we will build an intelligent robotic wheelchair with automatic obstacle-avoidance navigation, drawing on the ultrasonic sensor, besides completing automatic paint line detection tracking navigation.

ACKNOWLEDGMENT

For the results of this paper, we show our gratitude to the support from the Program Institute of National Science Council, the number is NSC-99-2632-E-324-001-MY3 and Ministry of Education technical colleges to establish a specialty model plan, the number is 0990045921n.

REFERENCES

[1]. The website of the Ministry of Interior Accounting office, http://www.moi.gov.tw/stat/.

[2]. The website of the Executive Yuan Economic development Committee, http://www.cepd.gov.tw/.

[3]. A. Rezoug and M. S. Djouadi, "Visual Based Lane Following for Non-holonomic Mobile Robot," *IEEE EUROCON'09*, pp. 902-907, 2009.

[4]. Y. Xu, K. Li, Yingma, Yuanyi, Wanjian, Chenjun, and Z Yufan, "General Design of the Lateral Control System Based on Monocular Vision on THASV-I," *2004 IEEE Intelligent Vehicles Symposium*, University of Parma. Parma, Italy June 14-17, 2004.

[5]. X. jiang, y motai, x. Zhu, "Prediction Fuzzy Logic Controller for Trajectory Tracking for Mobile Robot," *2005 IEEE Mid-Summer Workshop on Soft Computing in Industrial Applications*, Helsinki University of Technology, Espoo, Finland, June 28-30, 2005.

[6]. J-B. Coulaud, G. Campion, G. Bastin, and M. De Wan, "Stability Analysis of a Vision-Based Control Design for an Autonomous Mobile Robot," *IEEE trans. on Robotics*, vol. 22, no. 5, pp. 1062-1069, Oct. 2006.

[7]. G. Antonelli, S. Chiaverini, "Experiments of Fuzzy Lane Following for Mobile Robots," *in Proceeding of the 2004 American Control Conference*, Boston. Massachusetts, 2004.

[8]. Z. Hai-bo, Y. Kui, L. Jin-dong, "A Fast and Robust Vision System for Autonomous Mobile Robots," *in Proceeding of IEEE International*

Conference on Robotics, Intelligent Systems and Signal Processing, pp. 60-65, Oct. 2003.

[9]. Guilherme N. DeSouza and Avinash C. Kak, "Vision for Mobile Robot Navigation: A Survey" *IEEE Transactions on Pattern Analysis and Machine Intelligence*, vol. 24, no. 2, pp. 237-267, February 2002.

[10]. Q. Fang and C. Xie, "A Study on Intelligent Path Following and Control for Vision-based Automated Guided Vehicle," *in Proceedings of the 5th World Congress on Intelligent Control and Automation*, June 15-19, 2004, Hangzhou. P.R. China, 2004 IEEE.

[11]. K.Tomita, and S. Tsugawa, "Visual Navigation of Vehicle along Roads: The Algorithm and Experiments," *in proceedings of the IEEE conference on Vehicle Navigation and Information Systems,* 1994.

[12]. R. Martinez, A. Rodriguez, O. Castillo, L.T. Aguilar, "Fuzzy Logic Controllers Optimization Using Genetic Algoritms and Particle Swarm Optimization," *in Proceedings of the 9th Mexican International Conference on Artificial Intelligence*, pp. 475-486, 2010.

[13]. O. Castillo, P. Melin, F. Valdez, R. Martinez-Marroquin, "Handbook of Swarm Intelligence Adaptation, Learning, and Optimization," *Handbook of Swarm Intelligence Adaptation*, vol.8, part.3, pp. 389-417, 2010.

[14]. S. Tsugawa, "Vision-Based Vehicles in Japan: Machine Vision Systems and Driving Control Systems," *IEEE transactions on Industrial Electronics*, vol. 41, no. 4, pp. 398-405, Aug. 1994.

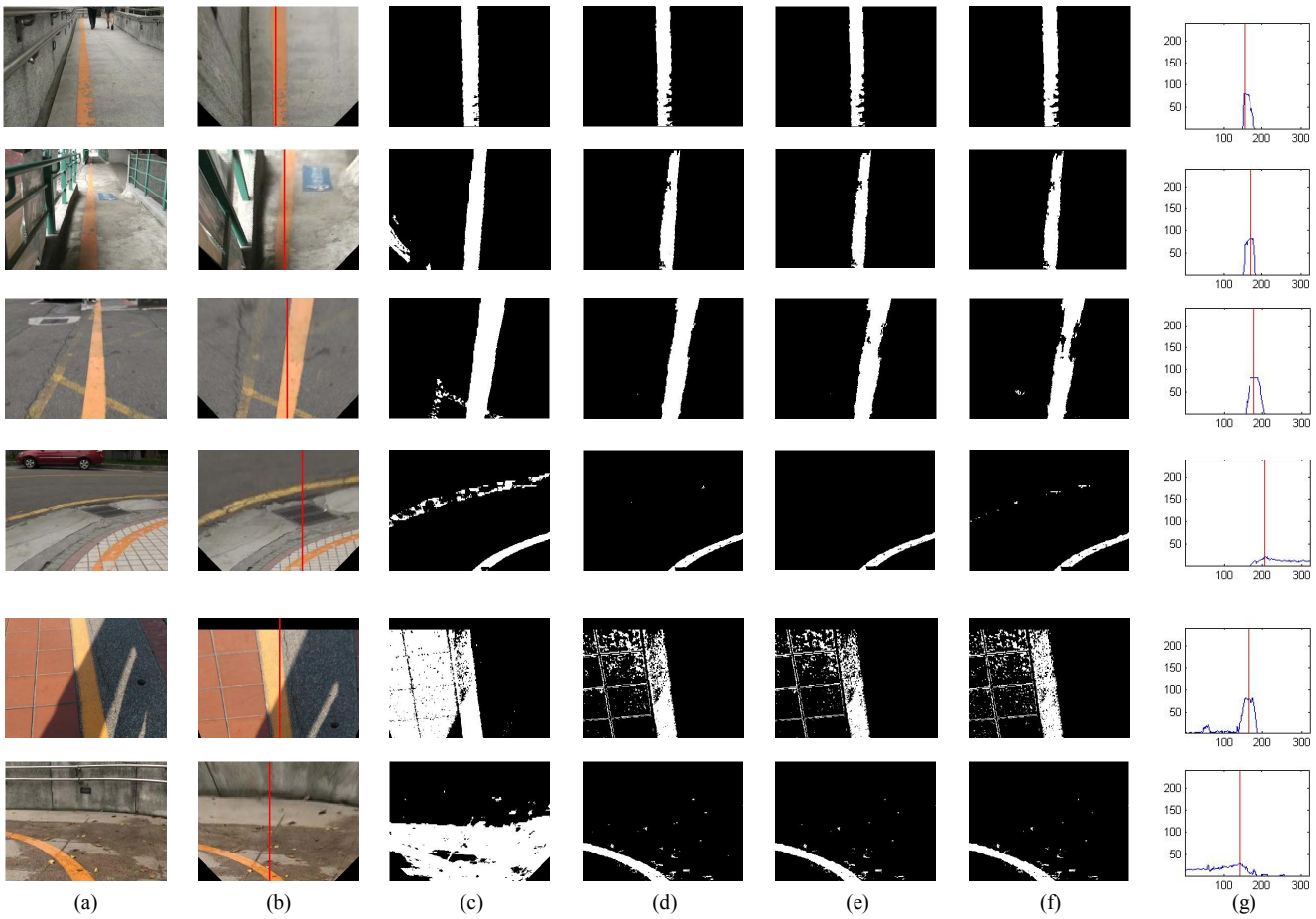

Figure 15. The some results of paint line detection, (a) input images, (b) aerial view of input images(c)-(f) K = 1, 3, 5, and 10 Gaussian mixture models, (g) paint line vertical accumulation values(K = 5).

2011 IEEE International Conference on Fuzzy Systems
June 27-30, 2011, Taipei, Taiwan

The Prediction of Trust Rating Based on the Quality of Services Using Fuzzy Linear Regression

M. Hadi Mashinchi, Lei Li, Mehmet A. Orgun, and Yan Wang

Department of Computing
Macquarie University
Sydney, NSW 2109, Australia
Emails: {hadi.mashinchi, lei.li, mehmet.orgun, and yan.wang}@mq.edu.au

***Abstract*—With the advent of service-oriented computing, the issue of trust and Quality of Service (QoS) have become increasingly important. In service-oriented environments, when there are a few service providers providing the same service, a service client would be keen to know the trustworthiness of each service provider in the forthcoming transaction. The trust rating of a delivered service from a service provider can be predicted according to a set of advertised QoS data collected by the trust management authority. Although trust and QoS are qualitative by nature, most data sets represent trust and QoS in the ordinal form for the sake of simplicity.**

This paper introduces a new approach based on Fuzzy Linear Regression Analysis (FLRA) to extract qualitative information from quantitative data and so use the obtained qualitative information for better modeling of the data. For verification purposes, the proposed approach can be applied for the trust prediction in the forthcoming transaction based on a set of advertised QoS in service-oriented environments.

***Index Terms*—Fuzzy linear regression; Trust prediction; Quality of service;**

I. Introduction

In Service-Oriented Computing (SOC), a service is an autonomous and platform-independent computational entity, which can be described, published, discovered and dynamically assembled for developing massively distributed systems [1]. In fact, any piece of code or application component deployed on a system can be taken as a service [1], [2].

In SOC environments, QoS (Quality of Service) refers to various nonfunctional characteristics. These specified characteristics should be measurable and constitute a description of what a service can offer. The QoS of an IT service is often expressed in terms of capacity, latency, bandwidth, the number of service requests, and the number of incidents [3]. QoS is essential when a set of quality metrics have to be achieved during service provision [3]. In contrast, in SOC environments, the general quality of a delivered service can be represented by a trust rating given by a service client. As trust and QoS both focus on the quality of service, the trust rating of a service or service provider can be taken as a function of a set of advertised QoS values reflecting the quality of the service or the service provider, and the trust rating can be predicted by the trust management authority.

When a service client looks for a service from a large set of services offered by different service providers, in addition to functionality and QoS, reputation-based trust is also a key factor for service selection. It is also critical for the trust management authority to be responsible for maintaining the list of reputable and trustworthy services and service providers with their advertised QoS values, and providing them to clients as required [2].

Conceptually, trust is the measure taken by one party on the willingness and ability of another party to act in the interest of the former party in a certain situation [4]. If the trust value is in the range of [0,1], it can be taken as the subjective probability with which, one party expects that another party performs a given action [5].

The trust issue has been widely studied in many applications. In e-commerce environments, a trust management system can provide valuable information to buyers and prevent certain typical attacks [6], [7]. In Peer-to-Peer information-sharing networks, binary ratings work pretty well as a file is either the definitively correct version or not [8]. In SOC environments, an effective trust management system is critical to identify potential risks, provide objective trust results to clients and prevent malicious service providers from easily deceiving clients [9]. Different from P2P information-sharing networks or the eBay reputation management system, where a binary rating system is used [8], in SOC environments, trust data is usually captured in its ordinal form, such as *5-star*, *gold* and *high-class*, due to the abstraction or even the simplicity of representation. This abstraction makes the trust value more understandable for the end users and service clients, but it is not really suitable for any further inference. An intuitively appealing approach towards trust, which is qualitative by nature, is to not quantize the trust but to take the uncertainty which comes from vagueness into consideration in the level of inference [10]. In contrast, the quantization only takes place for representing the trust to the end users or service clients when it is deemed to become necessary [10].

As mentioned above, the trust rating, representing the subjective belief of a service client on the general quality of the delivered service, is both subjective and qualitative. However, by quantization both subjective and qualitative information in the trust data set would be overlooked. For example, two

978-1-4244-7316-8/11/$26.00 ©2011 Crown

services with the same trust level of *5-star* may not be necessarily the same for a specific purpose or the requirement of a service client. In fact, one service could be much more suitable than the other one, but, due to the quantization process, such kind of important information may be ignored in the service selection process.

This paper proposes a QoS based approach to trust prediction using Fuzzy Linear Regression Analysis (FLRA). This approach is built up with the ordinal trust data which can be extracted, so that the hidden fuzzy information can be taken into consideration where it has been overlooked in the original trust data set. The motivations of applying FLRA for predicting trust are summarized as follows.

- Capturing the hidden fuzziness: we want to capture the fuzziness overlooked in the ordinal trust data set due to the reasons such as abstraction. The other machine learning approaches such as neural networks, decision trees and support vector machines in their original form, do not take the fuzziness into consideration and only model the original trust data set.
- Having a transparent model: we want to seek for a transparent relationship between the delivered trust rating and the advertised QoS values where the underlying function is extractable. In industry, neural networks or any other approaches, which have the black-box nature, are not suitable for marketing purposes.
- More detailed information: we want to provide more information than only a few trust levels. For example, a web service is not necessarily either *platinum* or *gold*; it could be for instance *better than gold,* but *worse than platinum* - which can be represented by a fuzzy value.

FLRA is a powerful tool to model the relationships in situations where the attributes are inexact. FLRA is widely applied in economy, finance, marketing, social sciences, healthcare and other domains [11], [12], [13]. In addition, trust is also a widely studied and complex issue, including many uncertain factors [6]. Hence, with the fuzziness, fuzzy regression based on fuzzy set theory can deal with QoS based trust prediction in a reasonable manner. In this paper, we propose a method for the prediction of trust rating based on fuzzy linear regression for building up a mapping from a set of advertised QoS values to the trust rating of the corresponding delivered service of a service provider. Then, the service client can predict the trustworthiness of the service provider in the forthcoming transaction with its advertised QoS values.

This paper is organized as follows. In Section II, we review trust management, trust evaluation and uncertainty. Section IV presents our QoS based trust prediction method with fuzzy regression. Some experiments are presented in Section V for illustrating how our proposed method can predict trust with QoS values. Finally Section VI concludes our work.

II. Related Work

A. Trust Evaluation in E-Commerce Environments

Trust is an important issue in e-commerce (EC) environments. At eBay [14], after each transaction, a buyer can give feedback with a rating of "positive", "neutral" or "negative" to the system according to the service quality of the seller. eBay calculates the feedback score $S = P - N$, where P is the number of positive ratings left by buyers and N is the number of negative ratings. Then the positive feedback rate $R = \frac{P}{P+N}$ (e.g., $R = 99.1\%$) is calculated and displayed on web pages. This is a simple trust management system providing valuable reputation information to buyers.

In [7], the Sporas system is introduced to evaluate the trust for EC applications based on the ratings of transactions over a recent time period. In this method, the ratings of later transactions are given higher weights as they are more important in trust evaluation. In [6], Wang *et al* propose an approach to evaluate the situational transaction trust, which binds the trust ratings of previous transactions with a new transaction. Since the situational trust includes service specific trust, service category trust, transaction amount category specific trust and price trust, it can deliver more accurate trust information to buyers and prevent some typical attacks.

B. Trust Evaluation in P2P Information Sharing Networks

The trust issue has been actively studied in Peer-to-Peer (P2P) information sharing networks as a client peer needs to know prior to download actions which serving peer can provide complete files. In [15], Damiani *et al* propose an approach for evaluating the reputation of peers through the use of the distributed polling algorithm and the *XRep* protocol before initiating any download action. This approach adopts a binary rating system and it is based on the Gnutella query broadcasting method. EigenTrust [16] adopts a binary rating system as well and aims to collect the local trust values of all peers to calculate the global trust value of a given peer.

Some other earlier studies also adopted the binary rating system. In [8], Xiong *et al* propose a *PeerTrust* model which has two main features. First, they introduce three basic trust parameters (i.e., the feedback that a peer receives from other peers, the total number of transactions that a peer performs, the credibility of the feedback sources) and two adaptive factors in computing trustworthiness of peers (i.e., transaction context factor and the community context factor). Second, they define some general trust metrics and formulas to aggregate these parameters into a final trust value.

C. Trust Evaluation in Service-Oriented Environments

In the literature, the issue of trust has also received much attention in the field of service-oriented computing (SOC). In [9], Vu *et al* present a model to evaluate the service trust by comparing the advertised service quality and the delivered service quality. If the advertised service quality is as good as the delivered service quality, the service is reputable.

The application of machine learning and soft-computing approaches for predicting the trust in service-oriented environments are suggested to be very successful in the literature. In [17], Wang *et al* propose several trust evaluation metrics and a formula for trust computation, with which a final trust value is computed. In addition, they propose a fuzzy logic based

approach for determining reputation ranks that particularly differentiate the service periods of new service providers and old (long-existing) ones. The aim is to provide incentives to new service providers and penalize those old service providers with poor service quality.

Other machine learning methods such as neural networks, decision trees, support vector machines and other classifiers are suggested and applied for predicting the ordinal trust rating based on the QoS data [18], [19].

D. Uncertainty

It is reported that the uncertainty in a system can be due to several reasons [20]:

- The high complexity of the environment, which necessitates the adaptation of abstraction (granulation of information) for generalization purposes [21].
- The influence of human subjective judgement in the decision process or the involvement of human-machine interactions [22], [23], [24].
- Partially available information [25], due to miss-recording or inaccurate measurements [26].

The trust terms in service-oriented environments come with uncertainty as they are derived from the *human subjective judgement* - one of the above reasons.

However, to the best of our knowledge, the application of FLRA for predicting the trust rating in service-oriented environments has only been studied in [13]. This approach applies FLRA to fit the ordinal data, however, it does not extract the fuzziness overlooked in the data set.

There are other approaches in different engineering applications where FLRA has been applied. However, a manual fuzzification of the data (by adding spreads) with some predefined variables estimated by experts is applied.

Therefore, there is a need to propose a novel fuzzy regression approach for QoS based trust prediction in service-oriented environments.

III. Fuzzy Regression Analysis

Regression analysis [27] is a statistical technique for modeling and investigating the relationship between two or more variables. For example, here regression analysis can be used to build up a model that represents the trust rating of the delivered service as a function of a set of advertised QoS values. Then this model can be used to predict the trust rating of the new delivered service with a new set of advertised QoS values.

A. Classical Regression Analysis

In the classical regression method, a set of parameters of an unknown function $f(x,\omega)$ can be estimated by making measurements of the function with uncertainty at any point x_i:

$$y_i = f(x_i,\omega) + \epsilon_i, \tag{1}$$

where the uncertain ϵ_i is independent of x and is distributed according to a known density $p_\omega(\epsilon)$. Based on the observed data sample $S = \{(x_i, y_i)|i = 1, 2, \ldots, n\}$, the likelihood is given by

$$P(S|\omega) = \sum_{i=1}^{n} \ln p_\omega(y_i - f(x_i,\omega)). \tag{2}$$

Assuming that uncertainty follows a normal distribution with the mean 0 and the variance δ, the likelihood is given by

$$P(S|\omega) = -\frac{1}{2\delta^2}\sum_{i=1}^{n}(y_i - f(x_i,\omega))^2 - n\ln(\sqrt{2\pi}\delta) \tag{3}$$

Maximizing the likelihood in Eq. (3) is equivalent to minimizing

$$E(\omega) = \frac{1}{n}\sum_{i=1}^{n}(y_i - f(x_i,\omega))^2, \tag{4}$$

which is in fact the same as the estimation by the method of least squares. Namely, the regression line is estimated so that the sum of squares of the deviations between the observations and the regression line is minimized.

Classical regression analysis [27] is a statistical technique for modeling and investigating the relationship for quantitative or homogeneous data. However, for qualitative heterogeneous data, an application of fuzzy regression analysis is more promising. In such systems, uncertainty arises usually not due to randomness but due to the phenomenon of fuzziness [20].

B. Fuzzy Regression Model Parameters

Prior to presenting the details of the fuzzy regression model, some definitions about the parameters of the model are introduced first in this section.

1) Membership Function: The fuzzy number mentioned in this paper is $\widetilde{A}(\alpha, C)$ with the following *membership function* [28],

$$\mu_{\widetilde{A}}(x) = \begin{cases} \begin{cases} 1 - \frac{|x-\alpha|}{C}, & |x-\alpha| \le C, \\ 0, & \text{otherwise}, \end{cases} & C > 0, \\ \begin{cases} 1, & x = \alpha, \\ 0, & \text{otherwise}, \end{cases} & C = 0. \end{cases} \tag{5}$$

According to Eq. (5), it is easy to prove that $\lambda\widetilde{A}$ is the fuzzy number $\widetilde{A}(\lambda\alpha, |\lambda|C)$ and $\widetilde{A}_1 + \widetilde{A}_2$ is the fuzzy number $\widetilde{A}(\alpha_1 + \alpha_2, C_1 + C_2)$. Therefore, if the following condition holds:

$$\widetilde{T}_i^* = \widetilde{A}_0 + q_{i1}\widetilde{A}_1 + \ldots + q_{in}\widetilde{A}_n, \tag{6}$$

then $\widetilde{T}_i^*$ is the fuzzy number

$$\widetilde{T}_i^*(\alpha_0 + \sum_{j=1}^{n} q_{ij}\alpha_j, C_0 + \sum_{j=1}^{n}|q_{ij}|C_j). \tag{7}$$

2) Goodness-of-fit:

Definition 1: Let A, B be the fuzzy sets in real space $\mathbf{R}$, then

$$h = \bigvee_{x\in\mathbf{R}} \{\mu_{\widetilde{A}}(x) \wedge \mu_{\widetilde{B}}(x)\} \tag{8}$$

is the *goodness-of-fit* from A to B.

In fact, the goodness-of-fit is defined as the inner product here. According to Definition 1, the goodness-of-fit from the fuzzy number $\widetilde{A}(\alpha_1, C_1)$ to the fuzzy number $\widetilde{B}(\alpha_2, C_2)$ is

$$h = \begin{cases} 1 - \frac{|\alpha_1 - \alpha_2|}{C_1 + C_2}, & |\alpha_1 - \alpha_2| \leq C_1 + C_2, \\ 0, & \text{otherwise.} \end{cases} \quad (9)$$

Hence, the goodness-of-fit h_i from $\widetilde{T}_i(T_i, e_i)$ to Eq. (7) $\widetilde{T}_i^*(\alpha_0 + \sum_{j=1}^n q_{ij}\alpha_j, C_0 + \sum_{j=1}^n |q_{ij}|C_j)$ is

$$h_i = \begin{cases} 1 - \frac{|T_i - (\alpha_0 + \sum_{j=1}^n q_{ij}\alpha_j)|}{C_0 + \sum_{j=1}^n |q_{ij}|C_j + e_i}, & |T_i - (\alpha_0 + \sum_{j=1}^n q_{ij}\alpha_j)| \\ & \leq C_0 + \sum_{j=1}^n |q_{ij}|C_j + e_i, \\ 0 & \text{otherwise.} \end{cases}$$

3) Fuzziness:

Definition 2: Let $A(\alpha, C)$ be a fuzzy number, then the *fuzziness* [28] of A is given as:

$$S_A = \frac{1}{2}C. \quad (10)$$

The fuzziness measures how fuzzy or vague the fuzzy set is or how clear it is not. According to Definition 2, the fuzziness of $\widetilde{T}_i^*$ in Eq. (6) is

$$S_{\widetilde{T}_i^*} = \frac{1}{2}(C_0 + \sum_{j=1}^{n} |q_{ij}|C_j). \quad (11)$$

C. Fuzzy Linear Regression Analysis (FLRA)

In the FLRA model, we are interested in finding a fuzzy function $\widetilde{y}$ in the form given below in Eq. (12) which fits a finite number of numeric input - fuzzy output data $\left((x_{1i}, x_{2i}, \cdots, x_{(n-1)i}, x_{ni}), \widetilde{y}_i^*\right)$ $i = 1, \cdots, k$ with a minimum uncertain [24].

$$\widetilde{y}_i = \quad (12)$$
$$\widetilde{A}_n x_{ni} + \widetilde{A}_{n-1} x_{(n-1)i} + \cdots + \widetilde{A}_j x_{ji} + \cdots + \widetilde{A}_1 x_{1i} + \widetilde{A}_0$$

In a more general situation, inputs and outputs are all treated as fuzzy numbers. In this case, we are looking for a function such as the one given by Eq. (13), to fit the fuzzy input and fuzzy output data $\left((\widetilde{x}_{1i}, \widetilde{x}_{2i}, \cdots, \widetilde{x}_{(n-1)i}, \widetilde{x}_{ni}), \widetilde{y}_i^*\right)$.

$$\widetilde{y}_i = \quad (13)$$
$$\widetilde{A}_n \widetilde{x}_{ni} + \widetilde{A}_{n-1} \widetilde{x}_{(n-1)i} + \cdots + \widetilde{A}_j \widetilde{x}_{ji} + \cdots + \widetilde{A}_1 \widetilde{x}_{1i} + \widetilde{A}_0$$

where in Eqs (12) and (13), $\widetilde{A}_j$ $(j = 0, \cdots, n)$ is the fuzzy coefficient (parameter) of the regression model. The parameters are optimized such that the differences between the observed outputs $\widetilde{y}_i^*$ and estimated ones $\widetilde{y}_i$ are as small as possible. All $\widetilde{y}_i$ $(i = 1, \cdots, k)$, $\widetilde{A}_j$ $(j = 0, \cdots, n)$ and $\widetilde{x}_{ji}$ are fuzzy numbers, and the operations used above are all treated as the multiplication and addition of fuzzy numbers.

The first FLR model, proposed by Tanaka *et al* [24], was based on the possibility theory and solved by Linear Programming (LP). Diamond [29] proposed a FR model based on the Least Square (LS) approach. According to the definition of the error, FR models are classified in two categories: probabilistic with LP, and LS approaches. In the former approach, the aim is to minimize the overall fuzziness by minimizing the total spread of the fuzzy coefficients while the estimated outputs and the observed ones are within a certain h-level of confidence [30]. The term h expresses the fitness between the estimated fuzzy outputs and the observed ones. On the other hand, in the LS-based model, a similarity measure between observed and estimated outputs, is used as the measurement for the fitness of the model.

In fuzzy mathematics, LP is a well-known technique used in probabilistic approaches to minimize the fuzziness of the coefficients. In the LP based approaches with additional observation data, two constraints are added to LP [20]. However, having extra constraints is not an issue in practice since the data sets for fuzzy regression are small and also, LP problems even with thousands of variables and constraints can be solved in a few seconds. The goal of LP based approaches is to cover the spreads of all the observations (up to an h-level). The goal of LS based approaches is to find a model which has the most similar estimated outputs to the observed ones based on the chosen similarity measure.

For example, here regression analysis can be used to build up a model that represents the trust rating of the delivered service as a function of a set of advertised QoS values. Then, this model can be used to predict the trust rating of the new delivered service with a new set of advertised QoS values in the forthcoming transaction.

IV. Trust Prediction Based on Fuzzy Regression

In this paper, we investigate the application of FLRA for the prediction of trust based on a set of advertised QoS values. The main goal in this paper is to predict the trust rating of a web-service, which could be represented by linguistic expressions such as platinum, gold, silver and bronze. So, a common approach is to seek the relationship between the independent attributes (the QoS attributes) and dependent attribute (the trust attribute). For doing so, a numeric form of the trust attribute is considered to construct the model - even if the QoS data comes with some imprecision or uncertainty. Hence, initially the linguistic expressions of trust are all considered to be ordinal data. Then, after they are quantized (defuzzified), classical approaches can be applied [10].

The critical issue here is that the quantization process causes some important information to be overlooked or neglected [20]. In environments with uncertain data, the best option is then to not defuzzify the data but to take the uncertainty in the data into consideration in the level of inference [10]. However, the final results could be defuzzified for the presentation purposes only if it becomes necessary [10].

A linear regression model in the form of

$$Y = a_0 + a_1 x_1 + \cdots + a_n x_n,$$

where n is the number of input variables, is applied for QoS based trust estimation for each web-service. However, we have

added an extra term to fuzzify the results. A triangular fuzzy value, like $\widetilde{B_i}$ which derives from

$$(\sum_{i=1}^{n} x_i) \cdot (b_1, b_2, b_3),$$

where $b_1 \leq b_2 \leq b_3$ is added to the above linear regression model given in Eq. (14).

$$\widetilde{Y_i} = a_0 + a_1 x_1 + \cdots + a_9 x_9 + \widetilde{B_i} \tag{14}$$

The coefficients $a_0, a_1, \cdots, a_n$ are estimated by statistical linear regression. The motivation of applying the model given in Eq. (14) is due to the fact that this model does not have the *spread increasing problem* - an issue which exists in the original models given in Eqs (12) and (13). A model with the spread increasing problem would increase the uncertainty of the trust of a service by an increase in the magnitude of the input QoS variables.

To derive the best values of the variables b_1, b_2 and b_3, tabu-harmony search is applied [20]. In order to measure the goodness of the individual models in tabu-harmony search, we need to count how many predictions of the model are correct. However, the models have a fuzzy estimation of the trust value which is hard to be compared with the actual trust values which are ordinal values. One way to tackle this issue is to defuzzify the estimation and then assign it to a class of trust which has the smallest distance to it. Basically by doing so, the fuzziness is taken into consideration for inference and the quantization process takes place only in the final stage for the sake of presentation [10].

In this paper, we have defined the same margin for all the classes by assigning a class for each estimation. For example, if the margin is 0.2, then in our example estimations will be in the bands of

$$(-\infty, 1.2],\ (1.2, 2.2],\ (2.2, 3.2],\ \text{and}\ (3.2, +\infty).$$

We introduce the variable b_4 to derive the best margin. Since the value of b_4 depends on the selection of b_1, b_2 and b_3, we optimize all the four variables in one phase.

In contrast to the other methods, with our method, the trust rating will be estimated in terms of a fuzzy number. In fact, trust is naturally an inexact concept. However, due to the abstraction, it is usually converted to a traditional classification problem and the fuzziness is overlooked.

V. Experiments

The most comprehensive data sets for web-services classification used by [19], [31], [32], include ten crisp independent attributes and one linguistic expression which represents the trust level of the web-service. To the best of our knowledge, in most studies in the literature, the trust terms (being platinum, gold, silver and bronze) are quantized to 1 to 4, respectively.

In the experiment, the web-services data set used for the simulation purposes is taken from [33]. The data set contains 365 real web service implementations extracted from the Web. These services were collected using the Web Service Crawler Engine (WSCE). The majority of the Web services were obtained from public sources on the Web including Universal Description, Discovery, and Integration (UDDI) registries, search engines, and service portals.[1] From the list of attributes given in Table I, we have excluded *WSRF* due to its high dominance [19].

The settings of experiments in this section are as follows.

- The introduced data set with the properties given in Table I is first normalized and then we perform 10-fold cross validation as used in [19].
- Tabu-harmony search with a population size of 100 for 2000 iterations is used.
- The migration and crossover fractions are set to 0.7 and 0.05, respectively.
- The lower and upper bounds of b_1, b_2, b_3 and b_4 are set to -1 and 1, respectively.

The comparison of the method and the results obtained from Support Vector Machines (SVM), decision tree and linear regression are given in Table II. We can observe the following results.

- The accuracy of the proposed method based on fuzzy linear regression is about 80%, which is superior to the other methods compared in this paper.
- The standard deviation is estimated to be 0.07, which reveals the robustness of the approach on different runs.
- Both the standard deviation and the performance of our proposed approach based on fuzzy linear regression is better than those of the one which applies the traditional linear regression.
- Moreover, as discussed earlier, our approach is able to regenerate the overlooked uncertainty in the trust of service and use it for inference.
- The standard deviations and the training performances of the other methods are not given in Table II, as they are not reported in [19].

As an example, we have estimated the trust ratings of two web services from the obtained model during training. The trust values are in the form of fuzzy triangular numbers as follows:

$$(1.5714, 3.4027, 4.1017),\ (1.9139, 3.8692, 4.6155).$$

Although after defuzzification both would be classified as *gold*, there are differences between them in terms of QoS. In fact, Figure 1 reveals that the second service is slightly better than the first one. Moreover, there is an uncertainty that the quality of both services depicted in Figure 1 might actually be silver, as the left spreads of both the fuzzy numbers are very wide.

As another example, we assume the trust of two web services given in Figure 2. In case of using traditional (exact) methods, it is deduced that service 2 is superior to service 1. However, as the left spread of service 2 goes all the way to the bronze quality, this may result in selecting service 1 over service 2.

[1]For more information visit:
http://www.uoguelph.ca/∼qmahmoud/qws/index.html#Service_Classification_

TABLE I
WEB-SERVICE DATASET; ATTRIBUTES AND DESCRIPTIONS [33]

ID	Attribute name	Description	Units
x_1	Response Time	Time taken to send a request and receive a response	ms
x_2	Availability	Number of successful invocations/total invocations	%
x_3	Throughput	Total Number of invocations for a given period of time	$\frac{invokes}{second}$
x_4	Successability	Number of response / number of request messages	%
x_5	Reliability	Ratio of the number of error messages to total messages	%
x_6	Compliance	The extent to which a documentation follows specification	%
x_7	Best Practices	The extent to which a Web service follows WS-I Basic Profile	%
x_8	Latency	Time taken for the server to process a given request	ms
x_9	Documentation	Measure of documentation (i.e. description tags) in WSDL	%
x_{10}	WSRF	Web Service Relevancy Function	%
y	Service Classification	Levels representing service offering qualities (1 through 4) (trust rating)	Type

TABLE II
ACCURACY OF THE CLASSIFIERS AFTER REMOVING WSRF

Classifier	Average performance on testing sets (%)	Standard deviation of the testing sets errors	Average performance on training sets (%)	Standard deviation of the training sets errors
Fuzzy linear regression (This work)	79.46	0.0756	83.36	0.0060
Decision Trees (CART) [19]	78.61	-	-	-
Linear regression (This work)	74.17	0.0816	79.91	0.0095
SVM [19]	60.55	-	-	-
Decision trees (J48) [19]	67.77	-	-	-

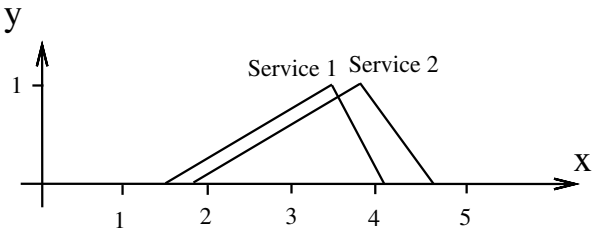

Fig. 1. The comparison of the trust of two web services before defuzzification

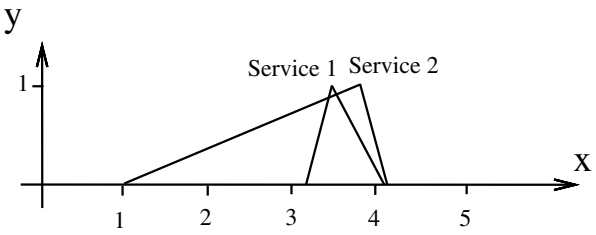

Fig. 2. An example where a traditional method and an inexact method may vary in the result

VI. CONCLUSIONS

In this paper, we have proposed an approach based on fuzzy linear regression to extract the qualitative information which may have been overlooked in the original data set. The extracted qualitative data is then used for modeling the data. The proposed approach is applied for the trust prediction of the delivered web-services based on a set of advertised QoS values. The method not only provides more detailed information of trust but it also has promising results. Although in order to quantitatively compare the performance of the method, the results are defuzzified, one could use the fuzzy results as they provide more information.

For future work, one may consider having different weights for each of the QoS variables. By doing so the number of variables for optimization increases, but the obtained model will be more generalized.

ACKNOWLEDGMENT

This research has been supported in part by an Australian Research Council (ARC) Discovery grant (DP1094799). The first author would like to thank the Macquarie University Postgraduate Research Fund for partially supporting this research.

REFERENCES

[1] M. P. Papazoglou, P. Traverso, S. Dustdar, and F. Leymann, "Service-oriented computing: a research roadmap," *Int. J. Cooperative Inf. Syst.*, vol. 17, no. 2, pp. 223–255, 2008.

[2] L. Li, Y. Wang, and E.-P. Lim, "Trust-oriented composite service selection and discovery," in *Proceedings of the International Conference on Service-Oriented Computing* (ICSOC/ServiceWave 2009), pp. 50–67, 2009.

[3] L. Li, Y. Wang, and E.-P. Lim, "Trust-oriented composite service selection with qos constraints," *Journal of Universal Computer Science (J. UCS)*, vol. 16, no. 13, pp. 1720–1744, 2010.

[4] L. Li and Y. Wang, "Subjective trust inference in composite services," in *Proceedings of the AAAI Conference on Artificial Intelligence* (AAAI 2010), pp. 1377–1384, 2010.

[5] A. Jøsang, R. Ismail, and C. Boyd, "A survey of trust and reputation systems for online service provision," *Decision Support Systems*, vol. 43, no. 2, pp. 618–644, 2007.

[6] Y. Wang and E.-P. Lim, "The evaluation of situational transaction trust in e-service environments," in *Proceedings of the IEEE International Conference on e-Business Engineering* (ICEBE 2008), pp. 265–272, 2008.

[7] G. Zacharia and P.Maes, "Trust management through reputation mechanisms," *Applied Artificial Intelligence*, vol. 14, no. 9, pp. 881–907, 2000.

[8] L. Xiong and L. Liu, "PeerTrust: Supporting reputation-based trust for peer-to-peer electronic communities," *IEEE Trans. Knowl. Data Eng.*, vol. 16, no. 7, pp. 843–857, 2004.

[9] L.-H. Vu, M. Hauswirth, and K. Aberer, "QoS-based service selection and ranking with trust and reputation management," in *Proceedings of the International Conference on Cooperative Information Systems* (CoopIS 2005), pp. 466–483, 2005.

[10] W. Näther, "Regression with fuzzy random data," *Computational Statistics & Data Analysis*, vol. 51, no. 1, pp. 235–252, 2006.

[11] R. M. Dom, *Fuzzy regression model for the prediction of oral cancer susceptibility*. PhD thesis, University of Malaya, 2009.

[12] C. Kao and C.-L. Chyu, "Least-squares estimates in fuzzy regression analysis," *European Journal of Operational Research*, vol. 148, no. 2, pp. 426–435, 2003.

[13] L. Li, Y. Wang, and V. Varadharajan, "Fuzzy regression based trust prediction in service-oriented applications," in *Proceedings of the 6th International Conference on Autonomic and Trusted Computing* (ATC '09), (Berlin, Heidelberg), pp. 221–235, Springer-Verlag, 2009.

[14] *eBay*. http://www.eBay.com/.

[15] E. Damiani, S. D. C. di Vimercati, S. Paraboschi, P. Samarati, and F. Violante, "A reputation-based approach for choosing reliable resources in peer-to-peer networks," in *ACM Conference on Computer and Communications Security* (CCS 2002), pp. 207–216, 2002.

[16] S. D. Kamvar, M. T. Schlosser, and H. Garcia-Molina, "The eigentrust algorithm for reputation management in p2p networks," in *Proceedings of the international conference on World Wide Web* (WWW 2003), pp. 640–651, 2003.

[17] Y. Wang, K.-J. Lin, D. S. Wong, and V. Varadharajan, "Trust management towards service-oriented applications," *Service Oriented Computing and Applications*, vol. 3, no. 2, pp. 129–146, 2009.

[18] E. Al-Masri and Q. H. Mahmoud, "Discovering the best web service: A neural network-based solution," in *Proceedings of the IEEE International Conference on Systems, Man and Cybernetics*, pp. 4250 – 4255, 2009.

[19] R. Mohanty, V. Ravi, and M. R. Patra, "Web-services classification using intelligent techniques," *Expert Syst. Appl.*, vol. 37, no. 7, pp. 5484–5490, 2010.

[20] M. H. Mashinchi, M. A. Orgun, M. Mashinchi, and W. Pedrycz, "Tabu-harmony search based approach to fuzzy linear regression," *IEEE Transactions on Fuzzy Systems*, 2011. DOI:10.1109/TFUZZ.2011.2106791.

[21] A. Bargiela, W. Pedrycz, and T. Nakashima, "Multiple regression with fuzzy data," *Fuzzy Sets and Systems*, vol. 158, no. 19, pp. 2169–2188, 2007.

[22] R. A. Aliev, B. Fazlollahi, and R. M. Vahidov, "Genetic algorithms-based fuzzy regression analysis," *Soft Computing*, vol. 6, no. 6, pp. 470–475, 2002.

[23] B. Kim and R. R. Bishu, "Evaluation of fuzzy linear regression models by comparing membership functions," *Fuzzy Sets and Systems*, vol. 100, no. 1-3, pp. 343–352, 1998.

[24] H. Tanaka, S. Uejima, and A. Asai, "Linear regression analysis with fuzzy model," *IEEE Transactions on Systems, Man and Cybernetics*, vol. 12, pp. 903–907, 1982.

[25] D. H. Hong and C. Hwang, "Support vector fuzzy regression machines," *Fuzzy Sets and Systems*, vol. 138, no. 2, pp. 271–281, 2003.

[26] D. T. Redden and W. H. Woodall, "Further examination of fuzzy linear regression," *Fuzzy Sets and Systems*, vol. 79, pp. 203–211, 1996.

[27] W. W. Hines, D. C. Montgomery, D. M. Goldsman, and C. M. Borror, *Probability and Statistics in Engineering*. John Wiley & Sons, Inc, 2003.

[28] A. T. Azar, *Fuzzy Systems*. Intech, 2010.

[29] P. Diamond, "Fuzzy least squares," *Information Sciences*, vol. 46, no. 3, pp. 141–157, 1988.

[30] J. Lu and R. Wang, "An enhanced fuzzy linear regression model with more flexible spreads," *Fuzzy Sets and Systems*, vol. 160, no. 17, pp. 2505–2523, 2009.

[31] E. Al-Masri and Q. H. Mahmoud, "Investigating web services on the world wide web," in *Proceeding of the 17th international conference on World Wide Web* (WWW '08), (New York, NY, USA), pp. 795–804, ACM, 2008.

[32] M. Alrifai, T. Risse, P. Dolog, and W. Nejdl, "Service-oriented computing — icsoc 2008 workshops," ch. A Scalable Approach for QoS-Based Web Service Selection, pp. 190–199, Berlin, Heidelberg: Springer-Verlag, 2009.

[33] E. Al-Masri and Q. H. Mahmoud, "Discovering the best web service," in *Proceedings of the 16th international conference on World Wide Web* (WWW '07), (New York, NY, USA), pp. 1257–1258, ACM, 2007.

2011 IEEE International Conference on Fuzzy Systems
June 27-30, 2011, Taipei, Taiwan

Observer-based Hybrid Fuzzy CMAC Controller for a Class of Uncertain Chaotic Systems

Chun-Sheng Chen
Department of Electronic Engineering
China University of Science and Technology
Taipei, Taiwan, R.O.C.

***Abstract*—This paper presents an observer-based hybrid fuzzy cerebellar model articulation controller (CMAC) neural network control with a supervisory controller for a class of uncertain chaotic systems. This proposed control system is integrating sliding mode control (SMC) theory and CMAC neural network into fuzzy controller design. The total states of the chaotic system are not assumed to be available for measurement. A state observer is used to estimate unmeasured states of the systems. The supervised control is appended to assure that the fuzzy CMAC controller achieve a stable closed-loop system through Lyapunov stability theory. Finally, simulation results show that the effect of the approximation error on the tracking error can be attenuated efficiently by the proposed method.**

Keywords- CMAC; fuzzy control; chaotic systems; observer; sliding mode control;

I. INTRODUCTION

Many different aspects of chaotic dynamics have attracted considerable attention in laser physics, digital communication, chemical reaction analysis and design, biological systems, power converters, circuit systems [1]-[5], etc. An interesting and challenging problem in the field is the control of chaotic systems. However, the chaotic systems have complex and unpredictable dynamical behavior. Inevitably, the constructed model comprises unmodeled nonlinearity and uncertain disturbance that conventional control strategies based on the accurate mathematical models of the controlled systems are difficult to derive.

The cerebellar model articulation controller (CMAC), developed by Albus in the 1970s [6]-[7], is a nonfully connected perceptron-like associative memory network with overlapping receptive-fields. The contents of these memory locations are referred as weights, and the output of this network is a linear combination of these weights in the memory addressed by the activated inputs [8]. Compared with the general multiplayer neural network with back-propagation algorithm, the CMAC has been applied to a wide variety of complex dynamical systems because of its simple computation, fast learning property and good generalization capability [9]-[10]. In the meantime, sliding mode control (SMC), or variable structure control, has successfully been developed as a popular robust strategy to a wide variety of systems having uncertainties and invariance to unknown disturbance [11]-[12]. Integrating CMAC neural network and SMC into fuzzy controller design have acquired superior performance [13]. However, these control methods are based on the assumption that the system states are known or available for feedback. If system states are not available for measurement, the conventional adaptive laws would be difficult to be realized. To treat this problem, an observer needs to estimate the unmeasured states and the SPR-Lyapunov design approach has been used to design an adaptive scheme [14]-[15]. The goal of this paper is to design a hybrid observer-based fuzzy CMAC controller with supervisory control for a class of uncertain chaotic systems under the constraint that only the system output is available for measurement.

II. PROBLEM FORMULATION

Consider the *n*th-order nonlinear system described in the following form:

$$\begin{aligned} x^{(n)} &= f(\boldsymbol{x}) + bu + d \\ y &= x \end{aligned} \tag{1}$$

where $f(\boldsymbol{x})$ is unknown real continuous function, $u \in R$ and $y \in R$ are the control input and output of the system, respectively, b is a positive constant, and $\boldsymbol{x} = [x, \dot{x}, \cdots, x^{(n-1)}]^T = [x_1, x_2, \cdots, x_n]^T$ is the state vector of system, d is the external disturbance with the properties of standard smoothness and it is assumed to have an upper bound D_N.

Rewriting (1) in the following form

$$\begin{aligned} \dot{\boldsymbol{x}} &= A\boldsymbol{x} + B(f(\boldsymbol{x}) + bu + d) \\ y &= C^T \boldsymbol{x} \end{aligned} \tag{2}$$

where $A = \begin{bmatrix} 0 & 1 & 0 & \cdots & 0 \\ 0 & 0 & 1 & \cdots & 0 \\ \cdots & \cdots & \cdots & \cdots & \vdots \\ 0 & 0 & 0 & \cdots & 0 \end{bmatrix}$, $B = \begin{bmatrix} 0 \\ \vdots \\ 0 \\ 1 \end{bmatrix}$, $C = \begin{bmatrix} 1 \\ 0 \\ \vdots \\ 0 \end{bmatrix}$

The control objective is to design an observer-based fuzzy CMAC controller such that the system output y follows a given desired trajectory y_d. The desired trajectory vector $\boldsymbol{y}_d$, the output tracking error vector $\boldsymbol{e}$ and the estimation error vector $\hat{\boldsymbol{e}}$ are defined as, respectively,

$$\boldsymbol{y}_d = [y_d \;\; \dot{y}_d \;\; \ddot{y}_d \;\; \cdots \;\; y_d^{(n-1)}]^T, \tag{3}$$

$$\boldsymbol{e} = \boldsymbol{y}_d - \boldsymbol{x} = [e \;\; \dot{e} \;\; \cdots \;\; e^{(n-1)}]^T = [e_1 \;\; e_2 \;\; \cdots \;\; e_n]^T \tag{4}$$

$$\hat{\boldsymbol{e}} = \boldsymbol{y}_d - \hat{\boldsymbol{x}} = [e \;\; \dot{\hat{e}} \;\; \cdots \;\; \hat{e}^{(n-1)}]^T \tag{5}$$

where $\hat{\boldsymbol{x}}$ and $\hat{\boldsymbol{e}}$ denote the estimates of $\boldsymbol{x}$ and $\boldsymbol{e}$, respectively. Set the sliding surface as

$$S(\boldsymbol{e}) = \boldsymbol{\lambda}^T \boldsymbol{e} \tag{6}$$

where $\boldsymbol{\lambda} = [\lambda_1, \lambda_2, \cdots, \lambda_n]^T$ is chosen such that $\lambda_n = 1$ and the polynomial $h(p)$

$$h(p) = \lambda_n p^{(n-1)} + \lambda_{n-1} p^{(n-2)} + \cdots + \lambda_1 p \tag{7}$$

is strictly Hurwitz [16].

Since (7) satisfies Hurwitz stability criterion, maintaining system states on surface $S(\boldsymbol{e},t)$ for all $t > 0$ is equivalent to the tracking problem $y = y_d$. The tracking control problem can be formulated by keeping the error vector $\boldsymbol{e}$ on the sliding surface defined as follows:

$$\dot{S} = y_d^{(n)} - f(\boldsymbol{x}) - bu - d + \sum_{i=1}^{n-1} \lambda_i e^{(i)} \tag{8}$$

In the design of the sliding mode controller, an equivalent control is given first such that each state Lyapunov-like condition holds for system stability [12]:

$$\frac{1}{2}\frac{d}{dt}(S^2) \le -\eta|S|, \;\; \eta > 0 \tag{9}$$

Therefore the control problem is to obtain the optimal control input u^* that guarantees the sliding condition (9).

If function $f(\boldsymbol{x})$ is known and the system is free of external disturbance *d*, the control law can be designed as

$$u^* = b^{-1}[-f(\boldsymbol{x}) + y_d^{(n)} + K_c^T \boldsymbol{e} + \eta \,\mathrm{sgn}(S)] \tag{10}$$

where $K_c = [k_{c1}, k_{c2}, \cdots, k_{cn}]^T$ is the feedback gain vector, $\eta > 0$ and $\mathrm{sgn}(S)$ is defined as

$$\mathrm{sgn}(S) = \begin{cases} 1 & S > 0 \\ 0 & S = 0 \\ -1 & S < 0 \end{cases} \tag{11}$$

By plugging u^* into (8), we will have $\dot{S} = -\eta \,\mathrm{sgn}(S)$. Thus, the sliding condition (9) can be easily verified. However, $f(\boldsymbol{x})$ is unknown, the control law (10) cannot be implement, and not all system state x_i are available. Therefore, to overcome such problems, we will design an observer to estimate the state $\boldsymbol{x}$ and the fuzzy CMAC systems are utilized to approximate unknown functions.

III. Description of the Fuzzy CMAC System

The CMAC is a simple and fast associative memory type neural network that is proposed as a well-established computational model based on the cerebellum in humans [6]-[7]. Fig. 1 depicts the structure of a two-dimensional CMAC. Each input variable, I_1 and I_2, must be quantized and the problem space is divided into discrete regions (called an *element*) and 3 elements are accumulated as a block. For each input variable, three kinds of segmentation are used, the variable I_1 is divided into blocks *A*, *B* and *C*, and the variable I_2 is divided into blocks *a*, *b* and *c*. Then, the areas formed by blocks, referred to as *Aa*, *Ab*, *Ac*, *Ba*, *Bb*, *Bc*, *Ca*, *Cb* and *Cc* are the addresses or the locations that store data which are called receptive-fields (or hypercubes). When each block is shifted by a small interval, different blocks will be obtained. For instance, blocks *D*, *E* and *F* in the second row for I_1 and *d*, *e* and *f* in the second column for I_2 are possible shifted regions. Then, *Dd*, *De*, *Df*, *Ed*, *Ee*, *Ef*, *Fd*, *Fe* and *Ff* are new hypercubes from the shifted regions. Similarly, hypercubes *Gg*, *Gh*, *Gi*, *Hg*, *Hh*, *Hi*, *Ig*, *Ih* and *Ii* are defined in the third layer. No hypercube is formed by the combination of different layers. Each activated element in each layer becomes a firing element, thus, the weight of each block can be obtained.

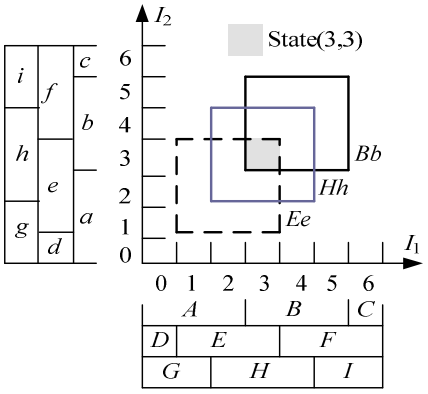

Figure 1. Block division of a 2-D CMAC.

CMAC uses a set of indices as an address in accordance with the current state to extract the stored data. Assume that N_n is the number of hypercubes; this is the same as the memory size in the case. Using the CMAC technique, a stored data y_i can be mathematically expressed as

$$y_i = \boldsymbol{a}_i \boldsymbol{w} = \sum_{j=1}^{N_n} a_{ij} w_j \tag{12}$$

where $\boldsymbol{w}$ indicates the column vector of memory contents and $\boldsymbol{a}_i$ is a memory element selection row vector that has N_e ones. Each hypercube is associated to an " arbitrary but deterministic" physical memory address. In Fig. 1, there are 27 hypercubes used to distinguish 49 different states in the 2-D CMAC. For example, let the hypercubes *Bb*, *Ee*, and *Hh* be addressed by the state $(v_1, v_2) = (3,3)$. Since each state addresses exactly N_n hypercubes, only these three hypercubes are set to 1, and the others are set to 0. Note that after the way of block division (see Fig. 1) is determined, the vector $\boldsymbol{a}_i$ for a specific quantized state is fixed.

A fuzzy CMAC controller system can be controlled by the following linguistic rules

$$R^{(j)}: \text{IF } x_1 \text{ is } F_1^j \text{ and} \cdots \text{and } x_n \text{ is } F_n^j, \text{ THEN } \hat{f} = \boldsymbol{a}_j \boldsymbol{w}_I \tag{13}$$

and

$$R^{(k)}: \text{IF } x_1 \text{ is } F_1^k \text{ and} \cdots \text{and } x_n \text{ is } F_n^k, \text{ THEN } u_D = \boldsymbol{a}_k \boldsymbol{w}_D \tag{14}$$

where $\hat{f}$ is the approximation of f, $\boldsymbol{a}_j$ and $\boldsymbol{a}_k$ are the memory element selection row vectors, $\boldsymbol{w}_I$ and $\boldsymbol{w}_D$ are the weighting column vectors of the CMAC. The FCMAC system with center-average defuzzifier, product inference and singleton fuzzifier is defined as [16]

$$\hat{f} = \sum_{l=1}^{N} \boldsymbol{a}_j \boldsymbol{w}_I \mu^l(\boldsymbol{x}) \Big/ \sum_{l=1}^{N} \mu^l(\boldsymbol{x}) = (\boldsymbol{A}_I \boldsymbol{w}_I)^T \boldsymbol{\Phi}(\boldsymbol{x}) \tag{15}$$

$$u_D = \sum_{k=1}^{N} \boldsymbol{a}_k \boldsymbol{w}_D \mu^l(\boldsymbol{x}) \Big/ \sum_{j=1}^{N} \mu^l(\boldsymbol{x}) = (\boldsymbol{A}_D \boldsymbol{w}_D)^T \boldsymbol{\Phi}(\boldsymbol{x}) \tag{16}$$

where $\mu^l(\boldsymbol{x}) = \prod_{i=1}^{n} \mu_{F_i^l}(x_i)$ is the matching degree of the lth, N is the number of the total IF-THEN rules,, $\boldsymbol{A}_I$ and $\boldsymbol{A}_d$ are matrix constituted from the memory element selection vector $\boldsymbol{a}_j$ and $\boldsymbol{a}_k$, respectively, and $\boldsymbol{\Phi} = (\phi_1, \phi_2, \cdots, \phi_N)^T$ is a column vector whose proper dimension depends on the number of fuzzy rules with ϕ_j is defined as

$$\phi_j(\boldsymbol{x}) = \left(\prod_{i=1}^{n} \mu_{F_i^j}(x_i) \right) \Big/ \sum_{l=1}^{N} \left(\prod_{i=1}^{n} \mu_{F_i^j}(x_i) \right) \tag{17}$$

IV. STATE OBSERVER SCHEME

In the previous section, due to assumption that the state vector $\boldsymbol{x}$ is immeasurable, $f(\boldsymbol{x})$ are unavailable, by replacing the function $f(\boldsymbol{x})$, system state $\boldsymbol{x}$, error vector $\boldsymbol{e}$ and sliding surface S in (10) with their estimates $\hat{f}(\hat{\boldsymbol{x}})$, $\hat{\boldsymbol{x}}$, $\hat{\boldsymbol{e}}$ and $\hat{S}(\hat{\boldsymbol{e}})$. Since the fuzzy CMAC systems have the property such that they can approximate any continuous functions on a compact set, utilize fuzzy CMAC systems $\hat{f}(\hat{\boldsymbol{x}})$ be of the form

$$\hat{f}(\hat{\boldsymbol{x}}) = \boldsymbol{w}_I^T \boldsymbol{A}_I^T \boldsymbol{\Phi}(\hat{\boldsymbol{x}}) \tag{18}$$

where $\boldsymbol{\Phi}(\hat{\boldsymbol{x}}) = [\phi_1(\hat{\boldsymbol{x}}), \cdots, \phi_N(\hat{\boldsymbol{x}})]^T$. An indirect controller is comprised of a fuzzy CMAC based certainty equivalent controller and is given by

$$u_I = b^{-1}[-\hat{f}(\hat{\boldsymbol{x}}) + y_d^{(n)} + K_c^T \hat{\boldsymbol{e}} + \eta \operatorname{sgn}(\hat{S})] \tag{19}$$

where $\hat{S} = \boldsymbol{\lambda}^T \hat{\boldsymbol{e}}$. The direct fuzzy CMAC controller is chosen as

$$u_D = \boldsymbol{w}_D^T \boldsymbol{A}_D^T \boldsymbol{\Phi}(\hat{\boldsymbol{x}}) \tag{20}$$

where u_D is the fuzzy CMAC system to directly approximate the control law (10). Thus, the resulting control law is

$$u = u_H + u_s = \alpha u_I + (1-\alpha) u_D + u_s \tag{21}$$

where $u_H = \alpha u_I + (1-\alpha) u_D$ is the hybrid fuzzy CMAC controller, u_I is the indirect fuzzy CMAC controller as (19), u_D is the direct fuzzy CMAC controller as (20), u_s is utilized to compensate the modeling error and external disturbance, and $\alpha \in [0,1]$. Substituting (21) into (2), after some manipulation, one has

$$\begin{aligned} \dot{\boldsymbol{e}} &= A\boldsymbol{e} - BK_c^T \hat{\boldsymbol{e}} + B[\alpha(\hat{f}(\hat{\boldsymbol{x}}) - f(\boldsymbol{x})) \\ &\quad - (1-\alpha) b(u_D(\hat{\boldsymbol{x}}) - u^*(\boldsymbol{x}))] - B[bu_s + \eta \operatorname{sgn}(\hat{S}) + d] \\ e_1 &= C^T \boldsymbol{e} \end{aligned} \tag{22}$$

where $u^*(\boldsymbol{x}) = b^{-1}[-f(\boldsymbol{x}) + y_d^{(n)} + K_c^T \hat{\boldsymbol{e}} + \eta \operatorname{sgn}(\hat{S})]$. Thus, the tracking problem has been converted to the regulation problem of designing a sate observer for estimating the state vector $\boldsymbol{e}$ in (22).

Design the following observer to estimate the error vector $\boldsymbol{e}$ in (22)

$$\begin{aligned} \dot{\hat{\boldsymbol{e}}} &= A\hat{\boldsymbol{e}} - B[K_c^T \hat{\boldsymbol{e}} + \eta \operatorname{sgn}(\hat{S})] + K_o(e_1 - \hat{e}_1) \\ \hat{e}_1 &= C^T \hat{\boldsymbol{e}} \end{aligned} \tag{23}$$

where $K_o = [k_{o1}, k_{o2}, \cdots, k_{on}]^T$ is the observer gain vector, which is selected such that the characteristic polynomial of $A - K_o C^T$ is strictly Hurwitz because (C, A) is observable. Define the observation errors $\tilde{\boldsymbol{e}} = \boldsymbol{e} - \hat{\boldsymbol{e}}$ and $\tilde{e}_1 = e_1 - \hat{e}_1$. Subtracting (23) from (22) yields

$$\begin{aligned} \dot{\tilde{\boldsymbol{e}}} &= (A - K_o C^T)\tilde{\boldsymbol{e}} + B[\alpha(\hat{f}(\hat{\boldsymbol{x}}) - f(\boldsymbol{x})) \\ &\quad - (1-\alpha) b(u_D(\hat{\boldsymbol{x}}) - u^*(\boldsymbol{x})) - bu_s - d] \\ \tilde{e}_1 &= C^T \tilde{\boldsymbol{e}} \end{aligned} \tag{24}$$

Since (C, A) is observable, there exist a positive-definite symmetric matrix P which satisfies the Lyapunov equation

$$\begin{aligned} &(A - BK_o^T)^T P + P(A - BK_o^T) = -Q \\ &PB = C \end{aligned} \tag{25}$$

where Q is a given positive-definite matrix.

V. ADAPTIVE LAW AND STABILITY ANALYSIS

This section is to use fuzzy CMAC system to approximate the nonlinear functions $f(\boldsymbol{x})$, $u_D(\boldsymbol{x})$ and derive the adaptive laws to adjust the weighting factors of the fuzzy CMAC system for the purpose of forcing the estimation error $\tilde{\boldsymbol{e}}$ to converge to zero.

First, replace the estimation $\hat{f}(\hat{\boldsymbol{x}})$ of the indirect control effort and the direct control effort $u_D(\hat{\boldsymbol{x}})$ in specific fuzzy CMAC systems as (13) and (14), i.e.

$$\hat{f}(\hat{\boldsymbol{x}}) = \hat{f}(\hat{\boldsymbol{x}} \mid \boldsymbol{w}_I) = \boldsymbol{w}_I^T \boldsymbol{A}_I^T \boldsymbol{\Phi}(\hat{\boldsymbol{x}}) \tag{26}$$

$$u_D(\hat{\boldsymbol{x}}) = u_D(\hat{\boldsymbol{x}} \mid \boldsymbol{w}_D) = \boldsymbol{w}_D^T \boldsymbol{A}_D^T \boldsymbol{\Phi}(\hat{\boldsymbol{x}}) \tag{27}$$

Suppose there exists constant optimal parameter vectors $\boldsymbol{w}_I^*$, $\boldsymbol{w}_D^*$

$$\boldsymbol{w}_I^* = \arg \min_{\boldsymbol{w}_I \in \Omega_f} \left[\sup_{\boldsymbol{x} \in U_1, \hat{\boldsymbol{x}} \in U_2} \left| f(\boldsymbol{x}) - \hat{f}(\hat{\boldsymbol{x}} \mid \boldsymbol{w}_I) \right| \right] \tag{28}$$

$$\boldsymbol{w}_D^* = \arg \min_{\boldsymbol{w}_D \in \Omega_D} \left[\sup_{\boldsymbol{x} \in U_1, \hat{\boldsymbol{x}} \in U_2} \left| u^*(\boldsymbol{x}) - u_D(\hat{\boldsymbol{x}} \mid \boldsymbol{w}_D) \right| \right] \tag{29}$$

where $\boldsymbol{x}$, $\hat{\boldsymbol{x}}$, $\boldsymbol{w}_I$ and $\boldsymbol{w}_D$ belong to compact sets U_1, U_2, Ω_f and Ω_D, respectively, which are defined as $U_1 = \{\boldsymbol{x} \in R^n : \|\boldsymbol{x}\| \le M_1\}$, $U_2 = \{\hat{\boldsymbol{x}} \in R^n : \|\hat{\boldsymbol{x}}\| \le M_2\}$, $\Omega_f = \{\boldsymbol{w}_I \in R^N : \|\boldsymbol{w}_I\| \le M_f\}$ and $\Omega_D = \{\boldsymbol{\theta}_D \in R^N : \|\boldsymbol{\theta}_D\| \le M_D\}$, where M_1, M_2, M_f and M_D are the designed parameters. Let the minimum approximation error be defined as

$$w = \alpha[\hat{f}(\hat{\boldsymbol{x}} \mid \boldsymbol{w}_I^*) - f(\boldsymbol{x})] - (1-\alpha)b[(u_D(\hat{\boldsymbol{x}} \mid \boldsymbol{w}_D^*) - u^*(\boldsymbol{x})] \quad (30)$$

Applying (28) and (29), the error dynamics (24) of the observation can be formulated as

$$\begin{aligned} \dot{\tilde{\boldsymbol{e}}} &= (A - K_o C^T)\tilde{\boldsymbol{e}} + B[\alpha \tilde{\boldsymbol{w}}_I^T \boldsymbol{A}_I^T \boldsymbol{\Phi}(\hat{\boldsymbol{x}}) \\ &\quad - (1-\alpha)b\tilde{\boldsymbol{w}}_D^T \boldsymbol{A}_D^T \boldsymbol{\Phi}(\hat{\boldsymbol{x}}) + w - bu_s - d] \\ \tilde{e}_1 &= C^T \tilde{\boldsymbol{e}} \end{aligned} \quad (31)$$

where $\tilde{\boldsymbol{w}}_I = \boldsymbol{w}_I - \boldsymbol{w}_I^*$, $\tilde{\boldsymbol{w}}_D = \boldsymbol{w}_D - \boldsymbol{w}_D^*$.

Assumption 1. We can choose K_c to guarantee $\boldsymbol{x} \approx \hat{\boldsymbol{x}}$. The bound function $f^U(\boldsymbol{x})$ is known such that

$$|f(\boldsymbol{x})| \le f^U(\boldsymbol{x}) \approx f^U(\hat{\boldsymbol{x}}) < \infty,$$

Considering the error dynamical equation (24), let the Lyapunov function candidate be

$$V_{\tilde{e}} = \frac{1}{2}\tilde{\boldsymbol{e}}^T P \tilde{\boldsymbol{e}} \quad (32)$$

Differentiating (32) with respect to time yields

$$\begin{aligned} \dot{V}_{\tilde{e}} &= \frac{1}{2}\dot{\tilde{\boldsymbol{e}}}^T P\tilde{\boldsymbol{e}} + \frac{1}{2}\tilde{\boldsymbol{e}}^T P\dot{\tilde{\boldsymbol{e}}} \\ &= \frac{1}{2}\tilde{\boldsymbol{e}}^T\{(A - K_o C^T)^T P + P(A - K_o C^T)\}\tilde{\boldsymbol{e}} + \tilde{\boldsymbol{e}}^T PB[\alpha(\hat{f}(\hat{\boldsymbol{x}}) \\ &\quad - f(\boldsymbol{x})) - (1-\alpha)b(u_D(\hat{\boldsymbol{x}}) - u^*(\boldsymbol{x})) - bu_s - d] \\ &\le -\frac{1}{2}\tilde{\boldsymbol{e}}^T Q\tilde{\boldsymbol{e}} - \tilde{\boldsymbol{e}}^T PBbu_s + \|\tilde{\boldsymbol{e}}^T PB\|(|\hat{f}(\hat{\boldsymbol{x}})| + |f(\boldsymbol{x})| + \\ &\quad |y_d^{(n)} + K_c^T \hat{\boldsymbol{e}}| + |bu_D(\hat{\boldsymbol{x}})| + \eta + |d|) \end{aligned} \quad (33)$$

Based on Assumption 1 and by observing (33), the supervisory control u_s is chosen as

$$\begin{aligned} u_s = I^* \operatorname{sgn}(\tilde{\boldsymbol{e}}^T PB)b^{-1}(&|\hat{f}(\hat{\boldsymbol{x}})| + f^U + |y_d^{(n)} + K_c^T \hat{\boldsymbol{e}}| \\ &+ |bu_D(\hat{\boldsymbol{x}})| + \eta + D_N) \end{aligned} \quad (34)$$

where $\hat{f}(\hat{\boldsymbol{x}})$ and $\hat{u}_D(\hat{\boldsymbol{x}})$ can be obtained from the output of the fuzzy CMAC system, sgn( ) is a sign function, I^* is defined as

$$I^* = \begin{cases} 1 & V_{\tilde{e}} > \overline{V} \\ 0 & V_{\tilde{e}} \le \overline{V} \end{cases} \quad (35)$$

where $\overline{V}$ is a pre-specific constant by designer. Consider the case $V_{\tilde{e}} > \overline{V}$, substituting (34) into (33) yields

$$\begin{aligned} \dot{V}_{\tilde{e}} &\le -\frac{1}{2}\tilde{\boldsymbol{e}}^T Q\tilde{\boldsymbol{e}} + |\tilde{\boldsymbol{e}}^T PB| \cdot [(|\hat{f}(\hat{\boldsymbol{x}})| + |f(\boldsymbol{x})| \\ &\quad + |y_d^{(n)} + K_c^T \hat{\boldsymbol{e}}| + |bu_D(\hat{\boldsymbol{x}})| + \eta + |d|) \\ &\quad - (|\hat{f}(\hat{\boldsymbol{x}})| + f^U + |y_d^{(n)} + K_c^T \hat{\boldsymbol{e}}| + |bu_D(\hat{\boldsymbol{x}})| + \eta + D_N)] \\ &\le -\frac{1}{2}\tilde{\boldsymbol{e}}^T Q\tilde{\boldsymbol{e}} \le 0 \end{aligned} \quad (36)$$

Theorem 1: Consider the nonlinear system (1) with control law (19), (21) and (34), $\hat{f}(\hat{\boldsymbol{x}} \mid \boldsymbol{w}_I)$ and $u_D(\hat{\boldsymbol{x}} \mid \boldsymbol{w}_D)$ are given by (26) and (27), and the parameter adaptation law are chosen as

$$\dot{\boldsymbol{\theta}}_f = -r_1 \tilde{\boldsymbol{e}}^T PB\boldsymbol{A}_I^T \boldsymbol{\Phi}(\hat{\boldsymbol{x}}) \quad (37)$$

$$\dot{\boldsymbol{\theta}}_D = r_2 b\boldsymbol{e}^T PB\boldsymbol{A}_D^T \boldsymbol{\Phi}(\hat{\boldsymbol{x}}) \quad (38)$$

where $r_1 > 0$ and $r_2 > 0$ are positive adaptive gain constants to be designed. If Assumption 1 is satisfied, the proposed control scheme can ensures that all the closed-loop signals are bounded, and the tracking errors converge to zero.

Proof:

Choose the Lyapunov-like function candidate as

$$V = \frac{1}{2}\tilde{\boldsymbol{e}}^T P\tilde{\boldsymbol{e}} + \frac{\alpha}{2r_1}\tilde{\boldsymbol{w}}_I^T \tilde{\boldsymbol{w}}_I + \frac{1-\alpha}{2r_2}\tilde{\boldsymbol{w}}_D^T \tilde{\boldsymbol{w}}_D \quad (39)$$

with $P = P^T > 0$. Taking the time derivative of V yields

$$\dot{V} = \frac{1}{2}(\dot{\tilde{\boldsymbol{e}}}^T P\tilde{\boldsymbol{e}} + \tilde{\boldsymbol{e}}^T P\dot{\tilde{\boldsymbol{e}}}) + \frac{\alpha}{r_1}\tilde{\boldsymbol{w}}_I^T \dot{\tilde{\boldsymbol{w}}}_I + \frac{1-\alpha}{r_2}\tilde{\boldsymbol{w}}_D^T \dot{\tilde{\boldsymbol{w}}}_D \quad (40)$$

Substituting (24) into (40) and the fact $\dot{\tilde{\boldsymbol{w}}}_I = \dot{\boldsymbol{w}}_I$, $\dot{\tilde{\boldsymbol{w}}}_D = \dot{\boldsymbol{w}}_D$, the above equation becomes

$$\begin{aligned} \dot{V} &= \frac{1}{2}[\tilde{\boldsymbol{e}}^T (A - K_o C^T)^T P\tilde{\boldsymbol{e}} + \tilde{\boldsymbol{e}}^T P(A - K_o C^T)\tilde{\boldsymbol{e}}] \\ &\quad + \tilde{\boldsymbol{e}}^T PB(w - bu_s - d) + \frac{\alpha}{r_1}\tilde{\boldsymbol{w}}_I^T (r_1 \tilde{\boldsymbol{e}}^T PB\boldsymbol{A}_I^T \boldsymbol{\Phi}(\hat{\boldsymbol{x}}) + \dot{\boldsymbol{w}}_I) \\ &\quad - \frac{1-\alpha}{r_2}\tilde{\boldsymbol{w}}_D^T (r_2 b\boldsymbol{e}^T PB\boldsymbol{A}_D^T \boldsymbol{\Phi}(\hat{\boldsymbol{x}}) - \dot{\boldsymbol{w}}_D) \end{aligned} \quad (41)$$

Using parameter adaptation law (37)-(38) and (25), and the definition of u_s in (34), then (41) can be formulated as

$$\dot{V} = -\frac{1}{2}\tilde{\boldsymbol{e}}^T Q\tilde{\boldsymbol{e}} + \tilde{\boldsymbol{e}}^T PB(w - bu_s - d) \le -\frac{1}{2}\tilde{\boldsymbol{e}}^T Q\tilde{\boldsymbol{e}} \le 0 \quad (42)$$

This means that the inequality $\dot{V}_i < 0$ is obtained and the whole closed-loop system is stable.

VI. SIMULATION RESULTS

Chaotic system is a nonlinear deterministic system that displays complex, noisy-like and unpredictable dynamical behavior. To illustrate the performance and efficiency of the proposed fuzzy CMAC control system, it is applied to control a Duffing forced oscillation system [16]. The oscillation system has chaotic phenomena if the control input equals zero. The dynamic equation of a Duffing forced oscillation system can be described as follows:

$$\begin{bmatrix}\dot{x}_1\\ \dot{x}_2\end{bmatrix}=\begin{bmatrix}0 & 1\\ 0 & 0\end{bmatrix}\begin{bmatrix}x_1\\ x_2\end{bmatrix}+\begin{bmatrix}0\\ 1\end{bmatrix}(f+bu+d),$$
$$y=\begin{bmatrix}1 & 0\end{bmatrix}\begin{bmatrix}x_1\\ x_2\end{bmatrix}. \tag{43}$$

where $f(x_1,x_2)=-0.1x_2-x_1^3+12\cos(t)$, y is the system output, u is the applied force (the control input) and d is the external disturbance. Also the external disturbance $d(t)$ is assumed to be a square wave with an amplitude ±1 and a period of 2π.

The control objective is to maintain the output x_1 of the system to track the desired trajectory $y_d=\sin(t)$ under the constraint that only the system output is available for measurement. In the implementation, the fuzzy sets of states $\hat{x}_1$ and $\hat{x}_2$ are defined as {*NB, NM, NS, ZE, PS, PM, PB*} and their membership functions are

$\mu_{NB}(\hat{x}_i)=1/(1+\exp(5(\hat{x}_i+3))$, $\mu_{NM}(\hat{x}_i)=\exp(-((\hat{x}_i+2)^2)$,
$\mu_{NS}(\hat{x}_i)=\exp(-(\hat{x}_i+1)^2)$, $\mu_{ZE}(\hat{x}_i)=\exp(-(\hat{x}_i)^2)$,
$\mu_{PS}(\hat{x}_i)=\exp(-(\hat{x}_i-1)^2)$, $\mu_{PM}(\hat{x}_i)=\exp((\hat{x}_i-2)^2)$,
$\mu_{PB}(\hat{x}_i)=1/(1+\exp(-5(\hat{x}_i-3)^2)$.

Select the positive matrices $Q=Diag[10\ 10]$ and choose the feedback and observer gain vector as $K_c^T=[30,50]$ and $K_o^T=[60,140]$. The sliding surface is selected as $\hat{S}=\Lambda^T\tilde{\boldsymbol{e}}$, where $\Lambda=[5,1]^{\mathrm{T}}$. The initial states are chosen as $\boldsymbol{x}(0)=[0.2,0.2]^T$, $\hat{\boldsymbol{x}}(0)=[1.5,1.5]^T$ and let adaptation gains as $r_1=r_2=100$. Consider three cases of prescribed adaptation levels $\alpha=1$, 0, 0.5, respectively, the simulation results are shown in Fig. 2 to Fig. 4. The simulation results show that the tracking error has been attenuated efficiently. Thus the proposed adaptive control scheme can control the system to follow the desired trajectory and achieve desired performance.

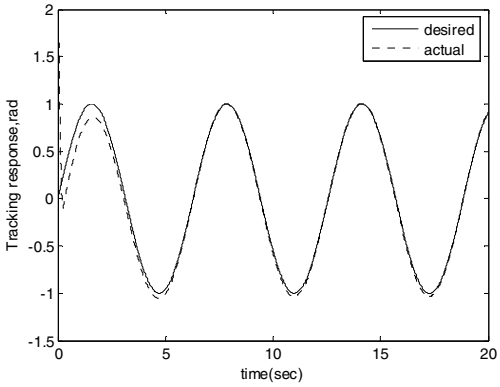

(a) Trajectories of the state x_1 (dash line)and desired y_d (solid line)

Figure 2 The responses of Duffing forced oscillation system for $\alpha=1$.

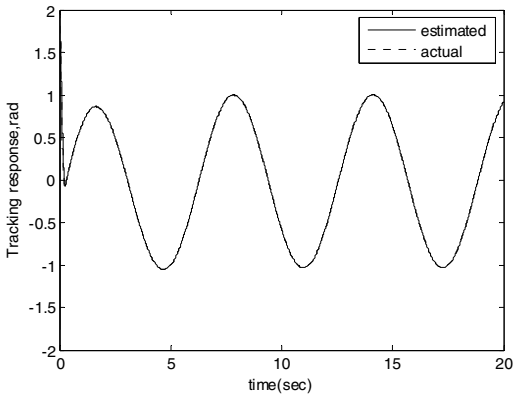

(b) Trajectories of the state x_1 (solid line) and estimated state $\hat{x}_1$ (dash line)

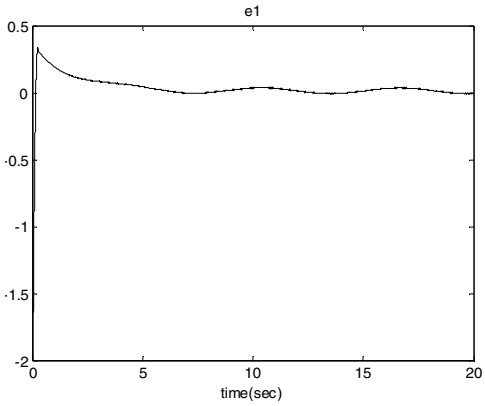

(c) The trajectory of the actual tracking error.

Figure 2 The responses of Duffing forced oscillation system for $\alpha=1$.

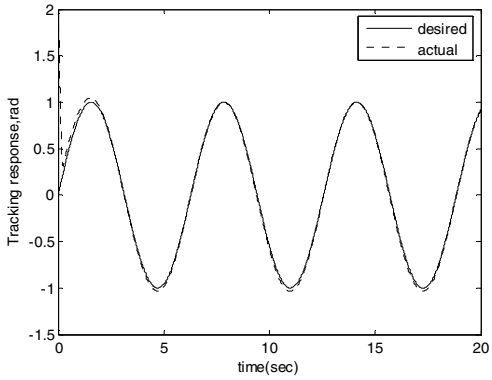

(a) Trajectories of the state x_1 (dash line)and desired y_d (solid line)

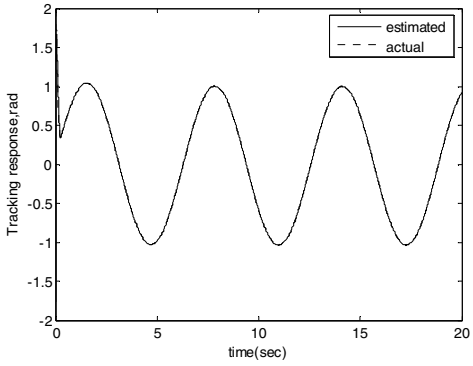

(b) Trajectories of the state x_1 (solid line) and estimated state $\hat{x}_1$ (dash line)

Figure 3 The responses of Duffing forced oscillation system for $\alpha=0.5$

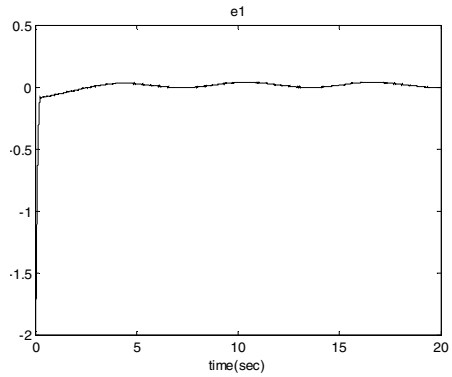

(c) The trajectory of the actual tracking error.

Figure 3 The responses of Duffing forced oscillation system for $\alpha = 0.5$

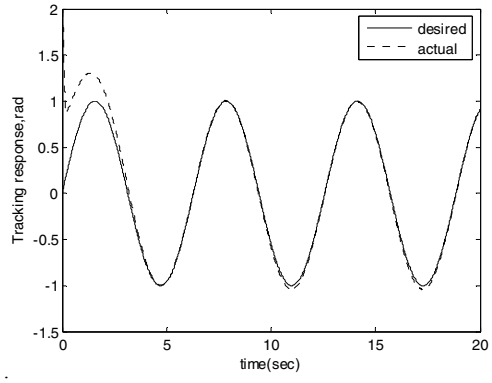

(a) Trajectories of the state x_1 (dash line)and desired y_d (solid line)

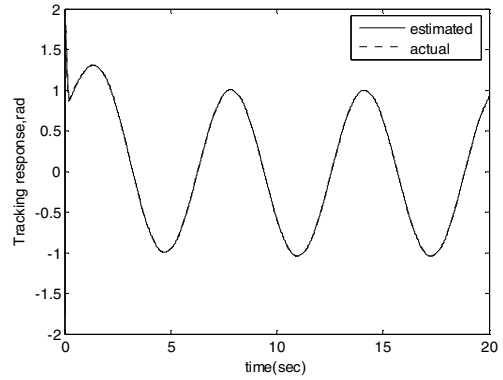

(b) Trajectories of the state x_1 (solid line) and estimated state $\hat{x}_1$ (dash line)

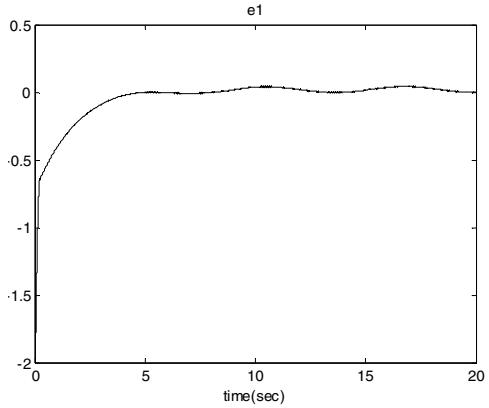

(c) The trajectory of the actual tracking error.

Figure 4 The responses of Duffing forced oscillation system for $\alpha = 0$.

VII. SIMULATION RESULTS

The goal of this work is the development and implementation of a hybrid fuzzy CMAC control based sliding mode control for the robust trajectory tracking of uncertain chaotic systems. This design obtains robustness in the sense that the self-tuning mechanism can automatically adapt the fuzzy CMAC controller by using a learning algorithm and the global asymptotic stability of the algorithm is established via Lyapunov stability criterion. The simulation presented in the Duffing forced oscillation system control indicates that the proposed approach is capable of achieving a good trajectory following performance without the knowledge of plant parameters. Although only the Duffing forced oscillation system has been studied in this paper, the proposed control scheme can also be used to address the other class of chaotic systems.

REFERENCES

[1] J. J. Yan, K. K. Shyu and J. S. Lin, "Adaptive variable structure control for uncertain chaotic systems containing dead-zone nonlinearity," Chaos, Solitons & Fractals, Vol. 35, No. 2, pp.347-355, 2005.

[2] C. M. Lin and C. H. Chen, "CMAC-based supervisory control for nonlinear chaotic systems," Chaos, Solitons & Fractals, Vol. 35, No.1, pp. 40-58, 2008.

[3] J. Wang, G. D. Qiao and B. Deng, "H∞ Variable universe adaptive fuzzy control for chaotic system", Chaos, Solitons & Fractals, Vol. 24, No.4, pp. 1075-1086, 2005.

[4] C. Hua and X. Guan, "Adaptive control for chaotic systems", Chaos, Solitons & Fractals, Vol. 22, No.1, pp. 55-60, 2004.

[5] Y. J. Cao, "A nonlinear adaptive approach to controlling chaotic oscillators", Physics Letters A, Vol. 270, No. 3-4, pp. 171-176, 2000.

[6] J. S. Albus, "A new approach to manipulator control: The cerebellar model articulation controller (CMAC)," Trans. ASME J. Dyn. Syst., Meas., Contr, , Vol. 97, pp. 220–227, Sept. 1975.

[7] J. S. Albus, "Data storage in the cerebellar model articulation controller (CMAC)," Trans. ASME J. Dyn. Syst., Meas., Contr., Vol. 97, pp. 228–233, 1975.

[8] S. H. Lane, D. A. Handelman, and J. J. Gelfand, "Theory and development of higher-order CMAC neural networks," IEEE Contr. Syst. Mag., Vol. 12, pp. 23–30, 1992.

[9] H. Shiraishi, S. L. Ipri, and D. D. Cho, "CMAC neural network controller for fuel-injection systems," IEEE Trans. Contr. Sys. Technology, Vol. 3, pp. 32–38, 1995.

[10] K. S. Hwang and C. S. Lin, "Smooth trajectory tracking of three-link robot: A self-organizing CMAC approach," IEEE Trans. Syst., Man, Cybern. B, Vol. 28, pp. 680-692, 1998.

[11] U. Itkis, Control Systems of Variable Structure, Wiley, New York, 1976.

[12] J. J. E. Slotine and J. A. Coetsee, "Adaptive sliding controller synthesis for non-linear systems," Int. J. Control, Vol. 43, No. 6, pp. 1631-1651, 1986.

[13] C. M. Lin and T.-Y.Chen, "Self-Organizing CMAC Control for a Class of MIMO Uncertain Nonlinear Systems," IEEE Trans. Neural Networks, Vol. 20, pp. 1377-1384, 2008.

[14] Y. G. Leu, T. T. Lee and W. Y. Wang, "Observer-based adaptive fuzzy-neural control for unknown nonlinear dynamical systems," IEEE Trans. Systems, Man, Cybernetics, Vol. 29, No. 5, pp. 583-591, 1999.

[15] J. H. Park and S. H. Kim, "Direct adaptive output feedback fuzzy observer for a nonaffine nonlinear system," IEE Proc. Control Theory Application, Vol. 151, No. 1, pp. 65-71, 2004.

[16] L. X. Wang, "Stable adaptive fuzzy control of nonlinear systems," IEEE Trans. Fuzzy Systems, Vol. 1, No. 2, pp. 146-155, 1993.

2011 IEEE International Conference on Fuzzy Systems
June 27-30, 2011, Taipei, Taiwan

Automated Boundary Extraction and Visualization System for Coronary Plaque in IVUS Image by Using Fuzzy Inference-based Method

Takanori Koga*, Eiji Uchino†‡, Noriaki Suetake†

*Department of Computer Science and Electronic Engineering
Tokuyama College of Technology, Gakuendai, Shunan 745–8585, JAPAN
Email: koga@tokuyama.ac.jp
†Graduate School of Science and Engineering
Yamaguchi University, 1677-1 Yoshida, Yamaguchi 753-8512, JAPAN
Email: {uchino@, suetake@sci.}yamaguchi-u.ac.jp
‡Fuzzy Logic Systems Institute (FLSI), 680-41 Kawazu, Iizuka 820-0067, JAPAN

***Abstract*—We propose a fully automatic plaque boundary extraction system for an intravascular ultrasound (IVUS) image aiming at practical use in clinic. The IVUS image, which is commonly used for a diagnosis of acute coronary syndromes (ACS) in the field of cardiology, has coarse-grained texture due to heavy speckle noise. A medical doctor's interpretation of the IVUS image is disturbed frequently by the heavy speckle noise. In the proposed system, the heavy speckle noise is reduced firstly by using an anisotropic diffusion filter. Secondarily, the plaque boundary is extracted by using the Takagi-Sugeno (T-S) type fuzzy inference with a weighted separability measure and some heuristic rules. Extraction of plaque boundary is achieved fully automatically. The proposed system substantially reduces the workload of medical doctors. The effectiveness of the proposed system has been verified by the experiments using the real IVUS images.**

***Index Terms*—Acute coronary syndromes, IVUS image, plaque boundary extraction, fuzzy inference.**

I. Introduction

Intravascular ultrasound (IVUS) method [1], [2] is a real-time computed tomographic imaging method for the visualization of coronary atherosclerotic plaque. It provides thousands of cross-sectional images of a coronary artery in vivo, and is employed especially for a diagnosis of the acute coronary syndromes (ACS) caused by a rupture of vulnerable plaque [3], [4]. For quantitative assessment of plaque [5], precise boundary extraction of plaque is strongly required in the interpretation of the tomographic images produced by the IVUS method. In particular, the inner and outer boundaries of the plaque and the cross-sectional area of the plaque are to be extracted and evaluated precisely in order to monitor the effect of medical treatment.

Frequently, medical doctors manually trace the boundaries of the plaque and then evaluate the area of that plaque for many IVUS images. After that, the volume of the plaque is estimated by integrating the extracted area. However, the boundary extraction task of plaque is tough and time-consuming for a medical doctor. This is not only because a large number of the IVUS images must be processed, but also because recognizing the boundaries of plaque is very hard due to a heavy blood speckle noise. A computer-aided full-automatic precise boundary extraction of plaque is thus strongly desired.

So far, in the representative boundary extraction methods [6], *e.g.*, curve interpolation method such as spline interpolation is used, where seed points are given manually by a medical doctor. Those methods and tools can reduce somewhat the workload of the tracing task on a medical doctor. However, the accuracy of the plaque boundary extraction by the curve interpolation is considerably affected by the number of the seed points and/or the positions of those points.

On the other hand, the methods based on automatic search algorithms, *e.g.*, an active contour (snake) model [7], genetic algorithm [8], and so on, have been proposed to date. However, those methods involve some iterative processes for optimizing evaluation function and take plenty of computing time. To meet with a demand for a practical use, a quick and fully automatic boundary extraction of plaque is definitely required.

In the past, to cope with this problem, the authors proposed some fundamental techniques for the plaque boundary extraction such as speckle noise reduction by using a modified anisotropic diffusion filter [9], [10] with a statistical discriminant measure (being called separability) [11], an automatic searching algorithm for the boundary extraction area based on some heuristic rules [12], boundary extraction method by using Takagi-Sugeno (T-S) type fuzzy inference [13], and so on. Then the authors furthermore advanced the method by employing an adaptive allocation rule of membership functions in the T-S fuzzy inference engine, and some of the performance of the proposed method has been presented in [14]. The fuzzy inference-based method realizes a fast, precise, robust, and automatic extraction of the boundary of plaque.

In this paper, we introduce an automatic boundary extraction system which combines all the above-mentioned fundamental techniques. The proposed system is implemented as

978-1-4244-7316-8/11/$26.00 ©2011 IEEE

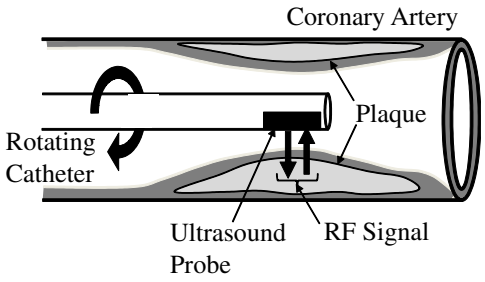

Fig. 1. Overview image of the intravascular ultrasound (IVUS) method.

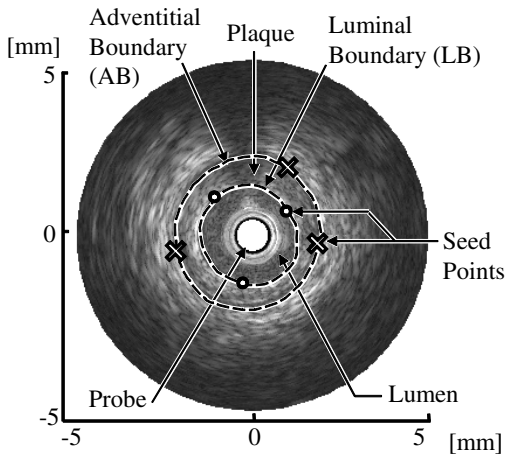

Fig. 2. An example of B-mode image obtained by the IVUS method. In the image, 4mm corresponds to 2,048 pixels.

a software with easy-to-use graphical user interface (GUI) aiming at the real practical use in clinic and at the research use.

In the proposed system, the plaque boundary extraction area is automatically searched and is found by an edge-preserved smoothing filter using anisotropic diffusion, weighted separability, the heuristic rules, and T-S type fuzzy inference. This system also has a semi-automatic boundary extraction function using the seed points allocated by the user, for the IVUS images with very complicated boundary of coronary plaque.

The validity and the effectiveness of the system are briefly reviewed by applying it to the practical problem of plaque boundary extraction in clinic. Finally, it is shown that a 3-dimensional image of the coronary plaque can be reconstructed.

II. Intravascular Ultrasound (IVUS) Method

Intravascular ultrasound (IVUS) method [1], [2] is one of the medical imaging techniques. It allows the application of ultrasound technology to observe from inside the blood vessels out through the surrounding blood column, visualizing the coronary plaque in vivo.

In the IVUS method, a specially designed thin catheter with the ultimately-miniaturized ultrasound probe attached to its distal end is used (see Fig. 1). To visualize the coronary arteries and plaques in vivo, angiographic techniques are used. A medical doctor steers the guidewire with very thin diameter from outside the body through angiography catheters into the coronary artery to be visualized. The ultrasound catheter tip is slid in over the guidewire and positioned, using angiography techniques so that the tip is at the farthest away position to be visualized. The guidewire is kept stationary and the ultrasound catheter tip is slid backwards, usually under motorized control.

The proximal end of the catheter is connected to a computerized ultrasound equipment. The ultrasound waves are emitted from the ultrasound probe, which are in the 40MHz range in this study, and the catheter also receives the reflected signal from the plaque tissue. It is sampled at 400 MHz and stored in the computerized ultrasound equipment.

An IVUS image is constructed of the amplitude information of the received radiofrequency (RF) signal. In order to visualize the inside of a coronary artery, the sampled RF signal is first transformed into an 8-bit luminal intensity signal by taking the absolute value of a signal, then by taking the envelope of a signal, and finally by taking its logarithmic value.

The luminal intensity signals in all radial directions are then formed to obtain a tomographic cross sectional image of a coronary artery as shown in Fig. 2. The IVUS image of Fig. 2 is called "B-mode image." A B-mode image displays a real time ultrasound cross-sectional image of a thin section of a blood vessel currently surrounding a catheter probe.

In this study, the B-mode image is constructed with 2,048 pixels in depth, and 256 lines in radial direction. Hence, the resolution of distance and angle are $1.95\mu m$/pixel and $1.41°$/line, respectively.

In the quantitative assessment of coronary plaque, the following two boundaries are extracted in the IVUS B-mode image as shown in Fig. 2. One is a luminal boundary (LB) between the lumen and the plaque, and the other is an adventitial boundary (AB) between the plaque and the vascular wall.

III. Proposed System

Figs. 3(a) and 3(b) show the overviews of the proposed diagnosis system. By applying a set of IVUS data obtained by IVUS instrument, the software extracts the boundaries of plaque by the full-automatic extraction algorithm and reconstructs the 3-D classified tissue structure of the plaque as shown in Fig. 3(b). In this section, we firstly describe the full-automatic search method for the area of boundary extraction without using any seed points and giving any initial boundary. Then semi-automatic (interactive) boundary extraction method, which is used for IVUS images with very complicated boundaries of plaque, is described.

A. Fully automatic plaque boundary extraction

In the present method, at first, an IVUS image is transformed from the polar coordinate system into the orthogonal coordinate system as shown in Fig. 4(a). Then the edge-preserved smoothing using anisotropic diffusion is performed

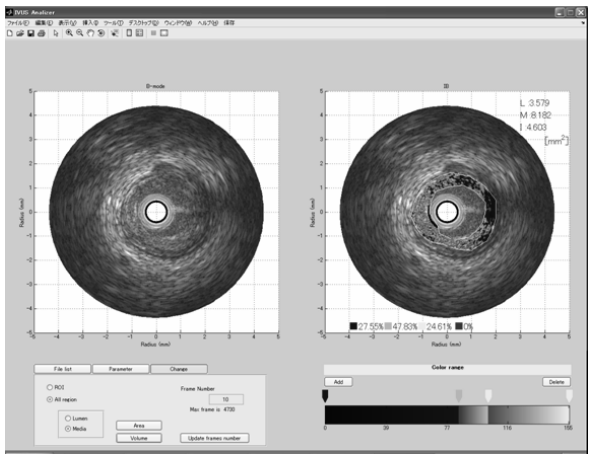

(a)

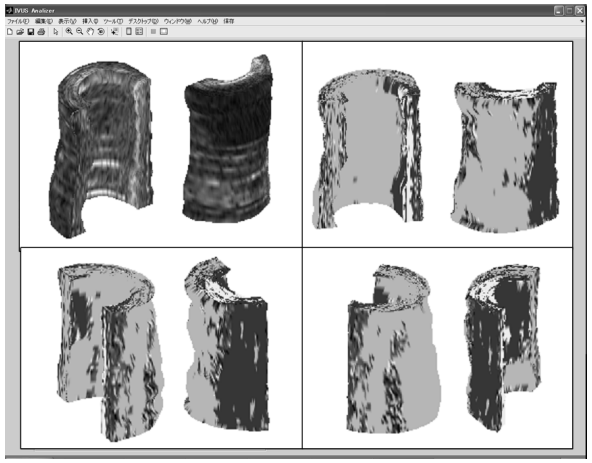

(b)

Fig. 3. Overview of the proposed diagnosis system. (a) Overview of main GUI. (b) 3-D viewing of the extracted plaque.

on the input image as shown in Fig. 4(b). An anisotropic diffusion filter is known as an effective edge-preserved smoothing method, and it is broadly used.

Then image processing using some heuristic rules are applied to find out the boundary extraction areas. Finally in the found areas, the objective boundaries are extracted by T-S type fuzzy inference with the weighted separability measure. The weighted separability is a modification of a separability measure with special consideration to an IVUS image.

1) Speckle Noise Reduction by Perona-Malik's anisotropic diffusion (PMD): The anisotropic diffusion filter proposed by Perona and Malik [9] is employed to realize an edge-preserved smoothing for an IVUS B-mode image. The discrete version of PMD is given as follows:

$$I_{\boldsymbol{s}}^{(n+1)} = I_{\boldsymbol{s}}^{(n)} + \frac{\lambda}{|\phi_{\boldsymbol{s}}|} \sum_{\boldsymbol{p}\in\phi_{\boldsymbol{s}}} g(\nabla I_{\boldsymbol{s},\boldsymbol{p}}^{(n)}) \cdot \nabla I_{\boldsymbol{s},\boldsymbol{p}}^{(n)}, \qquad (1)$$

where $\boldsymbol{s}$=(x, y) and $\boldsymbol{p}$ are the coordinates of the pixel of concern and its neighboring pixels, respectively. $I_s^{(n)}$ is an intensity at $\boldsymbol{s}$ with an iteration count n. $\phi_{\boldsymbol{s}}$ represents the four neighboring pixels in North, West, South and East diffusion

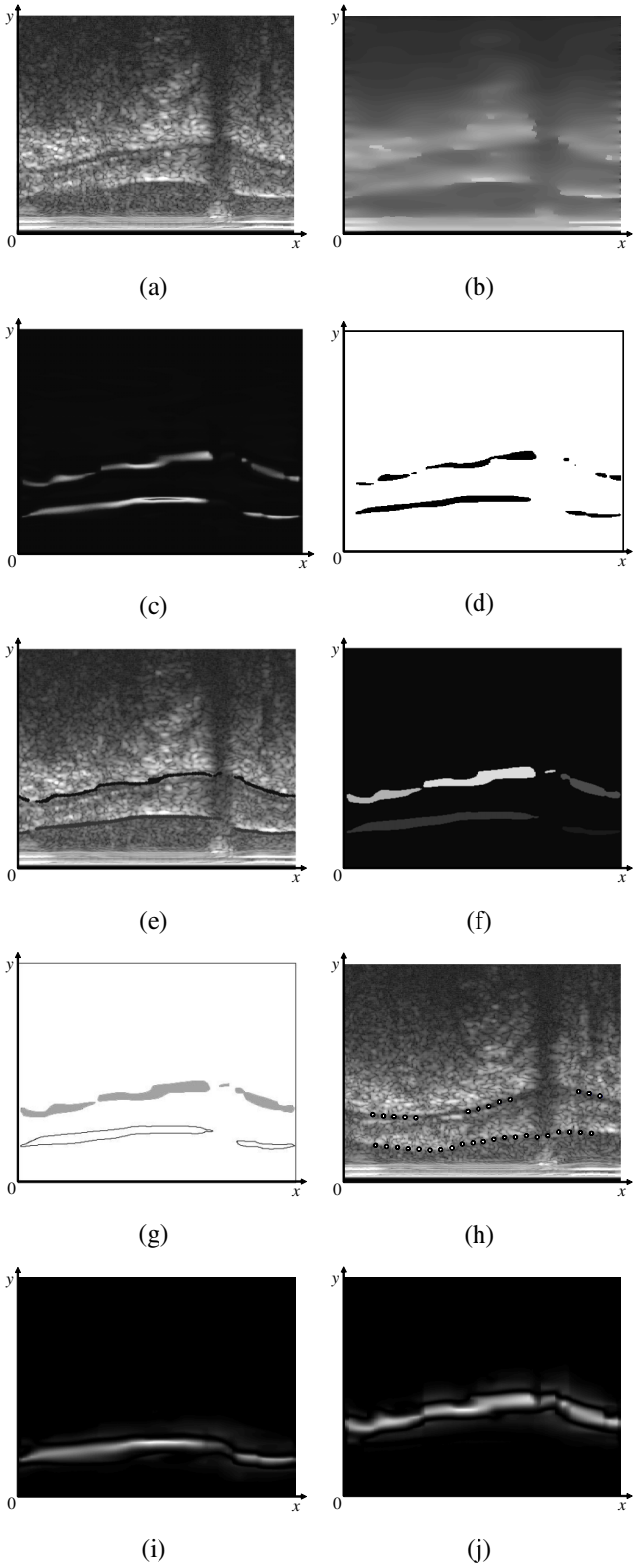

Fig. 4. Automatic placement of seed points and automatic partitioning of boundary extraction area. (a) Input image. (b) Edge-preserved and smoothed image by PMD. (c) Discriminant image of (b) by weighted separability. (d) Binary image obtained by threshold processing for (c). (e) Candidates of the seed points. (f) Regions for getting the final seed points. (g) Classified regions of (f) for LB or AB. (h) Final seed points automatically placed. (i) The plaque boundary extraction area for luminal boundary (LB). (j) The plaque boundary extraction area for adventitial boundary (AB).

directions. $|\phi_{\boldsymbol{s}}|$ is a number of the pixels in the neighborhood area, which is then $|\phi_{\boldsymbol{s}}|=4$ in this study. λ is a parameter. $g(\cdot)$ is called an edge stopping function. A monotonically decreasing function of the gradient of an image is usually adopted as $g(\cdot)$. The gradient of the image is calculated by:

$$\nabla I^{(n)}_{\boldsymbol{s},\boldsymbol{p}} = I^{(n)}_{\boldsymbol{p}} - I^{(n)}_{\boldsymbol{s}}. \tag{2}$$

In PMD, the edge stopping function is given by:

$$g(z) = \frac{1}{1+\left(\frac{z}{K}\right)^2}, \tag{3}$$

where K is a parameter which controls the strength of diffusion. $g(\cdot)$ takes large values at the regions where the intensity gradients are small. On the contrary, it takes small values at the regions where the intensity gradients are large.

By applying the PMD to an IVUS B-mode image as a pre-processing, the speckle patterns are reduced enough, and the edges corresponding to the luminal boundary and the adventitial boundary of plaque are preserved enough as shown in Fig. 4(b).

2) Detection of boundary extraction area by weighted separability measure: In order to distinguish the edge of plaque and that of the speckle pattern in an IVUS image, the proposed method employs a statistical discriminant measure of image separability [11]. Evaluation of image separability is very simple, and it has the following features:

i) Robust to noisy and blurred edge,
ii) Sensitive to an edge between different texture regions.

Separability is calculated by a linear discriminant analysis using the information of the two local regions. The separability $\eta_{\boldsymbol{s}}$ for the pixel $\boldsymbol{s}=(x,y)$ is calculated by:

$$\eta_{\boldsymbol{s}} = \frac{\sum_{k=1}^{k=L} \sigma^2_{bk}}{\sum_{k=1}^{k=L} \sigma^2_{Tk}}, \tag{4}$$

$$\sigma^2_{bk} = n_1(\bar{I}_{k1}-\bar{I}_k)^2 + n_2(\bar{I}_{k2}-\bar{I}_k)^2, \tag{5}$$

and

$$\sigma^2_{Tk} = \sum_{i=1}^{n_1+n_2} (I_{ki}-\bar{I}_k), \tag{6}$$

where $\bar{I}_{k1}$ and $\bar{I}_{k2}$ are the means of the intensities in the regions 1 and 2, respectively. $\bar{I}_k$ is the mean of the intensities in the combined two regions. n_1 and n_2 represent the numbers of the pixels in regions 1 and 2, respectively. $\eta_{\boldsymbol{s}}$ is $0 \le \eta_{\boldsymbol{s}} \le 1$, and it takes a large value when two regions are separated with each other in the meaning of separability.

The weighted separability, which is a modification of the original separability [11], detects the candidates of the inner (lower) and the outer (upper) boundaries of plaque by considering the following two conditions peculiar to an IVUS image. Those are: i) intensity in the outside area of a luminal boundary (LB) tends to be bigger than that in the inside area of LB; ii) intensity in the outside area of an adventitial boundary (AB) tends to be bigger than that in the inside area of AB.

The weighted separability for a pixel $\boldsymbol{s}=(i,j)$ is defined by:

$$\eta^w_{\boldsymbol{s}} = \eta_{\boldsymbol{s}} \cdot \left(\frac{\bar{I}_2(I_{Max}-\bar{I}_1)}{I_{Max}}\right)^2, \tag{7}$$

where I_{Max} is a maximum intensity on the whole IVUS image. $\bar{I}_1$ and $\bar{I}_2$ are the means of the intensities in the two discriminative regions 1 and 2, respectively [14].

Fig. 4(c) shows a discriminant image of Fig. 4(b) by using $\eta^w_{\boldsymbol{s}}$. Each pixel of the image represents the weighted separability $\eta^w_{\boldsymbol{s}}$. When $\eta^w_{\boldsymbol{s}}$ is large, high brightness is assigned to its corresponding pixel.

The weighted separability takes a large value around the regional edge of the IVUS image. That is, a chain of white pixels with high brightness can then be a candidate of a boundary of plaque.

Fig. 4(c) shows vividly the two candidates of plaque boundary. Furthermore, it is observed that the weighted separability in the area where the blood speckle noise exists (in the lumen area) is suppressed.

3) Automatic partitioning of boundary extraction area and placement of seed points by heuristic rules: Here, the candidates of boundaries of plaque shown in Fig. 4(c) are partitioned to the candidate for LB and that for AB. The following are the concrete processes of each step shown in Figs. 4(d)-(h).

Fig. 4(d) shows a binary image obtained by the threshold processing for the image of Fig. 4(c). Here, let the threshold value of the weighted separability be ζ. By changing the value of ζ from ζ_{low} to ζ_{high} at regular intervals, a binary image with each threshold value of ζ, such as Fig. 4(d), is obtained.

The points on the central line of each black-colored region of Fig. 4(d) are regarded as candidates of the seed points. The candidates are detected by line scanning in parallel to the x-axis. When two regions are detected by the line scanning, the centers of regions are regarded as the candidates. The candidates of the seed points for all the binary images are superimposed on Fig. 4(e).

The optimum threshold value of ζ has to be set to obtain the best binary image of Fig. 4(d) for detecting the final seed points. In this process, the binary images are evaluated by using the following score S:

$$G_1 = \begin{cases} \frac{1}{N_{r1}} \cdot n_r & 0 \le n_r < N_{r1} \\ -\frac{1}{N_{r2}-N_{r1}} \cdot n_r + \frac{N_{r2}}{N_{r2}-N_{r1}} & N_{r1} \le n_r < N_{r2} \\ 0 & N_{r2} \le n_r, \end{cases} \tag{8}$$

$$G_2 = \begin{cases} 0 & 0 \le n_p < N_{p1} \\ \frac{1}{N_{p2}-N_{p1}} \cdot n_p - \frac{N_{p1}}{N_{p2}-N_{p1}} & N_{p1} \le n_p < N_{p2} \\ -\frac{1}{N_{p3}-N_{p2}} \cdot n_p + \frac{N_{p3}}{N_{p3}-N_{p2}} & N_{p2} \le n_p < N_{p3} \\ 0 & N_{p3} \le n_p, \end{cases} \tag{9}$$

$$G_3 = \begin{cases} 0 & 0 \le l_r < L_{r1} \\ \frac{1}{L_{r2}-L_{r1}} \cdot l_r - \frac{L_{r1}}{L_{r2}-L_{r1}} & L_{r1} \le l_r < L_{r2} \\ -\frac{1}{L_{r3}-L_{r2}} \cdot l_r + \frac{L_{r3}}{L_{r3}-L_{r2}} & L_{r2} \le l_r < L_{r3} \\ 0 & L_{r3} \le l_r, \end{cases} \tag{10}$$

$$S = G_1 \cdot G_2 \cdot G_3, \tag{11}$$

where G_1, G_2 and G_3 are concerned with the membership functions for the number of regions n_r, the number of pixels n_p, and the total length of regions l_r, respectively.

The sets of parameters $\{N_{r1}, N_{r2}\}$, $\{N_{p1}, N_{p2}, N_{p3}\}$, $\{L_{r1}, L_{r2}, L_{r3}\}$ define the figure of each membership function. Those functions are empirically determined by analyzing hundreds of real IVUS images. The image with the maximum score of S is selected to obtain Fig. 4(f).

The color-coded regions in Fig. 4(f) are then classified either to the region for LB or that for AB as shown in Fig. 4(g) by majority decision by using the class information of the candidates of the seed points.

Finally, the points on the central line of each region of Fig. 4(g) are regarded as the final seed points to get Fig. 4(h). The selected seed points are linearly interpolated, and the boundary extraction areas are allocated around this linearly interpolated curve with weights of the following Gaussian kernel function:

$$f(y) = \exp(-\frac{(y - y(i))^2}{2\sigma^2}), \tag{12}$$

$$\sigma = (y_{out}(i) - y_{in}(i))/3, \tag{13}$$

where $y_{in}(i)$ and $y_{out}(i)$ are lines obtained by the interpolation for LB and AB, respectively. The allocated areas for the boundary extraction are shown in Fig. 4(i) and 4(j).

4) Plaque boundary extraction by T-S type fuzzy inference: By using the images obtained by the above-mentioned procedures shown in Figs. 4(i) and 4(j), the objective true boundaries of coronary plaque are extracted by T-S type fuzzy model [13] as shown in Figs. 5(a) and 5(b).

Concretely, the boundary is piecewise approximated by the polynomials in the orthogonal coordinates by a series of the following fuzzy if-then rules [15]:

$$\text{IF } x_i \text{ is } A_\ell \text{ THEN } f_\ell(x_i) = a_\ell x_i + b_\ell,$$

where A_ℓ is a fuzzy set with the membership function (MSF) μ_ℓ as shown in Fig. 5(b). Usually, four complementary triangular MSFs are uniformly allocated over the interval of concern. x_i corresponds to an angle index, and $f_\ell(x_i)$ is a linear function. The ℓ-th rule thus stands for a piecewise approximation of a plaque boundary by a linear function in the interval $[t_{\ell-1}, t_{\ell+1}]$. The inferred boundary $\hat{y}(x_i)$ is given by:

$$\hat{y}(x_i) = \mu_\ell(x_i) f_\ell(x_i) + \mu_{\ell+1}(x_i) f_{\ell+1}(x_i). \tag{14}$$

The optimum coefficients a_ℓ^* and b_ℓ^* of the ℓ-th fuzzy if-then rule are determined with use of the weighted least square method (WLSM) so as to minimize the following weighted error criterion:

$$E = \sum_{j=0}^{J-1} \sum_{i=0}^{I-1} \eta_{ij}^2 \{y_j - \hat{y}(x_i)\}^2, \tag{15}$$

where η_{ij} is a separability of pixel $\boldsymbol{s} = (i, j)$ [11].

In this method η_{ij} which lies in the specified boundary search area, *i.e.*, within the thin dotted lines in Fig. 5(a), are used as the weights of WLSM.

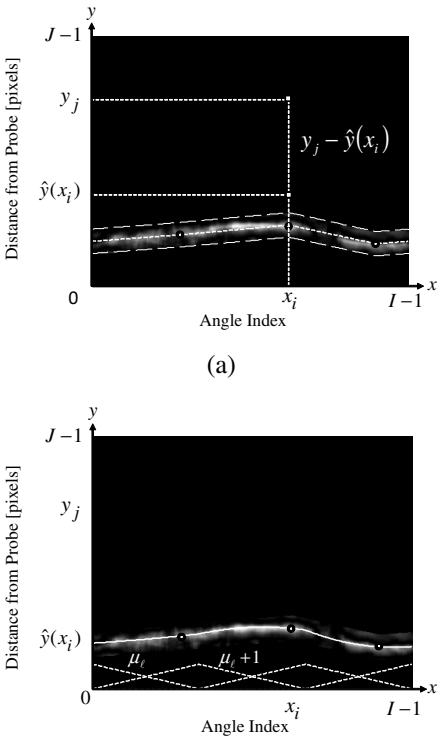

Fig. 5. Plaque boundary extraction scheme by the T-S type fuzzy inference. (a) A primitive boundary and a specified search area, which is within the two thin dotted lines. (b) The extracted luminal boundary (LB) by T-S type fuzzy inference.

B. Semi-automatic (interactive) plaque boundary extraction with adaptive allocation of membership functions

At first, Seed points are placed on the B-mode image by a medical doctor. The image is then transformed from the polar coordinates into the orthogonal coordinates.

The seed points are first linearly interpolated on the orthogonal coordinates to obtain a primitive boundary (the bold dotted line shown in Fig. 6. The true boundary is then searched by starting from this primitive boundary. The weighted separability is calculated for this image and the search area is restricted around this primitive boundary.

Let θ_n $(n = 1, \ldots, N)$ be a specified angle at the n-th seed point as shown in Fig. 6. If all θ_n are obtuse angles, four complementary triangular MSFs are uniformly allocated over the interval of concern. A plaque boundary is then extracted by

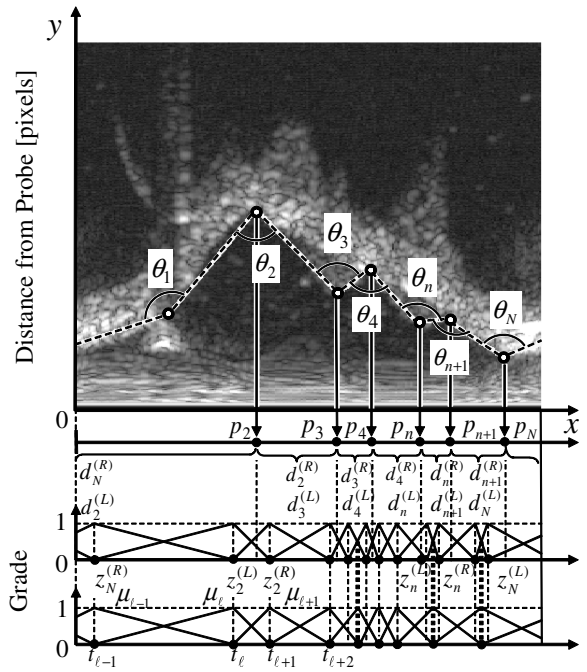

Fig. 6. Procedure of adaptive allocation of membership functions. Some θ_i angles look like to be obtuse, but they are acute. This is because of the length and width ratio of the Cartesian coordinates of the figure.

the T-S fuzzy model. In that case, a smooth plaque boundary is depicted along the obtuse seed points with a small number of MSFs.

In other cases, e.g., acute and obtuse angles coexist in the interval of concern, the following procedures are applied for the seed points with acute angles. The seed points with obtuse angles are left unprocessed.

i) Let p_n be an angle index of the n-th seed point, and $d_n^{(R)}$ and $d_n^{(L)}$ be the length between p_n and p_{n+1}, and between p_{n-1} and p_n, respectively. Note that the right-hand side edge and the left-hand side edge of the plaque boundary in Fig. 6 are linked.

ii) Two complementary and triangular MSFs are allocated on either side of each seed point. Let $z_n^{(R)}$ and $z_n^{(L)}$ be the tentative peak positions of the MSFs on the right-hand side and the left-hand side of p_n, which are given as:

$$\begin{cases} z_n^{(R)} = p_n + (1-\rho_n)[d_n^{(R)}/\{2+\beta(d_n^{(R)})\}] \\ z_n^{(L)} = p_n - (1-\rho_n)[d_n^{(L)}/\{2+\beta(d_n^{(L)})\}], \end{cases} \quad (16)$$

where ρ_n is a sharpness of the angle θ_n defined by:

$$\rho_n = \begin{cases} 1-\theta_n/T & \theta_n < T \\ 0 & \theta_n \geq T. \end{cases} \quad (17)$$

T is a constant value. The function $\beta(\cdot)$ compensates the peak position of $d_n^{(\cdot)}$ when it is extremely large, and is defined by:

$$\beta(d_n^{(\cdot)}) = 1/[1+\exp\{-a(d_n^{(\cdot)}-c)\}], \quad (18)$$

where a and c are parameters to fix the shape of $\beta(\cdot)$. Eq. (16) specifies that when θ_n is small, the MSFs are allocated close to the n-th seed point. This means that the MSFs around p_n are allocated densely, because when θ_n is small, the plaque boundary is complex. The MSFs' allocation map at the upper row in Fig. 6 is thus obtained.

iii) The tentatively allocated MSFs above are merged if the following three conditions are satisfied at the same time; (a) the seed point position p_n and the peak position of its right-hand side MSF $z_n^{(R)}$ are apart enough each other; (b) the seed point position p_{n+1} and the peak position of its left-hand side MSF $z_{n+1}^{(L)}$ are apart enough each other; (c) the positions of the peaks $z_n^{(R)}$ and $z_{n+1}^{(L)}$ are close each other. We now define the following criterion to reflect the above three merging conditions:

$$f_1 = 2\|p_n - z_n^{(R)}\|/d_n^{(R)}, \quad (19)$$

$$f_2 = 2\|p_{n+1} - z_{n+1}^{(L)}\|/d_n^{(R)}, \quad (20)$$

$$f_3 = \max(1 - 2\|z_n^{(R)} - z_{n+1}^{(L)}\|/d_n^{(R)}, 0), \quad (21)$$

$$S_{merge} = f_1 \cdot f_2 \cdot f_3. \quad (22)$$

If S_{merge} is greater than 0.5, the peaks $z_n^{(R)}$ and $z_{n+1}^{(L)}$ are merged. An example of merging is shown in the MSFs' allocation map at the bottom row of Fig. 6.

TABLE I
QUANTITATIVE EVALUATION FOR THE PLAQUE BOUNDARY EXTRACTION RESULTS.

(μm)

	Spline Function		Previous Method		Present Method	
	LB	AB	LB	AB	LB	AB
RMSE	14.5	16.9	36.5	52.1	37.5	63.2
SD	14.3	16.5	34.5	31.1	34.9	33.3

IV. EXPERIMENTAL RESULTS

In this section, experimental results of the full-automatic boundary extraction and of the semi-automatic boundary extraction are shown.

A. Fully automatic plaque boundary extraction

The proposed method is applied to real IVUS B-mode images. Extraction results are compared to those by spline function method and by our previous method. In those experiments, the threshold values of ζ_{Low} and ζ_{High} are set to be 0.1 and 0.2, respectively. The binary images are generated by changing ζ at 0.02 intervals. The other settings are the same as those in our previous paper [14].

The parameters of Eqs. (9)-(11) which define the figures of each membership function, are empirically set to be $\{N_{r1}, N_{r2}\} = \{4, 20\}$, $\{N_{p1}, N_{p2}, N_{p3}\} = \{5000, 15000, 25000\}$, $\{L_{r1}, L_{r2}, L_{r3}\} = \{256, 512, 640\}$.

Figs. 7(a)-7(d) show the plaque boundary extraction results for the IVUS image. The results show that the proposed

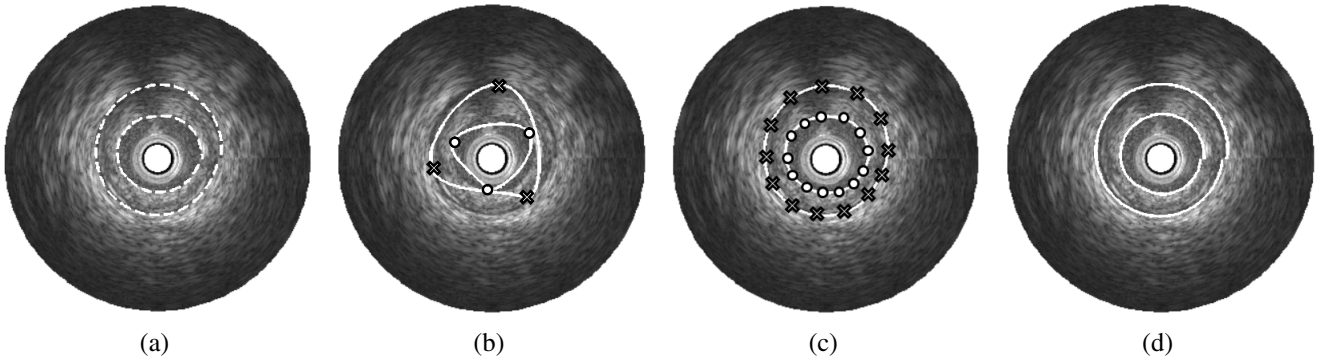

Fig. 7. Plaque boundary extraction results. ×: Given seed points for AB (Adventitial Boundary). ○: Given seed points for LB (Luminal Boundary). (a) B-mode image and objective true boundaries to be extracted. (b) Extracted boundaries by spline function method with a few seed points. (c) Extracted boundaries by spline function with many seed points. (d) Extracted boundaries by the proposed method without using any seed points (fully automatic boundary extraction).

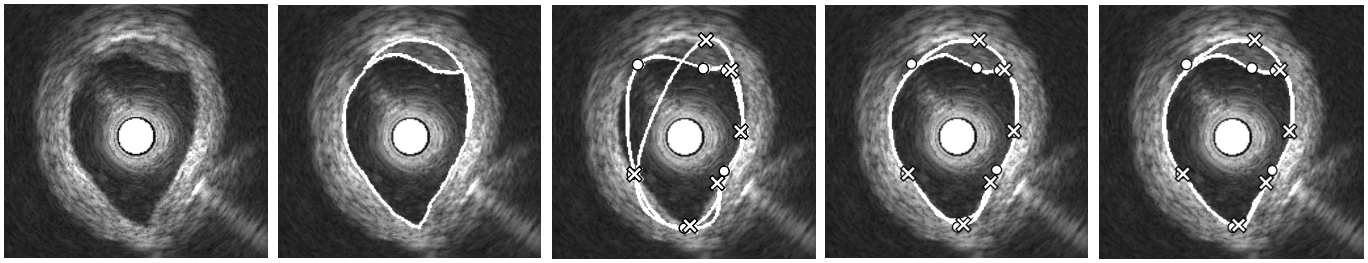

Fig. 8. Boundary extraction results. × : Given seed points for AB (Adventitial Boundary). ○: Given seed points for LB (Luminal Boundary). (a) B-mode image 4. (b) Objective true boundaries to be extracted. (c) Extracted boundaries by spline function method with a few seed points. (d) Extracted boundaries by the proposed method with the fixed membership functions uniformly allocated. (e) Extracted boundary by the proposed method with the membership functions adaptively allocated.

method works very well compared to the conventional methods, even if without using any seed points. Particularly, the spline function method requires many seed points though the accuracy of boundary extraction is good.

The root mean square errors (RMSEs) between the true boundary $y^*(x_i)$ and the extracted one $\hat{y}(x_i)$, and the standard deviations (SDs) calculated from 60 IVUS images are shown in Table I. The true boundary is calculated by a parametric spline-interpolation with a lot of seed points. It is observed that the proposed method, fully automatic, gives nearly equal extraction results to the previous method which uses some seed points given by a medical doctor.

With those results, the effectiveness of the proposed method has been verified.

B. Semi-automatic (interactive) plaque boundary extraction with user's assistance

The proposed method is applied to four IVUS B-mode images (Image 1 through Image 4). Extraction results are compared to those by the conventional method with fixed MSFs allocated at even intervals. In the experiments, the parameters in Eqs. (17) and (18) are empirically assigned to be T=45, a=0.05 and c=150.

The parameter T must be tuned by considering the figures of the boundaries of the objective IVUS images. In this experiment, T=45 is employed. On the other hand, the parameters a and c in Eq. (18) are not so sensitive for the extraction of plaque boundaries. This is because a function $\beta(\cdot)$ is used only for a compensation of a peak position of the MFS.

TABLE II
COMPARISON OF RMSES OF BOUNDARY EXTRACTION RESULTS UNDER THE SAME NUMBER OF MSFS.

(μm)

	Img. 1		Img. 2		Img. 3		Img. 4	
	LB	AB	LB	AB	LB	AB	LB	AB
No. of MSFs	4	3	10	4	12	9	9	6
Proposed Method	**33.2**	**27.3**	**44.5**	**46.4**	**30.6**	**34.5**	**72.7**	**29.4**
Fixed MSFs	**33.2**	43.3	49.3	68.3	38.0	41.9	89.9	78.8

Fig. 8 shows the boundary extraction results for Image 4, one of the four IVUS images employed for the experiments. The results show that the proposed method works very well compared to the conventional method with the fixed MSFs uniformly allocated.

The root mean square errors (RMSEs) between the objective boundary $y^*(x_i)$ and the extracted one $\hat{y}(x_i)$ are shown in Table II. The objective boundary is calculated by a parametric spline-interpolation using a lot of seed points given. It is observed that the proposed method gives better extraction results than the conventional methods with the fixed MSFs uniformly allocated. Table II shows the RMSEs of boundary extraction results in case of using the same number of MSFs in comparison with the method with the fixed MSFs and the

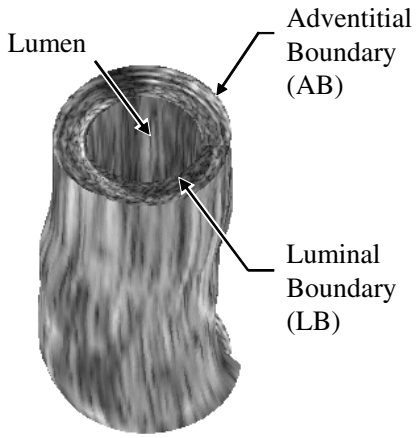

Fig. 9. 3-dimensional viewing of coronary plaque.

method with MSFs adaptively allocated (the proposed method). This implies that the position of each MSF is important for an accurate boundary extraction.

With those results the effectiveness of the proposed method has been verified.

C. 3-dimensional viewing of coronary plaque

Fig. 9 shows a 3-dimensional viewing of a coronary plaque which is reconstructed by interpolating the extracted boundary of 20 frames of B-mode image. By using the automatic plaque boundary extraction function of the proposed system, the 3-dimensional view is easily obtained. This 3-dimensional viewing is very useful and indispensable for analyzing the structure of coronary plaque. Particularly, the assessment of the objective response to therapeutic interventions by measuring the volume of plaque can be achieved by using this 3-D view of coronary plaque.

V. Conclusions

We have proposed fully automatic and semi-automatic plaque boundary extraction techniques for an IVUS image, and have implemented them as a software diagnosis system. In the present system, the plaque boundary extraction area is automatically found by using anisotropic diffusion, weighted separability, and some heuristic rules. T-S type fuzzy inference is used to extract the plaque boundary in that area.

The fully automatic present system has shown a nearly equal extraction performance to the previous method using seed points placed by a medical doctor, and thus the workload of a medical doctor is substantially reduced. After the boundary extraction, the proposed system can produce the 3-D view of coronary plaque which can be used for assessment of objective response to therapeutic interventions.

Future works are automatic adjustment of parameters and further speed up of each calculation process.

Acknowledgment

This work was supported by the strategic program for promoting research of Yamaguchi University, 2010. Many thanks are due to Mr. S. Ichiyama for his helpful assistance.

References

[1] J. B. Hodgson, S. P. Graham, A. D. Savakus, S. G. Dame, D. N. Stephens, P. S. Dhillon, D. Brands, H. Sheehan, and M. J. Eberle, "Clinical percutaneous imaging of coronary anatomy using an over-the-wire ultrasound catheter system," *Int. J. Cardiac Imaging*, vol. 4, pp. 187–193, 1989.

[2] B. N. Potkin, A. L. Bartorelli, J. M. Gessert, R. F. Neville, Y. Almagor, W. C. Roberts, and M. B. Leon, "Coronary artery imaging with intravascular high-frequency ultrasound," *Circulation*, vol. 81, pp. 1575–1585, 1990.

[3] E. Falk, "Why do plaques rupture?," *Circulation*, vol. 86, pp. 30–42, 1992.

[4] E. Falk, P. K. Shah, and V. Fuster, "Coronary plaque disruption," *Circulation*, vol. 92, no. 3, pp. 657–671, 1995.

[5] S. E. Nissen, J. C. Gurley, C. L. Grines, D. C. Booth, R. McClure, M. Berk, C. Fischer, and A. N. DeMaria, "Intravascular ultrasound assessment of lumen size and wall morphology in normal subjects and patients with coronary artery disease," *Circulation*, vol. 84, pp. 1087–1099, 1991.

[6] M. Sonka, X. Zhang, M. Siebes, M. S. Bissing, S. C. DeJong, S. M. Collins, and C. R. McKay, "Segmentation of intravascular ultrasound images: A knowledge-based approach," *IEEE Trans. Med. Imag.*, vol. 14, pp. 719–732, 1995.

[7] J. D. Klingensmith, D. G. Vince, B. D. Kuban, R. Shekhar, E. M. Tuzcu, S. E. Nissen, and J. F. Cornhill, "Assessment of coronary compensatory enlargement by three-dimensional intravascular ultrasound," *Int. J. Cardiac Imaging*, vol. 16, pp. 87–98, 2000.

[8] R. Kubota, T. Okamoto, N. Suetake, E. Uchino, G. Hashimoto, T. Hiro, and M. Matsuzaki, "Discrete genetic algorithm with Laplacian of Gaussian-based edge detector for plaque boundary extraction in intravascular ultrasound image," *Proc. of Int. Workshop on Nonlinear Circuits and Signal Processing*, pp. 329–332, 2009.

[9] P. Perona and J. Malik, "Scale-space and edge detection using anisotropic diffusion," *IEEE Trans. Pattern Anal. Mach. Intell.*, vol. 12, pp. 629–639, 1990.

[10] T. Koga, E. Uchino, N. Suetake, G. Hashimoto, T. Hiro, and M. Matsuzaki, "Speckle noise reduction and edge-enhancement of coronary plaque tissue in intravascular ultrasound image by using anisotropic diffusion filter," *Int. J. of Circuits, Syst. and Signal Processing*, vol. 2, pp. 239–248, 2008.

[11] K. Fukui, "Edge extraction method based on separability of image features," *IEICE Trans. Inf. Syst.*, vol. E78–D, pp. 1533–1538, 1995.

[12] T. Koga, S. Ichiyama, E. Uchino, N. Suetake, T. Hiro, and M. Matsuzaki, "Full automatic boundary extraction of coronary plaque on IVUS image by anisotropic diffusion and T-S type fuzzy inference," *Soft Computing in Industrial Applications, Advances in Intelligent and Soft Computing*, vol. 75, pp. 139–147, 2010.

[13] T. Takagi and M. Sugeno, "Fuzzy identification of systems and its applications to modeling and control," *IEEE Trans. Syst. Man Cybern.*, vol. 15, pp. 116–132, 1985.

[14] E. Uchino, N. Suetake, T. Koga, R. Kubota, S. Ichiyama, G. Hashimoto, T. Hiro, and M. Matsuzaki, "Fuzzy inference-based plaque boundary extraction using image separability for intravascular ultrasound image of coronary artery," *Electron. Lett.*, vol. 45, pp. 451–453, 2009.

[15] E. Uchino, T. Yamakawa, T. Miki, and S. Nakamura, "Fuzzy rule-based simple interpolation algorithm for discrete signal," *Fuzzy Sets and Systems*, vol. 59, no. 3, pp. 259–270, 1993.

2011 IEEE International Conference on Fuzzy Systems
June 27-30, 2011, Taipei, Taiwan

Multi-source Knowledge Based Unnormalized Interval Type-2 Fuzzy Logic Systems Design

Tiechao Wang and Jianqiang Yi
Institute of Automation
Chinese Academy of Sciences
Beijing 100190, China
Email: {tiechao.wang & jianqiang.yi}@ia.ac.cn

Tiechao Wang
College of Electrical Engineering
Liaoning University of Technology
Jinzhou 121001, China
Email: tiechao.wang@gmail.com

Chengdong Li
School of Info. and Electrical Engineering
Shandong Jianzhu University
Jinan 250101, China
Email: lichengdong@sdjzu.edu.cn

***Abstract*—In this paper we propose an effective method to design a Single-Input Single-Output (SISO) Unnormalized Interval Type-2 Takagi-Sugeno-Kang (TSK) Fuzzy Logic System (UIT2FLS) for noisy regression problems based on multi-source knowledge which includes here the information from sample data and the prior knowledge of bounded range, symmetry and monotonicity. The sufficient conditions are given which ensure that the prior knowledge can be embedded into the UIT2FLS, and then the UIT2FLS is designed so that the target function can be approached as accurately as possible via constrained least squares algorithm. The performance of the UIT2FLS is verified through comparisons with unnormalized type-1 Fuzzy Logic Systems (FLSs) and normalized interval type-2 FLSs under three different noisy circumstances. Simulation results verify the correctness of the sufficient conditions, and demonstrate that the UIT2FLS has the best overall performance.**

Keywords – interval type-2 fuzzy logic system; constrained least squares algorithm; prior knowledge

I. INTRODUCTION

In the past decades, there had been many excellent studies on the theory and application of type-2 FLSs [1] – [5]. Type-2 FLSs are extensions of type-1 FLSs, and more complex than type-1 FLSs due to using type-2 fuzzy sets in the antecedent and the consequent part of fuzzy rules. Interval Type-2 Fuzzy Logic Systems (IT2FLSs), a special case of type-2 FLSs, have obvious advantages for handling different sources of uncertainties, such as noisy data.

Although interval type-2 FLSs provide a powerful framework to represent and handle the uncertainties, the problem of how to design interval type-2 FLSs is still a heavily researched issue, especially when sample data are insufficient and noisy. In order to overcome the problem, we can utilize some prior knowledge of plants or systems, such as bounded range, symmetry, monotonicity, etc., to compensate the insufficiency of the information from sample data or to make the data invalid which are out of accord with the known prior knowledge. Recently, many researchers have incorporated prior knowledge into neural networks [6], type-1 FLSs [7] – [10] and normalized IT2FLSs [11], [12]. Lindskog [7] proposed a fuzzy model structure to ensure monotonic gain characteristics in identified models. In [8], Won gave sufficient conditions of monotonicity for normalized type-1 TSK fuzzy systems. In [11], [12], Li and Yi gave sufficient conditions to ensure that the prior knowledge of bounded range, symmetry and monotonicity can be incorporated into normalized IT2FLSs.

Unnormalized type-1 TSK FLSs are employed by K.Tanaka [13], and then Liang combined unnormalized TSK fuzzy systems with type-2 fuzzy logic in [4]. Unnormalizing the output of a TSK FLS can provide fast inference, reduce computational complexity, and may achieve the same performance as the normalized TSK in some specific applications [13]. At present, there are a few studies in the literature that incorporate prior knowledge. In [14], Wang and Yi gave the sufficient conditions to ensure that the prior knowledge of monotonicity and convexity can be integrated into UIT2FLSs, but did not present the method of designing an UIT2FLS. In this paper, we propose an effective method to design an UIT2FLS based on multi-source knowledge, and demonstrate the advantages of UIT2FLSs over type-1 FLSs and normalized IT2FLSs in simulation.

II. SISO ZEROTH-ORDER UIT2FLS

Consider an SISO zeroth-order type-2 FLS whose fuzzy rule base consists of M fuzzy rules. The ith rule R^i is denoted as

$$R^i: \text{ IF } x \text{ is } \widetilde{A}^i, \text{ THEN } Y^i = [\underline{w}^i, \overline{w}^i], \tag{1}$$

where $i = 1, 2, \ldots, M$; x is an input variable; $\widetilde{A}^i$s are the antecedent IT2FSs which can be completely depicted by the lower and the upper membership functions - $\underline{\mu}_{\widetilde{A}^i}(x)$ and $\overline{\mu}_{\widetilde{A}^i}(x)$, which are the trapezoidal membership functions formulated by (4) and (5) shown in Fig. 1, or the quadratic polynomial membership functions formulated by (6) and (7) shown in Fig. 2. The firing set F^i of rule R^i is an interval type-1 set, i.e., $F^i = [\underline{f}^i(x), \overline{f}^i(x)]$, in which $\underline{f}^i(x) = \underline{\mu}_{\widetilde{A}^i}(x)$ and $\overline{f}^i(x) = \overline{\mu}_{\widetilde{A}^i}(x)$.

Definition 2.1: If the computation method of the SISO zeroth-order type-2 FLS described by (1) follows that

$$\widehat{y}(x) = \int_{y^1 \in Y^1} \cdots \int_{y^M \in Y^M} \int_{f^1 \in F^1} \cdots \int_{f^M \in F^M} \frac{1}{\sum_{i=1}^{M} f^i y^i}, \tag{2}$$

then we refer to the fuzzy system as UIT2FLS.

978-1-4244-7316-8/11/$26.00 ©2011 IEEE

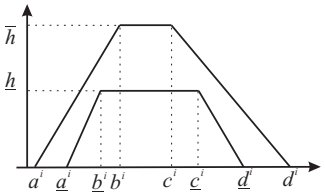

Fig. 1. Interval type-2 trapezoidal membership function.

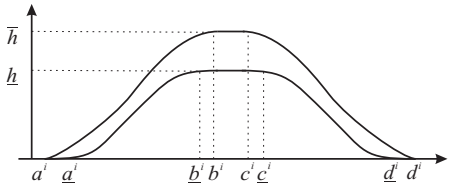

Fig. 2. Interval type-2 polynomial trapezoidal membership function.

According to Theorem 13-2 in [1], the final output $\widehat{y}(x)$ of the UIT2FLS is inferred as

$$\widehat{y}(x) = \frac{1}{2}\sum_{i=1}^{M}(\underline{f}^i(x)\underline{w}^i + \overline{f}^i(x)\overline{w}^i). \tag{3}$$

$$\underline{\mu}_{\widetilde{A}^i}(x) = \begin{cases} 0 & x < \underline{a}^i, \\ \underline{h}(\frac{x-\underline{a}^i}{\underline{b}^i-\underline{a}^i}) & \underline{a}^i \le x < \underline{b}^i, \\ \underline{h} & \underline{b}^i \le x < \underline{c}^i, \\ \underline{h}(\frac{\underline{d}^i-x}{\underline{d}^i-\underline{c}^i}) & \underline{c}^i \le x < \underline{d}^i, \\ 0 & x \ge \underline{d}^i. \end{cases} \tag{4}$$

$$\overline{\mu}_{\widetilde{A}^i}(x) = \begin{cases} 0 & x < a^i, \\ \overline{h}(\frac{x-a^i}{b^i-a^i}) & a^i \le x < b^i, \\ \overline{h} & b^i \le x < c^i, \\ \overline{h}(\frac{d^i-x}{d^i-c^i}) & c^i \le x < d^i, \\ 0 & x \ge d^i. \end{cases} \tag{5}$$

$$\underline{\mu}_{\widetilde{A}^i}(x) = \begin{cases} 0 & x < \underline{a}^i, \\ 2\underline{h}(\frac{x-\underline{a}^i}{\underline{b}^i-\underline{a}^i})^2 & \underline{a}^i \le x < \frac{\underline{a}^i+\underline{b}^i}{2}, \\ \underline{h} - 2\underline{h}(\frac{\underline{b}^i-x}{\underline{b}^i-\underline{a}^i})^2 & \frac{\underline{a}^i+\underline{b}^i}{2} \le x < \underline{b}^i, \\ \underline{h} & \underline{b}^i \le x < \underline{c}^i, \\ \underline{h} - 2\underline{h}(\frac{x-\underline{c}^i}{\underline{d}^i-\underline{c}^i})^2 & \underline{c}^i \le x < \frac{\underline{c}^i+\underline{d}^i}{2}, \\ 2\underline{h}(\frac{\underline{d}^i-x}{\underline{d}^i-\underline{c}^i})^2 & \frac{\underline{c}^i+\underline{d}^i}{2} \le x < \underline{d}^i, \\ 0 & x \ge \underline{d}^i. \end{cases} \tag{6}$$

$$\overline{\mu}_{\widetilde{A}^i}(x) = \begin{cases} 0 & x < a^i, \\ 2\overline{h}(\frac{x-a^i}{b^i-a^i})^2 & a^i \le x < \frac{a^i+b^i}{2}, \\ \overline{h} - 2\overline{h}(\frac{b^i-x}{b^i-a^i})^2 & \frac{a^i+b^i}{2} \le x < b^i, \\ \overline{h} & b^i \le x < c^i, \\ \overline{h} - 2\overline{h}(\frac{x-c^i}{d^i-c^i})^2 & c^i \le x < \frac{c^i+d^i}{2}, \\ 2\overline{h}(\frac{d^i-x}{d^i-c^i})^2 & \frac{c^i+d^i}{2} \le x < d^i, \\ 0 & x \ge d^i. \end{cases} \tag{7}$$

where $a^i \le \underline{a}^i$, $\underline{b}^i \le b^i$, $c^i \le \underline{c}^i$, $\underline{d}^i \le d^i$, $b^i \le m^i \le c^i$, and $\underline{\mu}_{\widetilde{A}^i}(x) \le \overline{\mu}_{\widetilde{A}^i}(x)$.

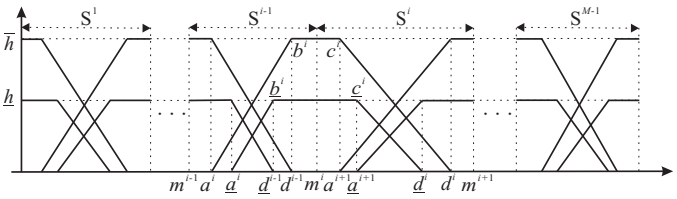

Fig. 3. Interval type-2 fuzzy partition of trapezoidal membership function.

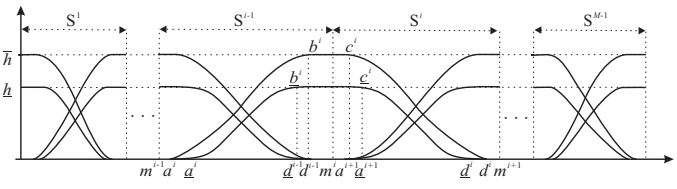

Fig. 4. Interval type-2 fuzzy partition of polynomial trapezoidal membership function.

III. Constraint conditions of Prior Knowledge

In this section, we will give some sufficient conditions to ensure that some prior knowledge can be integrated into an UIT2FLS. We will consider the prior knowledge of bounded range, symmetry and monotonicity.

A. Prior Knowledge of Bounded Range

For the prior knowledge of bounded range, we have the following results for an SISO zeroth-order UIT2FLS.

Theorem 3.1: Assume that the input domain $U = [\underline{u}, \overline{u}]$ is partitioned by M IT2FSs $\widetilde{A}^1, \widetilde{A}^2, \ldots, \widetilde{A}^M$ shown in Fig. 3 or Fig. 4. Then, the output $\widehat{y}(x)$ of the UIT2FLS is bounded on $[\underline{b}, \overline{b}]$, if the following conditions are satisfied:

1) No more than two fuzzy rules are fired.
2) Inequalities (8) and (9) hold.

$$\begin{aligned} &\frac{1}{2}\Big(\min_{p=1,\ldots,M-1}\{\underline{v}^p_{min}\}\min_{i=1,2,\ldots,M}\{\underline{w}^i\} \\ &+\min_{p=1,\ldots,M-1}\{\overline{v}^p_{min}\}\min_{i=1,2,\ldots,M}\{\overline{w}^i\}\Big) \ge \underline{b}, \end{aligned} \tag{8}$$

$$\begin{aligned} &\frac{1}{2}\Big(\max_{p=1,\ldots,M-1}\{\underline{v}^p_{max}\}\max_{i=1,2,\ldots,M}\{\underline{w}^i\} \\ &+\max_{p=1,\ldots,M-1}\{\overline{v}^p_{max}\}\max_{i=1,2,\ldots,M}\{\overline{w}^i\}\Big) \le \overline{b}, \end{aligned} \tag{9}$$

where

$$\begin{aligned} \underline{v}^p_{max} &= \sup\{\underline{\mu}_{\widetilde{A}^p}(x) + \underline{\mu}_{\widetilde{A}^{p+1}}(x) : x \in S^p\}, \\ \underline{v}^p_{min} &= \inf\{\underline{\mu}_{\widetilde{A}^p}(x) + \underline{\mu}_{\widetilde{A}^{p+1}}(x) : x \in S^p\}, \\ \overline{v}^p_{max} &= \sup\{\overline{\mu}_{\widetilde{A}^p}(x) + \overline{\mu}_{\widetilde{A}^{p+1}}(x) : x \in S^p\}, \\ \overline{v}^p_{min} &= \inf\{\overline{\mu}_{\widetilde{A}^p}(x) + \overline{\mu}_{\widetilde{A}^{p+1}}(x) : x \in S^p\}, \\ S^p &= [m^p, m^{p+1}] \quad (p = 1, 2, \ldots, M-1). \end{aligned}$$

Proof: Suppose that no more than two fuzzy IT2FSs are fired, and the ordinal numbers of the two fired rules are p and $p+1$.

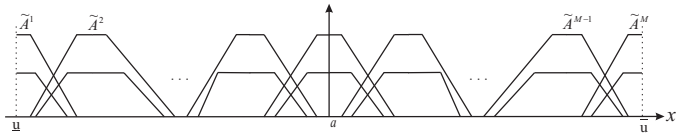

Fig. 5. Interval type-2 fuzzy partition symmetrically around a with trapezoidal membership functions.

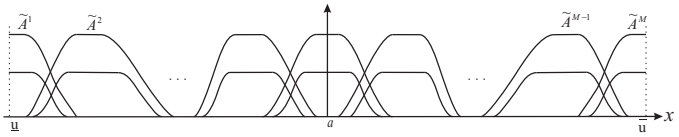

Fig. 6. Interval type-2 fuzzy partition symmetrically around a with quadratic polynomial membership functions.

Then, from (3), the final output can be rewritten as

$$\widehat{y}(x) = \frac{1}{2}\sum_{k=p}^{p+1}\big(\underline{\mu}_{\widetilde{A}^k}(x)\underline{w}^k + \overline{\mu}_{\widetilde{A}^k}(x)\overline{w}^k\big). \tag{10}$$

When x' is an input to the UIT2FLS, we get

$$\begin{aligned} y_l &= \sum\nolimits_{i=p}^{p+1}\underline{\mu}_{\widetilde{A}^i}(x')\underline{w}^i \\ &\geq \big(\underline{\mu}_{\widetilde{A}^p}(x') + \underline{\mu}_{\widetilde{A}^{p+1}}(x')\big)\min_{i=1,2,\ldots,M}\{\underline{w}^i\} \\ &\geq \underline{v}^p_{min}\min_{i=1,2,\ldots,M}\{\underline{w}^i\} \\ &\geq \min_{p=1,\ldots,M-1}\{\underline{v}^p_{min}\}\min_{i=1,2,\ldots,M}\{\underline{w}^i\}, \end{aligned} \tag{11}$$

and

$$\begin{aligned} y_l &= \sum\nolimits_{i=p}^{p+1}\underline{\mu}_{\widetilde{A}^i}(x')\underline{w}^i \\ &\leq \big(\underline{\mu}_{\widetilde{A}^p}(x') + \underline{\mu}_{\widetilde{A}^{p+1}}(x')\big)\max_{i=1,2,\ldots,M}\{\underline{w}^i\} \\ &\leq \underline{v}^p_{max}\max_{i=1,2,\ldots,M}\{\underline{w}^i\} \\ &\leq \max_{p=1,\ldots,M-1}\{\underline{v}^p_{max}\}\max_{i=1,2,\ldots,M}\{\underline{w}^i\}. \end{aligned} \tag{12}$$

In the similar way, we have

$$y_r \geq \min_{p=1,\ldots,M-1}\{\overline{v}^p_{min}\}\min_{i=1,2,\ldots,M}\{\overline{w}^i\} \tag{13}$$

and

$$y_r \leq \max_{p=1,\ldots,M-1}\{\overline{v}^p_{max}\}\max_{i=1,2,\ldots,M}\{\overline{w}^i\}, \tag{14}$$

From (11), (12), (13) and (14), it is obvious that

$$\begin{aligned} &\frac{1}{2}\Big(\min_{p=1,\ldots,M-1}\{\underline{v}^p_{min}\}\min_{i=1,2,\ldots,M}\{\underline{w}^i\} \\ &+ \min_{p=1,\ldots,M-1}\{\overline{v}^p_{min}\}\min_{i=1,2,\ldots,M}\{\overline{w}^i\}\Big) \\ &\leq \widehat{y}(x) \leq \frac{1}{2}\Big(\max_{p=1,\ldots,M-1}\{\underline{v}^p_{max}\}\max_{i=1,2,\ldots,M}\{\underline{w}^i\} \\ &+ \max_{p=1,\ldots,M-1}\{\overline{v}^p_{max}\}\max_{i=1,2,\ldots,M}\{\overline{w}^i\}\Big). \end{aligned} \tag{15}$$

As a result, if (8) and (9) hold, then $\underline{b} \leq \widehat{y}(x) \leq \overline{b}$.

Hence, the theorem holds. □

B. Prior Knowledge of Symmetry

For the prior knowledge of symmetry, we have the following results for an SISO zeroth-order UIT2FLS.

Theorem 3.2: An UIT2FLS is even symmetry around a, i.e. $\widehat{y}(x) = \widehat{y}(2a - x)$, if the following conditions are satisfied:

1) The input domain of $x \in [\underline{u}, \overline{u}]$ is partitioned symmetrically around a by IT2FSs $\widetilde{A}^1, \widetilde{A}^2, \ldots, \widetilde{A}^M$ shown in Fig. 5 or Fig. 6, where M is an odd number.
2) The consequent interval weights of the rules R^is satisfy that $[\underline{w}^i, \overline{w}^i] = [\underline{w}^{M+1-i}, \overline{w}^{M+1-i}]$ for $i = 1, 2, \ldots, \frac{M-1}{2}$.

Proof: when x' is an input, assume that t fuzzy IT2FSs can be fired, and the ordinal numbers of the fired rules are $i_1, i_2, \ldots, i_t$, here t is a positive integer.

As the fuzzy rule base is complete, and the input domain is partitioned symmetrically around a. Therefore, when $2a - x'$ is input to the UIT2FLS, the ordinal numbers of the fired rules is $M + 1 - i_1, M + 1 - i_2, \ldots, M + 1 - i_t$.

The conditions of Theorem 3.2 can also be stated as follows:

$$\underline{\mu}_{\widetilde{A}^{i_p}}(x') = \underline{\mu}_{\widetilde{A}^{M+1-i_p}}(2a - x'), \tag{16a}$$
$$\overline{\mu}_{\widetilde{A}^{i_p}}(x') = \overline{\mu}_{\widetilde{A}^{M+1-i_p}}(2a - x'), \tag{16b}$$

and

$$\underline{w}^{i_p} = \underline{w}^{M+1-i_p}, \tag{17a}$$
$$\overline{w}^{i_p} = \overline{w}^{M+1-i_p}, \tag{17b}$$

where $p = 1, 2, \ldots, t$.

Since

$$\underline{y}(x') = \sum\nolimits_{p=1}^{t}\underline{\mu}_{\widetilde{A}^{i_p}}(x')\underline{w}^{i_p}$$

and

$$\underline{y}(2a - x') = \sum\nolimits_{p=1}^{t}\underline{\mu}_{\widetilde{A}^{M+1-i_p}}(2a - x')\underline{w}^{M+1-i_p},$$

according to (16a) and (17a), we can derive that $\underline{y}(x') = \underline{y}(2a - x')$.

Similarly, according to (16b) and (17b), we can derive that

$$\overline{y}(x') = \overline{y}(2a - x').$$

Therefore,

$$\begin{aligned} y(x') &= \frac{1}{2}\big(\underline{y}(x') + \overline{y}(x')\big) \\ &= \frac{1}{2}\big(\underline{y}(2a - x') + \overline{y}(2a - x')\big) \\ &= y(2a - x') \end{aligned} \tag{18}$$

From (18), Theorem 3.2 holds. □

C. Prior Knowledge of Monotonicity

We consider the monotonicity of an SISO zeroth-order UIT2FLS. Firstly, the definition of SISO monotonic fuzzy systems is given as follows.

Definition 3.1: Let x be an input of a fuzzy system defined on $U = [a, b]$, where $U \subset \mathbb{R}$. And, $y = F(x)$ be the output of the fuzzy system in the set $V \subset \mathbb{R}$. Then, $F : U \mapsto V$ is said to be monotonically increasing if $a \leq x_1 \leq x_2 \leq b$ implies

$$F(x_1) \leq F(x_2). \tag{19}$$

If Inequality (19) is reversed, we obtain the definition of SISO monotonically decreasing fuzzy systems.

For the prior knowledge of monotonically increasing property, we have the following results for an SISO zeroth-order UIT2FLS.

Theorem 3.3: Assume that the fuzzy system is single-input single-output, and that the input domain $U = [\underline{u}, \overline{u}]$ which consists of $M-1$ intervals $S^i = [m^i, m^{i+1}]$ is partitioned by M IT2FSs $\widetilde{A}^1, \widetilde{A}^2, \ldots, \widetilde{A}^M$ shown in Fig. 3 or Fig. 4. Then, the UIT2FLS monotonically increases with respect to x, if the following conditions are satisfied:

1) No more than two fuzzy rules are fired, i.e. $a^1 = \underline{a}^1 = \underline{b}^1 = b^1 = m^1 = \underline{u}$, $m^M = c^M = \underline{c}^M = \underline{d}^M = d^M = \overline{u}$, $a^i \leq \underline{a}^i$, $\underline{b}^i \leq b^i$, $c^i \leq \underline{c}^i$, $\underline{d}^i \leq d^i$, $b^i \leq m^i \leq c^i$ for $2 \leq i \leq M-1$;
2) For any $x \in S^i$, $b^{i+1} = d^i$, $\underline{b}^{i+1} = \underline{d}^i$, $a^{i+1} = c^i$, $\underline{a}^{i+1} = \underline{c}^i$, so that $\overline{\mu}_{\widetilde{A}^i}(x) + \overline{\mu}_{\widetilde{A}^{i+1}}(x) = \overline{h}$, and $\underline{\mu}_{\widetilde{A}^i}(x) + \underline{\mu}_{\widetilde{A}^{i+1}}(x) = \underline{h}$ $(i = 1, 2, \ldots, M-1)$;
3) $\underline{w}^i \leq \underline{w}^{i+1}$ and $\overline{w}^i \leq \overline{w}^{i+1} (i = 1, 2, \ldots, M-1)$.

Proof: Assume that no more than two fuzzy IT2FSs can be fired, and the ordinal numbers of the fired rules are k and $k+1$.

Let

$$\underline{y}^k(x) = \sum\nolimits_{i=k}^{k+1} \underline{\mu}_{\widetilde{A}^i}(x)\underline{w}^i, \tag{20}$$

$$\overline{y}^k(x) = \sum\nolimits_{i=k}^{k+1} \overline{\mu}_{\widetilde{A}^i}(x)\overline{w}^i. \tag{21}$$

Hence, we have $\widehat{y}(x) = \frac{1}{2}\big(\underline{y}^k(x) + \overline{y}^k(x)\big)$.

1) When $x \in S^k$, $x' \in S^k$, $x' > x$, from the second condition of this theorem, (20) can be rewritten as

$$\begin{aligned}\underline{y}^k(x) &= \underline{\mu}_{\widetilde{A}^k}(x)\underline{w}^k + \underline{\mu}_{\widetilde{A}^{k+1}}(x)\underline{w}^{k+1} \\ &= (\underline{h} - \underline{\mu}_{\widetilde{A}^{k+1}}(x))\underline{w}^k + \underline{\mu}_{\widetilde{A}^{k+1}}(x)\underline{w}^{k+1} \\ &= \underline{h}\,\underline{w}^k + \underline{\mu}_{\widetilde{A}^{k+1}}(x)(\underline{w}^{k+1} - \underline{w}^k). \end{aligned} \tag{22}$$

Then, we get

$$\begin{aligned}&\underline{y}^k(x') - \underline{y}^k(x) = \\ &(\underline{\mu}_{\widetilde{A}^{k+1}}(x') - \underline{\mu}_{\widetilde{A}^{k+1}}(x))(\underline{w}^{k+1} - \underline{w}^k). \end{aligned} \tag{23}$$

Notice that $\underline{\mu}_{\widetilde{A}^{k+1}}(x)$ monotonically increases when $x \in S^k$, i.e.,

$$\underline{\mu}_{\widetilde{A}^{k+1}}(x') - \underline{\mu}_{\widetilde{A}^{k+1}}(x) \geq 0.$$

If the third condition of this theorem holds, we can deduce that

$$\underline{y}^k(x') - \underline{y}^k(x) \geq 0. \tag{24}$$

In the same way, we can also obtain that

$$\overline{y}^k(x') - \overline{y}^k(x) \geq 0. \tag{25}$$

According to (24) and (25), when $x \in S^k$, we can deduce that

$$\widehat{y}(x') \geq \widehat{y}(x) \tag{26}$$

2) When $x \in S^k$, $x' \in S^{k'}$, $k' > k$, and $k, k' = 1, 2, \ldots, M$, it is clear that $x' > x$ holds.
From Equations (20) and (21), when $x \in S^k$, we can see that

$$\begin{aligned}\underline{h}\,\underline{w}^k \leq \underline{y}^k(x) \leq \underline{h}\,\underline{w}^{k+1}, \\ \overline{h}\,\overline{w}^k \leq \overline{y}^k(x) \leq \overline{h}\,\overline{w}^{k+1}.\end{aligned}$$

With Condition 3) of this theorem holding, it follows that

$$\begin{aligned}\underline{y}^1(x^1) \leq \underline{y}^2(x^2) \leq \ldots \leq \underline{y}^M(x^M), \\ \overline{y}^1(x^1) \leq \overline{y}^2(x^2) \leq \ldots \leq \overline{y}^M(x^M),\end{aligned}$$

where $x^i \in S^i$, $i = 1, \ldots, M-1$. So, in this circumstances, we can deduce that

$$\widehat{y}(x') \geq \widehat{y}(x) \tag{27}$$

Therefore, from the discussion above, we can conclude that the theorem holds. □

Next, we give the sufficient conditions on the prior knowledge of monotonically decreasing property.

Theorem 3.4: Assume that the fuzzy system is single-input single-output, and that the input domain $U = [\underline{u}, \overline{u}]$ which consists of $M-1$ intervals $S^i = [m^i, m^{i+1}]$ is partitioned by M IT2FSs $\widetilde{A}^1, \widetilde{A}^2, \ldots, \widetilde{A}^M$ as shown in Fig. 3 or Fig. 4. Then, the UIT2FLS monotonically decreases with respect to x, if the following conditions are satisfied:

1) No more than two fuzzy rules are fired, i.e. $a^1 = \underline{a}^1 = \underline{b}^1 = b^1 = m^1 = \underline{u}$, $m^M = c^M = \underline{c}^M = \underline{d}^M = d^M = \overline{u}$, $a^i \leq \underline{a}^i$, $\underline{b}^i \leq b^i$, $c^i \leq \underline{c}^i$, $\underline{d}^i \leq d^i$, $b^i \leq m^i \leq c^i$ for $2 \leq i \leq M-1$;
2) For any $x \in S^i$, $b^{i+1} = d^i$, $\underline{b}^{i+1} = \underline{d}^i$, $a^{i+1} = c^i$, $\underline{a}^{i+1} = \underline{c}^i$, so that $\overline{\mu}_{\widetilde{A}^i}(x) + \overline{\mu}_{\widetilde{A}^{i+1}}(x) = \overline{h}$, and $\underline{\mu}_{\widetilde{A}^i}(x) + \underline{\mu}_{\widetilde{A}^{i+1}}(x) = \underline{h}$ $(i = 1, 2, \ldots, M-1)$;
3) $\underline{w}^i \geq \underline{w}^{i+1}$ and $\overline{w}^i \geq \overline{w}^{i+1} (i = 1, 2, \ldots, M-1)$.

Proof: The theorem can be proved in the similar way as Theorem 3.3. □

IV. Design of UIT2FLSs Using Multi-source Knowledge

Suppose that there exist r input-output data pairs (x_1, y_1), $\ldots$, (x_r, y_r). And our objective is that the parameters of the above-mentioned UIT2FLS can be optimized subject to the following training criteria (28) such that overall error measure E is minimal.

$$\min_{\boldsymbol{w}} E = \min_{\boldsymbol{w}} \sum_{k=1}^{r} \big(\widehat{y}(x_k) - y_k\big)^2. \tag{28}$$

Then, according to the objective, we design the UIT2FLS based on sample data and prior knowledge via constrained least squares algorithm.

A. Design of UIT2FLSs Using the Constrained Least Squares Algorithm

Firstly, we should determine whether the output of the UIT2FLS is linear with its consequent parameters.

Since (3) can be written as

$$\widehat{y}(x) = \boldsymbol{\phi}^{\mathrm{T}}(x)\boldsymbol{w}, \tag{29}$$

where

$$\begin{aligned}
\phi_i(x) &= \begin{cases} \frac{1}{2}\underline{\mu}_{\widetilde{A}^i}(x) & \text{if } i = 1, 2, \ldots, M, \\ \frac{1}{2}\overline{\mu}_{\widetilde{A}^i}(x) & \text{if } i = M+1, \ldots, 2M, \end{cases} \\
\boldsymbol{\phi}(x) &= [\phi_1(x), \phi_2(x), \ldots, \phi_{2M}(x)]^{\mathrm{T}}, \\
\boldsymbol{w} &= [\underline{w}^1, \ldots, \underline{w}^M, \overline{w}^1, \ldots, \overline{w}^M]^{\mathrm{T}},
\end{aligned}$$

we can deduce that the output of the UIT2FLS is linear with its consequent parameters. Then, the overall error measure E can be rewritten as the following form:

$$E = (\Phi\boldsymbol{w} - \boldsymbol{y})^{\mathrm{T}}(\Phi\boldsymbol{w} - \boldsymbol{y}), \tag{30}$$

where

$$\begin{aligned}
\boldsymbol{y} &= [y_1, y_2, \ldots, y_r], \\
\Phi &= \left[\boldsymbol{\phi}^{\mathrm{T}}(x_1), \boldsymbol{\phi}^{\mathrm{T}}(x_2), \ldots, \boldsymbol{\phi}^{\mathrm{T}}(x_r)\right]^{\mathrm{T}}.
\end{aligned}$$

Since the sample data should satisfy one or several kinds of prior knowledge such as bounded range, symmetry and monotonicity, we can use the sample data to train the consequent parameters of the UIT2FLS when the antecedent parameters are determined beforehand. From (30), according to our objective, the UIT2FLS design problem can be transformed into the following constrained least squares optimization problem (31). Therefore, we can solve (31) to design the UIT2FLS utilizing the multi-source knowledge which includes the information from both sample data and prior knowledge.

$$\begin{cases} \min\limits_{\boldsymbol{w}} (\Phi\boldsymbol{w} - \boldsymbol{y})^{\mathrm{T}}(\Phi\boldsymbol{w} - \boldsymbol{y}) \\ \text{subject to} \quad \boldsymbol{w} \in \Omega \end{cases}, \tag{31}$$

where Ω represents the constrained feasible parameter space.

Next, we will show that how to transform different kinds of prior knowledge description into the constraints of the consequent parameters of UIT2FLSs.

B. Constraints for Bounded Range

The constraints on the consequent interval weights of bounded UIT2FLSs in Theorem 3.1 can be expressed as

$$\begin{aligned}
\frac{1}{2}(\underline{v}_{min}\underline{w}^i + \overline{v}_{min}\overline{w}^i) &\geq \underline{b}, \\
\frac{1}{2}(\underline{v}_{max}\underline{w}^i + \overline{v}_{max}\overline{w}^i) &\leq \overline{b},
\end{aligned}$$

where

$$\begin{aligned}
\underline{v}_{min} &= \min_{p=1,\ldots,M-1}\{\underline{v}^p_{min}\}, \\
\overline{v}_{min} &= \min_{p=1,\ldots,M-1}\{\overline{v}^p_{min}\}, \\
\underline{v}_{max} &= \max_{p=1,\ldots,M-1}\{\underline{v}^p_{max}\}, \\
\overline{v}_{max} &= \max_{p=1,\ldots,M-1}\{\overline{v}^p_{max}\}, \\
i &= 1, 2, \ldots, M.
\end{aligned}$$

Therefore, there exist the $2M$ linear inequality constraints. It is convenient and brief to formulate these constraints as the following linear matrix inequality:

$$\begin{bmatrix} -\frac{1}{2}\underline{v}_{min}I_M & -\frac{1}{2}\overline{v}_{min}I_M \\ \frac{1}{2}\underline{v}_{max}I_M & \frac{1}{2}\underline{v}_{max}I_M \end{bmatrix}\boldsymbol{w} \leq \begin{bmatrix} -\underline{\boldsymbol{b}} \\ \overline{\boldsymbol{b}} \end{bmatrix}, \tag{32}$$

where I_M is the $M \times M$ identity matrix, $\underline{\boldsymbol{b}} = [\underline{b}, \ldots, \underline{b}]^{\mathrm{T}} \in \mathbb{R}^M$, and $\overline{\boldsymbol{b}} = [\overline{b}, \ldots, \overline{b}]^{\mathrm{T}} \in \mathbb{R}^M$.

C. Constraints for Symmetry

The constraints on the consequent parameters of symmetrical UIT2FLSs in Theorem 3.2 can be expressed as

$$\begin{aligned}
&\underline{w}^i - \underline{w}^{M+1-i} = 0, \\
&\overline{w}^i - \overline{w}^{M+1-i} = 0, \ (i = 1, \ldots, \tfrac{M-1}{2}) \\
&\underline{w}^j \leq \overline{w}^j, \ (j = 1, \ldots, M).
\end{aligned}$$

Hence, there exist $M-1$ equality and M inequality constraints for these parameters, and the matrix form of the constraints can be expressed as

$$\begin{bmatrix} I_{\frac{M-1}{2}} & \mathbf{0}_{\frac{M-1}{2}\times 1} & -I^{\mathrm{R}}_{\frac{M-1}{2}} & \mathbf{0}_{\frac{M-1}{2}} & \mathbf{0}_{\frac{M-1}{2}\times 1} & \mathbf{0}_{\frac{M-1}{2}} \\ \mathbf{0}_{\frac{M-1}{2}} & \mathbf{0}_{\frac{M-1}{2}\times 1} & \mathbf{0}_{\frac{M-1}{2}} & I_{\frac{M-1}{2}} & \mathbf{0}_{\frac{M-1}{2}\times 1} & -I^{\mathrm{R}}_{\frac{M-1}{2}} \end{bmatrix} \times \boldsymbol{w} = \mathbf{0}_{M-1\times 1}, \tag{33}$$

$$\begin{bmatrix} I_M & -I_M \end{bmatrix}\boldsymbol{w} \leq \mathbf{0}_{M\times 1}, \tag{34}$$

where I^{R}_M denotes the $M \times M$ matrix obtained by rotating I_M 90 degrees clockwise.

D. Constraints for Monotonicity

The constraints on the consequent parameters of monotonically increasing UIT2FLSs on U in Theorem 3.3 can be expressed as

$$\begin{aligned}
&\underline{w}^i - \underline{w}^{i+1} \leq 0, \\
&\overline{w}^i - \overline{w}^{i+1} \leq 0, \ (i = 1, 2, \ldots, M-1), \\
&\underline{w}^j - \overline{w}^j \leq 0, \ (j = 1, 2, \ldots, M).
\end{aligned}$$

Hence, there exist $3M - 2$ inequality constraints for these parameters, and the matrix form of the constraints can be expressed as

$$\begin{bmatrix} Y_{11} & \mathbf{0}_{(M-1)\times M} \\ \mathbf{0}_{(M-1)\times M} & Y_{22} \\ I_M & -I_M \end{bmatrix}\boldsymbol{w} \leq \mathbf{0}_{(3M-2)\times 1}, \tag{35}$$

where

$$Y_{11} = Y_{22} = \begin{bmatrix} 1 & -1 & 0 & \dots & 0 & 0 \\ 0 & 1 & -1 & \dots & 0 & 0 \\ \vdots & \vdots & \vdots & \ddots & \vdots & \vdots \\ 0 & 0 & 0 & \dots & 1 & -1 \end{bmatrix} \in \mathbb{R}^{(M-1)\times M}.$$

In a similar way, based on Theorem 3.4, there exist $3M-2$ inequality constraints for the consequent parameters, and when UIT2FLSs monotonically decrease, the matrix form of the constraints can be expressed as

$$\begin{bmatrix} Z_{11} & \mathbf{0}_{(M-1)\times M} \\ \mathbf{0}_{(M-1)\times M} & Z_{22} \\ I_M & -I_M \end{bmatrix} \boldsymbol{w} \leq \mathbf{0}_{(3M-2)\times 1}, \qquad (36)$$

where $Z_{11} = Z_{22} = -Y_{11} \in \mathbb{R}^{(M-1)\times M}$.

Remarks: Assume there exists a function $y = f(x)$, which is monotonically decreasing when $x < 0$, and monotonically increasing when $x > 0$. If the input variable x is partitioned as shown in Fig. 5, then we can deal with the circumstances as follows:

$$\begin{bmatrix} ZY & \mathbf{0}_{(M-1)\times M} \\ \mathbf{0}_{(M-1)\times M} & ZY \\ I_M & -I_M \end{bmatrix} \boldsymbol{w} \leq \mathbf{0}_{(3M-2)\times 1}, \qquad (37)$$

where

$$ZY = \begin{bmatrix} Z_{11} & \mathbf{0}_{\frac{M-1}{2}\times\frac{M-1}{2}} \\ \mathbf{0}_{\frac{M-1}{2}\times\frac{M-1}{2}} & Y_{11} \end{bmatrix} \in \mathbb{R}^{(M-1)\times M}.$$

where $Z_{11}, Y_{11} \in \mathbb{R}^{\frac{M-1}{2}\times\frac{M+1}{2}}$, and M is odd number.

V. Simulation

In this section, we use a simulation example to illustrate the advantages based on multi-source knowledge, as above mentioned, when the output of a target function is corrupted by white noise.

Consider the following SISO nonlinear function

$$y = \left(\frac{x}{3}\right)^2 \tanh(|x|), \qquad (38)$$

where $x \in U = [-3, 3]$. It is obvious that the function is even symmetry with respect to $x = 0$, bounded on interval [0,1], monotonically decreases on interval [-3,0], and monotonically increases on interval [0,3].

We can create 500-training-data set $\mathfrak{D}$ whose elements $(x_i, \widetilde{y}_i)$ $(i = 1, \dots, 500)$ are generated by $\widetilde{y} = y + Noise$, where $Noise \in [-n_b, n_b]$ is the uniformly distributed additive noise. From Equation (38), we can obtain 500 input-output data pairs (x_i, y_i) $(i = 1, \dots, 500)$ which are the elements of test data set $\mathfrak{E}$. In this simulation, we test three different levels of noisy disturbance including $n_b = 20\%, 30\%, 40\%$. For each level of noisy disturbance, five cases are considered. In case k $(k = 1, \dots, 5)$, the elements of training data subset $\mathfrak{D}_k$ and test data subset $\mathfrak{E}_k$ are randomly chosen from $\mathfrak{D}$ and $\mathfrak{E}$, respectively. The numbers of the training data subset and the test data subset r_k are 25, 40, 60, 80, 100, and all the values of input variable x_i in $\mathfrak{D}_k$ and $\mathfrak{E}_k$ are different in each case k.

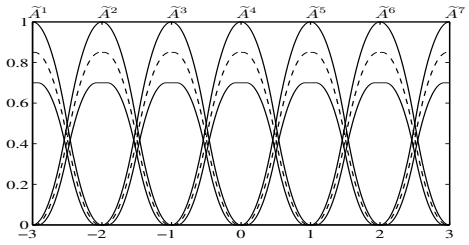

Fig. 7. Type-1 (dashed line) and type-2 (solid line) fuzzy partitions of the input domain.

In order to demonstrate the superiority of prior knowledge and type-2 FLSs, we use the following six FLSs to identify the target function: UIT2FLS with the monotonic, symmetric and bounded constraints (T2PFLS), UIT2FLS without the constraints (T2NPFLS), unnormalized type-1 FLS (UT1FLS) with the constraints (T1PFLS), UT1FLS without the constraints (T1NPFLS), normalized interval type-2 FLS (NT2FLS) with the constraints (NT2PFLS) and NT2FLS without the constraints (NT2NPFLS). For each FLS, we use seven membership functions equally distributed on input domain, and the fuzzy partitions which are shown in Fig. 7 satisfy the conditions on the parameters of the antecedent parts in Theorem 3.1 – 3.4.

Based on the training data and the test data, we use the following two RMSE performance indices in case k,

$$ap_k = \left(\frac{1}{r_k}\sum_{i=1}^{r_k}\left(\widehat{y}(x_k) - \widetilde{y}_k\right)^2\right)^{\frac{1}{2}}, \qquad (39)$$

$$gp_k = \left(\frac{1}{r_k}\sum_{i=1}^{r_k}\left(\widehat{y}(x_k) - y_k\right)^2\right)^{\frac{1}{2}}, \qquad (40)$$

where ap_k can reflect the approximation performance of the fuzzy systems for the training data, and gp_k can reflect the generalization performance of the fuzzy systems for the test data. From (39) and (40), we know that the less both indices are, the better the corresponding performances are. Furthermore, in order to avoid particularity, we calculate the statistical indices of the approximation performance and the generalization performance, ap_{sk} and gp_{sk}, which are the arithmetic mean of the corresponding indices obtained from 50 runs.

As mentioned above, three different levels of noise and five cases for each level of noise are considered. The comparisons between the six FLSs are drawn with respect to the size of data subsets and the noise level for the statistical RMSEs of the approximation performance and the generalization performance, ap_{is} and gp_{is}, which are shown in Fig. 8, Fig. 9 and Fig. 10, respectively. When the training data subset is comprised of 25 sample data, and the noise distributes uniformly in $[-40\%, 40\%]$, we obtain one of the identification results shown in Fig. 11. We can note that the data shown in Fig. 11 are consistent with the corresponding data in Fig.10

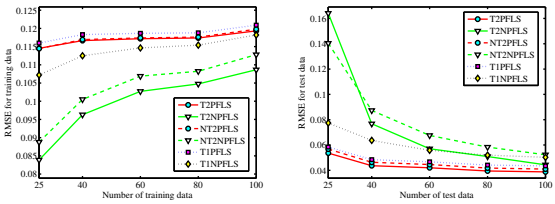

(a) (b)

Fig. 8. Performance comparisons of six different FLSs when $n_b = 20\%$: (a) approximation performance (b) generalization performance.

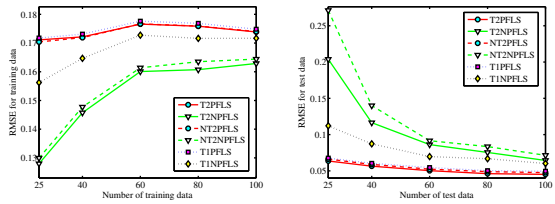

(a) (b)

Fig. 9. Performance comparisons of six different FLSs when $n_b = 30\%$: (a) approximation performance (b) generalization performance.

on the whole.

From these figures, we can compare and analyze the approximation performances and the generalization performances in terms of both the size of the data subsets and the level of noise for the six FLSs as follows:

(1) About approximation performance, from Fig. 8(a), Fig. 9(a) and Fig. 10(a), we observe that the unnormalized interval type-2 FLS without the prior knowledge constraints (T2NPFLS) performs better than the other five FLSs listed in the descending order of approximation performance, in general, as follows: NT2NPFLS, T1NPFLS, T2PFLS, NT2PFLS and T1PFLS. Also, it is can be observed that the FLSs without the constraints have better approximation capabilities than the FLSs with the constraints, whose performance indices are almost the same apparently. There exist the following two reasons to explain this. For one thing, the consequent parameters of T2NPFLS, NT2NPFLS and T1NPFLS are not constrained by the prior knowledge, so the three FLSs have a larger degree of freedom than the counterpart of T2PFLS, NT2PFLS and T1PFLS. For another, type-2 FLSs have more parameters than type-1 FLSs. Thus interval type-2 FLSs without constraints have best approximation capabilities among the six FLSs. In terms of the size of a training data subset, note that the smaller the size of the subset is, the better the approximation performance is in each case. As the level of noise increases, the approximation performances deteriorate for the six FLSs in each case.

(2) About generalization performance, from Fig. 8(b), Fig. 9(b) and Fig. 10(b), we observe that the unnormalized interval type-2 FLS with the prior knowledge constraints (T2PFLS) outperforms the other five FLSs listed in the descending order of generalization performance, in general,

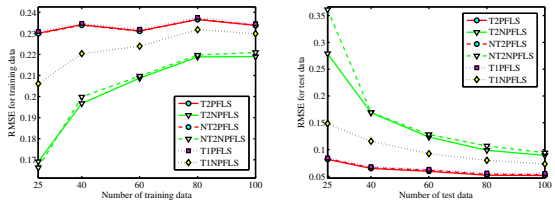

(a) (b)

Fig. 10. Performance comparisons of six different FLSs when $n_b = 40\%$: (a) approximation performance (b) generalization performance.

as follows: NT2PFLS, T1PFLS, T1NPFLS, T2NPFLS and NT2NPFLS. Also, it is can be observed that the FLSs with the constraints, whose performance indices are different slightly, have better generalization capabilities than the FLSs without the constraints. The reason for this is that the prior knowledge makes the FLSs with the constraints not be over-fitted to the target function so that their feasible parameters spaces are smaller than the counterpart of the FLSs without constraints. Thus, to some extent, T2PFLS, NT2PFLS and T1PFLS can overcome the effect of noise to approach better the original noise-free function. In terms of the size of a test data subset, note that the bigger the size of the subset is, the better the generalization performance is in each case. As the level of noise increases, the generalization performances deteriorate for the six FLSs in each case.

(3) About T2PFLS, NT2PFLS and T1PFLS, from Fig. 8 – Fig. 10, we observe that the performance curves of the three FLSs are in close proximity both for approximation capability and for generalization capability, and as the level of noise increases, they become closer. The following reasons can explain the fact. Since the consequent weights of the three kinds of FLSs are constrained identically, the performances of T2PFLS and NT2PFLS are almost the same as that of T1PFLS. However, the interval type-2 FLSs are formed by the linear combination of the two type-1 bounding FLSs [3]. This implies that type-2 FLSs have more parameters and more freedom degrees than type-1 FLSs. Thus, the approximation performances and the generalization performances of the two kinds of FLSs are better slightly than the counterpart of T1PFLS.

(4) From Fig. 8 – Fig. 10, we observe that unnormalized interval type-2 FLSs perform slightly better than normalized interval type-2 FLSs, and as the level of noise increases, the difference between the unnormalized T2FLSs and the normalized T2FLSs became smaller and smaller. On the other hand, since unnormalized T2FLSs do not need the operation of normalization, i.e., division operation, its elapsed time is less than that of normalized T2FLSs. Here, elapsed time of a type-2 FLS is defined as the time spent on computing the output $\widehat{y}(x)$ of the type-2 FLS for a data subset. Without loss of generality, in the simulation, we use arithmetic means of all the elapsed time obtained from 50 runs. For each case k of T2NPFLS and NT2NPFLS, the average values of the elapsed time are shown in Table I. From the table, we can know that if

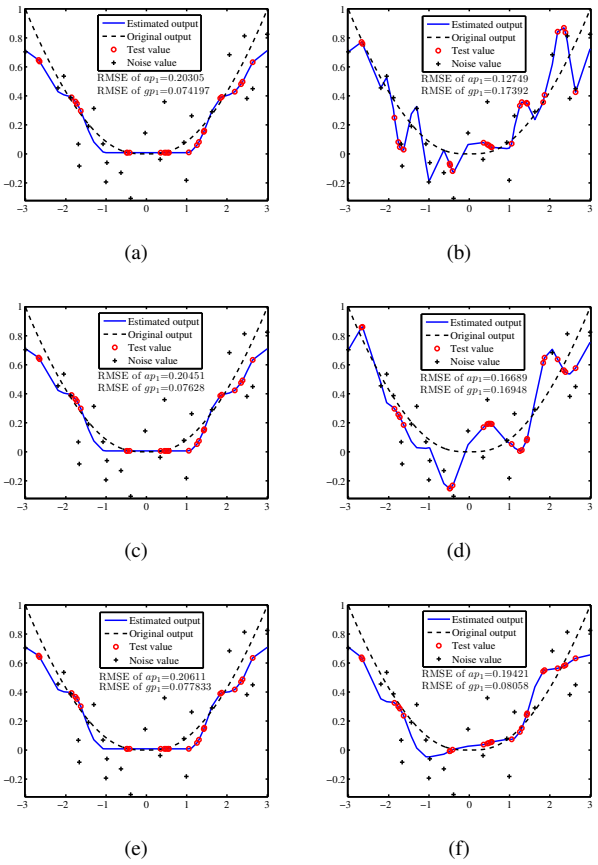

Fig. 11. one of identification results of the six FLSs when the $r_1 = 25$ and $n_b = 40\%$: (a) T2PFLS (b) T2NPFLS (c) NT2PFLS (d) NT2NPFLS (e) T1PFLS (f) T1NPFLS

TABLE I
ELAPSED TIME OF DIFFERENT SAMPLE NUMBER

FLS type	sample number 25	40	60	80	100
T2NPFLS	0.0052	0.0076	0.012	0.015	0.019
NT2NPFLS	0.0060	0.0088	0.013	0.017	0.021

we utilize UIT2FLS, we would save about 11% of the elapsed time of normalized IT2FLS.

In conclusion, based on multi-source knowledge, not only can the UIT2FLS obtain better performance than unnormalized type-1 FLSs on the whole, but also the UIT2FLS slightly outperform and need less computation time than normalized IT2FLSs.

VI. CONCLUSIONS

In this paper, we give some sufficient conditions on ensuring that the prior knowledge of bounded range, symmetry and monotonicity can be incorporated into UIT2FLSs. And then, we design an SISO zeroth-order UIT2FLS for noisy regression problems via constrained least squares algorithm. The simulation results have verified the validity of Theorem 3.1 – 3.4. The FLSs with prior knowledge description have better performances than the FLSs without prior knowledge description on the whole. In contrast with T1PFLS, T2PFLS have better overall performance for approximation capability and generalization capability. In contrast with NT2PFLS, T2PFLS can save more computation time, and have slightly better performance. Therefore, we can conclude that based on multi-source knowledge, the UIT2FLS performs best among all the six fuzzy logic systems.

ACKNOWLEDGMENT

This work was supported by the National Natural Science Foundation of China under Grant No. 60975060.

REFERENCES

[1] J. M. Mendel, Uncertain Rule-Based Fuzzy Logic Systems: Introduction and New Directions, New Jersey: Prentice-Hall, 2001.
[2] J. M. Mendel, "Advances in type-2 fuzzy sets and systems," Information Sciences, vol. 177, pp. 84–110, Jan. 2007.
[3] J. M. Mendel, "A Quantitative Comparison of Interval Type-2 and Type-1 Fuzzy Logic Systems: First Results" 2010 IEEE World Congress on Computational Intelligence, Barcelona, Spain, July. 2010, pp. 404–411.
[4] Q.Liang and J. M. Mendel, "Equalization of nonlinear time-varying channels using type-2 fuzzy adaptive filters," IEEE Transactions on Fuzzy Systems, vol. 8, pp. 551–563, Oct. 2000.
[5] O. Castillo and P. Melin, Type-2 Fuzzy Logic Theory and Applications, Berlin: Springer-Verlag, 2008.
[6] Wayne H. Joerding, and Jack L. Meador, "Encoding a priori information in feedback networks," Neural Networks, vol. 4, pp. 847–856, 1991.
[7] Peter Lindskog and Lennart Ljung, "Ensuring Monotonic Gain Characteristic in Estimated Models by Fuzzy Model Structures," Automatica, vol. 36, pp. 311–317, Jun. 2000.
[8] Jin M. Won, Sang Y. Park and Jin S. Lee, "Parameter conditions for monotonic Takagi-Sugeno-Kang fuzzy system," Fuzzy Sets and Sysems, vol. 132, pp. 135–146, Mar. 2002.
[9] Jinwook Kim and Jin S. Lee, "Single-input Single-ouput Convex Fuzzy Systems as Universal Approximators for Single-input Single-output Convex Functions," 2009 IEEE International Conference on Fuzzy Systems, Jeju Island, Korea, Aug. 2009, pp. 20–24.
[10] Tae-Wook Kim, Sang Y. Park and Jin S. Lee, "Parameter Conditions and Least Squares Identification of Single-input Single-output Convex Fuzzy System," SICE Annual Conference 2007, Kagawa University, Japan, Sep. 2007, pp. 568–573.
[11] Chengdong Li, Jianqiang Yi and Dongbin Zhao, "Analysis and design of monotonic type-2 fuzzy inference system," 2009 IEEE International Conference on Fuzzy Systems, Jeju Island, Korea, Aug. 2009, pp. 1193–1198.
[12] Chengdong Li, Jianqiang Yi and Dongbin Zhao, "Design of Interval Type-2 Fuzzy Logic System Using Sampled Data and Prior Knowledge," ICIC Express Letters, vol. 3, pp. 695–700 , Sep. 2009.
[13] K. Tanaka, M. Sano and H. Watanabe, "Modeling and control of carbon monoxide concentration using a neuro-fuzzy technique," IEEE Transactions on Fuzzy System, vol. 3, pp. 271–279, Aug. 1995.
[14] Tiechao Wang, Jianqiang Yi, and Chengdong Li, "The monotonicity and convexity of unnormalized interval type-2 TSK fuzzy logic systems", 2010 IEEE World Congress on Computational Intelligence, Barcelona, Spain,July, 2010, pp.3056-3061.

2011 IEEE International Conference on Fuzzy Systems
June 27-30, 2011, Taipei, Taiwan

On the Properties of SIRMs Connected Type-1 and Type-2 Fuzzy Inference Systems

Chengdong Li and Guiqing Zhang
School of Information and Electrical Engineering
Shandong Jianzhu University
Jinan 250101, China
Email: lichengdong@sdjzu.edu.cn

Jianqiang Yi, *Senior Member, IEEE*
Institute of Automation
Chinese Academy of Sciences
Beijing 100190, China
Email: jianqiang.yi@ia.ac.cn

Tiechao Wang
College of Electrical Engineering
Liaoning University of Technology
Jinzhou 121001, China
Email: tiechao.wang@gmail.com

***Abstract*—This paper tries to show some important properties of the single input rule modules (SIRMs) connected fuzzy inference systems (FIS), including both type-1 (T1) and interval type-2 (IT2) FISs. Three kinds of properties – continuity, monotonicity and robustness – are explored. First, conditions on the parameters are derived to ensure that the SIRMs connected FISs are continuous and monotonic. Then, a methodology for the robustness analysis of the SIRMs connected FISs are presented. At last, an example is given to show the correctness of the theorems on the continuity and monotonicity and to demonstrate the effectiveness of the proposed methodology for robustness analysis. These results can not only deepen our understanding of the SIRMs connected FISs, but also provide us guidelines for the design of the SIRMs connected FISs.**

Keywords — type-2 fuzzy; continuity; monotonicity; robustness analysis

I. Introduction

The single input rule modules (SIRMs) connected fuzzy inference system (FIS) is first proposed by J. Yi, et al. [1-3] to simplify the design process of the conventional type-1 (T1) FIS, and then studied by H. Seki, et al. [4, 5, 24]. Compared with the conventional FISs, the number of rules of the SIRMs connected FISs can be reduced greatly. And, this kind of FIS has been applied to many problems, such as the stabilization control of parallel-type double inverted pendulum systems [1], anti-swing and positioning control of overhead traveling crane [3], etc. Recently, we have extended the SIRMs connected T1 FISs to the interval type-2 (IT2) case [6]. Moreover, we have also utilized the SIRMs connected IT2 FISs to realize the stabilization control of the TORA system [7] and the inverted pendulum system [8].

However, little theoretical research has been conducted for the SIRMs connected FISs. To the best of the authors' knowledge, only two theoretical aspects of the SIRMs connected FISs have been explored. The first aspect is about the relationships between the SIRMs connected FISs and other types of FISs (e.g. Takagi-Sugeno FISs). Such issue has been explored by us [6] and Seki et al. [4, 5]. Recently, we have also studied another theoretical aspect – stability of the SIRMs connected FISs [9]. But, the theoretical research of the SIRMs connected FISs is still not profound enough. And, more properties of the SIRMs connected FISs should be derived to deepen our understanding of this kind of FIS.

Therefore, in this paper, we will study some new properties of the SIRMs connected FISs, such as continuity, monotonicity and robustness. First, we will derive parameter conditions to ensure the continuity and monotonicity of the SIRMs connected FISs. Then, we will present a methodology for the robustness analysis of the SIRMs connected FISs. At last, to show the correctness of the conditions for continuity and monotonicity and to demonstrate the effectiveness of the proposed methodology for robustness analysis, an example will be given. These results can help us to design more reasonable and robust SIRMs connected FISs.

The organization of this paper is as follows. In Section II, the SIRMs connected IT2 FIS is introduced briefly. In Section III, three properties – continuity, monotonicity and robustness – are explored. In Section IV, an example is given. At last, conclusions are drawn in Section V.

II. SIRMs Connected Fuzzy Inference System

As the SIRMs connected T1 FISs are special cases of the SIRMs connected IT2 FISs, in this paper, we will only consider the general case – the SIRMs connected IT2 FISs in detail. The presented results can be readily used for the SIRMs connected T1 FISs as well. In the following, we will give a brief introduction of the SIRMs connected IT2 FISs first.

A SIRMs connected IT2 FIS, which has n input variables x_1, x_2, ..., x_n, is composed of n IT2 SIRMs. The IT2 SIRM for the input variable x_i (IT2SIRM-i) can be expressed as [1-3, 6-9]

$$\text{IT2SIRM-}i: \quad \left\{ R_i^j: \quad x_i = \widetilde{A}_i^j \;\rightarrow\; y_i = \widetilde{C}_i^j \right\}_{j=1}^{M_i}, \qquad (1)$$

where $\widetilde{A}_i^j$s are IT2 fuzzy sets (FSs), $\widetilde{C}_i^j$s are interval weighting factors, and $\widetilde{C}_i^j = [\underline{c}_i^j, \overline{c}_i^j]$. IT2FSs $\widetilde{A}_i^j$s and interval weighting factors $[\underline{c}_i^j, \overline{c}_i^j]$s can be formed by blurring type-1 fuzzy sets A_i^js and crisp values c_i^js, respectively [10-16].

A IT2 SIRM can be seen as a single-input-single-output interval type-2 fuzzy logic system (IT2FLS) [10-16]. Therefore, the inference structure of the IT2 SIRM is the same as the inference structure of the IT2FLS, which consists of a fuzzifier, an inference engine, a rule base, a type-reducer and a defuzzifier [10-16].

978-1-4244-7316-8/11/$26.00 ©2011 IEEE

Once a crisp input x_i is applied to IT2SIRM-i, the firing strength of the jth rule can be expressed as

$$F_i^j(x_i) = \left[\underline{f}_i^j(x_i), \overline{f}_i^j(x_i)\right], \tag{2}$$

where

$$\underline{f}_i^j(x_i) = \underline{\mu}_{\widetilde{A}_i^j}(x_i), \quad \overline{f}_i^j(x_i) = \overline{\mu}_{\widetilde{A}_i^j}(x_i), \tag{3}$$

in which $\underline{\mu}(), \overline{\mu}()$ denote the grades of the lower membership functions (MFs) and upper MFs of IT2 FSs.

To generate a crisp output from IT2SIRM-i, different type-reduction and defuzzification methods can be used. Here, for the convenience of rigorous mathematical analysis, the following inference engine, which is an extension of the inference engine proposed in [16], is used:

$$y_i(x_i) = m_i \frac{\sum_{j=1}^{M_i} \underline{f}_i^j(x_i)\underline{c}_i^j}{\sum_{j=1}^{M_i} \underline{f}_i^j(x_i)} + n_i \frac{\sum_{j=1}^{M_i} \overline{f}_i^j(x_i)\overline{c}_i^j}{\sum_{j=1}^{M_i} \overline{f}_i^j(x_i)}, \tag{4}$$

where m_i and n_i, which satisfy that $m_i + n_i = 1$, are inference coefficient.

Once the fuzzy inference result $y_i(x_i)$ of IT2SIRM-i is already calculated, to express clearly the different role of each input varible on system performance, the output $y(\boldsymbol{x})$ of the SIRMs connected IT2 FIS will be computed as the summation of the products of the fuzzy inference result $y_i(x_i)$ and the importance degree w_i of the ith input varible x_i. In other words, the output $y(\boldsymbol{x})$ of the SIRMs connected IT2 FIS can be calculated as [6-9]

$$\begin{aligned} y(\boldsymbol{x}) &= \sum_{i=1}^{n} w_i y_i(x_i) \\ &= \sum_{i=1}^{n} w_i \left[m_i \frac{\sum_{j=1}^{M_i} \underline{f}_i^j(x_i)\underline{c}_i^j}{\sum_{j=1}^{M_i} \underline{f}_i^j(x_i)} + n_i \frac{\sum_{j=1}^{M_i} \overline{f}_i^j(x_i)\overline{c}_i^j}{\sum_{j=1}^{M_i} \overline{f}_i^j(x_i)} \right]. \end{aligned} \tag{5}$$

From (5), we can observe that the input-output mapping of the SIRMs connected FIS can be seen as a multi-variable function.

III. Properties of SIRMs Connected FISs

In this section, we will study the continuity, monotonicity and robustness of the SIRMs connected FISs. These properties always needs to be met in practical applications, e.g. the controller designed for the cart-pole system should be continuous, monotonic and robust. First, let us discuss the issue of continuity.

A. Continuity

As stated in [17], "*in many cases, continuous and smooth input-output mapping is desired for a FLS, because most physical systems are continuous*". Also in [17], the conditions have been derived to assure the continuity of the input-output mappings of IT2 FISs under six different type-reduction and defuzzification methods. From Section II, we can see that the type-reduction and defuzzification method adopted in the SIRMs is different from the six ones studied in [17], and the inference process of the SIRMs connected IT2 FISs differs from the inference process of conventional IT2 FISs. Hence, there is a need for us to study the continuity of the SIRMs connected FISs.

To begin, let us introduce the definition of continuity.

Definition 1 [17, 18]: A multi-variable function $f(\boldsymbol{x})$, where $\boldsymbol{x} = (x_1, ..., x_n) \in \mathbb{X}_1 \times \mathbb{X}_2 \times \cdots \times \mathbb{X}_n$, is continuous at $\boldsymbol{x}^* = (x_1^*, ..., x_n^*) \in \mathbb{X}_1 \times \mathbb{X}_2 \times \cdots \times \mathbb{X}_n$ if and only if it is defined at $\boldsymbol{x}^*$, and $\lim_{\boldsymbol{x} \to \boldsymbol{x}^*} f(\boldsymbol{x}) = f(\boldsymbol{x}^*)$. And $f(\boldsymbol{x})$ is said to be continuous if it is continuous at each point of the universe of discourse $\mathbb{X}_1 \times \mathbb{X}_2 \times \cdots \times \mathbb{X}_n$.

Definition 2 [17]: An IT2 FS A is continuous if and only if its lower MF $\underline{\mu}_{\widetilde{A}}(x)$ and upper MF $\overline{\mu}_{\widetilde{A}}(x)$ are continuous functions of x.

As T1 FSs are special cases of IT2 FSs, hence *Definition 2* is also valid for continuous T1 FSs. In this paper, all IT2 (T1) FSs used in the SIRMs connected IT2 (T1) FISs are supposed to be continuous IT2 (T1) FSs.

The following theorem and corollary show the conditions for the continuity of the SIRMs connected IT2 FISs and the SIRMs connected T1 FISs.

Theorem 1: The SIRMs connected IT2 FIS is continuous if and only if $\max_{j=1,2,...,M_i} \underline{\mu}_{\widetilde{A}_i^j}(x_i) > 0$ for $i = 1, 2, ..., n$, i.e., each point of $\mathbb{X}_i$ is covered by some lower MFs.

Proof: First, recall the following facts about continuous functions [17, 18]:

If both $f_1(\boldsymbol{x})$ and $f_2(\boldsymbol{x})$ are continuous, then,

a) for any constant k, the function $k \cdot f_1(\boldsymbol{x})$ is continuous;

b) the sum of finite continuous functions is also continuous;

c) $f_1(\boldsymbol{x})/f_2(\boldsymbol{x})$ is continuous if and only if $f_2(\boldsymbol{x}) \neq 0$.

Therefore, to prove that the input-output mapping of a SIRMs connected IT2 FIS is continuous, we just need to prove that $\frac{\sum_{j=1}^{M_i} \underline{f}_i^j(x_i)\underline{c}_i^j}{\sum_{j=1}^{M_i} \underline{f}_i^j(x_i)}$ and $\frac{\sum_{j=1}^{M_i} \overline{f}_i^j(x_i)\overline{c}_i^j}{\sum_{j=1}^{M_i} \overline{f}_i^j(x_i)}$ are continuous for $i = 1, 2, ..., n$.

Since all lower and upper MFs are continuous, so $\underline{f}_i^j(x_i)$ and $\overline{f}_i^j(x_i)$ $(j = 1, 2, ..., M_i)$ are continuous for the input variable x_i. Hence, from the above fact b), both $\sum_{j=1}^{M_i} \underline{f}_i^j(x_i)$ and $\sum_{j=1}^{M_i} \overline{f}_i^j(x_i)$ are continuous.

Then, from the above fact c), $\frac{\sum_{j=1}^{M_i} \underline{f}_i^j(x_i)\underline{c}_i^j}{\sum_{j=1}^{M_i} \underline{f}_i^j(x_i)}$ and $\frac{\sum_{j=1}^{M_i} \overline{f}_i^j(x_i)\overline{c}_i^j}{\sum_{j=1}^{M_i} \overline{f}_i^j(x_i)}$ are continuous if and only if $\sum_{j=1}^{M_i} \underline{f}_i^j(x_i) > 0$ and $\sum_{j=1}^{M_i} \overline{f}_i^j(x_i) > 0$. This implies that $\max_{j=1,2,...,M_i} \underline{\mu}_{\widetilde{A}_i^j}(x_i) > 0$.

From above discussions, we can conclude that the SIRMs connected IT2 FIS is continuous if and only if, for $i = 1, 2, ..., n$, $\max_{j=1,2,...,M_i} \underline{\mu}_{\widetilde{A}_i^j}(x_i) > 0$.

□

Corollary 1: The SIRMs connected T1 FIS is continuous if and only if $\max_{j=1,2,...,M_i} \mu_{\widetilde{A}_i^j}(x_i) > 0$ for $i = 1, 2, ..., n$, i.e., everywhere of the universe of discourse $\mathbb{X}_i$ is covered by some MFs.

In this subsection, conditions for the continuity of the SIRMs connected IT2 FISs and T1 FISs were derived. Such

results should be very useful in traditional control problems, where the input-output mappings of the designed controllers are usually required to be continuous.

B. Monotonicity

Many applications of fuzzy logic control requires monotonicity of the output with respect to inputs, e.g., in the cart-pole system, an appropriate controller for the cart-pole system needs to satisfy the monotonicity between the pole angle and the desired cart acceleration. Several papers have studied the monotonicity of traditional T1 FISs [19, 20] and traditional IT2 FISs [21-23]; however, only one paper has focused on the monotonicity of the SIRMs connected T1 FISs [24]. In the following, we will derive conditions to ensure the monotonicity between the inputs and outputs of the SIRMs connected IT2 FISs. As the SIRMs connected T1 FISs are the special SIRMs connected IT2 FISs, so our result is more general than that in [24].

To begin, let us give the definition of monotonicity.

Definition 2 [20]: A multi-variable function $f(\boldsymbol{x})$, where $\boldsymbol{x} = (x_1, ..., x_n) \in \mathbb{X}_1 \times \mathbb{X}_2 \times \cdots \times \mathbb{X}_n$, is said to be monotonically increasing with respect to (w.r.t) x_k if $\forall x_k^1 \leq x_k^2 \in \mathbb{X}_k$ implies that $f(x_1, ..., x_k^1, ..., x_n) \leq f(x_1, ..., x_k^2, ..., x_n)$ for all combinations of $(x_1, ..., x_{k-1}, x_{k+1}, ..., x_n)$.

In this study, we just take increasing monotonicity into account. Similar results can be obtained for decreasing monotonicity.

Theorem 2: The SIRMs connected IT2 FIS is monotonically increasing w.r.t x_k if the following conditions can be satisfied:

1): $\frac{\partial \underline{\mu}_{\widetilde{A}_k^i}(x_k)}{\partial x_k} \underline{\mu}_{\widetilde{A}_k^j}(x_k) \leq \frac{\partial \underline{\mu}_{\widetilde{A}_k^j}(x_k)}{\partial x_k} \underline{\mu}_{\widetilde{A}_k^i}(x_k)$ and $\frac{\partial \overline{\mu}_{\widetilde{A}_k^i}(x_k)}{\partial x_k} \cdot \overline{\mu}_{\widetilde{A}_k^j}(x_k) \leq \frac{\partial \overline{\mu}_{\widetilde{A}_k^j}(x_k)}{\partial x_k} \overline{\mu}_{\widetilde{A}_k^i}(x_k)$, where $1 \leq i \leq j \leq M_k$;

2): $\underline{c}_k^1 \leq \underline{c}_k^2 \leq ... \leq \underline{c}_k^{M_k}$ and $\overline{c}_k^1 \leq \overline{c}_k^2 \leq ... \leq \overline{c}_k^{M_k}$.

Proof: Denote that $\boldsymbol{x}^1 = (x_1, ..., x_k^1, ..., x_n)$ and $\boldsymbol{x}^2 = (x_1, ..., x_k^2, ..., x_n)$.

From (4) and (5), we can obtain that

$$\begin{aligned} y(\boldsymbol{x}^2) - y(\boldsymbol{x}^1) &= w_k[y_k(x_k^1) - y_k(x_k^2)] \\ &= w_k m_k \alpha_k + w_k n_k \beta_k. \end{aligned} \tag{6}$$

where $w_k > 0, 0 \leq m_k = 1 - n_k \leq 1$ and

$$\alpha_k = \frac{\sum_{j=1}^{M_k} \underline{f}_k^j(x_k^2)\underline{c}_k^j}{\sum_{j=1}^{M_k} \underline{f}_k^j(x_k^2)} - \frac{\sum_{j=1}^{M_k} \underline{f}_k^j(x_k^1)\underline{c}_k^j}{\sum_{j=1}^{M_k} \underline{f}_k^j(x_k^1)}, \tag{7}$$

$$\beta_k = \frac{\sum_{j=1}^{M_k} \overline{f}_k^j(x_k^2)\overline{c}_k^j}{\sum_{j=1}^{M_k} \overline{f}_k^j(x_k^2)} - \frac{\sum_{j=1}^{M_k} \overline{f}_k^j(x_k^1)\overline{c}_k^j}{\sum_{j=1}^{M_k} \overline{f}_k^j(x_k^1)}. \tag{8}$$

Therefore, to prove that the SIRMs connected IT2 FIS is monotonically increasing w.r.t x_k, we only need to prove that $\alpha_k \geq 0$ and $\beta_k \geq 0$.

Below, we will only prove that $\alpha_k \geq 0$.

Note that

$$\begin{aligned} \alpha_k &= \frac{\sum_{j=1}^{M_k} \underline{f}_k^j(x_k^2)\underline{c}_k^j}{\sum_{j=1}^{M_k} \underline{f}_k^j(x_k^2)} - \frac{\sum_{j=1}^{M_k} \underline{f}_k^j(x_k^1)\underline{c}_k^j}{\sum_{j=1}^{M_k} \underline{f}_k^j(x_k^1)} \\ &= \frac{\sum_{i=1}^{M_k}\sum_{j=1}^{M_k} \underline{f}_k^i(x_k^1)\underline{f}_k^j(x_k^2)\underline{c}_k^j - \sum_{i=1}^{M_k}\sum_{j=1}^{M_k} \underline{f}_k^i(x_k^1)\underline{f}_k^j(x_k^2)\underline{c}_k^i}{\sum_{j=1}^{M_k} \underline{f}_k^j(x_k^2) \sum_{i=1}^{M_k} \underline{f}_k^i(x_k^1)} \\ &= \frac{\sum_{i=1}^{M_k}\sum_{j=1}^{M_k} (\underline{c}_k^j - \underline{c}_k^i)\underline{f}_k^i(x_k^1)\underline{f}_k^j(x_k^2)}{\sum_{j=1}^{M_k} \underline{f}_k^j(x_k^2) \sum_{i=1}^{M_k} \underline{f}_k^i(x_k^1)} \\ &= \frac{\sum_{i=1}^{M_k-1}\sum_{j=i+1}^{M_k} (\underline{c}_k^j - \underline{c}_k^i)\left[\underline{f}_k^j(x_k^2)\underline{f}_k^i(x_k^1) - \underline{f}_k^i(x_k^2)\underline{f}_k^j(x_k^1)\right]}{\sum_{j=1}^{M_k} \underline{f}_k^j(x_k^2) \sum_{i=1}^{M_k} \underline{f}_k^i(x_k^1)}. \end{aligned} \tag{9}$$

Condition 2) implies that, if $j > i$, then

$$\underline{c}_k^j - \underline{c}_k^i \geq 0. \tag{10}$$

Condition 1) implies that $\frac{\partial}{\partial x_k}\left[\frac{\underline{\mu}_{\widetilde{A}_k^j}(x_k)}{\underline{\mu}_{\widetilde{A}_k^i}(x_k)}\right] \geq 0$, which means that $\frac{\underline{\mu}_{\widetilde{A}_k^j}(x_k)}{\underline{\mu}_{\widetilde{A}_k^i}(x_k)}$ is monotonically increasing w.r.t x_k.

Therefore,

$$\frac{\underline{\mu}_{\widetilde{A}_k^j}(x_k^2)}{\underline{\mu}_{\widetilde{A}_k^i}(x_k^2)} - \frac{\underline{\mu}_{\widetilde{A}_k^j}(x_k)}{\underline{\mu}_{\widetilde{A}_k^i}(x_k)} = \frac{\underline{f}_k^j(x_k^2)}{\underline{f}_k^i(x_k^2)} - \frac{\underline{f}_k^j(x_k^1)}{\underline{f}_k^i(x_k^1)} \geq 0, \tag{11}$$

which implies that

$$\underline{f}_k^j(x_k^2)\underline{f}_k^i(x_k^1) - \underline{f}_k^i(x_k^2)\underline{f}_k^j(x_k^1) \geq 0. \tag{12}$$

From (9), (10) and (12), we can conclude that $\alpha_k \geq 0$.

The result that $\beta_k \geq 0$ can be similarly proved.

In conclusion, this theorem holds.

□

In [20], Won et al. have derived parameter conditions of triangular, trapezoidal and Gaussian T1 MFs to satisfy that $\frac{\partial \underline{\mu}_{\widetilde{A}^i}(x)}{\partial x} \underline{\mu}_{\widetilde{A}^j}(x) \leq \frac{\partial \underline{\mu}_{\widetilde{A}^j}(x)}{\partial x} \underline{\mu}_{\widetilde{A}^i}(x)$, where $j \geq i$.

Similarly, parameter conditions of triangular, trapezoidal and Gaussian lower MFs and upper MFs of IT2 FSs can be derived to satisfy the first condition in *Theorem 2*. The related conclusions are listed in the following:

I): Suppose that the lower and upper MFs of IT2 FS $\widetilde{A}_k^t$ are triangular as depicted below

$$\underline{\mu}_{\widetilde{A}_k^t}(x_k) = \underline{\mu}_{\widetilde{A}_k^t}(x_k, \underline{a}_k^t, b_k^t, \underline{c}_k^t) = \begin{cases} \frac{x_k - \underline{a}_k^t}{b_k^t - \underline{a}_k^t}, & x_k \in (\underline{a}_k^t, b_k^t], \\ \frac{\underline{c}_k^t - x_k}{\underline{c}_k^t - b_k^t}, & x_k \in (b_k^t, \underline{c}_k^t], \\ 0, & else \end{cases} \tag{13}$$

$$\overline{\mu}_{\widetilde{A}_k^t}(x_k) = \overline{\mu}_{\widetilde{A}_k^t}(x_k, \overline{a}_k^t, b_k^t, \overline{c}_k^t) = \begin{cases} \frac{x_k - \overline{a}_k^t}{b_k^t - \overline{a}_k^t}, & x_k \in (\overline{a}_k^t, b_k^t], \\ \frac{\overline{c}_k^t - x_k}{\overline{c}_k^t - b_k^t}, & x_k \in (b_k^t, \overline{c}_k^t], \\ 0, & else \end{cases} \tag{14}$$

where $\overline{a}_k^t \leq \underline{a}_k^t \leq b_k^t \leq \underline{c}_k^t \leq \overline{c}_k^t$.

For triangular IT2 FSs, if $\underline{a}_k^i \leq \underline{a}_k^j$, $b_k^i \leq b_k^j$, $\underline{c}_k^i \leq \underline{c}_k^j$, $\overline{a}_k^i \leq \overline{a}_k^j$, and $\overline{c}_k^i \leq \overline{c}_k^j$, then the first condition in ***Theorem 2*** can be satisfied.

II): Suppose that the lower and upper MFs of IT2 FS $\widetilde{A}_k^t$ are trapezoidal as depicted below

$$\underline{\mu}_{\widetilde{A}_k^t}(x_k)=\underline{\mu}_{\widetilde{A}_k^t}(x_k,\underline{a}_k^t,\underline{b}_k^t,\underline{c}_k^t,\underline{d}_k^t)=\begin{cases}\frac{x_k-\underline{a}_k^t}{\underline{b}_k^t-\underline{a}_k^t}, & x_k\in(\underline{a}_k^t,\underline{b}_k^t],\\ 1, & x_k\in(\underline{b}_k^t,\underline{c}_k^t],\\ \frac{\underline{d}_k^t-x_k}{\underline{d}_k^t-\underline{c}_k^t}, & x_k\in(\underline{c}_k^t,\underline{d}_k^t],\\ 0, & else\end{cases} \tag{15}$$

$$\overline{\mu}_{\widetilde{A}_k^t}(x_k)=\overline{\mu}_{\widetilde{A}_k^t}(x_k,\overline{a}_k^t,\overline{b}_k^t,\overline{c}_k^t,\overline{d}_k^t)=\begin{cases}\frac{x_k-\overline{a}_k^t}{\overline{b}_k^t-\overline{a}_k^t}, & x_k\in(\overline{a}_k^t,\overline{b}_k^t],\\ 1, & x_k\in(\overline{b}_k^t,\overline{c}_k^t],\\ \frac{\overline{d}_k^t-x_k}{\overline{d}_k^t-\overline{c}_k^t}, & x_k\in(\overline{c}_k^t,\overline{d}_k^t],\\ 0, & else\end{cases} \tag{16}$$

where $\overline{a}_k^t\le\underline{a}_k^t$, $\overline{b}_k^t\le\underline{b}_k^t$, $\underline{c}_k^t\le\overline{c}_k^t$ and $\underline{d}_k^t\le\overline{d}_k^t$.

For trapezoidal IT2 FSs, if $\underline{a}_k^i\le\underline{a}_k^j$, $\underline{b}_k^i\le\underline{b}_k^j$, $\underline{c}_k^i\le\underline{c}_k^j$, $\underline{d}_k^i\le\underline{d}_k^j$, $\overline{a}_k^i\le\overline{a}_k^j$, $\overline{b}_k^i\le\overline{b}_k^j$, $\overline{c}_k^i\le\overline{c}_k^j$ and $\overline{d}_k^i\le\overline{d}_k^j$, then the first condition in ***Theorem 2*** can be satisfied.

III): Suppose that the lower and upper MFs of IT2 FS $\widetilde{A}_k^t$ are Gaussian as depicted below

$$\underline{\mu}_{\widetilde{A}_k^t}(x_k)=\underline{\mu}_{\widetilde{A}_k^t}(x_k,c_k^t,\underline{\delta}_k^t)=\exp\left(-\frac{1}{2}\frac{(x_k-c_k^t)^2}{{\underline{\delta}_k^t}^2}\right), \tag{17}$$

$$\overline{\mu}_{\widetilde{A}_k^t}(x_k)=\overline{\mu}_{\widetilde{A}_k^t}(x_k,c_k^t,\overline{\delta}_k^t)=\exp\left(-\frac{1}{2}\frac{(x_k-c_k^t)^2}{{\overline{\delta}_k^t}^2}\right), \tag{18}$$

where $0<\underline{\delta}_k^t\le\overline{\delta}_k^t$.

For Gaussian IT2 FSs, if $c_k^i\le c_k^j$, $\underline{\delta}_k^i=\underline{\delta}_k^j$ and $\overline{\delta}_k^i=\overline{\delta}_k^j$, then the first condition in ***Theorem 2*** can be satisfied.

When IT2 FSs become to T1 FSs, the SIRMs connected IT2 FIS become to the SIRMs connected T1 FIS, and the result in *Theorem 2* can be rewritten for the SIRMs connected T1 FIS as follows.

Corollary 2: The SIRMs connected T1 FIS is monotonically increasing w.r.t x_k if the following conditions can be satisfied:

1): $\frac{\partial\mu_{\widetilde{A}_k^i}(x_k)}{\partial x_k}\mu_{\widetilde{A}_k^j}(x_k)\le\frac{\partial\mu_{\widetilde{A}_k^j}(x_k)}{\partial x_k}\mu_{\widetilde{A}_k^i}(x_k)$, where $1\le i\le j\le M_k$;

2): $c_k^1\le c_k^2\le...\le c_k^{M_k}$.

In this subsection, parameter conditions were derived to ensure the monotonicity of the SIRMs connected FISs. These conditions can be easily satisfied in the design process of the SIRMs connected FISs. But we should notice that the above derived conditions are sufficient ones. It means that, if such conditions are not fulfilled, the SIRMs connected FIS may still be monotonic.

C. Robustness

Robustness is an interesting and important issue of FISs as discussed in [25]:

When a system is subjected to small deviations around the sampling points (operating points), it is essential to find the maximum tolerance of the system with respect to those perturbations, referred to herein as the systems robustness. Thus, in the context of modeling, robustness is a metric for measuring the impact of input deviations on the desired output.

In the following, we will first give the definition of the robustness of the SIRMs connected FISs as defined in [25], and then study how to compute the robustness of the SIRMs connected FISs.

Definition 3: the **robustness** of the SIRMs connected FIS at point $\boldsymbol{x}^*$ w.r.t x_k is defined as

$$R_k=\frac{\Delta_k}{\Delta y_d}, \tag{19}$$

where Δy_d is the given allowable output deviation, and Δ_k is the maximum allowable perturbation of the kth input variable at the sampling point $\boldsymbol{x}^*$ such that $|y(\boldsymbol{x}^*+\Delta\boldsymbol{x})-y(\boldsymbol{x}^*)|\le\Delta y_d$, i.e.

$$\Delta_k=\max\Big\{|\Delta x_k|\Big||y(\boldsymbol{x}^*+\Delta\boldsymbol{x})-y(\boldsymbol{x}^*)|\le\Delta y_d\Big\}.$$

Definition 4: the **robustness** of the SIRMs connected FIS at points $\{\boldsymbol{x}^{*1},\boldsymbol{x}^{*2},...,\boldsymbol{x}^{*L}\}$ w.r.t x_k is defined as

$$R_k=\frac{\min\limits_{j=1,2,...,L}\{\Delta_k^j\}}{\Delta y_d}, \tag{20}$$

where Δy_d is the given allowable output deviation, and Δ_k^j is the maximum allowable perturbation of the kth input variable at the sampling point $\boldsymbol{x}^{*j}$ such that $|y(\boldsymbol{x}^{*j}+\Delta\boldsymbol{x}^j)-y(\boldsymbol{x}^{*j})|\le\Delta y_d$, i.e.

$$\Delta_k^j=\max\Big\{|\Delta x_k^j|\Big||y(\boldsymbol{x}^{*j}+\Delta\boldsymbol{x}^j)-y(\boldsymbol{x}^{*j})|\le\Delta y_d\Big\}.$$

One thing deserves to be mentioned is that the definition of robustness is mathematically equivalent to the sub–additivity or output resolution properties studied in [26-29]. Such properties are proposed for the assessment problems.

Below, we will discuss how to compute the robustness of the SIRMs connected FISs.

First, let us derive the formula for the computation of $\Delta y(\boldsymbol{x}^*)=y(\boldsymbol{x}^*+\Delta\boldsymbol{x})-y(\boldsymbol{x}^*)$.

Note that

$$\begin{aligned}\Delta y(\boldsymbol{x}^*)&=y(\boldsymbol{x}^*+\Delta\boldsymbol{x})-y(\boldsymbol{x}^*)\\&=\sum_{i=1}^n w_i[y_i(x_i^*+\Delta x_i)-y_i(x_i^*)].\end{aligned} \tag{21}$$

Define

$$\Delta y_i(x_i^*)=y_i(x_i^*+\Delta x_i)-y_i(x_i^*). \tag{22}$$

It follows

$$\Delta y(\boldsymbol{x}^*)=\sum_{i=1}^n w_i\Delta y_i(x_i^*). \tag{23}$$

Assuming Δx_i is small and using a Taylor-series expansion, $y(x_i^*+\Delta x_i)$ can be expressed around x_i^* as

$$y_i(x_i^*+\Delta x_i)=y_i(x_i^*)+\left.\frac{\partial y_i(x_i)}{\partial x_i}\right|_{x_i=x_i^*}\Delta x_i+h.o.t, \tag{24}$$

where $h.o.t$ is short for higher order terms.

From (22) and (24), we obtain that

$$\Delta y_i(x_i^*) \simeq \left.\frac{\partial y_i(x_i)}{\partial x_i}\right|_{x_i=x_i^*} \cdot \Delta x_i. \tag{25}$$

From (4)

$$y_i(x_i) = m_i \underline{g}_i(x_i) + n_i \overline{g}_i(x_i). \tag{26}$$

where

$$\underline{g}_i(x_i) = \frac{\sum_{j=1}^{M_i} \underline{f}_i^j(x_i)\underline{c}_i^j}{\sum_{j=1}^{M_i} \underline{f}_i^j(x_i)}, \tag{27}$$

$$\overline{g}_i(x_i) = \frac{\sum_{j=1}^{M_i} \overline{f}_i^j(x_i)\overline{c}_i^j}{\sum_{j=1}^{M_i} \overline{f}_i^j(x_i)}. \tag{28}$$

It follows that

$$\frac{\partial y_i(x_i)}{\partial x_i} = m_i \frac{\partial \underline{g}_i(x_i)}{\partial x_i} + n_i \frac{\partial \overline{g}_i(x_i)}{\partial x_i}. \tag{29}$$

First, derive $\frac{\partial \underline{g}_i(x_i)}{\partial x_i}$ and $\frac{\partial \overline{g}_i(x_i)}{\partial x_i}$.

$$\begin{aligned}\frac{\partial \underline{g}_i(x_i)}{\partial x_i} &= \frac{\sum_{j=1}^{M_i}\sum_{s=1}^{M_i} \frac{\partial \underline{f}_i^j(x_i)}{\partial x_i} \cdot \underline{f}_i^s(x_i) \cdot [\underline{c}_i^j - \underline{c}_i^s]}{\left[\sum_{j=1}^{M_i} \underline{f}_i^j(x_i)\right]^2} \\ &= \frac{\sum_{j=1}^{M_i}\sum_{s=1}^{M_i} \frac{\partial \underline{\mu}_{\widetilde{A}_i^j}(x_i)}{\partial x_i} \cdot \underline{\mu}_{\widetilde{A}_i^s}(x_i) \cdot [\underline{c}_i^j - \underline{c}_i^s]}{\left[\sum_{j=1}^{M_i} \underline{\mu}_{\widetilde{A}_i^j}(x_i)\right]^2}, \end{aligned} \tag{30}$$

$$\begin{aligned}\frac{\partial \overline{g}_i(x_i)}{\partial x_i} &= \frac{\sum_{j=1}^{M_i}\sum_{s=1}^{M_i} \frac{\partial \overline{f}_i^j(x_i)}{\partial x_i} \cdot \overline{f}_i^s(x_i) \cdot [\overline{c}_i^j - \overline{c}_i^s]}{\left[\sum_{j=1}^{M_i} \overline{f}_i^j(x_i)\right]^2} \\ &= \frac{\sum_{j=1}^{M_i}\sum_{s=1}^{M_i} \frac{\partial \overline{\mu}_{\widetilde{A}_i^j}(x_i)}{\partial x_i} \cdot \overline{\mu}_{\widetilde{A}_i^s}(x_i) \cdot [\overline{c}_i^j - \overline{c}_i^s]}{\left[\sum_{j=1}^{M_i} \overline{\mu}_{\widetilde{A}_i^j}(x_i)\right]^2}. \end{aligned} \tag{31}$$

From (23) (25), and (29)-(31), we can conclude that, at the sampling point (operating point) $\boldsymbol{x}^*$,

$$\Delta y(\boldsymbol{x}^*) \simeq \sum_{i=1}^{n} w_i \eta_i(x_i^*) \Delta x_i, \tag{32}$$

where

$$\begin{aligned}\eta_i(x_i^*) = m_i &\frac{\sum_{j=1}^{M_i}\sum_{s=1}^{M_i} \frac{\partial \underline{\mu}_{\widetilde{A}_i^j}(x_i^*)}{\partial x_i} \cdot \underline{\mu}_{\widetilde{A}_i^s}(x_i^*) \cdot [\underline{c}_i^j - \underline{c}_i^s]}{\left[\sum_{j=1}^{M_i} \underline{\mu}_{\widetilde{A}_i^j}(x_i^*)\right]^2} \\ + n_i &\frac{\sum_{j=1}^{M_i}\sum_{s=1}^{M_i} \frac{\partial \overline{\mu}_{\widetilde{A}_i^j}(x_i^*)}{\partial x_i} \cdot \overline{\mu}_{\widetilde{A}_i^s}(x_i^*) \cdot [\overline{c}_i^j - \overline{c}_i^s]}{\left[\sum_{j=1}^{M_i} \overline{\mu}_{\widetilde{A}_i^j}(x_i^*)\right]^2}. \end{aligned} \tag{33}$$

For the T1 case, (33) can be rewritten as

$$\eta_i(x_i^*) = \frac{\sum_{j=1}^{M_i}\sum_{s=1}^{M_i} \frac{\partial \mu_{\widetilde{A}_i^j}(x_i^*)}{\partial x_i} \cdot \mu_{\widetilde{A}_i^s}(x_i^*) \cdot [c_i^j - c_i^s]}{\left[\sum_{j=1}^{M_i} \mu_{\widetilde{A}_i^j}(x_i^*)\right]^2}. \tag{34}$$

From Definition 3, to compute the robustness of the SIRMs connected IT2 FIS at point $\boldsymbol{x}^*$ w.r.t $x_1, x_2, ..., x_n$, we need to derive the maximum allowable perturbation $\Delta_1, \Delta_2, ..., \Delta_n$ at point $\boldsymbol{x}^*$, which can be computed as $(\Delta_1, \Delta_2, ..., \Delta_n) = \max\left\{\left(|\Delta x_1|, |\Delta x_2|, ..., |\Delta x_n|\right) \middle| \sum_{i=1}^{n} w_i \eta_i(x_i^*) \Delta x_i| \le \Delta y_d\right\}$

Therefore, $(\Delta_1, \Delta_2, ..., \Delta_n)$ can be obtained by solving the following optimization problem:

$$\begin{cases} maximize \quad \left(|\Delta x_1|, |\Delta x_2|, ..., |\Delta x_n|\right) \\ s.t. \left|w_1\eta_1(x_1^*)\Delta x_1 + \cdots + w_n\eta_n(x_n^*)\Delta x_n\right| \le \Delta y_d \end{cases} \tag{35}$$

From Definition 4, to compute the robustness of the SIRMs connected IT2 FIS at points $\{\boldsymbol{x}^{*1}, \boldsymbol{x}^{*2}, ..., \boldsymbol{x}^{*L}\}$ w.r.t $x_1, x_2, ..., x_n$, we just need to derive the maximum allowable perturbation $(\Delta_1^j, \Delta_2^j, ..., \Delta_n^j)$s at each point $\boldsymbol{x}^{j*}$ using the aforementioned optimization problem.

IV. Example

In this section, we will give an example to show the continuity and monotonicity of the SIRMs connected FISs. Also, the robustness of the SIRMs connected FISs will be computed in this example.

Consider the following SIRMs connected T1 and IT2 FISs:

SIRMs connected IT2 FIS

$$\text{IT2SIRM} - 1 = \begin{cases} x_1 = \widetilde{A}_1^1 \to y_1 = [8, 10] \\ x_1 = \widetilde{A}_1^2 \to y_1 = [14, 16] \\ x_1 = \widetilde{A}_1^3 \to y_1 = [20, 22] \end{cases}$$

$$\text{IT2SIRM} - 2 = \begin{cases} x_2 = \widetilde{A}_2^1 \to y_2 = [6, 10] \\ x_2 = \widetilde{A}_2^2 \to y_2 = [16, 20] \\ x_2 = \widetilde{A}_2^3 \to y_2 = [26, 30] \end{cases}$$

SIRMs connected T1 FIS

$$\text{T1SIRM} - 1 = \begin{cases} x_1 = \widetilde{A}_1^1 \to y_1 = 9 \\ x_1 = \widetilde{A}_1^2 \to y_1 = 15 \\ x_1 = \widetilde{A}_1^3 \to y_1 = 21 \end{cases}$$

$$\text{T1SIRM} - 2 = \begin{cases} x_2 = \widetilde{A}_2^1 \to y_2 = 8 \\ x_2 = \widetilde{A}_2^2 \to y_2 = 18 \\ x_2 = \widetilde{A}_2^3 \to y_2 = 28 \end{cases}$$

where the IT2 MFs and T1 MFs are shown in Fig. 1, and the importance degrees of IT2 (T1) SIRM-1 and IT2 (T1) SIRM-2 are 0.7 and 0.3, respectively. The coefficients used in the inference engine of the IT2 case are chosen as $m_1 = m_2 = 0.6$ and $n_1 = n_2 = 0.4$.

Fig. 2 shows the input-output mappings of the SIRMs connected T1 and IT2 FISs. We can observe from Fig. 2 that the corresponding input-output mappings are continuous and monotonically increasing. Such results are consistent with Theorem 1, Theorem 2 and their corollaries.

Now, let us compute the robustness of these two-input-one-output SIRMs connected FISs. To do so, we first need to solve the optimization problem below

$$\begin{cases} maximize \quad \left(|\Delta x_1|, |\Delta x_2|\right) \\ s.t. \quad \left|w_1\eta_1(x_1^*)\Delta x_1 + w_2\eta_2(x_2^*)\Delta x_2\right| \le \Delta y_d \end{cases} \tag{36}$$

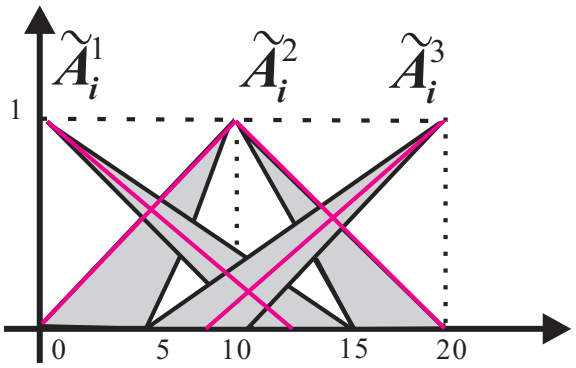

Fig. 1. IT2 MFs (grey areas) and T1 MFs (red lines)

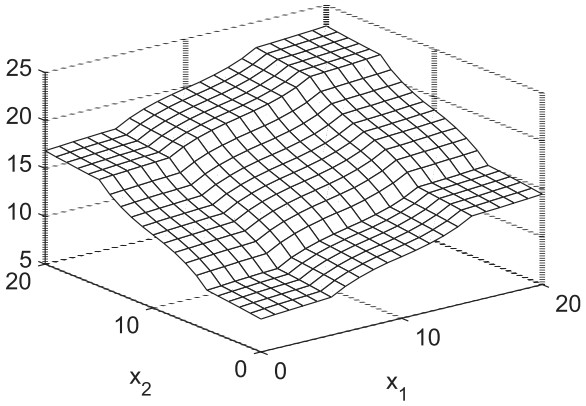

(a) SIRMs Connected IT2 FIS

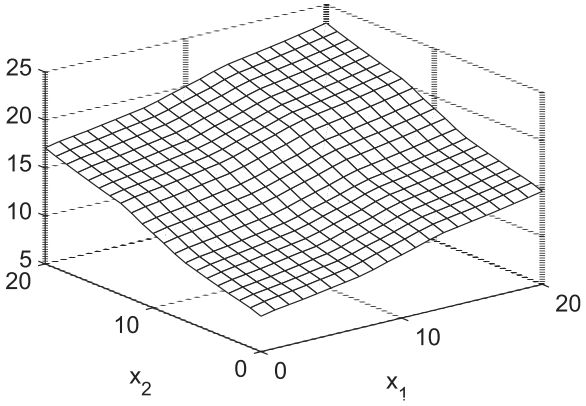

(b) SIRMs Connected T1 FIS

Fig. 2. Input-output mappings of the SIRMs connected FISs

The result of this optimization problem can be obtained as (details are omitted)

$$\Delta_1 = \frac{\Delta y_d}{2w_1|\eta_1(x_1^*)|}, \tag{37}$$

$$\Delta_2 = \frac{\Delta y_d}{2w_2|\eta_2(x_2^*)|}. \tag{38}$$

Hence, the robustness of such SIRMs connected FISs at

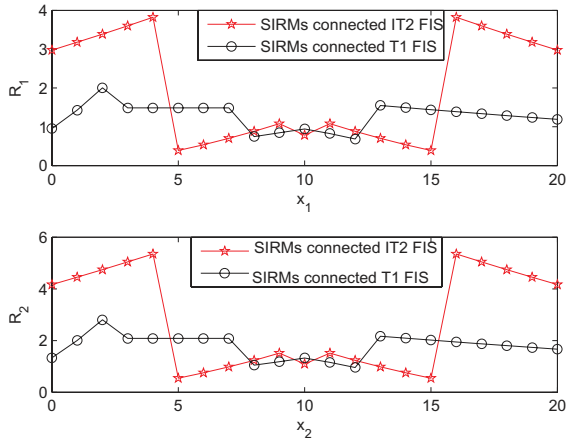

Fig. 3. Robustness indexes of the SIRMs connected FISs

point $\boldsymbol{x}^*$ w.r.t x_1, x_2 can be computed respectively as

$$R_1 = \frac{1}{2w_1|\eta_1(x_1^*)|}, \tag{39}$$

$$R_2 = \frac{1}{2w_2|\eta_2(x_2^*)|}. \tag{40}$$

It is easy to see that, in the two-input-one-output SIRMs connected FISs, R_1 and R_2 are only functions of the sampling points. Thus, the robustness R_i is constant for different desired output deviations.

The robustness of the SIRMs connected FISs at different sampling points w.r.t x_1, x_2 are shown in Fig. 3.

From Fig. 2 and Fig. 3, we can observe and conclude that:

1) The robustness of the SIRMs connected FISs w.r.t x_1, x_2 lies in the intervals $(0, 4]$ and $(0, 6]$, respectively. This means that, for the given allowable output deviation $\Delta y_d = 1$, the maximum allowable perturbation of the first and second input variables lies in $(0, 4]$ and $(0, 6]$ at different sampling points. This result is reasonable and also consistent with the input-output mappings.

2) The SIRMs connected IT2 FIS performs more robustly than the SIRMs connected T1 FIS when $x_1 \in [0, 4.5] \cup [15.5, 20]$ and $x_2 \in [0, 4.5] \cup [15.5, 20]$, although the input-output mapping of the SIRMs connected T1 FIS seems smoother than the IT2 one. The reason for this may be that the output of the SIRMs connected IT2 FIS changes more slowly in the neighbor of these sampling points.

3) For both SIRMs connected FISs, if their outputs change slowly in the neighbor of one sampling point, then the robustness at this point will be large. On the contrary, if the outputs change fast in the neighbor of one sampling point, then the robustness at this point will become small. This is also consistent with our intuition.

V. Conclusion

In this paper, new properties – continuity, monotonicity and robustness – of the SIRMs connected FISs, including both T1 and IT2 cases, are explored. Parameter conditions are derived to ensure the continuity and monotonicity of the

SIRMs connected FISs. These conditions can be easily satisfied in the design process of the SIRMs connected FISs. Also, a methodology for the robustness analysis of the SIRMs connected FISs is presented. The given example demonstrate that the proposed robustness analysis methodology is reasonable. However, how to design SIRMs connected FISs using the proposed methodology has not been studied. This will be one of our future research directions.

ACKNOWLEDGMENT

This work is supported by the National Natural Science Foundation of China under Grant No. 60975060 and 61074149. We also gratefully acknowledge the supports of the Shandong Provincial Key Laboratory of Intelligent Buildings Technology, Jinan 250101, China.

REFERENCES

[1] J. Yi, N. Yubazaki and K. Hirota, "A new fuzzy controller for stabilization of parallel-type double inverted pendulum system," Fuzzy Sets and Systems, vol. 126, pp. 105–119, 2002.

[2] J. Yi, N. Yubazaki and K. Hirota, "A proposal of SIRMs dynamically connected fuzzy inference model for plural input fuzzy control," Fuzzy Sets and Systems, vol. 125, pp. 79–92, 2002.

[3] J. Yi, N. Yubazaki and K. Hirota, "Anti-swing and positioning control of overhead traveling crane," Information Sciences, vol. 155, pp. 19–42, 2002.

[4] H. Seki, M. Mizumoto and N. Yubazaki, "On the property of single input rule modules connected type fuzzy reasoning method," IEICE Transactions on Fundamentals, vol. J89-A, pp. 557–565, June 2006.

[5] H. Seki, H. Ishii and M. Mizumoto, "On the generalization of single input rule modules connected type fuzzy reasoning method," IEEE Transactions on Fuzzy Systems, vol. 16, no. 5, pp. 1180–1187, 2008.

[6] C. Li and J. Yi, "SIRMs based interval type-2 fuzzy inference systems: properties and application," International Journal of Innovative Computing, Information and Control, vol. 6, no. 9, pp. 4019–4028, 2010.

[7] C. Li, J. Yi and D. Zhao, "Control of the TORA system using SIRMs based type-2 fuzzy logic," Proc. 2009 IEEE International Conference on Fuzzy Systems, Jeju Island, Korea, 2009, pp. 694–699.

[8] C. Li and J. Yi, "Design of SIRMs connected interval type-2 fuzzy logic controller based on prior knowledge," Journal of Southeast University (Natural Science Edition), vol. 39, no. suppl. 1, pp. 57–61, 2009.

[9] C. Li, J. Yi and T. Wang "Stability analysis of SIRMs based type-2 fuzzy logic control systems," Proc. 2010 IEEE World Congress on Computational Intelligence, Barcelona, Spain, 2010, pp. 2913–2918.

[10] Q. Liang and J. M. Mendel, "Interval type-2 fuzzy logic systems: theory and design," IEEE Transactions on Fuzzy Systems, vol. 8, no. 5, pp. 535–550, 2000.

[11] J. M. Mendel, Uncertain Rule-Based Fuzzy Logic Systems: Introduction and New directions, New Jersey : Prentice-Hall, 2001.

[12] J. M. Mendel, R. I. John and F. Liu, "Interval type-2 fuzzy logic systems made simple," IEEE Transactions on Fuzzy Systems, vol. 14, no. 6, pp. 808–821, 2006.

[13] J. M. Mendel, "Advances in type-2 fuzzy sets and systems," Information Sciences, vol. 177, pp. 84–110, 2007.

[14] J. M. Mendel, "On answering the question 'where do I start in order to solve a new problem involving interval type-2 fuzzy sets?'", Information Sciences, vol. 179, pp. 3418–3431, 2009.

[15] S. Coupland and R. John, "Geometric type-1 and type-2 fuzzy logic systems," IEEE Transactions on Fuzzy Systems, vol. 15, no. 1, pp. 3–15, 2007.

[16] M. Biglarbegian, W.W. Melek and J. M. Mendel, "On the stability of interval type-2 TSK fuzzy logic control systems," IEEE Transactions on Systems, Man, and Cybernetics, vol. 4, no. 3, pp. 798–818, 2010.

[17] D. Wu and J. M. Mendel, "On the continuity of type-1 and interval type-2 fuzzy logic systems," IEEE Transactions on Fuzzy Systems, vol. 19, no. 1, pp. 179–192, 2011.

[18] R. Courant and F. John, Introduction to Calculus and Analysis. vol. II/I, New York: Springer, 1999.

[19] V. S. Kouikoglou and Y. A. Phillis, "On the monotonicity of hierarchical sum-product fuzzy systems", Fuzzy Sets and Systems, vol. 160, pp. 3530–3538, 2009.

[20] J. Won, S. Park and J. Lee, "Parameter conditions for monotonic Takagi–Sugeno–Kang fuzzy system," Fuzzy Sets and Systems, vol. 132, pp. 135–146, 2002.

[21] C. Li, J. Yi and T. Wang, "Combing prior knowledge with data driven design of interval type-2 fuzzy logic systems," International Journal of Innovative Computing, Information and Control, vol. 7, no. 3, pp. 1133–1144, 2011.

[22] C. Li, J. Yi and D. Zhao, "Analysis and design of monotonic type-2 fuzzy inference systems," Proc. 2009 IEEE International Conference on Fuzzy Systems, Jeju Island, Korea, 2009, pp. 1193–1198.

[23] T. Wang, J. Yi and C. Li "Fuzzy identification based on monotonicity and interval type-2 fuzzy logic," ICIC Express Letters – An International Journal of Research and Surveys, vol. 5, no. 4(A), pp. 1107–1113, 2011.

[24] H. Seki, H. Ishii and M. Mizumoto, "On the monotonicity of single input type fuzzy reasoning methods," IEICE Transactions on Fundamentals, vol. E90-A, pp. 1462–1468, July 2007.

[25] M. Biglarbegian, W. Melek and J. M. Mendel, "On the robustness of type-1 and interval tpe-2 fuzzy logic systems in modeling," Information Sciences, vol. 181, pp. 1325–1347, 2011.

[26] K. M. Tay and C. P. Lim, "A fuzzy inference system-based criterion-referenced assessment model," Expert Systems With Applications, in press.

[27] K. M. Tay and C. P. Lim, "Enhancing the failure mode and effect analysis methodology with fuzzy inference techniques," Journal of Intelligent and Fuzzy systems, vol. 21, no. 1-2, pp. 135–146, 2010.

[28] K. M. Tay and C. P. Lim, "On the use of fuzzy inference techniques in assessment models: Part I: theoretical," Fuzzy Optimization and Decision Making: A Journal of Modeling and Computation Under Uncertainty, vol. 7, no. 3, pp. 269–281, 2008.

[29] K. M. Tay and C. P. Lim, "On the use of fuzzy inference techniques in assessment models: Part II: industrial applications," Fuzzy Optimization and Decision Making: A Journal of Modeling and Computation Under Uncertainty, vol. 7, no. 3, pp. 283–302, 2008.

2011 IEEE International Conference on Fuzzy Systems
June 27-30, 2011, Taipei, Taiwan

Digital Controller Design for Fuzzy Systems with Packet Loss: Intelligent Digital Redesign Approach

Geun Bum Koo
and Jin Bae Park
Department of Electrical
and Electronic Engineering,
Yonsei University,
Seoul 120-749, Korea
Email: {milbam, jbpark}@yonsei.ac.kr)

Young Hoon Joo
and Hyoung Seok Jeon
Department of Control
and Robotics Engineering,
Kunsan National University,
Kunsan, Chonbuk, 573-701, Korea,
Email: yhjoo, mnxcbv@kunsan.ac.kr

***Abstract*—In this paper, a novel digital controller is proposed for the nonlinear systems with packet loss using the intelligent digital redesign (IDR). For the fuzzy controller, the nonlinear system is represented by a Takagi–Sugeno (T–S) fuzzy model. The IDR technique is to convert a pre-designed analog controller into an equivalent digital controller. For this technique, the discretized models of the analog and digital closed-loop system are presented, respectively. The digital control gain is obtained to minimize the norm error between the state of the analog and digital closed-loop systems and stabilize the digital closed-loop system. Its sufficient conditions are derived in terms of linear matrix inequalities (LMIs). Finally, a numerical example is provided to verify the effectiveness of the proposed technique.**

***Index Terms*—intelligent digital redesign (IDR), Takagi–Sugeno (T–S) fuzzy model, packet loss, linear matrix inequality (LMI)**

I. Introduction

Networked control system (NCS) has been a very hot research topic over the past decade [1], [2], [3], [4], [5]. NCSs have attracted much attention because of their successful applications in modern complicated industry processes, e.g., aircraft and space shuttle, unclear power stations, high-performance automobiles, etc. Basically, NCS has wireless communication channels or networks between sensors, controllers, and actuators. Due to these structure, there are many problems, such as time delay, packet loss and so on. Also, the system is continuous, while the control law is discrete. For solving above problems, many studies were progressed. However, contrary to time delay and sampling study, there are not enough studies for packet loss problem. To solve the packet loss problem, it needs an stochastic approach.

Also, because of continuous system and discrete controller, the study for the digital control is essential for NCS. Among many digital control methods, a digital redesign (DR) is widely used as the predominant digital controller design technique [6], [7], [8]. It executes as a tool which converts an original analog controller into a new digital one maintaining the state-matching condition. However, there is a problem that the DR can be only used in linear systems.

In order to apply DR method in the nonlinear system, an intelligent digital redesign (IDR), which is merged with the fuzzy control scheme and the DR method, was proposed in [9]. Also, the robust IDR problem was studied for nonlinear systems with parametric uncertainties [10]. However, these papers dealt with the local state-matching without concerning the global one. The global approaches of the IDR problem were presented in [11], [12], [13], but they did not consider the packet loss problem of the nonlinear systems. The stochastic stability for the nonlinear systems with packet loss were proposed in [3], [4], [5]. But there were no studies about the IDR problem for the nonlinear systems with packet loss.

In this paper, we propose a novel digital controller design for the nonlinear systems which can be modelled by T–S fuzzy systems. For the digital controller design, we use the IDR approach which is to convert a pre-designed analong controller into an equivalent digital one. To develop the IDR technique, the discretized models of the analog and digital closed-loop system with the decentralized controller are presented, respectively. Based on discretized models, sufficient conditions are achieved for both the state-matching condition between analog and digital closed-loop systems and the stability of the digital closed-loop system. Its constructive conditions are presented in terms of linear matrix inequalities (LMIs). Finally, it shows the validity of the proposed ideas, techniques and procedures, through simple example.

This paper is organized as follows: Section 2 describes the discretized models of the T–S fuzzy systems. The stability and state-matching conditions are proposed with the LMI form in Section 3. In Section 4, simulation example is provided to demonstrate the design procedures. Finally, the conclusions are given in Section 5.

II. Preliminaries

Consider a T–S fuzzy system, in which the ith IF-THEN rule is represented by the following form:

$$R_i : \text{IF } z_1(t) \text{ is } \Gamma_{i1} \text{ and } \cdots \text{ and } z_p(t) \text{ is } \Gamma_{ip}$$
$$\text{THEN } \dot{x}(t) = A_i x(t) + B_i u(t) \quad (1)$$

where z_h, $h \in \mathcal{I}_p$ is the premise variable; $x \in \mathbb{R}^n$ and $u \in \mathbb{R}^m$ are the state and control input, respectively; Γ_{ih}, $(i,h) \in \mathcal{I}_r \times$

978-1-4244-7316-8/11/$26.00 ©2011 IEEE

$\mathcal{I}_p$, is a fuzzy set for $z_h(t)$; A_i and B_i denote nominal system matrices with appropriate dimensions for the ith rule.

Using the center-average defuzzification, product inference, and singleton fuzzifier, the global dynamics is inferred as

$$\dot{x}(t) = \sum_{i=1}^{r} \mu_i(z(t))\Big(A_i x(t) + B_i u(t)\Big) \tag{2}$$

where

$$\mu_i(z(t)) = \omega_i(z(t)) \Big/ \sum_{i=1}^{r} \omega_i(z(t)),$$
$$\omega_i(z(t)) = \prod_{h=1}^{p} \Gamma_{ih}(z_h(t))$$

in which $\Gamma_{ih}(z_h(t))$ is the fuzzy membership grade of $z_h(t)$ in Γ_{ih}.

Suppose the pre-designed analog and the digital fuzzy controller (2).

$$u_c(t) = \sum_{i=1}^{r} \mu_i(z(t)) K_i^c x_c(t) \tag{3}$$

$$u_d(t) = u_d(kT) = \alpha(kT) \sum_{i=1}^{r} \mu_i(z(t)) K_i^d x_d(kT) \tag{4}$$

where K_i^c and K_i^d denote the analog and the digital control gains, the subscript 'c' and 'd' mean the analog control and the digital control, respectively, and $\alpha(kT)$ is a Bernoulli random process to determine the packet loss with the following assumption:

Assumption 1: Bernoulli random process $\alpha(kT)$ is an independent, identically distributed (iid) random sequence specified by the following law:

$$\begin{cases} \mathbf{Prob}\{\alpha(kT) = 1\} = \mathbb{E}\{\alpha(kT)\} = \tilde{\alpha} \\ \mathbf{Prob}\{\alpha(kT) = 0\} = 1 - \mathbb{E}\{\alpha(kT)\} = 1 - \tilde{\alpha} \end{cases}$$

Substituting (3) and (4) into (2), respectively, the closed-loop systems are written as

$$\dot{x}_c(t) = \sum_{i=1}^{r}\sum_{j=1}^{r} \mu_i(z(t))\mu_j(z(t))\big(A_i + B_i K_j^c\big)x(t) \tag{5}$$

$$\dot{x}_d(t) = \sum_{i=1}^{r}\sum_{j=1}^{r} \mu_i(z(t))\mu_j(z(kT)) \times \big(A_i x(t) + \alpha(kT) B_i K_j^d x(kT)\big) \tag{6}$$

To obtain the discretized systems of (5) and (6), we have introduced the following assumption.

Assumption 2: Assume that $\mu_i(z(t)) \approx \mu_i(z(kT))$ for $t \in [kT,\ kT+T)$. Consequently, the nonlinear matrix functions $\sum_{i=1}^{r} \mu_i(z(t))A_i$ and $\sum_{i=1}^{r} \mu_i(z(t))B_i$ can be represented by constant matrices $\sum_{i=1}^{r} \mu_i(z(kT))A_i$ and $\sum_{i=1}^{r} \mu_i(z(t))B_i$, respectively, over any interval $[kT,\ kT+T)$, $k \in \mathbb{Z}_{\geq 0}$.

Supposing the sampling period T, closed-loop fuzzy system (5) and (6) are approximately discretized as

$$x_c(kT+T) \approx \sum_{i=1}^{r}\sum_{j=1}^{r} \mu_i(z(kT))\mu_j(z(kT))\Phi_{ij} x_c(kT) \tag{7}$$

where

$$\Phi_{ij} = \exp\Big(\big(A_i + B_i K_j^c\big)T\Big)$$

$$x_d(kT+T) \approx \sum_{i=1}^{r}\sum_{j=1}^{r} \mu_i(z(kT))\mu_j(z(kT)) \times \Big(\big(G_i + \alpha(kT) H_i K_j^d\big)T\Big) x_d(kT) \tag{8}$$

where

$$G_i = \exp(A_i T),$$
$$H_i = (G_i - I)(A_i)^{-1} B_i.$$

The objective of this paper is to obtain the LMI for the digital fuzzy control gain K_i^d which minimize the state-matching error between $x_c(kT)$ and $x_d(kT)$ and stabilize the digital closed-loop system (6).

III. Main results

In order to proceed to main results, the following definition and lemmas will be needed throughout the proof.

Definition 1: The equilibrium point $x(t) = 0$ is said to be stochastically stable in the nonlinear system if, for any $\epsilon > 0$ there exists a $\delta = \delta(\epsilon) > 0$, such that

$$\|x(0)\| < \delta \Rightarrow E\{\|x(t)\|\} < \epsilon, \qquad \forall t \geq 0$$

Lemma 1 ([14]): If there exist a Lyapunov functional and a non-decreasing convex function $a(r)$ satisfying the following conditions:

$$\begin{cases} V(0) = 0 \\ a(\|x(t)\|) \leq V(x(t)) \\ E\{V(x(t+1))\} - E\{V(x(t))\} < 0 \end{cases}$$

then the equilibrium point $x(t) = 0$ of the fuzzy system (8) is stochastically stable.

Lemma 2 ([15]): Given any matrices Y and $P = P^T \succ 0$, we have

$$-Y^T P^{-1} Y \preceq P - Y^T - Y\ .$$

Lemma 3 ([16]): : For any real matrices X_i, Y_i for $1 \leq i \leq N$, and $S \succ 0$ with appropriate dimensions, we have

$$2\sum_{i=1}^{N}\sum_{j=1}^{N}\sum_{k=1}^{N}\sum_{l=1}^{N} h_i h_j h_k h_l X_{ij}^T S Y_{kl} \leq \sum_{i=1}^{N}\sum_{j=1}^{N} h_i h_j (X_{ij}^T S X_{ij} + Y_{ij}^T S Y_{ij})$$

where h_i $(1 \leq i \leq N)$ are defined as $h_i \geq 0$, $\sum_{i=1}^{N} h_i = 1$.

Lemma 4 ([17]): : For real matrices X and Y with appropriate dimensions, the following inequality is always satisfied.

$$X^T Y + Y^T X \leq \sigma X^T X + \frac{1}{\sigma} Y^T Y$$

where σ is a positive constant.

Proposition 1: In (6), there exists some constant $\delta > 0$ such that

$$\mathbb{E}\{\|x(t)\|\} \le \delta \mathbb{E}\{\|x(kT)\|\} \tag{9}$$

where

$$\begin{aligned}\delta =&(1+T\beta)e^{\alpha T},\\ \alpha =& \sup_{i\in\mathcal{I}_r}\|A_i\|,\\ \beta =& \sup_{(i,j)\in\mathcal{I}_r\times\mathcal{I}_r}\|B_iK_j^d\|\end{aligned}$$

for $t \in [kT, kT+T)$.

Proof: Integrating (6) from kT to t, $t \in [kT, kT+T)$ and taking the norm on both sides of the results yields

$$\begin{aligned}&\|x(t)\|\\ &\le \|x(kT)\| + \int_{kT}^{t}\left(\left\|\sum_{i=1}^{r}\mu_i(z(t))A_i\right\|\|x(\tau)\|\right.\\ &\quad\left.+\left\|\sum_{i=1}^{r}\sum_{j=1}^{r}\mu_i(z(t))\mu_j(z(kT))\alpha(kT)B_iK_j\right\|\|x(kT)\|\right)d\tau\\ &\le \sup_{(i,j)\in\mathcal{I}_r\times\mathcal{I}_r}\left\{\big(1+T\|B_iK_j^d\|\big)\|x(kT)\| + \int_{kT}^{t}\|A_i\|\|x(\tau)d\tau\right\}\end{aligned}$$

An application of the Grownwall-Bellman inequality to $\|x(t)\|$ constructs the inequality

$$\|x(t)\| \le \delta\|x(kT)\| \tag{10}$$

where

$$\delta = \sup_{(i,j)\in\mathcal{I}_r\times\mathcal{I}_r}\left\{\big(1+T\|B_iK_j^d\|\big)e^{\|A_i\|T}\right\}$$

is independent of k. Taking the expectation of (10), we can obtain the inequality (1). ■

Theorem 1: If there exist some symmetric and positive matrix Q and some matrix M_i, such that the following LMIs have optimal solutions, then, $x_d(kT)$ of (8) closely matches $x_c(kT)$ of (7), and origin of (8) is stochastically stable.

$$\underset{Q,M_i}{\text{minimize}} \quad \gamma \quad \text{subject to}$$

$$\begin{bmatrix}-\gamma Q & * & *\\ \Phi_{ij}Q - G_iQ - \tilde{\alpha}H_iM_j & -\gamma I & *\\ \sqrt{(1-\tilde{\alpha})\tilde{\alpha}}H_iM_j & 0 & -\gamma I\end{bmatrix} \prec 0 \tag{11}$$

$$\begin{bmatrix}-Q & * & *\\ G_iQ + \tilde{\alpha}H_iM_i & -Q & *\\ \sqrt{(1-\tilde{\alpha})\tilde{\alpha}}H_iM_j & 0 & -Q\end{bmatrix} \prec 0 \tag{12}$$

$$\begin{bmatrix}-4Q & * & *\\ G_iQ + G_jQ + \tilde{\alpha}H_iM_j + \tilde{\alpha}H_jM_i & -Q & *\\ \sqrt{(1-\tilde{\alpha})\tilde{\alpha}}(H_iM_j + H_jM_i) & 0 & -Q\end{bmatrix} \prec 0 \tag{13}$$

for $\forall\{(i,j) \in \mathcal{I}_r \times \mathcal{I}_r | 1 \le i \le j \le r\}$.

Proof: In order to closely match $x_d(kT)$ of (8) to $x_c(kT)$ of (7), consider the norm minimization problem in the following form:

$$\left\|\Phi_{ij}^k - (G_i + \alpha(kT)H_iK_j^d)\right\| \le \hat{\gamma} \tag{14}$$

for some $\hat{\gamma} > 0$. Using the norm property, the above inequality holds

$$\begin{aligned}&\Big(\Phi_{ij} - (G_i + \alpha(kT)H_iK_j^d)\Big)^T\Big(\Phi_{ij} - (G_i + \alpha(kT)H_iK_j^d)\Big)\\ &\prec \gamma^2 P\end{aligned} \tag{15}$$

where $\gamma > 0$ and $P^k = (P)^T \succ 0$ with $\hat{\gamma}I \prec \gamma^2 P$. Taking the expectation, inequality (15) results in

$$\begin{aligned}(15) \Rightarrow& E\Big\{\Big(\Phi_{ij} - (\Psi_{ij} + \hat{\alpha}(kT)H_i^kK_j^d)\Big)^T\\ &\times\Big(\Phi_{ij} - (\Psi_{ij} + \hat{\alpha}(kT)H_i^kK_j^d)\Big) - \gamma^2 P\Big\}\\ =&\big(\Phi_{ij} - \Psi_{ij}\big)^T\big(\Phi_{ij} - \Psi_{ij}\big) - \gamma^2 P\\ &+ (1-\tilde{\alpha})\tilde{\alpha}(K_j^d)^TH_i^TH_iK_j^d\end{aligned} \tag{16}$$

where

$$\begin{aligned}\Psi_{ij} &= G_i + \tilde{\alpha}H_iK_j^d,\\ \hat{\alpha}(kT) &= \alpha(kT) - \tilde{\alpha}.\end{aligned}$$

Taking the Schur complement and the congruence transformation with $\mathrm{diag}\{\gamma^{-1}P^{-1}, I, I\}$ and denoting $K_j^dQ = M_j$, inequality (15) yields (11).

Apart from the state-matching problem, for solving the stability problem, we choose the Lyapunov function candidate $V(x(kT))$ for (8) as follows:

$$V(x(kT)) = x_d^T(kT)Px_d(kT)$$

The rate of increase of $E\{V(x(kT))\}$ along (8) is then

$$\begin{aligned}&E\{V(kT+T)\} - E\{V(kT)\}\\ &\le E\Big\{\frac{1}{4}\sum_{i=1}^{r}\sum_{j=1}^{r}\mu_i(z(kT))\mu_j(z(kT))\\ &\quad\times\Big(\Big((\Psi_{ij}+\Psi_{ji} + \hat{\alpha}(kT)H_iK_j^d + \hat{\alpha}(kT)H_jK_i^d)x_d\Big)^T\\ &\quad\times P^k\Big((\Psi_{ij}+\Psi_{ji} + \hat{\alpha}(kT)H_iK_j^d + \hat{\alpha}(kT)H_jK_i^d)x_d\Big)\\ &\quad - 4x_d^TP^kx_d\Big)\Big\}\end{aligned} \tag{17}$$

Because of $\mathbb{E}\{\hat{\alpha}(kT)\} = 0$ and $\mathbb{E}\{\hat{\alpha}^2(kT)\} = (1-\tilde{\alpha})\tilde{\alpha}$, inequality (17) is rearranged as follows:

$$\begin{aligned}&E\{V(kT+T)\} - E\{V(kT)\}\\ &\le \frac{1}{4}\sum_{i=1}^{r}\sum_{j=1}^{r}\mu_i(z(kT))\mu_j(z(kT))\\ &\quad\times\Big(\Big((\Psi_{ij}+\Psi_{ji})x_d\Big)^TP\Big((\Psi_{ij}+\Psi_{ji})x_d\Big) - 4x_d^TP^kx_d\\ &\quad + (1-\tilde{\alpha})\tilde{\alpha}x_d^T\big(H_iK_j^d + H_jK_i^d\big)^TP\big(H_iK_j^d + H_jK_i^d\big)x_d\Big)\end{aligned} \tag{18}$$

Form (18), if the following inequalities hold for any $1 \le i < j \le r$, we know that the closed-loop system (6) is

stochastically stable by Definition 1 and Proposition 1.

$$\Psi_{ii}^T P \Psi_{ii} - P + (1-\tilde{\alpha})\alpha (K_j^d)^T H_i^T P H_i K_j^d \prec 0 \tag{19}$$

$$\left(\frac{\Psi_{ij}+\Psi_{ji}}{2}\right)^T P \left(\frac{\Psi_{ij}+\Psi_{ji}}{2}\right) - P + (1-\tilde{\alpha})\alpha \left(\frac{H_i K_j^d + H_j K_i^d}{2}\right)^T P \left(\frac{H_i K_j^d + H_j K_i^d}{2}\right) \prec 0 \tag{20}$$

Using Schur complement and congruence transformation with $\mathrm{diag}\{P^{-1}, I, I\}$ to (19) and (20), we can obtain the LMI conditions (12) and (13) in the Theorem 1. ■

Remark 1: The inequalities for the pair (k, m) such that $\mu_{ik}(x_i(t) \times \mu_{im}(x_i(t)) = 0$, do not need to be solved to determine global stability.

IV. Numerical Examples

In this section, an example is given to validate the proposed method. We consider the fuzzy system which is called the chaotic Lorenz system. The dynamic equations of the system are described by [18]

$$\begin{aligned}\dot{w}(t) &= -\sigma w(t) + \sigma y(t)\\ \dot{y}(t) &= r w(t) - y(t) - w(t) z(t)\\ \dot{z}(t) &= w(t) y(t) - b z(t)\end{aligned}$$

where $\sigma = 10$, $r = 28$ and $b = -\frac{8}{3}$.

Assuming $w(t) \in [M_1, M_2]$ and choosing $x(t) = \begin{bmatrix} x_1(t) & x_2(t) & x_3(t)\end{bmatrix}^T = \begin{bmatrix} w(t) & y(t) & z(t)\end{bmatrix}^T$, the T–S fuzzy system can be constructed as follows:

$$\dot{x}(t) = \sum_{i=1}^{2} \mu_i(x_1(t))\big(A_i x(t) + B_i u(t)\big)$$

where

$$A_1 = \begin{bmatrix} -\sigma & \sigma & 0\\ r & -1 & -M_1\\ 0 & M_1 & -b\end{bmatrix}$$

$$A_2 = \begin{bmatrix} -\sigma & \sigma & 0\\ r & -1 & -M_2\\ 0 & M_2 & -b\end{bmatrix}$$

$$B_1 = B_2 = \begin{bmatrix} 1 & 0 & 0\end{bmatrix}$$

for $i \in \mathcal{I}_r$. The membership functions are

$$\mu_1(x_1(t)) = \frac{-x_1(t) + M_2}{M_2 - M_1}$$

$$\mu_2(x_1(t)) = \frac{x_1(t) - M_1}{M_2 - M_1}$$

We assume $M_1 = -20$, $M_2 = 30$, the initial sate conditions $x(0) = [10, -10, -10]^T$, packet loss probability $\tilde{\alpha} = 0.8$ and a sampling time $T = 0.05$s.

By using Theorem 1 and solving the corresponding LMIs, we obtain the control gains:

$$K_1^d = \begin{bmatrix} -25.0411 & -15.8009 & -11.6152\end{bmatrix}$$

$$K_2^d = \begin{bmatrix} -23.4177 & -10.0505 & 15.5128\end{bmatrix}$$

Time responses for each subsystem are shown in Figs. 1, 2 and 3. As shown in these figures, we can observe that the controlled state variables by IDR method follow the controlled analog ones and converge to the origin. Thus we can know that the proposed IDR technique satisfies an asymptotic stability of digitally closed-loop fuzzy system and the state-matching requirement with the originally closed-loop system.

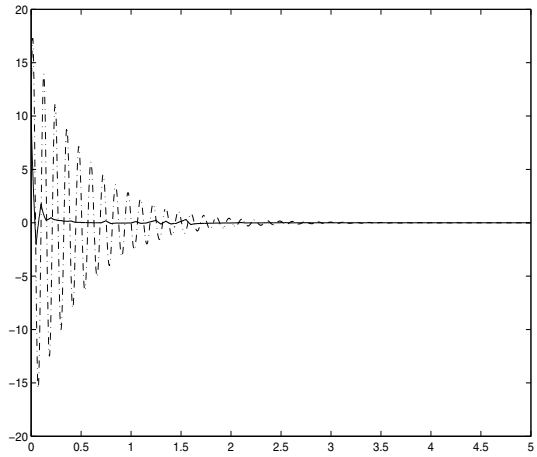

Fig. 1. The time responses x_1 of controlled system for $T = 0.2$s: analog (dash-dotted), proposed (solid).

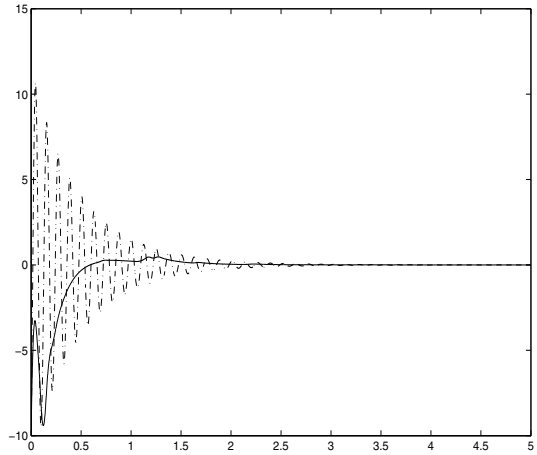

Fig. 2. The time responses x_2 of controlled system for $T = 0.2$s: analog (dash-dotted), proposed (solid).

V. Conclusion

This paper has established the IDR method for the fuzzy systems. Using the T–S fuzzy model, we has presented the analog and digital closed-loop fuzzy systems. For the IDR method, descritized models of each closed-loop systems are obtained. Based on the descritized systems, it was shown that the IDR technique can find the digital fuzzy gains to minimize the norm error between the state of analog system and digital system and stabilize the digital closed-loop system. Also, the sufficient design conditions were derived and formulated in the LMI format, and were therefore easily tractable by convex

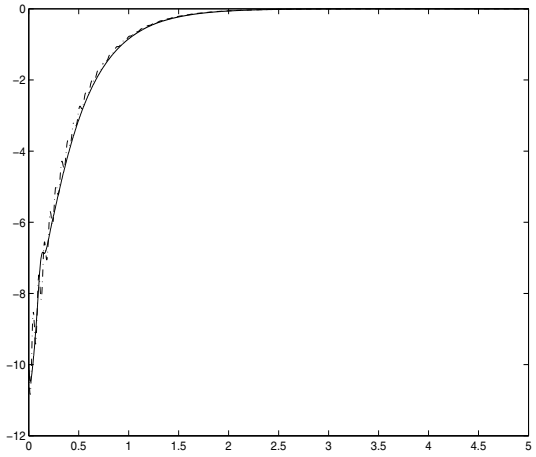

Fig. 3. The time responses x_3 of controlled system for $T = 0.2$s: analog (dash-dotted), proposed (solid).

optimization. Finally a simulation example has shown that the results of this paper are effective and valuable.

ACKNOWLEDGMENT

This research was supported by Basic Research Program through the National Research Foundation of Korea(NRF) funded by the Ministry of Education, Science and Technology(2010-0024352).

REFERENCES

[1] W. Zhang, M. S. Branicky and S. M. Phillips, "Stability of networked control system", *IEEE Control Systems Magazine*, vol. 21, no. 1, pp. 84-99, 2001.

[2] G. C. Walsh, H. Ye and L. G. Bushnell, "Stability analysis of networked control systems", *IEEE Control Systems Technology*, vol. 10, no. 3, pp. 436-446, 2002.

[3] D. Huang and S. K. Nguang, "State feedback control of uncertain networked control systems with random time delays", *IEEE Trans. on Automatic Control*, vol. 53, no. 3, pp. 829-834, 2008.

[4] J. Xiong and J. Lam, "Stabilization of linear systems over networked with bounded packet loss", *Automatica*, vol. 43, pp. 80-87, 2007.

[5] J. Wu and T. Chen, "Design of networked control systems with packet dropouts", *IEEE Trans. on Automatic Control*, vol. 52, no. 7, pp. 1314-1319, 2007.

[6] B. C. Kuo, "Digital Control System", *Holt, Rinehart and Winston, New York*, 1980.

[7] L. S. Shieh, W. M. Wang, and J. S. H. Tsai, "Digital modelling and digital redesign of sampled-data uncertain systems", *IEE Control Theory*, Vol. 142, pp. 585-594, 1995.

[8] L. S. Shieh, W. M. Wang, and J. B. Zheng, "Robust control of sampled-data uncertain systems using digitally redesigned observer-based controllers", *Int. J. Control*, Vol. 66, pp. 43-64, 1997.

[9] Y. H. Joo, G. Chen, and L. S. Shieh, "Hybrid state-space fuzzy model-based controller with dual-rate sampling for digital control of chaotic sysems", *IEEE Transactions on Fuzzy Systems*, Vol. 7, No. 4 pp. 394-408, 1999.

[10] W. Chang, J. B. Park, Y. H. Joo, and G. Chen, "Design of sampled-data fuzzy-model-based control systems by using intelligent digital redesign", *IEEE Transactions on Circuits and Systems*, Vol. 49, No. 4, pp. 509-517, 2002.

[11] H. J. Lee, H. B. Kim, Y. H. Joo, W. Chang, and J. B. Park, "A new intelligent digital redesign for T–S fuzzy systems: global approach", *IEEE Transactions on Fuzzy Systems*, Vol. 12, No. 2, pp. 274-284, 2004.

[12] D. W. Kim, J. B. Park, and Y. H. Joo, "Effective digital implementation of fuzzy control systems based on approximate discrete-time models", *Automatica*, Vol. 43, No. 10, pp. 1671-1683, 2007.

[13] H. C. Sung, D. W. Kim, J. B. Park, and Y. H. Joo, "Robust digital control of fuzzy systems with parametric uncertainties: LMI-based digital redesign approach", *Fuzzy Sets and Systems*, Vol. 161, pp. 919-933, 2010.

[14] B. Chen, Z. Wang, H. Shu and G. Wei, "On nonlinear H_∞ filtering for discrete-time stochastic systems with missing measurements", *IEEE Trans. on Automatic Control*, vol. 53, no. 9, pp. 2170-2180, 2008.

[15] J. V. D. Oliveira, J. Bernussou, and J. C. Geromel, "A new discrete-time robust stability condition", *Systems and Control Letters*, Vol. 37, pp. 261-265, 1999.

[16] X. P. Guan and C. L. Chen, "Delay-dependent guaranteed cost control for T–S fuzzy systems with time delay", *IEEE Trans. on Fuzzy Systems*, vol. 12, no. 2, pp. 236-249, 2004.

[17] L. Xie, "Output feedback H_∞ control of systems with parameter uncertainties", *Int. J. Contr.*, vol. 63, no. 4, pp. 741-750, 1996.

[18] H. J. Lee, J. B. Park and G. Chen, "Robust fuzzy control of nonlinear systems with parametic uncertainties", *IEEE Trans. on Fuzzy Systems*, vol. 9, no. 2, pp. 369-379, 2001.

2011 IEEE International Conference on Fuzzy Systems
June 27-30, 2011, Taipei, Taiwan

Mixed-Time T-S Fuzzy Optimal Estimator for Target Tracking

Sun Young Noh
Department of Electrical and Electronic Engineering, Yonsei University
Seodaemun-gu, Seoul, 120-749, Korea
Email: NohSunYoung@gmail.com

Jin Bae Park
Department of Electrical and Electronic Engineering, Yonsei University
Seodaemun-gu, Seoul 120-749, Korea
Email: jbpark@yonsei.ac.kr

Young Hoon Joo
Department of Electronic and Information, Kunsan National University
Kunsan, Chonbuk, 573-701, Korea
Email:yhjoo@kunsan.ac.kr

***Abstract*—This paper is concerned with the mixed-time fuzzy optimal estimator for the target tracking. The proposed method takes account of behaviour for target motion in continuous time and system measurement in discrete time. The overall dynamic of system in continuous-time is discretised by using Takagi-Sugeno(T-S) fuzzy models. Based on the fuzzy model the fuzzy estimation is studied. Then the error state of the filtering process is means square bounded. A basis dependent Lyapunov function approach is developed to design the fuzzy filter and a filter gain is minimized by using some linear matrix inequalities(LMIs) constraints. A numerical example is provided to demonstrate various aspects of theoretical results.**

***Index Terms*—T-S Fuzzy, Mixed-Time, LMI, Fuzzy Optimal Estimator, Lyapunov function**

I. Introduction

The purpose of target tracking is an accurate state estimation of a moving object. Estimating as accurately as possible of the state of a dynamic system have been a very important topic. Among the various approaches proposed in this topic, the estimation processes a relative states between a moving platform and a target as well as estimation of the target states[1], [2], [3]. In most cases, whether the target states are described in inertial, spherical, or modified spherical coordinates in[5]. The model-based adaptive filtering method was presented in [7], [9], [10], [11] that consider the motion of a target by using multiple sub-filters. Almost all maneuvering target tracking methods are model based. Research continues on techniques and applications to the target tracking problem each of these approaches has its own drawbacks. And all are approximate from sense in discrete-time domain and some do not apply to the tracking problem[6], [7], [9], [10]. They assume that the target motion and its observation can be represented by some known mathematical models accurately[8]. The most of thesis used target motion and measurement model in continuous-time(CT) domain or discrete-time(DT) domain.

However, the target motion is more accurately modeled in CT domain. They should not depend on how and when samples are taken. And measurements are usually available only at discrete time instants. To design the target motion in DT domain, the discretisation of it is usually first required. The discretisation methods of the fuzzy system have been studied[12], [13]. This method is directly discretise the global dynamics of the fuzzy model. And Takagi-Sugeno(T-S) fuzzy model have the important advantage of its universal approximation.

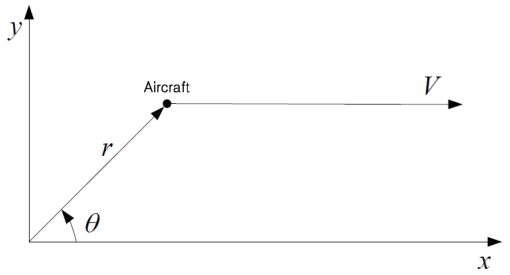

Fig. 1. Radar tracking geometry

In this paper, we concerned with the mixed-time fuzzy optimal estimator for the target tracking. We propose that take account of behavior for target motion in CT domain and system measurement in DT domain. The overall dynamic of system in CT is discretised by using T-S fuzzy models. Based on the fuzzy model, the fuzzy estimation is studied. Then the error state of the filtering process is mean square bounded. A basis dependent Lyapunov function approach is developed to design the fuzzy filter and a filter gain is minimized by using some linear matrix inequalities(LMIs) constraints. A numerical example is provided to demonstrate various aspects of theoretical results. This paper is organized as follows: Section 2 describes the conventional discretisation method of the continuous-time T-S fuzzy model. Section 3 describes the fuzzy filter design by using the discretizing system and measurement. In Section 4, a numerical example is provided to design the fuzzy filter. Finally, the conclusions are given in Section 5.

II. Preliminaries and problem description

We assume here that the target moves in a plane that is the two-dimensional radar tracking problem illustrated in Figure 1. In fact, the target motion is more accurately modeled in CT domain while observations are usually available only at DT instants. It is often more appropriate to use the following mixed-time models for most tracking problem.

978-1-4244-7316-8/11/$26.00 ©2011 IEEE

A. State and measurement models

The moving target[14] can be described as

$$\begin{aligned} r^2 &= x^2 + y^2 \\ 2r\dot{r} &= 2x\dot{x} + 2y\dot{y} \\ \dot{r} &= \frac{x}{r}\dot{x} + \frac{y}{r}\dot{y} \end{aligned} \tag{1}$$

where $x = rcos\theta$, $\dot{x} = V$, $\dot{y} = 0$, V is velocity, r is the radar measurement range and θ is azimuth, therefore

$$\dot{r} = Vcos\theta \tag{2}$$

Assume that the aircraft is not accelerating so that $\dot{V} = 0$. If r and θ do not change much during each scan of the radar(about 1-10s), we have $\ddot{r} \approx 0$ and $\ddot{\theta} \approx 0$.

Differentiating

$$\begin{aligned} \frac{d}{dt}\dot{r} &= \dot{V}cos\theta - V\dot{\theta}sin\theta \\ \frac{d}{dt}\theta &= -\left(\frac{\dot{V}r - V\dot{r}}{r^2}\right)sin\theta - \frac{V}{r}\dot{\theta}cos\theta \end{aligned} \tag{3}$$

We have the state equation as

$$\frac{d}{dt}\begin{bmatrix} r \\ \dot{r} \\ \theta \\ \dot{\theta} \end{bmatrix} = A\begin{bmatrix} r \\ \dot{r} \\ \theta \\ \dot{\theta} \end{bmatrix} + \begin{bmatrix} 0 \\ w_1(t) \\ 0 \\ w_2(t) \end{bmatrix} \tag{4}$$

where A is system matrix and $w_1(t), w_2(t)$ are random disturbances. From (4), we have the continuous-time state model.

$$\dot{X}(t) = AX(t) + BW(t) \tag{5}$$

$$y(k) = CX(k) + v(k) \tag{6}$$

where $X(t) = [r \quad \dot{r} \quad \theta \quad \dot{\theta}]^T$ denotes the state vector, $y(k)$ denotes measurement equation, A, B, C denote the system matrix, $W(t)$ is maneuver noise, $v(k)$ is measurement noise.

Remark 1: Measurements are available only at discrete-time instants because they are in fact from sensor. It is often more appropriate to use the following mixed-time models for most tracking problems.

The general solution to (5) excited by the initial state $X(t_0)$ is given by

$$\dot{X}(t) = \Phi(t, t_0) + \int_{t_0}^{t} \Phi(t, \tau)Bw(\tau)d\tau \tag{7}$$

where the state transition matrix $\Phi(t, t_0)$ satisfies $\Phi(t, t_0) = \Phi(t, t_1)\Phi(t_1, t_0)$ with initial condition $\Phi(t, t_0) = I$. The solution to (5) at $t = (k+1)T$ with $t_0 = kT$ is

$$\begin{aligned} X(kT+T) =& exp(AT)X(kT) \\ &+ \int_{kT}^{kT+T} exp(A(kT+T-\tau))BW(kT)d\tau \\ =& GX(kT) + HW(kT) \end{aligned} \tag{8}$$

where $G = exp(AT)$ and $H = (G - I)BA^{-1}$.

B. The discretizing the continuous-time T-S fuzzy model

The discretising the continuous-time T-S fuzzy model is to apply the discretisation method for system to the consequent parts of the fuzzy rules. The rule of the T-S fuzzy system is formulated in the following form

$$\begin{aligned} R_i &: \text{IF } z_1(t) \text{ is about } \Gamma_{i1} \text{ and } \cdots \text{ and } z_g(t) \text{ is about } \Gamma_{ig}, \\ &\text{THEN } \dot{X}(t) = A_iX(t) + B_iW(t) \end{aligned} \tag{9}$$

where $i \in \Re_g = \{1, 2, ..., g\}$, denotes the ith fuzzy rule; $z_h(t)$, $h \in \Re_p = \{1, 2, ..., p\}$, the hth premise variable; $\Gamma_{ih}, (i, h) \in \Re_q \times \Re_g$, the fuzzy set. If $z_h(t)$ for $t \in [kT, kT+T)$ is $z_h(kT)$, the rule of the corresponding discrete-time T-S fuzzy model is obtained as follows

$$\begin{aligned} R_i &: \text{IF } z_1(kT) \text{ is about } \Gamma_{i1} \text{ and } \cdots \text{ and } z_g(kT) \text{ is about } \Gamma_{ig}, \\ &\text{THEN } X(kT+T) = G_iX(kT) + H_iW(kT) \\ &\qquad y(kT) = C_iX(kT) + v(kT) \end{aligned} \tag{10}$$

where $G_i = exp(A_iT)$ and $H_i = (G_i - I)B_iA_i^{-1}$. Using the center-average defuzzification, product inference and singleton fuzzifier, the overall dynamics of this discrete-time T-S fuzzy model is described by

$$X(kT+T) = \sum_{i=1}^{g} \theta_i(z(kT))(G_iX(kT) + H_iW(kT)) \tag{11}$$

$$y(kT) = \sum_{i=1}^{g} \theta_i(z(kT))(C_iX(kT) + v(kT)) \tag{12}$$

where $\theta_i(z(kT)) = \frac{\mu_i(z(kT))}{\sum_{i=1}^{p}\mu_i(z(kT))}$,
$\mu_i(z(kT)) = \prod_j^q \Gamma_{ij}(z_j(kT))$ and $\Gamma_{ih}(z_h(kT))$ is the grade of membership of $z_h(kT)$ in Γ_{ih}.

Remark 2: In the target tracking, a target is usually treated as a point object a shape in tracking, The state is often approximated piecewise constant with $X(k) = X(t), t(k) \leq t < t(k+1)$ when discretizing a continuous time system. Note that $W(k) \neq W(t_k), X(k) \neq X(t_k)$.

We denote that

$$\begin{aligned} X(kT) &= G_{if}X(kT) + H_{if}W(kT) \\ y(kT) &= C_{if}X(kT) + v(kT) \end{aligned} \tag{13}$$

where

$$\begin{aligned} G_{if} &= \sum_{i=1}^{g} \theta_i(z(kT))G_i, \qquad H_{if} = \sum_{i=1}^{g} \theta_i(z(kT))H_i, \\ C_{if} &= \sum_{i=1}^{g} \theta_i(z(kT))C_i. \end{aligned} \tag{14}$$

In this paper, we use the discretizing fuzzy system for accurately model of the target motion. Because the target motion modeling is one of the first tasks for maneuvering target tracking.

III. T-S Fuzzy Model based Fuzzy Filter Design

This Section presents a fuzzy filter design method based on Lyapunov function. We present the proposed discretised version of the continuous-time T-S fuzzy system. The discretising fuzzy model is used to deal with the state estimation. Before proceeding, let us introduce the following lemma which will be essential for the proof of our main result.

Lemma 1: (Schur complement [4]) Given constant symmetric matrices N, O and L of appropriate dimensions, the following two inequalities are equivalent:

$$O > 0, \quad N + L^T O L < 0, \tag{15}$$

$$\begin{bmatrix} N & L^T \\ L & -O^{-1} \end{bmatrix} < 0 \quad \text{or} \quad \begin{bmatrix} -O^{-1} & L \\ L^T & N \end{bmatrix} < 0$$

The following fuzzy filter is proposed to deal with a state estimation.

Filter Rule R_j

IF $z_1(kT)$ is about Γ_{j1} and $\cdots$ and $z_g(kT)$ is about Γ_{jg},

THEN $\hat{X}(kT+T) = G_j\hat{X}(kT) + L_j(y(kT) - \hat{y}(kT))$ (16)

where $\hat{X}(kT)$ is an estimate of $X(kT)$, $G_j = exp(A_jT)$ and L_j is the filter parameter to be determined, $\hat{y}(kT) = \sum_{k=1}^{q}\theta(z(kT))C_k(kT)\hat{X}(kT)$ and L_j is the filter gain with jth filter rule. The defuzzified outputs are given by

$$\begin{aligned}\hat{X}(kT+T) =& \sum_{j=1}^{q}\theta_j(z(kT))\sum_{k=1}^{q}\theta(kT)(z(kT)) \\ & \times [G_j\hat{X}(kT) + L_j(y(kT) - \hat{y}(kT))] \\ =& \sum_{i=1}^{q}\theta_i(z(kT))\sum_{j=1}^{q}\theta_j(z(kT))\sum_{k=1}^{q}\theta_k(z(kT)) \\ & \{L_jC_iX(kT) + L_jv(kT) \\ & +(G_j - L_jC_k(kT))\hat{X}(kT)\Big\}\end{aligned} \tag{17}$$

For the notational convenience in the following discussions, we denote that

$$\begin{aligned}\hat{X}(kT+T) =& L_{jf}C_{if}X(kT) \\ & +(C_{jf} - L_{jf})\hat{X}(kT) + L_jv(kT)\end{aligned} \tag{18}$$

where

$$L_{jf} = \sum_{j=1}^{q}\theta_j(z(kT))L_j, \quad G_{jf} = \sum_{j=1}^{q}\theta_j(z(kT))G_j,$$
$$C_{kf} = \sum_{k=1}^{q}\theta_j(z(kT))C_k.$$

From (11) and (17), the augmented system can be expressed as

$$\eta(kT+T) = G_m\eta(kT) + B_md(kT+T) \tag{19}$$

where

$$\begin{aligned}\eta(kT+T) &:= \begin{bmatrix} X(kT+T) & \hat{X}(kT+T) \end{bmatrix}^T \\ d(kT+T) &:= \begin{bmatrix} W(kT+T) & \hat{v}(kT+T) \end{bmatrix}^T \\ G_m &:= \begin{bmatrix} G_{if} & 0 \\ L_{if}C_{if} & (C_{jf} - L_{jf}) \end{bmatrix} \\ B_m &:= \begin{bmatrix} H_{if} & 0 \\ 0 & L_{jf} \end{bmatrix}\end{aligned} \tag{20}$$

Before proceeding further, we define the estimation error as

$$\begin{aligned}e(kT+T) :=& X(kT+T) - \hat{X}(kT+T) \\ =& [I \ -I] \times \begin{bmatrix} X(k+T) \\ \hat{X}(kT+T) \end{bmatrix} \\ =& D_m\eta(kT).\end{aligned} \tag{21}$$

Then, the optimal fuzzy filter is concerned. We assume that the filter system is stochastically stable in the mean square with filter gain L_{jf} performance. The filter gain is to specify L_{jf} such that the following minimal problem is achieved in (22)

$$\min \sup_{d(kT)\in L_\infty} \frac{\|e(kT)\|_\infty}{\|d(kT)\|_\infty}. \tag{22}$$

However it is difficult to directly solve the minimax problem in (22). In this paper, the suboptimal approach via minimizing the upper bounded of the L_{jf} gain is obtained. The optimal L_{jf} gain fuzzy filter problem is the following minimax problem.

Theorem 1:

$$\begin{bmatrix} P & * & * & * \\ 0 & -\alpha^2 I & * & * \\ \left(\frac{G_{m_{ijk}}D_m + G_{m_{ikj}}D_m}{2}\right) & B_mD_m & P^{-1} & * \\ -D_m & 0 & 0 & I \end{bmatrix} \geq 0 \tag{23}$$

where P is symmetric positive-definite matrix and α is positive constant.

Proof: Using by the Tanaka disturbance rejection [15]; there exists a quadratic function $V(e(kT)) = e(kT)^TPe(kT)$, $P > 0$, and $\alpha \geq 0$, such that for all $t \in [kT, kT+T)$,

$$\begin{aligned}& V(e(kT)) = e^T(kT)Pe(kT), \\ & \triangle V(e(kT))_{\geq 0} + e^T(kT)e(kT) - \alpha^2 d^T(kT)d(kT) \leq 0 \\ & \xi(k) = [\eta(kT)^T \quad d(kT)^T],\end{aligned} \tag{24}$$

$$
\begin{aligned}
&\triangle V(e(kT)) \\
&= E\left\{V(e(kT+T))|\xi(k)\right\} - V(kT) \\
&= E\left\{(D_m\eta(kT+T))^T P(D_m\eta(kT+T))|\xi(kT)\right\} \\
&\quad - \eta^T(kT)D_m^T P D_m\eta(kT) \\
&= E\left\{[(G_m\eta(kT+T)+B_m d(kT+T)]^T D_m^T P\right. \\
&\quad \left.\times\, D_m[G_m\eta(kT+T)+B_m d(kT+T)]|\xi(kT)\right\} \\
&\quad - \eta^T(kT)D_m^T P D_m\eta(kT) \\
&= E\left\{\xi(kT)^T \begin{bmatrix} G_m^T D_m^T \\ B_m^T D_m^T \end{bmatrix} P \begin{bmatrix} D_m G_m & D_m B_m \end{bmatrix} \xi(kT)|\xi(kT)\right\} \\
&\quad - \eta^T(kT)D_m^T P D_m\eta(kT) \\
&= \xi(kT)^T \left(\begin{bmatrix} G_m^T D_m^T \\ B_m^T D_m^T \end{bmatrix} P \begin{bmatrix} D_m G_m & D_m B_m \end{bmatrix} \right) \xi(kT) \\
&\quad - \eta^T(kT)D_m^T P D_m\eta(kT). \qquad (25)
\end{aligned}
$$

Since $V(e(kT)) \geq 0$, this implies

$$
\frac{\|e(kT)\|}{\|d(kT)\|} \leq \alpha \qquad (26)
$$

and

$$
\begin{aligned}
&e^T(kT)e(kT) - \alpha^2 d^T(kT)d(kT) \\
&= \xi^T(kT) \begin{bmatrix} D_m^T D_m & 0 \\ 0 & -\alpha^2 I \end{bmatrix} \xi(kT). \qquad (27)
\end{aligned}
$$

Then we have

$$
\begin{aligned}
&\xi^T(kT) \left(\begin{bmatrix} G_m^T D_m^T \\ B_m^T D_m^T \end{bmatrix} P \begin{bmatrix} D_m G_m & D_m B_m \end{bmatrix} \right. \\
&\left. - \begin{bmatrix} D_m^T P D_m & 0 \\ 0 & \alpha^2 I \end{bmatrix} \right) \xi(kT) \leq 0. \qquad (28)
\end{aligned}
$$

Form the Schur complement [4], we obtain the LMIs condition;

$$
\begin{bmatrix} P & * & * & * \\ 0 & -\alpha^2 I & * & * \\ \left(\frac{G_{m_{ijk}} D_m + G_{m_{ikj}} D_m}{2}\right) & B_m D_m & P^{-1} & * \\ -D_m & 0 & 0 & I \end{bmatrix} \geq 0 \qquad (29)
$$

■

By multiplying both sides of (29) by block-diag$[X\ I\ I\ I]$, (23) is obtained, where $X = P^{-1}$, the subscript $\{i, j, k\}$ is fuzzy filter rule each. The proof is completed.

IV. Simulation

In this section, we demonstrate the results in Section 3 to discretise the continuous-time T-S system for the moving target like the Van der Pol oscillator. We first the dynamic state equations in CT are given by

$$
\begin{aligned}
\frac{d}{dt}x_1(t) &= x_2(t) \\
\frac{d}{dt}x_2(t) &= -x_1(t) + (1 - x_1^2(t))x_2(t) + w(t) \\
y(t) &= (1 + 0.25x_1(t)) + v(t) \qquad (30)
\end{aligned}
$$

The corresponding T-S fuzzy model of the system in (30) is expressed as follows:

$$
\begin{aligned}
R_1 &: \text{IF } x_1(t) \text{ is about } \Gamma_{11}, \\
&\quad \text{THEN } \dot{x}(t) = A_1 x(t) + B_1 w(t), \\
&\qquad y(t) = C_1 x(t) + v(t). \\
R_2 &: \text{IF } x_1(t) \text{ is about } \Gamma_{12}, \\
&\quad \text{THEN } \dot{x}(t) = A_2 x(t) + B_2 w(t), \\
&\qquad y(t) = C_2 x(t) + v(t). \qquad (31)
\end{aligned}
$$

where A_i, B_i, C_i are by the following as

$$
\begin{aligned}
&A_1 = \begin{bmatrix} 0 & 1 \\ -1 & 1-k^2 \end{bmatrix}, \quad A_2 = \begin{bmatrix} 0 & 1 \\ -1 & 1 \end{bmatrix}, \\
&C_1 = \begin{bmatrix} 1 + 0.2k^2 & 0 \end{bmatrix}, \quad C_2 = \begin{bmatrix} 1 & 0 \end{bmatrix}, \\
&B_i = \begin{bmatrix} 0 & 1 \end{bmatrix}^T, \qquad i = 1, 2, \qquad (32)
\end{aligned}
$$

and the membership function are

$$
\Gamma_{11} = x_1^2/k^2, \quad \Gamma_{12} = 1 - x_1^2/k^2 \qquad (33)
$$

where $k = 2.5$.

First, we simulate the continuous-time T-S fuzzy system. To obtain the corresponding discretised T-S fuzzy system for the sampling time $T = 0.01(s)$, Theorem 1 is applied. The discretised version of the continuous-time T-S fuzzy system is

$$
\begin{aligned}
R_1 &: \text{IF } x_1(kT) \text{ is about } \Gamma_{11} \\
&\quad \text{THEN } x(kT+T) = \Phi_1 x(kT) + B_1 w(kT) \\
&\qquad y(kT+T) = C_1 x(kT) + v(kT) \\
R_2 &: \text{IF } x_2(kT) \text{ is about } \Gamma_{12} \\
&\quad \text{THEN } x(kT+T) = \Phi_2 x(kT) + B_2 w(kT) \\
&\qquad y(kT+T) = C_2 x(kT) + v(kT) \qquad (34)
\end{aligned}
$$

By using Theorem 1 and solving the corresponding LMIs constraints, we obtain the filter gains L and P:

$$
\begin{aligned}
&P = \begin{bmatrix} 0.0277 & -0.0050 \\ -0.0050 & 0.0036 \end{bmatrix}, \\
&L_1 = \begin{bmatrix} 0.1496 \\ 1.3159 \end{bmatrix}, \quad L_2 = \begin{bmatrix} 0.2187 \\ 1.7408 \end{bmatrix}. \qquad (35)
\end{aligned}
$$

V. Conclusion

In this paper, we has been proposed for the mixed-time fuzzy optimal estimator design for the target tracking. The proposed method has taken account of behavior for target motion in CT domain and system measurement in DT domain. The overall dynamic system in DT domain has discretized by using T-S fuzzy models. Based on the fuzzy model, the fuzzy estimation has been studied. The error state of the filtering process have mean square bounded. In addition, a basis dependent Lyapunov function approach has developed to design the fuzzy filter and a filter gain has minimized by

using some LMIs constraints. A numerical example have been provided to demonstrate various aspects of theoretical results.

REFERENCES

[1] S. N. Balakrishnan, "Extension to modified polar coordinates and application with passive measurements", *Journal of Guidance, Control and Dynamics*, vol. 12, no. 6, pp. 906-912, 1989.

[2] P. L. Vergez and K. L. Randall, "Target acceleration modeling for tactical missile guidance", *Journal of Guidance, Control and Dynamics*, vol. 7, no. 3, pp. 315-321, 1984.

[3] M. S. Grewal and A. P. Andrews, *Kalman filtering: theory and practice*, Prentice Hall, 1984.

[4] R. W. Cottle, *Manifestations of the Schur complement*, Linear Algebra and its Applications, 8(1974), pp. 189-211.

[5] X. R. Li, V. P. Jilkov, "Survey of Maneuveirng Target Tracking: Part 1:Dynamic Models", *IEEE Transactions of Aerospace and Electronic Systems*, vol. 39, no. 4, pp.1333-1364, 2003.

[6] Y. Bar-Shalom and K. Birmiwal, "Variable dimension filter for maneuvering target tracking", *IEEE Transactions of Aerospace and Electronic Systems*, vol. 18, no. 5, pp. 621-629, 1982.

[7] J. K. Tugnait, "Detection and estimation for abruptly changing systems", *Automatica*, vol. 18, no. 5, pp. 607-615, 1982.

[8] X. R. Li and V. P. Jilkov,"Survey of Maneuvering Trarget Tracking. Part I: Dynamic Models", *IEEE Transactions of Aerospace and Electronic Systems*, vol. 39, no. 4, pp. 1333-1364, 2003.

[9] H. A. P. Blom and Y. Bar-Shalom, "The interaction multiple model algorithm for systems with a jump-linear smoothing application", *IEEE Transactions on Automatic Control*, vol. 33, no. 8, pp. 780-783, 1988.

[10] Y. Bar-Shalomand and X. Li, *Principles, Techniques and Software* Norwood, MA: Arteck House, 1993

[11] A. Munir and D. P. Atherton, "Adaptive interacting multiple model algorithm for tracking a maneuvering target", *IEE Proc. Radar Sonar Navig.*, vol. 142, no. 1, pp. 11-17, 1995.

[12] H. J. Lee, H. Kim, Y. H, Joo, W., Chang, and J. B. Park, "A new intelligent disital redisign for T-S fuzzy systems: global approach", *IEEE Transactions Fuzzy Syst.*, vol. 12, no. 2, pp. 274-284, 2004.

[13] Z. Li, J. B. Park, and Y. H, Joo, "Chaotifying continuous-time T-S fuzzy systems via discretization", *IEEE Transactions Circuits Syst. I*, vol. 48, no. 10, pp. 1237-1243, 2001.

[14] L. L. Frank, X. Lihua and P. Dan, *Optimal and Robust Estimation*, CRC Press, 2007.

[15] K. Tanaka, T. Ikeda, and H. O. Wang, "Fuzzy Regulators and Fuzzy Observers", *IEEE Trans, Fuzzy Syst.*, vol. 6, no. 2, pp. 250-265, 1998

2011 IEEE International Conference on Fuzzy Systems
June 27-30, 2011, Taipei, Taiwan

Generalized Projective Synchroization of Time-Delayed Chaotic Systems via Sliding Adaptive Fuzzy Control

Negin Farzbod
Engineering Department
Imam Khomeini International University of Qazvin
Qazvin, Iran
negin.farzbod@ yahoo.com

Hassan Zarabadipour
Faculty of Electrical Engineering, Engineering Department
Imam Khomeini International University of Qazvin
Qazvin, Iran
H_zarabadi@ikiu.ac.i

Mahdi Aliyari Shoorehdeli
Faculty of Electrical & Computer Engineering,
Mechatronics Department
K. N. Toosi University of Technology
Tehran, Iran
Aliyari@eetd.kntu.ac.ir

Faezeh Farivar
Faculty of Engineering, Mechatronics Department
Science and Research Branch, Islamic Azad University
Tehran, Iran
f.farivar@srbiau.ac.ir

Abstract— **In this paper, generalized projective synchronization (GPS) of two time-delayed chaotic systems using sliding adaptive fuzzy control (SAFC) is investigated. The proposed method combines the advantages of the adaptive control, fuzzy systems and sliding mode control theory. Lyapunov stability theory is employed to guarantee the stability of error dynamics. Assuming that the parameters of the chaotic drive system are unknown, recursive least square (RLS) method is applied to estimate these unknown parameters. Simulation results show the validity and effectiveness of the proposed method for synchronization of two identical and nonidentical time-delayed chaotic systems.**

Keywords: Generalized Projective Synchronization, Time-Delayed Chaotic Systems, Adaptive Fuzzy Control

I. INTRODUCTION

Since Pecora and Carroll observed the synchronization of two identical chaotic systems under different initial conditions in 1990 [1], chaos synchronization has attracted many interests, especially in secure communication. Moreover, it has been widely explored in a variety of fields such as physical, chemical and ecological process [2]. In previous researches, different types of synchronization have been found in interacting chaotic systems, such as complete synchronization (CS) [1,3,4,5,6], projective synchronization (PS)[2], generalized synchronization (GS) [7,8,9,10], phase synchronization [11,12], anti-phase synchronization [13,14,15] and so on. In PS, the drive-response system synchronizes up to a constant scaling factor α . CS is a special case of PS at $\alpha = 1$, as well as anti-phase synchronization at $\alpha = -1$ [16].

Many various synchronization methods such as backstepping design [17], active control [18], nonlinear control [19], adaptive control [20] and adaptive fuzzy control [21] have been applied for chaos synchronization in low-dimensional systems such as Lorenz and Duffing systems [22]. Since low-dimensional chaotic signals can be easily detected, they are not suitable for applications such as secure communications [22]. But, because of the infinite-dimensional of time-delayed chaotic systems, they are safety for secure communications.

Since Mackey and Glass first observed chaos in time-delayed system [23], many researchers interested in time-delayed chaotic systems. After that, the synchronization of time-delayed chaotic systems is also investigated by many researchers.

A few works have been done on synchronization of time-delayed chaotic systems. The problem of CS [24,25] and GS [26] of time-delayed systems have been studied for some special models. PS has been proposed to synchronize identical Logistic delayed models [27]. Fuzzy delayed output feedback synchronization for time-delayed chaotic systems is studied, too [28]. Sliding mode controller is applied for projective synchronization of time-delayed systems in [29].

In this paper, sliding adaptive fuzzy control (SAFC) is proposed for generalized projective synchronization (GPS) of two identical and nonidentical time-delayed chaotic systems. Furthermore, synchronization of time-delayed chaotic systems with unknown parameters is studied. It is shown that the speed of synchronization is appropriate and the performance of the proposed controller is well when the response system designed with the estimated parameters of the drive system.

This paper is organized as follows: in section 2, the model of time-delayed chaotic systems and its properties are described. The structure of proposed controller constitutes section 3. Stability analysis is studied in section 4. Simulation

978-1-4244-7316-8/11/$26.00 ©2011 IEEE

results and conclusion are given in section 5 and 6, respectively.

II. MODEL OF SYSTEM

A class of time-delayed systems is considered as follows:

$$\dot{x}(t) = -ax(t) + f_b(x(t-\tau)) + u(t) \tag{1}$$

where, $x, u \in R$ are the state variable and control input, respectively. a, b, τ are the system parameters , $\tau \succ 0$. Time-delayed system in (1) can show chaotic behavior when the nonlinear function $f_b(.)$ satisfies the following conditions [30,31]:

$(i) f_b(0) = 0;$

$(ii) \forall x \quad x f_b(x) \geq 0;$

$(iii) \exists x_{eq} \succ 0 \quad f_b(x_{eq}) = x_{eq};$

$(iiii) \exists r \in (0, x_{eq}) : \forall x \quad f_b(x) \leq f_b(r) = M \quad , M \succ 0.$

Some time-delayed chaotic systems satisfied above conditions are Mackey-Glass, Ikeda and Logistic models. These models are given as

Mackey-Glass Model [30]

$$f_b(z) = \frac{bz}{1 + |z|^C} \quad (C \succ 1) \tag{2}$$

Ikeda model [30]

$$f_b(z) = \begin{cases} b\sin(z) & |z| \leq \pi \\ 0 & otherwise \end{cases} \tag{3}$$

Logistic model [31]

$$f_b(z) = \begin{cases} bz(1-z) & 0 \leq z \leq 1 \\ 0 & otherwise \end{cases} \tag{4}$$

In this paper, Mackey-Glass and Logistic models are studied.

III. GENERALIZED PROJECTIVE SYNCHRONIZATION VIA SLIDING ADAPTIVE FUZZY CONTROL

In this section, SAFC is designed to chaos synchronization of time-delayed chaotic systems.

Now, the drive and response systems are considered as follows:

$$\text{Drive:} \quad \begin{cases} \dot{x}(t) = -ax(t) + f_b(x(t-\tau)) \\ x(t) = \varphi_1 \quad -\tau \leq t \leq 0 \end{cases} \tag{5}$$

$$\text{Response:} \quad \begin{cases} \dot{y}(t) = -ay(t) + g_\beta(y(t-\theta)) + u \\ y(t) = \varphi_2 \quad -\theta \leq t \leq 0 \end{cases} \tag{6}$$

where $f_b(.)$ and $g_\beta(.)$ have the properties described in section 2. a, b, β are systems parameters, and τ, θ are time delays. φ_1, φ_2 are initial values of drive and response systems, respectively. Notice that, if synchronization of two identical systems is considered, then $f = g$. Also f is not equal to g for synchronization of two nonidentical systems. For GPS, the synchronization error is defined as follows:

$$e = \alpha x - y \tag{7}$$

where α is the scaling factor of GPS, then

$$\dot{e} = -\alpha a x(t) + a y(t) - g_\beta(y(t-\theta)) + \alpha f_b(x(t-\tau)) - u \tag{8}$$

It is assumed that $f_b(.)$ and $g_\beta(.)$ are bounded and α is known. The control signal is defined as

$$u = u_1 + u_2 \tag{9}$$

Where u_2 is the output of fuzzy controller and u_1 is determined as follows

$$u_1 = -\alpha a x(t) + a y(t) - g_\beta(y(t-\theta)) + \alpha f_b(x(t-\tau)) \tag{10}$$

To design the proposed controller u_2, GD is applied to train the parameters of fuzzy controller. In the proposed method, minimizing the first derivation of Lyapunov function is considered, so that the stability is achieved. This derivation is applied as a cost function to determine unknown parameters utilized to design of the control system.

Sliding surface is defined as follows:

$$s = e = \alpha x - y \tag{11}$$

The fuzzy system used in this study has product inference engine, singleton fuzzifier, center average defuzzifier, and Gaussian membership function. So, the fuzzy system is given as

$$u_2 = \frac{\sum_{l=1}^{E} w^l \left[\prod_{i=1}^{n} \exp(-(\frac{s - c_i^l}{\sigma})^2) \right]}{\sum_{l=1}^{E} \left[\prod_{i=1}^{n} \exp(-(\frac{s - c_i^l}{\sigma})^2) \right]} = \hat{W}^T \phi \qquad (12)$$

where $\hat{W} = [w^1, ..., w^n]^T$, E is fixed, w^l, c_i^l and σ are free parameters. $s \in R^n$ is the input of the fuzzy system, and $u_2 \in R$ is the output of the fuzzy system. w^l is the center of fuzzy set. Parameters c_i^l and σ are centers and radius of basis function, respectively. In this paper, c_i^l and σ are chosen arbitrarily. Since this fuzzy system is considered with one input, n is equal to 1. To design the controller, the parameter w^l must be determined based on the reaching condition, $s\dot{s} < 0$. Thus, the GD method is applied to determine it as follows:

$$\dot{w}^l = -\gamma \frac{\partial s(t)\dot{s}(t)}{\partial w^l(t)} \qquad (13)$$

Equation (13) can be rewritten as

$$\begin{aligned} \dot{w}^l &= -\gamma \frac{\partial s(t)\dot{s}(t)}{\partial w^l(t)} = -\gamma \frac{\partial s(t)\dot{s}(t)}{\partial u(t)} \frac{\partial u(t)}{\partial w^l(t)} \\ &= -\gamma \frac{\partial s(t)\dot{s}(t)}{\partial u_2(t)} \frac{\partial u_2(t)}{\partial w^l(t)} \\ &= \gamma s(t) \frac{\exp(-(\frac{s - c^l}{\sigma})^2)}{\sum_{l=1}^{E} \exp(-(\frac{s - c^l}{\sigma})^2)} = \gamma s(t) \phi_l(s) \end{aligned} \qquad (14)$$

where γ is the learning rate parameter. Finally, w_i can be on-line adjusted as it is shown in (14).

Now, with defined control signal the synchronization is achieved. In the next section, the stability of the control system is investigated.

IV. STABILITY ANALYSIS

Lyapunov stability analysis is applied to prove the stability of error dynamics. From the theory of sliding mode control and (8), a perfect control law is obtained as

$$u_{eq} = -\dot{e} + \dot{s} + \lambda s \qquad (15)$$

where is presented in (11).

First, to analyze the stability, (9) and (10) are substituted in (8):

$$\dot{e} = -u_2 \qquad (16)$$

If u_2 is substituted with u_{eq} then $\dot{s}(t) + \lambda s(t) = 0$. Since λ is a positive constant parameter, the sliding surface variable s will converge to zero, gradually. So, will converge to zero. From (15) and (16):

$$\dot{s}(t) = -\lambda s(t) + (u_{eq} - u_2) \qquad (17)$$

Theorem [32]. *Suppose that the input universe of discourse U is a compact set in R^n. Then, for any given real continuous function $g(z)$ on U and arbitrary $\xi \succ 0$, there exists a fuzzy system $F(z)$ in the form of (10) such that*

$$\sup_{z \in U} \left\| g(z) - F(z) \right\| \le \xi$$

That is, the fuzzy systems with product inference engine, singleton fuzzifier, center average defuzzifier, and Gaussian membership functions are universal approximators.

Therefore, the control law u_2 can be btained via the optimal weighting vector $\overline{W}$ of the fuzzy system. The designed control is applied to estimate the u_{eq}. This approximation can be achieved with the error which is smaller than ξ

$$\max \left| \overline{u}(x, \overline{W}) - u_{eq}(x) \right| \prec \xi$$

where $\overline{u}(x, \overline{W}) = \sum_{k=1}^{n} \overline{w}_k \phi_k = \overline{W}^T \phi$ and $u_{eq}(x) = \overline{W}^T \phi + \xi$.

Define $\tilde{W} = \overline{W} - \hat{W}$ as the weighting error, and then (17) can be rewritten as

$$\dot{s}(t) = -\lambda s(t) + (\tilde{W}^T \phi + \xi) \qquad (18)$$

Notice that $\overline{W}$ and $\hat{W}$ are the optimal and estimated values of W, respectively.

Define the Lyapunov function as follows:

$$V(s, \tilde{W}) = \frac{1}{2} s^2 + \frac{1}{2\gamma} \tilde{W}^T \tilde{W} \qquad (19)$$

The first derivation of (19) with respect to time is obtained as

$$\dot{V} = s\dot{s} + \frac{1}{\gamma}\tilde{W}^T\dot{\tilde{W}} = s\dot{s} + \frac{1}{\gamma}\tilde{W}^T(-\dot{\hat{W}}) \quad (20)$$

Substituting (14) and (18) in to (20), then

$$\dot{V} = s(-\lambda s + \tilde{W}^T\phi + \xi) + \frac{1}{\gamma}\tilde{W}^T(-\gamma s\phi) = -\lambda s^2 + s\xi \quad (21)$$

Thus

$$\dot{V} \le |s|(-\lambda|s| + \xi) \quad (22)$$

So, if $|s| \ge \xi/\lambda$, then $\dot{V} \le 0$ which means that this Lyapunov function will decrease gradually. It can be concluded that the error of state variable will converge into a boundary layer ξ/λ around $e = s = 0$ in the phase plane.

Hence, the SAFC is stable and the error of state variable will converge into a small value.

V. SIMULATION RESULTS

A. Synchronization of two identical systems with known parameters

To synchronize two identical Mackey-Glass systems, the parameters of drive and response systems are chosen as $a = 1, b = 2, \varphi_1 = 0.1, \varphi_2 = 0.01, \tau = 10, \theta = 10$, and it is assumed that $\alpha = 0.5$ Fig. 1a,b shows the state trajectory of drive and response systems. Fig. 1c shows the phase plane $(\alpha x, y)$ and Fig. 1d shows the synchronization error.

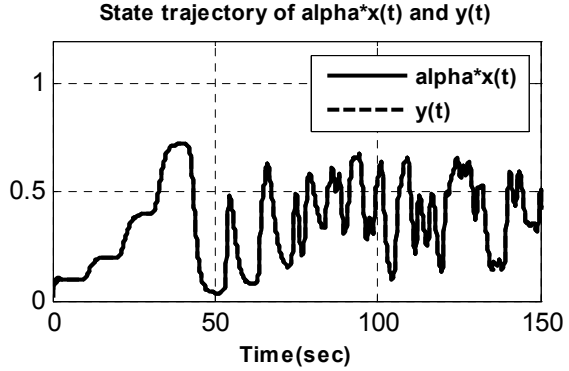

(a)

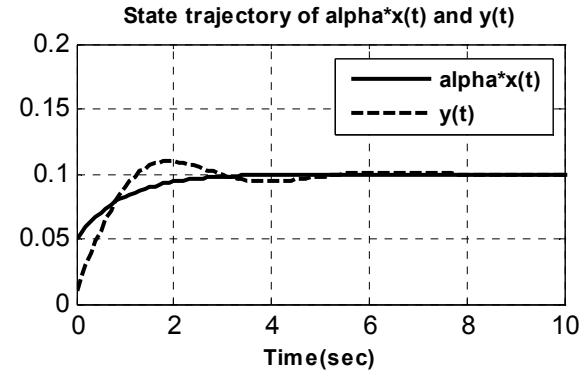

(b)

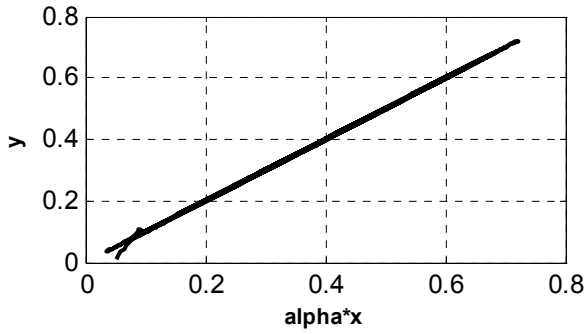

(c)

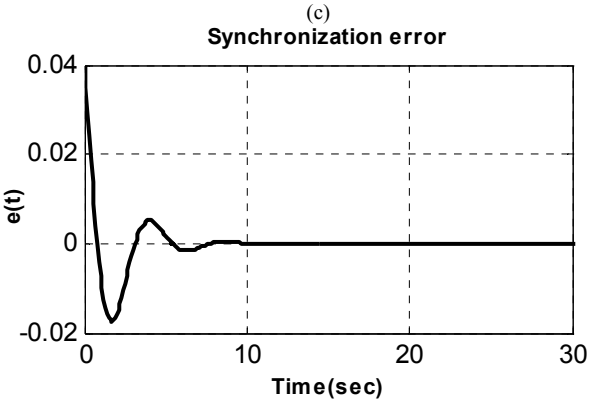

(d)

Figure 1. The state trajectory of Mackey-Glass system: (a, b) drive and response systems; (c) the phase plane; (d) the synchronization error.

B. Synchronization of two nonidentical systems with known parameters

In this section, Mackey-Glass and Logistic models are chosen as drive and response systems, respectively. The parameters of two considered systems are $a = 1, b = 2, \varphi_1 = 0.1, \quad \varphi_2 = 0.01, \tau = 20, \theta = 20$, and it is assumed that $\alpha = 0.5$. Fig. 2a,b shows the state trajectory of drive and response systems, Fig. 2c shows the phase plane $(\alpha x, y)$ and Fig. 2d shows the synchronization error.

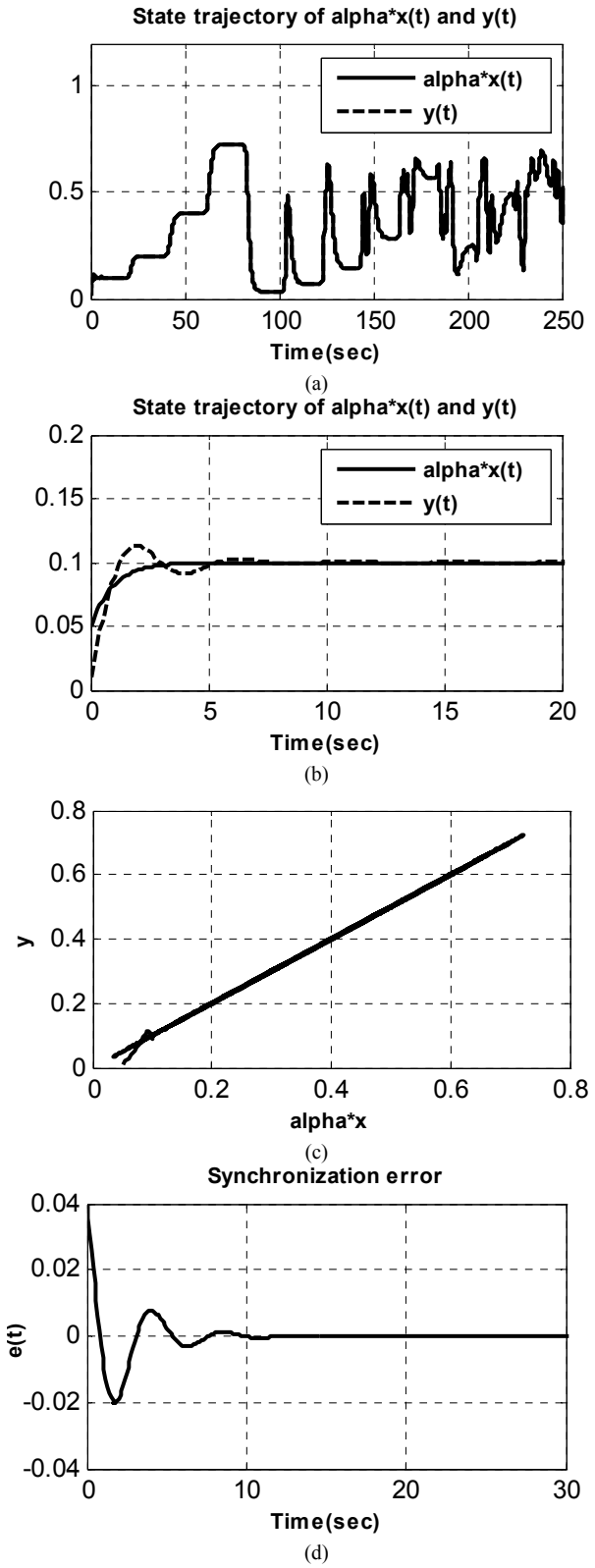

Figure 2. The state trajectory of Mackey-Glass and Logistic systems: (a, b) drive (Mackey-Glass) and response (Logistic) system; (c) the phase plane; (d) the synchronization error.

C. *Synchronization of two identical systems with unknown parameters*

In this section, synchronization is studied when the drive system has unknown parameters with known nonlinear part. To design a response system, the estimated parameters of the drive system is used. Mackey-Glass model is chosen as drive and response systems. The parameters of drive system are $a = 1, b = 2, \varphi_1 = 0.1, \tau = 10,$ and for response system, the parameters are considered as $\varphi_2 = 0.01, \theta = 10$ and it is assumed that $\alpha = 0.5$.

The recursive least square (RLS) method is applied to estimate $\hat{a}$, $\hat{b}$. Note that the estimated parameters affect the $s(t)$. The initial values of $\hat{a}, \hat{b}$ are considered as 0.1 and 0.5, respectively. Fig. 3a,b shows the state trajectory of drive and response systems, Fig. 3c shows the phase plane $(\alpha x, y)$, and Fig. 3d shows the synchronization error. The convergence of parameters $\hat{a}, \hat{b}$ to their actual values are shown in Figs. 5a and 5b.

In this section, the performance of SAFC for synchronization of delayed chaotic systems is compared with fuzzy model-based adaptive synchronization of time-delayed chaotic systems proposed in [22]. In this method, to design the fuzzy controller, the chaotic system is modeled by Takagi Sugeno fuzzy system considering the properties of the nonlinear part of the system [22].

Define $h_1(x)$ and $h_2(x)$ as

$$h_1(x) = \begin{cases} \dfrac{f(x)}{x} & x \neq 0 \\ 0 & x = 0 \end{cases} \tag{23}$$

$$h_2(x) = 1 - h_1(x) \tag{24}$$

The adaptation laws for $\hat{a}_i$ and $\hat{b}_i$ are chosen as

$$\dot{\hat{a}}_i = -\frac{h_i e(t) y(t)}{p_i} \tag{25}$$

$$\dot{\hat{b}}_i = \frac{h_i e(t) y(t-\tau)}{q_i} \tag{26}$$

where $p_i, q_i > 0$ (Vasegh and Johari Majd, 2009).

The parameters of Mackey-Glass model with the both controllers are assumed as it is considered in this section. Furthermore, we choose $p_i = q_i = 1/220, a_s = 10$ .The initial values of $\hat{a}, \hat{b}$ are chosen as 0.1 and 0.5, respectively. Simulation results are shown in Figs.4 and 5. From Figures.3,4 and 5, it is concluded that SAFC is better than the other considered method for chaos synchronization of two identical systems when the drive system has unknown parameters. The convergence of parameters with SAFC is faster and smoother than that with fuzzy model-based adaptive control. In summary, it is concluded that the speed of synchronization with the proposed method is better than that with fuzzy model-based adaptive control and it is an advantage of SAFC. Notice that the speed of synchronization with SAFC can be controlled and improved.

For better comparison, the performance of two considered controllers is compared with the following criteria:

1. Synchronization error variance after 10τ (EV).
2. Synchronization error settling time. It is the time at which $|e| < 0.005$ and e remains in this bound (EST).

As we know, the less the EV, the better synchronization is achieved. The less the EST, the sooner is the convergence. The results of these comparisons are given in Table 1.

It is resulted that SAFC performs better than fuzzy model-based adaptive control. Notice that the best performance of fuzzy model-based adaptive control was considered.

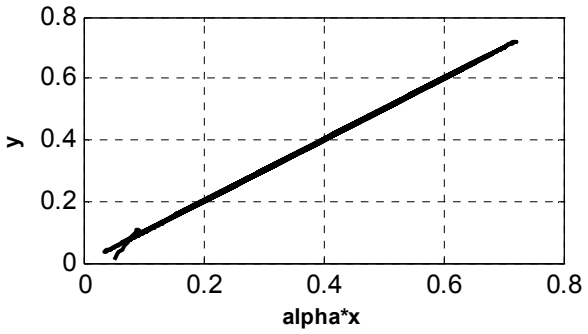

(c)

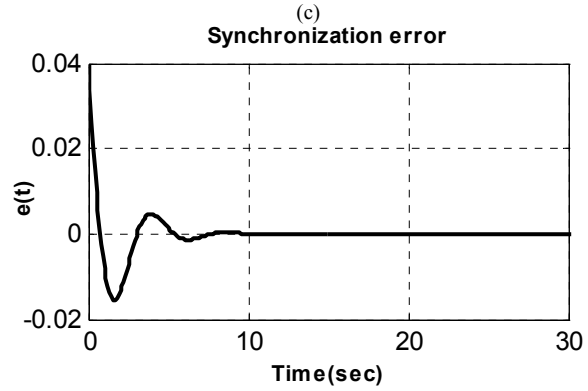

(d)

Figure 3. The state trajectory of two identical Mackey-Glass systems with SAFC: (a, b) drive and response systems; (c) the phase plane; (d) the synchronization error.

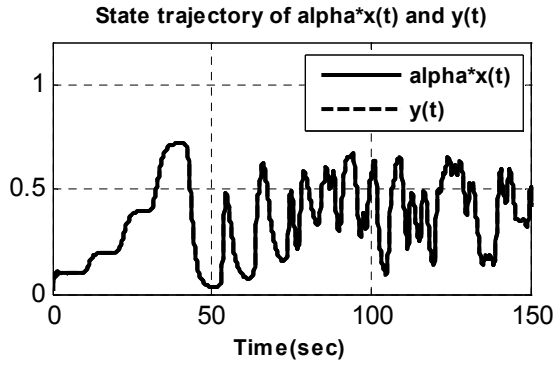

(a)

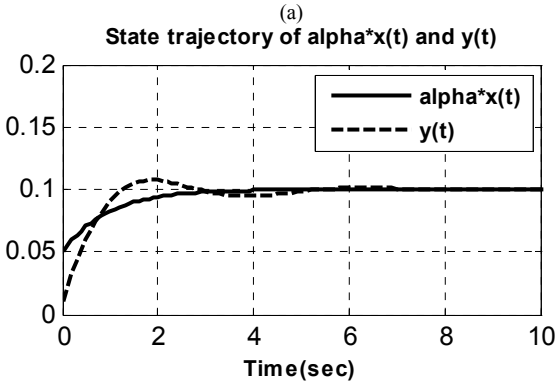

(b)

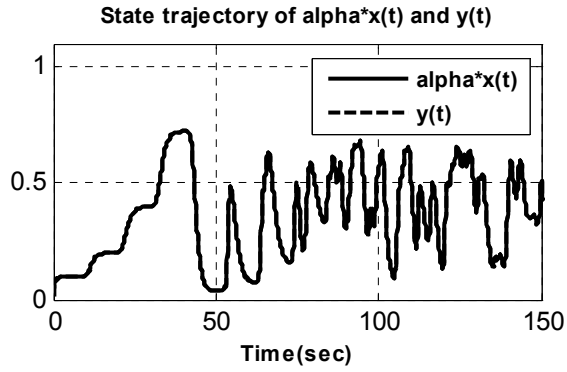

(a)

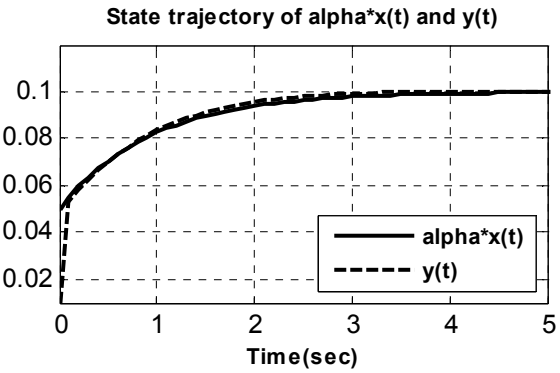

(b)

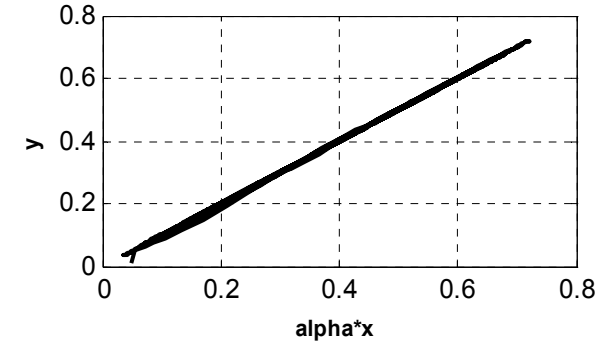

(c)

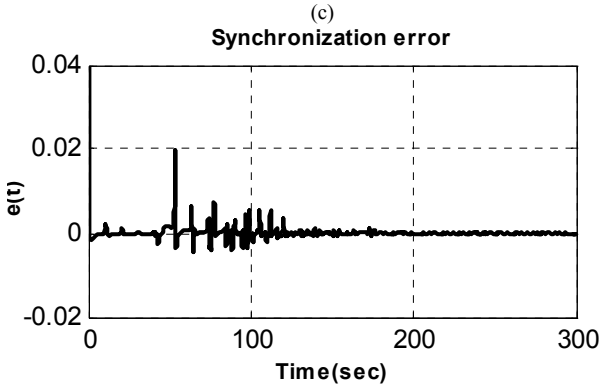

(d)

Figure 4. The state trajectory of two identical Mackey-Glass systems with FMBAC: (a, b) drive and response systems; (c) the phase plane; (d) the synchronization error.

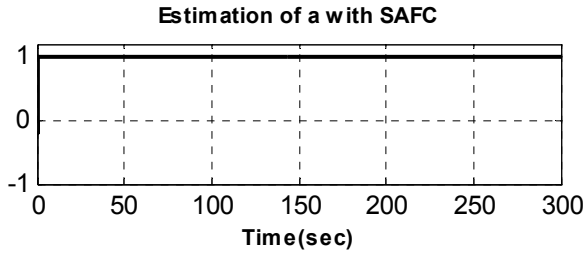

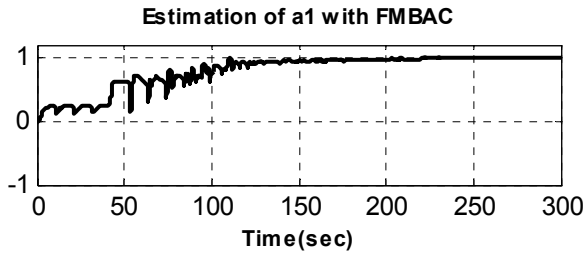

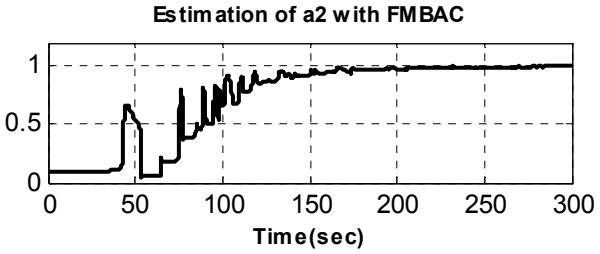

(a)

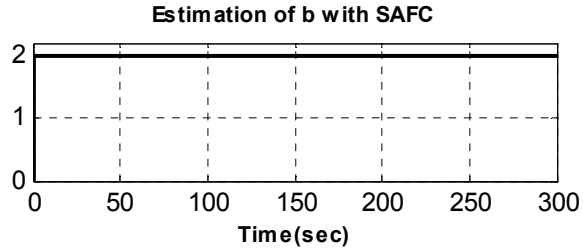

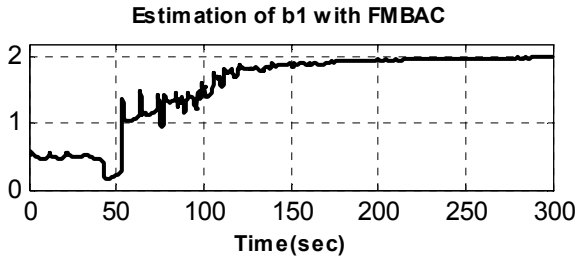

(b)

Figure 5. Estimation of parameters: (a) $\hat{a}$, $\hat{a}_1, \hat{a}_2$ (b) $\hat{b}, \hat{b}_1$ for Mackey-Glass model.

TABLE I. COMPARISONS BETWEEN DIFFERENT METHODS OF SYNCHRONIZATION

Criterion	Control Method	
	SAFC	***FMBAC***
EV	1.21e-15	2.18e-7
EST(sec)	2.7	112.1

VI. CONCOLUSION

In this paper, an effective control method was used for synchronization of scalar time-delayed chaotic systems. Using the Lyapunov stability theory, a sliding mode controller based on the fuzzy system was applied for synchronization of two identical and nonidentical chaotic systems. When synchronization with unknown parameters was considered, the drive system had unknown parameters with known nonlinear part. To design a response system, the estimated parameters of the drive system was used. Numerical simulations for Mackey-Glass and Logistic models are provided to show the effectiveness and feasibility of the proposed controller. The convergence of parameters to their actual values with SAFC is faster than that with FMBAC. These results are obtained from comparisons of these two methods with two criteria which show the quality of the performance of the control system.

REFERENCES

[1] L. M. Pecora, T. L.Carroll, "Synchronization in Chaotic Systems," Phys. Rev. Lett, vol. 64, p. 821, 1990.

[2] G. Chen, X. Dong, From chaos to order: Methodologies, Perspectives and applications, World Scientific, Singapore, 1998.

[3] H. T. Yau, "Design of adaptive sliding mode controller for chaos synchronization with uncertainties," Chaos Solitons & Fractals, vol. 22, p. 341, 2004.

[4] S. Bowong, "A new adaptive chaos synchronization principle for a class of chaotic systems," Int .J. Nonlinear Sci. Numerical Simulation, vol. 6, p. 399, 2005.

[5] J. H. Park, "Adaptive synchronization of a unified chaotic system with an uncertain parameter," Int .J. Nonlinear Sci. Numerical Simulation, vol. 6, p. 201, 2005.

[6] H. T. Yau, C. L. Kuo, J. J. Yan, "Fuzzy sliding mode control for a class of chaos synchronization with uncertainties," Int .J. Nonlinear Sci. Numerical Simulation, vol. 7, p. 333, 2005.

[7] Y. W. Wang, Z. H. Guan, "Generalized synchronization of continuous chaotic system," Chaos Solitons & Fractals, vol. 27, p. 97, 2006.

[8] K. Murali, M. Lakshmanan, "Secure communication using a compound signal from generalized synchronizable chaotic systems," Phys. Lett. A, vol. 241, p. 301, 1998.

[9] S. S. Yang, C. K. Duan, "Generalized synchronization in chaotic systems," Chaos Solitons & Fractals, vol. 10, p. 1703, 1998.

[10] L. Kocarev, U. Parlitz, "Generalized Synchronization, Predictability, and Equivalence of Unidirectionally Coupled Dynamical Systems," Phys. Rev. Lett, vol. 76,p. 1816, 1996.

[11] G. Santoboni, A. Y. Pogromski, H. Nijmeijer, "An observer for phase synchronization of chaos," Phys. Lett. A, vol. 291, p. 265, 2001.

[12] M. Rosenblum, A. Pikovsky, J. Kurths, "Phase synchronization of chaotic oscillators," Phys.Rev. Lett, vol. 76, p. 1804, 1996.

[13] G. H. Li, S. P. Zhou, "An observer-based anti-synchronization," Chaos Solitons & Fractals, vol. 9, p. 495, 2006.

[14] G. H. Li, "Synchronization and anti-synchronization of colpitts oscillators using active control," Chaos Solitons & Fractals, vol. 26, p. 87, 2005.

[15] J. Hu, S. Chen, L. Chen, "Adaptive control for anti-synchronization of Chua's chaotic system," Phys. Lett. A, vol. 339, p. 455, 2005.

[16] H. T. Yau, "Generalized projective synchronization of gyroscope systems subject to dead-zone nonlinear inputs," Phys. Lett. A, vol. 372, p. 2380, 2008.

[17] G. Tan, J. Zhang, Y. Yang, "Synchronizing chaotic systems using backstepping design," Chaos Solitons & Fractals, vol. 16, pp. 37-45, 2003.

[18] M. C. Ho, Y. C. Hung, "Synchronization of two different systems by using generalized active control," Phys. Lett. A, vol. 301, pp. 424-428, 2002.

[19] L. Huang, R. Feng, M. Wang, "Synchronization of chaotic systems via nonlinear control," Phys. Lett. A, vol. 320, pp. 271-275, 2004.

[20] S. Chen, J. Lu, "Synchronization of an uncertain chaotic system via adaptive control," Chaos Solitons & Fractals, vol. 14, pp. 643-647, 2002.

[21] N. Vasegh, V. Johari Majd, "Adaptive fuzzy synchronization of discrete-time chaotic systems," Chaos Solitons & Fractals, vol. 28, pp. 1029-1036, 2006.

[22] N. Vasegh, V. Johari Majd, "Fuzzy model-based adaptive synchronization of time-delayed chaotic systems," Chaos Solitons & Fractals, vol. 40, pp. 1484-1492, 2009.

[23] M. Mackey, L. Glass, "Oscillation and chaos in physiological control system," Science, vol. 197, pp. 287-289, 1977.

[24] B. Mensour, A. Longtin, "Synchronization of delay-differential equations with application to private communication," Phys. Lett. A, vol. 244, pp. 59-70, 1998.

[25] K. Pyragas, "Synchronization of coupled time-delay systems: analaytical estimations," Phys. Rev. E, vol. 58, pp. 3067-3071, 1998.

[26] M. Zhan, X. wang, X. Gong, G. W. Wei, C. H. Lai, "Complete synchronization and generalized synchronization of one-way coupled time-delay systems," Phys. Rev. E, vol. 68, pp. 36208-3621, 2003.

[27] C. F. Feng, Y. Zhang, J. T. Sun, W. Qi, Y. H. Wang, "Generalized projective synchronization in time-delayed chaotic systems," Chaos Solitons & Fractals, vol. 38, pp. 743-747, 2008.

[28] K. A. Choon, "Fuzzy delayed output feedback synchronization for time-delayed chaotic systems," Nonlinear Analysis: Hybrid Systems, vol. 4, pp. 16-24, 2010.

[29] N. Vasegh, F. Khellat, "Projective synchronization of time-delayed systems via sliding mode controller," Chaos Solitons & Fractals, vol. 42, pp. 1054-1061, 2009.

[30] Y. C. Tian, F. Gao, "Simple delay systems with chaotic dynamics," IEEE CDC, pp. 319-320, 1997, St. Petersburg, Russia.

[31] Y. C. Tian, F. Gao, "Adaptive control of chaotic continuous-time systems with delay," Physica D, vol. 117, pp. 1-12, 1998.

[32] L. X. Wang, A Course in Fuzzy Systems and Control, Prentice-Hall International, Inc, p. 124, 1997.

2011 IEEE International Conference on Fuzzy Systems
June 27-30, 2011, Taipei, Taiwan

Knowledge Management, Education and Firm's Performance

Yen-Tzu Chen
Department of Business and Management
National University of Tainan, Taiwan
yentzufl@gmail.com

Yun-Chia Yan
Department of Accounting
University of New Orleans
New Orleans,US
yyan1@uno.edu

Hsiao-Wen Huang
Department of Information Management
Chang Jung Christian University, Taiwan
victoria@mail.cjcu.edu.tw

Hua-Wei Huang
Department of Accounting and Business Law,
State University of New York at Old Westbury, US
huangh@oldwestbury.edu

***Abstract* - In this paper, we examine how new CIO's education affects the association between knowledge management and firm's operating performance. Using OLS regression analysis, we find that the positive relationship between the effectiveness of knowledge management and firm's operating performance is more prominent when the firm's new CIO has a PHD degree. Our results therefore provide evidence that CIO's education facilitates the application of knowledge management.**

Keywords - Knowledge Management, Education, Performance

Data Availability - Data is publicly available.

I. INTRODUCTION

Early studies indicate that effective knowledge management is positively associated with firm's value and operating performance [1, 2, 3]. Recent studies further suggest that individual level innovation may lead to knowledge management success in an organization (e.g. [4]). Extending from these findings, the purpose of this study is to expand the knowledge management literature by investigating how individual's professional ability affects the association between the effectiveness of knowledge management and firms' operating performance. More specifically, we examine the impact of new CIO's education on the association between the level of research and development expenses and firm's financial performance measurements.

By using OLS regression analysis on a sample of 103 firms that appointed new CIO from 2007 to 2008, we find that the positive relationship between the effectiveness of knowledge management and firm's operating performance is more prominent when the firm's new CIO has a PHD degree. Our study contributes to the knowledge management literature by providing empirical evidence that CIO's education facilitates the application of knowledge management. To our knowledge, this is the first study showing the CIO's education has influences on firms' knowledge and financial performance. Our study should therefore be of interest to researchers and academia since it provides evidence to suggest that education of the management plays a significant role in enhancing the knowledge management process and firm's financial performance.

The remainder of this paper is organized as follows. Section 2 discusses prior research and hypothesis development. Section 3 presents the research design. Section 4 describes the sample selection process. Section 5 presents the empirical results and Section 6 provides the conclusion and limitations.

II. PRIOR RESEARCH AND HYPOTHESIS DEVELOPMENT

A. Knowledge Management, Firm's Value and Operating Performance

Extant research shows that effective knowledge management has a positive effect on firm's value and financial performance. [1] examine the short-term impact of announcements of information technology based knowledge management efforts on firm value and find that firms' cumulative abnormal returns are positively associated with these knowledge management events. [2] investigates how knowledge management capability affects firm performance and suggests that the synergies created by the information technology relatedness and managerial knowledge resources increase the financial performance of the firm. [3] explore the introduction of knowledge management practices and find that these practices are able to improve firm's performance. In summary, firm's effective knowledge management is found to be associated with better financial performance.

B. Knowledge Management, CIO and Education

Prior research shows that hiring new managers with MBA degrees leads to short-term improvements in operating performance [5] and management change is an important factor of business performance [6]. Besides, education level is often employed as a measurement for intellectual capital in empirical research [7]. Knowledge management is largely driven by the information technology department, where CIO plays a critical role in the entire process. CIO is responsible to integrate firm's limited information technology resources as well as human capitals. In addition, CIO has to combine business operation and e-commerce for future knowledge formations, sharing and applications. Especially in today's global economy and complex business environment, the education level of CIO should be a suitable proxy for firm's ability of knowledge creation and innovation.

978-1-4244-7316-8/11/$26.00 ©2011 IEEE

[4] further suggest that individual's conceptual knowledge increases operational and contextual knowledge, and in turn improves operational knowledge. Since individual knowledge innovation is documented to help organizations to be more productive, CIO with better education should be more innovative in facilitating the effectiveness of knowledge management process and therefore enhances firm's financial performance.

C. Hypothesis Development

Since effective knowledge management has a positive effect on firm's performance, and better education of CIO is expected to strengthen this effect, we thus develop the following research hypothesis:

H: *The positive relationship between the effectiveness of knowledge management and firm's operating performance is more prominent when the firm's new CIO has a PHD degree.*

III. RESEARCH DESIGN

A. OLS Regression Test

We use a multivariate OLS regression model to test the impact of new CIO's education on the association between the effectiveness of knowledge management and firm's financial performance measurements. The effectiveness of knowledge management is measured by the level of research and development expenses in this study. The level of support for research and development activities has been documented as a major influencing factor (knowledge generation) of successful knowledge management process and infrastructure [8]. Additionally, [3] find that there is a positive relationship between the development of an innovative culture that encourages research and development projects and firm performance. Prior research also show that the level of research and development may decide the competitive advantage of firms in terms of higher quality, reduced cycle time and lowered costs [9]. In addition, a company invests lower research and development outlay than its competitors is more likely to lose its competitiveness of products and services which will shortly be reflected in its operating performance [10]. Further, [10] finds that firms experience a consistent five-year positive operating performance as well as positive stock returns following their research and development expenditures increase. Therefore, we expect that any new management occurring in IT firms will utilize IT advantages through promoting research and development use. In this study, we investigate whether new CIO with a PHD degree enhances individual level innovation in an organization and in turn strengthens the positive relationship between research and development projects and firm performance. Based on prior research, we also control for traditional variables related to firm's financial performance (e.g., [8, 10, 11]). We therefore use the following logistic regression model:

$$Performance = \alpha + \beta_1 NI/REV + \beta_2 RESTR + \beta_3 LEV + \beta_4 SQSEG + \beta_5 GROWTH + \beta_6 PHD + \beta_7 RD/REV + \beta_8 PHD*RD/REV + \varepsilon \quad (1)$$

Performance is measured by the following financial variables:
EPSDiluted = Diluted earnings per share[1];
EPSBasic = Basic earnings per share[2];
ROA = Returns on assets.

Control variables include:

NI/REV = Net income ratio measured by net income over total revenues;
RESTR = 1 if firm had restructuring, 0 otherwise;
LEV = Percentage of total debts over total assets;
SQSEG = Square root of the number of business segments reported on *Compustat*;
GROWTH = Sales growth (percent change in sales from prior year);
PHD = 1 if the new CIO has a PHD degree, else 0;
RD/REV = Ratio of research and development expense to total revenues;
*PHD*RD/REV* = Interaction of research and development activities and CIO's education.

We used several measures of financial performance to investigate our research question, resulting in three separate OLS regression models. We first control the company's profitability (NI/REV) which is expected to have positive influence on financial performance. Consistent with prior research, we use RESTR and LEV to proxy for firm's financial condition. Rapidly growing firms (GROWTH) and firms with diverse operations (SQSEG) which have higher business risks are also controlled. The positive effect of research and development expense on firm's performance is also controlled [3, 9, 10]. For our variable of interest, we expect CIO's better education may facilitate the effectiveness of research and development activities so the coefficient of PHD*RD/REV is positive.

IV. SAMPLE SELECTION PROCEDURES

We select our sample of 103 firms hiring new CIO reported in *AuditAnalytics* in the recent two years. The sample includes firms satisfying the following criteria: (1) the firm has CIO turnover data for 2007 and 2008 (2) the CIO's education data is presented, and (3) financial data are available on *Compustat*.

[1] This item represents basic earnings per share for common shares after allowing for the conversion of convertible senior stock and debt, and the exercise of warrants, options and agreements for issuance of common shares upon satisfaction of certain conditions.

[2] The basic earnings figures should be reported by the company (as outlined in Accounting Principles Board Opinion No. 15) after the effect of conversion of convertible preferred, convertible debentures and option and warrants that have been identified as common/ordinary stock (capital) equivalents and before extraordinary items.

Table 1 reports the sample distribution by industry. The 103 sample firms span several two-digit SIC codes, with the maximum number of firms being 30 (29.1%) in the computers industry.

< Insert Table 1 here >

V. Empirical Results

A. Descriptive Statistics

Table 2 reports the means, medians and standard deviations of the variables for our sample firms[3]. The means and medians of research and development level are 0.30 and 0.02, respectively.

< Insert Table 2 here >

In table 3, the descriptive data of research and development level is reported separately in two groups: CIO with a PHD degree and CIO without a PHD degree. The means and medians of research and development level in PHD group (non-PHD group) are 0.63 (0.28) and 0.11 (0.01), respectively. Table 3 also reports univariate tests of differences between the two groups using the parametric t-test and the Wilcoxon ranksum test. The median of research and development level is significantly higher in the PHD group than the non-PHD group ($p=0.01$, two-tailed). This is consistent with our expectation that CIO with a higher degree facilitates effective knowledge management applications.

< Insert Table 3 here >

B. Logistic Regression Results

Table 4 reports the OLS regression results for our three models. Model 1 measures financial performance using diluted earnings per share. Model 2 uses basic earnings per share, and Model 3 uses the returns on assets. All the three models are significant at $p < 0.01$ (two-tailed) and show satisfactory R-squares.

The interactive variable *PHD*RD/REV* is significantly positive at $p < 0.10$ (two-tailed) in all the three models. The variable *RD/REV* is also positively significant at conventional levels. The significantly positive coefficients indicate that the level of research and development benefits firm's financial performance and this relationship is further strengthened by the CIO's education level. This empirical result is consistent with our hypothesis.

Consistent with our expectations, NI/REV is significant and positive at $p < 0.01$ (two-tailed) in all the models. Besides, RESTR is negatively significant in model 1 and model 2 showing higher business risks may result in poorer financial outcomes.

< Insert Table 4 here >

VI. Conclusion and Limitations

In this paper, we examine how new CIO's education affects the association between knowledge management and firm's operating performance. Using OLS regression analysis, we find that the positive relationship between the effectiveness of knowledge management and firm's operating performance is more prominent when the firm's new CIO has a PHD degree. Our results therefore provide empirical evidence that CIO's education facilitates the application of knowledge management, which is never explored in prior studies.

Our study is subject to several limitations. First, while we control for factors we believe are associated with firm's financial performance in our models, there is still a possibility of omitted variables. Second, the power of our tests is subject to the small sample size of firms with available CIO and education data. Third, around one-third of our sample firms are in computer industry. The uneven distribution of numbers of company types may lead to sample selection bias. Future research could investigate if CIO education has similar effects on the other knowledge management proxies.

[3] In order to eliminate the outlier effects, we winsorize 5% for all control variables.

References

[1] Sabherwal R., S. Sabherwal. 2005. Knowledge management using information technology: Determinants of short-term impact on firm value. *Decision Sciences*: Vol. 36, Iss. 4; p. 531-548.

[2] Tanriverdi H. 2005. Information technology relatedness, knowledge management capacity, and performance of multi-business firms. *MIS Quarterly*: Vol. 29, Iss. 2; p. 311-335.

[3] Marqués D. P., F. J. G. Simón. 2006. The effect of knowledge management practices on firm performance. *Journal of Knowledge Management*: Vol. 10, Iss. 3; p. 143.

[4] Muhammed S., W. J Doll, X. Deng. 2009. A model of interrelationships among individual level knowledge management success measures. *International Journal of Knowledge Management*: Vol. 5, Iss. 1; p. 1-16.

[5] Bhagat S., B. J. Bolton and A. Subramanian. 2010. CEO education, CEO turnover, and firm performance. Working Paper at SSRN: http://papers.ssrn.com/sol3/papers.cfm?abstract_id=1670219.

[6] Muravyev, A. (2003). Turnover of senior managers in Russian privatised firms. *Comparative Economic Studies*: 45: 148-172.

[7] Barro, R. and J-W. Lee. 2010. A new data set of educational attainment in the world, 1950-2010, National Bureau of Economic Research: Working Paper.

[8] Zaim H., E. Tatoglu, S. Zaim. 2007. Performance of knowledge management practices: a causal analysis. *Journal of Knowledge Management*: Vol. 11, Iss. 6; p. 54.

[9] Mendelson, H. (2000). Organizational architecture and success in the information technology industry. *Management Science*: 46 (4): p. 513-529.

[10] Tubbs, M. 2007. The relationship between R&D and company performance. *Research Technology Management*: Vol. 50, Iss. 6; p. 23-31.

[11] Ohlson J. (1995). Earnings, book value, and dividends in security valuation. *Contemporary Accounting Research* 11: 161-82.

Table 1: Distribution of Sample Firms				
By Industry: Defined by SIC Code		N		%
Mining and Construction (1000-1999, excluding 1300-1399)		2		1.9%
Food (2000-2111)		1		1.0%
Textiles and Printing & Publishing (2200-2799)		4		3.9%
Chemicals (2800-2824, 2840-2899)		4		3.9%
Pharmaceuticals (2830-2836)		4		3.9%
Durable manufactures (3000-3999, excluding 3570-3579, and 3670-3679)		19		18.4%
Transportations (4000-4899, excluding 4810-4819)		4		3.9%
Telecommunications (4810-4819)		1		1.0%
Retail (5000-5999)		11		10.7%
Finance (600-6999)		12		11.7%
Services (7000-8999, excluding 7370-7379)		11		10.7%
Computers (3570-3579, 3670-3679, 7370-7379)		30		29.1%
Total		103		100.0%

Table 2: Descriptive Statistics											
N=103		ROA	EPSDiluted	EPSBasic	NI/REV	RESTR	LEV	SQSEG	GROWTH	PHD	RD/REV
Mean		-0.01	0.61	0.63	-0.06	0.43	0.49	1.38	0.11	0.07	0.30
Std. Deviation		0.16	1.60	1.61	0.29	0.50	0.25	0.49	0.21	0.25	1.25
Percentiles	25	-0.03	-0.25	-0.25	-0.08	0.00	0.25	1.00	0.02	0.00	0.00
	50	0.03	0.55	0.57	0.03	0.00	0.46	1.00	0.11	0.00	0.02
	75	0.08	1.42	1.45	0.10	1.00	0.67	1.73	0.22	0.00	0.16

Performance is measured by the following financial variables:
EPSDiluted = Diluted earnings per share;
EPSBasic = Basic earnings per share;
ROA = Returns on assets.
Control variables include:
NI/REV = Net income ratio measured by net income over total revenues;
RESTR = 1 if firm had restructuring, 0 otherwise;
LEV = Percentage of total debts over total assets;
SQSEG = Square root of the number of business segments reported on *Compustat*;
GROWTH = Sales growth (percent change in sales from prior year);
PHD = 1 if the new CIO has a PHD degree, else 0;
RD/REV = Ratio of research and development expense to total revenues;
*PHD*RD/REV* = Interaction of research and development activities and CIO's education.

Table 3: RD/REV Mean & Median Tests: PHD VS Non PHD				
RD/REV	PHD	Non PHD	T-test	Non-parametric Test
Mean	0.63	0.28	*0.47*	
Median	0.11	0.01		***0.01***
Std. Deviation	0.99	1.27		

Variables are the same as defined in Table 2.

Table 4: Regression Analysis: Knowledge Management, Education and Firm's Performance												
Dependent Variable		Performance-EPSDiluted				Performance-EPSBasic				Performance-ROA		
		Coefficients	t	p-value		Coefficients	t	p-value		Coefficients	t	p-value
(Constant)		-0.26	-0.54	*0.59*		-0.25	-0.50	*0.62*		0.01	0.37	*0.71*
PHD		-0.32	-0.52	*0.60*		-0.30	-0.49	*0.63*		-0.02	-0.63	*0.53*
RD/REV		0.36	2.43	***0.02***		0.37	2.47	***0.02***		0.02	2.08	***0.04***
PHD*RD/REV		1.02	1.73	***0.09***		1.01	1.70	***0.09***		0.07	1.82	***0.07***
NI/REV		4.00	5.82	***0.00***		4.04	5.82	***0.00***		0.53	12.2	***0.00***
RESTR		-0.53	-1.98	***0.05***		-0.54	-1.97	***0.05***		-0.03	-1.55	*0.13*
LEV		0.35	0.64	*0.52*		0.36	0.66	*0.51*		0.00	0.01	*0.99*
SQSEG		0.71	2.58	***0.01***		0.71	2.56	***0.01***		0.00	0.04	*0.97*
GROWTH		0.30	0.45	*0.65*		0.29	0.45	*0.66*		0.07	1.61	*0.11*
Adjusted R Square		34.3%				34.2%				72.9%		
F		7.7				7.6				35.3		
p-value		***0.00***				***0.00***				***0.00***		
N		103				103				103		

Variables are the same as defined in Table 2.

2011 IEEE International Conference on Fuzzy Systems
June 27-30, 2011, Taipei, Taiwan

A Fuzzy MCDM Method to Select The Best Company Based on Financial Report Analysis

Jung-Yuan Kung
Dept. of Information Management
Chinese Naval Academy
Kaohsiung, Taiwan
jykung@cna.edu.tw

Tzung-Nan Chuang
Dept. of Business and Management
National University of Tainan
Tainan, Taiwan
chua@mail.nutn.edu.tw

Chau Minh Ky
National University of Tainan
Graduate Institute of Machatronic System Engineering
minhky032003@gmail.com

***Abstract*—In this paper, based on financial report analysis, a multi-criteria decision-making approach for supporting decision is presented. There are five companies are evaluated by proposed method. Fuzzy AHP (Analytic Hierarchy Process) is utilized to evaluate weights of criteria for selecting company and fuzzy TOPSIS (technique for order preference by similarity to ideal solution) is used to determine the most suitable alternative with respect to various considered criteria. A numerical example is also included to demonstrate the proposed approach.**

Keywords-FAHP, FTOPSIS, Financial report

I. INTRODUCTION

Decision-making problem is a problem that one has to face in life. MCDM (multi-criteria decision-making) problem is the process that chooses the best preferred solution from all considered possible alternatives under evaluation criteria. It has been proved significant to numerous fields such as management science, engineering, education, public administration and military issues. In convention, the ratings of alternatives and the weights of criteria are treated as crisp values when one makes decisions. In real world, however, the used data in MCDM problems are very often imprecise and vague. As one knows, linguistic statements are usually used to evaluate alternatives and criteria. Fuzzy set theory is frequently utilized to deal with uncertainity. Numerous researches have paid attention to fuzzy MCDM problems. Investment issue can be regarded as a FMCDM problem without doubt. Somebody will deposit their money to bank, buy a land, real estate, stock, currency or/and gold for example. In this paper, we focus on how to choose a good stock of company. In addition, financial report is used to analyze the company's performance.

A hybrid model that incorporates FAHP and FTOPSIS methods is employed to solve MCDM problems in a fuzzy environment. According to the proposal model, we have to perform three stages in that the objectives of alternative and criterion will be determined from the investors and practitioners. After that the evaluation will be made by the experts who have much experience in finance fields. We will build hierarchy model include the criteria and alternatives. In next stage, fuzzy AHP is used to determine the preference weights of alternative. Finally, the fuzzy TOPSIS is employed to find out the best alternative for achieving the aspired/desired levels based on the proposed company

II. LITERATURE REVIEW

In the empirical studies, one of the widely used methods is financial report analysis. Tozum (2009) carried out the measurement of performances by using ratio analysis and performance evaluation of bank. He emphasized that traditional ratio analyses were not sufficient to measure company performance and they should be evaluated in a multilateral way. Another important method used in the measurement of bank performance is data envelopment analysis (DEA). This method is used for measuring the efficiencies of bank's branches. Demir and Astarcioglu (2007) analyzed Turkish commercial banks' performance with DEA by considering their total commercials, interest income and expenses, non-interest income and expense. Ravi *et. al* (2008) suggested some models to estimate banks' financial performances. Mercan *et. al* (2003) examined the impact of ownership and growth of the bank on performance with the selected financial ratios in the period between 1989 and 1999. Thai and Kumar (2008) developed some models for the estimation of banks' financial performances by financial variables and they combined these models with the neural networks and statistical techniques. Beccalli (2007) examined the relation between bank performances and the investment in informatics.

There are so many financial ratios that may be evaluated a company. It makes a difficult problem to evaluate the alternatives. So, I have made a Questionnaire for evaluating the important financial ratios. The aim of this questionnaire reduces a number of financial ratios and support to calculate more easily. This questionnaire has sent to 4 experts who have many experiences in field of finance to get the evaluation opinion. Questionnaire will be fill in the blank to express the important level of each financial ratio based on the linguistic value is presented in table 3.1. After 4 questionnaires have been collected, we have calculated the average value of each ratio (according to Appendix 1). If any average value of each ratio is larger than 7 (very strongly important), they will be

978-1-4244-7316-8/11/$26.00 ©2011 IEEE

selected. The result of this evaluation is selected 7 important financial ratios

TABLE I. THE IMPORTANT RATIOS

No.	Ratios	Sign	Criteria Direction	Measuring Units
1	Current ratios	S1	Max	Fraction
2	Debt ratio	S2	Min	Fraction
3	Equity/ Debt ratio	S3	Max	Fraction
4	Operation profit ratio	S4	Max	Percentage
5	Income before tax ratio	S5	Max	Percentage
6	Net income revenue	S6	Max	Percentage
7	Return on total assets	S7	Max	Percentage

III. RESEARCH METHOD

MCDM is a well-known method of decision making. It is a branch of a general class of operations research models, which deal with decision problems under the presence of a number of decision criteria. This part presents a Fuzzy MCDM model for criteria selection and evaluation. Fuzzy MCDM model are briefly reviewed combining the general Decision making process. Then Fuzzy sets, weighting method, FMCDM are presented

A. Fuzzy Set Theory

Linguistic expressions are usually used in daily life, and more or less represent some degree of uncertainly of human thought. The fuzzy set theory [1], proposed by Zadeh, is frequently used to treat uncertainity problems. Fuzzy number is a fuzzy subset of real number; they represent the expansion of the idea of a confidence interval. In this paper, we use triangle fuzzy number (TFN) to represent the importance weighting of criterion and rating of alternative. It can be represented by

$$\mu_A(x) = \begin{cases} \dfrac{(x-a)}{(b-a)}, a \le x \le b \\ \dfrac{(x-c)}{(b-c)}, b \le x \le c \\ 0, \ otherwise \end{cases} \quad (1)$$

Based on the characteristic of TFN and the extension definition proposed by Zadeh [1], given any two TFN and a positive real number *r*, some algebraic operation of TFN can be described as follow:

Addition of two TFN:

$$A_1 + A_2 = (a_1 + a_2, b_1 + b_2, c_1 + c_2) \quad (2)$$

Multiplication of two TFN

$$A_1 \otimes A_2 = (a_1 \times a_2, b_1 \times b_2, c_1 \times c_2) \quad (3)$$

Multiplication of any real number and a TFN:

$$r \otimes A_1 = (ra_1, ra_2, ra_3) \quad (4)$$

Subtraction of two TFNs:

$$A_1 - A_2 = (a_1 - c_2, b_2 - b_1, c_1 - a_2) \quad (5)$$

Division of two TFNs:

$$A_1 / A_2 = (a_1 / c_2, b_2 / b_1, c_1 / a_2) \quad (6)$$

Reciprocal of a TFN:

$$A_1^{-1} = (1/c_1, 1/b_1, 1/a_1) \quad (7)$$

Let two TFNs A_1 and A_2, then the vertex method is defined to calculate the distance between them [26]

$$d(\tilde{A}_1, \tilde{A}_2) = \sqrt{\frac{1}{3}[(a_1 - a_2)^2 + (b_1 - b_2)^2 + (c_1 - c_2)^2]} \quad (8)$$

B. Linguistic Variable

Linguistic variable represents crisp information in a form and precision appropriate for the problem. For example, to answer the question "How do you think about this clothe?" we can answer "it is "not bad" outside. So, "not bad" is linguistic variable. The computational technique is based on the following fuzzy numbers defined by Hsieh *et. al*. We have a table corresponding linguistic variable as follows.

TABLE II. FUZZY PREFERENCE USED IN THE STUDY

Fuzzy number	Linguistic variable	TFN	Reciprocal
$\tilde{9}$	Absolutely Important	(7,9,9)	(1/9,1/9,1/7)
$\tilde{7}$	Very strongly important	(5,7,9)	(1/9,1/7,1/5)
$\tilde{5}$	Essential important	(3,5,7)	(1/7,1/5,1/3)
$\tilde{3}$	Weakly important	(1,3,5)	(1/5,1/3,1)
$\tilde{1}$	Equally important	(1,1,3)	(1/3,1,1)
$\tilde{2},\tilde{4},\tilde{6},\tilde{8}$	Intermediate value between two adjacent judgments		

C. The AHP and Fuzzy AHP method

The AHP method, developed by Saaty (1980), addresses how to determine the relative importance of a set of activities in a multi-criteria decision problem its main characteristic is that it is based on pair-wise comparison judgments. However, the pure AHP model has some problems (Yang & Chen, 2004). They pointed out that the AHP method is mainly used in nearly crisp data applications, creates and deals with a very unbalanced scale of judgment, rather imprecise; and the subjective judgment, selection and preference of decision-makers have much influence on the AHP results. To overcome these problems, several researchers integrate fuzzy theory with AHP to improve the uncertainty.

Step 1: AHP uses several small problems to present a complex problem. Thus, the first ace decompose into a hierarchy with a goal at the top, criteria and sub-criteria at level and sub-level and decision alternative at the bottom of the hierarchy (Fig 3)

Step 2: Construct fuzzy pair-wise comparison matrices. Through expert questionnaires, each expert is asked to assign

linguistic terms by TFN (as shown in Table 2 and Fig. 2 to the pair-wise comparisons among all criteria in the dimensions of a hierarchy system

$$D = \begin{array}{c} \\ C_1 \\ C_2 \\ \vdots \\ C_i \\ \vdots \\ C_n \end{array} \begin{array}{c} \begin{array}{cccccc} C_1 & C_2 & \cdots & C_j & \cdots & C_m \end{array} \\ \begin{bmatrix} \tilde{a}_{11} & \tilde{a}_{12} & \cdots & \tilde{a}_{1j} & \cdots & \tilde{a}_{1m} \\ \tilde{a}_{21} & \tilde{a}_{22} & \cdots & \tilde{a}_{2j} & \cdots & \tilde{a}_{2m} \\ \vdots & \vdots & \cdots & \vdots & \cdots & \cdots \\ \tilde{a}_{i1} & \tilde{a}_{i2} & \cdots & \tilde{a}_{ij} & \cdots & \tilde{a}_{im} \\ \vdots & \vdots & \cdots & \vdots & \cdots & \cdots \\ \tilde{a}_{n1} & \tilde{a}_{n2} & \cdots & \tilde{a}_{nj} & \cdots & \tilde{a}_{nm} \end{bmatrix} \end{array}$$

The elements a_{ij} can be interpreted as the degree preference of ith criterion over jth criterion. The comparison matrix has to be normalized into the range of [0, 1] by Eq. (13)

$$\tilde{r}_{ij} = \frac{\tilde{a}_{ij}}{\sum_{i=1}^{n} \tilde{a}_{ij}} \quad (13)$$

$$R = \begin{bmatrix} r_{11} & r_{12} & \cdots & r_{1j} & \cdots & r_{1m} \\ r_{21} & r_{22} & \cdots & r_{2j} & \cdots & r_{2m} \\ \vdots & \vdots & \cdots & \vdots & \cdots & \cdots \\ r_{i1} & r_{i2} & \cdots & r_{ij} & \cdots & r_{im} \\ \vdots & \vdots & \cdots & \vdots & \cdots & \cdots \\ r_{n1} & r_{n2} & \cdots & r_{nj} & \cdots & r_{nm} \end{bmatrix}$$

Step 3: Examine the consistency of the fuzzy pair-wise comparison matrices like the AHP method

According to the research of Buckley (1985), it proves that if $A = [a_{ij}]$ is a positive reciprocal matrix then A^{-1} is a fuzzy positive reciprocal matrix. That is, if the result of the comparisons of $A = [a_{ij}]$ is consistent.

Step 4: in the next step, transform the real elements of matrix R into the fuzzy numbers

Step 5: before conducting all the calculation of vector of priorities, the comparison matrix D has to be normalized by Eq. (13)

Step 6: Compute the fuzzy geometric mean for each criterion.

The geometric technique is used to calculate the geometric mean of the fuzzy comparison values of criterion to each criterion, as shown in Eq. (20), where r_i is a fuzzy value of the pair-wise comparison of criterion *i* to criterion *n* (Buckley, 1985)

$$r_i = [r_{i1}, r_{i2}, \ldots r_{in}] \quad (14)$$

Step 7: compute the fuzzy weight by normalization. The fuzzy weight of the criterion can be derived as Eq. (15), where $\tilde{w}_i$ denoted as $\tilde{w}_i = (L_{w_i}, M_{w_i}, U_{w_i})$ by a TFN and $L_{w_i}, M_{w_i}, U_{w_i}$ represent a lower, middle, upper value of the fuzzy weight of the i-th criterion.

$$\tilde{w}_i = \tilde{r}_i \otimes (\tilde{r}_1 \oplus \tilde{r}_2 \oplus \ldots \tilde{r}_n)^{-1} \quad (15)$$

D. Fuzzy Topsis method

Topsis was developed by Hwang and Yoon (1980). Topsis method is based on choosing the best alternative, which has the shortest distance from the positive ideal-solution (PIS) and has the longest from the negative ideal-solution (NIS) for solving problem.In this study, the combination between Topsis and fuzzy number has been applied. The general step-by-step procedure using Fuzzy Topsis method is briefly listed as follow

Step 1: The Fuzzy MCDM can be concisely expressed in the matrix format as follow:

$$X = \begin{array}{c} \\ A_1 \\ A_2 \\ \vdots \\ A_i \\ \vdots \\ A_n \end{array} \begin{array}{c} \begin{array}{cccccc} C_1 & C_2 & \cdots & C_j & \cdots & C_m \end{array} \\ \begin{bmatrix} x_{11} & x_{12} & \cdots & x_{1j} & \cdots & x_{1m} \\ x_{21} & x_{22} & \cdots & x_{2j} & \cdots & x_{2m} \\ \vdots & \vdots & \cdots & \vdots & \cdots & \cdots \\ x_{i1} & x_{i2} & \cdots & x_{ij} & \cdots & x_{im} \\ \vdots & \vdots & \cdots & \vdots & \cdots & \cdots \\ x_{n1} & x_{n2} & \cdots & x_{nj} & \cdots & x_{nm} \end{bmatrix} \end{array}$$

$$\tilde{w} = (\tilde{w}_1, \tilde{w}_2, \ldots \tilde{w}_n)^t$$

If the expert's opinions are evaluated by *k*th persons, we will calculate the average value as the following Eq. (26)

$$x_{ij} = (1/k)(x_{ij}^1 + x_{ij}^2 + \ldots x_{ij}^k) \quad (26)$$

Where A_i denotes by the alternatives, i=1, 2…n; C_j denotes by the criteria, j=1, 2…m. The fuzzy linguistic rating x_{ij} is a fuzzy value indicating the performance rating of the alternative A_i with respect to each criterion C_j. If x_{ij} preserves the property that the range of normalized fuzzy number belong to [0, 1], there is no need for normalization. Decision matrix is normalized as following Eq. (19)

Step 2: calculated the weighted normalization fuzzy decision matrix by multiplying the normalized decision matrix by its association weighted. The weighted normalized value is $\tilde{v}_{ij}$ calculated by (26)

$$\tilde{v}_{ij} = \tilde{w}_i \times \tilde{r}_{ij} \quad (26)$$

$$\tilde{V} = [\tilde{v}_{ij}]_{nm} \quad (27)$$

Where *i*= 1, 2,….*n* and *j*= 1, 2, …*m*.

Step 3: calculate the distance of each alternative from A^* and A^- using the following equation:

$$D_j^* = \sum_j^m d(\tilde{v}_{ij}, \tilde{v}_i^*) \quad (28)$$

$$D_j^- = \sum_j^m d(\tilde{v}_{ij}, \tilde{v}_i^-) \quad (29)$$

where j= 1, 2, …m.

Step 4: Identify positive ideal A^* and negative ideal solution A^-. The fuzzy positive ideal and fuzzy negative ideal solution are shown in the following Equation.

$$A^* = \{\tilde{v}_1^*, \tilde{v}_2^*, \ldots \tilde{v}_i^*\} = \{(max_j\, v_{ij}\ i \in B), (min_j\, v_{ij}\ i \in C)\} \quad (30)$$

$$A^- = \{\tilde{v}_1^-, \tilde{v}_2^-, \ldots \tilde{v}_i^-\} = \{(min_j\, v_{ij}\ i \in B), (max_j\, v_{ij}\ i \in C)\} \quad (31)$$

where i= 1, 2,….i and j= 1, 2, …j.

Where ***B*** is associated with benefit criteria and C ***C*** is associated with cost criteria.

Step 5: calculate the relative closeness to the ideal solution

$$CC_j = \frac{D_j^-}{D_j^+ + D_j^-} \quad j\text{= 1, 2, …}m. \quad (32)$$

Step 6: Rank preference order. Rank alternatives according to CC_j in descending order.

IV. A NUMERICAL APPLICATION FROM THE TAIWAN STOCK EXCHANGE

In this research, we first base on the criteria and ratios of the financial statement to prepare a list of performance evaluation indicators, and then have a survey with the experts in related financial areas in Taiwan. A questionnaire is designed using the AHP and TOPSIS questionnaire format, the criteria and ratios of the financial statement and the selected companies are included. The results can provide some suggestions and orientation to investors in developing their investment strategies in the future.

For selecting operation system, four main criteria and seven sub-criteria are used in application. Regarding the evaluation of the firm's financial statement, three experts were invited to survey five alternatives. After the construction of hierarchy, the different priority weights of each criterion attribute and alternatives are calculated using the fuzzy AHP and Fuzzy TOPSIS approaches. The comparison of the importance or preference of one criterion, attribute or alternative over another can be done with the help of the survey questionnaire. The method of calculating priority weights of the difference decision alternatives is presented below.

We transfer the linguistic scales to the corresponding fuzzy numbers (as Appendix A). Computing the elements of synthetic pair-wise comparison matrix by using the geometric mean method suggested by Buckley (1985) that is:

$$\tilde{a}_{ij} = \left(\tilde{a}_{ij}^1 \otimes \tilde{a}_{ij}^2 \otimes \tilde{a}_{ij}^3\right)^{1/3} \tilde{a}_{12} = [(5,6,7) \otimes (6,7,8) \otimes (2,3,4)]^{1/3} = (3.91,5.01,6.07)$$

TABLE III. WEIGHT OF DIMENSIONS

No.	Criteria	Weights	BNP	Rank
S1	Current ratio	$(\mathbf{0.185, 0.284, 0.372})$	0.281	1
S2	Debt ratio	$(\mathbf{0.185, 0.234, 0.299})$	0.239	2
S3	Equity/Debt ratio	$(\mathbf{0.091, 0.123, 0.165})$	0.126	4
S4	Operation profit ratio	$(\mathbf{0.091, 0.122, 0.167})$	0.127	3
S5	Income before tax ratio	$(\mathbf{0.095, 0.115, 0.153})$	0.121	5
S6	Net income revenue	$(\mathbf{0.058, 0.072, 0.094})$	0.075	6
S7	Return on total asset ratio	$(\mathbf{0.054, 0.051, 0.068})$	0.058	7

It can be obtained the other matrix elements by the same computational procedure; therefore, the synthetic pair-wise comparison matrix of the five representatives will be constructed as follows matrix D

To apply the COA method to compare the BNP value of the fuzzy weights of each dimension: to take the BNP value of the weight of S1 (current ratio) as an example, the calculation process is as follows:

$$BNP_{S1} = \frac{[(U_{w1} - L_{w1}) + (M_{w1} - L_{w1})]}{3} + L_{w1} = \frac{[(0.372 - 0.185) + (0.284 - 0.185)]}{3} + 0.185 = 0.281$$

Then, the weights for the remaining dimensions can be found as shown in table 4. This table shows the relative weight of eight dimensions of the evaluation of the companies, which obtained by Fuzzy AHP method.

$$\begin{bmatrix} (1,1,1) & (3.91,5.01,6.07) & (4.64,5.65,6.65) & (2.88,4.12,5.24) & (1.49,1.82,2.19) & (0.79,1.17,1.55) & (1.10,1.44,1.82) \\ (0.25,0.20,0.26) & (1,1,1) & (3.78,4.82,5.85) & (5.19,6.21,7.23) & (1.67,1.69,2.08) & (1.91,1.71,1.98) & (4.31,5.31,6.32) \\ (0.26,0.18,0.22) & (0.28,0.21,0.26) & (1,1,1) & (2.62,3.83,4.93) & (0.83,1.49,2.08) & (1.14,1.33,1.59) & (2.62,3.63,4.64) \\ (0.150.24,0.35) & (0.24,0.16,0.19) & (0.30,0.26,0.38) & (1,1,1) & (3.91,5.01,6.07) & (3.63,4.72,5.77) & (2.88,4.12,5.24) \\ (0.48,0.55,0.67) & (0.48,0.59,0.75) & (0.48,0.67,1.00) & (0.31,0.20,0.26) & (1,1,1) & (6.21,7.23,8.24) & (2.88,2.00,2.38) \\ (0.61,0.85,1.26) & (0.51,0.58,0.69) & (0.63,0.75,0.94) & (0.26,0.21,0.28) & (0.22,0.14,0.16) & (1,1,1) & (1.82,2.11,2.43) \\ (0.87,0.69,0.91) & (0.29,0.19,0.23) & (0.37,0.28,0.38) & (0.35,0.24,0.35) & (0.42,0.50,0.60 & (0.85,0.47,0.55) & (1,1,1) \end{bmatrix}$$

In order to calculate the closeness coefficients of each of the alternatives. The values d_1^+ and d_1^- can be calculated as a follows:

$$\mathbf{d_1^+} = \sum\sqrt{[(\mathbf{0.074-1})^2+(\mathbf{0.170-1})^2+(\mathbf{0.289-1})^2]\frac{\mathbf{1}}{\mathbf{3}}}+\cdots$$

$$+\sqrt{[(\mathbf{0.021-1})^2+(\mathbf{0.030-1})^2+(\mathbf{0.055-1})^2]\frac{\mathbf{1}}{\mathbf{3}}}$$

$$=\mathbf{6.281}$$

$$\mathbf{d_1^-} = \sum\sqrt{[(\mathbf{0.074-0})^2+(\mathbf{0.170-0})^2+(\mathbf{0.289-0})^2]\frac{\mathbf{1}}{\mathbf{3}}}+\cdots$$

$$+\sqrt{[(\mathbf{0.021-0})^2+(\mathbf{0.030-0})^2+(\mathbf{0.055-0})^2]\frac{\mathbf{1}}{\mathbf{3}}}=\mathbf{0.799}$$

Once the distances from FPIS and FNIS are determined, the closeness coefficient can be obtained with (32). The index CC_1 of firstalternative is calculated as:

$$CC_1 = \frac{0.799}{0.799+6.281} = 0.113$$

The other results are shown in table 5.

TABLE IV. CLOSENESS COEFFICIENTS AMONG DIFFERENT COMPANIES

Company	d+	d-	Satisfaction of CC_1^-	Rank
China Steel	6.281	0.799	0.113	5
Cathay	6.277	0.805	0.114	4
TSMC	6.225	0.855	0.121	2
Acer	6.208	0.869	0.123	1
Asus	6.256	0.821	0.116	3

V. CONCLUSION

The result of this study can offer us the way to select the best company among the company group. It help the people to invest the best one based on analyzing the information from financial report and applying fuzzy MCDM method. The new point of this study is that the user only needs some basic knowledge of finance to construct the criteria hierarchy, and the necessary result will be obtained. This method used in the study can also be applied to other industries only the considered criteria may be different. For example, solvency ratios are very important with banks. However, they are less important than with manufacturing company. In the future, we will try to develop or use the fuzzy MCDM method to solve the decision problems.

REFERENCES

[1] L. A. Zadeh, "Fuzzy Sets," Information and Control, 8(3), pp. 338-356., 1965.

[2] Zimmermann H.J., , "Fuzzy Set Theory and its Applications", second ed., Kluwer Academic Publishers, Boston, 1991.

[3] S. J. Chen and C.L. Hwang, "Fuzzy Multiple Attribute Decision Making", Lecture notes in Economics and Mathematical System Series 375, Springer-Verlag, New York, 1992.

[4] P. J. M. Laarhoven and W. Pedrycz, "A Fuzzy Extension of Saaty's Priority Theory," Fuzzy Sets and Systems, 11(3), pp. 229-241, 1983.

[5] R. E. Bellmann and L.A. Zadeh, "Decision Making in Fuzzy environment," Management Science, 17(4), pp.141-164,1970.

[6] J. J. Buckley, "Fuzzy Hierarchical Analysis," Fuzzy Sets and Systems, 17(3), pp. 233-247, 1985.

[7] T. L. Saaty, "Decision making with the Analytical Hierarchy Process," 1980.

[8] C. L. Hwang and K. Yoon, "Multiple Attributes Decision Making Methods and Applications," Springer, Berlin Heidelberg, 1981.

[9] E. Triantaphyllou, "Multi – criteria Decision making methods: A comparative study," Kluwer Academic Publishers, London, 2000.

[10] J. Lu, G. Zhang, D. Ruan, and F. Wu, Series in Electrical and Computer Engineering Vol 6 Multi-Objective Group Decision Making Methods, Software and Applications with Fuzzy Set Techniques Imperial College Press, 2007.

[11] C.T. Chen, "Extensions of the TOPSIS for group decision-making under fuzzy environment," Fuzzy Sets and Systems, 114, pp. 1-9, 2001.

[12] Y. Huang, H. Lee, "A clustering method to identify representative a financial ratios," 178, pp. 1087-1097, 2009.

[13] P. Xidonasa, G. Mavrotasb, and J. Psarrasa, "A multi-criteria methodology for equity selection using financial analysis," Computers & Operations Research 36, pp. 3187 – 3203, 2009.

[14] J. Gallizo, F. Jim, and M. Salvado, "Adjusting financial ratios: a Bayesian analysis of the Spanish manufacturing sector," Omega 30, pp.185, 2002.

[15] E. K. Laitinen, "Financial statement data in assessing the future potential of a technology firm: The case of Nokia" International Review of Financial Analysis 15, pp. 256– 28, 2006.

[16] . E. O¨cal, E. L. Oral, E. Erdis, and G. Vural, "Industry financial ratios—application of factor analysis in Turkish construction industry," Building and Environment, 42, pp. 385–392, 2007.

[17] W. Shiue, S. T. Li, and K. J. Chen, "A frame knowledge system for managing financial decision knowledge," Expert Systems with Applications, 35, pp. 1068–1079, 2008.

[18] Y. Marinakis, M. Marinaki, M. Doumpos, and C. Zopounidis, "Ant colony and particle swarm optimization for financial classification problems," Expert Systems with Applications, 36, pp. 10604–10611, 2009.

[19] J. Sun, H. Li, "Financial distress prediction based on serial combination of multiple classifiers," Expert Systems with Applications, 36, pp. 8659-8666, 2009.

2011 IEEE International Conference on Fuzzy Systems
June 27-30, 2011, Taipei, Taiwan

Applying FML and Fuzzy Ontologies to Malware Behavioural Analysis

Hsien-De Huang
National Center for High-Performance Computing
NARL
Tainan, Taiwan
TonTon@ieee.org

Giovanni Acampora
Vincenzo Loia
Dept. Computer Science
University of Salerno
Italy
acampora@unisa.it

Chang-Shing Lee
Dept. Computer Science and Information Engineering
NUTN
Tainan, Taiwan
leecs@mail.nutn.edu.tw

Hung-Yu Kao
Dept. Computer Science and Information Engineering
NCKU
Tainan, Taiwan
hykuo@mail.ncku.edu.tw

***Abstract*—Antimalware applications represent one of the most important research topic in the area of information security threat. Indeed, most computer network issues have malwares as their underlying cause. As a consequence, enhanced systems for analyzing the behavior of malwares are needed in order to try to predict their malicious actions and minimize eventual computer damages. However, because the environments where malwares operate are characterized by high levels of imprecision and vagueness, the conventional data analysis tools lack to deal with these computer safety applications. This work tries to bridge this gap by integrating semantic technologies and computational intelligence methods, such as the Fuzzy Ontologies and Fuzzy Markup Language (FML), in order to propose an advanced semantic decision making system that, as shown by experimental results, achieves good performances in terms of malicious programs identification.**

Keywords-malware behavioural analysis; ontology; fuzzy ontology; fuzzy markup language

I. INTRODUCTION

In recent years, the rapid growth of information technology has strongly enhanced computer systems both in terms of computational and networking capabilities. However, these novel distributed computing scenarios, other than enabling the development of efficient computer applications, have raised important issues about the security and safety of the interconnected hardware systems. Indeed, computer threats, such as viruses and backdoor programs have created different economical and technological disasters all around the world. Internet fraud activities [1], users private data stealing, malwares damaging computer systems without the owner's informed consent [2], are only some examples of computer threats each day sabotage personal, academic and industrial computer equipments. As a consequence, enhanced systems for analyzing the behavior of malwares are needed in order to try to predict their malicious actions and minimize eventual computer damages [3]. However, because the environments where malwares operate are characterized by high levels of imprecision and vagueness, the conventional data analysis tools lack to deal with these computer safety applications. This work tries to bridge this gap by integrating different computational intelligence methods, such as the Fuzzy Ontologies [4] and Fuzzy Markup Language (FML) [5].

Ontologies are structural frameworks for modeling information by means of an explicit specification and a shared conceptualization [6]; they are mainly used as good knowledge representation and communication model for intelligent agents [4]. Nevertheless, in their conventional view, ontologies are not enough to deal with imprecise and vague knowledge. As a consequence, many researchers have explored the use of fuzzy ontologies, i.e., structural frameworks based on fuzzy logic used for modeling information characterized by high levels of imprecision and vagueness. For example, Lee *et al.* proposed a fuzzy ontology for designing an intelligent decision making system for summarization systems [4]; Quan *et al.* presented the automatic fuzzy ontology generation for semantic help desk support [7], and the automatic fuzzy ontology generation for semantic web [8]. Typically, the joint exploitation of Fuzzy Ontologies and FML is mainly used as support framework for designing intelligent fuzzy inference systems, one of the key topics in artificial and computational intelligence research [9].

The FML [10] is a novel computer language useful for modeling advanced fuzzy systems by means of a structural and taxonomic approach that improves fuzzy systems design from a twofold point of view: transparency and reliability (see section II.B). This paper presents an FML-based ontological agent for malware behavioral analysis. In particular, this agent uses a fuzzy ontology for modeling malware behavioral knowledge collected by domain experts and our homemade tool, Taiwan Malware Analysis Net (TWMAN) [1, 3]. An FML program is used in order to design an intelligent decision making system whose behavioral rules are used to detect viruses and malicious programs and, consequently, provide a better protection to computer equipments.

This paper contains five sections. Section II describes the literature survey about Web Ontology Language (OWL), FML and TWMAN. Section III describe the integration of a fuzzy ontology model and FML for modeling the knowledge about malware behaviors and propose an intelligent decision making system for detecting computer anomalies. Section IV discusses the experimental results of this study. Finally, some conclusive remarks are offered in Section V.

II. BASIC CONCEPTS AND BACKGROUND

Today, there is a growing interest in the development of systems based on knowledge representation by means of ontological approaches. Nevertheless, conventional ontology languages are not appropriate to deal with uncertainty [11],

978-1-4244-7316-8/11/$26.00 ©2011 IEEE

vagueness or imprecision which strongly characterize the real world scenarios . It is not surprising that fuzzy set theory and fuzzy logic are handle these types of knowledge and, indeed, fuzzy ontologies are emerging as a useful methodology for knowledge representation in several semantic-oriented applications. In this paper, a decision making system for analyzing malware system behavior is implemented by integrating the following technologies: Web Ontology Language (OWL), Fuzzy Markup Language (FML) and Taiwan Malware Analysis Net (TWMAN) .

A. Web Ontology Language (OWL)

When a malware behavioral analysis tool owns the malwares source code at its disposal, the analysis step becomes quite simple. Indeed, understanding the malicious program is as simple as reading, interpreting and looking for code fragments that reveal key information on the attacker and the attack. However, our approach does not own malwares source codes to detect eventual viruses or similar programs, but it exploits an ontological view of malwares behavior in order to define a more general and efficient detection platform. In order to express the ontological knowledge about malware behavior, our proposal uses the OWL2 language, a standard tool for modeling knowledge in a semantic way. In particular, our framework uses OWL for describing an ontological model for malware behavioral (see Fig. 1) composed by the following information: *File Hash (FH)*, *Connect IP (CI)*, *Files Change (FC) and Similarity (SI)* (see section II.C) [1]. Precisely, File Hash is a malware information (computed by the *ssdeep* program [12]) useful to detect the presence of malwares on the system under protection by comparing the hash code of a suspicious file with a collection of malware hash codes previously gathered. Connect Ip allow us to count the number of TCP/IP connection opened by a given program and, as a consequence, to detect anomalous network behaviors; this information is computed by INetSim [13], a software suite for simulating common internet services for analyzing the network behavior of unknown malware samples; File change is a malware information used to evaluate the number of changes occurred in the file system due to some eventual malware actions; it is computed by the Advanced Intrusion Detection Environment (AIDE) [14]. The Similarity concept is a cumulative information used to evaluate the level of maliciousness of a program; it is computed starting from FH, CI and FC. However, even though OWL enables a suitable representation of malwares knowledge, it is not able to apply advanced inference mechanisms to derive additional imprecise and vague knowledge in the scenario of malwares detection. For this reason, we exploit FML, an innovative fuzzy inference language bridging the gap shown by other methodologies.

B. Fuzzy Markup Language (FML)

FML is a domain-specific language proposed by Acampora and Loia [10] whose main aim is to model fuzzy systems by directly dealing with fuzzy concepts, fuzzy rules and fuzzy inference engines [9]. In particular, it is used to model two well-known kind of fuzzy controllers: Mamdani and Takagi-Sugeno-Kang (TSK). This language is XML-based, so FML programs are coded through a collection of correlated semantic XML tags, following an opportune XML Schema, capable of modeling the different components of a fuzzy controller. Some samples of FML tag are [15]:

- <FUZZYCONTROL> that models a whole fuzzy system;
- <KNOWLEDGEBASE> and <RULEBASE> that represent the main components of a fuzzy system: the knowledge base and the rule base.

However, since an FML program realizes only a static view of a fuzzy system, the so-called eXtensible Stylesheet Language Translator (XSLT) is provided to change this static view to a computable version. Therefore, in short, FML is essentially composed by three layers [9]:

- XML in order to create a new markup language for fuzzy logic control;
- a XML Schema Document (XSD) as grammar to define the legal building blocks;
- a XSLT in order to convert a fuzzy controller description into a general-purpose computer language.

Differently from other similar approaches used to describe fuzzy controllers such as Fuzzy Control Language or MATLAB Fuzzy Inference System (FIS) developed by the Math Works, FML allows fuzzy designers to simply code their ideas on heterogeneous hardware by exploiting abstraction benefits offered by XML tools. Indeed, thanks to FML it is possible to design a fuzzy controller in human-readable and hardware independent way by avoiding additional work and development phases. The exploitation of FML is resulted in a new fuzzy control design philosophy named *transparent fuzzy controller* based on the integration among fuzzy systems, labeled tree theory, and XML methodology. Fig. 2 shows the tree structure of FML.

C. Taiwan Malware Analysis Net (TWMAN)

TWMAN is an open source (GPL v2) project based on a real OS environment such as the Joe Stewart's Truman [1, 3, 16]. TWMAN is an automated behavioral malware analysis environment to analyze the malware and a client-server architecture. The server works on Linux, while the client is Microsoft Windows, which use PXE-Boot in a real environment . In a Windows environment, malware usually attempts to execute or to install other applications in the Windows. It also includes the WinSock-functions, which can be able to communicate with TCP/IP-networks, such as the Internet or an intranet system. Some important efforts are made to interpret the Winsock calls. It must detect HTTP, FTP, SMTP and IRC connections and extracts the important data (i.e. FTP and IRC login information). It is interesting to know what the malware can create or how it can modify files on the disk. Windows NT/2000/2003/XP stores configuration data in a registry. It is a central repository for data configuration which is stored in a hierarchical manner. Systems, users, applications, and hardware in Windows allow the registry to store their configuration especially when a registry run key has been modified by some programs to make itself auto-start. The Advanced Intrusion Detection Environment (AIDE) against the disk image after the malware is run and compare it to the clean image that was uploaded to the client before the process and

take note if files were added, modified, or deleted during the malware run.

In order to test and verify, we have completed analyze 4840 malwares and generated report by TWMAN (Please see Table I). Our approach can get correct malware behavioral information, which can be expanded to solve more complex, practical problems and exploited to malware behavioral by agents to infer additional information and provide advanced services to end users.

III. FUZZY ONTOLOGICAL MODEL FOR TWMAN

This section is devoted to integrate OWL and FML in order to design a semantic methodology for improving malware behavioral analysis. In particular, in this section, we will describe how to use fuzzy ontologies to model the knowledge related to malware behaviors and how to merge these fuzzy ontologies with FML in order to design the proposed intelligent system. The main tools used to achieve the proposed result are: OWL by Protégé and VisualFML.

Description Logic and Fuzzy set theory are well-known formalisms for representing complex knowledge related to different application domains. According to the FML, which can create a data-oriented markup language features, and combine fuzzy logic, then create a vague abstraction of the fuzzy controller. Fig. 3 shows structure of FML-based malware behavioral analysis, so we can see two parts, namely the left part of the Knowledge Base and the right half of the rule base, and Table III shows the part of example FML code.

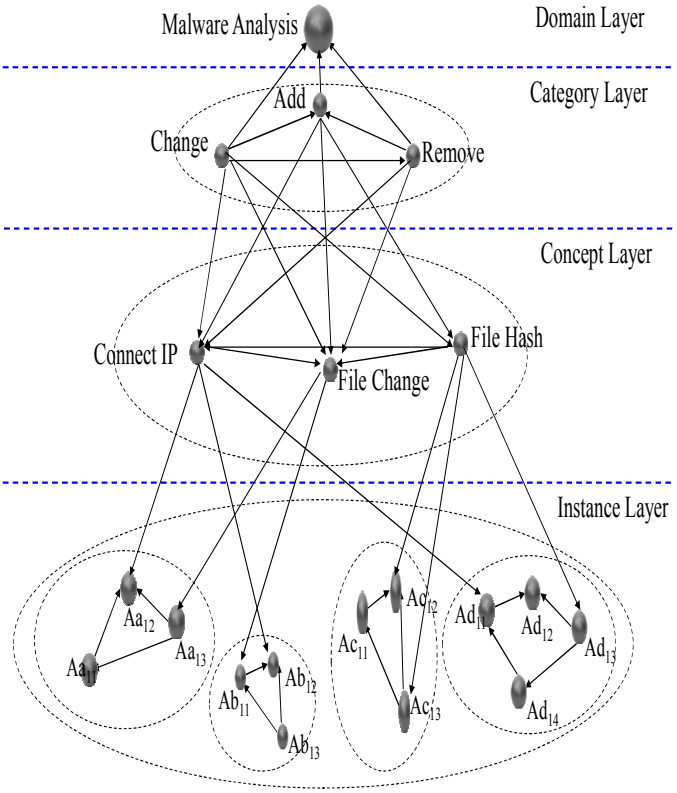

Figure 1. Structure of the malware behavioral ontology [1, 5].

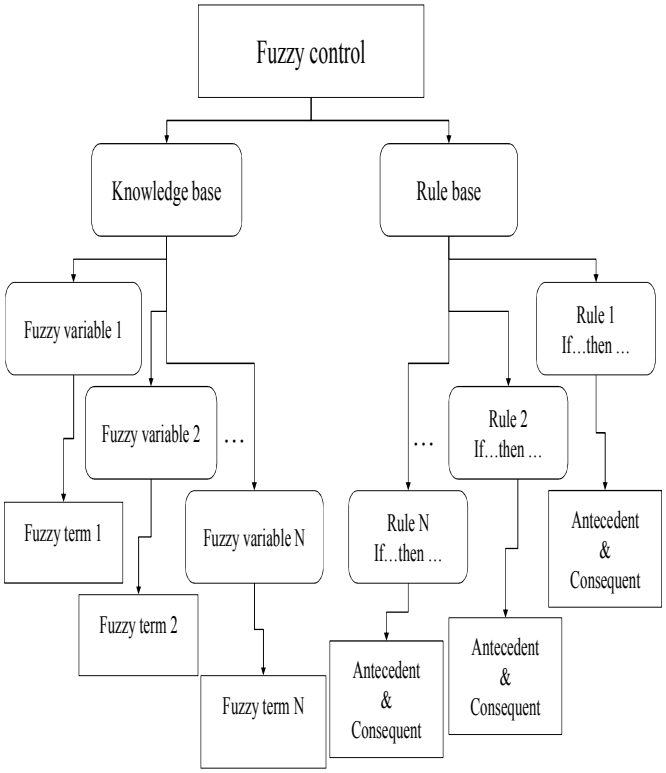

Figure 2. The tree structure of FML [10, 15].

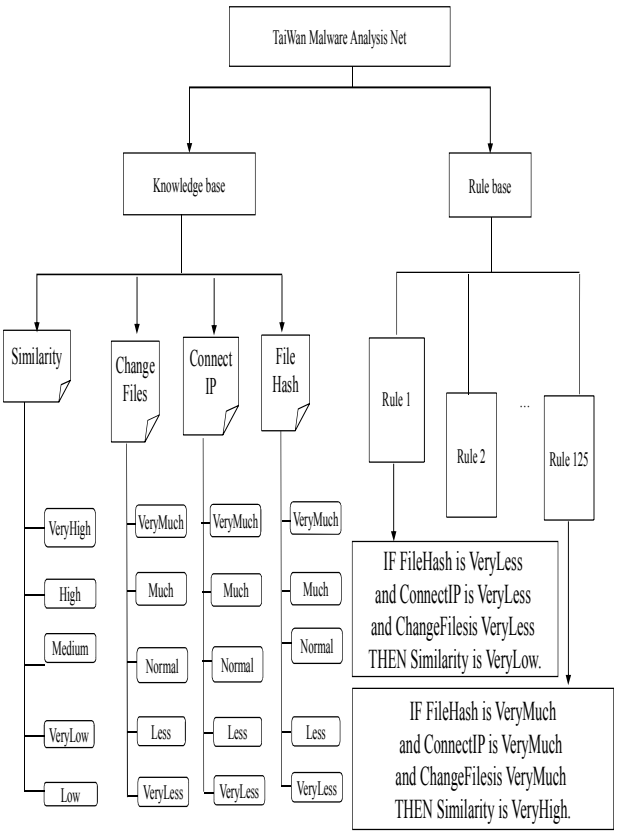

Figure 3. The structure of FML-based malware behavioral analysis.

TABLE I. EXAMPLE REPORT PART OF TWMAN [1, 3, 16].

```
Taiwan Malware Analysis Net, TWMAN - Analysis Report
>> Summary report for 7d99b0e9108065ad5700a899a1fe3441 created at Jan
12 14:06:37 CST 2011 <<
>> Host file changes <<
>> Registry Run Key changes<<
+++ /forensics/7d99b0e9108065ad5700a899a1fe3441/run-rip.txt    2010-07-
12 05:05:06.000000000 +0800
+Cryptographic Service|C:\WINDOWS\system32\enjqtk.exe
>> Registry Service Key changes <<
+{33F3B709-064F-4FF7-95BD-434D50D67CCC}
+{DAACA8DA-DD27-4F5F-8163-1AE2BF76188D}
>> ssdeep info (  Fuzzy Hashing )<<
192:5E0HVFnXlKyFMOJd1BPSXPe2T7GCkE80XuPH:KwznVKyqCvPSry
iZu/,"7d99b0e9108065ad5700a899a1fe3441"
7d99b0e9108065ad5700a899a1fe3441 matches
/forensics/ssdeep.db:96924b5583a0fa34a66d81257939a5d6 (65)
7d99b0e9108065ad5700a899a1fe3441 matches
 matches /forensics/ssdeep.db:33d8d205001b83f96a9480ce51d54b60 (60)
>> Connect IP <<
IP 192.168.0.110 > 131.80.82.30: ICMP echo request, id 512, seq 5376,
IP 192.168.0.110 > 131.80.120.13: ICMP echo request, id 512, seq 56
IP 192.168.0.110 > 201.196.11.244: ICMP echo request, id 512, length 41
IP 192.168.0.110 > 201.196.171.67: ICMP echo request, id 512, length 41
IP 192.168.0.110.123 > 207.46.197.32.123: UDP, length 48
IP 192.168.0.110 > 201.196.207.12: ICMP echo request, id 512, length 41
IP 192.168.0.110 > 201.196.202.32: ICMP echo request, id 512, length 41
IP 192.168.0.110 > 201.196.13.108: ICMP echo request, id 512, length 41
IP 192.168.0.110 > 201.196.85.157: ICMP echo request, id 512, length 41
IP 192.168.0.110 > 201.196.108.43: ICMP echo request, id 512, length 41
IP 192.168.0.110 > 131.80.82.30: ICMP echo request, id 512, seq 5376,
IP 192.168.0.110 > 131.80.120.13: ICMP echo request, id 512, seq 5632,
IP 192.168.0.110 > 131.80.120.13: ICMP echo request, id 512, seq 5632,
IP 192.168.0.110 > 131.80.57.246: ICMP echo request, id 512, seq 5888,
IP 192.168.0.110 > 131.80.57.246: ICMP echo request, id 512, seq 5888,
IP 192.168.0.110 > 131.80.120.13: ICMP echo request, id 512, seq 56
IP 192.168.0.110 > 131.80.136.224: ICMP echo request, id 512, seq 6656,
IP 192.168.0.110 > 131.80.136.224: ICMP echo request, id 512, seq 6656
IP 192.168.0.110 > 201.196.85.157: ICMP echo request, id 512, length 41
IP 192.168.0.110 > 201.196.108.43: ICMP echo request, id 512, length 41
IP 192.168.0.110 > 131.80.82.30: ICMP echo request, id 512, seq 5376,
IP 192.168.0.110 > 131.80.120.13: ICMP echo request, id 512, seq 5632,
IP 192.168.0.110 > 131.80.120.13: ICMP echo request, id 512, seq 5632
>> NPASCAN v1.7  <<
------------------Start Scan-----------------------
掃瞄完成!!未偵測到相關惡意程式!
------------------End Scan-------------------------
>> CWSandBox VirusScan Report  <<
VSCAN Version:3.2.1861.2 (Feb 22 2009  19:30:04);run at:: Jul 11 12:54:40
2010
defs version: 5444 (2009-10-12T17:47:12)
command line: c:\SBScanV3\vscan /l c:\virus.txt /def c:\SBDefsV3
C:\WINDOWS\system32\sandnet.exe
 [      53], Malicious      ,CRC8_BL ,          Trojan.Win32.Generic!BT,
4150696,C:\WINDOWS\system32\sandnet.exe
1 objects processed in 0 secs, 0 fps
1 threats detected, 0 suspicious files

>> Advanced Intrusion Detection Environment-檔案異動偵測 <<
Summary:
  Total number of files:        28292
  Added files:                  333
  Removed files:                664
  Changed files:                51
--------------------------------------------------------------------------------
Taiwan Malware Analysis Net, TWMAN - Analysis Report
Last Update 2011-01-01" E-Mail : TWMAN@nchc.narl.org.tw
Developed By TonTon | http://TWMAN.nchc.org.tw "
```

A. OWL and FML Model

There are several knowledge representation language, DLs and Fuzzy DLs have existed, e.g., Semantic Web Rule Language (SWRL), Java Environment Expert Systems (Jess), FUZZYDL and DELOREAN. Which provide a shared vocabulary of an application domain. Indeed, OWL can describe the relation between concept with instance and inference new instance, but the limitation of the first one must integrate SWRL language and Jess in Protégé 3, and the second one have to integrate Fuzzy OWL in Protégé 4. Table II shows the part of example OWL code. Therefore, we will introduce FML to model malware behavioral knowledge, are the following ones.

FML parser was used to extract the knowledge from the FML-based definition. The input is FML-based definition of the fuzzy controller which denoted by CFML. The output is composed of a set of Fin={FileHashVeryLess, FileHashLess, FileHashNormal, FileHashMuch, FileHashVeryMuch, ConnectIPVeryLess, ConnectIPLess, ConnectIPNormal, ConnectIPMuch, ConnectIPVeryMuch FileChangeLess, FileChangeVeryLess, FileChangeNormal, FileChangeMuch, FileChangeVeryMuch}, a set of Fout={ SimilarityVeryLow, SimilarityLow, SimilarityMedium, SimilarityHigh, SimilarityVeryHigh } and fuzzy inference rules set FS={Rule1, Rule2,..,Rule125}.

VisualFML Tool is a development environment for fuzzy-inference-based systems developed by Acampora and Loia [4]. The environment has been completely programmed in Java, so it can be executed on any platform with JRE (Java Runtime Environment) installed. Its functionalities cover the different stages of the fuzzy system design process, from their initial description to the final implementation [4]. It is possible to import a *.fml* file to build a fuzzy controller, and also to export a system created by the tool in a .fml file. The main functionalities the tool provides are the following ones: Fuzzy system description: define the system creating linguistic variables and rules; Verification: monitor the system behavior showing outputs corresponding to different inserted inputs; Tuning: apply algorithms based on neural network; Synthesis: generate high-level languages descriptions. Fig. 4 shows the fuzzy input variable editor in VisualFML and Fig. 5 shows the conceptual framework for the fuzzy controller.

B. Fuzzy Inference Mechanism

In order to design the our proposal of malware behavioral analysis tool, the main fuzzy components composing the system have to be defined. Fig. 6 show the membership functions of the fuzzy variables: File Hash (FH), Connect IP (CI), File Change (FC), and Similarity (SI) respectively. Fig. 7 shows the fuzzy variable control surface viewer. Table IV lists the parameters of the membership functions. Table V lists part of the fuzzy rules, which are constructed by the domain experts. Starting from this initial information, the proposed decision making system will be able to take opportune decisions about the malicious program detection. Next section is devoted to introduce a case study where our intelligent framework has been tested and validated.

TABLE II. THE PART OF EXAMPLE OWL CODE.

```
<?xml version="1.0"?>
<rdf:RDF
   xmlns:rdf="http://www.w3.org/1999/02/22-rdf-syntax-ns#"
   xmlns="file:/D:/TWMAN/TWMAN.owl#"
   xmlns:protege="http://protege.stanford.edu/plugins/owl/protege#"
   xmlns:xsp="http://www.owl-ontologies.com/2005/08/07/xsp.owl#"
   xmlns:owl="http://www.w3.org/2002/07/owl#"
   xmlns:sqwrl="http://sqwrl.stanford.edu/ontologies/built-
ins/3.4/sqwrl.owl#"
   xmlns:xsd="http://www.w3.org/2001/XMLSchema#"
   xmlns:swrl="http://www.w3.org/2003/11/swrl#"
   xmlns:swrlb="http://www.w3.org/2003/11/swrlb#"
   xmlns:rdfs="http://www.w3.org/2000/01/rdf-schema#"
   xmlns:swrla="http://swrl.stanford.edu/ontologies/3.3/swrla.owl#"
  xml:base="file:/D:/TWMAN/TWMAN.owl">
  <owl:Ontology rdf:about="file:/D:/TWMAN/TWMAN.owl">
  <owl:imports
rdf:resource="http://swrl.stanford.edu/ontologies/3.3/swrla.owl"/>
    <owl:imports
rdf:resource="http://sqwrl.stanford.edu/ontologies/built-
ins/3.4/sqwrl.owl"/>
  ...
                </swrl:argument1>
                <swrl:propertyPredicate
rdf:resource="file:/D:/TWMAN/TWMAN.owl#Has_Change"/>
              </swrl:IndividualPropertyAtom>
            </rdf:first>
          </swrl:AtomList>
        </rdf:rest>
      </swrl:AtomList>
    </rdf:rest>
  </swrl:AtomList>
  </swrl:body>
 </swrl:Imp>
 <MS_Win_XP rdf:ID="Win_XP-SP2"/>
 <America rdf:ID="IP_199.7.51.190.80"/>
 <System32 rdf:ID="tmp.edb"/>
 <MS_Win_XP rdf:ID="Win_XP"/>
 <Service_Key rdf:ID="xmlprov"/>
 <MS_Win_Vista rdf:ID="Win_Vista"/>
 <MS_Win_XP rdf:ID="Win_XP-SP1"/>
</rdf:RDF>
<!-- Created with Protege (with OWL Plugin 3.4.2, Build 562)
http://protege.stanford.edu -->
```

TABLE III. PARAMETERS OF THE MEMBERSHIP FUNCTIONS..

Symbol	Fuzzy Term	Membership Function
FH	Very Less	[0, 0, 851, 1276]
	Less	[851, 1276, 1702, 2128]
	Normal	[1702, 2128, 2553, 2979]
	Much	[2553, 2979, 3405, 3830]
	Very Much	[3405, 3830, 4682, 4682]
FC	Very Less	[0, 0, 1818, 2727]
	Less	[1818, 2727, 3636, 4545]
	Normal	[3636, 4545, 5454, 6363]
	Much	[5454, 6363, 7272, 8181]
	Very Much	[7272, 8181, 10000, 10000]
CI	Very Less	[0, 0, 1818, 2727]
	Less	[1818, 2727, 3636, 4545]
	Normal	[3636, 4545, 5454, 6363]
	Much	[5454, 6363, 7272, 8181]
	Very Much	[7272, 8181, 10000, 10000]
SI	Very Low	[0, 0.09, 0.18, 0.27]
	Low	[0.18, 0.27, 0.36, 0.45]
	Medium	[0.36, 0.45, 0.54, 0.63]
	High	[0.54, 0.63, 0.72, 0.81]
	Very High	[0.72, 0.81, 0.90, 1]

TABLE IV. THE PART OF EXAMPLE FML CODE.

```
<?xml version="1.0" encoding="UTF-8"?>
<FuzzyController name="TWMAN-3i5v-1o5v" ip="140.110.96.100">
  <KnowledgeBase>
    <FuzzyVariable name="ConnectIP" domainleft="0.0"
domainright="10000.0" scale="" type="input">
      <FuzzyTerm name="Less" complement="false">
        <TrapezoidShape Param1="1818.181818"
Param2="2727.272727" Param3="3636.363636"
Param4="4545.454545"/>
      </FuzzyTerm>
      <FuzzyTerm name="Much" complement="false">
        <TrapezoidShape Param1="5454.545455"
Param2="6363.636364" Param3="7272.727273"
Param4="8181.818182"/>
      </FuzzyTerm>
      <FuzzyTerm name="Normal" complement="false">
        <TrapezoidShape Param1="3636.363636"
Param2="4545.454545" Param3="5454.545455"
Param4="6363.636364"/>
      </FuzzyTerm>
      <FuzzyTerm name="VeryLess" complement="false">
        <TrapezoidShape Param1="0.0" Param2="0.0"
Param3="1818.181818" Param4="2727.272727"/>
      </FuzzyTerm>
      <FuzzyTerm name="VeryMuch" complement="false">
        <TrapezoidShape Param1="7272.727273"
Param2="8181.818182" Param3="10000.0" Param4="10000.0"/>
      </FuzzyTerm>
    </FuzzyVariable>
    <FuzzyVariable name="FileChange" domainleft="0.0"
domainright="10000.0" scale="" type="input">
      <FuzzyTerm name="Less" complement="false">
        <TrapezoidShape Param1="1818.181818"
Param2="2727.272727" Param3="3636.363636"
Param4="4545.454545"/>
      </FuzzyTerm>
      <FuzzyTerm name="Much" complement="false">
        <TrapezoidShape Param1="5454.545455"
Param2="6363.636364" Param3="7272.727273"
Param4="8181.818182"/>
      </FuzzyTerm>
      ...
      </Consequent>
    </Rule>
  <Rule name="RULE99" connector="and" operator="MIN"
weight="1.0">
      <Antecedent>
        <Clause>
          <Variable>FileHash</Variable>
          <Term>Less</Term>
        </Clause>
        <Clause>
          <Variable>FileChange</Variable>
          <Term>VeryLess</Term>
        </Clause>
        <Clause>
          <Variable>ConnectIP</Variable>
          <Term>Less</Term>
        </Clause>
      </Antecedent>
      <Consequent>
        <Clause>
          <Variable>Similarity</Variable>
          <Term>VeryLow</Term>
        </Clause>
      </Consequent>
    </Rule>
  </RuleBase>
</FuzzyController>
```

TABLE V. PART OF THE FUZZY RULES

Rule No	Fuzzy Variable			
	Input			Output
	FH	FC	CI	SI
1	Normal	Normal	Normal	Medium
2	Normal	Normal	Very Much	High
3	Normal	Normal	Much	Medium
4	Normal	Normal	Less	Low
5	Normal	Normal	Very Less	Very Low
6	Normal	Very Much	Normal	Medium
7	Normal	Very Much	Very Much	High
8	Normal	Very Much	Much	High
9	Normal	Very Much	Less	Medium
10	Normal	Very Much	Very Less	Medium
11	Normal	Much	Normal	Medium
12	Normal	Much	Very Much	High
13	Normal	Much	Much	High
		...		
114	Very Less	Normal	Less	Low
115	Very Less	Normal	Very Less	Low
116	Very Less	Less	Very Much	Low
117	Very Less	Less	Much	Medium
118	Very Less	Less	Normal	Low
119	Very Less	Less	Less	Low
120	Very Less	Less	Very Less	Very Low
121	Very Less	Very Less	Very Much	Low
122	Very Less	Very Less	Much	Medium
123	Very Less	Very Less	Normal	Medium
124	Very Less	Very Less	Less	Low
125	Very Less	Very Less	Very Less	Very Low

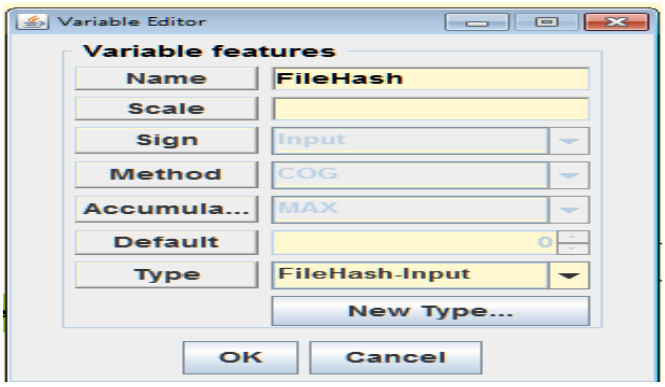

Figure 4. The fuzzy input variable editor in VisualFML .

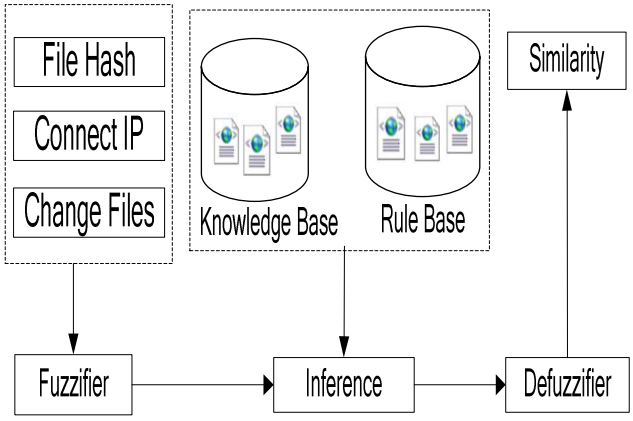

Figure 5. conceptual framework for the fuzzy controller

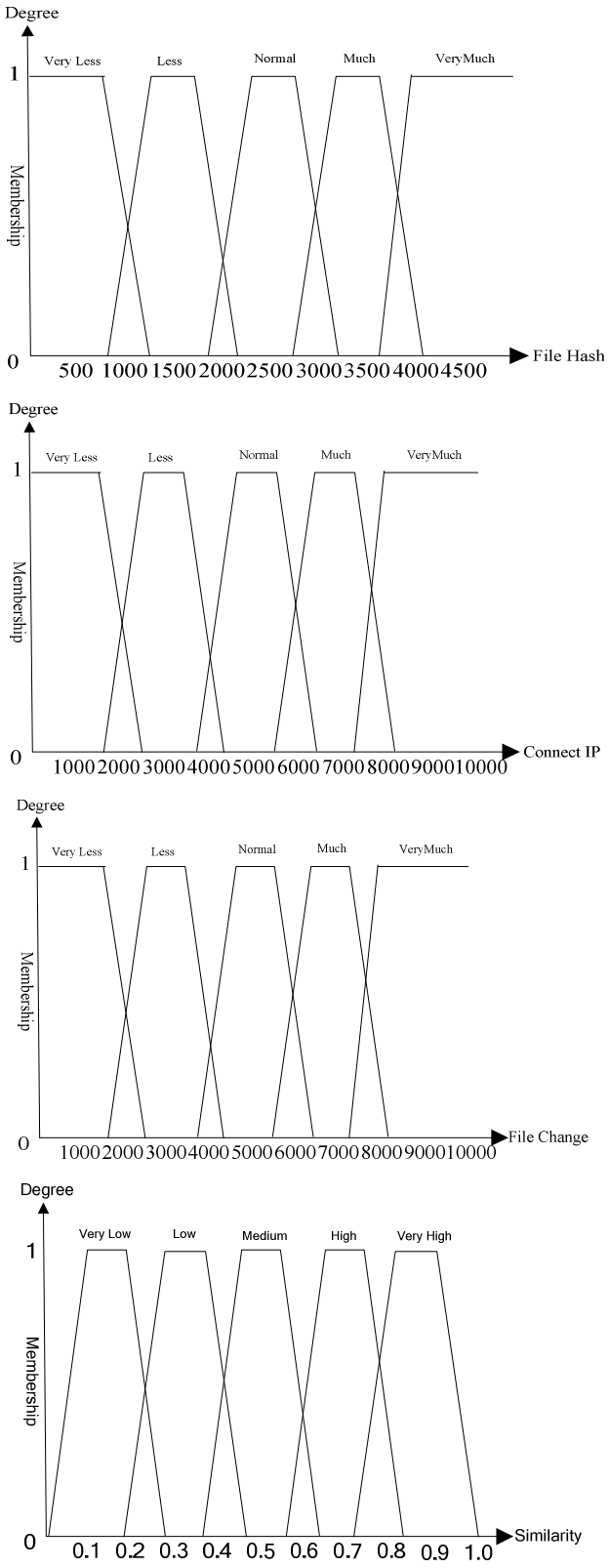

Figure 6. the membership functions of the fuzzy variables.

IV. EXPERIMENTAL RESULTS

In order to evaluate the effectiveness of the proposed approach, we adopt 30 attendance records retrieved from the malware repository of National Center for High Performance and Computing (NCHC) as the experimental data in Table VI. Fig. 7 shows a three-dimensional graphical representation of the system behavior and results of fuzzy inference process, which the values of the different output variables for a given set of input values.

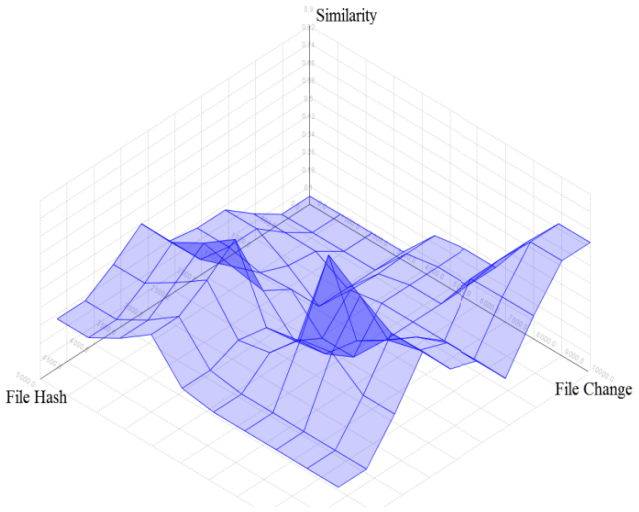

Figure 7. Fuzzy variable control surface viewer.

TABLE VI. EXPERIMENTAL DATA INPUT.

	Input			Output	
Unit	[0,4762]	[0,10000]	[0,10000]	[0,1]	
No	FH	CI	FC	SI	
				Desired	Inferred
01	40	0	998	0.977	0.136
02	0	8480	316	1	0.5
03	0	7332	194	0	0.5
04	0	10000	563	0.976	0.681
05	0	10000	2675	0	0.512
06	0	10000	2677	0	0.512
07	8	115	42	0	0.136
08	0	5726	553	0.951	0.375
09	12	10000	2586	0.951	0.5
10	6	10000	6198	0.951	0.681
11	0	10000	3375	0	0.5
12	195	0	1048	0.829	0.136
13	69	0	16	0.95	0.136
14	654	0	17	0.95	0.136
15	3522	7850	43	0.976	0.681
16	3140	7850	6450	0.976	0.681
17	3980	10000	10000	0.951	0.863
18	3540	10000	4357	0.951	0.727
19	2654	60	1423	0.976	0.364
20	3474	254	4750	0.95	0.318
21	941	10000	350	0.976	0.542
22	4112	10000	3456	1	0.863
23	50	930	132	0.976	0.136
24	359	10000	3246	0.976	0.5
25	298	339	6756	1	0.318
26	3728	0	2585	0.976	0.514
27	4	0	28	0.825	0.136
28	4613	947	6541	0.951	0.318
29	293	0	2831	0.951	0.136
30	4174	9543	7585	0.878	0.747

TABLE VII. VARIOUS PARAMETERS USED IN EQS. (1), (2) AND (3).

Actual results	Prediction results	
	YES	NO
YES	TP (true positive)	FN (false negative)
NO	FP (false positive)	TN (true negative)

$$Accuracy = (TN+TP)/(TP+TN+FP+FN) \times 100\% \quad (1)$$

$$Precision = TP/(TP+FP) \times 100\% \quad (2)$$

$$Recall = TP/(TP+FN) \times 100\% \quad (3)$$

The accuracy, precision and recall functions are shown by Eqs. (1), (2) and (3), respectively. The parameters of TP, FP, FN and TN are defined and listed in Table VII. The distribution of the accuracy, precision and recall are shown in Fig. 8.

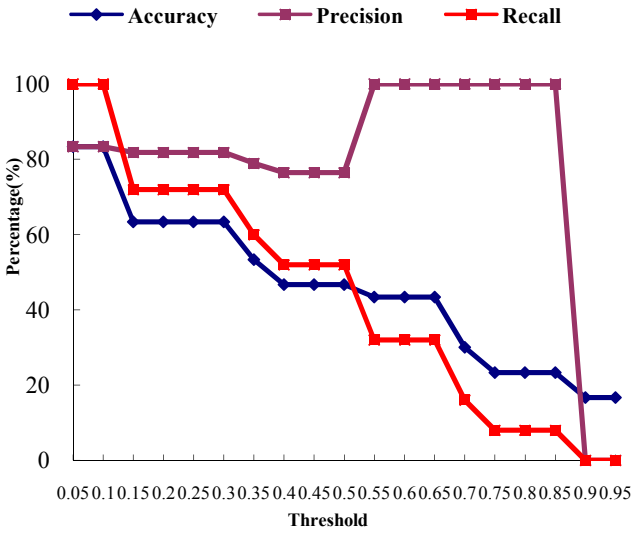

Figure 8. Results of the accuracy, precision and recall.

V. CONCLUSION

In this study, fuzzy ontology for malware behavioral analysis scheme based on FML has been presented. It is composed of a fuzzy inference and semantic decision-making mechanism to describe the changes of the registry key value, network connection and file to build the ontology and behavioral rules. The experimental results show that our approach will feasible and usable for malware behavioral analysis system. It can utilize them to determine the behaviors of virus or malicious program to provide better protection and services to end users.

In the future, there are more vague knowledge of OS platform with experimental data will be collected, and type-1 FML is not enough to deal with. Therefore, some upgradable technologies, like genetic algorithm and type-2 fuzzy set, will be update to be exercised for comparing with the current technology. We also compare the performance with other classification methods. In order to take prompt and appropriate measures, TWMAN can integrate with a human thinking semantic model. Therefore, we consider that TWMAN could be a powerful tool to improve the network safety.

ACKNOWLEDGMENT

The authors would like to thank the National Center for High Performance Center of Taiwan for financially supporting this open source research project. In addition, the authors would like to thank National Science Council of Taiwan for financially supporting this research under the Grant NSC 99-2923-E-024-003-MY3, NSC 98-2221-E-024-009-MY3, NSC 99-2911-I-024-004 and NSC 99-2218-E-492-006 .

REFERENCES

[1] H. D. Huang, T. Y. Chuang, Y. L. Tsai, and C. S. Lee, "Ontology-based Intelligent System for Malware Behavioral Analysis," in Proceeding of the *2010 IEEE World Congress on Computational Intelligence (WCCI2010)*, Barcelona, Spain, Jul. 18-23, 2010, pp. 1-6.

[2] H. Zhao, M. Xu, N. Zheng, J. Yao, and Q. Ho, "Malicious Executables Classification Based on Behavioral Factor Analysis," *2010 International Conference on e-Education, e-Business, e-Management and e-Learning*, Sanya, China, 2010.

[3] H. D. Huang, C. S. Lee, H. Y. Kao, Y. L. Tsai, and J. G. Chang, "Malware Behavioral Analysis System: TWMAN," in Proceeding of the *2011 IEEE Symposium on Computational Intelligence for Intelligent Agent (IEEE SSCI 2011)*, Paris, France, Apr. 11-15, 2011, pp. in press.

[4] C. S. Lee, Z. W. Jian, and L. K. Huang, "A fuzzy ontology and its application to news summarization," *IEEE Transactions on Systems, Man and Cybernetics Part B,* vol. 35, no. 5, pp. 859-880, 2005.

[5] M. H. Wang, C. S. Lee, K. L. Hsieh, C. Y. Hsu, G. Acampora, and C. C. Chang, "Ontology-based multi-agents for intelligent healthcare applications," *Journal of Ambient Intelligence and Humanized Computing,* vol. 1, no. 2, pp. 111-131, Jun. 2010.

[6] F. G. Sanchez, R. M. Bejar, L. Contreras, J. T. F. Breis, and D. C. Nieves, "An ontology-based intelligent system for recruitment," *Expert Systems with Applications,* vol. 31, no. 2, pp. 248-263, Aug. 2006.

[7] T. T. Quan, S. C. Hui, and A. C. M. Fong, "Automatic fuzzy ontology generation for semantic help-desk support," *IEEE Transactions on Industrial Informatics,* vol. 2, no. 3, pp. 155-164, Aug. 2006.

[8] T. T. Quan, S. C. Hui, A. C. M. Fong, and T. H. Cao, "Automatic fuzzy ontology generation for semantic web," *IEEE Transactions on Knowledge and Data Engineering,* vol. 18, no. 6, pp. 842 - 856, Jun. 2006.

[9] S. H. Ho, C. L. Yang, C. Y. Chen, C. Y. Hsu, and Y. K. Chang, "An Intelligent-Mamdani Inference Scheme for Healthcare Applications Based on Fuzzy Markup Language," in Proceeding of the *2009 10th International Symposium on Pervasive Systems, Algorithms, and Networks (ISPAN2009)*, Kaohsiung, Taiwan, Dec. 14-16, 2009, pp. 400-404.

[10] G. Acampora and V. Loia, "Using fml and fuzzy technology in ambient intelligent environments," *International Journal of Computational Intelligence Research,* vol. 1, no. 2, pp. 171-182, 2005.

[11] F. Bobillo and U. Straccia, "Representing fuzzy ontologies in OWL 2," in Proceeding of the *2010 IEEE International Conference on Fuzzy Systems (FUZZ-IEEE 2010)*, 18-23 July, 2010, pp. 1-6.

[12] J. Kornblum. (2010). *ssdeep*. Available: http://ssdeep.sourceforge.net

[13] T. Hungenberg and M. Eckert. (2010). *INetSim*. Available: http://www.inetsim.org

[14] R. Lehti and P. Virolainen. (2011). *AIDE*. Available: http://aide.sourceforge.net

[15] G. Acampora and V. Loia, "Fuzzy control interoperability and scalability for adaptive domotic framework," *IEEE Transactions Industrial Informatics,* vol. 1, no. 2, pp. 97-111, May 2005.

[16] J. Stewart, "Behavioural malware analysis using Sandnets," *Computer Fraud & Security,* vol. 2006, no. 12, pp. 4-6, Dec. 2006.

2011 IEEE International Conference on Fuzzy Systems
June 27-30, 2011, Taipei, Taiwan

Applying Fuzzy AHP to Study the KSFs of Information Security Management

Jen-Sheng Wang
Institute of Technology Management, National Chiao-Tung University
Hsinchu County, Taiwan
vincent.mt98g@nctu.edu.tw

Che-Hung Liu
Department of Business & Management, National University of Tainan
Tainan City, Taiwan
chehung@mail.nutn.edu.tw

Joseph Z. Shyu
Institute of Technology Management, National Chiao-Tung University
Hsinchu County, Taiwan
joseph@cc.nctu.edu.tw

Hsiao-Wen Huang
Department of Information Management
Chang Jung Christian University, Taiwan
victoria@mail.cjcu.edu.tw

***Abstract* - The launch of the digital era has made information security management a most significant and critical issue. However, perfect information security management requires certain factors for complete success. This study aims to collect Key Success Factors (KSFs) for information security management through literature review and design of a questionnaire survey. This comprises four major aspects: (1) External dimension, (2) Internal dimension, (3) Technology dimension, and (4) Execution dimension. Based on these, we proceed with categorization and analysis using Fuzzy Analytic Hierarchy Process (Fuzzy AHP or FAHP), which was applied to this study to overcome the seeming failure of general Analytical Hierarchy Process (AHP) in dealing with respondents' impersonal differences in paired comparison.**

The ordered ranking of objectives under each aspect is: system, human resource, security function, organization, performance, operation, market, and legislation. The results sifted from the FAHP approach suggest five top key success factors: "Training Plan", "MIS Staffing", "System Structure", "Regulation", and "Maintain Service".

***Keywords* - Information Security Management, Key Success Factors, Fuzzy Analytic Hierarchy Process**

I. INTRODUCTION

It has been recognized that due to the development of information and communication technology, most organizations now heavily rely on information systems to provide effective information for supporting operation and decision activities. This information is valuable and important capital for organizations. Porter and Millar stated that the complete information management keeps an enterprise competitive [1]. Information management also sustains an enterprise's competitive advantage [2], and contributes to its performance [3, 4]; Obviously, the key issue is how to manage information security systems to meet the requirements of all of organizations and achieve organization's goals [5]. Torres et al. also mentioned the importance of information security management to ensure an organization can take advantage of information management, with its criticality, openness and risk [6].

Gordon and Martin analyzed the role of information security based on the viewpoint of competition systems [7]. They regarded investment in information security to have extreme value, as it could help an organization occupy markets and upgrade competence. Organizations should make appropriate information security management policies in order to keep their information system safe [8, 9]. Information security management issues could be addressed through several dimensions and diverse means [10], but might be concluded to be the combination of information, technology, and people [11]. Another definition is that information security management is the detection and prevention of unauthorized actions from computer system users [12, 13]. There are many factors that will affect the organizational policies for information security management [14]. Austin et al. also pointed out that certain key items should be noted to implement information security management [15].

As discussed above, in order to realize the importance of information security management implementation through study, we use theories, key success factors (KSFs) and Fuzzy AHP. Identification of the KSFs of information security management implementation is a multiple-criteria decision making (MCDM) problem with many quantitative and qualitative attributes. We selected the analytic hierarchy process (AHP) method developed by Saaty [16], as it has been widely applied for affirming the issue of criteria importance [17]. However, conventional AHP uses pairwise comparisons at each level with respect to the importance of criteria for the goal, and judge by using a nine-degree scale. So there is a possibility that the application of Saaty's AHP might have some shortcomings [18].

In addition, respondent considerations on criteria priority and importance always contain ambiguity and multiplicity of meaning. It is also recognized that human assessment of qualitative attributes is always subjective and thus imprecise. Therefore, conventional AHP seems inadequate to explicitly capture the considerations of respondents. In order to model this uncertainty in human preference, fuzzy sets could be incorporated with pairwise comparison as an extension of AHP.

978-1-4244-7316-8/11/$26.00 ©2011 IEEE

This Fuzzy AHP was formerly proposed to solve the inevitable vagueness incident to AHP, and allows a more accurate description of the decision making process.

In this research, a fuzzy AHP approach is proposed to compensate for the vagueness and uncertainty of the attribute importance determination of respondents. This approach is used because the crisp pairwise comparison of conventional AHP seems too insufficient and imprecise in capturing the degree of importance of respondents' KSF evaluations. Our goal is to discover the KSFs of information security management implementation, and apply Fuzzy AHP to analyze them.

II. LITERATURE REVIEW

A. Key Success Factors (KSFs)

The perspective of KSFs was first proposed by Daniel [19], who stated that most successful organizations possess three to six fundamental elements. An organization that wants to succeed must focus and specialize on these essentialities. Most recently, the KSFs concept has been widely applied to management research. Many researchers apply it, especially in industrial analysis and strategy management where the concept of KSFs is interpreted and extended. This shows KSFs becoming explainable, durable, and consistent [20, 21, 22, 23, 24]

We concur with previous researchers who argued that KSFs are characters, criteria, or variables. If these factors are appropriately supported, maintained, and managed, they would be greatly beneficial to the success of organizations in certain industries [25]. KSFs would be a character, like price competence, and also a criterion, like capital structure or superior customer combination.

B. Fuzzy Analytic Hierarchy Process (FAHP)

The earliest research in fuzzy AHP was argued by van Laarhoven and Pedrycz [26], who compared fuzzy ratios described by triangular membership functions. In this research, Lootsma's logarithmic least square was used to derive local fuzzy priorities. Later, using geometric mean, Buckley determined fuzzy priorities of comparison ratios whose membership functions were trapezoidal [27]. Modifying van Laarhoven and Pedrycz's method, Boender et al. presented a more robust approach to the normalization of local priorities [28]. Taking the perspective, Chang [29] and Mikhailov [30] applied row mean method to obtain priorities for comparison ratios which were fuzzy triangular numbers.

All the aforementioned works compute fuzzy priorities based on arithmetic operations for fuzzy triangular (or trapezoidal) numbers. To be able to use fuzzy arithmetic operations, specific assumptions on the forms of membership functions are required. To date, there are only a limited number of membership-function forms that are computationally manageable. Moreover, the accuracy of the final ranking is inevitably weakened by the series of approximations required during the computation procedure. But the most important criticism on these works has to be their failure to address the issue of consistency.

The issue of consistency in fuzzy AHP was first tackled by Salo [31]. Departing from the fuzzy arithmetic approach, Salo derived fuzzy weights using an auxiliary programming formulation, which described relative fuzzy ratios as constraints on the membership values of local priorities. Expressing relative weights' feasible region in terms of linear inequalities was previously proposed by Arbel [32], and extended in Salo and Hämäläinen [33]. Requiring only quasi-concave and continuous fuzzy comparison ratios, Salo defined consistency in terms of the mean values of the fuzzy ratios (range of values with membership degree equal to one). Here, a fuzzy matrix was considered consistent if there were a set of crisp relative weights within the feasible region defined by the ranges of mean values. When the matrix was not consistent (no crisp weights existed), Salo proposed a simple heuristic which enlarged the feasible region and also guaranteed feasible weights.

After the above literature review, we found the fuzzy AHP method modified problems that might happen in the traditional AHP method, including imprecision, obscurity and disproportion of scales. Therefore, this research decided to use the fuzzy AHP method to study weights of the KSFs of information security management implementation. This is by using triangular fuzzy numbers, group integration, and fuzzy ranking to build fuzzy analytic hierarchy process.

III. FAHP RESEARCH APPROACH

The FAHP research approach for studying the KSFs of information security management is demonstrated in the following steps:

Step 1: Building the Hierarchy Model and Its Criteria

Based on literature review, we used KJ method to build the hierarchy model [34]. After revising both the hierarchy and descriptions of criteria, we finally developed a hierarchy KSFs model (refer to Figure 1). The first level is the goal, the KSFs of information security management. The second level is the four aspects of the KSFs. The third level is objectives which affect the success of information security management. The fourth level represents all involved and relevant criteria.

Step 2: Designing the Questionnaire

Using the hierarchy model built in Step 1, we adopt the concept of AHP to design the questionnaire as pairwise comparison of the relative importance of criteria, using a scale from 1 to 9, to form comparison matrices.

Based on the FAHP analysis, the variables were compared in pairs. The relative importance between two variables, from low to high, was mainly given five ranks: (1) for equally important, (3) for slightly important, (5) for very important, (7) for extremely important, and (9) for absolutely important. Ranks (2), (4), (6), and (8) in were also assigned between these ranks accordingly. In fuzzy sets, the interval value, instead of crisp value, was provided for filling in the questionnaires for the pairwise comparison.

Step 3: Building Fuzzy Converted Judgments $\tilde{M}_{ij}$ *Matrices*

We used the triangular membership function and cuts to convert the subjective judgments of the respondents to fuzzy judgments. We extracted the judgments of each criterion, objective and aspect, and use the triangular fuzzy number rules on Table I to convert.

Table Ⅰ. Triangular fuzzy numbers for the pairwise comparison scale

Linguistic Scale	Triangular fuzzy numbers
Equal Important	$\tilde{1}=(1,1,1)$
Between each ranks	$\tilde{2}=(1,2,3)$
Slightly Important	$\tilde{3}=(2,3,4)$
Between each ranks	$\tilde{4}=(3,4,5)$
Very Important	$\tilde{5}=(4,5,6)$
Between each ranks	$\tilde{6}=(5,6,7)$
Extremely important	$\tilde{7}=(6,7,8)$
Between each ranks	$\tilde{8}=(7,8,9)$
Absolutely important	$\tilde{9}=(8,9,10)$

We first formulated all initial individual fuzzy comparison matrices based on the triangular membership function, then used Microsoft Excel to calculate the fuzzy weight.

$$M=\left[\tilde{M}_{ij}\right]\ ;\quad \tilde{M}_{ij}=\left(L_{ij},M_{ij},R_{ij}\right)\ ;\quad \tilde{M}_{ij}=1\Big/\tilde{M}_{ji}\ ,\quad \forall i,j=1,2,\ldots,n \tag{1}$$

Step 4: Group Integration

We used the geometric approach of Buckley to integrate respondents' judgments into group fuzzy comparison matrices [27]. The formula is as follows:

$$\tilde{m}_{ij}=(1/N)\otimes(\tilde{m}_{ij}^{1}\oplus\tilde{m}_{ij}^{2}\oplus\ldots\oplus\tilde{m}_{ij}^{N}) \tag{2}$$

Step 5: Calculating Fuzzy Weights

We calculated fuzzy weights $\tilde{w}_i$ through the following formulas:

$$\tilde{Z}_i=\left(\tilde{a}_{i1}\otimes\tilde{a}_{i2}\otimes\ldots\otimes\tilde{a}_{in}\right)^{\frac{1}{n}},\forall i=1,2,\ldots,n \tag{3}$$

$$\tilde{w}_i=\tilde{Z}_i\otimes\left(\tilde{Z}_1\oplus\tilde{Z}_2\oplus\ldots\tilde{Z}_n\right)^{-1} \tag{4}$$

Step 6: Defuzzication

We took the algorithm developed by Teng & Tzeng to do defuzzication [54]. The equation of the weights of defuzzication, DF_{ij}, is as follows:

$$DF_{ij}=\left[\left(R_{ij}-L_{ij}\right)+\left(M_{ij}-L_{ij}\right)\right]/3+L_{ij} \tag{5}$$

Step 7: Normalization

The formula of normalization weights NW_i is as follows:

$$NW_i=DF_{ij}/\sum DF_{ij} \tag{6}$$

Step 8: Series of Hierarchical

Through the above steps, we got the weights NW_i of "i" aspect at level 2, and NW_{ij} of "j" objective at level 3 under certain level 2 aspect. NW_{ijk} is the weight of criterion "k" at level 4. If we want to get NW_k, the final weight of "k" criterion under level 1, the top goal of this research, we calculate per series of hierarchical using formula (7).

$$NW_K=NW_i\times NW_{ij}\times NW_{ijk} \tag{7}$$

With above illustration and calculus, we can get the weights to rank the priority of KSFs after series of hierarchical, achieving the goal of this research. This research mainly used Microsoft Excel to process data and analyze the questionnaire.

IV. EVALUATING HIERACHICAL STRUCTURE FOR KSFS

This research found the KSFs of information security management through literature review, then extracted and compiled the KSFs into 25 criteria, as Table Ⅱ illustrates. Next, we used KJ method to categorize these 25 criteria into 8 objectives, then conducted these 8 objectives into 4 aspects to fulfill the goal, the KSFs of information security management. The 4 aspects are: (1) External Dimension; (2) Internal Dimension, (3) Technology Dimension, and (4) Execution Dimension. KSFs could be inducted from the External and Internal Dimension of the organization, or the condition of the topic [22, 35, 36, 37]. A successful information security management results from the two dimensions Technology and Execution [38, 39, 40]. In this way, we completed the framework of the research hierarchy shown in Figure 1.

(Table Ⅱ. The criteria of KSFs and relative references)

(Figure 1. The hierarchy model of KSFs of information security management.)

V. DATA ANALYSIS

We released a total of 25 expertise questionnaires and collected results for all. Ten of the respondents are experts in the information security system industry, and the other 15 are information system managers in sizable companies. The following results were obtained through Fuzzy AHP analysis.

A. The Evaluation Results and the Analysis of the Measurement in Level 2

The level 2 aspects are: (1) External Dimension, (2) Internal Dimension, (3) Technology Dimension, and (4) Execution Dimension. The fuzzy weighted values and rankings are shown in Table Ⅲ.

Table Ⅲ. The fuzzy weights of the aspects

Aspects	Fuzzy weights	Ranking
External Dimension	0.12	4
Internal Dimension	0.21	3
Technology Dimension	0.38	1

Execution Dimension	0.29	2
CI=0.047 CR＝0.049		

Table Ⅲ states that the Technology Dimension is the most important aspect of the KSFs of information security management. The next in importance was the Execution Dimension. The Internal Dimension is the third most important factor, and the External Dimension is the last.

B. The Evaluation Results and the Analysis of the Measurement in Level 3

The level 3 objectives and their fuzzy weighted values and ranking are shown in Table Ⅳ.

Table Ⅳ. The fuzzy weights of the objectives

Level 2 Aspects	Level 3 Objectives	Fuzzy weights	Ranking	Tests
External Dimension	Legislation	0.46	2	CI=0.046 CR=0.080
	Market	0.54	1	
Internal Dimension	Organization	0.61	1	CI=0.049 CR=0.084
	Operation	0.39	2	
Technology Dimension	System	0.52	1	CI=0.034 CR=0.059
	Security Function	0.48	2	
Execution Dimension	Human Resource	0.65	1	CI=0.046 CR=0.079
	Performance	0.35	2	

C. The Evaluation Results and the Analysis of the Measurement in Level 4

The level 4 criteria and their fuzzy weighted values and ranking are shown in Table Ⅴ.

(Table Ⅴ. The fuzzy weights of the criteria)

D. The Weights of Series of Hierarchical

Using Tables 3, 4, and 5, we can calculate the weights after series of hierarchical to rank all criteria in the KSFs of information security management. This is shown in Table Ⅵ.

(Table Ⅵ. The weights after series of hierarchical)

Table 6 demonstrates the final results from using FAHP to rank the KSFs in order of importance, using the data on the 25 criteria received from respondents. The highest final weight is "Training Plan" under Human Resource, which accounts for about 8.1% and is therefore the most important factor. The second is "MIS Staffing", also under Human Resource, which accounts for 6.6%. The close relationship of these criteria to the "Human Resource" objective could obviously indicate that people are a critical aspect of information security management execution.

The third most important accounted for 6.2%, and is "System Structure" under System and the most important factor at Technology Dimension. However, since Technology Dimension is the most important aspect, its factors are comparatively unremarkable. The fourth most important factor, "Regulation", accounts for 5.5%. We understand that government policy has some affect on enterprises implementing information security management. The System's "Maintain Service" accounted for 5.3%, and is fifth in the ranking. It seems enterprises rely more on system suppliers' service.

VI. CONCLUSION

This research adopts Fuzzy AHP that ranks the KSFs of information security management per investigation of expert opinions in this field. By using the empirical analysis results, we verified the perspectives of previous research on factors affecting information security systems, and worked out systematic priority of these factors. The results can also be organized and interpreted to form suggestions to relevant people. This Fuzzy AHP approach makes this research capable of precisely disclosing the importance of factors and developing deep knowledge of them.

The research results of the KSFs of information security management analyze the 25 criteria listed previously in this paper, and suggest the more critical success factors for information security management. Although some weights are distributed averagely, we can still realize successful information security management through multi-aspect efforts to achieve the goal without neglecting anyone.

The "Technology Dimension" aspect conclusively takes the first position, and reveals that technology criteria all play considerably important roles in information security management. Although "Execution Dimension" does not rank as high as "Technology Dimension" in aspect comparison, its criteria under the Human Resource objective, "Training Plan" and "MIS Staffing", are the two most important criteria. This shows that reviewing KSFs from different levels may result in different answers, and this is evidently also pointed out by AHP analysis.

REFERENCES

[1] M.E. Porter, and V.E. Millar, "How Information Gives You Competitive Advantage," *Harvard Business Review*, Jul.-Aug., pp. 149-160, 1999.

[2] F.J. Mata, W.L. Fuerst, and J.B. Barney, "Information technology and sustained competitive advantage: A resource-based…," *MIS Quarterly*, vol. 19, no. 4, pp. 487-505, 1995.

[3] N. Melville, K. Kraemer, and V. Gurbaxani, "Review: Information technology and organizational performance: An integrative model of IT business value," *MIS Quarterly*, vol. 28, pp. 283-322, 2004.

[4] T.C. Powell, and A. Dent-Micallef, "Information Technology as Competitive Advantage: The Role of Human, Business, and Technology Resources," *Strategic Management Journal*, vol.18, no. 5, pp. 375-405, 1997.

[5] T.Jr. Dellecava, "In security: Is technology putting your company's primary asset it's information at risk?," *Sales and Marketing Management*, vol. 148, no. 4, pp. 39-50, 1996.

[6] J.M. Torres, J.M. Sarriegi, J. Santos, & N. Serrano, "Managing Information Systems Security: Critical Success Factors and Indicators to Measure Effectiveness," Lecture Notes in Computer Science 4176, *Springer-Verlag*, pp. 530-545, 2006.

[7] L.A. Gordon, and P. Maltin, "Using Information Security as a Response to Competitor Analysis Systems," *Communications of the ACM*, vol. 44, no. 9, pp. 70-75, 2001.

[8] A. Kankanhalli, H.H. Teo, B.C.Y. Tan, & K.K. Wei, "An integrative study of information system security effectiveness," *Internation Journal of Information Management*, vol. 23, pp. 139-154, 2003.

[9] P. Ward, and C.L. Smith, "The Development of Access Control Policies for Information Technology Systems," *Computers & Security*, vol. 21, no. 4, 356- 371, 2002.
[10] R.V. Solms, "Information Security Management: The Second Generation," *Computers & Security*, vol. 15, pp. 281-288, 1996.
[11] S. Hinde, "If you can meet with triumph and disaster, and treat those two impostors just the same," *Computers & Security*, vol. 20, no. 8, pp. 657-666, 2001.
[12] D. Gollmann, *Computer Security*, NY: John Wiley & Sons Ltd, 1999.
[13] D.B. Parker, *Fighting computer crime: a new framework for protecting information*, NY: John Wiley and Sons, 1998.
[14] C. Pounder, "The European Union Proposal for a Policy towards Network and Information Security," *Computers & Security*, vol. 20, no. 7, pp. 573-576, 1998.
[15] R.D. Austin, C.A. Darby, & A.R. Christopher, "The Myth of Secure Computing, " *Harvard Business Review*, vol. 81, no. 6, pp. 120-126, 2003.
[16] T.L. Saaty, *The Analytic Hierarchy Process*. New York: McGraw-Hill, 1980.
[17] Z. Ayăg, "An analytic-hierarchy-process based simulation model for implementation and analysis of computer-aided systems," *International Journal of Production Research*, vol. 40, pp. 3053–3073, 2002.
[18] T.L. Saaty, "Decision Making, Scaling, and number crunching," *Decision Science*, vol. 20, pp. 404–409, 1989.
[19] D.R. Dainel, "Management Information Crisis," *Harvard Business Review*, vol. 39, no. 5, pp. 107-118, 1961.
[20] D.A. Aakers, *Strategic Market Management*, New York; Wiley and Sons, 1984.
[21] A.C. Boynton, and R.W. Zmud, "An Assessment of Critical Success Factor," *Sloan Management Review*, Summer, pp. 19-21, 1984.
[22] C. Ferguson, and R. Dickinson, "Critical success factors for directors in the eighties," *Business Horizons,* vol. 25, no. 3, pp. 14-18, 1982.
[23] C.W. Hofer, and D. Schendle, *Strategy Formulation: Analytical Concepts*, St. Paul: West Publishing, 1978.
[24] J.F. Rockart, "Chief Executives Define Their Own Data Needs," *Harvard Business Review*, Mar.-Apr., pp. 85, 1979.
[25] A.A. Thompson, and A.J. Strickland, *Crafting and Implementing Strategy,* 10th ed. New York: McGraw Hill, 1998.
[26] P.J.M. van Laarhoven, and W. Pedrycz, "A fuzzy extension of Saaty's priority theory," *Fuzzy Sets and Systems*, vol. 11, pp. 229-241, 1983.
[27] J.J. Buckley, "Fuzzy Hierarchical Analysis," *Fuzzy Sets and Systems*, vol. 17, pp. 233-247, 1985.
[28] C.G.E. Boender, J.G. de Graan, & F.A. Lootsma, "Multicriteria decision analysis with fuzzy pairwise comparisons," *Fuzzy Sets and Systems*, vol. 29, pp. 133-143, 1989.
[29] D.Y. Chang, "Application of the extent analysis method on fuzzy AHP," *European Journal of Operational Research*, vol. 95, pp. 649-655, 1996.
[30] L. Mikhailov, "Deriving priorities from fuzzy pairwise comparison judgments," *Fuzzy Sets and Systems*, vol. 134, no. 3, pp. 365 -385, 2003.
[31] A.A., Salo, "On fuzzy ratio comparisons in hierarchical decision models," *Fuzzy Set and Systems*, vol. 84, pp. 21–32, 1996.
[32] A. Arbel, "Approximate articulation of preference and priority derivation," *European Journal of Operational Research*, vol. 43, pp. 317-326, 1989.
[33] A.A. Salo, and R.P. Hämäläinen, "Preference programming through approximate ratio comparisons," *European Journal of Operational Research*, vol. 82, pp. 458–475, 1995.
[34] H. Kawakita, *The KJ Method*. Tokyo: Chu-Ko-Sinsho, 1986.
[35] R.B. Duncan, "Characteristics of Organizational Environment and Perceived Environmental Uncertainty," *Admin. Sci. Quart.*, vol. 17, pp. 313-327, 1972.
[36] F. Zahedi, "Reliability of information systems based on the critical success factors-formulation," *MIS Quarterly*, vol. 11, no. 2, pp. 187-204, 1987.
[37] R. Sabherwal, A. Jeyaraj, & C. Chowa, "Information system success: Individual and organizational determinants," *Management Science*, vol. 52, pp. 1849-1864, 2006.
[38] D.L. Carter, and A.J. Katz, "Computer Crime and Security: the Perceptions and Experiences of Corporate Security Directors," *Security Journal*, vol. 7, pp. 101-108, 1996.
[39] M.M. Eloff, and V.S.H., Solms, "Information Security Management: An Approach to Combine Process Certification and Product Evaluation," *Computers & Security*, vol. 19, pp. 698-709, 2000.
[40] D. Trěek, "An Integral Framework for Information Systems Security Management," *Computers & Security*, vol. 22, no. 4, pp. 337-360, 2003.
[41] E.E. Anderson, and J. Choobineh, "Enterprise Information Security Strategies," *Computers & Security*, vol. 27, pp. 22-29, 2008.
[42] M. Caminada, "Internet security incidents, a survey with Dutch organizations," *Computer & Security*, vol. 17, pp. 417-433, 1998.
[43] A.J.T. Chang, and Q.J. Yeh, "On Security Preparations against Possible IS Threats across Industries," *Information Management & Computer Security*, vol. 14, no. 4, pp. 343-360, 2006.
[44] P. Chwelos, I. Benbasat, I. & A.S. Dexter, "Research report :empirical test of an EDI adoption model," *Information Systems Research*, vol. 12, no. 3, pp. 304-321, 2001.
[45] F. Cohen, "Information System Attacks : A Preliminary Classification Scheme," *Computers and Security*, vol. 16, no. 1, pp. 26-47, 1997.
[46] G. Dhillon, and J. Backhouse, "Current directions in IS security research: towards socio-organizational perspectives," *Information Systems Journal*, vol. 11, no. 2, pp. 127-153, 2001.
[47] L.A. Gordon, and M.P. Loeb, "Budgeting Process for Information Security Expenditures," *Communications of the ACM*, vol. 49, no. 1, pp. 121-125, 2006.
[48] T. Lillywhite, "How to protect your information - an introduction to BS7799," *Management Services*, vol. 43, no. 1, pp. 20-21, 1999.
[49] J. Olnes, "Development of Security Policies," *Computer & Security*, vol. 13, pp. 628-636, 1994.
[50] K. Osborne, "Auditing the IT security function," *Computers & Security*, vol. 17, no. 1, pp. 34-41, 1998.
[51] W. Ozier, "Generally Accepted System Security Principles (GASSP)," *Computer Security Journal*, vol. 13, no. 2, pp. 69-75, 1997.
[52] E.E. Schultz, R.W. Proctor, M.C. Lien, & G. Salvendy, "Usability and Security An Appraisal of Usability Issues in Information Security Methods," *Computer & Security*, vol. 20, no. 7, pp. 620-634, 2001.
[53] J.K. Tudor, *Information Security Architecture*. FL, Boca Raton: Auerbach Publications, 2001.
[54] J.Y. Teng, and G.H. Tzeng, "Transportation Investment Project Selection with Fuzzy Multi-objective," *Transportation Planning and Technology*, vol. 17, pp. 91-112, 1998.

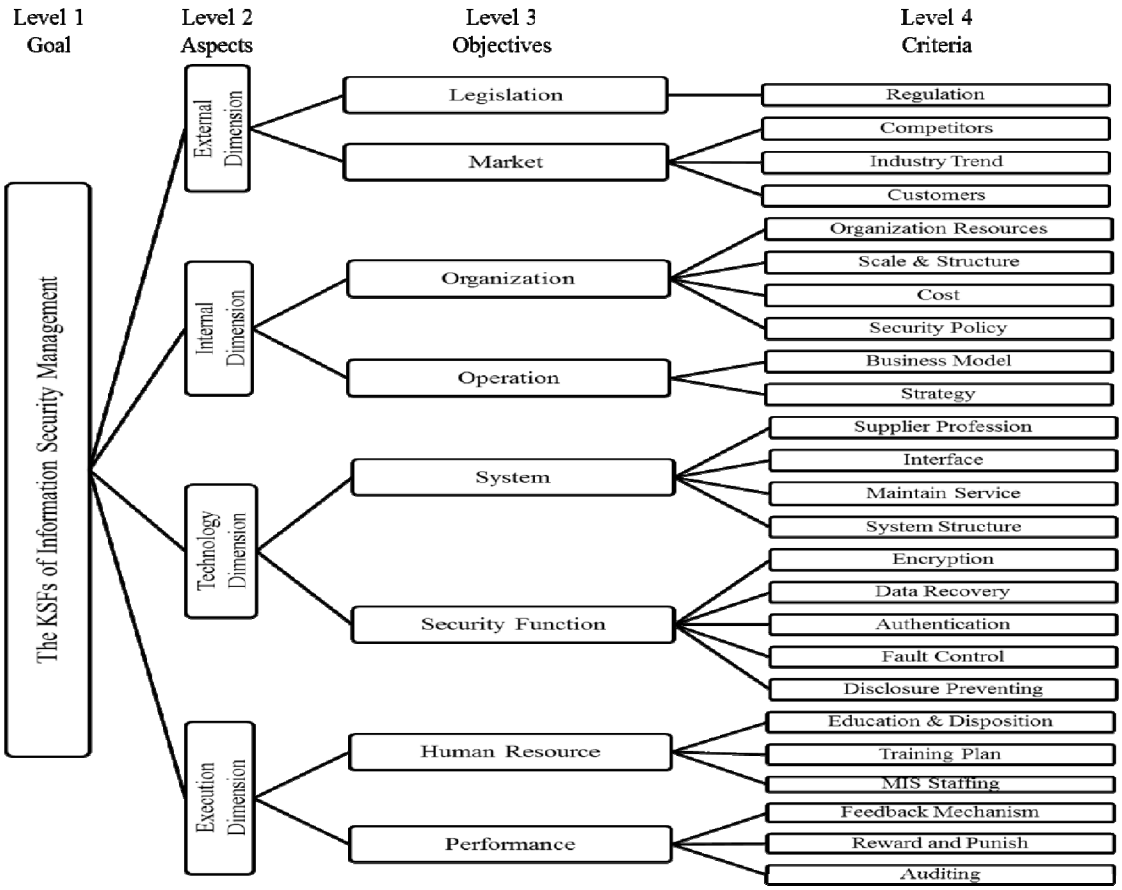

Figure 1. The hierarchy model of KSFs of information security management.

Table Ⅱ. The criteria of KSFs and relative references

Aspects	Objectives	Criteria	Reference Index	References
External Dimension	Legislation	Regulation	(17) (20) (22) (21) (23)	(1) Anderson & Choobineh (2008) [41] (2) Austin et al.(2003) [15] (3) Caminada (1998) [42] (4) Chang & Yeh (2006) [43] (5) Chwelos et al. (2001) [44] (6) Cohen (1998) [45] (7) Dhillon & Backhouse (2001) [46] (8) Eloff & Solms (2000) [39] (9) Gollmann (1999) [12] (10) Gordon & Loeb (2006) [47] (11) Gordon & Maltin (2001) [7] (12) Hinde (2001) [11] (13) Kankanhalli et al.(2003) [8] (14) Lillywhite (1999) [48] (15) Olnes (1994) [49] (16) Osborne (1998) [50] (17) Ozier (1997) [51] (18) Pounder (2001) [14] (19) Schultz et al. (2001) [52] (20) Solms (2001) [10] (21) Torres et al. (2006) [6] (22) Trěek (2003) [40] (23) Tudor (2001) [53] (24) Ward & Smith (2002) [9]
	Market	Competitors	(1) (4) (5) (6) (11) (14)	
		Industry Trend	(1) (4) (5) (6) (11) (13) (14)	
		Customers	(1) (4) (5) (14)	
Internal Dimension	Organization	Organization Resources	(2) (15) (17) (22) (23)	
		Scale & Structure	(2) (8) (15) (18) (23) (24)	
		Cost	(4) (13) (16) (21) (23) (24)	
		Security Policy	(3) (4) (15) (16) (18) (20) (21) (24)	
	Operation	Business Model	(1) (4) (12) (13) (15) (20) (24)	
		Strategies	(1) (4) (11) (12) (13) (18) (20) (24)	
Technology Dimension	System	Supplier Profession	(8) (10) (17) (21) (22)	
		Interface	(3) (9) (17) (22) (23)	
		Maintain Service	(8) (10) (21) (22) (23)	
		System Structure	(2) (9) (17) (21) (22)	
	Security Function	Encryption	(3) (17) (21) (22) (23)	
		Data Recovery	(9) (17) (20) (22) (23)	
		Authentication	(2) (8) (19) (22) (23)	
		Fault Control	(3) (15) (18) (19) (23)	
		Disclosure Preventing	(3) (9) (19) (22) (23)	
Execution Dimension	Human Resource	Education & Disposition	(3) (7) (12) (16) (17) (19)	
		Training Plan	(7) (12) (16) (17) (18) (19) (23)	
		MIS Staffing	(3) (7) (16) (19) (23)	
	Performance	Feedback Mechanism	(2) (8) (16) (18) (19)	
		Rewards and Punish	(7) (8) (12) (17) (19)	
		Auditing	(16) (19) (20) (22) (23)	

Table V. The fuzzy weights of the criteria

Level 2 Aspects	Level 3 Objectives	Level 4 Criteria	Fuzzy weights	Ranking	Tests
External Dimension	Legislation	Regulation	1	1	CI=0.002 CR=0.002
	Market	Competitors	0.44	1	CI=0.068 CR=0.075
		Industry Trend	0.19	3	
		Customers	0.37	2	
Internal Dimension	Organization	Organization Resources	0.19	4	CI=0.084 CR=0.093
		Scale & Structure	0.24	2	
		Cost	0.35	1	
		Security Policy	0.22	3	
	Operation	Business Model	0.37	2	CI=0.043 CR=0.048
		Strategies	0.63	1	
Technology Dimension	System	Supplier Profess ion	0.19	4	CI=0.071 CR=0.079
		Interface	0.22	3	
		Maintain Service	0.27	2	
		System Structure	0.32	1	
	Security Function	Encryption	0.20	3	CI=0.078 CR=0.087
		Data Recovery	0.23	2	
		Authentication	0.25	1	
		Fault Control	0.18	4	
		Disclosure Preventing	0.14	5	
Execution Dimension	Human Resource	Education & Disposition	0.22	3	CI=0.057 CR=0.063
		Training Plan	0.43	1	
		MIS Staffing	0.35	2	
	Performance	Feedback Mechanism	0.33	2	CI=0.068 CR=0.075
		Reward and Punish	0.26	3	
		Auditing	0.41	1	

Table VI. The weights after series of hierarchical

Level 1 Goal	Level 2 Aspects		Level 3 Objectives		Level 4 Criteria		Final Weights	Ranking
KSF of Information Security Management	**External**	0.12	Legislation	0.46	Regulation	1	0.0552	4
			Market	0.54	Competitors	0.44	0.0285	19
					Industry Trend	0.19	0.0123	25
					Customers	0.37	0.0240	24
	Internal	0.21	Organization	0.61	Organization Resources	0.19	0.0243	23
					Scale & Structure	0.24	0.0307	17
					Cost	0.35	0.0448	8
					Security Policy	0.22	0.0282	20
			Operation	0.39	Business Model	0.37	0.0303	18
					Strategies	0.63	0.0516	6
	Technology	0.38	System	0.52	Supplier Profess ion	0.19	0.0375	13
					Interface	0.22	0.0435	9
					Maintain Service	0.27	0.0534	5
					System Structure	0.32	0.0632	3
			Security Function	0.48	Encryption	0.20	0.0365	14
					Data Recovery	0.23	0.0420	10
					Authentication	0.25	0.0456	7
					Fault Control	0.18	0.0328	16
					Disclosure Preventing	0.14	0.0255	22
	Execution	0.29	Human Resource	0.65	Education & Disposition	0.22	0.0415	12
					Training Plan	0.43	0.0811	1
					MIS Staffing	0.35	0.0660	2
			Performance	0.35	Feedback Mechanism	0.33	0.0335	15
					Reward and Punish	0.26	0.0264	21
					Auditing	0.41	0.0416	11

2011 IEEE International Conference on Fuzzy Systems
June 27-30, 2011, Taipei, Taiwan

An Extension of a Fuzzy Ontology for Flexible Querying

Nouredine Tamani
IRISA/ENSSAT/Univ. de Rennes 1
BP 80518, 22305
Lannion Cedex, France
Email: tamani@enssat.fr

Ludovic Liétard
IRISA/IUT/Univ. de rennes 1
BP 30219, 22302
Lannion Cedex, France
Email: ludovic.lietard@univ-rennes1.fr

Daniel Rocacher
IRISA/ENSSAT/Univ de Rennes 1
BP 80518, 22305
Lannion Cedex, France
Email: rocacher@enssat.fr

***Abstract*—In this paper, we propose a personalized approach for flexible querying of information systems. This approach consists in the combination of the reasoning capabilities of the fuzzy DLR-Lite ontology and the expressivity of the SQLf language. The interpretation of the gradual inclusion (subsumption) axioms of the ontology is based on the Gödel fuzzy implication. Its generalization to a tree of inclusions is also proposed. This tree and its property of propagation of degrees are the basic theoretical elements of our application, which consists in querying of a multimodal transport information system which is embedded in a mobile terminal characterized by limited storage and processing capabilities.**

***Keywords*—Ontology, flexible querying, personalization, fuzzy DLR-Lite, SQLf, fuzzy sets theory, multimodal transportation.**

I. Introduction

The personalization of flexible querying of information systems dedicated to multimodal transportation networks is addressed in this paper. We propose an approach which consists in the development of a fuzzy semantic layer in order to extend the functionalities of information systems to reasoning. This layer is made of reasoning functions which combine domain application data with ontology axioms. Ontologies are able (i) to model the domain knowledge, (ii) to unify its vocabulary, (iii) to reason with available knowledge and (iv) to deduce implicit data from explicit data.

The proposed approach is developed in the framework of flexible querying of information systems which allows the user to express preferences in his/her queries. In such a system, the delivered answers are ranked from the most to the least preferred. In this context, user preferences can be expressed by vague or fuzzy predicates such as *fast*, *expensive*, *near*, etc. which are defined by fuzzy sets [16]. From the querying point of view, the SQLf language [4], [3] is a suitable language to express query with preferences. It is an extension of the SQL language to fuzzy predicates (conditions) and provides more expressive SQL-like statements.

From the reasoning point of view, several fuzzy ontologies (based on description logics [1]) have been developed (see [2], [8], [9], [10], [11], [12]) in which theoretical aspects have been widely studied (the definition of fuzzy concepts and relations, the definition and the interpretation of fuzzy inclusion or subsumption axioms, the fuzzy extension of subsumption algorithms, etc.). However, these ontologies are not suitable to address querying issue. Indeed, ontologies save axioms, individuals and related data in text files which are not appropriate for the needs of real applications. Ontology-based querying systems are faced with a large amount of data to such extent that the combination of ontologies and databases become an absolute necessity. In addition, the developed ontology-based querying systems, such as [15], [5], [10], [13], are based on limited description logics in terms of expressivity. To overcome this limitation, databases are combined with ontologies to provide DBMS functionalities such as data persistence and query evaluation. Ontology axioms are then used in the query rewriting process to take into account the logical relationships between concepts.

In this context, we consider the Description Logic extended to *m*-ary Relations [5] denoted DLR-Lite. More precisely, we are interested in the fuzzy extension of the DLR-Lite, called fuzzy DLR-Lite [7], [14], [15], which is made of a reduced set of fuzzy operators and abstraction rules which are connected to databases through SQL statements.

In this paper, we aim to design a flexible querying system that combines a fuzzy DLR-Lite knowledge base with the SQLf language, so as to take profit from the expressivity of the SQLf language and the reasoning mechanisms of the fuzzy DLR-Lite. Firstly, we show the relevance of the Gödel fuzzy implication to the interpretation of gradual inclusion (subsumption) axioms of the fuzzy ontology. Then, we consider the enrichment of the fuzzy DLR-Lite knowledge base with the SQLf language. The resulting knowledge base is finally applied on a sample mobile application in the field of multimodal transportation. The developed application is embedded in a lightweight terminal in which the accessible data are limited to a subset of the knowledge base. This restriction is due to the limited storage and processing capabilities of such terminals.

The remainder of the paper is structured as follows. Section II introduces the fuzzy DLR-Lite knowledge base. In section III, the Gödel fuzzy implication is used to define an interpretation to the gradual inclusion axiom; its contrapositive is also used to define a restricted form of the negation operator. We also show in section III the way in which our interpretation is extended to a tree of gradual inclusion axioms and its degree propagation property. Section IV introduces briefly the SQLf language and points out the relevance of the enrichment of

978-1-4244-7316-8/11/$26.00 ©2011 IEEE

the fuzzy DLR-Lite knowledge base with this language. Our sample application is described in section V. Section VI recalls our contributions and draws some lines for future works.

II. The Fuzzy DLR-Lite Ontology

In this section, we introduce some elements of both the fuzzy sets theory and the fuzzy DLR-Lite knowledge base.

A. The Fuzzy Sets Theory

The fuzzy sets theory is introduced by Zadeh [16] to express the gradual membership of an element to a set. Formally, a fuzzy set F is defined on a referential U by a membership function $\mu_F : U \mapsto [0,1]$ such that $\mu_F(x)$ denotes the membership grade of x in F.

In particular, $\mu_F(x) = 1$ denotes the full membership of x in F, $\mu_F(x) = 0$ expresses the absolute non-membership and when $0 < \mu_F(x) < 1$, it reflects a partial membership (the more $\mu_F(x)$ is close to 1, the more x is a member of F).

A fuzzy set generalizes a crisp set in which membership grades are in $\{0,1\}$. If a fuzzy set is a discrete set then it is denoted by $F = \{(x_1, \mu_F(x_1)), ..., (x_n, \mu_F(x_n))\}$, otherwise, it is characterized by its membership function.

The union $\cup$ and the intersection $\cap$ operators are defined with a couple of (t-norm, t-conorm) such as (min, max). Let F, G be two fuzzy sets; $\mu_{F\cup G}(x) = max(\mu_F(x), \mu_G(x))$, $\mu_{F\cap G}(x) = min(\mu_F(x), \mu_G(x))$ and the complement of F, noted F^c, is defined by $\mu_{F^c}(x) = 1 - \mu_F(x)$. The logical counterparts of $\cap$, $\cup$ and the complement are resp. $\wedge, \vee$ and $\neg$. Other operators are also defined such as fuzzy implications.

B. The Fuzzy DLR-Lite Knowledge Base

The fuzzy DLR-Lite knowledge base $\mathscr{K}$ consists of three components $(\mathscr{O}, \mathscr{F}, \mathscr{A})$ defined in what follows.

1) The Facts Component $\mathscr{F}$: It contains the extensions of relations made of tuples of the form $R(c_1, ..., c_n)[s]$, where R is an n-ary relation, $c_{i,i=1,...,n}$ are constants and $s \in]0,1]$ is a grade indicating in which extent the tuple $\langle c_1, ..., c_n \rangle$ is an instance of the relation R.

2) The Ontology Component $\mathscr{O}$: The ontology defines the concepts of the application domain by means of projection, intersection and inclusion axioms:

- *The gradual inclusion (subsumption) axiom* has the form $(R_1 \sqcap R_2 \sqcap ... \sqcap R_l \sqsubseteq R_r)[s]$, where $l \geq 1$ and all the involved relations are of the same arity and $s \in]0,1]$ is the truth degree of the axiom.
- *The projection axioms* allow to define new concepts and their attached facts by extracting one or more columns from other relations. Two kinds of projection axioms are defined in the ontology component: *the simple projection* and *the restricted projection*.
  The simple projection is of the form $\exists[i_1, ..., i_k]R$ that expresses the projection of the relation R on columns $i_1, ..., i_k$, and *the restricted projection* is of the form $\exists[i_1, ..., i_k]R.(Cond_1 \sqcap ... \sqcap Cond_h)$ which restricts the projection of $\exists[i_1, ..., i_k]R$ according to the boolean conditions $Cond_{j,j=1,...,h}$ of the form $([i]\theta v)$, where $[i]$ corresponds to a column number of the relation R, $\theta \in \{<, \leq, =, \neq, >, \geq\}$ and v is a value.

3) The Abstraction Component $\mathscr{A}$: It forms the set of statements that connect concepts and relations, defined in the ontology component, to physical relational tables defined in a database. Simple and complex abstraction statements are defined as follows:

- *Simple abstraction statement* has the form:
  $R_1 \longmapsto R_2(c_1[t_1], ..., c_n[t_n])[c_s]$ which states that the n-ary relation R_1 of the ontology component is mapped into the projection on columns $c_1, ..., c_n$ of the m-ary table R_2 $(n \leq m)$ each of which is of type t_i. The score of the delivered tuples is provided by the column c_s.
- *Complex abstraction statement* has the form:
  $R_1 \longmapsto (t_1, ..., t_n)[c_s].sql$ where R_1 is an n-ary relation of the ontology component and sql is an SQL query which returns the n-ary tuples $\langle t_1, ..., t_n \rangle$ ranked in decreasing order of their scores c_s.

C. Interpretation of the Ontology Axioms $\mathscr{O}$

An interpretation of the fuzzy DLR-Lite ontology, denoted $\mathscr{I} =< \Delta, \cdot^{\mathscr{I}} >$, consists of a finite interpretation domain Δ and of an interpretation function $\cdot^{\mathscr{I}}$ which associates for each relation R (of arity m) an interpretation $R^{\mathscr{I}} : \Delta^m \to [0,1]$ where $R^{\mathscr{I}}(c)$ denotes the grade of membership of the tuple c to the relation R.

It is worth noticing that the interpretation function $R^{\mathscr{I}}$ has the same meaning as the membership function μ_R as defined in the fuzzy sets theory. Therefore, both $R^{\mathscr{I}}(x)$ and $\mu_R(x)$ notations are identical.

For sake of clarity, we only introduce the interpretation of the gradual inclusion axiom; see [14] for more details about the interpretation of simple and restricted projection axioms.

The interpretation of the gradual inclusion axiom is defined as follows:

$$\mathscr{I} \models (R_1 \sqcap ... \sqcap R_l \sqsubseteq R_r)[n] \Leftrightarrow \forall c \in \Delta^m, n \otimes R_1^{\mathscr{I}}(c) \otimes ... \otimes R_l^{\mathscr{I}}(c) \leq R_r^{\mathscr{I}}(c), \quad (1)$$

where m is the arity of the relations $R_{i,i=1,...,m}$ and R_r and $\otimes$ is a t-norm.

The formula (1) states that if c is an instance of $R_{i,i=1,...,l}$ at the degree $s_i = R_i^{\mathscr{I}}(c)$ then c is an instance of R_r at the minimal degree $n \otimes s_1 \otimes ... \otimes s_l$.

D. The Query Language

A fuzzy DLR-Lite query consists in a conjunction query combined with a scoring function to rank answers. The query is of the following form:

$$\underbrace{q(x)[s]}_{head} \leftarrow \underbrace{\exists y R_1(z_1)[s_1], ..., R_l(z_l)[s_l],}_{body} \underbrace{OrderBy(s = f(s_1, ..., s_l))}_{scoring\ function},$$

where q is a k-ary relation, each R_i is a relation, x (resp. y) is a vector of distinguished (resp. non distinguished) variables, z_i is a tuple of constants or variables from x or y, f is a scoring

function which combines the scores $s_1,...,s_l$ and s is the degree of satisfaction of a tuple x to the query q.

Such a query is evaluated using the gradual inclusion axioms defined in the ontology component. Each query atom $(R_i(z_i)[s_i])$ appearing in the right-hand side of an inclusion axiom is substituted by its left-hand side. Each axiom substitution generates a new query which is added to a disjunctive query. Each subquery of the resulting disjunctive query is finally translated into an SQL query to be evaluated over the facts component.

Example 1. Let *Journey* be a relational table of journeys defined from a multimodal transportation system. We define the fuzzy relation *FastJourney* from the *Journey* relation and the following inclusion (subsumption) axiom:

$(FastJourney \sqsubseteq FavoriteJourney)[0.7]$,

which states that each *fast* journey is also a *favorite* journey at the minimal degree of 0.7.

Any query involving *favorite* journeys, such as:

$q(t)[s] \leftarrow FavoriteJourney(t), OrderBy(s)$

is rewritten, based on the above gradual inclusion axiom, in terms of *fast* journeys (the t-norm used is *min*) as follows:

$q'(t)[s] \leftarrow FastJourney(t)[s'], OrderBy(s = min(0.7, s'))$,

where $s' = fast^{\mathscr{I}}(t)$ is the grade which expresses in what extent the journey t is *fast*.

We obtain for each journey t a minimal grade of satisfaction to the query q equals to $min(0.7, fast^{\mathscr{I}}(t))$ since the interpretation of the gradual inclusion axiom means:

$\forall t, Favorite^{\mathscr{I}}(t) \geq min(0.7, fast^{\mathscr{I}}(t))$. ▪

III. The Gradual Inclusion Axiom and the Gödel Fuzzy Implication

In this section, we show that the interpretation of the gradual inclusion axioms of the fuzzy DLR-Lite ontology is based on the Gödel fuzzy implication. We also show the interest of its contrapositive for the definition of a restricted form of the negation operator. We finally generalize the Gödel fuzzy implication based interpretation to a tree of gradual inclusion axioms.

A. Gödel Fuzzy Implication Based Interpretation of the Gradual Inclusion (Subsumption) Axiom

Let $(A \sqsubseteq B)[\alpha]$ be a gradual inclusion axiom, denoted by $A \sqsubseteq^{\alpha} B$. It is interpreted in the framework of the fuzzy DLR-Lite [14] as follows:

$$\forall x \in \Delta, B^{\mathscr{I}}(x) \geq min(\alpha, A^{\mathscr{I}}(x)) \quad (2)$$

We can prove that this interpretation is based on a gradual inclusion defined by the Gödel fuzzy implication $(\mu_A(x) \Rightarrow_{G\ddot{o}} \mu_B(x) = 1 \ \ if \ \ \mu_A(x) \leq \mu_B(x); \mu_B(x), otherwise)$:

$$A \sqsubseteq^{\alpha}_{G\ddot{o}} B \Leftrightarrow min_x(\mu_A(x) \Rightarrow_{G\ddot{o}} \mu_B(x)) = \alpha \quad (3)$$

In the remainder of the paper, we use equally the notations $A \sqsubseteq^{\alpha} B$ and $A \sqsubseteq^{\alpha}_{G\ddot{o}} B$.

Proof: The Gödel fuzzy implication is an R-implication defined by:

$\mu_A(x) \Rightarrow_{G\ddot{o}} \mu_B(x) = \sup_{[0,1]}\{u | min(\mu_A(x), u) \leq \mu_B(x)\}$.
We denote $(\mu_A(x) \Rightarrow_{G\ddot{o}} \mu_B(x))$ by $I(\mu_A(x), \mu_B(x))$.
As $I(\mu_A(x), \mu_B(x))$ is a u value then:

$$\forall x, min(\mu_A(x), I(\mu_A(x), \mu_B(x))) \leq \mu_B(x) \quad (4)$$

having $\alpha = min_x(I(\mu_A(x), \mu_B(x)))$ then
$\forall x, \alpha \leq I(\mu_A(x), \mu_B(x)) \Rightarrow$
$\forall x, min(\mu_A(x), \alpha) \leq min(\mu_A(x), I(\mu_A(x), \mu_B(x)))$.
From the formula (4), we obtain: $\forall x, min(\mu_A(x), \alpha) \leq \mu_B(x)$. ■

This interpretation, based on the Gödel fuzzy implication, allows the definition of a minimal threshold of satisfaction to queries in which substitutions of the gradual inclusion axioms are performed.

In addition, the Gödel fuzzy implication provides effective means of computing the minimal grade of the gradual inclusion axioms (formula (1)).

B. The Gradual Inclusion Axiom and the Contrapositive of the Gödel Fuzzy Implication

The contrapositive of the Gödel fuzzy implication could be used to define a new type of fuzzy inclusion (subsumption) denoted $\sqsubseteq_{ContG}$:

$$A \sqsubseteq^{\beta}_{ContG} B \Leftrightarrow min_x(1 - \mu_B(x) \Rightarrow_{G\ddot{o}} 1 - \mu_A(x)) = \beta \quad (5)$$

The interpretation of this form of fuzzy inclusion axioms is deduced from the interpretation based on the Gödel fuzzy implication as follows:

$$A \sqsubseteq^{\beta}_{ContG} B \Rightarrow \forall x, \neg A^{\mathscr{I}}(x) \geq min(\beta, \neg B^{\mathscr{I}}(x)) \quad (6)$$

The proof of this interpretation is similar to the previous proof. This form of gradual inclusion axioms allows to express a restricted negation operator.

Example 2. Let $TouristJourney \sqsubseteq^{0.6}_{ContG} FavoriteJourney$ be a fuzzy inclusion (subsumption) axiom which means that the fuzzy set of *touristic* journeys is included in the fuzzy set of *favorite* journeys at the minimal degree of 0.6. In the case that the access is limited to *favorite* journeys, the system can answer queries about journeys which aren't *touristic*, based on the above fuzzy inclusion axiom, as follows:

$\neg TouristJourney(t) \geq min(1 - FavoriteJourney(t), 0.6)$ (formula (5)). ▪

Please notice that this negation is only applicable to relations involved in gradual inclusion axioms.

C. Interpretation of a Tree of Gradual Inclusion Axioms

The proposed interpretation of the gradual inclusion axiom is generalized in the case of a tree of inclusion axioms. This tree structure and its property of degree propagation are the basis of the developed application in section 5.

Without loss of generality, we restrict the tree structure to two levels of inclusion as depicted in Fig. 1a.

Such a tree structure means: $A \sqsubseteq^{\alpha}_{G\ddot{o}} B$ and $B \sqsubseteq^{\beta}_{G\ddot{o}} C$, where $\alpha, \beta \in]0,1]$.

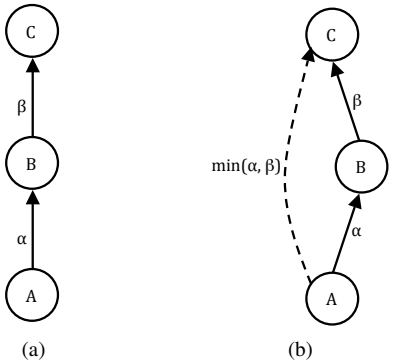

Fig. 1: A tree structure with two levels.

By applying the formula (2), we obtain:

$$\mu_B(x) \geq min(\mu_A(x), \alpha) \tag{7}$$

$$\mu_C(x) \geq min(\mu_B(x), \beta) \tag{8}$$

The propagation property allows the deduction of the grade of inclusion of the concept A in the concept C (see Fig. 1b).

Proof: From the formula (7), we deduce:

$$\mu_B(x) \geq min(\mu_A(x), \alpha) \Rightarrow$$
$$min(\beta, \mu_B(x)) \geq min(\beta, min(\mu_A(x), \alpha)) =$$
$$min(\alpha, \beta, \mu_A(x)) = min(min(\alpha, \beta), \mu_A(x)).$$

From $\begin{cases} min(\beta, \mu_B(x)) \geq min(min(\alpha, \beta), \mu_A(x)) \\ \mu_C(x) \geq min(\mu_B(x), \beta) \, (cf.\ formula\, 8) \end{cases}$

$$\Rightarrow \mu_C(x) \geq min(min(\alpha, \beta), \mu_A(x)).$$

■

This property of degree propagation can be generalized to a series of gradual inclusion axioms of the form:

$$A_1 \sqsubseteq_{G\ddot{o}}^{\alpha_1} A_2 \sqsubseteq_{G\ddot{o}}^{\alpha_2} \ldots \sqsubseteq_{G\ddot{o}}^{\alpha_{n-1}} A_n.$$

Effectively, transitive relationships of the form: $A_i \sqsubseteq_{G\ddot{o}}^{\alpha} A_j$, where $i < j$ can be interpreted as follows:

$\forall x : \mu_{A_j}(x) \geq min(\mu_{A_i}(x), \alpha)$,

where $\alpha = min(\alpha_i, \alpha_{i+1}, \ldots, \alpha_{j-1})$.

IV. The Enrichment of the Fuzzy DLR-Lite With the SQLf Language

The SQLf language [4], [3] is an extension of the SQL language to flexible querying by extending its statements to fuzzy conditions. An SQLf query delivers a fuzzy relation r which is a fuzzy set in which the grade of membership of tuple t to the relation r, denoted $\mu_r(t)$, expresses its level of satisfaction. The closer to 1 $\mu_r(t)$, the more t is preferred.

The SQLf language is based on the extension of the relational algebra operators to fuzzy conditions. The basic form of an SQLf query (fuzzy restriction) is as follows:

Select [distinct] *[n|t|n,t] attributes* ***From*** *relations*
Where *fuzzy_cond;*

The above query returns a set of ranked tuples with their grades of satisfaction, where n is a limitation of the size of the returned set and $t \in]0,1]$ is a minimal threshold of satisfaction.

Furthermore, the SQLf language allows more complex statements such as partitioning, fuzzy nesting, division involving fuzzy relations and queries based on fuzzy quantified propositions. These complex statements haven't any boolean counterpart [3].

The limitation of the fuzzy DLR-Lite lies in its inability to express complex preferences. This is due to the fact that abstraction statements, based on SQL queries, do not allow the user to define complex concepts such as *"journeys that satisfy almost all important criteria"*, which is based on a fuzzy quantified proposition.

In order to improve the expressiveness of the fuzzy DLR-Lite knowledge base, we propose the extension of the complex abstraction statements to the SQLf language. So that, it becomes possible to express preferences using complex SQLf statements. We redefine, then, the extended complex abstraction statements as follows:

$R_1 \mapsto (t_1, \ldots, t_k)[c_s].sqlf$, where R_1 is a concept from the ontology and *sqlf* is an SQLf query which delivers a fuzzy relation.

Example 3. The extended complex abstraction statements allow to define concepts and relations corresponding to complex preferences, such as *MyFastJourney* that corresponds to *"journeys having most of steps are fast"*, which is a fuzzy relation that can be defined by the following extended abstraction statement using an SQLf statement:

MyFastJourneys $\mapsto$ (int)$[c_s]$.(***Select*** *#Journey* ***From*** *Journey* ***Group By*** *#Journey* ***Having*** *most (#step) are fast(durLink)*); ▪

From the semantic point of view, our extension fits in well with the fuzzy DLR-Lite knowledge base and ensures backward compatibility, since the SQLf language covers the SQL language and the fuzzy sets theory is the common formal framework of interpretation of both SQLf queries and axioms of the fuzzy DLR-Lite, which is based on the Gödel fuzzy implication and the t-norm *min*.

V. Illustrative Example

In this section, a sample application is developed in the field of multimodal transportation, in order to show the interests of our approach, and to emphasize the benefit gained from the interpretation of the gradual inclusion axiom, using the Gödel fuzzy implication and the enrichment of the knowledge base with the SQLf language. The main features and the context of the application are described in following subsections.

A. The Context of the application

The considered application is developed in the context of mobile applications. The user terminal is a lightweight terminal which is limited in terms of main storage and processing capabilities. Therefore, the user terminal only embeds a subset of the knowledge base that consists of (i) fuzzy relations defined by the abstraction statements, (ii) fuzzy predicates and (iii) gradual inclusion axioms.

The user can query the embedded application with conjunctive queries which will be evaluated over the available data, based on the gradual inclusion axioms.

We assume that a user interface is provided to define membership functions corresponding to fuzzy concepts. The embedded system can deduce, from the gradual inclusion axioms, the minimal grade of inclusion of the already defined fuzzy concepts in the user-defined fuzzy concepts.

B. An Embedded Multimodal Transport Information System

We design a mobile application in the field of multimodal transportation. The conceptual data model of the system is consistent with the Transmodel standard [6]. Transmodel is an european standard defining a unified conceptual data model of multimodal transport networks which combine bus, tramway, trolley bus and underground networks. Transmodel provides operating data model for network management activities such as timetables, staff, fleet and rolling stock management, real time monitoring and user information circulation.

In practice, travelers are more interested in information about available networks, timetables and services. So, a subset of the database is enough, from the user point of view, to answer his/her queries which are generally about journeys.

For the sake of clarity, the knowledge base of our application is limited to one level of gradual inclusion enriched after that with a user defined fuzzy predicate.

We introduce below the 3 steps for the design of the embedded application: (i) data preprocessing, (ii) querying of the embedded system and (iii) the enrichment of the system.

1) Step 1. Data Preprocessing: Let the following relational tables be a subset of a database from a multimodal transport information system:

Network, Line, Station, Link and *LinkLine*.

We define the *Journey* relation as follows:

Journey (#journey, #link, departure, arrival, source, destination, duration, DepLink, ArrLink, modeLink, durLink, costLink, comfLink, waitLink).

It is assumed that journeys from source s to destination d are preprocessed.

Based on the SQLf queries, the following fuzzy relations are defined from the *Journey* relation:

1) *TouristJourney* $\mapsto$ [*#Journey*].***Select*** *#Journey* ***From*** *Journey* ***Group By*** *#Journey* ***Having*** *(most #Link are Touristic);*
2) *PleasantJourney* $\mapsto$ [*#Journey*].***Select*** *#Journey* ***From*** *Journey* ***Group By*** *#Journey* ***Having*** *(most #Link are Short(waitLink));*

The above extended complex abstraction statements state respectively that a *touristic* journey is a journey in which most of its steps (named link in the statements) cut across touristic sites and a *pleasant* journey is a journey in which the waiting time of most of its steps is *short*. Both *touristic* and *short* are fuzzy predicates.

The fuzzy predicate *MorningDeparture* is also defined by the membership function described in Fig. 2.

The following gradual inclusion axioms could be obtained by a processing using the formula (2) over the database:

- TouristJourney $\sqsubseteq^{0.7}_{G\ddot{o}}$ MorningDepartureJourney
- PleasantJourney $\sqsubseteq^{0.8}_{G\ddot{o}}$ MorningDepartureJourney

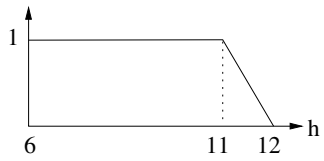

Fig. 2: The membership function of the fuzzy predicate *Morning*.

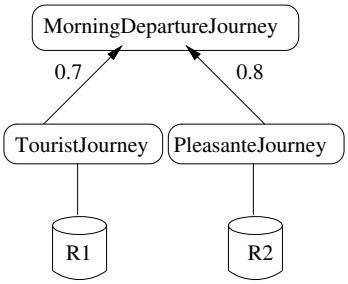

Fig. 3: The embedded concepts and data.

2) Step 2. Querying the Embedded System: The data embedded in the user terminal are illustrated in Fig. 3. The fuzzy relations $R_{i,i=1,2}(\#Journey)$ (in the sense of the SQLf language) are resulting from SQLf queries of the extended complex abstraction statements and mapped respectively to fuzzy concepts (relations in the sense of the fuzzy DLR-Lite) *TouristJourney* et *PleasantJourney*.

Due to the storage limitation of the user terminal, both the relations $R_{i,i=1,2}$ only contain the *#Journey* and the score columns. The membership function of the fuzzy predicate *MorningDeparture* is also embedded.

The user can query the system based on the embedded fuzzy predicates. The grade of satisfaction to both fuzzy conditions *Touristic* and *pleasant* are embedded within the relations $R_{i,i=1,2}$. About the fuzzy relation *MorningDepartureJourney*, a minimal grade of satisfaction can be obtained using the formula (2). For example:

$\forall t, \mu_{Morning}(t) \geq min(\mu_{Touristic}, 0.7) = min(\mu_{R_1}(t), 0.7)$,
and
$\forall t, \mu_{Morning}(t) \geq min(\mu_{Pleasant}(t), 0.8) = min(\mu_{R_2}(t), 0.8)$.
Finally, we can write:

$$\forall t, \mu_{Morning}(t) \geq max(min(\mu_{R_1}(t), 0.7), min(\mu_{R_2}(t), 0.8)).$$

3) Step 3. Enrichment of the Embedded System: The user can define his/her own fuzzy concepts to express his/her preferences. These concepts could be connected to the previously defined tree structure of concepts in order to personalize the embedded system. The query evaluation process is then made more accurate and close to user expectations.

Example 4. Through the fuzzy concept definition interface, the user can define *FavoriteDepartureJourney* as a fuzzy concept based on the favorite departure time (see Fig. 4). *FavoriteDepartureJourney* is then bound to *MorningDepartureJourney* fuzzy concept as follows:
$MorningDepartureJourney \sqsubseteq^{\alpha}_{G\ddot{o}} FavoriteDepartureJourney$.

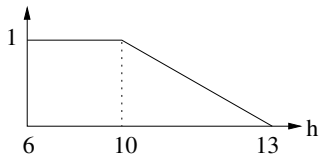

Fig. 4: The membership function of the fuzzy predicate *Favorite*.

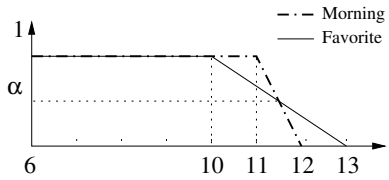

Fig. 5: Computation of the value of α.

The value of α in the above gradual inclusion axiom is $\alpha = min_t(\mu_{Morning}(t) \Rightarrow_{Gö} \mu_{Favorite}(t))$ and can be computed from the membership functions of both *Morning* and *Favorite* fuzzy predicates as depicted in Fig. 5.

Once the value of α is obtained ($\alpha = 0.5$ in this example), the embedded system, by applying the propagation property, deduces the grade of gradual inclusion links that bind the added concept to the existing ones as described in Fig. 6.

Any query which is about the fuzzy predicate *FavoriteDepartureJourney* is evaluated over the available data which covers *pleasant* and *touristic* journeys such that:

$\forall t, \mu_{Favorite}(t) \geq max(min(0.5, \mu_{R_1}(t)), min(0.5, \mu_{R_2}(t)))$. ▪

Remark. The deduction of the minimal grade of inclusion of a fuzzy concept in a user-defined fuzzy concept is based on both their respective membership function and the formula:

$$A \sqsubseteq^{\alpha}_{Gö} B \Leftrightarrow min_x(\mu_A(x) \Rightarrow_{Gö} \mu_B(x)) = \alpha.$$

This computation is only significant if the concept B generalizes the concept A (in the same way as concept hierarchies in ontologies) which means that $Support(A) \subseteq Support(B)$. Indeed, if $Support(A) \nsubseteq Support(B)$ then the grade of inclusion is equal to 0; which is in fact worthless.

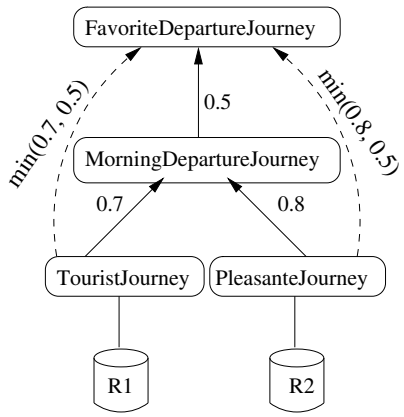

Fig. 6: Enrichment of the system.

VI. Conclusion and future works

The flexible querying approach developed in this paper is based on the combination of a fuzzy description logic (denoted fuzzy DLR-Lite) and the SQLf language that allows the expression of more complex fuzzy relations than those could be expressed by the SQL language. An interpretation of the gradual inclusion axiom based on the Gödel fuzzy implication is introduced. This interpretation provides a formal framework in which a restricted form of the negation operator is defined and a generalization to a tree of fuzzy relations is also proposed.

An implementation, based on algorithms for query evaluation introduced in [14], is in progress. It remains the development of an effective algorithm to compute the minimum grade of inclusion of fuzzy concepts added to the knowledge base. We also plan to extend the enrichment process to complex fuzzy predicates as those defined by division involving fuzzy relations.

Acknowledgments

This work is funded by the Brittany region and the department of Côtes-d'Armor and is partially supported by the National Agency of Research (AOC Ref. ANR-08-CORD- 009).

References

[1] F. Baader, D. Calvanese, D. L. M. Guinness, D. Nardi, and P. F. Patel-Schneider, editors. *The Description Logic Handbook : Theory, Implementation and Applications*. Cambridge University Press, 2003.

[2] F. Bobillo and U. Straccia. fuzzyDL : An expressive fuzzy description logic reasoner. In *IEEE International Conference on Fuzzy Systems*, pages 923–930, 2008.

[3] P. Bosc, L. Liétard, O. Pivert, and D. Rocacher. *Base de données - Gradualité et imprécision dans les bases de données Ensembles flous, requêtes flexibles et interrogation de données mal connues*. Technosup. 1 edition, 2004.

[4] P. Bosc and O. Pivert. SQLf: A relational database langage for fuzzy querying. *IEEE Transactions on Fuzzy Systems*, 3(1):1–17, Feb 1995.

[5] D. Calvanese, G. D. Giacomo, D. Lembo, M. Lenzerini, and R. Rosati. Data complexity of query answering in description logics. In *KR*, pages 260–270, 2006.

[6] O. Carles. Modèle conceptuel de données générique pour la représentation des réseaux intermodaux. Tech. report, INRETS, 2002.

[7] S. Colucci, T. D. Noia, A. Ragone, M. Ruta, U. Straccia, and E. Tinelli. *Semantic Web Information Management*, chapter 19 : Informative Top-k retrieval for advanced skill management, pages 449–476. Springer-Verlag Belin Heidelberg, 2010.

[8] C. Hudelot, J. Atif, and I. Bloch. Fuzzy spatial relation ontology for image interpretation. *Fuzzy Sets and Systems*, 159:1929–1951, 2008.

[9] J. Lu, Y. Li, B. Zhou, and D. Kang. Reasoning within extended fuzzy description logic. *Knowledge-Based Systems*, 22:28–37, 2009.

[10] J. Z. Pan, G. Stamou, G. Stoilos, and E. Thomas. Expressive querying over fuzzy DL-Lite ontologies. In *20th International workshop on description logics, Brixen-Bressanone, Italy*, 2007.

[11] G. Stoilos, G. Stamou, V. Tzouvaras, J. Z. Pan, and I. Horrocks. Fuzzy OWL: Uncertainty and the semantic web. In *International workshop on OWL: Experience and Directions*, 2005.

[12] U. Straccia. Towards a fuzzy description logic for the semantic web (preliminary report). *LNCS*, 3532:167–181, 2005.

[13] U. Straccia. Answering vague queries in fuzzy DL-lite. In *In Proceedings of the 11th. Inter. Conf. on Information Processing and Management of uncertainty in Knowledge-Based Systems*, pages 2238–2245, 2006.

[14] U. Straccia. Softfacts : a top-k retrieval engine for a tractable description logic accessing relational databases. Technical report, ISTI-CNR, 2009.

[15] U. Straccia and G. Visco. DLmedia: an ontology mediated multimedia information retrieval system. In *In Proceedings of DL 2007*, 2007.

[16] L. Zadeh. Fuzzy sets. *Information and control*, 8(3):338–353, 1965.

2011 IEEE International Conference on Fuzzy Systems
June 27-30, 2011, Taipei, Taiwan

A Computational Linguistic Approach for the Identification of Translator Stylometry using Arabic-English Text

Heba El-Fiqi
School of Engineering and Information Technology
University of New South Wales
ADFA campus
Canberra, Australia
H.El-Fiqi@student.adfa.edu.au

Eleni Petraki
Faculty of Arts and Design
University of Canberra
Canberra, Australia
Eleni.Petraki@canberra.edu.au

Hussein A. Abbass
School of Engineering and Information Technology
University of New South Wales
ADFA campus
Canberra, Australia
H.Abbass@adfa.edu.au

***Abstract*- Translator Stylometry is a small but growing area of research in computational linguistics. Despite the research proliferation on the wider research field of authorship attribution using computational linguistics techniques, the translator stylometry problem is more challenging and there is no sufficient literature on the topic. Some authors even claimed that this problem does not have a solution; a claim we will challenge in this paper. We present an innovative set of translator stylometric features that can be used as signatures to detect and identify translators. The features are based on the concept of network motifs: small graph local substructures which have been used successfully in characterizing global network dynamics. The text is transformed into a network, where words become nodes and their adjacencies in a sentence are represented through links. Motifs of size 3 are then extracted from this network and their distribution is used as a signature for the corresponding translator.**

We then investigate the impact of sample size, method of normalization and imbalance dataset on classification accuracy. We also adopt the Fuzzy Lattice Reasoning Classifier (FLR) among others, where FLR achieved the best performance with a classification accuracy reaching the 70% mark.

Keywords-component; Translator Stylometry; Authorship Attributions; Network Motifs; Decision Tree Analysis; Fuzzy Classifier; Computational linguistics; Arabic-English Corpus.

I. INTRODUCTION

Identifying the author of a text is an important area of research in *"Computational Linguistics"* [1, 2]. There are many studies in *"Authorship Attributions"* [1-14]. These studies use the stylometric features of the authors to identify the original authors. These stylometric features include lexical, character, syntactic, semantic, and application-specific features [1-14].

On the one hand, the problem of authorship attributions is a difficult one and research challenges remain to exist in this area. On the other hand, the sub-problem of translator attributions is even harder and no solution for it exists so far.

Translation is a fascinating topic. While the original writer of a text had a specific mental picture in her mind and an intended message to be communicated through the text, a translator faces a different type of challenge. Successful translation necessitates that the translator needs to form the same mental picture as the original author of the text. Good translation does not stop at the level of mapping words, but extends to mapping meaning, mental pictures, imagination, and feelings. This is called the "loyalty" dilemma, where a wide discussion in the literature exists on the importance of maintaining the spirit of the original work.

If we compare author attributions to translator attributions, we find that the former is expected to have more signatures or discriminatory factors representing the choices made by the authors. Authors have many more degrees of freedom, where they can build their own identity as authors. Translators have less. Being constrained with the original text is a non-trivial limitation. This feature alone makes translator attributions a more difficult problem than author attributions. Nevertheless, we conjecture that translators attempt to have their own touch, signatures that can be used to detect who translated what. This is the hypothesis we hold in this paper.

The problem of how to identify translator stylometry is under-studied in the literature; probably because it is a harder problem. Some argue that translated work is considered as the original author's literature work rather than the translator's own work; however, no one can ignore the fact that translators are individuals [15]; they make personal choices which can affect the translation process. This is what we call "*Translator Stylometry*".

In this paper, we are going to introduce a new method that uses network motifs to identify the difference in translator's style. Our hypothesis is reformulated as "network motifs can be used to differentiate between different translators based on their own writing stylometrics". To test this hypothesis, we represent our datasets as networks. This is done by generating a word adjacency network for each piece of work by a translator in the dataset. To analyze and compare two networks, we can use their global statistical features; these include Shortest-path length, global centrality, clustering coefficient, etc.., or their structural design principles like the network motifs. Network motifs which are initially introduced by Ron Milo et al. [16] are patterns

978-1-4244-7316-8/11/$26.00 ©2011 IEEE

(represented by small subgraphs) that are repeated in a real network more often than randomly generated networks.

Our method is an instance based approach, in which each sample generates its own network representing a single piece of work. After extracting the motifs, we use a classifier to classify the translated works. The accuracy of this classifier is used to test our hypothesis on a dataset comprising 30 chapters from the Holy Quran. We focus this paper on a text written in Arabic and translated into English.

II. BACKGROUND

A. Stylometry

The translator has to make many personal decisions while he is translating a piece of work. Examples of these decisions include the choice of words, discourse markers, modal verb selection, length of sentences, frames, and their own understanding of the original text.

In 2010, Winters discusses how a translator's attitude influences her translation [17]. He uses two German translations of the original novel "*The Beautiful and Damned*" (1922) written by F. Scott Fitzgerald. He shows that different translators' views affect the macro level of the novel, and how this from his point of view extended to influence the readers' attitude as well.

Xiumei uses relevance theory to explain the translator's style [18]. The findings demonstrated that, while the translator tries to balance between the original author's communicative intentions and the target reader's cognitive environment, she is still influenced by her own preferences and abilities; the outcome of all of that introduces her style.

The sample of papers reviewed above and others [17-19] demonstrate that studies in linguistics highlight that there are translator stylometric features existing in translated texts. However, the area of automatic identification and feature extraction of translator stylometric features has not seen an equivalent breed of research. The only attempt that we are aware of was in 2001 by Mikhailov and Villikka [15]. They tried to find *"stylistic fingerprints"* for translator by extracting three lexical features as: "Vocabulary richness", "Most frequent words" and "Favorite words". Their experiment was done on Russian fiction texts in addition to their Finnish translations. The lexical features that they used in the research failed to find stylistic fingerprints for different translators. Their conclusion was summed up in their title; that it is not possible to differentiate between translators. While this conclusion is inconsistent with traditional linguistic studies, it seems that it was sufficient to turn away researchers from this line of research over the last 10 years and since the publication of Mikhailov and Villikka paper in 2001.

B. Network analysis:

Newmann [20] defined a *Network* as "*a collection of points joined together in pairs by lines*"; these points are referred to as vertices or nodes and the lines are referred to as edges. Networks are everywhere; almost any system can be represented as a network. The traditional definition of a system is that it is a group of components interacting together for a purpose; this is a definition whereby network representation is paramount (components are nodes and interactions are through links). Many tools exist in the literature for analysing networks [21]. These tools vary from mathematical, computational, to statistical tools.

Network mining is the process whereby a problem is represented through networks and is searched to identify patterns. Examples of network mining problems include: link prediction, link type prediction, discovery of communities of interest, and discovery of infrequent or unusual patterns. Networks can be analyzed through measurements on the global and local level. Local measures attempt to capture from local constructs the global features of the network. A widely used local measure is network motifs. They are used to uncover network structural design principles [22]. Network motifs have been successfully used by different researchers in Biology [23, 24], Game theory [25], Electronic circuits [26], and Software [27].

C. Fuzzy classifier:

In our research, we are going to employ two fuzzy classifiers; the first one is *Unordered Fuzzy Rule Induction Algorithm* called FURIA [28], which is an extension to the well-known RIPPER algorithm [29] but using fuzzy rather than conventional rules. This algorithm is introduced in 2009 by Hühn and demonstrated promising results in some types of classification problems [28, 30].

The other fuzzy classifier is the Fuzzy Lattice Reasoning Classifier (FLR), which is initially introduced by Athanasiadis in 2003 [31] . This classifier uses the Fuzzy Lattices to create a Reasoning Environment. The rules are induced in a mathematical lattice data domain. FLR has the advantage that it can be incremental. It is also able to deal with missing data [32].

III. DATA

In our work, we are going to work on translation from Arabic to English. We choose the Arabic language as it is spoken by approximately 280 million native speakers [33]. It is also the official language for 26 countries[1]; it is the third most official language in the world after English and French. The Arabic language is gaining interest due to its socio-political importance. Millions of Muslims (both Arab and non-Arab) are studying the Arabic Language as the Holy Qur'an (the main religious text of Islam) is written in Arabic; also, all the Islamic terms are in Arabic. Therefore, the interpretation of the Arabic language has wider significance.

In our work, we are going to use "The Holy Qur'an" and the translation of its meaning as our corpus. The Holy Qur'an is a widely popular text as it is read on daily basis by Muslims. The total number of Muslims worldwide is more than 1.3 billions [34] but not all Muslims can read Arabic. Hence, there is a need to translate Qur'an meanings accurately that reflect and respect the original meaning. Despite the existence of many translations of this text, there is considerable dispute about the loss in the

1 As in World Atlas website http://www.worldatlas.com/ on 28th of January 2011

translation of Qur'an meanings due to the uniqueness of its textual characteristics. Another important consideration for the choice of this text was the expectation that given its religious significance, there would be minimal difference in the translations.

We obtained our corpus data from tanzil.net [2] website. This website introduces 14 different English translations for the meanings of Holy Qur'an. We choose two of them; the first one is by Muhammad Marmaduke Pickthall and the second one is by Abdullah Yusuf Ali. These two translations are among the few translations that have been assessed by Khaleel Mohammed in 2005 [35] as being among the most accurate translations.

IV. METHODOLOGY

A. Network formation

To establish the word-adjacency network from the dataset, we worked on Ayah (verse) level. Each word is represented by a node, and each ordered word adjacency is represented by edge going from the first occurring word to the following word. The frequency of two words adjacency is counted and represented by edges labels. The edges here represent an "occurring- before" binary relationship.

B. Features identification

Working on the lexical level, there are different features that can be extracted like word n-gram, vocabulary richness, word frequencies, and token-based [36]. We are trying to find the linkage between the words and how frequently they are used by different translators. We also attempt to extract the frequency of occurrence of patterns of ordered words –known in linguistics as 'lexical chunks'- in the text.

C. Motif extraction

The motifs are small subgraphs, usually 3, 4 or 5 nodes. For a subgraph with three connected nodes, we have only 13 distinguished possible subgraphs as shown in Fig. 1. While for four connected nodes, we have 199 distinguished possible subgraphs, and 9364 possible subgraphs for five nodes. This study uses 3-node motifs.

To illustrate how we can extract these 13 motifs, we give an example using a sample translation by "Yousif Ali"[2] for chapter 112 in the Holy Qura'n in Fig. 1. The sample text is "Say: He is Allah, the One and Only; (1) Allah, the Eternal, Absolute; (2) He begetteth not, nor is He begotten; (3) And there is none like unto Him. (4)".

For example, motif 7 (M7) represent the relationship between three nodes; two way relationship between the left and upper nodes, and one way relationship between the right and upper nodes. The first relationship is represented by the ordered appearance of words "is" and "He" in Aya (3), and the other direction where "He" before "is" in Aya (1). The second relationship is represented by the ordered appearance of words "nor" and "He" in Aya (3).

In motif 8 (M8), the first relationship that appeared in motif 7 is the same, while we has another two way relationship between the upper and right nodes, represented in Aya (3) where the word "He" appeared once before "not" and the second time after it.

We scanned the network for all of these possible subgraphs and counted each of them. All matches are counted, even if there are overlapping counts. We used ***MAVisto***[37] for pre-processing.

M1		Aya (1): "Say: **He** is **Allah**, **the** One and Only"	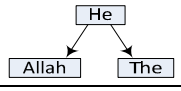
M2		Aya (1): "Say: **He** is **Allah**, the One and **Only**;"	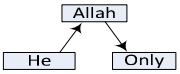
M3		Aya (3): "**He begetteth not**, nor is **He** begotten;"	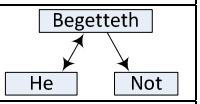
M4		Aya (1):"Say: He is **Allah**, the One **and Only**;"	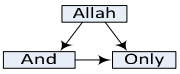
M5		Aya(1): "Say: **He is Allah**, the One and Only". Aya(3): "He begetteth not, nor **is He** begotten;"	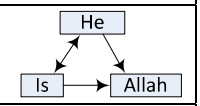
M6		Aya(2):" **Allah**, the **Eternal**, **Absolute**	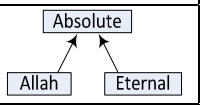
M7		Aya(1): "Say: **He is** Allah, the One and Only" Aya(3): "He begetteth not, **nor is He** begotten;"	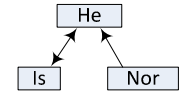
M8		Aya(1):" Say: **He is** Allah, the One and Only" Aya(3):" **He** begetteth **not**, nor **is He** begotten;"	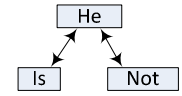
M9		Aya(3):"He begetteth not, nor **is He** begotten;" Aya(1):"Say: **He** is Allah, the One **and** Only;" Aya(4):"**And** there **is** none like unto Him"	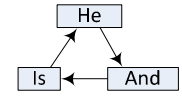
M10		Aya(3):" He begetteth not, nor **is He** begotten;" Aya(1):" Say: **He is** Allah, the One **and** Only;" Aya(4):" **And** there **is** none like unto Him"	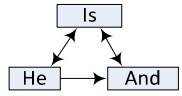
M11		Aya(3): "He begetteth not, nor **is He** begotten;" Aya(1): " Say: **He is** Allah, the One **and** Only;" Aya(4): "**And** there **is** none like unto Him"	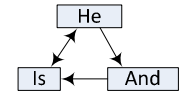
M12		Aya(3): "**He begetteth** not, nor **is He** begotten;" Aya(1): "Say: **He is** Allah, the One and Only;"	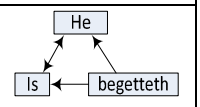
M13		Not applicable for this sample text	

Figure 1. All possible 3-nodes connected Subgraph

[2] ***Tanzil*** is a quranic project launched in early 2007 to produce a highly verified Unicode quran text to be used in quranic websites and applications. www.*tanzil.net*

D. Randomization:

To randomize the network, a random local rewiring algorithm is used. This algorithm keeps the degrees of the vertices constant. This is done by reshuffling the links: If A is connected to B (A->B), and C is connected to D (C->D).

Then, it makes a link from A to D and from C to B instead of the old links. But before applying the new links, it checks if these links already exist in the network. If so, this process is skipped and the algorithm attempts to find other links. This check is necessary to prevent having multiple links connecting the same vertices [38]. This process is repeated several times in excess of the total number of edges in the system to generate a randomized network [39]. We considered 500 randomized networks for each sample when conducting our experiments.

E. Significance test

To calculate Z-score, we need to calculate the average and standard deviation of occurrences of a motif in all randomized networks. The z-score is calculated as the difference between the frequency of this motif in the target network and the mean frequency of the generated randomized networks divided by the standard deviation of the frequency values for these randomized networks.

Since we are testing for confidence level %95, the z normal range is from -1.96 to +1.96. If the z-score is within this range, it is not significant. If it is outside this range, it is significant.

V. EXPERIMENTS

A. Research questions

The main question we attempt to answer in this paper is: Can we use network motifs to detect translator's style? The sub-questions of our research include:

- How can data normalization affect the bias of the sample?
- What is an appropriate sample size for detecting translator stylometry?
- How can class distribution balance/imbalance affect the results?

B. Expiremneal design

For all tests we used 30 parallel samples for two translators in addition to their original texts, so that we have 30 chapters from the Qur'an with their corresponding translations for two translators.

First: to address the normalization problem, we conduct 5 different tests considering the parameters as in Table 1: In the first test, we consider absolute values: The attributes of motifs represent f(xi) and f(yi). So, we have 13 attributes representing the 13 motifs and one attribute representing class label for 40 samples for training and 20 samples for testing considering class balance. The second test, using the same configuration of the first test but we tried to minimise the translator bias to her own writing; thus, we used the attributes of motifs to represent f(xi)/Σ(f(xi)) for the first translator, and f(yi)/Σ(f(yi)). In the third Test: The attributes of motifs represent f(xi)/f(zi) and f(yi)/f(zi). The conjecture behind this is to minimise the bias regarding the original text. While in the fourth test; we used the attributes of motifs to represent f(x)/(Σ(f (xi)* f(zi)) as a conjecture for minimising both the original text bias and translator bias. For tests 3 and 4, we need to divide by the frequency of Arabic motifs, which is sometimes zero, so we increment the number of motifs for Arabic text by 1. In the fifth test, we used 16 attributes which are the 13 motifs in addition to the number of nodes and edges and one attribute for class label.

Second: to address the sample size problem, we repeated the previous experiments with 10 sample chapters for each translator for training and 10 samples for testing, and compared these results to their corresponding results from the first experiment. The comparison is between an experiment with 10 samples as the training size and the other with 20 samples for the training size. In both cases, we maintained the test sample constant to have a fair comparison. The test size is 10 sample chapters, forming a total of 20 chapters covering both translators.

The third question was about class balance. To address such question we repeated the first experiment but considered randomizing the choice of the classes for training and testing purposes, and compared the results to the balanced experiment. Since we have 30 samples which introduce 60(30x2) instances, and we are considering an imbalance problem, we choose randomly 40 out of the 60 instances for training and the rest are used for testing.

C. Classifiers:

We used six different classifiers in our experiments to study which of them can produce more accurate results in our problem. These classifiers are:

1. FT: Functional Tree (FT) is a classifier that was introduced by João in 2004 [40]. This classifier uses decision tests based on a combination of attributes. FT is used with its default parameters using WEKA where the minimum number of instances at which a node is considered for splitting is set to 15, and the number of fixed LogitBoost iterations is set to 15 with no weight trimming.
2. NBTree**:** This decision tree uses Naive Bayes classifiers at the leaves. This hyperid classifier is firstly presented by Kohavi in 1996 [41].
3. Random Forest: This classifier generates a random number of decision trees that represent a forest to be used for classification[42].

TABLE 1 EXPERIMENTS PARAMETERS

$f(x_i)$	is the frequency of each motif in a sample i for the first translator
$\Sigma(f(x_i))$	is the summation of all frequencies of motifs in a sample i for the first translator
$F(y_i)$	is the frequency of each motif in a sample i for the second translator
$\Sigma(f(y_i))$	is the summation of all frequencies of motifs in a sample i for the second translator
$F(z_i)$	is the frequency of each motif in a sample i for the original Arabic text

We used this classifier with no constraints on the maximum depth of the trees and the number of attributes to be used, while the number of trees in limited to 10.

4. Random Tree: While constructing decision trees, a random number of attributes is chosen at each node to introduce a Random Tree classifier. We used the defaults parameters for this classifier which includes no backfitting or pruning.
5. FURIA: Fuzzy Unordered Rule Induction algorithm (FURIA) is discussed in detail in section II(C) of this paper; the parameters for applying this algorithm includes setting the minimum total weight of the instances in a rule to two, with two runs of an optimization procedure, and to use check for error rate that >= 0.5 for the stopping criterion.
6. FLR: Fuzzy Lattice Reasoning Classifier (FLR) is discussed earlier in section II(C) as well. The vigilance parameter value is set to 0.5 while running our experiments.
7. Multiclass Classifier: This classifier uses multi-class datasets with 2-class classifiers. In these experiments we used a logistic classifier. It applies error correcting output codes to increase the accuracy.

VI. Results and Analysis

Looking at Fig. 2; when we calculated the means of the 30 sample that we have for each translator, we found that the appearance of the motifs is different for each author. The second translator has the highest average for all motifs.

A. Paired T-test:

We applied paired t-test on the frequencies of motifs for each paired sample text, where the pair here represents two translations of the same original text. Two tail t-critical for alpha=0.05 and sample size of 30 is 2.04523.

Table 2 displays the t-calculated for each motif. All of them show that the differences between the frequencies for the two translators are significant.

B. Correlation between motifs:

We calculated the Pearson correlation coefficient between the motifs for each translator to find how often these motifs appeared concurrently, and then compared them to each other. We summarized the important differences in Table 3.

Since these motifs represent links between words in the text, and the correlation represents how often these motifs occur together, the difference between these correlations indicates difference in translator's style.

C. Experiment 1:

For Experiment 1; as Table 4 shows the best results are obtained using the functional tree classifier and multiclass classifier with test 5 which includes the number of nodes and edges with the motif frequency as inputs. The accuracy of these classifiers is 70%, which is the same accuracy of NBTree and FLR when applied to test 3, where the data is normalised against the original text bias.

D. Experiment 2:

For experiment 2, we test using smaller training sample size, which are 10 for each translator. We noticed that the results for the multiclass classifier are enhanced compared to the first experiment, while the functional tree accuracy decreased. The best accuracy obtained for this experiment remained at 70% as shown in

Table 5. This level of accuracy is obtained using Random Tree classifier and FLR classifier for test2 where the data is normalized against the translator bias. It is also obtained by the multiclass classifier with test5 which is the same result for this classifier in the first experiment.

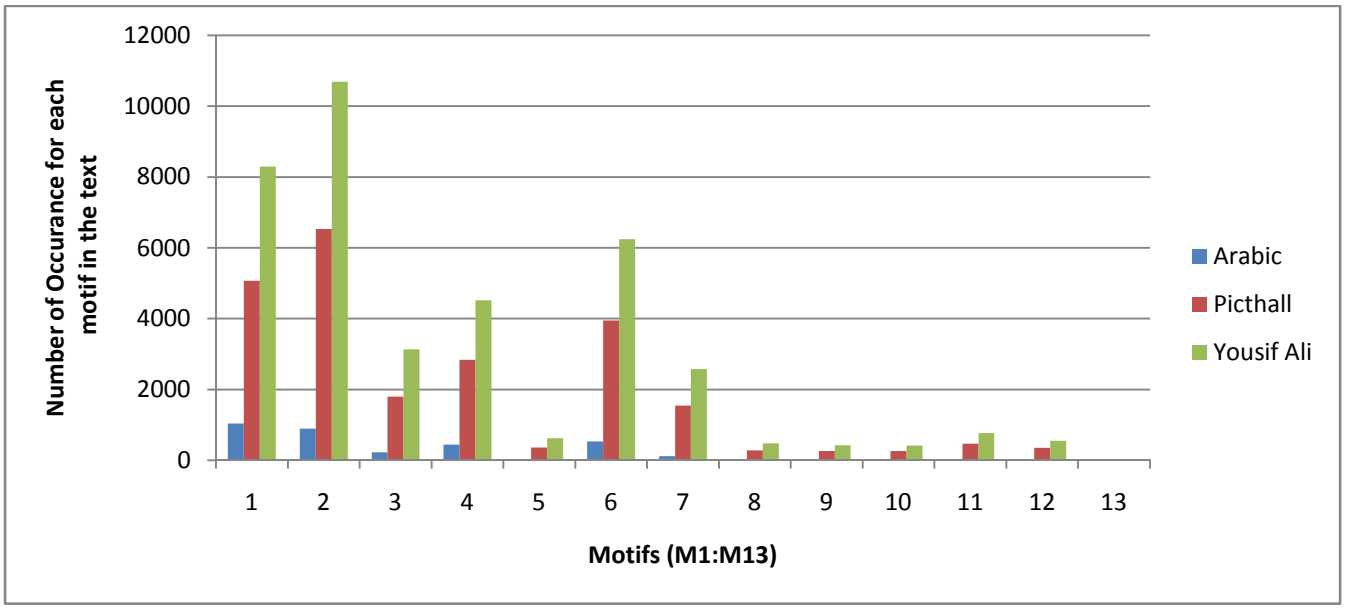

Figure 2. Comparison between the average of the 13 motifs for the Arabic, First English Translation, Second Translation

E. Experiment 3:

In the third experiment, we addressed the imbalance class problem. We used the 40 instances for training as 24 instances for the first translator "Pitchall" and 16 instances for the second translator "Yousif Ali". For testing, we used 20 instances, where 6 instances for "Pitchall" and 14 for "Yousif Ali". We noticed that most of the results were only 30% as shown in

Table 6 where the classifiers classified all the instances to belong to the first translator. The only classifier that gives acceptable results was FLR, where we got 70% accuracy for test 3 where data is normalized against the original text.

In general, the Random Forest classifier and FURIA consistently failed to detect the differences between translator's styles. On the other hand, the FLR classifier introduced acceptable results in the three experiments. Test 1 and test 4 failed to identify the translator's style, where in test 1 the data is not normalized, and in test 4 it is normalized against both the translator bias and the original text bias.

Both test 3 and test 5 introduced acceptable classifiers three times in the overall experiments. That indicates the importance of normalizing the data against its original text bias and the importance of including the number of nodes and edges into the attributes as it may help the classifier to normalize the data implicitly.

TABLE 2 PAIRED T-TEST BETWEEN FREQUENCIES OF MOTIFS FOR THE TWO TRANSLATORS

Motif	t-test
M1	-5.21757
M2	-5.36426
M3	-4.71189
M4	-5.48586
M5	-4.39642
M6	-5.46861
M7	-5.28081
M8	-4.65985
M9	-4.42133
M10	-3.93762
M11	-4.36377
M12	-4.94248
M13	-2.75729

TABLE 3 CORRELATION BETWEEN FREQUENCIES OF MOTIFS

Motifs	First Translator "Pitchall"	Second Translator "Yousif Ali"
(M2, M13)	0.768	0.523
(M4 , M13)	0.910	0.550
(M6, M13)	0.816	0.495
(M7, M13)	0.911	0.640
(M9, M13)	0.946	0.711
(M11, M13)	0.978	0.751
(M12, M13)	0.975	0.752

TABLE 4 ACCURACY OF THE DIFFERENT CLASSIFIERS FOR EXPIREMENT1

Classifier	Functional Tree	NBTree	Random Tree	Random Forest	FURIA	FLR	Multiclass Classifier
Test1	60%	50%	55%	25%	50%	50%	55%
Test2	65%	50%	65%	65%	50%	60%	45%
Test3	65%	70%	45%	60%	55%	70%	60%
Test4	50%	50%	50%	50%	55%	60%	45%
Test5	70%	50%	60%	50%	50%	50%	70%

TABLE 5 ACCURACY OF THE DIFFERENT CLASSIFIERS FOR EXPIREMENT2

Classifier	Functional Tree	NBTree	Random Tree	Random Forest	FURIA	FLR	Multiclass Classifier
Test1	50%	50%	60%	55%	50%	50%	65%
Test2	50%	50%	70%	60%	60%	70%	60%
Test3	50%	50%	60%	65%	55%	65%	60%
Test4	50%	50%	60%	45%	50%	55%	60%
Test5	50%	50%	50%	65%	60%	50%	70%

TABLE 6 ACCURACY OF THE DIFFERENT CLASSIFIERS FOR EXPIREMENT3

Classifier	Functional Tree	NBTree	Random Tree	Random Forest	FURIA	FLR	Multiclass Classifier
Test1	45%	30%	25%	60%	30%	30%	40%
Test2	60%	30%	30%	20%	30%	30%	50%
Test3	45%	45%	45%	50%	55%	70%	35%
Test4	30%	30%	40%	30%	45%	40%	40%
Test5	45%	30%	50%	35%	30%	30%	45%

VII. CONCLUSION

Studying *"Translator Stylometry"* is a non-trivial task. While there has been research in linguistics and social sciences discussing the characteristics of each translator, this line of research is limited in computational linguistics. Contrary to previous findings that this problem does not have an automatic solution, this paper presented a first attempt to counteract this belief. We demonstrated that translators cannot disappear under the skin of the original authors; they have their own identities. Different translators represent the same idea in different ways. Although some existing authorship attributions couldn't capture these differences [15], this work shows that we can use social network analysis to differentiate between translators' styles. Detecting network motifs shows that each author is using certain patterns while writing. The proposed method introduces a classifier that can classify translated texts into their translators with accuracy of 70%. Fuzzy Lattice Reasoning Classifier (FLR) introduces the best results among seven tested classifiers. Normalising the data against its original text and the network size offers promising results. Further analysis is needed to explore this research area.

VIII. REFERENCES

[1] M. Koppel, J. Schler, and S. Argamon, *Computational methods in authorship attribution.* Journal of the American Society for Information Science and Technology, 2009. **60**(1): p. 9-26.

[2] E. Stamatatos, *A survey of modern authorship attribution methods.* Journal of the American Society for Information Science and Technology, 2009. **60**(3): p. 538-556.

[3] S. Argamon. *Measuring the usefulness of function words for authorship attribution*. in *In Proceedings of the 2005 ACH/ALLC Conference*. 2005.

[4] P. Fuchun, S. Dale, W. Shaojun, and K. Vlado, *Language independent authorship attribution using character level language models*, in *Proceedings of the tenth conference on European chapter of the Association for Computational Linguistics - Volume 1*. 2003, Association for Computational Linguistics: Budapest, Hungary.

[5] A.M. García and J.C. Martín, *Function words in authorship attribution studies.* Literary Linguist Computing, 2007. **22**(1): p. 49-66.

[6] J. Grieve, *Quantitative authorship attribution: An evaluation of techniques.* Literary and Linguistic Computing, 2007. **22**(3): p. 251-270.

[7] H.V. Halteren, *Author verification by linguistic profiling: An exploration of the parameter space.* ACM Transactions on Speech and Language Processing (TSLP) 2007. **4**(1): p. 1-17.

[8] P. Juola, *Authorship attribution.* Foundations and Trends in Information Retrieval, 2006. **1**(3): p. 233–334.

[9] P. Juola, *Future trends in authorship attribution*, in *Advances in digital forensics iii*, P. Craiger and S. Shenoi, Editors. 2007, Springer Boston. p. 119-132.

[10] P. Juola, J. Sofko, and P. Brennan, *A prototype for authorship attribution studies.* Literary and Linguistic Computing, 2006. **21**(2): p. 169-178.

[11] D. Labbe`, *Experiments on authorship attribution by intertextual distance in english.* Journal of Quantitative Linguistics, 2007. **14**(1): p. 33 - 80.

[12] D. Madigan, et al. *Author identification on the large scale*. in *In Proc. of the Meeting of the Classification Society of North America*. 2005.

[13] J. Rudman and B. Keith, *Authorship attribution: Statistical and computational methods*, in *Encyclopedia of language & linguistics*. 2006, Elsevier: Oxford. p. 611-617.

[14] S. Urszula and A.C. Krzysztof, *Application of artificial neural networks to stylometric analysis*, in *Proceedings of the 8th conference on Systems theory and scientific computation*. 2008, World Scientific and Engineering Academy and Society (WSEAS): Rhodes, Greece.

[15] M. Mihailov and M. Villikka. *Is there such a thing as a translator's style?* . in *Proceedings of the Corpus Linguistics*. 2001. Lancaster.

[16] R. Milo, et al., *Network motifs: Simple building blocks of complex networks.* Science, 2002. **298**(5594): p. 824-827.

[17] M. Winters, *From modal particles to point of view a theoretical framework for the analysis of translator attitude.* Translation and Interpreting Studies, 2010. **5**: p. 163-185.

[18] X. Xiumei, *Style is the relationship a relevance-theoretic approach to the translator's style.* Babel, 2006. **52**: p. 334-348.

[19] P.S. Angermeyer, *Translation style and participant roles in court interpreting.* Journal of Sociolinguistics, 2009. **13**(1): p. 3-28.

[20] M. Newman, *Networks: An introduction*. 2010, New York: Oxford University Press.

[21] S. Wasserman and K. Faust, *Social network analysis: Methods and applications (structural analysis in the social sciences)*. 1994: Cambridge University Press.

[22] U. Alon, *Network motifs: Theory and experimental approaches.* Nat Rev Genet, 2007. **8**(6): p. 450-461.

[23] O. Sporns and R. Kötter, *Motifs in brain networks.* PLoS Biol, 2004. **2**(11): p. e369.

[24] N. Puig, I. Pournara, and L. Wernisch, *Statistical model comparison applied to common network motifs.* BMC Systems Biology, 2010. **4**(1): p. 18.

[25] A. Ghoneim, H. Abbass, and M. Barlow, *Characterizing game dynamics in two-player strategy games using network motifs.* Systems, Man, and Cybernetics, Part B: Cybernetics, IEEE Transactions on, 2008. **38**(3): p. 682-690.

[26] S. Itzkovitz, et al., *Coarse-graining and self-dissimilarity of complex networks.* Phys Rev E Stat Nonlin Soft Matter Phys, 2005. **71**(1 Pt 2).

[27] S. Valverde and R.V. Solé, *Network motifs in computational graphs: A case study in software architecture.* Physical Review E, 2005. **72**(2): p. 026107.

[28] J. Hühn and E. Hüllermeier, *Furia: An algorithm for unordered fuzzy rule induction.* Data Mining and Knowledge Discovery, 2009. **19**(3): p. 293-319.

[29] W.C. William, *Fast effective rule induction*, in *Proceedings of the 12th international conference on machine learning (ICML)*. 1995: Tahoe City. p. 115–123.

[30] J. Hühn and E. Hüllermeier, *An analysis of the FURIA algorithm for fuzzy rule induction*, in *Advances in machine learning i*, J. Koronacki, et al., Editors. 2010, Springer Berlin / Heidelberg. p. 321-344.

[31] I.N. Athanasiadis, V.G. Kaburlasos, P.A. Mitkas, and V. Petridis. *Applying machine learning techniques on air quality data for real-time decision support*. in *First International NAISO Symposium on Information Technologies in Environmental Engineering (ITEE'2003)*. 2003. Gdansk, Ploand: ICSC-NAISO Publishers.

[32] I. Jenhani, N.B. Amor, and Z. Elouedi, *Decision trees as possibilistic classifiers.* International Journal of Approximate Reasoning, 2008. **48**(3): p. 784-807.

[33] S. Procházka, *Arabic*, in *Encyclopedia of language & linguistics*, B. Keith, Editor. 2006, Elsevier: Oxford. p. 423-431.

[34] M. Abdel Haleem, *Islam and Arabic*, in *Encyclopedia of language & linguistics*, B. Keith, Editor. 2006, Elsevier: Oxford. p. 34-37.

[35] K. Mohammed, *Assessing English translations of the Qur'an.* The Middle East Quarterly, 2005. **XII**(2): p. 58-71.

[36] A. Abbasi and H. Chen, *Applying authorship analysis to extremist-group web forum messages.* 2005. **20**(5): p. 67-75.

[37] F. Schreiber and H. Schwöbbermeyer, *MAVisto: A tool for the exploration of network motifs.* Bioinformatics, 2005. **21**(17): p. 3572-3574.

[38] S. Maslov and K. Sneppen, *Specificity and stability in topology of protein networks.* Science, 2002. **296**(5569): p. 910-913.

[39] S. Maslov, K. Sneppen, and U. Alon, *Correlation profiles and motifs in complex networks*. Handbook of graphs and networks. 2005: Wiley-VCH Verlag GmbH & Co. KGaA. 168-198.

[40] G. João, *Functional trees.* Machine Learning, 2004. **55**(3): p. 219-250.

[41] R. Kohavi. *Scaling up the accuracy of naive-bayes classifiers: A decision-tree hybrid*. 1996.

[42] L. Breiman, *Random forests.* Mach. Learn., 2001. **45**(1): p. 5-32.

2011 IEEE International Conference on Fuzzy Systems
June 27-30, 2011, Taipei, Taiwan

Genetic-Fuzzy Association Rules for Network Intrusion Detection Systems

Ming-Yang Su
Department of Computer Science and Information Engineering,
Ming Chuan University, Taiwan
*minysu@mail.mcu.edu.tw

Chun-Yuen Lin
Department of Computer and Communication Engineering,
Ming Chuan University, Taiwan
o1o1o1o1o.safe@gmail.com

Sheng-Wei Chien, Han-Chung Hsu
Department of Computer Science and Information Engineering,
Ming Chuan University, Taiwan
lancehtm@hotmail.com,
s110552178@gmail.com

***Abstract*—A network intrusion detection system (NIDS) based on genetic-fuzzy association rules is presented in the paper, which mines rules in an incremental manner in order to meet the real-time requirement of a NIDS. More precisely, the proposed NIDS adopts the incremental mining of fuzzy association rules from network traffic, in which membership functions of fuzzy variables are optimized by a genetic algorithm. The proposed online system belongs to anomaly detection, not misuse detection. Some denial-of-service (DoS) attacks were experimented in this study to show the performance of the proposed NIDS. The results show that the proposed NIDS can detect DoS attacks in both effectiveness and efficiency.**

Keywords-Genetic-fuzzy association rules; incremental mining; membership functions; genetic algorithm; anomaly detection; denial-of-service (DoS) attacks

I. INTRODUCTION

Misuse detection, such as SNORT [1], aims to detect known attacks by characterizing the rules that govern these attacks. Thus, a rules update is most important and is frequently released by IDS vendors. However, the rapid emergence of new vulnerabilities and exploits makes misuse detection difficult to trust day after day. Anomaly detection is designed to capture any deviation from the profiles of normal behavior patterns. It is much more suitable than misuse detection for detecting unknown or novel attacks, but it has the potential to generate too many false positives. Many approaches have been proposed in previous literature concerning the design of anomaly NIDSs, such as neuro-fuzzy [2], support vector machine [3], decision tree [4], Bayesian Neural Networks [5], Naïve Nayes [6], genetic-fuzzy [7, 8], and fuzzy association rules [9, 10, 11, 12, 13, 14].

For a NIDS, effectiveness is usually measured by detection rate, false alarm rate, etc., and efficiency is measured by response time when an attack has occurred. This study focuses on how to create an anomaly NIDS, based on genetic optimized mining of fuzzy association rules, which can detect and react to a flooding attack in real-time. In contrast to traditional static mining for NIDS designs [9, 10, 11, 12, 13, 14], which can only be applied to offline NIDS, this system was designed based on an incremental mining approach, which enables the system to make a decision per time unit. In addition, a genetic algorithm was applied to help select the best membership functions for the fuzzy variables of mining. Consequently the performance of the proposed response system can be improved.

The remainder of this paper is organized as follows: Section 2 states fuzzy association rules and membership functions of a genetic algorithm; Section 3 introduces the genetically optimized incremental mining algorithm for fuzzy association rules; Section 4 describes the proposed NIDS by genetic-fuzzy association rules; Section 5 shows some experimental results; and Section 6 is the conclusions.

II. FUZZY ASSOCIATION RULES

Agrawal and Srikant proposed the well-known Apriori algorithm [15] in 1994 in which, given two thresholds of *mini_sup* and *mini_conf*, the algorithm will find all such rules as "$X \Rightarrow Y$" with *support* $\geq$ *mini_sup* and *confidence* $\geq$ *mini_conf*, where X and Y are subsets of the set of items, and $X \cap Y = \varnothing$. The rule $X \Rightarrow Y$ in the database D has *support* s if the percentage of records in D that contain $X \cup Y$ is s, and has *confidence* c if the ratio of the number of records in D that contain $X \cup Y$ to the number of records in D that contain X is c. Since the Apriori algorithm was designed for mining in databases with binary items, fuzzy association rules mining [16, 17, 18] has been one of the variations which has dealt with quantitative items.

While applying fuzzy association rules to an IDS (intrusion detection system) design, the term item, is replaced by the term feature, and thus, the term itemset is equivalent to the term feature-set, which is a set of features. Let $D = \{r_1, r_2, \ldots, r_n\}$ be the database and $I = \{x_1, x_2, \ldots, x_m\}$ represent all features appearing in D. The record r_i represents the ith m-tuple in D. Each quantitative feature x_k, $1 \leq k \leq m$, is associated with some fuzzy variables, say $v_1, v_2, \ldots, v_t$. Every fuzzy variable is represented by a membership function. For easy representation in the following, $MFx_i.v_j$, $1 \leq i \leq m$ and $1 \leq j \leq t$, is used to uniquely denote the jth membership function of feature x_i. In the mining of fuzzy association rules [18, 19], a fuzzy itemset consists of two parts: items and fuzzy variables, say $<X, U>$, where $X = (x_1, x_2, \ldots, x_k) \subset I$ is a collection of items (or features) and $U = (v_1, v_2, \ldots, v_k)$ is the collection of corresponding fuzzy variables to X in order. Suppose there are totally n records in the database. Then the support of $<X, U>$ is computed as:

978-1-4244-7316-8/11/$26.00 ©2011 IEEE

$$\text{Sup}(\langle X, U\rangle) = \frac{\sum_{i=1}^{n}\prod_{j=1}^{k} MF_{x_j \cdot v_j}(r_i[x_j])}{n}, \quad (1)$$

where $r_i[x_j]$ denotes the value of feature x_j of the ith record. For example, suppose four features, *#packet*, *#SYN*, *#ACK*, and *#connection,* are of concern in a NIDS, and each feature has three fuzzy variables, say *low*, *medium* and *high*, then 4 × 3 = 12 membership functions are involved, i.e., $MF_{\#packet.low}$ denotes the low function of feature *#packet*, $MF_{\#ACK.high}$ denotes the high function of feature *#ACK*, etc. Suppose there are three records in the database, as shown in Table 1. Then the support of the fuzzy itemset <(*#packet*, *#SYN*, *#connection*), (*low*, *medium*, *low*)> is computed as ($MF_{\#packet.low}(3260)$ × $MF_{\#SYN.medium}(135)$ × $MF_{\#connection.low}(27)$ + $MF_{\#packet.low}(2170)$ × $MF_{\#SYN.medium}(75)$ × $MF_{\#connection.low}(65)$ + $MF_{\#packet.low}(6123)$ × $MF_{\#SYN.medium}(213)$ × $MF_{\#connection.low}(89)$) / 3.

TABLE I. RECORDS IN DATABASE, FOR AN EXAMPLE

#packet	*#SYN*	*#ACK*	*#connection*
3260	135	75	27
2170	75	43	65
6123	213	27	89

A fuzzy association rule has the form of "<*X*, *U*> ⇒ <*Y*, *V*>", where <*X*, *U*> and <*Y*, *V*> are two fuzzy itemsets and $X \cap Y = \varnothing$. Let $Z = X \oplus Y$ and $W = U \oplus V$, where ⊕ is the concatenation operation. The support of the fuzzy association rule "<*X*, *U*> ⇒ <*Y*, *V*>" is computed as Sup (<*Z*, *W*>), and the confidence of the rule is computed as Sup (<*Z*, *W*>) / Sup (<*X*, *U*>). For example, let us consider the following fuzzy association rule.

<(*#SYN*, *#ACK*), (*high*, *low*)> ⇒ <(*#connection*), (*medium*)>.

//if *#SYN* is high and *#ACK* is low, then *#connection* is medium

Its support is computed as Sup(<(*#SYN*, *#ACK*, *#connection*), (*high*, *low*, *medium*)>), and its confidence is computed as Sup(<(*#SYN*, *#ACK*, *#connection*), (*high*, *low*, *medium*)>) / Sup(<(*#SYN*, *#ACK*), (*high*, *low*)>).

III. FUZZY ASSOCIATION RULES THROUGH INCREMENTAL MINING WITH GENETIC OPTIMIZATION ON MEMBERSHIP FUNCTIONS

Two important keys need to be addressed for a successful NIDS based on fuzzy association rules. One is applying incremental mining, instead of static mining, to meet real-time demands. The other is a deliberate design for membership functions. We have proposed an incremental mining algorithm [20] to derive fuzzy association rules from network traffic. Based on the incremental mining algorithm, the paper further extends the algorithm to design an online detection system with genetic optimization in membership functions.

According to the proposed algorithm [20], packet information was collected to form one record every short time unit, and to mine out the newest rule set as the latest record was being gathered. Each current support value of a fuzzy itemset was kept in the memory for a time unit. As the next record was being gathered, the algorithm used the current support value to compute the next one, and then replaced it with the new one, as shown in the example below. Suppose the quantitative values of the four features, *#packet*, *#SYN*, *#ACK* and *#connection*, are measured for each time unit, and in sequence they are t_1 = (97, 310, 66, 311), t_2 = (215, 208, 75, 210), t_3 = (62, 710, 41, 88), …, t_i = (230, 86, 31, 720), …. For the fuzzy itemset <*X*, *U*> = <(*#packet*, *#SYN*, *#connection*), (*low*, *medium*, *low*)>, its support value *s* at t_1, t_2, t_3, …, t_i, …, is computed individually as:

s_{t1} = ($MF_{\#packet.low}(97)$ × $MF_{\#SYN.medium}(310)$ × $MF_{\#connection.low}(311)$) /1 → *tmp*;

s_{t2} = (*tmp* × 1 + ($MF_{\#packet.low}(215)$ × $MF_{\#SYN.medium}(208)$ × $MF_{\#connection.low}(210)$)) / 2 → *tmp*;

s_{t3} = (*tmp* × 2 + ($MF_{\#packet.low}(62)$ × $MF_{\#SYN.medium}(710)$ × $MF_{\#connection.low}(88)$)) / 3 → *tmp*;

…

s_{ti} = (*tmp* × (*i*-1) + ($MF_{\#packet.low}(230)$ × $MF_{\#SYN.medium}(86)$ × $MF_{\#connection.low}(720)$)) / *i* → *tmp*.

…

Since the contribution of previous records to the current support of a fuzzy itemset is ephemerally saved in the variable, i.e, *tmp*, the cost of mining time will not be prolonged as the aggregate records increase. The whole algorithm can be found in [20].

Membership functions design is important, and they usually have profound affects on the mined rules. This research adopts a genetic algorithm to select the best membership functions for the features applied in the proposed NIDS system. The membership functions applied in this paper are listed below, in which abs( ) is the absolute function, ^ is the power operation, and *a*, *b*, *c*, *d*, *e*, *f*, *g*, and *h* are the constants. The output value of a membership function falls in the interval of [0, 1]. Each feature has its own membership functions, i.e., with different constants from feature to feature. The goal of a genetic algorithm is to derive the most appropriate membership functions for every feature. As shown in Figure 1, for a feature, its membership functions before and after genetic evolution, are depicted by solid lines and dashed lines, respectively.

Fuzzy membership functions:

Low: $f(x) = 1 / (1 + \text{abs}((x - a) / b) \text{ ^ } c)$

Medium: $f(x) = 1 / (1 + \text{abs}((x - d) / e)^{\wedge} f)$

High: $f(x) = 1 / (1 + \exp(-g(x - h)))$

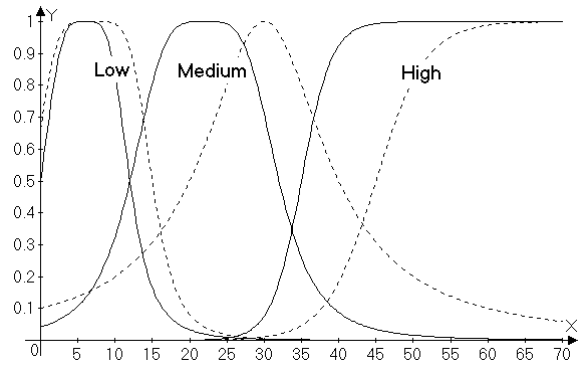

Figure 1 Fuzzy membership functions before and after genetic optimization

Suppose *n* features are considered in the NIDS design, then one chromosome in the genetic algorithm contains the *n* features' membership functions, as defined in Figure 2. The first chromosome in the experiment was constructed heuristically. An initial population, containing 30 chromosomes, was derived from the first chromosome by repeated application of the mutation process. In each generation, the fitness of each new chromosome was evaluated according to the performance of the proposed NIDS, using the fuzzy membership functions represented by the chromosome, i.e., the fitness function of the genetic algorithm was to maximize the overall accuracy in a given labeled dataset. A specified percentage of the chromosomes with high fitness were retained for the next generation. Then, parent chromosomes were repeatedly selected from the current generation, and new chromosomes were generated from these parents by crossover and mutation. One generation ended when the number of chromosomes for the next generation had reached the original population, i.e., 30 chromosomes. The evolution process was repeated for 250 generations.

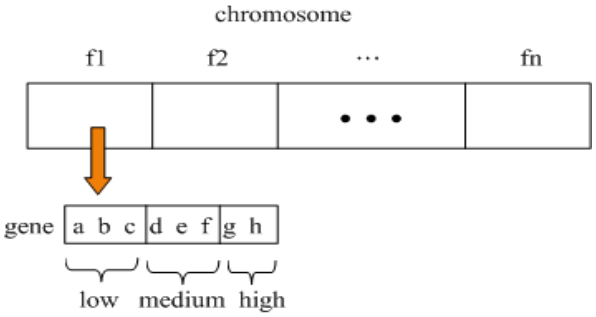

Figure 2 Gene and chromosome structures of evolution

IV. THE PROPOSED NIDS

The proposed system was designed for online detection and response to flooding attacks. A short time unit was defined, thus, the reaction of the system must be performed once every time unit. Two seconds defined one unit in this research, i.e., one record was generated regardless of the number of captured packets. In the training stage, attack-free network traffic information was collected at the rate of one record every two seconds, and the genetic optimized membership functions were derived in advance from a labeled dataset. The online response system consists of four modules. Module_A collected run-time network traffic information online, at the rate of one record every two seconds, and consistently sent the records to module_B. Module_B applied the genetically optimized incremental mining algorithm to generate the newest fuzzy rule set every two seconds. At the same time, module_C also performed the algorithm every 2 seconds on the attack-free data records, i.e., adding one new attack-free record every 2 seconds to the set of mined data records. The two newest rule sets from module_C and module_B were then sent to module_D for comparison, again, once every two seconds. If their similarity was below the threshold, an anomaly of network traffic could be found. Once an attack had been detected, three actions resulted: an alarm was inserted into the database, module_A was required to gather more detailed information about the attack and, finally, the filtering rule in the firewall could be changed dynamically. In the implementation, a round-robin strategy was applied on the attack-free records in module_C.

In this paper, the similarity between the two rule sets was defined as follows. Let $S1$ and $S2$ be two rule sets. The similarity between them was computed as:

$$sim(S_1, S_2) = \frac{SCORE1}{|S_1|} \times \frac{SCORE2}{|S_2|}, \quad (2)$$

where $|S_1|$, $|S_2|$ represent the number of rules in the sets, $SCORE1 = \sum_{\forall r \in S_1} score(r, S_2)$ and $SCORE2 = \sum_{\forall r \in S_2} score(r, S_1)$. For a single rule r with support s and confidence c and a rule set S, $score(r, S)$ was defined as:

If there is a rule $r' = r$ in S with support s' and confidence c', then $score(r, S) = 1 - \max(\frac{|c - c'|}{\max(c, c')}, \frac{|s - s'|}{\max(s, s')})$, else $score(r, S) = -\max(c, s)$. (3)

Two rules, r and r', are regarded as $r = r'$, if they have the same antecedents and consequents. Finally, let SCORE1 or SCORE2 be 0 if it was a negative value. In our system, for any fuzzy itemset, its support was computed by:

Current support = support due to the latest record * k + support due to all historical records * $(1 - k)$, where k is a constant between 0 and 1. (4)

V. SIMULATION RESULTS

In the experiments of this section, a commercial application named IP Traffic [21] was applied to produce background traffic which can generate any amount of TCP/UDP/ICMP packets by hardware limit. Two hosts running IP Traffic played sender and receiver, respectively, and the receiver in the LAN and the sender transmitting packets was deployed through the Internet. During the experiments of this study, the amount of network traffic remained from 0 to 80 Mbps through random connection and random flow size. One laptop launched flooding attacks against the victim located in the LAN through the Internet. Our system, deployed in the LAN, was coded by Microsoft Visual C++ - MFC and run on a laptop with Windows XP. A total of 1000 attack-free traffic records were derived from IP Traffic in advance and stored in the database, one at a time for every two seconds. As these records in the database were exhausted, they were cyclically reused.

TABLE II. 15-FEATURE LIST

IP:D.IP slots hit	TCP:checksum_error count
IP:MF_Flag count	IP:checksum_error count
TCP:S.IP+URG_Flag+URG data count	ARP:Size error count
IGMP:checksum_error count	TCP:URG_Flag+URG_data count
ARP:S.IP+ARP count	UDP:Same_length_interval count
IGMP:Length>1000 count	ICMP:Length>1000 count
TCP:Sequence_number==0 count	IP:(Total length>1400 || <40)&&TTL == 64 count
ICMP: Type error count	

All of the 15 features applied in this research are listed in Table 2, which were all derived from IP, TCP, UDP, ICMP, ARP, and IGMP headers. They were adopted to collect packet information and generate one record every two seconds. Some of the features were single condition, e.g., *D.IP slots hit*, and some were compound, e.g., *S.IP + ARP count*. The example, *D.IP slots hit*, for instance denoted how many slots of IP addresses were hit by network packets, according to their destination IP addresses. This study mapped a 32-bit IP address to one of 256 slots by its twice-folded IP address, i.e., mapping IP:x1.x2.x3.x4 to slot (x1⊕x2)⊕(x3⊕x4). The first three features in Table 2 before and after genetic optimization on membership functions are depicted in Figure3, Figure 4, and Figure 5, respectively. The before functions that were adopted in [20] are obtained by manually heuristic selections.

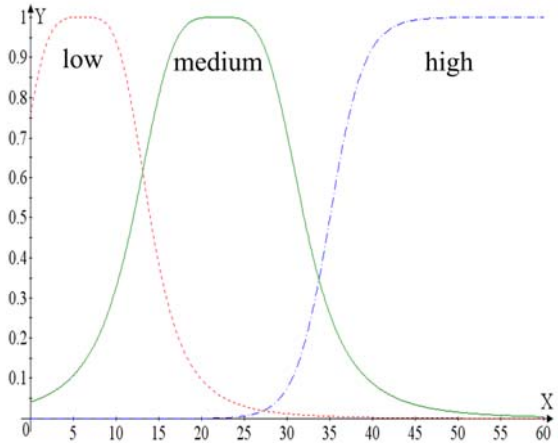

(a) Before

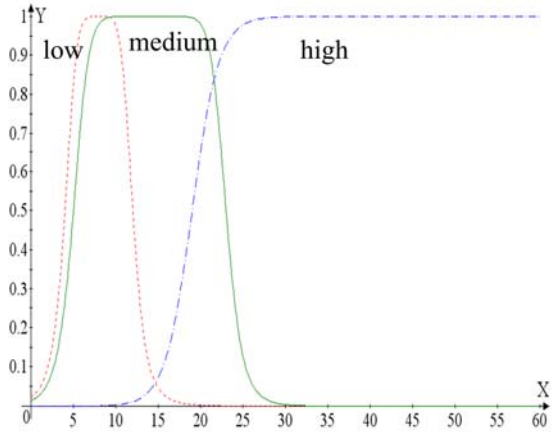

(b) After

Figure 3 Fuzzy membership functions of the feature "IP:D.IP slots hit" before and after genetic optimization

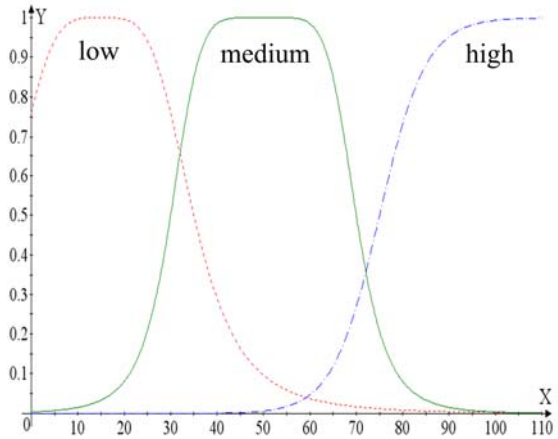

(a) Before

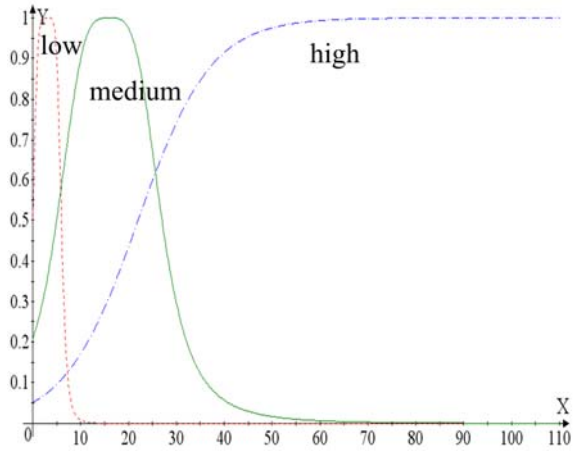

(b) After

Figure 4 Fuzzy membership functions of the feature " IP:MF_Flag count" before and after genetic optimization

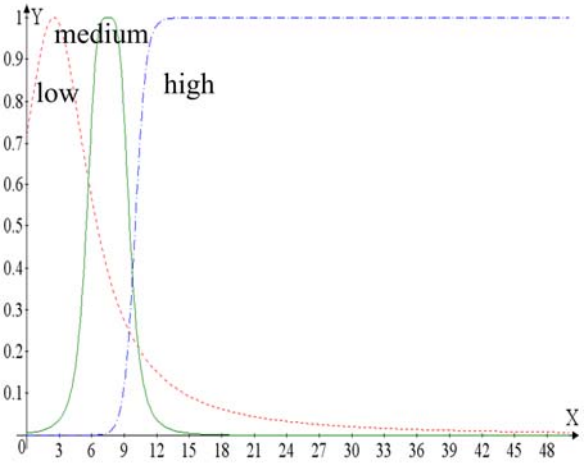

(a) Before

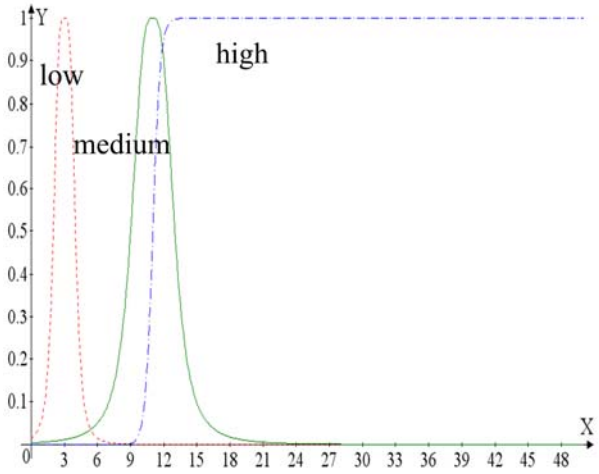

(b) After

Figure 5 Fuzzy membership functions of the feature " TCP:S.IP+URG_Flag+URG data count " before and after genetic optimization

As all 15 features' membership functions after genetic optimization were used to replace that in the original NIDS system [20], the similarity degradation at DoS attacks are more apparent than ever had in [20], as shown in Figures 6-8 for Angryping Attack, ChinBomb Attack, and DeepThroat Attack, respectively. This represents that the modified NIDS, proposed in this paper, can be more precisely than its predecessor, because false positives can be reduced. The two red vertical lines in each figure denote the attack starting and ending time.

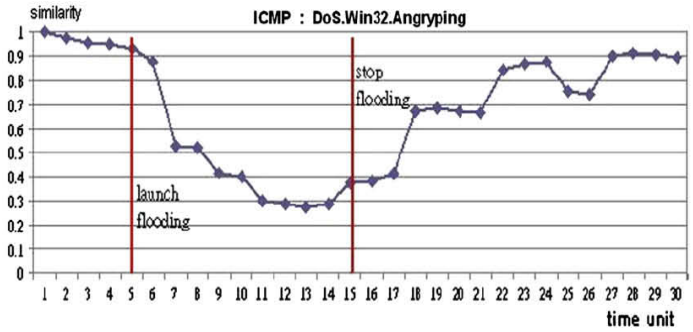

(a) without membership functions genetic optimization

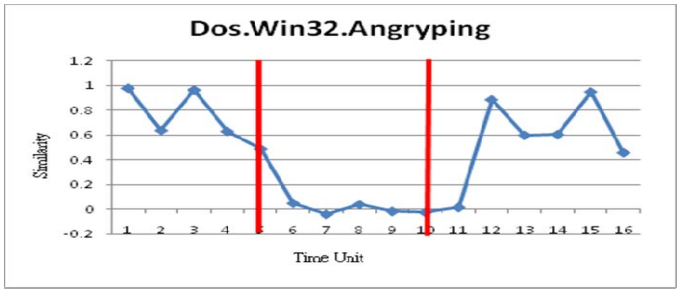

(b) with membership functions genetic optimization

Figure 6 NIDS performance for Angryping Attack with and without fuzzy membership functions being genetic optimized

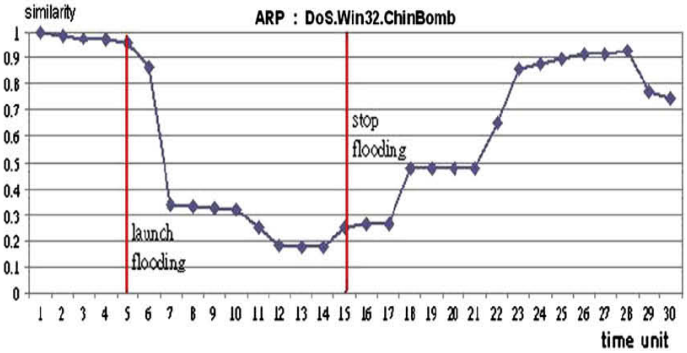

(a) without membership functions genetic optimization

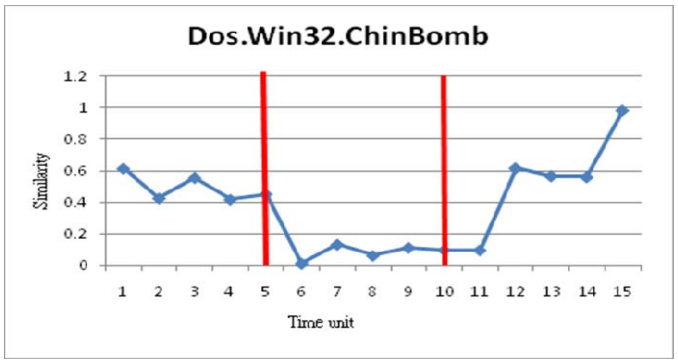

(b) with membership functions genetic optimization

Figure 7 NIDS performance for ChinBomb Attack with and without fuzzy membership functions being genetic optimized

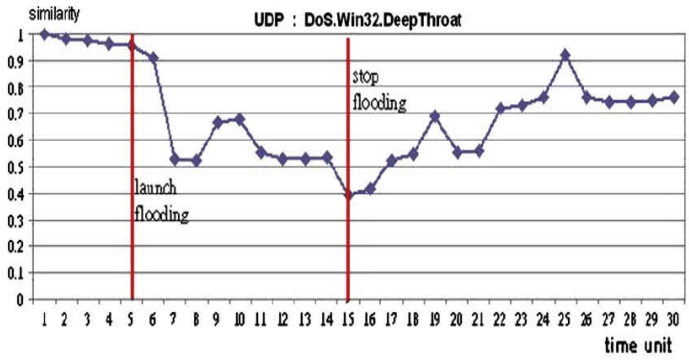

(a) Without membership functions genetic optimization

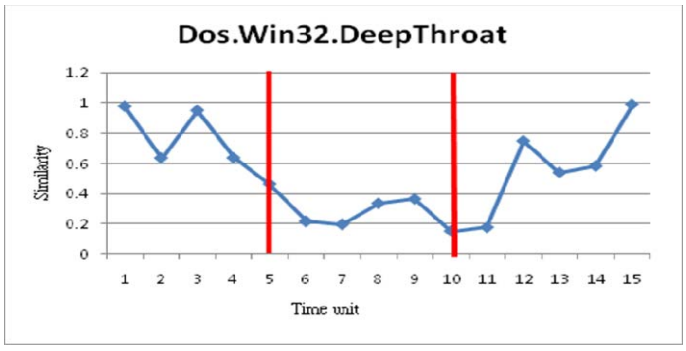

(b) Without membership functions genetic optimization

Figure 8 NIDS performance for DeepThroat Attack with and without fuzzy membership functions being genetic optimized

Three cases of k in Eq. (4), k = 0.2, k = 0.5, and k = 0.8, were considered separately in the experiments. Detail of the similarity in degradation from the *win32.fakeping* attack is illustrated in Figure 9. A *win32.fakeping* attack was remotely launched at the fifth time unit lasting for 10 time units of flooding; the attack was stopped at the fifteenth time unit. This system deployed in the LAN showed that the similarity began to degrade at the sixth time unit, even more so during the next ten units, and then started to upgrade at the sixteenth time unit. If the threshold of similarity is set to 0.5, the system, for the case of k = 0.2, would generate the first alarm at the seventh time unit (similarity value = 0.483554) and the last alarm at the twentieth time unit (similarity value = 0.478354). Ideally, the NIDS system in the LAN should show an alarm at the sixth time unit because an attack has occurred and to end the alarm at the sixteenth time unit because the attack has disappeared. Since historical data records are taken into consideration in the incremental design, it may be difficult for the similarity to immediately go down below the threshold as an attack occurs, and immediately go up above the threshold as the attack disappears. The smallest similarity value was 0.124654 for the case of k = 0.2 in Figure 9, occurred at the fifteenth time unit. It also can be concluded from Figure 9 that during the incremental mining the larger ratio of the latest record, i.e. k value, causes the system to become more susceptible. *Win32.fakeping* ceaselessly pings the victim machine with an abnormal size of payload.

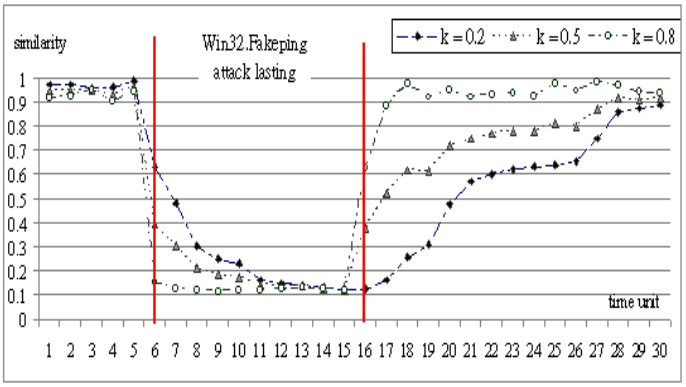

Figure 9 Similarity degradations while being Win32.Fakeping attacked

VI. CONCLUSION REMARKS

In the design, this proposed system has adopted incremental mining of fuzzy association rules, with genetic optimization on the membership functions. Experiments were conducted which demonstrated the effectiveness and efficiency of this intrusion detection system in detecting DoS attacks by an anomaly detection approach.

ACKNOWLEDGMENTS

This work was supported in part by the National Science Council, project no.: NSC 96-2221-E-130-009 and 97-2221-E-130-014.

REFERENCES

[1] B. Caswell, J. C. Foster, R. Russell, J. Beale and J. Posluns, Snort 2.0 Intrusion Detection, Syngress Press, 2003.

[2] A. N. Toosj and M. Kahani, "A New Approach to Intrusion Detection Based on An Evolutionary Soft Computing Model Using Neuro-fuzzy

Classifiers," Computer Communications, Vol. 30, No. 10, pp. 2201-2212, 2007.

[3] G. Zhang, J. Yin, Z. Liang, and Y.-G. Cai1, "Prior Knowledge SVM-based Intrusion Detection Framework," in Proc. of the third Int'l Conf. on Natural Computation, pp. 489-493, 2007.

[4] N. B. Amor, S. Benferhat, and Z. Elouedi, "Naive Bayes vs Decision Trees in Intrusion Detection Systems," in Proc. of the ACM Symp. on Applied Computing, pp. 420-424, 2004.

[5] T. Auld, A. W. Moore, and S. F. Gull, "Bayesian Neural Networks for Internet Traffic Classification", IEEE Transactions on Neural Networks, Vol. 18, No. 1, pp. 223-239, 2007.

[6] D. Zuev and A. W. Moore, "Traffic Classification using a Statistical Approach", in Proc. of the Sixth Passive and Active Measurement Workshop, 2005.

[7] C.-H. Tsang, S. Kwong, and H. Wang, "Genetic-Fuzzy Rule Mining Approach and Evaluation of Feature Selection Techniques for Anomaly Intrusion Detection," Pattern Recognition, Vol. 40, No. 9, pp. 2373-2391, 2007.

[8] M. S. Abadeh, J. Habibi, Z. Barzegar, and M. Sergi, "A Parallel Genetic Local Search Algorithm for Intrusion Detection in Computer Networks," Engineering Applications of Artificial Intelligence, Vol. 20, No. 8, pp. 1058-1069, 2007.

[9] A. El–Semary, J. Edmonds, J. Gonz alez-Pino and M. Papa, "Applying Data Mining of Fuzzy Association Rules to Network Intrusion Detection," in Proc. of the IEEE Workshop on Information Assurance United States Military Academy, 2006.

[10] S. M. Bridges, R. B. Vaughn, "Intrusion Detection via Fuzzy Data Mining," in Proc. of the Canadian Information Technology Security Symposium, 2000.

[11] G. Florez, S. M. Bridges, and R. B. Vaughn, "An Improved Algorithm for Fuzzy Data Mining for Intrusion Detection," in Proc. of the IEEE Fuzzy Information, 2002.

[12] J. E. Dickerson and J. A. Dickerson, "Fuzzy Network Profiling for Intrusion Detection," in Proc. of the Int'l Conf. on North American Fuzzy Information Processing, pp. 301-306, 2000.

[13] M. Hossain, S. M. Bridges, R. B. Vaughn, Jr., "Adaptive Intrusion Detection with Data Mining," in Proc. of the IEEE Conf. on Systems, Man and Cybernetics, pp. 3097-3103, 2003.

[14] B. Shanmugam and N. B. Idris, "Improved Hybrid Intelligent Intrusion Detection System Using AI Technique," Neural Network World, Vol. 17, Issue 4, pp. 351-362, 2007.

[15] R. Agrawal, T. Imielinski and A. Swami, "Mining Association Rules Between Sets of Items in Large Databases," in Proc. of the ACM SIGMOD, pp. 207-216, 1993.

[16] D. (Walter) Xie, "Fuzzy Association Rules discovered on Effective Reduced Database Algorithm," in Proc. of the IEEE Conf. on Fuzzy Systems, pp. 779-784, 2005.

[17] Y. Gao, J. Ma, and L. Ma, "A New Algorithm for Mining Fuzzy Association Rules," in Proc. of the Conf. on Machine Laming and Cybemetics, pp. 1635-1640, 2004.

[18] C. Kuok, A. Fu, and M. Wong, "Mining Fuzzy Association Rules in Databases," in Proc. of the ACM SIGMOD, pp. 41-46, 1998.

[19] M. Kaya and R. Alhajj, "A Clustering Algorithm with Genetically Optimized Membership Functions for Fuzzy Association Rules Mining," in Proc. of the IEEE Conf. on Fuzzy Systems, pp. 881-886, 2003.

[20] M.-Y. Su, G.-J. Yu, and C.-Y. Lin, "A Real-Time Network Intrusion Detection System for Large-Scale Attacks Based on an Incremental Mining Approach," Computers & Security, Vol. 28, No. 5, pp. 301-309, July 2009.

[21] IP Traffic, http://www.omnicor.com/netest.htm.

2011 IEEE International Conference on Fuzzy Systems
June 27-30, 2011, Taipei, Taiwan

Personalized Recommendation for Web-based Learning Based on Ant Colony Optimization with Segmented-goal and Meta-Control Strategies

Feng-Hsu Wang
Department of Computer Science and Information Engineering
Ming Chuan University,
Taoyuan County, Taiwan
fhwang@mail.mcu.edu.tw

***Abstract*—Personalized web-based learning has become an important learning form in the 21st century. An earlier research result showed that a fuzzy knowledge extraction model can be established to extract personalized recommendation knowledge by discovering effective learning paths from an access database through an ant colony model. However, critical limitations arose when considering its applications in real world situations. In this paper, the aim is to improve the model by devising more efficient algorithms that requires a reasonable number of learners and training cycles to find satisfying good results. The key approaches to resolving the practical issues include revising the global update policy, an adaptive search policy and a segmented-goal training strategy. Based on simulation results, it is shown that these new ingredients added to the original knowledge extraction algorithm result in more efficient ones that can be applied in practical situations.**

Keywords- Web-based learning ;personalized recommendatio; learning style; fuzzy set theory; ant colony optimization

I. INTRODUCTION

As the explosion of information due to the Internet in modern age, it becomes more important and more difficult to retrieve information adapted to user preferences. Therefore, personalized recommendation systems are in need to provide proper recommendations based on users' requirements and preferences [10]. Recommendation systems also find their applications in the eLearning area, especially as personalized web-based learning has become an important learning paradigm in the 21st century. Since learning resources grow so abundant on the Internet that the problem of how to help learners get appropriate learning materials to fit their learning needs has become a popular research subject in the area of adaptive content delivery.

A challenging work of this research lies in how to discover recommendation knowledge efficiently from a huge access database of a web-based learning platform [1][2]. An earlier research of ours [6] showed that a fuzzy knowledge extraction model can be established to extract personalized recommendation knowledge by discovering effective learning paths from the access database through a novel approach that is inspired by the experience sharing mechanism of natural ants. This approach imitates the experience sharing mechanism of natural ants, which share the paths they have found leading to food by scattering pheromone along the paths. In this approach, learners play the role of ants, scattering trail marks in a proper way according to their learning performances along the learning paths characterized by appropriate learning contexts. These trail marks can then be used to discover effective learning paths for learners with specific learning styles and competency.

However, though the research results [6] revealed the theoretical potential of the proposed method in discovering effective learning paths for learners, critical limitations arose when considering its application in real world situations, such as the requirement of a large amount of learners and a long period of training cycles in order to discover good learning paths for learners. That requirement is impractical for large classes in life and the reasonable time for a course to accumulate good learning experiences should be as short as possible. Therefore, the aim of this research is to resolve the aforementioned issues by devising more efficient algorithms that basically run on the same ant colony model yet requiring only a reasonable number of learners and training cycles to find satisfactory good results.

II. LITERATURE REVIEW

In the context of personalized recommendation on the Internet, web usage mining has been used as a potential approach to fulfill the requirement of web personalization [4][11][12][13][14][15]. In some commercial applications, the problem is approached by building an anticipation model through analyzing the content of items that a user has purchased in the past or were in his personal preference list. Sometimes, the items can be those in the user's navigation history. However, this content-based approach has several shortcomings and critical issues, including that only a very shallow analysis of specific kinds of content (text documents, etc.) are available; users can receive only recommendations similar to their earlier experiences; and the sparseness problem of item rating information [16][17].

This research was supported by National Science Council of Taiwan under contract NSC 98-2221-E-130 -023

On the other hand, in the approach of collaborative filtering [10], items are recommended to a particular user when other similar users also prefer them. The definition of 'similarity' between users depends on applications. For example, it may be defined as users having similar ratings of items or users having similar navigation behavior. However, a pure collaborative filtering system also has several shortcomings and critical issues, including that the coverage of item ratings could be very sparse, hence yielding poor recommendation efficiency; it is difficult to provide services for users who have unusual tastes; and the user clustering and classification problems for users with changing and/or evolving preferences [18].

As far as learning on the web is concerned, the experiences that learners have left need to be further distinguished into good and bad ones in terms of learning effectiveness. Therefore, the aforementioned approaches to personalized recommendation have to be extended in some way so that they can distinguish good experiences from bad ones in terms of some performance measurement. Another fact that distinguishes recommendation systems for eLearning from other fields is that intrinsic characteristics of a learner, such as learning style and competency, need to be considered to deliver appropriate contents to his/her needs. From this view point, our approach can deal with the recommendation problem for personalized learning by considering all the special demands in a seamless way.

Finally, a research area that relates to this research is the development of a new paradigm for computational optimization algorithms, called ACO (Ant Colony Optimization) in computer science. The ant algorithm proposed by Dorigo (1996) [9] generated an artificial wisdom (heuristic) which was developed based on the behavior of nature ants to control the direction of finding good solutions to optimization problems. Computational threads, called artificial ants, are executed separately to find solutions based on their individual states. At each move of an artificial ant, the choice is made in a certain probabilistic distribution, which is determined by a proper combination of a priori information of the structure of good solutions and a posteriori information of the structure of previously found solutions. A posteriori information of the structure of previously found solutions is accumulated by the amount of "pheromone" spread over the moves of the solutions previously found. The better quality of a found solution is of, the more pheromone it will spread over its moves. In order to avoid the phenomena of "local optimization", evaporation of pheromone in a proper rate is allowed. It was also found that a global update of the pheromone amount along the moves of the best solution only is useful to speed the convergence of solutions.

Compared with the problem to be dealt with in this research, the problems to be solved by ACO algorithms are simpler in the sense that there is only one goal to be solved for all artificial ants, and the goal to be solved is independent of the internal states of the artificial ants during the search of solutions. In contrast, the problem addressed in this research considers different goals pursued by individuals with different and changing internal states. For example, a learner who is a beginner pursues a more achievable learning goal that is easier than the one pursued when s/he becomes an advanced learner.

III. THE ANT-COLONY MODEL

In the following, to facilitate a better understanding of the problem dealt with in this research, we first give a brief explanation about the term "learning experience". Learning experience is defined as the sequence of resource accesses, where resources refer to those in a web-based learning platform that are helpful for student learning, such as contents, assessments, learning activities and so on. Another term for learning experience we use interchangeably here is "learning path". Furthermore, "good" learning experiences refer to those that can help certain types of students (with specific learning styles and competency) to achieve significant improvement in learning performance. In other words, good learning experiences mean different for different types of learners. Finally, learning performance is assumed to be measurable by assessment tools such as those developed in [7]. Therefore, the "value" of a learning experience can be measured by the degree to which it can help students to improve their learning performance. Next, we present the main idea of our approach in the following sections.

In the context of web-based learning, learners learn through accessing online materials and doing self-assessments to evaluate their performance. Learners with different characteristics such as competency and learning styles may need different kinds of materials to meet their current learning needs. The problem here is how to provide appropriate recommendations for learners matching their individual characteristics so that they can learn to achieve optimal performance.

In this research, individual characteristics are described in terms of competency and learning styles. As for learning styles, categories developed by researchers can be a represented as a discrete symbolic set like $\{L_1, L_2, L_3, L_4\}$ for the Kolb styles [3]. Competency is represented as a numerical value, coding the level of a learner's proficiency in a certain concept of a specific domain. Furthermore, the competency level is divided into a fixed set of linguistic categories using fuzzy classifications. Without loss of generality, three linguistic categories of competency are used, that is, the "Novice", "Experienced" and "Master". For the limitation of the size of the paper, readers could refer to [19] for more details about fuzzy sets.

The problem is modeled as finding solution paths for different types of learners in a multiple-dimensional knowledge space consisting of nodes and edges, dictating the learning paths of learners with particular learning contexts, forming knowledge subspaces indexed by competency levels and learning styles. Specifically, each node in a knowledge subspace represents an online resource. An edge, labeled as *e*, linking from one node to another node represents the transition of the corresponding nodes caused by accessing a resource *e*. The knowledge space plays the role of recording, accumulating and sharing learning experiences with learner characteristics, including learner competency and learning styles, encoded appropriately.

For example, consider the knowledge subspaces illustrated in Figure 1, where a learner with learning style L_x and competency level *c* has the fuzzy competency levels

represented as $\mu_{Novice}(c) = 0.4$, $\mu_{Experienced}(c) = 0.8$, and $\mu_{Master}(c) = 0.2$. Suppose the learner is now in the knowledge node of $\{e\}$. When the learner accesses a resource f, it will lead him to the knowledge node of $\{f\}$. In this situation, the system will mark the learner's trail by adding an edge linking from $\{e\}$ to $\{f\}$ with a strength proportional to the learner's membership in the corresponding knowledge subspaces. After updating the trail marks in the knowledge subspaces, the learner's current state is relocated at the knowledge node of $\{f\}$. This event is called a "local" update of the trails in the knowledge subspaces.

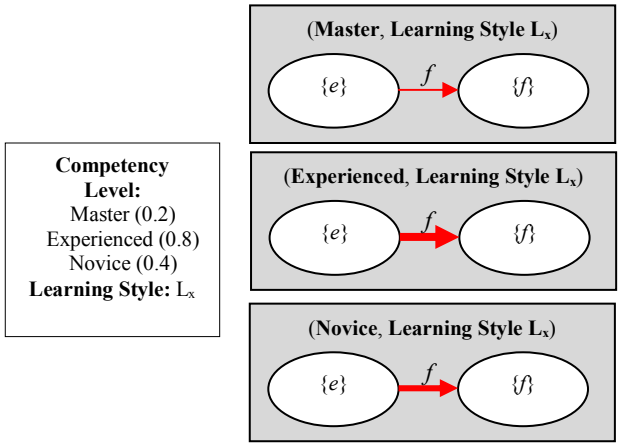

Figure 1. State transitions and local update in fuzzy knowledge subspaces.

Specifically, for a given learner x, the local update formula on the pheromone of an edge in a subspace S is given by (1):

Local update:

$$\tau = (1-\lambda)\tau + \lambda\Delta\tau$$
$$\Delta\tau = \mu_S(x) * \tau_0 \quad (1)$$

where τ is the current pheromone of an edge, λ is the evaporation parameter, $\triangle\tau$ is the change amount of pheromone, which is specified by $\mu_S(x)$ the user membership degree of the learner in the subspace S, and τ_0 is a fixed amount of pheromone.

On the other hand, Figure 2 shows how the trails in the knowledge subspaces are reinforced in the situation when changes of a learner's competency are affirmed through feedbacks obtained from either a self-assessment test or by a self-evaluation questionnaire. (It is assumed that learning styles are not changed during the learning course. Otherwise, the trail reinforcement also happens for changes of learning styles). Specifically, the edges of the path passed through in-between the change of learner states are updated in each knowledge subspace with an appropriate amount of trail marks dependent on the learner's membership in the corresponding knowledge subspaces. This is called a "global" update of the trails in the knowledge subspaces. The global update formula on the pheromone of a path in a subspace S is given by (2):

Global update:

$$\tau_{path} = (1-\rho)\tau_{path} + \Delta\tau_{path} \quad (2)$$

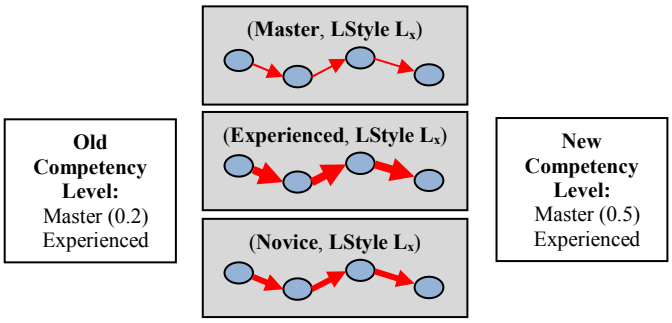

Figure 2. Learner state change and global update in fuzzy knowledge subspaces.

where τ_{path} is a set of pheromone values of the edges in a path, and ρ is the evaporation parameter, and $\triangle\tau_{path}$ is the change of pheromone values on the edges of the path, which is given by (3):

$$\Delta\tau_{path} = \mu_S(x) * \Delta D$$
$$\Delta D = effectiveness * \Delta Q \quad (3)$$

where $\triangle Q$ is a constant value, and $\triangle D$ increases when the learner's performance (effectiveness) in that session is better. The effectiveness of a learner's performance can be defined in a certain form dependent on applications. For example, the competency estimated by the assessment tool developed in [7] can be used to measure the learner's performance.

Now, as far as personalized recommendation is concerned, a knowledge subspace provides recommendations for a learner of certain characteristics by considering the membership degree to which s/he belong to it and the knowledge node that s/he is currently in. The transitions (resource) that leads out from the current node in each subspace are candidates for recommendation, and they are associated with a strength (amount of pheromone) that is computed as the product of the transition strength and the membership degree of the learner in the subspace. Different recommendation policies can be used in this phase. For example, recommendations can be given by selecting the top R-ranked transitions under the transition strength, where R is a number chosen by the system designer.

IV. The Revised Method

As shown in [6], the method has the theoretical potential in discovering effective learning paths for learners. Table I shows one of the results.

TABLE I. Number of Cycles Required for Different Effectiveness and Numbers of Learners [6]

Effectiveness	0.5	0.6	0.7	0.8	0.9
100 人	48	55	95	172	251
200 人	23	28	47	86	115
500 人	9	11	18	33	45
1000 人	5	6	10	17	33

However, critical limitations arose when considering its applications in real world situations. For example, for a large class of 100-200 students, it would take almost 300 training cycles to discover good learning paths for learners. Though increasing the number of students to 1000 might help, it is still impractical for real large classes in life, where the number of students is often limited by 200 to 300.

Three observations are worth mentioning from the research of [6]:

1. The more number of virtual ants involved, the sooner the network gets staged (the situation of being unable to improve paths easily).

2. Another fact is that during the searching of good paths, the memory of those good paths are apt to lost if more number of virtual ants are passing through them due to the local-update effect. This means that in certain situations, adding more virtual ants might cause the system to lose memory of its good paths due to the fading pheromone on the edges.

3. One last fact is that in situations of low global evaporation rates, newly found good paths are apt to hold the pheromones it had during global updates. That is, they temped to be dominated by their old states. In contrast, in situations of high global evaporation rates, newly found good paths are apt to be dominated by their current states.

The key approaches to resolving the practical issues will include (1) revising the ant exploration and global update policy, (2) adopting segmented-goal training strategy, and (3) adopting an adaptive randomness control policy, In the following, we describe the rationale behind each new approach to solving the practical issues of the problem.

A. Revise the ant exploration and global update policy

The original global update policy is to activate the global update mechanism once a virtual ant has produced its evaluation feedback. That is, the system updates the pheromone trail using all the solutions produced by the ant colony. As indicated in [8][9], it would be more effective if only the best solution found since the beginning of the computation is used to globally update the pheromone, since it avoids long convergence time by directly concentrate the search in a neighborhood of the best path found up to the current iteration of the algorithm.

B. Adopt segmented-goal training strategy

It was also observed in [6] that the length of the goal path also affect the convergence time of the algorithm. As the length increased, the convergence time also increased in an exponential way. To handle this problem, one possible way is to divide a learning session into more but a reasonable number of stages, with a sub goal specified in each stage.

C. Adopt an adaptive randomness control policy

In our previous work [6], the exploration policy is a two-fold decision. First, a random number in-between 0 and 1 is generated, and if it is larger than a threshold (say 0.1) the virtual ant would explore a visited neighboring node according to the accumulated probability distribution formed from the out-going edge weights of its current knowledge node. Otherwise, it will randomly choose an unvisited neighboring node. In other words, the decision about whether to explore a new edge or follow existing good (more weighted) edges is determined by a randomness control parameter, which was set to 0.1.

The original exploration policy in [6] may incur another problem when quality of the good paths is in good situations. In that circumstance, it should be better to deterministically follow the edges of the paths. On the other hand, when the quality of the good paths is poor, exploration of unvisited edges should be encouraged. Therefore, the new ant exploration policy is updated so that it will prefer choosing best nodes if the quality of the current best paths is good enough. To achieve this goal we adopt the "value" of the best-found solutions computed by (5) as an indicator of the system's solution quality.

V. DESIGN OF SIMULATION

To investigate whether the proposed method is useful for extracting effective recommendation knowledge, a simulation program was developed that simulates learners of different competency levels and learning styles exploring a web-based knowledge space consisted of material documents based on the aforementioned path finding model. In one simulation run, simulated learners explore the knowledge space by receiving system recommendations of documents or choose a document as they wish to explore. The decision about whether to explore a new edge (document) or follow existing edges (documents) is determined by a randomness control parameter, which can be fixed (say 0.1) or adaptive.

In the program, we predefined a set of "good" learning paths to be found for simulated learners of different competency levels and learning styles. The competency of a simulated learner gets an increment to a degree proportional to the similarity between its current learning path and the "hidden" good learning paths. The increment of competency will be fed back to the ant colony model according to the global update mechanism. In particular, the similarity between a learner's learning path and a "hidden" good learning path is calculated as follows [5]:

$$\text{Similarity}: S = S_1 + S_2 + \ldots + S_i + \ldots + S_n$$
$$\text{hidden good path}: X = X_1 X_2 \ldots X_j \ldots X_n$$
$$\text{user's path}: Y = Y_1 Y_2 \ldots . Y_i \ldots . Y_m$$
$$\text{for } i = 1, \ldots, n,$$
$$(1) \exists j, j = 1, \ldots, m, \text{such that } X_i = Y_j \text{ and } i = j \Rightarrow S_i = \frac{1}{n}$$
$$(2) \exists j, j = 1, \ldots, m, X_i = Y_j \text{ but } i \neq j \Rightarrow S_i = \frac{1}{n} * \frac{1}{|i - j|}$$
$$(3) \forall j, j = 1, \ldots, m, X_i \neq Y_j \Rightarrow S_i = 0$$

As a result, for a learner with a learning path of $Y = Y_1 Y_2 \ldots . Y_i \ldots . Y_m$, its effectiveness regarding to the hidden good path of $X=X_1X_2\ldots X_j\ldots X_n$, is defined as (5):

$$effctiveness(s, A) = \mu_A(s) \times Sim \quad (5)$$

where $\mu_A(s)$ is the degree that the learner belongs to the subspace of competency level of A.

The simulation program runs iteratively for a number of training cycles, and in each cycle a virtual learner can give a number of self-evaluation feedbacks as is given by (5) to the system. The effectiveness of one simulation run is defined as the best similarity between user learning paths and the "hidden" good paths.

VI. Results and Discussion

The simulations are run under different combinations of strategies and parameter settings. Specifically, the ant number can be 50, 100, and 200; and the GE (Global Evaporation) rate can be 0.01, 0.1 and 0.9; and the goal structure can be single-goal or segmented-goal; and the meta-control for search can be fixed or adaptive. The local evaporation rate is set to 0.01 for all simulations. All the simulations are run within 100 cycles and three times of intermediate feedbacks for each cycle. The size of the search space is determined by 30 resource items with the maximum length of the goal sequence set to 10.

Figure 3 shows the effectiveness of the algorithm under "fixed" randomness control and single-goal strategies with different number of ants (50, 100, 200) and GE settings (0.01, 0.1, 0.9); while Figure 4 shows the effectiveness of the algorithm under "adaptive" randomness control and segmented-goal strategies with the counter-parameter settings. From the figures, it can be seen that the algorithms get convergent quite fast, and as is common in ACO algorithms, the phenomena of "stagnation" appears in the algorithms. It also seems that different combinations of the ant number and GE settings have higher impacts on the effectiveness for algorithms under "adaptive" randomness control and segmented-goal strategies than those under "fixed" randomness control and single-goal strategies.

To further investigate the effect of the proposed strategies on the effectiveness of the algorithms, look at Figures 5-7. From Figure 5, it can be seen that under the fixed randomness control strategy, the algorithm equipped with segmented-goal strategy works comparable with the one equipped with the single-goal strategy.

From Figure 6, it can be seen that under the adaptive randomness control strategy, the new algorithm equipped with segmented-goal strategy outperforms the one equipped with the single-goal strategy in effectiveness.

From Figure 7, it can be seen that the new algorithm under the segmented-goal and adaptive randomness strategies has higher effectiveness than the one with the single-goal and fixed randomness strategies.

Furthermore, as shown in Table II and III, the new algorithm under the segmented-goal and adaptive randomness strategies requires few cycles than the one with the single-goal and fixed randomness strategies. And they are both much better than the original one reported in [6], as shown in Table I. As a result, the combinations of the new ingredients added to the original knowledge extraction algorithm can result in more efficient algorithms in the long run.

VII. Conclusion

In this paper, an improved ACO algorithm is devised to handle the problem of personalized recommendation for Web-based learning. It was verified through simulation that the segmented-goal training and meta-search control strategies proposed in this paper are useful for extracting personalized recommendation knowledge with a smaller amount of learners and training cycles. This makes our algorithm more suitable for practical situations. In the future, we will conduct experiments on real students to investigate its effectiveness in sharing good learning experiences among learners.

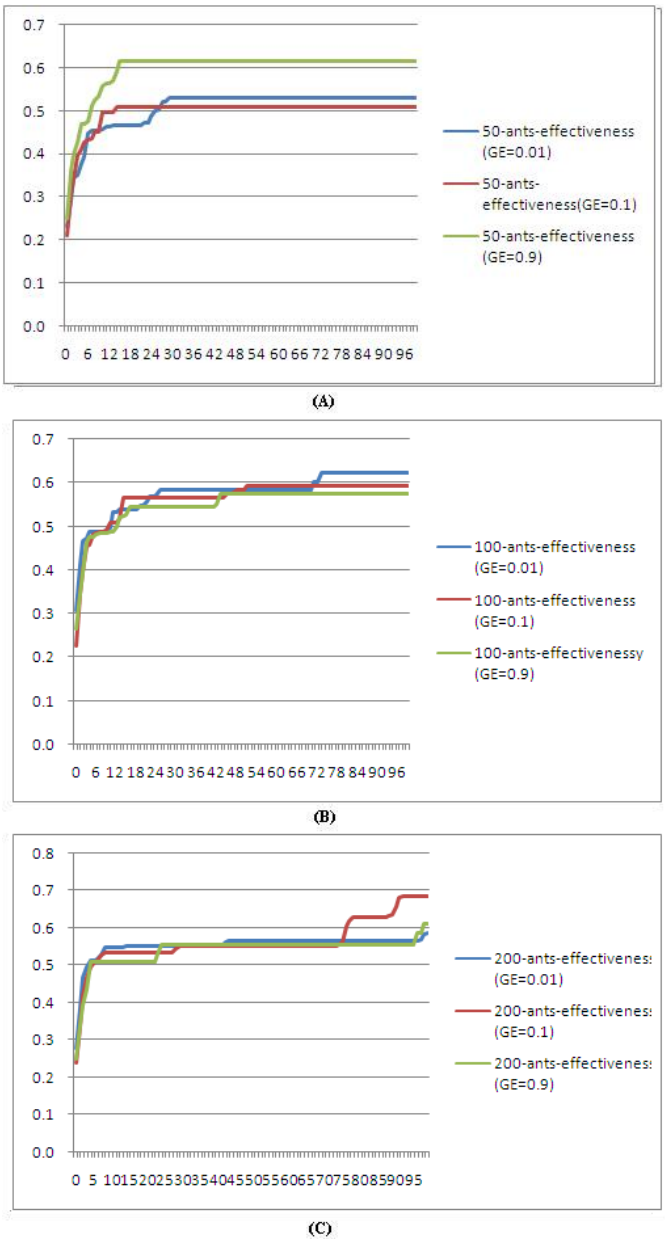

Figure 3. The performance under "fixed" randomness control and single-goal strategies with different number of ants and GE settings.

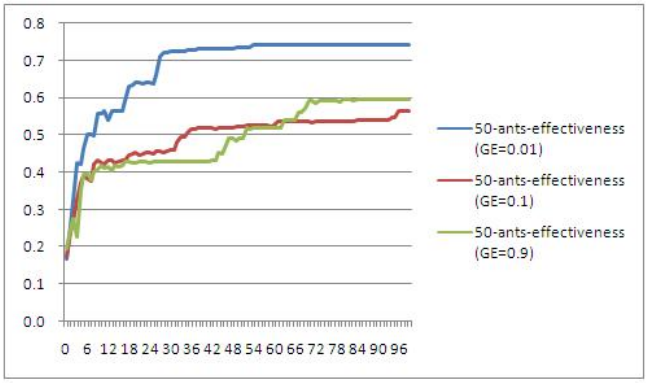

(A)

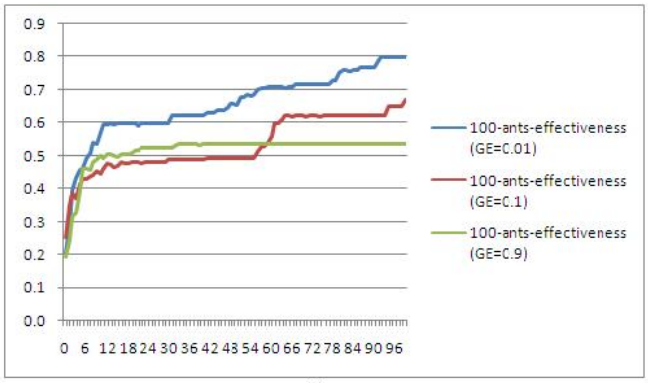

(B)

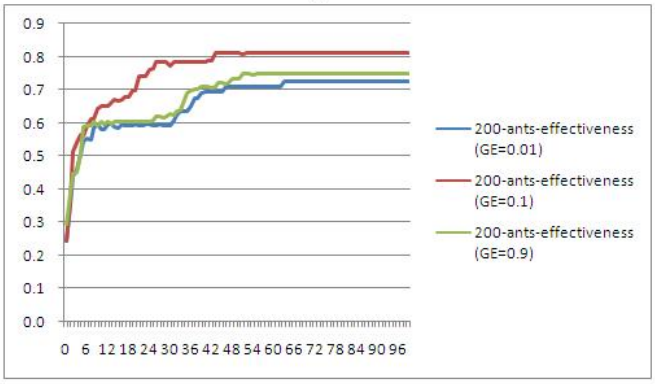

(C)

Figure 4. The performance under "adaptive" randomness control and segmented-goal strategies with different number of ants and GE settings..

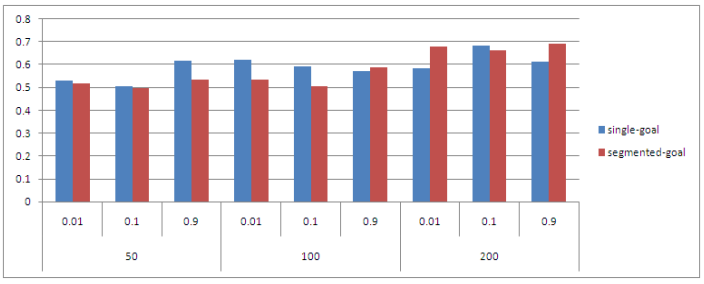

Figure 5. The performance under "fixed" randomness with single-goal and segmented-goal strategies.

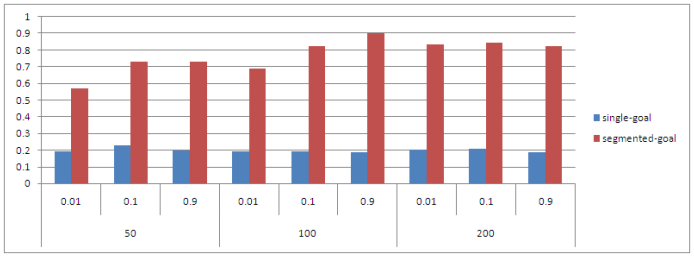

Figure 6. The performance under "adaptive" randomness with single-goal and segmented-goal strategies.

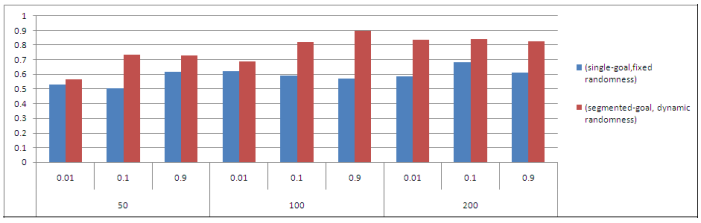

Figure 7. The performance under (single-goal, fixed randomness) and (segmented-goal, adaptive randomness) strategies with different number of ants (50, 100, 200) and global evaporation rates (0.01, 0.1, 0.9).

TABLE II. NUMBER OF CYCLES REQUIRED FOR DIFFERENT EFFECTIVENESS AND NUMBERS OF LEARNERS FOR THE ALGORIHM UNDER (SINGLE-GOAL, FIXED RANDOMNESS) CONFIGURATIONS WITHIN 100 CYCLES

Effectiveness	0.5	0.6	0.7	0.8	0.9
50 人	8	15	-	-	-
100 人	3	15	-	-	-
200 人	3	15	91	-	-

TABLE III. NUMBER OF CYCLES REQUIRED FOR DIFFERENT EFFECTIVENESS AND NUMBERS OF LEARNERS FOR THE ALGORIHM UNDER (SEGMENTED-GOAL, ADAPTIVE RANDOMNESS) CONFIGURATIONS WITHIN 100 CYCLES

Effectiveness	0.5	0.6	0.7	0.8	0.9
50 人	6	10	27	-	-
100 人	5	12	49	81	-
200 人	4	5	11	25	-

REFERENCES

[1] T. Y. Tang and G. Mccalla, "Smart Recommendation for an Evolving E-learning System," London, Ontario, Canada,2004.

[2] E. Mor and J. Minguillon, "E-learning Personalization based on Itineraries and Long-term Navigational Behavior" ACM,1-58113-912-8/04/0005,2004.

[3] "Kolb learning styles", available on: http://www.businessballs.com/kolblearningstyles.htm.2005.

[4] X. Fu, J. Budzik,and K. J. Hammond, "Mining Navigation History for Recommendation,"ACM 2000 1-58113-134-8/00/1,2000.

[5] C-M Chen, L-J Dunm and C-Y Liu, "A personalized Courseware Recommendation System Based on Fuzzy Item Response Theory,"IEEE International Conference on e-Technology,e-Commerce and e-Service,2004.

[6] F-H Wang, C-C Lin, "On Extracting Personal Recommendation Knowledge Based On the Experience Sharing Mechanism of Natural Ants," in Proceedings of International Conference on eLearning, Freiburg, German, 2010.

[7] F-H Wang, “Design of an Online Diagnostic Test Tool for Personalized Learning Based on Componential IRT Approach,” International Journal of Digital Learning Technology, in press.

[8] M. Dorigo and L. M. Gambardella, “Ant colony system: a cooperative learning approach to the traveling salesman problem,” IEEE Transaction on Evolutionary Computation vol. 53-66, 1997.

[9] L. M Gambardella and M. Dorigo, “Solving Symmetric and Asymmetric TSPs by Ant Colonies,” Proceedings of the IEEE Conference on Evolutionary Computation, ICEC96, Nagoya, Japan, May 20-22, 1996, pp. 622-627.

[10] D. Riecken, “Personalized views of personalization”, Communications of the ACM, 43(8), 27–28, 2000.

[11] R. Cooley, B. Mobasher and J. Srivastava, “Web mining: Information and pattern discovery on the World Wide Web,” in Proceedings of IEEE international conference tools with AI, 1997, pp. 558–567.

[12] B. Mobasher, R. Cooley and J. Srivastava, “Automatic personalization based on Web usage mining,” Communications of the ACM, 43(8), 142–151, 2000.

[13] M. D. Mulvenna, S. S. Anand and A. G. Buchner, “Personalization on the net using Web mining,” Communications of the ACM, 43(8), 123–125, 2000.

[14] M. Eirinaki and M. Vazirgiannis, “Web mining for Web personalization,” ACM Transactions on Internet Technology, 3(1), 1–27, 2003.

[15] M. Gery and H. Haddad, “Evaluation of Web usage mining approaches for user’s next request prediction,” in proceedings of the fifth ACM international workshop on Web information and data management, 2003, pp. 74–81.

[16] M. Kwak and D. S. Cho, “Collaborative filtering with automatic rating for recommendation,” in Proceedings of ISIE 2001 IEEE international symposium on industrial electronics, 2001, pp. 625–628.

[17] C. H. Lee, Y. H. Kim and P. K. Rhee, “Web personalization expert with combining collaborative filtering and association rule mining technique,” Expert Systems with Applications, vol. 21, 131–137, 2001.

[18] J. A. Konstan, B. N. Miller, D. Maltz, J. L. Herlocker, L. R. Gordon, and J. Reial, “GroupLens: Applying collaborative filtering to Usenet news,” Communications of the ACM, vol.40, no. 3, 77–87, 1997.

[19] L. A. Zadeh, “Fuzzy sets. In Information and Control,” vol. 8, no. 3, 338-353, 1965.

2011 IEEE International Conference on Fuzzy Systems
June 27-30, 2011, Taipei, Taiwan

A Novel Fuzzy Recommendation System Integrated the Experts' Opinion

Li-Chen Cheng
Department of Computer Science and Information Management, Soochow University,
Taipei 100, Taiwan, ROC
lijencheng@cism.scu.edu.tw

Hua-An Wang
Department of Computer Science and Information Management, Soochow University,
Taipei 100, Taiwan, ROC
stone.wwf@gmail.com

***Abstract*—Collaborative Filtering (CF) has been applied to many commercial systems successfully, such as IMDB, Netflix and son on. The basic idea of a CF system is to generate recommendations based on the experiences of past similar users. The users' option can be categorized into objective and subject information. The former was furnished by the common users and the later represents solicit opinions provided by experts (such as film critics). Both information types are valuable and important for the CF system. This study attempts to propose a novel collaborative filtering framework based on fuzzy set theory which integrates the subjective and objective information. The new methodology not only provides a comprehensive result but also solve the problems of traditional CF system, new user and new item. Finally, an experiment is performed, and the result indicates that the proposed methodology produces high-quality recommendations.**

Keywords- Data mining, recommender system, collaborative filtering, fuzzy set theory, objective evaluation, subjective evaluation

I. INTRODUCTION

E-commerce (EC) has been growing rapidly in the last decade. More and more items, however, result in an information overloading problem. In other words, consumers have to browse a huge of product lists to determine their final needs. In response to the above issue, an idea of the online product recommendation systems is proposed to assist customers for reducing these redundant information and offer advice to find suitable products for facilitating online decision-making [9, 15].

Generally, the study of recommender systems can be divided into three categories: (1) content based recommendation, (2) collaborative recommendation and (3) hybrid approaches [1]. Collaborative filtering (CF) is the most successful technologies among the above-mentioned systems and has been applied in many applications such as Amazon.com, Netflix, and MovieLens [8, 14, 15]. Basically, the idea of CF is to provide the users the recommendation based on their personal profile of previous rentals and the rentals of other similar customers. That is, the CF systems use historical data on user preferences or behavior to predict how new/old users will act.

The recommender system is the most useful way to help consumers to purchase products in an EC system. The information generated from the experiences of past similar users in a traditional recommender system is called the objective information. This kind of information does not include the influence of domain experts or opinion leaders on the customers' purchasing decision. Consider the following scenario: someone goes to see a movie on Saturday; he will check the film review from many difference ways, such as: Yahoo movie and IMDB. Because the influence of domain expert on consumers is self-evident, it will be better if the opinion from domain expert can be involved in the recommender system. Therefore, this research proposes a new integrated approach, which combines the subjective and objective information to generate recommendations for an active consumer. The subjective information solicits opinion from domain experts or option leaders [5, 12, 22]. The objective information clarifies the active user's preference based on the similar users' preference or the perdition from his past experience.

There are some common limitations in the traditional CF systems: (1) the new user, (2) new item and (3) sparsity problems [1]. They may cause the system to provide the lower quality recommendations. Therefore, this study attempts to propose a novel recommendation methodology which aggregates both the subjective and objective information to recommend items to address these limitations. In addition, if a user's preference to be provided in systems is not sufficient, the proposed method still can give recommendations from the subjective information.

Also noted herein, most previous methods are based on users' ratings which suffer from the effects of personal differences in scoring behavior. Generally, assessing users' preference by assigning precise values (rating) is difficult for users. Therefore, a fuzzy linguistic assessment (called fuzzy set theoretic method, FTM) is adopted in the proposed methodology. Linguistic assessment is based on words rather than numbers. This assessment can approach human perception, making it easier to evaluate qualitative problems [8, 20].

The proposed approach has the following two major advantages for recommender systems. First, the proposed algorithm aggregates the subjective and objective information to generate recommendations. The processing of opinion merged is more natural for the consumer decision process.

978-1-4244-7316-8/11/$26.00 ©2011 IEEE

Second, we present a new idea by applying the fuzzy linguistic model. Use of linguistic terms to present human beings' mind is a better way to understand the users' preference.

This paper is organized in the following sections. First, this study will formally define the problem in Section 2 and propose the algorithms in Section 3. Then, we evaluate the effectiveness of the proposed methods in Section 4. Finally, conclusions and valuable discussions are stated in Section 5.

II. Related Work

In a recent survey of state-of-the-art recommender systems they can be classified into collaborative, content-based and hybrid approaches. The classification is dependent on how recommendations are made.

Collaborative filtering is widely used and is the preferred method for personal recommendation. Recommendations are made for items that people with similar tastes and preferences have liked in the past. Many systems, such as that of Amazon.com [13], Sarwar [14], Hofmann [11], and GroupLens [16], have adopted this technique.

CF algorithms can be divided into two main categories [1]: User-based and Item-based. The former combines the similar users' previous preferences to make rating predications. The later is to compute the similarity between items, and then selects the most similar one.

The basic purpose for the CF algorithm is to generate recommendations from the experiences of past similar users. Most CF-based algorithms recommend items for users based on the nearest-neighborhood method [7, 10, 11]. A typical nearest-neighborhood procedure can be separated into three steps. The first step is to determine a neighborhood for the active user or item through the similarity value, which is usually defined by the Pearson correlations. Then, a prediction is calculated from a weighted combination of selected neighbors' ratings for the active user or given item. Finally, a descending sorted list is made from these predications. Recommendations are generated by choosing the top N items on this list.

Yager gives a methodology for using fuzzy set methods to represent the content knowledge in a content-based recommender system[18]. He assumes the availability of a representation scheme for each object that allows the development of an appropriate tool to calculate the similarity relationship for the set of objects. A different approach is to use fuzzy values to represent the attributes of an item. The proposed recommendation strategies are purely content-based. Zenebe followed the concepts of Yager to propose a new approach which uses items features such as background data and user feedback as input [22].

III. Problem Statement and Definitions

A. Problem Description

Let $U = \{u_1, u_2, ..., u_m\}$ and $I = \{i_1, i_2, ..., i_n\}$ denote all users and the set of all distinct items, respectively. A preference function, $\mathrm{P}_{u_i}(i_p)$, represents user u_i's preference for the item i_p. The active user is defined as u_a and the domain expert can be a subjective user denoted us. The goal of this study is to propose new algorithms which aggregate both the subjective and the objective information to make prediction for unrated items. After having the predicted information, the top-N recommendations will be derived for the active user.

B. Problem Definitions

1) User's Preference Representation Using Fuzzy Set

As stated previously, it is nature for users to assess their preference function based on words rather than numbers [2, 4, 22]. The preference function can be defined by a linguistic term. The semantic meaning of each term can be quantified by fuzzy numbers.

The preference function illustrates user u_i's preference for the items i_p. The number of users is m and the number of items is n. The preference function $\mathrm{P}_{u_i}(i_p)$ is determined as follows:

$$P_{u_i}(i_p) = \langle q_{ip}^1, q_{ip}^2, q_{ip}^3, q_{ip}^4, q_{ip}^5 \rangle, \quad q_{ip}^k \in [0,1],\ 1 \le k \le 5,\ 1 \le i \le m,\ 1 \le p \le n \tag{1}$$

In Eq. (1), $\langle q_{ip}^k \rangle$ denotes 5-touples used for the user u_i preference degree on item i_p by mapping the linguistic terms listed in Table 1. As shown in Table 1, the linguistic terms "highly recommend", "very like", "like", "somewhat like", "no comment", "somewhat dislike", "dislike", "very dislike" and "hate" are used to represent the degree of user's preference in this study.

TABLE I. The mapping of linguistic terms and 5-touples.

Linguistic term	5-tuples
highly recommend very like	< 1, 0, 0, 0, 0> < 0.8, 0.2, 0, 0, 0 >
like somewhat like	< 0.3, 0.6, 0.1, 0, 0> < 0.1, 0.5, 0.4, 0, 0 >
no comment	< 0, 0.25, 0.5, 0.25, 0 >
somewhat dislike dislike	< 0, 0, 0.2, 0.6, 0.2 > < 0, 0, 0.1, 0.7, 0.2 >
very dislike hate NULL	< 0, 0, 0, 0.2, 0.8 > < 0, 0, 0, 0, 1 > <0, 0, 0, 0, 0 >

For example:

If user u_a likes item 1 very much, we may set $P_{u_a}(i_1)$ = "very like" = <0.8, 0.2, 0, 0, 0>. In other words, $P_{u_a}(i_2)$ will be NULL if user u_a does not provide rating for item 2.

2) Similarity Measure

The user's preference function is expressed by a fuzzy number. The Euclidean fuzzy near compactness is widely used to assess the distance of similarity between two fuzzy numbers. While the Euclidean near compactness is close to 1, the degree of similarity becomes higher.

The preference function of user u_i and u_j can be expressed as $P_{u_i}(i_p)=\langle q_{ip}^1, q_{ip}^2, q_{ip}^3, q_{ip}^4, q_{ip}^5\rangle$ and $P_{u_j}(i_p)=\langle q_{jp}^1, q_{jp}^2, q_{jp}^3, q_{jp}^4, q_{jp}^5\rangle$

The similarity $S_{u_i,u_j}(i_p)$ between u_i and u_j for the item i_p is defined as Eq. (2).

$$S_{u_i,u_j}(i_p)=1-\frac{1}{\sqrt{5}}\left(\sum_{k=1}^{5}\left(q_{ip}^k-q_{jp}^k\right)^2\right)^{1/2} \tag{2}$$

For example: if user u_a likes item 1 very much, we may set $P_{u_1}(i_1)$ = "very like" = <0.8, 0.2, 0, 0, 0>. In other words, $P_{u_2}(i_1)$ = "like" =< 0.3, 0.6, 0.1, 0, 0>

$$S_{u_1,u_2}(i_1)=1-\frac{1}{\sqrt{5}}\left(\sum_{j=1}^{5}(0.8-0.3)^2+(0.2-0.6)^2+(0-0.1)^2+(0)^2+(0)^2\right)^{1/2}=0.71$$

The average degree of similarity S(u_i , u_j) between u_i and u_j is defined as

$$S(u_i,u_j)=\frac{\sum_{q=1}^{|Z|}S_{u_i,u_j}(i_q)}{|Z|}, \tag{3}$$

where Z is the set of items for which users u_i and u_j provide ratings simultaneously and $|Z|$ is the number of items .

3) Generate The Prediction for Unrated Item

Once the neighbors are found, we can combine the preference value of neighbors to compute a prediction value on unrated items for the active user. The influence of different neighbor will not be equal. The following weight function denotes the influence of user u_j on the active user u_a It is expressed as:

$$w_{u_j,u_a}=\frac{S(u_j,u_a)}{\sum_{N}S(u_k,u_a)} \tag{4}$$

As shown Eq. (4), each neighbor should be weighted by the similarity value. The higher similarity value between a neighbor and the active user will cause the larger weight to account for the prediction value. Therefore, we can derive a weight vector W^a based on the normalized similarity from neighbors.

To generate the perdition for the active user's preference degree on item i_p, the process can be implemented through the composition matrix operation $W^a \circ E^a$. The matrix E^a, called evaluation matrix, contains the linguistic term of each neighbor's preference.

Let the number of neighbors be n. The prediction for the preference of u_a for item i_p is defined as follows:

$$\begin{aligned}Y^a &= W^a \circ E^a \\ &= \begin{bmatrix}w_1^a & \dots & w_n^a\end{bmatrix}\circ\begin{bmatrix}P_{u_k}(i_p)\\ .\\ .\\ .\\ P_{u_n}(i_p)\end{bmatrix} \\ &= \begin{bmatrix}w_1^a & \dots & w_n^a\end{bmatrix}\circ\begin{bmatrix}q_{kp}^1 & q_{kp}^2 & q_{kp}^3 & q_{kp}^4 & q_{kp}^5\\ . & . & . & & \\ q_{kn}^1 & q_{kn}^2 & q_{kn}^3 & q_{kn}^4 & q_{kn}^5\end{bmatrix} \\ &= \begin{bmatrix}y_1^a & \dots & y_n^a\end{bmatrix}\end{aligned} \tag{5}$$

Where $y_j^a=(w_j^a \bullet q_{kp}^j)\oplus\dots\oplus(w_n^a \bullet q_{kn}^j)$ and "$\bullet$", "$\oplus$" are defined as algebraic product (a $\bullet$ b = ab), bounded sum (a$\oplus$b = *min* {1, a + b}), respectively.

For example, Let the weight vector W be [0.36 0.33 0.31] and the preference matrix of item i_p be expressed as:

$$E=\begin{bmatrix}0.8 & 0.2 & 0 & 0 & 0\\ 0.6 & 0.3 & 0.1 & 0 & 0\\ 1 & 0 & 0 & 0 & 0\end{bmatrix}$$

Finally, user ua's preference for item i_p can be conducted

$$Y = W \circ E = \begin{bmatrix}0.36 & 0.33 & 0.31\end{bmatrix}\circ\begin{bmatrix}0.8 & 0.2 & 0 & 0 & 0\\ 0.6 & 0.3 & 0.1 & 0 & 0\\ 1 & 0 & 0 & 0 & 0\end{bmatrix}$$

= [0.796 0.171 0.033 0 0]

The proposed system will recommend item i_p for user u_a.

A defuzzification process is necessary in order to generate a ranked list of recommendations for the active user u_a. There are several defuzzification methods, such as center of gravity, center of sum, maximum method and so on. The most popular is the center of gravity method which can be defined as follows:

$$y^*=\frac{\sum_{i=1}^{5}y_i^a\times(5-i+1)}{\sum_{i=1}^{5}y_i^a} \tag{6}$$

If the defuzzification value y^* of the prediction for item i_p is larger than 4, the framework will put the item i_p into the recommendation list.

IV. SOLUTION FRAMEWORK

This section details the proposed algorithm which is similar in spirit to the classical memory-based CF approach. To model the users' perceptions of preference, the system defines nine linguistic terms shown in table 1 to represent the degrees of preference. Each user has his/her own perception of the approximate value of each linguistic term. The proposed framework is illustrated in Fig.1.

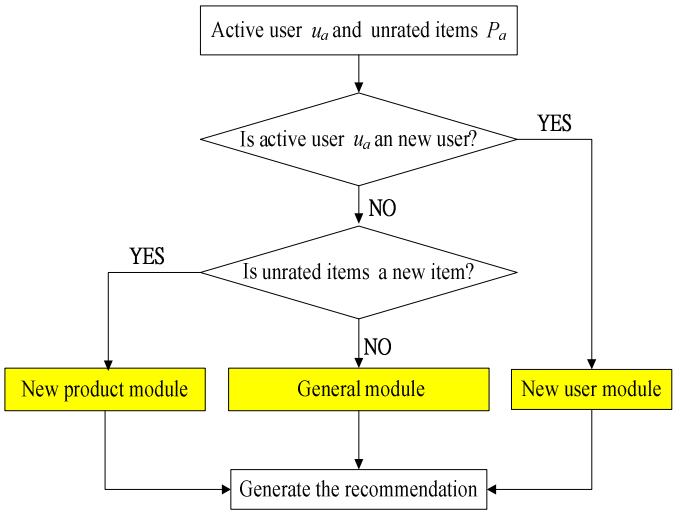

Figure 1 The flowchart of the proposed framework.

Fig. 1 shows the flowchart of the proposed framework. When the active user is an old user and the unrated item has been rated by other users, the framework will use the general module to make prediction. If the active user is an old user and the unrated item is new, the system will use the new item module. However, if the active user is a new user, the system will furnish the subjective information to make a prediction. We will explain each step in detail as follows.

A. New Product Module

New products are added regularly to recommender systems. When the new product launch, some domain experts will write the product review. For example, when a new movie launch, there are some film review written by famous film critic. To calculate the similarity between the active user and the subjective user, the result will demonstrate whether the active user like mainstream films. We compute the average similarity $S_{u_s,u_a}(i_q)$ between subjective user u_s and u_a for the item i_q based on Eqs. (2) and (3). Then the proposed algorithm will use Eqs. (4) and (5) to predict the value.

B. New User Modeule

For users that are new to the recommender system, information about their preferences is initially unknown. We can furnish the subjective user's information to the new user.

C. General Modeule

There are four steps in this module. The nearest-neighbor technique and user-based approach are applied to find the users similar to active user u_a. Neighborhood, *Neighbor* (u_a), is a set of users who are similar to u_a. The aggregated information from all neighbors' preference could be represented as the objective users' opinion. The proposed algorithm will make prediction based on the aggregation of objective and the subjective users' information.

Input:
Set of items: I, Set of users: U, Subjective user: u_s, Active user: u_a
Subjective users' preference, objective users' preference
Active user's preference, Set of unrated items for u_a: P_a
Output: Top N recommendations
Method:
// Subjective module
for each $u \in U$
Use Eq. (3) to compute average degree of similarity S(u, u_s)
According to the average similarity S(u, u_s), we rank all users into a rank list RL
// Objective module
Based on S(u_a, u_s) and choose $k+v$ nearest neighbors from RL to *Neighbors*
for each $u \in$ *Neighbors*
Use Eq. (3) to compute average degree of similarity S(u, u_a)
Select the best k nearest neighbors from *Neighbors* to *Neighbor* (u_a)
Use Eq. (4) to compute the weight of influence in *Neighbor* (u_a)
Construct a weight vector W^a
Call *Generate the predictions and recommendations procedure*

■ Subjective Procedure:

The subjective procedure is a preprocessing phase, a special procedure in the proposed algorithm. This job is usually performed offline and the results are stored in a database. Let the subjective user be denoted by u_s. When we input one user's preference data, the system automatically computes the average similarity between this user and subjective user using Eq. (3). We will generate a ranking list which contains all users, based on the average similarity between each user and the subjective user.

■ Objective Procedure:

(1) Creating Possible Neighborhoods for an Active User u_a

According to the similarity between the active user and the subjective user S(u_a, u_s), the system filters the nearest $k + v$ neighbors to a temporary buffer *Neighbors*. Eq. (3) will be used to compute the average degree of similarity of each user to the active user. Next, we choose the best k nearest neighbors to form *Neighbor* (u_a). We use Eq. (4) to compute each user's weight of influence in *Neighbor* (u_a) and then determine a weight vector W^a based on the normalized similarity of the neighbors.

(2) Compute the Influence for Each User in Neighbor (u_a)

Once the best k neighbors are found, we can aggregate the preference value of neighbors to compute a prediction value for unrated items for the active user. Evaluators may want to assign some level of importance when the top k users'

information is considered. The influence of different neighbors will not be equal. Therefore, we determine a weight vector W^a based on the normalized similarity of neighbors from Eq. (4). The evaluation matrix E^a contains a linguistic term for each neighbor's preference.

(3) Generate the Predictions and Recommendations Procedure

The process of generating a prediction for item i_p can be implemented through the composition matrix operation $W^a \circ E^a$. The result is a fuzzy vector giving user u_a preference for item i_p. The prediction for u_a's preference for item i_p is defined as

$$Y^a = W^a \circ E^a.$$

The prediction y^* is a fuzzy number which should lead to defuzzification by Eq. (6). After predicting all the unrated items, the top N recommendations, a set of ordered items with a higher predicted value is identified.

V. Experiment Evaluation

To evaluate the performance of the proposed model, we collected preference data about movies from IMDB. One hundred different movies from IMDB are collected for 618 users. Therefore, the dataset consisted of ratings from 618 users on 100 items. The subjective information is the film review from Yahoo! Movies. Four popular metrics are adopted to evaluate the effectiveness of recommendations in this study. Precision is defined as the ratio of relevant items selected to number items selected. It can be expressed as follow：

$$precision = \frac{\text{recommend items that are relevant}}{\text{total recommend items}} \tag{7}$$

Recall represents the probability that a relevant item will be selected. It can be expressed as follow：

$$recall = \frac{\text{relevant items that are recommended}}{\text{total known relevant items}} \tag{8}$$

F1 combines precision and recall into a single number. It can be expressed as follow：

$$F1 = \frac{2 \times precision \times recall}{(precision + recall)} \tag{9}$$

Mean absolute error (MAE) measures the average absolute deviation between a predicted rating and the true one. It can be expressed as follow：

$$E = \frac{\sum_{i=1}^{N} | p_i - r_i |}{N} \tag{10}$$

where N is the number of all items; p_i and r_i represent the predicted rating and the true rating, respectively.

In this experiment we evaluate the effect of neighbor size with the proposed algorithms. It is useful to select a subset of users to use in computing prediction instead of the entire user database. We compare the accuracy of the proposed algorithms based on two kinds of datasets, rich and sparse. The results are shown in Figs. 2, 3, 4. In these figure, the x-axis and y-axis represent the size of the neighborhood and the measures of accuracy, respectively. The size of the neighborhood will be 5, 10, 15, 20, 25 or 30. An examination of the results in these figures indicates that the best performance will be met when the size of the neighborhood is fifteen.

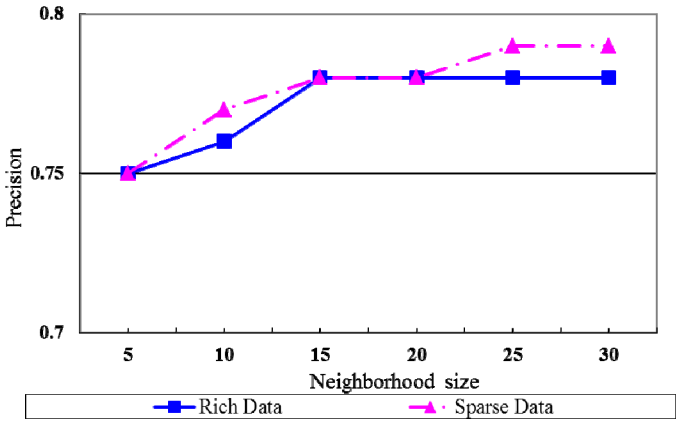

Figure 2 Precision for the proposed algorithms as neighborhood size grows.

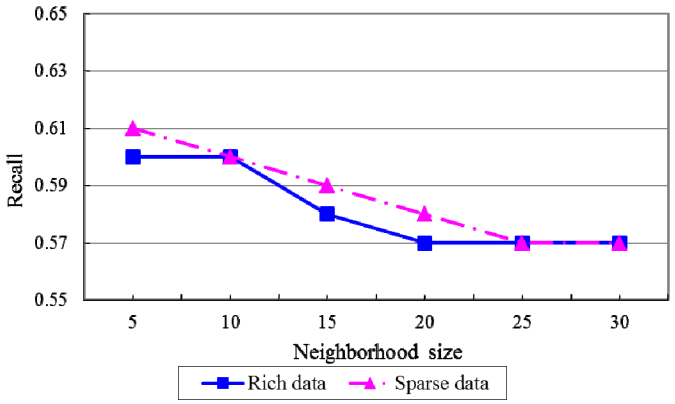

Figure 3 Recall for the proposed algorithms as neighborhood size grows.

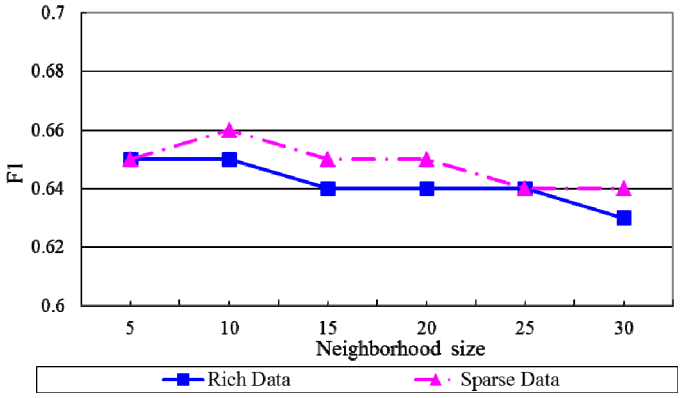

Fig. 4 F1 for the proposed algorithms as neighborhood size grows

There is no significant difference in the accuracy of the proposed algorithm between the sparse and rich dataset, as illustrated in Figs. 2, 3 and 4. When the users' preferences are insufficient (sparse dataset), most recommender systems suffer from neighbor forming bias so that those neighbors are not really similar to the active user. However, the accuracy of the proposed algorithm is not influenced by the sparsity problem. We also observe that the subjective module plays an important role. This is because the subjective user's information is always sufficient. The similarity between the subjective user and active user is always reliable.

VI. Conclusion

Traditional CF methods suffer from some limitations which are new user, new item and sparsity. This study proposes a novel CF framework based on fuzzy set theory. The proposed algorithm which combines the subjective and objective information can overcome the limitations. Experimental results show that the proposed method not only can provide reasonable recommendations as traditional CF methods, but also can solve the traditional limitations.

Acknowledgment

This research was supported in part by the National Science Council of the Taiwan (Republic of China) under the grant NSC 99-2410-H-031-051.

References

[1] G. Adomavicius, A. Tuzhilin,"Toward the next generation of recommender systems: A survey of the state-of-the-art and possible extensions." IEEE Transactions on Knowledge and Data Engineering, vol.17(6), pp. 734-749 , 2005.

[2] P. du Boucher-Ryan, D. Bridge, "Collaborative Recommending using Formal Concept Analysis", Knowledge-Based Systems, vol. 19(5) , pp. 309-315 , 2006.

[3] J. Breese, D. Heckerman, and C. Kadie, Empirical Analysis of Predictive Algorithms for Collaborative Filtering, in Proceedings of the14th Annual Conference on Uncertainty in Artificial Intelligence (UAI98) , pp. 43-52 1998.

[4] Y. Cao, Y. Li, "An intelligent fuzzy-based recommendation system for consumer electronic products", Expert Systems with Applications, vol. 33(1) , pp.230-240, 2007.

[5] Z. Duanning, M. Jian, E. Turban, "Journal quality assessment: an integrated subjective and objective approach", IEEE Transactions on Engineering Management , vol. 48(4) , pp. 479-490, 2001.

[6] D. Dubois, H. Prade, Fuzzy Sets and Systems, Theory and Applications, Academic Press, New York, 1980.

[7] D. Goldberg, D. Nichols, B. M. Oki, D. Terry, "Using collaborative filtering to weave an information tapestry". Communications of the ACM, , vol. 35(12), pp.61-70, 1992.

[8] L. Greg, S. Brent, Y. Jeremy, "Amazon.com Recommendations: Item-to-Item Collaborative Filtering", IEEE Internet Computing, vol. 7(1) , pp.76-80, 2003.

[9] P. Kotler ,K. Keller, Marketing Management, 13th , Prentice-Hall, 2008.

[10] J. L. Herlocker, J. A. Konstan, K. Terveen, J. T. Riedl," Evaluating collaborative filtering recommender systems". AC

[11] T. Hofmann, "Latent semantic models for collaborative filtering", ACM Transactions on Information Systems, vol. 22(1) , pp.89-115, 2004.

[12] T. C.K. Huang, C.H. Huang, "An integrated decision model for evaluating educational web sites from the fuzzy subjective and objective perspectives", Computers & Education, vol. 55(2) , pp. 616-629, 2010.

[13] G. Linden, B. Smith, J. York,"Amazon.com recommendation Item-to-item collaborative filtering". IEEE Internet Computing, vol. 7(1) , pp.76-80 , 2003.

[14] B. Sarwar, G. Karypis, J. Konstan, J. Riedl, "Item-based collaborative filtering recommendation algorithms". Proceedings of the 10th international conference on World Wide Web (pp. 285-295), Hong Kong , 2001.

[15] J. B. Schafer, J. A. Konstan, J. Riedl," E-commerce recommendation applications." Data Mining and Knowledge Discovery, vol. 5(1-2) , pp. 115-153, 2001.

[16] P. Resnick, N. Iacovou, M. Suchak, P. Bergstrom, J. Riedl, "GroupLens: An open architecture for collaborative filtering of netnews", in Proceedings of ACM Conference on Computer-Supported Cooperative Work, 1994, pp. 175-186.

[17] J.-M. Yang, K. F. Li, "Recommendation based on rational inferences in collaborative filtering", Knowledge-Based Systems, vol. 22(1) , pp. 105-114, 2009.

[18] R. R. Yager, "Fuzzy logic methods in recommender systems", Fuzzy Sets and Systems, vol. 136(2) , pp. 133-149, 2003.

[19] L.A. Zadeh, The concept of a linguistic variable and its application to approximate reasoning, parts 1, 2, and 3. Information Sciences, vol. 8 (2) pp.199–249, 1975; vol. 8 (3) pp. 301–357, 1975; vol. 9 (1) pp. 43–80 , 1975.

[20] D. Zhou, , D. Ma, M. Efraim,"Journal quality assessment: an integrated subjective and objective approach," IEEE Transactions on Engineering Management, vol.48(4), pp. 479-490 , 2001

[21] A. Zenebe, A. F. Norcio, "Representation, similarity measures and aggregation methods using fuzzy sets for content-based recommender systems", Fuzzy Sets and Systems, vol. 160(1), pp. 76-94 , 2009.

2011 IEEE International Conference on Fuzzy Systems
June 27-30, 2011, Taipei, Taiwan

Fuzzy Rule-Based Stock Trading System

I-Cheng Yeh
Department of Information Management,
Chung-Hua University,
Hsin Chu 30067, Taiwan
icyeh@chu.edu.tw

Che-hui Lien
Department of Management,
Thompson Rivers University,
Kamloops, BC, Canada
elien@tru.ca

Abstract— **Our study investigates the generalization capability of fuzzy rule-based trading systems and conducted an empirical study on Taiwan's stock market during 1991/1/1-2010/12/31. The empirical conclusions are as follows (1) The investment performance in the training period is much better than that in the testing period, which exhibits over-learning. (2) The symmetry rules approach demonstrates that the pure price trend trading system is better than the pure volume trend trading system and hybrid price-volume trend trading system. The pure volume trend trading system is the poorest system. (3) The asymmetry rules approach demonstrates that the trading system optimized in one period may be performed poorer in another period. The pure price trend buy-rule combined with the pure volume trend sell-rule has good performance in 1991-2000 but acts poorly in 2001-2010.**

Keywords-fuzzy rule; market timing; stock market; moving average; over-learning

I. INTRODUCTION

The stock market is a high-risk market. The reason is that too many factors affect the stock prices, making them hard to predict. Nearly a dozen years, many artificial intelligence methods, such as artificial neural networks [1], genetic algorithms [2,3], and hybrid approach [4], have been applied to the stock price forecast and the buy-sell decision-making. These studies first attempt to establish a stock price forecast system, and then use the forecast system to develop the buy-sell decision system. Because of the unpredictability of the stock prices, the effect of such a study has its limitations [5-15].

Recently, some studies [16, 17] adopted new ways of thinking to directly construct the buy-sell decision system, instead of developing a stock price forecast system, and indicated that this strategy can effectively enhance investment performance. Although this thinking may seem unreasonable, but it is feasible if we consider it from the perspective of control theory. Just like most people can learn driving through practice, but very few people really understand vehicle dynamics. In other words, most people can't accurately predict the movement of the vehicle, but still capable of making decisions (control the steering wheel).

The fuzzy rule-based systems (FRBS) are decision-making systems combining the non-linear model of fuzzy rules and the stock trading simulation mechanism. FRBS use the strategy of optimization to skip the construction of stock price forecast system and directly develop the buy-sell decision system. The rationale is to employ the fuzzy rule-based system as the decision system. The technical indicators based on daily stock prices and trading volume are employed as the system inputs, and the buy-sell decision indicator as the system output. When these technical indicators trigger the fuzzy buy-rule, a buying decision is recommended; when these indicators trigger the fuzzy sell-rule, a selling decision is suggested. This study adjusted the parameters in these fuzzy rules to optimize the performance to produce the decision-making system. The steps of building FRBS are detailed as follows:

1. Build the fuzzy rule-based trading system

There are the buy-rule and the sell-rule in the system. Each rule has some adjustable parameters, such as membership function shape parameters, rule trigger thresholds, and weights of conditions.

2. Optimize the fuzzy rule-based trading system

Alter the adjustable parameters in the system to maximize the profits under the simulated environment of using the historical stock market data in the training period.

3. Evaluate the fuzzy rule-based trading system

Use the optimized adjustable parameters in the system, and evaluate the profits under the simulated environment in the testing periods.

4. Determine the best parameters

Choose the parameters that have the best performance during testing periods.

Because of the changing nature of stock markets, the decision-making system generated from the fuzzy rule-based approach can only be guaranteed for generating good profits in the training period, but it is not guaranteed to produce good profits in the future. The future performance of this original decision-making system is suspicious. Therefore, to objectively prove that the generated decision-making system has good performance in the future, the historical stock market data must

978-1-4244-7316-8/11/$26.00 ©2011 IEEE

be divided into several parts, for example, four parts. Every time we use one of the parts as the "training period" and the others as the "testing periods" as shown in Fig. 1. In the second step of FRBS, several fuzzy rule-based systems are generated, according to the profits, in the training period. In step three of FRBS, the profits produced in the testing periods are used to evaluate which systems can be generalized to the testing periods. That is, if we can generate a system that not only has good performance in the training periods but also has good performance in the testing periods, then we can expect this system will generate good profits in the future.

Our study aims to examine whether FRBS have the generalization capability. Section 2 describes the rationale of fuzzy rule-based stock trading decision system. Section 3 examines the investment performance of FRBS in the testing periods. Section 4 contains concluding remarks.

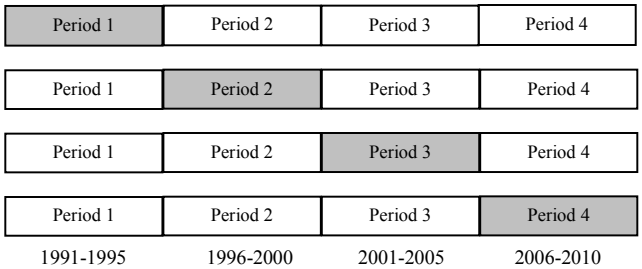

Figure 1. Cross-Evaluation Approach (the gray boxes represent the training periods, and the white ones are testing periods)

II. FUZZY RULE-BASED STOCK TRADING SYSTEM

A. *The calculation of technical indicators*

Although there are thousands of technical indicators can be used in the stock market, the moving averages of price and volume are essential. A moving average is calculated by adding the security's prices for the most recent N time periods and then divided by N. It smooths out a data series, making it easier to spot trends.

The Moving Average Indicator (MAI) and Moving Average Volume Indicator (MVI) are defined as follows

$$MAI_{m,n} = \frac{MA_m}{MA_n} \tag{1}$$

$$MVI_{m,n} = \frac{MV_m}{MV_n} \tag{2}$$

where MA_m and MA_n = *m*-day and *n*-day moving average of closing prices; MV_m and MV_n = *m*-day *n*-day moving average of trading volume. In this study, we adopted m=1 and n=50.

B. *The fuzzy rules*

There are two rules in the system

Buy-rule: IF MAI is big and MVI is big Then buy

Sell-rule: IF MAI is small and MVI is small Then sell

The membership functions are defined as follows

$$\mu(MAI\ is\ big) = \frac{1}{1+\exp(-MAI)} \tag{3}$$

$$\mu(MVI\ is\ big) = \frac{1}{1+\exp(-MVI)} \tag{4}$$

$$\mu(MAI\ is\ small) = 1-\mu(MAI\ is\ big) \tag{5}$$

$$\mu(MVI\ is\ small) = 1-\mu(MVI\ is\ big) \tag{6}$$

where

$$MAI = \frac{MAI_{m,n}-1}{k\cdot\sigma_{MAI}} \tag{7}$$

$$MVI = \frac{MVI_{m,n}-1}{k\cdot\sigma_{MVI}} \tag{8}$$

where σ_{MAI} and σ_{MVI} are the standard deviations of $MAI_{m,n}$ and $MVI_{m,n}$ in the recent n days, and k is the membership function shape parameter.

We use the weighted summation instead of minimization for the "and" operation; that is the fuzzy rules triggered based on the following rules

$$If\ w_{MAI-Buy}\cdot\mu(MAI\ is\ big)+w_{MVI-Buy}\cdot\mu(MVI\ is\ big) > \theta_{buy}\quad Then\ Buy \tag{9}$$

$$If\ w_{MAI-Sell}\cdot\mu(MAI\ is\ small)+w_{MVI-Sell}\cdot\mu(MVI\ is\ small) > \theta_{sell}\quad Then\ Sell \tag{10}$$

where θ_{buy} and θ_{sell} are the rule trigger thresholds, and we assumed

$$\theta_{sell} = \theta_{buy} = \theta \tag{11}$$

and $w_{MAI-Buy}$ and $w_{MVI-Buy}$ are the weights of conditions in the Buy-rule; $w_{MAI-Sell}$ and $w_{MVI-Sell}$ are the weights of conditions in the Sell-rule, , and we assume

$$w_{MVI-Buy} = 1 - w_{MAI-Buy} \tag{12}$$

$$w_{MVI-Sell} = 1 - w_{MAI-Sell} \tag{13}$$

The fuzzy rule response surfaces are shown in Fig. 2. When the k, membership function shape parameter, is close to 0, then the system is close to crisp system instead of fuzzy system. The weights of conditions control the slope direction of the response surface.

III. The Results of FRBS in Taiwan Stock Market

We use daily data of the Taiwan Stock Market Index (TAIEX) from 1 Jan 1991 to 31 Dec 2010 as shown in Figure 3. Totally 5297 individual data were collected. The data are divided into four parts by timing and are shown in Figure 1. This research considers the profit or loss in the training period and in the testing period.

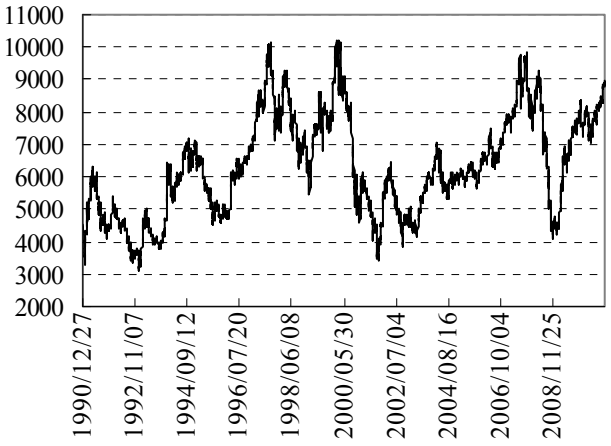

Figure 3. TAIEX (1991/1/1-2010/12/31)

Figure 3 exhibits the stock market fluctuating in the training and in the testing periods, which show the representativeness of the data. Every time we use one of the parts as the "training period" and the remaining ones as the "testing periods". Several fuzzy rule-based systems are produced based on the profits generated in the training period, and then the profits in the testing period are used to evaluate which systems can be generalized to the testing periods.

Because the objective of this study is to develop a decision-making system with high investment performance in Taiwan's stock market; therefore, the transaction costs refer to the practical stock transaction costs in Taiwan. These costs include transaction fees of purchasing accounting for 0.1425% of the buying price; the transaction fees and trading tax of selling account for 0.1425% and 0.3% of the selling price, respectively. The profits (annual return) of buy-and-hold strategy in the 4 parts are 4.0%, -1.7%, 6.7%, 6.5%, respectively.

A. The symmetry rules approach

In this approach, we assume that the weights of conditions of the buy-rule and the sell-rule are the same.

$$w_{MAI-Buy} = w_{MAI-Sell} = w_{MAI} \tag{14}$$

We firstly use 0, 0.3, 0.5, 0.7, 1 for the w_{MAI}, and change the rest of adjustable parameters, the membership function shape parameters k (0.1, 0.2, …, 1) and rule trigger threshold θ (0.5, 0.55, …, 0.95), in the system to maximize the profits under the simulated environment of using the historical stock market data in the training period. To avoid the profit comes form few trades, we eliminated all the results whose number of trade is less than 60 times in the 20 years (60 times for buy and 60 times for sell). Then we use the optimized adjustable parameters in the system and evaluate the profits under the simulated environment in the testing periods. The results are shown in Table 1. In this table, we use the profit gain, the gap between the annual return of the system and the buy-and-hold strategy, to evaluate these systems.

To objectively prove that the generated decision-making system has good performance in the training period, we use the average profit gain produced in the testing periods to evaluate the system. Because we exclude the profit gain generated in the training periods, the average profit gain can objectively be used to evaluate the performance of the system. If we can generate a system that not only has good performance in the training periods, but also has good performance in all the testing periods, then we can expect this system will generate good profits in the future. We also use the standard deviation of profit gain to evaluate the stability of the system. Finally, we use the ratio of the average profit gain to the standard deviation of profit gain to measure the total performance for a specific weight. The results show that when the weight is varied (0, 0.3, 0.5, 0.7, and 1), the generated profit gains in the training periods are 8.0, 7.1, 7.0, 7.3, and 6.8, and the ratios are 2.14, 1.20, 1.51, 1.85, and 3.40, respectively. On the other hand, in the testing periods, when the weight is changed (0, 0.3, 0.5, 0.7, and 1), the produced profit gains are 3.0, 1.8, 2.6, 3.6, and 5.5, and the ratios are 0.74, 0.54, 0.56, 1.03, and 3.09, respectively. The investment performance in the training period is much better than that in the testing period, which exhibits over-learning.

The results show that 1.0 is the best weight of conditions. That is, the best fuzzy rule is the rule containing only the MAI conditions, and the MVI conditions are not included in the system. Figure 4-7 show its performance. The initial capital is 10000. All these four optimized fuzzy rule sets can obtain fairly high final cumulated capital.

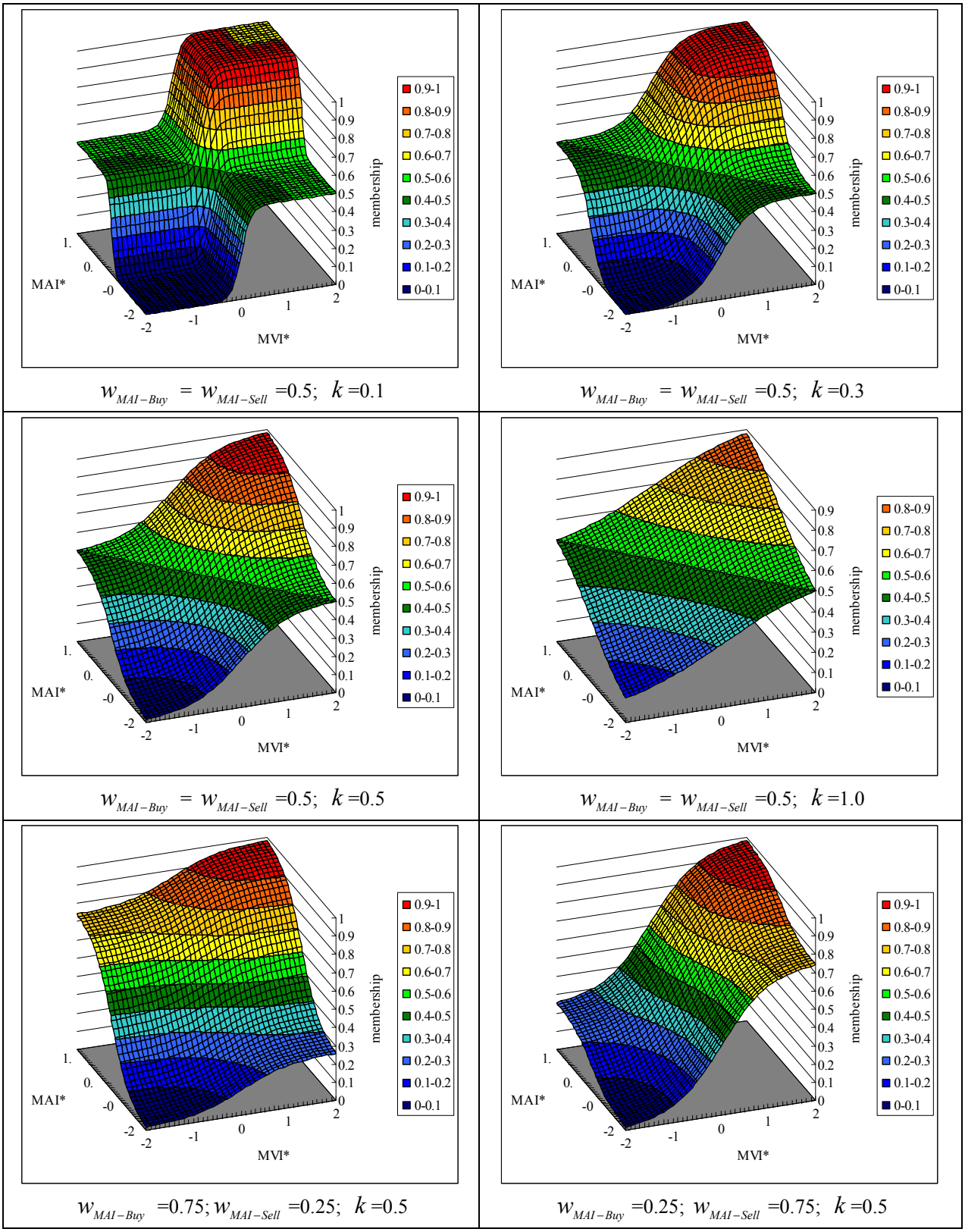

$w_{MAI-Buy} = w_{MAI-Sell} = 0.5;\ k = 0.1$ | $w_{MAI-Buy} = w_{MAI-Sell} = 0.5;\ k = 0.3$

$w_{MAI-Buy} = w_{MAI-Sell} = 0.5;\ k = 0.5$ | $w_{MAI-Buy} = w_{MAI-Sell} = 0.5;\ k = 1.0$

$w_{MAI-Buy} = 0.75; w_{MAI-Sell} = 0.25;\ k = 0.5$ | $w_{MAI-Buy} = 0.25;\ w_{MAI-Sell} = 0.75;\ k = 0.5$

Figure 2. Fuzzy rule response surface

TABLE 1. The Results of FRBS: Symmetry Rules Approach

weight pair	Train Period	Opt. θ	Opt. k	Test period 1	2	3	4	Avg profit gain	Std of profit gain	Ratio
(0,0)	1	0.7	1	**8.5**	5.9	2.7	2.4	**8.0** 3.0	**3.7** 4.0	**2.14** 0.74
	2	0.65	1	1.4	**12.8**	0.2	-6.0			
	3	0.7	0.9	6.7	8.0	**3.9**	1.4			
	4	0.8	0.7	3.1	8.8	1.1	**6.7**			
(0.3,0.3)	1	0.75	0.6	**12.4**	7.6	-0.9	-2.0	**7.1** 1.8	**5.9** 3.3	**1.20** 0.54
	2	0.75	0.1	4.5	**12.0**	-1.3	-0.1			
	3	0.65	1	3.5	3.2	**2.1**	-2.9			
	4	0.9	0.1	4.5	5.0	0.5	**1.8**			
(0.5,0.5)	1	0.6	1	**9.0**	5.2	-1.6	-2.5	**7.0** 2.6	**4.6** 4.6	**1.51** 0.56
	2	0.6	0.3	6.7	**12.4**	-6.5	-0.6			
	3	0.85	0.1	3.9	4.7	**2.0**	4.1			
	4	0.9	0.1	8.5	7.5	1.1	**4.5**			
(0.7,0.7)	1	0.7	0.3	**10.6**	5.4	0.6	5.1	**7.3** 3.6	**4.0** 3.4	**1.85** 1.03
	2	0.55	0.5	6.7	**10.2**	0.1	-2.3			
	3	0.6	0.3	4.9	9.2	**2.1**	0.5			
	4	0.85	0.1	6.4	4.7	1.1	**6.4**			
(1,1)	1	0.8	0.1	**8.7**	5.8	3.3	6.0	**6.8** 5.5	**2.0** 1.8	**3.40** 3.09
	2	0.7	0.2	8.2	**7.0**	4.0	4.5			
	3	0.7	0.2	8.2	7.0	**4.0**	4.5			
	4	0.6	0.3	6.4	5.4	2.7	**7.6**			

(The bold values are based on the training period; the rest of the values are based on the testing periods.)

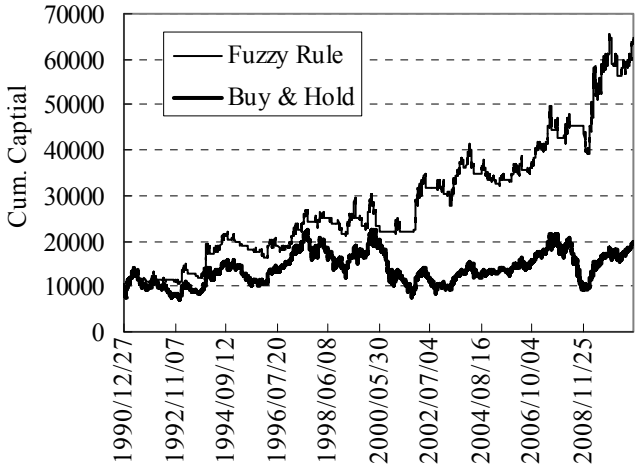

Figure 4. The cumulated capital employing the optimized fuzzy rule set with the weight pair (1,1) in the 1st period (1991-95).

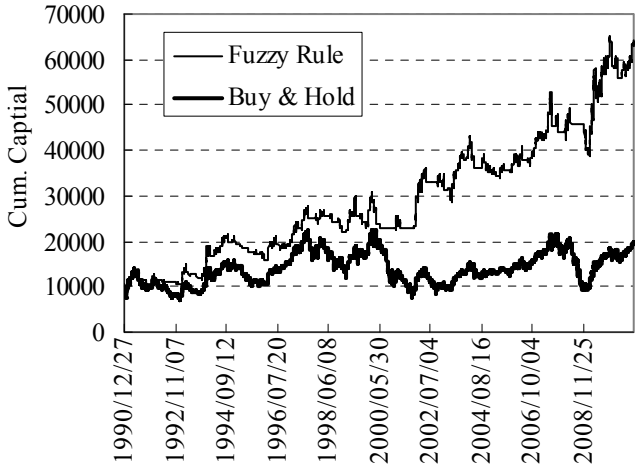

Figure 5. The cumulated capital employing the optimized fuzzy rule set with the weight pair (1,1) in the 2nd period (1996-00).

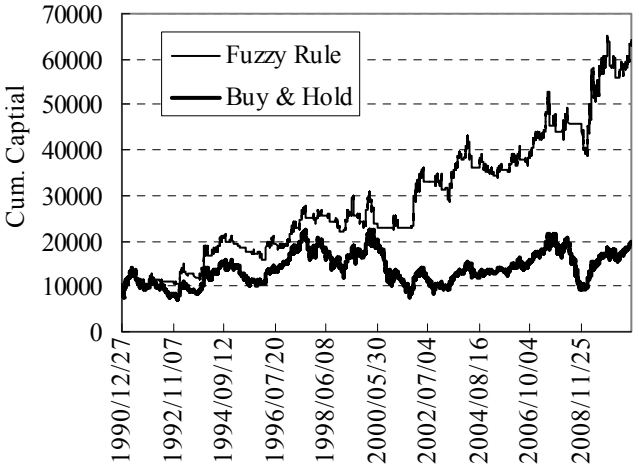

Figure 6. The cumulated capital employing the optimized fuzzy rule set with the weight pair (1,1) in the 3rd period (2001-05).

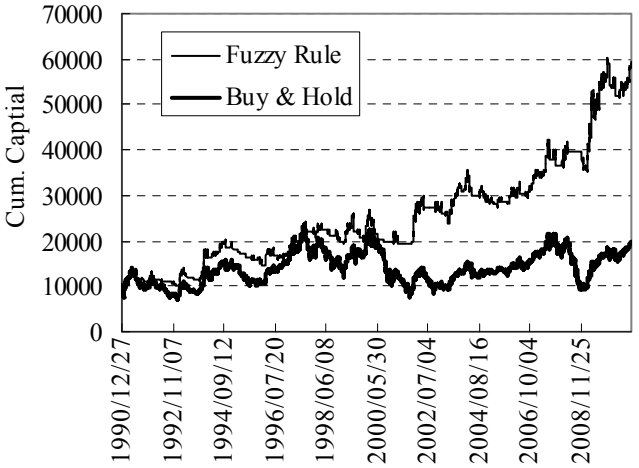

Figure 7. The cumulated capital employing the optimized fuzzy rule set with the weight pair (1,1) in the 4th period (2006-10).

B. The asymmetry rules approach

In this approach, we assume that the weights of conditions of the buy-rule and the sell-rule are different. We try the buy weight and the sell weight pair=(0,1) and (1,0). The results are shown in Table 2. Figure 8-11 show the cumulated capital employing the optimized fuzzy rule set with the weight pair (1, 0), which is the pure price trend buy-rule combined with the pure volume trend sell-rule, in the four different periods. Although these four optimized fuzzy rule sets can obtain rather high final cumulated capital, but he systems generated from the period 1 (1991-1995) and period 2 (1996-2000) have relatively poor performance in period 3 (2001-2005) and period 4 (2006-2010), which demonstrates that the optimized trade system produced from one period may be performed poorer in another period. We also use different weights such as 0, 0.05, 0.1, 0.15, 0.2,…, 1. Therefore, there are totally 21x21=441 weight pairs. The pair of (0.8, 1) has the highest ratio of the average profit gain to the standard deviation of profit gain. However, it also exhibits over-learning.

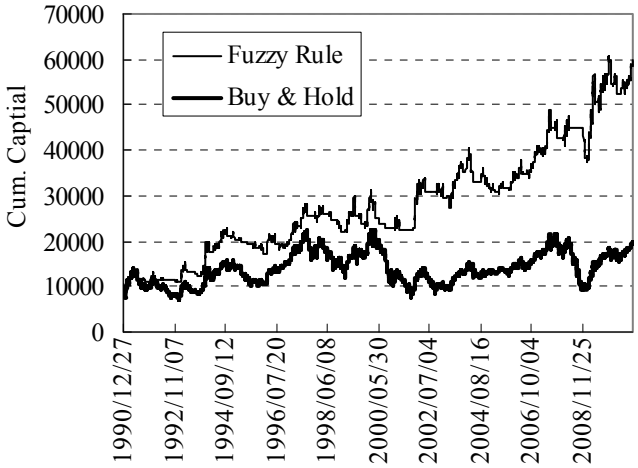

Figure 8. The cumulated capital employing the optimized fuzzy rule set with the weight pair (1,0) in the 1st period (1991-95).

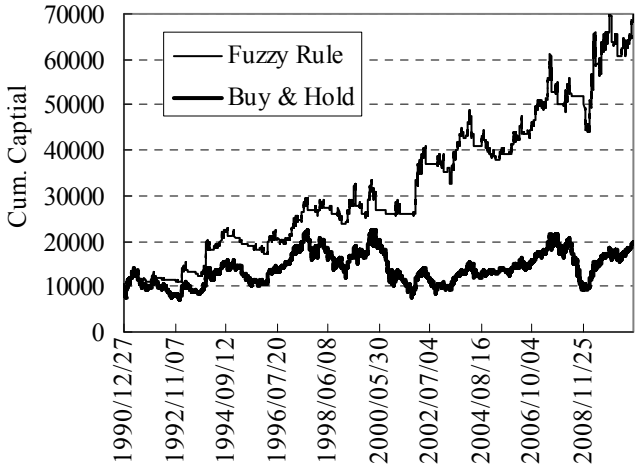

Figure 9. The cumulated capital employing the optimized fuzzy rule set with the weight pair (1,0) in the 2nd period (1996-00).

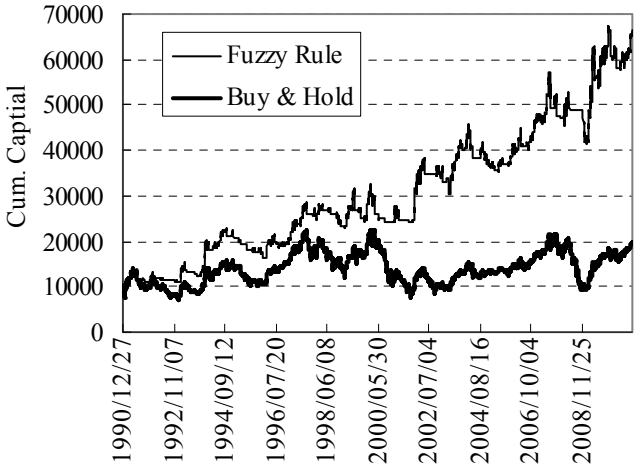

Figure 10. The cumulated capital employing the optimized fuzzy rule set with the weight pair (1,0) in the 3rd period (2001-05).

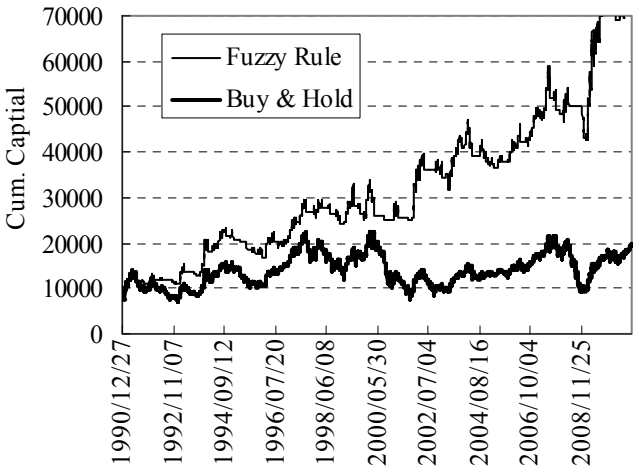

Figure 11. The cumulated capital employing the optimized fuzzy rule set with the weight pair (1,0) in the 4th period (2006-10).

IV. CONCLUSION

Our study investigates the generalization capability of fuzzy rule-based trading systems and conducted an empirical study on Taiwan's stock market during 1991/1/1-2010/12/31. The empirical conclusions are as follows:

1. The investment performance in the training period is much better than that in the testing period, which exhibits over-learning.
2. The symmetry rules approach demonstrates that the pure price trend trading system performs better than the pure volume trend trading system and hybrid price-volume trend trading system. The pure volume trend trading system has the poorest performance.

TABLE 2. The Results of FRBS: Asymmetry Rules Approach

weight pair	Train Period	Opt. θ	Opt. k	Test period 1	2	3	4	Avg profit gain	Std of profit gain	Ratio
(0,1)	1	0.55	1	**7.2**	7.1	1.9	3.3	**5.9** 3.1	**2.7** 3.0	**2.18** 1.03
	2	0.95	0.1	3.2	**9.1**	-0.1	0.0			
	3	0.65	0.4	5.2	9.0	**3.2**	2.4			
	4	0.65	0.2	3.5	2.8	-1.5	**4.2**			
(1,0)	1	0.95	0.1	**13.3**	8.4	0.8	-2.7	**7.7** 4.7	**6.4** 5.0	**1.20** 0.95
	2	0.7	0.2	11.7	**13.1**	-0.3	0.2			
	3	0.7	0.1	6.2	10.9	**1.7**	2.6			
	4	0.7	0.1	6.2	10.9	1.7	**2.6**			
(0.8, 1)	1	0.8	0.1	**10.9**	6.7	1.5	4.7	**7.9** 5.6	**3.26** 2.7	**2.50** 2.04
	2	0.7	0.2	5.6	**9.7**	1.8	6.1			
	3	0.6	0.4	9.4	8.5	**3.7**	5.9			
	4	0.6	0.5	7.9	7.1	1.4	**7.4**			

(The bold values are based on the training period; the rest of the values are based on the testing periods)

3. The asymmetry rules approach demonstrates that the optimized trading system in one period might act poorer in another period. The pure price trend buy-rule combined with the pure volume trend sell-rule has fairly good performance in the period of 1991-2000, but has poor performance in 2001-2010.

The deterioration of the investment performance may be resulted from that the 5-year training period is not long enough to gather sufficient patterns to build general model; or maybe the 5-year testing period is too long and the stock market structure has been changed during the time, which also makes the developed trading system cannot be applied to the testing period. Apparently, it is not easy to use the current framework to overcome the problem of over-learning. Researchers have to solve this problem through different approaches.

ACKNOWLEDGMENT

This study is sponsored by the National Science Council (Project No. 99-2221-E-216-040).

REFERENCES

[1] S. Haykin, Neural Networks: A Comprehensive Foundation, Prentice Hall PTR, NJ, 2004.

[2] L. B. Booker, D. E. Goldberg, and J. H. Holland, "Classifier systems and genetic algorithms," Artificial Intelligence, vol. 40, pp. 235-282, 1989.

[3] J. H. Holland, Adaptation in Natural and Artificial Systems, University of Michigan, Ann Arbor, MI, 1975.

[4] L. C. Lien and I. C. Yeh, "Building trading system for Taiwan stock market using genetic neural networks," Journal of Information Management, vol.15, no.1, pp. 29-52, 2008.

[5] G. Armano, A. Murru, and F. Roli, "Stock market prediction by a mixture of genetic-neural experts," International Journal of Pattern Recognition and Artificial Intelligence, vol. 16, no.5, pp. 501-526, 2002.

[6] G. Armano, M. Marchesi, and A. Murru, "A hybrid genetic-neural architecture for stock indexes forecasting," Information Sciences, vol.170, no.1, pp. 3-33, 2005.

[7] D. Enke and S. Thawornwong, "The use of data mining and neural networks for forecasting stock market returns," Expert Systems With Applications, vol. 29, no. 4, pp. 927-940, 2005.

[8] S. Hayward, "Setting up performance surface on an artificial neural network with genetic algorithm optimization: in search of an accurate and profitable prediction for stock trading," Proceedings, 2004 Congress on Evolutionary Computation, pp. 948-954, 2004.

[9] K. Kim and I. Han, "Genetic algorithms approach to feature discretization in artificial neural networks for the prediction of stock price index," Expert Systems with Applications, vol. 19, no.2, 125-132, 2000.

[10] Y. K. Kwon and B. R. Moon, "Daily Stock Prediction Using Neuro-Genetic Hybrids," Genetic and Evolutionary Computation Conference 2003, pp. 2203-2214, 2003.

[11] M. Lam, "Neural network techniques for financial performance prediction: integrating fundamental and technical analysis," Decision Support Systems, vol. 37, no. 4, pp. 567-581, 2004.

[12] R. S. T. Lee, "iJADE stock advisor: An intelligent agent based stock prediction system using hybrid RBF recurrent network," IEEE Transactions on Systems, Man, and Cybernetics Part A, vol. 34, no. 3, pp. 421-428, 2004.

[13] V. Massimiliano, B. Rushi, H. Oliver, and S. Mark, "Predicting the exchange traded fund DIA with a combination of genetic algorithms and neural networks," Expert Systems with Applications, vol. 27, no.3, pp. 417-425, 2004.

[14] D. Olson and C. Mossman, "Neural network forecasts of Canadian stock returns using accounting ratios," International Journal of Forecasting, vol. 19, no. 3, pp. 453-465, 2003.

[15] H. P. K. Phua, D. Ming, and W. Lin, "Neural network with genetically evolution algorithms for stocks prediction," Asia-Pacific Journal of Operation Research, vol. 18, no. 1, pp. 103-108, 2001.

[16] F. Allen and R. Karjalainen, "Using genetic algorithms to find technical trading rules," Journal of Financial Economics, vol. 51, pp. 245-271, 1999.

[17] R. J. Kuo, C. H. Chen, and Y. C. Hwang, "An intelligent stock trading decision support system through integration of genetic algorithm based fuzzy neural network and artificial neural network," Fuzzy Sets and Systems, vol. 118, pp. 21-45, 2001.

2011 IEEE International Conference on Fuzzy Systems
June 27-30, 2011, Taipei, Taiwan

Towards Application of FML in Suspicion of Non-Common Diseases

Giovanni Acampora*, Tatiana Kiseliova†, Karaman Pagava‡ and Autilia Vitiello*
*Dept. of Computer Science
University of Salerno, Fisciano, Salerno 84084
Email: {gacampora, avitiello}@unisa.it
†Dept. of Computer Sciences
Ivane Javakhishvili Tbilisi State University, Tbilisi, Georgia 0143
Email: t.kiseliova@web.de
‡ Child and Adolescent Medicine
Tbilisi Medical State University, Tbilisi, Georgia 0177

***Abstract*—In this paper we present the preliminary results of application of Fuzzy Markup Language (FML) to suspect a non-common disease. Under non-common diseases we understand rare diseases. From the broad point of view this problem belongs to the computer-assisted decision support in medical diagnostics and can be supported by fuzzy logic controllers. We can use conventional methods to diagnose a rare disease if it can be exhibited by outstanding symptoms. For example, there are several search machines and data banks that allow to find a rare disease clearly exhibited by a patient's symptoms/signs. But it is very difficult to diagnose a rare disease if it masks as a common disease. Diagnostic of rare diseases is connected with lack, uncertainty and imprecision of knowledge, medical mistake and even medical failure. Additionally, very often a common disease is also established with some degree of belief, thus, the expressions such as "it is possible that a patient has a particular disease" rather often present in the daily medical practice. It is clear that if we would know the common diseases, then deviations from them can be considered as a sign of non-common diseases. In this paper we investigate such deviations with the help of FML. We show how FML mechanism can be adjusted to suspect a rare disease, and discuss the appropriateness of the available operators.**

***Index Terms*—Fuzzy Systems, Fuzzy Markup Language, Medical Diagnosis, Rare diseases.**

I. Introduction

In this paper we present the preliminary results of application of Fuzzy Markup Language (FML) to suspect a non-common disease. Under non-common diseases we understand rare diseases. A rare disease is any disease that affects a small percentage of the population. There is no single, widely accepted definition for rare diseases (RD)[1]. According to different definitions the prevalence of RD should be between $1/200000$ and $1/1000$, usually about $1/2000$. There are several thousand rare diseases. Their total number is quite significant: the 5-6% of population have some rare diseases[2].

From the broad point of view this problem belongs to the computer-assisted decision support in medical diagnostics and can be supported by fuzzy logic controllers. It is possible to diagnose a rare disease if it can be exhibited by outstanding symptoms. For example, there are several search machines and data banks that allow to find a rare disease clearly exhibited by a patient's symptoms/signs[3]. But it is very difficult to diagnose a rare disease if it masks as a common disease. Diagnostic of rare diseases is connected with lack, uncertainty and imprecision of knowledge, medical mistake and even medical failure. From another side, a common disease also is established with some degree of belief, so the expressions such as "it is possible that a patient has a particular disease" rather often present in the daily medical practice.

It is clear that if we would know the common diseases, then deviations from them can be considered as a sign of non-common diseases. If these deviations reach a certain level, a suspicious of a rare disease exists. Thus, a physician obtains a sign of "non-normality" of a case in hand. Then a search of a rare disease can be continued in the specific databases, cited above.

In our approach we use a methodology based on fuzzy logic, because the elements of the diagnostic process (symptoms, diagnoses, connections between both) and a diagnostic process itself are mostly described imprecisely and approximately. First, we define what we understand under common (normal) diseases and then consider possible deviations from them. Our description of common (normal) diseases is based on the terminology used in CADIAG-like systems [1], [2], [3], [4], [5], [6], [7], [8], [9], [10], [11], [12], whereas, we investigate the deviations from normal diseases with the help of FML [13], [14]. In the last years, FML (Fuzzy Markup Language) is emerging as one of the most efficient and useful language to define fuzzy control thanks to its capability of modeling Fuzzy Logic Controllers in a human-readable and hardware inde-

[1] http://en.wikipedia.org/wiki/Rare_disease
[2] http://rarediseases.info.nih.gov/
http://rarediseases.about.com/
http://ec.europa.eu/health-eu/health_problems/rare_diseases/index_en.htm/

[3] http://www.orpha.net/consor/cgi-bin/index.php?lng=EN
http://www.crdnetwork.org/
http://www.rarediseases.org/search/rdblist.html

978-1-4244-7316-8/11/$26.00 ©2011 IEEE

pendent way, i.e., the so-called Transparent Fuzzy Controllers (TFCs) [15]. We show how FML mechanism can be adjusted to suspect a rare disease, and discuss the appropriateness of the available operators.

In next Section we recall some necessary definition and denotations. In the Section III we present a brief FML description. The results of FML applications to suspect a rare disease on examples are reported in the Section IV. Section V concludes our work.

II. Preliminaries. Notions and denotations

We present a medical decision support mechanism based on the fuzzy approach generally as follows. Three components take part in the process: symptoms/signs of the patient to whom a diagnosis should be established, medical knowledge (written as "IF S THEN D", but formalized as fuzzy relations) available before the process starts and diagnosis that we are trying to find. A schema of the process is presented below.

Symptoms		Medical Knowledge	Diagnosis
$\Downarrow$			
Symptoms +		Medical Knowledge	= Diagnosis
$\Downarrow$		$\Downarrow$	$\Downarrow$
S_p	$\circ$	R_{SD}	$=D_p$

R_{SD} is a fuzzy relation between symptoms/signs and diseases is defined as

$$R_{SD} : \Sigma \times \Delta \to [0,1] \tag{1}$$

$$S_p : \Sigma \to [0,1] \tag{2}$$

$$D_p : \Delta \to [0,1] \tag{3}$$

where $\Sigma = \{s_1, \ldots, s_m\}$ is the crisp set of symptoms/signs, $\Pi = \{p_1, \ldots, p_r\}$ is the crisp set of patients, $\Delta = \{d_1, \ldots, d_n\}$ is the crisp set of diseases, each element of the fuzzy set S_p shows to which degree it is true, that a patient $p \in \Pi$ has symptom/sign s_i, or a degree of possibility of the presence of the symptom, or its severity; symbol D_p is used for the final diagnosis for a patient $p \in \Pi$ and each element of the fuzzy set D_p shows to which degree it is true, that a patient $p \in \Pi$ has a given disease d_j, or a degree of possibility with which we can attach each relevant diagnostic label to the patient [16]. R_{SD} can be of different types, it depends what information is available from experts or manuals. For example, R_{SD} can be considered as *confirmation* relation (R^c_{SD}), *occurrence* relation (R^o_{SD}), *exclusion* relation (R^e_{SD}) , *temporal* or *time of manifestation* relation (R^t_{SD}). R^c_{SD} shows the degree to which a symptom/sign confirms the presence of disease, R^o_{SD} shows the frequency of occurrence of symptom/sign with disease, R^e_{SD} indicates the degree in which the present symptom/sign (combination) excludes (or disconfirms) the disease, R^t_{SD} relation shows to which degree it is true that exhibition of a symptom leads to immediate manifestation of a disease (or a disease is manifested after some period of time).

	d_1	d_2	$\ldots$	d_n
s_1	$f(s_1\|d_1)$	$f(s_1\|d_2)$	$\ldots$	$f(s_1\|d_n)$
s_2	$f(s_2\|d_1)$	$f(s_2\|d_2)$	$\ldots$	$f(s_2\|d_n)$
$\vdots$	$\vdots$	$\vdots$	$f(s_i\|d_j)$	$\vdots$
s_m	$f(s_m\|d_1)$	$f(s_m\|d_2)$	$\ldots$	$f(s_m\|d_n)$

TABLE I: Numerical representation of symptom/sign - disease connections for R^o_{SD}

never,	very seldom,	seldom,
sometimes,	unspecified,	occasionally,
often,	very often,	always

TABLE II: Linguistic values

$R^o_{SD}(s_i, d_j)$ and $R^c_{SD}(s_i, d_j)$ can be derived from relative frequencies, i.e., numerically [5]:

$$R^o_{SD}(s_i, d_j) = f(s_i|d_j) \tag{4}$$

and

$$R^c_{SD}(s_i, d_j) = f(d_j|s_i) \tag{5}$$

where $f(s_i|d_j) = \frac{f(d_j \cap s_i)}{f(d_j)}$, $f(d_j|s_i) = \frac{f(d_j \cap s_i)}{f(s_i)}$; $f(s_i|d_j)$ is a conditional frequency of s_i given d_j, $f(d_j|s_i)$ is a conditional frequency of d_j given s_i, $f(d_j \cap s_i)$ is the absolute frequency of joint occurrence of d_j and s_i, $f(d_j)$ and $f(s_i)$ are absolute frequencies of d_j and s_i, correspondingly. We call this numerical interpretation.

An example of a numerical description is presented in the Table I.

A linguistic way opens a possibility to estimate relations R^o_{SD}, R^c_{SD}, R^e_{SD}, R^t_{SD} (linguistic variables) using fuzzy sets (values of linguistic variables), e.g., presented in the Table II.

The fuzzy sets (Table II) are defined as mappings from $[0,1]$ to $[0,1]$. An example of a linguistic description of symptom/sign - disease connection is presented in the Table III. Each linguistic value can be defined by an expert [17]. For example, an expert can define his own fuzzy set *often* and supports the interpretation with the following sentence: symptom/sign and disease meet each other often, if it happens in, approximately, 60%. Such way fuzzy relations of type II [16] are defined. An example of linguistic values from the scale (Table II) as triangular fuzzy sets is shown in the Table IV.

Another possibility to define linguistic values (simple one) is to assign to them an ordered set of numbers, e.g, from $[0,1]$ as shown in the Table V.

	d_1	d_2	$\ldots$	d_n
s_1	`often`	`always`	$\ldots$	`never`
s_2	`never`	`often`	$\ldots$	`always`
$\vdots$	$\vdots$	$\vdots$	f_{ij}	$\vdots$
s_m	`often`	`seldom`	$\ldots$	`always`

TABLE III: Linguistic representation of symptom/sign - disease connections

never	*very seldom*	*seldom*
$(0, 0.1, 0.2)$	$(0.1, 0.2, 0.3)$	$(0.2, 0.3, 0.4)$
sometimes	*unspecified*	*occasionally*
$(0.3, 0.4, 0.5)$	$(0.4, 0.5, 0.6)$	$(0.5, 0.6, 0.7)$
often	*very often*	*always*
$(0.6, 0.7, 0.8)$	$(0.7, 0.8, 0.9)$	$(0.8, 0.9, 1)$

TABLE IV: Representation of linguistic terms as triangular fuzzy sets

never	*very seldom*	*seldom*
0	0.2	0.3
sometimes	*unspecified*	*occasionally*
0.4	0.5	0.6
often	*very often*	*always*
0.7	0.8	1.0

TABLE V: Representation of linguistic terms as numbers

In our work we use the scale (shown in Table II) to estimate the relationships of the symptoms/signs and diseases.

A $\max - \min$ composition of fuzzy relations [18], [19] or its generalised version t-conorm-t-norm composition can be used for medical diagnosing. Thus,

$$D_p = S_p \circ R_{SD} \tag{6}$$

is a composition of a fuzzy set and a fuzzy relation.

Moreover $\forall d_j \in \Delta$

$$D_p(d_j) = \vee_{s_i \in \Sigma} \wedge \{S_p(s_i); R_{SD}(s_i, d_j)\} \tag{7}$$

where $D_p : \Delta \to [0, 1]$ are inferred possible diagnoses for the patient $p \in \Pi$, $\vee$ is a t-conorm and $\wedge$ is a t-norm.

In general, the aggregation operators can be used in this inference mechanism [16].

Working with a decision-support system, a physician expects from a computer program a tip, a help, what diagnosis it can be for a patient at hand. In this way, the system should alarm if some things are outside of its normal functioning, i.e., if the case is neither confirmed nor possible, or has "strange" values. Thus, such behaviour of a system could be considered as a sign of a possible rare disease.

It is obvious that conclusions about the patient's diagnosis with a help of a computer program is made based on the information available, in particular, what initial information is contained in the knowledge base and what information about a patient at hand we have. It is possible to investigate how to suspect a rare disease under the presence of different initial information, in our denotation R^o_{SD}, R^c_{SD}, R^e_{SD} or R^t_{SD}. In the section IV we consider relation R^o_{SD} and simulate the inference process with FML. For this reason, a description of this novel language is provided in the following section.

III. Fuzzy Markup Language: A Description

Fuzzy Markup Language (FML) is a XML-based domain-specific language proposed by Acampora and Loia [13] whose main aim is to model fuzzy systems by directly dealing with fuzzy concepts, fuzzy rules and fuzzy inference engines [8]. In particular, it is used to model two well-known kind of fuzzy controllers: Mamdani and Takagi-Sugeno-Kang (TSK). FML programs are coded through a collection of correlated semantic tags capable of modeling different components of a controller by exploiting abstraction benefits offered by XML tools. Differently from other similar approaches used to describe fuzzy controllers such as Fuzzy Control Language (FCL) or MATLAB Fuzzy Inference System (FIS) developed by the Matworks, FML allows fuzzy designers to simply code their ideas on heterogeneous hardware without understanding details related to the different platforms. In short, thanks to FML it is possible to model a fuzzy controller in human-readable and hardware independent way. The exploitation of FML is resulted in a new fuzzy control design philosophy named *transparent fuzzy controller* [20] based on the integration among fuzzy systems, labeled tree theory [21], and XML methodology.

In the following, a brief description of the used FML tags is given. The root tag of FML program is <FuzzyController> which has two attributes: name and ip. The *name* attribute permits to specify the name of fuzzy controller and *ip* is used to define the location of controller in a computer network. The fuzzy knowledge base is defined by means of the tag <KnowledgeBase> which maintains the set of fuzzy concepts used to model the fuzzy system. In order to define a fuzzy concept, the following set of nested tags is used:

- <FuzzyVariable> defines the fuzzy concept;
- <FuzzyTerm> defines a linguistic term describing the fuzzy concept;
- a set of tags defining a shape of fuzzy sets related to fuzzy terms.

The attributes of <FuzzyVariable> tag are: name, scale, domainLeft, domainRight, type and, for only output concept, accumulation, defuzzifier and defaultValue. The *name* attribute defines the name of fuzzy concept; *scale* is employed to define the scale used to measure the fuzzy concept, *domainLeft* and *domainRight* are used to model the universe of discourse of fuzzy concept, i.e, the set of real values related to fuzzy concept; the position of fuzzy concept into rule (consequent part or antecedent part) is defined by *type* attribute (input/output); *accumulation* attribute defines the method of accumulation that is a method that permits the combination of results of a variable of each rule in a final result; *defuzzifier* attribute defines the method used to execute the conversion from a fuzzy set, obtained after aggregation process, into a numerical value to give it in output to system; *defaultValue* attribute defines a real value used only when no rule has fired for the variable at issue. <FuzzyTerm> uses two attributes: *name* used to identify the linguistic value associate with fuzzy concept and *complement*, a boolean attribute that defines, if it is true, it is necessary to consider the complement of membership function defined by given parameters. Fuzzy shape tags, used to complete the definition of fuzzy concept, are several, in our case of study, the triangular membership functions has been used through <TriangularShape> tag. Each shaping tag uses a set of attributes which defines the real outline of corresponding

fuzzy set. In particular, the <TriangularShape> tag uses three parameters. The rule base is modeled by <RuleBase> tag which defines a fuzzy rule set. The <RuleBase> tag uses five attributes: name, type, activationMethod, andMethod and orMethod. Obviously, the *name* attribute uniquely identifies the rule base. The *type* attribute permits to specify the kind of fuzzy controller (Mamdani or TSK) respect to the rule base at issue. The *activationMethod* attribute defines the method used to implication process; the *andMethod* and *orMethod* attribute define, respectively, the and and or algorithm to use by default. In order to define the single rule the <Rule> tag is used. The attributes used by the <Rule> tag are: name, connector, operator and weight. The *name* attribute permits to identify the rule; *connector* is used to define the logical operator used to connect the different clauses in antecedent part (and/or); *operator* defines the algorithm to use for chosen connector; *weight* defines the importance of rule during inference engine time. The definition of antecedent and consequent rule part is obtained by using <Antecedent> and <Consequent> tags. <Clause> tag is used to model the fuzzy clauses in antecedent and consequent part. This tag use the attribute *modifier* to describe a modification to term used in the clause. To complete the definition of fuzzy clause the nested <Variable> and <Term> tag have to be used.

The FML tags represent the set of lexemes used to build a fuzzy controller. However, in order to realize a well-formed XML-based language, an FML context-free grammar is necessary. The FML context-free grammar is modeled by XML file in the form of a XML Schema Document (XSD). Moreover, since an FML program realizes only a static view of a fuzzy system, the so-called eXtensible Stylesheet Language Translator (XSLT) is provided to change this static view to a computable version. In particular, the XSLT technology is used to convert a fuzzy controller description into a general-purpose computer language to be computed on several hardware platforms.

Finally, the FML is essentially composed by three layers:

- XML in order to create a new markup language for fuzzy logic control;
- a XML Schema Document in order to define the legal building blocks;
- extensible stylesheet language transformations (XSLT) in order to convert a fuzzy controller description into a specific programming language.

IV. FML IN SIMULATION

In this section, the simulation with FML of the inference process used to suspect a rare disease under the presence of the initial information R^o_{SD} is shown and discussed.

In particular, we illustrate the use of FML to suspect a rare disease by means of an example. Assume, that a knowledge base contains R^o_{SD} as, for example, in the Table VI and corresponding numerical form (due to the scale Table V) as singletons and/or triangular fuzzy sets. In this case $\Delta = \{d_1, d_2\}$, $\Sigma = \{s_1, s_2, \ldots, s_6\}$. We assume that a rare disease is not in the knowledge base, it means that it is not in Δ.

	Bronchitis	*Pneumonia*
wheezing	sometimes	occasionally
breathlessness	very seldom	often
anosmia	seldom	seldom
fever	sometimes	often
sinusitis	sometimes	sometimes
chronicotitis	seldom	seldom

TABLE VI: Linguistic descriptions for "normal" diseases *Bronchitis*/*Pneumonia*

	d_1	d_2
s_1	0.4	0.6
s_2	0.2	0.8
s_3	0.3	0.3
s_4	0.4	0.8
s_5	0.4	0.4
s_6	0.3	0.3

TABLE VII: Corresponding numerical descriptions for "normal" diseases (see Table VI)

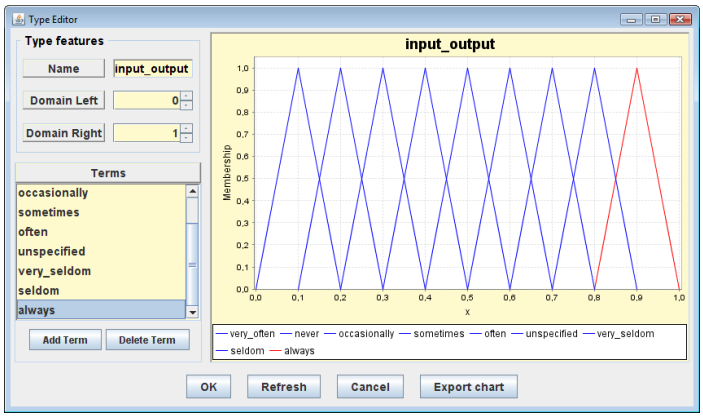

Fig. 1: Presentation of linguistic values from Table V in FML

We define nine linguistic values from Table IV as shown in Figure 1.

Thus, we use the same type of input and output variables in FML, in particular, triangular shape.

As input variables we consider 6 symptoms: wheezing, breathlessness, anosmia, fever, sinusitis, chronicotitis. As output variables we consider two diseases: Bronchitis and Pneumonia. Due to the Table VI we have constructed the following rule base (see Figure 2).

In the listing 1, a portion of the FML-based fuzzy controller to suspect a rare disease is presented.

As we speak about a rare disease, we consider how "far" is this case from the common representation.

In the Table VII we present corresponding singletons for linguistic values from Table VI for the explanation reason.

We can predefined an excluded diagnoses in the case if a symptom is fully present/absent with a corresponding full

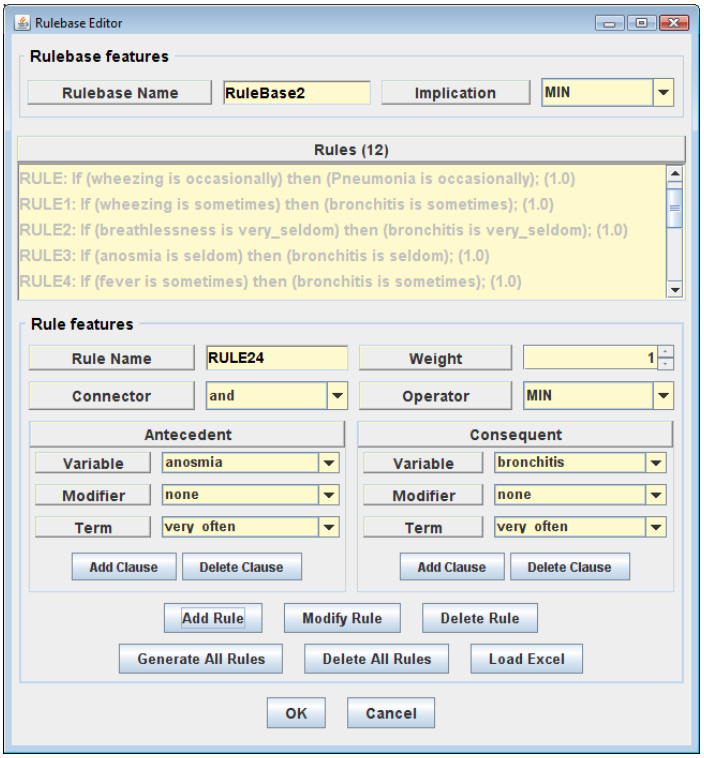

Fig. 2: 12 rules describing relation of six symptoms and two diseases in FML

occurrence/absent of occurrence. Simply speaking, at least one element of the Table VII should be 1 or 0 and at least one membership degree of fuzzy set S_p should be 1 or 0 as well. It means, that, to define such case, we need a crisp information. It is a clear situation, but is not always a case.

As we have already mentioned, the difficulty to suspect a rare disease is because of its symptomatic similarity to the "normal cases" and, of course, absence of the necessary information. If a physician has enough experience with a computer program, s/he usually has been working, and s/he mentions that the values for possible diagnoses are much below or much above the usual representation, it can be also the sign of alarm "a rare disease" for a physician.

We need to define appropriate operations and thresholds (that allow to detect a deviation from the "normal" case). If we take max-min composition of fuzzy relations (7), it restricts the maximum membership degree of possible diseases for a patient by values in Table VII. For example, if a patient at hand has

$$S_p^1 = \{(s_1, 0.4), (s_2, 0.2), (s_3, 0.3), (s_4, 0.4), (s_5, 0.4), (s_6, 0.2)\}$$

the possible diagnosis d_1 has the membership degree 0.4 (see (8)). If a patient at hand has

$$S_p^2 = \{(s_1, 1.0), (s_2, 1.0), (s_3, 0.2), (s_4, 0.3), (s_5, 0.2), (s_6, 0.2)\}$$

the possible diagnosis d_1 has the membership degree 0.4

```
<?xml version="1.0" encoding="UTF-8"?>
<FuzzyController name="Mamdani_controller" ip="127.0.0.1">
    <KnowledgeBase>
        <FuzzyVariable name="wheezing" domainleft="0.0" domainright="1.0" scale=""
                       type="input">
            <FuzzyTerm name="always" complement="false">
                <TriangularShape Param1="0.8" Param2="0.9" Param3="1.0"/>
            </FuzzyTerm>
            <FuzzyTerm name="never" complement="false">
                <TriangularShape Param1="0.0" Param2="0.1" Param3="0.2"/>
            </FuzzyTerm>
            <FuzzyTerm name="occasionally" complement="false">
                <TriangularShape Param1="0.5" Param2="0.6" Param3="0.7"/>
            </FuzzyTerm>
            <FuzzyTerm name="often" complement="false">
                <TriangularShape Param1="0.6" Param2="0.7" Param3="0.8"/>
            </FuzzyTerm>
            <FuzzyTerm name="seldom" complement="false">
                <TriangularShape Param1="0.2" Param2="0.3" Param3="0.4"/>
            </FuzzyTerm>
            <FuzzyTerm name="sometimes" complement="false">
                <TriangularShape Param1="0.3" Param2="0.4" Param3="0.5"/>
            </FuzzyTerm>
            <FuzzyTerm name="unspecified" complement="false">
                <TriangularShape Param1="0.4" Param2="0.5" Param3="0.6"/>
            </FuzzyTerm>
            <FuzzyTerm name="very_often" complement="false">
                <TriangularShape Param1="0.7" Param2="0.8" Param3="0.9"/>
            </FuzzyTerm>
            <FuzzyTerm name="very_seldom" complement="false">
                <TriangularShape Param1="0.1" Param2="0.2" Param3="0.3"/>
            </FuzzyTerm>
        </FuzzyVariable>
        .....
        <FuzzyVariable name="bronchitis" domainleft="0.0" domainright="1.0"
                       scale="" defaultValue="0.0" accumulation="MEAN"
                       defuzzifier="MOM" type="output">
            <FuzzyTerm name="always" complement="false">
                <TriangularShape Param1="0.8" Param2="0.9" Param3="1.0"/>
            </FuzzyTerm>
            <FuzzyTerm name="never" complement="false">
                <TriangularShape Param1="0.0" Param2="0.1" Param3="0.2"/>
            </FuzzyTerm>
            <FuzzyTerm name="occasionally" complement="false">
                <TriangularShape Param1="0.5" Param2="0.6" Param3="0.7"/>
            </FuzzyTerm>
            <FuzzyTerm name="often" complement="false">
                <TriangularShape Param1="0.6" Param2="0.7" Param3="0.8"/>
            </FuzzyTerm>
            <FuzzyTerm name="seldom" complement="false">
                <TriangularShape Param1="0.2" Param2="0.3" Param3="0.4"/>
            </FuzzyTerm>
            <FuzzyTerm name="sometimes" complement="false">
                <TriangularShape Param1="0.3" Param2="0.4" Param3="0.5"/>
            </FuzzyTerm>
            <FuzzyTerm name="unspecified" complement="false">
                <TriangularShape Param1="0.4" Param2="0.5" Param3="0.6"/>
            </FuzzyTerm>
            <FuzzyTerm name="very_often" complement="false">
                <TriangularShape Param1="0.7" Param2="0.8" Param3="0.9"/>
            </FuzzyTerm>
            <FuzzyTerm name="very_seldom" complement="false">
                <TriangularShape Param1="0.1" Param2="0.2" Param3="0.3"/>
            </FuzzyTerm>
        </FuzzyVariable>
        .....
    </KnowledgeBase>
    <RuleBase name="RuleBase1" andMethod="MIN" orMethod="MAX"
              activationMethod="MIN" type="mamdani">
        <Rule name="RULE1" connector="and" operator="MIN" weight="1.0">
            <Antecedent>
                <Clause>
                    <Variable>wheezing</Variable>
                    <Term>sometimes</Term>
                </Clause>
            </Antecedent>
            <Consequent>
                <Clause>
                    <Variable>bronchitis</Variable>
                    <Term>sometimes</Term>
                </Clause>
            </Consequent>
        </Rule>
        .....
    </RuleBase>
</FuzzyController>
```

Listing 1: FML code to model a portion of the FML-based fuzzy controller to suspect a rare disease

as well. It means, that the values from the initial tabel (in our case R^o_{SD}) bound from above the possible exhibitions of symptoms/signs of the patient. With operator min is not possible to see deviations.

	d_1	d_2
S_p^1	0.4	0.4
S_p^2	0.4	0.8
S_p^3	0.4	0.7

TABLE VIII: Possible degrees for "normal" diseases under max-min composition

.

$$D_p(d_1) = \max \left\{ \begin{array}{l} \min\{0.4, 0.4\}; \\ \min\{0.2, 0.2\}; \\ \min\{0.3, 0.3\}; \\ \min\{0.4, 0.4\}; \\ \min\{0.4, 0.4\}; \\ \min\{0.3, 0.3\}; \end{array} \right\} = 0.4 \qquad (8)$$

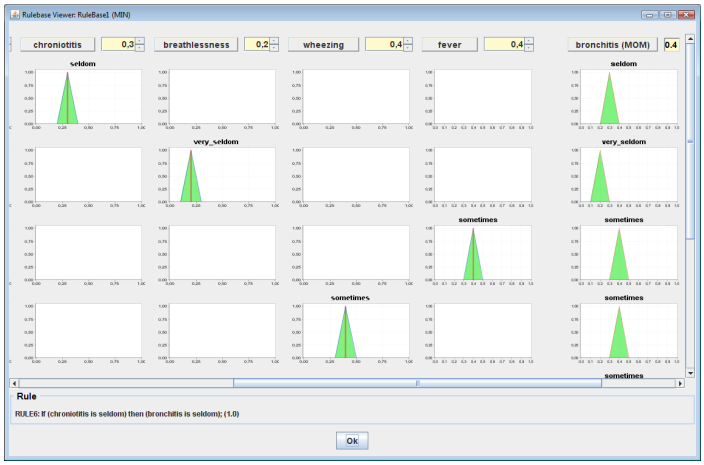

Fig. 3: Results of execution of FML under S_p^1 for d_1

This standard $\max - \min$ composition in our case guarantees that the degree of occurrence can be less than 0.4, but not more (see Figure 3, Table VIII). Using FML, the antecedent and consequent of a rule in the rule base should be defined as fuzzy sets. We, however, consider R_{SD} relation is a given one, we do not construct it from fuzzy sets described symptoms/signs and diseases. The omission of this step can be solved by assigning the same linguistic values to the antecedent variable and the consequent variable. In general, due to our approach to define deviations from "common" diseases as a sign of non-normality, and consequently, a suspicious of a rare disease, we need operators, that allow to estimate such deviation. For example, in controllers, realized in the FML, an input value and antecedent value are connected by 'min' operator, but if we need to know, how far is an input value from the antecedent value, we need a corresponding operator that estimates the distance between two fuzzy sets.

Let us continue to discuss our considerations on examples.

If we take the *absolute difference* (for two numbers a and b their *absolute difference* is defined as $|a - b|$) instead of min-operation (max-operation remains unchanged) we obtain more flexibility to detect deviations. For example, for S_p^1 the

	d_1	d_2
S_p^1	0.0	0.13
S_p^2	0.23	0.24
S_p^3	0.40	0.26

TABLE IX: Possible degrees for "normal" diseases under $mean - absolute\ difference$ composition

membership degree of d_1 in this case is 0 and for S_p^2 we obtain 0.8. If instead of the max operator we take another aggregation operator, such as the *arithmetic mean* of deviations (the *arithmetic mean* of $a_1, a_2, \ldots, a_n$ is $\frac{a_1+a_2+\cdots+a_n}{n}$), for d_1 in the case of S_p^1 we obtain 0 as well and 0.23 in the case of S_p^2. We interpret 0 as a sign of most believable diagnosis, and every deviation from 0 points less believable diagnosis. The question is, as always in applications, how to detect a threshold, under (or above) which a suspicious of a rare disease arises. If we take $max - absolute\ difference$ composition of S_p and R_{SD} and a result is different from 0, the final value shows that at least one symptom/sign differs from the normal case, but does not say anything about the rest of symptoms. When a rare disease can be pointed by a representative symptom (i.e., such symptom which presence/absence is a sure sign of the non-normality of a diagnosis) $\max$- *absolute difference* is suitable.

The $mean - absolute\ difference$ composition of S_p and R_{SD} shows the mean value of all deviations. As it is often with rare diseases, they are described with the same symptoms/signs as "normal" diseases and only a certain deviation can point a rare disease, the application of $mean - absolute\ difference$ composition of S_p and R_{SD} seems to be reasonable. Notice, that in general, a $p - mean$, and/or other distance metrics can be considered.

$$S_p^3 = \{(s_1, 0.7), (s_2, 0.7), (s_3, 0.7), \\ (s_4, 0.7), (s_5, 0.8), (s_6, 0.7)\}$$

The possible degrees for d_1, d_2 under S_p^1, S_p^2, S_p^3 using $\max - \min$ composition are presented in the Table VIII.

The possible degrees for d_1, d_2 under S_p^1, S_p^2, S_p^3 using $mean - absolute\ difference$ composition are presented in the Table IX.

For this particular example 0.25 can be chosen as a threshold to point a suspicion of a rare disease, i.e., if all numbers in one string in the Table IX are above 0.25 a physician should think about "non-normality" of a possible diagnosis for a patient at hand. It means, that we found an approach to suspect a rare disease if the diagnoses from the initially defined list seems to be possible. The choice of a threshold remains on experts. There are many ways to formalise this procedure[22], [23], [24], which approach has to be used is a subject of a separate investigation.

Notice, that the difference between symptoms of a given patient and the predefined symptoms/signs picture of a disease may be also calculated as ratio $\frac{a}{b}$ and then also a mean value of these ratios may be calculated. In this case a value for a normal case will be 1.

So, we need an operation that will calculate a distance

between two fuzzy sets in the inference mechanism. It is a subject of our future applications.

It can be also argued that one number, as a threshold, does not reflect a flexibility in diagnostics. In forthcoming time we investigate interval- and fuzzy sets estimations of linguistic expressions for a rare disease diagnostic problem. In this paper our intend was to discuss the principal approach to diagnostics of rare diseases and show the first steps for its realisation with the help of FML.

V. Conclusions

The problem to suspect a rare disease (in particular, in pediatrics) with a help of computer - assisted system is an important problem and till now is not well investigated. This problem is connected with absence, insufficiency, uncertainty and imprecision of information and, therefore, belongs to the category of problems, that can be solved by fuzzy logic approaches.

Our main idea to suspect a rare disease is based on the assumption, that deviation from a "normal" disease is a sign to warn a rare disease. Thus, well acquaintance with normal diseases involves a recognition of a rare disease. We suppose, that a physician has already established a preliminary diagnosis for a patient, but s/he hesitates about its correctness. Then a physician, based on the patient's data, checks the deviations from the "normal" cases, and if these deviations reach certain level, a suspicion of a rare disease arises.

We test our approach on FML and preliminary results have shown that we are able successfully model the process of suspicious of a rare disease, but for flexibility we need additional operators, that allow to estimate a deviation of one fuzzy set from another. It is a subject of our recent collaborative work.

Acknowledgment

This work was supported by Georgia National Science Foundation, Ministry of Education and Science of Georgia, Grant GNSF/ST08/6-460, Grant STCU-GNSF #5015 and the Grant #GNSF(ST08/1-361), Georgian National Science Foundation. Any idea in this publication is possessed by the authors and may not represent the opinion of the Georgian National Science Foundation itself.

References

[1] K.-P. Adlassnig and G. Kolarz. CADIAG-II: computer-assisted medical diagnosis using fuzzy subsets. In M.M. Gupta and E. Sanchez, editors, *Approximate Reasoning in Decision Analysis*, pages 495–505. North Holland Publishing Company, 1982.

[2] K. Boegl. *Design and Implementation of a Web-Based Knowledge Acquisition Toolkit for Medical Expert Consultation Systems*. PhD thesis, Technische Universität Wien, 1997.

[3] K. Boegl, K.-P. Adlassnig, Y. Hayashi, T. Rothenfluh, and H. Leitich. Knowledge acquisition in the fuzzy knowledge representation framework of a medical consultation system. *Artificial Intelligence in Medicine*, 30:1–26, 2004.

[4] M. Daniel. Theoretical comparison of inference in CADIAG and MYCIN-like systems. *Tatra Mountains Mathematical Publications*, 16:255–272, 1999.

[5] M. Daniel, P. Hájek, and H. Nguyen. CADIAG-2 and MYCIN-like systems. *Artificial Intelligence in Medicine*, 9:241–259, 1997.

[6] P. Hájek, T. Havránek, and R. Jiroušek. *Uncertain Information Processing in Expert Systems*. CRC Press, 1992.

[7] P. Hájek and J. Valdés. An analysis of MYCIN-like expert systems. *Mathware and Soft Computing*, 1:45–68, 1994.

[8] T. Kiseliova. A theoretical comparison of Disco and CADIAG-II-like systems for medical diagnoses. *Kybernetika*, 42(6):723–748, 2006.

[9] T. Kiseliova and K. Pagava. New approach to estimate different drugs and/or other medical interventions effectiveness based on fuzzy logic principles. *Georgia Medical News*, 3(156):65–68, March 2008.

[10] T. Kiseliova and K. Pagava. Modelling uncertainty in the connection of socio-economic factors and health-related behavior of adolescents in Georgia. In *Proceedings of the 28th North American Fuzzy Information Processing Society Annual Conference (NAFIPS2009)*, Cincinnati, OH, USA, June 14–17, 2009.

[11] H. Leitich, K.-P. Adlassnig, and G. Kolarz. Evaluation of two different models of semi-automatic knowledge acquisition for the medical consultant system CADIAG-II/RHEUMA. *Artificial Intelligence in Medicine*, 25:215–225, 2002.

[12] R. Seising, C. Schuh, and K.-P. Adlassnig. Medical knowledge, fuzzy sets and expert systems. In *Workshop on Intelligent and Adaptive Systems in Medicine*, Prague, http://cyber.felk.cvut.cz/EUNITE03-BIO, March 31 - April 1, 2003.

[13] G. Acampora and V. Loia. Fuzzy control interoperability and scalability for adaptive domotic framework. In *IEEE Transac- tions on Industrial Informatics*, volume 1.

[14] Mei-Hui Wang, Chang-Shing Lee, Kuang-Liang Hsieh, Chin-Yuan Hsu, Giovanni Acampora, and Chong-Ching Chang. Ontology-based multi-agents for intelligent healthcare ap- plications. *Journal of Ambient Intelligence and Humanized Computing*, 1(2), 2010. DOI: 10.1007/s12652-010-0011-5.

[15] D. Acampora, V. Loia, and A. Vitiello. Enhancing Transparent Fuzzy Controllers through Temporal Concepts: An Application to Computer Games. In *2010 International Conference on Technologies and Applications of Artificial Intelligence*, pages 405–412, 2010.

[16] G. J. Klir and B. Yuan. *Fuzzy Sets and Fuzzy Logic. Theory and Applications*. Prentice Hall PTR, 1995.

[17] H. Phagava. Numerical estimates of probability expressions to be used in medical expert programs. In *Georgian Medical News*, volume 2, pages 130–134. February 2002.

[18] E. Sanchez. Medical diagnosis and composite fuzzy relations. In M. M. Gupta, R. K. Ragade, and R. R. Yager, editors, *Advances in Fuzzy Set Theory and Applications*, pages 437–444. North-Hollands, New York, 1979.

[19] L. A. Zadeh. The concept of a linguistic variable and its application to approximate reasoning, Part I, Part II, Part III. *Information Sciences*, 8,9:199–249, 301–357, 43–80, 1975.

[20] G. Acampora and V. Loia, "Using fml and fuzzy technology in ambient intelligent environments," *International Journal of Computational Intelligence Research*, vol. 1, no. Issue, pp. 171-182, 2005.

[21] G.Acampora, V. Loia, "An Open Integrated Environment for Transparent Fuzzy Agents Design," *Open Source Development, Communities and Quality, IFIP International Federation for Information Processing*, Springer Boston, vol. 275/2008, pp. 1571-5736, 2008.

[22] C. Naylon. How to build an inferencing engine. In R. Forsyth, editor, *Expert Systems, Principles and Case Studies*, chapter 5, pages 85–105. Champman and Hall, 1989.

[23] J. W. Grzymala-Busse. *Managing Uncertainty in Expert Systems*. The Kluwer International Series in Engineering and Computer Science. Kluwer Academic Publishers Boston/Dordrecht/London, University of Kansas, 1991.

[24] A. Kandel. *Fuzzy expert systems*. CRC Press, Inc, 2000 Corporate Blvd., N.W., Boca Raton, Florida 33431, 1991.

2011 IEEE International Conference on Fuzzy Systems
June 27-30, 2011, Taipei, Taiwan

Linguistic Summarization Of Long-Term Trends For Understanding Change In Human Behavior

María Ros, Manuel Pegalajar, Miguel Delgado and Amparo Vila
Computer Science and Artificial Intelligent
University of Granada
Granada, Spain
{marosiz, manupc, mdelgado, vila}@decsai.ugr.es

Derek T. Anderson, James M. Keller and Mihail Popescu
Electrical and Computer Engineering
University of Missouri
Columbia, MO 65211 USA
{andersondt, kellerj, popescum}@missouri.edu

***Abstract*—In this paper, we propose a linguistic summarization procedure for describing long-term trends of change in human behavior. Our objective consists of defining methods that provide information to elders, caregivers, social workers or even family in an understandable language. We adapt a measure that we defined in previous work on soft cluster partition similarity for comparing behaviors that are adapted over time. From that measure, we are able to produce a time series that numerically describes change in behavior over time. In this article, the resulting time series is partitioned and linguistically summarized depending on a user's (caregiver, social worker, etc.) desired time resolution. Simulated resident behavior is used in order to explore a range of different scenarios and the response of the proposed linguistic summarization process is investigated.**

Keywords- comparing soft partitions, human behavior, anomaly detection, fuzzy linguistic summarization

I. INTRODUCTION

In recent years, successful aging has become one of the most important problems in our society. Life expectancy has improved, and along with it the resources required to maintain quality and style of life. Emerging applications combining *technology* and *medicine* provide one possible solution. Multiple large scale projects combine these subjects. One such project is the center for Eldercare and Rehabilitation Technology (CERT) [1] and the TigerPlace facility [2]. This effort is a large interdisciplinary collaboration between electrical and computer engineers, gerontological nurses, social workers, physical therapists and others at the University of Missouri. This group has installed multiple sensing technologies in the homes of elders. One goal of these technologies includes assisting residents with "aging in place" as independently as possible. Other projects include the MavHome project [3], iDorm [4], CASAS [5] and the Georgia Tech Aware Home [6]. In addition, in [7] eight other relevant projects in this field are summarized.

Important advantages of behavior analysis in the eldercare domain include: reducing dependency, enhancing personal comfort and safety and delaying the process of moving to a nursing home. Many projects are centered around Activities of Daily Living (ADL) [8]. From the set that focus on the ADL, we emphasize [9], an approach based on multiple behavioral hidden Markov models (MBHMM). The authors propose the creation of multiple HMMs for each variation of an action. The most important advantage of this proposal is that the system is able to determine which tasks are currently active, even if the user has not yet completed the activity.

A related fuzzy approach is [10]. In that work, the authors propose an AmI fuzzy computing system, which is a multilayer architecture to learn and model human behavior. They attempt to join the advantages of a multi-agent based framework with fuzzy control techniques to improve the recognition process and continuously enrich the knowledge about the user and environment.

The majority of existing efforts are focused on the detection of normal and abnormal behaviors at the moment the resident is performing them. In previous work [11], we introduced a method to identify changes in patterns of behavior over longer periods of time (days, weeks or months). Identification of changes in behavior over such time frames is significant in the regard that it can be used to help predict cognitive and/or functional decline that affects overall quality of life [12, 13, 14]. If significant change in human behavior can be recognized early, then caregivers can take action to help avoid or postpone catastrophic events. However, the information obtained is a numerical data set. In this article our objective consists of developing a method to produce linguistic information that is of greater use to users. Our approach is based on the concept of linguistic summarization. A linguistic data summary is a concise, human-consistent description of a (numerical) data set [15, 16, 17]. This process allows us to summarize a data time series by segmenting and describing long-terms trends of change in behavior.

In the existing literature, there are different approaches to deal with time series summarization. The application range is very assorted, but the business field stands out over the rest. In [18, 20] Kacprzyk and Wilbik deals with time series used for an analysis of the past performance of investment (mutual) funds and extracts summaries to help to make future investment decisions. Focusing on human activities, in [19] the authors propose a novel method for recognizing human

978-1-4244-7316-8/11/$26.00 ©2011 IEEE

activity from linguistic summarizations of temporal fuzzy inference curves representing the states of a three-dimensional object called voxel person. However, the approach taken in this article is most similar to that of Kacprzyk et al. [20]. Primarily, they focus on stock market analysis and finance applications. They propose a way to summarize trends identified with straight line segments of a piecewise defined linear approximation of time series of change in long-term human behavior. They employ a set of features (attributes) to characterize the trends such as the slope of the line segment. They then use a linguistic quantifier driven aggregation of trends to perform the linguistic summary. In addition, they also study the description of duration and variability.

Herein, we introduce a method to obtain a natural language description about change in long-term adapted behavior. The user selects a time period amount (resolution) to summarize, e.g., day, week, month, etc. A resident history is partitioned according to this time window and we extract features to characterize the change. In particular, we look for decreasing, constant, or increasing change (similarity) in behavior. This makes it possible to monitor cases such as a degenerative disease or a rehabilitation process without the need to continuously bother an elder.

This paper is organized as follows. Section 2 is previous work, which is required in order to understand this article. Next, in section 3 we introduce the linguistic summarization process, specifying the parameters used and the structure of the sentences. Section 4 is experiments. We present simulated user behavior in order to demonstrate a wide range of different possible scenarios and the response of our proposed approach.

II. Related Work

A. Modeling Human Behavior

Modeling human behavior in eldercare is a field that studies computational techniques to represent and analyze human daily activities in order to provide people with services if required, but without loss of independence. In this article, our objective is to extract a linguistic description of trends in long-term change of human behavior. This approach depends on the choice of representation. Here, we focus on a computational framework investigated by our research team in unpublished [21, 22]. The choice of representation is a sequence of cascaded AND gates with an underlying probability distribution that characterizes temporal dependency requirements over a set of actions for the different ways in which a user can perform a behavior. The work in [21, 22] is summarized in this subsection.

An abnormal situation occurs when a person does not perform the behavior as expected, i.e., forgetting things, performing actions in a dangerous order, etc. Example 1 demonstrates the role of detecting abnormal situations in the context of the goals of this work.

Example 1: Suppose that every morning a resident wakes up, goes to the bathroom, takes his pajamas off, takes a shower, washes his face, gets dressed and returns to the bedroom. All of these actions could be embraced as a single behavior concept, "morning routine". However, suppose that for a period of time the person does not take a shower. This is considered as a change in the "morning routine" behavior. This abnormal situation needs to be identified and the behavior model needs to be updated accordingly.

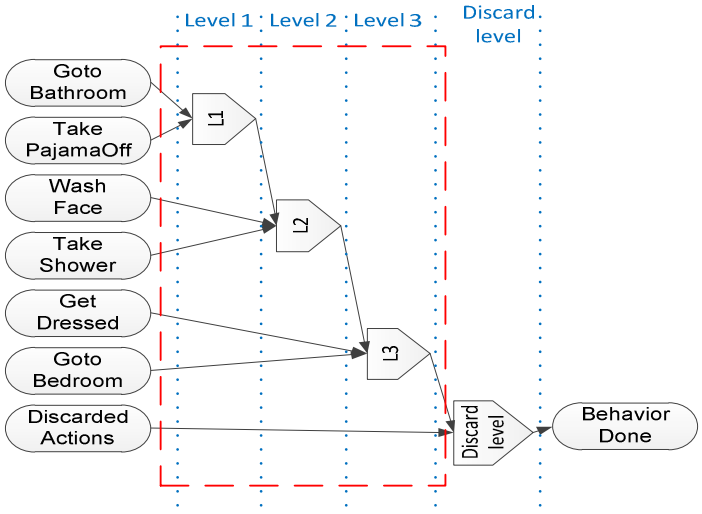

Fig.1. Morning routine behavior model (example 1).

In example 1, two important concepts are introduced, *action* and *behavior*. Informally, an action is the output of a sensor or a low-level algorithm interpreting sensor firings, e.g., the refrigerator door is closed, the front door is opened, a person is sitting on the couch, etc. Behavior is the set of actions and the order in which the actions need be performed. Formally, these concepts are characterized as follows.

Definition 1 (Human Action) [21, 22]: A human action h_i is a triple $h_i =< l_i, s_i, t_i >$, where l_i is a label used to identify the action, s_i is a sensor event and t_i is a time stamp in which the action occurs.

Definition 2 (Behavior) [21, 22]: A human behavior B_i is a quadruple $B_i =< H, R_i, C_i, \prec >$, where $H = \{h_1, h_2, \dots, h_n\}$ is a set of available human tasks, $R_i = \{r_1^i, r_2^i, \dots, r_{|R_i|}^i\} \subseteq H$ is the subset of available human tasks that are required to complete the behavior, and C_i is a set of temporal constraints between the tasks in R_i defined over a partial order relationship operator $\prec$. The partial order relationship $\prec$ defines the temporal dependency requirements over the actions of a behavior, and its formal definition is

$$r_a^i \prec r_b^i \leftrightarrow t_a \prec t_b. \quad (1)$$

Thus, a behavior is represented as a set of relevant actions, which maintain a specific order of performance between them. In [21, 22], we demonstrated that a behavior can be represented as a set of cascaded AND gates. An action in the system corresponds to an input of a specific AND gate. Each input is true if the action has been performed, or false if not. On the other hand, although all the tasks in the H set may be taken into consideration for a specific behavior, only those

actions that are included in the R set are really required for it. To handle this situation, we introduced a discard-level in which those actions that are irrelevant are assigned.

Besides relevant actions, this representation contains more knowledge about a specific behavior, such as the order relationship between diverse actions. As previously pointed out, a behavior is designed as a set of actions that maintains an order relationship between them. The level-representation for a behavior simulates the order relationship between the actions in such a way that those actions that are the input to an AND gate in Level_n have to be done previously to those that are the inputs to the following AND gate, in Level_{n+1}. Fig. 1 shows the sequence of AND gates obtained from example 1.

Nevertheless, a behavior does not have a single way to be performed. Hence, there may be several combinations of the same set of actions for a behavior, i.e., that some tasks may be performed in different levels of the structure without loss of meaning. For instance, in example 1, the action "wash face" could be performed either in level 2 or in the level 3 and be a legitimate Morning Routine. To deal with this disparity, in [21, 22] a probability matrix, $P(i,j)$, was computed, whose rows, $1 \le i \le |H|$, are actions, H set, and columns, $1 \le j \le |L|$, are available levels in the sequence of ANDs. Each element represents the probability of an action being performed in a particular level. Therefore, the behavior model represents, for each action, the most expected level for it being carried out. Next, keeping on with the prior example, an achievable matrix is presented below.

Continuation of example 1: Let us suppose that we want to study a "morning routine" behavior. In addition, let us suppose that we have the actions presented in example 1, plus the action "go to kitchen". Then, if the maximum number of levels was fixed to four, a possible P matrix to represent the model presented in fig. 1 could be

$$\begin{bmatrix} & L_1 & L_2 & L_3 & L_4 & L_5(discard\ level) \\ go\ to\ bathroom & 0.7 & 0.2 & 0 & 0 & 0 \\ take\ pajama\ off & 0.6 & 0.4 & 0 & 0 & 0 \\ take\ shower & 0.2 & 0.7 & 0.1 & 0 & 0 \\ wash\ face & 0 & 0.5 & 0.3 & 0 & 0.2 \\ get\ dressed & 0 & 0.2 & 0.6 & 0.2 & 0 \\ go\ to\ bedroom & 0 & 0.1 & 0.5 & 0.3 & 0.1 \\ go\ to\ kitchen & 0 & 0 & 0 & 0 & 1 \end{bmatrix}$$

Among the advantages of our approach, the independence between the behavior representation and the method used to learn, recognize or adapt is the most important. This separation allows us to achieve better system modularization and to use a higher number of learning methods for the same activity model [21]. In [21, 22] we constructed a learning and recognition/adaptation process that will be used in this article to obtain the input to the process presented here. However, as this is not the focus of our article, we refer the reader to our previous work [11, 21, 22].

B. Comparing Soft Partitions

The next tool used in this investigation comes from the field of clustering. This method is used herein to compute the similarity between two behaviors according to how closely actions group into levels. Let $O = \{o_1, \ldots, o_n\}$ denote n objects. When each object in O is represented by a (column) vector x, the set $X = \{x_1, \ldots, x_n\} \subset \Re^p$ is an *object data representation* of O. When each object in $o_i \in O$ has a *physical label*, O is a set of *labeled data*; otherwise, O is unlabeled. Let integer c denote the number of groups, $1 < c < n$. Clustering in unlabeled data is the assignment of one of four types of labels to each object in O. After clustering, the label vectors of the objects are the columns of c-partitions of O, which are sets of (cn) values $\{ u_{ik} \}$ that can be conveniently arrayed as $(c \times n)$ matrices, $U = [u_{ik}]$. These labels can be crisp, probabilistic, fuzzy, or possibilistic.

When clustering produces more than one candidate for partitioning a finite set of objects O, there are two approaches to validation, i.e., selection of a "best" partition, and implicitly, a best value for c, the number of clusters in O. First, one could use an internal index, which evaluates each partition separately. Second, one could compare pairs of candidate partitions to each other, or to a reference partition that purports to represent the "true" cluster structure in the objects. In [23], we generalized many of the classical indices that have been used with outputs of crisp clustering algorithms so that they are applicable for candidate partitions of any type, i.e. crisp or soft, soft comprising the fuzzy, probabilistic and possibilistic cases. In particular, we concentrated on the Rand index and its modifications. We showed that our extension of the Rand index is $\boldsymbol{O}(n)$.

Let U and V be crisp partitions of O. Here, U and V need not possess the same number of clusters, i.e., r need not equal to c ($r \neq c$). The four classical combinations for pairs of objects from $O \times O$ in clusters of U and V are: (a) paired in U and V; (b) not paired in U nor in V; (c) paired in V but not in U; and (d) paired in U but not in V [24]. The comparison of U to V with a similarity measure s begins with the $r \times c$ contingency matrix $N = UV^T$ that contains counts of the number of occurrences of each of the four types over the $n(n-1)/2$ distinct, unordered pairs in $O \times O$. Entry n_{ij} is the number of objects common to subgroups U_i and V_j. The building blocks of many similarity measures for $s(U,V)$ are the four expressions (a)-(d) below. These four calculations count the number of occurrences amongst the $n(n-1)/2$ pairs of each of the four types of unordered pairs:

$$a = \frac{1}{2} \sum_{i=1}^{r} \sum_{j=1}^{c} n_{ij}(n_{ij} - 1); \quad (2)$$

$$d = \frac{1}{2} \left(n^2 + \sum_{i=1}^{r} \sum_{j=1}^{c} n_{ij}^2 - \left(\sum_{i=1}^{r} n_{i\bullet}^2 + \sum_{j=1}^{c} n_{\bullet j}^2 \right) \right); \quad (3)$$

$$b = \frac{1}{2} \left(\sum_{j=1}^{c} n_{\bullet j}^2 - \sum_{i=1}^{r} \sum_{j=1}^{c} n_{ij}^2 \right); \quad (4)$$

$$c = \frac{1}{2} \left(\sum_{i=1}^{r} n_{i\bullet}^2 - \sum_{i=1}^{r} \sum_{j=1}^{c} n_{ij}^2 \right). \quad (5)$$

where $n_{i\bullet}$ and $n_{\bullet j}$ referring respectively to the number of objects in classes U_i and V_j, using standard "dot" notation for row and column sums.

The sums $(a+d)$ and $(b+c)$ are usually interpreted, respectively, as (the total number of) *agreements* and *disagreements* between U and V. Anderson et al. [23] tabulate a (non-exhaustive) list of 14 coefficients that have been proposed for $s(U,V)$ based on functions of a, b, c and d; Sokal and Sneath list many others [25]. In addition, Anderson et al. also present a scaling value in the case of possibilistic labels. Here, we focus on the Rand, the classical form of which is

$$s_R(U,V) = (a+d)\,/\,(a+b+c+d). \quad (6)$$

The measure $s(U,V)$ can be used to address a variety of clustering problems [23]. For example, it can be used to compare a *clustering* to a reference partition that purports to represent the "true cluster structure", measure the effect of noise or missing data with respect to a specific clustering algorithm, study the convergence of a clustering algorithm at successive iterations, perform prediction (regression), as well as compare two different clustering algorithms.

C. Similarity measure for comparing human behavior

In [11], a similarity measure is introduced for comparing pairs of learned behavior and subsequently anomaly detection. Our new measure for analyzing long term human activity tends includes three different components: (1) comparing partitions, (2) subsethood of non-discarded actions, and the (3) similarity of partial order relations.

- *Comparing soft partitions*
  We determine the similarity between pairs of behaviors according to the strength of actions grouping into similar levels. Specifically, $s(U,V)$ is used, where U and V are behavior probability matrices acquired using the procedures described in subsection IIA, i.e. $U(i,j)$ is the probability that action i belongs to level j. In [11], we presented a scaling of $s(U,V)$ to produce a [0,1] value that is more appealing to human interpretation. The formula used to compare two different behaviors is

$$s_{cp}(U,V) = s(U,V)\,/\,maximum(\,s(U,U)\,,s(V,V)\,) \quad (7)$$

- *Subsethood of Non-Discarded Actions*
  This term is included to reduce the influence of the discarded level on $s_{cp}(U,V)$. This is because U and V generally share many actions in that level, independently of the represented behavior. First, the most likely level, $L_{i,max} = argmax_j\, P(i,j)$, for each action is found. Next, the crisp sets, $R_U \subseteq H_U$ and $R_V \subseteq H_V$, of actions in which $L_{i,max}$ does not equal the discard level is found. The matrix P contains evidence about the importance of actions to a behavior and the criteria of picking all actions that are not most likely in the discard level is feature selection. The subsethood measure of non-discarded actions over R_U and R_V is

$$s_{sub}(U,V) = |R_U \wedge R_V| \,/\, |R_U \vee R_V| \quad (8)$$

where $\wedge$ is intersection, $\vee$ is union and $|\bullet|$ is cardinality. The resulting similarity is

$$s_{cp_sub}(U,V) = s_{cp}(U,V) \times s_{sub}(U,V). \quad (9)$$

- *Similarity of Partial Order Relations*
  The definition of $s_{cp_sub}(U,V)$ does not take into account the similarity between the partial order relations. That is, two behaviors may share a set of non-discarded actions and have a strong similarity of actions grouping into levels (clusters), but the order of levels is not consistent. Hence, to truly compare two behaviors, the partial order relations need to be factored into the measure. We resolve this by counting the number of disagreements between U and V and weight the disagreements by their individual importance.

  First, a $|H|x|H|$ matrix, E_U, is created for behavior matrix U. For each action, the level with the greatest probability (most likely explanation) is found, i.e. $L_{i,max}$. Next, $E_U(i,j)$ is assigned a label from the set $\{B,A,S\}$, where 'B' (before) means $L_{i,max} < L_{j,max}$, 'A' (after) means $L_{i,max} > L_{j,max}$, and 'S' (same) means $L_{i,max} = L_{j,max}$. Cell $E_U(i,i) =$ *'S'* and if $E_U(i,j)$ is 'B' ('A') then $E_U(j,i)$ is 'A' ('B'). Remember, $L_{i,max}$ is the most likely level that action i belongs to. For that reason, we cannot just count the number of disagreements in E_U. Instead, we calculate an importance value per action. For action i, $\mathrm{P_{U,i}}$ measures the ability to decide that action i belongs to some particular level,

$$\mathrm{P_{U,i}} = \max_j(\mathrm{P_U(i,j)}) - \max_{\substack{k \\ j\neq k}} \big(\mathrm{P_U}(i,k)\big) \quad (10)$$

The significance weighted calculation of the similarity of partial order relations, $s_{por}(U,V)$, is based on the set of off-diagonal upper triangular indices of E_U, i.e. all (i,j) where $j > i$. In particular, the measure uses only the subset of indices, I', in which actions i and j are not most likely discarded. Based on $P_{U,i}$ and $E_U(\mathrm{i,j})$, the similarity of partial order relations is now defined as

$$s_{por}(U,V) = 1 - \left(\textstyle\sum_{(i,j)\in I'} \emptyset(\,\mathrm{E_U(i,j)}\,,\mathrm{E_V(i,j)}\,)\right)/|I'|, \quad (11)$$

where

$$\emptyset\big(\mathrm{E(i,j)},\mathrm{E_V(i,j)}\big) = \begin{cases} 0 & if\ \mathrm{E_U(i,j)} = \mathrm{E_V(i,j)} \\ \min\,(\mathrm{P_{U,i}},\mathrm{P_{V,i}}) & else \end{cases}, \quad (12)$$

and the final measure for comparing human behaviors is

$$s_{final}(U,V) = s_{cp}(U,V) \times s_{sub}(U,V) \times s_{por}(U,V) \quad (13)$$

With this measure, we are able to detect longer time period changes in the *same* behavior (days, weeks, months, etc). The anomaly detection approach in this article is independent of the success of any short time period recognition algorithm. That is, if a serious short-term event is undetected, we still expect significant change in longer time period behavior. In [11], we also presented a time series normalization of $s(U,V)$,

$$norm_1(U,V) = maximum(\, s(U,U)\,, s(V,V)\,), \quad (14)$$

$$norm_2(U,\{V_1,\dots,V_n\}) = maximum(\,\{\, norm_1(U,V_1)\,,\dots\,, norm_1(U,V_n)\,\}\,), \quad (15)$$

$$s_{cp2}(U,V_i) = s(U,V_i) \,/\, norm_2(U,\{V_1,\dots,V_n\}), \quad (16)$$

where U is the reference behavior and V_i $(1 \le i \le N)$ is an adapted behavior. We update the behavior model each day. The final measure presented in [11] is

$$s_{final2}(U,V_i) = s_{cp2}(U,V_i) \times s_{sub}(U,V_i) \times s_{por}(U,V_i) \quad (17)$$

Fig. 2 is an example time series from [11] for the behavior 'Wake up". The annotations describe what the person was doing during the one year time period. We see that the proposed similarity measure captures these important changes.

III. LINGUISTIC SUMMARIZATION

Using the measure discussed in section 2c, we are able to study longer time period changes in behavior. However, this representation is not the most understandable by nurses, social workers, families or residents. Our objective is to produce linguistic summarizations of the time series. Example summarizations include *"the quality of the 'wake up' behavior is decreasing in the last month"*, *"the quality of the 'have breakfast' behavior is slowly increasing in the last week"*, or *"the quality of 'morning routine' is constant but highly unstable in the last month"*. These examples illustrate cases in which less information is more useful. That is, summarization identifies the important trends and it is understandable by a domain expert. In the following sections, we present a method to measure the type and amount of change as well as the stability in comparing behavior time series. We then present a fuzzy set theoretic approach for linguistically interpreting the numeric values for the eldercare problem domain.

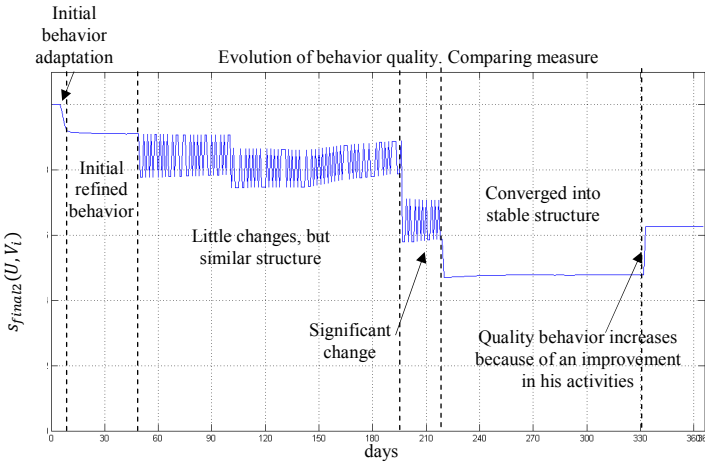

Fig 2. Output of our comparing behavior approach [10] for 360 days of adapted behavior for the activity "Wake up" (which is reported in table 1). Annotations show what happened in this year. Each day is compared to an initial base refined behavior (the base-line behavior).

A. Temporal resolution of summarization

As already discussed, in Kacprzyk et al. [20] a time series is algorithmically segmented. The proposed technique can address identifying trends that take varying amounts of time to occur, but only one set of summarizations are produced. That is, different summarizations could be produced if the problem is viewed in different ways, like being sampled differently. For example, a summary of increasing might be produced if we analyzed day by day, while a summarization of constant might be produced if the time scale is month. Our objective is not to study automatically segmented global trends, rather trends for a user specified time scale. We are interested in detecting gradual changes in the elder's behavior as soon as possible. Kacprzyk et al. differentiate between global trends, which concern the entire time series (or some, probably large, part of it), and partial trends concerning a smaller time span (e.g. a window). Our focus is on the second (partial trends). We provide the person with the option of selecting the time period that he/she would like summarized. That defined time window has a considerable influence on the linguistic summarizations produced. Thus, the user will select it based on a specific hypothesis to be tested. For example, has there been change this week, this month, etc.

B. Partial trend summarization using linear regression

The global trend segmentation and resulting variability calculations of Kacprzyk et al. did not work particulary well for our problem domain. Their focus is stock market analysis and financial domains. The particular trends that we are looking to identify are not reliably segmented using their technique. Instead, we rely on the well-known method of linear regression in order to numerically summarize a partial trend time window. Linear regression is used here to fit a predicted model (linear equation) to observed data, a window of our time series. We calculate the slope of the estimated linear equation, which resides in $[-90°, 90°]$. Additionally, we compute the mean squared error (mse), which varies in [0, 1]. This simple but effective method provides us with the two desirable quantities, the angle of the line segment that characterizes the rate of change of the time series and the variability of the samples to the estimated linear equation.

Herein, linguistic summarization of change in human

behavior over long time periods according to a reference baseline model for a given user time resolution consists of the generation of understandable sentences of the form:

Behavior [X] is [angle] with [mse] in a time period equal to [time window].

C. Fuzzy sets

In this article, we leverage the concept of *dynamics of change* (or speed of change) identified by Kacprzyk et al [20]. The authors propose linguistic terms corresponding to various inclinations of a trend line: *quickly decreasing, decreasing, slowly decreasing, constant, slowly increasing, increasing and quickly increasing*. Each term represents a fuzzy granule of direction. Following the authors' indication, we define the following trapezoidal fuzzy sets on the angle domain in degrees, and illustrated in fig. 3:

- *Quickly decreasing* [-90 -90 -80 -60]
- *Decreasing* [-75 -60 -40 -25]
- *Slowly decreasing* [-40 -30 -20 -10]
- *Constant* [-20 -10 10 20]
- *Slowly increasing* [10 20 30 40]
- *Increasing* [25 40 60 75]
- *Quickly increasing* [60 80 90 90].

Next, we define a linguistic variable for the concept stability of a time series in a user defined time window. While this is similar to Kacprzyk's notion of variability, they are calculated differently. Our terms for stability are defined using linear regression, specifically mse. The fuzzy sets represent the possible levels of instability existing in a time window. We define five terms: *no instability, low instability, medium instability, high instability* and *extreme instability*. The trapezoidal membership functions for these fuzzy sets are (see fig. 4 for a graphical representation):

- *no instability* [0 0 0.0001 0.0012]
- *low instability* [0.0001 0.0005 0.001 0.0014]
- *medium instability* [0.0001 2 0.002 0.004 0.0048]
- *high instability* [0.004 0.009 0.04 0.07]
- *extreme instability* [0.05 0.071 1 1].

These fuzzy sets have been defined as a generalization of a wide range of cases studied, using the trial and error technique.

IV. EXPERIMENTS

Our experiments study different common elderly behaviors, such as Wake Up, Morning Routine or Have Breakfast. Here, we show results for *Wake Up* and *Morning Routine*, but more results can be found in [11].

As previously indicated, the behavior model is an abstract architecture completely independent of method used to learn, recognize or adapt it. Therefore, our outcomes will be also independent of the type of sensors used to detect the user activities required to those processes. In order to test a wide range of human behavior scenarios, we have developed an

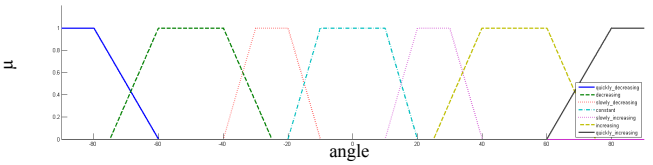

Fig. 3: Fuzzy sets for the angle of the estimated linear equation.

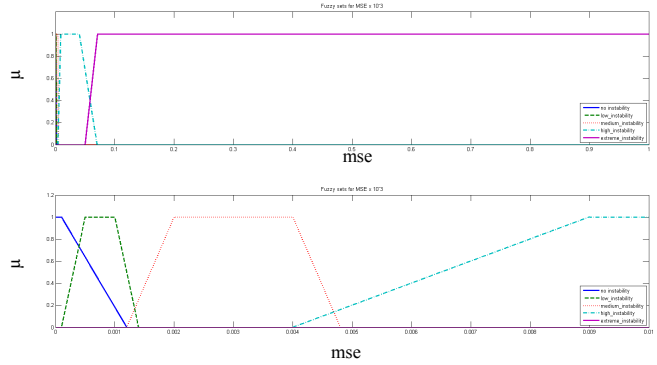

Fig. 4: Fuzzy sets for the mse in the user specified time window.

algorithm that takes action and temporal constraints and generates *synthetic data sets* [21, 22]. The input to this algorithm consists of a set of constraints (table 1), where the partial order relations between the actions are defined. These data sets are used in both learning and recognition [21]. We generated the following data sets to explore how the proposed measure responds to different scenarios.

- DS_1: The resident always performs the behavior correctly, i.e. normal behaviors. Herein, DS_1 is used to learn the initial baseline model. It has 365 days worth of behavior.
- DS_2: The resident has a degenerative disease, and his behavior deteriorates continuously and slowly.
- DS_3: The resident has a *catastrophic event*, e.g. a fall. This event is severe and it results in restricted mobility. After the event, a user's routine has changed significantly as a result. However, after a period of time the user is able to start *rehabilitation*, and his behavior improves. There

TABLE 1: BEHAVIOR AND TEMPORAL CONSTRAINTS

Behavior	Order relationship constraints	Temporal constraints
B_1 (Wake up)	AsleepInBed ≺ AwakeInBed AwakeInBed ≺ GetOutOfBed GetOutOfBed ≺ GetSlippers GetSlippers ≺ GotoBathroom	6:50 to 7:10
B_2 (Morning Routine)	GotoBathroom ≺ { UseToilet, TurnShowerOn} {UseToilet, TakePijamaOff , TurnShowerOn } ≺ TakeShower TakeShower ≺ { TurnShowerOff, UseTowel, BrushTeeth, WashFace, CombHair} UseTowel ≺ GetDressed {TurnShowerOff, UseToilet, BrushTeeth, CombHair, WashFace } ≺ GotoBedroom	7:00 to 7:40

TABLE 2: BEHAVIOR CONSTRAINTS AFTER CATASTROPHIC EVENT

Behavior	Order relationship constraints
B_1^* (Wake up)	AsleepInBed ≺ AwakeInBed AwakeInBed ≺ GetOutOfBed GetOutOfBed ≺ GotoBathroom
B_2^* (Morning Routine)	GotoBathroom ≺ { GetDressed, UseToilet, BrushTeeth, CombHair, WashFace} { UseToilet, BrushTeeth, CombHair, WashFace} ≺ GotoBedroom

are 110 days before the event, 1 day in which the event occurred (day 111), 139 days of convalescence and others 115 days of different behavior afterwards when the user is undergoing rehabilitation. During the rehabilitation, his behavior is improving slowly.

The changes in behavior due to the catastrophic event are shown in table 2.

A. *Experiment 1. Degenerative disease*

In the first experiment, we show how our system is able to detect a degenerative disease. First, we learn a correct behavior using DS_1. After that, we use DS_2 as input to the recognition and adaptation process. Once the process has finished, the evolution graph is generated using the method in [11]. This time series is used as input to our linguistic summarization method. First of all, we define the *time window resolution*. Although the system is able to deal with different resolutions, here we study the results monthly in order to simplify the problem.

The results for *Wake up* behavior are shown in fig. 5. The graph represents the measured change in behavior. The continuous curve is the similarity measure, while the discontinuous lines are the linear regression results at each non-overlapping window. The related linguistic summarization is presented in table 3.

Fig. 5 shows a behavior whose quality is decreasing very slowly. This corresponds to a resident with a degenerative disease reducing the resident mobility and, therefore, changing his normal activity. However, there are time periods when his/her behavior is considered constant although not stable. Our summary is able to detect those moments of instability, describing it as medium in *February* or low in *November,* when the behavior has a little decrease and later an increase.

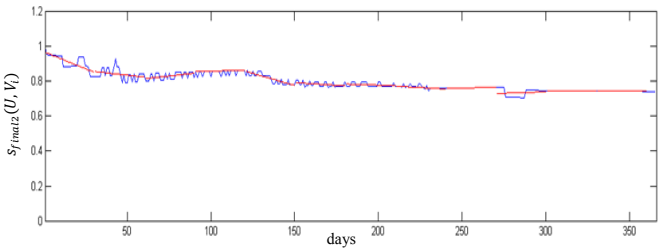

Fig. 5: Similarity of adapted behavior to a learned reference behavior for "Wake up" behavior. In this situation, we simulate a user with a degenerative disease. The rate of change for this behavior is slow.

TABLE 3: LINGUISTIC SUMMARIZATION OF TIME SERIES IN FIGURE 5

Days	Linguistic Summarization
1-30	B_1 is *slowly decreasing* in a time period equal to *30 days*
31-60	B_1 *is constant* with *medium instability* in a time period equal to *30 days*
61-90	B_1 *is constant* with *low Instability* in a time period equal to *30 days*
91-120	B_1 *is constant* with *no instability* in a time period equal to *30 days*
121-150	B_1 *is slowly decreasing* in a time period equal to *30 days*
151-180	B_1 *is constant*, with *no instability* in a time period equal to *30 days*
181-210	B_1 *is constant*, with *no instability* in a time period equal to *30 days*
211-240	B_1 *is constant*, with *no instability* in a time period equal to *30 days*
241-270	B_1 *is constant*, with *no instability* in a time period equal to *30 days*
271-300	B_1 *is constant*, with *low Instability* in a time period equal to *30 days*
301-330	B_1 *is constant*, with *no instability* in a time period equal to *30 days*
331-365	B_1 *is constant*, with *no instability* in a time period equal to *30 days*

B. *Experiment 2. Catastrophic event and rehabilitation*

For the second experiment, once again DS_1 is used to learn a reference behavior. However, DS_3 is used during the recognition and adaptation process. The database represents user activities for a year. The user suffers a *catastrophic event*, as a fall. This event provokes the elder to change his/her activity significantly, and then undergo *rehabilitation*. The linguistic summarization for *Morning Routine* behavior obtained from these results is presented in table 4 regarding fig. 6.

We would like to emphasize how the linguistic summarization is able to delineate the important changes occurring during the year. During the first three months, the behavior is *constant* because the elder maintains his/her normal activities. When the catastrophic event happens, at the middle of the fourth month, the behavior model adapts to the new normal. The model requires some time period to adapt completely. However, it does reflect those little changes, as does the linguistic summary. The forth month is characterized as *medium instability*, since the behavior is summarized as *constant*. During the fifth and sixth months, the behavior changes significantly (declines), resulting in *behavior decreasing* and *behavior slowly decreasing* respectively. These months are included in the convalescence period: the user stabilizes her behavior and she recovers from the catastrophic event. The ninth month is when the elder starts rehabilitation. As expected, rehabilitation is not an instant process, it requires effort and time. During the ninth and tenth months, she is changing her behavior slowly without great advance (*behavior constant* and *low instability*). Nevertheless, after two months undergoing rehabilitation, the elder improves her behavior more rapid than before (*behavior increasing*), until a point where the behavior is stable again (*behavior constant* and *low instability*).

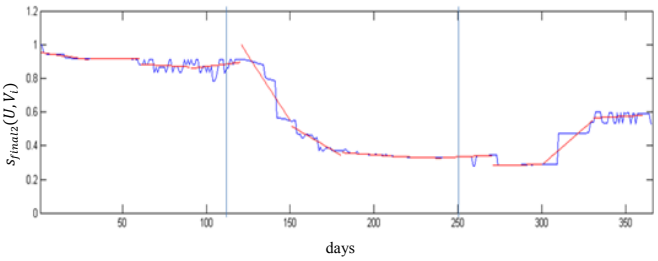

Fig. 6: Similarity of adapted behavior to a learned reference behavior for "Morning Routine" behavior. This event, e.g. a fall, results in a large change in subsequent behavior (i.e. table 2). We also simulate a scenario in which the user undergoes rehabilitation and his/her behavior improves but never goes back to what it was before.

TABLE 4: LINGUISTIC SUMMARIZATION OF TIME SERIES IN FIG. 6

Days	Linguistic Summarization
1-30	B_2 is *constant*, with *no instability* in a time period equal to *30 days*
31-60	B_2 is *constant*, with *no instability* in a time period equal to *30 days*
61-90	B_2 is *constant* with *low Instability* in a time period equal to *30 days*
91-120	B_2 is *constant* with *medium instability* in a time period equal to *30 days*
121-150	B_2 is *decreasing* in a time period equal to *30 days*
151-180	B_2 is *slowly decreasing* in a time period equal to *30 days*
181-210	B_2 is *constant*, with *no instability* in a time period equal to *30 days*
211-240	B_2 is *constant*, with *no instability* in a time period equal to *30 days*
241-270	B_2 is *constant* with *low Instability* in a time period equal to *30 days*
271-300	B_2 is *constant* with *low Instability* in a time period equal to *30 days*
301-330	B_2 is *increasing* in a time period equal to *30 days*
331-365	B_2 is *constant* with *low Instability* in a time period equal to *30 days*

V. CONCLUSIONS

In this paper, we presented a method to produce a linguistic summarization about the quality of an elder's behavior as it adapts over time. In previous work, we presented a method to obtain behavior representations [21, 22] and a measure to analyze change in behavior models [11]. This paper is focused on defining a fuzzy set-based method to summarize the measured information, with the goal of reporting information in a natural language to nurses, doctors or social workers, which makes it simpler for them to understand what is going on. We introduced a user-defined time resolution approach that allows the expert to investigate different time specific health queries. In addition, we defined a set of features that allows us to detect if the behavior is changing, the speed of the change and the stability of the behavior. Finally, we tested our method in a simulated resident scenario to show how the method helps a person (e.g. elder, caregiver, social workers or even family member) to monitor the activities of an elderly resident.

Future work includes the following. First, a synthetic data set was used to test different behavior scenarios. We will investigate using the LA approach from the University of Granada, Spain on real sensor data collected from the assisted living facility, TigerPlace [2], in Columbia MO, USA. Secondly, we propose to obtain the expert opinion to evaluate the method and improve it by adding more attributes. Both the membership functions and the methods of producing the linguistic summarization can be learned.

VI. ACKNOWLEDGMENT

This work has been partially supported by TIN2009-14538-C02-01 project, I+D+I national program from Spain Government and by National Science Foundation NFS IIS-0428420.

REFERENCES

[1] M. Skubic and M. Rantz. (2011) Active elders: Center for eldercare and rehabilitation technology. [Online]. Available: http://eldertech.missouri.edu/

[2] M. Rantz, M. Aud, G. Alexander, D. Oliver, D. Minner, M. Skubic, J. Keller, Z. He, M. Popescu, G. Demiris, , and S. Miller, "Tiger place: An innovative educational and research environment," AAAI in Eldercare: New Solutions to Old Problems, Tech. Rep, November 2008.

[3] D. Cook, M. Youngblood, I. Heierman, E.O., K. Gopalratnam, S. Rao, A. Litvin and F. Khawaja. "Mavhome: An agent-based smart home", in *Pervasive Computing and Communications, 2003. (PerCom 2003). Proceedings of the First IEEE International Conference on*, march 2003, pp. 521 – 524.

[4] F. Doctor, H. Hagras, and V. Callaghan, "A fuzzy embedded agentbased approach for realizing ambient intelligence in intelligent inhabited environments," *Systems, Man and Cybernetics, Part A: Systems and Humans. IEEE Transactions on*, vol. 35, no. 1, pp. 55–65, jan. 2005.

[5] P. Rashidi and D. Cook. "Keeping the resident in the loop: Adapting the smart home to the user". *Systems,Man and Cybernetics,Part A:Systems and Humans. IEEE Transactions on*, vol.39, no.5, pp.949 –959. sept.2009

[6] J.A. Kientz, S.N.Patel, B. Jones, E. Price,E.D. Mynatt, G.D. Abowd, "The georgia tech aware home", in *CHI '08: CHI '08 extended abstracts on Human factors in computing systems*, ser CHI EA '08. New York, NY, USA: ACM, 2008, pp. 3675–3680.

[7] R.-M. Droes, M. Mulvenna, C. Nugent, D. Finlay, M. Donnelly, M. Mikalsen, S. Walderhaug, T. v. Kasteren, B. Krose, S. Puglia, F. Scanu, M. O. Migliori, E. Ucar, C. Atlig, Y. Kilicaslan, O. Ucar, and J. Hou, "Healthcare systems and other applications," *Pervasive Computing, IEEE*, vol. 6, no. 1, pp. 59 –63, jan.-march 2007.

[8] M. Philipose, K. P. Fishkin, M. Perkowitz, D. J. Patterson, D. Fox, H. Kautz, and D. Hahnel, "Inferring activities from interactions with objects," *Pervasive Computing, IEEE*, vol. 3, no. 4, pp. 50 – 57, oct.-dec. 2004.

[9] U. Naeem and J. Bigham, "A comparison of two hidden markov approaches to task identification in the home environment," in *Proceedings of the 2nd International Conference on Pervasive Computing and Applications*, 2007, pp. 383–388.

[10] Acampora, G., Loia, V. "Fuzzy control interoperability and scalability for adaptive domotic framework". *Industrial Informatics, IEEE Transactions on,* vol. 1, no. 2, pp. 97 – 111, may 2005.

[11] Derek T. Anderson, María Ros, James M. Keller, Manuel P.Cuéllar, Mihail Popescu, Miguel Delgado and Amparo Vila. Similarity measure for anomaly detection and comparing human behaviors. Submitted to IEEE Transactions on Knowledge and Data Engineering, 2011.

[12] Stone E, Anderson D, Skubic M & Keller J, "Extracting Footfalls from Voxel Data," *Engineering in Medicine and Biology Society(EMBC), 2010 Annual International Conference of the IEEE,*vol.1, no. 1, sept. 2010, pp. 1119 –1122.

[13] Wang F, Skubic M, Abbott C & Keller J, "Body Sway Measurement for Fall Risk Assessment Using Inexpensive Webcams," *Engineering in Medicine and Biology Society(EMBC), 2010 Annual International Conference of the IEEE,*vol.1, no.1, sept 2010, pp. 2225 –2229.

[14] Wang F, Stone E, Dai W, Skubic M & Keller J, "Gait Analysis and Validation Using Voxel Data," in *Engineering in Medicine and Biology Society, 2009 EMBC. Annual International Conference of the IEEE*, sept, 2009, pp. 6127–6130.

[15] R.R. Yager. "A new approach to the summarization of data". *Information Sciences*, vol. 28, no. 1, pp. 69 – 86, 1982.

[16] J. Kacprzyk, RR. Yager, "Linguistic summaries of data using fuzzy logic". *International Journal of General Systems* vol. 30, no. 2, pp. 133 – 154, 2001.

[17] J. Kacprzyk, RR. Yager, S. Zadrozny, "A fuzzy logic based approach to lingusitic summaries of database". *International Journal of Applied Mathematics and Computer Science*, vol. 10, pp. 813–834, 2000.

[18] Kacprzyk, Janusk and Wilbik, Anna. "Temporal Linguistic Summaries of Time Series Using Fuzzy Logic", in *Information Processing and Management of Uncertainty in Knowledge-Based Systems. Theory and Methods,* ser. Communications in Computer and Information Science, 2010, vol. 80, pp. 436–445.

[19] Derek Anderson, Robert H. Luke, James M. Keller, Marjorie Skubic, Marilyn Rantz, and Myra Aud. "Linguistic summarization of video for fall detection using voxel person and fuzzy logic". *Computer Vision and Image Understanding,* vol. 113, no. 1, pp. 80 – 89, 2009

[20] J. Kacprzyk, A. Wilbik, and S. Zadrony. "Linguistic summarization of time series using a fuzzy quantifier driven aggregation". *Fuzzy Sets Syst.*, vol. 159, pp. 1485–1499, June 2008

[21] Cuellar, MP., Ros M., Delgado M, Vila A, Detection of abnormal human activities by means of learning automata. Submitted to IEEE Trans. on Systems, Man and Cybernetics, Part A .

[22] Ros M., Cuellar, MP., Delgado M, Vila A, Online recognition of human activities and adaptation to habit changes by means of learning automata and fuzzy temporal windows. Submitted to Spec. Iss.: On-Line Fuzzy ML and DM. Information Sciences.

[23] D. T. Anderson, J. C. Bezdek, M. Popescu, and J. M. Keller, "Comparing Fuzzy, Probabilistic, and Possibilistic Partitions," *Fuzzy Systems, IEEE Transactions on*, vol. 18, no. 5, pp. 906 –918, oct. 2010.

[24] Hubert, L. and Arabie, P., "Comparing partitions". *Journal of Classification*, vol. 2, pp. 193–218, 1985.

[25] Sneath, P. H. A. and Sokal, R. R.. *Numerical Taxonomy - The Principles and Practice of Numerical Classification*, Freeman, 1973.

2011 IEEE International Conference on Fuzzy Systems
June 27-30, 2011, Taipei, Taiwan

Fuzzy Knowledge Approach to Automatic Disease Diagnosis

Carmen De Maio, Vincenzo Loia
Dipartimento di Informatica
Università degli Studi di Salerno
Fisciano (SA), Italy
{cdemaio, loia}@unisa.it

Giuseppe Fenza, Mariacristina Gallo
CORISA
Università degli Studi di Salerno
Fisciano (SA), Italy
{gfenza, mcgallo}@corisa.it

Roberto Linciano, Aldo Morrone
Azienda Ospedaliera San Camillo-Forlanini
Roma, Italy
rlinciano@yahoo.it,
amorrone@scamilloforlanini.rm.it

Abstract— **Applying best available evidences to clinical decision making requires medical research sharing and (re)using. Recently, computer assisted medical decision making is taking advantage of Semantic Web technologies. In particular, the power of ontologies allows to share medical research and to provide suitable support to the physician's practices. This paper describes a system, named ODINO (Ontological DIsease kNOwledge), aimed at supporting medical decision making through semantic based modeling of medical knowledge base. The system defines an ontology model able to represent relations between medical disease and its symptomatology in a qualitative manner by using fuzzy labels. Medical knowledge is defined according with physician experts members of INMP[1] (National Institute for Health Migration and Poverty). The main aim of ODINO is to provide an effective user interface by using ontologies and controlled vocabularies and by allowing faceted search of diseases. In particular, this work mashes the capabilities of Description Logic reasoners and information retrieval techniques in order to answer to physician's requests. Some experimental results are given in the field of dermatological diseases.**

Keywords- Semantic Web, Ontology, Clinical DSS, Diagnosis

I. INTRODUCTION

Traditional approaches to the medical diagnosis practice have many drawbacks, like as: the huge growth of biomedical information has made difficult the retraining for the individual doctors; the poor dissemination of effective research results; and so on.

New trend is the Evidence-Based Medicine (EBM) which aims to apply the best available evidences gained from the scientific methods to clinical decision making. The challenge of EBM is to define a systematic approach to integrate research results with clinical expertise and patient preferences, and exploit them during the medical diagnosis. So, it is necessary to provide a suitable model to structure medical results and to perform the knowledge spreading and sharing.

There are several ongoing efforts aimed at developing formal models of medical knowledge and reasoning to design decision support systems. These efforts have focused on representing content of clinical guidelines and their logical structure. Semantic Web technologies and ontologies are enabling elements to achieve these aims. In fact, today ontologies are assuming increasingly important role in the area of knowledge based decision support systems by introducing capabilities in terms of logic based reasoning.

This work presents ODINO, a multilingual web based application, that addresses the aim to use semantic web technologies in order to support medical practices through an effective user interface. In particular, ontologies are used to model available medical diseases features (e.g., skin diseases), symptomatologies, treatment protocols and so on. The relations between symptomatologies (i.e., symptoms and signs) and available diseases are represented by using fuzzy labels resulting from the analysis of medical expertise included in [1]. Standard formalisms, like OWL and SKOS, are used to specify domain knowledge and controlled vocabularies, i.e., diseases, symptomatology, active ingredients and clinical tests according to standard specifications, like as ICD-9-CM[2].

Ontologies, controlled vocabularies and information retrieval techniques are exploited to provide typical capabilities of Semantic Web portals [2] and medical decision support. Some of the main features of the system are:

- disease catalogue browsing including images, symptoms and signs, treatments, etc. to support rapid training;
- preliminary medical diagnosis, indeed medical knowledge querying by specifying symptoms, signs and complications, to find eligible diseases;
- faceted search of diseases by enabling multi-criteria selections (i.e., symptomatologies, complications, active ingredients, etc.) to support differential diagnosis.

ODINO results are explained to physician by highlighting symptoms/signs/complications that match the retrieved diagnosis and by suggesting other important features of founded diseases.

The paper is organized as follows. Section II introduce some related works in the applicative domain. Section III describe the knowledge layer of ODINO. The medical decision support methodology is described in Section IV. Then, Section V details features of system and provides the results of the case

[1] http://www.inmp.it/

[2] International Statistical Classification of Diseases, 9th Revision, Clinical Modification

study. Finally, there are conclusions of the paper.

II. Related Works

A medical diagnosis problem consists of the identification of a disease and corresponding treatments that treat it.

In the past years, a great deal of artificial intelligence research has been directed towards the development of expert systems for problem solving in medical diagnosis domain. As examples of developed medical expert systems, we mention: Mycin [3], DXplain [4], Puff [5], Cadiag2 [6], Gideon [7] and Casnet [8]. In particular, interesting approach is used in Cadiag2 that exploits fuzzy set theory to model medical concepts, and fuzzy logic to emulate diagnostic processes. As argued in [9], [10], fuzzy sets offer linguistic label that well approximate medical texts. In addition, fuzzy logic provides reasoning methods capable of making approximate inference [11],[12]. So, fuzzy set theory provides appropriate basis for the development of a computer-based diagnosis system [13]. Nevertheless, there are some problems related with these expert systems consisting in their limited [14],[15]: flexibility, adaptability, extendibility and cooperation capability. Strictly related to our approach, some works, such as [16] and [17], highlight benefits of mashing semantic and fuzzy logic in healthcare. Analogously, ODINO exploits: Semantic Web formalism to represent fuzzy relations between diseases and symptomatologies; and soft computing techniques to arrange diseases that share these relations.

Conversely, solutions like MEDBOLI [18] and ODDIN [19] use Semantic Web Technologies to develop a software that allows users to make diagnosis. In fact, since in medical discipline homogeneity of terminology is mostly problematic, the semantic technologies can be exploited to make known machine-readable latent relationships [20]. Ontologies allow users to understand meaning of each element, and improve reasoning [21], [22]. Regarding efforts which apply semantic techniques, initiatives such as OpenGalen [23] should be mentioned, a not-for-profit organization which provides downloadable open source medical terminology. Other initiatives include, for example, OBO Foundries [24], a collaborative experiment among developers of science-based ontologies. Within the scope of this research there are many resources in use such as Biological Ontologies [25], Ontology-based Support for Human Disease Study and Medical Ontologies to support human disease research and control [26], "relations in biomedical ontologies" [27], and SNOMED CT, a concept-oriented controlled vocabulary [28].

However, today, semantic annotation of Web content with metadata is not very common on health websites, but it is sometimes mandated by, e.g., government standards. The annotation processes are often tedious and require capability in the use of large vocabularies, such as Medical Subject Headings (MeSH)[3]. In this perspective, one of the major contribution of ODINO is that diseases are semantically annotated by using typical standards and controlled vocabularies of medical domain, as well as ICD9. These standards are exploited in order to provide feature of faceted based navigation of diseases. Furthermore, thanks to the benefits of semantic technologies usage (flexibility and configurability of the system), faceted navigation supports multi-criteria selection to discover right diseases. In this sense, ODINO was inspired by previous semantic portals such as SWED [2], the MultimediaN E-culture demonstrator [28] and HealthFinland [30]. Another contribution of ODINO is the definition of sharable *Medical Disease Ontology* model capable to represent relation degree between disease and symptoms coming from statistical analysis included in the book [1].

[3] http://www.nlm.nih.gov/mesh/

III. Knowledge Layer

ODINO is a knowledge based system that provides capabilities in terms of clinical decision support system and medical semantic web portal. In particular, ODINO makes an intensive usage of ontologies, controlled vocabularies and other standards typical in the medical domain. This section provides details about medical knowledge modeling of ODINO.

A. Technologies and Standards

Following sections provide some references to used technologies and standards, and introduce their roles in ODINO. Semantic technologies (i.e., OWL and SKOS) have been used to represent medical diseases. On the other hand, knowledge developed in ODINO have been aligned with international standard classification of medical diseases available in ICD9-CM.

1) OWL

Ontologies play an important role in ODINO. Generally, ontologies enable knowledge sharing, exchanging and reusing. Standardization of ontology languages has been an important issue in W3C for years. OWL[4] (Web Ontology Language) is their result and is the standard for ontology definition in the last decade. OWL can be used to explicitly represent the meaning of terms and their relationships. Furthermore, OWL has more facilities for expressing meaning and semantics than others W3C's standards and thus fosters availability of machine interpretable content on the Web. In particular, OWL has three sublanguages with different expressive power: OWL Lite, OWL DL, and OWL Full, respectively. OWL is based on XML and RDF and all data in an OWL file can be represented as a set of RDF triples.

In this work, we follow W3C's recommendation to build ontologies and construct knowledge bases according to the OWL-DL restrictions. In particular, a *Medical Disease Ontology* has been defined as described in Section III.C.

2) SKOS

SKOS[5] (Simple Knowledge Organization System) is a common data model for knowledge organization systems such as thesauri, classification schemes, subject heading systems and taxonomies. Using SKOS, a knowledge organization system can be expressed as machine-readable data. It can be exchanged between computer applications and published in a machine-readable format in the Web.

[4] http://www.w3.org/TR/owl-features/

[5] http://www.w3.org/TR/skos-reference/#L895

SKOS is used in our system together with OWL in order to express and share knowledge about medical domain. In particular, ODINO exploits SKOS to write vocabularies and taxonomies, like as: symptomatologies, diseases, drugs, etc. (as described in Section III.B). On the other hand, OWL is used to represent the formal model of disease ontology by defining axioms and constraints.

3) ICD-9-CM

The International Statistical Classification of Diseases and Related Health Problems (ICD) is a way to code and organize diseases and a wide variety of signs, symptoms, abnormal findings, complaints, and external causes of injury or disease, published by the World Health Organization [6] (WHO). It assigns a unique up to six characters long code to every health condition.

In this work, the ninth version of ICD (ICD-9) has been used. In particular, ODINO uses ICD9 - Clinical Modification (ICD-9-CM) that provides additional morbidity details than ICD9. ICD9-CM has been applied to align controlled vocabularies deployed during the knowledge base design. This alignment provides shareability of the knowledge base deployed for ODINO.

B. Controlled Vocabularies & Taxonomies

Some controlled vocabularies and taxonomies (i.e., diseases, symptomatology, clinical tests, active ingredients) have been deployed in ODINO by using SKOS technology. Generally, following SKOS properties have been used to represent vocabularies:

- *preferredLabel* (in both Italian and English languages), to define the favorite name of concept;
- *alternateLabels* (in both Italian and English languages), to associate alternative terms to the same concept in order to specify synonym, and so on;
- *hiddenLabel*, to associate the right ICD-9-CM code to the defined concepts (i.e., disease, symptom, etc.) taking into account results from the alignment process;
- *exactMatch,* to eventually specify relation between concepts with equivalent meaning;
- *broader* and *narrower* to specify hierarchical relations among concepts. These properties are enabling elements to create taxonomies and to support faceted navigation as described below in Section V.C;
- *prefSymbol* and *altSymbol* properties, to join one or more images to concept.

In particular, *exactMatch* allows to maintain ICD9-CM coding and to update the knowledge base with alignment to others classification systems (such as ICD-10 or ICD-11).

Controlled vocabularies and taxonomies developed in ODINO are:

- *Symptomatology* – that contains definitions of concept concerning symptoms and signs, like as: paresthesia, anhidrosis, plaque of psoriasis, etc.. Fig. 1 shows an example of SKOS concept modeling a symptomatology and their hierarchical relations;
- *Disaeses* – that contains medical diseases, their characteristics and hierarchical relations, like as: leprosy, malaria, AIDS, etc.. In particular, broader and narrower properties, in SKOS, allow to define a hierarchy of diseases;
- *Clinical Tests* – that models clinical and laboratory tests useful in diagnostic process, like as: haemochrome, urinalysis, specific blood tests for syphilis, etc.
- *Active ingredients* – that defines the drugs suitable for a specific disease treatment, like as: Dapsone, Rifampicin, Antacids, etc.. Since, ICD9 doesn't contain any drug classification, this vocabulary is not aligned with it.

C. Medical Disease Ontology

This section describes main aspects of knowledge models developed in ODINO. An ontology named *Medical Disease Ontology* has been defined. Through a set of properties and concepts, this ontology models disease characteristics and relations. In particular, *Medical Disease Ontology* includes the definition of a correlation degree between disease and its symptomatology by using fuzzy labels. These properties lead system's diagnosis processes and aid disease information consultation.

One of the main class defined is the concept of Disease which identifies condition of medical disease that causes pain, dysfunction, distress, social problems, and/or death, to afflicted person. Fig. 2 shows a sketch of the ontology by illustrating the relations between *Disease*, *Symptom/Sign* and *Complication* classes. In particular:

- *Symptom/Sign* is the class identifying symptom or sign that influences a disease. Many instances of *Symptom/Sign* may be associated to the same *Disease*. So, the relation *"has symptom"* hasn't any cardinality restriction.
- *Complication* is a medical disease or symptom that represents an unfavorable evolution of disease, health condition or medical treatment. Analogously with *"has symptom",* the relation *"has complication"* hasn't any

```
<owl:Thing rdf:about="#Sin157">
  <rdf:type rdf:resource="&skos;Concept"/>
  <skos:prefLabel xml:lang="en">Hand swelling</skos:prefLabel>
  <skos:prefLabel xml:lang="it">Edema delle mani<skos:prefLabel>
  <skos:altLabel xml:lang="en">Hand edema</skos:altLabel>
   <skos:hiddenLabel>729.81</skos:hiddenLabel>
   <skos:prefSymbol>edema1.jpg</skos:prefSymbol>
   <skos:altSymbol>edema2.jpg</skos:altSymbol>
   <skos:inScheme rdf:resource="#Symptomatology "/>
</owl:Thing>
```

Figure 1. An *example* of symptom specification in SKOS.

[6] http://www.who.int/en/

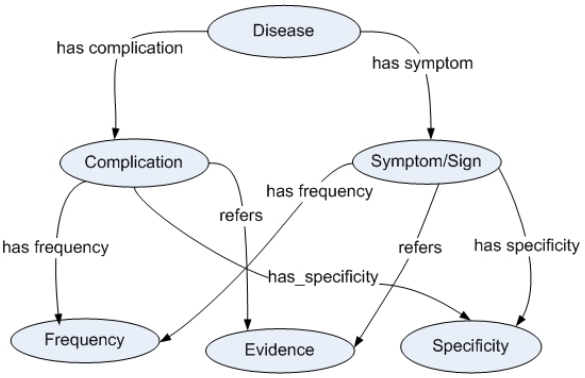

Figure 2. A sketch of *Medical Disease Ontology: Disease, Complication* and *Symptom/Sign.*

cardinality restriction.

Complication and *Symptom/Sign* are themselves related with other classes:

- *Evidence,* that represents the bridging element with the *Symptomatology* SKOS vocabulary;
- *Specificity* and *Frequency,* that allow to indicate how much *Complication* or *Symptom/Sign* implies the presence of that disease.

Furthermore, as shown in Fig. 3, *Disease* is also related with *Clinical test* class. *Clinical test* identifies each possible clinical, laboratory and diagnostic test. Analogously with *Symptom/Sign* and *Complication*, the model foresees the specification of *Precision* degree between a *Clinical test* and a *Disease* (see Fig. 3). In particular, the *Precision* defines how much a *Clinical test* result determines the presence of specific disease.

Frequency, Specificity and *Precision* are enumeration classes defined by using *oneOf* construct available in OWL. More precisely, we have defined, for each of them, some individuals that identify fuzzy labels. Values assumed by these relations are obtained from the analysis of medical practice and experience included in [1]. Specifically:

- *Frequency* - is the rate with a symptom/sign or complication is present in a given disease. Identified levels are: *very frequent, very frequent/frequent, frequent, frequent/occasional, occasional*;
- *Specificity* - is the measure with which manifestation implies a specific disease. Identified levels are: *high, high/medium, medium, medium/low, low;*
- *Precision* - is the level with which *Clinical test* result allows to include or exclude a diagnosis. Identified levels are: *high, high/medium, medium, medium/low, low*.

Furthermore, the model foresees other concepts and relations useful to define additional information of diseases, and recommendation), etiology, epidemiology, transmission of disease, prophylaxis, and so on.

Code listed in Fig. 4 shows an individual definition of Disease as an example. In particular, "Sin189" is of type

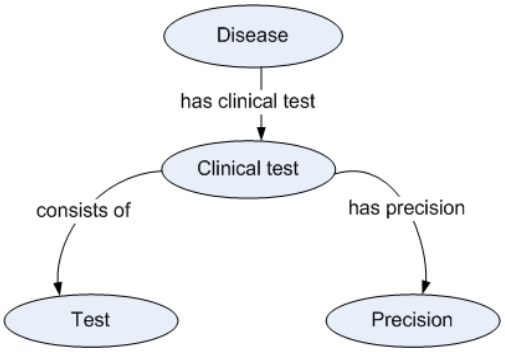

Figure 3. A sketch of some classes of *Medical Disease Ontology*: *Disease* and *Clinical test*.

Evidence and is associated with "*Medium/Low*" specificity and "*Frequent*" frequency degree to disease "*Mal002*". Furthermore, we have associated a complication (*infertility*) and a *NMR (Nuclear Magnetic Resonance)* test.

As detailed in the following section, *Medical Disease Ontology* is the baseline to build our medical diagnosis methodology.

IV. MEDICAL DIAGNOSYS METHODOLOGY

A. Mathematical model to support preliminary diagnosis

One of the main features supported by ODINO is preliminary medical diagnosis. During medical practices, physician submits a query by specifying one or more evidences that may be symptoms, signs and/or complications. So, the system evaluates correlation degree among incoming query and available diseases by means of an approach based on Information Retrieval techniques and Fuzzy Formal Concept Analysis (FFCA) [31]. Furthermore, system is capable to use relations among concepts in order to augment query results by using a Description Logic reasoner.

As described above, *Specificity* and *Frequency* are the main features to include or exclude diagnosis results. Specifically, a mathematical model of *Disease* and its correlation with *Symptom/Sign* and *Complication* may be obtained in order to perform FFCA.

```
<owl:Thing rdf:about="&Symptomatology ;Sin189">
  <rdf:type rdf:resource="#Evidence"/>
</owl:Thing>
                                ...
<owl:Thing rdf:about="#Sem_fever">
  <rdf:type rdf:resource="#Symptom/Sign"/>
  <refers rdf:resource="&Symptomatology ;Sin189"/>
  <frequency rdf:resource="#Frequent"/>
  <specificity rdf:resource="#Medium-Low"/>
</owl:Thing>
                                ...
<owl:Thing rdf:about="&Diseases;Mal002">
  <rdf:type rdf:resource="#Disease"/>
  <has_semeiotics rdf:resource="#Sem_fever"/>
  <has_complication rdf:resource="#Com_infertility"/>
  <has_clinical_test rdf:resource="#Acc_RMN"/>
</owl:Thing>
```

Figure 4. *Medical Disease Ontology*: individual disease example.

The FFCA, informally, exploits a matrix that represents the fuzzy relation between objects of the input data (i.e., *Diseases*) and some attributes (i.e., *Symptoms/Signs* and *Complications*). The relation is calculated by assessing both *Frequency* and *Specificity* degree between *Disease*, *Symptom/Sign* and *Complication*. In particular, the value of relation, $\mu_{i,j}$, between $Disease_i$ and $Symptoms/Signs_j$ or $Complications_j$ is calculated by performing a linear combination (a weighted sum) of *Specificity* and *Frequency* with parameters λ_1 e λ_2. These parameters consist of constant values chosen based on medical experience, depicted in [1], which shows that, during preliminary diagnosis, *Frequency* is less important than *Specificity*. Formally:

$$\mu_{i,j} = (Specificity * \lambda_1) + (Frequency * \lambda_2), \lambda_1 > \lambda_2 \quad (1)$$

Taking into account the matrix created according to these criteria, FFCA arrange data in a corresponding lattice [31]. Specifically, diseases that share symptoms/signs or complications are arranged together. As argued, the lattice is used to retrieve concepts closer to the incoming query in order to retrieve eligible set of diseases.

B. Identification of candidate disease

In this process the main aim is to get a synthetic value which represents how each resource is relevant with respect to the user query. By revising some Information Retrieval measures (i.e., Precision and Recall), we determine what is the concept (or concepts) most related to the incoming symptoms/signs or complications in the query. In particular, the standard measures of Precision, Recall and F-measure have been adapted to our objective.

Formally, let us consider the following notions:

- $A = \{a_1, a_2, \ldots, a_n\}$ the whole set of attributes (i.e., symptoms, signs, complications) belonging to object;
- $O = \{o_1, o_2, \ldots, o_t\}$ the whole set of objects (i.e., diseases);
- $C_i = (A_i, O_i)$ *i-th* formal concept of a lattice (where A_i and O_i represent, respectively, terms and resources for the concept C_i);
- $Q_i = \{q_1, q_2, \ldots, q_m\}$ a query (e.g., set of symptoms/signs, etc.).

Thus, given a formal concept C_i, we calculate the values of precision P_i and recall R_i as follows:

$$P_i = \frac{|Q_i \cap A_i|}{|A_i|} \qquad R_i = \frac{|Q_i \cap A_i|}{|Q_i|} \quad (2)$$

where Pi is computed as ratio between the number of relevant attributes in C_i and all the attributes belonging to C_i. And, R_i represents the number of relevant attributes in C_i divided by the total number of query terms.

Consequently, F-measure value F_i, relative to concept C_i, is computed as follows:

$$F_i = 2 \times \frac{P_i \times R_i}{P_i + R_i} \quad (3)$$

Final result of this computation is the list of the F-measure values $F = \{F_1, \ldots, F_s\}$ for all formal concepts in the lattice, given a query.

In order to evaluate diagnosis results, for each object (disease), $o_i \in O$ the system evaluate score as follows:

$$score(o_i) = \sum_{j=1}^{s} \left(\mu_j(o_i) \times F_j \right) \quad (4)$$

where $\mu_j(o_i)$ represents the membership of object o_i (in according to definition of *Fuzzy Formal Context* in FFCA theory [31]). The score represents correlation degree between query and available diseases. Then, a ranked list of diseases may be retrieved in order to answer to a given query.

V. CASE STUDY

Taking into account our experimental results, next subsections detail main features of ODINO. Actually, ODINO has been tested with dermatological disease knowledge. Defined vocabularies include: 700 symptoms/signs; 150 diseases; 125 clinical tests; 260 active ingredients.

A. Disease Catalogue Browsing.

This feature accomplishes the aim to provide rapid training on specific diseases. In fact, ODINO knowledge base includes many multimedia information, such as: definition and historical data, etiological agents, disease transmission, large set of pictures revealing specific symptomatology, complications, clinical tests and treatment protocols, and so on.

B. Preliminary medical diagnosis

This functionality allows to assist physician during preliminary diagnosis practice. Physician starts the process by selecting some clinical manifestations (i.e., symptoms, signs and/or complications). As shown in Fig. 5, ODINO supports selection through two alternative interactions, namely: by browsing ICD-9 tree and specifying ICD-9 categories; by using text based search.

The matching algorithm (described in Section IV.B) allows the system to retrieve eligible diseases. So, taking into account clinical manifestations selected by the user (e.g., *Gangrene* and *Physical decay*), as highlighted in Fig. 6, the system retrieves a ranked list of eligible diagnosis. In particular, the system shows correlation degree useful to rank the results (see Fig. 6(a)) and it allows to access to motivations of each result (in Fig. 6(b)).

Result motivations consist of hints to the physicians about distinctive symptomatology of retrieved disease. These hints may be useful to suggest eventually escaped factors. For example, as shown in Fig. 7, system highlights: submitted symptoms in the request (red outlined box) and *pathognomonic signs* (green outlined box) for the retrieved disease (i.e., in the picture *"Venereal ulcer"*). This is a useful information because the presence of a *pathognomonic sign* means, beyond any doubt, that particular disease is present.

In order to validate preliminary diagnosis performed by ODINO, several queries and relevance sets have been defined with physician experts of dermatological diseases.

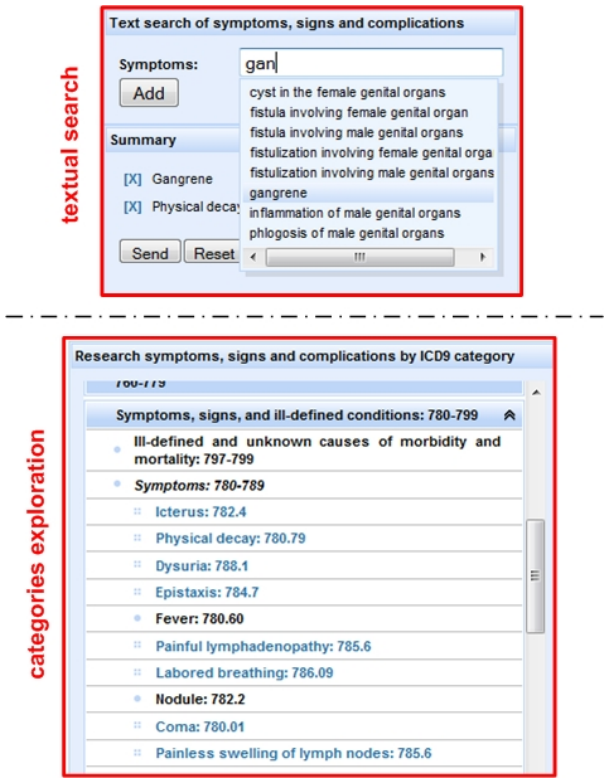

Figure 5. Selection of clinical manifestation by mean textual search (with autocomplete) or categories exploration.

In particular, through the analysis of retrieval performance, we have measured: *Average Uninterpolated Precision* (AUP) [32] and *Precision*. The AUP is defined as the ratio between the sum of the precision value at each point of hierarchical structure (or node of lattice) where a relevant item appears, and the total number of relevant items. The performance for Precision and AUP are shown in Fig. 8, considering a different number N of the clinical manifestations (e.g., *Fever*, *Headache*, *Anemia*, etc.). Let us note that, for N larger than 6, the values of Precision and AUP provide good performance results (between 0.7 and 1). Considering these results we can say that knowledge base and methodology are enough selective for available diseases.

More generally, by analyzing system usage and physician expectancy, experimental results reveal that 86% of diseases retrieved by the system are coherent with results expected by the physicians; just the remaining 14% of results emerge to be too vague. Specifically, by considering wrong results, we have identified that the problem is strictly related to ambiguous clinical manifestations. More precisely, two weakness have been revealed: cases in which huge number of clinical manifestations characterize the same disease (i.e., *AIDS*); and cases in which the same clinical manifestation characterizes many disease with similar *Frequency* and *Specificity* degree (i.e., *Fever*).

C. *Faceted search*

ODINO also provides a faceted search of diseases through taxonomy constraints (i.e., Symptomatology, etc.). Faceted search [33] is an exploration technique for structured datasets based on the facet theory.

As described in [34], in faceted search the information space is partitioned using orthogonal conceptual dimensions of the data. Each dimension is called facet and represent important disease partitioning feature. The facet has multiple restriction values and the user selects a restriction value to filter relevant items in the information space. The facet based approach can be directly mapped to navigation in semi-structured data, as well as in *Medical Diseases Ontology* model deployed in ODINO. Specifically, available facets are: symptoms, complications, clinical tests and active ingredients. All of these facets are associated with controlled vocabulary defined according to the SKOS formalism.

Obviously, items that ODINO filters step-by-step are diseases. Fig. 9 shows an example of faceted search in ODINO. The left side of Fig. 9 shows constraint "step-by-step" selection to filter diseases (constraints are highlighted with box outlined in green color). At each step of the facet-based search, the system returns an ordered list of eligible diagnosis allowing also further filtering.

With respect to text based search, a faceted search is more useful because allows navigation of an unknown dataset through system suggested restriction values at each step. Additionally, facets provide an intuitive user interface eliminating the need to write exact queries; and prevent empty query results by including restriction values that certainly lead to true results.

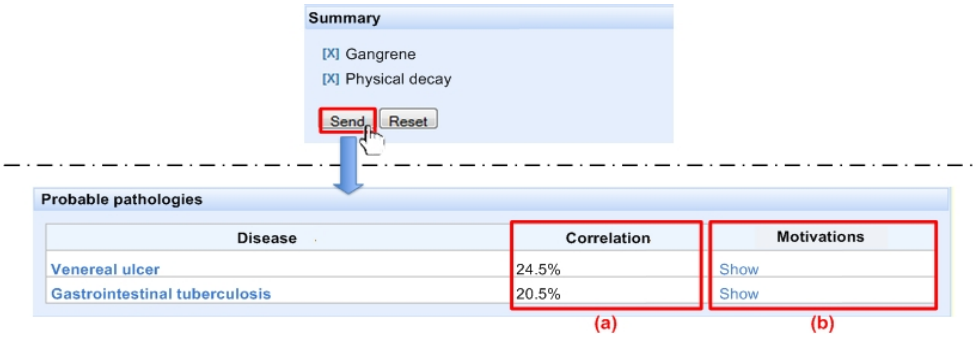

Figure 6. Preliminary diagnosis retrieved results: (a) correlation degree, (b) links to motivations of results.

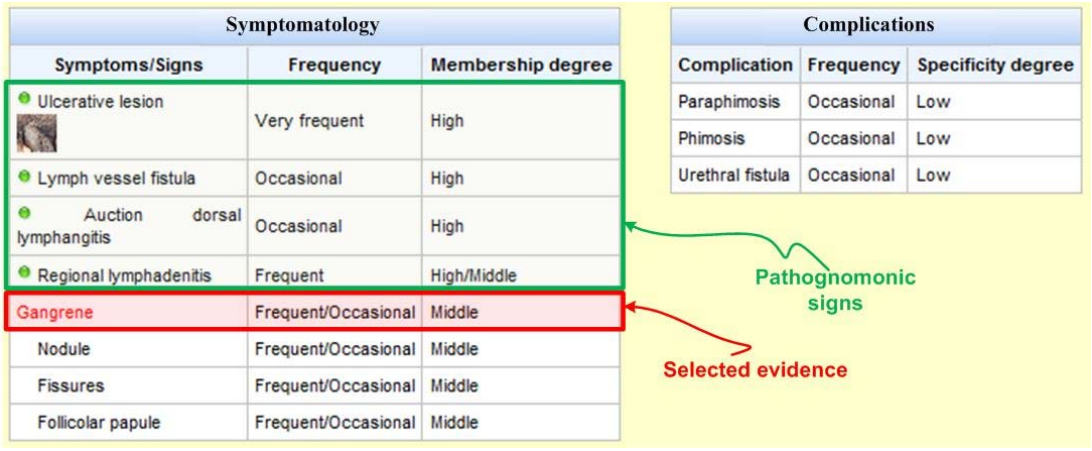

Figure 7. Example of result motivation interface.

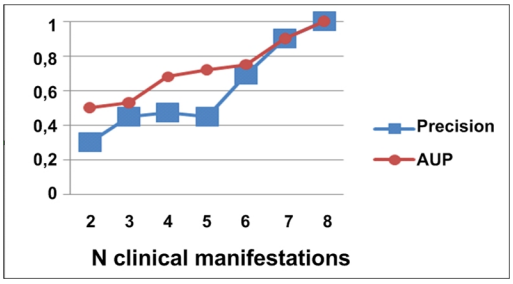

Figure 8. Performance evaluation on Precision and AUP.

VI. Conclusion & Future Works

This paper presents a project named ODINO, an ontology based web application that provides features to daily support medical practices. In particular, ODINO exploits Semantic Web formalisms in order to model medical knowledge. On the other hand, Fuzzy Formal Concept Analysis and ontology inference are applied to support preliminary medical diagnosis.

The availability of rich set of multimedia information allows to provide rapid training feature. Moreover, thanks to the semantic modeling of knowledge base, a faceted search of diseases has been developed.

Benefits deriving from the applied approach are especially related to the reusability of the knowledge layer, scalability and flexibility of the main features, like as faceted search.

The main goal of ODINO is to introduce an effective user interface to provide second opinion especially for the developing country, such as: Etiopia, Kenya, etc. where the availability of economic and human resources are limited. Future works are related to introduce support to improve the exploitation of multimedia information, available in the knowledge base, during faceted search and preliminary diagnosis.

Acknowledgment

The results of the present work have been achieved thanks to the intensive contribution of physician members of INMP that are also involved as authors of [1].

References

[1] A. Morrone. GLOBAL DERMATOLOGY ricerca clinica e logica matematica in Medicina delle Migrazioni, Manuale pratico.

[2] D. Reynolds, P. Shabajee, S. Cayzer, Semantic Information Portals, in: Proceedings of WWW 2004, Alternate track papers & posters, ACM Press, New York, New York, 2004.

[3] E. H. Shortliffe. Computer-Based Medical Consultations: MYCIN. Elsevier, New York, 1976.

[4] Barnett GO, Cimino JJ, Hupp JA, Hoffer EP. DXplain: an evolving diagnostic decision-support system. JAMA 1987;258:67-74.

[5] J. S. Aikins, J. C. Kunz, E. H. Shortliffe, R. J. Fallat. Puff: An expert system for interpretation of pulmonary function data. Comput. Biomed. Res., 3(16):199–208, 1983.

[6] K. Adlassing. Cardiag 2 expert system. IEEE Transactions on Systems, Man and Cybernetics, SMC-16(2), 1986.

[7] Edberg SC. Global infectious diseases and epidemiology network (GIDEON): a world wide Web-based program for diagnosis and informatics in infectious diseases. Clin Infect Dis. 2005; 40(1): 123-126.

[8] S. M. Kulikowski, C. A. Weiss. Representation of expert knowledge for consultation: the CASNET and EXPERT projects. Artificial Intelligence in medicine. Szolovits, P. (Ed.), Boulder: Westview Press, pages 21–56, 1982.

[9] H. Bossel, S. Klaczko, and N. Muller, A fuzzy-algorithmic approach to the definition of complex or imprecise concepts, in Systems Theory in the Social Sciences, , Eds. Stuttgart: Birkhauser Verlag, 1976, pp. 202-282.

[10] L. A. Zadeh, Linguistic variables, approximate reasoning and dispositions, Med. Iniform, vol. 8, pp. 173-186, 1983.

[11] L. A. Zadeh, Lotfi A., Outline of a new approach to the analysis of complex systems and decision processes, IEEE Trans. Svst., Man, Cybern., vol. 3, pp. 28-44, 1973.

[12] R. E. Bellman and L. A. Zadeh, Local and fuzzy logics, memo. ERL-M584, Electronics Research Laboratory, College of Engineering, University of California, Berkeley 94720, May 11, 1976.

[13] K. -P. Adlassnig, A survey on medical diagnosis and fuzzy subsets, in Approximate Reasoning in Decision Analysis. M. M. Gupta and E. Sanchez Eds. New York: North-Holland, 1982, pp. 203-217.

[14] B. Iantovics, C. Chira, D. Dumitrescu. Principles of the Intelligent Agents. Casa Cartii de Stiinta Press, Cluj-Napoca, 2007.

[15] J. Kuhl, E.J. Graham. Esagent: Expert system control of simulated agent-based mobile robots. Intelligent Systems Research Laboratory, Technical Report TR-ISRL-04-02 University of Louisville, Louisville, 2004.

[16] Acampora, Giovanni; Lee, Chang-Shing; Wang, Mei-Hui; , FML-Based Ontological Agent for Healthcare Application with Diabetes. *Web Intelligence and Intelligent Agent Technologies, 2009. WI-IAT '09.* vol.3,

Figure 9. An example of faceted search of diseases.

no., pp.413-416, 15-18 Sept. 2009.

[17] Chang-Shing Lee; Mei-Hui Wang; Acampora, G.; Loia, V.; Chin-Yuan Hsu; , "Ontology-based intelligent fuzzy agent for diabetes application," *Intelligent Agents, 2009. IA '09. IEEE Symposium on* , 2009.

[18] Rodríguez A., Mencke M., Alor Hernandez G., Posada Gómez R. and J. M. Gomez., Medboli: Medical Diagnosis Based on Ontologies and Logical Inference. The Third International Conference on Digital Society, ICDS 2009 (accepted, to appear), 2008

[19] García-Crespo Á., Rodríguez González A., Mencke M., J. M. Gomez., Colomo Palacios R.: ODDIN: Ontology-driven differential diagnosis based on logical inference and probabilistic refinements. Expert Syst. Appl. 37(3): 2621-2628 (2010)

[20] Fuentes-Lorenzo, D., Morato, J., & Gómez, J. M. (2009). Knowledge management in biomedical libraries: A Semantic Web approach. Information Systems Frontiers, 11(4), 471–480.

[21] García Sanchez, F., Fernandez Breis, J., Valencia García, R., Gómez, J. M., & Martínez- Bejar, R. (2008). Combining Semantic Web technologies with multi-agent systems for integrated access to biological resources. Journal of Biomedical Informatics, 41(5), 848–859.

[22] Gomez, J. M., Colomo-Palacios, R., Mayoral, M. R., & Garcia-Crespo, A. (2008). Microarray information and data integration using SAMIDI. In J. R. Rabuñal, J. Dorado, & A. Pazos (Eds.), Encyclopedia of artificial intelligence. Hershey, PA: IGI Global.

[23] Rector, A. L., Rogers, J. E., Zanstra, P. E., & Van Der Haring, E. (2003). OpenGALEN: Open source medical terminology and tools. In Proceedings of the American medical informatics association symposium 2003 (pp. 982–985).

[24] Smith, B., Ashburner, M., Rosse, C., Bard, J., Bug, W., Ceusters, W., et al. (2007). The OBO Foundry: Coordinated evolution of ontologies to support biomedical data integration. Nature Biotechnology, 25(11), 1251–1255.

[25] Lambrix, P., Tan, H., Jakoniene, V., & Strömbäck, L. (2007). Biological ontologies. In C. J. O. Baker & K. H. S. Cheung (Eds.), Semantic Web revolutionizing knowledge discovery in the life sciences (pp. 85–89). Berlin: Springer.

[26] Hadzic, M., & Chang, E. (2005). Medical Ontologies to support human disease research and control. International Journal of Web and Grid Services, 1(2), 139–150.

[27] Smith, B., Ceusters, W., Klagges, B., Köhler, J., Kumar, A., Lomax, J., et al. (2005). Relations in biomedical ontologies. Genome Biology, 6(5), 1425–1433.

[28] Schulz S, Hanser S, Hahn U, Rogers, J. The semantics of procedures and diseases in SNOMED CT, Methods Inf Med. 2006; 45(4): 354-358.

[29] A. Schreiber, A. Amin, M. van Assem, V. de Boer, L. Hardman, M. Hildebrand, L. Hollink, Z. Huang, J. Kersen, M. Niet, B. Omelayenko, J. Ossenbruggen, R. Siebes, J. Taekema, J. Wielemaker, B. Wielinga, MultimediaN E-Culture demonstrator, in: Proceedings of ISWC 2006, Athens, GA, Springer–Verlag, Berlin, 2006.

[30] Suominen, O., Hyvönen, E., Viljanen, K. and Hukka, E.: HealthFinland-A National Semantic Publishing Network and Portal for Health Information. Web Semantics: Science, Services and Agents on the World Wide Web, 7(4), pp. 287--297 (2009).

[31] De Maio, C., Fenza, G., Loia, V. and Senatore, S. (2010), Knowledge structuring to support facet-based ontology visualization. International Journal of Intelligent Systems, 25: 1249–1264. doi: 10.1002/int.20451.

[32] N.Nanas, V.Uren and A. de Roeck, "Building and Applying a Concept Hierarchy Representation of a User Profile", In Proceedings of the 26th annual international ACM SIGIR Conference on Research and Development in Information Retrieval, ACM Press, 2003.

[33] K.-P. Yee, K. Swearingen, K. Li, and M. Hearst. Faceted metadata for image search and browsing. In *CHI* 2003.

[34] Eyal Oren, Renaud Delbru, and Stefan Decker. Extending Faceted Navigation for RDF Data. ISWC 2006, volume 4273 of Lecture Notes in Computer Science, chapter 40, pages 559–572.

2011 IEEE International Conference on Fuzzy Systems
June 27-30, 2011, Taipei, Taiwan

Predicting Laboratory Testing in Intensive Care using Fuzzy and Neural Modeling

Federico Cismondi*†‡, André S. Fialho*†‡,
Susana M. Vieira‡, João M.C. Sousa‡, Shane R. Reti§,
Leo A. Celi‖, Michael D. Howell¶ and Stan N. Finkelstein*
*Massachusetts Institute of Technology, Engineering Systems Division,
77 Massachusetts Avenue, 02139 Cambridge, MA, USA (email: cismondi@mit.edu)
†MIT Portugal Program, 77 Massachusetts Avenue, E40-221, 02139 Cambridge, MA, USA
‡Technical University of Lisbon, Instituto Superior Técnico, Dept. of Mechanical Engineering,
CIS/IDMEC – LAETA, Av. Rovisco Pais, 1049-001 Lisbon, Portugal
§Division of Clinical Informatics, Department of Medicine,
Beth Israel Deaconess Medical Center, Harvard Medical School, Boston, MA, USA
¶Silverman Institute for Healthcare Quality and Safety,
Beth Israel Deaconess Medical Center, Harvard Medical School, Boston, MA, USA
‖Beth Israel Deaconess Medical Center, Harvard Medical School, Boston, MA, USA

***Abstract*—Laboratory testing is a frequent activity for patients in intensive care units (ICU). Recent studies demonstrate that frequent laboratory testing does not necessarily relate to better outcomes. We hypothesize that unnecessary laboratory testing can be reduced by predicting which tests are unlikely to influence clinical management. Reducing unnecessary tests could reduce morbidity and hospitalization costs. We analyzed an ICU database containing 26,665 patient records at Beth Israel Deaconess Medical Center, Boston, and selected a subset of patients with gastrointestinal bleeding. Database knowledge discovery was applied involving data preprocessing, feature selection, and classification. Conventional soft computing tools such as fuzzy models and neural networks were utilized in this work, combined with statistical and mathematical tools. The input variables included bedside monitor trends, lab tests, arterial/central catheter information, urine collections, transfusions, indexes and scores calculated for the patients. The outcome variable was a binary classification based on falling levels of hematocrit. Feature selection was performed by a bottom-up strategy, maximizing the area under the ROC curve (AUC), the integrated discrimination improvement (IDI) and a multiobjective function primarily pondering the sensitivity of the models. A leave-one-out cross validation process was used to evaluate the overall models' performance, as well as the additional predictive value of the variables selected. Urine output was selected by all models as the best predictor of useful hematocrit testing. Our results show that it is possible to correctly classify the usefulness of a hematocrit lab test up to 81% of the time by using fuzzy models and neural networks.**

***Index Terms*—Knowledge Discovery in Databases, Classification, Intensive Care Unit, Laboratory testing, Modeling, ICD9, Neural Networks, Fuzzy Models**

I. Introduction

Laboratory testing occurs frequently in hospitalized patients [1]. This is especially so for patients in intensive care where frequent blood draws may cause increased general phlebotomy complications such as blood loss [2], [3]. Although many lab tests are performed during the hyperacute first day of the patient's ICU stay, about two-thirds of laboratory studies are ordered later in the stay. While part of this testing reflects the intrinsic critical status of ICU patients, other tests are run almost by default, following general guidelines and not patient specific characteristics [4].

Recent data demonstrate that patients who have received more frequent laboratory tests do not necessarily have better outcomes [5]. On a cost comparative basis, patients with the highest discretionary laboratory costs are around US$273 higher per ICU stay than the lowest spenders, even when corrected for different ICU lengths of stay and hospital mortality [2]. The highest spenders also spend more on other discretionary costs, which could be driven by increased laboratory use, including pharmacy costs and blood banking costs (e.g., red blood cell transfusion in a patient with anemia attributable to laboratory testing).

A further laboratory risk is false positives associated with over-testing [6]. The probability of false positives (lab results out of the normal range, when in fact the real values are normal) depends on the laboratory equipment, employees training and correct blood draws. However, the incidence of false positives increases with the number of tests run [7]. For example, if a given lab test randomly misclassifies people as *diseased* at a 1% rate (i.e. the test is 99% *accurate*), then the probability of having a false positive in the healthy population after an arbitrary 50 lab tests is

$$P_{wrong(n)} = 1 - (P_{right})^n \tag{1}$$

$$P_{wrong(50)} = 1 - (0.99)^{50} = 0.40$$

where n is the number of lab tests, $P_{wrong(n)}$ is the probability of obtaining one wrong result (in this case, a false positive) in n lab tests and P_{right} is the probability of obtaining an

978-1-4244-7316-8/11/$26.00 ©2011 IEEE

accurate result in a given lab test. One strategy to reduce this increasing probability of obtaining false positives is to avoid testing when no additional information is expected or, in other words, to reduce n.

In [3], it was shown that the introduction of new laboratory testing guidelines in an ICU setting resulted in a significant decrease in the number of tests performed (37%), and a significant increase in the number of tests obtained with a proper physician order (38%). These results were sustained over time, and were associated with no detectable morbidity and possibly to a decrease in red blood cell transfusions.

To prove that it is possible to model and classify the usefulness of a given lab test using information from other variables, this work focuses specifically in classifying the need for a hematocrit lab test. This measurement was chosen as a starting point because its dynamics are well understood, and specifically related to other measurable phenomena, like bleeding, transfusions, urine output and red blood cell count lab tests [8]. Also the impact of its prediction may be high, since it would be one step forward into reducing the amount of complete blood count (CBC) tests run and therefore, the amount of blood draws. We hypothesize that it is possible to reduce hematocrit laboratory testing by predicting when further testing is unlikely to provide new information that would change treatment strategy. This reduction would be achieved by assessing a range of physiological variables, and predicting when significant variations in hematocrit are likely to occur.

We apply a Knowledge Discovery in Databases (KDD) process to find the classification models on an ICU database named MIMIC II. Conventional soft computing techniques, namely fuzzy modeling and neural networks, combined with bottom-up feature selection were used to classify the usefulness of hematocrit lab tests. Other mathematical and statistical tools were also applied during data preprocessing.

This work is organized as follows. Section 2 formally describes the MIMIC II database and the methods used to preprocess, reduce and classify the outcome proposed. Section 3 describes and discusses the results obtained from these methods. Conclusions are presented in Section 4.

II. Methods

Knowledge Discovery in Databases (KDD) is an interactive and iterative process [9], involving numerous steps, which aims to discover hidden patterns and/or useful information in large datasets that do not express those patterns easily.

According to the steps described by Figure 1 for the KDD process, the following subsections define the approaches used in this work to tackle each step.

A. Application domain and target dataset

The application domain identified for this work is in the field of critical care medicine, specifically, a medical ICU. Laboratory testing guidelines are generally created according to evidence based medicine informed by different population studies. However, lab tests are frequently run by default, without considering an individual patient's condition. The main role of the KDD process in this work is to classify the relevance of hematocrit lab testing for ICU patients based on existing data specific to the patient, and whether a given test would then add information that could change management.

For this study, an ICU database named MIMIC II was used. MIMIC II was created as part of a Bioengineering Research Partnership (BRP) grant from the National Institute of Biomedical Imaging and Bioengineering entitled Integrating Data, Models and Reasoning in Intensive Care (RO1-EB001659). MIMIC II has been collected since 2001 at Beth Israel Deaconess Medical Center in Boston, MA, USA, including high frequency sampled data of bedside monitors, clinical data (laboratory tests, physicians' and nurses' notes, imaging reports, medications and other input/output events related to the patient) and demographic data [10]. All data is appropriately de-identified. As this is being written, MIMIC II continues to evolve with new versions being posted on the PhysioNet web site (http://www.physionet.org/). The version 2.5, used in this work, contains 26,665 ICU patients.

The target dataset used in this work was created using the following inclusion criteria:

- patients with Gastrointestinal (GI) bleeding were selected from MIMIC II, according to GI bleeding-related ICD9 (International Classification of Diseases) codes registered for them during their whole ICU stay [11];
- patients were required to be in the ICU for 7 days or more in order to have useful time series for analysis;
- data collection was considered to start when the first heart rate value was stored in the database, and ended with the last recorded heart rate, or a gap of 24 hours or more;
- only first ICU stays were considered, mainly to avoid patients that could have had several ICU admissions during the same hospitalization, reflecting a more complex state;
- only patients 18 years or older were included as MIMIC II also includes neonates and infants [10];
- bedside monitor trends, lab tests, ventilator variables, indexes, scores, arterial/central/catheter line monitoring were considered, while medications and demographic information were discarded (Table I).

B. Data Preprocessing

Data preprocessing is a complex and crucial step as it defines the information that will be used later in the classification process, and it has to be carefully carried out in order to obtain clean data without altering the real information contained therein. Noise and outliers removal, misalignment correction and missing data treatment are considered as substeps of the preprocessing, accounting for up to 60% of the effort in a knowledge discovery process [12], [13].

The nature and occurrence of noise in MIMIC II is difficult to manage mainly due to the low sampling frequency of most variables, and to the broad band of frequencies that originally compose them. Consequently, it was not considered during the preprocessing.

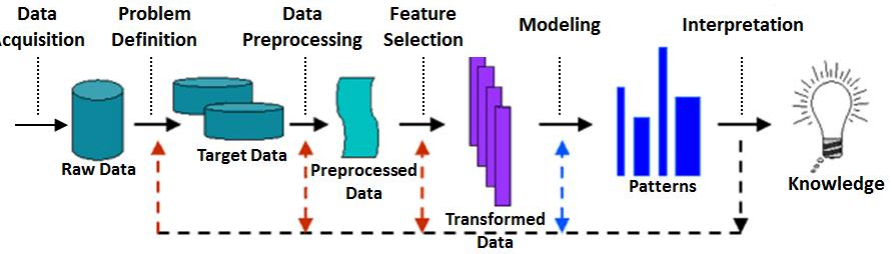

Fig. 1. Overview of the steps that compose the KDD process.

TABLE I
VARIABLES USED FOR THE MODELING PURPOSES.

Bedside monitor trends							
Heart Rate		Temperature		Respiratory Rate		Oxygen Saturation (SpO2)	
Arterial/Central/Catheter Line							
Arterial Blood Pressure (ABP)	ABP Mean	Arterial pH	Arterial CO2	Arterial PaCO2	Arterial PaO2	Arterial Base Excess	Central Venous Pressure
Laboratory results							
Hematocrit	Potassium	Glucose	Creatinine	Sodium	Chloride	Lactic Acid	Uric Acid
Carbon Dioxide	Magnesium	Ionized Calcium	Phosphorous	Calcium	SaO2	CaO2	Albumin
Ventilator monitored variables							
PEEP Set		Respiratory Rate		Minute Volume (Observed)		Low Exhaled Minute Volume	
High Inspiratory Pressure		Plateau Pressure		Mean Airway Pressure		Respiratory Rate Set	
Resp Rate (Spontaneous)		Peak Inspiratory Pressure		Tidal Volume (Observed)		Tidal Volume (Set)	
Indexes calculated for combination of variables							
Cardiac Output		Systemic Vascular Resistance		Left Ventricular Cardiac Work		Right Ventricular Cardiac Work	
Scores							
SAPS-I	SAPS-II	APACHE					
Other variables collected							
Non-invasive Blood pressure (NBP)		NBP Mean	Blood transfusions				

An outlier is defined as an observation that is markedly different in value from the others of the sample or, in other words, a value out of the normal range of occurrence. The standard approach to identify and eliminate outliers is to filter the signal by amplitude, which means that specific upper and lower thresholds are defined for the signal. Those values above or below the threshold are considered outliers and therefore, removed from the signal. Another approach is to analyze every value in its context, comparing it with its neighbors to assess the likelihood of that point of being an outlier. Since it is sometimes possible for hematocrit to change quite drastically in a short period of time (e.g. hemorrhage) and then very rapidly rebound closer to their prior value (e.g. with massive transfusion), the second approach cannot be used in this work and, because of that, a filter with upper and lower amplitude thresholds was designed considering as possible extreme values those clinically accepted as possible for humans. This was reviewed and validated under medical assessment. Those values identified as outliers were assigned as missing data for further preprocessing.

According to [14], misalignments can be corrected using one variable in the dataset as a template, and shifting the data points of other variables to align sampling times. In this work, the outcome variable (*Hematocrit*) was used as the template to unshift the values of all the other variables, as it defines the points for which the model is meant to give a classification result. Although [14] proposes to use the variable with the highest sampling rate (in this dataset it corresponds to *Heart Rate*, with a mean sampling time of 0.76±0.2 hours), in this work it would create an excessive amount of points for which the outcome is not expected to be measured (*Hematocrit* has a mean sampling time of 9.15±1.24 hours). As shown in Figure 2, all the existing entries are shifted to the closest template alignment location, and values are then obtained through an interpolation strategy using the template variable as a time reference. No new points were created in this step to fill otherwise blank values. The values for the new time positions were obtained through cubic interpolation, as suggested by [14].

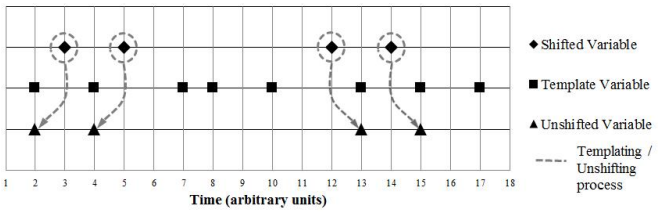

Fig. 2. Simplified representation of a *template variable*, together with the *shifted* and *unshifted* version of a second variable.

To differentiate true missing values from lack of sampling [14], a 95% confidence interval was defined for the sampling time of every variable, and absent segments inside those intervals were recovered by cubic interpolation.

In order to assess whether true missing values were recoverable or not in each specific variable, a method based in fuzzy models, which classifies every missing point according to the ability to find information about the missingness contained in other variables [15], was used. For each point of a specific variable, a binary outcome is created containing a 1 if the variable is missing or a 0 if it has a value. Using the other variables of the dataset as inputs and the binary outcome as the output, if the fuzzy model is able to correctly classify a missing point as missing it is because it found information in the other variables that explain the missingness. In [15] it was pointed out that when there is an underlying medical reason for the missingness, the value should not be imputed; information in other variables may be considered as medical reasons. After classifying missing data, those missing segments identified as *recoverable* were recovered using expectation maximization [16], [17]; those classified as *not-recoverable* caused the deletion of all the variables for that sampling time.

C. Data Reduction. Bottom-Up Feature Selection.

Data reduction involves finding those variables with useful information to model and predict the pursued outcome. A bottom-up feature selection process to reduce data dimensionality was use in this work.

A detailed description of the bottom-up approach used here may be encountered in [18]. However, it is important to note that a more recent algorithm that minimizes the computational time with similar performance has been proposed in [19]. The bottom-up approach looks for single inputs that may influence the output, and combines them in order to achieve the model with the best performance criterion. Two subsets of data are used in this stage, train and test. Using the train set, a model is built for each of the n features in consideration, and evaluated using the performance criterion upon the test set. The feature that returns the best value of the performance criterion is the one selected. Next, other feature candidates are added to the previous best model, one at a time, and evaluated. Again, the combination of features that maximizes the performance criterion is selected. When this second stage finishes, the model has two features. This procedure is repeated until the value of the performance criterion stops increasing. In the end, all the relevant features for the considered process should be obtained.

Three different performance criteria were separately tried in this work:

- the area under the ROC curve (AUC), as used by [20]
- the integrated discrimination improvement (IDI) [21], calculated in a simplified form as follows

$$IDI = (Sensitivity_{new} - Sensitivity_{old}) \quad (2)$$
$$-(Specificity_{new} - Specificity_{old})$$

  where $Sensitivity$ and $Specificity$ refer to the true positive (hematocrit correctly classified as relevant) and true negative (hematocrit correctly classified as not relevant) classification rate of a model[1], subscript new refers to the model with the new feature selected and subscript old to the model without it. The IDI can be viewed as a difference between improvement in average sensitivity and any potential increase in average specificity.
- the sensitivity, as part of a multi-objective function in which the specified criterion is considered together with specificity and percentage of correct classifications[2] (PCC), but with a higher degree of consideration through different membership functions of a fuzzy model [22].

D. Classification strategy

The data mining strategy used in this work was defined for a binary classification of every hematocrit lab test as:

- Relevant, with a value of 1, when there is a drop d (varied between 1 and 5) in the value of hematocrit, or when those values are under a certain critical threshold T (varied between 15 and 40). Both d and T were varied to find the best classification point, and then reviewed with clinicians to check their practical significance and management influence on events such as triggering a decision of start or stop a blood transfusions or medications.
- Not relevant, with a value of 0, if the variations were below the previously defined thresholds.

The preprocessed data subset was randomly divided into two equal parts, one for the feature selection process (FS dataset) and the other for the model selection (MS dataset). This was done to assess select the relevant features and to assess the model's performances over independent datasets.

The subsets of features were defined over the FS dataset by randomly selecting the train (60%), test (30%) and validation (10%) sets from the FS dataset; the subset of features resulting in the highest PCC for the validation set was selected.

A leave-one-out cross-validation (LOOCV) process was used to select the best model, by using a subset 10% of the MS dataset, defined as the validation set, and the remaining 90% as the training set. To reduce variability, 10 rounds of cross-validation were performed using different partitions, and the validation results were averaged over the rounds. The model with the best performance criteria was selected.

E. Modeling and Data Mining

The classification previously defined was performed using two different soft computing techniques and their results were compared. Namely, fuzzy models and neural networks were independently used, due to their universal approximators nature and previous results showing their performance in medical

[1]Sensitivity = TP / (TP + FN); true positives over true positives and false negatives, or total positives.
Specificity = TN / (TN + FP); true negatives over true negatives and false positives, or total negatives.

[2]The percentage of correct classifications is equal to the number of true positives (TP) together with the number of true negatives (TN) divided by the total number of patients, and then multiplied by 100.

databases [20]. For the specific case of fuzzy models, an additional motivation for their use was the easy-understandable rules they generate after classifying data, which could be useful for medical interpretation.

1) Fuzzy Models: Fuzzy modeling is a tool that allows an approximation of nonlinear systems when there is few or no previous knowledge of the system to be modeled. The fuzzy modeling approach has several advantages compared to other nonlinear modeling techniques ([23],[24]). In general, fuzzy models provide not only a more transparent model, but also a linguistic interpretation in the form of rules. A fuzzy classifier contains a rule base consisting of a set of fuzzy if–then rules together with a fuzzy inference mechanism.

In this work, Takagi-Sugeno (TS) fuzzy models [24] were used, which consist of fuzzy rules where each rule describes a local input-output relation. When TS fuzzy systems are used, each discriminant function consists of rules of the type

$$\begin{aligned} \text{Rule } R_i^c \quad : \quad & \text{If } x_1 \text{ is } A_{i1}^c \text{ and } \ldots \text{ and } x_M \text{ is } A_{iM}^c \\ & \text{then } d_i^c(\mathbf{x}) = f_i^c(\mathbf{x}),\ i = 1, 2, \ldots, K, \end{aligned}$$

where f_i^c is the consequent function for rule R_i^c. In these rules, the index c indicates that the rule is associated with the output class c. Note that the antecedent parts of the rules can be for different discriminants, as well as the consequents. Therefore, the output of each discriminant function $d_c(\mathbf{x})$ can be interpreted as a score (or evidence) for the associated class c given the input feature vector $\mathbf{x}$. The degree of activation of the ith rule for class c is given by:

$$\beta_i = \prod_{j=1}^{M} \mu_{A_{ij}^c}(\mathbf{x}) \tag{3}$$

where $\mu_{A_{ij}^c}(\mathbf{x}) : \mathbb{R} \rightarrow [0, 1]$. The discriminant output for each class c, with $c = 1, \ldots, C$, is computed by aggregating the individual rules contribution:

$$d_c(\mathbf{x}) = \frac{\sum_{i=1}^{K} \beta_i f_i^c(\mathbf{x})}{\sum_{i=1}^{K} \beta_i} \tag{4}$$

The classifier assigns the class label corresponding to the maximum value of the discriminant functions, i.e

$$\max_c d_c(\mathbf{x}) \tag{5}$$

2) Neural Networks: Artificial Neural Networks (ANN) have been largely used as input-output mapping for different applications including modeling and classification. There are typically three parts in a neural network: an input layer with neurons representing the input variables, one or more hidden layers with a definable number of neurons, and an output layer with one or more units representing the output variables(s). The neuron output signal is given by the following relationship:

$$\sigma = f\left(\mathbf{w}^T x\right) = f\left(\sum_{j=1}^{n} (w_j x_j)\right) \tag{6}$$

where $\mathbf{w} = (w_1, \ldots, w_n)^T \in \mathbb{R}^n$ is the weight vector, and $x = (x_1, \ldots, x_n)^T \in \mathbb{R}^n$ is the vector of neuron inputs. The function $f\left(\mathbf{w}^T x\right)$ is often referred to as the activation (or transfer) function. Its domain is the set of activation values, net, of the neuron model, and is often represented by $f(net)$. The variable net is defined as a scalar product of the weight and input vectors:

$$net = \sum_{j=1}^{n} (w_j x_j) = w_1 x_1 + \ldots + w_n x_n \tag{7}$$

In this work, a feed forward multilayer perceptron (FF MLP) neural network was used, with 10 neurons and logarithmic activation functions in the hidden layer, and tangential activation function in the output layer, following the structure proposed by [20].

III. Results and Discussion

A subset of GI bleeding patients was selected from MIMIC II database according to ICD9 (International Classification of Diseases) codes. After the outliers were removed and misalignment correction and missing data recovery/deletion, the resulting dataset consisted of 235 patients with 50 variables present in all of them, summing up a total of 9382 records. The variables considered for posterior modeling within this dataset were bedside monitor trends, ventilator acquired/set values, indexes, scores, urine output and blood transfusions. All lab tests were included, excluding red and white blood cell counts, hemoglobin and platelets, since they are considered to be tested together with hematocrit in a complete blood count (CBC) [25]. Hematocrit was excluded from the inputs, since it was used as the outcome to classify. After the preprocessing, a complete dataset was obtained for modeling purposes.

The outcome was created as a binary variable, taking the value 1 when the hematocrit was below a threshold T or when a drop of d points occurred on it. T was varied between 15 and 40, and d was varied between 1 and 5. Tables II and III show the values of AUC obtained when using neural networks and fuzzy modeling in the classification the resulting outcome. The maximum AUC obtained when classifying the outcomes generated with fuzzy models and neural networks agreed, and corresponded to T = 35 and d = 3. These values were validated by clinical co-authors as significant for influencing clinical management. In other words, both a drop of 3 points in the hematocrit value or a sustained hematocrit value below 35 would be triggers for urgent diagnostic activities exploring causes of blood loss (e.g. endoscopy) and urgent therapeutic activities such as insertion of a central line, cross matching blood and increased laboratory testing. The resulting outcome can be seen in Figure 3 for an arbitrarily chosen patient.

After defining the outcome, the complete dataset was randomly divided into two equal parts, one for the feature selection process (FS dataset) and the other for the model selection (MS dataset). This was done to assess model performances and to select the best model over an independent dataset not used during any step of model construction.

TABLE II

AUC FOR FUZZY AND NEURAL MODELS WHEN CLASSIFYING DIFFERENT HEMATOCRIT LOWER THRESHOLDS T, VARIED FROM 15 TO 40. FM - FUZZY MODELING; NN – NEURAL NETWORKS; HCT – HEMATOCRIT

	AUC	
HCT threshold T	NN	FM
15	0.52 ± 0.09	0.53 ± 0.03
20	0.54 ± 0.04	0.60 ± 0.04
25	0.61 ± 0.05	0.67 ± 0.02
30	0.65 ± 0.02	0.72 ± 0.04
35	0.82 ± 0.03	0.84 ± 0.02
40	0.60 ± 0.06	0.61 ± 0.04

TABLE III

AUC FOR FUZZY AND NEURAL MODELS WHEN CLASSIFYING DIFFERENT HEMATOCRIT DROPS d, VARIED FROM 1 TO 5. FM - FUZZY MODELING; NN – NEURAL NETWORKS; HCT – HEMATOCRIT

	AUC	
HCT Drop d	NN	FM
1	0.55 ± 0.02	0.55± 0.01
2	0.64 ± 0.01	0.66± 0.03
3	0.71 ± 0.03	0.75± 0.04
4	0.65 ± 0.02	0.63± 0.01
5	0.60 ± 0.01	0.59± 0.02

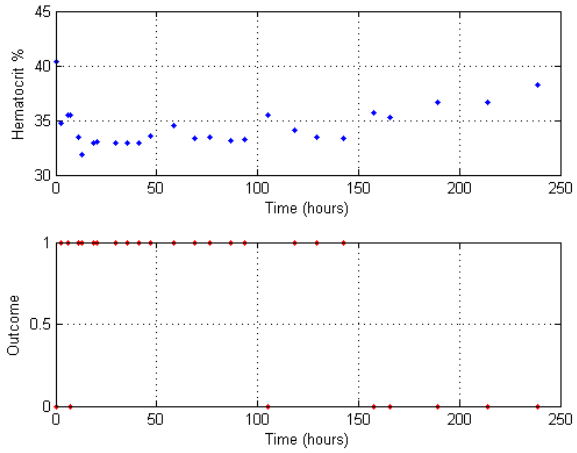

Fig. 3. Outcome generation from the original hematocrit time series for an arbitrarily chosen patient.

The subsets of features were defined over the FS dataset by maximizing AUC, IDI or sensitivity (considered in a multiobjective function). This process was performed 10 times for each maximization criterion, randomly selecting the train (60%), test (30%) and validation (10%) sets from the FS dataset, using neural networks and fuzzy models to classify the outcome; the subset of features resulting in the highest percentage of correct classifications (PCC) for the validation set was selected.

Variables selected with AUC, IDI and sensitivity maximization criteria and their respective PCC values, obtained with neural networks and fuzzy models are shown in Table IV. For both neural networks and fuzzy models, it is possible to see that when AUC was used as the maximization criterion, variables selected result in the highest PCC values. Although

TABLE IV

PCC AND VARIABLES SELECTED WHEN USING AUC, IDI AND SENSITIVITY AS THE MAXIMIZATION CRITERIA DURING A BOTTOM-UP FEATURE SELECTION, PERFORMED WITH FUZZY AND NEURAL MODELS. FM - FUZZY MODELING; NN – NEURAL NETWORKS; IDI – INTEGRATED DISCRIMINATION IMPROVEMENT

Model	Maximization	PCC	Variables Selected
NN	AUC	81.3	Urine Output Creatinine NBP Sodium
	IDI	60.1	Urine Output Creatinine Chloride
	Sensitivity	77.5	Urine Output NBP
FM	AUC	85.2	Urine Output SpO2 Creatinine
	IDI	59.7	Urine Output Chloride Blood Transfusion SpO2 Arterial CO2
	Sensitivity	78.8	Urine Output NBP Blood Transfusion Heart Rate

there was always a coincidence in the first variable selected by all models, the other features seem to respond to minor variations of the subsets used to create the models, since they varied a lot even for different runs of the same modeling technique.

Although it was expected that the use of sensitivity, as the maximization criterion, could increase the final sensitivity and maybe the AUC too, the results obtained showed no improvements (Table V). Moreover, the computational time (not shown in the results) increased for this approach. In the case of IDI, it was expected for it to result in values similar to AUC, since it integrates both sensitivity and specificity in one measurement in a similar way than AUC. However, its use resulted in the lowest PCC values.

The three resulting features subsets, one for each maximization criterion, were separately used in a leave-one-out cross-validation (LOOCV) process. A subset 10% of the MS dataset was defined as the validation set, and the remaining 90% as the training set.

Figure 4a and 4b show an accumulative representation of the results for each additional variable used as input, when AUC was previously used as the maximization criterion to obtain the subset of variables, averaged over the ten runs of cross validation. It can be seen that no improvement is obtain by the use of any variable after *Urine Output*. This, together with the variability reflected in the variables selected under the same maximization criterion (not shown in the results), suggests that only *Urine Output* has predictive value for the outcome defined, while the other variables are selected responding to the variability of the subsets used to create the models. Some other frequently selected variables such as *Non-invasive Blood Pressure* (NBP) and *Creatinine*, could relate to

TABLE V

AUC, SENSITIVITY, SPECIFICITY AND PCC OF FUZZY AND NEURAL MODELS OBTAINED DURING THE LEAVE-ONE-OUT CROSS VALIDATION PROCESS, WHEN USING THE FEATURES SELECTED BY AUC, IDI AND SENSITIVITY MAXIMIZATION CRITERIA. FM - FUZZY MODELING; NN – NEURAL NETWORKS

	NN				FM			
Criterion	AUC	Sensitivity	Specificity	PCC	AUC	Sensitivity	Specificity	PCC
AUC	0.78±0.03	0.77±0.03	0.75±0.01	79±3	0.79±0.05	0.79±0.04	0.80±0.03	81±3
IDI	0.59±0.07	0.62±0.05	0.55±0.04	59±6	0.60±0.03	0.63±0.01	0.58±0.07	58±5
Sensitivity	0.72±0.04	0.71±0.01	0.70±0.02	67±2	0.73±0.04	0.70±0.03	0.74±0.02	73±2

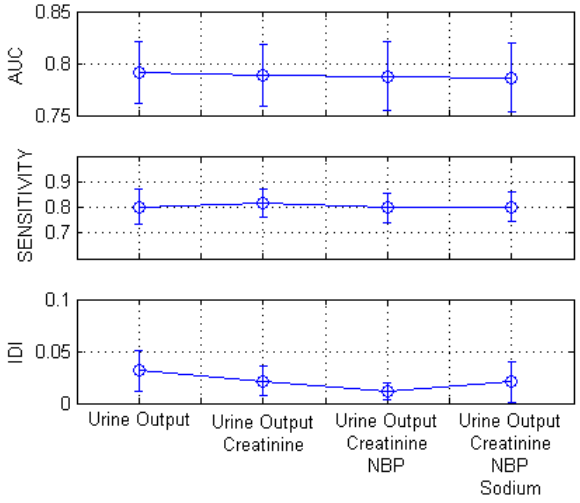

(a) Neural networks

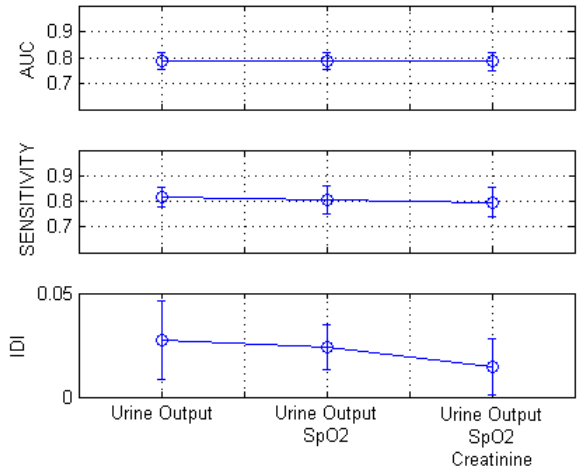

(b) Fuzzy models

Fig. 4. Accumulative AUC, Sensitivity and IDI when each variable selected, using AUC as the maximization criterion, is added during the LOOCV.

specific conditions of some patients that are not shared by the whole dataset.

Table V summarizes the results obtained for fuzzy and neural networks modeling, when the three maximization criteria were separately used to select the features, averaged during the LOOCV process. It can be seen that fuzzy models perform slightly better than neural networks, expressed in higher values for almost all performance measurements.

The fuzzy models gave best results when 2 clusters were

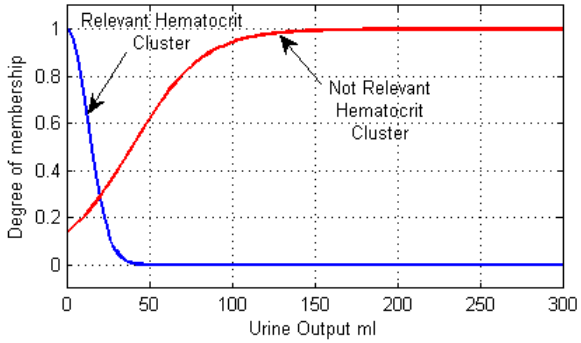

Fig. 5. Membership function for Urine Output obtained with a fuzzy model, maximizing the AUC, during the validation.

used during their training, testing and validation. Neural networks presented their best performance for one hidden layer composed by 10 neurons with logarithmic activation functions, and a linear summation in the output layer.

The selection of *Urine Output* as the primary variable in all models was reviewed and validated under medical assessment. Due to the selection of GI bleeding patients during the creation of the dataset used in this work, the presence of hemorrhage was someway proved for all patients during their ICU stay. Blood volume can be significantly affected by hemorrhage, and so the urine output. If the hematocrit is low enough or presents sudden drops, poor urine collection will reflect those states with some accuracy. This can be seen in one membership function obtained from the fuzzy models, illustrated in Figure 5. This is a positive finding since, by using a simple variable that is collected by the nurse in an hourly assessment of the patient, phlebotomy associated risks and complete blood count (CBC) testing can potentially be avoided.

IV. CONCLUSIONS

Increasing health trends towards improved efficiency seek to align evidence based medicine with cost efficient medicine, both underpinned by a drive to quality. Unnecessary phlebotomy increases clinical and fiscal risks at many levels. In this work, hematocrit lab testing usefulness was evaluated by modeling and classifying the relevance of the results when other collected variables are assessed. A properly de-identified ICU database collected at Beth Israel Deaconess Medical Center, named MIMIC II, was used to develop the models. A subset of gastrointestinal bleeding patients were selected along

with their associated physiological ICU variables, including bedside monitor trends, ventilator records, scores, indexes, lab tests, urine output and blood transfusion information.

Informed by clinical decision making, hematocrit was defined as the positive binary outcome variable set to threshold levels of hematocrit less than 35% or a drop of 3 points. All other measures were represented as the negative binary outcome.

Three maximization criteria, namely the area under the ROC curve (AUC), integrated discrimination improvement (IDI) and sensitivity, were used in a bottom-up feature selection process, combined with neural networks and fuzzy models.

A leave-one-out cross validation process was used to evaluate the overall models' performance, as well as the additional predictive value of the variables selected. Urine output was selected by all models as the most predictive variable for hematocrit levels, and consequently for potential diagnostic and therapeutic interventions. This is consistent with known physiological processes whereby deteriorating renal function occurs as a result of falling blood volume due to factors such as hemorrhage. Results showed that it was possible to correctly classify the usefulness of a hematocrit lab test up to 81% of the time by using fuzzy models and neural networks.

This work is offered as a proof of concept for the use of artificial intelligence models in predicting the usefulness of diagnostic testing. Although the dynamics of hematocrit values are used here on the basis that they are supported by a deeper body of knowledge, the results obtained showed that other routinely variables collected could also be used for predicting diagnostic testing requirements in critical care patients. Future work will focus on:

- expanding the models to a broader population of patients, under different medical conditions
- predicting/classifying different and more complex lab tests currently run on ICU patients
- creating dynamical models to perform future predictions of lab tests usefulness based on present and previous data acquired.

ACKNOWLEDGMENT

The author would like to acknowledge the assistance of the Division of Clinical Informatics at the Beth Israel Deaconess Medical Center and the Massachusetts Institute of Technology. Both human and technical resources were made available, both of which were critical for the development of this work. This work is supported by the Portuguese Government under the programs: project PTDC/SEM-ENR/100063/2008, Fundação para a Ciência e Tecnologia (FCT), and by the MIT-Portugal Program and FCT grants SFRH/BPD/65215/2009, SFRH/43043/2008 and SFRH/43081/2008, Fundação para a Ciência e a Tecnologia, Ministério do Ensino Superior, da Ciência e da Tecnologia, Portugal.

REFERENCES

[1] D. E. Roberts, D. D. Bell, T. Ostryzniuk, K. Dobson, L. Oppenheimer, D. Martens, N. Honcharik, H. Cramp, E. Loewen, and S. Bodnar., "Eliminating needless testing in intensive care: An information-based management approach," *Crit Care Med*, vol. 10, pp. 1452–1458, 1993.

[2] M. E. Ezzie, S. K. Aberegg, and J. M. OBrien, "Laboratory testing in the intensive care unit," *Crit Care Clin*, no. 23, pp. 435–465, 2007.

[3] K. Kumwilaisak, A. Noto, U. H. Schmidt, C. I. Beck, C. Crimi, K. Lewandrowski, and L. M. Bigatello., "Effect of laboratory testing guidelines on the utilization of tests and order entries in a surgical intensive care unit," *Crit Care Med*, vol. 36, no. 11, 2008.

[4] S. M. Mehari and J. H. Havill., "Written guidelines for laboratory testing in intensive care," *Critical Care Resicitation*, vol. 3, pp. 158–162, 2001.

[5] A. Garland, Z. Shaman, J. Baron, and J. A. F. Connors, "Physician-attributable differences in intensive care unit costs," *American Journal of Resp and Crit Care Medicine*, vol. 174, pp. 1206–1210, 2006.

[6] R. J. Woolley, "Drug testing of physicians: the danger of false positives," *JAMA*, vol. 264, no. 24, p. 3148, 1990.

[7] D. W. Bates, L. Goldman, and T. H. Lee, "Contaminant blood cultures and resource utilization: The true consequences of false-positive results," *JAMA*, vol. 265, pp. 365–369, 1991.

[8] W. L. Lee and G. P. Downey, "Icu cornerstone: Changing our view of blood transfusions," *Crit. Care*, vol. 6, no. 4, pp. 291–292, 2002.

[9] U. Fayyad, G. P.-Shapiro, and P. Smyth., "From data mining to knowledge discovery in databases," *AI Magazine*, vol. 17(3), pp. 37–54, 1996.

[10] G. D. Clifford, D. J. Scott, and M. Villarroel, "User guide and documentation for the mimic ii database," 2009, version 2.1.

[11] N. C. for Health Statistics (NCHS), the Centers for Medicare, and M. S. (CMS), *The Int Class Diseases, 9th Rev, Clinical Modification*. NCHS, 2008.

[12] K. Cios, L. Kurgan, K. J. Cios, and L. A. Kurgan, "Trends in data mining and knowledge discovery," in *In: Pal N.R., Jain, L.C. and Teodoresku, N. (Eds.), Knowledge Discovery in Advanced Information Systems*. Springer, 2005, pp. 200–202.

[13] D. Pyle, *Data Preparation for Data Mining*. San Francisco, CA: Morgan Kaufmann, 1999.

[14] F. Cismondi, A. S. Fialho, S. M. Vieira, J. M. C. Sousa, S. R. Reti, M. D. Howell, and S. N. Finkelstein, "New methods to processing misaligned, unevenly sampled time series containing missing data," *IEEE Symposium Series on Computational Intelligence - SSCI 2011*, 2011.

[15] A. S. Fialho, F. Cismondi, S. M. Vieira, J. M. C. Sousa, S. R. Reti, M. D. Howell, R. Welch, and S. N. Finkelstein, "Missing data in large intensive care units databases," in *Soc of Crit Care Med (SCCM) 40th Crit Care Con*, vol. 38, San Diego, California, USA, 2011, pp. A1–A285.

[16] N. M. L. A. P. Dempster and D. B. Rubin, "Maximum likelihood estimation from incomplete data via the em algorithm," *J. Roy. Stat. Soc.*, vol. 39, pp. 1–38, 1977.

[17] R. J. Little and D. B. Rubin, *Statistical Analysis with Missing Data. Series in Probability and Mathematical Statistics*. Wiley, 1987.

[18] M. Sugeno and T. Yasukawa, "A fuzzy-logic-based approach to qualitative modeling," *IEEE Trans. on Fuzzy Systems*, vol. 1, pp. 7–31, 1993.

[19] L. F. Mendonça, S. M. Vieira, and J. M. C. Sousa, "Decision tree search methods in fuzzy modeling and classification," *International Journal of Approximate Reasoning*, vol. 44, pp. 106–123, 2007.

[20] A. S. Fialho, F. Cismondi, S. M. Vieira, J. M. C. Sousa, S. R. Reti, M. D. Howell, and S. N. Finkelstein, "Predicting outcomes of septic shock patients using feature selection based on soft computing techniques," in *Applications 13th International Conference, IPMU 2010, Proceedings, Part II*, ser. Communications in Computer and Information Science (CCIS), R. K. E. Huellermeier and F. Hoffmann, Eds., vol. 81. Springer-Verlag Berlin Heidelberg, 2010, pp. 65–74.

[21] M. Pencina, R. D. Sr., R. D. Jr., and R. Vasan, "Evaluating the added predictive ability of a new marker: From AUC to reclassification and beyond," *Statistics in Medicine*, vol. 27, pp. 157–172, 2008.

[22] A. L. Horn, F. Cismondi, A. S. Fialho, S. M. Vieira, J. M. C. Sousa, S. R. Reti, M. D. Howell, and S. N. Finkelstein, "Multi-objective performance evaluation using fuzzy criteria: Increasing sensitivity prediction for outcome of septic shock patients," in *18th World Congress of the International Federation of Automatic Control (IFAC)*, Italy, 2011.

[23] J. M. C. Sousa and U. Kaymak, *Fuzzy Decision Making in Modeling and Control*. Singapore: World Scientific Pub. Co., 2002.

[24] T. Takagi and M. Sugeno, "Fuzzy identification of systems and its applications to modelling and control," *IEEE Trans. on Systems, Man and Cybernetics*, vol. 15, pp. 116–132, 1985.

[25] W. K. Purves, D. Sadava, G. H. Orians, and H. C. Heller, *Life: The Science of Biology*, 7th ed. Sunderland, Mass, USA: Sinauer Associates, 2004.

2011 IEEE International Conference on Fuzzy Systems
June 27-30, 2011, Taipei, Taiwan

A Fuzzy Inference System for Sleep Staging

Sheng-Fu Liang, Ying-Huang Chen, Chih-En Kuo, Jyun-Yu Chen
Dept. of Computer Science and Information
National Cheng Kung University
Tainan,Taiwan
sfliang@mail.ncku.edu.tw

Sheng-Che Hsu
Department of Electrical Engineering
Ta Hwa Institute of Technology
Hsinchu, Taiwan
eehsu@et4.thit.edu.tw

***Abstract*—In this paper, a fuzzy inference system for sleep staging was developed. Nine input variables including temporal and spectrum analyses of the EEG, EOG, and EMG signals were extracted and normalization was applied to these variables to reduce the effect of individual variability. A fuzzy inference system contains fourteen fuzzy rules was designed to classify the 30-s sleep epochs as five sleep stages. Finally, a smoothing process was applied to the scoring results for fine-tuning. The average accuracy of the proposed method applied to 16 all-night polysomnography (PSG) recordings compared with the manual scorings can reach 87 %. This method can integrate with various PSG systems for sleep monitoring in clinical or homecare applications.**

Keywords-Automatic sleep staging; sleep staging, fuzzy inference systems, sleep minitoring, fuzzy rules.

I. INTRODUCTION

Sleep diseases, such as insomnia and obstructive sleep apnea, seriously affect patients' quality of life. The prevalence of insomnia symptoms is approximately 33% in the general population [1]. There are over 4% of adult men and 3% adult women be affected by obstructive sleep apnea [2]. These sleep issues may cause daytime sleepiness, irritability, depression or anxiety. For the diagnosis of sleep issues, all night polysomnographic (PSG) recordings, including electroencephalogram (EEG), electrooculogram (EOG) and electromyogram (EMG), are usually taken from the patients and the recordings are scored by a well-trained expert according to the Rechtschaffen & Kales (R&K) rules presented in 1968 [3].

According to the R&K rules, each epoch (i.e., 30 s of data) is classified into one of the sleep stages, including wakefulness (Wake), non-rapid eye movement (stages 1-4, from light to deep sleep) and rapid eye movement (REM). Recently, stages 3 and 4 were combined and are now known as the slow wave sleep stage (SWS) [4].

Because visual sleep scoring is a time consuming and subjective process, automatic sleep staging methods, including rule-based methods [5-6], numerical classification methods [7-8] and the hybrid system, that take advantage of both approaches [9], were developed. In rule-based methods, signal information and human knowledge are combined to deduce a reasonable sleep state. In contrast, numerical classification methods do not require a set of rules or any human knowledge. The overall agreement of these methods is in the range of 80% to 85%.

In this paper, a fuzzy inference system for sleep staging was proposed. The central EEG (C3-A2), the difference between two EOG and the chin EMG were analyzed, and nine features were extracted for each 30-s epoch. The features were normalized to reduce the individual variability, so that the system parameters were subject-independent. Finally, a smoothing process was applied to the scoring results for fine-tuning. In future, this method can integrate with various PSG systems for sleep monitoring in homecare applications.

II. METHOD AND MATERIALS

A. Subjects and recordings

All-night polysomnographic sleep recordings were obtained from 20 healthy subjects (12 males and 8 females) ranging from 19 to 23 years in age (mean = 21.2 ± 1.1). The data from four subjects were used to train the system, and data from 16 subjects were used for testing. The recordings included six EEG channels (F3-A2, F4-A1, C3-A2, C4-A1, P3-A2, and P4-A1, according to the international 10-20 standard system), two EOG channels (positioned 1 cm lateral to the left and right outer canthi), and a chin EMG channel (Siesta 802 PSG, Compumedics, Inc.). The sampling rate was 1 KHz with 16-bit resolution. The 20 PSG sleep recordings were visually scored by a sleep specialist using the R&K rules with a 30-s interval (termed the epoch).

B. Feature extraction

The automatic sleep staging system analyzes the data for three channels: the central EEG (C3-A2), the difference of the two EOGs, and the chin EMG. After downsampling the signals to 256 Hz, the EEG and EOG data were filtered with an eighth-order Butterworth band-pass filter with a cutoff frequency of 0.5–30 Hz, and the EMG data were filtered with a 5–100 Hz eighth-order Butterworth band-pass filter. The continuous time signals were segmented with every 30-s epoch.

This work was supported by the National Science Council of Taiwan under grant NSC 98-2221-E-006-161-MY3, 99-2220-E-009-072, 99-2632-E-233-001-MY3.

Before extracting spectral features, the signal was segmented into non-overlapping intervals of 2 seconds for a 512-point fast Fourier transformation (FFT) calculation. The spectrums corresponding to the 15 2-s segments were averaged to represent the spectrum for a 30-s epoch. Table I lists the nine features used in this paper [7-8, 10-11].

After feature extraction, normalization of features was employed to reduce the effects of individual variability. For each feature, the mean of maximal 10% data was calculated as the maximum value of the feature, and the mean of minimal 10% data was calculated as the minimum value of the feature for the subject. This process can prevent extremely high or low values from influencing any conclusions. The procedure for normalization is summarized in the following steps:

Step 1: Calculate the means of the 10% minimal and maximal values for the feature as the min and max values, respectively.
Step 2: Set the min and max values as 0 and 1, and then normalize other values from 0 to 1.
Step 3: If the value is higher than 1, the value is specified as 1. If the value is lower than 0, the value is specified as 0.

TABLE I. The features for sleep scoring

No.	Type	Feature	Source	Label
1	PS	Total power of 0-30 Hz	EEG	0-30 E
2	PS	Total power of 0-30 Hz	EMG	0-30 M
3	PR	0-4 Hz/0-30 Hz	EEG	0-4 E
4	PR	22-30 Hz/0-30 Hz	EEG	22-30 E
5	PR	0-4 Hz/0-30 Hz	EOG	0-4 O
6	SF	Mean frequency of 0-30 Hz	EEG	Mean(fre.) E
7	DR	Alpha ratio	EEG	Alpha E
8	DR	Spindle ratio	EEG	Spindle E
9	EMG energy	Mean amplitude	EMG	Amp M

*PS(=Power spectrum), PR(=Power ratio), SF(=Spectral frequency), DR(=Duration ratio)

C. Fuzzy inference system

In the proposed method, the fuzzy inference system includes 14 fuzzy rules. We use nine features as the input of the fuzzy system to build the fuzzy sets as show in Figure 1.

According to the R&K rules and distributions of the features with respect to various sleep stages, 14 fuzzy rules were constructed. Taking rule 1 as an example, during wake stage, we can observe high frequency activity of EEG such as abundant alpha activity (8-13 Hz) and gamma activity (>20 Hz) in EEG with higher muscle tone. So, The concept of rule 1 is that, when alpha EEG is high (*Alpha E* is G_3) and EMG is high (*0-30 M* is B_2) and low frequency (delta, 0-4 Hz) EEG is low (*0-4 E* is C_1); then the rule concludes that the stage is wake.

The followings are the summary of the 14 fuzzy rules:

R_1: *IF Alpha E is G_3 AND 0-30 M is B_2 AND 0-4 E is C_1 THEN out is WAKE*

R_2: *IF Alpha E is G_3 AND 0-30 M is B_2 AND Spindle E is H_3 AND (0-4 E is C_2 OR 0-4 E is C_3 OR 0-4 E is C_4) THEN out is S2*

R_3: *IF Alpha E is G_3 AND 0-30 M is B_2 AND (Spindle E is H_1 OR Spindle E is H_2) AND Mean(fre.) E is F_2 THEN out is WAKE*

R_4: *IF Alpha E is G_3 AND 0-30 M is B_2 AND (Spindle E is H_1 OR Spindle E is H_2) AND Mean(fre.) E is F_1 THEN out is S1*

R_5: *IF Alpha E is G_3 AND 0-30 M is B_1 AND Amp E is I_1 AND (Spindle E is H_1 OR (Spindle E is H_2 AND 0-30 E is A_1)) THEN out is REM*

R_6: *IF Alpha E is G_3 AND 0-30 M is B_1 AND Amp E is I_1 AND (((Spindle E is H_2 OR Spindle E is H_3) AND (0-30 E is A_2 OR 0-30 E is A_3)) OR (Spindle E is H_3 AND 0-30 E is A_1)) THEN out is S2*

R_7: *IF Alpha E is G_3 AND 0-30 M is B_1 AND Amp E is I_2 AND (Spindle E is H_1 OR Spindle E is H_2) THEN out is S1*

R_8: *IF Alpha E is G_3 AND 0-30 M is B_1 AND Amp E is I_2 AND Spindle E is H_3 THEN out is S2*

R_9: *IF (Alpha E is G_1 OR Alpha E is G_2) AND (22-30 E is D_1 AND (0-4 E is C_3 OR 0-4 E is C_4)) AND 0-4 O is E_2 THEN out is SWS*

R_{10}: *IF (Alpha E is G_1 OR Alpha E is G_2) AND (22-30 E is D_1 AND (0-4 E is C_3 OR 0-4 E is C_4)) AND 0-4 O is E_1 THEN out is S2*

R_{11}: *IF (Alpha E is G_1 OR Alpha E is G_2) AND (22-30 E is D_2 OR (22-30 E is D_1 AND (0-4 E is C_1 OR 0-4 E is C_2))) AND Amp E is I_1 AND (Spindle E is H_1 OR (Spindle E is H_2 AND 0-30 E is A_1)) THEN out is REM*

R_{12}: *IF (Alpha E is G_1 OR Alpha E is G_2) AND (22-30 E is D_2 OR (22-30 E is D_1 AND (0-4 E is C_1 OR 0-4 E is C_2))) AND Amp E is I_1 AND (((Spindle E is H_2 OR Spindle E is H_3) AND (0-30 E is A_2 OR 0-30 E is A_3)) OR (Spindle E is H_3 AND 0-30 E is A_1)) THEN out is S2*

R_{13}: *IF (Alpha E is G_1 OR Alpha E is G_2) AND (22-30 E is D_2 OR (22-30 E is D_1 AND (0-4 E is C_1 OR 0-4 E is C_2))) AND Amp E is I_2 AND (Spindle E is H_1 OR Spindle E is H_2) THEN out is S1*

R_{14}: *IF (Alpha E is G_1 OR Alpha E is G_2) AND (22-30 E is D_2 OR (22-30 E is D_1 AND (0-4 E is C_1 OR 0-4 E is C_2))) AND Amp E is I_2 AND Spindle is H_3 THEN out is S2*

The operations "AND" and "OR" in the fuzzy rules take the minimum and maximum values of the activations, respectively. For each epoch, the inference output is the determined stage that has the maximum activation value among all of the 14 rules.

D. Classification:

The classification process comprises three steps:

1) Movement epochs detection:

The movement (MT) epochs were detected with the following rules: if over 1/3 of the epoch of the absolute EMG amplitude was higher than double of Th1, or if the difference between the two consecutive epochs was higher than Th2, the epoch was defined as MT. Th1 is the mean value of the feature Amp M in Wake epochs of the training data, and Th2 is the mean value of the Amp M difference between every two consecutive epochs of the training data.

2) Fuzzy inference system:

For each epoch, the inference output is the determined stage that has the maximum activation value among all of the 14 rules.

3) Contextual rule smoothing

After classifying the sleep stage, a smoothing process, considering the temporal contextual information, was applied for continuity. Eleven rules [9][12] that refer to the relationship between epochs prior to and posterior to the current epoch were utilized for smoothing.

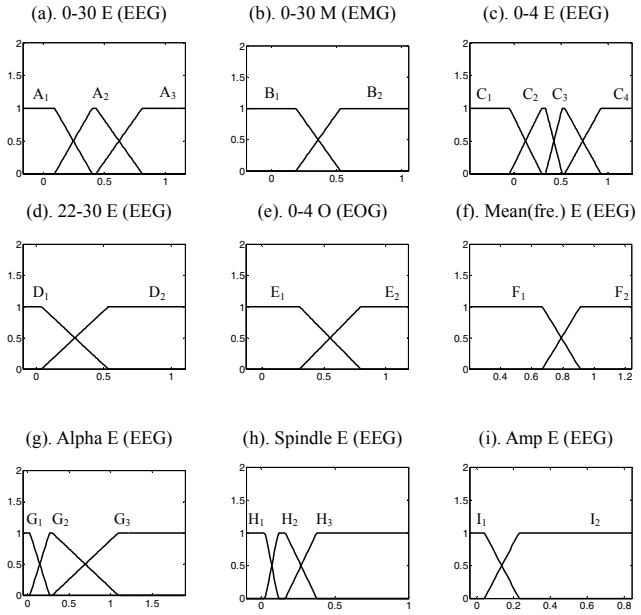

Fig 1. Fuzzy sets in our proposed method

III. EXPERIMENTAL RESULTS

To evaluate the performance of the proposed sleep staging method, 16 all-night PSG recordings from 16 subjects were used for testing. The performance was evaluated in the following aspects: the average performance of the method with smoothing and the sleep staging result of subject's overnight sleep data.

A. Performance of accuracy

TABLE II shows the confusion matrices of the five-stage epoch classification by the proposed sleep staging method. The rows and column are the results staged by expert and our fuzzy inference system, respectively. The testing dataset for performance estimation was comprised of 13,626 30-second epochs. As shown in Table 1, the overall sensitivity was 87.05% for the proposed fuzzy inference system.

B. Performance evaluation of consecutive staging

Figure 2 shows the hypnograms of one subject, including the manual scoring by the expert, the automatic staging without smoothing, and the automatic staging with smoothing.

It was observed that the hypnogram of our proposed method followed the changes in sleep stages of the subject. After smoothing, the resultant hypnogram is closer to the hypnogram scored by the expert.

TABLE II. Confusion table for comparison between computer scoring with smoothing and visual scoring for all 16 subjects.

		Computer						
		Wake	S1	S2	SWS	REM	Total	SE(%)
Expert	Wake	**323**	30	12	0	3	368	87.77
	S1	60	**194**	79	2	118	452	42.92
	S2	111	205	**6591**	258	241	7406	89
	SWS	5	17	239	**2216**	19	2496	88.78
	REM	38	172	118	38	**2538**	2904	87.4
	Overall						**13626**	87.05

* SE = sensitivity

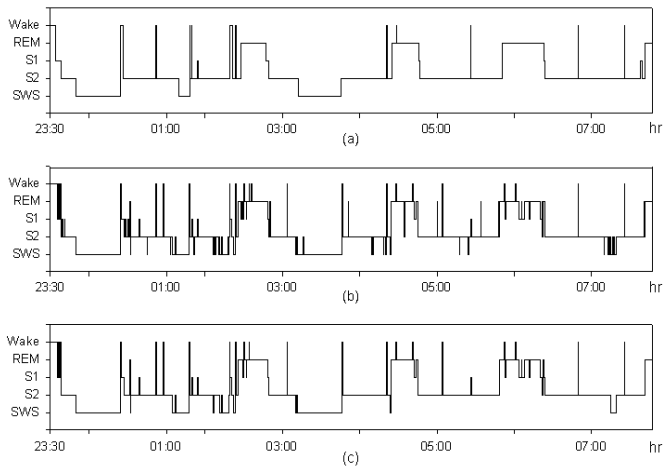

Fig 2. The sleep hypnogram of a subject: (a) the original manually score, (b) the automatic staging without smoothing, and (c) the automatic staging with smoothing.

IV. DISCUSSION

In this paper, an automated sleep staging system based on the fuzzy inference system was proposed. Temporal and spectral features of the EEG, EOG, and EMG signals were extracted and normalization was applied to these features to reduce the effect of individual variability. Experimental results show that the overall accuracy of the proposed fuzzy inference

system can reach 87.05%. Except for S1, the sensitivities of each stage are higher than 87%. The performance is superior to the previous studies [5-9, 12].

In the observation of the PSG signal for each stage, we found that there are many types of signals present in one stage, particularly during S1. So the developed multi-rule staging method that considers various kinds of situations according to the features of frequency and time domain is better than only referring to the R&K rules.

In previous studies, the sensitivity of expert and automatic sleep staging has high accuracy, but the sensitivity of S1 was about only 20% [8, 14]. Some previous studies try to improve the sensitivity of S1 to about 35% [7] [12], but the overall accuracy is about only 80%. S1 is easily mistakenly categorized as one of the other stages, except for SWS, and the number of S1 epochs is significantly lower than that of other stages. So, it is difficult to train a model with a high sensitivity for S1.

The proposed sleep staging method has high sensitivity and the resultant hypnogram is closer to the results scored by the expert. In future, we expect this method can integrate with various PSG systems for sleep monitoring in homecare applications.

REFERENCES

[1] M.M. Ohayon, "Epidemiology of insomnia: what we know and what we still need to learn," Sleep Medicine Reviews, 6: 97-111, 2002.

[2] M.W. Mahowald and C.H. Schenck, "Insights from studying human sleep disorders," Nature, 437: 1279-1285, 2005.

[3] A. Rechtschaffen, A. Kales, eds. A manual of standardized terminology, techniques and scoring system for sleep stages of human subjects, CA: BI/BR, Los Angeles, 1968.

[4] C. Iber, S. Ancoli-Israel, A. Chesson, and S.F. Quan, "The AASM manual for the scoring of sleep and associated events," 1st ed. Westchester, IL: American Academy of Sleep Medicine, 2007.

[5] G.H. Jansen and B.M. Dawant, "Knowledge-based approach to sleep EEG analysis-a feasibility study," IEEE Trans. Biomed. Eng., 36: 510-518, 1989.

[6] J.R. Smith, M. Negin, and A.H. Nevis, "Automatic analysis of sleep electroencephalograms by hybrid computation," IEEE Trans. on Systems Science, and Cybernetics, SSC-5: 278-284, 1969.

[7] R. Agarwal and J. Gotman, "Computer-assisted sleep staging," IEEE Trans. Biomed. Eng., 48: 1412-1423, 2001.

[8] N. Schaltenbrand, R. Lengelle, M. Toussaint, et al., "Sleep stage scoring using the neural network model: Comparison between visual and automatic analysis in normal subjects and patients," Sleep, 19: 26-35, 1996.

[9] H.J. Park, K.S. Park and D.U. Jeong, "Hybrid neural-network and rule-based expert system for automatic sleep stage scoring," in Proc. 22th Annual EMBS Int. Conf., Chicago, pp. 1316-1319, 2000.

[10] C. Berthomier, J. Prado, and O. Benoit, "Automatic sleep EEG analysis using filter banks," Biomed. Sci. Instrum., 35: 241-246, 1999.

[11] F. Duman, A. Erdamar, O. Erogul, Z. Telatar, and S. Yetkin, "Efficient sleep spindle detection algorithm with decision tree," Expert Systems with Applications, 36: 9980-9985, 2009.

[12] J. Virkkala, J. Hasan, A. Värri, S. Himanen, and K. Müller, "Automatic sleep stage classification using two-channel electro-oculography,"J. Neurosci. Methods, 166: 109-115, 2007.

[13] D.G. Altman, Practical statistics for medical research, Chapman & Hall, London, 1991.

[14] A. Flexer, G. Gruber, and G. Dorffner, "A reliable probabilistic sleep stager based on a single EEG signal," Artificial Intelligence in Medicine, 33: 199-207, 2005.

2011 IEEE International Conference on Fuzzy Systems
June 27-30, 2011, Taipei, Taiwan

Fusion of Fuzzy Logic and PD Control for a Five-Fingered Smart Prosthetic Hand

Cheng-Hung Chen
Measurement and Control
Engineering Research Center
Department of Biological Sciences
College of Science and Engineering
Idaho State University
Pocatello, ID 83209, USA
Email: chenchen@isu.edu

D. Subbaram Naidu
Measurement and Control
Engineering Research Center
Department of Electrical Engineering
School of Engineering
Idaho State University
Pocatello, ID 83209, USA
Email: naiduds@isu.edu

***Abstract*—A hybrid of soft control technique of adaptive neuro-fuzzy inference system (ANFIS) and fuzzy logic (FL) and hard control technique of proportional-derivative (PD) for a five-fingered, smart prosthetic hand is presented. The ANFIS is used for inverse kinematics and FL is used for tuning the PD parameters with two input layers (error and error change) using 7 triangular membership functions and 49 fuzzy logic rules. Simulation results with FL-tuned PD controller exhibit superior performance compared to the PD and PID control alone.**

***Index Terms*—Prosthetic Hand, Fuzzy Logic, PD Control, Adaptive Neuro-Fuzzy Inference System, Hybrid Control**

I. Introduction

During the recent wars in Afghanistan and Iraq, "at least 251,102 people have been killed and 532,715 people have been seriously wounded" [1]. Further, in the United States, the Amputee Coalition of America (ACA) [2] reports that there are approximately 1.9 million people living with limb loss, due to combat operations (such as conflicts, wars etc.), and non-combat operations such as accidents, or birth defects. According to a study of the 1996 National Health Interview Survey (NHIS) published by Vital and Health Statistics [3], it is estimated that one out of every 200 people in the U.S. has had an amputation. In other words, about one in every 2,000 new born babies will have limb deficiency and over 3,000 people lose a limb every week in America. By the year 2050, the projected number of Americans living with limb amputation will become 3.6 million [4]. In the past several decades, prosthetic hands have been developed by various researchers in the field [5]–[9], but reproducing the human hand in all its various functions, appearance, visibility, and weight is still a challenging task [5].

Hard computing/control (HC) techniques are used at lower levels for accuracy, precision, stability and robustness. HC comprises proportional-derivative (PD) control [10], proportional-integral-derivative (PID) control [11], [12], optimal control [12]–[15], adaptive control [16]–[19] etc. with specific applications to prosthetic devices. However, our previous works [10]–[12], [20] for a smart prosthetic hand showed that PID controller resulted in overshooting and oscillation. Soft computing (SC) or computational intelligence (CI) [21] is an emerging field based on synergy and seamless integration of neural networks (NN), fuzzy logic (FL) and optimization methods, such as genetic algorithms (GA), particle swarm (PS) [10], [22], [23], tabu search (TS) [23] and so on. The methodology based on SC can be used, in particular with FL, at upper levels of the overall mission where human involvement and decision making is of primary importance, whereas the HC can be used at lower levels for accuracy, precision, stability and robustness. Hence, we present the integration of SC and HC to solve problems that cannot be solved satisfactorily by using either HC or SC methodology alone with specific applications to prosthetics.

In this paper, we first consider briefly trajectory planning and kinematics problems associated with a five-fingered prosthetic hand. Then, adaptive neuro-fuzzy inference system (ANFIS) is used to solve inverse kinematics problem for three-link fingers (index, middle, ring, and little). Next, the dynamics of the hand is derived and feedback linearization technique is used to obtain *linear* tracking error dynamics. Then we propose the fuzzy logic-based PD (hybrid) controller, which uses fuzzy logic with 7 triangular membership functions in each input/output layer and 49 logic rules to tune PD gain parameters. The resulting overall hybrid system incorporating both soft and hard control techniques is simulated with practical data for the hand and found the performance to be superior to PD or PID alone. Finally, we provide conclusions and future work.

II. Modeling

A. Trajectory Planning and Kinematics

The trajectory planning using cubic polynomial was discussed in our previous work [10], [11], [14], [18], [19], [24] for a two-fingered (thumb and index finger) smart prosthetic hand.

Kinematics is the study of geometry in motion and is restricted to a natural geometrical description of motion by

978-1-4244-7316-8/11/$26.00 ©2011 IEEE

the manners, including positions, orientations, and their derivatives (velocities and accelerations) [25], [26]. Forward and inverse kinematics of articulated systems study the analytical relationship between the angular positions of joints and the positions and orientations of the fingertips. A desired trajectory is usually specified in *Cartesian* space and the trajectory controller is easily performed in the *joint* space. Therefore, conversion of Cartesian trajectory planning to the joint space [26] is necessary. Using inverse kinematics, the joint angular positions of each finger need to be obtained from the known fingertip positions. Then the angular velocities and angular accelerations of joints can be obtained from the linear and angular velocities and accelerations of fingertips by differential kinematics. The inverse and differential kinematics of two-link thumb and three-link fingers were discussed in our previous publications [10], [11], [14], [18], [19], [24] for a two-fingered (thumb and index finger) smart prosthetic hand.

For five fingers shown in Figure 1, X^G, Y^G, and Z^G are

Fig. 1. Relationship between Global Coordinate and Local Coordinates: Local coordinate x^t-y^t-z^t of thumb can be reached by rotating through angles α and β to X^G and Y^G of global coordinate, subsequently. Local coordinate x^i-y^i-z^i of index finger can be obtained by rotating through angle α to X^G and then translating a vector $\mathbf{d^i}$ of the global coordinate.

the three axes of global coordinate. Local coordinate x^t-y^t-z^t of thumb can be reached by rotating through angles α and β to X^G and Y^G of the global coordinate, subsequently. Local coordinate x^i-y^i-z^i of index finger can be obtained by rotating through angle α to X^G and then translating a vector $\mathbf{d^i}$ of the global coordinate; similarly, the local coordinate x^j-y^j-z^j of middle finger ($j = m$), ring finger ($j = r$), and little finger ($j = l$) can be obtained by rotating through angle α to X^G and then translating the vector $\mathbf{d^j}$ ($j = m$, r and l) of the global coordinate.

B. Adaptive Neuro-Fuzzy Inference System (ANFIS)

The inverse kinematics problems can be solved by using adaptive neuro-fuzzy inference system (ANFIS) method [27] where the input of fuzzy-neuro system is the Cartesian space and the output is the joint space. ANFIS is a fuzzy inference system implemented in the framework of adaptive networks which provides the best optimization algorithm to find parameters in order to fit the data. ANFIS includes *premise parameters*, that defines membership functions, and *consequent parameters*, that defines the coefficients of each output equation. ANFIS tunes the membership function and identifies the coefficients by the backpropagation gradient descent and least-squares methods, respectively. ANFIS uses a hybrid learning algorithm to identify parameters of Sugeno-type fuzzy inference systems for fuzzy modeling procedures to learn information about a data set in order to compute the membership function and track the given input/output data. Figure 2 (a) shows a two input first-order Sugeno fuzzy model with two rules and Figure 2 (b) depicts the equivalent ANFIS structure for all the computation below. Sugeno-type fuzzy

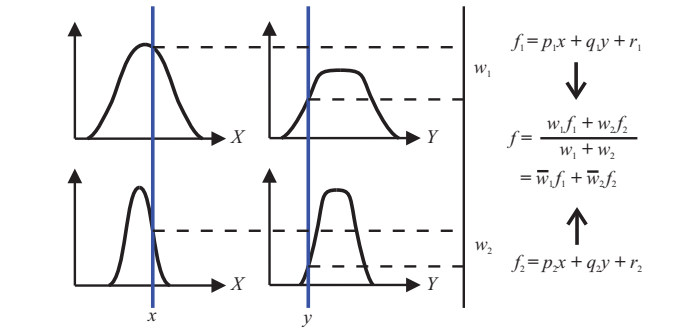

(a) A Two Input First-OrderSugeno Fuzzy Model with Two Rules

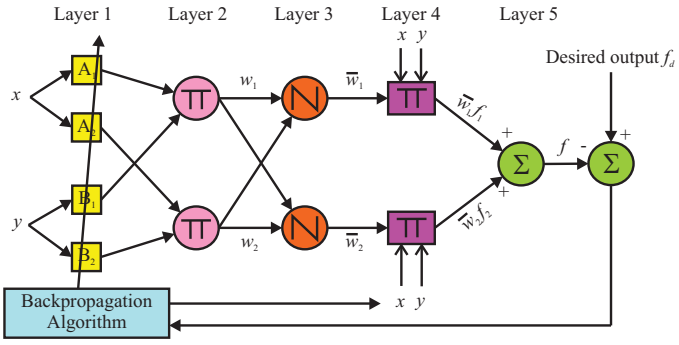

(b) Equivalent ANFIS Structures

Fig. 2. ANFIS Architecture: (a) A Two Input First-Order Sugeno Fuzzy Model with Two Rules (b) Equivalent ANFIS Structure [27]. The inverse kinematics problems are solved by using adaptive neuro-fuzzy inference system (ANFIS) method where the input of fuzzy-neuro system is the Cartesian space and the output is the joint space. ANFIS is a fuzzy inference system implemented in the framework of adaptive networks which provides the best optimization algorithm to find parameters in order to fit the data.

system has the following **Rule Base** [27]–[31].
If x is A_1 and y is B_1, then $f_1 = p_1x + q_1y + r_1$.
If x is A_2 and y is B_2, then $f_2 = p_2x + q_2y + r_2$.
Here, x and y are inputs to constitute the premise parameters A_1, A_2, B_1, and B_2 (Layer 1 in Figure 2 (b)). p_i, q_i, and r_i (i = 1,2) are the consequent parameters. We evaluate the rules by choosing *product* $\prod$ for T-Norm (Layers 2 and 3) which results in

$$w_i = \mu_{A_i}(x)\ \mu_{B_i}(y),\ i = 1, 2. \quad (1)$$

Here, $\mu_{A_i}(x)$ and $\mu_{B_i}(y)$ are designed fuzzy membership functions. Now after leaving the arguments (Layer 4), we get the output $f(x,y)$ by **Rule Consequences**.

$$f(x,y) = \frac{w_1(x,y)f_1(x,y) + w_2(x,y)f_2(x,y)}{w_1(x,y) + w_2(x,y)}. \quad (2)$$

f (Layer 5) can be written as

$$\begin{aligned} f &= \frac{w_1 f_1 + w_2 f_2}{w_1 + w_2} \\ &= \bar{w}_1 f_1 + \bar{w}_2 f_2, \end{aligned} \quad (3)$$

where

$$\bar{w}_1 = \frac{w_1}{w_1 + w_2}, \quad \bar{w}_2 = \frac{w_2}{w_1 + w_2}. \quad (4)$$

C. Dynamics of Hand

The dynamic equations of hand motion are derived via Lagrangian approach using kinetic energy and potential energy as [17], [24]–[26], [32]

$$\frac{d}{dt}\left(\frac{\partial \mathcal{L}}{\partial \dot{\mathbf{q}}}\right) - \frac{\partial \mathcal{L}}{\partial \mathbf{q}} = \boldsymbol{\tau}, \quad (5)$$

where $\mathcal{L}$ is the Lagrangian; $\dot{\mathbf{q}}$ and $\mathbf{q}$ represent the angular velocities and angle vectors of joints, respectively; $\boldsymbol{\tau}$ is the given torque vector at joints. The Lagrangian $\mathcal{L}$ can be expressed as

$$\mathcal{L} = T - V, \quad (6)$$

where T and V denote kinetic and potential energies, respectively. Substituting (6) into (5), dynamic equations of thumb can be obtained as below.

$$\mathbf{M}(\mathbf{q})\ddot{\mathbf{q}} + \mathbf{C}(\mathbf{q}, \dot{\mathbf{q}}) + \mathbf{G}(\mathbf{q}) = \boldsymbol{\tau}, \quad (7)$$

where $\mathbf{M}(\mathbf{q})$ is the inertia matrix; $\mathbf{C}(\mathbf{q}, \dot{\mathbf{q}})$ is the Coriolis/centripetal vector and $\mathbf{G}(\mathbf{q})$ is the gravity vector. (7) can be also written as

$$\mathbf{M}(\mathbf{q})\ddot{\mathbf{q}} + \mathbf{N}(\mathbf{q}, \dot{\mathbf{q}}) = \boldsymbol{\tau}, \quad (8)$$

where $\mathbf{N}(\mathbf{q}, \dot{\mathbf{q}}) = \mathbf{C}(\mathbf{q}, \dot{\mathbf{q}}) + \mathbf{G}(\mathbf{q})$ represents nonlinear terms. The dynamic relations for the two-link thumb and the remaining three-link fingers are quite lengthy and omitted here due to lack of space [24], [33], [34].

III. Control Techniques

A. Feedback Linearization

The nonlinear dynamics represented by (8) is to be converted into a linear state-variable system using feedback linearization technique [17]. Alternative state-space equations of the dynamics can be obtained by defining the position/velocity state $\mathbf{x}(t)$ of the joints as

$$\mathbf{x}(t) = \left[\mathbf{q}'(t) \quad \dot{\mathbf{q}}'(t)\right]'. \quad (9)$$

Let us repeat the dynamical model and rewrite (8) as

$$\frac{d}{dt}\dot{\mathbf{q}}(t) = -\mathbf{M}^{-1}(\mathbf{q}(t))\left[\mathbf{N}(\mathbf{q}(t), \dot{\mathbf{q}}(t)) - \boldsymbol{\tau}(t)\right]. \quad (10)$$

Thus, from (9) and (10), we can derive a linear system in *Brunovsky canonical form* as

$$\dot{\mathbf{x}}(t) = \begin{bmatrix} \mathbf{0} & \mathbf{I} \\ \mathbf{0} & \mathbf{0} \end{bmatrix}\mathbf{x}(t) + \begin{bmatrix} \mathbf{0} \\ \mathbf{I} \end{bmatrix}\mathbf{u}(t) \quad (11)$$

with its control input vector given by

$$\mathbf{u}(t) = -\mathbf{M}^{-1}(\mathbf{q}(t))\left[\mathbf{N}(\mathbf{q}(t), \dot{\mathbf{q}}(t)) - \boldsymbol{\tau}(t)\right]. \quad (12)$$

Let us suppose the prosthetic hand is required to track the desired trajectory $\mathbf{q}_d(t)$ described under path generation or tracking. Then, the tracking error $\mathbf{e}(t)$ is defined as

$$\mathbf{e}(t) = \mathbf{q}_d(t) - \mathbf{q}(t). \quad (13)$$

Here, $\mathbf{q}_d(t)$ is the *desired* angle vector of joints and can be obtained by trajectory planning [10], [11], [14], [18], [24]; $\mathbf{q}(t)$ is the *actual* angle vector of joints. Differentiating (13) twice, to get

$$\dot{\mathbf{e}}(t) = \dot{\mathbf{q}}_d(t) - \dot{\mathbf{q}}(t), \quad \ddot{\mathbf{e}}(t) = \ddot{\mathbf{q}}_d(t) - \ddot{\mathbf{q}}(t). \quad (14)$$

Substituting (10) into (14) yields

$$\ddot{\mathbf{e}}(t) = \ddot{\mathbf{q}}_d(t) + \mathbf{M}^{-1}(\mathbf{q}(t))\left[\mathbf{N}(\mathbf{q}(t), \dot{\mathbf{q}}(t)) - \boldsymbol{\tau}(t)\right] \quad (15)$$

from which the control function can be defined as

$$\mathbf{u}(t) = \ddot{\mathbf{q}}_d(t) + \mathbf{M}^{-1}(\mathbf{q}(t))\left[\mathbf{N}(\mathbf{q}(t), \dot{\mathbf{q}}(t)) - \boldsymbol{\tau}(t)\right]. \quad (16)$$

This is often called the *feedback linearization* control law, which can also be inverted to express it as

$$\boldsymbol{\tau}(t) = \mathbf{M}(\mathbf{q}(t))\left[\ddot{\mathbf{q}}_d(t) - \mathbf{u}(t)\right) + \mathbf{N}(\mathbf{q}(t), \dot{\mathbf{q}}(t)\right]. \quad (17)$$

Using the relations (14) and (16), and defining state vector $\mathbf{x}(t) = [\mathbf{e}'(t) \quad \dot{\mathbf{e}}'(t)]'$, the *tracking error dynamics* can be written as

$$\dot{\mathbf{x}}(t) = \begin{bmatrix} \mathbf{0} & \mathbf{I} \\ \mathbf{0} & \mathbf{0} \end{bmatrix}\mathbf{x}(t) + \begin{bmatrix} \mathbf{0} \\ \mathbf{I} \end{bmatrix}\mathbf{u}(t). \quad (18)$$

Note that this is in the form of a *linear* system such as

$$\dot{\mathbf{x}}(t) = \mathbf{A}\mathbf{x}(t) + \mathbf{B}\mathbf{u}(t). \quad (19)$$

B. Fuzzy Logic-Based PD Hybrid Control

Figure 3 shows the block diagram of the hybrid fuzzy logic-based PD controller for the presented five-fingered prosthetic hand with control signal as

$$\mathbf{u}(t) = -\mathbf{K_P}(t)\mathbf{e}(t) - \mathbf{K_D}(t)\dot{\mathbf{e}}(t) \quad (20)$$

with the proportional $\mathbf{K_P}(t)$ and derivative $\mathbf{K_D}(t)$ diagonal gain matrices with time varying. We then rewrite (17) as

$$\begin{aligned} \boldsymbol{\tau}(t) = \; & \mathbf{M}(\mathbf{q}(t))[\ddot{\mathbf{q}}_d(t) + \mathbf{K_P}(t)\mathbf{e}(t) + \mathbf{K_D}(t)\dot{\mathbf{e}}(t)) + \\ & \mathbf{N}(\mathbf{q}(t), \dot{\mathbf{q}}(t)]. \end{aligned} \quad (21)$$

Then we use mamdani fuzzy inference system to tune the time-varying parameters $\mathbf{K_P}(t)$ and $\mathbf{K_D}(t)$ of PD controller. Figure 4 shows the structural characteristics of proposed fuzzy inference system, which includes two inputs (error $\mathbf{e}$ and error change $\dot{\mathbf{e}}$) on the left and one output ($\mathbf{K_P}$) on the right. Each input or output layer contains seven triangular membership

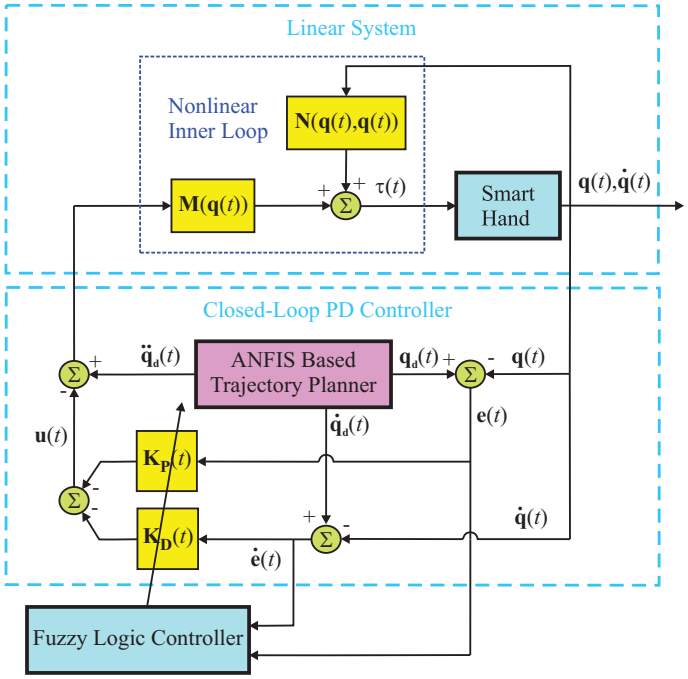

Fig. 3. Block Diagram of the Presented Hybrid Fuzzy Logic-Based Proportional-Derivative (PD) Controller for a Five-Fingered Prosthetic Hand: Errors and error changes are calculated by actual and desired angles, which are based on adaptive neuro-fuzzy inference system (ANFIS) trajectory planner. Then fuzzy logic controller tunes all parameters of closed-loop PD control so that the required torque of the prosthetic hand nonlinear system is computed by control input.

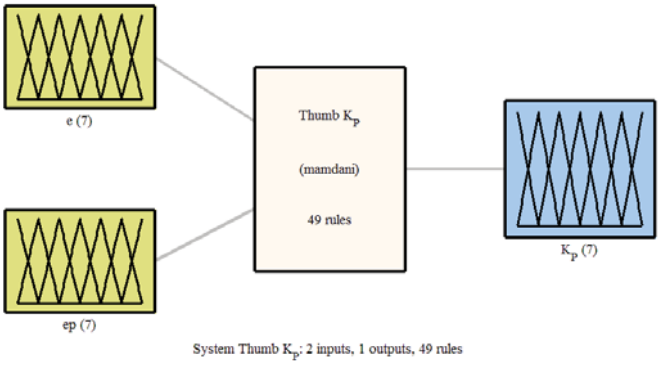

Fig. 4. The Structural Characteristics of Proposed Fuzzy Inference System: Two inputs (error $\mathbf{e}$ and error change $\dot{\mathbf{e}}$) on the left and one output (tuned $\mathbf{K_P}$) on the right with 49 logic rules

functions as shown in Figure 5 and 49 logic rules as listed in Table I. After using 49 logic rules, the output surface $\mathbf{K_P}$ of fuzzy inference system is generated as shown in Figure 6. Similarly, $\mathbf{K_D}$ can be computed by the same way.

IV. Simulation Results and Discussion

Figure 7 shows that a five-fingered prosthetic hand with 14 DOFs is reaching a rectangular rod in order to grasp the object. When thumb and the other four fingers are performing extension/flexion movements, the workspace of fingertips is restricted to the maximum angles of joints. Referring to inverse

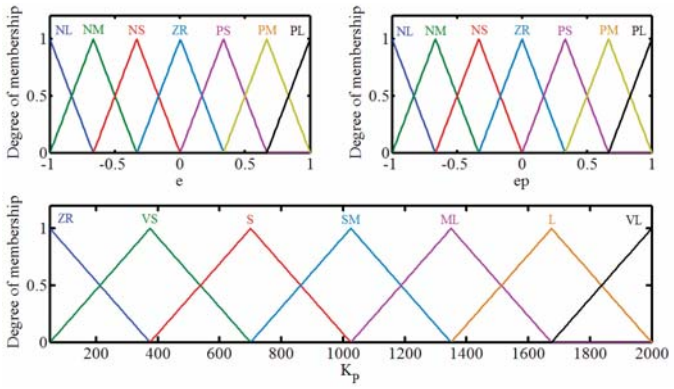

Fig. 5. All Membership Functions: Each of Two Inputs (Upper Panel) and One Output (Lower Panel) Uses 7 Triangular Membership Functions

TABLE I
A Complete Fuzzy Logic Rule Base

ė\e	NL	NM	NS	ZR	PS	PM	PL
NL	ZR	ZR	ZR	ZR	VS	S	SM
NM	ZR	ZR	ZR	VS	S	SM	ML
NS	ZR	ZR	VS	S	SM	ML	L
ZR	ZR	VS	S	SM	ML	L	VL
PS	VS	S	SM	ML	L	VL	VL
PM	S	SM	ML	L	VL	VL	VL
PL	SM	ML	L	VL	VL	VL	VL

N: negative; P: positive; ZR: zero; L: large; M: medium; S: small; V: very

kinematics, the first and second joint angles of the thumb fingertip are constrained in the ranges of [0,90] and [-80,0] (degrees). The first, second, and third joint angles of the other four fingers are constrained in the ranges of [0,90], [0,110] and [0,80] (degrees), respectively [35].

Next, we present simulations with PD and PID controllers and fuzzy inference system tuned PD controller for the 14 DOFs five-fingered smart prosthetic hand. The parameters of the two-link thumb/three-link fingers [36] were related to desired trajectory. All parameters of the smart prosthetic hand selected for the simulations are given in Table II and the

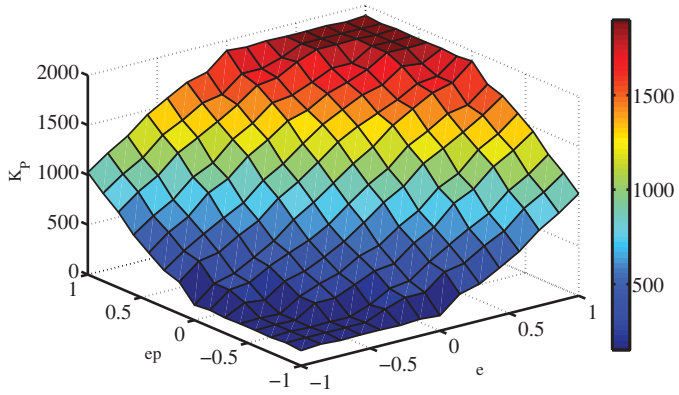

Fig. 6. The Output Surface of Fuzzy Inference System with Two Inputs and 49 Logic Rules

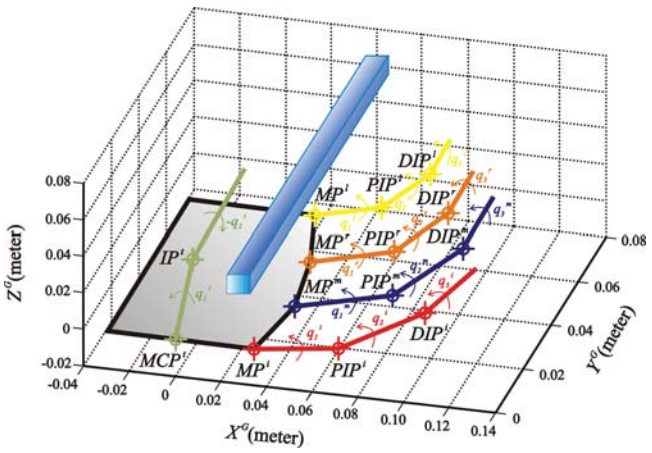

Fig. 7. Five-Fingered Prosthetic Hand Grasping a Rectangular Object

side length and length of the target rectangular rod are 0.010 and 0.100 (m), respectively. The relating parameters between the global coordinate and the local coordinates are defined in Table III. Moreover, in this work, we assumed that each link

TABLE II
PARAMETER SELECTION OF THE SMART HAND

Parameters	Values
Thumb	
Time $(t_0,t_f)^*$	0, 20 (sec)
Desired Initial Position $(X_0^t,Y_0^t)^{**}$	0.035, 0.060 (m)
Desired Final Position $(X_f^t,Y_f^t)^{**}$	0.0495, 0.060 (m)
Desired Initial Velocity $(\dot{X}_0^t,\dot{Y}_0^t)^*$	0, 0 (m/s)
Desired Final Velocity $(\dot{X}_f^t,\dot{Y}_f^t)^*$	0, 0 (m/s)
Length (L_1^t,L_2^t)	0.040, 0.040 (m)
Mass (m_1^t,m_2^t)	0.043, 0.031 (kg)
Index Finger	
Desired Initial Position $(X_0^i,Y_0^i)^{**}$	0.065, 0.080 (m)
Desired Final Position $(X_f^i,Y_f^i)^{**}$	0.010, 0.060 (m)
Length (L_1^i,L_2^i,L_3^i)	0.040, 0.040, 0.030 (m)
Mass (m_1^i,m_2^i,m_3^i)	0.045, 0.025, 0.017 (kg)
Middle Finger	
Desired Initial Position $(X_0^m,Y_0^m)^{**}$	0.065, 0.080 (m)
Desired Final Position $(X_f^m,Y_f^m)^{**}$	0.005, 0.060 (m)
Length (L_1^m,L_2^m,L_3^m)	0.044, 0.044, 0.033 (m)
Mass (m_1^m,m_2^m,m_3^m)	0.050, 0.028, 0.017 (kg)
Ring Finger	
Desired Initial Position $(X_0^r,Y_0^r)^{**}$	0.065, 0.080 (m)
Desired Final Position $(X_f^r,Y_f^r)^{**}$	0.010, 0.060 (m)
Length (L_1^r,L_2^r,L_3^r)	0.040, 0.040, 0.030 (m)
Mass (m_1^r,m_2^r,m_3^r)	0.041, 0.023, 0.014 (kg)
Little Finger	
Desired Initial Position $(X_0^l,Y_0^l)^{**}$	0.055, 0.080 (m)
Desired Final Position $(X_f^l,Y_f^l)^{**}$	0.020, 0.060 (m)
Length (L_1^l,L_2^l,L_3^l)	0.036, 0.036, 0.027 (m)
Mass (m_1^l,m_2^l,m_3^l)	0.041, 0.023, 0.014 (kg)

*All fingers use same parameters
**All parameters are in local coordinates

of all fingers is a circular cylinder with the radius (R) 0.010 (m), so the inertia I_{zzk}^j of each link k of all fingers j (= t, i, m, r and l) can be calculated as

$$I_{zzk}^j = \frac{1}{4} m_k^j R^2 + \frac{1}{3} m_k^j {L_k^j}^2. \quad (22)$$

All initial actual angles are zero and the diagonal coefficients, $\mathbf{K_P}$, $\mathbf{K_I}$ and $\mathbf{K_D}$, for the PD or PID controller alone are arbitrarily chosen as 100. From the derived dynamic and control models, after the parameters ($\mathbf{K_P}$ and $\mathbf{K_D}$) are selected, the control signal $\boldsymbol{u}$ and torque $\boldsymbol{\tau}$ can be calculated.

Figure 8 shows tracking errors (e_1^t and e_2^t on the left

TABLE III
PARAMETER SELECTION OF CONVERSION BETWEEN GLOBAL AND LOCAL COORDINATES

Parameters	Values
Rotating α	90 (deg)
Rotating β	45 (deg)
Translating $\mathbf{d^i}$	(0.035, 0, 0) (m)
Translating $\mathbf{d^m}$	(0.040, 0, -0.020) (m)
Translating $\mathbf{d^r}$	(0.035, 0, -0.040) (m)
Translating $\mathbf{d^l}$	(0.025, 0, -0.060) (m)

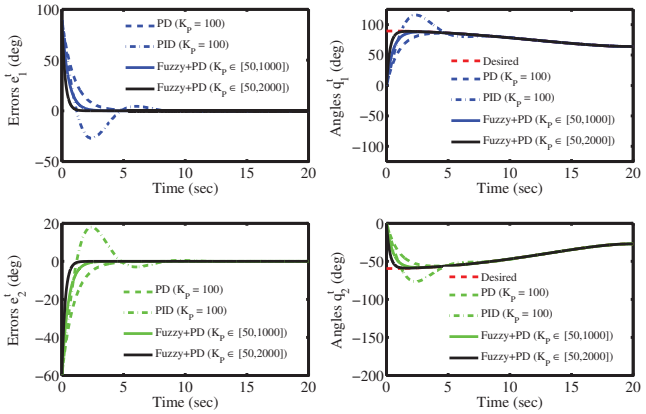

Fig. 8. Tracking Errors (Left) and Desired/Actual Angles (Right) of Joints 1 (Upper) and 2 (Lower) for Two-Link Thumb Using PD (Dash Line), PID (Dot Line) and Fuzzy Logic Based PD (Solid Line) Controllers

column) and desired/actual angles (q_1^t and q_2^t on the right column) of joints 1 (the top row) and 2 (the bottom row) for two-link thumb using PD (dash line), PID (dot line) and fuzzy logic based PD (solid line) controllers. The tracking errors for PD control are convergent within 5 seconds without overshooting, but PID control acts longer (approximate 10 seconds) with overshooting and oscillation. The proposed hybrid fuzzy logic PD control using parameters $\mathbf{K_P} \in [50, 1000]$ and $\mathbf{K_D} \in [50, 500]$ provides faster convergence than both PD and PID controllers. To further study whether the parameter range influences tracking errors, we found that the larger parameter range, the faster convergent speed after altering $\mathbf{K_P} \in [50, 2000]$ without additional computational time. We also used fuzzy logic controller with two inputs (error and error rate) and one output (control signal), but the control system could not obtain convergent tracking errors (data not shown). These data suggest that fusion of soft computing (SC) and

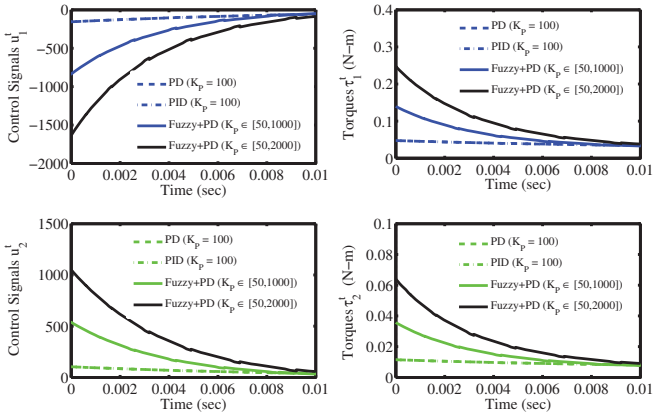

Fig. 9. Control Signals (Left) and Actuated Torques (Right) of Joints 1 (Upper) and 2 (Lower) for Two-Link Thumb Using PD (Dash Line), PID (Dot Line) and Fuzzy Logic Based PD (Solid Line) Controllers in 0.01 Second

hard control (HC) is superior to either HC or SC methodology alone.

The time-variant computed control signals (u_1^t and u_2^t) and torques (τ_1^t and τ_2^t) for two-link thumb within the first 0.01 second are shown in Figure 9, suggesting that the presented hybrid fuzzy logic PD controller requires more power (torque) than PD and PID controllers in order to obtain faster convergent tracking errors.

Similarly, Figures 10, 12, 14 and 16 show tracking errors and desired/actual angles for all remaining three-link fingers. Figures 11, 13, 15 and 17 show control signals and torques for the mapping three-link fingers.

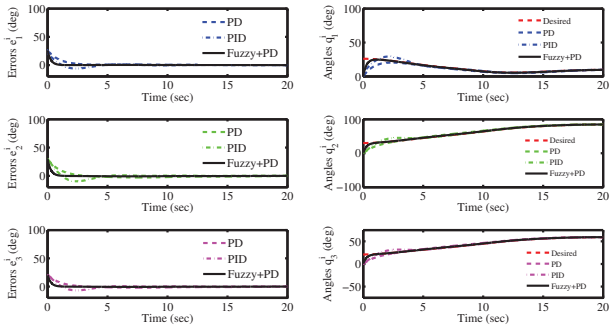

Fig. 10. Tracking Errors (Left) and Desired/Actual Angles (Right) of Joints 1 (Top), 2 (Middle) and 3 (Bottom) for Three-Link Index Finger Using PD (Dash Line), PID (Dot Line) and Fuzzy Logic Based PD (Solid Line) Controllers

V. Conclusions and Future Work

For a five-fingered smart prosthetic hand, a hybrid control technique involving soft control with adaptive neuro-fuzzy inference system (ANFIS) and fuzzy logic (FL) and hard control with proportional-derivative (PD) was presented. The ANFIS is used for inverse kinematics and FL is used for tuning the PD parameters with two input layers (error and

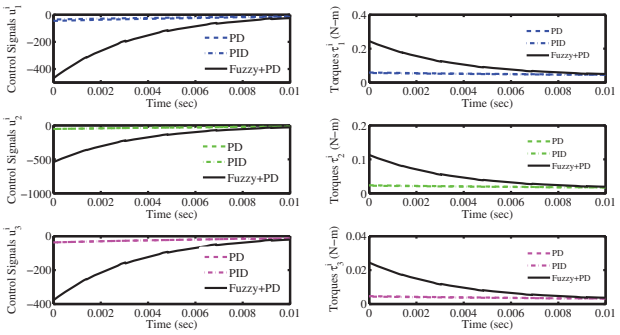

Fig. 11. Control Signals (Left) and Actuated Torques (Right) of Joints 1 (Top), 2 (Middle) and 3 (Bottom) for Three-Link Index Finger Using PD (Dash Line), PID (Dot Line) and Fuzzy Logic Based PD (Solid Line) Controllers in 0.01 Second

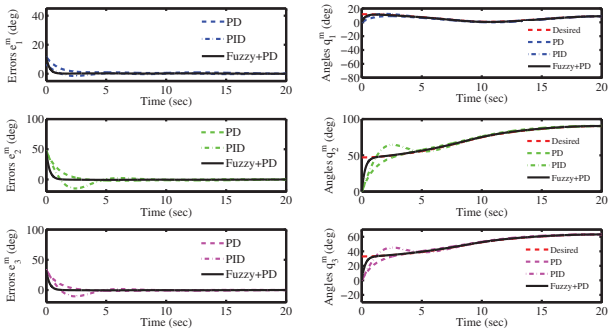

Fig. 12. Tracking Errors (Left) and Desired/Actual Angles (Right) of Joints 1 (Top), 2 (Middle) and 3 (Bottom) for Three-Link Middle Finger Using PD (Dash Line), PID (Dot Line) and Fuzzy Logic Based PD (Solid Line) Controllers

error change) using 7 triangular membership functions and 49 fuzzy logic rules. Simulation results with FL-tuned PD (hybrid) controller showed superior performance compared to the PD and PID control alone. Work is underway to extend this methodology to a real-time implementation on the prototype of a prosthetic hand.

Acknowledgment

The research was sponsored by the U.S. Department of the Army, under the award number W81XWH-10-1-0128 awarded and administered by the U.S. Army Medical Research Acquisition Activity, 820 Chandler Street, Fort Detrick, MD 21702-5014. The information does not necessarily reflect the position or the policy of the Government, and no official endorsement should be inferred. For purposes of this article, information includes news releases, articles, manuscripts, brochures, advertisements, still and motion pictures, speeches, trade association proceedings, etc.

References

[1] "Casualties in Afghanistan & Iraq," www.unknownnews.net, June 5 2006.

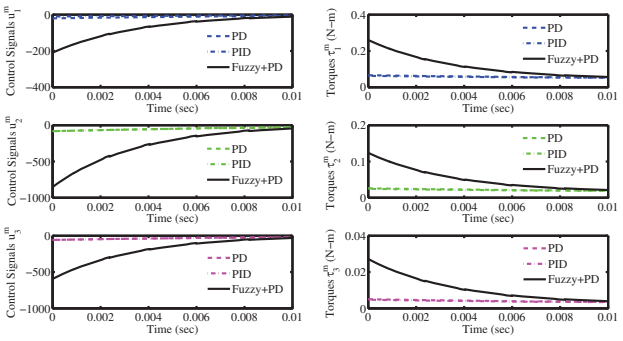

Fig. 13. Control Signals (Left) and Actuated Torques (Right) of Joints 1 (Top), 2 (Middle) and 3 (Bottom) for Three-Link Middle Finger Using PD (Dash Line), PID (Dot Line) and Fuzzy Logic Based PD (Solid Line) Controllers in 0.01 Second

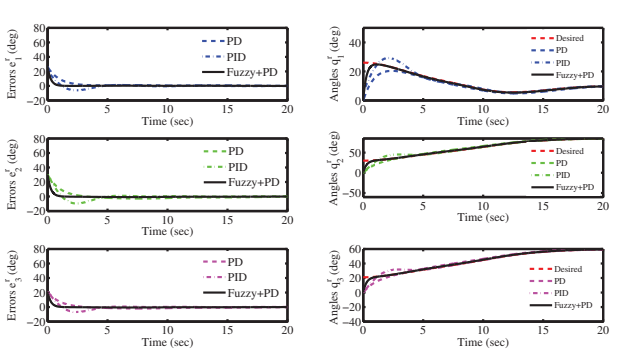

Fig. 14. Tracking Errors (Left) and Desired/Actual Angles (Right) of Joints 1 (Top), 2 (Middle) and 3 (Bottom) for Three-Link Ring Finger Using PD (Dash Line), PID (Dot Line) and Fuzzy Logic Based PD (Solid Line) Controllers

[2] "Amputee Coalition of America (ACA) National Limb Loss Information Center (NLLIC) Limb Loss Facts in the United States," http://www.amputee-coalition.org, 2006.

[3] P. F. Adams, G. E. Hendershot, and M. A. Marano, "Current estimates from the national health interview survey, 1996." *National Center for Health Statistics. Vital and Health Statistics*, vol. 200, no. 10, pp. 1–203, 1999.

[4] K. Ziegler-Graham, E. J. MacKenzie, P. L. Ephraim, T. G. Travison, and R. Brookmeyer, "Estimating the prevalence of limb loss in the united states: 2005 to 2050," *Archives of Physical Medicine and Rehabilitation*, vol. 89, pp. 422–429, March 2008.

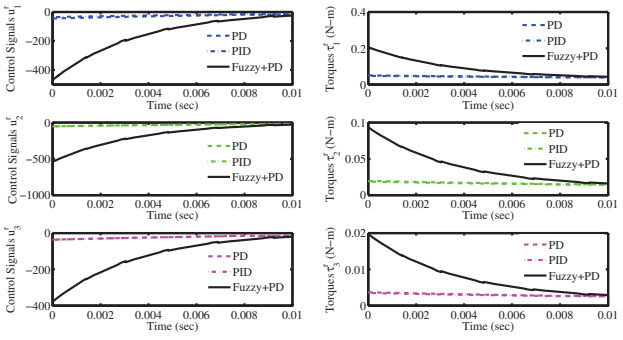

Fig. 15. Control Signals (Left) and Actuated Torques (Right) of Joints 1 (Top), 2 (Middle) and 3 (Bottom) for Three-Link Ring Finger Using PD (Dash Line), PID (Dot Line) and Fuzzy Logic Based PD (Solid Line) Controllers in 0.01 Second

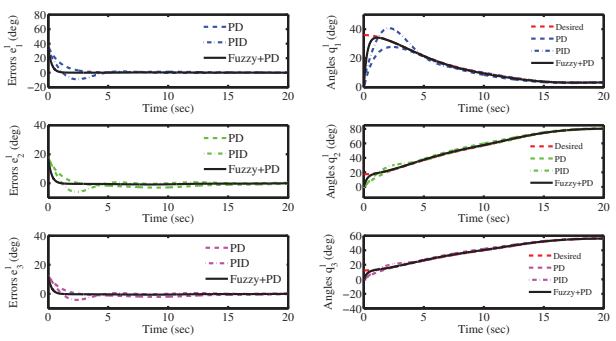

Fig. 16. Tracking Errors (Left) and Desired/Actual Angles (Right) of Joints 1 (Top), 2 (Middle) and 3 (Bottom) for Three-Link Little Finger Using PD (Dash Line), PID (Dot Line) and Fuzzy Logic Based PD (Solid Line) Controllers

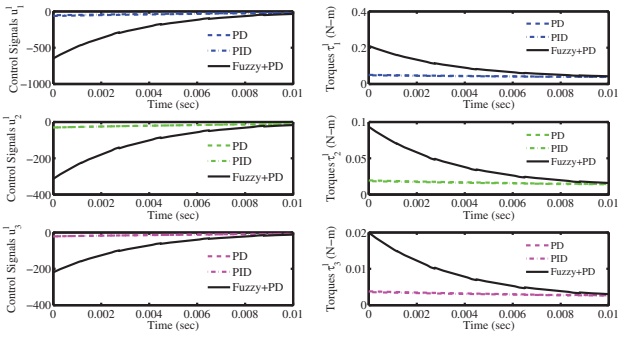

Fig. 17. Control Signals (Left) and Actuated Torques (Right) of Joints 1 (Top), 2 (Middle) and 3 (Bottom) for Three-Link Little Finger Using PD (Dash Line), PID (Dot Line) and Fuzzy Logic Based PD (Solid Line) Controllers in 0.01 Second

[5] M. Zecca, S. Micera, M. Carrozza, and P. Dario, "Control of multifunctional prosthetic hands by processing the electromyographic signal," *Critical Reviews^{TM} in Biomedical Engineering*, vol. 30, pp. 459–485, 2002, (Review article with 96 references).

[6] J. C. K. Lai, M. P. Schoen, A. Perez-Gracia, D. S. Naidu, and S. W. Leung, "Prosthetic devices: Challenges and implications of robotic implants and biological interfaces," *Proceedings of the Institute of Mechanical Engineers (IMechE), Part H: Journal of Engineering in Medicine*, vol. 221, no. 2, pp. 173–183, January 2007, special Issue on Micro and Nano Technologies in Medicine.

[7] L. Zollo, S. Roccella, E. Guglielmelli, M. C. Carrozza, and P. Dario, "Biomechatronic design and control of an anthropomorphic artificial hand for prosthetic and robotic applications," *IEEE/ASME Transactions on Mechatronics*, vol. 12, no. 4, pp. 418–429, August 2007.

[8] D. S. Naidu, C.-H. Chen, A. Perez, and M. P. Schoen, "Control strategies for smart prosthetic hand technology: An overview," in *Proceedings of the 30th Annual International IEEE EMBS Conference*, Vancouver, Canada, August 20-24 2008, pp. 4314–4317.

[9] D. S. Naidu and C.-H. Chen., *Automatic Control Techniques for Smart Prosthetic Hand Technology: An Overview, book chapter 12, to appear in a book titled "Distributed Diagnosis and Home Healthcare (D2H2): Volume 2"*. California, USA: American Scientific Publishers, 2011, (in printed).

[10] C.-H. Chen, K. W. Bosworth, M. P. Schoen, S. E. Bearden, D. S. Naidu, and A. Perez, "A study of particle swarm optimization on leukocyte adhesion molecules and control strategies for smart prosthetic hand," in *2008 IEEE Swarm Intelligence Symposium (IEEE SIS08)*, St. Louis, Missouri, USA, September 21-23 2008.

[11] C.-H. Chen, D. S. Naidu, A. Perez, and M. P. Schoen, "Fusion of hard and soft control techniques for prosthetic hand," in *Proceedings of the International Association of Science and Technology for Development (IASTED) International Conference on Intelligent Systems and Control (ISC 2008)*, Orlando, Florida, USA, November 16-18 2008, pp. 120–125.

[12] C.-H. Chen, D. S. Naidu, A. Perez-Gracia, and M. P. Schoen, "A hybrid control strategy for five-fingered smart prosthetic hand," in *Joint 48th IEEE Conference on Decision and Control (CDC) and 28th Chinese Control Conference (CCC)*, Shanghai, P. R. China, December 16-18 2009, pp. 5102–5107.

[13] D. Naidu, *Optimal Control Systems*. Boca Raton, FL: CRC Press, 2003.

[14] C.-H. Chen, D. S. Naidu, A. Perez-Gracia, and M. P. Schoen, "A hybrid optimal control strategy for a smart prosthetic hand," in *Proceedings of the ASME 2009 Dynamic Systems and Control Conference (DSCC)*, Hollywood, California, USA, October 12-14 2009, (No. DSCC2009-2507).

[15] C.-H. Chen and D. S. Naidu, "Optimal control strategy for two-fingered smart prosthetic hand," in *Proceedings of the International Association of Science and Technology for Development (IASTED) International Conference on Robotics and Applications (RA 2010)*, Cambridge, Massachusetts, USA, November 1-3 2010, pp. 190–196.

[16] F. Lewis, S. Jagannathan, and A. Yesildirek, *Neural Network Control of Robotic Manipulators and Nonlinear Systems*. London, UK: Taylor & Francis, 1999.

[17] F. Lewis, D. Dawson, and C. Abdallah, *Robot Manipulators Control: Second Edition, Revised and Expanded*. New York, NY: Marcel Dekker, Inc.,, 2004.

[18] C.-H. Chen, D. S. Naidu, A. Perez-Gracia, and M. P. Schoen, "A hybrid adaptive control strategy for a smart prosthetic hand," in *The 31st Annual International Conference of the IEEE Engineering Medicine and Biology Society (EMBS)*, Minneapolis, Minnesota, USA, September 2-6 2009, pp. 5056–5059.

[19] C.-H. Chen, D. S. Naidu, and M. P. Schoen, "An adaptive control strategy for a five-fingered prosthetic hand," in *The 14th World Scientific and Engineering Academy and Society (WSEAS) International Conference on Systems, Latest Trends on Systems (Volume II)*, Corfu Island, Greece, July 22-24 2010, pp. 405–410.

[20] C.-H. Chen, M. P. Schoen, and K. W. Bosworth, "A condensed hybrid optimization algorithm using enhanced continuous tabu search and particle swarm optimization," in *Proceedings of the ASME 2009 Dynamic Systems and Control Conference (DSCC)*, Hollywood, California, USA, October 12-14 2009, (No. DSCC2009-2526).

[21] A. Konar, *Computational Intelligence: Principles, Techniques and Applications*. Berlin, Germany: Springer-Verlag, 2005.

[22] C.-H. Chen, K. W. Bosworth, and M. P. Schoen, "Investigation of particle swarm optimization dynamics," in *Proceedings of International Mechanical Engineering Congress and Exposition (IMECE) 2007*, Seattle, Washington, USA, November 11-15 2007, (No. IMECE2007-41343).

[23] C.-H. Chen, K. Bosworth, and M. P. Schoen, "An adaptive particle swarm method to multiple dimensional problems," in *Proceedings of the International Association of Science and Technology for Development (IASTED) International Symposium on Computational Biology and Bioinformatics (CBB 2008)*, Orlando, Florida, USA, November 16-18 2008, pp. 260–265.

[24] C.-H. Chen, "Hybrid control strategies for smart prosthetic hand," Ph.D. dissertation, Measurement and Control Engineering, Idaho State University, May 2009.

[25] R. N. Jazar, *Theory of Applied Robotics. Kinematics, Dynamics, and Control*. New York, USA: Springer, 2007.

[26] B. Siciliano, L. Sciavicco, L. Villani, and G. Oriolo, *Robotics: Modelling, Planning and Control*. London, UK: Springer-Verlag, 2009.

[27] J.-S. Jang, C.-T. Sun, and E. Mizutani, *Neuro-Fuzzy and Soft Computing: A Computational Approach to Learning and Machine Intelligence*. Upper Saddle River, NJ: Prentice Hall PTR, 1997.

[28] F. Karray and C. De Silva, *Soft Computing and Intelligent Systems Design: Theory, Tools and Applications*. Harlow, England, UK: Pearson Educational Limited, 2004.

[29] H. Nguyen, N. Prasad, C. Walker, and E. Walker, *A First Course in Fuzzy and Neural Control*. Boca Raton, FL: Chapman & Hall/CRC, 2003.

[30] V. Nandikolla and D. Naidu, "Blood glucose regulation for diabetic mellitus using a hybrid intelligent technique," in *Proceedings of the 2005 ASME International Mechanical Engineering Congress and Exposition (IMECE)*, Orlando, FL, November 5-11 2005, pp. 1–6.

[31] V. Nandikolla, "Fusion of hard and soft control techniques in biomedical engineering," Ph.D. dissertation, Measurement and Control Engineering, Idaho State University, Pocatello, Idaho, December 2005, thesis Supervisor: D.S. Naidu.

[32] R. Kelly, V. Santibanez, and A. Loria, *Control of Robot Manipulators in Joint Space*. New York, USA: Springer, 2005.

[33] A. Nikoobin and R. Haghighi, "Lyapunov-based nonlinear disturbance observer for serial n-link robot manipulators," *Journal of Intelligent and Robotic Systems*, 2008, (Published online on 11 December 2008).

[34] Y. Z. Arslan, Y. Hacioglu, and N. Yagiz, "Prosthetic hand finger control using fuzzy sliding modes," *Journal of Intelligent and Robotic Systems*, vol. 52, pp. 121–138, 2008.

[35] P. K. Lavangie and C. C. Norkin, *Joint Structure and Function: A Comprehensive Analysis, Third Edition*. Philadelphia, PA: F. A. Davis Company, 2001.

[36] S. Arimoto, *Control Theory of Multi-fingered Hands: A Modeling and Analytical-Mechanics Approach for Dexterity and Intelligence*. London, UK: Springer-Verlag, 2008.

2011 IEEE International Conference on Fuzzy Systems
June 27-30, 2011, Taipei, Taiwan

Hierarchical-interpolative Fuzzy System Construction by Genetic and Bacterial Programming Algorithms

Krisztián Balázs
Department of Telecommunications and Media Informatics
Budapest University of Technology and Economics
Budapest, Hungary
Email: balazs@tmit.bme.hu

László T. Kóczy
Institute of Informatics, Electrical and Mechanical Engineering
Faculty of Engineering Sciences
Széchenyi István University
Győr, Hungary
Email: koczy@sze.hu

***Abstract*—In this paper a method is proposed for constructing hierarchical-interpolative fuzzy rule bases in order to model black box systems defined by input-output pairs, i.e. to solve supervised machine learning problems. The resulting hierarchical rule base is the knowledge base, which is constructed by using evolutionary techniques, namely, Genetic and Bacterial Programming Algorithms. Applying hierarchical-interpolative fuzzy rule bases is an advanced way of reducing the complexity of the knowledge base, whereas evolutionary methods ensure a relatively efficient learning process. This is the reason of the investigation of this combination.**

***Index Terms*—Hierarchical-interpolative fuzzy systems, Genetic Programming, Bacterial Programming, supervised machine learning**

I. Introduction

This paper proposes a method for constructing hierarchical-interpolative fuzzy rules in order to model black box systems based on input-output pairs, i.e. to solve a certain type of supervised machine learning problem. The resulting hierarchical rule base is constructed by using evolutionary techniques, namely, Genetic and Bacterial Programming Algorithms.

There are two key elements in machine learning systems: the learning architecture including the structure of the knowledge base and the learning algorithm applied during the learning process, i.e. the technique that optimizes the knowledge base according to the particular problem. Hence, in order to establish a learning system having favorable properties (low knowledge complexity, high accuracy, fast learning process, etc.) these elements must be chosen so that they outperform other alternatives of knowledge bases and learning algorithms.

For interpretability purposes, i.e. after the learning process to have a quasi-interpretable knowledge base, this paper considers only knowledge bases realized in the form of fuzzy rule bases.

The classical approaches of fuzzy control deal with dense rule bases where the universe of discourse is fully covered by the antecedent fuzzy sets of the rule base in each dimension, thus for every input there is at least one activated rule. The main problem is the high computational complexity of these traditional approaches.

If a fuzzy model contains k variables and maximum T linguistic terms in each dimension, the order of the number of necessary rules is $\mathcal{O}(T^k)$. This expression can be decreased either by decreasing T, or k, or both. Of course, these are very different in terms of the efficiency of the complexity reduction. The first way (decreasing T) leads to sparse rule bases and rule interpolation, see e.g. [1], [2]. The second, more effective way (decreasing k) aims at reducing the dimension of the sub-rule bases by using meta-levels or hierarchical fuzzy rule bases (e.g. [3], [4]). The combination of these two methods leads to decreasing of both T and k, and was introduced in [5].

The scope of this paper focuses on this combination of complexity reduction approaches, namely, the application of hierarchical-interpolative fuzzy rule bases as previous papers [6], [7], [8] considered the other ways of complexity reduction.

Nature inspired evolutionary optimization algorithms are suitable for the global optimization of even non-linear, high-dimensional, multi-modal, and non-continuous problems. The original Genetic Algorithm (GA) was developed by Holland [9] and was based on the process of the evolution of biological organisms. Recognized as a powerful global search technique, genetic algorithms have been applied to a wide variety of problems. They exhibit a remarkable balance between search domain exploration and exploitation [10]. On one hand, every part of the domain is searched and on the other hand, the search effort is concentrated around the best solutions and their neighborhood, producing even better solutions. Bacterial Evolutionary Algorithm (BEA) [11] inspired by the microbial evolution phenomenon is similar, but based on results in the literature appearing more effective technique than GA (e.g. [12], [13], [6]). Approaches like Genetic Programming (GProg) [14] and Bacterial Programming (BProg) [15], present an alternative to the former algorithms. These techniques use the same operators as GA and BEA, respectively, though they require expression trees for gene representation, which could model hierarchical fuzzy rule bases, for example.

Evolutionary algorithms are useful tools for identification problems, they can help with finding a good compromise between the accuracy and the complexity of the model. In case of hierarchical but non-interpolative (i.e. dense) rule bases, genetic and bacterial approaches were successfully applied for fuzzy rule based learning during our previous work [7], [8]. This is the reason why Genetic and Bacterial Programming

978-1-4244-7316-8/11/$26.00 ©2011 IEEE

is applied in our present work as the learning approaches that optimize the knowledge base (instead of using e.g. fuzzy clustering for this purpose like proposed in [16]).

Since so far no method has been invented to obtain the main properties (efficiency, accuracy, etc.) of such complex systems exactly, they can be figured out mostly by simulation. Therefore, in order to discover the capabilities of the established hierarchical-interpolative fuzzy rule based learning systems, simulation runs were carried out.

The next section gives a brief overview of the algorithms and techniques used. The third section proposes a method for constructing and optimizing hierarchical-interpolative fuzzy rule bases by Genetic and Bacterial Programming approaches. The simulation results and the observed behavior will be discussed in the fourth section. Finally, in the last section we will summarize our work and draw some conclusions.

II. Overview of the techniques and algorithms

In order to carry out this investigation, it is necessary to have familiarity with some theoretical fields including the concept of interpolative, hierarchical and hierarchical-interpolative fuzzy rule bases, structure constructing evolutionary optimization techniques (GProg, BProg) and machine learning.

The following subsections aim at giving a brief overview of some important points of these theoretical aspects, which will be repeatedly referred to later in the paper.

A. Interpolative fuzzy systems

In case of classical inference techniques (e.g. Mamdani-[17] or Takagi-Sugeno-inference [18]) in order to obtain any conclusion for an arbitrary observation, the fuzzy rules must cover the whole input space in the following sense. For every observation ($x \in X$) there must be at least one rule (in the form 'R_i: if x_1 is A_{i1} and x_2 is A_{i2} and ...and x_k is A_{ik} then y is B_i') in the rule base ($R = \{R_i\}$) so that $\wedge_{j=1}^{k} A_{ij}(x) \geq \alpha > 0$, i.e. the rule base must be α-*dense*.

Interpolative fuzzy systems calculate the conclusion by using interpolation, hence the input space need only be partially covered by the rules in the sense that there can be observations ($x \in X$) for which there is no rule in the rule base so that $\wedge_{j=1}^{k} A_{ij}(x) \geq \alpha > 0$, i.e. the rule base can be *sparse*.

The interpolative inference technique considered in this paper is the stabilized KH-interpolation [19]. This method is based on a certain interpolation of a family of distances between fuzzy sets in the rules and in the observation. Unlike the original linear KH-interpolation (cf. [1], [2]), it does not consider only the two closest surrounding rules, but it takes all the rules and computes the conclusion based on the consequent parts weighted by the distances. Furthermore, it contains an exponent determined by the number of input dimensions in the denominator in order to stabilize the interpolation function.

B. Hierarchical fuzzy rule based systems

The basic idea of using hierarchical fuzzy rule bases is the following ([3], [4]). Often the multi-dimensional input space $X = X_1 \times X_2 \times \cdots \times X_m$ can be decomposed, so that some of its components, e.g. $Z_0 = X_1 \times X_2 \times \cdots \times X_p$ determine a subspace of $X (p < m)$, so that in Z_0 a partition $\Pi = D_1, D_2, \ldots, D_n$ can be determined: $\bigcup_{i=1}^{n} D_i = Z_0$.

In each element of Π, i.e. in each D_i, a sub-rule base R_i can be constructed with local validity. In the worst case, each sub-rule base refers to exactly $X/Z_0 = X_{p+1} \times \cdots \times X_m$. The complexity of the whole rule base $\mathcal{O}(T^m)$ is not decreased, as the size of R_0 is $\mathcal{O}(T^p)$, and each R_i, $i > 0$, is of order $\mathcal{O}(T^{m-p})$, $\mathcal{O}(T^p) \times \mathcal{O}(T^{m-p}) = \mathcal{O}(T^m)$.

A way to decrease the complexity would be finding in each D_i a proper subset of $X_{p+1} \times \cdots \times X_m$, so that each R_i contains only less than $m-p$ input variables. In some concrete applications in each D_i a proper subset of $X_{p+1}, \ldots, X_m$ can be found so that each R_i contains only less than $m - p$ input variables, and the rule base has the structure shown in Table I., where $z_i \in Z_i$, $Z_0 \times Z_i$ being a proper subspace of X for $i = 1, .., n$.

TABLE I
HIERARCHICAL RULE BASE

R_0:	**If** z_0 is D_1 **then** use R_1
	If z_0 is D_2 **then** use R_2
	...
	If z_0 is D_n **then** use R_n
R_1:	**If** z_1 is A_{11} **then** y is B_{11}
	If z_1 is A_{12} **then** y is B_{12}
	...
	If z_1 is A_{1r_1} **then** y is B_{1r_1}
R_2:	**If** z_2 is A_{21} **then** y is B_{21}
	If z_2 is A_{22} **then** y is B_{22}
	...
	If z_2 is A_{2r_2} **then** y is B_{2r_2}
...	
R_n:	**If** z_n is A_{n1} **then** y is B_{n1}
	If z_n is A_{n2} **then** y is B_{n2}
	...
	If z_n is A_{nr_n} **then** y is B_{nr_n}

If the number of variables in Z_i is $k_i < m - p$ and $\max_{i=1}^{n} k_i = K < m - p$, then the resulting complexity will be $\mathcal{O}(T^{p+K}) < \mathcal{O}(T^m)$, so the structured rule base might lead to a reduction of the complexity.

The task of finding such a partition is often difficult, if not impossible, (sometimes such a partition does not even exist), however there are cases when, locally, some variables unambiguously dominate the behavior of the system, and consequently the omission of the other variables allows an acceptably accurate approximation.

C. Hierarchical-interpolative fuzzy systems

Based on [20], [21] and [22] the reduction of both the maximum number of the linguistic terms (T), and the number of variables (k) can be performed as follows when applying stabilized KH-interpolation. Let us assume that the observation on X is A^* and its projections are $A_0^* = A^*/Z_0$, $A_1^* = A^*/Z_1$,

$A_2^* = A^*/Z_2$, ..., $A_n^* = A^*/Z_n$. Using stabilized KH-interpolation, the sub-conclusions, obtained from the sub-rule bases R_1, R_2, ..., R_n are ${}^{SKH}B^{(1)*}$, ${}^{SKH}B^{(2)*}$, ..., ${}^{SKH}B^{(n)*}$, respectively. (The superscript shows the reference to the rule bases.) Then, by substituting the sub-conclusions into the meta-rule base we obtain ${}^{SKH}B_k^*$, the conclusion. The steps of the algorithm are as follows:

1) determine the projection A_0^* of the observation A^* to the subspace of the fuzzy partition Π
2) determine the distances between A_0^* and the meta-rule antecedents
3) for each R_i determine A_i^* the projection of A^* to Z_i and determine the distances between A_i^* and the rule antecedents
4) determine the sub-conclusions for each sub-rule base R_i by applying stabilized KH-interpolation
5) using the sub-conclusions from step 4, compute the final conclusion ${}^{SKH}B^*$ by applying stabilized KH-interpolation again

Fig. 1 shows a simple example of the algorithm. In step 3 and 4, in each sub-rule base, a different inference engine can be applied, e.g., if the sub-rule base itself is dense, the Mamdani-algorithm (or one of its variations), or in any case one of the interpolation algorithms can be used.

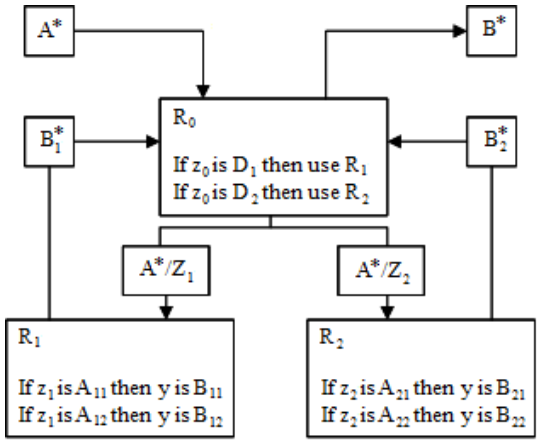

Fig. 1. Interpolation in a hierarchical-interpolative fuzzy system

D. Structure building evolutionary techniques

1) Genetic Programming: There are various optimization algorithms, which were inspired by processes in the nature. The advantage of these algorithms is their ability to solve and quasi-optimize problems with non-linear, high-dimensional, multimodal, and discontinuous character. These processes can easily be applied in optimization problems where one individual corresponds to one possible solution of the problem. In the original Genetic Algorithm (GA) [9] an individual is represented by a sequence of numbers, for example a sequence of bits. This sequence is called chromosome. GA uses three operators: selection, crossover, and mutation. A more recent approach is Genetic Programming (GProg) [14], which uses the same operators as GA, though the individuals are represented by the so called expression tree. This tree is composed of the non-terminal nodes (also called as inner or function nodes) and the terminal nodes (leaves).

The evolutionary process involves the following steps:

a) creation of an initial population
b) evaluation of the candidates
c) application of genetic operators:
   - **selection**: pairs of trees are selected based on their fitness for reproduction
   - **crossover**: nodes in the trees are selected at random and the sub-trees belonging to the selected nodes are exchanged producing a pair of offspring trees
   - **mutation**: this is performed by either replacing a node selected at random by a sub-tree generated randomly or by changing the inner properties of the node
   - **replacement**: substituting the created offsprings to the population
d) test of the termination criteria (e.g. reaching the maximum number of generations, or the time limit) and if any of the termination criteria is achieved, the algorithm stops, otherwise it continues from step b)

The cycle of evolution is summarized in Fig. 2.

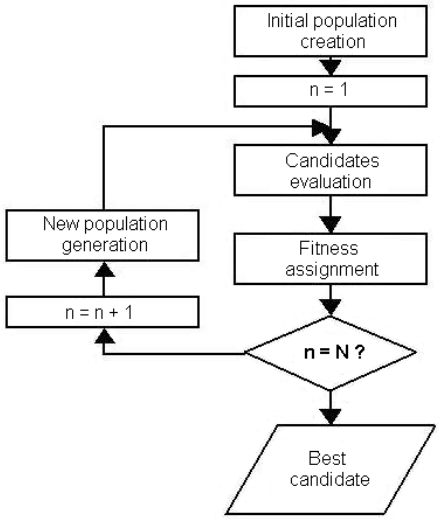

Fig. 2. Flowchart of Genetic Programming

2) Bacterial Programming: An evolutionary technique being slightly different compared to GA is called Bacterial Evolutionary Algorithm (BEA). This algorithm was introduced by Nawa and Furuhashi in [11]. The first version of this algorithm was called Pseudo-Bacterial Genetic Algorithm (PBGA) [23] which proposed a modified mutation operator called bacterial mutation, based on the natural phenomenon of microbial evolution. Bacterial Evolutionary Algorithm introduced a new operator called gene transfer operator. While PBGA incorporates

bacterial mutation and crossover operator, the BEA substitutes the classical crossover with the gene transfer operation. Both of these new operators were inspired by bacterial evolution. Bacteria can transfer genes to other bacteria. The bacterial mutation performs local optimization whilst the gene transfer allows the bacteria to directly transfer information to the other individuals in the population.

Based on these bacterial operations, but using the tree structures similar to the ones in the Genetic Programming, a new technique was proposed, named Bacterial Programming (BProg) [15].

The evolutionary process of BProg involves the following steps:

a) creation of an initial population
b) application of bacterial operators:
   - **bacterial mutation**: this is performed by either replacing a node selected at random by a sub-tree generated randomly or by changing the inner properties of the node
   - **gene transfer**: nodes in the trees are selected at random in the selected superior individual and the sub-trees belonging to the selected nodes are copied to the selected inferior individual
c) test of the termination criteria (e.g. reaching the maximum number of generations, or the time limit) and if any of the termination criteria is achieved, the algorithm stops, otherwise it continues from step b)

The cycle of evolution is summarized in Fig. 3.

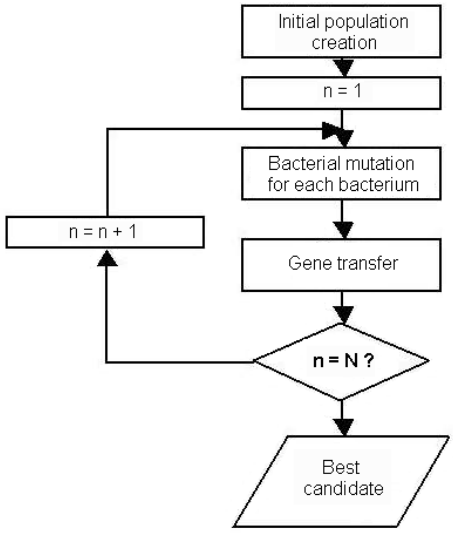

Fig. 3. Flowchart of Bacterial Programming

E. Supervised machine learning

Supervised machine learning [24] means a process where parameters of a 'model' are being adjusted so that its behavior becomes similar to the behavior of the 'system', which is to be modeled. Since the behavior can be characterized by input-output pairs, the aim of the learning process can be formulated so that the model should give similar outputs for the input as the original system does.

The model can be, for example, a simple function (e.g. a polynomial function), where the parameters are the coefficients, or it can be a neural network, where the parameters are the weights, or it can be a hierarchical fuzzy rule base together with an inference engine [25]. In this case the parameters determine the structure of the rule base as well as the membership functions of the rules in the rule base. In our work we applied a hierarchical fuzzy rule base containing trapezoidal membership functions.

If the system is denoted by $\phi(\boldsymbol{x})$ and the model is denoted by $f(\boldsymbol{x}, \boldsymbol{p})$, where $\boldsymbol{x} \in X$ is the input vector and $\boldsymbol{p}$ is the adjustable parameter vector, the previous requirement can be expressed as follows:

$$\forall \boldsymbol{x} \in \boldsymbol{X}: \ \phi(\boldsymbol{x}) \overset{!}{\approx} f(\boldsymbol{x}, \boldsymbol{p}) \tag{1}$$

In a supervised case the learning happens using a set of training samples (input-output pairs). If the number of samples is m, the input in the ith sample is $\boldsymbol{x}_i$, the desired output is $d_i = \phi(\boldsymbol{x}_i)$ and the output of the model is $y_i = f(\boldsymbol{x}_i, \boldsymbol{p})$, the following formula can be used:

$$\forall i \in [1, m]: \ d_i \overset{!}{\approx} y_i \tag{2}$$

The error (ε) shows how similar the model to the system is (see Fig. 4). It is the function of the parameter vector, so it can be denoted by $\varepsilon(\boldsymbol{p})$. A widely applied definition for the error is the Mean Squared Error (MSE):

$$\varepsilon(\boldsymbol{p}) = \frac{\sum_{i=1}^{m} (d_i - y_i)^2}{m} \tag{3}$$

Obviously, the task is to minimize this $\varepsilon(\boldsymbol{p})$ function. It can be done by numerical optimization algorithms.

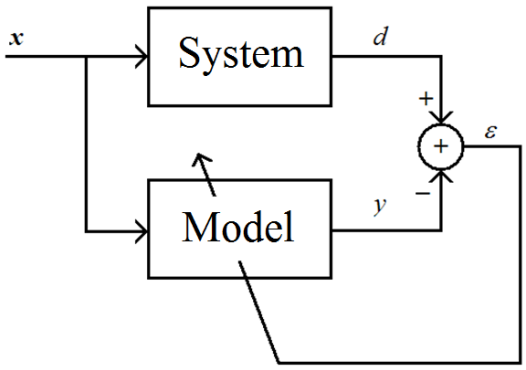

Fig. 4. Supervised machine learning

This way machine learning problems can be traced back to optimization problems.

III. The encoding method

This section describes the method how the hierarchical fuzzy rule bases are represented by the individuals, i.e. how the rule bases are encoded.

The non-terminal (inner) nodes hold the antecedent parts of one or more rules. In case of each non-terminal node the number of considered input dimensions (number of *decision variables*) is a random value, whose maximum can be parameterized. A decision variable can only be such a dimension, which has not been decision variable in the ancestors of the current node. (This way the size of the expression tree becomes limited.) The consequent part of a rule is a child node of the particular node, which can be either a non-terminal or a terminal node. Thus, the number of rules a non-terminal node holds is determined by the number of the children of the particular node. The number of children of the nodes is a random value, whose maximum, i.e. the maximum number of rules belonging to a node, can be parameterized.

Each terminal node (leaf) holds one single fuzzy set, as a conclusion (output) set.

There can be non-terminal nodes as well as terminal nodes on the same level, hence meta-rules and rules can appear together (see Fig. 5).

Since a decision variable cannot be such a dimension, which has already been a decision variable in any ancestor of the current node, in case of crossover in GProg the transfered nodes change their decision variables so that the new decision variables be such dimensions, which have not been decision variables in the ancestors. The same solution of this technical difficulty is applied in gene transfer in BProg, too.

In case of mutation in GProg and bacterial mutation in BProg there are no technical difficulties: only new sub-trees or nodes must be generated with the consideration of the above described encoding rules.

The applied inference algorithm is a simple extension of one of the first interpolation techniques, namely the stabilized KH-interpolation method [19]. This extension is necessary, because there are child nodes in the consequent parts of the rules. Since the conclusions of sub-trees are fuzzy sets (specially, the contents of terminal nodes can also be considered as conclusions), they can be substituted into the consequent parts of the rules of the parent nodes. This can be performed recursively.

IV. Simulation results

Simulation runs were carried out in order to discover the important properties of the established learning systems (speed of learning, accuracy of the resultant knowledge base, etc.).

In our work a six dimensional learning problem was applied that was also used in [11] to evaluate the performance of Bacterial Evolutionary Algorithm. This problem is to approximate the following function:

$$f_{6dim} = x_1 + \sqrt{x_2} + x_3 x_4 + 2e^{2(x_5 - x_6)} \tag{4}$$

$$x_1, x_2 \in [1, 5], \quad x_3 \in [0, 4], \quad x_4 \in [0, 0.6],$$

$$x_5 \in [0, 1], \quad x_6 \in [0, 1.2].$$

In the simulations the parameters had the following values, because after a number of test runs these values seemed to be suitable. The number of individuals in a generation was 8 in both Genetic and Bacterial Programming algorithms. The maximum number of rules belonging to a node, i.e. the maximum number of children of a node, was set to 4 and the maximum number of decision variables in a node was 3. In case of genetic techniques the selection rate was 0.3 and the mutation rate was 0.1, in case of bacterial techniques the number of clones was 5 and 4 gene transfers were carried out in each generation. The genetic methods applied elitist strategy.

The numbers of training samples were 200 in the learning processes.

Two type of simulation were carried out, which differed in the termination criteria. The runs applying the first criterion stopped after reaching the maximum number of generations, which was 2000 generations, whereas the other optimization processes stopped after reaching the time limit, which was 2000 seconds.

At the end of each optimization processes the accuracy of the resultant rule bases was measured by using three error definitions:

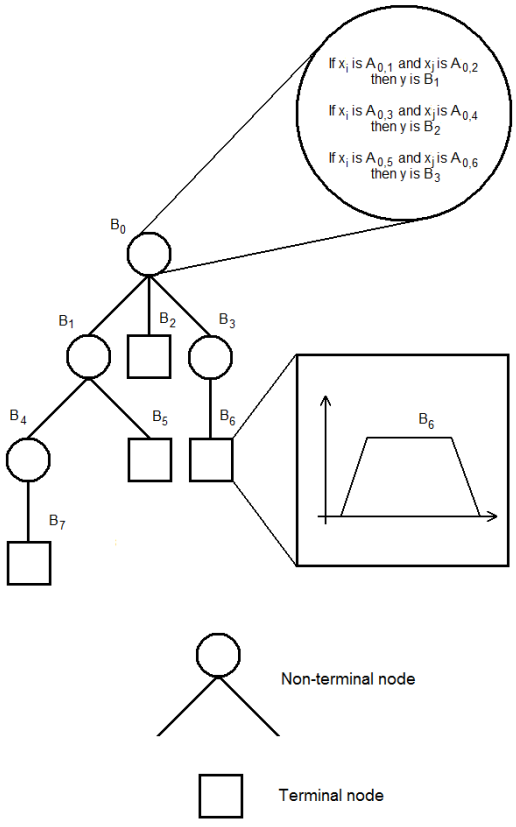

Fig. 5. Tree of a hierarchical rule base (rules and meta-rules appear together on the same levels)

- *Mean Squared Error* (*MSE*):

$$\frac{1}{m}\sum_{i=1}^{m}(d_i - y_i)^2 \tag{5}$$

- *Mean Squared Relative Error* (*MSRE*):

$$\frac{1}{m}\sum_{i=1}^{m}\frac{(d_i - y_i)^2}{y_i^2} \tag{6}$$

- *Mean Relative Error Percentage* (*MREP*):

$$\frac{100}{m}\sum_{i=1}^{m}\left|\frac{d_i - y_i}{y_i}\right| \tag{7}$$

The MSE, MSRE, and MREP values were calculated on the test samples.

The computation time and the number of executed generations were also observed.

In case of both algorithms for each parameterization 10 runs were carried out. Then we took the mean of the obtained values.

During the runs the fitness values of the best individuals were monitored. These fitness values were calculated based on the MSE values (measured on the training samples) as follows:

$$F = \frac{10}{\mathrm{MSE} + 1} = \frac{10m}{\sum_{i=1}^{m}(d_i - y_i)^2 + m} \tag{8}$$

The means of the fitness values of the best individuals during the runs were presented in Fig. 6 and Fig. 7 to get a better overview. The horizontal axes show the executed number of generations and the elapsed computation time in seconds, respectively, and the vertical axes show the fitness values of the best individuals at the current time.

In the figures the dashed lines show the results of GProg and the solid lines present the graph of BProg. For comparing purposes the results obtained in case of non-interpolative (dense) hierarchical rule bases (which can be found in our previous work [7]) are also presented in the figures (drawn with dotted and dotted-dashed lines).

The results of the simulation runs are presented in Table II and Table III. In Table II 'Comp. time' denotes the mean of the computation time (in seconds) the optimization processes required and in Table III 'No. of gen.' denotes the mean of the number of executed generations. In both tables 'No. of rules' denotes the mean of the number of rules in the resulting hierarchical rule bases (including meta-rules).

Again, for comparing purposes the results obtained in case of non-interpolative hierarchical rule bases are also presented in the tables (in columns named 'Hierarchical').

Observing the results given by the hierarchical-interpolative systems it can be seen that BProg outperformed GProg in both simulation types from the point of view of both fitness values (see Fig. 6 and Fig. 7) and the final error values (see Table II and Table III).

Compared to previous results produced by dense hierarchical, Mamdani-inference based learning systems [7], the results

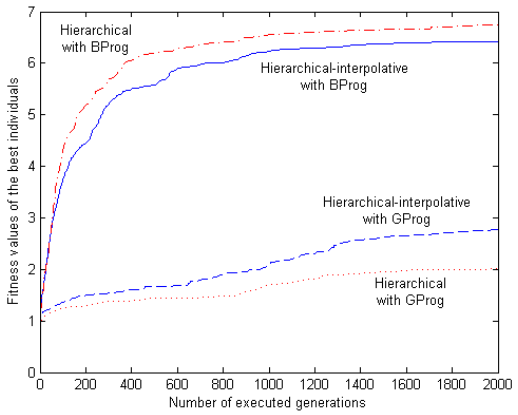

Fig. 6. Results for the six-dimensional learning problem in case of generation limit

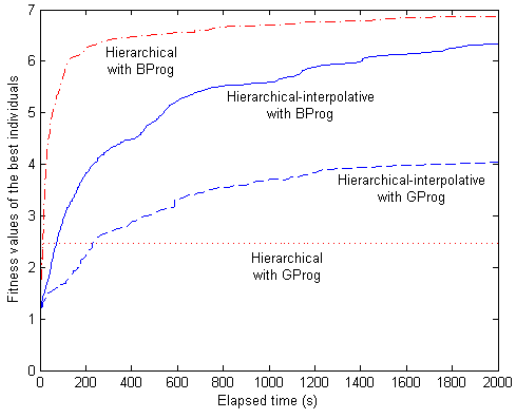

Fig. 7. Results for the six-dimensional learning problem in case of time limit

TABLE II
RESULTS FOR THE SIX DIMENSIONAL LEARNING PROBLEM IN CASE OF 2000 GENERATIONS

	Hierarchical		Hierarchical-interpolative	
	GProg	BProg	GProg	BProg
MSE	4.7773	1.2189	3.7690	**1.2176**
MSRE	0.0711	0.0161	0.0500	**0.0159**
MREP	19.8608	9.5621	16.8610	**9.3132**
Comp. time	1.4	182.7	90.2	3601.6
No. of rules	3	6.8	5.4	7.2

TABLE III
RESULTS FOR THE SIX DIMENSIONAL LEARNING PROBLEM IN CASE OF THE 2000 SECONDS TIME LIMIT

	Hierarchical		Hierarchical-interpolative	
	GProg	BProg	GProg	BProg
MSE	3.4850	**1.0240**	1.5846	1.0335
MSRE	0.0558	0.0155	0.0202	**0.0136**
MREP	17.7449	9.4368	11.0189	**8.8223**
No. of gen.	1914618	34627	52685	1611
No. of rules	4.2	6.4	6	6.8

given by the established hierarchical-interpolative learning systems are convincingly better in case of GProg, however it is not so unambiguous in case of BProg, because the non-interpolative hierarchical system gave higher fitness values during the learning processes (see Fig. 6 and Fig. 7), but most often the hierarchical-interpolative system had lower errors on the test samples after learning (see Table II and Table III, where bold numbers present the best error values).

In case of the time limited runs GProg with the dense hierarchical system stuck in local optima and its convergence speed became zero in 20 seconds, whereas the other combinations had a positive convergence speed even after 2000 seconds and continued advancing to better fitness values (see Fig. 7).

V. Conclusion

Our work proposed a method for constructing hierarchical-interpolative fuzzy rule bases in order to solve supervised machine learning problems. The rule bases were constructed by using Genetic and Bacterial Programming algorithms.

Simulation runs were carried out in order to discover the properties of the obtained learning systems and to compare them with previous results on non-interpolative hierarchical systems [7]. Bacterial Programming outperformed Genetic Programming in both executed simulation types. The results given by the established hierarchical-interpolative learning systems combined with GProg were unambiguously better than previous results produced by the corresponding non-hierarchical, Mamdani-inference based learning system, however in case of the systems with BProg optimization technique neither the interpolative nor the non-interpolative system showed overwhelmingly better properties.

Further research may aim at improving both the encoded learning architecture and the applied optimization methods (e.g. using gradient steps during the optimization process) and to compare the established hierarchical fuzzy systems with non-hierarchical ones.

Acknowledgment

This paper was supported by the National Scientific Research Fund Grant OTKA K75711, a Széchenyi István University Main Research Direction Grant and the Social Renewal Operation Programmes TÁMOP-4.2.2 08/1-2008-0021 and 421 B.

References

[1] L. T. Kóczy and K. Hirota, "Approximate reasoning by linear rule interpolation and general approximation", *International Journal of Approximate Reasoning*, 9, 1993, pp. 197–225.

[2] L. T. Kóczy and K. Hirota, "Interpolative reasoning with insufficient evidence in sparse fuzzy rule bases", *Information Sciences*, 71, 1993, pp. 169–201.

[3] M. Sugeno, T. Murofushi, J. Nishio, and H. Miwa, "Helicopter control based on fuzzy logic", *Second Fuzzy Symposium on Fuzzy Systems and Their Applications to Human and Natural Systems*, Tokyo – Ochanomizu, Japan, 1991.

[4] M. Sugeno, M. F. Griffin, and A. Bastian, "Fuzzy hierarchical control of an unmanned helicopter", Proceedings of the *5th IFSA World Congress (IFSA93)*, Seoul, South Korea, 1993, pp. 1262-1265.

[5] L. T. Kóczy and K. Hirota, "Interpolation in structured fuzzy rule bases", Proceedings of the *IEEE International Conference on Fuzzy Systems, FUZZ-IEEE'93*, San Francisco, 1993, pp. 803–808.

[6] K. Balázs, J. Botzheim, L. T. Kóczy, "Comparative analysis of interpolative and non-interpolative fuzzy rule based machine learning systems applying various numerical optimization methods", *World Congress on Computational Intelligence, WCCI 2010*, Barcelona, Spain, 2010, pp. 875–982.

[7] K. Balázs, J. Botzheim, L. T. Kóczy, "Hierarchical fuzzy system modeling by genetic and bacterial programming approaches", *World Congress on Computational Intelligence, WCCI 2010*, Barcelona, Spain, 2010, pp. 1866-1871.

[8] K. Balázs, J. Botzheim, L. T. Kóczy, "Hierarchical fuzzy system construction applying genetic and bacterial programming algorithms with expression tree building restrictions", *World Automation Congress, WAC 2010*, Kobe, Japan, 2010.

[9] J. H. Holland, "Adaption in natural and artificial systems", The MIT Press, Cambridge, Massachusetts, 1992.

[10] D. E. Goldberg, "Genetic algorithms in search, optimization, and machine learning", Addison-Wesley, Reading, Massachusetts, 1989.

[11] N. E. Nawa and T. Furuhashi, "Fuzzy system parameters discovery by bacterial evolutionary algorithm", *IEEE Transactions on Fuzzy Systems*, vol. 7, no. 5, 1999, pp. 608–616.

[12] K. Balázs, J. Botzheim and L. T. Kóczy, "Comparative analysis of various evolutionary and memetic algorithms", Proceedings of the *10th International Symposium of Hungarian Researchers on Computational Intelligence and Informatics, CINTI 2009*, Budapest, Hungary, 2009, pp. 193–205.

[13] K. Balázs, J. Botzheim, L. T. Kóczy, "Comparison of various evolutionary and memetic algorithms", Proceedings of the *International Symposium on Integrated Uncertainty Management and Applications, IUM 2010*, Ishikawa, Japan, 2010, pp. 431–442.

[14] J. R. Koza, "Genetic programming: On the programming of computers by means of natural selection", The MIT Press, 1992.

[15] J. Botzheim, C. Cabrita, L. T. Kóczy, and A. E. Ruano, "Genetic and bacterial programming for B-spline neural networks design", *Journal of Advanced Computational Intelligence and Intelligent Informatics*, vol. 11, no. 2, 2007, pp. 220–231.

[16] A. Chong, T. D. Gedeon, L. T. Kóczy, "Hierarchical fuzzy modeling", *International Fuzzy System Association World Congress, IFSA 2003*, Istanbul, 2003, pp. 236–240.

[17] E. H. Mamdani, "Application of fuzzy algorithms for control of simple dynamic plant", IEEE Proc., vol. 121, no. 12, 1974, pp. 1585–1588.

[18] T. Takagi and M. Sugeno, "Fuzzy identification of systems and its applications to modeling and control", *IEEE Transactions on Systems, Man and Cybernetics*, vol. 15, no. 1, 1985, pp. 116-132.

[19] D. Tikk, I. Joó, L. T. Kóczy, P. Várlaki, B. Moser and T. D. Gedeon, "Stability of interpolative fuzzy KH-controllers", *Fuzzy Sets and Systems*, 125, 2002, pp. 105–119.

[20] L. T. Kóczy and K. Hirota, "Interpolation in hierarchical fuzzy rule bases with sparse meta-levels", Technical Report 97-3, Tokyo Institute of Technology, Yokohama, 1997.

[21] L. T. Kóczy, K. Hirota and L. Muresan, "Interpolation in hierarchical fuzzy rule bases", *International Journal of Fuzzy Systems*, vol. 1, no. 2, 1999, pp. 77–84.

[22] L. T. Kóczy, J. Botzheim, T. D. Gedeon, "Fuzzy models and interpolation", Forging New Frontiers: Fuzzy pioneers I and II, Heidelberg, Springer-Verlag, 2007. pp. 111-131.

[23] N. E. Nawa, T. Hashiyama, T. Furuhashi, and Y. Uchikawa, "Fuzzy logic controllers generated by pseudo-bacterial genetic algorithm", Proceedings of the *IEEE International Conference on Neural Networks, ICNN97*, Houston, 1997, pp. 2408–2413.

[24] E. Alpaydin, "Introduction to machine learning", The MIT Press, 2004, 445 p.

[25] D. Driankov, H. Hellendoorn, M. Reinfrank, "An introduction to fuzzy control", Springer, New York, 316 p.

2011 IEEE International Conference on Fuzzy Systems
June 27-30, 2011, Taipei, Taiwan

Study on Various Defuzzification Methods for Fuzzy Clustering Algorithms to Improve ROIs Detection in Lung CTs

Alberto Rey
Faculty of Computer Science
University of A Coruna
A Coruna, Spain
Email: alberto.rey@udc.es

Bernardino Arcay
Faculty of Computer Science
University of A Coruna
A Coruna, Spain
Email: bernardino.arcay@udc.es

Alfonso Castro
Faculty of Computer Science
University of A Coruna
A Coruna, Spain
Email: alfonso.castro@udc.es

***Abstract*—The detection of pulmonary nodules is one of the most studied areas and challenging task in the field of medical image analysis, due the current relevance of the lung carcinoma. The difficulty and complexity of this task has led to the development of CAD systems for the automated detection of lung nodules in CT scans, which provides valuable assistance for radiologists and could improve the detection rate. A common phase of these systems is the detection of regions of interest (ROIs) that could be marked as nodules, in order to reduce the searching space problem. In this paper, we evaluate and compare the combination of various approaches of supervised vector machines (SVMs) with different kinds of fuzzy clustering algorithms, so as to improve the detection and segmentation of ROIs that could represent lung nodules in high resolution CT scans. These images are provided by the LIDC database (Lung Internet Database Consortium).**

***Keywords*—Fuzzy Clustering, Support Vector Machines, Medical Image Analysis, Computer Aided Detection.**

I. Introduction

The high complexity of the lung structure, with 23 airway subdivisions between trachea and alveolar sacs, and numerous lung diseases represented in images by pathological structures such as nodules, tumors, etc., have encouraged the analysis of computer pulmonary images. In this area, one of the most studied diseases is lung carcinoma, one of the most mortal carcinomas for which early detection is essential. The survival rate after 5 years for patients who were diagnosed and had surgery in a early stage is over 60%, but drops to 10% if the patients do not have surgery during these five years.[1]

Both primary and metastatic lung carcinoma most commonly manifest as pulmonary nodules, so researchers are focusing on the detection of these structures as a previous step for an early diagnosis.

The development of new modalities of image acquisition, such as high resolution CTs, has improved the detection and diagnosis of early nodules that, at their initial stage, may have a diameter below 3mm [2]. This technique offers a non-invasive way to observe the lung structure with great definition. Nevertheless, it is rarely used due to the high cost of the technology.

High resolution CTs studies may contain up to 600 images [2] whose examination and interpretation by radiologist is a very tedious and time-consuming task. Moreover, lung nodules are difficult to detect in CT images because they may appear attached to other non-pathological elements such as blood vessels or pleura, or have a small size and different shapes. For these reasons, currently new CADs (Computer Aided System) systems are being developed [3] [4] for the automated detection of lung nodules, providing support to the diagnosis of the experts. Our research group is developing such a system.

The first stage for these systems usually consists in preprocessing the CT images in order to isolate the lungs and reduce the search area where nodules could appear, removing those external elements that could interfere with the detection task. Lungs are therefore the only elements on each image of the CT scan. Our system follows this approach.

The second step consists in the detection of ROIs that could be treated as possible nodules. This paper presents the results obtained with a combination of different fuzzy clustering algorithms with various approaches of the SVM technique. The analysed fuzzy algorithms represent the state of the art in this field, obtaining good results for the detection of ROIs in lung CTs [5] [6]. The non-defuzzified output of these algorithms provides membership factors for each image pixel that represents with which grade they are classified into each segmented cluster. The principal aim of the study is to improve these results by applying the SVM technique to the membership factors, so as to obtain a better defuzzification phase with fewer rates of false positives in the segmentation of lung CT images. As this step is included in a CAD system, the analysis focuses on achieving a good method that reduces the false nodule candidate area, minimizing the deficiencies in the classification of the pixels provided by the fuzzy algorithms.

II. Materials

In this paper, we used a training and simulation set that consists in several high-resolution CT lung images, provided

This work was supported by project 09SIN006PR from the I+D Suma Call of the Galician Plan for Research, Development and Technological Innovation (INCITE) from Xunta de Galicia.

978-1-4244-7316-8/11/$26.00 ©2011 IEEE

by the LIDC (Lung Image Database Consortium) database. This project, developed by the NCI (National Cancer Institute), mainly aims at developing and publishing a reference repository for the evaluation and implementation of CAD systems in lung nodules detection.[7]

The database consists in a repository of images in which each has associated relevant data regarding the presence or absence and the characteristics of the observed nodule(s) if present. This information is obtained from a process whereby four expert thoracic radiologists analyse and mark, regardless, each image. Later, if discrepancies in observations exist, they can be revised and corrected. The data is provided in a XML file that indicates its type and contour, specified by the pixels coordinates that conform it.

The provided studies are stored using the DICOM standard and have a size of 512x512 pixels, with a pixel size varying from 0,5 to 0,8 mm. The grayscale is of 12 bits in Hounsfiled Units (HU).

The implementations of the different multi-class SVM approaches is provided by the BSVM library [8], that can be used freely for research purposes. The fuzzy algorithms were implemented with the ITK library, focused mainly on medical image analysis.

III. Analysed fuzzy algorithms

We selected three fuzzy clustering algorithms to carry out the detection task of the initial ROIs. They all provide less sensitivity to noise and outliers, are able to easily handle multidimensional problems, and provided the best results during the previous analysis [5] and [6] carried out on LIDC data sets.

A. SFCM (Spatial Fuzzy C-Means)

This algorithm [9] is a modified version of the FCM (Fuzzy C-Means) that incorporates spatial information in such a way that it alters the membership weighting value of each cluster after considering the distribution in the neighborhood. This spatial information provides the possibility to obtain more homogeneous regions and reduce the effect of noise.

In the first step, the algorithm calculates the initial membership values for each pixel, applying the standard FCM algorithm. Then, the spatial relationship is introduced by the following function:

$$h_{ij} = \sum_{k \in NB(x_j)} u_{ik} \tag{1}$$

where $NB(x_j)$ represents a resizable square window, centered on each pixel x_j under consideration. Therefore, the greater the value of this function, the greater the probability that pixel x_j belongs to cluster ith.

The next step calculates the new membership function using the previous spatial information:

$$u'_{ij} = \frac{u_{ij}^p h_{ij}^q}{\sum_{k=1}^{C} u_{kj}^p h_{kj}^q} \tag{2}$$

where p and q control the relevance of functions u_{ij} and h_{ij}.

In the last step, the new centroids are obtained following the same FCM procedure:

$$c_j = \frac{\sum_{i=1}^{N} u'^m_{ij} x_i}{\sum_{i=1}^{N} u'^m_{ij}} \tag{3}$$

The iteration process will stop when the maximal difference between two centroids lies below a determined threshold.

B. SKFCM (Spatial Kernelized Fuzzy C-Means)

This algorithm [11] introduces a penalty factor that contains spatial neighborhood information to the KFCM (Kernelized Fuzzy C-Means) algorithm proposed in the same work. Kernelized methods introduce a kernel function that allows us to transform the original low dimension input space into a higher dimensional feature space, where complex nonlinear problems can be treated and solved in a better way as probed by Cover [12]. The present paper only considers the Gaussian radial basis function kernel:

$$K(x, y) = exp\left(\frac{\|x - y\|^2}{\sigma^2}\right) \tag{4}$$

Therefore, modifying the objective function of the FCM in order to introduce the kernel function and add the penalty factor, we obtain the final objective function:

$$JS_m^{\phi} = \sum_{i=1}^{c}\sum_{k=1}^{N} u_{ik}^m (1 - K(x_k, v_i)) + \frac{\alpha}{N_R}\sum_{i=1}^{c}\sum_{k=1}^{N} u_{ik}^m \sum_{r \epsilon N_k} (1 - u_{ir})^m \tag{5}$$

where N_k represents the square window which includes the neighbors of pixel x_k (without considering it), N_r is the cardinality of N_k, and α ($0<\alpha<1$) is a parameter that controls the effect of the penalty term. Deriving the Eq. 5 respect the variables u_{ik} and v_i obtains the following two conditions that minimize the function. An iterative algorithm can be derived from the above conditions.

In the initialization of the algorithm, the parameters c, i.e. the number of clusters, the initial class centroids, the initial memberships, and the threshold epsilon, must be determined.

In the first step of the iterative process, the memberships are calculated as follows:

$$u_{ik} = \frac{\left((1 - K(x_k, v_i)) + \frac{\alpha}{N_R}\sum_{r \epsilon N_k}(1 - u_{ir})^m\right)^{\frac{-1}{(m-1)}}}{\sum_{j=1}^{c}\left((1 - K(x_k, v_j)) + \frac{\alpha}{N_R}\sum_{r \epsilon N_k}(1 - u_{jr})^m\right)^{\frac{-1}{(m-1)}}} \tag{6}$$

Finally, the centroids are updated as follows:

$$v_i = \frac{\sum_{k=1}^{n} u_{ik}^m K(x_k, v_i) x_k}{\sum_{k=1}^{n} u_{ik}^m K(x_k, v_i)} \tag{7}$$

As in the other algorithms, repeat these steps until condition $\max_{i,k} \|u_{ik}^t - u_{ik}^t\| \leq \epsilon$ is satisfied, where epsilon is a determined threshold.

C. MKSFCM (Modified Kernelized Spatial Fuzzy C-Means)

This algorithm was proposed by Castro et Al. in [6], and consists in the combination of the algorithms SFCM, introduced in section III-A, and the FKCM (Fuzzy Kernel C-Means) proposed in [13]. The principal purpose is to join the main advantages of both methods: homogeneity and robustness.

Initially, this algorithm calculates the kernelized membership function, using the same equation as the FKCM:

$$u_{jk} = \frac{(1/d^2(x_j, V_k))^{1/(q-1)}}{\sum_{j=1}^{C}(1/d^2(x_j, V_k))^{1/(q-1)}} \tag{8}$$

where $d^2(x_j, V_k) = K(x_j, x_j) - 2K(x_j, V_k) + K(V_k, V_k)$, q is a fuzzy index that determines the fuzziness of the clusters, C is the number of clusters, V are the centroids, and K is the kernelized function.

The second step introduces the spatial information as in the SFCM procedure through the spatial function h_{ij} in Eq. 1, after which the Eq. 2 is applied to obtain the membership factors.

Finally, the new kernel matrix $K(x_j, \hat{V}_k)$ and $K(\hat{V}_k, \hat{V}_k)$ is calculated as follows:

$$K(x_j, \hat{V}_k) = \phi(x_j) \cdot \phi(\hat{V}_k) = \frac{\sum_{i=1}^{N}(u_{ik})^q K(x_i, x_j)}{\sum_{i=1}^{N}(u_{ik})^q} \tag{9}$$

To halt the iteration process, the error must lie below a determined threshold, otherwise a new iteration will start and Eq. 8 is again applied.

IV. Support vector machine for classification problems

The standard Support Vector Machines (SVM) were designed specifically for binary classification and regression estimation. However, they have also been extended to multi-class problems [14]. We opted for the multi-class approach in order to realize a more refined classification of the lung structures segmented in the previous stages, rather than dividing the marked zones into nodule or non-nodule.

These problems are usually solved by two different approaches. One consists of decomposing and combining several binary classifiers that the binary SVM can solve, the other consists of solving it directly by considering all data in one formulation. This paper compares the two methods outlined above. In the first approach, we selected the one-against-one Kreβel implementation [15], in the other we selected the one proposed by Weston and Watkins [16]. Note that there are other implementations for multi-class SVM [14], but the proposal of this paper is not so much to compare different SVMs but rather to obtain an idea of the improvements that these SVM approaches can provide us.

A. One-against-one

This method constructs $k(k-1)/2$ classifiers, where k is the number of classes. The ith SVM is trained on data from two classes, resulting in l training data (x_1, y_1),...,(x_l, y_l), where $x_i \in R^n$, i=1,...,l and $y_i \in \{1,\ldots,k\}$ is the class of x_i. Training data from the ith and the jth classes are solved according to the following classification problem:

$$\begin{aligned} \overset{min}{w^{ij}, b^{ij}, \xi^{ij}} \quad & \frac{1}{2}(w^{ij})^T w^{ij} + C\sum_t \xi_t^{ij}(w^{ij})^T \\ & (w^{ij})^T\phi(x_t) + b^{ij} \geq 1 - \xi_t^{ij}, \quad if y_t = i \\ & (w^{ij})^T\phi(x_t) + b^{ij} \leq -1 + \xi_t^{ij}, \quad if y_t = j \\ & \xi_t^{ij} \geq 0 \end{aligned} \tag{10}$$

where the training data x_t are mapped to a higher dimensional space applying function ϕ, and parameter C represents the penalty.

The decision of the ensemble is made using the max-wins voting strategy, in which each classifier is considered to be a voting. In this approach, Hsu and Lin use $f_{ij}(x) = ((w^{ij})^T\phi(x) + b^{ij})$ as a decision function. Let us denote the voting function by:

$$V_i(x) = \sum_{j=1,\ldots,q \;\; j\neq i} s(f_{ij}(x)) \tag{11}$$

where the function s(t) maps the decision value to {0,1}

$$s(t) = \begin{cases} 1, & if \quad t \geq 0 \\ 0, & otherwise \end{cases} \tag{12}$$

Therefore, when element x_t is in the ith class ($f_{ij}(x_t) > 0$) rather than class j, the vote for this element will increase its value by one in accordance with Eq. 11; otherwise it contributes 0. At the end of the voting process, the value of $V_i(x)$ will be the sum of all votes made by all classifiers that cast one vote for the ith class.

Consequently, the final decision is made as follows:

$$\text{Class Label of i}^*(x) = argmax_{i=1,\ldots,q} V_i(x) \tag{13}$$

i.e element x is classified into class i, which is the class with most votes from the classifiers. Remark that if two or more classes have the same number of votes, the class with the smallest index is selected.

B. Multi-class SVM

This kind of approach was introduced simultaneously by Vapnik [17] and Weston and Watkins [16]. In essence, these formulations are essentially identical and propose an approach to solve multi-class problems in a single optimization.

Like the one-against-one approach, this approach constructs k two-class decision rules where the mth function $w_m^T\phi(x)+b$ separates training vectors of the m class from the other are constructed. However, unlike the previous method, even though there are k decisions functions, all are obtained by solving a single optimization problem. The formulation of this is as follows:

$$\begin{aligned} \overset{min}{w^{ij}, b^{ij}, \xi^{ij}} \quad & \frac{1}{2}\sum_{m=1}^{k} w_m^T w_m + C\sum_{i=1}^{l}\sum_{m\neq y_i} \xi_i^m w_{y_i}^T\phi(x_i) \\ & + b_{y_i} \geq w_m^T\phi(x_i) + b_m + 2 - \xi_i^m, \\ & \xi_t^{ij} \geq 0, \quad i = 1,\ldots,l, \quad m \in \{1,\ldots,k\}\setminus y_i \end{aligned} \tag{14}$$

The decision function is:

$$argmax_{m=1,\ldots,k}(w_m^T \phi(x) + b_m) \quad (15)$$

V. Methodology

For this paper we selected 23 preprocessed images of CT scans with isolated lungs, containing a representation of different kinds of lung nodules (initial phase, juxtapleural or wall-attached, isolated, etc.), as well as examples from different thoracic zones. These images, provided by LIDC database, each have an XML file with the nodule information, as specified in the material section. These files are converted into mask images so as to facilitate the measurement task of the quality results.

The process to combine the different techniques is initiated by the execution of the clustering algorithms, who perform a classification of the preprocessed images, obtaining the initial ROIs. Attending to the results in [5] and [6], it can be observed that the better results are obtained from partitioning the image into 3 clusters that represent lung tissue, regions marked as nodules, and background.

The construction of the training set, formed by the non-defuzzified output of the fuzzy algorithms as indicated in section I, follows a process that consists of several steps:

1) Select a set of pixels of each cluster, proportional to the percentage of each cluster in the segmented image. For example, if one cluster represents 20% of a segmented image, select only 20% of pixels of this cluster. Thereby, not only the training set is reduced in size, but the original characteristics of the input space are maintained as well. We observed during this analysis that better results were obtained by separating the ROI marked as nodule into two sets: one set with the true nodule pixels, another set with the remaining marked pixels, representing the false positives. Note that the results of this analysis follow this approach.
2) Obtain the membership factors for the previously selected pixels, using the non-defuzzified output of the fuzzy algorithms. These factors for each pixel are disposed as a row in the train set and represent one input for the SVM.
3) Repeat steps 1 and 2 for each image that serves as an input for the training set.

The training set used in the SVMs analysis is constructed, following this strategy, with three images of the dataset that represent different kinds of lung nodules. Since initially the dataset is not bigger, this number is sufficient to represent the input space, but it should be increased to boost the generalization capacity in the case of a bigger dataset.

The feature vector is defined as numerical values ranging from 1 to 4, and is associated to the appropriate train row, depending on the cluster that it represents.

The quality of the obtained results is quantified by means of true positives (TP) and false positives (FP), because the mask images only have information about the nodule region, omitting the information referring to the other elements of the CT image.

The comparative is divided into two approaches: first, analyse each fuzzy algorithm along with its possible combinations with the two SVM implementations, in order to select the optimal parameters; then, compare all combinations methods, to form an idea of the general improvements.

The results are represented in the form of charts and tables that summarize the best results obtained with different selections of parameters of the analysed algorithms. The principal aim is to observe the enhancement capacity of the fuzzy algorithms and its stability when they are combined with the SVM technique.

VI. Results

Table I presents the optimal parameters values obtained for the different combinations of the fuzzy algorithms with SVMs and their respective kernels. For each method, we search the optimal parameters for the SVM executions, focusing on the regularization cost C and the kernel parameter gamma. These were estimated by varying their values into the ranges of [0.05, 2] and [10, 600], respectively. Moreover, we adopt 3 different kernels for each kind of SVM: RBF, Sigmoid, and Polynomial with grade 3. Therefore, for each method we try 264 combinations.

We started by analysing the SFCM algorithm with its SVM combinations. The true and false positive rates for this algorithm can be observed in the first row of each image represented on the x-axis of Fig. 1 and Fig. 2. The success rates are 100% in most cases and 76% for the worst result. Even though the false positives rate is not too high in general, in seven images this rate is above 15%-20%, reaching 36% in image number 20.

In order to select the best combination for each SVM approach with the SFCM algorithm, we compare the results obtained for a selected group of images that are more representative of the dataset and present a significant variability in our problem. The results obtained for the remaining images are represented in the charts because of limited space and their smaller relevance in the decisions.These results are given in Table II.

This table shows that the rates obtained for the different approaches and kernels are quite similar, except for the sigmoid kernels, which obtain a better true positive rate, the improvement being approximately 12% for images 5 and 7, as well as a slightly higher false positive rate than the other kernels

TABLE I
Optimal values for (C,GAMMA) for each algorithm combination

Svm Approaches	**Fuzzy Algorithms**		
	SFCM	SKFCM	MKSFCM
OAO[1]RBF	(0.05,10)	(0.3,500)	(0.05,10)
OAO-SIGMOID	(0.8,10)	(0.5,500)	(0.05,10)
OAO-POLYNOMIAL	(0.1,10)	(0.08,150)	(0.1,400)
MSVM[2]RBF	(0.05,10)	(0.5,300)	(0.1,10)
MSVM-SIGMOID	(0.5,10)	(1.5,10)	(0.05,100)
MSVM-POLYNOMIAL	(0.05,150)	(0.08,200)	(0.1,300)

[1] one-against-one
[2] multi-class svm (Weston's approach)

TABLE II
RESULTS OBTAINED FOR SOME REPRESENTATIVE IMAGES FOR THE SFCM COMBINATIONS

Image		SVM Approaches					
		OAO -RBF	OAO -SIG.[1]	OAO -POLY.[1]	MSVM -RBF	MSVM -SIG.	MSVM -POLY.
5	TP	77.08	95.83	77.08	85.42	95.83	77.08
	FP	8.2	9.08	7.95	8.62	8.9	7.93
7	TP	50	64.29	52.86	50	62.86	51.43
	FP	9.02	11.78	8.96	9.67	11.03	8.72
13	TP	59.26	70.37	59.26	59.26	62.96	59.26
	FP	6.79	8.49	6.54	7.33	8.1	6.37
18	TP	88.89	95.68	91.98	89.51	93.21	90.74
	FP	14.19	18.5	14.11	14.73	16.94	13.67
20	TP	82.86	82.86	80	82.86	82.86	80
	FP	18.88	25.19	17.95	19.57	22.81	17.47
21	TP	81.69	94.37	90.14	83.1	92.96	84.51
	FP	12.14	16.7	12.14	12.72	14.94	11.76

[1] Sigmoid
[2] Polynomial

(less than 4% for most cases). These results are extended to the one-against-one approach and the approach presented by Weston and Watkins. Therefore, Fig. 1 and Fig. 2 compare the initial rates for the fuzzy algorithm with the best results obtained for each approach of the SVM, in this case, using the sigmoid kernel.

Fig. 1 shows that, in general, the success rate is good and maintains the fuzzy results with values above 80%. The worst true positive rate is for images 7 and 13, reducing the success rate with respect to the initial segmentation above 20%.

In Fig. 2 it can be observed that the false positive rates is reduced for all the datasets, except for image 5, where the rate is slightly higher but still below 0.2%, so it is not relevant. For five images, the reduction reaches 10%.

Therefore, this combination provides good results, maintaining the true positives rate of the initial fuzzy segmentation, and realizes a significant reduction of the false positive ratio for most images.

The second analysed algorithm was the SKFCM and its combinations with the approaches of the SVM. The results, indicated in the first row of each image in Fig. 3, show a high

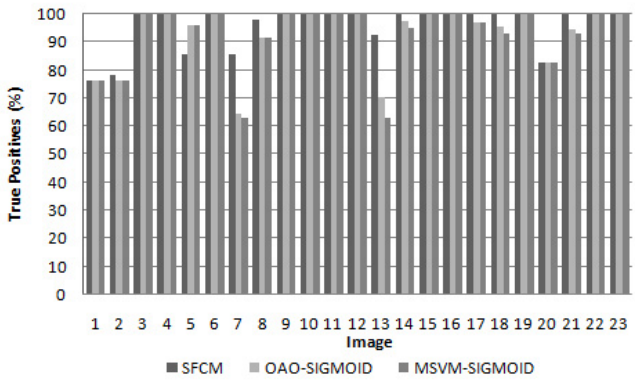

Fig. 1. True positive rates for the SFCM algorithm and the best combinations.

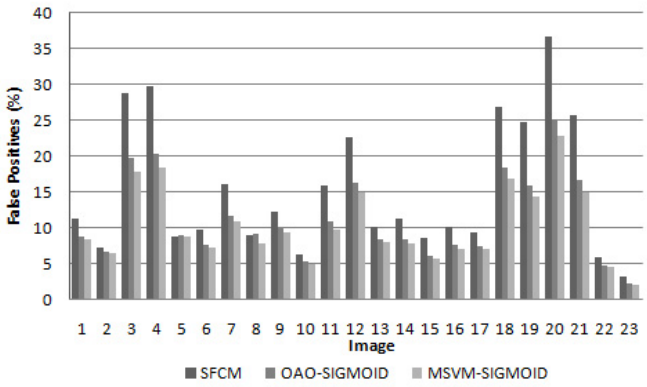

Fig. 2. False positive rates for the SFCM algorithm and the best combinations.

true positive rate for most images, the results being almost identical to those results of the SFCM method, except for small variations. Nonetheless, the false positive rate, illustrated in Fig. 4, has increased for all the images that do not fall in the 10%-20% range and reach 37% and 42% for images 22 and 2, respectively.

Table III shows the results obtained for the group of variability images. These reveal a classification problem with images number 7 and 21 in most SVM combinations with their different kernels, because the success rate decreases below 10%. This indicates that the nodules are misclassified in other cluster, probably because these images have smooth nodules with small intensity variations that are difficult to detect and distinguish form the other structures.

The best combinations for the SKFCM algorithm are the one-against-one approach with polynomial kernel and the Weston and Watkins approach with sigmoid kernel. For the one-against-one methods, the results are not good because the tests with RBF and sigmoid kernels have misclassification problems (cf. above); for the polynomial kernel, the false positive rates for some images (e.g image 20) have very high value that nullify our goals. In the same way, note that for

TABLE III
RESULTS OBTAINED FOR SOME REPRESENTATIVE IMAGES FOR THE SKFCM COMBINATIONS

Image		SVM Approaches					
		OAO -RBF	OAO -SIG.	OAO -POLY.	MSVM -RBF	MSVM -SIG.	MSVM -POLY.
5	TP	83.33	81.25	93.75	83.33	70.83	97.92
	FP	24.43	24.05	28.19	24.39	23.58	28.87
7	TP	4.29	1.43	22.89	4.29	54.29	28.57
	FP	6.74	6.53	14.56	6.9	6.47	15.64
13	TP	55.56	51.58	77.78	55.56	29.63	88.89
	FP	8.31	7.99	14.23	8.38	7.74	15.11
18	TP	26.54	24.07	43.21	26.54	61.11	48.77
	FP	11.79	11.14	25.76	11.55	10.34	27.99
20	TP	82.86	82.86	82.86	82.86	65.71	82.86
	FP	33.14	30.16	47.77	30.53	14.2	45.81
21	TP	8.45	5.63	26.76	7.04	71.83	35.21
	FP	9.61	9.02	21.4	9.43	6.1	23.78

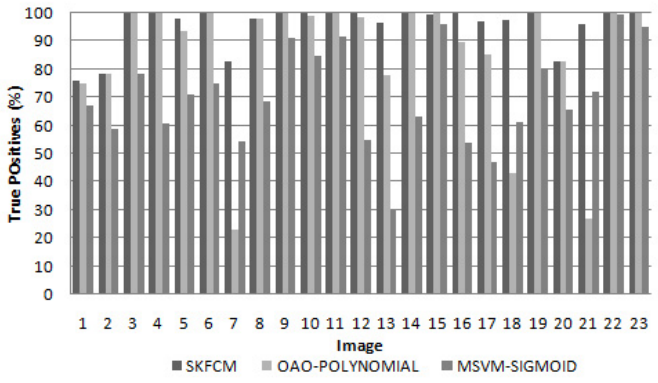

Fig. 3. True positive rates for the SKFCM algorithm and the best combinations.

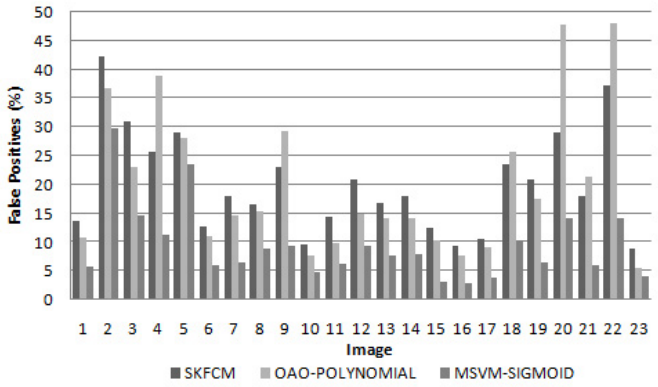

Fig. 4. False positive rates for the SKFCM algorithm and the best combinations.

this last approach, image 20 has very high false positive rates except for the sigmoid kernel; hence we choose this combination instead of others with better true positive rates.

The results obtained for the Weston approach with sigmoid kernel (Fig. 3 and Fig. 4) show the success rates for the selected variability images. These decrease in a high percentage, 54% and 29% being the true positive rate of images 7 and 13, respectively. The remaining images have rates up to 60%. In Fig. 4, the false positive rate experiments a high decrease, reaching 23% in the case of image 22, and 5%-15% for the remaining images.

In essence, the SKFCM algorithm does not function well for data sets with high variability because of the misclassification problems; it is therefore not a good election for the CAD system.

Finally, the results obtained by the MKSFCM algorithm, shown in Fig. 5 and Fig. 6, reveal success rates of approximately 100% for most images; even though in this case the worst rate is 68% rather than 76% for the previous methods, this reduction is not critical. It compensates for the decrease of the false positive ratio in all images, most of them falling into the 5%-15% rates and none above 21%.

Table IV introduces the results of the combinations for this fuzzy algorithm. These manifest a stable behavior of the

TABLE IV
RESULTS OBTAINED FOR SOME REPRESENTATIVE IMAGES FOR THE MKSFCM COMBINATIONS

Image		SVM Approaches					
		OAO -RBF	OAO -SIG.	OAO -POLY.	MSVM -RBF	MSVM -SIG.	MSVM -POLY.
5	TP	62.5	68.75	72.92	64.58	62.5	77.08
	FP	17.11	17.37	17.92	17.24	16.81	17.99
7	TP	60	62.86	64.29	62.86	58.57	64.29
	FP	10.25	10.52	11.13	10.41	9.83	11.04
13	TP	81.48	81.48	92.59	81.48	74.07	81.48
	FP	10.2	10.51	11.04	10.36	9.87	10.98
18	TP	82.72	84.57	87.04	82.72	79.63	85.8
	FP	11.42	11.81	12.51	11.65	11.03	12.39
20	TP	80	81.43	82.86	81.43	80	81.43
	FP	7.14	7.41	8.19	7.25	6.87	8.06
21	TP	66.2	70.42	77.46	70.42	61.97	77.46
	FP	8.89	9.23	9.81	9.07	8.85	9.73

different SVM approaches, highlighting those obtained by the polynomial kernel with a slightly better success rate and a restrained false positive ratio. Fig. 5 and Fig. 6 analyse the two SVM approaches with polynomial kernel.

Fig 5 indicates a maintenance of the true positive ratio in concordance with the initial fuzzy segmentation; in some

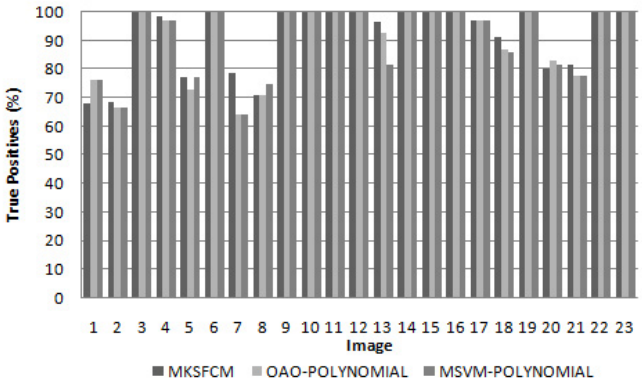

Fig. 5. True positive rates for the MKSFCM algorithm and the best combinations

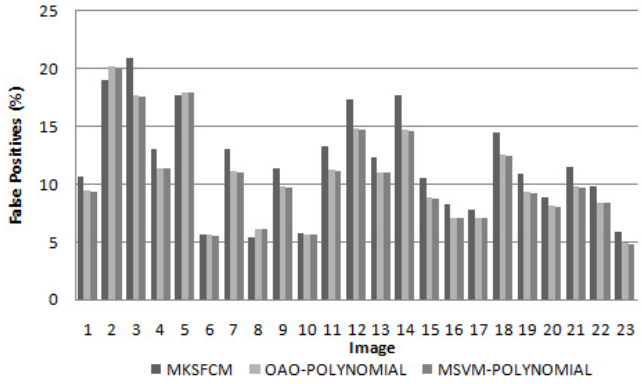

Fig. 6. False positive rates for the MKSFCM algorithm and the best combinations.

images (e.g. images 1,8, and 20) this rate is improved with an increase of up to 8% for the first image. The false positive ratio, in Fig. 6, decreases for most images in terms of a stable 2%. There are some images (e.g 2 and 8) for which this rate increases, but less than 0.5%, so the worsening is slightly marked.

The two analysed polynomial combinations of this algorithm present a stable behaviour with good rates for true and false positives, although the decrease of this final rate is not high because the initial fuzzy segmentation presented low values and it is difficult to realize a better classification.

VII. Conclusions

This paper presents an analysis of the combination of various fuzzy clustering algorithms with different approaches of the SVM technique. The principal aim of the study is to improve the defuzzification phase of the analysed fuzzy algorithms, obtaining better segmentations with fewer rates of false positives, by applying the SVM technique to the membership factors obtained in the initial ROIs classification.

The best combinations obtained for the SFCM and MKSFCM algorithms provide good results, being able to maintain and increase in some cases the fuzzy success rate and decrease the false positive ratio in a significant value for most of the images.

In the case of SFCM, the better combination was that provided by the one-against-one approach with sigmoid kernel obtaining a general true positive ratio above 80% for most images and reducing the false positives rate up to 10% for various images. Fig. 7 shows a comparative of the improvements introduced by this approach applied to an image of the dataset. The left upper image represents the preprocessed image, where the lungs are isolated, the right upper image is the output obtained by the fuzzy algorithm without any combination, and finally, the image below them is the defuzzification result provided by the best combination.

The best combination for MKFSCM was the one-against-one approach, as for SFCM, but in this case with the polynomial kernel. This obtains the best and most robust results, improving even the success rates for some images up to 8% and preserving it for the rest of images. In the case of false positive rate, the combination reduces the good rates of false positives (already obtained by previous results of the fuzzy algorithm) for all images but in a minor way if compared with the better SFCM combination. As in the previous case, Fig. 8 indicates the results obtained by this approach.

Once again, the SKFCM fuzzy combinations have classifications problems with data sets with high variability, due to the presence of images with nodules in early stages or that are hard to differentiate from the other lung structures. In this case, the results are not good for our problem, because the low true positive rate is less than 10% in some images and the high true positive rate is above 40%.

As a result, the SFCM and MKFSCM fuzzy clustering algorithms with their optimal SVM combinations can serve to improve the defuzzification phase in the task of ROIs detection.

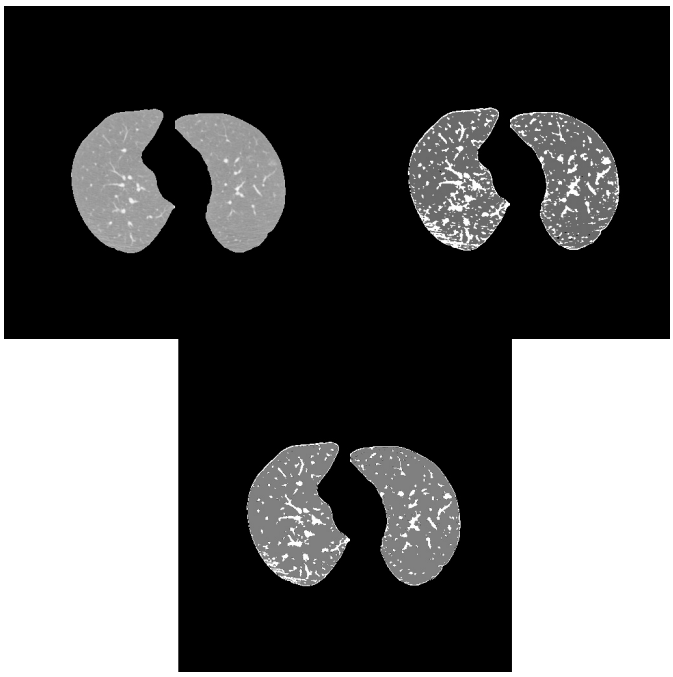

Fig. 7. Example of result obtained with the best combination of SFCM with SVM.

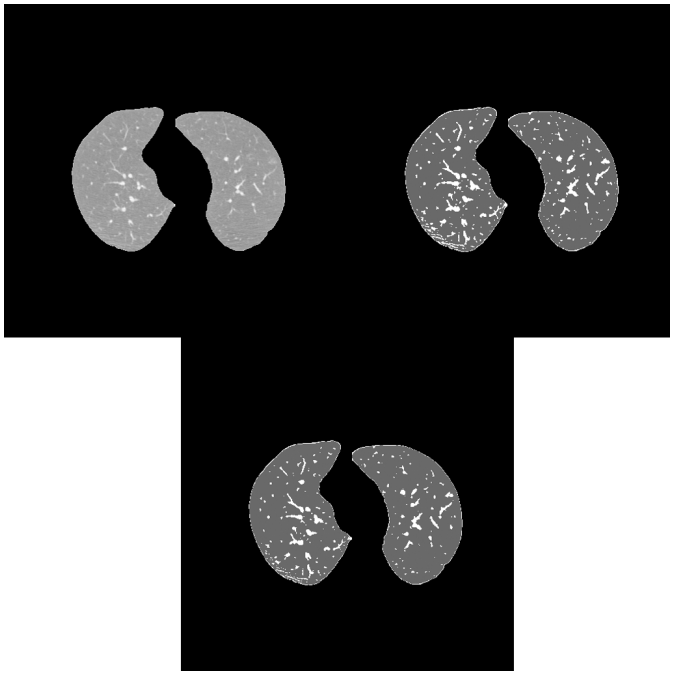

Fig. 8. Example of result obtained with the best combination of MKSFCM with SVM.

In our opinion, this result can be incorporated into the lung nodule detection CAD system.

References

[1] H. K. Weir et al., "Annual report to the nation on the status of cancer, 1975-2000," J. Natl. Cancer Inst., vol. 95, no. 17, pp. 1276-1299, 2003.

[2] X. Lu, G. Wei, J. Qian, and A. K. Jain, "Learning-based Pulmonary Nodule Detection from Multislice CT Data," in Proc. CARS, 2004.

[3] Y. Lee, T. Hara, H. Fujita, S. Itoh, and T. Ishigaki, "Automated detection of pulmonary nodules in helical CT images based on an improved template-matching technique," IEEE Trans. Med. Imaging, vol. 27, no. 7, pp. 595-604, July 2001.
[4] C. Lei, L. Xiaojian, Z. Jie, and C. Wufan, "Automated lung segmentation algorithm for CAD system of thoracic CT," J. Med. of PLA, vol. 23, no. 4, pp. 215-222, August 2008.
[5] A. Castro, C. Boveda, A. Rey and B. Arcay, "An analysis of various clustering algorithms for ROI detection in high resolution CT lung images," Lect. Notes Comput. Sc., vol. 6374, Warsaw, Poland, 2010.
[6] A. Castro and B. Arcay, "Comparison of various fuzzy clustering algorithms in the detection of ROI in lung CT and a modified kernelized-spatial fuzzy c-means algorithm," Proc. of 10th IEEE Int. Conf. on Inf. Tech. and Appl. in Biom., Corfu, Greece, 2010.
[7] S.G. Armato III, G. McLennan, M.F. McNitt-Gray for the Lung Image Database Consortium Research Group, "Lung Image Database Consortium: Developing a Resource for the Medical Imaging Research Community," Radiology, 232, pp. 739-748, 2004.
[8] C.W. Hsu and C. J. Lin. (April, 2006). BSVM: A Library for Support Vector Machines. [Online]. Available: http://www.csie.ntu.edu.tw/ cjlin/bsvm.
[9] K. Chuang, H. Tzeng,S. Chen, J. Wu, and T.Chen, "Fuzzy C-means clustering with Spatial information for image segmentation," Comput. Med. Imaging Grap., no. 30, pp. 9-15, 2006.
[10] S. Chen, D. Zhang, "Robust image segmentation using FCM with spatial constraints based on new kernel-induced distance measure," IEEE Trans. Syst. Man Cybern. Part B-Cybern., vol.34, no.4, pp.1907-1916, Aug. 2004.
[11] D. Q. Zhang and S. C. Chen, "A novel kernelized fuzzy C-means algorithm with application in medical image segmentation," Artif. Intell. Med., vol. 32, no. 1, pp. 37-50, Sept. 2004.
[12] T.M. Cover, "Geomeasureal and statistical properties of systems of linear inequalities in pattern recognition," IEEE Trans. Electron. Comput. vol. EC-14, pp. 326-334, Mar. 1965.
[13] W.D. Zhong, X.X. Wei, and Y.P. Jian, Fuzzy C-Means clustering algorithm based on kernel method," Proc. of 5th Int. Conf. on Comp. Intell. and Mult. Appl., Xi'an, China, 2003, pp. 49-54.
[14] C. Hsu, and C. Lin, "A comparison of methods for multiclass support vector machines," IEEE Trans. on Neural Netw., vol. 13, no. 2, pp. 415-425, March 2002.
[15] U. Kreβel, "Pairwise classification and support vector machines," in Advances in Kernel Methods: Support Vector Learning, B. Schölkopf, C.J. C. Burges, and A. J. Smola, Eds. Cambridge, MA: MIT Press, 1999, ch. 15, pp. 255-268.
[16] J. Weston and C. Watkins, "Multi-class support vector machines," Proc. 7th Eur. Symp. On Artif. Neural Netw., Burges, Belgium, 1999, pp. 219-224.
[17] V. Vapnik, Statistical Learning Theory, New York:John Wiley&Sons, 1998.

2011 IEEE International Conference on Fuzzy Systems
June 27-30, 2011, Taipei, Taiwan

Comparison and Practical Implementation of Type-Reduction Algorithms for Type-2 Fuzzy Sets and Systems

Dongrui Wu
Industrial Artificial Intelligence Laboratory
GE Global Research, Niskayuna, NY, USA
E-mail: wud@ge.com

Maowen Nie
Department of Electrical and Computer Engineering
National University of Singapore, Singapore
E-mail: g0700223@nus.edu.sg

***Abstract*—Type-reduction algorithms are very important for type-2 fuzzy sets and systems. The earliest one, and also the most popular one, is the Karnik-Mendel Algorithm, which is iterative and computationally intensive. In the last a few years researchers have proposed several other more efficient type-reduction algorithms. In this paper we also propose a new algorithm which improves over the latest results. Experiments show that it is the most efficient one to use in practice. Particularly, when the number of elements in type-reduction is smaller than 100, which is true in most practical type-reduction computations, our proposed algorithm can save over 50% computational cost over the Karnik-Mendel Algorithms. We also give the Matlab implementation of our most efficient algorithm in the Appendix. It includes preprocessing steps to eliminate numerical problems, and also improved testing criteria to prevent possible infinite loops. This program will be very helpful in promoting the popularity of type-2 fuzzy sets and systems.**

***Keywords*—Interval type-2 fuzzy sets, interval type-2 fuzzy logic systems, type-reduction, Karnik-Mendel Algorithm, Enhanced Karnik-Mendel Algorithm, computational cost**

I. Introduction

As introduced in [1], the following optimization problem is frequently met in (but not limited to) fuzzy logic theory:

Given

$$x_n \in X_n \equiv [\underline{x}_n, \overline{x}_n], \qquad n = 1, 2, \ldots, N \tag{1}$$

$$w_n \in W_n \equiv [\underline{w}_n, \overline{w}_n], \qquad n = 1, 2, \ldots, N \tag{2}$$

where

$$\underline{x}_n \leqslant \overline{x}_n, \qquad n = 1, 2, \ldots, N \tag{3}$$

$$\underline{w}_n \leqslant \overline{w}_n, \qquad n = 1, 2, \ldots, N \tag{4}$$

compute

$$Y = \frac{\sum_{n=1}^{N} X_n W_n}{\sum_{n=1}^{N} W_n} \equiv [y_l, y_r], \tag{5}$$

where

$$y_l = \min_{\substack{\forall x_n \in [\underline{x}_n, \overline{x}_n] \\ \forall w_n \in [\underline{w}_n, \overline{w}_n]}} \frac{\sum_{n=1}^{N} x_n w_n}{\sum_{n=1}^{N} w_n} \tag{6}$$

$$y_r = \max_{\substack{\forall x_n \in [\underline{x}_n, \overline{x}_n] \\ \forall w_n \in [\underline{w}_n, \overline{w}_n]}} \frac{\sum_{n=1}^{N} x_n w_n}{\sum_{n=1}^{N} w_n} \tag{7}$$

For instance, in computing the centroid of an interval type-2 fuzzy sets (IT2 FS) $\tilde{A}$ [2]–[4], $\underline{x}_n = \overline{x}_n = x_n$ represent discretizations of the primary variable x, and interval $[\underline{w}_n, \overline{w}_n]$ is the membership grade of x_n. Y is the centroid of $\tilde{A}$. In center-of-sets type-reduction of IT2 fuzzy logic systems (FLSs) [4], X_n represents the centroid of the consequent IT2 FS of the n^{th} rule, W_n is the firing level of that rule, and Y is the type-reduced set. In computing the linguistic weighted average [5]–[8], X_n and W_n are α-cuts of the upper membership functions (or lower membership functions) of the inputs signals and the weights, both of which are IT2 FSs, and Y is the corresponding α-cut on the upper membership function (or lower membership function) of the linguistic weighted average, which is also an IT2 FS.

Equation (5) is usually solved by the iterative Karnik-Mendel algorithms (KMA) [2], [4], which is computationally intensive. In the last a few years several more efficient algorithms[1] have been proposed, e.g., the enhanced Karnik-Mendel algorithm (EKMA) [1], [7], a fast recursive method for computing the generalized centroid of IT2 FSs [17], an iterative algorithm with stop condition[2] (IASC) for computing the generalized centroid[3] [18], and, an enhanced algorithm for computing the generalized centroid of general type-2 FSs [19]. For simplicity these algorithms are all referred to as type-reduction algorithms in this paper.

In this paper we focus on more efficient type-reduction algorithms. Our contributions are: 1) We propose an enhanced version of IASC and compare it with several other type-reduction algorithms; and, 2) We give an Matlab implementation of our most efficient type-reduction algorithm, which can be used freely by other researchers.

The rest of this paper is organized as follows: Section II introduces KMA. Section III introduces four more efficient type-reduction algorithms, including EKMA, EKMA with new

[1]There are also many approximations to KMA [9]–[15]. As pointed out in [16], these approximations are fundamentally different from the original KMA, and hence they are not considered in this paper.

[2]This algorithm is called IASCO in [18].

[3]Though the two algorithms in [17], [18] were initially proposed for computing the generalized centroid of IT2 FSs, they can also be used in type-reduction of IT2 FLSs.

978-1-4244-7316-8/11/$26.00 ©2011 IEEE

initialization (EKMANI), IASC, and enhanced IASC (EIASC). Section IV compares the performances of these five algorithms under three different scenarios. Finally, Section V draws conclusions. Matlab implementation of EIASC is given in the Appendix.

II. Karnik-Mendel Algorithms (KMA)

KMA consists of two parts, one for computing y_l in (6) and the other for computing y_r in (7). Define

$$f_l(k) = \frac{\sum_{n=1}^{k} \underline{x}_n \overline{w}_n + \sum_{n=k+1}^{N} \underline{x}_n \underline{w}_n}{\sum_{n=1}^{k} \overline{w}_n + \sum_{n=k+1}^{N} \underline{w}_n} \tag{8}$$

$$f_r(k) = \frac{\sum_{n=1}^{k} \overline{x}_n \underline{w}_n + \sum_{n=k+1}^{N} \overline{x}_n \overline{w}_n}{\sum_{n=1}^{k} \underline{w}_n + \sum_{n=k+1}^{N} \overline{w}_n} \tag{9}$$

where $\{\underline{x}_n\}$ and $\{\overline{x}_n\}$ have been sorted in ascending order, respectively. Furthermore, in this paper it is assumed that $\{\underline{x}_n\}$ ($\{\overline{x}_n\}$) has no duplicate elements, which can be easily achieved by combining the weights for duplicate elements. Then, y_l in (6) and y_r in (7) can also be re-expressed as [4]:

$$y_l = \min_{k=1,\ldots,N-1} f_l(k) \equiv f_l(l) \tag{10}$$

$$= \frac{\sum_{n=1}^{l} \underline{x}_n \overline{w}_n + \sum_{n=l+1}^{N} \underline{x}_n \underline{w}_n}{\sum_{n=1}^{l} \overline{w}_n + \sum_{n=l+1}^{N} \underline{w}_n} \tag{11}$$

$$y_r = \max_{k=1,\ldots,N-1} f_r(k) \equiv f_r(r) \tag{12}$$

$$= \frac{\sum_{n=1}^{r} \overline{x}_n \underline{w}_n + \sum_{n=r+1}^{N} \overline{x}_n \overline{w}_n}{\sum_{n=1}^{r} \underline{w}_n + \sum_{n=r+1}^{N} \overline{w}_n} \tag{13}$$

where l and r are switch points satisfying

$$\underline{x}_l \leqslant y_l < \underline{x}_{l+1} \tag{14}$$

$$\overline{x}_r < y_r \leqslant \overline{x}_{r+1}. \tag{15}$$

Note that in [4] these two inequalities are

$$\underline{x}_l \leqslant y_l \leqslant \underline{x}_{l+1} \tag{16}$$

$$\overline{x}_r \leqslant y_r \leqslant \overline{x}_{r+1} \tag{17}$$

because there $\{\underline{x}_n\}$ and $\{\overline{x}_n\}$ can have duplicate elements. When duplicate elements are combined, it follows that $\underline{x}_l < \underline{x}_{l+1}$ for $\forall l \in [1, N-1]$ and $\overline{x}_r < \overline{x}_{r+1}$ for $\forall r \in [1, N-1]$, and hence the two equalities in (16) or (17) cannot be satisfied simultaneously.

KMA for Computing y_l:

1) Sort $\underline{x}_n$ $(n = 1, 2, \ldots, N)$ in increasing order and call the sorted $\underline{x}_n$ by the same name, but now $\underline{x}_1 < \underline{x}_2 < \cdots < \underline{x}_N$. Match the weights W_n with their respective $\underline{x}_n$ and renumber them so that their index corresponds to the renumbered $\underline{x}_n$.
2) Initialize w_n by setting
$$w_n = \frac{\underline{w}_n + \overline{w}_n}{2}, \qquad n = 1, 2, \ldots, N \tag{18}$$
and then compute
$$y = \frac{\sum_{n=1}^{N} \underline{x}_n w_n}{\sum_{n=1}^{N} w_n}. \tag{19}$$
3) Find switch point l $(1 \leqslant l \leqslant N-1)$ such that
$$\underline{x}_l < y \leqslant \underline{x}_{l+1} \tag{20}$$
4) Set
$$w_n = \begin{cases} \overline{w}_n, & n \leqslant l \\ \underline{w}_n, & n > l \end{cases} \tag{21}$$
and compute
$$y' = \frac{\sum_{n=1}^{N} \underline{x}_n w_n}{\sum_{n=1}^{N} w_n} \tag{22}$$
5) If $y' = y$, stop and set $y_l = y$; otherwise, set $y = y'$ and go to Step 3.

KMA for Computing y_r:

1) Sort $\overline{x}_n$ $(n = 1, 2, \ldots, N)$ in increasing order and call the sorted $\overline{x}_n$ by the same name, but now $\overline{x}_1 < \overline{x}_2 < \cdots < \overline{x}_N$. Match the weights W_n with their respective $\overline{x}_n$ and renumber them so that their index corresponds to the renumbered $\overline{x}_n$.
2) Initialize w_n by setting
$$w_n = \frac{\underline{w}_n + \overline{w}_n}{2}, \qquad n = 1, 2, \ldots, N \tag{23}$$
and then compute
$$y = \frac{\sum_{n=1}^{N} \overline{x}_n w_n}{\sum_{n=1}^{N} w_n}. \tag{24}$$
3) Find switch point r $(1 \leqslant r \leqslant N-1)$ such that
$$\overline{x}_r < y \leqslant \overline{x}_{r+1} \tag{25}$$
4) Set
$$w_n = \begin{cases} \underline{w}_n, & n \leqslant r \\ \overline{w}_n, & n > r \end{cases} \tag{26}$$
and compute
$$y' = \frac{\sum_{n=1}^{N} \overline{x}_n w_n}{\sum_{n=1}^{N} w_n} \tag{27}$$
5) If $y' = y$, stop and set $y_r = y$; otherwise, set $y = y'$ and go to Step (3).

The main idea of KMA is to find the switch points for y_l and y_r. Take y_l as an example. y_l is the minimum of Y. Since $\underline{x}_n$ increases from the left to the right along the horizontal axis of Fig. 1(a), we should choose a large w_n for $\underline{x}_n$ on the left and a small w_n for $\underline{x}_n$ on the right. KMA for y_l finds the switch point l. For $n \leqslant l$, $\overline{w}_n$ is used to calculate y_l; for $n > l$, $\underline{w}_n$ is used. This ensures y_l is the minimum.

Note that the above KMA works well in most practical cases; however, sometimes due to roundoff error y' can never be equal to y and hence KMA runs into infinite loops. Special attentions need to be paid to these cases, as we have done in the Matlab program in the Appendix.

III. More Efficient Type-Reduction Algorithms

Three existing more efficient type-reduction algorithms are introduced in this section, and a new algorithm is also proposed.

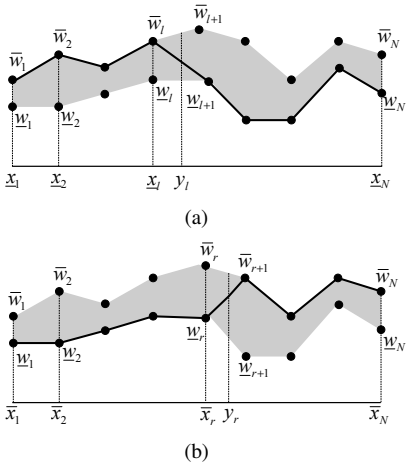

Fig. 1. Illustration of the switch points in computing y_l and y_r. (a) Computing y_l: switch from $\overline{w}_l$ to $\underline{w}_{l+1}$; (b) Computing y_r: switch from $\underline{w}_r$ to $\overline{w}_{r+1}$.

A. Enhanced Karnik-Mendel Algorithms (EKMA)

EKMA [1] has three improvements over KMA. First, a better initialization is used to reduce the number of iterations. Then, the termination condition of the iterations is changed to remove one unnecessary iteration. Finally, a subtle computing technique is used to reduce the computational cost of each iteration.

EKMA for computing y_l:

1) The same as Step (1) of KMA for computing y_l.
2) Set $l = [N/2.4]$ (the nearest integer to $N/2.4$), and compute

$$a = \sum_{n=1}^{l} \underline{x}_n \overline{w}_n + \sum_{n=l+1}^{N} \underline{x}_n \underline{w}_n \tag{28}$$

$$b = \sum_{n=1}^{l} \overline{w}_n + \sum_{n=l+1}^{N} \underline{w}_n \tag{29}$$

$$y = a/b \tag{30}$$

3) Find $l' \in [1, N-1]$ such that

$$\underline{x}_{l'} < y \leqslant \underline{x}_{l'+1} \tag{31}$$

4) If $l' = l$, stop; otherwise, continue.
5) Compute $s = \text{sign}(l' - l)$, and

$$a' = a + s \sum_{n=\min(l,l')+1}^{\max(l,l')} \underline{x}_n (\overline{w}_n - \underline{w}_n) \tag{32}$$

$$b' = b + s \sum_{n=\min(l,l')+1}^{\max(l,l')} (\overline{w}_n - \underline{w}_n) \tag{33}$$

$$y' = a'/b' \tag{34}$$

6) Set $y = y'$, $a = a'$, $b = b'$ and $l = l'$. Go to Step 3.

EKMA for computing y_r:

1) The same as Step (1) of KMA for computing y_r.
2) Set $r = [N/1.7]$ (the nearest integer to $N/1.7$), and compute

$$a = \sum_{n=1}^{r} \overline{x}_n \underline{w}_n + \sum_{n=r+1}^{N} \overline{x}_n \overline{w}_n \tag{35}$$

$$b = \sum_{n=1}^{r} \underline{w}_n + \sum_{n=r+1}^{N} \overline{w}_n \tag{36}$$

$$y = a/b \tag{37}$$

3) Find $r' \in [1, N-1]$ such that

$$\overline{x}_{r'} < y \leqslant \overline{x}_{r'+1} \tag{38}$$

4) If $r' = r$, stop; otherwise, continue.
5) Compute $s = \text{sign}(r' - r)$, and

$$a' = a - s \sum_{n=\min(r,r')+1}^{\max(r,r')} \overline{x}_n (\overline{w}_n - \underline{w}_n) \tag{39}$$

$$b' = b - s \sum_{n=\min(r,r')+1}^{\max(r,r')} (\overline{w}_n - \underline{w}_n) \tag{40}$$

$$y' = a'/b' \tag{41}$$

6) Set $y = y'$, $a = a'$, $b = b'$ and $r = r'$. Go to Step (3).

Note that similar to KMA, sometimes due to roundoff error $l' = l$ and/or $r' = r$ cannot be achieved and EKMA runs into infinite loops. Special attentions need to be paid to these cases, as done in the Appendix.

B. Enhanced Karnik-Mendel Algorithm with New Initialization (EKMANI)

Yeh et al. [19] proposed Enhanced Karnik-Mendel Algorithm with new initialization (EKMANI) to compute the generalized centroid of general T2 FSs. It is based on the observation that for two α-planes [20] close to each other, the centroids of the resulting two IT2 FSs are also close to each other. So, it may be advantageous to use the switch points obtained from the previous α-plane to initialize the switch points in the next α-plane. Though EKMANI was primarily designed for computing the generalized centroid, it may also be used in type-reduction of IT2 FLSs, especially IT2 fuzzy logic controllers (FLCs), because usually the output of an IT2 FLC changes only a small amount each step.

EKMANI for computing y_l is identical to EKMA for computing y_l, except that in Step (2), if there is a switch point obtained from previous computation, then set l to it; otherwise, set $l = [N/2.4]$.

EKMANI for computing y_r is identical to EKMA for computing y_r, expect that in Step (2), if there is a switch point obtained from previous computation, then set r to it; otherwise, set $r = [N/1.7]$.

C. Iterative Algorithm with Stop Condition (IASC)

Melgarejo and his co-authors [17], [18] proposed two efficient algorithms for computing the generalized centroid of IT2 FSs, which can also be used in type-reduction of IT2 FLSs.

The faster one, called iterative algorithm with stop condition (IASC) [18], is introduced in this subsection[4]. It is based on the fact [4] that y_l in (10) first monotonically decreases and then monotonically increases with the increase of k, and y_r in (12) first monotonically increases and then monotonically decreases with the increase of k.

IASC for computing y_l:

1) The same as Step (1) of KMA for computing y_l.
2) Initialize

$$a = \sum_{n=1}^{N} \underline{x}_n \underline{w}_n, \qquad b = \sum_{n=1}^{N} \underline{w}_n$$
$$y_l = \underline{x}_N, \qquad l = 0$$

3) Compute

$$l = l + 1$$
$$a = a + \underline{x}_l(\overline{w}_l - \underline{w}_l)$$
$$b = b + \overline{w}_l - \underline{w}_l$$
$$c = a/b$$

4) If $c > y_l$, set $l = l - 1$ and stop; otherwise, set $y_l = c$ and go to Step (3).

IASC for computing y_r:

1) The same as Step (1) of KMA for computing y_r.
2) Initialize

$$a = \sum_{n=1}^{N} \overline{x}_n \overline{w}_n, \qquad b = \sum_{n=1}^{N} \overline{w}_n$$
$$y_r = \overline{x}_1, \qquad r = 0$$

3) Compute

$$r = r + 1$$
$$a = a - \overline{x}_r(\overline{w}_r - \underline{w}_r)$$
$$b = b - \overline{w}_r + \underline{w}_r$$
$$c = a/b$$

4) If $c < y_r$, set $r = r - 1$ and stop; otherwise, set $y_r = c$ and go to Step (3).

D. Enhanced Iterative Algorithm with Stop Condition (EIASC)

An Enhanced IASC (EIASC) is proposed in this subsection. It uses the following theorem:

Theorem 1: $f_l(k)$ in (8) satisfies:

$$f_l(k) \begin{cases} \geqslant \underline{x}_k, & k \leqslant l \\ < \underline{x}_k, & k > l \end{cases} \tag{42}$$

Similarly, $f_r(k)$ in (9) satisfies:

$$f_r(k) \begin{cases} \leqslant \overline{x}_k, & k > r \\ > \overline{x}_k, & k \leqslant r \end{cases} . \quad \square \tag{43}$$

Proof: Because the proof for (43) is very similar to that for (42), we only provide the proof for (42) in this paper.

[4] [18] did not give the complete IASC presented in this subsection. It is the authors' integration of the ideas in [17] and [18].

From (10) and (14) it follows that

$$f_l(l) \geqslant \underline{x}_l. \tag{44}$$

For $\forall k \in [1, N-1]$, it is always true that

$$f_l(k) \geqslant f_l(l) \tag{45}$$

because by definition $f_l(l) = \min\limits_{k=1,\ldots,N-1} f_l(k)$. When $k \leqslant l$, it is also true that

$$\underline{x}_l \geqslant \underline{x}_k \tag{46}$$

because $\{\underline{x}_n\}$ has been sorted in ascending order and $k \leqslant l$. Considering (44)-(46) together, it follows that

$$f_l(k) \geqslant f_l(l) \geqslant \underline{x}_l \geqslant \underline{x}_k \tag{47}$$

which is the first line of (42). Next we focus on the second line of (42).

Beginning with (8), we see that

$$f_l(l)\left[\sum_{n=1}^{l} \overline{w}_n + \sum_{n=l+1}^{N} \underline{w}_n\right] = \sum_{n=1}^{l} \underline{x}_n \overline{w}_n + \sum_{n=l+1}^{N} \underline{x}_n \underline{w}_n \tag{48}$$

Let $k > l$ and add $\sum\limits_{n=l+1}^{k} \underline{x}_n(\overline{w}_n - \underline{w}_n)$ to both sides of (48), in order to see that

$$f_l(l)\left[\sum_{n=1}^{l} \overline{w}_n + \sum_{n=l+1}^{N} \underline{w}_n\right] + \sum_{n=l+1}^{k} \underline{x}_n(\overline{w}_n - \underline{w}_n)$$
$$= \sum_{n=1}^{k} \underline{x}_n \overline{w}_n + \sum_{n=k+1}^{N} \underline{x}_n \underline{w}_n \tag{49}$$

Because $k > l$, $\underline{x}_k > f_l(l)$, $\sum\limits_{n=1}^{k} \overline{w}_n + \sum\limits_{n=k+1}^{N} \underline{w}_n > 0$ and $\overline{w}_n - \underline{w}_n > 0$,

$$f_l(l)\left[\sum_{n=1}^{l} \overline{w}_n + \sum_{n=l+1}^{N} \underline{w}_n\right] < \underline{x}_k\left[\sum_{n=1}^{l} \overline{w}_n + \sum_{n=l+1}^{N} \underline{w}_n\right] \tag{50}$$

$$\sum_{n=l+1}^{k} \underline{x}_n(\overline{w}_n - \underline{w}_n) < \underline{x}_k \sum_{n=l+1}^{k} (\overline{w}_n - \underline{w}_n) \tag{51}$$

We obtain the following inequality from the above three inequalities:

$$\sum_{n=1}^{k} \underline{x}_n \overline{w}_n + \sum_{n=k+1}^{N} \underline{x}_n \underline{w}_n$$
$$< \underline{x}_k\left[\sum_{n=1}^{l} \overline{w}_n + \sum_{n=l+1}^{N} \underline{w}_n\right] + \underline{x}_k \sum_{n=l+1}^{k} (\overline{w}_n - \underline{w}_n)$$
$$= \underline{x}_k\left[\sum_{n=1}^{k} \overline{w}_n + \sum_{n=k+1}^{N} \underline{w}_n\right] \tag{52}$$

Because $\sum\limits_{n=1}^{k} \overline{w}_n + \sum\limits_{n=k+2}^{N} \underline{w}_n > 0$, it follows that

$$\underline{x}_k > \frac{\sum_{n=1}^{k} \underline{x}_n \overline{w}_n + \sum_{n=k+1}^{N} \underline{x}_n \underline{w}_n}{\sum_{n=1}^{k} \overline{w}_n + \sum_{n=k+1}^{N} \underline{w}_n} = f_l(k). \quad \square \tag{53}$$

Our proposed EIASC makes the following two improvements over the IASC:

1) New stopping criterion based on Theorem 1.
2) Both the IASC for computing y_l and the IASC for computing y_r start from switch point 1 and increase it gradually to find the correct switch points. This is reasonable for y_l, since it has been shown in [1] that for a variety of scenarios, its switch point l is smaller than $N/2$; so, it is more efficient to search from $l = 1$ instead of from $l = N - 1$. However, setting the initial switch point $r = 1$ may not be efficient for y_r, since it has been shown in [1] that generally its switch point $r > N/2$. So, it would be more efficient if for y_r one initializes the switch point as $r = N - 1$ and then gradually decreases it until the correct r is found.

In summary, the EIASC for computing y_l and y_r are:

EIASC for computing y_l:

1) The same as Step (1) of KMA for computing y_l.
2) Initialize

$$a = \sum_{n=1}^{N} \underline{x}_n \underline{w}_n, \qquad b = \sum_{n=1}^{N} \underline{w}_n$$
$$y_l = \underline{x}_N, \qquad l = 0$$

3) Compute

$$l = l + 1, \qquad a = a + \underline{x}_l(\overline{w}_l - \underline{w}_l)$$
$$b = b + \overline{w}_l - \underline{w}_l, \qquad c = a/b$$

4) If $c > y_l$, set $l = l - 1$ and stop; otherwise, set $y_l = c$ and go to Step (3).

EIASC for computing y_r:

1) The same as Step (1) of KMA for computing y_r.
2) Initialize

$$a = \sum_{n=1}^{N} \overline{x}_n \underline{w}_n, \qquad b = \sum_{n=1}^{N} \underline{w}_n$$
$$y_r = \overline{x}_1, \qquad r = N$$

3) Compute

$$a = a + \overline{x}_r(\overline{w}_r - \underline{w}_r), \qquad b = b + \overline{w}_r - \underline{w}_r$$
$$c = a/b, \qquad r = r - 1$$

4) If $c < y_r$, set $r = r + 1$ and stop; otherwise, set $y_r = c$ and go to Step (3).

Clearly, based on Theorem 1, given an initialization of l (or r), one can easily tell whether it is on the left or right of the true l (or r), and hence the new initialization idea in EKMANI can also be used in EIASC. We implemented the corresponding algorithm, where the user can specify an initial l (or r); otherwise, l is initialized to $[N/2.4]$ (r to $[N/1.7]$), the same as EKMA. Interestingly, this new algorithm only outperforms EIASC when $N > 1000$. Since in practice usually $k < 1000$, this new algorithm is not included in this paper. However, it can be downloaded from the first author's website at http://www-scf.usc.edu/~dongruiw/files/TR_Algorithms.zip.

IV. Experimental Comparison

In this section we compare the performance of the five type-reduction algorithms (KMA, EKMA, EKMANI, IASC, and EIASC) using three simulations. The platform is a Lenovo Thinkpad T500 with Intel Core2 Duo CPU P8600@2.40Hz and 3GB memory, running Windows 7 32-bit Home Premium and Matlab R2009a. The computational cost is measured by the computation time, obtained from Matlab *tic* and *toc* functions.

A. Comparison 1: Uniformly Distributed X_n and W_n

In this comparison, we assume the elements in X_n and W_n are uniformly distributed, $\underline{x}_n = \overline{x}$, and $N = \{3, 4, ..., 10, 20, ..., 100, 200, ..., 1000, 1500, 2000\}$ were used. For each N, 5000 Monte Carlo simulations were used to compute y. The results are shown in Fig. 2. Observe that:

1) All four efficient algorithms outperformed KMA.
2) The performances of EKMA and EKMANI were almost identical in this simulation because for each N all 5000 Monte Carlo simulations were independent, so it does not make sense to initialize a switch point from a previous simulation. We did not supply the new initial switch points in EKMANI in this simulation, so it reduced to EKMA. Also, the performance improvement of EKMA over KMA is not as large as that reported in [1] since for each algorithm in this paper we added the same preprocessing steps to eliminate possible numerical problems and the preprocessing time was included in the computational cost, whereas in [1] preprocessing time was not considered.
3) Both IASC and EIASC significantly outperformed KMA, especially when N is small ($N \leqslant 100$). And, EIASC slightly outperformed IASC. The computational cost of both IASC and EIASC increase rapidly as N increases since they need to evaluate many possible switch points before finding the correct ones.

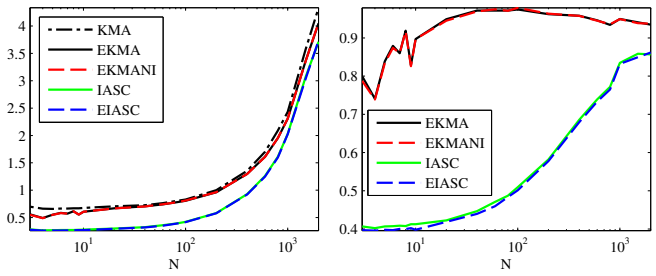

(a) (b)

Fig. 2. (a) Total computation time (seconds) of the 5000 Monte Carlo simulations of uniformly distributed X_n and W_n ($n = 1, 2, ..., N$) for different N. (b) The ratio of the computation time of the four efficient algorithms with respect to KMA.

B. Comparison 2: Computing the Generalized Centroid of A General Type-2 FS

In this simulation, we compare the performance of the five type-reduction algorithms in computing the generalized

centroid of a general type-2 FS, which is originally defined in [20] as:

$$\mu_{\tilde{A}}(x) = \begin{cases} \frac{z-d(x)}{p(x)-d(x)}, & d(x) \leqslant z \leqslant p(x) \\ \frac{u(x)-z}{u(x)-p(x)}, & p(x) \leqslant z \leqslant u(x) \\ 0 & \text{otherwise} \end{cases} \tag{54}$$

$$u(x) = \max(f_1(x), f_2(x)) \tag{55}$$

$$d(x) = \max(g_1(x), g_2(x)) \tag{56}$$

$$f_1(x) = \exp\left(-\frac{(x-3)^2}{8}\right) \tag{57}$$

$$f_2(x) = 0.8\exp\left(-\frac{(x-6)^2}{8}\right) \tag{58}$$

$$g_1(x) = 0.5\exp\left(-\frac{(x-3)^2}{2}\right) \tag{59}$$

$$g_2(x) = 0.4\exp\left(-\frac{(x-6)^2}{2}\right) \tag{60}$$

$$p(x) = d(x) + w(x)(u(x) - d(x)) \tag{61}$$

where $\mu_{\tilde{A}}(x)$ is the secondary membership grade, $z \in [d(x), u(x)]$ is the primary membership grade, and $w(x)$ is a random number in [0, 1]. An example of the type-2 FS is shown in Fig. 3.

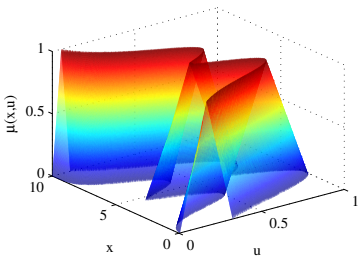

Fig. 3. An example of the type-2 FS in Comparison 2.

In [19] it has been shown that EKMANI achieved a much better performance than KMA and EKMA. As in [19], we fixed $N = 200$ and took the number of α-planes as $\{5, 10, 20, 50, 75, 100\}$. For each number of α-planes, we repeated the experiment 1000 times to get a more accurate computation time. The results are shown in Fig. 4. Observe that:

1) All four efficient algorithms outperformed KMA.
2) EKMANI outperformed EKMA significantly since in EKMANI the switch points from the previous α-plane were used as the initial switch points in the next α-plane. As usually y_l and y_r change very slightly from one α-plane to the next (especially when the number of α-planes is large), the switch points in two α-planes are very close to each other, and hence the new initialization strategy is better than that in EKMA.
3) Both IASC and EIASC significantly outperformed all other three algorithms, and EIASC also outperformed IASC slightly.

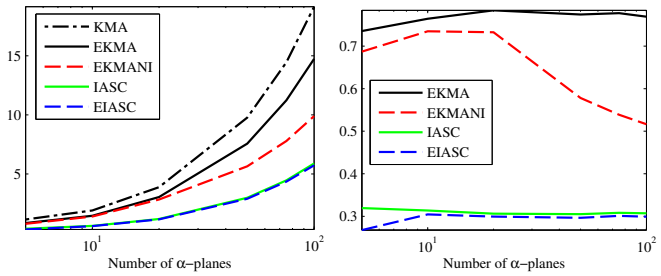

Fig. 4. (a) Total computation time (seconds) of the 1000 runs of centroid computation for different number of α-planes. (b) The ratio of the computation time of the four efficient algorithms with respect to KMA.

C. Comparison 3: IT2 Fuzzy Logic Controller Design

In this subsection we compare the performance of the five algorithms in FLC design using evolutionary computation [21], where the performance of a large number of (usually randomly generated) FLCs are evaluated. The following simple first-order plus dead-time plant is employed as the nominal system [22]:

$$G(s) = \frac{K}{\tau s + 1}e^{-Ls} = \frac{1}{10s+1}e^{-2.5s} \tag{62}$$

The goal is to design an IT2 fuzzy PI controller

$$\dot{u} = k_P\dot{e} + k_I e \tag{63}$$

where $\dot{u}$ is the change in control signal, e is the error, $\dot{e}$ is the change of error, and k_P and k_I are proportional and integral gains. Assume there are M Gaussian IT2 FSs in each domain (e and $\dot{e}$), and each IT2 FSs is determined by three parameters (one mean, m_m, and two standard deviations, σ_m^1 and σ_m^2, $m = 1, 2, ..., M$). Each of the M^2 rule consequents is represented by a crisp number y_n, $n = 1, ..., M^2$. Then, for each input pair $(e, \dot{e})$, all $N = M^2$ rules are fired, and a type-reduction algorithm is needed to compute the output of the IT2 FLC.

Assume the population consists of 100 randomly generated IT2 FLCs (all m_m, σ_m^1, σ_m^2, and y_n are random), and the performance of each FLC is evaluated by a step response in the first 100 seconds with sampling frequency 1 Hz. We recorded the time that the five algorithms were used to perform type-reduction for these $100 \times 100 = 10000$ input pairs. $M = \{3, 4, ..., 10, 20, ..., 100\}$ were used. The results are shown in Fig. 5. Observe that:

1) All four efficient algorithms outperformed KMA.
2) EKMANI outperformed EKMA significantly since in EKMANI the switch points from the previous step were used as the initial switch points in the next step. As usually e and $\dot{e}$ change very slightly from one step to the next (especially when the sampling frequency is high, and/or during steady state), the switch points in two steps are very close to each other, and hence the new initialization strategy is better than that in EKMA.

3) Both IASC and EIASC significantly outperformed all other three algorithms when M is small ($M \leqslant 20$), and EIASC also outperformed IASC slightly.

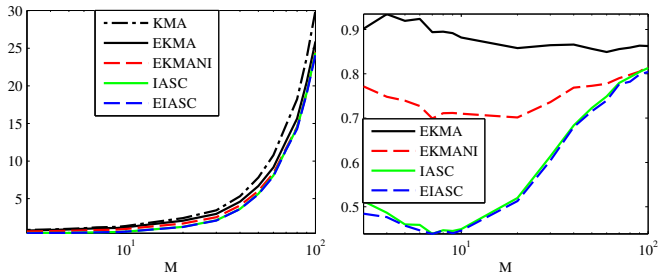

(a) (b)

Fig. 5. (a) Total computation time (seconds) of the 100 IT2 FLCs for different M, the number of IT2 FSs in each input domain. Note that $N = M^2$. (b) The ratio of the computation time of the efficient algorithms with respect to KMA.

V. Conclusions

Type-reduction algorithms are very important for type-2 fuzzy sets and systems. However, the most popular Karnik-Mendel Algorithms is computationally intensive. In this paper we have reviewed several more efficient type-reduction algorithms, and also improved over one of them. Experimental results showed that our proposed algorithm is the most efficient one to use. Particularly, when $N \leqslant 100$, which is true in most practical type-reduction computations, our proposed algorithm (EIASC) can save over 50% computational cost over the Karnik-Mendel Algorithms. An Matlab implementation of EIASC is also given. It includes preprocessing steps to eliminate numerical problems. This algorithm will be very helpful in promoting the popularity of type-2 fuzzy sets and systems.

Appendix A
Matlab Implementation of EIASC

This appendix presents an Matlab implementation of EIASC. Note that it is more complex than the algorithm presented in Section III-D since here we include the following preprocessing steps to eliminate possible numerical problems:

1) When all $\underline{w}_n$ are zero or all $\overline{w}_n$ are very close to zero, e.g., $\overline{w}_n < 10^{-10}$ for $\forall n$, we return $y_l = \min_n \underline{x}_n$ and $y_r = \max_n \overline{x}_n$.
2) All very small $\overline{w}_n$, e.g., $\overline{w}_n < 10^{-10}$, and their associated $\underline{x}_n$, $\overline{x}_n$, and $\underline{w}_n$, are removed to prevent numerical instability.
3) $\{\underline{x}_n\}$ and $\{\overline{x}_n\}$ are made unique respectively to prevent possible infinite loops.

A user can easily modify the codes for additional computational cost saving. For example, Step (3) above may be done only once *a priori* in an FLC. Additionally, $\{\underline{x}_n\}$ and $\{\overline{x}_n\}$ can be sorted only once *a priori* in an FLC, and they do not need to be sorted in computing the generalized centroid of type-2 fuzzy sets.

The following four input parameters are mandatory:

- *Xl*: A row vector containing $\underline{x}_n$, $n = 1, 2, ..., N$.
- *Xr*: A row vector containing $\overline{x}_n$, $n = 1, 2, ..., N$. If $\underline{x}_n = \overline{x}_n$ $\forall n$, then use [] as input for *Xr*.
- *Wl*: A row vector containing $\underline{w}_n$, $n = 1, 2, ..., N$.
- *Wr*: A row vector containing $\overline{w}_n$, $n = 1, 2, ..., N$.

The following input is optional:

- *needSort*: "1" if at least one of *Xl* and *Xr* is not in ascending order. "0" if both *Xl* and *Xr* are in ascending order. Default "1."

The outputs are:

- *y*: Mid-point of Y in (5). $y = (yl + yr)/2$.
- *yl*: y_l in (6).
- *yr*: y_r in (7).
- *l*: Switch point l for computing *yl*.
- *r*: Switch point r for computing *yr*.

Matlab implementations of all other algorithms introduced in this paper can be found from the first author's website at http://www-scf.usc.edu/~dongruiw/files/TR_Algorithms.zip.

```
function [y,yl,yr,l,r]=EIASC(Xl,Xr,...
                         Wl,Wr,needSort)

ly=length(Xl);
XrEmpty=isempty(Xr);
if XrEmpty; Xr=Xl; end

if max(Wl)==0
    yl=min(Xl);  yr=max(Xr);
    y=(yl+yr)/2;
    l=1;   r=ly-1;
    return;
end

index=find(Wr<10^(-10));
if length(index)==ly
    yl=min(Xl);  yr=max(Xr);
    y=(yl+yr)/2;
    l=1;  r=ly-1;
    return;
end

Xl(index)=[]; Xr(index)=[];
Wl(index)=[]; Wr(index)=[];

if nargin==4; needSort=1; end

% Compute yl
if  needSort
    [Xl,index]=sort(Xl);
    Xr=Xr(index);
    Wl=Wl(index);
    Wr=Wr(index);
end
Wl2=Wl;  Wr2=Wr;
```

```
for i=length(Xl):-1:2 % Make Xl unique
    if Xl(i)==Xl(i-1)
        Wl(i)=Wl(i)+Wl(i-1);
        Wr(i)=Wr(i)+Wr(i-1);
        Xl(i)=[];
        Wl(i-1)=[]; Wr(i-1)=[];
    end
end

ly=length(Xl);
if ly==1
    yl=Xl;  l=1;
else
    yl=Xl(end); l=0;
    a=Xl*Wl'; b=sum(Wl);
    while yl > Xl(l+1)
        l=l+1;
        a=a+Xl(l)*(Wr(l)-Wl(l));
        b=b+Wr(l)-Wl(l);
        yl=a/b;
    end
end

% Compute yr
if ~XrEmpty && needSort==1
    [Xr,index]=sort(Xr);
    Wl=Wl2(index); Wr=Wr2(index);
end

if ~XrEmpty
    for i=length(Xr):-1:2 % Make Xr unique
        if Xr(i)==Xr(i-1)
            Wl(i)=Wl(i)+Wl(i-1);
            Wr(i)=Wr(i)+Wr(i-1);
            Xr(i)=[];
            Wl(i-1)=[]; Wr(i-1)=[];
        end
    end
end

ly=length(Xr);
if ly==1
    yr=Xr; r=1;
else
    r=ly; yr=Xr(1);
    a=Xr*Wl'; b=sum(Wl);
    while yr < Xr(r)
        a=a+Xr(r)*(Wr(r)-Wl(r));
        b=b+Wr(r)-Wl(r);
        yr=a/b; r=r-1;
    end
end

y=(yl+yr)/2;
```

REFERENCES

[1] D. Wu and J. M. Mendel, "Enhanced Karnik-Mendel Algorithms," *IEEE Trans. on Fuzzy Systems*, vol. 17, no. 4, pp. 923–934, 2009.

[2] N. N. Karnik and J. M. Mendel, "Centroid of a type-2 fuzzy set," *Information Sciences*, vol. 132, pp. 195–220, 2001.

[3] J. M. Mendel and F. Liu, "Super-exponential convergence of the Karnik-Mendel Algorithms for computing the centroid of an interval type-2 fuzzy set," *IEEE Trans. on Fuzzy Systems*, vol. 15, no. 2, pp. 309–320, 2007.

[4] J. M. Mendel, *Uncertain Rule-Based Fuzzy Logic Systems: Introduction and New Directions*. Upper Saddle River, NJ: Prentice-Hall, 2001.

[5] D. Wu and J. M. Mendel, "Aggregation using the linguistic weighted average and interval type-2 fuzzy sets," *IEEE Trans. on Fuzzy Systems*, vol. 15, no. 6, pp. 1145–1161, 2007.

[6] ——, "Corrections to 'Aggregation using the linguistic weighted average and interval type-2 fuzzy sets'," *IEEE Trans. on Fuzzy Systems*, vol. 16, no. 6, pp. 1664–1666, 2008.

[7] J. M. Mendel and D. Wu, *Perceptual Computing: Aiding People in Making Subjective Judgments*. Hoboken, NJ: Wiley-IEEE Press, 2010.

[8] D. Wu and J. M. Mendel, "Computing with words for hierarchical decision making applied to evaluating a weapon system," *IEEE Trans. on Fuzzy Systems*, vol. 18, no. 3, pp. 441–460, 2010.

[9] H. Wu and J. M. Mendel, "Uncertainty bounds and their use in the design of interval type-2 fuzzy logic systems," *IEEE Trans. on Fuzzy Systems*, vol. 10, no. 5, pp. 622–639, 2002.

[10] D. Wu and W. W. Tan, "Computationally efficient type-reduction strategies for a type-2 fuzzy logic controller," in *Proc. IEEE Int'l Conf. on Fuzzy Systems*, Reno, NV, May 2005, pp. 353–358.

[11] M. Nie and W. W. Tan, "Towards an efficient type-reduction method for interval type-2 fuzzy logic systems," in *Proc. IEEE Int'l Conf. on Fuzzy Systems*, Hong Kong, June 2008, pp. 1425–1432.

[12] M. Begian, W. Melek, and J. Mendel, "Stability analysis of type-2 fuzzy systems," in *Proc. IEEE Int'l Conf. on Fuzzy Systems*, Hong Kong, June 2008, pp. 947–953.

[13] X. Du and H. Ying, "Control performance comparison between a type-2 fuzzy controller and a comparable conventional mamdani fuzzy controller," in *Proc. Annual Meeting of the North American Fuzzy Information Processing Society*, San Diego, CA, June 2007, pp. 100–105.

[14] S. Greenfield, F. Chiclana, S. Coupland, and R. John, "The collapsing method of defuzzification for discretised interval type-2 fuzzy sets," *Information Sciences*, 2008, in press.

[15] R. Sepulveda, O. Castillo, P. Melin, and O. Montiel, "An efficient computational method to implement type-2 fuzzy logic in control applications," in *Analysis and Design of Intelligent Systems using Soft Computing Techniques*, P. Melin, O. Castillo, E. Ramirez, J. Kacprzyk, and W. Pedrycz, Eds. Berlin/Heidelberg: Springer, 2007, pp. 45–52.

[16] D. Wu, "An interval type-2 fuzzy logic system cannot be implemented by traditional type-1 fuzzy logic systems," in *Proc. World Conference on Soft Computing*, San Francisco, CA, May 2011.

[17] M. Melgarejo, "A fast recursive method to compute the generalized centroid of an interval type-2 fuzzy set," in *Proc. Annual Meeting of the North American Fuzzy Information Processing Society*, San Diego, CA, June 2007, pp. 190–194.

[18] K. Duran, H. Bernal, and M. Melgarejo, "Improved iterative algorithm for computing the generalized centroid of an interval type-2 fuzzy set," in *Proc. Annual Meeting of the North American Fuzzy Information Processing Society*, New York, May 2008, pp. 1–5.

[19] C.-Y. Yeh, W.-H. Jeng, and S.-J. Lee, "An enhanced type-reduction algorithm for type-2 fuzzy sets," *IEEE Trans. on Fuzzy Systems*, 2011, in press.

[20] F. Liu, "An efficient centroid type-reduction strategy for general type-2 fuzzy logic system," *Information Sciences*, vol. 178, no. 9, pp. 2224–2236, 2008.

[21] D. B. Fogel, *Evolutionary computation: Toward a new philosophy of machine intelligence*, 3rd ed. Hoboken, NJ: Wiley-IEEE Press, 2006.

[22] D. Wu and W. W. Tan, "Interval type-2 fuzzy PI controllers: Why they are more robust," in *Proc. IEEE Int'l. Conf. on Granular Computing*, San Jose, CA, August 2010, pp. 802–807.

2011 IEEE International Conference on Fuzzy Systems
June 27-30, 2011, Taipei, Taiwan

Interpreting Fuzzy Set Operations and Multi Level Agreement in a Computing with Words Context

Christian Wagner
Computational Intelligence Centre
University of Essex
United Kingdom
christian AT wagnerweb.net

Hani Hagras
Computational Intelligence Centre
University of Essex
United Kingdom
hani AT essex.ac.uk

***Abstract*—Computing with Words (CWW) aims to investigate the possibility of imitating the unique ability of humans for approximate reasoning on the basis of approximately defined classes and concepts in the form of words. Type-2 fuzzy sets have been used to provide an adequate modeling basis for words in a fuzzy logic context. In the context of type-2 fuzzy sets employed as part of CWW, a variety of research efforts have been made to investigate approaches to model the meaning of specific words using type-2 fuzzy sets. In this paper we start by focusing on the interpretation of classical set-theoretical operations (complement, union and intersection) for crisp and type-1 fuzzy sets. We proceed by extending the interpretations to the results of the union and intersection operations of interval type-2 fuzzy sets, specifically indicating their effect on the uncertainty representation in the sets. We note the impact of the choice of t-norms and t-conorms in particular in the context of CWW applications where the interpretation of the resulting sets and its resemblance to the human intuitive meaning of the concept or word is essential. Finally, we provide the interpretation and reasoning behind the Multi Level Agreement (MLA) operation based on zSlices which was previously introduced and discuss the requirement for the selection of the right operations for the amalgamation of individual fuzzy sets and the potential for investigating this choice in particular in a CWW context.**

Keywords: Multi Level Agreement (MLA); zSlices; intersection; union; interpretation; Computing With Words (CWW)

I. INTRODUCTION

Fuzzy Logic Sets were initially introduced in 1965 by Zadeh [1] in order to provide a framework "which may be of use in dealing with "classes"" that are imprecisely defined such as for example "the class of tall men" or "the class of beautiful women". Since 1965, fuzzy sets and resulting fuzzy logic systems have become widely popular both in research terms as well as through a large number and variety of applications.

Further to the original concept of what is today referred to as type-1 fuzzy sets, Zadeh in 1975 introduced the concept of a linguistic variable and its application to approximate reasoning [2], providing the basis for what is referred to today as type-2 fuzzy sets and systems.

While the main focus of fuzzy logic (systems) in terms of their applications has been what could be called "traditional areas of fuzzy logic application" such as control applications (e.g.: [3],[4]), medical applications (e.g. [5]) and applications in business (e.g. [6]), in recent years a new body of research centered around the concept of "Computing With Words" (CWW) has been raising interest (e.g. [7], [8] and [9]).

At the basis of CWW is the renewed effort of investigating the possibility of imitating the unique (in the sense of outstanding, especially compared to computers) ability of humans for approximate reasoning or more specifically the reasoning with, or on the basis of approximately defined classes and concepts in the form of words. Language and the use of "words" encapsulates this human ability and as such, the "word" or more specifically, *the meaning of a word* and how it can be represented, manipulated, stored and in a general sense be computed with (including for inference purposes) is a "hot" topic of research. Type-2 fuzzy sets and specifically interval type-2 fuzzy sets have been used to provide an adequate modeling basis for words in a fuzzy logic context as their Footprint Of Uncertainty (FOU) allows for expressing a degree of uncertainty about a specific degree of membership. In the context of type-2 fuzzy sets employed as part of CWW, a variety of research efforts have been made to investigate approaches to model the meaning of specific words using type-2 fuzzy sets based on (usually survey based) data (e.g. [10], [11] [12]).

In our recent work we have developed the notion of agreement in the sense of zSlices [13] based general type-2 fuzzy sets [14], [15] with a specific focus on its application in the context of Ambient Intelligent Environment (AIE) applications. As part of our research, we have investigated the combination of several interval type-2 fuzzy sets (originating from different sources (e.g.: people) but describing the same linguistic label or word) to form an "agreement" zSlices based set which aims to preserve the interpretation of the specific concept (word) by the individual while assigning higher importance to interpretations shared amongst multiple sources (e.g. individual people). While this work was application-oriented, it is clear that the application of fuzzy sets to model human-centered concepts such as words requires a far more general investigation into the actual meaning of words and how this meaning can be captured based on individual interpretations of a given meaning. Incidentally, the role of classes and concepts in human perception and decision making has been subject to considerable study in sociology and psychology. For example, recent work has considered the investigation into whether humans categorize (make categories) according to exemplar or rule-based theories [16].

978-1-4244-7316-8/11/$26.00 ©2011 IEEE

If fuzzy logic is to model human concepts and words, it is not farfetched to believe that it is essential to investigate the formation of such concepts in humans in order to replicate fuzzy set based models that truly reflect the human notion of concepts and/or words.

It is clear that the adoption - of existing knowledge in - and cooperation with - other fields such as social and psychological sciences is a long term endeavor. In the current paper we, are aiming to present some early and in comparison basic findings based on the previously mentioned notion of agreement for zSlices based general type-2 fuzzy sets as well the more general question of the interpretation of the "aggregation" of multiple samples of a specific concept (i.e. through finding agreement, intersection, etc.). We are not addressing the question of how individual fuzzy sets can be designed (through manual or automatic means) in order for them to represent the meaning of a specific word or concept. Instead, we focus on the investigation of the operation(s) required to extract or represent meaning based on multiple interpretations (sets) of the same concept. As an example, consider the concept of "tall people" expressed as a fuzzy set. Further, consider that this concept would most likely be expressed differently depending on the subject expressing it, i.e. a basketball player is likely to have a different interpretation of the concept than a normal citizen. The questions we are investigating as part of this paper is the following:

- How can individual interpretations (one, two, …, many) of a concept be "combined" in a useful way? I.e. how can the two interpretations of "tall men" be combined to get a better understanding of what "tall men" means – and what does "better" mean in this context?
- If the classical set theoretic operations union and intersection are employed, how can the resulting sets be interpreted? I.e. if we were to compute the intersection of the two fuzzy sets representing "tall men" – what would be the interpretation of the resulting set? (The latter is not straightforward – in particular for type-2 sets.)
- How can general type-2 fuzzy sets be employed to preserve information in "combined concepts" and how can for example zSlices based agreement sets be interpreted? I.e. If we were to employ zSlices based agreement to combine the two sets representing "tall men" – what would be the interpretation (meaning) of the resulting set?
- What is the scope to elicit existing / define new operations for (type-2) fuzzy sets that allow the "combination" of individual concept interpretations in different ways in order to imitate human concept creation? I.e. are there operations other than intersection and union that allow us to combine for example the two sets representing individual interpretations of "tall men" and is there a need or case for introducing new operations specifically for CWW?

In order to address the individual points, we will briefly review basic set theoretic operations and their interpretation as part of Section II. Section III will focus on the interpretation of the intersection and union operations of interval type-2 fuzzy sets while Section IV will focus on the agreement operation based on zSlices and their interpretation, specifically in contrast to the interval type-2 operations. Subsequently, Section V provides a discussion of the individual points and the potential for the elicitation of other operations with the view to generating representative and meaningful fuzzy set representations from series of individual fuzzy set based interpretations, specifically in a CWW context. Section VI finally provides some conclusions and describes future work.

II. Basic Set Operations and their Interpretation

A. Overview

As fuzzy logic is an extension of classical set theory, the most fundamental operations are themselves extensions of the fundamental set theoretic operations of complement, union and intersection. In the current section we revisit each of these operations by referring to both crisp sets as well as type-1 fuzzy sets and briefly discuss their interpretation with the specific aim of investigating their potential for building "agreement fuzzy set model" which incorporate multiple individual fuzzy set sources.

B. The Complement Operation

In classical crisp sets, the standard complement $\bar{A}$ of a set A describes the set of all elements which are not part of A. In fuzzy logic, the complement $\bar{A}$ of a set A describes the membership for any element to not be part of A. Fig. 1 illustrates the complement operation for both crisp and type-1 fuzzy sets. Equation (1) describes the complement operation in terms of the membership values for type-1 fuzzy sets.

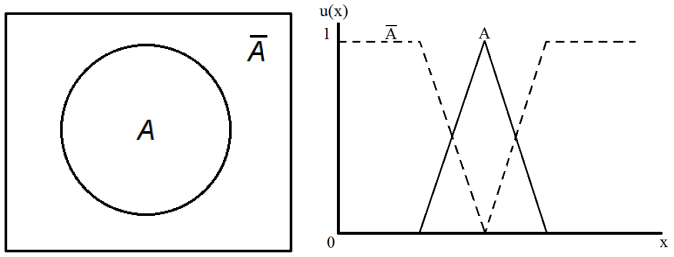

Figure 1. (a) The complement of a crisp set. (b) The complement of a fuzzy set (dashed).

$$u_{\bar{A}} = 1 - u_A \tag{1}$$

The complement operation is straightforward in the logical sense, in terms of its interpretation in a CWW context however it should be considered with caution. For example consider in Fig. 1 the set A describing the concept "*tall people*" as defined by an individual – a person. It is not clear that $\bar{A}$ in this case reflects that person's interpretation of the concept "*not tall people*". For instance, the person may only consider shorter people as "*not tall*", while $\bar{A}$ includes for example includes "*very tall people*". The investigation of this question of what the actual meaning is or should be doubtlessly involves the incorporation of existing knowledge from the areas of psychology and social sciences - we are not addressing it in further detail as part of this paper and we merely include the review of the complement operation for completeness.

C. The Union Operation

The union operation in classical set theory results in a new set that comprises all elements of the initial sets as shown in Fig. 2a. The union of two type-1 fuzzy sets A and B is described by taking the t-conorm of the sets' membership values. One passible t-conorm is the maximum operator as used in Equation (2) and shown in Fig. 2b.

$$u_A \vee u_B = \max(u_A, u_B) \quad (2)$$

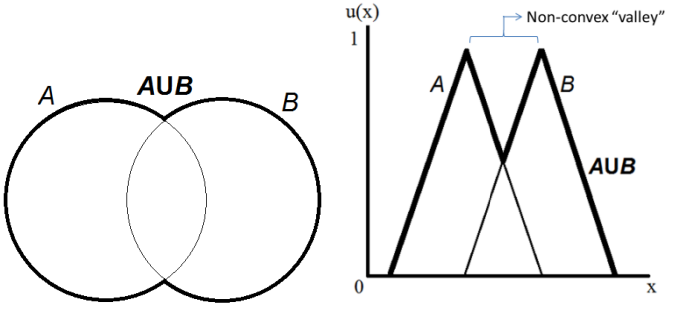

(a) (b)

Figure 2 (a) The union of two crisp sets. (b) The union of two type-1 fuzzy sets.

In terms of interpretation, the union implements the logical OR, thus reflecting that any member of the union belongs to either (one or many) of its constituting sets. In fuzzy logic the union operation is generally applied to individual sets qualifying a specific linguistic variable such as *height of people*, where for example the union of the adjacent sets *tall* and *very tall* could be computed to reflect the membership of people who are tall ***or*** very tall.

In contrast to computing the union on different sets describing a linguistic label, in this paper we are focusing on the union of different instances of the same fuzzy set or more precisely, different interpretations (expressed through a fuzzy set) of the same linguistic label, for example: *tall people*. Further, we are specifically aiming to investigate how a useful and meaningful model of a specific label can be extracted from a series of individual models/interpretations. In other words – what is an appropriate general model for *tall people* based on the sample interpretations gathered?

In this context, where for example the type-1 fuzzy sets A and B in Fig. 2b describe different interpretations of the same concept (e.g. *tall people*), the union can be interpreted as a summary of all individual interpretations or opinions in terms of the meaning of the actual concept. While this may be useful, it is clear that as the number of "opinions" (i.e. fuzzy set interpretations of the concept) increases, the resulting model (the union of the individual sets) tends to grow in terms of its support. This in turn means that the precision of the model for *tall people* decreases or perhaps more appropriately the generality of the model increases. This effect may not be desirable as part of CWW applications as a very general concept is often less useful when attempting to reason based on specific data. For example, what information can be gathered from *tall people* if the fuzzy set model covers a very large range from 1 meter – 2.5 meters? Further, applying the union operation does not allow for the modeling of where more candidate sets are in agreement. For example, the resulting union membership function does not allow differentiating between a union set formed by many similar sets or potential outliers. While one could aim to remedy this effect by pre-selecting candidate sets for *tall people* and removing outliers, we are aiming to investigate a more transparent approach to aggregating all individual interpretations while also modeling "agreement" between individual sets (i.e. to model where many sets overlap, rather than just few).

Finally, in terms of employing the union operation in CWW applications, it can be noted that in terms of its meaning / interpretation, it can be difficult to explain the usually resulting area of non-convexity or "valley" which is shown for example in Fig. 2b. Referring to our example of multiple interpretations of the concept "*tall people*", one may expect that if A and B depict two interpretations, that their union should cover the entire space between the sets (thus incorporating the range between the individual interpretations). Interestingly, replacing the most common t-conorm *maximum* to implement the union operation by the equally valid but less popular Łukasiewicz t-conorm [17] (more precisely the dual to the Łukasiewicz t-norm) for strong disjunction shown in Equation (3) results in sets which generally more closely represent the expected result as shown for example for sets A and B in Fig. 3.

$$u_A \vee_{Ł} u_B = \min(1, (u_A + u_B)) \quad (3)$$

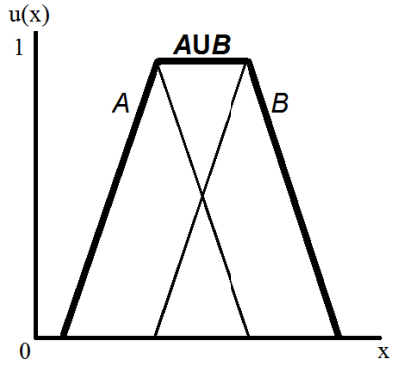

Figure 3 The union of two fuzzy sets when employing the Łukasiewicz t-conorm.

It should be noted that we are not recommending the replacement of the *t-conorm* maximum by the *Łukasiewicz t-conorm* in a general fashion. However, the example above serves the purpose to show that when considering the modeling of human concepts and words (as part of CWW), it may be appropriate to revisit the choice of t-conorms (and t-norms) with the aim of producing fuzzy sets which closely mimic the human interpretation of a given concept or word. In particular in type-2 fuzzy logic, less common t-conorms and t-norms have so far only been explored in a very limited fashion, in particular in CWW applications.

D. The Intersection Operation

While the union operation implements the logical OR, the intersection operation implements the logical AND, i.e. the conjunction operation. The intersection operation in classical set theory results in a new set that comprises the elements in common between the initial sets as shown in in Fig. 4a. The intersection of two type-1 fuzzy sets A and B is described by taking the t-norm of the sets' membership values. One possible

t-norm is the minimum operator as used in Equation (4) and shown in in Fig. 4b.

In terms of interpretation, the intersection operation extracts the "common ground" between two concepts or words. As such, following our example of two interpretations of the concept "*tall people*" expressed as sets *A* and *B* in Fig. 4, their intersection (also in Fig. 4) describes the set representing the area where both interpretations *A* and *B* "agree", i.e. where both interpretations overlap.

$$u_A \vee u_B = \min(u_A, u_B) \quad (4)$$

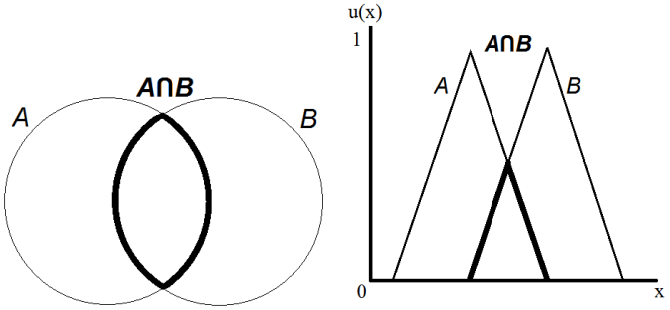

Figure 4 (a) The intersection of two crisp sets. (b) The intersection of two type-1 fuzzy sets.

Incidentally, Fig. 4 also indicates the common tendency of intersections to decrease generality in terms of support. In other words, the support of the intersection of two sets is always smaller or equal to the support of either set. This in turn can be interpreted as a "homing in" on the core meaning of the concept. In other words, the intersection in Fig. 4b can be interpreted as the core meaning of "*tall people*" in the sense that the interpretations of two individuals overlap (agree). If one imagines further sets (interpretations by other individuals), the intersection's support will tend to decrease further in size.

As exemplified in Fig. 4, the intersection of two type-1 fuzzy sets tends to result in a set with low degrees of membership **if** the sets are significantly different. This reflects the intuitive notion that the common ground between two people with vastly differing opinions tends to be small. Reciprocally, in terms of employing the intersection to extract a global meaning of many individual interpretations of a specific concept (e.g. *tall people*) rapidly tends to result in an empty set if the sample sets show any significant degree of variation. Of course, one could identify and eliminate so called outliers but by doing so one specifically excludes individual interpretations which while convenient, may not reflect the globally valid meaning. In this context, it should be noted that what "the globally valid meaning" actually is, is itself an open question and quickly leads to research in democracy and the role of an individual in a society. We are not making any claims in the direction of what a "globally valid meaning" is in reality, but as part of this paper we are considering the "globally valid meaning" as a fuzzy set which incorporates all individual interpretations of a concept and at the same time reflects the potential common ground between several interpretations where it exists.

For completeness it should be noted that, analogous to the union operation, a selection of different t-norm operations are available which slightly alter the resulting intersection and thus allow for the capturing of different interpretations.

E. Discussion

While the review of the complement, union and intersection operations can be considered trivial, their interpretation, in particular in a CWW context becomes highly significant. It lays the foundations of the idea of "agreement" as established using zSlices [15]. Specifically, considering the generalization properties of the union and the constraining properties of the intersection (in terms of the support of the resulting sets), it is clear how the latter two operations capture two very important aspects in the definition of a "globally valid meaning" in the form of a fuzzy set.

In the following section we proceed by considering the union and the intersection of interval type-2 fuzzy sets. We briefly discuss some at first glance non-intuitive properties of these basic operations when applied to type-2 fuzzy sets and provide our attempt at interpreting the sets resulting from these operations in a CWW context.

III. Interpretation of the Union and Intersection Operations for Interval Type-2 Fuzzy Sets

A. Overview

Both the union and intersection operations of interval type-2 fuzzy sets can be reduced to applying t-conorms and t-norms respectively to the upper and lower membership functions of the sets upon which the operations are to be performed [18]. Thus, it is reasonable to expect similar interpretations of the resulting sets as were described in Section II for type-1 fuzzy sets. However, while the basic properties such as the generalizing effect of the union (in terms of the support) hold both in the type-1 and in the interval type-2 case, the resulting effects on the fuzzy set Footprints Of Uncertainty (FOUs) are far less intuitive and warrant a directed effort to establish their interpretation. In the following two sections we review both the union and intersection operations for interval type-2 fuzzy sets and provide our attempt at their interpretations with a specific focus on the resulting FOUs.

B. The Union Operation for Interval Type-2 Fuzzy Sets

As noted, the union operation for interval type-2 fuzzy sets is based on computing the chosen t-conorm on the upper and lower membership functions of the specific sets. As expected, the resulting sets exhibit the same generalization tendency (i.e. a widening of the support) as was identified for their type-1 counterparts in Section II. This observation can also clearly be made in the two examples of union operations performed on different interval type-2 fuzzy sets provided in Fig. 5 and Fig. 6.

However, while it may be intuitive that the union of two interval type-2 fuzzy sets (i.e. the logical OR) should include the whole FOU of both initial interval type-2 fuzzy sets, Fig. 5 and Fig. 6 clearly indicate (by example) that this is clearly not the case.

The interpretation of this observation is not immediately straightforward. By definition, the FOU of an interval type-2 fuzzy set describes the uncertainty in terms of the degree of

membership for a given input. Consider for example the sets $\tilde{A}$ and $\tilde{B}$ as two interpretations of the concept *tall people*. As we noted, the union operation can generally be interpreted as a summary of both "opinions", i.e. in classical sets the union includes all elements of the underlying sets. In interval type-2 fuzzy sets however, the result of the union operation does not necessarily include the lower membership functions (and thus associated values) of both sets (see Fig. 5 and Fig. 6). The most obvious interpretation of this is that the union operation does not extract a "summary" of the individual sets' memberships which could be expected to include the full range from the lowest to the highest witnessed degrees of membership but actually extracts the highest degrees of membership.

In terms of our example of the union of two sets describing *tall*, the resulting set $\tilde{A} \cup \tilde{B}$ combines both individual interpretations. As a consequence the resulting model of *tall* becomes more general (wider support) and has a new uncertainty model (FOU) associated with it. Incidentally, the uncertainty (FOU) of the resulting set $\tilde{A} \cup \tilde{B}$ is generally neither the uncertainty of any one of the original interpretations (sets) but a combination of both uncertainty models.

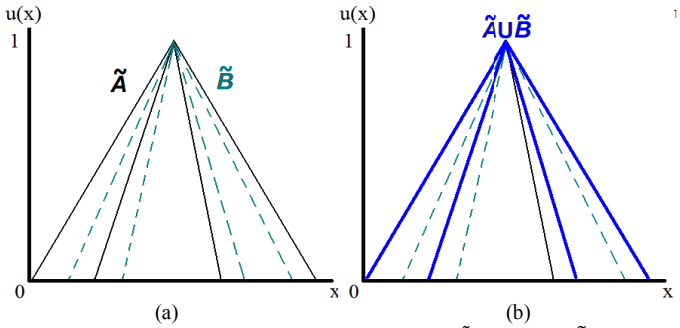

Figure 5 (a) Two example interval type-2 fuzzy sets $\tilde{A}$ (solid) and $\tilde{B}$ (dashed). (b) The union of $\tilde{A}$ and $\tilde{B}$ (bold).

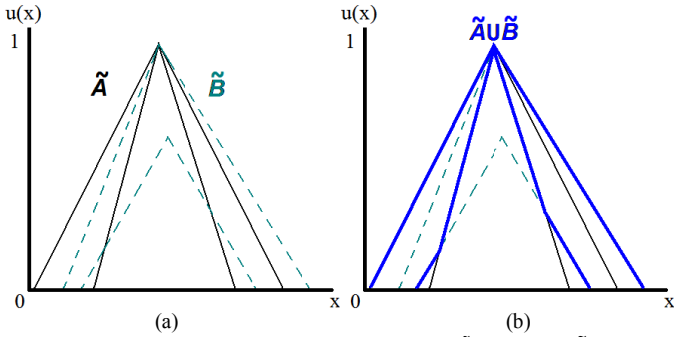

Figure 6 (a) Two example interval type-2 fuzzy sets $\tilde{A}$ (solid) and $\tilde{B}$ (dashed). (b) The union of $\tilde{A}$ and $\tilde{B}$ (bold).

In terms of CWW, the interesting question that arises is if such a recombination of "opinions" (expressed as interval type-2 fuzzy sets) indeed reflects the expected interpretation of "OR-ing" the two opinions. In the same context, to which extent can the union operation with its described results be employed as part of CWW to reflect the notion of agreement (where the incorporation of all "opinions" can be considered crucial) when computed over multiple instances (sets) describing the same concept?

The following section will review the intersection operation for interval type-2 fuzzy sets before we proceed and review the zSlices based "agreement" operation in Section IV in order to address some of the posed questions.

C. *The Intersection Operation for Interval Type-2 Fuzzy Sets*

Analogous to the union operation, the intersection operation for interval type-2 fuzzy sets can be achieved by applying a t-norm operation to the upper and lower membership functions respectively of the given candidate interval type-2 fuzzy sets.

As noted in Section II, the intersection operation, reflecting the logical AND, can be interpreted as extracting the "common ground" between the individual interval type-2 fuzzy sets. We provide two examples of the intersection operation on two interval type-2 fuzzy sets as illustrated in Fig. 7 and Fig. 8.

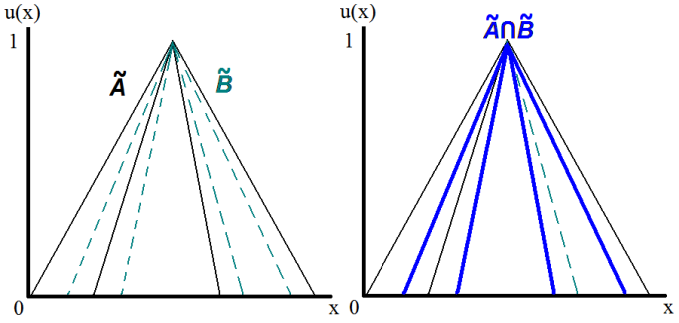

Figure 7 (a) Two example interval type-2 fuzzy sets $\tilde{A}$ (solid) and $\tilde{B}$ (dashed). (b) The intersection of $\tilde{A}$ and $\tilde{B}$ (bold).

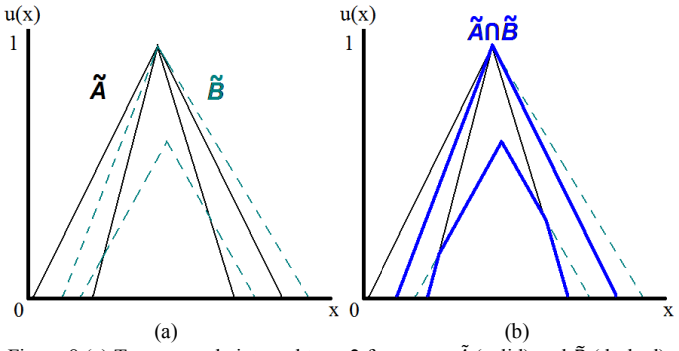

Figure 8 (a) Two example interval type-2 fuzzy sets $\tilde{A}$ (solid) and $\tilde{B}$ (dashed). (b) The intersection of $\tilde{A}$ and $\tilde{B}$ (bold).

While the fundamental interpretation of the intersection operation is straightforward and analogous to that of the intersection operation of type-1 fuzzy sets described in Section II, it is noteworthy that the results in terms of the FOU of the interval type-2 intersection are far less straightforward/intuitive to interpret. As can easily be seen in the examples in Fig. 7 and Fig. 8, the intersection operation does not result in a FOU that solely includes areas of membership that belong to both sets $\tilde{A}$ and $\tilde{B}$ but moreover it results in an FOU that ranges from the lowest lower membership function to the lowest upper membership function. To illustrate the difference in what could be considered an intuitive result of the intersection operation, consider Fig. 9 which depicts the "common ground" in terms of FOU of both fuzzy sets $\tilde{A}$ and $\tilde{B}$, while Fig. 7 shows the actual results of the intersection operation.

If we refer to our example of *tall people,* the computation of the intersection of two interpretations of this concept (i.e.

two interval type-2 fuzzy sets) could be expected to result in the overlap of the FOUs of the specific sets (as in Fig. 9). As shown, the actual result (Fig. 7) however is a set that while sharing the upper membership function with the expected result, preserves the lowest witnessed (in an input set) degree of membership.

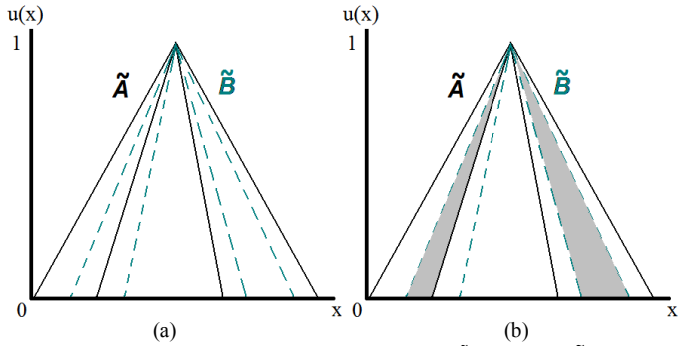

Figure 9 (a) Two example interval type-2 fuzzy sets $\tilde{A}$ (solid) and $\tilde{B}$ (dashed). (b) The potentially intuitive result of an intersection of the FOUs of $\tilde{A}$ and $\tilde{B}$ (shaded).

As for the union operation, the reason for pointing out this potential difference in the actual result of the intersection and the expected result is not to question the intersection operation as a mathematically correct operation but to provide an example of the increased complexity that results from using and particularly amalgamating (through set theoretic operations) higher order fuzzy sets. If such sets are used as part of CWW to represent and encode human-centered concepts such as words, it is essential that:

- The operations (such as intersection) employed result in sets that match our expectation – respectively reality (i.e. the concepts that are being modeled).
- We are able to accurately interpret the resulting sets in a given context.

Having explored the basic operations of union and intersection for interval type-2 fuzzy sets and briefly reflecting on their respective interpretations, we proceed in the following section to providing the underlying reasoning for introducing the agreement operation based on zSlices, followed by an overview of the actual operation and its interpretation.

IV. The Agreement Operation Based on zSlices

A. Overview

zSlices based agreement was conceptually introduced in [14] (where it was largely based around overlapping FOUs as for example in Fig. 9) and recently developed further by basing it firmly on classical set theoretical operations of union and intersection [15] (as for example in Fig. 5 and Fig. 7). While both publications addressed the operation in terms of its functionality and applicability, in this paper we are reviewing the underlying concept and need for expanding on the "basic" amalgamation operations offered by interval type-2 fuzzy set operations (specifically the union and intersection as described in Section III) which underpins the creation of the "zSlices based agreement" operation. We briefly review the operation itself in Section IV.B and proceed by focusing on its interpretation in Section IV.C.

B. Review of zSlices based notion of Agreement.

While an initial approach to developing agreement focused on overlapping FOUs was mentioned in [14] (as shown in Fig. 9), in this paper we exclusively focus on the notion of Multi Level Agreement (MLA) based firmly on the sole use of the classical set-theoretic operations of union and intersection as detailed in [15]. It is worth mentioning that the two slightly different approaches were developed as a result of the discussion raised in this paper – the requirement to employ classical firmly established set theoretical operations versus the need to develop interpretable models of agreement.

MLA describes an operation which transforms a series of interval type-2 fuzzy sets into a zSlices based set. Each of the initial interval type-2 sets is generally *one individual interpretation* of a specific concept or word, such as *tall people*. MLA subsequently aims to provide a general model which reflects all individual interpretations while considering the agreement (common ground) between multiple individual interpretations (modeled in the third dimension). In other words, it aims to preserve all "interpretation inputs" but to weight specific areas on the final MLA output set in terms of the number of input sets that intersect. An MLA zSlices based set $\tilde{Z}_{MLA}$ based on K source interval type-2 fuzzy sets $\widetilde{S_k}$, where $k \in \{1, \dots, K\}$ has a number of zLevels I equal to K (and as such zSlices $\tilde{Z}_i$, where $i \in \{1, \dots, I\}$). At low zLevels, the MLA set models the most general information provided by the individual interpretations while with increasing zLevel (third dimension), higher levels of agreement are represented. We do not repeat the full detail of the operation here for space reasons, but for a full account of the detailed steps of computing an MLA set, please see [15].

It is crucial to note the difference between MLA and employing interval type-2 fuzzy set based operations (such as union or intersection). The latter only allow for the focus on the common ground (intersection) or a generalization (union). Further, they do not allow for a modeling of the information in terms of the number of interpretations (interval type-2 sets) that are in agreement (i.e. a single outlier is weighted the same as a series of highly similar sets). MLA addresses both issues by combining union and intersection and utilizing the third dimension to weight areas of agreement where many interval type-2 sets (interpretations) are similar. As such it could be said that MLA aims to model the interpretation which the majority can agree on (and weighting it accordingly) but still preserving other interpretations (with an associated lower weight).

C. Interpretation of zSlices based Agreement.

In order to facilitate the interpretation of MLA we provide an example detailing the computation of an MLA model based on three individual "input" interval type-2 fuzzy set interpretations. The example sets have been reproduced from [15] as the in-depth review of the MLA sets in terms of their interpretation completes the theoretical background introduced in [15]. Fig. 10 depicts the three example "input" sets.

Fig. 11 shows the results of applying the basic operations of union and intersection to the "input" sets shown in Fig. 10a and Fig. 10b. The results of both operations have been included to reflect the review of the said operations in Section III and to

allow the contrasting of the resulting sets with the MLA set (Fig. 12a) computed on two interval type-2 "input" sets shown in Fig. 10a and Fig. 10b.

Fig. 12b finally shows the MLA set based on computing MLA on all three "input" sets shown in Fig. 10.

In order to interpret the MLA based sets shown in Fig. 12 it is worth recapitulating the MLA based sets are zSlices based and that higher zLevels (i.e. the third dimension) are to represent higher levels of agreement.

Considering the example of a MLA set in Fig. 12a computed on the "input" sets in Fig. 10a and Fig. 10b, it first of all becomes clear that the MLA set indeed reflects the union of both "input" sets as primary zSlices (front / dark blue). The union as a simple interval type-2 fuzzy set is provided for comparison in Fig. 11a. Further, as we have two "input" sets, the second zLevel should represent the agreement of both "input" sets which as part of MLA is modeled through the intersection operation. Considering the second zLevel (rear / light blue) in Fig. 12a and comparing it to the basic intersection shown in Fig. 11b it is clear that the MLA set reflects the expected intersection at the second zLevel.

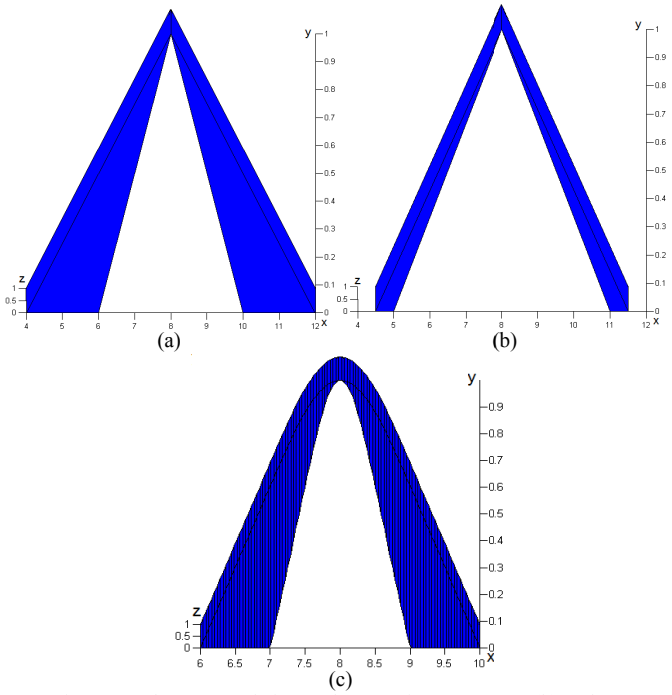

Figure 10 Three example interval type-2 fuzzy sets: (a), (b) and (c).

In terms of interpretation, the resulting MLA sets reflect the generalized amalgamation (union – see Section III.B) of the "input" sets at the lower zLevels while the common ground of the individual "input" sets is modeled (through the intersection – see Section III.C) at higher zLevels. With the zLevels acting as weights it is clear that "common ground" is weighted more heavily which is in line with the intuition that common ground between individuals should be reflected strongly in any model of agreement. The fact that levels of low "common ground", i.e. the very general low zLevels incorporate all "input set" interpretations is also in line with the intuition that an agreement model should not disregard interpretations made by only one or a few members.

Considering the common operations of union and intersection performed on interval type-2 fuzzy sets (Fig. 11), it is clear that the resulting interval type-2 sets cannot achieve both aims – the union by itself allows only to generalize while the intersection solely focuses on the common ground.

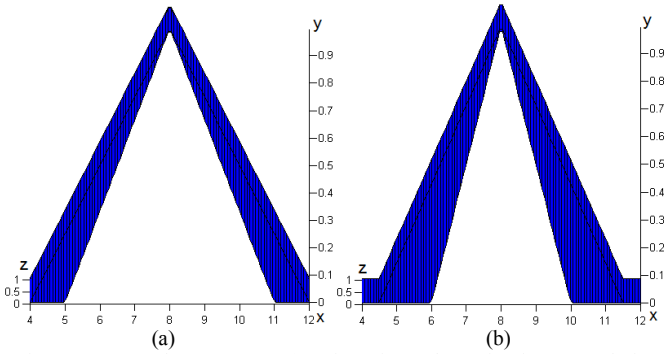

Figure 11 Interval type-2 sets: (a) Union of sets shown in Fig. 10a and Fig. 10b. (b) Intersection of sets shown in Fig. 10a and Fig. 10b.

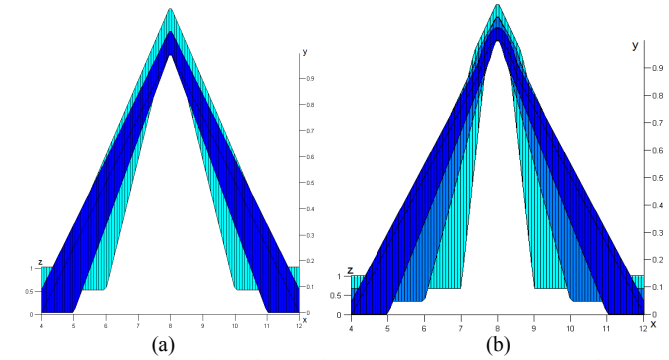

Figure 12 MLA zSlices based general type-2 sets. (a) MLA computed on sets shown in Fig. 10a and Fig. 10b. (b) MLA computed on sets shown in Fig. 10a, Fig. 10b Fig. 10c.

Finally, it is worth noting that the shape of the MLA sets as shown for two and three "input" interval type-2 fuzzy sets in Fig. 12a and Fig. 12b respectively reflects the basic properties of the underlying union and intersection operations (see Section III): a generalization effect and as such a widening of the support at lower zLevels and an increasing precision in terms of the concept (narrowing of support) as the zLevels increase.

V. Discussion and Scope for Other Operations.

This paper has mainly focused on the classical set theoretical operations of intersection and union and on their most common implementations – using the minimum t-norm and maximum t-conorms. These operations and their effect and have been shown and MLA has been interpreted being based on these classical implementations. However, as we indicated with the example of the Łukasiewicz t-conorm in Section II.C, it is clear that the common t-norms/t-conorms are by far not the only possible ones. Indeed, as was shown for the example of the Łukasiewicz t-conorm, other operations, or at the very least, the use of other t-norms and t-conorms to implement the classical set-theoretical operations of union and intersection promises great potential in the aim of actually reflecting the meaning of concepts as they are perceived by humans. In terms

of interval type-2 operations the use of different t-norm / t-conorm operations for the upper and lower membership functions could also be investigated.

As such, we believe that the choice of operation (union, intersection, …) as well as the choice of the underlying t-norm and t-conorm can be an essential component in designing CWW applications. The selection of what the "right" operations are for which application and if there are common indicators across CWW applications promises to be a fruitful ground for future multi-disciplinary research, firmly based on collaboration between human-centred sciences such as the social sciences and the fuzzy logic field.

VI. Conclusions and Future Work

As part of this paper we have reviewed the classical set-theoretical operations of complement, union and intersection for classical and type-1 fuzzy sets. Specifically, we have focused on investigating the interpretation of the latter two operations, laying the groundwork for subsequently considering the interpretation of said operations for interval type-2 fuzzy sets. We have briefly reviewed the concept of MLA based zSlices sets and have proceeded to detail their interpretation in the light of the interval type-2 operation interpretations that form the basis of MLA. We have indicated how MLA allows a more comprehensive representation of agreement compared to interval type-2 based operations through the weighting of highly similar interpretations (sets) in the third dimension while still preserving all, including infrequent interpretations (sets) at lower weights. By employing the third dimension, MLA can combine both the concept "narrowing" and "generalization" provided by the intersection and union operations.

Importantly, our efforts of interpreting the given operations and sets were focused on their use in CWW applications. As CWW aims to "compute with words", it is paramount to investigate whether the individual sets and operations really reflect words, or more explicitly, whether they reflect the interpretation that is intuitively made by humans.

As such, this paper is not aimed at providing novel results or operations, it is merely aimed at:

- Providing details on the motivation of using MLA sets based on zSlices rather than interval type-2 fuzzy sets (based on either the union or intersection) for agreement modeling.
- Providing the interpretation of MLA sets in the context of the underlying operations.
- Indicating that the choice of operations and indeed the choice of implementation of operations (t-norm / t-conorm) has a significant impact on the resulting sets and interpretations. This is of particular importance in the context of CWW application which aim to imitate the human.

The scope of this paper has only allowed for a comparatively shallow investigation of the interpretations of the sets and the additional questions raised (such as the choice of t-norm /t-conorm). A remaining question is for example the application of different t-norms and t-conorms as part of MLA. Further, in the future we aim to deepen our investigation, in particular through multi-disciplinary collaboration with the aim of advancing the goal of "imitating" human concepts and reasoning though the application of fuzzy logic in a CWW context.

References

[1] L.A. Zadeh, "Fuzzy sets", Information and Control, 8 (3), 1965, pp. 338—353.

[2] L.A. Zadeh, "The Concept of a Linguistic Variable and Its Application to Approximate Reasoning-I," Information Sciences, vol. 8, no. 3, pp. 199-249, 1975.

[3] A. Homaifar and E. McCormick, "Simultaneous design of membership functions and rule sets for fuzzy controllers using genetic algorithms," IEEE Transactions Fuzzy Systems, vol. 3, no. 2, pp. 129-139, May 1995.

[4] C. Lynch. H. Hagras and V. Callaghan, "Embedded Interval type-2 Neuro-Fuzzy Speed Controller for Marine Diesel Engines," Proceedings of the 2006 Information Processing and Management of Uncertainty in Knowledge-based Systems conference, Paris, France, July 2006, pp. 1340-1347.

[5] J. M. Garibaldi, T. Ozen, "Uncertain Fuzzy Reasoning: A Case Study in Modelling Expert Decision Making," IEEE Transactions Fuzzy Systems, vol. 15, no. 1, pp. 16-30 February 2007.

[6] G. Bojadziev, M. Bojadziev, *Fuzzy Logic for Business, Finance, and Management,* Advances in Fuzzy Systems: Applications and Theory – Vol. 23. Singapore: World Scientific Publishing Co. Pte. Ltd., 2007.

[7] L.A. Zadeh, "Fuzzy logic = computing with words," IEEE Transactions Fuzzy Systems, vol.4, no.2, pp.103-111, May 1996.

[8] J.M. Mendel, "Computing with words and its relationships with fuzzistics," Information Sciences, vol. 177, no. 4, pp. 988-1006, February 2007.

[9] F. Herrera, E. Herrera-Viedma, S. Alonso, and F. Chiclana, *Computing with words and decision making*, Fuzzy Optimization and Decision Making. Hingham, USA: Kluwer Academic Publishing, December 2009.

[10] F. Liu, J. M. Mendel, "Encoding Words Into Interval Type-2 Fuzzy Sets Using an Interval Approach," IEEE Transactions Fuzzy Systems, vol. 16, no. 6, pp. 1503-1521 December 2008.

[11] S. Coupland, J. M. Mendel, D. Wu, "Enhanced Interval Approach for encoding words into interval type-2 fuzzy sets and convergence of the word FOUs," Proceeding of the 2010 IEEE International Conference on Fuzzy Systems, Barcelona, Spain, July 2010, pp. 1-8.

[12] C. Wagner and H. Hagras, "Novel methods for the design of general type-2 fuzzy sets based on device characteristics and linguistic labels surveys", Proceedings of the 2009 International Fuzzy Systems Association World Congress and the 2009 European Society for Fuzzy Logic and Technology Conference, pp. 537-543, Lisbon, Portugal, July 2009

[13] C. Wagner and H. Hagras, "Towards general type-2 fuzzy logic systems based on zSlices," IEEE Transactions Fuzzy Systems, vol. 18, no. 4, pp. 637-660, August 2010.

[14] C. Wagner and H. Hagras, "An Approach for the Generation and Adaptation of zSlices based General Type-2 Fuzzy Sets from Interval Type-2 Fuzzy Sets to Model Agreement with Application to Intelligent Environments," Proceedings of the IEEE International Conference of Fuzzy Systems, Barcelona,Spain, July 2010.

[15] C. Wagner and H. Hagras, "Employing zSlices Based General Type-2 Fuzzy Sets to Model Multi Level Agreement," Proceedings of the 2011 IEEE Symposium on Advances in Type-2 Fuzzy Logic Systems, Paris, France, April 2011, In Press.

[16] J. N. Rouder, R. Roger, "Comparing Exemplar- and Rule-based Theories of Categorization," Current Directions in Psychological Science, vol. 15, no. 1, pp. 9-13, February 2006.

[17] L. Borkowski, *Selected works by Jan Łukasiewicz*, North–Holland, Amsterdam, 1970.

[18] J. Mendel, Uncertain Rule-Based Fuzzy Logic Systems: Introduction and New Directions. Upper Saddle River, NJ, Prentice Hall, 2001.

2011 IEEE International Conference on Fuzzy Systems
June 27-30, 2011, Taipei, Taiwan

An Adaptive Type-2 Fuzzy Logic Controller for Dynamic Positioning

Xue Tao Chen
Department of Electrical and Computer Engineering
National University of Singapore
Singapore 117576
Email: g0800483@nus.edu.sg

Woei Wan Tan
Department of Electrical and Computer Engineering
National University of Singapore
Singapore 117576
Email: wwtan@nus.edu.sg

***Abstract*—This paper presents an indirect adaptive type-2 fuzzy logic controller (FLC) for dynamic positioning (DP) vessels with attached thrusters under various time-varying hydrodynamic disturbances. Approximation-based adaptive control technique in combination with type-2 fuzzy logic system (FLS) is employed in the design of the control. The stability of the design is demonstrated through Lyapunov analysis where globally asymptotical convergence of the regulation error is guaranteed. Rigorous analysis shows the resultant closed-loop system is passive. The proposed adaptive type-2 FLC is able to reject the hydrodynamic disturbances without exact information on them. Comparative simulations with linear proportional derivative (PD) controller and adaptive type-1 FLC are carried out. The proposed technique is found to be effective, robust, and has better performance.**

***Index Terms*—Adaptive control, type-2 fuzzy logic system, function approximation, dynamic positioning.**

I. Introduction

The offshore exploration and exploitation of hydrocarbons have opened up an era of dynamic positioning (DP) vessels. DP systems are widely used in situations where mooring or anchoring is not feasible due to deep water, congested structures such as pipelines on the sea bottom or other economical issues. DP systems maintain floating structures in fixed position and heading for marine operation purpose exclusively by means of active propellers and thrusters. In the 1960s the first DP system was introduced for horizontal modes of motion (surge, sway, and yaw) using PID controllers in cascaded with low-pass or notch filter. In the 1970s more advanced control techniques based on optimal control and linear Kalman filter theory was proposed in [1]. This work was later improved and extended [2], [3]. In the 1990s nonlinear control techniques were employed in several works [4]. More recently, supervisory switched hybrid controllers for DP from calm to extreme sea conditions and from transit to station keeping operation were presented [5].

In parallel with the developments in control techniques, vessel modeling techniques have been improving as well [3]. One of the newest vessel models was presented in [6], [7], and there is still a lack of effective controller for this model due to the complex time-varying hydrodynamic disturbances presented in this model. One intuitive solution is adaptive control technique. For this model, traditional model-based adaptive control technique is not applicable since it is generally useful only when dealing with systems in which the dynamics are linear in the parameters, the regressors are exactly known, and the uncertainties are parametric and time-invariant [8]. As these disturbances are time-varying and changing for different sea conditions, approximation-based adaptive control technique [9], [10] is adopted to compensate for the disturbances and functional uncertainties. Such approximators can utilize a standard regressor function whose structure is independent of the disturbances' dynamic characteristics.

Type-1 fuzzy logic system (FLS) has been found to be able to approximate continuous nonlinear functions to any desired accuracy over a compact set [11]–[14], thus could be such an approximator. In recent years, studies on type-2 fuzzy sets and FLSs have drawn much attention [15]–[18]. A type-2 fuzzy set is characterized by a fuzzy membership function whose membership value for each element is a fuzzy set in [0,1], unlike a type-1 fuzzy set whose membership value is a crisp number in [0,1]. The membership functions of type-2 fuzzy sets are three dimensional, and it is the new third dimension that provides additional degrees of freedom that equip type-2 FLS with the potential to outperform its type-1 counterpart. Type-2 FLS is a fuzzy system where at least one of the antecedent or consequent fuzzy sets is a type-2 fuzzy set. The type-2 FLS has already been successfully applied to several engineering problems [19]–[22] and studied from lots of points of view. One interesting research point of view is whether the type-2 FLS could be a universal approximator for different application, and this paper is an effort along this direction.

By combining approximation-based adaptive control technique and type-2 FLS, an indirect adaptive type-2 fuzzy logic controller (FLC) is proposed. It overcomes the limitations of model-based adaptive control to provide an effective control algorithm for the newly developed vessel model [6], [7]. And the DP problem is treated as an application to investigate the approximation property of type-2 FLS.

The rest of the paper is organized as follows. Section II describes the singleton interval type-2 (IT2) FLS and expresses it in the linear in the parameters form. Next, the modeling of marine vessels in two complexity levels is introduced in

978-1-4244-7316-8/11/$26.00 ©2011 IEEE

Section III. Then the design and stability analysis of the adaptive type-2 FLC is delineated in Section IV, the passivity property of the resultant closed-loop system is illustrated in this section as well. After that, Section V describes the simulation results of the closed-loop system. Comparisons with other controllers are also shown in this section. Finally, conclusions are drawn in Section VI.

II. Description of Singleton IT2 FLS

In this paper, we consider a singleton IT2 FLS whose basic configuration is depicted in Fig. 1. It consists of fuzzifier, rule base, fuzzy inference engine, type-reducer, and defuzzifier. Here, a multi-input, single-out fuzzy system is described. And a multi-output system can always be separated into a group of single-output systems.

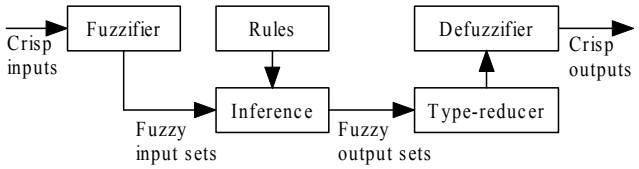

Fig. 1. A singleton interval type-2 FLS.

1) Fuzzification: The fuzzifier maps a crisp point $\mathbf{x} = (x_1, \ldots, x_n) \in \mathbf{U} \subset R^n$ into a fuzzy set $\tilde{A}_{\mathbf{x}}$ in $\mathbf{U}$. Since singleton fuzzification is employed, the membership grade of an input $\mathbf{x}$ in the fuzzy set $\tilde{A}_{\mathbf{x}}$ is as follows.

$$\mu_{\tilde{A}_{\mathbf{x}}}(\mathbf{x}) = \begin{cases} 1; & \mathbf{x} = \mathbf{x}' \\ 0; & \mathbf{x} \neq \mathbf{x}' \end{cases} \tag{1}$$

2) Rules: Rules are the heart of a FLS, and can be extracted from numerical data or provided by experts. Consider a FLS having n inputs and one output, then the lth rule in the rule base of the IT2 FLS is

$$R^l : \text{IF } x_1 \text{ is } \tilde{F}_1^l \text{ and } \cdots \text{and } x_n \text{ is } \tilde{F}_n^l \text{ THEN } y \text{ is } \tilde{G}^l \tag{2}$$

where $l = 1, 2, \ldots, M$, x_i $(i = 1, 2, \ldots, n)$ and y are the input and output variables to the fuzzy system respectively, $\tilde{F}_i^l$ and $\tilde{G}^l$ are labels of fuzzy sets in $\mathbf{U}_i$ and R, respectively.

3) Fuzzy Inference Engine: The fuzzy inference engine combines fuzzy rules with fuzzy logic principles to provide a mapping from fuzzy input sets in $\mathbf{U}$ to fuzzy output sets in R. For the singleton IT2 FLS, based on the sup-star compositional rule of inference, the output consequent set corresponding to rule R^l can be represented as

$$\mu_{\tilde{B}^l}(y) = \mu_{\tilde{G}^l}(y) \sqcap \left[\sqcap_{i=1}^n \mu_{\tilde{F}_i^l}(x_i') \right]. \tag{3}$$

where the firing set $\sqcap_{i=1}^n \mu_{\tilde{F}_i^l}(x_i') \equiv F^l(\boldsymbol{x}')$ is an interval type-1 set, i.e.,

$$F^l(\boldsymbol{x}') = \left[\underline{f}^l(\boldsymbol{x}'), \overline{f}^l(\boldsymbol{x}') \right] \tag{4}$$

$$\underline{f}^l(\boldsymbol{x}') = \underline{\mu}_{\tilde{F}_1^l}(x_1') \bigstar \cdots \bigstar \underline{\mu}_{\tilde{F}_1^n}(x_n') \tag{5}$$

$$\overline{f}^l(\boldsymbol{x}') = \overline{\mu}_{\tilde{F}_1^l}(x_1') \bigstar \cdots \bigstar \overline{\mu}_{\tilde{F}_1^n}(x_n'). \tag{6}$$

Here $\underline{\mu}_{\tilde{F}_i^l}(x_i')$ is the lower membership grade of $\tilde{F}_i^l$, whereas $\overline{\mu}_{\tilde{F}_i^l}(x_i')$ is the upper membership grade of $\tilde{F}_i^l$, symbol $\bigstar$ denotes the t-norm, which corresponds to the conjunction "and" in (2). The fired output consequent set, $\mu_{\tilde{B}^l}(y)$, for the l th rule is the IT2 fuzzy set

$$\mu_{\tilde{B}^l}(y) = \int_{b^l \in \left[\underline{f}^l \bigstar \underline{\mu}_{\tilde{G}^l}(y), \overline{f}^l \bigstar \overline{\mu}_{\tilde{G}^l}(y) \right]} 1/b^l \tag{7}$$

where $\underline{\mu}_{\tilde{G}^l}$ and $\overline{\mu}_{\tilde{G}^l}$ are the lower and upper membership grades of consequent IT2 fuzzy set, $\tilde{G}^l$.

4) Type-Reduction and Defuzzification: The outputs of the inference engine are IT2 fuzzy sets which need to be type-reduced and then defuzzified to produce a crisp output. Assume maximum t-conorm, product t-norm, product implication, and center of sets type reduction are used. Then in the type-reduction, the type-reduced set is an interval type-1 fuzzy set $[y_l', y_r']$. The outputs y_l' and y_r' can be computed using the Karnik-Mendel iterative procedure. In this procedure, assume singleton consequent sets are used, the consequent parameters are reordered in ascending order. Let $\mathbf{y} = (y^1, \ldots, y^M)^{\mathrm{T}}$ denote the original rule-ordered consequent values, and let $\hat{\mathbf{y}} = (\hat{y}^1, \ldots, \hat{y}^M)^{\mathrm{T}}$ denote the reordered sequences, where $\hat{y}^1 \leq \hat{y}^2 \leq \ldots \leq \hat{y}^M$. The relationship between $\mathbf{y}$ and $\hat{\mathbf{y}}$ is

$$\hat{\mathbf{y}} = \mathbf{Q}\mathbf{y} \tag{8}$$

where $\mathbf{Q}$ is $M \times M$ permutation matrix with elementary vectors as columns, and these vectors are arranged to move elements in $\mathbf{y}$ to new locations in ascending order in the transformed vector $\hat{\mathbf{y}}$. The original rule firing strength orders $\underline{\mathbf{f}} = (\underline{f}^1, \underline{f}^2, \ldots, \underline{f}^M)^{\mathrm{T}}$ and $\overline{\mathbf{f}} = (\overline{f}^1, \overline{f}^2, \ldots, \overline{f}^M)^{\mathrm{T}}$ are reordered accordingly. And the new orders for $\underline{\mathbf{f}}$ and $\overline{\mathbf{f}}$ are $\mathbf{Q}\underline{\mathbf{f}}$ and $\mathbf{Q}\overline{\mathbf{f}}$ respectively. According to [23], [24], the output y_l' can be computed as

$$\begin{aligned} y_l' =& \frac{\sum_{i=1}^{L} (\mathbf{Q}\overline{\mathbf{f}})_i \hat{y}^i + \sum_{i=L+1}^{M} (\mathbf{Q}\underline{\mathbf{f}})_i \hat{y}^i}{\sum_{i=1}^{L} (\mathbf{Q}\overline{\mathbf{f}})_i + \sum_{i=L+1}^{M} (\mathbf{Q}\underline{\mathbf{f}})_i} \\ =& \frac{\overline{\mathbf{f}}^{\mathrm{T}} \mathbf{Q}^{\mathrm{T}} \mathbf{E}_1^{\mathrm{T}} \mathbf{E}_1 \mathbf{Q}\mathbf{y} + \underline{\mathbf{f}}^{\mathrm{T}} \mathbf{Q}^{\mathrm{T}} \mathbf{E}_2^{\mathrm{T}} \mathbf{E}_2 \mathbf{Q}\mathbf{y}}{\mathbf{p}_l^{\mathrm{T}} \mathbf{Q}\overline{\mathbf{f}} + \mathbf{g}_l^{\mathrm{T}} \mathbf{Q}\underline{\mathbf{f}}} \end{aligned} \tag{9}$$

where L and R denote the left and right crossover points respectively,

$$\begin{aligned} \mathbf{p}_l &= (\underbrace{1, 1, \ldots, 1}_{L}, 0, \ldots, 0)^{\mathrm{T}} \in R^{M \times 1} \\ \mathbf{g}_l &= (0, \ldots, 0, \underbrace{1, 1, \ldots, 1}_{M-L})^{\mathrm{T}} \in R^{M \times 1} \\ \mathbf{E}_1 &= (\mathbf{e}_1, \mathbf{e}_2, \ldots, \mathbf{e}_L, \mathbf{0}, \ldots, \mathbf{0})^{\mathrm{T}} \in R^{L \times M} \\ \mathbf{E}_2 &= (\mathbf{0}, \ldots, \mathbf{0}, \boldsymbol{\varepsilon}_1, \boldsymbol{\varepsilon}_2, \ldots, \boldsymbol{\varepsilon}_{M-L})^{\mathrm{T}} \in R^{(M-L) \times M} \end{aligned}$$

and where $\mathbf{e}_i \in R^L$ and $\boldsymbol{\varepsilon}_i \in R^{M-L}$ are elementary vectors. Similarly, the output y'_r can be expressed as

$$\begin{aligned} y'_r =& \frac{\sum_{i=1}^{R}(\mathbf{Q}\underline{\mathbf{f}})_i \hat{y}^i + \sum_{i=R+1}^{M}(\mathbf{Q}\overline{\mathbf{f}})_i \hat{y}^i}{\sum_{i=1}^{R}(\mathbf{Q}\underline{\mathbf{f}})_i + \sum_{i=R+1}^{M}(\mathbf{Q}\overline{\mathbf{f}})_i} \\ =& \frac{\underline{\mathbf{f}}^{\mathrm{T}}\mathbf{Q}^{\mathrm{T}}\mathbf{E}_3^{\mathrm{T}}\mathbf{E}_3\mathbf{Q}\mathbf{y} + \overline{\mathbf{f}}^{\mathrm{T}}\mathbf{Q}^{\mathrm{T}}\mathbf{E}_4^{\mathrm{T}}\mathbf{E}_4\mathbf{Q}\mathbf{y}}{\mathbf{p}_r^{\mathrm{T}}\mathbf{Q}\underline{\mathbf{f}} + \mathbf{g}_r^{\mathrm{T}}\mathbf{Q}\overline{\mathbf{f}}} \end{aligned} \tag{10}$$

where

$$\begin{aligned} \mathbf{p}_r &= (\underbrace{1,1,\ldots,1}_{R},0,\ldots,0)^{\mathrm{T}} \in R^{M\times 1} \\ \mathbf{g}_r &= (0,\ldots,0,\underbrace{1,1,\ldots,1}_{M-R})^{\mathrm{T}} \in R^{M\times 1} \\ \mathbf{E}_3 &= (\mathbf{e}_1,\mathbf{e}_2,\ldots,\mathbf{e}_R,\mathbf{0},\ldots,\mathbf{0})^{\mathrm{T}} \in R^{R\times M} \\ \mathbf{E}_4 &= (\mathbf{0},\ldots,\mathbf{0},\boldsymbol{\varepsilon}_1,\boldsymbol{\varepsilon}_2,\ldots,\boldsymbol{\varepsilon}_{M-R})^{\mathrm{T}} \in R^{(M-R)\times M} \end{aligned}$$

and where $\mathbf{e}_i \in R^R$ and $\boldsymbol{\varepsilon}_i \in R^{M-R}$ are elementary vectors. Finally, by computing the average of y'_l and y'_r, the interval set is defuzzified to generate the system output as

$$y' = \frac{y'_l + y'_r}{2}. \tag{11}$$

View $\boldsymbol{\theta} = \mathbf{y} = (y^1,\ldots,y^M)^{\mathrm{T}}$ as adjustable parameters, then (11) can be written as

$$y' = \boldsymbol{\phi}^{\mathrm{T}}\boldsymbol{\theta} \tag{12}$$

where

$$\begin{aligned} \boldsymbol{\phi}^{\mathrm{T}} =& \frac{\overline{\mathbf{f}}^{\mathrm{T}}\mathbf{Q}^{\mathrm{T}}\mathbf{E}_1^{\mathrm{T}}\mathbf{E}_1\mathbf{Q} + \underline{\mathbf{f}}^{\mathrm{T}}\mathbf{Q}^{\mathrm{T}}\mathbf{E}_2^{\mathrm{T}}\mathbf{E}_2\mathbf{Q}}{2(\mathbf{p}_l^{\mathrm{T}}\mathbf{Q}\overline{\mathbf{f}} + \mathbf{g}_l^{\mathrm{T}}\mathbf{Q}\underline{\mathbf{f}})} \\ &+ \frac{\underline{\mathbf{f}}^{\mathrm{T}}\mathbf{Q}^{\mathrm{T}}\mathbf{E}_3^{\mathrm{T}}\mathbf{E}_3\mathbf{Q} + \overline{\mathbf{f}}^{\mathrm{T}}\mathbf{Q}^{\mathrm{T}}\mathbf{E}_4^{\mathrm{T}}\mathbf{E}_4\mathbf{Q}}{2(\mathbf{p}_r^{\mathrm{T}}\mathbf{Q}\underline{\mathbf{f}} + \mathbf{g}_r^{\mathrm{T}}\mathbf{Q}\overline{\mathbf{f}})} \end{aligned} \tag{13}$$

is a regressive vector. Now as shown in (12), the singleton IT2 FLS is expressed as linear in the parameters.

III. Modeling of Marine Vessels

The model of positioned vessels may be divided into two groups [25], namely process plant model and control plant model. The process plant model is used for numerical analysis of the performance and stability of the closed-loop system by simulating the real plant dynamics as closely as possible. It includes process disturbance, sensor outputs and control inputs. The control plant model, which is used for controller design and theoretical stability analysis (e.g., in the sense of Lyapunov), is a simplified form of the process plant model.

A. Process Plant Model

1) Kinematics: In DP, the motions and state variables of the system are conventionally defined and measured with respect to two reference frames as shown in Fig. 2, namely earth-fixed frame and body-fixed frame. The earth-fixed frame, denoted as $\mathrm{X_E Y_E Z_E}$, is used for global guidance and navigation. The body-fixed frame, denoted as XYZ, is fixed to the vessel with its origin located at the vessel's center of gravity. Let

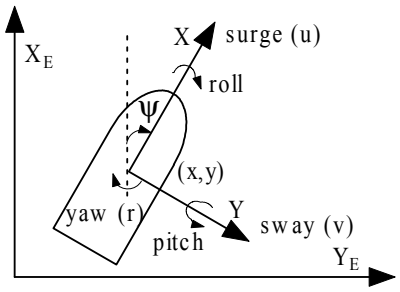

Fig. 2. 2D Earth-fixed and body-fixed reference frames.

$\boldsymbol{\eta}' = [x, y, z, \phi, \theta, \psi]^{\mathrm{T}}$ be the vector denoting the position and orientation of the vessel relative to an earth-fixed frame, and let $\boldsymbol{\nu}' = [u, v, w, p, q, r]^{\mathrm{T}}$ represent the translation and rotation velocities of the vessel decomposed in a body-fixed frame. These six modes are referred to as the surge, sway, heave, roll, pitch, yaw modes of a vessel. Then, the transformation between the earth-fixed and body-fixed velocity vectors is

$$\dot{\boldsymbol{\eta}}' = \mathbf{J}'(\boldsymbol{\eta}')\boldsymbol{\nu}'. \tag{14}$$

where $\mathbf{J}'(\boldsymbol{\eta}')$ is a state dependent transformation matrix, whose definition can be found in [3].

2) Dynamics: The six degrees of freedom (DOF) model formulation is based on [6], [7]. The equation of motion, which is in body-fixed frame, for the nonlinear low frequency model of a floating vessel traveling in low speed is given by

$$\mathbf{M}'\dot{\boldsymbol{\nu}}' + \bar{\mathbf{B}}'\boldsymbol{\nu}'_r + \mathbf{G}'\boldsymbol{\eta}' + \boldsymbol{\mu}' = \boldsymbol{\tau}' + \boldsymbol{\tau}'_{\text{CFD}} + \boldsymbol{\tau}'_{\text{wave}} \tag{15}$$

where $\mathbf{M}' = \mathbf{M}'_{RB} + \bar{\mathbf{A}}' \in R^{6\times 6}$ is the sum of the system inertia matrix and added mass matrix, $\bar{\mathbf{B}}' \in R^{6\times 6}$ is the potential damping matrix, $\mathbf{G}' \in R^{6\times 6}$ is the restoring matrix, $\boldsymbol{\mu}' \in R^6$ is computed using a state space model to represent the fluid memory effect,

$$\dot{\boldsymbol{\chi}} = \mathbf{A}_r\boldsymbol{\chi} + \mathbf{B}_r\boldsymbol{\nu}'_r \tag{16}$$

$$\boldsymbol{\mu}' = \mathbf{C}_r\boldsymbol{\chi} + \mathbf{D}_r\boldsymbol{\nu}'_r \tag{17}$$

and where $(\mathbf{A}_r, \mathbf{B}_r, \mathbf{C}_r, \mathbf{D}_r)$ are constant matrices of appropriate dimensions. $\boldsymbol{\tau}' \in R^6$ is control force vector produced by thruster system, $\boldsymbol{\tau}'_{\text{CFD}} \in R^6$ is cross-flow drag and surge resistance vector, $\boldsymbol{\tau}'_{\text{wave}} \in R^6$ is wave load vector, which is computed according to Response Amplitude Operator tables, and $\boldsymbol{\nu}'_r = \boldsymbol{\nu}' - \boldsymbol{\nu}'_c \in R^6$ is the relative velocity vector between vessel velocity vector $\boldsymbol{\nu}'$ and sea current velocity vector $\boldsymbol{\nu}'_c$. All the detailed definition and computation of the above matrices and vectors can be found in [3], [6] and references therein.

B. Control Plant Model

To facilitate the controller design and analytical stability analysis, the process plant model presented in previous subsection is simplified based on the following assumptions.

Assumption 1: The motions along heave, roll, and pitch directions are ignored. In fact, this is an appropriate assumption since a conventional ship is metacentric stable which implies that there exist restoring force and moments along those

directions. As a result of this assumption, the dimension of the restoring matrix $\mathbf{G}' \in R^{6\times 6}$ in (15) is reduced to yield $\mathbf{G} \in R^{3\times 3} = \mathbf{0}$.

Assumption 2: The state variables, i.e. displacements and velocities along surge, sway, and yaw directions, are measured by on-board devices such as GPS, gyro system, and accelerometers. This is a acceptable assumption due to the development of integration system of inertial sensors and satellite navigation system.

Assumption 3: The effect of sea current is ignored. This assumption is for the convenience of theoretical analysis.

Assumption 4: The various kinds of time-varying hydrodynamic disturbances, i.e. $\boldsymbol{\mu}'$, $\boldsymbol{\tau}'_{\text{CFD}}$, and $\boldsymbol{\tau}'_{\text{wave}}$ in (15), could be estimated by singleton IT2 FLSs in the form of

$$\begin{aligned} \boldsymbol{\tau}'_d &= -\Phi'(\boldsymbol{\nu}')\Theta' \\ &= \boldsymbol{\tau}'_{\text{CFD}} + \boldsymbol{\tau}'_{\text{wave}} - \boldsymbol{\mu}' \end{aligned} \tag{18}$$

where

$$\Theta' = (\boldsymbol{\theta}_1'^{\mathrm{T}}, \boldsymbol{\theta}_2'^{\mathrm{T}}, \ldots, \boldsymbol{\theta}_6'^{\mathrm{T}})^{\mathrm{T}} \in R^{6M\times 1} \tag{19}$$

is a weighting vector and

$$\Phi'(\boldsymbol{\nu}') = \text{diag}[\boldsymbol{\phi}_1'^{\mathrm{T}}, \boldsymbol{\phi}_2'^{\mathrm{T}}, \ldots, \boldsymbol{\phi}_6'^{\mathrm{T}}] \in R^{6\times 6M} \tag{20}$$

is a regressive matrix, M is the number of rules for each sub-FLS. So far, this assumption is not well established, since there is still a lack of rigorous proof that singleton IT2 FLS is universal approximator, but the assumption will be checked by subsequent simulations. The situation is different for type-1 case, as there has been a lot of works showing that type-1 FLS is universal approximator [11]–[14].

Application of Assumptions 1-4 to (14) and (15) yields the following control plant model for DP.

$$\dot{\boldsymbol{\eta}} = \mathbf{J}(\boldsymbol{\eta})\boldsymbol{\nu} \tag{21}$$

$$\mathbf{M}\dot{\boldsymbol{\nu}} + \bar{\mathbf{B}}\boldsymbol{\nu} = \boldsymbol{\tau} - \Phi(\boldsymbol{\nu})\Theta \tag{22}$$

where $\boldsymbol{\eta} = [x, y, \psi]^{\mathrm{T}}$ and $\boldsymbol{\nu} = [u, v, r]^{\mathrm{T}}$ are the vectors representing displacement and velocity along surge, sway, and yaw, $\mathbf{J}(\boldsymbol{\eta}) \in R^{3\times 3}$ is the rotation matrix, note that $\mathbf{J}\mathbf{J}^{\mathrm{T}} = \mathbf{I}$ ($\mathbf{I}$ is the identity matrix), $\mathbf{M} \in R^{3\times 3}$ is the system inertia matrix including added mass, $\bar{\mathbf{B}} \in R^{3\times 3}$ is the potential damping matrix,

$$\Theta = (\boldsymbol{\theta}_1^{\mathrm{T}}, \boldsymbol{\theta}_2^{\mathrm{T}}, \boldsymbol{\theta}_3^{\mathrm{T}})^{\mathrm{T}} \in R^{3M\times 1} \tag{23}$$

is the weighting vector and

$$\Phi(\boldsymbol{\nu}) = \text{diag}[\boldsymbol{\phi}_1^{\mathrm{T}}(\boldsymbol{\nu}), \boldsymbol{\phi}_2^{\mathrm{T}}(\boldsymbol{\nu}), \boldsymbol{\phi}_3^{\mathrm{T}}(\boldsymbol{\nu})] \in R^{3\times 3M} \tag{24}$$

is the regressive matrix. Thus, here three sub-FLSs are used to estimate the hydrodynamic disturbances.

IV. Adaptive Fuzzy Logic Controller Design

The control objective for DP is to position and orientate the vessel to a fixed placement via attached thruster system, which actually is a regulation problem. In this section, an indirect adaptive fuzzy logic controller for DP is proposed, the regulation error is proved to globally asymptotically converge to zero. Rigorous analysis shows the resultant closed-loop system is passive.

A. Control and Adaptive Law

The proposed control and adaptive law for plant (21), (22) are as follows.

$$\boldsymbol{\tau} = -\lambda_1\boldsymbol{\nu} - \lambda_2\mathbf{J}^{\mathrm{T}}(\boldsymbol{\eta})\boldsymbol{e} + \Phi(\boldsymbol{\nu})\hat{\Theta} \tag{25}$$

$$\dot{\hat{\Theta}} = \lambda_3\Phi^{\mathrm{T}}(\boldsymbol{\nu})(\lambda_4\boldsymbol{\nu} + \frac{2\mathbf{J}^{\mathrm{T}}(\boldsymbol{\eta})\boldsymbol{e}}{1+2\boldsymbol{e}^{\mathrm{T}}\boldsymbol{e}}) \tag{26}$$

where $\boldsymbol{e} = \boldsymbol{\eta} - \boldsymbol{\eta}_d \in R^3$ is the control error vector between vessel displacement vector $\boldsymbol{\eta}$ and the desired vessel placement vector $\boldsymbol{\eta}_d$, $\tilde{\Theta} = \Theta - \hat{\Theta} \in R^{3M}$ is the error vector between true Θ in (22) and adapted $\hat{\Theta}$, and λ_i $(i = 1, \ldots, 4)$ are positive constant.

Application of control and adaptive law (25), (26) to the plant (21), (22) yields the resultant closed-loop system

$$\mathbf{M}\dot{\boldsymbol{\nu}} + \bar{\mathbf{B}}\boldsymbol{\nu} = -\lambda_1\boldsymbol{\nu} - \lambda_2\mathbf{J}^{\mathrm{T}}(\boldsymbol{\eta})\boldsymbol{e} - \Phi(\boldsymbol{\nu})\tilde{\Theta} \tag{27}$$

$$\dot{\tilde{\Theta}} = \lambda_3\Phi^{\mathrm{T}}(\boldsymbol{\nu})(\lambda_4\boldsymbol{\nu} + \frac{2\mathbf{J}^{\mathrm{T}}(\boldsymbol{\eta})\boldsymbol{e}}{1+2\boldsymbol{e}^{\mathrm{T}}\boldsymbol{e}}) \tag{28}$$

$$\dot{\boldsymbol{e}} = \dot{\boldsymbol{\eta}} = \mathbf{J}(\boldsymbol{\eta})\boldsymbol{\nu}. \tag{29}$$

B. Stability Analysis

Theorem 1: The states $(\boldsymbol{e}, \boldsymbol{\nu})$ of the closed-loop system (27)-(29) globally asymptotically converge to $(\mathbf{0}, \mathbf{0})$ if

$$\lambda_4 > \max\{\frac{2\lambda_M}{\sqrt{\lambda_2\lambda_m}}, \frac{(\lambda_d + 2\lambda_1)^2 + 16\lambda_2\lambda_M}{4\lambda_2\lambda_d + 8\lambda_1\lambda_2}\}, \tag{30}$$

where λ_m and λ_M are the minimum and maximum eigenvalue of matrix $\mathbf{M}$ respectively, and λ_d is the minimum eigenvalue of matrix $\bar{\mathbf{B}} + \bar{\mathbf{B}}^{\mathrm{T}}$.

Proof: Consider the following Lyapunov function candidate.

$$V = \frac{\lambda_2\lambda_4}{2}\boldsymbol{e}^{\mathrm{T}}\boldsymbol{e} + \frac{\lambda_4}{2}\boldsymbol{\nu}^{\mathrm{T}}\mathbf{M}\boldsymbol{\nu} + \frac{2\boldsymbol{\nu}^{\mathrm{T}}\mathbf{M}\mathbf{J}^{\mathrm{T}}\boldsymbol{e}}{1+2\boldsymbol{e}^{\mathrm{T}}\boldsymbol{e}} + \frac{1}{2\lambda_3}\tilde{\Theta}^{\mathrm{T}}\tilde{\Theta} \tag{31}$$

To make sure the Lyapunov function candidate V positive definite, due to the fact $\|\mathbf{J}\| = 1$ and $\lambda_m\mathbf{I} \le \mathbf{M} \le \lambda_M\mathbf{I}$, we have

$$\begin{aligned} V_1 =& \frac{\lambda_2\lambda_4}{2}\boldsymbol{e}^{\mathrm{T}}\boldsymbol{e} + \frac{\lambda_4}{2}\boldsymbol{\nu}^{\mathrm{T}}\mathbf{M}\boldsymbol{\nu} + \frac{2\boldsymbol{\nu}^{\mathrm{T}}\mathbf{M}\mathbf{J}^{\mathrm{T}}\boldsymbol{e}}{1+2\boldsymbol{e}^{\mathrm{T}}\boldsymbol{e}} \\ \ge& \frac{\lambda_2\lambda_4}{2}\boldsymbol{e}^{\mathrm{T}}\boldsymbol{e} + \frac{\lambda_4\lambda_m}{2}\boldsymbol{\nu}^{\mathrm{T}}\boldsymbol{\nu} - \frac{2\lambda_M}{1+2\boldsymbol{e}^{\mathrm{T}}\boldsymbol{e}}\boldsymbol{\nu}^{\mathrm{T}}\boldsymbol{e}, \end{aligned}$$

If $4\lambda_M^2 - \lambda_4^2\lambda_2\lambda_m < 0$ i.e., $\lambda_4 > 2\lambda_M/\sqrt{\lambda_2\lambda_m}$, then V_1 is positive definite, additionally,

$$V_2 = \frac{1}{2\lambda_3}\tilde{\Theta}^{\mathrm{T}}\tilde{\Theta}$$

is positive definite, thus $V = V_1 + V_2$ is positive definite.

Differentiation of V along the trajectory of the closed-loop system (27)-(29) yields

$$\begin{aligned} \dot{V} =& -\lambda_4\boldsymbol{\nu}^{\mathrm{T}}\bar{\mathbf{B}}\boldsymbol{\nu} - \lambda_1\lambda_4\boldsymbol{\nu}^{\mathrm{T}}\boldsymbol{\nu} + \frac{2\boldsymbol{\nu}^{\mathrm{T}}\mathbf{M}\boldsymbol{\nu}}{1+2\boldsymbol{e}^{\mathrm{T}}\boldsymbol{e}} - \frac{2\mathbf{e}^{\mathrm{T}}\mathbf{J}\bar{\mathbf{B}}\boldsymbol{\nu}}{1+2\boldsymbol{e}^{\mathrm{T}}\boldsymbol{e}} \\ & - \frac{2\lambda_1\mathbf{e}^{\mathrm{T}}\mathbf{J}\boldsymbol{\nu}}{1+2\boldsymbol{e}^{\mathrm{T}}\boldsymbol{e}} - \frac{2\lambda_2\boldsymbol{e}^{\mathrm{T}}\boldsymbol{e}}{1+2\boldsymbol{e}^{\mathrm{T}}\boldsymbol{e}} - \frac{8\boldsymbol{e}^{\mathrm{T}}\boldsymbol{\nu}\boldsymbol{\nu}^{\mathrm{T}}\mathbf{M}\boldsymbol{e}}{(1+2\boldsymbol{e}^{\mathrm{T}}\boldsymbol{e})^2}. \end{aligned}$$

Applying $\lambda_d\mathbf{I} \le \bar{\mathbf{B}} + \bar{\mathbf{B}}^{\mathrm{T}}$, we have

$$\dot{V} \le -(\frac{\lambda_4\lambda_d}{2} + \lambda_1\lambda_4 - 2\lambda_M)\boldsymbol{\nu}^{\mathrm{T}}\boldsymbol{\nu} - (\lambda_d + 2\lambda_1)\boldsymbol{e}^{\mathrm{T}}\boldsymbol{\nu} - 2\lambda_2\boldsymbol{e}^{\mathrm{T}}\boldsymbol{e},$$

If $(\lambda_d + 2\lambda_1)^2 - 8\lambda_2((\lambda_4\lambda_d)/2 + \lambda_1\lambda_4 - 2\lambda_M) < 0$ i.e.,

$$\lambda_4 > \frac{(\lambda_d + 2\lambda_1)^2 + 16\lambda_2\lambda_M}{4\lambda_2\lambda_d + 8\lambda_1\lambda_2}$$

then $\dot{V} \leq 0$, which means the derivative of the Lyapunov function candidate is semi-negative definite. Moreover, the largest invariant set contained in the set $\dot{V} \equiv 0$ is contained in the set $(\boldsymbol{e}, \boldsymbol{\nu}) = (\mathbf{0}, \mathbf{0})$.

Now, according to Krasovskii-La Salle Theorem, we may conclude the point $(\boldsymbol{e}, \boldsymbol{\nu})$ globally asymptotically converges to $(\mathbf{0}, \mathbf{0})$, and $\dot{\tilde{\Theta}} = 0$, which means $\hat{\Theta}$ is bounded, if

$$\lambda_4 > \max\{\frac{2\lambda_M}{\sqrt{\lambda_2\lambda_m}}, \frac{(\lambda_d + 2\lambda_1)^2 + 16\lambda_2\lambda_M}{4\lambda_2\lambda_d + 8\lambda_1\lambda_2}\}.$$

■

Remark 1: For plant (21), (22), an intuitive adaptive law may be

$$\dot{\tilde{\Theta}} = \lambda_5 \Phi^{\mathrm{T}}(\boldsymbol{\nu})\boldsymbol{\nu}, \tag{32}$$

but rigorous analysis indicates that the regulation error using such adaptive law cannot be asymptotically convergence.

Remark 2: Here, the theorem is developed for the case where the gains λ_i $(i = 1, \ldots, 4)$ are scalar, the case where the gains are matrices can be easily extended to in a similar approach.

C. Passivity Interpretation

Passivity theory gives a framework for the design and analysis of control systems using an input-output description according to energy-related considerations. And the input-output description further allows for a modular approach to control systems design and analysis [26]. As illustrated in Fig. 3, the closed-loop system (27)-(29) can be interpreted as the negative feedback interconnection of two subsystems with respective inputs u_1, u_2 and outputs y_1 and y_2, with $y_1 = u_2$ and $y_2 = -u_1$, and the two subsystems as follows.

Subsystem 1:

$$\begin{cases} \mathbf{M}\dot{\boldsymbol{\nu}} + \bar{\mathbf{B}}\boldsymbol{\nu} = -\lambda_1\boldsymbol{\nu} - \lambda_2\mathbf{J}^{\mathrm{T}}(\boldsymbol{\eta})\boldsymbol{e} + u_1 \\ y_1 = \lambda_4\boldsymbol{\nu} + \frac{2\mathbf{J}^{\mathrm{T}}(\boldsymbol{\eta})\boldsymbol{e}}{1+2\boldsymbol{e}^{\mathrm{T}}\boldsymbol{e}} \end{cases} \tag{33}$$

Subsystem 2:

$$\begin{cases} \dot{\tilde{\Theta}} = \lambda_3 \Phi^{\mathrm{T}}(\boldsymbol{\nu}) u_2 \\ y_2 = \Phi(\boldsymbol{\nu})\tilde{\Theta} \end{cases} \tag{34}$$

Theorem 2: The closed-loop system (27)-(29) is passive if (30) is satisfied.

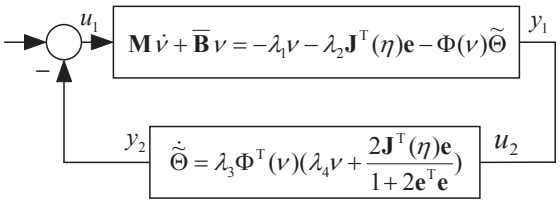

Fig. 3. Closed-loop equivalent representation.

Proof: For subsystem 1, its supply rate is

$$\begin{aligned} &\int_0^t u_1^{\mathrm{T}} y_1 ds \\ &= \int_0^t (\lambda_4\boldsymbol{\nu} + \frac{2\mathbf{J}^{\mathrm{T}}\boldsymbol{e}}{1+2\boldsymbol{e}^{\mathrm{T}}\boldsymbol{e}})^{\mathrm{T}}(\mathbf{M}\dot{\boldsymbol{\nu}} + \bar{\mathbf{B}}\boldsymbol{\nu} + \lambda_1\boldsymbol{\nu} + \lambda_2\mathbf{J}^{\mathrm{T}}\boldsymbol{e})ds \\ &= \int_0^t [\lambda_2\lambda_4\boldsymbol{\nu}^{\mathrm{T}}\mathbf{J}^{\mathrm{T}}\boldsymbol{e} + \frac{d}{ds}(\frac{\lambda_4}{2}\boldsymbol{\nu}^{\mathrm{T}}\mathbf{M}\boldsymbol{\nu} + \frac{2\boldsymbol{\nu}^{\mathrm{T}}\mathbf{M}\mathbf{J}^{\mathrm{T}}\boldsymbol{e}}{1+2\boldsymbol{e}^{\mathrm{T}}\boldsymbol{e}})]ds \\ &+ \int_0^t [\lambda_4\boldsymbol{\nu}^{\mathrm{T}}\bar{\mathbf{B}}\boldsymbol{\nu} + \lambda_1\lambda_4\boldsymbol{\nu}^{\mathrm{T}}\boldsymbol{\nu} - \frac{2\boldsymbol{\nu}^{\mathrm{T}}\mathbf{M}\boldsymbol{\nu}}{1+2\boldsymbol{e}^{\mathrm{T}}\boldsymbol{e}} + \frac{2\mathbf{e}^{\mathrm{T}}\mathbf{J}\bar{\mathbf{B}}\boldsymbol{\nu}}{1+2\boldsymbol{e}^{\mathrm{T}}\boldsymbol{e}} \\ &+ \frac{2\lambda_1\mathbf{e}^{\mathrm{T}}\mathbf{J}\boldsymbol{\nu}}{1+2\boldsymbol{e}^{\mathrm{T}}\boldsymbol{e}} + \frac{2\lambda_2\boldsymbol{e}^{\mathrm{T}}\boldsymbol{e}}{1+2\boldsymbol{e}^{\mathrm{T}}\boldsymbol{e}} + \frac{8\boldsymbol{e}^{\mathrm{T}}\boldsymbol{\nu}\boldsymbol{\nu}^{\mathrm{T}}\mathbf{M}\boldsymbol{e}}{(1+2\boldsymbol{e}^{\mathrm{T}}\boldsymbol{e})^2}]ds, \end{aligned}$$

if (30) is satisfied,

$$\int_0^t u_1^{\mathrm{T}} y_1 ds \geq V_1(t) - V_1(0),$$

which means the subsystem 1 is passive with supply rate $\int_0^t u_1^{\mathrm{T}} y_1 ds$ and storage function V_1, which has been defined during the proof for Theorem 1.

For subsystem 2 its supply rate is

$$\begin{aligned} \int_0^t u_2^{\mathrm{T}} y_2 ds &= \int_0^t \tilde{\Theta}^{\mathrm{T}}\Phi^{\mathrm{T}}(\boldsymbol{\nu}) u_2 ds \\ &= \int_0^t \tilde{\Theta}^{\mathrm{T}} \frac{1}{\lambda_3}\dot{\tilde{\Theta}} ds \\ &\geq V_2(t) - V_2(0) \end{aligned}$$

which means the subsystem 2 is passive with supply rate $\int_0^t u_2^{\mathrm{T}} y_2 ds$ and storage function V_2.

According to the fact that the negative feedback interconnection of two passive systems is passive, the closed-loop system (27)-(29) is passive. ■

V. Simulation Studies

The simulation studies are performed on the platform of Marine System Simulator developed in Norwegian University of Science and Technology [27]. The S-175 container ship is used as case study. The subsequent simulation results are obtained for following seas with the International Towing Tank Conference (ITTC) wave spectrum using significant wave height $H_s = 5$ m and peak frequency $\omega_0 = 0.56$ rad/s. The significant wave height H_s is used to classify the type of sea, $H_s = 5$ m corresponds to very rough sea with large waves. Even though ignored during Lyapunov analysis, the sea current is set with speed $V_c = 2$ m/s and direction $\beta_c = 30^\circ$

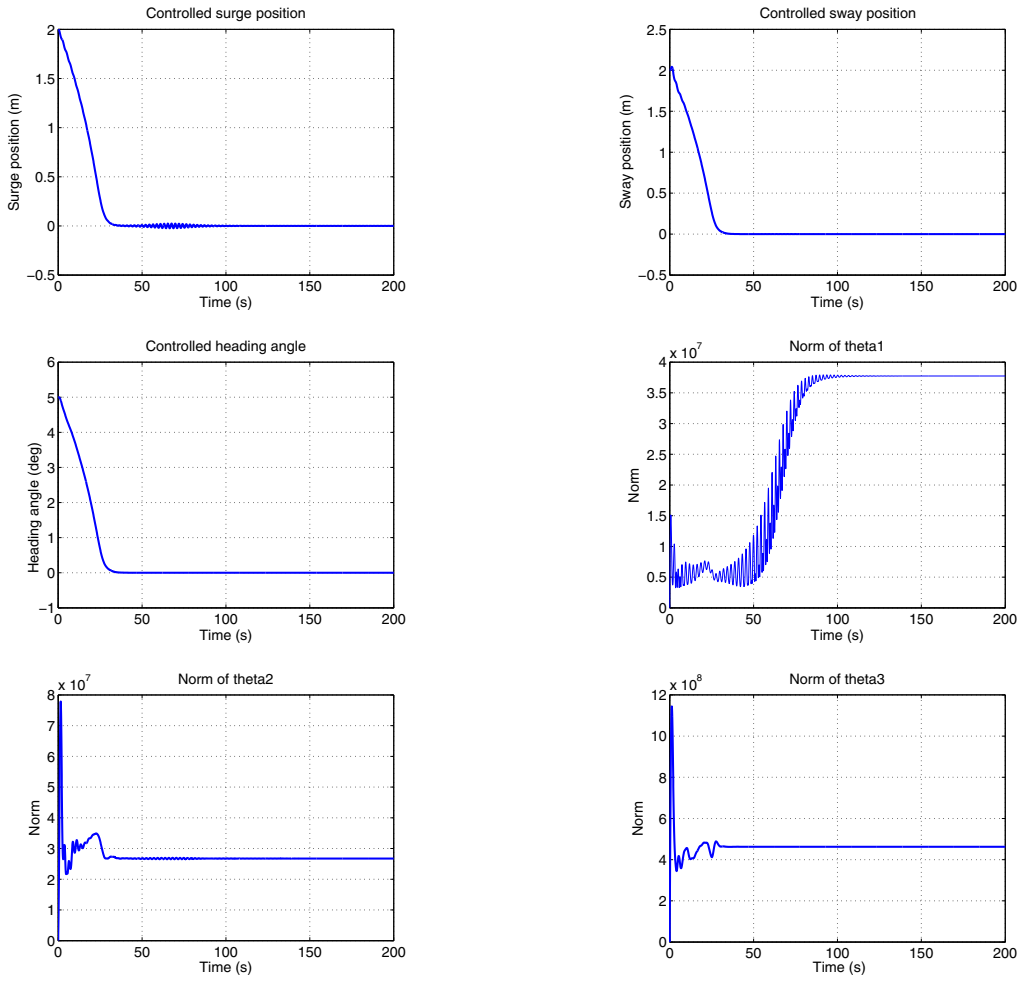

Fig. 4. Plots 1-3 show the controlled position and heading angle of the vessel. Plots 4-6 show the norms of the adapted weighting vectors.

in the following simulations. The control objective is set to regulate the vessel to state $[\boldsymbol{\eta}_d^{\mathrm{T}}, \boldsymbol{\nu}_d^{\mathrm{T}}] = [\mathbf{0}, \mathbf{0}]$ from initial state $[\boldsymbol{\eta}_0^{\mathrm{T}}, \boldsymbol{\nu}_0^{\mathrm{T}}] = [2, 2, 5^\circ, 0, 0, 0]$.

A. Closed-loop Performance

Although the controller (25), (26) is designed based on the control plant model (21), (22), it is tested with the process plant model (14), (15). As indicated in (12), (23), and (24), three singleton IT2 sub-FLSs are used to approximate the complex hydrodynamic disturbances. In each sub-system, each of the input domain is partitioned by three fuzzy membership functions labeled as **N**, **Z**, and **P**, thus there are 27 rules and 27 adjustable consequent parameters accordingly. The primary membership functions of the antecedent IT2 fuzzy sets are chosen to be Gaussian function with uncertain standard deviation, i.e.,

$$\mu_{\tilde{F}_i^j}(x_j) = \exp[-\frac{1}{2}(\frac{x_j - m_i}{\sigma})^2] \quad \sigma \in [\underline{\sigma}, \overline{\sigma}] \qquad (35)$$

where $i = 1, 2, 3$ is the index of three fuzzy membership functions for jth input and $j = 1, 2, 3$ is the index of three inputs. The inputs to each sub-system is scaled properly so that the means for the Gaussian functions are fixed at $m_1 = -1$, $m_2 = 0$, and $m_3 = 1$ for each input, and the standard deviation for all of the lower membership function is fixed at $\underline{\sigma} = 0.6$, whereas the one for all of the upper membership function is $\overline{\sigma} = 0.8$. Set $\lambda_1 = 4.3 \times 10^6$, $\lambda_2 = 4.3 \times 10^5$, $\lambda_3 = 5 \times 10^8$, and $\lambda_4 = 5$ in (25) and (26). The controlled position and heading angle of the vessel are shown in plot 1-3 of Fig. 4, from which it can be observed that the closed-loop system is stable, the control performance is satisfactory despite the time-varying hydrodynamic disturbances, and the sub-FLSs efficiently approximate the complex disturbances although universal approximation property for IT2 FLS has not been established yet. Plot 4-6 of Fig. 4 show the norms of the adapted weighting vectors $\|\hat{\boldsymbol{\theta}}_i\|$ $(i = 1, 2, 3)$, they verify the boundedness of $\hat{\boldsymbol{\Theta}}$. Note that the norm of weighting vector $\hat{\boldsymbol{\theta}}_1$ shows fluctuation during the simulation, it is because the disturbances along the surge direction fluctuate heavily at the start of the simulation.

B. Comparison with a PD Controller

Comparative study between the designed controller and a linear proportional derivative (PD) controller is presented. The

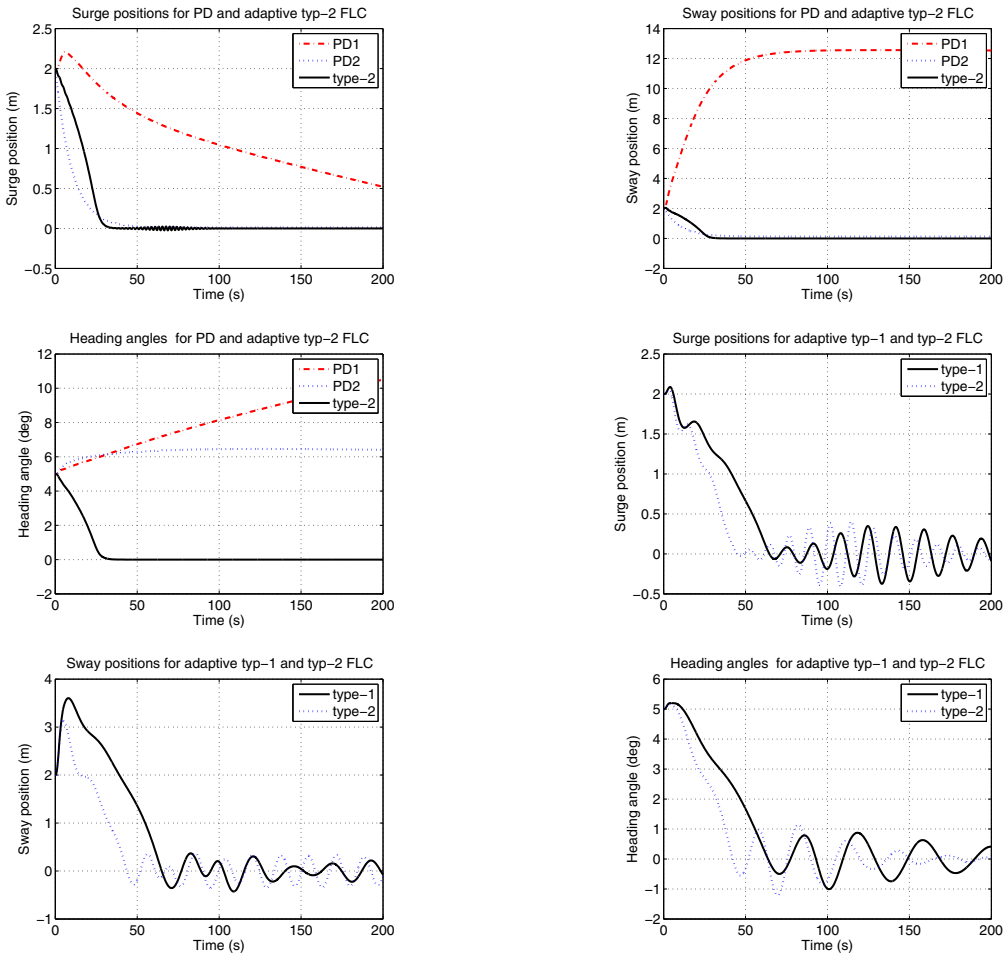

Fig. 5. Plots 1-3 show the positions and heading angles of the vessel for two PD controllers and the adaptive type-2 FLC. Plots 4-6 show the positions and heading angles of the vessel for the adaptive type-1 and type-2 FLC.

PD controller is in the form of

$$\boldsymbol{\tau} = -\lambda_5 \boldsymbol{\nu} - \lambda_6 \mathbf{J}^{\mathrm{T}}(\boldsymbol{\eta}) \boldsymbol{e}. \tag{36}$$

Two sets of control gains are implemented for the PD controller, $\lambda_5^1 = 4.3 \times 10^6$, $\lambda_6^1 = 4.3 \times 10^5$ and $\lambda_5^2 = 4.3 \times 10^8$, $\lambda_6^2 = 4.3 \times 10^7$, meanwhile the parameter settings for the adaptive type-2 FLC are kept same as the one in previous subsection. The results are shown in plot 1-3 of Fig. 5, from which it can be seen that with same proportion and derivative gains, the designed controller achieves satisfactory performance, whereas the PD controller is unstable. With its proportion and derivative gains increasing, the PD controller can be stable, but still with large steady state error due to disturbances. Besides, large control gains are not recommended in practice as they reduce robustness and cause large overshoots. Hence, the designed controller performs much better than the PD controller and has better disturbance rejection property.

C. Comparison with an Adaptive Type-1 FLC

Replace the components in (24) and correspondingly in (25) and (26) with fuzzy basis function vector [10], [11],

$$\boldsymbol{\phi}^{\mathrm{T}} = (\phi^1(\mathbf{x}), \ldots, \phi^M(\mathbf{x})) \tag{37}$$

where fuzzy basis function is defined as

$$\phi^l(\mathbf{x}) = \frac{\Pi_{i=1}^n \mu_{F_i^l}(x_i)}{\Sigma_{l=1}^M (\Pi_{i=1}^n \mu_{F_i^l}(x_i))}, \tag{38}$$

the controller (25), (26) becomes an adaptive type-1 FLC. In this subsection, the adaptive type-2 FLC is compared with such an adaptive type-1 FLC. For each sub-system in the adaptive type-2 FLC, the parameter settings are kept identical as the one in previous subsection, whereas for each sub-system in type-1 case, each of the input domain is partitioned by five fuzzy membership functions labeled as **NL**, **NS**, **Z**, **PS**, and **PL**, thus there are 125 rules and 125 adjustable consequent parameters accordingly in contrast to 27 rules and parameters for type-2 case. The membership functions of the antecedent sets for each input are chosen as Gaussian functions, i.e.,

$$\mu_{F_i^j}(x_j) = \exp[-\frac{1}{2}(\frac{x_j - m_i}{\sigma})^2]. \tag{39}$$

where $i = 1, \ldots, 5$ is the index of five fuzzy membership functions for jth input and $j = 1, 2, 3$ is the index of three inputs. While the means are set as $(m_1, \ldots, m_5) =$

$(-1, -0.5, 0, 0.5, 1)$, the standard deviations for all the Gaussian functions are fixed at $\sigma = 0.4$. Set $\lambda_1 = 4.3 \times 10^6$, $\lambda_2 = 4.3 \times 10^5$, $\lambda_3 = 1.5 \times 10^7$, and $\lambda_4 = 5$ in (25) and (26) for both adaptive type-1 and type-2 FLCs, the resultant positions and heading angles of the vessel are shown in plot 4-6 of Fig. 5, from which it can be observed that the rising and settling time for adaptive type-2 FLC is shorter than that for type-1 case, even though type-1 case uses more rules. To quantify the performance differences between adaptive type-1 and type-2 FLCs, the integral of time-weighted absolute errors (ITAE) for both cases in the following form are calculated.

$$P_x = \int_0^T t|x|dt \tag{40}$$

$$P_y = \int_0^T t|y|dt \tag{41}$$

$$P_\psi = \int_0^T t|\psi|dt \tag{42}$$

where T is the total simulation time. The results are shown in Table I, and the ITAE for the type-2 case are smaller than those for type-1 case along all the three degrees of freedom. Regarding the computational burden, type-reduction for type-2 case does take some time, but the time is very little as only a few rules are fired simultaneously and it has been proved Karnik-Mendel algorithm is super-exponentially convergent [28]. In addition, the real-time application of the type-2 FLS has been reported [29]. Thus, type-reduction should not be an issue that causes any stability problem. In a word, it seems that the type-2 FLS has better approximation property with less rules than its type-1 counterpart, and rigorous theoretical examination is needed.

TABLE I
ITAE FOR ADAPTIVE TYPE-1 AND TYPE-2 FLCS

ITAE	P_x	P_y	P_ψ
Type-1	4604	5960	210
Type-2	3252	4951	121

VI. CONCLUSIONS

In this paper, an indirect adaptive type-2 FLC has been designed for DP vessels with attached thrusters in the presence of complex hydrodynamic disturbances. It has been proved that the regulation error under the proposed control globally asymptotically converges to zero and the closed-loop system under the proposed control is passive. Simulation results have demonstrated that the adaptive type-2 FLC is effective and robust. When compared against a PD controller, the proposed controller has better control performance and disturbance rejection property. Comparison with its type-1 counterpart suggests type-2 FLS has better approximation property, but rigorous theoretical examination is necessary.

REFERENCES

[1] J. G. Balchen, N. A. Jensen, and S. Sælid, "Dynamic positioning using kalman filtering and optimal control theory," in *IFAC/IFIP Symp. Autom. Offshore Oil Field Oper.*, Amsterdam, The Netherlands, 1976, pp. 183–186.

[2] A. J. Sørensen, S. I. Sagatun, and T. I. Fossen, "Design of a dynamic positioning system using model based cotrol," *J. Control Eng. Practice*, vol. 4, no. 3, pp. 359–368, 1996.

[3] T. I. Fossen, *Marine Control Systems: Guidance Navigation and Control of Ships Rigs and Underwater Vehicles*. Trondheim, Norway: Marine Cybernetics, 2002.

[4] ——, "A survey on nonlinear ship control: From theory to practise," in *Proc. 5th IFAC Conf. on Manoeuvring and Control of Marine Craft*, Aalborg, Denmark, 2000.

[5] T. D. Nguyen, "Design of hybrid marine control systems for dynamic positioning," Ph.D dissertation, Dept. Civil Eng., NUS, Singapore, 2006.

[6] T. I. Fossen, "Nonliear time-domain strip theory formulation for low speed manoeuving and station-keeping," *Modelling, Id. Control*, vol. 25, no. 4, pp. 201–221, 2004.

[7] T. Perez and T. I. Fossen, "Kinematic models for manoeuvring and seakeeping of marine vessels," *Modelling, Id. Control*, vol. 28, no. 1, pp. 19–30, 2007.

[8] K. S. Narendra and A. M. Annaswamy, *Stable Adaptive Systems*. Englewood Cliffs, NJ: Prentice-Hall, 1989.

[9] S. S. Ge, C. C. Hang, T. H. Lee, and T. Zhang, *Stable Adaptive Neural Network Control*. Boston, MA: Kluwer, 2001.

[10] L. X. Wang, "Stable adaptive fuzzy control of nonlinear systems," *IEEE Trans. Fuzzy Syst.*, vol. 1, no. 2, pp. 146–155, May 1993.

[11] L. X. Wang and J. M. Mendel, "Fuzzy basis functions, universal approximation, and orthogonal least-squares learning," *IEEE Trans. Neural Netw.*, vol. 3, no. 5, pp. 807–814, Sep. 1992.

[12] J. L. Castro, "Fuzzy logic controllers are universal approximators," *IEEE Trans. Syst., Man, Cybern.*, vol. 25, no. 4, pp. 629–635, Apr. 1995.

[13] X. J. Zeng and M. G. Singh, "Approximation accuracy analysis of fuzzy systems as function approximators," *IEEE Trans. Fuzzy Syst.*, vol. 4, no. 1, pp. 44–63, Jan. 1996.

[14] H. Ying, *Fuzzy Control and Modeling: Analytical Foundations and Applications*. New York: IEEE Press, 2000.

[15] N. N. Karnik, J. M. Mendel, and Q. Liang, "Type-2 fuzzy logic systems," *IEEE Trans. Fuzzy Syst.*, vol. 7, no. 6, pp. 643–658, Dec. 1999.

[16] J. M. Mendel, *Uncertain Rule-Based Fuzzy Logic System: Introduction and New Directions*. Upper Saddle River, NJ: Prentice-Hall, 2001.

[17] J. M. Mendel and R. I. John, "Type-2 fuzzy sets made simple," *IEEE Trans. Fuzzy Syst.*, vol. 10, no. 2, pp. 117–127, Apr. 2002.

[18] R. John and S. Coupland, "Type-2 fuzzy logic: a historical view," *IEEE Comput. Intell. Mag.*, vol. 2, no. 1, pp. 57–62, Feb. 2007.

[19] H. Hagras, "A hierarchical type-2 fuzzy logic control architecture for autonomous mobile robots," *IEEE Trans. Fuzzy Syst.*, vol. 12, no. 4, pp. 524–539, Aug. 2004.

[20] D. R. Wu and W. W. Tan, "A type-2 fuzzy logic controller for the liquid-level process," in *Proc. IEEE Int. Conf. on Fuzzy Syst.*, Budapest, 2004, pp. 953–958.

[21] C. Wagner and H. Hagras, "Slices based general type-2 flc for the control of autonomous mobile robots in real world environments," in *Proc. IEEE Int. Conf. on Fuzzy Syst.*, Jeju Island, Korea, 2009, pp. 718–725.

[22] X. T. Chen and W. W. Tan, "A type-2 fuzzy logic controller for dynamic positioning systems," in *Proc. IEEE Int. Conf. on Control and Automation*, Xiamen, China, 2010, pp. 1013–1018.

[23] J. M. Mendel, "Computing derivatives in interval type-2 fuzzy logic system," *IEEE Trans. Fuzzy Syst.*, vol. 12, no. 1, pp. 84–98, Feb. 2004.

[24] C. F. Juang, R. B. Huang, and Y. Y. Lin, "A recurrent self-evolving interval type-2 fuzzy neural network for dynamic system processing," *IEEE Trans. Fuzzy Syst.*, vol. 17, no. 5, pp. 1092–1105, Oct. 2009.

[25] A. J. Sørensen, *Marine Cybernetics: Modelling and Control*, 5th ed. Trondheim, Norway: Dept. Marine Technology, NTNU, 2005.

[26] B. Brogliato, R. Lozano, B. Maschke, and O. Egeland, *Dissipative Systems Analysis and Control: Theory and Applications*, 2nd ed. London: Springer Verlag, 2007.

[27] MSS. (2010, Aug.) Marine Systems Simulator (2010). [Online]. Available: http://www.marinecontrol.org/

[28] J. Mendel and F. Liu, "Super-exponential convergence of the Karnik-Mendel algorithms for computing the centroid of an interval type-2 fuzzy set," *IEEE Trans. Fuzzy Syst.*, vol. 15, no. 2, pp. 309–320, Apr. 2007.

[29] C. Lynch and H. Hagras, "Developing embedded type-2 fuzzy logic controllers for handling the uncertainties in marine diesel engine speed control," *International Journal of Computational Intelligence Research*, vol. 4, no. 4, pp. 402–420, Oct. 2008.

2011 IEEE International Conference on Fuzzy Systems
June 27-30, 2011, Taipei, Taiwan

Interval Type-2 Recurrent Fuzzy Neural System Desing via Stable Simultaneous Perturbation Stochastic Approximation Algorithm

Feng-Yu Chang
Department of Electrical Engineering
Yuan Ze University
Chungli, Taoyuan, Taiwan

Ching-Hung Lee
Department of Electrical Engineering
Yuan Ze University
Chungli, Taoyuan, Taiwan
E-mail: chlee@saturn.yzu.edu.tw

Abstract— **This paper proposes a new type fuzzy neural systems, denotes IT2RFNS-A (interval type-2 recurrent fuzzy neural system with asymmetric membership function), for nonlinear systems control. To enhance the performance and approximation ability, the TSK-type consequent part is adopted for IT2RFNS-A. The gradient information of the IT2RFNS-A is not easy to obtain due to the asymmetric membership functions and interval valued sets. The corresponding stable learning is derived by simultaneous perturbation stochastic approximation (SPSA) algorithm which guarantees the convergence and stability of the closed-loop systems. Simulation and comparison on the control of Chua's chaotic circuit is done to show the feasibility and effectiveness of proposed method.**

Keywords- Nonlinear systems, fuzzy neural system, type-2 fuzzy system, Lyapunov theorem, SPSA algorithm

I. INTRODUCTION

In past few decades, the fuzzy neural network (FNN) which provides the advantages of both neural network and fuzzy system is successfully applied to nonlinear system identification and control [1-4]. In the FNN, the symmetric and fixed membership functions are commonly adopted to simplify the design procedure. However, a large number of fuzzy rules should be used to achieve the specified performance [5, 6]. Thus, an asymmetric fuzzy membership function (AFMF) has been proposed to solve this problem. The AFMF is discussed and analyzed that it can effectively improve the accuracy and achieve the specific performance with fewer fuzzy rules [7, 8].

Recently, the type-2 fuzzy sets (T2 FSs) are gaining more and more in popularity [9, 10]. The T2 FSs are described by membership functions (MFs) that are characterized by more parameters than the type-1 fuzzy sets (T1 FSs). Hence, the T2 FSs provide us with more design degree of freedom. Nevertheless, due to the computational complexity of using the T2 FS, most people only use interval type-2 fuzzy sets (IT2 FSs) [10]. The computations associated with IT2 FSs are very manageable which makes it quite practical [11]. Many results has been shown that the interval type-2 fuzzy logic system (IT2 FLS) can successfully apply to cope with the control problems and perform well [12-17]. In our previous research [18-21], we proposed a type-2 fuzzy neural network with asymmetric membership function (T2FNN-A) which combines the IT2 FLS with neural network. Then, in order to improve the efficiency of the T2FNN-A, we proposed an interval type-2 fuzzy neural system with asymmetric membership function (IT2FNS-A) which utilizes several enhanced techniques such as Takagi-Sugeno-Kang fuzzy logic system (TSK FLS) and embedded type-reduction network layer [22]. These modifications not only improve the approximation accuracy of the T2FNN-A, but also achieve the specific performance with fewer fuzzy rules. However, a major drawback of the IT2FNS-A is that its application domain is limited to static problem due to its feedforward network structure. Using IT2FNS-A to process dynamic problems is inefficient. Thus, in this paper, we propose an interval type-2 recurrent fuzzy neural system with asymmetric membership functions (IT2RFNS-A) which provides the memory elements and extends the basic ability of the IT2FNS-A to include the dynamic problems. In addition, since the feedback layer captures the dynamic response of the system, the approximation accuracy of the network is improved.

In training of the neural network, the back-propagation (BP) algorithm is widely used. There is, however, a critical problem where the differential information of the system is very difficult to obtain because there are too many adjustable parameters in the IT2RFNS-A. Herein, we adopt the simultaneous perturbation stochastic approximation (SPSA) algorithm which is proposed by Spall [23-25]. This algorithm is based on the approximation to gradient formed from the measurements of the objective function. Hence, a great deal of computational effort is saved. Nevertheless, there still remains a problem. Because of the stochastic characteristic of SPSA algorithm, we cannot guarantee that every search step length is appropriate which may lead to the invalid search. To overcome this situation, we employ the Lyapunov stability analysis to derive the optimal learning step length for guaranteeing the stability of the closed-loop system. In addition, the efficient training is also ensured.

The remainder of this paper is organized as follows. In Section II, we cover the prerequisite material to be used in the study. Section III illustrates the proposed IT2RFNS-A. The

978-1-4244-7316-8/11/$26.00 ©2011 IEEE

simulation results on chaotic system control of the Chua's chaotic circuit are shown in Section IV. Finally, the conclusion is given in Section V.

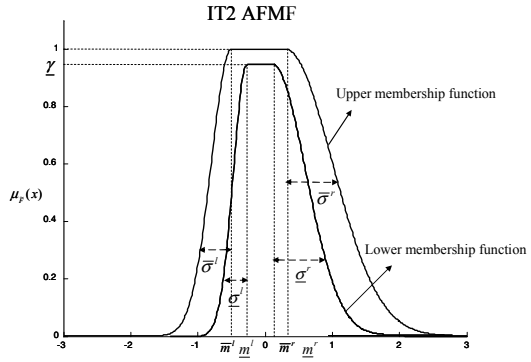

Figure 1. Construction of interval type-2 asymmetric fuzzy membership function.

II. PRELIMINARIES

A. Interval Type-2 Asymmetric Fuzzy Membership Function

Several literatures indicate that using AFMFs can improve the approximation accuracy and for effectively reducing the number of fuzzy rules [5-8]. It also provides better performance than traditional fuzzy systems on application of function approximation, modeling, and control. The learning capability and flexibility can be upgraded [5-8]. Here, we introduce the IT2 AFMFs. According to previous results [8], Gaussian functions are used to construct IT2 AFMFs, as shown in Fig. 1. Each IT2 AFMF is constructed by parts of four Gaussian functions. The upper and lower membership functions (MFs) are constructed by using two Gaussian MFs and one segment. The superscripts "l" and "r" denote the left and right curves of MF. The parameters of the lower and upper MFs are denoted by "$\underline{\ }$" and "$\overline{\ }$", respectively. Accordingly, the upper AFMF is constructed as:

$$\overline{\mu}_{\tilde{F}}(x)=\begin{cases} e^{-\frac{1}{2}\left(\frac{x-\overline{m}^{l}}{\overline{\sigma}^{l}}\right)^{2}}, \text{for } x\le \overline{m}^{l} \\ 1 \qquad\quad , \text{for } \overline{m}^{l}<x<\overline{m}^{r} \\ e^{-\frac{1}{2}\left(\frac{x-\overline{m}^{r}}{\overline{\sigma}^{r}}\right)^{2}}, \text{for } \overline{m}^{r}\le x \end{cases} \tag{1}$$

where $\overline{m}^{l}$ and $\overline{m}^{r}$ denote the means of two Gaussian MFs satisfying $\overline{m}^{l}\le\overline{m}^{r}$, and $\overline{\sigma}^{l}$ and $\overline{\sigma}^{r}$ denote the deviations (width) of two Gaussian MFs. Similarly, the lower AFMF is

$$\underline{\mu}_{\tilde{F}}(x)=\begin{cases} \lambda\cdot e^{-\frac{1}{2}\left(\frac{x-\underline{m}^{l}}{\underline{\sigma}^{l}}\right)^{2}}, \text{for } x\le \underline{m}^{l} \\ \lambda \qquad\quad , \text{for } \underline{m}^{l}<x<\underline{m}^{r} \\ \lambda\cdot e^{-\frac{1}{2}\left(\frac{x-\underline{m}^{r}}{\underline{\sigma}^{r}}\right)^{2}}, \text{for } \underline{m}^{r}\le x \end{cases} \tag{2}$$

where $\underline{m}^{l}\le\underline{m}^{r}$. To avoid a small activation value, λ is chosen to be $0.5\le\lambda\le1$. Thus, the following restrictions should be added to avoid unreasonable MFs:

$$\overline{m}^{l}\le\underline{m}^{l}\le\underline{m}^{r}\le\overline{m}^{r},\ \underline{\sigma}^{l}\le\overline{\sigma}^{l},\ \underline{\sigma}^{r}\le\overline{\sigma}^{r},\quad 0.5\le\lambda\le1. \tag{3}$$

B. Simultaneous Perturbation Stochastic Approximation Algorithm

This section introduces the SPSA algorithm briefly. The detail description can be found in literature [25]. Consider a problem of finding the minimum of objective function $f(W)$. The SPSA algorithm computes the parameter W at next iteration as

$$W(k+1)=W(k)-a_k g(W(k)) \tag{4}$$

where $g(.)$ is estimated gradient result for objective function $f(.)$, i.e., $\frac{\partial f(W)}{\partial W}\approx g(W)$. a_k is the learning step length which is decreased over iterations with $a_k=a/(k+A)^{\alpha}$, where a, A, and α are positive configuration coefficients [25]. The SPSA approach estimates the gradient $g(.)$ using following method. Assume that the dimension of parameter W is p. Let $\Delta_k=[\Delta_{k1}\ \Delta_{k2}\ \ldots\ \Delta_{kp}]$ be a p-dimensional vector whose element is mutually independent zero-mean random variable. Then, the estimation of the gradient at kth iteration can be computed by SPSA algorithm

$$g(W(k))=\frac{f(W(k)+c_k\Delta_k)-f(W(k))}{c_k}\left[\Delta_{k1}^{-1}\ \Delta_{k2}^{-1}\ \ldots\ \Delta_{kp}^{-1}\right]^{T} \tag{5}$$

$c_k=c/(k+1)^{\gamma}$ is gain sequence, where c and γ are nonnegative configuration coefficients. Obviously, all the elements of the parameter W are perturbed simultaneously, and only two measurement of the objective function are needed to estimate the gradient. In addition, Δ_k is usually obtained using Bernoulli ±1 distribution with equal probability for each value.

In general, the gradient information of neural fuzzy system is not easy to obtain due to the asymmetric membership functions and interval valued sets. Herein, we adopt the SPSA algorithm to derive the stable learning rule which guarantees the convergence and stability of the closed-loop systems.

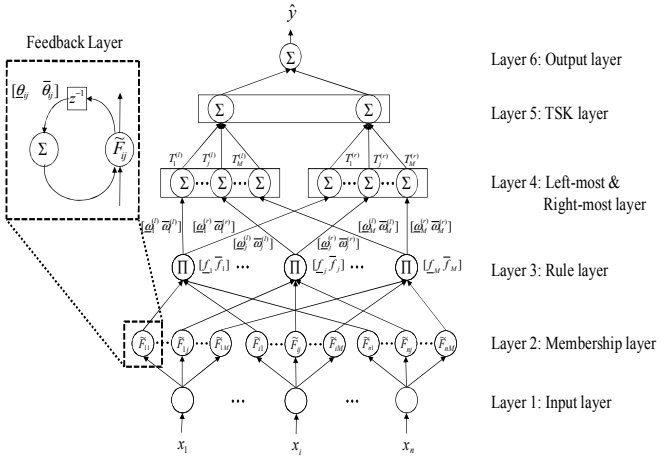

Figure 2. Diagram of the proposed interval type-2 recurrent fuzzy neural system with asymmetric membership functions.

III. Interval Type-2 Recurrent Fuzzy Neural System with Asymmetric Membership Function

A. Fuzzy Reasoning of IT2RFNS-A

The proposed IT2RFNS-A realizes the fuzzy inference into the IT2RFNS-A systems. Assume that an IT2RFNS-A system has M rules and n inputs, the jth rule can be expressed as

$$\begin{aligned} R^j &: \text{IF } z_{1j} \text{ is } \widetilde{F}_{1j} \text{ and } ... \text{ and } z_{nj} \text{ is } \widetilde{F}_{nj}, \\ &\text{THEN } Y_j = C_{j0} + C_{j1}x_1 + C_{j2}x_j + ... + C_{jn}x_n \end{aligned} \tag{6}$$

where z_{ij} is input linguistic variable of the jth rule, $\widetilde{F}_{ij}$ is interval type-2 antecedent fuzzy set, C_{ji} is type-1 consequent fuzzy set, x_i is the network input, and Y_j is the output of the jth rule and is also a type-1 fuzzy set (because it is the linear combination of type-1 fuzzy sets). Note that the input linguistic variable z_{ij} has the system input term and the past information which is introduced in Section III.B. Due to the IT2 FSs are used for the antecedent part and the interval type-1 fuzzy sets are used for the consequent part of the type-2 TSK rule, $\mu_{\widetilde{F}_{ij}}$ and C_{ji} are interval sets, i.e.,

$$\mu_{\widetilde{F}_{ij}}(z_{ij}) = \left[\underline{\mu}_{\widetilde{F}_{ij}}(z_{ij}) \quad \overline{\mu}_{\widetilde{F}_{ij}}(z_{ij}) \right] \tag{7}$$

$$C_{ji} = [c_{ji} - s_{ji} \quad c_{ji} + s_{ji}] \tag{8}$$

where c_{ji} denotes the center (mean) of C_{ji}, and s_{ji} denotes the spread of C_{ji}. Therefore, using the product t-norm, the firing strength associated with the jth rule is

$$F_j(\mathbf{z}) = [\underline{f}_j(\mathbf{z}) \quad \overline{f}_j(\mathbf{z})] \tag{9}$$

where

$$\underline{f}_j(\mathbf{z}) = \underline{\mu}_{\widetilde{F}_{1j}}(z_{1j}) * \cdots * \underline{\mu}_{\widetilde{F}_{nj}}(z_{nj}) \tag{10}$$

and

$$\overline{f}_j(\mathbf{z}) = \overline{\mu}_{\widetilde{F}_{1j}}(z_{1j}) * \cdots * \overline{\mu}_{\widetilde{F}_{nj}}(z_{nj}) . \tag{11}$$

The consequent of rule R^j, Y_j is also an interval set, i.e., $Y_j = [y_j^l \quad y_j^r]$, where

$$y_j^l = (c_{j0} + \sum_{i=1}^{n} c_{ji}x_{ij}) - (s_{j0} + \sum_{i=1}^{n} s_{ji}|x_{ij}|) \tag{12}$$

and

$$y_j^r = (c_{j0} + \sum_{i=1}^{n} c_{ji}x_{ij}) + (s_{j0} + \sum_{i=1}^{n} s_{ji}|x_{ij}|) . \tag{13}$$

By applying the Extension principle [26], the output of the FLS is

$$\begin{aligned} Y_{TSK}(\mathbf{z}) &= [y^l \quad y^r] \\ &= \int_{y_1 \in [y_1^l \ y_1^r]} \cdots \int_{y_M \in [y_M^l \ y_M^r]} \int_{f_1 \in [\underline{f}_1 \ \overline{f}_1]} \cdots \int_{f_M \in [\underline{f}_M \ \overline{f}_M]} 1 \Big/ \frac{\sum_{j=1}^{M} f_j y_j}{\sum_{j=1}^{M} f_j} \end{aligned} \tag{14}$$

where $\underline{f}_j$, $\overline{f}_j$, y_j^l, and y_j^r are computed using (10)-(13). To compute $Y_{TSK}(\mathbf{z})$, we need to compute its two end-points y^l and y^r by type-reduction operation [26]. Finally, we defuzzify it using the average of y^l and y^r. Hence, the defuzzified output of IT2RFNS-A is

$$y(\mathbf{z}) = \frac{y^l + y^r}{2} . \tag{15}$$

B. Network Structure of IT2RFNS-A

The IT2RFNS-A consists of six feed-forward layers and a feedback one. Layer 1 accepts input variables. Layer 2 is used to calculate the interval type-2 AFMF grade. Feedback layer which is embedded in Layer 2 is used to store the past information. Layer 3 forms the fuzzy rule base. Layer 4 is used for type-reduction. The TSK consequent part is implemented into Layer 5. Layer 6 is the output layer.

Next, we would indicate the signal propagation and the operation functions of the node in each layer. For convenience, the multi-input-single-output (MISO) case is considered here. The schematic diagram of the proposed IT2RFNS-A is shown in Fig. 2. In the following description, $O_i^{(l)}$ denotes the ith output node in layer l.

Layer 1: Input Layer

For the ith node of layer 1, the net input and the net output are represented as:

$$O_i^{(1)} = x_i . \tag{16}$$

The x_i represents the ith input to the ith node of layer 1. The nodes in this layer only transmit input values to the next layer directly.

Layer 2: Membership Layer

In this layer, each node performs the interval type-2 asymmetric fuzzy membership function, i.e.,

$$\begin{aligned} O_{ij}^{(2)} &= \mu_{\widetilde{F}_{ij}}(O_i^{(1)} + O_i^{(f)}) \\ &= [\underline{O}_{ij}^{(2)} \quad \overline{O}_{ij}^{(2)}]^T \\ &= [\underline{\mu}_{\widetilde{F}_{ij}}(O_i^{(1)} + O_i^{(f)}) \quad \overline{\mu}_{\widetilde{F}_{ij}}(O_i^{(1)} + O_i^{(f)})]^T \end{aligned} \tag{17}$$

where subscript $_{ij}$ indicates the jth term of the ith input $O_i^{(1)}$, $\mu_{\widetilde{F}_{ij}}$ is an IT2 AFMF as shown in Fig. 1. Note that the output of layer 2 and the feedback weight are interval values. According to the results of [27], the type-reduction can be integrated into the network, $O_i^{(f)}$ is the output of feedback layer

$$O_i^{(f)}(k) = \frac{\underline{O}_{ij}^{(2)}(k-1) \cdot \underline{\theta}_{ij} + \overline{O}_{ij}^{(2)}(k-1) \cdot \overline{\theta}_{ij}}{\underline{\theta}_{ij} + \overline{\theta}_{ij}} \tag{18}$$

where $\underline{\theta}_{ij}$ and $\overline{\theta}_{ij}$ denote the link weight of the feedback unit. Clearly, the input of this layer contains the memory terms $\underline{O}_{ij}^{(2)}(k-1)$ and $\overline{O}_{ij}^{(2)}(k-1)$ which store the past information of the network.

Layer 3: Rule Layer

This layer is used for computing firing strength of the rule. From (9)-(11), we obtain

$$\underline{f}_j = \underline{\mu}_{\widetilde{F}_{1j}}(O_1^{(1)} + O_1^{(f)}) * \cdots * \underline{\mu}_{\widetilde{F}_{nj}}(O_n^{(1)} + O_n^{(f)}) \tag{19}$$

$$\overline{f}_j = \overline{\mu}_{\tilde{F}_{1j}}(O_1^{(1)} + O_1^{(f)}) * \cdots * \overline{\mu}_{\tilde{F}_{nj}}(O_n^{(1)} + O_n^{(f)}) \quad (20)$$

where $\underline{\mu}_{\tilde{F}_{ij}}(\cdot)$ and $\overline{\mu}_{\tilde{F}_{ij}}(\cdot)$ are the lower and upper membership grades of $\mu_{\tilde{F}}(\cdot)$. Therefore, for the jth rule, the operation function of the node in this layer is

$$O_j^{(3)} = \left[\underline{O}_j^{(3)} \quad \overline{O}_j^{(3)}\right]^T = \left[\prod_{i=1}^{n} \underline{O}_{ij}^{(2)} \quad \prod_{i=1}^{n} \overline{O}_{ij}^{(2)}\right]^T \quad (21)$$

Layer 4: Left-most & Right-most layer

According to [27], the type-reduction can be integrated into the network layer by calculating their left-most and right-most value. That is, the complicated type-reduction method such as KM algorithm can be reduced as

$$O_j^{(4)} = \left[O_{jl}^{(4)} \; O_{jr}^{(4)}\right]^T = \left[\frac{\overline{\omega}_j^l \overline{O}_j^{(3)} + \underline{\omega}_j^l \underline{O}_j^{(3)}}{\overline{\omega}_j^l + \underline{\omega}_j^l} \quad \frac{\overline{\omega}_j^r \overline{O}_j^{(3)} + \underline{\omega}_j^r \underline{O}_j^{(3)}}{\overline{\omega}_j^r + \underline{\omega}_j^r}\right]^T \quad (22)$$

where the link weights are $\underline{\omega}^l = [\underline{\omega}_1^l \cdots \underline{\omega}_M^l]^T$, $\overline{\omega}^l = [\overline{\omega}_1^l \cdots \overline{\omega}_M^l]^T$, $\underline{\omega}^r = [\underline{\omega}_1^r \cdots \underline{\omega}_M^r]^T$, and $\overline{\omega}^r = [\overline{\omega}_1^r \cdots \overline{\omega}_M^r]^T$. Note that $\underline{\omega}_j^l < \overline{\omega}_j^l$ and $\underline{\omega}_j^r < \overline{\omega}_j^r$.

Layer 5: TSK Layer

From (12) and (13), we can obtain

$$\begin{aligned} T_j &= \left[T_j^l \; T_j^r\right]^T \\ &= \left[\left(c_{j0} + \sum_{i=1}^{n} c_{ji} x_i\right) - \left(s_{j0} + \sum_{i=1}^{n} s_{ji} |x_i|\right)\right. \\ &\quad \left.\left(c_{j0} + \sum_{i=1}^{n} c_{ji} x_i\right) + \left(s_{j0} + \sum_{i=1}^{n} s_{ji} |x_i|\right)\right]^T. \end{aligned} \quad (23)$$

Then, the output of this layer is

$$O^{(5)} = \left[O_l^{(5)} \; O_r^{(5)}\right]^T = \left[\frac{\sum_{j=1}^{M} O_{jl}^{(4)} T_j^l}{\sum_{j=1}^{M} O_{jl}^{(4)}} \quad \frac{\sum_{j=1}^{M} O_{jr}^{(4)} T_j^r}{\sum_{j=1}^{M} O_{jr}^{(4)}}\right]^T. \quad (24)$$

Layer 6: Output Layer

Layer 6 is the output layer which is used to implement the defuzzification operation. Each node is the actual output that will be pumped out this system. From (15), the crisp output is

$$O^{(6)} = \frac{O_l^{(5)} + O_r^{(5)}}{2}. \quad (25)$$

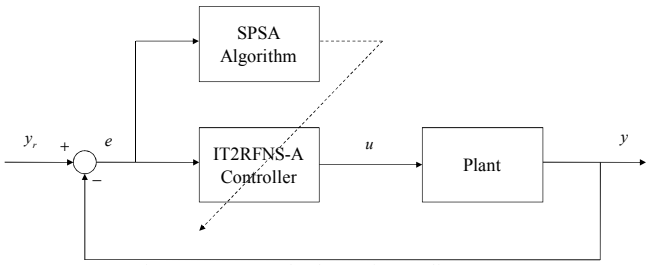

Figure 3. Control scheme for nonlinear system.

C. Training of IT2RFNS-A by A Stable SPSA Algorithm

Consider the nonlinear control problem, our goal is to generate a proper control signal $u(k)$ such that the system output $y(k)$ follows the desired trajectory $y_r(k)$, where k is the time index of discrete-time case. The IT2RFNS-A with the stable SPSA algorithm plays the role of controller for nonlinear plant, the adaptive control scheme is shown in Fig. 3. For convenience, we consider the single-output case and the tracking error is defined as

$$e(k) = y_r(k) - y(k). \quad (26)$$

Then, we define the objective function (error cost function) as

$$E(k) = \frac{1}{2} e^2(k) = \frac{1}{2}\left(y_r(k) - y(k)\right)^2. \quad (27)$$

Our goal is to generate the control signal $u(k)$ such that the tracking error approaching to zero, i.e., minimize the objective function $E(k)$. By using the SPSA algorithm, the parameters of IT2RFNS-A is adjusted such that the error defined in equation (27) is minimized. From the well-known gradient descent method and equation (5), the parameter update law can be written as

$$W(k+1) = W(k) + \Delta W(k) = W(k) + a_k\left(-\frac{\partial E(k)}{\partial W}\right) \quad (28)$$

where W is the tuning parameters of IT2RFNS-A. Then,

$$\frac{\partial E(k)}{\partial W} = -e(k)\frac{\partial e(k)}{\partial W}. \quad (29)$$

Herein, we adopt the SPSA algorithm to reduce the computational complexity of parameters update. The parameters update laws can be represented as

$$W(k+1) = W(k) + a_k e(k) g(W(k)) \quad (30)$$

where

$$g(W(k)) = \frac{e(W(k) + c_k\Delta_k) - e(W(k))}{c_k}\left[\Delta_{k1}^{-1} \; \Delta_{k2}^{-1} \; \ldots \; \Delta_{kp}^{-1}\right]^T. \quad (31)$$

$e(W(k) + c_k\Delta_k)$ denotes the tracking error between desired output and system output resulted by the IT2RFNS-A with perturbed tuning parameters. Note that equation (31) does not need to calculate the system gradient information, this simplifies the computational effort of nonlinear control.

D. Stability Analysis

Herein, we develop the stable theorem for selecting appropriate learning step length a_k. The choice of learning step length is very important for convergence. Hence, we employ the Lyapunov stability analysis approach to have convergence condition and the optimal learning step length for IT2RFNS-A.

Theorem 1. Let a_k be the learning step length of tuning parameters for the IT2RFNS-A. Consider the nonlinear control problem using IT2RFNS-A (shown in Fig. 3), the asymptotic convergence of the closed-loop system is guarantee if the learning step length is chosen satisfying

$$0 < a_k < \frac{2}{\left|g(k)\right|^2}, \text{ for all } k \quad (32)$$

where $g(W(k)) = \dfrac{e(W(k)+c_k\Delta_k)-e(W(k))}{c_k}\left[\Delta_{k1}^{-1}\ \Delta_{k2}^{-1}\ \ldots\ \Delta_{kp}^{-1}\right]^T$ is the gradient estimation using SPSA approach. In addition, the faster convergence can be obtained by using the following optimal time-varying learning step length

$$a_k^* = \frac{1}{\left|g(k)\right|^2}. \tag{33}$$

Proof: First, we define the discrete-time Lyapunov function as follows

$$V(k) = E(k) = \frac{1}{2}e^2(k) = \frac{1}{2}\left(y_r(k) - y(k)\right)^2 \tag{34}$$

where $e(k)$ represents the tracking error. Then, the change of the Lyapunov function is

$$\Delta V(k) = V(k+1) - V(k) = \frac{1}{2}\left(e^2(k+1) - e^2(k)\right). \tag{35}$$

According to the Lyapunov stability theorem, if the change of the positive definite Lyapunov function, denoted $\Delta V(k)$, satisfies the condition $\Delta V(k) < 0$, $\forall k$, then the asymptotical stability is guaranteed [1, 2]. Hence, our objective is to select the proper learning step length such that $\Delta V(k) < 0$, $\forall k$. This implies that $V(k)$ will converge to zero when k approaches to infinity. By [1, 2, 28], the error difference can be represented as

$$\Delta e(k) = e(k+1) - e(k) \cong \left[\frac{\partial e(k)}{\partial W}\right]^T \Delta W \tag{36}$$

where ΔW denotes the change of W. From equations (28) and (30), we obtain

$$\Delta W \equiv -a_k e(k)\frac{\partial e(k)}{\partial W} \cong a_k e(k) g(k). \tag{37}$$

Thus,

$$\begin{aligned}
\Delta V(k) &= \frac{1}{2}\left[e^2(k+1) - e^2(k)\right] \\
&= \frac{1}{2}\left[e(k+1) - e(k)\right]\cdot\left[e(k+1) + e(k)\right] \\
&= \frac{1}{2}\Delta e(k)\cdot\left[2e(k) + \Delta e(k)\right] \\
&= \Delta e(k)\cdot\left(e(k) + \frac{1}{2}\Delta e(k)\right) \\
&= \left[\frac{\partial e(k)}{\partial W}\right]^T a_k e(k) g(k)\cdot\left\{e(k) + \frac{1}{2}\left[\frac{\partial e(k)}{\partial W}\right]^T a_k e(k) g(k)\right\} \\
&= -a_k e^2(k)\left|g(k)\right|^2\left(1 - \frac{1}{2}a_k\left|g(k)\right|^2\right).
\end{aligned} \tag{38}$$

Note that $P(k)$ is positive for all k>0 and let $P(k) = a_k\left|g(k)\right|^2$. Thus,

$$\Delta V(k) = -e^2(k)P(k)\left(1 - \frac{1}{2}P(k)\right). \tag{39}$$

Recall that the asymptotical stability of the IT2RFNS-A is guaranteed if $\Delta V(k) < 0$, $\forall$ k>0. Thus, $\left(1 - \frac{1}{2}P(k)\right)$ should be positive such that $\Delta V(k) < 0$, $\forall k$. Therefore, we obtain the stability condition for a_k

$$0 < a_k < \frac{2}{|\,g(k)\,|^2}. \tag{40}$$

The asymptotic stability is guaranteed if a_k is chosen to satisfy equation (40). In addition, we would like to find a condition for a_k that guarantees the fast convergence. From (38) and (39), we have

$$\begin{aligned}
e^2(k+1) &= e^2(k) - e^2(k)P(k)\left(2 - P(k)\right) \\
&= e^2(k)\left[1 - 2P(k) + P^2(k)\right] \\
&= e^2(k)\left[P(k) - 1\right]^2.
\end{aligned} \tag{41}$$

The minimum of $e^2(k+1)$ is achieved when $P(k) = 1$. Hence, the time-varying optimal learning step length is

$$a_k^* = \frac{1}{\left|g(k)\right|^2}. \tag{42}$$

■

IV. Simulation Results

Consider the control problem of Chua's chaotic circuit. Our purpose is to develop an IT2RFNS-A controller to generate the proper control signal such that the system output y can follow a given reference trajectory y_r by the scheme as shown in the Fig. 3.

The typical Chua's chaotic circuit consists of one inductor, two capacitors, one linear resistor, and one piecewise-linear resistor [30, 31]. It has been shown that this circuit holds very rich nonlinear dynamics such as chaos and bifurcations. The dynamic equation of Chua's circuit are described as

$$\begin{aligned}
\frac{dv_{C_1}}{dt} &= (C_1)^{-1}\left(\frac{v_{C_2} - v_{C_1}}{R} - \lambda\right) \\
\frac{dv_{C_2}}{dt} &= (C_2)^{-1}\left(\frac{v_{C_1} - v_{C_2}}{R} - i_L\right) \\
\frac{di_L}{dt} &= (L)^{-1}\left(-v_{C_1} - R_O i_L\right)
\end{aligned} \tag{43}$$

where voltages v_{C_1}, v_{C_2}, and current i_L are state variables; R_O is a constant; λ denotes the nonlinear resistor which is a function of voltage across two terminals of C_1. The is λ defined as a cubic function as

$$\lambda = aV_{C_1} + c(v_{C_1})^3 \quad (a > 0, c < 0). \tag{44}$$

According to [31], equation (43) can be transferred into the canonical form as

$$\begin{bmatrix}\dot{x}_1\\ \dot{x}_2\\ \dot{x}_3\end{bmatrix}=\begin{bmatrix}0&1&0\\0&0&1\\0&0&0\end{bmatrix}\cdot\begin{bmatrix}x_1\\x_2\\x_3\end{bmatrix}+\begin{bmatrix}0\\0\\1\end{bmatrix}\cdot\left(f+g\cdot u+d\right)$$
$$y=x_1 \tag{45}$$

where $f=\frac{14}{1805}x_1-\frac{168}{9025}x_2+\frac{1}{38}x_3-\frac{2}{45}\left(\frac{28}{361}x_1+\frac{7}{95}x_2+x_3\right)^3$, $g=1$, and d is the external disturbance and is assumed to be a square-wave with amplitude ± 0.5 and period 2π. Herein, the objective is to track the reference trajectory $y_r=1.5\sin(t)$. We choose the initial state value as $x(0)=[0\ \ 0\ \ 1]^T$ and sampling time as 0.01 second.

For comparison, the same simulations are done by using IT2FNS-A and the case without optimal learning step length. The used coefficients are listed in Table I. The simulation results of trajectories are shown in Fig. 4. Figure 4(a) shows the phase plant trajectory after controlled, Fig. 4(b)-4(d) shows the state trajectories x_1, x_2, and x_3, respectively (solid line: actual system output; dashed line: reference trajectory). Figure 5 depicts the control effort of the IT2RFNS-A controller. The final fuzzy rules are

R^1: IF z_{11} is $\widetilde{F}_{11}$ and z_{21} is $\widetilde{F}_{21}$ and z_{31} is $\widetilde{F}_{31}$,
THEN $Y_1=[-7.6414\ -0.2130]+[-5.6236\ -0.3833]x_1$
$+[8.5389\ 9.0126]x_2+[-0.7853\ 1.6596]x_3$

where $\theta_{11}=[-4.3323\ 9.3274]$, $\theta_{21}=[-2.0292\ 2.6543]$, $\theta_{31}=[-8.0895\ 4.3461]$, $\overline{\omega}_1=[-10.0520\ -9.9033]$, and $\underline{\omega}_1=[-10.2740\ -9.3170]$.

R^2: IF z_{12} is $\widetilde{F}_{12}$ and z_{22} is $\widetilde{F}_{22}$ and z_{32} is $\widetilde{F}_{32}$,
THEN $Y_2=[0.4022\ 14.6956]+[-0.7847\ 13.4972]x_1$
$+[4.2989\ 5.6034]x_2+[14.6956\ 2.0163]x_3$

where $\theta_{12}=[-10.2843\ 1.1492]$, $\theta_{22}=[-2.1777\ 9.1312]$, $\theta_{32}=[-6.9073\ -0.5194]$, $\overline{\omega}_2=[-9.6955\ 2.2647]$, and $\underline{\omega}_2=[-5.7276\ -7.5890]$.

R^3: IF z_{13} is $\widetilde{F}_{13}$ and z_{23} is $\widetilde{F}_{23}$ and z_{33} is $\widetilde{F}_{33}$,
THEN $Y_1=[-8.4356\ -6.3436]+[-9.0422\ -4.7307]x_1$
$+[4.5459\ 9.6610]x_2+[-9.1732\ 2.0163]x_3$

where $\theta_{13}=[-2.0828\ 3.3525]$, $\theta_{23}=[-6.9332\ -2.3628]$, $\theta_{33}=[-7.1283\ -7.4267]$, $\overline{\omega}_3=[-9.5861\ -0.3531]$, and $\underline{\omega}_3=[-9.9473\ -8.7061]$.

R^4: IF z_{14} is $\widetilde{F}_{14}$ and z_{24} is $\widetilde{F}_{24}$ and z_{34} is $\widetilde{F}_{34}$,
THEN $Y_1=[3.9646\ 11.7177]+[5.1486\ 9.3539]x_1$
$+[-4.5256\ 6.0764]x_2+[-0.9234\ 6.5402]x_3$

where $\theta_{14}=[-7.7789\ -7.6991]$, $\theta_{24}=[-8.7967\ -5.7106]$, $\theta_{34}=[-7.1095\ -6.3978]$, $\overline{\omega}_4=[-8.7774\ 1.2302]$, and $\underline{\omega}_3=[-7.3826\ -4.7145]$.

The corresponding MFs are depicted in Fig. 6.

We can observe that the proposed method is valid to control a nonlinear dynamic system. The comparison results are shown in Table II which is obtained by 10 independent runs. From Table II, we can easily find that the IT2RFNS-A performs better than IT2FNS-A. This result shows that the IT2RFNS-A has ability to cope with dynamic problems. Observe the performance of the case with optimal learning step length from Table II, we again demonstrate that adopting optimal learning step length guarantees the efficient training of IT2RFNS-A.

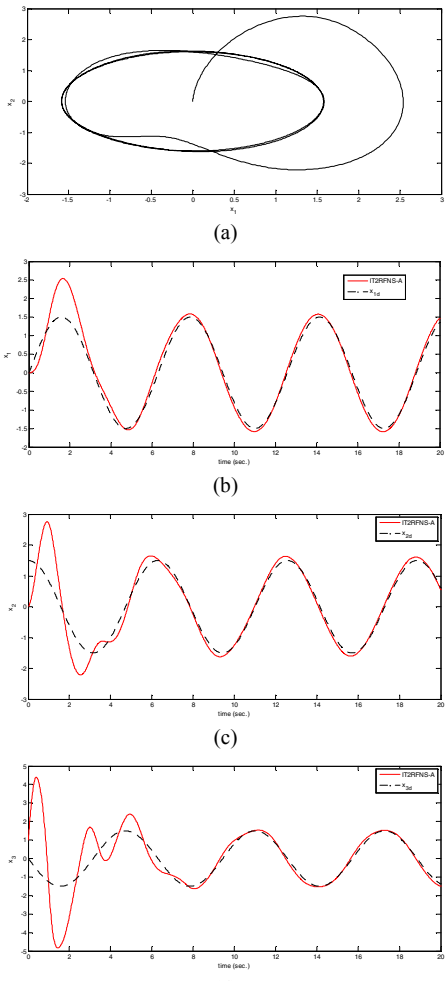

Figure 4. Simulation results: (a) phase plant trajectory of IT2RFNS-A, (b) state x_1 and reference trajectory y_r, (c) state x_2 and reference trajectory $\dot{y}_r$, and (d) state x_3 and reference trajectory $\ddot{y}_r$.

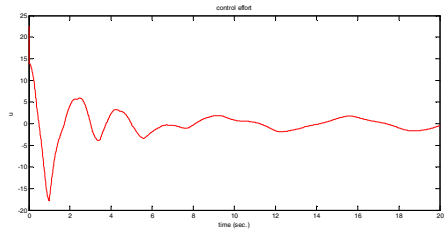

Figure 5. Control effort of IT2RFNS-A controller of Chua's chaotic circuit.

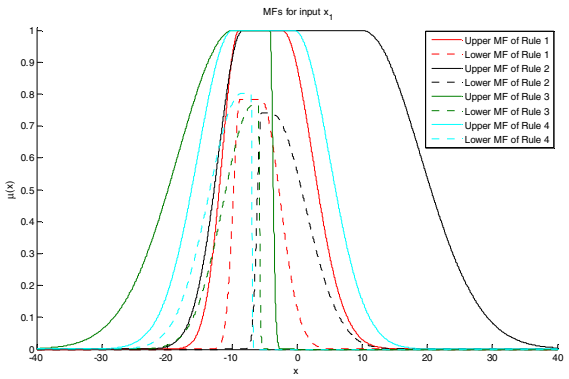

(a)

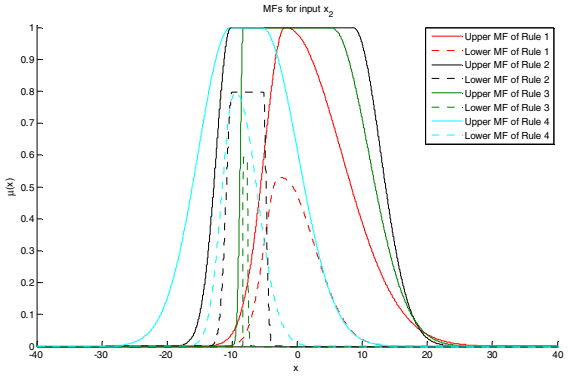

(b)

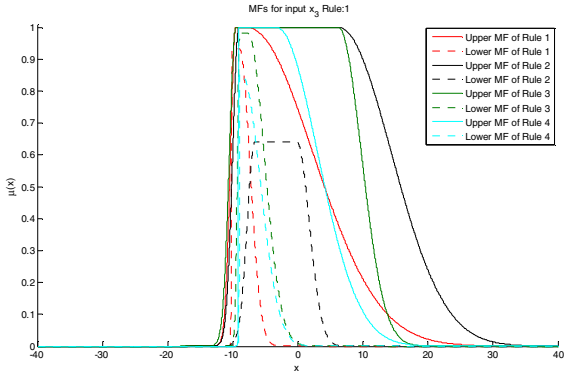

(c)

Figure 6. Final membership functions: (a) MFs for x_1, (b) MFs for x_2, and (c) MFs for x_3.

TABLE I. THE USED COEFFICIENTS.

	IT2FNS-A	IT2RFNS-A	**IT2RFNS-A**
a	0.01	0.01	optimal learning step length (33)
α	0.602	0.602	
A	200	200	
c	1	1	1
γ	0.101	0.101	0.101
rule number	4	4	4

TABLE II. COMPARISON RESULTS OF CONTROL PERFORMANCE.

MSE	IT2FNS-A	IT2RFNS-A	IT2RFNS-A (optimal a_k)
Worst	2.5485	2.1833	0.0663
Average	0.9189	0.3265	0.0661
Best	0.2474	0.0675	0.0659

V. CONCLUSION

In this paper, we have proposed an interval type-2 recurrent fuzzy system with asymmetric membership functions (IT2RFNS-A) and its training scheme using the proposed stable SPSA algorithm. In addition, we adopt the Lyapunov theorem to derive the appropriate range of learning step length for SPSA to guarantee the stability of the closed-loop system for nonlinear control. In addition, we also derive the optimal learning step length which can ensure the efficient training for IT2RFNS-A. The feasibility and the effectiveness of the proposed method have been demonstrated by illustration example. The simulations on the control of the Chua's chaotic circuit are done and shows the following advantages of proposed approach; (a) The IT2RFNS-A can reduce the fuzzy rules, that is, only few rules can achieve the specific performance or even better; (b) The IT2RFNS-A can catch the dynamic response of the system, i.e., it is capable of coping with dynamic problems; (c) By using the proposed SPSA algorithm, the gradient information is unnecessary. In other words, a great deal of computational effort is saved. (d) For control problems, the proposed method avoids approximating the system sensitivity which leads to inaccuracy. (e) Adopting optimal learning step length improves the performance of training IT2RFNS-A.

ACKNOWLEDGMENT

This work was partially supported by the National Science Council, Taiwan, R.O.C., under contract No: NSC-97-2221-E-155-033-MY3.

REFERENCES

[1] Y. C. Chen and C. C. Teng, "A model reference control structure using a fuzzy neural network," *Fuzzy Sets Syst.*, Vol. 73, pp. 291–312, 1995.

[2] C. H. Lee and C. C. Teng, "Identification and control of dynamic systems using recurrent fuzzy neural networks," *IEEE Trans. on Fuzzy Systems*, Vol. 8, No. 4, pp. 349-366, 2000.

[3] Y. Gao and M. J. Er, "Online adaptive fuzzy neural identification and control of a class of MIMO nonlinear systems," *IEEE Trans. Fuzzy Syst.*, Vol. 11, No. 4, pp. 462–477, Aug. 2003.

[4] R. J. Wai and P. C. Chen, "Intelligent tracking control for robot manipulator including actuator dynamics via TSK-type fuzzy neural network," *IEEE Trans. Fuzzy Syst.*, Vol. 12, No. 4, pp. 552–560, Aug. 2004.

[5] A. Lotfi and A. C. Tsoi, "Learning fuzzy inference systems using an adaptive membership function scheme," *IEEE Trans. On Systems, Man, and, Cybernetics, Part B*, Vol. 26, No. 2, pp. 326-331, 1996.

[6] C. H. Lee and C. C. Teng, "Fine tuning of membership functions for fuzzy neural systems," *Asian Journal of Control*, Vol. 3, No. 3, pp. 216-225, 2001.

[7] P. Z. Lin and T. T. Lee, "Robust self-organizing fuzzy-neural control using asymmetric Gaussian membership functions," *International Journal of Fuzzy Systems*, Vol. 9, No. 2, pp. 77-86, 2007.

[8] C. H. Lee and H. Y. Pan, "Performance enhancement for neural fuzzy systems using asymmetric membership functions," *Fuzzy Sets and Systems,* Vol. 160, No. 7, pp. 949-971, 2009.

[9] L. A. Zadeh, "The concept of a linguistic variable and its application to approximate reasoning-1," *Information Sciences*, Vol. 8, pp. 199-249, 1975.

[10] Q. Liang and J. M. Mendel, "Interval type-2 fuzzy logic systems: Theory and design," *IEEE Trans. Fuzzy Syst*., Vol. 8, No. 5, pp. 535-550, Oct. 2000.

[11] J. M. Mendel, "On the importance of interval sets in type-2 fuzzy logic systems," in *Proc*. *Joint 9th IFSA World Congr*. *20th NAFIPS Int*. *Conf*., Vancouver, BC, Canada, pp. 1647-1652, Jul. 25-28, 2001.

[12] O. Castillo, N. Cazarez, and P. Melin, "Design of Stable Type-2 Fuzzy Logic Controller based on a Fuzzy Lyapunov Approach," *IEEE International Conference on Fuzzy Systems*, pp. 2331-2336, 2006.

[13] O. Castillo, "Interval Type-2 Fuzzy Logic for Control Application," *IEEE International Conference on Granular Computing*, pp. 79-84, 2010.

[14] H. A. Hagras, "A Hierarchical Type-2 Fuzzy Logic Control Architecture for Autonomous Mobile Robot," *IEEE Trans. on Fuzzy Systems*, Vol. 12, No. 4, 2004.

[15] H. A. Hagras, "Type-2 Fuzzy Control: A New Generation of Fuzzy Controllers," *IEEE Comput. Intell. Mag*., Vol. 2, No. 1, pp. 30-43, Feb. 2007.

[16] D. Wu and W. W. Tan, "A Simplified Architecture for Type-2 FLSs and Its Application to Nonlinear Control," *IEEE Conf. on Cybern. and Intell. Syst.*, pp. 485-490, Dec. 2004.

[17] X. T. Chen and W. W. Tan, "A Type-2 Fuzzy Logic Controller for Dynamic Positioning Systems," *IEEE International Conference on Control and Automation*, pp. 1013-1018, June 2010.

[18] C. H. Lee, J. L. Hong, Y. C. Lin, and W. Y. Lai, "Type-2 fuzzy neural network systems and learning," *International Journal of Computational Cognition*, Vol. 1, No. 4, pp. 79-90, 2003.

[19] C. H. Lee, Y. C. Lin, and W. Y. Lai, "Systems identification using type-2 fuzzy neural Network (type-2 FNN) systems," *IEEE International Sym*. *On Computational Intelligence in Robotics and Automation*, Vol. 3, pp. 1264-1269, 2003.

[20] C. H. Lee and Y. C. Lin, "Control of nonlinear uncertain system using type-2 fuzzy neural network and adaptive filter," *IEEE International Conf*. *on Networking*, *Sensing*, *and Control*, Vol. 2, pp. 1177-1182, 2004.

[21] C. H. Lee, Y. C. Lin, "An adaptive type-2 fuzzy neural controller for nonlinear uncertain systems," *International Journal of Control and Intelligent systems*, Vol. 12, No. 1, pp. 41-50, 2005.

[22] C. H. Lee, F. Y. Chang, and C. T. Lee, "Species-based hybrid of electromagnetism-like mechanism and back-propagation algorithms for an interval type-2 fuzzy system design," *Lecture Notes in Engineering and Computer Science: Proceedings of The International MultiConference of Engineers and Computer Scientists 2010*, IMECS 2010, 17-19 March, 2010, Hong Kong, pp. 140-145.

[23] J. C. Spall, "Multivariate stochastic approximation using a simultaneous perturbation gradient approximation," *IEEE Trans. Autom. Control,* Vol. 37, No. 3, pp. 332–341, Mar. 1992.

[24] J. C. Spall and J. A. Cristion, "Model free control of nonlinear stochastic systems with discrete-time measurements," *IEEE Trans. Autom. Control*, Vol. 43, No. 9, pp. 1198–1210, Sep. 1998.

[25] J. C. Spall, Introduction to Stochastic Search and Optimization: Estimation, Simulation, and Control, John Wiley and Sons, Hoboken, NJ, 2003.

[26] J. M. Mendel, Uncertain Rule-based Fuzzy Logic Systems: Introduction and New Directions, Upper Saddle River, Prentice-Hall, NJ, 2001.

[27] J. R. Castro, O. Castillo, P. Melin, and A. R. Díaz, "A hybrid learning algorithm for a class of interval type-2 fuzzy neural networks," *Information Sciences*, Vol. 179, No. 13, pp. 2175-2193, 2009.

[28] T. Yabuta and T. Yamada, "Learning control using neural networks," *Proc. IEEE Int. Conf. Robotics and Automation*, Sacramento, CA, Apr. pp. 740-745, 1991.

[29] K. S. Narendra and K. Parthasarathy, "Identification and control of dynamical system using neural network," *IEEE Trans. On Neural Networks*, Vol. 1, No. 1, pp. 4-27, 1990.

[30] Y. H. Joo, L. S. Shieh, and G. R. Chen, "Hybrid state space fuzzy model based controller with dual-rate sampling for digital control of chaotic systems," *IEEE Trans. on Fuzzy Systems*, Vol. 7, No. 4, pp. 394-408, 1999.

[31] C. H. Wang, T. C. Lin, T. T. Lee, and H. L. Liu, "Adaptive hybrid intelligent control for uncertain nonlinear dynamical systems," *IEEE Trans*. *on Systems*, *Man*, *Cybernetics Part-B*, Vol. 32, No. 5, pp. 583-597, 2002.

2011 IEEE International Conference on Fuzzy Systems
June 27-30, 2011, Taipei, Taiwan

Efficient Centroid Computation of General Type-2 Fuzzy Sets with Linear Secondary Membership Function

Xinwang Liu
School of Economics and Management
Southeast University, Nanjing, Jiangsu, 210096
Email: xwliu@seu.edu.cn

***Abstract*—This paper provides root finding methods for the centroid computation of interval type-2 fuzzy sets and general type-2 fuzzy sets with linear secondary membership function. When the FOUs of the type-2 fuzzy sets are provided, the centroid computation methods in this paper is accurate and computational efficient, which provide new methods for the type-2 fuzzy systems computation.**

***Keywords*—Type-2 fuzzy set (IT2 FS) , Karnik-Mendel (KM) algorithms, centroid computation, root finding.**

I. Introduction

Type-2 fuzzy logic system (FLS) allows for better modeling of uncertainty as type-2 fuzzy set (T2 FS) encompass a Footprint of Uncertainty (FOU) which, associated with its third dimension, gives more degrees of freedom to T2 FS in comparison to type-1 fuzzy set (T1 FS) [1], [14], [20], [30]. Interval type-2 fuzzy set (IT2 FS) is a simplified version of general T2 FS where the membership grade is crisp interval rather than functions. Most applications on type-2 fuzzy FLS involve only interval type-2 systems applications, and it has been shown that interval type-2 FLSs can outperform their type-1 FLSs counterparts in a variety of fields including information processing, fuzzy control and decision making [10], [28], [21], [6], [16]. General type-2 FLSs has only recently been investigated in more detail [19], [25], [11], [3], [24], [4], [23]. It is expected that the general T2 FSs will have the ability to model uncertainty more accurately than IT2 FSs which in turn will result in the potential for a superior performance in comparison to type-1 and interval type-2 FLSs. But the high complexity associated with their design and their computational requirements made them appear unsuitable for real-world use. One of the major obstacles to the use of generalized type-2 FLSs on real-world problems is the type reduction of general T2 FSs [19], [25], [3], [11], which is consisted of the steps of type reduction from general T2 FS into T1 FS, and T1 FS defuzzification to the final crisp output. Calculating the centroid of a general T2 FS typically requires a large amount of computation.

To date, type-reduction methods have been developed by Karnik and Mendel [9] and are elaborated upon in [14]. The efficient algorithms, called the Karnik-Mendel (KM) algorithms, have been developed for centroid type reduction for interval type-2 FLSs. The KM algorithms have been applied to many applications of T2 FSs and play an important role in type-2 FLSs [20], [14], [7], [15], [16]. Mendel and Liu [18] proved monotonicity and super-exponential convergence of the algorithms. The iteration number of KM algorithm is usually less than seven for accuracies of 10^{-2}. Because of the iterative natures of the KM algorithms, there may be a computational bottleneck in real-time applications. So, Wu and Mendel [29] proposed an uncertainty bound method to approximate type reduction of ITS without computation burden. Greenfield, Chiclana, Coupland and Robert John [5] proposed a collapsing method of defuzzification for discretised IT2 FSs, which claimed can be outperformed the KM algorithms both in accuracy and speed. Finally, Wu and Mendel [27] proposed Enhanced KM (EKM) algorithms to reduce the computational cost of the standard KM algorithm.

However, no efficient strategies exist to date for centroid type-reduction of general T2 FLSs [11], [19], [25]. John and Czarnecki [8] and Lucas et al. [13] proposed the general centroid computation as the centroids of all vertical slices (each of which is a T1 FS). Liu [11] developed an efficient strategy to implement centroid type-reduction for general type-2 FLSs by decomposing a general T2 FS into IT2 FS α-planes with $\alpha \in [0, 1]$. Mendel, Liu and Zhai [19] use this method for the computation of general type-2 sets, which seems to be the first practical choices for extension of IT2 FSs to general T2 FSs. The centroid type reduction is performed using KM algorithms individually for each α-plane. A quasi-T2 fuzzy logic system with two α-plane sets are designed. Starczewski [24] also designed triangular type-2 fuzzy logic systems. A new efficient approximate iterative procedure based on the KM type-reduction is proposed. Wagner and Hagras [25] introduced the zSlices-based representation, and proposed a similar type reduction method with the repetitive KM algorithm for the centroid of general T2 FSs. Except the α-plane (zslice) based centroid computation method mentioned [19], [25], which takes samples from the two dimensional directions of the membership function, and obtains approximate solution with repetitive computation and iterations, Coupland and John [2], [3], [4] presented a geometric representation of general type-2 sets. The geometric method [4], [3], [2] uses more simplified

978-1-4244-7316-8/11/$26.00 ©2011 IEEE

and rough approximation method than the α-plane method with KM-algorithm, and it is claimed faster than the KM algorithm in computation. More recently, Zhai and Mendel [31] proposed introduced a centroid-flow (CF) algorithm, which only utilizes the KM/EKM algorithms to compute the centroid of the general type-2 fuzzy sets, which only need to compute the α-plane of the beginning. It should be noted that in all of the general T2 FSs publications for the authors [19], [11], [10], [3], [25], [4], [24], the second membership function are often assumed linear (triangular or trapezoidal), there seems no much justification to adopt other forms of second membership functions forms in general type-2 FLSs, especially in control and decision applications.

Up till now, in contrast to the centroid defuzzification of type-1 fuzzy sets, that is usually computed integral of the membership function of the output fuzzy set, almost all the current type reduction methods of T2 FS are discrete based, that is we take sampling data from the T2 FS, and compute the general centroid values approximately. This not only make the computation accuracy becomes very low but also make the computation complexity increases very fast, e. g. for 100 samples on the α-plane and x-domain respectively, we should compute 100 times iterate computation with $10,000$ data; if we want a one more digit accuracy of the general centroid values, we have to take 1000 samples on two dimensions, and compute 1000 times iterate computation with $1,000,000$ data. Some computational analysis of these methods can be found in [19], [11], [25]. In the present paper, we will extend the KM algorithm to the general root finding method. The KM algorithm iteration process become a part of rooting finding with Newton-Raphson method. In which, the centroid values can be computed directly and the accurately, and can integrate other numerical integral and root finding techniques in practice. For general T2 FSs under linear second membership function, the centroid value computation is only two times of the case of IT2 FSs, the repetitive IT2 FS slices computation can be avoided, and the computation is accurate.

The organization of the paper is as follows. Section II gives preliminaries about T2 FSs and the centroid computation of T2 FSs. Section III provides the root finding methods for the centroid of IT2 FS and the analytical method for the centroid computation of general T2 FS. Section IV illustrates the proposed methods with numerical examples. Section **??** summarizes the main results and draws conclusions.

II. Preliminaries

A. The centroid of interval type-2 fuzzy set and general type-2 fuzzy set

Definition 1: [17] A T2 FS, denoted as $\tilde{A}$, is characterized by a type-2 membership function $\mu_{\tilde{A}}(x,u)$, where $x \in X$ and $u \in J_x \subseteq [0,1]$, i. e.

$$\tilde{A} = \{((x,u), \mu_{\tilde{A}}(x,u) | \forall x \in X, \forall u \in J_x \subseteq [0,1]\} \quad (1)$$

where $0 \leq \mu_{\tilde{A}(x,u)} \leq 1$, X is the domain of the fuzzy set, and J_x is the domain of the secondary membership function at x. $\tilde{A}$ can also be expressed as

$$\tilde{A} = \int_{x \in X} \int_{u \in J_x} \mu_{\tilde{A}}(x,u)/(x,u) \quad \forall u \in J_x \subseteq [0,1] \quad (2)$$

where $\int\int$ denotes union over all admissible x and u. J_x is called the primary membership of x in $\tilde{A}$. At each value of x say $x = x'$, the 2-D plane whose axes are u and $\mu_{\tilde{A}}(x',u)$ is called a vertical slice of $\tilde{A}$. Besides the vertical slice representation mentioned above, a general T2 FS can also be represented as a series of wavy slices where for discrete universes of discourse X and U [14] .

The footprint of uncertainty, denoted $FOU(\tilde{A})$ is the union of all primary memberships, i.e., $FOU(\tilde{A}) = \bigcup_x \in X J_x$, which represents the uncertainty in the primary memberships of a T2 FS $\tilde{A}$.

Definition 2: [14] An IT2 FS $\tilde{A}$ is completely described by its lower and upper MFs, $\underline{\mu}_{\tilde{A}}(x)$ and $\overline{\mu}_{\tilde{A}}(x)$, respectively. The footprint of uncertainty (FOU) of an IT2 FS is described in terms of these MFs:

$$FOU(\tilde{A}) = \bigcup_{x \in X} \left[\underline{\mu}_{\tilde{A}}(x), \overline{\mu}_{\tilde{A}}(x)\right]$$

Definition 3: [19] An α-plane FOU, i.e., $FOU(\tilde{A}_\alpha)$ is

$$FOU(\tilde{A}_\alpha) = \alpha I_{\tilde{A}_\alpha}(x,u|\alpha). \quad (3)$$

where $I_{\tilde{A}_\alpha}$ is an indicator function

$$I_{\tilde{A}_\alpha}(x,u|\alpha) = \begin{cases} 1 & (x,u) \in \tilde{A}_\alpha \\ 0 & (x,u) \notin \tilde{A}_\alpha \end{cases}$$

The α-plane representation (theorem) for $\tilde{A}$ is

$$\tilde{A} = \bigcup_{\alpha \in [0,1]} FOU(\tilde{A}_\alpha)$$

Definition 4: The centroid $c(A)$ of the T1 FS A is defined as

$$C(A) = \frac{\sum_{i=1}^{N} x_i \mu_A(x_i)}{\sum_{i=1}^{N} \mu_A(x_i)} \quad (4)$$

The centroid of a T2 FS, which was developed by Karnik and Mendel [9], has turned out to be a very important concept for IT2, as well as general T2 FSs and their associated FLSs.

Definition 5: [26] The centroid $C_{\widetilde{A}}$ of an IT2 FS $\widetilde{A}$ is the union of the centroids of all its embedded T1 FSs A_e, i.e.,

$$C(\widetilde{A}) = \bigcup_{\forall A_e} c(A_e) = [c_l(\widetilde{A}), c_r(\widetilde{A})] \quad (5)$$

where $\bigcup$ is the union operation, and

$$c_l(\widetilde{A}) = \min_{\forall A_e} c(A_e) \quad (6)$$

$$c_r(\widetilde{A}) = \max_{\forall A_e} c(A_e) \quad (7)$$

Definition 6: [19] The centroid of general T2 FS $\tilde{A}$, is the union of the centroids of all the embedded T1 sets. With the α-plane representation method [19], [11], $C_{\tilde{A}}$ can be computed using the α-plane decomposition of $\tilde{A}$, the centroid of general

T2 FS $C_{\tilde{A}}(x)$ is the union of a series of IT2 FS at every α-plane, i.e.,

$$C_{\tilde{A}}(x) = \bigcup_{\alpha \in [0,1]} \alpha / C_{\tilde{A}_\alpha}(x)$$

where $C_{\tilde{A}_\alpha}(x)$ is the centroid of the α-plane $\tilde{A}$. Because each $\tilde{A}_\alpha$ is an interval-valued set, its centroid is an interval set, i.e.,

$$C_{\tilde{A}_\alpha}(x) = [l_{\tilde{A}_\alpha}, r_{\tilde{A}_\alpha}]$$

B. The centroid computation with KM algorithms

Let $x_i (i = 1, 2 \ldots, N)$ represent the discretization of an IT2 FS $\widetilde{A}$; $\underline{\mu}_{\widetilde{A}}(x_i)$ and $\overline{\mu}_{\widetilde{A}}(x_i)$ are the lower and upper membership functions that are associated with $\widetilde{A}$ respectively. Using the representation theorem for a T2 FS [17], the centroid of IT2 FS $\widetilde{A}$, $c_{\widetilde{A}} = [c_l, c_r]$, can be computed as the optimal solutions of the following interval weighted average problems [9], [18]:

$$c_l = \min_{\forall \theta_i \in [\underline{\mu}_{\widetilde{A}}(x_i), \overline{\mu}_{\widetilde{A}}(x_i)]} \frac{\sum_{i=1}^{N} x_i \theta_i}{\sum_{i=1}^{N} x_i \theta_i} \tag{8}$$

$$c_r = \max_{\forall \theta_i \in [\underline{\mu}_{\widetilde{A}}(x_i), \overline{\mu}_{\widetilde{A}}(x_i)]} \frac{\sum_{i=1}^{N} x_i \theta_i}{\sum_{i=1}^{N} x_i \theta_i} \tag{9}$$

It is well known that c_l and c_r can be expressed, as:

$$c_l = \frac{\sum_{i=1}^{L} x_i \overline{\mu}_{\widetilde{A}}(x_i) + \sum_{i=L+1}^{N} x_i \underline{\mu}_{\widetilde{A}}(x_i)}{\sum_{i=1}^{L} \overline{\mu}_{\widetilde{A}}(x_i) + \sum_{i=L+1}^{N} \underline{\mu}_{\widetilde{A}}(x_i)} \tag{10}$$

$$c_r = \frac{\sum_{i=1}^{R} x_i \underline{\mu}_{\widetilde{A}}(x_i) + \sum_{i=R+1}^{N} x_i \overline{\mu}_{\widetilde{A}}(x_i)}{\sum_{i=1}^{R} \overline{\mu}_{\widetilde{A}}(x_i) + \sum_{i=L+1}^{N} \underline{\mu}_{\widetilde{A}}(x_i)} \tag{11}$$

where L and R are called switch points with $x_L \le c_l \le x_{L+1}$ and $x_R \le c_r \le x_{R+1}$. The determination of L and R can be performed by using the KM algorithms [20].

Currently, the centroid of general T2 FS $\tilde{A}$ is computed with α-plane (or zslices) [19], [25] with $\alpha \in [0, 1]$, which decomposes the general T2 FS into a series of IT2 FS. The centroid of T2 FS is computed by the process in Table I.

III. The Analytical Direct Centroid Computation of General Type-2 Fuzzy Set with Linear Secondary Membership Function

A. Direct centroid computation of Interval type-2 sets

We assume all the x_is are different, and they are bounded in $[a, b]$, where $a = \min_{1 \le i \le n} \{x_i\}$ and $b = \max_{1 \le i \le n} \{x_i\}$, which denote the smallest and the largest sampled values of x respectively*. Then, the continuous versions of (10) and (11) are

$$c_l = \frac{\int_a^{c_l} x \overline{\mu}_{\widetilde{A}}(x) dx + \int_{c_l}^{b} x \underline{\mu}_{\widetilde{A}}(x) dx}{\int_a^{c_l} \overline{\mu}_{\widetilde{A}}(x) dx + \int_{c_l}^{b} \underline{\mu}_{\widetilde{A}}(x) dx} \tag{12}$$

*As noted in [22, p. 363], if Gaussian MFs are used, one can extend the theoretical results to $a \to -\infty$, $b \to +\infty$; but, in practice, when truncations are used, a and b are again finite numbers.

$$c_r = \frac{\int_a^{c_r} x \underline{\mu}_{\widetilde{A}}(x) dx + \int_{c_r}^{b} x \overline{\mu}_{\widetilde{A}}(x) dx}{\int_a^{c_r} \underline{\mu}_{\widetilde{A}}(x) dx + \int_{c_r}^{b} \overline{\mu}_{\widetilde{A}}(x) dx} \tag{13}$$

From (12) and (13), we have

$$\int_a^{c_l} (c_l - x) \overline{\mu}_{\widetilde{A}}(x) dx + \int_{c_l}^{b} (c_l - x) \underline{\mu}_{\widetilde{A}}(x) dx = 0 \tag{14}$$

$$\int_a^{c_r} (c_r - x) \underline{\mu}_{\widetilde{A}}(x) dx + \int_{c_r}^{b} (c_r - x) \overline{\mu}_{\widetilde{A}}(x) dx = 0 \tag{15}$$

Let

$$\varphi(\xi) = \int_a^{\xi} (\xi - x) \overline{\mu}_{\widetilde{A}}(x) dx + \int_{\xi}^{b} (\xi - x) \underline{\mu}_{\widetilde{A}}(x) dx \tag{16}$$

$$\psi(\xi) = \int_a^{\xi} (\xi - x) \underline{\mu}_{\widetilde{A}}(x) dx + \int_{\xi}^{b} (\xi - x) \overline{\mu}_{\widetilde{A}}(x) dx \tag{17}$$

Consider (14), (15), then $\varphi(c_l) = 0$ and $\psi(c_r) = 0$. The computation of the centroid values of c_l and c_r can be transformed in the root finding problems of $\varphi(\xi) = 0$ and $\psi(\xi) = 0$. The equivalence of KM Algorithm and Newton-Raphson root-finding method and some more theoretical analysis were given in [12]. We can use the centroid finding equations (16) and (17) as the direct centroid computation methods.

B. Direct centroid computation of general type-2 sets

The centroid of general T2 FS is the combination of a series of α-plane IT2 FS with $\alpha \in [0, 1]$, which is in fact a normal type-1 fuzzy set with type reduction [19], [11]. It is natural that the centroid computation is the centroid of general T2 FS is more complicated, which is obtained by solving the centroids of a series of IT2 FS repeatedly [19], [25]. As the T2 FSs are obtained from T1 FS with an additional dimension, there is not common principle for the secondary membership determination. We often assume the secondary membership function of T2 FS to be assumed linear (triangular or trapezoidal membership function) [19], [11], [10], [3], [25], [4], [24]. It is very lucky that under such assumptions the centroid of a T2 FS can be obtained directly without solving every α-plane and we also get the type-1 centroid function analytically, which is convenient for final defuzzification.

If the second membership function of general T2 FS is linear, then α-plane decomposition of general T2 FS $\tilde{A}$ can be expressed as:

$$\underline{\mu}_{\widetilde{A}_\alpha}(x) = (1 - \alpha) \underline{\mu}_{\widetilde{A}_0}(x) + \alpha \underline{\mu}_{\widetilde{A}_1}(x) \tag{18}$$

$$\overline{\mu}_{\widetilde{A}_\alpha}(x) = (1 - \alpha) \overline{\mu}_{\widetilde{A}_0}(x) + \alpha \overline{\mu}_{\widetilde{A}_1}(x) \tag{19}$$

where $\underline{\mu}_{\widetilde{A}_\alpha}(x)$ and $\overline{\mu}_{\widetilde{A}_\alpha}(x)$ are the LMF and UMF of α-plane IT2 FS respectively.

We usually have $\forall x$, $\underline{\mu}_{\widetilde{A}_0}(x) \le \underline{\mu}_{\widetilde{A}_1}(x)$ and $\overline{\mu}_{\widetilde{A}_0}(x) \ge \overline{\mu}_{\widetilde{A}_1}(x)$, so that $\underline{\mu}_{\widetilde{A}_\alpha}(x)$ is increasing with α and $\overline{\mu}_{\widetilde{A}_\alpha}(x)$ is decreasing with α. We can compute the centroid values of IT2 FS with FOU $\underline{\mu}_{\widetilde{A}_\alpha}(x)$ and $\overline{\mu}_{\widetilde{A}_\alpha}(x)$, in which α is a parameter of the IT2 FSs.

TABLE I
THE CENTROID COMPUTATION OF GENERAL TYPE-2 FUZZY SET

Step	The computation process
1	Sample $\alpha \in [0,1]$ with $0 = \alpha_1 < \alpha_2 < \cdots < \alpha_m = 1$, where m can be determined by the tolerance error bound of the problem. Then the general T2 FS is decomposed into a serial of α-planes in the form of IT2 FS $\tilde{A}_{\alpha_j}$, $j = 1, 2, \ldots, m$.
2	For every $\tilde{A}_{\alpha_j}$, $j = 1, 2, \ldots, m$, compute the general centroid values $c_l(\alpha_j)$ and $c_r(\alpha_j)(j = 1, 2, \ldots, m)$ with the KM algorithms respectively.
3	Connect the points $c_l(\alpha_j)$ and $c_r(\alpha_j)$ for all $j = 1, 2, \ldots, m$ together, thereby obtaining any approximate solution for $c_l(\alpha)$ and $c_r(\alpha)$ for $\alpha \in [0,1]$.

With (16),

$$\begin{aligned}\varphi(\alpha, l) &= \int_a^l (l-x)\overline{\mu}_{\widetilde{A}_\alpha}(x)dx + \int_l^b (l-x)\underline{\mu}_{\widetilde{A}_\alpha}(x)dx \\ &= \int_a^l (l-x)\left((1-\alpha)\overline{\mu}_{\widetilde{A}_0}(x) + \alpha\overline{\mu}_{\widetilde{A}_1}(x)\right)dx \\ &\quad + \int_l^b (l-x)\left((1-\alpha)\underline{\mu}_{\widetilde{A}_0}(x) + \alpha\underline{\mu}_{\widetilde{A}_1}(x)\right)dx \\ &= -\alpha\left(\int_a^l (l-x)\left(\overline{\mu}_{\widetilde{A}_0}(x) - \overline{\mu}_{\widetilde{A}_1}(x)\right)dx \right. \\ &\quad \left. + \int_l^b (l-x)\left(\underline{\mu}_{\widetilde{A}_0}(x) - \underline{\mu}_{\widetilde{A}_1}(x)\right)dx\right) \\ &\quad + \left(\int_a^l (l-x)\overline{\mu}_{\widetilde{A}_0}(x)dx + \int_l^b (l-x)\underline{\mu}_{\widetilde{A}_0}(x)dx\right)\end{aligned}$$

Let $\varphi(\alpha, l) = 0$, we have

$$\begin{aligned}\alpha_l = &\left(\int_a^l (l-x)\overline{\mu}_{\widetilde{A}_0}(x)dx + \int_l^b (l-x)\underline{\mu}_{\widetilde{A}_0}(x)dx\right) \\ &\Big/ \left(\int_a^l (l-x)\left(\overline{\mu}_{\widetilde{A}_0}(x) - \overline{\mu}_{\widetilde{A}_1}(x)\right)dx \right. \\ &\left. + \int_l^b (l-x)\left(\underline{\mu}_{\widetilde{A}_0}(x) - \underline{\mu}_{\widetilde{A}_1}(x)\right)dx\right) \qquad (20)\end{aligned}$$

This expression shows the relationship between l and α, if we have an additional restrict value of α with $\alpha \in [0,1]$, then it can be regard the reverse function of $c_l(\alpha)$.

Similarly, with

$$\begin{aligned}\psi(\alpha, r) = &\int_a^r (r-x)\underline{\mu}_{\widetilde{A}_\alpha}(x)dx \\ &+ \int_r^b (l-x)\overline{\mu}_{\widetilde{A}_\alpha}(x)dx \qquad (21)\end{aligned}$$

Let $\psi(\alpha, r) = 0$, we can also get that

$$\begin{aligned}\alpha_r = &\left(\int_a^r (r-x)\underline{\mu}_{\widetilde{A}_0}(x)dx + \int_l^b (r-x)\overline{\mu}_{\widetilde{A}_0}(x)dx\right) \\ &\Big/ \left(\int_a^r (r-x)\left(\underline{\mu}_{\widetilde{A}_0}(x) - \underline{\mu}_{\widetilde{A}_1}(x)\right)dx \right. \\ &\left. + \int_r^b (r-x)\left(\overline{\mu}_{\widetilde{A}_0}(x) - \overline{\mu}_{\widetilde{A}_1}(x)\right)dx\right) \qquad (22)\end{aligned}$$

This provides a direct computation for the centroid of T2 FS with linear second membership function.

According to (20), solving $\alpha_l(l) = 0$ and $\alpha_l(l) = 1$ about l respectively. Suppose the solutions are l_0 and l_1, then $\alpha_l(l)$ with $l \in [l_0, l_1]$ will be the left centroid. Similarly, according to (22), solving $\alpha_r(r) = 0$ and $\alpha_l(r) = 1$ about r respectively. Suppose the solutions are r_0 and r_1, then $\alpha_r(r)$ with $r \in [r_1, r_0]$ will be the right centroid. The solution of $\alpha_l(l) = 0$ and $\alpha_l(l) = 1$, $\alpha_r(r) = 0$ and $\alpha_l(r) = 1$ can be obtained by the direct root finding method of Subsection III-A.

In summary, for general T2 FS with linear second membership function, the centroid function can be computed in a very simple way comparing to the α-plane method in Table I, which is given in Table II.

So, the type-1 centroid function of general T2 FS $\tilde{A}$ should be:

$$C_{\tilde{A}}(x) = \begin{cases}\alpha_l(x) & x \in [l_0, l_1] \\ 1 & x \in [l_1, r_1] \\ \alpha_r(x) & x \in [r_1, r_0]\end{cases} \qquad (23)$$

With the centroid defuzzification method of type-1 set, the final defuzzification value can be computed:

$$c(\tilde{A}) = \frac{\int_{l_0}^{l_1} x\alpha_l(x)dx + \int_{l_1}^{r_1} xdx + \int_{r_1}^{r_0} x\alpha_r(x)dx}{\int_{l_0}^{l_1} \alpha_l(x)dx + \int_{l_1}^{r_1} dx + \int_{r_1}^{r_0} \alpha_r(x)dx} \qquad (24)$$

IV. NUMERICAL EXAMPLES

Some numerical examples are provided to illustrate our proposed methods. If the membership functions is expressed with elementary function, the centroid function of T2 FS can even be expressed analytically. Here is an examples.

Example 1: Here is a T2 FS with non symmetrical FOU.

$$\overline{\mu}_{\widetilde{A}_0}(x) = -\frac{4}{9}x^2 + \frac{4}{3}x \qquad (25)$$

$$\underline{\mu}_{\widetilde{A}_0}(x) = -\frac{4}{9}x^2 + \frac{8}{9}x \qquad (26)$$

where $x \in [0, 2]$, which is shown in Figure 1.

The secondary MF of $\widetilde{A}$ is chosen to be a triangular membership function whose base equals $\overline{\mu}_{\widetilde{A}_0}(x) - \underline{\mu}_{\widetilde{A}_0}(x)$ and whose apex is determined by a randomly generated value $w(x) \in [0,1]$ as

$$Apex(x) = \underline{\mu}_{\widetilde{A}_0}(x) + w(x)\left[\overline{\mu}_{\widetilde{A}_0}(x) - \underline{\mu}_{\widetilde{A}_0}(x)\right] \qquad (27)$$

Here, we set $w = \frac{3}{5}$ and the domain is $x \in [0, 2]$.

TABLE II
THE CENTROID COMPUTATION OF GENERAL T2 FS WITH LINEAR SECOND MEMBERSHIP FUNCTION

Step	The computation process
1	Compute the centroid functions $\alpha_l(l)$ and $\alpha_r(r)$ without considering the domain of α-plane level value α with (20) and (22) respectively.
2	Find the corresponding bounds of l and r for $\alpha \in [0,1]$ by solving equations $\alpha_l(l) = 0$ and $\alpha_l(l) = 1$ about l, and $\alpha_r(r) = 0$ and $\alpha_l(r) = 1$ about r respectively. Suppose the solutions are l_0, l_1 and r_0, r_1 respectively.
3	Replacing $\alpha_l(l)$, $\alpha_r(r)$ with $\alpha_l(x)$, $\alpha_r(x)$, then $\alpha_l(x)$ with $x \in [l_0, l_1]$ and $\alpha_r(x)$ with $x \in [r_0, r_1]$ will be the left and right centroid functions of general T2 FS respectively.

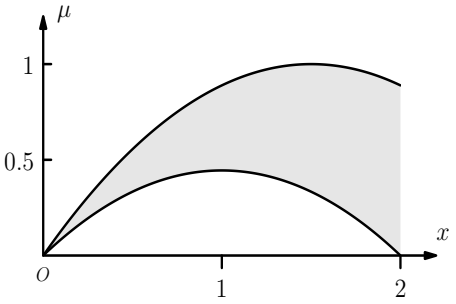

Fig. 1. The FOU of Example 1

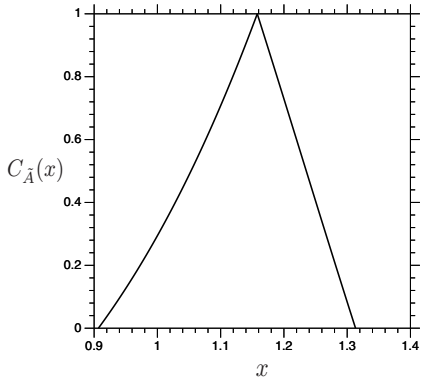

Fig. 2. The centroid function of Example 1

The left centroid function and right centroid function can be computed respectively:

$$\alpha_l(l) = \frac{5(l^3 + 8l - 8)}{5l^3 - 36l + 48} \tag{28}$$

$$\alpha_r(r) = \frac{5(r^3 - 20r + 24)}{5r^3 - 24r + 32)} \tag{29}$$

Find the solutions for $\alpha_l(l) = 0, \alpha_l(l) = 1$ for l and $\alpha_r(r) = 0, \alpha_r(r) = 1$ for r respectively. We can get that $l_0 = 0.907$, $l_1 = 1.158$, $r_1 = 1.158$, $r_0 = 1.313$.

Then the left centroid function of $\widetilde{A}$ is the function α_l in the domain $l \in [l_0, l_1]$. The right centroid function of $\widetilde{A}$ is the function α_r in the domain $r \in [r_1, r_0]$. The centroid of this T2 FS is in triangular shape, which can be expressed as (30) if the variables l and r are replaced with x.

$$\alpha(x) = \begin{cases} \frac{5(x^3+8x-8)}{5x^3-36x+48} & 0.907 \le x \le 1.158 \\ \frac{5(x^3-20x+24)}{5x^3-24x+32} & 1.158 \le x \le 1.313 \end{cases} \tag{30}$$

The results is plotted in Fig 2. It is shown that the centroid function is also in triangular shape. With (24), the final centroid defuzzification value is 1.1327.

Here are two more complicated examples.

Example 2: Piecewise linear LMF and UMF, and triangle secondary MFs [19], which is also similar to the example of [11]:

$$\underline{\mu}_{\widetilde{A}_0}(x) = \max\left\{ \begin{bmatrix} (x-1)/2, & 1 \le x \le 3 \\ (7-x)/4, & 4 \le x \le 7 \\ 0, & \text{otherwise} \end{bmatrix}, \begin{bmatrix} (x-2)/5, & 2 \le x \le 6 \\ (16-2x)/5, & 6 \le x \le 8 \\ 0, & \text{otherwise} \end{bmatrix} \right\} \tag{31}$$

$$\overline{\mu}_{\widetilde{A}_0}(x) = \max\left\{ \begin{bmatrix} (x-1)/6, & 1 \le x \le 4 \\ (7-x)/6, & 4 \le x \le 7 \\ 0, & \text{otherwise} \end{bmatrix}, \begin{bmatrix} (x-3)/6, & 2 \le x \le 5 \\ (8-x)/9, & 5 \le x \le 8 \\ 0, & \text{otherwise} \end{bmatrix} \right\} \tag{32}$$

which is shown in Figure 3. In this example, each secondary MF is chosen to be a triangle of height one whose base equals $\overline{\mu}_{\tilde{A}}(x) - \underline{\mu}_{\tilde{A}}(x)$ and whose apex location Apex(x) is parameterized as

$$Apex(x) = \underline{\mu}(\tilde{A})(x) + w[\overline{\mu}(\tilde{A})(x) - \underline{\mu}(\tilde{A})(x)] \tag{33}$$

where $w = 0, 0.25, 0.5, 0.75, 1$.

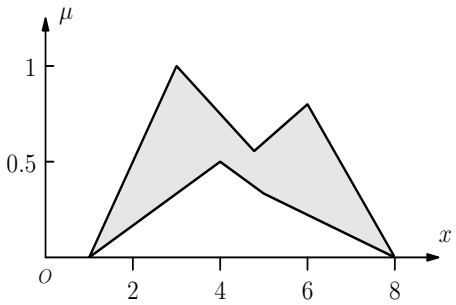

Fig. 3. The FOU of Example 2

Set $w = 0$, let $\alpha_l = 0, 1$ for (20), $\alpha_r = 0, 1$ for (22), then we can get $l_0 = 3.6605$, $l_1 = 4.2667$ and $r_0 = 4.9917, r_1 = 4.2667$, respectively. Then the left centroid function $\alpha_l(l)$ with $l \in [l_0, l_1]$ and right centroid function $\alpha_r(r)$ with $r \in [r_1, r_0]$

can be obtained. Replacing l, r with the same variable x, $\alpha_l(x)$ and $\alpha_r(x)$ can be plotted together.

The other cases for $w = 0.25, 0.5, 0.75, 1$ can also be obtained in a similar way. The two pairs of end points for the left centroid and right centroid functions for the different cases of w are listed in Table III. The left and right centroid functions are plotted in Fig. 4. These are almost the same as the results of [19] which are computed with $N = 10000$, $m = 100$ respectively.

TABLE III
THE CENTROID FUNCTIONS BOUNDS OF EXAMPLE 2

w	$[l_0, l_1]$	$[r_1, r_0]$
0	[3.6605, 4.2667]	[4.2667, 4.9917]
0.25	[3.6605, 4.3008]	[4.3008, 4.9917]
0.5	[3.6605, 4.3208]	[4.3208, 4.9917]
0.75	[3.6605, 4.3340]	[4.3340, 4.9917]
1	[3.6605, 4.3433]	[4.3433, 4.9917]

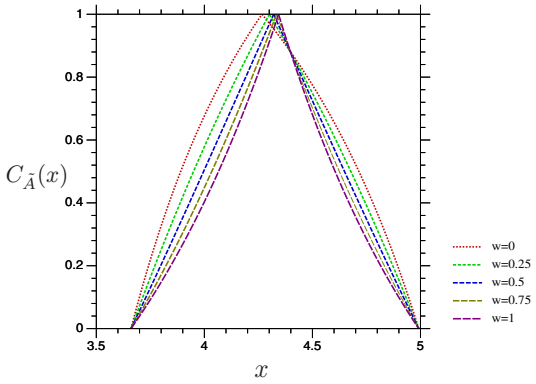

Fig. 4. The centroid functions of Example 2

All the centroid functions are kept in triangular shape with $l_1 = r_1$. With (24), the final centroid defuzzification values of these fuzzy sets are $4.4640, 4.4800, 4.4918, 4.5012, 4.5090$ respectively.

Example 3: Gaussian LMF and UMF, and trapezoidal secondary MFs [19], which is also similar to the example of [11]:

$$\overline{\mu}_{\widetilde{A}_0}(x) = \max\left\{\exp\left[-\frac{(x-3)^2}{8}\right], 0.8\exp\left[-\frac{(x-6)^2}{8}\right]\right\} \quad (34)$$

$$\underline{\mu}_{\widetilde{A}_0}(x) = \max\left\{0.5\exp\left[-\frac{(x-3)^2}{2}\right], 0.4\exp\left[-\frac{(x-6)^2}{2}\right]\right\} \quad (35)$$

which is shown in Figure 5. The secondary MF of $\widetilde{A}$ is chosen to be a trapezoid whose base equals $\overline{\mu}_{\widetilde{A}_0}(x) - \underline{\mu}_{\widetilde{A}_0}(x)$ and whose top is defined by left and right endpoints, which are $\underline{\mu}_{\widetilde{A}_1}(x)$ and $\overline{\mu}_{\widetilde{A}_1}(x)$, and both are parameterized as

$$\underline{\mu}_{\widetilde{A}_1}(x) = \underline{\mu}_{\widetilde{A}_0}(x) + 0.6w\left[\overline{\mu}_{\widetilde{A}_0}(x) - \underline{\mu}_{\widetilde{A}_0}(x)\right] \quad (36)$$

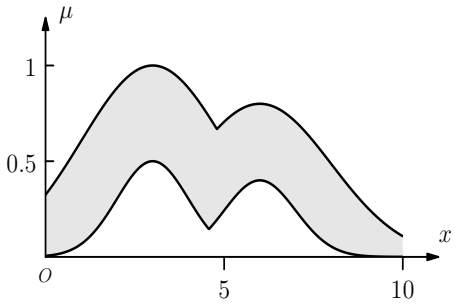

Fig. 5. The FOU of Example 3

$$\overline{\mu}_{\widetilde{A}_1}(x) = \overline{\mu}_{\widetilde{A}_0}(x) - 0.6(1-w)\left[\overline{\mu}_{\widetilde{A}_0}(x) - \underline{\mu}_{\widetilde{A}_0}(x)\right] \quad (37)$$

where $w = 0, 0.25, 0.5, 0.75, 1$, and the domain is $x \in [0, 10]$.

Set $w = 0$, let $\alpha_l = 0, 1$ for (20), $\alpha_r = 0, 1$ for (22), then we can get $l_0 = 3.156$, $l_1 = 3.680$, $r_1 = 5.059$, $r_0 = 5.675$, respectively. Then the left centroid function $\alpha_l(l)$ with $l \in [l_0, l_1]$ and right centroid function $\alpha_r(r)$ with $r \in [r_1, r_0]$ can be obtained. Replacing l, r with the same variable x, $\alpha_l(x)$ and $\alpha_r(x)$ can be plotted together.

The other cases for $w = 0.25, 0.5, 0.75, 1$ can also be obtained in a similar way. The two pairs of end points for the left centroid and right centroid functions for the different cases of w are listed in Table IV. The left and right centroid functions are plotted in Fig. 6. These are almost the same as the results of [19] which are computed with KM algorithms of $N = 10000$, $m = 100$ and Table I respectively.

TABLE IV
THE CENTROID FUNCTIONS BOUNDS OF EXAMPLE 3

w	$[l_0, l_1]$	$[r_1, r_0]$
0	[3.1557, 3.6800]	[5.0589, 5.6747]
0.25	[3.1557, 3.8281]	[4.9454, 5.6747]
0.5	[3.1557, 3.9286]	[4.8686, 5.6747]
0.75	[3.1557, 4.0013]	[4.8131, 5.6747]
1	[3.1557, 4.0565]	[4.7711, 5.6747]

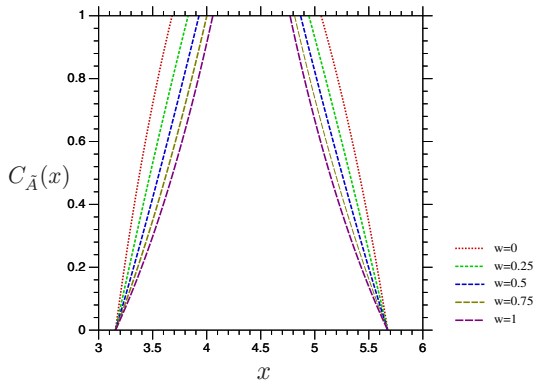

Fig. 6. The centroid functions of Example 3

All the centroid functions are kept in trapezoidal shape. With (24), the final centroid defuzzification values of these fuzzy sets are $4.9080, 4.8721, 4.8565, 4.8490, 4.8454$ respectively.

This general type-2 defuzzification method not only utilizes the rooting finding method in centroid computation of the IT2 FSs, and also avoid in the data sampling in the second membership function, the repetitive iterate computation can be avoided, which can greatly reduce the amount of computation in application. In fact, except the possible root finding iteration at the two end points $\alpha = 0, 1$, there is no iteration in our method at all, which is helpful to loose the computation bottleneck for defuzzification applications, even for realtime implementation requirements.

Another advantage of our method is that, we use the integral operation of the membership function instead of the sum operation of the sampling data, the centroid value is the exact solution of the original problem, which is different from current approximate data sampling methods in essence. We can also use numerical integral method from the same sampling data of current sampling methods where computation error can be greatly reduced, and the error bound can be estimated in advance with the theory in numerical analysis.

Note that, both in the IT2 FS and general T2 FS centroid computation, we do not pay much attention on the lower level implementation of the algorithms. As we have mentioned, this can be done through the proper use of software packages or the programming of computer languages directly. The numerical integration and root finding methods in numerical analysis and the computation cost reduction techniques such as Enhanced KM algorithms [27] can be applied, but this is beyond the main topic of this paper.

V. Conclusion

With the continuous form of the centroid computation of interval type-2 (IT2 FS) fuzzy sets (IT2 FSs), this paper transforms the centroid computation of IT2 Fs into root finding problems. When the FOUs of the IT2 FS are given, the centroid of the IT2 Fs can be computed directly and accurately. Then efficient methods for the centroid computation of general type-2 fuzzy sets with linear membership function are provided. Numerical examples illustrate the proposed approaches.

Acknowledgment

The work is supported by the National Natural Science Foundation of China (NSFC) under project 70771025.

References

[1] O. Castillo and P. Melin, *Type-2 Fuzzy Logic Theory and Applications*. Berlin: Springer-Verlag, 2008.

[2] S. Coupland and R. I. John, "Geometric type-1 and type-2 fuzzy logic systems," *IEEE Transactions on Fuzzy Systems*, vol. 15, no. 1, pp. 3–15, Feb. 2007.

[3] ——, "A fast geometric method for defuzzification of type-2 fuzzy sets," *IEEE Transactions on Fuzzy Systems*, vol. 16, no. 4, pp. 929–941, Aug. 2008.

[4] ——, "New geometric inference techniques for type-2 fuzzy sets," *International Journal of Approximate Reasoning*, vol. 49, no. 1, pp. 198–211, Sep. 2008.

[5] S. Greenfield, F. Chiclana, S. Coupland, and R. John, "The collapsing method of defuzzification for discretised interval type-2 fuzzy sets," *Information Sciences*, vol. 179, no. 13, pp. 2055–2069, Jun. 2009.

[6] H. Hagras, "Type-2 FLCs: A new generation of fuzzy controllers," *IEEE Computational Intelligence Magazine*, vol. 2, no. 1, pp. 30–43, Feb. 2007.

[7] R. I. John and S. Coupland, "Type-2 fuzzy logic: A historical view," *IEEE Computational Intelligence Magazine*, vol. 2, no. 1, pp. 57–62, Feb. 2007.

[8] R. I. John and C. Czarnecki, "An adaptive type-2 fuzzy system for learning linguistic membership grades," in *Proc. IEEE FUZZ Conf*, Seoul, Korea, 1999, pp. 1552–1556.

[9] N. N. Karnik and J. M. Mendel, "Centroid of a type-2 fuzzy set," *Information Sciences*, vol. 132, no. 1-4, pp. 195–220, 2001.

[10] C. S. Lee, M. H. Wang, and H. Hagras, "A type-2 fuzzy ontology and its application to personal diabetic-diet recommendation," *IEEE Transactions on Fuzzy Systems*, vol. 18, no. 2, pp. 374–395, Apr. 2010.

[11] F. Liu, "An efficient centroid type-reduction strategy for general type-2 fuzzy logic system," *Information Sciences*, vol. 178, no. 9, pp. 2224–2236, May 2008.

[12] X. Liu and J. M. Mendel, "Connect Karnik-Mendel algorithms to root-finding for computing the centroid of an interval type-2 fuzzy set," *IEEE Transactions on Fuzzy Systems*, 2011, in press.

[13] L. Lucas, T. Centeno, and M. Delgado, "General type-2 fuzzy inference systems: analysis, design and computational aspects," in *IEEE International Fuzzy Systems Conference, 2007*, 2007, pp. 1107–1012.

[14] J. M. Mendel, *Uncertain Rule-Based Fuzzy Logic Systems: Introduction and New Directions*. Upper Saddle River, NJ: Prentice-Hall, 2001.

[15] ——, "Type-2 fuzzy sets and systems: An overview," *IEEE Computational Intelligence Magazine*, vol. 2, no. 1, pp. 20–29, Feb. 2007.

[16] ——, "On answering the question 'where do I start in order to solve a new problem involving interval type-2 fuzzy sets?'," *Information Sciences*, vol. 179, no. 19, pp. 3418–3431, Sep. 2009.

[17] J. M. Mendel and R. I. John, "Type-2 fuzzy sets made simple," *IEEE Transactions on Fuzzy Systems*, vol. 10, no. 2, pp. 117–127, Apr. 2002.

[18] J. M. Mendel and F. Liu, "Super-exponential convergence of the Karnik-Mendel algorithms for computing the centroid of an interval type-2 fuzzy set," *IEEE Transactions on Fuzzy Systems*, vol. 15, no. 2, pp. 309–320, 2007.

[19] J. M. Mendel, F. Liu, and D. Zhai, "α-plane representation for type-2 fuzzy sets: Theory and applications," *IEEE Transactions on Fuzzy Systems*, vol. 17, no. 5, pp. 1189–1207, Oct. 2009.

[20] J. M. Mendel and D. Wu, *Perceptual Computing: Aiding People in Making Subjective Judgments*. Hoboken, NJ: Wiley-IEEE Press, 2010.

[21] ——, "Perceptual reasoning for perceptual computing," *IEEE Transactions on Fuzzy Systems*, vol. 16, no. 6, pp. 1550–1564, Dec. 2008.

[22] J. M. Mendel and H. Wu, "New results about the centroid of an interval type-2 fuzzy set, including the centroid of a fuzzy granule," *Information Sciences*, vol. 177, no. 2, pp. 360–377, 2007.

[23] A. Niewiadomski, "A type-2 fuzzy approach to linguistic summarization of data," *IEEE Transactions On Fuzzy Systems*, vol. 16, no. 1, pp. 198–212, Feb. 2008.

[24] J. T. Starczewski, "Efficient triangular type-2 fuzzy logic systems," *International Journal of Approximate Reasoning*, vol. 50, no. 5, pp. 799–811, May 2009.

[25] C. Wagner and H. Hagras, "Toward general type-2 fuzzy logic systems based on zslices," *IEEE Transactions on Fuzzy Systems*, vol. 18, no. 4, pp. 637–660, 2010.

[26] D. Wu and J. M. Mendel, "Uncertainty measures for interval type-2 fuzzy sets," *Information Sciences*, vol. 177, no. 23, pp. 5378–5393, 2007.

[27] ——, "Enhanced Karnik-Mendel algorithms," *IEEE Transactions on Fuzzy Systems*, vol. 17, no. 4, pp. 923–934, 2009.

[28] ——, "Perceptual reasoning for perceptual computing: A similarity-based approach," *IEEE Transactions on Fuzzy Systems*, vol. 17, no. 6, pp. 1397–1411, 2009.

[29] H. Wu and J. M. Mendel, "Uncertainty bounds and their use in the design of interval type-2 fuzzy logic systems," *IEEE Transactions on Fuzzy Systems*, vol. 10, no. 5, pp. 622–639, 2002.

[30] D. Y. Zhai and J. M. Mendel, "Uncertainty measures for general type-2 fuzzy sets," *Information Sciences*, vol. 181, no. 3, pp. 503–518, Feb. 2011.

[31] ——, "Computing the centroid of a general type-2 fuzzy set by means of the centroid-flow algorithm," *IEEE Transactions on Fuzzy Systems*, 2011, in press.

2011 IEEE International Conference on Fuzzy Systems
June 27-30, 2011, Taipei, Taiwan

Type-2 Fuzzy Airplane Altitude Control:

A Comparative Study

Sheir Afgen Zaheer and Jong-Hwan Kim
RIT Lab, Dept. of Electrical Engineering
KAIST
Daejeon, Republic of Korea
{sheir, johkim}@rit.kaist.ac.kr

Abstract— **The standard fuzzy logic controllers, also known as type-1 fuzzy logic controllers, have often been criticized for their inability to handle uncertainties in the control processes. Therefore, a lot of attention is being focused on type-2 fuzzy logic controllers, especially, the interval type-2 fuzzy logic controllers. This paper aims at developing both type-1 and type-2 fuzzy logic controllers for an airplane altitude control problem and comparing their performances. Both the controllers have similar knowledge bases, and both of them are tested in two simulation setups, an ideally modeled setup and a setup with uncertainties. The results show that the type-2 fuzzy logic controller outperforms the type-1 fuzzy logic controller, especially, in the environment with uncertainties. Therefore, this research seems to validate the superiority of type-2 fuzzy logic control in making the controllers independent of uncertainties in intricate model details.**

Keywords — **Type-2 fuzzy logic control, altitude control, fuzzy airplane control.**

I. INTRODUCTION

The popularity of type-2 fuzzy systems has risen enormously during the past few years. Though the theoretical concepts of type-2 fuzzy sets date back to 1975 [1], the limitation of computational resources limited their practical applications. However, with the massive improvements in computational capabilities in the recent years, type-2 fuzzy systems are being widely used in various control and decision making problems.

Moreover, the type-2 fuzzy systems also answer the skepticism regarding the fuzziness of type-1 fuzzy systems. Type-1 fuzzy sets have a crisp membership value which means that each element in a set has a predefined fixed value; this violates the notion of fuzziness regarding uncertainties. A two-layered architecture to improve nonlinearity handling in type-1 fuzzy controller for the systems with dead-zones has been proposed [2]. However, the causes of nonlinearities and uncertainties in real systems are not always known. Such problems associated with uncertainties in systems or the fuzzy rules are solved in type-2 fuzzy systems by assigning a secondary membership function, to each element in the fuzzy set, rather than a crisp membership value [1], [3]. This type of type-2 fuzzy systems, known as the general type-2 fuzzy sets, are computationally very complex. Therefore, interval type-2 fuzzy systems (IT2FS) have been developed to provide a satisfactory compromise between the uncertainty handling of type-2 systems and the computational complexity [3], [4]. The IT2FS assigns a range of membership values to each element in such a way that every value in the specified range has a full secondary membership grade. Fig. 1 gives a graphical depiction of a typical triangular interval type-2 fuzzy set. The shaded region that defines the range of membership values for a particular element is called the foot of uncertainty (FoU) [3].

Type-2 fuzzy systems have been used in many research problems. Type-2 fuzzy logic has been widely used in mobile robot control and navigation applications [5]-[10]. A simplified real time controller for a coupled-tank liquid-level control has also been developed [11]. Moreover, type-2 fuzzy logic has also been used in medical diagnosis [12], [13]; human machine interaction [14]; traffic control systems [15], etc. Apart from the above mentioned contributions, type-2 fuzzy systems have also been used in management surveys [16] and human resource management [17]. However, there has been a very little research about the performance comparison of the type-1 and type-2 fuzzy systems developed through similar rules and membership functions, and subjected to identical testing conditions.

This paper compares the performances of the type-1 fuzzy and the interval type 2 fuzzy logic (IT2FLC) control systems for a multi-input multi-output (MIMO) airplane altitude control simulation. Type-1 fuzzy control systems have been widely used in the airplane altitude control problem. Different kinds of fuzzy altitude and/or flight controllers have been developed. Complete type-1 fuzzy flight control system has been developed [18]. Another research was aimed at developing decoupled PID controllers for speed and heading control, and a type-1 fuzzy altitude controller [19]. However, none of the

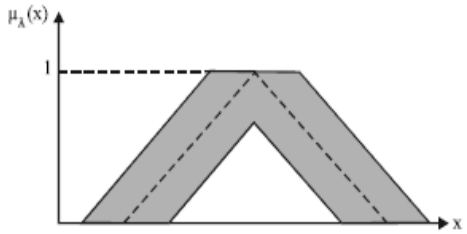

Fig. 1. Interval type-2 triangular fuzzy set.

This research was supported by Basic Science Research Program through the National Research Foundation of Korea (NRF) funded by the Ministry of Education, Science and Technology (2010-0000831)

previous researches at flight control systems have employed type-2 fuzzy control systems.

The proposed system aims at developing a fuzzy flight control system (FFCS) with two decoupled controllers: a fuzzy heading controller (FHC) and a fuzzy altitude controller (FAC). FHC is designed as a type-1 fuzzy control system and its major functions are to control airplane's heading and lateral stability. FAC, on the other hand, is developed, first by employing a type-1 fuzzy altitude controller (T1FAC) and then by an interval type-2 fuzzy altitude controller (IT2FAC). Two sets of simulations are conducted: one with ideally modeled system and the other with a system with uncertainties. These simulations put both the T1FAC and the IT2FAC under test for each of the simulation scenarios. The resulting responses are then compared.

The paper is organized as follows: Section II describes the airplane model. Section III gives an overview of the overall control scheme and the FHC, and section IV explains the two altitude controllers, T1FAC and IT2FAC. Section V describes the results of T1FAC and IT2FAC. Finally the discussions and conclusion follow in section VI.

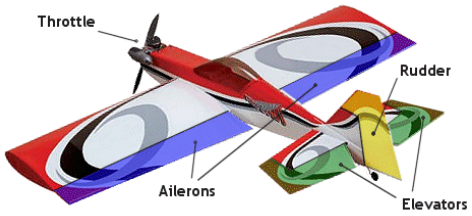

Fig. 2. Basic airplane controls.

II. The Airplane Model

In order to assess the performances of the developed controllers, an airplane model is required. A propulsion based RC airplane is modeled. The control surfaces for a typical RC airplane are shown in Fig. 2. The throttle is used to regulate the speed of the airplane by varying the rotational speed of the propeller, the elevator is used to control the airplane's ascent and descent, the ailerons are used for airplane's lateral stabilization and mid air turning, and the rudder is used for the on-ground taxiing of the airplane. The specific RC model used as a control problem in this research is the Kadet MK-II RC airplane model. The aerodynamic parameters for MK-II RC airplane used are the same as in the previous research [19].

Aerosim Blockset in Simulink environment is a simulation tool for modeling and control of airplanes [20]. The Aereosim Blockset is configured for the Kadet MK-II RC airplane by using the aerodynamic configuration file consisting of aerodynamic coefficients and parameters for the Kadet MK-II RC airplane [19]. A snapshot of the Simulink control model is shown in Fig. 3. As evident from Fig. 3, any airplane can be modeled by plugging in the corresponding airplane parameters to each block.

III. The Fuzzy Flight Control System

The fuzzy flight control system (FFCS) consists of two decoupled controllers: A fuzzy heading controller (FHC) and a fuzzy altitude controller (FAC). The goal of FFCS, schematically shown in Fig. 4, is to autonomously track the desired altitude and the heading, and then maintain the desired

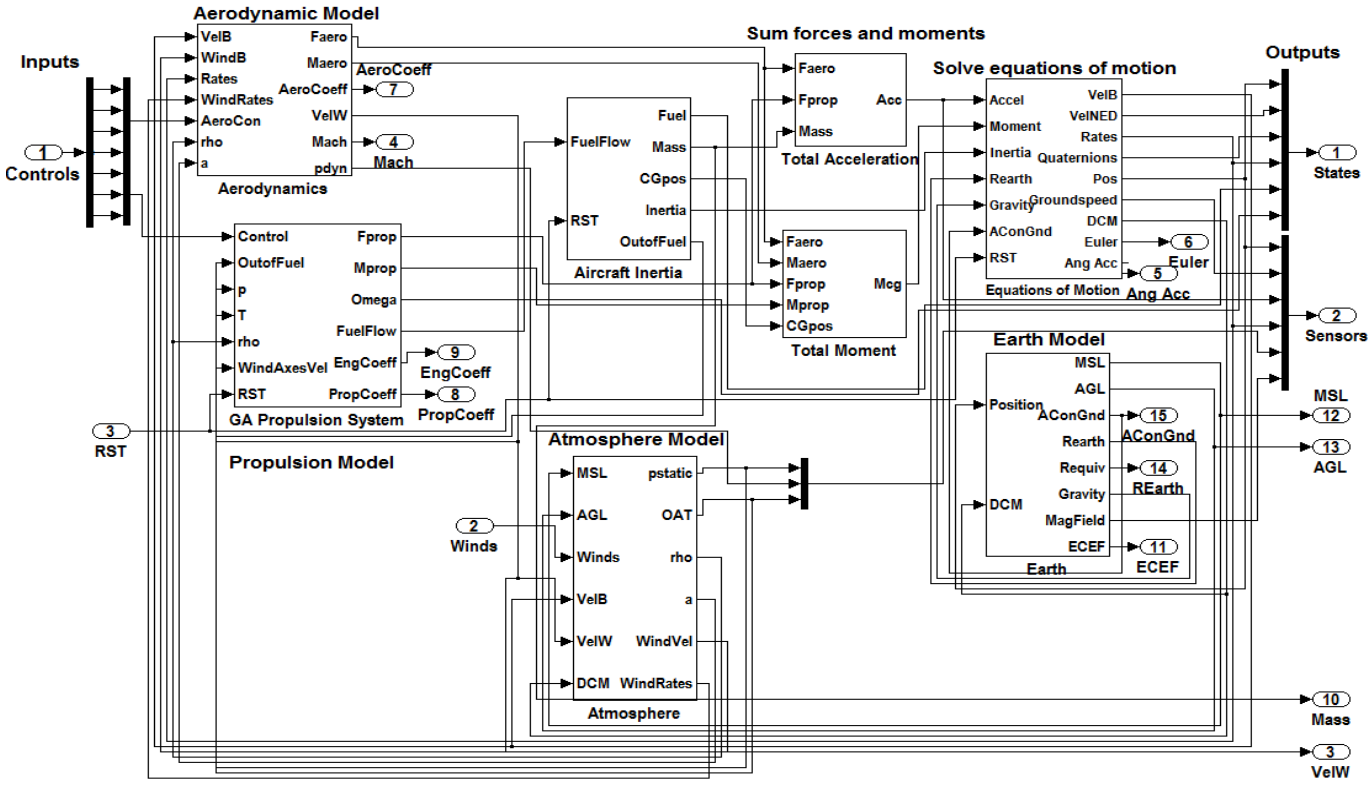

Fig. 3. The block diagram of Simulink based airplane model.

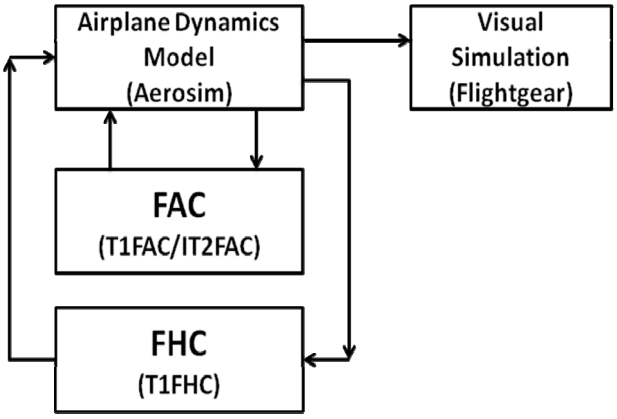

Fig. 4. Overall FFCS architecture.

values once they are achieved. The desired altitude and heading are calculated using the three desired position co-ordinates specified by the user. The overall system is also linked with Flightgear for the visual simulation of the airplane behavior.

A. *The Fuzzy Heading Controller*

Though this research is aimed at the performance comparison of type-1and type-2 fuzzy systems in altitude control, designing a heading controller is imperative because of the following two reasons:

- The heading controller is in charge of the ailerons, thus providing the in-flight lateral stability essential for the airplane to track the desired altitude.
- The airplane, while ascending, descending or maintaining altitude, also experiences some horizontal displacement; the heading controller ensures that the horizontal displacement is in the required direction.

The heading controller employed in this research is a FHC. The FHC is a type-1 fuzzy controller; the schematics along with the membership functions are shown in Fig. 5. The bank angle calculated by FHC is then transformed to the control surface level command to the ailerons by using the following proportional compensator:

$$Aeleron = (0.55\pi/180) * BankAngle. \quad (1)$$

IV. The Fuzzy Altitude Controllers

The FACs have been widely implemented by researchers for controlling the altitude of both manned and unmanned aerial vehicles. The altitude controller is a multi-input and multi-output (MIMO) system, generally developed by considering altitude error, change in altitude error and airspeed as the controller's inputs while elevator/angle of attack and throttle level are the controller's output. The throttle is linked with the FAC because throttle regulates the amount of thrust required by an ascending or descending airplane.

The similar control schematics are considered in this paper. The rule base for the controller is developed using the expert knowledge based on literature review and personal experiences with RC airplane control [19]. The fuzzy set representation and the membership functions for the inputs

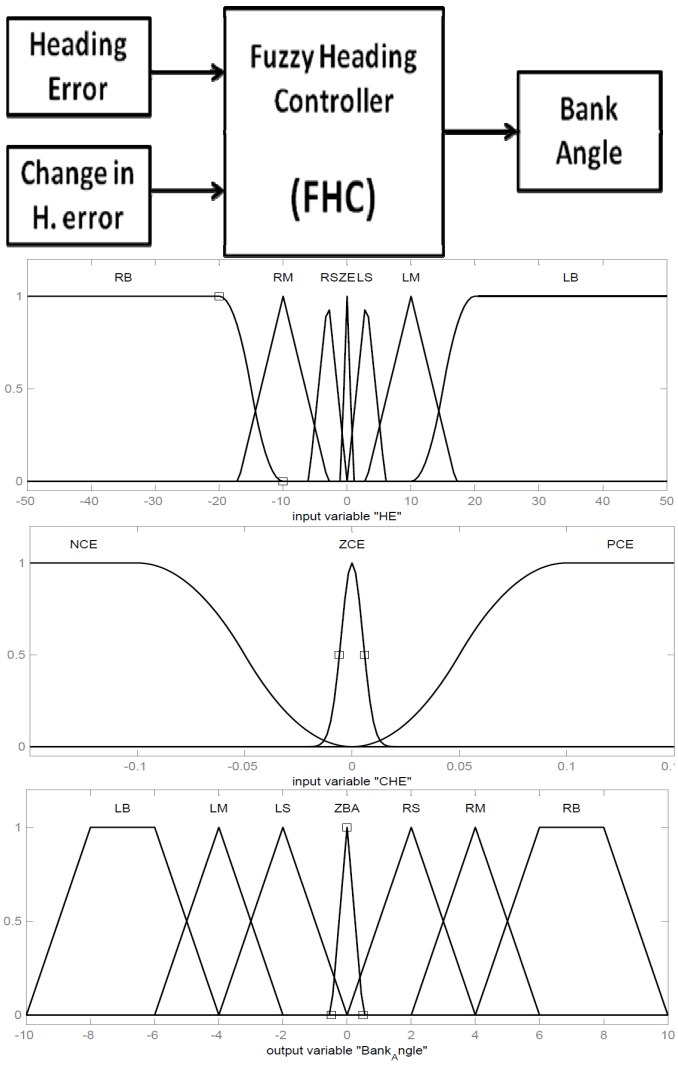

Fig. 5. (Top to Bottom) The schematics of FHC, and the membership functions of inputs and output respectively.

and outputs for the T1FAC and the IT2FAC are discussed in the following subsections.

A. *The Type-1 Fuzzy Altitude Controller*

The first controller developed for altitude control is T1FAC. T1FAC was developed as a Mamdani type-1 fuzzy logic controller. This 3-input 2-output controller was tuned via simulations. Fig. 6 shows the architecture of the T1FAC along with the membership functions for inputs and outputs, respectively. The t-Norm and s-Norm operators used are "min" and "max", respectively, with "min" implication and "max" aggregation. The centroid method is employed for defuzzification.

B. *The Interval Type-2 Fuzzy Altiude Control*

The layout of the IT2FAC and the membership functions for inputs and outputs, respectively are shown in Fig. 7. The interval type-2 fuzzy sets are defined using a principal membership function (similar to T1FAC) with a certain footprint of uncertainty (FoU). The principal membership

function and FoU are transformed into the left and right membership functions (LMF and RMF) according to the following membership definitions for triangular membership functions:

LMF = triangular MF [*A-FoU*N, B-FoU*N, C-FoU*N*]

RMF = triangular MF [*A+FoU*N, B+FoU*N, C+FoU*N*] (2)

where *A*, *B*, and *C* are the three index parameters for the primary triangular member ship functions. *N* is the normalization factor given as:

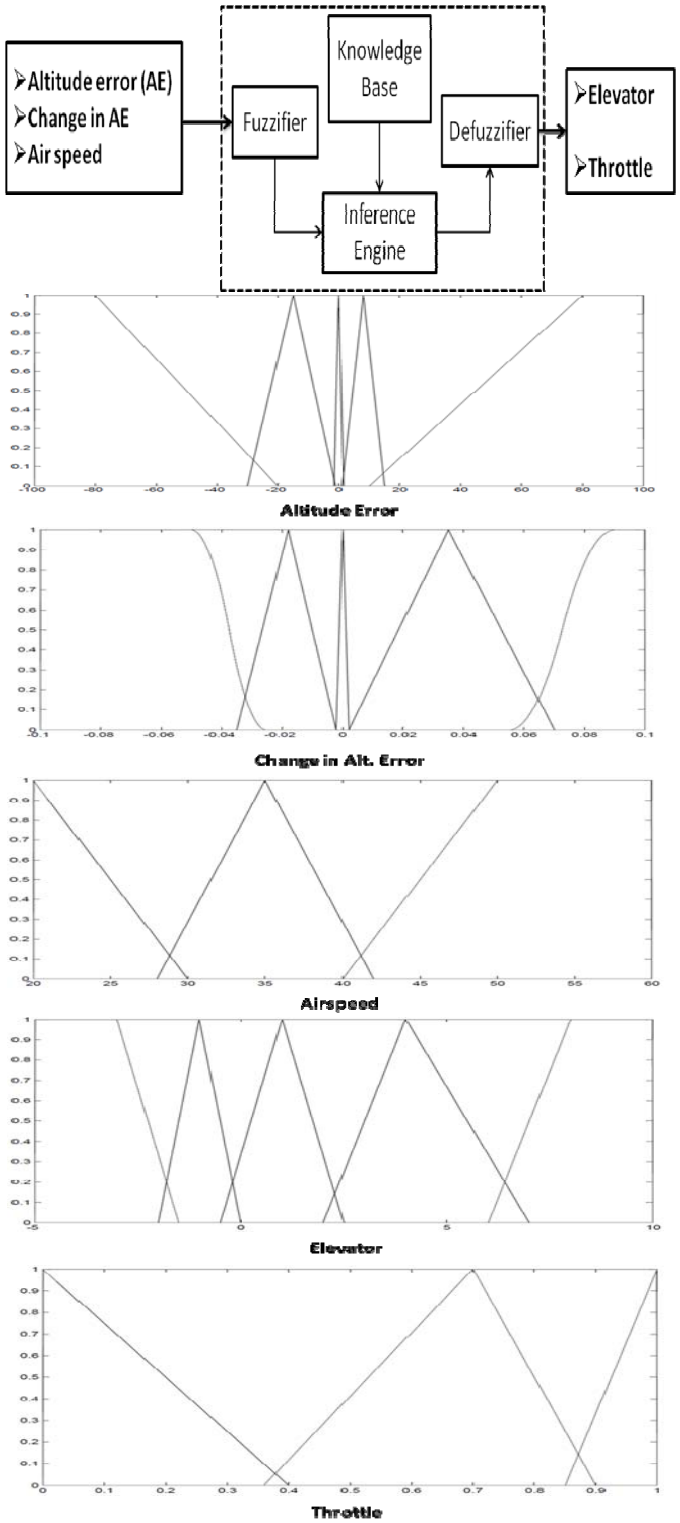

Fig. 6. (Top to Bottom) The schematics of T1FAC, and the membership functions of inputs and outputs respectively.

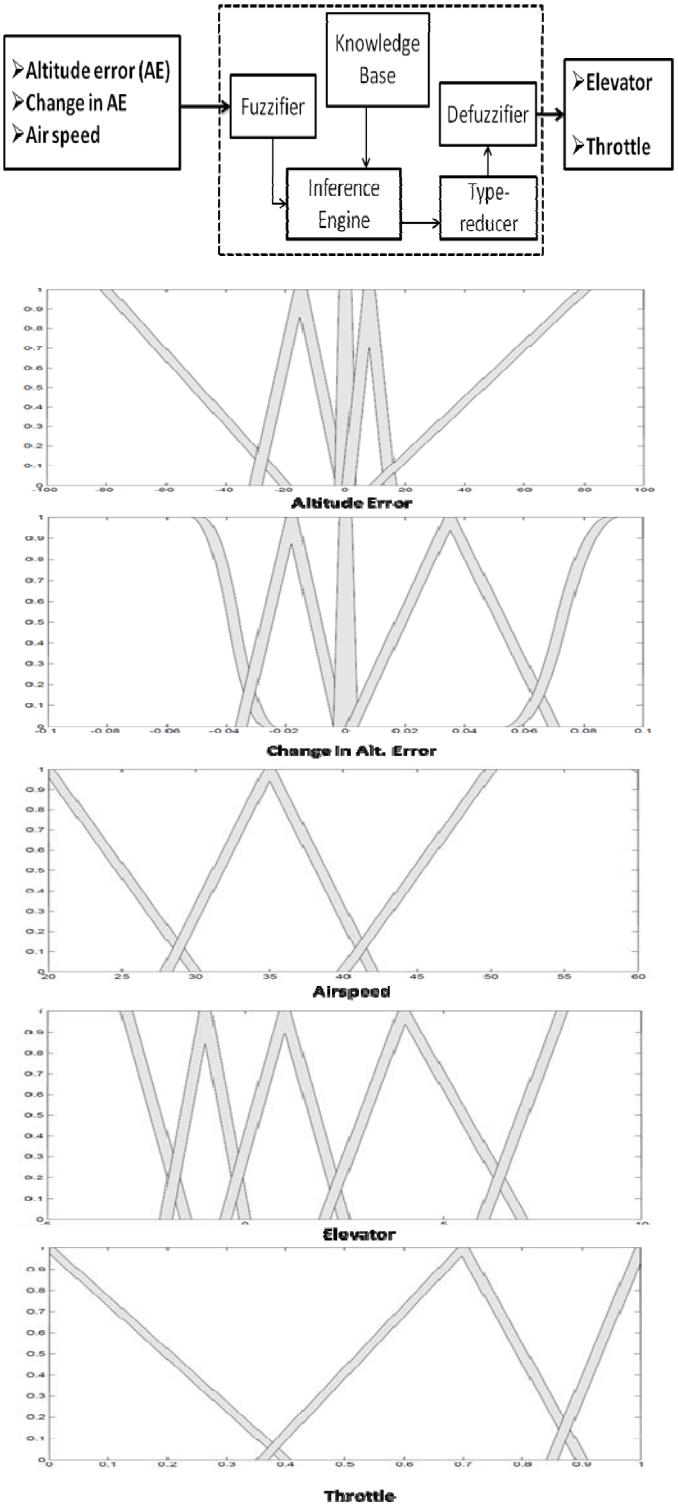

Fig. 7. (Top to Bottom) The schematics of IT2FAC, and the membership functions of inputs and outputs respectively.

$$N = (UoD_{max} - UoD_{min})/200 \quad (3)$$

where UoD_{max} and UoD_{min} are the maximum and minimum values, respectively, of the universe of discourse (UoD). Whereas, for Gaussian membership functions, the FoU defined is used to convert the membership functions to a pair of LMFs and RMFs with same variance but variable means. The conversion is defined by the following equations:

$$LMF = gauss\ MF\ [\sigma, \mu - FoU*N]$$
$$RMF = gauss\ MF\ [\sigma, \mu + FoU*N] \quad (4)$$

where σ and μ are the variance and the mean of the primary membership functions, respectively. The fuzzy operations used are similar to those used in T1FAC but with an addition of "KM type reduction" [3], [21].

V. Simulations and Results

Two types of simulations were conducted to gauge the performances of both the controllers. The first simulation setup was conducted under an ideal environment with no noises and uncertainties. However, the second setup had a level of random noise associated with both the actuator model and the sensory model. The introduction of this noise made the airplane model uncertain, i.e., the system no longer was exactly the same for which the altitude controller was designed. The performances in both the simulation setups were evaluated by their success in tracking the reference altitudes. In the particular scenario discussed here, the airplane, initially at an altitude of 500m, was required to ascend to a height of 700m. Once a steady state was achieved the airplane was then required to descend to an altitude of 300m. Additionally, simulations to observe the response of the developed IT2FAC under the ramp reference input were also conducted. The setup for this simulation scenario is explained in section V-D The simulation setup was also linked with a visual simulator to observe the airplane response in a 3D simulated environment. Flightgear was used as a visual simulator. Flightgear is an open-source flight simulator development project licensed under the GNU General Public Liscence. A snapshot of the visual simulation is shown in Fig. 8.

Fig. 8. A snapshot of the visual simulation in Flightgear.

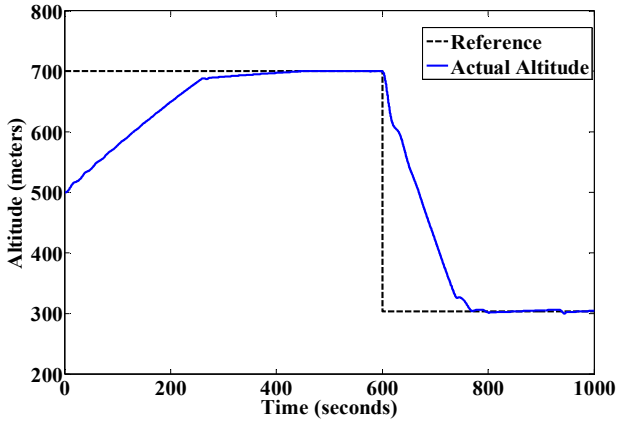

Fig. 9(a). Results of T1FAC in the ideal simulation setup.

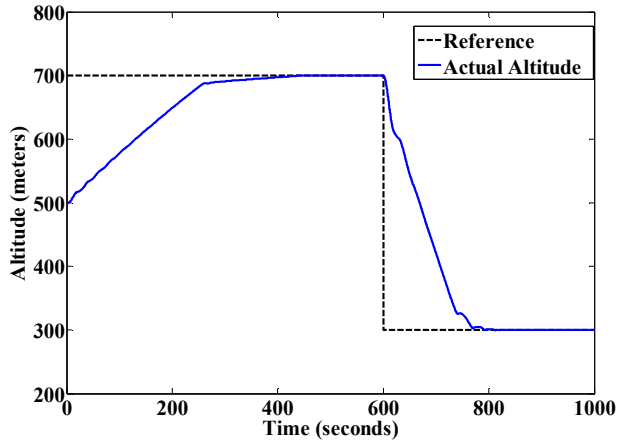

Fig. 9(b). Results of IT2FAC in the ideal simulation setup.

A. The Ideal Simulation Environment

The simulation results are shown in Fig. 9 (9(a) for T1FAC and 9(b) for IT2FAC). As evident from the figure, both the controllers were able to perform the job at the hand. However, when analyzed in detail, the steady state response under T1FAC had a slight measure of unwanted oscillations. Moreover, the mean steady state error over a number of simulations, in case of T1FAC, was up to 0.17 meter; while in case of IT2FAC, the steady state error was under 0.03 meter.

B. The Uncertain Simulation Environment

In this setup, a level of uncertainty was introduced in the plant model. This uncertainty was introduced to slightly perturb the airplane model and to propagate uncertainty to the actuator and sensor modules. This arrangement provided a system whose behavior differed from the actual model for which the controller was designed and tuned. Moreover, it also provided with the opportunity to validate the often advocated hypothesis about the superiority of the interval type-2 fuzzy logic controllers, as compared to the type-1 fuzzy logic controllers, in handling uncertainties. The results of these simulations are summarized graphically in Fig. 10 (10(a) for T1FAC and 10(b) for IT2FAC). It can be seen that the steady state response generated by T1FAC is not satisfactory.

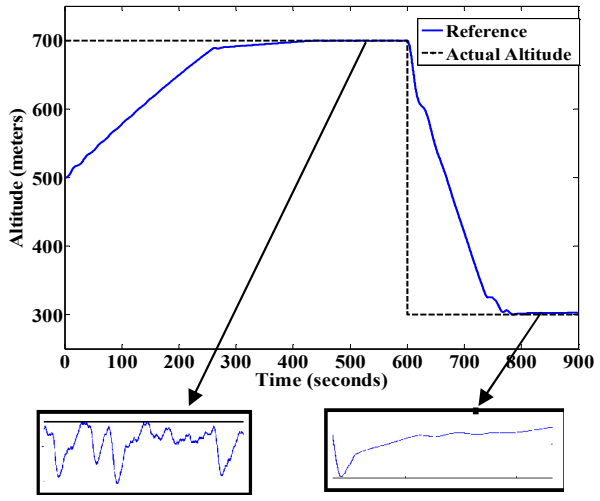

Fig. 10(a). Results of T1FAC in the simulation setup with uncertainties (Bottom blocks are the magnified steady state responses, (RMSE = 3.58 m)).

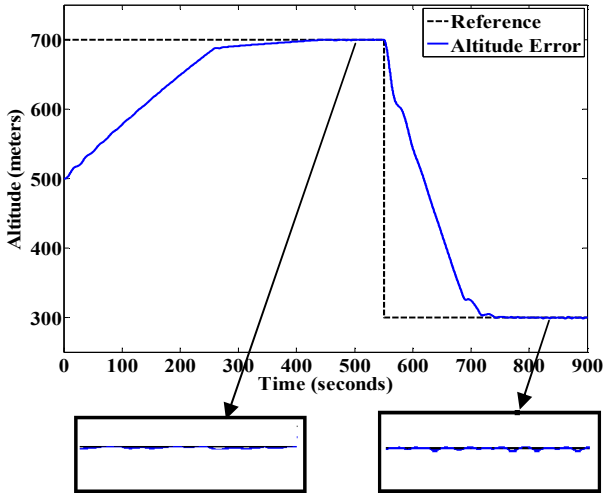

Fig. 10(b). Results of IT2FAC in the simulation setup with uncertainties (Bottom blocks are the magnified steady state responses (RMSE = 0.43 m)).

C. *Effects of Different Values for Footprint of Uncertainties*

The IT2FAC had an additional parameter that required tuning; this parameter was the footprint of uncertainty (FoU), given in (2). An appropriate value for FoU was thus needed. The optimization of FoU is out of the scope of this paper. However, the effects of different values of FoU, in the neighborhood of the FoU*s* in the previous simulations, on the steady state performance were studied. The study state performances, for different FoU values, in terms of steady state root mean squared errors (RMSE) are summarized in Fig. 11. In each of the cases in Fig. 11, the FoU was assumed to be the same for all the fuzzy membership functions. It is evident from these simulation results that a balanced level of FoU value is essential for the desired performance of the system. Therefore, the value of the FoU should not be too large to

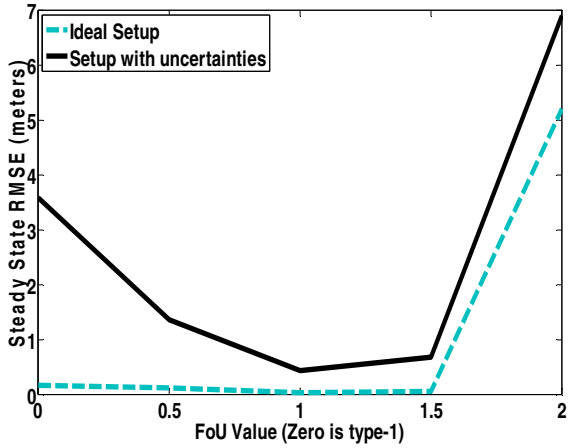

Fig. 11. Steady state RMSE as the result of simulations with different values of FoUs

vanquish the minimum level of preciseness required for the distinctive identifications of the fuzzy sets.

D. *Ramp response of the IT2FAC*

All the results and analysis in the previous subsections were based on the step response of the developed IT2FAC. This subsection deals with the response of the IT2FAC when subjected to a reference input with a ramp (sloped) profile. The results of the simulation, with ramp as a reference input, are shown in Fig. 12. In this setup, the airplane was made to track the reference altitude trajectory that linearly ascended to an altitude of 600 meters, then stayed there for a while, and finally, descended linearly to the altitude of 475 meters. As evident from the figure, a successful tracking response was observed.

VI. Discussions and Conclusion

The purpose of this paper was to compare the performances of the T1FAC and the IT2FAC in an airplane altitude control problem. In the ideal simulation environment, both the controllers were able to track the desired altitude. However in the second simulation environment that had some modeling uncertainties, IT2FAC was the clear winner because

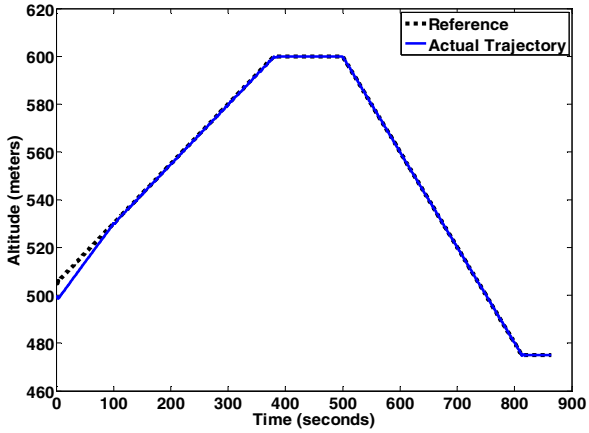

Fig. 12. Tracking response of IT2FAC to a ramp input

the system with T1FAC showed oscillatory behavior around the reference altitude set-points.

This success of IT2FAC can be attributed to its non-crisp membership functions. These non-crisp membership values make IT2FAC more robust than its simpler counterpart with crisp membership values, i.e., T1FAC. The control problem in this study, however, emphasized only on stability and steady state response. Therefore, the control problems and studies emphasizing transient response characteristics like rise time, settling time, etc., might limit the extent to which these results can be generalized. However, considering the current problem, it can be safely deduced that interval type-2 fuzzy logic controller outperforms type-1 fuzzy controller, especially, in handling uncertainties. This finding also seems to be consistent with most of the research done on type-2 fuzzy logic controllers.

The IT2FAC can be further improved by optimizing the controller for desired transient and steady state responses, such as rise time and settling time, etc. Moreover, the FHC can also be upgraded to type-2 fuzzy control for a complete type-2 fuzzy flight control system.

REFERENCES

[1] L. A. Zadeh, "The Concept of a Linguistic Variable and Its Application to Approximate Reasoning–1," *Information Sciences*, vol. 8, pp. 199-249, 1975.

[2] J.-H. Kim, J.-H. Park, S.-W. Lee and Edwin K.P.Chong, "A Two-Layered Fuzzy Logic Controller for Systems with Deadzones," IEEE Trans. on Industrial Electronics, vol. 41, no. 2, pp. 155-162, Apr. 1994.

[3] J. M. Mendel, Uncertain Rule-Based Fuzzy Logic Systems: Introduction and New Directions, Prentice-Hall, Upper-Saddle River, NJ, 2001.

[4] J. M. Mendel, R. I. John and F. Liu, "Interval type-2 fuzzy logic systems made simple," *IEEE Trans. on Fuzzy Systems*, vol. 14, pp. 808-821, December 2006.

[5] N. Baklouti and A. M. Alimi, "Motion Planning in Dynamic and Unknown Environment Using an Interval Type-2 TSK Fuzzy Logic Controller," *Proc. IEEE FUZZ Conference*, pp. 1848-1853, London, UK, July 2007

[6] J. Figueroa, J. Posada, J. Soriano, M. Melgarejo and S. Rojas, "A Type-2 Fuzzy Controller for Tracking Mobile Objects in the Context of Robotic Soccer Games," *Proc. IEEE FUZZ Conference*, pp. 359-364, Reno, NV, May 2005.

[7] H. Hagras, "A Type-2 Fuzzy Logic Controller For Autonomous Mobile Robots," *Proc. IEEE FUZZ Conference*, Budapest, Hungary, July 2004.

[8] H. Astudillo, O. Castillo, L. T. Aguilar and R. Martinez, "Hybrid control for an autonomous wheeled mobile robot under perturbed torques," in Foundations of Fuzzy Logic and Soft Computing (P. Melin et al, Eds.), *Proc. of IFSA 2007*, Cancun, Mexico, June 2007, Springer-Verlag, Berlin, Heidelberg, pp. 594-603.

[9] Yuan-Shiu Chen and L. Yao, "Robust Type-2 Fuzzy Control of an Automatic Guided Vehicle for Wall-Following," *Soft Computing and Pattern Recognition, 2009. SOCPAR '09. International Conference of* , vol., no., pp.172-177, 4-7 Dec. 2009.

[10] R. Martínez, O. Castillo and L. T. Aguilar, "Optimization with Genetic Algorithms of Interval Type-2 Fuzzy Logic Controllers for an Autonomous Wheeled Mobile Robot Using Genetic Algorithms," *Studies in Computational Intelligence*, 2008, Volume 154/2008, pp. 3-18

[11] Dongrui Wu Woei Wan Tan, "A simplified type-2 fuzzy logic controller for real-time control," *ISA Transactions*, Volume 45, Issue 4, October 2006, pp. 503-516, ISSN 0019-0578.

[12] P.R. Innocent and R. I. John, "Type-2 Fuzzy Medical Diagnosis." *Proc. IEEE FUZZ Conference*, pp. 1326-1331, 2002

[13] L. Di Lascio, A. Gisolfi and A. Nappi, "Medical Differential Diagnosis Through Type-2 Fuzzy Sets," *Proc. IEEE FUZZ Conference*, pp. 371-376, Reno, NV, May 2005.

[14] P. Herman, G. Prasad and T.M. McGinnity, "Designing a robust type-2 fuzzy logic classifier for non-stationary systems with application in brain-computer interfacing," *Systems, Man and Cybernetics, 2008. SMC 2008. IEEE International Conference on* , vol., no., pp.1343-1349, 12-15 Oct. 2008

[15] P.G. Balaji and D. Srinivasan, "Type-2 fuzzy logic based urban traffic management," *Engineering Applications of Artificial Intelligence*, Volume 24, Issue 1, February 2011, pp. 12-22, ISSN 0952-1976.

[16] S. Auephanwiriyakul, A. Adrian and J. M. Keller, "Type-2 Fuzzy Set Analysis in Management Surveys," *Proc. IEEE FUZZ Conference*, Honolulu, HI, May 2002, pp. 1321-1325.

[17] F. Doctor, H. Hagras, D. Roberts and V. Callaghan, "A Type-2 Fuzzy Based System for Handling the Uncertainties in Group Decisions for Ranking Job Applicants within Human Resources Systems," *Proc. IEEE FUZZ Conference*, Hong Kong, China, June 2008.

[18] L. Doitsidis, K.P. Valavanis, N.C. Tsourveloudis and M. Kontitsis, "A framework for fuzzy logic based UAV navigation and control," *Robotics and Automation, 2004. Proceedings. ICRA '04. 2004 IEEE International Conference on* , vol.4, no., pp. 4041- 4046 Vol.4, April 26-May 1, 2004.

[19] A. Awan, S. A. Zaheer, N. Ahsan, A. Mushtaq, M. Qasim, U. Mushtaq, A. Ijaz, J. Iqbal and K. Munawwar, "Autonomous control for a Kadet MKII RC airplane,"*Emerging Technologies, 2008. ICET 2008. 4th International Conference on* , vol., no., pp.50-55, 18-19 Oct. 2008.

[20] Aerosim, Aeronautical Simulation Blockset v1.2, Users Guide.

[21] N. N. Karnik and J. M. Mendel, "Centroid of a type-2 fuzzy set," *Information Sciences*, vol. 132, pp. 195-220, 2001.

2011 IEEE International Conference on Fuzzy Systems
June 27-30, 2011, Taipei, Taiwan

Solving Zadeh's Magnus Challenge Problem on Linguistic Probabilities via Linguistic Weighted Averages

Mohammad Reza Rajati
Department of Electrical Engineering
University of Southern California
Los Angeles, California 90089-2560
Email: rajati@usc.edu

Jerry M. Mendel
Department of Electrical Engineering
University of Southern California
Los Angeles, California 90089-2560
Email: mendel@sipi.usc.edu

Dongrui Wu
Industrial Artificial Intelligence Lab
GE Global Research
1 Research Circle, Niskayuna, NY 12309
Email: wud@ge.com

***Abstract*—In this paper, we present a solution to Zadeh's Magnus challenge problem on linguistic probabilities. First, we implement Zadeh's solution to this problem. Then, we use the intersection-product syllogism and a syllogism based on the entailment principle to interpret the problem so that it can be solved via Linguistic Weighted Averages. We show that the problem can be solved by calculation of pessimistic (lower) and optimistic (upper) probabilities via Linguistic Weighted Averages. Then, we choose vocabularies for quantifiers and linguistic probabilities that are involved in the problem statement. The vocabularies are modeled using interval type-2 fuzzy sets. We calculate optimistic (upper) and pessimistic (lower) probabilities, which naturally would be interval type-2 fuzzy sets. Finally, we map the pessimistic and optimistic probabilities to linguistic probabilities present in the vocabularies, so that the results can be comprehended by a human.**

***Index Terms*—Computing with words, interval type-2 fuzzy sets, linguistic weighted average, lower and upper probabilities**

I. Introduction

Computing with words (CWW) is believed to play a pivotal role in the mainstream of research on automation of everyday reasoning and decision-making [8], [10], [15], [32]. Everyday reasoning exploits information stated in natural language; therefore, pertinent techniques are needed to describe and interpret information stated in natural language propositions, combine information coming from multiple sources with different degrees of reliability, and make decisions based on such information.

In essence, CWW can be viewed as a computational theory of perceptions [29]. Human perceptions are about physical and mental objects like length, color, speed, time, direction, strength, likelihood, truth, intent, etc. The key challenge for building a computational theory of perceptions is that perceptions of such objects are imprecise, due to the limited accuracy of human's sensorimotor system. As a result, one of the central concepts of CWW is "precisiation of meaning," which calls for building a computational model pertinent to the semantics of a statement in a natural language. This is mainly performed by assigning fuzzy sets to linguistic attributes, be they possibilistic, probabilistic, or veristic [27]. It is also believed that for CWW, a viable method of completing this task is collecting data about a linguistic constraint from subjects, and building type-2 fuzzy sets based on the empirical data [11].

Recently, Zadeh proposed that two levels of CWW could be distinguished [13]: In *basic* (level 1) CWW, information carriers are numbers, intervals, and words. Propositions are usually simple "assignment" ones like: X *is between 3 and 4* ($X \in [3,4]$), X *is very small*, or *If* X *is high, then* Y *is low*. In *advanced* (level-2) CWW, information carriers can also be more complicated natural language propositions involving modifiers, truth values, possibilistic constraints, linguistic probabilities, usuality constraints, etc.

Essentially, in level-2 CWW, assignment of constraints in such statements can be implicit, e.g., using a modifier "Some" in the statement "Some PhD students at the University of Southern California are Iranian" implies assigning a linguistic value (Some) to the portion of USC's PhD students who are Iranian.

Zadeh asserts that in level-2 CWW, propositions (and not just words) are precisiated, i.e. the *whole statement* is reduced down to the assignment of generalized constraints to some variables; therefore, level-2 CWW must exploit techniques for capturing the semantics of a proposition in a natural language in terms of the semantics of its building blocks.

It is worth noting that the existing approaches to rule-based fuzzy systems mainly deal with level-1 CWW, since they employ the calculi of fuzzy if-then rules.

As stressed in [12], a scientifically correct first order model for a word is a type-2 fuzzy set. Zadeh also predicts that type-2 fuzzy sets will play a central role in level-2 CWW [13]; thus, it can be envisioned that type-2 fuzzy sets will be used as the rudiments of advanced CWW in the forthcoming years. In essence, we view CWW as the interactions between a group of people and at least another person (or computer). Henceforth,

978-1-4244-7316-8/11/$26.00 ©2011 IEEE

the group's perception of a word needs to affect the uncertainty about the word in the word's fuzzy set model. This can be viewed as the main motivation for using type-2 fuzzy sets in CWW. Moreover, as will be seen in the sequel, type-2 fuzzy sets provide a natural framework to provide uncertain numeric values like "about 20% " as solutions to CWW problems, and the term "about" captures the inter-person and intra-person uncertainties propagated via information aggregation methods.

One of the most important problems in CWW is aggregation of linguistic information for hierarchical multi-criteria decision making. Linguistic Weighted Averages are believed to provide an appropriate framework for performing this task [19], [20], especially when we deal with words precisiated with type-2 fuzzy sets.

A set of challenge problems for testing CWW methodologies has been proposed in [25], [28], [30], [33]. Perhaps the most famous challenge problem in this set is the so-called "tall Swedes" problem: *Most Swedes are tall. What is the average height of Swedes?*

We examined the solution to the "tall Swedes" challenge problem in [18]. One of the most challenging problems in level-2 CWW is manipulation of propositions containing linguistic and imprecise probabilities [31], [13], and some of Zadeh's challenge problems deal with linguistic probabilities.

In this paper, we focus on the following problem (called the "Magnus problem") involving linguistic quantifiers: *Most Swedes are tall. Most tall Swedes are blond. What is the probability that Magnus (a Swede picked at random) is blond?*

It is worth noting that although these kinds of problems may appear to be "toy problems," serious consideration of them leads to solution of totally new classes of CWW problems. As will be seen in this paper, the solution of the Magnus problem calls for calculation of linguistic lower and upper probabilities, which are closely related to Dempster-Shafer theory of evidence [5]. We will demonstrate that the Linguistic Weighted Average method can contribute to the solution of this problem via manipulating linguistic probabilities.

It is worth noting that we believe that there is no unique solution to Advanced CWW problems, including the Magnus problem. There might be different methodologies for solving a particular problem, and additionally, one can choose different vocabularies to decode the solution so that it can be comprehended by humans. However, the solutions should be linguistically similar.

The rest of this paper is organized as follows: Section II elaborates on Zadeh's methodology for solving the Magnus problem; Section III implements Zadeh's solution to the Magnus problem, and maps it into a linguistic probability via linguistic approximation; Section IV is a critique of Zadeh's solution; Section V uses some standard reasoning tools to interpret the Magnus problem so that it can be solved via Linguistic Weighted Averages, and demonstrates that this gives rise to the calculation of type-2 fuzzy lower and upper probabilities; Section VI studies the effect of the size of the vocabularies on the solution, and shows that when the size of the vocabulary of linguistic probabilities is small, the linguistic lower and upper probabilities are translated to the same word through linguistic approximation; and, Section VII presents some conclusions and suggestions for future research.

II. Zadeh's Methodology for Solving The Magnus Problem

Zadeh solves the Magnus problem by utilizing the following intersection-product syllogism [28]:

$Q_1 A$'s are B's
$Q_2(A$ and $B)$'s are C's

$Q_1 \otimes Q_2 A$'s are (B and C)'s

At least $(Q_1 \otimes Q_2)$ A's are C's

in which Q_1 and Q_2 are linguistic quantifiers, A, B, C are linguistic attributes, and $\otimes$ denotes fuzzy multiplication determined by:

$$\mu_{Q_1 \otimes Q_2}(u) = \sup_{u=xy} (\min(\mu_{Q_1}(x), \mu_{Q_2}(y)) \tag{1}$$

At least is an operator acting on a fuzzy quantifier Q, and can be seen as the order relation $\leq$ extended by the extension principle as follows:

$$\mu_{At\ least(Q)}(x) = \sup_{y \leq x} \mu_Q(y), \quad x, y \in [0,1] \tag{2}$$

The intersection-product syllogism is a fuzzy extension of a simple calculation involving numeric quantifiers. Consider the following example: 50% of the students of the EE Department at USC are graduate students. 80% of the graduate students of the EE Department at USC are on F1 visa. Therefore, 50% $\times$ 80% of the graduate students of the EE Department at USC are on F1 visa. Consequently, *at least* 40% of the students of the EE Department at USC are on F1 visa (since some undergraduate students may be on F1 visa, we use the term *at least*).

It can easily be observed that in the Magnus problem, $Q_1 = Most$, $Q_2 = Most$, $A = Swede$, $B = tall$, and $C = blond$; therefore, it can be inferred that $At\ least$ $(Q = Most \otimes Most)$ Swedes are both tall and blond. On the other hand for a *(non-decreasing) monotonic quantifier* Q, i.e. one whose membership function $\mu_Q(u)$ is monotonically non-decreasing, $At\ least(Q) = Q$ [26]. For a proof of this proposition see Appendix A.

Zadeh views $Most$ as a monotonic quantifier, and hence $Most \otimes Most$ is monotonic. Therefore, the portion of Swedes who are both blond and tall is $Most \otimes Most$. Zadeh interprets a linguistic constraint on the portion of a population as a linguistic probability (LProb), and directly concludes that:

$$\text{LProb}(\text{Magnus is blond}) = Most \otimes Most \tag{3}$$

III. Implementation of Zadeh's Solution

Zadeh's elaboration on the Magnus problem does not include some components of CWW engines. He does not provide the exact membership functions of the fuzzy quantifier $Most$, the linguistic approximation method, or the vocabulary

of linguistic probabilities through which the result could be communicated with humans.

We believe that although a linguistic quantifier has the same mathematical nature as a linguistic probability (both of them are fuzzy subsets of the unit interval $[0, 1]$), they are semantically different: A linguistic quantifier imposes an elastic constraint on the *portion of a population having a specific attribute*, but a linguistic probability (e.g., *Very likely*) imposes a linguistic constraint on the more objective concept of *likelihood of a particular event*. This issue can be viewed as analogous to the difference between two ways of defining probability: the relative frequency definition and the axiomatic definition. The relative frequency approach defines the probability of an event in an experiment as the limit of the ratio of the number of occurrences of that event to the total number of repetitions of the experiment, when this number tends to infinity. The linguistic quantifier *Most* imposes a linguistic constraint on such a ratio. On the other hand, a set of linguistic probabilities (e.g., *Unlikely, Likely, Very likely, Very unlikely*) obeys a fuzzy version of axioms pertinent to probability theory [1]. The relative frequency approach is based on heuristics and the axiomatic approach bears more mathematical rigor.

In any solution of the Magnus problem (be it in a type-1 or a type-2 fuzzy logic framework) not only must one therefore construct a fuzzy set for modeling (precisiating) the quantifier $Most$, but one must also employ a vocabulary of fuzzy probabilities for linguistic approximation of the solution $Most \otimes Most$ containing a linguistic probability that is understandable by human beings. To do the latter, we choose a member of the vocabulary of linguistic probabilities whose Jaccard's similarity [4], [9] with $Most \otimes Most$ is the largest. Recall that the Jaccard's similarity measure between two type-1 fuzzy sets A and B, $s_J(A, B)$, is:

$$s_J(A, B) = \frac{\int_X \mu_{A \cap B}(x) dx}{\int_X \mu_{A \cup B}(x) dx} \tag{4}$$

We chose a right shoulder type-1 fuzzy set to model (precisiate) the linguistic quantifier $Most$[1], whose membership function is depicted in Fig. 1. We also constructed a nine word vocabulary of type-1 fuzzy sets to model the linguistic probabilities. The members of the vocabulary are: *Absolutely improbable, Almost improbable (AI), Very unlikely (VU), Unlikely (UL), Moderately likely (ML), Likely (L), Very likely (VL), Almost certain (AC), Absolutely certain*. Their membership functions are shown in Fig. 2. The extreme words *Absolutely improbable* and *Absolutely certain*[2] are naturally modeled via singletons, and hence are not shown in the figure.

Following Zadeh's philosophy of precisiation of $Most$ as a monotonic quantifier (which could be interpreted as $All \subset Most$), we chose the membership functions so that: $Almost\ improbable \subset Very\ unlikely \subset Unlikely$ and $Likely \subset Very\ likely \subset Almost\ certain$.

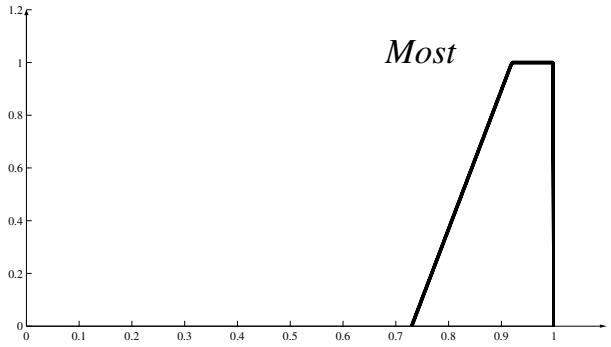

Fig. 1. The membership function of the type-1 fuzzy quantifier $Most$.

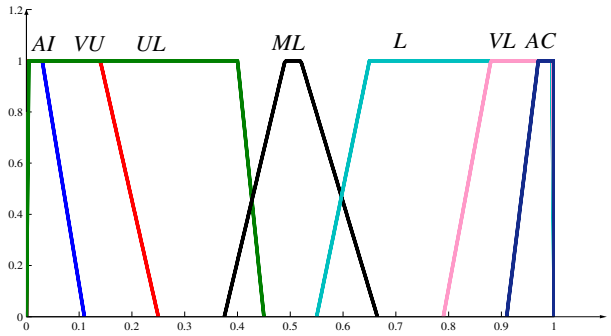

Fig. 2. The membership functions of the vocabulary of type-1 linguistic probabilities.

Computation of Zadeh's solution to the Magnus problem involves a fuzzy multiplication. Since we have chosen a trapezoidal membership function for $Most$, it is easy to compute $Most \otimes Most$ by (1). Assume that one has two trapezoidal fuzzy numbers $A = (a_1, b_1, c_1, d_1)$ and $B = (a_2, b_2, c_2, d_2)$; then, $A \otimes B = (a_1 a_2, b_1 b_2, c_1 c_2, d_1 d_2)$. The computed $Most \otimes Most$ corresponding to the membership function of Fig. 1 is shown in Fig. 3. Note that the center of gravity of the solution is 0.8304. Later, this will be compared to the average centroid of the type-2 solution(s).

In the next step of our interpretation of Zadeh's solution, we calculate Jaccard's similarity measure between $Most \otimes Most$ and each member of the vocabulary of type-1 linguistic probabilities P_i, $(i = 1, \ldots, 9)$, and denote them by $s_J(Most \otimes Most, P_i)$. The results are shown in Table I.

It can be concluded that decoding Zadeh's methodology yields the following solution to the Magnus problem, given

[1]In practice, we can collect data from a group of subjects about all words and then use the Interval Approach [11] or the Enhanced Interval Approach [2] to construct the IT2 FS models. Our hypothetical T1 FSs could then correspond to the upper membership functions of these IT2 FSs. The membership functions used here are for illustrative purposes only.

[2]Note that from (4), it is obvious that the Jaccard's similarity of a singleton and any fuzzy set is always zero. Hence, no solution would map to the extreme words in the decoding procedure. The extreme words are included in the vocabulary because their presence is crucial for an axiomatic approach to fuzzy probabilities, as will be seen in the sequel.

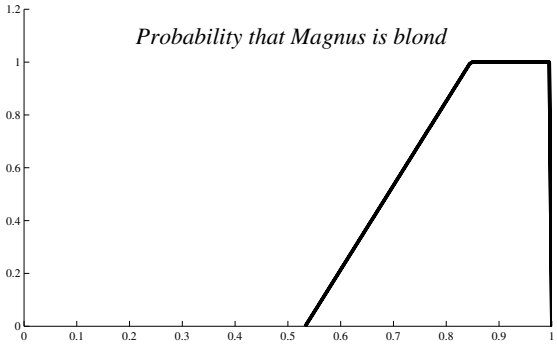

Fig. 3. The membership functions of $Most \otimes Most$.

the aforementioned fuzzy sets for the type-1 linguistic probabilities:

"It is *Likely* that Magnus (a Swede picked at random) is blond."

IV. Critique of Zadeh's Solution

As stressed by [7], although Zadeh's treatment of fuzzy probabilities is very interesting and can be applied to data-centered applications, it needs to be mathematically rigorized so that it is more appropriate from the viewpoint of a probability theorist. As a result, the following linguistic probability measure is defined in [7]: Assume that Ω is a sample space, and $\mathcal{B}$ is the σ-algebra of events associated with Ω, i.e:

1) $\mathcal{B} \subseteq \mathcal{P}_\Omega$
2) $\mathcal{B} \neq \emptyset$
3) $A \in \mathcal{B} \Rightarrow A' \in \mathcal{B}$
4) $\{A_i\}_{i=1}^{\infty} \subseteq \mathcal{B} \Rightarrow \bigcup_{i=1}^{\infty} A_i \in \mathcal{B}$

in which $\mathcal{P}_\Omega$ is the family of subsets of Ω, and $A' = \Omega - A$ is the complement of A.

A function $\mathrm{LProb} : \mathcal{B} \rightarrow \mathscr{N}_{[0,1]}$ is called a *linguistic probability measure* if and only if, for any $A \in \mathcal{B}$:

1) $0 \preceq \mathrm{LProb}(A) \preceq 1$
2) $\mathrm{LProb}(\emptyset) = 0$ and $\mathrm{LProb}(\Omega) = 1$
3) If $\{A_i\}_{i=1}^{\infty} \subseteq \mathcal{B}$ and $i \neq j \Rightarrow A_i \cap A_j = \emptyset$ (i.e. A_i's are mutually disjoint), then $\mathrm{LProb}\left(\bigcup_{i=1}^{\infty} A_i\right) \subseteq \bigoplus_{i=1}^{\infty} \mathrm{LProb}(A_i)$
4) $\mathrm{LProb}(A') = 1 \ominus \mathrm{LProb}(A)$

TABLE I
Similarities between Zadeh's solution $Most \otimes Most$ and linguistic probabilities

Linguistic probability (P_i)	$s_J(Most \otimes Most, P_i)$
Absolutely improbable	0
Almost improbable	0
Very unlikely	0
Unlikely	0
Moderately likely	0.0435
Likely	**0.7499**
Very likely	0.4857
Almost certain	0.1166
Absolutely certain	0

in which $\mathscr{N}_{[0,1]}$ is the set of all fuzzy numbers over the unit interval, $\preceq$ is the order relation induced by the fuzzy minimum operator (and is equivalent to the α-cut ranking method), $\oplus$ represents a special addition for fuzzy numbers [6], and $\ominus$ is the fuzzy subtraction operation.

Zadeh's approach to solving the Magnus problem does not obey the axioms of linguistic probability theory. In his approach, he only considers the events "tall" and "blond". Nevertheless, the above axiomatic approach requires the σ-algebra of events to contain the complement of those events (i.e. "not tall" and "not blond") as well. As will be seen in the sequel, using syllogisms proposed by Zadeh, we consider the events "not tall" and "not blond" and the linguistic probabilities assigned to them in our model. We solve the Magnus problem using type-2 fuzzy sets as models for linguistic probabilities, and we can show [17] that our treatment of linguistic probabilities obeys a set of axioms which are similar to those stated for type-1 fuzzy sets in above.

V. Fuzzy Reasoning and Calculation of Linguistic Upper and Lower Probabilities via Linguistic Weighted Averages

Heuristically, when one assigns a linguistic attribute to *Most of a population*, it can be concluded that the *rest* of that population does not have that attribute. Such an intuition can be derived formally from the following rule obtained from the entailment principle [26] :

QA's are B's

$\neg QA$'s are B''s

in which $\neg Q$ is the antonym of the fuzzy quantifier Q, and its membership function [26] is given by:

$$\mu_{\neg Q}(u) = \mu_Q(1-u),\ u \in [0,1] \tag{5}$$

and B' is the complement of the fuzzy set B, characterized by:

$$\mu_{B'}(u) = 1 - \mu_B(u) \tag{6}$$

Exploiting the aforementioned rule, we have: "A few Swedes are not tall," in which Few is an antonym of the linguistic quantifier $Most$. Consequently, applying this rule to the statement "Most tall Swedes are blond," one concludes that: "A few tall Swedes are not blond."

It is worth noting that the semantics of the fuzzy quantifier $Most$ suggests that it is more appropriately modeled by an interior fuzzy set. As we insisted earlier, when *Most of a population* have a linguistic attribute, it means that there are some members of that population who *do not* have such an attribute. It is reasonable, therefore, to assume that $\mu_{Most}(1) \neq 1$ (i.e. the membership value of 100% in $Most$ is not 1); thus, we choose an interior fuzzy set to model the quantifier $Most$, and its antonym to model the quantifier Few, as shown in Fig. 4.

One has linguistic information about the distribution of blond Swedes among those who are tall, i.e. one knows that most of tall Swedes are blond. Unfortunately, one does not know anything about the distribution of blond Swedes

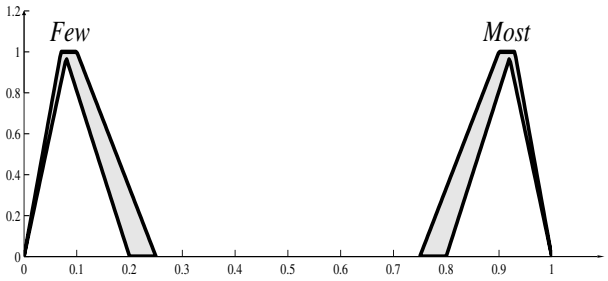

Fig. 4. Type-2 fuzzy sets for modeling $Most$ and Few.

among those (few) Swedes who are not tall. This situation is summarized in the tree of Fig. 5.

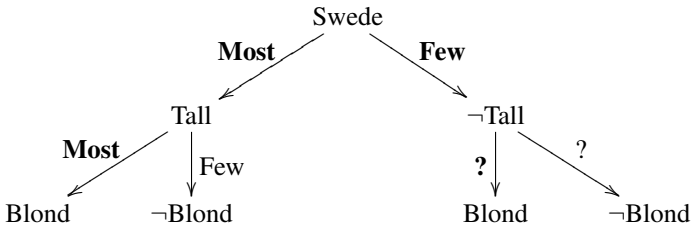

Fig. 5. Linguistic information about the distribution of blond people among Swedes.

Because of one's total ignorance about the distribution of blonds among the Swedes who are not tall, one can take two different approaches to calculate the linguistic probability that Magnus is blond: The first approach assumes that the distribution of blonds among Swedes who are not tall is similar to the case of tall Swedes i.e., *Most Swedes who are not tall are blond; few of them are not blond;* however, such a methodology does not seem to be quite plausible, because it completely neglects our total ignorance about the situation, and assumes additional *world knowledge*, which may not always be available.

The second approach calculates a linguistic lower and a linguistic upper probability corresponding respectively to the pessimistic case, when *none of Swedes who are not tall are blond* and the optimistic case when *all of Swedes who are not tall are blond*.

To calculate the linguistic lower and upper probabilities, we use a *normalized version* of the intersection-product syllogism, so that the problem can be solved using Linguistic Weighted Averages [19], [20]. The linguistic lower probability $\mathrm{LProb}^{-}(\cdot)$ is determined as:

$$\mathrm{LProb}^{-}(\text{Magnus is blond}) = \frac{\mathit{Most} \times \mathit{Most} + \mathit{Few} \times \mathit{None}}{\mathit{Most} + \mathit{Few}} \tag{7}$$

Similarly, the linguistic upper probability $\mathrm{LProb}^{+}(\cdot)$ is determined as:

$$\mathrm{LProb}^{+}(\text{Magnus is blond}) = \frac{\mathit{Most} \times \mathit{Most} + \mathit{Few} \times \mathit{All}}{\mathit{Most} + \mathit{Few}} \tag{8}$$

In (7) and (8), All and $None$ are singletons, respectively represented by:

$$\mu_{All}(u) = \begin{cases} 1 & u = 1 \\ 0 & \text{otherwise} \end{cases} \tag{9}$$

$$\mu_{None}(u) = \begin{cases} 1 & u = 0 \\ 0 & \text{otherwise} \end{cases} \tag{10}$$

A Linguistic Weighted Average $\widetilde{Y}_{LWA}$ of interval type-2 fuzzy sets $\widetilde{X}_i$ with interval type-2 fuzzy weights $\widetilde{W}_i$, $(i = 1, \cdots, n)$ is characterized by the following *expressive formula*[3] [14]:

$$\widetilde{Y}_{LWA} = \frac{\sum_{i=1}^{n} \widetilde{W}_i \times \widetilde{X}_i}{\sum_{i=1}^{n} \widetilde{W}_i} = [\underline{Y}_{LWA}, \overline{Y}_{LWA}] \tag{11}$$

in which:

$$\underline{Y}_{LWA} = \min_{\forall W_i \in [\underline{W}_i, \overline{W}_i]} \frac{\sum_{i=1}^{n} W_i \underline{X}_i}{\sum_{i=1}^{n} W_i} \tag{12}$$

$$\overline{Y}_{LWA} = \max_{\forall W_i \in [\underline{W}_i, \overline{W}_i]} \frac{\sum_{i=1}^{n} W_i \overline{X}_i}{\sum_{i=1}^{n} W_i} \tag{13}$$

in which the underlined and overlined quantities denote lower and upper membership values of $\widetilde{Y}_{LWA}$. Observe that LProb^{-} and LProb^{+} in (7) and (8) are Linguistic Weighted Averages that can be computed by (12) and (13).

By analogy with classical probability theory, one can observe that the weighted average solutions in (7) and (8) can be derived from the following conditional fuzzy probability calculation which is a generalization of the calculations of [7] to type-2 fuzzy sets:

$$\begin{aligned} &\mathrm{LProb}(\text{blond}|\text{Swede}) = \\ &\mathrm{LProb}(\text{tall}|\text{Swede}) \times \mathrm{LProb}(\text{blond}|\text{tall and Swede}) + \\ &\mathrm{LProb}(\neg\text{tall}|\text{Swede}) \times \mathrm{LProb}(\text{blond}|\neg\text{tall and Swede}) \end{aligned} \tag{14}$$

$\mathrm{LProb}^{-}(\text{Magnus is blond})$ is obtained by assuming in (14) that:

$$\mathrm{LProb}(\text{blond}|\neg\text{tall and Swede}) = \mathit{None} = 0 \tag{15}$$

and $\mathrm{LProb}^{+}(\text{Magnus is blond})$ is obtained by assuming in (14) that:

$$\mathrm{LProb}(\text{blond}|\neg\text{tall and Swede}) = \mathit{All} = 1 \tag{16}$$

It can be shown [16] that the intrinsic normalization present in the linguistic weighted average contributes to interactive addition of fuzzy probabilities, which avoids obtaining counter-intuitive linguistic probabilities whose membership functions are non-zero outside $[0, 1]$ [6], [24].

One can argue that when there is no assumption on the distribution of blonds among Swedes who are not tall, based

[3]This means that although $\widetilde{Y}_{LWA}$ can be expressed by (11), it is not computed by adding/multiplying interval type-2 fuzzy sets.

on the principle of maximum entropy [3], one should assume that:

$$\begin{aligned}&\text{LProb}(\text{blond}|\neg\text{tall and Swede}) = \\ &\text{LProb}(\text{not blond}|\neg\text{tall and Swede}) = 0.5\end{aligned} \quad (17)$$

It can easily be shown that the linguistic probability calculated by (17) is exactly $(\text{LProb}^+ + \text{LProb}^-)/2$. This is a direct result of the fact that $(All + None)/2 = 0.5$, and the nature of the average. The linguistic upper and lower probabilities provide more flexibility when such an assumption cannot be made.

We calculate LProb^- and LProb^+ exploiting a method based on alpha-cuts [21], [23]. The results are shown in Figs. 6 and 7, respectively. The centroid and average centroid of the lower probability are $[0.7966, 0.8150]$ and 0.8058, respectively. The centroid and average centroid for the upper probability are $[0.8888, 0.9002]$ and 0.8945, respectively. The centroid can be used to report a solution in terms of the uncertain numeric upper and lower probabilities for the problem: "the probability that Magnus is blond is between around 80% and around 89%." Note that 80% and 89% are the average centroids of the type-2 fuzzy lower and the upper probabilities, and the term "around" reflects the uncertainty represented by the centroids, and reflects the inter-person and intra-person uncertainties about the words. Such uncertainties are propagated by the linguistic weighted average, and can be captured when reporting a numeric value for the lower and the upper probabilities, by calculation of centroid and average centroid. This cannot be done by any solution involving type-1 fuzzy sets, including Zadeh's solution.

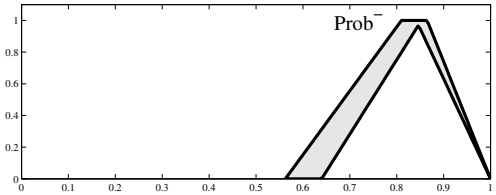

Fig. 6. Linguistic lower probability that Magnus is blond.

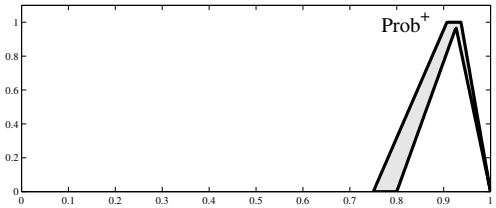

Fig. 7. Linguistic upper probability that Magnus is blond.

In order to communicate the results to people via linguistic probabilities (e.g., very likely), we computed Jaccard's similarities of the linguistic lower probability and the linguistic upper probability with the vocabulary of linguistic probabilities ($\widetilde{P}_i,\ i = 1, \cdots, 9$) whose membership functions are shown in Fig. 8. The results are shown in Table II. The vocabulary of type-2 linguistic probabilities contains the same words as the vocabulary of type-1 linguistic probabilities. As done previously, we modeled the extreme words *Absolutely improbable* and *Absolutely certain* as singletons, and hence they are not shown in the figure.

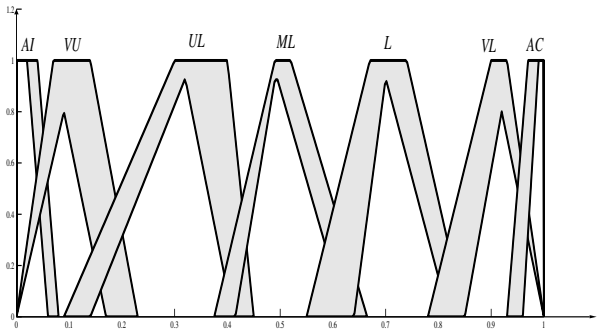

Fig. 8. The membership functions of the vocabulary of type-2 linguistic probabilities.

Note that the Jaccard's similarity between interval type-2 fuzzy sets $\widetilde{A}$ and $\widetilde{B}$ is calculated by [22], [23]:

$$s_J(\tilde{A}, \tilde{B}) = \frac{\int_X (\min(\bar{\mu}_{\tilde{A}}(x), \bar{\mu}_{\tilde{B}}(x)) + \min(\underline{\mu}_{\tilde{A}}(x), \underline{\mu}_{\tilde{B}}(x)))dx}{\int_X (\max(\bar{\mu}_{\tilde{A}}(x), \bar{\mu}_{\tilde{B}}(x)) + \max(\underline{\mu}_{\tilde{A}}(x), \underline{\mu}_{\tilde{B}}(x)))dx} \quad (18)$$

in which $\bar{\mu}_{\tilde{A}}(x)$ and $\underline{\mu}_{\tilde{A}}(x)$ are upper membership and lower membership functions of $\tilde{A}$.

Since we have obtained a pessimistic and an optimistic probability, we can make the following statement: "The probability that Magnus is blond is between likely and very likely."

TABLE II
SIMILARITIES BETWEEN THE LINGUISTIC LOWER AND UPPER PROBABILITIES WITH THE MEMBERS OF THE VOCABULARY OF LINGUISTIC PROBABILITIES

Linguistic probability ($\widetilde{P}_i$)	$s_J(\text{LProb}^-, \widetilde{P}_i)$	$s_J(\text{LProb}^+, \widetilde{P}_i)$
Absolutely improbable	0	0
Almost improbable	0	0
Very unlikely	0	0
Unlikely	0	0
Moderately likely	0.0191	0
Likely	**0.3117**	0.0332
Very likely	0.2997	**0.7657**
Almost certain	0.0435	0.1108
Absolutely certain	0	0

VI. A Study on The Effect of The Size of Vocabulary on The Results

Linguistic approximation is essentially the fuzzy counterpart of rounding numeric values. In conventional rounding, one approximates a numerical value with the "nearest" number that is meaningful for available computing machinery. In linguistic approximation, analogously, a member of the vocabulary that

is most similar to the result of a reasoning procedure is selected so that the result is perceivable by a person.

It is therefore appropriate to investigate the issue of "resolution," when performing linguistic approximation. More specifically in the Magnus problem, if the vocabulary of linguistic probabilities is not of a sufficient resolution, both the linguistic upper and lower probabilities map to the same word, removing the effect of considering total ignorance about the distribution of blonds among the Swedes who are not tall. On the other hand, precision makes communication more difficult, e.g. the statement " It is very likely that Magnus is blond" is more comprehensible by a human than the statement "The probability that Magnus is blond is between likely and very likely." Consequently, it is of interest to investigate the conditions which lead to a more precise linguistic answer.

The main factor affecting the resolution of a CWW system is the size of its vocabularies, because the size of the vocabulary is influential on the shape of the fuzzy set modeling a word [14]. As the size of a vocabulary increases, the "fuzziness" [34] of fuzzy sets modeling each word decreases.

To examine the dependence of the solution on the resolution of the vocabulary of the linguistic probabilities, we chose vocabularies containing 3, 5, and 7 words, and calculated Jaccard's similarities of the linguistic lower and the upper probabilities with the words of each vocabulary, in the following manner:

Vocabulary 1: *Absolutely improbable, Likely, Absolutely certain* (see Fig. 9). Vocabulary 2: *Absolutely improbable, Unlikely, Likely, Very likely, Absolutely certain* (see Fig. 10). Vocabulary 3: *Absolutely improbable, Almost Improbable, Unlikely, Likely, Very likely, Almost certain, Absolutely certain* (see Fig. 11). Note that the singletons are not shown in Figs. 9-11.

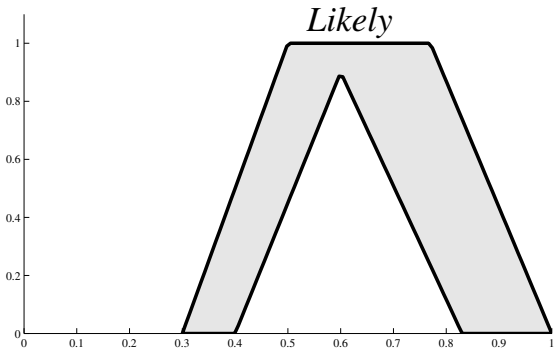

Fig. 9. The membership functions of the 3-word vocabulary of linguistic probabilities.

The similarities between the linguistic lower and upper probabilities with the members of each of the vocabularies are shown in Tables III-V. Interestingly, the linguistic lower and upper probabilities are decoded into the same word in the cases where we have 3, 5, and 7 words in the vocabulary. For the three-word vocabulary, the word is "Likely", whereas in the five-word and seven-word vocabularies, it is "Very likely".

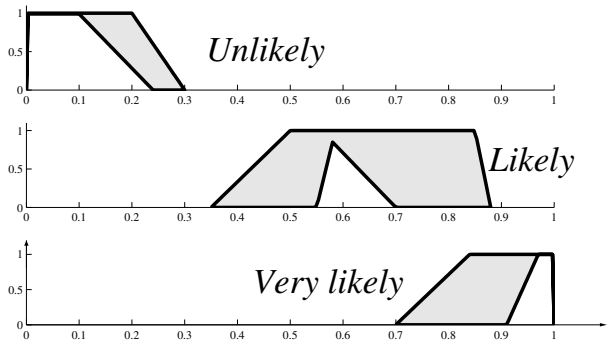

Fig. 10. The membership functions of the 5-word vocabulary of linguistic probabilities.

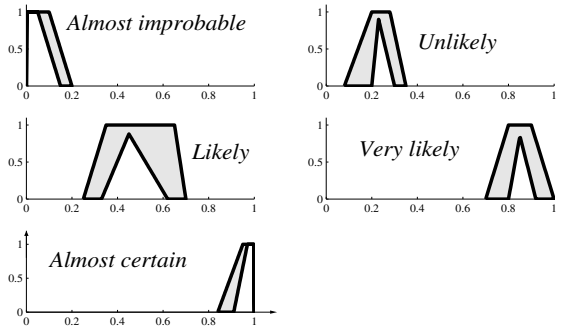

Fig. 11. The membership functions of the 7-word vocabulary of linguistic probabilities.

TABLE III
SIMILARITIES BETWEEN THE LINGUISTIC LOWER AND UPPER PROBABILITIES WITH THE MEMBERS OF THE 3-WORD VOCABULARY OF LINGUISTIC PROBABILITIES

Linguistic probability ($\widetilde{P}_i$)	$s_J(\mathrm{LProb}^-, \widetilde{P}_i)$	$s_J(\mathrm{LProb}^+, \widetilde{P}_i)$
Improbable	0	0
Likely	**0.2946**	**0.1122**
Absolutely certain	0	0

TABLE IV
SIMILARITIES BETWEEN THE LINGUISTIC LOWER AND UPPER PROBABILITIES WITH THE MEMBERS OF THE 5-WORD VOCABULARY OF LINGUISTIC PROBABILITIES

Linguistic probability ($\widetilde{P}_i$)	$s_J(\mathrm{LProb}^-, \widetilde{P}_i)$	$s_J(\mathrm{LProb}^+, \widetilde{P}_i)$
Improbable	0	0
Unlikely	0	0
Likely	0.2949	0.0894
Very likely	**0.3387**	**0.6051**
Absolutely certain	0	0

VII. CONCLUSIONS

In this paper, we applied Linguistic Weighted Averages to the calculation of linguistic probabilities to solve Zadeh's "Magnus" challenge problem. We demonstrated that applying syllogisms related to linguistic quantifiers to this problem

TABLE V
SIMILARITIES BETWEEN THE LINGUISTIC LOWER AND UPPER PROBABILITIES WITH THE MEMBERS OF THE 7-WORD VOCABULARY OF LINGUISTIC PROBABILITIES

Linguistic probability ($\widetilde{P}_i$)	$s_J(\mathrm{LProb}^-, \widetilde{P}_i)$	$s_J(\mathrm{LProb}^+, \widetilde{P}_i)$
Improbable	0	0
Almost improbable	0	0
Unlikely	0	0
Likely	0.0390	0.0421
Very likely	**0.5410**	**0.5684**
Almost certain	0.0984	0.1102
Absolutely certain	0	0

gives rise to the derivation of linguistic upper and lower probabilities. This is in accord with the existing landscape of Dempster-Shafer theory of evidence, which has been used for manipulation of imprecise probabilities in decision making problems. Our forthcoming efforts will be devoted to developing a new linguistic evidence theory.

The use of Linguistic Weighted Averages appears to be promising in solving more complicated CWW problems which involve implicit assignment of linguistic constraints to variables like probability (and truth). This is mainly due to the inherent normalization done by them, which prevents them from resulting in fuzzy probabilities whose membership functions are non-zero outside the interval $[0, 1]$.

ACKNOWLEDGMENT

Mohammad Reza Rajati would like to sincerely acknowledge the support of Annenberg Fellowship Program of the University of Southern California.

APPENDIX A
PROOF FOR $At\ least(Q) = Q$ WHEN Q IS MONOTONICALLY NON-DECREASING

The operator *At least* is defined by:

$$\mu_{At\ least(Q)}(x) = \sup_{y \le x} \mu_Q(y), \quad x, y \in [0, 1] \tag{19}$$

Since $\mu_Q(x)$ is non-decreasingly monotonic, $\forall y \le x,\ \mu_Q(y) \le \mu_Q(x)$. Therefore, $\sup_{y \le x} \mu_Q(y) = \mu_Q(x)$, and $\mu_{At\ least(Q)}(x) = \mu_Q(x)$.

REFERENCES

[1] J. J. Buckley, *Fuzzy Probability and Statistics, Studies in Fuzziness and Soft Computing*, Berlin, Heidelberg: Springer-Verlag, 2006.

[2] S. Coupland, J. M. Mendel, and D. Wu, "Enhanced interval approach for encoding words into interval type-2 fuzzy sets and convergence of the word fous," in *Proc. IEEE World Congress on Computational Intelligence*, July 2010.

[3] T. M. Cover and J. A. Thomas, *Elements of Information Theory*, John Wiley & Sons, 1991.

[4] V. V. Cross and T. A. Sudkamp, *Similarity and Compatibility in Fuzzy Set Theory: Assessment and Applications*. Heidelberg, NY: Physica-Verlag, 2002.

[5] A. P. Dempster, "The Dempster-Shafer Calculus for Statisticians," *International Journal of Approximate Reasoning*, vol. 48, no. 2, pp. 365-377, June 2008.

[6] D. Dubois and H. Prade, "Various kinds of interactive addition of fuzzy numbers. Applications to decision analysis in presence of linguistic probabilities," *Proceedings of 1979 18th IEEE Conference on Decision and Control, CDC'79*, 1979, pp. 783 – 787.

[7] J. Halliwell and Q. Shen, "Linguistic probabilities: theory and applications," *Soft Computing*, vol. 13, pp. 169–183, 2009.

[8] T. C. Havens, J. M. Keller, and M. Popescu, "Computing with words with the ontological self-organizing map," *IEEE Transactions on Fuzzy Systems*, vol. 18, no. 3, pp. 473–485, April 2010.

[9] P. Jaccard, "Ètude comparative de la distribution florale dans une portion des Alpes et des Jura," *Bulletin de la Societè Vaudoise des Sciences Naturelles*, vol. 37, pp. 547–579, 1901.

[10] J. Lawry, "A methodology for CWW," *International Journal of Approximate Reasoning*, vol. 28, pp. 5189, 2001.

[11] F. Liu and J. M. Mendel "Encoding words into interval type-2 fuzzy sets using an interval approach," *IEEE Transactions on Fuzzy Systems*, vol. 16, no. 6, pp. 1503–1521, December 2008.

[12] J. M. Mendel, "Computing with words: Zadeh, Turing, Popper, and Occam," *IEEE Computational Intelligence Magazine*, vol. 2, no. 4, pp. 10–17, November 2007.

[13] J. M. Mendel, J. Lawry, and L. A. Zadeh, "Foreword to the special section on computing with words," *IEEE Transactions on Fuzzy Systems*, vol. 18, no. 3, pp. 437–440, June 2010.

[14] J. M. Mendel and D. Wu, *Perceptual Computing: Aiding People in Making Subjective Judgements,* Hoboken, NJ: John Wiley & Sons, Inc., 2010.

[15] W. Pedrycz and S. H. Rubin, "Data compactification and computing with words," *Engineering Applications of Artificial Intelligence*, vol. 23, no. 3, pp. 346–356, April 2010.

[16] M. R. Rajati and J. M. Mendel, "Linguistic Dempster-Shafer theory of evidence: A computing with words perspective," *In preparation*.

[17] M. R. Rajati and J. M. Mendel, "Interval type-2 fuzzy sets as linguistic probabilities," *In preparation*.

[18] M. R. Rajati, D. Wu, and J. M. Mendel, "On solving Zadeh's tall Swedes problem," *To be presented in 2011 World Congress on Soft Computing*, San Francisco, CA, May 2011.

[19] D. Wu and J. M. Mendel, "Aggregation using the linguistic weighted average and interval type-2 fuzzy sets," *IEEE Transactions on Fuzzy Systems*, vol. 15, no. 6, pp. 1145–1161, 2007.

[20] ——, "Corrections to 'Aggregation using the linguistic weighted average and interval type-2 fuzzy sets'," *IEEE Transactions on Fuzzy Systems*, vol. 16, no. 6, pp. 1664–1666, 2008.

[21] ——, "Perceptual reasoning for perceptual computing," *IEEE Transactions on Fuzzy Systems*, vol. 16, no. 6, pp. 1550–1564, 2008.

[22] ——, "A comparative study of ranking methods, similarity measures and uncertainty measures for interval type-2 fuzzy sets," *Information Sciences*, vol. 179, pp. 1169–1192, 2009.

[23] ——, "Perceptual reasoning for perceptual computing: A similarity based approach," *IEEE Transactions on Fuzzy Systems*, vol. 17, no. 6, pp. 1397–1411, 2008.

[24] L. A. Zadeh,"Fuzzy sets and information granularity," in *Advances in Fuzzy Set Theory and Applications,* M. Gupta et al., Eds. North-Holland Publishing Company, 1979, pp. 3–18.

[25] ——, "Fuzzy sets versus probability," *Proceedings of the IEEE*, vol. 68, no. 3, p. 421, March 1980.

[26] ——, "A computational approach to fuzzy quantifiers in natural languages," *Computers and Mathematics with Applications*, vol. 9, no. 1, pp. 149-184, 1983.

[27] ——,"Precisiation of meaning via translation into PRUF," in *Cognitive Constraints in Communication*, L. Vaina and J. Hintikka, Eds., Kluwer Academic Publishers, 1984, pp. 373–402.

[28] ——, "Fuzzy logic=computing with words," *IEEE Transactions on Systems, Man, and Cybernetics*, vol. 4, no. 2, pp. 103–111, May 1996.

[29] ——, "A new direction in AI–toward a computational theory of Perceptions," *AI Magazine*, vol. 22, no. 1, pp. 73–84, November 2001.

[30] ——,"Precisiated natural language (PNL)," *AI Magazine*, vol. 25, no. 3, pp. 74–91, 2004.

[31] ——,"From imprecise to granular probabilities," *Fuzzy Sets and Systems*, vol. 154, pp. 370–374, 2005.

[32] ——, "Precisiation of meaning–toward computation with natural language," in *Proceedings of 2010 IEEE International Conference on Information Reuse and Integration (IRI)*, 2010, pp. 1–4.

[33] ——, "Computing with words – A paradigm shift." [Online]. Available: http://www.cs.berkeley.edu/˜zadeh/presentations.html. April 2010.

[34] D. Zhai and J. M. Mendel,"Uncertainty measures for general type-2 fuzzy sets," *Information Sciences*, vol. 181, pp. 503–518, 2011.

2011 IEEE International Conference on Fuzzy Systems
June 27-30, 2011, Taipei, Taiwan

Linguistic Weighted Power Means

Comparison with the Linguistic Weighted Average

John T. Rickard
Distributed Infinity, Inc.
Larkspur, CO, USA
terry.rickard@gmail.com

Janet Aisbett
School of Science and IT
University of Newcastle
Newcastle, NSW, Australia
janet.aisbett@newcastle.edu.au

Ronald R. Yager
Machine Intelligence Institute, Iona College
New Rochelle, NY, USA
yager@panix.com

Greg Gibbon
School of Science and IT
University of Newcastle
Newcastle, NSW, Australia
greg.gibbon@newcastle.edu.au

***Abstract* – We have introduced the linguistic weighted power mean and its computation via a generalization of the Karnick-Mendel algorithm. This new family of aggregation operators admits interval type-2 fuzzy membership functions for both its inputs and its weights to account for imprecise knowledge of these quantities. The simplest member of this family, the linguistic weighted average, is the primary instantiation of a "perceptual computing" engine in Mendel and Wu's recent book by this title. This paper presents a comparison of the linguistic weighted power mean and the linguistic weighted average on one of the examples they describe in detail—the "investment judgment advisor". Our results illustrate the flexibility and range of logical inference provided by this very versatile aggregation operator for computing with words applications.**

Keywords-aggregation operators; type-2 fuzzy logic; computing with words; perceptual computing

I. INTRODUCTION

The recent book by Mendel and Wu entitled *Perceptual Computing* [1] presents an approach to "computing with words" (CWW), a problem area originally suggested by Zadeh [2] that remains of high interest. (See, for example, the recent special section of the *IEEE Transactions on Fuzzy Systems* on CWW [3] and publications [4]-[7].)

Mendel and Wu's approach to CWW is motivated by the premise that "words mean different things to different people," and therefore the inputs, computational engine and outputs of a perceptual computer (Per-C) must explicitly take account of this inherent imprecision. Inputs to the Per-C are modeled as interval type-2 (IT2) fuzzy membership functions (MFs) spanning an appropriate range (e.g., a 0-10 scale), which is perhaps the simplest method for representing imprecise knowledge of membership values.

The Per-C is proposed to have three components: an *encoder*, a *computational engine* and a *decoder*. Mendel and Wu's strategy for the encoder is to develop a code book of input and output *words* that are also represented by IT2 MFs. Inputs to the Per-C computational engine are selected from this vocabulary of input words. The IT2 fuzzy input variables and importance weights are mapped to code book words via similarity comparisons. The computational engine logically aggregates the imprecision represented in these word MFs into corresponding output IT2 MFs. These output IT2 MFs are decoded by an analogous similarity mapping into corresponding word outputs.

Two architectures for the Per-C computational engine are proposed in [1]: 1) a bank of parallel *if-then rules*, and 2) a "*linguistic weighted average*" (LWA). The first of these relies upon results summarized in Mendel's earlier book [8] on type-2 fuzzy rule-bases systems, where input variables are represented by IT2 MFs and the implication operation performed by the rules results in an output IT2 MF. In fuzzy control applications, this output MF is generally type-reduced to an interval whose midpoint describes the defuzzified scalar output of the computational engine. In CWW applications, the output IT2 MF is typically mapped into an output word in the code book vocabulary using the decoder described above.

The LWA Per-C architecture is employed in three of the four chapters in [1] presenting detailed examples of Per-C applications. It is a generalization of the traditional weighted average, first to a type-1 *fuzzy weighted average* (FWA) and then to a IT2 fuzzy weighted average in which all inputs and importance weights are represented by IT2 MFs. The latter generalization applies the celebrated Karnick-Mendel algorithm [9] for computing the centroid of an IT2 MF to the α-cuts of the upper and lower MFs (UMF and LMF, respectively) of the input variables and weights, resulting in the corresponding α-cuts of the LWA UMF and LMF. The output UMF and LMF are then constructed (in approximation) using the well-known α-cut Representation Theorem [10].

The LWA is perhaps the simplest aggregation operator $L(\tilde{\mathbf{x}}, \tilde{\mathbf{w}})$ mapping IT2 MFs of scores $\tilde{\mathbf{x}} = (\tilde{x}_1, ..., \tilde{x}_n)$ and associated importance weights $\tilde{\mathbf{w}} = (\tilde{w}_1, ..., \tilde{w}_n)$ into an output IT2 MF. These operators represent a form of data fusion in which both scores and weights are generally taken to lie within a common interval range and are characterized by IT2 MFs. Although the LWA is the primary computational method featured for computing with words in [1], it is limited in its ability to represent how humans aggregate preference scores. For example, it cannot model a mandatory requirement. Therefore it is highly desirable to develop more powerful and computationally feasible aggregation operators that can be applied to IT2 inputs.

978-1-4244-7316-8/11/$26.00 ©2011 IEEE

The LWA is but one member of the class of aggregation operators generally referred to as the p-norm [11]. When the power r in the p-norm is allowed to vary over the entire real line, it is called a weighted power mean (WPM), defined by

$$L_r(\tilde{\mathbf{x}},\tilde{\mathbf{w}}) \triangleq \lim_{q\to r}\left(\frac{\sum_{i=1}^{n}\tilde{w}_i\tilde{x}_i^q}{\sum_{i=1}^{n}\tilde{w}_i}\right)^{1/q}. \quad (1)$$

While it is no longer always a norm, the WPM is a flexible operator that is used in information retrieval and other ranked decision applications [12]. As r ranges over the real line, L_r ranges from logical conjunction $x_1\wedge\cdots\wedge x_n$ of the inputs (in the limit as $r\to-\infty$) to logical disjunction $x_1\vee\cdots\vee x_n$ (in the limit as $r\to\infty$). L_r is thus an *orand* operator. Other special cases of the weighted power mean include the LWA ($r=1$), geometric mean ($r=0$), harmonic mean ($r=-1$) and Euclidean mean ($r=2$). Dujmovi [13] suggests (in a type-1 setting) that the WPM performs best of a general class of parameterised aggregation operators that range continuously between the extremes of conjunction and disjunction.

In a current paper [14], we have generalized the Karnick-Mendel algorithm to compute the output interval of the WPM given input intervals for $\tilde{\mathbf{x}}$ and $\tilde{\mathbf{w}}$, for arbitrary values of the power r. We denote this as the Weighted Power Mean Enhanced Karnick-Mendel (WPMEKM) algorithm, since it makes use of performance enhancements over the original Karnick-Mendel algorithm as described in [15]-[16]. By employing the α-cut Representation Theorem, we use the WPMEKM algorithm to compute the output IT2 MF of $L_r(\tilde{\mathbf{x}},\tilde{\mathbf{w}})$, given IT2 MFs for the inputs and weights. We denote this new aggregation operator as the *linguistic weighted power mean* (LWPM).

The primary contribution of this paper is to provide a comparison of Per-C computational engines using the LWPM aggregation operator $L_r(\tilde{\mathbf{x}},\tilde{\mathbf{w}})$ with the LWA Per-C engine described by Mendel and Wu (which is $L_1(\tilde{\mathbf{x}},\tilde{\mathbf{w}})$), using the detailed example of an Investment Judgment Advisor presented in [1] and described below. This example illustrates the flexibility and range of logical inferences available using the LWPM as compared to the LWA. Thus the LWPM represents a significant generalization and extension of the choices of Per-C computational engines available for CWW applications.

The remainder of this paper is organized as follows: first, we summarize the WPMEKM algorithm of [14]. Then we review the Investment Judgment Advisor (IJA) example of [1]. Next, we compare the IJA outputs using the LWPM versus the LWA, and discuss the advantages of the LWPM. Finally, we describe how even more useful logical aggregation operators can be constructed hierarchically using combinations of LWPM components.

II. SUMMARY OF WPMEKM ALGORITHM

Suppose initially that we have interval-valued scores $[\underline{x}_i,\overline{x}_i]$ and weights $[\underline{w}_i,\overline{w}_i]$, where $\overline{x}_i,\underline{x}_i\in[0,1]$, $\overline{w}_i,\underline{w}_i\geq 0$, $i\in\{1,\ldots,n\}$ are inputs to the LWPM $L_r(\tilde{\mathbf{x}},\tilde{\mathbf{w}})$. We summarize below the WPMEKM algorithm for computing corresponding output intervals of the LWPM [14].

First we consider the exceptional cases $r=\pm\infty$, for which $L_r(\mathbf{x},\mathbf{w})$ is independent of w_i. The interval endpoints then are determined solely by the x_i interval boundaries, with

$$\begin{aligned}\underline{L}_{-\infty}(\mathbf{x},\mathbf{w}) &= \min_{i:\ w_i>0}\{\underline{x}_i\},\ \overline{L}_{-\infty} = \min_{i:\ w_i>0}\{\overline{x}_i\}\\ \underline{L}_{\infty}(\mathbf{x},\mathbf{w}) &= \max_{i:\ w_i>0}\{\underline{x}_i\},\ \overline{L}_{\infty} = \max_{i:\ w_i>0}\{\overline{x}_i\}\end{aligned}. \quad (2)$$

Next, consider the weighted power mean for a finite power r. Then (1) can be rewritten as

$$L_r(\mathbf{x},\mathbf{w}) = h_r\left(\sum_{i=1}^{n}w_i h_r^{-1}(x_i)\Big/\sum_{i=1}^{n}w_i\right) = h_r\left(y_r(\mathbf{x},\mathbf{w})\right) \quad (3)$$

where

$$h_r(z)=\begin{cases} z^{1/r}, & r\neq 0\\ \exp(z), & r=0\end{cases}, \quad (4)$$

$$y_r(\mathbf{x},\mathbf{w}) = \sum_{i=1}^{n}w_i h_r^{-1}(x_i)\Big/\sum_{i=1}^{n}w_i. \quad (5)$$

Note that h_r and h_r^{-1} are strictly increasing on the non-negative reals if $r\geq 0$ and are strictly decreasing if $r<0$.

With (3), the value of the weighted power mean applied to intervals $[\underline{x},\overline{x}_i],[\underline{w}_i,\overline{w}_i]$ can be written as the interval

$$[\underline{L}_r,\overline{L}_r] = \left[\min h_r\left(\sum_{i=1}^{n}w_i h_r^{-1}(x_i)\Big/\sum_{i=1}^{n}w_i\right), \max h_r\left(\sum_{i=1}^{n}w_i h_r^{-1}(x_i)\Big/\sum_{i=1}^{n}w_i\right)\right] \quad (6)$$

where min and max are taken over $\{x_1,\ldots x_n,w_1,\ldots w_n : x_i\in[\underline{x}_i,\overline{x}_i], w_i\in[\underline{w}_i,\overline{w}_i],\ i=1,\ldots,n\}$.

From (6), we have

$$[\underline{L}_r,\overline{L}_r] = \begin{cases}[h_r(\underline{y}_r),h_r(\overline{y}_r)] & r\geq 0\\ [h_r(\overline{y}_r),h_r(\underline{y}_r)] & r<0\end{cases}, \quad (7)$$

where

$$\left[\underline{y}_r, \overline{y}_r\right] = \left[\min\left\{ \frac{\sum_{i=1}^{n} w_i h_r^{-1}(x_i)}{\sum_{i=1}^{n} w_i} \right\}, \max\left\{ \frac{\sum_{i=1}^{n} w_i h_r^{-1}(x_i)}{\sum_{i=1}^{n} w_i} \right\} \right]. \quad (8)$$

Now for any $i \in \{1,...,n\}$, $h_r^{-1}\left(\underline{x}_i\right) \le h_r^{-1}\left(\overline{x}_i\right)$ if h_r is strictly increasing and $h_r^{-1}\left(\underline{x}_i\right) \ge h_r^{-1}\left(\overline{x}_i\right)$ if h_r is strictly decreasing. So to compute (8), we compute the LWA of input intervals $\left[h_r^{-1}\left(\underline{x}_i\right), h_r^{-1}\left(\overline{x}_i\right)\right]$ when $r \ge 0$ and $\left[h_r^{-1}\left(\overline{x}_i\right), h_r^{-1}\left(\underline{x}_i\right)\right]$ when $r < 0$. Then we apply h_r to the resulting interval LWA, where the upper and lower bounds are transposed at this step if h_r is strictly decreasing. Thus in all cases, the bounds in (7) are given by:

$$\begin{aligned} \underline{L}_r &= h_r\left(\sum_{i=1}^{n} \underline{z}_i h_r^{-1}\left(\underline{x}_i\right) \Big/ \sum_{i=1}^{n} \underline{z}_i \right), \\ \underline{z}_i &= \begin{cases} \overline{w}_i, & \underline{x}_i < h_r\left(y_r\left(\underline{\mathbf{x}}, \underline{\mathbf{z}}\right)\right) = \underline{L}_r \\ \underline{w}_i, & \underline{x}_i > h_r\left(y_r\left(\underline{\mathbf{x}}, \underline{\mathbf{z}}\right)\right) = \underline{L}_r \end{cases} \\ \overline{L}_r &= h_r\left(\sum_{i=1}^{n} \overline{z}_i h_r^{-1}\left(\overline{x}_i\right) \Big/ \sum_{i=1}^{n} \overline{z}_i \right), \\ \overline{z}_i &= \begin{cases} \underline{w}_i, & \overline{x}_i < h_r\left(y_r\left(\overline{\mathbf{x}}, \overline{\mathbf{z}}\right)\right) = \overline{L}_r, \\ \overline{w}_i, & \overline{x}_i > h_r\left(y_r\left(\overline{\mathbf{x}}, \overline{\mathbf{z}}\right)\right) = \overline{L}_r \end{cases} \end{aligned} \quad . \quad (9)$$

The EKM algorithms [15]-[16] can be adapted to compute $\left[\underline{y}, \overline{y}\right] = \left[\min h\left(\frac{\sum_{i=1}^{n} w_i h^{-1}(x_i)}{\sum_{i=1}^{n} w_i} \right), \max h\left(\frac{\sum_{i=1}^{n} w_i h^{-1}(x_i)}{\sum_{i=1}^{n} w_i} \right) \right]$ for any strictly monotonic function h, which in the present case we take to be h_r. We call the resulting algorithm WPMEKM for the special case of weighted power means, while recognizing the more general application.

WPMEKM Algorithm

1) If the minimum $L_r\left(\mathbf{x}, \mathbf{w}\right) = \underline{L}_r$ is to be computed, set $k = \left[n / 2.4 \right]$ where $[x]$ is the nearest integer to x. Set $x_i = \underline{x}_i$, $u_i = \underline{w}_i$ and $v_i = \overline{w}_i$ for each $i = 1,\ldots,n$. If the maximum $L_r(\mathbf{x}, \mathbf{w}) = \overline{L}_r$ is to be computed, set $k = \left[n / 1.7 \right]$, $x_i = \overline{x}_i$, $u_i = \overline{w}_i$ and $v_i = \underline{w}_i$ for $i = 1,\ldots,n$.

2) Sort the x_i for $i = 1,\ldots,n$ in ascending order so that $x_{i_1} \le x_{i_2} \le \cdots \le x_{i_n}$ where i_j, $j = 1,\ldots,n$ represents the original index values. Rearrange the weight interval endpoints u_i and v_i using the same permutation of index values i_j, $j = 1,\ldots,n$ that result from the x_i sort. Now refer to x_i, u_i, v_i, $i = 1,\ldots,n$ as the sorted sets of inputs and weights.

3) Compute

$$a = \sum_{i=1}^{k} h^{-1}(x_i) v_i + \sum_{i=k+1}^{n} h^{-1}(x_i) u_i, \quad (10)$$

$$b = \sum_{i=1}^{k} v_i + \sum_{i=k+1}^{n} u_i, \quad y = \left(\frac{a}{b} \right). \quad (11)$$

4) Find $k' \in \{0,1,...,n\}$ such that $x_{k'} \le h(y) < x_{k'+1}$. Check if $k' = k$. If yes, set $L_r(\mathbf{x}, \mathbf{w}) = h(y)$, stop. If no, continue.

5) Set $s = sign\left(k' - k\right)$, and compute

$$a' = a + s \sum_{i=\min(k,k')+1}^{i=\max(k,k')} h^{-1}(x_i)\left(v_i - u_i\right), \quad (12)$$

$$b' = b + s \sum_{i=\min(k,k')+1}^{i=\max(k,k')} \left(v_i - u_i\right), \; y = \left(\frac{a'}{b'} \right). \quad (13)$$

6) Set $a = a'$, $b = b'$ and $k = k'$. Go to step 4).

Note that because h is strictly monotonic, the sort on x_i results in either an ascending or descending sort on $h^{-1}(x_i)$ depending on whether h is increasing or decreasing.

With the WPMEKM algorithm, the weighted power mean interval boundaries can be computed for any value of r. These interval-valued results enable us directly to compute arbitrarily accurate approximations to the weighted power mean membership function for scores and weights that are fuzzy sets, using the α-cut representation theorem [10]. In this case the interval computation is applied to α-cuts of the input variables to determine the corresponding α-cuts of the output variable. In the IT2 case, this computation is applied to both the upper and lower bounding functions for the scores and weights to determine the corresponding upper and lower bounding functions of the global score.

III. INVESTMENT JUDGMENT ADVISOR REVIEW

The IJA example in [1] originated with Tong and Bonissone [17], who considered the decision confronting an individual with a moderately large amount of capital who wishes to select among five investment sector alternatives, using four investment criteria. The five alternatives are commodities (a_1), stocks (a_2), gold (a_3), real estate (a_4) and long-term bonds (a_5). The four investment criteria are:

risk of losing capital (c_1),inflation vulnerability (c_2), anticipated profit (c_3) and liquidity (c_4). The investor's goal is to rate each investment with respect to the four criteria and then aggregate these ratings into a decision statistic that can be used for ranking (or for capital allocation among the different alternatives to achieve an appropriately diversified portfolio.)

Through a process of interval analysis [18] using inputs from real subjects, Mendel and Wu derive three descriptive vocabularies of eight, seven and four words that are represented using IT2 MFs. The UMF and LMF of each vocabulary word MF is a trapezoid disposed on the domain interval $[0,10]$, with the extreme words in each vocabulary typically represented by left- or right-shoulder MFs, while the intermediate words are represented by mid-range MFs. (For details, see [1], Tables 7.13, 7.14 and 7.15.) The eight-word vocabulary expresses *amount*, characterized by None to Very Little (NVL) , Very Low (VL), Low (L), More or Less Low (MLL), Fair to More or Less High (FMLH), More or Less High (MLH), High (H) and Extremely High (EH). This vocabulary is used to grade each alternative with respect to the first three criteria, where in keeping with [1] a simple *antonym* $\mu_{10-\tilde{A}}(x)$ of the respective IT2 MF is used for criteria 1 and 2 in the aggregation, i.e., $\mu_{10-\tilde{A}}(x) = \mu_{\tilde{A}}(10-x)$. Alternative forms for the membership functions antonyms which exhibit more intuitive behaviour are discussed in [19].

The seven-word vocabulary expresses *quality*, characterized by Very Bad (VB), Bad (B), Somewhat Bad (SB), Fair (F), Somewhat Good (SG), Good (G) and Very Good (VG). This vocabulary is used in grading the alternatives with respect to criterion 4. The four-word vocabulary expresses *importance*, characterized by Unimportant (U), More or Less Unimportant (MLU), More or Less Important (MLI) and Very Important (VI). Table 1 (replicated from [1]) presents three hypothetical word evaluation matrices grading each investment alternative from the perspectives of speculative, conservative and in-between investors, respectively.

TABLE 1 LINGUISTIC RATINGS AND WEIGHTS OF INVESTMENT ALTERNATIVES WRT CRITERIA

(a) Speculative Investor

Ratings	c_1	c_2	c_3	c_4
a_1	FMLH	FMLH	EH	G
a_2	MLH	FMLH	H	SG
a_3	VL	L	VL	SB
a_4	MLL	MLH	MLH	SG
a_5	NVL	MLL	VL	VB
Weight	U	MLU	VI	MLU

(b) Conservative Investor

Ratings	c_1	c_2	c_3	c_4
a_1	EH	MLH	MLL	F
a_2	H	H	MLH	SG
a_3	MLL	FMLH	FMLH	F
a_4	MLH	MLH	H	F
a_5	NVL	MLL	MLH	SG
Weight	VI	MLI	VI	MLI

(c) In-between Investor

Ratings	c_1	c_2	c_3	c_4
a_1	H	H	MLH	SB
a_2	FMLH	FMLH	H	VG
a_3	L	MLL	MLL	SB
a_4	FMLH	FMLH	H	SG
a_5	L	L	L	F
Weight	MLI	MLI	VI	MLI

Mendel and Wu use the LWA to aggregate the criteria evaluations and importance evaluations for each alternative into corresponding output IT2 MFs, which are then ranked to determine the order of appropriateness of the investment categories for each of the three types of investors. In the next section we generalize these results using the LWPM with different power exponents on the same input data, which will illustrate the versatility of this aggregation operator as a function of the power exponent.

IV. COMPARISON OF AGGREGATION OPERATORS

When a parameterized aggregation operator such as the LWPM ranges between conjunction and disjunction, we define its similarity to conjunction as the degree of *andness* and its similarity to disjunction as the degree of *orness*, where andness is the complement to orness. The weighted arithmetic mean is equi-similar to conjunction and disjunction, with both andness and orness equal to 1/2. Andness of an aggregator L for which $x_1 \wedge \cdots \wedge x_n \le L(\mathbf{x},\mathbf{w}) \le x_1 \vee \cdots \vee x_n$ everywhere is defined in [13] to be:

$$\alpha_g = \frac{\overline{x_1 \vee \cdots \vee x_n} - \overline{L(\mathbf{x},\mathbf{w})}}{\overline{x_1 \vee \cdots \vee x_n} - \overline{x_1 \wedge \cdots \wedge x_n}} = \frac{n-(n+1)\left(\overline{L(\mathbf{x},\mathbf{w})}\right)}{n-1}, \quad (14)$$

where the overbar denotes averaging over the hypercube $[0,1]^n$ in which $\mathbf{x}$ lies. An aggregator L that is more similar to conjunction than disjunction is referred to as *partial conjunction*, and if vice versa, as *partial disjunction* [13]. Properties are partially substitutable if L is a partial

disjunction, and must be partially simultaneous if L is a partial conjunction.

When L is the weighted power mean with fixed weights and input scores, $L_r(\mathbf{x},\mathbf{w})$ is a continuous and increasing function of r. Therefore from (14), the andness $\alpha_g^{(r)}$ of $L_r(\mathbf{x},\mathbf{w})$ is a monotonically decreasing function of r. When $-\infty < r < 1$, $L_r(\mathbf{x},\mathbf{w})$ represents partial conjunction (i.e., $\alpha_g^{(r)} > 0.5$) whereas for $1 < r < +\infty$, $L_r(\mathbf{x},\mathbf{w})$ represents partial disjunction. For $r \le 0$, $L_r(\mathbf{x},\mathbf{w}) = 0$ if $x_i = 0$ for any $i \in \{1,\ldots,n\}$. Therefore $r = 0$ is the upper bound on r when all inputs are mandatory.

When the inputs are represented by IT2 MFs, the notions of substitutable and mandatory are no longer crisp, but the qualitative aspects of partial disjunction/conjunction are still preserved. To illustrate the range of behaviors for the LWPM as compared with the LWA, we plot in the following sequences of figures the output IT2 MF footprint of uncertainty (FOU) of the LWPM for different values of the power exponent r. In each figure we also plot the FOU of the LWA where $r = 1$, with andness $\alpha_g^{(1)} = 0.5$. The "+" crosshatch corresponds to the LWA MF, while the "x" crosshatch corresponds to the LWPM MF; the UMF is shown as a solid line, while the LMF is shown as a dashed line. The solid vertical line indicates the defuzzified centroid of the LWPM IT2 MF, and the two dashed vertical lines indicate the left and right endpoints of the LWPM centroid interval. Note that our purpose in the choices of alternatives shown below is to illustrate the cases where the LWPM is qualitatively the *most* similar and the *least* similar to the LWA results for a given value of the parameter r.

Consider first the extreme cases of $r = \pm\infty$, where the andness of the LWPM is 1 ($r = -\infty$) or 0 ($r = +\infty$). Figs. 1-6 are for $r = +\infty$, with andness $\alpha_g^{(\infty)} = 0$ (pure disjunction), where the LWPM MF lies generally to the right of the LWA MF. Odd numbered figures correspond to the alternatives for which the LWPM MF FOU is most similar qualitatively to that of the LWA, and even numbered figures correspond to alternatives for which it is most dissimilar to the LWA.

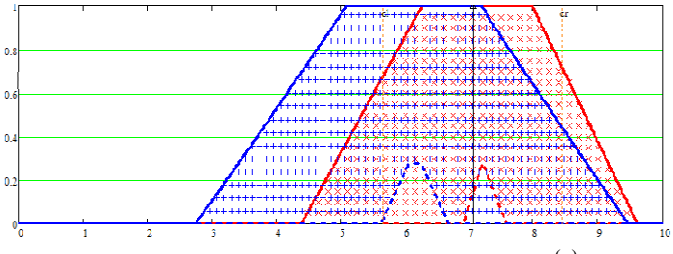

Figure 1 Speculative investor FOUs for a_4, $r = +\infty$, $\alpha_g^{(\infty)} = 0$

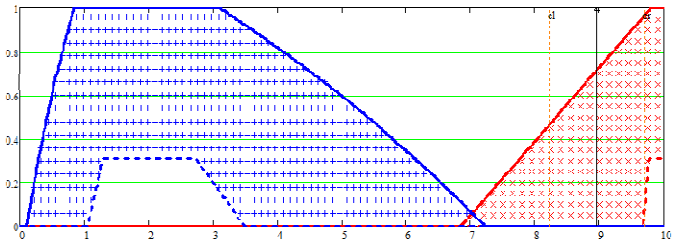

Figure 2 Speculative investor FOUs for a_5, $r = +\infty$, $\alpha_g^{(\infty)} = 0$

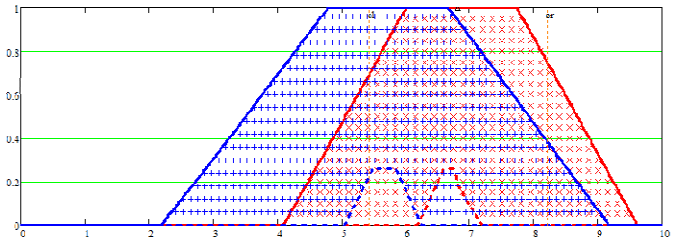

Figure 3 Conservative investor FOUs for a_3, $r = +\infty$, $\alpha_g^{(\infty)} = 0$

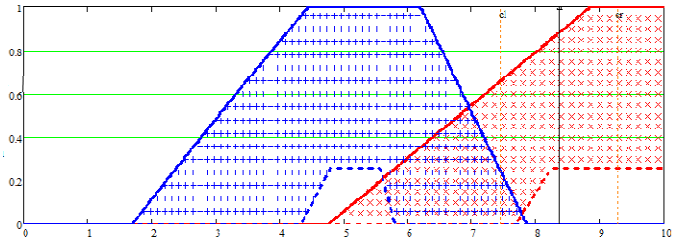

Figure 4 Conservative investor FOUs for a_4, $r = +\infty$, $\alpha_g^{(\infty)} = 0$

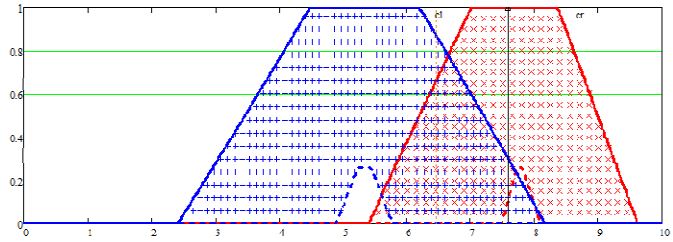

Figure 5 In-between investor FOUs for a_5, $r = +\infty$, $\alpha_g^{(\infty)} = 0$

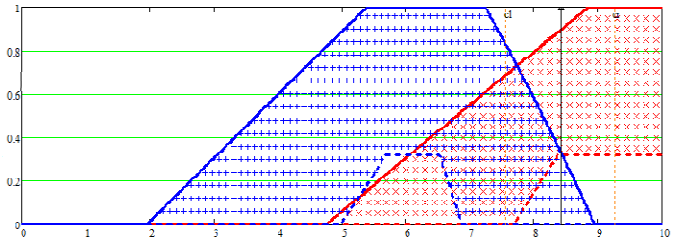

Figure 6 In-between investor FOUs for a_4, $r = +\infty$, $\alpha_g^{(\infty)} = 0$

We observe a dramatic range of differences between the LWPM and LWA over different alternatives, which is a function of the *dispersion* of the evaluation words' IT2 MFs over the 0-10 scale with respect to the various criteria. The LWA smooths these differences, resulting in an interior

trapezoidal IT2 MF in all cases, while the LWPM for $r = +\infty$ often results in a right-shoulder trapezoidal IT2 MF.

Figs. 7-12 show analogous results for the case $r = -\infty$ (pure conjunction), which corresponds to andness $\alpha_g^{(-\infty)} = 1$.

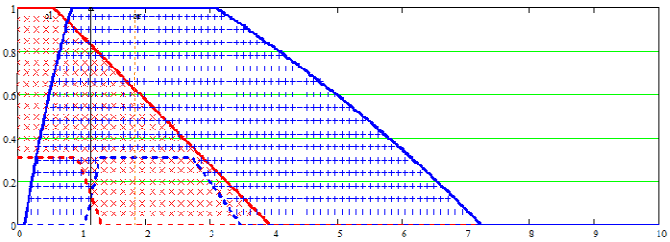

Figure 7 Speculative investor FOUs for a_5, $r = -\infty$, $\alpha_g^{(-\infty)} = 1$

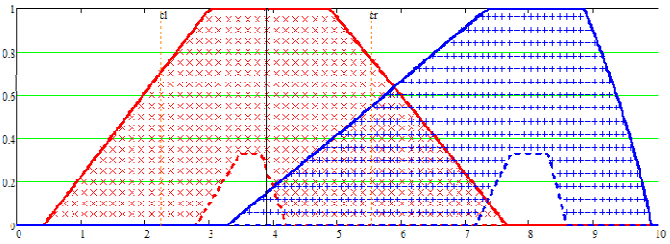

Figure 8 Speculative investor FOUs for a_1, $r = -\infty$, $\alpha_g^{(-\infty)} = 1$

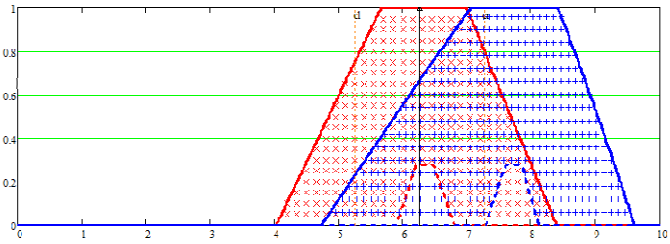

Figure 9 Conservative investor FOUs for a_5, $r = -\infty$, $\alpha_g^{(-\infty)} = 1$

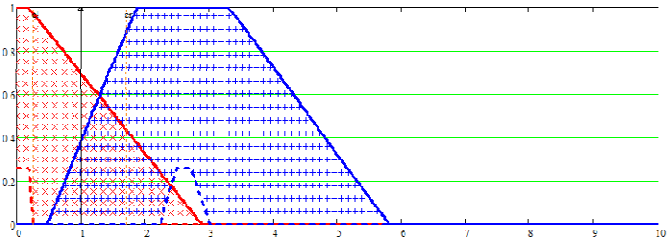

Figure 10 Conservative investor FOUs for a_1, $r = -\infty$, $\alpha_g^{(-\infty)} = 1$

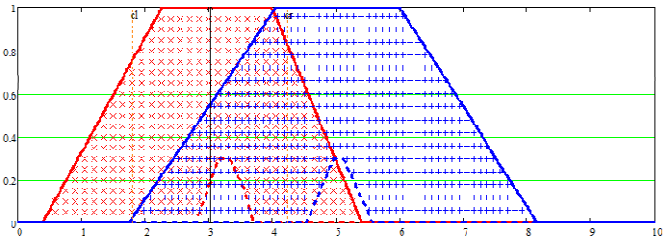

Figure 11 In-between investor FOUs for a_3, $r = -\infty$, $\alpha_g^{(-\infty)} = 1$

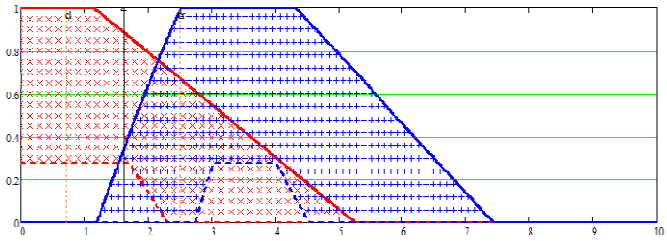

Figure 12 In-between investor FOUs for a_1, $r = -\infty$, $\alpha_g^{(-\infty)} = 1$

Here, the LWPM MF lies generally to the left of the LWA MF, since the LWPM for $r = -\infty$ selects the *minimum* left and right endpoints over the input MFs for each α-cut. Again we observe a substantial range of differences between the LWPM and LWA IT2 MFs, with the LWPM often transitioning to a left-shoulder trapezoidal IT2 MF.

These examples serve to illustrate the substantially greater aggregation versatility of the LWPM over the LWA. By the choice of r, we impart different perspectives to the fuzzy IT2 decision process, ranging from the most optimistic view having an orness of 1, to the most pessimistic view having an andness of 1, with a continuous range of andness/orness between these extremes. This compares with the single value of andness = orness = 0.5 available with the LWA, which averages out the more extreme inputs and thus might be termed a "consensus" view.

Figs. 13-18 show the analogous results for the case $r = -1$ (i.e., the harmonic mean), for which $\alpha_g^{(-1)} = 0.773$. Here, we observe considerably more overlap between the LWPM and LWA MFs, since the power exponents of the two aggregation operators are closer in value. However, even in this case, we observe instances (i.e., Figs. 16 and 18) where the LWPM transitions into a left-shoulder trapezoidal IT2 MF, whereas the LWA has a midrange trapezoidal IT2 MF in all cases.

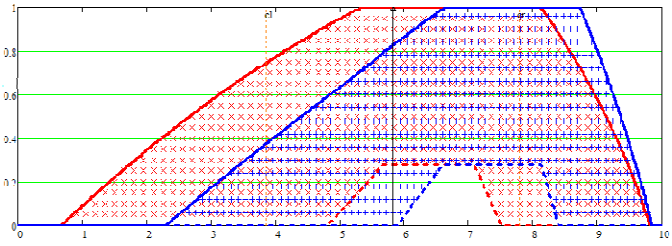

Figure 13 Speculative investor FOUs for a_2, $r = -1$, $\alpha_g^{(-1)} = 0.773$

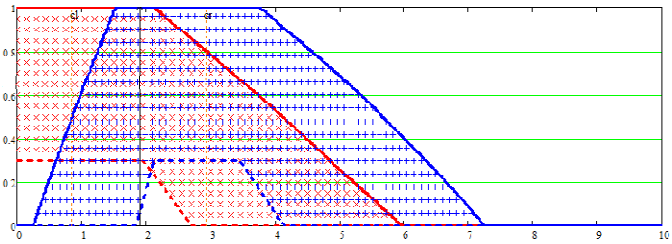

Figure 14 Speculative investor FOUs for a_3, $r = -1$, $\alpha_g^{(-1)} = 0.773$

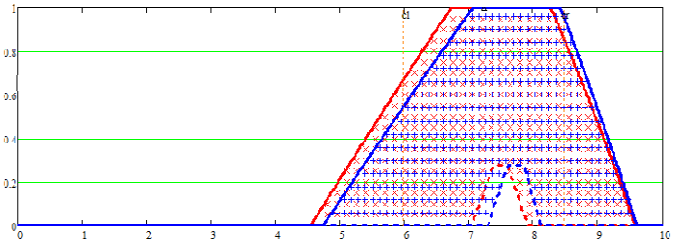

Figure 15 Conservative investor FOUs for a_5, $r=-1$, $\alpha_g^{(-1)}=0.773$

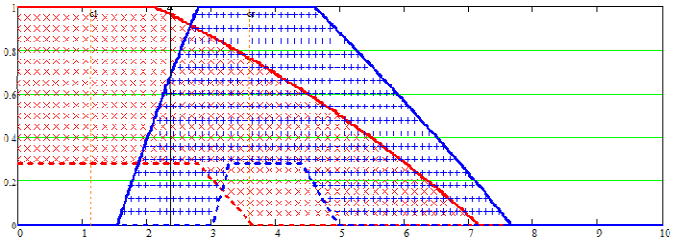

Figure 16 Conservative investor FOUs for a_2, $r=-1$, $\alpha_g^{(-1)}=0.773$

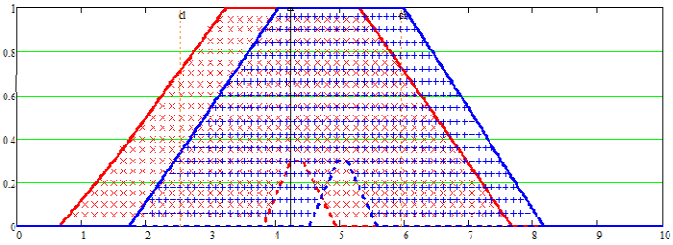

Figure 17 In-between investor FOUs for a_3, $r=-1$, $\alpha_g^{(-1)}=0.773$

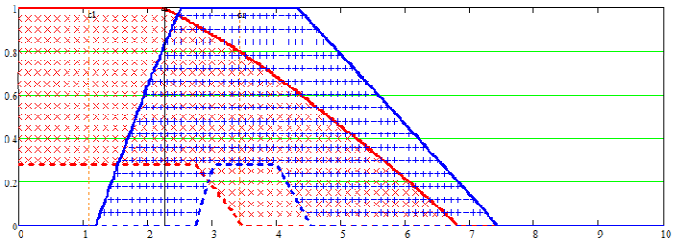

Figure 18 In-between investor FOUs for a_1, $r=-1$, $\alpha_g^{(-1)}=0.773$

In other examples in [1], Mendel and Wu employ hierarchical LWAs in a decision tree to aggregate subcategories of criteria scores into higher-level criteria. Use of the LWPM enables us further to generalize these hierarchical aggregations. For example, to aggregate a mandatory fuzzy input x_1 with a desired fuzzy input x_2, Dujmovi [20] composes bivariate operators denoted by $x_1\Delta(x_1\nabla x_2)$ and called *conjunctive partial absorption* (CPA) aggregators (see also [13]). CPA aggregators apply a WPM partial disjunction (denoted ∇, where $r\geq 1$) to the two inputs, and then take a partial conjunction (denoted Δ, where $r\leq 0$) of that output with the mandatory input.

In a type-1 fuzzy context, $x_1\Delta(x_1\nabla x_2)$ necessarily is zero if x_1 is zero, and $x_1\Delta(x_1\nabla x_2)-x_1$ is positive (resp. negative) when x_2 is greater (resp. less) than x_1. The absolute difference $\left|x_1\Delta(x_1\nabla x_2)-x_1\right|$ is called the *reward* when x_2 is greater than x_1, and is otherwise called a *penalty* [13]. We construct the operator $x_1\Delta(x_1\nabla x_2)$ from weighted power means as

$$CPA_2(\mathbf{x},\mathbf{w}',\mathbf{w})=L_r\left(\left(x_1,L_s(\mathbf{x},\mathbf{w})\right),\mathbf{w}'\right), \qquad (15)$$

with $r\leq 0, 1\leq s<\infty$. Here, $\left(x_1,L_s(\mathbf{x},\mathbf{w})\right)$ are 2-dimensional scores, and $\mathbf{w}'$ is a 2-dimensional weight vector. However $\mathbf{x}$ and $\mathbf{w}$ may be of higher dimension if we have multiple partially substitutable inputs.

As an illustration of the application of IT2 CPA operators, suppose the speculative investor places a mandatory (in a type-1 context) requirement on high investment returns (criterion c_3 in Table 1), making it analogous to x_1 in (15), with a LWPM aggregation of the remaining criteria scores constituting x_2 using a power exponent of -1, as in Figs. 13-18. Suppose further that we specify a maximum reward of +15%, with a maximum penalty of -25%, and set $r=-10$ and $s=1.449$ (the latter corresponding to an andness of 7/16) in (15). Using the techniques of [20], we compute corresponding type-1 weights $\mathbf{w}=(0.347,0.653)$ and $\mathbf{w}'=(0.935,0.065)$ in (15) that achieve these reward/penalty values, and then calculate the LWPMs for ∇ and Δ on the IT2 input variables, with singleton weights.

Fig. 19 shows the CPA IT2 FOU (X crosshatch) and the LWA FOU (+ crosshatch) for investment alternative a_1 (commodities). Comparing this with Fig. 20, where we used a LWPM on all four inputs with $r=-1$, we observe that the CPA FOU is substantially narrower, and is disposed over considerably higher values, than the LWPM FOU. This is understandable from inspection of Table 1, where we observe that the potential for high investment returns in commodities is graded as "extremely high" by a speculative investor. Thus we would expect an enhanced score for commodities when this criterion is elevated to mandatory.

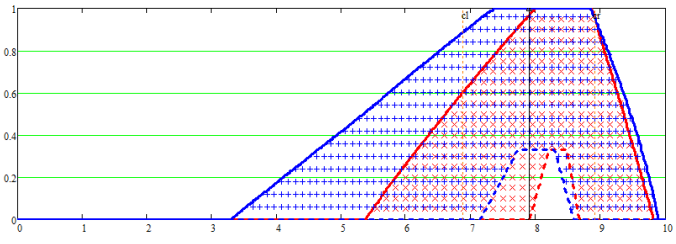

Figure 19 Speculative investor CPA for a_1, with c_3 mandatory.

On the other hand, Figs. 21-22 show the same comparison for investment alternative a_5 (long-term bonds), whose potential for high returns is graded "very low" by the speculative investor. The CPA FOU differs relatively little from the comparable LWPM FOU, since alternative a_5 is in fact scored relatively low with respect to *all* criteria by the speculative investor.

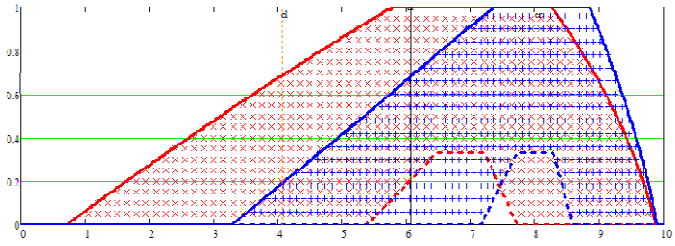

Figure 20 Speculative investor LWPM for a_1, $r=-1$, $\alpha_g^{(-1)}=0.773$.

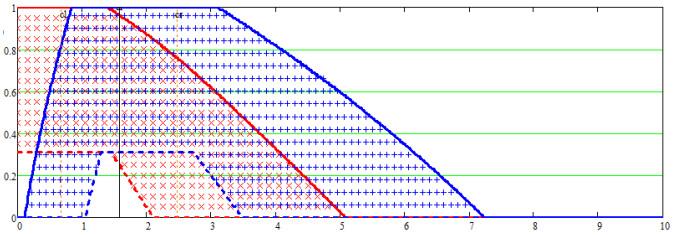

Figure 21 Speculative investor CPA for a_5, with c_3 mandatory.

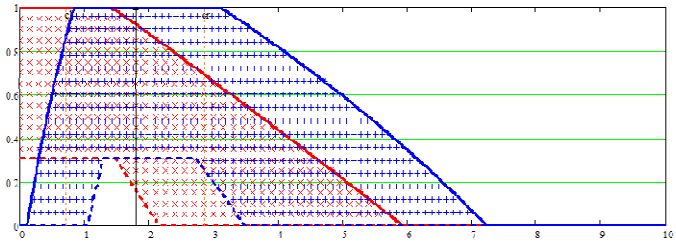

Figure 22 Speculative investor LWPM for a_5, $r=-1$, $\alpha_g^{(-1)}=0.773$.

V. CONCLUSION

We introduce a new family of Per-C computational engines based on the LWPM, and compare it with the LWA using an extended example described in [1]. The WPMEKM algorithm is presented for the computation of LWPM aggregations with interval input and weight variables. This can be extended to inputs and weights described by IT2 MFs using the α-cut Representation Theorem. The LWPM is shown to be a much more versatile aggregation operator, and thus it provides a significant extension to the suite of tools available for CWW applications. We also show how LWPM modules can be used to produce conjunctive partial absorption operators, and illustrate their differences with respect to a straightforward LWPM. These operators enable far more general hierarchical logic functions to be constructed than are available with simple hierarchies of LWAs.

REFERENCES

[1] Mendel, J.M. and D. Wu, *Perceptual Computing*, Hoboken, N.J.: John Wiley & Sons, Inc., 2010.

[2] Zadeh, L.A., "Fuzzy logic = computing with words," *IEEE Trans. Fuzzy Syst*., vol. 4, pp. 103-111, 1996.

[3] Special Section on Computing with Words, *IEEE Trans. Fuzzy Syst*., vol. 18, June 2010.

[4] Mendel, J.M., "Computing with words: Zadeh, Turing, Popper and Occam," *IEEE Computational Intelligence Magazine*, vol. 2, pp. 10-17, Nov. 2007.

[5] Yager, R.R., "Approximate reasoning as a basis for computing with words, in L.A. Zadeh and J. Kacprzyk (Eds.) *Computing with Words in Information/Intelligent Systems I: Foundations*, Heidelberg: Physica-Verlag, pp. 50-77, 1999.

[6] Yager, R.R., "On the retranslation process in Zadeh's paradigm of computing with words," *IEEE Trans. On Systems, Man, and Cybernetics—Part B: Cybernetics*, vol. 34, pp. 1184-1195, March 2004.

[7] Zadeh, L.A., "Toward human-level machine intelligence—Is it achievable? The need for a new paradigm shift," *IEEE Computational Intelligence Magazine*, vol. 3, pp. 11-22, August 2008.

[8] Mendel, J.M., *Uncertain Rule-Based Fuzzy Logic Systems: Introduction and New Directions*, Upper Saddle River, NJ: Prentice-Hall, 2001.

[9] Karnick, N. and J.M. Mendel, "Centroid of a type-2 fuzzy set," *Information Sciences*, vol. 132, pp. 195-220, 2001.

[10] Klir, G. and B. Yuan, *Fuzzy Sets and Fuzzy Logic*, Upper Saddle River, NJ: Prentice-Hall, 1995.

[11] Salton, G., E.A. Fox and H. Wu, "Extended Boolean information retrieval," *Communications of the ACM*, vol. 26, pp. 1022–1036, Dec. 1983.

[12] Hong W.S., Chen S.J. and Wang L.H., et al. "A new approach for fuzzy information retrieval based on weighted power-mean averaging operators," *Computers & Mathematics with Applications*, vol. 53, pp.1800-1819, June 2007.

[13] Dujmović, J., "Continuous preference logic for system evaluation," *IEEE Trans. on Fuzzy Systems*, vol. 15, pp. 1082-1099, Dec. 2007.

[14] Rickard, J.T., J. Aisbett, R.R. Yager and G. Gibbon, "Fuzzy weighted power means in evaluation decisions," to be presented at *World Conf. on Soft Computing*, San Francisco, CA, May 2011.

[15] Wu, D. and J.M. Mendel, "Aggregation using the linguistic weighted average and interval type-2 fuzzy sets," *IEEE Trans. on Fuzzy Systems*, vol. 15, pp. 1145-1161, Dec. 2007.

[16] Wu, D. and J.M. Mendel, "Corrections to 'Aggregation using the linguistic weighted average and interval type-2 fuzzy sets'," *IEEE Trans. on Fuzzy Systems*, vol. 16, pp. 1664-1666, Dec. 2008.

[17] Tong, R.M. and P.P. Bonissone, "A linguistic approach to decision making with fuzzy sets," *IEEE Trans. Syst., Man, Cybern*., vol. SMC-10, pp.716–723, Nov. 1980.

[18] Liu F. and J.M. Mendel, "Aggregation using the fuzzy weighted average as computed using the Karnick-Mendel algorithms," *IEEE Trans. Fuzzy Syst.*, vol.17, Dec. 2009.

[19] Trillas E., C. Moraga, S. Guadarrama, S. Cubillo and E. Castiñeira, "Computing with Antonyms", in M. Nikravesh et al., (eds.), Forging New Frontiers: Fuzzy Pioneers I. *Studies in Fuzziness and Soft Computing*, vol. 217, pp. 133-153, 2007.

[20] Dujmović, J., "Partial absorption functions,", *J. Univ. Belgrade, EE Dept.* ser. Math & Physics, no. 659, pp. 156-163, 1979.

2011 IEEE International Conference on Fuzzy Systems
June 27-30, 2011, Taipei, Taiwan

Finding the Capacity of Fuzzy Neural Networks (FNNs) via Its Equivalent Fully Connected Neural Networks (FFNNs)

Jing Wang
Faculty of Science and Technology
University of Macau
MSAR, People Republic of China
wj_adr@163.com

Chi-Hsu Wang, FIEEE
Department of Electrical Engineering
National Chiaotung University
Hsinchu, Taiwan
cwang@cn.nctu.edu.tw

C. L. Philip Chen, FIEEE
Faculty of Science and Technology
University of Macau
MSAR, People Republic of China
philip.chen@ieee.org

***Abstract*—The capacity of Fuzzy Neural Network (FNN) is explored in this paper. The FNN is first transformed into an equivalent fully connected three layer neural network, or FFNN, via a new approach proposed in this paper. Then the lower and upper bounds of FNN can be found. To check the validity of the theoretical bounds, an example is illustrated with the trainings to yield excellent capacity matching with the theoretical bounds. This new finding has its emerging values in all engineering applications using FNN, such as intelligent adaptive control, pattern recognition, and signal processing, …, etc.**

Keywords-Neural Networks, Fuzzy Logic, Fuzzy Neural Networks, Back Propagations, Universal Approximation Theorem, Capacity of Neural Networks

I. INTRODUCTION

During the past decade, fuzzy neural networks (FNNs) have been proposed and successfully applied to solve problems in various fields, such as intelligent adaptive control, system identification, pattern classification and image processing,…, etc [1-4]. FNN can utilize human experience and knowledge by incorporating linguistic fuzzy information. FNN consists of a set of if-then fuzzy rules. The rules are built up by human experts as linguistic knowledge. To obtain better performance, some training algorithms such as back-propagation(BP) algorithm is adopted to tune the parameters of fuzzy system and the weights of neural network. Training algorithm attempts to minimize the training error, which is the difference between the desired and actual outputs [5]. If FNN is properly constructed, it follows Universal Approximate Theorem (UAT), i.e., the properly constructed FNN can approximate any functions [6-7]. However, the UAT does not point out how to properly construct the fuzzy system and neural network. This is to say that the FNN designed for certain applications by human experts cannot be ideal, which will lead to the discussion of the constraints of FNN, i.e., the capacity of FNN, so that engineering applications via FNN can be achieved. Similar to the discussions of the capacity of multilayer neural networks [8], the capacity of FNN is defined as the maximum number of desired input vectors that can be mapped to desired output vectors without error. This is also to say that the number of training samples has significant impact on training process. Excessive samples size may lead training process to be diverged. The capacity of associative memory and multilayer perceptron (MLP) has been conducted in the past decade, assuming a fully connected neural network [8-15]. However, the capacity of FNN has never been found in the literatures. This is due to fact that the FNN is not a fully connected directed graph and the intermediate layer is defined as a product layer, instead of a summing layer in a NN.

To apply the techniques in finding the capacity of three layers NN, a new approach is proposed to transform the four layers FNN into a fully connected directed graph with all summing nodes. This is achieved in this paper by also combining a systematic fuzzy rule generation for FNN [16] so as to obtain a fully indexed equivalent three layer NN for FNN, or FFNN. By using this new FFNN, the lower and upper bounds of the capacity of FNN can be found in this paper. An example is illustrated this paper to validate the theoretical bounds by back propagation trainings. Excellent matching is achieved between the theoretical bounds and training simulation.

978-1-4244-7316-8/11/$26.00 ©2011 IEEE

II. THE FNN WITH SYSTEMATIC RULE GENERATION

Given the training input data vectors $\{x_q^*, q = 1, 2, 3, \cdots, n\}$, and the desired output vectors $\{y_p^*, p = 1, 2, \ldots, m\}$, the inference rules of simplified fuzzy reasoning can be established by the expert. The l^{th} control rule has the following form:

Rule l: IF x_1 is $A_1^{r_1}$ and ….. and x_n is $A_n^{r_n}$ THEN y_1 is W_{l1} and …. and y_m is W_{lm}

where l is a rule number, the $A_q^{r_i}$ are membership functions of antecedent part, and W_{lp} are real numbers of the consequent part. When the inputs are given, the truth value μ_l of the premise of the l^{th} rule is defined by

$$\mu_l = A_1^{r_1}(x_1)\times\cdots\times A_n^{r_n}(x_n); \{l = 0,1,2,\ \ldots, L;\ r_i = 0,1,2,\ldots,R_{i-1}\} \quad \text{趙} \tag{1}$$

where L is total number of fuzzy rules and R_i is the number of MFs for fuzzy variable x_i , and r_i is the ordinal index of MFs for fuzzy variable x_i . Among the commonly used defuzzification strategies, the simplified fuzzy reasoning yields a superior result. The output yp of the fuzzy reasoning can be derived from the following equation:

$$y_p = \frac{\sum_i \mu_i w_{ip}}{\sum_i \mu_i}, (p = 1,2,\cdots,m) \tag{2}$$

Where μ_l is the truth value of the premise of the l^{th} rule, equations (1) and (2) describe the simplified fuzzy reasoning methods, through which the membership functions of the antecedent part are chosen. Then the fuzzy neural network (FNN) can be constructed and is shown in Fig. 1. [1]

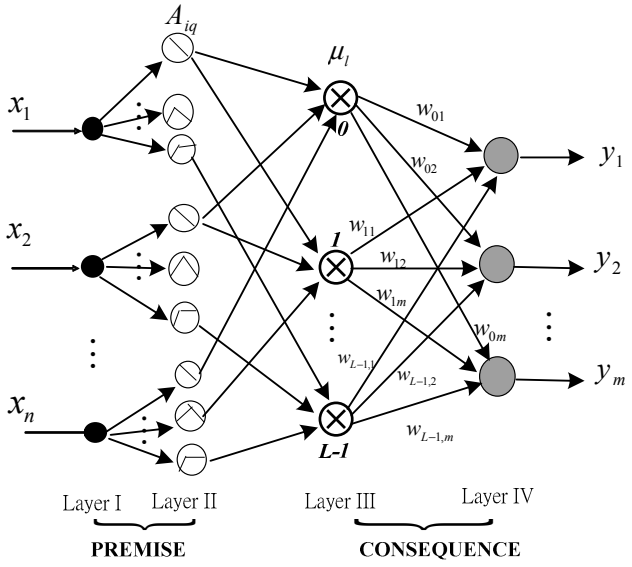

Figure. 1 The configuration of FNN

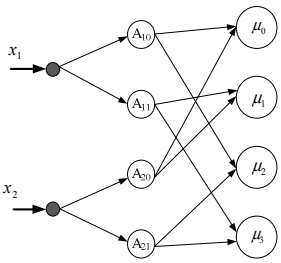

Figure. 2. Simple Illustration of Layers 1, 2 and 3 in FNN

TABLE I. SYSTEMATIC GENERATION OF RULES FROM MFS

r_1	r_2	$l(=r_1+2r_2)$	μ_l
0	0	0	$A_{10}(x_1)A_{20}(x_2)$
1	0	1	$A_{11}(x_1)A_{20}(x_2)$
0	1	2	$A_{10}(x_1)A_{21}(x_2)$
1	1	3	$A_{11}(x_1)A_{21}(x_2)$

Figure. 1 shows that the system has a total of four layers. Nodes at Layer I are input nodes, which represent input linguistic variables. Nodes at Layer II are term nodes, which represent the terms of the respective linguistic variables. Each node at Layer III is a fuzzy rule. All the layer-three nodes form the fuzzy rule base. Layer IV is the output layer. The links between Layer III and IV are fully connected by the weighting factors w_{lp}. Further a systematic generation of the fuzzy rule in Layer III has been derived in [16] which can reduce the programming effort with less execution time in real-time applications. In [16], a systematic generation of fuzzy rules in Layer III of the FNN in Figure 1 has been presented. In particular, the ordinal index l of the l^{th} fuzzy rule is:

$$l = r_1 + \sum_{i=2}^{n}\left(\prod_{j=1}^{i-1} R_j\right) r_i \tag{3}$$

where R_i is the total number of MFs for fuzzy variable x_i , and r_i ($0 \le r_i \le R_i - 1$) is the ordinal index for the r_i th MF for fuzzy variable x_i . Equation (3) can produce all the $l's$ in the range of $0 \le l \le (\prod_{i=1}^{n} R_i) - 1$ with a one-to-one mapping from MFs to fuzzy rules. This will provide us with a complete indexing of the equivalent fully connected fuzzy neural network for FNN in the following sections. For two fuzzy variables $\{x_1, x_2\}$ with two MFs for $\{x_1, x_2\}$, i.e., $\{A_{10}(x_1), A_{11}(x_1)\}$ for x_1 , $\{A_{20}(x_2), A_{21}(x_2)\}$ for x_2 , with $\{R_1 = R_2 = 2\}$, as shown in Fig. 2. From (3), the ordinal index of four fuzzy rules can be generated using $\{l = r_1 + 2r_2, l = 0,1,2,3\}$. Table I shows the result.

III. THE EQUIVALENT FULLY CONNECTED NEURAL NETWORK FOR FNN

As can be seen from the above discussion of FNN, the FNN is not a fully connected graph between Layer II and Layer III. This will hinder the discussion of the capacity of FNN. Therefore, in order to find the capacity of FNN, we need to convert the FNN into a fully connected neural network. There are two obstacles to be resolved. The first obstacle is that the links between Layer II and Layer III of FNN are not fully connected. The second obstacle is that computation unit in Layer III of FNN is a product unit rather than a summing unit. From Fig. 1, we can see the transitions from Layer II to Layer III can be simplified by arranging the links between Layer I to Layer III using equivalent weights. This can be more easily observed from Fig. 2 that there are links from each input node (x_1 or x_2) to every fuzzy rule, all through one of the MFs of every input node. Figures 3-1 & 3-2 show these cases for x_1 and x_2 with proper link weights. This is to say that we can suppress Layer II (MF layer) in the original FNN and replace new links between Layer I and Layer III, so that we can have a fully connected FNN (FFNN) as shown in Fig. 3-3.

This can be generalized to a general case of fully connected FNN, or FFNN as shown in Figure 4. This can resolve the first obstacle of not-fully connected property of the original FNN shown in Figure 1. The $\{V_{ij}(i=1,2,...,n; j=1,2,...,L)\}$ in Fig. 4 is defined as the link weight between the i^{th} node of Input Layer and the j^{th} node of Hidden Layer, or the fuzzy rule layer.

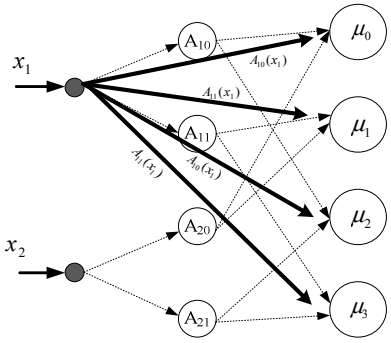

Figure. 3-1. Suppressing the MF Layer for x_1

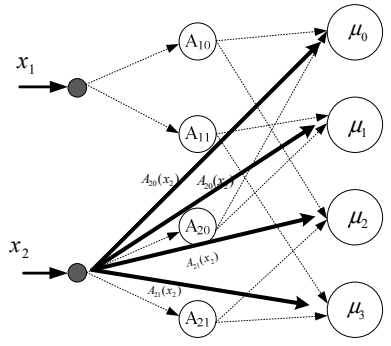

Figure. 3-2. Suppressing the MF Layer for x_2

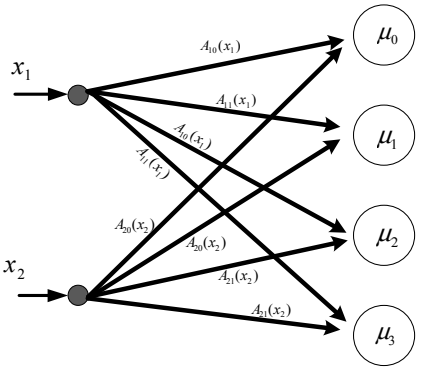

Figure 3-3. Suppressing the MF Layer with proper link weights

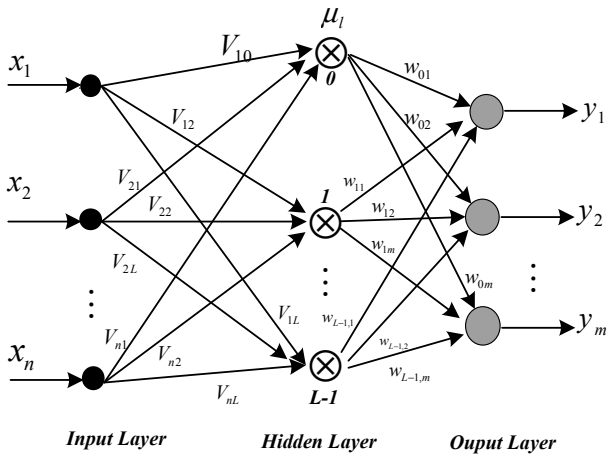

Figure 4. The equivalent fully connected neural network for FNN

However, the V_{ij} links between Input Layer and Hidden Layer in Figure 4 are still not well specified to yield μ_l in the Hidden Layer. We only know that each input node is only allowed to contribute one link weight form μ_l. Therefore μ_l is expressed in term of the product of n V_{ij} weights. Fortunately, a systematic way to generate the fuzzy rules in Hidden Layer has been proposed in [16]. This is to say that, given the fuzzy rule μ_l, we can determine its related links from all input nodes in a systematic way. From (3), we can reversely find all the r_i's for a specific l (fuzzy rule number in Layer III) as follows:

$$r_1(l) = l\%R_1;$$
$$r_i(l) = (l / \prod_{k=1}^{i-1} R_k)\%R_i, i = 2,...,n \quad (4)$$

where A % B represents the remainder of the division of A over B, A/B represents the quotient of the division of A over B. From (4) we can get n ordinal index $r_i(l)(i=1, 2, ..., n)$ of membership functions corresponding to rule l, then the $V_{ij}(i=1, 2, ..., n; j=1,2,...,L)$ can be set as:

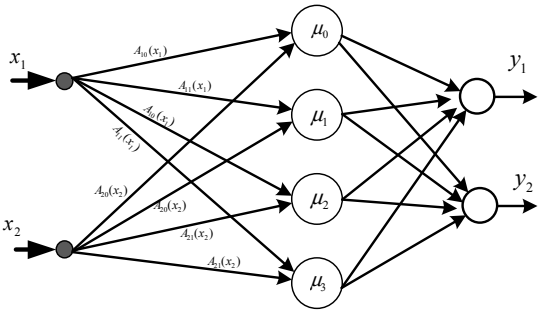

Figure 5. The FFNN with two input variables, two output variables

$$V_{ij} = A_{ir_i(j)}(x_i),\ i = 1, 2,\ ..., n; j = 1, 2, ..., L \qquad (5)$$

For two fuzzy variables $\{x_1, x_2\}$ with two MFs for each input variable i.e. $\{A_{10}(x_1), A_{11}(x_1)\}$ for x_1, $\{A_{20}(x_1), A_{21}(x_1)\}$ for x_2, then there are four hidden nodes (i.e., four rules), eight weights from input nodes to hidden nodes $V_{ij}(i = 1,\ 2; j = 1, 2, 3, 4)$. Table II shows the result. Fig. 5 shows the FFNN.

Therefore we have resolved the issue of not-fully connected MF layer in the original FNN, as shown in Figure 4. The next task will be to transform the product unit in Layer III (fuzzy rule layer) of FNN, or Layer II in Fig. 4 into an equivalent summing unit. To do so, we need to change the V_{ij} defined in (5) into the following new weight:

$$V_{ij} = Ln(A_{ir_i(j)}(x_i)) \qquad (6)$$

The output of hidden Layer is:

$$\mu_j = \sigma(\sum_{i=1}^{n} Ln(A_{ir_i(j)}(x_i))) = \sigma(Ln(\prod_{i=1}^{n} A_{ir_i(j)}(x_i)) \qquad (7)$$

where σ is any activation function, Ln is natural logarithm. If we take exponential function as activation function, we have

$$\mu_j = Exp(Ln(\prod_{i=1}^{n} A_{ir_i(j)}(x_i)) = \prod_{i=1}^{n} A_{ir_i(j)}(x_i) \quad 趙趙趙 \qquad (8)$$

Fig. 6 illustrates this transformation via (6) to (8).

It is important to note that the exponential activation function in Fig. 6 has limit zero when the input argument is a negative number, or the exponential activation function has limit at one infinite direction. This does match the requirement for finding the capacity of the three layers NN [15]. Figure 7 shows the complete fully connected FNN, or FFNN. It is obvious that the FFNN shown in Figure 7 is equivalent to the original FNN shown in Fig. 1. However, the FFNN is a fully connected three layer directed graph, which is the basis of finding the capacity of FFNN, or FNN. This will be discussed in the following sections.

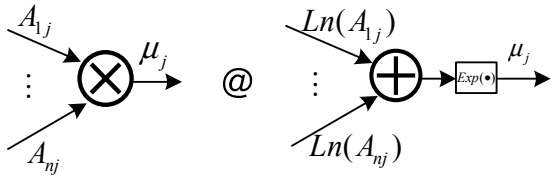

Figure 6. Transforming the product unit into summing unit in FNN

TABLE II FFNN WEIGHTS GENERATED FROM MFS AND RULE NUMBER

$l(=j-1)$	$r_1(l)$	$r_2(l)$	V_{1j}	V_{2j}
0	0	0	$A_{10}(x_1)$	$A_{20}(x_2)$
1	1	0	$A_{11}(x_1)$	$A_{20}(x_2)$
2	0	1	$A_{10}(x_1)$	$A_{21}(x_2)$
3	1	1	$A_{11}(x_1)$	$A_{21}(x_2)$

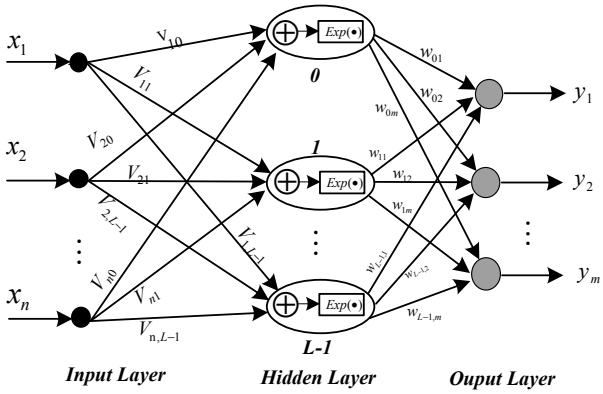

Figure 7. The complete fully connected FNN, or FFNN

IV. THE CAPACITY OF FNN OR FFNN

As mentioned in section 3, the original FNN has the same capacity as that of the equivalent FNNN with three layers. In this section, we will discuss the capacity of the three layers FNNN with exponential activation functions in the hidden layer. The following Theorem 1 shows lower and upper bounds of the FNN, or the three layer FFNN.

Theorem 1. For the FNN defined in Figure 1, where there are n inputs, m outputs, and L neurons in fuzzy layer (or hidden layer), each fuzzy variable x_i has R_i MFs, each MFs has N_{cp} control parameters, then the capacity P of the FNN can be bounded by the following inequality:

$$L \le P \le (\sum_{i=1}^{n} R_i N_{cp} + Lm) / m \qquad (9)$$

Proof:

In [15], it has been shown that standard single-hidden layer feed-forward networks (SLFN) with at most L hidden neurons and with any bounded nonlinear activation function which has a limit at one infinity can learn L distinct samples with zero

error. This implies that the SLFN with L hidden units can memorize at least L distinct patterns. For the FFNN, the exponential activation function in the hidden layer satisfies the condition of activation function in [15], so the lower bound on the capacity *P* is the number of hidden nodes L, i.e.,

$$P \geq L \tag{10}$$

Further, it has been shown in [8] that the upper bound for the capacity of feed-forward networks with arbitrary hidden unit activation functions can be found. For a feed-forward network (without bias) with n inputs, m outputs, *L* hidden units and arbitrary hidden activation functions, the number of patterns P that can be memorized with no error is less than or equal to $L(n+m)$, divided by the number of outputs m. Then the upper bound for the capacity P of SLFN is

$$P \leq L(n+m)/m \tag{11}$$

In the right hand side of (11), *nL* represents the number of links between input layer and hidden layer and *mL* represents the number of links between hidden layer and output layer. The *nL* and *mL* links should have the weights which are independent of input variables. However the link weights between layer I and layer II of FFNN depends on input variables, we should find another kind of control parameters between layer I and layer II to find the upper bound of the capacity of the FFNN. Assume that each MF in FNN has identical N_{cp} control parameters, such as the mean and variance in Gaussian MFs. In this popular case, $N_{cp} = 2$. So the total number of independent control parameters between layer I and layer II is $\sum_{i=1}^{n} R_i N_{cp}$. Replacing *nL* in (11) with $\sum_{i=1}^{n} R_i N_{cp}$, we have the following upper bound for the capacity *P* of FFNN:

$$P \leq (\sum_{i=1}^{n} R_i N_{cp} + Lm)/m \tag{12}$$

From (10) and (12), we can conclude that:

$$L \leq P \leq (\sum_{i=1}^{n} R_i N_{cp} + Lm)/m \qquad \text{Q.E.D.}$$

For Gaussian or any triangular membership functions, the number of control parameters N_{cp} is 2. From (1) we have $L = \prod_{i=1}^{n} R_i$, so if $n \geq 2$ and $R_i \geq 2$, then we have $nL = n\prod_{i=1}^{n} R_i > N_{cp}\sum_{i=1}^{n} R_i$. Therefore, from (11) and (12),

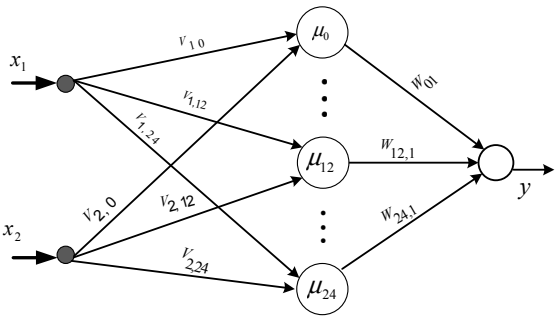

Figure. 8. FFNN with two input variables, each variable with five MFs

we find that the upper bound for capacity of FNN is less than that of MLP with the same configuration for larger *n*.

V. ILLUSTRATED EXAMPLE

In this section, Theorem 1 will be adopted to decide the theoretical upper and lower bounds of a particular FNN. In order to check the validity of the theoretical results, detailed BP trainings of the FNN are also conducted. The FFNN shown in Fig. 8 has two input nodes ($n = 2$) and one output node ($m = 1$), each linguistic variable has five items, so there are 25 nodes in hidden layer ($L = 25$). According to Theorem 1, the capacity P of the FNN should be bounded by $L \leq P \leq (\sum_{i=1}^{n} R_i N_{cp} + Lm)/m$, which is $25 \leq P \leq 45$. The membership functions are Gaussian functions (= $Exp(\frac{-(x-\mu)^2}{2\sigma^2})$), the output node is a linear unit. The training data is generated by $y = \sin(x_1\pi)\cos(x_2\pi)$, x_1 and x_2 are both in the range of [-1, 1] with 0.1 as the step-size. The FNN can be trained by the following BP algorithm as described in [5]:

$$\begin{cases} m_i(t+1) = m_i(t) - k_m \dfrac{\partial e_p}{\partial m_i}, i = 1,...,K \\ \sigma_i(t+1) = \sigma_i(t) - k_\sigma \dfrac{\partial e_p}{\partial \sigma_i}, i = 1,...,K \\ w_{jp}(t+1) = w_{jp}(t) - k_w \dfrac{\partial e_p}{\partial w_{jp}}, j = 1,...,L, p = 1,...,m \end{cases} \tag{13}$$

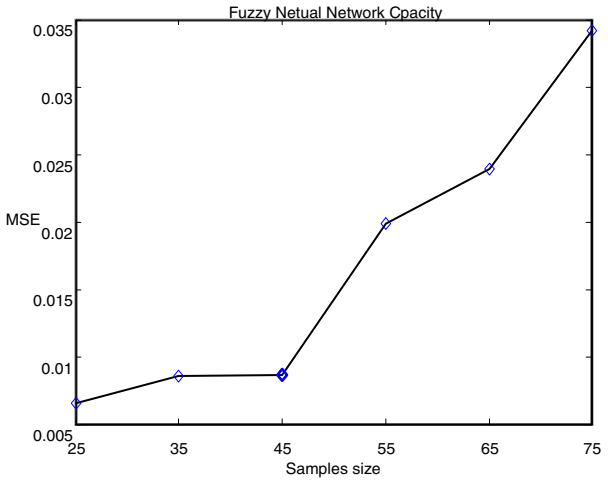

Figure 9. Relationship between training error and patterns number of FNN

Where $e_p = \frac{1}{2}(y_p - y_p^*)^2$, $K = \sum_{i=1}^{n} R_i$ is the number of MFs. From Fig. 9, we can see that if the number of training patterns is near the lower bound (=25),the MSE can be made as close as possible to zero. When the number of training patterns reach upper bound (=45),the MSE values start to deviate from zero rapidly, which will be very difficult for the training process to converge. Therefore the theoretical bounds are in excellent agreement with the real BP training results

VI. CONCLUSION

This paper proposes a new approach to find the lower and upper bounds of the capacity of FNN. By transforming the conventional four layers FNN into an equivalent fully connected three layer feed-forward NN, or FFNN, we can obtain the lower and upper bounds of FNN. An illustrated example is proposed to demonstrate the validity of theoretical bound using real BP trainings. Excellent agreement has been obtained between the theoretical bounds and real BP trainings. The impact of this paper is that all engineering application via FNN should have the capacity of their imperfect FNN in mind to complete the successful implementations. This will be our future research directions.

VII. ACKNOWLEDGEMENT

This research is supported by the research fund of the National Grand Fundamental Research 973 Program of China under Grant 2011CB302801.

REFERENCES

[1] Chi-Hsu Wang, Wei-Yen Wang, Tsu-Tian Lee, Pao -Shun Tseng, "Fuzzy B-spline Membership Function and Its Applications in Fuzzy-Neural Control," IEEE Trans. on Systems, Man, and Cybernetics , pp. pp. 841-851, Vol. 25, No. 5, May, 1995.

[2] Yih-Guang Leu, Tsu-Tian Lee and Wei-Yen Wang, "On-Line Tuning of Fuzzy-Neural Network for Adaptive Control of Nonlinear Dynamical Systems," IEEE Trans.on System Man and Cybernetics Part B, Vol. 27, No. 6, pp. 1034-1043, Dec. 1997.

[3] Jeffrey T. Spooner and Kevin M. Passino, "Stable Adaptive Control Using Fuzzy Systems and Neural Networks," IEEE Trans. on Fuzzy System, Vol. 4, No. 3, pp. 339-359, Aug. 1996.

[4] Wen Yu and Xiaoou Li,"Fuzzy Identification Using Fuzzy Neural Networks With Stable Learning Algorithms," IEEE on Fuzzy System, Vol. 12, No. 3, pp. 339-359, Jun. 2004.

[5] Kevin M. Passino and Stephen Yurkovich, Fuzzy Control, Addison Wesley Longman, Menlo Park, CA, 1998.

[6] Liu, Puyin and Li, Hongxing, Fuzzy Neural Network Theory and Application, River Edge, NJ : World Scientific, 2004.

[7] V. Kreinovich, H. T. Nguyen, and Y. Yam, "Fuzzy systems are universal approximators for a smooth function and its derivatives," International Journal of Intelligent Systems, Volume 15, Issue 6, pages 565–574, June 2000.

[8] Pramod L. Narasimha, Michael T. Manry and Francisco Maldonado, "Upper Bound on Pattern Storage in Feedforward Networks, " Proceedings of International Joint Conference on Neural Networks, Orlando, Florida, USA, August 12-17, 2007.

[9] Robert J. Mceliece,"The Capacity of the Hopfield Associative Memory," IEEE Trans. on Information Theory, Vol. IT-33, NO. 4, July,1987.

[10] Anthony Kuh and Bradley W. Dickson, "Information Capacity of Associative Memories" IEEE Trans. on Information Theory , Vol. 35, No. 1, Jan., 1989.

[11] Thomas M. Cover, "Capacity Problems for Linear Machines," in Pattern Recognition, L. Kanal ed., Thompson Book Co., pp. 283-289. 1968.

[12] Shin'ichi Tamura, "Capabilities of a three-layer feedforward neural network," in Proc. IJCNN91, pp. 2757–2762, Nov. 1991.

[13] Shih-Chi Huang and Yih-Fang Huang, " Bounds on the Number of Hidden Neurons in Multilayer Perceptrons," IEEE Transaction on Neural Networks. Vol.2. No.1, pp. 47 -55, Jan. 1991.

[14] M.A. Sartori and P.J. Antsaklis, "A simple method to derive bounds on the size and to train multilayer neural networks," IEEE Tran. on Neural Networks, vol. 2,No.4, pp. 467-471, July 1991.

[15] Guang-Bin Huang and Haroon A. Babri, "Upper Bounds on the Number of Hidden Neurons in Feedforward Networks with Arbitrary Bounded Nonlinear Activation Function," IEEE Trans. on Neural Networks, vol. 9, no. 1, pp. 224-229, Jan. 1998.

[16] Chi-Hsu Wang and Jung-Sheng Wen,"On the Equivalence of a Table Lookup (TL)Technique and Fuzzy Neural Network (FNN) With Block Pulse Membership Functions (BPMFs) and Its Application to Water Injection Control of an Automobile," IEEE Trans on Systems, Man, and Cybernetics- Part C: Applications and Reviews, Vol. 38, NO. 4, pp. 574-580, July 2008.

2011 IEEE International Conference on Fuzzy Systems
June 27-30, 2011, Taipei, Taiwan

On the Classification of Cancer Cell Gene via Expressive Value Distance (EVD) Algorithm and Its Comparison to the Optimally Trained ANN Method

Tong Zhang[1]
Faculty of Science and Technology, University of Macau
MSAR, PROC
ma96530@umac.mo

Chi-Hsu Wang[2]
Department of Electrical Engineering, National Chiaotung University
Hsinchu, Taiwan
cwang@cn.nctu.edu.tw

Sik Chung Tam[2*]
Faculty of Science and Technology, University of Macau
MSAR, PROC
fstsct@umac.mo
[2*]*Corresponding author*

C.L. Philip Chen[3]
Faculty of Science and Technology, University of Macau
MSAR, PROC
philipchen@umac.mo

***Abstract*—In recent years, cancer can be detected and recognized by analyzing the sample's expression profile. The cancer gene expression data are high dimensional, high variable dependent, and very noisy. The dimension reduction method is often used for processing the high dimensional data. In this study, a new statistical dimension reduction method called Expressive Value Distance (EVD) is developed and proposed for the practical high-dimensional gene expression cancer data. The feature genes data extracted by EVD are arranged for training the optimally trained Artificial Neural Network (ANN). The trained ANN is then used to classify whether the unseen gene data is cancer or not. In comparison of ANN classification with and without EVD, it is found that both of the ANN can classify the cancer data in good accuracy. With the EVD method, the great amount of data (2000 genes) can be effectively reduced to 16 genes. Therefore, EVD is an effective dimension reduction method. Even the EVD method is not used, the optimally trained ANN is also an advanced method for classifying the high dimensional and complicated cancer data. Briefly, it proves that optimally trained ANN is a very robust classification technique.**

Keywords-Gene expression profile; Dimension reduction; Artificial neural network; Expressive value distance; Classification of cancer;

I. INTRODUCTION

Classification has become one of the most promising learning techniques. It is crucial in many applications such as cancer classification [1]. Such classifications have an immense impact on cancer prognosis and therapy. In contrast with clustering, classification techniques start with a collection of labeled (pre-classified) expression patterns. The purpose is to train a classification model that would be able to classify a new expression pattern. In recent years, the development of microarray technology has allowed the simultaneous monitoring of thousands of genes [2, 3], which have motivated the progress in cancer classification by using gene expression [4, 5, 6].

Known as a parallel distributed processing network, artificial neural network is a robust tool recently used as classification. It has been applied to a very broad range of tasks in many different disciplines. It consists of interconnected processing elements called nodes or neurons that work together to produce an output function. The output of a neural network relies on the cooperation of the individual neurons within the network.

It becomes a reality to apply neural network with bioinformatics technology to cancer diagnosis for the development of DNA microarray technology. It has attracted tremendous interest in both the scientific community and in industry. Several studies have recently reported on the application of microarray gene expression analysis for the classification of cancer [7]. Most of these applications assumed a predefined network architecture (including connectivity and node transfer functions) and used a training algorithm to the learn weights.

In this study, 62 colon cells with 2000 genes expression data are analyzed (22 normal and 40 cancer cells). On the basis of the feature of gene expression data (high dimensional, high variable dependent, and very noisy), feature extraction by dimension reduction is necessary before the classification from the original data set [8, 9]. To classify the high dimensional gene expression cancer data, the dimension reduction methods were often used, such as principal component analysis (PCA), generalized topographic mapping, projection pursuit and so on [10]. After the dimension is reduced, the feature genes can be obtained and analyzed more easily. A new dimension reduction method (EVD) based on the concept of probability distribution and hierarchical clustering method is proposed for cancer data. After the feature gene data is obtained, the feature genes data will be arranged as the input for training the optimal trained Artificial Neural Network (ANN) [11]. The trained ANN is

978-1-4244-7316-8/11/$26.00 ©2011 IEEE

used to classify whether the unseen gene data is cancer or not. The benchmark classification tests have been performed to show that the EVD can yield a slightly better result than that of the optimally trained ANN method. For computational complexity comparison, it is obvious that the optimally trained ANN has less computational complexity than that of EVD, and yet provides a very robust classification technique with good accuracy.

II. THE ALGORITHMS

2.1 Classification method

The structure of two layers ANN is shown in Fig. I, which will be used as a cancer gene classifier in this paper.

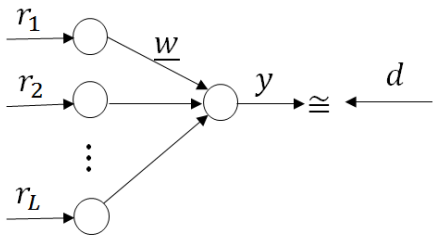

Fig. I. Two-layers ANN

Where

$$\underline{r} = [r_1, r_2, \dots, r_L]^T \in \mathbb{R}^L \quad (2.1)$$

is the input vector of the network

$$\underline{w} = [w_1, w_2, \dots, w_L]^T \in \mathbb{R}^L \quad (2.2)$$

is the weighting vector $y \in \mathbb{R}$ is the network output, and "T" is the transpose operator of matrices.

Hence, according to the structure of the two layers ANN, we obtain the following formula

$$y = \sum_{l=1}^{L} r_l w_l = \underline{r}^T \underline{w} \quad (2.3)$$

Given a training dataset with P samples

$$\{(\underline{r}_1, d_1), (\underline{r}_2, d_2), \dots, (\underline{r}_P, d_P)\},$$

We define the sum of square error which is a function of the weight vector $\underline{w}$ by

$$J(\underline{w}) = \frac{1}{2P}\left(\underline{y} - \underline{d}\right)^T \left(\underline{y} - \underline{d}\right)$$
$$= \tfrac{1}{2P}\left(R^T\underline{w} - \underline{d}\right)^T \left(R^T\underline{w} - \underline{d}\right) \quad (2.4)$$

Where

$$R = \left[\underline{r}_1, \underline{r}_2, \dots, \underline{r}_P\right] \in \mathbb{R}^{L\times P} \quad (2.5)$$
$$\underline{y} = [y_1, y_2, \dots, y_P] \in \mathbb{R}^P \quad (2.6)$$
$$\underline{d} = [d_1, d_2, \dots, d_P] \in \mathbb{R}^P \quad (2.7)$$

Indeed to train the ANN is to minimize the error function $J(w)$ in equation (2.4). The classical approach to find the minimum weight vector is using steepest descent method. Precisely, we will construct an iteration sequence which is expected to converge to the minimum weight vector as below:

$$\underline{\mathrm{w}}(t+1) = \underline{\mathrm{w}}(t) - \beta(t)\left.\frac{\partial J(\underline{w})}{\partial \underline{w}}\right|_{\underline{\mathrm{w}}(t)} \quad (2.8)$$

Where t denotes the t th iteration and the number $\beta(t)$is the learning rate. By chain rule, the gradient $\frac{\partial J(\underline{w})}{\partial \underline{w}}$ is equal to $\frac{1}{P}R(R^T\underline{w} - \underline{d})$. Hence, we have

$$\underline{w}(t+1) = \underline{w}(t) - \frac{\beta(t)}{P}R\left(R^T\underline{w}(t) - \underline{d}\right) \quad (2.9)$$

It was shown that the relatively large or small learning rates may affect the learning progress and even may lead to failure of the process [12]. So, to avoid these situations, dynamic optimal learning rate training for ANN is employed to train the two layers ANN in this paper. It is not only guaranteed that the maximum error reduction can be achieved by choosing the optimal learning rate for the next training iteration, but also that the initial choice of the weights become not essential. According to Theorem 1 in [11], the optimal learning rate $\beta_{opt}(t)$ can be found from the minimum of a quadratic polynomial $A\beta^2 + B\beta$ where

$$A = \frac{1}{2P^3}R^T R\underline{e}_t\underline{e}_t^T R^T R$$
$$B = \frac{1}{P^2}R^T\underline{e}_t^T\underline{e}_t R$$
$$\underline{e}_t = R^T\underline{w}(t) - \underline{d} \quad (2.10)$$

The dynamic optimal learning rate training is summarized as follow:

Algorithm 1: Classification by using ANN with Dynamic Optimal Learning Rates

1) Training the classifier

step1. Given P training data and obtain R and $\underline{d}$ as above.

step2. Set the iteration counter $t = 0$ and the initial weight to be $\underline{w}(0)$. Find the optimal learning rate $\beta_{opt}(0)$. Start the steepest descend to the error function $J(\underline{w})$.

step3. Find if the error function $J(\underline{w})$ is smaller than a given tolerant ε? If yes, go to Step 7.

step4. Update the weighting matrix to yield $\underline{w}(t+1)$ according to (2.9)

step5. Find the optimal learning rate $\beta_{opt}(t+1)$ for the next iteration.

step6. Set $t = t + 1$.Go back to Step 3.

step7. Store the current $\underline{w}(t)$ to $\underline{w}_{opt}$ and end.

2) Testing the classifier:

step8. Given another set of testing data and form R_{test} and $\underline{d}_{test}$ as if in step 1 of the training process.

step9. Obtain the trained network output vector $\underline{y}_{test}$ by using the formula $\underline{y}_{test} = R^T\underline{w}_{opt}$.

step10. Convert the output $\underline{y}_{test}$ into the classification label (1/-1).

step11. Compare $\underline{y}_{test}$ and $\underline{d}_{test}$ and have the diagnostic accuracy.

step12. End.

2.2 Dimension reduction method

Gene expression profile of a DNA is very complicated and it can be represented by a high dimensional vector. For example, in this paper, the dimension of such vector is up to 2000. However, most the genes within DNAs are not relevant

for cancer classification and they should be eliminated [13, 14]. Besides, the rest of the genes can be grouped into clusters. The genes within a cluster actually are highly correlated. Therefore, one of the genes in a cluster can be chosen as its representative. Based on this theory, we are able to reduce the dimension of the gene expression profile vectors. In our study, we have actually implemented such dimension reduction by vertical process and horizontal process. The vertical process is to eliminate those irrelevant genes by using EVD method, while the horizontal process is to classify the resulted genes from vertical process into clusters by the hierarchical clustering method and to choose one representative gene from each cluster [15].

A. *Vertical process*

First of all, we assume that the condition distribution of a gene expression given that it is from a normal DNA (or a cancer DNA) follows normal distribution. Therefore, the conditional probability density function of a gene expression is

$$f(x|normal) = \frac{1}{\sigma_1\sqrt{2\pi}} e^{-\frac{1}{2}(\frac{x-\mu_1}{\sigma_1})^2}$$

and

$$f(x|cancer) = \frac{1}{\sigma_2\sqrt{2\pi}} e^{-\frac{1}{2}(\frac{x-\mu_2}{\sigma_2})^2}$$

Note that practically, the mean and the variance can be replaced by its sample mean and sample variance respectively in order to obtain the above density functions.

Definition 1: The expressive value distance between $f(x|normal)$ and $f(x|cancer)$ of a gene expression is defined to be **EVD**:

$$EVD = \int_{min(x)-\delta}^{max(x)+\delta} |f(x|normal) - f(x|cancer)|dx \quad (2.11)$$

Where δ is called the generalization error of the distribution area and

$$\delta = \frac{\min(x) - \min(x)}{5} \quad (2.12)$$

Algorithm 2: Vertical process of EVD

step1. Calculate the EVD of all the gene expressions by using equation (2.11).

step2. Set the EVD threshold α.

step3. Select the i^{th} gene if its EVD is bigger than α to form a new feature gene set and its size is denoted by L_1.

step4. End.

B. *Horizontal process*

In order to have further reduction of the numbers of genes, we are going to group the genes with similar gene expression. Assume a gene expression profile x_k of the resulted dataset of vertical process. Therefore,

$$x_k = (x_{k1}, x_{k2}, \dots, x_{kL_1}) \in \mathbb{R}^{L_1}$$

Where $k = 1,2, \dots, n$ and n is the number of samples.

The correlation between i^{th} genes and j^{th} gene is defined as below

$$r_{ij} = \frac{\sum_{k=1}^{n}(x_{ki} - \bar{x_i})(x_{kj} - \bar{x_j})}{[\sum_{k=1}^{n}(x_{ki} - \bar{x_i})^2 \sum_{k=1}^{n}(x_{kj} - \bar{x_j})^2]^{\frac{1}{2}}} \quad (2.13)$$

Where $\bar{x_i}$ and $\bar{x_j}$ are the sample means of the gene expression of i^{th} and j^{th} genes respectively.

Then, we get the relation matrix of the feature genes as below (2.14):

$$RM = \begin{bmatrix} r_{11} & r_{12} & \cdots & r_{1L_1} \\ r_{21} & r_{22} & \cdots & r_{2L_1} \\ \vdots & \vdots & \ddots & \vdots \\ r_{L_1 1} & r_{L_1 2} & \cdots & r_{L_1 L_1} \end{bmatrix} \quad (2.14)$$

The average related value represent as (2.15)

$$\overline{RM}(C_1, C_2) = \frac{1}{n_{C_1} \times n_{C_2}} \sum_{x_k \in C_1} \sum_{x_m \in C_2} r_{km} \quad (2.15)$$

Where C_1 and C_2 stand for two classes of genes and n_{C_1} and n_{C_2} are the sizes of C_1 and C_2 respectively.

Algorithm 3: Horizontal process of EVD

step1. Fix a integer number L_2

step2. Clustering the output gene set of vertical process by classical hierarchical clustering method (bottom-up), refer to [15], with distance function $\overline{RM}(C_1, C_2)$ and $K = L_2$.

step3. Choose one gene from every sample of the final L_2 clusters to form a reduce list of genes for ANN classification.

step4. End.

III. EXAMPLE

In this paper, the expression of colon dataset of 62 cells were used, 22 normal cells and 40 cancer cells (Fig. II and Table I). The dataset was free for download in the website [16].

Fig. II. Colon cancer dataset

TABLE I

COLON CANCER DATASET

Name / Sample		1_Has.3004	…	2000_Hsa.9683
S1	**N**	12.77219	…	5.888287
S2	**N**	10.90289	…	4.252098
S3	**N**	11.83636	…	4.942221
⋮	⋮	⋮	⋮	⋮
S61	**C**	13.15361	…	5.007476
S62	**C**	12.60609	…	4.540089

Then 6 of 22 normal cells and 16 of 40 cancers randomly was selected as the training set. The remains were arranged into the testing set (see Fig. III).

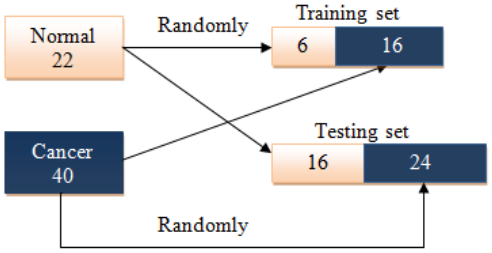

Fig. III. Colon cancer dataset

For comparison purpose, we did two kinds of methods experiments with ANN for classification in this study. The first method, the ANN was treated as the classifier directly. The second method, apply the dimension reduction method EVD before classification by ANN. (See Fig. IV).

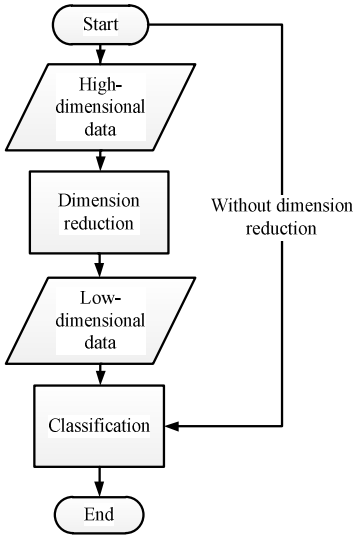

Fig. IV. Flow chart of two groups of classification

By using algorithm 1, the variables were listed as below:

R: refers to the expression dataset matrix of colon cancer, treated as the input matrix. And $L = 2000, P = 22$.

$\underline{d}$: refers to the desired output vector. $\underline{d} = [d_1, d_2, \ldots, d_P]$ $d_1 \sim d_6$ equal to 1, $d_7 \sim d_{22}$ equal to -1. 1 stand for normal, and -1 stands for cancer.

R_{test} : refers to the testing data. And $L = 2000, P_{test} = 40$.

$\underline{d}_{test}$: refers to desired output of the testing input R_{test}. $\underline{d}_{test} = [d'_1, d'_2, \ldots, d'_{40}]$, $d'_1 \sim d'_{16}$ equal to 1, $d'_{17} \sim d'_{40}$ equal to -1.

The tolerant ε=0.008, i.e. when $J(\underline{w})$<=0.008, $\underline{d}$ and y are closed enough. Then, the current $\underline{w}(t)$ was stored to $\underline{w}_{opt}$.

Thus, we test the classifier by comparing $\underline{y}_{test}$ and $\underline{d}_{test}$ we have the diagnostic accuracy of classification using ANN listed in Table IV.

By using dimension reduction method mentioned as EVD, we get the EVD bar chart (see Fig. V) of the initial genes.

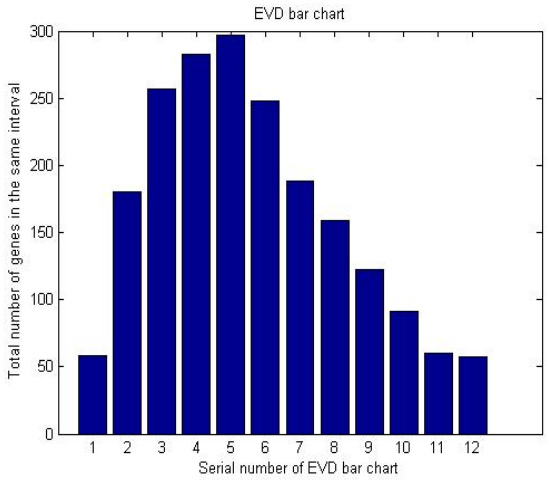

Fig. V. Statistical graph of EVD

Considering the statistical result of the EVD, in Table II, the threshold of the genes was set as α=0.8. Thus, L_1 (L_1 =330) genes (EVD>0.8) were selected and form the feature dataset in the vertical process.

TABLE II

THE STATISTICAL DATA OF EVD

EVD	0~0.1	0.1~0.2	0.2~0.3	0.3~0.4
Number of genes	58	180	257	283
EVD	0.4~0.5	0.5~0.6	0.6~0.7	0.7~0.8
Number of genes	297	248	188	159
EVD	0.8~0.9	0.9~1.0	1.0~1.1	1.1~1.5
Number of genes	122	91	60	57

In horizontal process, dimensions of the feature genes from the vertical process were reduced by using algorithm 3. Here, L_2 was set to be 16. That is to say, 16 clusters were clustered in the final. Then, choose the gene, whose EVD is the largest in each cluster.

Since the indexes of the genes have been stored in every step, the sequence number of the genes was lain out in Table III, i.e. these 16 genes form the feature genes dataset.

Then we apply algorithm 1 by using ANN as a cancer gene classifier. Here, $\underline{d'}$ and $\underline{d'}_{test}$ are same with $\underline{d}$ and $\underline{d}_{test}$ in the first experiment. However, L has been reduced to L_2 applying the EVD algorithm. Then, the variables were listed as below:

R': refers to the expression dataset matrix of colon cancer, treated as the input matrix. And $L_2 = 16, P' = 22$.

$\underline{d'}$: refers to the desired output vector. $\underline{d'} = \underline{d}$.

R'_{test} : refers to the testing data. And $L_2 = 16, P'_{test} = 40$.

$\underline{d'}_{test}$: refers to desired output of the testing input R'_{test}, $\underline{d'}_{test} = \underline{d}_{test}$.

Thus, the trained network output vector $\underline{y'}_{test}$ can be obtained by using the formula $\underline{y'}_{test} = R'^{T}\underline{w'}_{opt}$. By comparing $\underline{y'}_{test}$ and $\underline{d'}_{test}$ we have the diagnostic accuracy of classification using ANN with EVD. (Refer to Table IV).

TABLE III

SEQUENCE NUMBER OF THE FEATURE GENES IN THE INITIAL DATASET

sequence number	1680	177	1559	260
name	Hsa.1380	Hsa.8831	Hsa.1731	i
sequence number	686	1792	1655	1895
name	Hsa.1920	Hsa.1057	Hsa.30310	Hsa.8192
sequence number	1025	715	673	1636
name	Hsa.3215	Hsa.44686	Hsa.10908	Hsa.345
sequence number	765	1505	1504	1732
name	Hsa.692	Hsa.862	Hsa.44244	Hsa.888

TABLE IV

THE ACCURACY FOR CLASSIFICATION OF THE TWO METHODS

Method / Test times	Accuracy of classification use ANN	Accuracy of classification using ANN with EVD
1	0.9000	0.9500
2	0.9000	0.9750
3	0.9500	0.9000
4	0.8500	0.8750
5	0.9500	0.9500
6	0.9000	0.9000
7	0.9500	0.9500
8	0.8750	0.8750
9	0.8500	0.9000
10	0.9000	0.9500
11	0.9500	0.9000
12	0.8750	0.8750
13	0.9000	0.9250
14	0.9500	1.0000
15	0.9000	0.9500
16	0.8500	0.9000
17	0.9250	0.8500
18	0.9000	0.9500
19	0.9250	0.9250
20	0.8750	0.8750
Average accuracy	0.9038	0.91875

IV. EXPERIMENTAL RESULTS

The program in this study was written in the Matlab® code and operated in the laptop PC with Windows® platform. The accuracy of classification is described as Table IV.

We compute 20 times by using optimal trained Artificial Neural Network (ANN) and ANN method with the Expressive Value Distance (EVD) algorithm separately. Then we get the results of the accuracy respectively (see Table IV). It suggests that both of the two kinds of methods could be used for colon cancer classification efficiently. By the comparison of these two ways of training methods, we found that the average accuracy is slightly better by using EVD. So, it has been shown that EVD is an effective method in the area of dimension reduction. For computational complexity comparison, it is obvious that the optimally trained ANN has less computational complexity, and yet provides a very robust classification technique with good accuracy.

V. CONCLUTION

In this study, the new statistical dimension reduction algorithm EVD is developed successfully. It is applied to the practical colon cancer dataset. After using the EVD method, the dimension of the input data to ANN was largely reduced from 2,000 to 16. The reduction of the number of inputs does not affect the subsequent optimally trained ANN approach because both of the ANNs with or without the EVD method can provide the very accurate classification results. It is also represented that the important feature of the data can be extracted by the EVD method, although the optimally trained ANN approach can provide less computational complexity.

ACKNOWLEDGMENT

This research is supported by the research grant of the National Grand Fundamental Research 973 Program of China under Grant 2011CB302801.

REFERENCES

[1] Rong-En Fan, Kai-Wei Chang, Cho-Jui Hsieh, Xiang-Rui Wang, Chih-Jen Lin, "LIBLINEAR: A Library for Large Linear Classification," Journal of machine leaning, pp. 1871-1874, Sept. 2008.

[2] A. A. Alizadeh, M. B. Eisen, R. E. Davis, C. Ma, I. S. Lossos, A. Rosenwald, J. C. Boldrick, H. Sabet, T. Tran, X. Yu, et al., "Distinct types of diffuse large B-cell lymphoma identified by gene expression profiling," Nature, vol. 403, pp. 503-511, 2000.

[3] X. Ma, R. Salunga, J. T. Tuggle, J. Gaudet, E. Enright, P. McQuary, T. Payette, M. Pistone, K. Stecker, B. M. Zhang, et al., "Gene expression profiles of human breast cancer progression," in Proc. Natl. Acad. Sci. USA, vol. 100, pp. 5974-5979, 2003.

[4] J. M. Khan, J. S. Wei, M. Ringner, L. H. Saal, M. Ladanyi, F. Westermann, F. Berthold, M. Schwab, C. R. Antonescu, C. Peterson, et al., "Classification and diagnostic prediction of cancers using gene expression profiling and artificial neural networks," Nature Medicine, vol. 7, pp. 673-679, 2001.

[5] A. B. Olshen, and A. N. Jain, "Deriving quantitative conclusions from microarray expression data," Bioinformatics, vol. 18, pp. 961-970, 2002.

[6] R. Tibshirani, T. Hastie, B. Narashiman, and G. Chu, "Diagnosis of multiple cancer types by shrunken centroids of gene expression," in Proc. Natl. Acad. Sci. USA, vol. 99, pp. 6567-6572, 2002.

[7] Sridhar Ramaswamy, Pablo Tamay, Ryan Rifkin, Sayan Mukherjee, Chen-Hsiang Yeang, Michael Angelo, et al., Multiclass cancer diagnosis using tumor gene expression signatures, the national academy of sciences of the United States of America, 2001. 98(26): pp. 15149-15154.

[8] Kyeong Eun Lee, Naijun Sha, Edward R. Dougherty, Marina Vannucci and Bani K. Mallick, "Gene selection: a Bayesian variable selection approach," BIOINFORMATICS, 2003. 19(1): pp. 90-97.

[9] Deutsch, J.M., "Evolutionary algorithms for finding optimal gene sets in microarray prediction," BIOINFORMATICS, 2003. 19(1): pp. 45-52.

[10] M. C. Mozer, M. I. Jordan, and T. Petsche, eds., A principled alternative to the self-organizing map, in Advances in Neural Information Processing Systems, vol. 9, MIT Press, Cambridge,MA, 1997.

[11] Chi-Hsu Wang, Han-Leih Liu, and Chin-Teng Lin, "Dynamic Optimal Learning Rates of a Certain Class of Fuzzy Neural Networks and its Applications with Genetic Algorithm," IEEE transactions on Systems, Man, and Cybernetics—Part B: Cybernetics, VOL. 31, NO. 3, JUNE 2001.

[12] Xiao-Hu Yu, Guo-An Chen, and Shi-Xin Cheng, "Dynamic learning rate optimization of the back propagation algorithm," IEEE Trans. Neural Networks, vol. 6, pp. 669–677, May 1995.

[13] U. Alon, N. Barkai, D. A. Nottierman, K. Gish, S. Ybarra, D. Mack, AND A. J. Levine, Broad patterns of gene expression revealed by clustering analysis of tumor and normal colon tissues probed by oligonucleotide arrays, national academy of sciences of the United States of America, 1999, 96(12): pp. 6745-6750.

[14] Zhang H, Yu C-Y, Singer B, Xiong M., Recursive partitions for tumor classification with gene expression microarray data, the national academy of sciences of the United States of America, 2001. 98(12): pp. 6730-6735.

[15] Jain, A. and Dubes, R., Algorithms for Clustering Data, Prentice-Hall, Englewood Cliffs, NJ, 1988.

[16] Kaufman, L. and Rousseeuw, P., Finding Groups in Data: An Introduction to Cluster Analysis. John Wiley and Sons, New York, NY. 1990.

[17] (2011)The Princeton University website. [Online]. Available: http://genomics-pubs.princeton.edu/oncology/

[18] P. Berkhin, A Survey of Clustering Data Mining Techniques, Grouping Multidimensional Data, Springer, 2006, 25-71.

[19] R. Tibshirani, T. Hastie, B. Narasimhan, G. Chu, Class predication by nearest shrunken centroids with applications to DNA microarrays, Statistical Science, 2003, vol. 18, pp. 104-117.

[20] M. Schena, D. Shalon, R. W. Davis, and P. O. Brown, Quantitative monitoring of gene expression patterns with a complementary DNA microarray, Science, 1995, vol. 270, pp. 467-470.

[21] T. R. Golub, D. K. Slonim, P. Tamayo, C. Huard, M. Gaasenbeek, J. P. Mesirov, H. Coller, et al., Molecular classification of cancer: Class discovery and class prediction by gene expression monitoring, Science, 1999. 286(5439): pp. 531-537.

[22] M. P. Brown, W. N. Grundy, D. Lin, N. Cristianini, C. W. Sugnet, T. S. Furey, M. Jr. Ares, D. Haussler, Knowledge-based analysis of microarray gene expression data by using support vector machines, the national academy of sciences of the United States of America, 2000, vol. 97, pp. 262-267.

[23] Lillian Y. Chang, Nancy S. Pollard, Tom M. Mitchell, and Eric P. Xing, "Feature selection for grasp recognition from optical markers," in Proc. IEEE International conference on Intelligent Robots Systems, VOLS 1-9, 2007: pp. 2950-2956.

2011 IEEE International Conference on Fuzzy Systems
June 27-30, 2011, Taipei, Taiwan

Adaptive Neural-Fuzzy Inference System for Classification of Rail Quality Data with Bootstrapping-Based Over-Sampling

Y. Y. Yang, M. Mahfouf, G. Panoutsos, Q. Zhang
Dept. of Automatic Control and Systems Eng.
IMMPETUS, The University of Sheffield
Mappin Street, Sheffield S1 3JD, United Kingdom
y.y.yang@sheffield.ac.uk

S. Thornton
Teesside Technology Centre
Tata Steel Europe
Eston Rd., Middlesbrough, TS6 6US, UK
Steve.Thornton@Tatasteel.com

Abstract— **An iterative bootstrapping-based data over-sampling strategy is presented in this paper together with an adaptive neural-fuzzy inference system (ANFIS) to deal with a severely imbalanced data modelling problem. As real industrial data are often very large, containing hundreds of process variables and a huge number of data records, the selection of a compact set of input variables becomes critical for any successful modelling and analysis operations. Significant efforts have been devoted to identifying the most relevant input variables through correlation analysis and neural network based forward input selection. An optimal majority to minority class data ratio, which controls the level of data imbalance for model training, is then determined through the iterative bootstrapping process such that the combined sensitivity and specificity performance is optimised. The iterative bootstrapping ANFIS modelling strategy is then applied to a real industrial case study for rail quality classification, with the original data being provided by Tata Steel Europe. Preliminary results show a good overall performance through the iterative bootstrapping data over-sampling ANFIS modelling.**

Keywords: Imbalance data; bootstrapping, data resampling; fuzzy c-means clustering, ANFIS, steel manufacturing, rail.

I. INTRODUCTION

Data-driven modelling has gathered pace and gained much popularity due the rapid growth in computing power and the wide availability of data/information. Modelling tools and algorithms have also evolved into more complex structures capable of dealing with highly non-linear and multi-dimensional input/output mappings. However, in many real-world modelling scenarios, the available data are often highly imbalanced, such as product quality data and patient-disease data, where the data ratio of the majority class (the 'good' data) towards the minority class (the 'bad' data) can be very high. The data imbalance problem is prevalent in many applications, including fraud detection, risk management, quality classification, and medical diagnosis. Due to the overwhelming dominance of the majority class, the resulting model is often heavily biased to the majority cases while ignoring the minority class if the imbalance is not adequately dealt with [1]. Research in imbalanced data modelling has grown rapidly [2-4] as more researchers realized that imbalance entails more often than not sub-optimal modelling. Research methods for imbalanced data modelling can be classified into two major categories: using data resampling so that the resampled data are more balanced [5]; and modifying the learning algorithm or the cost criteria so that the classifier is biased towards the minority class [6, 7].

In this paper, a modelling strategy of integrated bootstrapping [8] data resampling and adaptive neural-fuzzy inference system (ANFIS) is proposed. The core of the ANFIS model is developed using fuzzy C-means clustering [9] on the resampled data. This modelling strategy is then applied to a case study for a large scale industrial problem provided by Tata Steel Europe, relating through process manufacturing data to finished steel rail ultrasonic test results. The remainder of the paper is organized as follows. Section 2 provides an overview of the data which are extracted from the sequential steelmaking, casting, rolling and finishing processes of the large multi-product manufacturing complex. Section 3 is devoted to data pre-processing, which deals with data consolidation, input selection, and feature extraction. As the data set is very large, containing over two hundred process variables in more than sixty-five thousand data records, the data pre-processing task becomes essential and critical toward any successful modelling practices. In Section 4, an iterative bootstrapping data resampling algorithm is developed, together with an ANFIS based classification scheme. It is found that the majority to minority class data ratio, which controls the level of data imbalance in the bootstrapping resampled data, plays a pivotal role in optimising the overall classification performance over the two different categories. Finally, concluding remarks and discussions are outlined in Section 5.

Financial support from the UK-EPSRC is acknowledged under Grant EP/F023464/1.

978-1-4244-7316-8/11/$26.00 ©2011 IEEE

II. Overview of the Rail Production Data

A. Brief Description of the Rail Production Route

The rail manufacturing data used for this study were collected from an integrated steel manufacturing complex belonging to Tata Steel Europe. The production line which manufactures a range of steel products including rail, consists of steelmaking, continuous casting, rolling, and finishing sub-processes, as sketched in Fig. 1. A basic oxygen furnace takes molten iron from upstream blast furnaces as well as additional scraps and refines them into steel by blowing high purity oxygen through the lance onto the surface of the hot metal. The oxidation process generates heat and removes excessive carbon and other chemical impurities (a batch process lasting approximately 30 minutes). The liquid steel is then tapped into a ladle, for further secondary steelmaking, going through a ladle metallurgical furnace where the steel chemical compositions are adjusted through alloy addition and desulphurization, and a vacuum de-gasser where harmful hydrogen and other gas inclusions are removed to improve steel cleanness. The rail grade liquid steel is then transferred to the multi-strand continuous casting machine where steel blooms of about 8-tonne are produced. These steel blooms are subsequently heated in a reheating furnace and processed to rail via multi-pass hot rolling and straightening operations to produce rails upto 120 metres in length. The final stage of manufacture entails comprehensive Non-Destructive Testing (NDT) of every rail to ensure adherence to strict standards for internal and surface quality, as well as for dimensional accuracy, before dispatch to customers. This study focuses on the small number of rails which are rejected due to internal flaws and analytical approaches to find root causes and thus by introduction of appropriate control measures, to improve product yields.

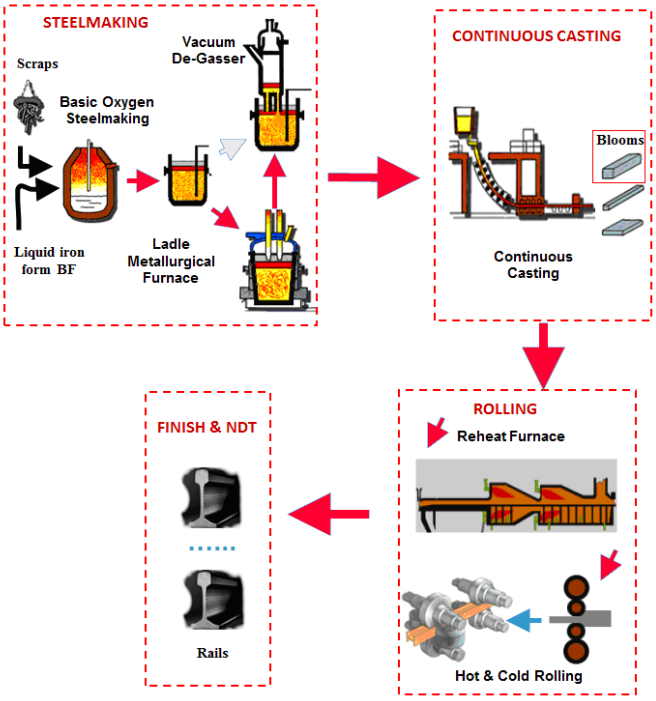

Figure 1. Overview of the rail production route

B. Overview of the Rail Manufacturing Data

In a modern rail production line, there exists extensive instrumentation for online process monitoring and control, as well as offline production management and administration. An integrated data infrastructure, which includes multiple online data servers for collecting real-time variables, process parameters, management information, key unit production time histories, and quality inspection data, is installed through the production line. These original data, which are stored in various databases, are further processed and aggregated before being stored in a master data mining server where higher level data analysis and mining tasks can be conducted. The data can also be easily accessed in this environment for other advanced modelling and optimisation tasks.

The data collected from the rail production route described above cover a two-year production period, including over 65000 data records with up to 200 variables. Preliminary investigations of the rail data revealed many challenges for modelling and analyses. Due to the large scale of the data, even simply processing the data can prove to be resource intensive, and algorithms and procedures need to be planned with great care. Basic tasks such as plotting, copying and paste are not straightforward, as they often break commonly used software specifications and norms. Often, responses become prohibitive sluggish, hence an adequate choice of analysis tools becomes a necessity as a single computing tool cannot best serve the diversified requirements demanded in the data modelling cycle. Hence, an integrated software environment has been established to deal with the large scale rail data modelling, as shown in Fig. 2.

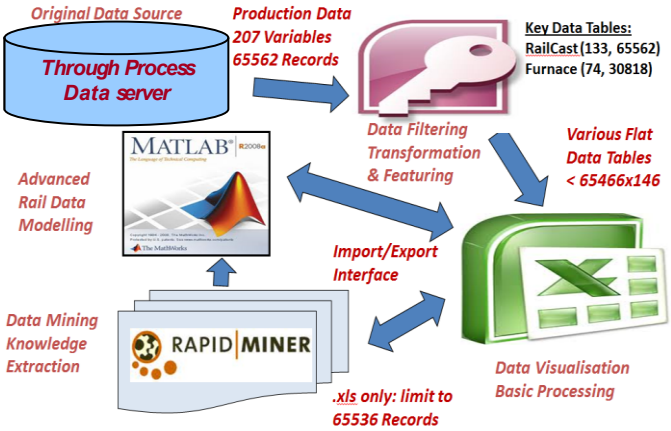

Figure 2. An integrated database and software environment

An initial inspection of the data revealed that some variables were redundant, and others contained conflicting information. A few records included also a significant amount of missing values and could not hence be used for modelling. Furthermore, many of the variables are primarily relevant to production management, hence should be eliminated for the rail quality analysis.

Based on this initial perspective, a data pre-processing strategy has been carefully designed in order to form a parsimonious model data set from the original rail production route data. As pointed out in [10-11], pre-processing is an

important step in any complicated data modelling process, and its function normally includes data cleaning, normalization, transformation, feature selection, etc. In this study, the focus of the data pre-processing operation is directed mainly towards identifying data outliers, correcting wrong data entries, checking data conflicts, missing value decision, and identifying relevant inputs. A process expert from Tata Steel was closely involved in the data pre-processing task providing essential knowledge input to explain and advise about inter variable correlations, apparent redundancy and relevance of data items. After the initial data pre-processing stage, the original rail data are reduced in both dimension and length by eliminating non-relevant variables and deleting data records with too many missing values or conflict data items. The resulting rail data set, after the pre-processing stage, consists of 140 process variables and 39687 records.

This pre-processed data set remained very large and the data dimension was still too high for any meaningful feature classification. The input dimension needed to be reduced further in order for a manageable data classification model to be elicited. Hence, the reduction of the input space dimension and the selection of the most suitable input variables will be tackled in the next section.

III. Model Input Selection

Input variable selection is a vital step in complex system modelling where the input–output relationship is often not too well understood. An unnecessarily large number of inputs can be detrimental to effective modelling, not only that the high dimensional space will cause the difficulty due to 'the curse of dimensionality', but also the irrelevant and redundant inputs tend to confuse and distort the true input-output outcomes. It is a well-known fact that the data examples needed to tune a model grow exponentially with the number of inputs, and the resources required for an increasing large data set soon become prohibitive. The central task in input selection is to identify and remove variables that have little influence on the output, so that the main emphasis can be put on the important input variables. As pointed out in [12], the objective of input variable selection is three-fold: improving the prediction performance of the predictors, providing faster and more cost-effective predictors, and providing a better understanding of the underlying process that generated the data. Many different methods have been proposed to deal with the input selection problem, including fuzzy logic based approaches [13-14], statistical test or correlation analysis [15-16], and direct objective optimisation based approaches [17].

A. Correlation Analysis

The correlation coefficient analysis can prove sufficient enough to help identify the input/output dependency if the process under investigation is linear [18]. Even though the rail production line is complex and certainly nonlinear, it is believed that some preliminary correlation analysis will be worthwhile. Correlation coefficient analysis can help to reach a better understanding of the data to be modelled. The Pearson's correlation coefficient can be calculated via the following equation:

$$\rho_{ij} = \frac{\sum_{k=1}^{N}(x_i(k)-\bar{x}_i)(x_j(k)-\bar{x}_j)}{\sqrt{\sum_{k=1}^{N}(x_i(k)-\bar{x}_i)^2 \sum_{k=1}^{N}(x_j(k)-\bar{x}_j)^2}} \quad (1)$$

Where $\rho_{ij} \in [-1, 1]$ is the correlation coefficient between variable x_i and x_j, $x_i(k)$ is the value of the kth x_i sample, N is the total number of samples, and $\bar{x}_i$ is the sample mean. When one of the variables is the output, ρ_{ij} represents the linear dependency between the output and the given input, otherwise it indicates the co-linearity between the two given inputs.

When a significant number of variables are involved in the data set, there will be a very large number of correlation coefficients. A compact form to summarize all the correlation coefficients is a correlation matrix $\boldsymbol{R}$, defined as follows:

$$\boldsymbol{R} = [\rho_{ij}]_{n\times n} = \begin{pmatrix} \rho_{11} & \cdots & \rho_{1n} \\ \vdots & \ddots & \vdots \\ \rho_{n1} & \cdots & \rho_{nn} \end{pmatrix} \quad (2)$$

Where ρ_{ij} is the correlation coefficient defined in (1), n is the total number of data variables in the data set. $\boldsymbol{R}$ is a symmetric and with $\rho_{ii} = 1$, $i = \{1, 2, \ldots, n\}$.

For this study, data variables are limited to steelmaking and continuous casting sub-processes (named as rail-cast data, with process variables $x_1 \sim x_{70}$), as it is known that these two sub-processes have strong influences on the internal rail quality. Correlation analysis of the rail-cast data revealed that there is little linear correlation between inputs and the output (the number of rejected rails), with the top-10 correlation coefficients being listed in Table I. The correlation coefficient values are rather small, with the maximum being 0.144 related to the 9th input. The results are not constructive enough to help identify the relevant inputs for data modelling. However, the resulting correlation matrix revealed significant correlations among various potential inputs, as many correlation coefficients exceeded 0.95, as outlined in the last two columns of Table 1. Highly correlated inputs indicate significant redundant information contained in the corresponding variables, which need to be eliminated for parsimonious data modelling.

TABLE I. Top 10 significant Correlation coefficients

Rank	*Output Corr.*	*Var*	*Input Corr.*	*Vars (I, J)*
1	0.144	x_9	0.982	x_{50}, x_{53}
2	0.133	x_{10}	0.981	x_{24}, x_{25}
3	0.111	x_8	0.979	x_{11}, x_{40}
4	0.106	x_{13}	0.979	x_{12}, x_{40}
5	-0.097	x_7	0.978	x_{24}, x_{26}
6	-0.074	x_6	0.975	x_{52}, x_{53}
7	-0.071	x_{30}	0.967	x_{51}, x_{52}
8	0.060	x_3	0.966	x_{67}, x_{68}
9	-0.050	x_{37}	0.965	x_{68}, x_{69}
10	-0.047	x_{54}	0.953	x_{66}, x_{67}

B. Input Selection using a Neural Network Model

As is clear from the previous correlation analysis that the input-output relation is highly nonlinear, a neural network (NN) based forward selection procedure is proposed here to identify the most relevant input variables. A simple 3-layer feed-forward neural network possesses very powerful input-output mapping capability and can approximate any continuous non-linear function with arbitrary accuracy provided that enough hidden neurons have been used [19]. The output of such an NN can be expressed as follows [20]:

$$\hat{y}(k) = \sum_{j=1}^{M} w_j \varphi_j(\sum_{i=1}^{n} w_{ij} x_i(k) + w_{j0}) + w_0 \qquad (3)$$

where $\hat{y}(k)$ is the NN output prediction for the kth sample, w_j and w_{ji} are the relevant NN weighting coefficients at the output layer and hidden layer, respectively, w_0 and w_{j0} are the corresponding bias, ϕ_j is the nonlinear activate function of the jth hidden neuron, and M is the total number of hidden neurons.

A forward input selection procedure is proposed with the above NN model as a performance evaluator. The input selection is implemented through an iterative process, starting from selecting a single input for the NN modelling. All the potential inputs are sampled as the single input candidate, and the neural network model with the minimum root mean squared error (RMSE) is identified as NN*. The inputs corresponding to the ones used in NN* are ranked as the most important inputs identified so far. In the next round of input selection, the inputs of the NN is increased by one from the identified input set, with the newly increased input selected from all remaining potential input candidates. The above forward input selection procedure was repeated until either a sufficient number of inputs identified or no performance improvement achieved by adding more inputs. The NN training procedure used here is adapted from the one used in [22], with critical training parameters fixed via trial-and-error tuning. The number of hidden neurons is determined by the number of NN model inputs by using empirical rules, as optimisation in this scenario will be computationally too expensive. The iterative forward input selection algorithm is summarized as follows:

Step i: Initialisation of the forward input selection: i = 1, $\boldsymbol{x}^{\boldsymbol{0}} = \{\}$, put all the variables into the potential input candidate set $\boldsymbol{X}^0 = [x_1, x_2, \ldots, x_n]$

Step ii: Start a new round of input selection. For each of the potential input candidate $x_j \in \boldsymbol{X}^0$, perform neural network modelling with extended input $\boldsymbol{x}^{\boldsymbol{0}} = [\boldsymbol{x}^{\boldsymbol{0}}, x_j]$. Computing the corresponding model performance $J_j, j = \{1, 2, \ldots, dim(\boldsymbol{X}^0)\}$.

Step iii: Identify the best neural network model NN_{j*} using the corresponding RMSE (Root mean square error) performance, and electing x_{j*} as the most important input in the current round. Expanding the fixed input set $\boldsymbol{x}^{\boldsymbol{0}} = [\boldsymbol{x}^{\boldsymbol{0}}, x_{j*}]$, and eliminate it from $\boldsymbol{X}^0$ ($\boldsymbol{X}^0 = \boldsymbol{X}^0 \setminus x_{j*}$).

Step iv: If the best NN performance in the current round does not improve over the previous one, or if $dim(\boldsymbol{x}^{\boldsymbol{0}}) >= n_{max}$, or if $\boldsymbol{X}^0$ is empty, then go to Step v, otherwise return to Step ii.

Step v: The elements in $\boldsymbol{x}^{\boldsymbol{0}}$ are the most important input variables identified by the NN forward selection procedure. The importance ranking is the order of inclusion of the elements.

Table II summarises the results obtained from the aforementioned forward input selection procedure. As the neural network model is very powerful for input-output mapping, the nonlinear behaviour in the data set can be better dealt with. However, the computation involved in this NN based forward input ranking is quite heavy, especially when a large data set is involved. For the current input ranking task with 70 potential inputs, a maximum number of 2450 neural networks need to be trained via some kind of error back-propagation algorithm, and each neural network need to be trained over more than 20000 samples. Extra in-loop optimisations, for the hidden neuron number or learning parameters, are not computationally feasible. Hence, key training parameters and network structure parameters are fixed based on the modelling experience.

TABLE II. INPUT RANKING USING THE NN FORWARD SELECTION

No	Var	No	Var	No	Var	No	Var
1	x_8	11	x_{24}	21	x_{51}	31	x_{23}
2	x_2	12	x_{46}	22	x_{63}	32	x_{20}
3	x_9	13	x_{13}	23	x_{54}	33	x_{48}
4	x_{53}	14	x_{34}	24	x_{58}	34	x_{59}
5	x_{16}	15	x_{67}	25	x_{12}	35	x_{61}
6	x_{47}	16	x_{22}	26	x_{25}	36	x_{50}
7	x_3	17	x_{28}	27	x_{37}	37	x_{15}
8	x_{68}	18	x_{19}	28	x_{62}	38	x_{55}
9	x_{11}	19	x_{41}	29	x_1	39	x_7
10	x_{65}	20	x_6	30	x_{57}	40	x_{35}

IV. BOOTSTRAPPING RESAMPLING AND DATA CLASSIFICATION

The number of model inputs has been reduced to 39 by selecting the first 39 variables listed in Table 2 obtained by using the NN forward input ranking scheme described in Section 3. The original output, $y \in \{0, 1, 2, 3\}$, is chosen as the feature variable originating from the NDT ultrasonic testing, with y=0 representing a good rail and $y = \{1, 2, 3\}$ indicating a rejected rail. The non-zero discrete value of y indicates the presence of single or multiple flaws. An adaptive neural-fuzzy modelling approach was developed based on the *ANFIS* framework [21], however the success rate for the rejected rail classification is very poor with less that 10% correctly classified, when the imbalanced data is used for training the model. Further investigations revealed that the main cause of such poor classification is the severe data imbalance in the training data set.

A. Boostrapping for Data Resampling

Since samples belonging to the minority class are fewer than those belonging to the majority class in the current modelling scenario, a direct approach for data resampling is adopted here in order to change the class distributions. A more balanced data can be obtained through different resampling

strategies, such as under-sampling, over sampling, or the combination of both, as is briefly discussed in [22]. In order to avoid unnecessary information loss, the resampling scheme used here is over-sampling of the minority class data, with the resampling implemented via bootstrapping [23]. In order to carry out the over-sampling, the original rail-cast data are first segregated into two data subsets, each containing data samples from a single class. The data subset corresponding to the minority class is then fed into the bootstrapping resampling algorithm, which produces a multiple randomly resampled subsets, each with the same size as the original minority subset. Those resampled subsets are then combined into an over-sampled minority class data, and then mixed with the majority class data to form the final resampled training data. The level of imbalance for the resampled training data can be controlled via a design parameter R_{MM}, defined as the ratio of the number of samples belong to the majority class to that belong to the minority class. As a price paid to avoid information loss during the resampling, the size of the resampled training data set is increased. Fig. 3 shows the effect of the R_{MM} on the size of the resampled training data.

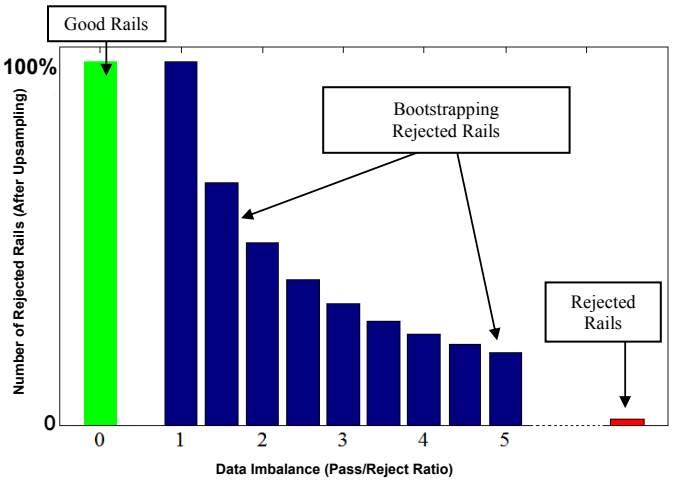

Figure 3. Effect of R_{MM} to the size of resampled training data

B. Fuzzy C-means Clustering based Classification

An adaptive neural-fuzzy inference system can be viewed as a fuzzy logic system whose rules are generated through fuzzy neural network training from a carefully assembled training data set [24-25]. A generic fuzzy inference model can be presented as a collection of fuzzy rules in the following form:

R_i: **If** x_1 is A_{i1} **and** x_2 is A_{i2} ... **and** x_n is A_{in} **then** $y = z_i(\boldsymbol{x})$

where $\boldsymbol{x} = [x_1, x_2, \ldots, x_n] \in U$ and $y \in V$ are linguistic variables, A_{ij} are fuzzy sets defined on the universe U, and $z_i(\boldsymbol{x})$ is a function of $\boldsymbol{x}$. Fig. 4 shows a simplified ANFIS architecture with two rules, where Layer 1 is for fuzzy membership mapping of the input, Layer 2 implements the fuzzy 'and' operation, Layer 3 normalises the firing strength of each fuzzy rule, Layer 4 performs the then part function $y = z_i(\boldsymbol{x})$ of the corresponding fuzzy rule, and Layer 5 computes the overall output of the fuzzy system for the given input.

In this study, the fuzzy membership takes a form of a Gaussian function, and the fuzzy rule is trained using fuzzy c-means clustering through a Matlab built-in fuzzy logic toolbox routine *genfis3* [21]. Fuzzy c-means clustering (FCM) is a well-recognized paradigm to generate fuzzy models, due to its efficiency and simplicity. After the number of clusters p (equivalent to the number fuzzy rules) is chosen, the FCM algorithm partitions all the data samples $\{\boldsymbol{x}(1), \boldsymbol{x}(2), \ldots, \boldsymbol{x}(N)\}$ into p fuzzy clusters such that the following objective function is minimized:

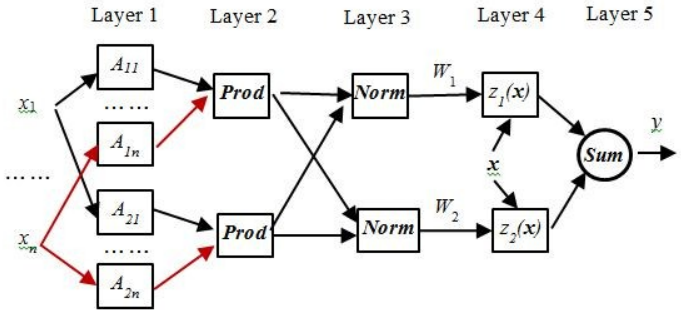

Figure 4. A simplified ANFIS architecture with 2 rules [21]

$$J_m = \sum_{k=1}^{N} \sum_{i=1}^{p} \mu_{ik}^{\alpha} ||\boldsymbol{x}(k) - \boldsymbol{c}_i||^2 \quad (4)$$

where $\boldsymbol{c}_i$ is the centre of the ith cluster generated by fuzzy clustering, μ_{ik} is the membership degree of the kth data belonging to the ith cluster, and α is the exponent of μ_{ik}. The fuzzy membership μ_{ik} normally satisfies the following constraints:

$$\sum_{i=1}^{p} \mu_{ik} = 1, \ \forall k \in \{1, N\}; \ 0 \le \mu_{ik} \le 1, \forall k, i \in \{1, p\} \quad (5)$$

In this study, a hybrid learning algorithm is used to optimise the parameters of the fuzzy inference systems. It applies a combination of the 'least-squares' method and the error back-propagation gradient descent method for training the membership function and other ANFIS parameters using the inputs-outputs in the training data set.

The number of fuzzy rules p and the majority-to-minority ratio R_{MM} are two critical parameters which will influence the ultimate modelling performance. We have developed an iterative optimisation procedure in order to identify the 'best' combination of these two critical design parameters under the paradigm of bootstrapping over-sampling and adaptive neural-fuzzy classification. Fig. 5 shows the diagram for the iterative optimisation scheme.

C. Preliminary Results

The pre-processed rail-cast data need to be divided into two data sets, one used for training and another for testing and with the training/testing data ratio set to 70:30. 39 inputs are used for modelling, as specified by the forward NN input selection scheme discussed in Section 3. The training data set will be used for bootstrapping resampling in order to generate a balanced training set for data modelling. The range of majority to minority case data ratio R_{MM} is selected as $[R_{min} \sim R_{max}] = [1.0, 5.0]$ with an increment step length of 0.5. The range for p, the number of fuzzy rules, is chosen as $[p_{min}, p_{max}] = [2, 10]$ with

incremental step of 1. The maximum training epoch is 100. Some preliminary modelling results are shown in Fig. 6.

In a classification problem, the performance of misclassification gives a better measure of the quality of the developed model than the RMSE based performance. In order to calculate such misclassification performance, the continuous outputs of the optimised ANFIS model are transformed into binary outputs, with 1 indicating the minority class ('Reject') and 0 for the majority class ('Good'). Specificity, sensitivity and accuracy performances originated in medical research [26] are adopted in this paper as the binary classification performances. 'Specificity' measures the proportion of 'negative' samples (majority class) which are correctly identified, while 'sensitivity' measures the proportion of 'positive' samples (minority class) which are correctly identified. In other words, sensitivity represents the true 'negative' rate, while specificity is the true 'positive' rate. 'Accuracy' is the overall percentage that both categories are correctly classified.

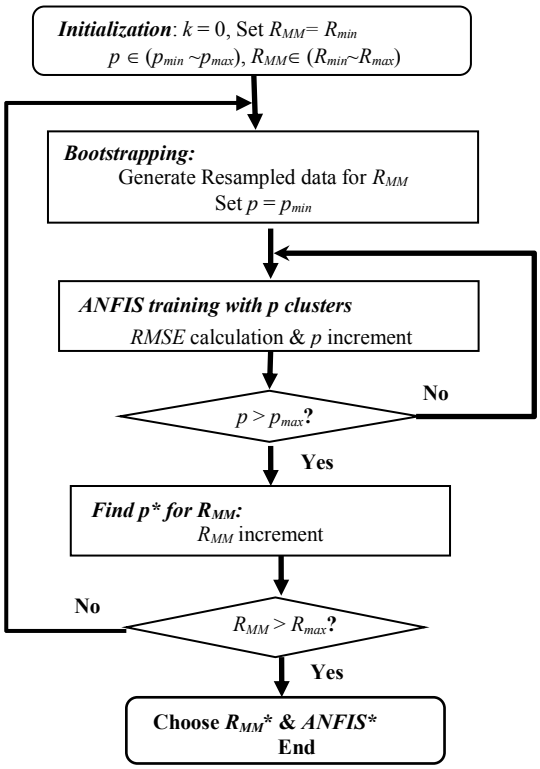

Figure 5. Iterative optimisation for p & R_{MM} in bootstrapping-ANFIS scheme

Fig. 6 shows a clear trend of the three different performances against the variation of the R_{MM} data ratio, which is used to control the data imbalance level in bootstrapping. The data over-sampling is carried out on the original training data alone, so the whole testing data remain to be 'unseen' for the model to be developed using the resampled training data. A large R_{MM} value indicates more dominance for the majority class in the resampled training data, and hence is beneficial to the performance related to the majority class, i.e., the specificity. In contrast, a small R_{MM} value indicates a reduced dominance of the majority class, and hence tends to benefit the performance for the minority class, i.e., sensitivity. There exists an optimal R_{MM} such that the overall classification performance reaches its optimum. Simulation results show that, the optima R_{MM} * value is approximately 2.5 for the current study.

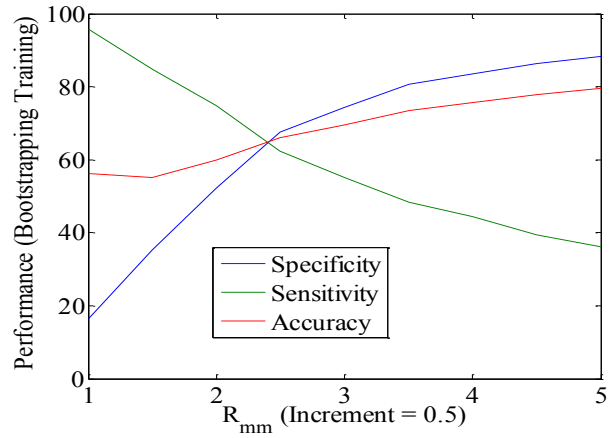

(a). Measured by the over-sampled training data (Train-Original)

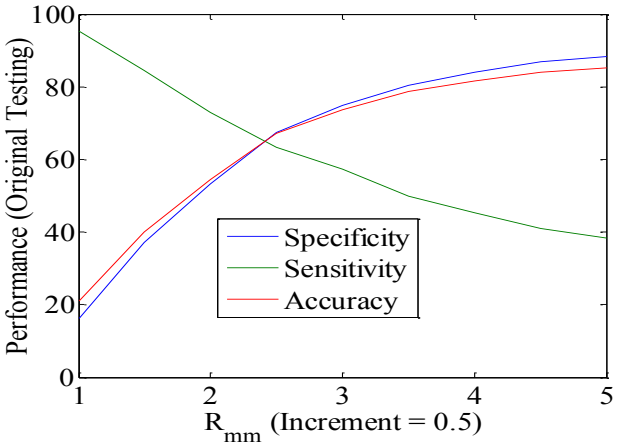

(b). Measured by the original testing data (Test-Original)

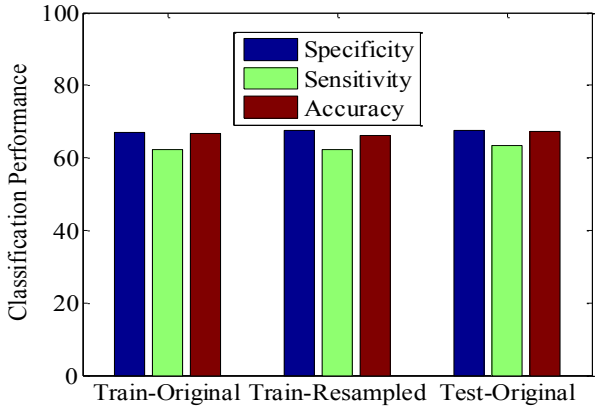

(c). Classification performance for R_{MM} *= 2.5

Figure 6. Performance of bootstrapping ANFIS scheme

The iterative bootstrapping ANFIS model produced a good balance between the data fitting and generalisation performance, as exemplified by the results shown in Fig. 6. In

the original data modelling without resampling applied (see Fig. 7), the success rate for rejected rail classification (sensitivity) was very poor at less than 10% for the testing data set and about 16% for the trainiing data set. Although in that case, the specificity performance was very good (over 96% for both the training and testing data sets), the model was of little practical value as the concern in the production route is to identify robust relationships that support identification and elimination of root causes for rail rejection. The sensitivity of the optimal model (discovered through the iterative procedure presented in Fig. 5) is much better at 65% for the resampled training data (Fig. 6a), and when this optimal model is applied to the original training data set (without resampling) similar results are observed. Furthermore, when the model is applied for the previously unused testing portion from the original data set the same performance results are observed (Fig. 6b) indicating that the matched performance for familiar data and for 'unseen' data are consistent. Fig. 6c shows the sensitivity, specificity and accuracy performances for the ANFIS model developed under the optimal resampled training data set corresponding to R_{MM} *= 2.5.

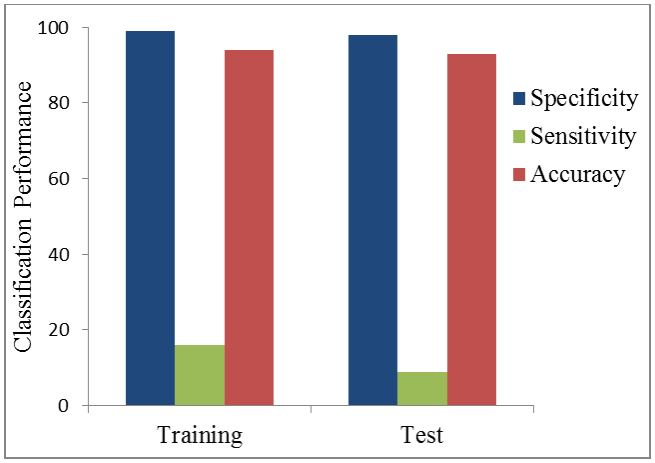

Figure 7. Classification performance using the rail data without resampling

V. Conclusions

In this paper an integrated bootstrapping-ANFIS modelling scheme has been developed to deal with severely imbalanced data classification. The fuzzy classification is implemented through an iterative process of generating oversampling training data and learning the ANFIS model parameters using the resampled training data through fuzzy c-means clustering. Since the case study involves large scale industrial data, data pre-processing plays a significant role for effective data modelling. One of the key objectives of the data pre-processing is to form a compact data set by selecting the most relevant optimal input variables, thus minimising redundancy and eliminating data conflicts. Correlation analysis and forward NN-based input ranking have been incorporated in the data pre-processing stage. Preliminary results show that the integrated bootstrapping-ANFIS modelling scheme developed is very promising, with significant performance improvement especially in terms of the sensitivity. Moreover, the developed classification model achieved a good balance between data fitting and data generalisation.

One disadvantage of using bootstrapping-based over-sampling is that the resampled training data set includes a significant level of redundancy related to the minority class data. The increase in the overall training data set size may also pose difficulties for large scale data modelling and classification, due to the relatively big increase in computing resources. We will investigate new methodologies to overcome these shortcomings in future research.

Acknowledgment

Financial support from the UK-EPSRC is acknowledged under Grant EP/F023464/1. The authors wish to thank Tata Steel Europe for providing the data used in this research as well as expert knowledge to guide the data consolidation.

References

[1] N. V. Chawla, N. Japkowicz, and A. Kolcz, "Editorial: Special issue on learning from imbalanced data sets", ACM SIGKDD Explorations, vol. 6, no. 1, pp. 1–6, 2004.

[2] S. Kotsiantis, D. Kanellopoulos, and P. Pintelas, "Handling imbalanced datasets: A review", GESTS International Transactions on Computer Science and Engineering, vol. 30, no. 1 , pp 25-36, 2006.

[3] G. Weiss, "Mining with rarity: A unifying framework", SIGKDD Explorations, vol. 6, no.1, pp. 7-19, 2004.

[4] N. V. Chawla, N. Japkowicz, and A. Kotcz, Eds., ICML'2003 Workshop on Learning from Imbalanced Data Sets, Washington DC, 21 August 2003.

[5] N. V. Chawla, L. O. Hall, K. W. Bowyer, and W. P. Kegelmeyer, "SMOTE: Synthetic minority oversampling technique", Journal of Artificial Intelligence Research, vol. 16, pp. 321-357, 2002.

[6] P. Domingos, "MetaCost: A general method for making classifiers cost-sensitive", Proceedings of the Fifth International Conference on Knowledge Discovery and Data Mining, pp. 155-164, 1999.

[7] K. Huang, H. Yang, I. King, and M. R. Lyu, "Learning classifiers from imbalanced data based on biased minimax probability machine", Proceedings of IEEE Computer Society Conference on Computer Vision and Pattern Recognition, Washington, DC, pp. 558–563, 2004.

[8] D. S. Moore, G.P. McCabe, W.M. Duckworth, and S.L. Sclove, "Bootstrap methods and permutation tests", The Practice of Business Statistics, Ch18, pp.1-73, W. H. Freeman Eds., 2003. http://bcs.whfreeman.com/pbs/cat_140/chap18.pdf

[9] F. Höppner, F. Klawonn, R. Kruse, and T. Runkler, Fuzzy Cluster Analysis: Methods for Classification, Data Analysis and Image Recognition, John Wiley & Sons, Inc., 1999.

[10] S. Kotsiantis, D. Kanellopoulos, P. Pintelas, "Data preprocessing for supervised leaning", International Journal of Computer Science, vol. 1, no. 2, pp.111-117, 2006.

[11] C. M. Bishop, Pattern Recognition and Machine Learning, Springer. London, 2006.

[12] I. Guyon, and A. Elisseeff, "An introduction to variable and feature selection", Journal of Machine Learning Research, vol. 3, pp. 1157-1182, 2003.

[13] Y. Hou, J. M. Zurada, W. Karwowski, W. S. Marras, and K. Davis, "Identification of key variables using fuzzy average with fuzzy cluster distribution", IEEE Transactions On Fuzzy Systems, vol. 15, no. 4, pp. 673-685. 2007.

[14] R. Sindelár, and R. Babuska, "Input selection for nonlinear regression models", IEEE Transactions On Fuzzy Systems, vol. 12, no. 5, pp. 688-696. 2004.

[15] A. Miller, Subset Selection in Regression, 2nd ed., Chapman & Hall/CRC, 2002.

[16] L. Yu, and H. Liu, “Feature selection for high-dimensional data: A fast correlation-based filter solution”, Proceedings of the 20th International Conference on Machine Learning (ICML-2003), Washington DC, 2003.

[17] S. Perkins, K. Lacker, and J. Theiler, “Grafting: Fast incremental feature selection by gradient descent in function space”, Journal of Machine Learning Research, vol. 3, pp. 1333–1356, 2003.

[18] M. P. C. Couto, “Review of input determination techniques for neural network models based on mutual information and genetic algorithms”, Neural Comput & Application, vol. 18: pp. 891–901, 2009.

[19] K. Hornik, “Approxiation capabilities of multilayer feedforward networks”, Neural Networks; vol. 4, no. 2, pp. 251-257. 1991.

[20] M. Mahfouf, and Y. Y. Yang, “A GA-optimised ensemble neural network model for charpy impact energy predictions”, IFAC MMM2010, The 13th Symposium on Automation in Mining, Mineral and Metal Industry, 2-4 August 2010, Cape Town, South Africa.

[21] The MathWorks Inc., Fuzzy Logic Toolbox 2 User's Guide, http://www.mathworks.com/help/pdf_doc/fuzzy/fuzzy.pdf, 2010.

[22] X. Guo, Y. Yin , C. Dong, G. Yang, and G. Zhou, “On the class imbalance problem”, Fourth International Conference on Natural Computation (ICNC'08), pp. 192-201, 25-27 August 2008, Jinan, China.

[23] M. R. Chernick, Bootstrap Methods: A Guide for Practitioners and Researchers. 2nd ed., Wiley Series in Probability and Statistics, New Jersey, 2008.

[24] J.-S. Roger Jang, “ANFIS: Adaptive-Network-Based Fuzzy Inference Systems”, IEEE Transactions on Systems, Man, and Cybernetics, vol. 23, no. 03, pp. 665-685, 1993.

[25] M. Y. Chen, D. A. Linkens, D. J. Howarth, and J. H. Beynon, “Fuzzy model-based charpy impact toughness assessment for ship steels”, ISIJ International, vol. 44, no. 6, pp. 1108–1113. 2004.

[26] A. J. Saah, and D. R. Hoover. “’Sensitivity’ and ‘Specificity’ Reconsidered: The Meaning of These Terms in Analytical and Diagnostic Settings”, Ann Intern Med , vol. 126, pp. 91-94.

2011 IEEE International Conference on Fuzzy Systems
June 27-30, 2011, Taipei, Taiwan

Passive Fuzzy Control for Uncertain Nonlinear Stochastic Inverted Pendulum Robot System

Wen-Jer Chang
Department of Marine Engineering
National Taiwan Ocean University
Keelung 20224, Taiwan, R.O.C.
e-mail: wjchnag@mail.ntou.edu.tw

Sin-Sian Jheng
Department of Marine Engineering
National Taiwan Ocean University
Keelung 20224, Taiwan, R.O.C.
e-mail: M98660024@mail.ntou.edu.tw

Cheung-Chieh Ku
Department of Electrical Engineering
National Taiwan Ocean University
Keelung 20224, Taiwan, R.O.C.
e-mail: D95530001@mail.ntou.edu.tw

***Abstract*—This paper presents a passive fuzzy controller design method for stabilizing the uncertain nonlinear stochastic inverted pendulum robot system. Through Takagi-Sugeno (T-S) fuzzy modeling approach, the complex nonlinear properties can be described by combining several linear sub-systems and determined membership functions. The Itô stochastic differential equation is employed to represent dynamics of systems in this paper. Appling the modeling approach, the T-S fuzzy model with multiplicative noise can be built for describing the nonlinear stochastic system. Besides, the uncertainties of the controlled system are considered in this paper for dealing with molding errors and varying parameters. Hence, the robust control problem is also discussed and investigated in this paper. Finally, the numerical simulations are proposed to show the effectiveness of the present design approach.**

Keywords-passive; uncertain; T-S fuzzy model; multiplicative noise

I. INTRODUCTION

There have been many researches on control of a two wheeled inverted pendulum system. Over the past few years, the inverted pendulum robot control problem has been investigated in many literatures [1-2]. And, the researchers have applied the pendulum system to simulate human stance and walk behaviors. However, the human stance and walk behaviors control problem is a complicated and difficult problem due to the nonlinearities of system.

In some circumstances, we may encounter real systems with random noise which makes the systems stochastic. When the stochastic behavior exists in the system, the related model can be called as systems with multiplicative noise [3]. Since stochastic modeling approach plays important role, many efforts have been proposed for stochastic system. Furthermore, parameter uncertainty often also appears in the real system due to the model inaccuracies and/or changes in the environment. With the parameter uncertainties, the control problem of the system considered in this paper are more difficult and challenger to be solved and investigated, than the same problems of deterministic systems. Based on the above motivation, the control problem of the inverted pendulum robot model with multiplicative noise is studied in this paper.

As well known that the stability of complex nonlinear systems is hard to be analyzed and synthesized. Recently, the fuzzy logic has been widely applied to approximate the nonlinearities of the system. And then, since Takagi-Sugeno [4], proved a model-based fuzzy approximating matched called T-S model, there have been dramatic progress in stability analysis and control design of nonlinear systems this model-based fuzzy systems. Referring to [4], many practical nonlinear systems have been successful represented via T-S fuzzy model. Thus, the inverted pendulum robot system with multiplicative noise is represented by T-S fuzzy model in this paper. Besides, the Parallel Distributed Compensation (PDC) concept [5] is applied to design the fuzzy controller for T-S fuzzy models. Through the T-S fuzzy model and PDC design concept, the linear control criteria can be applied to analyze the complex nonlinear systems.

Furthermore, consider the attenuation performance, the passivity theory [6] provides a useful tool to discuss the effect of disturbance on the systems. With the passivity theory, many efforts [7-8] have been proposed to design fuzzy controller for T-S fuzzy model with external disturbance. And, based on Lyapunov function, the stability conditions were derived into Linear Matrix Inequality (LMI) problems. According to the literatures [9], we can find that passivity theory provides several kinds of the performance: for example, H_∞ control and L_2 control. Based on the definition of supply rate, the different performance can be determined with passivity theory.

The purpose of this paper is to concentrate on the passive fuzzy controller design problem for uncertain nonlinear stochastic inverted pendulum robot system with multiplicative noises. The proposed fuzzy controller design methodology is developed by using the concept of PDC and the Lyapunov stability criterion. And the passivity theory is employed to guarantee disturbance attenuation performance of the system. Based on the LMI technique [10], one can find a suitable common positive definite matrix and feedback gains for satisfying the derived stability conditions. Then, the PDC-based passive fuzzy controller can be designed by obtained feedback gains. Thus, according to the proposed stability criterion, the nonlinear stochastic inverted pendulum robot system driven by designed fuzzy controller is strictly input passive and robustly asymptotically mean square stable.

978-1-4244-7316-8/11/$26.00 ©2011 IEEE

Finally, a simulations result is proposed to show the effectiveness and application of the proposed design method of this paper.

The organization of this paper is structured as follows. The dynamic model of simple human stance system with multiplicative noise is described in Section II. The discrete-time stochastic T-S fuzzy system of the nonlinear system is described in Section III. The fuzzy controller design method is proposed in Section IV. Through applying the proposed design approach, simulation results are provided in Section V. Finally, concluding remarks are made in Section VI.

II. The Dynamic Model of Simple Human Stance System

In this section, the inverted pendulum robot system is introduced. Referring to Fig. 1, a simplified mathematical dynamic model for describing inverted pendulum robot system is proposed to simulate the stance of human [11] as follows.

$$
\begin{aligned}
x_1(\mathrm{k}+1) &= x_1(\mathrm{k}) + T\,x_2(\mathrm{k}) + 0.1\,v(\mathrm{k}) \\
x_2(\mathrm{k}+1) &= x_2(\mathrm{k}) + \frac{T}{M + m\left(sin\,x_3(\mathrm{k})\right)^2}\Big(u(\mathrm{k}) + ml\,x_4^2(\mathrm{k}) \\
&\quad \times sin\,x_3(\mathrm{k}) - b\,x_2(\mathrm{k}) - mg\,cos\,x_3(\mathrm{k})\,sin\,x_3(\mathrm{k})\Big) \\
x_3(\mathrm{k}+1) &= x_3(\mathrm{k}) + T\,x_4(\mathrm{k}) \\
x_4(\mathrm{k}+1) &= x_4(\mathrm{k}) + \frac{T}{l\left(M + m\left(sin\,x_3(\mathrm{k})\right)^2\right)}\Big((M+m)\,g \\
&\quad \times sin\,x_3(\mathrm{k}) - u(\mathrm{k})\,cos\,x_3(\mathrm{k}) + b\,x_2(\mathrm{k})\,cos\,x_3(\mathrm{k}) \\
&\quad - ml\,x_4^2(\mathrm{k})\,sin\,x_3(\mathrm{k})\,cos\,x_3(\mathrm{k})\Big) \\
y(\mathrm{k}) &= x_1(\mathrm{k}) + v(\mathrm{k})
\end{aligned}
\tag{1}
$$

where

m	is the mass of black on the pendulum.
l	is the length of pendulum.
g	is the acceleration due to gravity.
b	is coefficient of viscous friction for motion of cart.
u	is the applied force.
v	is the external disturbance input.
M	is the mass of the cart.
T	is the sampling period.

The four state variables stand for $x_1(\mathrm{k}) = x$, $x_2(\mathrm{k}) = \dot{x}$, $x_3(\mathrm{k}) = \theta$, $x_4(\mathrm{k}) = \dot{\theta}$ with x the position of the cart, $y(\mathrm{k})$ is the system output, $v(\mathrm{k})$ is the external disturbance, and θ the angle of pendulum makes with vertical. This model is obtained by discretizing the continuous time model via Euler's method with $T = 0.1$ s, $b = 12.98$ Kg/s, $M = 1.378$ Kg, $l = 0.325$ m, $g = 9.8$ m/s^2, $m = 0.051$ Kg.

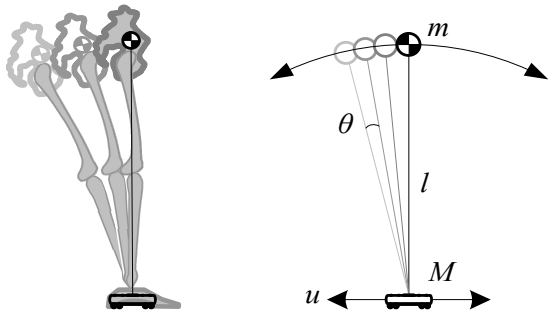

Fig. 1 Inverted pendulum robot system

Considering parameter uncertainties and stochastic behaviors, the modified dynamic model for the inverted pendulum robot system can be described as follows:

$$
\begin{aligned}
x_1(\mathrm{k}+1) &= x_1(\mathrm{k}) + 0.1\,x_2(\mathrm{k}) + 0.01\,x_1(\mathrm{k})\,w(\mathrm{k}) + \delta_1\,x_1(\mathrm{k}) \\
&\quad + 0.1\,v(\mathrm{k}) + 0.001\mathrm{v}(\mathrm{k})\,w(\mathrm{k}) + \delta_2\,u(\mathrm{k}) + \delta_3\,v(\mathrm{k}) \\
x_2(\mathrm{k}+1) &= x_2(\mathrm{k}) + \frac{0.1}{1.378 + 0.051\left(sin\,x_3(\mathrm{k})\right)^2}\Big(u(\mathrm{k}) - 12.98\,x_2 \\
&\quad + 0.0166\,x_4^2(\mathrm{k})\,sin\,x_3(\mathrm{k}) - 0.4998\,cos\,x_3(\mathrm{k}) \\
&\quad \times sin\,x_3(\mathrm{k})\Big) + 0.1\,x_2(\mathrm{k})\,w(\mathrm{k}) + 0.000726\,u(\mathrm{k})\,w(\mathrm{k}) \\
x_3(\mathrm{k}+1) &= x_3(\mathrm{k}) + 0.1\,x_4(\mathrm{k}) + 0.1\,x_3(\mathrm{k})\,w(\mathrm{k}) \\
x_4(\mathrm{k}+1) &= x_4(\mathrm{k}) + \frac{0.1}{0.4478\left(0.0166\left(sin\,x_3(\mathrm{k})\right)^2\right)} \\
&\quad \times\Big(14.0042\,sin\,x_3(\mathrm{k}) - u(\mathrm{k})\,cos\,x_3(\mathrm{k}) \\
&\quad + 12.98\,x_2(\mathrm{k})\,cos\,x_3(\mathrm{k}) \\
&\quad - 0.0166\,x_4^2(\mathrm{k})\,sin\,x_3(\mathrm{k})\,cos\,x_3(\mathrm{k})\Big) \\
&\quad + 0.1\,x_4(\mathrm{k})\,w(\mathrm{k}) - 0.002233\,u(\mathrm{k})\,w(\mathrm{k}) \\
y(\mathrm{k}) &= x_1(\mathrm{k}) + v(\mathrm{k})
\end{aligned}
\tag{2}
$$

where δ_1, δ_2 and δ_3 are the perturbation, which denoted by $\delta_1 \in [-0.001,\ \ 0.001]$, $\delta_2 = \delta_3 \in [-0.0002,\ \ 0.0002]$, and $w(\mathrm{k})$ is discrete Brownian Motion [12]. Using fuzzy modeling technique one can obtain T-S fuzzy model of (2) in the following section.

III. The Discrete Stochastic T-S Fuzzy Models

In order to build the T-S fuzzy model of the considered inverted pendulum robot system (2), two operating points are chosen to obtain the linearized models with the sector linearization technique [10]. The operating points are chosen as follows.

$\left(x_1(\mathrm{k}),\ x_2(\mathrm{k}),\ x_3(\mathrm{k}),\ x_4(\mathrm{k}),\ u(\mathrm{k})\right)_{\text{oper1}} = \left(0 \quad 0 \quad \pm 88^\circ \quad 0 \quad 0\right)$
and
$\left(x_1(\mathrm{k}),\ x_2(\mathrm{k}),\ x_3(\mathrm{k}),\ x_4(\mathrm{k}),\ u(\mathrm{k})\right)_{\text{oper2}} = \left(0 \quad 0 \quad 0 \quad 0 \quad 0\right)$.

In the points $\left(x_1(\mathrm{k}),\ x_2(\mathrm{k}),\ x_3(\mathrm{k}),\ x_4(\mathrm{k}),\ u(\mathrm{k})\right)_{\text{oper2}}$ is the equilibrium point and the others is the off-equilibrium point. According to the points, the membership function can be determined as Fig. 2. Through the above two linear subsystems and defining membership functions as Fig. 2, one can obtain the following T-S fuzzy model for the inverted pendulum robot system (2) such as.

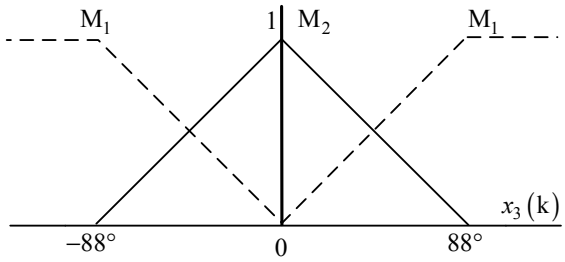

Fig. 2 Membership functions of $x_3(\mathrm{k})$

Rule 1: IF $x_3(\mathrm{k})$ is about M_1 THEN

$$x(\mathrm{k+1}) = \mathbf{A}_1(\mathrm{k})x(\mathrm{k}) + \mathbf{B}_1(\mathrm{k})u(\mathrm{k}) + \mathbf{D}_1(\mathrm{k})v(\mathrm{k}) + \left(\bar{\mathbf{A}}_1 x(\mathrm{k}) + \bar{\mathbf{B}}_1 u(\mathrm{k}) + \bar{\mathbf{D}}_1 v(\mathrm{k})\right) w(\mathrm{k})$$
$$y(\mathrm{k}) = \mathbf{C}_1 x(\mathrm{k}) + \mathbf{E}_1 v(\mathrm{k}) \tag{3}$$

Rule 2: IF $x_3(\mathrm{k})$ is about M_2 THEN

$$x(\mathrm{k+1}) = \mathbf{A}_2(\mathrm{k})x(\mathrm{k}) + \mathbf{B}_2(\mathrm{k})u(\mathrm{k}) + \mathbf{D}_2(\mathrm{k})v(\mathrm{k}) + \left(\bar{\mathbf{A}}_2 x(\mathrm{k}) + \bar{\mathbf{B}}_2 u(\mathrm{k}) + \bar{\mathbf{D}}_2 v(\mathrm{k})\right) w(\mathrm{k})$$
$$y(\mathrm{k}) = \mathbf{C}_2 x(\mathrm{k}) + \mathbf{E}_2 v(\mathrm{k}) \tag{4}$$

where $x(\mathrm{k}) = \left[x_1(\mathrm{k}) \quad x_2(\mathrm{k}) \quad x_3(\mathrm{k}) \quad x_4(\mathrm{k})\right]^{\mathrm{T}}$,
$\mathbf{A}_{\mathrm{i}}(\mathrm{k}) = \mathbf{A}_{\mathrm{i}} + \Delta\mathbf{A}_{\mathrm{i}}(\mathrm{k})$, $\mathbf{B}_{\mathrm{i}}(\mathrm{k}) = \mathbf{B}_{\mathrm{i}} + \Delta\mathbf{B}_{\mathrm{i}}(\mathrm{k})$,
$\mathbf{D}_{\mathrm{i}}(\mathrm{k}) = \mathbf{D}_{\mathrm{i}} + \Delta\mathbf{D}_{\mathrm{i}}(\mathrm{k})$,

$$\left[\Delta\mathbf{A}_{\mathrm{i}}(\mathrm{k}) \quad \Delta\mathbf{B}_{\mathrm{i}}(\mathrm{k}) \quad \Delta\mathbf{D}_{\mathrm{i}}(\mathrm{k})\right] = \mathbf{H}_{\mathrm{i}}\Delta(\mathrm{k})\left[\mathbf{R}_{\mathrm{i}} \quad \mathbf{R}_{\mathrm{Bi}} \quad \mathbf{R}_{\mathrm{Di}}\right], \tag{5}$$
$$\Delta(\mathrm{k})^{\mathrm{T}}\Delta(\mathrm{k}) \le \mathbf{I} \tag{6}$$

and

$$\mathbf{A}_1 = \begin{bmatrix} 1 & 0.1 & 0 & 0 \\ 0 & 0.0916 & -0.0008 & 0 \\ 0 & 0 & 1 & 0.1 \\ 0 & 0.0975 & 1.9622 & 1 \end{bmatrix},$$

$$\mathbf{A}_2 = \begin{bmatrix} 1 & 0.1 & 0 & 0 \\ 0 & 0.0581 & -0.0363 & 0 \\ 0 & 0 & 1 & 0.1 \\ 0 & 2.8983 & 3.127 & 1 \end{bmatrix},\ \mathbf{B}_1 = \mathbf{B}_2 = \begin{bmatrix} 0 \\ 0.0726 \\ 0 \\ -0.2233 \end{bmatrix},$$

$$\mathbf{D}_1 = \mathbf{D}_2 = \begin{bmatrix} 0.1 \\ 0 \\ 0 \\ 0 \end{bmatrix},\ \bar{\mathbf{A}}_1 = \bar{\mathbf{A}}_2 = \begin{bmatrix} 0.01 & 0 & 0 & 0 \\ 0 & 0.1 & 0 & 0 \\ 0 & 0 & 0.1 & 0 \\ 0 & 0 & 0 & 0.1 \end{bmatrix},$$

$$\bar{\mathbf{B}}_1 = \bar{\mathbf{B}}_2 = 0.01\times\begin{bmatrix} 0 \\ 0.0726 \\ 0 \\ -0.2233 \end{bmatrix},\ \bar{\mathbf{D}}_1 = \bar{\mathbf{D}}_2 = 0.01\times\begin{bmatrix} 0.1 \\ 0 \\ 0 \\ 0 \end{bmatrix},$$

$$\Delta\mathbf{A}_1 = \Delta\mathbf{A}_2 = \begin{bmatrix} \delta & 0 & 0 & 0 \\ 0 & 0 & 0 & 0 \\ 0 & 0 & 0 & 0 \\ 0 & 0 & 0 & 0 \end{bmatrix} = \mathbf{H}\Delta(\mathrm{k})\mathbf{R},\ \mathbf{E}_1 = \mathbf{E}_2 = 1$$
$$\mathbf{H} = [0.02 \quad 0 \quad 0 \quad 0]^{\mathrm{T}},\ \mathbf{R} = \left[0.05 \quad 0 \quad 0 \quad 0\right],$$
$$\mathbf{R}_{\mathrm{B1}} = \mathbf{R}_{\mathrm{B2}} = \mathbf{R}_{\mathrm{D1}} = \mathbf{R}_{\mathrm{D2}} = 0.01,\ \mathbf{C}_1 = \mathbf{C}_2 = \left[1 \quad 0 \quad 0 \quad 0\right]. \tag{7}$$

where $\mathbf{I}$ is identity matrix and the notation $\Delta(\mathrm{k})$ is time-varying matrix function. In this simulation, we assume that $\Delta(\mathrm{k}) = \sin(\mathrm{k})$. $E\{w(\mathrm{k})\} = 0$, $E\left\{w(\mathrm{k})^2\right\} = 1$, the noise $w(\mathrm{k})$ is assumed independent with $x(\mathrm{k})$. Furthermore, $E\{\bullet\}$ denotes standard expected operator. The uncertain matrices $\Delta\mathbf{A}_{\mathrm{i}}(\mathrm{k})$, $\Delta\mathbf{B}_{\mathrm{i}}(\mathrm{k})$, $\Delta\mathbf{D}_{\mathrm{i}}(\mathrm{k})$ are said to be admissible if both (5) and (6) hold. Given a pair of $\left(x(\mathrm{k}), u(\mathrm{k})\right)$, the final outputs of the fuzzy system can be inferred as follows.

$$x(\mathrm{k+1}) = \sum_{\mathrm{i}=1}^{2} h_{\mathrm{i}}\left(x_3(\mathrm{k})\right)\left(\mathbf{A}_{\mathrm{i}}(\mathrm{k})x(\mathrm{k}) + \mathbf{B}_{\mathrm{i}}(\mathrm{k})u(\mathrm{k}) + \mathbf{D}_{\mathrm{i}}(\mathrm{k})\mathrm{v}(\mathrm{k}) + \left(\bar{\mathbf{A}}_{\mathrm{i}}x(\mathrm{k}) + \bar{\mathbf{B}}_{\mathrm{i}}u(\mathrm{k}) + \bar{\mathbf{D}}_{\mathrm{i}}v(\mathrm{k})\right)w(\mathrm{k})\right)$$
$$y(\mathrm{k}) = \sum_{\mathrm{i}=1}^{2} h_{\mathrm{i}}\left(x_3(\mathrm{k})\right)\left(\mathbf{C}_{\mathrm{i}}x(\mathrm{k}) + \mathbf{E}_{\mathrm{i}}v(\mathrm{k})\right) \tag{8}$$

where $h_{\mathrm{i}}\left(x_3(\mathrm{k})\right) = \dfrac{M_{\mathrm{i}}\left(x_3(\mathrm{k})\right)}{\sum_{\mathrm{i}=1}^{2} M_{\mathrm{i}}\left(x_3(\mathrm{k})\right)}$, $h_{\mathrm{i}}\left(x_3(\mathrm{k})\right) \ge 0$,

$M_{\mathrm{i}}\left(x_3(\mathrm{k})\right) = \prod_{\mathrm{j}=1}^{\mathrm{r}} \mathrm{M}_{\mathrm{j}}\left(x_3(\mathrm{k})\right)$ and $\sum_{\mathrm{i}=1}^{2} h_{\mathrm{i}}\left(x_3(\mathrm{k})\right) = 1$. And the classical PDC law is given by

$$u(\mathrm{k}) = \sum_{\mathrm{i}=1}^{2} h_{\mathrm{i}}\left(x_3(\mathrm{k})\right)\mathbf{F}_{\mathrm{i}}x(\mathrm{k}) \tag{9}$$

Substituting (9) into (8), the closed-loop model can be written as

$$x(\mathrm{k+1}) = \sum_{\mathrm{i}=1}^{2}\sum_{\mathrm{j}=1}^{2} h_{\mathrm{i}}\left(x_3(\mathrm{k})\right) h_{\mathrm{j}}\left(x_3(\mathrm{k})\right)\left(\mathbf{G}_{\mathrm{ij}}(\mathrm{k})x(\mathrm{k}) + \mathbf{D}_{\mathrm{i}}(\mathrm{k})\right.$$
$$\left.\times v(\mathrm{k}) + \left(\bar{\mathbf{G}}_{\mathrm{ij}}x(\mathrm{k}) + \bar{\mathbf{D}}_{\mathrm{i}}v(\mathrm{k})\right)w(\mathrm{k})\right)$$
$$y(\mathrm{k}) = \sum_{\mathrm{i}=1}^{2} h_{\mathrm{i}}\left(x_3(\mathrm{k})\right)\left(\mathbf{C}_{\mathrm{i}}x(\mathrm{k}) + \mathbf{E}_{\mathrm{i}}v(\mathrm{k})\right) \tag{10}$$

where $\mathbf{G}_{\mathrm{ij}}(\mathrm{k}) = \mathbf{A}_{\mathrm{i}}(\mathrm{k}) + \mathbf{B}_{\mathrm{i}}(\mathrm{k})\mathbf{F}_{\mathrm{j}}$, $\bar{\mathbf{G}}_{\mathrm{ij}} = \bar{\mathbf{A}}_{\mathrm{i}} + \bar{\mathbf{B}}_{\mathrm{i}}\mathbf{F}_{\mathrm{j}}$. (11)

In the following, we introduce the following lemma and definition, which will be used in the derivation of our main results in the next sections.

Definition 1 [8]

Considering the system (1), then the disturbance $v(\mathrm{k})$ and output $y(\mathrm{k})$ are said to be strictly input passive if

$$E\left\{2\sum_{\mathrm{k}=0}^{\mathrm{k_q}} y^{\mathrm{T}}(\mathrm{k})v(\mathrm{k})\right\} > E\left\{\sum_{\mathrm{k}=0}^{\mathrm{k_q}} \gamma v^{\mathrm{T}}(\mathrm{k})v(\mathrm{k})\right\} \tag{12}$$

where $\gamma \geq 0$ and terminal time $\mathrm{k_q} > 0$. #

Lemma 1 [13]

Let $\mathbf{Q}$, $\mathbf{H}$, $\mathbf{S}$, $\boldsymbol{\beta}$ and $\boldsymbol{\psi}$ be real matrices with appropriate dimensions such that $\boldsymbol{\beta} > 0$ and $\boldsymbol{\psi}^{\mathrm{T}}\boldsymbol{\psi} \leq \mathbf{I}$. Then, for any scalar $\varepsilon > 0$ such that $\boldsymbol{\beta} - \varepsilon\mathbf{H}\mathbf{H}^{\mathrm{T}} > 0$, one has

$$\left(\mathbf{Q} + \mathbf{H}\boldsymbol{\psi}\mathbf{S}\right)^{\mathrm{T}}\boldsymbol{\beta}^{-1}\left(\mathbf{Q} + \mathbf{H}\boldsymbol{\psi}\mathbf{S}\right) \leq \mathbf{Q}^{\mathrm{T}}\left(\boldsymbol{\beta} - \varepsilon\mathbf{H}\mathbf{H}^{\mathrm{T}}\right)^{-1}\mathbf{Q} + \varepsilon^{-1}\mathbf{S}^{\mathrm{T}}\mathbf{S}. \tag{13}$$

#

IV. Robust Passive Control Design

In this section, for analyzing and synthesizing the stability of closed-loop system (10), the sufficient stability condition is developed via passivity theory and Lyapunov function.

Theorem 1

Given a dissipative rate $\gamma \geq 0$, if there exists a positive definite matrix $\mathbf{P} > 0$, and scalar $\varepsilon_{\mathrm{i}} > 0$ for satisfying the following conditions, then the closed-loop system (10) is strictly input passive and robustly asymptotically mean square stable.

$$\begin{bmatrix} \bar{\boldsymbol{\Phi}}_{11} & \bar{\boldsymbol{\Phi}}_{21}^{\mathrm{T}} \\ \bar{\boldsymbol{\Phi}}_{21} & \bar{\boldsymbol{\Phi}}_{22} \end{bmatrix} < 0 \text{ for } \mathrm{i, j} = 1, 2 \tag{14}$$

where

$$\bar{\boldsymbol{\Phi}}_{11} = \mathbf{G}_{\mathrm{ij}}^{\mathrm{T}}\left(\mathbf{P}^{-1} - \varepsilon_{\mathrm{i}}\mathbf{H}_{\mathrm{i}}\mathbf{H}_{\mathrm{i}}^{\mathrm{T}}\right)^{-1}\mathbf{G}_{\mathrm{ij}} + \varepsilon_{\mathrm{i}}^{-1}\mathbf{R}_{\mathrm{ij}}^{\mathrm{T}}\mathbf{R}_{\mathrm{ij}} + \bar{\mathbf{G}}_{\mathrm{ij}}^{\mathrm{T}}\mathbf{P}\bar{\mathbf{G}}_{\mathrm{ij}} - \mathbf{P}$$
$$\bar{\boldsymbol{\Phi}}_{21} = \boldsymbol{\Phi}_{21} - \mathbf{C}_{\mathrm{i}},\ \bar{\boldsymbol{\Phi}}_{22} = \boldsymbol{\Phi}_{22} - \mathbf{E}_{\mathrm{i}}^{\mathrm{T}} - \mathbf{E}_{\mathrm{i}} + \gamma\mathbf{I}$$
$$\boldsymbol{\Phi}_{21} = \mathbf{D}_{\mathrm{i}}^{\mathrm{T}}\left(\mathbf{P}^{-1} - \varepsilon_{\mathrm{i}}\mathbf{H}_{\mathrm{i}}\mathbf{H}_{\mathrm{i}}^{\mathrm{T}}\right)^{-1}\mathbf{G}_{\mathrm{ij}} + \varepsilon_{\mathrm{i}}^{-1}\mathbf{R}_{\mathrm{Di}}^{\mathrm{T}}\mathbf{R}_{\mathrm{ij}} + \bar{\mathbf{D}}_{\mathrm{i}}^{\mathrm{T}}\mathbf{P}\bar{\mathbf{G}}_{\mathrm{ij}}$$
$$\boldsymbol{\Phi}_{22} = \mathbf{D}_{\mathrm{i}}^{\mathrm{T}}\left(\mathbf{P}^{-1} - \varepsilon_{\mathrm{i}}\mathbf{H}_{\mathrm{i}}\mathbf{H}_{\mathrm{i}}^{\mathrm{T}}\right)^{-1}\mathbf{D}_{\mathrm{i}} + \varepsilon_{\mathrm{i}}^{-1}\mathbf{R}_{\mathrm{Di}}^{\mathrm{T}}\mathbf{R}_{\mathrm{Di}} + \bar{\mathbf{D}}_{\mathrm{i}}^{\mathrm{T}}\mathbf{P}\bar{\mathbf{D}}_{\mathrm{i}} \tag{15}$$

Proof :

Les us choose the Lyapunov function $V\left(x(\mathrm{k})\right) = x^{\mathrm{T}}(\mathrm{k})\mathbf{P}x(\mathrm{k})$. Firstly, by calculating difference and taking mathematical expectation of $V\left(x(\mathrm{k})\right)$ one has.

$$E\left\{\Delta V\left(x(\mathrm{k})\right)\right\} = E\left\{x^{\mathrm{T}}(\mathrm{k+1})\mathbf{P}x(\mathrm{k+1}) - x^{\mathrm{T}}(\mathrm{k})\mathbf{P}x(\mathrm{k})\right\}$$
$$= E\left\{\sum_{\mathrm{i}=1}^{2}\sum_{\mathrm{j}=1}^{2} h_{\mathrm{i}}\left(x_3(\mathrm{k})\right)h_j\left(x_3(\mathrm{k})\right)\left(\left(\mathbf{G}_{\mathrm{ij}}(\mathrm{k})x(\mathrm{k}) + \mathbf{D}_{\mathrm{i}}(\mathrm{k})v(\mathrm{k})\right)^{\mathrm{T}}\right.\right.$$
$$\times\mathbf{P}\left(\mathbf{G}_{\mathrm{ij}}(\mathrm{k})x(\mathrm{k}) + \mathbf{D}_{\mathrm{i}}(\mathrm{k})v(\mathrm{k})\right) + \left(\bar{\mathbf{G}}_{\mathrm{ij}}x(\mathrm{k}) + \bar{\mathbf{D}}_{\mathrm{i}}v(\mathrm{k})\right)^{\mathrm{T}}$$
$$\left.\left.\times\mathbf{P}\left(\bar{\mathbf{G}}_{\mathrm{ij}}x(\mathrm{k}) + \bar{\mathbf{D}}_{\mathrm{i}}v(\mathrm{k})\right) - x^{\mathrm{T}}(\mathrm{k})\mathbf{P}x(\mathrm{k})\right)\right\} \tag{16}$$

Using the Lemma 1, the following relations can be obtained.

$$\left(\mathbf{G}_{\mathrm{ij}}(\mathrm{k})x(\mathrm{k}) + \mathbf{D}_{\mathrm{i}}(\mathrm{k})v(\mathrm{k})\right)^{\mathrm{T}}\mathbf{P}\left(\mathbf{G}_{\mathrm{ij}}(\mathrm{k})x(\mathrm{k}) + \mathbf{D}_{\mathrm{i}}(\mathrm{k})v(\mathrm{k})\right)$$
$$\leq \xi^{\mathrm{T}}(\mathrm{k})\left(\begin{bmatrix}\mathbf{G}_{\mathrm{ij}}^{\mathrm{T}} \\ \mathbf{D}_{\mathrm{i}}^{\mathrm{T}}\end{bmatrix}\left(\mathbf{P}^{-1} - \varepsilon_{\mathrm{i}}\mathbf{H}_{\mathrm{i}}\mathbf{H}_{\mathrm{i}}^{\mathrm{T}}\right)^{-1}\begin{bmatrix}\mathbf{G}_{\mathrm{ij}} & \mathbf{D}_{\mathrm{i}}\end{bmatrix}\right.$$
$$\left.+\varepsilon_{1\mathrm{i}}^{-1}\begin{bmatrix}\mathbf{R}_{\mathrm{ij}}^{\mathrm{T}} \\ \mathbf{R}_{\mathrm{Di}}^{\mathrm{T}}\end{bmatrix}\begin{bmatrix}\mathbf{R}_{\mathrm{ij}}^{\mathrm{T}} \\ \mathbf{R}_{\mathrm{Di}}^{\mathrm{T}}\end{bmatrix}^{\mathrm{T}}\right)\xi(\mathrm{k}), \tag{17}$$

where $\mathbf{G}_{\mathrm{ij}}(\mathrm{k}) = \mathbf{G}_{\mathrm{ij}} + \mathbf{H}_{\mathrm{i}}\Delta\mathbf{R}_{\mathrm{ij}}$, $\mathbf{R}_{\mathrm{ij}} = \mathbf{R}_{\mathrm{i}} + \mathbf{R}_{\mathrm{Bi}}\mathbf{F}_{\mathrm{j}}$ and $\xi(\mathrm{k}) = \begin{bmatrix}x(\mathrm{k}) \\ v(\mathrm{k})\end{bmatrix}$.

From (17), one has following inequality from (16)

$$E\left\{\Delta V\left(x(\mathrm{k})\right)\right\}$$
$$\leq E\left\{\sum_{\mathrm{i}=1}^{2}\sum_{\mathrm{j}=1}^{2} h_{\mathrm{i}}\left(x_3(\mathrm{k})\right)h_{\mathrm{j}}\left(x_3(\mathrm{k})\right)\left\{\xi^{\mathrm{T}}(\mathrm{k})\begin{bmatrix}\bar{\boldsymbol{\Phi}}_{11} & \boldsymbol{\Phi}_{21}^{\mathrm{T}} \\ \boldsymbol{\Phi}_{21} & \boldsymbol{\Phi}_{22}\end{bmatrix}\xi(\mathrm{k})\right\}\right\} \tag{18}$$

Let us introduce the following performance function

$$J = E\left\{\sum_{\mathrm{k}=0}^{\mathrm{k_q}}\left(\gamma v^{\mathrm{T}}(\mathrm{k})v(\mathrm{k}) - 2y^{\mathrm{T}}(\mathrm{k})v(\mathrm{k})\right)\right\} \tag{19}$$

for all $v(k) \neq 0$ with zero initial condition. From (19), one has

$$J \le E\left\{\sum_{k=0}^{k_q}\left(\gamma v^{T}(k)v(k)-2y^{T}(k)v(k)+\Delta V(x(k))\right)\right\}$$
$$\equiv E\left\{\sum_{k=0}^{k_q}\Theta(k)\right\} \tag{20}$$

where

$$\Theta(k)=\Delta V(x(k))+\gamma v^{T}(k)v(k)-2y^{T}(k)v(k) \tag{21}$$

From (18) and (10), one has

$$\Theta(k)\le\sum_{i=1}^{r}\sum_{j=1}^{r}h_i(x_3(k))h_j(x_3(k))\{\xi^{T}(k)\Psi\xi(k)\} \tag{22}$$

where $\Psi=\begin{bmatrix}\bar{\Phi}_{11} & \bar{\Phi}_{12}\\ \bar{\Phi}_{21} & \bar{\Phi}_{22}\end{bmatrix}$. Obviously, if the stability condition (14) holds, then one has $\Psi<0$ and $\Theta(k)<0$. According to $\Theta(k)<0$, one has the following relations from (20).

$$J<0 \text{ and } E\left\{2\sum_{k=0}^{k_q}y^{T}(k)v(k)\right\}>E\left\{\sum_{k=0}^{k_q}\gamma v^{T}(k)v(k)\right\} \tag{23}$$

Since the (23) is equivalent to (12) of Definition 1, the closed-loop system (10) is strictly input passive. Besides, the stability of system is necessary performance for controlled system. Hence, in the following, the stability of system is discussed. If the condition (14) of Theorem 1 is held i.e., $\Psi<0$, thus $\Theta(k)<0$ from (22). By assuming the $v(k)=0$, the $\Delta V(x(k))<0$ can be found from (21) due to $\Theta(k)<0$. Referring to [14], one can find that the system is robustly asymptotically mean square stable due to $E\{\Delta V(x(k))\}<0$. So, if the stability condition (14) holds then the closed-loop system (10) is strictly input passive and robustly asymptotically mean square stable. The proof is completed.

#

In Theorem 1, the stability condition (14) is not strict LMI problem for applying convex optimization algorithm. For the reason, one can directly convert (14) into LMI form with Schur complement and variables setting technique. Since the limitation of paper, the convention process is omitted here. In the following section, the proposed method of this paper is employed to design PDC-based fuzzy controller for stabilizing system (2).

V. Simulation Results

Consider the closed-loop system (10), and choose the dissipative rate $\gamma=1$. Applying Theorem 1 and using the MATLAB LMI toolbox, one can obtain

$$\mathbf{P}=\begin{bmatrix}16.8513 & 6.4704 & 22.3447 & 4.3105\\ 6.4704 & 3.6448 & 12.0250 & 2.2749\\ 22.3447 & 12.0250 & 45.1505 & 8.6407\\ 4.3105 & 2.2749 & 8.6407 & 1.6566\end{bmatrix},$$

$\varepsilon_1=3.6974$ and $\varepsilon_2=3.4109$. Subsequently, one can obtain the feedback gain

$\mathbf{F}_1=[17.6175 \quad 3.5721 \quad 53.3833 \quad 11.3578]$ and
$\mathbf{F}_2=[17.5728 \quad 24.1477 \quad 61.6890 \quad 11.3458]$.

According to the PDC concept, the fuzzy controller can be structured via state feedback gains with control law (9) designed controller, the responses of considered system are stated in Figs. 3-6 with initial condition $x(0)=[0 \quad 0 \quad 0.8 \quad 0]^{T}$ and $v(k)$ is a zero-mean white nose with variance 0.01. From the simulation results of Figs. 3-6, one can find that the closed-loop system is robustly asymptotically mean square stable. Besides, the following equation is introduced to check the strictly input passive of system.

$$\frac{E\left\{\sum_{k=0}^{k_q}v^{T}(k)v(k)\right\}}{E\left\{2\sum_{k=0}^{k_q}y^{T}(k)v(k)\right\}}=0.4958 \tag{24}$$

Based on Definition 1, the strictly input passivity of system (2) can be achieved by fuzzy controller (9) due to the value in (24) is less than one. From the Figs. 3-6 and (24), the strictly input passivity and robustly asymptotically mean square stability of system (2) is achieved by employing the designed PDC-based fuzzy controller (9).

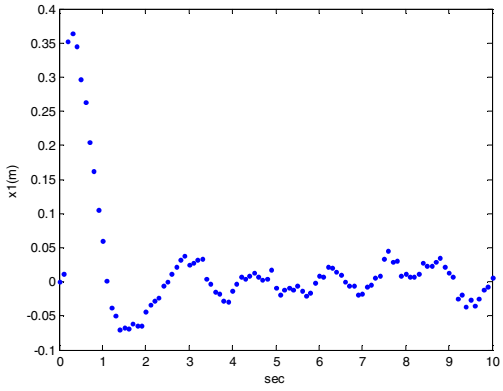

Fig. 3 Responses of $x_1(k)$

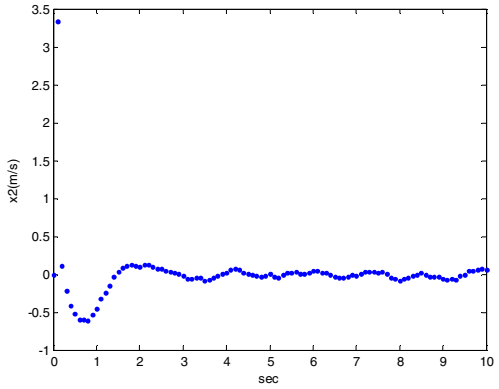

Fig. 4 Responses of $x_2(k)$

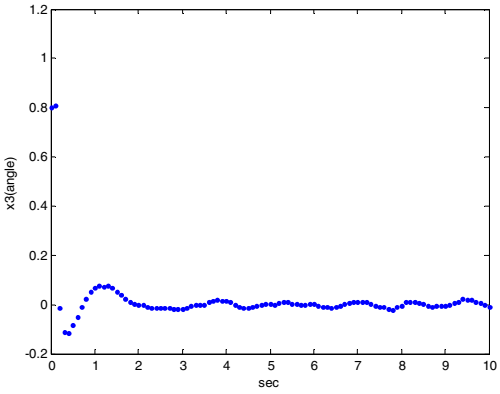

Fig. 5 Responses of $x_3(k)$

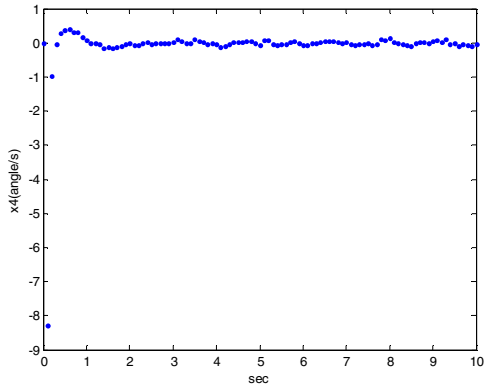

Fig. 6 Responses of $x_4(k)$

VI. CONCLUSIONS

In this paper, the control problem of nonlinear inverted pendulum system with multiplicative noises has been studied. The T-S fuzzy model was build to represent the original complex nonlinear system. In order to simulate the practical operation conditions, the stochastic behavior and uncertainties of system have been considered during investigation and discussion in this paper. Expect for stability of system, the attenuation performance was also concerned in this paper. Referring to the simulation results, the strictly input passivity and robustly asymptotically mean square stability of nonlinear inverted pendulum robot system with multiplicative noise can be achieved designed PDC-based fuzzy controller.

REFERENCES

[1] H. J. Lee and S. Jung, "Control of a Mobile Inverted Pendulum Robot System," Proc. IEEE International Conf. on Control, Automation and Syst., pp. 217–222, Oct., 2008.

[2] L. F. Lupian and R. Avila, "Stabilization of a Wheeled Inverted Pendulum by a Continuous-Time Infinite-Horizon LQG Optimal Controller," Proc. IEEE Latin American Robotic Symposium, pp. 65–70, Oct., 2008.

[3] L. E. Ghaoui, "State-Feedback Control of Systems with Multiplicative Noise via Linear Matrix Inequalities," Syst. and Control Letters, vol. 24, pp. 223–228, Feb. 1995.

[4] H. O. Wang, K. Tanaka and M. Griffin, "An Approach to Fuzzy Control of Nonlinear System: Stability and Design Issues," IEEE Trans. on Fuzzy syst., vol. 4, pp. 14–23, Feb., 1996.

[5] K. Tanaka and M. Sano, "A Robust Stabilization Problem of Fuzzy Control Systems and Its Application to Backing Up Control of a Truck-Trailer," IEEE Trans. Fuzzy syst., vol. 2, pp. 119–134, May, 1994.

[6] C. I. Byrnes and W. Lin, "Discrete-Time Lossless Systems, Feedback Equivalence and Passivity," Proc. IEEE Conf., Decision and Control, vol. 2, pp. 1775–1781, Dec., 1993.

[7] H. J. Uang, "On the Dissipativity of Nonlinear Systems: Fuzzy Control Approach," Fuzzy Sets and Syst., vol. 156, pp. 185–207, Dec., 2005.

[8] W. J. Chang, M. W. Chen and C. C. Ku, "Passive Fuzzy Controller Design for a Model Car via Discrete T-S Fuzzy Model with Multiplicative Noise," Proc. IEEE International Conf. on Information and Automation, pp. 1193–1198, June, 2009.

[9] R. Lozano, B. Brogliato, O. Egeland and B. Maschke, Dissipative Systems Analysis and Control Theory and Application, Springer, London, 2000.

[10] K. Tanaka and H. O. Wang, Fuzzy Control Systems Design and Analysis: A Linear Matrix Inequality Approach, John Wiley and Sons, Inc., New York, 2001.

[11] D. Wang and J. Huang, "A Neutral-Network-Based Approximation Method for Discrete-Time Nonlinear Servomechanism Problem," IEEE Trans. on Neural Networks, vol. 12, pp. 591–597, May, 2001.

[12] J. Liang, Z. Wang, Y. Liu, and X. Liu, "Global Synchronization Control of General Delayed Discrete-Time Networks with Stochastic Coupling and Disturbances," IEEE Trans. Syst., Man, Cybern. B, Cybern., vol. 38, pp. 1073–1083, Aug., 2008.

[13] Y. Wang, L. Xie, and C. E. de Souza, "Robust Control of a Class of Uncertain Nonlinear Systems," Syst. and Control Letters, vol. 19, pp. 139–149, Aug., 1992.

[14] G. Eli, S. Uri and Y. Isaac, H_∞ Control and Estimation of State–Multiplicative Linear Systems, Springer, London, 2005.

2011 IEEE International Conference on Fuzzy Systems
June 27-30, 2011, Taipei, Taiwan

Economic Load Dispatch using Intelligent Optimization with Fuzzy Control

Johnny C.Y. Lai
Centre for Signal Processing, Dept of Electronic & Information Engg., The Hong Kong Polytechnic University, Hung Ham, Hong Kong
08900438r@polyu.edu.hk

Frank H.F. Leung
Centre for Signal Processing, Dept. of Electronic and Information Engg., The Hong Kong Polytechnic University, Hung Ham, Hong Kong
enfrank@inet.polyu.edu.hk

Sai-Ho Ling
Centre for Health Technologies, Faculty of Engineering and Information Technology, University of Technology, Sydney, NSW, Australia
steve.ling@uts.edu.au

Edwin C. Shi
Centre for Signal Processing, Dept. of Electronic and Information Engg., The Hong Kong Polytechnic University, Hung Ham, Hong Kong
forseeking@gmail.com

***Abstract*— In this paper, Differential Evolution (DE) that incorporates fuzzy control and k-nearest neighbors algorithm is proposed to tackle the economic load dispatch problem. To provide the self-terminating ability, a technique called Iteration Windows (IW) is introduced to govern the number of iteration in each searching stage during the optimization. The size of IW is controlled by a fuzzy controller, which uses the information provided by the k-nearest neighbors system to analyze the population during the searching process. The controller keeps controlling the IW till the end of the searching process. A wavelet based mutation process is embedded in the DE searching process to enhance the searching performance. The weight *F* of DE is also controlled by the fuzzy controller to further speed up the searching process. The proposed method is employed to solve the Economic Load Dispatch with Valve-Point Loading (ELD-VPL) Problem. It is shown empirically that the proposed method can terminate the searching process with a reasonable number of iteration and performs significantly better than the conventional methods in terms of convergence speed and solution quality.**

Keywords-Fuzzy Control, Economic Load Dispatch, Differential Evolution

I. INTRODUCTION

Differential Evolution (DE) [1] is a population based stochastic optimization algorithm that searches the solution space for the best solution by using a group of particles. It uses the weighted difference between two particles to determine the third particle. Because of the population based searching strategy, DE is less possibly getting trapped in local optima [3]. DE guides the particles to move toward the best solution by using evolutionary operations. Comparing with other optimization algorithms, DE is relatively easy to implement. It requires fewer parameters for tuning, and has a relatively fast convergence speed. It can also offer a high degree of exploration for the population, and has been successfully applied in many optimization problems such as data clustering [4], power plant control [5], optimization of non-linear functions [6], etc.

On applying DE to real-world problems, the maximum number of iteration is usually needed to be provided as the stopping criterion of the algorithm. Different problems might require different numbers of iteration and there is no strong proof for the best number of iteration for a given problem. The maximum number of iteration often is determined by trial and error and/or the user's experience. To tackle this problem, much research work have been done to test the convergence criteria for different search methods [7][8]. In this paper, a new technique called Iteration Windows is embedded into the searching process of DE. On searching, the searching stage of DE can be analyzed based on the distribution of the population in the search domain. By monitoring the distribution of the population, we can get an idea of the state of the searching process. One method for analyzing the population behavior is clustering. In this paper, an improved DE that incorporates fuzzy control and k-nearest neighbors to determine the terminating condition is proposed to handle the problem of Economic Load Dispatch with Valve-Point Loading (ELD-VPL).

ELD is a method to schedule or control the power generator outputs with respect to the load demands, and to operate the power system economically [9]. The goal is to minimize the operation cost of the power generating system. Because of the valve-point loadings and rate limits, the input-output characteristics of modern generators are nonlinear by nature. As a result, the characteristics of ELD-VPL problems are multimodal, discontinuous, and highly nonlinear. Owing to its complexity, we cannot determine the maximum number of iteration easily.

This paper is organized as follows: Section II presents the operation of the DE with self-terminating ability. The problem formulation of ELD-VPL is given in Section III. Experimental study and analysis are given in Section IV. A conclusion will be drawn in Section V.

978-1-4244-7316-8/11/$26.00 ©2011 IEEE

II. DE WITH SELF-TERMINATING ABILITY

First, a population of solution vectors will be randomly generated over the solution space. They move on the solution space by addition, subtraction and component swapping; until the population converges to the best solution after a number of iteration. The pseudo code for the standard DE (SDE) process is shown in Fig.1. In this paper, DE with self-terminating ability using k-nearest neighbors and fuzzy control is proposed. The pseudo code is shown in Fig. 2.

```
begin
   Initialize the population;
   While (not the maximum number of iteration)
   {
         Mutation operation by equation (2);
         Crossover operation by equation (3);
         Evaluation of the fitness function;
         Selection of the best vector by equation (4);
   }
end
```

Figure 1. Pseudo code for SDE.

```
begin
Initialize the population;
   While (control not equal to 0) do
   {
        While (Iteration window not equal to 0)
        {
              Mutation operation by equation (2);
              Crossover operation by equation (3);
              Modifying the trial population vectors by
              equation (5);
              Evaluation of the fitness function;
              Select the best vector by equation (4);
              Iteration window =Iteration window – 1;
        }
        Analyze the population by k-NN by equation (10);
        Count the number of local clusters;
        Determine the new k , the new F and iteration
            window size by the fuzzy controller;
        If iteration window size> 6 then control = 1;
        If iteration window size< = 6 then control = 0;
          }
end
```

Figure 2. Pseudo code for the proposed system.

A. Standard Differential Evolution (SDE)

DE attempts to control a set of population of N_p vectors for each generation of evolution, with each vector contains D elements of parameters. Let $P_{x,g}$ be the population of the current generation g, and $\mathbf{x}_{i,g}$ be the i-th vector in this population:

$$\begin{aligned} P_{x,g} &= (\mathbf{x}_{i,g}), i = 0,1,...,N_p - 1; g = 0,1,...,g_{\max} \\ \mathbf{x}_{i,g} &= (x_{j,i,g}), j = 0,1,...,D-1. \end{aligned} \tag{1}$$

where $g_{\max}$ is the maximum number of generation. The population should be initialized as uniformly and randomly distributed over the solution space, which should have a specified boundary. DE generates a mutated vector $\mathbf{v}_{i,g}$ for each target vector $\mathbf{x}_{i,g}$ by using the mutation operation:

$$\mathbf{v}_{i,g} = \mathbf{x}_{i,g} + F \cdot (\mathbf{x}_{r_1,g} - \mathbf{x}_{r_2,g}) \tag{2}$$

where F is the scaling factor, which is a user-defined value; r_1 and r_2 are two different integers randomly generated from {0, 1, ..., N_p−1}. After the mutation operation, uniform crossover is employed to enhance the differential mutation search strategy and increase the diversity of the perturbed parameter vectors. Each vector element pair $x_{j,i,g}$ and $v_{j,i,g}$ generates a new trial vector element $u_{j,i,g}$:

$$\mathbf{u}_{i,g} = (u_{j,i,g}) = \begin{cases} (v_{j,i,g}) & \text{if } (rand_j(0,1) \le Cr \\ (x_{j,i,g}) & \text{otherwise.} \end{cases} \tag{3}$$

where $Cr \in [0, 1]$ is the crossover rate, which is a user-defined value that controls the number of parameters that are copied from the mutant. $rand_j(0,1)$ generates a random value between 0 and 1 for the j-th parameter. The algorithm also ensures $u_{j,i,g}$ gets at least one parameter value as $x_{j,i,g}$ [1]. Then the population is updated by comparing each trial vector to the corresponding target vector $\mathbf{x}_{i,g}$. For finding the global minimum, if the fitness value of the trial vector is lower than that the target vector, DE will replace the target vector in the next generation; otherwise the target vector retains its original place in the population for at least one generation. The selection operation is therefore given by:

$$\mathbf{x}_{i,g+1} = \begin{cases} \mathbf{u}_{i,g} & \text{if } f(\mathbf{u}_{i,g}) \le f(\mathbf{x}_{i,g}) \\ \mathbf{x}_{i,g} & \text{otherwise.} \end{cases} \tag{4}$$

where $f(\cdot)$ is the fitness function. When the condition to stop further evolution is satisfied, for example, the preset maximum number of iteration has been reached, the algorithm ends with the best solution as the final solution.

B. Wavelet mutation in crossover operation

To enhance the searching performance, we can embed a wavelet mutation in the DE crossover operation [19], which exhibits a fine-tuning ability. Let the i-th vector after crossover for the wavelet mutation be $\mathbf{u}_{i,g} = (u_{0,i,g}, u_{1,i,g}, ..., u_{D-1,i,g})$. Its element value is inside the vector element's boundary [$para^j_{\min}$, $para^j_{\max}$]. The mutated crossover vector is given by $\bar{\mathbf{u}}_{i,g} = (\bar{u}_{0,i,g}, \bar{u}_{1,i,g}, ..., \bar{u}_{D-1,i,g})$, and

$$\bar{u}_{j,i,g} = \begin{cases} u_{j,i,g} + \sigma \times (para^j_{\max} - u_{j,i,g}) \text{ if } \sigma > 0 \\ u_{j,i,g} + \sigma \times (u_{j,i,g} - para^j_{\min}) \text{ if } \sigma \le 0 \end{cases}, \tag{5}$$

$$\sigma = \frac{1}{\sqrt{a}} e^{-\left(\frac{\varphi}{a}\right)^2 / 2} \cos\left(5\left(\frac{\varphi}{a}\right)\right), \quad (6)$$

where

$$a = e^{-\ln(\lambda)\times\left(1-\frac{t}{T}\right)^{\zeta_{wm}}+\ln(\lambda)}. \quad (7)$$

T is the total number of iteration and t is the current iteration number; ζ_{wm} is the shape parameter of the monotonic increasing function, λ is the upper limit of the parameter a. At the early stage, a larger value of $|\sigma|$ gives a larger searching space; at the later stage, $|\sigma|$ is smaller and the algorithm gives a smaller searching space for fine-tuning. After the operation of the wavelet mutation, the population is updated by comparing each trial vector $\bar{\mathbf{u}}_{i,g}$ to the corresponding target vector $\mathbf{x}_{i,g}$ using the method of standard DE as given by (4). A new population is generated and the same DE evolution process is repeated.

C. K-Nearest Neighbors (K-NN)

The k-nearest neighbor algorithm (k -NN) algorithm is used to identify the number of groups of vectors (clusters) in the searching domain. It is a method for classifying and grouping data based on closest training data samples in a multidimensional feature space, and a class label is assigned with each training data sample [10][11][12]. By counting the majority class of its neighbors, a data element can be classified with a class label. The value of k is used to control the number of training data samples being considered in one group.

In the proposed system, a user-defined threshold T is introduced for controlling the size of the cluster. Firstly, the entire population is evaluated by the k-NN algorithm, where k is a value controlled by a fuzzy controller. Then, the k nearest vectors would be determined by k-NN. The total distance between those nearest vectors and the current test vector is:

$$D_{total} = \sum_{i=1}^{k} d_i(\mathbf{p}, \mathbf{q}_i) \quad (8)$$

where $d_i(\cdot)$ is the Euclidean distance between two points; $\mathbf{p}$ is the current testing point and $\mathbf{q}_i$ is one of the k nearest elements in the searching domain. The Euclidean distance is given by:

$$d_i(\mathbf{p},\mathbf{q}_i) = \sqrt{(p_1 - q_{i1})^2 + (p_2 - q_{i2})^2 + \cdots + (p_n - q_{in})^2} = \sqrt{\sum_{j=1}^{n} (p_j - q_{ij})^2} \quad (9)$$

The average distance d_{average} of a group (cluster) is:

$$d_{average} = \frac{D_{total}}{k} \quad (10)$$

If $d_{\text{average}} < T$, a local cluster is obtained. If $d_{\text{average}} \geq T$, a cluster is not present. The system will count the number of clusters obtained, which is passed to the fuzzy controller to determine the size of the next iteration window.

D. Iteration Windows

In the proposed system, the DE algorithm will first run for a small number of iteration (i.e. the first stage), and then the evolution will be paused (Fig. 3). After going through this iteration window, the population will be saved. The population distribution information (i.e. the number of local clusters) obtained from k-NN will be passed to the fuzzy controller to determine the size of the next-stage iteration window. One advantage of using the iteration window is that it can reduce the computation power for reaching the final solution, since the fuzzy controller is not operating during the evolution within a stage. It operates between stages only. Moreover, the total number of iteration is governed by the fuzzy controller instead of fixed by the user.

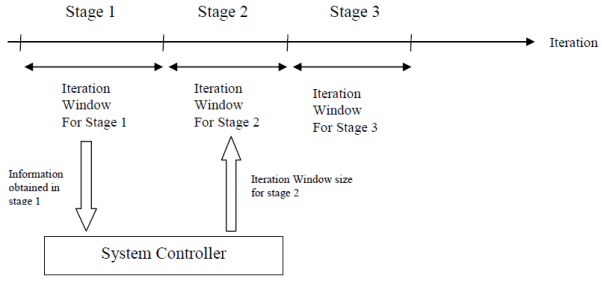

Figure 3. Operation of Iteration Windows.

The relation of the next iteration window's size (the next number of iteration) to the population distribution could be described by some heuristic rules. As a result, the fuzzy controller is modeling this relation. Hence, the total number of iteration could be controlled with respect to the nature of the problem. It does not require the user to determine the total number of iteration, but the system has its own ability to stop the system when it has reliably converged to the real optimum point.

E. Fuzzy Controller

A fuzzy controller realizes fuzzy inference [13]. Its applications include climate control [14], medicine [15], relational database [16], scheduling [17], etc. The process of fuzzy inference involves membership functions, logical operations and fuzzy if-then rules. Implementing fuzzy inference systems can be in Mamdani-type and Sugeno-type [18]. The Mamdani-type fuzzy inference method is used in this paper to construct the fuzzy controller. It uses linguistic control rules obtained from experienced human experts to perform decision making. The output variables must be fuzzy sets. To map the fuzzy set to some crisp output value, the system needs to do defuzzification. In this paper, the method

of center of gravity (COG) is used to perform defuzzification. Fig. 4 shows how the fuzzy inference system works.

The evolution of population-based searching algorithms, including DE, will not be the same for different experiments of a given problem because the algorithms themselves contain a lot of uncertainties. On analyzing the population distribution in the searching process, the derivation of the next iteration window's size from the population distribution should best be described as some heuristic rules. The aforementioned fuzzy controller can then be employed to determine the window's size together with the value of k for the k-NN in the next stage. The fuzzy controller takes the current k value and the population distribution information (i.e. the number of local clusters obtained) provided by k-NN as inputs, and maps this information into the fuzzy membership functions. The fuzzy controller also controls the value of F in the DE operation to enhance the searching process. An overview of the proposed system is shown in Fig. 5.

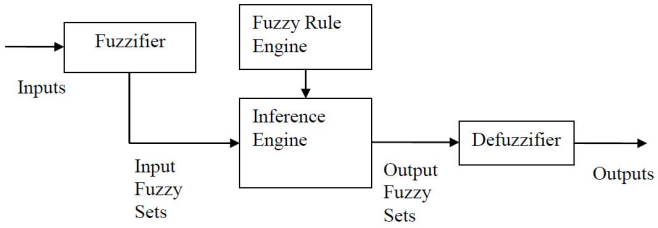

Figure 4. Operation of fuzzy inference system.

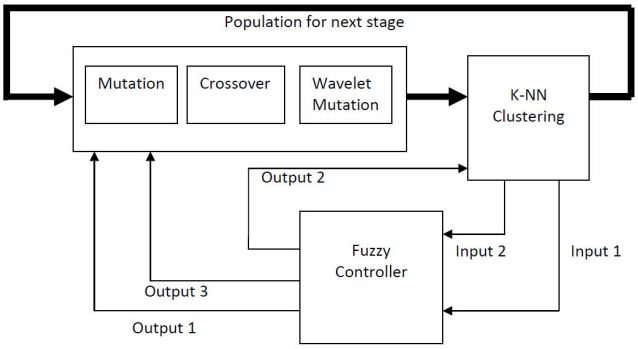

Figure 5. Overview of the proposed system.

III. ELD-VPL PROBLEM

The Economic Load Dispatch with Valve-Point Loading (ELD-VPL) is a method to control or schedule a group of power generator outputs with respect to the load demands, and operate a power system economically so as to minimize the operation cost of the power generating system. The problem can be formulated into the following objective function:

$$\min \sum_{i=1}^{n} C_i(P_{L_i}) \tag{11}$$

where $C_i(P_{L_i})$ is the operation fuel cost of generator i, and n denotes the number of generators. The problem is subject to balance constraints and generating capacity constraints:

$$D_L = \sum_{i=1}^{n} P_{L_i} - P_{Loss} \tag{12}$$

$$P_{L_{i,min}} \le P_{L_i} \le P_{L_{i,\max}}, i = 1,2,\cdots,n \tag{13}$$

where D_L is the load demand, P_{L_i} is the output power of the i-th generator, P_{Loss} is the transmission loss, and $P_{L_{i,\max}}$ and $P_{L_{i,min}}$ are the maximum and minimum output power of the i-th generator, respectively. The operation fuel cost function with valve-point loadings of the generators is given by

$$C_i(P_{L_i}) = a_i P_{L_i}^2 + b_i P_{L_i} + c_i + \left| e_i \times \sin(f_i \times (P_{L_{i,\min}} - P_{L_i})) \right| \tag{14}$$

where a_i, b_i, and c_i are the coefficients of the cost curve of the i-th generator, and e_i and f_i are the coefficients of the valve point loadings. The generating units with multivalve steam turbines exhibit a greater variation in the fuel cost functions. The valve-point effects introduce ripples in the heat-rate curves. To solve the ELD-VPL problem by using the proposed system, the solution representation of elements in the population is defined as follows:

$$\mathbf{P} = [P_{L_1} P_{L_2} P_{L_3} \cdots P_{L_{n-1}}] \tag{15}$$

where n is the number of generators. From (11), we have

$$P_{L_n} = D_L - \sum_{i=1}^{n-1} P_{L_i} + P_{Loss} \tag{16}$$

In this paper, the power loss is not considered, so

$$P_{L_n} = D_L - \sum_{i=1}^{n-1} P_{L_i} \tag{17}$$

To ensure that P_{L_n} falls within the range [$P_{L_{n,\min}}$, $P_{L_{n,\max}}$],

$$\text{If } P_{L_n} > P_{L_{n,\max}} \begin{cases} P_{L_1} = P_{L_1} + (P_{L_n} - P_{L_{n,\max}}) \\ P_{L_n} = P_{L_{n,\max}} \end{cases} \tag{18}$$

$$\text{If } P_{L_n} < P_{L_{n,\min}} \begin{cases} P_{L_1} = P_{L_1} - (P_{L_n} - P_{L_{n,\min}}) \\ P_{L_n} = P_{L_{n,\min}} \end{cases} \tag{19}$$

It should be noted that (18) and (19) are used to control each individual power generator. If the value of P_{L_1} is outside the constraint boundary (i.e. the safety range), the exceeding portion of the power required will be shared by other generators to ensure that the output power of all individual generators are working within the safety range.

IV. EXPERIMENT AND RESULT

Different kinds of DE methods are applied to a 40-generator system, which is adopted as an example in [19]. The load demand (D) of the problem is 10500 MW. Standard DE [20], DE/local-to-best/1 [20], DE/rand/1 with per-vector-dither [22] and the proposed system are used to solve the ELD-VPL problem. The following simulation conditions are used:

- The shape parameter of the wavelet mutation (ζ_{wm}): It is chosen by trial and error. ζ_{wm} = 1 is used in this paper;
- The parameter λ in (7): 10000;
- The number of population vectors: N_p = 30;
- Initial population: It is generated uniformly at random.
- Crossover rate: C_r= 0.5;
- The mutation weight factor (For standard DE, DE/local-to-best/1, DE/rand/1 with per-vector-dither): F=0.6;
- The number of iteration: 2000;
- Threshold T for k-NN: 5;
- Membership functions: As shown in Fig. 6 and Fig. 7;
- Fuzzy rule: Listed in Table 1. (Input 1 is the current number of local clusters; Input 2 is the k value of the current iteration window; Output 1 is the next F value for DE; Output 2 is k for the next stage; Output 3 is the next iteration window size.)

TABLE 1. THE FUZZY RULE TABLE

1	If (Input1 is Too Low) then (Output1 is Large).
2	If (Input1 is Low) then (Output1 is Average).
3	If (Input1 is Average) then (Output1 is Low).
4	If (Input1 is Large) then (Output1 is Too Low).
5	If (Input1 is Too Large) then (Output is Too Low).
6	If (Input1 is Too Low) or (Input2 is Too Low) then (Output1 is Large).
7	If (Input1 is Low) or (Input2 is Low) then (Output1 is Large).
8	If (Input1 is Average) or (Input2 is Average) then (Output1 is Average).
9	If (Input1 is Large) or (Input2 is Large) then (Output1 is Too Low).
10	If (Input1 is Too Large) or (Input2 is Too Large) then (Output1 is Too Low).
11	If (Input1 is Too Low) then (Output2 is Too Low).
12	If (Input1 is Low) then (Output2 is Low).
13	If (Input1 is Average) then (Output2 is Average).
14	If (Input1 is Large) then (Output2 is Large).
15	If (Input1 is Too Large) then (Output2 is Too Large).
16	If (Input1 is Too Low) then (Output3 is Too Large).
17	If (Input1 is Low) then (Output3 is Large).
18	If (Input1 is Average) then (Output3 is Average).
19	If (Input1 is Large) then (Output3 is Large).
20	If (Input1 is Too Large) then (Output3 is Too Large).
21	If (Input1 is Too Low) or (Input2 is Too Low) then (Output3 is too Large).
22	If (Input1 is Low) or (Input2 is Low) then (Output3 is Large).
23	If (Input1 is Average) or (Input2 is Average) then (Output3 is Average).
24	If (Input1 is Large) or (Input2 is Large) then (Output3 is Low).
25	If (Input1 is Too Large) or (Input2 is Too Large) then (Output3 is Too Low).

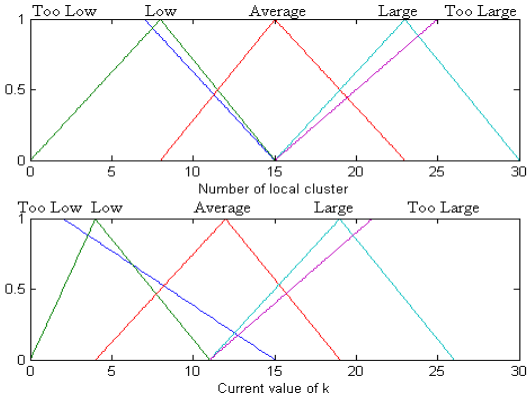

Figure 6. Output Membership Functions.

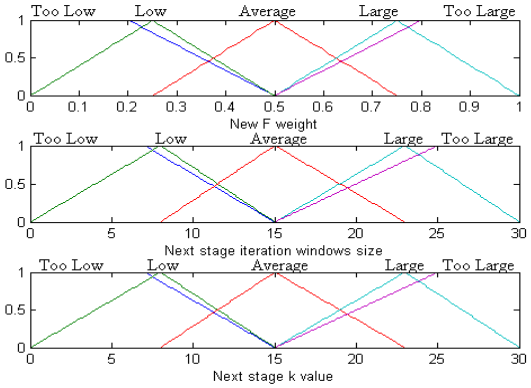

Figure 7. Input Membership Functions.

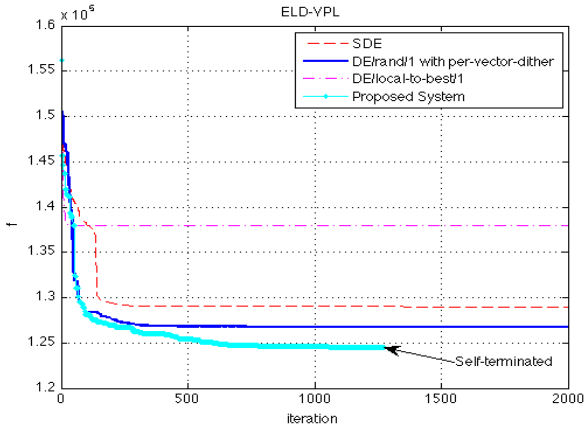

Figure 8. Fitness curve of ELD Problem

The dimension of ELD-VPL problem is 39. The result in terms of the cost value is shown in Table 2. All results shown are averaged data out of 50 trials. The convergence curves of different tested methods are shown in Fig. 8. We can see that the proposed system performs much better than the other methods in terms of convergence rate and cost value. The proposed system can offer the best (minimum) cost among the methods, which is $124559.87. The proposed system is able to terminate itself at the 1376-th iteration.

The comparison between the Delta method with standard DE, Delta method with DE/local-to-best/1, Delta method with

DE/rand/1 with per-vector-dither and the proposed system with Iteration Window is shown in Fig. 9. The Delta method is a common method for terminating the searching process in evolution algorithms. In the experiments, if the fitness value of the current iteration is less the 10^{-6} of the previous 10-th iteration, the searching process will be terminated. It shows that when using the Delta method, most of the algorithms will terminate very early with a very poor result, while the proposed system can terminate the searching process with much better solution quality.

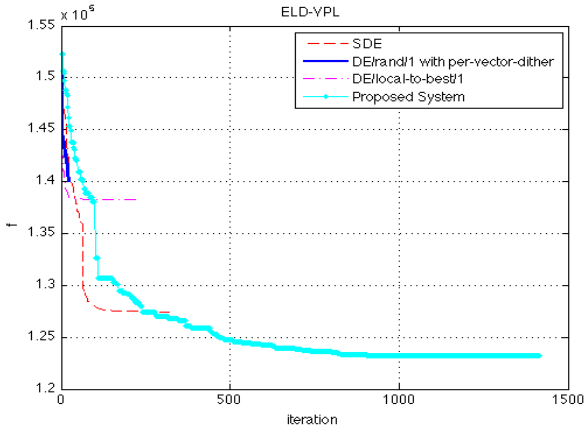

Figure 9. Comparison between the Delta method and the proposed system.

TABLE II. THE RESULT

	Proposed System	standard DE	DE/local-to-best/1	DE/rand/1 with per-vector-dither
Costs	**124559.87**	128982.54	137924.53	126753.64

V. CONCLUSION

In this paper, DE that incorporates fuzzy control and *k*-nearest neighbor algorithm has been proposed to handle the ELD-VPL Problem. To provide the self-terminating ability, the technique called Iteration Windows has been introduced to govern the number of iteration in each searching stage during the optimization. The size of the iteration windows is controlled by a fuzzy controller, which uses the information provided by the *k*-NN algorithm to analyze the population during the searching process. The controller keeps controlling the iteration windows until the end of the searching process. The wavelet based mutation process is embedded in the DE searching process to enhance the searching performance. The *F* weight of DE is also controlled by the fuzzy controller to further speed up the searching process. For the ELD-VPL problem, it is shown empirically that the proposed method out-performs significantly the conventional methods in terms of convergence speed and solution quality. The proposed system can terminate itself with a reasonable number of iteration.

ACKNOWLEDGMENT

The work described in this paper was substantially supported by a grant from The Hong Kong Polytechnic University (Project No. RP9L).

REFERENCES

[1] J. Brest, S. Greiner, B. Boskovic, M. Mernik, and V. Zumer "Self-Adapting Control Parameters in Differentail Evolution: Comparative Study on Numerical Benchmark Problems," *IEEE Trans. Evol. Comput.*, vol. 10, no. 6,pp 646-657, Dec. 2006.

[2] R. Storn and K. Price "Differential evolution–a simple and efficient heuristic for global optimization over continuous spaces," *Journal of Global Optimization*, vol. 11, pp. 341–359, 1997.

[3] U.K. Chakraborty (Ed.), *Advances in Differential Evolution*. Springer, Heidelberg, 2008.

[4] S. Paterlini and T. Krink, "High performance clustering with differential evolution," in *Proc. IEEE Congress on Evolutionary Computation*, vol. 2, 2004, pp. 2004–2011.

[5] J.H. van Sickel, K.Y. Lee, and J.S. Heo, "Differential evolution and its applications to power plant control," in *Proc. Intelligent Systems Applications to Power Systems 2007*, (ISAP 2007), 5-8 Nov. 2007, pp.1 – 6.

[6] B. Babu and R. Angira, "Optimization of non-linear functions using evolutionary computation," in *Proc. 12th ISME International Conference on Mechanical Engineering*, India, 2001, pp. 153–157.

[7] D. Greenhalgh and S. Marshall, "Convergence criteria for genetic algorithms," *SIAM J. Computer*, vol. 30, no. 1, pp. 260-282, 2000.

[8] H. Aytug and G.J. Koehler, "New stopping criterion for genetic algorithms," *European Journal of Operational Research*, Vol. 126, Issue 3, pp. 662-674, 2000.

[9] P.H. Chen and H.C. Chang, " Large-scale economic dispatch by genetic algorithms," *IEEE Trans. Power Syst.*, vol. 10, no. 1, pp. 117–124, Feb. 1995.

[10] D. Bremner, E. Demaine, J. Erickson, J. Iacono, S. Langerman, P. Morin, and G. Toussaint, "Output-sensitive algorithms for computing nearest-neighbor decision boundaries," *Discrete and Computational Geometry*, vol. 33, no. 4, pp. 593-604, 2005.

[11] T.M. Cover and P.E. Hart, "Nearest neighbor pattern classification," *IEEE Transactions on Information Theory*, vol. 13, no. 1, pp. 21-27, 1976.

[12] G.T. Toussaint, "Geometric proximity graphs for improving nearest neighbor methods in instance-based learning and data mining," *International Journal of Computational Geometry and Applications*, vol. 15, no. 2, pp. 101-150, April 2005.

[13] G.J. Klir and T.A. Folger, *Fuzzy Sets, Uncertainty, and Information*. Prentice-Hall, 1988.

[14] M.M. Eftekhari and L.D. Marjanovic. "Application of fuzzy control in naturally ventilated buildings for summer conditions," *Energy and Buildings*, vol. 35, issue 7, Aug. 2003.

[15] S. Zahan, C. Micheal, and S. Nikolakeas. *Fuzzy and Neuro-Fuzzy Systems in Medicine, chapter Fuzzy Expert Systems for Myocardial Ischemia Diagnosis*. CRC, 1999.

[16] P. Bosc and O. Pivert, "Extending SQL retrieval feature for the handling of flexible queries," *Fuzzy Information Engineering: A Guided Tour of Applications*, pp 233 -251. Wiley, 1997.

[17] B. Grabot, L. Geneste, and A. Dupeux, "Tuning of fuzzy rules for multiobjective scheduling," *Fuzzy Information Engineering: A Guided Tour of Applications*, pp. 695-703. Wiley, 1997.

[18] Mamdani, E.H. and S. Assilian, "An experiment in linguistic synthesis with a fuzzy logic controller," *International Journal of Man-Machine Studies*, vol. 7, no. 1, pp. 1-13, 1975.

[19] S.H. Ling, H.H.C. Iu, K.Y. Chan, H.K. Lam, C.W. Yeung, and F.H.F. Leung, "Hybrid particle swarm optimization with wavelet mutation and its industrial applications," *IEEE Trans. Syst., Man and Cybern., Part B: Cybernetics*, vol. 38, no. 3, pp. 743-763, Jun. 2008.

[20] X. Yao and Y. Liu, "Evolutionary programming made faster," *IEEE Trans. Evolutionary Computation*, vol. 3, no. 2, pp. 82-102, July 1999.

[21] S. Rahnamayan, H.R. Tizhoosh, and M.M.A. Salama, "Opposition-based differential evolution," *IEEE Trans. Evol. Comput.*, vol. 12, no. 1,pp 64-79, Feb. 2008.

[22] Y. Ao, and H. Chi, "Experimental study on differential evolution strategies," in *Proc. Global Congress on Intelligent Systems.*, vol. 2, pp. 19-24, May. 2009.

2011 IEEE International Conference on Fuzzy Systems
June 27-30, 2011, Taipei, Taiwan

Hypoglycemia Detection using Fuzzy Inference System with Genetic Algorithm

Sai Ho Ling
Faculty of Engineering
and Information Technology,
University of Technology, Sydney,
NSW 2007, Australia
Email: Steve.Ling@uts.edu.au
Telephone: (61)2-95142390
Fax: (61)2-95142435

Hung T. Nguyen
Faculty of Engineering
and Information Technology,
University of Technology, Sydney,
NSW 2007, Australia
Email: Hung.Nguyen@uts.edu.au

Frank Hung Fat Leung
Centre for Signal Processing,
Department of Electronic and
Information Engineering,
The Hong Kong Polytechnic University,
Hong Kong
Email: Frank.H.Leung@inet.polyu.edu.hk

***Abstract*—In this paper, we develope a genetic algorithm based fuzzy inference system to recognize hypoglycemic episodes based on heart rate and corrected QT interval of the electrocardiogram (ECG) signal. Genetic algorithm is introduced to optimize the membership functions and fuzzy rules. A practical experiment based on data from 15 children with T1DM is studied. All the data sets are collected from the Department of Health, Government of Western Australia. To prevent the phenomenon of overtraining (over-fitting), a validation strategy that may adjust the fitness function is proposed. Thus, the data are organized into a training set, a validation set, and a testing set randomly selected. The classification results in term of sensitivity, specificity, and receiver operating characteristic (ROC) analysis show that the proposed classification method performs well.**

***Index Terms*—Diabetes, Fuzzy logic, Genetic algorithm, Hypoglycemia.**

I. Introduction

Episodes of hypoglycemia for Type 1 diabetes mellitus (T1DM) patients, which can result in unconsciousness, seizures or even death, are common and can cause serious side effect in insulin therapy [1]. At least 50% of all severe episodes of hypoglycemia occur during night time [2] because usual insulin preparations do not adequately mimic the normal patterns of endogenous insulin secretion [3]. However, it is impossible in practice to monitor the episodes of hypoglycemia by measuring the blood glucose levels around the clock. Based on the physiological parameters of heart rate and QT interval of the ECG signal, the glucose levels of the T1DM patients can be determined and thus the episodes of hypoglycemia can be diagnosed [4].

A significant contribution is made by the use of fuzzy inferencing to realize the modeling and design of a non-invasive hypoglycemia monitoring system based on physiological responses. The classification models for numerous medical diagnosis such as diabetic nephropathy [5], acute gastrointestinal bleeding [6] and pancreatic cancer [7] have been developed by the use of the statical regression methods [8]. However, statical regression models are only accurate over the range of patients' data. In addition, it can only be applied if the patents' data are distributed based on the developed regression model, and the correlation between dependent and independent variables does not exist. If the patients' data are irregular, the developed regression models would have an unnaturally too wide possibility range.

To carry out modeling and classification for medical diagnosis purposes using the ECG and EEG signals [9]–[11], much attention has been devoted to computational technologies such as fuzzy system [12], support vector machine [13], and neural networks [14]. Apart from EEG and ECG classification, advanced computational intelligence techniques have been applied to cardiovascular response [15], breast cancer and blood cell [16], skull and brain [17], etc. Each technology has its own advantages; for example, fuzzy system is famous for its decision-making ability. Thanks to its ability of representing expert knowledge, the system's output can be determined by a set of linguistic rules which can be understood easily. As discussed in [18], neural networks (NNs) have been used as universal function approximators thanks to their good approximation capability. To develop classification models for medical diagnosis purpose [19], NNs are good to use because of their ability in addressing both the nonlinear and fuzzy nature of patients' data. In [20], the support vector machine (SVM) has shown good performance for doing classification. It has been used in many applications. Thanks to its capability of tackling binary classification problems, SVM has been used in classifying the features of the cardiac signal [21].

Since traditional optimization methods like the least square algorithm and gradient descent methods have the potential problem of trapping in local optima, evolutionary algorithms such as particle swarm optimization (PSO) [22], genetic algorithm (GA) [23], differential evolution (DE) [24], and ant colony optimization [25] were considered. They are efficient global optimization algorithms particularly good for handling multimodal problems. As discussed in [10], [26], [27], the combination of optimization methods and evolutionary algorithms can eventually give good performance in clinical applications.

In this paper, a genetic algorithm based fuzzy inference system is developed for the detection of hypoglycemic episodes using the physiological parameters of heart rate (HR), cor-

978-1-4244-7316-8/11/$26.00 ©2011 IEEE

rected QT interval (QTc) of the electrocardiogram (ECG) signal, change of heart rate, (ΔHR), and change of corrected QT interval of the electrocardiogram signal (ΔQT_c). Fuzzy inference system (FIS) [12], [28] is good at representing expert knowledge in linguistic rules that can be easily understood by human beings. In this paper, we prove that the overall performance of the hypoglycemia detection system is distinctly improved in terms of sensitivity and specificity by using an FIS. To optimize the fuzzy rules and fuzzy membership functions of the FIS, the global searching algorithm of Genetic Algorithm (GA) [23] is investigated. GA is a powerful random global search technique to handle optimization problems. It can help find the globally optimal solution over a domain. A real application is given to show the proposed algorithm is useful to detect the hypoglycaemic episodes in T1DM children. Besides, a validation strategy is introduced to reduce the effects of overtraining [29].

The organization of this paper is as follows: In Section II, the details of the development of the genetic algorithm based fuzzy inference system are presented. To show the effectiveness of our proposed methods, the results of detecting nocturnal hypoglycemic episodes in T1DM patients are discussed in Section III. A conclusion is drawn in Section IV.

II. Methodology

To realize the detection of hypoglycemic episodes in T1DM patients, a GA based fuzzy inference system (FIS) is developed. The 4-input 1-output system is shown in Fig. 1. The physiological inputs are the heart rate (HR), corrected QT interval of the electrocardiogram signal (QT_c), change of heart rate (ΔHR), and change of corrected QT interval of the electrocardiogram signal (ΔQT_c). The output is the binary status of hypoglycemia (h), with +1 representing hypoglycemia and -1 representing non-hypoglycemia. The FIS plays a main role in modeling the correlation between the physiological parameters (HR, QT_c, ΔHR, and ΔQT_c) and the presence of hypoglycemia (h).

In this system, the fuzzy membership functions and fuzzy rules are optimized by GA. The details of the GA-based FIS, the performance measurement, and the fitness function that is associated with a validation strategy are discussed as follows:

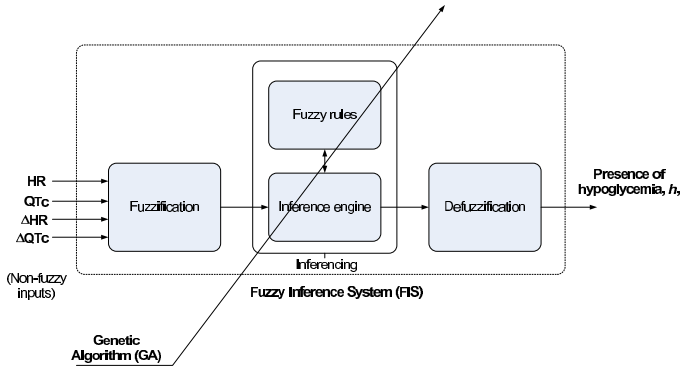

Fig. 1. Hypoglycemia detection system.

A. Fuzzy Inference System

Referring to Fig. 1, an FIS is used to model the hypoglycemic detection based on the physiological inputs (HR, QT_c, ΔHR, and ΔQT_c). The physiological inputs are treated as linguistic variables and given membership values that allow fuzzy detection. The fuzzy detection system consists of three components: fuzzification, inferencing, and defuzzification.

1) Fuzzification: The first step is to take the inputs, and determine the degree of membership they belong to each of the appropriate fuzzy sets. The membership function is defined as $\mu_{N_z^k}(z(t))$, which is a bell-shaped function given by:

$$\mu_{N_z^k}(z(t)) = e^{\frac{-(z(t)-m_z^k)^2}{2\varsigma_z^k}}, \tag{1}$$

where $z(t)$ is any one of the following 4 signals: $HR(t)$, $QT(t)$, $\Delta HR(t)$, $\Delta QT_c(t)$; $z(t)$ denotes the non-fuzzy input, $k = 1, 2, ..., m_f$; m_f denotes the number of membership functions, $t = 1, 2, ..., n_d$; n_d denotes the number of input-output data pairs. The parameters m_z^k and ς_z^k are the mean value and the standard deviation of the k-th membership function, respectively. If the input value is less than the minimum of the mean value or higher than the maximum of the mean value, the corresponding degree of membership is set as 1.

2) Inferencing: The task of the inferencing process is to map the fuzzified inputs to the rule base, and to produce a fuzzified output for each rule. The fuzzy if-then rules in the rule base are of the following format:

$$\begin{aligned} \text{Rule } \gamma : \textbf{IF} HR(t) \text{ is } N_{HR}^k(HR(t)) \textbf{ AND} \\ QT_c(t) \text{ is } N_{QT_c}^k(QT_c(t)) \textbf{ AND} \\ \Delta HR(t) \text{ is } N_{\Delta HR}^k(\Delta HR(t)) \textbf{ AND} \\ \Delta QT_c(t) \text{ is } N_{\Delta QT_c}^k(\Delta QT_c(t)) \textbf{ THEN } y(t) \text{ is } w_\gamma. \end{aligned} \tag{2}$$

where $N_{HR}^k(HR(t))$, $N_{QT_c}^k(QT_c(t))$, $N_{\Delta HR}^k(\Delta HR(t))$, and $N_{\Delta QT_c}^k(\Delta QT_c(t))$ are fuzzy terms, γ=1, 2, ...,n_r; n_r denotes number of rules and n_r is set to $(m_f)^{n_{in}}$, where $n_{in} = 4$ is the number of inputs to the FIS. From the fuzzification process, the inference engine obtains the values of $\mu_{N_{HR}^k}(HR(t))$, $\mu_{N_{QT_c}^k}(QT_c(t))$, $\mu_{N_{\Delta HR}^k}(\Delta HR(t))$, $\mu_{N_{\Delta QT_c}^k}(\Delta QT_c(t))$. Aggregation is then used to obtain the output of each rule γ as a fuzzy value. The output for each rule is defined as:

$$\begin{aligned} \mu_\gamma = (\mu_{N_{HR}^k}(HR(t))) \times (\mu_{N_{QT_c}^k}(QT_c(t))) \\ \times(\mu_{N_{\Delta HR}^k}(\Delta HR(t))) \times (\mu_{N_{\Delta QT_c}^k}(\Delta QT_c(t))), \\ \gamma = 1, 2, ..., n_r. \end{aligned} \tag{3}$$

3) Defuzzification: Defuzzification is the process of translating the outputs of the fuzzy rules into a value. The output of the defuzzication process is given by:

$$y(t) = \frac{\sum_{\gamma=1}^{n_r} w_\gamma \mu_\gamma}{\sum_{\gamma=1}^{n_r} \mu_\gamma}, \tag{4}$$

where $w_\gamma \in [0, 1]$ is the fuzzy singleton in Rule γ. If the output $y(t)$ is positive, hypoglycemia is present $(h(t) = +1)$.

B. Genetic Algorithm

To optimize the fuzzy membership functions and rules (the values of m, ς and w), the Genetic Algorithm (GA) is investigated. The GA process is shown in Algorithm II.1. First, a population of chromosomes P is created. Each chromosome $\mathbf{p}_i$ contains a set of genes p_{ij}, where $i = 1, 2, ..., n_p$, $j = 1, 2, ..., n_g$; n_p and n_g denote the population size (number of chromosomes) and the number of genes respectively. Second, the chromosomes are evaluated by a defined fitness function $f(\mathbf{p}_i)$. The form of the fitness function depends on the application. The better chromosomes are those returning higher fitness values in this process. Third, some of the chromosomes are selected to undergo genetic operations for reproduction by the method of normalized geometric ranking [30]. It is a selection based on a non-stationary penalty function which is a function of the generation number. As the number of generation increases, the penalty increases that puts more and more selective pressure on the GA to find the feasible solution. In general, a higher-rank chromosome will have a higher chance to be selected. Fourth, the genetic operation of crossover is performed. The crossover operation is mainly for exchanging information from the two parents, chromosomes $\mathbf{p}_1$ and $\mathbf{p}_2$, obtained in the selection process with a defined probability of crossover μ_c. This probability gives an expected number of chromosomes that undergo the crossover. In this paper, Blend-α [31] is used as the operation of crossover, which has a good searching ability and can handle multimodal and separability problem effectively. For the Blend-α crossover, the resulting offspring is chosen randomly from the interval $[X_j^1, X_j^2]$ following the uniform distribution, where

$$\begin{aligned} X_j^1 &= \min(p_{1j}, p_{2j}) - \alpha d_j \\ X_j^2 &= \max(p_{1j}, p_{2j}) + \alpha d_j \end{aligned}, \tag{5}$$

$d_j = |p_{1j} - p_{2j}|$, p_{1j} and p_{2j} are the j-th element of $\mathbf{p}_1$ and $\mathbf{p}_2$, respectively, and α is a positive constant.

After the crossover operation, the mutation operation follows. The mutation operation is to change the genes of the chromosomes in the population such that the features inherited from their parents can be changed. A probability of mutation, μ_m, is defined to govern the operation. It gives an expected number of genes that undergo the mutation. Non-uniform mutation [23] is used, which is an operation with a fine-tuning capability. The mutated gene is given by,

$$\hat{p}_{ij} = \begin{cases} p_{ij} + \Delta(\tau, \delta^j_{\max} - p_{ij}) & \text{if } r_d = 0 \\ p_{ij} + \Delta(\tau, p_{ij} - \delta^j_{\min}) & \text{if } r_d = 1 \end{cases}, \tag{6}$$

where r_d is a random number equal to 0 or 1 only. $\delta^j_{\max}$ and $\delta^j_{\min}$ are the upper and lower boundary of the gene. The function $\Delta(\tau, y)$ return a value in the range $[0, y]$ approaches 0 as τ increases. It is defined as follows.

$$\Delta(\tau, y) = y\left(1 - r^{(1-\tau/T)^{\zeta}}\right), \tag{7}$$

where r is a random number in range of [0,1], τ represents the current generation number, T represents the total number of iteration and ζ is a shape parameter that determines the degree of non-uniformity. After going through the mutation operation, the new offspring will be evaluated using the fitness function. The new population will be formed when the new offspring replaces the chromosome with the smallest fitness value. A global best chromosome $\hat{\mathbf{p}}_g$ that has the best fitness value will be stored if the current best chromosome $\hat{\mathbf{p}}(\tau)$ is better than the global one in the current generation. The newly formed population will repeat the same process. Such an iterative process will be terminated when a defined termination condition is met. Finally, the best chromosome (solution) $\hat{\mathbf{p}}_g$ will be found.

Algorithm II.1: PSEUDO CODE FOR GA()

```
τ ← 0
Initialize P(τ)
output (f(P(τ)))
while <not termination condition>
  do { τ ← τ + 1
       Select 2 parents, p_1 and p_2 from P(τ − 1)
       Perform crossover operation (5) with μ_c
       Perform mutation operation (6) − (7) with μ_m
       if p̂(τ) > p̂_g
         then p̂_g = p̂(τ)
       output (P(τ))
       output (f(P(τ)))
return (p̂_g)
comment: return the best chromosome (solution)
```

C. Performance Evaluation and Fitness Function

In this system, GA is employed to optimize the fuzzy rules and membership functions by finding out the best parameters m, ς and w. The function of the fuzzy inference system is to detect the hypoglycemic episodes accurately. To measure the performance of the biomedical classification test, sensitivity and specificity are introduced [32]. The sensitivity measures the proportion of actual positives which are correctly identified and the specificity measures the proportion of actual negatives which are correctly identified. The definitions of the sensitivity (ξ) and the specificity (η) are given as follows:

$$\xi = \frac{N_{TP}}{N_{TP} + N_{FN}}, \tag{8}$$

$$\eta = \frac{N_{TN}}{N_{TN} + N_{FP}}, \tag{9}$$

where N_{TP} is number of true positives which means the sick people are correctly diagnosed as sick; N_{FN} is number of false negative which means the sick people are wrongly diagnosed as healthy; N_{FP} is number of false positives which means healthy people are wrongly diagnosed as sick; and N_{TN} is number of true negatives which means the healthy people are correctly diagnosed as healthy. The values of ξ and η are within 0 to 1.

The objective of the system is to maximize the sensitivity and the specificity; thus, the fitness function is designed to maximize both values. A fitness function with a constant value and a penalty function is given in [33]. The constant value is used to control the balance between the sensitivity and specificity. The penalty function is used to force the sensitivity and the specificity to a required condition. However, on using this approach, only the training set and testing set are considered, which will risk the occurrence of overtraining [29]. Overtraining refers to the reduction of the generalization ability that can occur as the system is trained. To overcome this problem, a validation strategy that may adjust the fitness function is proposed in this paper to reduce the risk of overtraining.

Fig. 2 shows the idea of the proposed method to solve the overtraining problem. In this figure, the two curves represent the training performance and validation performance respectively. To overcome the overtraining problem, a validation set is introduced for the proposed fitness function. The x-axis represents the iteration number and T denotes the total number of iteration (as introduced in (7)), the y-axis represents the classification performance (in this paper, the performance is governed by sensitivity and specificity). The objective of the proposed validation strategy is to train the training set and test the trained results with the validation set with respect to a target region. The target region is a performance requirement related to sensitivity and specificity, for example, $\xi > 0.7$ and $\eta > 0.5$. As illustrated in Fig. 2 at T_a, we can see the performance of the training set has reached a very good result; however, the performance of the validation set cannot meet the minimum requirement of the target region. The testing performance will have a high chance to be out of the target region. It is an overtraining phenomenon; the model is over-fit with the training set and has the generalization performance reduced. At time T_b, the performance of both the training set and the validation set are within the target region; the testing result will have a good chance meeting the performance requirement. The parameters of the FIS will be stored at this time. In this paper, the termination condition of the GA is met when τ=T. When both sets have reached the target region and $\tau < T$, such as $\tau = T_b$, we will update the target region (increase the requirement level). For example, increase $\xi > 0.7$ to $\xi > 0.75$. At time T_c, both the training and validation performance are in the updated target region, the model parameters will then be updated.

Algorithm II.2: FITNESS FUNCTION($\bar{\xi}_t, \bar{\eta}_t, \bar{\xi}_v, \bar{\eta}_v$)

$\eta_l \leftarrow \eta_d$
$\xi_l \leftarrow \xi_d$
output $(\bar{\xi}_t, \bar{\eta}_t, \bar{\xi}_v, \bar{\eta}_v)$ based on (8) and (9)
output (f_{fit}) based on (10)
if $(\xi_t > \xi_l$ & $\eta_t > \eta_l$ & $\xi_v > \xi_l$ & $\eta_v > \eta_l)$
  then $\xi_d = \xi_d + \sigma$

Based on the above concept, the process of formulating the fitness function is shown in Algorithm II.2. First, a target region will be defined, the lower boundary of the sensitivity and specificity are defined as ξ_l and η_l respectively; the upper boundary for them is 1 (maximum performance). The initial values of the lower boundary for ξ_d and η_d are given. Second, based on (8) and (9), the training sensitivity ξ_t, the training specificity η_t, the validation sensitivity ξ_v, and the validation specificity η_v are evaluated. Referring to Fig. 2, the training performance is the result of ξ_t and η_t. Similarly, the validation performance is the result of ξ_v and η_v. Next,the fitness function, f_{fit} is calculated as follow:

$$f_{fit} = \bar{\xi}_t + \bar{\eta}_t + \bar{\xi}_v + \bar{\eta}_v, \tag{10}$$

where

$$\bar{\xi}_t = \begin{cases} 1 & \text{if } \xi_t \geq \xi_l \\ 1 - \frac{\xi_l - \xi_t}{\xi_l} & \text{if } \xi_t < \xi_l \end{cases},$$

and

$$\bar{\xi}_v = \begin{cases} 1 & \text{if } \xi_v \geq \xi_l \\ 1 - \frac{\xi_l - \xi_v}{\xi_l} & \text{if } \xi_v < \xi_l \end{cases},$$

and

$$\bar{\eta}_t = \begin{cases} 1 & \text{if } \eta_t \geq \eta_l \\ 1 - \frac{\eta_l - \eta_t}{\eta_l} & \text{if } \eta_t < \eta_l \end{cases},$$

and

$$\bar{\eta}_v = \begin{cases} 1 & \text{if } \eta_v \geq \eta_l \\ 1 - \frac{\eta_l - \eta_v}{\eta_l} & \text{if } \eta_v < \eta_l \end{cases}.$$

In (10), the maximum fitness value is equal to 4 (when $\bar{\xi}_t$, $\bar{\eta}_t$, $\bar{\xi}_v$, $\bar{\eta}_v$ all equal 1), which implies that both the training and validation performance have met the defined requirement. Finally, if the target region ($\xi_t > \xi_l$ and $\eta_t > \eta_l$ and $\xi_v > \xi_l$ and $\eta_v > \eta_l$) is reached, ξ_d will be updated by $\xi_d + \sigma$, where the value of σ is normally between 0.01 and 0.05. For finding out the optimal sensitivity with a fixed specificity value, only ξ_d will be updated during the training process.

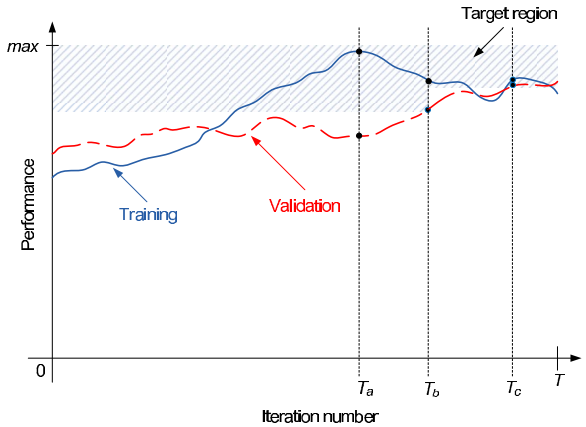

Fig. 2. Fitness function with validation strategy

III. Results and Discussion

Fifteen children with T1DM (14.6 ± 1.5 years) volunteered for the 10-hour overnight hypoglycemia study at the Princess Margaret Hospital for Children in Perth, Western Australia, Australia. Each patient was monitored overnight for the natural occurrence of nocturnal hypoglycemia. Data were collected with approval from Women's and Children's Health Service, Department of Heath, Government of Western Australia, and with informed consent.

A comprehensive patient information and consent form was formulated and approved by the Ethics Committee. The consent form included the actual consent and a revocation of consent page. Each patient received this information consent form at least two weeks prior to the start of the studies. He/She had the opportunity to raise questions and concerns with any medical advisers, researchers and the investigators. For the children participating in this study, the parent or guardian signed the relevant forms. We measured the required physiological parameters, while the actual blood glucose levels (BGL) were collected as reference using Yellow Spring Instruments. The main parameters used for the detection of hypoglycemia are the heart rate, corrected QT interval, change of heart rate and change of corrected QT interval. The responses from 15 T1DM children exhibited significant changes during the hypoglycemia phase against the non-hypoglycemia phase. Normalization is used to reduce patient-to-patient variability and to enable group comparison. The normalization is done by dividing the patient's heart rate and corrected QT interval by his/her corresponding values at time zero.

In this paper, the meaning of hypoglycemia is suggested as BGL $<$ 3.3 mmol/l. The detection of hypoglycemic episodes using these variables is based on the proposed GA-based fuzzy inference system developed using the obtained clinical data. In effect, it estimates the presence of hypoglycaemia at sample period k_s based on the data at sampling period k_s and the previous data at sampling period $k_s - 1$. In general, the sampling period is 5 minutes and approximately 35-40 data points are used for each patient. The whole data set consists of a training set, a validation set and a testing set, each with 5 patients randomly selected. With these 15 patients, the number of data points for training, validation, and testing is 199, 177, and 193 respectively. The whole data set, which includes both the hypoglycemia data part and non-hypoglycemia data part, is used to build the classification and measure the classification performance in terms of sensitivity and specificity.

For comparison and analysis purposes, 4 approaches are used to tackle the same T1DM problem. They are: i) Evolved fuzzy inference system with 4 inputs (EFIS4) (4 inputs: HR, QT_c, ΔHR, and ΔQT_c) with the proposed fitness function and validation strategy considered; ii) Evolved fuzzy inference system with 2 inputs (EFIS2) (2 inputs: HR and QT_c only) with the proposed fitness function and validation strategy considered; iii) Evolved fuzzy inference system with 4 inputs without the proposed fitness function and validation strategy (EFIS4-V), the fitness function in [33] is applied; and iv) Evolved multiple regression with 4 inputs (EMR4).

GA is used to find the optimized fuzzy rules and membership functions of EIFS4, EFIS2, EFIS4-V, and the model parameters of EMR4. The parameter values of the GA are shown as follows.

- Population size θ: 100;
- Probability of crossover μ_c: 0.8;
- Constant value of crossover α: 0.5;
- Probability of mutation μ_m: 0.3;
- Shape parameter of mutation ζ: 2;
- Number of iteration T : 1000;
- Number of runs : 20.

In the fuzzy inference system, the number of the membership functions is set at 3 (m_f = 3); thus, the total number of fuzzy rules n_r is equal to 81 ($n_r = {n_f}^{n_{in}} = 3^4 = 81$). The best training, validation and testing results in term of the sensitivity (ξ) and specificity (η) are tabulated in Table I. For the proposed fitness function, the initial ξ_l and η_l are set at 0.7 and 0.4 respectively. The σ for sensitivity is set at 0.02. From Table I, we can see that the testing performance of EFIS4 outperform the other approaches, and the testing sensitivity is 86.05% with 42.73% specificity. The sensitivity of EFIS4 (86.05%) is significantly better than the sensitivity of EMR4 (67.44%). To illustrate the effectiveness of the proposed fitness function and validation strategy, evolved fuzzy inference system with 4 inputs (EFIS4-V) without the proposed fitness function and validation strategy is used. In EFIS4-V, there are only 2 data set (training and testing), 10 patients (combining the training and validation set of EFIS4) are selected for training and 5 patients are selected for testing. We can see from the results that the testing sensitivity of EFIS4 shows an increase from 81.40% to 86.05%. Furthermore, on comparing EFIS4 and EFIS2, the testing sensitivity with 4 inputs is better, which reflects that ΔHR; ΔQT_c are useful physiological information to enhance the sensitivity.

The Receiver Operating Characteristic (ROC) [34] analysis is tabulated in Table II and the ROC plot is shown in Fig. 3. ROC analysis is commonly used in medical decision making, and is a useful technique for visualizing the diagnostic performance of a test. In an ROC curve the sensitivity is plotted against the false positive rate (1−specificity). A test with perfect discrimination has an ROC plot that passes through the upper left corner (100% sensitivity, 100% specificity). Thus, the closer the ROC plot is to the upper left corner, the higher the overall accuracy of the test. In Table II, the corresponding Area Under the Curve (AUC) of EFIS4 for testing is 0.7502 with a 95% confidence interval of (0.6578, 0.8426). With these results, we can see that the diagnostic performance of EFIS4 for testing is the best.

IV. Conclusion

A genetic algorithm based fuzzy inference system is developed to detect hypoglycemia. Experimental results indicate that hypoglycemia can be detected from the physiological responses of heart rate, corrected QT interval, change of heart rate and change of corrected QT interval. To optimize the fuzzy rules and membership functions, the genetic algorithm is

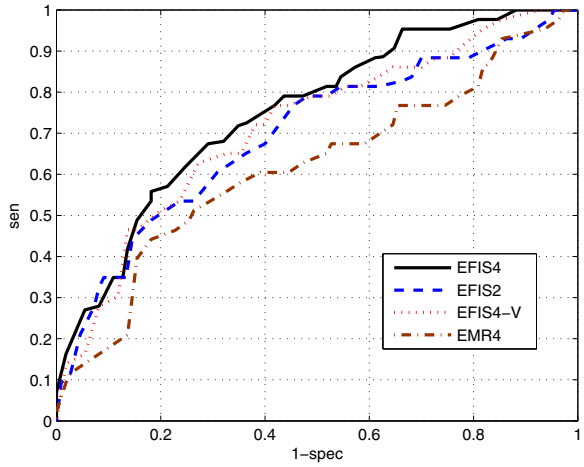

Fig. 3. ROC curve for testing.

		Method			
		EFIS4	EFIS2	EFIS4-V	EMR4
Training	ξ	82.76%	79.31%	89.23%	62.07%
	η	40.59%	38.82%	39.87%	39.41%
Validation	ξ	97.22%	97.22%	-	86.11%
	η	43.97%	41.84%	-	39.72%
Testing	ξ	86.05%	81.40%	81.40%	67.44%
	η	42.73%	40.91%	41.82%	40.91%

TABLE I
SIMULATION RESULT FOR EFIS4, EFIS2,EFIS4-V AND EMR4 AS $\eta_l = 0.4$ (ξ-SENSITIVITY, η-SPECIFICITY).

used. To avoid the over-training problem, a validation strategy that may adjust the fitness function is proposed. A clinical study is given to illustrate that the system with the proposed fitness function and validation strategy offers better results as compared with those from a fuzzy inference system of only 2 inputs, a fuzzy inference system without considering the over-training problem, and an evolved multiple regression algorithm in terms of sensitivity and specificity.

ACKNOWLEDGMENT

This work was supported by a grant from Juvenile Diabetes Research Foundation, US, and a grant from the Hong Kong Polytechnic University (Project No. G-U748).

	AUC	Standard Error (S.E)	95% Confidence Interval	
			min	max
EFIS4	0.7502	0.0472	0.6578	0.8426
EFIS2	0.6976	0.0498	0.6001	0.7952
EFIS4-V	0.7146	0.0490	0.6185	0.8107
EMR4	0.6183	0.0520	0.5164	0.7203

TABLE II
ROC CURVE ANALYSIS.

REFERENCES

[1] D. R. Group, "Adverse events and their association with treatment regimens in the Diabetes Control and Complications Trial," *Diabetes Care*, vol. 18, pp. 1415–1427, 1995.
[2] J. C. Pickup, "Sensitivity glucose sensing in diabetes," *Lancet*, vol. 355, pp. 426–427, 2000.
[3] J. F. Yale, "Nocturnal hypoglycemia in patients with insulin-treated diabetes," *Diabetes Research and Clinical Practice*, vol. 65, no. 1, pp. S41–S46, 2004.
[4] N. D. Harris, S. B. Baykouchev, and J. L. B. Marques, "A portable system for monitoring physiological responses to hypoglycaemia," *Journal of Medical Engineering and Technology*, vol. 20, no. 6, pp. 196–202, 1996.
[5] B. H. Cho, H. Yu, K. Kim, T. H. Kim, I. Y. Kim, and S. I. Kim, "Application of irregular and unbalanced data to predict diabetic nephropathy using visualization and feature selection methods," *Artificial Intelligence in Medicine archive*, vol. 42, no. 1, pp. 37–53, 2008.
[6] A. Chu, H. Ahn, B. Halwan, B. Kalmin, E. L. V. Artifon, A. Barkun, M. G. Lagoudakis, and A. Kumar, "A decision support system to facilitate management of patients with acute gastrointestinal bleeding," *Artificial Intelligence in Medicine archive*, vol. 42, no. 3, pp. 247–259, 2008.
[7] C. L. Chang and C. H. Chen, "Applying decision tree and neural network to increase quality of dermatologic diagnosis," *Expert Systems with Applications*, vol. 36, no. 2, pp. 4035–4041, 2009.
[8] G. A. F. Seber, *Linear regression analysis*. Hoboken, NJ: Wiley, 2003.
[9] C. M. Fira and L. Goras, "An ECG signals compression method and its validation using NNs," *IEEE Transactions on Biomedical Engineering*, vol. 55, no. 4, pp. 1319–1326, 2008.
[10] W. Jiang, S. G. Kong, and G. D. Peterson, "ECG signal classification using block-based neural networks," *IEEE Transactions on Neural Networks*, vol. 18, no. 6, pp. 1750–1761, 2007.
[11] A. H. Khandoker, M. Palaniswami, and C. K. Karmakar, "Support vector machines for automated recognition of obstructive sleep apnea syndrome from ECG recordings," *IEEE Transactions on Information Technology in Biomedicine*, vol. 13, no. 1, pp. 37–48, 2009.
[12] J. S. R. Jang, C. T. Sun, and E. Mizutani, *Neuro-Fuzzy and Soft Computing: A Computational Approach to Learning and Machine Intelligence*. Upper Saddle River, NJ: Prentice Hall, 1997.
[13] C. Cortes and V. Vapnik, "Support-vector networks," *Machine Learning*, vol. 20, no. 3, pp. 1573–1565, 1995.
[14] A. K. Jain, J. Mao, and K. M. Mohiuddin, "Artificial neural networks: a tutorial," *IEEE Computer Society*, vol. 29, no. 3, pp. 31–44, 1996.
[15] W. W. Melek, Z. Lu, A. Kapps, and B. Cheung, "Modeling of dynamic cardiovascular responses during G-transition-induced orthostatic stress in pitch and roll rotations," *IEEE Transactions on Biomedical Engineering*, vol. 49, no. 12, pp. 1481–1490, 2002.
[16] S. Wang and W. Min, "A new detection algorithm (NDA) based on fuzzy cellular neural networks for white blood cell detection," *IEEE Transactions on Information Technology in Biomedicine*, vol. 10, no. 1, pp. 5–10, 2006.
[17] S. Kobashi, Y. Fujiki, M. Matsui, and N. Inoue, "Genetic programming for classification and feature selection: analysis of 1H nuclear magnetic resonance spectra from human brain tumour biopsies," *IEEE Transactions on Systems, Man, and Cybernetics, Part B*, vol. 36, no. 1, pp. 74 – 86, 2006.
[18] M. Brown and C. Haris, *Neuro-Fuzzy Adaptive Modeling and Control*. Eaglewood Clifts, NJ: Prentice Hall, 1994.
[19] J. A. Reggia and S. S. Sutton, "Self-processing networks and their biomedical implications," *Proceedings of the IEEE*, vol. 76, no. 6, pp. 580–592, 1988.
[20] D. Meyer, F. Leisch, and K. Hornik, "The support vector machine under test," *Neurocomputing*, vol. 55, no. 6, pp. 169–186, 2003.
[21] N. Acir, "A support vector machine classifier algorithm based on a perturbation method and its application to ECG beat recognition systems," *Expert Systems with Applications*, vol. 31, no. 1, pp. 150–158, 2006.
[22] J. Kennedy and R. Eberhart, "Particle swarm optimization," in *Proceedings of IEEE International Conference on Neural Networks*, 1995, pp. 1942–1948.
[23] Z. Michalewicz, *Genetic algorithms + data structures = evolution programs (3rd, extended ed.)*. Berlin: Springer, 1996.
[24] R. Storn and K. Price, "Differential evolution - a simple and efficient heuristic for global optimization over continuous spaces," *Journal of Global Optimization*, vol. 11, pp. 341–359, 1997.

[25] M. Dorigo and T. Stuzle, *Ant Colony Optimization*. Cambridge, Mass: MIT Press, 2004.
[26] A. Keles, S. A. Hasiloglu, K. Ali, and Y. Aksoy, "Neuro-fuzzy classification of prostate cancer using NEFCLASS-J," *Computers in Biology and Medicine*, vol. 37, no. 11, pp. 1617–1628, 2007.
[27] R. J. Oentaryo, M. Pasquier, and C. Quek, "GenSoFNN-Yager: A novel brain-inspired generic self-organizing neuro-fuzzy system realizing Yager inference," *Expert Systems with Application*, vol. 35, no. 4, pp. 1825–1840, 2008.
[28] H. Mamdani and S. Assilian, "An experiment in linguistic synthesis with a fuzzy logic controller," *International Journal of Man-Machine Studies*, vol. 7, no. 1, pp. 1–13, 1975.
[29] M. L. Astion, M. H. Wener, R. G. Thomas, and G. G. Hunder, "Overtraining in neural networks that interpret clinical data," *Clinical Chemistry*, vol. 39, no. 9, pp. 1998–2004, 1993.
[30] J. Joines and C. Houck, "On the use of non-stationary penalty functions to solve constrained optimization problems with genetic algorithm," in *Proc. 1994 International Symposium evolutionary computation*, 1994, pp. 579–584.
[31] L. J. Eshelman and J. D. Schaffer, "Real-coded genetic algorithms and interval-schemata," *Foundations of Genetic Algorithms*, vol. 2, pp. 187–202, 1993.
[32] D. G. Altman and J. M. Bland, "Statistics notes: Diagnostic tests 1: sensitivity and specificity," *Clinical chemistry*, no. 308, pp. 1552–1552, 1994.
[33] S. H. Ling, Nuryani, and H. T. Nguyen, "Evolved fuzzy reasoning model for hypoglycaemic detection," in *Proc. 32nd Annual International conference of the IEEE Engineering in Medicine and Biology Society*, 2010, pp. 4662–4665.
[34] M. H. Zweig and G. Campbell, "Receiver-operating characteristic (ROC) plots: a fundamental evaluation tool in clinical medicine," *Clinical Chemistry*, vol. 39, pp. 561–577, 1993.

2011 IEEE International Conference on Fuzzy Systems
June 27-30, 2011, Taipei, Taiwan

An Approach for Stability Analysis of Polynomial Fuzzy Model-Based Control Systems

Mohammand Narimani, H.K. Lam, K. Althoefer, R. Dilmaghani, Charles Wolfe and C. Deters
Division of Engineering, Kings College London, Strand,
London, WC2R 2LS, UK
E-mails: mohammad.narimani@kcl.ac.uk, hak-keung.lam@kcl.ac.uk

***Abstract*—Stability analysis of polynomial fuzzy model-based (PFMB) control systems under the parallel distributed compensation (PDC) design technique is investigated. A new polynomial fuzzy controller (PFC) is introduced to release conservativeness in the existing approaches. Compared to the conventional (PFC), the controller under consideration in this paper has a favorable property which introduces some more variables in the stability conditions such that, the solution of the derived stability conditions can be explored in a larger group of potential solutions. This property may lead to further relax stability conditions. However, the stability conditions will not be in the form of SOS conditions. Hence, particle swarm optimization (PSO) is employed to explore the solution of the derived stability conditions which are in the form of state-dependent BMI. It is shown that the conventional PFC is a special case of that of proposed one. Finally, a simulation example is given to illustrate the effectiveness of the proposed approach.**

***Index Terms*—polynomial fuzzy model(PFM), state-dependent Bilinear Matrix Inequality (BMI), stability conditions, sum of squares (SOS), particle swarm optimization (PSO).**

I. Introduction

Recently, fuzzy model-based (FMB) control approach has become a popular system control analysis methodology. It provides a systematic way for handling of nonlinear control systems [1]. To demonstrate complex nonlinear systems in a fuzzy frame, T-S fuzzy model [2], [3], introduces a mathematical framework. This model portrays a nonlinear system by a set of fuzzy rules. Each rule contains a linear model, so-called subsystem, that represents the dynamics of the nonlinear plant in a specific local operating domain. The overall T-S fuzzy model is constructed as an average weighted sums of some subsystems. To control a nonlinear plant, a fuzzy controller is employed to close the feedback loop. The design strategy of fuzzy controller is based on the T-S fuzzy model so that, a FMB control system [4]–[6] is formed.

At early stage of research on the FMB control approach, lack of a rigorous theoretical basis for stability analysis had drawn a great deal of attention to this area. Recently, based on the Lyapunov stability theory [7] for nonlinear control systems, sufficient conditions to guarantee the stability of the FMB control system are derived. In most of the proposed approaches, stability analysis and control design problems are formulated to Linear Matrix Inequality (LMI) problems [8]. Then, utilizing convex programming techniques, LMI MATLAB Toolbox [9], numerical solutions are obtained. Some of the well-known LMI-based stability conditions have been reported in [1], [5], [10]–[18]. *Parallel Distributed Compensation* (PDC) [5] design technique, for which the fuzzy controller shares the same membership functions as T-S fuzzy model, is employed to further relax the stability conditions [1], [11], [12], [18]. When the fuzzy controller does not follow the PDC design, it is called non-PDC fuzzy controller.

Very recently, nonlinear control systems have been represented by polynomial fuzzy model (PFM) [19], which is a generalized form of the T-S fuzzy model. PFMs have the same structure as the T-S fuzzy model, but polynomials are allowed to be considered in the subsystems. To close the feedback loop, polynomial fuzzy controller (PFC) which is similar to the traditional fuzzy controller [6], but with polynomials in its structure, is employed and polynomial fuzzy model-based (PFMB) control system is constructed.

To deal with the stability analysis and performance design of the PFMB control systems, sum of squares (SOS) approach is employed [19]. Based on the SOS approach, polynomials are allowed to be incorporated in the stability conditions. These conditions can be regarded as state-dependent LMI conditions. Semi-definite programming software SOSTOOLS [20] is the computational method to be employed to solve numerically these SOS (state-dependent LMI) conditions, based on the SOS decomposition. Compared to the LMI approach, SOS approach has some advantages in dealing with stability analysis of fuzzy control systems. Since, polynomials are allowed to be incorporated in the PFM, it is more effective in representing nonlinear control systems. Moreover, when various polynomials of state variables are allowed to be considered in the PFC, solution of stability conditions can be searched in a larger group of candidates, which may result in the relaxation of stability conditions. In addition, to investigate stability of these systems, polynomial Lyapunov function (PLF) which is a generalized form of quadratic Lyapunov function, can be implemented. It should be noted that PLF can be utilized in the LMI-based stability conditions.

Conservatism is one of the drawbacks that most of the existing stability conditions suffer from it. In [21], to relax

The work described in this paper was partially supported by COSMOS project grant from the European Communities Seventh Framework Programme (FP7-NMP-2009-SMALL-3, NMP- 2009-3.2-2) under grant agreement 246371-2, and a grant from the Modernisation Initiative with the support of the Guys and St Thomas Hospitals Charity.

978-1-4244-7316-8/11/$26.00 ©2011 IEEE

the stability conditions under the non-PDC paradigm for FMB control systems, a fuzzy controller has been considered, for which the feedback gains were time-varying nonlinear functions. Due to introducing more decision variables in the structure of the stability conditions, feedback gains can be searched in a wider domain of potential solution for the conditions under consideration. However, the derived stability conditions were in the form of bilinear matrix inequality (BMI). Therefore, numerical solution were found by employing genetic algorithm (GA) [22] and LMI MATLAB Toolbox.

In this paper, stability of PFMB control systems under the PDC design technique is investigated. To release conservativeness resulting from considering conventional form for PFC [19], PFC with similar structure to the controller in [21] is introduced. Compared to the conventional PFC, the PFC under consideration introduces some more decision variables in the stability conditions such that, the solution of the derived stability conditions can be explored in a larger group of potential solutions which may lead to relaxed stability conditions. However, the resulting conditions will be in the form of state-dependent BMI. Then, utilizing searching algorithms say, particle swarm optimization (PSO) [23], the solution of derived conditions can be searched in a wider domain.

The rest of this chapter is organized as follows. In section II, PFM, PFC and PFMB control system are presented. In section III, stability analysis of PFMB control system is presented. In section IV, a simulation example is given to illustrate the validity of the proposed approach. Section V concludes this paper.

II. PFM, PFC AND PFMB CONTROL SYSTEM

Consider a nonlinear system described by

$$\dot{\mathbf{x}} = \mathbf{f}\big(\mathbf{x}(t), \mathbf{u}(t)\big), \tag{1}$$

where $\mathbf{f}\big(\mathbf{x}(t), \mathbf{u}(t)\big)$ is a nonlinear function in which $\mathbf{x}(t) \in \mathbb{R}^{\rho}$ is the system state vector and $\mathbf{u}(t) \in \mathbb{R}^{\omega}$ is the input vector. Using the sector nonlinearity concept [6], the nonlinear system (1) is represented by the following polynomial fuzzy model [19], [24],

Plant Rule *i*:

$$\begin{aligned} &\text{IF } z_1(\mathbf{x}(t)) \text{ is } M_1^i \text{ AND ... AND } z_p(\mathbf{x}(t)) \text{ is } M_p^i \\ &\text{THEN } \dot{\mathbf{x}}(t) = \mathbf{A}_i(\mathbf{x}(t))\hat{\mathbf{x}}(\mathbf{x}(t)) + \mathbf{B}_i(\mathbf{x}(t))\mathbf{u}(t) \\ &\qquad\qquad\qquad\qquad\qquad\qquad i = 1, \cdots, r, \end{aligned} \tag{2}$$

for which $z_{\alpha}(\mathbf{x}(t))$ is the premise variable; M_{α}^i is a fuzzy term corresponding to i^{th} rule; $\mathbf{A}_i(\mathbf{x}(t)) \in \mathbb{R}^{\rho \times N}$ and $\mathbf{B}_i(\mathbf{x}(t)) \in \mathbb{R}^{\rho \times \omega}$ are the polynomial system and polynomial input matrices respectively, for $i = 1, ..., r$, $\alpha = 1, ..., p$; In addition, $\hat{\mathbf{x}}(t) = [\hat{x}_1(t), \hat{x}_2(t), ..., \hat{x}_N(t)]^T \in \mathbb{R}^N$ is a vector of monomials in $\mathbf{x}(t)$ with assumption that $\hat{\mathbf{x}}(t) = \mathbf{0}$ *iff* $\mathbf{x}(t) = \mathbf{0}$. A monomial in $\mathbf{x}(t)$ is a function of the form $x_1^{\alpha_1}(t)x_2^{\alpha_2}(t)...x_n^{\alpha_{\rho}}(t)$, where $\alpha_1, \alpha_2, ..., \alpha_{\rho}$ are nonnegative integers. In this case, the degree of the monomial is given by $\alpha_1 + \alpha_2 + ... + \alpha_{\rho}$.

The overall system dynamics is represented by

$$\dot{\mathbf{x}}(t) = \sum_{i=1}^{r} \mu_i(\mathbf{z}(\mathbf{x}(t)))\Big(\mathbf{A}_i(\mathbf{x}(t))\hat{\mathbf{x}}(\mathbf{x}(t)) + \mathbf{B}_i(\mathbf{x}(t))\mathbf{u}(t)\Big). \tag{3}$$

where

$$\begin{aligned} &\mu_i(\mathbf{z}(\mathbf{x}(t))) \in [0, \ \ 1], \\ &\sum_{i=1}^{r} \mu_i(\mathbf{z}(\mathbf{x}(t))) = 1. \end{aligned}$$

To control nonlinear system represented by the polynomial fuzzy model (3), a polynomial fuzzy controller is introduced, which is described by following fuzzy rules.

Control Rule *j* :

$$\begin{aligned} &\text{IF } g_1(\mathbf{x}(t)) \text{ is } N_1^j \text{ AND ... AND } g_q(\mathbf{x}(t)) \text{ is } N_q^j \\ &\text{THEN } \mathbf{u}(t) = \frac{\mathbf{F}_j(\mathbf{x}(t))}{H(\mathbf{x}(t))}\hat{\mathbf{x}}(\mathbf{x}(t)) \\ &\qquad\qquad\qquad\qquad\qquad\qquad j = 1, ..., c, \end{aligned} \tag{4}$$

where $g_{\theta}(\mathbf{x}(t))$ is the premise variable; N_{θ}^j is a fuzzy term corresponding to the j^{th} control rule, $j = 1, ..., c$, $\theta = 1, ..., q$; $\mathbf{F}_j(\mathbf{x}(t)) \in \mathbb{R}^{\omega \times N}$ is the polynomial feedback gain of the j^{th} rule to be determined and $H(\mathbf{x}(t))$ is defined as follows.

$$H(\mathbf{x}(t)) = \sum_{k=1}^{c} \lambda_k(\mathbf{g}(\mathbf{x}(t)))a_k(\mathbf{x}) \tag{5}$$

in which

$$a_k(\mathbf{x}(t)) = a_k^1\hat{x}_1 + ... + a_k^{l-1}\hat{x}_{l-1} + a_k^l,$$

where $\hat{x}_1, ..., \hat{x}_{l-1}$ are monomials and $a_k^1, ..., a_k^l$ are scalars.

Then, regarding to (5), the overall PFC is defined as

$$\begin{aligned} \mathbf{u}(t) &= \sum_{j=1}^{c} \lambda_j(\mathbf{g}(\mathbf{x}(t)))\frac{\mathbf{F}_j(\mathbf{x}(t))}{H(\mathbf{x}(t))}\hat{\mathbf{x}}(\mathbf{x}(t)) \\ &= \sum_{j=1}^{c} \lambda_j(\mathbf{g}(\mathbf{x}(t)))\frac{\mathbf{F}_j(\mathbf{x}(t))}{\sum_{k=1}^{c} \lambda_k(\mathbf{g}(\mathbf{x}(t)))a_k(\mathbf{x}(t))}\hat{\mathbf{x}}(\mathbf{x}(t)) \end{aligned} \tag{6}$$

where

$$\begin{aligned} &\lambda_j(\mathbf{g}(\mathbf{x}(t))) \in [0, \ \ 1], \\ &\sum_{j=1}^{c} \lambda_j(\mathbf{g}(\mathbf{x}(t))) = 1. \end{aligned} \tag{7}$$

$$\dot{\mathbf{x}}(t) = \frac{\sum_{i=1}^{r}\sum_{j=1}^{c}\mu_i(\mathbf{x}(t))\lambda_j(\mathbf{x}(t))\Big(a_j(\mathbf{x}(t))\mathbf{A}_i(\mathbf{x}(t)) + \mathbf{B}_i(\mathbf{x}(t))\mathbf{F}_j(\mathbf{x}(t))\Big)}{\sum_{k=1}^{c}\lambda_k(\mathbf{x}(t))a_k(\mathbf{x}(t))}\hat{\mathbf{x}}(\mathbf{x}(t)). \tag{8}$$

Considering the PFM (3) and the PFC (6) connected in a closed loop, we have

$$\dot{\mathbf{x}}(t) = \sum_{i=1}^{r}\mu_i(\mathbf{x})(t)\Big(\mathbf{A}_i(\mathbf{x}(t))\hat{\mathbf{x}}(\mathbf{x}(t)) + \mathbf{B}_i(\mathbf{x}(t))\sum_{j=1}^{c}\lambda_j(\mathbf{x})(t) \times \frac{\mathbf{F}_j(\mathbf{x}(t))}{\sum_{k=1}^{c}\lambda_k(\mathbf{x}(t))a_k(\mathbf{x}(t))}\hat{\mathbf{x}}(\mathbf{x}(t))\Big)$$

Then, the PFMB control system is obtained as (8).

For brevity, $\mathbf{x}$, $\hat{\mathbf{x}}(\mathbf{x})$, $\mu_i(\mathbf{x})$, $\lambda_j(\mathbf{x})$ and $\mathbf{u}$ are used to denote $\mathbf{x}(t)$, $\hat{\mathbf{x}}(\mathbf{x}(t))$, $\mu_i(\mathbf{z}(t))$, $\lambda_j(\mathbf{s}(\mathbf{x}(t)))$, and $\mathbf{u}(t)$, respectively, in the following analysis.

III. Stability Analysis of PFMB Control Systems

Based on the Lyapunov stability theory, the stability of the PFMB control system (8) is investigated. Consider the following polynomial quadratic Lyapunov function candidate [19]

$$V(\mathbf{x}) = \hat{\mathbf{x}}(\mathbf{x})^T\mathbf{X}^{-1}(\tilde{\mathbf{x}})\hat{\mathbf{x}}(\mathbf{x}), \tag{9}$$

where $\mathbf{X}^{-1}(\tilde{\mathbf{x}}) \in \mathbb{R}^{N\times N}$ is a symmetric positive definite polynomial matrix and $\tilde{\mathbf{x}} = [x_{k_1}, x_{k_2}, ..., x_{k_d}]$ is a vector to be chosen such that $\mathbf{K} = \{k_1, k_2, ..., k_d\}$ denotes the indices of the corresponding zero rows in $\mathbf{B}_i(\mathbf{x})$ for all i. Denoting the k^{th} row in $\mathbf{A}_i(\mathbf{x})$ and $\mathbf{B}_i(\mathbf{x})$ as $\mathbf{A}_i^k(\mathbf{x})$ and $\mathbf{B}_i^k(\mathbf{x})$ respectively, we have

$$\mathbf{B}_i^k(\mathbf{x}) = \mathbf{0} \qquad \text{for } k \in \mathbf{K}. \tag{10}$$

To avoid introducing non-convex condition, we assume that $\mathbf{X}(\tilde{\mathbf{x}})$ only depends on state vector $\tilde{\mathbf{x}}$. Hence $\frac{\partial\mathbf{X}^{-1}(\tilde{\mathbf{x}})}{\partial x_k} = \mathbf{0}$ for $k \notin \mathbf{K}$. For more details readers are referred to [19], [25]. According to the Lyapunov stability theory, if $\mathbf{X}(\tilde{\mathbf{x}})$ and $\mathbf{X}^{-1}(\tilde{\mathbf{x}})$ are positive definite matrices in $\tilde{\mathbf{x}}$ and $\dot{V}(t) \leq 0$ (equality holds when $\mathbf{x} = \mathbf{0}$), then the polynomial FMB control system (8) is asymptotically stable. Following the approach in [19]:

$$\dot{V}(\mathbf{x}) = \dot{\hat{\mathbf{x}}}^T(\mathbf{x})\mathbf{X}^{-1}(\tilde{\mathbf{x}})\hat{\mathbf{x}}(\mathbf{x}) + \hat{\mathbf{x}}^T(\mathbf{x})\mathbf{X}^{-1}(\tilde{\mathbf{x}})\dot{\hat{\mathbf{x}}}(\mathbf{x}) + \hat{\mathbf{x}}^T(\mathbf{x})\dot{\mathbf{X}}^{-1}(\tilde{\mathbf{x}})\hat{\mathbf{x}}(\mathbf{x}) \tag{11}$$

in which

$$\begin{aligned}\dot{\hat{\mathbf{x}}}(\mathbf{x}) &= \begin{pmatrix}\dot{\hat{\mathbf{x}}}_1(\mathbf{x})\\ \vdots \\ \dot{\hat{\mathbf{x}}}_N(\mathbf{x})\end{pmatrix}\\ &= \begin{pmatrix}\frac{\partial\hat{x}_1}{\partial x_1} & \cdots & \frac{\partial\hat{x}_1}{\partial x_\rho}\\ \vdots & \ddots & \vdots \\ \frac{\partial\hat{x}_N}{\partial x_1} & \cdots & \frac{\partial\hat{x}_N}{\partial x_\rho}\end{pmatrix}\begin{pmatrix}\frac{\partial x_1}{\partial t}\\ \vdots \\ \frac{\partial x_\rho}{\partial t}\end{pmatrix}\\ &= \mathbf{\Phi}(\mathbf{x})\dot{\mathbf{x}}\end{aligned}$$

where $\mathbf{\Phi}(\mathbf{x}) \in \mathbb{R}^{N\times\rho}$ is a polynomial matrix defined as follows

$$\mathbf{\Phi}(\mathbf{x}) = \begin{pmatrix}\frac{\partial\hat{x}_1}{\partial x_1} & \cdots & \frac{\partial\hat{x}_1}{\partial x_\rho}\\ \vdots & \ddots & \vdots \\ \frac{\partial\hat{x}_N}{\partial x_1} & \cdots & \frac{\partial\hat{x}_N}{\partial x_\rho}\end{pmatrix}. \tag{12}$$

Then, (11) is derived as follows.

$$\dot{V}(\mathbf{x}) = \dot{\mathbf{x}}^T\mathbf{\Phi}^T(\mathbf{x})\mathbf{X}^{-1}(\tilde{\mathbf{x}})\hat{\mathbf{x}}(\mathbf{x}) + \hat{\mathbf{x}}^T(\mathbf{x})\mathbf{X}^{-1}(\tilde{\mathbf{x}})\mathbf{\Phi}(\mathbf{x})\dot{\mathbf{x}} + \hat{\mathbf{x}}^T(\mathbf{x}) \times \left(\sum_{k=1}^{\rho}\frac{\partial\mathbf{X}^{-1}(\tilde{\mathbf{x}})}{\partial x_k}\dot{x}_k\right)\hat{\mathbf{x}}(\mathbf{x}). \tag{13}$$

Since $\frac{\partial\mathbf{X}^{-1}(\tilde{\mathbf{x}})}{\partial x_k} = \mathbf{0}$ for $k \notin \mathbf{K}$, and according to (10), $\dot{V}(\mathbf{x})$ is written as follows.

$$\dot{V}(\mathbf{x}) = \dot{\mathbf{x}}^T\mathbf{\Phi}^T(\mathbf{x})\mathbf{X}^{-1}(\tilde{\mathbf{x}})\hat{\mathbf{x}}(\mathbf{x}) + \hat{\mathbf{x}}^T(\mathbf{x})\mathbf{X}^{-1}(\tilde{\mathbf{x}})\mathbf{\Phi}(\mathbf{x})\dot{\mathbf{x}} + \hat{\mathbf{x}}^T(\mathbf{x}) \times \left(\sum_{k\in\mathbf{K}}\frac{\partial\mathbf{X}^{-1}(\tilde{\mathbf{x}})}{\partial x_k}\sum_{i=1}^{r}\mu_i(\mathbf{x})\mathbf{A}_i^k(\mathbf{x})\hat{\mathbf{x}}(\mathbf{x})\right)\hat{\mathbf{x}}(\mathbf{x}). \tag{14}$$

Also, $\mathbf{X}(\tilde{\mathbf{x}})$ is invertible, then we have $\mathbf{X}^{-1}(\tilde{\mathbf{x}})\mathbf{X}(\tilde{\mathbf{x}}) = \mathbf{I}$. Differentiating both sides with respect to x_k yields

$$\frac{\partial\mathbf{X}^{-1}(\tilde{\mathbf{x}})}{\partial t}\mathbf{X}(\tilde{\mathbf{x}}) + \mathbf{X}^{-1}(\tilde{\mathbf{x}})\frac{\partial\mathbf{X}(\tilde{\mathbf{x}})}{\partial t} = \mathbf{0}.$$

Hence the following relation holds.

$$\frac{\partial\mathbf{X}^{-1}(\tilde{\mathbf{x}})}{\partial t} = -\mathbf{X}^{-1}(\tilde{\mathbf{x}})\frac{\partial\mathbf{X}(\tilde{\mathbf{x}})}{\partial t}\mathbf{X}^{-1}(\tilde{\mathbf{x}}) \tag{15}$$

Denoting $\mathbf{y}(\mathbf{x}) = \mathbf{X}^{-1}\hat{\mathbf{x}}(\mathbf{x})$ and according to (15), $\dot{V}(\mathbf{x})$ can be written in the following form.

$$\dot{V}(\mathbf{x}) = \sum_{i=1}^{r}\sum_{j=1}^{c} \mu_i(\mathbf{x})\lambda_j(\mathbf{x})\mathbf{y}^T(\mathbf{x}) \frac{\mathbf{T}_{ij}(\mathbf{x})}{\sum_{k=1}^{c}\lambda_k(\mathbf{x})a_k(\mathbf{x})}\mathbf{y}(\mathbf{x}), \quad (16)$$

where

$$\begin{aligned}\mathbf{T}_{ij}(\mathbf{x}) = &\Big(a_j(\mathbf{x})\mathbf{A}_i(\mathbf{x})\mathbf{X}(\tilde{\mathbf{x}}) + \mathbf{B}_i(\mathbf{x})\mathbf{M}_j(\mathbf{x})\Big)^T\mathbf{\Phi}^T(\mathbf{x}) \\ &+ \mathbf{\Phi}(\mathbf{x})\Big(a_j(\mathbf{x})\mathbf{A}_i(\mathbf{x})\mathbf{X}(\tilde{\mathbf{x}}) + \mathbf{B}_i(\mathbf{x})\mathbf{M}_j(\mathbf{x})\Big) \\ &- \sum_{k\in\mathbf{K}}\frac{\partial\mathbf{X}(\tilde{\mathbf{x}})}{\partial x_k}a_j(\mathbf{x})\mathbf{A}_i^k(\mathbf{x})\hat{\mathbf{x}}(\mathbf{x}) \quad (17)\end{aligned}$$

in which the local feedback gains are defined as

$$\mathbf{F}_j(\mathbf{x}) = \mathbf{M}_j(\mathbf{x})\mathbf{X}^{-1}(\tilde{\mathbf{x}}), \qquad j = 1, ..., c. \quad (18)$$

Utilizing the PDC design technique, (16) can be written as

$$\begin{aligned}\dot{V}(\mathbf{x}) &= \sum_{i=1}^{r}\sum_{j=1}^{r} \mu_i(\mathbf{x})\mu_j(\mathbf{x})\mathbf{y}^T(\mathbf{x}) \frac{\mathbf{T}_{ij}(\mathbf{x})}{\sum_{k=1}^{r}\mu_k(\mathbf{x})a_k(\mathbf{x})}\mathbf{y}(\mathbf{x}) \\ &= \sum_{i=1}^{r} \mu_i(\mathbf{x})\mu_i(\mathbf{x})\mathbf{y}^T(\mathbf{x}) \frac{\mathbf{T}_{ii}(\mathbf{x})}{\sum_{k=1}^{r}\mu_k(\mathbf{x})a_k(\mathbf{x})}\mathbf{y}(\mathbf{x}) \\ &+ \sum_{i=1}^{r}\sum_{i<j} \mu_i(\mathbf{x})\mu_j(\mathbf{x})\mathbf{y}^T(\mathbf{x}) \frac{\mathbf{T}_{ij}(\mathbf{x}) + \mathbf{T}_{ji}(\mathbf{x})}{\sum_{k=1}^{r}\mu_k(\mathbf{x})a_k(\mathbf{x})}\mathbf{y}(\mathbf{x}) \quad (19)\end{aligned}$$

Choosing $a_j(\mathbf{x}) > 0$, $j = 1, ..., c$ and regarding to the properties of the membership functions in (4),

$$\sum_{k=1}^{c}\lambda_k(\mathbf{x})a_k(\mathbf{x}) > 0. \quad (20)$$

Referring to the Lyapunov stability theory, the PFMB control system (8) is asymptotically stable if $\dot{V}(\mathbf{x}) < 0$. If $\mathbf{T}_{ii}(\mathbf{x}) < 0$ for $i = 1, ..., r$ and $\mathbf{T}_{ij}(\mathbf{x}) < 0$ for $i = 1, ..., r, i < j$ in (19), then $\dot{V}(\mathbf{x}) < 0$ and thus, resulting in asymptotically stability of PFMB control system (8).

The stability analysis result is proposed as the following theorem.

Theorem 1. *The PFMB control system* (8) *consisting of the PFM* (3) *and the PFC* (6) *is asymptotically stable if there exist pre-defined polynomials* $a_k(\mathbf{x}) > 0$ $k = 1, ..., r$, *and matrices* $\boldsymbol{X}(\tilde{\mathbf{x}})$ *and* $\boldsymbol{M}_j(\mathbf{x})$ *such that, the following SOS-based conditions are satisfied,*

$$\upsilon^T\Big(\mathbf{X}(\tilde{\mathbf{x}}) - \epsilon_1(\mathbf{x})\mathbf{I}\Big)\upsilon \text{ is SOS}, \quad (21)$$

$$-\upsilon^T\Big(\mathbf{T}_{ii}(\mathbf{x})) + \epsilon_{2ii}(\mathbf{x})\mathbf{I}\Big)\upsilon \text{ is SOS}, \qquad \text{for } i = 1, ..., r, \quad (22)$$

$$-\upsilon^T\Big(\mathbf{T}_{ij}(\mathbf{x}) + \mathbf{T}_{ji}(\mathbf{x}) + \epsilon_{2ij}(\mathbf{x})\mathbf{I}\Big)\upsilon \text{ is SOS}, \qquad \forall\, i < j, \quad (23)$$

where $\mathbf{T}_{ij}(\mathbf{x})$ *is defined in* (17), $\upsilon(t) \in \mathbb{R}^\rho$ *is an arbitrary vector independent of* $\mathbf{x}$ *and* $\epsilon_1(\mathbf{x}) > 0$, $\epsilon_{2ij}(\mathbf{x}) > 0$ *for* $\mathbf{x} \neq \mathbf{0}$ *are pre-defined polynomial scalars and the local feedback gains are defined in* (18).

Remark 1: To derive the numerical solution of state-dependent BMI conditions in Theorem 1, the searching algorithm, PSO technique, is exploited. The procedure for finding numerical solution is illustrated in Fig. 1 and summarized in the following stages:

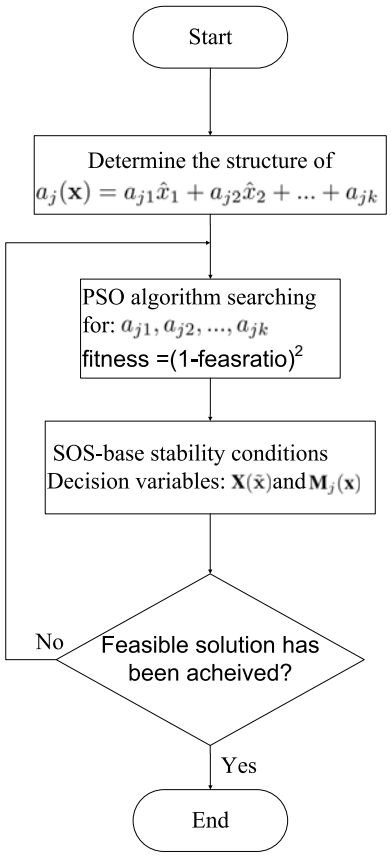

Fig. 1. Flowchart of the proposed PSO and SOS-based technique

Stage 1: The $a_j(\mathbf{x})$ $j = 1, ..., r$, are polynomials containing monomials with various degrees. As the first step, proper monomials which have contribution in relaxation of stability conditions are determined. The coefficients of these monomials

are considered as decision variables to be determined by the PSO in the next steps.

Stage 2: The PSO assigns initial values to the coefficients of $a_j(\mathbf{x})$ $j = 1, ..., r$. These values are kept fixed during stage 3.

Stage 3: Since the values of $a_j(\mathbf{x})$ are fixed then, the stability conditions in Theorem 1 convert to SOS-based stability conditions. Numerical solution for the derived SOS-based stability conditions are obtained by SOSTOOLS [25].

Stage 4: If the derived parameters for the SOSTOOLS show feasibility of solution for the SOS-based stability conditions then, the searching procedure will stop. Otherwise, if the stopping criterion, which is a predefined number of iteration has not been reached, return to *Step 2*. It should be noted that, in the PSO searching algorithm, finding of solution is formulated as a minimization problem for a fitness function. In this paper, fitness function for the PSO algorithm is chosen as $-(1-\text{feasratio})^2$. A more closer value of 'feasratio' to '1' leads to minimization of the fitness function and implies more accurate solution for the SOS-based stability conditions.

IV. Simulation Example

The effectiveness of the proposed stability analysis approach is illustrated by following simulation example.

Consider a three-rule PFM with the following system and input relations.

$$\mathbf{A}_1(\mathbf{x}) = \begin{pmatrix} 1.59 + x_1^2 - 2x_2^2 - x_1x_2 & -7.29 + 2x_1x_2 \\ 0.01 & -x_1^2 - x_2^2 \end{pmatrix},$$

$$\mathbf{A}_2(\mathbf{x}) = \begin{pmatrix} 0.02 + x_1^2 - 2x_2^2 - x_1x_2 & -4.64 + 2x_1x_2 \\ 0.35 & 0.21 - x_1^2 - x_2^2 \end{pmatrix},$$

$$\mathbf{A}_3(\mathbf{x}) = \begin{pmatrix} -\alpha + x_1^2 - 2x_2^2 - x_1x_2 & -4.33 + 2x_1x_2 \\ 0 & 0.05 - x_1^2 - x_2^2 \end{pmatrix},$$

$$\mathbf{B}_1(\mathbf{x}) = \begin{pmatrix} 1 + x1 + x1^2 \\ 0 \end{pmatrix},$$

$$\mathbf{B}_2(\mathbf{x}) = \begin{pmatrix} 8 + x1 + x1^2 \\ 0 \end{pmatrix},$$

$$\mathbf{B}_3(\mathbf{x}) = \begin{pmatrix} -\beta + 6 + x1 + x1^2; 0 \\ -1 \end{pmatrix},$$

where α and β are constant parameters. Based on the PDC design technique, a three-rule PFC in the form of (6) is employed to close the feedback loop. Then, the PFMB control system in the form of (8) is obtained.

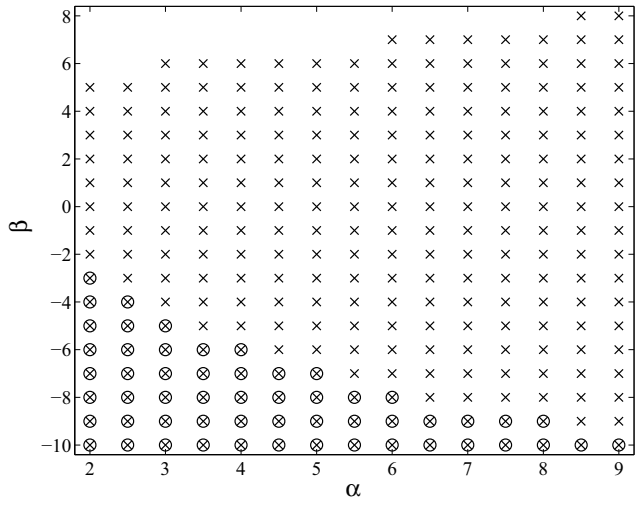

Fig. 2. Stability regions given by [19] (×), and Theorem 1 (○) for the Simulation Example.

To investigate the stability of the aforementioned PFMB control system, the stability conditions proposed in Theorem 1 are employed. However, as it mentioned in Remark 1, $a_j(\mathbf{x})$ are decision variables that means the derived stability conditions are in the form of state-dependent BMI. Then, implementing algorithm shown in Fig. 1, the solution for the derived stability conditions are achieved.

In this simulation example the following format is chosen for $a_j(\mathbf{x})$

$$a_j(\mathbf{x}) = a_j^1 x_1^2 + a_j^2, \tag{24}$$

where a_j^1 and a_j^2 are scalars to be chosen via PSO searching algorithms. The lower and upper bounds of a_j^1 and a_j^2, are chosen as 10^{-3} and 3 respectively.

For comparison purposes the stability conditions proposed in [19], is employed to investigate the system stability for $2 \leq a \leq 9$, $7.4 \leq b \leq 9$. The stability regions given by SOS-based stability conditions in [19] and Theorem 1 are demonstrated in Fig. 2. It can be seen that comparing to the stability conditions in [19], the proposed SOS-based stability conditions in Theorem 1 are able to offer a larger stability region.

For reference, according to Theorem 1 with considering the relaxation expressions, for $a = 5$ and $b = 6$, $\mathbf{X}(\tilde{\mathbf{x}})$ and the feedback gains are obtained as the above of this page.

V. Conclusion

Stability analysis of PFMB control systems has been proposed. Introducing a new form of PFC which is the generalized form of the conventional one, relaxed stability conditions have been achieved. Compared to the conventional PFC, the fuzzy controller under consideration has a favorable property which introduces some more variables in the stability conditions such that, the solution of the derived stability conditions can be explored in a larger group of potential solutions. The

$$\mathbf{X}(\tilde{\mathbf{x}}) = \begin{bmatrix} 10.807 & -1.5579 \\ -1.5579 & 1.4054 \end{bmatrix}$$

$$\mathbf{F}_1 = [-1.0414 - 0.5533x_1 + 0.0287x_1^2 + 0.1159x_1^3 - 0.1741x_1^4 - 0.0201x_1x_2 + 0.0450x_2 - 0.2055x_2^2 \\ 0.9848 - 1.6206x_1 + 0.0919x_1^2 + 0.1286x_1^3 - 0.1929x_1^4 - 0.0435x_1x_2 + 0.0393x_2 - 0.2276x_2^2],$$

$$\mathbf{F}_2 = [-2.7283 + 0.2983x_1 + 0.2779x_1^2 - 0.0339x_1^3 - 0.3559x_1^4 + 0.3844x_1x_2 - 0.0088x_2 - 0.3004x_2^2 \\ - 0.3482 - 0.0861x_1 + 0.2112x_1^2 - 0.0380x_1^3 - 0.3945x_1^4 + 0.0470x_1x_2 + 0.0137x_2 - 0.3329x_2^2],$$

$$\mathbf{F}_3 = [-0.7934 + 0.0610x_1 + 0.0461x_1^2 - 0.1019x_1^3 - 0.1316x_1^4 - 0.0088x_1x_2 - 0.0019x_2 - 0.1139x_2^2 \\ 0.5162 - 0.6742x_1 + 0.3559x_1^2 - 0.1129x_1^3 - 0.1459x_1^4 - 0.0731x_1x_2 + 0.0594x_2 - 0.1263x_2^2],$$

achieved stability conditions are in the form of state-dependent BMI conditions. The PSO algorithm has been employed to search for the numerical solution of the derived conditions. A simulation example has been presented to confirm the validity of the proposed approach.

REFERENCES

[1] C. H. Fang, Y. S. Liu, S. W. Kau, L. Hong, and C. H. Lee, "A new LMI-based approach to relaxed quadratic stabilization of Takagi–Sugeno fuzzy control systems," *IEEE Trans. Fuzzy Systems*, vol. 14, no. 3, pp. 386–397, Jun. 2006.

[2] T. Takagi and M. Sugeno, "Fuzzy identification of systems and its applications to modelling and control," *IEEE Trans. Sys., Man., Cybern.*, vol. smc-15, no. 1, pp. 116–132, Jan. 1985.

[3] M. Sugeno and G. T. Kang, "Structure identification of fuzzy model," *Fuzzy sets and systems*, vol. 28, no. 1, pp. 15–33, Oct. 1988.

[4] K. Tanaka and M. Sugeno, "Stability analysis and design of fuzzy control systems," *Fuzzy Sets and Systems*, vol. 45, no. 2, pp. 135–156, Jan. 1992.

[5] H. O. Wang, K. Tanaka, and M. F. Griffin, "An approach to fuzzy control of nonlinear systems: Stability and design issues," *IEEE Trans. Fuzzy Systems*, vol. 4, no. 1, pp. 14–23, Feb. 1996.

[6] K. Tanaka and H. O. Wang, *Fuzzy control systems design and analysis: A linear matrix inequality approach*. John Wiley & Sons, Inc. New York, NY, USA, 2001.

[7] H. K. Khalil, *Nonlinear Systems*. Prentice Hall Upper Saddle River, NJ, 1996.

[8] S. P. Boyd, *Linear matrix inequalities in system and control theory*. Society for Industrial & Applied, 1994.

[9] P. Gahinet, A. Nemirovskii, A. J. Laub, and M. Chilali, "The LMI control Toolbox," in proceedings of *the 33rd IEEE Conference on Decision and Control*, vol. 3, pp. 2038–2041, 1994.

[10] C. L. Chen, P. C. Chen, and C. K. Chen, "Analysis and design of fuzzy control system," *Fuzzy Sets and Systems*, vol. 57, no. 2, pp. 125–140, Jan. 1993.

[11] E. Kim and H. Lee, "New approaches to relaxed quadratic stability condition of fuzzy control systems," *IEEE Trans. Fuzzy Systems*, vol. 8, no. 5, pp. 523–534, Oct. 2000.

[12] X. Liu and Q. Zhang, "New approaches to H_∞ controller designs based on fuzzy observers for Takagi–Sugeno fuzzy systems via LMI," *Automatica*, vol. 39, no. 9, pp. 1571–1582, Sep. 2003.

[13] ——, "Approaches to quadratic stability conditions and H_∞ control designs for Takagi–Sugeno fuzzy systems," *IEEE Trans. Fuzzy Systems*, vol. 11, no. 6, pp. 830–839, Dec. 2003.

[14] T. M. Guerra and L. Vermeiren, "LMI-based relaxed nonquadratic stabilization conditions for nonlinear systems in the Takagi–Sugeno's form," *Automatica*, vol. 40, no. 5, pp. 823–829, May 2004.

[15] T. Taniguchi, K. Tanaka, and H. O. Wang, "Fuzzy descriptor systems and nonlinear model following control," *IEEE Trans. Fuzzy Systems*, vol. 8, no. 4, pp. 442–452, Aug. 2000.

[16] M. C. M. Teixeira, E. Assuncao, and R. G. Avellar, "On relaxed LMI-based designs for fuzzy regulators and fuzzy observers," *IEEE Trans. Fuzzy Systems*, vol. 11, no. 5, pp. 613–623, Oct. 2003.

[17] H. K. Lam and F. H. F. Leung, "Stability analysis of fuzzy control systems subject to uncertain grades of membership," *IEEE Trans. Systems, Man, and Cybernetics, Part B*, vol. 35, no. 6, pp. 1322–1325, Dec. 2005.

[18] A. Sala and C. Ariño, "Asymptotically necessary and sufficient conditions for stability and performance in fuzzy control: Applications of Polya's theorem," *Fuzzy Sets Syst.*, vol. 158, no. 24, pp. 2671–2686, Jul. 2007.

[19] K. Tanaka, H. Yoshida, H. Ohtake, and H. O. Wang, "A Sum-of-Squares approach to modeling and control of nonlinear dynamical systems with polynomial fuzzy systems," *IEEE Trans. Fuzzy Systems*, vol. 17, no. 4, pp. 911–922, Aug. 2009.

[20] S. Prajna, A. Papachristodoulou, P. Seiler, and P. A. Parrilo, "SOSTOOLS: Sum of squares optimization toolbox for MATLAB," URL:http://www.cds.caltech.edu/sostools.

[21] H. K. Lam and F. H. F. Leung, "Stability analysis and performance design for fuzzy model-based control systems using a BMI-based approach," *Foundations of Generic Optimization*, vol. 24, pp. 261–281, 2008.

[22] Z. Michalewicz, *Genetic algorithms + data structures = Evolution Programs*. 2nd extended Edition ed., Springer, 1996.

[23] J. Kennedy, R. C. Eberhart, *et al.*, "Particle swarm optimization," in *Proceedings of IEEE international conference on neural networks*, vol. 4. Perth, Australia, 1995, pp. 1942–1948.

[24] A. Sala and C. Ariño, "Polynomial fuzzy models for nonlinear control: A taylor series approach," *IEEE Trans. Fuzzy Systems*, vol. 17, no. 6, pp. 1284–1295, Dec. 2009.

[25] S. Prajna, A. Papachristodoulou, and F. Wu, "Nonlinear control synthesis by sum of squares optimization: a Lyapunov-based approach," in proceedings of *Control Conference, 2004. 5th Asian*, vol. 1, pp. 157–165, Jul. 2004.

2011 IEEE International Conference on Fuzzy Systems
June 27-30, 2011, Taipei, Taiwan

A Distributed Smart Routing Scheme for Terrestrial Sensor Networks with Hybrid Neural Rough Sets

Frank Jiang and Michael Frater
Department of Engineering and IT
The University of New South Wales
Email: Frank.Jiang@unsw.edu.au

Steve S.H. Ling
Faculty of Engineering and IT
University of Technology, Sydney.
Email: Steve.Ling@uts.edu.au

Abstract— **The limited power consumption, as a major constraint, presents challenges in improving the network throughput for Wireless Sensor Networks (WSNs). Due to the limited computational power, the applications of WSNs in Terrestrial Networks require the capability to pre-process the observation data so as to remove irrelevant features or factors from multi-dimensional dataset. This paper proposes a intelligent distributed energy efficient routing algorithm inspired from natural learning and adaptation process with the aid of hybrid Neural Rough Sets theory, which is used to efficiently reduce the dimensionality of input dataset. The algorithmic implementation and experimental validation are described in this paper. Details of the algorithm and its testing procedures are presented in comparison with the other power-aware protocols, e.g., mini-hop. The validation of the proposed model is carried out via a wireless sensor network test-bed implemented in Castalia Simulator. The experimental results show the network performance measurements such as delay, throughput and packet loss that have been greatly improved as the outcome of applying this integration with Neural Rough Sets.**

Keywords-Neural Rough Set; Wireless Sensor Networks (WSNs); Biologically Inspired System; Ant Colony Optimisation (ACO); Swarm Intelligence (SW)

I. INTRODUCTION

Wireless Sensor Networks (WSNs) have drawn considerable attention recently in both terrestrial and underwater network research community [1-2], [14-15]. Specifically, WSNs consist of a number of sensor devices (MOTEs), which are normally inexpensive, portable, having communication and limited computational power. It potentially enlists our daily life with such characteristics as required by pervasive computing, ubiquitous communication and monitoring, which enables to establish on-demand interactions with data devices, services and applications without spacial and time limitations. Portable wireless communication devices, microprocessors as well as communication protocols and wireless techniques including WiMAX all contribute to the construction of WSNs.

The MOTEs are interconnected to each other via the network grid. Routing schemes play an important role in maintaining efficient data communications across this network grid. Whereas, routing algorithms are required to consider the constraints of MOTEs such as limited energy supply, limited computational power. Huge amount of data are produced to be processed in this regard, it is desirable to have the reduced data dimensions in a pre-processing stage. In this paper, we explore the possibility of using a new Neural Rough Set process to fulfill this purpose.

Current and future computing environments will be of massive scale and complexity. They have heterogeneous products, services, devices and platforms of ever growing scale. Intensive research has recently gone into developing a robust distributed smart algorithms and protocols for decentralised cases.

At the meantime, there are a number of routing protocols that have been proposed so far, such as Low Energy Adaptive Clustering Hierarchy (LEACH), Data-centric SPIN and Direct diffusion. LEACH relies heavily on the regular routing structure, which cannot flexibly adapt to changeable network environment. While the Direct diffusion does not build up a regular routing structure and SPIN even does not maintain a structural hierarchy at all, even no state information. These protocols cannot satisfy the practical requirements with these disadvantages under various circumstances. In fact, there are two major aspects for a routing scheme to consider (1) energy efficiency and (2) self-healing. Based on this consideration, a *self-governed* bio-inspired routing scheme is proposed in this paper. This algorithm is designed to solve the *packet* routing problem with minimal energy consumption for each hop communication and aims to maximise the lifetime of nodes in the network. Meanwhile, the new self-healing algorithm well reduce the possibility of node failures and satisfy the need for various levels of dynamic packets routing when routing decisions can be made locally at each node.

The remainder of the paper is organized as follows: Section II reviews the background of Neural Rough Set theory and the new bio-inspired scheme initiated by the swarm behavior. Section III presents the new routing algorithm details including algorithmic steps, and its implementation details. Simulation results of the new algorithm are presented in Section IV. As a validation experiment, the performance analysis shows the efficiency of our proposed routing scheme that potentially to small sized networks in WSNs. Finally, we conclude the contributions of this paper and look into the future work.

978-1-4244-7316-8/11/$26.00 ©2011 IEEE

II. PROPOSED NEURAL ROUGH SETS AND ANT COLONY BIOLOGICAL MODEL

A. Related Rough Set Preliminaries

The rough set theory is an extension of set theory for the study of intelligent system with indiscernible, ambiguous and imperfect data information. Rough-set theory appeared two decades ago. Its main thrust is used in attribute reduction, rule-generation and prediction. For instance, by applying a mathematical approach to solve the data reduction problem, it is good at finding out the discernity, vagueness and uncertainty in data analysis. The rough-set concept was introduced by Pawlak and his colleagues [16]. This theory became very popular among scientists around the world in the last decade, and it is now one of the most developed AI methods. The primary goal of this new emerging theory is to classify the information from incomplete information. Its successful application to a variety of problems has shown its usefulness and versatility[18].

As we know, the decision table in a rough set scheme plays an important role in clarifying a discretized feature values. Applying rough-neural bundled computation has proved to be more efficient in discovering emergence and hidden order of control area as an approach to knowledge discovery and data mining. The integration of such an approach with telecommunication complex scenario, the goal of having a more robust internet tolerating the nonstationary anomalies can be achieved. Below are some definitions and domain descriptions [18].

The information system is The information system is formed as a pair of IS=(U, A, V, f), where U is a *non-empty* finite set of objects (formed as an universe), and A is a set of finite attributes, V is the domain limitation of A, and $f:U\times A\rightarrow V$ is an information function. $\forall a\in A$, $x\in U$, $f(x,a)\in V$. Each non-empty subset $B\subseteq A$, Let $H\subseteq U\times U$ denote an indiscernibility relation on U that can be defined as:

$$H=\{(x,y)\in U\times U:b(x)=b(y),\forall b\in B\} \quad (1)$$

Objects x and y satisfying the relationship H are indiscernible by attributes from B.

Definition 1 *Given an information system S, let $B\subset A$, and $x(i), x(j)\in U$, a binary relation $[x]_B\triangleq\{(x(i), x(j))\in U\times U /\forall a\in B, f(x(i),a)=f(x(j),a)\}$ is an indiscernibility relationship.*

Let U/H denote the equivalent class of H.For any $x\in U$, we denote the set,$[x]_B\triangleq\{(x(i),x(j))\in U\times U|\forall a\in B,f(x(i),a)=f(x(j),a)\}$ is called the equivalent class in B. The empty set φ and the elements in U/H are called elementary sets. Any subsets $X\subset U$ from the given data can be approximated by the elementary sets. Let $X\in U$, We define two sets $S_{LB}(X)$ and $S_{HB}(X)$ as the *lower approximation* and *upper approximation* of the set of objects X as:

$$S_{LB}(X)=\{x\in U:[x]_B\subseteq X\} \quad (2)$$

$$S_{HB}(X)=\{x\in U:[x]_B\}\cap X\neq\varphi\} \quad (3)$$

where $[x]_B$ denotes the set of all objects indiscernible with x by attributes from B. In Pawlak's definition of indiscernibility relations, for $x,y\in U$, it is called that y is indiscernible to x with respect to $B\subseteq A$ if $f(x,a)=f(y,a)$, $\forall a\in B$. Where f(x,a) means a mapping of value x with respect to attribute a [18].

B. Neural Rough Sets and BP Training

The concept of lower and upper approximation has been applied in many applications of computational intelligence. Successive research shows that the general concepts of lower and upper bound offer a broader application field in various types of industrial fields. In particular, rough set theory has demonstrated the power of using these bounds in rule generation [18].

Although there are plenty of classifications of recurrent neural networks, Zhang, et al [19] make a good performance comparison among the main algorithm i.e. BP, Perceptron-Back propagation Hybrid (PBH), Fuzzy ARTmap and Radial-Basis Function Network (RBF), their results reveal that BP and PBH nets outperform Perceptron, Fuzzy ARTmap and RBF by the criteria of classification errors. Hence we will apply BP nets in our design. The input datasets with all features are filtered by rough-sets logic and subsequently the models based on the minimum feature sets are built with the integration of rough neurons into Neural Rough networks. In this part, our network architecture is Ninput : Nhidden:1 three layer feed-forward rough neural network for processing. During this process, the error in the output neuron is propagated back from one layer to the previous layer by altering the weights of the connections, i.e. Back-Propagation (BP) algorithm. A rule of thumb, known as the Baum-Haussler rule [17], is used to determine the number of hidden neurons to be used:

$$N_{\text{hidden}}=\frac{Ntrain*Etolerance}{Npts+Noutput} \quad (4)$$

where N_{train} is the number of hidden neurons, E_{tolerance} is the error tolerance, N_{pts} is the number of data points per training example, N_{output} is the number of output neurons, in our architecture, $N_{output}=1$. In our case, for example, Let $E_{tolerance}=0.001$; $N_{train}=4000\times N_{pts}$; then the above equation becomes:

$$N_{\text{hidden}}\leq\frac{4Npts}{Npts+1} \quad (5)$$

Hence, the number of neurons in the hidden layer should be no more than 4. Now, we are ready to start the rough neural multilayer sets process to reduce the dimensionality of inputs datasets [18].

C. Proposed Bio-inspired Algorithm

We apply the metaphor of ant food foraging behavior into network routing system. As stated in the literature, ant colony optimization metaheuristic (ACO) was first systematically

introduced by Dorigo in 1992 in his PhD dissertation [6]. ACO is a probabilistic technique for solving computational problems which can be reduced to finding good paths through graphs. They are inspired by the behavior of ants in finding paths from the colony to food. The early attempts of biological researches on ants were conducted by Dorigo and Gambardella [7] for routing in wired and wireless mobile environments.

In addition, Stutzle and Hoos proposed MAX-MIN ant system, namely MMAS, it is an improvement version of ACO. MMAS differs from standard ACO in that (i) only the best ant adds pheromone trails, and (ii) the minimum and maximum values of the pheromone are explicitly limited [8]. Agassounon 9], [10] proposed interesting work based on ACO to solve information retrieval and resource allocation issues. A good review of available ACO basis, models and new trends can be found in Oscar's work [11].

ACO algorithms can be applied to find the near-optimal multihop routing path in mobile ad hoc networks, namely AntHocNet, the experimental results indicate AntHocNet algorithm outperforms the other popular Ad hoc On-Demand Distance Vector Routing (AODV) algorithm in terms of *end-to-end delay* and *delivery* ratio. Related problems such as load-balance and routing in computer networks are also investigated in the work by Hsiao et. al, by use of ACO [12]. In sum, performance comparisons between ACO-based algorithm and other routing algorithm show better performance by use of ACO metaheuristics.

The most important feature of ACO metaheuristic is inspired from the *stigmergy,* which mimics the indirect communication behaviors adopted by social insects. The proposed algorithm, termed iACO, especially for WSNs, each packet are regarded as an individual ant, communicating with each other via "pheromone" values stored in each wireless sensor node's pheromone table.

Three main steps are included in the flowchat of the proposed algorithms for the routing scheme of WSNs. In brief, the steps include (1) Generate local solutions based on the path (i,j) selection probability; (2) Pheromone update; (3) Decision making.Maintaining the Integrity of the Specifications

Figure 2 depicts the overall integration process where Rough set process and the proposed algorithm are attached together to solve the routing path in network environment.

III. ROUTING ALGORITHM IN WSNS

Suppose the ant is randomly placed on node i, the probability of an ant k choosing the next adjacent node j is as depicted in Equation 6. And the pheromone table helps to choose the next neighbor in the process.

$$P_{ij} = \begin{cases} \dfrac{[\tau(i,j)]^{\alpha} \cdot [\eta(j)]^{\beta}}{\sum_{u \notin M_k} [\tau(i,j)]^{\alpha} \cdot [\eta(j)]^{\beta}} & if\ j \notin M_k \\ 0 & \text{otherwise} \end{cases} \qquad (6)$$

where P_{ij} = probability of packet going from node i to j,
τ (i,j) = pheromone level in the table of node i for node j,
η (j) = energy level of node j,
M_k = identifier of every visited node,
α = parameter that denotes pheromone level,
β = parameter that denotes energy level heuristics.

Two categories of ants are in use, they are termed as forward ants and backward ants. We adopted this concept from the relating work of ant algorithm routing such as T-ant, antNet [2] and EEABR [3]. We further develop the definitions as used in the literature. The forward ants are defined as the ants that are sent from the source. The forward ants will carry the information such as (1) the required sensor type, (2) the sensor region of interest, (3) the data rate and (4) the time period of the interest. More details can be seen in table I where both categories of ants are described in functions.

Parameters and variables formatted in the packet of the experiment are described here in Table I. The header and data are carried by each packet. The packet is sent from source node, taking the form as backward and forward ants

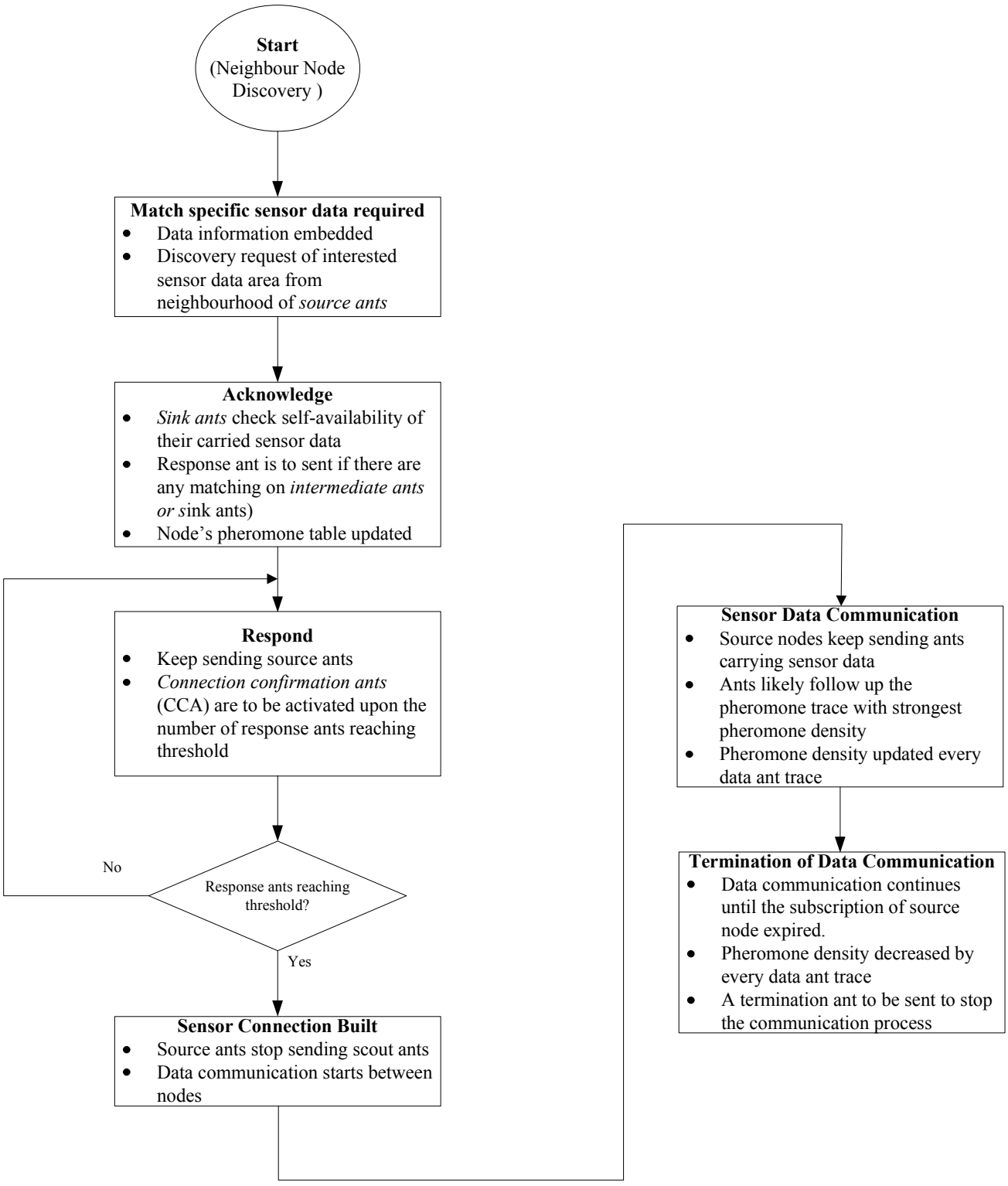

Figure 1. Flowchart of the proposed algorithms for the routing scheme of WSNs

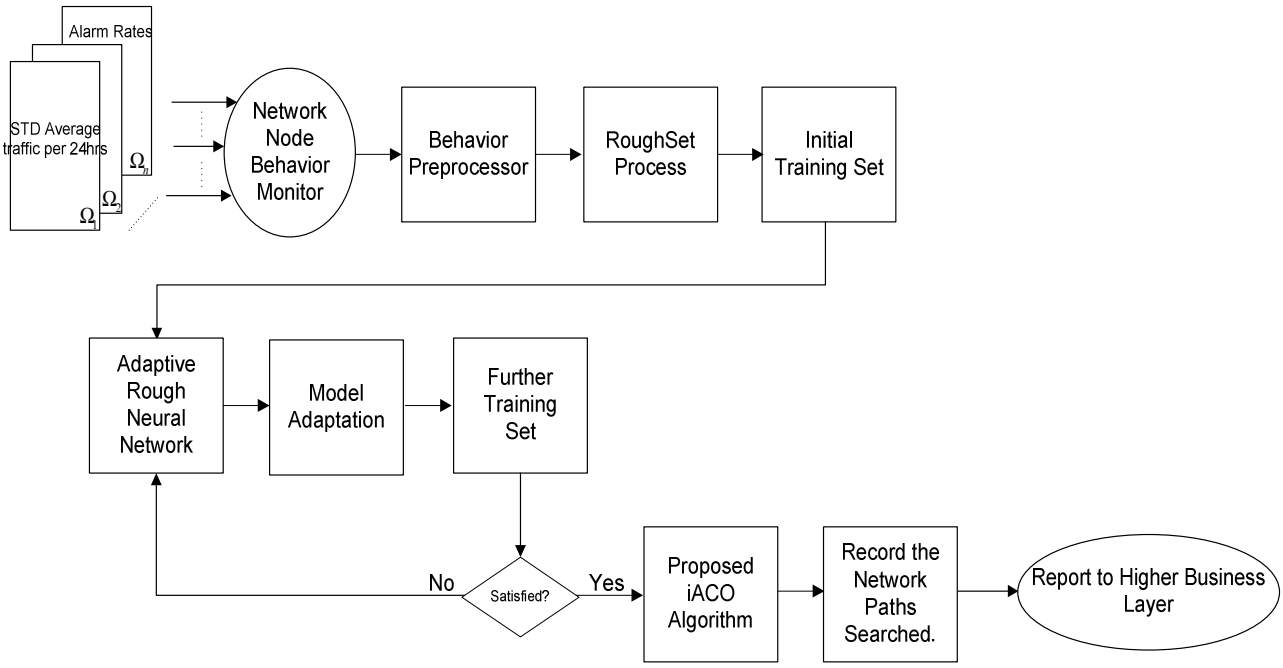

Figure 2. Illustration Schematic of The Overall Process

Pheromone Update:

Pheromone plays an important role in searching for a suitable node. In our algorithm, only the pheromone along our successfully recorded paths (usually more than one) is intensified, instead, pheromone in those incomplete paths evaporates. The pheromone increases and reductions will influence the searching process in next iteration. We adopt the conventional ACO pheromone update rule as [20]:

- Intensify pheromone: an absolute amount of pheromone $\Delta\tau_{i,j}^{k} > 0$ is added to the existing pheromone values on the paths completed by k -th ant

$$\Delta\tau_{i,j}^{k} = \begin{cases} \frac{Q}{Z_{\min(k)}} if \ (i, \ j) \in T_k \\ 0 \qquad if \notin T_k \end{cases} \qquad (7)$$

where T_k are the paths having been traversed by k -th ant. Q is a constant. More research on Q value have been done in Dorigo [6].

- Evaporate pheromone: pheromone on the edges of incomplete traversing paths is reduced in order to minimize the chances of being selected by other ants.

$$\tau_{i,j} = (1-\rho)\times\tau_{i,j} \qquad \forall i, \ j \in [1:52] \quad (8)$$

where $\rho \in [0, \ 1)$ is the pheromone evaporation rate. $\tau_{i,j}$ is the current pheromone density on the trail $a(i, \ j)$.

Mutate pheromone update process: In order to increase the convergence speed of the algorithm, we combine the *mutation* parameter into our pheromone update rules, where the concept of *threshold* is also involved. The mutation parameter in our algorithm are partly based on *Best-worst Ant Colony Algorithm* (BWACA) as well as *Max-min* Ant system.

IV. EXPERIMENT

A. Simulation Platform and Configuration Parameters

The simulation is conducted on the platform called Castalia network simulator [5]. Being a specially designed network simulator, Castalia contains models for realistic wireless channels, MAC layers, radio, physical sensor and resource management. Moreover, it contains modules that can simulate the different functionality and behaviours of wireless sensors and hence is regarded as a good simulation of the real behaviour in the research society for WSNs [4].

The dataset preprocessed by Neural Rough Set process is further processed in this simulation section.

The most commonly used algorithm for routing label witched Paths (LSPs) is the min-hop algorithm [13] The nature of this algorithm has been adopted by many routing protocols. Therefore, it is reasonable to compare our proposed algorithm with min-hop algorithm.

To evaluate two algorithms, we define the following parameter metrics in use in the simulation.

1) *Energy consumption*
2) *Delay*
3) *Throughput*

With regards to these metrics, Figure 3 and 4 depict the comparison view of *energy consumption* and *delay* exhibited by various node density levels. As shown, the small number of nodes would not make a significant impact on the energy consumption and delays.

When the interactive nodes increasing till 145, an energy peak occurs, and new routing algorithm proposed consumes less 1/3 energy than min-hop algorithm though the similar curve trend is observed. For the larger network, this difference tends to be more significant.

As shown in Figure 4, the impacts of delays for algorithms are trivial, though the proposed routing produces a slightly less delays than the min-hop. *Max-min* Ant system.

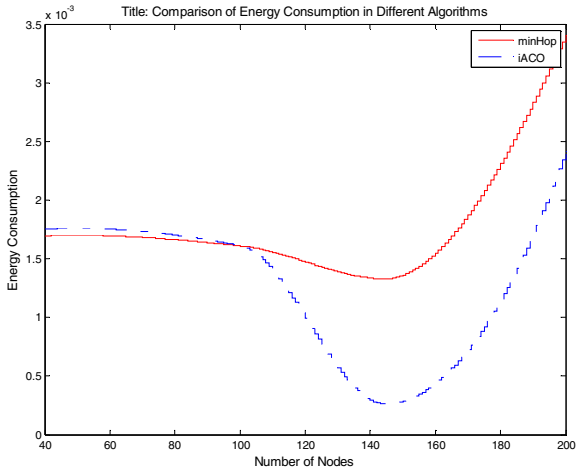

Figure 3 Comparison of Energy Consumption of Ant Population Levels

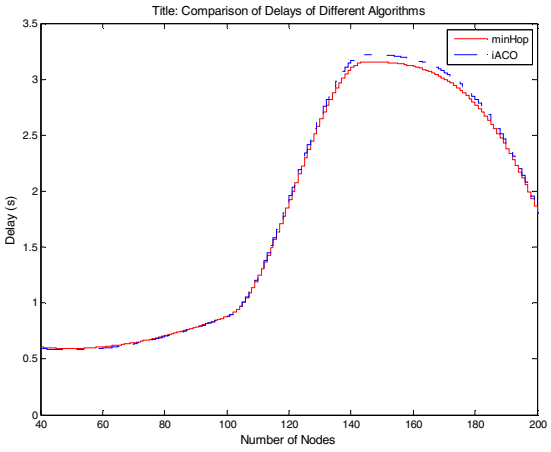

Figure 4 Comparison of Delays Between Two Algorithms

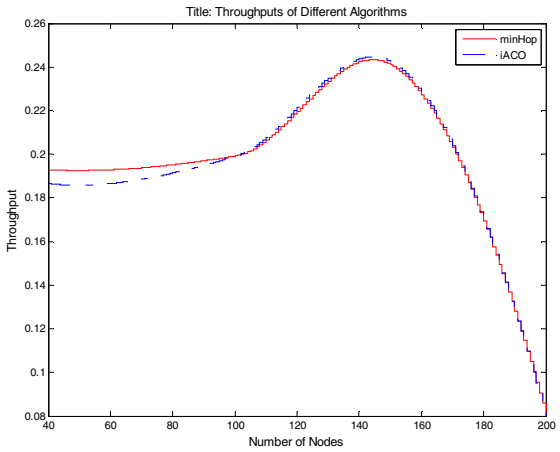

Figure 5 Comparison of Throughputs Between Two Algorithms

With regards to the throughput, as shown in Figure 5, when the number of nodes increase till 145, there are not much differences between min-hop algorithm and enhance ant-based protocol. The experience data and literature prove it is difficult for the traditional ACO achieve the marginal performance as min-hop routing scheme. The proposed protocol demonstrates the similar performance in this regard, so it can be regarded as a good improvement.

Figure 6, 7 and 8 shows the impacts of various node densities towards energy consumption, delays and throughput. It is shown there is an obvious effect on the efficiency of various node densities, but it seems not a linear relationship. There is a few optimal node densities at which the lowest energy consumption is observed. Similarly, it comes to the delay in Figure 7 and throughput in Figure 8. Specifically, the density is 0.005 when the minimum delay occurs, but the maximum delay occurs when the density is 0.1. This is also the case for throughput.

In particular, the minimum energy consumption, maximum

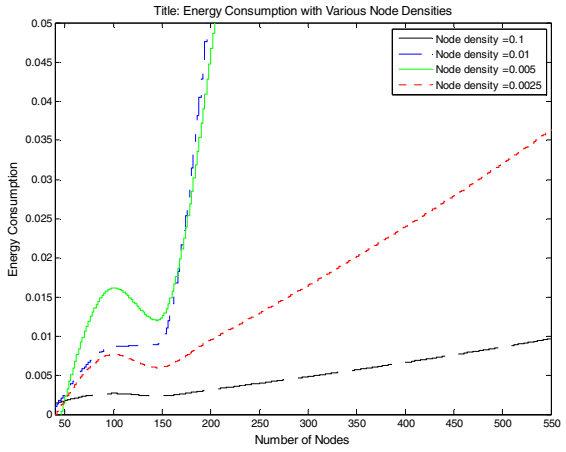

Figure 6 Energy Consumption with Various Node Densities

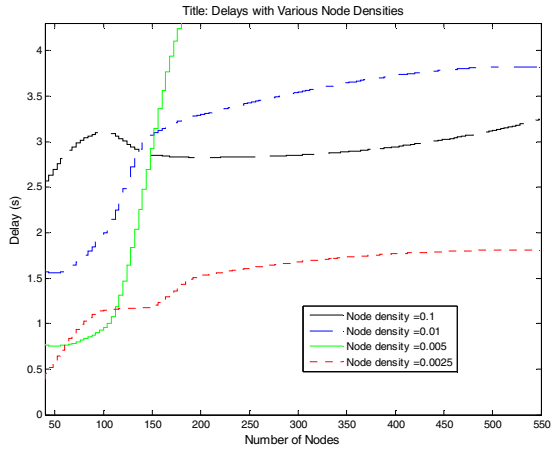

Figure 7 Delays with Various Node Densities

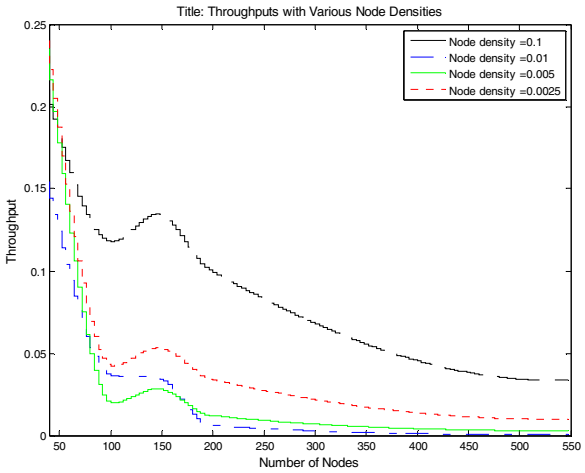

Figure 8 Throughputs with Various Node Densities

when the network has 50 nodes. The current good results are well compliance with the expected network size less than 100.

V. CONCLUSION AND FUTURE WORK

In this paper, a distributed, reliable nature-inspired routing algorithm for terrestrial sensor networks is presented. This routing process occurs after the dataset feature reduction via neural rough set theory. The swarm algorithm is partly based on the efficient *Max-Min* algorithm and it is suitable for flexible structure of wireless sensor networks. This new distributed scheme performs generally not worse than other standard routing algorithm, and in some occasions, it outperforms than conventional *min-hop* algorithm. More work in the future includes conducting further performance comparison work with other sensor network routing algorithms, as well as identifying and validating the best parameters configurations for the proposed algorithm under various network environment to guide real productive practices in the networking industry.

REFERENCES

[1] S. Selvakennedy, S. Sinnappan, and Yi Shang, "Data dissemination based on ant swarms for wireless sensor networks," in *Proc. Consumer Communications and Networking Conference,* 2006, pp. 132 – 136.

[2] D. Caro and M. Dorigo, "AntNet: Distributed Stigmergetic Control for Communications Networks." *Journal of Artificial Intelligence Research,* vol. 9, pp. 317-365, 1998.

[3] T. Camilo, C. Carreto, C. Silva, and J. S. Boavida, "An Energy-Efficient Ant-Based Routing Algorithm for Wireless Sensor Networks" *Lecture Notes In Computer Science,* pp. 49-59, 2006.

[4] H. N. Pham, D. Pediaditakis, and B. Athanassios, "From Simulation to Real Deployments in WSN and Back," in *IEEE International Symposium on World of Wireless, Mobile and Multimedia Networks,* 2007, pp. 1-6.

[5] NICTA. "Castalia: http://castalia.npc.nicta.com.au/ [Feb. 6, 2010].

[6] M. Dorigo, "Optimization, learning and natural algorithms (in italian)," Ph.D. dissertation, 1992.

[7] R. Montemanni and L. Gambardella, "Swarm approach for a connectivity problem in wireless networks," in *Proc. IEEE Swarm Intelligence Symposium,* 2005, pp. 265 – 272.

[8] M. Dorigo and T. Stuzle, *Ant Colony Optimization*. MIT Press, 2004.

[9] R. Montemanni, L. M. Gambardella, "Exact algorithms for the minimum power symmetric connectivity problem in wireless networks," *Journal Computers and Operations Research,* vol. 32, issue 11, pp. 2891-2904, 2005.

[10] W. Agassounon, "Distributed information retrieval and dissemination in swarm-based networks of mobile, autonomous agents," in *Proc. of IEEE Swarm Intelligence Symposium*, 2003, pp. 152—159.

[11] O. Cordon, F. Herrera and T. Stuzle, "A review on the ant colony optimization metaheuristic: Basis, models and new trends," *Mathware and software computing,* vol. 30, no. 9, pp. 1 - 35, 2002.

[12] Y. t. Hsiao, C. L. Chuang and C. C. Chien, "Computer network load-balancing and routing by ant colony optimization," in *12th IEEE International Conference on Networks,* 2004, pp. 313 - 318.

[13] M. Zhu, M., Y. Wu, and F. Suili, "A New Dynamic Routing Algorithm Based on Minimum Interference in MPLS Networks," in *4th International Conference on Wireless Communications, Networking and Mobile Computing,* 2008, pp. 1-4.

[14] M. Ismail and M.Y. Sanavullah, "Security topology in wireless sensor networks with routing optimization," in *4th International Conference on Wireless Communication and Sensor Networks,* 2008, pp. 7-15.

[15] K. Yamasaki and T. Ohtsuki, "Design of energy-efficient wireless sensor networks with censoring, on-off, and censoring and on-off sensors based on mutual information," in *Vehicular Technology Conference,* vol. 2, 2005, pp. 1312 – 1316.

[16] Z. Pawlak, "Why rough sets?," in *Proc. of the Fifth IEEE International Conference on Fuzzy Systems,* vol. 2, pp. 738 - 743, 1996.

[17] E. Baum and D. Haussler, "What size net gives valid generalization?," *Neural Computation*, vol. 1, no. 1, pp. 151-160, 1989.

[18] F. Jiang and R. Braun, "Intelligent Failure Domain Prediction in Complex Telecommunication Networks with Hybrid Rough Sets and Adaptive Neural Nets", *in International Information and Telecommunication Technologies Symposium*, pp. 45-52, 2004.

[19] Z. Zhang., C. Manikopoulos, "Hide: a hierarchical network intrusion detection system using statistical pre-processing and neural network classification," in *Proc. the 2001 IEEE Workshop on information Assurance and security United States Military Academy,* 2001, pp. 85–90.

[20] F. Jiang, and V. Mahadevan, "Towards the Distributed Autonomy in Complex Environments", in *Proc. International Conference on information and Multimedia Technology,* 2009, pp. 169-172.

2011 IEEE International Conference on Fuzzy Systems
June 27-30, 2011, Taipei, Taiwan

P2P Traffic Identification and Optimization Using Fuzzy C-means Clustering

Duo Liu
Department of Systems and Computer Engineering
Carleton University
Ottawa, Ontario, Canada K1S 5B6
duoliu@sce.carleton.ca

Chung-Horng Lung
Department of Systems and Computer Engineering
Carleton University
Ottawa, Ontario, Canada K1S 5B6
chlung@sce.carleton.ca

***Abstract*—Accurate identification of P2P traffic is critical for efficient network management and reasonable utilization of network resources, as P2P applications have been growing dramatically. Fuzzy clustering is more flexible than hard clustering and is practical for P2P traffic identification because of the natural treatment of data using fuzzy clustering. Fuzzy c-means clustering (FCM) is an iteratively optimal algorithm normally based on the least square method to partition data sets, which has high computational overhead. This paper proposes modifications to the objective function and the distance function that greatly reduces the computational complexity of FCM while keeping the clustering accurate. The proposed FCM clustering technology can be incorporated into a Fuzzy Inference System (FIS) to implement real-time network traffic classification by updating the training data set continuously and efficiently.**

Keywords-network traffic identification; peer-to-peer communications; machine learning; fuzzy c-means clustering; statistical analysis; data transformation

I. INTRODUCTION

Network traffic that could be administered through traffic measurement, traffic control, and traffic simulation consists of flows from a great variety of users using different applications on diverse utilities. Network traffic management plays a key role in optimizing network performance, improving latency, and scheduling network resources for adjusting bandwidth based on traffic engineering. Network traffic measurement measures the amount of different types of traffic on a specific device, an individual port, or a particular application; network control prioritizes and optimizes traffic. Both network measurement and control are key processes for network traffic management [1].

Internet protocol-based network traffic classification (also know as IP traffic identification or characterization) has become one of the major challenges in network management. The main roles of network management are to provide information for capacity planning and provisioning, traffic engineering, fault diagnosis, application performance optimization, anomaly detection and pricing to Internet Service Providers (ISPs) and their equipment vendors. Based on network traffic measurement, appropriate features selection, and classification methods, traffic classification relies on an in-depth understanding of the contents of Internet traffic dynamically [2].

Peer-to-peer (P2P) networking is a distributed application architecture that mainly relies on the computing power and bandwidth of the participants in the network and uses application software to search for shared files of users connected to the network. Every participant in the network plays both roles of provider (server) and consumer (client) without requiring to be coordinated by a central server or file hosting services. Compared to Web browsing, e-mail or many other non-P2P applications, where data is only transferred in short intervals and with relative small quantities, P2P file-sharing could utilize significant network resources, resulting in network jams and affecting the quality of service (QoS). Classifying P2P traffic could support ISPs to increase overall availability and reliability of connection by offering less bandwidth to specific users or definite P2P applications while maintaining QoS to other users or applications. P2P traffic classification is a key element for network traffic management, network resource scheduling, and performance enhancement.

P2P traffic classification is getting more sophisticated as P2P communications are continuously changing from TCP layers using well known ports to disguising themselves by using port numbers for commonly used protocols such as HTTP and FTP and implementing dynamic port numbers. The accurate identification is proved to be more complicated with the enormous emerging P2P applications. Traditional P2P traffic classification mechanisms depend on mapping applications to well-known port numbers and have been very successful in the past. However, they are becoming obsolete as new P2P applications began using dynamic port numbers. Payload based analyses which inspect application packet payloads to determine if they contain characteristic signatures of known applications overcome the shortcomings of port-based classification. However, their performance is greatly reduced and inefficient with P2P applications using plain-text ciphers, variable-length padding, and encryption. The payload-independent statistical identification based on network layer and data link layer utilizes machine learning techniques such as neural networks, unsupervised machine learning, support vector machine, and hybrid mechanism with much flexibility, self-learning and self-adaptive and is gained much attention in academic and industrial areas [3].

Clustering is one of the machine learning techniques that has been used for network traffic classification. Fuzzy

978-1-4244-7316-8/11/$26.00 ©2011 IEEE

clustering is more flexible than hard clustering and is practical for P2P traffic identification because of the natural treatment of data [2]. Traditional FCM (Fuzzy c-means) clustering technique has the advantage of quantifying a level of membership of elements to detected clusters. GK-FCM (Gustafson-Kessel FCM) can generate clusters that adapt themselves to the shape and location of data [4]. However, the computational complexity of FCM or GK-FCM is high. Our proposed modification for the objective function and distance can decrease computational complexity greatly while keeping the classification accurate, which is crucial for high volume real-time P2P traffic applications.

The remainder of the paper is structured as follows: Section II discusses various network traffic analysis categories. Different machine learning techniques with supervised, un-supervised, and hybrid learning are described in Section III. Section IV illustrates FCM and the proposed method for P2P traffic identification. Some simulations and comparison of simulating results are provided in Section V. We conclude the research and outline future work in Section VI.

II. NETWORK TRAFFIC ANALYSIS

Network traffic analysis is the process of observing and identifying network traffic. The ultimate goal of traffic analysis is to classify the traffic into definite groups, which is defined by network administrators. The classification could be based on users recognized by sources or destinations, or applications identified by a protocol. Traffic classification typically starts with network measurements and extracts traffic attributes later, and finally groups the traffic based on the selected strategies. The following sub-sections briefly describe various techniques that have been used for traffic analysis.

A. Traffic Measurement

Network traffic measurement measures traffic flows of observing devices such as routers, switches and dedicated probes to capture traffic attributes such as port numbers, payload and statistical characteristics. Traffic measurements are conducted on a continuous basis and the results are used for network management and temporary routing, maintenance, or long-term network deployment depending on the sampling period. They can be categorized into active and passive measurements. External traffic is injected to the network during the measurement in active measurements, whereas no enhanced injection is adopted for passive measurements. Active measurements are mainly used to detect the vulnerability of a specific network or a device, and examine the performance of a network to a particular application. Active measurements are not suitable to check the influence by users because user-independent packets are injected to network continuously. Passive measurements based on users connected to a specific network observe network connections, packets and flows to find source and destination addresses, port numbers and transport protocols. Passive measurements are the fundamentals for traffic identification and optimization [2, 5, 6]. This paper focuses on passive network flow-level-based measurements.

B. Port Number Analysis

Port-based analysis rests on the fact that many traditional P2P applications have default ports (assigned by the Internet Assigned Numbers Authority (IANA) and can be classified by looking up the TCP SYN packets for TCP traffic). This is the most straightforward and most successful method in the early time for identifying P2P network traffic. This method is easy and fast because it only accesses the header of the packets to get the data required for classification. The port-based classification system does not apply sophisticated strategy and can be easily extended by adding new application-port match pairs to its database. For example, HTTP traffic uses port 80, FTP uses 20, 21, DNS uses 53, and E-mail uses 25, 110, and etc.

However, for P2P applications, the accuracy of port-based classification is decreased abruptly as modern networks exceedingly carry more and more traffic that use dynamically allocated port numbers. Some applications may not have their ports registered with IANA or use ports other than well-known ports to prevent them from being detected. IP layer encryption may confuse the traffic headers also, making it impractical to identify network traffic through port-based approaches [7].

C. Payload-based Analysis

To avoid total reliance on the port numbers, a more reliable approach, payload-based analysis, a.k.a. DPI (Deep Packet Inspection), is to inspect the packet payload for characteristic signature of known applications. Payload-based identification based on some knowledge about the payload formats of specific applications checks particular features present in the application traffic to see whether it contains some characteristic signatures or not.

Payload-based classification works well for Internet traffic, including P2P traffic, when the payload is not encrypted. But payload-based classification is gradually becoming ineffective or impossible as new P2P applications use encryption, variable-length padding and other more advanced routing techniques to avoid being detected. The lack of openly reliable protocol specifications, especially for enormous emerging applications, the demand for high computing and storage capacities, the application signatures changing with the corresponding applications, and their protocol evolution are key challenges for developing application signatures [8, 9].

D. Statistical Analysis

To overcome the drawbacks of heavily relying on fixed port numbers or deep inspection of packet contents of network traffic, the approaches that take advantage of the statistical properties at the network layer and data link layer are attracting much attention to academic researchers, industrial developers and network administrators. The statistical analysis relies on the fact that traffic at the network layer has statistical properties (such as the distribution of flow duration, flow idle time, packet inter-arrival time and packet lengths, and etc.) and that similar applications typically have similar behavior patterns. For example, FTP normally used for large file transferring have a longer connection duration and larger average packet size, while some P2P applications such as BitTorrent typically are persistent and send data bi-directionally.

Exploiting distinct characteristics of traffic flow for specific applications, network traffic classifier can identify network traffic using only flow statistics. P2P nodes are possibly located within a domain of common data link layer switch; however, detecting the traffic is a minor concern because it does not consume network resources outside the local switch.

Based on the statistical parameters, machine learning which automatically builds a classifier by learning the inherent structure of network traffic dataset can automatically identify traffic flows. The classifier has the ability of continually gaining new knowledge based on the data newly acquired and modifies the model structure to adapt to the whole data and get the overall performance optimized [10, 11].

E. Feature selection and reduction

Feature selection techniques normally based on the actual performance of the learning algorithms are critical to build a machine learning classifier by which the network traffic can be identified using the smallest necessary set of features to reduce the demand for storage capacity and computational complexity. It can be broadly classified into filter method based on general characteristics of traffic data and wrapper method based on the comparison of different subsets and selection of the best one using machine learning techniques. Transformations of features such as Log or Gaussian are sometimes very effective to get higher levels of classification accuracy.

Appropriate feature reduction algorithms can reduce the number of features needed to identify traffic flows drastically, which in turn can greatly reduce the computational complexity without affecting classification accuracy apparently. Feature reduction can be achieved by using machine learning techniques to get the best combination of attributes that provide the most contrasting application classes. Although the total number of packets in the flow, the average packets size of a flow, and the duration of the flow are all valid features, there is still a need to transform some features to increase classification accuracy and reduce feature sets as much as possible using correlation-based or consistency-based approaches to decrease the computation overhead [12].

III. MACHINE LEARNING TECHNIQUES

Machine learning techniques can map instances of network traffic flows into different traffic classes based on selected features. Features are descriptive statistic variables that can be calculated from one or more packets. For example, mean packet length is a scientific discipline that focuses on the design and development of solutions. The discipline allows computers to evolve characteristics based on empirical data. As a subset of the wider Artificial Intelligence, it is closely related to probability theory, statistics, and fuzzy systems and neural networks.

The application of machine learning approaches usually starts by defining features based on calculation of multiple packets to identify and distinguish future unknown IP traffic. The next step is to train the established classifier to match traffic classes and feature sets. Finally, the last step is to classify unknown traffic using previously learned rules. Machine learning techniques can be categorized into three subsets: *supervised learning* which generates a function that maps inputs to desired outputs, *unsupervised learning*, such as clustering which seeks the structure of data and organizes them orderly, and *hybrid* also called semi-supervised which combines supervised and unsupervised machine learning algorithms. The following sub-sections describe the three subsets briefly.

A. Supervised machine learning

In network traffic classification, supervised machine learning generates knowledge structures to classify new traffic flow into pre-defined classes based on the training of the classifier for the matches of known traffic to definite classes. The classifier is provided with a collection of traffic datasets and their pre-identified classes. The result of classifying the known traffic into specific classes becomes more accurate with the progress of training and the ultimate goal for the classifier is to classify the unknown traffic into the suitable classes as accurately as possible. Two major steps in supervised machine learning are matching training datasets with classes and classifying unknown new captured datasets into classes. Artificial neural network and Naïve Bayes classifier are two important algorithms used in traffic classification.

Based on independent presence and absence of distinct features, the Naïve Bayes classifier greatly simplifies the training procedure [12], although independence is generally a poor practice. The Naïve Bayes method calculates the Gaussian distribution of the features for each class based on labeled training dataset. The maximum likelihood algorithm classifies data into definite classes based on conditional probabilities.

Neural networks have attracted more attention compared to other approaches in many application areas, including network traffic classification. Neural networks with a built-in ability to modify their synaptic connections and weights to adapt in surrounding environment have the potential to address many of the problems encountered by rule-based algorithms. Their attributes of non-linearity and adaptiveness are especially desirable for P2P traffic identification. However, neural networks, like other supervised machine learning approaches, normally require a large diversity of training for real world operations since they need sufficient representative examples in order to capture the underling structure in which generalization of cases is occurred. The complexity of calculation may also limit its applications in some categories, especially in data pre-processing while clustering techniques have advantages on those [13].

B. Unsupervised machine learning (clustering)

Compared to supervised machine learning techniques in which training datasets match pre-defined classes before testing, unsupervised machine learning algorithms explore natural classes using internalized heuristics to group data. Clustering methods classify data based on the similarity which can be measured by distance functions such as Euclidean, Tchebychev, or City Block. A good set of clusters should have intra-similarity and inter-dissimilarity. As an algorithmic framework for data analysis and interpretation, clustering has been widely used in understanding data, revealing fundamental phenomenon, and visualizing major tendencies. Clustering can be categorized into two types: *hierarchical clustering* uses previously established clusters to find successive clusters; and

partitioning clustering determines all clusters at once based on iterative procedures. Subspace clusters, correlation clustering and bi clustering are new emerging algorithms and have been adapted to practical applications. Density-based algorithms, such as DBSCAN (Density Based Spatial Clustering of Applications with Noise), probabilistic model-based techniques, for instance, AutoClass and K-means clustering have become popular.

DBSCAN is based on density-reachability. Density-connectivity is an example of density-based algorithms which find clusters starting from the estimated density distribution of corresponding nodes. In this approach, all points in a specific cluster are mutually density-connected. It requires two parameters: epsilon (the distance around an object that defines its eps-neighborhood) and minPts (minimum number of points to classify data into distinct classes) [14].

Expectation Maximization (EM) approach focuses on finding maximum likelihood. EM is used to group data into a small number of classes and then generates classification rules from distinct classes. The probabilistic model-based AutoClass allows automatic selection of the number of classes and soft clustering of the data, which allows data to be fractionally assigned to more than one cluster. It is effective for first step of classification or individual applications identification in network traffic engineering [3].

K-means clustering approaches partition data into classes based on distances and try to maximize the homogeneity intra-cluster by minimizing the error overall and heterogeneity inter-cluster by maximizing the error. The distance and objective functions are fundamental elements for clustering. The iteration changes the clusters' centers and alters the belongingness of data to distinct clusters until specifications are met. It can classify different types of TCP-based applications using the first few packets of the traffic flow [11].

C. Hybrid approaches

Semi-supervised machine learning approaches (also called Hybrid approaches) combine unsupervised and supervised learning techniques. Hybrid approaches use both a small quantity of labeled and a large amount of unlabelled data. This approach partitions training dataset into classes first using clustering algorithms, then maps unlabelled traffic data into identified classes with the existence of empty classes for further use. The approach is flexible, especially for new emerging unknown network traffic classification [15].

IV. FUZZY C-MEANS CLUSTERING AND PROPOSED MODIFICATIONS

Conventional hard clustering methods classify each data point into one cluster. Nevertheless, the observation of P2P traffic characteristics could be imprecise because of the ever-changing nature of IP network traffic. Fuzzy clustering, however, can classify a piece of data point, such as network traffic data information, into two or more clusters with different belongingness. Based on the fuzzy logic, which has a great resemblance with human decision making ability, FCM generates precise solutions and results from either a certain or an approximate set of input information. It can achieve optimal through iterations with the simultaneous change of cluster centers and the membership values which are definitions of one data belonging to one class. Fuzzy clustering is more flexible than hard clustering and is practical for P2P traffic identification because of the natural treatment of data [2].

This section first describes FCM and GK FCM clustering methods. Both FCM and GK FCM methods can effectively generate clusters, but with high overhead. The modifications to FCM are then proposed to simplify the calculation and complexity, which is vital for real-time P2P applications that could consist of a large number of real-time traffic flows.

A. Fuzzy c-means clustering

Fuzzy c-means clustering has three requirements [16]:

1. Membership degree (pattern *k* belongs to cluster *i*):

$$0 \le \mu_{ik} \le 1, i = 1,..., C(clusters), k = 1,..., N(patterns)$$

2. Total Membership (the sum of all membership degrees is constrained to 1):

$$\sum_{i=1}^{C} \mu_{ik} = 1, k = 1,..., N \quad (1)$$

3. No empty clusters are allowed and no cluster may contain all the data examples.

$$0 < \sum_{k=1}^{N} \mu_{ik} < N, i = 1,..., C \quad (2)$$

The procedure of clustering is an iterative process of minimizing the objective function,

$$J(X;U,V) = \sum_{i=1}^{C}\sum_{k=1}^{N} (\mu_{ik})^m d^2(x_k, v_i) \quad (3)$$

Where m: [1, ∞] is a weighting exponent that determines the fuzziness of the clusters (fuzziness parameter). If m=1 the sets are crisp not fuzzy. $d^2(x_k,v_i)$is the distance measurement.

The data are typically in geometric forms, such as lines or points. When points are used, the general form of the distance measurement between a point x_k and a cluster center v_i is given by:

$$d_{ik}^2 = (x_k - v_i)^T A_i (x_k - v_i) \quad (4)$$

When A_i=I, the measurement is based on the Euclidean distance and the clusters are with the spherical shape (traditional FCM or FCM).

When $A_i=F_i^{-1}$, the measurement is based on the Mahalanobis distance and the clusters are with the ellipsoidal shape where F_i is the Fuzzy Covariance Matrix of cluster *i*. The method is called GK FCM [4].

The objective of the FCM clustering is to find spherical clusters of approximately the same size. Its input is a data matrix X = (N, M) and the number of clusters C; its outputs are cluster centers V and fuzzy partition matrix U. Cluster centers V are initialized randomly.

The iterative procedure of the FCM algorithm is as follows,

1) *Compute distances from x_k to each clsuter center v_i:*

$$d_{ik}^2 = (x_k - v_i)^T (x_k - v_i) \quad (5)$$

2) *Compute partition matrix U (membership values):*

$$\mu = \frac{1}{\sum_{i=1}^{C} (d_{ik}^2 / d_{jk}^2)^{1/(m-1)}} \quad (6)$$

3) *Compute new cluster centers V based on U:*

$$v_i = \frac{\sum_{k=1}^{N} (\mu_{ik})^m x_k}{\sum_{k=1}^{N} (\mu_{ik})^m} \quad (7)$$

These three steps will be repeated until a criterion is satisfied, typically a pre-configured threshold is reached.

B. Gustafson-Kessel FCM clustering

The Gustafson-Kessel (GK) clustering algorithm [4] is commonly used in various domains including image processing, classification and system identification. Contrast to the FCM algorithm, its main feature is the local adaptation of the distance metric to the shape of the cluster. In addition, it is relatively insensitive to the data scaling and initialization of the partition matrix.

The objective of the GK FCM clustering is to find ellipsoidal clusters of approximately the same size. Its inputs and outputs are exactly same with traditional FCM except the distance function.

The iterative procedure of the GK FCM algorithm is the same as the traditional FCM, except that the distance computation uses Equation (4) instead of (5). A_i used in Equation (4) is defined as:

$$A_i = \left|F_i^{1/M}\right| F_i^{-1} \quad (8)$$

$$F_i = \frac{\sum_{k=1}^{N} (\mu_{ik})^m (x_k - v_i)^T (x_k - v_i)}{\sum_{k=1}^{N} (\mu_{ik})^m}$$

The procedure repeats the computations with the simultaneous change of cluster centers, membership values, and belongingness until a criterion is satisfied.

C. Modification to FCM clustering

The FCM has been shown to be an effective data clustering algorithm [13]. It is an iteratively optimal algorithm usually based on the least square method to make a fuzzy partition of the data set. The objective function of the traditional FCM is described in (3). However, it was found out that the modified linear distance, suggested by Bezdek [17], and as shown in (9) produced almost the same results in practice, with the clustering center values identical to those from the least square method [18].

$$J(X;U,V) = \sum_{i=1}^{C} \sum_{k=1}^{N} (\mu_{ik})^m d(x_k, v_i) \quad (9)$$

Additionally, in this paper, the linear distance measurement using City Block distance instead of Euclidean distance is adopted to reduce the computational overhead. City Block distance is calculated as:

$$d_{ik} = \left|x_k - v_i\right| \quad (10)$$

for a data point x_k and a cluster center v_i.

The proposed modifications to FCM reduce the complexity of the objective function from quadratic in (3) to linear in (9). Moreover, the complexity of the distance function also is reduced from quadratic plus square root calculations used in Euclidean distance to simply linear used for City Block distance, as shown in (10). The calculation is needed for each data point. Therefore, the total computation overhead for the entire dataset could be significant. The reduction of calculation time is vital for real-time P2P traffic applications, as the number of P2P flows could be huge and the response time needs to be very short.

V. SIMULATIONS AND COMPARISONS

The major role of FCM is to cluster data into different groups (classes or clusters). When the objects in the same clusters share more similar characteristics and the objects in different clusters are with more different features, the clustering result is considered to be better. Our experiments showed that the proposed method using simplified objective function and distance function can generate results and classification accuracy similar to that of the conventional FCM, while the method improves the computational speed. For the traditional FCM, the time complexity is $O(\mathrm{NDC}^2\mathrm{I})$, where N is the number of patterns and C is the number of clusters (see section IV), D stands for data dimensions, and I equals the number of iterations of calculations. The modified FCM has time complexity of $O(\mathrm{NDCI})$. With more emerging P2P applications, the complexity reduction from proportional of C^2 to C would greatly enhance the efficiency of this approach. As a result, the proposed method has the potential to be used for online network traffic monitoring or pre-processing for network management [19].

The following two sub-sections demonstrate the results generated by traditional FCM and the modified FCM, respectively, for a comparison. The application of the proposed FCM to P2P traffic classification was then demonstrated.

A. Results of FCM clustering

The results produced by traditional FCM clustering are presented in Fig. 1. The quasi-random two-dimensional data, as depicted in Fig. 1(a), were used for demonstration. Fig. 1(b) shows the result for two clusters, while Fig. 1(c) present the result for three clusters. The black labels (×, ○, and Δ) in the figures are cluster centers.

The membership values of the data points to the cluster centers are shown in Fig. 2. The vertical axis illustrates the

membership values for data presented on the horizontal 2-dimensional plane. Fig. 2(a) presents the membership values for cluster 1 after those three clusters, as shown in Fig. 1(c), were generated; Fig. 2(b) is for cluster 2, and Fig. 2(c) is for cluster 3. Threshold values were to determine which cluster each data point belongs to.

B. Results of modified FCM

As stated in the previous section, this paper modifies the objective function from quadratic to linear, and changes the distance function from Euclidean distance to City Block. The modifications were implemented in Matlab by changing the related M-functions.

Using the same data as the FCM, the clustering results with three clusters for the modified FCM methods are shown in Fig. 3. In Fig. 3(a), only the objective function was changed from quadratic to linear; Fig. 3(b) only the distance function was altered from Euclidean to City Block; and Fig. 3(c) both the objective function and the distance function have been modified.

Compared with Fig.1(c) which depicts results generated from the traditional FCM, there is not much clustering difference. The cluster centers for the modified FCM remain unchanged, the belongingness of objects to clusters are almost the same as the traditional FCM. Only a few boundary points were grouped into different clusters. In addition, Fig. 3 also reveals that the difference between the variations (a), (b), and (c) is also small.

The experiments were used to study the feasibility of the proposed changes to FCM and to compare the results for both approaches. The results demonstrated that the proposed FCM is feasible from the clustering accuracy perspective; the next step is to apply the proposed FCM to P2P traffic classification.

C. P2P traffic classification using modified FCM clustering

We used the data captured in an empirical platform and extracted the features from traffic flows. Many features can be obtained directly from packet headers or their statistic characteristics such as average, min, max, and standard deviation. The dataset consists of 41 features. Some features are correlated with each other, while others are independent. Feature reduction was adapted to closely related features. Feature selection is crucial for clustering techniques. For P2P traffic clustering, after feature reduction, we grouped features into two categories: traffic flow and packet statistics.

From the traffic flow perspective, features that are essential for flow identification and flow characteristics include:

- number of packets sent for a flow
- number of packets received for a flow
- duration of the flow
- protocol
- source and destination ports (2 features)

From the perspective of packet statistics, we consider:

- total number of packets
- mean packet length
- mean payload length
- mean packet inter-arrival time the average sent packet size
- average received packet size
- variances of average sent packet size
- variances of average received packet size
- byte ratio of sent packets
- byte ratio of received packets

We examined those 15 features listed above and applied the clustering to the experimental data using those 15 features. We did not find significant clustering difference using the modified distance function from Euclidean to City Block and the changed objective function. This demonstrates that the proposed modifications to FCM would generate clusters that are comparable with those created with the traditional FCM. However, the computational speed has improved significantly.

On the other hand, when we used different feature combinations, we obtained apparently different clustering results, so feature selection can have direct impact not only on the efficiency for network traffic data clustering, but also clustering accuracy as well. This is also true for other clustering methods.

For Fuzzy clustering, the selection of the number of clusters is also crucial; otherwise the clustering results may be absurd. We applied the modified FCM on simulated P2P network traffic, as illustrated in Fig. 4 (a). The data consist of four simulated P2P traffic types: PPLive, BitTorrent, QQ, and Skype.

Fig. 4(b) shows the clustering results for four clusters, each representing one P2P traffic type. The results for four clusters were consistent for 8-10 experiments. Running the same data using the traditional FCM method generates similar results, i.e., there was no significant difference between the traditional and the modified approaches. This demonstrates that the modified FCM generates very comparable results to the traditional FCM.

On the other hand, the experiments also demonstrate that the selection of the number of clusters has a direct effect on the clustering outcome. For instance, Fig. 4(c) and 4(d) illustrate results of selecting five clusters for the simulated P2P traffic which has only four different traffic types: PPLive, BitTorrent, QQ, and Skype.

As presented in Fig. 4(c) and Fig. 4 (d), the results are very different if the number of clusters is set to five for the clustering process. Obtaining very different results using the same number of clusters is an indication that the number of clusters is incorrect or does not represent the actual data.

The effect of the number of clusters is further explained here. If Fig. 4(d) represents the actual traffic data and Fig. 4(b) is the results when we choose four clusters in the beginning of the clustering, then only the data in the yellow region of Fig. 4(d) would be misclassified. If Fig. 4(c) represents the actual traffic data and we obtain the results shown in Fig. 4(b) when four clusters are chosen, it means that more data have been misclassified. In both cases, the clustering errors are caused by

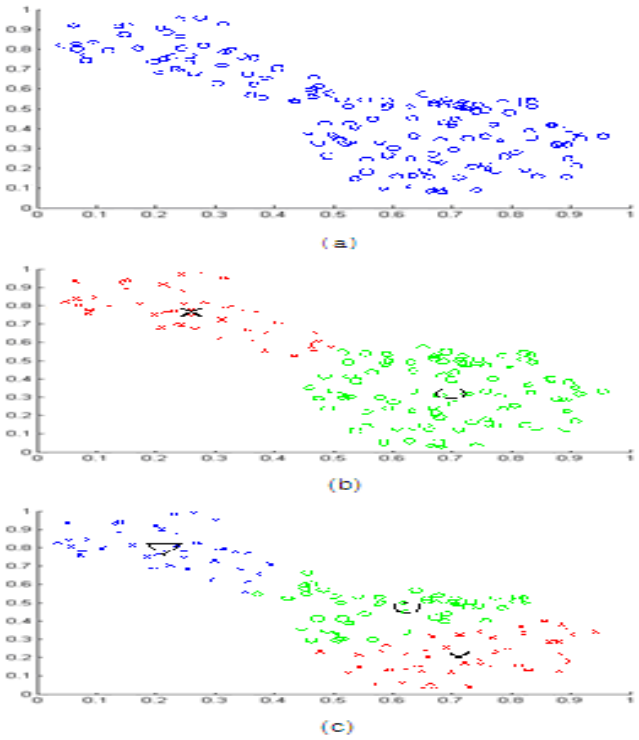

Figure 1. Clustering results of traditioal FCM: (a) quasi-random data to be clustered, (b) clustering result with 2 clusters, (c) clustering result with 3 clusters

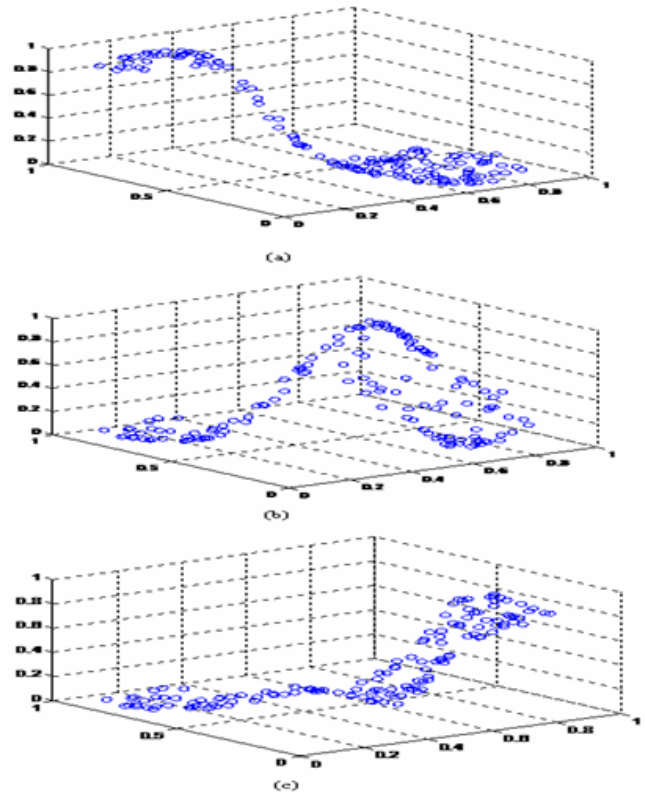

Figure 2. Membership values for: (a) cluster 1, (b) cluster 2, (c) cluster 3 after being grouped into 3 clusters

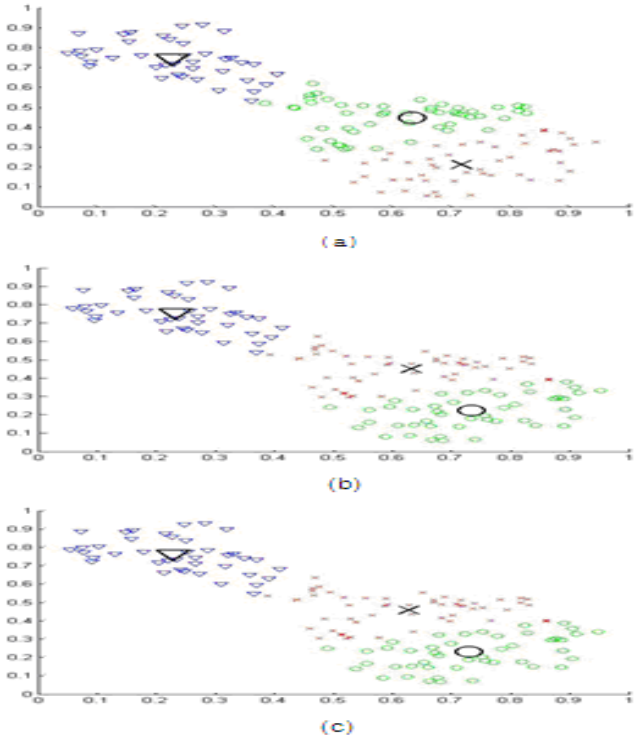

Figure 3. Clustering results of modified FCM: (a) modified objective function, (b) modified distance function, (c) modified objective and distance functions

the inappropriate selection of the number of clusters, which is crucial for FCM-based clustering.

If we obtain different results, e.g., results illustrated in Fig. 4(c) and Fig. 4(d), for different runs using the same number of clusters, cross-examination is needed. In this case, more data may be needed to validate the classification. Normally FCM does not generate reasonable or correct results if the number of clusters is wrong or inappropriate. We can also examine the membership values to determine if the clustering results should be accepted or rejected, or if more data are needed for verification.

In real-time classification for P2P traffic in which new applications are emerging, re-clustering is likely needed. With the modified FCM method, the speed is much faster than the traditional FCM, which is another important factor to consider for comparison for frequent re-clustering.

VI. CONCLUSIONS AND FUTURE WORK

The feasibility of automatic P2P traffic classification using machine learning techniques was explored in this paper. Classification accuracy and computational overhead are critical factors to consider for the high dimensional network traffic dataset. The fewer the features we select, the lower the computational overhead is with possibly lower accuracy. We compared different feature combinations for feature selection and reduced the feature set to 15 critical ones for analysis. Further, this paper modified the distance function from Euclidean (involving square and square root calculations) to City Block (linear calculations only) and changed the objective

function from quadratic to linear to decrease the computational complexity. Computational overhead is crucial for a large volume of real-time P2P traffic monitoring. With the proposed modifications to FCM, the efficiency is improved, while the results obtained from our data were very similar to the traditional FCM.

Performance estimation of the modified FCM clustering based on overall accuracy, precision, and recall can be conducted in the future. We are also working on getting real traffic data using tcpdump on campus for further investigation.

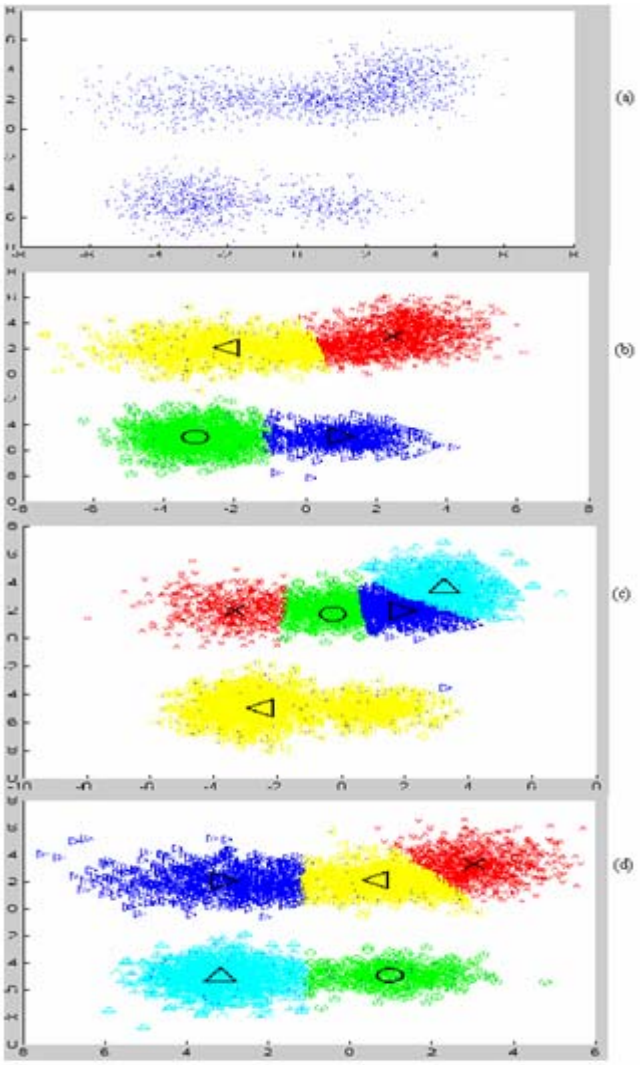

Figure 4. Simulated P2P traffic classification using modified FCM: (a) traffic data 2D visulization, (b) results for 4 clusters, (c)-(d) results for 5 clusters

REFERENCES

[1] T. T. Nguyen and G. Armitage, "A survey of techniques for Internet traffic classification using machine learning," IEEE Communications Surveys & Tutorials, vol. 10, no. 3, pp. 56–76, 2008.

[2] A. Callado, C. Kamienski, G. Szabo, B. P. Gero, J. Kelner, and D. Sadok, "A survey on Internet traffic identification," IEEE Communication Surveys & Tutorials, vol. 11, no. 3, pp. 37-52, 2009.

[3] J. Erman, M. Arlitt, and A. Mahanti, "Traffic classification using clustering algorithms," Proc. of SIGCOMM'06 Workshops, 2006.

[4] D. E. Gustafson and W. C. Kessel, "Fuzzy clustering with fuzzy covariance matrix," Proc. of IEEE CDC, pp.761-766, 1979.

[5] WIKIPEDIA, Traffic measurement (telecommunications), Dec. 2010, http://en.wikipedia.org/wiki/Traffic_measurement_(telecommunications)

[6] M. Crovella and B. Krishnamurty, Internet Measurement: Infrastructure, Traffic and Applications, Wiley, 2006.

[7] IANA, Port Numbers, http://www.iana.org/assignments/port-numbers

[8] P. Haffner, S. Sen, O. Spatscheck, and D. Wang, "ACAS: Automated construction of application signatures," Proc. of SIGCOMM'05 Workshops, 2005.

[9] S. Sen, O. Spatscheck, and D. Wang, "Accurate, scable in-network identification of P2P traffic using application signatures," Proc. of WWW 2004.

[10] S. Zander, T. Nguyen, and G. Armitage, "Automated traffic classification and application identification using machine learning," Proc. of the IEEE Conference on Local Computer Networks, 2005.

[11] Y. Liu, W. Li, and Y. Li, "Network traffic classification using K-means clustering," Proc. of the 2nd International Multisymposium on Computer and Computational Sciences, IEEE 2007.

[12] N. Williams, S. Zander, and G. Armitage, "A preliminary performance comparison of five machine learning algorithms for practical IP traffic flow classification," ACM SIGCOMM Computer Communication Review, vol. 36, no. 5, pp. 7-15, October, 2006.

[13] W. Pedrycz, Knowledge-Based Clustering, John Wiley & Sons. 2005.

[14] M. Ester, H. Kriegel, J. Sander, and X. Xu, "Adensite-based algorithm for discovering clusters in large spatial database with noise," Proc. of the 2nd International Conference on Knowledge Discovery and Data Mining (KDD), 1996.

[15] J. Erman, A. Mahanti, M. Arlitt, and C Williamson, "Semi-supervised network traffic classification," Proc. of SIGMETRICS'07, June 12-16, 2007.

[16] J. V. Oliveira and W. Pedrycz, Advances in Fuzzy Clustering and its Applications, John Wiley & Sons, 2007.

[17] J. C. Bezdek, "A convergence theorem for the fuzzy ISODATA clustering algorithms," IEEE Pattern Analysis and Machine Intelligence 2 (1), 1980.

[18] L. Ma, R.C. Staunton, "A modified fuzzy c-means image segmentation algorithm for use with uneven illumination patterns," Pattern Recognition, Vol. 40, 2007.

[19] V. S. Rao, "Comparative Investigations and Performance Analysis of FCM and MFPCM Algorithms on IRIS Dats," Indian Journal of Computer Science and Engineering, vol. 1, no. 2, pp. 145-151, 2010.

2011 IEEE International Conference on Fuzzy Systems
June 27-30, 2011, Taipei, Taiwan

Determination Of Process Conditions Of Epoxy Dispensing Processes Using A Genetic Algorithm Based Neural Fuzzy Networks

K.Y. Chan
Digital Ecosystems and Business Intelligence Institute,
Curtin University of Technology, Perth, Australia
kit.chan@curtin.edu.au

T.S. Dillon
Digital Ecosystems and Business Intelligence Institute,
Curtin University of Technology, Perth, Australia
Tharam.dillon@cbs.curtin.edu.au

S.H. Ling,
Department and Electrical and Electronic Engineering,
University of Technology, Sydney, Australia
Steve.Ling@uts.edu.au

C.K.. Kwong
Department of Industrial and Systems Engineering,
The Hong Kong Polytechnic University, Hong Kong
C.K.Kwong@inet.polyu.edu.hk

Abstract— **In this paper, process conditions of epoxy dispensing processes are determined by the proposed genetic algorithm based neural fuzzy networks, which consists of two tasks: a) the approach of neural fuzzy networks, which was shown to be better than the other existing approaches, is proposed to develop models in relating between process parameters and quality characteristics for the epoxy dispensing processes; b) the approach of genetic algorithm is used to determine process parameters with respect to pre-defined quality requirements based on the developed neural fuzzy network models. The results indicate that, based on the proposed genetic algorithm based neural fuzzy network, estimated process parameters can achieve specified requirements of microchip encapsulations with high and robust qualities.**

Keywords- Epoxy dispensing process, microchip encapsulation, neural fuzzy networks

I. INTRODUCTION

Epoxy dispensing is one of the most popular processes for microchip encapsulation on chip-on-board packages. In traditional semiconductor manufacturing, a trial-and-error method is usually used to identify proper process parameters setting so as to achieve the required quality characteristics. However, epoxy dispensing processes involve extremely complex inter-relationships among the fluid properties, process conditions, needle design parameters and overall encapsulation quality. Also cognitive uncertainties exist in the epoxy dispensing processes such as the human handling of substrate for measurement, insufficient data for process model development, and human judgment on qualities of the microchip encapsulation. Recently, various approaches have been attempted to model epoxy dispensing process including analytical approach [1], statistical regression [9], artificial neural networks [9] and fuzzy regression [7].

Statistical regression [14] is a commonly used empirical approach to develop manufacturing process models. However, statistical regression can only be applied if the given data are distributed along the developed statistical regression models, and the relationship between dependent and independent variables is crisp [2]. Artificial neural networks can transform a nonlinear mathematical model into simplified black-box structures for various manufacturing processes [10]. They can be used for modeling nonlinear, complex and noisy manufacturing processes, but they are not recommendable by engineering users, as the models developed are in black-box nature and no information can be obtained within the models. Unlike these two approaches which required certain amount of data to develop models, fuzzy regression [13] has a distinct advantage that it can develop models using incomplete data sets or smaller amount of data. However, linear fuzzy regression models, which can only address linearity but not address nonlinearity, can only be generated by the fuzzy regression approaches.

Neural fuzzy networks have been used to develop models for various manufacturing processes which are both nonlinear and complex [15, 11]. The approach has the capability to transform a nonlinear mathematical model into a simplified input-output structure. Kang et al. [8] have proved that neural fuzzy networks outperform statistical regression in modeling of highly nonlinear systems. Compared with conventional fuzzy logic modeling, neural fuzzy systems can achieve better performance in mathematical function approximations, while the same number of fuzzy sets is used in input variables [5].

In this paper, a genetic algorithm based neural fuzzy networks is proposed to determine process condition for epoxy dispensing process of microchip encapsulation. First the approach of neural fuzzy networks is used to model epoxy dispensing for microchip encapsulation based on a set of experimental data. Validation results show that the process models developed based on neural fuzzy networks outperform those developed based on statistical regression, neural network and fuzzy regression. The developed process models are then used to formulate an optimization problem, which aims at specifying the optimal process parameters for the required quality characteristics. The process optimization is performed

978-1-4244-7316-8/11/$26.00 ©2011 IEEE

by a genetic algorithm, which involves with the developed process models. The solutions of the optimization problem allow the optimal settings for the parameters of the epoxy dispensing process to be obtained. Validation tests are performed to evaluate the proposed approach to the modeling and optimization of the fluid dispensing process, and the results indicate that effective process parameter settings can be obtained that achieve the specified product quality requirements.

II. EPOXY DISPENSING PROCESS

In electronic packaging, normally, silicon chips are covered using an X-Y numerically controlled dispensing system that delivers epoxy encapsulant through a needle. The epoxy material is commonly dispensed in a pattern, working from the center out. A fluid dam around the die site and second wire bond points can be made to contain the flow of material and make a more uniform looking part as shown in Figure 1. The process is called the epoxy dispensing of microchip encapsulation. Two quality characteristics of encapsulation were also identified as

a) encapsulation weight (mg), *y*

b) encapsulation thickness (mm), *z*.

Three significant process parameters and their normal operating ranges were identified by the company supporting this research as:

c) the compressed air pressure (1 bar to 4 bar) x_1;

d) the pump motor speed (400 rpm to 1000 rpm), x_2;

e) the height between the substrate and the needle (250 to 2000 steps of stepping motor), x_3.

96 experiments were carried out based on a full factorial design with 4 levels in x_1, 6 levels in x_2 and 4 levels in x_3. 88 of the 96 experimental data were used to develop the model in relating the process parameters and the quality characteristics, and the rest 8 experimental data were used for the validation test.

To evaluate prediction accuracy of the process model, the mean error (Me) was used as defined below:

$$\text{Merror} = \frac{1}{n}\sum_{k=1}^{n}\frac{\left|t(k) - y(x(k))\right|}{t(k)} \qquad (1)$$

where $t(k)$ is the actual value of the quality requirement for the *k-th* experimental data; $y(x(k))$ is the estimated quality requirement with the recommended process parameters $x(k)$ obtained from the process model; n is the number of experimental data sets used for the validation tests.

The variance of errors (Var) was also involved in the validation as shown below:

$$\text{Var} = \frac{1}{n-1}\sum_{k=1}^{n}\left(\frac{\left|t(k) - y(x(k))\right|}{t(k)} - \text{Merror}\right)^2 \qquad (2)$$

III. MODELLING OF EPOXY DISPENSING USING NEURAL FUZZY NETWORK

Figure 2 shows the structure of a neural fuzzy network (NFN) which was used to develop models of the epoxy dispensing process in which the relationship between process parameters (x_1, x_2 and x_3) and the quality characteristics (y and z) is addressed. NFN consists of an input layer which feds in an input vector containing x_1, x_2 and x_3, and the output layer which produces the output response, y or z. Two hidden layers are connected between the input and output layers. The functions of the four layers of the NFN are described below:

Input layer: Each node in this layer which corresponds to a process parameter transmits input values to the next layer.

Hidden layer 1: Each node in this layer corresponds to one linguistic label (i.e. small, medium or large) with respect to x_1, x_2 and x_3. The membership value which specifies the degree to which an input value belongs to fuzzy set, is calculated in Layer 2. The j^{th} membership function of the input variable x_i is a bell-shaped function and is given by

$$A_{ij}(x_i) = e^{\frac{-(x_i - \bar{x}_{ij})^2}{2\sigma_{ij}^2}} \qquad (3)$$

where parameters $\bar{x}_{ij}$ and σ_{ij} with i=1,2,3 and j=1,2,3 are the mean value and the standard deviation of the j^{th} membership function of the input variable x_i respectively.

Hidden layer 2: The node in this layer represents one fuzzy logic rule and performs precondition matching of a rule. For instance, a fuzzy rule $R_{g_1g_2g_3}$ can be given as:

$R_{g_1g_2g_3}$: IF x_1 is $A_{1g_1}(x_1)$ AND x_2 is $A_{2g_2}(x_2)$ AND x_3 is $A_{3g_3}(x_3)$ THEN $y(x_1,x_2,x_3)$ is $\mu_{g_1g_2g_3}$,

where $\mu_{g_1g_2g_3}$ is an output singleton y of the rule $R_{g_1g_2g_3}$, and it can be represented as:

$$\mu_{g_1g_2g_3} = A_{1g_1}(x_1)\cdot A_{2g_2}(x_2)\cdot A_{3g_3}(x_3) \qquad (4)$$

As the number of membership functions of each input variable is 3 and the number of input variables is 3, the total number of fuzzy rules is 27 (i.e. 3^3).

Output layer: The nodes in this layer corresponds to the output variable y. The node integrates all the outputs of hidden layer 2 and it acts as a defuzzifier with defined in (5).

$$y(x_1,x_2,x_3)=\frac{1}{\sum_{g_1,g_2,g_3=1}^{3}\mu_{g_1,g_2,g_3}}\cdot \sum_{g_1,g_2,g_3=1}^{3}\mu_{g_1,g_2,g_3}\left(w_1^{g_1,g_2,g_3}x_1+w_2^{g_1,g_2,g_3}x_2+w_3^{g_1,g_2,g_3}x_3+w_0^{g_1,g_2,g_3}\right) \quad (5)$$

where the weights $w_0^{g_1,g_2,g_3}$, $w_1^{g_1,g_2,g_3}$, $w_2^{g_1,g_2,g_3}$ and $w_3^{g_1,g_2,g_3}$ with $g_1,g_2,g_3=1,2,3$ are the neural fuzzy parameters.

$w_0^{g_1,g_2,g_3}$, $w_1^{g_1,g_2,g_3}$, $w_2^{g_1,g_2,g_3}$ and $w_3^{g_1,g_2,g_3}$ with $g_1,g_2,g_3=1,2,3$ $\bar{x}_{ij}$ and σ_{ij} with *i*=1,2,3 and *j*=1,2,3 (namely NFN parameters) were searched by using a genetic algorithm (GA) [6]. The objective of the genetic algorithm is to minimize the training error of the NFN model by searching the NFN parameters setting. The fitness function is defined as:

$$fitness=\frac{1}{1+err} \quad (6)$$

where $err=\frac{1}{N}\sum_{\mathbf{x}=X}\frac{\left|y(\mathbf{x})-y^t(\mathbf{x})\right|}{y^t(\mathbf{x})}\times 100\%$; $\mathbf{x}=(x_1,x_2,x_3)$, $y^t(\mathbf{x})$ is the actual output, **X** is the domain of all the training data, and *N* is the total number of training data. The range of *fitness* in (6) is between 0 and 1.

The GA starts with a population of randomly generated chromosomes, while each chromosome is set to be a set of neural fuzzy parameters. The length of each chromosome is equal to the number of neural fuzzy parameters which is 45. Thereafter, the GA further processes a fixed number of generations using the evolutionary operations (i.e. selection, crossover and mutation). The selection is performed in two steps, chromosome selection and survival. The selection on chromosomes decides who parents become and how many children the parents have. The children are created through crossover which exchanges information between parents, and the mutation which further perturbs the children. The fitness of each child is then evaluated based on the fitness function (6). Finally, the survival step decides who survives in the population. After the operations of selection, crossover and mutation, a new population is generated. The chromosome with the highest fitness is selected to be the setting of the neural fuzzy parameters.

The following parameter values have been used in the GA for searching the neural fuzzy parameters; crossover rate = 0.8; mutation rate =1/45, where 45 is the length of the chromosome; number of generations = 1000; population size = 200. The GA were implemented using Matlab programming software. The training errors of the NFNs for the encapsulation weight and encapsulation thickness were found as 6.0263% and 5.2591% respectively.

Eight validation tests were carried out in order to evaluate the effectiveness of the developed NFN models in modelling the epoxy dispensing process. Table 1 shows the validation results are compared with those based on our previously developed statistical regression, artificial neural networks and fuzzy regression for modelling the epoxy dispensing process [9]. Row 1 and Row 3 show the comparisons of the mean testing errors for the encapsulation weight and thickness respectively. Row 2 and Row 4 show that the comparisons of the variances of the testing errors for the encapsulation weight and thickness respectively. It can be seen that the NFN based process models can achieve the smallest mean testing errors and the smallest variance of mean errors compared with other methods. Therefore the NFN based process models for encapsulation weight and thickness predictions were used to perform the process optimization of the epoxy dispensing.

IV. PROCESS OPTIMIZATION USING GENETIC ALGORITHM

Process optimization aims at determining a setting of the process parameters so as to achieve the required encapsulation weight (β mg) and encapsulation thickness (γ mm). To determine the process parameter setting, the following objective function is used:

$$Min\ \ \rho=\lambda_1\frac{|y-\beta|}{\beta}+\lambda_2\frac{|z-\gamma|}{\gamma} \quad (7)$$

subject to: $1\le x_1\le 4$, $400\le x_2\le 1000$ and $250\le x_3\le 2000$, where λ_1 and λ_2 are the weights of the two quality characteristics, encapsulation weight and encapsulation thickness respectively. As the two quality characteristics are supposed to be equal importance, $\lambda_1=\lambda_2=0.5$ were used.

Figure 3 shows a GA for determining process parameters setting for the epoxy dispensing, and it shows how the GA is interconnected to the NFN for modeling the epoxy dispensing process. The GA aims at minimizing the objective function (7) from which the optimal values of x_1, x_2 and x_3 can be obtained to achieve the required encapsulation weight β mg and encapsulation thickness γ mm. The main operations of the GA are described below.

A. Representation of strings

The first step of GA is to randomly generate strings which represent the population of GA. Real and binary encoding representations are two commonly used approaches for representing strings in GA. In binary encoding representation, strings need to be encoded to real values for fitness evaluation and also they need to be decoded again for reproduction operation. However, in real encoding representation, there is no need for string encoding and decoding, which would save a considerable amount of computational time and would lead to a much faster searching process than that of the binary encoding representation. Therefore, real encoding was adopted in GA, and each string contains three real values, which correspond to x_1, x_2 and x_3. The generated random values have the ranges associated with the operating ranges of the process parameters.

B. Fitness function

The objective function (7) was formulated to determine how close the randomly generated strings are to the required values of encapsulation weight (β mg) and encapsulation thickness (γ mm). Based on a string with the three process parameters, the quality measures of encapsulation weight y and encapsulation thickness z can be predicted by the NFN based process models. The fitness function of the GA is defined as follows:

$$\text{fitness} = \frac{1}{1+\text{error}} \tag{8}$$

where $\text{error} = \lambda_1 \frac{|y-\beta|}{\beta} + \lambda_2 \frac{|z-\gamma|}{\gamma}$.

Based on the fitness function (8), the fitness of a string with x_1, x_2 and x_3 can be evaluated. The objective is to maximize the fitness value of the fitness function (8) by searching the optimal x_1, x_2 and x_3.

C. Crossover operation

The intermediate crossover [12] for real encoding representation is used in the GA. It is a method of producing a new string around and between the process parameters of the two selected parent strings. The new string $\left[x_1^3, x_2^3, x_3^3\right]$ is produced based on the following formulation:

$$\left[x_1^3, x_2^3, x_3^3\right] = \left[x_1^2, x_2^2, x_3^2\right] \times \alpha \left\{\left[x_1^2, x_2^2, x_3^2\right] - \left[x_1^1, x_2^1, x_3^1\right]\right\} \tag{9}$$

where α is a scaling factor chosen uniformly at random over some interval typically $[-0.25, 1.25]$, and $\left[x_1^1, x_2^1, x_3^1\right]$ and $\left[x_1^2, x_2^2, x_3^2\right]$ are the two selected parent strings. The process parameters in the new string are the result of combining the values of the process parameters in the parent strings according to (9) with a scaling factor α chosen for each process parameter. In geometric terms, intermediate crossover is capable of producing new parameter values within a slightly larger hypercube than that defined by the parent strings but constrained by the range of the scaling factor α.

D. Mutation operation

Mutation is carried out by randomly changing one or more process parameter values of the selected string between its pre-defined upper and lower bound. The mutation operator of Gaussian perturbation of individual parameters is used. For example, the parameter x_j is selected to be mutated. After performing mutation, its value becomes:

$$x_j' = x_j + \text{MutMx} \times R_j \times \delta \tag{10}$$

where MutMx = +1 or -1 with equal probability; R_j = 0.5 × searching domain of the process parameter x_j; δ = a value in the range [0,1] for shrinking the mutation range based on Gaussian perturbation.

E. Selection of strings

The population is evolved and improved iteratively until a stopping condition is met. In evolutionary computation, there are several stopping conditions. In this GA, the stopping criterion is met when the number of generations is equal to a pre-defined number of generations. Otherwise, the population is evolved in the next generation. The approach of roulette-wheel, which is one of the most common selection methods used for selecting strings to perform reproduction operations [6], is used for strings selection in the GA. For example, the fitness of the j-th string in a population is assigned a value $fitness_j$. The fitness values are used to assign a probability value prob_j to the j-th string. The probability value prob_j is defined as:

$$\text{prob}_j = \frac{\text{fitness}_j}{\sum_{j=1}^{\text{Popsize}} \text{fitness}_j} \tag{10}$$

where Popsize is the population size of GA. Equation (10) shows that the string with a larger fitness value has higher probability to be selected. The updated population is produced by reinserting the new reproduced strings into the old population. It can be produced by replacing the least fitness strings in the old population with the new reproduced strings. However, pre-mature convergence likely occurs in early generations of evolution. To avoid the problem, random reinserting approach is used in the GA.

The population size, crossover rate and the mutation rate of the GA are set as 200, 0.8 and 0.001 respectively, which are suggested by DeJong [4]. The pre-defined number of generations is set at 1000. The GA toolbox coded in Matlab [3], which exists in the public domain, has been employed to search the process parameters of the epoxy dispensing process.

Eight validation tests were performed to evaluate the effectiveness of the GA. For each test, required values of encapsulation weight and thickness are input and it is expected that a setting of process parameters can be obtained from the optimization model. Table 2 shows the eight settings of process parameters recommended by the GA corresponding to the eight sets of quality requirements. The second and third columns show the required values of encapsulation weight and encapsulation thickness. The last three columns show the settings of the process parameters recommended by the GA.

V. CONCLUSION

In this paper, a genetic algorithm based neural fuzzy networks was proposed to determine process parameters setting of epoxy dispensing process for microchip encapsulation. 96 experiments based on a full factorial design were conducted in which the parameters of compressed air pressure, pump motor speed, distance between substrate and needle, and two quality characteristics, encapsulation weights and encapsulation thickness, are involved. 88 experimental data were used to develop the NFN based process models. 8 validation tests were carried out to evaluate the effectiveness and robustness of the process parameters settings recommended by the GA. The validation results indicate that, for each test, a setting of process parameters can be obtained to achieve the required quality requirement based on the proposed approaches.

Further work involves the validation of the searched process parameters obtained by the genetic algorithm based

neural fuzzy networks in a real world environment using experiments.

REFERENCES

[1] D.X. Chen, Modeling and off-line control of fluid dispensing for electronics packaging. PhD thesis, The University of Saskatchewan, 2002.

[2] Y. Chen, J. Tang, R.Y.K. Fung, and Z. Ren, "Fuzzy regression based mathematical programming for QFD", International Journal of Production Research, vol. 42, no. 5, pp. 3583-3604, 2004.

[3] A. J. Chipperfield, P.J. Fleming, H. Pohlheim, C.M. Fonseca, Genetic Algorithm Toolbox User's Guide. ACSE Research Report No. 512, University of Sheffield, 1994

[4] K.A. DeJong, An analysis of the behaviour of a class of genetic adaptive systems. PhD thesis, Department of Computer and Communication Science, University of Michigan, 1975.

[5] A. Fiordaliso, "A constrained Takagi-Sugeno fuzzy system that allows for better interpretation and analysis. Fuzzy Sets and Systems", vol. 118, pp. 307-318, 2001..

[6] D.E. Goldberg, Genetic Algorithms in Search, Optimization and Machine Learning. United States of America: Addison Wesley Longman, Inc, 1989.

[7] K.W. Ip, C.K. Kwong, H. Bai and Y.C. Tsim, "Process modelling of epoxy dispensing for microchip encapsulation using fuzzy linear regression with fuzzy intervals", International Journal of Advanced Manufacturing Technology, vol. 22, pp. 417–423, 2003.

[8] S.Y. Kang, H. Xie, and Y.C. Lee, "Physical and fuzzy logic modeling of a flip-chip thermocompression bonding process", Journal of Electronic Packaging, vol. 115, pp. 63–70, 1993.

[9] C.K. Kwong, K.Y. Chan and H. Wong, "An empirical approach to modeling fluid dispensing for electronic packaging", International Journal of Advanced Manufacturing Technology, vol. 34, pp. 111-121, 2007.

[10] H.L. Li and C.P. Chou., "Optimization of resistance spot welding process using Taguchi method and a neural network", Experimental Techniques, vol. 31, no. 5, pp. 30-36, 2007.

[11] C.H. Ling, F.H.F. Leung, H.K. Lam and P.K.S. Tam, "Short-term electric load forecasting based on a neural fuzzy network", IEEE Transactions on Industrial Electronics, vol. 50, no. 6, pp. 1305-1316, 2003.

[12] H. Muhlenbein and D.S. Voosen, "Predictive models for the breeder genetic algorithm: I. Continuous parameter optimization", Evolutionary Computation, vol. 1, no. 1, pp. 25-49, 1993.

[13] B. Schaible and Y.C. Lee, "Fuzzy Logic Based Regression Models for electronics manufacturing applications", Advances in Electronic Packaging, vol. 1, pp. 147-155, 1997.

[14] G.A.F. Seber, Linear regression analysis, Wiley, 2003.

[15] S. G. Tzafestas and K.C. Zikidis, "NeuroFAST: on-line neuro-fuzzy ART-based structure and parameter learning TSK model", IEEE Transactions on Systems, Man and Cybernetics—Part B: Cybernetics vol. 31, no. 5, pp. 797–802, 2001.

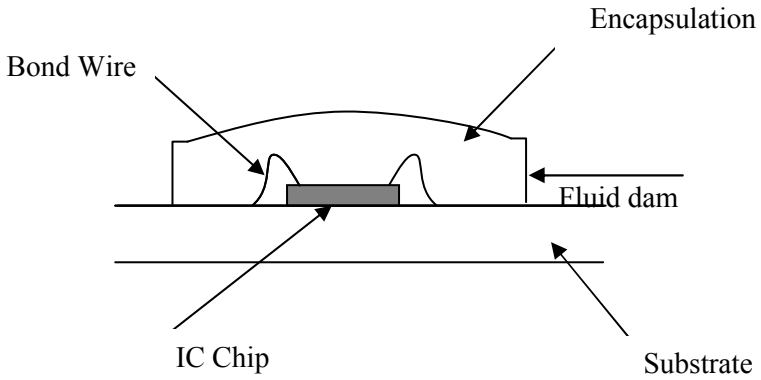

Figure 1 Encapsulation of IC chip using epoxy dispensing

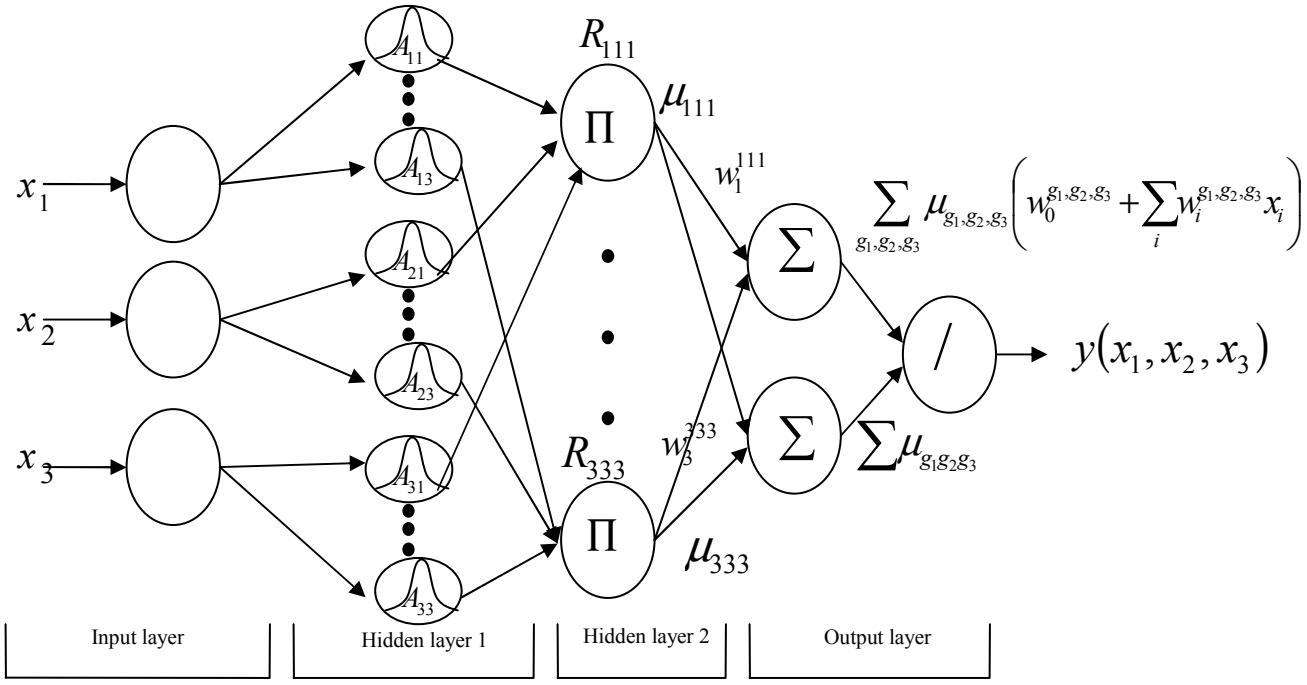

Figure 2 NFN based process model

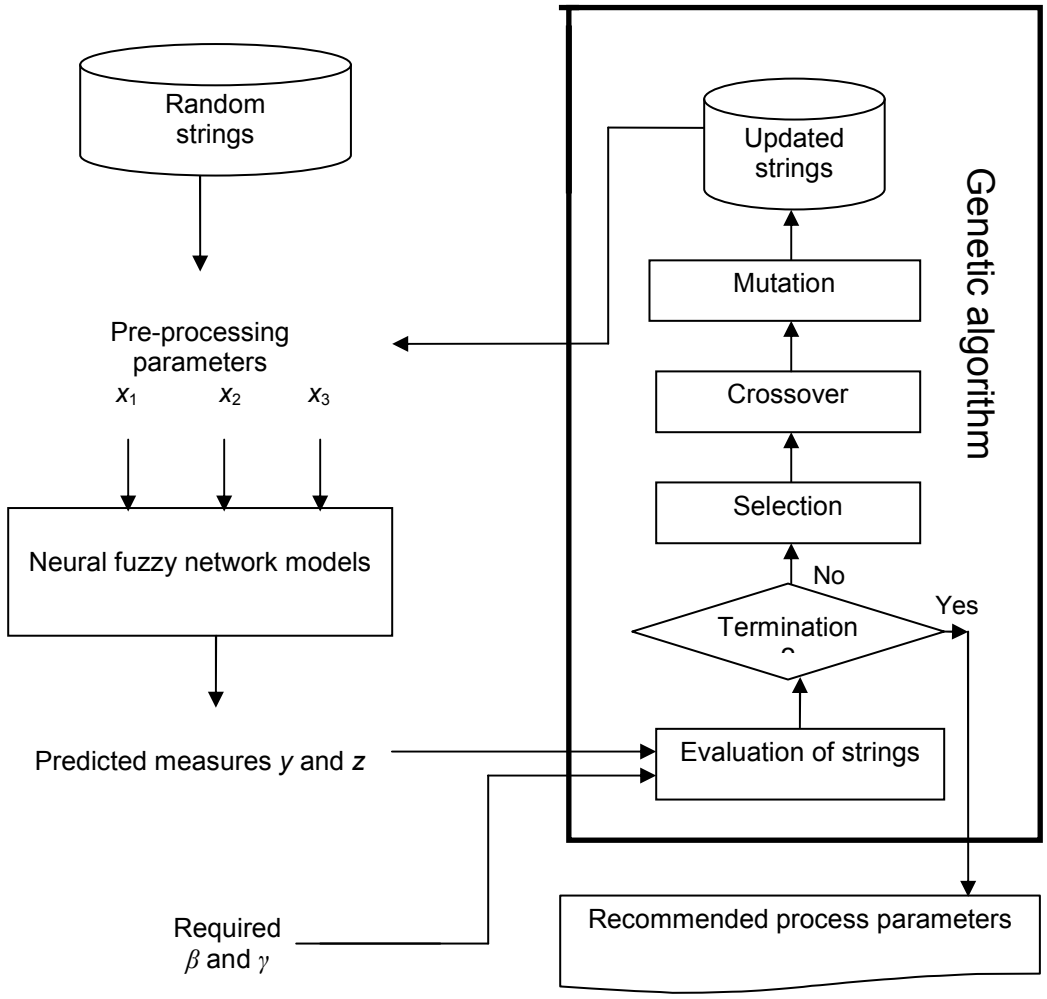

Figure 3 The genetic algorithm for determining optimal process parameters

Table 1 Mean testing errors and variances of testing errors for the various models

	Statistical regression model	Neural network model	Fuzzy regression model	TS neural fuzzy model
Encapsulation weight (mean)	5.3128	5.4532	6.5615	1.5409
Encapsulation weight (variance)	4.8835	3.8691	3.483	3.0637
Encapsulation thickness (mean)	5.3481	3.8271	18.4161	1.6947
Encapsulation thickness (variance)	20.318	4.7447	13.089	5.0879

Table 2 Recommended process conditions with respect to the pre-defined quality requirements

	Requirements of quality characteristics		**Recommended process condition**		
Validation test	***Weight*** β ***(mg)***	***Thickness*** γ ***(mm)***	x_3 ***(bar)***	x_2 ***(steps)***	x_3 ***(rpm)***
1	72.3	0.58	2.2275	250	561.71
2	43.2	0.48	1.0653	404.15	807.75
3	87.4	0.67	4	2000	666.38
4	37.2	0.46	1.0118	550.75	890.19
5	75.1	0.62	2.5239	2000	635.45
6	59.3	0.57	3.2162	1377.5	855.07
7	62.4	0.53	1.6594	250	613.77
8	53.1	0.53	1.4084	1099.4	734.5

2011 IEEE International Conference on Fuzzy Systems
June 27-30, 2011, Taipei, Taiwan

Manufacturing Modeling Using An Evolutionary Fuzzy Regression

K.Y. Chan
Digital Ecosystems and Business Intelligence Institute,
Curtin University of Technology, Perth, Australia
kit.chan@curtin.edu.au

T.S. Dillon
Digital Ecosystems and Business Intelligence Institute,
Curtin University of Technology, Perth, Australia
Tharam.dillon@cbs.curtin.edu.au

S.H. Ling,
Department and Electrical and Electronic Engineering,
University of Technology, Sydney, Australia
Steve.Ling@uts.edu.au

C.K.. Kwong
Department of Industrial and Systems Engineering,
The Hong Kong Polytechnic University, Hong Kong
C.K.Kwong@inet.polyu.edu.hk

Abstract— **Fuzzy regression is a commonly used approach for modeling manufacturing processes in which the availability of experimental data is limited. Fuzzy regression can address fuzzy nature of experimental data in which fuzziness is not avoidable while carrying experiments. However, fuzzy regression can only address linearity in manufacturing process systems, but nonlinearity, which is unavoidable in the process, cannot be addressed. In this paper, an evolutionary fuzzy regression which integrates the mechanism of a fuzzy regression and genetic programming is proposed to generate manufacturing process models. It intends to overcome the deficiency of the fuzzy regression, which cannot address nonlinearities in manufacturing processes. The evolutionary fuzzy regression uses genetic programming to generate the structural form of the manufacturing process model based on tree representation which can address both linearity and nonlinearities in manufacturing processes. Then it uses a fuzzy regression to determine outliers in experimental data sets. By using experimental data excluding the outliers, the fuzzy regression can determine fuzzy coefficients which indicate the contribution and fuzziness of each term in the structural form of the manufacturing process model. To evaluate the effectiveness of the evolutionary fuzzy regression, a case study regarding modeling of epoxy dispensing process is carried out.**

Keywords- fuzzy regression, manufacturing process modeling

I. INTRODUCTION

In manufacturing processes, process variables at each of the many processing steps in a manufacturing line need to be controlled, and all process variables related to the desired output need to be optimized to maintain tight control. Development of a manufacturing process model, which represents relationship between process variables and desired outputs, is essential.

While only a small amount of experimental data is available, fuzzy regression [1, 4, 10, 21-23] has the distinct advantage of being able to generate models in manufacturing process systems, which have a high degree of fuzziness. For examples, Schaiable and Lee used the fuzzy linear regression method to model the vertical CVD process [20]. Lai and Chang applied fuzzy regression to model the die casting process [1]. Ip et al. introduced the fuzzy linear regression to develop models for epoxy dispensing [8]. Three different approaches of fuzzy linear regression were summarized in Chang and Ayyub [2]. However, the existing fuzzy regression approaches cannot be used to develop manufacturing process models which are nonlinear in nature. In fact, nonlinear behaviors of manufacturing process commonly exist. If nonlinearities are integrated into the approach of fuzzy regression, more accurate models can be developed.

Furthermore, it is widely recognized that the quality of model development declines when outliers in experimental data exist, but very few studies have attempted to detect outliers when developing fuzzy regression models. Chen [6] proposed a method to detect outliers involving crisp inputs and fuzzy outputs. The method detects the difference in width between the spread of fuzzy data and the spread of fuzzy output. However, experimental data and the results of manufacturing processes involve crisp values of experimental settings and crisp values of experimental responses. Therefore, this method cannot be applied to manufacturing process modeling.

To overcome these deficiencies, we propose a genetic fuzzy regression, which can be used to generate manufacturing process models with nonlinear nature. The genetic fuzzy regression uses the general outcomes of genetic programming to construct models based on a tree structure representation in which both the interaction and higher order terms can be considered so as to address nonlinearity. Then it uses the mechanism of fuzzy regression to detect the outliers from experimental data sets based on an indicator of outliers. The fuzzy regression then estimates the contribution of each branch of the tree in order to determine the fuzzy coefficient of each term of the model by using the experimental data sets excluding the outliers. As nonlinear terms can be generated and represented in the branches of the tree based on the

978-1-4244-7316-8/11/$26.00 ©2011 IEEE

genetic fuzzy regression, nonlinear terms can be generated in the manufacturing process models. Furthermore, as the fuzzy regression is used to determine fuzzy coefficients of the manufacturing process model, only a small amount of data is required, which is practical in the manufacturing process.

The effectiveness of the proposed genetic fuzzy regression approach is evaluated by modeling the epoxy dispensing process for electronic packages, which is used in various electronic packaging processes such as integrated circuit (IC) encapsulation and die-bonding [16]. Epoxy dispensing is a highly non-linear process that involves extremely complex inter-relationships among the epoxy properties, process conditions and overall encapsulation quality [7]. The genetic fuzzy regression is used to develop models for this manufacturing process. Modeling results based on genetic fuzzy regression is compared with those based on the fuzzy linear regression methods of Tanaka [9] and Peters [8], which have been employed to model the epoxy dispensing processes.

II. GENETIC FUZZY REGRESSION

The genetic fuzzy regression approach generates the manufacturing process model which relates output responses and process variables in fuzzy regression form. When defining, the genetic fuzzy regression needs to:

a) specify the form of the manufacturing process model in fuzzy regression form
b) determine the fuzzy coefficients which characterize the model
c) define the algorithm of genetic fuzzy regression

A. Form of process model

The general form of the manufacturing process models, which involves nonlinear terms between process variables are represented as fuzzy regression form as follows:

$$\tilde{y} = \tilde{f}_0 + \sum_{i=1}^{N} \tilde{f}_i(x_i) + \sum_{i=1}^{N}\sum_{j=1}^{N} \tilde{f}_{ij}(x_i, x_j) + \ldots + \tilde{f}_{1,2,\ldots N}(x_1, x_2, \ldots x_N) \tag{1}$$

where $\tilde{y}$ is the output response, x_i is the i-th process variable, $\tilde{f}_0$ is a fuzzy bias term and $\tilde{f}_i(x_i)$, $\tilde{f}_{ij}(x_i, x_j)$, … represent univariate fuzzy components and bivariate fuzzy components respectively. A higher order high-dimensional Kolmogorov-Gabor polynomial is one of the forms of (1), which can be written as follows:

$$\tilde{y} = \tilde{f}_{NR}(x) = \tilde{A}_0 + \sum_{i_1=1}^{N} \tilde{A}_{i_1} x_{i_1} + \sum_{i_1=1}^{N}\sum_{i_2=1}^{N} \tilde{A}_{i_1 i_2} x_{i_1} x_{i_2} + \ldots + \sum_{i_1=1}^{N} \ldots \sum_{i_d=1}^{N} \tilde{A}_{i_1 \ldots i_d} \prod_{j=1}^{d} x_j \tag{2}$$

where $\tilde{A}_0 = (a_0^c, a_0^s)$, $\tilde{A}_1 = (a_1^c, a_1^s)$, $\tilde{A}_2 = (a_2^c, a_2^s)$, … $\tilde{A}_N = (a_N^c, a_N^s)$, $\tilde{A}_{11} = (a_{11}^c, a_{11}^s)$, $\tilde{A}_{12} = (a_{12}^c, a_{12}^s)$, … $\tilde{A}_{NN} = (a_{NN}^c, a_{NN}^s)$, … $\tilde{A}_{N\ldots N} = (a_{N\ldots N}^c, a_{N\ldots N}^s)$.

The fuzzy regression model (2) can be rewritten as follows:

$$\tilde{y} = \tilde{A}'_0 x'_0 + \tilde{A}'_1 x'_1 + \tilde{A}'_2 x'_2 \ldots \tilde{A}'_{N_{NR}} x'_{N_{NR}} \tag{3}$$

or $$\tilde{y} = (a_0^c{}', a_0^s{}')x'_0 + (a_1^c{}', a_1^s{}')x'_1 + (a_2^c{}', a_2^s{}')x'_2 + \ldots (a_{N_{NR}}^c{}', a_{N_{NR}}^s{}')x'_{N_{NR}} \tag{4}$$

where $1+N_{NR}$ is the number of terms of (1), (2) and (3); $\tilde{A}'_0 = \tilde{A}_0$, $\tilde{A}'_1 = \tilde{A}_1$, $\tilde{A}'_2 = \tilde{A}_2$, … $\tilde{A}'_{N_{NR}} = \tilde{A}_{N\ldots N}$; $x'_0 = 1$, $x'_1 = x_1$, $x'_2 = x_2$, … $x'_{N_{NR}} = x_1 \cdot x_2 \cdot \ldots x_d$; and $\tilde{A}'_0 = (a_0^c{}', a_0^s{}')$, $\tilde{A}'_1 = (a_1^c{}', a_1^s{}')$, … $\tilde{A}'_{N_{NR}} = (a_{N_{NR}}^c{}', a_{N_{NR}}^s{}')$. $\tilde{A}'_i$ and x'_i are called the fuzzy coefficients and the transformed variables respectively, where i=0,1,2,…N_{NR}.

The vectors of the fuzzy coefficients are defined as follows:

$$\tilde{A}' = (\tilde{A}'_0, \tilde{A}'_1, \ldots \tilde{A}'_{N_{NR}}) = ((a_0^c{}', a_0^s{}'), (a_1^c{}', a_1^s{}'), \ldots (a_{N_{NR}}^c{}', a_{N_{NR}}^s{}')), \tag{5}$$

$$a^c{}' = (a_0^c{}', a_1^c{}', \ldots a_{N_{NR}}^c{}'), \tag{6}$$

and $$a^s{}' = (a_0^s{}', a_1^s{}', \ldots a_{N_{NR}}^s{}'). \tag{7}$$

The vector of the transformed variables is defined as follows:

$$x' = (x'_0, x'_1, x'_2, \ldots x'_{N_{NR}}). \tag{8}$$

Using the vectors of the fuzzy coefficients and the vector of the transformed variables, (3) can be rewritten as follows:

$$\tilde{y} = \tilde{A}' \cdot x'^T \tag{9}$$

B. Determination of fuzzy coefficients

The fuzzy regression is proposed to determine the fuzzy coefficients of the manufacturing process models which are structured in the form of (4). Based on Peters' fuzzy regression [19], the fuzzy coefficients of the manufacturing process model are determined by solving the linear programming (LP) problem formulated as (10a) to (10f):

$$\max \bar{\lambda} = \frac{1}{M} \sum_{i=1}^{M} \lambda_i \tag{10a}$$

$$\text{s.t. } (1 - \bar{\lambda}) p_0 - \sum_{i=1}^{M}\sum_{j=0}^{N} a_j^S{}' |x_{ij}| \geq -d_0 \tag{10b}$$

$$(1 - \lambda_i) p_i - \sum_{j=0}^{N} a_j^c{}' x_{ij} - \sum_{j=0}^{N} a_j^S{}' |x_{ij}| \leq y_i, i = 1,2,\ldots,M \tag{10c}$$

$$(1 - \lambda_i) p_i + \sum_{j=0}^{N} a_j^c{}' x_{ij} + \sum_{j=0}^{N} a_j^S{}' |x_{ij}| \geq y_i, i = 1,2,\ldots,M \tag{10d}$$

$$\lambda_i \leq 1, \; i=1,2,\ldots,M \tag{10e}$$

$$a_j^S{}' \geq 0, j = 0,1,\ldots,N_{NS} \tag{10f}$$

where d_0 represents the desired value of the objective function, p_0 is the tolerance of the desired lower bound and p_i is the width of the tolerance interval of y_i. $\bar{\lambda}$ is the arithmetic mean of all λ_i. The parameters p_0 and p_i are determined in a context-dependent way according to the decision maker's experience and knowledge. A very low value of the special λ_i

)

in a Peters' fuzzy linear regression model indicates that the corresponding data set y_i is far outside the interval and can be treated as an outlier. Therefore λ_i (i=1,2,…,M) can be employed to determine whether or not the ith data set is an outlier [11]. With a threshold value of λ_0, the y_i is defined as an outlier if $\lambda_i \le \lambda_0$ for i=1,2,…,M, and the outliers are removed one by one from the training data sets during the process of developing manufacturing process models. The pseudocode of the fuzzy regression is shown below:

Determine the values of d_0, p_0 and p_i;
Select an appropriate threshold value λ_0;
Solve the LP problem (10a)-(10f) using the 1-st to the M-th data sets;
While ($\min_{i=1,...M} \lambda_i \le \lambda_0$) **do {**
Solve the LP problem (10a)-(10f) using the 1-st to the M-th data sets excluding the k–th data set;
// where λ_k is the small one among all the λ_i with i=1, 2, …M;
Remove the k-th data set from the M data sets
M=M-1;
}
Return the final fuzzy coefficients

In the fuzzy regression, the first step is to determine the values of d_0, p_0 and p_i [19], which can be used to control the spread of the interval of the fuzzy regression model. A threshold value λ_0 is then defined as follows:

$$\lambda_0 = \frac{1}{2}\left(\max_{i=1,...,M} \lambda_i + \min_{i=1,...,M} \lambda_i\right) \qquad (11)$$

where $\max_{i=1,...,M} \lambda_i$ and $\min_{i=1,...,M} \lambda_i$ are calculated using all the data sets. In the while-loop of the fuzzy regression, all λ_i with i = 1,2, …M, are found by solving the linear programming problem (10a)-(10f). If all λ_i are larger than λ_0, the fuzzy coefficients are returned as the final solution, and the fuzzy regression is terminated. Otherwise, the LP problem (10a)-(10f) is solved by excluding the k-th data set, where λ_k are the smallest among all the λ_i with i=1,…M. The k-th data set is then removed from the M data sets, and the number of data sets becomes M-1. The operations in the while-loop continues until all λ_i with i=1,…M are larger than λ_0.

In the fuzzy regression, the dependent data belongs to a certain range based on the mechanism of Peters' fuzzy regression [19]. Outliers are compensated for by data that lies within the interval, and the estimated interval is determined by using all of the data rather than using only the "worst" data. Therefore a new variable is introduced to represent the degree to which the solution belongs to the set of "good solutions" (i.e. degree of membership).

Since some terms in (1) may be redundant, prudent selection of significant terms or orders is advisable if a more economical and adequate model is desired. In the intelligent fuzzy regression approach, genetic programming is used to generate the fuzzy regression model which consists of significant terms.

C. Pseudocode of Evolutionary Fuzzy Regression

Genetic programming is proposed to determine the structures of process models in the evolutionary fuzzy regression, and its pseudocode is shown as follows.

t=0
Initialize $\Omega(t)$=[$\theta_1(t)$, $\theta_2(t)$,… $\theta_{POP}(t)$]
Assign fuzzy coefficients to all $\theta_i(t)$
// $\Omega(t)$ is the population of the t-th generation.
// $\theta_i(t)$ is the i-th individual of $\Omega(t)$.
Evaluate all $\theta_i(t)$ according to a fitness function
while (termination condition not fulfilled) **do {**
Parent Selection $\Omega(t$+1)
Crossover $\Omega(t$+1)
Mutation $\Omega(t$+1)
Determine fuzzy coefficients in all $\theta_i(t$+1) by using
Fuzzy regression discussed in Section 2B
Evaluate all $\theta_i(t$+1)
$\Omega(t)$= $\Omega(t$+1)
t=t+1
}

The evolutionary fuzzy regression begins by creating a random initial population $\Omega(t)$ with POP individuals $\theta_i(t)$, while t=0. Each individual $\theta_i(t)$ is in the form of a tree structure [12, 13], which can be used to represent the structure of the manufacturing process model as defined in (4). Hierarchical trees are composed of functions F and terminals T [12, 13]. The manufacturing process model (4) contains only the three arithmetic operations, +, - and *, thus F is represented as F = {+, -, *}. The set of terminals is defined as T = { x_1, x_2, … x_N}. In the tree, operations from the function set F are used as internal nodes, and arguments from the terminal set T are used as terminal nodes. For example, a hierarchical tree can be expressed as:

(x_1*x_1) - (x_2*x_2) + $(x_1*x_2*x_4)$

which is equivalent to:

$x_1^2 - x_2^2 + x_1 x_2 x_4$

The fuzzy regression as described in Section IIB is used to assign the fuzzy coefficients to each individual $\theta_i(t)$. All individuals are evaluated according to a defined fitness function, which is aimed at evaluating the goodness-of-fitness of the manufacturing process model. The mean absolute error (MAE) of the *j-th* individual can be calculated based on (12).

$$MAE_j = 100\% \times \sqrt{\frac{1}{M}\sum_{k=1}^{M}\left|\frac{y_k - F_j(\mathbf{x_k})}{y_k}\right|}, \qquad (12)$$

where F_j is the fuzzy regression model represented by the *j-th* individual, $(y_k, \mathbf{x_k}) = (y_k, (x_{k1}, x_{k2}, ...x_{kN}))$ is the *k-th* training data set which excludes the outliers detected by the fuzzy regression, and M is the number of training data sets excluding the outliers used to develop the manufacturing process model.

(12) is commonly known as an indicator of training error in a model. It reflects how well the model fits the training data sets. However, a model may contain many unnecessary and complex terms. A complex over-parameterized model with a large number of parametrical terms reduces the transparency

and interpretation of the model. To prevent the evolutionary fuzzy regression from generating models that are too complex, a fitness function is designed to balance the trade-off between the reduction of complexity and the model accuracy. In this paper, penalty terms are introduced into the fitness function of the evolutionary fuzzy regressions [17]. The fitness of the *j-th* individual is denoted as follows:

$$fitness_j = \frac{1 - MAE_j}{\left(1 + \exp\left(c_1\left(L_j - c_2\right)\right)\right)} \quad (13)$$

where $fitness_j$ is the fitness value, L_j is the number of nodes of the *j-th* individual, and c_1 and c_2 are both penalty terms.

The parent selection process then uses the goodness-of-fitness of each individual to determine the selection of potential individuals to perform crossover or mutation. Finally, the new individuals with the determined fuzzy coefficients are evaluated using the fitness function to create a new population $\Omega(t+1)$. The process continues until the pre-defined termination condition has been fulfilled.

III. EVALUATION OF GENETIC FUZZY REGRESSION

In this section, the evaluation of the performance of the proposed evolutionary fuzzy regression is illustrated by modeling a fluid dispensing process [34] for the encapsulation of IC chips for electronic packages. The modeling results are compared with those based on Tanaka and Watada's fuzzy regression (FR-Tanaka) [43] and Peters' fuzzy regression (FR-Peters) [36]. All the algorithms, GP-FR, FR-Tanaka and FR-Peters were implemented using Matlab. The GP parameters in evolutionary fuzzy regression are shown as follows: population size =50; maximum number of evaluated individuals =5000; generation gap = 0.9; probability of crossover = 0.5; probability of mutation = 0.5.

Epoxy dispensing is a common process for performing the encapsulation of IC chips for electronic packages [15]. Modeling the epoxy dispensing process is critical to understanding the behavior of the process and to achieving optimization of the process. However, the epoxy dispensing process is difficult to characterize due to the complex behavior of the epoxy encapsulant and the existence of uncertainties inherent to epoxy dispensing systems [3, 5, 7]. In the following, the modeling of epoxy dispensing for IC chip encapsulation is described. In the epoxy dispensing machines for IC chip encapsulation, normally, silicon chips are covered using an X-Y numerically controlled dispensing system that delivers epoxy encapsulant through a needle by a pump. The material is commonly dispensed in a pattern, working from the center out. An epoxy dam around the die site and the second wire bond points can be made to contain the flow of material and produce a uniform-looking part as shown in Figure 1 in the appendix.

The epoxy dispenser consists of three essential parts, the syringe with epoxy, the time-pressure dispensing machine and the nozzle's head. The epoxy was injected from the syringe vertically by the time-pressure dispensing machine. The dropped epoxy paste was collected horizontally on the grinded plastic block. To minimize the discrepancies of the experiments, the vertical distance between the syringe and glass slides was kept identically at 1.5cm in all the experiments. The quality characteristic, encapsulation weight (mg), was investigated. The weights of the epoxy pastes were measured by a precise electronic weighing instrument.

With the assistance of the company supporting this research, three process parameters, which are significant to the encapsulation weight *y*, were identified as follows:

- the dispensing time (5s to 9s), x_1 , which is the duration of the air pressure controlled by the time-pressure dispensing machine;
- the compressed air pressure (0.4Mpa to 0.6Mpa), x_2 which is the amount of pressurized air compressed by the time-pressure dispensing machine; and
- the diameters of the nozzle head (0.61mm , 0.84 mm or 0.137 mm), x_3 .

Fifty-four experiments were carried out based on a 3^k full factorial design with 2. In the factorial design, 3 levels of dispensing time (x_1), 3 levels of compressed air pressure (x_2) and 3 levels of nozzle head diameters of (x_3) were adopted. Forty-eight out of the fifty-four experimental data sets and results were used to develop the process models of the epoxy dispensing process while the remaining seven were used to test the developed models. The outliers were included in all the training data sets. The 1st, 18th, 28th and 45th data sets were considered outliers in modeling the encapsulation weight. Both the training and testing data sets of the epoxy dispensing process are shown in Table 1 in the appendix.

Using the 47 training data sets for the encapsulation weight as shown in Table 4, the manufacturing process model for encapsulation weight as determined by FR-Tanaka is as follows:

$$y = (-0.70,-0.00) + (0.24,-0.00) \cdot x_1 + (0.03,0.16) \cdot x_2 + (0.63,0) \cdot x_3 \quad (14)$$

The manufacturing process model for encapsulation weight found by FR-Peters is as follows:

$$y = (-0.54, 0.15) + (0.20, 0.87) \cdot x_1 + (0.01,0.14) \cdot x_2 + (0.55,0.56) \cdot x_3 \quad (15)$$

Using the same experimental data sets shown in Table 4, the model for the encapsulation weight found by the GP-FR is shown as follows:

$$y = (-0.03,1.42) + (0.06, 0.01) \cdot x_1 \cdot x_2 \cdot x_3^4 \quad (16)$$

It can be found that only linear terms can be generated by the FR-Tanaka and FR-Peters, and the higher order and interaction terms of the process models can be generated by the proposed evolutionary fuzzy regression. Therefore nonlinearity can be addressed by the manufacturing process models generated the proposed evolutionary fuzzy regression. To evaluate the effectiveness of the three fuzzy regression methods, 6 validation tests were conducted. Tables 2 show the results of the validation tests yielded by the developed models for the epoxy dispensing process. From the table, it can be found that the smallest errors can be obtained by the proposed evolutionary fuzzy regression rather than the other two methods in all the validation tests of both models of the

encapsulation weight. In addition, the mean errors and variances of errors obtained by the evolutionary fuzzy regression are the smallest.

IV. CONCLUSION

In this paper, an evolutionary fuzzy regression approach which integrates the mechanisms of genetic programming and fuzzy regression is proposed for modeling manufacturing processes. The proposed evolutionary fuzzy regression intends to compensate the limitation of the traditional fuzzy regression which can only address linearity in manufacturing systems but cannot address nonlinearity. Apart from this, the proposed evolutionary fuzzy regression approach can also be used to detect outliers from data sets such that models with better capability of prediction can be developed. To evaluate the effectiveness of the proposed evolutionary fuzzy regression approach, the evolutionary fuzzy regression, FR-Tanaka and FR-Peters were all applied to model the epoxy-dispensing process in which outliers exist in the data sets. Modeling results based on the three approaches were compared. The results indicate that the smallest prediction errors and errors in variance can be achieved by evolutionary fuzzy regression than by the commonly used fuzzy regression methods, FR-Peters, and FR-Tanaka. The achievement of better results can be explained by the introduction of nonlinear terms in the manufacturing process models developed based on evolutionary fuzzy regression, and the exclusion of outliers.

REFERENCES

[1] Celikyilmaz A. and Turksen B., Fuzzy functions with support vector machines, Information Sciences, vol. 177, pp. 5163-5177, 2007.

[2] Chang Y.H.O. and Ayyub B.M., Fuzzy regression methods – a comparative assessment, Fuzzy Sets and Systems, vol. 119, pp. 187-203, 2001.

[3] Chen D.X., Modeling and off-line control of fluid dispensing for electronics packaging. PhD thesis, The University of Saskatchewan, 2002.

[4] Chen S.P. and Dang J.F. A variable spread fuzzy linear regression model with higher explanatory power and forecasting accuracy, Information Sciences, vol. 178, pp. 3973-3988, 2008.

[5] Chen X.B. and Ke H., Effect of fluid properties on dispensing processes for electronic packaging, IEEE Transactions on Electronic Packaging Manufacturing, vol. 29, no. 2, pp. 75-82, 2006.

[6] Chen Y.S. Outliers detection and confidence interval modification in fuzzy regression, Fuzzy sets and systems, vol. 119, pp. 259-272, 2001.

[7] Hong Y.P. and Li H.X., Comparative study of fluid dispensing modeling. IEEE Transactions of Electronic Packaging Manufacturing, vol. 26, no. 4, pp. 273-280, 2003.

[8] Ip C.K.W, Kwong C.K., Bai H. and Tsim Y.C., The process modeling of epoxy dispensing for microchip encapsulation using fuzzy linear regression with fuzzy intervals, International Journal of Advanced Manufacturing Technology, vol. 22, pp. 417-423, 2003.

[9] Ip C.K.W., Kwong C.K. and Wong Y.W., Fuzzy regression approach to modeling transfer moulding for microchip encapsulation, Journal of Materials Processing Technology, vol. 140, pp. 147-151, 2003.

[10] Kim H.K., Yoon J.H. and Li Y., Asymptotic properties of least squares estimation with fuzzy observations, Information Sciences, vol. 178, pp. 439-451, 2008.

[11] Kwong C.K., Chen Y., Wong H., Modeling manufacturing processes using fuzzy regression with the detection of outliers, International Journal of Advanced Manufacturing Technologies, vol. 36, no. 5-6, pp. 547-557, 2008.

[12] Koza J., Genetic Programming: On the Programming of Computers by Means of Natural Evolution, MIT Press: Cambridge, 1992.

[13] Koza J., Genetic Programming II: automatic discovery of reusable programs, MIT Press, 1994.

[14] Lai Y.J. and Chang S.I., A fuzzy approach for Multiresponse optimization: an off-line quality engineering problem, Fuzzy Sets and Systems, vol. 63, pp. 117-129, 1994.

[15] Li H.X., Tso S.K. and Deng H., A concept approach to integrate design and control for the epoxy dispensing process, International Journal of Advanced Manufacturing Technology, vol. 17, pp. 677-682, 2001.

[16] Li H.L., Chou T. and Chou C.P., Optimization of resistance spot welding process using Taguchi method and a neural network, Experimental Techniques, vol. 31, no. 5, pp. 30-36, 2007.

[17] McKay B., Willis M.J., and Barton G.W., Steady-state modeling of chemical processes using genetic programming, Computers and Chemical Engineering, vol. 21, no. 9, pp. 981-996, 1997.

[18] Ng K.Y., Process modeling of epoxy dispensing, BEng Final Year Report, The Hong Kong Polytechnic University, April 2005.

[19] Peters G., Fuzzy linear regression with fuzzy intervals, Fuzzy Sets and Systems, vol. 63, pp. 45-55, 1994.

[20] Schaiable B. and Lee Y.C., Fuzzy logic based regression models for electronics manufacturing applications, Advances in Electronic Packaging, vol. 1, pp. 147-155, 1997.

[21] Takagi T. and Sugeno M., Fuzzy identification of systems and its application to modeling and control, IEEE Transactions on Systems, Man and Cybernetics, vol. 15, no. 1, pp. 116-132, 1985.

[22] Tanaka H., Uejima S. and Asai K., Linear regression analysis with fuzzy model, IEEE Transactions on Systems, Man, and Cybernetics, vol. 12, pp. 903-907, 1982.

[23] Tanaka H. and Watada J., Possibilistic linear systems and their application to the linear regression model, Fuzzy Sets and Systems, vol. 272, pp. 275-289, 1988.

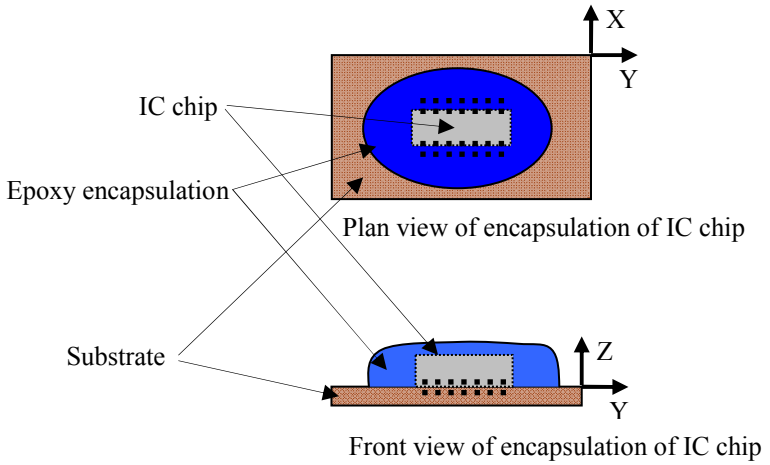

Figure 1 Encapsulation of IC chip

Table 1 Validation tests of the models of the encapsulation weight

Data set	Actual value	FR-Tanaka		FR-Peters		GP-FR	
		Predicted value	Abs error (%)	Predicted value	Abs error (%)	Predicted value	Abs error (%)
9	0.60	0.46	22.93	0.37	38.79	0.60	0.16
13	0.47	0.40	13.24	0.34	27.14	0.46	0.64
21	0.05	0.14	166.56	0.11	110.87	0.05	6.39
32	0.07	0.16	142.67	0.13	92.52	0.07	12.92
42	0.38	0.42	8.50	0.33	13.98	0.39	2.62
52	0.50	0.44	11.52	0.35	29.79	0.50	0.20
Mean relative error (%)		60.90		52.18		3.82	
Variance of relative errors (%)		5.35×10^3		1.57×10^3		25.50	

Table 2 Data sets for the epoxy dispensing system

Experimental data	Pressure (Mpa)	Dispensing time (sec)	Diameter of nozzle (mm)	Weight of epoxy (g)
1	0.5	5	1.19	0.278
2	0.4	9	1.19	0.383
3	0.6	7	0.61	0.025
4	0.5	5	0.61	0.015
5	0.4	9	0.61	0.023
6	0.5	9	0.84	0.075
7	0.6	5	0.84	0.045
8	0.4	7	0.84	0.05
9	0.5	9	0.61	0.022
10	0.6	5	0.61	0.019
11	0.4	5	0.84	0.033
12	0.5	7	0.84	0.066
13	0.6	9	0.84	0.096
14	0.4	5	1.19	0.215
15	0.5	7	1.19	0.405
16	0.6	9	1.19	0.612
17	0.6	7	0.84	0.075
18	0.5	5	0.84	0.046
19	0.4	9	0.84	0.06
20	0.6	7	1.19	0.4845
21	0.6	5	1.19	0.341
22	0.4	7	1.19	0.31
23	0.4	5	0.61	0.014
24	0.5	7	0.61	0.018
25	0.6	9	0.61	0.027
26	0.4	7	0.84	0.051
27	0.5	9	0.61	0.029
28	0.6	5	0.61	0.021
29	0.4	7	0.61	0.02
30	0.5	9	1.19	0.492
31	0.5	5	0.84	0.042
32	0.4	9	0.84	0.062
33	0.6	7	1.19	0.466
34	0.5	5	1.19	0.274
35	0.4	9	1.19	0.381
36	0.6	7	0.61	0.022
37	0.5	5	0.61	0.017
38	0.4	9	0.61	0.017
39	0.5	9	0.84	0.083
40	0.6	5	0.84	0.059
41	0.4	5	0.61	0.0075
42	0.5	7	0.61	0.022
43	0.6	9	0.61	0.027
44	0.4	5	0.84	0.038
45	0.5	7	0.84	0.064
46	0.6	9	0.84	0.1
47	0.4	5	1.19	0.214
48	0.5	7	1.19	0.381
49	0.6	9	1.19	0.602
50	0.6	7	0.84	0.078
51	0.6	5	1.19	0.337
52	0.4	7	1.19	0.298
53	0.4	7	0.61	0.018
54	0.5	9	1.19	0.497

2011 IEEE International Conference on Fuzzy Systems
June 27-30, 2011, Taipei, Taiwan

A Heuristic Search and its Roughness

Chun-Hung Tzeng
Computer Science Department
Ball State University
Muncie, Indiana 47306
Email: tzeng@bsu.edu

Fu-Shing Sun
Computer Science Department
Ball State University
Muncie, Indiana 47306
Email: fsun@bsu.edu

***Abstract*—This paper introduces an abstract model of heuristic search for handling uncertainty. In the search, heuristic information and evaluation are precisely defined mathematically. As special cases, the model includes a previous probabilistic game-tree search and a pattern search. This paper also considers the relationship between the model and the rough set approach. Each rough set formulation can be reformulated as a special case of the abstract model.**

***Index Terms*—Heuristic information, game-tree search, pattern recognition, tolerance relation, tolerance representative, rough set.**

I. Introduction

This paper reports a preliminary result of a recent study on uncertainty based on probability theory. The study of uncertainty often includes search and evaluation([7]). For the evaluation, the information returned by the search usually is incomplete. In this paper, the incomplete information is called heuristic information and the corresponding search is called a heuristic search. This paper introduces an abstract model of heuristic search. Special cases include a probabilistic game-tree search and a pattern search in a pattern recognition. This paper also considers the relationship between the abstract model and the rough set approach in handling uncertainty.

The rough set approach ([8]) of handling uncertainty can be interpreted as a task of classifying some objects in a universe of discourse, denoted by U. The information for U is usually provided by a set of attributes. An indiscernibility relation R is an equivalent relation on U, which is usually defined by a subset of attributes. Each R-equivalent class $[x]_R$ is an R-exact elementary set. Any subset $Y \subseteq U$ is R-exact if it is a union of R-exact elementary sets. Any subset $X \subseteq U$ which is not R-exact is R-rough. The R-lower and R-upper approximation of X are defined, respectively, as follows:

$$\begin{aligned} \underline{R}X &= \{\omega \in \Omega \mid [\omega]_R \subseteq X\}. \\ \overline{R}X &= \{\omega \in \Omega \mid [\omega]_R \cap X \neq \emptyset\}. \end{aligned}$$

The rough set is extended by use of a tolerance relation instead of an equivalent relation ([9]). A tolerance relation ([19]) is a reflexive and transitive binary relation on U.

For a game-tree search, the goal is to estimate the game values at certain nodes of the game tree. The information provided by a search is usually incomplete to determine the game values. Intuitively, a deeper search returns more precise information and the decision can be improved. However, there is a pathological phenomenon ([6]), in which the minimax algorithm may degrade the information provided by a static evaluation in a deeper search.

A probabilistic formulation of heuristic information in game-tree search has been introduced ([11], [12]). The goal of the game search is to estimate the game values at a certain nodes for a given game $\omega \in \Omega$. The set Ω of all possible games is a probability space. Let M be one of the game values, which is a random variable. A search returns a piece of information about ω, which is a subset X ($\subset \Omega$) containing ω. The theoretical evaluation of M is the conditional expectation $E_X(M)$. A deeper search returns more precise information about ω, which corresponds to a more accurate estimation of M. The actual algorithm depends on each individual game structure. The minimax algorithm does not compute $M_X(M)$ in general, even if M is the minimax value of a node.

Uncertain information also appears in a pattern recognition, which is to classify certain objects. For a given element ω, a two-class recognition problem can be formulated as a determination of the predicate $\omega \in X$, where X is the set of all elements of one class.

The classical probabilistic formulation of pattern recognition on a Euclidean space $\Re^n$ ([3]) is extended to general probability spaces ([14], [15], [16]). This approach uses a tolerance relation as a similarity. The heuristic information is generated by a non-crispy ([18]) representative data clustering which is defined by a set of representative elements. The cluster of a representative is the set of all similar elements to the representative. A conditional probability given a piece of heuristic information is used to estimate the pattern of the given element.

This paper introduces a general abstract model for heuristic search based on probability theory. A search task consists of a probability space $(\Omega, \mu, \mathcal{F})$ and a random variable M. The goal is to approximate the random variable M. A heuristic search is to find heuristic information I about a given element ω. The heuristic information I is a measurable set containing ω: $\omega \in I$. The set of all such possible I's forms a partition of Ω. The partition generates a Borel subfield $F \subseteq \mathcal{F}$. The evaluation of M is the conditional expectation $E_F(M)$.

The heuristic game-tree search and the pattern recognition mentioned above are special cases of this abstract model. Each rough set formulation can also be formulated in a special heuristic search model.

978-1-4244-7316-8/11/$26.00 ©2011 IEEE

The rest of this paper is organized as follows: Section 2 defines the abstract heuristic search model, using a game-tree search as an example. Section 3 discusses the relationship between this model and the rough set approach. Section 4 introduces a pattern recognition model by use of representative data clustering. Section 5 considers an example. The rough set properties in a representative data clustering are computed for different similarities in this section. Section 6 is the conclusion.

II. Heuristic Information and Evaluation

Based on probability theory, this section introduces a mathematical model for heuristic information and heuristic search. The heuristic information in a game-tree search ([11], [12]) and the heuristic search by use of representative coverings ([16]) are special cases.

Definition 2.1. A *search model* is a probability space with a random variable, denoted by $(\Omega, \mathcal{F}, \mu, M)$, where Ω is a sample space of all possible elements, $\mathcal{F}$ is a Borel field on Ω, μ is a probability measure on $\mathcal{F}$, and M is a random variable of the probability space $(\Omega, \mathcal{F}, \mu)$.

For simplicity, we assume that Ω is a finite set. Let $F \subseteq \mathcal{F}$ be any Borel subfield. A non-empty set $A \in F$ is F-minimal if there is no non-empty F-measurable set properly contained in A. Suppose that $P_F = \{I_1, .., I_n\}$ consists of all F-minimal sets. Then P_F forms a partition of Ω and any F-measurable set is a union of F-minimal sets.

Definition 2.2. A *heuristic search* of a search model $(\Omega, \mathcal{F}, \mu, M)$, is a pair (F, f) where F is a Borel subfield $F \subseteq \mathcal{F}$ and f is a function on Ω. For any given element $\omega \in \Omega$, f returns the F-minimal set I containing ω: $\omega \in I$. The function f is the *heuristic search function* and I is the *heuristic information* about the element ω.

In a heuristic search, we consider an evaluation of the random variable M.

Definition 2.3. The estimator of M, based on the heuristic search $S = (F, f)$, is the conditional expectation M_S of M with respective to F:

$$M_S = E_F(M). \tag{1}$$

The estimator is also a random variable. For any $\omega \in \Omega$, let $I = f(\omega)$, the heuristic information about ω. Then $M_S(\omega)$ is the conditional expectation of M relative to I:

$$M_S(\omega) = E_I(M) = \frac{1}{\mu(I)} \int_I M d\mu. \tag{2}$$

That is, M_S has a constant value in I, which is the average of M. Here we assume I has a positive measure.

Let $P_F = \{I_i \mid i = 1, ..., n\}$ be the partition corresponding to the heuristic search S. Then M_S is a linear combination:

$$M_S = \sum_i E_{I_i}(M) \mathbf{1}_{I_i}, \tag{3}$$

where $\mathbf{1}_{I_i}$ is the indicator function of I_i: $\mathbf{1}_{I_i}(\omega) = 1$ if $\omega \in I_i$, 0 otherwise.

Consider two heuristic searches $S_1 = (F_1, f_1)$ and $S_2 = (F_2, f_2)$. If F_1 is a subfield of F_2: $F_1 \subset F_2$, then we say that S_2 is *more precise* than S_1. In this case, each F_1-minimal set is a union of F_2-minimal sets. The corresponding estimators have the following property([2]).

Theorem 2.1. If S_2 is more precise than S_1, then the estimator M_{S_1} is also an estimator of M_{S_2}:

$$M_{S_1} = (M_{S_2})_{S_1}. \tag{4}$$

In each F_1-minimal set, the value of M_{S_1} is the average of M_{S_2}. That is, M_{S_2} is more accurate than M_{S_1} in estimating M.

To illustrate the idea of the heuristic information formulation, we consider a uniform binary game tree of four levels([11], [12]), where each terminal node has independently the value 1 (a win for MAX) or 0 (a loss for MAX) with a probability p $(0 < p < 1)$ and $1 - p$, respectively. The space $\Omega = \{0, 1\}^8$ of all leaf patterns forms a probability space. The game value at each internal node is the minimax value at that node, which is a random variable. We consider the task of estimating the minimax value at the root, denoted by M. Then the probability space Ω and M form a search model.

We consider two searches. First, consider the heuristic searches $S_1 = (F_1, f_1)$ where the function f_1 counts the number of 1's at the leaves under the root. The corresponding partition of F_1 consists of 9 members: $I_k = \{(x_1, .., x_8) \in \Omega \mid \sum_1^8 x_i = k\}$, $k = 0, 1, ..., 8$. For a given game $x' = (x'_1, .., x'_8)$, the heuristic information is I_k, where $k = \sum_1^8 x'_i$, based on which the estimation of M is the conditional probability:

$$M_{F_1}(x') = P(M = 1 \mid x' \in I_k).$$

The second heuristic search is $S_2 = (F_2, f_2)$. The function f_2 counts the numbers of 1's at the leaves under each of the two nodes of level 2. The Borel field F_2 is generated by the partition consisting of following 25 sets:

$$I_{ij} = \{(x_1, .., x_8) \in \Omega \mid \sum_1^4 x_k = i, \sum_5^8 x_k = j\}, 0 \le i, j \le 4.$$

For the given game $x' = (x'_1, .., x'_8)$, the heuristic information is I_{ij}, where $i = \sum_1^4 x'_k$ and $j = \sum_5^8 x'_j$, based on which the estimation of M is

$$M_{F_2}(x') = P(M = 1 \mid x' \in I_{ij}).$$

The search S_2 is more precise than S_1 because $I_k = \cup_{i+j=k} I_{ij}$ for each I_k in F_1. The both estimators have the following relation:

$$P(M = 1 \mid x' \in I_k) = \sum_{i+j=k} \mu(I_{ij}) P(M = 1 \mid x' \in I_{ij}).$$

III. Heuristic Search and Rough Set

This section shows that in a heuristic search any measurable set of probability space may be treated as a rough set ([8], [9]) . And each rough set formulation can be reformulated as a heuristic search.

Suppose that X is a measurable set in a given a probability space $(\Omega, \mathcal{F}, \mu)$. Let $M = \mathbf{1}_X$, the indicator of X, which is a random variable because X is measurable. Let $S = (F, f)$ be a heuristic search for the search model $(\Omega, \mathcal{F}, \mu, M)$. Consider the corresponding partition of Ω: $P_F = \{I_1, .., I_n\}$, which consists of all F-minimal sets. The partition defines an indiscernibility relation (also denoted by F) in the rough set terminology ([8], [9]), : two elements ω_1 and ω_2 are indiscernible if $f(\omega_1) = f(\omega_2)$; that is, for the two elements, the heuristic search returns the same heuristic information I_i: $\omega_1 \in I_i$ and $\omega_2 \in I_i$. Based on this indiscernibility relation, all F-exact elementary sets are those I_i's in P_F. The F-lower and F-upper approximations of X are, respectively,

$$\underline{F}X = \{\omega \in \Omega \mid M_F(\omega) = 1\} \tag{5}$$

$$\overline{F}X = \{\omega \in \Omega \mid M_F(\omega) > 0\} \tag{6}$$

That is, $\underline{F}X$ consists of all F-minimal sets contained in X and $\overline{F}X$ consists of all F-minimal sets which has a non-empty intersection with X and the intersection has a positive measure. If $\underline{F}X = \overline{F}X$, then X is F-exact. Any member in the Borel field F is F-exact.

Conversely, each rough set formulation ([8], [9]) can be treated as a special heuristic search. In a rough set formulation, let Ω be the universe of objects and R the equivalence relation on Ω. The R-exact elementary sets are the R-equivalence classes $[x]_R$, $x \in \Omega$. Any union of R-exact elementary sets is R-exact. Any set $X \subseteq \Omega$ which is not R-exact is R-rough. The lower and upper approximation of X are defined, respectively, as follows:

$$\underline{R}X = \{\omega \in \Omega \mid [\omega]_R \subseteq X\} \tag{7}$$

$$\overline{R}X = \{\omega \in \Omega \mid [\omega]_R \cap X \neq \emptyset\} \tag{8}$$

Consider the universe of objects (i.e., Ω) as a probability space, where the Borel field $\mathcal{F}$ is the set of all subsets of Ω and each object $\omega \in \Omega$ is measurable and has the same probability measure $\mu(\omega) = \frac{1}{|\Omega|}$. Then the indicator $M = \mathbf{1}_X$ of X is a random variable. For the search model $(\omega, \mathcal{F}, \mu, M)$, we consider the following heuristic search. Let F be the Borel field generated by the R-exact elementary sets. That is, the F-minimal sets are the R-exact elementary sets and the members of F are R-exact. The function $f(\omega) = [\omega]_R$ is a heuristic function. The lower and upper approximation of X are, respectively, $\underline{F}X = \{\omega \in \Omega \mid M_F(\omega) = 1\}$ and $\overline{F}X = \{\omega \in \Omega \mid M_F(\omega) > 0\}$. The estimator M_F at an element ω is the conditional probability $M_F(\omega) = P(\omega \in X \mid \omega \in [\omega]_R)$; that is, it is the rough membership function defined in ([9]):

$$M_F(\omega) = \mu(\omega, X) = \frac{|[\omega]_R \cap X|}{|[\omega]_R|}.$$

Therefore each rough set formulation is a special heuristic search for a search model.

IV. Heuristic Search Using Representatives

This section introduces a heuristic information computed by comparing an element with representatives. First, we consider a pattern recognition model on a probability space $(\Omega, \mathcal{F}, \mu)$, ([14], [15], [16]), which is an extension of the classical model ([3]).

A. Pattern Recognition and Classifiers

Pattern recognition is about guessing or predicting the unknown nature of an observation. Formally, we use ω to denote an observation and Ω to denote the space of all possible observations. For simplicity, we considers only two classes (e.g., normal and anomaly), denoted by 0 and 1.

We assume the observation is probabilistic. Consider the probability space $(\Omega, \mathcal{F}, \mu)$. Let (X, Y) be a random pair taking their respective values from Ω and $\{0, 1\}$. The random pair is defined by a pair (μ, η), where μ is the probability measure of X and η is the posterior probability, given the value of X. That is, for any $A \in \mathcal{F}$, $P(X \in A) = \mu(A)$, and for any $\omega \in \Omega$, $\eta(\omega) = P(Y = 1 \mid X \in [\omega]_{\mathcal{F}})$, where $[\omega]_{\mathcal{F}}$ is the $\mathcal{F}$-minimal set containing ω. Note that η is measurable (relative to $\mathcal{F}$) and the 4-tuple $(\Omega, \mathcal{F}, \mu, \eta)$ forms a search model defined in Section 1.

In pattern recognition, one creates a classifier $g : \Omega \to \{0, 1\}$ to represent one's guess of y, the class of a given observation ω. The classifier errs on ω when $g(\omega) \neq y$. We only consider measurable classifiers, which always assign indistinguishable observations (i.e., elements in the same $\mathcal{F}$-minimal set) to a same class.

Definition 4.1. A classifier on the search model $(\Omega, \mathcal{F}, \mu, \eta)$ is an F-measurable function $g : \Omega \to \{0, 1\}$, where $\{0, 1\}$ is treated as a discrete space.

The probability of error $L(g) = P(g(X) \neq Y)$ is the *error rate* of g:

$$L(g) = P(g(X) \neq Y) = \int_{\Omega} P(g(X) \neq Y | X \in [\omega]_{\mathcal{F}}) d\mu(\omega). \tag{9}$$

The *false positive rate* $L^{(0)}(g)$ and the *false negative rate* $L^{(1)}(g)$ are

$$L^{(0)}(g) = P(g(X) = 1 | Y = 0), \tag{10}$$

and

$$L^{(1)}(g) = P(g(X) = 0 | Y = 1). \tag{11}$$

The relation among the three types of error is

$$L(g) = L^{(0)}(g)P(Y = 0) + L^{(1)}(g)P(Y = 1).$$

Let $0 \leq \theta < 1$. The classifier g_θ is defined as follows

$$g_\theta(\omega) = \begin{cases} 1 \text{ if } \eta(\omega) > \theta, \\ 0 \text{ otherwise.} \end{cases} \tag{12}$$

Note that, if $\eta(\omega) \in \{0, 1\}$, then $L(g_\theta) = L^{(0)}(g_\theta) = L^{(1)}(g_\theta) = 0$ for $0 < \theta < 1$. The classifier $g_{0.5}$ is the *Bayes classifier* and $L(g_{0.5})$ is the *Bayes Error*. Similarly to the classical theory [3], we have following theorems.

Theorem 4.1. (Bayes) For any classifier g, $L(g_{0.5}) \leq L(g)$.

Theorem 4.2. (Neyman-Pearson) For any classifier g and θ $(0 < \theta < 1)$, if $L^{(0)}(g) \leq L^{(0)}(g_\theta)$, then $L^{(1)}(g) \geq L^{(1)}(g_\theta)$.

The Bayes classifier is an optimal classifier if we are required to minimize the error rate. If the false positive rate $L^{(0)}$ is required to be kept under a certain level, then g_θ minimizes the false negative rate $L^{(1)}$ for some θ.

B. Representative data clustering and heuristic information

First we consider a tolerance relation ξ on the search model $(\Omega, \mathcal{F}, \mu, \eta)$, which is a reflexive and symmetric binary relation; that is, $(\omega, \omega) \in \xi$ for any $\omega \in \Omega$, and $(\omega_1, \omega_2) \in \xi$ implies $(\omega_2, \omega_1) \in \xi$. A space with a tolerance relation is called a tolerance space.

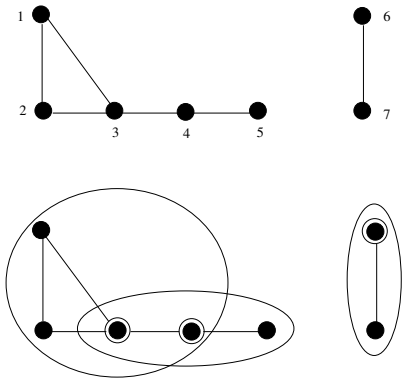

Fig. 1. A tolerance space and a minimal representative clustering.

We also use ξ as a predicate: $\xi(\omega_1, \omega_2)$ iff $(\omega_1, \omega_2) \in \xi$. If $\xi(\omega_1, \omega_2)$, we say that ω_1 is ξ-similar to ω_2, or ω_1 and ω_2 are ξ-similar. We may omit ξ when there is no ambiguity. Any undirected graph is a tolerance space (and vice versa), where Ω is the set of all vertices, and two vertices are similar if they are the same vertex or they are adjacent (e.g., Fig. 1).

For each $\omega \in \Omega$, the set $\xi(\omega) = \{u \in \Omega \mid \xi(\omega, u)\}$ is called the neighborhood of ω. Here we assume that each neighborhood is measurable (i.e., an element of $\mathcal{F}$). We consider a data clustering of the search model by use of the neighborhoods (e.g., [13], [15], [16]). Each $\omega \in \Omega$ is called a *representative* of its neighborhood $\xi(\omega)$. A set of elements $\{r_1, ..., r_k\}$ is a representative system of Ω if the corresponding neighborhoods cover the whole space Ω . The representative system is minimal ([4], [10]) if there is no other representative system with less than k members.

A representative system forms a clustering of Ω, in which the clusters are the corresponding neighborhoods. Note that each cluster is measurable. We call such a clustering a representative clustering. The clustering is in general not a partition (e.g., Fig. 1).

An element $\omega \in \Omega$ is called a *surprise* ([15], [16]) if ω is not similar to any other element in Ω; that is, $\xi(\omega) = \{\omega\}$. Therefore, each surprise is always in any representative system. Let the numbers of the surprises be denoted by α_ξ, which is independent of the choice of representative systems. The similarity ξ does not provide any pattern about surprises. In application, searching a similarity should eliminate or reduce the number of surprises.

Let $\mathbf{R}_\xi = \{r_1, ..., r_k\}$ be a minimal representative system. Let the neighborhoods of r_i's generate the Borel subfield D $(D \subseteq \mathcal{F})$, and the corresponding partition be $P_D = \{A_i \mid i = 1, ..., n\}$. For example, in Fig. 1 there are three representatives and the corresponding partition is $\{\{1, 2\}, \{3, 4\}, \{5\}, \{6, 7\}\}$. For an $\omega \in \Omega$, the member A_i containing ω, denoted by $f(\omega)$, is computed as follows. We compare ω with the k representatives. Let S_ω be the set of all representatives similar to ω and $N_\omega = \mathbf{R}_\xi - S_\omega$. Then

$$f(\omega) = A_i = \cap_{r \in S_\omega} \xi(r) - \cup_{r \in N_\omega} \xi(r). \tag{13}$$

The pair $S = (D, f)$ is a heuristic search for the search model $(\Omega, \mathcal{F}, \mu, \eta)$. The estimator of η is $\eta_D = E(\eta|D)$. Given ω, $\eta_D(\omega)$ is the conditional probability:

$$\eta_D(\omega) = \frac{1}{\mu(A_i)} \int_{A_i} \eta(t) d\mu(t) = P(Y = 1 | X \in A_i). \tag{14}$$

We define classifiers based on the heuristic search $S = (D, f)$. A *D-classifier* is a D-measurable function $g^D : \Omega \longrightarrow \{0, 1\}$. Note that g^D is constant on each A_i. As in Section 1, any *D-classifier* g^D is a linear combination of the indicators $\mathbf{1}_{A_i}$'s. Any D-classifier is also $\mathcal{F}$-measurable and hence a classifier on the search model $(\Omega, \mathcal{F}, \mu, \eta)$, but not vice versa.

For D-classifiers, we have following similar definitions and properties. The D-classifier $g^D_\theta = 1$ iff $\eta_D(x) > \theta$, $0 \leq \theta < 1$. The Bayes D-classifier $g^D_{0.5}$ minimizes the error rate of all $\mathcal{D}$-classifiers. The Neyman-Pearson Theorem is also true; that is, for any D-classifier g^D, if $L^{(0)}(g^D) \leq L^{(0)}(g^D_\theta)$, then $L^{(1)}(g^D) \geq L^{(1)}(g^D_\theta)$. Since the Bayes classifier $g_{0.5}$ minimizes the error rate, $L(g^D_{0.5}) \geq L(g_{0.5})$.

To search for a minimal representative system is intractable in general. A heuristic method to search for sub-minimal representative system has been introduced ([13], [14]).

C. Application in Supervised Learning

This subsection briefly summarizes an application of heuristic search in a supervised learning, which has been introduced in ([16]). Suppose a supervised learning process consists of two sets: a training data set and a testing data set. The goal of the process is to classify each element in the testing data set. We assume that there are two classes, 0 and 1. We treat the training data set as the space Ω. We assign each element in Ω the same probability measure $\frac{1}{|\Omega|}$ if there is no previously given probability. From the given class label in the training data set, the posterior probability η can be computed. That is, we formulate the training data set into a search model $(\Omega, \mathcal{F}, \mu, \eta)$, where $\mathcal{F}$ is the Borel field corresponding to the probability measure.

The training process is to search for a suitable similarity ξ (i.e., a tolerance relation) and to compute a sub-minimal representative system $\mathbf{R}_\xi$, which defines a heuristic search $S = (D, f)$. Based on $\mathbf{R}_\xi$ the estimator η_D is computed. Then the classifier g^D_θ $(0 \leq \theta < 1)$ is defined by use of η_D.

For each element ω in the testing data set, the heuristic information about ω in the training data set is computed by comparing ω with the representatives, as discussed above. Then we use the value of η_D on the searched heuristic information as an evaluation of the element: $\eta_D(\omega)$. Based on this evaluation, each classifier g_θ^D is extended to the testing data set. If ω is an unknown surprise (i.e, not similar to any representative), then the evaluation is not defined. In this case, ω may be evaluated by the distribution of surprises in the training data set.

The training result can be studied by use of different type of errors and the receiver operating characteristic analysis ([5]). In the training process, the Bayes error $L(g_{0.5}^D)$ should be as near to the original Bayes error $L(g_{0.5})$ as possible. To be a typical pattern, each representative should be similar to as many records as possible because surprising elements predict existence of unknown surprises in the testing data set which are not similar to any representatives. There is no heuristic information for the unknown surprise. One the other hand, for the computational purpose, the number of representatives should be small relative to the training data set size $|\Omega|$.

V. Examples

The section uses the Breast Cancer Wisconsin (Original) Data Set ([1], [17]) as an example data set. The data set consists of 699 Instances. The instances have 10 attributes and a class attribute. Except the first attribute which is the sample code number, there are 9 attributes to consider for a pattern search task. The domain for the attributes are integers from 1 to 10. There are few instances that contain a single missing (i.e., unavailable) attribute value. For the class attribue, there are two classes: 2 for benign and 4 for malignant. There are 458 benign instances and 241 malignant instances. Let X be the set of malignant instances. We consider the approximations of X in the rough set terminology by use of representative clusterings.

Let $(x_1^\omega, ..., x_9^\omega)$ represent the 9 attributes of an instance ω. We consider three different kinds of similarities. In the following we assume that $|x_i^{\omega_1} - x_i^{\omega_2}| = 5$ if one of the values is missing.

The first similarity is:

$$\xi_1(\omega_1, \omega_2) \text{ if } |x_i^{\omega_1} - x_i^{\omega_2}| \leq 3, \quad i = 1, ..., 9. \tag{15}$$

That is, for two instances if the difference of each attribute values is less than or equal to 3, then they are ξ_1-similar.

The second one is:

$$\xi_2(\omega_1, \omega_2) \text{ if } |x_i^{\omega_1} - x_i^{\omega_2}| \leq 2 \text{ for a least } 8 \text{ attributes.}$$

That is, ω_1 and ω_2 are ξ_2-similar if there are 8 attributes for which the differences are less than or equal to 2.

The third one is:

$$\xi_2(\omega_1, \omega_2) \text{ if } \sum_{i=1}^{9} |x_i^{\omega_1} - x_i^{\omega_2}| \leq 15. \tag{16}$$

That is, ω_1 and ω_2 are ξ_3-similar if the sum of of all differences is less than or equal to 15.

TABLE I
Summaries of the examples

	$\lvert\mathbf{R}_\xi\rvert$	α_ξ	$\lvert\mathbf{P}_\xi\rvert$	$\lvert L_\xi\rvert$	$\lvert\mathbf{B}_\xi\rvert$	b_ξ	m_ξ	B-error
ξ_1	97	36	229	167	7	20	10	0.0114
ξ_2	66	12	224	185	5	9	6	0.0027
ξ_3	32	3	176	153	10	59	24	0.0172

For each similarity ξ, we compute a sub-minimal representative system $\mathbf{R}_\xi$ and the corresponding partitions $\mathbf{P}_\xi$. The number of surprises is α_ξ. The set of the exact elementary sets in the lower approximation of X is represented by L_ξ. The set of boundary exact elementary sets is denoted by $\mathbf{B}_\xi$. A boundary exact elementary set is an exact elementary set which is in the upper approximation but not in the lower approximation. Let b_ξ and m_ξ be the numbers of benign and malignant instances in the boundary, respectively.

The results are summarized in the Table 1, where B-error represents the Bayes error. For example, in the first similarity ξ_1, there are 97 representatives, 229 exact elementary sets. There are 10 malignant instances in the boundary; that is 231 malignant instances are in the lower approximation of X. The similarity ξ_2 gives a better result, where 235 malignant instances are in the lower approximation of X and there are only 15 (i.e., $9+6$) instances in the boundary. The Bayes error is 0.0027.

VI. Conclusion

This paper introduces an abstract model of heuristic search based on probability. Both the previous probabilistic game-tree search and the pattern search are special cases of the abstract model. Each rough set formulation can also be reformulated as a special case of the abstract model. Further research on the abstract model is needed in order to understand more about the theoretical properties of heuristic search and heuristic information.

References

[1] Breast Cancer Wisconsin (Original) data set, 1992 http://archive.ics.uci.edu/ml/datasets/Breast+Cancer+Wisconsin+(Original).

[2] K. L. Chung. *A Course in Probability Theory*. Academix Press, New York, 1974.

[3] L. Devroye and G. L. Gyoerffi. *A Probabilistic Theory of Pattern Recognition*. Springer, 1996.

[4] W. Maak. *Fastperiodische Funktionen*. Springer-Verlag, 1967.

[5] M. A. E. Maloof. *Machine Learning and Data Mining for Computer Security*. Springer-Verlag, 2006.

[6] J. Pearl. On the nature of pathology in game tree searching. *Artificial Intelligence* 20, 1983, pages 427–453.

[7] J. Pearl. *Heuristics: intelligent search strategies for computer problem solving*. Addison-Wesley, Reading, MA, 1984.

[8] L. Polkowski. *Rough Sets*. Springer-Verlag, 2002.

[9] A. Skowron and J. Stepaniuk. Tolerance Approximation Spaces. *Fundamenta Informaticae*, 27, pages 245–253, 1996.

[10] C.-H. Tzeng and O. C.-S. Tzeng. Tolerance Spaces and Almost Periodic Functions. *Bulletin of the Institute of Mathematics Academia Sinica.* Vol. 6, No. 1, pages 159–173, 1978.

[11] C.-H. Tzeng and P. W. Purdom, Jr. A Theory of Game Tree. *Proceedings of the National Conference on Artificial Intelligence AAAI-83*, pages 416-419, William Kaufmann, Los Altos, CA. 1983.

[12] C.-H. Tzeng. *A Theory of Heuristic Information in Game-Tree Search*. Springer-Verlag, 1988.

[13] C.-H. Tzeng and F.-S. Sun. Data clustering in tolerance space. *Berthold, Lenz, Bradley, Kruse, and Borgelt, editors, Advances in Intelligent Data Analysis V*, pages 297–306. Springer-Verlag, 2003.

[14] C.-H. Tzeng. Similarity and pattern recognition. *Proc. Intern. Conf. on Data Mining and Appl.*, 2008, pages 584–590

[15] C.-H. Tzeng A Probabilistic Model of Pattern Recognition on Abstract Data. *Proceedings of the 2009 Intern. Conf. on Data Mining* CSREA Press 2009, pages 319-325

[16] C.-H. Tzeng and F.-S. Sun. A Pattern Search in Data Analysis. *International Journal of Electronic Commerce Studies* Vol. 1, No. 2, 2010, pages 117-138.

[17] W. H. Wolberg and O. L. Mangasarian. Multisurface method of pattern separation for medical diagnosis applied to breast cytology. *Proceedings of the National Academy of Sciences, U.S.A.*, Vol 87, pages 9193–9196, 1990.

[18] L. Zadeh. A New Direction in AI Toward a Computational Theory of Perceptions, *AI Magazine*, Spring 2001, pages 73–84.

[19] E. C. Zeeman. The topology of the brain and visual perception. *Topology of 3-Manifolds and related Topics*, pages 240–256. Proc. The Univ. of Georgia Institute, 1962.

2011 IEEE International Conference on Fuzzy Systems
June 27-30, 2011, Taipei, Taiwan

Linguistic Description of Adult Skeletal Age-at-Death Estimations from Fuzzy Integral Acquired Fuzzy Sets

Derek T. Anderson and James M. Keller
Electrical and Computer Engineering
University of Missouri
Columbia, MO, USA
andersondt@missouri.edu and kellerj@missouri.edu

Melissa Anderson and [1]Daniel J. Wescott
[1]Department of Biological Sciences
Florida International University
Miami, FL, USA
dwescott@fiu.edu and melissafanderson@gmail.com

***Abstract*—Previously, we introduced a novel method to estimate adult skeletal age-at-death using the Sugeno fuzzy integral (FI). Specifically, we took a multi-hypothesis testing approach to make the classical FI yield a fuzzy set (FS)-valued result, which is not guaranteed to be normal or convex, based on interval-valued sources of information (aging methods). We showed quantitative results for summarizing the FS and comparing the single decision to a known age-at-death. In this article, we extend our prior work and present formulas to measure the uncertainty in the resultant FSs. We generate linguistic descriptions to establish domain standardization for the goal of assisting forensic and biological anthropologists. Specifically, we introduce fuzzy class definitions for age-at-death FSs and we present an OWA contrast approach to measure the degree of specificity in age-at-death FSs.**

Keywords; Sugeno fuzzy integral; linguisitic description; skeletal age-at-death; anthropology

I. INTRODUCTION

Age-at-death estimation of an individual skeleton is important to forensic and biological anthropologists for identification and demographic analysis. It has been shown that current individual aging methods are often unreliable because of skeletal variation and taphonomic factors. In [1], we demonstrated that the fuzzy integral (FI) can be used for age-at-death estimation. Our algorithm produces a decision regarding age-at-death using multiple interval-valued aging methods while taking into account the numeric accuracies of the methods and the condition of the bone being examined. Advantages of this FI approach are that it does not require a population, it can (quantitatively) produce a single age-at-death estimate and it (qualitative) produces a fuzzy set (FS).

Forensic and biological anthropology is rooted heavily in definitions, methods and standardization. It is important that techniques are well established and that their findings be reproducible and understandable by different scientists. Our prior work is based on a set of accepted aging methods, their documented reliabilities and the weathering or quality of the skeletal remains. However, while our quantitative procedure is well established in [1], the qualitative component, i.e. interpretation of the FSs, is currently based on a set of crisp rules. Herein, we assert that the (linguistic) anthropological desired results are not crisp but instead fuzzy. Therefore, we require a mathematical (fuzzy) way to model these concepts and their associated uncertainties. We focus on the FSs and we introduce a systematic way to interpret the discoveries.

This article is important to anthropology because it makes the qualitative FS analysis procedure explicit and researchers can therefore better understand how to interpret results acquired from different investigators on different types of skeletal remains. This article is important to the FS community because it demonstrates a real-world application of the classical number-valued FI to construct (potentially non-normal and non-convex) FSs. In addition, we present a feature-based method to determine different age-at-death FS anthropological classes and the degree of FS specificity. This work is a case in which it is useful to maintain as much uncertainty as possible throughout the entire analysis procedure, exemplifying Marr's Principle of Least Commitment [2]. That is, one should not stop with the production of a single quantitative result. Instead, we show that it is possible to generate linguistic descriptions of FSs, and that analysis of this information results in different knowledge than what the quantitative approach yields.

II. BACKGROUND

A. Related Work in the FS Community

In [1], we show how the classical FI with a number-valued integrand and number-valued fuzzy measure (FM) can be used to produce FS-valued results based on interval-valued sources of information. Our approach, which is summarized later in this article, is one of multiple hypotheses testing. Grabisch et al. [3] previously demonstrated a *literal* extension of the number-valued FI to FS-valued integrands and number-valued FMs. Grabisch's FI, for a FS-valued integrand and number-valued FM, is comprised of a series of interval-valued integrand and number-valued FM calculations (based on the work of Dubois [4]), which in return is decomposed into the classical FI for a number-valued integrand and FM. While it might initially appear to be possible to cast our anthropological problem into one of a FI with a FS-valued integrand and number-valued measure, the problem is that Grabisch's approach requires that the FSs be normal and convex. As we discuss later, while our FSs are usually convex they are generally not normal.

978-1-4244-7316-8/11/$26.00 ©2011 IEEE

Table 1. Morphological Stages and Age Ranges for Pubic Symphysis, Auricular Surface, and Cranial Suture Closure

Pubic Symphysis[1]		Auricular Surface[2]		Ectocranial Lateral-Anterior Suture Closure[3]		Ectocranial Vault Suture Closure[3]	
Stage	Age Range (yrs)	Stage	Age Range (yrs)	Composite Score	Age Range (yrs)	Composite Score	Age Range (yrs)
1	18-19	1	20-24	0	<50	0	<49
2	20-21	2	25-29	1	19-48	1,2	18-45
3	22-24	3	30-34	2	25-49	3,4,5,6	22-48
4	25-26	4	35-39	3,4,5	23-68	7,8,9,10,11	24-60
5	27-30	5	40-44	6	23-63	12,13,14,15	24-75
6	30-35	6	45-49	7,8	32-65	16,17,18	30-71
7	35-39	7	50-59	9,10	33-76	19,20	23-76
8	39-44	8	60+	11,12,13,14	34-68	21	Closed (40-)
9	45-50			15	Closed		
10	50+						

[1]Todd 1920 [2]Lovejoy et al. 1985b [3]Meindl and Lovejoy 1985

Yager and Klir [5, 6], to name two, have previously presented various specificity measures for FSs. To the best of our knowledge, our approach to linguistically measuring the specificity of an age-at-death FS, based on the OWA [7] and contrast in different regions of a FS is new.

B. *Aging Methods*

Forensic investigators rely on the accuracy of age indicators for personal identification purposes, whereas biological anthropologists generally have a broader area of applicability for accurate age estimation, such as paleodemographic studies [8]. In general, all skeletal remains are not guaranteed to be present in a forensic case. Different aging methods have been established in the field in order to approximate age-at-death based on the analysis of different skeletal remains. The aging methods used in our prior work and herein include the pubic symphysis morphology [9], auricular surface morphology [10], and ectocranial suture closure [11] used for adult age estimation. The intervals that these techniques produce are shown in table 1. For the methods used here, researchers compare the skeletal remains to a discrete set of stages, or use a composite score and lookup the age-range (interval) in a table.

C. *Uncertainity in Age-at-Death Estimation and Prior Work*

It is well known that there is uncertainty in age-at-death estimation [12, 13, 14, 15]. Causes of uncertainty come from actual death age, the amount of exposure to various unknown elements, and cause and timing of death. Even more specifically, we know: (1) skeletally immature and young adult individuals are likely to be aged more precisely than older adult individuals, (2) bones are in a continual process of change, usually degenerative and influenced by the habitual activities and health of the individual as well as the age of the individual, (3) skeletal age assessment produces (crisp) age ranges instead of a specific age or fuzzy intervals, and (4) aging methods have varying accuracies.

Due to the inherent uncertainty in this domain, some have developed procedures to aggregate information acquired from multiple aging methods in order to improve age-a-death estimation. Prior approaches in the field are all statistical and are generally based on populations. Existing multifactorial aging methods include Acsádi and Nemeskéri, [16]; Lovejoy et al. [17]; Boldsen et al. [18]. Our method, [1], however can incorporate more information. In addition to the (objective) strength in a hypothesis, we also take into account the variable (subjective) accuracies associated with each method and the weathering or quality of remains.

D. *Accuracy and Quality Indicies*

Because of the various stated uncertainties, it is important to include as much known or observable information as possible about the skeleton so that all factors available can be taken into consideration when determining skeletal age-at-death. The accuracy of the methods and condition or quality of the skeleton becomes important because they are related to the overall assessment of the skeleton.

Accuracy index. Accuracy in age estimation is defined as how well the estimated or biological age conforms to the real chronological age, and relies on how strongly correlated the biological and chronological ages are to each other. We use the correlation coefficient of the chronological and biological age indicator that is associated with each adult aging method (Katz and Suchey [18]; Meindl and Lovejoy [11]; Meindl et al. [15]).

Quality. Bone quality is an additional piece of information that can be taken into consideration when analyzing a skeleton. Because the condition of the skeleton is dependent on environmental factors, the quality of a skeleton affects determining age-at-death. Previously, we evaluated and scored the bone quality using a modified version of Behrensmeyer [19] weathering stages provided in Standards [20], but with a stage 6 added to take into account the absence of an age indicator. Quality values are assigned, based on the weathering stages, and are associated specifically with the part of the skeleton for which the aging methods are being applied. If the bone is deteriorated but can still be used, the aging method will still be applied but the decision reached will respectively be associated with a lower support value. The quality indices are ordinal and arbitrarily assigned values. They must be decreasing values and no greater than one and no less than 0. They were assigned in this manner to indicate the least weathering as producing the best results (1) and the most weathering as producing poor or no results (0). A score of 0 is assigned if the bone is not present. Previously, we assigned Stage 0 a quality value of 1.0, Stage 1 a value of 0.8, Stage 2 is 0.6, Stage 3 is 0.4, Stage 4 is 0.2, Stage 5 is 0.1, and Stage 6 is 0. However, the data used in this study were collected on museum specimens and therefore the quality index does not vary considerably.

E. Sugeno Fuzzy Integral

The fusion of information using the fuzzy integral (Sugeno or Choquet) has a rich history. Much of the theory and several applications can be found in [21, 3, 22]. With respect to this problem, we consider a finite set of sources of information, $X = \{x_1, x_2, \cdots, x_E\}$ and a function that maps X into some domain (initially [0,1]) that represents the partial support of a hypothesis from the standpoint of each source of information. Depending on the problem domain, X can be a set of experts, sensors, features, pattern recognition algorithms, etc. The hypothesis is usually thought of as an alternative in a decision process or a class label in pattern recognition. Both Sugeno and Choquet integrals take partial support for the hypothesis from the standpoint of each source of information and fuse it with the (perhaps subjective) worth of each subset of X in a non-linear fashion. This worth is encoded into a fuzzy measure [23]. Initially, the function $h: X \to [0,1]$, and the measure $g: 2^X \to [0,1]$ take real number values in [0,1]. Certainly, the output range for both function and measure can be (and have been) defined more generally, but it is convenient to think of them in the unit interval for confidence fusion.

More formally, for a finite set $X = \{x_1, x_2, \cdots, x_E\}$, a (numeric) fuzzy measure is a function $g: 2^X \to [0,1]$, (a real valued set function) such that

1. $g(\phi) = 0$ and $g(X) = 1$;
2. If $A, B \subseteq X$ with $A \subseteq B$, then $g(A) \leq g(B)$.

Note that if X is an infinite set, a third condition guaranteeing continuity is required, but it is a moot point for finite X. In this article, we use the Sugeno λ-fuzzy measure [23]. The Sugeno λ-fuzzy measure builds the measure, all 2^N-1 values, given a set of densities (the measure for all singletons). Alternatively, for a few number of sources, one can define the fuzzy measure by hand or learn it from training data.

Given a finite set X, a fuzzy measure $g: 2^X \to [0,1]$ and a function $h: X \to [0,1]$, the (numeric) Sugeno integral of h with respect to g is given by

$$\int h \circ g = \bigvee_{i=1}^{E} \left(h(x_{(i)}) \wedge g(\{x_{(1)}, \cdots, x_{(i)}\}) \right),$$

where $X = \{x_{(1)}, \cdots, x_{(E)}\}$ has been sorted so that $h(x_{(1)}) \geq h(x_{(2)}) \geq \cdots \geq h(x_{(E)})$. This finite realization of the actual definition highlights the fact that the Sugeno integral represents the best pessimistic agreement between the objective evidence in support of a hypothesis (h function) and the (possibly subjective) worth of the supporting evidence as provided by the fuzzy measure g.

F. Sugeno FI for Adult Skeletal Age-at-Death Estimation

After the age, accuracy, and quality indices are collected, a hypothesis is tested. The hypothesis is "the skeleton is age _ (a specific age, not range)". The Sugeno integral is repeatedly applied, once for each possible age using the respective accuracy, range and quality information. Every age, in discrete one year increments from 1 to 110 is tested. The age indicators provide input based on if the age tested is in their respective interval. The $h(x_i)$ values are a function (t-norm) of the quality, a [0,1] value, and if the aging method indicates that the age tested falls in the age interval, either a 0 for false or 1 for true. The result of this procedure is a collection of (age tested, FI result) pairs, which is a FS defined over the age domain. In this respect, we are able to address the case of sub-normal FSs.

G. Prior Method to Classify Age-at-Death FSs

As shown in figures 1 and 4, at least four different potential FS classes are possible; specific, figure 1(a), interval, figure 1(b), reconsideration, figure 1(c), and inconclusive, figure 1(d).

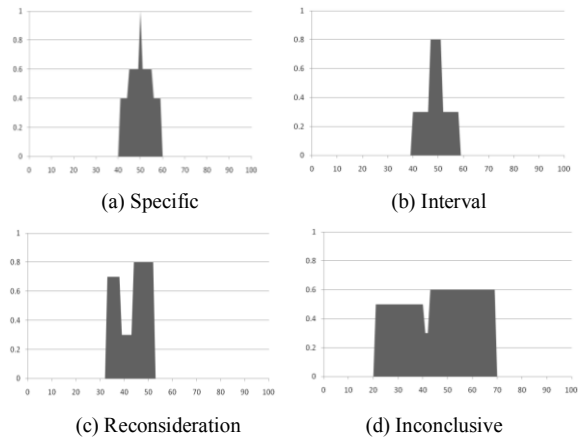

(a) Specific (b) Interval

(c) Reconsideration (d) Inconclusive

Fig. 1. Illustration of age-at-death FS classes for the FI results.

In [1], 'Specific' means that the procedure has identified an exact age-at-death, e.g. 25 years old. Class 'Interval' indicates that the procedure has identified a range (interval) of possible ages, e.g. 25-30. Class 'Reconsideration' means that there are multiple similar age-at-death ranges (intervals). Therefore, a researcher needs to decide how to resolve the conflict. Class 'Inconclusive' means that there is too little solid evidence to indicate any age-at-death.

Initially, an age-at-death FS was classified into one of the four just mentioned classes according to the characteristics of its intervals. A plateau is defined here to be an interval such that the interval directly before it and the interval directly after it (if they exist) have smaller FI values. For example, figure 1(a) has one plateau while figure 1(c) has two plateaus. The following tests, analyzed in the order specified below, were used in [1] to determine the type of FS. Each test is a yes or no question.

- *Test 1*: Is the length of the maximum plateau greater than or equal to 30 years? If the answer is yes, then the FS is placed in the category inconclusive, if not, then the next test is conducted.
- *Test 2*: Is there a single plateau and is its length equal to one? If yes, the result is specific age.

- *Test 3*: Is there a single plateau and is its length 29 or less years? If yes, the result is age interval.

In the case that the FS does not pass one of the above three tests then it is labeled as type reconsideration.

III. Fuzzy Set Approach to Class Determination

A shortcoming of [1] is it's crisp class definitions. Initially, this set of definitions appeared to be suitable. However, after investigating different results, it was discovered that these initial definitions do not capture the inherent fuzziness that exists in age-at-death FS classes. Figure 2 contains example age-at-death FSs illustrating the inherent fuzziness of the classes.

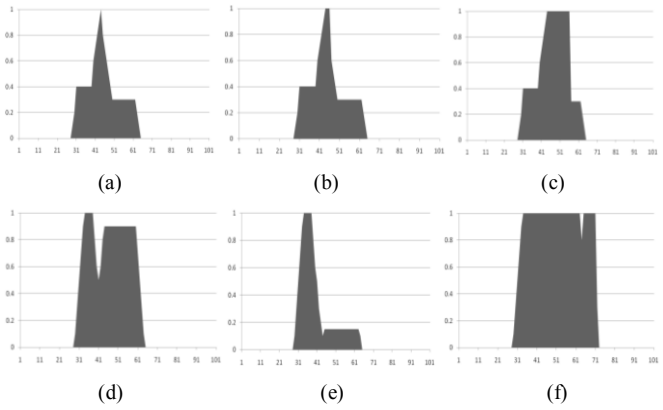

Fig. 2. FSs showing the fuzziness inherent to defining age-at-death FS classes.

We begin this discussion with the comparison of figure 2(a) to figure 2(b). In figure 2(a), the maximum plateau has a width of 1. In figure 2(b), the maximum plateau has a width of 3. The old definitions classify figure 2(b) as type 'Interval'. As it turns out, figure 2(a) is an interval, just with a small (length 1) width. We assert that there is little difference between figures 2(a) and 2(b). Figure 2(b) should instead have the highest membership in 'Specific' instead of 'Interval'. In comparison, figure 2(c) should have the highest membership in the class 'Interval'. The question is to what degree do these examples belong to these concepts?

Next, consider figures 2(d) and 2(e). The prior definitions in [1] classify these FSs as type 'Reconsideration'. However, the second (smaller) plateau in figure 2(e) has a very low (0.15) membership degree. Should these two FSs have the same membership degree in class 'Reconsideration'? Should figure 2(e) not have a higher degree in 'Interval' or 'Specific'?

On a final note, figure 2(f) is classified as 'Inconclusive' by the old set of definitions. The maximum plateau has a width of 30. Should this FS have the same membership degree as a FS with a maximum plateau with width 35, 40, or higher? What about a FS with a maximum plateau with width of 28? The recurring theme between these different examples is that the definitions provided prior do not accurately take into account the fuzziness that exists in determining the class of age-at-death FSs.

What is needed is a set of measurements of age-at-death FSs and FS class definitions. In this respect, a baseline for analysis can be established and a common understanding of age-at-death FS interpretation can take place.

First, we extract all plateau, $I = \{I_1,...,I_N\}$, where $I_n = [I_{n,start}, I_{n,end}]$ and $I_{n,start} \le I_{n,end}$. Herein, we restrict our analysis to a discrete set of ages, $I_{n,start}, I_{n,end} \in \{1,2,...,110\}$. Each interval is also associated with a membership degree, $\mu_{FI,n}$, which is the output of our FI procedure.

The first feature is the width, $|I_n|$, of the plateau that has the largest $\mu_{FI,n}$ value. The width of the maximum plateau is important for our understanding of how well the FI procedure singled out an age-at-death. The linguistic variable 'Maximum Plateau Width' (MPW) is defined and has the terms 'little', 'some', and 'big' (reported in table 2). The FSs used herein are trapezoidal membership functions (MFs), which are defined with respect to four ordered points, [a b c d]. These four numbers specify an interval in which the membership is value 1, i.e. between [b c], a linearly increasing interval, i.e. [a b], a linearly decreasing interval, i.e. [c d], and any point that is less than a, or greater than d, has a membership value of zero.

Table 2. Linguistic variable and terms for 'Maximum Plateau Width'.

	little	moderate	big
MF	[0 1 4 6]	[1 5 29 35]	[25 30 110 110]

The next feature is the distance (in terms of membership value) between the maximum plateau and the second largest plateau. The calculation is

$$\beta = \begin{cases} 1 & \text{if } |I| == 1 \\ (f_{max\,1} - f_{max\,2}) & \text{else} \end{cases},$$

where

$$f_{max\,1} = \max_{n} \mu_{FI,n},$$

$$f_{max\,2} = \max_{k \neq n} \mu_{FI,k}.$$

Table 3 reports the set of terms for the linguistic variable 'Plateau Separation' (PS), defined on the domain β.

Table 3. Linguistic variable and terms for 'Plateau Separation'.

	little	moderate	big
MF	[0 0 .3 .5]	[.3 .5 .7 .9]	[.5 .7 1 1]

Based on these two features, we are now able to define the four age-at-death FS classes. The definitions are no longer crisp. The confidence (membership degree) that an age-at-death FS belongs to the category (concept) 'Specific' is

$$\mu_{\text{Specific}} = \mu_{\text{little}}^{\text{MPW}} * \mu_{\text{big}}^{\text{PS}},$$

'Interval' is

$$\mu_{\text{Interval}} = \mu_{\text{moderate}}^{\text{MPW}} * \mu_{\text{big}}^{\text{PS}},$$

'Inconclusive' is

$$\mu_{\text{Inconclusive}} = \mu_{\text{big}}^{\text{MPW}},$$

and 'Reconsideration' is

$$\mu_{\text{Reconsideration}} = \mu_{\text{small}}^{\text{PS}}.$$

For the example FSs in figure 2, the membership values for the above four terms are provided in table 4.

Table 4. FS class memberships for the FSs in figure 2.

	$\mu_{Specific}$	$\mu_{Interval}$	$\mu_{Inconclusive}$	$\mu_{Reconsideration}$
2(a)	1*1=1	0*1=0	0	0
2(b)	1*1=1	0.5*1=0.5	0	0
2(c)	0*1=0	1*1=1	0	0
2(d)	0.5*0=0.5	1*0=0	0	1
2(e)	0.5*1=0.5	1*1=1	0	0
2(f)	0*0=0	0.83*0=0	1	0

Table 4 shows what we expect. Figure 2(a) is 'Specific', figure 2(b) is more 'Specific' than 'Interval', figure 2(c) is 'Interval', figure 2(d) is somewhat 'Specific' but more of type 'Reconsideration', figure 2(e) is somewhat 'Specific', but mostly 'Interval', and figure 2(f) is 'Inconclusive'.

IV. Measuring Age-at-Death FS Specificitiy

While the last section detailed a feature and FS-based approach to determining the membership degree of an age-at-death FS in the four anthropological classes, a question still remains regarding how *specific* the FS is with respect to being able to narrow the age-at-death to a single value? For example, even if the method indicates a single age-at-death, i.e. class 'Specific', how specific are the findings in terms of there being evidence that the skeletal remains might be a different age? Figure 3 and figure 2(a) illustrate this concept.

Figure 3 illustrates what we already know. The smaller the area in the age-at-death FS, the greater our confidence is that the aging methods agreed on a specific age-at-death. That is, the less fuzzy the age-at-death FS, the more *specific* the age. In reality, figure 3(b) is unlikely because aging methods produce intervals and not a single age-at-death. Because a specific age is not expected to ever be encountered using current crisp aging methods, it is important that we include a measure of age-at-death FS specificity. The first thought was to use the standard FS scalar-cardinality to measure age-at-death specificity,

$$\text{sc}(A) = \sum_{i=1}^{110} A(x_i).$$

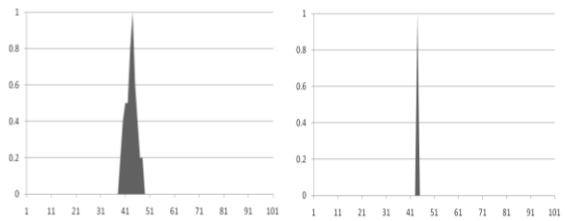

(a) (b)

Fig. 3. Differences in age-at-death *specificity* for age-at-death FSs. Compared to figure 2(a), figure 3(a) is more specific, while figure 3(b) is the most specific.

However, it turns out that we need something tailored specifically to age-at-death FSs. If the goal is to have a low sc(A), namely a FS with value 1 at one domain location and zero elsewhere, i.e. figure 3(b), then in return we open the door for other types of age-at-death FSs that could acquire a low sc(A) values. Namely, this can occur because our FI procedure can yield FSs that are not normal. For example, if there is significant disagreement between all of the aging methods, then sc(A) can have a near zero value.

Instead, we address age-at-death FS specificity using an ordered weighted average (OWA) approach [7]. The OWA begins by sorting (in descending order) the membership values. The OWA also takes a set of weights that generally sum to one (or the calculation is weighted by the sum of the weights). The first weight is for the largest sorted value, the second weight is for the second largest value, etc. The OWA is capable of producing many familiar order statistics, i.e. the weighted average, maximum, minimum, etc. For example,

$$\text{OWA}(0, \underbrace{\frac{1}{10}, \ldots, \frac{1}{10}}_{10}, \underbrace{0, \ldots, 0}_{99}))$$

is an OWA operator with a weight of 0 for the maximum value, the average of the next 10 largest values and weights of 0 for all the remaining values.

We use different OWAs to calculate the membership of the age-at-death specificity for the terms 'Exact', 'High', 'Moderate' and 'Low'. The membership of 'Exact' is

$$\mu_{\text{Exact}} = \text{OWA}(1, \underbrace{0, \ldots 0}_{109}) - \text{OWA}(0, \underbrace{\frac{1}{10}, \ldots, \frac{1}{10}}_{10}, \underbrace{0, \ldots, 0}_{99})),$$

'High' is

$$\mu_{\text{High}} = \text{OWA}(1, \underbrace{0, \ldots 0}_{109}) *$$

$$\frac{\left(\text{OWA}(0, \underbrace{\frac{1}{10}, \ldots, \frac{1}{10}}_{10}, \underbrace{0, \ldots, 0}_{99})\right) - \left(\text{OWA}(\underbrace{0, \ldots, 0}_{11}, \underbrace{\frac{1}{20}, \ldots, \frac{1}{20}}_{20}, \underbrace{0, \ldots, 0}_{79})\right)}{\left(\text{OWA}(0, \underbrace{\frac{1}{10}, \ldots, \frac{1}{10}}_{10}, \underbrace{0, \ldots, 0}_{99})\right)},$$

'Moderate is

$$\mu_{\text{Moderate}} = \text{OWA}(1, \underbrace{0,\ldots 0}_{109}) * \left(\frac{\left(\text{OWA}(\underbrace{0,\ldots,0}_{20}, \underbrace{\frac{1}{20},\ldots,\frac{1}{20}}_{20}, \underbrace{0,\ldots,0}_{70})) \right) - \left(\text{OWA}(\underbrace{0,\ldots,0}_{30}, \underbrace{\frac{1}{20},\ldots,\frac{1}{20}}_{30}, \underbrace{0,\ldots,0}_{50})) \right)}{\left(\text{OWA}(\underbrace{0,\ldots,0}_{20}, \underbrace{\frac{1}{20},\ldots,\frac{1}{20}}_{20}, \underbrace{0,\ldots,0}_{70})) \right)} \right),$$

and 'Low' is

$$\mu_{\text{Low}} = \text{OWA}(1, \underbrace{0,\ldots 0}_{109}) * \left(\text{OWA}(\underbrace{0,\ldots,0}_{30}, \underbrace{\frac{1}{10},\ldots,\frac{1}{10}}_{10}, \underbrace{0,\ldots,0}_{70}) \right).$$

These formulas take into the account the maximum membership value and 'contrast' between different parts of the FS. For the example FSs in figures 2 and 3, the membership values for the above four terms are provided in table 5.

Table 5. Age-at-death specificity value for the FSs in Figure 2.

	μ_{Exact}	μ_{High}	μ_{Moderate}	μ_{Low}
2(a)	0.36	0.6	0.78	0
2(b)	0.31	0.63	0.78	0
2(c)	0	0.34	0.81	0
2(d)	0.06	0.39	0.85	0
2(e)	0.2	0.84	0.75	0
2(f)	0	0.05	0.63	.89
3(a)	0.62	1	0	0
3(b)	1	0	0	0

Again, table 5 reports what we expect. Figure 2(a) is mostly 'Moderate' but also somewhat 'High', figure 2(b) is essentially the same as figure 2(a), figure 2(c) is more 'Moderate' and less 'High' than figure 2(a-b), figure 2(e) has a higher specificity than figure 2(d), figure 2(f) has a very low specificity, while figure 3(b) is the most specific.

V. Confidence

Formulas have now been presented for age-at-death FS classification and determination of the amount of specificity. The final component of this article is interpretation of the FI output degree. No new procedure is presented here in terms of measurements. The importance is establishing a vocabulary for the concept 'Confidence in Age-at-Death'. Table 6 reports the terms and their values.

Table 6. Linguistic variable and terms for 'Confidence in Age-at-Death'.

	High	moderate	low	no
MF	[.8 .9 1 1]	[.4 .6 .8 1]	[0 .2 .4 .6]	[0 0 .1 .2]

VI. Data Set and Experiments

Most of the skeletal aging methods are based on collections with known aged individuals, such as the Terry Anatomical Collection [24, 25]. This collection contains mainly black and white adult skeletons with dates of birth ranging from 1822-1943. It contains 1,728 individuals with the majority between 20 to 80 years of age. The data used here, which is the same data used in our prior FI article, was collected as part of another study by L. Konigsberg, N. Herrmann, and D. Wescott. It is available at http://konig.la.utk.edu/paleod.htm. Skeletal remains of known age from the Terry Collection were scored for pubic symphysis morphology [9], auricular surface morphology [10] and ectocranial suture closure [11]. Our data set is comprised of 735 individuals, specifically 323 females and 412 males. There are too many skeletons to report all findings, so a select set are shown to emphasize the proposed method. We use the same examples from our prior article [1]. The first four results in figure 4, (a-d), are the findings of the procedure introduced in this article for four skeletal cases from the Terry Anatomical Collection.

The Terry collection only contains skeletal remains with a quality value of 1. If any wearing is present, it is most likely due to researchers working on the skeletal remains. Because of this, in [1] we introduced 4 hypothetical cases (HCs) based on individuals from the Terry collection in which the quality value was varied and additional methods were simulated to test scenarios outside of the data set analyzed (figure 4 e-h). These experiments are summarized here, while the full information is contained in [1].

Figure 4 tells the following story. Skeleton 208 (4a) is clearly of type specific, has a low specificity, and there is a high FI confidence. This reinforces the class label that we found prior in [1]. Discoveries for skeletons 25R and 635 also reinforce what we found earlier (figures 4b and 4d). However, for skeleton 779R (4c), we now discover two class labels with high membership value, inconclusive and reconsideration. According to our definitions, it is inconclusive due to the length of the maximum plateau, however, there is also very little difference (in confidence) between the maximum plateau and the second largest. Even if one could reduce the width of the interval for the maximum plateau, there would still remain substantial disagreement between it and the second largest.

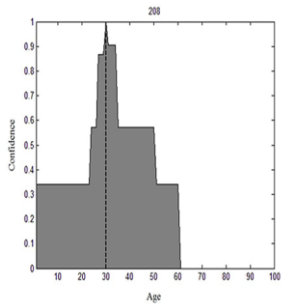

Skeleton	208
Chronological Age	30 yrs
Sex	Female
Sugeno Age Range	30 yrs
Pubic Symphysis	27-30 yrs
Auricular Surface	30-34 yrs
Ectocranial Suture – Vault	24-60 yrs
Ectocranial Suture - Lateral-Anterior	< 50 yrs

a: class=(1,0,0,0), specificity=(0,0.17,0.38,0.57) and conf=(1,0,0,0)

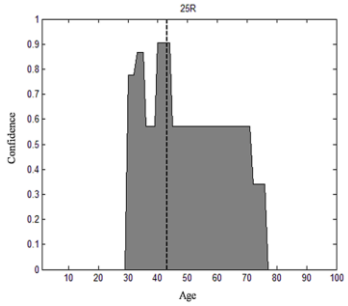

Skeleton	25R
Chronological Age	43 yrs
Sex	Female
Sugeno Age Range 1	40-44 yrs
Sugeno Age Range 2	33-35 yrs
Pubic Symphysis	30-35 yrs
Auricular Surface	40-44 yrs
Ectocranial Suture – Vault	30-71 yrs
Ectocranial Suture - Lateral-Anterior	33-76 yrs

b: class=(0,0,0,1), specificity=(0.05,0.3,0.45,0.31) and conf=(1,0.48,0,0)

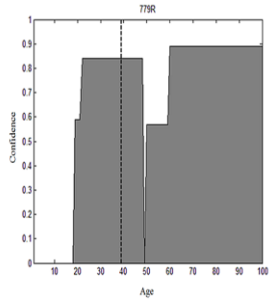

Skeleton	779R
Chronological Age	39 yrs
Sex	Male
Sugeno Age Range 1	60-100 yrs
Sugeno Age Range 2	22-48 yrs
Pubic Symphysis	50+ yrs
Auricular Surface	60+ yrs
Ectocranial Suture – Vault	22-48 yrs
Ectocranial Suture - Lateral-Anterior	19-48 yrs

c: class=(0,0,1,1), specificity=(0,0,0.03,0.79) and conf=(0.89,0.55,0,0)

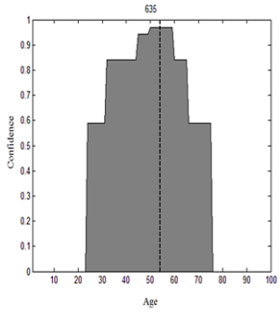

Skeleton	635
Chronological Age	54 yrs
Sex	Male
Sugeno Age Range	50-59 yrs
Pubic Symphysis	45-49 yrs
Auricular Surface	50-59 yrs
Ectocranial Suture – Vault	24-75 yrs
Ectocranial Suture - Lateral-Anterior	32-65 yrs

d: class=(0,1,0,0), specificity=(0,0.17,0.38,0.57) and conf=(1,0.15,0,0)

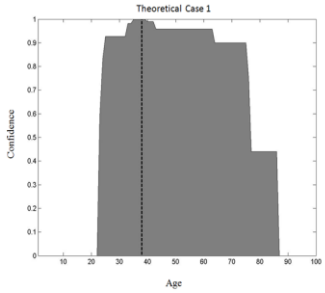

Aging Method	Age Range
Pubic Symphysis	35-39
Auricular Surface	35-39
Ectocranial Sutures – vault	24-75
Ectocranial Sutures- lateral	23-63
Sternal Rib Ends	33-42
Endocranial Sutures	35-39
Proximal Humerus	37-86
Proximal Femur	25-76

e: class=(0.5,1,0,0), specificity=(0.01,0.04,0.16,0.90) and conf=(1,0,0,0)

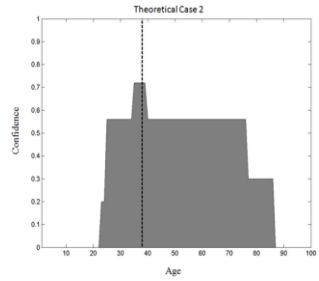

Aging Method	Quality	Age Range
Pubic Symphysis	0.6	35-39
Auricular Surface	0.8	35-39
Ectocranial Sutures	0.2	24-75
Sternal Rib Ends – vault	0.5	23-63
Sternal Rib Ends – lateral	0.5	33-42
Endocranial Sutures	0.4	35-39
Proximal Humerus	0.3	37-86
Proximal Femur	0.7	25-76

f: class=(0.5,1,0,0), specificity=(0.1,0.07,0.1,0.40) and conf=(0,1,0,0)

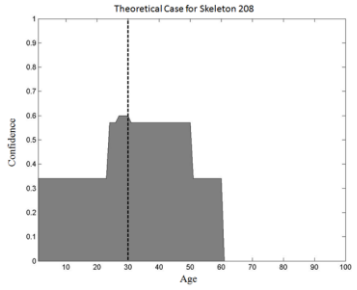

Skeleton	208
Chronological Age	30 yrs
Sex	Female
Sugeno Age Range	30 yrs
Pubic Symphysis	27-30 yrs (quality 0.6)
Auricular Surface	30-34 yrs (quality 0.4)
Ectocranial Suture - Vault	24-60 yrs (quality 0.8)
Ectocranial Suture - Lateral-Anterior	< 50 yrs (quality 0.8)

g: class=(0.5,0.38,0,0), specificity=(0.02,0.12,0.13,0.21) and conf=(0,1,0,0)

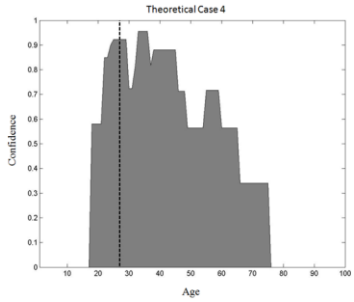

Aging Method	Age Range
Pubic Symphysis	22-24
Auricular Surface	25-29
Ectocranial Sutures - vault	24-75
Ectocranial Sutures - lateral	32-65
Sternal Rib Ends	33-36
Endocranial Sutures	55-59
Proximal Humerus	38-48
Proximal Femur	18-45

h: class=(0,0,0,1), specificity=(0.03,0.21,0.3,0.52) and conf=(1,0.22,0,0)

Fig. 4. Four skeletal examples from the Terry Anatomical Collection (a-d) and four hypothetical examples from [1] (e-h). For each age-at-death FS, we present the membership values in (1) the type of FS, (Specific, Interval, Inconclusive, Reconsideration), (2) the specificity, (Exact, High, Moderate, Low), and (3) the confidence interpretation, (High, Moderate, Low, No).

In HC1 (figure 4e), numerous (8) aging methods are simulated and the result is a single plateau of FI value 1 between ages 37-39. The highest membership in 'Interval', but there is also support in 'Specific'. In HC2 (figure 4f), the qualities of the skeletal remains were varied and the result was a single plateau of FI value 0.7 and age between ages 35 to 39. We see the same basic trend for HC2 as seen in HC1. In HC3 (figure 4g), the quality of the skeleton 208 (figure 4a) were varied. The result is a value of 0.6 for the ages 27 to 30. For HC3, there is little support for any class label. The measurements do not match our models to any high degree. There is more support in 'Specific', however almost the same confidence amount in 'Interval'. Additionally, the specificity degree has decreased between HCs 2 and 3. In part, this is because our OWA approach takes into account the maximum

FI value. Thus, as the maximum FI value decreases, so does our confidence in the amount of attainable specificity of the FS.

Lastly, for HC4 (figure 4h), we showed a case in which the quality value is 1 but the aging methods were in extreme disagreement. Multiple plateaus are discovered. The maximum plateau has a FI value of 0.95 for the ages 33 to 36 and the second largest is of FI value 0.91 for ages 25 to 29. In this case, there is a distinct class label of 'Reconsideration' with a high confidence and indication of 'Low' FS specificity.

VII. Conclusions

In this article, we extended our previous anthropological FI-based adult skeletal age-at-death estimation research [1]. This work is important to anthropology because it makes the prior qualitative procedure of manually analyzing age-at-death FSs now explicit. Therefore, researchers can better understand how to interpret results acquired from different investigators on different types of skeletal remains. This work is important to the fuzzy set community because we show how the FI for a number-valued integrand and number-valued measure can produce FS-valued results We also demonstrate a feature-based method of defining and measuring classes of different FSs in the context of anthropology. Lastly, we demonstrate an OWA-based contrast approach to measure the amount of specificity in an age-at-death FS. The method proposed in this article both reinforces many findings from our earlier work as well as shedding light on new discoveries. The proposed method makes the previous process of qualitatively analyzing the FI produced FSs explicit and understandable by others.

References

[1] M. F. Anderson, D. T. Anderson and D. Wescott, "Estimation of Adult Skeletal Age-at-Death Using the Sugeno Fuzzy Integral," in *American Journal of Physical Anthropology*, 142 (1), 30-41, 2010.

[2] D. Marr, Vision. W. H. Freeman and Company, NY, 1982.

[3] M. Grabisch, H. Nguyen and E. Walker, "Fundamentals of uncertainty calculi, with applications to fuzzy inference," Kluwer Academic, 1995.

[4] D. Dubois and H. Prade, "Fuzzy Numbers: An Overview," in *readings in Fuzzy Sets for Intelligent Systems*, Morgan Kauffman, 1, 3-39, 1993.

[5] R. Yager, "On the Specificity of a Possibility Distribution," in *Fuzzy Sets and Systems,* 50, 279-292, 1990.

[6] G. Klir and B. Yuan, "Fuzzy Sets and Fuzzy Logic Theory and Applications," Prentice Hall, 1995.

[7] R. Yager, "Applications and Extensions of OWA Aggregations," in *International Journal of Man-Machine Studies,* 37 (1), 103-122, 1992.

[8] A. Schmitt, P. Murail, E. Cunha and D. Rouge, "Variability of the pattern of aging on the human skeleton: evidence from bone indicators and implications on age at death estimation," in *Journal of Forensic Science*, 47, 1203-1209, 2002.

[9] T. Todd, "Age changes in the pubic bone: I: the male white pubis," in *American Journal of Physical Anthropology*, 3, 285-334, 1920.

[10] C. Lovejoy, R. Meindl, T. Pryzbeck, R. Mensforth, "Chronological metamorphosis of the auricular surface of the ilium: a new method for the determination of adult skeleton age at death," in *American Journal of Physical Anthropology*, 68, 15-28, 1985.

[11] R. Meindl and C. Lovejoy, "Ectocranial suture closure: a revised method for the determination of skeletal age at death based on the lateral-anterior sutures," *American Journal of Physical Anthropology*, 68, 57-66, 1985.

[12] J. Boldsen, G. Milner, L. Konigsberg J. Wood, "Transitional analysis: a new method for estimating age from skeletons," Hoppa RD and Vaupel JW, Cambridge Press, 73-106, 2002.

[13] R. Hoppa, "Population variation in osteological aging criteria: an example from the pubic symphysis," in *American Journal of Physical Anthropology*, 111, 185-191, 2000.

[14] R. Hoppa and J. Vaupel, "Paleodemography: age distributions from skeletal samples," Cambridge University Press, 2002.

[15] R. Meindl, C. Lovejoy, R. Mensforth, R. Walker, "A revised method of age determination using the os pubis, with a review and test of accuracy of other current methods of pubic symphseal aging," in *American Journal of Physical Anthropology*, 68, 29-46, 1985.

[16] G. Acsádi and J. Nemeskéri, "History of human life span and mortality," Akadémiai Kiadó, 1970.

[17] C. Lovejoy, R. Meindl, R. Mensforth, T. Barton, "Multifactorial determination of skeletal age at death: a method and blind test of its accuracy," *American Journal of Physical Anthropology*, 68, 1-14, 1985.

[18] J. Boldsen, G. Milner, L. Konigsberg and J. Wood, "Transitional analysis: a new method for estimating age from skeletons," in Hoppa RD, Vaupel JW, Cambridge Press, 73–106, 2002.

[19] A. Behrensmeyer, "Taphonomic and ecologic information from bone weathering," in *Paleoecology*, 4, 150-162, 1978.

[20] J. Buikstra and D. Uelaker, "Standards for data collection from human skeletal remains," Research Series 44. Fayetteville: Arkansas Archaeological Survey, 1994.

[21] H. Tahani and J. Keller, "Information fusion in computer vision using the fuzzy integral," in *IEEE Transactions System Man Cybernetics*, 20, 733–741, 1990.

[22] M. Grabisch, T. Murofushi and M. Sugeno, "Fuzzy Measures and Integrals: Theory and Applications," Physica-Verlag, Heidelberg, 2000.

[23] M. Sugeno, "Theory of fuzzy integrals and its applications," Ph.D. thesis, Tokyo Institute of Technology, 1974.

[24] M. Trotter and R. J. Terry, *American Journal of Physical Anthropology*, 56, 503-508, 1981.

[25] D. Hunt and J. Albanese, "History and demographic composition of the Robert J. Terry Anatomical Collection," *American Journal of Physical Anthropology*, 127, 406-417, 2005.

2011 IEEE International Conference on Fuzzy Systems
June 27-30, 2011, Taipei, Taiwan

Moving Pattern-based Approach to Modeling of a Class of Complex Production Processes

Xu Zhengguang, *Member,IEEE and* Sun Changping*
Department of Automation
University of Science and Technology Beijing
Beijing, China
sunchangping2000@sina.com.cn

***Abstract*—For a class of complex production processes, based on the actual running status data, a new modeling approach based on moving pattern is presented by constructing pattern moving space and defining moving variable-pattern class variable in it. The dynamics of a class of complex production processes is characterized by the movement of pattern class variable in pattern moving space. For characterizing pattern class variable quantitatively , in this paper, interval number is used as its metric form, and our previous proposed interval T-S fuzzy model (ITSFM) is adapted to model its movement in pattern moving space. Experimental results are then presented that indicate the validity and applicability of the proposed approach.**

Keywords: moving pattern, pattern moving space, pattern class variable, interval arithmetic, Takagi–Sugeno fuzzy model, interval time series

I. INTRODUCTION

In real world, there are many complex production processes in metallurgy, chemical industry and building materials etc （e.g. blast furnace, sintering machine, cement rotary kiln and so on.）For this class of production processes, there are the same characteristics as follows[1]. Therein, there is a series of physical chemistry reactions of heat transfer and matter transfer, burning thermodynamics and chemistry reaction dynamics, moving boundary, hydrodynamics and aerodynamics. It is difficult to characterize the dynamics. In addition, the mapping relationships between inputs and outputs can't be described by classic Newton's laws of mechanics, but be described only by statistics. For example, even under the same experimental conditions, the obtained data usually differ from one to another. Thus, the traditional modeling approach based on input/output data characterized in Euclidean space is not appropriate for modeling the relationship between inputs and outputs of a complex industrial process.

For this class of complex production process systems, there is lack of effective dynamics description methods. We try to give a new method to describe the movement law obeying statistics by using statistical principal, pattern recognition and control theory.

For modeling of complex dynamical systems, an pattern-based process identification approach emulating human in dealing with process response was originally introduced in [2]. Generally, the existing methods for pattern-based process identification can be divided into four classes [3], namely the key-values approach [4][5], the qualitative evaluation approach [6], the elementary pattern recognition approach [7], and the cure fitting approach [8] [9]. In these methods, Pattern recognition is mainly used to solve system model identification or system state estimation problems. After that, the design of control law is still based on the time-domain model. Here pattern is not considered as a moving variable.

In this paper, in contrast to traditional modeling approach to characterizing dynamical systems in Euclidean space, the dynamics of complex production processes is characterized by the moving of running status patttern from one pattern class to another in pattern moving space. First, the collected multi-dimensional actual running status data of complex production processes are reduced to one dimensional data . Then, the one dimensional data are partitioned into C pattern classes constructing the pattern moving space, and pattern class variable is defined in it. Each pattern class represented by an interval number can be considered as a scale value of pattern moving space. The pattern samples belonging to the same pattern class have the same scale value in pattern moving space, and are represented by the same interval number. That is, we view the considered systems at the level of pattern class and capature only the dominant characteristics of the process. We are not concerned about the exact value of the running status data of the complex production processes, but concerned about the pattern classes which the running status data of complex production processes belong to. After pattern moving space is constructed and pattern class variable is defined in this space, the prediction model is built as follows:

$$\begin{aligned} dx(k) &= F(d\tilde{x}(k)) \\ &= F(f(dx(k-1), dx(k-2)\cdots dx(k-m_y), \\ &\qquad u(k-1), u(k-2), \cdots, u(k-m_u))) \end{aligned} \tag{1}$$

Where $dx(k)$ is pattern class variable, $F(\cdot)$ denotes classification, $d\tilde{x}(k)$ is the initial prediction output of pattern class variable and $d\tilde{x}(k) = f(\cdot)$ is a kind of initial prediction model. This is a prediction process including two steps. The first step is to obtain the initial prediction output $d\tilde{x}(k)$ based

*Corresponding Author.

on the initial prediction model $d\tilde{x}(k) = f(\cdot)$ modeled by our previous proposed interval T-S fuzzy model (ITSFM). The second step is to obtain the finial output pattern class variable $dx(k)$ by classifying the initial prediction output $d\tilde{x}(k)$.

This paper is organized as follows. After the introduction the preliminary knowledege about interval arithmetic is presented in Section II. In Section III, moving pattern-based modeling approach of a class of complex production process is proposed. In Section IV, the example is considered to demonstrate the validity and applicability of the proposed approach. Finally, Section V concludes this paper.

II. PRELIMINARY KNOWLEDGE

In this section, we briefly look at some important formulations in interval arithmetic[10] .

A. Interval arithmetic

An interval number can be represented by its lower and upper bounds as $A=[a^L, a^U]$, or, equivalently, by its midpoint and radius as $A=(a^C, a^R)$, where $a^C=(a^L+a^U)/2$ and $a^R=(a^U-a^L)/2$. Let A and B be two intervals represented by its lower and upper bounds, the operations defined on the interval numbers are, respectively.

$$A+B=[a^L+b^L, a^U+b^U] \quad (2)$$

$$A-B=[a^L-b^U, a^U-b^L] \quad (3)$$

$$\lambda \cdot A=[\lambda \cdot a^L, \lambda \cdot a^U] \quad (4)$$

Where λ is a constant and $\lambda>0$.

If the interval number A and B are represented by its midpoint and radius, the operations defined on the interval numbers are respectively:

$$A+B=(a^C+b^C, a^R+b^R) \quad (5)$$

$$A-B=(a^C-b^C, a^R+b^R) \quad (6)$$

$$\lambda \cdot A=(\lambda \cdot a^C, |\lambda| \cdot a^R) \quad (7)$$

B. Hausdorff distance

The Hausdorff distance is often used to measure the distance between two interval data. The concept of Hausdorff distance is stated as follows. Assume that two interval numbers X_1 and X_2 , $X_1=(a_1, c_1)$, $X_2=(a_2, c_2)$, a_1 and c_1 are the center and radius of interval number X_1 , respectively, a_2 and c_2 are the center and radius of interval number X_2 , respectively. The distance between X_1 and X_2 is defined as:

$$D(X_1, X_2)=|a_1-a_2|+|c_1-c_2|$$

III. MODELING OF COMPLEX PRODUCTION PROCESSES BASED ON MOVING PATTERN

In this paper, the dynamics of complex production processes is characterized by the move of operating condition patterns in pattern moving space. So, we need to construct pattern moving space firstly.

A. Construction of pattern moving space

Firstly, the multi-dimensional running status data are reduced to one dimensional data using principal component analysis. This can be considered as a process of feature extraction. Then, by fuzzy c-mean (FCM) clustering algorithm, the one-dimensional running status samples are partitioned into C pattern classes, that is, $P_1, P_2, \cdots, P_C$. The collection of those classes forms pattern moving space which corresponds to the considered complex production process. An explanatory example for demonstrating the constructed pattern moving space is shown in Fig.1. Each pattern class in pattern moving space can be considered as a qualitative "scale". The pattern samples belonging to the same pattern class have same "scale" value in pattern moving space

If the data is collected in a long enough period of time, the pattern moving space constructed based on these actual running status data can be considered as the running subspace of the system. Dynamics description and control problems can be discussed in this space. When the actual running status sample is out of the pattern moving space, the pattern moving space can be expanded by using the following method.

When a new pattern sample is classified into its belonging class, the distance between the pattern sample and this class center is calculated. If this distance is more than the class radius, then a new pattern class generates. In this paper, the new pattern sample is used as a new class center and the membership function can be computed for the new pattern class.

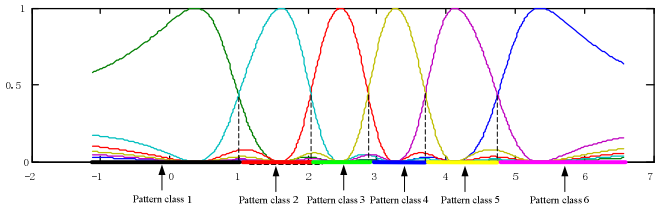

Fig.1 Pattern moving space composed of six pattern classes. The horizontal axis denotes the values of dimension reduced running status samples, and vertical axis denotes membership function values corresponding to dimension reduced running status samples.

B. The representation of pattern classes

In fact, each pattern class obtained in the above section is a qualitative description about pattern. In order to characterize quantitatively the dynamics of complex production processes in pattern moving space, each pattern class must be represented quantitatively. In this paper, we adopt interval numbers to represent pattern classes.

First, finding the maximum I_i^U and minimum I_i^L among the samples belonging to the same pattern class P_i , $i=1,\cdots,C$, where C is the number of pattern classes constructing the pattern moving space. Then, the maximum I_i^U and minimum I_i^L are used to construct an interval number

$I_i = [I_i^L, I_i^U]$. Thus, $I_i = [I_i^L, I_i^U]$ is the interval number characterizing pattern class P_i quantitatively. Let $I = \{I_1, I_2, \cdots, I_C\}$, it is the quantitative pattern moving space corresponding to pattern moving space P defined in above section. Here, quantified pattern classes are ordered from small to big in terms of the center values of I_i s. That is, $a_1 < a_2 < \cdots < a_C$, where $a_i = \dfrac{I_i^L + I_i^U}{2}$, $i = 1, \cdots, C$.

C. The definition of pattern class variable

In order to describe the movement of system in pattern moving space, a variable called pattern class variable is defined.

Assuming that $\{sx(k)\}$ and $\{mx(k)\}$ denotes measurement sample time series and pattern sample time series, respectively. Then pattern class variable must satisfy the following transformation:

$$mx(k) = T(sx(k)) \tag{8}$$

$$dx(k) = F(mx(k)) \tag{9}$$

Where $T(\cdot)$ and $F(\cdot)$ denote feature extraction and classification, respectively, $dx(k)$ is the pattern class variable.

Obviously, pattern class variable has two main characteristics:

(i) It is a variable over time.

(ii) It has the class attribute.

Pattern class variable is used to describe the variation of pattern class to which running status data belong over time in pattern moving space. And it together with pattern moving space forms the basis of the proposed modeling approach. The pattern class variable's metric form is not unique. In this paper, interval number is used as its metric form. That is, given at time instant *t*, $mx(k)$ is classified into pattern class i, and then let $dx(t) = I_i = [I_i^L, I_i^U]$. Thus, a pattern sample time series in Euclidean space is transformed into a pattern class variable time series in pattern moving space.

D. Modeling of Complex Production Processes based on moving pattern

In this paper, as interval numbers is used as the pattern class variable's metric form, so, in fact pattern class variable time series is an interval number time series. The dynamics of complex production processes is characterized by the transition of pattern class variable $dx(k)$ in pattern moving space. The dynamic model based on moving pattern is as follows:

$$\begin{aligned} dx(k) &= F(d\tilde{x}(k)) \\ &= F(f(dx(k-1), dx(k-2) \cdots dx(k-m_y) \\ &\qquad u(k-1), u(k-2), \cdots, u(k-m_u))) \end{aligned} \tag{10}$$

m_y and m_u, the orders of the considered dynamic systems; in this paper, m_y and m_u are assumed to be known priorly. $dx(t)$ is the pattern class variable, $F(\cdot)$ denotes classification, $d\tilde{x}(t)$ is the initial prediction output of pattern class variable and $d\tilde{x}(t) = f(\cdot)$ is a kind of initial prediction model. $u(k)$ is general system input represented by crisp real numbers, $u(k) \in R$.

The proposed moving pattern based modeling approach is composed of two steps.

1) Constructing the initial prediction model using the adapted interval T-S fuzzy model (ITSFM).

For modeling the moving of pattern class variable in pattern moving space, our previous proposed interval T-S fuzzy model (ITSFM) [11] is adapted and applied to moving pattern based modeling of complex production processes. The adapted ITSFM used to model of complex production complex in pattern moving space is as follows:

R^i : If $dx_c(k-1)$ is A_1^i and $dx_c(k-2)$ is A_2^i , $\cdots$, $dx_c(k-m_y)$ is $A_{m_y}^i$ and $u(k-1)$ is B_1^i , and $u(k-2)$ is B_2^i,…, $u(k-m_u)$ is $B_{m_u}^i$

then

$$\begin{aligned} dx^i(k) = \theta_0^i + \theta_1^i dx_c(k-1) + \cdots + \theta_{m_y}^i dx_c(k-m_y) + \\ + \theta_{m_y+1}^i u(k-1) + \theta_{m_y+2}^i u(k-2) + \cdots \\ + \theta_{m_y+m_u}^i u(k-m_u) \end{aligned} \tag{11}$$

Where A_j^i , B_q^i are the corresponding fuzzy sets. $dx_c(k-j)$ represents the center of pattern class variable $dx(k-j)$ at time instant $k-j$, that is, if the value of $dx(k-j)$ is equal to $I_i = [I_i^L, I_i^U]$ at time instant $k-j$, then $dx_c(k-j)$ is equal to $\dfrac{I_i^L + I_i^U}{2}$. $\theta_l^i = (a_l^i, c_l^i)$ is an interval number, a_l^i and c_l^i are the center and radius of θ_l^i , respectively. The membership grade $A_j^i(dx_c(k-j))$ and $B_q^i(u(k-q))$ are obtained by fuzzy *c*-means clustering algorithm in this paper, $l = 0,1,2,\cdots, m_y + m_u$, $j = 1,2,\cdots, m_y$, $q = 1,2,\cdots, m_u$, $i = 1,2,\ldots, r$, r denotes the number of rules.

The predicted interval output of the improved ITSFM, that is, $d\tilde{x}(k)$ is inferred as

$$d\tilde{x}(k) = \frac{\sum_{i=1}^{r} \omega_i dx^i(k)}{\sum_{i=1}^{r} \omega_i}, \tag{12}$$

Where $\omega_i = \prod_{j=1}^{m_y} A_j^i(dx_c(k-j)) \prod_{q=1}^{m_u} B_q^i(u(k-q))$

Let $\tilde{\omega}_i = \dfrac{\omega_i}{\sum_{i=1}^{r}\omega_i}$, then

$$
\begin{aligned}
d\tilde{x}(k) &= \sum_{i=1}^{r}\tilde{\omega}_i dx^i(k) \\
&= \sum_{i=1}^{r}\tilde{\omega}_i[\theta_0^i + \theta_1^i dx_c(k-1) + \cdots + \theta_{m_y}^i dx_c(k-m_y) \\
&\quad + \theta_{m_y+1}^i u(k-1) + \theta_{m_y+2}^i u(k-2) + \cdots \\
&\quad + \theta_{m_y+m_u}^i u(k-m_u)] \\
&= \sum_{i=1}^{r}\tilde{\omega}_i[(a_0^i, c_0^i) + (a_1^i, c_1^i)dx_c(k-1) + \cdots \\
&\quad + (a_{m_y}^i, c_{m_y}^i)dx_c(k-m_y) + (a_{m_y+1}^i, c_{m_y+1}^i)u(k-1) \\
&\quad + (a_{m_y+2}^i, c_{m_y+2}^i)u(k-2) + \cdots \\
&\quad + (a_{m_y+m_u}^i, c_{m_y+m_u}^i)u(k-m_u)] \\
&= \sum_{i=1}^{r}\omega_i(\mathbf{A}_i^t\mathbf{x}(k), \mathbf{C}_i^t \mid \mathbf{x}(k)\mid) \\
&= (\sum_{i=1}^{r}\omega_i\mathbf{A}_i^t\mathbf{x}(k), \sum_{i=1}^{r}\omega_i\mathbf{C}_i^t \mid \mathbf{x}(k)\mid)
\end{aligned}
\tag{13}
$$

Where

$$
\begin{aligned}
&\mathbf{A}_i = (a_0^i, a_1^i, \cdots, a_{m_y+m_u}^i)^t,\ \mathbf{C}_i = (c_0^i, c_1^i, \cdots, c_{m_y+m_u}^i)^t, \\
&\mathbf{x}(k) = (1, dx_c(k-1), dx_c(k-2), \cdots, dx_c(k-m_y), \\
&\qquad u(k-1), u(k-2), \cdots, u(k-m_u))^t, \\
&\mid \mathbf{x}(k)\mid = (1, \left|dx_c(k-1)\right|, \left|dx_c(k-2)\right|, \cdots, \left|dx_c(k-m_y)\right|, \\
&\qquad \left|u(k-1)\right|, \left|u(k-2)\right|, \cdots, \left|u(k-m_u)\right|)^t
\end{aligned}
$$

Furthermore, $\hat{p}(k)$ can be expressed as

$$
d\tilde{x}(k) = (\mathbf{A}^t\tilde{\mathbf{x}}(k),\ \mathbf{C}^t\left|\tilde{\mathbf{x}}(k)\right|) \tag{14}
$$

Where $\mathbf{A} = (\mathbf{A}_1^t, \mathbf{A}_2^t, \cdots, \mathbf{A}_r^t)^t$, $\mathbf{C} = (\mathbf{C}_1^t, \mathbf{C}_2^t, \cdots, \mathbf{C}_r^t)^t$

$$
\begin{aligned}
\tilde{\mathbf{x}}(k) &= (\tilde{\omega}_1\mathbf{x}(k)^t, \tilde{\omega}_2\mathbf{x}(k)^t, \cdots \tilde{\omega}_r\mathbf{x}(k)^t)^t \\
\left|\tilde{\mathbf{x}}(k)\right| &= (\tilde{\omega}_1\left|\mathbf{x}(k)\right|^t, \tilde{\omega}_2\left|\mathbf{x}(k)\right|^t, \cdots, \tilde{\omega}_r\left|\mathbf{x}(k)\right|^t)^t
\end{aligned}
$$

$\mathbf{A}^t\tilde{\mathbf{x}}(k)$ and $\mathbf{C}^t\left|\tilde{\mathbf{x}}(k)\right|$ are the center and radius of the initial predicted interval output $d\tilde{x}(k)$, respectively.

Different from our previous work [13], the parameters in (14) are obtained by minimizing the following objective function J in (15) subject to the constraints $c_j^i \geq 0$ as the radius of an interval is greater than or equal to zero, $i = 1, 2, \ldots, r$, $j = 0, 1, 2, \cdots, m_y + m_u$. Where $d\tilde{x}^L(k)$, $d\tilde{x}^U(k)$ are the lower and upper bound of the initial prediction output $d\tilde{x}(k)$, respectively, $dx^L(k)$, $dx^U(k)$ are the lower and upper bound of real pattern class variable $dx(k)$ at time instant k, respectively.

$$
\begin{aligned}
&\underset{\mathbf{A},\mathbf{C}}{Min} \quad J = \sum_{k=1}^{N}[dx^L(k) - d\tilde{x}^L(k)]^2 + \sum_{k=1}^{N}[dx^U(k) - d\tilde{x}^U(k)]^2 \\
&\text{subject to } c_j^i \geq 0, i = 1,2,\cdots,r,\ j = 0,1,2,\cdots,m_y + m_u
\end{aligned}
\tag{15}
$$

2) After obtaining the initial prediction output $d\tilde{x}(k)$, the finial prediction output $d\hat{x}(k)$ can be obtained by classifying the initial prediction output $d\tilde{x}(k)$ into the pattern class which is nearest to the initial prediction output $d\tilde{x}(k)$ by calculating the Hausdorff distance between the initial prediction output $d\tilde{x}(k)$ and each pattern class I_i in pattern moving space. That is, if $j = \underset{i=1,2,\cdots,C}{\arg\min}\left(D(d\tilde{x}(k), I_i)\right)$, then the final prediction output $d\hat{x}(k)$ is equal to I_j, where $I_i = [I_i^L, I_i^U]$ is the quantified value of pattern class i, $i = 1,2,\cdots,C$, C is the number of pattern class in pattern moving space. $D(d\tilde{x}(k), I_i)$ denotes the Hausdorff distance between interval number $d\tilde{x}(k)$ and I_i.

IV. NUMERICAL EXAMPLE

In this chapter, one practical example- sintering process of Anyang (one city of Henan Province of China) iron and steel plant is given to verify the validity of the proposed moving pattern-based modeling approach.

In the example, the actual running status data collected from sintering process of Anyang (one city of Shandong Province of China) iron and steel plant are used. The data consist of 864 pairs of input-output samples of a sintering process: the input $u(k)$ is the temperature of ignition hood and the output $y(k)$ is the first principal component of exhaust gas temperatures of three wind boxes, and the sampling time is 25s. In this example, the input and output data are normalized by statistical normalization, that is, $Z = \dfrac{X - \mu}{\sigma}$, where μ and σ are the mean and standard deviation of X, respectively. Fig.2 shows the 864 pairs of input-output samples. In this example, 864 running status samples $y(k)$ are used to constructing the pattern moving space by fuzzy c-means (FCM) clustering algorithm. Here, the cluster number is set to 20. The 20 pattern classes P_i represented by interval numbers are shown in Table I. The running status time series $y(k)$ in Euclidean space and the corresponding pattern class variable time series $\tilde{p}(k)$ characterized by intervals in pattern moving space are shown in Fig.3, $k = 1,2,\cdots,100$. From Fig.3, we can see that the transition of pattern class variable from one pattern class to another in pattern moving space can also characterize change of running status $y(k)$ in general.

In this example, the first 500 pairs of input-output samples are used to train the proposed initial prediction model, the

others are used to validate the model. The initial prediction model based on ITSFM is as follows:

R^i : If $dx_c(k-1)$ is A_1^i and $dx_c(k-2)$ is A_2^i and $dx_c(k-3)$ is A_3^i and $dx_c(k-4)$ is A_4^i and $u(k-1)$ is B_1^i

Then:

$$dx^i(k) = \theta_0^i + \theta_1^i dx_c(k-1) + \theta_2^i dx_c(k-2) + \theta_3^i dx_c(k-3) + \theta_4^i dx_c(k-4) + \theta_5^i u(k-1)$$

Where $dx_c(k-1)$ is the center of $dx(k-1)$. The membership grade $A_1^i(dx_c(k-1))$ and $B_1^i(u(k-1))$ is obtained by fuzzy *c*-means clustering algorithm which was adopted in [12] for determining the premise structure of T-S fuzzy model. $\boldsymbol{\theta}^i = [\theta_0^i, \theta_1^i, \theta_2^i, \theta_3^i, \theta_4^i, \theta_5^i]$ is the interval parameter vector in consequent part of ITSFM. Based on formula (15), the interval parameters in the consequent part of ITSFM are obtained and shown in Table II.

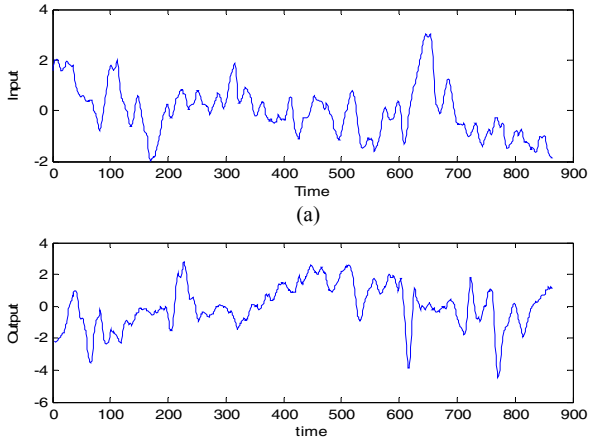

Fig.2 The input and output signals of the sintering process: (a) input $u(k)$; (b) output $y(k)$

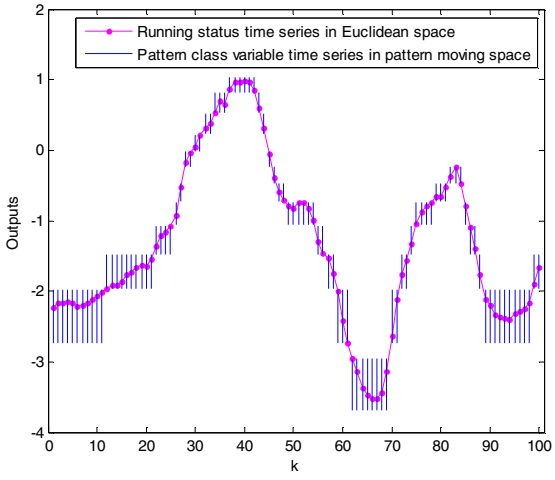

Fig.3 The running status time series $y(k)$ (dots) and the corresponding pattern class variable time series $dx(k)$ (segments) characterized by intervals

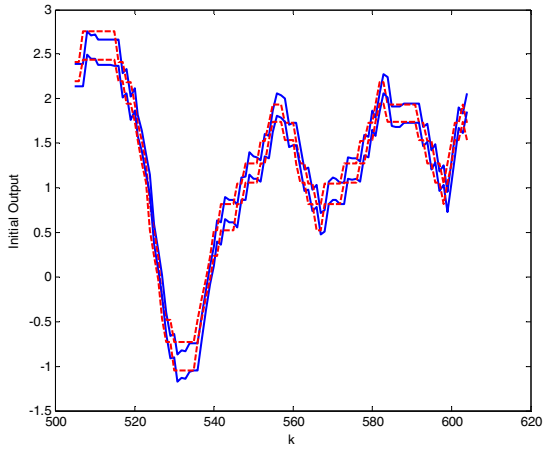

Fig.4 The initial prediction outputs $d\tilde{x}(k)$ (solid line) obtained by ITSFM and the real pattern class variable time series $dx(k)$ (dashed line).

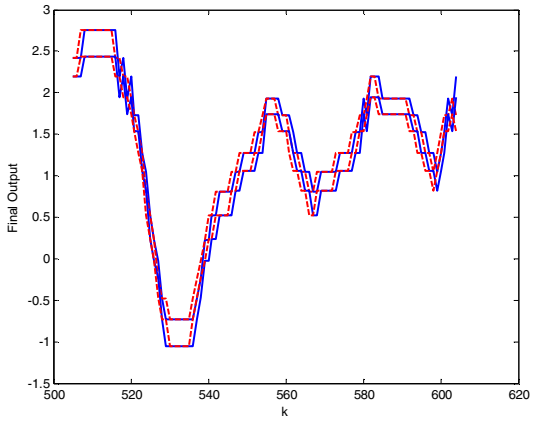

Fig.5 The final prediction outputs $d\hat{x}(k)$ (solid line) of the proposed model and the real pattern class variable time series $dx(k)$ (dashed line).

In Fig.4, the solid lines represent the initial prediction output $d\tilde{x}(k)$ obtained by the ITSFM with 4 fuzzy rules, and the dashed lines represent the real pattern class variable time series $dx(k)$ with time from 505 to 600. After the initial prediction output $d\tilde{x}(k)$ is classified, the final outputs $d\hat{x}(k)$ of the proposed model are obtained. In Fig.5, the solid lines represent the final outputs of the proposed model, the dashed lines represent the pattern class variable time series $dx(k)$ with time from 505 to 600. By comparing Fig.4 with Fig.5, we can see that the small difference between initial prediction output $d\tilde{x}(k)$ and the corresponding real pattern class variable time series $dx(k)$ at some time instant (for example *k*=508-515, 530-535, 585-591) is eliminated after $d\tilde{x}(k)$ is classified.

V. CONCLUSION

In this paper, in contrast to traditional modeling approach to characterizing dynamical systems in Euclidean space, the dynamics of complex production processes is characterized by

TABLE II
THE IDENTIFIED INTERVAL PARAMETERS IN CONSEQUENT PART OF ITSFM

Interval parameters \ Rule i	i=1	i=2	i=3	i=4
θ_0^i	(0.1433, 0.0738)	(0.0001, 0.1217)	(-0.0558, 0.0644)	(-0.1388, 0.0373)
θ_1^i	(1.2793, 0.0068)	(1.1292, 0.0000)	(1.1333, 0.1147)	(0.8526, 0.1251)
θ_2^i	(-0.1925, 0.0000)	(0.0711, 0.0039)	(0.0932, 0.0000)	(0.3105, 0.0021)
θ_3^i	(0.0274,0.0000)	(-0.0864,0.0000)	(0.0757,0.0000)	(-0.0547,0.0000)
θ_4^i	(-0.1913,0.0112)	(-0.1268, 0.0068)	(-0.3706,0.0000)	(-0.2143,0.0000)
θ_5^i	(-0.0102,0.0000)	(-0.0352, 0.0082)	(0.0445,0.0000)	(-0.0408, 0.0081)

TABLE I
REPRESENTION OF PATTERN CLASSES BY INTERVAL NUMBER

P_i	$I_i = [\underline{I_i}, \overline{I_i}]$
1	[-4.4856, -3.8815]
2	[-3.6970, -2.9504]
3	[-2.7281, -1.9855]
4	[-1.9612, -1.4761]
5	[-1.4707, -1.0692]
6	[-1.0535, -0.7335]
7	[-0.7262, -0.4766]
8	[-0.4681, -0.2368]
9	[-0.2304, -0.0229]
10	[-0.0215, 0.2212]
11	[0.2330, 0.5212]
12	[0.5257, 0.8140]
13	[0.8200, 1.0430]
14	[1.0558, 1.2733]
15	[1.2774, 1.5243]
16	[1.5413, 1.7245]
17	[1.7445, 1.9327]
18	[1.9451, 2.1911]
19	[2.1939, 2.4154]
20	[2.4309, 2.7607]

movement of pattern class variable in pattern moving space. That is, we view the considered complex production the processes at the level of pattern class and capture only the dominant characteristics of the process. Each pattern class in pattern moving space can be considered as a "scale". Running status patterns belonging to the same pattern class are characterized (quantified) by the same pattern class label (interval number). Running status time series in Euclidean space is transformed into pattern class time series in pattern moving space.

REFERENCES

[1] S.D.Qu, "Pattern recognition approach to intelligent automation for complex industrial processes," *Journal of University of Science and Technology Beijing*, vol.20, pp.385-389, Aug.1998.

[2] E.H.Bristol, "Pattern recognition: An alternative to parameter identification in adaptive control," *Automatica*, vol.13,pp.197-202, Mar.1977.

[3] Kar-Ann Toh and R.Devanathan, "Pattern-based identification for control applications," *IEEE Trans.on Control Systems Technology*, vol.4, pp.641-648, Nov.1996.

[4] Yu-Chu Tian, Futao Zhao, B.H.Bisowarno, and Moses O. Tade, "Pattern-based predictive control for ETBE reactive distillation," *Journal of Process Control*, vol.13, pp.57-67, Feb.2003.

[5] Rachelle Howard and Douglas Copper, "A novel pattern-based approach for diagnostic controller performance monitoring," *Control Engineering Practice*, vol.18, pp.279-288, Mar.2010.

[6] B. Porter, A. H. Jones and C. B. McKeown, "Real-time expert tuners for PI-controllers," *IEE Proc., Part D*, vol. 134, pp. 260-263, Jul.1987..

[7] M.Klein, T.Marczinkowsky, and M.Pandit, "An elementary pattern recognition self-tuning PI-controller," *in Proc.IFAC Int.Symp.Intell.Tuning and Adaptive Contr*, Singapore, Jan.1991, pp.17-21.

[8] M.S.Caceci and W.P.Cacheris, "Fitting curves to data," *BYTE*, pp.340-362, May.1984.

[9] A.G.Hill and W.Raksakij, "Process and disturbance identification by curve fitting the closed loop response," in *Proc.Amer.Contr.Conf.,* Pittsburgh, PA, USA, Jun. 1989, pp.2206-2209.

[10] Moore R E. Methods and Applications of Interval analysis, Englewood Cliffs: Prentice-Hall, 1979. 9-17

[11] C.P.Sun and Z.G.Xu, "Extended T-S Fuzzy Model based on Interval Arithmetic and Its Application to Interval Nonlinear Regression Analysis," in *Proc.18th IEEE Int. Conf. Fuzzy Syst*., Jeju, South Korea, Aug. 2009, pp.1773-1778.

[12] L.Wang and R.Langari, "Complex systems modeling via fuzzy logic," *IEEE Transactions on System Man,and Cybernetics*, vol. 26,pp.100-106, Feb.1996.

2011 IEEE International Conference on Fuzzy Systems
June 27-30, 2011, Taipei, Taiwan

Multiple Characterisation Modelling of Friction Stir Welding Using a Genetic Multi-objective Data-driven Fuzzy Modelling Approach

Qian Zhang, Mahdi Mahfouf, George Panoutsos
Department of Automatic Control and Systems Engineering
The University of Sheffield
Sheffield, UK
{qian.zhang, m.mahfouf, g.panoutsos}@sheffield.ac.uk

Kathryn Beamish, Ian Norris
TWI Ltd
Cambridge, UK
{kathryn.beamish, ian.norris}@twi.co.uk

***Abstract*—Friction Stir Welding (FSW) is a relatively new solid-state joining technique, which is versatile, environment friendly, and energy and time efficient. For a comprehensive understanding of the effects of process conditions, such as tool rotation speed and traverse speed, on characterisations of welded materials, it is essential to establish prediction models for different aspects of the materials' behaviours. Because of the high complexity of the FSW process, it is often difficult to derive accurate and yet transparent enough mathematical models. In such a situation, a systematic data-driven fuzzy modelling approach is developed and implemented in this paper to model FSW behaviour relating to AA5083 aluminium alloy, consisting of microstructural features, mechanical properties, as well as overall weld quality. This methodology allows constructing transparent fuzzy models considering both accuracy and interpretability attributes of fuzzy systems. The elicited models proved to be accurate, interpretable and robust and can be further applied to facilitate the optimal design of process parameters, with the aim of finding the optimal combinations of process parameters to achieve desired welding properties.**

Keywords-friction stir welding; aluminium alloy; mechanical property; microstructure; weld quality; fuzzy; modelling; multi-objective; NSGA-II

I. INTRODUCTION

Friction Stir Welding (FSW) is a practical solid-state joining technique, which was invented at The Welding Institute (TWI), UK in 1991 [1]. It was initially developed for welding aluminium alloys, and nowadays has been extended to be implemented in a variety of materials, including magnesium alloys [2], steels [3], copper alloys [4], titanium alloys [5], etc.

In a standard FSW process, a non-consumable rotating tool with a shoulder and a pin is inserted into the abutting edges of two rigidly clamped plates to be joined, as shown in Fig. 1 [6]. The tool moves along the joint line of the butting surfaces while the shoulder makes firm contact with the top surface of the work-piece. With the tool rotation, heat generated by friction between the tool and the work-piece softens the material being welded. Severe plastic deformation and flow of this plasticised metal occurs as the tool is rotating and travelling along the welding direction. Material is transported from the front of the tool to the trailing edge where it is forged into a joint.

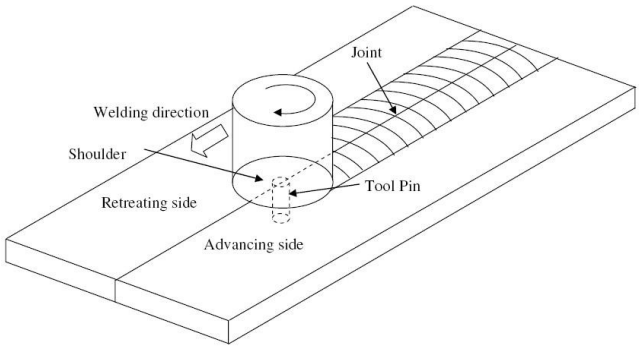

Figure 1. A schematic drawing of friction stir welding [6].

The FSW process involves intense plastic deformation and complex thermo-mechanical processes, which result in recrystallisation and development of texture within and around the stirred zone [7]. A typical cross-section of the FSW joint consists of three distinct zones, stirred (nugget) zone, Thermo-Mechanically Affected Zone (TMAZ), and Heat-Affected zone (HAZ), which can be identified in Fig. 2 [7].

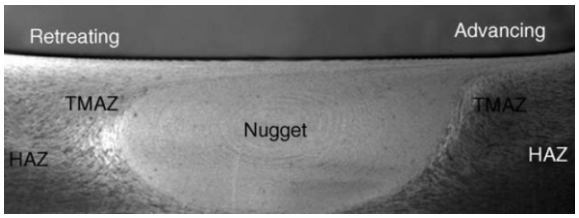

Figure 2. A cross-section macrograph of FSW showing various micro-structural zones [7].

During the FSW process, the material undergoes intense plastic deformation at elevated temperature, resulting in generation of fine and equiaxed recrystallised grains [8]. This fine microstructure produces good mechanical properties for the welded material. In addition, FSW demonstrates its

978-1-4244-7316-8/11/$26.00 ©2011 IEEE

versatility as it is able to weld dissimilar alloys and dissimilar composites [9], for various types of joints, such as butt joints, lap joints, fillet joints, etc. FSW is also considered to be a "green" technology due to its energy efficiency and environment friendliness [7]. Compared to conventional welding methods, FSW consumes considerably less energy and it does not need shielding gas or flux, thereby making the process environmentally friendly. Since its invention in 1991 [1], FSW has found widespread applications in diverse industries, for example, aerospace, shipbuilding, automotive and railway industries [10].

For a comprehensive understanding of the effects of process conditions, such as tool rotation speed and traverse speed, on characterisations of welded materials, it is essential to construct accurate and reliable prediction models. Because of the high complexity of the FSW process, it is often 'tricky' to derive practical physical models. In such a situation, a systematic data-driven fuzzy modelling strategy is developed in this paper to elicit adequate prediction models based on experimental data, which include the micro-structural features, mechanical properties, as well as overall weld quality relating to AA5083 aluminium alloy.

Compared with analytically based methods, fuzzy systems are simpler in structure and easier to apply. They are capable of learning from data without needing much prior knowledge about the materials and processing [11], [12]. Fuzzy models are also convenient when combined with optimisation techniques to identify the input parameters that will provide a desirable behaviour profile [13], [14]. On the other hand, compared with black-box modelling approaches, such as Artificial Neural Networks (ANNs), fuzzy systems have transparent characteristics and the relationships between inputs and outputs are more interpretable, because of their use of descriptive language, such as linguistic 'IF-THEN' rules.

The proposed fuzzy modelling methodology allows to generate fuzzy models considering not only accuracy (precision) but also transparency (interpretability) of fuzzy systems via applying multi-objective optimisation techniques. As a result, a set of so-called 'Pareto-optimal' [15] models, in terms of different accuracy and interpretability levels, are constructed, which provide a wide range of choices for practitioners or users. In this paper, a hierarchical optimisation structure is proposed to improve the modelling efficiency, where two learning methods are systematically combined in order to improve various attributes of fuzzy systems: One multi-objective optimisation algorithm, the Non-dominated Sorting Genetic Algorithm II (NSGA-II) [16], is used to optimise the model's structure; Based on a fixed model structure, the other single-objective learning paradigm, the Gradient Descent (GD) method is employed to improve the model's parameters.

The remaining parts of this paper are organised as follows. Section II introduces the proposed modelling framework. Section III presents the experimental studies on modelling the FSW-related properties in detail. Finally, conclusions in relation to the whole study are drawn in Section IV.

II. THE MODELLING METHODOLOGY

A. Introduction to fuzzy systems

Fuzzy rule-based systems are viewed as robust 'universal approximators' capable of performing nonlinear mappings between inputs and outputs. It is an approach that allows a system to be represented using a descriptive language (linguistic 'IF-THEN' rules), which can easily be understood and explained by humans to allow them to gain a deeper insight into uncertain, complex and ill-defined systems.

Generally, a fuzzy system consists of four fundamental components: fuzzy rule-base, fuzzy inference engine, fuzzifier and defuzzifier. Fig. 3 shows the diagram of a fuzzy system. The central part of a fuzzy system is the knowledge-base (rule-base) consisting of the fuzzy rules. A fuzzy rule is an IF-THEN statement in which some words are characterised by continuous membership functions. Specifically, the fuzzy rule-base comprises the following fuzzy rules:

Rule$_l$: IF x_1 is A_1^l AND … AND x_n is A_n^l, THEN y is B^l,

where l = 1, 2, …, m; m is the number of rules in the fuzzy rule-base; A_i^l and B^l are fuzzy sets in $U_i \subset R$ and $V \subset R$, respectively, and $\boldsymbol{x} = (x_1, x_2, \ldots, x_i)^T \in U$ and $y \in V$ are the input and output (linguistic) variables of the fuzzy system, respectively.

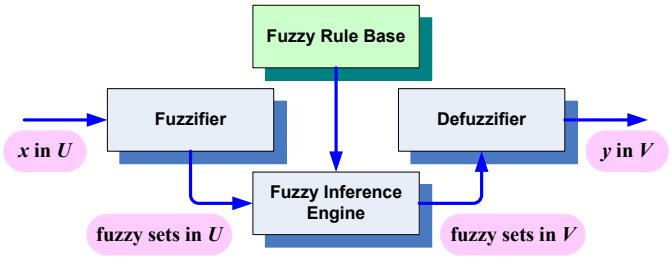

Figure 3. Basic configuration of fuzzy systems.

The fuzzifier is defined as a mapping from a real-valued point $\boldsymbol{x}^* \in U \subset R^i$ to a fuzzy set A^* in U. Normally, three types of fuzzifiers are used, which are singleton fuzzifier, Gaussian fuzzifier and triangular fuzzifier. They correspond to three types of fuzzy sets with different shapes of membership functions. In a fuzzy inference engine, fuzzy logic principles direct how to employ the fuzzy rules into a mapping from an input fuzzy set A^* to an output fuzzy set B^*. The defuzzifier is a mapping from the output fuzzy set B^* in $V \subset R$ to a real-valued point $y^* \in V$. Conceptually, the purpose of the defuzzifier is to specify a point in V that best represents B^*. Three widely used defuzzifiers are centre of gravity defuzzifier, centre average defuzzifier and maximum defuzzifier [17].

Fuzzy modelling is a systems modelling approach with fuzzy rule-based systems. In most of the fuzzy modelling methods, the fuzzy inference engine and the defuzzifier are predefined. Thus, the primary work is to generate appropriate fuzzy sets and right fuzzy rules.

B. A hierarchical multi-objective fuzzy modelling approach

Generally, data-driven fuzzy modelling can be viewed as a two-step process. The first step aims to generate a 'crude'

approximation of the fuzzy model. The second step consists of optimising the initial fuzzy rules and fuzzy sets to lead to a final 'optimised' fuzzy model.

For the first step, it can be achieved via two different methods: the grid-partitioning based method or the clustering based method. For the first method, the grid-partitioning defines a number of evenly distributed fuzzy sets for each variable. These fuzzy sets are shared by all the fuzzy rules. The main disadvantage of this method, in its basic version, lies in the large number of generated fuzzy rules when dealing with a high-dimensional modelling problem. In contrast, the second method employs data clustering information to define fuzzy sets. The fuzzy sets are not shared by all the rules, but each set is only mapped into one particular fuzzy rule. In this method, each fuzzy rule is associated to one cluster. In this paper, the clustering based method is employed, which includes a previously developed high-performance clustering algorithm, an agglomerative complete-link clustering algorithm [18].

For the second step, the main learning and optimisation techniques include linear least squares, gradient descent methods, neuro-fuzzy training methods, and some evolutionary optimisation techniques (evolutionary fuzzy systems). Compared with the fuzzy systems using other learning techniques, evolutionary fuzzy systems are able to realise improvements on not only the parameters but also the structure of the fuzzy systems. Moreover, multi-objective optimisation techniques within the evolutionary computation can prove very helpful in studying the trade-off between the accuracy and the interpretability of fuzzy systems. Some recent works in the literature [19], [20] have employed multi-objective optimisation techniques to tackle the trade-off issue of fuzzy models, while most of them were carried out based on grid-partitioning-type fuzzy sets.

In the previously proposed modelling approach [18], [21], a multi-objective optimisation algorithm was used to improve fuzzy models' structure and tune their parameters at the same time. This method would use relatively more calculation and would take longer to converge, where a large number of decision variables need to be adjusted and optimised simultaneously.

In this paper, a hierarchical optimisation structure is proposed, where two learning techniques conduct sequentially and iteratively to improve the different aspects of fuzzy systems: the multi-objective optimisation algorithm NSGA-II [16] is mainly employed to optimise the model's structure; while the gradient descent method is employed to improve the model's parameters. The NSGA-II algorithm has been demonstrated as one of the most efficient algorithms for multi-objective optimisation on a number of benchmark problems and applications. Two of the most important features in NSGA-II lie in its fast non-dominated sorting procedure and an elitist strategy. The detailed implementation procedure can be found in [16]. Gradient descent is a first-order optimisation algorithm that can quickly find a local minimum of a function. It has widely been employed in fuzzy modelling for tuning the membership functions [17] and shown to perform efficiently in improving the accuracy of fuzzy models.

Fig. 4 illustrates the proposed fuzzy modelling approach. This approach will be referred to throughout as a Fast Hierarchical Multi-Objective Fuzzy Modelling (FHMO-FM) approach. It can be divided into several components and the execution steps can be described as follows:

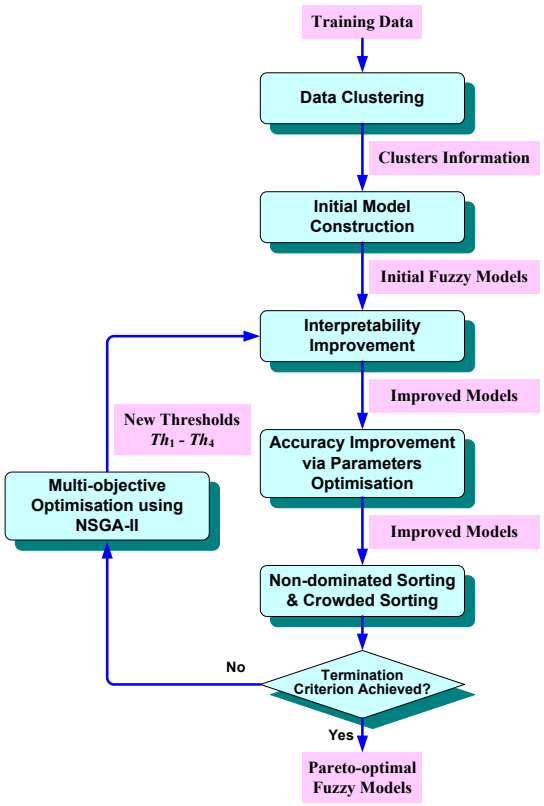

Figure 4. The flow chart of the proposed fuzzy modelling approach.

1. Data clustering: A modified agglomerative complete-link clustering algorithm [18] is employed to process training data in order to obtain the information relating to clusters. This algorithm has been shown to be more efficient and perform better than other well-known clustering algorithms, such as the fuzzy c-means (FCM) clustering algorithm [22].

2. Initial model construction: The information that these clusters provide is then used to construct an initial fuzzy model. In this approach, one cluster corresponds directly to one fuzzy rule; the centres of membership functions are defined using the information of their corresponding clusters' centre positions; other parameters relating to the membership functions are defined under the principle that one membership function must cover all the training data, which are included in its corresponding cluster. More details about this step have been introduced in [11].

3. Interpretability improvement: The fuzzy system is improved in structure, including the variation of the fuzzy rules and fuzzy sets, considering the interpretability issue. This task can be achieved using a four-step operation, including (1) removing redundant fuzzy rules, (2) merging similar fuzzy rules, (3) removing redundant fuzzy sets and (4) merging similar fuzzy sets. These four steps are controlled by 4

threshold parameters, Th_1 – Th_4. The details relating to the whole operation have been explained in [18], [21].

4. Accuracy improvement: The fuzzy models are improved by the gradient descent method [17] in terms of accuracy based on a fixed modelling structure.

5. Non-dominated sorting and crowed sorting: The non-dominated fuzzy models with a good diversity are found using the non-dominated sorting and crowed sorting mechanism, which are introduced in the algorithm NSGA-II [16].

6. Termination check: If the termination criterion is achieved, the modelling process is stopped and the final Pareto-optimal solutions are obtained; if not, all the modelling and performance information are passed to the algorithm NSGA-II. Normally, the termination criteria are designed so that the number of function evaluations achieves a predefined value.

7. Multi-objective optimisation using NSGA-II: The algorithm generates new control parameters (Th_1 – Th_4) for interpretability improvement based on the multi-objective optimisation strategy, then return to Step 3. It should been noted that the structure of a fuzzy model is not directly coded into the optimisation procedure, but is rather varied and optimised via controlling the thresholds. The accuracy of a fuzzy model can be evaluated using the Root Mean Square Error (RMSE) index, which is described as follows:

$$RMSE = \sqrt{\frac{\sum_{l=1}^{N}\left(y_l^m - y_l^p\right)^2}{N}} \tag{1}$$

where y_l^m is the measured output data and y_l^p is the predicted output data, l = 1, 2, …, N; N is the total number of data. The interpretability of a fuzzy model is affected by the number of fuzzy rules (*Nrule*), the number of fuzzy sets (*Nset*) and the total length of fuzzy rules (*Lrule*). To normalise these two objectives and make them similar and comparable in scale, they are formulated as follows:

$$\text{Objective 1: } \frac{RMSE}{RMSE_1} \tag{2}$$

$$\text{Objective 2: } \frac{Nrule}{Nrule_1} + \frac{Nset}{Nset_1} + \frac{Lrule}{Lrule_1} \tag{3}$$

where $RMSE_1$ is the root mean square error of the fuzzy model that is not optimised using the multi-objective optimisation mechanism; $Nrule_1$, $Nset_1$ and $Lrule_1$ represent the number of fuzzy rules, the number of fuzzy sets and the total rule length of this fuzzy model, respectively.

In the next section, this method will be further applied to predict the multiple properties for the friction stir welded materials. In those experiments, the initial number of clusters was set to 9, which means that the initial fuzzy model was generated using 9 rules. For the NSGA-II algorithm, the population size and the archive size were set to be 50 and the number of generation was set to be 200. Every single experiment was carried out over 20 runs. Only one set of typical results out of the 20 runs is selected and shown in the following paragraphs.

III. EXPERIMENTAL STUDIES

AA5083 is a non-heat treatable aluminium alloy that has excellent corrosion resistance and weldability combined with good strength and formability [23]. In this paper, 5.8 mm AA5083 plates were friction stir processed using the MX-Triflute^{TM} tool [24].

For FSW, two independent variables are used to control the process: tool Rotation Speed (RS) (rpm) in clockwise or counter-clockwise direction and Forward Movement per revolution (FM) (mm/rev) along the line of joint. The rotation of tool results in stirring and mixing of material around the rotating pin and the translation of tool moves the stirred material from the front to the back of the pin. Normally, a higher tool rotation speed generates higher temperature because of higher friction heating and results in more intense stirring and mixing of material. In this work, the welds were conducted at five different tool rotation speeds, typically between 200 and 600 rpm and five different traverse feed rates of 0.6, 0.8, 1.0, 1.2, and 1.4 mm/rev.

A. Mechanical properties

First, all the welds being tested for tensile properties at room temperature, including Yield Strength (YS), Ultimate Tensile Strength (UTS), Reduction Of Area (ROA) and elongation, where a two-dimensional Digital Image Correlation (DIC) system (LaVision 2D system running a 2MP monochrome camera) was used for data acquisition and displacement measurements. For each weld profile, 5 separate specimens were produced and tested. Based on these testing data, the intelligent modelling approach is then employed to construct the prediction models for the above mechanical properties.

Tensile specimens were machined from the nugget zone in transverse orientation to the weld. It should be emphasized that the strength obtained in the transverse tensile test represents the weakest region of the weld and the observed ductility is an average strain over the gage length including various zones.

In these tensile tests, failures mainly occurred as shear fracture in the HAZ (see Fig. 5 (a)), because the HAZ has the lowest strength due to significantly coarsened precipitates and the development of the Precipitate-Free Zones (PFZs) [7]. For the welds with defects, failures may also occur in the nugget zone (see Fig. 5 (b)), where porosity voids are produced.

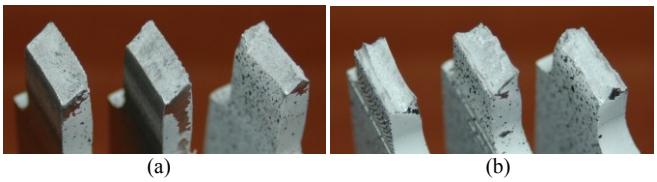

(a) (b)

Figure 5. Fracture surfaces of tensile specimens: fracture occurring in the (a) HAZ and (b) nugget zone.

In the following case relating to the yield strength, 16 data were used for training and 4 data were used for final testing. Fig. 6 demonstrates the trade-offs among the Pareto-optimal models respect to the multiple objectives and various criteria, including the Root Mean Square Error (RMSE), the number of

fuzzy rules, the number of fuzzy sets and the total length of fuzzy rules.

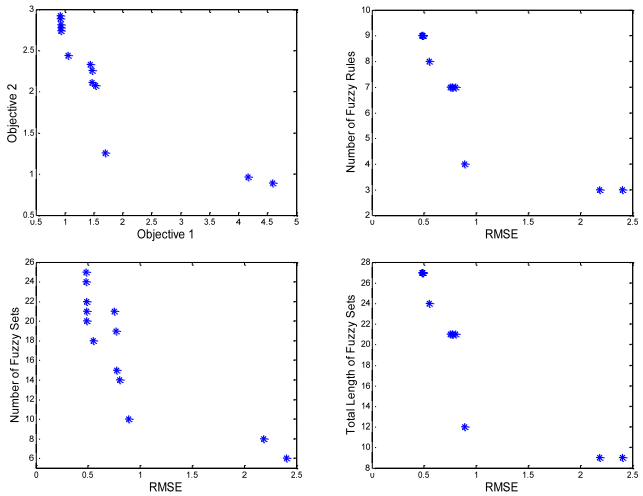

Figure 6. The performance of one set of optimised Pareto-optimal fuzzy models for the yield strength modelling problem.

Table I includes the main parameters of three optimised fuzzy models, which are selected from all the Pareto-optimal models and with 9, 7 and 4 rules respectively. Fig. 7 shows the prediction performance of these models. It can be seen that, for these optimised models, more fuzzy rules and more parameters will bring more accuracy while the models with fewer fuzzy rules and parameters are simpler in structure and easier to understand.

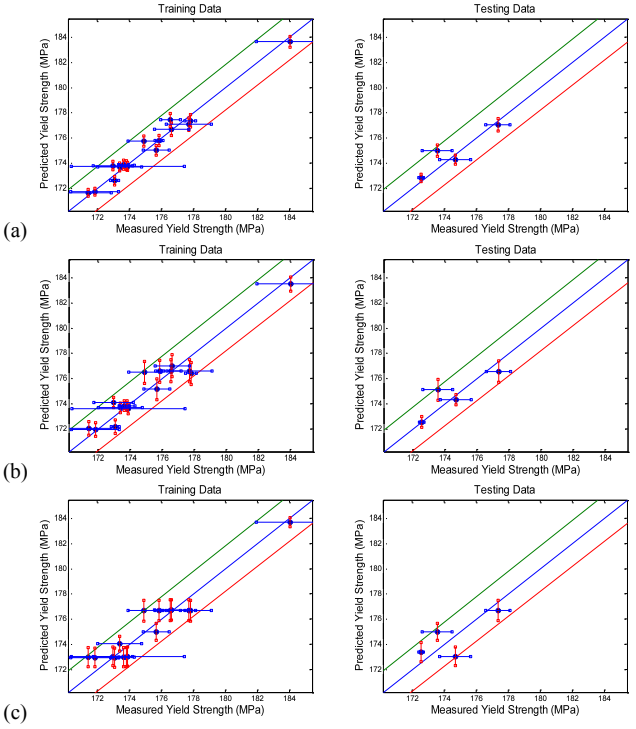

Figure 7. The yield strength models' predicted outputs versus measured outputs (with +1% and -1% error bands): (a) an optimised model with 9 rules, (b) an optimised model with 7 rules, and (c) an optimised model with 4 rules.

TABLE I. MAIN PARAMETERS OF SOME OBTAINED YIELD STRENGTH MODELS

Fuzzy model	*Number of fuzzy sets for each variable*	*Rule length of each fuzzy rule*	*RMSE of training*	*RMSE of testing*
Yield strength model with 9 rules	Inputs: [6; 7] Output: 9	[3; 3; 3; 3; 3; 3; 3; 3; 3]	0.4846	0.7676
Yield strength model with 7 rules	Inputs: [6; 7] Output: 6	[3; 3; 3; 3; 3; 3; 3]	0.7707	0.8878
Yield strength model with 4 rules	Inputs: [3; 4] Output: 3	[3; 3; 3; 3]	0.8901	1.2190

To provide more details about the obtained fuzzy models, Fig. 8 shows the fuzzy rule-base of the 4-fuzzy-rule model. For these fuzzy rules, they can be rewritten as the following approximate linguistic rules using the linguistic hedges approach [25]:

R_1: IF *RS* is *medium small* AND *FM* is *medium large*, THEN *YS* is *small*.
R_2: IF *RS* is *small* AND *FM* is *large*, THEN *YS* is *large*.
R_3: IF *RS* is *large* AND *FM* is *small*, THEN *YS* is *small*.
R_4: IF *RS* is *large* AND *FM* is *medium*, THEN *YS* is *medium*.

By inspecting these linguistic rules, one can understand more about the system's behaviour.

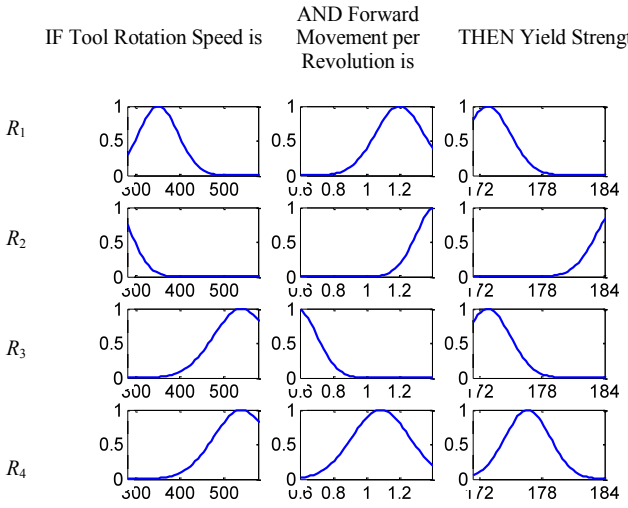

Figure 8. The rule-base of the 4-rule yield strength model.

To verify the physical interpretation of the obtained model, Fig. 9 shows three-dimensional response surfaces of the obtained models. From these surfaces, it can be seen that the models with more fuzzy rules can catch more details from the training data. It can also be observed that, with increasing forward movement per revolution, the yield strength tends to increase. This trend is considered to be consistent with the expected behaviour from the knowledge experts.

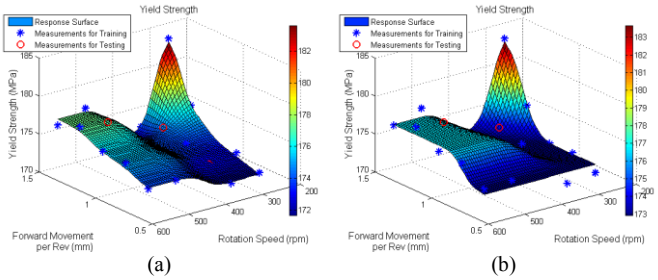

(a) (b)

Figure 9. Response surfaces of the yield strength models: (a) the 9-rule model and (b) the 4-rule model.

B. *Weld quality*

Common defects in friction stir welds include porosity and surface defects [6]. To evaluate the quality of welds, three independent tests were conducted, including a bend test, a surface inspection, and a cross-section inspection. Based on these tests, four sub-indexes are designed to express the various aspects relating to the weld quality, i.e. the face flaws and root flaws in the bend test, the flaws on the surface, and the flaws within the cross-section. The values of such sub-indexes are integers from 0 to 3, where 0 means free from identifiable flaws and 3 represents complete failure or significant number of voids. By summing these sub-indexes together, an overall Weld Quality index (WQ) is obtained to represent the general situation for weld quality, whose value could be from 0 to 12 (0: excellent quality).

In this case, 20 overall weld quality index data were employed in the training phase and the remaining 5 data were used for testing. Fig. 10 demonstrates the trade-offs respect to the multiple criteria within these Pareto-optimal fuzzy models. It can be observed that these Pareto-optimal models exhibit fuzzy sets pattern behaviour, which means that they provide a wider choice of different solutions to users.

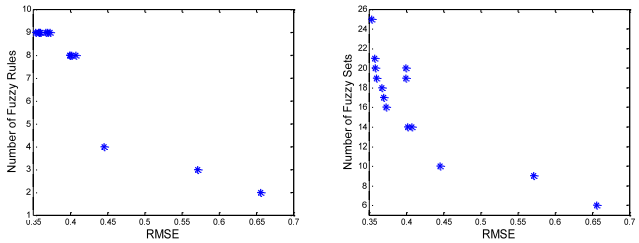

Figure 10. The performance of one set of optimised Pareto-optimal fuzzy models for the weld quality modelling problem.

Table II includes the main parameters of three optimised fuzzy models, which are selected from all the Pareto-optimal models and with 9, 8 and 4 rules respectively. Fig. 11 shows the prediction performance of these models. It can be seen that, for these optimised models, more rules and more parameters will bring more accuracy while the models with fewer rules and parameters are simpler in structure and easier to understand (interpret).

Fig. 12 shows the 3-D response surfaces of these models. From it, one can observe that, at a constant rotational speed, an increase in the travel speed favours the formation of wormhole defects. This shows a consistency with the phenomena reported in other literatures [6], [26].

TABLE II. MAIN PARAMETERS OF SOME OBTAINED WELD QUALITY MODELS

Fuzzy model	*Number of fuzzy sets for each variable*	*Rule length of each fuzzy rule*	*RMSE of training*	*RMSE of testing*
Weld quality model with 9 rules	Inputs: [5; 7] Output: 6	[3; 3; 3; 3; 3; 3; 3; 3; 3]	0.3751	0.3047
Weld quality model with 8 rules	Inputs: [4; 6] Output: 6	[3; 3; 3; 3; 3; 3; 3; 3]	0.3993	0.3313
Weld quality model with 4 rules	Inputs: [5; 4] Output: 5	[3; 3; 3; 3; 3]	0.4452	0.5165

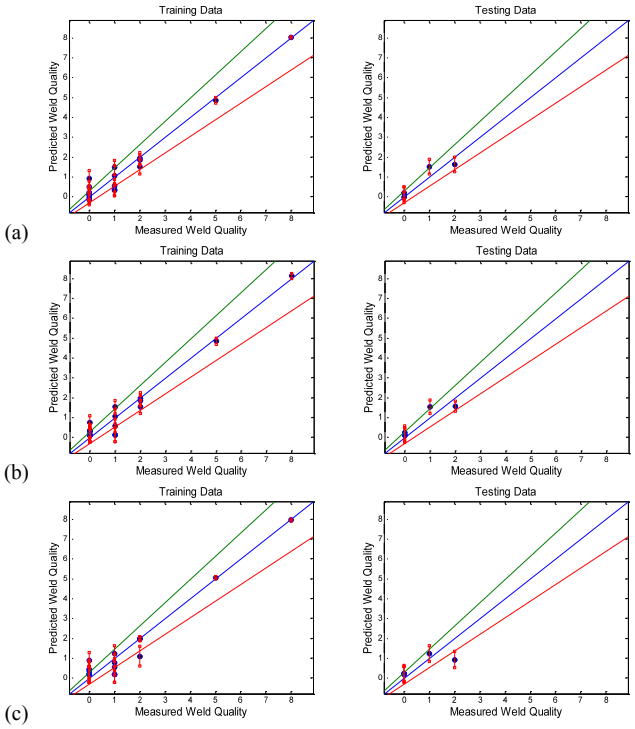

Figure 11. The weld quality models' predicted outputs versus measured outputs (with +10% and -10% error bands): (a) an optimised model with 9 rules, (b) an optimised model with 8 rules, and (c) an optimised model with 4 rules.

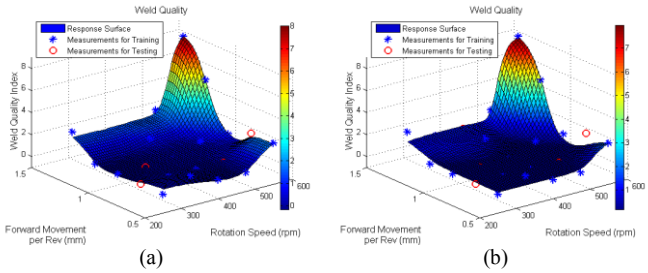

(a) (b)

Figure 12. Response surfaces of the weld quality models: (a) the 9-rule model, (b) the 8-rule model, and (c) the 4-rule model.

For more details about these Pareto-optimal models, Fig. 13 shows the rule-base of the 4-rule fuzzy model. It can be further represented as the following approximate linguistic rules using the linguistic hedges approach [25]:

R_1: IF *RS* is *medium small* AND *FM* is *large*, THEN *WQ* is *medium small*.
R_2: IF *RS* is *more or less medium large* AND *FM* is *medium small*, THEN *WQ* is *small*.
R_3: IF *RS* is *very large* AND *FM* is *small*, THEN *WQ* is *medium small*.
R_4: IF *RS* is *very large* AND *FM* is *large*, THEN *WQ* is *more or less large*.

It is clear that such linguistic fuzzy rules allow for a better insight into the FSW process.

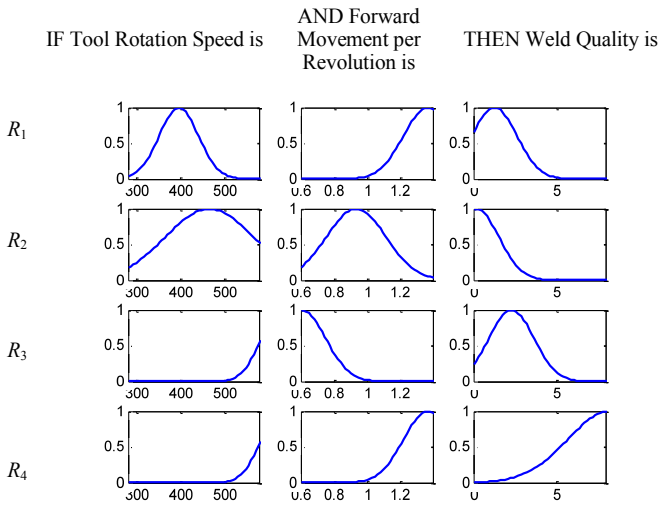

Figure 13. The rule-base of the 4-rule weld quality model.

C. *Grain size*

The FSW process results in significant micro-structural evolution, including grain size, grain boundary character, dissolution and coarsening of precipitates, breakup and redistribution of dispersoids, and texture [7]. In this paper, Average Grain Size (AGS) in the nugget zone is studied. Fig. 14 shows the micrographs of the pre-weld and post-weld materials, where one can identify different grain sizes.

In this experiment, 20 data points were used for training and 5 data points were reserved for testing. Fig. 15 shows the trade-offs among the multiple criteria within the non-dominated fuzzy solutions.

Fig. 16 shows the prediction performance of the model with 5 fuzzy rules and its response surface is displayed in Fig. 17. This surface has been confirmed to indeed follow the expected behaviour as predicted by theory and by knowledge experts. It should also be noted that the elicited fuzzy models reveal good generalisation ability from the smooth input-output response surface.

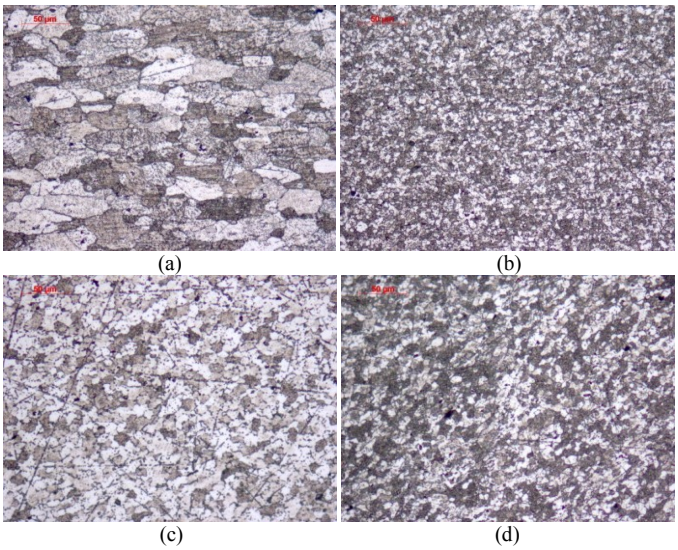

Figure 14. Micrographs of (a) the parent material, (b) the weld with *RS* = 280 rpm and *FM* = 1.4 mm/rev, (c) the weld with *RS* =580 rpm and *FM* =0.6 mm/rev, and (d) the weld with *RS* =580 rpm and *FM* =1.4 mm/rev.

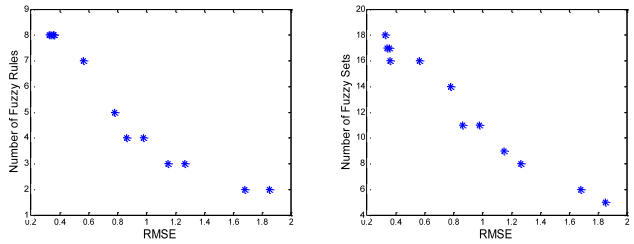

Figure 15. The performance of one set of optimised Pareto-optimal fuzzy models for the grain size modelling problem.

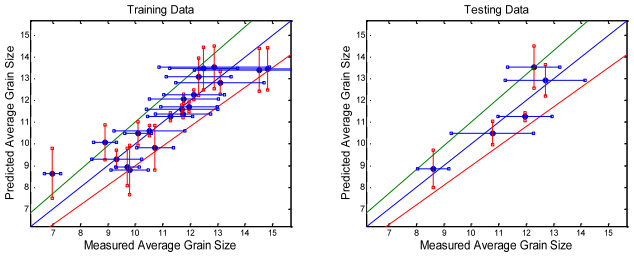

Figure 16. The 5-rule average grain size model's predicted outputs versus measured outputs(with +20% and -20% error bands).

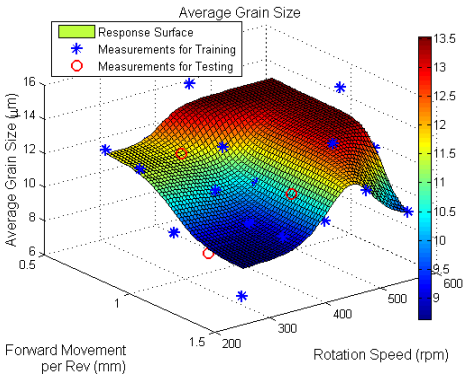

Figure 17. The response surface of the 5-rule average grain size model.

IV. CONCLUSION

In spite of the relatively short history of friction stir welding, it has found widespread applications in various industries. FSW can also lead to significant improvements in the mechanical properties of the welded materials (weld and parent material) over the more conventional welding techniques. However, the fundamental physical understanding about the process is still lacking, as the material flow and micro-structural evolution within the weld is very complex. To achieve a comprehensive understanding of the effects of process conditions on characterisations of welded materials, a systems modelling framework, FHMO-FM, was successfully applied in this paper within the context of predicting multiple properties for the FSW processed material, including mechanical properties, weld quality, and average grain size. In the derived modelling method, the multi-objective optimisation technique has been employed to improve both the accuracy and the interpretability attributes of fuzzy models, and a hierarchical optimisation structure, including two learning techniques (NSGA-II and gradient descent), has also been included to improve the modelling efficiency. In future, the developed models will be exploited to serve as the core module for 'reverse-engineering' designs that are able to suggest optimal process conditions (process routes) by taking into account a set of desired objectives relating to achieving structurally sound, defect free, and reliable welds.

REFERENCES

[1] W.M. Thomas, E.D. Nicholas, J.C. Needham, M.G. Murch, P. Templesmith, and C.J. Dawes, G.B. Patent Application No. 9125978.8, December 1991.

[2] N. Afrin, D.L. Chen, and M. Jahazi, "Microstructure and tensile properties of friction stir welded az31b magnesium alloy," Materials Science and Engineering A, vol. 472, pp. 179–186, 2008.

[3] H. Fujii, L. Cui, N. Tsuji, M. Maeda, K. Nakata, and K. Nogi, "Friction stir welding of carbon steels," Materials Science and Engineering A, vol. 429, pp. 50–57, 2006.

[4] T. Sakthivel and J. Mukhopadhyay, "Microstructure and mechanical properties of friction stir welded copper," Journal of Materials Science, vol. 42, pp. 8126–8129, 2007.

[5] A.J. Ramirez and M.C. Juhas, "Microstructural evolution in Ti-6Al-4V friction stir welds," Materials Science Forum, vol. 426–432, pp. 2999–3004, 2003.

[6] R. Nandan, T. DebRoy and H.K.D.H. Bhadeshia, "Recent advances in friction stir welding-process," Weldment Structure and Properties, Progress in materials science, vol. 53, pp. 980–1023, 2008.

[7] R.S. Mishra and Z.Y. Ma, "Friction stir welding and processing," Materials Science and Engineering R: Reports, vol. 50, no. 1-2, pp. 1–78, 2005.

[8] K.V. Jata and S.L. Semiatin, "Continuous dynamic recrystallization during friction stir welding of high strength aluminium alloys," Scripta Materialia. vol. 43, pp. 743–749, 2000.

[9] L.E. Murr, Y. Li, E.A. Trillo, and J.C. McClure, "Fundamental issues and industrial applications of friction-stir welding," Materials Technology, vol. 15, no. 1, pp. 37–48, 2000.

[10] W.M. Thomas and E.D. Nicholas. "Friction stir welding for the transportation industries," Materials and Design, vol. 18, pp. 269–273, 1997.

[11] Q. Zhang and M. Mahfouf, "Fuzzy predictive modelling using hierarchical clustering and multi-objective optimisation for mechanical properties of alloy steels," in Proceedings of the 12th IFAC symposium on automation in mining, mineral and metal processing, 2007, DOI: 10.3182/20070821-3-CA-2919.00059.

[12] Q. Zhang, M. Mahfouf, L. de Leon, S. Boumaiza, J.R. Yates, C. Pinna, and R.J. Greene, "Prediction of machining induced residual stresses in aluminium alloys using a hierarchical data-driven fuzzy modelling approach," in Proceedings of the 13th IFAC workshop on automation in mining, mineral and metal industry, 2009, DOI: 10.3182/20091014-3-CL-4011.00042.

[13] Q. Zhang and M. Mahfouf, "A Modified PSO with a Dynamically Varying Population and Its Application to the Multi-Objective Optimal Design of Alloy Steels," in Proceedings of the 2009 IEEE Congress on Evolutionary Computation, pp. 3241-3248, 2009.

[14] Q. Zhang and M. Mahfouf, "A nature-inspired multi-objective optimisation strategy based on a new reduced space searching algorithm - special application to the design of alloy steels," Engineering applications of artificial intelligence, vol. 23, no. 5, pp. 660–675, 2010.

[15] C.A. Coello Coello and R.L. Becerra, "Evolutionary Multiobjective Optimization in Materials Science and Engineering," Materials and Manufacturing Processes, vol. 24, no. 2, pp. 119-129, 2009.

[16] K. Deb, A. Pratap, and S. Agarwal, and T. Meyarivan, "A Fast and Elitist Multiobjective Genetic Algorithm: NSGA-II," IEEE Transactions on Evolutionary Computation, vol. 6, no. 2, pp. 182-197, 2002.

[17] L.-X. Wang, A course in fuzzy systems and control. Englewood Cliffs, NJ: Prentice-Hall, 1997.

[18] Q. Zhang and M. Mahfouf, "Mamdani-type fuzzy modelling via hierarchical clustering and multi-objective particle swarm optimisation (FM-HCPSO)," International Journal of Computational Intelligence Research, vol. 4, no. 4, pp. 314–328, 2008.

[19] H. Ishibuchi and Y. Nojima, "Analysis of interpretability-accuracy tradeoff of fuzzy systems by multiobjective fuzzy genetics-based machine learning," International Journal of Approximate Reasoning, vol. 44, no. 1, pp. 4-31, 2007.

[20] R. Alcala, P. Ducange, F. Herrera, B. Lazzerini, and F. Marcelloni, "A multiobjective evolutionary approach to concurrently learn rule and data bases of linguistic fuzzy-rule-based systems," IEEE Transactions on Fuzzy Systems, vol. 17, no. 5, pp. 1106–1122, 2009.

[21] Q. Zhang, and M. Mahfouf, "A hierarchical Mamdani-type fuzzy modelling approach with new training data selection and multi-objective optimisation mechanisms: A special application for the prediction of mechanical properties of alloy steels," Applied Soft Computing, vol. 11, no. 2, pp. 2419–2443, 2011.

[22] Q. Zhang, Nature-Inspired Multi-Objective Optimisation and Transparent Knowledge Discovery via Hierarchical Fuzzy Modelling. PhD Thesis, The Department of Automatic Control and Systems Engineering, The University of Sheffield, UK, 2008.

[23] E.A. El-Danaf, M.M. El-Rayes, and M.S. Soliman, "Friction stir processing: An effective technique to refine grain structure and enhance ductility," Materials and Design, vol. 31, pp. 1231–1236, 2010.

[24] W.M. Thomas and M.F. Gittos, "Development of friction stir tools for the welding of thick (25mm) aluminium alloys", TWI Members Report 694/1999, December 1999.

[25] L.A. Zadeh, "A fuzzy-set-theoretic interpretation of linguistic hedges," Journal of Cybernetics, vol. 2, pp. 4–34, 1972.

[26] X. Long and S.K. Khanna, "Modelling of electrically enhanced friction stir welding process using finite element method," Science and Technology of Welding and Joining, vol. 10, pp. 482–487, 2005.

2011 IEEE International Conference on Fuzzy Systems
June 27-30, 2011, Taipei, Taiwan

Fuzzy Modeling to Predict Administration of Vasopressors in Intensive Care Unit Patients

André S. Fialho*†‡, Federico Cismondi*†‡,
Susana M. Vieira‡, João M. C. Sousa‡, Shane R. Reti§,
Leo A. Celi¶, Michael D. Howell‖ and Stan N. Finkelstein*
*Massachusetts Institute of Technology, Engineering Systems Division,
77 Massachusetts Avenue, 02139 Cambridge, MA, USA (email: afialho@mit.edu)
†MIT Portugal Program, 77 Massachusetts Avenue, E40-221, 02139 Cambridge, MA, USA
‡Technical University of Lisbon, Instituto Superior Técnico, Dept. of Mechanical Engineering,
CIS/IDMEC – LAETA, Av. Rovisco Pais, 1049-001 Lisbon, Portugal
§Division of Clinical Informatics, Department of Medicine,
Beth Israel Deaconess Medical Centre, Harvard Medical School, Boston, MA, USA
¶ Division of Pulmonary, Critical Care and Sleep Medicine, Beth Israel Deaconess Medical Center, Boston, MA USA
‖Silverman Institute for Healthcare Quality and Safety,
Beth Israel Deaconess Medical Center, Harvard Medical School, Boston, MA, USA

***Abstract*—Vasopressors belong to a powerful class of drugs used in the management of systemic shock in ill patients. The administration of a vasopressor involves the non-trivial process of inserting a central venous catheter. This procedure carries with it inherent risks which are increased when done under urgency such as in the case of unexpected systemic shock. The ability to predict the transition to vasopressor dependence could be expected to improve overall outcomes associated with the procedure. We use three different approaches combining fuzzy modeling with bottom-up (BU), top-town (TD) and ant feature selection (AFS), to classify requirements for vasopressors in shock. We observe that fuzzy models combined with BU feature selection return higher values of sensitivity; fuzzy models with no feature selection and fuzzy models with TD feature selection return higher values of AUC and specificity; features most commonly selected to classify impending use of vasopressores in pancreatitis patients include levels of Sodium and White Blood Cell counts, while for pneumonia patients include levels of Lactid Acid and White Blood Cell Count; and finally, fuzzy models combined with BU and fuzzy models combined with AFS demonstrate the lowest number of selected variables with no significant loss in accuracy.**

Keywords: Feature selection, Fuzzy models, Vasopressors, Shock

I. Introduction

Systemic shock is defined as "an acute clinical syndrome initiated by ineffective blood perfusion, resulting in severe dysfunction of organs vital to survival" [1]. The signs and symptoms of shock include hypotension, tachycardia, cool and clammy extremities, oliguria, dysglycemia, and delirium [1]. Depending on the etiology, mortality figures vary from 23% to 75% [2].

Early recognition and intervention are critical to prevent irreversible organ injury and failure. Unlike other conditions where the clinical diagnosis is made before the treatment is initiated, the treatment of shock often occurs concurrently or ahead of the diagnostic process [3]. This treatment entails three main steps - ventilate, infuse and pump [4] - consisting respectively of supplying oxygen to the patient until blood gas test results are available, infusion of fluids in order to increase plasma volume and cardiac output, and finally, when fluid administration fails to restore an adequate arterial pressure and organ perfusion, administration of vasopressors [5].

Vasopressors belong to a powerful class of drugs which are extremely useful for managing low blood pressure (hypotension) in patients with systemic shock. In critically ill patients, these drugs are often administered through central venous (CV) lines as they provide a fast and direct access to the central venous circulation [6]. However, inserting this type of line requires significant amounts of time (up to 1 hour, including radiologic imaging to evaluate placement), personnel resources, and can be associated with risks such as bloodstream infection. In the US only, catheter-related blood–stream infections have been reported to occur in 3 to 8% of inserted catheters and are the main cause of nosocomial bloodstream infection in intensive care units, with 80,000 cases annually at a cost of $300 million to $2.3 billion [7], [8]. Non-sterile central venous line insertion is more likely in urgent rather than elective scenarios. Simultaneously, there is a growing body of evidence supporting early commencement of vasopressor therapy as the key contributor to improved patient outcomes in certain disease states [9].

Bearing this in mind, being able to predict, within a certain time window, a patient's transition to vasopressor dependence could have great impact in a hospital, and particularly within the ICU environment, where patients are among the sickest in the hospital, for two main reasons: (i) a central line would only be inserted if the patient needs it in fact in the future (reduction in the performance of this procedure) (ii) the central line insertion protocol could be initiated with enough time, prior to the moment of need of vasopressors.

The present work will be a first step towards this major

978-1-4244-7316-8/11/$26.00 ©2011 IEEE

goal. We will perform a classification task where, for a given set of clinical variables in a specific instant of the patient stay in the ICU, we will try to classify whether the patient was on vasopressors or not, as well as to find which subset of variables allows its better classification. This task will involve the application of soft computing techniques to a de-identified publicly available ICU database - MIMIC II [10]. As with other real-world databases, the dataset dealt with here, contains a relatively large number of non-linear features. Thus, from the engineering point of view, input selection is a crucial step in order to reduce models' complexity and remove inputs that do not improve the classification performance. From the clinical point of view, this feature selection process may bring to light new variables not been previously considered relevant to a given medical condition. In this paper, three different combinations of modeling and feature selection approaches are proposed and compared: fuzzy modeling with bottom-up tree search [11], with top-down tree search [11] and with ant colony feature selection [12].

Some studies have already explored this issue. In [13], a fuzzy-logic based algorithm was developed, taking arterial blood pressure and heart rate as inputs to generate a 'vasopressor advisability index'. In 2009, following Physionet/Computers in Cardiology Challenge, several algorithms were proposed to predict which patients would experience an acute hypotensive episode beginning within the forecast window. Finally, in [14] the application of some of the knowledge based methods as presented here was used to estimate outcomes in septic shock.

The paper is organized as follows. Section 2 briefly describes the modeling technique and proposed feature selection algorithms. A description of the database, its preprocessing as well as the obtained results are presented in Section 3. Conclusions are drawn in Section 4.

II. Methods

A. Fuzzy Modeling

Fuzzy modeling is a tool that allows an approximation of nonlinear systems when there is few or no previous knowledge of the system to be modeled [15]. Fuzzy models have several advantages compared to other non-linear modeling techniques. For clinical related classification systems, this approach is particularly appealing as it provides not only a more transparent model, but also a linguistic interpretation in the form of rules. These rules and logical connectives are used to establish relations between the defined features in order to derive a model. A fuzzy classifier contains a rule base consisting of a set of fuzzy if-then rules together with a fuzzy inference mechanism.

There are three general methods to design a fuzzy classifier that can be distinguished [16]: the regression method, the discriminant method and the maximum compatibility method. Given that the classification decision does not change by taking a monotonic transformation of the discriminant function [17], we used in this work the discriminant method. Here, the classification is based on the largest discriminant function, which is associated with a certain class, regardless of the values or definitions of other discriminant functions. In the discriminant method, a separate discriminant function $d_c(x)$ is associated with each class ω_c, $c = 1, \ldots, C$. The discriminant functions can be implemented as fuzzy inference systems. In this work, we use Takagi-Sugeno (TS) fuzzy models [18], which consist of fuzzy rules where each rule describes a local input-output relation. When TS fuzzy systems are used, each discriminant function consists of rules of the type

$$R_i^c : \textbf{If } x_{i1} \text{ is } A_{i1}^c \textbf{ and ... and } x_M \text{ is } A_{iM}^c$$

$$\textbf{then } d_i^c(\mathbf{x}) = f_i^c(\mathbf{x}),\ i = 1, 2, ..., K \tag{1}$$

where f_i^c is the consequent function for rule R_i^c. In these rules, the index c indicates that the rule is associated with the output class c. Note that the antecedent parts of the rules can be for different discriminants, as well as the consequents. Therefore, the output of each discriminant function $d_c(x)$ can be interpreted as a score (or evidence) for the associated class c given the input feature vector x. The degree of activation of the ith rule for class c is given by: $\beta_i = \prod_{j=1}^{M} \mu_{A_{ij}^c}(x)$, where $\mu_{A_{ij}^c}(x) : \mathbb{R} \rightarrow [0, 1]$. The discriminant output for each class c, is computed by aggregating the individual rules contribution: $d_c(x) = \frac{\sum_{i=1}^{K} \beta_i f_i^c(x)}{\sum_{i=1}^{K} \beta_i}$. The classifier assigns the class label corresponding to the maximum value of the discriminant functions, i.e

$$\max_c d_c(x). \tag{2}$$

The number of rules K, the antecedent fuzzy sets A_{ij}, and the consequent parameters $f_i^c(x)$ are determined using fuzzy clustering in the product space of the input and output variables. The number of fuzzy rules (or clusters) that best suits the data must be determined for classification. The following criterion, as proposed in [19], is used in this paper to determine the optimum number of clusters:

$$S(K) = \sum_{k=1}^{N} \sum_{i=1}^{K} (\mu_{ik})^m (\|x_k - v_i\|^2 - \|v_i - \bar{x}\|^2)^2 \tag{3}$$

Values of $S(K)$ were calculated by varying K from 2 to 20. The final number of clusters corresponded to a local minimum where the differences between the values of the criterion are minor. In our case we used a 10% threshold for this difference between two values. A fuzzy clustering and data analysis toolbox was used in this step [20].

B. Feature Selection

Feature selection is generally used to reduce computational complexity, to eliminate features with high mutual correlation [21], and required generalization properties of the model [22]. From the clinical point of view, this process may bring to light new variables that had not been previously considered for a given medical condition.

1) Bottom-up: A detailed description of the bottom-up approach used here is reported in [11]. Briefly, the bottom-up approach starts by looking for single features that may influence the process output and works to assemble these single relevant features, to achieve a model with the best performance. This approach deals with feature redundancy in a simple way. Once the features are added one by one, if a feature is redundant it means that it will not improve the model prediction, and for that reason it will not be incorporated in the previously selected subset of features. Considering X the vector containing n features, this feature selection process is described by Algorithm 1. The model evaluation method was generalized by using AUC – Area Under the ROC Curve – as the most suitable performance criteria.

According to [23], a Receiver–Operator Characteristics (ROC) curve can be used to study the behaviour of two–class classifiers. This is a function of the true positive ratio versus the false positive ratio. Consequently, in order to compare the performance of various classifiers, the AUC can be used. It corresponds to the total performance of a two-class classifier integrated over all thresholds:

$$AUC = 1 - \int_0^1 FP(FN)dFN \tag{4}$$

where FP and FN represent, respectively, the false positive rate the false negative rate. The true positive rate and true negative rate are respectively named as Sensitivity and Specificity and, in this particular scenario, correspond to the cases where the patient was correctly classified as being on vasopressors and the cases where the patient was correctly classified as not being on vasopressors.

Algorithm 1 Bottom-Up Feature Selection

For each feature in the feature vector X that does not belong to the features of the model:
repeat
  Build model using previous features of the model combined with each feature in the feature vector X that does not belong to the features of the model
  Compute AUC;
  Select the combination of features with the highest value of AUC as the new features of the model;
until AUC does not increase or the end of the feature vector is reached.
Select the final features;

2) Top-Down: A different approach based on a top-down tree search method was also used to select the most relevant features. This approach begins with all the available features, and removes those with the worst performance. The proposed top-down approach is described in Algorithm 2.

This algorithm differs from the bottom-up approach, as it begins with all the features and starts discarding features from stage to stage. Advantages include the reduction of the number of iterations per stage and, in some cases, of the number of stages, which, in lower dimension problems, ultimately leads to the overall reduction of the computational time. However, when the number of features is large, given that this approach will use more inputs to build each model from the beginning, the identification of each model can be computationally intensive.

Algorithm 2 Top-Down Feature Selection

$i = 0$, where i is the stage number;
repeat
  if $Stage = 0$ **then**
    Build a model using all the available features;
    $m = n$; where n is the number of initial features
  else
    $i = i + 2$
    Build a model using the features not discarded at the previous stage;
  end if
  Compute AUC_i;
  for $j = 1$ **to** m **do**
    Build model using all the features except feature j;
    Compute $AUC_{i+1,j}$
    if $AUC_{i+1,j} < AUC$ **then**
      Discard the feature j not used in modeling;
    end if
  end for
  $m = m - p$, where p is the number of discarded features;
until (no feature is discarded) OR (model has only one feature) OR ($AUC_i > AUC_{i-2}$)

3) Ant Colony: Ant Colony Optimization (ACO) a method suited to find minimum cost paths in optimization problems described by graphs [24]. This paper uses the ant feature selection algorithm (AFS) proposed in [12], where the best number of features is determined automatically by considering two objectives: minimizing the number of features (*feature cardinality* - N_f) and maximizing the prediction performance. Two cooperative ant colonies formed by g ants, optimize each objective. The first colony determines the number (cardinality) of features and the second selects the features based on the cardinality given by the first colony. Thus, two pheromone matrices and two different heuristics are used.

The objective function of this optimization algorithm aggregates both criteria, the maximization of the model performance and the minimization of the feature cardinality:

$$J^k = w_1(1 - AUC^k) + w_2 \frac{N_f^k}{n} \tag{5}$$

where $k = 1, \ldots, g$, AUC is the performance criterion previously defined in [23] and n is the total number of features. The weights w_1 and w_2 are selected based on experiments.

The heuristic value used for each feature (ants visibility) for the second colony, is computed as $\eta_{f_j} = AUC_j$ for $j = 1, \ldots, n$, where AUC_j quantifies the relevance of each feature in the prediction model.

For the feature cardinality (first colony), the heuristic value is computed using the Fisher discriminant criterion for feature

selection [25]. Considering a classification problem with two possible classes, class 1 and class 2, the Fisher discriminant criterion is described as

$$F(i) = \frac{|\mu_1(i) - \mu_2(i)|^2}{\sigma_1^2 + \sigma_2^2} \quad (6)$$

where $\mu_1(i)$ and $\mu_2(i)$ are the mean values of feature i for the samples in class 1 and class 2, and σ_1^2 and σ_2^2 are the variances of feature i for the samples in class 1 and 2. The score aims to maximize the between-class difference, minimize the within a given class spread and thus to limit the number of features chosen by the AFS algorithm, which can be particularly useful when the number of available features is large. Other currently proposed rank-based criteria generally come from similar considerations and show similar performance [25].

III. Results

A. MIMIC II Database

This paper used a de-identified publicly available ICU database named MIMIC II (Multiparameter Intelligent Monitoring in Intensive Care), containing data from 26,655 admitted patients. Data was collected over a six-year period, from Boston's Beth Israel Deaconess Medical Center, commencing in 2001. This database has two distinctive groups of data: the clinical database consisting of data integrated from different information systems in the hospital (patient demographics, medications, laboratory tests, etc), and a second group containing high resolution waveforms recorded from the bedside monitors in the intensive care units [10].

In this work we focused exclusively on the clinical data for two specific subsets of patients – pancreatitis and pneumonia. Given that these patients are usually treated differently – surgically and medically – we hypothesized that the circumstances related to the initiation of vasopressors are also distinct. In order to select these subsets, ICD9 (International Classification of Diseases) codes were used. These data included a total of 154 pancreatitis and 820 pneumonia patients, and 32 input variables, including vital signs, laboratory tests and urine output, sampled from one to every twelve hours, during the length of stay of the patient in the ICU. The output was formed as a binary classification with value one if, the patient was on vasopressors, and zero if not. The list of vasopressors for which the classification was performed included: phenylephrine, norepinephrine and dopamine. Their use represented 75% of all vasopressor administration events in the database. Other data inclusion criteria included: only data regarding the first stay of a patient in the ICU was considered; a period of at least six hours had to exist between the admission of the patient to the ICU (and commencement of the acquisition of data) and the administration of vasopressors; and only patients that were on vasopressors for more than two hours were included.

B. Data Preprocessing

Modern intensive care units are undergoing a significant evolution that is being driven by rapid improvements in technology as well as changes in healthcare policy. The growth of computer networking and information storage technologies has been accompanied by an increase in the complexity and number of biosensors used in the ICU, thus generating large amounts of data [26]. However, this has also contributed to issues of what to do when data are collected in different frequencies or when it is partially lost or absent. In this way, data preprocessing represents a crucial step since it defines the reliability of the information that will be used in later stages of the knowledge discovery process.

In the present work, in order to manage differences in frequency of collection, Heart Rate samples were used as a template to align the remaining variables. This choice is based on being the most frequently measured variable. A detailed description of this alignment process is presented in [27].

In general, ICU data can be missing either because they are perceived to be irrelevant for the current clinical problems (thus, not recorded), or because exogenous interventions or endogenous activities have rendered the data useless [26]. When it is possible to prove that a variable was not measured during a certain period of time because of an intentional reason (e.g. ventilator parameters when a patient is extubated), this missing segment is considered as non-recoverable. In this work, these non-recoverable missing segments were deleted. On the other hand, if the variable was suppose to exist, but for some unintentional reason (e.g. cable disconnection) it is missing, this absent segment is considered recoverable and thus, proper imputation techniques can be applied [27], [28]. In this work, a cubic interpolation was used to impute values to the recoverable missing segments.

C. Simulation and Results

The general goal of this work entailed classifying, for a specific time point of a patient stay in the ICU, whether vasopressors were being administered or not, as well as to find which subset of variables allows its better classification. Classification methods were used combining fuzzy modeling with three feature selection techniques: bottom-up (BU), top-down (TD) and ant feature selection (AFS). For purposes of comparison, a fourth method using fuzzy modeling without feature selection (No FS) was also used. In order to evaluate the performance of these models, three different criteria were used: AUC, specificity and sensitivity. The entire algorithm was run in two separate sections: feature selection and 10-fold cross-validation. Ten iterations were used during the feature selection step, thus obtaining ten different combinations of features. The combination returning the best value of AUC was selected and used on a 10-fold cross-validation step to assess how the built fuzzy model would perform. Final results are presented as an average of all these 10 folds.

Before analysing the obtained results, it is important to note some of the issues found during simulation. In determining the optimum number of fuzzy rules (clusters), in most cases, the number of clusters returned by the criterion described in equation 3 was between five and eight. However, in a few cases, the number of clusters was higher then eight, which also

TABLE I

MEAN AUC, SENSITIVITY, SPECIFICITY USING FUZZY MODELING COMBINED WITH BOTTOM-UP (BU), TOP-DOWN (TD), ANT FEATURE SELECTION (AFS), NO FEATURE SELECTION (NO FS) AND FEATURES MANUALLY SELECTED IN [13] (MANUAL FS) TO CLASSIFY THE USE OF ALL THREE VASOPRESSORS

	[13]			**Pancreatitis**			**Pneumonia**		
Method	AUC	Specificity	Sensitivity	AUC	Specificity	Sensitivity	AUC	Specificity	Sensitivity
BU	-	-	-	0.87 ± 0.02	0.83 ± 0.05	0.90 ± 0.03	0.80 ± 0.02	0.78 ± 0.02	0.81 ± 0.03
TD	-	-	-	0.87 ± 0.02	0.89 ± 0.03	0.85 ± 0.05	0.80 ± 0.01	0.81 ± 0.03	0.80 ± 0.03
AFS	-	-	-	0.83 ± 0.02	0.84 ± 0.06	0.82 ± 0.04	0.76 ± 0.01	0.81 ± 0.04	0.71 ± 0.05
No FS	-	-	-	0.90 ± 0.02	0.92 ± 0.02	0.87 ± 0.05	0.80 ± 0.02	0.82 ± 0.02	0.79 ± 0.03
Manual FS	(0.77)	0.84	0.70	0.63 ± 0.01	0.55 ± 0.02	0.72 ± 0.02	0.63 ± 0.01	0.62 ± 0.02	0.64 ± 0.02

TABLE II

NUMBER OF SELECTED FEATURES (NO. SEL. FEATURES) AND LIST OF MOST COMMONLY SELECTED FEATURES (MOST SELECTED) WHEN USING FUZZY MODELING COMBINED WITH BOTTOM-UP (BU), TOP-DOWN (TD), ANT FEATURE SELECTION (AFS) AND THE FEATURES MANUALLY SELECTED IN [13] TO CLASSIFY THE USE OF ALL THREE VASOPRESSORS

	[13]		**Pancreatitis**		**Pneumonia**	
Method	No. Sel. Features	Most Selected	No. Sel. Features	Most Selected	No. Sel. Features	Most Selected
BU	-	-	2–3	14, 10, 12	3–5	28, 12, 18, 22
TD	-	-	26–29	All except 16, 5, 32, 7, 4	29–31	All except 6, 13
AFS	-	-	4–5	14, 30, 29, 12	8	7, 12, 16, 28, 8, 2, 31
Manual FS	2	1, 3	2	1, 3	2	1, 3

meant significantly higher computational times. Comparing the three feature selection methods regarding their execution times, fuzzy modeling combined with BU was the fastest (20 minutes in average for ten iterations), followed by fuzzy modeling combined with AFS and, finally, taking almost twice as the first, fuzzy modeling combined with TD.

In the first part of this work, we focused on comparing our results with other studies [13], where the classification of whether vasopressors were being administered or not, was made without distinguishing between them. In the second part of the work, we do distinguish and explore each of the vasopressors individually, i.e. a specific output was defined for each of the three vasopressors (phenylephrine, norepinephrine and dopamine).

1) Classification of general use of vasopressors: In [13], a fuzzy-logic based algorithm was developed to predict the need for vasopressor therapy, using the same MIMIC II database but with different criteria for patient selection. These models were built using as inputs two manually selected features - arterial blood pressure and heart rate. As shown in Table I, their algorithm achieved a specificity of 0.84 and a sensitivity of 0.69. The 0.77 value for AUC was estimated by us based on the respective values of specificity (0.84) and sensitivity (0.70). As mentioned, a comparison between the performance of our models with [13] was carried. However, it is important to note that it was not possible to identify which specific vasopressor(s) were included in their work, neither the criteria used to select patients. Furthermore, the conditions in which the values of specificity and sensitivity were obtained were not clear. Accordingly, some caution is needed when analysing and comparing the two approaches.

Main results follow: using the same two variables as in [13], the proposed fuzzy models returned lower values of AUC, specificity and sensitivity; however, when applying them to all variables or when combining them with any of the proposed automated feature selection processes, both AUC, specificity and sensitivity were shown to be significantly higher than in [13]. This indicates that for the specific models and data subsets chosen in this work, the two features used in [13], do not contain information that allows the correct classification of the outcome (the use of vasopressors). This is confirmed by Table II, where it is possible to observe that the features most commonly selected to classify impending use of vasopressores in pancreatitis patients include levels of Sodium (feature no. 14) and White Blood Cell counts (feature no. 12), while for pneumonia patients include levels of Lactid Acid (feature no. 28) and White Blood Cell Count (feature no. 12). These sets of features differ completely from the ones chosen in [13]. Despite the limitations, these results suggest that for the purpose of classifying whether vasopressors were being administered or not, both the proposed fuzzy model approach without feature selection and the fuzzy model approach combined with any of the automated feature selection processes, significantly outperformed previous approaches [13].

Additional comments can be made regarding the results obtained in Table I. First, higher values of AUC, specificity and sensitivity were in general obtained for the pancreatitis subset than for the pneumonia one. This might be related to the size of these subsets. As mentioned, the first contained 154 patients while the second contained 820. Most likely, the smaller subset contained a more homogeneous group of patients whose clinical condition was similar during the periods when vasopressors were being administrated or not. Secondly, it is also possible to observe that fuzzy modeling with No FS and fuzzy modeling combined with TD feature selection returned the highest values of AUC and specificity. However, these models did not return the best values of sensitivity. In other words, they performed the best in classifying when patients were not on vasopressors, but the worst in correctly classifying which patients were on vasopressors. The best values of sensitivity were given by fuzzy modeling combined with BU feature selection.

From the analysis of Table II, it can be pointed out that:

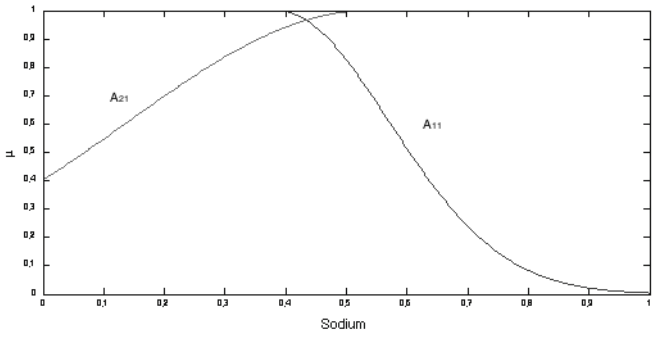

Fig. 1. Sodium's membership functions for cluster 1 (A_{11}) and 2 (A_{21})

BU and AFS techniques selected fewer features than the TD approach; in general, less features were selected for the pancreatitis subset than for the pneumonia subset; and finally, a certain consistency seems to exist between the variables most commonly selected by BU and AFS within each subset, but little or no agreement exists between the variables selected in the two subsets. In other words, this means that different variables were selected as being able to correctly classify the same outcome, between the pancreatitis and pneumonia subset of patients, thus pointing that the use of patient-specific models should be considered in future studies. In future works, it would be interesting to include a penalty for models with large numbers of features. This will reduce the number of features in the final model.

Finally, as an example, the rules built for the specific case of classifying the impending use of vasopressors in pancreatitis patients when using fuzzy modeling combined with BU, are presented:

1. **If** Sodium is A_{11} & White Blood Cell is A_{12} & BUN is A_{13} & Chloride is A_{14} **Then** $y(k) = 1.9 \cdot Sodium - 1.4 \cdot WhiteBloodCell - 3.2 \cdot BUN + 0.36 \cdot Chloride + 2.2$

2. **If** Sodium is A_{21} & White Blood Cell is A_{22} & BUN is A_{23} & Chloride is A_{24} **Then** $y(k) = -0.52 \cdot Sodium + 0.23 \cdot WhiteBloodCell + 0.073BUN + 0.55 \cdot Chloride - 0.094$

Given that two clusters were defined, two rules were obtained. The variables used to build the rules (Sodium, White Blood Cell, BUN and Chloride) were pre-selected by the BU feature selection process. A_{kj} corresponds to the membership function of cluster k for variable j. For example, in Figure 1, A_{11} and A_{21} correspond respectively to Sodium's membership functions for cluster 1 and 2. $y(k)$ corresponds the output of the model for cluster k. After the defuzzification step, all clusters outputs are combined into a single output, by averaging them. This final output takes a real value between 0 and 1 which, by using a pre-determined threshold (in this work defined as 0.12), is set to 1 if it is over this threshold, and 0 if it is below.

2) Classification of the specific use of phenylephrine, norepinephrine or dopamine: In the second part of this work, as previously mentioned, we tried to explore the individual use of each of the three vasopressors. First, in accordance to what was found in Table I, by comparing Table III and IV it is possible to observe that better results were obtained for the pancreatitis than for the pneumonia subset of patients. Second, developed models seem to perform the best in classifying when dopamine is administered, followed by phenylephrine and lastly in classifying the use of norepinephrine. Finally, fuzzy modeling with No FS and fuzzy modeling combined with TD returned again the best values of AUC and specificity, while fuzzy modeling combined with BU returned the best values of sensitivity.

From Tables V and VI several comments can be made regarding the set of selected features. First, contrarily to what was expected, having more features selected did not mean that models would perform better. For example, in classifying if dopamine was being administered to a pneumonia patient, after ten iterations of fuzzy modeling combined with BU, an average of two to four variables were selected. However, the model with the best values of AUC was the one where only two variables allowed to classify this outcome. Another interesting finding is that there is a certain agreement between the variables most commonly selected by BU and AFS. Most obvious examples include levels of Sodium (Table VII - Feature no. 14) and BUN (Table VII - Feature no. 10) in explaining the use of phenylephrine in pacreatitis patients, and levels of INR (Table VII - Feature no. 21) in explaining the use of dopamine in pneumonia patients. However, there are still a few cases (e.g. norepinephrine in pneumonia patients) where

TABLE VII
LIST OF FEATURES

Feature Name	Feature Number
Heart Rate	1
Temperature C	2
Arterial BP (Systolic)	3
Respiratory Rate	4
SpO2	5
Hematocrit	6
Potassium	7
Glucose	8
Creatinine	9
BUN	10
Platelets	11
White Blood Cell	12
Red Blood Cell	13
Sodium	14
Chloride	15
Arterial CO2	16
Magnesium	17
NBP	18
NBP Mean	19
PTT	20
INR	21
Arterial PaCO2	22
Arterial PaO2	23
Arterial pH	24
Arterial Base Excess	25
Ionized Calcium	26
Phosphorous	27
Lactic Acid	28
Calcium	29
CVP	30
Urine Out Foley	31
Arterial BP (Dyastolic)	32

TABLE III

PANCREATITIS SUBSET: MEAN AUC, SENSITIVITY, SPECIFICITY USING FUZZY MODELING COMBINED WITH BOTTOM-UP (BU), TOP-DOWN (TD), ANT FEATURE SELECTION (AFS) AND NO FEATURE SELECTION (NO FS) TO CLASSIFY THE USE OF EACH OF THE THREE VASOPRESSORS

	Phenylephrine			**Norepinephrine**			**Dopamine**		
Method	AUC	Specificity	Sensitivity	AUC	Specificity	Sensitivity	AUC	Specificity	Sensitivity
BU	0.92 ± 0.02	0.89 ± 0.03	0.94 ± 0.04	0.86 ± 0.01	0.84 ± 0.04	0.89 ± 0.05	0.99 ± 0.01	0.99 ± 0.02	1 ± 0.00
TD	0.94 ± 0.03	0.95 ± 0.03	0.93 ± 0.04	0.87 ± 0.02	0.92 ± 0.03	0.83 ± 0.05	0.99 ± 0.01	0.99 ± 0.01	1 ± 0.00
AFS	0.87 ± 0.03	0.85 ± 0.05	0.88 ± 0.04	0.81 ± 0.02	0.87 ± 0.04	0.77 ± 0.04	0.97 ± 0.02	0.97 ± 0.02	0.98 ± 0.05
No FS	0.94 ± 0.03	0.95 ± 0.03	0.94 ± 0.05	0.90 ± 0.02	0.94 ± 0.03	0.85 ± 0.00	0.98 ± 0.05	0.99 ± 0.01	0.96 ± 0.08

TABLE IV

PNEUMONIA SUBSET: MEAN AUC, SENSITIVITY, SPECIFICITY USING FUZZY MODELING COMBINED WITH BOTTOM-UP (BU), TOP-DOWN (TD), ANT FEATURE SELECTION (AFS) AND NO FEATURE SELECTION (NO FS) TO CLASSIFY THE USE OF EACH OF THE THREE VASOPRESSORS

	Phenylephrine			**Norepinephrine**			**Dopamine**		
Method	AUC	Specificity	Sensitivity	AUC	Specificity	Sensitivity	AUC	Specificity	Sensitivity
BU	0.80 ± 0.02	0.76 ± 0.03	0.83 ± 0.03	0.80 ± 0.01	0.80 ± 0.03	0.81 ± 0.03	0.90 ± 0.01	0.95 ± 0.03	0.85 ± 0.04
TD	0.83 ± 0.01	0.85 ± 0.01	0.81 ± 0.03	0.79 ± 0.01	0.80 ± 0.01	0.77 ± 0.03	0.91 ± 0.02	0.98 ± 0.01	0.84 ± 0.05
AFS	0.80 ± 0.02	0.81 ± 0.05	0.80 ± 0.04	0.77 ± 0.01	0.78 ± 0.04	0.76 ± 0.04	0.85 ± 0.03	0.93 ± 0.04	0.78 ± 0.05
No FS	0.85 ± 0.03	0.88 ± 0.04	0.81 ± 0.03	0.82 ± 0.02	0.83 ± 0.02	0.80 ± 0.03	0.91 ± 0.03	0.97 ± 0.02	0.85 ± 0.05

TABLE V

PANCREATITIS SUBSET: NUMBER OF SELECTED FEATURES (NO. SEL. FEATURES) AND LIST OF MOST COMMONLY SELECTED FEATURES (MOST SELECTED) WHEN USING FUZZY MODELING COMBINED WITH BOTTOM-UP (BU), TOP-DOWN (TD), ANT FEATURE SELECTION (AFS) AND NO FEATURE SELECTION (NO FS) TO CLASSIFY THE USE OF EACH OF THE THREE VASOPRESSORS

	Phenylephrine		**Norepinephrine**		**Dopamine**	
Method	No. Sel. Features	Most Selected	No. Sel. Features	Most Selected	No. Sel. Features	Most Selected
BU	3–4	14, 10, 15	4–5	12, 9, 20, 15	2–3	28, 6
TD	30–32	All except 32	31–32	All except 25	31–32	All except 25
AFS	4–5	14, 10, 29, 15	4–5	11, 2, 12, 24	3–5	20, 2, 4, 8, 18

TABLE VI

PNEUMONIA SUBSET: NUMBER OF SELECTED FEATURES (NO. SEL. FEATURES) AND LIST OF MOST COMMONLY SELECTED FEATURES (MOST SELECTED) WHEN USING FUZZY MODELING COMBINED WITH BOTTOM-UP (BU), TOP-DOWN (TD), ANT FEATURE SELECTION (AFS) AND NO FEATURE SELECTION (NO FS) TO CLASSIFY THE USE OF EACH OF THE THREE VASOPRESSORS

	Phenylephrine		**Norepinephrine**		**Dopamine**	
Method	No. Sel. Features	Most Selected	No. Sel. Features	Most Selected	No. Sel. Features	Most Selected
BU	9–13	18, 19	9–12	15, 28, 12, 9	2–4	21, 6
TD	29–31	All except 2,32	30–32	All except 32	29–31	All except 32
AFS	10–12	19, 15, 17, 22, 32, 2	10–13	19, 32, 10, 16, 24, 12	2–4	21, 12

a total disagreement exists between the two sets of selected features. This may be an indicator that for this specific problem of classifying the use of vasopressors, different and specific rules should be determined in order to explain the use of each of the three vasopressors. This highlights the importance and applicability of combining feature selection techniques with predictive models.

IV. CONCLUSIONS

Evidence based medicine firstly requires medicine based evidence. Modern intensive care units fill databases with large amounts of data which go some way to addressing this. However, these databases commonly contain large amounts of data acquired from different sources, and require reliable tools to process the information and integrate results in a human-understandable way. Given the particularly appealing feature for clinicians of providing transparent models and a linguistic interpretation in the form of rules, fuzzy models were used in the present work. In order to reduce the number of rules and bring to light new variables not previously thought relevant, a feature selection process was added to the models.

A classification task was performed to determine which set of clinical variables best predicted the likely administration of vasopressors. It was demonstrated that all the proposed approaches outperform previous works. Fuzzy models combined with BU feature selection returned higher values of sensitivity (i.e. perform better in classifying when a vasopressor was being administered), while fuzzy models with No FS and fuzzy models with TD feature selection returned higher values of AUC and specificity (i.e. performed better in classifying when a vasaprossor was not being administered). The fact that different features were selected to classify the same vasopressor in two different subsets of patients (pancreatitis and pneumonia), points to the future exploration of patient-specific models. Finally, fuzzy models combined with BU and fuzzy models combined with AFS utilize less variables with no significant loss in accuracy. Given the advantage of model ease of interpretation while maintaining high levels of accuracy, we believe that fuzzy modeling combined with these last two feature selection techniques provide opportunities for further studies in this area.

ACKNOWLEDGMENT

The author would like to acknowledge the assistance of the Division of Clinical Informatics at Beth Israel Medical Center. Both human and technical resources were made available and were critical for the development of this work.

This work is supported by the Portuguese Government under the programs: project PTDC/SEM-ENR/100063/2008, Fundação para a Ciência e Tecnologia (FCT), by the MIT-Portugal Program, and by FCT grants SFRH/43043/2008, SFRH/43081/2008 and SFRH/BPD/65215/2009.

REFERENCES

[1] *Shock. In: Critical Care, 3rd Ed.* Lippincott Williams & Wilkins, 1997, pp. 359–387.

[2] T. J. Ellender and J. C. Skinner, "The use of vasopressors and inotropes in the emergency medical treatment of shock," *Emerg Med Clin N Am*, vol. 26, no. 3, pp. 759–786, 2008.

[3] S. Herget-Rosenthal, F. Saner, and L. S. Chawla, "The vip approach to the bedside management of shock," *JAMA*, vol. 207, pp. 337–340, 1969.

[4] M. Weil and H. Shubin, "Approach to hemodynamic shock and vasopressors," *Clin J Am Soc Nephrol*, vol. 26, pp. 546–553, 1969.

[5] S. Hollenberg, T. Ahrens, D. Annane, M. Astiz, D. Chalfin, J. Dasta, S. Heard, C. Martin, L. Napolitano, G. Susla, R. Totaro, J. Vincent, and S. Zanotti-Cavazzoni, "Practice parameters for hemodynamic support of sepsis in adult patients: 2004 update," *Critical Care Medicine*, vol. 32, no. 9, pp. 1928–48, 2004.

[6] *Definition, Monitoring, and Management of Shock States. In: Intensive and Critical Care Medicine*. SpringerLink, 2009, pp. 143–150.

[7] L. A. Mermel, "Prevention of intravascular catheter–related infections," *Ann Intern Med*, vol. 132, pp. 391–402, 2000.

[8] D. Frasca, C. Dahyot-Fizelier, and O. Mimoz, "Prevention of central venous catheter–related infection in the intensive care unit," *Critical Care*, vol. 14, pp. 212–220, 2010.

[9] A. Kumar, D. Roberts, K. E.Wood, B. Light, J. E. Parrillo, S. Sharma, R. Suppes, D. Feinstein, S. Zanotti, L. Taiberg, D. Gurka, A. Kumar, and M. Cheang, "Duration of hypotension before initiation of effective antimicrobial therapy is the critical determinant of survival in human septic shock." *Crit Care Med*, vol. 34, no. 6, pp. 1589–96, 2006.

[10] M. Saeed, C. Lieu, and R. Mark, "MIMIC II: A massive temporal icu database to support research in intelligence patient monitoring." *Computers in Cardiology*, vol. 29, pp. 641–644, 2002.

[11] L. F. Mendonça, S. M. Vieira, and J. M. C. Sousa, "Decision tree search methods in fuzzy modeling and classification," *International Journal of Approximate Reasoning*, vol. 44, pp. 106–123, 2007.

[12] S. M. Vieira, J. M. C. Sousa, and T. A. Runkler, "Two cooperative ant colonies for feature selection using fuzzy models," *Expert Systems with Applications*, vol. 37, no. 4, pp. 2714 – 2723, 2010.

[13] W. Zong, M. Saeed, and L. Nielsen, "A vasopressor advisability index for hemodynamic monitoring." *AMIA Annu Symp Proc*, p. 1198, 2008. [Online]. Available: http://www.biomedsearch.com/nih/vasopressor-advisability-index-hemodynamic-monitoring/18998959.html

[14] A. S. Fialho, F. Cismondi, S. M. Vieira, J. M. C. Sousa, S. R. Reti, M. D. Howell, and S. N. Finkelstein, "Predicting outcomes of septic shock patients using feature selection based on soft computing techniques," in *Applications 13th International Conference, IPMU 2010, Proceedings, Part II*, ser. Communications in Computer and Information Science (CCIS), R. K. E. Huellermeier and F. Hoffmann, Eds., vol. 81. Springer-Verlag Berlin Heidelberg, 2010, pp. 65–74.

[15] J. M. C. Sousa and U. Kaymak, *Fuzzy Decision Making in Modeling and Control*. Singapore: World Scientific Pub. Co., 2002.

[16] L. I. Kuncheva, *Fuzzy Classifier Design*. Heidelberg: Springer, 2000.

[17] J. van den Berg, U. Kaymak, and W. van den Bergh, "Fuzzy classification using probability based rule weighting." in *Proceedings of the 2002 IEEE International Conference on Fuzzy Systems, FUZZ-IEEE'02*, vol. 2, pp. 991–996.

[18] T. Takagi and M. Sugeno, "Fuzzy identification of systems and its applications to modelling and control," *IEEE Transactions on Systems, Man and Cybernetics*, vol. 15, pp. 116–132, 1985.

[19] M. Sugeno and T. Yasukawa, "A fuzzy-logic-based approach to qualitative modeling," *IEEE Transactions on Fuzzy Systems*, vol. 1, pp. 7–31, 1993.

[20] B. Balasko, J. Abonyi, and B. Feil, "Fuzzy clustering and data analysis toolbox - for use with matlab," 2010. [Online]. Available: http://www.fmt.vein.hu/softcomp/

[21] R. Jensen and Q. Shen, "Are more features better? a response to attributes reduction using fuzzy rough sets," *IEEE Transactions on Fuzzy Systems*, vol. 17, no. 6, pp. 1456–1458, 2009.

[22] I. Guyon and A. Elisseeff, "An introduction to variable and feature selection," *Journal of Machine Learning Research*, vol. 3, pp. 1157–1182, 2003.

[23] E. Pekalska and R. Duin, *The Dissimilarity Representation for Pattern Recognition: Foundations And Applications (Machine Perception and Artificial Intelligence)*. World Scientific Publishing Co., Inc., 2005.

[24] M. Dorigo, M. Birattari, and T. Stützle, "Ant colony optimization," *IEEE Computational Intelligence Magazine*, vol. 1, no. 4, pp. 28–39, 2006.

[25] R. O. Duda, P. E. Hart, and D. G. Stork, *Pattern Classification, Second Edition*. Wiley–Interscience Publication, 2001.

[26] G. D. Clifford, W. J. Long, G. B. Moody, and P. Szolovits, "Robust parameter extraction for decision support using multimodal intensive care data," *Philosophical transactions. Series A, Mathematical, physical, and engineering sciences*, vol. 367, no. 1887, pp. 411–429, 2009.

[27] F. Cismondi, A. S. Fialho, S. M. Vieira, J. M. C. Sousa, S. R. Reti, M. D. Howell, and S. N. Finkelstein, "New methods to processing misaligned, unevenly sampled time series containing missing data." *IEEE Symposium Series on Computational Intelligence - SSCI 2011*, 2011.

[28] A. S. Fialho, F. Cismondi, S. M. Vieira, J. M. C. Sousa, S. R. Reti, R. E. Welsch, M. D. Howell, and S. N. Finkelstein, "Missing data in large intensive care units databases," *Crit Care Med*, no. 38, pp. A1–A285, 2010.

2011 IEEE International Conference on Fuzzy Systems
June 27-30, 2011, Taipei, Taiwan

Probing Performance Evaluation for NPD Process by Using Fuzzy MCDM Approach

Chia-Chun Hsiang[1], Meng-Jong Kuan[2]
[1, 2]Graduate Institute of Project Management,
Kainan University, Taiwan
[1]kv05210403@hotmail.com;
[2]mjkuan@mail.knu.edu.tw

Gwo-Hshiung Tzeng[3,4]
[3]Graduate Institute of Project Management,
Kainan University, Taiwan
[4]Institute of Management of Technology,
National Chiao Tung University, Taiwan
ghtzeng@mail.knu.edu.tw; ghtzeng@cc.nctu.edu.tw

Abstract: **Due to the rapid changing marketplace, technology, equipment and raw materials, companies pursuit competitiveness by the new product and new product development (NPD) process for the purpose of innovation, high quality, and speed to the market. It is a gradual trend that the product life cycle is becoming shorter. The product manager intends to achieve the highest customer satisfaction, product value and product continuity. Therefore, to evaluate performance of NPD becomes a critical issue on the NPD process selection which is considered in many different uncertain aspects. Thus, this situation can be regarded as a fuzzy multiple criteria decision-making (FMCDM) problem, so the vagueness and uncertainty of subjective perception could be considered. In this paper, the non-additive (called super-additive) fuzzy integral is used to deal with evaluation of fuzzy MCDM problems particularly while there is dependence among the selected criteria. We can evaluate the quality performance of NPD process according to the result of empirical analysis. Consequently, DEMATEL is used to explore the relevance for the selected criteria of NPD process which is used to find the directions of problem-solving. The results of this study will provide NPD project team a guidance to satisfy the customer needs and creative the value of enterprise business.**

Keywords: New product development (NPD), fuzzy multiple criteria decision-making (FMCDM), fuzzy integral, DEMATEL

I. INTRODUCTION

Due to the rapid changing marketplace, technology, equipment and raw materials, companies try to seek competitiveness by the product and new product development (NPD) process for the purpose of innovation, high quality, and speed to the market. It is a gradual trend that the product life cycle is becoming shorter. The manager intends to achieve the highest customer satisfaction, product value and product continuity. For the company, to select and evaluate is greatly critical on the NPD process which needs to be considered in different aspects [1]. As a result the high quality of NPD process has become the critical success factors of new product development.

Garvin (1984) thinks quality improvement is beneficial for market expansion and cost reduction, so the appropriate and high quality NPD process can provide the enterprise sustainable business. Its can increase the sense of reliance of product for obtaining the positive impression to create a good product (brand) image [5]. In 1987, the International Organization for Standardization (ISO) released ISO 9000 series of quality management system and quality assurance standards, most companies are using this standard to improve the process quality of enterprise. The enterprises of various fields that can review standard of ISO quality management through the procedures and conduct a series mission of the "process quality" for supervision, control, tracking and continuous improvement according to the design review standards and ISO quality management.

The development of new products and services involves an integrated set of unique activities. U.S. Product Development and Management Association (PDMA) proposed the NPD process with a clear definition as "a clear mission and the steps show that is from the concept to the marketable products or services required standardized methods". The manager should plan, check and execute a formal written review of the mission results under the appropriate stage of NPD process [27].

This study is based on ISO 9000:2008 quality management system to explore the evaluation indexes for the quality of NPD process [25]. The purpose here is to construct a model that not only considers in the presence of intangible attributes and uncertainty such has inter-dependent characteristics between attributes. First, a fuzzy integral is applied to integrate the performance rating of attributes in each criterion. The results can obtain the total performance of each dimension for the case study. Second, DEMATEL is used to construct the relevance for the evaluated criteria. Then, the manager can find the direction of problem-solving from DEMATEL. The results of this study will provide NPD team a guidance to satisfy the customer needs and create the value of sustainable business.

The reminder of this paper is organized as follows. In Section 2, literature review on quality of NPD process is introduced. In Section 3, NPD process performance evaluation model is developed. An empirical case analysis for NPD process is illustrated to show our proposed model in Section 4. The result and discussions is in Section 5. Finally, conclusion is presented in Section 6.

II. LITERATURE RELATED ON NPD PROCESS

This section is aimed to understand the evaluation indexes related to NPD process. It is collected, selected, analyzed, simulated and tested by the literature of the past new product development with expert questionnaires to find problems that requires strict quality management as a basis. We use ISO9000 series of quality management system standards to explore the related evaluation indexes of process quality.

A. The new product development (NPD)

Sampson (1970) proposed the view of consumer to explain the new product that is defined as "it has to meet new demands, requirements or desires that is more significant than other products" [2]. Souder (1988) defined the new product is based

on the view of business as "it has never owned products in previous" [7]. Kolter (1994) proposed the view of product characteristic to explain the new product who divided the types of new product as: (1) internal development of original product; (2) improved product; (3) modified product; (4) new brand. Overview of the scholar defines the new product to explain that opens up an entirely new market and adapts or replaces an existing product [8]. In addition, it is including an old product introduced in a new market or packaged and marketed in different way.

According to above all, the new product development (NPD) is a process which is designed to develop, test and consider the viability of products which are new to the market in order to ensure the growth or survival of the organization. The primary impact of the environment is to drive the types of new product changes which help speed products through development, and improve process efficiency and overall NPD effectiveness [12].

NPD involves a series of organization and connects the activities closely which is significantly for the input of manpower and financial capability. They believe the quality and up to 80% of NPD costs that has decided in the product design stage [13]. Therefore, the managers reduce and control the uncertainty activities before the next phase is implemented according to the integrity of information. It can ensure to improve the performance and quality of NPD.

B. New product development (NPD) process

From the past product idea to the new product development starts with the cumulative ideas. The idea generation is a NPD process in which creative thinking is used to produce large amount of ideas for new products. Therefore, NPD process may be accepted as a dynamic process in which each decision-making on each stage must be evaluated, selected, and prioritized. All the stages of the process are affected by uncertain, changing information and dynamic opportunities [18]. It is greatly complex and widely which is combined by many different aspects. The NPD process not only evaluates the gathered ideas but also has a specific purpose, which involve the whole of the enterprise including its customer, cost, time, technical, raw materials, regulatory requirement and the person in charge. Furthermore, the management of ideas is also very important at this stage due to the large number of ideas to be selected and their diversity.

Urban and Hauser (1980) defined the NPD process as: (1) opportunity identification phase; (2) design phase; (3) testing phase; (4) listed phase [4]. Cooper (1994, 1996) proposed the definition of NPD process as: (1) the ideas of product; (2) initial assessment; (3) concept design; (4) product development; (5) product testing; (6) engineering trial production; (7) mass production and listed [9][11]. To overview of the NPD process concept which is extended by the concept of stage and gate. A "Stage-Gate Process" is a conceptual and operational roadmap for moving a new-product project from idea to launch. Stage-Gate divides the effort into distinct stages separated by management decision gates. Cross-functional teams must successfully complete a prescribed set of related cross-functional tasks in each stage prior to obtaining management approval to proceed to the next stage of product development [14].

Today organizations have developed many different variations and varieties from the original concept of NPD process. In this paper, we propose a critical NPD process according to the NPD process definition from the concept of stage and gate, which is divided into five parts for ten phases as: (1) customer needs analysis; (2) conceptual design; (3) conceptual development; (4) preliminary design; (5) design and evaluation; (6) detail design; (7) product run and test; (8) pre-mass production run and test; (9) mass production listing; (10) transference, these NPD phases combine with the design review [3,10,13,14].

C. The evaluation indexes for NPD process

We explore the evaluation indexes of NPD process according to the ISO 9000:2008 quality management system [23][15]. Through the expert questionnaires select and evaluate the evaluation indexes according to its properties which is selected and divided into fifteen criteria, the result as shown in Table 1.

III. DEVELOPING AN EVALUATION MODEL FOR NPD PROCESS

In this paper, the fuzzy integral is used to combines the efficient value of those related attributes and to develop a new combining performance value [20]. Then, DEMATEL is used to explore the affect and relevance for the criteria of each dimension respectively which can provide the product manager to find the directions of problem-solving for the performance gaps of NPD process [28].

A. Regrouping the evaluation indexes of NPD process by fuzzy integral

The traditional multi-criteria decision-making evaluation is based on the assumption that each attribute is independent with the evaluation of multiple attributes executed by simply weighting the relative importance and performance of each [20][10]. The integrated performance is measured by weighting and performance for each attribute. In the real world, there are some inter-dependent characteristics between attributes. Therefore, partitioning the type of fuzzy integral has to be applied on these related attributes to regroup a new hierarchy system [20][3].

TABLE I. THE EVALUATION INDEXES OF NPD PROCESS [23][15]

Criteria for the process quality
C_1 Product specifications and customer needs analysis
C_2 Compatibility of safety and environment
C_3 The regulatory requirements of business practices, national and international standards
C_4 To compare with the competitive products
C_5 Consideration of improper use and misuse
C_6 The requirements of reliability, service and maintainability
C_7 The allowed tolerance and process capability assessment
C_8 The criteria of product acceptance and rejection
C_9 Installable features and easy assembly
C_{10} To review and use the standard components
C_{11} The manufacturability of product design and development
C_{12} The examination and experimentation of product design and development
C_{13} The specification of materials and components
C_{14} The requirements of packaging, handling, storage and storage life
C_{15} Confirmation of customer needs and assessment of production costs

B. λ-Fuzzy measure

Fuzzy measure is a set function, let g_λ be a λ fuzzy measure which is defined on a power set $P(x)$, for the finite set $X=\{x_1,x_2,\ldots,x_n\}$ [16].The fuzzy measure has the following property [19] [22]:

$$\forall A,B\in P(x),\quad A\cap B=\varnothing,$$
$$g_\lambda(A\cup B)=g_\lambda(A)+g_\lambda(B)+\lambda g_\lambda(A)g_\lambda(B) \quad \text{for } -1<\lambda<\infty \tag{1}$$

The density of the fuzzy measure $g_i=g_\lambda(\{x_i\})$ can be formulated as

$$\begin{aligned} g_\lambda(\{x_1,x_2,\ldots,x_n\}) &= \sum_{i=1}^{n} g_i+\lambda\sum_{i_1=1}^{n-1}\sum_{i_2=i_1+1}^{n} g_{i_1}g_{i_2} \\ &\quad +\cdots+\lambda^{n-1}g_1,g_2,\ldots,g_n, \\ &= \frac{1}{\lambda}\left|\prod_{i=1}^{n}(1+\lambda g_i)-1\right| \\ &\quad \text{for } -1<\lambda<\infty \end{aligned} \tag{2}$$

Base on these properties, one of the three following situations will be sustained for a specific case with two attributes, x_1 and x_2.

(a) If $\lambda>0$, then $g_\lambda(A\cup B)>g_\lambda(A)+g_\lambda(B)$: this implies that x_1 and x_2 have multiplicative effect in $\{A,B\}$.

(b) If $\lambda=0$, then $g_\lambda(A\cup B)=g_\lambda(A)+g_\lambda(B)$: this implies that x_1 and x_2 have additive effect in $\{A,B\}$.

(c) If $\lambda<0$, then $g_\lambda(A\cup B)<g_\lambda(A)+g_\lambda(B)$: this implies that x_1 and x_2 have substitutive effect in $\{A,B\}$.

C. Fuzzy integral

Let h be a measurable set function defined on the fuzzy measurable space, and supposing that $h(x_1)\ge h(x_2)\ge\cdots\ge h(x_n)$, then the fuzzy integral of fuzzy measure $g(\cdot)$ with respect to $h(\cdot)$ can be defined as Eq. (3) [6] and the concept of fuzzy integral as shown in Fig. 1 [20][22]:

$$\begin{aligned} \int h\,\mathrm{d}g &= h(x_n)g(H_n)+[h(x_{n-1})-h(x_n)] \\ &\quad g(H_{n-1})+\cdots+[h(x_1)-h(x_2)]g(H_1) \\ &= h(x_n)[g(H_n)-g(H_{n-1})]+h(x_{n-1}) \\ &\quad [g(H_{n-1})-g(H_{n-2})]+\cdots+h(x_1)g(H_1), \end{aligned} \tag{3}$$

where $H_1=\{x_1\}, H_2=\{x_1,x_2\},\ldots,H_n=\{x_1,x_2\ldots,x_n\}=X$.

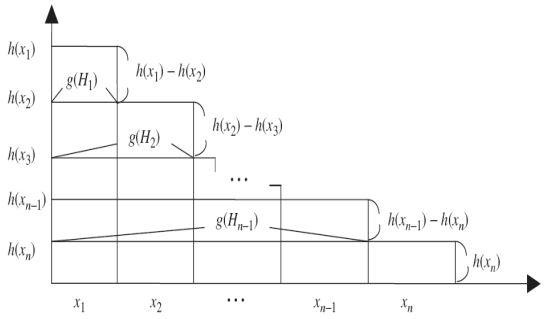

Figure 1. Concept of fuzzy integral [20] [22]

Using the fuzzy integral to formulae the original data, not only can fewer and more representative factors be extracted to describe the system, but the interactions between attributes can be considered. Furthermore, we used $\int h\,\mathrm{d}g=a_i(d)$ as the integrated performance value of the common-factor C_d for the case study.

D. Building a network relationship by DEMATEL

DEMATEL is an analytical method of structural model. It is mainly used to solve all kinds of complex problems to clarify the essential of the problem that can effectively understand the complex structure and provide viable options of problem-solving [21].

DEMATEL is divided into five steps. The first step is to confirm the system has n elements and develop the evaluating scale, using pair of dimensions to compare and also using evaluating scale 0, 1, 2, 3, 4, which in turn represents no effect (0), low effect (1), medium effect (2), high effect (3), and extremely high effect (4) as measuring standard. The second step is to calculate initial matrix, using pair of degree of interaction to obtain directly effecting matrix $\boldsymbol{Z}=[z_{ij}]_{n\times n}$, where z_{ij} represents the degree of effect on i factor effects j factor [24][26].

$$\boldsymbol{Z}=\begin{bmatrix} z_{11} & \cdots & z_{1j} & \cdots & z_{1n} \\ \vdots & & \vdots & & \vdots \\ z_{i1} & \cdots & z_{ij} & \cdots & z_{in} \\ \vdots & & \vdots & & \vdots \\ z_{n1} & \cdots & z_{nj} & \cdots & z_{nn} \end{bmatrix} \tag{4}$$

When the elements of *i* have a direct effect on the elements of *j*, then $z_{ij}\neq 0$, opposite $z_{ij}=0$. The third step is to normalize the matrix. It can be obtained from Eqs. (2) and (3). Its diagonal is 0, and maximum sum of row or column is 1.

$$\boldsymbol{X}=s\,\boldsymbol{Z} \tag{5}$$

$$s=\min\left[\frac{1}{\max_i\sum_{j=1}^{n}|z_{ij}|},\frac{1}{\max_j\sum_{i=1}^{n}|z_{ij}|}\right] \quad i,j=1,2,\ldots,n \tag{6}$$

The forth step is to obtain the total influence matrix $\boldsymbol{T}$. Its can be obtained by $\boldsymbol{T}=\boldsymbol{X}+\boldsymbol{X}^2+\cdots+\boldsymbol{X}^m=\boldsymbol{X}(\boldsymbol{I}-\boldsymbol{X})^{-1}$, where $\boldsymbol{I}$ is the identity matrix. The fifth step is to obtain prominence and

relation. To sum of each row and column of the total influence matrix $\boldsymbol{T}=[t_{ij}]$. Its will obtain the sum of all rows (vector $\boldsymbol{r}=(r_1,...,r_i,...,r_n)$) and the sum of all columns (vector $\boldsymbol{d}=(d_1,...,d_j,...,d_n)$).

If r_i represents the sum of all rows of the total influence matrix $\boldsymbol{T}$, meaning directly or indirectly influence degree; d_j represents the sum of all columns of the total influence matrix $\boldsymbol{T}$, meaning influence or be influenced other criteria. r_i represents the factor *i* which will influence other factors, d_j represents the factor *j* that is influenced by other factors. According to the definition, r_i+d_j presents the degree of relationship between the factors, meaning "prominence"; r_i-d_j presents the degree of influence and influenced for the factors, meaning "relation" [21][17].

IV. Empirical analysis for the case study

In this section, we evaluate the performance of NPD processes within a case study of company A. We will consider the overall impact in product manufacturing and developing that may have potential problems and risks in the NPD process. Through the expert questionnaires, we classify the evaluation indexes according to its properties which is selected and divided into five dimensions of fifteen criteria, as shown in Fig.2.

A. To obtain the assessment value by fuzzy measure

Here fuzzy measure and fuzzy integral are used to determine the problem of NPD performance evaluation for human subjective decision-making issues. In the table2, we obtain the results of fuzzy measure which illustrates that the criterion "Confirmation of customer needs and assessment of production costs (C_{13})" is most important attribute of customer needs included (C_{13}=0.74). And the set values are obtained respectively according to those evaluated value of attributes.

Consequently, the non-additive fuzzy integral model is used to calculate the assessment value (C_d) for each dimension. Furthermore, the performance value for each dimension is calculated as shown in Table 3. The result shows dimension "Customer needs (D_1)" is the highest performance value (D_1=0.920) than others; "Product design (D_3)" is the lowest performance value than others (D_3=0.865). The priority of performance value for each dimension is following: D_1 (Customer needs) > D_4 (Process planning) > D_5 (Product Logistics) > D_2 (Environment) > D_3 (Product design).

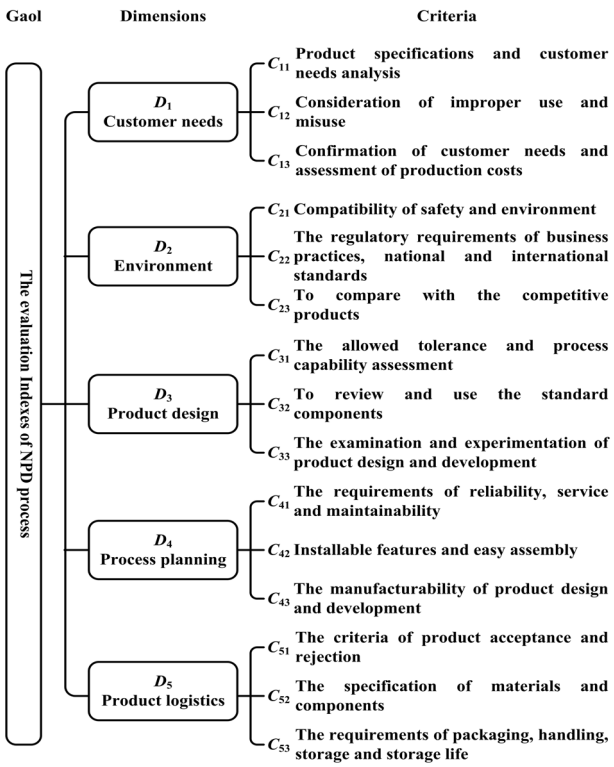

Figure 2. The assessment hierarchy system

TABLE II. FUZZY MEASURE $g(\cdot)$ OF EACH CRITERIA

Fuzzy measure of criteria	
D_1 Customer needs (λ =-0.91)	
$C_{11}=0.63$	$\{C_{11},C_{12}\}=0.79$
$C_{12}=0.38$	$\{C_{12},C_{13}\}=0.87$
$C_{13}=0.74$	$\{C_{11},C_{13}\}=0.95$
	$\{C_{11},C_{12},C_{13}\}=1$
D_2 Environment (λ =-0.85)	
$C_{21}=0.57$	$\{C_{21},C_{22}\}=0.82$
$C_{22}=0.49$	$\{C_{22},C_{23}\}=0.84$
$C_{23}=0.60$	$\{C_{21},C_{23}\}=0.88$
	$\{C_{21},C_{22},C_{23}\}=1$
D_3 Product design (λ =-0.81)	
$C_{31}=0.62$	$\{C_{31},C_{32}\}=0.83$
$C_{32}=0.43$	$\{C_{32},C_{33}\}=0.77$
$C_{33}=0.52$	$\{C_{31},C_{33}\}=0.88$
	$\{C_{31},C_{32},C_{33}\}=1$
D_4 Process planning (λ =-0.92)	
$C_{41}=0.65$	$\{C_{41},C_{42}\}=0.90$
$C_{42}=0.63$	$\{C_{42},C_{43}\}=0.87$
$C_{43}=0.58$	$\{C_{41},C_{43}\}=0.88$

Fuzzy measure of criteria	
	$\{C_{41}, C_{42}, C_{43}\} = 1$
D_5 Product logistics (λ =-0.94)	
$C_{51} = 0.55$	$\{C_{51}, C_{52}\} = 0.87$
$C_{52} = 0.66$	$\{C_{52}, C_{53}\} = 0.93$
$C_{53} = 0.72$	$\{C_{51}, C_{53}\} = 0.90$
	$\{C_{51}, C_{52}, C_{53}\} = 1$

B. To obtain the total performance by fuzzy integral

We used fuzzy integral to obtain the total performance base on the assessment value from fuzzy measure. The result demonstrates that dimensions "Environment (D_2)" and "Product design (D_3)" are the performance gaps with total performance 0.907 from Fuzzy Integral as illustrated in Table 3.

TABLE III. TO OBTAIN THE TOTAL PERFORMANCE BY FUZZY INTEGRAL

The case study of company A			
Dimensions	***Fuzzy measure of dimensions***	***Assessment value (C_d)***	***Performance ranking***
	λ=-0.99		
D_1	0.584	0.920	1
D_2	0.556	0.874	4
D_3	0.524	0.865	5
D_4	0.619	0.890	2
D_5	0.642	0.887	3
Total performance	**0.907**		
{D1,D2}=0.82	{D2,D4}=0.84		
{D1,D3}=0.81	{D2,D5}=0.85		
{D1,D4}=0.85	{D3,D4}=0.82		
{D1,D5}=0.86	{D3,D5}=0.83		
{D2,D3}=0.79	{D4,D5}=0.87		
{D1,D2,D3}=0.92	{D2,D3,D5}=0.93		
{D1,D2,D4}=0.94	{D3,D4,D5}=0.94		
{D1,D2,D5}=0.94	{D1,D2,D3,D4}=0.94		
{D1,D3,D4}=0.93	{D1,D2,D3,D5}=0.94		
(D1,D3,D5)=0.93	{D1,D2,D4,D5}=0.99		
{D1,D4,D5}=0.95	{D2,D3,D4,D5}=0.77		
{D2,D3,D4}=0.93	{D1,D2,D3,D4,D5}=1		

C. Constructing the network by DEMATEL

In this section, DEMATEL is applied to explore the inter-relationship between the criteria. According to the empirical analysis, we obtain the influence degree of each criterion as shown in Table 4. Based on the results of fuzzy integral, we build the network about "Environment (D_2)" and "Product design (D_3)" which are proved by the empirical analysis from DEMATEL as illustrated in Fig. 3 and Fig. 4.

TABLE IV. THE DEGREE OF INFLUENCE FOR EACH CRITERION

T	r	d	$r + d$	$r - d$
C_{11}	8.861	8.701	17.562	0.160
C_{12}	8.378	8.096	16.474	0.282
C_{13}	8.636	7.846	16.482	0.791
C_{21}	8.426	8.643	17.069	-0.218
C_{22}	7.737	9.209	16.947	-1.472
C_{23}	9.083	8.506	17.589	0.577
C_{31}	9.310	8.571	17.881	0.739
C_{32}	8.074	8.282	16.357	-0.208
C_{33}	8.418	8.504	16.922	-0.086
C_{41}	9.038	9.446	18.484	-0.409
C_{42}	8.848	8.564	17.412	0.285
C_{43}	8.351	8.818	17.169	-0.468
C_{51}	8.873	8.443	17.316	0.429
C_{52}	7.028	9.225	16.253	-2.197
C_{53}	8.563	6.770	15.333	1.793

Within the dimension "environment (D_2)", criterion C_{23} is the highest impact of the strength of relation that means the most important influencing factors; C_{22} is all the factors that affects the least degree of other factors according to the total influential prominence $(r_i + d_i)$. Furthermore, we also found that C_{23} is the highest degree of impact relationship which affects other factors directly; and C_{22} is the most vulnerable influence factor to compare with other criteria according to the influential relation $(r_i - d_i)$.

The result also illustrates that criterion "The regulatory requirements of business practices, national and international standards (C_{22})" needs for prior improvement. The product manager can improve the performance gap form the criterion "To compare with the competitive products (C_{23})" which could then effectively improve the entire performance of this dimension.

In the dimension "product design (D_3)", the criterion C_{31} is the highest impact of the strength of relation that means the most important influencing factors; C_{32} is all the factors that affects the least degree of other factors according to the total influential prominence $(r_i + d_i)$. Furthermore, we also found that C_{31} is the highest degree of impact relationship that affect

other factors directly; and C_{32} is the most vulnerable impact factor to compare with other criteria according to the influential relation $(r_i - d_i)$.

The result illustrates that criterion "To review and use the standard components (C_{32})" needs for prior improvement. The product manager can improve the performance gap begin with the criterion "The allowed tolerance and process capability assessment (C_{31})" which can effectively improve the entire performance of this dimension D_3.

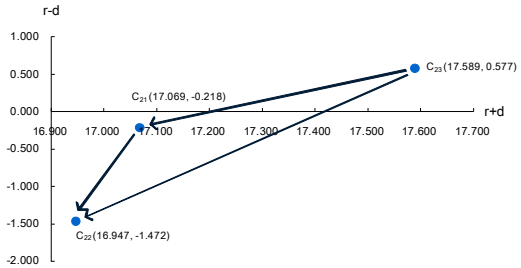

Figure 3. the Shown the interrelationship of D_2

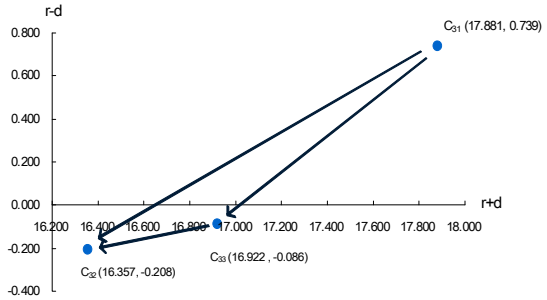

Figure 4. the Shown the interrelationship of D_3

V. Results and discussions

In this paper, we use fuzzy integral to integrate the performance rating of attributes for performance evaluation quality of the NPD process. Furthermore, we combine with the results of to obtain the total performance of NPD process for the case study. Consequently, we use DEMATEL to explore the relevance for the considered criteria of NPD process which is used to find the directions of problem-solving respectively.

According to the results of empirical analysis and the literature review to the past research, the study illustrates that shows "customer needs (D_1)", "process planning (D_4)" and "product logistics (D_5)" are the critical dimensions in NPD process quality [28]. In addition, we can know D_2 (Environment) and D_3 (Product design) both are the lowest performance value than others. The manager can improve the performance through the criteria of "To compare with the competitive products (C_{23})" and "The allowed tolerance and process capability assessment (C_{31})" which can improve the performance efficiency.

VI. Conclusion

In our study, we find that "customer needs", "process planning" and "product logistics" are still the critical indexes for performance assessment of the NPD process according to the empirical analysis. In case study of company A, we obtain the total performance is greatly near to the highest expect value, but the performance for the dimension of "environment (D_2)" and "product design (D_3)" are low. In the real word, the manager may take into those dimensions which can support the company to improve the entire NPD process efficiency in order to exceed the aspire level. The results from this study will provide an NPD project team a guidance to satisfy the customer needs and create the value of sustainable business.

ACKNOWLEDGEMENTS: NSC 99-2632-H-424-001-MY3

References

[1] Levitt, T. "Exploit the Product Life Cycle", Harvard Business Review, 43(6), 81-94, 1965.

[2] Sampson, P. "Can Consumer Create New Products", Journal of the Market Research Society, 12(1), 42-52, 1970.

[3] Sugeno M. "Theory of fuzzy integrals and its applications", PhD dissertation, Tokyo Institute of Technology, Tokyo, Japan, 1974.

[4] Urban, G. L. and Hauser, J. R. "Design and Marketing of new products", New Jersey: Prentice-Hall Inc., Englewood Cliffs, 538-551, 1980.

[5] Garvin, D. A. "What does product quality really mean", Sloan Management Review, 26(1), 25-39, 1984.

[6] Ishii, K. and Sugeno, M. "A model of human evaluation process using fuzzy integral", International Journal of Man-Machine Studies, 22(1), 19-38, 1985, 1985.

[7] Souder, W. E. "Managing relations between R&D and marketing in new product development projects", Journal of Product Innovation Management, 5(1), 6-19, 1988.

[8] Kotler "Marketing Management: Analysis, Planning, Implementation, and Control", New Jersey: Prentice-Hall Inc., Englewood Cliffs, 1994.

[9] Cooper, R. G. "Perspective: Third-Generation New Product Processes", Journal of Product Innovation Management, 11(1), 3-14, 1994.

[10] Grabisch M. "Fuzzy integral in multi criteria decision making", Fuzzy Sets and Systems, 69(3), 279–298, 1995.

[11] Cooper, R. G. "Overhauling the New Product Process", Industrial Marketing Management, 25(6), 465-482, 1996.

[12] Poolton, J. and Barclay, I. "New product development from past research to future application", Industrial Marketing Management, 27(3), 197-212, 1998.

[13] Swink, M. "Threats to New Product Manufacturability and the Effects of Development Team Integration Processes", Journal of Operations Management, 17(6), 691-709 1999.

[14] Cooper, R. G. and Kleinschmidt, E. J. (2001), "Stage-Gate process for new product success", edited by Jens Arleth, Innovation Management, 2001.

[15] Lu, C. C. and Tian, M. C. "International quality management – ISO : 2000 establishment and audit quality control system", Taipei: Hsinglu press, 2001.

[16] Chen, Y. W. and Tzeng, G. H. "Using fuzzy integral for evaluating subjectively perceived travel cost in traffic assignment model", European Journal of Operation Research, 130(3), 653-664, 2001.

[17] Tamura, M., Nagata, H., and Akazawa, K. "Extraction and systems analysis of factors that prevent safety and security by structural models", In 41st SICE annual conference, Osaka, Japan, 2002.

[18] Büyüközkan, G. G. and Feyzolu, O. (2004), "A fuzzy-logic-based decision-making approach for new product development", International Journal of Production Economics, 90(1), 27-45.

[19] Tzeng, G. H., Ou Yang, Y. P., Lin, C. T. and Chen, C. B (2005), "Hierarchical MCDM with fuzzy integral for evaluating enterprise intranet web sites", Information Science, 169(3/4), 409-426, 2005.

[20] Liou, J. H. and Tzeng, G. H. "A non-additive model for evaluating airline service quality", Journal of Air Transport management, 13(3), 131-138, 2007.

[21] Tzeng, G. H., Chiang, C. H. and Li, C. W. "Evaluating Intertwined Effects in E-learning Programs: A Novel Hybrid MCDM Model Based

on Factor Analysis and DEMATEL", Expert Systems with Applications, 32(4), 1028-1044, 2007.
[22] Yang, J. L., Chiu, H. N., Tzeng, G. H. and Yeh, R. H. "Vendor Selection by integrated fuzzy MCDM techniques with independent and interdependent relationships", Information Science, 178(21), 4166-4183, 2008.
[23] ISO official website , http://www.iso.org/iso/en/ISOOnline.frontpage, 2010.
[24] Lin, C. L. and Tzeng, G. H. "A value-created system of science (technology) park by using DEMATEL", Expert Systems with Applications, 36(6), 9683-9697, 2009.
[25] Kuan, C. M. "ISO 9001: 2008 quality management system and system documentation", Taiwan of society for quality, 2009.
[26] Chen, Y. C., Lien, H. P. and Tzeng, G. H. "Measures and evaluation for environment watershed plans using a novel hybrid MCDM model", Expert Systems with Applications, 37(2), 926-938, 2010.
[27] Product Development and Management Association (PDMA) official website, http://www.pdma.org/, 2010.
[28] Tzeng, G. H., Kuan M. J. and Hsiang C. C. "Exploring the Quality Assessment System for New Product Development Process by combining DANP with MCDM model", International Symposium on Management Engineering, Waseda University, Kitakyushu, Japan, 2010.

2011 IEEE International Conference on Fuzzy Systems
June 27-30, 2011, Taipei, Taiwan

Application of Adaptive Self-Organizing CMAC_GBF to Aircraft Landing System

Chung-Ju Cheng
Department of Communications, Navigation and Control Engineering, National Taiwan Ocean University
Keelung, Taiwan
M98670011@mail.ntou.edu.tw

Jih-Gau Juang
Department of Communications, Navigation and Control Engineering, National Taiwan Ocean University
Keelung, Taiwan
jgjuang@mail.ntou.edu.tw

***Abstract*—This paper presents an intelligent control scheme that uses an adaptive self-organizing cerebellar model articulation controller with general basis function (CMAC_GBF) in aircraft automatic landing system (ALS). During landing phase if the flight condition is out of the desired or preset environments, such as encountering severe turbulence, the ALS is disabled. The proposed intelligent controller can act as an experienced pilot and guide the aircraft landed safely in the serious condition. Lyapunov theory is applied to obtain adaptive learning rule and stability analysis is also provided. The performance of the proposed controller is better than conventional CMAC_GBF.**

Keywords-self-organizing CMAC; automatic landing system; general basis function; turbulence; PID control

I. INTRODUCTION

On March 1, 2008, at Hamburg airport, a Lufthansa Airbus A320 tried to land in crosswind conditions which exceeded the limit for the aircraft and made the left wing touch ground. The pilots then performed a go around and successfully saved the aircraft from crashing. The atmospheric disturbance causes the problem of flight safety and reduces the flying quality. According to International Air Transport Association (IATA) classification, aircraft accident contributing factor is divided into five categories as human factor, technical, environment, organization factor and insufficient. An aircraft accident survey of 19562 aircraft accidents from 1994 through 2003, weather was a contributing factor. The percentage of weather related to total accidents is 21.3% [1]. Percentage of weather related accidents by weather conditions is shown in Fig. 1. The first automatic landing system (ALS) was developed in England during 1965. Since then, most aircraft have had this system installed. The ALS relies on the instrument landing system (ILS) to guide the aircraft into the proper altitude, position, and approach angle during the landing phase. According to Federal Aviation Administration (FAA) regulations [2], environmental conditions considered in the determination of dispersion limits are: headwinds up to 25 knots, tailwinds up to 10 knots, crosswinds up to 15 knots, moderate turbulence, and wind shear of 8 knots per 100 feet from 200 feet to touchdown. Conventional automatic landing systems can provide a smooth landing, which is essential to the comfort of passengers. However, these systems work only within a specified operational safety envelope. When the conditions, such as turbulence or wind shear, are beyond the envelope, they often cannot be used. Most conventional control laws generated by the ALS are based on the gain scheduling method [3]. Control parameters are preset for different flight conditions within a specified safety envelope, which is relative defined by FAA regulation. When the conditions, such as turbulence, are beyond the envelope, the ALS is disabled and manual operation is engaged. An inexperience pilot may not be able to guide the aircraft safely. Therefore it is desirable to develop an intelligent ALS that expands the operational envelope to include more safe responses under a wider range of conditions. The goal of this study is to show that the proposed intelligent ALS can relieve human operation and guide the aircraft to a safe landing in wind-disturbance environment.

In recent years, intelligent control is more and more popular in control engineering applications. Many intelligent concepts have been applied into various scientific and engineering researches. There are also obvious achievements in flight control domain [4]-[9]. CMAC_GBF has attracted researchers' attentions for the following advantages: rapid learning speed, guarantee of learning convergence, good generalization, and low computational load. A simplified addressing technique procedure, S_CMAC_GBF, is presented by C.T. Chiang [10]. The simplified model not only provides fixed addressing procedure for CMAC_GBF but also reduces the usage of memory. The S_CMAC_GBF still posses the same learning convergence characteristics of CMAC_GBF, but with more enhanced accurate system performance. The calculation speed of S_CMAC_GBF is faster than conventional CMAC_GBF. It is very useful in on-line control system. But it is hard to decide the number of layers and the value of learning rate of the S_CMAC_GBF. In this study, we utilize a self-organizing CMAC_GBF (SOCM) [11] by judging error rate to add or delete layer and introduce a SOCM with adaptive learning rate to automatic landing system. Because adaptive control theory has been successfully employed in various fields, more and more researchers integrated the adaptive concept into the intelligent control system. The performance of the intelligent ALS under severe environment can be improved by the advantages of the SOCM with adaptive learning rate, and

978-1-4244-7316-8/11/$26.00 ©2011 IEEE

the advantages are local generalization, rapid learning convergence, and environment adaptive capability.

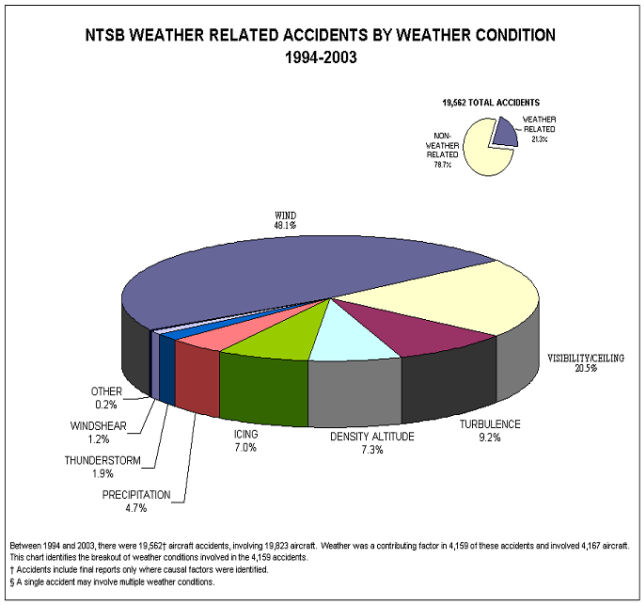

Figure 1. NTSB weather related accidents by weather condition.

II. LANDING SYSTEM MODEL

At the aircraft landing phase, the pilot descends from the cruise altitude to an altitude of approximately 1200 ft above the ground. The pilot then positions the aircraft so that the aircraft is on a heading towards the runway centerline. When the aircraft approaches the outer airport marker, which is about 4 nautical miles from the runway, the glide path signal is intercepted, as shown in Fig. 2 [12]. As the airplane descends along the glide path, its pitch, attitude, and speed must be controlled. The descent rate is about 10 ft/sec and the pitch angle is between -5 to +5degrees. Finally, as the airplane descends 20 to 70 feet above the ground, the glide path control system is disengaged and a flare maneuver is executed. The vertical descent rate is decreased to 2 ft/sec so that the landing gear may be able to dissipate the energy of the impact at landing. The pitch angle of the airplane is then adjusted, between 0 to 5 degrees for most aircraft, which allows a soft touchdown on the runway surface.

A simplified model of a commercial aircraft that moves only in the longitudinal and vertical plane is used in the simulations for implementation ease [7]. The motion equations of the aircraft are given as follows:

$$\Delta\dot{u} = X_u(\Delta u - u_g) + X_w(\Delta w - w_g) + X_q\Delta q - g(\frac{\pi}{180})\cos(\gamma_0)\Delta\theta + Z_E\delta_E + Z_T\delta_T \quad (1)$$

$$\Delta\dot{w} = Z_u(\Delta u - u_g) + Z_w(\Delta w - w_g) + (Z_q - \frac{\pi}{180}U_0)\Delta q - g(\frac{\pi}{180})\sin(\gamma_0)\Delta\theta + Z_E\delta_E + Z_T\delta_T \quad (2)$$

$$\Delta\dot{q} = M_u(\Delta u - u_g) + M_w(\Delta w - w_g) + M_q\Delta q + M_E\delta_E + M_T\delta_T \quad (3)$$

$$\Delta\dot{\theta} = \Delta q \quad (4)$$

$$\Delta\dot{h} = -\Delta w + \frac{\pi}{180}U_0\Delta\theta \quad (5)$$

where u is the aircraft longitudinal velocity (ft/sec), w is the aircraft vertical velocity (ft/sec), q is the pitch rate (rate/sec), θ is the pitch angle (deg), h is the aircraft altitude (ft), δ_E is the incremental elevator angle (deg), δ_T is the throttle setting (ft/sec), γ_o is the flight path angle (-3deg), and g is the gravity (32.2 ft/sec^2). The parameters X_i , Z_i and M_i are the stability and control derivatives.

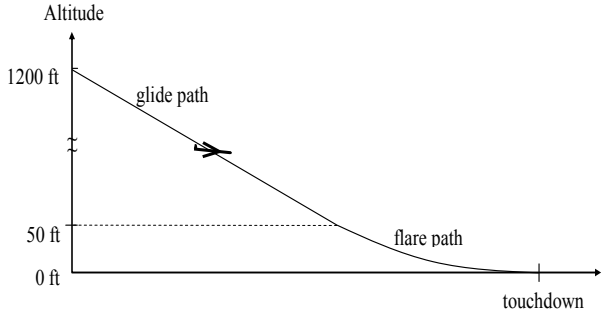

Figure 2. Glide path and flare path.

To make the ALS more intelligent, reliable wind profiles are necessary. Two spectral turbulence models by von Karman and Dryden are mostly used for aircraft response studies. In this study the Dryden form [7] was used for its demonstration ease. The model is given by:

$$u_g = u_{gc} + N(0,1)\sqrt{\frac{1}{\Delta t}\left(\frac{\sigma_u\sqrt{2a_u}}{s+a_u}\right)} \quad (6)$$

$$w_g = N(0,1)\sqrt{\frac{1}{\Delta t}\left(\frac{\sigma_w\sqrt{3a_w}(s+b_w)}{(s+a_u)^2}\right)} \quad (7)$$

where $u_{gc} = -u_{wind\,510}[1 + \frac{\ln(h/510)}{\ln(51)}]$, $a_u = \frac{U_o}{L_u}$, $L_w = h$, $a_u = \frac{U_o}{L_u}$, $a_w = \frac{U_o}{L_w}$, $b_w = \frac{U_o}{L_w\sqrt{3}}$, $L_u = 100h^{1/3}$ for $h > 230$, $L_u = 600$ for $h \le 230$, $\sigma_u = 0.2|u_{gc}|$ for $h > 500$, $\sigma_w = 0.2|u_{gc}|(0.5 + 0.00098*h)$ for $0 \le h \le 500$. The parameters are: u_g is the horizontal wind velocity (ft/sec), w_g is the vertical wind velocity (ft/sec), u_0 is the nominal aircraft speed (ft/sec), $u_{wind510}$ is the wind speed at 510 ft altitude, L_u and L_w are scale lengths (ft), σ_u and σ_w are RMS values of turbulence velocity (ft/sec), Δt is the simulation time step (sec), $N(0,1)$ is the Gaussian white noise with zero mean and unity standards deviation, u_{gc} is the constant component of u_g, and h is the aircraft altitude (ft). Fig. 3 shows a turbulence profile with a wind speed of 30 ft/sec at 510 ft altitude.

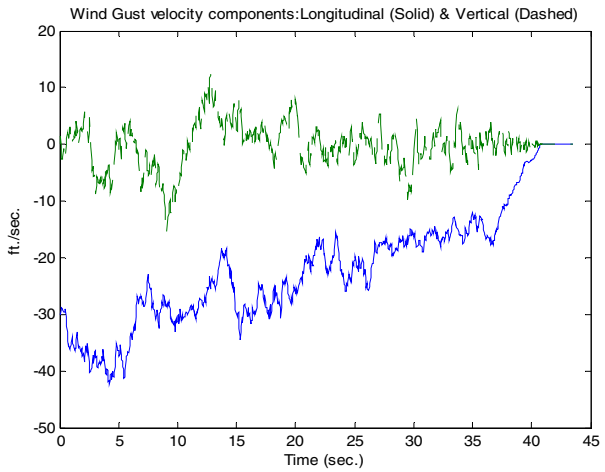

Figure 3. Turbulence profile.

III. INTELLIGENT CONTROL

A simplified PID control structure is applied to aircraft landing control as shown in Fig. 4. Its inputs consist of altitude and altitude rate commands along with aircraft altitude and altitude rate. Via aircraft landing controller we can obtain the pitch command θ_c. Then, the pitch autopilot is controlled by pitch command. The pitch autopilot is shown in Fig. 5. Detail descriptions can be found in [7]. In order to enable aircraft to land more steady when an aircraft approaches to the flare path, a constant pitch angle is added to the controller. In general, the PID controller is simple and effective but there are some drawbacks such as apparent overshoot and sensitive to external noise and disturbance. When severe turbulence is encountered the PID controller may not be able to guide the aircraft to land safely. With SOCM compensator the proposed controller can overcome these disadvantages. The control scheme utilizes a conventional PID controller to stabilize the controlled system and train the SOCM to provide precise control. The gains of PID controller are adjusted based on experiences, what it provides are tolerable solutions, not desired solutions. The SOCM can effectively meliorate these disadvantages.

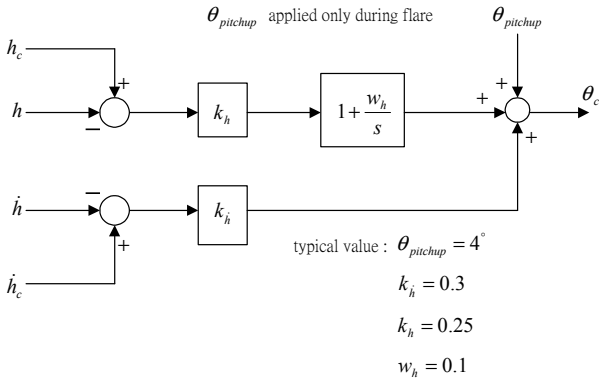

Figure 4. PID-controller.

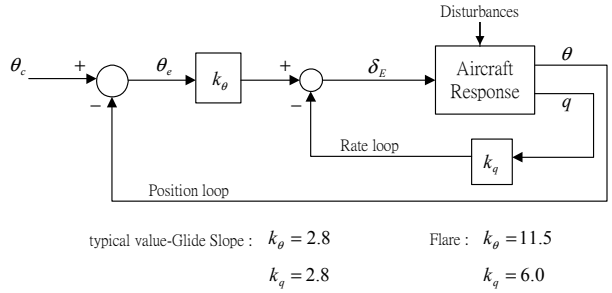

Figure 5. Pitch autopilot.

The output of CMAC is the sum of several values of hypercube and the input vector is the values of the aircraft status. The overall control scheme is described in Fig. 6, in which the control signal U is the sum of the PID controller output and the SOCM output. The inputs of the SOCM and PID controller are: altitude, altitude command, altitude rate, and altitude rate command. The PID controller provides tolerable solutions. In each time step k, the SOCM involves a recall process and a learning process. In the recall process, it uses the desired system output of the next time step and the actual system output as the address to generate the control signal U_{SOCM}. In the learning process, the control signal of the pitch autopilot, U, is treated as a desired output. It is used to modify the weights of SOCM stored at desired location which is addressed by the actual system output and the system output of the next time step. The output of the SOCM is the compensation for pitch command. When the wind turbulence is too strong, the ALS can not control the aircraft to land safely. In here we use a SOCM control scheme to improve the ability of turbulence resistance of the ALS.

A. CMAC_GBF

The CMAC represents one kind of associative memory technique. In the addressing technique, each input space (state variable) is quantized and the output space is divided into discrete states. A quantized input vector specifies a discrete state and is used to generate addresses for retrieving information from memory for this state. There is no big difference on the structure and quantization method and the mapping process between CMAC-GBF and original CMAC. The difference is that while the input vector maps the hypercube by way of the association in Fig. 7, the stored data can be the differential basis function value. Fig. 8 illustrates the block division of the CMAC-GBF for a two-variable case. This simple example has two state variables (x_1 and x_2) with each quantized into four discrete regions, called blocks. For instance, x_1 can be divided into *A*, *B*, *C,* and *D* and x_2 can be divided into *a*, *b*, *c,* and *d*. Areas *Aa*, *Ab*,...*Dd* formed by quantized regions are called hypercubes. By shifting each block a small interval (called an element) different hypercubes can be obtained. For instance, *E*, *F*, *G*, and *H* in the second row for x_1 and *e*, *f*, *g*, and *h* in the second row for x_2 are possible shifted regions. *Ee*, *Ef*, ...*Hh* are new hypercubes from the shifted regions. With this kind of decomposition, if there are *Ne* elements in a complete block, we will have *Ne* layers of hypercubes. In the given example there are four

layers as shown in Fig. 8. The state is covered by *Ne* different hypercubes, one from each layer. In the original CMAC, a constant value is assigned to each hypercube. By inputting these values into hypercubes, no matter what the positions are, they are treated as memory addresses. Therefore, the output is irrelevant to input and the differential of output to input is also not obtainable. Thus, in the CMAC-GBF, a general basis function (GBF) is used to replace constants in every hypercube. In this way, the positions of input vectors are related to output value, and the learning precision is also increased.

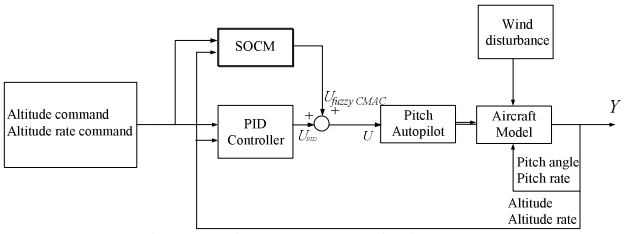

Figure 6. The SOCM control scheme.

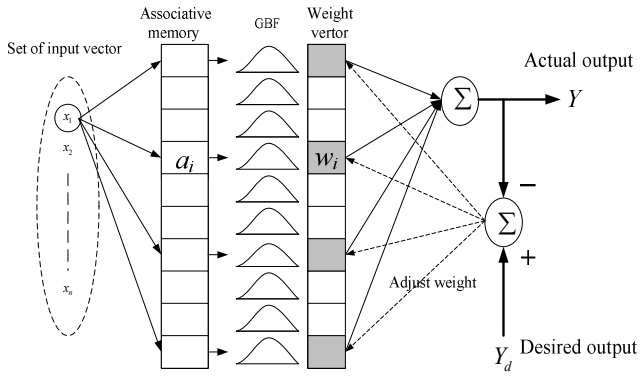

Figure 7. The structure of CMAC-GBF.

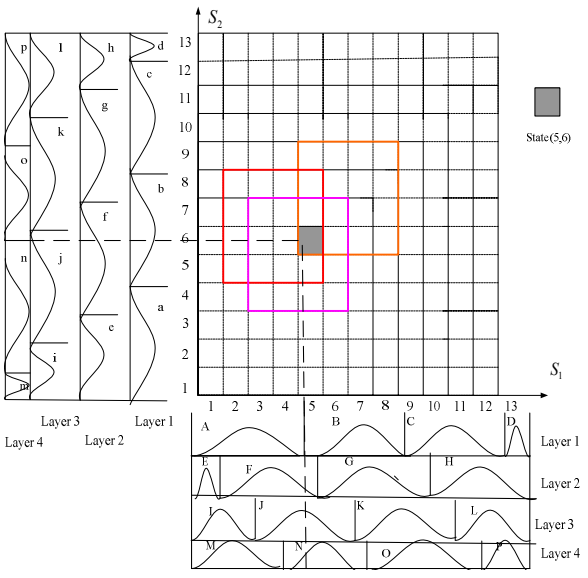

Figure 8. Block division of CMAC-GBF for a two-variable case.

In the CMAC_GBF, the content of hypercube can be expressed as $w_i(x_s) = v_i b_i(x_s)$, where $b_i(x_s)$ is a general basis function and v_i is a weight to be obtained through learning. The output of the CMAC-GBF can be written as below.

$$y(x_s) = \boldsymbol{a}_s^T w(x_s) = \sum_i^N [a_{s,i} v_i . b_i(x_s)] \tag{8}$$

where $\boldsymbol{a}_s^T = [a_{s,1} \quad a_{s,2} ..... a_{s,N}]$ is a basis function selection vector (or so-called association cells) and $W^T = [w_1 \quad w_2 ..... w_N]$ is the vector of memory contents of CMAC_GBF. The Gaussian functions are employed as the basis functions

$$b_i(x_s) \equiv \prod_{j=1}^N \phi_{ij}(x_{s,j}) \tag{9}$$

with

$$\phi_{ij}(x_{s,j}) = \exp[-\frac{(x_{s,j} - m_{ij})^2}{\sigma_{ij}^2}] \tag{10}$$

m_{ij} is the mean, σ_{ij} is the variance and N is the number of variables in the target function. Consequently, the weight function is

$$w_i(x_s) = v_i \prod_{j=1}^N \phi_{ij}(x_{s,j}) \tag{11}$$

The output from the CMAC with Gaussian basis functions can be mathematically expressed as

$$E = \frac{1}{2}(\hat{y}_s - y_s)^2 \tag{12}$$

The updated amount for v_i can be set to

$$\begin{aligned} \Delta v_i &= -\frac{\alpha_v}{N_e}\frac{\partial E}{\partial v_i} \\ &= -\frac{\alpha_v}{N_e}\frac{\partial E}{\partial e_s}\frac{\partial e_s}{\partial y(x_s)}\frac{\partial y(x_s)}{\partial w_i(x_s)}\frac{\partial w_i(x_s)}{\partial v_i} \\ &= \frac{\alpha_v}{N_e}(\hat{y}_s - \boldsymbol{a}_s^T w(x_s)) a_{s,i} b_i(x_s) \end{aligned} \tag{13}$$

where α_v is the learning rate for v. The mean and variables of the Gaussian function can also be adjusted to increase the approximation capability. The updating rules for these parameters can be derived as

$$\begin{aligned} \Delta m_{ij} &= -\frac{\alpha_m}{N_e}\frac{\partial E}{\partial m_{ij}} \\ &= -\frac{\alpha_m}{N_e}\frac{\partial E}{\partial e_s}\frac{\partial e_s}{\partial y(x_s)}\frac{\partial y(x_s)}{\partial w_i(x_s)}\frac{\partial w_i(x_s)}{\partial \phi_{ij}}\frac{\partial \phi_{ij}}{\partial m_{ij}} \\ &= \frac{\alpha_m}{N_e}(\hat{y}_s - \boldsymbol{a}_s^T w(x_s)) a_{s,i} v_i b_i(x_s) \frac{2(x_{s,i} - m_{ij})}{\sigma_{ij}^2} \end{aligned} \tag{14}$$

$$\Delta\sigma_{ij} = -\frac{\alpha_\sigma}{N_e}\frac{\partial E}{\partial \sigma_{ij}}$$
$$= -\frac{\alpha_\sigma}{N_e}\frac{\partial E}{\partial e_s}\frac{\partial e_s}{\partial y(x_s)}\frac{\partial y(x_s)}{\partial w_i(x_s)}\frac{\partial w_i(x_s)}{\partial \phi_{ij}}\frac{\partial \phi_{ij}}{\partial \sigma_{ij}} \quad (15)$$
$$= \frac{\alpha_\sigma}{N_e}(\hat{y}_s - \boldsymbol{a}_s^T w(x_s))a_{s,i}v_i b_i(x_s)(\frac{2(x_{s,i}-m_{ij})^2}{\sigma_{ij}^3})$$

where α_m and α_σ are the learning rates for mean and variance.

B. Self Organizing CMAC_GBF (SOCM)

The learning method for S_CMAC_GBF [10] and CMAC_GBF are the same, but they are different in the structures. The quantified method of input variables is different from the quantified conventional CMAC_GBF. In S_CMAC_GBF, each layer has only one block, and each block has different basis function. The weighting of each layer can be obtained by multiplying basis function of each layer with its height. Fig. 9 shows a two variables case, from recall process of S_CMAC_GBF, the output is the sum of the weights of 20 layers. The learning method of S_CMAC_GBF is just like the one for CMAC_GBF. In S_CMAC_GBF, the output equation is the same as CMAC_GBF. $a_{s,i}$ (element of selection vector) is either 1 (selected) or 0 (not selected) for CMAC_GBF, but in S_CMAC_GBF each element in the hypercube selection vector is equal to 1. It is noted that the learning rules of S_CMAC_GBF are also the same as CMAC_GBF. Adjust the required parameters in the recall process, and after repeated learning processes, the output of S_CMAC_GBF can reach the same accurate level as of CMAC_GBF.

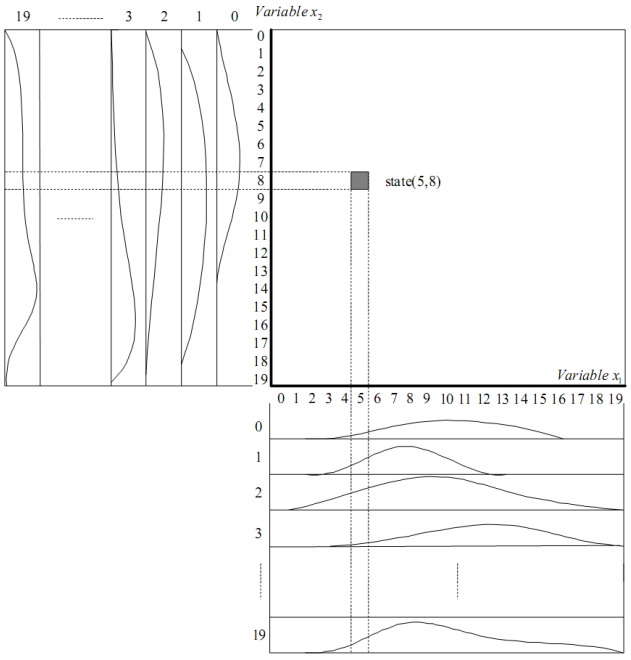

Figure 9. Block division of S_CMAC_GBF for two-variable case [10].

The difference of S_CMAC_GBF and SOCM [11] is that SOCM can create a new layer and delete a layer. The first process of the structure learning is to determine whether to add a new layer in association memory and to create its hypercube and weight memory, simultaneously. In the layer generating process, the mathematical description of the existing layers can be expressed as clusters. The firing strength of a rule for each incoming data can be represented as the degree to which the incoming data belong to the cluster. If a new input data falls within the boundary of clusters, SOCM will not generate a new layer but update parameters of the existing rules. Before SOCM decides which layer should be added or deleted, we have to choose the upper threshold (UT) (layer should be added) and lower threshold (LT) (layer should be deleted). The error rate can be expressed as

$$E_{rate} = \left|\frac{E(t)}{E(t-1)}\right| \quad (16)$$

If $E_{rate} > UT$ then $n_k(t+1) = n_k(t)+1$ (17)

where $n_k(t)$ is the number of the existing layers at time t. In the meanwhile, for the new layer, the initial mean and variance of Gaussian basis function in association memory space are defined as $m_{ink} = x_s$ and $\sigma_{ink}(t) = \sigma_{ink}(t\text{-}1)$, respectively.

If $E_{rate} < LT$ then $n_k(t+1) = n_k(t)\text{-}1$ (18)

We choose the least contribution layer of the SOCM output to be deleted. Using the ratio of the output from every layer

$$LO_i = \frac{v_i . b_i(x_s)}{v_{SOCM}}, \; i = 1 \; \ldots\ldots\ldots n_k \quad (19)$$

The layer which has minimum output ($\min_{i=1\sim nk} LO_i$) should be deleted.

IV. Stability Analysis of SOCM

In order to improve the shortcoming of conventional CMAC-GBF on the crisp relation, adaptive learning rule is introduced. Here, we use the discrete-time Lyapunov function to define the adaptive learning rate α. Let the tracking error e_s be

$$e_s(t) = \hat{y}_s - y_s \quad (20)$$

where t is the time index. A discrete-type Lyapunov function can be expressed as

$$V = \frac{1}{2}e_s^2(t) \quad (21)$$

Thus, the change in the Lyapunov function is obtained by

$$\Delta V = V(t+1) - V(t) = \frac{1}{2}\left[e_s^2(t+1) - e_s^2(t)\right] \quad (22)$$

The error difference can be represented by [13]

$$\Delta e_s(t) = e_s(t+1) - e_s(t) \approx \left[\left(\frac{\partial e_s(t)}{\partial v_i(t)}\right) \left(\frac{\partial e_s(t)}{\partial m_{ij}(t)}\right) \left(\frac{\partial e_s(t)}{\partial \sigma_{ij}(t)}\right) \right] \begin{bmatrix} \Delta v_i(t) \\ \Delta m_{ij}(t) \\ \Delta \sigma_{ij}(t) \end{bmatrix} \tag{23}$$

From (13) to (15) we have

$$\frac{\partial e_s(t)}{\partial v_i(t)} = \frac{\partial e_s}{\partial y}\frac{\partial y}{\partial w_i}\frac{\partial w_i}{\partial v_i} = -a_{s,i} b_i(x_s) \tag{24}$$

$$\frac{\partial e_s(t)}{\partial m_{ij}(t)} = \frac{\partial e_s}{\partial y}\frac{\partial y}{\partial w_i}\frac{\partial w_i}{\partial \phi_{ij}}\frac{\partial \phi_{ij}}{\partial m_{ij}} = -a_{s,i} v_i b_i(x_s)\frac{2(x_{s,i} - m_{ij})}{\sigma_{ij}^2} \tag{25}$$

$$\frac{\partial e_s(t)}{\partial \sigma_{ij}(t)} = \frac{\partial e_s}{\partial y}\frac{\partial y}{\partial w_i}\frac{\partial w_i}{\partial \phi_{ij}}\frac{\partial \phi_{ij}}{\partial \sigma_{ij}} = -a_{s,i} v_i b_i(x_s)\frac{2(x_{s,i} - m_{ij})^2}{\sigma_{ij}^3} \tag{26}$$

From (22) to (24), with respect to v_i, we have

$$\Delta V = \frac{1}{2}\left[e_s{}^2(t+1) - e_s{}^2(t) \right]$$
$$= \frac{1}{2}\left[e_s(t+1) - e_s(t) \right]\left[e_s(t+1) + e_s(t) \right]$$
$$= \frac{1}{2}\left[\Delta e_s(t) \right]\left[2 \cdot e_s(t) + \Delta e_s(t) \right]$$
$$= \Delta e_s(t)\left[e_s(t) + \frac{1}{2}\Delta e_s(t) \right]$$
$$= \left[-a_{s,i} b_i(x_s)\frac{\alpha_v}{N_e} e_s(t) a_{s,i} b_i(x_s) \right]$$
$$\left\{ e_s(t) + \frac{1}{2}\left[-a_{s,i} b_i(x_s)\frac{\alpha_v}{N_e} e_s(t) a_{s,i} b_i(x_s) \right] \right\}$$
$$= \left\{ -\frac{1}{2}\frac{\alpha_v}{N_e} e_s(t)\left[a_{s,i} b_i(x_s) \right]^2 \right\}$$
$$\left[2e_s(t) - \frac{\alpha_v}{N_e} e_s(t)\left[a_{s,i} b_i(x_s) \right]^2 \right]$$
$$= \left[-\frac{1}{2}\frac{\alpha_v}{N_e} e_s{}^2(t)\left[a_{s,i} b_i(x_s) \right]^2 \right]\left[2 - \frac{\alpha_v}{N_e}\left[a_{s,i} b_i(x_s) \right]^2 \right] \tag{27}$$

Let $\left[2 - \frac{\alpha_v}{N_e}\left[a_{s,i} b_i(x_s) \right]^2 \right] > 0$ then $\Delta V < 0$, i.e., we can select the learning rate α_v in the following range

$$\frac{2N_e}{\left[a_{s,i} b_i(x_s) \right]^2} > \alpha_v > 0 \tag{28}$$

From (22), (23), and (25), with respect to m_{ij}, we have

$$\Delta V = \frac{1}{2}\left[e_s{}^2(t+1) - e_s{}^2(t) \right] = \Delta e_s(t)\left[e_s(t) + \frac{1}{2}\Delta e_s(t) \right]$$
$$= \left\{ -\frac{1}{2}\frac{\alpha_m}{N_e} e_s(t)\left[a_{s,i} v_i b_i(x_s)\frac{2(x_{s,i} - m_{ij})}{\sigma_{ij}^2} \right]^2 \right\}$$
$$\left[2e_s(t) - \frac{\alpha_m}{N_e} e_s(t)\left[a_{s,i} v_i b_i(x_s)\frac{2(x_{s,i} - m_{ij})}{\sigma_{ij}^2} \right]^2 \right] \tag{29}$$
$$= \left[-\frac{1}{2}\frac{\alpha_m}{N_e} e_s{}^2(t)\left[a_{s,i} v_i b_i(x_s)\frac{2(x_{s,i} - m_{ij})}{\sigma_{ij}^2} \right]^2 \right]$$
$$\left[2 - \frac{\alpha_m}{N_e}\left[a_{s,i} v_i b_i(x_s)\frac{2(x_{s,i} - m_{ij})}{\sigma_{ij}^2} \right]^2 \right]$$

Let $\left[2 - \frac{\alpha_m}{N_e}\left[a_{s,i} v_i b_i(x_s)\frac{2(x_{s,i} - m_{ij})}{\sigma_{ij}^2} \right]^2 \right] > 0$ then $\Delta V < 0$, i.e., we can select the learning rate α_m in the following range

$$\frac{2N_e}{\left[a_{s,i} v_i b_i(x_s)\frac{2(x_{s,i} - m_{ij})}{\sigma_{ij}^2} \right]^2} > \alpha_m > 0 \tag{30}$$

From (22), (24), and (26), with respect to σ_{ij}, we have

$$\Delta V = \frac{1}{2}\left[e_s{}^2(t+1) - e_s{}^2(t) \right] = \Delta e_s(t)\left[e_s(t) + \frac{1}{2}\Delta e_s(t) \right]$$
$$= \left\{ -\frac{1}{2}\frac{\alpha_\sigma}{N_e} e_s(t)\left[a_{s,i} v_i b_i(x_s)\left(\frac{2(x_{s,i} - m_{ij})^2}{\sigma_{ij}^3}\right) \right]^2 \right\}$$
$$\left[2e_s(t) - \frac{\alpha_\sigma}{N_e} e_s(t)\left[a_{s,i} v_i b_i(x_s)\left(\frac{2(x_{s,i} - m_{ij})^2}{\sigma_{ij}^3}\right) \right]^2 \right] \tag{31}$$
$$= \left[-\frac{1}{2}\frac{\alpha_\sigma}{N_e} e_s{}^2(t)\left[a_{s,i} v_i b_i(x_s)\left(\frac{2(x_{s,i} - m_{ij})^2}{\sigma_{ij}^3}\right) \right]^2 \right]$$
$$\left[2 - \frac{\alpha_\sigma}{N_e}\left[a_{s,i} v_i b_i(x_s)\left(\frac{2(x_{s,i} - m_{ij})^2}{\sigma_{ij}^3}\right) \right]^2 \right]$$

Let $\left[2 - \frac{\alpha_\sigma}{N_e} \cdot \left[a_{s,i} v_i b_i(x_s)\left(\frac{2(x_{s,i} - m_{ij})^2}{\sigma_{ij}^3}\right) \right]^2 \right] > 0$ then $\Delta V < 0$, i.e., we can select the learning rate α_σ in the following range

$$\frac{2N_e}{\left[a_{s,i} v_i b_i(x_s)\left(\frac{2(x_{s,i} - m_{ij})^2}{\sigma_{ij}^3}\right) \right]^2} > \alpha_\sigma > 0 \tag{32}$$

ΔV becomes negative definite. This implies that $E(t) \to 0$ for $t \to \infty$. The convergence of the adaptive SOCM learning process is then guaranteed. The aircraft landing control system is locally asymptotically stable.

V. Simulations

The aircraft starts the initial states of the ALS as follows: the flight height is 500 ft, the horizontal position before touching the ground is 9240 ft, the flight angle is -3 degrees, the speed of the aircraft is 234.7 ft/sec. Successful touchdown landing conditions are defined as follows:

$$-3 \le \dot{h}_{TD} \text{ ft/sec} \le 0, \quad 200 \le V_{TD}(t) \text{ ft/sec} \le 270,$$
$$-300 \le x_{TD} \text{ ft} \le 1000, \quad -1 \le \theta_{TD} \text{ degree} \le 5,$$

where T is the time at touch down, $\dot{h}_{TD}$ is the vertical speed of the aircraft at touch down, x_{TD} is the position at touch down, $V_{TD}(t)$ is horizontal speed, θ_{TD} is the pitch angle at touch down.

Table I shows the result of conventional PID controller with different wind turbulence speeds. The conventional controller can only successfully guide an aircraft flying through wind speeds of 0 ft/sec to 30 ft/sec. The situations at wind turbulence 30 ft/sec are that the pitch angle is -0.1115 degrees, vertical speed is -2.1704/sec, horizontal velocity is 234.6779 ft/sec, and horizontal position at touchdown is 902.6000 ft, as shown in Fig. 10 to Fig. 12. If the wind speed is higher than 30 ft/sec, the ALS will be unable to guide the aircraft to land safely.

TABLE I. Results from using conventional PID controller (k1=2.8; k2=2.8; k3=11.5; k4=6.0)

Wind Speed (ft/sec)	Landing Point (ft)	Vertical Speed (ft/sec)	Pitch angle (degree)
0	785.2610	-2.8449	-1.3511
10	853.9561	-2.5786	-0.9523
20	910.0164	-2.3443	-0.4800
30	902.6000	-2.1704	-0.1115
40	1090.3424	-1.7348	0.3873

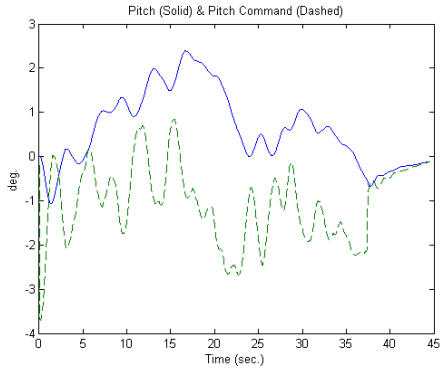

Figure 10. Aircraft pitch and pitch command.

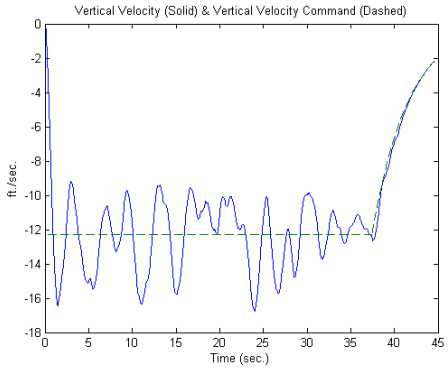

Figure 11. Aircraft vertical velocity and command.

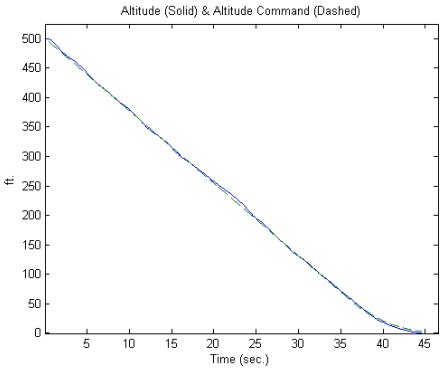

Figure 12. Aircraft altitude and command.

For the safe landing of an aircraft using the adaptive SOCM control scheme under different wind turbulence speeds are tested. The simulations show that the adaptive SOCM controller has well adaptive capability against severe wind disturbance. It is more robust than conventional PID type controller, as shown in Table II. The adaptive SOCM control scheme can successfully guide the aircraft flying through wind speeds of 0 ft/sec to 96 ft/sec. The situations at wind turbulence 96 ft/sec are that the pitch angle is 1.5011 degrees, vertical speed is -1.4125 ft/sec, horizontal velocity is 234.6779 ft/sec, and horizontal position at touchdown is 937.8017 ft, as shown in Fig.13 to Fig. 15. The layer variance is shown in Fig. 16.

TABLE II. Results from using adaptive SOCM control scheme (k1=2.8; k2=2.8; k3=11.5; k4=6.0)

Wind Speed (ft/sec)	Landing Point (ft)	Vertical Speed (ft/sec)	Pitch angle (degree)
20	937.8017	-1.9125	-0.3762
40	867.3983	-1.8542	-0.1497
60	949.5356	-1.4679	1.0374
80	738.3255	-1.4031	2.4873
90	926.0678	-1.5081	1.8440
96	937.8017	-1.4125	1.5011
97	1278.085	-0.7979	2.0038

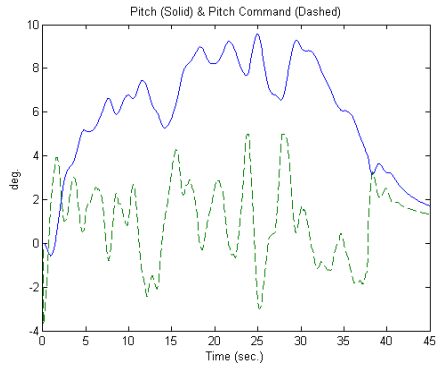

Figure 13. Aircraft pitch and pitch command.

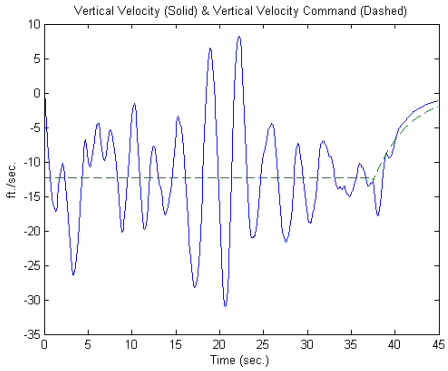

Figure 14. Aircraft vertical velocity and command.

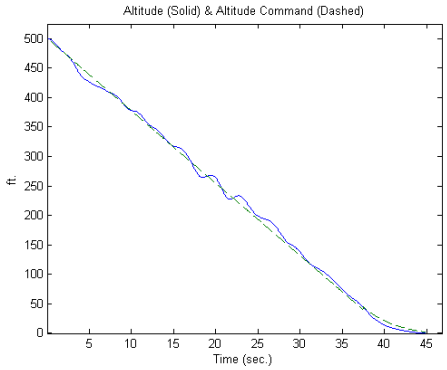

Figure 15. Aircraft altitude and command.

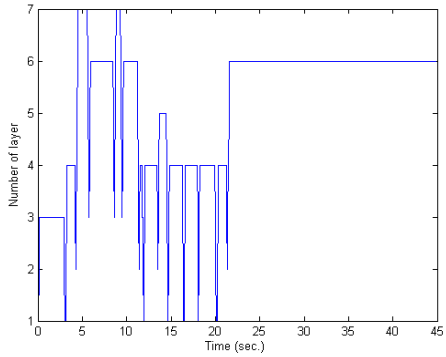

Figure 16. The layer variance of adaptive SOCM.

VI. CONCLUSION

The purpose of this paper is to investigate the use of adaptive SOCM in aircraft automatic landing system and to make the automatic landing system more intelligent. Current flight control law is adopted in the intelligent controller design. Tracking performance and adaptive capability are demonstrated through software simulations. For the safe landing of an aircraft using a conventional controller, CMAC or a conventional fuzzy CMAC, the wind speed of turbulence limits are 30, 58, and 90 ft/sec [14], respectively. In this study, a well-trained adaptive SOCM control scheme can reach 96 ft/sec. The proposed controllers have better performance than previous works, and it can act as an experienced pilot and guide the aircraft to a safe landing in severe wind turbulence environment.

REFERENCES

[1] NASDAC Review of TSB Weather-Related accidents, http://www.asias.faa.gov/aviation_studies/weather_study/windcond.html

[2] Federal Aviation Administration, "Automatic Landing Systems," AC 20-57A, Jan. 1971.

[3] H. Buschek and A. J. Calise, "Uncertainty Modeling and Fixed-Order Controller Dsign for Hypersonic Vehicle Model," *Journal of Guidance, Control, and Dynamics*, vol. 20, no. 1, pp. 42-48, 1997.

[4] M.G. Cooper, "Genetic Design of Rule-Based Fuzzy Controllers," Ph.D. dissertation, University of California, Los Angeles, 1995.

[5] Y. Iiguni, H. Akiyoshi, and N. Adachi, "An Intelligent Landing System Based on Human Skill Model," IEEE Transactions on Aerospace and Electronic Systems, 34(3), pp.877-882, 1998.

[6] H. Izadi, M. Pakmehr, and N. Sadati, "Optimal Neural-Controller in Longitudinal Autolanding of a Commercial Jet Transport," *Proc. IEEE International Conference on Control Applications*, CD-000202, 1-6, Istanbul, Turkey, 2003.

[7] C.C. Jorgensen, and C. Schley, "A Neural Network Baseline Problem for Control of Aircraft Flare and Touchdown," *Neural Networks for Control*, pp.403-425, 1991.

[8] J.G. Juang, and J.Z. Chio, "Fuzzy Modeling Control for Aircraft Automatic Landing System," *International Journal of Systems Science*, 36(2), pp.77–87, 2005.

[9] S.M.B. Malaek, N. Sadati, H. Izadi, and M. Pakmehr, "Intelligent autolanding controller design using neural networks and fuzzy logic," *Proc. IEEE 5th Control Conference*, 1, pp.365–373, 2004.

[10] C.T. Chiang, T.S. Chiang, and C.K. Li, "A Simple and Converged Structure of Addressing Technique for CMAC_GBF", *Proc. IEEE International Conference on Systems, Man and Cybernetics*, pp. 6097~6101,10-13 Oct. 2004.

[11] C.M. Lin and T.Y. Chen, "Self-Organizing CMAC Control for a Class of MIMO Uncertain Nonlinear Systems", *IEEE Transaction on Neural Network*, pp. 1377~1384, Sep. 2009.

[12] Flight Safety Foundation-Taiwan, http://www.flightsafety.org.tw/news1.php?Code=1&main_id=3&pages=5

[13] D.E. Rumelhart, G.E. Hinton, and R.J. Williams, "Learning Internal Representations by Error Propagation," in D.E. Rumelhart, J.L. McMclelland, et al., *Parallel Distributed Processing,* vol. 1, Chap. 8, Cambridge, MA : MIT Press, 1986.

[14] J.G. Juang and W.P. Lin, "Aircraft Landing Control Based on CMAC and GA Techniques," *Proc. of IFAC WC 2008*, P1173, 2008.

2011 IEEE International Conference on Fuzzy Systems
June 27-30, 2011, Taipei, Taiwan

Optimal Necessary Conditions for General SISO Mamdani Fuzzy Systems as Function Approximators within a Given Accuracy

Fuchun Sun, Jin Yang, Minnan Luo, Huaping Liu
Department of Computer Science and Technology
Tsinghua University
Beijing , P. R. China
fcsun@mail.tsinghua.edu.cn

Abstract — **In this paper, necessary conditions are investigated for a single input/single output (SISO) Mamdani fuzzy systems as function approximators of continuous functions within a given accuracy. Since general SISO Mamdani fuzzy systems are monotonic on subintervals, the optimal configuration of fuzzy systems is that the number of division points is at least the times of its monotonicity changes. Thus with the extreme of the desired continuous function, necessary conditions are obtained through generating intervals that contain division points and pruning redundant intervals. Furthermore, a dynamically constructive method is proposed to show the conditions are optimal. It has been shown that existing results concerning necessary conditions are only special cases of our results. Finally, simulation examples are given to illustrate the conclusions, the strength of the fuzzy systems as function approximators are analyzed.**

Keywords- fuzzy systems; necessary conditions; fuzzy rules; approximation accuracy

I. INTRODUCTION

In the past decades, fuzzy systems were widely used and extensively studied for a variety of applications, especially in control applications because of their excellent performance in representing nonlinear functions in an intuitive and informative manner. In many applications of fuzzy theory, fuzzy systems involved can be viewed as rule-based function approximators. Many scholars have proved that fuzzy systems are universal approximators in different aspects [1-5]. To our knowledge, the smaller the approximation accuracy, the more fuzzy rules are required in order to approximate a certain continuous function, especially in high dimensions. Large numbers of rules render difficulty in designing fuzzy systems, such as high storage consumption, increased computational complexity, etc.

One always wants to construct a fuzzy system using less fuzzy rules to approximate a continuous function within a given accuracy. Therefore, many efforts have been made to reduce fuzzy rules. Some methods of these include orthogonal transformation, singular value decomposition[6-8] and heuristic methods such as genetic algorithms[9-10], clustering methods [11,12], and tree search[13], etc. Sufficient conditions for fuzzy systems have also been defined and solved by many scholars in term of the function approximation, which are mainly based on the uniform approximate polynomial [14-16] and the derivative of the object function[17-18, 23]. However, from a practical viewpoint, necessary conditions for fuzzy systems are more important since they place restrictions on selection components for fuzzy systems. Despite its importance, only a few papers [19-22] have dealt with this problem. Generally, the number of the fuzzy rules needed increases with the number of extreme of the desired function. However, the existing conclusions are only available for the fuzzy system with perfect approximation to a continuous function. In most cases of fuzzy system applications, the core part is to design a fuzzy system to approximate a prospective continuous function within certain accuracy. As a result, necessary conditions for fuzzy systems as function approximators within a given accuracy deserve deep study.

In this paper, we will establish new necessary conditions for general SISO Mamdani fuzzy systems as function approximator within a prescribed accuracy. By generating the intervals that contain division points and pruning redundant intervals, a novel constructive algorithm is proposed to obtain the necessary conditions. Furthermore, it has been shown that the conditions are optimal and the existing results given in [19] are only a special case of ours. Finally, illustrative examples are used to demonstrate the strength and limitation of the general SISO Mamdani fuzzy systems.

II. PROBLEM FORMULATION

A. Configuration of general SISO Mamdani fuzzy systems

The interval $[a,b]$, on which the object function $f(x)$ is defined, is divided into N subintervals (S_i is endpoint of sub-intervals):

$$a = S_0 < S_1 < S_2 < \cdots < S_N = b$$

Then there are $N+1$ normal, consistent and continuous input fuzzy sets defined on $[a,b]$ to fuzzify the input variable (Fig. 1). Each input fuzzy set denoted by A_i ($0 \le i \le N$) has a membership function $\mu_i(x)$ defined as follows:

This work was jointly supported by the National Science Foundation of China (Grants No.60625304, 60716021) and the National Key Project for Basic Research of China (Grants No.G2007cb311003, 2009cb724002).

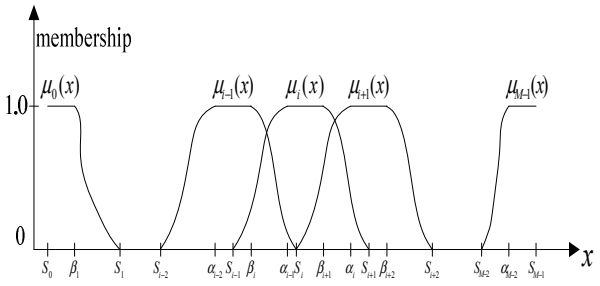

Figure 1. Illustrative definitions of input fuzzy sets.

$$\mu_i(x)=\begin{cases} I_i(x) & x\in[S_{i-1},\alpha_{i-1}] \\ 1 & x\in[\alpha_{i-1},\beta_{i+1}] \\ D_i(x) & x\in[\beta_{i+1},S_{i+1}] \\ 0 & x\in[a,b]/[S_{i-1},S_{i+1}] \end{cases} \tag{1}$$

where $I_i(x)$ equals to zero at $x=S_{i-1}$ and increases monotonically to one at $x=\alpha_{i-1}$, $D_i(x)$ equals to one at $x=\beta_{i+1}$ and decreases monotonically to zero at $x=S_{i+1}$, and

$$S_{-1}=S_0, S_{N+1}=S_N,\ S_{i-1}<\alpha_{i-1}\le S_i, S_i\le\beta_{i+1}<S_{i+1}.$$

The $N+1$ fuzzy rules used in the fuzzy system are in the form:

$$R_i: \text{IF } x \text{ is } A_i, \text{ THEN } y \text{ is } B_i,\ i=0,1,\cdots,N. \tag{2}$$

where B_i is a singleton output fuzzy set, whose membership function is one only at $y=y_i$ (an arbitrary constant) and is zero elsewhere. Using product inference engine and center-average defuzzifier, the output of the SISO Mamdani fuzzy system is

$$F(x)=\sum_i \mu_i(x)y_i \Big/ \sum_i \mu_i(x) \tag{3}$$

B. The approximation problems for fuzzy systems

The objective function $f(x)$ is defined on the compact domain Θ, which can be approximated by a fuzzy system $F(x)$ defined in sub-section II. A. The necessary condition of the fuzzy system for universal approximation is to find the minimal system configuration that the fuzzy system $F(x)$ can approximate the continuous function $f(x)$ within a given accuracy $\varepsilon\ge 0$ using smallest fuzzy rules, i.e.

$$\left\|F(x)-f(x)\right\|_\infty \le \varepsilon \tag{4}$$

III. Necessary Conditions for General SISO Mamdani Fuzzy Systems

A. Necessary Conditions for General SISO Mamdani Fuzzy Systems

The following lemmas are given for the subsequent development of necessary conditions for general SISO Mamdani fuzzy systems.

Lemma 1[19]: The fuzzy system $F(x)$ defined in (3) is continuous, and monotonic on $[S_{i-1},S_i]$ for all $i=1,2,\cdots,N$.

Lemma 2: Suppose $F(x)$ defined in (3) can approximate $f(x)$ within a given accuracy ε, for each subinterval $[S_j,S_{j+1}]$ there does not exist $S_j\le\xi_1<\xi_2<\xi_3\le S_{j+1}$ (ξ_1, ξ_2 and ξ_3 are extremes of $f(x)$ on $[S_j,S_{j+1}]$), such that

$$\begin{aligned} &f(\xi_1)-f(\xi_2)>2\varepsilon,\ f(\xi_2)-f(\xi_3)<-2\varepsilon \\ \text{or}\ &f(\xi_1)-f(\xi_2)<-2\varepsilon,\ f(\xi_2)-f(\xi_3)>2\varepsilon \end{aligned} \tag{5}$$

Proof: Without losing generality, assume that there exists $S_j\le\xi_1<\xi_2<\xi_3\le S_{j+1}$, such that

$$f(\xi_1)-f(\xi_2)>2\varepsilon,\ f(\xi_2)-f(\xi_3)<-2\varepsilon \tag{6}$$

Firstly, using reduction to absurdity, it can be proved that there exists $[x_{t1},x_{t2}]\subseteq[\xi_1,\xi_2]$, such that $F(x)$ strictly decreases on $[x_{t1},x_{t2}]$. It is assumed that the interval $[x_{t1},x_{t2}]$, on which $F(x)$ strictly decreases, does not exist. Then $F(x)$ increases monotonically on $[\xi_1,\xi_2]$ so that we can get

$$F(x_2)\ge F(x_1) \tag{7}$$

for arbitrary $\xi_1\le x_1<x_2\le\xi_2$. Since $F(x)$ can approximate $f(x)$ within a given accuracy $\varepsilon>0$, we have

$$-\varepsilon\le f(x_1)-F(x_1)\le\varepsilon \tag{8}$$

$$-\varepsilon\le f(x_2)-F(x_2)\le\varepsilon \tag{9}$$

Subtracting (9) from (8) yields

$$f(x_1)-f(x_2)\le 2\varepsilon+F(x_1)-F(x_2) \tag{10}$$

Similarly, subtracting (7) from (10) leads to

$$f(x_1)-f(x_2)\le 2\varepsilon \tag{11}$$

Eq. (11) is contradictory with Eq. (6). This contradiction means that there exists $[x_{t1},x_{t2}]\subseteq[\xi_1,\xi_2]$, on which $F(x)$ strictly decreases. Similarly, we can also prove that there exists $[x_{t3},x_{t4}]\subseteq[\xi_2,\xi_3]$, such that $F(x)$ strictly increases. Therefore, there exists two subintervals $[x_{t1},x_{t2}]$ and $[x_{t3},x_{t4}]$ in $[S_j,S_{j+1}]$, such that $F(x)$ strictly decreases and increases

respectively. By derivative's property, there must exist division points on $[S_j, S_{j+1}]$, which contradicted with Lemma 1. The proof is completed.

Lemma 2 has established some necessary conditions for Mamdani fuzzy systems as function approximators within a given approximation accuracy. In order to construct the necessary conditions in an intuitive manner, the construction algorithm is presented as follows, which consists of generating the intervals that contain division points and pruning redundant intervals.

Construction algorithm:

Step 1: Calculate the object function's extreme set $\boldsymbol{\xi}$ and create an empty set P.

Step 2: Traverse the extreme set $\boldsymbol{\xi}$,

WHILE there exist $\xi_p, \xi_e, \xi_q \in \xi$ with $\xi_p < \xi_e < \xi_q$ such that

$$f(\xi_p) - f(\xi_e) > 2\varepsilon,\ f(\xi_e) - f(\xi_q) < -2\varepsilon$$
$$\text{or } f(\xi_p) - f(\xi_e) < -2\varepsilon,\ f(\xi_e) - f(\xi_q) > 2\varepsilon$$

DO $P = P \bigcup \{[\xi_p, \xi_q]\}$.

Step 3: $Q = P$,

WHILE there exists $C_1, C_2 \in Q$, such that $C_1 \subset C_2$.

DO remove C_2 from Q.

Step 4: The algorithm ends and the characteristic set Q is got.

The characteristic set Q determined by construction algorithm above has the following properties:

(i) Given the extreme set $\boldsymbol{\xi}$, Q is unique.

(ii) There does not exist $C_j \in Q$ such that $P_i \subset C_j$ for arbitrary $P_i \in P$.

(iii) There also does not exist $C_1, C_2 \in Q$ such that $C_1 \subset C_2$.

To analyze the characteristics of the elements in set Q, the following definitions are given.

Definition 1: For an interval $C_t = [\xi_j, \xi_k]$, let $C_t^{\min} = \xi_j$, $C_t^{\max} = \xi_k$.

Definition 2 (interval correlation): For arbitrary $C_1, C_2 \in Q$, C_1 and C_2 are said to be correlative if there exist extremes ξ_1 and ξ_2 with $\xi_1 < \xi_2$ such that $\xi_1, \xi_2 \in C_1$, $\xi_1, \xi_2 \in C_2$,

Definition 3 (interval consistency): For arbitrary $C_1, C_2 \in Q$, C_1 and C_2 are said to be consistent if there exist extremes $\xi_1 \in C_1$ and $\xi_2 \in C_2$ such that

$$f(C_1^{\min}) - f(\xi_1) > 2\varepsilon,\ f(C_1^{\max}) - f(\xi_1) > 2\varepsilon$$
$$f(C_2^{\min}) - f(\xi_2) > 2\varepsilon,\ f(C_2^{\max}) - f(\xi_2) > 2\varepsilon$$
$$\text{or } f(\xi_1) - f(C_1^{\min}) > 2\varepsilon,\ f(\xi_1) - f(C_1^{\max}) > 2\varepsilon$$
$$f(\xi_2) - f(C_2^{\min}) > 2\varepsilon,\ f(\xi_2) - f(C_2^{\max}) > 2\varepsilon;$$

or else inconsistent.

Definition 4: For arbitrary $C_1, C_2 \in Q$, it is said $C_1 < C_2$ if $C_1^{\min} < C_2^{\min}$.

According to the construction algorithm, the following four corollaries could be obtained easily.

Corollary 1: For arbitrary $C_1, C_2 \in Q$, C_1 and C_2 could only be consistent or inconsistent exclusively.

Corollary 2: $C_1^{\min} \neq C_2^{\min}$, $C_1^{\max} \neq C_2^{\max}$ for arbitrary $C_1, C_2 \in Q$.

Corollary 3: For arbitrary $C_1, C_2 \in Q$, $C_1^{\max} < C_2^{\max}$ if $C_1^{\min} < C_2^{\min}$.

Corollary 4: For the elements $C_1, C_2, \cdots, C_n$ in Q, there exists a new sorting $C_{i_1}, C_{i_2}, \cdots, C_{i_n}$, such that $C_{i_1} < C_{i_2} < \cdots < C_{i_n}$

$$C_{i_1} < C_{i_2} < \cdots < C_{i_n} \tag{12}$$

In the following, relationship among elements in Q would be analyzed using reduction to absurdity.

Lemma 3: For arbitrary $C_1, C_2 \in Q$ with $C_1 < C_2$, C_1 and C_2 are not correlative if C_1 and C_2 are consistent.

Proof: Suppose C_1 and C_2 are correlative, we have $C_1^{\min} < C_2^{\min} < C_1^{\max} < C_2^{\max}$ by Corollary 3. Without losing generality, there exist extremes $\xi_1 \in C_1$, $\xi_2 \in C_2$ such that

$$f(C_1^{\min}) - f(\xi_1) > 2\varepsilon,\ f(C_1^{\max}) - f(\xi_1) > 2\varepsilon;$$
$$f(C_2^{\min}) - f(\xi_2) > 2\varepsilon,\ f(C_2^{\max}) - f(\xi_2) > 2\varepsilon \tag{13}$$

Let $\xi_e = \arg_{\xi_i} \min\{f(\xi_1), f(\xi_2)\}$. If $\xi_e \in [C_1^{\min}, C_2^{\min}]$, we have

$$f(C_1^{\min}) - f(\xi_e) > 2\varepsilon, f(C_2^{\min}) - f(\xi_e) > 2\varepsilon.$$

Thus $[C_1^{\min}, C_2^{\min}] \in P$ is obtained. This contradicted with $[C_1^{\min}, C_2^{\min}] \subset C_1$ and $C_1 \in Q$ based on property (ii). Assuming $\xi_e \in [C_2^{\min}, C_1^{\max}]$ or $\xi_e \in [C_1^{\max}, C_2^{\max}]$ yields a similar contradiction. Therefore C_1 and C_2 are not correlative.

Lemma 4: For arbitrary $C_1 < C_2 \in Q$, if C_1 and C_2 are correlative,

(1) C_1 and C_2 are inconsistent.

(2) Extremes ξ_1 and ξ_2 defined in Definition 3 satisfy $C_1^{\min} < \xi_1 \le C_2^{\min} < C_1^{\max} \le \xi_2 < C_2^{\max}$.

(3) There exist at least two division points in $[C_1^{\min}, C_2^{\max}]$ to achieve the approximation accuracy requirement in Eq. (4).

Proof: Conclusion (1) is obvious by Lemma 3. We now use a contradiction argument to show the other conclusions are also satisfied. Since C_1 and C_2 are correlative and $C_1 < C_2$, we can easily get

$$C_1^{\min} < C_2^{\min} < C_1^{\max} < C_2^{\max} \tag{14}$$

according to Corollary 3, Without losing generality, there is extreme $\xi_1 \in C_1$ such that

$$f(C_1^{\min}) - f(\xi_1) > 2\varepsilon,\ f(C_1^{\max}) - f(\xi_1) > 2\varepsilon \tag{15}$$

Because C_1 and C_2 are inconsistent, there exists $\xi_2 \in C_2$ such that

$$f(\xi_2) - f(C_2^{\min}) > 2\varepsilon,\ f(\xi_2) - f(C_2^{\max}) > 2\varepsilon \tag{16}$$

Assuming $C_2^{\min} < \xi_1 < C_1^{\max}$ and $\xi_1 < \xi_2$, we have

$$\begin{aligned} &\max\{f(C_1^{\max}), f(\xi_2)\} - f(\xi_1) > 2\varepsilon, \\ &\max\{f(C_1^{\max}), f(\xi_2)\} - f(C_2^{\max}) > 2\varepsilon \end{aligned} \tag{17}$$

Thus $[\xi_1, C_2^{\min}] \in P$ is obtained. This contradicted with $[\xi_1, C_2^{\min}] \subset C_2$ and $C_2 \in Q$ based on property (ii). Assuming $C_2^{\min} < \xi_2 < C_1^{\max}$ yields a similar contradiction. As a result, the conclusion (2) is satisfied.

Subsequently, let us analyze the conclusion (3). Without losing generality, there exist extremes $\xi_1 \in C_1$, $\xi_2 \in C_2$ such that

$$\begin{aligned} &f(C_1^{\min}) - f(\xi_1) > 2\varepsilon,\ f(C_1^{\max}) - f(\xi_1) > 2\varepsilon \\ &f(\xi_2) - f(C_2^{\min}) > 2\varepsilon,\ f(\xi_2) - f(C_2^{\max}) > 2\varepsilon \end{aligned} \tag{18}$$

By conclusion (2), we have

$$\begin{aligned} &f(C_1^{\min}) - \min\{f(\xi_1), f(C_2^{\min})\} > 2\varepsilon, \\ &\min\{f(\xi_1), f(C_2^{\min})\} - \max\{f(C_1^{\max}), f(\xi_2)\} < -2\varepsilon, \\ &\max\{f(C_1^{\max}), f(\xi_2)\} - f(C_2^{\max}) > 2\varepsilon. \end{aligned}$$

As a result, there exists at least two division points in $[C_1^{\min}, C_2^{\max}]$ according to Lemma 2.

From Lemma 4, we can conclude that two correlative intervals in Q could not have a common division point. Furthermore, the following Lemma which will help founding the relationship between the number of the elements in Q and the number of the division points for fuzzy systems could be obtained.

Lemma 5: Each element in Q determined by the construction algorithm has division point of its own if the fuzzy system $F(x)$ defined in (3) can approximate $f(x)$ within a given approximation accuracy ε.

Proof: For arbitrary $C_i \in Q$, if C_i is not correlative with the other element in Q, there exists division point in C_i according to Lemma 2. If C_i is correlative with $C_k \in Q$, C_i and C_k have their own division points by Lemma 4. Hence each element in Q determined by the proposed construction algorithm has division point of its own.

Suppose that the objective function $f(x)$ is defined on the interval $[a, b]$ in the framework of SISO Mamdani fuzzy system. If there are n elements in Q which is determined by the construction algorithm with respect to the function $f(x)$ above, n division points exist in the interval $[a, b]$ based on Lemma 5.

Furthermore, the interval is divided into at least $n+1$ subintervals, and at least $n+2$ fuzzy rules are needed to approximate the object function within a given approximation accuracy ε. Thus the necessary conditions for general SISO Mamdani fuzzy systems could be established intuitively.

Theorem 1: (Necessary conditions for fuzzy systems) Suppose there are n elements in Q determined by the construction algorithm. In order to approximate the object function within a given approximation accuracy, the input interval of the fuzzy system should be divided into at least $n+1$ subintervals; at least $n+2$ fuzzy rules are needed.

We will prove that the conditions established in Theorem 1 are also optimal.

Lemma 6: If $f(x_1) - f(x_2) \geq -2\varepsilon$ or $f(x_1) - f(x_2) \leq 2\varepsilon$ for arbitrary x_1, $x_2 \in [S_j, S_{j+1}]$ with $x_1 < x_2$, there exists a fuzzy system $F(x)$ in Eq.(4) which can approximate the object function $f(x)$ within a given approximation accuracy ε on subinterval $[S_j, S_{j+1}]$.

Proof: A constructive method will be used here to prove this lemma.

(a) If $f(x_1) - f(x_2) \geq -2\varepsilon$ for arbitrary $x_1, x_2 \in [S_j, S_{j+1}]$ with $x_1 < x_2$, the output $F(x)$ of a fuzzy system that can approximate $f(x)$ within a given accuracy ε on $[S_j, S_{j+1}]$ can be constructed as Fig. 2. And the output $F(x)$ of a fuzzy system can be constructed in details as follows.

Step 1 Calculate the extremes $\xi_0, \xi_1, \cdots, \xi_{n+1}$ of the object function $f(x)$ on $[S_j, S_{j+1}]$ with $\xi_0 = S_j, \xi_{n+1} = S_{j+1}$. Let $i = 0$, $e = \xi_0$.

Step 2 WHILE $i < n$ DO

$$F(x) = \min(f(x) + \varepsilon, f(e) + \varepsilon),\ x \in [\xi_i, \xi_{i+1}].$$

If $f(e) - f(\xi_{i+1}) \geq 0$

$e = \xi_{i+1}$.

$i = i + 1$.

Step 3 If $f(\xi_n) - f(\xi_{n+1}) \geq 0$, on $[\xi_n, \xi_{n+1}]$

$$F(x) = f(x) - \varepsilon + \frac{\xi_{n+1} - x}{\xi_{n+1} - \xi_n}(f(e) - f(\xi_n) + 2\varepsilon),$$

else

$$F(x) = f(e) + \varepsilon + \frac{x - \xi_n}{\xi_{n+1} - \xi_n}(f(\xi_{n+1}) - f(e) - 2\varepsilon).$$

(b) If $f(x_1) - f(x_2) \leq 2\varepsilon$ for arbitrary x_1, $x_2 \in [S_j, S_{j+1}]$ with $x_1 < x_2$. The corresponding fuzzy system output $F(x)$ on $[S_j, S_{j+1}]$ can be constructed in a similar way:

Step 1. Calculate the extremes $\xi_0, \xi_1, \cdots, \xi_{n+1}$ of the object function $f(x)$ on $[S_j, S_{j+1}]$ with $\xi_0 = S_j, \xi_{n+1} = S_{j+1}$. Let $i = 0$, $e = \xi_0$.

Step 2. WHILE $i < n$ DO

$F(x) = \max(f(x) - \varepsilon, f(e) - \varepsilon)$ on $x \in [\xi_i, \xi_{i+1}]$.

If $f(e) - f(\xi_{i+1}) \leq 0$

$e = \xi_{i+1}$.

$i = i + 1$.

Step 3. If $f(\xi_n) - f(\xi_{n+1}) \leq 0$, on $[\xi_n, \xi_{n+1}]$,

$$F(x) = f(x) + \varepsilon + \frac{\xi_{n+1} - x}{\xi_{n+1} - \xi_n}(f(e) - f(\xi_n) - 2\varepsilon).$$

else

$$F(x) = f(e) - \varepsilon + \frac{x - \xi_n}{\xi_{n+1} - \xi_n}(f(\xi_{n+1}) - f(e) + 2\varepsilon).$$

Furthermore, the input/output fuzzy sets can be constructed as: $\mu_1(x) = (\sup F - F(x)) / (\sup F - \inf F)$, $\mu_2(x) = 1 - \mu_1(x)$, $y_1 = F(S_j)$ and $y_2 = F(S_{j+1})$. The proof is completed.

Remark 1: The constructive methods in Lemma 6 just show that there exists fuzzy system that can approximate the object function within a given approximation accuracy in Eq. (4). Since the output constructed above in the first case is $f(S_j) - \varepsilon$ at $x = S_j$ and decreases monotonically to $f(S_{j+1}) + \varepsilon$ at $x = S_{j+1}$, while the second output constructed above is $f(S_j) + \varepsilon$ at $x = S_j$ and increases monotonically to $f(S_{j+1}) - \varepsilon$ at $x = S_{j+1}$, this two cases can be used alternately on subintervals to form a continuous output on the whole domain.

Lemma 7: Arbitrary two adjacent $C_{i_j}, C_{i_{j+1}} \in Q$ $(1 \leq j < n)$ in Corollary 4 are inconsistent.

Proof: If C_{i_j} and $C_{i_{j+1}}$ are correlative, C_{i_j} and $C_{i_{j+1}}$ are inconsistent according to Lemma 5. Otherwise, we have

$$C_{i_j}^{\max} \leq C_{i_{j+1}}^{\max} \tag{19}$$

If C_{i_j} and $C_{i_{j+1}}$ are consistent. Without losing generality, assume there exist extremes $\xi_1 \in C_1$, $\xi_2 \in C_2$ such that

$$\begin{aligned} &f(C_{i_j}^{\max}) - f(\xi_1) > 2\varepsilon,\ f(C_{i_j}^{\min}) - f(\xi_1) > 2\varepsilon \\ &f(C_{i_{j+1}}^{\max}) - f(\xi_2) > 2\varepsilon,\ f(C_{i_{j+1}}^{\min}) - f(\xi_2) > 2\varepsilon \end{aligned} \tag{20}$$

With (19) and (20),

$$\begin{aligned} &\max\{f(C_{i_j}^{\max}), f(C_{i_{j+1}}^{\min})\} - f(\xi_1) > 2\varepsilon, \\ &\max\{f(C_{i_j}^{\max}), f(C_{i_{j+1}}^{\min})\} - f(\xi_2) > 2\varepsilon. \end{aligned}$$

Thus $[\xi_1, \xi_2] \in P$ is obtained. It means there exists $C_s \in Q$ and $C_s \subseteq [\xi_1, \xi_2]$ such that $C_{i_j} < C_s < C_{i_{j+1}}$. It contradicted with Corollary 4. Therefore C_{i_j} and $C_{i_{j+1}}$ are inconsistent.

With Lemma 6 and Lemma 7, the optimal necessary condition for SISO Mamdani fuzzy systems is established as follows.

Theorem 2 (Optimal necessary conditions for fuzzy systems): To approximate a continuous function within a given accuracy, a general SISO Mamdani fuzzy system established on the number n of the characteristic set Q is optimal.

Proof: Let $C_j \in Q$ ($j = 1, \cdots, n$), where Q is determined by the construction algorithm with respect to the function $f(x)$ defined on $[a, b]$. n division points exist in the interval $[a, b]$ by Lemma 5. Without losing generality, we select all the division points $S_j \in C_j$ ($j = 1, \cdots, n$) at extremes of the function $f(x)$. And S_j satisfies

$$\begin{aligned} &f(C_j^{\min}) - f(S_j) > 2\varepsilon,\ f(C_j^{\max}) - f(S_j) > 2\varepsilon, \\ &\text{or } f(S_j) - f(C_j^{\min}) > 2\varepsilon,\ f(S_j) - f(C_j^{\max}) > 2\varepsilon. \end{aligned}$$

Suppose that the approximation accuracy ε can't be achieved on subinterval $[S_j, S_{j+1}]$. With Lemma 6, there exist extremes of $f(x)$ ξ_1, ξ_2, ξ_3 on $[S_j, S_{j+1}]$ with $S_j \leq \xi_1 < \xi_2 < \xi_3 \leq S_{j+1}$ such that

$$\begin{aligned} &f(\xi_1) - f(\xi_2) > 2\varepsilon,\ f(\xi_2) - f(\xi_3) < -2\varepsilon \\ &\text{or } f(\xi_1) - f(\xi_2) < -2\varepsilon,\ f(\xi_2) - f(\xi_3) > 2\varepsilon \end{aligned} \tag{21}$$

Thus $[\xi_1, \xi_3] \in P$ is obtained. It means there exists $C_t \in Q$, $C_t \subseteq [\xi_1, \xi_3]$ such that $C_j < C_t < C_{j+1}$ .This contradicted with Corollary 4. Therefore the fuzzy system can achieve approximation accuracy on each subinterval. In other words , the inequality $f(x_1) - f(x_2) \geq -2\varepsilon$ or $f(x_1) - f(x_2) \leq 2\varepsilon$ holds for arbitrary $x_1, x_2 \in [S_j, S_{j+1}]$ with $x_1 < x_2$.

According to Lemma 7, if there exist $x_1, x_2 \in [S_j, S_{j+1}]$ with $x_1 < x_2$ such that $f(x_1) - f(x_2) > 2\varepsilon$, there must exist $x_3, x_4 \in [S_j, S_{j+1}]$ with $x_3 < x_4$ such that $f(x_3) - f(x_4) < -2\varepsilon$.

Hence, for arbitrary two adjacent subintervals $[S_{j-1}, S_j]$ and $[S_j, S_{j+1}]$, if $f(x_1) - f(x_2) \geq -2\varepsilon$ holds for arbitrary $x_1, x_2 \in [S_j, S_{j+1}]$ with $x_1 < x_2$; $f(x_3) - f(x_4) \leq 2\varepsilon$ holds for arbitrary $x_3, x_4 \in [S_j, S_{j+1}]$ with $x_3 < x_4$. A continuous output for fuzzy system can be constructed using the constructive methods in Lemma 6 alternately. It means that there exists a fuzzy system which can achieve the given approximation accuracy in Eq. (4). Therefore the necessary conditions are optimal under the same condition.

Remark 2: If *n* division points in Theorem 1 are selected appropriately, none other division points are necessary for the fuzzy systems to achieve the given approximation accuracy in Eq. (4).

Remark 3: In Theorems 1 and 2, the following assumptions are assumed to be known for the necessary conditions of the SISO Mamdani fuzzy system on a given approximation accuracy ε:

(a) Approximation accuracy $\varepsilon \geq 0$;

(b) The values of $f(x) \in C[a,b]$ at extremes $\xi_i : v_i = f(\xi_i)$, $1 \leq i \leq m$;

(c) The values of $f(x)$ at endpoints: $v_0 = f(a)$, $v_{m+1} = f(b)$.

These prerequisite conditions (a)-(c) will be the minimum information required to describe a well-behaved continuous function so that the fuzzy systems performs more efficiently than other classical functional approximators. And these conditions can be gained easily in practical process.

B. Comparision study on necessary conditions

Ying [19, 20] pointed out that, a fuzzy system as approximator, the number of division points is at least the number of extremes of the continuous function for the necessary condition. However, these results are not available for the fuzzy system as universal approximator within a given accuracy. In most cases, the necessary conditions for the fuzzy system as universal approximator within a given accuracy are more practical and useful. Here we will show that Ying's conclusion is only a special case of our results given above.

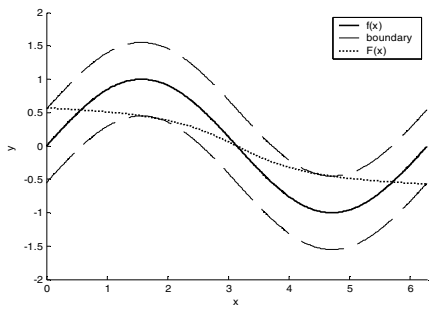

Figure 2. The fuzzy system using only two rules approximates $f(x)$.

Consider the function $f(x) = \sin x$, $x \in [0, 2\pi]$ in Fig. 3 with error bound 0.55 (dashed lines). A fuzzy system $F(x)$ with 2 fuzzy rules could be constructed (the dotted line) to achieve the given approximation accuracy by Lemma 7. However, according to Ying's conclusion, the fuzzy system requires at least 4 rules to achieve the given approximation accuracy. Consequently, necessary conditions proposed by Ying hold no longer when the approximation accuracy is prescribed.

In the construction algorithm, when the given approximation accuracy $\varepsilon \to 0$, we have

$$f(\xi_{i-1}) - f(\xi_i) > 2\varepsilon, f(\xi_i) - f(\xi_{i+1}) < -2\varepsilon$$
$$\text{or } f(\xi_{i-1}) - f(\xi_i) < -2\varepsilon, f(\xi_i) - f(\xi_{i+1}) > 2\varepsilon \quad (23)$$

for arbitrary $\xi_{i-1}, \xi_i, \xi_{i+1} \in \xi$, $i = 1, 2, \cdots, m$, and $Q = \{[\xi_0, \xi_2], [\xi_1, \xi_3], \cdots, [\xi_{m-1}, \xi_{m+1}]\}$.

According to Theorem 1, the input interval $[a,b]$ must be divided into at least $m+1$ subintervals, and the number of the fuzzy rules is $m+2$. This is just the necessary conditions for fuzzy systems as universal approximates proposed in [19]. As a result, the approach in [19] is a special case of our necessary conditions when ε approaches zero.

IV. ILLUSTRATIVE EXAMPLES

In this section, the developed approaches above will be illustrated by examples.

Example: Design a Mamdani fuzzy system to uniformly approximate the continuous function shown in Fig. 4. We can find easily that the extreme set of $f(x)$ is $\{0, 4, 6, 8, 12, 12.5, 13, 14.5, 16, 20, 21, 22, 26\}$ whose values are $\{1, -1, -0.4, -1, 1, 0.9, 1, 0.7, 1, -1, -0.8, -1, 1\}$.

The necessary conditions for a fuzzy system on various kinds of approximation accuracy are given as follows:

(1) $0 \leq \varepsilon < 0.05$

Using the construction algorithm, the characteristic set Q is

$$Q=\{[0,6],[4,8],[6,12],[8,12.5],[12,13],[12.5,14.5],[13,16],$$
$$[14.5,20],[16,21],[20,22],[21,26]\}.$$

By using the necessary conditions for fuzzy systems in Theorem 1, 13 fuzzy rules are required to achieve approximation accuracy.

(2) $0.05 \le \varepsilon < 0.1$

Using the construction algorithm, the characteristic set Q is

$$Q=\{[0,6],[4,8],[6,12],[8,14.5],[13,16],[14.5,20],$$
$$[16,21],[20,22],[21,26]\}.$$

We can conclude that 11 fuzzy rules can be used to achieve the given approximation accuracy by Theorem 1. Take $\varepsilon = 0.08$ as an example, the upper and lower boundaries of $f(x)$ are obtained by moving it vertically by ε upwards and downwards (the dashed lines in Fig. 5). A fuzzy system output whose monotonicity changes 9 times, is constructed in the tunnel encircled by the boundaries to approximate $f(x)$ (dotted line). Therefore 11 fuzzy rules are necessary for achieving the given accuracy.

(3) $0.1 \le \varepsilon < 0.15$

Using the construction algorithm, the characteristic set Q is

$$Q=\{[0,6],[4,8],[6,12],[8,14.5],[13,16],[14.5,20],[16,26]\}$$

And 9 fuzzy rules are required to achieve the given approximation accuracy by Theorem 1.

(4) $0.15 \le \varepsilon < 0.2$

The construction algorithm is used to determine the characteristic set as

$$Q=\{[0,6],[4,8],[6,12],[8,20],[16,26]\}.$$

And 7 fuzzy rules are required to achieve the given approximation accuracy by Theorem 1. Take $\varepsilon = 0.18$ as an example, the upper and lower bounds of $f(x)$ are obtained by moving it vertically by ε upwards and downwards (the dashed lines in Fig. 6). A fuzzy system output whose monotonicity changes 5 times, is constructed in the tunnel encircled by the boundaries to approximate $f(x)$ (dotted line). Therefore 7 fuzzy rules are necessary for achieving the given accuracy.

(5) $0.2 \le \varepsilon < 0.5$

Using the construction algorithm, the characteristic set Q is

$$Q=\{[0,12],[8,20],[16,26]\}.$$

5 fuzzy rules are required to achieve the given approximation accuracy by Theorem 1.

(6) $\varepsilon \ge 0.5$

The construction algorithm is used to determine the characteristic set Q as $Q=\Phi$. 2 fuzzy rules are required to achieve approximation accuracy by Theorem 1.

The strength as well as limitation of the general SISO Mamdani fuzzy system as function approximator is showed in the example. It is observed that the minimal number of fuzzy rules M increases with the number Ω of the desired continuous function's extremes whose swings are larger than the approximation accuracy. That is to say, on one hand, a small number of fuzzy rules suffice to achieve the approximat ion if Ω is a small number, even the desired function has a complicated formulation. On the other hand, large numbers of fuzzy rules are required to approximate a simple function with large Ω. It means that fuzzy systems are not ideal function approximators for applications involving highly oscillatory continuous functions with large amplitudes. And the necessary conditions are local constant with accuracy. These may be used to explain practical fuzzy models only use a small number of fuzzy rules to achieve successful applications.

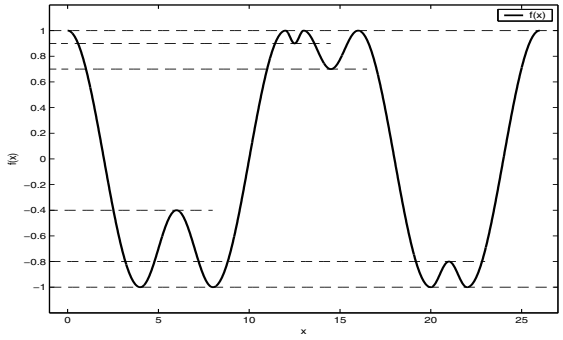

Figure 3. The desired function $f(x)$ in example 2.

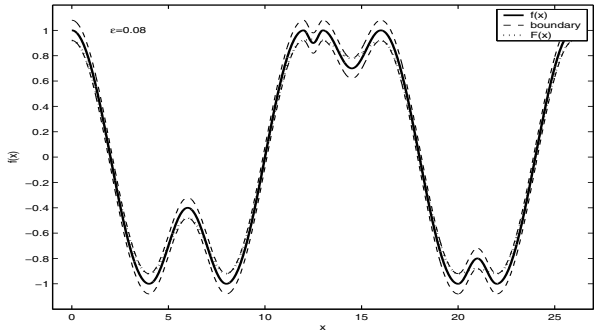

Figure 4. A fuzzy system $F(x)$ is constructed to approximate $f(x)$ in example 2 with accuracy 0.08.

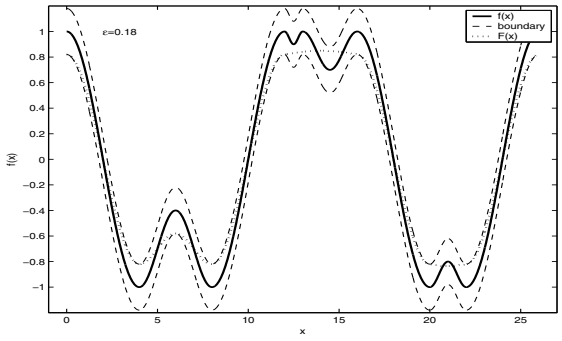

Figure 5. A fuzzy system $F(x)$ is constructed to approximate $f(x)$ in example 2 with accuracy 0.18.

V. CONCLUSIONS

This paper is concerned with the necessary conditions for general SISO Mamdani fuzzy systems as approximators within a given accuracy. The necessary conditions proposed in this paper expand the existing ones so that new conclusions are suitable for more practical cases. It has been proved that the proposed conditions are optimal. Finally, some examples are used to demonstrate the strength and limitation of the general SISO Mamdani fuzzy systems.

REFERENCES

[1] J. J. Buckley, "Universal fuzzy controllers", Automatica, vol. 28, no. 6, pp. 1245-1248, 1992.

[2] B. Kosko, "Fuzzy systems as universal approximators", IEEE Trans. Computers, vol. 43, no. 11, pp. 1329-1333, 1994.

[3] G. C. Mouzouris and J. M. Mendel, "Nonsingleton fuzzy logic systems: theory and application", IEEE Trans. Fuzzy Systems, vol. 5, no. 1, pp. 56-71, 1997.

[4] H. T. Ngugen, V. Kreionovich and O. Sirisaengtaksin, "Fuzzy control as universal control tool", Fuzzy Sets and Systems, vol. 80, no. 1, pp. 71-86, 1997.

[5] X. J. Zeng and M. G. Singh, "Approximation theory of fuzzy systems-MIMO case", IEEE Trans. Fuzzy Systems, vol. 3, no. 2, pp. 219-235, 1995.

[6] Y. Yam, P. Baranyi and C.T. Yang, "Reduction of fuzzy rule base via singular value decomposition", IEEE Trans. Fuzzy Systems, vol. 7, no. 2, pp. 120–132, 1999.

[7] J. Yen and L. Wang, "Simplifying fuzzy rule-based models using orthogonal transformation methods", IEEE Trans. Systems Man Cybernetics. B vol. 29, no. 1, pp. 13-24, 1999.

[8] T. Sudkamp, A. Knapp and J. Knapp, "Rule base reduction: some comments on the use of orthogonal transforms", IEEE Trans. Systems Man Cybernetics. C, vol. 31, no. 3, pp. 199-206, 2001.

[9] H. Ishibuchi, K. Nozaki, N. Yamamoto and H. Tanaka, "Selecting fuzzy if-then rules for classification problems using genetic algorithms", IEEE Trans. Fuzzy Systems, vol. 3, no. 4, pp. 260-270, 1995.

[10] H. Roubos and M. Setnes, "Compact and transparent fuzzy models and classifiers through iterative complexity reduction", IEEE Trans. Fuzzy Systems, vol. 9, no. 4, pp. 516-524, 2001.

[11] M. Setnes, "Supervised fuzzy clustering for rule extraction", IEEE Trans. Fuzzy Systems, vol. 8, no. 4, pp. 416-424, 2000.

[12] T. Sudkamp, A. Knapp and J. Knapp, "Model generation by domain refinement and rule reduction", IEEE Trans. Systems Man Cybernetics. B, vol. 33, no. 1, pp. 45-55, 2003.

[13] P. Manley-Cooke and M. Razaz, "An efficient approach for reduction of membership functions and rules in fuzzy systems", IEEE International Conference on Fuzzy Systems, pp. 1 -5, 2007.

[14] H. Ying, "Sufficient conditions on general fuzzy systems as function approximations", Automatica, vol. 30, no.3, pp. 521-525, 1994.

[15] X. J. Zeng and M. G. Singh, "Approximation accuracy analysis of fuzzy systems as function approximators", IEEE Trans. Fuzzy Systems, vol. 4, no. 1, pp. 44-63, 1996.

[16] K. Zeng, N. Y. Zhang and W. L. Xu, "A comparative study on sufficient conditions for Takagi–Sugeno fuzzy systems as universal approximators", IEEE Trans. Fuzzy Systems, vol. 8, no. 6, pp. 773-780, 2000.

[17] H. Ying, "General SISO Takagi-Sugeno fuzzy systems with linear rule consequent are universal approximators", IEEE Trans. Fuzzy System, vol. 6, pp. 582–587, 1998.

[18] H. Ying, "Sufficient conditions on uniform approximation of multivariate functions by general Takagi-Sugeno fuzzy systems with linear rule consequent", IEEE Trans. System, Man, Cybernetics, vol. 28, pp. 515–520, 1998.

[19] H. Ying and G. R. Chen, "Necessary conditions for some typical fuzzy systems as universal approximators", Automatica, vol. 33, no. 7, pp. 1333-1338, 1997.

[20] H. Ying, Y. S. Ding, S. K. Li and S. H. Shao, "Comparison of necessary conditions for typical Takagi-Sugeno and Mamdani fuzzy systems as universal approximators", IEEE Trans. Man, System, Cybernetics, vol. 29, no.5, pp. 508–514, 1999.

[21] Y. S. Ding, H. Ying and S. H. Shao, "Necessary conditions on minimal system configuration for general MISO Mamdani fuzzy systems as universal approximators", IEEE Trans. on Systems, Man and Cybernetics, vol. 30, no. 6, pp.857 -864, 2000.

[22] F. Wan, H. L. Shang, L. X. Wang and Y. X. Sun, "How to determine the minimum number of fuzzy rules to achieve given accuracy: a computational geometric approach to SISO case", Fuzzy Sets and Systems, vol. 150, 199–209, 2005.

[23] F. C. Sun and N. Zhao,"Universal approximation for Takagi-Sugeno fuzzy systems using dynamically constructive method-SISO cases", IEEE 22nd International Symposium on Intelligent Control, pp. 150-155, 2007.

2011 IEEE International Conference on Fuzzy Systems
June 27-30, 2011, Taipei, Taiwan

A Fuzzy Stochastic Programming Approach to Solve the Capacitated Lot Size Problem Under Uncertainty

Navid Sahebjamnia, S. Ali Torabi
Department of Industrial Engineering, College of Engineering
University of Tehran
Tehran, Iran
n.sahebjamnia@ut.ac.ir, satorabi@ut.ac.ir

Abstract— **This paper develops a fuzzy stochastic multi-objective linear programming (FSMOLP) model for a multi-level, multi-item capacitated lot sizing problem (CLSP) in a multi assembly shop. The proposed model attempts to minimize the total cost consisting of total production variation cost, inventory cost, backlog cost and total setup cost while maximizing the resource utilization simultaneously. To cope with the uncertainty associated with the most of the input data, e.g., the demand and process-related parameters they are treated as fuzzy stochastic parameters with identical stochastic membership function during the planning horizon. To show the usefulness of the proposed solution method, a numerical example is first solved. Then, the usefulness of the proposed model is validated over a set of randomly generated test problems.**

Keywords; Multi-level, multi-item capacitated lot sizing problem, Fuzzy Stochastic Multi-Objective Linear Programming, Multi assembly shop

I. INTRODUCTION

Shops, in which several assembly products are mounted simultaneously, are called Multi-Assembly Shops (MSA). In these shops, the raw material after being converted to sub-components by initial operations enters the main assembly line with different lot sizes. In such environments, many products with various sub-assemblies are assembled in different levels and then changed into final products (see [1]-[3]). MSA production planning models involves multiple items, restrictive capacities and setup times and/or cost. In this multi-level, multi-item production system, assumes a serial item structure with one or more final products that requires a multiple component. Each item is produced on a resource.

The multi-item multi-period CLSP with dynamic demand is a well known optimization problem that finds a wide variety of applications in real-world problems. Due to its vast industrial applicability, researchers have devoted special attention to it (see [4]-[5]). The problem arises in production environments where the changeover of a resource from one product type to another causes setup time and/or setup costs. Numerous models to support dynamic lot sizing for multi-level production systems have been presented over the last decades. Reviews of the literature on dynamic lot sizing are given by [6]-[8]. Big-bucket model formulations multi-level CLSP determines production quantities and periods only, without consideration of the actual production sequence of the orders within a time period [9]. The problem is complicated by the existence of setup costs as well as inventory holding costs [10].

The deterministic multi-item dynamic capacitated lot-sizing problem has been studied for a long time (For recent overviews see [11]-[13]). However, only a limited number of researchers have considered dynamic capacitated lot sizing under imprecise parameters. Industrial planning practice usually applies a forecasting procedure that provides a deterministic time series of expected future parameters. Uncertainty is taken into consideration by developing stochastic or fuzzy programming methods.

However, only a limited number of researchers have considered dynamic CLSP under uncertain demand. A literature overview is presented in Sox et al. [14]. Sox and Muckstadt [15] solve a variant of the stochastic dynamic CLSP, where item and period specific backorder costs as well as extendible production capacities are considered. Brandimarte [16] considers the stochastic CLSP where the uncertainty of the demand is represented through a scenario tree. In this case, the period demands are modeled as discrete random variables. Tempelmeier [17] consider the stochastic version of the dynamic multi-item CLSP. The problem is to determine lot sizes to satisfy demands for multiple products over a finite discrete time horizon.

Another imprecision is that, in actual practice, the capacity is frequently vague and difficult to predict. Moreover only a limited amount of (production, space, or budget) capacity might be available for a type of product, and this capacity might vary over time due to its own or other products seasonality. The fuzzy set theory, which can represent this vague future capacity easily, is an ideal approach. Pai [18] extended the work of Florian and Klein [l9] by using fuzzy capacity. Various investigators have used fuzzy set theory to investigate the lot-sizing problem. Lee and Yao [20] used the fuzzy concept to deal with lot sizing problem while demand and production quantity are uncertain. Chang et al. [21] modified the economic reorder point problem by introducing a fuzzy backorder quantity. The results offered a better sense of using economic fuzzy quantities. Chen and Wang [22] proposed a functional principle to deal with the lot sizing problem in a fuzzy environment. Yao and Lee [23] used a triangular fuzzy number to represent the fuzzy order quantity. Pappis and Karacapilidis [24] derived an appropriate number of production runs and lot sizes for multi-products with fuzzy

978-1-4244-7316-8/11/$26.00 ©2011 IEEE

demands. Several methods have been developed in the literature to deal with the possibilistic models involving the imprecise coefficients in both objective functions and constraints. Notably, the main part of proposed method is based on Jimenez et al. [25], Jimenez, [27] and Torabi and Hassini [26] because of their several advantages as follow:

1. Jimenez, [27] introduced general ranking method which can be applied to different kinds of membership functions such as triangular, trapezoidal and nonlinear ones in both symmetric and a symmetric forms.
2. The Jimenez et al. [25] method is based on the strong mathematical concepts such as expected interval and expected value of fuzzy numbers.
3. By increasing the size of problem, the complexity of proposed model should not be increased exponentially.
4. TH method [26] is very promising fuzzy multi-objective approach which can produce efficient solutions based on the decision maker's preferences along with offering appropriate flexibility to provide different solutions to help the decision maker in selecting the final preferred compromise solution.

However, the most popular approach to convert the fuzzy linear program (FLP) into the conventional deterministic linear program (LP) is the method of ordering fuzzy numbers such as area compensation method [28], the expected mid-point of fuzzy numbers [29], the grade of possibility and necessity [30] and the signed distance method [31].

Similarly, the fuzzy stochastic linear program has also been handled by defuzzifying and derandomizing fuzzy stochastic variables in two manner as sequential or simultaneously. In the sequential approaches, the defuzzifying process is performed first. Then the derandomizing process is done later (see [32]-[33]).

In this paper, we develop a fuzzy stochastic formulation for CLSP in which an optimal production plan is provided for multi products with imprecise dynamic demands over a given planning horizon. The production system is capacitated and setup times/costs occur when changing from one product to another while the model's parameters are vague. The objective is to find an optimal production plan that minimizes production variation, setup, and backlog and inventory cost while maximizes the resource utilization. Compared with deterministic models, fuzzy stochastic CLSP models are even more important in practice. In many real-world problems, customer demands, inventory bounds, and costs are all subject to uncertainty, and to make things worse, they could be dependent on each other in consecutive periods. The study of lot-sizing began with Wagner and Whitin [33], and there is now a sizeable literature in this area extending the basic model to consider capacity constraints, multiple items, multiple levels, etc. However, most previous work on lot-sizing has been directed towards the deterministic case. The practical problem is that in general much, if not all, of the future demands, capacity, resource consumption and costs (i.e. setup, production variation, holding and backorder cost) have to be forecast. However, the existence of forecast errors radically affects the behavior of the lot sizing procedures [34]. In contrast to the deterministic CLSP, we assume that every parameters such as cost multiple, demand, available resource and consumption resource are fuzzy stochastic variable. The period demands are non stationary (to permit dynamic effects such as seasonal variations, promotions, or general mixtures of known customer orders with random portions of period demands). Because they depend on many factors. Thus, it is difficult to determine exactly the values of these parameters. Moreover, the factors, which are fluctuating due to uncertain environment, could make these parameters vary. These circumstances often happen in long term planning, development strategies and engineering design, in which the described conditions (objectives, constraints, and coefficients) cannot be determined precisely and certainly.

In addition, we developed a new fuzzy stochastic multi-objective linear programming (FSMOLP) approach to solve the proposed model. We first convert the imprecise constraints into the crisp ones by using the expected value of corresponding imprecise parameters as well as the imprecise nature of the objective function by using upper and lower bound of the fuzzy stochastic objective functions coefficients. Then, after applying appropriate strategies for converting this possibilistic model into an auxiliary crisp multi-objective linear model (MOLP), we apply an interactive fuzzy approach to solve this MOLP and finding a preferred compromise solution. The main contributions of this paper could be highlight as follows:

1. Proposing a new bi-objective multi item, multi level CLSP model.
2. Developing a new CLSP model based on the structure of multi assembly shops.
3. Considering the imprecision and ambiguousness of CLSP parameters and modeling a fuzzy stochastic CLSP.
4. Proposing a new algorithm to find the efficient solutions of the proposed fuzzy stochastic CLSP.

II. PROPOSED MODEL

We classified the parameters of the proposed CLSP into two categories as supplier-related and demand-related parameters. Demand-related parameters include demand, backorder cost which are related (or set) to the costumers, while supplier-related parameters are determined by the supplier. Production variation, holding and setup cost, the amount of needed resource to produce one item and the available resource at each level in each period are fallen in the second category. CLSP is a multi period, big-time bucket, production planning problem that lot sizes of the product should be determined for long planning horizon. Thus, it is difficult to determine exactly the values of supplier-related and demand –related parameters. Moreover, the factors, which are fluctuating due to uncertain environment, could make these parameters vary. These circumstances often are different for each category that could introduce as follows:

1. Long planning horizon

2. Risk
3. Impact of the environmental factors
4. Change shops and workers situation
5. Vagueness and imprecise parameters

According to the above mentioned, many researchers focus on the stochastic or fuzzy techniques to deal with the vagueness and imprecision nature of the real case problems. Although both of stochastic and fuzzy approach separately are worthful techniques. According to the nature of problem parameters, fuzzy stochastic parameters are more desirable than stochastic or fuzzy parameters, because the parameters of the model determined based on the incomplete historical data (or ill-known data). In addition considering the input parameter as fuzzy stochastic variable could help the decision makers to close into the real problem. Consequently, due to the unavailability or incompleteness of data in real world circumstances, especially in big-time bucket production planning problem, every parameters embedded in such CLSP model have an imprecise and vague nature. So, in order to model the lack of knowledge about these parameters we use appropriate fuzzy stochastic membership function. The following assumption has been considered to formulate proposed CLSP model.

A. Assumptions

1. Each item needs just an identical resource.
2. The amounts of available resources in shop floor are imprecise and consider as fuzzy stochastic variable.
3. At the end of each period available resource will be retrieved.
4. Several products are produced, each of which is assembled from two or more item from upper level.
5. The considered CLSP problem is a multi period big-time bucket problem.
6. When all tasks of a level are finished, the tasks of the lower level could be started.
7. The demand of the product is non deterministic parameter with identical fuzzy stochastic membership function.
8. Costumers demand should be satisfied completely at the end of planning horizon.
9. The backorder and inventory holding is allowed, while both of them are equal to zero at the begging and ending of the planning horizon.
10. The production system has been designed as multi-level that in each level various item should be assembled.
11. In terms of number of products is a multi-item production planning that there are several products should be organized during planning horizon.
12. The capacity constraint is considered on available resource.
13. Setup time is considered as constraint in model and setup cost appeared as cost in objective function.

The following notations are used in the formulation of the proposed CLSP model:

B. Notations

Indices:

i: End product, $i=1,\ldots,P$
v: Item, $v=1,\ldots,V$
l: level. $l=1,\ldots,L$
j: Machine, $j=1,\ldots,J$
h: period(Time bucket), $h=1,\ldots,H$

Parameters:

$\widetilde{\widetilde{C}}_{ihj}^{Sh}$: Setup cost of item *v* of level *l*, from end product *i* on machine *j* in period *h*

$\widetilde{\widetilde{C}}_{i}^{Hh}$: Holding cost of end product *i* in period *h*

$\widetilde{\widetilde{C}}_{i}^{Bh}$: Back order cost of product *i* in period *h*

$\widetilde{\widetilde{d}}_{i}^{h}$: Demand of end product *i* at the end of period *h*

RT_{ihj} : The rate of production item *v* at level *l* of end product *i* on machine *j*

t_{ihj}^{h} : The processing time of item *v* at level *l* of end product *i* on machine *j* at period *h*

b_{ilv} : The number of item *v* at level *l* needed for producing product *i*.

ST_{ihj} : Setup time of item *v* at level *l* of end product *i* on machine *j*

$\widetilde{\widetilde{a}}_{ihv}$: The amount of resource needed to produce one unit of item *v* of level *l* from end product *i*

$\widetilde{\widetilde{R}}_{j}$: The accessible amount of resource *j*

λ_{ihj} :1, If item *v* of level *l*, from end product *i is* need machine j,0 otherwise

Decision variable:

I_{i}^{h} : Inventory level of end product i at the end of period h

B_{i}^{h} : Back order level of end product i at the end of period h

Q_{i}^{h} : The lot size of end product i at period h

C. Fuzzy Stochastic CLSP formulation

The objective of the proposed CLSP model is to determine the lot-sizes of the products whereas satisfying the cost and utility of the multi assembly shop. There are two objectives associated with the model: one is to minimize the costs related to the assembling operations, resource setups, backorder and inventory holding; the other is to maximize the utilization of the available resource. The two objectives are described below.

The first objective function is:

$$\text{Min} \sum_{h=1}^{H}\sum_{i=1}^{P}\sum_{l=1}^{L}\sum_{v=1}^{V}\widetilde{\widetilde{C}}_{ihv}^{Sh}.Y_{i}^{h}+\sum_{h=1}^{H}\sum_{i=1}^{P}\widetilde{\widetilde{C}}_{i}^{Hh}.I_{i}^{h}+\sum_{h=1}^{H}\sum_{i=1}^{P}\widetilde{\widetilde{C}}_{i}^{Bh}.B_{i}^{h}+\sum_{h=1}^{H}\sum_{i=1}^{P}\sum_{l=1}^{L}\sum_{v=1}^{V}\widetilde{\widetilde{C}}_{ihv}^{Ph}.Q_{i}^{h}.b_{ilv} \quad (1)$$

The four terms indicate, respectively, resource setup cost, inventory holding cost, backorder cost and production variation cost. In the first term, $\widetilde{\widetilde{C}}_{ihj}^{Sh}$ is the setup cost of

resource j and Y_i^h is an auxiliary 0-1 integer variable which assumes a value of one if product i is produced in period, and zero otherwise. In the second and third term, $\widetilde{\widetilde{C}}_i^{Hh}$ and $\widetilde{\widetilde{C}}_i^{Bh}$ are the holding and backorder cost for a unit of product i that holding or non delivery at the end of period. In the forth term, $\widetilde{\widetilde{C}}_{ilv}^{Ph}$ is per unit cost of performing operation item (ilv). This includes both the assembling and consumed resource cost.

The second objective function is formulated as follows:

$$\text{Min} \sum_{h=1}^{H}\sum_{l=1}^{L}\sum_{j=1}^{J}\left(\widetilde{\widetilde{R}}_j - R_{lj}^h\right) \tag{2}$$

where,

$$R_{lj}^h = \sum_{i=1}^{P}\sum_{v=1}^{V} b_{ilv}.Q_i^h.\widetilde{\widetilde{a}}_{ilv}.\lambda_{ilvj} \qquad \forall h,l,j$$

The $\widetilde{\widetilde{R}}_j$ is the total amount of resource j that is available during planning horizon. We split the multi assembly shop into a number of the level including various item from different products. When any level is started, all related item will be assembled until the next level begin. At the start of next level all resources will be retrieved and $\widetilde{\widetilde{R}}_j$ resource is available again. In the second objective, we try to close the amount of total available resource with consuming resource ($\widetilde{\widetilde{R}}_{lj}^h$) for each resource at each level in each period. The following constraint sets are in effect:

The demand of the customers should be satisfied during planning horizon, while according to the assumption the backorder and holding are allowed. So the demand balance constraints are defined as three equations.

$$I_i^{h-1} - B_i^{h-1} + Q_i^h = I_i^h - B_i^h + \widetilde{\widetilde{d}}_i^h \qquad \forall i, h \geq 2,3,...,H \tag{3}$$

$$Q_i^1 - I_i^1 + B_i^1 - \widetilde{\widetilde{d}}_i^h = 0 \qquad \forall i \tag{4}$$

$$I_i^H = B_i^H = I_i^0 = B_i^0 = 0 \qquad \forall i \tag{5}$$

The first and second equation balance the amount of the backorder, holding and lot sizes of all products from h=2 to end of the planning horizon and h=*1* respectively. The third formulation shows that at the start and end of the planning horizon backorder and holding is equal to zero.

The capacity constraint, ensure that the overall consumption must remain lower than the available capacity. The available resource $\widetilde{\widetilde{R}}_j$ would be retrieve at the end of each level for each resource at each level in each period.

$$\sum_{i=1}^{P}\sum_{v=1}^{V} b_{ilv}.Q_i^h.\widetilde{\widetilde{a}}_{ilv}.\lambda_{ilvj} \leq \widetilde{\widetilde{R}}_j \qquad \forall h,l,j \tag{6}$$

Production equation, grantee that if any product is produced in each period ($Q_i^h > 0$) the decision variable Y_i^h is become one, and zero otherwise.

$$Q_i^h \leq M.Y_i^h \qquad \forall i,h \tag{7}$$

$$Y_i^h = \{0,1\} \qquad \forall i,h \tag{8}$$

$$Q_i^h, B_i^h, I_i^h \in \text{Integer} \qquad \forall i,h \tag{9}$$

Variable constraint, show the type of each decision variable

$$Y_i^h = \{0,1\} \qquad \forall i,h \tag{10}$$

$$Q_i^h, B_i^h, I_i^h \in \text{Integer} \qquad \forall i,h \tag{11}$$

III. RANKIN OF FUZZY STOCHASTIC VARIABLE

There are several types of definition of fuzzy stochastic variable. Here, the attention is restricted to the concepts of Luhandjula [35] for the definition of the fuzzy stochastic variable and its characteristics (see [36]) as shown in figure 1.

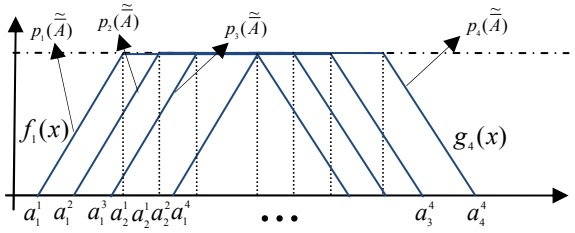

Figure 1. Fuzzy Stochastic number

When $\widetilde{A}$ is an uncertain value parameter, the membership degree $\mu_{\widetilde{A}}(x)$ can be viewed as the credibility degree of $\widetilde{A}$ taking value x [37]. $\widetilde{A}$ ($\widetilde{A} = (a_1, a_2, a_3, a_4)$) is a trapezoidal fuzzy number with membership degree $\mu_{\widetilde{A}}(x)$ as (12) if $f_a(x)$ and $g_a(x)$ are the linear function.

$$\mu_{\widetilde{A}}(x) = \begin{cases} 0 & (-\infty, a_1] \\ f(x) & [a_1, a_2] \\ 1 & [a_2, a_3] \\ g(x) & [a_3, a_4] \\ 0 & [a_4, +\infty) \end{cases} \tag{12}$$

According to the $\widetilde{A}$ definition, the expected interval of $\widetilde{A}$ was define by Heilpern, [38] as (13).

$$EI(\widetilde{A}) = [E_1^{\widetilde{A}}, E_2^{\widetilde{A}}] \tag{13}$$

where

$$E_1^{\widetilde{A}} = \int_0^1 f_{\widetilde{A}}^{-1}(y)dy = \int_0^1 ((a_2 - a_1).y + a_1)dy = \frac{a_2 + a_1}{2}$$

$$E_2^{\widetilde{A}} = \int_0^1 g_{\widetilde{A}}^{-1}(y)dy = \int_0^1 ((a_3 - a_4).y + a_4)dy = \frac{a_3 + a_4}{2}$$

From (13), the expected interval of fuzzy stochastic variable $\widetilde{\widetilde{A}}$ is obtained by (14). Moreover the expected value is define as the average of the $E_1^{\widetilde{A}}$ and $E_2^{\widetilde{A}}$.

$$EI(\widetilde{\widetilde{A}}) = [E_1^{\widetilde{\widetilde{A}}}, E_2^{\widetilde{\widetilde{A}}}] = [\frac{\overline{a}_1 + \overline{a}_2}{2}, \frac{\overline{a}_3 + \overline{a}_4}{2}] \tag{14}$$

where

$$\overline{a}_i = E(a_i) = \sum_k p_k(\widetilde{\widetilde{A}}) \times a_i$$

While there is existed wide range of ranking approach to rank fuzzy numbers in the literature, notably some issued should be considered to choose efficient ranking method as follow:

1. Due to the complicated structure of the mathematical models, the applied method should not increase the size of the problem (neither variable nor constraints).
2. The ranking method should not be approximated approach while we prefer to find the best solution if possible.

Definition 1. Assuming $\tilde{\tilde{A}}_1$ and $\tilde{\tilde{A}}_2$ are two fuzzy stochastic variable. The membership degree $\mu_{\tilde{\tilde{A}}_1 \geq \tilde{\tilde{A}}_2}(x)$ can be viewed as the credibility degree of $\tilde{\tilde{A}}_1 \geq \tilde{\tilde{A}}_2$ taking value x and as follow:

$$\mu_{\tilde{\tilde{A}}_1 \geq \tilde{\tilde{A}}_2} = \begin{cases} 0 & E_2^{\tilde{\tilde{A}}_1} - E_1^{\tilde{\tilde{A}}_2} < 0 \\ \dfrac{E_2^{\tilde{\tilde{A}}_1} - E_1^{\tilde{\tilde{A}}_2}}{E_2^{\tilde{\tilde{A}}_1} - E_1^{\tilde{\tilde{A}}_2} - (E_1^{\tilde{\tilde{A}}_1} - E_2^{\tilde{\tilde{A}}_2})} & 0 \in [E_1^{\tilde{\tilde{A}}_1} - E_2^{\tilde{\tilde{A}}_2}, E_2^{\tilde{\tilde{A}}_1} - E_1^{\tilde{\tilde{A}}_2}] \\ 1 & E_1^{\tilde{\tilde{A}}_1} - E_2^{\tilde{\tilde{A}}_2} > 0 \end{cases} \quad (14)$$

where $[E_1^{\tilde{\tilde{A}}_1}, E_2^{\tilde{\tilde{A}}_1}]$ and $[E_1^{\tilde{\tilde{A}}_2}, E_2^{\tilde{\tilde{A}}_2}]$ are the expected interval of $\tilde{\tilde{A}}_1$ and $\tilde{\tilde{A}}_2$. When $\mu_m(\tilde{\tilde{A}}_1, \tilde{\tilde{A}}_2) \geq \chi$ we will say that $\tilde{\tilde{A}}_1$ is bigger than, or equal, to $\tilde{\tilde{A}}_2$ at least in a degree a and we will represent it by $\tilde{\tilde{A}}_1 \geq_\chi \tilde{\tilde{A}}_2$.

Definition 2 [36]. Given a decision vector $x \in R^n$ we will say that it is feasible in degree χ if

$$\min_{m=1,\ldots,M} \{\mu_m(\tilde{\tilde{A}}_1 x, \tilde{\tilde{A}}_2)\} = \chi \quad (15)$$

That is to say

$$\tilde{\tilde{A}} x_1 \geq_\chi \tilde{\tilde{A}}_2 \quad (16)$$

It is equivalent to (from (14)),

$$[\chi E_1^{\tilde{\tilde{A}}_1} + (1-\chi) E_2^{\tilde{\tilde{A}}_1}] x \leq \chi E_2^{\tilde{\tilde{A}}_2} + (1-\chi) E_1^{\tilde{\tilde{A}}_2} \quad (17)$$

IV. OBJECTIVE FUNCTION WITH FUZZY STOCHASTIC COEFFICIENT

In this section we try to convert the fuzzy stochastic coefficient of the objective functions into the crisp ones such that using maximum performance of the fuzzy stochastic number. Assumed that P is a fuzzy stochastic programming problem as follow:

$$P: \min \ Z_h = \tilde{\tilde{c}}_n x \quad \text{for } n = 1,\ldots,N$$
$$\text{s.t.}$$
$$x \in X$$

$\tilde{\tilde{c}}_n$ is a fuzzy stochastic coefficient of the objective function (n^{th}) and X is feasible space of the problem.

Definition 3. For fuzzy stochastic number ($\tilde{\tilde{c}}_h$) we define the upper and lower bound of $\tilde{\tilde{c}}$ ($\tilde{c}_n^l$ and $\tilde{c}_n^u$) as follow:

Lower bound of $\tilde{\tilde{c}}_n$ *(*$\tilde{c}_n^l$*):* The maximum movement that $\tilde{\tilde{c}}_n$ could move to left hand side as follows:

$$\tilde{c}_n^l = \min a_{ni}^k = (\min a_{n1}^k, \min a_{n2}^k, \min a_{n3}^k, \min a_{n4}^k) \quad (18)$$

Upper bound of $\tilde{\tilde{c}}$ *(*$\tilde{c}_n^u$*):* The maximum movement that $\tilde{\tilde{c}}$ could move to right hand side as follows:

$$\tilde{c}_n^l = \max a_{ni}^k = (\max a_{n1}^k, \max a_{n2}^k, \max a_{n3}^k, \max a_{n4}^k) \quad (19)$$

According to $\tilde{c}_n^l$ and $\tilde{c}_n^u$ the membership function of each objective function would be obtained (20) and (21) for minimizing and maximizing respectively.

$$\mu_n^z(z) = \begin{cases} 0 & Z > z_u^{n(NIS)} \\ \dfrac{z_l^{n(PIS)} - Z}{z_u^{n(NIS)} - z_l^{n(PIS)}} & z_l^{n(PIS)} \leq Z \leq z_u^{n(NIS)} \\ 1 & Z \leq z_l^{n(PIS)} \end{cases} \quad (20)$$

$$\mu_n^z(z) = \begin{cases} 1 & Z > z_u^{n(PIS)} \\ \dfrac{Z - z_u^{n(PIS)}}{z_u^{n(PIS)} - z_l^{n(NIS)}} & z_l^{n(NIS)} \leq Z \leq z_u^{n(PIS)} \\ 0 & Z \leq z_l^{n(NIS)} \end{cases} \quad (21)$$

Often the researchers to find the positive ideal solution (PIS) and negative ideal solution (NIS) solve the MOLP problem 2N time (N number of the objective functions). To avoid iterative procedure and reduce running time, we define $z_l^{n(PIS)}$ and $z_u^{n(NIS)}$ and $z_u^{n(PIS)}$ and $z_l^{n(NIS)}$ for minimizing and maximizing objective functions respectively as definition 6 and 7.

Definition 4. Define $z_l^{n(PIS)}$ and $z_u^{n(NIS)}$ for minimization:

$z_l^{n(PIS)} = \min z_l^n(x)$ (For each *h* individually)

$z_u^{n(NIS)} = \max_{\hat{x}_n} \{z_u^n(\hat{x}_n)\}$ ($\hat{x}$ is the solution of z_u^n, for maximizing each n individually)

Definition 5. Define $z_u^{n(PIS)}$ and $z_l^{n(NIS)}$ for maximization:

$z_u^{n(PIS)} = \max z_u^n(x)$ (For each *h* individually)

$z_l^{n(NIS)} = \min_{\hat{x}_n} \{z_l^n(\hat{x}_n)\}$ ($\hat{x}$ is the solution of z_l^n, for minimizing each *n* individually)

where z_l^n and z_u^n is formulated as (22) and (23).

$$Z_\cdot^n = \min \ E\mathrm{V}(\tilde{\tilde{c}}_l^n).x$$
$$\text{s.t.} \quad (22)$$
$$x \in X$$

$$Z_\cdot^n = \min \ E\mathrm{V}(\tilde{\tilde{c}}_u^n).x$$
$$\text{s.t.} \quad (23)$$
$$x \in X$$

Torabi and Hassini, [26], proposed a novel interactive fuzzy approach to solve multi objective linear programming (MOLP) problem and finding a preferred compromise solution. We applied their aggregate function to solve P as follow:

$$\max \ \eta(z) = \varsigma\eta_0 + (1-\varsigma)\sum_n \theta_n \mu_n(z)$$
$$s.t.$$
$$\eta_0 \leq \mu_n(z) \quad n = 1,\ldots,N \quad (24)$$
$$z \in F(z)$$
$$\varsigma \in [0,1]$$

where $\mu_n(z)$ and $\eta_0 = \min_n \{\mu_n(z)\}$ denote the satisfaction degree and minimum satisfaction degree of objective functions, respectively. This formulation has a new achievement function defined as a convex combination of the lower bound for satisfaction degree of objectives (η_0), and the weighted sum of these achievement degrees ($\mu_n(z)$) to ensure yielding an adjustably balanced compromise solution.

Moreover, θ_n and ς indicate the relative importance of the n^{th} objective function and the coefficient of compensation, respectively. The θ_n parameters are determined by the decision maker based on her/his preferences such that $\sum_n \theta_n = 1,\ \theta_n > 0$. Also, ς controls the minimum satisfaction level of objectives as well as the compromise degree among the objectives implicitly. That is, the proposed formulation is capable of yielding both unbalanced and balanced compromised solutions for a given problem instance based on the decision maker's preferences through adjusting the value of parameter ς [17].

By defining upper and lower bound of fuzzy stochastic coefficient (definition 3) we convert the imprecision objective function into crisp one for single or multi objective fuzzy stochastic programming problem.

V. THE PROPOSED FUZZY SOLUTION APPROACH

To solve the proposed MOLP models with fuzzy stochastic parameters several methods have been developed in the literature. By considering the imprecision situation as fuzzy stochastic parameters, both experimentally nature of the data and satisfaction level of decision makers are take into account simultaneously. But it would increase the complexity of the solution method. Hop, [16] convert the fuzzy stochastic MOLP into the corresponding deterministic MOLP problem by using superiority and inferiority measures of the fuzzy stochastic variables. In another work, he presented a model to measure attainment value of fuzzy stochastic goals and then applied it to de-randomize and defuzzify the fuzzy stochastic goal programming problem and obtain a standard linear program [39]. Although in both paper he obtained acceptable results, two issues could be discussed A) he consider fuzzy stochastic number as different fuzzy number with identical probability (discrete distribution). B) He changed the structure of the model by adding the imprecise constraint into objective function. However, in this paper to solve the proposed fuzzy stochastic MOLP model of CLSP, we proposed an interactive fuzzy stochastic solution approach by combining the [25], [26], [36]. The proposed hybrid approach is as follows:

Step 1: Determine the appropriate fuzzy stochastic membership function for imprecise parameters and forming the fuzzy stochastic CLSP model.

Step 2: Convert the uncertain constraints into the crisp ones by using the expected value of corresponding imprecise parameters as equation (17).

Step 3: Convert fuzzy stochastic coefficient of the objective functions into the fuzzy ones by using upper and lower bound of coefficient (equations (18) and (19)).

Step 4: Convert fuzzy objective functions into the crisp ones by using the expected value of the upper and lower bound of the coefficients and find the Z_*^n , Z_*^n

Step 5: Determine the membership function of the objective functions by using (20)-(21) and definition 6 and 7.

Step 6: Convert the equivalent crisp MOLP model into a single ones using TH aggregation functions [26], (24) which resulting the efficient solutions.

To run the proposed algorithm the decision maker should specify the value of the: feasibility degree of the constraints (χ); the deviation of the objective function coefficient (γ); coefficient of compensation (ς); relative importance of the fuzzy goals θ_n . Jimenez, [25] proposed a three steps procedure to maximize the satisfaction (feasibility) degree. The deviation of the objective function coefficient (γ) is set by the DM. Also, the coefficient of compensation and relative importance of the fuzzy goals are specified by decision makers generally. If the decision makers are not satisfied with the obtained results, another solution will be provided by changing these values.

VI. NUMERICAL ILLUSTRATION

To illustrate the efficiency of the proposed method, we consider Luhandjula's example. The results are compared with Luhandjula [35] and Hop [36] results. In this example a triangular fuzzy number ($(m-0.5, m, m+0.5)$) with a discrete distribution $p_1 = 0.25$ and $p_2 = 0.75$ has been considered. The results show the capability of the proposed model in against of existed method [36] and [35] as reported in table 1.

$$\max \quad \left(\begin{matrix}\tilde{3}\\ \tilde{4}\end{matrix}\right)x_1 + \left(\begin{matrix}\tilde{2}\\ \tilde{3}\end{matrix}\right)x_2$$
$$s.t.$$
$$\tilde{\tilde{A}}x \le \tilde{\tilde{b}}$$
$$x \ge 0,$$

$$(\tilde{\tilde{A}}, \tilde{\tilde{B}}) = \begin{cases} (\tilde{A}_1, \tilde{B}_1) = \left\{\left(\begin{matrix}\tilde{1} & \tilde{1}\\ \tilde{2} & \tilde{1}\end{matrix}\right), \left(\begin{matrix}\tilde{3}\\ \tilde{4}\end{matrix}\right)\right\} \\ (\tilde{A}_2, \tilde{B}_2) = \left\{\left(\begin{matrix}\tilde{1} & \tilde{3}\\ \tilde{1} & \tilde{2}\end{matrix}\right), \left(\begin{matrix}\tilde{5}\\ \tilde{4}\end{matrix}\right)\right\} \end{cases}$$

According to the step 1 to 6 the model would be rewritten as follow:

$$\max \quad \eta_0$$
s.t.
$$\eta_0 \le \mu_n(z) \quad n = 1$$
$$[0.75\chi + (1-\chi)1.25]x_1 + [2.25\chi + (1-\chi)2.75]x_2 \le [4.25\chi + (1-\chi)4.75]$$
$$[\chi + (1-\chi)1.5]x_1 + [1.5\chi + (1-\chi)2]x_2 \le [3.75\chi + (1-\chi)4.25]$$

where

$$\mu_1(z) = \begin{cases} 1 & z > 15 \\ \dfrac{x - 11.25}{3.75} & 11.25 \le z \le 15 \\ 0 & z < 11.25 \end{cases}$$

Table 1. Obtained results

Method	Decision vector	Objective function
Proposed method	$x_1 = 3.6\ x_2 = 0.1$	15
Hop [16]	$x_1 = 4\ x_2 = 1$	14
Luhandjula [25]	$x_1 = 1.34\ x_2 = 1$	6.02

From the obtained results, it is clear that the proposed method gives acceptable solution based on the Luhandjula [35] and Hop [36] results. In addition, the proposed methodology is also superior considering the amount of calculations and complexities embedded in other methodology, especially, the Hop's method because of a few number of constraints and the simplicity of conversion. Moreover, the proposed method compares fuzzy stochastic variables based on their relative relationships. This comparison will relax the constraints from the deterministic ones. Thus, the larger spreads of fuzzy numbers led to the more relaxation amount [36].

To illustrate the validity of the proposed model, a numerical experiment is solved and results are reported in table 2. The characteristics of the problem are as follows:

1. Membership function of each fuzzy stochastic parameter (FSP) is trapezoidal with discrete uniform distribution.
2. Setup and production variation costs are a FSP with trapezoidal fuzzy membership function and are generated randomly with uniform distribution. Similarly, Backorder and holding cost of product are $\tilde{\tilde{C}}_{ilv}^{Hh} = 0.55 \times \tilde{\tilde{C}}_{ilv}^{Ph}$ and $\tilde{\tilde{C}}_{ilv}^{Bh} = 1.2 \times \tilde{\tilde{C}}_{ilv}^{Ph}$ respectively.
3. b_{ilv} were generated from a uniform distribution U [1,5].
4. $\tilde{\tilde{a}}_{ilv}$ were generated randomly from uniform distribution U [3,5].
5. $\tilde{\tilde{R}}_{j}$ were generated randomly from uniform distribution U [4000,16000].

Based on the structure of the proposed CLSP model, problem dimensions has been obtained according to five parameters as period, product, level, item and resource and is equal to $(h \times i \times l \times v \times j) = (3 \times 3 \times 4 \times 3 \times 3)$.

The test problem is carried out with a branch-and-bound (B&B) method by using the LINGO 9.0 software. We have considered a problem with three products, four levels, three item which should be produced during three periods with three resources. According to the step 1 to 4 of proposed method the Fuzzy stochastic CLSP model is reformulated and the solution of $Z_{\cdot}^{n}$, $Z_{\cdot}^{n}$, $z_{l}^{n(PIS)}$, $z_{u}^{n(NIS)}$ has been calculated firstly. We determine the membership function of the each objective function and then convert the equivalent MOLP model into a single crisp ones based on the step 6 and obtaining results as Z_1=6971 and Z_2=288 with $\varsigma = 0.1$, $\vec{\theta} = (0.7, 0.3)$ as reported in table 2.

VII. CONCLUSION

We develop a fuzzy stochastic multi-objective linear programming model for big bucket multiple periods lot-sizing problems in which an optimal production plan is provided for multiple products with dynamic demands over a given planning horizon. The significance of accounting for uncertainty and risk in such networks spurs an interest to develop appropriate production planning tools to cope with uncertain and imprecise parameters in multi assembly shop lot sizing. To deal with imprecise and ambiguous nature of data, we introduce appropriate fuzzy stochastic membership functions for imprecise parameters.

Then an interactive fuzzy stochastic approach has been developed. Uncertain constraints as well as imprecise objective functions are converted into their crisp one by using the expected interval and value of the ill-known parameters, respectively. Finally, the equivalent crisp MOLP model is transferred into a single objective model using an appropriate aggregation function which ensures yielding efficient solutions. The proposed solution method is validated over a number of test problem and the corresponding results seem to be promising. This approach can also be used for solving other fuzzy stochastic MOLP models due to its computationally advantages.

REFERENCES

[1] C. K. Tsai, "Enhancing disassembly and recycling planning using life cycle analysis," Robotics and computer-integrated manufacturing, vol. 22, Issue 5, 2006, pp. 420–428.

[2] C. K. Tsai and H. C. Zhang, "A graph-based disassembly planning for end-of-life electromechanical products," International journal of production research, Vol. 38, Issue 5, 2000, pp. 993–1007.

[3] I. Mahdavi, B. Shirazi, M. Solimanpur and N. Sahebjamnia, "Lot size approximation based on minimizing total delay in a shop with multi-assembly products," International Journal of Production Research, Vol. 47, No. 10, 15, 2009, pp. 2685–2703

[4] Y. Pochet and L.A. Wolsey, "Polyhedra for lot sizing with Wagner–Within costs," Mathematical Program, vol. 67, 1994, pp. 297–323.

[5] M. Constantino, "A cutting plane approach to capacitated lot-sizing with start-up costs," Mathematical Program, vol. 75, 1996, pp. 353–376.

[6] Y.P. Gupta and Y. Keung, "A review of multi-stage lot-sizing models," International Journal of Operations and Production Management, vol. 10, 1990, pp. 57–73.

[7] M. Salomon, L.G. Kroon, R. Kuik and L.N. Van Wassenhove, "Some extensions of the discrete lot sizing and scheduling problem," Management Science, vol. 37, 1991, pp. 801–812.

[8] L. Buschkuhl, F. Sahling, S. Helber and H. Tempelmeier, "Dynamic capacitated lot-sizing problems a classification and review of solution approaches," Operations Research Spectrum, DOI:10.1007/s00291-008-0150-7.

[9] F. Sahling, L. Buschkuhl, H.Tempelmeier and S. Helber, "Solving a multi-level capacitated lot sizing problem with multi-period setup carry-over via a fix-and-optimize heuristic," Computers & Operations Research, vol. 36, 2009, pp. 2546-2553.

[10] M. Caserta and E. Quinonez Ricob, "A cross entropy-Lagrangean hybrid algorithm for the multi-item capacitated lot-sizing problem with setup times," Computers & Operations Research, vol. 36, 2009, pp. 530-548.

[11] B. Karimi, S.M.T. Fatemi Ghomi and J.M. Wilson, "The capacitated lot sizing problem: a review of models and algorithms," Omega, vol. 31, 2003, pp. 365–78.

[12] R. Jans and Z. Degraeve, "Modeling industrial lot sizing problems: a review," International Journal of Production Research, vol. 46, 2008, pp. 1619–43.

[13] P. Robinson, A. Narayanan and F. Sahin, "Coordinated deterministic dynamic demand lot-sizing problem: a review of models and algorithms," Omega, vol. 37, 2009, pp. 3–15.

[14] C. Sox, P. Jackson, A. Bowman and J. Muckstadt, "A review of the stochastic lot scheduling problem," International Journal of Production Economics, vol. 62, 1999, pp. 181–200.

[15] C. Sox and J. Muckstadt, "Optimization-based planning for the stochastic lot- scheduling problem," IIE Transactions, vol. 29, 1997, pp. 349–57.

[16] P. Brandimarte, "Multi-item capacitated lot-sizing with demand uncertainty," International Journal of Production Research, vol. 44, issue 15, 2006, pp. 2997–3022.

[17] H. Tempelmeier, "A column generation heuristic for dynamic capacitated lot sizing with random demand under a fill rate constraint," Omega, doi:10.1016/j.omega.2011.01.003.

[18] P. F. Pai, "Capacitated Lot Size Problems with Fuzzy Capacity," Mathematical and Computer Modeling, vol. 38, 2003, pp. 661-669.

[19] M. Florian and M. Klein, "Deterministic production planning with concave cost and capacity constraint," Management, vol. 5, issue 18, 1971, pp. 12-20.

[20] H.M. Lee and J.S. Yao, "Economic production quantity for fuzzy demand quantity and fuzzy production quantity," European Journal of Operational &search, vol. 109, 1998, pp. 203-211.

[21] S.C. Chang, J.S. Yao and H.M. Lee, "Economic reorder point for fuzzy backorder quantity," European Journal of Operational Research, vol. 109 1998, pp. 183-202.

[22] S.H. Chen and C.C. Wang, "Backorder fuzzy inventory model under function principle," Information Sciences, vol. 95, 1996, pp. 71-79.

[23] J.S. Yao and H.M. Lee, "Fuzzy inventory with backorder for fuzzy order quantity," Information Sciences, vol. 93, 1996, pp. 283-319.

[24] C.P. Pappis and N.I. Karacapilidis, "Lot size scheduling using fuzzy numbers, ht. Trans. Opl. Res, vol. 2, issue 2, 1995, pp. 205-212.

[25] M. Jimenez, M. Arenas, A. Bilbao and M.V. Rodriguez, "Linear programming with fuzzy parameters: an interactive method resolution," European Journal of Operational Research, vol. 177, 2007, pp. 1599–1609.

[26] S.A. Torabi and E. Hassini, "An interactive possibilistic programming approach for multiple objective supply chain master planning," Fuzzy Sets and Systems, vol. 159, 2008, pp. 193–214.

[27] M. Jimenez, "Ranking fuzzy numbers through the comparison of its expected intervals," International Journal of Uncertainty, Fuzziness and Knowledge Based Systems, vol. 4, issue 4, 1996, pp. 379–388.

[28] P. Fortemps and M. Roubens, "Ranking and defuzzification methods based on area compensation," Fuzzy Sets and Systems, vol. 82, 1996, pp. 319–330.

[29] K.D. Jamison and W.A. Lodwick, "Fuzzy linear programming using a penalty method," Fuzzy Sets and Systems, vol. 119, 2001, pp. 97–110.

[30] L. Campos and J.L. Verdegay, "Linear programming problems and ranking of fuzzy numbers," Fuzzy Sets and Systems, vol. 32, 1989, pp. 1–11.

[31] J. Chiang, "Fuzzy linear programming based on statistical confidence interval and interval-valued fuzzy set," European Journal of Operational Research, vol. 129, 2001, pp. 65–86.

[32] M.G. Iskander, "A suggested approach for possibility and necessity dominance indices in stochastic fuzzy linear programming," Applied Mathematics Letters, vol. 18, 2005, pp. 395–399.

[33] B. Liu and Y.K. Liu, "Expected value of fuzzy variable and fuzzy expected value models," IEEE Transactions on Fuzzy Systems, vol. 10, 2003, pp. 445–450.

[33] H.M. Wagner and T.M. Whitin, "Dynamic version of the economic lot size model," Management Science, vol. 5, 1958, pp. 89–96.

[34]S.A. Tarim and B.G. Kingsman, "The stochastic dynamic production/inventory lot-sizing problem with service-level constraints," International Journal of Production Economics, vol. 88, 2004, pp. 105–119.

[35] M.K. Luhandjula, "Fuzziness and randomness in an optimization framework," Fuzzy Sets and Systems, vol. 77, 1996, vol. 291–297.

[36] N.V. Hop, "Solving fuzzy (stochastic) linear programming problems using superiority and inferiority measures," Information Sciences, vol. 177, 2007, pp. 1977–1991.

[37] L. Zadeh, "Fuzzy sets as a basis for a theory of possibility," Fuzzy Sets and Systems, vol. 1, 1978, pp. 3–28.

[38] S. Heilpern, "The expected value of a fuzzy number," Fuzzy Sets and Systems, vol. 47, 1992, pp. 81–86.

[39] N.V. Hop, "Fuzzy stochastic goal programming problems," European Journal of Operational Research, vol. 176, 2007, pp. 77–86.

Table 2. Obtained results

Objective function			Period								
			h=1 Products			h=2 Products			h=3 Products		
	Cost	Utility	Q	B	I	Q	B	I	Q	B	I
Lower	6971	288	23-24-24	0-0-0	14-14-14	0-0-0	0-0-0	6-6-7	0-0-0	0-0-0	0-0-0
Upper	8769	352	0-0-0	9-10-9	0-0-0	0-0-0	17-17-16	0-0-0	23-24-24	0-0-0	0-0-0

2011 IEEE International Conference on Fuzzy Systems
June 27-30, 2011, Taipei, Taiwan

Look-Ahead Intelligent Energy Management of A Parallel Hybrid Electric Vehicle

Behnam Ganji
School of Engineering
Deakin University
Geelong, Australia
bganj@deakin.edu.au

Abbas Z. Kouzani
School of Engineering
Deakin University
Geelong, Australia
kouzani@deakin.edu.au

Hamid Khayyam
School of Engineering
Deakin University
Geelong, Australia
h.khayyam@deakin.edu.au

***Abstract*—Improving fuel efficiency in vehicles can reduce the energy consumption concerns associated with operating the vehicles. This paper presents a model for a parallel hybrid electric vehicle. In the model, the flow of energy starts from wheels and spreads toward engine and electric motor. A fuzzy logic based control strategy is implemented for the vehicle. The controller manages the energy flow from the engine and the electric motor, controlling transmission ratio, adjusting speed, and sustaining battery's state of charge. The controller examines the vehicle speed, demand torque, slope difference, state of charge of battery, and engine and electric motor rotation speeds. It then determines the best values for continuous variable transmission ratio, speed, and torque. A slope window method is formed that takes into account the look-ahead slope information, and determines the best vehicle speed. The developed model and control strategy are simulated using real highway data relating to Nowra-Bateman Bay in Australia, and SAE Highway Fuel Economy Driving Schedule. The simulation results are presented and discussed. It is shown that the use of the proposed fuzzy controller reduces the fuel consumption of the vehicle.**

Keywords: Hybrid electric vehicles, backward modeling, look-ahead fuzzy control system, fuel efficiency.

I. INTRODUCTION

The demand for petroleum continues to increase whilst oil supplies remain finite [1]. According to a report published in 2006 [2], 80 million barrels of petrol is used per day around the world. The transportation sector consumes 66% of this petrol, and the portion of the land transportation is 56% of this quantity. Consuming this amount of fuel continues to aggravate the economical and environmental concerns around the world.

When it comes to energy utilisation and climate change concerns, cars and trucks are considered one of the principal problems. They consume a large portion of the oil and emit a large amount of greenhouse gas. In response to the impacts of the vehicles on environment and energy security, improving fuel efficiency in vehicles can play a massive role. There exist many techniques to improve the fuel efficiency in vehicles. Over the past few decades, there has been significant development in automobile engine and body technology. Thus, there are little gains achievable in fuel economy through vehicle engine and body. This has resulted in the emergence of innovative technologies for automotive industry. Since pure electric vehicles do not have adequate source of energy for propulsion in relatively long distance ranges, and because their recharging process requires several hours, hybrid electric vehicles (HEVs) can be considered as a better means of transportation. In comparison with conventional vehicles, fuel economy and reduced emissions have been achieved by HEVs [3-5]. The general concept of a HEV is the combination of an electric drive with an internal combustion engine (ICE), where both engine and motor can work in their optimal operating range.

A HEV is a complex system consisting of many components. The necessary propulsion energy is generated and converted in the component known as powertrain or propulsion system. The ways of arrangement of these components determine the configuration of the powertrain. There are a vast range of feasible configurations for a HEV. Based on the configuration of its powertrain, a HEV can be classified into series hybrid, parallel and series parallel hybrid. In this study, a parallel hybrid electric configuration is considered.

Although HEVs have made it possible to improve fuel efficiency and reduce emissions, considerable energy effectiveness can be achieved also by using driving profile, environmental effects, driving behaviour and control strategy. In this study, a control strategy that takes into account road geometry is developed.

II. ENERGY MANAGEMENT AND CONTROL IN HYBRID ELECTRIC VEHICLES

The overall performance of a HEV depends on how its individual components are efficiently designed and how the operation of the components is coordinated with each other.

Respectively, the control in HEVs can be classified in two levels: coordinate control and component control. In a HEV, the driver demand via accelerator is translated into power as the input of the coordinate control. Accordingly, the coordinate control system manages the components to achieve certain objectives.

There are two approaches in HEVs coordinate control, heuristic methods and classical optimal methods. The major feature of the former is its success in real-time control. The deterministic rule based control and fuzzy logic control can be classified in the heuristic approaches. The applied rules are designed based on heuristic knowledge of expert and even mathematical model.

978-1-4244-7316-8/11/$26.00 ©2011 IEEE

Usually the rule based coordinate controllers in HEVs benefit from "load-leveling" concept. This approach is applied by Hochgraf et al. [6]. They used engine, alternator and battery characteristics for determining an appropriate engine control strategy for a series hybrid electric vehicle. Their examination revealed that a load-levelling strategy applied to the engine would provide better fuel economy than a power-tracking scheme. Their idea became a fundamental for some other works. Jalil et al. [7] defined a rule-based control strategy based on the engineering knowledge. Rule-based control is the foundation of the fuzzy logic which translates linguistic representation of control inputs into numerical representation with membership function in the fuzzification and defuzzification process. The knowledge of expert in controlling the process is expressed in the form of rules. Schouten et al. [8] proposed a fuzzy-logic control system in order to optimise the fuel consumption in a parallel HEV. Accordingly, the power-split strategy through fuzzy rules is formulated to manage the possible ways of power to wheels: (1) only the ICE; (2) only the EM; (3) both the ICE and the EM at the same time; (4) charge the battery, using portion of the ICE power to drive the EM as a generator and using the remainder power to drive the wheels; and (5) regenerative braking by slowing down the vehicle and letting the wheels drive the EM as a generator that provides power to the battery.

Despite the fact that, the applied controllers have enhanced the fuel efficiency the effects of in-advance information from the road has not been used in the existing works. Thereafter, we will show how real road data can be applied in a HEV model, and the impact of in-advance knowledge of road slope on fuel economy will be investigated.

III. PARALLEL HYBRID ELECTRIC POWER TRAIN

HEVs usually consist of two sources of energy. In order to achieve the part of energy which in conventional vehicle is wasted in the form of heat, the electrical part of drive train has bidirectional energy sources and converters. In a parallel hybrid electric vehicle (PHEV), the engine supplies the mechanical power to the wheels and generator during the charge of battery. The power can be supplied by only electric motor to the wheels, or engine can be assisted by the electric motor. The engine and electric motor are coupled together by mechanical coupling. A configuration and power flow in a PHEV is illustrated in Fig. 1.

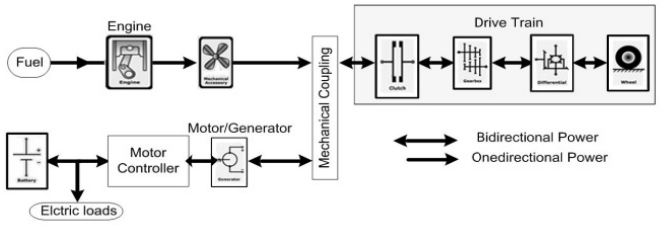

Figure 1. Parallel hybrid vehicle configuration and power flow diagram.

For a given HEV and road, the speed and torque at the output of mechanical coupling for providing the required force in the wheels can be calculated from the forces acting on vehicle.

The various longitudinal forces in a vehicle are expressed as acceleration, rolling, gravitational and drag. Accordingly, the traction force, F_{tr} is derived from the equation of solid body motion in the following form:

$$F_{tr} = M\dot{v}(t) + C_{rr}MgCos\alpha + MgSin\alpha + \frac{1}{2}C_D A\rho(v(t) + v_w(t))^2 \quad (1)$$

where the traction force parameters are listed in Table I.

TABLE I. TRACTION FORCE PARAMETERS

M vehicle mass	C_{rr} rolling Coe.	C_D drag Coe.
v vehicle speed	g gravitational acc.	A frontal area
v_w wind speed	α road slope	ρ air density

Equation (1) describes the dynamic of vehicle, and determines the amount of power that can be provided by the two sources of energy, battery and petrol. In the quasi-static HEV model, the engine can be modeled by the efficiency map model. The engine model is described by the following equation and Fig. 2.

$$\eta_{ice} = \frac{P_m}{P_{ch}} = \frac{P_m}{\dot{m}\,(T_m,\omega)\,Q_{lhv}} = \frac{3600\times10^3}{Q_{lhv}BSFC(T_m,\omega)} \quad (2)$$

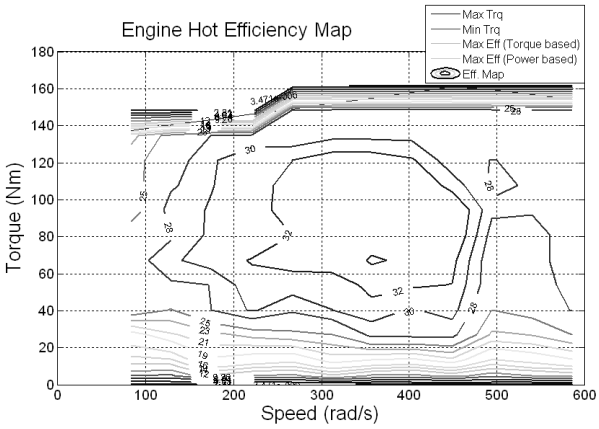

Figure 2. Engine efficiency map.

where ηice is the engine efficiency, which is a function of internal combustion engine torque and crankshaft rotational speed, Pm is the mechanical power at the crankshaft, Pch is the delivered mechanical power to the engine, and Qlhv [J/g] is chemical energy of fuel which is defined as "the amount of heat released by combusting a specified quantity (initially at 25 °C or another reference state) and returning the temperature of the combustion products to 150 °C". Typically, Qlhv=42.5[kJ/g] for petrol [9].

Similar to the engine efficiency map, there exists an efficiency map for an electric machine (EM) which presents empirical data of its efficiencies as a function of torque and speed. These efficiencies can be presented as contours on a torque-speed map. The applied motor/generator efficiency map in this study is illustrated in the Fig. 3.

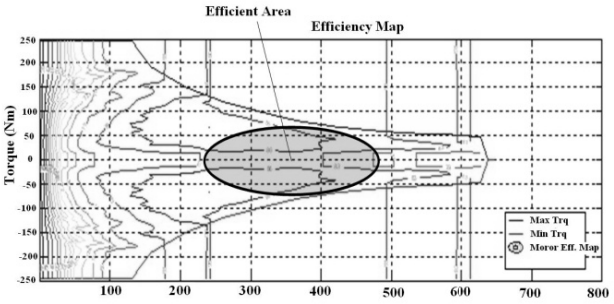

Figure 3. Efficiency map of a 33 kW (peak power) induction AC motor.

The input-output power in EM can be calculated as follows:

$$P_{in}(t) = V(t)I(t) \quad (3)$$

$$P_{out}(t) = T_{em}(t)\omega_{em}(t) \quad (4)$$

$$\eta_{em}(T_{em}(t), \omega_{em}(t)) = \frac{P_{out}(t)}{P_{in}(t)} \quad (5)$$

Where I is the EM input current in ampere, V is the input voltage in volt, and η_{em} is the EM efficiency. As presented in Fig. 3, according to the speed and the torque, there is an efficient area. Respectively, EM should be controlled to operate in this region. Consequently, in order to obtain the maximum efficiency when we are using the engine to charge the battery, the optimal speed range is considered in the applied fuzzy controller of this study.

Many types of battery have been modeled thus far. An overview of the battery models is available in literature [10]. Typically used batteries in HEVs are the lead acid and the Nickel metal batteries. In our modeling, we used the introduced lead acid model in [11].

IV. POSITIONING METHOD

In the proposed model, the drive train is represented by using the backward looking method. An overview of the different approaches in HEV modelling is available in literature [12]. A desired speed is fed to the longitudinal block. The desired speed can be a constant speed as the input of a conventional cruise control or a variable speed. The variable speed can be a drive cycle, an optimiser output or an adaptive cruise controller output [13]. We consider that the origin and destination of travel is known in advance and its information can be obtained from GIS. In order to simplify the problem, the road points are considered in a plane in two dimensions, x and y (distance and altitude) [14]. From the variation of altitude and distance, the slopes are determined for the entire path.

Assume that a moving vehicle at time t is at place $\vec{x_i}(t)$ and its velocity is $\vec{v_i}(t)$. The position vector between two consequent points can be calculated from following relation:

$$\vec{r}_i(t) = \vec{x_i}(t + \Delta t) - \vec{x_i}(t) \quad (6)$$

where, $\vec{x_i}$ is the position vector in the x-y coordinates. The distance between two consequent points can be written as:

$$s_i(t) = \|\vec{x_i}(t + \Delta t) - \vec{x_i}(t)\| \quad (7)$$

where $\| \ \|$ represent the norm of the specified vector.

The direction toward the forward point can be easily calculated from the following equation:

$$\vec{e}_i(t) = \frac{\vec{x_i}(t+\Delta t) - \vec{x_i}(t)}{\|\vec{x_i}(t+\Delta t) - \vec{x_i}(t)\|} \quad (8)$$

The velocity, $\vec{v_i}(t)$ can be found as follow:

$$\vec{v}_i(t) = \frac{s_i(t)}{\Delta t}\vec{e}_i(t) \quad (9)$$

Therefore, instantaneous velocity has two orthogonal terms in vertical and horizontal directions whose scalar can be presented in the following form:

$$v_x(t) = \left\|\frac{s_i(t)}{\Delta t}\vec{e}_i(t)\right\| Cos\alpha(t) = \|\vec{v}_i(t)\| Cos\alpha(t) \quad (10)$$

$$v_y(t) = \left\|\frac{s_i(t)}{\Delta t}\vec{e}_i(t)\right\| Sin\alpha(t) = \|\vec{v}_i(t)\| Sin\alpha(t) \quad (11)$$

where α(t) is the instantaneous slope angle between the direction vector, $\vec{e}_i(t)$ and x axis, and can be calculated from following relation:

$$\alpha(t) = \tan^{-1}\left(\frac{y(t+\Delta t) - y(t)}{x(t+\Delta t) - x(t)}\right) \quad (12)$$

A moving average method is used, and the samples are averaged to estimate the future slopes. With the movement of vehicle in each meter, a new sample is entered to the look-ahead window and the oldest sample is eliminated from the sampling space (see Fig. 4).

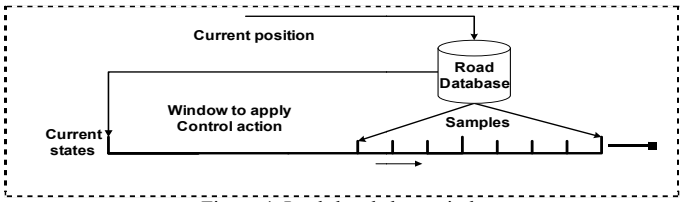

Figure 4. Look-head slope window.

$$\alpha(look_{ahead}) = \frac{\sum_{K=1}^{n}(\text{sampled date})}{n} - \frac{\text{oldest sample}}{n} + \frac{\text{new sample}}{n} \quad (13)$$

As in the backward facing model, the flow of energy starts from wheels and spreads toward ICE and EM. This facilitates the necessary calculations.

V. LOOK-AHEAD FUZZY LOGIC CONTROLLER

This section presents the proposed control strategy and the fuzzy controller, whose rules are based on the empirical knowledge of the expert, which is developed in this study. The main objectives of the controller are to manage the energy flow between ICE and EM, control the transmission ratio, adjust the optimal speed and sustain the battery state of charge (SOC) at an optimal level. The advantage of this system is its robustness, since it is tolerant to imprecise measurements and component variations. The fuzzy rules can be easily tuned, if required, therefore adaptation is an additional benefit of this controller. The main idea behind the fuzzy-logic controller is to employ logic-based control strategy. The look-ahead control is a strategy that relies on logical reasoning of how the vehicle should behave in certain circumstances.

In this paper, it is assumed that the environment is represented by the road slope. The longitudinal forces on a vehicle, "(1)" is associated with road slopes. Since the required propulsive energy is provided by ICE, EM or both using the road slope, making intelligent decisions can improve the fuel economy.

The operation of the modeled PHEV based on the controller commands can be electric only, engine traction, hybrid propulsion, regenerative braking and battery charging using the energy due to gravity. The controller acts such that the required torque is always met. Control in HEVs can be divided in two levels: coordinate control and components control. The coordinate controller (CC) is at the higher level and should mange the lower level controllers such as ICE controllers, EM controller, speed controller, mechanical brake controller and battery SOC controller. The inputs to CC are the demand torque, the difference between the existing slope and the future slope, SOC, the engine speed, the motor speed, and the resistive force.

From the stand point of the control problem, it is desired to find such control outputs that optimize the fuel consumption. In the proposed CC, there are inputs such as future slope, vehicle speed, demand torque, SOC, rotational speed and resistive force. From the expert knowledge, it is known that fuel saving can be made during uphill or downhill. During moderate uphill travel, vehicle loses speed and engine works in its inefficient region. During downhill travel because of the gravity, the acceleration of vehicle will increase. An expert driver will speed up before an uphill and slow down before a downhill drive. Therefore, driving can be classified into three main states: driving on level, uphill or downhill roads. This classification is not crisp (or precise) and can be best modeled using fuzzy logic. Therefore, the difference of current slope and the calculated one from the look-ahead slope estimator is considered as an input to CC. With respect to the engineering considerations of the road structure, and in order to generate the geographical fuzzy set of the road, the linguistic interpretation of slope is considered from a very high negative (-30%) to a very high positive (30%) slope. Based on the variation of this input, the controller output is the speed that manipulates the current speed with respect to the future slopes. The range of operation is from -10 to 10 km/h.

The design criteria for controlling the power split between ICE, EM and charging of battery is based on the efficiency maps. In other words, ICE and EM are confined to operate in the high efficiency area of the map. The inputs to the controller such as demand torque, shaft rotational speed and resistive force are converted to fuzzy values. These fuzzified inputs are demonstrated in Fig. 5. The fuzzy logic controller maps the inputs to the outputs with a set of logic rules. Fuzzy control rules are characterized as a collection of fuzzy IF-THEN rules whose conditions and consequences involve linguistic variables. The IF-part of the rules refers to attributes that express fuzzy set of the input variables. A particular input value, which belongs to this set to a certain degree, is demonstrated by the degree of membership. For instance, the membership functions that define the degree of membership of the speed are Pi functions. They determine the degree of memberships to the fuzzy set, from very low speed to very high speed. The defined membership functions for road slope are Gaussians which show the degree of membership to the fuzzy set from very steep down to very steep up. Fuzzy speed is considered from zero speed to very high speed (150 km/h). Taking into consideration the linguistic representation of all of the numerical inputs, the fuzzifications which have been done are illustrated in Fig. 5.

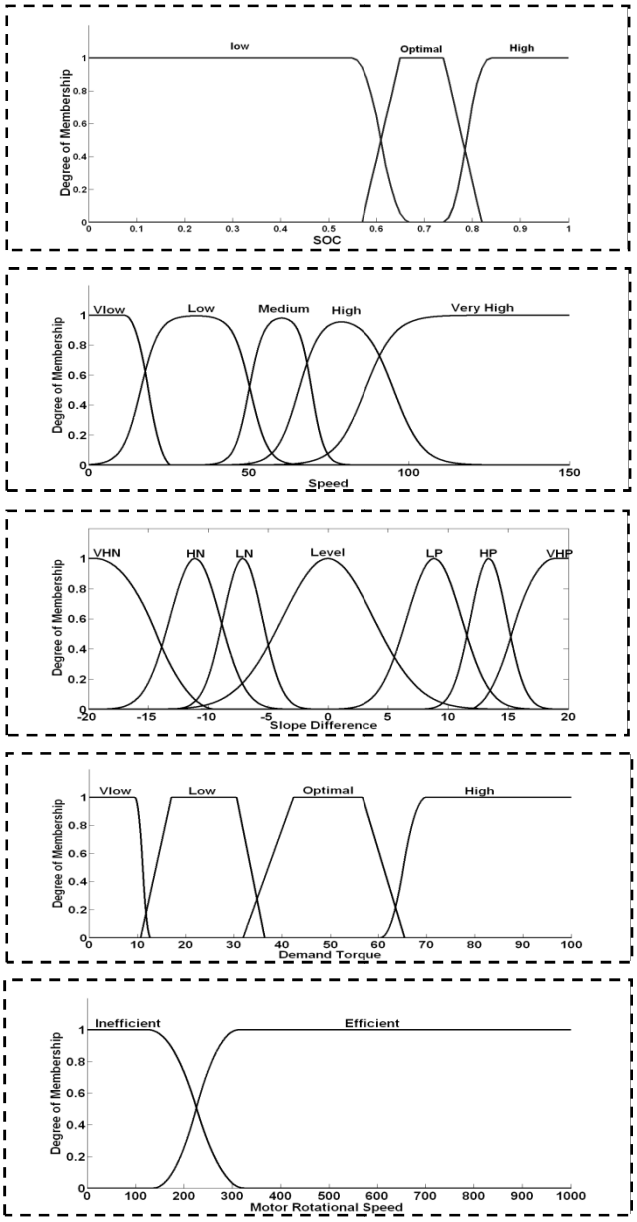

Figure 5. Input membership functions.

The THEN-part of the rules of the controller refers to the values of the output variable. To achieve the output of the controller, the degrees of membership of the IF-parts of rules are evaluated, and the THEN-parts of the rules are weighted by these degrees of membership. For example, in the membership functions that define this degree of membership for the input speed are Pi functions which establish the degree of membership to the fuzzy set, from very high shift to low shift. We implemented the most frequently used method generally known as the Mamdani's minimum operation [15]. In this

method, if the inputs are fuzzy singletons, A'=u0 and B'=v0, then the results C' can be obtained from the following relation:

$$\mu_{C'}(w) = \bigvee_{i=1}^{n}[\mu_{A_i}(u_0) \wedge \mu_{B_i}(v_0)] \wedge \mu_{C_i}(w) \quad (14)$$

In order to obtain a crisp control output from an inferred fuzzy inference engine, the most common method called the centroid area is used:

$$Z_{COA} = \frac{\int_z \mu_C(z) Z dz}{\int_z \mu_C(z) dz} \quad (15)$$

where Z is the output from the given inputs and their fuzzy relation, and μC(Z) is the aggregated output membership function. For instance, the crisp output of the fuzzy controller to the adaptive cruise controller increases the vehicle speed before an uphill or decreases it before a downhill. The extended or diminished speed is proportional to the fuzzified angle of slope.

For the engine considered in this model, from the ICE efficiency map, the optimal operation of engine occurs from the rotational speed of 250 rad/sec to 400 rad/sec and torque of 45 Nm to 60 Nm. Maintaining the crankshaft rotational speed in the efficient section can be achieved by the gear ratio transmission which is controlled by the controller according to the fuzzified vehicle speed. EM can be used as a load regulator to sustain ICE in the efficient torque area. Since there are two stages in the energy conversion, EM should be controlled to operate in the efficient speed range. This mater has been considered in the control strategy so far. When we are using the regenerative braking, or the energy from the gravitational force, SOC is the only parameter which is considered. During battery's charging and discharging, the efficiency of the battery can be defined as:

$$\eta_{discharge} = \frac{V}{V_o} \quad (16)$$

$$\eta_{charge} = \frac{V_o}{V} \quad (17)$$

where V is the cell operating voltage, and Vo is the thermodynamic voltage. In the discharging mode, a higher efficiency is obtained in high SOC, and in the charging mode, a higher efficiency is obtained in lower SOC. Enhancing net cycle efficiency and considering the state of health of battery, the fuzzy controller controls the battery in its middle SOC range of 0.6 - 0.8.

Beside the shift ratio and adaptive speed, the engine torque is the other output of the fuzzy controller. The membership functions of the fuzzy outputs are shown in Fig. 6.

If the vehicle speed is very low, or the demand torque is very low, SOC will be examined. If SOC is in its normal condition, the vehicle will work in electric only mode. The negative resistive force and brake will also be examined, and with the condition of SOC less than 0.8, the battery will be charged. Because of the certainty in these situations, regenerative braking and electric only mode of operation of the HEV have been controlled with crisp rules. For the other states of the fuzzy controller outputs, the engine is maintained in its optimal operation mode. Correspondingly, the fuzzy controller rules are performed. For instance, when SOC is not high and the demand torque is low and the motor rotational speed is efficient, the engine is controlled to deliver optimal torque, EM will be controlled to work in the generator mode, and the difference between the engine torque and the demand torque will be used in the generator to produce electrical energy. The produced electrical energy will be stored in the battery.

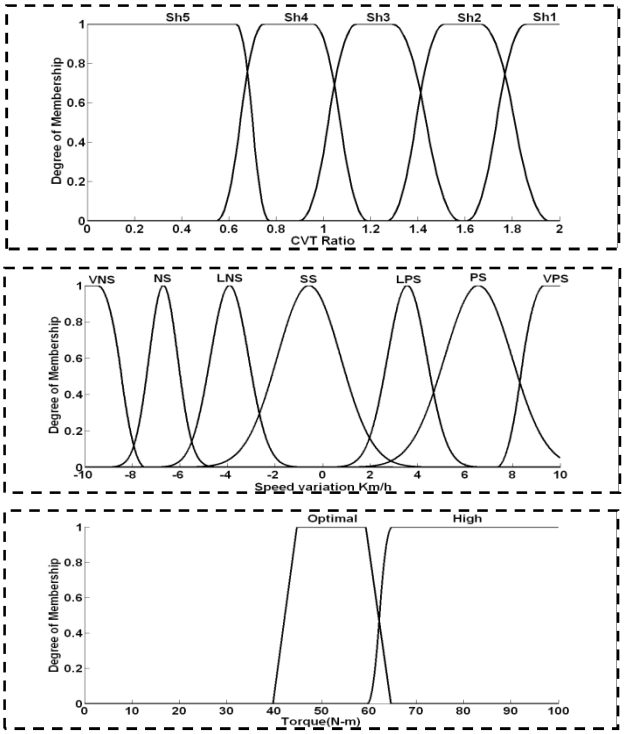

Figure 6. Output membership functions.

VI. SIMULATION AND RESULTS

The described controller and the PHEV are modeled in SIMULINK. The recommended Highway Fuel Economy Driving Schedule (HFEDS) by SAE J1711 standard [16] and real road data are applied to evaluate the proposed model.

To present the simulation results, the information of a highway, 50km of Nowra-Bateman Bay in Australia, is implemented in the model. The Cartesian coordinate's of the data is presented in Table II.

TABLE II. REAL CARTESIAN COORDINATES FOR NOVARA TO BATMAN BAY, AUSTRALIA

Road location	DIST D(km)	EAST X(km)	NORTH Y(km)	ALT Z(km)
R[1,10,C1,0.009]	0.0085	9687.63	4421.904	0.0155
R[1,10,C1,0.019]	0.0188	9687.599	4421.895	0.0158
R[1,10,C1,0.029]	0.0291	9687.596	4421.885	0.0162
R[1,10,C1,0.039]	0.0386	9687.592	4421.876	0.0164

Accordingly, the slope is calculated based on the rate of change in altitudes of distances. The graph of the used slope data is demonstrated in Fig. 7.

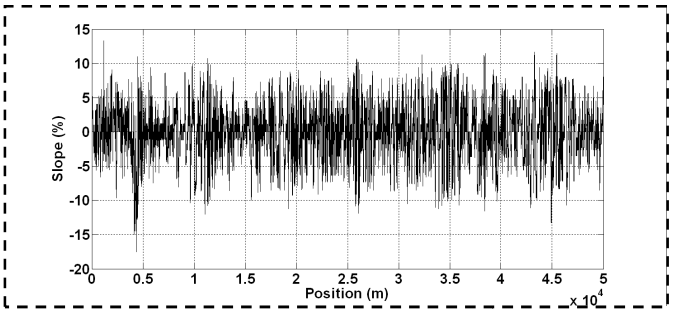

Figure 7. Slope of highway.

The use of real road data in the model distinguishes this approach from the former ones which use only the drive cycle and a constant grade. In order to evaluate the model and its fuzzy controller, simulation is run through the highway fuel economy test (HWFET). Three circumstances are considered: look-ahead information and adaptation the speed based on the future slope on the applied drive cycle, fuzzy controller with the applied drive cycle, and the default control strategy in PSAT [17]. As can be seen from the operating points of the engine on the efficiency map, which are presented in Fig. 8 for the first controller, the operation points are more controlled in the efficient area than the second and the third controllers. It means that the fuzzy controller with adaptive cruise control leads a better fuel consumption than the other controllers. Define abbreviations and acronyms the first time they are used in the text, even after they have been defined in the abstract. Abbreviations such as IEEE, SI, MKS, CGS, sc, dc, and rms do not have to be defined. Do not use abbreviations in the title or heads unless they are unavoidable.

The results of the proposed controller in comparison with the other controllers, from the standpoint of fuel economy are summarised in the Table III.

VII. CONCLUSIONS

This paper presented an approach for PHEV modelling based on the real road geographical data. From the model, the dynamic position of vehicle is achievable. The applied method uses a combination of the calculated data (distance, altitude and slope) and the static information from GIS. Instantly, the calculated data is compared with the road geographical information (length and altitude). The instantaneous position and slope are extracted. The new information is applied to determine various longitudinal forces, rolling resistance, gravitational and aerodynamic drags. The future states for a look-ahead window are extracted. Accordingly, a moving average calculator is implemented to estimate the future slopes. The deference between future and instant slopes is expressed as a fuzzy value which is applied to a fuzzy controller. The control output from the fuzzy inference engine is the amount of speed change with respect to the alteration of slope ahead. The control output is added to the reference speed which is the HWEFT drive cycle.

Considering the optimal operation of ICE, EM and SOC of battery, the fuzzy controller commands PHEV to achieve optimal fuel consumption. Simulations were carried out. The results show that good improvements on fuel consumption (6%) in comparison with the PSAT default controller. The comparison has been done with the fuzzy controller without look-ahead information, where fuel saving of 2.62% was recorded.

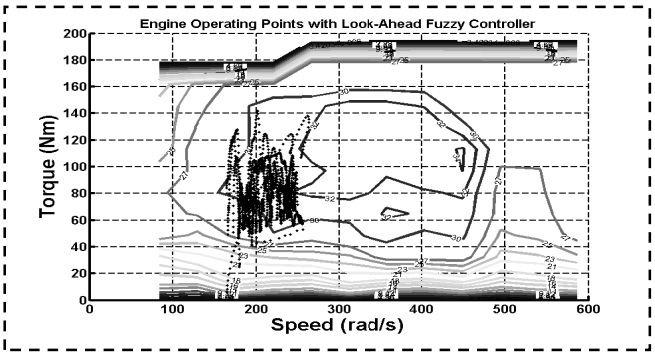

(a)

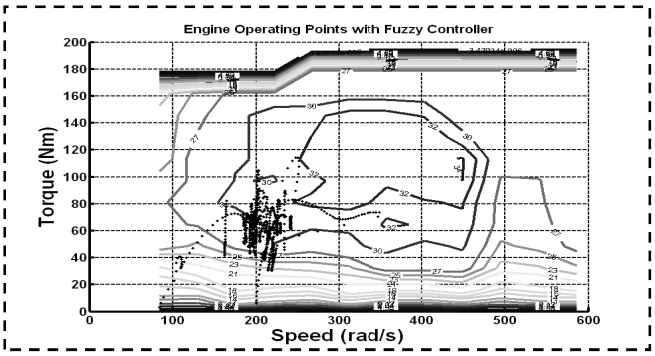

(b)

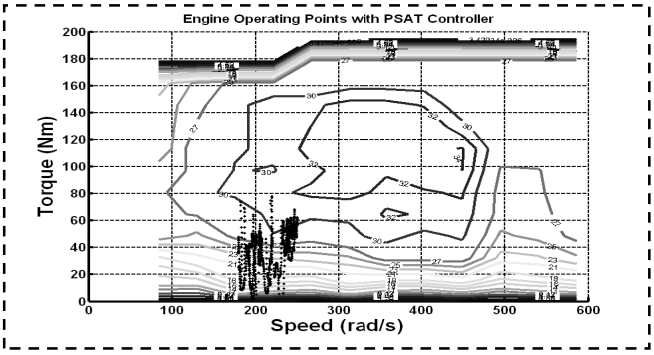

(c)

Figure 8. Engine operation points on the efficiency map. (a) Look-ahead fuzzy controller. (b) Fuzzy controller. (c) PSAT default controller.

TABLE IIII. FUEL CONSUMPTION FOR THREE SIMULATION MODE

The simulated model with HWFET drive cycle	FC (lit/100km)
PHEV with look-ahead fuzzy controller and real road data	4.83
PHEV with fuzzy controller and real road data	4.96
PHEV in PSAT with its default control strategy	5.14

ACKNOWLEDGMENT

The authors would like to thank AUTOCRC and Commonwealth of Australia which provide financial support for this research.

REFERENCES

[1] L. Hirch, H. Bezdek, and M. Wendling. "Peaking Oil Production: Sooner Rather Than Later?" Accessible on: http://www.issues.org/21.3/hirsch.html.

[2] A. Fuhs, "Hybrid vehicles and the future of personal transportation," CRC Press.

[3] M. R. Cuddy, and K. B. Wipke, "Analysis of the fuel economy benefit of drivetrain hybridization," SAE Special Publications, vol. 1243, pp. 101-111, 1997.

[4] M. J. Riezenman, "Engineering the EV future," IEEE Spectrum, vol. 35, no. 11, pp. 18-20, 1998.

[5] V. Wouk, "Hybrids: then and now," IEEE Spectrum, vol. 32, no. 7, pp. 16-21, 1995.

[6] G. C. Hochgraf, J. M. Ryan, and L. H. Wiegman, "Engine Control Strategy for a Series Hybrid Electric Vehicle Incorporating Load-Leveling and Computer Controlled Energy Management," SAE International, February 1996.

[7] N. Jalil, N. A. Kheir, and M. Salman, "Rule-based energy management strategy for a series hybrid vehicle," Proceedings of the 1997 American Control Conference. Part 3 (of 6). pp. 689-693.

[8] N. J. Schouten, M. A. Salman, and N. A. Kheir, "Energy management strategies for parallel hybrid vehicles using fuzzy logic," Control Engineering Practice, vol. 11, no. 2, pp. 171-177, 2003.

[9] Ulf Bossel:, " Well-to-Wheel Studies, Heating Values, and the Energy Conservation Principle," Proceedings of Fuel Cell Forum, Feb. 2003.

[10] P. Singh, and A. Nallanchakravarthula, "Fuzzy logic modeling of Unmanned Surface Vehicle (USV) hybrid power system." pp. 261-267.

[11] R. A. Jackey, "A Simple, Effective Lead-Acid Battery Modeling Process for Electrical System Component Selection," SAE Transaction, vol. 116, pp. 219-227, 2007.

[12] D. W. Gao, C. Mi, and A. Emadi, "Modeling and simulation of electric and hybrid vehicles," Proceedings of the IEEE, vol. 95, no. 4, pp. 729-745, 2007.

[13] S. Moon, I. Moon, and K. Yi, "Design, tuning, and evaluation of a full-range adaptive cruise control system with collision avoidance," Control Engineering Practice, vol. 17, no. 4, pp. 442-455, 2009.

[14] B. Ganji, and A. Z. Kuzani, "A Powertrain Vehicle Model for Look-ahead Control " International Review on Modelling and Simulation, vol. 3, no. 5, October 2010.

[15] E. H. Mamdani, and S. Assilian, "An experiment in linguistic synthesis with a fuzzy logic controller," International Journal of Man-Machine Studies, vol. Vol. 7, No. 1, pp. 1-13, 1975.

[16] S. J1711, "Recommended Practice for Measuring the Exhaust Emissions and Fuel Economy of Hybrid-Electric Vehicles, Including Plug-in Hybrid Vehicles," SAE, 2010.

[17] "PSAT Vehivle Simulation Software," Information accesible on: http://www.transportation.anl.gov/software/PSAT/.

2011 IEEE International Conference on Fuzzy Systems
June 27-30, 2011, Taipei, Taiwan

Dynamic Window with Fuzzy Controller in Wireless Sensor Networks for Elliptic Curve Cryptography

Xu Huang
Faculty of Information Sciences and Engineering,
University of Canberra, 2601, Australia
Xu.Huang@canberra.edu.au

Dharmendra Sharma
Faculty of Information Sciences and Engineering,
University of Canberra, 2601, Australia
Dharmendra.Sharma@canberra.edu.au

Pritam Gajkumar Shah
Faculty of Information Sciences and Engineering,
University of Canberra, 2601, Australia
Pritam.Shah@canberra.edu.au

***Abstract*—Elliptic curve cryptosystem (ECC) was proposed by Miller [10] and Koblitz [9] which relies on the difficulty of elliptic curve discrete logarithmic problem (ECDLP). It is gaining wide acceptance as an alternative to the conventional public key cryptosystem such as RSA [24], DSA [25], DH [26]. Also it is noted that the wireless sensor networks (WSN) based on the rapid progress of wireless communications and embedded micro electro mechanical systems technologies are becoming important part in our daily life. The security of the WSN becomes one of the major concerns in its applications. Even ECC prominently offers great potential benefits for WSN security there is still a lot of work needs to be done due to WSN has very restraint running conditions such as limited energy source, capability of computing, etc. It is well known that scalar multiplication operation in ECC accounts for about 80% of key calculation time on wireless sensor network motes. In this paper we present an optimized dynamic window based on our previous research works. The whole quality of service (QoS) has been improved under this algorism in particularly the power consuming is more efficiently. The simulation results showed that the average calculation time, due to fuzzy conditions decreased from previous 26 to current 9 as a whole the calculation time, decreased by approximately 18% in comparison to our previous algorithms in an ECC wireless sensor network [23].**

Keywords-Elliptic curve cryptography (ECC), scalar multiplication, non-adjacent form, slide window, fuzzy control

I. INTRODUCTION

The high demand for various applications shows the fact that the rapid progress of wireless sensor networks has become popular in our daily life. With the growth in very large scale integrated (VLSI) technology, embedded systems and micro electro mechanical systems (MEMS) has enabled production of inexpensive sensor nodes, which can transmit data over a distances with free media and efficient use of power [1, 22, 23]. In the WSN systems, the sensor node will detect the interested information, processes it with the help of an in-built microcontroller and communicates results to a sink or base station. Normally the base station is a more powerful node, which can be linked to a central station via satellite or internet communication to form a network. There are many deployments for wireless sensor networks depending on various applications such as environmental monitoring e.g. volcano detection [2,3], distributed control systems [4], agricultural and farm management [5], detection of radioactive sources [6], and computing platform for tomorrows' internet [7]. Generally speaking, a typical WSN architecture can be shown in Figure 1.

Contrast to traditional networks, a wireless sensor network normally has many resource constraints [4] due to the limited size. As an example, the MICA2 mote consists of an 8 bit ATMega 128L microcontroller working on 7.3 MHz. As a result nodes of WSN have limited computational power. Radio transceiver of MICA motes can normally achieve maximum data rate of 250 Kbits/s, which restricts available communication resources. The flash memory that is available on the MICA mote is only 512 Kbyte. Apart from these limitations, the on board battery is 3.3.V with 2A-Hr capacity. Therefore, the above restrictions with the current state of art protocols and algorithms are expensive for sensor networks due to their high communication overhead.

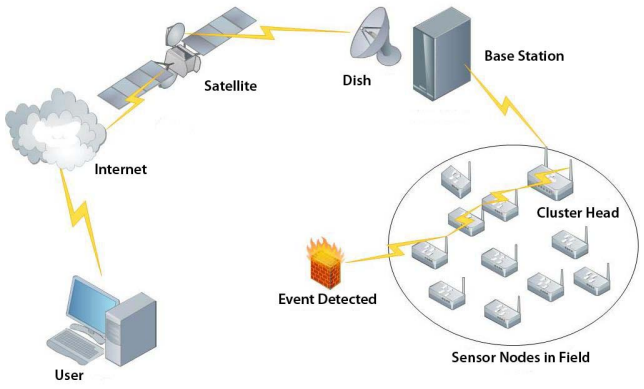

Figure 1: A Typical WSN architecture

Recalled that the Elliptic Curve Cryptography was first introduced by Neal Koblitz [9] and Victor Miller [10] independently in the early eighties. The advantage of ECC over other public key cryptography techniques such as RSA, Diffie-Hellman is that the best known algorithm for solving elliptic curve discrete logarithm problem (ECDLP) which is the underlying hard mathematical problem in ECC which will take the fully exponential time. On the other hand the best algorithm for solving RSA and Diffie-Hellman takes sub exponential time [11]. ECC offers the same level of security with smaller key size and it leads to the better performance in limited environments like cellular phones, PDA, sensor networking, etc. For example, ECC with a key size of 160 bits provides the same level of security as RSA [24], DSA [25] and DH [26] with a key size of 1024 bits. In summary, the ECC problem can only be solved in exponential time and, to date, there is a lack of sub exponential methods to attack ECC.

An elliptic curve E over $GF(p)$ can be defined by

$$y^2 = x^3 + ax + b$$

where $a, b \in GF(p)$ and

$$4a^3 + 27b^2 \neq 0$$

in the $GF(p)$.

The point (x, y) on the curve satisfies the above equation and the point at infinity denoted by ∞ is said to be on the curve.

If there are two points on the curve namely, $P(x_1, y_1)$, $Q(x_2, y_2)$ and their sum is given by point $R(x_3, y_3)$ the algebraic formulas for point addition and point doubling are given by following equations:

We have:

$$x_3 = \lambda^2 - x_1 - x_2$$

$$y_3 = \lambda(x_1 - x_3) - y_1$$

$$\lambda = \frac{y_2 - y_1}{x_2 - x_1}, \quad \text{if } P \neq Q$$

$$\lambda = \frac{3x^2 + a}{2y_1}, \quad \text{if } P = Q$$

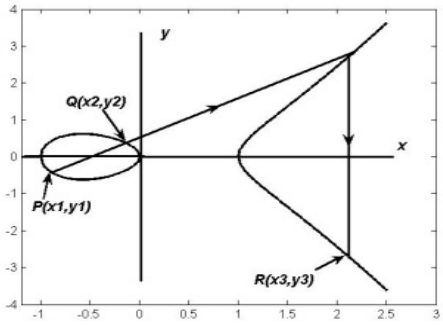

(a) Addition: $P + Q = R$

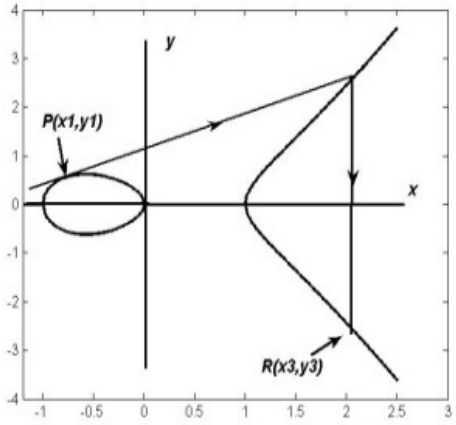

(b) Doubling: $P+P = R$

Figure 2: Point addition and point doubling on elliptic curve.

Here, the addition, subtraction, multiplication and inverse are the arithmetic operations over $GF(p)$, which can be shown in Figure 2.

II. Elliptic Curve Diffie-Hellman Scheme Proposed for WSN

Before we get into our innovation method, we need to have a closer look at the popular legacy scheme for WSN. As per [13] the original Diffie-Hellman algorithm with RSA requires a key of 1024 bits to achieve sufficient security but *Diffie Hellman based on ECC* can achieve the same security level with only 160 bit key size.

The classical Elliptic Curve Diffie Hellman scheme operates as shown in the Figure 3.

Initially Alice and Bob agree on a particular curve with base point P. They generate their public keys by multiplying P with their private keys namely K_A and K_B. After sharing public keys, they generate a shared secret key by multiplying public keys by their private keys. The secret key is $R = K_A * Q_A = K_B * Q_B$. With the known values of Q_A, Q_B and P, it is computationally intractable for an eavesdropper to calculate K_A and K_B which are the private keys of Alice and Bob. As a result, adversaries cannot calculate R the shared secret key.

In ECC, two heavily used operations are involved: scalar multiplication and modular reduction. Gura *et. al.* [14] showed that 85% of execution time is spent on scalar multiplication. Scalar Multiplication is the operation of multiplying point P on an elliptic curve E defined over a field $GF(p)$ with positive integer k which involves point addition and point doubling. Operational efficiency of kP is affected by the type of coordinate system used for point P on the elliptic curve and the algorithm used for recoding of integer k in scalar multiplication.

This research paper proposes an innovative algorithm based on one's complement for representation of integer k which

accelerates the computation of scalar multiplication in wireless sensor networks.

The number of point doubling and point addition operations in scalar multiplication depends on the recoding of integer *k*. Expressing integer *k* in binary format highlight this dependency.

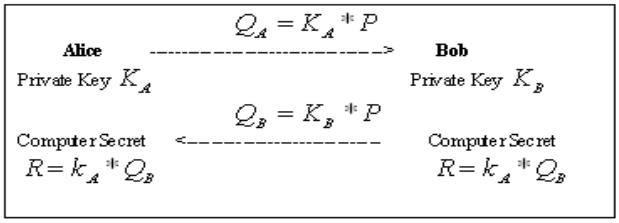

Figure 3: Diffie-Hellman protocol based on ECC

The number of zeros and number of ones in the binary form, their places and the total number of bits will affect the computational cost of scalar multiplications. The Hamming weight as represented by the number of non-zero elements, determines the number of point additions and bit length of integer *K* determines the number of point doublings operations in scalar multiplication.

One point addition when $P \neq Q$ requires one field inversion and three field multiplications [13]. Squaring is counted as regular multiplication. This cost is denoted by $1I + 3M$, where *I* denotes the cost of inversion and *M* denotes the cost of multiplication.

One point doubling when $P = Q$ requires $1I + 4M$ as we can neglect the cost of field additions as well as the cost of multiplications by small constant 2 and 3 in the above formulae.

Binary Method

Scalar multiplication is the computation of the form $Q = kP$, where *P* and *Q* are the elliptic curve points and *k* is positive integer. This is obtained by repeated elliptic curve point addition and doubling operations. In binary method the integer *k* is represented in binary form:

$$k = \sum_{j=0}^{l-1} K_j 2^j, \; K_j \in \{0,1\}$$

The binary method scans the bits of *K* either from left-to-right or right-to-left. The binary method for the computation of *kP* is given in the following *algorithm 1*, as shown below:

The cost of multiplication when using binary method depends on the number of non-zero elements and the length of the binary representation of *k*. If the representation has $k_{l-1} \neq 0$ then binary method require $(l - 1)$ point doublings and $(W-1)$ where *l* is the length of the binary expansion of *k*, and *W* is the Hamming weight of *k* (i.e., the number of non-zero elements in expansion of *k*). For example, if $k = 629 = (1001110101)_2$, it will require $(W-1) = 6 - 1 = 5$ point additions and $l - 1 = 10 - 1 = 9$ point doublings operations.

Algorithm 1: Left to right binary method for point multiplication

Input: A point $P \in E(F_q)$, an

$$k = \sum_{j=o}^{l-1} K_j 2^j, \;\; K_j \in \{0,1\}$$

l bits integer

Output: $Q = kP$

1. $Q \leftarrow \infty$
2. For $j = l$ □ 1 to 0 do:
   2.1 $Q \leftarrow 2Q$,
   2.2 if $k_j = 1$ the $Q \leftarrow Q + P$.
3. Return Q.

Signed Digit Representation Method

The subtraction has virtually the same cost as addition in the elliptic curve group. The negative of point (x, y) is $(x, -y)$ for odd characters. This leads to scalar multiplication methods based on addition–subtraction chains, which help to reduce the number of curve operations. When integer *k* is represented with the following form, it is a *binary signed digit representation*.

$$k = \sum_{j=0}^{l} S_j 2^j, \;\; S_j \in \{1,0,-1\}$$

When a signed-digit representation has no adjacent non zero digits, i.e. $S_j S_{j+1} = 0$ for all $j \geq 0$ it is called a non-adjacent form (NAF).

The following *algorithm 2* computes the NAF of a positive integer given in binary representation.

Algorithm 2: Conversion from Binary to NAF

$$k = \sum_{j=0}^{l-1} K_j 2^j, \; K_j \in \{0,1\}$$

Input: An integer

$$k = \sum_{j=0}^{l} S_j 2^j, \;\; S_j \in \{1,0,-1\}$$

Output: NAF

1. $C_0 \leftarrow 0$
2. *For j = 0 to l do:*
3. $C_{j+1} \leftarrow [(K_j + K_{j+1} + C_j)/2]$
4. $S_j \leftarrow K_j + C_j - 2C_{j+1}$
5. *Return* $(S_l \ldots S_0)$

NAF usually has fewer non-zero digits than binary representations. The average hamming weight for NAF form is $(n-1)/3.0$. So generally it requires $(n-1)$ point doublings and $(n-1)/3.0$ point additions. The binary method can be revised accordingly and is given another algorithm for NAF, and this modified method is called the *Addition Subtraction* method.

III. FUZZY CONTROLLER FOR DYNAMITIC WINDOW IN ECC- PROPOSED ALGORITHM BASED

We are going to use the algorithm, based on *subtraction by utilization of the 1's* complement, is most common in binary arithmetic. The 1's complement of any binary number may be found by the following equation [19-22]:

$$C_1 = (2^a - 1) - N \quad (1)$$

where C_1 = 1's complement of the binary number, a = number of bits in N in terms of binary form, N = binary number.

From a closer observation of the equation (1), it reveals that any positive integer can be represented by using minimal non-zero bits in its 1's complement form provided that it has a minimum of 50% Hamming weight. The minimal non-zero bits in positive integer scalar are very important to reduce the number of intermediate operations of multiplication, squaring and inverse calculations used in elliptical curve cryptography as we have seen in previous sections.

The equation (1) can therefore be modified as per below:

$$N = (2^a - C_1 - 1) \quad (2)$$

For example, we may take N =1788 then it appears

N= $(11011111100)_2$ in its binary form

C_1= 1's Complement of the number of N= $(00100000011)_2$

a is in binary form so we have a = 11

After putting all the above values in the equation (2) we have:

$1788 = 2^{11} - 00100000011 - 1$, this can be reduced as below:

$$1788 = 100000000000 - 00100000011 - 1 \quad (3)$$

So we have

$1788 = 2048 - 256 - 2 - 1 - 1$

As is evident from equation (3), the Hamming weight of scalar N has reduced from 8 to 5 which will save 3 elliptic curve addition operations.

The above recoding method based on one's complement subtraction combined with sliding window method provides a more optimized result.

Let us compute [763] P (in other words k = 763) as an example, with a *sliding window algorithm* with K recoded in binary form and window sizes ranging from 2 to 10. It is observed that as the window size increases the number of pre-computations also increases geometrically. At the same time number of additions and doubling operations decrease.

Now we present the details for the different window size to find out the optimal window size using the following example:

Window Size w = 2

$763 = (1011111011)_2$

No of pre-computations = $2^w - 1 = 2^2 - 1 = [3]\ P$

763 = 10 11 11 10 11

The intermediate values of Q are

P, 2P 4P, 8P, 11P, 22P, 44P, 47P, 94P, 95P, 190P, 380P, 760P, 763P

Computational cost = 9 doublings, 4 additions, and 1 pre-computation.

Window Size w = 3

No of pre-computations = $2^w - 1 = 2^3 - 1 = [7]\ P$

So all odd values: [3]P, [5]P, [7]P

763 = 101 111 101 1

= [5]P [7]P [5]P [1]P

The intermediate values of Q are

5P, 10P, 20P, 40P, 47P, 94P, 188P, 376P, 381P, 762P, 763P

Computational cost = 7 doublings, 3 additions, and 3 pre-computations.

We continue to derive the remaining calculations for Window Size w = 6, Window Size w = 7, Window Size w = 8, Window Size w = 9, and Window Size w = 10. The results for all calculations are presented in Table 1.

Table 1: WINDOW SIZE VS NO OF DOUBLINGS, ADDITIONS AND PRE COMPUTATIONS

Window Size	No of Doublings	No of Additions	No of Pre computations
2	9	4	1
3	7	3	3
4	6	2	7
5	5	1	15
6	4	1	31
7	3	1	61
8	3	1	127
9	1	1	251
10	0	0	501

It is interesting to have some information from Figure 4, which shows the charts obtained from table 1 (in order to see the relation clearly, we used so-called amplified chart because of the range is only limited 0 to 10 in window size).

As we are interested in the further details about the relations between "Doubling" and "Addition", from Figure 4 it clearly shows that the "Pre-computation" and "doubling" are the dominated factors hence we need to focus on this factor in our future discussion for the window size.

Algorithm for sliding window scalar multiplication on elliptic curves.

1. $Q \leftarrow P_{\infty}$ *and* i $\leftarrow l$ - 1
2. while i $\geq$ 0 do
3. if $n_i = 0$ then Q $\leftarrow$ [2]Q and i $\leftarrow$ i - 1
4. else
5. s $\leftarrow \max(i - k + 1, 0)$
6. *while* $n_s = 0$ do s $\leftarrow$ s + 1
7. for h = 1 to i - s + 1 do Q $\leftarrow$ [2]Q
8. u $\leftarrow (n_i \ldots\ldots n_s)_2$ [$n_i = n_s = 1$ and i - s + 1 $\leq$ k]
9. Q $\leftarrow$ Q $\oplus$ [u]P [u is odd so that [u]P is precompute d]
10. i $\leftarrow$ s - 1
11. return Q

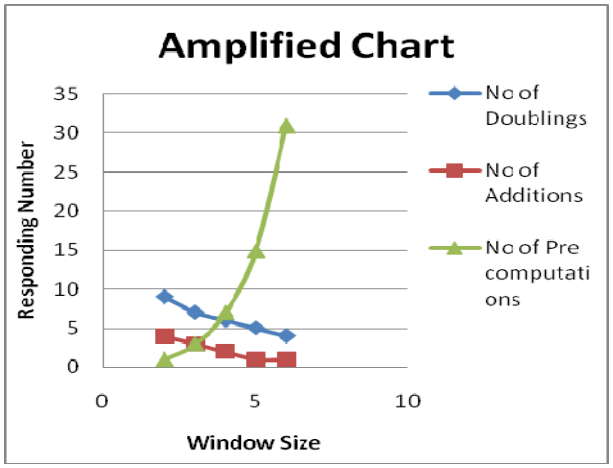

Fig. 4: amplified chart (focus on limited range) for the Table 1

IV. FUZZY CONTROLLER SYSTEM IN ECC

It is clear, from above description, that there is a tradeoff between the computational cost and the window size as shown in Table 1. However, this tradeoff is underpinned by the balance between computing cost (or the RAM cost) and the pre-computing (or the ROM cost) of the node in the network.

It is obviously to observe that the variety of wireless network working states will make this control complex and calculations could be relatively more expensive.

Therefore, we propose a fuzzy dynamic control system, to provide dynamic control to ensure the optimum window size is obtained by tradeoff between pre-computation and computation cost.

The fuzzy decision problem introduced by Bellman and Zadeh has as a goal the maximization of the minimum value of the membership functions of the objectives to be optimized.

Accordingly, the fuzzy optimization model can be represented as a multi-objective programming problem as follows [21]:

$$Max : \min\{\mu_s(D)\} \,\&\, \min\{\mu_l(U_l)\} \quad \forall s \in S \,\&\, \forall l \in L$$

$$\text{such that} \quad A_l \le C_l \qquad \forall l \in L,$$

$$\sum_{r \in R_p} x_{rs} = 1 \qquad \forall p \in P \,\&\, \forall s \in S,$$

$$x_{rs} = 0 \text{ or } 1 \qquad \forall r \in R \,\&\, \forall s \in S$$

In above equation, the objective is to maximize the minimum membership function of all delays, denoted by D, and the difference between the recommend value and the measured value, denoted by U.

The Fuzzy control system is extended from our previous design and shown in Figure 5. For the accurate control, we designed a three inputs fuzzy controller. The first input is *storage room*, which has three statuses, showing storage room in one of the three, namely (a) low, (b) average, and (c) high. The second input is pre-computing working load (*PreComputing*) in one of three states, namely (a) low, (b) average, and (c) high. The third input is *Doubling*, expressing how much working load for the calculation "doubling" which has three cases, namely (a) low, (b) average, and (c) high. The output is one, called *WindowSize,* to express the next window size should be moved in which way, which has three states for the window sizes, namely (a) down, (b) stay, and (c) up.

There are 26 *Fuzzy Rules* listed as shown in Table 2 (weights are unit). Note: H=high; A=average; L= low; U=up; S= stay; D1= down.

TABLE 2 26 Fuzzy rules for Figure 1

StorgeRoom	PreComputing	Doubling	WindSize
L	L	L	U
L	L	A	U
L	L	H	S
L	A	L	U
L	A	A	U
L	A	H	S
L	H	L	U
L	H	A	S
L	H	H	S
A	L	L	U
A	L	A	U
A	L	H	S
A	A	L	U
A	A	A	S
A	A	H	D1
A	H	A	S
A	H	H	S
H	L	L	S
H	L	A	S
H	L	H	D1
H	A	L	S
H	A	A	S
H	A	H	D1
H	H	L	D1
H	H	A	D1
H	H	H	D1

It is noted that above 26 fuzzy rules did work in our previous designed system, but it is noted that there are only 9 *Fuzzy Rules* listed in above table will be dominated the whole fuzzy control procedure (if we still keep the weights are unit) due to the fact that *StorageRoom* in Figure 5 can be ignored because of that the results shown in Figure 4 even it is a factor (with little impact on the outcome of this fuzzy system) needs to be appeared in this control system.

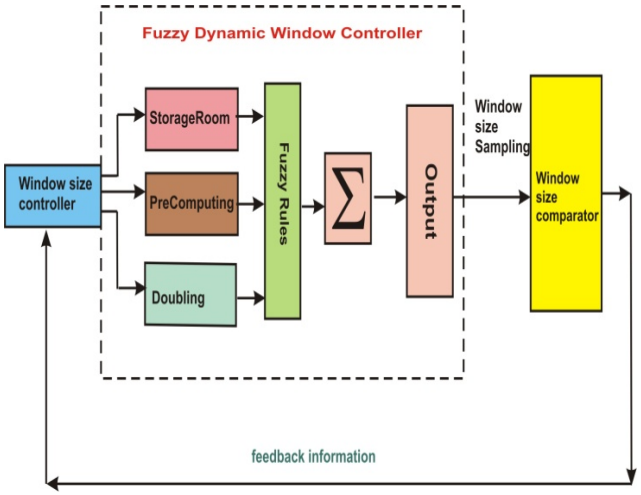

Figure 5: Three inputs fuzzy window control system

Therefore, the above 26 fuzzy rules become the major 9 fuzzy rules, which will decrease the system latency and improve the quality of service (QoS). The 9 fuzzy rules can be described as below:

1. If 1·(PreComputing is low) and 1·(Doubling is low) then 1·(WindowSize is Up)
2. If 1·(PreComputing is low) and 1·(Doubling is average) then 1· (WindowSize is Up)
3. If 1·(PreComputing is low) and 1·(Doubling is high) then 1· (WindowSize is stay)
4. If 1·(PreComputing is average) and 1·(Doubling is low) then 1· (WindowSize is Up)
5. If 1·(PreComputing is average) and 1·(Doubling is average) then 1· (WindowSize is Up)
6. If 1·(PreComputing is average) and 1·(Doubling is high) then (WindowSize is stay)
7. If 1·(PreComputing is high) and 1·(Doubling is low) then 1· (WindowSize is Up)
8. If 1·(PreComputing is high) and 1·(Doubling is average) then 1· (WindowSize is stay)
9. If 1·(PreComputing is high) and 1·(Doubling is high) then 1· (WindowSize is stay)

The number at each fuzzy condition being with a bracket is defined as "the weight number", currently it is unit. Later we shall change it with different weight according to the running situations as described in the next. The three inputs with 9 fuzzy rules in *Mamdani model* running fuzzy controller part. The three inputs are *StorageRoom*, *PreComputing* and *Doubling* as shown in Figure 6.

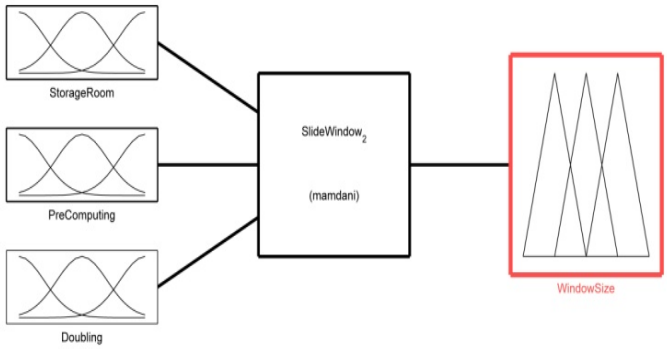

Figure 6: The block diagram of current fuzzy controller

As our target is to making window size at closer to or sitting on the optimum "window size," the output is taking *WindowSize*. It is noted that the "*StorageRoom*" has low, average, high with other two parameters's combinations.

The output with *StorageRoom* and *PreComputing* is shown in Figure 7. The surface *StorageRoom* vs. *Doubling* is shown in Figure 8.

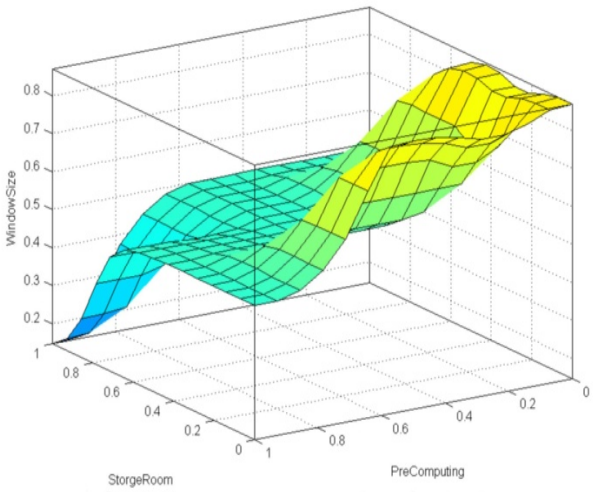

Figure 7: The output of the surface for the *StorageRoom* vs. *PreComputing*.

From above figures, it is clearly observed that in the low window size side, if the storage room is low the dominated function of "doubling" will play role as Figure 7 shown but if the window size is at the high side, the storage room will be fairly stay at the middle either for PreComputing or Doubling, which is the doubling will sharply increased when window size a little bit larger that also can be shown from Table 1.

From Figure 8 it is clearly to show when the storage room is getting big, it would be nice to have larger window size for the "doubling".

Now if we change the weight for above fuzzy rules as such the rules 1,5 10, 13, 14, 15, 16, 18, 20 ,21, 22, 23, 25, and 26 are set in 0.5 (the rest will keep the same) due to the major functions are controlled by the storage room, and doubling

will rapidly increasing by the window size larger. The outputs will changed as the average storage room will increased 0.04% and the other two inputs are decreased by 0.02% the output become window staying a little wider side by 0.003%.

It is clear that this fuzzy controller for the dynamic window is also involved a tradeoff between accuracy and control costs. For example the same system may go further for the second order parameters, i.e. not just check the changes about the input variables but also check the change tendencies of the variables, which will be discussed in another paper.

If we keep the *StorageRoom* constant, e.g. *StorageRoom* = 0.4, and the output of the "*PreComputing*" vs. "*Doubling*" is shown in Figure 9. Now in order to show the "StorageRoom" is not dominated factor as we discussed above, we took another value, "StorageRoom" = 0.8 and the output of the "*PreComputing*" vs. "*Doubling*" is shown in Figure 10.

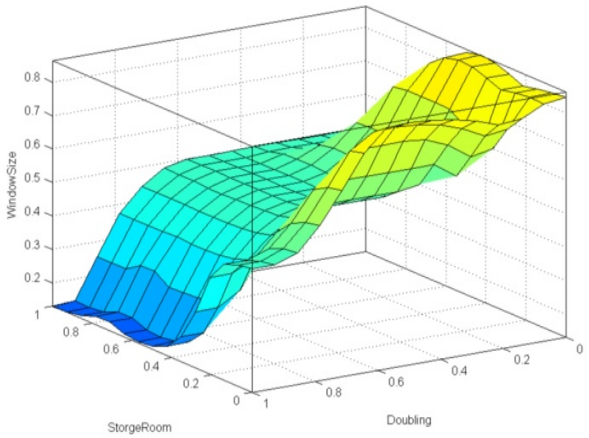

Figure 8: The output of the surface for the *StorageRoom* vs. *Doubling*.

It is observed that the output of the "*PreComputing*" vs. "*Doubling*" is not much difference between Figures 8 and 9.

From Figures 7 and 8 we can observe that the "dominated factor" is not the members of the "*StorageRoom*" in Figure 8 due to the fact that the *StorageRoom* goes to large than 40% (or 0.4) the factors *PreComputing* and *Doubling* are dominated in Figure 7 and Figure 8 separately.

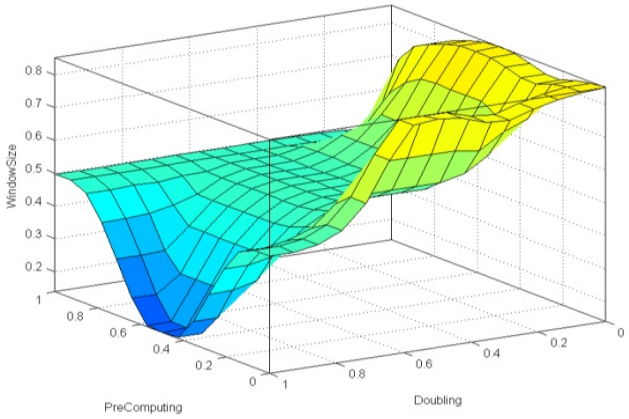

Figure 9: The output of the surface for the *StorageRoom* = constant (0.4) and *PrecComputing* vs. *Doubling*.

The *StorageRoom* cannot play a role in the process of the dynamic window, which is underpinned by the fact that has been shown in Figures 4. The simulations of the example described in above were implemented. Also it is noted that with equation (2), the computational cost has been reduced from 3 additions as in the binary method to only 1 addition in one's complement subtraction form. The number of pre-computations has remained the same.

In our simulations, the proposed method together with a fuzzy window size controller makes the ECC calculation in the current algorism is about 18% more efficient (in terms of average) than the methods in [23] with the same QoS level.

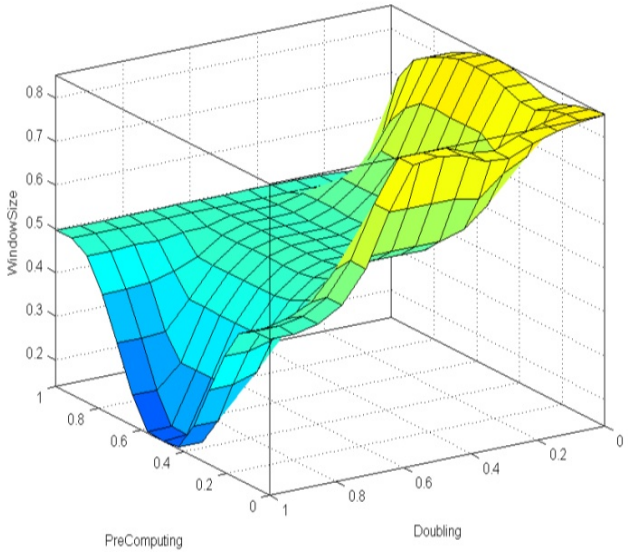

Figure 10: The output of the surface for the *StorageRoom* = constant (0.8) and *PreComputing* vs. *Doubling*.

V. CONCLUSION

In this paper, it has been investigated that the positive integer in point multiplication may be recorded with *one's complement subtraction* to reduce the computational cost involved in this heavy mathematical operation for wireless sensor network platforms. As the NAF method involves modular inversion operation to get the NAF of binary number, the one's complement subtraction can provide a very simple way of recoding the integer. There is always a decision between pre-computing and computing, the former is related to the storage and the latter is associated with computing capability and capacity. The window size may be the subject of trade-off between the available RAM and ROM at a particular instance on a sensor node, which can be controlled by fuzzy controller. The final simulation in a sensor wireless network shows that about 18% more efficient than our previous method [23] can be obtained with an ECC sensor network.

REFERENCES

[1] I. F. Akyildiz, W. Su, Y. Sankarasubramaniam, and E. Cayirci, "Wireless sensor networks: a survey," *Computer Networks,* vol. 38, pp. 393-422, 2002.

[2] C. Chung-Kuo, J. M. Overhage, and J. Huang, "An application of sensor networks for syndromic surveillance," 2005, pp. 191-196.

[3] G. Werner-Allen, K. Lorincz, M. Ruiz, O. Marcillo, J. Johnson, J. Lees, and M. Welsh, "Deploying a wireless sensor network on an active volcano," *IEEE Internet Computing,* vol. 10, pp. 18-25, 2006.

[4] B. Sinopoli, C. Sharp, L. Schenato, S. Schaffert, and S. S. Sastry, "Distributed control applications within sensor networks," *Proceedings of the IEEE,* vol. 91, pp. 1235-1246, 2003.

[5] P. Sikka, P. Corke, P. Valencia, C. Crossman, D. Swain, and G. Bishop-Hurley, "Wireless ad hoc sensor and actuator networks on the farm," 2006, pp. 492-499.

[6] D. L. Stephens, Jr. and A. J. Peurrung, "Detection of moving radioactive sources using sensor networks," *Nuclear Science, IEEE Transactions on,* vol. 51, pp. 2273-2278, 2004.

[7] Z. Feng, "Wireless sensor networks: a new computing platform for tomorrow's Internet," 2004, pp. I-27 Vol.1.

[8] I. F. Akyildiz, Weilian Su, Yogesh Sankarasubramaniam, and E. Cayirci, "A Survey on Sensor Networks" in *IEEE Communication Magazine*. vol. 40, August 2002, pp. 102-116.

[9] N.Koblitz, "Elliptic Curve Cryptosystems," *Mathematics of Computation,* vol. 48, pp. 203-209, 1987.

[10] V. S. Miller, "Use of Elliptic Curves in Cryptography," in *Advances in Cryptology - CRYPTO '85: Proceedings*. vol. 218: Springer-Verlag, 1986, pp. 417-426.

[11] J. Lopez and R. Dahab., " An overview of elliptic curve cryptography," Technical report ,Institute of Computing, Sate University of Campinas, Sao Paulo, Brazil, May 2000.

[12] K. Lauter, "The advantages of elliptic curve cryptography for wireless security," *Wireless Communications, IEEE [see also IEEE Personal Communications],* vol. 11, pp. 62-67, 2004.

[13] H. Wang, B. Sheng, and Q. Li, "Elliptic curve cryptography-based access control in sensor networks," *Int. J. Security and Networks,,* vol. 1, pp. 127-137, 2006.

[14] N. Gura, A. Patel, and A. Wander, "Comparing elliptic curve cryptography and RSA on 8-bit CPUs," in *Proceedings of the 2004 Workshop on Cryptographic Hardware and Embedded Systems (CHES)* August 2004.

[15] http://csrc.nist.gov/CryptoToolkit/dss/ecdsa/NISTReCur.pdf."

[16] D. J. Malan, M. Welsh, and M. D. Smith, "A public-key infrastructure for key distribution in TinyOS based on elliptic curve cryptography," in *2nd IEEE International Conference on Sensor and Ad Hoc Communications and Networks (SECON 2004)2nd IEEE International Conference on Sensor and Ad Hoc Communications and Networks (SECON 2004)*, 2004, pp. 71-80.

[17] I. Blake, G. Seroussi, and N. Smart, *Elliptic Curves in Cryptography* vol. 265, 1999.

[18] D. Hankerson, J. L. Hernandez, and A. Menezes, "Software Implementation of Elliptic Curve Cryptography over Binary Fields, CHES," 2000.

[19] Angelo C Gillie, "Binary Arithmetic and Boolean algebra," McGRAW-HILL Book Company, 1965. pp53.

[20] H R. Bellman and L.A. Zadeh, Decision-making in a fuzzy environment, Management Science 17 (1970),141-164.

[21] Xu Huang, Shirantha Wijesekera, and Dharmendra Sharma, "Fuzzy Dynamic Switching in Quantum Key Distribution for Wi-Fi Networks," 6th International Conference on Fuzzy Systems and Knowledge Discovery, 14-16 August 2009, Tianjin, China. Proceeding pp302-306.

[22] Xu Huang, Pritam Gajkumar Shah and Dharmendra Sharma, "Multi-Agent System Protecting from Attacking with Elliptic Curve Cryptography," the 2nd International Symposium on Intelligent Decision Technologies, Baltimore, USA, 28-30 July 2010. Accepted to be published.

[23] Xu Huang and Dharmendra Sharma, "Fuzzy Controller for a Dynamic Window in Elliptic Curve Cryptography Wireless Networks for Scalar Multipication" APCC 2010. The 16th Asia-Pacific Conference on Communications, 31 October – 3 November 2010, Langham Hotel, Auckland, New Zealand, ISBN: 978-1-4244-8127-9 pp.509-514.

[24] R.L. Rivest, A. Shamir, L.M. Adleman, A Method for obtaining digital signatures and public key cryptosystem, Communications of the ACM 21 (1978) 120–126.

[25] T. ElGamal, Public key cryptosystem and a signature scheme based on discrete logarithms, IEEE Transactions on Information Theory 31 (4) (1985) 469–472.

[26] W. Diffie, M.E. Hellman, New directions in cryptography, IEEE Transactions on Information Theory 22 (6) (1976) 644–654.

2011 IEEE International Conference on Fuzzy Systems
June 27-30, 2011, Taipei, Taiwan

Regulation for Wind Generation System Using Ant system Based Takagi Sugeno Fuzzy PID

A.H.Besheer
Electrical Engineering Department
Faculty of Engineering – University of Tabuk
Tabuk - Kingdom of Saudi Arabia
abesheer@ut.edu.sa

T. M. Abdo, M. M. Halouda
Electrical Power & Machines Department
Faculty of Engineering, Cairo University
Giza - Egypt
tam2k0@gmail.com

Abstract— **This paper introduces a new tuning technique for the PID control scheme that is adopted for regulating the magnitude and frequency of the wind energy conversion system (WECS) output voltage which presents interesting control demands and exhibits intrinsic non-linear characteristics. The developed technique is stem from blending the ant system optimization method with Takagi Sugeno fuzzy system approach. The optimum relationship between the PID controller gains and the parameters of fuzzy modules is explored using Ant system algorithm; hence a satisfactory dynamic performance of the WECS is obtained.**

Keywords-Takagi - Sugeno fuzzy control; PID control; Ant system optimization; Wind energy conversion systems

I. INTRODUCTION

In the world of today there is a need for alternatives to the large coal and oil fired power plants. Renewable energy is one way to go, and in particular wind turbines have proven to be a solution [1]. The arrival of the new power devices technologies, new circuit topologies and novel control strategies are contributing to the success of the wind generation technology.

In wind energy standalone generation systems, the frequency and the magnitude of the terminal voltage for the Self Excited Induction generators (SEIG) vary with load even when the rotor speed is maintained constant. An increase in the rotor speed due to the increase of wind speed will result in a proportionate increase in frequency, often accompanied by severe overvoltage and excessive current.

Although the slip-ring machine is more expensive and requires more maintenance, it permits rotor slip-power control when driven by a variable-speed turbine. When a grid connection is permissible, the slip-ring machine may be operated as a double-output induction generator (DOIG) using the slip-energy recovery technique. In the case of Self Excited Slip Ring Induction Generator (SESRIG), the system cost can be further reduced by the use of a simple rotor resistance controller [2], [3]. Since only a capacitor bank needs to be connected to the stator terminals, the SESRIG provides a good quality ac source with little harmonic distortion to the stator load. Another advantageous feature of the SESRIG is that independent control of the voltage and frequency can be achieved easily. Even with a wide variation in speed, the generator frequency can be maintained reasonably constant by rotor resistance control, while the voltage can be controlled by varying the excitation capacitance. The rating of the rotor resistance controller is small compared with the generator rating; hence, the cost saving is quite significant.

Fuzzy control and tuning methodologies have emerged in last years as promising ways to approach nonlinear control problems and to deal with difficulties of conventional PID controllers [4]. The area of auto-tuning of PID controller using fuzzy systems has attracted many authors [5][6]. However, a common bottleneck encountered in fuzzy controller design is that derivation of fuzzy rules is often difficult and time-consuming, and relies on expert knowledge. To overcome this disadvantage, many automatic methods for fuzzy system design and optimization algorithms have been proposed, such as neural fuzzy systems [7]and evolutionary fuzzy systems [8].

Recently, the social inspired optimization algorithms become a successful alternative for the conventional tuning method to adapt the PID controllers. Using these new methods, the global optimal or suboptimal solutions of the optimized control scheme are found. These algorithms are adopted by many researchers for tuning PID controller in its classical and intelligent forms. One such approach is Ant System Optimization (ASO) which is founded on the foraging behavior of ants and their indirect communication based on pheromones see for instance [9]. ASO has been applied to several combinatorial problems such as job scheduling, routing optimization in data communication networks and telephone networks [10].

One of the widely used methods for optimizing a fuzzy logic controller is to modify the rule base using this self-organizing algorithm automatically according to previous responses until the desired control performance is achieved. Many works studied this problem such as [11], [8] and [12]. In [11], a tracking control problem is assumed to develop a self tuning PID control scheme with application to antilock braking system via combinations of fuzzy and genetic algorithms. While in [13], the approximation of analytical test function is performed using ant colony algorithm to tune the parameters of Takagi Sugeno (T-S) fuzzy rule base. The authors simplified their work by assuming constant

Deanship of Scientific Research – University of Tabuk. *(sponsors)*

consequence part instead of the ordinary linear function consequent part of T-S fuzzy system. In [12], incremental fuzzy PID controller is used which is slightly different from the T-S fuzzy PID controller where, the scaling factors for input/output Macvicar-Whelan based fuzzy system are addressed in the ant colony optimization framework. In T-S fuzzy systems design, one challenging design task is the determination of the parameters of the consequent part. In this paper, ASO is employed to design the consequent part of a Takagi Sugeno fuzzy PID controller. The paper presents design procedures for a model free T-S fuzzy PID controller. Three independent T-S fuzzy systems are combined to tune different gains of PID controller. The optimum relationship between the PID controller parameters and the parameters of T-S fuzzy modules is explored. Using Ant system algorithm, the parameters of each T-S fuzzy system are optimally determined. The idea is to start with a tuned, conventional PID controller, replace it with an equivalent Takagi-Sugeno fuzzy PID controller and eventually fine-tune the T-S fuzzy tuner. This is relevant whenever a PID controller is possible or already implemented.

In the proposed T-S Fuzzy Ant System PID, structure of T-S fuzzy system is well adapted via defining the optimum parameters of its consequence part. Once new rules are generated, the PID controller parameters are calculated from the defuzzification process. This paper has two main contributions. Firstly, a PID controller has been designed for WECS using a blending tuning mechanism namely Takagi – Sugeno fuzzy Ant system algorithm. Secondly, a satisfactory closed loop performance is achieved with respect to the conventional ZN frequency response tuning method. The objective of Ant System Optimization in this paper is to improve both the design efficiency of Takagi – Sugeno fuzzy systems and its performance to get optimal PID parameters. In this paper the voltage and frequency control of a three phase SESRIG is investigated by varying the external rotor resistance and the excitation capacitance using the proposed Ant Takagi Sugeno Fuzzy PID controller.

This paper is organized as follows: section II shows the main feature of the control characteristic for SESRIG used in the proposed standalone WECS. Takagi Sugeno fuzzy tuner for PID controller is presented in section III. Section IV introduces ant system optimization algorithm for optimal parameter determination for Takagi Sugeno fuzzy systems. The proposed control strategy is applied to WECS in section V. Finally, a conclusion is set in section VI.

II. SESRIG VOLTAGE AND FREQUENCY CONTROL

Normalized equivalent circuit of the steady state model of SESRIG can be proposed as seen in Fig. 1 [14]. Where a is per unit frequency (actual frequency/base frequency), b per-unit speed (rotor speed/synchronous speed) corresponding to base frequency, C excitation capacitance per phase, E_1 air-gap voltage per phase referred to base frequency, R_1 & R_2 stator and rotor winding resistances per phase. R_L stator load resistance per phase. V_1 Load voltage per phase, X_1& X_2 Stator and rotor leakage reactances per phase, X_c Excitation capacitive reactance per phase and X_L Load reactance per phase.

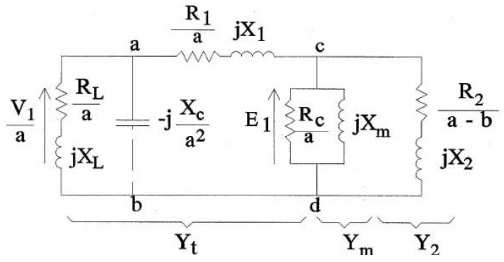

Figure 1 Normalized equivalent circuit of SESRIG[14]

For convenience, all of the machine parameters, except the excitation capacitance, are expressed in per unit. The solution of the SEIG equivalent circuit have been developed using various methods. Among them, the nodal admittance method [15], is considered very simple and easy to follow, hence it will be adopted in this paper. The main feature of the control characteristic for SESRIG used in standalone WECS is deduced in this section by performing laboratory experiments on 1.1 KW machine. The effect of changing the external rotor resistance with constant excitation capacitance and vice versa on the output terminal voltage and frequency at loading condition is presented. Fig's. 2 &3 show the effect of changing the external rotor resistance with constant excitation capacitance at loading conditions (R_L = 8 p.u) on the SESRIG output terminal voltage and frequency.

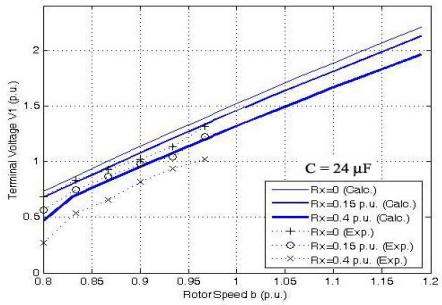

Figure 2 Terminal Voltage (V_1) versus Rotor Speed (b) at different external resistance (R_x) at R_L= 8 p.u.

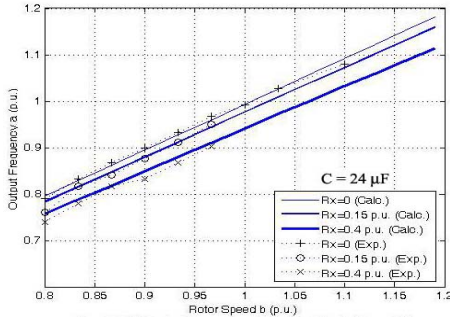

Figure 3 Output Frequency (a) versus Rotor Speed (b) at different external resistance (R_x) at R_L= 8 p.u.

Fig. 4, shows that as the rotor speed (b) increase the external rotor resistance (R_x) required to maintain the frequency constant at 1 p.u. increases. It is noted that unity per-unit frequency is only achievable at rotor speeds above 1 p.u.

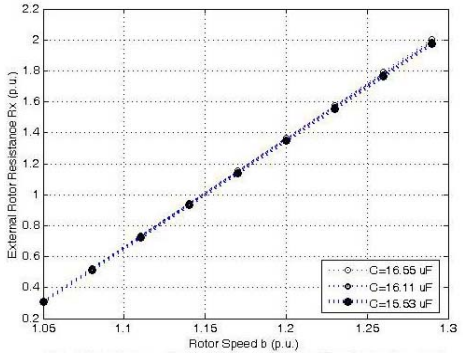

Figure. 4 External Rotor Resistance (R_x) required to maintain rated frequency as the rotor speed varies at different excitation capacitance (R_L=8)

Fig. 5 shows the corresponding terminal voltage. The terminal voltage (V_1) is constant as the rotor speed increases. At the same rotor speed, increasing the excitation capacitance increases the voltage. At a certain value of excitation capacitance, unity per-unit voltage can be obtained. For example, at rotor speed b = 1.1 p.u. and load resistance R_L= 8 p.u., the external rotor resistance required to achieve a = 1 p.u. is 0.66 p.u. To keep the voltage at 1 p.u. at the same time, the external capacitance is adjusted to 16.11 μF.

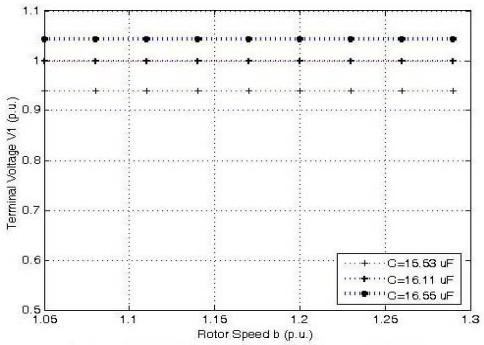

Figure 5 Terminal voltage (V_1) at rated frequency as the rotor speed varies at different excitation capacitance (R_L=8)

Fig.'s 6&7, show the external resistance and excitation capacitance needed to maintain nominal voltage and frequency at a constant rotor speeds (b) of 1.1 p.u. and 1.2 p.u. as the load current increases. For example, when rotor speed (b) is 1.1 and load current (I_L) is 0.25 p.u., the values of the external resistance and excitation capacitance which are needed to maintain the frequency and voltage at 1 p.u. are 0.7 p.u. and 16.55 μF respectively.

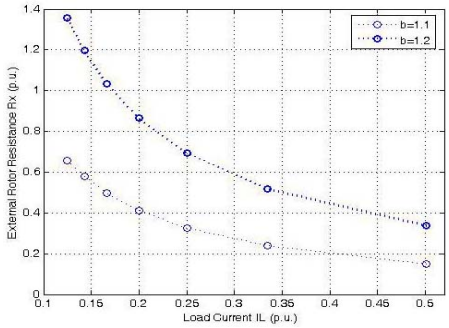

Figure 6 Variation of external resistance (R_x) to operate at rated voltage and frequency as the load current increases

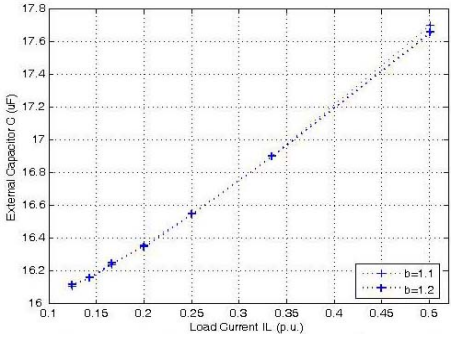

Figure 7 Variation of excitation capacitance (C) to operate at rated voltage and frequency as the load current increases

From the above figures and discussions the following points can be concluded:

Remark 1:

(1) Comparison between the computed and experimental results reflects their close matching that reflects the adequateness of the circuit model and the solution method proposed in [16] and [17].

(2) At constant load conditions, changing the external rotor resistance will affect the standalone WECS terminal output voltage and frequency while the excitation capacitance remains unchanged (i.e. increasing rotor speed (i.e. wind speed) should accompany with increasing the external rotor resistance while the excitation remains nearly constant)

(3) At variable load conditions, simultaneous change in the external rotor resistance and the excitation capacitance is required in order to keep the standalone WECS working at the rated voltage and frequency (i.e. increasing the loading condition (the output power required from the standalone WECS) to be delivered to the load) should accompany with decreasing the external rotor resistance and increasing the excitation capacitance).

III. T – S FUZZY TUNER FOR PID CONTROLLER

Many PID controllers were presented in literature, the expression of PID control law for a continuous time system is given as follows:

$$\boldsymbol{u(t) = K_p e(t) + \frac{K_p}{T_i}\int_0^t e(t)dt + K_p T_d \frac{de(t)}{dt}} \quad (1)$$

where *e(t)* is the error between the input and the output of the system; *u(t)* is the control action generated by the PID controller; K_p is the proportional gain; T_i is the integral time constant; and T_d is the derivative time constant.

In this section, three independent T-S fuzzy systems are used to tune different gains of PID controller. Each fuzzy module is assigned to obtain each PID gains. The typical T-S fuzzy systems studied in this paper have two inputs and one output. The input variables are error and rate of change of the error. We denote *e(t)*, $\dot{e(t)}$ and *y(t)* as error, rate of change of error and system output, respectively. A fuzzy set for *e(t)* (or $\dot{e}(t)$) is denoted as *M* (or *L*) and the corresponding membership is designated as $\mu_i(e(t))$ or ($\mu_i(\dot{e}(t))$). Throughout this work, a Gaussians membership functions for the two inputs of the premise part of T-S fuzzy system are used. The error *e(t)* and the rate of change of the error $\dot{e}(t)$ are normalized using three Gaussian membership functions; negative *N*, zero *Z*, and positive *P*, so that nine rules constitute the rule base for each module. For simplicity, the consequent part has been chosen to be a first order function of *e(t)* and $\dot{e}(t)$. The rule bases have the following form:

Rule j: **If *e(t)* is *M* and $\dot{\mathbf{e}}(\mathbf{t})$ is *L* then $k_i = a_{ij}e(t) + b_{ij}\dot{e}(t)$**

where $k_i = f(e(t), \dot{e}(t))$ is the gain to be tuned, i.e. K_p , K_i or K_d . a_{ij} and b_{ij} are the constants, and *j=1, 2, ...9* is the rule number. In this paper, the weighted average technique is utilized to get the overall fuzzy output as follows:

Given a pair of *e(t)*, $\dot{e}(t)$, the final output of the fuzzy system is inferred as follows [18]:

$$\boldsymbol{k^i = \frac{\sum_{j=1}^{r} w_j(e(t), \dot{e}(t))\left(a_{ij}e(t) + b_{ij}\dot{e}(t)\right)}{\sum_{j=1}^{r} w_j(e(t), \dot{e}(t))}}$$

$$k^i = \sum_{j=1}^{r} h_j\left(e(t), \dot{e}(t)\right)\left(a_{ij}e(t) + b_{ij}\dot{e}(t)\right) \quad (2)$$

$$w_j\left(e(t), \dot{e}(t)\right) = \prod_{j=1}^{2} \mu_{A_j^i}(e(t), \dot{e}(t)),$$

$$\boldsymbol{h_j\left(e(t), \dot{e}(t)\right) = \frac{w_j\left(e(t), \dot{e}(t)\right)}{\sum_{j=1}^{r} w_j\left(e(t), \dot{e}(t)\right)}}$$

Where $\mu_{A_j^i}(e(t), \dot{e}(t))$ is the grade of membership of $(e(t), \dot{e}(t))$ in *A* and *B*. In this paper, we assume that,

$w_j\left(e(t), \dot{e}(t)\right) \geq 0 \quad for\ j = 1,2, \dots, r$

$\sum_{j=1}^{r} w_j(e(t), \dot{e}(t)) > 0$ for all *t*. Therefore we obtain

$h_j\left(e(t), \dot{e}(t)\right) \geq 0 \quad for\ j = 1,2, \dots, r$ and

$\sum_{j=1}^{r} h_j\left(e(t), \dot{e}(t)\right) = 1$

Remark 3: Our approach is different from those of [11], [13] and [12] in the following ways.

i. A Takagi – Sugeno type of the fuzzy PID control system is assumed instead of incremental fuzzy PID control system.
ii. The input Gaussian membership functions of T-S fuzzy tuner are assumed to be constant (i.e. the membership function's center *"c"* and its spread *"σ"* are constant over each rules and fuzzy system).
iii. The total no. of free parameters to be tuned in is 117 parameters while in our proposed design procedures are 54 parameters (i.e. smaller computational burden).

IV. ASO ALGORITHM BASED T-S FUZZY OPTIMAL PARAMETER DETERMINATION

A. Ant System Optimization

The ant system is the first member of a class of algorithms called Ant Colony Optimization (ACO) that was initially proposed by Colorni, Dorigo and Maniezzo [19]. This technique is adopted in this paper due to its simplicity. The main underlying idea, loosely inspired by the behavior of real ants, is that of a parallel search over several constructive computational threads based on local problem data and on a dynamic memory structure containing information on the quality of previously obtained result. In this algorithm, computational resources are allocated to a set of artificial ants that exploit a form of indirect communication mediated by the environment to find the shortest path from the ant nest to a set target. Ant algorithms have been proved to be a quick global optimal solution finder when compared to other heuristic methods such as simulated annealing and genetic algorithms. It also states that the ant algorithms have the quality to find new optimal solution without reinitiating the computations from scratch.

B. T-S Fuzzy PID optimization problem

Usually, the optimization process consists of finding the controller parameters such as to minimize or maximize a given cost function of the closed loop system consisting of a fuzzy PID controller and an unknown plant. The optimization of step response of the system under control by minimizing a suitable performance criterion is the aim of this work.

Each T-S fuzzy module consists of constant premise parameters (that is needn't to be optimized) and 18 free consequence parameters (that will be optimized). The total number of free parameters to be optimized for the overall fuzzy system is 54. The AS algorithm is applied to optimize two different parameter matrices (*A* & *B*). These parameters matrices are driven by the consequence parts of fuzzy rule base. The dimension of both parameter matrices is "*3x9*". The effectiveness of the proposed T-S Fuzzy controller is quantified by the following performance criteria that are evaluated at the end of a step response experiment. It includes the overshoot ζ, settling time t_s and steady state error e_{ss} of the system unit step response. The performance criterion of the system F is designed as follows:

$$\boldsymbol{F = \lambda_\zeta f_1 + \lambda_{t_s} f_2 + \lambda_{e_{ss}} f_3} \quad (3)$$

where $\lambda_\zeta, \lambda_{t_s} and\ \lambda_{e_{ss}}$ are three weighting coefficients and f_1, f_2 & f_3 are defined as follows:

$$f_1 = \frac{\zeta}{\zeta_o}, f_2 = \frac{t_s}{t_{so}}\ and\ f_3 = \begin{cases} \frac{e_{ss}}{e_{sso}}\ if\ e_{sso} \neq 0 \\ 0\ ,\quad if\ e_{sso} = 0 \end{cases}, \quad (4)$$

Where $\zeta_o, t_{so}\ and\ e_{sso}$ are the performance values obtained from ZN tuning formula. The parameters matrices for the problem of tuning T-S fuzzy PID controller are defined as:

$$\boldsymbol{A} = \begin{bmatrix} \boldsymbol{a_{11}} & \cdots & \boldsymbol{a_{19}} \\ \vdots & \ddots & \vdots \\ \boldsymbol{a_{31}} & \cdots & \boldsymbol{a_{39}} \end{bmatrix} \& B = \begin{bmatrix} \boldsymbol{b_{11}} & \cdots & \boldsymbol{b_{19}} \\ \vdots & \ddots & \vdots \\ \boldsymbol{b_{31}} & \cdots & \boldsymbol{b_{39}} \end{bmatrix} \quad (5)$$

Now, the control problem in this paper can be formulated as follows:

Given a plant *G(s)* to be controlled (Fig.8), ***determine*** the optimum values of the parameters in (2) using ant system algorithm, hence, ***find*** the optimal PID parameters K_p, T_i and T_d ***so that*** the control system has the minimum value of given performance criterion "*F*" (3).

Fig. 8 depicts the closed loop control system used in this paper.

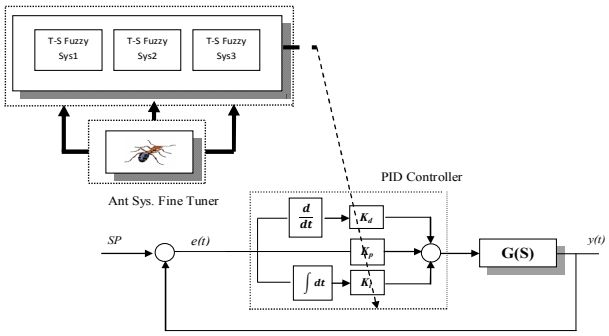

Figure 8 The Proposed Closed loop Control System

A. Proposed Algorithm

Using the same technique used in [20] or the ant system optimization, we can modify the design algorithm presented in [12] to take into account the presence of T-S fuzzy system. The proposed AS Algorithm based T-S Fuzzy optimal PID parameter determination can be summarized as follows:

Step 1: Determine K_{po}, K_{io} and K_{do} using the classical Ziegler-Nichols tuning formula for a given control system with a PID controller and compute the system's performance indexes $\zeta_o, t_{so}\ and\ e_{sso}$.

Step 2: Specify the initialization parameters of our proposed problem that contain the following:

- Values of $\alpha, \beta, \rho, \tau_o\ and\ m$.
- The maximum number of iterations t_{max}.
- A one-dimensional array $Path_k$ with 108 elements. Array $Path_k$ can be used to denote the moving path of ant *k*.

Step 3: Set the iteration counter *t=1* and then place all of the m ants at the origin O.

Step 4: Set *i=1*.

Step 5: Set *k=1*.

Step 6: Compute the transition probability of each node on line L_i using the following formula

$$P_k(i,j,t) = \frac{\tau^\alpha(i,j,t)\eta^\beta(i,j,t)}{\sum_{j=0}^{9}\tau^\alpha(i,j,t)\eta^\beta(i,j,t)}$$

Where $\eta(i,j,t)$ is the visibility of node *(i, j)* and defined as:

$$\eta(i,j,t) = \frac{10 - |j - j^*|}{10}$$

Where the values of j^* are set in the following way:

- In the first iteration of the AS algorithm, the values of j^* (*i=1-108, j=0-9*) are assigned from the different values of the one dimensional array $Path_{k\text{-}initial}$.
- In each of the following iterations, j^* are determined from the calculated one dimensional array $Path_k$ (it contains different entities of matrices *A* & *B*) that is corresponding to optimal traveling path generated in the previous iteration by the ant

$\alpha\&\beta$ represent respectively the relative importance of the pheromone concentration and visibility in transition probability

Step 7: Based on the calculated transition probability in the previous step and using Roulette wheel selection method, select a node on line L_i for ant *k* and move ant *k* to this node, then save the *y* coordinate of the node into the i^{th} element of $Path_k$.

Step 8: Set *k*←*k+1*. If $k \leq m$, go to Step 6; Otherwise, continue.

Step 9: Set *i*←*i+1*. If $i \leq 108$, go to Step 5; Otherwise, continue.

Step 10: For each ant *k* (*k=1, 2, ..., m*): according to Pathk, compute different entities values of matrices *A* & *B* using formula (5).

Step 11: For each ant *k* (*k=1, 2, ..., m*): evaluate the PID gain values from the T-S fuzzy system according to formula (2).

Step 12: For each ant *k* (*k=1, 2, ..., m*): perform a simulation experiment using the calculated matrices *A* & B and compute the system's performance indexes $\zeta^k, t_s^k\ and\ e_{ss}^k$ then compute the performance criterion F_k using formula (3).

Step 13: Compare all of the obtained F_k values and find the optimal ant path of this iteration ($Path_{k\text{-}optimal}$), that has minimum value of the performance criterion (i.e. $min_k F_k$, *k=1,2,...,m*). Save the $Path_{k\text{-}optimal}$ and the corresponding optimal PID gains.

Step 14: Set each element of $Path_k$ to zero, *k=1, 2,..., m*.

Step 15: Update the pheromone concentration of each node on the moving ant path using the following updating rule:

$$\tau(i,j,t+1) = \rho\tau(i,j,t) + \Delta\tau(i,j)$$

$$\Delta\tau(i,j) = \sum_{k=1}^{m}\Delta\tau(i,j)$$

Where $0 < \rho < 1$ is the pheromone decay parameter; $\tau(i,j)$ is the amount of pheromone laid at n_{ij} by ant *k* in the iteration just completed and computed by the following formula:

$$\Delta\tau_k(i,j) = \begin{cases} \frac{Q}{F_k}\ if\ ant\ k\ passed\ through\ n_{ij}\ in\ previous\ iterat. \\ 0 \qquad\qquad\qquad\qquad\qquad Otherwise \end{cases}$$

Where Q is a positive constant, F_k is the value of performance criterion of ant k in the iteration just completed and computed by (3).

Step 16: Set $t \leftarrow t+1$. If $t < t_{max}$ and all of the m ants do not make the same tour, place all the ants at the origin O and go to Step 4; if $t < t_{max}$ but all of the m ants make the same tour or $t = t_{max}$, ; stop.

V. Standalone WECS Simulation Using the Proposed Technique

In this section, based on the results drawn from the above sections, the proposed technique namely Ant System based Takagi Sugeno Fuzzy PID (ASTSFPID) Control is applied to the standalone WECS configured in Fig. (9) to automatically control the terminal output voltage and frequency of SESRIG when either the stator load impedance or the rotor speed changes. The goal is to keep the voltage and frequency at the value of 1 p.u. This is achieved by simultaneously changing the excitation capacitor and the added rotor resistance.

A. Closed loop control

The stator terminal voltage and the output frequency are chosen as the feedback variable since any change in speed and stator load impedance will result in a corresponding change in the terminal voltage and output frequency. The stator terminal voltage signal is compared with the voltage reference signal. The voltage error signal is fed to a proportional-plus-integral (PI) controller that outputs a signal for the firing angle of the thyristor controlled inductor (TCR). The output frequency signal is compared with the frequency reference signal. The frequency error signal is fed to another PI controller that outputs a signal for the duty cycle of the chopper controlled resistance.

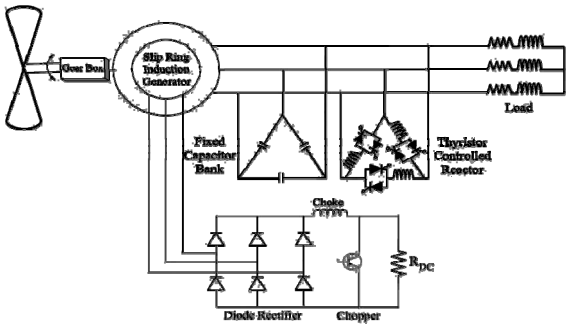

Figure 9 Schematic Diagram for the system configuration

In [17], since no electrical dynamics is involved the SESRIG was approximated as a first-order delayed system, the parameters of the proposed transfer function were determined using the open-loop step response method. Proper tuning of the PI controller is required in order to give satisfactory dynamic performance of the proposed standalone WECS. Hence, same approximation for SESRIG performed in [17] will be adopted in this paper.

Among different traditional tuning methods, the Ziegler-Nichols (ZN) technique has been very influential. The idea is to start the proposed algorithm with ZN PI gains then enhance the dynamic response of the closed loop system according to the performance index in (3) via the steps of the algorithm. Finally, the algorithm will reach to the optimal parameters of the PI controller that can be used in controlling the voltage and the frequency of the standalone WECS.

B. Closed Loop Control Simulation Results

This section contains the results of three simulation experiments using MATLAB/SIMULINK environment to study the dynamic response of SESRIG based standalone WECS with Takagi Seguno Fuzzy based Ant System PI closed loop control. For the sack of comparison, the results with ZN-PI controller designed in [17] are also presented. Firstly the response for changing the rotor speed (b) while the stator load resistance kept constant is presented. Secondly the response for changing the stator load resistance (R_L) while the rotor speed (b) kept constant is studied. Thirdly the response for changing the rotor speed (b) followed with a change in the stator load resistance (R_L) is introduced. Fig's. (10-15) show the dynamic response (output voltage and frequency) of the standalone WECS subjected to the proposed and traditional control method. The proposed PI controllers (ASTSFPI) after a short transient time restored both the output terminal voltage and frequency to the reference value (i.e. 1 p.u.) with reasonable overshoot and zero steady state error irrespective of changing the rotor speed and the stator load resistance. As seen from the following figures, the proposed control method outperforms the traditional control method.

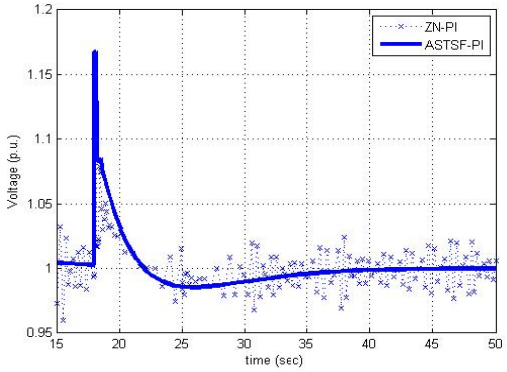

Figure 10 Dynamic Response of the voltage as the rotor speed increases from 1.2 to 1.3 p.u at R_L= 4 p.u. with the proposed and the traditional control

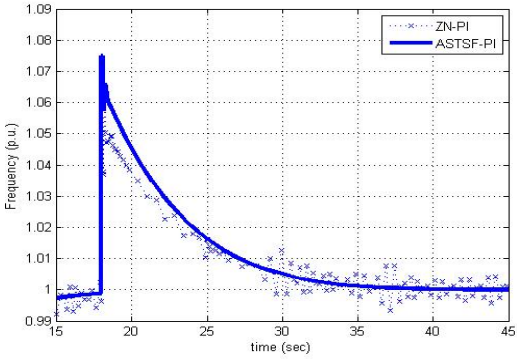

Figure 11 Dynamic Response of the frequency as the rotor speed increases from 1.2 to 1.3 p.u at R_L= 4 p.u. with the proposed and the traditional control

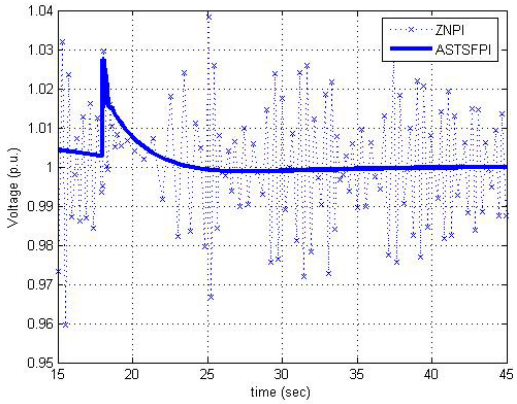

Figure 12 Dynamic Response of the voltage as the load increases from 4 to 4.3 p.u at *b*= 1.2 p.u. with the proposed and the traditional control

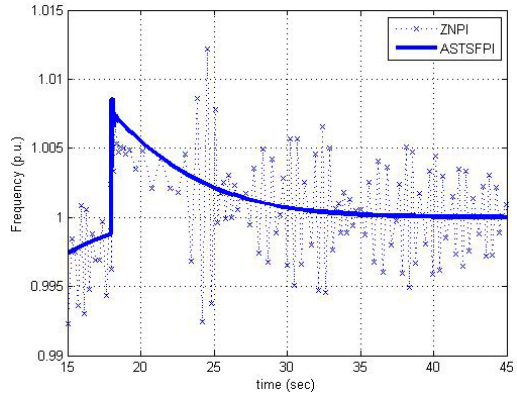

Figure 13 Dynamic Response of the frequency as the load increases from 4 to 4.3 p.u at *b*= 1.2 p.u. with the proposed and the traditional control

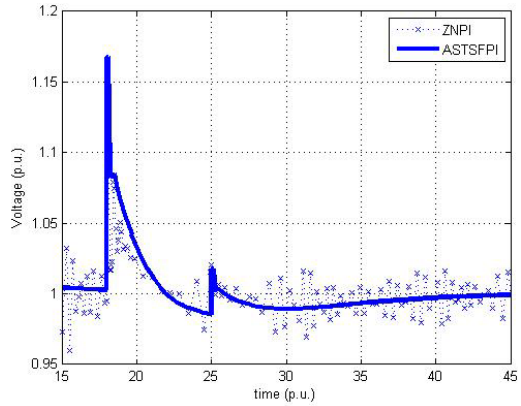

Figure 14 Dynamic response for the voltage as rotor speed & Stator load resistance change from b = 1.15 to 1.3 p.u and from R_L= 4.5 to R_L= 4.3 p.u. with the proposed and the traditional control

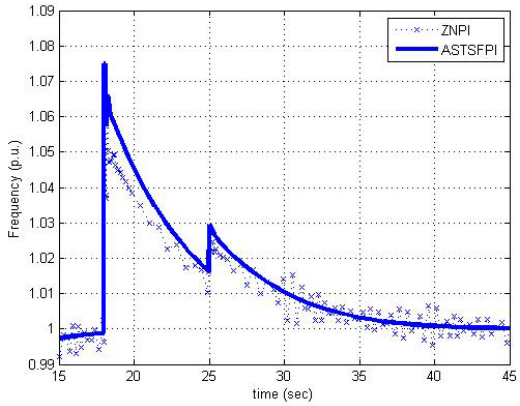

Figure 15 Dynamic response of the frequency as rotor speed change &stator load resistance change from *b*= 1.15 to 1.3 p.u and from R_L= 4.5 to R_L= 4.3 p.u. with the proposed and the traditional control

VI. CONCLUSION

In this paper, an optimal Takagi Seguno fuzzy PID controller is determined using ant system algorithm. The proposed controller is used to control the output voltage and frequency for standalone WECS at the sending end of self-excited slip-ring induction generator. The ant system algorithm search for the optimal parameters of the consequent part of the Takagi Seguno fuzzy system that is in turn produces the optimal PID gains. It is shown that with varying rotor speed and load impedance both the frequency and the output voltage of the SESRIG can be maintained constant by rotor resistance control and excitation capacitance control over a wide range of speeds without exceeding the stator current limit. The proposed algorithm is easily implemented, has a good convergence property and has an efficient searching ability for the optimal PID controller. Moreover the proposed technique is very effective and useful for making the self excited induction generator feasible for remote windy areas.

ACKNOWLEDGMENT

The authors gratefully acknowledge the financial support by the Deanship of Scientific Research at the University of Tabuk - Grant No. 41/50/1432.

REFERENCES

[1] J.F.Manwell, J.G. McGowan, A.L. Rogers, Wind Energy Explained Theory, Design and Application, John Wiley & sons LTD, England, 2002.

[2] A. A. Shaltout and A. F. El-Ramahi , " Maximum power tracking for a wind driven induction generator connected to a utility network", Applied Energy, Volume 52, Issues 2-3, pp. 243-253, 1995.

[3] Badrul H. Chowdhury and Srinivas Chellapilla, " Double-fed induction generator control for variable speed wind power generation ", Electric Power Systems Research, Volume 76, Issues 9-10, pp. 786-800, June 2006.

[4] S.R.Vaishnav and Z.J.Khan, "Design and performance of PID and fuzzy logic controller with smaller rule set for higher order system", Proceedings of the World Congress on Engineering and Computer Science 2007, WCECS 2007, San Francisco, USA October 24-26, 2007.

[5] A. Visioli, “Tuning PID controllers with fuzzy logic,” IEE Proc. Control Theory and Applications, Vol. 148, No. 1, pp. 1-8, 2001.

[6] S. Bhattacharya, A. Chatterjee and S. Munshi, “An improved PID-type fuzzy controller employing individual fuzzy P, fuzzy I and fuzzy PID controllers,” Transaction of the Institute of Measurements and Control Vol. 25, pp. 352-372, No. 4, 2003.

[7] Lin, C.T. and Lee, C.S.G., “Neural Fuzzy Systems: A Neural-Fuzzy Synergism to Intelligent Systems”, Englewood Cliffs: Prentice Hall, 1996.

[8] Cordon, O., Herrera, F., Hoffmann, F. and Magdalena, L., “Genetic fuzzy systems: evolutionary tuning and learning of fuzzy knowledge bases” (Singapore: World Scientific), 2001.

[9] A.H.Besheer, “Tuning method for PID control scheme: A blended ant system optimization technique with Takagi Sugeno fuzzy system”, ICFC 2010 - International Conference on Fuzzy Computation, Valencia, Spain 24-26 October, 2010.

[10] Karl O. Jones, André Bouffet’ “Comparison of ant colony optimisation and differential evolution”, International Conference on Computer Systems and Technologies – CompSysTech, 2007.

[11] Abdel Badie Sharkawy, "Genetic fuzzy self tuning PID controllers for antilock braking systems", Alexandria Engineering Journal, Vol. 45, No. 6, pp. 657-673, 2006.

[12] Tan Guan-zheng and Dou Hong-quan, “ACS algorithm-based adaptive fuzzy PID controller and its application to CIP-I intelligent leg”, J.Cent. South Univ. Technol. (2007)04-0528-09, Springer, DOI: 10.1007/s11771-007-0103-3.

[13] Hadi Nobahari, Seid H. Pourtakdoust, "Optimization of fuzzy rule bases using continuous ant colony system", Proceeding of the first International Conference on Modeling, Simulation and Applied optimization, Sharjah, U.A.E, February 1-3, 2005.

[14] M. G. Say, Alternating Current Machines, 5th ed. London, U.K.: Pitman Publishers (ELBS), 1983.

[15] T.F.Chan, “Analysis of self excited induction generators using an iterative method”, IEEE Transaction on Energy Conversion Vol. 10, No. 3, pp. 502-507, September 1995.

[16] T. F. Chan, "Steady state analysis of self excited induction generators", *IEEE Transactions on Energy Conversion*, Vol. 9. No. 2, June, 1994.

[17] T. F. Chan, K. A. Nigim, and L. L. Lai, “Voltage and frequency control of self-excited slip-ring induction generators”, IEEE Transactions on Energy Conversion, vol. 19, No. 1, pp. 81-87, March 2004.

[18] A.H.Besheer and H.R.Emara “Relaxed LMI based designs for Takagi Sugeno fuzzy regulators and observers; poly-quadratic lyapunov function approach”, Proceedings of the 2009 IEEE International Conference on Systems, Man, and Cybernetics San Antonio, TX, USA – October, 2009.

[19] DORIGO M, V. Maniezzo and A. Colorni, “Ant system optimization by a colony of cooperating agents”, IEEE Transaction on Systems Man and cybernetics – part B, 26 (1), pp. 29-41, 1996.

[20] Guanzheng Tan, Qingdong Zeng, Shengjun He and Guangchao, “Adaptive and robust design for PID controller based on ant system algorithm”, Advances in Natural Computation, Lecture Notes in Computer Science, 2005, Volume 3612/2005, 915-924, DOI: 10.1007/11539902_113

2011 IEEE International Conference on Fuzzy Systems
June 27-30, 2011, Taipei, Taiwan

Actuator Delayed Active Vehicle Suspension Control: A T-S Fuzzy Approach

Hongyi Li Honghai Liu
Intelligent Systems & Biomedical Robotics Group,
School of Creative Technologies, University of Portsmouth,
Eldon Building, Portsmouth, PO1 2DJ
Email: hongyi.li@port.ac.uk
honghai.liu@port.ac.uk

Huijun Gao
Research Institute of Intelligent Control and Systems,
Harbin Institute of Technology, Harbin 150001, China
Email: hjgao@hit.edu.cn

***Abstract*—This paper focuses on fuzzy H_∞ controller design for uncertain active suspension systems with actuator delay based on Takagi-Sugeno (T-S) model approach. This dynamic system is presented by taking into account the sprung and unsprung mass variations, the actuator delay, and the suspension performance. The fuzzy H_∞ controller is designed such that the resulting T-S fuzzy system is asymptotically stable and guarantees H_∞ performance, and simultaneous satisfying the constraint performance. The existence condition of fuzzy H_∞ control is obtained in terms of linear matrix inequalities (LMIs) and can be solved by using the standard software. A quarter-car suspension model is provided to validate the effectiveness of the proposed design procedures.**

Keywords: Fuzzy control, T-S model, H_∞ control, actuator delay, uncertain active suspension systems.

I. Introduction

The vehicle suspension is a crucial component that is used to support the vehicle weight, to provide effective isolation of the chassis from road excitations, to keep tyre contact with the ground, and to maintain the wheels in appropriate position on the road surface. Recently, considerable attention has been paid to the hot issue how to achieve the required suspension performances, namely, ride comfort, road handling, and suspension deflection [1]. Recently, many active suspension control approaches have been presented to handle the tradeoff [2]–[7]. It has been proved that H_∞ control method is feasible to achieve a compromised vehicle performance in [6], [7].

For active suspension systems, the vehicle sprung and unsprung masses may vary according to the different loading conditions, such as the payload and number of vehicle passengers. If we do not take into account the varying vehicle sprung and unsprung masses in the control design process, the performance of the vehicle suspension systems will be affected. More recently, the authors in [8], [9] used the polytopic parameter uncertainties to model the varying vehicle sprung or unsprung masses. Among [8], [10], the parameter-dependent controllers has been proposed for the quarter-car suspension systems with sprung mass variation. The parameter-independent sampled-data H_∞ controller design strategy has been provided in [9] for quarter-car suspension systems with both sprung and unsprung mass variations. In particular, the authors in [11] presented T-S model-based fuzzy control design approach for electrohydraulic active suspension systems with input constraint.

This paper is concerned with the problem of fuzzy H_∞ control for uncertain active suspension systems with actuator delay based on T-S model approach. The parallel-distributed compensation (PDC) scheme is used to develop fuzzy H_∞ performance analysis condition for the proposed T-S fuzzy systems presenting the uncertain active suspension systems. Then, the fuzzy H_∞ controller is designed to ensure the resulting T-S fuzzy system is asymptotically stable and satisfy H_∞ performance, and guarantee the suspension performance. The linear matrix inequality (LMI)-based condition of fuzzy H_∞ controller is derived and can be solved by using the standard software. Finally, a quarter-car suspension model is provided to demonstrate the effectiveness of the proposed design approach.

II. Problem Formulation

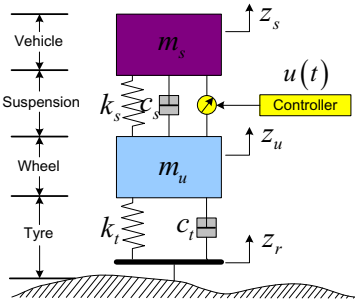

Fig. 1. Quarter-car model

Over the past years, many researchers became to investigate the modeling and control design for active suspension systems since these systems play an important role in guaranteeing the suspension performance, such as ride comfort, road holding, and suspension deflection. A quarter-car model has been used widely for the research in the literature and is shown in Fig. 1, in which m_s is used to denote the sprung mass, which represents the car chassis; m_u is the unsprung mass, which represents mass of the wheel assembly; $u(t)$ is used to stand for the active input of the suspension system; z_s and z_u are used to

978-1-4244-7316-8/11/$26.00 ©2011 IEEE

denote the displacements of the sprung and unsprung masses, respectively; z_r is used to denote the road displacement input; c_s and k_s are damping and stiffness of the suspension system, respectively; k_t and c_t stand for compressibility and damping of the pneumatic tyre, respectively. Then, the dynamic equation of the suspension model is established as:

$$\begin{aligned} & m_u\ddot{z}_u(t)+c_s[\dot{z}_u(t)-\dot{z}_s(t)]+k_s[z_u(t)-z_s(t)] \\ & +k_t[z_u(t)-z_r(t)]+c_t[\dot{z}_u(t)-\dot{z}_r(t)] \\ = \; & -u\left(t\right), \\ & m_s\ddot{z}_s(t)+c_s[\dot{z}_s(t)-\dot{z}_u\left(t\right)]+k_s[z_s(t)-z_u(t)] \\ = \; & u\left(t\right). \end{aligned} \tag{1}$$

Denote $x_1(t)=z_s(t)-z_u(t)$ as the suspension deflection, $x_2(t)=z_u(t)-z_r(t)$ as the tire deflection, $x_3(t)=\dot{z}_s(t)$ as the sprung mass speed, $x_4(t)=\dot{z}_u(t)$ as the unsprung mass speed, and $w(t)=\dot{z}_r(t)$ as the disturbance input, respectively. The equations in (1) can be rewritten as:

$$\dot{x}(t)=A\left(t\right)x(t)+B_1\left(t\right)w(t)+B\left(t\right)u\left(t\right), \tag{2}$$

where

$$\begin{aligned} A\left(t\right) &= \begin{bmatrix} 0 & 0 & 1 & -1 \\ 0 & 0 & 0 & 1 \\ -\frac{k_s}{m_s} & 0 & -\frac{c_s}{m_s} & \frac{c_s}{m_s} \\ \frac{k_s}{m_u} & -\frac{k_t}{m_u} & \frac{c_s}{m_u} & -\frac{c_s+c_t}{m_u} \end{bmatrix}, \\ B\left(t\right) &= \begin{bmatrix} 0 \\ 0 \\ \frac{1}{m_s} \\ -\frac{1}{m_u} \end{bmatrix}, \quad B_1\left(t\right)=\begin{bmatrix} 0 \\ -1 \\ 0 \\ \frac{c_t}{m_u} \end{bmatrix}, \\ x(t) &= \begin{bmatrix} x_1(t) & x_2(t) & x_3(t) & x_4(t) \end{bmatrix}^T. \end{aligned}$$

For suspension systems control design problems, their performance, such as ride comfort and suspension deflection, road holding should be taken into account. For quarter car suspension model showed in Fig. 1, it is extensively accepted that ride comfort can be generally quantified by the body acceleration in the vertical direction, hence it is practically acceptable to choose body acceleration, $\ddot{z}_s(t)$, as the first control output. Therefore, one of our main objectives is to minimize the vertical acceleration $\ddot{z}_s(t)$, which means that the passengers feel comfortable. Here we recall H_∞ control method since the value of H_∞ norm is defined as an upper bound of the root-mean-square gain. Our main goal is to minimize the H_∞ norm of the transfer function from the disturbance $w(t)$ to the control output $z_1(t)=\ddot{z}_s(t)$ with an emphasis on ride comfort improving. Meanwhile the following required performance should be taken into account:

I) The suspension deflection cannot exceed a maximum value constrained due to mechanical structure, that is,

$$|z_s(t)-z_u(t)|\le z_{\max}, \tag{3}$$

where $z_{\max}$ is the maximum suspension deflection.

II) The dynamic tyre load has to be less than the static tyre load in order to ensure a firm uninterrupted contact of the wheels on the road,

$$k_t\left(z_u(t)-z_r(t)\right)<\left(m_s+m_u\right)g. \tag{4}$$

Based on the above discussion, we choose the body acceleration $\ddot{z}_s(t)$ as performance control output, the suspension stroke $z_s(t)-z_u(t)$ and relative dynamic tire load $k_t\left(z_u(t)-z_r(t)\right)/\left(m_s+m_u\right)g$ as constrained control output $z_2(t)$. Therefore, we can use the following system to present the active vehicle suspension system:

$$\begin{aligned} \dot{x}(t) &= A\left(t\right)x\left(t\right)+B_1\left(t\right)w\left(t\right)+B\left(t\right)u\left(t\right), \\ z_1(t) &= C_1\left(t\right)x(t)+D_1\left(t\right)u\left(t\right), \\ z_2(t) &= C_2\left(t\right)x(t), \end{aligned} \tag{5}$$

where $A\left(t\right)$, $B_1\left(t\right)$ and $B\left(t\right)$ are defined in (2), and

$$\begin{aligned} C_1\left(t\right) &= \begin{bmatrix} -\frac{k_s}{m_s} & 0 & -\frac{c_s}{m_s} & \frac{c_s}{m_s} \end{bmatrix}, \\ D_1\left(t\right) &= \frac{1}{m_s}, \\ C_2\left(t\right) &= \begin{bmatrix} \frac{1}{z_{\max}} & 0 & 0 & 0 \\ 0 & \frac{k_t}{(m_s+m_u)g} & 0 & 0 \end{bmatrix}. \end{aligned}$$

It can be found that the suspension suspension system in (5) is an uncertain model in that the sprung mass m_s and the unsprung mass m_u vary in given ranges. When carrying out the modeling the suspension systems, the actuator time delay should be taken into account, which can be expressed as:

$$\begin{aligned} \dot{x}(t) &= A\left(t\right)x\left(t\right)+B_1\left(t\right)w\left(t\right)+B\left(t\right)u\left(t-d\left(t\right)\right), \\ z_1(t) &= C_1\left(t\right)x(t)+D_1\left(t\right)u\left(t-d\left(t\right)\right), \\ z_2(t) &= C_2\left(t\right)x(t), \\ x(t) &= \phi(t), \quad t\in\left[-\bar{d},0\right], \end{aligned} \tag{6}$$

where $\phi(t)$ is a vector-valued initial continuous function defined on $t\in\left[-\bar{d},0\right]$. $d\left(t\right)$ denotes the time-varying delay satisfying

$$0\le d\left(t\right)\le\bar{d}, \quad d\left(t\right)\le\mu. \tag{7}$$

The sprung mass m_s and the unsprung mass m_u are assumed to be uncertainties and replaced by $m_s\left(t\right)$ and $m_u\left(t\right)$, which vary in a given range, i.e. $m_s\left(t\right)\in\left[m_{s\min},m_{s\max}\right]$ and $m_u\left(t\right)\in\left[m_{u\min},m_{u\max}\right]$. This means the uncertain mass $m_s\left(t\right)$ is bounded by its minimum value $m_{s\min}$ and its maximum value $m_{s\max}$. In addition, the uncertain mass $m_u\left(t\right)$ is bounded by its minimum value $m_{u\min}$ and its maximum value $m_{u\max}$. Next, we can obtain the values of $\frac{1}{m_s(t)}$ and $\frac{1}{m_u(t)}$ from $m_s\left(t\right)\in\left[m_{s\min},m_{s\max}\right]$ and $m_u\left(t\right)\in\left[m_{u\min},m_{u\max}\right]$. Then we have

$$\begin{aligned} \text{maximum}\frac{1}{m_s\left(t\right)} &= \frac{1}{m_{s\min}}=:\hat{m}_s, \\ \text{minimum}\frac{1}{m_s\left(t\right)} &= \frac{1}{m_{s\max}}=:\check{m}_s, \\ \text{maximum}\frac{1}{m_u\left(t\right)} &= \frac{1}{m_{u\min}}=:\hat{m}_u, \\ \text{minimum}\frac{1}{m_u\left(t\right)} &= \frac{1}{m_{u\max}}=:\check{m}_u. \end{aligned}$$

We can represent $\frac{1}{m_s(t)}$ and $\frac{1}{m_u(t)}$ by

$$\begin{aligned}\frac{1}{m_s(t)} &= M_1(\xi_1(t))\hat{m}_s + M_2(\xi_1(t))\check{m}_s,\\ \frac{1}{m_u(t)} &= N_1(\xi_2(t))\hat{m}_u + N_2(\xi_2(t))\check{m}_u,\end{aligned}$$

where $\xi_1(t) = \frac{1}{m_s(t)}$ and $\xi_2(t) = \frac{1}{m_u(t)}$,

$$\begin{aligned}M_1(\xi_1(t)) + M_2(\xi_1(t)) &= 1,\\ N_1(\xi_2(t)) + N_2(\xi_2(t)) &= 1.\end{aligned}$$

The membership functions can be calculated as

$$\begin{aligned}M_1(\xi_1(t)) &= \frac{\frac{1}{m_s(t)} - \check{m}_s}{\hat{m}_s - \check{m}_s}, \quad M_2(\xi_1(t)) = \frac{\hat{m}_s - \frac{1}{m_s(t)}}{\hat{m}_s - \check{m}_s},\\ N_1(\xi_2(t)) &= \frac{\frac{1}{m_u(t)} - \check{m}_u}{\hat{m}_u - \check{m}_u}, \quad N_2(\xi_2(t)) = \frac{\hat{m}_u - \frac{1}{m_u(t)}}{\hat{m}_u - \check{m}_u}.\end{aligned}$$

We name the member functions **Heavy**, **Light**, **Heavy** and **Light**. Then, the uncertain systems in (6) is represented by the following fuzzy model.

Model Rule 1: **IF** $\xi_1(t)$ is **Heavy** and $\xi_2(t)$ is **Heavy**, **THEN**

$$\begin{aligned}\dot{x}(t) &= A_1x(t) + B_1u(t-d(t)) + B_{11}w(t),\\ z_1(t) &= C_{11}x(t) + D_{11}u(t-d(t)),\\ z_2(t) &= C_{21}x(t),\end{aligned}$$

matrices A_1, B_1, B_{11}, C_{11}, D_{11} and C_{21} are obtained by replacing $\frac{1}{m_s(t)}$ and $\frac{1}{m_u(t)}$ with matrices $A(t)$, $B(t)$, $B_1(t)$, $C_1(t)$, $D_1(t)$ and $C_2(t)$ with $\hat{m}_s$ and $\hat{m}_u$ respectively.

Model Rule 2: **IF** $\xi_1(t)$ is **Heavy** and $\xi_2(t)$ is **Light**, **THEN**

$$\begin{aligned}\dot{x}(t) &= A_2x(t) + B_2u(t-d(t)) + B_{12}w(t),\\ z_1(t) &= C_{12}x(t) + D_{12}u(t-d(t)),\\ z_2(t) &= C_{22}x(t),\end{aligned}$$

matrices A_2, B_2, B_{12}, C_{12}, D_{12} and C_{22} are obtained by replacing $\frac{1}{m_s(t)}$ and $\frac{1}{m_u(t)}$ with matrices $A(t)$, $B(t)$, $B_1(t)$, $C_1(t)$, $D_1(t)$ and $C_2(t)$ with $\hat{m}_s$ and $\check{m}_u$ respectively.

Model Rule 3: **IF** $\xi_1(t)$ is **Light** and $\xi_2(t)$ is **Heavy**, **THEN**

$$\begin{aligned}\dot{x}(t) &= A_3x(t) + B_3u(t-d(t)) + B_{13}w(t),\\ z_1(t) &= C_{13}x(t) + D_{13}u(t-d(t)),\\ z_2(t) &= C_{23}x(t),\end{aligned}$$

matrices A_3, B_3, B_{13}, C_{13}, D_{13} and C_{23} are obtained by replacing $\frac{1}{m_s(t)}$ and $\frac{1}{m_u(t)}$ with matrices $A(t)$, $B(t)$, $B_1(t)$, $C_1(t)$, $D_1(t)$ and $C_2(t)$ with $\check{m}_s$ and $\hat{m}_u$ respectively.

Model Rule 4: **IF** $\xi_1(t)$ is **Light** and $\xi_2(t)$ is **Light**, **THEN**

$$\begin{aligned}\dot{x}(t) &= A_4x(t) + B_4u(t-d(t)) + B_{14}w(t),\\ z_1(t) &= C_{14}x(t) + D_{14}u(t-d(t)),\\ z_2(t) &= C_{24}x(t),\end{aligned}$$

matrices A_4, B_4, B_{14}, C_{14}, D_{14} and C_{24} are obtained by replacing $\frac{1}{m_s(t)}$ and $\frac{1}{m_u(t)}$ with matrices $A(t)$, $B(t)$, $B_1(t)$, $C_1(t)$, $D_1(t)$ and $C_2(t)$ wit $\check{m}_s$ and $\check{m}_u$ respectively.

By fuzzy blending, the overall fuzzy model is inferred as follows:

$$\begin{aligned}\dot{x}(t) &= \sum_{i=1}^{4} h_i(\xi(t))\left[A_ix(t) + B_iu(t-d(t)) + B_{1i}w(t)\right],\\ z_1(t) &= \sum_{i=1}^{4} h_i(\xi(t))\left[C_{1i}x(t) + D_{1i}u(t-d(t))\right],\\ z_2(t) &= \sum_{i=1}^{4} h_i(\xi(t))C_{2i}x(t),\end{aligned} \tag{8}$$

where

$$\begin{aligned}h_1(\xi(t)) &= M_1(\xi_1(t)) \times N_1(\xi_2(t)),\\ h_2(\xi(t)) &= M_1(\xi_1(t)) \times N_2(\xi_2(t)),\\ h_3(\xi(t)) &= M_2(\xi_1(t)) \times N_1(\xi_2(t)),\\ h_4(\xi(t)) &= M_2(\xi_1(t)) \times N_2(\xi_2(t)).\end{aligned}$$

It is obvious that the fuzzy weighting functions $h_i(\xi(t))$ satisfy

$$h_i(\xi(t)) \geq 0, \quad \sum_{i=1}^{4} h_i(\xi(t)) = 1.$$

In this study, we consider the design of fuzzy controllers. By using parallel distributed compensation, we suppose the following fuzzy controller:

Control Rule j: **IF** $\xi_1(t)$ is **Heavy** (**Light**) and $\xi_2(t)$ is **Heavy** (**Light**),

THEN $u(t) = K_jx(t)(j = 1, 2, 3, 4)$.

Hence, the overall fuzzy control law is represented by

$$u(t) = \sum_{j=1}^{4} h_j(\xi(t))K_jx(t) \tag{9}$$

where K_j $(j = 1, 2, 3, 4)$ are the local control gains and $u(t-d(t)) = \sum_{j=1}^{4} h_j(\xi(t-d(t)))K_jx(t-d(t))$. Therefore, in this paper, we assume that $h_j(\xi(t-d(t)))$ is well defined for $t \in \left[-\bar{d}, 0\right]$, and $h_j(\xi(t-d(t))) \geq 0$, $(j = 1, 2, 3, 4)$ $\sum_{j=1}^{4} h_j(\xi(t-d(t))) = 1$. For simplicity, the following notations will be used:

$$h_i =: h_i(\xi(t)), \quad h_j^d =: h_j(\xi(t-d(t))).$$

Applying the fuzzy controller (9) to system (8) yields the closed-loop system:

$$\begin{aligned}\dot{x}(t) &= \sum_{i=1}^{4}\sum_{j=1}^{4} h_ih_j^d\left[A_ix(t) + B_iK_jx(t-d(t)) + B_{1i}w(t)\right],\\ z_1(t) &= \sum_{i=1}^{4}\sum_{j=1}^{4} h_ih_j^d\left[C_{1i}x(t) + D_{1i}K_jx(t-d(t))\right],\\ z_2(t) &= \sum_{i=1}^{4} h_iC_{2i}x(t).\end{aligned} \tag{10}$$

It should be pointed out that the T-S fuzzy system in (10) can be established due to the sprung $m_s(t)$ and unsprung $m_u(t)$ can be measured in practice. In our study, the sector nonlinearity method [12] is used to analysis the variations of the sprung $m_s(t)$ and unsprung $m_u(t)$ to present the T-S fuzzy system in (10).

Without loss of generality, It is assumed, $w \in L_2[0,\infty)$, and $\|w\|_2^2 \leq w_{\max} < \infty$. The main object of this subsection is just to design the feedback gain matrices K_j $(j = 1,2,3,4)$ such that the following requirements are satisfied: the closed-loop system is asymptotically stable; under zero initial condition, the closed-loop system guarantees that $\|z_1\|_2 < \gamma \|w\|_2$ for all nonzero $w \in L_2[0,\infty)$, where $\gamma > 0$ is a prescribed scalar; the following control output constraints are guaranteed:

$$|\{z_2(t)\}_q| \leq 1, \quad q = 1,2. \tag{11}$$

III. Fuzzy Controller Design

In this section, fuzzy H_∞ state-feedback controller is derived for the active suspension system with actuator delay such that the closed-loop system in (10) is asymptotically stable and can also guarantee a prescribed gain from disturbance $w(t)$ to performance output z_1 while keeping the suspension stroke and tire deflection constraints satisfied. Based on the Lyapunov stability, we have the following theorem.

Theorem 1: Consider the closed-loop system in (10). For given scalars $\bar{d} > 0$, μ and matrices K_j, if there exist matrices $P > 0$, $Q > 0$, $S > 0$, $R > 0$, N_j, and M_j with appropriate dimensions $(j = 1,2,3,4)$ such that the following LMIs hold for $q = 1,2$:

$$\begin{bmatrix} \Phi_{11}^{ij} & \Phi_{12}^{1ij} & \Phi_{13}^{ij} & \Phi_{14}^{ij} \\ 0 & -R & 0 & 0 \\ 0 & 0 & -I & 0 \\ 0 & 0 & 0 & -R \end{bmatrix} < 0, \tag{12}$$

$$\begin{bmatrix} \Phi_{11}^{ij} & \Phi_{12}^{2ij} & \Phi_{13}^{ij} & \Phi_{14}^{ij} \\ 0 & -R & 0 & 0 \\ 0 & 0 & -I & 0 \\ 0 & 0 & 0 & -R \end{bmatrix} < 0, \tag{13}$$

$$\begin{bmatrix} -P & \sqrt{\rho}\{C_{2i}\}_q^T \\ * & -I \end{bmatrix} < 0, \tag{14}$$

where

$$\Phi_{11}^{ij} = \begin{bmatrix} \Xi_{11}^{ij} & \Xi_{12}^{ij} & \Xi_{13}^{ij} & \Xi_{14}^{ij} \\ * & \Xi_{22}^{ij} & \Xi_{23}^{ij} & \Xi_{24}^{ij} \\ * & * & \Xi_{33}^{ij} & -N_4^T \\ * & * & * & -\gamma^2 I \end{bmatrix},$$

$$\Phi_{12}^{1ij} = \begin{bmatrix} \sqrt{\bar{d}}M_1 \\ \sqrt{\bar{d}}M_2 \\ \sqrt{\bar{d}}M_3 \\ \sqrt{\bar{d}}M_4 \end{bmatrix}, \Phi_{12}^{2ij} = \begin{bmatrix} \sqrt{\bar{d}}N_1 \\ \sqrt{\bar{d}}N_2 \\ \sqrt{\bar{d}}N_3 \\ \sqrt{\bar{d}}N_4 \end{bmatrix},$$

$$\Phi_{13}^{ij} = \begin{bmatrix} C_{1i}^T \\ K_j^T D_{1i}^T \\ 0 \\ 0 \end{bmatrix}, \Phi_{14}^{ij} = \begin{bmatrix} \sqrt{\bar{d}}A_i^T R \\ \sqrt{\bar{d}}K_j^T B_i^T R \\ 0 \\ \sqrt{\bar{d}}B_{1i}^T R \end{bmatrix},$$

$$\begin{aligned} \Xi_{11}^{ij} &= PA_i + A_i^T P + Q + S + M_1 + M_1^T, \\ \Xi_{12}^{ij} &= PB_iK_j - M_1 + M_2^T + N_1, \\ \Xi_{13}^{ij} &= M_3^T - N_1, \Xi_{14}^{ij} = PB_{1i} + M_4^T, \\ \Xi_{22}^{ij} &= -(1-\mu)S + N_2 + N_2^T - M_2 - M_2^T, \\ \Xi_{23}^{ij} &= N_3^T - N_2 - M_3^T, \Xi_{24}^{ij} = N_4^T - M_4^T, \\ \Xi_{33}^{ij} &= -Q - N_3 - N_3^T. \end{aligned}$$

Then,

(1) the closed-loop system is asymptotically stable;

(2) the performance $\|T_{z_1 w}\|_\infty < \gamma$ is minimized subject to output constraints (11) with the disturbance energy under the bound $w_{\max} = (\rho - V(0))/\gamma^2$, where $T_{z_1 w}$ denotes the closed-loop transfer function from the road disturbance $w(t)$ to the control output $z_1(t)$.

Proof. Considering the Lyapunov-Krasovskii functional as follows:

$$\begin{aligned} V(t) &= x^T(t)Px(t) + \int_{t-\bar{d}}^{t} x^T(s)Qx(s)\,\mathrm{d}s \\ &\quad + \int_{t-d(t)}^{t} x^T(s)Sx(s)\,\mathrm{d}s \\ &\quad + \int_{-\bar{d}}^{0}\int_{t+\alpha}^{t} \dot{x}^T(s)R\dot{x}(s)\,\mathrm{d}s\mathrm{d}\alpha. \end{aligned} \tag{15}$$

For any appropriately dimensioned matrices M and N, the following equalities hold directly according to Newton-Leibniz formula:

$$\begin{aligned} \eta_1(t) &= 2\bar{\xi}^T(t)M \\ &\quad \left(x(t) - x(t-d(t)) - \int_{t-d(t)}^{t} \dot{x}(s)\,\mathrm{d}s\right) = 0, \\ \eta_2(t) &= 2\bar{\xi}^T(t)N \\ &\quad \left(x(t-d(t)) - x\left(t-\bar{d}\right) - \int_{t-\bar{d}}^{t-d(t)} \dot{x}(s)\,\mathrm{d}s\right) = 0, \end{aligned}$$

where

$$\begin{aligned} M &= \begin{bmatrix} M_1^T & M_2^T & M_3^T & M_4^T \end{bmatrix}^T, \\ N &= \begin{bmatrix} N_1^T & N_2^T & N_3^T & N_4^T \end{bmatrix}^T \\ \bar{\xi}^T(t) &= \begin{bmatrix} x^T(t) & x^T(t-d(t)) & x^T\left(t-\bar{d}\right) & w^T(t) \end{bmatrix}. \end{aligned}$$

We first establish the H_∞ performance of the system in (10) under zero initial conditions. Adding $\eta_1(t)$ and $\eta_2(t)$ into $\dot{V}(t)$, we have

$$\begin{aligned} &\dot{V}(t) + z_1^T(t)z_1(t) - \gamma^2 w^T(t)w(t) \\ \leq\ & \sum_{i=1}^{4}\sum_{j=1}^{4} h_i h_j^d \bar{\xi}^T(t) \left[\frac{d(t)}{\bar{d}}\left(\bar{\Xi}_{ij} + \bar{d}MR^{-1}M^T\right)\right. \\ & \left. + \frac{\bar{d}-d(t)}{\bar{d}}\left(\bar{\Xi}_{ij} + \bar{d}NR^{-1}N^T\right)\right]\bar{\xi}(t), \end{aligned}$$

where

$$\breve{\Xi}_{ij} = \begin{bmatrix} \Xi_{11}^{ij} & \hat{\Xi}_{12}^{ij} & \Xi_{13}^{ij} & \Xi_{14}^{ij} \\ * & \Xi_{22}^{ij} & \Xi_{23}^{ij} & \Xi_{24}^{ij} \\ * & * & \Xi_{33}^{ij} & -N_4^T \\ * & * & * & -\gamma^2 I \end{bmatrix} + \begin{bmatrix} C_{1i}^T \\ K_j^T D_{1i}^T \\ 0 \\ 0 \end{bmatrix} \begin{bmatrix} C_{1i}^T \\ K_j^T D_{1i}^T \\ 0 \\ 0 \end{bmatrix}^T + \begin{bmatrix} A_i^T \\ K_j^T B_i^T \\ 0 \\ B_{1i}^T \end{bmatrix} \bar{d}R \begin{bmatrix} A_i^T \\ K_j^T B_i^T \\ 0 \\ B_{1i}^T \end{bmatrix}^T.$$

According to Schur complement and the above method, we develop

$$\dot{V}(t) + z_1^T(t) z_1(t) - \gamma^2 w^T(t) w(t) < 0, \tag{16}$$

for all nonzero $w \in L_2[0,\infty)$. Under zero initial conditions, we have $V(0) = 0$ and $V(\infty) \geq 0$. Integrating both sides of (16) yields $\|z_1\|_2 < \gamma \|w\|_2$ for all nonzero $w \in L_2[0,\infty)$, and the H_∞ performance is established. Then, we can show that system (10) is stable with $w(t) = 0$ after using above similar proof.

The rest proof of Theorem 1 is cut off due to space limitation. Please refer to the proof of [9].

In what follows, the fuzzy H_∞ controller existence condition for the active suspension system in (10) is presented based on fuzzy H_∞ performance analysis criterion in Theorem 1.

Theorem 2: Consider the closed-loop system in (10). For given scalars $\bar{d} > 0$ and μ, if there exist matrices $\bar{P} > 0$, $\bar{Q} > 0$, $\bar{S} > 0$, $\bar{R} > 0$, Y_j, $\bar{N}_j$, and $\bar{M}_j$ with appropriate dimensions such that the following LMIs hold for $q = 1, 2$:

$$\begin{bmatrix} \bar{\Phi}_{11}^{ij} & \bar{\Phi}_{12}^{1ij} & \bar{\Phi}_{13}^{ij} & \bar{\Phi}_{14}^{ij} \\ 0 & \bar{R} - 2\bar{P} & 0 & 0 \\ 0 & 0 & -I & 0 \\ 0 & 0 & 0 & -R \end{bmatrix} < 0, \tag{17}$$

$$\begin{bmatrix} \bar{\Phi}_{11}^{ij} & \bar{\Phi}_{12}^{2ij} & \bar{\Phi}_{13}^{ij} & \bar{\Phi}_{14}^{ij} \\ 0 & \bar{R} - 2\bar{P} & 0 & 0 \\ 0 & 0 & -I & 0 \\ 0 & 0 & 0 & -R \end{bmatrix} < 0, \tag{18}$$

$$\begin{bmatrix} -\bar{P} & \sqrt{\rho}\bar{P}\{C_{2i}\}_q^T \\ * & -I \end{bmatrix} < 0, \tag{19}$$

where

$$\bar{\Phi}_{11}^{ij} = \begin{bmatrix} \bar{\Xi}_{11}^{ij} & \bar{\Xi}_{12}^{ij} & \bar{\Xi}_{13}^{ij} & \bar{\Xi}_{14}^{ij} \\ * & \bar{\Xi}_{22}^{ij} & \bar{\Xi}_{23}^{ij} & \bar{\Xi}_{24}^{ij} \\ * & * & \bar{\Xi}_{33}^{ij} & -\bar{N}_4^T \\ * & * & * & -\gamma^2 I \end{bmatrix},$$

$$\bar{\Phi}_{12}^{1ij} = \begin{bmatrix} \sqrt{\bar{d}}\bar{M}_1 \\ \sqrt{\bar{d}}\bar{M}_2 \\ \sqrt{\bar{d}}\bar{M}_3 \\ \sqrt{\bar{d}}\bar{M}_4 \end{bmatrix}, \bar{\Phi}_{12}^{2ij} = \begin{bmatrix} \sqrt{\bar{d}}\bar{N}_1 \\ \sqrt{\bar{d}}\bar{N}_2 \\ \sqrt{\bar{d}}\bar{N}_3 \\ \sqrt{\bar{d}}\bar{N}_4 \end{bmatrix},$$

$$\bar{\Phi}_{13}^{ij} = \begin{bmatrix} \bar{P}C_{1i}^T \\ Y_j^T D_{1i}^T \\ 0 \\ 0 \end{bmatrix} \bar{\Phi}_{14}^{ij} = \begin{bmatrix} \sqrt{\bar{d}}A_i^T \\ \sqrt{\bar{d}}Y_j^T B_i^T \\ 0 \\ \sqrt{\bar{d}}B_{1i}^T \end{bmatrix},$$

$$\begin{aligned} \bar{\Xi}_{11}^{ij} &= A_i\bar{P} + \bar{P}A_i^T + \bar{Q} + \bar{S} + \bar{M}_1 + \bar{M}_1^T, \\ \bar{\Xi}_{12}^{ij} &= B_i Y_j - \bar{M}_1 + \bar{M}_2^T + \bar{N}_1, \\ \bar{\Xi}_{13}^{ij} &= \bar{M}_3^T - \bar{N}_1, \bar{\Xi}_{14}^{ij} = B_{1i} + \bar{M}_4^T, \\ \bar{\Xi}_{22}^{ij} &= -(1-\mu)\bar{S} + \bar{N}_2 + \bar{N}_2^T - \bar{M}_2 - \bar{M}_2^T, \\ \bar{\Xi}_{23}^{ij} &= \bar{N}_3^T - \bar{N}_2 - \bar{M}_3^T, \bar{\Xi}_{24}^{ij} = \bar{N}_4^T - \bar{M}_4^T, \\ \bar{\Xi}_{33}^{ij} &= -Q - \bar{N}_3 - \bar{N}_3^T. \end{aligned}$$

Then a controller in the form of (9) exists, such that

(1) the closed-loop system is asymptotically stable;

(2) the performance $\|T_{z_1 w}\|_\infty < \gamma$ is minimized subject to output constraint (11) with the disturbance energy under the bound $w_{\max} = (\rho - V(0))/\gamma^2$.

Moreover, if inequalities (17)–(19) have a feasible solution, then the control gain K_j in (9) is given by $K_j = Y_j \bar{P}^{-1}$.

The proof is cut off due to space limitation. Contact the authors for the detailed proof.

IV. Simulation Results

In this section, a quarter vehicle active suspension system is exploited to demonstrate the effectiveness of the proposed approach. The quarter-car suspension model parameters are listed in Table I for the following controller design. The sprung

TABLE I
QUARTER-CAR MODEL PARAMETERS

k_s	k_t	c_s	c_t
42720N/m	101115N/m	1095Ns/m	14.6Ns/m

mass $m_s(t)$ is assumed to belong to the range $[873\text{kg}, 1073\text{kg}]$ and the unsprung mass $m_u(t)$ is assumed to belong to $[104\text{kg}, 124\text{kg}]$. In this study, the maximum allowable suspension stroke is assumed as $z_{\max} = 0.08$ m with $\rho = 1$. For the actuator delay $d(t) = 5 + 5\sin(\frac{1}{50})$ms satisfying $\bar{d} = 10$ms and $\mu = 0.1$, we consider fuzzy H_∞ controller design for the uncertain active suspension systems in (10). By using the convex optimization, it is found that the minimum guaranteed closed-loop H_∞ performance index γ_{min} is 5.9805 and the fuzzy controller gain matrices

$$K_j = 10^4 \times \begin{bmatrix} -8.0250 & 4.0130 & -3.3667 & 0.2256 \end{bmatrix}, \tag{20}$$

where $j = 1, 2, 3, 4$.

It is expected that the desired the fuzzy H_∞ controller with the parameters in (20) can be designed such that: 1) the sprung mass acceleration $z_1(t)$ is as small as possible; 2) the suspension deflection is below the maximum allowable suspension stroke $z_{\max} = 0.08$m, which means that $x_1(t)/z_{\max}$ below 1; 3) the relation dynamic tire load $k_t x_2(t)/(m_s(t) + m_u(t))g < 1$. We first consider the following test road disturbance as

$$z_r(t) = 0.0254\sin 2\pi t + 0.005\sin 10.5\pi t + 0.001\sin 21.5\pi t(\text{m}) \tag{21}$$

As discussed in [11], this road disturbance is close to the car body resonance frequency (1Hz), with high-frequency disturbance added to simulate the rough road surface. In order to carry out the simulation for the fuzzy H_∞ controller for the system in (10), the variational sprung mass $m_s(t)$ and the variational unsprung mass $m_u(t)$ are regards as $m_s(t) = 973+100\sin(t)$kg and $m_u(t) = 114+10\cos(t)$kg for deriving the fuzzy membership functional $h_i(\xi(t))$ $(i = 1, 2, 3, 4)$. By using the fuzzy H_∞ controller with the parameters in (20), we derive the corresponding closed-loop fuzzy system. Fig. 2 (a) depicts the responses of body vertical accelerations for the open- (passive) and closed-loop (active) systems and Fig. 2 (b) plots the responses of suspension stroke and tire deflection constraint for the passive and active systems. It is observed from Fig. 2 (a) that the proposed fuzzy H_∞ control strategy reduces the sprung mass acceleration significantly compared to the passive suspension under the same road disturbance. The designed fuzzy H_∞ controller can achieve the less value of the maximum body acceleration for the active suspension system than the passive system, and passenger acceleration in the active suspension system is reduced significantly, which guarantee better ride comfort. In addition, we can see from Fig. 2 (b) that the suspension deflection constrain $x_1(t)/z_{\max} < 1$ and the relation dynamic tire load $k_t x_2(t)/(m_s(t)+m_u(t))g < 1$ are guaranteed, which implies the road holding capability is ensured by the desired fuzzy controller. These two figures confirm that the designed standard state-feedback fuzzy H_∞ controller can achieve much better ride comfort and road handling, guarantee constrain suspension deflection for the active suspension system.

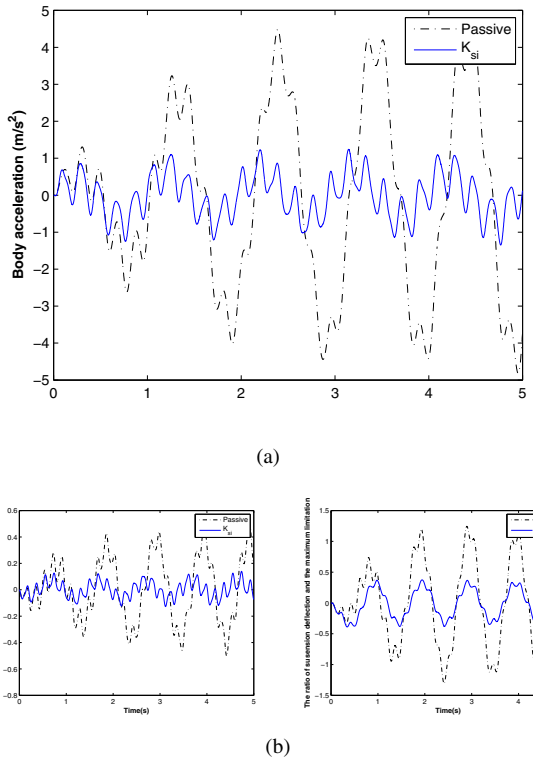

(a)

(b)

Fig. 2. (a) Responses of body vertical acceleration (b) Responses of suspension deflection constrain; Responses of tire stroke constrain.

V. Conclusions

This paper has investigated the problem of fuzzy H_∞ control for T-S fuzzy-model-based active suspension systems with actuator delay. The sprung and unsprung mass variations, the actuator delay, and the suspension performance have been taken into account to establish the T-S fuzzy system for the control design objective. Based on the PDC scheme and stability theory, the fuzzy H_∞ performance analysis condition has been presented for the proposed T-S fuzzy system presenting the uncertain active suspension system. Then, the fuzzy H_∞ controller has been designed such that the resulting closed-loop T-S fuzzy system is asymptotically stable with H_∞ performance, and simultaneous satisfy the constraint suspension performance. A quarter-car suspension model has been given to validate the effectiveness of the proposed design method.

VI. Acknowledgements

This work was partially supported by a joint PhD scholarship of Portsmouth University and Protean Electric Ltd.

References

[1] M. Yamashita, K. Fujimori, K. Hayakawa, and H. Kimura, "Application of H_∞ control to active suspension systems," *Automatica*, vol. 30, no. 11, pp. 1717–1729, 1994.

[2] N. Al-Holou, T. Lahdhiri, D. Joo, J. Weaver, and F. Al-Abbas, "Sliding mode neural network inference fuzzy logic control foractive suspension systems," *IEEE Transactions on Fuzzy Systems*, vol. 10, no. 2, pp. 234–246, 2002.

[3] C. Sivrioglu and I. Cansever, "LPV gain-scheduling controller design for a non-linear quarter-vehicle active suspension system," *Transactions of the Institute of Measurement and Control*, vol. 31, no. 1, pp. 71–95, 2009.

[4] M. ElMadany and Z. Abduljabbar, "Linear quadratic Gaussian control of a quarter-car suspension," *Vehicle System Dynamics*, vol. 32, no. 6, pp. 479–497, 1999.

[5] I. Fialho and G. Balas, "Road adaptive active suspension design using linear parameter-varying gain-scheduling," *IEEE transactions on Control Systems Technology*, vol. 10, no. 1, pp. 43–54, 2002.

[6] H. Chen and K. Guo, "Constrained H_∞ control of active suspensions: an LMI approach," *IEEE Transactions on Control Systems Technology*, vol. 13, no. 3, 2005.

[7] H. Du and N. Zhang, "H_∞ control of active vehicle suspensions with actuator time delay," *Journal of Sound and Vibration*, vol. 301, no. 1-2, pp. 236–252, 2007.

[8] H. Gao, J. Lam, and C. Wang, "Multi-objective control of vehicle active suspension systems via load-dependent controllers," *Journal of Sound and Vibration*, vol. 290, no. 3-5, pp. 654–675, 2006.

[9] H. Gao, W. Sun, and P. Shi, "Robust sampled-data H_∞ control for vehicle active suspension systems ," *IEEE Transactions on Control Systems Technology*, vol. 18, no. 1, pp. 238–245, 2010.

[10] H. Du, N. Zhang, and J. Lam, "Parameter-dependent input-delayed control of uncertain vehicle suspensions," *Journal of Sound and Vibration*, vol. 317, no. 3-5, pp. 537–556, 2008.

[11] H. Du and N. Zhang, "Fuzzy control for nonlinear uncertain electrohydraulic active suspensions with input constraint," *IEEE Transactions on Fuzzy Systems*, vol. 17, no. 2, pp. 343–356, 2009.

[12] K. Tanaka and H. Wang, *Fuzzy Control Systems Design and Analysis: A Linear Matrix Inequality Approach*. Wiley-Interscience, 2001.

2011 IEEE International Conference on Fuzzy Systems
June 27-30, 2011, Taipei, Taiwan

H_∞ Disturbance Attenuation of Fuzzy Large-Scale Systems

Mehdi Hosseinzadeh
Department of Electrical Engineering
Sharif University of Technology
Tehran, Iran
Emails: mehdi_hosseinzadeh@ee.sharif.edu,

Nasser Sadati
Department of Electrical Engineering
Sharif University of Technology
Tehran, Iran
Email: sadati@sina.sharif.edu

Iman Zamani
Department of Electrical Engineering
Amirkabir University of Technology
(Tehran Polytechnique)
Tehran, Iran
Email: zamaniiman@aut.ac.ir

***Abstract*—This paper is concerned with the disturbance attenuation problem of fuzzy large-scale systems which consist of N interconnected subsystems which are represented by Takagi-Sugeno fuzzy models. Using Lyapunov function and linear matrix inequalities (LMIs), a criterion is proposed to have a prescribed level of disturbance attenuation. A numerical example is given to illustrate the control design procedure and its effectiveness.**

***Index Terms*—Fuzzy large-scale systems, Stability, Disturbance attenuation, Linear matrix inequalities (LMIs).**

I. Introduction

A "large-scale system" could be considered as a system which consists of several subsystems. These subsystems serve particular functions, share resources, and are usually connected by a set of interconnections [1]-[3]. Electrical power system, nuclear reactors, aerospace systems, economic systems, and process control systems, etc., are examples of large-scale systems. Since most of the real systems are complex and huge in size, many researchers are interested to study the stability problem of large-scale systems [4]-[12].

Nowadays, most complex systems are modeled as a fuzzy system with IF-THEN rules. By using fuzzy modeling, we can model complex nonlinear systems to arbitrary degrees of accuracy [13],[14]. There are too many approaches to model a process using fuzzy rules. One of them is the so-called T-S fuzzy model which is proposed by Takagi and Sugeno [15],[16]. Suppose that the large-scale system consists of a number of subsystems with interconnections, the nonlinear model of each subsystem can be modeled as a T-S fuzzy model such that each subsystem has a number of fuzzy regions having local linear dynamic in each region. The global model of large-scale system can be then achieved by connecting these local models by the use of membership functions.

Motivated from the work in [17],[18], the main task of this paper is to investigate the disturbance attenuation problem of fuzzy large-scale systems. Instead of conventional fuzzy parallel distribute compensation (PDC) design [19], nonlinear state feedback controllers are used in the stabilization of the whole system with a good disturbance attenuation.

This paper is organized as follows. Section II introduces the fuzzy large-scale model. An H_∞ controller design method for fuzzy large-scale systems is presented in Section III. An example which illustrate the effectiveness of the proposed approach is given in Section IV. Finally, some concluding remarks are given in Section V .

II. Fuzzy Large-scale Systems Model

Consider a fuzzy large-scale system (S) which consists of N interconnected subsystems $S_i (i = 1,2,\ldots,N)$. The ith fuzzy subsystem S_i can be described by:

$$S_i^l = \begin{cases} \dot{x}_i(t) = \sum_{l=1}^{r_i} \mu_i^l (A_i^l x_i(t) + B_i^l u_i(t) + E_i^l v_i(t)) \\ \qquad\qquad + \sum_{\substack{j=1 \\ j\neq i}}^{N} \sum_{l=1}^{r_i} \mu_i^l f_{ij}^l (x_j(t)) \\ y_i(t) = \sum_{l=1}^{r_i} \mu_i^l C_i^l x_i(t) \end{cases} \quad (1)$$

where S_i^l is the lth rule of S_i, $u_i(t) \in \mathbb{R}^{m_i}$ is the control input of S_i at time t with appropriate dimension, $x_i(t) \in \mathbb{R}^{n_i}$ is the state vector of the ith subsystem, $v_i(t) \in \mathbb{R}^{q_i}$ is the disturbance that belongs to $L_2[0,\infty)$, $f_{ij}^l(x_j(t))$ is the interconnection between the ith and jth subsystem in the lth rule of S_i, r_i is the number of rules in subsystem S_i, $(A_i^l, B_i^l, E_i^l, C_i^l)$ is the system matrices of rule l, in subsystem S_i, such that (A_i^l, B_i^l) is controllable, and μ_i^l is normalized membership function defined in in the following, in which $M_i^k(x_{ik}(t))$ is the grade of membership of $x_{ik}(t)$ in M_i^k.

$$\begin{aligned} &\mu_i^l(x_i(t)) = {}^{w_i^l}\!/_{\sum_{k=1}^{n_i} w_i^j} \\ &w_i^j = \prod_{k=1}^{n_i} M_i^k(x_{ik}(t)) \geq 0 \end{aligned} \quad (2)$$

As it can be seen in Fig. 1, $\sum_{l=1}^{r_i} \mu_i^l = 1, i = 1,2,\ldots,N$.

The jth rule of the isolated subsystem S_i, which is represented by a T-S fuzzy model, is of the following form:

$$\begin{aligned} &\text{Rule } j: \\ &\text{if } x_{i1}(t) \text{ is } M_i^l \text{ and } \ldots\ x_{in_i}(t) \text{ is } M_i^{n_i} \\ &\text{then } \dot{x}_i = A_i^l x_i(t) + B_i^l u_i(t) + E_i^l v_i(t) \\ &\qquad\qquad + \sum_{\substack{j=1 \\ j\neq i}}^{N} f_{ij}^l (x_j(t)) \\ &y_i(t) = C_i^l x_i(t) \end{aligned} \quad (3)$$

where $x_i(t) = [x_{i1}(t), x_{i2}(t), \ldots, x_{in_i}(t)]^T$, and M_i^ls are the fuzzy sets.

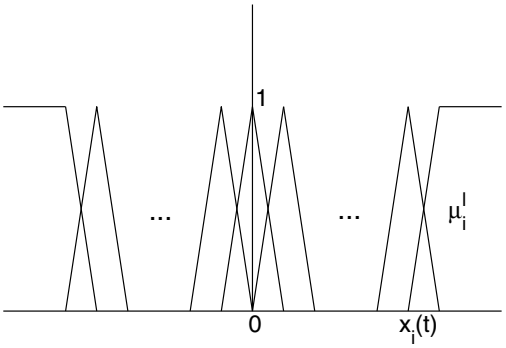

Fig. 1. Normalized membership function

III. H_∞ Controller Design with Nonlinear State Feedback Controller

In this section, based on Lyapunov functions we consider the H_∞ controller design for the large-scale fuzzy system (1). The objective is to find a fuzzy control law $u_i(t)$ such that the system (1) has a good level of disturbance attenuation, i.e., to have a good level of performance in the H_∞ sense. The H_∞ norm of a transfer function like $F(s)$, with output $y(t)$ and input $v(t)$, can be defined as follows [20]:

$$\|F(s)\|_\infty := \sup_{Re(s)>0} \bar{\sigma}[F(s)] = \sup_{\omega \varepsilon R} \bar{\sigma}[F(j\omega)] \tag{4}$$

Now, by defining the H_2 norm of $y(t)$ and $v(t)$ as

$$\|y\|_2^2 = \int_{-\infty}^{+\infty} y^T(t)y(t)dt$$
$$\|v\|_2^2 = \int_{-\infty}^{+\infty} v^T(t)v(t)dt$$

it can be concluded that

$$\frac{\|y\|_2}{\|v\|_2} \leq \|F\|_\infty$$

In the large-scale fuzzy system (1), by defining $F(s)$ the transfer function from the disturbance $v(t)$ to the output as $y(t)$, having a disturbance attenuation γ is equal to have $\|F\|_\infty \leq \gamma$, or equally:

$$\|y(t)\|_2 < \gamma \|v(t)\|_2 \tag{5}$$

for all non-zero $v(t) \in L_2$, where $y(t) = [y_1^T(t), y_2^T(t), \ldots, y_N^T(t)]^T$ and $v(t) = [v_1^T(t), v_2^T(t), \ldots, v_N^T(t)]^T$. Now, the closed-loop control system is said to be stable with disturbance attenuation γ. For this purpose, a nonlinear state feedback controller is considered as follows

$$u_i(t) = -\sum_{k=1}^{c_i} m_i^k(t) K_i^k(t) x_i(t) \tag{6}$$

in which

$$\sum_{k=1}^{c_i} m_i^k(t) = 1 \quad , \quad 0 \leq m_i^k(t) \leq 1$$

$$(i = 1,2,\ldots,N)(k = 1,2,\ldots,c_i) \tag{7}$$

and K_i^k is the state feedback gain with appropriate dimension. $m_i^k(t)$ is a nonlinear function defined by (9) and (10), c_i is an optimal number of controller in each subsystem. $M_i^{l,\acute{l},h}$s and $|M_i^{l,\acute{l},h}|$s are given in (11) and (12), in which, P_is are symmetric positive definite matrices, ε_{i1} and ε_{i2} are positive scalars, $f_{ij}^l(x_j(t)) = G_{ij}^l x_j(t)$, and n_{ij} is either 0 or 1. Now, by proposing the nonlinear state feedback controller, the closed-loop fuzzy subsystem becomes

$$\dot{x}_i(t) = \sum_{l=1}^{r_i}\sum_{k=1}^{c_i} \mu_i^l(t) m_i^k(t) \left\{ (A_i^l - B_i^l K_i^k) x_i(t) + E_i^l v_i(t) \right\} + \sum_{l=1}^{r_i}\sum_{\substack{j=1 \\ j\neq i}}^{N} \mu_i^l(t) f_{ij}^l(x_j(t))$$

$$y_i(t) = \sum_{l=1}^{r_i} \mu_i^l C_i^l x_i(t) \tag{8}$$

in which

$$m_i^1(t) = \begin{cases} 1 - \frac{\sum_{k=2}^{c_i} M_i^{l,\acute{l},k}}{\sum_{h=2}^{c_i} abs(M_i^{l,\acute{l},h})} & ,if \ \sum_{h=2}^{c_i} |M_i^{l,\acute{l},h}| \neq 0 \\ \frac{1}{c_i} & ,if \ \sum_{h=2}^{c_i} |M_i^{l,\acute{l},h}| = 0 \end{cases} \tag{9}$$

and

$$m_i^k(t) = \begin{cases} \frac{\sum_{k=2}^{c_i} M_i^{l,\acute{l},k}}{\sum_{h=2}^{c_i} |M_i^{l,\acute{l},h}|} & ,if \ \sum_{h=2}^{c_i} |M_i^{l,\acute{l},h}| \neq 0 \\ \frac{1}{c_i} & ,if \ \sum_{h=2}^{c_i} |M_i^{l,\acute{l},h}| = 0 \end{cases} \tag{10}$$

where

$$M_i^{l,\acute{l},k} = \sum_{l=1}^{r_i} \mu_i^l \mu_i^{\acute{l}} x_i^T(t) \Big(\left(A_i^l - B_i^l K_i^k\right)^T P_i + P_i \left(A_i^l - B_i^l K_i^k\right) + C_i^{lT} C_i^{\acute{l}} + \varepsilon_{i1}^{-1} P_i^T P_i + \sum_{j=1}^{N} \varepsilon_{i2}^{-1} n_{ij} P_i^T P_i + \sum_{j=1}^{N} \varepsilon_{i2} n_{ji} G_{ji}^{lT} G_{ji}^l \Big) x_i(t) \tag{11}$$

and

$$|M_i^{l,\acute{l},k}| = \sum_{l=1}^{r_i} |\mu_i^l \mu_i^{\acute{l}} x_i^T(t) \Big(\left(A_i^l - B_i^l K_i^k\right)^T P_i + P_i \left(A_i^l - B_i^l K_i^k\right) + C_i^{lT} C_i^{\acute{l}} + \varepsilon_{i1}^{-1} P_i^T P_i + \sum_{j=1}^{N} \varepsilon_{i2}^{-1} n_{ij} P_i^T P_i + \sum_{j=1}^{N} \varepsilon_{i2} n_{ji} G_{ji}^{lT} G_{ji}^l \Big) x_i(t)| \tag{12}$$

Now, our task is to design K_i^k in such a way that the whole fuzzy large-scale system satisfies the condition (5). This condition is summarized by the following theorem.

Theorem 3.1: The fuzzy large-scale system (1) has a guaranteed performance in H_∞ sense, if there exist symmetric positive definite matrices P_i, positive scaler ε_{i1} and ε_{i2}, and state gain K_i^1, such that the following condition is satisfied:

$$\begin{bmatrix} \Omega_1 & 0 \\ 0 & \Omega_2 \end{bmatrix} < 0 \tag{13}$$

where

$$\begin{aligned}\Omega_1 &= m_i^1\left(A_i^l - B_i^l K_i^1\right)^T P_i + P_i\left(A_i^l - B_i^l K_i^1\right)\\ &\quad + C_i^{lT} C_i^{\acute{l}} + \varepsilon_{i1}^{-1} P_i^T P_i + \textstyle\sum_{j=1}^N \varepsilon_{i2} n_{ji} G_{ji}^{lT} G_{ji}^l \\ \Omega_2 &= \varepsilon_{i1} E_i^{lT} E_i^l - \gamma^2 I.\end{aligned} \tag{14}$$

Proof: Consider a Lyapunov function $V(t)$ for the fuzzy large-scale system (1), given by

$$V(t) = \sum_{i=1}^N V_i(t) = \sum_{i=1}^N x_i^T(t) P_i x_i(t) \tag{15}$$

Now, by taking the derivative of $V_i(t)$ along the trajectories of ith subsystem, we get

$$\dot{V}_i(t) = \dot{x}_i^T P_i x_i(t) + x_i^T(t) P_i \dot{x}_i(t) \tag{16}$$

where, under zero conditions

$$\begin{aligned}&\textstyle\int_0^{+\infty}\left\{y^T(t)y(t) - \gamma^2 v^T(t)v(t)\right\}dt\\ &= \textstyle\int_0^{+\infty}\left\{y^T(t)y(t) - \gamma^2 v^T(t)v(t) + \frac{d}{dt}V(t)\right\}dt\\ &\quad - V(+\infty)\\ &\le \textstyle\int_0^{+\infty}\left\{y^T(t)y(t) - \gamma^2 v^T(t)v(t)\right.\\ &\quad \left. + \textstyle\sum_{i=1}^N\left[\dot{x}_i^T P_i x_i(t) + x_i^T(t) P_i \dot{x}_i(t)\right]\right\}dt\\ &\le \textstyle\int_0^{+\infty}\sum_{i=1}^N\left\{\sum_{\acute{l}=1}^{r_i}\mu_i^l\mu_i^{\acute{l}} x_i^T(t) C_i^{lT} C_i^{\acute{l}} x_i(t)\right.\\ &\quad - \gamma^2 v_i^T(t) v_i(t)\\ &\quad + \textstyle\sum_{l=1}^{r_i}\sum_{k=1}^{c_i}\mu_i^l m_i^k x_i^T(t)\left(\left(A_i^l - B_i^l K_i^k\right)^T P_i\right.\\ &\quad \left. + P_i\left(A_i^l - B_i^l K_i^k\right)\right) x_i(t)\\ &\quad + \textstyle\sum_{l=1}^{r_i}\mu_i^l\left(v_i^T(t) E_i^{lT} P_i x_i(t) x_i^T(t) P_i E_i^l v_i(t)\right)\\ &\quad \left. + 2\textstyle\sum_{l=1}^{r_i}\sum_{j=1}^N \mu_i^l f_{ij}^{lT} P_i x_i(t)\right\}dt\end{aligned} \tag{17}$$

Using the following matrix inequalities for all $a, b \in \mathbb{R}^n$, and any positive constant $\varepsilon > 0$

$$2a^T b \le \varepsilon a^T a + \varepsilon^{-1} b^T b \tag{18}$$

Now, let $f_{ij}^l(x_j(t)) = G_{ij}^l x_j(t)$, then we get

$$\begin{aligned}&\le \textstyle\int_0^{+\infty}\sum_{i=1}^N\left\{\sum_{\acute{l}=1}^{r_i}\sum_{k=1}^{c_i}\mu_i^l\mu_i^{\acute{l}} m_i^k x_i^T(t)\left(\left(A_i^l\right.\right.\right.\\ &\quad \left.\left.\left. - B_i^l K_i^k\right)^T P_i + P_i\left(A_i^l - B_i^l K_i^k\right)\right.\right.\\ &\quad \left.\left. + C_i^{lT} C_i^{\acute{l}}\right) x_i(t) - \gamma^2 v^T(t) v(t)\right.\\ &\quad + \textstyle\sum_{l=1}^{r_i}\mu_i^l \varepsilon_{i1} v_i^T(t) E_i^{lT} E_i^l v_i(t)\\ &\quad + \textstyle\sum_{l=1}^{r_i}\mu_i^l \varepsilon_{i1}^{-1} x_i^T(t) P_i^T P_i x_i(t)\\ &\quad + \textstyle\sum_{l=1}^{r_i}\sum_{j=1}^N \mu_i^l \varepsilon_{i2} x_j^T(t) G_{ij}^{lT} G_{ij}^l x_j(t)\\ &\quad \left. + \textstyle\sum_{l=1}^{r_i}\sum_{j=1}^N \mu_i^l \varepsilon_{i2}^{-1} x_i^T(t) P_i^T P_i x_i(t)\right\}dt\end{aligned} \tag{19}$$

By defining n_{ij} as follows

$$n_{ij} = \begin{cases} 1 & \text{if } G_{ij}^l \neq 0 \\ 0 & \text{if } G_{ij}^l = 0 \end{cases} \tag{20}$$

we get

$$\begin{aligned}&= \textstyle\int_0^{+\infty}\sum_{i=1}^N\left\{\sum_{l=1}^{r_i}\sum_{k=1}^{c_i}\mu_i^l\mu_i^{\acute{l}} m_i^k x_i^T(t)\left(\left(A_i^l\right.\right.\right.\\ &\quad \left.\left.\left. - B_i^l K_i^k\right)^T P_i + P_i\left(A_i^l - B_i^l K_i^k\right)\right.\right.\\ &\quad \left.\left. + C_i^{lT} C_i^{\acute{l}} + \varepsilon_{i1}^{-1} P_i^T P_i\right.\right.\\ &\quad \left.\left. + \textstyle\sum_{j=1}^N \varepsilon_{i2}^{-1} n_{ij} P_i^T P_i\right.\right.\\ &\quad \left.\left. + \textstyle\sum_{j=1}^N \varepsilon_{i2} n_{ji} G_{ij}^{lT} G_{ij}^l\right) x_i(t)\right.\\ &\quad \left. + \textstyle\sum_{l=1}^{r_i}\mu_i^l v_i^T(t)\left(\varepsilon_{i1} E_i^{lT} E_i^l - \gamma^2 I\right) v_i(t)\right\}dt\end{aligned} \tag{21}$$

Now, by using the definition of m_i^k, we have

$$\begin{aligned}&\textstyle\int_0^{+\infty}\left\{y^T(t)y(t) - \gamma^2 v^T(t)v(t)\right\}dt\\ &\le \textstyle\int_0^{+\infty}\sum_{i=1}^N\sum_{\acute{l}=1}^{r_i}\mu_i^l\mu_i^{\acute{l}} \times \left\{\begin{bmatrix} x_i(t) \\ v_i(t)\end{bmatrix}^T\right.\\ &\quad \left.\times \begin{bmatrix} \Omega_1 & 0 \\ 0 & \Omega_2\end{bmatrix} \times \begin{bmatrix} x_i(t) \\ v_i(t)\end{bmatrix}\right\}dt\end{aligned} \tag{22}$$

where

$$\begin{aligned}\Omega_1 &= m_i^1\left(A_i^l - B_i^l K_i^1\right)^T P_i + P_i\left(A_i^l - B_i^l K_i^1\right)\\ &\quad + C_i^{lT} C_i^{\acute{l}} + \varepsilon_{i1}^{-1} P_i^T P_i + \textstyle\sum_{j=1}^N \varepsilon_{i2} n_{ji} G_{ji}^{lT} G_{ji}^l \\ \Omega_2 &= \varepsilon_{i1} E_i^{lT} E_i^l - \gamma^2 I\end{aligned} \tag{23}$$

now if $\begin{bmatrix} \Omega_1 & 0 \\ 0 & \Omega_2\end{bmatrix} < 0$, we get

$$\int_0^{+\infty}\left\{y^T(t)y(t) - \gamma^2 v^T(t)v(t)\right\}dt < 0 \tag{24}$$

which implies that when $x_i(0) = 0; i = 1, 2, \ldots, N$, $\|y(t)\|_2 < \gamma\|v(t)\|_2$. ■

Now, it can be easily seen that if inequality (13) is satisfied, then the closed-loop fuzzy large-scale system is asymptotically stable, with disturbance attenuation γ.

According to the above theorem, the following algorithm can be developed for designing the controller.

Algorithm

1) Set a value for $\varepsilon_{ij}; j = 1, 2$.
2) Solve the matrix inequality (13). This can be solved by using the MATLAB LMI toolbox.
3) If the solution is feasible, the controller parameter K_i^1 will be obtained and the procedure can be stopped. In this case $K_i^k; k \neq 1$ can be chosen according to the type of the response. That is, $K_i^k; k \neq 1$ affects the response features, like: settling time, overshoot , etc. If the solution is not feasible, set $\varepsilon_{ij} = \frac{\varepsilon_{ij}}{2}$ [18], and go to step 2.

IV. Numerical Example

Here, an example is presented to verify the results of the proposed stabilization procedure of fuzzy large-scale system composed of two subsystems described by

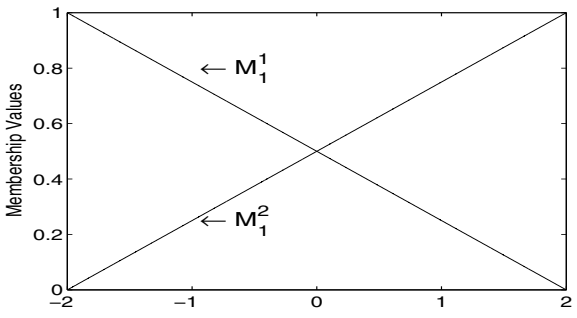

Fig. 2. Membership functions of subsystem S_1

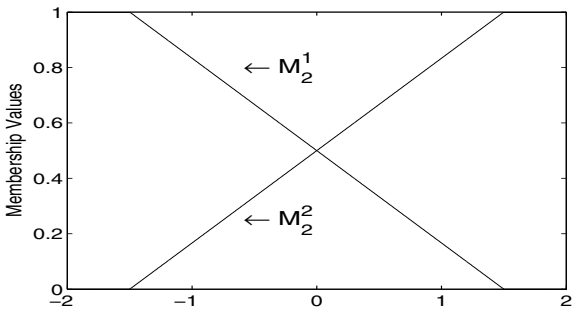

Fig. 3. Membership functions of subsystem S_2

Subsystem S_1

$$
\begin{aligned}
\text{Rule1}: \ & \text{if } x_{11}(t) \text{ is } M_1^2 \text{ and } x_{12}(t) \text{ is } M_1^1 \\
& \text{then } \dot{x_1}(t) = A_1^1 x_1(t) + B_1^1 u_1(t) \\
& \quad + E_1^1 v_1(t) + \textstyle\sum_{j=1}^{2} G_{1j}^1 x_j(t) \\
& y(t) = C_1^1 x_1(t) \\
\text{Rule2}: \ & \text{if } x_{11}(t) \text{ is } M_1^2 \text{ and } x_{12}(t) \text{ is } M_1^2 \\
& \text{then } \dot{x_1}(t) = A_1^2 x_1(t) + B_1^2 u_1(t) \\
& \quad + E_1^2 v_1(t) + \textstyle\sum_{j=1}^{2} G_{1j}^2 x_j(t) \\
& y(t) = C_1^2 x_1(t)
\end{aligned}
$$

in which $A_1^1 = \begin{bmatrix} -0.1 & 0 \\ 0 & -1 \end{bmatrix}$, $A_1^2 = \begin{bmatrix} 0 & 1 \\ -1.2 & -1 \end{bmatrix}$, $B_1^1 = \begin{bmatrix} 2.2 \\ 0 \end{bmatrix}$, $B_1^2 = \begin{bmatrix} 1.2 \\ -0.6 \end{bmatrix}$, $D_1^1 = D_1^2 = \begin{bmatrix} 0 \\ 0.5 \end{bmatrix}$, $C_1^1 = C_1^2 = \begin{bmatrix} 1 & 0 \end{bmatrix}$. Moreover, the interconnection matrices among the two subsystems are given by $G_{12}^1 = \begin{bmatrix} 0.1 & 0 \\ 0 & 0 \end{bmatrix}$, $G_{12}^2 = \begin{bmatrix} 0.1 & 0.1 \\ 0.1 & 0.1 \end{bmatrix}$. Membership functions of subsystem S_1 are shown in Fig. 2.

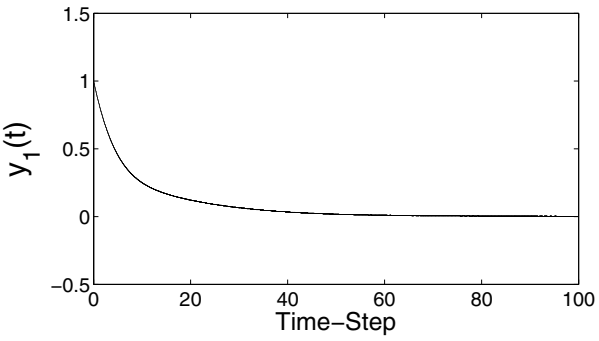

Fig. 4. $y_1(t)$, the output of the subsystem S_1

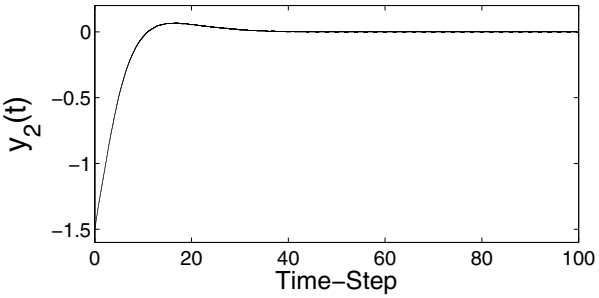

Fig. 5. $y_2(t)$, the output of the subsystem S_2

Subsystem S_2

$$
\begin{aligned}
\text{Rule1}: \ & \text{if } x_{21}(t) \text{ is } M_2^1 \text{ and } x_{22}(t) \text{ is } M_2^1 \\
& \text{then } \dot{x_2}(t) = A_2^1 x_2(t) + B_2^1 u_2(t) \\
& \quad + E_2^1 v_2(t) + \textstyle\sum_{j=1}^{2} G_{2j}^1 x_j(t) \\
& y(t) = C_2^1 x_2(t) \\
\text{Rule2}: \ & \text{if } x_{21}(t) \text{ is } M_2^2 \text{ and } x_{22}(t) \text{ is } M_2^1 \\
& \text{then } \dot{x_2}(t) = A_2^2 x_2(t) + B_2^2 u_2(t) \\
& \quad + E_2^2 v_2(t) + \textstyle\sum_{j=1}^{2} G_{2j}^2 x_j(t) \\
& y(t) = C_2^2 x_2(t)
\end{aligned}
$$

in which $A_2^1 = \begin{bmatrix} -1 & 0 \\ -0.8 & -2 \end{bmatrix}$, $A_2^2 = \begin{bmatrix} 0.08 & 1 \\ -2.5 & -0.6 \end{bmatrix}$, $B_2^1 = \begin{bmatrix} 1.2 \\ 1.2 \end{bmatrix}$, $B_2^2 = \begin{bmatrix} 2.2 \\ -0.8 \end{bmatrix}$, $D_2^1 = D_2^2 = \begin{bmatrix} 0 \\ 0.4 \end{bmatrix}$, $C_2^1 = C_2^2 = \begin{bmatrix} 1 & 0 \end{bmatrix}$. Moreover, the interconnection matrices among the two subsystems are given by $G_{21}^1 = \begin{bmatrix} 0 & 0.1 \\ 1 & 0 \end{bmatrix}$, $G_{21}^2 = \begin{bmatrix} 0.3 & 0 \\ -0.9 & 0 \end{bmatrix}$. The normalized membership functions of subsystem S_2 are shown in Fig. 3. To design, first, we design a nonlinear state feedback controller for each subsystem so to make the fuzzy large-scale have a good performance in H_∞ sense. By choosing $\varepsilon_{11} = \varepsilon_{21} = 2$ and $\varepsilon_{12} = \varepsilon_{22} = \frac{100}{0.15}$ and

using the above procedure, we can have

$$Q_1 = P_1^{-1} = \begin{bmatrix} 0.162 & 0.0066 \\ 0.0066 & 0.1626 \end{bmatrix},$$
$$Q_2 = P_2^{-1} = \begin{bmatrix} 0.1137 & 0.0157 \\ 0.0157 & 0.1851 \end{bmatrix},$$
$$K_1^1 = K_2^1 = \begin{bmatrix} 1 & 0 \end{bmatrix}$$

Since K_1^2 and K_2^2 don't affect the stability, by choosing $K_1^2 = \begin{bmatrix} 1 & 1 \end{bmatrix}$ and $K_2^2 = \begin{bmatrix} 0.01 & 0.01 \end{bmatrix}$, the procedure is completed. The initial conditions are $x_1(0) = \begin{bmatrix} 1 & -1.5 \end{bmatrix}^T$, $x_2(0) = \begin{bmatrix} -1.5 & 1 \end{bmatrix}^T$.

The simulation results using $v_1(t) = 5\sin(2\pi t)$, $v_2(t) = 5\sin(\pi t)$, 100 steps of $\Delta t = 0.01$, and $\gamma = 0.0036$ are shown in Figs. 4 and 5. It can be observed that the controller proposed in this paper based on the fuzzy dynamic model not only stabilizes the original nonlinear system but also effectively attenuates the disturbances as expected.

V. Conclusion

This paper investigates the disturbance attenuation problem of fuzzy large-scale systems. Under some sufficient conditions, the nonlinear state feedback controller is designed to have a desired disturbance attenuation. LMI tools play a key role to find the symmetric positive matrices P_i. It is shown that using the method presented in this paper, the stability condition can be checked by K_i^1. That is, K_i^k (for $k \neq 1$) does not affect the stability. An example is also presented to illustrate the effectiveness of the proposed method.

References

[1] M. Jamshidi, Large-scale system modeling and control, New York: Elsevier, 1983.

[2] M. S. Mahmoud, "Multilevel systems control and application: a survey,"IEEE Trans. Syst., Man, Cybern.,vol. SMC-7, pp. 125-143, 1977.

[3] A. N. Michel, and R. K. Miller, Qualitative analysis of large-scale system, New York: Academic, 1977.

[4] T. N. Lee, and U. L. Radovic, "General decentralized stabilization of large-scale linear continuous and discrete time-delay systems," Int. J. Control, vol. 46, no. 6, pp. 2127-2140, 1987.

[5] W. J. Wang, and L. G. Mau, "Decentralized PDC for large-scale T-S fuzzy systems," IEEE Trans. Fuzzy Syst., vol. 13, no. 6, pp. 779-786, 2005.

[6] W. J. Wang, and W. W. Lin, "Stabilization and estimation for perturbed discrete time-delay large-scale systems," IEEE Trans. Fuzzy Syst., vol. 13, no. 6, pp. 779-786, 2005.

[7] W. J. Wang, and L. Luoh, "Stability and stabilization of fuzzy large-scale systems," IEEE Trans. Autom. Control., vol. 42, no. 9, pp. 1277-1282, 1997.

[8] J. C. Tsay, P. L. Liu, and T. J. Su, "Robust stability for perturbed large-scale time-delay systems," Proc. Inst. Elec. Eng., Control Theory Appl., vol. 143, no. 3, pp. 233-236, 1996.

[9] F. H. Hsiao, and J. D. Hwang, "Stability analysis of fuzzy large-scale systems," IEEE Trans. Syst., Man, Cybern., vol. 32, no. 1, pp. 122-126, 2001.

[10] H. K. Lam, F. H. Leung, and P. K. S. Tam, "Nonlinear state feedback controller for nonlinear systems: stability analysis and design based on fuzzy plant model," IEEE Trans. Fuzzy Syst., vol. 9, no. 4, pp. 657-661, 2001.

[11] Z. Hu, "Decentralized stabilization of large-scale interconnection systems with delay," IEEE Trans. Autom. Control.,vol. 39, no. 1, pp. 180-182, 1994.

[12] K. Tanaka, and M. Sano, "Fuzzy stability criterion of a class of nonlinear systems," Inf. Sci., vol. 71, no. 1/2, pp. 3-26, 1993.

[13] J. J. Buckley, "Universal fuzzy controllers ," Automatica., vol. 28, pp. 1245-1248, 1992.

[14] L. X. Wang, "Fuzzy systems are universal approximators," Proc. IEEE Int. Conf. Fuzzy Systems, San Diego, CA, 1992, pp. 1163-1170.

[15] K. Takagi, and M. Sano, "Fuzzy indentification of systems and its application to modeling and control," IEEE Trans. Syst. Man. Cybern., vol. SMC-15, no. 1, pp. 116-132, 1985.

[16] K. Tanaka, and M. Sugeno, "Stability analysis and design of fuzzy control systems," Fuzzy Sets Syst., vol. 45, no. 2, pp. 135-156, 1992.

[17] I. Zamani, and N. Sadati, "Fuzzy large-scale systems stabilization with nonlinear state feedback controller," Proceeding of the 2009 IEEE International Conference on Systems, Man, and Cybernetics, San Antonio, TX, USA, Oct. 2009.

[18] H. Zhang, C. Li, and X. Liao, "Stability analysis and H_∞ controller design of fuzzy large-scale systems based on piecewise Lyapunov functions," IEEE Trans. Syst., Man, Cybern., B, Cybern., vol. 36, no. 3, pp. 685-697, 2006.

[19] H. K. Khalil, Nonlinear Systems, Upper saddle River, NJ: Prentice-Hall, third edition, 2002.

[20] K. Zhou, and J. Doyle, Essentials of robust control, Prentice-Hall, 1998.

2011 IEEE International Conference on Fuzzy Systems
June 27-30, 2011, Taipei, Taiwan

Dualities and Isomorphisms between Indistinguishabilities and Related Concepts

Gabriel Mattioli
Sec. Matemàtiques i Informàtica
ETS Arquitectura del Vallès
Universitat Politècnica de Catalunya
C. Pere Serra 1-15
Sant Cugat del Vallès 08190
Spain
Email: gabriel.mattioli@upc.edu

Jordi Recasens
Sec. Matemàtiques i Informàtica
ETS Arquitectura del Vallès
Universitat Politècnica de Catalunya
C. Pere Serra 1-15
Sant Cugat del Vallès 08190
Spain
Email: j.recasens@upc.edu

***Abstract*—Given a T-indistinguishability operator, the corresponding set H_E of extensional sets and the operators ϕ_E and ψ_E that provide upper and lower approximations of a fuzzy subset by extensional ones can be defined. Reciprocally, given any of these, the initial indistinguishability operator can be retrieved. In order to understand in depth how this relation works, it will be shown that there is an isomorphism between the corresponding lattices and how this isomorphism acts over the operations and orderings of the lattices will be studied.**

Keywords*: *indistinguishability operator; extensional set; upper approximation, lower approximation; transitive closure; extensional closure

I. Introduction

The set H_E of extensional fuzzy subsets of an indistinguishability operator E has been widely studied in the literature. In [1] it has been studied from an algebraic point of view and in [2] its topological behaviour has been analyzed. It has also been characterized as the set of generators of E [3], the set of logical states and the set of fixed points of two operators known as ϕ_E and ψ_E [2]. These two operators give upper and lower approximations respectively of a fuzzy subset by extensional ones with respect to E. Although the results obtained in relation to H_E, ϕ_E and ψ_E show a very similar family of properties these concepts fulfill separately, up to this point a real study of the depth of this relation has not been done yet.

In [4] the operators that can be upper and lower approximations of an indistinguishability operators have been characterized and [1] did the same for a set of fuzzy subsets of a universe to be the extensional set of an indistinguishability operator providing as a consequence bijections between the set $\mathcal{E}$ of indistinguishability operators on a given universe X, the set $\mathcal{H}$ of sets of extensional sets with respect to indistinguishability operators on X and the sets $\mathcal{U}$ and $\mathcal{L}$ of upper and lower approximations of fuzzy subsets by extensional ones with respect to an indistinguishability operator on X. Taking this into account and also the fact that these concepts verify a very similar collection of properties, it seems natural to ask if the connection between these sets is more than a simple bijection or if some kind of structure is kept.

This work has focused on this point and the results obtained have been that these bijections are actually isomorphisms, as the ordering and the structure given by the operations is kept. Furthermore, these sets can be regarded as lattices and, therefore, what we obtain is that all these lattices are isomorphic.

This fact has both a theoretical and practical relevance. It is theoretically interesting because this work provides some order and relation between the studies on indistinguishability operators, extensional sets, and upper and lower approximations that have been done up to this point. Furthermore, as all these concepts are isomorphic, the result shows that the only difference between them is the way in which are approached and the notation; this fact allowing us to translate all the results obtained on one lattice to the others through the isomorphisms presented on this paper.

From a practical point of view these isomorphisms are interesting too because several times multiple attributes are considered in a given problem and some kind of aggregation has to be done between them. This problem has been studied in [8] restricted to the aggregation of different indistinguishability operators. What if some attributes are more easily modelled by an indistinguishability operator, as they come from matching objects with a prototype, for instance, while other attributes are better seen as extensional sets because they come from direct observation? The isomorphisms we present in this paper allow us to codify different attributes into the concept that shows less difficulty to do so, and translate them into the same concept through these isomorphisms.

This work is structured in the following way:

In the next section of preliminaries the concepts related with the work are defined and the main properties and results related to them are given.

In Section III the main results of this work are proved. It is separated into three subsections that will show separately the isomorphisms between the sets $\mathcal{E}$, $\mathcal{H}$, $\mathcal{U}$ and $\mathcal{L}$.

978-1-4244-7316-8/11/$26.00 ©2011 IEEE

The isomorphisms will be explicitly given and how they work on the operations will be showed.

Finally, the main results of this work are summarized at the Conclusion.

II. Preliminaries

In this section the basic definitions and results that underly the present work will be provided. Firstly the concepts related to indistinguishability operators will be given: the definition of an indistinguishability operator and the transitive closure of a reflexive and symmetric fuzzy relation. Furthermore, the definition and basic properties of the set H_E of extensional fuzzy subsets sets of an indistinguishability operator E and the upper and lower approximations (ϕ_E and ψ_E respectively) related to E will be given.

Definition II.1. *Let T be a t-norm.*

- *The residuation $\overrightarrow{T}$ of T is defined for all $x, y \in [0,1]$ by*
$$\overrightarrow{T}(x|y) = \sup\{\alpha \in [0,1] | T(\alpha, x) \leq y\}.$$
- *The birresiduation $\overleftrightarrow{T}$ of T is defined for all $x, y \in [0,1]$ by*
$$\overleftrightarrow{T}(x,y) = \min\{\overrightarrow{T}(x|y), \overrightarrow{T}(y|x)\} = T(\overrightarrow{T}(x|y), \overrightarrow{T}(y|x)).$$

Definition II.2. *Let T be a t-norm. A fuzzy relation E on a set X is a T-indistinguishability operator if and only if for all $x, y, z \in X$*

a) $E(x,x) = 1$ *(Reflexivity)*
b) $E(x,y) = E(y,x)$ *(Symmetry)*
c) $T(E(x,y), E(y,z)) \leq E(x,z)$ *(T-transitivity).*

It is well known that given two indistinguishability operators E, F, the intersection $E \cap F$ is also an indistinguishability operator. On the contrary, the union $E \cup F$ is not generally an indistinguishability operator. The concept of transitive closure will prove to be useful further to be able to use the union operator as well.

Definition II.3. *Let T be a t-norm and R a fuzzy proximity (a reflexive and symmetric fuzzy relation) on a set X. The transitive closure $\overline{R}$ of R is the T-indistinguishability operator defined by*

$$\overline{R} = \bigcap_{E \in A} E$$

where A is the set of T-indistinguishability operators on X greater than or equal to R.

Now we can give a lattice structure to the set $\mathcal{E}$ of T-indistinguishability operators on a set X, with the natural ordering $\leq$, and two operations: the intersection $E \cap F$ and the closed union $\overline{E \cup F}$.

Indistinguishability operators can be generated in several ways. The simplest way is by obtaining the indistinguishability related to a fuzzy subset.

Definition II.4. *Let X be a set, T a t-norm and μ a fuzzy subset of X. The fuzzy relation E on X defined by*

$$E_\mu(x,y) = \overleftrightarrow{T}(\mu(x), \mu(y))$$

for all $x, y \in X$ is a T-indistinguishability operator.

One of the main results of the theory of indistinguishability operators is the Representation Theorem. This theorem proves that any family of fuzzy subsets on a set X generates a T-indistinguishability operator E on X and, reciprocally, that every T-indistinguishability operator on X can be generated by a family of fuzzy subsets.

Theorem II.5. [12] *Representation Theorem. Let R be a fuzzy relation on a set X and T a continuous t-norm. Then R is an T-indistinguishability operator if and only if there exists a family $(\mu_i)_{i \in I}$ of fuzzy subsets of X such that for all $x, y \in X$*

$$R(x,y) = \inf_{i \in I} E_{\mu_i}(x,y).$$

An indistinguishability operator E determines a set of observable sets or granules. These are given by the generators of E in the sense of the Representation Theorem and it is well known that they coincide with the set of extensional sets we define now.

Definition II.6. *Let X be a set and E a T-indistinguishability operator on X. A fuzzy subset μ of X is called extensional if and only if:*

$$\forall x, y \in X \quad T(E(x,y), \mu(y)) \leq \mu(x).$$

We will denote H_E the set of all extensional fuzzy subsets of X with respect to E.

Proposition II.7. *Let X be a set, E a T-indistinguishability operator on X and μ a fuzzy subset of X. Then:*

$$\mu \in H_E \Leftrightarrow E_\mu \geq E$$

As it has been proved in [1], extensional fuzzy subsets verify the properties of the next proposition. Furthermore, these properties completely determine the set of extensional fuzzy subsets.

Proposition II.8. *Let E be a T-indistinguishability operator and H_E its set of extensional fuzzy sets. Then, $\forall \mu \in H_E, (\mu_i)_{i \in I}$ a family of extensional sets and $\forall \alpha \in [0,1]$ the following properties hold:*

1) $\bigvee_{i \in I} \mu_i \in H_E$
2) $\bigwedge_{i \in I} \mu_i \in H_E$
3) $T(\alpha, \mu) \in H_E$
4) $\overrightarrow{T}(\mu|\alpha) \in H_E$
5) $\overrightarrow{T}(\alpha|\mu) \in H_E$

Given a fuzzy subset $\mu \in [0,1]^X$, it is an interesting topic to find the closest extensional set that contains μ. This is done using the operator ϕ_E, defined below. This operator can be also seen as a topological closure operator on the set $[0,1]^X$ [2].

Definition II.9. *Let X be a set and E a T-indistinguishability operator on X. The map ϕ_E: $[0,1]^X \to [0,1]^X$ is defined $\forall x \in X$ by:*

$$\phi_E(\mu)(x) = \sup_{y \in X} T(E(x,y), \mu(y)).$$

The operator ϕ_E verifies the following properties.

Proposition II.10. *For all μ, $\mu' \in [0,1]^X$ the following properties are satisfied:*

1) $\mu \leq \mu' \Rightarrow \phi_E(\mu) \leq \phi_E(\mu')$
2) $\mu \leq \phi_E(\mu)$
3) $\phi_E(\mu \vee \mu') = \phi_E(\mu) \vee \phi_E(\mu')$
4) $\phi_E(\phi_E(\mu)) = \phi_E(\mu)$
5) $\phi_E(\{x\})(y) = \phi_E(\{y\})(x)$
6) $\phi_E(T(\alpha, \mu)) = T(\alpha, \phi_E(\mu))$

Analogously, given a T-indistinguishability operator E, the operator ψ_E can be defined that provides extensional lower approximations of fuzzy subsets of X with respect to E. The operator ψ_E is dual to ϕ_E and can be seen topologically as an opening or interior operator.

Definition II.11. *Let E be a T-indistinguishability operator on a set X. The map ψ_E: $[0,1]^X \to [0,1]^X$ is defined $\forall x \in X$ by:*

$$\psi_E(\mu)(x) = \inf_{y \in X} \overrightarrow{T}(E(x,y) | \mu(y)).$$

ψ_E satisfies the properties below (dual to Properties II.10) and is determined by them.

Proposition II.12. *For all μ, $\mu' \in [0,1]^X$ the following properties are satisfied:*

1) $\mu \leq \mu' \Rightarrow \psi_E(\mu) \leq \psi_E(\mu')$
2) $\psi_E(\mu) \leq \mu$
3) $\psi_E(\mu \wedge \mu') = \psi_E(\mu) \wedge \psi_E(\mu')$
4) $\psi_E(\psi_E(\mu)) = \psi_E(\mu)$
5) $\psi_E(\overrightarrow{T}(x|\alpha)(y) = \psi_E(\overrightarrow{T}(y|\alpha)(x)$
6) $\psi_E(\overrightarrow{T}(\alpha|\mu)) = \overrightarrow{T}(\alpha, \psi_E(\mu))$

An interesting issue concerning the operators ϕ_E and ψ_E is that $Im(\phi_E) = Im(\psi_E) = H_E$, and hence the set of extensional fuzzy subsets H_E can also be characterized as the set of fixed points of ϕ_E and ψ_E. This fact is actually a direct consequence of the definitions and is very natural when ϕ_E and ψ_E is regarded from the topological approach.

Finally, we remind the concept of Galois connection between two ordered sets, as it will be used further to understand the relations between the concepts introduced previously:

Definition II.13. *Let $(A, \leq)$, $(B, \leq)$ two partially ordered sets. A Galois connection between these sets is a pair (F, G) of functions $F : A \to B$ and $G : B \to A$ satisfying:*

$$F(a) \leq b \quad \Leftrightarrow \quad a \leq G(b) \text{ (monotone Galois connection)}$$
$$b \leq F(a) \quad \Leftrightarrow \quad a \leq G(b) \text{ (antitone Galois connection)}$$

III. Isomorphisms and Dualities between Indistinguishability Operators, Extensional Sets, Upper and Lower Approximations

It is noticeable that the three concepts introduced (extensional sets, upper approximations and lower approximations) related to an indistinguishability operator E satisfy very similar families of properties. It is natural to ask then what is exactly the relation between these concepts.

In this section it will be shown that there actually exist bijections between the four stated concepts ($\mathcal{E}$, $\mathcal{H}$, $\mathcal{U}$, $\mathcal{L}$) and furthermore the structure of these is preserved through these bijections. This will lead us to the final fact that there are isomorphisms of lattices between the stated concepts, and these isomorphisms will be explicitly given.

This section is divided intro three subsections. The first one will study the isomorphism between indistinguishability operators and extensional sets. The second one will face indistinguishability operators and upper approximations and the third one will deal with lower approximations.

A. Indistinguishability Operators and Extensional Sets

This section will focus on studying the isomorphism between the lattice $\mathcal{E}$ of indistinguishability operators on a set X and the lattice $\mathcal{H}$ of sets of extensional fuzzy subsets.

Analogously as in the case of indistinguishability operators, given H_E and H_F two collections of extensional sets, the intersection of them $H_E \cap H_F$ is also the set of extensional sets of a certain indistinguishability operator, but the union of them $H_E \cup H_F$ is not. In order to close the set of extensional sets under the union operator, and therefore give to it the structure of a lattice, we have to introduce, as done with indistinguishability operators, the concept of extensional closure of a subset of $[0,1]^X$.

Definition III.1. *Let $J \subseteq [0,1]^X$. Its extensional closure $\overline{J}$ is defined by:*

$$\overline{J} := \bigcap_{H \in [0,1]^X, J \subseteq H} H$$

where H is a set of fuzzy subsets of X satisfying the properties of Proposition II.8:

1) $\bigvee_{i \in I} \mu_i \in H$
2) $\bigwedge_{i \in I} \mu_i \in H$
3) $T(\alpha, \mu) \in H$
4) $\overrightarrow{T}(\alpha|\mu) \in H$
5) $\overrightarrow{T}(\mu|\alpha) \in H$

The lattice $\mathcal{E}$ of indistinguishability operators on a set X has a natural ordering given by $\leq$, while the lattice $\mathcal{H}$ of sets extensional fuzzy subsets is ordered by the inclusion $\subseteq$. The following proposition states how these orders are inverted when we pass from one lattice to the other one.

Proposition III.2. *Let E, F be two indistinguishability operators on X with extensional sets H_E and H_F respectively. Then:*

$$E \leq F \Leftrightarrow H_F \subseteq H_E$$

Proof: $E \leq F \Leftrightarrow \forall x,y \in X\ E(x,y) \leq F(x,y)$, which is equivalent to $\forall x,y\ \forall \mu \in H_F\ T(E(x,y),\mu(y)) \leq T(F(x,y),\mu(y)) \leq \mu(x) \Leftrightarrow H_F \subseteq H_E$ ∎

The following theorem proves that there is a bijection between both lattices. This theorem was proved in [1].

Theorem III.3. *Let H be a subset of $[0,1]^X$ satisfying the properties of Proposition II.8. Then there exists a unique T-indistinguishability operator E such that $H = H_E$.*

Proof: Let E be the indistinguishability operator generated by H using the Representation Theorem (Theorem II.5).

Let us proof first that $H = H_E$.

Since H is a generating family, its fuzzy subsets are extensional with respect to E and $H \subseteq H_E$.

Let us see the other inequality.

Given $\mu \in H_E$ and $y \in X$, we define the fuzzy subset $\mu_y(x) = T(E(x,y),\mu(y))$. We will show that $\mu = \sup_{y\in X} \mu_y$.

$$\begin{aligned}\mu_y(x) &= T(\inf_{\nu\in H} E_\nu(x,y),\mu(y)) \\ &= \inf_{\nu\in H} T(\min\{\overrightarrow{T}(\nu(x)|\nu(y)),\overrightarrow{T}(\nu(y)|\nu(x))\},\mu(y)).\end{aligned}$$

Since $\mu(y)$ and $\nu(y)$ are constants, applying properties 2, 3, 4 and 5 of Proposition II.8 we have $\mu_y \in H$.

Since μ is extensional, $\mu_y(x) = T(E(x,y),\mu(y)) \leq \mu(x)$. As $\mu_y(y) = \mu(y)$ we obtain $\mu = \sup_{y\in x} \mu_y$ which belongs to H due to property 1 of Proposition II.8. So, $H_E \subseteq H$).

The uniqueness is a direct consequence of Proposition III.2. ∎

Corollary III.4. *$(\Gamma : E \to H_E, \Sigma : H_E \to E)$ define an antitone Galois connection between $\mathcal{E}$ and $\mathcal{H}$.*

We have shown that there is a bijection between $\mathcal{E}$ and $\mathcal{H}$ and how the orderings of the lattices are affected by it. Let us finally show how the structure is preserved (inverting the order) and therefore we will have proved that the bijection is an isomorphism of lattices. In fact we will have proved that given an indistinguishability operator E on X, H_E is actually its dual space.

Theorem III.5. *Let E, F be two indistinguishability operators on a set X with sets of extensional fuzzy subsets sets H_E and H_F respectively. Then:*

1) $H_{\overline{E\cup F}} = H_E \cap H_F$
2) $H_{E\bigcap F} = \overline{H_E \cup H_F}$

Proof:

1) $\mu \in H_E \cap H_F \Leftrightarrow \mu \in H_E$ and $\mu \in H_F$. This is equivalent to $E_\mu \geq E$ and $E_\mu \geq F$ or $E_\mu \geq E \cup F$ and by the definition of the extensional closure, this is equivalent to $E_\mu \geq \overline{E \cup F} \Leftrightarrow \mu \in H_{\overline{E\cup F}}$
2) $\supseteq$)
   $E \cap F \leq E \Rightarrow H_E \subseteq H_{E\cap F}$.
   $E \cap F \leq F \Rightarrow H_F \subseteq H_{E\cap F}$.
   Then $H_E \cup H_F \subseteq H_{E\cap F} \Rightarrow \overline{H_E \cup H_F} \subseteq H_{E\cap F}$.
   $\subseteq$)
   Let $\mu \in H_{E\cap F}$. Let us suppose $\mu \notin \overline{H_E \cup H_F}$. Then there exists an extensional set H_G with indistinguishability operator G such that $H_G \supseteq H_E \cup H_F$ and $\mu \notin H_G \Rightarrow \exists (x,y)$ such that $E_\mu(x,y) < G(x,y)$. Without loss of generality we can assume $E(x,y) \leq F(x,y)$. As $H_G \supseteq H_E \cup H_F$, $H_E \subseteq H_G$ and $H_F \subseteq H_G \Rightarrow G \leq E$ and $G \leq F$. So
   $E_\mu(x,y) < G(x,y) \leq E(x,y) \leq F(x,y)$. Hence
   $E_\mu(x,y) < (E \cap F)(x,y)$.
   Therefore, $\mu \notin H_{E\cap F}$ which contradicts our hypothesis!
   So $\mu \in \overline{H_E \cup H_F}$.

∎

B. Indistinguishability Operators and Upper Approximations

This subsection will be faced on proving that the lattice $\mathcal{U}$ is isomorphic to the lattice $\mathcal{E}$ of indistinguishability operators on a set X. The path that will take us to this result will be analogous to the one followed in the previous subsection.

As we did with $\mathcal{E}$ and $\mathcal{H}$, to give the set $\mathcal{U}$ of upper approximations ϕ_E ($E \in \mathcal{E}$) a lattice structure, we have to define a ϕ-closure.

Definition III.6. *Let f be a map defined on $[0,1]^X \to [0,1]^X$. The ϕ-closure $\overline{f}$ of f is defined as:*

$$\overline{f} = \bigwedge_{f\leq\phi,\phi\in U} \phi$$

where U is the set of maps $\phi : [0,1]^X \to [0,1]^X$ satisfying the properties of Proposition II.10:

1) $\mu \leq \mu' \Rightarrow \phi(\mu) \leq \phi(\mu')$
2) $\mu \leq \phi(\mu)$
3) $\phi(\mu \vee \mu') = \phi(\mu) \vee \phi(\mu')$
4) $\phi(\phi(\mu)) = \phi(\mu)$
5) $\phi(\{x\})(y) = \phi(\{y\})(x)$
6) $\phi(T(\alpha,\mu)) = T(\alpha,\phi(\mu))$

On the contrary with respect to what happened with extensional sets, in the case of upper approximations the ordering relation is directly preserved, instead of dually.

Proposition III.7. *Let E, F be two T-indistinguishability operators on X with upper approximations ϕ_E and ϕ_F respectively. Then:*

$$E \leq F \Leftrightarrow \phi_E \leq \phi_F$$

Given a ϕ operator, one can define an indistinguishability operator in the following way.

Proposition III.8. *Let $\phi : [0,1]^X \to [0,1]^X$ be a map satisfying the properties of Proposition II.10. Then the fuzzy relation E_ϕ defined by*

$$E_\phi(x,y) = \phi(\{x\})(y)$$

is a T-indistinguishability operator on X.

Proof: Straightforward ■

The following theorem proves that there is a bijection between indistinguishability operators and upper approximations.

Theorem III.9. *There is a bijection between the set $\mathcal{E}$ of T-indistinguishability operators on X and the maps $\phi : [0,1]^X \to [0,1]^X$ satisfying the properties of Proposition II.10.*

Proof: We have to prove that $\phi_{E_\phi} = \phi$ and $E_{\phi_E} = E$

- Let ϕ be a map satisfying the properties of Proposition II.10. For all $x, y \in X$ and for any fuzzy subset $\mu \in [0,1]^X$ we have:

$$\begin{aligned} \phi_{E_\phi}(\mu)(x) &= \sup_{y\in X} T(E_\phi(x,y), \mu(y)) \\ &= \sup_{y\in X} T(\phi(\{y\})(x), \mu(y)) \\ &= \phi(\mu)(x). \end{aligned}$$

- Let E be a T-indistinguishability operator. Then for all $x, y \in X$ we have:

$$\begin{aligned} E_{\phi_E}(x,y) &= \phi(\{x\})(y) \\ &= \sup_{z\in X} T(E(y,z), \{x\}(z)) \\ &= E(x,y). \end{aligned}$$

■

Corollary III.10. *$(\Gamma : E \to \phi_E, \Sigma : \phi_E \to E)$ define a monotone Galois connection between $\mathcal{E}$ and $\mathcal{U}$.*

Proof: Trivial due to the monotonicity of a t-norm ■

We have construct a bijection between $\mathcal{E}$ and $\mathcal{U}$ and analyzed how the order was affected by it. Again, let us finish by studying how the structure of the operations is directly preserved and therefore by proving that the bijection is an isomorphism.

Theorem III.11. *Let E, F be two indistinguishability operators with upper approximations ϕ_E and ϕ_F respectively. Then:*

1) $\phi_{\overline{E\cup F}} = \overline{\phi_E \vee \phi_F}$
2) $\phi_{E\cap F} = \phi_E \wedge \phi_F$

Proof:

1) $\geq$)
   Let $\mu \in [0,1]^X$.
   $\phi_{\overline{E\cup F}}(\mu)(x) = \sup_{y\in X} T(\overline{E \cup F}(x,y), \mu(y))$.
   As $\overline{E \cup F} \geq E, F \Rightarrow \phi_{\overline{E\cup F}}(\mu)(x) \geq \phi_E(\mu)(x)$ and $\phi_{\overline{E\cup F}}(\mu)(x) \geq \phi_F(\mu)(x)$. Hence:
   $\phi_{\overline{E\cup F}}(\mu)(x) \geq (\phi_E \vee \phi_F)(\mu(x)) \Rightarrow \phi_{\overline{E\cup F}} \geq \overline{\phi_E \vee \phi_F}$.
   $\leq$)
   By Definition III.6 and Proposition II.10, there exists a T-indistinguishability operator G on X such that $\overline{\phi_E \vee \phi_F} = \phi_G$. We have to prove that $\overline{E \cup F} \leq G$.
   Indeed, $\phi_E \leq \overline{\phi_E \vee \phi_F} = \phi_G$ and by Lemma III.7 $E \leq G$. Analogously we get $F \leq G$, and then $E \cup F \leq G \Rightarrow \overline{E \cup F} \leq G$, which proves the inequality.
2) $\phi_{E\cap F}(\mu)(x) = \sup_{y\in X} T(\min\{E(x,y), F(x,y)\}, \mu(y))$
   $= \sup_{y\in X} \min\{T(E(x,y), \mu(y)), T(F(x,y), \mu(y))\}$.
   And, as the min and the sup operators are interchangeable in the previous expression, this is equal to $(\phi_E \wedge \phi_F)(\mu)(x)$

■

C. Indistinguishability Operators and Lower Approximations

This subsection will deal with indistinguishability operators and lower approximations. The final result of the subsection will be, analogously as the previous subsections, the construction of the isomorphism between both lattices.

Firstly, to give the set $\mathcal{L}$ of lower approximations a lattice structure we have to introduce the ψ-closure of a map.

Definition III.12. *Let f be a map defined on $[0,1]^X \to [0,1]^X$. The ψ-closure $\widetilde{f}$ of f is defined as:*

$$\widetilde{f} = \bigwedge_{\psi\in L, f\leq\psi} \psi$$

where L is the set of maps $\psi : [0,1]^X \to [0,1]^X$ satisfying the properties of Proposition II.12:

1) $\mu \leq \mu' \Rightarrow \psi_E(\mu) \leq \psi_E(\mu')$
2) $\psi_E(\mu) \leq \mu$
3) $\psi_E(\mu \wedge \mu') = \psi_E(\mu) \wedge \psi_E(\mu')$
4) $\psi_E(\psi_E(\mu)) = \psi_E(\mu)$
5) $\psi_E(\overrightarrow{T}(x|\alpha)(y) = \psi_E(\overrightarrow{T}(y|\alpha)(x)$
6) $\psi_E(\overrightarrow{T}(\alpha|\mu)) = \overrightarrow{T}(\alpha, \psi_E(\mu))$

This way, the lattice structure is obtained with the ordering $\leq$, and the operations $\wedge$ and $\widetilde{\vee}$.

Let us prove now that the ordering of the lattices is directly preserved when we pass from one to the other.

Proposition III.13. *Let E, F be two indistinguishability operators on X with upper approximations ψ_E and ψ_F respectively. Then:*

$$E \leq F \Leftrightarrow \psi_E \leq \psi_F.$$

Analogously to the case of upper approximations, an indistinguishability operator can be defined given a lower approximation ψ.

Proposition III.14. *Let $\psi : [0,1]^X \to [0,1]^X$ be a map satisfying the properties of Proposition II.12. Then the fuzzy relation E_ψ defined by*

$$E_\psi(x,y) = \inf_{\alpha\in[0,1]} \overrightarrow{T}(\psi(\overrightarrow{T}(\{x\}|\alpha)(y)|\alpha)).$$

is a T-indistinguishability operator on X.

From this proposition, it can be proved that there is a bijection between the lattices $\mathcal{E}$ and $\mathcal{L}$.

Theorem III.15. [4] *There is a bijection between the set of T-indistinguishability operators and the maps ψ satisfying the properties of Proposition II.12.*

Corollary III.16. *($\Gamma : E \to \psi_E, \Sigma : \psi_E \to E$) define a monotone Galois connection between $\mathcal{E}$ and $\mathcal{L}$.*

Proof: Trivial by applying the properties of the residuation. ∎

We finally have to see that the stated bijection between the lattice of indistinguishability operators on X and the lattice of lower approximations on X preserves the structure given by $\wedge$ and $\overline{\vee}$. This is proved in the following Theorem. With this result, we have the stated isomorphism between both lattices.

Theorem III.17. *Let E, F be two T-indistinguishability operators on X with lower approximations ψ_E and ψ_F respectively. Then:*

1) $\psi_{\overline{E\cup F}} = \widetilde{\psi_E \vee \psi_F}$
2) $\psi_{E\cap F} = \phi_E \wedge \psi_F$

Proof:

1) $\geq$)
   $E \leq \overline{E \cup F} \Rightarrow \psi_E \leq \psi_{\overline{E\cup F}}$
   $F \leq \overline{E \cup F} \Rightarrow \psi_F \leq \psi_{\overline{E\cup F}}$
   Therefore, $\psi_E \vee \psi_F \leq \psi_{\overline{E\cup F}} \Rightarrow \widetilde{\psi_E \vee \psi_F} \leq \psi_{\overline{E\cup F}}$
   $\leq$)
   Let us assume that there exist $x \in X$ and a fuzzy subset μ of X such that:
   $\psi_{\overline{E\cup F}}(\mu)(x) > \widetilde{\psi_E \vee \psi_F}(\mu)(x)$. Then there exists a T-indistinguishability operator G on X such that $\widetilde{\psi_E \vee \psi_F} \leq \psi_G$ and $\psi_G(\mu)(x) < \psi_{\overline{E\cup F}}(\mu)(x)$.
   But $\psi_E \leq \widetilde{\psi_E \vee \psi_F} \leq \psi_G$. By Lemma III.13 we have $E \leq G$. Analogously $F \leq G$. So $E \cup F \leq G \Rightarrow \overline{E \cup F} \leq G$, which contradicts $\widetilde{\psi_G}(\mu)(x) < \psi_{\overline{E\cup F}}(\mu)(x)$. So we have $\psi_{\overline{E\cup F}} \leq \widetilde{\psi_E \cup \psi_F}$.
2) $(\psi_E \wedge \psi_F)(\mu)(x) =$
   $\min\{\inf_{y\in X} \overrightarrow{T}((E(x,y)|\mu(x)),$
   $\quad \inf_{y\in X} \overrightarrow{T}((F(x,y)|\mu(x)))\}$
   $= \inf_{y\in X} \overrightarrow{T}(\min\{E(x,y), F(x,y)\}|\mu(x)) =$
   $\psi_{E\cap F}(\mu)(x)$.

∎

IV. Conclusion

In this work, the relation between the set $\mathcal{E}$ of T-indistinguishability operators on a set X, the set $\mathcal{H}$ of sets of extensional fuzzy subsets with respect to a T-indistinguishability operator E on X and the sets $\mathcal{U}$ and $\mathcal{L}$ of upper and lower approximations of fuzzy subsets by extensional ones with respect to a T-indistinguishability operator respectively has been studied and stated. It has been proved that these sets are in fact isomorphic lattices and the isomorphisms have been given explicitly. These results are summarized bellow.

$$\begin{array}{ccccccc} \mathcal{L} & \approx & \mathcal{U} & \approx & \mathcal{E} & \approx & \mathcal{H} \\ \psi_E \wedge \psi_F & \leftrightarrow & \phi_E \wedge \phi_F & \leftrightarrow & E \cap F & \leftrightarrow & \overline{H_E \cup H_F} \\ \widetilde{\psi_E \vee \psi_F} & \leftrightarrow & \overline{\phi_E \vee \phi_F} & \leftrightarrow & \overline{E \cup F} & \leftrightarrow & H_E \cap H_F \end{array}$$

Acknowledgment

Research partially supported by project number TIN2009-07235.

The first author is supported by the Universitat Politècnica de Catalunya (UPC).

References

[1] Castro, J.L., Klawonn, F.: "Similarity in Fuzzy Reasoning," Mathware & Soft Computing, vol. 2, 1996, pp. 197-228.
[2] Jacas, J., Recasens, J.: "Fuzzy T-transitive relations: eigenvectors and generators," Fuzzy Sets and Systems, vol. 72, 1995, pp. 147-154.
[3] Jacas, J., Recasens, J.: "Fixed points and generators of fuzzy relations," J. Math. Anal. Appl., vol. 186, 1994, pp. 21-29.
[4] Morsi, N.N., Yakout, M.M.: "Axiomatics for fuzzy rough sets," Fuzzy Sets and Systems, vol. 100, 1998, pp. 327-342.
[5] Boixader, D., Jacas, J., Recasens, J.: "Upper and lower approximation of fuzzy sets," Int. J. of General Systems, vol. 29, 2000, pp. 555-568.
[6] Bělohlvek, R.: Fuzzy Relational Systems: Foundations and Principles. Kluwer Academic Publishers, New York, 2002.
[7] Boixader, D., Jacas, J., Recasens, J.: Fuzzy equivalence relations: advanced material. In: Dubois, D., Prade, H. (eds.) Fundamentals of Fuzzy Sets, pp. 261-290. Kluwer Academic Publishers, New York, 2000
[8] Jacas, J., Recasens, J.: "Aggregation of T-Transitive Relations," Int J. of Intelligent Systems, vol. 18, 2003, pp. 1193-1214.
[9] Klement, E.P., Mesiar, R., Pap E.: Triangular norms. Kluwer Academic Publishers, Dordrecht, 2000.
[10] Recasens, J. Indistinguishability Operators. Modelling Fuzzy Equalities and Fuzzy Equivalence Relations Series: Studies in Fuzziness and Soft Computing, vol. 260,,2011.
[11] Trillas, E.: "Assaig sobre les relacions d'indistingibilitat," Proc. Primer Congrés Català de Lògica Matemàtica, Barcelona, 1982, pp. 51-59. (In Catalan).
[12] Valverde, L.: "On the Structure of F-indistinguishability Operators," Fuzzy Sets and Systems, vol. 17, 1985, pp. 313-328.
[13] Zadeh. L.A. "Similarity relations and fuzzy orderings," Inform. Sci., vol. 3, 1971, pp. 177-200.
[14] Zadeh, L.A.: Fuzzy sets and information granularity. In: Gupta, M.M., Ragade, R.K., Yager, R.R. (eds.) Advances in Fuzzy Set Theory and Applications, pp. 3-18. Amsterdam, North-Holland, 1979
[15] Zadeh, L.A.: "Toward a theory of fuzzy information granulation and its centrality in human reasoning and fuzzy logic," Fuzzy Sets and Systems, vol. 90, 1997, pp. 111-127.

2011 IEEE International Conference on Fuzzy Systems
June 27-30, 2011, Taipei, Taiwan

Graded Equipollence And Fuzzy C-measures Of Finite Fuzzy Sets

Michal Holčapek
Institute for Research and Applications of Fuzzy Modeling
University of Ostrava, 30. dubna 22, 701 03 Ostrava 1, Czech Republic
michal.holcapek@osu.cz

***Abstract*—In the classical set theory, there is the well known correspondence between the equipollence of finite sets and the equality of natural numbers expressing their cardinalities. In the fuzzy set theory, an equivalent correspondence between the equipollence of finite fuzzy sets and the equality of generalized cardinals has been proposed in [1]. This paper is devoted to the situation when we consider the mentioned relations to be graded, that means, the crisp equipollence of fuzzy sets is replaced now by the graded equipollence of fuzzy sets and the equality of fuzzy sets by their similarity.**

***Index Terms*—residuated-dually residuated lattice; graded equipollence; fuzzy c-measure**

I. Introduction

In the classical set theory, two sets have the same number of elements if and only if there exists a one-to-one mapping of one set onto the second one. Thus, there is a nice relation between the functional approach to the cardinality of sets, which does not suppose any knowledge about the numbers of elements in sets, and the approach based on the ordinal numbers expressing the numbers of elements of sets.

The above two mentioned approaches to the cardinality for (finite) fuzzy sets have been also studied in the fuzzy set theory. Nevertheless, for fuzzy sets, the situation is much more complicated by the graduation of membership of elements of fuzzy sets.

The classical-like approaches to the cardinality of fuzzy sets based on the notion of the equipollence of fuzzy sets were proposed by D. Klaua [2] and S. Gottwald [3], [4]. In the second case, a degree in which two fuzzy sets are equipollent is defined using fuzzy uniqueness of fuzzy mappings. Equivalence classes (fuzzy sets) are *fuzzy cardinals*. Note that fuzzy mappings are here defined as special fuzzy relations. Since these approaches are purely theoretical, a further substantial research in this direction has not been realized yet. Another approach was suggested by M. Wygralak [5], where the notion of equipollence of fuzzy sets is introduced using the cardinality of α-cuts of fuzzy sets. More precisely, two fuzzy sets A and B are equipollent, if

$$\bigvee\{\alpha \in [0,1] \mid |A_\alpha| \geq i\} = \bigvee\{\alpha \in [0,1] \mid |B_\alpha| \geq i\} \quad (1)$$

for any cardinal number i. Some modifications of (1) can be found in [1], [6], [7], [8]. In [9] (see also [10], [11]), we proposed a new approach to the equipollence of fuzzy sets over a universe of sets (e.g., a universe of all finite or countable sets, or all sets, or a Grothendieck universe). Analogously to the Gottwald's approach, a graded equipollence is considered, where, however, the degrees of being equipollent are obtained by a simpler way than in the Gottwald's approach. More precisely, this approach is based on a graded one-to-one correspondence between fuzzy sets where the crisp mappings between universes are considered.

The approaches to the cardinality of finite fuzzy sets based on objects expressing the number of elements in fuzzy sets can be divided to two directions, namely, to the scalar and fuzzy approaches. In this contribution, we are interested in the second approach, where the cardinality of fuzzy sets is expressed by special fuzzy sets defined over the set of natural numbers $\mathbb{N}$ or over universes containing a class of cardinal numbers. In this case, convex fuzzy sets over a class of cardinals have a dominant role. These fuzzy sets are usually called *generalized natural numbers* or *generalized cardinals* (see e.g. [12], [13], [14]). This type of cardinality of fuzzy sets is usually referred to the *fuzzy cardinality*.

Let us mention that the first definition of fuzzy cardinality of finite fuzzy sets, by means of functions from $\mathbb{N}$ to $[0,1]$, was done by L.A. Zadeh in [15]. A substantial improvement of the original definition was done again by L.A. Zadeh in [16] and gave rise to three types of cardinality, namely, $FGCount$, $FLCount$ and $FECount$. A generalization of FGCount, FLCount and FECount using t-norms and t-conorms was proposed by M. Wygralak in [14] and further developed in [1]. Both publications are an attempt to develop the cardinal theory for fuzzy sets including a relation between equipollence and equality of cardinal numbers. An axiomatic approach to fuzzy cardinality of finite fuzzy sets covering some of the well-known definition, defined by means of the generalized natural numbers, was proposed by J. Casasnovas and J. Torrens [17].

In [18], we generalized the Casasnovas-Torrens axiomatic approach and defined "fuzzy measures" extending the cardinality of finite sets to a cardinality finite fuzzy sets.[1] Although, the proposed system of fuzzy measures generalizes the cardinality of sets, some properties like the valuation property or, as will be seen later, the fundamental correspondence between the graded equipollence of fuzzy sets and the equality of their generalized cardinals are failed in general. Therefore, we call these measures as the *c-measures*, where the letter "c" is an

[1]Note that, in contrast to the cardinality of finite sets, we can define a large scale of fuzzy measures expressing the number of elements of finite fuzzy sets.

978-1-4244-7316-8/11/$26.00 ©2011 IEEE

abbreviation of "cardinal".

The aim of this contribution is to show relations between functional approach based on the graded equipollence introduced in [9] (see also [10], [11]) and the approach based on the fuzzy c-measures proposed in [18], where the cardinality of finite fuzzy sets is expressed by generalized cardinals.

The paper is structured as follows. In Preliminaries, we propose a residuated-dually residuated lattice as an algebraical structure of membership degrees of fuzzy sets and (countable and finite) fuzzy sets defined in the class of all countable sets. The graded equipollence of (countable) fuzzy sets is introduced in Section III. The section IV is devoted to fuzzy c-measures including the important properties as a representation of fuzzy c-measures by suitable homomorphisms between reducts of the rdr-lattices. In Section V, we shows the relation between the graded equipollence of finite fuzzy sets and the similarity of generalized cardinals obtained by fuzzy c-measures. The last section is the conclusion.

II. Preliminaries

A. Algebraic Structures of Membership Degrees of Fuzzy Sets

In this paper, the membership degrees of fuzzy sets are interpreted in a complete residuated lattice which is, moreover, extended by an adjoint pair of dual operations. We shall say that an algebra $\mathbf{L} = \langle L, \wedge, \vee, \otimes, \rightarrow, \oplus, \ominus, \bot, \top \rangle$ with six binary operations and two constants is a *residuated-dually residuated lattice* (shortly, an rdr-lattice), if

(i) $\langle L, \wedge, \vee, \bot, \top \rangle$ is a bounded lattice, where $\bot$ is the least element and $\top$ is the greatest element of L, respectively,
(ii) $\langle L, \otimes, \top \rangle$ and $\langle L, \oplus, \bot \rangle$ are commutative monoids,
(iii) the pairs $\langle \otimes, \rightarrow \rangle$ and $\langle \oplus, \ominus \rangle$ form adjoint pairs, i.e.

$$a \leq b \rightarrow c \quad \text{if and only if} \quad a \otimes b \leq c, \tag{2}$$
$$a \leq b \oplus c \quad \text{if and only if} \quad a \ominus b \leq c \tag{3}$$

hold for each $a, b, c \in L$ ($\leq$ denotes the corresponding lattice ordering).

The operations $\otimes$, $\rightarrow$, $\oplus$ and $\ominus$ are called *multiplication*, *residuum*, *addition* and *difference*, respectively.[2] We shall say that an rdr-lattice is *complete* (*linearly ordered*), if $\langle L, \wedge, \vee, \bot, \top \rangle$ is a complete (linearly ordered) lattice, respectively. Further, an rdr-lattice is *divisible*, if $a \otimes (a \rightarrow b) = a \wedge b$ holds for all $a, b, c \in L$, and *dually divisible*, if $(a \ominus b) \oplus b = a \vee b$ holds for all $a, b, c \in L$.

EXAMPLE 1 Let T and S be a left continuous t-norm and a right continuous t-conorm, respectively, and define $\rightarrow_T$ and $\ominus_S$ by

$$a \rightarrow_T b = \bigvee \{c \in [0,1] \mid T(a,c) \leq b\},$$
$$a \ominus_S b = \bigwedge \{c \in [0,1] \mid S(b,c) \geq a\}.$$

The algebra $\mathbf{L} = \langle [0,1], \min, \max, T, \rightarrow_T, S, \ominus_S, 0, 1 \rangle$ is a complete rdr-lattice. If T and S is the product (or the Łukasiewicz conjunction) and the probabilistic sum (or the Łukasiewicz disjunction), respectively, then we shall use $\mathbf{L}_\Pi$ ($\mathbf{L}_Ł$) to denote the Goguen (Łukasiewicz) rdr-lattice.

Let us define the following additional operations for any $a, b \in L$ and set $\{a_i \mid i \in I\}$ of elements from L over a countable (possibly empty) index set I:

$$a \leftrightarrow b = (a \rightarrow b) \wedge (b \rightarrow a), \qquad \textit{(biresiduum)}$$
$$\neg a = a \rightarrow \bot, \qquad \textit{(negation)}$$
$$\bigotimes_{i \in I} a_i = \begin{cases} \top, & I = \emptyset, \\ \bigwedge_{K \in \mathfrak{Fin}(I)} \bigotimes_{i \in K} a_i, & \text{otherwise}, \end{cases} \qquad \textit{(countable multiplication)}$$
$$\bigoplus_{i \in I} a_i = \begin{cases} \bot, & I = \emptyset, \\ \bigvee_{K \in \mathfrak{Fin}(I)} \bigoplus_{i \in K} a_i, & \text{otherwise}, \end{cases} \qquad \textit{(countable addition)}$$

where $\mathfrak{Fin}(I)$ denotes the set of all finite subsets of I. If $|I| = n$ is a finite index set and $a_i = a$ for any $i \in I$, then we will write $a^n = \bigotimes_{i \in I} a_i$ or $na = \bigoplus_{i \in I} a_i$.

To integrate some of alternative constructions based on the operations of $\wedge$ and $\otimes$, we shall use the common symbol $\odot$ (or $\bigodot$) for them. Analogously, we shall use $\overline{\odot}$ (or $\overline{\bigodot}$) to denote one of the operations $\vee$ or $\oplus$.

B. Fuzzy Sets

Since we are interested in finite fuzzy sets and consequently also denumerable fuzzy sets, let us consider the class $\mathfrak{Count}$ of all countable sets as a framework for our theory.[3] Further, we shall use $\mathfrak{Fin}$ to denote the class of all finite sets. A fuzzy set in $\mathfrak{Count}$ is defined as follows.

DEFINITION 1 A mapping $A : x \rightarrow L$ is called a fuzzy set in $\mathfrak{Count}$, if x is a set in $\mathfrak{Count}$.

In what follows, we shall use $\mathfrak{Fcount}$ to denote the class of all fuzzy sets in $\mathfrak{Count}$. Although, the fuzzy sets in $\mathfrak{Fcount}$ may be referred to "countable" fuzzy sets, we shall not use this notation and say only fuzzy sets. Notice that, for example, each fuzzy set or pair of fuzzy sets belong to $\mathfrak{Count}$. Hence, we obtain that $\mathfrak{Fcount} \subseteq \mathfrak{Count}$ and $\mathfrak{Fcount} \times \mathfrak{Fcount} \subseteq \mathfrak{Count}$.

Let us summarize several well known notions of the fuzzy set theory and suppose that $A : z \rightarrow L$ is a fuzzy set from $\mathfrak{Fcount}$. The set $z = \mathrm{Dom}(A)$ is called a *universe of discourse of* A, $\mathrm{Supp}(A) = \{x \in z \mid A(x) > \bot\}$ is called a *support of fuzzy set* A and $A_a = \{x \in z \mid A(x) \geq a\}$ is called an *a-cut of fuzzy set* A. The fuzzy set A is *crisp*, if $A(x) \in \{\bot, \top\}$ for any $x \in z$, and is called a *singleton*, if $A(x) > \bot$ for some $x \in z$ and $A(y) = \bot$ for any $y \in z$ with $y \neq x$. For simplicity, we shall use the same symbol to denote a crisp set as a fuzzy set (e.g., $\emptyset$ denotes the empty set as well as the empty fuzzy

[2] Notice that if the adjoint pair $\langle \oplus, \ominus \rangle$ (or $\langle \otimes, \rightarrow \rangle$) is forgotten in the rdr-lattice $\mathbf{L}$ we obtain the *residuated lattice* (or *dually residuated lattice*).

[3] Note that we need to deal with the set $\mathbb{N}$ of all natural numbers and fuzzy sets defined on it, and, therefore, the countable sets are considered. In general, we can consider an arbitrary universe of sets containing $\mathbb{N}$ satisfying the axioms U1-U5 of the definition of a universe of sets over $\mathbf{L}$ (see e.g. [9], [18], [10]). Note that the entire set theory can be introduced inside such universes of sets.

set) and $\{a/x\}$ to denote a singleton A with $A(x) = a > \bot$. Finally, if $f : z \to z'$ and $A : z \to L$ be a fuzzy set, then the *image of A under f* is denoted by $f^{\rightarrow}(A)$ and defined by $f^{\rightarrow}(A)(y) = \bigvee_{x \in z : f(x) = y} A(x)$ for any $y \in z'$.

An essential predicate in our theory is a binary relation saying that two fuzzy sets are the same or equivalent fuzzy sets. In the classical set theory, we say that two sets are the same sets, if they have the same elements. In our theory, we define the analogical notion as follows.

DEFINITION 2 We shall say that fuzzy sets A and B are *equivalent* (symbolically, $A = B$), if $\mathrm{Supp}(A) = \mathrm{Supp}(B)$ and $A(x) = B(x)$ for any $x \in \mathrm{Supp}(A)$.

For example, $A = \{0.9/a, 0/b\}$ and $B = \{0.9, /a\}$ are the equivalent fuzzy sets. We shall use $\mathrm{cls}(A)$ to denote the class of all fuzzy sets from $\mathfrak{Fcount}$ which are equivalent with A. A graded generalization of this relation may be given as follows.

DEFINITION 3 We shall say that fuzzy sets A and B are *the equivalent fuzzy sets* in the degree a (symbolically, $[A \approx B] = a$), if

$$a = \bigwedge_{x \in \mathrm{Dom}(A) \cup \mathrm{Dom}(B)} (A'(x) \leftrightarrow B'(x)), \tag{4}$$

holds for $A' \in \mathrm{cls}(A)$, $B' \in \mathrm{cls}(B)$ with $\mathrm{Dom}(A') = \mathrm{Dom}(B') = \mathrm{Dom}(A) \cup \mathrm{Dom}(B)$.

One can simply prove that $[A \approx B] = [A' \approx B']$ holds for any $A' \in \mathrm{cls}(A)$ and $B' \in \mathrm{cls}(B)$ and, hence, the previous definition is correct. Moreover, $[A \approx B] = \top$ if and only if $A = B$. For our investigation, we need only the operations of union and intersection defined as follows.[4] Let $A, B \in \mathfrak{Fcount}$, $x = \mathrm{Dom}(A) \cup \mathrm{Dom}(B)$ and $A' = A$, $B' = B$ such that $\mathrm{Dom}(A') = \mathrm{Dom}(B') = x$. Then

- *the union* of A and B is a mapping $A \cup B : x \to L$ defined by

$$(A \cup B)(a) = A'(a) \vee B'(a) \tag{5}$$

  for any $a \in x$,
- *the intersection* of A and B is a mapping $A \cap B : x \to L$ defined by

$$(A \cap B)(a) = A'(a) \wedge B'(a) \tag{6}$$

  for any $a \in x$,

One can check easily that our definition is correct, i.e., there is no dependence on the choice of fuzzy sets A' and B' in the previous definitions.

As one could notice, the major object of our theory is a finite fuzzy set. We propose the following definition based on the finiteness of universes of discourse (cf. [1], [14]).

DEFINITION 4 We shall say that a fuzzy set A from $\mathfrak{Fcount}$ is *finite*, if there exists $A' \in \mathrm{cls}(A)$ such that $\mathrm{Dom}(A')$ is a finite set.

[4]Further definitions of operations between fuzzy sets and also a definition of a fuzzy power set can be found in [10].

We shall use $\mathfrak{Ffin}$ to denote the class of all finite fuzzy sets in $\mathfrak{Count}$. Obviously, A is a finite fuzzy set if and only if $\mathrm{Supp}(A)$ is a finite set, $\mathfrak{Ffin}$ is a subclass of $\mathfrak{Fcount}$, the union or intersection of finite fuzzy sets is again a finite fuzzy set.

To define measures of finite fuzzy sets which are similar to the cardinality for finite sets, we need to introduce a concept of generalized cardinal over $\mathbb{N}$. A reasonable condition (see e.g. [1], [14]) for this concept is a "convexity" of fuzzy sets. The convexity of fuzzy sets may be defined over linearly ordered sets as follows. Recall that $\odot \in \{\wedge, \otimes\}$.

DEFINITION 5 Let x be a set in $\mathfrak{Count}$ equipped with a linear ordering $\leq$. We shall say that $A : x \to L$ is an *$\odot$-convex fuzzy set*, if $A(a) \odot A(c) \leq A(b)$ holds for any $a, b, c \in x$ with $a \leq b \leq c$.

DEFINITION 6 *A generalized cardinal* A (over $\mathbb{N}$) is an $\odot$-convex fuzzy set $A : \mathbb{N} \to L$.

One can see that generalized cardinals need not be finite fuzzy sets. We shall use $\mathfrak{N}$ to denote the set of all generalized cardinals. To be able to manipulate with generalized cardinals, we establish, by the Zadeh' extension principle, the operation of addition on $\mathfrak{N}$ as

$$(A + B)(i) = \bigvee_{\substack{k,l \in \mathbb{N} \\ k+l=i}} (A(k) \odot B(l)). \tag{7}$$

Let us define $\mathbf{0} : \mathbb{N} \to L$ by $\mathbf{0}(k) = \top$, if $k = 0$, and $\mathbf{0}(k) = \bot$, otherwise. One can easily prove the following statement saying that our definition of addition is correct.

THEOREM 1 *The triplet $(\mathfrak{N}, +, \mathbf{0})$ is a commutative monoid, where the divisibility of the rdr-lattice $\mathbf{L}$ has to be supposed for $\odot = \wedge$.*

III. GRADED EQUIPOLLENCE OF FUZZY SETS

In order to introduce a graded equipollence for fuzzy sets, we shall follow the classical idea and use "one-to-one mappings between fuzzy sets". Nevertheless, contrary to the classical approach, it seems to be reasonable to distinguish what one-to-one mapping is better than another one. This motivates us to introduce a degree in which a one-to-one mapping between suitable sets is a one-to-one mapping between fuzzy sets as follows.

DEFINITION 7 Let $A, B \in \mathfrak{Fcount}$, $x, y \in \mathfrak{Count}$ and $f : x \to y$ be a one-to-one mapping of x onto y in $\mathfrak{Count}$. We shall say that f is a *one-to-one mapping of A onto B in the degree a* with respect to $\odot$, if $\mathrm{Supp}(A) \subseteq x \subseteq \mathrm{Dom}(A)$ and $\mathrm{Supp}(B) \subseteq y \subseteq \mathrm{Dom}(B)$ and

$$a = \bigodot_{z \in x} (A(z) \leftrightarrow B(f(z))). \tag{8}$$

We shall write $[A \sim_f^{\odot} B] = a$, if f is a one-to-one mapping of A onto B in the degree a with respect to $\odot$. Before we introduce the definition of being equipollent in

the degree α, let us denote $\mathrm{Bij}(A,B)$ the set of all one-to-one correspondences between A and B. Obviously, the set $\mathrm{Bij}(A,B)$ can be characterized as follows.

THEOREM 2 *Let $A, B \in \mathfrak{Fcount}$. A mapping $f : x \to y$ belongs to the set $\mathrm{Bij}(A,B)$, if*

(i) f is a one-to-one mapping of x onto y,
(ii) $\mathrm{Supp}(A) \subseteq x \subseteq \mathrm{Dom}(A)$, and
(iii) $\mathrm{Supp}(B) \subseteq y \subseteq \mathrm{Dom}(B)$.

In what follows, we shall use some results on the graded equipollence for fuzzy sets to simplify the original definition (see [9], [11]). Moreover, we shall consider a more general case, when the operation $\bigwedge$ is replaced by $\bigodot$.[5]

Let $z \in \mathfrak{Count}$. We shall use $\mathrm{Perm}(z)$ to denote the set of all permutations on z, that is, the one-to-one mappings of z onto z.

DEFINITION 8 Let $A, B \in \mathfrak{Fcount}$. We shall say that A is equipollent with B in a degree a with respect to $\odot$ (symbolically, $[A \sim^{\odot} B] = a$), if

$$a = \bigvee_{f \in \mathrm{Perm}(z)} [C \sim_f^{\odot} D] \tag{9}$$

where $C \in \mathrm{cls}(A)$, $D \in \mathrm{cls}(B)$ are arbitrary fuzzy sets with $z = \mathrm{Dom}(C) = \mathrm{Dom}(D)$ such that $|\mathrm{Supp}(A)| \leq |z \setminus \mathrm{Supp}(B)|$ and $|\mathrm{Supp}(B)| \leq |z \setminus \mathrm{Supp}(A)|$.

One could be surprised that the degree in which fuzzy sets are equipollent is not dependent on the choice of fuzzy sets C and D. As we have mentioned above, the previous definition uses the results presented in [9], [11]. More precisely, we use the fact (described for the case $\odot = \wedge$) that the degree of equipollence of A and B can be obtained by fuzzy sets C and D being equivalent with A and B, respectively, for which it is sufficient to suppose that their domains have the same cardinality, or even, their domains are identical (after a suitable extension). Analogously, one could prove the sufficiency of this presumption on $\mathrm{Dom}(C) = \mathrm{Dom}(D)$ for $\odot = \otimes$.

The following useful lemma shows that the degree in which finite fuzzy sets are equipollent can be derived from finite sets.

THEOREM 3 *Let $A, B \in \mathfrak{Ffin}$ and $C \in \mathrm{cls}(A)$, $D \in \mathrm{cls}(B)$ be such that $z = \mathrm{Dom}(C) = \mathrm{Dom}(D)$ and $|z| = n$. Then*

$$[A \sim^{\odot} B] = \bigvee_{f \in \mathrm{Perm}(z)} [C \sim_f^{\odot} D]. \tag{10}$$

As we have mentioned above, the class $\mathfrak{Fcount} \times \mathfrak{Fcount}$ is a subclass of $\mathfrak{Count}$. Hence, we can define the following "fuzzy class" (or also "fuzzy class relation") in $\mathfrak{Count}$, which is analogous to the equivalence relation "to be equipollent" on the class of all sets (for details about fuzzy classes in a universe of sets, we refer to [9], [10]).

[5]For interesting readers, we refer to [9], [10], [11].

THEOREM 4 *The fuzzy class relation $\sim^{\odot}$: $\mathfrak{Fcount} \times \mathfrak{Fcount} \to L$ is a similarity relation ($\otimes$-equivalence) on the class $\mathfrak{Fcount}$, i.e.,*

$$[A \sim^{\odot} A] = \top, \tag{11}$$
$$[A \sim^{\odot} B] = [B \sim^{\odot} A], \tag{12}$$
$$[A \sim^{\odot} B] \otimes [B \sim^{\odot} C] \leq [A \sim^{\odot} C] \tag{13}$$

hold for arbitrary finite fuzzy sets $A, B, C \in \mathfrak{Fcount}$.

The fuzzy class relation $\sim^{\odot}$ is called the *graded equipollence* of finite fuzzy sets.

The rest of this section is devoted to the mappings (fuzzy classes) which can well characterize under some condition the finite fuzzy sets from the graded equipollence perspective.

Let $A \in \mathfrak{Ffin}$ be a finite fuzzy set and define a fuzzy class $p_A^{\odot} : \mathbb{N} \times \mathfrak{Fin} \to L$ by

$$p_A^{\odot}(i,y) = \bigvee_{\substack{z \subseteq y, \\ |z| = i}} \bigodot_{x \in z} A(x) \tag{14}$$

for any $i \in \mathbb{N}$. For simplicity, we shall omit the symbol $\odot$ in $p_A^{\odot}(-,y)$ in such cases, when we consider both interpretations of $\odot$, and thus no confusion can arise. Several properties of the fuzzy sets $p_A(-,y)$ are summarized in the following lemma.

LEMMA 5 *Let $A \in \mathfrak{Ffin}$. Then, for $i, j \in \mathbb{N}$, we have*

$$p_A(i,y) \leq p_A(j,y), \text{ if } i \geq j, \tag{15}$$
$$p_A(i,y) = \bot, \text{ if } i > \min(|y|, |\mathrm{Supp}(A)|), \tag{16}$$
$$p_A(0,y) = \top, \tag{17}$$
$$p_A(1,y) = \bigvee_{x \in y \cap \mathrm{Supp}(A)} A(x). \tag{18}$$

According to the previous lemma, one can see that $p_A(-,y)$ is a generalized cardinal which is a finite fuzzy set. The following statement shows an interesting relation between the equipollence of finite fuzzy sets and the equivalence of generalized cardinals derived from them.

THEOREM 6 *Let $A, B \in \mathfrak{Ffin}$ and $y \in \mathfrak{Fin}$ such that $\mathrm{Supp}(A) \cup \mathrm{Supp}(B) \subseteq y$. Then*

$$[A \sim^{\odot} B] \leq [p_A^{\odot}(-,y) \approx p_B^{\odot}(-,y)]. \tag{19}$$

Simple consequences of the inequality (19) are

$$p_A^{\odot}(-,y) = p_B^{\odot}(-,y), \tag{20}$$
$$[p_A^{\odot}(-,y) \sim^{\odot} p_B^{\odot}(-,y)] = \top, \tag{21}$$

whenever $A \in \mathrm{cls}(B)$ and $\mathrm{Supp}(A) \subseteq y$.

Let us suppose in the rest of this section that $\mathbf{L}$ be a complete linearly ordered rdr-lattice. Then one may simply prove the following equality for $\odot = \wedge$.

THEOREM 7 *Let $\mathbf{L}$ be a complete linearly ordered rdr-lattice, $A, B \in \mathfrak{Ffin}$ and $y \in \mathfrak{Fin}$ such that $\mathrm{Supp}(A) \cup \mathrm{Supp}(B) \subseteq y$. Then*

$$[A \sim^{\wedge} B] = [p_A^{\wedge}(-,y) \approx p_B^{\wedge}(-,y)]. \tag{22}$$

A straightforward consequence of the previous theorem is the following lemma shows that under some presumption on domains of considered finite fuzzy sets there exists a permutation determining the degree in which these fuzzy sets are equipollent.

COROLLARY 8 *Let* $\mathbf{L}$ *be a linearly ordered residuated lattice and* $A, B \in \mathfrak{Ffin}$ *be such that* $z = \mathrm{Dom}(A) = \mathrm{Dom}(B)$. *Then there exists a permutation* f *on* z *such that*

$$[A \sim^{\wedge} B] = [f^{\rightarrow}(A) \approx B]. \tag{23}$$

EXAMPLE 2 Let $\mathbf{L}$ be the Łukasiewicz algebra and $z = \{c_1 \ldots, c_5\}$ be a set of criterion. Let us suppose that the following fuzzy sets

$$A = \{0.3/c_1, 0.8/c_2, 0.4/c_3, 0/c_4, 0/c_5\}$$
$$B = \{0/c_1, 0.6/c_2, 0.9/c_3, 0/c_4, 0.7/c_5\}$$

express the satisfaction of all criterion by two applicants and our goal is to determine, whether the numbers of satisfied criterion are more or less the same for both applicants. According to (14), we can establish

$$p^{\wedge}_A(-, z) = \{1/0, 0.8/1, 0.4/2, 0.3/3, 0/4, 0/5, \ldots\},$$
$$p^{\wedge}_B(-, z) = \{1/0, 0.9/1, 0.7/2, 0.6/3, 0/4, 0/5, \ldots\}$$

and, using Theorem 7, we obtain

$$[A \sim^{\wedge} B] = \bigwedge_{i \in N} (p^{\wedge}_A(i, z) \leftrightarrow p^{\wedge}_B(i, z)) = 0.7.$$

Hence, we can conclude that both applicants have more or less the same number of satisfied criterion.

In the end of this section, we shall introduce an analogous notion to $p^{\odot}_A(i, y)$ for $\overline{\odot}$. Let $A \in \mathfrak{Ffin}$ be a finite fuzzy set and define a fuzzy class $p^{\overline{\odot}}_A : \mathbb{N} \times \mathfrak{Ffin} \to L$ by

$$p^{\overline{\odot}}_A(i, y) = \bigwedge_{\substack{z \subseteq y, \\ |z| = i}} \overline{\bigodot_{x \in z}} A(x) \tag{24}$$

for any $i \in \mathbb{N}$. Again, for simplicity, we shall omit the symbol $\overline{\odot}$ in $p^{\overline{\odot}}_A$ in such cases, when we consider both interpretations of $\overline{\odot}$, and thus no confusion can arise.

LEMMA 9 *Let* $A \in \mathfrak{Ffin}$. *Then, for* $i, j \in \mathbb{N}$, *we have*

$$p_A(i, y) \geq p_A(j, y), \ \textit{if} \ \ i \geq j, \tag{25}$$
$$p_A(i, y) = \top, \ \textit{if} \ \ i > \min(|y|, |\mathrm{Supp}(A)|), \tag{26}$$
$$p_A(0, y) = \bot, \tag{27}$$
$$p_A(1, y) = \bigwedge_{x \in y \cap \mathrm{Supp}(A)} A(x). \tag{28}$$

In contrast to $p^{\odot}_A(-, y)$, the mappings $p^{\overline{\odot}}_A(-, y)$ are denumerable fuzzy sets, i.e., $|\mathrm{Supp}(p^{\overline{\odot}}_A(-, y))| = \aleph_0$. Nevertheless, one can simply check that

$$[p^{\overline{\odot}}_A(-, y) \approx p^{\overline{\odot}}_B(-, y)] = \top, \tag{29}$$

whenever $A \in \mathrm{cls}(B)$ and $\mathrm{Supp}(A) \subseteq y$.

IV. FUZZY C-MEASURES

In the following text, we shall suppose that $\mathbf{L}$ is a complete rdr-lattice which is, moreover, divisible, whenever $\wedge$ is considered as $\odot$.

DEFINITION 9 A class mapping $\mathfrak{C} : \mathfrak{Ffin} \to \mathfrak{N}$ is a *fuzzy c-measure of finite fuzzy sets* with respect to $\odot$, if, for arbitrary $A, B \in \mathfrak{Ffin}$, it satisfies the following axioms

C1: if $A \cap B = \emptyset$, then $\mathfrak{C}(A \cup B) = \mathfrak{C}(A) + \mathfrak{C}(B)$,
C2: if $i, j \in N$ and $i > |\mathrm{Supp}(A)|$, $j > |\mathrm{Supp}(B)|$, then $\mathfrak{C}(A)(i) = \mathfrak{C}(B)(j)$,
C3: if A is a crisp set, then $\mathfrak{C}(A)$ is a crisp set and $\mathfrak{C}(A)(|A|) = \top$,
C4: if $a \in L$, $x, y \in \mathcal{U}$ and $i \in N$, then $\mathfrak{C}(\{a/x\})(i) = \mathfrak{C}(\{a/y\})(i)$,
C5: if $a, b \in L$ and $x \in \mathcal{U}$, then

$$\mathfrak{C}(\{a \,\overline{\odot}\, b/x\})(0) = \mathfrak{C}(\{a/x\})(0) \odot \mathfrak{C}(\{b/x\})(0),$$
$$\mathfrak{C}(\{a \odot b/x\})(1) = \mathfrak{C}(\{a/x\})(1) \odot \mathfrak{C}(\{b/x\})(1).$$

The axioms C1-C5 are called the *additivity, variability, consistency, singleton independency, preservation of non-existence* and *existence*, respectively. In the following text, for simplicity, we shall often speak only about "c-measure" instead of "fuzzy c-measure of finite fuzzy sets" and we shall omit "with respect to $\odot$", when no confusion can arise.

The first three axioms are adopted from [17] and their motivation is as follows. The additivity of c-measure is the standard property of cardinality of sets. The variability states that the c-measure of fuzzy sets is not influenced by the elements that do not belong to supports. A consequence of this axiom is correctness of our axiomatic system, it means, the equivalent finite fuzzy sets[6] have the same c-measure. The axiom of consistency ensures the fact that the c-measures are extensions of the cardinality measure (for finite sets). The singleton independency ensures that a form of elements does not influence the value of a c-measure. Finally, a value $\mathfrak{C}(\{A(x)/x\})(0)$ expresses a degree to which $\{A(x)/x\}$ may be considered as the empty set $\{0/x\}$, i.e. x does not belong to A. Analogously, a value $\mathfrak{C}(\{A(x)/x\})(1)$ determines a degree to which $\{A(x)/x\}$ may be considered as a singleton $\{1/x\}$, i.e. x belongs to A. Since $a \,\overline{\odot}\, b \geq a \vee b$, then one could deduce that the singletons $\{a/x\}$ and $\{b/x\}$ are closer to the empty set $\{0/x\}$ than the singleton $\{a \,\overline{\odot}\, b/x\}$ and, hence,

$$\mathfrak{C}(\{a \,\overline{\odot}\, b/x\})(0) \leq \mathfrak{C}(\{a/x\})(0) \wedge \mathfrak{C}(\{b/x\})(0).$$

Since $a \odot b \leq a \wedge b$, we may obtain

$$\mathfrak{C}(\{a/x\})(0) \odot \mathfrak{C}(\{b/x\})(0) \leq \mathfrak{C}(\{a \,\overline{\odot}\, b/x\})(0),$$

but this is in a contradiction with the relation mentioned above. A compromise is the first "strong" relation of the axiom C5.

[6] See Definition 2.

Analogously, one could deduce the second "strong" relation of the axiom C5. [7]

The following proposition shows the FGCount, FLCount and FECount by means of c-measures of finite fuzzy sets for $\odot = \wedge$ (cf. [17], [8], [1]). Define a complement of A by $\overline{A}(x) = A(x) \to \bot$ for any $x \in \mathrm{Supp}(A)$ and $\overline{A}(x) = \bot$ for any $x \in \mathrm{Dom}(A) \setminus \mathrm{Supp}(A)$.[8]

PROPOSITION 10 *The mappings $\mathfrak{C}_k : \mathfrak{Ffin} \to \mathfrak{N}$, $k = 1, 2, 3$, defined by*

$$\mathfrak{C}_1(A)(i) = \bigvee\{a \mid a \in L \text{ and } |A_a| \geq i\}, \tag{30}$$

$$\mathfrak{C}_2(A)(i) = \mathfrak{C}_1(\overline{A})(\bar{i}), \tag{31}$$

$$\mathfrak{C}_3(A)(i) = \mathfrak{C}_1(A)(i) \wedge \mathfrak{C}_2(A)(i) \tag{32}$$

are c-measures of finite fuzzy sets with respect to $\wedge$, where $\bar{i} = \max(0, |\mathrm{Dom}(A)| - i)$.

EXAMPLE 3 Let $\mathbf{L}$ be the Łukasiewicz algebra, i.e. $a \otimes b = \max(0, a + b - 1)$ and $A = \{0.5/a, 0.8/b, 0.1/c, 0.4/d, 0/e\}$. Then

$$\mathfrak{C}_1(A) = \{1/0, 0.8/1, 0.5/2, 0.4/3, 0.1/4, 0/5, 0/6 \dots\},$$
$$\mathfrak{C}_2(A) = \{0/0, 0.2/1, 0.5/2, 0.6/3, 0.9/4, 1/5, 1/6, \dots\},$$
$$\mathfrak{C}_3(A) = \{0/0, 0.2/1, 0.5/2, 0.4/3, 0.1/4, 0/0, 0/6 \dots\}.$$

Note that $\mathfrak{C}_1$ does not define a c-measure with respect to $\otimes$ in general. Two examples of c-measures with respect to $\otimes$ are given below.

PROPOSITION 11 *Let $\mathfrak{C}_1$ be the c-measure with respect to $\wedge$ defined above. Then mappings $\mathfrak{C}_k : \mathfrak{Ffin} \to \mathfrak{N}$ defined by*

$$\mathfrak{C}_4(A)(i) = \mathfrak{C}_1(A_\top)(i), \tag{33}$$

$$\mathfrak{C}_5(A)(i) = \begin{cases} \top, & i = 0, \\ \mathfrak{C}_5(A)(i-1) \otimes \mathfrak{C}_1(A)(i), & i > 0 \end{cases} \tag{34}$$

are c-measures with respect to $\otimes$.

EXAMPLE 4 Let A be the fuzzy set from Example 3. Then

$$\mathfrak{C}_4(A) = \{1/0, 0/1, 0/2, \dots\},$$
$$\mathfrak{C}_5(A) = \{1/0, 0.8/1, 0.3/2, 0/3, 0/4, 6 \dots\},$$

where, for example, $0.3 = 0.8 \otimes 0.5 = \max(0, 0.8 + 0.5 - 1)$.

The following proposition shows that the form of the c-measure can be various. Recall that $\mathbf{0}$ is the neutral element in the monoid $(\mathfrak{N}, +, \mathbf{0})$ and $\mathbb{N}$ can also denote the fuzzy set of all natural numbers, i.e., $\mathbb{N}(n) = \top$ for any $n \in \mathbb{N}$.

[7]Note that one could imagine a weaker relation, where the equalities in C5 are replaces by the inequality $\leq$. Nevertheless, this inequality does not lead to nicer results.

[8]One can verify that $A = B$ implies $\overline{A} = \overline{B}$ and thus $=$ is a congruence with respect to the complement in $\mathcal{U}$. Note that the same result cannot be obtained for a definition of $\overline{A}$ where $\overline{A}(x) = \top$ for any $x \in \mathrm{Dom}(A) \setminus \mathrm{Supp}(A)$.

PROPOSITION 12 *Let $\mathfrak{C} : \mathfrak{Ffin} \to \mathfrak{N}$ be a c-measure. Then $\mathfrak{C}(\emptyset) = \mathbf{0}$ or $\mathfrak{C}(\emptyset) = \mathbb{N}$. If $\mathfrak{C}(\emptyset) = \mathbb{N}$, then $\mathfrak{C}(A)$ is a non-decreasing mapping.*

A simple consequence of this proposition is the fact that $\mathfrak{C}(A)(i) \in \{\bot, \top\}$ for any $i \in \mathbb{N}$ such that $i > |\mathrm{Supp}(A)|$.

A consequence of the additivity of c-measure is the following theorem.

THEOREM 13 *Let $\mathfrak{C} : \mathfrak{Ffin} \to \mathfrak{N}$ be a c-measure and $A \in \mathfrak{Ffin}$ such that $\mathrm{Supp}(A) = \{x_1, \dots, x_m\}$. Then*

$$\mathfrak{C}(A)(i) = \bigvee_{\substack{i_1, \dots, i_m \in \{0,1\} \\ i_1 + \cdots + i_m = i}} \bigodot_{k=1}^{m} \mathfrak{C}(\{A(x_k)/x_k\})(i_k) \tag{35}$$

for each $i \in N$. Moreover, $\mathfrak{C}(A)(i) = \bot$ or $\mathfrak{C}(A)(i) = \top$ hold for any $m < i$.

In [17], a representation of cardinalities of finite fuzzy sets using two monotonic mappings $f, g : [0,1] \to [0,1]$ was shown. In order to introduce an analogical representation for the c-measures, we need to establish a generalization of monotonic mappings.

Let $\mathbf{L}_1, \mathbf{L}_2$ be complete rdr-lattices. We shall say that $h : L_1 \to L_2$ is an *$\odot$-homomorphism* of $\mathbf{L}_1$ to $\mathbf{L}_2$, if h is a homomorphism of the reduct $(L_1, \odot_1, \top_1)$ of $\mathbf{L}_1$ to the reduct $(L_2, \odot_2, \top_2)$ of $\mathbf{L}_2$, i.e., $h(a \odot_1 b) = h(a) \odot_2 h(b)$ and $h(\top_1) = \top_2$.[9] Further, we shall say that $h : L_1 \to L_2$ is an *$\overline{\odot}_{\mathrm{d}}$-homomorphism*, if h is a homomorphism from the reduct $(L_1, \overline{\odot}_1, \bot_1)$ of $\mathbf{L}_1$ to the reduct $(L_2, \odot_2, \top_2)$ of $\mathbf{L}_2$, i.e. $h(a \,\overline{\odot}_1\, b) = h(a) \odot h(b)$ and $h(\bot_1) = \top_2$.

The following lemma gives a characterization of c-measures using $\odot$- and $\overline{\odot}_{\mathrm{d}}$-homomorphisms.

LEMMA 14 *Let $f, g : L \to L$ be $\odot$- and $\overline{\odot}_{\mathrm{d}}$-homomorphisms from $\mathbf{L}$ to $\mathbf{L}$ such that $f(\bot) \in \{\bot, \top\}$ and $g(\top) \in \{\bot, \top\}$, respectively. Let $\mathfrak{C}_{f,g} : \mathfrak{Ffin} \to \mathfrak{N}$ be a mapping defined by the induction:*

$$\mathfrak{C}_{f,g}(\{a/x\})(0) = g(a),\ \mathfrak{C}_{f,g}(\{a/x\})(1) = f(a),$$
$$\mathfrak{C}_{f,g}(\{a/x\})(k) = f(\bot),\ k > 1$$

hold for each singleton $\{a/x\} \in \mathfrak{Ffin}$ and

$$\mathfrak{C}_{f,g}(A) = \mathfrak{C}_{f,g}(\{A(x_1)/x_1\}) + \cdots + \mathfrak{C}_{f,g}(\{A(x_m)/x_m\})$$

holds for each $A \in \mathfrak{Ffin}$ with $\mathrm{Supp}(A) = \{x_1, \dots, x_m\}$. Then $\mathfrak{C}_{f,g}$ is a c-measure of finite fuzzy sets with respect to $\odot$.

THEOREM 15 (REPRESENTATION OF C-MEASURES) *Let $\mathfrak{C} : \mathfrak{Ffin} \to \mathfrak{N}$ be a mapping satisfying the additivity axiom. Then the following statements are equivalent:*

(i) $\mathfrak{C}$ is a c-measure of finite fuzzy sets with respect to $\odot$,

[9]Note that each homomorphism between rdr-lattices (or residuated lattices which are the reducts of original rdr-lattices) is also an $\odot$-homomorphism.

(ii) there exist an $\odot$-homomorphism $f : L \to L$ and an $\overline{\odot}_{\mathrm{d}}$-homomorphism $g : L \to L$, such that $f(\bot) \in \{\bot, \top\}$, $g(\top) \in \{\bot, \top\}$ and

$$\mathfrak{C}(\{a/x\})(0) = g(a),\ \mathfrak{C}(\{a/x\})(1) = f(a),$$
$$\mathfrak{C}(\{a/x\})(k) = f(\bot)$$

hold for arbitrary $a \in L$, $x \in \mathfrak{Count}$ and $k \in \mathbb{N}$, $k > 1$.

We shall use $\mathfrak{C}_{f,g}$ to denote a c-measure which is determined by an $\odot$-homomorphism $f : L \to L$ and an $\overline{\odot}_{\mathrm{d}}$-homomorphism $g : L \to L$ satisfying (ii). Moreover, we shall use $\mathfrak{C}_f$ or $\mathfrak{C}_g$, if g or f are the trivial $\overline{\odot}_{\mathrm{d}}$-homomorphism or $\odot$-homomorphism (i.e., $g(a) = \top$ or $f(a) = \top$ for any $a \in L$), respectively. Note that the trivial homomorphisms have no influence on the form of a c-measure.

V. Graded equipollence and c-measures

Let $\mathbf{L}$ be a complete rdr-lattice, $f : L \to L$ be a mapping and $A : x \to L$ be a fuzzy set. We shall use $f(A)$ to denote a fuzzy set of x to L defined by $f(A)(z) = f(A(z))$ for any $z \in x$. Note that $f(A) = f \circ A$ and thus $\mathrm{Dom}(A) = \mathrm{Dom}(f(A))$.

The first theorem shows a relation between the degrees in which there exist one-to-one correspondences between fuzzy sets (under f and g) and the similarity of generalized cardinals obtained by the corresponding c-measure.

Theorem 16 *Let $\mathfrak{C}_{f,g} : \mathfrak{Ffin} \to \mathfrak{N}$ be a c-measure determined by $\odot$- and $\overline{\odot}_d$-homomorphisms f and g, respectively, $A, B \in \mathfrak{Ffin}$ and $h \in \mathrm{Bij}(A, B)$. Then*

$$a_{gh} \odot a_{fh} \leq [\mathfrak{C}_{f,g}(A) \approx \mathfrak{C}_{f,g}(B)], \tag{36}$$

where a_{gh} and a_{fh} are the degrees in which h is a one-to-one mapping of $g(A)$ and $f(A)$ onto $g(B)$ and $f(B)$, respectively.

A straightforward consequence of the previous theorem is the following corollary.

Corollary 17 *Let $f : L \to L$ be a $\odot$-homomorphism and $g : L \to L$ be a $\overline{\odot}_d$-homomorphism. Then*

(i) $[f(A) \sim^{\odot} f(B)] \leq [\mathfrak{C}_f(A) \approx \mathfrak{C}_f(B)]$,
(ii) $[g(A) \sim^{\odot} g(B)] \leq [\mathfrak{C}_g(A) \approx \mathfrak{C}_g(B)]$

hold for any $A, B \in \mathfrak{Ffin}$.

Let $\mathbf{L}$ be a complete rdr-lattice and $h : L \to L$ be a mapping. We shall say that h is $(k, \odot)$-compatible with $\leftrightarrow$, if

$$\underbrace{(a \leftrightarrow b) \odot \cdots \odot (a \leftrightarrow b)}_{\text{k-times}} \leq h(a) \leftrightarrow h(b). \tag{37}$$

Obviously, h is $(k, \wedge)$-compatible with $\leftrightarrow$, if $(a \leftrightarrow b) \leq h(a) \leftrightarrow h(b)$. For example, $h(a) = (\neg a)^k$ is $(k, \otimes)$-compatible with $\leftrightarrow$.

Corollary 18 *Let $\mathfrak{C}_{f,g} : \mathfrak{Ffin} \to \mathfrak{N}$ be a c-measure determined by $\odot$- and $\overline{\odot}_d$-homomorphisms f and g which are $(k, \odot)$- and $(l, \odot)$-compatible with $\leftrightarrow$, respectively, $A, B \in \mathfrak{Ffin}$ and $h \in \mathrm{Bij}(A, B)$. Then*

$$a_h^{k+l} \leq [\mathfrak{C}_{f,g}(A) \approx \mathfrak{C}_{f,g}(B)], \tag{38}$$

where a_h is the degree in which h is a one-to-one mapping of A onto B and $a^n = a$ for $\odot = \wedge$. Especially, we have

$$(A \sim^{\odot} B)^k \leq [\mathfrak{C}_f(A) \approx \mathfrak{C}_f(B)] \tag{39}$$
$$(A \sim^{\odot} B)^l \leq [\mathfrak{C}_g(A) \approx \mathfrak{C}_g(B)], \tag{40}$$

where $a^n = a$ for $\odot = \wedge$.

In the previous section, we have introduce the fuzzy classes $p_A^{\odot}$ and $p_A^{\overline{\odot}}$. The following theorems show the relation between the c-measures and some expressions obtained by the fuzzy sets $p_A^{\odot}(-, y)$ and $p_A^{\overline{\odot}}(-, y)$.

Theorem 19 *Let $\mathfrak{C}_{f,g} : \mathfrak{Ffin} \to \mathfrak{N}$ be a c-measure determined by $\odot$- and $\overline{\odot}_d$-homomorphisms f and g, respectively, $A \in \mathfrak{Ffin}$ and $y \in \mathfrak{Fin}$ such that $\mathrm{Supp}(A) \subseteq y$ and $|y| = m$. Then*

$$\mathfrak{C}_{f,g}(A)(i) \leq g(p_A^{\overline{\odot}}(m - i, y)) \odot f(p_A^{\odot}(i, y)) \tag{41}$$

holds for any $i = 0, \ldots, m$.

Theorem 20 *Let $\mathbf{L}$ be linearly ordered, $\mathfrak{C}_{f,g} : \mathfrak{Ffin} \to \mathfrak{N}$ be a c-measure determined by $\odot$- and $\overline{\odot}_d$-homomorphisms f and g, respectively, $A \in \mathfrak{Ffin}$ and $y \in \mathfrak{Fin}$ such that $\mathrm{Supp}(A) \subseteq y$ and $|y| = m$. Then*

$$\mathfrak{C}_{f,g}(A)(i) = g(p_A^{\overline{\odot}}(m - i, y)) \odot f(p_A^{\odot}(i, y)), \tag{42}$$
$$\mathfrak{C}_{f,g}(A)(i) = p^{\overline{\odot}}_{g(A) \cap y}(m - i, y) \odot p^{\odot}_{f(A)}(i, y) \tag{43}$$

hold for any $i = 0, \ldots, m$ and $\mathfrak{C}_{f,g}(A)(i) = f(\bot)$ for any $i > m$.

Corollary 21 *Let $\mathbf{L}$ be linearly ordered, $\mathfrak{C}_{f,g} : \mathfrak{Ffin} \to \mathfrak{N}$ be a c-measure determined by $\odot$- and $\overline{\odot}_d$-homomorphisms f and g, respectively, and $A \in \mathfrak{Ffin}$ such that $|\mathrm{Supp}(A)| = m$. Then*

$$\mathfrak{C}_{f,g}(A)(i) = g(p_A^{\wedge}(i + 1)) \wedge f(p_A^{\wedge}(i)) \tag{44}$$

holds for any $i = 0, \ldots, m$ and $\mathfrak{C}_{f,g}(A)(i) = f(\bot)$ for any $i > m$, where $p_A^{\wedge}(i) = p_A^{\wedge}(i, \mathrm{Supp}(A))$ for any $i \in \mathbb{N}$.

In the following example, we shall introduce three c-measures based on Theorem 20.

Example 5 Let us suppose that the membership degrees of fuzzy sets are interpreted in the Goguen rdr-lattice $\mathbf{L}_{\mathrm{P}}$ or Łukasiewicz rdr-lattice $\mathbf{L}_{\mathrm{Ł}}$ (see Ex. 1) and

$$A = \{0.5/x_1, 0.2/x_2, 0.9/x_3, 1/x_4,$$
$$0.8/x_5, 0.9/x_6, 1/x_7, 0.6/x_8\}$$

is a finite fuzzy set. Further, let us define $f, g : [0, 1] \to [0, 1]$ by $f(a) = a$ (the identity mapping) and $g(a) = 1 - a$ for any $a \in [0, 1]$. Obviously, both mappings are homomorphisms

between the corresponding structures. Let us put $\odot = T_{\mathrm{M}}$, $\odot = T_{\mathrm{P}}$ and $\odot = T_{\mathrm{L}}$ (the minimum, product and Łukasiewicz conjunction). Then we can construct three c-measures of finite fuzzy sets denoted by $\mathfrak{C}_{T_{\mathrm{M}}}$, $\mathfrak{C}_{T_{\mathrm{P}}}$ and $\mathfrak{C}_{T_{\mathrm{L}}}$. In particular, if T is one of the mentioned t-norms, then c-measure determined by the corresponding homomorphisms has the following form (due to Theorem 20)

$$\mathfrak{C}_T(A)(i) = T(1 - p_A^S(8-i, y), p_A^T(i, y)), \tag{45}$$

where $y = \{x_1, \ldots, x_8\}$, S is the corresponding t-conorm to T and $i = 1, \ldots, 8$. One can simply verify that $p_A^T(-, y)$ and $p_A^S(-, y)$ can be expressed by

$$p_A^T(i, y) = T(p_A^{T_{\mathrm{M}}}(0), \ldots, p_A^{T_{\mathrm{M}}}(i)),$$
$$p_A^S(i, y) = S(p_A^{S_{\mathrm{M}}}(0), \ldots, p_A^{S_{\mathrm{M}}}(i)),$$

where S_M denotes the maximum, for any $i = 0, \ldots, 8$, and $p_A^T(i, y) = \bot$ and $p_A^T(i, y) = \top$ for any $i \in \mathbb{N}$ such that $i > 8$ (see Lemmas 5 and 9). Hence, we can write the sequences

$$p_A^{T_{\mathrm{M}}} = \{1, 1, 1, 0.9, 0.9, 0.8, 0.6, 0.5, 0.2, 0, 0, \cdots\},$$
$$p_A^{S_{\mathrm{M}}} = \{0, 0.2, 0.5, 0.6, 0.8, 0.9, 0.9, 1, 1, 1, 1, \cdots\}$$

and, after a simple computation, we obtain

$$\mathfrak{C}_{T_{\mathrm{M}}}(A) = \{0/0{,}0/1, 0.1/2, 0.1/3, 0.2/4, 0.4/5, 0.5/6, 0.5/7, 0.2/8, 0/9, \ldots\},$$

$$\mathfrak{C}_{T_{\mathrm{P}}}(A) = \{0/0{,}0/1, 0.00032/2, 0.00288/3, 0.02592/4, 0.10368/5{,}0.15552/6, 0.15552/7, 0.03888/8, 0/9, \ldots\},$$

$$\mathfrak{C}_{T_{\mathrm{L}}}(A) = \{0/0{,}0/1, 0/2, 0/3, 0/4, 0/5, 0/6, 0/7, 0/8, \ldots\}.$$

Up till now all relationships between the graded equipollence and the similarity of c-measures of finite fuzzy sets have been in the form of the inequality. The following corollary shows that the equality can arise only in very special cases.

COROLLARY 22 *Let* $\mathbf{L}$ *be linearly ordered and* $\mathfrak{C}_{f,g} : \mathfrak{Fin} \to \mathfrak{Count}$ *be a c-measure determined by* $\odot$*- and* $\overline{\odot}_{\mathrm{d}}$*-homomorphisms* f *and* g*, respectively. Then*

$$(g(A) \sim^{\odot} g(B)) \odot (f(A) \sim^{\odot} f(B)) \leq [\mathfrak{C}_{f,g}(A) \approx \mathfrak{C}_{f,g}(B)] \tag{46}$$

for any $A, B \in \mathfrak{Fin}$*. Especially, we have*

$$g(A) \sim^{\wedge} g(B) = [\mathfrak{C}_g(A) \approx \mathfrak{C}_g(B)], \tag{47}$$
$$f(A) \sim^{\wedge} f(B) = [\mathfrak{C}_f(A) \approx \mathfrak{C}_f(B)] \tag{48}$$

for any $A, B \in \mathfrak{Fin}$*.*

VI. CONCLUSION

In this paper, we presented two approaches to the cardinality of finite fuzzy sets. In the first approach, the cardinality of fuzzy sets was expressed using the fuzzy (class) relation called the graded equipollence. In the second one, the number of elements in fuzzy sets was obtained by a fuzzy c-measure with respect to an operation $\odot$ as a generalized cardinal. Although, both approaches seem to be different, we showed that there exist several natural relations between them. Nevertheless, a desired relation which interconnects both approaches analogously to the classical relations between the equipollence of finite sets and finite ordinals can be proved only in the special cases, when $\odot = \wedge$ and some other presumptions on the form of fuzzy c-measures have to be satisfied (see Corollary 22).

ACKNOWLEDGMENT

This paper has been supported by the Grant IAA108270901 of the GA AV ČR.

REFERENCES

[1] M. Wygralak. *Cardinalities of Fuzzy Sets*. Kluwer Academic Publisher, Berlin, 2003. isbn: 3-5400-0337-1.
[2] D. Klaua. Zum kardinalzahlbegriff in der mehrwertigen mengenlehre. In G. Asser, J. Flashmayers, and W. Rinow, editors, *Theory of Sets and Topology*, pages 313–325. Deutsher Verlag der Wissenshaften, Berlin, 1972.
[3] S. Gottwald. Fuzzy uniqueness of fuzzy mappings. *Fuzzy Sets and Systems*, 3:49–74, 1980.
[4] S. Gottwald. A note on fuzzy cardinals. *Kybernetika*, 16:156–158, 1980.
[5] M. Wygralak. A new approach to the fuzzy cardinality of finite fuzzy sets. *BUSEFAL*, 15:72–75, 1983.
[6] K. Dyczkowski and M. Wygralak. On triangular norm-based generalized cardinals and singular fuzzy sets. *Fuzzy Sets and Systems*, 133(2):211–226, 2003.
[7] M. Wygralak. An axiomatic approach to scalar cardinalities of fuzzy sets. *Fuzzy Sets and Systems*, 110(2):175–179, 2000.
[8] M. Wygralak. Fuzzy sets with triangular norms and their cardinality theory. *Fuzzy Sets and Systems*, 124(1):1–24, 2001.
[9] M. Holčapek and M. Turčan. Graded equipollence of fuzzy sets. In Carvalho J.P., Kaymak D.U., and Sousa J.M.C., editors, *Proceedings of IFSA/EUSFLAT 2009*, pages 1565 –1570. European Soc Fuzzy logic & Technology, Johannes Kepler univ, Austria, 2009.
[10] M. Holčapek. Graded equipollence of fuzzy sets, part I: Basic definitions. *submitted to Fuzzy Sets and Systems*.
[11] M. Holčapek. Graded equipollence of fuzzy sets, part II: Properties. *submitted to Fuzzy Sets and Systems*.
[12] M. Wygralak. Fuzzy cardinals based on the generalized equality of fuzzy subsets. *Fuzzy Sets and Systems*, 18:143–158, 1986.
[13] M. Wygralak. Generalized cardinal numbers and operations on them. *Fuzzy Sets and Systems*, 53(1):49–85, 1993.
[14] M. Wygralak. *Vaguely defined objects. Representations, fuzzy sets and nonclassical cardinality theory*, volume 33 of *Theory and Decision Library. Series B: Mathematical and Statistical Methods*. Kluwer Academic Publisher, Dordrecht, 1996.
[15] L.A. Zadeh. Similarity relations and fuzzy orderings. *Inf. Science*, 3:177–200, 1971.
[16] L.A. Zadeh. A computational approach to fuzzy quantifiers in natural languages. *Comp. Math. with Applications*, 9:149–184, 1983.
[17] J. Casasnovas and J. Torrens. An axiomatic approach to fuzzy cardinalities of finite fuzzy sets. *Fuzzy Sets and Systems*, 133:193–209, 2003.
[18] M. Holčapek. An axiomatic approach to fuzzy measures like set cardinality for finite fuzzy sets. Hüllermeier, E. (ed.) et al., Information processing and management of uncertainty in knowledge-based systems. Theory and methods. IPMU 2010, Dortmund, Germany. Proceedings. Part I. Berlin: Springer. Communications in Computer and Information Science 80, 505-514., 2010.

2011 IEEE International Conference on Fuzzy Systems
June 27-30, 2011, Taipei, Taiwan

On Monotonicity Of Type $\langle 1, 1\rangle$ Fuzzy Quantifiers Determined By Fuzzy Measures

Michal Holčapek Antonín Dvořák
Institute for Research and Applications of Fuzzy Modeling
University of Ostrava, 30. dubna 22, 701 03 Ostrava 1, Czech Republic
{michal.holcapek,antonin.dvorak}@osu.cz

***Abstract*—In this contribution, we study a very important semantic property of generalized quantifiers called the monotonicity for fuzzy quantifiers of type $\langle 1, 1\rangle$ defined using fuzzy measures and Sugeno type of fuzzy integrals. We show that fuzzy integrals can ensure under some natural conditions the monotonicity of fuzzy quantifiers. Finally, we propose the concept of concave fuzzy quantifiers and prove that each concave fuzzy quantifier is expressible as the conjunction of a non-increasing and a non-decreasing fuzzy quantifier.**

***Index Terms*—fuzzy quantifier; fuzzy measure; residuated lattice operation; monotonicity of fuzzy quantifiers**

I. Introduction

This contribution continues our study of semantic properties of type $\langle 1, 1\rangle$ fuzzy quantifiers defined by fuzzy integrals published in [7] (see also [4]) and presents some results on the monotonicity which belongs among the basic semantic properties as, e.g., the isomorphism invariance, extension, conservativity, investigated in the theory of generalized quantifiers (Boolean theory) as well as fuzzy quantifiers theory (many valued theory). For more information, we refer to [8], [13], [26].

Generalized quantifiers evolved, from pioneering works of Mostowski [20], Lindström [17], Barwise and Cooper [1], into quite large research field with deep results. For overview as well as new results see the recent monograph [26].

Research in the field of fuzzy quantifiers started with works of Zadeh [31], Thiele [29], Ralescu [28] and others, see also [18], [19], [22]. Important contribution was made by Hájek in [12], where he considers especially quantifier "many" using relative frequencies. He also points out interconnections between generalized quantifiers and modalities. A comprehensive study of fuzzy quantifiers was undertaken by Glöckner [8] (see also [9]). In paper [24], Novák studies so-called intermediate quantifiers, mainly from syntactic point of view in the frame of fuzzy type theory [23]. This research has been continued in [21], where all of generalized Aristotelian syllogisms (from Peterson's book [27]) has been syntactically proved using slightly different definition of fuzzy quantifiers than ours.

The semantic interpretation of many generalized quantifiers is often connected to measurement of "size" of sets in concern. Consider e.g. the quantifier "many". The truth value of proposition "many books have a red cover" clearly depends on the "size" of the set of red books. Therefore, it is natural to consider measures (and integrals) of (fuzzy) sets as natural tools for the modeling of important classes of generalized quantifiers. This motivated us to introduce fuzzy quantifiers of type $\langle 1\rangle$, which are denotations of important noun phrases of natural language, e.g. "something" in "Something is broken.", "everyone" in "Everyone likes Bob.", "nobody" in "Nobody knows everything.", using tools of fuzzy measure theory ([30], see also [10], [15]). More precisely, we used a Sugeno type of fuzzy integrals and defined fuzzy integrals of type $\langle 1\rangle$ in [5].

A natural extension of this research was to study quantifiers of type $\langle 1, 1\rangle$, e.g. "every" in "Every book has leaves.", "most" in "Most birds fly.", which take two arguments. These type $\langle 1, 1\rangle$ quantifiers are claimed to be the most important from the point of view of natural language semantics [26]. To introduce this type of fuzzy quantifiers by fuzzy integrals, we had to work with slightly different definition of fuzzy measures and integrals than in [5]. Note that the first argument of $\langle 1, 1\rangle$ quantifier is called *restriction* and the second one is *scope* (i.e., in "Every book has leaves", "to be a book" is the restriction and "to have leaves" is the scope). It is natural to think of the restriction as of a *new universe* for the quantifier (in our example, for the determination of truth value of this sentence, only these objects fulfilling the restriction condition are important, i.e., books). Because we are working with fuzzy subsets of some universe M, we in effect should be able to define quantifiers on *fuzzy universes*. Therefore, we defined a new type of fuzzy measure spaces on algebras of subsets of a *fuzzy* set A and a fuzzy integral on these fuzzy measure spaces (see [3], [6], [7]).

In [5], we have showed that type $\langle 1\rangle$ fuzzy quantifiers determined by fuzzy measures are monotone fuzzy quantifiers. The type of monotonicity, i.e., whether a fuzzy quantifier is monotone increasing (non-decreasing) or monotone decreasing (non-increasing), depends on the type of the fuzzy integral,[1] e.g., the fuzzy quantifier "many" defined using a fuzzy measure is monotone increasing, but the fuzzy quantifier "few" defined using complementary fuzzy measure is monotone decreasing. For type $\langle 1, 1\rangle$ fuzzy quantifiers, the situation is more complicated, since operations between restriction and scope are used in our modeling.

[1] In [5], we proposed two types of fuzzy integrals defined on fuzzy and complementary fuzzy measure spaces to model, e.g., "many" and "few". Note that under some conditions both types can be interconnected by the operation of negation.

978-1-4244-7316-8/11/$26.00 ©2011 IEEE

The paper is structured as follows. In the following section, we recall basic notions from the fuzzy set theory and fuzzy measures and integrals. The third section is devoted to the residuated lattice operations using them operations between fuzzy sets are defined. Such operations between fuzzy sets are subsequently used as a means for a combination of two arguments of type $\langle 1,1\rangle$ fuzzy quantifiers. Fuzzy quantifiers defined using fuzzy integrals are introduced in the fourth section. The monotonicity of fuzzy quantifiers is studied in the fifth section. The last section is a conclusion.

II. Preliminaries

A. Structures of truth values

In this paper, we suppose that the structure of truth values is a *complete residuated lattice* (see e.g. [2]), i.e., an algebra $\mathbf{L} = \langle L, \wedge, \vee, \to, \otimes, \bot, \top\rangle$ with four binary operations and two constants such that $\langle L, \wedge, \vee, \bot, \top\rangle$ is a complete lattice, where $\bot$ is the least element and $\top$ is the greatest element of L, respectively, $\langle L, \otimes, \top\rangle$ is a commutative monoid (i.e., $\otimes$ is associative, commutative and the identity $a \otimes \top = a$ holds for any $a \in L$) and the adjointness property is satisfied, i.e.,

$$a \le b \to c \quad \text{iff} \quad a \otimes b \le c \tag{1}$$

holds for each $a, b, c \in L$, where $\le$ denotes the corresponding lattice ordering. A residuated lattice is *divisible*, if $a \otimes (a \to b) = a \wedge b$ holds for arbitrary $a, b \in L$, and satisfies the *law of double negation*, if $(a \to \bot) \to \bot = a$ holds for any $a \in L$. A divisible residuated lattice satisfying the law of double negation is called an *MV-algebra*. For more information about residuated lattices we refer to [2], [25].

Example 1 One can easily prove (see also [12]) that the algebra

$$\mathbf{L}_{\mathrm{T}} = \langle [0,1], \min, \max, T, \to_T, 0, 1\rangle,$$

where T is a left continuous t-norm and $a \to_T b = \bigvee\{c \in [0,1] \mid T(a,c) \le b\}$ defines the residuum, is a complete residuated lattice. Moreover, if T is the Łukasiewicz t-norm, i.e., $T(a,b) = \max(a+b-1, 0)$ for all $a, b \in [0,1]$, then $\mathbf{L}_{\mathrm{T}}$ is a complete MV-algebra called a *Łukasiewicz algebra (on* $[0,1]$*)*.

Let us define two additional operations for all $a, b \in L$:

$$a \leftrightarrow b = (a \to b) \wedge (b \to a), \qquad \text{(\textit{biresiduum})}$$
$$\neg a = a \to \bot. \qquad \text{(\textit{negation})}$$

B. Fuzzy sets

Let $\mathbf{L}$ be a complete residuated lattice and M be a universe of discourse (possibly empty). A mapping $A : M \to L$ is called an *fuzzy set on* M. A value $A(m)$ is called a *membership degree of* m *in the fuzzy set* A. The set of all fuzzy sets on M is denoted by $\mathcal{F}(M)$. Obviously, if $M = \emptyset$, then the empty mapping $\emptyset$ is the unique fuzzy set on $\emptyset$ and thus $\mathcal{F}(\emptyset) = \{\emptyset\}$. A fuzzy set A on M is called *crisp*, if there is a subset X of M such that $A = 1_X$, where 1_X denotes the characteristic function of X. Particularly, $1_\emptyset$ denotes the empty fuzzy set on M, i.e., $1_\emptyset(m) = \bot$ for any $m \in M$. This convention will be also kept for $M = \emptyset$. The set of all crisp fuzzy sets on M is denoted by $\mathcal{P}(M)$. A fuzzy set A is *constant*, if there is $c \in L$ such that $A(m) = c$ for any $m \in M$. For simplicity, a constant fuzzy set is denoted by the corresponding element of L, e.g., a, b, c.[2] Let us denote $\mathrm{Supp}(A) = \{m \mid m \in M \ \&\ A(m) > \bot\}$ and $\mathrm{Core}(A) = \{m \mid m \in M \ \&\ A(m) = \top\}$ the *support* and *core* of a fuzzy set A, respectively. Obviously, $\mathrm{Supp}(1_X) = \mathrm{Core}(1_X) = X$ for any crisp fuzzy set. A fuzzy set A is called *normal*, if $\mathrm{Core}(A) \neq \emptyset$.

Let $\{A_i \mid i \in I\}$ be a non-empty family of fuzzy sets on M. Then the *union of* A_i is defined by

$$\left(\bigcup_{i\in I} A_i\right)(m) = \bigvee_{i\in I} A_i(m) \tag{2}$$

for any $m \in M$ and the *intersection of* A_i is defined by

$$\left(\bigcap_{i\in I} A_i\right)(m) = \bigwedge_{i\in I} A_i(m) \tag{3}$$

for any $m \in M$. Let A, B be fuzzy sets on M. The *difference* of A and B is a fuzzy set $A \setminus B$ on M defined by

$$(A \setminus B)(m) = A(m) \otimes (B(m) \to \bot) \tag{4}$$

for any $m \in M$ and the *complement* of A is a fuzzy set $\overline{A} = 1_M \setminus A$. Finally, an extension of the operations $\otimes$ and $\to$ on L to the operations on $\mathcal{F}(M)$ is given by

$$(A \otimes B)(m) = A(m) \otimes B(m), \tag{5}$$
$$(A \to B)(m) = A(m) \to B(m) \tag{6}$$

for any $A, B \in \mathcal{F}(M)$ and $m \in M$, respectively.

Since we will deal with fuzzy sets over different universes, let us introduce the ordering relation between fuzzy sets on arbitrary universes. We say that a fuzzy set A on M is an *fuzzy subset of* a fuzzy set B on M' and denote by $A \subseteq B$, if $A(m) \le B(m)$ for any $m \in \mathrm{Supp}(A)$. The set of all fuzzy subsets of A on M is denoted by $\mathcal{F}(A)$. Thus

$$\mathcal{F}(A) = \{B \mid B \in \mathcal{F}(M) \text{ and } B \subseteq A\}. \tag{7}$$

Further, we say that a fuzzy set A on M is *equal* to a fuzzy set B on M' and denote by $A = B$, if $A \subseteq B$ and $B \subseteq A$. Obviously, if A and B are fuzzy sets on the same universe M, then the proposed relations coincide with the common definitions of the ordering and equality relations.

C. Fuzzy measures and integrals

In the following, we will consider algebras of fuzzy sets as a base for defining fuzzy measures of fuzzy sets.

Definition 1 Let A be a non-empty fuzzy set on M. A subset $\mathcal{F}$ of $\mathcal{F}(A)$ is an *algebra of fuzzy sets on* A, if the following conditions are satisfied

[2]We suppose that the meaning of this symbol will be unmistakable from the context, that is, it should be clear when an element of L is considered and when a constant fuzzy set is assumed.

(i) $1_\emptyset, A \in \mathcal{F}$,
(ii) if $X \in \mathcal{F}$, then $A \setminus X \in \mathcal{F}$,
(iii) if $X, Y \in \mathcal{F}$, then $X \cup Y \in \mathcal{F}$.

We denote $\mathbf{Alg}(A)$ the set of all algebras of fuzzy sets on A. A pair $(A, \mathcal{F})$ is called a *fuzzy measurable space* (on A), if $\mathcal{F}$ is an algebra of fuzzy sets on A. Let $(A, \mathcal{F})$ be a fuzzy measurable space and $X \in \mathcal{F}(A)$. We say that X is $\mathcal{F}$-*measurable*, if $X \in \mathcal{F}$.

REMARK 2 In order to refer to the universe of discourse M of A, we will sometimes write $\mathrm{Dom}(A)$ instead of M.

REMARK 3 For a non-empty set M, one checks easily that the proposed definition of algebra of fuzzy sets on 1_M coincides with the standard definition of algebra of fuzzy sets on M (cf. [30]).

EXAMPLE 4 $\{1_\emptyset, A\}$ and $\mathcal{F}(A)$ are trivial examples of algebras of fuzzy sets on A. The set of all crisp subsets of a fuzzy set A is not, in general, an algebra of fuzzy sets on A.

Let us introduce the concept of fuzzy measure as follows. The definition is a modification of the definition of a normed measure with respect to truth values (see e.g. [10]).

DEFINITION 2 Let $(A, \mathcal{F})$ be a fuzzy measurable space. A mapping $\mu : \mathcal{F} \to L$ is called a *fuzzy measure* on $(A, \mathcal{F})$, if
(i) $\mu(1_\emptyset) = \bot$ and $\mu(A) = \top$,
(ii) if $B, C \in \mathcal{F}$ such that $B \subseteq C$, then $\mu(B) \leq \mu(C)$.
A triplet $(A, \mathcal{F}, \mu)$ is called the *fuzzy measure space*, if $(A, \mathcal{F})$ is a fuzzy measurable space and μ is a fuzzy measure on $(A, \mathcal{F})$.

In the following text, a fuzzy measure space $(A, \mathcal{F}, \mu)$ may be shortly denoted by the same bold symbol $\mathbf{A}$, i.e. $\mathbf{A} = (A, \mathcal{F}, \mu)$. We denote $\mathbf{Fms}(M)$ the class of all fuzzy measure spaces defined on a non-empty universe M, i.e. a fuzzy measure space $(A, \mathcal{F}, \mu)$ belongs to $\mathbf{Fms}(M)$, if $A \in \mathcal{F}(M)$.

EXAMPLE 5 Let $\mathbf{L}_\mathrm{T}$ be an algebra from Example 1, where T is a continuous t-norm. Let M be a finite non-empty set and $A \in \mathcal{F}(M)$, $A \neq 1_\emptyset$. Then we can define fuzzy measure space $\mathbf{A}^\sigma = (A, \mathcal{F}(A), \mu^\sigma)$, where

$$\mu^\sigma(X) = \frac{\sum_{m \in M} X(m)}{\sum_{m \in M} A(m)}$$

for all $X \in \mathcal{F}(A)$. For motivation and more general definition of this fuzzy measure, we refer to Example 3.5 of our paper [5].

Now, we can introduce a type of fuzzy integral that is definable on an arbitrary fuzzy measure space $(A, \mathcal{F}, \mu)$. The integrated functions are fuzzy sets on $\mathrm{Dom}(A)$. For a convention with the classical measure theory, we will prefer, in this part, the denotation f, g for the integrated functions instead of X, Y. This integral is defined over a general operation $\odot$ which substitutes one of the operations $\wedge$ and $\otimes$, i.e., $\odot \in \{\wedge, \otimes\}$. This integral will be used as a basis for the definition of fuzzy quantifiers of type $\langle 1, 1\rangle$ determined by fuzzy measures.

DEFINITION 3 Let $(A, \mathcal{F}, \mu)$ be a fuzzy measure space with $M = \mathrm{Dom}(A)$, $f : M \to L$ be a mapping and X be an $\mathcal{F}$-measurable fuzzy set. Then $\odot$-fuzzy integrals of f on X is given by

$$\int_X^\odot f \, d\mu = \bigvee_{Y \in \mathcal{F}_X^-} \bigwedge_{m \in \mathrm{Supp}(Y)} (f(m) \odot \mu(Y)), \qquad (8)$$

where $\mathcal{F}_X^- = \{Y \mid Y \in \mathcal{F} \text{ and } 1_\emptyset \neq Y \subseteq X\}$. If $X = A$, then we write $\int^\odot f \, d\mu$.

One may see that no measurability of the mapping f is supposed in the definition, in contrast to the standard definition of fuzzy integral (cf. [16], [15]).

III. OPERATIONS BETWEEN FUZZY SETS DETERMINED BY RL-OPERATIONS

In this section, we will define so-called residuated lattice (rl-)operations and operations between fuzzy sets determined by them, which will subsequently be used as a means for a combination of two arguments (the restriction and scope, see Introduction) of a type $\langle 1, 1\rangle$ fuzzy quantifier. For example, the standard quantifier some is defined using the intersection operation, i.e.,

$$\mathsf{some}(A, B) = \bigvee_{m \in M} (A \cap B)(m), \qquad (9)$$

and every by the residuum operation $\to$, i.e.,

$$\mathsf{every}(A, B) = \bigwedge_{m \in M} (A \to B)(m). \qquad (10)$$

Hence, for the modeling of various natural language quantifiers we need different operations on fuzzy sets (cf. [11]).

DEFINITION 4 Let L be a set of constants. The set $\mathbf{P}(L)$ of *binary (residuated lattice) polynomials* with constants from L is the smallest set satisfying the following conditions
(i) $c \in \mathbf{P}(L)$ for any $c \in L$,
(ii) $x, y \in \mathbf{P}(L)$,
(iii) if $\psi_1, \psi_2 \in \mathbf{P}(L)$, then $\psi_1 \,\square\, \psi_2 \in \mathbf{P}(L)$ for any $\square \in \{\wedge, \vee, \otimes, \to\}$.

REMARK 6 In the previous definition, we refer the polynomials to a set L of constants. In our work, the set L will be identified with a support of a residuated lattice to deal with its elements and, hence, to extend the scale of models of fuzzy quantifiers.

Polynomials are abstract expressions of functions in all residuated lattices in which the considered constants are interpretable. As we have mentioned above, we identify a set L of

constants with a support L of a residuated lattice. Thus, if we write $\mathbf{P}(L)$, then we understand that all values of the support L are constants used in the constructions of polynomials of $\mathbf{P}(L)$. For simplicity, the support of a residuated lattice will be always denoted by the italic letter corresponding to the bold denotation of the residuated lattice. For example, the support of $\mathbf{L}$ is denoted by L. Using polynomials we can define operations on residuated lattices as follows (cf. [11]).

DEFINITION 5 Let $\mathbf{L}$ be a residuated lattice (with the support L). A binary residuated lattice polynomial $\psi \in \mathbf{P}(L)$ defines a binary *residuated lattice operation* (shortly rl-operation) on L by the following rules ($a, b, c \in L$)

(i) if $\psi = c$, then $\psi(a, b) = c$,
(ii) if $\psi = x$ or $\psi = y$, then $\psi(a, b) = a$ or $\psi(a, b) = b$, respectively,
(iii) if $\psi = \psi_1 \,\square\, \psi_2$, then $\psi(a, b) = \psi_1(a, b) \,\square\, \psi_2(a, b)$ for any operation $\square \in \{\wedge, \vee, \otimes, \rightarrow\}$.

The set of all rl-operations in a residuated lattice $\mathbf{L}$ will be denoted by $\mathbf{Ldo}(\mathbf{L})$ or shortly $\mathbf{Ldo}$, if the residuated lattice $\mathbf{L}$ is unmistakably determined by the context and thus no confusion can occur.

DEFINITION 6 Let $\psi_1, \psi_2 \in \mathbf{P}(L)$. We say that ψ_1 *is equal to* ψ_2 *in* $\mathbf{L}$ and denote it by $\psi_1 = \psi_2$, if $\psi_1(a, b) = \psi_2(a, b)$ holds for any $a, b \in L$.

EXAMPLE 7 The unary operation of the negation can be defined by the polynomial $\psi_1 = x \rightarrow \bot$ and thus $\neg a = \psi_1(a, b) = a \rightarrow \bot$ for any $a, b \in L$. The binary operation of the meet can be obtained from the polynomial $\psi_2 = x \wedge y$ and thus, $\psi_2(a, b) = a \wedge b$ for any $a, b \in L$. The difference between a and b can be defined using $\psi_3 = x \otimes (y \rightarrow \bot)$ and $a \setminus b = \psi_3(a, b) = a \otimes (b \rightarrow \bot)$.

DEFINITION 7 Let M be a non-empty universe and $\psi \in \mathbf{Ldo}(\mathbf{L})$. We say that an operation $\varphi_M : \mathcal{F}(M) \times \mathcal{F}(M) \rightarrow \mathcal{F}(M)$ is *determined by* ψ, if

$$\varphi_M(A, B)(m) = \psi(A(m), B(m)) \tag{11}$$

holds for any $A, B \in \mathcal{F}(M)$ and $m \in M$.

In this paper, we will suppose that all operations between fuzzy sets are determined by rl-operations.

IV. TYPE $\langle 1, 1\rangle$ FUZZY QUANTIFIERS DETERMINED BY $\odot$-FUZZY INTEGRALS

This section is devoted to fuzzy quantifiers that are defined using fuzzy measures and integrals introduced in [3] and summarized in Subsection II-C. Before commencing our introduction of fuzzy quantifiers, let us recall a common definition of limited and unlimited type $\langle 1, 1\rangle$ fuzzy quantifiers presented in [8], [9], [13].

In general, a mapping $Q_M : \mathcal{F}(M) \times \mathcal{F}(M) \rightarrow L$ is called the *monadic fuzzy quantifier of type* $\langle 1, 1\rangle$ *limited to* M, where M is a (possibly empty[3]) universe. A value of a fuzzy quantifier on fuzzy sets $A, B \in \mathcal{F}(M)$ is written as $Q_M(A, B)$.[4] A type $\langle 1, 1\rangle$ *unlimited (finite, countable) monadic fuzzy quantifier* is a functional Q assigning to each (finite, countable) universe M a type $\langle 1, 1\rangle$ monadic fuzzy quantifier Q_M limited to M.

In order to define fuzzy quantifiers determined by fuzzy measures in a reasonable generality, let us consider a functional $\mathcal{S}$ assigning to each non-empty universe M a mapping

$$\mathcal{S}(M) : \mathcal{F}(M) \times \mathcal{F}(M) \rightarrow \mathbf{Fms}(M). \tag{12}$$

For example, we can define $\mathcal{S}(M)(A, B) = (M, \mathcal{M}, \mu)$, where $(M, \mathcal{M}, \mu)$ is an arbitrary fuzzy measure space from $\mathbf{Fms}(M)$. One can see that $\mathcal{S}(M)$ is a constant mapping and the fuzzy sets A, B do not play any role in this definition. Further examples are $\mathcal{S}(M)(A, B) = (A, \mathcal{M}_A, \mu_A)$ or $\mathcal{S}(M)(A, B) = (A \cap B, \mathcal{M}_{A\cap B}, \mu_{A\cap B})$. Here, the fuzzy sets A, B have an active role in the definition of these fuzzy measure spaces.

To exclude a confusion, let us denote by

$$\int^{\odot}_{(A,\mathcal{F},\mu)} f \; d\mu \quad \text{or simply} \quad \int^{\odot}_{\mathbf{A}} f \; d\mu$$

the fuzzy integral from Subsection II-C defined on a fuzzy measure space $\mathbf{A} = (A, \mathcal{F}, \mu)$.

DEFINITION 8 Let M be a non-empty universe, $\mathcal{S}(M)$ be a mapping of the form (12) and φ_M be an operation on $\mathcal{F}(M)$ determined by an rl-operation ψ. A *fuzzy quantifier of type* $\langle 1, 1\rangle$ *limited to* M *determined by* $(\mathcal{S}(M), \varphi_M)$ is a mapping

$$Q_M : \mathcal{F}(M) \times \mathcal{F}(M) \rightarrow L$$

defined by

$$Q_M(A, B) = \int^{\odot}_{\mathcal{S}(M)(A,B)} \varphi_M(A, B) \; d\mu. \tag{13}$$

Since there is no fuzzy measure space on the empty (fuzzy) set, an extension of limited quantifiers to quantifiers over arbitrary universes cannot comprise a reasonably general stipulation how the quantifiers have to look for the empty universe. Therefore, we omit this situation in the following definition and introduce unlimited fuzzy quantifiers determined by fuzzy measures for the non-empty universes, whereas these fuzzy quantifiers can take arbitrary values for the empty universe.

[3]To define the behavior of generalized quantifiers for the empty universe is important in some situations. It happens, for example, when we study type $\langle 1, 1\rangle$ quantifiers which are obtained from type $\langle 1\rangle$ quantifiers by means of *relativization*. Then it is vital to have values of e.g. $\mathsf{some}_\emptyset(1_\emptyset)$ defined, see discussion in [26], p. 137.

[4]Note that, in the literature (see e.g. [13], [26]), we can also find the denotation $Q_M(A)(B)$ to emphasize what is the property modifying a common noun like "*to be a young student*" (A) and what is the considered predicate like "*to have a good result*" (B) in the sentence "*Many young students have good results*". In this conception, a type $\langle 1, 1\rangle$ fuzzy quantifier limited to M is a mapping $Q_M : \mathcal{F}(M) \rightarrow [\mathcal{F}(M) \rightarrow L]$, where $[\mathcal{F}(M) \rightarrow L]$ denotes the set of all mappings (type $\langle 1\rangle$ fuzzy quantifiers) of $\mathcal{F}(M)$ to L characterizing the predicates like "*to have a good result*".

DEFINITION 9 Let $\mathcal{S}$ and φ be functionals assigning to each non-empty universe M a mapping $\mathcal{S}(M)$ of the form (12) and an operation φ_M determined by an rl-operation ψ, respectively. An *unlimited fuzzy quantifier of type* $\langle 1,1\rangle$ *determined by* $(\mathcal{S},\varphi)$ is an unlimited fuzzy quantifier Q of type $\langle 1,1\rangle$ assigning a fuzzy quantifier Q_M limited to M determined by $(\mathcal{S}(M),\varphi_M)$ to each *non-empty* universe M.

Let us consider the sentence *"Many young students have good results"*,. Obviously, the fuzzy quantifier "many" expresses a quantity on the fuzzy set of "young students" and would be independent, in some sense, from the property "to have good results". More precisely, if we replace the property "to have good results" by "to have bad results", the interpretation of the fuzzy quantifier "many" would stay the same. This motivate us to establish the fuzzy quantifiers definable by fuzzy measures as follows.

DEFINITION 10 We say that an unlimited fuzzy quantifier Q is *definable by fuzzy measures*, if there exists a pair of functionals $(\mathcal{S},\varphi)$ such that Q is determined by $(\mathcal{S},\varphi)$ and $\mathcal{S}(M)(A,-)$ is a constant mapping for any non-empty universe M and $A\in\mathcal{F}(M)$.

REMARK 8 We can see that the class of fuzzy quantifiers definable by fuzzy measures is a subclass of the class of fuzzy quantifiers determined by $(\mathcal{S},\varphi)$. Hence, if a property is satisfied by fuzzy quantifiers determined by $(\mathcal{S},\varphi)$, then it is also satisfied by fuzzy quantifiers definable by fuzzy measures. In what follows, we will usually formulate statements for fuzzy quantifiers determined by $(\mathcal{S},\varphi)$.

Before we show several examples and start our study of monotonicity of fuzzy quantifiers definable by fuzzy measures (or determined by a pair of functionals $(\mathcal{S},\varphi)$ in general), let us introduce two important notions saying when one fuzzy quantifier is less than or equal to the second one, and when two fuzzy quantifiers are equal.

DEFINITION 11 Let P,Q be two quantifiers. We say that Q is *less than or equal to* P and denote it by $Q\le P$, if

$$Q_M(A,B)\le P_M(A,B) \tag{14}$$

holds for arbitrary non-empty universe M and $A,B\in\mathcal{F}(M)$. Further, we say that Q is *equal to* P and denote it by $Q=P$, if $Q\le P$ and $P\le Q$.

A reason why the empty universe is omitted in the previous definition is that fuzzy quantifiers determined by $(\mathcal{S},\varphi)$ are not a priori defined for the empty universe. In the following part, for simplicity, we will write only "Q is determined by $(\mathcal{S},\varphi)$" instead of "Q is a fuzzy quantifier of type $\langle 1,1\rangle$ determined by $(\mathcal{S},\varphi)$".

EXAMPLE 9 Let M be a non-empty universe and $\mathcal{S}_i(M)(A,B)=\{(M,\mathcal{F}(M),\mu_i)\}$, where, for $i=1,2$, we have

$$\mu_1(X)=\begin{cases}\bot, & \text{if } X=1_\emptyset,\\ \top, & \text{otherwise}\end{cases} \tag{15}$$

and

$$\mu_2(X)=\begin{cases}\top, & \text{if } X=M,\\ \bot, & \text{otherwise.}\end{cases} \tag{16}$$

If Q is determined by (S_1,φ_1), where $\varphi_{M,1}(A,B)=A\cap B$, then $Q=\mathsf{some}$, i.e., it is the interpretation of the standard quantifier some A are B. If Q is determined by (S_2,φ_2) for all $M\neq\emptyset$, where $\varphi_{M,2}(A,B)=A\to B$, then it is equal to every.

EXAMPLE 10 Let φ be a functional assigning φ_M to each non-empty universe and $\mathcal{S}_i$, $i=1,2$, be functionals defined in the previous example. We may introduce "boundary" fuzzy quantifiers $\forall_\varphi$ and $\exists_\varphi$ as follows

$$\forall_{\varphi,M}(A,B)=\bigwedge_{m\in M}\varphi_M(A,B)(m), \tag{17}$$

$$\exists_{\varphi,M}(A,B)=\bigvee_{m\in M}\varphi_M(A,B)(m). \tag{18}$$

Obviously, $\mathsf{every}=\forall_\varphi$ for $\varphi_M(A,B)=A\to B$ and $\mathsf{some}=\exists_\varphi$ for $\varphi_M(A,B)=A\cap B$. One can see that $\forall_\varphi\le\exists_\varphi$.

EXAMPLE 11 Let $\mathbf{L}_Ł$ be the Łukasiewicz algebra from Example 1. Let M be a finite non-empty set and $A\in\mathcal{F}(M)$, $A\neq 1_\emptyset$ and $\mathbf{A}^\sigma=(A,\mathcal{F}(A),\mu^\sigma)$ be a fuzzy measure space from Example 5. Let us define $S(M)(A,B)=\mathbf{A}^\sigma$ for $A\neq 1_\emptyset$, $S(M)(1_\emptyset,B)=(M,\mathcal{F}(M),\mu_2)$ and $\varphi_M(A,B)=A\to B$. Then, for any $A,B\in\mathcal{F}(M)$, we may define an interpretation of fuzzy quantifier many as

$$\begin{aligned}Q_M^{\mathsf{many}}(A,B)&=\int^{\otimes}_{S(M)(A,B)}\varphi_M(A,B)\;d\mu^\sigma=\\ &=\int^{\otimes}_{(A,\mathcal{F}(A),\mu^\sigma)}A\to B\;d\mu^\sigma=\\ &=\bigvee_{Y\in\mathcal{F}(A)^-}(\mu^\sigma(Y)\otimes\bigwedge_{m\in\mathrm{Supp}(Y)}(A\to B)(m)),\end{aligned}$$

if $A\neq 1_\emptyset$, and $Q_M^{\mathsf{many}}(1_\emptyset,B)=1$.

EXAMPLE 12 We can construct important fuzzy quantifiers, e.g., *few, no, at most half, etc.*, from already defined quantifiers using so-called external and inner negations (see [13], Definition 14). Let Q be a fuzzy quantifier of type $\langle 1,1\rangle$. The external or inner negation of Q is the fuzzy quantifier $\sim Q$ or $Q\sim$ defined as $(Q\sim)_M(A,B)=\neg Q_M(A,B)$ or $(Q\sim)_M(A,B)=Q_M(A,\overline{B})$, respectively. Hence, we can define fuzzy quantifiers, e.g., $\mathsf{no}=\sim\mathsf{some}$ and $\mathsf{few}=\mathsf{many}\sim$, where some and many are defined in Examples 9 and 11, respectively.

V. MONOTONICITY

The concept of monotonic quantifiers belongs among the basic properties which is observed for a large scale of natural language quantifiers as *all, some, few, many, nearly all, at least five, at most ten* etc. Of course, not all fuzzy quantifiers are monotonic. Typical examples are *about half, at least one and at most ten*. The monotonicity for the type $\langle 1,1\rangle$ fuzzy quantifiers is defined as follows.[5]

DEFINITION 12 Let Q be a fuzzy quantifier. We say that Q is monotonically non-decreasing in its first (second) component, if

$$Q_M(A,C) \leq Q_M(B,C) \quad (Q_M(C,A) \leq Q_M(C,B)) \quad (19)$$

holds for any universe M, $A,B,C \in \mathcal{F}(M)$, $A \subseteq B$, and Q is monotonically non-increasing in its first (second) component, if

$$Q_M(A,C) \geq Q_M(B,C) \quad (Q_M(C,A) \geq Q_M(C,B)) \quad (20)$$

holds for any universe M, $A,B,C \in \mathcal{F}(M)$, $A \subseteq B$.

REMARK 13 Notice that the mentioned inequalities are trivially satisfied for the empty universe. Hence, the empty universe can be excluded from our investigation of the monotonicity of fuzzy quantifiers.

One can see that *all, some, many, at least k* are monotonically non-decreasing and *not all, no, few, at most k* are monotonically non-increasing in the second component. Analogously to [26], we will use, for simplicity, the denotation $\uparrow$Mon, $\downarrow$Mon and Mon$\uparrow$, Mon$\downarrow$ to denote that a fuzzy quantifier is monotonically non-decreasing, non-increasing in the first component and monotonically non-decreasing, non-increasing in the second component, respectively. Sometimes it is useful a combination of the previous denotations as $\uparrow$Mon$\downarrow$ saying that a quantifier is non-decreasing in the first component and non-increasing in the second one. In general, the monotonicity of fuzzy quantifiers determined by $(\mathcal{S},\varphi)$ is closely related to the monotonicity of φ. Let us denote the monotonicity of the functional φ analogously by Mon$\uparrow$, Mon$\downarrow$ and $\uparrow$Mon, $\downarrow$Mon and similarly for their combinations, e.g. $\uparrow$Mon$\downarrow$.

THEOREM 1 *A fuzzy quantifier definable by fuzzy measures determined by $(\mathcal{S},\varphi)$ is Mon$\uparrow$ (Mon$\downarrow$) if and only if φ is Mon$\uparrow$ (Mon$\downarrow$).*

Proof: Let Q be a fuzzy quantifier definable by fuzzy measures determined by $(\mathcal{S},\varphi)$ which is Mon$\uparrow$. Let M be a non-empty universe and suppose that φ_M is determined by an rl-operation ψ. From the definition of φ, one can derive that the monotonicity of ψ implies the same form of the monotonicity of φ. Moreover, if a and b denote the constant fuzzy sets in $\mathcal{F}(M)$ with values a and b, respectively, then we may write $\varphi(a,b)(m) = \psi(a,b)$ for any $m \in M$. Recall that $\mathcal{S}(A,-)$ is a constant mapping from $\mathcal{F}(M)$ to $\mathbf{Fms}(M)$. Let a,b,c be constant fuzzy sets such that $b \leq c$. Since $\int^{\odot} c\ d\mu = c$, we obtain

$$\psi(a,b) = \varphi_M(a,b)(m) = \int^{\odot}_{\mathcal{S}(M)(a,b)} \varphi_M(a,b)\ d\mu =$$

$$Q_M(a,b) \leq Q_M(a,c) =$$

$$\int^{\odot}_{\mathcal{S}(M)(a,c)} \varphi_M(a,c)\ d\mu = \varphi_M(a,c)(m) = \psi(a,c),$$

where m is an arbitrary element of M. Hence, ψ is a monotonically non-decreasing mapping and, from the consideration above, we obtain that φ is Mon$\uparrow$. Analogously, we can prove Mon$\downarrow$ of φ under the presumption that Q is Mon$\downarrow$.

The opposite implication is a trivial consequence of the fact that the fuzzy integral is a non-decreasing mapping. ■

In the previous theorem, we cannot suppose the cases of $\uparrow$Mon and $\downarrow$Mon, since $\mathcal{S}(M)(b,-)$ and $\mathcal{S}(M)(c,-)$ are different fuzzy measure spaces and thus the presented inequality cannot be guarantied here. Nevertheless, supposing that $\mathcal{S}(M)(-,-)$ is a constant mapping, we may state the analogous result also for $\uparrow$Mon and $\downarrow$Mon.

THEOREM 2 *A fuzzy quantifier determined by $(\mathcal{S},\varphi)$ such that $\mathcal{S}(-,-)$ is a constant mapping for any non-empty universe M is $\uparrow$Mon ($\downarrow$Mon) if and only if φ is $\uparrow$Mon ($\downarrow$Mon).*

Proof: This is analogous to the proof of the cases Mon$\uparrow$ and Mon$\downarrow$. ■

REMARK 14 It is easy to see that the operations $\wedge$, $\vee$, $\otimes$ are $\uparrow$Mon$\uparrow$ and $\rightarrow$ is $\downarrow$Mon$\uparrow$. One can simply verify that, for example, $\varphi_1 \Box \varphi_2$ is Mon$\uparrow$, whenever φ_1 and φ_2 are Mon$\uparrow$ and $\Box$ is $\uparrow$Mon$\uparrow$.

REMARK 15 Obviously, the external negation and the inner negation of fuzzy quantifiers mentioned in the first part of our contribution (see also [8], [9], [13], [14], [26]) change the polarity of monotonicity in both components and in the second component, respectively. For example, let us consider every and some defined in Example 3.2. of the first part. Then every is $\downarrow$Mon$\uparrow$ and some is $\uparrow$Mon$\uparrow$, but $\sim$every $=$ some$\sim$ $=$ not every is $\uparrow$Mon$\downarrow$ and every$\sim$ $=\sim$ some $=$ no is $\downarrow$Mon$\downarrow$.

In [5], we showed that each type $\langle 1\rangle$ fuzzy quantifier determined by a fuzzy measure lays among the fuzzy quantifiers all and some. The question is, which boundaries hold for fuzzy quantifiers determined by $(\mathcal{S},\varphi)$, especially, for fuzzy quantifiers definable by fuzzy measures.

THEOREM 3 *For each fuzzy quantifier Q determined by $(\mathcal{S},\varphi)$, we have $\forall_\varphi \leq Q \leq \exists_\varphi$.*

Proof: This is a straightforward consequence of the definition of fuzzy measures on which the fuzzy quantifiers $\forall_\varphi$ and $\exists_\varphi$ are defined. ■

[5] A more general definition for monadic fuzzy quantifiers of type $\langle 1^n,1\rangle$ can be found in [13]. .

Naturally, we can find out fuzzy quantifiers (definable by fuzzy measures) which are not monotonic. For example, let us consider the Łukasiewicz algebra and operations between fuzzy sets determined by the following rl-operations

$$\psi_1(a,b) = a \otimes (a \rightarrow (b \vee \neg b)),$$
$$\psi_2(a,b) = a \leftrightarrow b.$$

Then fuzzy quantifiers which use the operations ψ_1 and ψ_2 are not monotonic. In fact, it is sufficient to consider the constant fuzzy sets $0 \subset 0.5 \subset 1$ defined on a non-empty universe. Since $\int^{\odot} c \, d\mu = c$, we may write, for ψ_1,

$$Q_M(1,0) = Q_M(1,1) = 1 > 0.5 = Q_M(1,0.5)$$

and, for ψ_2,

$$Q_M(0.5,0) = Q_M(0.5,1) = 0.5 < 1 = Q_M(0.5,0.5).$$

The proposed operations could be used in the evaluation of the quantified sentences:

"Every students is or is not prepared on the exam."
"Only blondes are pretty."

Obviously, the first statement is trivially fulfilled in the classical logic, but practically there are many students who know something but we cannot say that they are perfectly prepared on the exam. Hence, this statement has a sense in fuzzy logic.

Although, we are able to find some "reasonable" models of non-monotonic linguistic quantifiers definable by fuzzy measures, much more natural it is to define non-monotonic fuzzy quantifiers as a conjunction of two fuzzy quantifiers (definable by fuzzy measures), where one is Mon↑ (↑Mon) and the second one is Mon↓ (↓Mon). For example, a fuzzy quantifier *roughly between eight and ten* is a conjunction of *about eight or more than eight* (Mon↑) and *about ten or less than ten* (Mon↓).

An interesting question is, which non-monotonic fuzzy quantifiers can be described by the conjunction of two fuzzy quantifiers (not necessary definable by fuzzy measures) having the opposite polarity, i.e., one is Mon↑ and the second one Mon↓. In the generalized quantifier theory, such quantifiers are called *continuous*.[6] A generalization of the continuity for fuzzy quantifiers is a concavity defined as follows.

DEFINITION 13 We say that a fuzzy quantifier Q is concave in the first or the second component, if

$$Q_M(A',B) \wedge Q_M(A'',B) \leq Q_M(A,B) \tag{21}$$

or

$$(Q_M(B,A') \wedge Q_M(B,A'') \leq Q_M(B,A) \tag{22}$$

hold for any non-empty universe M and fuzzy sets $A, A', A'', B \in \mathcal{F}(M)$ such that $A' \subseteq A \subseteq A''$, respectively.

Let Q be a fuzzy quantifier and denote $Q_{M,a} : \mathcal{F}(M) \times \mathcal{F}(M) \rightarrow \{\bot, \top\}$ a fuzzy quantifier defined by $Q_{M,a}(A,B) = \top$ if and only if $Q_M(A,B) \geq a$. A fuzzy quantifier Q_a is the a-cut of the fuzzy quantifier Q.[7] The following lemma shows a relation between the concavity of fuzzy quantifiers and the continuity of a-cut fuzzy quantifiers.

LEMMA 4 *A fuzzy quantifier Q is concave in the first (second) component if and only if each a-cut fuzzy quantifier Q_a is continuous in the first (second) component.*

Proof: Here, we will prove only the concavity in the first component. The proof for the second component is analogous. Let Q be a concave in the first component fuzzy quantifier, $a \in L$, M be a non-empty universe and B be arbitrary fuzzy set of $\mathcal{F}(M)$. If $Q_{M,a}(A',B) = Q_{M,a}(A'',B) = \top$ and $A' \subseteq A \subseteq A''$, then $Q_M(A',B) \wedge Q_M(A'',B) \geq a$ and using the concavity of Q we obtain $Q_M(A,B) \geq a$ which implies $Q_{M,a}(A,B) = \top$. Hence, Q is continuous in the first component for any $a \in L$.

On the contrary, let Q_a be continuous fuzzy quantifier for any $a \in L$, $A' \subseteq A \subseteq A''$ and B be arbitrary fuzzy sets of $\mathcal{F}(M)$. Denote $a = Q_M(A',B) \wedge Q_M(A'',B)$. From the definition of Q_a, we obtain $Q_{M,a}(A',B) = Q_{M,a}(A'',B) = \top$. Since Q_a is continuous in the first component for any $a \in L$, then also $Q_{M,a}(A,B) = \top$. Hence, $Q_M(A,B) \geq a = Q_M(A',B) \wedge Q_M(A'',B)$ which means that Q is concave. ■

THEOREM 5 *Let Q and Q' be ↑Mon and ↓Mon (Mon↑ and Mon↓). Then $Q \wedge Q'$ is concave in the first (second) component.*

Proof: We restrict ourselves to the proof of the case of the first component. For any non-empty universe M and $A, A', A'', B \in \mathcal{F}(M)$ such that $A' \subseteq A \subseteq A''$, we have $Q_M(A',B) \leq Q_M(A,B) \leq Q_M(A'',B)$ and $Q'_M(A'',B) \leq Q'_M(A,B) \leq Q'_M(A',B)$. Hence, we obtain

$$(Q \wedge Q')_M(A',B) \wedge (Q \wedge Q')_M(A'',B) =$$
$$Q_M(A',B) \wedge Q'_M(A',B) \wedge Q_M(A'',B) \wedge Q'_M(A'',B) \leq$$
$$Q_M(A',B) \wedge Q'_M(A'',B) \leq Q_M(A,B) \wedge Q'_M(A,B) =$$
$$(Q \wedge Q')_M(A,B).$$

and thus $Q \wedge Q'$ is concave fuzzy quantifier. ■

THEOREM 6 *Let $\mathbf{L}$ be a distributive residuated lattice. Each concave in the first (second) component fuzzy quantifier is expressible as the conjunction of fuzzy quantifiers which are ↑Mon and ↓Mon (Mon↑ and Mon↓).*

Proof: Again, we restrict ourselves to the proof of the case of the first component. Let Q be concave in the first

[6] Note that a quantifier Q of type $\langle 1 \rangle$ is continuous, if the following holds: if $Q_M(A) = Q_M(C) = \top$ for a non-empty universe M and $A, C \in \mathcal{F}(M)$ such that $A \subseteq C$, then $Q_M(B) = \top$ for any $B \in \mathcal{F}(M)$ with $A \subseteq B \subseteq C$ (cf. [26]). For other types, one can analogously define the continuity of quantifiers in the given component as in the definition for the type $\langle 1 \rangle$.

[7] Obviously, each fuzzy quantifier can be simply derived from its a-cuts by $Q_M(A,B) = \bigvee \{a \mid a \in L \text{ and } Q_{M,a}(A,B) = \top\}$.

component. Put

$$P_M(A,B) = \bigvee_{A' \in \mathcal{F}(M),\ A' \subseteq A} Q_M(A',B).$$

$$P'_M(A,B) = \bigvee_{A'' \in \mathcal{F}(M),\ A \subseteq A''} Q_M(A'',B).$$

One can verify easily that P and P' are $\uparrow$Mon and $\downarrow$Mon, respectively. Moreover, $P \wedge P'$ is a concave fuzzy quantifier in the first component according to the previous theorem. Let M be an arbitrary non-empty universe and $A' \subseteq A \subseteq A''$ be arbitrary fuzzy sets from $\mathcal{F}(M)$. Obviously, we have

$$(P \wedge P')_M(A,B) = P_M(A,B) \wedge P'_M(A,B) =$$

$$\bigvee_{\substack{A' \in \mathcal{F}(M) \\ A' \subseteq A}} Q_M(A',B) \wedge \bigvee_{\substack{A'' \in \mathcal{F}(M) \\ A \subseteq A''}} Q_M(A'',B) \geq Q_M(A,B).$$

Since $\mathbf{L}$ is a distributive residuated lattice and $Q_M(A,B) \geq Q_M(A',B) \wedge Q_M(A'',B)$ for any $A' \subseteq A \subseteq A''$, then we may write

$$Q_M(A,B) \geq \bigvee_{\substack{A' \in \mathcal{F}(M) \\ A' \subseteq A}} \bigvee_{\substack{A'' \in \mathcal{F}(M) \\ A \subseteq A''}} (Q_M(A',B) \wedge Q_M(A'',B))$$

$$= \bigvee_{\substack{A' \in \mathcal{F}(M) \\ A' \subseteq A}} Q_M(A',B) \wedge \bigvee_{\substack{A'' \in \mathcal{F}(M) \\ A \subseteq A''}} Q_M(A'',B) =$$

$$P_M(A,B) \wedge P'_M(A,B) = (P \wedge P')_M(A,B).$$

Hence, Q is expressible as the conjunction $P \wedge P'$, where P is Mon$\uparrow$ and P' is Mon$\downarrow$. ■

VI. Conclusion

In this contribution, we defined fuzzy quantifiers of type $\langle 1,1 \rangle$ using fuzzy integrals and studied their monotonicity. Aside from the theoretical importance of generalized fuzzy quantifiers, we are also motivated by the applications of fuzzy logic e.g. in time series analysis, decision making and other fields where it can be advantageous to be able to use other than classical quantifiers "for all" and "exists". For example, in time series analysis and modeling, we can use quantifiers like "many" for filtering off of outliers, i.e. values that are numerically distant from (the course of) the data.

Acknowledgment

This paper has been supported by the Grant IAA108270901 of the GA AV ČR.

References

[1] J. Barwise and R. Cooper. Generalized quantifiers and natural language. *Linguistics and Philosophy*, 4:159–219, 1981.

[2] R. Bělohlávek. *Fuzzy Relational Systems: Foundations and Principles*. Kluwer Academic Publisher, New York, 2002.

[3] A. Dvořák and M. Holčapek. Fuzzy measures and integrals defined on algebras of fuzzy subsets. *submitted to Information Sciences*.

[4] A. Dvořák and M. Holčapek. Type $\langle 1,1 \rangle$ fuzzy quantfiers determined by fuzzy measures defined on residuated lattices, Part I.: Basic definitions and examples. *submitted to Fuzzy Sets and Systems*.

[5] A. Dvořák and M. Holčapek. $\mathbf{L}$-fuzzy quantifiers of type $\langle 1 \rangle$ determined by fuzzy measures. *Fuzzy Sets and Systems*, 160(23):3425–3452, 2009.

[6] A. Dvořák and M. Holčapek. Fuzzy measure spaces generated by fuzzy sets. Hüllermeier, Eyke (ed.) et al., Information processing and management of uncertainty in knowledge-based systems. Theory and methods. 13th international conference, IPMU 2010, Dortmund, Germany, June 28–July 2, 2010. Proceedings. Part I. Berlin: Springer. Communications in Computer and Information Science 80, 490-499 (2010)., 2010.

[7] A. Dvořák and M. Holčapek. Type $\langle 1,1 \rangle$ fuzzy quantifiers determined by fuzzy measures. In *Proceedengs of WCCI 2010 IEEE World Congress on Computational Intelligence*, pages 3168–3175. CCIB, Barcelona, Spain, July, 18-23 2010.

[8] I. Glöckner. *Fuzzy Quantifiers in Natural Language: Semantics and Computational Models*. Der Andere Verlag, Osnabrück, Germany, 2004.

[9] I. Glöckner. *Fuzzy Quantifiers: A Computational Theory*. Springer-Verlag, Berlin, 2006.

[10] M. Grabisch, T. Murofushi, and M. Sugeno, editors. *Fuzzy Measures and Integrals. Theory and Applications*. Studies in Fuzziness and Soft Computing. Physica Verlag, Heidelberg, 2000.

[11] George Grätzer. *General lattice theory*. Basel: Birkhäuser, 1998.

[12] P. Hájek. *Metamathematics of Fuzzy Logic*. Kluwer Academic Publishers, Dordrecht, 1998.

[13] M. Holčapek. Monadic $\mathbf{L}$-fuzzy quantifiers of the type $\langle 1^n, 1 \rangle$. *Fuzzy Sets and Systems*, 159(14):1811–1835, 2008.

[14] E.L. Keenan and Westerståhl. Generalized quantifiers in linguistics and logic. In J. van Benthem and A. ter Meulen, editors, *Handbook of Logic and Language*, pages 837–893. Elsevier, Amsterdam, 1996.

[15] E.P. Klement, R. Mesiar, and E. Pap. A universal integral as common frame for Choquet and Sugeno integral. *IEEE Transactions on Fuzzy Systems*, 18:178–187, 2010.

[16] G.J. Klir and Bo Yuan. *Fuzzy Sets and Fuzzy Logic: Theory and Applications*. Prentice Hall, New Jersey, 1995.

[17] P. Lindström. First ordered predicate logic with generalized quantifiers. *Theoria*, 32:186–195, 1966.

[18] Y. Liu and E.E. Kerre. An overview of fuzzy quantfiers. part I: Interpretation. *Fuzzy Sets and Systems*, 95(1):1–21, 1998.

[19] Y. Liu and E.E. Kerre. An overview of fuzzy quantfiers. part II: Reasoning and applications. *Fuzzy Sets and Systems*, 95(2):135–146, 1998.

[20] A. Mostowski. On a generalization of quantifiers. *Fundamenta Mathematicae*, 44:12–36, 1957.

[21] P. Murinová and V. Novák. A formal theory of generalized intermediate syllogisms. *submitted to Fuzzy Sets and Systems*.

[22] V. Novák. Antonyms and linguistic quantifiers in fuzzy logic. *Fuzzy Sets and Systems*, 124(3):335–351, 2001.

[23] V. Novák. On fuzzy type theory. *Fuzzy Sets and Systems*, 149:235–273, 2005.

[24] V. Novák. A formal theory of intermediate quantifiers. *Fuzzy Sets and Systems*, 159(10):1229 1246, 2008.

[25] V. Novák, I. Perfilieva, and J. Močkoř. *Mathematical Principles of Fuzzy Logic*. Kluwer Academic Publisher, Boston, 1999.

[26] S. Peters and D. Westerståhl. *Quantifiers in Language and Logic*. Oxford University Press, New York, 2006.

[27] P. Peterson. *Intermediate Quantifiers. Logic, Linguistics, and Aristotelian Semantics*. Ashgate, Aldershot, 2000.

[28] D. Ralescu. Cardinality, quantifiers and the aggregation of fuzzy criteria. *Fuzzy Sets and Systems*, 69:355–365, 1995.

[29] H. Thiele. On fuzzy quantifiers. In Z. Bien and K.C. Min, editors, *Fuzzy Logic and its Applications, Information Sciences, and Intelligent Systems*, pages 343–352. Kluwer Academic Publisher, Dordrecht, 1996.

[30] Z. Wang and G.J. Klir. *Fuzzy measure theory*. Plenum Press, New York, 1992.

[31] L.A. Zadeh. A computational approach to fuzzy quantifiers in natural languages. *Computers & Mathematics with Applications*, 9:149–184, 1983.

2011 IEEE International Conference on Fuzzy Systems
June 27-30, 2011, Taipei, Taiwan

Generalized Fuzzy Imaginary Ideals of Rings

Zuhua Liao^{+} , Shu Cao，Qinghe Tian , Miaohan Hu, Yang Zhang
School of Science, Jiangnan University Wuxi Jiangsu 214122, China
+Corresponding author :liaozuhua57@yahoo.cn , caoshu198709@yahoo.com.cn

***Abstract*—Our aim in this paper is to introduce and study the new type of fuzzy ideals of a ring called generalized fuzzy imaginary right (resp . left) ideals and the direct products of them . The equivalence relation of them is given , besides , the properties of their intersection, union and level sets are discussed . Finally, we also give the properties of their homomorphic preimage.**

Keywords-fuzzy imaginary ideals ;generalized fuzzy imaginary ideals ; $(\in,\in\vee q_{(\lambda,\mu)})-$ ***fuzzy imaginary ideals ; level sets ;homomorphic preimage***

I. INTRODUCTION

The theory of fuzzy sets which was introduced by Zadeh in 1965[1] is applied to many mathematical branches. Rosenfeld inspired the fuzzification of algebraic structures and introduced the notion of fuzzy subgroups in 1971 [2] . Since then, many scholars studied the theory of fuzzy algebra and have published a series of papers [3-6]. In 1982, W. J. Liu defined and studied fuzzy subrings as well as fuzzy ideals in rings [7]. In 1990, H.C.Ma gave the definition of imaginary ideals of rings and obtained some results[8] , then in 1992, he discussed the relation between the imaginary ideals, pseudo ideals and ideals of rings [9], besides, some relevant examples were also given by him.

In 1992, Indian scholar S. K. Bhakat and P. Das introduced the concept of (α,β) -fuzzy subgroup[10] by using "belong to ($\in$)" relation and "quais-coincident with(q)"relation between the fuzzy point and the fuzzy sets. In fact ,it's an important and useful generalization of Rosenfeld's fuzzy subgroup. In 1996, S. K. Bhakat and P .Das introduced the concept of (α,β) -fuzzy subring in [11], B . J .Zhao and H. G .Chi has introduced the concept of (λ,μ) -generalized fuzzy subring in [12]. Z . H. Liao et al extended Rosenfeld's fuzzy algebra, Bhakat and Das's fuzzy algebra and $(\overline{\in},\overline{\in}\vee\overline{q})$ -fuzzy algebra to ($\in$, $\in\vee q_{(\lambda,\mu)}$)- fuzzy algebra, and do series of researches [13-16] .

This paper is the continuation of the above work, we give the definition of $(\in,\in\vee q_{(\lambda,\mu)})-$ fuzzy imaginary right (resp. left) ideals of rings, generalized fuzzy imaginary right (resp. left) ideals of rings.The properties of their intersection, union and level sets et al are also discussed. Besides , we find the equivalence relation between $(\in,\in\vee q_{(\lambda,\mu)})-$ fuzzy imaginary right (resp. left) ideals and generalized fuzzy imaginary right (resp. left) ideals . Finally ,the property of homomorphic preimage is given .

II. PRELIMINARIES

From now on , we write R and H for rings.

Definition 2.1[8] Let A be a subring of R , then A is said to be a imaginary right (resp. left) ideal of R if for all $x\in A$ and $y\in R$, $xy\in A$ (resp. $yx\in A$) implies $y\in A$.

We say A a imaginary ideal of R if A is both a imaginary right ideal and a imaginary left ideal of R .

Definition2.2[14] Let $\alpha,\lambda,\mu\in[0,1]$ and $\lambda<\mu$, if $A(x)\geq\alpha$ then a fuzzy point x_α belongs to a fuzzy subset A , denoted by $x_\alpha\in A$; if $\lambda<\alpha$ and $A(x)+\alpha>2\mu$ then a fuzzy point x_α generalized quasicoincident with a fuzzy subset A , denoted by $x_\alpha q_{(\lambda,\mu)}A$ .If $x_\alpha\in A$ or $x_\alpha q_{(\lambda,\mu)}A$, then $x_\alpha\in\vee q_{(\lambda,\mu)}A$.

Definition2.3 [3] Let $R_i(1\leq i\leq n)$ be rings and the direct product:

$$\prod_{1\leq i\leq n}R_i=\{(a_1,a_2,....a_n)|a_i\in R_i\}\ .$$

Then $\prod_{1\leq i\leq n}R_i$ is a ring under the operations as follows:

$(a_1,a_2,....a_n)+(b_1,b_2,...b_n)=(a_1+b_1,a_2+b_2,...a_n+b_n)$;

$(a_1,a_2,....a_n)(b_1,b_2,...b_n)=(a_1b_1,a_2b_2,...a_nb_n)$.

Definition2.4 [3] Let $A_i(1\leq i\leq n)$ be fuzzy subsets of R_i ,then a fuzzy subset $\prod_{1\leq i\leq n}A_i$ is defined as $(\prod_{1\leq i\leq n}A_i)(x_1,x_2,...x_n)=\inf_{1\leq i\leq n}A_i(x_i)$ called fuzzy direct product.

Definition 2.5[3] A fuzzy subset A of R is called a generalized fuzzy subring of R if for all $x,y\in R$, the following conditions are satisfied ,

(1) $A(x+y)\vee\lambda\geq A(x)\wedge A(y)\wedge\mu$;

(2) $A(-x)\vee\lambda\geq A(x)\wedge\mu$;

(3) $A(xy)\vee\lambda\geq A(x)\wedge A(y)\wedge\mu$.

Theorem 2.1[3] Let A be a fuzzy subset of R , then A is a generalized fuzzy subring of R if and only if $A_\alpha\neq\Phi$ is a sub - ring of R for all $\alpha\in(\lambda,\mu]$.

Theorem 2.2[6] Let A and B be generalized fuzzy subrings of R , then $A\cap B$ is a generalized fuzzy subring of R.

Theorem 2.3 [6] A is a subring of R if and only if χ_A is a generalized fuzzy subring of R.

Theorem 2.4[3] Let $f: R \to H$ be a homomorphism, if B is a generalized fuzzy subring of H, then $f^{-1}(B)$ is a generalized fuzzy subring of R.

III. $(\in, \in \vee q_{(\lambda,\mu)})$- FUZZY IMAGINARY IDEALS OF RINGS

Definition 3.1 Let A be a generalized fuzzy subring of R, then A is called a generalized fuzzy imaginary right (resp. left) ideal of R if for all $x, y \in R$, $A(y) \vee \lambda \geq A(x) \wedge A(xy) \wedge \mu$ ($A(y) \vee \lambda \geq A(x) \wedge A(yx) \wedge \mu$).

We say A a generalized fuzzy imaginary ideal of R if A is both a generalized fuzzy imaginary right ideal and a generalized fuzzy imaginary left ideal of R.

Definition 3.2 Let A be an $(\in, \in \vee q_{(\lambda,\mu)})$ – fuzzy subring of R, $\alpha \in (\lambda, 1]$, then A is called an $(\in, \in \vee q_{(\lambda,\mu)})$ – fuzzy imaginary right (resp. left) ideal of R, if $x_\alpha \in A$, $y \in R$ and $(xy)_\alpha \in A$ (resp . $(yx)_\alpha \in A$)implies $y_\alpha \in \vee q_{(\lambda,\mu)} A$.

We say A an $(\in, \in \vee q_{(\lambda,\mu)})$ – fuzzy imaginary ideal of R if A is both an $(\in, \in \vee q_{(\lambda,\mu)})$ – fuzzy imaginary right ideal and an $(\in, \in \vee q_{(\lambda,\mu)})$ – fuzzy imaginary left ideal of R.

Theorem 3.1 A fuzzy subset A is an $(\in, \in \vee q_{(\lambda,\mu)})$ – fuzzy subring of R if and only if A is a generalized fuzzy subring of R.

The proof is omitted .

Theorem 3.2 Let A be a fuzzy subset of R, then the following conditions are equivalent:

(1) A is an $(\in, \in \vee q_{(\lambda,\mu)})$ – fuzzy imaginary right (resp. left) ideal of R ;

(2) A is a generalized fuzzy imaginary right (resp. left) ideal of R ;

(3) Nonempty set A_α is a imaginary right (resp . left) ideal of R for all $\alpha \in (\lambda, \mu]$.

Proof. We prove the theorem for imaginary right ideal. Analogous arguments apply to imaginaryleft ideal.

$(1) \Rightarrow (2)$

We obtain that A is a generalized fuzzy subring of R based on theorem 3.1. Assume that there exists $x_0, y_0 \in R$ such that $A(y_0) \vee \lambda < A(x_0) \wedge A(x_0 y_0) \wedge \mu$,choose α such that $A(y_0) \vee \lambda < \alpha < A(x_0) \wedge A(x_0 y_0) \wedge \mu$,then $A(y_0) < \alpha$, $A(x_0) > \alpha$, $A(x_0 y_0) > \alpha$ and $\lambda < \alpha < \mu$,so $(x_0)_\alpha \in A$, $(x_0 y_0)_\alpha \in A$,thus $(y_0)_\alpha \in \vee q_{(\lambda,\mu)} A$ based on definition 3.2 .But $A(y_0) < \alpha$,therefore $A(y_0) + \alpha < \alpha + \alpha \leq 2\mu$, a contradiction . So A is a generalized fuzzy imaginary right ideal of R .

$(2) \Rightarrow (1)$

From theorem 3.1 , we know that A is an $(\in, \in \vee q_{(\lambda,\mu)})$ – fuzzy subring of R. For all $x, y \in R$ and $\alpha \in (\lambda, 1]$,if $x_\alpha \in A$ and $(xy)_\alpha \in A$,then $A(x) \geq \alpha$ and $A(xy) \geq \alpha$ .Since A is a generalized fuzzy imaginary right ideal of R, then $A(y) \vee \lambda \geq A(x) \wedge A(xy) \wedge \mu \geq \alpha \wedge \mu$ .If $\alpha > \mu$,then $A(y) \vee \lambda \geq \mu$, by $\lambda < \mu$,so $A(y) \geq \mu$,then $A(y) + \alpha \geq \mu + \alpha > 2\mu$,i.e., $y_\alpha q_{(\lambda,\mu)} A$. On the other hand , if $\alpha \leq \mu$,then we can obtain that $A(y) \geq \alpha$,i.e., $y_\alpha \in A$, so $y_\alpha \in \vee q_{(\lambda,\mu)} A$. Thus A is an $(\in, \in \vee q_{(\lambda,\mu)})$ – fuzzy imaginary right ideal of R.

$(2) \Rightarrow (3)$

we know that A_α is a subring of R based on theorem 2.1 . For all $x \in A_\alpha$ and $y \in R$,if $xy \in A_\alpha$,then $A(x) \geq \alpha$ and $A(xy) \geq \alpha$ .Since A is a generalized fuzzy imaginary right ideal of R , then for all $\alpha \in (\lambda, \mu]$,we have $A(y) \vee \lambda \geq A(x) \wedge A(xy) \wedge \mu \geq \alpha \wedge \mu = \alpha$, by $\lambda < \alpha$, so $A(y) \geq \alpha$,i.e., $y \in A_\alpha$. Thererore A_α is a imaginary right ideal of R for all $\alpha \in (\lambda, \mu]$.

$(3) \Rightarrow (2)$

We obtain that A is a generalized fuzzy subring of R based on theorem 2.1 . Assume that there exists $x_0, y_0 \in R$ such that $A(y_0) \vee \lambda < A(x_0) \wedge A(x_0 y_0) \wedge \mu$,choose α such that $A(y_0) \vee \lambda < \alpha < A(x_0) \wedge A(x_0 y_0) \wedge \mu$,then $A(y_0) < \alpha$, $A(x_0) > \alpha$, $A(x_0 y_0) > \alpha$ and $\lambda < \alpha < \mu$ i.e., $x_0 \in A_\alpha$ and $x_0 y_0 \in A_\alpha$, since A_α is a imaginary right ideal of R, then $y_0 \in A_\alpha$, i.e., $A(y_0) \geq \alpha$, a contradiction to $A(y_0) < \alpha$. Therefore A is a generalized fuzzy imaginary right ideal of R .

Theorem 3.3 Let A and B be generalized fuzzy imaginary right

(resp. left) ideals of R,then $A \cap B$ is a generalized fuzzy imaginary right (resp. left) ideals of R.

Proof. We prove the theorem for imaginary right ideal. Analogous arguments apply to imaginary left ideal.

We obtain that $A \cap B$ is a generalized fuzzy subring of R based on theorem 2.2, for all $x, y \in R$,we have $(A \cap B)(y) \vee \lambda = (A(y) \wedge B(y)) \vee \lambda = (A(y) \vee \lambda) \wedge (B(y) \vee \lambda) \geq (A(x) \wedge A(xy) \wedge \mu) \wedge (B(x) \wedge B(xy) \wedge \mu) = (A \cap B)(x) \wedge (A \cap B)(xy) \wedge \mu$ .Therefore $A \cap B$ is a generalized fuzzy imaginary right ideal of R.

Corollary 3.1 Let $A_i (i \in I)$ be generalized fuzzy imaginary right (resp. left) ideals of R,then $\bigcap_{i \in I} A_i$ is a generalized fuzzy imaginary right (resp. left) ideal of R.

Theorem 3.4 Let $A_i (i \in I)$ be generalized fuzzy imaginary right (resp . left) ideals of R and for all $i, j \in I$, $A_i \subseteq A_j$ or $A_j \subseteq A_i$,then $\bigcup_{i \in I} A_i$ is a generalized fuzzy imaginary right (resp. left) ideal of R .

Proof. We prove the theorem for imaginary right ideal. Analogous arguments apply to imaginary left ideal.

Firstly , we prove that $\vee_{i \in I}(A_i(x) \wedge A_i(y) \wedge \mu) = (\bigcup_{i \in I} A_i)(x) \wedge (\bigcup_{i \in I} A_i)(y) \wedge \mu$. Obviously , $\vee_{i \in I}(A_i(x) \wedge A_i(y) \wedge \mu) \leq (\bigcup_{i \in I} A_i)(x) \wedge (\bigcup_{i \in I} A_i)(y) \wedge \mu$ .Assume that $\vee_{i \in I}(A_i(x) \wedge A_i(y) \wedge \mu) \neq (\bigcup_{i \in I} A_i)(x) \wedge (\bigcup_{i \in I} A_i)(y) \wedge \mu$, then there exists r such that $\vee_{i \in I}(A_i(x) \wedge A_i(y) \wedge \mu) < r < (\bigcup_{i \in I} A_i)(x) \wedge (\bigcup_{i \in I} A_i)(y) \wedge \mu$ .Since $A_i \subseteq A_j$ or $A_j \subseteq A_i$ for all $i, j \in I$,then exists $k \in I$ such that $r < A_k(x) \wedge A_k(y) \wedge \mu$ .On the other hand , $A_i(x) \wedge A_i(y) \wedge \mu < r$ for all $i \in I$,a contradiction . Therefore $\vee_{i \in I}(A_i(x) \wedge A_i(y) \wedge \mu) = (\bigcup_{i \in I} A_i)(x) \wedge (\bigcup_{i \in I} A_i)(y) \wedge \mu$.

Next , for all $x, y \in R$,

(1) $(\bigcup_{i \in I} A_i)(x + y) \vee \lambda = \vee_{i \in I} A_i(x + y) \vee \lambda = \vee_{i \in I}(A_i(x + y) \vee \lambda) \geq \vee_{i \in I}(A_i(x) \wedge A_i(y) \wedge \mu) = (\bigcup_{i \in I} A_i)(x) \wedge (\bigcup_{i \in I} A_i)(y) \wedge \mu$;

(2) $(\bigcup_{i \in I} A_i)(-x) \vee \lambda = \vee_{i \in I} A_i(-x) \vee \lambda = \vee_{i \in I}(A_i(-x) \vee \lambda) \geq \vee_{i \in I}(A_i(x) \wedge \mu) = (\bigcup_{i \in I} A_i)(x) \wedge \mu$;

(3) $(\bigcup_{i \in I} A_i)(xy) \vee \lambda = \vee_{i \in I} A_i(xy) \vee \lambda = \vee_{i \in I}(A_i(xy) \vee \lambda) \geq \vee_{i \in I}(A_i(x) \wedge A_i(y) \wedge \mu) = (\bigcup_{i \in I} A_i)(x) \wedge (\bigcup_{i \in I} A_i)(y) \wedge \mu$;

(4) $(\bigcup_{i \in I} A_i)(y) \vee \lambda = \vee_{i \in I} A_i(y) \vee \lambda = \vee_{i \in I}(A_i(y) \vee \lambda) \geq \vee_{i \in I}(A_i(x) \wedge A_i(xy) \wedge \mu) = (\bigcup_{i \in I} A_i)(x) \wedge (\bigcup_{i \in I} A_i)(xy) \wedge \mu$. Therefore $\bigcup_{i \in I} A_i$ is a generalized fuzzy imaginary right ideal of R.

Theorem 3.5 Let A_1 and A_2 be generalized fuzzy imaginary right (resp . left) ideals of R_1 and R_2 respectively , then $A_1 \times A_2$ is a generalized fuzzy imaginary right (resp . left) ideal of $R_1 \times R_2$.

Proof. We prove the theorem for imaginary right ideal. Analogous arguments apply to imaginary left ideal.

Firstly,we prove that $A_1 \times A_2$ is a generalized fuzzy subring of $R_1 \times R_2$ .For all $x, y \in R_1 \times R_2$, where $x = (x_1, x_2)$ and $y = (y_1, y_2)$ .Since A_1 and A_2 are generalized fuzzy subrings of R_1 and R_2 respectively,so we have $(A_1 \times A_2)(x + y) \vee \lambda = (A_1 \times A_2)((x_1, x_2) + (y_1, y_2)) \vee \lambda = (A_1 \times A_2)((x_1 + y_1, x_2 + y_2)) \vee \lambda = (A_1(x_1 + y_1) \wedge A_2(x_2 + y_2)) \vee \lambda = (A_1(x_1 + y_1) \vee \lambda) \wedge (A_2(x_2 + y_2) \vee \lambda) \geq (A_1(x_1) \wedge A_1(y_1) \wedge \mu) \wedge (A_2(x_2) \wedge A_2(y_2) \wedge \mu) = (A_1 \times A_2)((x_1, x_2)) \wedge (A_1 \times A_2)((y_1, y_2)) \wedge \mu = (A_1 \times A_2)(x) \wedge (A_1 \times A_2)(y) \wedge \mu$ .Similarly,we can prove that $(A_1 \times A_2)(-x) \vee \lambda \geq (A_1 \times A_2)(x) \wedge \mu$ and $(A_1 \times A_2)(xy) \vee \lambda \geq (A_1 \times A_2)(x) \wedge (A_1 \times A_2)(y) \wedge \mu$ .So $A_1 \times A_2$ is a generalized fuzzy subring of $R_1 \times R_2$.

Next, for all $x, y \in R_1 \times R_2$, where $x = (x_1, x_2)$ and $y = (y_1, y_2)$, $(A_1 \times A_2)(y) \vee \lambda = (A_1 \times A_2)((y_1, y_2)) \vee \lambda = (A_1(y_1) \wedge A_2(y_2)) \vee \lambda = (A_1(y_1) \vee \lambda) \wedge (A_2(y_2) \vee \lambda) \geq (A_1(x_1) \wedge A_1(x_1 y_1) \wedge \mu) \wedge (A_2(x_2) \wedge A_2(x_2 y_2) \wedge \mu) = (A_1 \times A_2)((x_1, x_2)) \wedge (A_1 \times A_2)((x_1 y_1, x_2 y_2)) \wedge \mu = (A_1 \times A_2)((x_1, x_2)) \wedge (A_1 \times A_2)((x_1, x_2)(y_1, y_2)) \wedge \mu = (A_1 \times A_2)(x) \wedge (A_1 \times A_2)(xy) \wedge \mu$.

Therefore $A_1 \times A_2$ is a generalized fuzzy imaginary right ideal of $R_1 \times R_2$.

Theorem 3.6 Let A_i be generalized fuzzy imaginary right (resp . left) ideals of R_i , then $\prod_{1 \leq i \leq n} A_i$ is a generalized fuzzy imaginary right (resp . left) ideal of $\prod_{1 \leq i \leq n} R_i$.

Proof. We prove the theorem for imaginary right ideal. Analogous arguments apply to imaginary left ideal.

Firstly ,we prove that $\prod_{1 \leq i \leq n} A_i$ is a generalized fuzzy subring of $\prod_{1 \leq i \leq n} R_i$ .For all $x, y \in \prod_{1 \leq i \leq n} R_i$,where $x = (x_1, x_2, \ldots x_n)$ and $y = (y_1, y_2, \ldots y_n)$,then $(\prod_{1 \leq i \leq n} A_i)(x + y) \vee \lambda = \inf A_i(x_i + y_i) \vee \lambda = \inf(A_i(x_i + y_i) \vee \lambda) \geq \inf(A_i(x_i) \wedge A_i(y_i) \wedge \mu) = \inf A_i(x_i) \wedge \inf A_i(y_i) \wedge \mu$

$= (\prod_{1\le i\le n} A_i)(x) \wedge (\prod_{1\le i\le n} A_i)(y) \wedge \mu$ .Similarly , $(\prod_{1\le i\le n} A_i)(-x) \vee \lambda = \inf A_i(-x_i) \vee \lambda = \inf(A_i(-x_i) \vee \lambda) \ge \inf(A_i(x_i) \wedge \mu) = \inf A_i(x_i) \wedge \mu = (\prod_{1\le i\le n} A_i)(x) \wedge \mu$. We can prove $\prod_{1\le i\le n} A_i(xy) \vee \lambda \ge (\prod_{1\le i\le n} A_i)(x) \wedge (\prod_{1\le i\le n} A_i)(y) \wedge \mu$ using the same method.Therefore $\prod_{1\le i\le n} A_i$ is a generalized fuzzy subring of $\prod_{1\le i\le n} R_i$.

Next , For all $x, y \in \prod_{1\le i\le n} R_i$,where $x = (x_1, x_2, ...x_n)$ and $y = (y_1, y_2, ...y_n)$, then $(\prod_{1\le i\le n} A_i)(y) \vee \lambda = \inf A_i(y_i) \vee \lambda = \inf(A_i(y_i) \vee \lambda) \ge \inf(A_i(x_i) \wedge A_i(x_i y_i) \wedge \mu) = \inf A_i(x_i) \wedge \inf A_i(x_i y_i) \wedge \mu = (\prod_{1\le i\le n} A_i)(x) \wedge (\prod_{1\le i\le n} A_i)(xy) \wedge \mu$.

Thus $\prod_{1\le i\le n} A_i$ is a generalized fuzzy imaginary right ideal of $\prod_{1\le i\le n} R_i$.

Theorem 3.7 Let A be a subset of R ,then χ_A is a generalized fuzzy imaginary right (resp . left) ideal of R if and only if A is a imaginary right (resp . left) ideal of R.

Proof. We prove the theorem for imaginary right ideal . Analogous arguments apply to imaginary left ideal.

We know that A is a subring of R based on theorem 2.3 .

For all $x \in A$ and $y \in R$,if $xy \in A$,then $\chi_A(xy) = 1$ and $\chi_A(x) = 1$ .Since χ_A is a generalized fuzzy imaginary right ideal of R , so $\chi_A(y) \vee \lambda \ge \chi_A(x) \wedge \chi_A(xy) \wedge \mu = \mu$, by $\lambda < \mu$,so $\chi_A(y) \ge \mu = 1$,then $y \in A$ .Therefore A is a imaginary right ideal of R.

Conversely , we can easily obtain that χ_A is a generalized fuzzy subring of R based on theorem 2.3 . Assume that there exists $x_0, y_0 \in R$ such that $\chi_A(y_0) \vee \lambda < \chi_A(x_0) \wedge \chi_A(x_0 y_0) \wedge \mu$, choose α such that $\chi_A(y_0) \vee \lambda < \alpha < \chi_A(x_0) \wedge \chi_A(x_0 y_0) \wedge \mu$,then $\chi_A(y_0) < \alpha$, $\chi_A(x_0) > \alpha$, $\chi_A(x_0 y_0) > \alpha$ and $\lambda < \alpha < \mu$ i.e., $x_0 \in A$ and $x_0 y_0 \in A$, since A is a imaginary right ideal of R , then $y_0 \in A$, so $\chi_A(y_0) = 1 > \alpha$, a contradiction . Thus χ_A is a generalized fuzzy imaginary right ideal of R.

Theorem 3.8 Let A be a generalized fuzzy imaginary right (resp . left) ideal of R , then $A_{\underline{\lambda}} = \{x \mid A(x) > \lambda\}$ is a imaginary right (resp . left) ideal of R .

Proof. We prove the theorem for imaginary right ideal . Analogous arguments apply to imaginary left ideal.

Since A is a generalized fuzzy imaginary right ideal of R , then for every $x, y \in A_{\underline{\lambda}}$,we have $A(x+y) \vee \lambda \ge A(x) \wedge A(y) \wedge \mu > \lambda$, $A(-x) \vee \lambda \ge A(x) \wedge \mu > \lambda$, and $A(xy) \vee \lambda \ge A(x) \wedge A(y) \wedge \mu > \lambda$,i.e., $A(x+y) > \lambda$, $A(-x) > \lambda$ and $A(xy) > \lambda$,so $x+y, xy, -x \in A_{\underline{\lambda}}$. Therefore $A_{\underline{\lambda}}$ is a subring of R .

For all $x \in A_{\underline{\lambda}}$ and $y \in R$, if $xy \in A_{\underline{\lambda}}$,then $A(xy) > \lambda$ and $A(x) > \lambda$ .Since A is a generalized fuzzy imaginary right ideal of R , then $A(y) \vee \lambda \ge A(x) \wedge A(xy) \wedge \mu > \lambda$,so $A(y) > \lambda$,i.e., $y \in A_{\underline{\lambda}}$ .Therefore $A_{\underline{\lambda}} = \{x \mid A(x) > \lambda\}$ is a imaginary right ideal of R.

Theorem 3.9 Let $f : R \to H$ be a homomorphism , if B is a generalized fuzzy imaginary right (resp . left) ideal of H , then $f^{-1}(B)$ is a generalized fuzzy imaginary right (resp . left) ideal of R.

Proof. We prove the theorem for imaginary right ideal. Analogous arguments apply to imaginary left ideal.

Based on theorem 2.4 , we obtain that $f^{-1}(B)$ is a generalized fuzzy subring of R . For all $x, y \in R$, $f(x), f(y) \in H$, since B is a generalized fuzzy imaginary right ideal of H, then

$$\begin{aligned} & f^{-1}(B)(y) \vee \lambda \\ &= B(f(y)) \vee \lambda \\ &\ge B(f(x)) \wedge B(f(x)f(y)) \wedge \mu \\ &= B(f(x)) \wedge B(f(xy)) \wedge \mu \\ &= f^{-1}(B)(x) \wedge f^{-1}(B)(xy) \wedge \mu \end{aligned}$$

Therefore $f^{-1}(B)$ is a generalized fuzzy imaginary right ideal of R .

IV. CONCLUSIONS

In this paper,we gave the definition of $(\in, \in \vee q_{(\lambda,\mu)})$ – fuzzy imaginary right (resp . left) ideals of rings and generalized fuzzy imaginary right (resp . left)ideals of rings. Moreover , we found the equivalence relation between $(\in, \in \vee q_{(\lambda,\mu)})$ – fuzzy imaginary right (resp . left) ideals and generalized fuzzy imaginary right (resp . left) ideals. The properties of their intersection, union and level sets were also discussed. Finally , we gave the properties of their homomorphic preimage.

ACKNOWLEDGMENT

This work is supported by Program for Innovative Research Team of Jiangnan University (Applied Mathematics No: 200902).

REFERENCES

[1] L. A. Zadeh, “Fuzzy sets”, Information and Control, vol. 8, pp. 338-353, Jun 1965.

[2] A. Rosenfeld, “Fuzzy groups”, Journal of Mathematical Analysis and Applications, vol. 35, pp. 512-517, September 1971.

[3] B. X. Yao, “Fuzzy theory on groups and rings”, Beijing: Science Press, 2008, pp.1-125.

[4] M. AtiMishref, “Normal fuzzy subgroups and fuzzy normal series of finite groups”, Fuzzy Sets and Systems, vol. 72, pp. 379-383, Jun 1995.

[5] X. H.Yuan, C. Zhang, and Y. H. Ren, “Generaized fuzzy subgroups and many valued implications”, Fuzzy Sets and Systems, vol. 138, pp. 205-211, October 2003.

[6] Z. H. Liao, X. L. Li, and H. Q. Sheng, “On (λ,μ) - generalized fuzzy subrings”, Journal of Jiangnan University (Natural Science), vol. 3, pp. 622-624, December 2004.

[7] W. J. Liu, “The character of fuzzy ideals and field”, Fuzzy Mathematics, vol. 1, pp. 101-101, September 1981.

[8] H.C.Ma , “ About imaginary ideals of rings ” , Journal of Xuchang Colledge , vol. 9, pp. 8-10 , September 1990 .

[9] H.C.Ma ,F .Z.Chen , Y.Z.Wu , “ About pseudo ideals and imaginary ideals of rings ” , Journal of Harbin Normal University (Natural Science) , vol. 8 , pp.23-26 , September 1992 .

[10] S. K. Bhakat and P. Das, “On the defenition of a fuzzy subgroup”, Fuzzy Sets and Systems, vol. 51, pp. 235-241, October 1992.

[11] S. K. Bhakat and P. Das, “Fuzzy subrings and ideals redefined”, Fuzzy Sets and Systems, vol. 81, pp. 383-393, August 1996.

[12] B .J .Zhao, H .G .Chi. “ Fuzzy subrings and ideals redifind”, Journal of Liaoning normal University (Natural Science), vol. 24, pp. 340-343. Jun 2001.

[13] Z.Y.Guo, Z.H.Liao, “ $(\in',\in'\vee q'_{(\lambda,\mu)})$ -Fuzzy subgroups ”, Lhasa, Tibet.The sixth International Conference on Information and Management Sciences ,Lhasa, Tibet, p. 570,2007.

[14] Z. H. Liao, H .Gu, “ $(\in,\in\vee q_{(\lambda,\mu)})$ -fuzzy normal subgroup” , Fuzzy Systems and Mathematics, vol. 20, pp. 340-343. October 2006.

[15] Z. H. Liao and M .Chen, “ $(\in,\in\vee q_{(\lambda,\mu)})-$ fuzzy subsemigroup and $(\in,\in\vee q_{(\lambda,\mu)})-$ fuzzy completely regular subsemigroup” , Journal of Jiangnan University (Natural Science), vol. 8, pp. 242-244, April 2009.

[16] J Zhou , Z. H.Liao , “Generalized (α,β) - convex Fuzzy Cones ” , 2008 IEEE International Conference on Fuzzy Systems (FUZZ 2008) , Hongkong , pp.439-442 , 2008.

2011 IEEE International Conference on Fuzzy Systems
June 27-30, 2011, Taipei, Taiwan

Cellular Fuzzy Networks

Koosha Sadeghi Oskooyee[1], Mohammad Mansour Riahi Kashani[2], and Mehrdad Jangjou[3]

[1,2]Dept. of Computer Engineering,
Islamic Azad University, North Tehran Branch,
Tehran, Iran

[3]Dept. of Computer Engineering,
Islamic Azad University, U.A.E. Branch,
Dubai, Emirates

e-mail: { [1]K_Sadeghi_Oskooyee, [2]M_Riahi_Kashani}@iau-tnb.ac.ir, and [3]Mehrdadjangjou@live.com

***Abstract*—A formal representation of the mutual information processing among the cognitive processes of the brain provides a real impression of the mechanisms of a Natural Intelligence (NI) system. The nature of information processing in the human brain is fuzzy. In this article, a new formal model, namely Cellular Fuzzy Networks (CFNs), is introduced to model the real characteristics of NI-Systems and especially the human mind. CFNs can effectively manipulate the interactions among natural concepts in an NI-system. The detailed definitions of CFNs and related theorems are provided. Then, CFNs are exploited to model a feasibility analysis of the human brain in the cognitive process of decision making. Finally, it is posited that CFNs have great potential to be applied in modeling the complex interrelationships in large-scale natural systems.**

Keywords- Cognitive informatics; natural intelligence system; fuzzy sets theory; cellular fuzzy networks; human mind

I. INTRODUCTION

The contemporary form of cybernetics is known as Cognitive Informatics (CI), which attempts to discover the mechanisms of natural intelligence and the cognitive processes of the brain [1]. CI applies many disciplines such as philosophy, physiology, psychology, and computer science to study the human brain as the most complicated organism in the universe [2, 3]. Natural intelligence, like other natural phenomena, is involved with vague concepts. An average brain in daily life thinks and proceeds with imprecise information and facts, and the nature of information processing in the human brain is fuzzy. Fuzzy sets theory provides a formal method to capture and process vague data from the natural world in a precise form [4].

The human brain proceeds through nonstop performance causal relationships among cognitive functions. Imitation of the real characteristics of the human mind requires the composition of an ultimately accurate harmony among the cognitive functions of the brain [5]. Subsequently, analyzing the complex interactions among a set of cognitive processes requires a formal method that can be easily adapted to the nature of information processing in an NI-System. The method can be exploited more effectively as one of the most vital issues in CI and AI research through the representation of mind flows [6].

In this paper, the concept of CI is used to make a relevant connection between psychological studies of NI and methodological models in computer engineering to develop a casual network in light of fuzzy sets theory. In this way, a new concept of cellular fuzzy networks is proposed to manipulate the mutual information processing among cognitive processes of the brain. The idea comes from the theorems of Cellular Bayesian Networks (CBNs) proposed in [7] and the fuzzy sets theory. Actually, CFNs acquire and merge the structure and mathematical background of CBNs and the principles of fuzzy inference systems [8].

This paper is arranged as follows: in Section II, a brief description of fuzzy sets theory is proposed, and then in Section III the cellular fuzzy network is developed on the basis of casual network and fuzzy sets theory. In Section IV, feasibility testing in NI-systems is modeled and simulated according to CFN in a MATLAB workspace. In this case, the psychological models for integrating new information into the existing knowledge are exploited to manipulate the feedback information to the NI-system. Finally, the paper is concluded in Section V.

II. FUZZY SETS THEORY

In cognitive psychology, vagueness and uncertainty regarding perception are properties of concepts which are inevitable in human thought processes. The origin of fuzzy concepts is due partly to the fact that the nature of information processing in the human brain is fuzzy.

The theory of fuzzy sets was proposed by L.A. Zadeh and provides an efficient basis for the model the cognitive capabilities of the human brain under uncertain circumstances. Currently, fuzzy sets is an extension of the classical notion of sets in which the membership of elements or objects in a set is assessed in binary terms according to a bivalent condition [9, 10]. In contrast, fuzzy sets theory permits the gradual assessment of the membership of elements in a set, which is determined by a membership function valued in the real unit interval [0, 1].

Fuzzy sets theory can be used in a wide range of domains in which information is incomplete or imprecise, such as bioinformatics [11]. In this way, fuzzy sets theory provides fuzzy production rules in order to reason and infer properly

978-1-4244-7316-8/11/$26.00 ©2011 IEEE

with real world information. Fuzzy systems apply linguistic identifiers and rules to mimic NI-System behaviors and thought mechanisms more effectively.

III. CELLULAR FUZZY NETWORKS

In this section, cellular fuzzy networks and their related theorems are defined and explained in detail to determine a formal framework for representing an accurate depiction of the information flow in an NI-system.

A *causal network* is an acyclic digraph arising from an evolution of a substitution system, and representative of its history. In the evolution of a multi-way system, each substitution event is a vertex in a causal network. The existence of an edge between two vertices in the casual network indicates the order of the corresponding events, which are related by causal dependence. More precisely, the edge is a directed edge leading from the past event to the future event [11]. In a causal network, if the variables A and B become the parents of the variable C independently, there is no information on how impacts from variable A and variable B interact, and more specification is required. In addition, causal networks do not support the domain to be modeled contains feedback cycles. In this way, to eliminate these restrictions, some modifications to the structure of causal networks are performed according to the following definitions.

Definition 1. A *Fuzzy Network* (FN) is a fuzzy graphical model that represents a set of natural variables and their causal dependencies via a Directed Acyclic Graph (DAG). More particularly, an FN is a kind of casual network with the following characteristics:

- There is a set of variables and a set of directed edges between the variables;
- Each set contains a finite set of mutually exclusive states;
- The variables coupled with the directed edges construct a directed acyclic graph;
- Each variable A with parents $B_1, B_2 \ldots B_n$ is associated with a set of fuzzy production rules table comprised of the fuzzy rules in the form of IF B_1 AND B_2 AND…B_n THEN A.

In fact, each node in an FN presents a fuzzy inference system. If the variable A has no parent, then the table can be replaced by the degree of membership. A fuzzy network provides a graphical model of information passing among nodes to mimic the behaviors of an NI-system.

In a directed acyclic graph $G = (V, E)$, a node $C \in V$ is called a *center node* if and only if for any node $X \in V \backslash \{C\}$, the condition $\langle X, C \rangle \in E$ is satisfied. For example, in Fig. 1, the node n_3 in graph G_1 and the node n_2 in G_2 are the center nodes in their graphs, respectively. A directed acyclic graph is a *centered graph* if and only if it has only one center node, and there are no edges ending at non-center nodes [7].

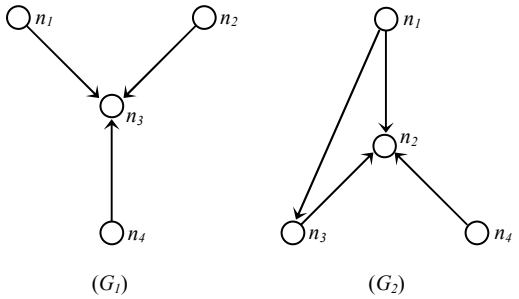

Figure 1. The sample graphs

For example, graph G_1 is a centered graph, and graph G_2 is not due to its containing extra edges between non-center nodes. The center node of a centered graph is specified shortly to C (G). Hence, in Fig. 1, we have $C(G_1) = n_3$.

Definition 2. A *cellular fuzzy network* is a pair (G, R), where $G = (V, E)$ is a centered graph, and R is a set of fuzzy production rules for the center node of G given its parents. For convenience, the center of G is also called, C (G), the center of the CFN, short for C (CFN).

In a CFN, each node acts as a fuzzy inference system, following five steps: (1) fuzzification of the input variables from the parents, (2) application of the fuzzy operator (AND or OR) in the antecedent, (3) implication from the antecedent to the consequent, (4) aggregation of the consequents across the rules, and, finally, (5) defuzzification and the outputs their passing onto the childs. For any two given cellular fuzzy networks $F_1 = (G_1, R_1)$ and $F_2 = (G_2, R_2)$, if C (B_1) ≠ C (B_2), the *union* $F = F_1 \cup F_2$ of the CFN F_1 and CFN F_2 is a pair (G, R), where G is the union of G_1 and G_2, and R is the union of R_1 and R_2. As shown in Fig. 2, two fuzzy cells (i.e. F_1, F_2) are linked through their center nodes (i.e. n_2, n_4) with directed edges. The union of two CBNs is also a graph model but according to the definitions it is no longer a CBN.

Definition 3. A *Cellular Fuzzy Networks* (CFNs) is a union, CFNs = $F_1 \cup F_2 \cup \ldots \cup F_n$, where F_i (i = 1, …, n) is cellular fuzzy network, and they are subject to the following constraints:

$$C(F_i) \neq C(F_j),\ 1 \leq i < j \leq n \tag{1}$$

and

$$C(F_i) \in (\bigcup_{i \neq j} V_j),\ i = 1, ..., n, \tag{2}$$

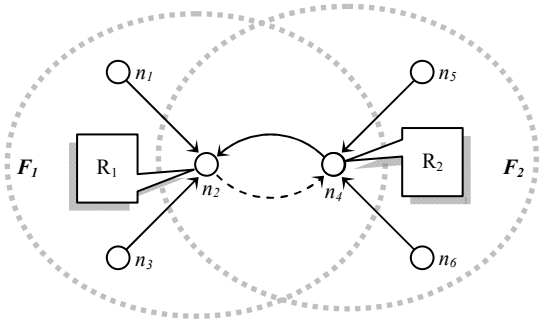

Figure 2. The union of cellular fuzzy networks (F_1andF_2)

where V_j is the node set of F_j. The first constraint indicates the uniqueness of every cell in the networks and the second constraint indicates that the center nodes are the only path for connection among the cells. CFNs can be developed like fractals by substituting every node with CFNs and so on. This attribute makes CFNs more flexible to model natural systems with dynamic scales.

IV. THE NATURAL INTELLIGENCE SYSTEM

An artificial mind system attempts to imitate cognitive mechanisms of the human brain in dealing with a wide variety of physical and mental incidents in the natural world. In cognitive psychology, vagueness and uncertainty are inevitable in human thought processes [12]. In many everyday situations, an average person thinks largely in an intuitive and associative manner, which is calculated or identified by qualitative or verbal measures within the range of interpretation for a given phrase. Particularly, it is recognized that people's internal representations of uncertainty are verbal.

Human brain as the most complex organism in the universe is the faculty of any kind of intelligent behaviors. Human behavior is directly generated by behavioral intensions, which are controlled by the attitude consisting of personal experiences and social norms [7].

Attitude or perceptual feasibility in which uncertainty is a substantial issue generally focuses on decision making processes. Attitude has a considerable impact on behavior and influences the ways a person thinks and feels. The direct relationship between attitude and behavior intention is shown in Table II. Furthermore, attitude of a person is affected by the environmental results of the related behavior. In this case, in order to manage the feedback of new information, in [18], a psychological model was developed which adjusted membership functions toward predicting the impact of new information on the existing body of knowledge. According to this model, newly acquired information from the environment about the possibility of doing an action has an impact on the modification of the perceptual feasibilities, as can be seen in Table I.

Now, the interactions between perceptual feasibility and behavior intention [18] as two fuzzy concepts in an NI-Sys are modeled with CFNs. Fuzzy concepts are characterized by generalized bell-shaped membership functions according to prevalent psychological and linguistic disciplines, as seen in Fig. 3 [8]. Psychological experiments [19] indicate that the amount of above-mentioned specifications is sufficient for practical purposes. As shown in Fig. 4, a CFNs model is developed which accounts for the verbal thinking orientation for decision making, or behavior modeling through logically describing the imprecision of the mind's activities ([10], [19]).

Tables I and II indicate the production rules of the fuzzy inference system on each node in the model in Fig. 4. As mentioned before, some natural and psychological attributes are extracted for the purpose of defining fuzzy rules. In fact, in the proposed model, perceptual feasibility is in charge of the evaluation or belief of a person about the difficulty of carrying out a designated behavior.

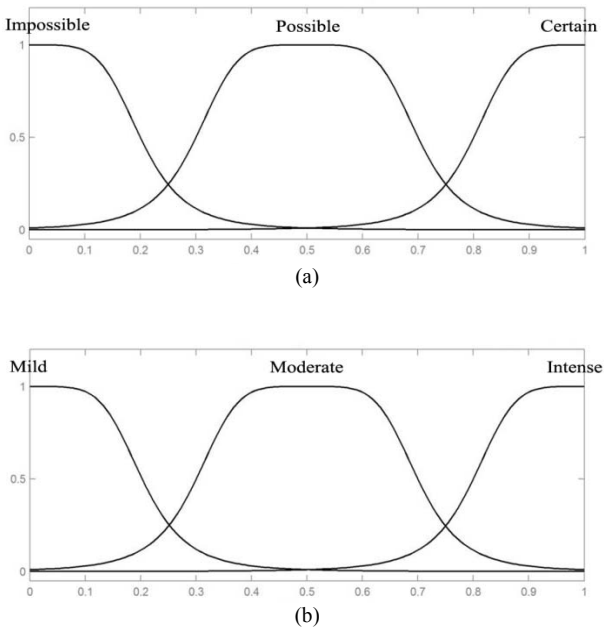

Figure 3. Diagrams of the membership functions of (a) feasibility analysis, and (b) behavior intention

For simulation, the fuzzy logic toolbox of Matlab was used to describe each node (in Fig. 4) efficiently as a fuzzy inference system and the plots of the fuzzy inference systems are shown in Figs. 5 and 6 [14]. In Fig. 5, the effect of the outcome of the behavior (i.e. the feedback) on the current belief about the feasibility of success in carrying out the behavior can be seen.

TABLE I. THE EFFECT OF FEEDBACK OF NEW INFORMATION ON OLD KNOWLEDGE

	New information		
Old knowledge	Impossible	Possible	Certain
Impossible	Impossible	Impossible	Possible
Possible	Impossible	Possible	Certain
Certain	Possible	Certain	Certain

TABLE II. THE EFFECT OF A FEASIBILITY ANALYSIS ON BEHAVIOR INTENTION

Feasibility analysis	Behavior intention
Impossible	Mild
Possible	Moderate
Certain	Intense

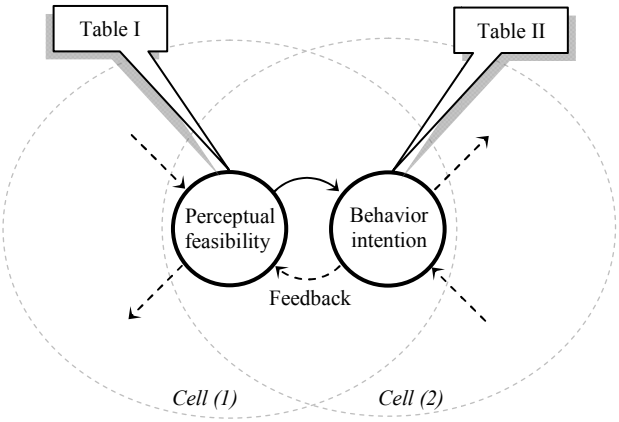

Figure 4. CFNs model of the interactions between feasibility analysis and behavior intention

In this case, the fuzzified inputs from the natural world are processed through IF-THEN rules and the Mamdani's max-min composition [17]. The simulated CFNs model provides a formal explanation for the mechanism and relationship between attitude and behavior. Also, it can be used for describing the way attitude helps to regulate the behavioral intention with a positive or negative judgment.

As a result, CFNs provide relevant specifications to freely determine the relationships among fuzzy inference systems, whether as aforementioned, a causal network has some restrictions in this way, such as a lack of information on how impacts from parent systems interact, and also the domain which contains feedback cycles are not supported. In addition, the model can be easily expanded to cover other factors involved in forming behavior in natural intelligent systems, like emotion and motivation. The designed CFNs can be used to control the behavior of an intelligent system with autonomous decision making ability according to the rules of feedback information and natural intelligence [15, 16].

V. CONCLUSION

A formal method is required to analyze the complex interactions among a set of cognitive processes of the brain

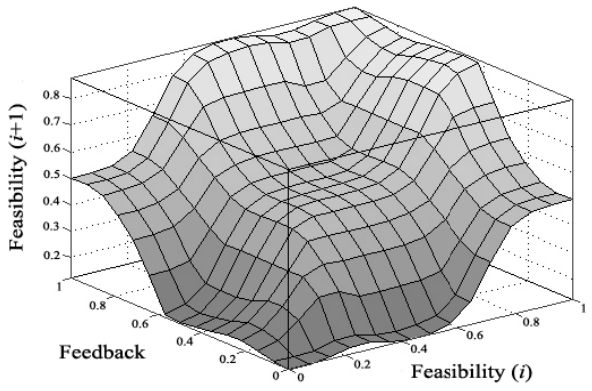

Figure 5. Surface plot of the fuzzy inference system of the left node in the CFNs model (in Fig. 4) that illustrates the influence of feedback as new information on the current feasibility analysis

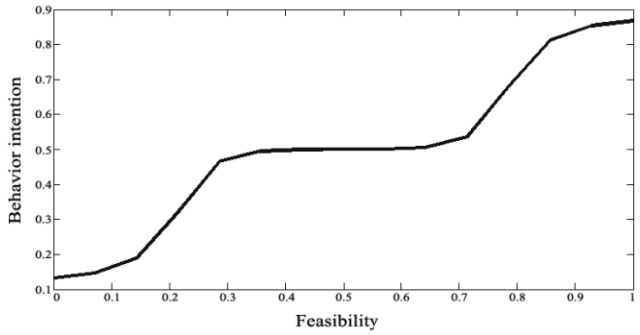

Figure 6. The plot of the fuzzy inference system of the right node in the CFNs model (in Fig. 4) that illustrates the influence of the feasibility analysis on the behavior intention

that can be easily adapted to the nature of information processing in a natural intelligence system. The brain works continuously through a life time; in such a dynamic organism, considering the effects of every stimulus and process becomes very complicated.

In the present work, a new concept of cellular fuzzy networks is proposed to model the real characteristics of NI-Systems, especially those of the human mind. The detailed definitions of CFNs and related theorems are provided. Subsequently, CFNs are exploited to model the feasibility analysis of the human brain in the cognitive process of decision making and behavior intention. The proposed model can be applied to simulate the transmission of mind flows toward implementing an intelligent humanoid behavior mechanism and other mental phenomena as well. The model offers the real possibility of humanoid behavior through developing an artificial mind system and future generation intelligent systems.

The authors propose future research on the theme, including the concepts of learning and inference in cellular fuzzy networks. CFNs have great potential to be applied to model the complex interrelationships in large-scale natural systems. Finally, it is expected that such methods will be able to establish more natural characteristics of the human mind and brain in the operation of artificial intelligence systems.

REFERENCES

[1] Y. Wang, W. Kinsner, and D. Zhang, "Contemporary Cybernetics and Its Facets of Cognitive Informatics and Computational Intelligence," IEEE Transactions on Systems, Man and Cybernetics—part B: Cybernetics, vol. 39, no. 4, Aug. 2009.

[2] Y. Wang and Ying Wang, "Cognitive Informatics Models of the Brain," IEEE Transactions on Systems, Man and Cybernetics—part: C, Applications and Reviews, vol. 36, no. 2, pp. 203-207, Mar. 2006.

[3] Z. Shi and J. Shi, "Perspectives on Cognitive Informatics," Proceedings of the Second IEEE International Conference on Cognitive Informatics (ICCI'03), 2003.

[4] X. Li, W. Yu, and F. Lara-Rosano, "Dynamic Knowledge Inference and Learning under Adaptive Fuzzy Petri Net Framework," IEEE Transactions on Systems, Man and Cybernetics—part: C, Applications and Reviews, vol. 30, no. 4, Nov. 2000.

[5] G. Baciu, Y. Wang, Y.Y. Yao, W. Kinsner, K. Chan and L.A. Zadeh (Eds.), "Perspectives on cognitive informatics and cognitive computing: Summary of the Panel of IEEE ICCI'09," Proc. of the 8th IEEE Int.

Conf. on cognitive informatics (ICCI'09), IEEE CS Press, Kowloon, Hong Kong, pp. 9-27, Jun. 2009.

[6] L. I. Perlovsky, "Neural Mechanisms of the Mind, Aristotle, Zadeh, and fMRI," IEEE Transactions on Neural Networks, vol. 21, no. 5, May. 2010.

[7] Y. Wang, Discoveries and Breakthroughs in Cognitive Informatics and Natural Intelligence, IGI global, pp. 428-435, Nov. 2009.

[8] J. C. Canales, X. Li, and W. Yu, "Fuzzy Knowledge Learning via Adaptive Fuzzy Petri Net with Triangular Function Model, Proceedings of the 6th World Congress on Intelligent Control and Automation, Dalian, china, Jun. 2006.

[9] G. Giangiacomo, "Effectiveness and Multivalued Logics". Journal of Symbolic Logic, Vol. 71, No. 1, pp. 137–162, 2006.

[10] P. D. Windschitl and G. L. Wells, "Measuring Psychological Uncertainty: Verbal Versus Numeric Methods," Journal of Experimental Psychology: Applied, vol. 2, no. 4, pp. 343-364, 1996.

[11] J. Pearl, Causality: Models, Reasoning, and Inference, Cambridge University Press, 2000.

[12] T. Hoya, Artificial Mind System – Kernel Memory Approach, Studies in Computational Intelligence (SCI), Springer-Verlag Berlin Heidelberg, Sep. 2005.

[13] L. R. Liang, S. Lu, X. Wang, Y. Lu, V. Mandal, D. Patacsil and D. Kumar, "FM-test: A Fuzzy-Set-Theory-Based Approach to Differential Gene Expression Data Analysis," BMC Bioinformatics, Jun. 2006.

[14] A. Che Soh, L. Guan Rhung, and H. Md. Sarkan, "MATLAB Simulation of Fuzzy Traffic Controller for Multilane Isolated Intersection," International Journal on Computer Science and Engineering, vol. 2, no. 4, pp. 924-933, 2010.

[15] D. Borrie, S. Isnandar, and C.S. Özveren, "Simulation of Complex Environments: The Fuzzy Cognitive Agent," IEEE Proceedings of the Sixth International Conference on Intelligent Systems Design and Applications (ISDA'06), 2006.

[16] K. S. Park, D. S. Kwon, M. Park, "A Design of the Mental Model of a Cognitive Robot," 16th IEEE International Conference on Robot & Human Interactive Communication, pp. 26 - 29, Aug. 2007.

[17] C. W. Hong, G. J. Choi, and D. S. Ahn, "Integrated Development Platform for Design of Fuzzy Inference System using RecurDyn and SIMULINK," SICE-ICASE International Joint Conference 2006, pp. 18-21, Bexco, Busan, Korea, Oct. 2006.

[18] Y. Wang, novel approaches in cognitive informatics and natural intelligence (Advances in Cognitive Informatics and Natural Intelligence), Information Science Reference, pp. 65-76, Dec. 2008.

[19] A. C. Zimmer, "A model for the interpretation of verbal predictions," International Journal of Man-Machine Studies, vol. 20, no. 1, pp. 121-134, Jan. 1984.

2011 IEEE International Conference on Fuzzy Systems
June 27-30, 2011, Taipei, Taiwan

Expatriate Manager Selection for an Overseas Manufacturing Site by Using FMCDM Methods

Chi-Yo Huang
Dept. of Industrial Education
Nat. Taiwan Normal University, No. 162, Ho-Ping East Road I, Taipei, Taiwan
cyhuang66@ntnu.edu.tw

Chih-Wei Wan
Dept. of Industrial Education
Nat. Taiwan Normal University, No. 162, Ho-Ping East Road I, Taipei, Taiwan
carollin829@gmail.com

Gwo-Hshiung Tzeng
Inst. of Project Management
Kainan University
No. 1, Kainan Road, Luchu, Taiwan
ghtzeng@mail.knu.edu.tw

Abstract — **The human resources is playing a daily important role in modern globalized firms. Appropriate staffing strategies are critical for coordinating and controlling international human resource management related issues across widely distributed business units or subsidiaries over various geographic areas. However, very few researches tried to uncover how the expatriate managers can be selected, especially when the evaluation criteria influence each other. Thus, this research aims to develop a decision framework for selecting appropriate expatriate managers. A multiple criteria decision making (MCDM) framework consisting of the Decision Making Trial and Evaluation Laboratory (DEMATEL) for structuring the decision problem, the Analytical Network Process (ANP) for deriving weights versus each criterion, and finally, the VlseKriterijumska Optimizacija I Kompromisno Resenje (VIKOR) for ranking the alternatives have been proposed. An empirical study based on a globalized high technology firm will be leveraged for verifying the usefulness of this proposed analytic framework on staff selections.**

Keywords - Multinational Enterprises (MNE); ***International Human Resource Management***; ***Staffing Strategies***; ***Multiple Criteria Decision Making (MCDM)***; ***Decision Making Trial and Evaluation Laboratory (DEMATEL)***; ***Analytic Network Process (ANP)***; ***VlseKriterijumska Optimizacija I Kompromisno Resenje (VIKOR).***

I. INTRODUCTION

In the era of globalization, multinational enterprises (MNEs) have gradually expanded their operations in order to maximize the profitability and enhance the competitive advantages. International trade may occur anywhere in the value chain. Meanwhile, new technologies are enabling global manufacturing activities and service deliveries with the world-class quality and prices [9].

Due to the local and global competitions, MNEs are always seeking lower costs, higher quality as well as products or service discrepancy [2]. The lower costs are including lower-cost materials and lower-cost inputs such as land, utilities, and labor. In addition, the matured markets and limited opportunities in the developed countries further drive many MNEs to seek markets in other countries [22]. Therefore, MNEs in general and high technology MNEs in special usually set up different functional units, including manufacturing, marketing and R&D overseas. Appropriate human resources for managing overseas operations are essential for the final success.

The major purposes for establishing overseas operations of a high technology MNE are three folds: (1) limitations by strict host country government's regulations, higher labor consciousness, and scarce raw materials, (2) attractiveness being provided by foreign countries' preferential policies, well potential markets or plenty raw materials, and (3) leading the relating industries to create the competitive advantage and reduce the managing cost [14]. Consequently, in order to compete in the global marketplace, high technology MNEs must develop business strategies which can take advantage of global resources and markets. Since high technology MNEs differ in the scale and scope of their international operations, international human resource managers must assist in the global operations no matter what their scale and scope are [20].

However, the international human resource management is not easy. The challenges include of how the thousands of MNE employees in many different countries can effectively be attracted, engaged and retained to achieve the strategic objectives [24]. Therefore, appropriate strategies, including expatriates, inpatriates, and flexpatriates [2] should be designed and executed

To achieve this purpose, a hybrid multiple criteria decision making (MCDM) framework consisting of the Decision Making Trial and Evaluation Laboratory (DEMATEL), the Analytic Network Process (ANP) and the VlseKriterijumska Optimizacija I Kompromisno Resenje (VIKOR) will be proposed. At first, literature being related to high technology MNEs, international human resource management strategies for MNEs, and criteria for expatriate manager selections will be reviewed. The validity of the derived criteria will be confirmed by using the Delphic Oracle's Skills of Interpretation and Foresight (Delphi). The structure of the entire decision making problem will be developed based on the influence relationships between the criteria by using the DEMATEL. Weights versus the criteria will be derived based on the influence relation map (IRM) being derived by using the ANP. Finally, the VlseKriterijumska Optimizacija I Kompromisno Resenje (VIKOR) will be leveraged to rank the criteria.

The rest of this research is organized as follows. In Section 2, literature on MNE and criteria definitions for staffing policies will be reviewed. In Section 3, the hybrid MCDM framework for selecting the appropriate expatriate managers will be defined and demonstrated. In Section 4, an empirical study on a world-leading information technology (IT) company with several overseas manufacturing sites will be illustrated. Discussion and implications will be presented in Section 5. The last section is the conclusion in Section 6.

II. LITERATURE REVIEW

A MNE can be defined as a firm which produces and/or distributes products and/or services across national borders. MNEs have repeatedly been identified as the drivers of globalization [23]. MNEs achieve future successes based on appropriate international assignments. First this section takes a look at a number of criteria that are used by various global firms to select their international assignees [30]. Then the section examines the consequences of making mistakes either

978-1-4244-7316-8/11/$26.00 ©2011 IEEE

in choosing international assignees or in preparing and supporting their assignments or in helping them make a successful return to home at the end of their international assignments [3].

Most MNEs base their choices for international assignments on candidates' technical expertise. The primary focus is on their ability to perform the target job requirements [9]. MNE makes the choice of individual to be sent on an international assignment and that choice is usually based on the individual's perceived ability to fill a perceived functional or technical need in the foreign operation [2]. The cultural adaptability is at least as important to the successful completion of an overseas assignment as is the individual's technical ability. Expatriates must be able to adjust to their new and often alien environments while effectively delivering their technical and managerial expertise [30]. They must graciously accept their new cultures but not at the expense of not getting their job done. While technical expertise is usually important, the principal difficulty faced by most expatriates lies in the inability of the managers and their families to adapt to the foreign cultures. Since adaptation to the foreign culture is so important to an international assignees performance, his desire for that foreign assignment is critical to their willingness to make the necessary efforts to adjust [17]. Sometimes MNEs need to recruit such people from the outside or acquire the expertise from consulting firms and the expertise could be recruited from overseas countries.

The selection decision for international assignees is critically important. Errors in the selection can have a major negative impact on the success of overseas operations as well as on the careers of relocated managers [17]. From the perspective of headquarters, it is most important that potential international assignees be seen as able to perform both the specific tasks to which they are assigned as well as to perform well in a different national culture. Because of the nature of most international assignments, selections for international transfer are most successful when based on factors such as the following: the maturity of the candidate; ability to handle foreign language; possession of a favorable outlook on the international assignment and locale by the expatiate and his family; possessing appropriate personal characteristics [13]. In order to convince the expatiates to take on the international assignments, some issues like dual families, disruption of their lives, work-life balance issues, and the uncertainty about the impact of the assignment on their careers, employees are becoming increasing reluctant. MNEs should pay attention to these factors when making selections for international assignments [21].

III. Research Methods

The analytical framework consists of five phases: reviewing related literature on MNEs staffing policy, establishing evaluation criteria for MNEs staffing policy by using the modified Delphi and the Cronbach's alpha coefficient; building the structure between evaluation criteria by using the DEMATEL; analyzing and ranking the interrelationship among the factors by using the VIKOR and finally, and deciding the strategies being suitable for each category of MNEs.

A. Modified Delphi

The modified Delphi method was designed by Dalkey and Helmer [19], try to identify issues and problems were collected from a group of technology education professionals using the modified-delphi Technique [12]. The primary objective of a Delphi inquiry is to obtain a consensus as a minimum of 75 percent agreement on any particular item at of opinion from a group of respondents. Meanwhile, it is possible to develop consensus on a common core of management assessment criteria which, when combined with the institution, unit, and position-specific criteria, can form a comprehensive management audit instrument.

B. DEMATEL

The DEMATEL method was developed by the Battelle Geneva Institute (1) to analyze complex 'world problems' dealing mainly with interactive man-model techniques; and (2) to evaluate qualitative and factor-linked aspects of societal problems [1]. The applicability of the method (e.g. [4; 5; 11; 31]) is widespread. Furthermore, a hybrid model combining the two methods has been widely used in various fields, for example, e-learning evaluation [7], airline safety measurement [11], and innovation policy portfolios for Taiwan's SIP Mall [5]. Therefore, in this paper we use DEMATEL not only to detect complex relationships and build a NRM of the criteria, but also to obtain the influence levels of each element over others; we then adopt these influence level values as the basis of the normalization supermatrix for determining ANP weights to obtain the relative importance. To apply the DEMATEL method smoothly, the authors refined the definitions based on above authors, and produced the essential definitions indicated below. The DEMATEL method is based upon graph theory, enabling us to plan and solve problems visually, so that we may divide multiple criteria into a relationship of cause and effect group, in order to better understand causal relationships. Directed graphs (also called digraphs) are more useful than directionless graphs, because digraphs will demonstrate the directed relationships of sub-systems. A digraph typically represents a communication network, or a domination relationship between individuals, etc. Suppose a system contains a set of elements, $S = \{s_1, s_2, \ldots, s_n\}$, and particular pair-wise relationships are determined for modeling, with respect to a mathematical relationship, MR. Next, portray the relationship MR as a direct-relation matrix that is indexed equally in both dimensions by elements from the set S . Then, extract the case for which the number 0 appears in the cell (i, j) , if the entry is a positive integral that has the meaning of: the ordered pair (s_i, s_j) is in the relationship MR; it has the kind of relationship regarding that element such that s_i causes element s_j . The digraph portrays a contextual relationship between the elements of the system, in which a numeral represents the strength of influence. The elements s_1 , s_2 , s_3 and s_4 represent the factors that have relationships in Fig. 1. The number between factors is influence or influenced degree. For example, an arrow from s_1 to s_2 represents the fact that s_1 influences s_2 and its influenced degree is two. The DEMATEL method can convert the relationship between the causes and effects of criteria into an intelligible structural model of the system [2].

Definition 1: The pair-wise comparison scale may be designated as eleven levels, where the scores 0,1,2,…,10 represent the range from 'no influence' to 'very high influence'.

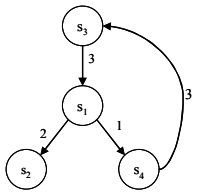

Fig. 1. An example of the directed graph

Definition 2: The initial direct relation/influence matrix $\boldsymbol{A}$ is an $n \times n$ matrix obtained by pair-wise comparisons, in terms of influences and directions between the determinants, in which a_{ij} is denoted as the degree to which the i^{th} determinant affects the j^{th} INC.

$$\mathrm{A} = \begin{bmatrix} a_{11} & a_{12} & \cdots & a_{1n} \\ a_{21} & a_{22} & \cdots & a_{2n} \\ \vdots & \vdots & \vdots & \vdots \\ a_{n1} & a_{n2} & \cdots & a_{nn} \end{bmatrix}$$

Definition 3: The normalized direct relation/influence matrix $\boldsymbol{N}$ can be obtained through Equations (1) and (2), in which all principal diagonal elements are equal to zero.

$$\boldsymbol{N} = z\mathrm{A}. \tag{1}$$

$$\text{where } z = 1 \Big/ \max_{1 \le i \le n} \sum_{j=1}^{n} a_{ij}. \tag{2}$$

In this case, $\boldsymbol{N}$ is called the normalized matrix. Since $\lim_{k \to \infty} \boldsymbol{N}^k = [0]$.

Definition 4: Then, the total relationship matrix $\boldsymbol{T}$ can be obtained using Equation (3), where $\boldsymbol{I}$ stands for the identity matrix.

$$\boldsymbol{T} = \boldsymbol{N} + \boldsymbol{N}^2 + \ldots + \boldsymbol{N}^k = \boldsymbol{N}(\boldsymbol{I} - \boldsymbol{N})^{-1}, \tag{3}$$

where $k \to \infty$ and $\boldsymbol{T}$ is a total influence-related matrix; $\boldsymbol{N}$ is a direct influence matrix and $\boldsymbol{N} = [x_{ij}]_{n \times n}$; $\lim_{k \to \infty} \left(\boldsymbol{N}^2 + \cdots + \boldsymbol{N}^k \right)$ stands for a indirect influence matrix and $0 \le \sum_{j=1}^{n} x_{ij} < 1$ or $0 \le \sum_{i=1}^{n} x_{ij} < 1$, and only one $\sum_{j=1}^{n} x_{ij}$ or $\sum_{i=1}^{n} x_{ij}$ equal to 1 for $\forall i, j$. So $\lim_{k \to \infty} \boldsymbol{N}^k = [\boldsymbol{0}]_{n \times n}$. The (i, j) element t_{ij} of matrix $\boldsymbol{T}$ denotes the direct and indirect influences of factor i on factor j.

Definition 5: The row and column sums are separately denoted as $\boldsymbol{r}$ and $\boldsymbol{c}$ within the total-relation matrix $\boldsymbol{T}$ through Equations (4), (5), and (6).

$$\boldsymbol{T} = [t_{ij}], \quad i, j \in \{1, 2, \ldots, n\} \tag{4}$$

$$\boldsymbol{r} = [r_i]_{n \times 1} = \left[\sum_{j=1}^{n} t_{ij} \right]_{n \times 1} \tag{5}$$

$$\boldsymbol{c} = [c_j]_{1 \times n} = \left[\sum_{i=1}^{n} t_{ij} \right]_{1 \times n} \tag{6}$$

where the $\boldsymbol{r}$ and $\boldsymbol{c}$ vectors denote the sums of the rows and columns, respectively.

Definition 6: Suppose r_i denotes the row sum of the i^{th} row of matrix $\boldsymbol{T}$. Then, r_i is the sum of the influences dispatching from factor i to the other factors, both directly and indirectly. Suppose that c_j denotes the column sum of the j^{th} column of matrix $\boldsymbol{T}$. Then, c_j is the sum of the influences that factor i is receiving from the other factors. Furthermore, when $i = j$ (i.e., the sum of the row sum and the column sum $(r_i + c_i)$ represents the index representing the strength of the influence, both dispatching and receiving), $(r_i + c_i)$ is the degree of the central role that factor i plays in the problem. If $(r_i - c_i)$ is positive, then factor i primarily is dispatching influence upon the strength of other factors; and if $(r_i - c_i)$ is negative, then factor i primarily is receiving influence from other factors [5; 11; 18].

C. Analytic Network Process (ANP)

The ANP method, a multi criteria theory of measurement developed by Saaty [26] provides a general framework to deal with decisions without making assumptions about the independence of higher-level elements from lower level elements and about the independence of the elements within a level as in a hierarchy. Compared with traditional MCDM methods [26], e.g. AHP (Analytic Hierarchy Process), TOPSIS, ELECTRE, etc [26; 27], which usually assume the independence between criteria, ANP, a new theory that extends AHP to deal with dependence in feedback and utilizes the supermatrix approach [28], is a more reasonable tool for dealing with complex MCDM problems in the real world. In this section, concepts of the ANP are summarized based on Saaty's earlier works [26-29].

The ANP is a coupling of two parts. The first consists of a control hierarchy or network of criteria and subcriteria that control the interactions. The second is a network of influences among the elements and clusters. The network varies from criterion to criterion and a different supermatrix of limiting influence is computed for each control criterion. Finally, each of these supermatrices is weighted by the priority of its control criterion and the results are synthesized through addition for all the control criteria [26]. A control hierarchy is a hierarchy of criteria and subcriteria for which priorities are derived in the usual way with respect to the goal of the system being considered.

The criteria are used to compare the components of a system, and the subcriteria are used to compare the elements. The criteria with respect to which influence is presented in individual supermatrices are called control criteria. Because all such influences obtained from the limits of the several supermatrices will be combined in order to obtain a measure of the priority of overall influences, the control criteria should be grouped in a structure to be used to derive priorities for them. These priorities will be used to weight the corresponding individual supermatrix limits and add. Analysis of priorities in a system can be thought of in terms of a control hierarchy with dependence among its bottom-level alternatives arranged as a network as shown in Fig. 2. Dependence can occur within the components and between them.

A control hierarchy at the top may be replaced by a control network with dependence among its components, which are

collections of elements whose functions derive from the synergy of their interaction and hence has a higher-order function not found in any single element. The criteria in the control hierarchy that are used for comparing the components are usually the major parent criteria whose subcriteria are used to compare the elements need to be more general than those of the elements because of the greater complexity of the components.

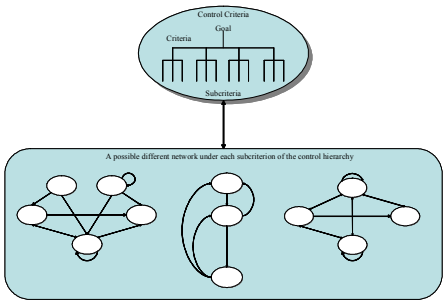

Source: [26]
Fig. 2. The control hierarchy

A network connects the components of a decision system. According to size, there will be a system that is made up of subsystems, with each subsystem made up of components, and each component made up of elements. The elements in each component interact or have an influence on some or all of the elements of another component with respect to a property governing the interactions of the entire system, such as energy, capital, or political influence. Figure 3 demonstrates a typical network. Those components which no arrow enters are known as source components such as $\boldsymbol{C}_1$ and $\boldsymbol{C}_2$. Those from which no arrow leaves are known as sink component such as $\boldsymbol{C}_5$. Those components which arrows both enter and exit leave are known as transient components such as $\boldsymbol{C}_3$ and $\boldsymbol{C}_4$. In addition, $\boldsymbol{C}_3$ and $\boldsymbol{C}_4$ form a cycle of two components because they feed back and forth into each other. $\boldsymbol{C}_2$ and $\boldsymbol{C}_4$ have loops that connect them to themselves and are inner dependent. All other connections represent dependence between components which are thus known to be outer dependent.

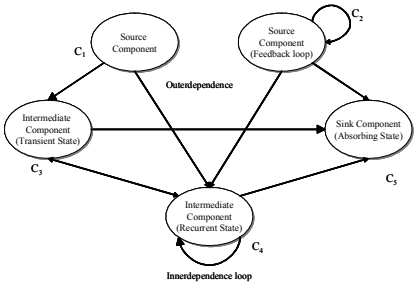

Source: [26]
Fig. 3. Connections in a network

A component of a decision network which was derived by the DEMATEL, it will be denoted by $\boldsymbol{C}_i, i=1,\cdots,m,$ and assume that it has n_h elements, which we denote by $e_{h1}, e_{h2},\cdots, e_{hm}$. The influences of a given set of elements in a component on any element in the decision system are represented by a ratio scale priority vector derived from paired comparisons of the comparative importance of one criterion and another criterion with respect to the interests or preferences of the decision makers. This relative importance value can be determined using a scale of 1–9 to represent equal importance to extreme importance [26-29]. The influence of elements in the network on other elementsin that network can be represented in the following supermatrix:

$$\boldsymbol{W} = \begin{array}{c} \\ \boldsymbol{C}_1 \\ \\ \\ \boldsymbol{C}_2 \\ \\ \\ \boldsymbol{C}_2 \\ \\ \end{array} \begin{array}{c} \begin{array}{cccccccccc} \boldsymbol{C}_1 & & & \boldsymbol{C}_2 & & & \cdots & \boldsymbol{C}_m & & \\ e_{11} & \cdots & e_{1n_1} & e_{21} & \cdots & e_{2n_2} & \cdots & e_{m1} & \cdots & e_{mn_m} \end{array} \\ \begin{bmatrix} \boldsymbol{W}_{11} & & \boldsymbol{W}_{12} & & \cdots & \boldsymbol{W}_{1m} \\ \boldsymbol{W}_{21} & & \boldsymbol{W}_{22} & & \cdots & \boldsymbol{W}_{2m} \\ \vdots & & \vdots & & \ddots & \vdots \\ \boldsymbol{W}_{m1} & & \boldsymbol{W}_{m2} & & \cdots & \boldsymbol{W}_{mm} \end{bmatrix} \end{array}$$

A typical entry $\boldsymbol{W}_{ij}$ in the supermatrix, is called a block of the supermatrix in the following form where each column of $\boldsymbol{W}_{ij}$ is a principal eigenvector of the influence of the elements in the i^{th} component of the network on an element in the j^{th} component. Some of its entries may be zero corresponding to those elements that have no influence.

$$\boldsymbol{W}_{ij} = \begin{bmatrix} w_{i_1 j_1} & w_{i_1 j_2} & \cdots & w_{i_1 j_{n_j}} \\ w_{i_2 j_2} & w_{i_2 j_2} & \cdots & w_{i_2 j_{n_j}} \\ \vdots & \vdots & \ddots & \vdots \\ w_{i_{n_i} j_1} & w_{i_{n_i} j_2} & \cdots & w_{i_{n_i} j_{n_j}} \end{bmatrix}$$

After forming the supermatrix, the weighted supermatrix is derived by transforming all columns sum to unity exactly. This step is very much similar to the concept of the Markov chain in terms of ensuring that the sum of these probabilities of all states equals 1. Next, the weighted supermatrix is raised to limiting powers, such as Equation (5) to get the global priority vector or called weights [4].

$$\lim_{\theta\to\infty} \boldsymbol{W}^{\theta} \tag{7}$$

In addition, if the supermatrix has the effect of cyclicity, the limiting supermatrix is not the only one. There are two or more limiting supermatrices in this situation, and the Cesaro sum would need to be calculated to get the priority. The Cesaro sum is formulated as follows.

$$\lim_{\psi\to\infty} (\frac{1}{\nu}) \sum_{j=1}^{\nu} \boldsymbol{W}_j^{\psi} \tag{8}$$

To calculate the average effect of the limiting supermatrix (i.e. the average priority weights) where $\boldsymbol{W}_j$ denotes the j^{th} limiting supermatrix. Otherwise, the supermatrix would be raised to large powers to get the priority weights [10] The weights of the k^{th} criterion derived by using the above ANP processes, namely ω_k, $k \in \{1,2,...,n\}$, will be regard as the weight of the k^{th} criterion.

D. VIKOR

VIKOR was proposed by Opricovic [6] and is a method to develop for multi-criteria optimization of complex systems. It determines the compromise ranking list and the compromise solution obtained with the initial (given) weights [16]. For

example from Figure 3-6, f_1^* (the ideal value of the first assessment criterion) and f_2^* (the ideal value of the second criterion) cannot reach f^* (ideal solution) at the same time. And the compromised solution is a point on the curve. f^c is closest to the ideal solution (f^*) among all non-inferior solutions. And therefore, the optimum compromised solution is: $f^c = f_1^c, f_2^c$. The steps of applying VIKOR are shown as follows [25]:

Step 1: Determine the ideal (best) solution (f_1^*) and the negative (worst) ideal solution (f_i^-) values of all criterion functions, $i = 1,2,\ldots n$. If the i th function represents a benefit then:

$$f_i^* = [(\max_j f_{ij} | i \in I_1) , (\min_j f_{ij} | i \in I_2)] , \forall_i \quad (9)$$

$$f_i^- = [(\min_j f_{ij} | i \in I_1) , (\max_j f_{ij} | i \in I_2)] , \forall_i \quad (10)$$

Step 2: Compute the values S_j and R_j , $j = 1,2,\ldots J$, by the relations

$$S_j = \sum_{i=1}^{n} w_i (f_i^* - f_{ij}) / (f_i^* - f_i^-) \quad (11)$$

$$R_j = \max_i \left[w_i (f_i^* - f_{ij}) / (f_i^* - f_i^-) \right] , \ j = 1,2,\ldots.J \quad (12)$$

where w_i are the weights of criteria, expressing their relative importance.

Step 3: Compute the values Q_j , $j = 1,2,\ldots J$, by the relation

$$Q_j = v(S_j - S^*) / (S^- - S^*) + (1-v)(R_j - R^*) / (R^- - R^*) \quad (14)$$

where $S^* = \min_j S_j$ $S^- = \max_j S_j$, $R^* = \min_j R_j$, $R^- \max_j R_j$

and v is introduced as a weight for the strategy of maximum group utility, whereas 1- v is the weight of the individual regret.

Step 4: Rank the alternatives, sorting by the values S , Q and R , in decreasing order. The results are three ranking lists.

Step 5: Propose as a compromise the alternative ($a^{'}$) which is ranked the best by the measure Q (minimum) if the following two conditions are satisfied:

C1. Acceptable advantage: $Q(a'')-Q(a') \geqq DQ$ where $a^{''}$ is the alternative with second position in the ranking list by Q ; $DQ = 1/(J-1)$; J is the number of alternatives.

C2. Acceptable stability in decision making: Alternative a′ must also be the best ranked by S or/and R . This compromise solution is stable within a decision making process, which could be: "voting by majority rule" (when $v > 0.5$ is needed), or "by consensus" $v \approx 0.5$, or "with veto" $v < 0.5$ .Here, v is the weight of the decision making strategy "the majority of criteria" (or "the maximum group utility").

If one of the conditions is not satisfied, then a set of compromise solutions is proposed, which consists of:

- Alternatives a′ and a″ if only condition C2 is not satisfied.
- Alternatives a′, a″,… $a^{(M)}$ if condition C1 is not satisfied; and $a^{(M)}$ is determined by the relation $Q(a^{(M)}) - Q(a^{'}) < DQ$ for maximum M (the positions of these alternatives are "in closeness").

According to Tzeng [8], the compromise solution is determined by the compromise-ranking method; the obtained compromise solution could be accepted by the decision makers because it provides maximum group utility of the majority (represented by min S , Eq. (11)), and minimum individual regret of the opponent (represented by min Q , Eq. (12)). The VIKOR algorithm determines the weight stability intervals for the obtained compromise solution with the input weights given by the experts.

IV. EMPIRICAL STUDY IN R&D FUNCTION

Following, an empirical study based on one of the world's leading IT company will be used for demonstrating the feasibility of the proposed hybrid MCDM framework. Managers for manufacturing sites will be evaluated and expatriated.

Ten experts with more than five years working experiences in globalized IT firms were invited to evaluate each of the first sixteen criteria. Those sixteen criteria include work experience (c_1), educational degree (c_2), language skill (c_3), age and sexuality (c_4), creativity (c_5), execution (c_6), communication (c_7), leadership (c_8), personal willingness (c_9), personal health (c_{10}), compensation (c_{11}), family support (c_{12}), loyalty (c_{13}), integrity (c_{14}), social skill (c_{15}) and cross-culture skill (c_{16}). The IRM can be derived then based on the DEMATEL. Furthermore, based on the ANP being introduced in Section 3, the weights versus each criterion can be derived. Based on the IRM being derived by the DEMATEL, the ANP method can be applied for calculating the weight versus each criterion. Pair-wise comparison results for the importance level of criteria being connected to the same goal are deprived according to experts' opinions and were provided as inputs for the ANP. The Super Decision [26] was used for deriving the weights (TABLE I).

TABLE I. The weights versus the criteria

Criteria	c_1	c_2	c_3	c_4	c_5	c_6	c_7	c_8
Weight	0.061	0.059	0.138	0.000	0.039	0.105	0.109	0.082
Criteria	c_9	c_{10}	c_{11}	c_{12}	c_{13}	c_{14}	c_{15}	c_{16}
Weight	0.113	0.037	0.000	0.021	0.056	0.054	0.126	0.000

Finally, the manager for an overseas manufacturing site can be evaluated and prioritized. According to Table II, the ranking results between all alternatives. The candidate C is the best one due to its lowest value in R-measure.

TABLE II. Results of ranking alternatives

Candidate	A	B	C
S	0.582	1.065	0.466
Q	0.138	0.808	0.109
R	0.118	1.000	0.000
Rank	2	3	1

V. DISICUSSION

In order to develop and sustain the global competitive advantage, appropriate international human resources management strategies should be adopted by MNEs. The appropriate expatriate manager selection is the very beginning step for the success of the international human resources management.

Based on the empirical study results, the language skill (0.138), social skills (0.126), personal willingness (0.113), communication skills (0.109), and execution capabilities (0.105) were regarded as the most important criteria. Except for the well-recognized including language skill et al., execution was selected as one of the important criteria albeit very little literature mentioned this criterion.

The criteria being neglected are worth discussing also. In this research, age, sexuality, creativity, personal health, compensation, as well as cross-culture skill was neglected. For the high technology firms being located in both Taiwan and China, since most managers got graduate degrees, their tendency to despise younger or female managers are less significant. Further, since the most Taiwanese IT company mainly focuses on process innovation aiming at cost reduction instead of product innovation, creativity is regarded as an non-important factor. For the neglect of health, compensation and family support, since most Taiwanese or mainland Chinese IT firms usually adopt the low cost strategy instead of differentiation, since there is almost nothing to be differentiated. Managers in such Asian firms usually neglected their personal health and family life.

Based on the results, the expatriates need to constantly enhance their professional skills and develop the potential energy by MNE training. The integrated training of the expatriates should be included manpower development, management development, career development, pre-departure training, and preview of the expatriate position, cultural awareness, language training and pre-departure practices.

In comparison with the traditional Fuzzy AHP based MCDM framework, the hybrid MCDM model consisting of the Delphi, the DEMATEL, the ANP, and the VIKOR was designed to overcome (1) the global expatriate selection issue, (2) traditional MCDM approaches for evaluating the global expatriate selection problem based on the wrong assumptions on the independence between the determinants, (3) the concept of the VIKOR which can be used to derive the optimal strategy which is closest to the ideal solution. Through the case study, we found the hybrid MCDM model to be applicable.

VI. CONCLUSSIONS

In the era of globalization, appropriate expatriate manager selections are critical conditions for the success of overseas operations. In this research, a hybrid MCDM framework consisting of the DEMATEL, the ANP and the VIKOR was proposed for selecting an appropriate expatriate manager for overseas manufacturing sites. An empirical study being modified from a real situation of a leading IT firm was introduced for verifying the feasibility of the proposed framework. In the future, the proposed framework can be applied on other expatriate selection problems. Meanwhile, further researches on the criteria being neglected during the evaluation process, including age, sexuality, compensation, cross-culture skill and etc. worth investigations.

REFERENCES

[1] A. Gabus and E. Fontela, *World Problems, an Invitation to Further Thought Within the Framework of DEMATEL*. Geneva, Switzerland: Batelle Geneva Research Center, 1972.

[2] C. A. Bartlett and S. Ghoshal, *Transnational management: text, cases and readings in cross-border management*. Boston: McGraw-Hill, 2000.

[3] C. Solomon, "Helping hand pulls global inpatriates onboard" *Personnel Journal*, vol. 74, no.1, pp. 40-49, 1995.

[4] C. J. Lin and W. W. Wu, "A causal analytical method for group decision-making under fuzzy environment," *Expert Systems with Applications,* vol. 34, no.1, pp. 205-213, 2008.

[5] C. Y. Huang, J.Z. Shyu and G.H. Tzeng, "Reconfiguring the Innovation Policy Portfolios for Taiwan 's SIP Mall Industry," *Technovation,* vol. 27, pp. 744-765, 2007.

[6] E. Ofek and M. Sarvary, "R&D, marketing, and the success of next-generation products," *Marketing Science,* vol. 22, no. 3, pp. 355-370, 2003.

[7] G. H. Tzeng, C. W. Lin and S. Opricovic, "Multi-criteria analysis of alternative-fuel buses for public transportation," *Energy Policy*, vol. 33, pp. 1373-1383, 2005.

[8] G. H. Tzeng, M. H. Teng, J. J. Chen and S. Opricovicc, et al., "Multicriteria selection for a restaurant location in Taipei," *International Journal of Hospitality Management*, vol. 21, pp. 171-187, 2002.

[9] J. Calof and P. Beamish, "The right attitude for international success," *Business Quality,* vol. 59, pp. 105-110, 1994.

[10] J.-J. Huang, G.H. Tzeng and C.S. Ong, "Multidimensional data in multidimensional scaling using the analytic network process," *Pattern Recognition Letters,* vol. 26, pp. 755-767, 2005.

[11] J. J. H. Liou, G. H. Tzeng & H. C. Chang, "Airline safety measurement using a hybrid model," Journal of Air Transport Management, vol.13, no. 4, pp.243-249, 2007.

[12] J. W. Murry and J. O. Hammons, "Delphi: A versatile methodology for conducting qualitative research. ," *The Review of Higher Education,* vol. 18, pp. 423-436, 1995.

[13] L. G. Mejia and R. M. Wiseman, "Reframing executive compensation: An assessment and outlook," *Journal of Management*, vol. 23, no.3, pp. 291-374, 1997.

[14] L. K. Stroh and P. M. Caligiuri, "Strategic human resource: A new source for competitive advantage in the global arena," *International Journal of Human Resource Management,* vol. 9, pp. 13-17, 1998.

[15] M. A. Hitt, B. B. Tyler, C. Hardee & D. Park, "Understanding the differences in Korean and U.S. executives' strategic orientations," *Academy of Management Executive*, vol. 9, no. 2, pp. 12-19, 1997.

[16] M. K. Sayadi, M. Heydari and K. Shahanaghi, "Extension of VIKOR method for decision making problem with interval numbers," *Applied Mathematical Modelling*, vol. 33, no. 5, pp. 2257-2262, 2009.

[17] M. Janssens, "Evaluating international managers' performance: Parent company standards as a control mechanism," *The International Journal of Human Resource Management,* vol. 5, pp. 853-873, 1994.

[18] M. Tamura, H. Nagata and K. Akazawa, "Extraction and systems analysis of factors that prevent safety and security by structural models," in *Proceedings of the 41st SICE Annual Conference, Volume 3.*, Osaka, Japan, 2002, pp. 1752-1759.

[19] N. Dalkey and O. Helmer, "An experimental application of the Delphi method to the use of experts," *Management Science,* vol. 9, pp. 458-467, 1963.

[20] N. Adler and F. Ghadar, "Strategic human resource management: A global perspective," *Human Resource Management,* vol. 11, pp. 205-206, 1990.

[21] P. M. Wright and G. C. McMahan, "Theoretical perspectives for strategic human resource management," *Journal of Management,* vol. 18, pp. 295-320, 1992.

[22] R. L. Tung and S. J. Haviovic, "Human resource management in transitional economies: The case of Poland the Czech Republic," *The International Journal of Human Resource Management,* vol. 7, pp. 1-17, 1996.

[23] S. A. Snell and M. A. Youndt, "Human resource management and finn performance: Testing a contingency model of executive control," *Journal of Management*, vol. 21, no. 4, pp. 711-737, 1995.

[24] S. Ferkertich, "Focus on psychometrics: internal consistency estimates of reliability," *Research in Nursing & Health,* vol. 13, pp. 437-440, 1990.

[25] S. Opricovic and G. H. Tzeng, "Extended VIKOR method in comparison with outranking methods," *European Journal of Operational Research,* vol. 178, pp. 514-529, 2007.

[26] T. L. Saaty, *Decision Making with Dependence and Feedback: The Analytic Network Process*. Pittsburgh: RWS Publication, 1996.

[27] T. L. Saaty, *Theory and Applications of the Analytic Network Process - Decision Making with Benefits, Opportunities, Costs, and Risks*. Pittsburg, PA: RWS Publications, 2005.

[28] T. L. Saaty, "Fundamentals of the analytic network process - dependence and feedback in decision-making with a single network," *Journal of Systems Science and Systems Engineering,* vol. 13, pp. 71-91, 2004.

[29] T. L. Saaty, "Fundamentals of the Analytic Network Process," *in Proceedings of International Symposium on Analytical Hierarchy Process,* Japan, Kobe, 1999.

[30] T.W. Malnight, "The transition from decentralized to network-based MNC structures: An evolutionary perspective," *Journal of International Business Studies*, vol. 27, no. 1, pp. 43-65, 1996.

[31] Y.-J. Chiu, H.C. Chen, J.Z. Shyu and G.H. Tzeng, "Marketing strategy based on customer behaviour for the LCD-TV," *International Journal of Management and Decision Making*, vol. 7, pp. 143-165, 2006.

2011 IEEE International Conference on Fuzzy Systems
June 27-30, 2011, Taipei, Taiwan

On the Geometry of Join and Meet Calculations for General Type-2 Fuzzy Sets

Jerry M. Mendel, *Life Fellow, IEEE*
Signal and Image Processing Institute
University of Southern California
Los Angeles, CA, USA
mendel@sipi.usc.edu

***Abstract*—The union and intersection of general type-2 fuzzy sets (T2 FSs) are fundamental computations for such FSs. In the past, algorithms were developed for the union and intersection computations using vertical-slice and horizontal-slice representations of T2 FSs. The vertical-slice representation of a T2 FS traces its origins back to Zadeh [32] and requires computing the join or meet, whereas the horizontal-slice representation of a T2 FS is very recent, traces its origins to Liu [14], and requires computing the join and meet only for interval T2 FSs that are raised to level alpha, for which closed-form formulas are available [15]. In this paper, by studying the join and meet geometrically for general T2 FSs, we show that for many situations closed-form formulas exist for them. We also show that the formulas for computing the union and intersection of general T2 FSs that were derived from the horizontal-slice representation of a T2 FS [19] can also be obtained directly from geometrical interpretations of formulas that were derived by Karnik and Mendel [12] for the vertical-slice representation of a T2 FS.**

Keywords-Type-2 fuzzy sets, union, intersection, join, meet

I. INTRODUCTION

The use of general type-2 fuzzy sets (T2 FSs) in T2 fuzzy systems has the potential to let such fuzzy systems outperform comparable T2 fuzzy systems that only use interval type-2 fuzzy sets (IT2 FSs). This is because a general T2 FS makes full use of its third dimension, whereas an interval T2 FS does not. Consequently, there is now renewed attention at all aspects of general T2 FSs and fuzzy systems, including the computations of the three basic set-theoretic operations of intersection, union and complement [1]-[32]. This paper focuses only on the intersection and union operations, because they can be difficult to compute for general T2 FSs, whereas the complement is straightforward to compute.

Consider two T2 FSs sets [1] $\tilde{A}$ ($\mu_{\tilde{A}}: X\times[0,1]\rightarrow[0,1]$) and $\tilde{B}$ ($\mu_{\tilde{B}}: X\times[0,1]\rightarrow[0,1]$). $\tilde{A}$ and $\tilde{B}$ are described by 3D membership functions $\mu_{\tilde{A}}(x,u)$ ($x\in X$, $u\in U=[0,1]$) and $\mu_{\tilde{B}}(x,w)$ ($x\in X$, $w\in W=[0,1]$), respectively. They can also be expressed in terms of their respective *secondary membership functions*, $\mu_{\tilde{A}}(u\,|\,x)$ and $\mu_{\tilde{B}}(w\,|\,x)$, and *secondary grades*, $f_x(u)$ and $g_x(w)$, as:

$$\tilde{A}=\int_X \mu_{\tilde{A}}(u\,|\,x)/x=\int_X\left[\int_{U=[0,1]} f_x(u)/u\right]/x \tag{1}$$

and[1]

$$\tilde{B}=\int_X \mu_{\tilde{B}}(w\,|\,x)/x=\int_X\left[\int_{W=[0,1]} g_x(w)/w\right]/x \tag{2}$$

Note that $\mu_{\tilde{A}}(u\,|\,x)$ and $\mu_{\tilde{B}}(w\,|\,x)$ are T1 FSs, and are also called *vertical slices* of $\tilde{A}$ and $\tilde{B}$, respectively; hence (1) and (2) are called *vertical-slice representations of* $\tilde{A}$ and $\tilde{B}$.

It is well-known[2] [20] that the union of $\tilde{A}$ and $\tilde{B}$ is another T2 FS whose MF can be computed from:

$$\tilde{A}\cup\tilde{B}=\int_X \mu_{\tilde{A}\cup\tilde{B}}(v\,|\,x)/x \tag{3}$$

where

$$\begin{aligned}\mu_{\tilde{A}\cup\tilde{B}}(v\,|\,x)&=\int_{U=[0,1]}\int_{W=[0,1]} f_x(u)\bigstar g_x(w)/(v=u\vee w)\\ &\equiv \mu_{\tilde{A}}(u\,|\,x)\sqcup\mu_{\tilde{B}}(w\,|\,x)\quad x\in X\end{aligned} \tag{4}$$

in which $\sqcup$ denotes the *join* operation. The use of the notation $\mu_{\tilde{A}}(u\,|\,x)\sqcup\mu_{\tilde{B}}(w\,|\,x)$ to indicate the join between the secondary MFs $\mu_{\tilde{A}}(u\,|\,x)$ and $\mu_{\tilde{B}}(w\,|\,x)$ is, of course, a *shorthand notation* for the operations in the middle of (4). What (4) says is that to perform the join between two secondary MFs, $\mu_{\tilde{A}}(u\,|\,x)$ and $\mu_{\tilde{B}}(w\,|\,x)$, $v=u\vee w$ must be computed between every possible pair of primary memberships u and w, such that $u\in U$ and $w\in W$, and that the secondary grade of $\mu_{\tilde{A}\cup\tilde{B}}(v\,|\,x)$ must be computed as the *t*-norm operation between the corresponding secondary grades of $\mu_{\tilde{A}}(u\,|\,x)$ and $\mu_{\tilde{B}}(w\,|\,x)$, $f_x(u)$ and $g_x(w)$, respectively. Note that at each value of x the join involves T1 FSs (i.e.,

[1] When a secondary MF, e.g. $\mu_{\tilde{A}}(u\,|\,x)$, has support that does not have gaps (the support of a T1 FS is the set of values of its primary variable for which that MF is > 0), then it has been customary in the past to denote that support as J_x^u, and to call it the *primary membership*. This notation, which has been called into question in [1], is not used herein because it is not needed. Note, also, that in the past the notation $\mu_{\tilde{A}}(x)$ has been used (e.g., [15]) as a shorthand notation for $\mu_{\tilde{A}}(u\,|\,x)$. We now prefer to use $\mu_{\tilde{A}}(u\,|\,x)$ because it shows the explicit dependence of $\mu_{\tilde{A}}$ on its functional argument u.

[2] Some of the material in this section is taken from [16] and [19].

secondary MFs), and that the join must be computed for $\forall x \in X$. If more than one combination of u and w gives the same point $u \vee w$, then in the join we keep the one with the largest membership grade. Usually, the maximum *t*-conorm is used, as suggested in [32] and [20].

In general, evaluating the join is difficult to do for arbitrary T2 FSs. Karnik and Mendel [12] have shown that for n convex and normal (secondary) T1 FSs, $F_1,...,F_n$, characterized by MFs $f_1(\theta \mid x)$,...,$f_n(\theta \mid x)$, respectively, where $f_1(v_1 \mid x) = \ldots = f_n(v_n \mid x) = 1$, and the $f_i(\theta \mid x)$ are re-ordered so that $v_1 \le v_2 \le \cdots \le v_n$, the MF of $\sqcup_{i=1}^{n} F_i$, using maximum *t*-conorm ($\vee$) and either minimum or product *t*-norm (T), can be expressed as ($\forall x \in X$):

$$\mu_{\sqcup_{i=1}^{n} F_i}(\theta \mid x) = \begin{cases} T_{i=1}^{n} f_i(\theta \mid x) & \theta < v_1 \\ T_{i=k+1}^{n} f_i(\theta \mid x) & v_k \le \theta \le v_{k+1} \\ \vee_{i=1}^{n} f_i(\theta \mid x) & \theta > v_n \end{cases} \quad 1 \le k \le n-1 \quad (5)$$

Coupland and John [4]-[8] have taken a very new and novel approach to computing the join. Because their approach is also used for computing the meet, we describe it later in this section.

It is also well known [20] that the intersection of $\tilde{A}$ and $\tilde{B}$ is another T2 FS whose MF can be computed from:

$$\tilde{A} \cap \tilde{B} = \int_X \mu_{\tilde{A} \cap \tilde{B}}(v \mid x) / x \quad (6)$$

where

$$\begin{aligned} \mu_{\tilde{A} \cap \tilde{B}}(v \mid x) &= \int_{U=[0,1]} \int_{W=[0,1]} f_x(u) \bigstar g_x(w) / (v = u \wedge w) \\ &\equiv \mu_{\tilde{A}}(u \mid x) \sqcap \mu_{\tilde{B}}(w \mid x) \quad x \in X \end{aligned} \quad (7)$$

in which $\sqcap$ denotes the *meet* operation. The use of the notation $\mu_{\tilde{A}}(u \mid x) \sqcap \mu_{\tilde{B}}(w \mid x)$ to indicate the meet between the secondary MFs $\mu_{\tilde{A}}(u \mid x)$ and $\mu_{\tilde{B}}(w \mid x)$ is another *shorthand notation*, but this time for the operations in the middle of (7). What (7) says is that to perform the meet between two secondary MFs, $\mu_{\tilde{A}}(u \mid x)$ and $\mu_{\tilde{B}}(w \mid x)$, $v = u \wedge w$ must be performed between every possible pair of primary memberships u and w, such that $u \in U$ and $w \in W$, and the secondary grade of $\mu_{\tilde{A} \cap \tilde{B}}(v \mid x)$ must be computed as the *t*-norm operation between the corresponding secondary grades of $\mu_{\tilde{A}}(u \mid x)$ and $\mu_{\tilde{B}}(w \mid x)$, $f_x(u)$ and $g_x(w)$, respectively. This must be done for $\forall x \in X$. If more than one combination of u and w gives the same point $u \wedge w$, then in the meet (just as in the join) we keep the one with the largest membership grade.

Note that in (7) there are two t-norms, $\bigstar$ and $\wedge$. Although they are usually chosen to be the same, they do not have to be. See Starczewski [23] for very interesting discussions about this.

In general, evaluating the meet is also difficult to do for arbitrary T2 FSs, especially when the product *t*-norm is used in both places in (7). Karnik and Mendel [20] have also shown that for n convex and normal T1 FSs, $F_1,...,F_n$, characterized by MFs $f_1(\theta \mid x)$,...,$f_n(\theta \mid x)$, respectively, where $f_1(v_1 \mid x) = \ldots = f_n(v_n \mid x) = 1$, and the $f_i(\theta \mid x)$ are re-ordered so that $v_1 \le v_2 \le \cdots \le v_n$, the MF of $\sqcap_{i=1}^{n} F_i$ using maximum *t*-conorm and minimum *t*-norm can be expressed as ($\forall x \in X$):

$$\mu_{\sqcap_{i=1}^{n} F_i}(\theta \mid x) = \begin{cases} \vee_{i=1}^{n} f_i(\theta \mid x) & \theta < v_1 \\ \wedge_{i=1}^{k} f_i(\theta \mid x) & v_k \le \theta \le v_{k+1} \\ \wedge_{i=1}^{n} f_i(\theta \mid x) & \theta > v_n \end{cases} \quad 1 \le k \le n-1 \quad (8)$$

The usual derivations of (4) and (7) utilize Zadeh's extension principle. Mendel and John [18] show how (4) and (7) can easily be derived without having to use the Extension Principle.

Because (4) and (7) compute the join and meet of T2 FSs one vertical slice at a time, we shall refer to them as *vertical-slice computations*.

Coupland and John [7, 8] have shown how to compute the join and meet of $\tilde{A}$ and $\tilde{B}$ using methods from computational geometry (e.g., a modified Weiler-Atherton clipping algorithm, and a Bentley-Ottman plane sweep algorithm). Their approach is based on modeling a secondary MF geometrically as a [9] "set of connected straight line segments that need not be equally-spaced across the domain," and is limited so far to the minimum t-norm and the maximum *t*-co-norm.

Even more recently, Greenfield and John [9] presented an optimized grid method for computing the join and meet, one that is much more computationally efficient than a direct approach to using (5) and (8).

A limitation of the geometric and grid methods is they do not obtain closed-form formulas for the join and meet operations. Such formulas can be very useful when a type-2 fuzzy logic system is designed by optimizing an objective function with respect to MF parameters, and explicit derivatives of that function have to be computed so that optimal values of those parameters can be found.

When secondary MFs are triangular (an interesting compromise between interval secondary MFs and general secondary MFs, and one that is also considered by Coupland and John [7]) then Starczewski [22, 24] has shown that "extended *t*-norms[3] of triangular fuzzy truth values may be approximated by triangular fuzzy truth values as well." One of the most interesting aspects of Starczewski's [24] approach is it "… reduces calculations of extended *t*-norms (a similar approach can be rearranged for *s*-norms) to computing only the three characteristic functions: principal, upper and lower. Arbitrary traditional *t*-norms (or *s*-norms) can be used to calculate these functions. A tremendously useful feature of this approach is that the resultant MF preserves triangular shapes of the two arguments, and this way the approximate *t*-norms can be expanded to multi-argument form. Moreover, for

[3] An extended *t*-norm is a *t*-norm obtained by applying the Extension Principle to a T1 *t*-norm. It was the basis for Mizumoto and Tanaka's [20] works.

each triangular fuzzy membership grade only three parameters have to be stored and processed by [a] FLS, instead of tabularized functions as in the general approach." Another very useful feature of this approach is that formulas are given for the operations, so that explicit derivative formulas can be obtained if a triangular T2 FLS is designed (optimized) using a method that requires such derivatives (e.g., steepest descent).

Recently, Liu [14] presented a horizontal-slice[4] α-plane representation for a general T2 FS. This was further elaborated upon in [19, 17]. Related works are in [27], [29] and [30]. Using this new representation, described next, it is possible to compute the union and intersection of general T2 FSs one α-plane at a time.

Definition 1. An *α-plane* for the general T2 FS $\tilde{A}$, denoted $\tilde{A}_\alpha$, is the union of all primary memberships of $\tilde{A}$ whose secondary grades are greater than or equal to α ($0 \le \alpha \le 1$), i.e. [14]

$$\begin{aligned}\tilde{A}_\alpha &= \left\{(x,u), \mu_{\tilde{A}}(x,u) \ge \alpha \,\middle|\, \forall x \in X, \forall u \in U = [0,1]\right\} \\ &= \int_{\forall x \in X} \int_{\forall u \in U=[0,1]} \{(x,u) \,|\, f_x(u) \ge \alpha\}\end{aligned} \quad \blacksquare \quad (9)$$

Let[5] $S_{\tilde{A}_\alpha}(x)$ denote an α-cut of the secondary MF $\mu_{\tilde{A}}(u \,|\, x)$, i.e.,

$$S_{\tilde{A}_\alpha}(x) = [\underline{\mu}_{\tilde{A}_\alpha}(x), \overline{\mu}_{\tilde{A}_\alpha}(x)] \quad (10)$$

where $\underline{\mu}_{\tilde{A}_\alpha}(x)$ is the lower MF of $\tilde{A}_\alpha$ at x and $\overline{\mu}_{\tilde{A}_\alpha}(x)$ is the upper MF of $\tilde{A}_\alpha$ at x, i.e.:

$$\underline{\mu}_{\tilde{A}_\alpha}(x) = \inf\left\{u \,|\, u \in [0,1], \mu_{\tilde{A}}(x,u) \ge \alpha\right\} \quad (11)$$

$$\overline{\mu}_{\tilde{A}_\alpha}(x) = \sup\left\{u \,|\, u \in [0,1], \mu_{\tilde{A}}(x,u) \ge \alpha\right\} \quad (12)$$

Then, another way to express $\tilde{A}_\alpha$ is:

$$\tilde{A}_\alpha = \int_{\forall x \in X} S_{\tilde{A}_\alpha}(x)/x = \int_{\forall x \in X} \left(\int_{\forall u \in [\underline{\mu}_{\tilde{A}_\alpha}(x), \overline{\mu}_{\tilde{A}_\alpha}(x)]} u \right) / x \quad (13)$$

Definition 2. The *α-plane Representation* for $\tilde{A}$ is [14]:

$$\tilde{A} = \bigcup_{\alpha \in [0,1]} \alpha / \tilde{A}_\alpha \quad \blacksquare \quad (14)$$

In (14), $\alpha / \tilde{A}_\alpha$ denotes $\tilde{A}_\alpha$ raised to level α, is called[6] an α-level T2 FS, and is an IT2 FS whose secondary grades equal α instead of 1 (as would be the case for the usual IT2 FS). This suggests, and is indeed the case, that operations involving T2 FSs can be performed using readily available operations for IT2 FSs. Note that $\alpha / \tilde{A}_\alpha$ is called a *zSlice* by Wagner and Hagras [29, 30].

Let $(\tilde{A} \cup \tilde{B})_\alpha$ and $(\tilde{A} \cap \tilde{B})_\alpha$ be the α-planes of $\tilde{A} \cup \tilde{B}$ and $\tilde{A} \cap \tilde{B}$, respectively. For the minimum t-norm [i.e., the star in (4) and (7)], it is true that [14], [19]:

$$\tilde{A} \cup \tilde{B} = \bigcup_{\alpha \in [0,1]} \alpha / (\tilde{A} \cup \tilde{B})_\alpha = \bigcup_{\alpha \in [0,1]} \alpha / \tilde{A}_\alpha \cup \tilde{B}_\alpha \quad (15)$$

$$\tilde{A} \cap \tilde{B} = \bigcup_{\alpha \in [0,1]} \alpha / (\tilde{A} \cap \tilde{B})_\alpha = \bigcup_{\alpha \in [0,1]} \alpha / \tilde{A}_\alpha \cap \tilde{B}_\alpha \quad (16)$$

To-date, comparable results for other star t-norms, such as the product, are not available; however, any conjunction can be used in the meet, e.g., minimum or product.

To compute, e.g., $\tilde{A}_\alpha \cup \tilde{B}_\alpha$, for each value of α and $\forall x \in X$:

1. Compute $\tilde{A}_\alpha$ and $\tilde{B}_\alpha$, the results of which are two planes that are bounded by their respective lower and upper MFs, $\underline{\mu}_{\tilde{A}_\alpha}(x)$, $\overline{\mu}_{\tilde{A}_\alpha}(x)$, $\underline{\mu}_{\tilde{B}_\alpha}(x)$ and $\overline{\mu}_{\tilde{B}_\alpha}(x)$
2. *Compute $\tilde{A}_\alpha \cup \tilde{B}_\alpha$, as:*

$$\tilde{A}_\alpha \cup \tilde{B}_\alpha = [\underline{\mu}_{\tilde{A}_\alpha \cup \tilde{B}_\alpha}(x), \overline{\mu}_{\tilde{A}_\alpha \cup \tilde{B}_\alpha}(x)] \quad (17)$$

where

$$\underline{\mu}_{\tilde{A}_\alpha \cup \tilde{B}_\alpha}(x) = \underline{\mu}_{\tilde{A}_\alpha}(x) \vee \underline{\mu}_{\tilde{B}_\alpha}(x) \quad (18)$$

$$\overline{\mu}_{\tilde{A}_\alpha \cup \tilde{B}_\alpha}(x) = \overline{\mu}_{\tilde{A}_\alpha}(x) \vee \overline{\mu}_{\tilde{B}_\alpha}(x) \quad (19)$$

To compute $\tilde{A}_\alpha \cap \tilde{B}_\alpha$, simply replace $\tilde{A}_\alpha \cup \tilde{B}_\alpha$ in (17) – (19) by $\tilde{A}_\alpha \cap \tilde{B}_\alpha$, and $\vee$ in (18) and (19) by $\wedge$.

Because (15) and (16) compute the union and intersection of T2 FSs one horizontal slice at a time (i.e., one α-plane at a time), we shall refer to them as either *horizontal-slice* or *α-plane computations*.

In this paper we connect results that can be obtained from using (5) and (15) for the union of two T2 FSs, and (8) and (16) for the intersection of two T2 FSs, i.e. we connect the vertical-slice and horizontal-slice computations. In order to do this, we first study the geometry of the join and meet when (5) and (15) are used. Our purpose for doing these things is to *provide more insight into computations of the join and meet* and to *provide a new derivation of (15) and (16) directly from (5) and (8)*.

[4] Because a horizontal slice is analogous to an α-cut of a T1 FS, it is called the *α-plane representation* for a T2 FS.

[5] [19] uses the notations $S_{\tilde{A}}(x \,|\, \alpha)$, $s_L(x \,|\, \alpha)$ and $s_R(x \,|\, \alpha)$ for $S_{\tilde{A}_\alpha}(x)$, $\underline{\mu}_{\tilde{A}_\alpha}(x)$ and $\overline{\mu}_{\tilde{A}_\alpha}(x)$, respectively. Our notation is more consistent with the notation that has been proposed in [1], which is why we use it.

[6] In [19] $\alpha / \tilde{A}_\alpha$ is called the *footprint of uncertainty (FOU) of the α-plane*. As explained in [17], this is a misnomer, because an FOU lies on the 2D support of the MF of $\tilde{A}$, which corresponds to the $\tilde{A}_0$-plane.

II. GEOMETRY OF THE JOIN AND MEET: VERTICAL-SLICE COMPUTATIONS

It is straightforward to re-express (5) and (8) recursively, so that their computations are done two type-2 fuzzy sets at a time; hence, in order to study the geometry of join and meet, we focus on (5) and (8) at *any* $x \in X$ for two T2 FSs, $\tilde{A}$ and $\tilde{B}$, as defined in (1) and (2), respectively. For two T2 FSs, letting $F_1 \equiv F$ and $F_2 \equiv G$, and using the minimum[7] t-norm, minimum for the conjunction operation and maximum for the disjunction operation, (5) and (8) simplify[8] to:

$$\mu_{F \sqcup G}(\theta) = \begin{cases} \min[f(\theta), g(\theta)] & \theta < v_0 \\ g(\theta) & v_0 \le \theta \le v_1 \\ \max[f(\theta), g(\theta)] & \theta > v_1 \end{cases} \tag{20}$$

$$\mu_{F \sqcap G}(\theta) = \begin{cases} \max[f(\theta), g(\theta)] & \theta < v_0 \\ f(\theta) & v_0 \le \theta \le v_1 \\ \min[f(\theta), g(\theta)] & \theta > v_1 \end{cases} \tag{21}$$

A. Geometry of the Join

To illustrate the geometry of the join, we chose triangle MFs for both $f(\theta)$ and $g(\theta)$, and then used (20) to compute $\mu_{F \sqcup G}(\theta)$. Note, however, that *our results are valid for all convex secondary MFs*.

It is easy to use (20) to obtain $\mu_{F \sqcup G}(\theta)$ for the (e.g.) nine different relative locations of $f(\theta)$ and $g(\theta)$ that are summarized in Table I. Additional cases can be obtained by interchanging $f(\theta)$ and $g(\theta)$, and this is left to the reader. Observe from these nine cases, that:

1. When $v_1 > v_0$, and $f(\theta)$ and $g(\theta)$ either do not intersect [cases (a) and (e)], or have exactly one intersection [cases (b) and (f)], then $\mu_{F \sqcup G}(\theta) = g(\theta)$, the right-most secondary MF.
2. When $v_1 = v_0 = 0$, and $g(\theta) \subseteq f(\theta)$ [case (d)], then $\mu_{F \sqcup G}(\theta) = f(\theta)$, the right-most secondary MF; if $f(\theta) \subseteq g(\theta)$ re-label $f(\theta)$ as $g(\theta)$ and vice-versa.
3. When $v_1 = v_0 \neq 0$, and $g(\theta) \subseteq f(\theta)$ [case (h)], then $\mu_{F \sqcup G}(\theta)$ involves both $f(\theta)$ and $g(\theta)$.
4. When $v_1 = v_0 \neq 0$, and the left leg of $f(\theta)$ is to the left of the left leg of $g(\theta)$, and the right leg of $f(\theta)$ is to the left of the right leg of $g(\theta)$ [case (i)], then $\mu_{F \sqcup G}(\theta) = g(\theta)$, the right-most secondary MF.
5. When $v_1 > v_0$ and $f(\theta)$ and $g(\theta)$ intersect at exactly two points [cases (c) and (g)], then $\mu_{F \sqcup G}(\theta)$ involves both $f(\theta)$ and $g(\theta)$. This is also true if $f(\theta)$ and $g(\theta)$ intersect at three points (see Fig. 2(a)).

Situations 1, 2 and 4 are interesting because solutions for the join are completely given and require no further computation. While this is interesting from an educational point of view, it may not be possible to easily carry out the tests for these cases in order to use these results in a computer implementation of these cases.

Situations 3 and 5 are also interesting because they let us focus on the situations when a computer solution for $\mu_{F \sqcup G}(\theta)$ will be required. It is only these situations that will be examined in Section III.

B. Geometry of the Meet

Table II summarizes $\mu_{F \sqcap G}(\theta)$ (computed from (21)) for triangle MFs for both $f(\theta)$ and $g(\theta)$, and for the same nine different relative locations of these MFs as in Table I. Observe from these nine cases, that:

1. When $v_1 > v_0$, and $f(\theta)$ and $g(\theta)$ either do not intersect [cases (a) and (e)], or have exactly one intersection [cases (b) and (f)], then $\mu_{F \sqcap G}(\theta) = f(\theta)$, the left-most secondary MF.
2. When $v_1 = v_0 = 0$, and $g(\theta) \subseteq f(\theta)$ [case (d)], then $\mu_{F \sqcap G}(\theta) = g(\theta)$, the left-most secondary MF; if $f(\theta) \subseteq g(\theta)$ re-label $f(\theta)$ as $g(\theta)$ and vice-versa.
3. When $v_1 = v_0 \neq 0$, and $g(\theta) \subseteq f(\theta)$ [case (h)], then $\mu_{F \sqcap G}(\theta)$ involves both $f(\theta)$ and $g(\theta)$.
4. When $v_1 = v_0 \neq 0$, and the left leg of $f(\theta)$ is to the left of the left leg of $g(\theta)$, and the right leg of $f(\theta)$ is to the left of the right leg of $g(\theta)$ [case (i)], then $\mu_{F \sqcap G}(\theta) = f(\theta)$, the left-most secondary MF.
5. When $v_1 > v_0$ and $f(\theta)$ and $g(\theta)$ intersect at exactly two points [cases (c) and (g)], then $\mu_{F \sqcap G}(\theta)$ involves both $f(\theta)$ and $g(\theta)$. This is also true if $f(\theta)$ and $g(\theta)$ intersect at three points (see Fig. 2(b)).

As for the join, Situations 1, 2 and 4 are interesting because solutions for the meet are completely given and require no further computation; however, it may not be possible to easily carry out the tests for these cases in order to use these results in a computer implementation of these cases.

Situations 3 and 5 are also interesting because they let us focus on the situations when a computer solution for $\mu_{F \sqcap G}(\theta)$

[7] It is straightforward to use the product t-norm in (5), something we leave to the readers [see also [26], in which (20) and (21) are re-derived; they are also extended to the product t-norm, but (21) is not extended to both the product t-norm and conjunction, a very difficult case that is considered in [12] but for which simple formula like (21) does not exist].

[8] In the rest of this paper, in order to be consistent with the notation in [15, Appendix A], we let $v_1 \to v_0$ and $v_2 \to v_1$. Additionally, f_x and g_x are shortened to f and g, and $\theta \mid x$ is shortened to θ, because we are focusing on (5) and (8) at *any* $x \in X$.

TABLE I

GEOMETRY OF THE JOIN: THE HEAVY LINES DENOTE $\mu_{F \sqcup G}(\theta)$

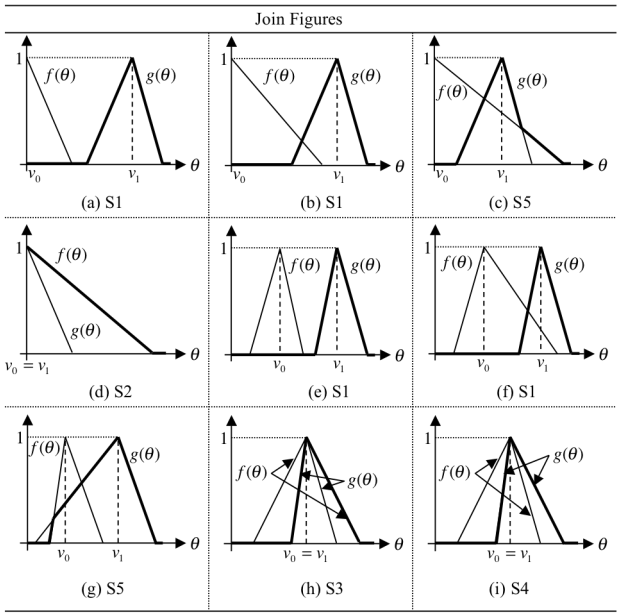

TABLE II

GEOMETRY OF THE MEET: THE HEAVY LINES DENOTE $\mu_{F \sqcap G}(\theta)$

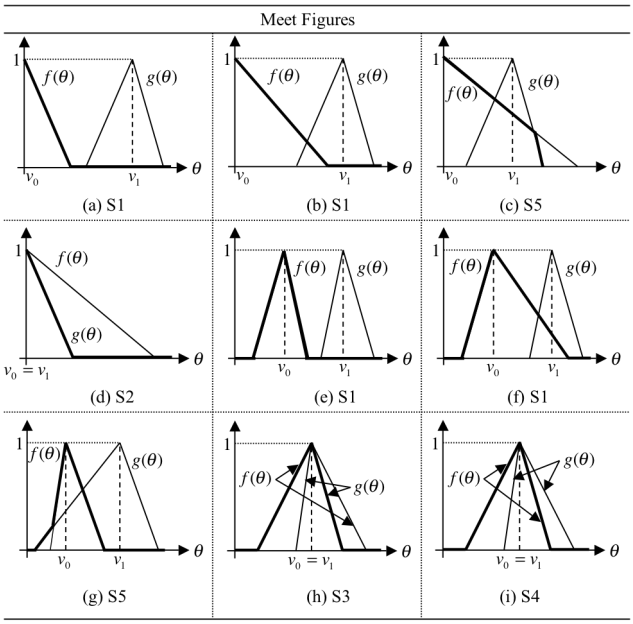

will be required. It is only these situations that will be examined in Section III.

C. Simple Rules

Based on the results in Tables I and II and the rules extracted from their figures that are given in Sections A and B, it is possible to arrive at the following simple rules:

1. If $v_1 > v_0$ and $f(\theta)$ and $g(\theta)$ do not intersect or only have one intersection, or, if $v_1 = v_0 = 0$ and $f(\theta) \subseteq g(\theta)$ [if $f(\theta) \subseteq g(\theta)$ re-label $f(\theta)$ as $g(\theta)$ and vice-versa], or if $v_1 = v_0 \neq 0$, and the left leg of $f(\theta)$ is to the left of the left leg of $g(\theta)$, and the right leg of $f(\theta)$ is to the left of the right leg of $g(\theta)$, then:

$$\begin{cases} \mu_{F \sqcup G}(\theta) = g(\theta) \\ \mu_{F \sqcap G}(\theta) = f(\theta) \end{cases} \tag{22}$$

2. If $v_1 = v_0 \neq 0$, and $g(\theta) \subseteq f(\theta)$, then, although $\mu_{F \sqcup G}(\theta)$ and $\mu_{F \sqcap G}(\theta)$ involve both $f(\theta)$ and $g(\theta)$, no computer solutions are needed to compute them.
3. If $v_1 > v_0$ and $f(\theta)$ and $g(\theta)$ intersect at exactly two or more points, that $\mu_{F \sqcup G}(\theta)$ and $\mu_{F \sqcap G}(\theta)$ involve both $f(\theta)$ and $g(\theta)$, and require computer solutions.

Although these rules are obtained above for triangle secondary MFs, it is straightforward to show that they are applicable for all convex T1 FSs (Klir and Yuan (1995)).

III. CONNECTING VERTICAL-SLICE CALCULATIONS TO HORIZONTAL-SLICE (α-PLANE) COMPUTATIONS

In Section II.C, Rule 3 establishes when it is necessary to pursue the computations of $\mu_{F \sqcup G}(\theta)$ and $\mu_{F \sqcap G}(\theta)$ in more detail. In this section we study these detailed computations from different perspectives so as to connect the vertical-slice and horizontal slice computations. This is done geometrically, first for the join and then for the meet, both for the two T1 secondary MFs that intersect each other at three points, as depicted in Fig. 1. We leave it to the reader to verify that our conclusions are also applicable to two convex secondary T1 MFs that intersect at exactly two points, or for two convex secondary T1 MFs for which $v_1 = v_0 \neq 0$, and $g(\theta) \subseteq f(\theta)$ (Rule 2).

A. Join Computations

Using (20), the join of the two secondary MFs in Fig. 1 is depicted in Fig. 2a using heavy lines.

Next, we show how $\mu_{F \sqcup G}(\theta)$ can be obtained using the α-cuts of $f(\theta)$ and $g(\theta)$ raised to level α, denoted $f(\theta \mid \alpha)$ and $g(\theta \mid \alpha)$, respectively. From Fig. 3, for $\alpha_0 = 0$, observe the following:

$$\begin{cases} f(\theta \mid \alpha_0) = [a_0, b_0] \\ g(\theta \mid \alpha_0) = [c_0, d_0] \end{cases} \tag{23}$$

$$\mu_{F \sqcup G}(\theta \mid \alpha_0) = [a_0, b_0] = \left[\max(a_0, c_0), \max(b_0, d_0)\right] \tag{24}$$

For α_1, observe that:

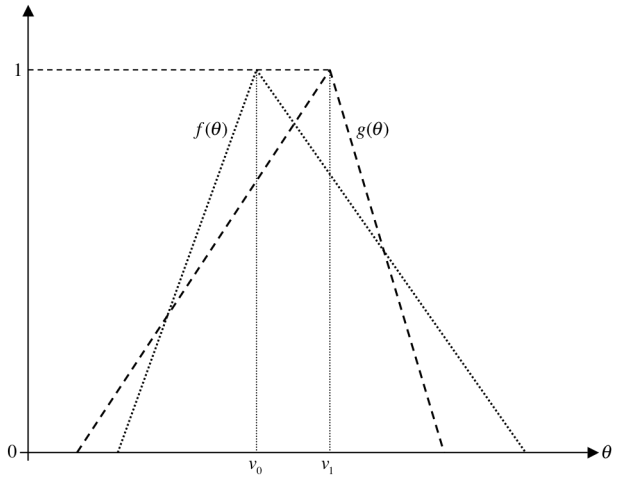

Figure 1. Two overlapping T1 secondary MFs.

$$\begin{cases} f(\theta \mid \alpha_1) = [a_1, b_1] \\ g(\theta \mid \alpha_1) = [c_1, d_1] \end{cases} \tag{25}$$

$$\mu_{F \sqcup G}(\theta \mid \alpha_1) = [a_1, b_1] = \left[\max(a_1, c_1), \max(b_1, d_1)\right] \tag{26}$$

Proceeding in a similar manner for the remaining α_i that are depicted on Fig. 3, it is straightforward to show that:

$$\begin{cases} f(\theta \mid \alpha_i) = [a_i, b_i] \\ g(\theta \mid \alpha_i) = [c_i, d_i] \end{cases}, \forall \alpha_i \tag{27}$$

$$\mu_{F \sqcup G}(\theta \mid \alpha_i) = \left[\max(a_i, c_i), \max(b_i, d_i)\right], \forall \alpha_i \tag{28}$$

The results in (27) and (28) are the same as the results that would be obtained from computing $\tilde{A}_\alpha \cup \tilde{B}_\alpha$, when (17)-(19) are used.

B. Meet Computations

Using (21), the meet of the two secondary MFs in Fig. 1 is depicted in Fig. 2b using heavy lines.

Next, we show how $\mu_{F \sqcap G}(\theta)$ can be obtained using $f(\theta \mid \alpha)$ and $g(\theta \mid \alpha)$. $f(\theta \mid \alpha_i)$ and $g(\theta \mid \alpha_i)$, for i = 0 and 1 are given in (23) and (25). From Fig. 4, for $\alpha_0 = 0$, observe that

$$\mu_{F \sqcap G}(\theta \mid \alpha_0) = [c_0, d_0] = \left[\min(a_0, c_0), \min(b_0, d_0)\right] \tag{29}$$

and, for α_1, observe that:

$$\mu_{F \sqcap G}(\theta \mid \alpha_1) = [c_1, d_1] = \left[\min(a_1, c_1), \min(b_1, d_1)\right] \tag{30}$$

Proceeding in a similar manner for the remaining α_i that are depicted on Fig. 4, it is straightforward to show that:

$$\mu_{F \sqcap G}(\theta \mid \alpha_i) = \left[\min(a_i, c_i), \min(b_i, d_i)\right], \forall \alpha_i \tag{31}$$

The result in (31) is the same as the result that would be obtained from computing $\tilde{A}_\alpha \cap \tilde{B}_\alpha$, when the well - known

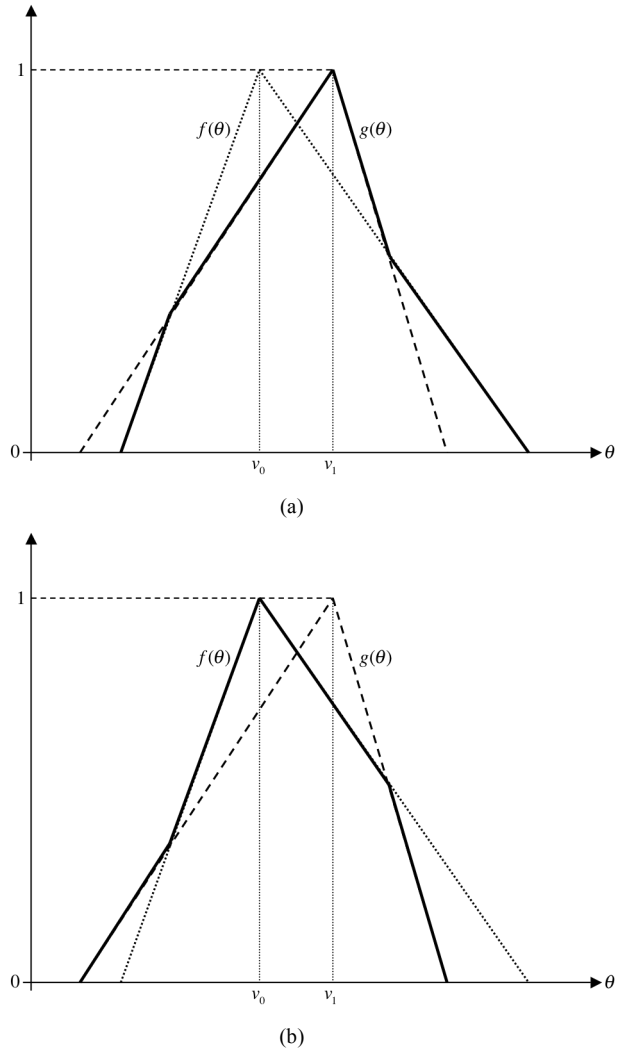

Figure 2. (a) Join and (b) meet of the two overlapping secondary MFs in Figure 1.

results for computing the intersection of IT2 FSs are used [described just below (19)].

C. Discussion

The results in (28) and (31) are, of course, not new. What is new is that they have been derived directly from the well-known vertical-slice computational results instead of from the α-plane representation. This provides an alternative way to obtain these results, which may be useful when teaching about general T2 FSs when time is limited.

IV. Conclusions

The union and intersection of general type-2 fuzzy sets (T2 FSs) are fundamental computations for such FSs. In the past, algorithms were developed for the union and intersection computations using vertical-slice and horizontal-slice representations of T2 FSs. The vertical-slice representation of a T2 FS traces its origins back to Zadeh [32] and requires computing the join or meet, whereas the horizontal-slice representation of a T2 FS is very recent, traces its origins to Liu [14], and requires computing the join and meet only for

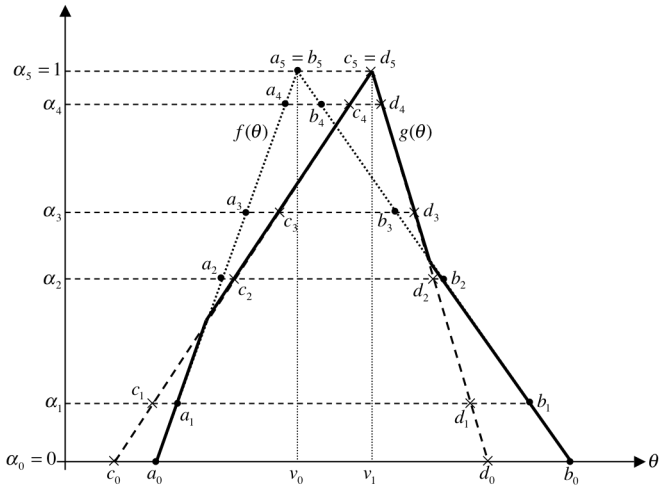

Figure 3. Join of the two overlapping secondary MFs in Fig. 1 and some α-cuts raised to level-α [9].

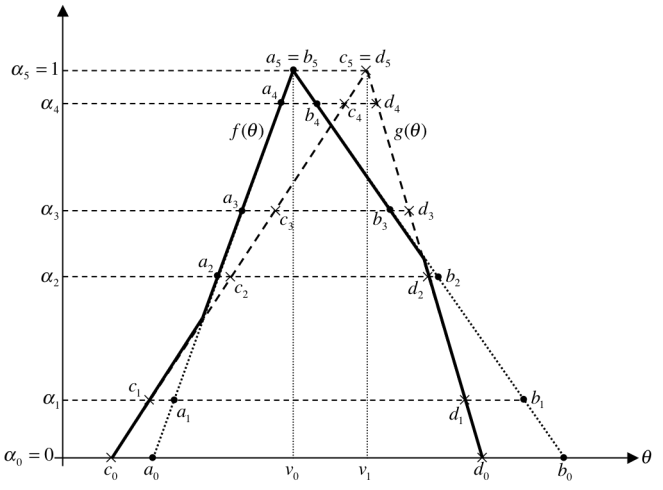

Figure 4. Meet of the two overlapping secondary MFs in Fig. 1 and some α-cuts raised to level-α. See footnote 9.

interval T2 FSs that are raised to level alpha, for which closed-form formulas are available [15]. In this paper, by studying the join and meet geometrically for general T2 FSs, we have shown that for many situations closed-form formulas exist for them. We have also shown that the formulas for computing the union and intersection of general T2 FSs that were derived from the horizontal-slice representation of a T2 FS [19] can also be obtained directly from geometrical interpretations of formulas that were derived by Karnik and Mendel [12] for the vertical-slice representation of a T2 FS.

How to turn the simple rules that are given in Section II.C into practical algorithms for computing the join and meet remains to be done. It was not done in this paper, because the purpose of this paper was to provide an alternative way to obtain these results, which may be useful when teaching about general T2 FSs when time is limited. We believe that this purpose has been accomplished.

REFERENCES

[1] J. Aisbett, T. Rickard and D. G. Morgenthaler, "Type-2 fuzzy sets as functions on spaces," *IEEE Trans. on Fuzzy Systems*," vol. 18, pp. 841-844, August 2010.

[2] J. Aisbett, J. Rickard and D. Morgenthaler, "Intersection and union of type-n fuzzy sets," *Proc. FUZZ-IEEE*, WCCI 2010 IEEE World Congress on Computational Intelligence, pp. 2043-2050, Barcelona, Spain, July 2010.

[3] C.-H. Chiu and W.-J. Wang, "A Simple computation of MIN and MAX operations for fuzzy numbers," *Fuzzy Sets and Systems*, vol. 126, pp. 273-276, 2002.

[4] S. Coupland and R. I. John, "An approach to type-2 fuzzy arithmetic," *Proc. UK Workshop on Computational Intelligence*, pp. 107-114, 2003.

[5] S. Coupland and R. I. John, "A new and efficient method for the type-2 meet operation," *Proc. of IEEE FUZZ Conf.*, pp. 959-964, Budapest, Hungary, July 2004.

[6] S. Coupland and R. I. John, "Towards more efficient type-2 fuzzy logic systems," *Proc. IEEE FUZZ Conf.*, pp. 236-241, Reno, NV, May 2005.

[7] S. Coupland and R. I. John, "Geometric type-1 and type-2 fuzzy logic systems," *IEEE Trans. on Fuzzy Systems*, vol. 15, pp. 3-15, February 2007.

[8] S. Coupland and R. I. John, "Geometric logical operations for type-2 fuzzy sets," *Proc. of IPMU 2008*, pp. 1274-1281, Malaga, Spain, June 2008.

[9] S. Greenfield and R. John, "Optimised generalized type-2 join and meet operations," *Proc. IEEE FUZZ Conference*, pp. 141-146, London, UK, July 2007.

[10] H. Hamrawi and S. Coupland, "Type-2 fuzzy arithmetic using alpha-planes," *Proc. IFSA/EUSFLAT*, pp. 606-611, Lisbon, Portugal, July 2009.

[11] H. Hamrawi, S. Coupland and R. John, "Extending operations on type-2 fuzzy sets," *Proc. UKCI*, Nottingham, UK, Sept. 2009.

[12] N. N. Karnik and J. M. Mendel, "Operations on type-2 fuzzy sets," *Fuzzy Sets and Systems*, vol. 122, pp. 327-348, 2001.

[13] M. F. Kawaguchi and M. Miyakoshi, "Extended triangular norms in type 2 fuzzy logic, *EUFIT '99 7th European Congress on Intelligent Techniques & Soft Computing*, Aachen, Germany, Sept., 1999.

[14] F. Liu, "An efficient centroid type-reduction strategy for general type-2 fuzzy logic system," *Information Sciences*, vol. 178, pp. 2224-2236, 2008.

[15] J. M. Mendel, *Uncertain Rule-Based Fuzzy Logic Systems: Introduction and New Directions*, Prentice-Hall, Upper-Saddle River, NJ, 2001.

[16] J. M. Mendel, "Advances in type-2 fuzzy sets and systems," *Information Sciences*, Vol. 177, pp. 84-110, 2007.

[17] J. M. Mendel, "Comments on 'α-plane representation for type-2 fuzzy sets: theory and applications'," *IEEE Trans. on Fuzzy Systems*, vol. 18, pp. 229-230, February 2010.

[18] J. M. Mendel and R. I. John, "Type-2 fuzzy sets made simple," *IEEE Trans. on Fuzzy Systems*, vol. 10, pp. 117-127, April 2002.

[19] J. M. Mendel, F. Liu and D. Zhai, "Alpha-plane representation for type-2 fuzzy sets: theory and applications," *IEEE Trans. on Fuzzy Systems*, vol. 17, pp. 1189-1207, October 2009.

[20] M. Mizumoto and K. Tanaka, "Some properties of fuzzy sets of type-2," *Information and Control*, vol. 31, pp. 312-340, 1976.

[9] Note that the heavy lines for the join (or for the meet in Figure 4) only exist as $\Delta\alpha \to 0$ and that for non-zero $\Delta\alpha$ they can be obtained by using piecewise linear approximations that connect the join (meet) from one α-level to the next.

2011 IEEE International Conference on Fuzzy Systems
June 27-30, 2011, Taipei, Taiwan

A Fuzzy-Based Output Power Smoothing of WECS using Short-Term Ahead Prediction of Wind Speed

Yuya Izumi
Alok Pratap
Yoshihisa Kinjyo
Akie Uehara
Atsushi Yona
and Tomonobu Senjyu
The Department of Electrical and Electronics Engineering,
Faculty of Engineering, University of the Ryukyus, Japan.
E-mail: b985542@tec.u-ryukyu.ac.jp.

Toshihisa Funabashi
Meidensha Corporation, Tokyo 141-8565, Japan.
E-mail: funabashi-t@mb.meidensha.co.jp.

Endusa Billy Muhando
Alaska Center for Energy and Power,
the University of Alaska Fairbanks USA.
E-mail: ebmuhando@alaska.edu.

Abstract— **This paper presents a fuzzy-based output power smoothing method for a wind energy conversion system (WECS) using short-term ahead prediction of wind speed. The WECS is based on a permanent magnet synchronous generator (PMSG) and transmits its electrical power to an AC grid through an IGBT pulse-width modulation (PWM) converter. The power converter controls the torque of the PMSG according to the torque command, which is determined by using the fuzzy logic. The inputs of the fuzzy logic are the predicted wind speed and the difference between the wind turbine torque and the generator torque. By means of the proposed method, the generator torque is smoothed and the kinetic energy stored by the inertia of the wind turbine can be utilized to smooth the output power fluctuations of the PMSG. In addition, the wind turbine's shaft stress is mitigated compared to a conventional maximum power point tracking (MPPT) control. The effectiveness of the proposed method is verified by numerical simulations.**

keywords–fuzzy logic, power smoothing, wind energy conversion system, wind speed prediction, wind turbine inertia.

I. Introduction

In recent years, there have been problems such as exhaustion of fossil fuels, e.g., coal and oil, and environmental pollution resulting from consumption of these fuels. For cleaner and economical energy characteristics, the world has been turning to alternatives of fossil fuels and wind energy conversion systems (WECS) have received increasing attention. Especially, variable speed wind turbine (VSWT) systems with power electronics interfaces have attracted interest. VSWT systems are usually based on doubly fed induction generators (DFIG) and permanent magnet synchronous generators (PMSG) [1]-[6]. Currently, the use of PMSGs has increased because of its simple structure and efficient energy production. Therefore, it is expected that more large size wind turbine generator (WTG) systems will adopt the PMSG [1]-[4]. Usually, the WECS with a PMSG is connected to the grid via an AC-DC-AC converter system. In this system, the WECS does not need to synchronize its rotational speed with the grid frequency. Besides, the gearbox can be omitted due to the low rotational speed of the WTG. On the other hand, wind energy is not constant and the wind turbine's power fluctuates. Since the output power fluctuations may cause grid frequency deviations, several literatures regarding the output power smoothing have been published such as the use of pitch angle control or the inertia of VSWTs [3]-[7].

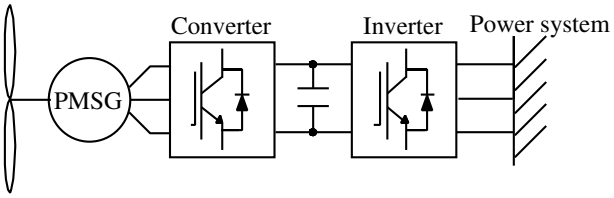

Fig. 1. Wind energy conversion system using PMSG.

This paper presents a fuzzy-based output power smoothing method for a WECS using short-term ahead prediction of wind speed. The WECS is based on a PMSG and transmits its electrical power to an AC grid through a IGBT pulse-width modulation (PWM) converter. The power converter controls the torque of the PMSG according to the torque command, which is determined by using the fuzzy logic. The inputs of the fuzzy logic are the predicted wind speed and the difference between the wind turbine torque and the generator torque. The short-term ahead wind speed is predicted by using least-squares method [7] and it is used to achieve more effective torque control of the PMSG for the wind speed variations. For high wind speed condition, the power fluctuations of the PMSG is smoothed with the pitch angle control. By using the proposed method, the torque of the PMSG is smoothed and the kinetic energy stored by the inertia of the wind turbine can be utilized to smooth the output power fluctuations of the PMSG. In addition, the wind turbine's shaft stress and the pitch action are mitigated compared to a conventional maximum power point tracking (MPPT) control. The effectiveness of the proposed method is verified by numerical simulations.

978-1-4244-7316-8/11/$26.00 ©2011 IEEE

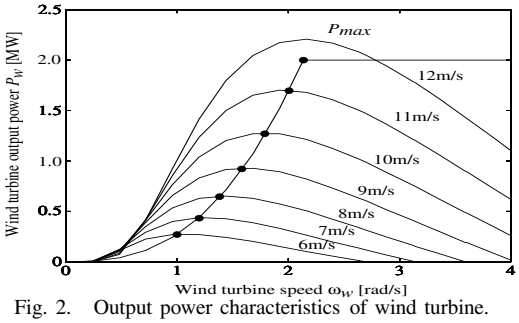

Fig. 2. Output power characteristics of wind turbine.

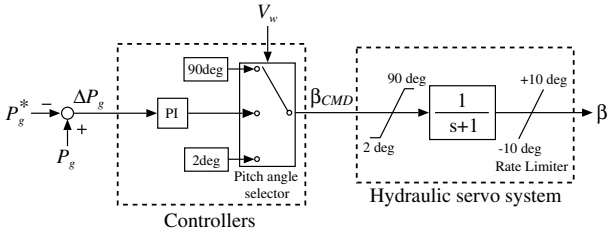

Fig. 3. Pitch angle control system.

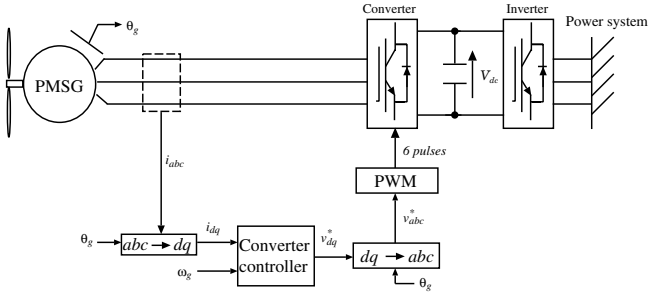

(a) Configuration of power converter system

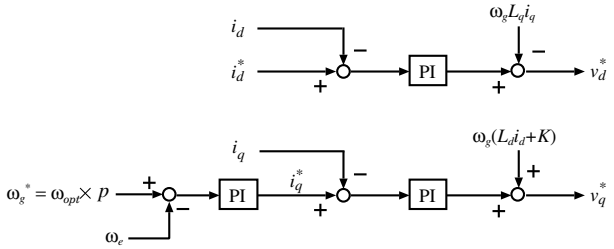

(b) Configuration of converter control system

Fig. 4. Configuration of PMSG control system.

II. Conventional WECS

A. System Configuration

The system of the WECS is shown in Fig. 1. Wind energy obtained from the wind turbine is sent to the PMSG. To generate maximum power, rotational speed of the PMSG is controlled by a pulse width modulation (PWM) converter. The output power of the PMSG is supplied to the grid through a generator-side converter and a grid-side inverter.

B. Wind Turbine Model

Wind turbine output power, P_w, and wind turbine torque, T_w, are given by the following equations:

$$P_w = 0.5 C_p(\lambda, \beta) \rho \pi R^2 V_w^3 \tag{1}$$

$$T_w = 0.5 C_p(\lambda, \beta) \rho \pi R^3 V_w^2 / \lambda \tag{2}$$

where V_w is the wind speed, ρ is the air density, R is the radius of the wind turbine, C_p is the wind turbine power coefficient, $\lambda = \omega_w R / V_w$ is the tip speed ratio, ω_w is the angular rotor speed of the wind turbine and β is the pitch angle. C_p is given by the following equations [3]:

$$C_p = 0.22 \left(\frac{116}{\Gamma} - 0.4\beta - 5 \right) \exp^{-\frac{12.5}{\Gamma}} \tag{3}$$

$$\Gamma = \frac{1}{\frac{1}{\lambda + 0.08\beta} - \frac{0.035}{\beta^3 + 1}}. \tag{4}$$

C. Maximum Power Point Tracking Control

The output power characteristics of the wind turbine are depicted in Fig. 2. Here, the pitch angle, $\beta = 2°$. From this figure, it can be seen that there is a rotational speed, ω_{opt}, dotted by the black circles, for any particular wind speed. ω_{opt} is called the optimum rotational speed and generates the maximum power, P_{max} (MPPT control). ω_{opt} is approximated as follows [1]-[3]:

$$\omega_{opt} = 0.1874 V_w. \tag{5}$$

Generally, the MPPT control is applied when the wind speed, V_w, is smaller than the rated speed. If V_w is greater than the rated speed, then output power of the PMSG is controlled by the pitch angle control system as shown in Fig. 3 [3]. The pitch angle is controlled in the region between the rated wind speed (12m/s) and the cut-out wind speed (24m/s). Subtraction of the output power command the the PMSG, P_g^*, from the output power of the PMSG, P_g, gives the output error of the PMSG, ΔP_g, that evaluates the pitch angle command, β_{CMD}, via the pitch angle control system. The output power of the PMSG is controlled by a hydraulic servo system that drives the blades according to the pitch angle command, β_{CMD}. The output power command of the PMSG, P_g^*, is constant at the rated power (2MW).

D. PMSG Model

Basically, the mass model of a PMSG is the same as that of a permanent magnet synchronous motor (PMSM). The voltage and torque equations of the PMSM in the d-q reference frames are given by the following equations:

$$v_d = R_a i_d + L_d \frac{di_d}{dt} - \omega_g L_q i_q \tag{6}$$

$$v_q = \omega_g L_d i_d + R_a i_q + L_q \frac{di_q}{dt} + \omega_g K \tag{7}$$

$$T_g = p\{K i_q + (L_d - L_q) i_d i_q\} \tag{8}$$

where v_d and v_q are the d-q axis voltages, i_d and i_q are the d-q axis currents, R_a is the stator resistance, L_d and L_q are the d-q axis inductances, ω_g is the generator rotational speed, K is the permanent magnetic flux, and p is the number of pole pairs. Generating operation starts when the electromagnetic torque, T_g, is negative. The motion equation of the PMSG is given as

follows:

$$J_{eq}\frac{d\omega_g}{dt} = T_w - T_g. \tag{9}$$

where $J_{eq}(= J_g + J_w)$ is the equivalent inertia, T_w is the wind turbine torque.

E. Configuration of Power Converter System

The configuration of the power converter control system is shown in Fig. 4(a). The power converter is standard 3-phase two-level unit, composed of six IGBTs and controlled by triangle-wave PWM law.

The conventional configuration of the power converter is shown in Fig. 4(b). By using vector control scheme, the power converter controls the rotational speed of the PMSG to achieve variable speed operation with the MPPT control. The speed control of the PMSG is realized on a rotating reference frame, where the rotational speed error is used as the input to a speed controller which produces q axis stator current command, i_q^*. A salient-pole synchronous machine is used in this paper. To achieve efficient operation of the PMSG, d axis stator current command, i_d^*, is determined by [8] and given as follows:

$$i_d^* = \frac{K}{2(L_d - L_q)} - \sqrt{\frac{K^2}{4(L_q - L_d)^2} + i_q^2}. \tag{10}$$

The error between the command d-q axis currents, i_d^*, i_q^*, and the actual d-q axis currents are used as inputs to the current controllers. The current controllers produce d-q axis voltage commands v_d^*, v_q^* after the decoupling. The angle θ_g, for the Park transformation, is calculated from the rotational speed of the PMSG.

III. Proposed WECS

This section presents the proposed fuzzy-based output power smoothing method using the inertia of the wind turbine.

A. Power and Torque Characteristics in WECS

The wind turbine output, P_w, the wind turbine torque, T_w, and the generator torque, T_g, versus the wind turbine speed, ω_w, curves are shown in Figs. 5 and 6, respectively [2, 5, 6]. Here, the wind speed is assumed as 12m/s. If a constant output power command, $P_{ref} = kP_{rated}$, is given for the PMSG, then the generator torque is expressed as $T_g = P_{ref}/\omega_g$, where, k is a multiplying factor. The generator torque for $k = 1.0$ and 0.7 is shown in Fig. 6. In the conventional MPPT control, the operating point of the wind turbine speed becomes the optimum rotational speed, ω_{opt}, as shown in Fig. 5. However, in the output power smoothing method using the inertia of the wind turbine, the wind turbine speed changes around ω_{opt} according to the actual wind speed. In Fig. 6, if the rotational speed of the wind turbine changes from ω_{min} to ω_{max}, then the kinetic energy stored by the wind turbine, ΔE, is expressed as follows [2]:

$$\Delta E = \frac{1}{2}J_{eq}(\omega_{max}^2 - \omega_{min}^2). \tag{11}$$

By controlling the rotational speed of wind turbine in the region of $\omega_{min} \sim \omega_{max}$, ΔE can be used for output power smoothing. Since stable operation of the wind turbine is

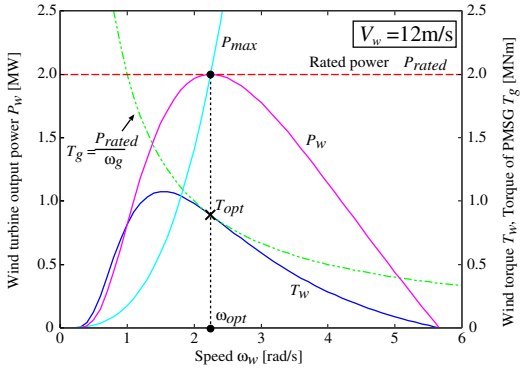

Fig. 5. Speed characteristics of WECS.

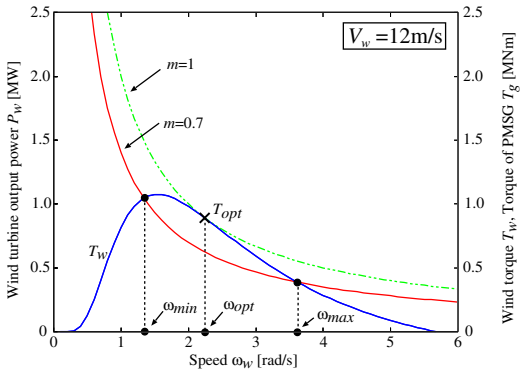

Fig. 6. Torques of PMSG for each output power.

achieved within a proper range, the upper and lower limits of the operation region are set to 0.6 pu and 1.4 pu. The rotational speed of the wind turbine is controlled within this region. Although Figs. 5 and 6 show the wind turbine characteristics at V_w=12m/s, wind turbine characteristics at $V_w = 5 \sim$12m/s can be obtained by using a lookup table which has prestored values of T_g and T_w as described in Fig. 6. Here, for the case of the constant power control, the rotational speed variations of the wind turbine will become large and will lead to the unstable operating of the WECS, increase of wind turbine's shaft stress. Therefore, this paper aims at the smoothing and controlling of the generator torque, T_g.

B. Torque Control Method using Fuzzy Logic

As described before, the generator-side converter smooths the generator torque for output power smoothing. The power fluctuations of the WECS can be leveled by smoothing the generator torque. For the proposed method, the generator torque command is determined by using the fuzzy logic. The fuzzy rules and membership functions are shown in Table 1 and Fig. 7, respectively. The inputs of the fuzzy logic are given by the following equations:

$$\Delta T = T_w - T_{g_opt} \tag{12}$$

$$\Delta \hat{V}_w = \frac{1}{T}\int_{t-T}^{t} \hat{V}_w dt - \hat{V}_w \tag{13}$$

where $\hat{V}_w$ is the predictive wind speed and it will be explained in next section. The output of the fuzzy logic is the torque

Table I. Fuzzy Rules

$\Delta\hat{V}_w$ \ ΔT	NB	NM	NS	NZ	PZ	PS	PM	PB
NB	PB	PB	PM	PS	NS	NM	NB	NB
NM	PB	PM	PS	PS	NS	NS	NM	NB
NS	PM	PM	PS	PZ	NZ	NS	NM	NM
NZ	PM	PS	PZ	PZ	NZ	NZ	NS	NM
PZ	PM	PS	PZ	PZ	NZ	NZ	NS	NM
PS	PM	PM	PS	PZ	NZ	NS	NM	NM
PM	PB	PM	PS	PS	NS	NS	NM	NB
PB	PB	PB	PM	PS	NS	NM	NB	NB

NB=Negative Big NM=Negative Medium NS=Negative Small
PB=Positive Big PM=Positive Medium PS=Positive Small
NZ=Negative Zero PZ=Positive Zero

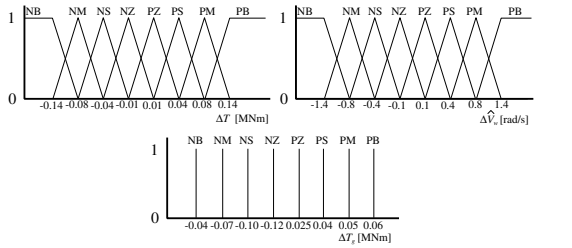

Fig. 7. Membership functions.

fluctuation index, ΔT_g. The increase and decrease of ΔT_g is determined by the input of ΔT, while the amount of ΔT_g is determined by the input of $\Delta\hat{V}_w$.

The reason for the use of (12) is based on (9) which is the system dynamics equation [6]. For (9), operating points, ω_{g0}, V_{w0}, T_{g0}, and T_{w0} are assumed. At the operating speed, ω_{g0}, if $d\omega_{g0}/dt = 0$ then $T_{w0} - T_{g0} = 0$. If the operating point, V_{w0}, increases and $T_{w0} - T_{g0} > 0$, then ω_{g0} should increase. The acceleration continues until $T_{w0} - T_{g0} = 0$. When $T_{w0} - T_{g0} = 0$, the operating speed, ω_{g0}, should remain at the operating point. If a decrease in wind speed occurs and $T_{w0} - T_{g0} < 0$, then ω_{g0} should decrease. The deceleration continues until $T_{w0} - T_{g0} = 0$. From these operations, by (12), if ΔT is increases, it means that the wind turbine torque, T_w, increases due to a increase in the wind speed. Therefore, the generator speed, ω_g, should increase, i.e., the generator torque, T_g, should decrease. On the other hand, if ΔT decreases, it means that T_w decreases due to a decrease in the wind speed. Therefore, ω_g should decrease, i.e., T_g should increase. Here, T_{g_opt} of (12) is the optimum generator torque in the MPPT control and can be calculated by the following equation [1]:

$$T_{g_opt} \approx T_{w_opt} = 1453.3\omega_g^2 \tag{14}$$

Here, T_{w_opt} is the optimum torque of wind turbine. (14) is derived assuming the wind rotor and the generator characteristics are at steady-state.

Equation (13) is used to evaluate the amount of ΔT_g. The first term of (13) is an average value of the predicted wind speed. To smooth the power fluctuations in the high frequency domain (above 0.1Hz), the value of T is set to 10s [2, 6]. If $\Delta\hat{V}_w$ is large, then it is seen that the wind speed variation is also large. Therefore, the amount of ΔT_g should be increased, and *vice-versa*. By using the predicted wind speed as the input of the fuzzy logic, more effective torque control can be achieved. Finally, the generator torque command, T_g^*, is determined by adding ΔT_g with T_{g_opt} as

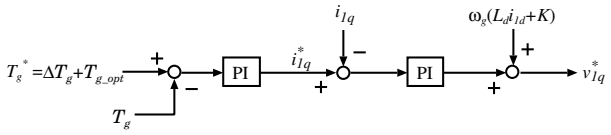

Fig. 8. Proposed configuration of converter.

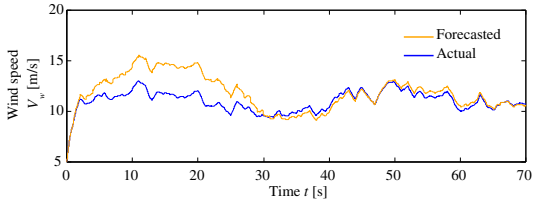

Fig. 9. Predicted and actual wind speeds.

shown in Fig. 8. In the proposed method, the fuzzy control is determined based on the motion equation of PMSG and the operating rotational speed. These are the fundamentals for the operations of WECS, and therefore, the fuzzy control can be used regardless of the kind of WECSs. On the other hand, the membership functions are needed to tune according to the specifications of generators and turbines. However, this is simple and flexible. The torque fluctuation index, ΔT_g, is determined by using several wind speed profiles in simulations. When using the proposed method in practical systems, one can simply determine the membership functions and the values of ΔT_g according to WECS's specifications and wind profiles.

C. Wind Speed Prediction by Least-Squares Method

In this paper, a short-term ahead wind speed is predicted by using the least-squares method [7].

The wind speed slope, $a(k)$, is derived by the wind speed from the past T_{pre} seconds (the sampling-period is 1s) as the following equation:

$$a(k) = \frac{T_{pre}\sum_{n=1}^{T_{pre}} nV_w(k-n) - \sum_{n=1}^{T_{pre}} n \sum_{n=1}^{T_{pre}} V_w(k-n)}{T_{pre}\sum_{n=1}^{T_{pre}} n^2 - \left(\sum_{n=1}^{T_{pre}} n\right)^2} \tag{15}$$

where k is the present time and $V_w(k-n)$ is the wind speed value of n intervals ago. If T_{pre} is set to 30s, then (15) is calculated as follows:

$$a(k) = \sum_{n=1}^{30} \frac{29 - 2(n-1)}{4495} V_w(k-n). \tag{16}$$

The predicted wind speed, $V_{wf}(k+T_f)$, is expressed as

$$V_{wf}(k+T_f) = V_w(k) + T_f a(k) \tag{17}$$

where T_f is the prediction time and set to 5s.

To investigate the effectiveness of the proposed prediction method, the simulation result of wind speed prediction is shown in Fig. 9. From this figure, it is seen that the prediction error is large by around $t = 30$ s because of the past wind

data is less than 30 points. After that, however, the prediction accuracy is improved and the percentage error becomes small.

IV. Power Smoothing Simulation

A. Simulation Model

The system model used for the simulation is shown in Fig. 10. Here, the grid-side inverter is connected to an infinite bus through a LC filter, three-phase transformer, and single circuit transmission line in parallel with load. The parameters of the PMSG and the power converters are listed in Table II.

B. Simulation Results

To evaluate the effectiveness of the proposed method, WECS operation is examined by using the both methods (conventional and proposed). In the conventional method, the MPPT control described in Section II is employed. In the proposed method, the WECS initially operates as the MPPT control by regulating the optimum generator torque. At $t = 40$ s, the WECS starts the proposed method for output power smoothing. The simulation results are shown in Fig. 11. The wind speed shown in Fig. 9 is used for the both methods. Figs. 11(a)$\sim$(d) show the generator torque and the input-output of the fuzzy logic, respectively. From these figures, it is confirmed that the generator torque is smoothed by the proposed torque control method compared with that of the MPPT control. Around $t = 40 \sim 60$ s, short term variations of the wind speed frequently occur. However, the predicted wind speed is used as the input of the fuzzy logic, and therefore, the control performance is improved as shown in Fig. 11(d). The generator speed and its d-q axis currents are shown in Figs. 11(e) and (f). By smoothing the generator torque, the generator speed accelerates/decelerates according to the wind speed increasing/decreasing. The kinetic energy of wind turbine, the pitch angle, the power coefficient, the active power of the PMSG and its maximum energy function with the both methods are shown in Figs. 11(g)$\sim$(k), respectively. Here, the maximum energy function, P_{max}, is expressed as follows [10]:

$$P_{max} = \int_0^t P_g(t)dt. \tag{18}$$

In the conventional MPPT method, the pitch action increases when the wind speed fluctuates around the rated speed (see Fig. 11(h)). This results is the reduction of the power coefficient as shown in Fig. 11(i). On the other hand, the kinetic energy stored by the wind turbine is utilized for power smoothing, and therefore, the pitch action can be decreased. Consequently, as can be seen in Fig. 11(k), the maximum energy function, P_{max}, increases compared with the MPPT control. Fig. 11(l) shows the torque difference between the wind turbine and the generator. From this figure, it is found that the torque difference is smaller than that of the MPPT control and the mitigation of the wind turbine's shaft stress is achieved.

V. Conclusion

This paper presents a fuzzy-based output power smoothing method for a WECS using short-term ahead prediction of wind speed. In the WECS, the power converter controls the generator torque according to the torque command, which is determined by using the fuzzy logic. By using the proposed method, the generator torque is smoothed and the kinetic energy stored by the inertia of the wind turbine can be utilized for power smoothing. The effectiveness of the proposed method is verified by numerical simulations.

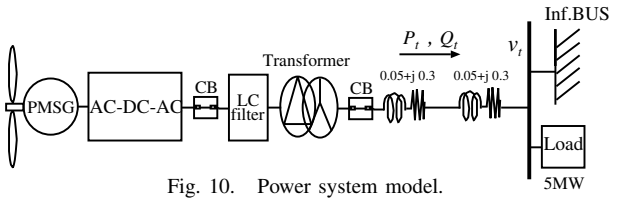

Fig. 10. Power system model.

Table II. Simulation Parameters

Parameters of windmill	
blade radius R	39 m
air density ρ	1.205 kg/m^3
rated wind speed V_{w_rated}	12m/s
Parameters of PMSG	
rated output P_g	2 MW
armature resistance R_a	50 $\mu\Omega$
d axis inductance L_d	5.5 mH
q axis inductance L_q	3.75 mH
number of pole pairs p	11
field flux K	136.25 V·s/rad
equivalent inertia J_{eq}	300,000 kg·m^2
rotational damping D	0
Parameters of power converter	
PWM carrier frequency f_p	10 kHz
rated DC-link voltage V_{dc_rated}	7.1 kV
DC-link capacitor C	15,000 μF

References

[1] S. Morimoto, H. Nakayama, M. Sanada, and Y. Takeda, "Sensorless Output Maximization Control for Variable-Speed Wind Generation System Using IPMSG," *IEEE Trans. on Industry Applications,* vol. 41, pp. 1, Jan/Feb. 2005.

[2] A. Abedini, G. Mandic, and A. Nasiri, "Wind Power Smoothing using Rotor Inertia Aimed at Reducing Grid Susceptibility", *The 34th Annual Conference of IEEE Industrial Electronics Society*, pp. 1445-1451, 10-13 Nov. 2008.

[3] T. Senjyu, N. Nakasone, A. Yona, S. A. Yousuf, T. Funabashi, and H. Sekine, "Operation Strategies for Stability of Gearless Wind Power Generation Systems," *Proceedings of IEEE/PES General Meeting 2008 (GM 2008),* CD-ROM, pp. 1-7, 20-24 July 2008, Pittsburgh, USA.

[4] D. Sato, and H. Saitoh, "Smoothing Control of Wind Farm Output by Using Kinetic Energy of Variable Speed Wind Power Generators",*T. IEE Japan*, Vol. 129-B, No. 5, pp. 580-590, 2009. (in Japanese)

[5] B. G. Rawn, P. W. Lehn, and M. Maggiore, "Control Methodology to Mitigate the Grid Impact of Wind Turbine", *IEEE Trans. Energy Conversion*, vol. 22, no. 2, pp. 431-438, 2007.

[6] C. Luo, H. Banakar, B. Shen, and B. T. Ooi, "Strategies to Smooth Wind Power Fluctuations of Wind Turbine Generator," *IEEE Trans. Energy Conversion*, vol. 22, no. 2, pp. 341-349, 2007.

[7] T. Kaneko, A. Uehara, T. Senjyu, A. Yona, and N. Urasaki, "An integrated control method for a wind farm to reduce frequency deviations in a small power system", *Applied Energy* (In Press).

[8] K. Matsuse, "Motor control engineering -Basic of variable-speed drive-, " Corona Publishing Co., Ltd, pp. 150, 2007 (in Japanese).

[9] L. R. Chang-Chien and Y. C. Yin, "Strategies for Operating Wind Power in a Similar Manner of Conventional Power Plant," *IEEE Trans. on Energy Conversion,* vol. 24, no. 4, pp. 926-934, Dec. 2009.

[10] T. Senjyu, R. Sakamoto, N. Urasaki, T. Funabashi, H. Fujita, and H. Sekine, "Output Power Leveling of Wind Turbine Generator for All Operating Regions by Pitch Angle Control", *IEEE Trans. on Energy Conversion*, vol. 21, no. 2, pp. 467-475, 2006.

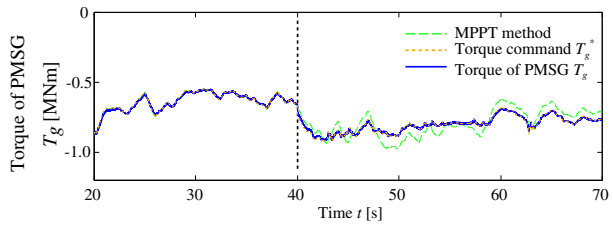

(a) Torque of PMSG.

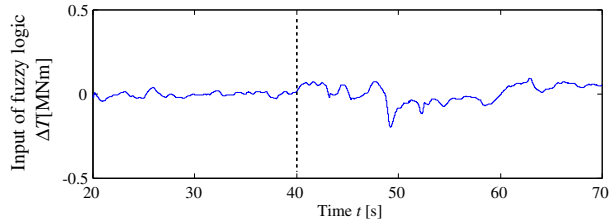

(b) Input of fuzzy logic ΔT.

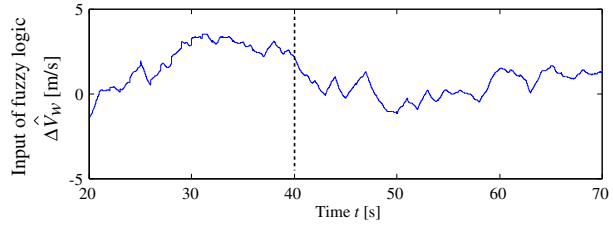

(c) Input of fuzzy logic $\Delta \hat{V}_w$

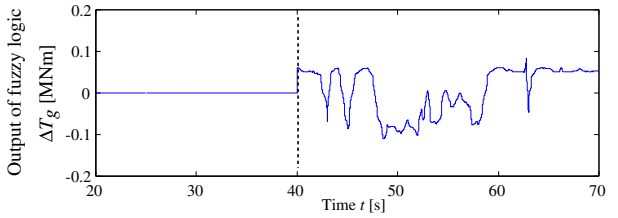

(d) Output of fuzzy logic.

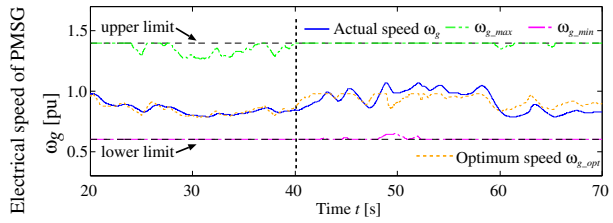

(e) Electrical speed of PMSG.

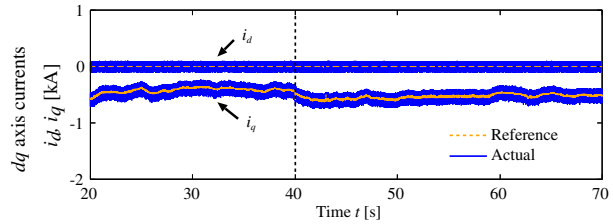

(f) d-q axis currents.

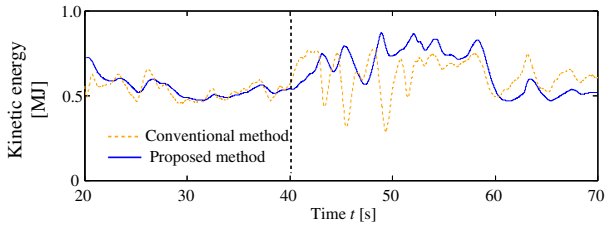

(g) Kinetic energy.

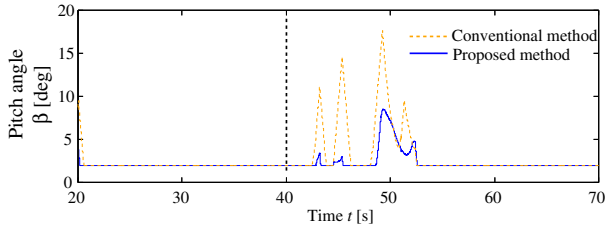

(h) Pitch angle.

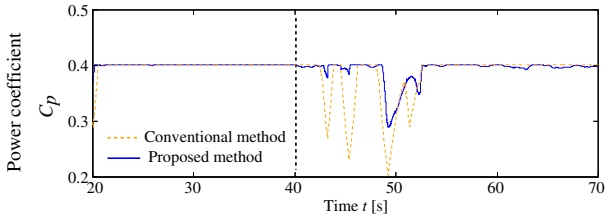

(i) Power coefficient.

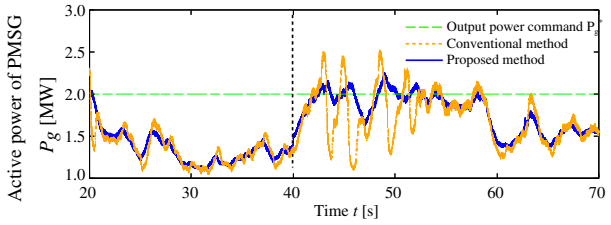

(j) Active power of PMSG.

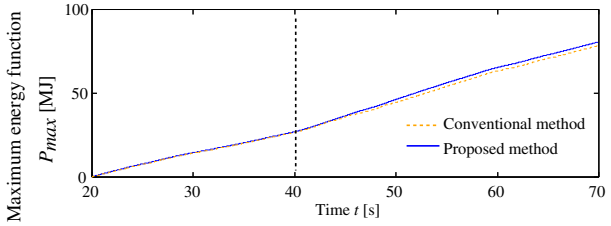

(k) Maximum energy function.

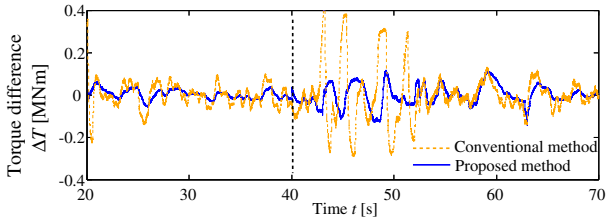

(l) Torque difference.

Fig. 11. Simulation results.

2011 IEEE International Conference on Fuzzy Systems
June 27-30, 2011, Taipei, Taiwan

Frequency and Voltage Control by Decentralized Controllable Loads with Fuzzy Control

Yoshihisa Kinjyo
Atsushi Yona
Naomitsu Urasaki
and Tomonobu Senjyu
The Department of Electrical and Electronics Engineering,
Facultyof Engineering, University of the Ryukyus, Japan.
E-mail: b985542@tec.u-ryukyu.ac.jp.

Toshihisa Funabashi
Meidensha Corporation, Tokyo 141-8565, Japan.
E-mail: funabashi-t@mb.meidensha.co.jp.

***Abstract*— In recent years, amount of renewable energy facilities using wind turbine generator and photovoltaic power system have been increased due to natural environment and resource depletion. Moreover, all electrification apartment houses or residences and electric vehicles have been increased. However, due to the fluctuating power from renewable energy sources and loads, fluctuations of grid frequency and voltage become problematic. This paper presents a methodology of control system frequency and voltage by distributed controllable loads such as heat pump and electric vehicles. By applying power consumption controller using distributed fuzzy control for HP and H_∞ control for battery, fluctuations of grid frequency and voltage are suppressed around a desired value. In order to verify the effectiveness of the proposed system, MATLAB/Simulink is used for computed simulations.**

keywords–frequency and voltage fluctuation, autonomous control, heat pump, distributed control, battery, H_∞ control.

I. Introduction

The amount of power generation utilizing renewable energy has shown an upward trend due to depletion of energy sources and consideration about environment [1, 2]. But, there are important issues of electric power quality due to change conditions of the weather. Additionally, the relation between power supply and demand becomes more complex by installing photovoltaic equipment in house and transition to all electric equipments. In small power system such as island, diesel generator is used as major source of electricity but it has high environmental issue and high unit price of power energy. Diesel generators have their limits with respect to maintaining the balance of supply and demand because diesel generators with governors have mechanical constraint. Moreover, due to the fluctuating power generation from renewable energy sources, frequency and voltage fluctuation are problematic in island power systems. Therefore provision is needed to control the system frequency and voltage.

As provision in supply side, installation of storage equipment and pitch angle control for wind generator have been proposed to control dispersed power system [3, 4]. However the installation of storage equipment that needs large storage capacity, and the cost of maintenance with quality degradation is expensive. In addition, wind generator is an obstacle for output power leveling due to mechanical constraint of control mechanism and irregularity of energy. Hence, in case of large amount of renewable energy is connected to the power system, the electricity quality degrades by measuring only supply side.

In recent years, smart grid technology with power consumption control at the power demand side becomes an active area of new research. This technology allows bidirectional information transmission between supply side and demand side [5∼7]. On the demand side, the transition to all-electritication in consideration of economy, safety, and use of heat pump water heater (HP) and electric vehicle (EV) that is suitable for the environment. Thus, power conditioning ability is increasing by these large capacity load connected to power system in the demand side [8, 9]. In addition, increase of equipment capacity for frequency and voltage control are not used for the electric power supplier.

This paper presents a method for system frequency control and voltage control using decentralized loads in a small power system based on smart grid. Decentralized controllable loads (HP, battery) are controlled to maintain the supply-demand balance, thereby suppressing frequency deviation. Also, terminal voltage control becomes possible by reactive power control of inverter connected to controllable loads that is introduced on the demand side. Since HP is limited by heating medium stabilization, it is necessary for each HP to starts and stops separately at different timing. As the control method, HP is controlled with the probability distribution of storage water temperature and system frequency that are local information. By applying H_∞ control theory which makes controller design possible by considering a response characteristic of frequency domain of battery operate in super high-frequency domain. On frequency domain, diesel generator operates in low-frequency domain because of mechanical constraint. Within the low-frequency domain, HP operates separately at different timing, and suppressing frequency fluctuations. That helps to diesel generator is operated with rated output power, and it can operate with high efficiency. In addition, controllable load is operated with system frequency, terminal voltage and storage water temperature. Thus the control method are achieved without any communications. The effectiveness of the pro-

978-1-4244-7316-8/11/$26.00 ©2011 IEEE

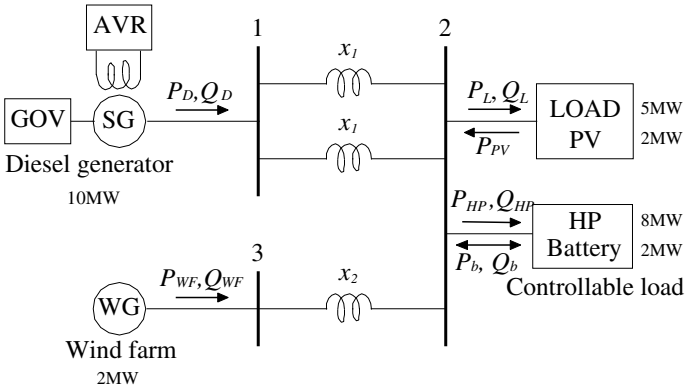

Fig. 1. Power system model.

Table 1. System constants.

Diesel generator
$H = 1.07$ s, $x_d = 1.5$ pu, $x'_d = 0.30$ pu
$x_q = 1.06$ pu, $x'_q = 0.3$ pu, $T'_{d0} = 3.7$ s,
$T'_{q0} = 0.21$ s, $T_G = 0.22$ s, $T_A = 0.329$ s
Transmission lines
$x_1 = 0.8$ pu, $x_2 = 0.3$ pu
HP and Battery
$K_{HP} = 0.00012$ pu, $T_B = 0.2$ s

posed control system is validated by simulation results in MATLAB$^{\mathrm{TM}}$.

II. MODELING

Fig. 1 illustrates a small power system. There are diesel generator, wind farm and photovoltaic in power system which supply electricity for load demand. They operate independently without communication large-scale power system. The system capacity is 10MW which is the base rule in Per Unit method. The system frequency is maintained constant at 60Hz by a diesel generator with governor. The diesel generator is modeled as a synchronous generator. The electrical and mechanical characteristics of the synchronous generator can be described by the following differential equations:

$$2H\frac{d\Delta\omega}{dt} = P_m - P_e \tag{1}$$

$$\frac{d\delta}{dt} = \Delta\omega \tag{2}$$

$$\frac{de'_q}{dt} = \frac{1}{T'_{do}}\left[e_{fd} - (x_d - x'_d)i_d - e'_q\right] \tag{3}$$

$$\frac{de'_d}{dt} = \frac{1}{T'_{q0}}\left[e'_d - (x_q - x'_q)i_q\right] \tag{4}$$

where H is the inertia constant, T_m is the mechanical input into generator, P_e is the generator output, δ is the angular phase difference, $\Delta\omega$ is the angular speed deviation, e'_d, e'_q are the transient voltage for the direct and quadrature-axis

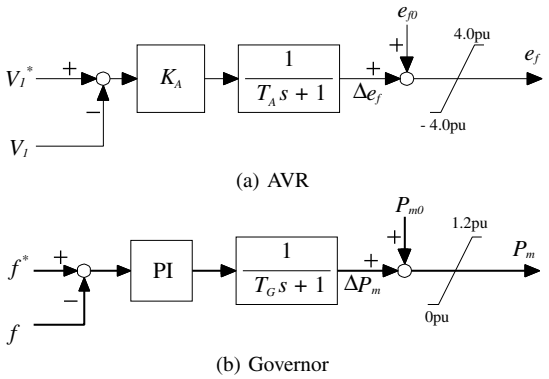

Fig. 2. Control block diagram of diesel generator.

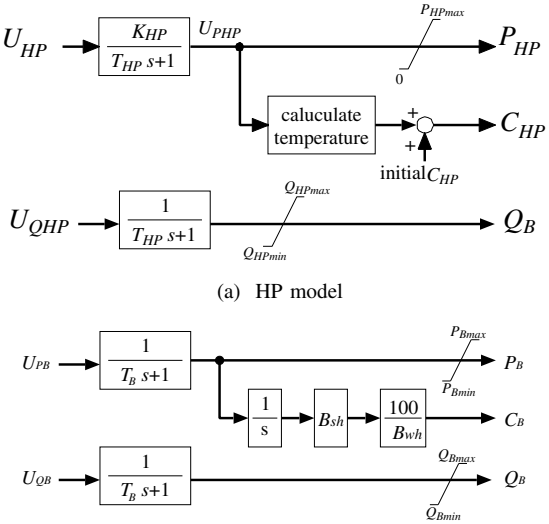

Fig. 3. Controllable load model.

of synchronous generator, e_{fd} is the excitation voltage converted to the q-axis, x_d, x_q are the d-and q-axis synchronous reactances, x'_d, x'_q are the d- and q-axis transient reactances, i_d, i_q are the generator terminal currents for the d-q axes, T'_{do}, T'_{qo} are the d-and q-axis open circuit transient time constant, respectively. The parameter values for each element are shown in Table 1. Fig. 2 illustrates control block diagram of diesel generator. Excitation using automatic voltage regulator (AVR) is modeled by first-order lag element shown in Fig. 2(a). Control composition of governor of diesel generator is shown in Fig. 2(b). System frequency control is achieved by mechanical input T_m of generator. The wind turbine generator and photovoltaic are modeled as fluctuation source because of output power is fluctuated by weather conditions. On supply side, wind farm (2MW) is introduced, and 800 photovoltaic panels (2MW) are introduced on demand side. As controllable load, heat pump (HP) group (8MW) and battery group (2MW) are introduced in power system, and its control system is explained in the next chapters.

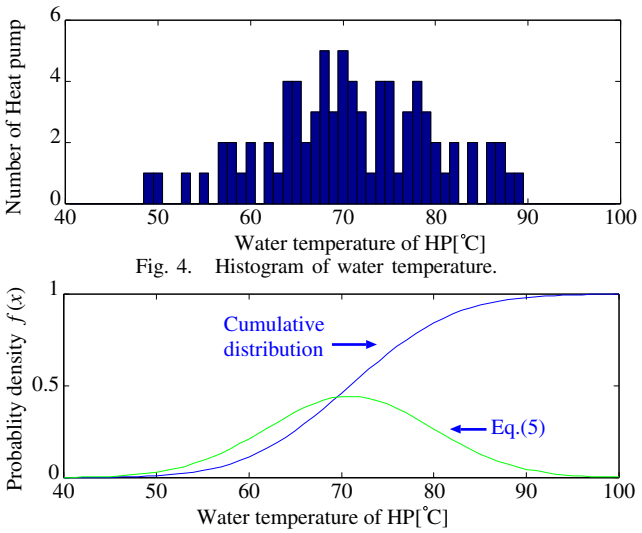

Fig. 4. Histogram of water temperature.

Fig. 5. Normal probability density distribution and cumulative distribution of water temperature.

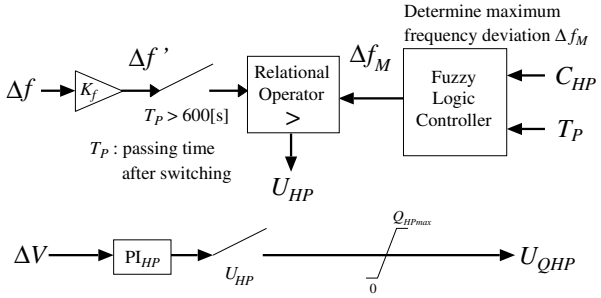

Fig. 6. Control block diagram of HP.

Table 2. Fuzzy rules

		C_{HP}			
		LR	L	H	HR
T_P	SR	LT	LR	L	ML
	S	LR	L	ML	MS
	L	ML	MS	S	SR
	LR	MS	S	SR	ST

LR=Lower HR=Higher SR=Shorter LR=Longer
ST=Smallest SR=Smaller MS=Middle Small ML=Middle Large
LR=Larger LT=Largest

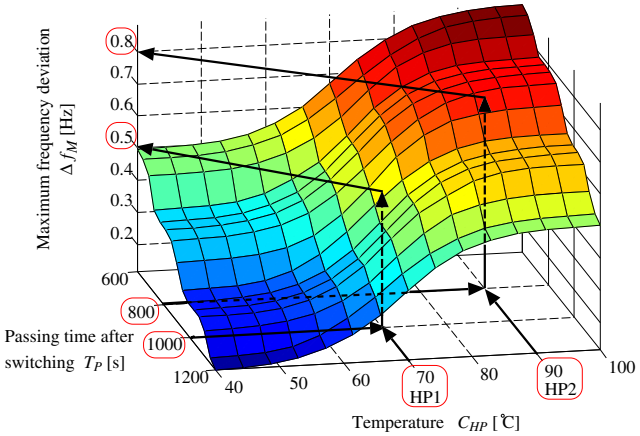

Fig. 7. maximum frequency deviation by fuzzy output response.

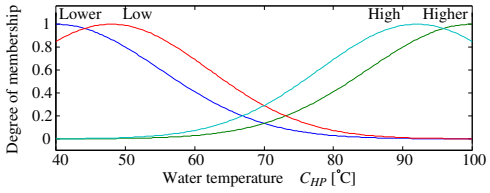

(a) Input variable of water temperature

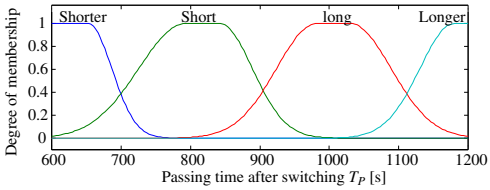

(b) Input variable of passing time after switching

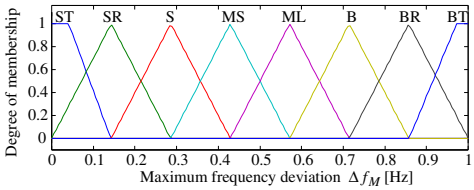

(c) Output variable of maximum frequency deviation

Fig. 8. Membership functions.

III. Controllable Load

The system frequency and terminal voltage fluctuations are suppressed by active and reactive power control with controllable loads. HPs and batterise are used as controllable load in this research. These electric appliances can be used as controllable load because their power consumption are adjustable and expend only during a given period of time. The decentralized HP model for houses is illustrated in Fig. 3(a). The water temperature of HP is controlled by feedback control with integral of power consumption under COP (coefficient of performance) is 4.0. The control block diagram is explained in the next section. The decentralized battery model is illustrated in Fig. 3(b). The discharge and charge operation are modeled as a first-order lag system, and charging rate is calculated by feedback control with integral of discharge and charge power consumption.

IV. Decentralized Autonomous Control of HP

A. Cumulative Distribution of Water Temperature

Each decentralized HP hold a unique water temperature, respectively, in power system. Those water temperature are produced by normal distribution random numbers shown in Fig. 4 as an average of 70 degrees °C. It can express the distribution of water temperature as a normal probability density distribution. The normal probability density distribution of water temperature is described by the following equation, and the normal probability density and its cumulative distribution are shown in Fig. 5.

$$f(x) = \frac{1}{\sigma\sqrt{2\pi}} \exp\left[-\frac{1}{2}\left(\frac{x-\mu}{\sigma}\right)^2\right] \tag{5}$$

where σ is the standard deviation ($\sigma > 0$), x (C_{HP}) is sample, and μ is the mean value.

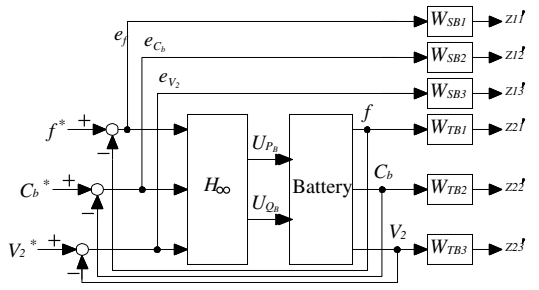

Fig. 9. Controller design of battery.

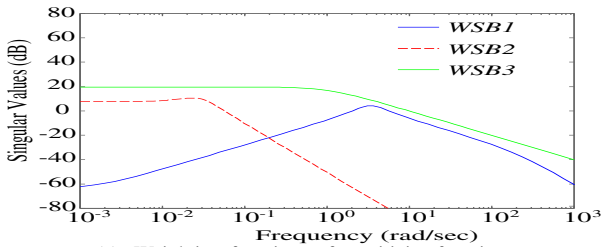

(a) Weighting functions of sensitivity function

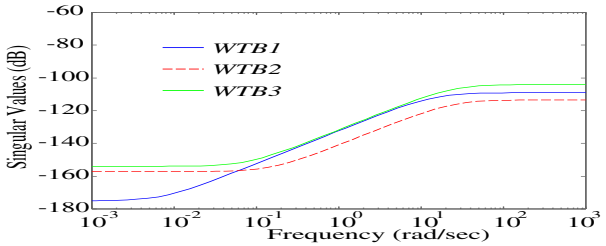

(b) Weighting functions of complementary sensitivity function

Fig. 10. Weighting function for control of battery.

B. Control System of HP

First, it is necessary to show property of HP before saying about control method. HP provides heat to the storage water with compressing and inflating heating medium. Because of this process, HP needs a time that heating medium stabilize. In fact, it cannot be turn off for 10 minutes if it turns on once. For above-mentioned constrained behavior, each HP is switched on/off separately at different timing, and control frequency. In this study, decentralized autonomous control of HP is entertained by Fuzzy Logic Toolbox$^{\mathrm{TM}}$. By two input function of water temperature C_{HP} and passing time after switching T_P, each HP decides a maximum frequency deviation Δf_M shown in Fig. 6. Each HP switch to frequency fluctuation based on these maximum frequency deviations, and control frequency. And these passing time are produsedby uniformly distributed pseudorandom numbers from 0 s to 1,200 s. Fuzzy output response is shown in Fig. 7. It is seen that switching priority is so high that water temperature is low, and passing time is long. Maximum frequency deviations respectively are decided as above, and when a signal $\Delta f'$ from Δf is approached to the maximum frequency deviation, HP control system of Fig.6 commands HP to switch. With this system, each HP is switched separately at different timing, and suppress frequency fluctuation. Fig. 8 illustrate fuzzy membership functions. Fig. 8(a) is designed to analogizing

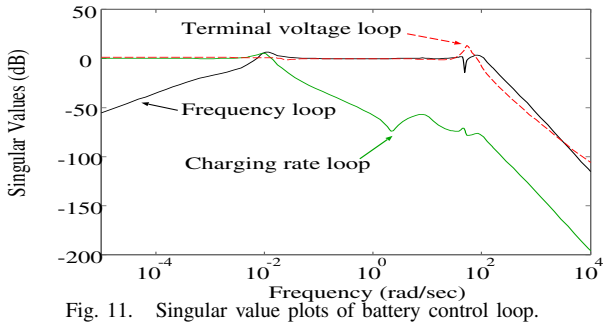

Fig. 11. Singular value plots of battery control loop.

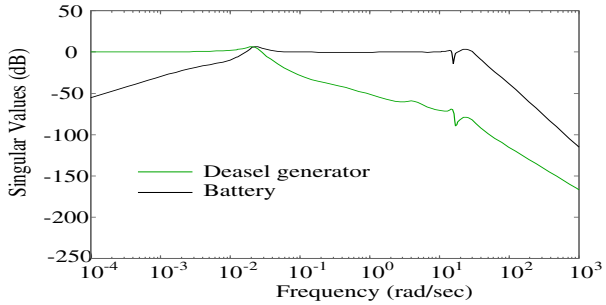

Fig. 12. Singular value plots of each control loop.

to cumulative distribution curve of water temperature, and it corresponds to distribution of water temperature. And Fig. 8(b) is designed that a maximum frequency deviation becomes smaller with increasing passing time.

V. Battery Control Method

H_∞ control block diagram of battery is shown in Fig. 9. The weighting function W_{SB1}, W_{SB2} and W_{SB3} for frequency deviation e_f, the charging rate deviation e_{C_B} and terminal voltage deviation V_2 in battery are shown in Fig. 10(a). To suppress only high frequency component of frequency deviation, W_{SE1} for battery discharge and charge behavior is designed to have high gain in high frequency domain and is designed low in low frequency domain. W_{SB2} for charging rate control of battery is designed to have low gain against W_{SB1}. W_{SB3} is designed to suppress the terminal voltage. Where charging rate reference and terminal voltage reference are 50% and 1.0 pu, respectively. Weighting functions of complementary sensitivity function is decided the robustness against the disturbance as illustrated in Fig. 10(b). The linear matrix inequality (LMI) approach is applied to the design of the H_∞ controller [10∼12]. The singular value plots of diesel generator and battery are illustrated in Fig. 11. It is seen that battery operates in high-frequency domain. Frequency loop of each controller are shown in Fig. 12. It is seen that diesel generator and battery operate in low-frequency and high-frequency domain, respectively.

VI. Simulation Results

The simulation results show the effectiveness of system frequency control and voltage control by the power consumption control of decentralized controllable loads in demand side. Because of a simulation time, 160 HP operate in simulation, and all output of HP are adjusted to the realistic value

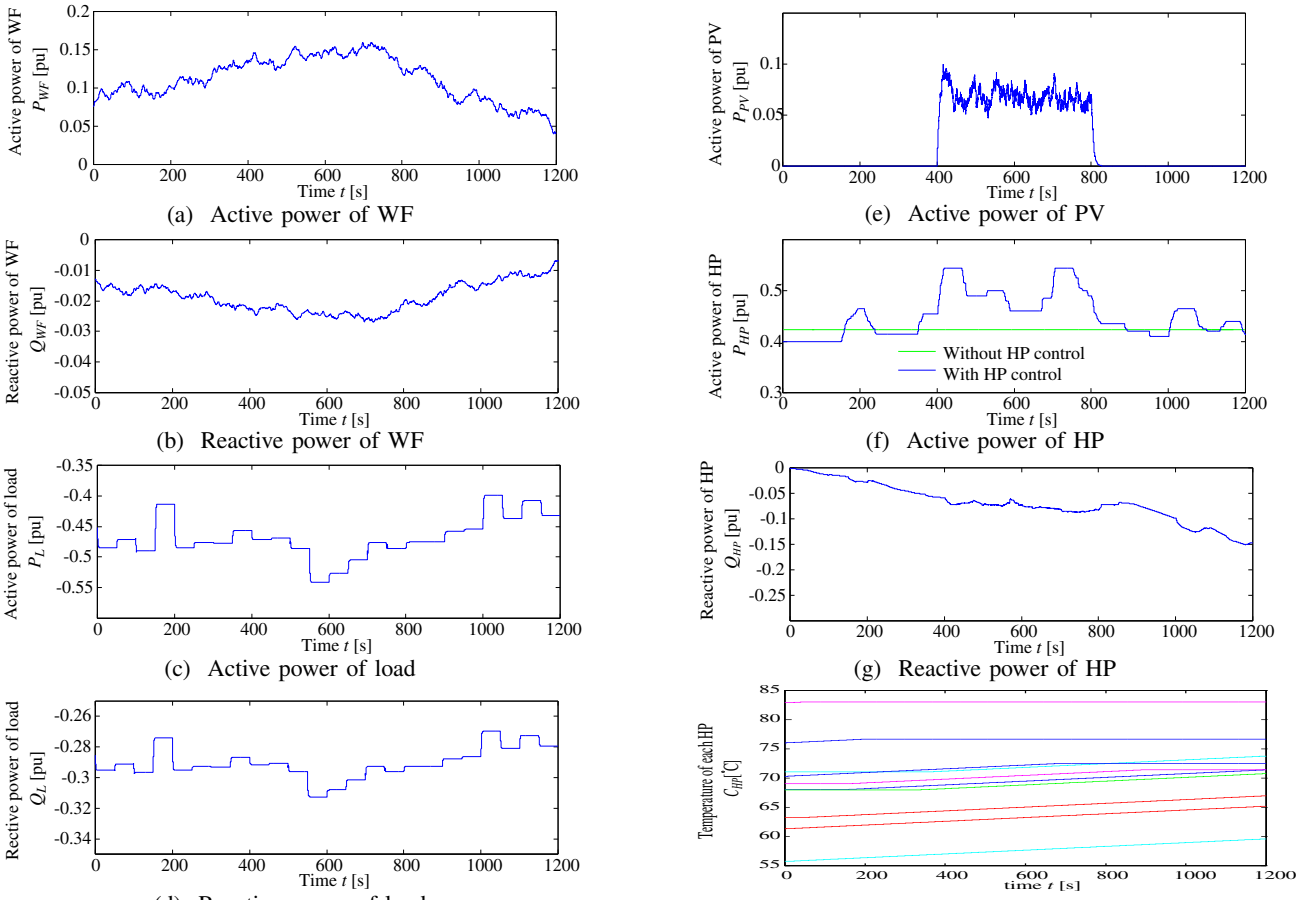

(a) Active power of WF
(b) Reactive power of WF
(c) Active power of load
(d) Reactive power of load
(e) Active power of PV
(f) Active power of HP
(g) Reactive power of HP
(h) Water temperature of 10HPs of all HPs

Fig. 13. Simulation results.

with gain multiple. The variation of wind farm output, non-controllable loads and photovoltaic outputs are assumed in this paper are shown in Fig. 13 (a)∼(e), respectively. The wind farm output is assumed by long-period fluctuation in 40-minute and short-period fluctuation in seconds as shown in Fig. 13(a), (b). The non-cantrollable load power consumptions P_l, Q_l are changed to assume the on/off operation of electric appliance as shown in Fig. 13(c), (d). The white noise is used to represent drastic change of photovoltaic output P_{pv} as shown in Fig. 13(e). The power consumption P_{HP} of HP is changed to suppress low-frequency component of frequency fluctuation in power system as seen in control results of Fig. 13(f). The reactive power Q_{HP} of HP is changed to suppress voltage fluctuation at bus 2 as shown in Fig. 13(g). Also the water temperature C_{HP} of 10 HPs are raised up respectively as seen in control result of Fig. 13(h). Fig. 14(a) show number of HP on each states that waiting states to stabilized and controllable states. The discharge and charge power P_b of battery are changed to suppress high-frequency component of frequency fluctuation in power system as seen in control results of Fig. 14(b). It can be seen that charged rate of battery stays constant as shown in Fig. 14(c). The reactive power Q_b of battery is changing to suppress voltage fluctuation at bus 2 as shown in Fig. 14(d). In case of without control, the active power P_d and reactive power Q_d of diesel generator fluctuate due to wind farm, photovoltaic and load variation are shown in Figs. 14(e), (f). Alternatively, when controllable loads are controlled, the diesel generator output P_d becomes smooth. The reactive power Q_d (Fig. 14(f)) also becomes smooth as well as active power. Therefore, it is seen that HP suppresses frequency fluctuation from low-frequency domain of diesel generator to low-frequency component in battery operating domain. Terminal voltage V2 of bus 2 is illustrated in Fig. 14(g). Although theterminal voltage fluctuates for the case where controllable load withoutcontrol and with control, the voltage becomes smooth and are kept in rated range as seen in same figure. It can be seen that the system frequency deviation df stays constant in Fig. 14(h). Therefore, the effectiveness of system frequency control and voltage control by power consumption control of decentralized controllable load in demand side is confirmed.

VII. Conclusion

This paper presents a control system to achieve suppression of frequency deviation and voltage fluctuation by using controllable load that may steadily increase in demand side in future. The power fluctuation occurred due to disperse power system is suppressed by active and reactive power control of controllable loads. Therefore, controllable loads are

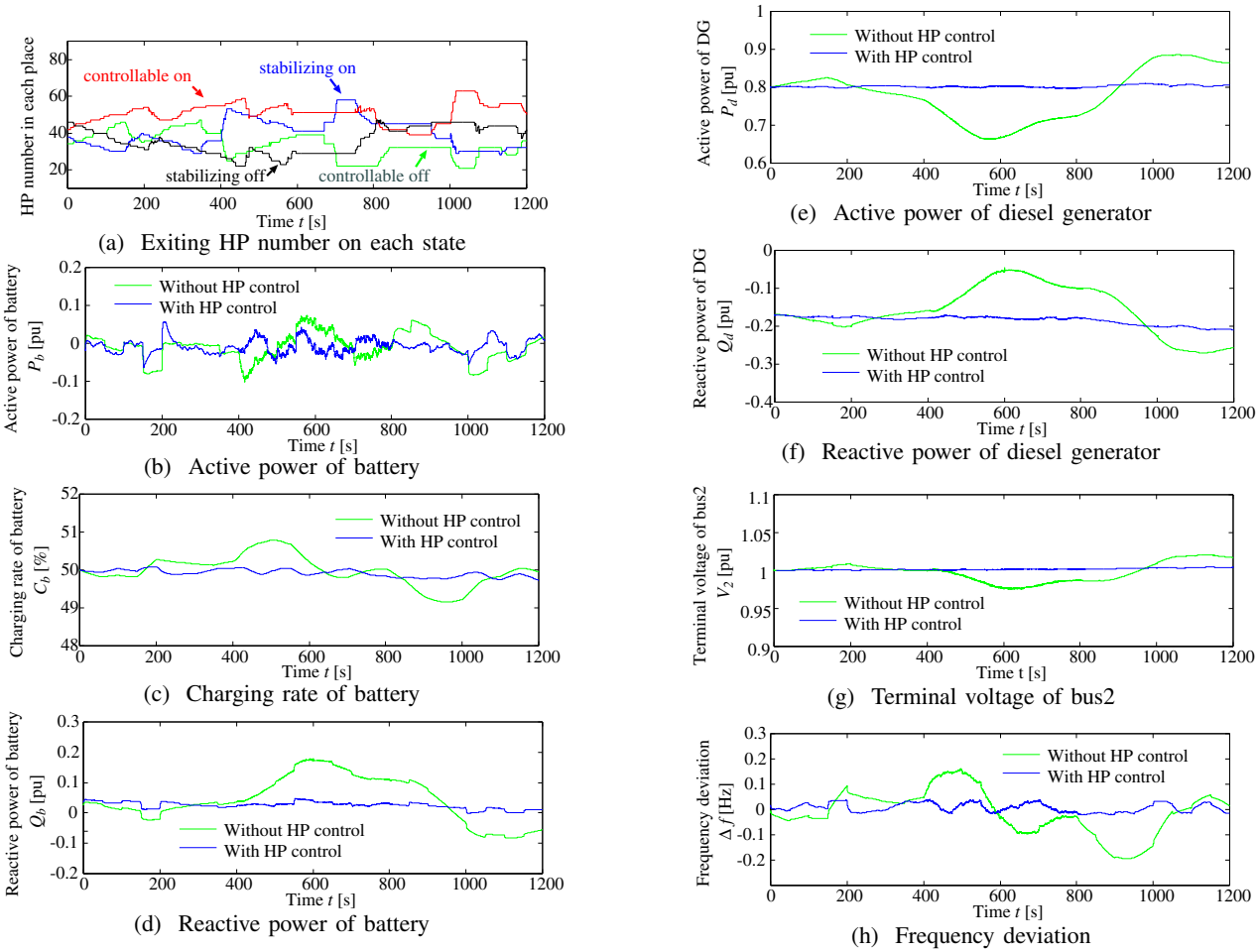

(a) Exiting HP number on each state

(b) Active power of battery

(c) Charging rate of battery

(d) Reactive power of battery

(e) Active power of diesel generator

(f) Reactive power of diesel generator

(g) Terminal voltage of bus2

(h) Frequency deviation

Fig. 14. Simulation results.

operated to suppress the power fluctuation, and the following are achieved without any communication: balancing of the supply-demand, generating power leveling of output power of diesel generator, and suppressing frequency fluctuation. There are advantages that wind turbine generator and photovoltaic generation enable to operate in maximum power point, equipment cost of battery is reduced and the ability to control the frequency is ensured. Consequently, electricity companies can expect to supply the high quality power and to reduce the capital cost.

REFERENCES

[1] N. Duic and M. G. Carvalho, "Increasing renewable energy sources in island energy supply: case study Porto Santo," *Renewable and sustainable energy*, vol. 8, pp. 383-399, 2004.

[2] D. A. Katsaprakakis, N. Paradakis, G. Kozirakis, Y. Minadakis, D. Christakis, and K. Kondaxakis, "Electricity supply on the island of Dia based on renewable energy sources(R. E. S)," *Applied Energy*, vol. 86, pp. 516-527, 2009.

[3] J. L. Rodriguez-Amenedo, S. Arnalte,and J. C. Burgos, "Automatic Generation Control of a Wind Farm With Variable Speed Wind Turbines," *T. IEEE Trans. on Energy Conversion*, vol 17, no. 2, pp. 279-284, 2002.

[4] Akie Uehara, Tomonobu Senjyu, Atsushi Yona, and Toshihisa Funabashi, "A Frequency Control Method by Wind Farm & Battery using Load Estimation in Isolated Power System," *International Journal of Emerging Electric Power Systems*,Vol. 11, Iss. 2, Article 2 , 2010.

[5] A. S. Yilmaz and Z. Ozer, "Pitch angle control in wind turbines above the rated wind speed by multi-layer percepton and radial function neural networks," *Expert Systems with Applications*, vol. 36, pp. 9767-9775, 2009.

[6] J. A. Momoh, "Smart Grid Design for Efficient and Flexible Power Networks Operation and Control," Power Systems Conference and Exposition 2009, pp. 1-8, 2009.

[7] M. Pipattanasomporn, H. Feroze, and S. Rahman, "Multi-Agent Systems in a Distributed Smart Grid: Design and Implementation," PSCE 2009, pp. 1-8, 2009.

[8] A. Molderink, V. Bakker, M. G. C. Bosman, J. L. Hurink, and G. J. M. Smit, "Domestic Energy Managemant Methodology for Optimizing Efficiency in Smart Grids," 2009 IEEE Power Tech Conference, pp. 1-7, 2009.

[9] P. Taylor, "Increased Renewable Energy Penetration on Island Power Systems through Distributed Fuzzy Load Control," *Int. Conf. Renewable Energies for Islands Toward 100% RES Supply, Greece*, June. 2001.

[10] M. Chilali and P. Gahinet, "H_∞ Design with Pole Placement Constraints: An LMI Approach," *IEEE Trans. on Automatic Control*, vol. 41, no. 3, pp. 358-367, 1996.

[11] C. Scherer, P. Gahinet, and M. Chilali, "Multiobjective Output Feedback Control via LMI Optimization," *IEEE Trans. on Automatic Control*, vol. 42, no. 7, pp. 896-911, 1997.

[12] P. Gahinet, A. Nemirovski, A. J. Laub, and M. Chilali, *"LMI Control Toolbox For Use with MATLAB,"* The Mathworks Inc. 2000.

2011 IEEE International Conference on Fuzzy Systems
June 27-30, 2011, Taipei, Taiwan

Short-Term Load Forecasting Via Fuzzy Neural Network With Varied Learning Rates

Rong-Jong Wai [1], Yi-Chang Chen [1] and Yung-Ruei Chang [2]

[1] Department of Electrical Engineering, Yuan Ze University, Chung Li, Taiwan, R.O.C.
[2] Institute of Nuclear Energy Research, Atomic Energy Council, Taoyuan, Taiwan, R.O.C.

***Abstract*–Due to the lack of natural resources, the majority of energy in many countries must depend on import, and the corresponding cost is expensive and affected by international market fluctuation and control. In recent years, an intelligent micro- grid system composed of renewable energy sources is becoming one of the interesting research topics. The forecasting of short-term loads enables the intelligent micro-grid system to manipulate an optimized loading and unloading control by measuring the electrical supply each hour for achieving the best economical and power efficiency. Therefore, this study investigates a fuzzy neural network (FNN) with varied learning rates for the short-term load forecasting (STLF), and compares its better forecasting performance with a conventional neural network (NN) by numerical simulations of a real case in Taiwan campus.**

***Keywords*–Fuzzy neural network, varied learning rates, short-term load forecasting.**

I. INTRODUCTION

Nowadays, the research topic of short-term load forecasting (STLF) becomes an important issue for power system operations. In general, the objective of high-precision STLF is difficult to reach due to complex effects on load by a variety of factors. In the past researches, various STLF methods have been investigated [1], including exponential smoothing [2], regression [3], Box-Jenkins models [4], Kalman filter [5], state space model [6], and time series techniques [6]. These frameworks were developed based on statistical methods and proven to work well under normal conditions. However, these methods show some deficiency in the presence of an abrupt change in environment or sociological variables, which are believed to affect load patterns. Besides, the employed techniques for these models in [1]–[6] use a large number of complex relationships and require a long computational time, so that the desired forecasting accuracy can not be achieved.

In recent years, artificial intelligent methods have attracted more attention in application to load forecasting, such as pattern recognition [7], expert system techniques [8]–[10], neural network (NN) [11]–[14] and fuzzy logic system [15], [16]. Amjady, Daraeepour, and Keynia [11] comprised a modified version of a relief algorithm for the feature selection and a hybrid neural network to forecast the day-ahead electricity price. Bashir and El-Hawary [12] proposed adaptive artificial neural networks with particle swarm optimization to forecast the hourly load. In the previous literatures [15], [16], fuzzy logic was designed for short-term and midterm load forecasting. Unfortunately, the detailed action behavior in the NN is difficult to handle clearly, and how to build appropriate rules in the fuzzy system is the major problem to be solved. Therefore, the concept of incorporating fuzzy logic into a neural network has grown into a popular research topic [17]. The integrated fuzzy-neural-network (FNN) system possesses the merits of both fuzzy systems (e.g., humanlike IF-THEN rules thinking and ease of incorporating expert knowledge) and neural networks (e.g., learning and optimization abilities, and connectionist structures). By this way, one can bring the low-level learning and computational power of neural networks into fuzzy systems and also high-level, humanlike IF-THEN rule thinking and reasoning of fuzzy systems into neural networks [18]–[20].

This study investigates a FNN forecaster with varied learning rates for the STLF model, and compares its better forecasting performance with a conventional NN forecaster. The back-propagation algorithm is used to train the FNN on line. Moreover, to guarantee the convergence of forecasting error, analytical methods based on a discrete-type Lyapunov function are proposed to determine the varied learning rates of the FNN. This study is organized into five sections. Following the introduction, the network structure of a four-layer FNN is described, and the on-line training algorithm for the FNN with varied learning rates is derived in Section II. Moreover, the proposed STLF model via the FNN forecaster is illustrated in Section III. In Section IV, numerical simulations are given to verify the effectiveness of the proposed strategy in terms of mean average percentage error (MAPE). Finally, some conclusions are drawn in Section V.

II. FUZZY NEURAL NETWORK

A. Description of Network Structure

A general four-layer fuzzy neural network (FNN) as shown in Fig. 1, which is composed of the input (the *i* layer), membership (the *j* layer), rule (the *k* layer) and output layers (the *o* layer), is adopted to implement the proposed FNN forecaster. Nodes in the input layer represent the input linguistic variables. Nodes in the membership layer act as the membership functions. Moreover, all the nodes in the rule layer form a fuzzy rule base. The signal propagation and the basic function of each layer are introduced as follows.

This work was supported by the Institute of Nuclear Energy Research of Taiwan, R.O.C. through grant number 1002001INER065.

978-1-4244-7316-8/11/$26.00 ©2011 IEEE

Layer 1: input layer

For every node *i* in this layer, the net input and the net output can be represented as

$$net_i^1 = x_h^1, \quad y_i^1 = f_i^1(net_i^1) = net_i^1 \tag{1}$$

where x_h^1 represents the *i*th input to the node of layer 1.

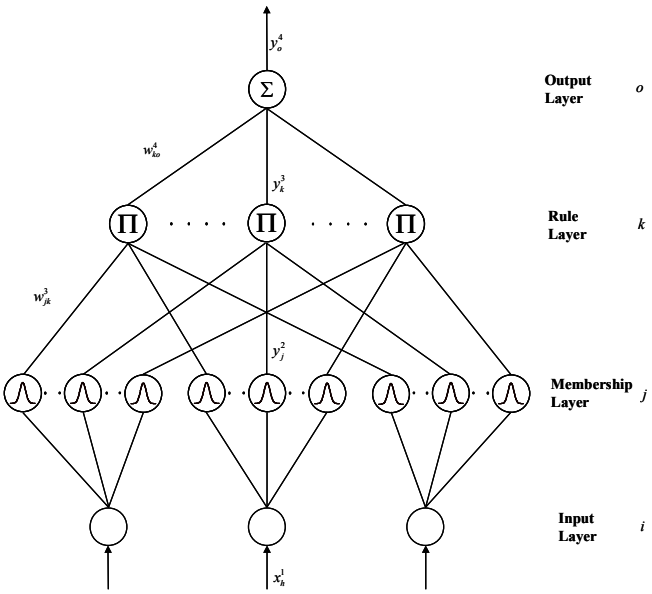

Fig. 1. Structure of four-layer fuzzy neural network (FNN).

Layer 2: membership layer

In this layer, each node performs a membership function. The Gaussian function is adopted as the membership function. For the *j*th node

$$net_j^2 = -\frac{(x_i^2 - m_{ij})^2}{(\sigma_{ij})^2}, \quad y_j^2 = f_j^2(net_j^2) = exp(net_j^2) \tag{2}$$

where m_{ij} and σ_{ij} are, respectively, the mean and the standard deviation of the Gaussian function in the *j*th term of the *i*th input linguistic variable x_i^2 to the node of layer 2.

Layer 3: rule layer

Each node *k* in this layer is denoted by $\prod$, which multiplies the incoming signal and outputs the result of product. For the *k*th rule node

$$net_k^3 = \prod_j w_{jk}^3 x_j^3, \qquad y_k^3 = f_k^3(net_k^3) = net_k^3 \tag{3}$$

where x_j^3 represents the *j*th input to the node of layer 3, and w_{jk}^3 is assumed to be unity.

Layer 4: output layer

The single node *o* in this layer is labeled as Σ, which computes the overall output as the summation of all incoming signals.

$$net_o^4 = \sum_k w_{ko}^4 x_k^4, \qquad y_o^4 = f_o^4(net_o^4) = net_o^4 \tag{4}$$

where the link weight w_{ko}^4 is the output action strength of the *o*th output associated with the *k*th rule; x_k^4 represents the *k*th input to the node of layer 4, and y_o^4 is the output of the FNN forecaster.

B. On-Line Learning Algorithm

The central part of the learning algorithm for an FNN concerns how to recursively obtain a gradient vector in which each element in the learning algorithm is defined as the derivative of an energy function with respect to a parameter of the network. This is done by means of the chain rule, and the method is generally referred to as the back-propagation learning rule, because the gradient vector is calculated in the direction opposite to the flow of the output of each node [17]. To describe the on-line learning algorithm of the FNN using the supervised gradient decent method, first the energy function *E* is defined as

$$E = (x_f - x_l)^2 / 2 = e^2 / 2 \tag{5}$$

where x_f and x_l represent the forecasting load and the actual load, and *e* denotes the output error between the forecasting load and the actual load. Then, the learning algorithm is described as follows.

Layer 4:

The error term to be propagated is given by

$$\delta_o^4 = -\frac{\partial E}{\partial y_o^4} = \left[-\frac{\partial E}{\partial e}\frac{\partial e}{\partial y_o^4}\right] = \left[-\frac{\partial E}{\partial e}\frac{\partial e}{\partial x_l}\frac{\partial x_l}{\partial y_o^4}\right] \tag{6}$$

and the weight is updated by the amount

$$\Delta w_{ko}^4 = -\eta_w \frac{\partial E}{\partial w_{ko}^4} = \left[-\eta_w \frac{\partial E}{\partial y_o^4}\right]\left(\frac{\partial y_o^4}{\partial net_o^4}\frac{\partial net_o^4}{\partial w_{ko}^4}\right) = \eta_w \delta_o^4 x_k^4 \tag{7}$$

The weights of the output layer are updated according to the following equation:

$$w_{ko}^4(N+1) = w_{ko}^4(N) + \Delta w_{ko}^4 \tag{8}$$

where the factor η_w is the learning-rate parameter of the weight, and N denotes the number of iteration.

Layer 3:

Since the weights in this layer are unity, only the error term needs to be calculated and propagated.

$$\delta_k^3 = -\frac{\partial E}{\partial net_k^3} = \left[-\frac{\partial E}{\partial y_o^4}\right]\left(\frac{\partial y_o^4}{\partial net_o^4}\frac{\partial net_o^4}{\partial y_k^3}\frac{\partial y_k^3}{\partial net_k^3}\right) = \delta_o^4 w_{ko}^4 \tag{9}$$

Layer 2:

The multiplication operation is done in this layer. The error term is computed as follows:

$$\begin{aligned}\delta_j^2 &= -\frac{\partial E}{\partial net_j^2} \\ &= \left[-\frac{\partial E}{\partial y_o^4}\frac{\partial y_o^4}{\partial net_o^4}\frac{\partial net_o^4}{\partial y_k^3}\frac{\partial y_k^3}{\partial net_k^3}\right]\left[\frac{\partial net_k^3}{\partial y_j^2}\frac{\partial y_j^2}{\partial net_j^2}\right] = \sum_k \delta_k^3 y_k^3\end{aligned} \tag{10}$$

Moreover, the variations of m_{ij} and σ_{ij} can be expressed as

$$\Delta m_{ij} = -\eta_m \frac{\partial E}{\partial m_{ij}} = \eta_m \delta_j^2 \frac{2(x_i^2 - m_{ij})}{(\sigma_{ij})^2} \tag{11}$$

$$\Delta \sigma_{ij} = -\eta_\sigma \frac{\partial E}{\partial \sigma_{ij}} = \eta_\sigma \delta_j^2 \frac{2(x_i^2 - m_{ij})^2}{(\sigma_{ij})^3} \tag{12}$$

where η_m and η_σ are the learning-rate parameters of the mean and the standard deviation of the Gaussian function. The mean and standard deviation of the membership layer are updated as follows:

$$m_{ij}(N+1) = m_{ij}(N) + \Delta m_{ij} \tag{13}$$

$$\sigma_{ij}(N+1) = \sigma_{ij}(N) + \Delta \sigma_{ij} \tag{14}$$

C. Convergence Analyses

Selection of the values for the learning-rate parameters has a significant effect on the network performance. In order to train the FNN effectively, three varied learning rates, which guarantee convergence of the output error based on the analyses of a discrete-type Lyapunov function, are derived in this section. The convergence analyses in this study are to derive specific learning-rate parameters for specific types of network parameters to assure convergence of the output error.

Theorem 1: Let η_w be the learning-rate parameter of the FNN weights and let P_{wmax} be defined as $P_{wmax} \equiv max_N \left\| P_w(N) \right\|$, where $P_w(N) = \partial y_o^4 / \partial w_{ko}^4$ and $\|\cdot\|$ is the Euclidean norm in $\Re^n$. The convergence is guaranteed if η_w is chosen as $\eta_w = \lambda / (P_{wmax}{}^2) = \lambda / R_u$, in which λ is a positive constant gain, and R_u is the number of rules in the FNN.

Proof: Since

$$P_w(N) = \frac{\partial y_o^4}{\partial w_{ko}^4} = x_k^4 \tag{15}$$

Thus

$$\left\| P_w(N) \right\| < \sqrt{R_u} \tag{16}$$

Then, a discrete-type Lyapunov function is selected as

$$V(N) = e^2(N)/2 \tag{17}$$

The change in the Lyapunov function can be obtained by

$$\Delta V(N) = V(N+1) - V(N) = [e^2(N+1) - e^2(N)]/2 \tag{18}$$

The error difference can be represented by

$$e(N+1) = e(N) + \Delta e(N) = e(N) + \left[\frac{\partial e(N)}{\partial w_{ko}^4} \right]^T \Delta w_{ko}^4 \tag{19}$$

where Δw_{ko}^4 represents a weight change in the output layer. By using (6), (7) and (19), then

$$\frac{\partial e(N)}{\partial w_{ko}^4} = \frac{\partial e(N)}{\partial y_o^4} \frac{\partial y_o^4}{\partial w_{ko}^4} = -\frac{\delta_o^4}{e(N)} P_w(N) \tag{20}$$

$$e(N+1) = e(N) - \left[\frac{\delta_o^4}{e(N)} P_w(N) \right]^T \eta_w \delta_o^4 P_w(N) \tag{21}$$

Then

$$\left\| e(N+1) \right\| \le \left\| e(N) \right\| \left\| 1 - \eta_w \left(\delta_o^4 / e(N) \right)^2 P_w^T(N) P_w(N) \right\| \tag{22}$$

If η_w is chosen as $\eta_w = \lambda / (P_{wmax}{}^2) = \lambda / R_u$, the term $\left\| 1 - \eta_w \left(\delta_o^4 / e(N) \right)^2 P_w^T(N) P_w(N) \right\|$ in (22) is less than 1. Therefore, the Lyapunov stability of $V > 0$ and $\Delta V < 0$ is guaranteed. The output error between the forecasting load and the actual load will converge to zero as $t \to \infty$. This completes the proof of Theorem 1.

In order to prove Theorem 2, the following lemmas [18] will be used.

Lemma 1 : Let $p(z) = z\, exp(-z^2)$. Then $|p(z)| < 1$, $\forall z \in \Re$.

Lemma 2 : Let $q(z) = z^2\, exp(-z^2)$. Then $|q(z)| < 1$, $\forall z \in \Re$.

Theorem 2: Let η_m and η_σ be the learning-rate parameters of the mean and the standard deviation of the Gaussian function for the FNN; let P_{mmax} be defined as $P_{mmax} \equiv max_N \left\| P_m(N) \right\|$, where $P_m(N) = \partial y_o^4 / \partial m_{ij}$; let $P_{\sigma max}$ be defined as $P_{\sigma max} \equiv max_N \left\| P_\sigma(N) \right\|$, where $P_\sigma(N) = \partial y_o^4 / \partial \sigma_{ij}$; $\|\cdot\|$ is the Euclidean norm in $\Re^n$. The convergence is guaranteed if η_m and η_σ is chosen as $\eta_m = \eta_\sigma = \eta_w [\left| w_{ko\,max}^4 \right| (2/\sigma_{ij\,min})]^{-2}$, in which $\eta_w = \lambda / R_u$; λ is a positive constant gain; $w_{ko\,\max}^4 = max_N [w_{ko}^4(N)]$; $\sigma_{ij\,\min} = max_N [\sigma_{ij}(N)]$; $|\cdot|$ is the absolute value.

Proof: According to lemma 1, $\left| [(x_i^2 - m_{ij})/\sigma_{ij}] exp\{ -\left[(x_i^2 - m_{ij})/\sigma_{ij} \right]^2 \} \right| < 1$. Since

$$\begin{aligned} P_m(N) &= \frac{\partial y_o^4(N)}{\partial m_{ij}} = w_{ko}^4 \frac{\partial y_j^2}{\partial m_{ij}} \\ &< w_{ko}^4 \left\{ max \left(\frac{2}{\sigma_{ij}} \right) \right\} = w_{ko}^4 \left(\frac{2}{\sigma_{ij\,min}} \right) \end{aligned} \tag{23}$$

Thus,

$$\left\| P_m(N) \right\| < \sqrt{R_u} \left| w_{ko\,max}^4 \right| (2/\sigma_{ij\,min}) \tag{24}$$

The error difference can also be represented by

$$e(N+1) = e(N) + \Delta e(N) = e(N) + \left[\frac{\partial e(N)}{\partial m_{ij}} \right]^T \Delta m_{ij} \tag{25}$$

where Δm_{ij} represents a change of the mean of the Gaussian function in the membership layer. By using (6), (11) and (25), then

$$\frac{\partial e(N)}{\partial m_{ij}} = \frac{\partial e(N)}{\partial y_o^4} \frac{\partial y_o^4}{\partial m_{ij}} = -\frac{\delta_o^4}{e(N)} P_m(N) \tag{26}$$

$$e(N+1) = e(N) - \left[\frac{\delta_o^4}{e(N)} P_m(N) \right]^T \eta_m \delta_o^4 P_m(N) \tag{27}$$

Then

$$\left\| e(N+1) \right\| \le \left\| e(N) \right\| \left\| 1 - \eta_m \left(\delta_o^4 / e(N) \right)^2 P_m^T(N) P_m(N) \right\| \tag{28}$$

If η_m is chosen as $\eta_m = \lambda / R_u [\left| w_{ko\,max}^4 \right| (2/\sigma_{ij\,\min})]^{-2} = \eta_w [\left| w_{ko\,max}^4 \right| (2/\sigma_{ij\,\min})]^{-2}$, $\left\| 1 - \eta_m \left(\delta_o^4 / e(N) \right)^2 P_m^T(N) P_m(N) \right\|$ in (28) is less than 1. Therefore, the Lyapunov stability of $V > 0$ and $\Delta V < 0$ by (17) and (18) is guaranteed. The output error between the forecasting load and the actual load will converge to zero as $t \to \infty$.

According to lemma 2, $\left\| [(x_i^2 - m_{ij}) / \sigma_{ij}]^2 \, exp\{-[(x_i^2 - m_{ij}) / \sigma_{ij}]^2\} \right\| < 1$. Since

$$\begin{aligned} P_\sigma(N) &= \frac{\partial y_o^4(N)}{\partial \sigma_{ij}} = w_{ko}^4 \frac{\partial y_j^2}{\partial \sigma_{ij}} \\ &< w_{ko}^4 \left\{ max\left(\frac{2}{\sigma_{ij}} \right) \right\} = w_{ko}^4 \left(\frac{2}{\sigma_{ij\,min}} \right) \end{aligned} \tag{29}$$

Thus,

$$\left\| P_\sigma(N) \right\| < \sqrt{R_u} \left| w_{ko\,max}^4 \right| (2/\sigma_{ij\,min}) \tag{30}$$

The error difference can also be represented by

$$e(N+1) = e(N) + \Delta e(N) = e(N) + \left[\frac{\partial e(N)}{\partial \sigma_{ij}} \right]^T \Delta \sigma_{ij} \tag{31}$$

where $\Delta \sigma_{ij}$ represents a standard deviation change of the Gaussian function in membership layer. By using (6), (12) and (31), then

$$\frac{\partial e(N)}{\partial \sigma_{ij}} = \frac{\partial e(N)}{\partial y_o^4} \frac{\partial y_o^4}{\partial \sigma_{ij}} = -\frac{\delta_o^4}{e(N)} P_\sigma(N) \tag{32}$$

$$e(N+1) = e(N) - \left[\frac{\delta_o^4}{e(N)} P_\sigma(N) \right]^T \eta_\sigma \, \delta_o^4 \, P_\sigma(N) \tag{33}$$

Then

$$\left\| e(N+1) \right\| \le \left\| e(N) \right\| \left\| 1 - \eta_\sigma \left(\delta_o^4 / e(N) \right)^2 P_\sigma^T(N) P_\sigma(N) \right\| \tag{34}$$

If η_σ is chosen as $\eta_\sigma = \lambda / R_u [\left| w_{ko\,max}^4 \right| (2/\sigma_{ij\,\min})]^{-2} = \eta_w [\left| w_{ko\,max}^4 \right| (2/\sigma_{ij\,\min})]^{-2}$, $\left\| 1 - \eta_\sigma (\delta_o^4 / e(N))^2 P_\sigma^T(N) P_\sigma(N) \right\|$ in (34) is less than 1. Therefore, the Lyapunov stability of $V > 0$ and $\Delta V < 0$ by (17) and (18) is guaranteed. The output error between the forecasting load and the actual load will converge to zero as $t \to \infty$. This completes the proof of Theorem 2.

III. Short-Term Load Forecasting Model

In general, the historical load data are usually used as the input for the short-term load forecasting (STLF) model. However, how to properly select characteristic data is a key question. To forecast the load at the next hour, the common practice is to use the most recently available load data, i.e., the yesterday load on the same hour. In the past research, the load data at the closed hour was selected to be the input for the STLF model. But, this selection method is not enough to completely appear the features for the forecasting hour. In order to improve the forecasting performance, a similar hour method is used to select the input variable for the STLF model.

The load patterns for weekdays are almost similar while those for weekends are different from weekdays due to social activities. Therefore, load information data for an entire week are considered. Moreover, all hours for a day will be considered because the daytime and night have different load features. In addition, a sudden load variation has a large influence for the forecasting performance. In order to prevent decreasing the forecasting accuracy from the sudden load variation, the data at the closed hours have to be considered.

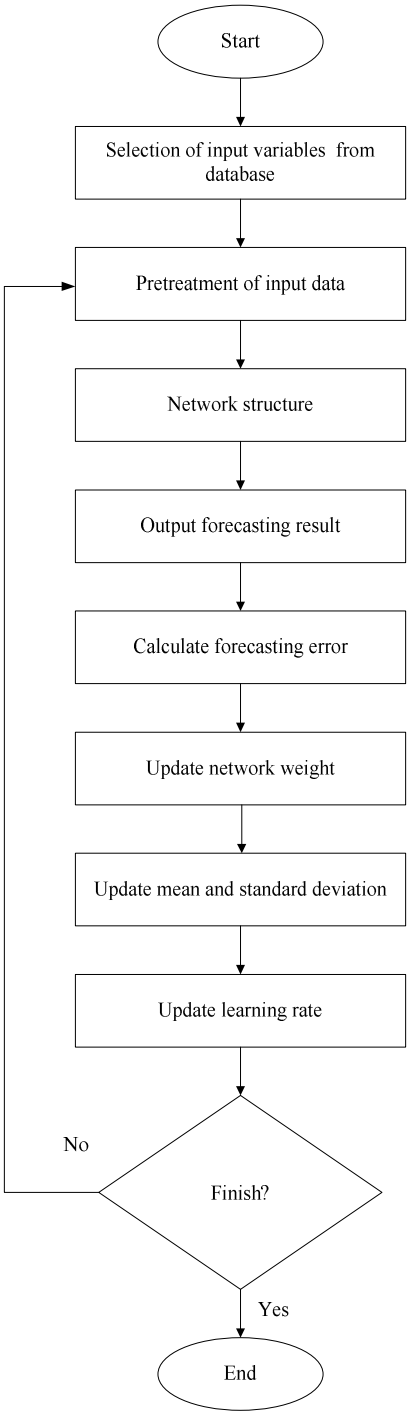

Fig. 2. Flowchart of neural-network-based short-term load forecasting (STLF).

According to the aforementioned consideration, a similar hour-based fuzzy neural network (FNN) forecaster as shown in Fig. 1 is designed to forecast the next hour's load. The flowchart of the proposed STLF model is depicted in Fig. 2. Three major factors including the load data at the same hour with the forecasting hour for yesterday, the load data at the same hour with the forecasting hour for the last week, and the load data at the closed hour with the forecasting hour are considered for the FNN forecaster. It will be helpful for simplifying the FNN structure and reducing the computation burden. In the proposed STLF model, the pretreatment of input data is to use the corresponding change rate in place of real data for normalizing input signals.

In this study, there are three input signals including the load data at the same hour with the forecasting hour for yesterday, and the load data at the same hour with the forecasting hour for the last two week, and one output signal for the FNN forecaster.

$$x_1^1 = [x_l(t-24) - x_l(t-25)] / x_l(t-25) \quad (35)$$

$$x_2^1 = [x_l(t-168) - x_l(t-169)] / x_l(t-169) \quad (36)$$

$$x_3^1 = [x_l(t-336) - x_l(t-337)] / x_l(t-337) \quad (37)$$

where t is the present hour. Because the main target in the proposed STLF model is to forecast the change rate between $x_l(t-1)$ and $x_l(t)$, the forecasting load $x_f(t)$ at the next hour can be represented as

$$x_f(t) = (1 + y_1^4)\, x_l(t-1) \quad (38)$$

The output error between $x_f(t)$ and $x_l(t)$ is continuously calculated to update the weights, the means, the standard deviations and the learning rates of the FNN forecaster until this program is finished. The effectiveness of the proposed STLF model is verified by the following numerical simulations.

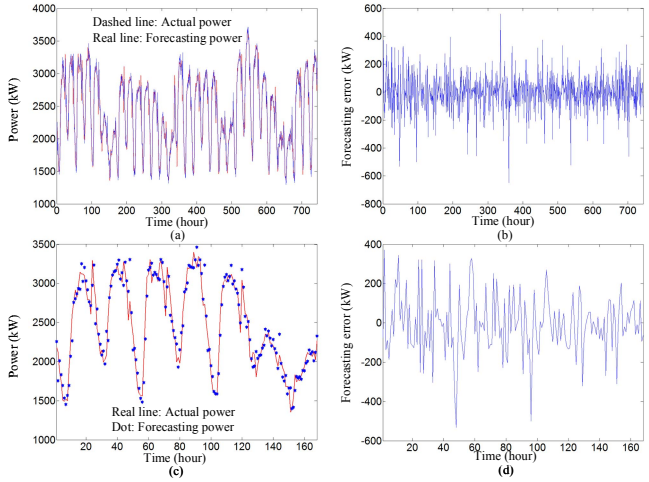

Fig. 3. Numerical simulations of STLF model with FNN forecaster in March: (a) Month forecasting performance; (b) Month forecasting error; (c) Week forecasting performance; (d) Week Forecasting error.

IV. Numerical Simulations

Numerical simulations of the proposed short-term load forecasting (STLF) model are implemented via the MATLAB software based on the schemes as shown in Figs. 1 and 2. In this study, the following mean absolute percentage error (MAPE) is adopted to measure the forecasting performance:

$$MAPE = \frac{1}{M}\sum_{t=1}^{M}\left[\frac{|x_f(t) - x_l(t)|}{x_l(t)}\right] \times 100\% \quad (39)$$

where M is the number of forecasting loads. In the numerical simulations, real data came from the energy management system in Yuan Ze University, Taiwan is used for examining the forecasting performance. In the fuzzy neural network (FNN) forecaster, there are three inputs in the input layer, nine neurons in the membership layer, twenty-seven neurons in the rule layer, one output in the output layer, and the learning rates are tuned according to Theorems 1 and 2 in Section II-C. For exhibiting the superiority of the proposed FNN forecaster with varied learning rates, a conventional neural network (NN) with the back-propagation learning algorithm is also examined here. In the NN forecaster, there are three inputs in the input layer, nine neurons in the hidden layer, one output in the output layer, and the learning rates are fixed at 0.5. The input and output signals of the NN forecaster are the same as the FNN forecaster as shown in (35)–(38).

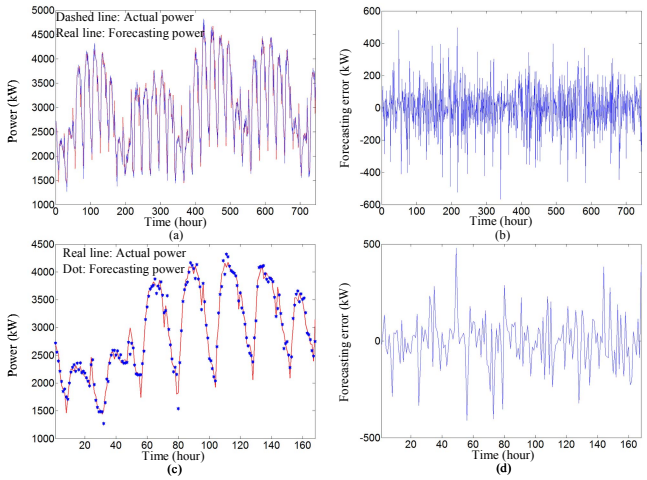

Fig. 4. Numerical simulations of STLF model with FNN forecaster in May: (a) Month forecasting performance; (b) Month forecasting error; (c) Week forecasting performance; (d) Week Forecasting error.

According to season factor and campus environment, the load data at four months (March, May, October and November in 2010) are selected. Numerical illustrations of the STLF model with the proposed FNN forecaster are depicted in Figs. 3–6. For all illustrations given in Figs. 3–6, the sub-figure (a) is the forecasting performance for a month; the sub-figure (b) is the forecasting error for a month; the sub-figure (c) is the forecasting performance for a week; the sub-figure (d) is the forecasting error for a week. The corresponding MAPE records of the STLF model with the conventional NN forecaster and the proposed FNN forecaster for different months are summarized in Table I. From these records, the MAPE value of the proposed STLF model with the FNN forecaster at different testing months is lower than 4.1%, and the average improvement rate in comparison with the conventional NN forecaster is 13.2%.

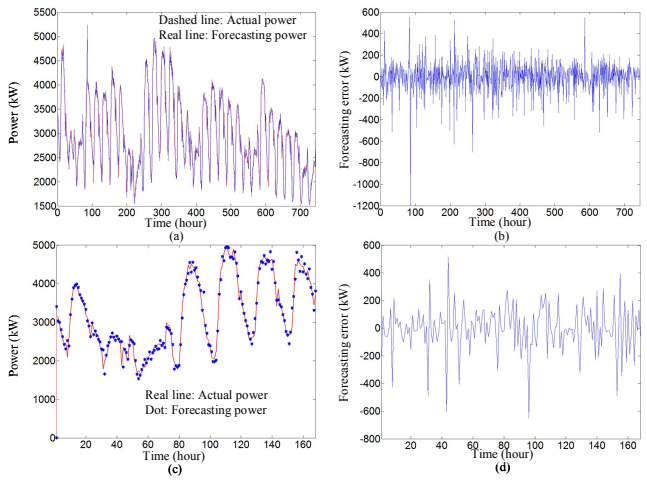

Fig. 5. Numerical simulations of STLF model with FNN forecaster in October: (a) Month forecasting performance; (b) Month forecasting error; (c) Week forecasting performance; (d) Week Forecasting error.

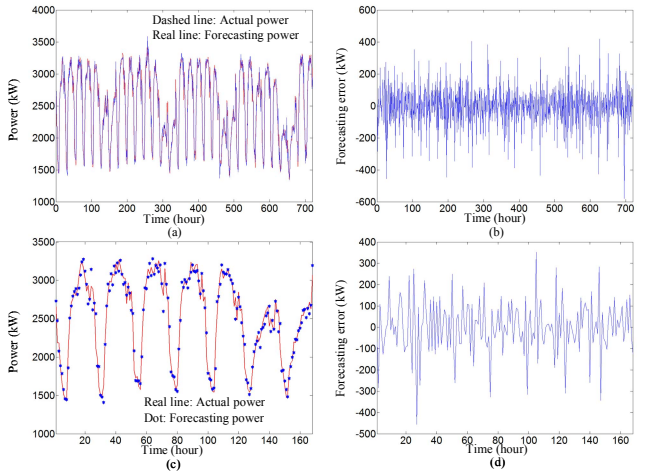

Fig. 6. Numerical simulations of STLF model with FNN forecaster in November: (a) Month forecasting performance; (b) Month forecasting error; (c) Week forecasting performance; (d) Week Forecasting error.

TABLE I. MAPE OF FORECASTING RECORDS FOR DIFFERENT MONTHS

Network structure	March	May	October	November
Fuzzy neural network	3.97%	4.04%	3.69%	3.98%
Neural network	4.8%	4.38%	4.41%	4.48%

V. CONCLUSIONS

This study has successfully developed a short-term load forecasting (STLF) model with a fuzzy neural network (FNN), and applied well to a real case in Taiwan campus. Due to the selection of similar hour data, the network structure can be simplified, and the computation time can be shortened. In order to guarantee the convergence of forecasting error, analytical methods based on a discrete-type Lyapunov function are proposed to determine varied learning rates for the on-line learning algorithm of the FNN forecaster. According to simulated results, the proposed STLF model with the FNN forecaster indeed yields better performance than the one with the conventional NN forecaster, and the average improvement rate is 13.2%. In the future, the proposed STLF model could be modified and extended to midterm and long-term load forecasting.

REFERENCES

[1] N. Amjady and F. Keynia, "Short-term load forecasting of power systems by combination of wavelet transform and neuro-evolutionary algorithm," *Energy*, vol. 34, no. 1, pp. 46–57, Jan. 2009.

[2] B. Billah, M. L. King, R. D. Snyder, and A. B. Koehler, "Exponential smoothing model selection for forecasting," *Int. J. Forecast.*, vol. 22, no. 2, pp. 239–247, June 2006.

[3] E. E. Elattar, J. Y. Goulermas, and Q. H. Wu, "Electric load forecasting based on locally weighted support vector regression," *IEEE Trans. Syst., Man, Cybern.*, vol. 40, no. 4, pp. 438–447, Jul. 2010.

[4] Y. Lu and S. M. AbouRizk, "Automated Box – Jenkins forecasting modelling," *Automation in Construction,* vol. 18, no. 5, pp. 547–558, Aug. 2009.

[5] S. C. Huang, "Online option price forecasting by using unscented Kalman filters and support vector machines," *Expert Systems with Applications,* vol. 34, no. 4, pp. 2819–2825, May 2008.

[6] M. Shahidehpour, H. Yamin, and Z. Li, *Market Operations in Electric Power Systems*. New York: John Wiley & Sons, 2002.

[7] A. S. Dehdashti, J. R. Tudor, and M. C. Smith, "Forecasting of hourly load by pattern recognition-a deterministic approach," *IEEE Trans Power Syst*., vol. 101, no. 9, pp. 3290–3294, Sept. 1982.

[8] S. Rahman and R. Bhatnagar, "An expert system based algorithm for short term load forecast," *IEEE Trans Power Syst.*, vol. 3, no. 2, pp. 392–399, May 1988.

[9] S. Rahman and O. Hazim, "Generalized knowledge-based short-term load forecasting technique," *IEEE Trans Power Syst.*, vol. 8, no. 2, pp. 508–514, May 1993.

[10] K. L. Ho, Y. Y. Hsu, C. F. Chen, T. E. Lee, C. C. Liang, T. S. Lai, and K. K. Chen, "Short term load forecasting of Taiwan power system using a knowledge-based expert system," *IEEE Trans Power Syst.,* vol. 5, no. 4, pp. 1214–1221, Nov. 1990.

[11] N. Amjady, A. Daraeepour, and F. Keynia, "Day-ahead electricity price forecasting by modified relief algorithm and hybrid neural network," *IET Gener. Transm. Distrib.,* vol. 4, no. 3, pp. 432–444, July 2010.

[12] Z. A. Bashir and M. E. El-Hawary, "Applying wavelets to short-term load forecasting using PSO-based neural networks," *IEEE Trans Power Syst.*, vol. 24, no. 1, pp. 20–27, Feb. 2009.

[13] E. González-Romera, M. A. Jaramillo-Morán, and D. Carmona-Fernández, "Monthly electric energy demand forecasting based on trend extraction," *IEEE Trans. Power Syst.*, vol. 21, no. 4, pp.1946–1953, Nov. 2006.

[14] P. C. Chang, C. Y. Fan, and C. H. Liu, "Integrating a piecewise linear representation method and a neural network model for stock trading points prediction," *IEEE Trans. Syst., Man, and Cybern.*, vol. 39, no. 1, pp. 80–92, Jan. 2009.

[15] V. H. Hinojosa and A. Hoese, "Short-term load forecasting using fuzzy inductive reasoning and evolutionary algorithms," *IEEE Trans. Power Syst.*, vol. 25, no. 1, pp. 565–574, Feb. 2010.

[16] N. E. Charalambos and D. H. Nikos, "An annual midterm energy forecasting model using fuzzy logic," *IEEE Trans. Power Syst.*, vol. 24, no. 1, pp. 469–478, Feb. 2009.

[17] C. T. Lin and C. S. George Lee, *Neural Fuzzy Systems*. New Jersey: Prentice-Hall, 1996.

[18] F. J. Lin, R. J. Wai, and C. C. Lee, "Fuzzy neural network position controller for ultrasonic motor drive using push-pull DC-DC converter," *IEE Proc. Control Theory Appl.*, vol. 146, no. 1, pp. 99–107, Jan. 1999.

[19] R. J. Wai, H. H. Lin, and F. J. Lin, "Hybrid controller using fuzzy neural networks for identification and control of induction servo motor drive," *Neurocomputing*, vol. 35, no. 4, pp. 91–112, Nov. 2000.

[20] F. J. Lin and R. J. Wai , "Adaptive fuzzy-neural-network control for induction spindle motor drive," *IEEE Trans. Energy Conversion*, vol. 17, no. 4, pp. 507–513, Dec. 2002.

2011 IEEE International Conference on Fuzzy Systems
June 27-30, 2011, Taipei, Taiwan

A Fuzzy Control Maximum Power Point Tracking Photovoltaic System

Irwan Purnama, Yu-Kang Lo, *IEEE Member*, Huang-Jen Chiu, *IEEE Senior Member*
Department of Electronic Engineering
National Taiwan University of Science and Technology
Taipei, Taiwan
E-mail: irpurnama@yahoo.co.id

***Abstract* -- Conventional maximum power point tracking (MPPT) method, e.g. perturbation and observation (P&O) and incremental conductance (INC), have the drawbacks such as oscillation at the MPP during power fast tracking and power divergence under rapidly changing atmospheric condition. Thus, a fuzzy logic controller (FLC) is implemented in the PV system to avoid the conventional problem. FLC method has not only fast response under rapidly changing atmospheric conditions but also small oscillation at the maximum power point (MPP). However, FLC presents tuning difficulty of membership function, scaling factor and control rules. The FLC disadvantages can be reduced using single-fuzzy logic controller (S-FLC) without degrading its performance. The experiment results are shown to verify the studied S-FLC MPPT method.**

Keywords: Maximum Power Point Tracking, Photovoltaic Module, Single-Fuzzy Logic Control

I. INTRODUCTION

Worldwide energy consumption has increased rapidly due to world population growth. Since amount of fossil energy source has no longer enough, renewable energy sources such as solar power, wind power, geothermal power, and fuel cell are considered to meet the global demand for energy. Aside from the unlimited amount of the sources, renewable energy has advantages such as no or low pollution emissions compared with fossil energy. Among these renewable energy sources, solar energy is one of the most appropriate and primary renewable energy [1, 2]. Although the first PV cell was developed in 1954 [3], the researcher began to conduct its further development in the 1970s. They have improved device efficiency and reliability with lowered cost by using new material and fabrication process [4]. Currently, improvement of PV system performance is the goal of the development.

Development of PV system is generally focused on two areas: the PV cell manufacturing process and materials and the PV power management strategy. Techniques in manufacturing have had significant progress in terms of higher efficiency with lower cost. Regarding to PV power management, implementation of PV system with inappropriate strategy will result in low efficiency. Thus, PV power management strategy including energy conversion system is a very important part in efficiency improvement. One of the energy conversion strategies being developed is method to find maximum power of the PV module that known as maximum power point tracking (MPPT) method. The MPPT method automatically finds the maximum voltage or maximum current of a PV module at which it will operate to reach the maximum power output under certain temperature and irradiance. To obtain good performance, numerous methods are proposed to be implemented in the PV system. Based on the control algorithm, these proposed MPPT methods can be categorized into conventional and intelligent methods. The conventional MPPT method includes perturbation and observation (P&O), incremental conductance (INC), voltage-feedback methods, and so on. Fuzzy logic control (FLC), neural network, genetic algorithm, and so on is based on intelligent algorithm, thus it categorized into intelligent method.

The P&O and INC method are commonly used in the MPPT system because of their simple implementation. However, the P&O method has two drawbacks regarding its performance. The first is power oscillation at the maximum power point (MPP) and the other one is divergence of the MPP under rapid atmospheric change [5, 6, 7, 8]. The problem of power oscillation at the MPP also occurs in the INC method when fast tracking of the maximum power is desired. In the case of solar vehicle which its load consist mainly of batteries, these two methods are not suitable to be implemented. Therefore, an appropriate MPPT method that can quickly converge to MPP without oscillation problem is needed to maximize load current or voltage. One of alternative method to be implemented in this case is FLC MPPT method [8]. The implementation of FLC method in the MPPT system is referred to [9, 10, 11]. Some Improvements of FLC MPPT method has been proposed but it still with complex control rules [10, 11]. Consequently, FLC presents difficulty of modification and tuning of control rules. Due to this reason, B.J. Choi e.t. [12, 13] simplified the inputs of FLC to only one input that known as single-fuzzy logic controller (S-FLC). Besides simplicity of tuning of membership function, scaling factor and control rules, S-FLC present some other advantages such as the control rule table is built in one-dimensional space, the computational complexity is reduced, it is equivalent to the sliding mode control with a boundary layer and so on [13].

II. PV MODULE CHARACTERISTIC

A PV module is composed of PV cells connected in series to achieve required output voltage within a certain range of the system voltage under condition of average irradiance and temperature. The simplest circuit model of PV cell is represented by a current source paralleled with an ideal diode as shown in Fig.1. The current source I_p represents a current source generated by solar radiation. This current source is also called as the photo generated current.

978-1-4244-7316-8/11/$26.00 ©2011 IEEE

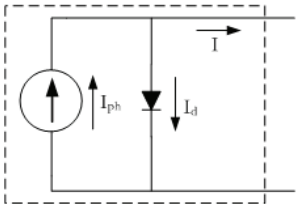

Fig.1. The equivalent circuit of ideal PV cell

The corresponding *I-V* characteristic can be described by the Kirchhoff's Current Law (KCL) where the output current I is the subtraction result of the current source I_p and the diode saturation current I_d. This characteristic can be written as:

$$I = I_p - I_d\left(e^{\frac{qV}{k_B T}} - 1\right) \quad (1)$$

where k_B is the Boltzman constant (1.381×10^{-23} J/K), T is the absolute temperature (in Kelvin), q(>0) is the electron charge (1.602×10^{-19}C), and V is the voltage at the terminal of the cell (in Volt).

In an ideal case, the open circuit voltage V_{oc} is calculated where the short circuit current I_{sc} is equal to the current source I_p. It can be written as:

$$V_{oc} = \frac{k_B T}{q} \ln\left(1 + \frac{I_p}{I_d}\right) \quad (2)$$

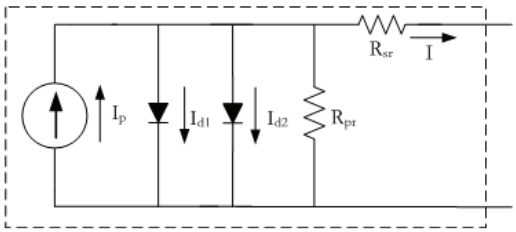

Fig.2. The equivalent circuit of non-ideal PV cell

In practice, a non-ideal circuit is used to model the PV cell represented by a two-diode, shunt resistance R_{pr}, and series resistance R_{sr} as shown in Fig. 2. These components relates to the maximum power which can be generated by the PV cell. In details, the two-diode is used to correct an ideal characteristic curve and the two-resistor is leading to a characteristic of the form where the photo generated current may depend on the voltage. Instead of the equation (1), the characteristic equation is now written by incorporating ideality factor of two which appeared in the exponential term of the second diode. The equation becomes [14]:

$$I = I_p - I_{d1}\left\{\exp\left(\frac{V + IR_{sr}}{k_B T}\right) - 1\right\} - I_{d2}\left\{\exp\left(\frac{V + IR_{sr}}{2k_B T}\right) - 1\right\} - \frac{V + IR_s r}{R_{pr}} \quad (3)$$

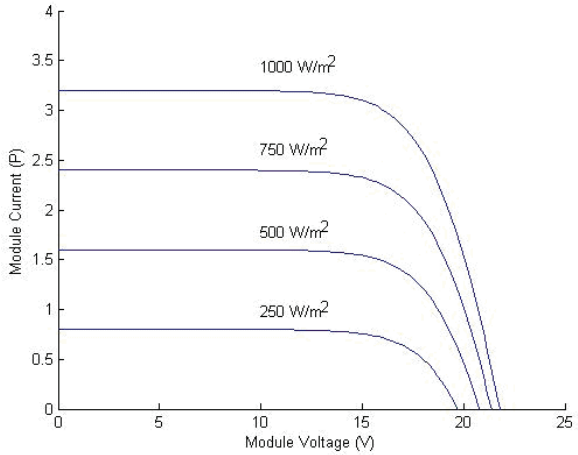

(a)

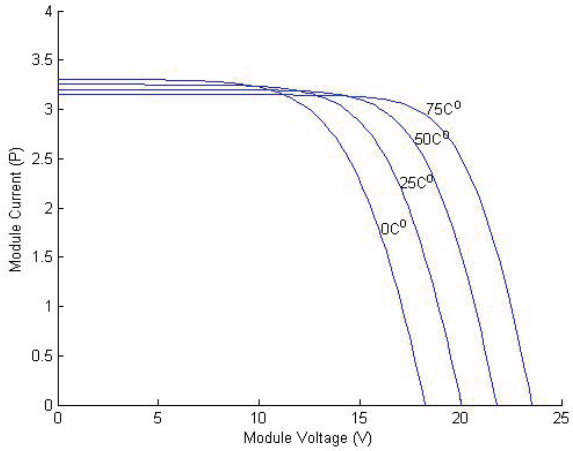

(b)

Fig.3. The *I-V* characteristic of BP350 PV module (a) under different levels of irradiance and (b) under different levels of temperature

The relationship among power P, current I and voltage V produced by the PV module is shown in Fig. 3. The figure shows if the PV module generates power maximum P_{max} at the maximum voltage V_{max} and the maximum current I_{max} and it is varying with present temperature and irradiance.

III. Fuzzy-Logic MPPT Controller

A. Conventional Fuzzy-Logic Controller

Based on fuzzy-logic system (FLS) as shown in Fig.4, fuzzy logic controller (FLC) MPPT method consists of four components: fuzzification, rules and inference engine, and defuzzifier [15, 16, 17]. The input signal is measured from the output of PV power and then processed to generate signal control in the FLS. In the process, each of these signal, either input signal or output signal, are defined by one or more variable (s).

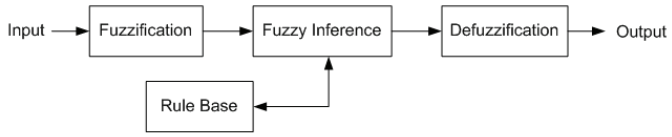

Fig.4. Fuzzy logic system (FLS)

Generally, FLC MPPT method has two input variables, error e and change in error Δe, and an output variable. The two input variables are described by:

$$e(k) = \frac{P_p(k) - P_p(k-1)}{I_p(k) - I_p(k-1)} \tag{4}$$

$$\Delta e(k) = e(k) - e(k-1) \tag{5}$$

where $P_{pk}(k)$ and $I_{pk}(k)$ are the power and current of the PV module, respectively [9]. Therefore, a fast convergence with a small oscillation at the steady state can be achieved. As for the output variable, the output of duty cycle step is expressed by dD.

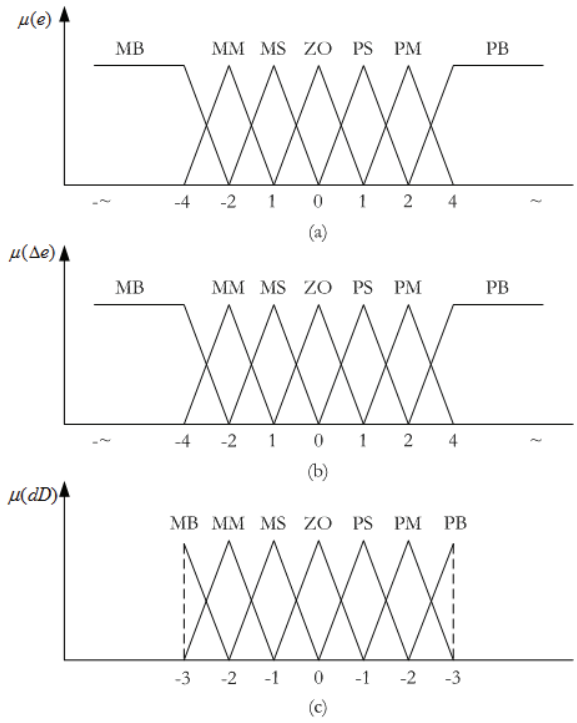

Fig.5. Membership function for (a) input, (b) input $e\Delta$ and (c) output dD

These two input and output variables are represented by fuzzy subsets. As shown in Fig.5, each fuzzy set has seven basic fuzzy subsets for variables of input and output which declared in terms of linguistic variables such as PB (plus big), PM (plus medium), PS (plus small), ZO (zero), MS (minus small), MM (minus medium), NB (minus big).

Fuzzy rules are designed to achieve zero error at the steady state of the MPP. As shown in the Table 1, the main idea of the rule is to bring operating point to the MPP by increasing or decreasing the duty ratio depending on the position of the operating point from the MPP. If the operating point is distant from the MPP, the duty ratio will be increased or decreased largely.

TABLE 1. FUZZY RULES BASE

Δe \ e	ML	MM	MS	ZO	PS	PM	PB
MB	MB	MB	MB	MB	MM	MS	ZO
MM	MB	MB	MB	NM	MS	ZO	PS
MS	MB	MB	MM	MS	ZO	PS	PM
ZO	MB	MM	MS	ZO	PS	PM	PB
PS	MM	MS	ZO	PS	PM	PB	PB
PM	MS	ZO	PS	PM	PB	PB	PB
PB	ZO	PS	PM	PB	PB	PB	PB

Since the rules table has seven linguistic variables of error e and change in error Δe respectively. The fuzzy-logic system has 49 rules as follows:

Rule^{1}*:* IF e is *MB* and Δe is *MB* THEN dD is *MB*

Rule^{2}*:* IF e is *MM* and Δe is *MB* THEN dD is *MB*

...

Rule^{49}*:* IF e is *PB* and Δe is *PB* THEN dD is *PB*

To get the output of inference, many methods are proposed by the researchers. There are some known methods such as Mandani, Sugeno, Larsen, and so on but the Mandani's method is commonly used. Its description is shown in Fig.6.

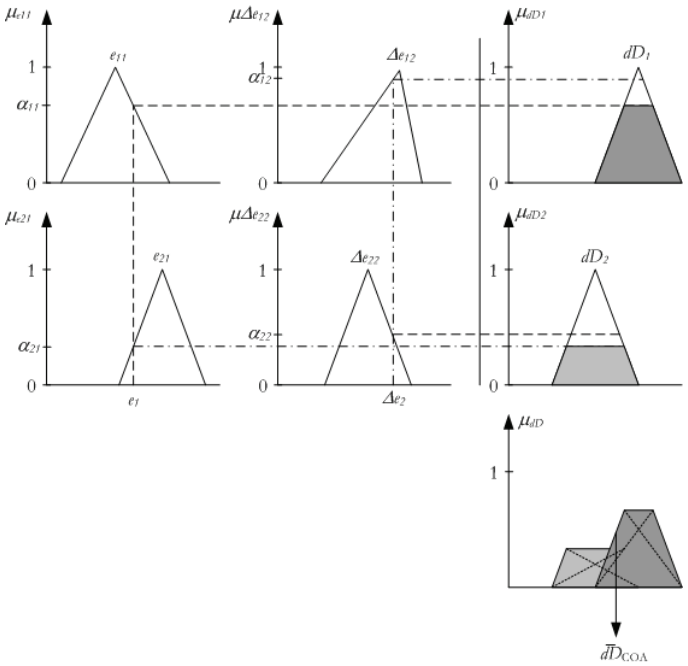

Fig.6. Mandani's inference method with COA defuzzification [17]

The output of fuzzy inference is a fuzzy control subset, such that it must be converted to the crisp value. By using the centroid (COA) defuzzifier, the output control *dD* can be calculated by:

$$dD = \frac{\sum_{k=1}^{I} dD_k \mu_{dD}(dD_k)}{\sum_{k=1}^{I} \mu_{dD}(dD_k)} \quad (6)$$

The value of *dD* is the duty step added to the previous duty cycle of PWM control signals.

B. Single Fuzzy-Logic Controller

S-FLC was published in [12, 13] as the controller of the inverted pendulum system tracking. The experiment proves that the performance and stability of S-FLC are similarly to that of FLC. The standalone MPPT system with S-FLC MPPT method is shown in Fig.7.

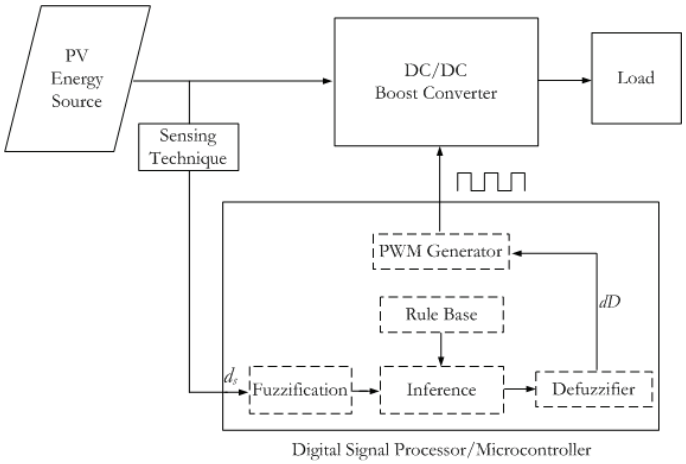

Fig.7. Stand-alone MPPT system with S-FLC MPPT method

As shown in Table 1, The FLC rules have a skew-symmetric property, thus the diagonal lines can be drawn following output variable shapes. The quantization level of the independent variables can be divided into two parts, such that the number of boundaries of control region is two times the numbers of output variables. Because the quantization level of the independent variables becomes infinitesimal, the boundaries become straight lines. Also the absolute magnitude of the input variables is proportional to the distance from the main diagonal line called the switching line *s*. It is written by [12, 13]:

$$s: \Delta e + \quad e = 0 \quad (7)$$

The value of the control input is measured as the distance from the main diagonal line or the distance between *H(e,Δe)* and *P(e,Δe)* called as the signed distance. It is described clearly in Fig. 8. This signed distance is written by:

$$d_s = \mathrm{sgn}(s) \frac{|\Delta e + \lambda e|}{\sqrt{1+\lambda^2}} = \frac{|\Delta e + \lambda e|}{\sqrt{1+\lambda^2}} \quad (8)$$

where:

$$\mathrm{sgn}(s) = \begin{cases} 1 & for\ s > 0 \\ -1 & for\ s < 0 \end{cases} \quad (9)$$

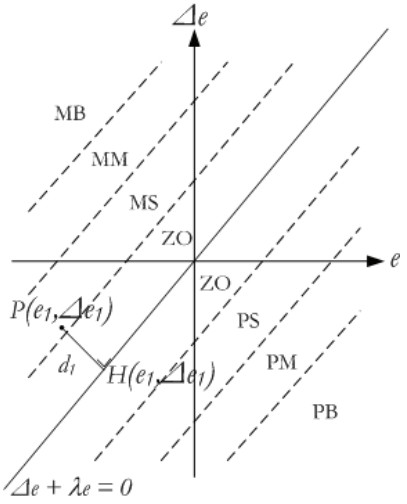

Fig.8. Derivation of a signed distance [12, 13]

Since the sign of a control input depends on the value of switching line *s* as described by equation (9), the absolute magnitude of control input is proportional to the distance from main diagonal line (*s*=0). It can be concluded that:

$$dD \sim -d_s \quad (10)$$

Instead of the fuzzy rules in Table 1, the single-fuzzy rules can be constructed to one dimensional space of d_s as shown in Table 2.

TABLE 2. SINGLE-FUZZY RULES BASE

d_s	MB	MM	MS	ZO	PS	PM	PB
dD	PB	PM	PS	ZO	MS	MM	MB

As shown in Table 2, the fuzzy-logic system has only 7 rules instead of 49 rules of Table 1. These 7 rules of S-FLC is shown as follows:

$Rule^1$: IF d_s is MB THEN *dD* is *PB*

$Rule^2$: IF d_s is MM THEN *dD* is *PM*

...

$Rule^7$: IF d_s is PB THEN *dD* is *MB*

Now, each of input variable *ds* and output variable *dD* is represented by seven basic fuzzy subsets as shown in Fig.9.

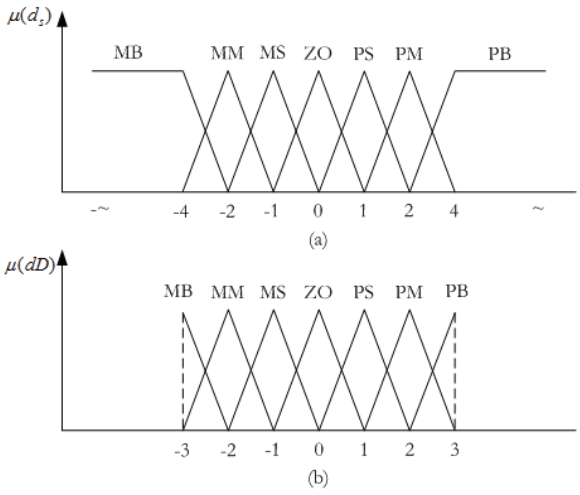

Fig.9. Membership functions for (a) input d_s and (b) output dD

IV. System Design

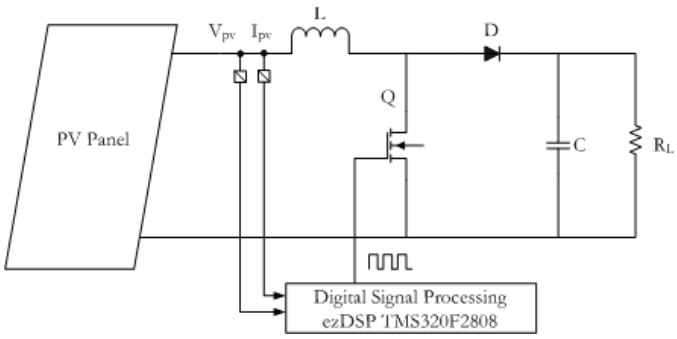

Fig.10. MPPT system with the boost converter and ezDSP TMS320F2800 controller

A design example of the studied MPPT PV system is shown in Fig.10. The design of standalone PV system consists of a PV panel, DC/DC boost converter and DSP controller. The design includes the boost converter which its component selection following the specification in Table 3. As the controller, DSP TMS320F2808 is used where a MPPT algorithm is implemented.

TABLE 3. Design Specifications of the Boost Converter

Specifications	
Nominal input voltage	17.5V
Maximum input voltage	21.8V
Nominal output voltage	24V
Maximum output voltage	50V
Maximum solar power	50Watt
Switching frequency	50kHz
Maximum inductor current ripple	10%
Maximum output voltage ripple	0.50%
Efficiency	>90%

To meet the specification required in Table 3, inductance L and output capacitance value C follows the calculation in Table 4 [18].

TABLE 4. List of the Selection Components: Inductance and Capacitance

Description	Values
Inductance L	$L = \frac{V_{pv} D}{2\Delta i_L f_s} = 165.885 \mu H$
Output capacitance C	$C = \frac{I_o D}{2\Delta v_o f_s} = 47.02 \mu F$

Regarding to diode selection, diode reverse voltage rating is one of the considerations. The diode is used as a current path for the inductor to the output at the off-state power switch and its forward current rating is calculated from the maximum output current. Therefore, a Schottky diode is chosen because it has fast switching characteristics, low reverse–recovery, and low forward voltage drop. The super fast recovery diode rectifier D10LC20U, with $200V$ maximum off-state voltage stresses and $10A$ average current handling, meets the requirement.

In selecting a power MOSFET and driver, the requirements is related to the ability to handle the maximum current and voltage stresses. This maximum voltage stress and the maximum current stress is considered from the maximal PV output voltage, and the maximum output current of PV module with its ripple, respectively. MOSFET IRFZ44N with $55V$ maximum drain-source voltage and $49A$ maximum drain current is selected in this design.

V. Experimental Result

A laboratory prototype of MPPT system is built to validate the performance of the S-FLC MPPT method. The prototype setup consists of a boost DC/DC converter, DSP controller, resistive load and a solar array simulator SAS Agilent E4360 (instead of PV module). The SAS Agilent E4360 simulates PV power source following the specification of BP350 solar module as shown in Table 5.

TABLE 5. The Specification of BP350 Solar Module [19]

Specifications	
Maximum Power (Pmax)	50W
Voltage at Pmax (Vmp)	17.5V
Current at Pmax (Imp)	2.9A
Short-circuit current (Isc)	3.17A
Open-circuit voltage (Voc)	21.8V

The experimental results include not only comparison between S-FLC MPPT method and FLC MPPT method, but also comparison between P&O methods and INC MPPT method. In detail, the results of measurement are described as follows:

a) No MPPT controller

The characteristics of MPPT system when the controller is not activated are shown in Fig. 11. A load of 50 Ω is connected to the system. The SAS voltage and current delivered to the converter is around 21.3*V* and 0.4*A,* respectively. Consequently, the SAS power reached by the system is only 8.7*W* or in the other hand 83% of PV maximum power is lost.

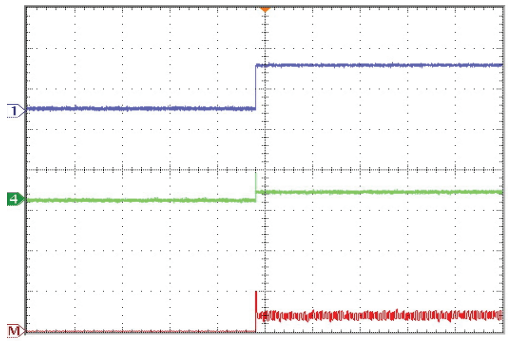

Fig.11. Maximum power reached by the system without any MPPT controller; Scale: [1]-Voltage (20V/div), [4] - Current (2A/div), [M]-Power (20W/div), Time 2s/div.

b) MPPT response time to the steady state

The characteristic of system response to the steady state (MPP) is shown is Fig. 12 when the controller is activated. The initial PWM duty cycle of 50% is set in the controller and a resistive load of 50Ω is connected to the system. It shows that the P&O and INC with 0.2% duty step are slower to reach the MPP than the others. The time required by the S-FLC method to reach the steady state of the MPP is close to the time needed by the P&O and INC with 0.9% duty step.

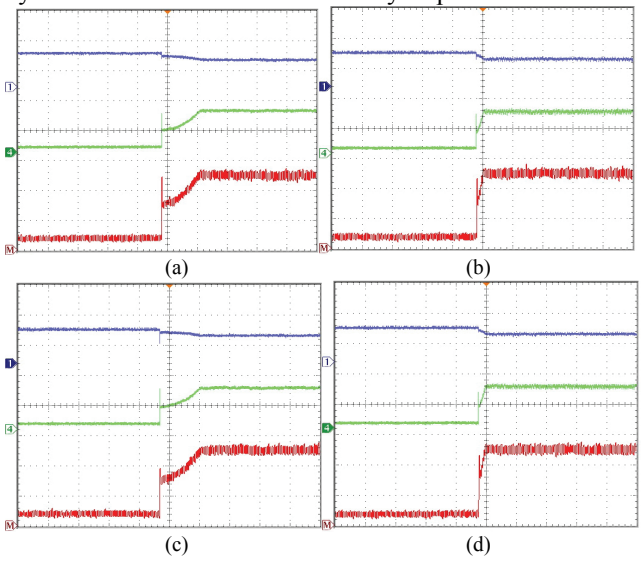

(a) (b) (c) (d)

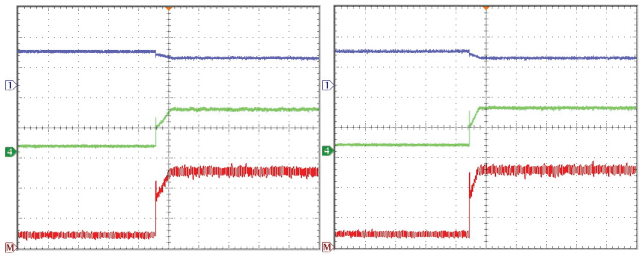

(e) (f)

Fig.12. Time response from no-MPPT to Load R=50Ω (a) P&O with duty step 0.2% (b) P&O with duty step 0.9% (c) INC with duty step 0.2% (d) INC with duty step 0.9% (e) FLC with duty step 0%-0.9% (f) S-FLC with duty step 0%-0.9%; Scale: [1]-Voltage (20V/div), [4]- Current (2A/div), [M]-Power (20W/div), Time 2s/div.

c) MPPT response time to load changing at the steady state

To validate the MPPT system response to the changing atmospheric condition, the system is tested by changing the loads. The value of load changing is 50 Ω to 100Ω and then 100Ω to 50Ω. Both FLC and S-FLC method have a fast response to reach the steady state condition. Fig. 13 shows the characteristics of the response time.

The response time of the MPPT system with respect to big load changing is shown in Fig. 14. The load changing of 25-110Ω is connected to the system. As shown in the Fig. 14, FLC and S-FLC methods are robust to handle big load changing that it means an extreme change in atmospheric conditions can be handled by the system.

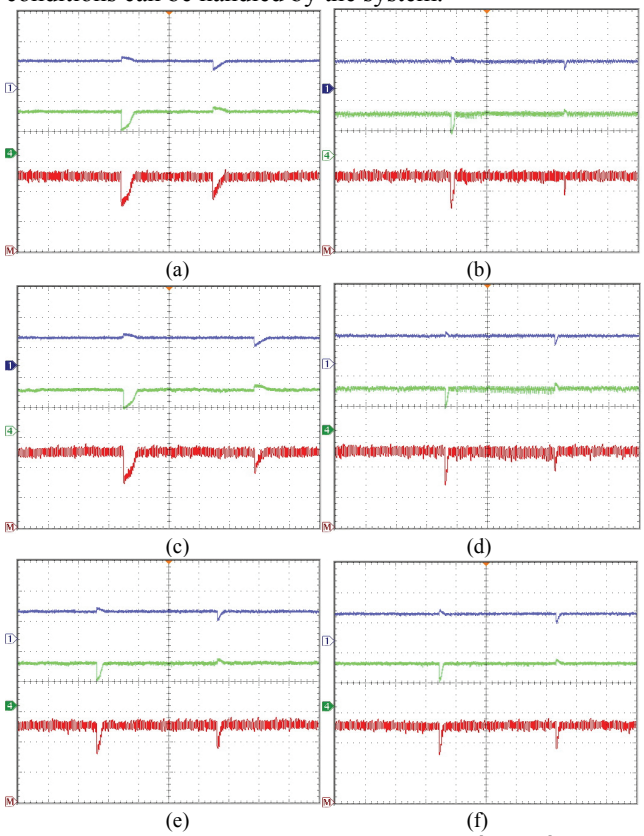

(a) (b) (c) (d) (e) (f)

Fig.13. Time response to small load change R=50Ω→100Ω→50Ω (a) P&O with duty step 0.2% (b) P&O with duty step 0.9% (c) INC with duty step 0.2% (d) INC with duty step 0.9% (e) FLC with duty step 0%-0.9% (f) S-FLC with duty step 0%-0.9%; Scale: [1]-Voltage (20V/div), [4]- Current (2A/div), [M]-Power (20W/div), Time 2s/div.

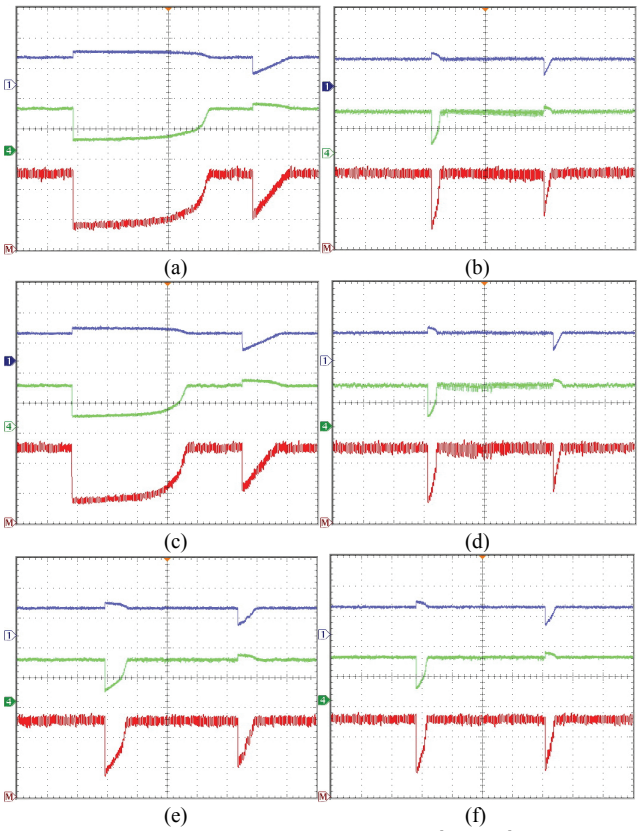

Fig.14. Time response to big load change R=25Ω→110Ω→25Ω (a) P&O with duty step 0.2% (b) P&O with duty step 0.9% (c) INC with duty step 0.2% (d) INC with duty step 0.9% (e) FLC with duty step 0%-0.9% (f) S-FLC with duty step 0%-0.9%; Scale: [1]-Voltage (20V/div), [4]- Current (2A/div), [M]-Power (20W/div), Time 2s/div.

d) MPPT oscillation at the steady state

Small oscillation at the steady state of the MPP is one of the criterions of the MPPT method. Regarding to this criteria, experimental comparison of all methods is shown in Fig.15. The system is connected to resistance load of 50Ω, and then the oscillation is measured at the MPP. It can be seen in the figure, similar to P&O and INC method with 0.2% duty step, the FLC and S-FLC method has a small power oscillation at the MPP. However, a big power oscillation at the MPP cannot be avoided by the P&O and INC method with 0.9% duty step.

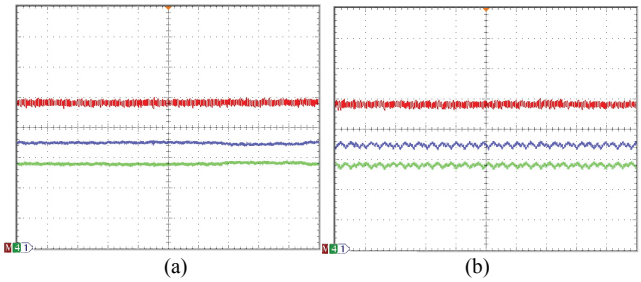

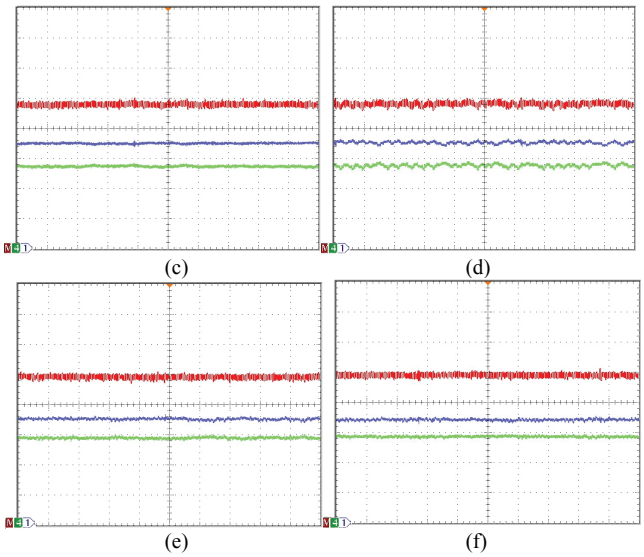

Fig.15. Power oscillation at the MPP (a) P&O with duty step 0.002% (b) P&O with duty step 0.009% (c) INC with duty step 0.2% (d) INC with duty step 0.9% (e) FLC with duty step 0%-0.9% (f) S-FLC with duty step 0%-0.9%; Scale: [1]-Voltage (5V/div), [4]- Current (1A/div), [M]-Power (10W/div), Time 400ms/div.

VI. Conclusion

A single-fuzzy logic controller (S-FLC) MPPT method is successfully implemented in a MPPT PV system. Due to control algorithm simplicity, it is easier to implement, modify and tune the control rules. The performance of S-FLC method has been validated in the MPPT system with a boost DC/DC converter and resistive load. A fast convergence with small oscillation at the MPP can be achieved by this method such that it has similar performance to FLC MPPT method. At the MPP tracking, both S-FLC and FLC, has a characteristic which similar to the conventional method, P&O and INC, with a high duty step and at the steady state of the MPP, they have a characteristic which similar to the conventional method with a low duty step.

To achieve more robust performance of S-FLC MPPT method, it is necessary to find appropriate membership function and sampling strategy without avoiding computation simplicity. Therefore, it is the most difficult part in the S-FLC design as well as the FLC design.

References

[1] A. Goetzberger, V.U. Hoffmann,"Photovoltaic Solar Energy Generation,"Springer-Verlag Berlin Heidelberg 2005.

[2] Y.K. Lo, H. J. Chiu, T.P. Lee, I. Purnama, and J.M. Wang, "Analysis and Design of a Photovoltaic System DC Connected to the Utility with a Power Factor Corrector," *IEEE Transaction on Industrial Electronics*, Vol. 56, No. 11, November 2009, page 4354-4362.

[3] Chapin, D.M., C.S. Fuller, & G.L. Pearson, "A New Silicon p-n junction Photocell for Converting Solar Radiation into Electrical Power", Journal of Applied Physics, Volume 25, Issue 5, May 1954, page 676-677.

[4] Thomas Surek, "Progress in U.S. Photovoltaics: Looking back 30 Years and Looking Ahead 20," *Proceedings of 3rd World Conference on Photovoltaic Energy Conversion*, Osaka, Japan, May 2003, page 2507-2512.

[5] K. H. Hussein, I. Muta, T. Hoshino, and M. Osakada, "Maximum Photovoltaic Power Tracking: An Algorithm for Rapidly Changing Atmospheric Conditions," *IEE Proceedings– Generation, Transmission and Distribution*, Vol. 142, No. 1, January 1995, page 59-64.

[6] G. M. S. Azevedo, M. C. Calvalcanti, K. C. Oliveira, F.A.S. Neves, and Z.D. Lins, "Comparative Evaluation of Maximum Power Point Tracking Methods for Photovoltaic Systems*," Journal of Solar Energy Engineering*, August 2009, Vol. 131, page 031006-1 - 031006-8.

[7] R. Faranda, S. Leva and V. Maugeri, "MPPT Techniques for PV Systems: Energetic and Cost Comparison," *IEEE Power and Energy Society General Meeting – Conversion and Delivery of Electrical Energy in the 21st Century*, 2008, page 1-6.

[8] T. Esram and P. L. Chapman, "Comparison of Photovoltaic Array Maximum Power Point Tracking Techniques," *IEEE Transaction on Energy Conversion*, Vol. 2, Issue 2, 2007, page 439-449.

[9] C.Y. Won, D.H. Kim, S.C. Kim, W.S. Kim, and H.S. Kim, "A New Maximum Power Point Tracker of Photovoltaic Arrays Using Fuzzy Controller," *25th Annual IEEE Power Electronic Specialist Conference*, Jun 1994, Vol 1, page 396-403.

[10] Guohui Zeng and Qizhong Liu, "An Intellegent Fuzzy Method for MPPT of Photovoltaic Arrays," *Second International Symposium on Computational Intellegence and Design*, 2009, page 356-359.

[11] X.B. Li, Ke Dong, Hao Wu, "Study on the Intelligent Fuzzy Control Method for MPPT in Photovoltaic Voltage Grid System," *3rd IEEE Conference on Industrial Electronics and Applications*, 2008, ICIEA, page 708-711.

[12] B.J. Choi, S.W. Kwak, and B.K. Kim, "Design of a Single-Fuzzy Logic Controller and Its Properties," *Fuzzy Sets and Systems 106*, 1999, page 299-308.

[13] B.J. Choi, S.W. Kwak, and B.K. Kim, "Design and Stability Analysis of Single-Input Fuzzy Logic Controller," *IEEE Transactions on Systems, Man, and Cybernetics, Part B: Cybernetics*, April 2000, Volume 30, Issue 2, page 303-309.

[14] Tom Markvart and Luis Castaner, "*Solar Cell Materials, Manufacture and Operation*," Elsevier, 2005.

[15] S. N. Sivanandam, S. Sumathi, and S.N. Deepa, "*Introduction to Fuzzy Logic using Matlab*," Springer, 2007.

[16] Jerry M. Mendel, "Fuzzy Logic System for Engineering: A tutorial," *Proceedings of IEEE*, Vol. 83, March 1995, page 345-377.

[17] Kwang H. Lee,"First Course on Fuzzy Theory and Applications," Springer-Verlag Berlin Heidelberg 2005.

[18] Mohan, Undeland, and Robbins, "*Power Electronics: Converter, Applications, and Design*," John Willey & Sons, Third Edition, 2003.

[19] bp Solar, "*BP350-High-efficiency photovoltaic module using silicon nitride multi-crystalline silicon cells*," 6802.0036 BP350J Rev. C Datasheet, 2007

2011 IEEE International Conference on Fuzzy Systems
June 27-30, 2011, Taipei, Taiwan

Fuzzy Control of MW-class PV Generation to Reduce Frequency and Tie-line Power Fluctuations in Three Control Area Power System

Manoj Datta, Tomonobu Senjyu, Atsushi Yona
Faculty of Engineering and Science
University of the Ryukyus
Okinawa, Japan
E-mail: manoj.eee.kuet@gmail.com

Toshihisa Funabashi
Power Systems Solutions Sales Engineering Department
Meidensha Corporation
Tokyo, Japan
E-mail: funabashi-t@mb.meidensha.co.jp

Abstract—**This paper presents a fuzzy based frequency control strategy by grid-connected MW class PV generation. The frequency control is proposed from the view point of the frequency fluctuation problem produced by the large penetration of PV power. The fuzzy control has three inputs: average insolation, change of insolation and system frequency deviation. Following these three inputs, a frequency control system of the PV inverters is proposed. For the case of different insolations, a coordinated inverter and battery control method is presented. The proposed method is simulated in three control area power system by considering dual power and information flows between supply and demand sides and is found satisfactory to provide frequency control and to reduce tie-line power fluctuations.**

Keywords-fuzzy control, frequecny deviations, MW-class PV, tie-line power fluctuations

I. INTRODUCTION

PV systems are expected to play a vital role in the future energy efficient and zero emission society. Recently, along with the smart grid, large PV power generation is getting enormous attraction. The penetration of PV systems in Japan is rising. Two factors have been boosting this: improved generation efficiency of PV modules and governmental subsidies [1]. However, PV power fluctuates depending on the weather conditions, season, and geographic location and causes problems like voltage fluctuation and large frequency deviation in an electric power system operation [2]-[4].

The integration of a large number of embedded PV generators will have far reaching consequences not only on the distribution networks but also on the national transmission and generation system. If the PV generators are built on the roof and sides of buildings, most of them will be located in urban areas and will be electrically close to loads. On the other hand, these PV generating units may be liable to common mode failures that might cause the sudden or rapid disconnection of a large proportion of operating PV capacity. However, considering the recent grid codes in Germany and Spain [5], PV generators should provide dynamic grid support e.g. voltage stability during voltage drops which is often referred to as Fault-Ride-Through (FRT) capability and frequency control.

Whether many studies are dedicated to the voltage control by PV inverters, this paper provides a strategy of frequency control by the grid-connected PV systems. The frequency control strategy is developed based on fuzzy logic [6] and is tested by simulation in a three control area power system and is compared with a conventional energy storage system (ESS) based smoothing method of PV output power fluctuations [1]. From the simulation results, it is found that the proposed frequency control method shows satisfactory performances and reduces the tie-line power fluctuations.

II. SYSTEM DESCRIPTION AND METHODOLOGY

To illustrate, frequency control performance by MW-class PV generation in a multi-area power system, three identical interconnected control areas are considered and is shown in Fig. 1. A generalized load frequency model in the presence of frequency control from PV generation is shown in Fig. 2[7]. The simulation parameters are given in Table I.

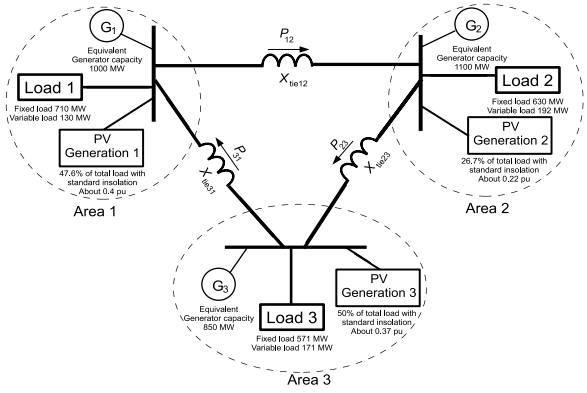

Fig 1. Three control area power system.

TABLE I. SIMULATION PARAMETERS FOR FIG. 2

Area	*K(s)*	*D* (pu/Hz)	2H (pu s)	R (Hz/s)	T_g (s)	T_t (s)	β (pu/Hz)	T_{ij} (pu/Hz)	Generation Capacity	Load	PV Penetration
Area1	-0.3	0.015	0.1667	3.00	0.08	0.40	0.3483	T_{12}=0.20 T_{13}=0.25	1000 MW	Fixed 710 MW Variable 130 MW	47.60% of total load
Area 2	-0.2	0.016	0.2917	2.73	0.06	0.44	0.3827	T_{21}=0.20 T_{23}=0.12	1100 MW	Fixed 630 MW Variable 192 MW	26.70% of total load
Area 3	-0.4	0.015	0.1247	2.82	0.07	0.30	0.3692	T_{31}=0.25 T_{32}=0.12	850 MW	Fixed 571 MW Variable 171 MW	50.00% of total load

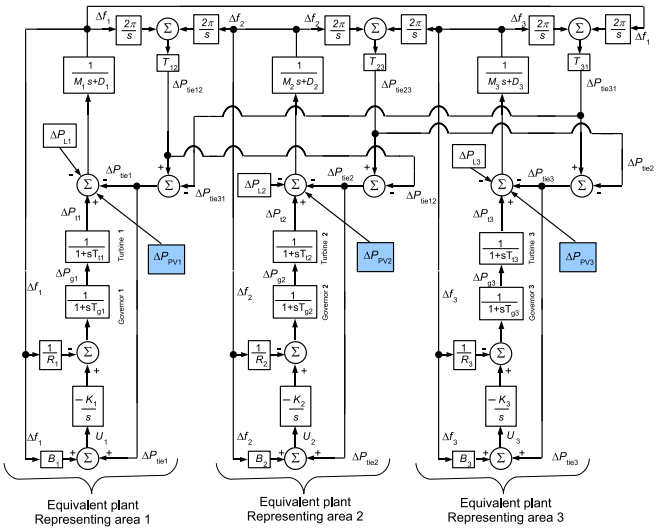

Fig. 2. Frequency control model with considering frequency control from PV generation.

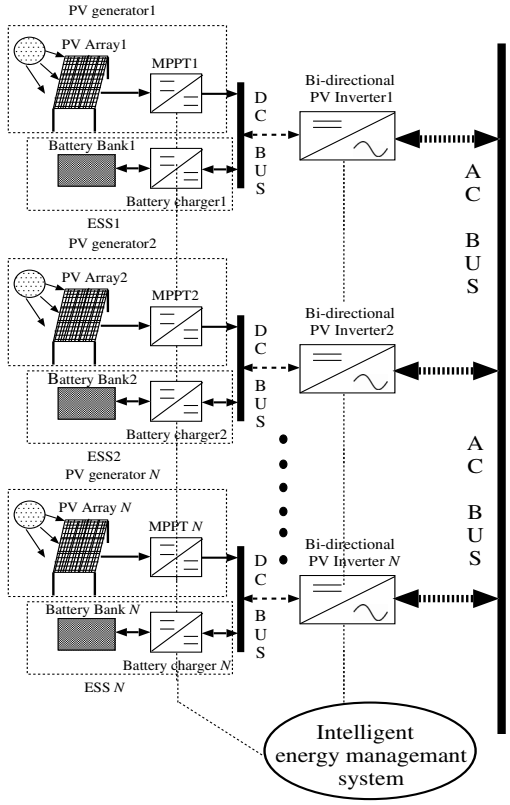

Fig. 3. Multiple PV generators are connected in coordinated control mode.

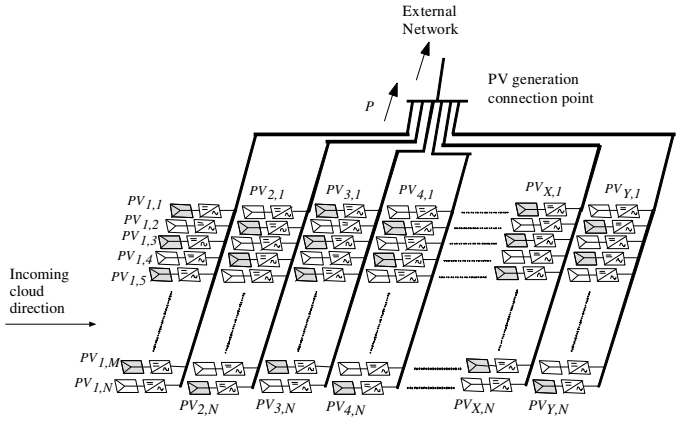

Fig. 4. The aggregate model of large PV plant connected to the power grid.

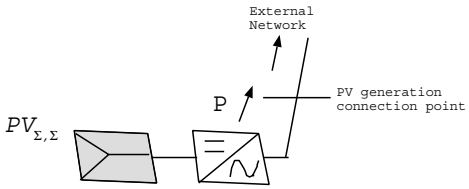

Fig. 5. One-PV generator equivalent.

A. Simplification of aggregate model of grid-connected PV generation

Commonly, grid-connected PV generation consist of a large number of relatively small PV units. This distributed generation can be represented by an equivalent PV generation plant whose rating is equal to the sum of the ratings of the individual PV generating units. A distributed PV generation systems with multiple PV generators is show in Fig. 3. An individual PV generator is consisted of a large PV array, a MPPT controller, and an ESS. The operational points of the individual PV generating units are determined by the insolation value and the frequency control algorithm. The aggregate model of the large-scale PV plant thus comprises $N \times Y$ PV generating units of G MW power capacity each where N is the number of PV generating unit in row and Y is the number of PV generating unit in column. The installed capacity of the equivalent PV plant is thus $N \times Y \times G$ MW. The model is shown in Fig. 4. However, the MPPT module and battery module of each PV system are not shown.

Uniform Insolation Distribution

In this case the PV generating units within the plant are assumed to have the same operating points. When reducing the

aggregate model of the large PV plant, the following assumptions are made:

- The MVA rating of the large PV plant equivalent, $S_{\Sigma,\Sigma}$ is the sum of the MVA ratings of the PV generating units:

$$S_{\Sigma,\Sigma} = \sum_{i=1}^{Y}\sum_{j=1}^{N} S_{i,j} \tag{1}$$

  Where $S_{i,j}$ is the MVA-rating of the PV generating unit j being in the column i.
- The equivalent PV generating plant supplies the same amount of electric power to the grid:

$$P_{\Sigma,\Sigma} = \sum_{i=1}^{Y}\sum_{j=1}^{N} P_{i,j} \tag{2}$$

  where $P_{i,j}$ is the electric power supplied by the PV generating unit j being in the column i and $P_{\Sigma,\Sigma}$ is the electric power supplied by the whole PV plant.

(1) and (2) imply that the equivalent PV plant can be defined by a simple addition of the MVA ratings and an addition of the electric power output of the individual generating units. Fig. 5 shows this one-PV generator equivalent. The incoming cloud shown in Fig. 4 is assumed to cover all the individual PV generating units in the equivalent plant at the same time.

Non-uniform Insolation Distribution

In this case the incoming cloud is such that:

- Its direction is as shown in Fig. 4.
- The cloud takes k seconds time to move from the first column to the second column of the PV generating units. In other words, the insolation is shifted by k seconds for each column of PV generating units.

Since the operating points of the PV units in each column are identical, the outputs of the PV units in each column are added and a multi-machine equivalent comprising of Y PV generating units is obtained. This multi-generators equivalent is shown in Fig. 6. The MVA ratings, $S_{\Sigma,\Sigma}$ the electric powers, $P_{\Sigma,\Sigma}$ of the equivalent PV plants are given by:

$$S_{\Sigma,\Sigma} = \sum_{i=1}^{Y} S_{i,\Sigma} \tag{3}$$

$$P_{\Sigma,\Sigma} = \sum_{i=1}^{Y} P_{i,\Sigma} \tag{4}$$

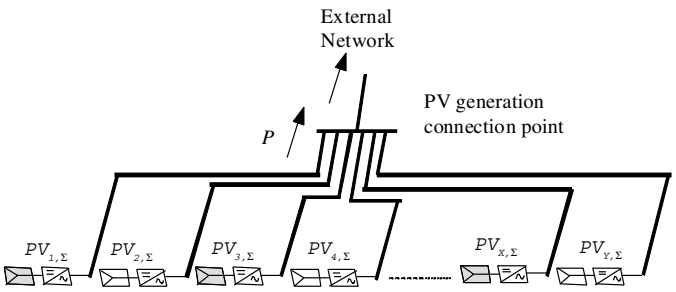

Fig. 6. The multi-PV generator equivalent.

B. Fuzzy based command power generation consdering uniform insolation to all PV inverters

In order to control output power of all PV systems considering power system condition, output power command P_{inv}^{*} is decided by output power command system shown in Fig. 7. Output power command system consists mainly of two fuzzy control blocks and the rate of rated output power for PV system is decided by these fuzzy controls. Fuzzy reasoning is described by a set of "if-then" rules based on fuzzy rules. Fuzzy reasoning is effective when mathematical expressions are difficult by inherent complexity or nonlinearity.

Firstly, fuzzy control I is explained. There are two inputs of fuzzy control I. One is frequency deviation Δf and the other is average insolation $\overline{S}_i$. Average insolation $\overline{S}_i$ is defined by

$$\overline{S}_i = \frac{1}{T}\int_{t-T}^{t} S_i dt \,. \tag{5}$$

where t is present time, T is integral interval, and S_i is instantaneous insolation. Fuzzy rules and membership functions of fuzzy control I are shown in TABLE II and Fig. 8, respectively. Fuzzy rules and membership functions that yield an output to reduce frequency deviations are defined by trial-and-error. The ith fuzzy rule is expressed as

$$\text{Rule } i: \text{if } \Delta f \text{ is } L_x \text{ and } \overline{S}_i \text{ is } M_y \text{ then } \gamma_I \text{ is } Z_l \tag{6}$$
$$x = 1,2,\cdots,7,\ y = 1,2,\cdots,7,\ l = 1,2,\cdots,7$$

where L_x , M_y denote the antecedents and Z_l are consequent part.

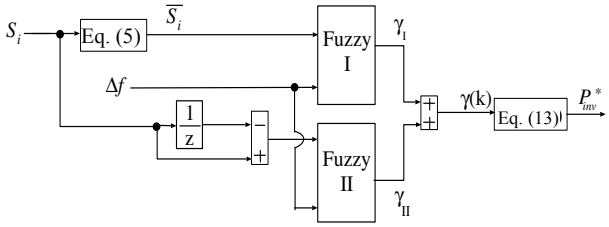

Fig. 7. Output power command generation system.

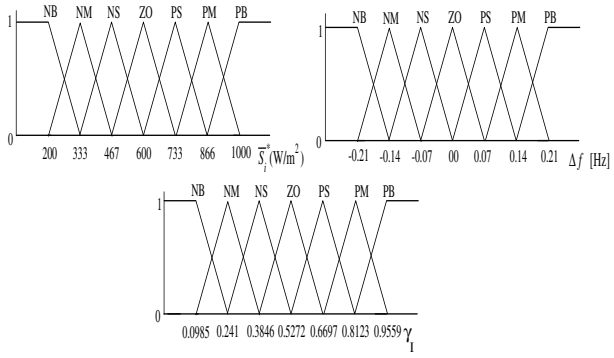

Fig. 8. Membership Functions of fuzzy control I.

TABLE II. FUZZY RULES OF FUZZY CONTROL I

$\overline{S_i}$ \ Δf	NB	NM	NS	ZO	PS	PM	PB
NB	NB	NB	NB	NB	NM	NS	ZO
NM	NB	NB	NB	NM	NS	ZO	PS
NS	NB	NB	NM	NS	ZO	PS	PM
ZO	NB	NM	NS	ZO	PS	PM	PB
PS	NM	NS	ZO	PS	PM	PB	PB
PM	NS	ZO	PS	PM	PB	PB	PB
PB	ZO	PS	PM	PB	PB	PB	PB

NB=Negative Big NM=Negative Medium NS=Negative Small
PB=Positive Big PM=Positive Medium PS=Positive Small
ZO=Zero

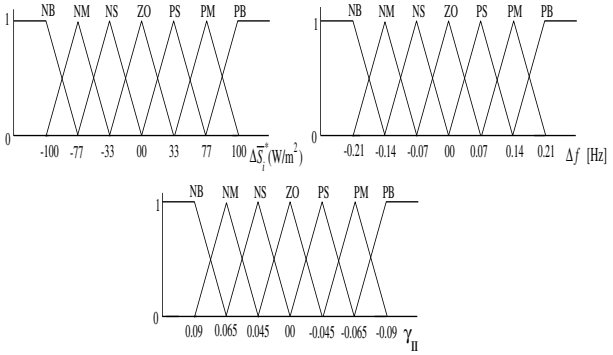

Fig. 9. Membership Functions of fuzzy control II.

TABLE III. FUZZY RULES OF FUZZY CONTROL II

ΔS_i \ Δf	NB	NM	NS	ZO	PS	PM	PB
NB	NB	NB	NB	NM	NM	NS	ZO
NM	NB	NB	NM	NM	NS	ZO	PS
NS	NB	NM	NM	NS	ZO	PS	PM
ZO	NM	NM	NS	ZO	PS	PM	PM
PS	NM	NS	ZO	PS	PM	PM	PB
PM	NS	ZO	PS	PM	PM	PB	PB
PB	ZO	PS	PM	PM	PB	PB	PB

NB=Negative Big NM=Negative Medium NS=Negative Small
PB=Positive Big PM=Positive Medium PS=Positive Small
ZO=Zero

Fuzzy reasoning output γ_I is calculated by

$$\gamma_I = \sum_{i=1}^{49} w_i Z_I \Big/ \sum_{i=1}^{49} w_i \tag{7}$$

where w_i denotes the grade for the antecedent and is obtained by

$$w_i = w_{\Delta fi} w_{\overline{s}_i i} \tag{8}$$

where $w_{\Delta fi}$ and $w_{\overline{s}_i i}$ are the grade of antecedents for each rule.

Secondly, fuzzy control II is explained. Frequency deviation Δf and change of insolation ΔS_i are used as inputs of Fuzzy control II, where change of insolation ΔS_i is expressed as

$$\Delta S_i = S_i(t-1) - S_i(t) \tag{9}$$

Output power command that depends on power system condition rather than insolation condition is decided by using frequency deviation Δf as input for both fuzzy reasoning I and fuzzy reasoning II. Fuzzy rules and membership functions of fuzzy control II are shown in TABLE III and Fig. 9, respectively. Setup of fuzzy rules and parameters of membership functions are determined by prioritizing to prevent boosting of frequency deviation. The *o*th of fuzzy rules is expressed as

$$\text{Rule } o: \text{if } \Delta f \text{ is } H_c \text{ and } \Delta S_i \text{ is } I_z \text{ then } \gamma_{II} \text{ is } Q_h \tag{10}$$

$$c = 1,2,\cdots,7,\ z = 1,2,\cdots,7,\ h = 1,2,\cdots,7$$

where H_c , I_z denote the antecedents and Q_h are consequent part. Fuzzy reasoning output γ_I is calculated by

$$\gamma_{II} = \sum_{i=1}^{49} w_o Q_h \Big/ \sum_{i=1}^{49} w_o \tag{11}$$

where w_o denotes the grade for the antecedent and is obtained by

$$w_o = w_{\Delta fo} w_{\Delta S_i o} \tag{12}$$

where $w_{\Delta fo}$ and $w_{\Delta S_i o}$ are the grade of antecedents for each rule.

The sum of outputs of fuzzy control I, γ_I , and fuzzy control II, γ_{II} become output power command by using the following equation:

$$P_{inv}^* = P_{rated}\left\{\gamma(k) + \frac{\gamma(k+1)-\gamma(k)}{T_s} f(t)\right\} \tag{13}$$

where P_{rated} is the rated output power of PV power generation system, T_s is sampling time, *f(t)* is periodic function such that $f(t) = t(0 < t < T_s)$.

C. Fuzzy based coordinated command power generation consdering different insolations todifferent PV inverters

In order to control the combined output power of multiple PV systems considering power utility and different insolation conditions, output power command is generated in two levels: central and local. Individual local output power commands are given to each of the PV power systems by maintaining coordination between central and local levels to produce combined PV output power same as the central output power command. Central output power command P_{inv}^* is decided by the previously described fuzzy based central output power command generation system and shown in Fig. 10. This central output power command system consists of mainly two fuzzy controls. There are two inputs of fuzzy control I. One is frequency deviation Δf and the other is average insolation $\overline{S}_i^*$. Average insolation $\overline{S}_i^*$ is defined by

$$\overline{S}_i^* = \frac{1}{T} \int_{t-T}^{t} S_i^* dt \tag{14}$$

where $S_i^* = \frac{1}{N}\sum_{N=1}^{N} S_{iN}$, t is present time, T is integral interval, N is the total number of PV power generation systems, S_{iN} is instantaneous insolation of each PV power generation system, and $\overline{S}_i^*$ is summation of insolation of each PV power generation system divided by N.

Frequency deviation Δf and change of insolation $\Delta\overline{S}_i^*$ are used as inputs of Fuzzy control II, where variance $\Delta\overline{S}_i^*$ is expressed as

$$\Delta\overline{S}_i^* = \overline{S}_i^*(t-1) - \overline{S}_i^*(t) \tag{15}$$

The sum of outputs of Fuzzy control I, γ_I , and Fuzzy control II, γ_{II} become central output power command by using the following equation:

$$P_{inv}^* = NP_{rated}\left\{\gamma(k) + \frac{\gamma(k+1)-\gamma(k)}{T_s} f(t)\right\} \tag{16}$$

where P_{rated} is the rated output power of a single PV power generation system, N is the total number of PV power generation systems, T_s is sampling time, *f(t)* is periodic function such that $f(t) = t(0 < t < T_s)$.

After generating central output power command, local output power command for each of the PV power generation systems is produced by a simple coordinated control. The N PV power generation systems with coordinated control are shown in Fig. 11. Here the combined PV output power P_A is expressed as

$$P_A = \sum_{N=1}^{N} P_{AN} \tag{17}$$

where P_{AN} is the output power of each PV power generation system. In order to achieve combined output power P_A equal to the central output power command P_{inv}^* coordinated control method for each of the PV power generation systems is needed.

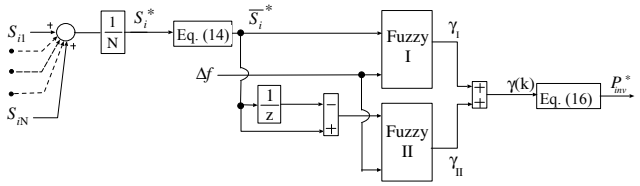

Fig. 10. Fuzzy based central output power generation.

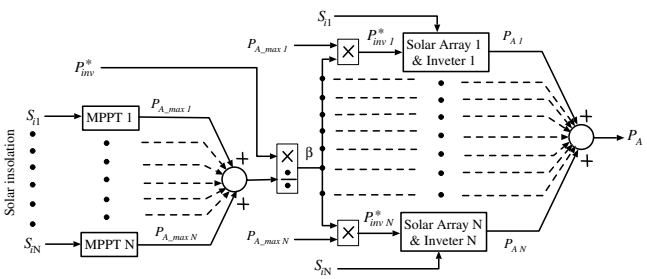

Fig. 11. Proposed coordinated control.

To generate coordination between central power command and individual local power command, a common tuning factor β is formulated. The tuning factor β can be expressed as

$$\beta = \frac{P_{inv}^*}{\sum_{N=1}^{N} P_{A\max\ N}} \tag{18}$$

where $P_{A\max N}$ is maximum power point tracking (MPPT) command of each PV power generation system. The P& O algorithm is used to generate the MPPT output power command considering instant insolation, PV array voltage, and PV array current. The individual local output power command for each of the PV power generation systems can be obtained by the following equation

$$P_{invN}^* = P_{A\max N} \times \beta \tag{19}$$

D. ESS charging/discharging

ESS power command P_{ESSi}^* for charging, discharging, and neutral modes can be expressed as follows

$P_{ESSi}^* = P_{\max i}^* - P_{invi}^*$ (Charging mode, if $P_{\max i}^* > P_{invi}^*$),

$P_{ESSi}^* = P_{invi}^* - P_{\max i}^*$ (Discharging mode, if $P_{\max i}^* < P_{invi}^*$),

$P_{ESSi}^* = 0$ (Neutral mode, if $P_{\max i}^* = P_{invi}^*$)

III. NUMERICAL SIMULATION RESULTS

Numerical simulation results of control area 1, 2, and 3 are shown in Figs. 12, 13, and 14 respectively. Figs. 12(a), 13(a), and 14(a) show the insolations. Different insolations are used for each of the control areas. Figs. 12(b), 13(b), and 14(b) show the average insolations. Figs. 12(c), 13(c), and 14(c) show the change of insolations. Figs. 12(d), 13(d), and 14(d) show the load of each area.

Figs. 12(e), 13(e), and 14(e) show the generator powers with the conventional smoothing method. Figs. 12(f), 13(f), and 14(f) show the generator powers with the proposed method. From Figs. 12(e), 12(f), 13(e), 13(f), and 14(e), 14(f), it is observed that the generator powers with the proposed method are smoother than those of the conventional method as PV inverters are taken part in the frequency control. As conventional generators stay far away from consumer loads and typically the PV systems are installed at the consumers' side, less fluctuating generator powers are easy to be produced by the conventional generators. This will also helps to reduce burden on the energy storages available on the consumer side.

Figs. 12(g), 13(g), and 14(g) show the PV powers with the conventional smoothing method. Figs. 12(h), 13(h), and 14(h) show the PV powers with the proposed method. From Figs. 12(g), 12(h), 13(g), 13(h), and 14(g), 14(h), it is seen that the PV powers with the proposed method are varying according to the load variation to provide frequency control. However, PV powers with the conventional method are smooth which means they cannot take part in frequency regulation and they are just trying to reduce the fluctuation of PV power by smoothing.

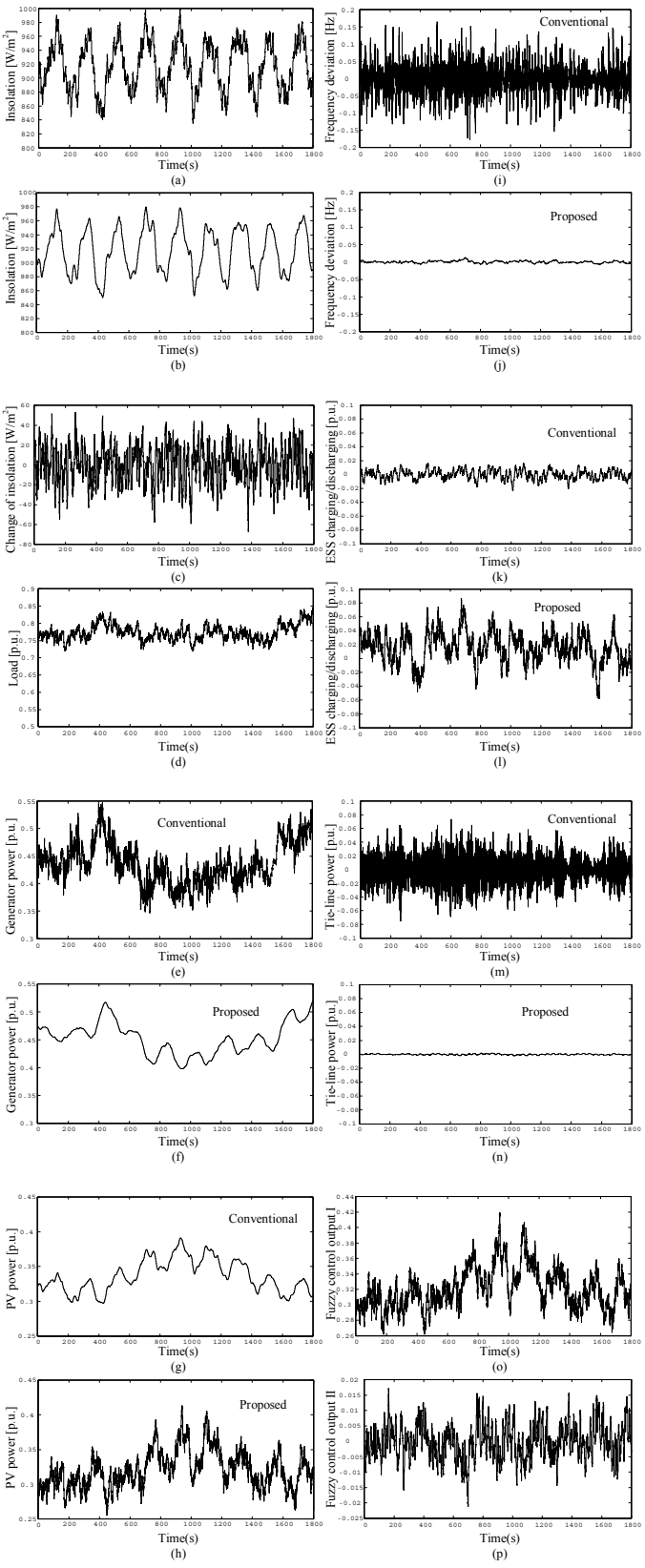

Fig. 12. Comparative simulation results of the proposed methods and the conventional smoothing based method [1] for control area 1.

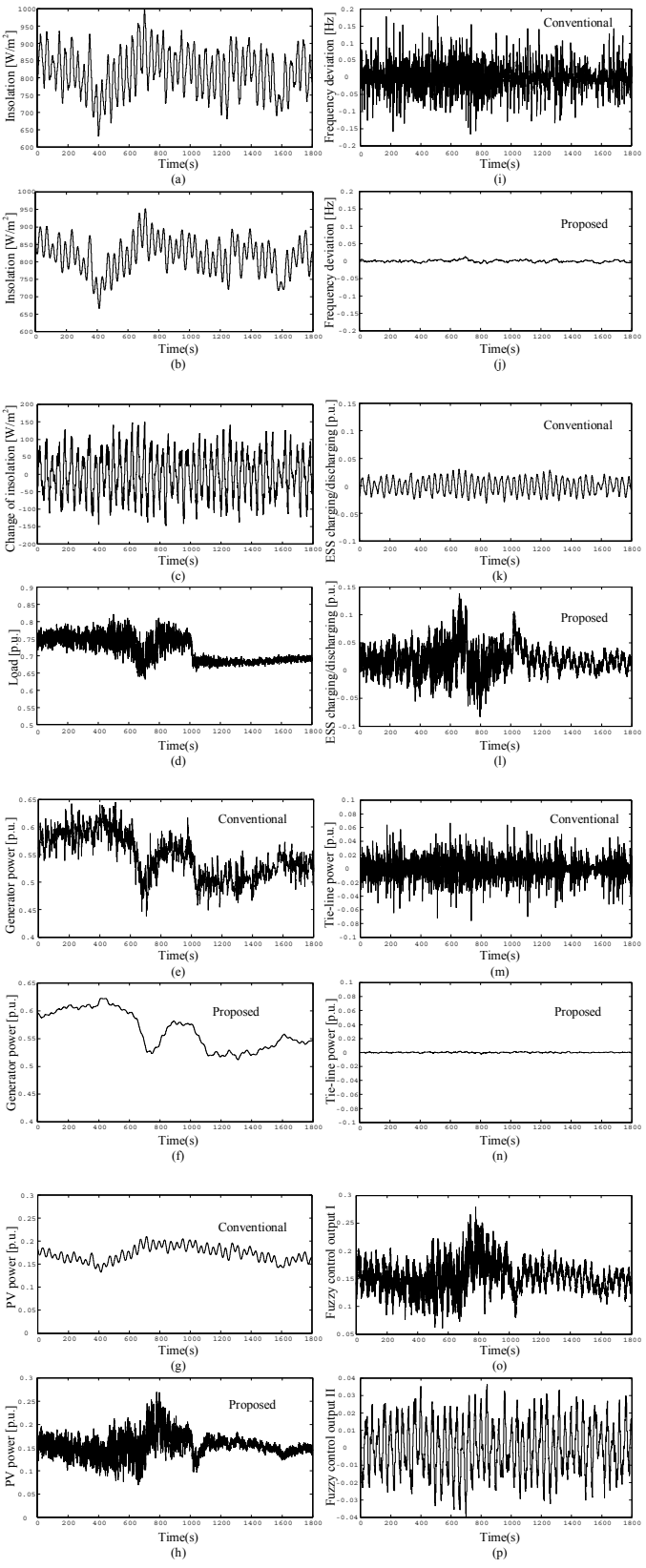

Fig. 13. Comparative simulation results of the proposed methods and the conventional smoothing based method [1] for control area 2.

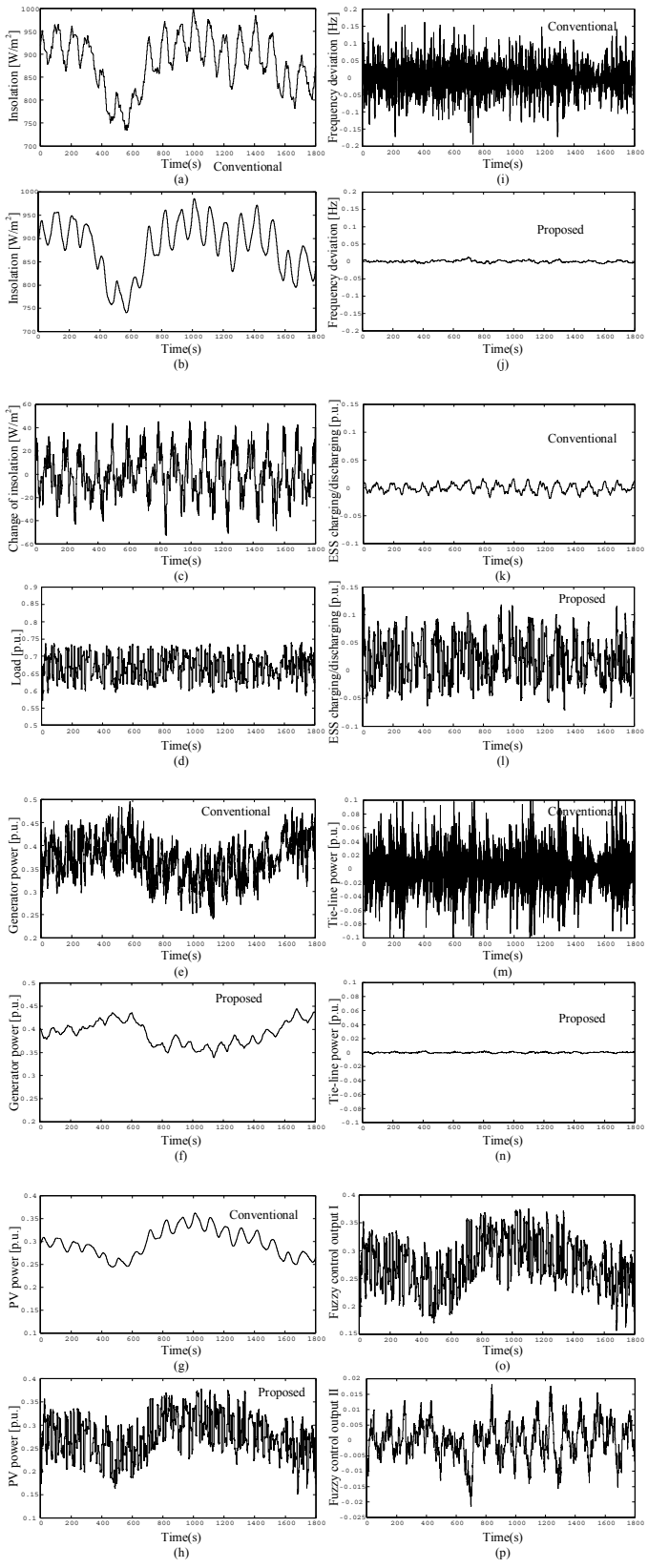

Fig. 14. Comparative simulation results of the proposed methods and the conventional smoothing based method [1] for control area 3.

Figs. 12(i), 13(i), and 14(i) show the frequency deviations with the conventional smoothing method. Figs. 12(j), 13(j), and 14(j) show the frequency deviation with the proposed method. From Figs. 12(i), 12(j), 13(i), 13(j), and 14(i), 14(j), it can be said the frequency control performances are better achieved by the proposed method as the frequency deviations with the proposed method are almost zero. This happens as the PV inverters acted like virtual generators by responding to a low frequency with the increase in their active power output and to a high frequency with the decrease in their active power output.

Figs. 12(k), 13(k), and 14(k) show the ESS charging/discharging powers with the conventional smoothing method. Figs. 12(l), 13(l), and 14(l) show the ESS charging/discharging powers with the proposed method. From Figs. 12(k), 12(l), 13(k), 13(l), and 14(k), 14(l), it can be said that the ESS powers required for the proposed method are higher than those of the conventional method. Considering the plug-in-electric vehicles and other energy storage systems, these can easily be maintained in the future smart power systems.

Figs. 12(m), 13(m), and 14(m) show the tie-line power fluctuations with the conventional smoothing method. Figs. 12(n), 13(n), and 14(n) show tie-line power fluctuations with the proposed method. From Figs. 12(m), 12(n), 13(m), 13(n), and 14(m), 14(n), it can be said that tie-line power fluctuations reduction are better achieved by the proposed method as the tie-line power fluctuations with the proposed method are almost zero. This happens as the PV inverters acted like virtual generators and try to address the issue of tie-line power fluctuations.

Figs. 12(o), 13(o), and 14(o) show the outputs of the fuzzy control I. Figs. 12(p), 13(p), and 14(p) show the outputs of the fuzzy control II. It can be observed that the outputs are changed in accordance to their inputs.

IV. CONLCUSIONS

This paper presents a fuzzy based frequency control approach by the grid-connected MW class PV generators. From the simulation results, it is seen that the proposed method works efficiently in the case of insolation and load variations.

In the proposed method, fuzzy controls are used as fuzzy controls are effective when mathematical expressions are difficult by inherent complexity or nonlinearity or uncertainty. Load and insolation variations are typical problems to be solved for large penetration of PV power in the utility. So, fuzzy control of PV inverters can be an intelligent solution towards the smart grid.

The current practice of smoothing PV power with the help of batteries cannot provide frequency control or ramp control according to the frequency deviations. Therefore by using the proposed method power consumers can play a vital role in the control of power system and can also reduce the burden on conventional generators far away.

In the proposed method, only active power controls of OV inverters for the purpose of frequency control are shown. In the future research, voltage control will also be included with the proposed frequency control and the response of the proposed frequency and voltage controller in the case of power system fault will be presented.

ACKNOWLEDGMENT

The authors would like to thank the Japan Society for the Promotion of Science (JSPS) and the Power Academy of Japan for availing resources in the execution of this research.

REFERENCES

[1] R. Hara, H. Kita, T. Tanabe, H. Sugihara, A. Kuwayama, S. Miwa, "Testing the technologies," IEEE Power & Energy Magazine, vol. 7, no. 3, 2009, pp. 77-85.

[2] S. Yanagawa, T. Kato, K. Wu, A. Tabata, and Y. Suzuoki, "Evaluation of LFC capacity for output fluctuation of photovoltaic generation systems based on multi-point observation of insolation," in Proc. IEEE Power Engineering Society Summer Meeting, 2001, pp. 1652-1657.

[3] A. Woyte, V.V. Thong, R. Belmans, and J. Nijs, "Voltage fluctuation on distribution level introduced by photovoltaic systems," IEEE Trans. Energy Convers., vol. 21, no. 1, 2006, pp. 202-209.

[4] H. Asano, K. Yajima, and Y. Kaya, "Influence of photovoltaic power generation on required capacity for load frequency control," IEEE Trans. Energy Convers., vol. 11, no. 1, 1996, pp. 188-193.

[5] E. Troester, "New German grid codes for connecting PV systems to the medium voltage power grid," in Proceedings of the 2nd Int. Work shop on Concentrating Photovoltaic Power Plants: Optical Design, Production, Grid Connection, Darmstadt, Germany, 9-10 March 2009, pp. 1-4

[6] V. Avatchanakorn, A. Ueda, Y. Gotoh, and Y. Mizutani, "Load frequency control using power demand estimation and fuzzy control," Electrical Engineering in Japan, vol. 111. no. 6, pp. 47-57, 1991.

[7] H. Bevrani, A. Ghosh, and G. Ledwich, "Renewable energy sources and frequency regulation: survey and new perspectives," IET RPG, vol. 4, no. 5, pp. 438-457, 2010.

2011 IEEE International Conference on Fuzzy Systems
June 27-30, 2011, Taipei, Taiwan

A Fuzzy-Rule Based Power Restoration Approach for a Distribution System with Renewable Energies

Hong-Tzer Yang, Jian-Tang Liao, and Xiang-He Su
Department of Electrical Engineering
National Cheng Kung University
Tainan, TAIWAN
htyang@mail.ncku.edu.tw

***Abstract*—Based on heuristic fuzzy rules, a new power restoration approach is presented in this paper. The restoration approach developed can be used to deal with different fault cases in a distribution system (DS) with sources of renewable energies. This paper introduces "Load Path" as the main framework for restoration. The proposed strategy can achieve the advantages of simple decision criterions, balance of backup feeders, fast execution time, and applicability for different fault cases. Depending on fault situations, the number of load paths is different. With more than two load paths existing, the proposed fuzzy rules infer the best main load path with one of its switches operated as the restoration strategy (RS) for the specific case. To consider the distributed generations (DGs) of renewable energies, the proposed approach has been validated in a test system adapted from Taipower distribution system for different scenario studies.**

Keywords-Restoration Strategies, Fuzzy Rules, Renewable Energies, Distribution System

I. INTRODUCTION

Due to rapid increases in demand and consumption of electrical energy, safe and reliable power supplies in an electrical system are drawing much more important than before. However, the growing size of power systems increases the complexity of its supervision, control, and energy demand supply management, especially as the DGs of renewable energies are taken into account.

Effective service RSs are very important when there is a fault occurring in the power system. The primary task of restoration is to find appropriate backup feeders to restore the outage zones (loads) as much as possible. For a large system, as a fault happens, the outage zones would be large and restoration of the outage zones appears relatively complicated.

There have been many studies focused on the RSs for the power systems. Heuristics based search methods [1-3] collect the operators' practical manipulation experiences to derive the restoration scheme. Expert system approaches [4-7] build a rule-based data system composed of operators' empirical rules and documents. Under occurrence of a fault, RSs would be automatically generated via the inference engine. Fuzzy theory [8-12] translates the problem's variables and objective functions into membership functions. By using the fuzzy inference value, feasible RSs are obtained. Petri-net algorithm [13, 14] constructs into a net the feeders of a distribution system and the switches' states and the locations. With combination of empirical rules and evaluation function, the searching process infers a restoration plan. These methods above can be roughly regarded as heuristic-based restoration strategies. They can find appropriate RSs fast; however it needs a large data base to handle different fault cases, and it can't ensure if the obtained RS is the best one for the fault case.

On the other hand, the RSs are derived on the basis of optimization algorithms. Genetic algorithm [15-18] has been employed to generate optimal restoration plan through imitating the evolution process. Particle-swarm optimization [19-21] and ant-colony optimization [22] are alternative optimization approaches. They are all inspired from the swarm or colony of creatures, such as fish, birds, and ants. Though these methods can deal with multi-objective optimization problem and achieve a near-optimal solution, the results are influenced by different parameters given. Besides, far more computational time is needed to generate an optimal restoration plan. Plus, in the optimization process, most of the switches considered as variables to determine may be unrelated to the restoration of the outage zones, a fact which wastes the searching time a lot.

In this paper, a fuzzy-rule based power restoration approach is proposed. For different types of faults occurring, a corresponding inference procedure is performed to create the restoration strategies. By using the "Load Path" notion, the developed RS transfers appropriate amount of outage loads to backup feeders based on backup feeders' capacity and their loads at the instance of restoration. Balanced loads of the backup feeders are expected with overloads avoided as much as possible. As more than one load paths are considered, a fuzzy-rule based inference process is used to achieve an appropriate restoration scheme. Load transferring or shedding would be used, as there is no enough margin of capacity on the backup feeders. With DGs of renewable energies existing in the distribution system, the developed RS can also take the influences of DGs into consideration.

II. PROPOSED FUZZY RULE BASED RESTORATION APPROACH

The proposed restoration approach to be detailed in this section is based on simple decision fuzzy rules. The algorithm developed is described in the flowchart of Figure 1. The

This work supported in part by National Science Council of R.O.C. under Grant NSC 100-3113-E-194 -001 is greatly acknowledged.)

following assumption is made before the restoration algorithm proceeds:

- The fault and the outage zones have been identified and isolated from the grid.
- The loads of each zone and the available output of DGs of renewable energy are well known enough at the instance of restoration in a smart-grid system.

In the proposed approach described below, the load transferring process will be used to make the backup feeder have more capacity to supply the loads. The load transferring process is to choose the secondary backup feeder with the largest capacity margin to supply appropriate amount of loads originally belonging to some backup feeder. The secondary backup feeders with smaller capacity margin are then considered. If capacity margin of the secondary backup feeder is smaller than the amount of loads needed to transfer, the transferring load process would not be performed.

A. Proposed Restoration Approach

The proposed restoration algorithm is described step by step as follows.

Step 1) Detect the fault, and open the isolation switch(es) to isolate the fault. The outage zones are recognized.

Step 2) Find out the set of available tie switches for restoring the outage zones.

Step 3) Based on the number of available tie switches, the sub-steps next are followed:

Step 3-1) For number of available tie switches, n_{TSW}**=1.**

Step 3-1-1) Check if the backup feeder has enough capacity margin. If it is, then go to **Step 3-1-5**; otherwise go to **Step 3-1-2**.

Step 3-1-2) Execute the load transferring process of the backup feeder.

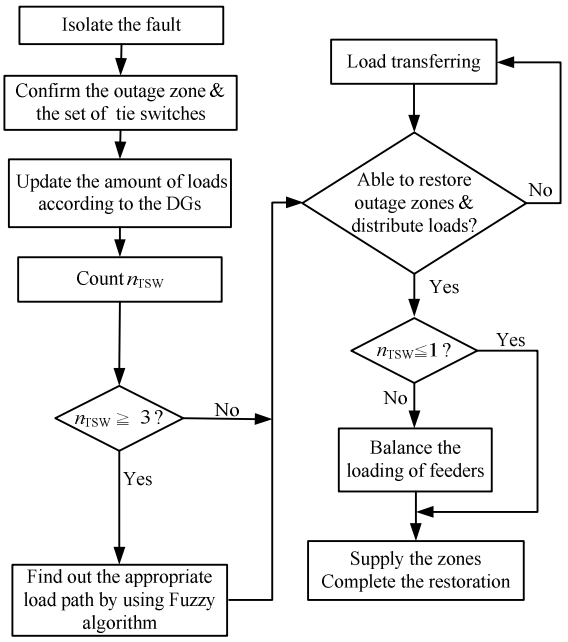

Figure 1. Flowchart of the proposed RS

Step 3-1-3) Check again whether the backup feeder has enough capacity margin. If it is, then go to **Step 3-1-5**; otherwise go to **Step 3-1-4**.

Step 3-1-4) Supply the loads in the outage zones by the backup feeder as much as possible; shed the loads still not restored in the remaining outage zones.

Step 3-1-5) Restore the outage zones by the backup feeder and finish the restoration process.

Step 3-2) For number of available tie switches**,** n_{TSW}**=2**

Step 3-2-1) Construct the only one load path between the two tie switches (for example, the load path is Z_5-Z_6-Z_7-Z_8-Z_9 in Figure 5).

Step 3-2-2) Identify and integrate the outage zones which would be integrated into a load path (for example, Z_4 in Figure 5).

Step 3-2-3) Check if the total capacity margin of the two backup feeders is enough to supply the outage loads. If it is, then go to **Step 3-2-6**; otherwise go to **Step 3-2-4**.

Step 3-2-4) Perform the load transferring process.

Step 3-2-4-1) Perform load transferring of the backup feeder with less capacity margin until the total capacity margin of the two backup feeders can meet the outage loads. If it cannot meet, then go to Step 3-2-5; otherwise go to Step 3-2-6.

Step 3-2-4-2) Perform load transferring of the backup feeder which cannot supply its corresponding loads. After the load transferring, if the backup feeder still doesn't have enough capacity margin, then go to **Step 3-2-5**; otherwise go to **Step 3-2-6**.

Step 3-2-5) Supply the outage zones as much as possible by the backup feeders individually; shed the remaining outage loads in the zones, if there still are.

Step 3-2-6) According to backup feeders' loading ratios of capacity margin, as shown in (1), divide appropriately the loads into two parts by opening a switch on the load path to be supplied by individual backup feeders.

$$\text{Min}\left(\left|\frac{LS_1}{MC_1}-\frac{LS_2}{MC_2}\right|\right) \quad (1)$$

where LS_i is the load supplied by backup feeder i, and MC_j is the capacity margin of backup feeder i. If both backup feeders can supply the corresponding loads individually, finish the restoration process; otherwise go to **Step 3-2-4-2**.

Step 3-3) For number of available tie switches, $n_{TSW} \geqq 3$

Step 3-3-1) Determine and integrate the outage zones into load paths.

Step 3-3-2) Determine the main load path based on the

proposed fuzzy inference rules, to be illustrated further below.

Step 3-3-3) Integrate the remaining outage zones other than those on the main load path into the main load path.

Step 3-3-4) Check whether the total capacity margin of the two backup feeders on the main load path is enough to supply all the outage loads. If it is, then go to **Step 3-3-9**; otherwise go to **Step 3-3-5**.

Step 3-3-5) Have the integrated outage zones (not belonging to the original main load path) be supplied by the other backup feeder as much as possible.

Step 3-3-6) Check again whether the total capacity margin of the two backup feeders on the main load path is enough to supply the outage loads. If it is, then go to **Step 3-3-9**; otherwise go to **Step 3-3-7**.

Step 3-3-7) Perform the load transferring process.

Step 3-3-7-1) Perform load transferring of the backup feeder with less capacity margin until the total capacity margin of backup feeders can supply the outage loads. If it cannot, go to **Step 3-3-8**; otherwise go to **Step 3-3-9**.

Step 3-3-7-2) Perform load transferring of the backup feeder which cannot supply its corresponding loads. After the load transferring, if the backup feeder still doesn't have enough capacity margin, go to **Step 3-3-8**; otherwise go to **Step 3-3-9**.

Step 3-3-8) Supply the outage zones as much as possible individually by two backup feeders; shed the remaining outage loads of the zones, if there are.

Step 3-3-9) According to backup feeders' loading ratios of capacity margin as shown in Eq. (1), allocate appropriate amounts of loads into two parts to open a switch on the load path. If both backup feeders can supply the corresponding loads individually, finish the restoration process; otherwise **Step 3-3-7-2**.

B. Update of Loads and DGs in Outage Zones

DGs of renewable energies may have discontinuous output due to weather conditions, such as PV, wind-turbine (WT), combined heat and power (CHP), and fuel cell (FC) generation systems in the DS. To restore the loads in the outage zones, the loads of the still energized area and the available power output of the DGs can be updated before the restoration process under the assumption of an established smart-grid system. At the same time, information on number of available tie switches n_{TSW} in the outage zone is needed.

C. Restoration Process

Figure 2 shows the example DS diagram used for illustration of the restoration process. In description of the proposed restoration approach below, cases of different numbers of available tie switches that can be used in restoration are discussed.

1) Case 1: Number of available tie switch = 1

In Figure 3, suppose there was a fault occurring at Z7, switches S_9 and S_{10}, therefore, were opened to isolate the fault. Then, the load path of Z_8-Z_9 is defined. This is the simplest case where to close S12 is the strategy to restore the outage zones. If the backup feeder, Feeder4, doesn't have enough capacity to supply the outage zones, the backup feeder transfers load to the other feeder (secondary backup feeder) to obtain more capacity.

However, if it still fails to restore outage zones after the load transferring process, the restoration process will start to shed the loads. As many loads as possible are supplied by the backup feeder (Feeder4) with the remaining loads in the outage zones being shed.

2) Case 2: Number of available tie switches = 2

a) Type 1: No outage zones to be integrated

Suppose there was a fault occurring in Z_4 as shown in Figure 4. Switches S_5 and S_6 were opened to isolate the fault. Load path of Z_5-Z_6-Z_7-Z_8-Z_9 is defined. It is clear to see that the outage zones have two backup feeders: Feeder2 and Feeder4. The RS will choose one switch of S_8, S_9, S_{10}, and S_{11} to separate the load path into two parts. Appropriate amount of loads is allocated to the two backup feeders according to the loading ratios of capacity margin of the individual backup feeder as shown in Eq. (1).

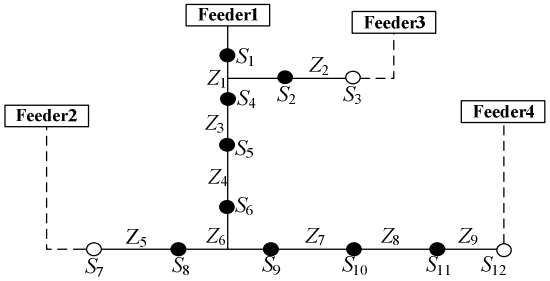

Figure 2. An example DS diagram

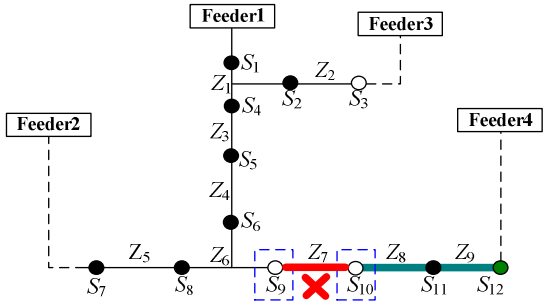

Figure 3. The DS diagram with one tie switch

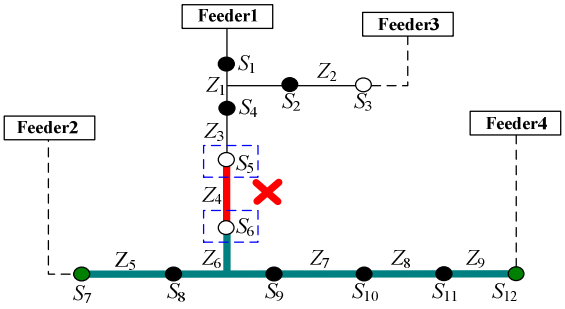

Figure 4. The DS diagram with two tie switches & no outage zones be integrated

The purpose is to make the loads of backup feeders balanced to avoid overloading for either of the backup feeders.

If the backup feeders, Feeder2 or Feeder4, don't have enough capacity margin to supply the outage zones, the backup feeders will proceed to the load transferring process trying to obtain more capacity. If it still fails to restore outage zones after their own load transferring process, the strategy will start to shed the loads to have as most loads supplied.

b) Type 2: Outage zones to be integrated

If the fault occurred at Z_3 as shown in Figure 5, S_4 and S_5 were opened to isolate the fault. The load path of Z_5-Z_6-Z_7-Z_8-Z_9 is defined. However, it is noted that Z_4 should be integrated into the load path, otherwise it cannot be restored. In this case, the outage zones also have two backup feeders: Feeder2 and Feeder4. The same steps are followed as in Type 1 above to restore the outage zones.

3) Case 3: Number of available tie switches ≧3

Suppose a fault occurred at Feeder1 as shown in Figure 6, S1 was opened to isolate the fault. Based on the proposed algorithm, three tie switches of S3, S7, and S12 are available for the restoration in this case. Accordingly, three load paths in Figure 6are defined below:

- Load Path 1 (S_3 to S_7): Z_2-Z_1-Z_3-Z_4-Z_6-Z_5
- Load Path 2 (S_3 to S_{12}): Z_2-Z_1-Z_3-Z_4-Z_6-Z_7-Z_8-Z_9
- Load Path 3 (S_7 to S_{12}): Z_5-Z_6-Z_7-Z_8-Z_9

The RS will find out the main load path by using the following fuzzy inference process. Two membership functions of the following fuzzy variables are used as illustrated in Figure 7 for the fuzzy inference rules.

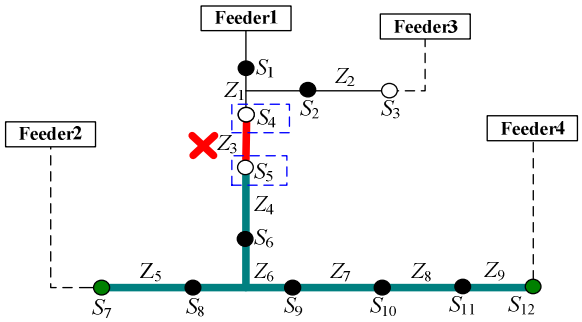

Figure 5. The DS diagram with two tie switches & outage zones to be integrated

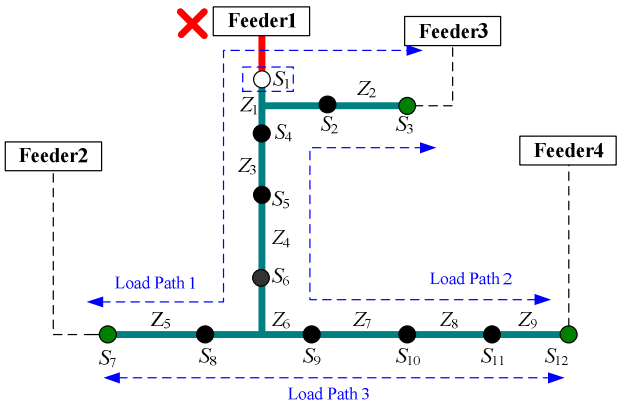

Figure 6. The DS diagram with more than three tie switches

- The total capacity margin of two backup feeders on the load path
- The total outage loads of the load path

The fuzzy rules are showed in Table. I. Take "Load Path 1" in Figure 6 for example, the inputs of the fuzzy inference engine are defined as the total capacity margin of Feeder3 and Feeder2 and the total outage loads of "Load Path 1." Based on the fuzzy inference and defuzzification process, the main load path with highest output value will be determined, whose outage zones will be restored with priority.

With the main load path determined, loads of the rest outage zones are integrated into the zone of the main load path. For example, if the "Load Path 2" is the determined main load path, the restoration process will integrate Z_5 into Z_6, and the outage zones will be restored by Feeder3 and Feeder4. Then, the restoration process will choose one switch among S_2, S_4, S_5, S_6, S_9, S_{10}, S_{11}, or S_{12} to separate the load path into two parts. The objective is to allocate appropriate amount of loads to different backup feeders.

If the backup feeders have no enough capacity margin , the proposed algorithm will check whether the integrated outage zones (e.g. Z_5) can be supplies by its connecting backup feeder (e.g. Feeder2) or not. In case the margin for restoration of the outage loads is still not enough, the load transferring process will proceed. However, if the load transferring process fails restoration of all the outage zones, the algorithm will start to shed the loads of the remaining outage zones, as the backup feeders (Feeder3 & 4) supply as many loads as they can.

III. Simulation Results

The proposed algorithm is implemented in MATLAB 7.1 on a windows-XP based PC with Intel Core 2, Duo E7200, 2.53-GHz CPU and 2GB of RAM. The proposed restoration approach was applied to a practical 6-feeder DS of Taipower Company (TPC) [23].

A. Scenario 1: Large Outage Zone Situation

Suppose that there was a fault occurring at Feeder5 as in Figure 8. The system opened S_{59} (CB_5) first to isolate the fault. Because the number of corresponding available tie switches is three, including S_{38}, S_{41} and S_{44}, with three load paths existing.

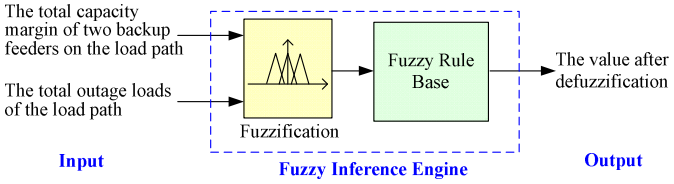

Figure 7. The fuzzy inference process in determining the main load path

TABLE I. THE FUZZY RULES USED IN THE INFERENCE ENGINE

B \ A	Low	Medium	High
Low	Medium	Low	Medium
Medium	Medium	Medium	High
High	Low	Medium	High

Note: A: total capacity margin of the backup feeders on the load path
B: the total outage loads on load path

The proposed algorithm determined the main load path based on the fuzzy inference rules described. Then the process proceeded to restore the outage zones to have balanced loading of feeders. The final result is showed in TABLE II. Through this scenario, it shows that the proposed restoration can deal with serious fault cases with large outage zones and achieve load balancing as much as possible.

B. *Scenario 2: Comparison with the Method in* [23]

In this scenario, the proposed approach was compared with the method in [23]. It was assumed that there was a fault occurring at Z_{43} as shown in Figure 9. The restoration algorithm opened S_{47} and S_{48} first to isolate the fault. The corresponding two available tie switches are S_4 and S_{41} for only one load path existing.

The proposed restoration approach determined whether outage zones were needed to be integrated or not. In this scenario, Z_{44} and Z_{45} must be integrated into Z_{46} for restoration. Then the process proceeded to restore the outage zones and balance the loading of feeders as much as possible simultaneously. The final result is showed in TABLE III, the proposed approach can achieve a solution with all outage zones restored with balanced loads of the backup feeders.

In comparison, the solution obtained by the expert system proposed in [23] still has the outage zones of Z_{49} and Z_{50} un-restored, and all the restored zones are supplied by single feeder instead of balancing the loads via two backup feeders as in the proposed method.

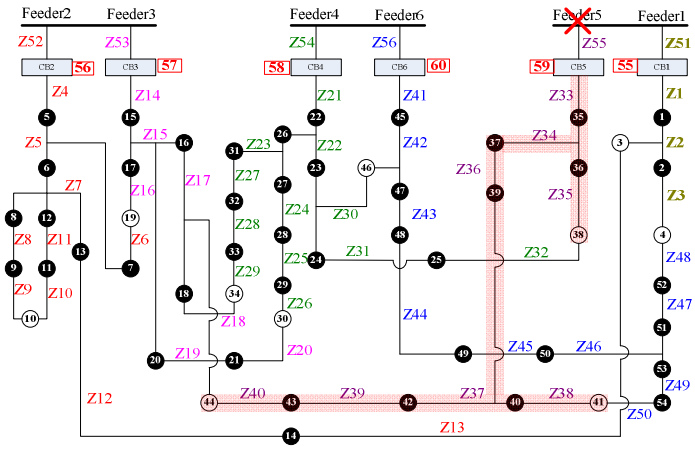

Figure 8. TPC 6-feeder system with fault at Feeder5

TABLE II. THE FINAL RESULTS FOR SCENARIO 1 AFTER RESTORATION

Items \ Scenario	Scenario 1	
Fault Location	Feeder5	
Isolation Switch	CB5 (S_{59})	
Total Outage Zones Before Restoration	Z_{33}, Z_{34}, Z_{35}, Z_{36}, Z_{37}, Z_{38}, Z_{39}, Z_{40}	
Backup Feeder (FD)	Feeder3	Feeder4
Supplied Zones	Z_{37}, Z_{38}, Z_{39}, Z_{40}	Z_{33}, Z_{34}, Z_{35}, Z_{36}
Switch Operation	Close: S_{44}, S_{38}; Open: S_{39}	
Outage Zones After Restoration	None	
Execution Time (s)	1.367136	

C. *Scenario 3: Comparison with/without DGs Considered*

In this scenario, the purpose is to find out influence of DGs considered on restoration strategies. The DS without DGs considered was compared with that with DGs. To consider the DGs, the fault situation is assumed the same as Scenario 1 as shown in Figure 8, but having some zones installed generators of renewable energies.

TABLE IV summarizes the zone conditions with DGs considered for Scenario 3. Accordingly, capacities of all feeders were also adjusted to lower values to make the restoration more difficult in recovering the loads.

TABLE V show the results obtained with and without DGs considered. It was supposed in a smart-grid system the loading conditions are updated periodically. Different switching operations for the two cases are shown in TABLE V. The case without DGs considered needs more switching operations to transfer the loads for the system restoration.

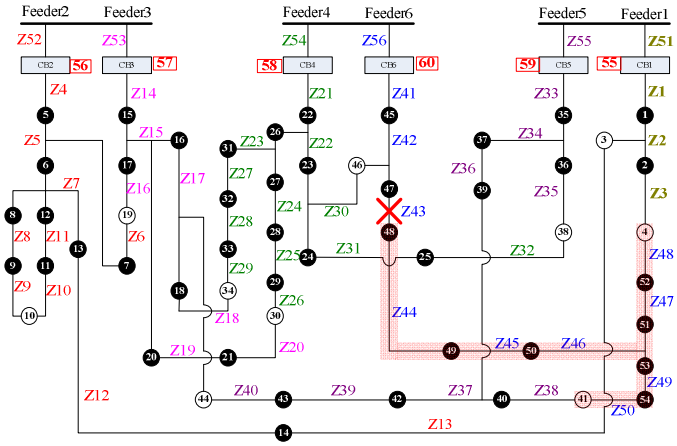

Figure 9. TPC 6-feeder system with fault at Z_{43}

TABLE III. THE FINAL RESULTS FOR SCENARIO 2 AFTER RESTORATION

Items \ Method	Proposed strategy		Expert system [23]
Fault Location	Z_{43}		
Isolation Switch	S_{48}		
Total Outage Zones Before Restoration	Z_{44}, Z_{45}, Z_{46}, Z_{47}, Z_{48}, Z_{49}, Z_{50}		
Backup Feeder	Feeder1	Feeder5	Feeder1
Supplied Zones	Z_{47}, Z_{48}	Z_{44}, Z_{45}, Z_{46}, Z_{49}, Z_{50}	Z_{44}, Z_{45}, Z_{46}, Z_{47}, Z_{48}
Switch Operation	Close: S_4, S_{41}, Open: S_{51}		Close: S_4 Open: S_{53}
Outage Zones After Restoration	None		Z_{49}, Z_{50}
Execution Time (s)	1.005192		N/A

TABLE IV. THE ZONE CONDITIONS FOR DGS IN SCENARIO 3

Zone	Type of DG	Capacity
33	PV+WT	60kW (5kW×8+2kW×10)
34	PV	40kW (5kW×8)
35	PV+FC	50kW (5kW×2+20kW×2)
36	WT	40kW (2kW×20)

TABLE V. THE RESULTS FOR SCENARIO 3 AFTER RESTORATION

Case / Items	With DGs		Without DGs	
Fault Location	Feeder5			
Isolation Switch	S_{59}			
Total Outage Zones Before Restoration	Z_{33}, Z_{34}, Z_{35}, Z_{36}, Z_{37}, Z_{38}, Z_{39}, Z_{40}			
Backup Feeder	Feeder3	Feeder4	Feeder3	Feeder4
Supplied Zones	Z_{37}, Z_{38}, Z_{39}, Z_{40}	Z_{33}, Z_{34}, Z_{35}, Z_{36}	Z_{36}, Z_{37}, Z_{39}, Z_{40}	Z_{33}, Z_{34}, Z_{35}
Switch Operation	Close: S_{44}, S_{38} Open: S_{39}		Close: S_{44}, S_{38}, S_{41} Open: S_{37}, S_{40}	
Outage Zones After Restoration	None		None	
Execution Time (s)	1.374077		1.359812	
Remark	None		Z_{38} is transferred to Feeder6	

IV. CONCLUSIONS

In this paper, a heuristic fuzzy-rule based system was proposed for restoration of a DS with/without existing DGs of renewable energies. Based on the concept of load path, loads in the outage zones are supplied as much as possible by backup feeders. Through the proposed process, balanced feeders' loading can thus be achieved. For large outage zones, the main load path is determined for more than two load paths via the proposed fuzzy inference rules. With different types of DGs and fault conditions existing in the DS, the proposed algorithm can also deal with the corresponding restoration problem easily based on the simple fuzzy decision rules.

The test results by using a practical Taipower distribution system showed different faulty situations can be well dealt with by using the proposed approach. Further, the proposed approach can have better restoration results (without loads un-restored in the outage zones) as compared with the expert system tested on the same system. The influence of DGs of renewable energies on restoration of a DS was also evaluated through the proposed approach.

ACKNOWLEDGMENT

This work supported in part by National Science Council of R.O.C. under Grant NSC 100-3113-E-194-001 is greatly acknowledged.

REFERENCES

[1] V. Susheela Devi, D. P. Sen Gupta, and G. Anandalingam, "Optimal restoration of power supply in large distribution systems in developing countries," *IEEE Trans. Power Del.*, vol. 10, no. 1, pp. 430-438, Jan. 1995.

[2] Y. Y. Hsu, H. M. Hung, C. H. Kuo, S. K. Peng, and H. S. Yu," Distribution System Service Restoration Using a Heuristic Search Approach," *IEEE Trans. Power Del.*, vol. 7, no. 2, pp. 734-740, April 1992.

[3] W. M. Lin and H. C. Chin," A New Approach for Distribution Feeder Reconfiguration for Loss Reduction and Service Restoration," *IEEE Trans. Power Del.*, vol. 13, no. 3, pp. 845-870, July 1998.

[4] H. J. Lee and Y. M. Park," A Restoration Aid Expert System for Distribution Substations," *IEEE Trans. Power Del.*, vol. 11, no. 4, pp. 1765-1769, Oct. 1996.

[5] C. C. Liu, S. J. Lee, and S. S. Venkata," An Expert System for Operational Aid for Restoration and Loss Reduction of Distributions," *IEEE Trans. Power Syst.*, vol. 3, no. 2, pp. 619-626, May 1988.

[6] S. J. Lee, K. H. Kim, H. Y. Kim, J. K. Lee, and K. Y. Nam," Expert System-Aided Service Restoration in Distribution Automation," *IEEE International Conference on Systems, Man and Cybernetics*, vol. 1, pp. 157-161, 1992.

[7] S. J. Lee, K. H. Kim, K. Y. Nam, and J. K. Lee," Service restoration expert system adopting branch pattern based grouping strategy in distribution systems ," *Expert Syst. Appl. Power Syst. IV*, pp. 423-427, Jan. 1994.

[8] H. C. Kuo, and Y. Y. Hsu, "Distribution System Load Estimation and Service Restoration Using A Fuzzy Set Approach," *IEEE Trans. Power Del.*, vol. 8, no. 4, pp. 1950-1957, Oct. 1993.

[9] Y. Y. Hsu, and H. C. Kuo, "A Heuristic Based Fuzzy Reasoning Approach for Distribution System Service Restoration," *IEEE Trans. Power Del.*, vol. 9, no. 2, pp. 948-953, Apr. 1994.

[10] Q. Zhou, D. Shirmohammadi, and W. H. Edwin Liu, "Distribution Feeder Reconfiguration for Service Restoration and Load Balancing," *IEEE Trans. Power Syst.*, vol. 12, no. 2, pp. 724-729, May. 1997.

[11] S. J. Lee, S. I. Lim, and B. S. Ahn, "Service Restoration of Primary Distribution Systems Based on Fuzzy Evaluation of Multi-Criteria," *IEEE Transactions on Power Syst.*, vol. 13, no. 3, pp. 1156-1163, Aug. 1998.

[12] C. M. Hung, "Multiobjective Service Restoration of Distribution Systems Using Fuzzy Cause-Effect Networks," *IEEE Transactions on Power Syst.*, vol. 18, no. 2, pp. 867-874, May 2003.

[13] J. S. Wu, "A Petri-Net Algorithm for Multiple Contingencies of Distribution System Operation," *IEEE Transactions on Power Syst.*, vol. 13, no. 3, pp. 1164-1171, Aug. 1998.

[14] C. S. Chen, C. H. Lin, and H. Y. Tsai, "A Rule-based Expert System with Colored Petri Net Models for Distribution System Service Restoration," *IEEE Transactions on Power Syst.*, vol. 17, no. 4, pp. 1073-1080, Nov. 2002.

[15] Y. Fukuyama, H. Endo, and Y. Nakanishi, "A Hybrid System for Service Restoration Using Expert System and Genetic Algorithm," *International Conference on Intelligent Systems Applications to Power Systems.*, pp. 394-398, 1996.

[16] Y. Fukuyama, and H. D. Chiang, "A Parallel Genetic Algorithm for Service Restoration in Electric Power Distribution System," *International Joint Conference of the Fourth IEEE International Conference on Fuzzy System and The Second International Fuzzy Engineering Symposium.*, vol. 1, pp. 275-282, 1995.

[17] Y. T. Hsiao and C. Y. Chien, "Enhancement of Restoration Service in Distribution Systems Using a Combination Fuzzy-GA Method," *IEEE Transactions on Power Syst.*, vol. 15, no. 4, pp. 1394-1400, Nov. 2000

[18] Sakae Toune, Hiroyuki Fudo, Takamu Genji, Yoshikazu Fukuyama, and Yosuke Nakanishi, "Comparative Study of Modern Heuristic Algorithms to Service Restoration in Distribution Systems," *IEEE Transactions on Power Del.*, vol. 17, no. 1, pp. 173-181, Jan. 2002

[19] Y. Liu, and Z. Gu, "Reconfiguration of network skeleton based on discrete particle-swarm optimization for black-start restoration," *IEEE Power Engineering Society General Meeting*, pp. 7, 2006

[20] Y. Liu, and X. Gu., "Skeleton-Network Reconfiguration Based on Topological Characteristics of Scale-Free Networks and Discrete Particle Swarm Optimization," *IEEE Trans. on Power Systems*, vol. 22, no. 3, Aug. 2007.

[21] G. Lambert-Torres, H. G. Martins, M. P. Coutinho, and C. P. Salomon, and F. C. Vieira, "Particle Swarm Optimization Applied to System Restoration," *IEEE Bucharest Power Tech Conference*, June 2009.

[22] H. C. Chin, and Y. S. Su, "Application of The Ant-Based Network for Power System Restoration," *IEEE /PES Transmission and Distribution Conference & Exhibition: Asia and Pacific Dalian, China*, 2005.

[23] M. S. Tsai, "Development of an Object-Oriented Service Restoration Expert System With Load Variations," *IEEE Transactions on Power Syst.*, vol. 23, no. 1, pp. 219-225, Feb. 2008.

2011 IEEE International Conference on Fuzzy Systems
June 27-30, 2011, Taipei, Taiwan

Neuro-Fuzzy Predictive Model for PV Energy Production based on Weather Forecast

Francesco Grimaccia
Politecnico di Milano
Energy Department
20156 Milano - Italy
Email: francesco.grimaccia@polimi.it

Marco Mussetta
Politecnico di Milano
Energy Department
20156 Milano - Italy
Email: marco.mussetta@polimi.it

Riccardo Zich
Politecnico di Milano
Energy Department
20156 Milano - Italy
Email: riccardo.zich@polimi.it

***Abstract*—This paper introduces an evolutionary optimization algorithm as a tool for training an Artificial Neural Network used for production forecasting of solar energy PV plants. This optimized procedure essentially represent a bio-inspired heuristic search technique which is used to solve complex forecasting problems modeled on the concepts of biological neurons. Some simulation results are reported to highlight advantages and drawbacks of the proposed method in order to suitably apply this algorithm to a neuro-fuzzy system application in solar energy production. The weather forecast data related to the PV plants are supplied by the airport service close to the production site and relative data are pre-processed using Fuzzy Logic techniques.**

***Index Terms*—PV energy prediction, Neural Networks.**

I. Introduction

In recent years solar power is getting more and more important as an alternative and renewable energy source, especially for small autonomous electrical power systems, villages and also rural areas. Photo-voltaic (PV) plants can also be connected to the traditional grid for energy distribution, but variations in solar power can cause, in general, voltage and frequency fluctuations.

Load and energy production forecasting has always been crucial for the effectiveness of power system planning and operation. Lots of electric power companies are now forecasting power load based on traditional prediction methods [1]. However, since the relationship between power load and factors influencing power production is nonlinear, it is difficult to identify its nonlinearity by using traditional prediction methods.

Moreover, renewable energy sources have increased the complexity of this scenario, thus requiring the capability to predict the dynamics of the system and to offer an optimal management; therefore, it has been proposed the application of advanced forecasting techniques integrated with an optimization algorithm in order to create a predictive model of the physical system and to provide an efficient control of resources and information. To implement this approach, evolutionary optimization procedures adaptively and dynamically analyzing consumer profiles have been defined in the so called digital energy environment [2].

Advanced forecasting techniques provide utilities with reliable production predictions and the opportunity to plan for additional power supply and to make proactive actions. This aspect can have an impact on the economic balance of the systems especially in an integrated smart grid solution perspective. In fact, in this way the system-plant management is capable for example to plan appropriate preventive maintenance strategies in order to minimize energy losses due to unproductive suspensions. It can be estimated in the order of million dollars per MW per year adopting predictive strategies in the renewable energy sector and just the 10% of these are due to an optimized operating efficiency [3].

Increased solar power penetration is possible if measures are taken concerning solar radiation forecasting. This procedure may also affect the energy efficiency of the conventional power stations, since it affects the operation point of the power units. Prediction of solar power is therefore of importance for efficient load management and operation of the system. It has been suggested in literature [4], [5], [6] that solar power forecast could be based on the use of Artificial Neural Networks (ANNs). They are particularly appealing because of their ability to model an unspecified nonlinear relationship between production and weather variables.

II. Artificial Neural Networks

Computation techniques play an important role in most engineering applications in which optimization problems have to be solved. Usually the complex nature of many practical problems involves an effective use of Artificial Neural Networks to solve them. ANNs are useful tools when it is necessary to understand the complex and nonlinear relationships among data, without any a-priori assumption concerning the nature of these correlations.

ANN is an effective computing method, in order to easily process the dynamic behavior of time-varying variable, as previously presented by the authors in [7]. It is a computational model that simulates the features and behavior of the human brain neural networks. It consists of an interconnected group of artificial neurons that suitably processes information according to the strength of connections among them. In more practical terms neural networks are non-linear statistical data modeling tools used to model complex relationships between inputs and outputs or to find patterns in data.

For the considered forecasting application, a multilayered

978-1-4244-7316-8/11/$26.00 ©2011 IEEE

perceptron (MLP) has been utilized. The MLP is a well-known universal approximator and has been extensively used in engineering applications, as well as other kind of ANN.

Training algorithms are used to train the network by learning the nonlinear behavior between input and output data. Therefore the learning process should result in finding the weights configuration associated to the minimum output error, namely the optimized weights configuration.

In other words, since ANN wish to infer the mapping implied by the data, the weights of the network have to be optimized in order to reach a good and accurate desired output: usually these tasks are associated to an objective function to be optimized. This function, called cost or energy function, provides the interface between the physical problems and the optimization algorithm itself. The cost function, in particular, is related to the mismatch between the proposed mapping and the data and for this reason it must contains prior knowledge about the problem domain.

A commonly used cost is the mean-squared error which tries to minimize the average squared error between the network's output, $f(x)$, and the target value y over all the example pairs.

There are often many problems related to this task: generally finding a solution in an optimization process means to reach a balance among different and often conflicting goals; as a consequence such a search could be extremely difficult. The huge number of variables is the first difficulty when dealing with one of these optimizing issues. Secondly, there are lots of weights configurations with different values of the cost function which are quite similar each other and very close to the global optimum case, even if these configurations are sub-optimal.

In particular, the approaches used to optimize and train a MLP may be divided into two main categories: the ones that need to calculate derivatives in order to optimize the objective function, such as gradient descent based strategies, e.g. the Error Back-Propagation (EBP) algorithm, and those that, starting from an initial position in the solution space, explore iteratively this space without requiring any derivatives calculation, e.g. evolutionary methods, like Genetic Algorithm (GA) or Particle Swarm Optimization (PSO) [7].

Error Back Propagation algorithm is a well known analytical algorithm used for neural networks training. In literature, there are several forms of back-propagation, all of them requiring different levels of computational efforts; the conventional back-propagation method is, however, the one based on the gradient descent algorithm.

One of the drawbacks of this method is the strong dependence upon the initial guess. A bad choice of the starting point may result in the possibility to get stuck in a local minimum and consequently to find a solution that is not the best one. Besides, most of the typical problems requiring optimization often have non-differentiable or/and discontinuous regions in the solution domain and this fact introduces difficulties in the application of these traditional methods based on derivatives calculations. These aspects are often overcome by evolutionary methods, like the one chosen by the authors, the Genetical Swarm Optimization (GSO) algorithm [8].

GSO essentially represent a bio-inspired heuristic search technique, which can be used to solve combinatorial optimization problems, modeled on the concepts of natural selection and evolution (GA), but also based on cultural and social behaviours derived from the analysis of the swarm intelligence and interaction among particles (PSO) [9]. Previously performed analyses highlighted some advantages of the proposed technique in order to suitably apply this algorithm to neural network applications in engineering problems [10].

III. Implementation

As shown in Figure 1, weather forecasts are a key input when the ANN is used for forecasting. Nevertheless in case of rapid changes in solar radiation or temperature at the forecast day, produced power changes greatly and forecast error would sensibly increase. In traditional prediction methods the ANN uses all similar days data to learn the trend of similarity. However, learning all similar days' data is quite complex, and it does not help if weather conditions change suddenly during the same day. Therefore, it is necessary to integrate into the neuro-fuzzy system real time information coming from local meteorological stations and, in particular, from surrounding regions and cities, where the weather change has already occurred.

In this paper a real-world case study with a proposed approach of fuzzy filtering is suitable for dealing with the complexity of inputs involved in the available weather forecast data. Over the last decades fuzzy models have been used to replace conventional methods for engineering applications, especially in control systems, making easier the solution to many problems by introducing an unconventional set of rules. System analysis and control design for nonlinear systems based on fuzzy system approaches have been very active in the scientific community [11], [12], [13]. In this context fuzzy models, due to their intrinsic capability of approximating nonlinear data mappings, could be exploited for the preprocessing of a subset of weather data in order to filter the inputs for the ANN. As shown in detail in Figure 1 a fuzzy preprocessing toolbox is introduced into the neural system to find data correlation between UV index, cloud cover and specific time/season with irradiance value useful to perform production forecast.

IV. Simulation Results

In order to compare the different optimization approaches for training the ANN, a production forecasting problem has been considered with a different perspective compared to [1]. The focus is to highlight how fast and accurate the methods are in determining and optimizing the neural networks weights associated to the considered problem.

After a trial campaign, the network architecture which have provided better results present two hidden layers, as shown in Figure 1. In particular, the number of neurons in the input layer is 16, as reported in Table I, which describes the meteorological parameter provided from the weather forecast service.

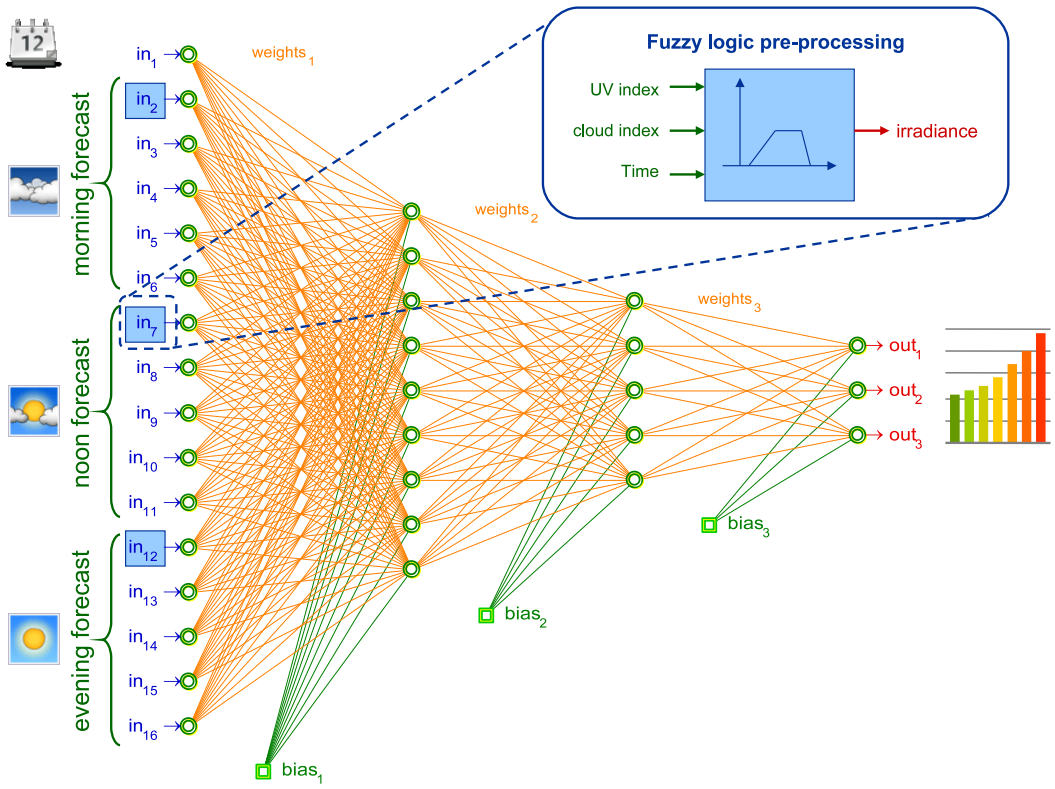

Fig. 1. Simplified view of the implemented feed-forward ANN with Fuzzy pre-processing.

TABLE I
STRUCTURE OF INPUT LAYER

Neuron	Variable name	Time	Range
i_1	Day		(1–366)
i_2	Irradiance	at 6:00	(0–1350) W/m^2
i_3	Air temperature	”	(0–30) °C
i_4	Wind speed	”	(0–20) km/h
i_5	Air humidity	”	(0–100) %
i_6	Air pressure	”	(1000–1040) mbar
i_7	Irradiance	at 12:00	(0–1350) W/m^2
i_8	Air temperature	”	(0–30) °C
i_9	Wind speed	”	(0–20) km/h
i_{10}	Air humidity	”	(0–100) %
i_{11}	Air pressure	”	(1000–1040) mbar
i_{12}	Irradiance	at 18:00	(0–1350) W/m^2
i_{13}	Air temperature	”	(0–30) °C
i_{14}	Wind speed	”	(0–20) km/h
i_{15}	Air humidity	”	(0–100) %
i_{16}	Air pressure	”	(1000–1040) mbar

The neurons in the two hidden layers are, respectively, 9 and 5, while the output layer is composed of 3 neurons, since 3 different produced-power forecasts are considered: in fact, the authors performed simulations for three different photovoltaic power plants in order to test their method at various scale, since they have different productive capacity, as shown in Table II. To compare the numerical results it is important to underline that the three plant locations present exactly the same GPS reference points. Therefore the weather conditions can be assumed identical for the three PV plants at each time.

Different time horizons was considered in load forecasting: short term (day and several days), medium term (week and several weeks), long term (year and several years), and forecasts for different lead time can potentially be used for different aims. We finally chose a short term time base for this specific application. The neuro-fuzzy system optimized by GSO exhibit good predictive performances in all the operative conditions, in a complete sunny day, a partly cloudy one and even a plant

TABLE II
STRUCTURE OF OUTPUT LAYER

Neuron	Variable name	Range
o_1	SM 4200S-2 Produced power	(0–4) kW
o_2	SM 4200S-3 Produced power	(0–4) kW
o_3	SM 35C-4 Produced power	(0–35) kW

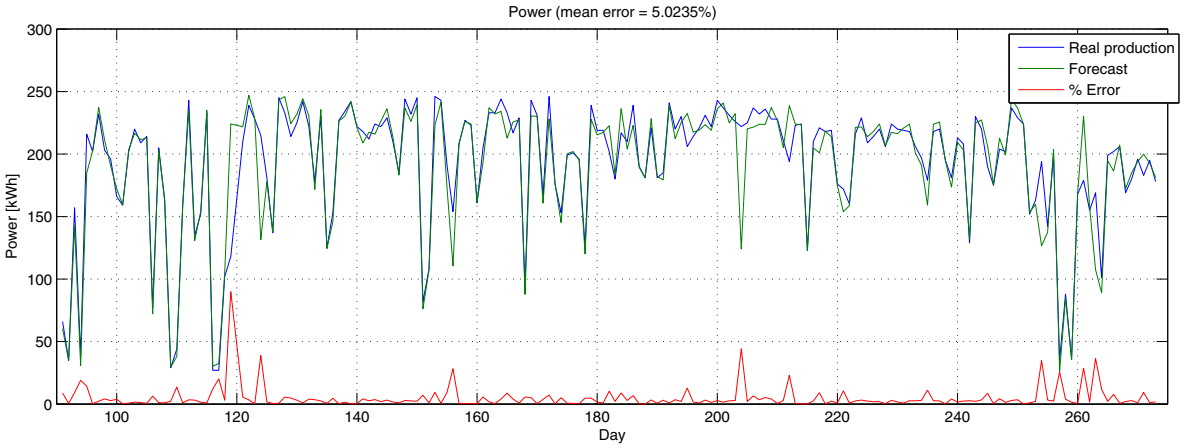

Fig. 2. Results of the forecasting over a six-months time frame and comparison with actual data.

maintenance day.

Figure 2 shows the complete data set simulations around six months and the average error is around 5% . The considered ANN behaviour does not change with respect to the plant power size.

V. Conclusions

Energy plant prediction is very important in industrial applications. An accurate prediction enables to mitigate the price risk associated with the power exchange, for instance signing more bilateral contracts. Besides, a good estimate of the load profile results in avoiding economic penalties on the balancing market. In this work the authors presented an effective and robust implementation of an Neuro-fuzzy model for forecasting of photo-voltaic energy production.

ACKNOWLEDGMENT

This work was supported by Regione Lombardia, ICT-Metadristretti Action, under grant ID5109 - DGR N.6735 [14].

References

[1] T. Senjyu, H. Takara, K. Uezato, and T. Funabashi, "One-hour-ahead load forecasting using neural network,", *IEEE Transactions on Power Systems*, Vol. 17, No. 1, February 2002, pp. 113-118.

[2] M. Simonov, M. Mussetta, R.E. Zich, "Digital Energy: Clustering Micro Grids for Social Networking", *International Journal of Virtual Communities and Social Networking*, Vol. 1, No. 3, 2009, pp. 75–93.

[3] M. Simonov, M. Mussetta, A. Pirisi, F. Grimaccia, D. Caputo, R.E. Zich, "Real time energy management in smart cities by Future Internet", in: G. Tselentis et al. (Eds.), *Towards the Future Internet–Emerging Trends from European Research*, IOS Press, Amsterdam, NL, 2010, pp. 173–182.

[4] W. Taylor, and R. Buizza, Neural network load forecasting with weather ensemble predictions, *IEEE Transactions on Power Systems*, Vol. 17, No. 3, 2002, pp. 626–632.

[5] H. S. Hippert, C. E. Pedreira, R. C. Souza, "Neural networks for short-term load forecasting: a review and evaluation," *IEEE Transactions on Power Systems*, Vol. 16, No. 4, November 2001, pp. 798–805.

[6] F. Grimaccia, M. Mussetta, R.E. Zich, "Photovoltaic plants predictive model by means of artificial neural networks", *Proceedings of the Solar Energy Tech 2010*, July 2010, Milano, Italy, pp. 95–102.

[7] E. Grimaldi, F. Grimaccia, M. Mussetta, R.E. Zich, "Pso as an effective learning algorithm for neural network applications", *Proceedings of the 3rd International Conference on Computational Electromagnetics and Its Applications ICCEA 2004*, 2004, pp. 557–560.

[8] F. Grimaccia, M. Mussetta, R.E. Zich, "Genetical Swarm Optimization: Self-Adaptive Hybrid Evolutionary Algorithm for Electromagnetics", *IEEE Transactions on Antennas and Propagation*, Vol.55, No.3, March 2007, pp. 781–785.

[9] A. Gandelli, F. Grimaccia, M. Mussetta, P. Pirinoli, R.E. Zich, "Development and Validation of Different Hybridization Strategies between GA and PSO", *Proc. of the 2007 IEEE Congress on Evolutionary Computation*, Sept. 2007, Singapore, pp. 2782–2787.

[10] D. Caputo, F. Grimaccia, M. Mussetta, R.E. Zich, "Photovoltaic Plants Predictive Model by means of ANN trained by a Hybrid Evolutionary Algorithm", *Proceedings of the 2010 IEEE World Congress on Computational Intelligence, WCCI 2010*, July 2010, Barcelona.

[11] M. Kumar, N. Stoll, D. Kaber, K. Thurow, R. Stall, Fuzzy Filtering for an Intelligent Interpretation of Medical Data *IEEE International Conference on Automation Science and Engineering*, 2007,pp. 225–230.

[12] F. Russo, Evolutionary neural fuzzy systems for data filtering *IEEE Conference Proceedings on Instrumentation and Measurement Technology Conference, IMTC'98*,2008, Vol. 2, pp. 826–830.

[13] Jin Ying, S. Veerappan, A fuzzy XML database system: Data storage and query processing, *IEEE International Conference on Information Reuse and Integration*, 2010, pp. 318–321.

[14] www.futurenergy.it

2011 IEEE International Conference on Fuzzy Systems
June 27-30, 2011, Taipei, Taiwan

Improving Estimation Accuracy of the COCOMO II Using an Adaptive Fuzzy Logic Model

Iman Attarzadeh, Siew Hock Ow
Department of Software Engineering, Faculty of Computer Science & Information Technology,
University of Malaya, 50603 Kuala Lumpur, MALAYSIA
attarzadeh@siswa.um.edu.my, show@um.edu.my

***Abstract*—Software development time and cost estimation are the process of estimating the most realistic use of time and cost required for developing a software. It is one of the biggest challenges in the area of software engineering and project management, in the last decades. The software estimates are difficult to obtain due to incomplete software information is available in the early phase of software development process. Insufficient software information causes inaccuracy in software attributes. Thus, the vagueness and uncertainty of the software attributes is the main reason of inaccuracy of software estimates. Software cost estimation models such as regression model, expert judgment, SLIM, and COCOMO require accurate software attributes and long term estimation process, which are not completely achievable in early phase of software development process. Soft computing techniques such as fuzzy logic can reduce the vagueness and uncertainty of software attributes. Therefore, it may consider as alternative to decrease the inaccuracy of software estimates. This research aims to utilise an adaptive fuzzy logic model to improve the accuracy of software time and cost estimation. Using advantages of fuzzy set and fuzzy logic can produce accurate software attributes which result in precise software estimates. The Two-Dimension Gaussian Membership Function (2-D GMF) was used in the fuzzy model to make software attributes smoother in terms of the range of values. The COCOMO I, NASA98 data sets; and four project data from a software company in Malaysia were used in the evaluation of the proposed Fuzzy Logic COCOMO II (FL-COCOMO II). The evaluation of the obtained results, using Mean of Magnitude of Relative Error (MMRE) and PRED(25%) evaluation techniques, showed that the FL-COCOMO II produced the MMRE less than the original COCOMO and the value of PRED(25%) in the Fuzzy-COCOMO II is higher than the original COCOMO. Furthermore, the FL-COCOMO II showed 8.03% improvement in terms of estimation accuracy using MMRE when compared with the original COCOMO. Using advantages of fuzzy logic such as accurate estimation; adaption; understandability, and etc., can improve the accuracy of software estimates.**

Keyword—Software project management, software cost estimation models, COCOMO II, soft computation techniques, fuzzy logic

I. INTRODUCTION

The number of project failures and those projects completed over cost and over schedule has been a significant issue for software project managers. Poor estimates have not only led projects to exceed budget and go over schedule but also, in many cases, to be terminated entirely. Although between 30% and 40% of software projects are ultimately completed despite going over budget or schedule, and many more projects are cancelled or failed [1]. Among the many reasons for failure, inaccuracy in software estimates has been identified as a root cause of a high percentage of failures in the software development [1, 2]. Software cost estimation is the set of techniques and procedures that organisations use to arrive at an estimate for proposal bidding, project planning, and probability estimates [3, 4]. As such, estimation accuracy is a very significant issue for executives, managers, technical staff, and, particularly, practitioners who perform or rely on cost estimation [5]. Accurate estimation of software development cost also continues to challenge software engineering researchers due to the continued lack of accurate estimates [2]. The reasons that software cost estimation is difficult and error prone include [3]:

- Software cost estimation requires a significant amount of cost to perform correctly;
- The process is often done hurriedly, without an appreciation for the cost required to perform the estimate;
- Experience is required for developing estimates, especially for large projects, and;
- Human bias

There are several software cost estimation models which can be classified as algorithmic and non-algorithmic models. The algorithmic models are based on the statistical analysis of historical data [6, 7], for example, Software Life Cycle Management (SLIM) [8] and Constructive Cost Model (COCOMO) [9]. Non-algorithmic techniques are based on new approaches such as, Parkinson, Expert Judgment, Price-to-Win, and Machine Learning approaches [10, 11]. The Machine learning approach is used to group together a set of techniques that represent some of the facts of human mind [12], for example regression trees, rule induction, fuzzy systems, genetic algorithms, artificial neural networks, Bayesian networks, and evolutionary computation. The last five of these approaches are classified as soft computing group. The importance of algorithmic and non-algorithmic estimation techniques discuss in the following sections, briefly.

978-1-4244-7316-8/11/$26.00 ©2011 IEEE

A. Algorithmic models

The famous algorithmic cost estimation models are: Boehm's COCOMO I and II [10]; Albrecht's Function Point; and Putnam's SLIM [8]. These models require inputs, accurate estimate of specific attributes, such as source line of code (SLOC), number of user screen, interfaces, complexity, etc. which are not easy to obtain in the early phase of software development. The formula and calculation of these models are easy to understand, also, they provide fast estimates when compared with non-algorithmic models. Besides, attributes and relationships used to estimate software development cost could change over time, and/or differ for software development environments [9]. The limitations of the algorithmic models led to the exploration of the non-algorithmic models.

B. Non-algorithmic models

In 1990's, the non-algorithmic models was born and have been proposed to software cost estimation. Software researchers have turned their attention to the new approaches that were based on soft computing approach such as artificial neural networks, fuzzy logic, and genetic algorithms. Fuzzy Logic (FL) offers a powerful linguistic representation that able to represent imprecision in the model inputs and outputs, while providing a more knowledge base approach to establish an effective model. Research shows that using FL can result in good performance in terms of reducing imprecision of inputs and outputs parameters.

This paper proposed an effective fuzzy logic model for embedding in the COCOMO II to overcome the vagueness and uncertainty of software attributes which resulted in producing more accurate estimation results.

II. Related work

Gray and MacDonell [2] compared popular techniques in software cost estimation such as regression techniques, function point analysis (FPA), fuzzy logic, and artificial neural networks. Their results showed that fuzzy logic model produced better performance than the other models. They introduced an application of fuzzy logic to cost estimation which resulted in developing a tool, FUzzy logic SOftware MEasuring (FULSOME) [2], to assist software managers in decision making. In the FULSOME model, the two important variables were selected: complexity adjustment factor and unadjusted function point. Then a triangular membership functions were defined for the small, medium, and large intervals of size, complexity, and software effort. Fei and Liu attempted to apply fuzzy logic to the algorithmic cost estimation models in order to handle uncertainty and imprecision problems in such models [13]. They proposed a fuzzy software size model for the COCOMO I. They found that it is unreasonable to assign determinate values for the software size attributes in the COCOMO I, because an accurate estimate of delivered source instruction (KDSI) cannot be made before starting the project. Ryder [14] applied fuzzy modeling technique to the COCOMO I and Function Points model. Idri et al and Huang et al [15, 16] investigated the application of fuzzy logic to the EMs in the intermediate COCOMO I. Also, the fuzzification of the COCOMO I without considering the adjustment factor, then they introduced the f-COCOMO. They assigned a new software size to the COCOMO I, also, the coefficients related to the development mode were assigned to a fuzzy set. In another research, Kumar et al [17] applied fuzzy logic to manpower buildup index (MBI) of Putnam estimation model. The MBI is based upon 64 different rules. The results showed that fuzzy logic can be effectively applied to software cost estimation.

Fuzzy logic also had been applied to the non-algorithmic models to overcome the uncertainly of the models. Molokken and Jorgensen, proposed a combination of a fuzzy logic model with the estimation by analogy technique [1]. Estimation by analogy is one of the classified techniques of expert-based estimation. It is a type of Case-based Reasoning (CBR) method. Besides, the fuzzy analogy for software cost estimation had also been applied to web-based software.

In summary, fuzzy logic has been applied to algorithmic and non-algorithmic cost estimation models in the pursuit of achieving better estimation results. Nevertheless, there is still much uncertainty as to what estimation technique suits which type of estimation problem [16]. Choosing between the different techniques is a difficult decision that requires the support of a well-defined evaluation method to show each estimation technique as it applies to any estimation problem.

III. Problem Statement

Inaccurate software cost estimation has plagued software projects for decades. Poor estimates have not only led projects to exceed budget and schedule but also, in many cases, be terminated entirely. The ability to accurately estimate software development time, cost, and manpower, changes as newer methodologies replace old ones. Therefore, an accurate software cost estimation model is highly required in software project management.

IV. Research Method

This section, first, introduces the characteristics and strength of the COCOMO II and fuzzy logic, briefly, then the new FL-COCOMO II is explained.

A. The COCOMO II

The COCOMO I model is a regression-based software cost estimation model, which was developed by Boehm in 1981 [9] and thought to be the most cited, best known, and the most plausible model among all traditional cost estimation models. The COCOMO I was a stable model on that time. One of the problems with the use of COCOMO I today is that it does not match the development environment of the late 1990's. Therefore, in 1997, Boehm was developed the COCOMO II to solve most of the COCOMO I problems [11]. Equation (1) and

Figure 1 show the formula and the process of software schedule, cost, and manpower estimation in the COCOMO II. The COCOMO II includes several software attributes such as: 17 Effort Multipliers (EMs), 5 Scale Factors (SFs), Software Size (SS), and Effort estimation that are used in the Post Architecture Model of the COCOMO II [20]. The description of the 17 EMs and 5 SFs based upon their numerical values and productivity ranges are shown in Table 1 [11].

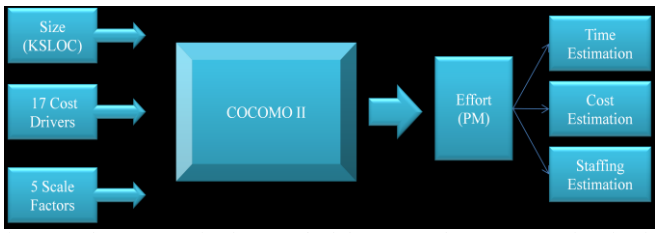

Figure 1: The process of software schedule, cost, and manpower estimation in the COCOMO II

$$\begin{cases} \text{Effort}_{\text{PM}} = \text{A} \times [\text{Size}]^{\text{B}+0.01\times\sum_{j=1}^{5}\text{SF}_j} \times \prod_{i=1}^{17}\text{EM}_i \\ \text{Schedule}_{\text{Months}} = \text{C} \times (\text{Effort})^{\text{D}+0.2\times 0.01\times\sum_{j=1}^{5}\text{SF}_j} \\ \text{Average staffing}_{\text{People}} = \dfrac{\text{Effort}}{\text{Schedule}} \\ \text{COST} = \text{Effort} \times (\text{Payment}_{\text{Month}}) \\ \text{A} = 2.94;\quad \text{B} = 0.91;\quad \text{C} = 3.67;\quad \text{D} = 0.28 \\ \text{Size: Software Size (SLOC)} \end{cases} \quad (1)$$

Vagueness and uncertainty of the software attributes can impact the software estimates. Thus, accurate software attributes resulted in producing accurate software estimates that is most desired for software project managers and organisations.

Table 1: The range of COCOMO II EMs

Effort Multiplier	Range
Required software reliability (RELY)	0.82-1.26
Database size (DATA)	0.90-1.28
Product complexity (CPLX)	0.73-1.74
Developed for reusability (RUSE)	0.95-1.24
Documentation match to life-cycle needs (DOCU)	0.81-1.23
Execution time constraint (TIME)	1.00-1.63
Main storage constraint (STOR)	1.00-1.46
Platform volatility (PVOL)	0.87-1.30
Analyst capability (ACAP)	1.42-0.71
Programmer capability (PCAP)	1.34-0.76
Personnel continuity (PCON)	1.29-0.81
Applications experience (APEX)	1.22-0.81
Platform experience (PLEX)	1.19-0.85
Language and tool experience (LTEX)	1.20-0.84
Use of software tools (TOOL)	1.17-0.78
Multi site development (SITE)	1.22-0.80
Required development schedule (SCED)	1.43-1.00

The value of SFs, are based on the rationale that they are a significant source of exponential variation on a project's effort or productivity variation.

B. *Fuzzy Logic*

In 1965, Lofti Zadeh formally developed multi-value set theory, and introduced the term fuzzy into the technical literature [18]. Fuzzy Logic (FL) starts with the concept of fuzzy set theory. It is a theory of classes with un-sharp boundaries, and considered as an extension of the classical set theory [19]. The membership $\mu_A(x)$ of an element x of a classical set A, as subset of the universe X, is defined by (2), as follows:

$$\mu_A(x) = \begin{cases} 1 & if \quad x \in A \\ 0 & if \quad x \notin A \end{cases} \quad (2)$$

A system based on FL has a direct relationship with fuzzy concepts (such as fuzzy sets, linguistic variables, etc.) and fuzzy logic. The popular fuzzy logic systems can be categorised into three types: Pure fuzzy logic systems, Takagi and Sugeno's fuzzy system, and fuzzy logic system with fuzzifier and defuzzifier [19]. Since most of the engineering applications produce crisp data as input and expects crisp data as output, the last type is the most widely used type of fuzzy logic systems. Fuzzy logic system with fuzzifier and defuzzifier, first, proposed by Mamdani and it has been successfully applied to a variety of industrial processes and consumer products [19]. The main three steps of applying fuzzy logic to a model are:

- Step 1:
  - Fuzzification: It converts a crisp input to a fuzzy set
- Step 2:
  - Fuzzy Rule-Based System: Fuzzy logic systems use fuzzy IF-THEN rules
  - Fuzzy Inference Engine: Once all crisp input values are fuzzified into their respective linguistic values, the inference engine accesses the fuzzy rule base to derive linguistic values for the intermediate and the output linguistic variables
- Step 3:
  - Defuzzification: It converts fuzzy output into crisp output

C. *The Fuzzy Logic COCOMO II (FL-COCOMO II)*

The new FL-COCOMO II is established based on the COCOMO II and FL. The COCOMO II includes a set of input software attributes: 17 EMs, 5 SFs, 1 SS and one output, Effort estimation. The architecture of the FL-COCOMO II is shown in Figure 2.

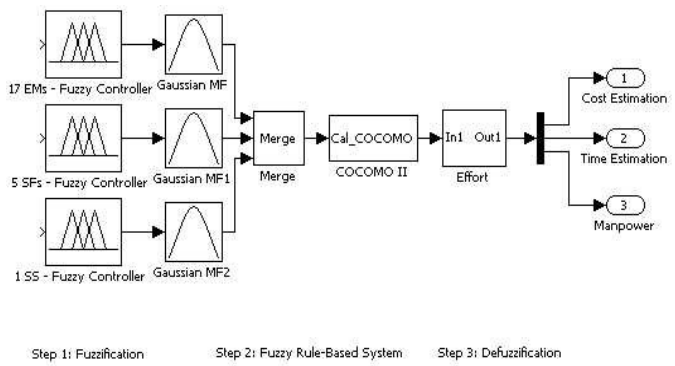

Figure 2: The architecture of the FL-COCOMO II includes: 17 EMs, 5SFs, 1 SS, and effort estimation

In the COCOMO II effort is expressed as Person Months (PM). It determines the efforts required for a project based on software project's size in Thousand Source Line of Code (KSLOC). Traditionally, the problem of software effort estimation relies on the single (numeric) values of the EMs, SFs, and software size that given as software attributes to estimate the effort. However, the size of the software may compute based on previously developed software that are similar to the current one (especially at the beginning of the project). Obviously, correctness and precision of such estimates are limited. It is essentially important to recognise this situation and come up with a technique which can evaluate the associated imprecision residing within the final results of cost estimation. Using fuzzy sets in EMs, SFs, and software size attributes can be specified by distribution of their possible values instead of using fixed values. Commonly, this form of distribution is represented in the form of a fuzzy set. It is important to clarify that vagueness and uncertainty at the input level of the COCOMO II yields uncertainty at the output level [10]. Converting the software attributes to respective fuzzy set causes improving the accuracy of the software attributes which resulted in estimation accuracy. Obviously, a certain monotonicity property holds, which is less precise estimate of inputs give rise to less detailed effort estimates. Overlapped symmetrical the Two-Dimension Gaussian Membership Function (2-D GMF) improves fuzzy model to a precise model.

Furthermore, there is a possibility when using the 2-D GMF that some attributes are assigned the maximum degree of compatibility instead of assigning to lower degrees. In order to avoid this linearity it is proposed to use more superior function, the 2-D GMF, for representing inputs of the model. The 2-D GMF is represented by (3) as follows:

$$\mu_{A_i}(x) = Gaussian\,(x, c_i, \sigma_i) = e^{\frac{-(x-c_i)^2}{2\sigma_i^2}} \quad (3)$$

Where c_i is the center of the i^{th} fuzzy set and σ_i is the width of the i^{th} fuzzy set.

The processes involved in applying fuzzy logic to the COCOMO II to establish the FL-COCOMO II are described as follows. The three main processes in the FL-COCOMO II are: Fuzzification, Fuzzy Rule-Based/ Fuzzy Inference Engine, and Defuzzification. The software attributes in the COCOMO II converted to the fuzzy variables based on the fuzzification process and terms Extra Low (XL), Very Low (VL), Low (L), Nominal (N), High (H), Very High (VH), and Extra High (XH) were defined for the 23 software attributes (17 EMs, 5 SFs, and 1 SS) were defined for each software attribute. The fuzzy sets corresponding to the various associated linguistic values for each software attribute were defined using the 2-D GMF. For example, the fuzzification of the Applications Experience (AEXP) EM based on the 2-D GMF function μ, using Fuzzy Inference System tool in the MATLAB software, is defined as shown in Table 2 and Figure 3. The Fuzzy Inference System (FIS) is a fuzzy tool in the MATLAB software which was used in the fuzzification, fuzzy calculations, fuzzy rule generation, and defuzzification process of the FL-COCOMO II. The FIS supports Mamdani and Sugeno fuzzy methods. The FL-COCOMO II was established based upon the Sugeno fuzzy interface system which is more accurate than the Mandani FIS method.

Table 2: Applications Experience (AEXP) EM Description

Effort Multiplier: Applications Experience (AEXP)						
Descriptors	2 months	6 months	1 year	3 years	6 years	-
Effort Multipliers	1.42	1.19	1	0.85	0.71	-
Rating	VL	L	N	H	VH	EX

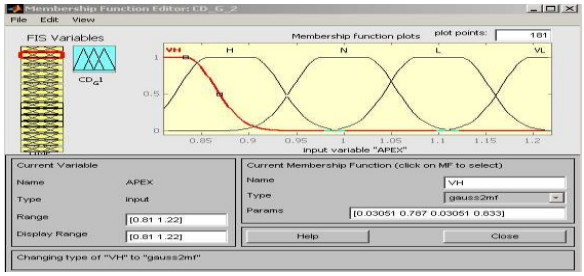

Figure 3: The fuzzification of the AEXP EM using FIS tool in the MATLAB software

At the first step, all the software attributes of the COCOMO II converted to the responding fuzzy sets and variables ($Fuzzy_{EMij}$) rather than using the fixed values of EM_{ij}. The $Fuzzy_{EMij}$ were calculated using equation (4) and the original EM_{ij} values and the 2-D MGF μ was defined for the various fuzzy sets associated with the EMs, SFs, and SS. This process helps to reduce the vagueness and uncertainty of the software attributes at this level.

$$Fuzzy_{EM_{ij}} = F\left(\mu^{V_1}{}_{A1}, \ldots \mu^{V_i}{}_{Ai}, EM_{i1} \ldots EM_{ij}\right) \quad (4)$$

For ease, F is taken as a linear function, where the $\mu^{Vi}{}_{Aj}$ is the membership function of the fuzzy set Aj associated with the cost driver V_i as shown in equation (5).

$$Fuzzy_{EM_{ij}} = \sum_{j=1}^{k_i} \mu_{A_i}{}^{v_i} * EM_{ij} \quad (5)$$

The fuzzy rules for the FL-COCOMO II were defined through the linguistic variables in the fuzzification process. It

is important to take note that these fuzzy rules were adjusted as well as all pertinence level functions, in accordance with the tests and the characteristics of the project. The fuzzy rules were defined based on the connective "AND" and "OR" or combination of them between input variables, as shown as follows.

Fuzzy rules:
IF TOOL is Low TEHN effort is Low
IF PCAP is Very Low THEN effort is Very High
IF RESUE is Nominal THEN effort is Nominal
IF DATA is Very High THEN effort is Very High
…

The number of rules which were defined for the FL-COCOMO II is more than 193 based on the input variables. In the process of fuzzy rule generation of the FL-COCOMO II, the FIS tool in the MATLAB software was used as shown in Figure 4.

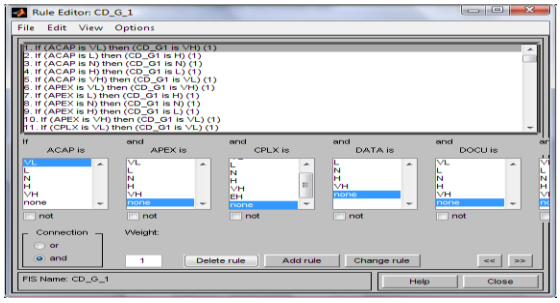

Figure 4: The fuzzy rule generation using FIS tool in the MATLAB software

The last step is defuzzification of the effort variable using defuzzification techniques such as Mean of Maximum (MOM), Center of Area (COA), and First of Maximum (FOM). The defuzzification of the output "Effort" performed using the Mean of Maximum (MOM) technique because the results obtained are more accurate when compared with the other defuzzification techniques.

V. RESULTS AND DICUSSION

The FL-COCOMO II was evaluated through three sources: two public domain data sets (Data set 1 and 2) and 4 software project data from software companies in Malaysia (Data set 3). The descriptions of these data sets are discussed as follows.

A. Data set 1

The COCOMO I data set—Boehm [10] was the first researcher which looked at software engineering from an economic point of view then he came up with a cost estimation model from a dataset, the COCOMO I data set. The COCOMO I dataset includes 63 historical project data. This data set is in public domain and available in http://promisedata.org.

B. Data set 2

The NASA93 data set—the NASA93 data set includes 93 project data from NASA Manager Measurement Benchmarking Element. This data set is in public domain and available in http://promisedata.org.

C. Data set 3

Four real project data from two software companes A and B in Malaysia. These project data were collected through a direct data collection from software companes A and B in the COCOMO data set fromat.

Therefore, in this research three different data sets (160 project data) were used for evaluation of the FL-COCOMO II.

D. Evaluation Method

In the evaluation of software cost estimation models, the most widely used evaluation criterion are the Mean Magnitude of Relative Error (MMRE) and the probability of a project having a relative error of less than or equal to L (PRED(L)). The Magnitude of Relative Error (MRE) is defined in equaton (6) as follows:

$$MRE_i = \frac{|Actual\ Effort_i - Predicted\ Effort_i|}{Actual\ Effort_i} \quad (6)$$

The MRE value was calculated for each observation i that effort is estimated at that observation. The aggregation of MRE over multiple observations (N) can be achieved through the Mean MRE (MMRE) in equation (7) as follows:

$$MMRE = \frac{1}{N} \sum_i^N MRE_i \quad (7)$$

A complementary criterion is the prediction at level L, PRED(L) = k/N, where k is the number of observations where MRE is less than or equal to L, and N is the total number of observations. Thus, PRED(25%) gives the percentage of projects which are predicted with a MRE less or equal than 25%. This value, 25%, is a realistic value for evaluation of models.

The FL-COCOMO II was evaluated through the three data sets (1, 2, and 3), separately, using the MMRE and PRED (25%). These data sets were applied to the COCOMO II and FL-COCOMO II, separately, and then the value of MRE and PRED (25%) were calculated for each data set. The comparison between obtained results from the COCOMO II and FL-COCOMO II using data set 1 to 3 are shown in Table 3 and Figure 5.

Table 3: Comparison between obtained results from the COCOMO II and FL-COCOMO II using the MRE and PRED(25%)

Data set	Model	Evaluation	
		MMRE	PRED(25%)
Data set 1	COCOMO II	0.366149358	37%
	FL-COCOMO II	0.393812753	34%
Data set 2	COCOMO II	0.341561862	33%
	FL-COCOMO II	0.280274946	38%
Data set 3	COCOMO II	0.38219836	29%
	FL-COCOMO II	0.32824384	33%
Mean	COCOMO II	0.363303193	33%
	FL-COCOMO II	0.334110513	35%

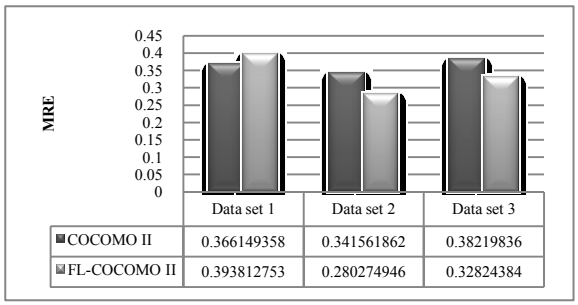

(a)

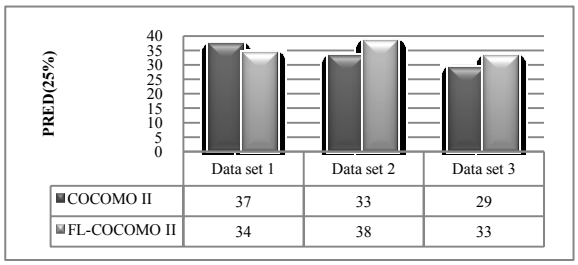

(b)

Figure 5: Comparison between the COCOMO II and FL-COCOMO II using the (a) MRE and (b) PRED (25%) evaluation techniques

The row labelled in "Mean" represents the average result for the data sets 1 to 3 based upon the evaluation criterion in the models.

For the data set 1, the value of MRE and PRED(25%) evaluation criterion for the COCOMO II and FL-COCOMO II are 0.366149358 and 0.393812753; 37 and 34, respectively. These values show that in terms of MRE, the COCOMO II shows less value for MRE and higher value for PRED (25%) when compared with the FL-COCOMO II. Therefore, in this case, the COCOMO II produced more accurate results for data set 1.

For the data set 2, the value of MRE and PRED(25%) evaluation criterion for the COCOMO II and FL-COCOMO II are 0.341561862 and 0.280274946; 33 and 38, respectively. These values show that in terms of MRE, the FL-COCOMO shows less value for MRE and higher value for PRED (25%) when compared with the COCOMO II. Therefore, in this case, the FL-COCOMO II produced more accurate results than the COCOMO II.

For the data set 3, the value of MRE and PRED(25%) evaluation criterion for the COCOMO II and FL-COCOMO II are 0.38219836 and 0.32824384; 29 and 33, respectively. These values show that in terms of MRE, the FL-COCOMO shows less value for MRE and higher value for PRED (25%) when compared with the COCOMO II.

Finally, The values of MMRE for COCOMO II and FL-COCOMO II based upon data sets 1 to 3 are 0.363303193 and 0.334110513, respectively, and the value of PRED (25%) are 33 and 35, respectively.

By comparing these results, a software cost estimation model with a lower value of MMRE gives better estimates than a model with a higher value. The best cost estimation model shows a value 0 for MMRE evaluation criterion. Also, a software cost estimation model with a higher value of PRED(25%) gives better estimates than a model with a lower value. The best cost estimation model shows a value 0 for MMRE and 100% for PRED(25%) evaluation criterion. Between these two estimation models (COCOMO II and FL-COCOMO II), the use of FL-COCOMO II for software development cost estimate can produce better estimates in terms of MMRE, and PRED (25%) than the COCOMO II based on the data sets 1 to 3.

The percentage of improvement of FL-COCOMO II is calculated based on the difference between the two models divided by the value of the COCOMO II. Table 4 shows the comparison of the improvement based upon estimation accuracy in COCOMO II and FL-COCOMO II.

Table 4: Comparison of improvement of the COCOMO II and FL-COCOMO II

Model		Evaluation	
		MMRE	PRED (25%)
COCOMO II vs. FL-COCOMO II			
	COCOMO II	0.363303193	33
	FL-COCOMO II	0.334110513	35
	Improvement (%)	8.03	6.06

According to the Table 4, in terms of MMRE, the percentage of improvement based upon estimation accuracy for the FL-COCOMO II is 8.03% and based on PRED (25%) is 6.06% when compared to the COCOMO II, respectively. It shows that using FL can improve the estimation accuracy and it can be used as alternative to apply to the other software cost estimation models to improve estimation accuracy.

VI. CONCLUSION

One of the important issues in software project management is accurate and reliable estimation of software time, cost, and manpower, especially in the early phase of software development. Software attributes usually have properties of uncertainty and vagueness when they are measured by human judgment. A software cost estimation model incorporates fuzzy logic can overcome the uncertainty and vagueness of software attributes. However, determination of the suitable fuzzy rule sets for fuzzy inference system plays an important role in coming up with accurate and reliable software estimates. The objective of this research was to examine the application of applying fuzzy logic in software cost estimation that can perform more accurate result. This paper presented an adaptive software cost estimation model incorporates fuzzy logic technique to handle imprecision and uncertainty of software attributes. The results obtained from applying three different data sets 1 to 3 to the models, showed that the FL-COCOMO II produced better estimation results than the COCOMO II using evaluation criterion MMRE=0.334110513 and PRED(25%)=35. Furthermore, the percentage of improvement for the FL-COCOMO is from 6.06 to 8.03, which shows the performance of the FL-COCOMO

when compared with the COCOMO II based on the estimation accuracy. The application of fuzzy logic in other software cost estimation models can also be explored in the future.

REFERENCES

1. K. Molokken and M. Jorgensen, "A review of software surveys on software effort estimation," Proceedings of IEEE International Symposium on Empirical Software Engineering (ISESE 2003). Rome, Italy, September 30 – October 1, 2003, pp: 223 – 230.
2. S.G. MacDonell and A.R. Gray, "A comparison of modeling techniques for software development effort prediction," Proceedings of the International Conference on Neural Information Processing and Intelligent Information Systems, Dunedin, New Zealand, November 12-14, 1997, pp. 869-872.
3. R. Agarwal, M. Kumar, M. Yogesh, S. Mallick, R. M. Bharadwaj, and D. Anantwar, "Estimating software projects," SIGSOFT Software Engineering Notes, 26(4), 60-67, 2001.
4. M . Jorgensen, "Practical guidelines for expert-judgment-based software effort estimation," IEEE Software Engineering, 22(3), pp. 57-63, 2005.
5. C. F. Kemerer, "An empirical validation of software cost estimation models," Communications of the ACM, 30(5), pp. 416-429, 1987.
6. K. Strike, K. El-Emam, and N. Madhavji, "Software cost estimation with incomplete Data," IEEE Transactions on Software Engineering, 27(10), pp. 215-223, 2001.
7. A. C. Hodgkinson and P.W. Garratt, "A neurofuzzy cost estimator," Proceedings of the 3rd International Conference on Software Engineering and Applications (SAE-1999), NJ, USA, 1999, pp. 401-406.
8. L. H. Putnam, "A general empirical solution to the macro software sizing and estimating problem," IEEE Transactions on Software Engineering, 4(4), pp. 345 – 361, 1978.
9. B. W. Boehm, Software engineering economics. Englewood Cliffs, NJ, Prentice-Hall, 1981.
10. B. W. Boehm, C. Abts, and S. Chulani, "Software development cost estimation approaches – A survey", University of Southern California Center for Software Engineering, Technical Reports, USC-CSE-2000-505, 2000.
11. B. W. Boehm, "Cost models for future software life cycle processes: COCOMO 2.0," Annals of Software Engineering Special Volume on Software Process and Product Measurement, Science Publisher, Amsterdam, Netherlands, 1(3) , pp. 45 – 60., 1995.
12. K. Srinivasan, and D. Fisher, "Machine learning approaches to estimating software development effort," IEEE Transactions on Software Engineering, 21(2), 1995.
13. Z. Fei, and X. Liu, "F-COCOMO: Fuzzy constructive cost model in software engineering," Proceedings of the IEEE International Conference on Fuzzy Systems, IEEE Press, New York, pp. 331–337, 1992.
14. J. Ryder, "Fuzzy modeling of software effort prediction," Proceedings of IEEE Information Technology Conference, Syracuse, NY, pp 102-114, 1998.
15. A. Idri, A. Zahi, and A. Abran, "Software cost estimation by fuzzy analogy for web hypermedia applications," Proceedings of the International Conference on Software Process and Product Measurement, Cadiz, Spain, pp. 53 – 62, 2006.
16. X. Huang, D. Ho, J. Ren, and F. Capretz, "A soft computing framework for software effort estimation," Soft Computing, A Fusion of Foundations, Methodologies and Applications Journal, 10(2), pp. 170-177, 2009.
17. S. Kumar, A. Krishna, and P. Satsangi, "Fuzzy systems and neural networks in software engineering project management," Journal of Applied Intelligence, 4(1), pp. 31-52, 1994.
18. A. Lotfi Zadeh, "Fuzzy logic, neural networks, and soft computing," Communication of ACM, 37(3), pp.77-84, 1994.
19. A. Lotfi Zadeh, "The future of soft computing," The 9th IFSA World Congress and 20th NAFIPS International Conference, Vancouver, Canada, pp. 217-228, 2001.

2011 IEEE International Conference on Fuzzy Systems
June 27-30, 2011, Taipei, Taiwan

Fuzzy-Rough Set based Semi-Supervised Learning

Neil Mac Parthaláin
Dept. of Computer Science
Aberystwyth University
Aberystwyth, Ceredigion, Wales. UK
Email: ncm@aber.ac.uk

Richard Jensen
Dept. of Computer Science
Aberystwyth University
Aberystyth, Ceredigion, Wales. UK
Email: rkj@aber.ac.uk

***Abstract*—Much work has been carried out in the area of fuzzy-rough sets for supervised learning. However, very little has been accomplished for the unsupervised or semi-supervised tasks. For many real-word applications, it is often expensive, time-consuming and difficult to obtain labels for all data objects. This often results in large quantities of data which may only have very few labelled data objects. This paper proposes a novel fuzzy-rough based semi-supervised self-learning or self-training approach for the assignment of labels to unlabelled data. Unlike other semi-supervised approaches, the proposed technique requires no subjective thresholding or domain information. An experimental evaluation is performed on artificial data and also applied to a real-world mammographic risk assessment problem with encouraging results.**

***Index Terms*—Rough sets, fuzzy sets, mammographic analysis, semi-supervised learning**

I. Introduction

Each year worldwide, more and more data is collected. In fact, it is estimated that the amount of data collected and stored at least doubles every two years. This collection and storage is facilitated by the fact that the actual process of doing so has become easier in recent times. The result is enormous collections of data. Of this data, a large percentage is unlabelled or has labels which are incomplete or missing. It is because this data is so large that it becomes very difficult, time-consuming and expensive for humans to manually assign labels to data objects. Additionally, many real-world application datasets (such as gene expression data, text classification, etc.) are also of large dimensionality. This further frustrates the process of label assignment for domain experts as large dimensionality can make the task of label assignment intractable.

Supervised learning operates on labelled data and attempts to learn its underlying functional relationships. It is the most common paradigm in machine learning and is typically concerned with the learning of classifiers which can accurately reflect the predictive regularities of the underlying model from the feature values and decision class labels. In unsupervised learning, decision class labels are unavailable and the task is to construct/reconstruct the class information from some inherent structure in the data (also known as cluster analysis). These techniques attempt to find groups in the data such that objects in the same group are similar to each other in some way. The notion of similarity is however subjective and as such unsupervised learning approaches are forced to make subjective assumptions about groupings as well as the number of groups into which objects belong. Semi-supervised learning (SSL) [1] lies somewhere between supervised learning and unsupervised learning. SSL is typically employed when some (but not all) of the data is labelled. The primary aim of SSL is to try to combine both the labelled and the unlabelled data. SSL has attracted much interest in the field of machine learning due (as mentioned previously) to the abundance of unlabelled data which is available for many real-world problems. The problem with of course with traditional classification methods is that they cannot use unlabeled data to train classifiers. SSL can also play an important part as a quantitative method in trying to reason about human category-learning, where most of the data is obviously unlabelled [24].

There have been many attempts to adapt existing supervised and unsupervised methods for use in the semi-supervised paradigm. These include typical approaches such as neural networks [3], EM algorithm [4], FCM clustering [5], Support Vector Machines [6], Fuzzy Systems [7], and others [8]. One of the main drawbacks of many of the existing semi-supervised approaches however is that they require the specification of at least one additional subjective tunable parameter.

Rough sets [9] and fuzzy-rough sets [10] have enjoyed much attention for the task of supervised learning [11], due to their domain independence and in the case of fuzzy-rough sets the additional ability to handle real-valued data. The vast majority of the work that has been carried out in the areas of rough sets and fuzzy-rough sets has been focused on supervised learning approaches, i.e. where the class labels are known. Very little work has been carried out which employs fuzzy-rough sets for the task of unsupervised learning, and even less still for that of semi-supervised learning. Although there has been some use of rough sets for the task of semi-supervised learning [12] as well as the use of fuzzy sets and rough sets in isolation of each other [13], no use has been made of *fuzzy-rough* sets. The motivation for a fuzzy-rough based semi-supervised approach is based on the success of the supervised approaches [11], [14], and the fact that no additional user-supplied thresholding is required.

This paper presents a novel fuzzy-rough based semi-supervised algorithm for the task of predicting labels for unlabelled data. The algorithm is based on the well-known self-training approach [15], [16], and uses the upper and lower approximation membership values of fuzzy-rough sets for each of the concepts of the labelled objects to iteratively label

978-1-4244-7316-8/11/$26.00 ©2011 IEEE

unlabelled objects.

The remainder of this paper is structured as follows. Section 2 summarises the theoretical basis and concepts of rough sets and fuzzy-rough sets. Section 3 describes the fuzzy-rough semi-supervised self learning approach and corresponding algorithm. Section 4 shows the results of applying the fuzzy-rough semi-supervised self-learning approach to a number of artificial datasets, as well as a real-world mammographic risk assessment task. Section 5 concludes the paper with some suggestions, as well as a discussion of ideas for future work.

II. Rough Set and Fuzzy Set Hybridisation

Rough set theory (RST) [9] provides a means by which knowledge can be extracted from a domain in a concise manner. RST can retain information content whilst reducing the amount of information involved. At the core of RST is the concept of indiscernibility. Let $I = (\mathbb{U}, \mathbb{S})$ be an information system, where $\mathbb{U}$ is a non-empty set of finite objects (the universe of discourse) and $\mathbb{S}$ is a non-empty finite set of attributes so that $a : \mathbb{U} \rightarrow V_a$ for every $a \in \mathbb{S}$. V_a is the set of values that a can take. For any $P \subseteq \mathbb{S}$, there exists an associated equivalence relation $IND(P)$:

$$IND(P) = \{(x, y) \in \mathbb{U}^2 | \forall a \in P, a(x) = a(y)\} \quad (1)$$

The partition generated by $IND(P)$ is denoted $\mathbb{U}/IND(P)$ and is calculated as follows:

$$\mathbb{U}/IND(P) = \otimes\{\mathbb{U}/IND(\{a\}) : a \in P\} \quad (2)$$

where,

$$P \otimes Q = \{X \cap Y : \forall X \in P, \forall Y \in Q, X \cap Y \neq \emptyset\} \quad (3)$$

If $(x, y) \in IND(P)$, then x and y are indiscernible by attributes from P. The equivalence classes of the P-indiscernibility relation are denoted $[x]_p$. Let $X \subseteq \mathbb{U}$. X can be approximated using only the information contained in P by constructing the P-*lower* and P-*upper* approximations of X:

$$\underline{P}X = \{x | [x]_p \subseteq X\} \quad (4)$$

$$\overline{P}X = \{x | [x]_p \cap X \neq \emptyset\} \quad (5)$$

The tuple $\langle \underline{P}X, \overline{P}X \rangle$ is known as a rough set. The problem with RST however, is that because of the definite equivalence imposed by the equivalence relation, it cannot be used effectively on real-valued data. As most data is real-valued, this usually involves a discretisation step prior to the application of RST. Discretisation usually results in a loss of information however and this has prompted the development of a more intuitive and flexible approach by hybridising fuzzy sets and rough sets to give fuzzy-rough sets [10].

A fuzzy-rough set [10] is defined by two fuzzy sets, fuzzy lower and upper approximations, obtained by extending the corresponding crisp rough set notions. In the crisp case, elements that belong to the lower approximation (i.e. have a membership of 1) are said to belong to the approximated set with absolute certainty. In the fuzzy-rough case, elements may have a membership in the range [0,1], allowing greater flexibility in handling uncertainty.

Definitions for the fuzzy lower and upper approximations can be found in [17], where a T-transitive fuzzy similarity relation is used to approximate a fuzzy concept X:

$$\mu_{\underline{R_P}X}(x) = \inf_{y \in \mathbb{U}} \mathcal{I}(\mu_{R_P}(x, y), \mu_X(y)) \quad (6)$$

$$\mu_{\overline{R_P}X}(x) = \sup_{y \in \mathbb{U}} \mathcal{T}(\mu_{R_P}(x, y), \mu_X(y)) \quad (7)$$

Here, $\mathcal{I}$ is a fuzzy implicator and $\mathcal{T}$ a t-norm. A fuzzy implicator is any $[0, 1]^2 \rightarrow [0, 1]$-mapping $\mathcal{I}$ satisfying $\mathcal{I}(0, 0) = 1, \mathcal{I}(1, x) = x$ for all x in $[0, 1]$. R_P is the fuzzy similarity relation induced by the subset of features P:

$$\mu_{R_P}(x, y) = \mathcal{T}_{a \in P}\{\mu_{R_a}(x, y)\} \quad (8)$$

$\mu_{R_a}(x, y)$ is the degree to which objects x and y are similar for feature a, and may be defined in many ways, for example:

$$\mu_{R_a}(x, y) = 1 - \frac{|a(x) - a(y)|}{|a_{max} - a_{min}|} \quad (9)$$

$$\mu_{R_a}(x, y) = \max(\min(\frac{(a(y) - (a(x) - \sigma_a))}{\sigma_a}, \frac{((a(x) + \sigma_a) - a(y))}{\sigma_a}, 0) \quad (10)$$

where ${\sigma_a}^2$ is the variance of feature a. As these relations do not necessarily display $\mathcal{T}$-transitivity, the fuzzy transitive closure can be computed for each attribute [2]. The choice of relation is largely determined by the intended application. For example, for the task of feature selection, a relation such as (10) may be best suited, as this allows only small differences between feature values of differing objects. For the task of classification however, a more gradual and inclusive relation such as (9) can be employed. Indeed, this is the relation which is used in the semi-supervised approach described in this paper.

III. Fuzzy-Rough Semi-Supervised Learning

The algorithm employed in this paper is a variation of the popular semi-supervised self-learning or self-training approach [15], [16]. Self learning has been widely employed for the task of semi-supervised learning in text mining applications [8], [12], [15], [16]. It is fast and converges sooner than most other semi-supervised approaches. The basis for the algorithm is that given a set of labelled objects and a set of unlabelled objects, the labelled objects are used to make predictions about the class membership of the unlabelled objects. In self learning/training a classifier (or induction method) is initially trained with a (usually small) amount of labelled data. The classifier is then used to predict labels for the unlabelled data. Typically the most 'confident' unlabelled points, along with their corresponding predicted labels, are then added

to the training set. The classifier is then re-trained and the procedure is repeated. Notice that the classifier uses its own predictions in order to 'train' itself. One of the criticisms that is often levelled at self-learning approaches is that they can reinforce classification errors that are made early-on in the label assignment. However, it is shown in [15] that this is not strictly the case and the self-learning algorithm can perform equally as well as co-training [18] - another well-known SSL approach. In this paper, a variation of self-learning is employed in that only objects which belong fully to the fuzzy-rough lower approximation of any of the decision classes are added to the labelled data at each iteration, and therefore no subjective confidence level threshold is employed. It should be emphasised at this point that the task at hand is the labelling of unlabelled data using a semi-supervised learning method rather than the building of models for unseen objects.

A. Fuzzy-Rough Semi-supervised Self Learning Algorithm

The rationale behind the fuzzy-rough self learning (FRSL) algorithm is that the fuzzy-rough lower and the upper approximation memberships of each of the (labelled) decision classes, (calculated by means of all of the labelled objects) to the unlabelled test object y, provide good clues in order to predict class membership.

In practice, the algorithm starts out by examining each object in the unlabelled data. If the unlabelled object belongs to the lower approximation of a given class with fuzzy-rough dependency equal to 1.0, then the label of that class is assigned to that object. The object is then added to the training data and will be included when generating the fuzzy-rough partitions in the following iterations. The algorithm continues until either: 1) all unlabelled objects have been labelled, or 2) until any of the remaining unlabelled objects do not belong to the lower approximation of any of the labelled decision classes with certainty (fuzzy-rough dependency < 1.0). If there are remaining unlabelled objects, a naive approach is adopted in order to assign labels by calculating the combination of lower and upper approximation memberships and using this value to assign class labels. Adopting such a strategy means that labels are (as far as possible) propagated via only those objects which are 'certain' thus minimising the risk of reinforcement of classification errors at an early stage in the algorithm.

It is important to note that the propagation of labels happens through the addition of previously unlabelled objects to the labelled training data. This has the effect of altering the fuzzy-rough lower and upper approximation memberships of the remaining unlabelled objects.

B. Worked Example

In order to demonstrate the fuzzy-rough concepts employed in the previous section, a small worked example is presented. Note that only a small dataset is included in this example, and as such the formal concepts are only demonstrated rather than the execution of the algorithm. The example dataset has 3 real-valued conditional attributes (a,b, and c) and a single crisp discrete-valued decision attribute (q) as the *labelled training data*, shown in Table I. A further dataset shown in Table II containing 2 objects is used as the *unlabelled* data, again with the same number of conditional attributes but with unknown decision attribute values.

FRSL(L, UL, C, y)
L, the set of all labelled data objects; UL, the set of all unlabelled data objects; C, the set of decision classes in L; y, the unlabelled data object to be labelled

```
(1)  while (∃y ∈ UL : μ_RC(y) == 1.0)
(2)     buildFuzzyRoughPartition(L)
(3)      ∀C ∈ L
(4)        if (μ_RC(y) == 1.0)
(5)          y ← y ∪ {C}
(6)          L ← L ∪ {y}
(7)  while UL ≠ ∅
(8)     buildFuzzyRoughPartition(L)
(9)     γ_best ← 0, γ_prev ← 0, bestClass ← ∅
(10)     ∀C ∈ L
(11)       if (μ_RC(y) + μ_R̄C(y))/2 > γ_best)
(12)       γ_best ← γ_prev, C ← bestClass
(13)       y ← y ∪ {bestClass}
(14)       L ← L ∪ {y}
(15)  end
```

Fig. 1. The FRSL Algorithm

TABLE I
EXAMPLE LABELLED TRAINING DATA

Object	a	b	c	q
1	-0.4	-0.2	-0.5	yes
2	-0.4	0.1	-0.1	no
3	0.2	-0.3	0	no
4	0.2	0	0	yes

TABLE II
UNLABELLED DATA

Object	a	b	c	q
$ul1$	0.3	-0.3	0	-
$ul2$	-0.4	0	-0.3	-

Referring to the FRSL algorithm described in the previous section, the first step is to calculate the fuzzy upper and lower approximations for all decision classes. In Table I there are 4 objects and as noted previously a decision attribute which has 2 classes ($\{yes\}$, and $\{no\}$).

Using the fuzzy similarity measure as defined in 9 the similarity of each unlabelled object is compared to all of the objects in the training data. For instance, consider the unlabelled object $ul1$:

$$\mu_{R_P}(ul1, 1) = T(\mu_{R_{\{a\}}}(ul1, 1), \mu_{R_{\{b\}}}(ul1, 1), \mu_{R_{\{c\}}}(ul1, 1)) = 0$$

$$\mu_{R_P}(ul1, 2) = T(\mu_{R_{\{a\}}}(ul1, 2), \mu_{R_{\{b\}}}(ul1, 2), \mu_{R_{\{c\}}}(ul1, 2)) = 0$$

$$\mu_{R_P}(ul1, 3) =$$

$$T(\mu_{R_{\{a\}}}(ul1,3), \mu_{R_{\{b\}}}(ul1,3), \mu_{R_{\{c\}}}(ul1,3)) = 0.83$$

$$\mu_{R_P}(ul1,4) =$$
$$T(\mu_{R_{\{a\}}}(ul1,4), \mu_{R_{\{b\}}}(ul1,4), \mu_{R_{\{c\}}}(ul1,4)) = 0.23$$

These similarity values can then be used to generate the lower and upper approximations. Note that the fuzzy connectives chosen for this example are the Lukasiewicz t-norm ($\max(x+y-1,0)$), and Lukasiewicz fuzzy implicator ($\min(1-x+y,1)$). For the labelled data decision concept $X = yes$ these are:

$$\mu_{\underline{R_P}}X(ul1) = \inf_{y\in\mathbb{U}} \{I(\mu_{R_P}(ul1,y), \mu_X(y)\}$$
$$= \inf\{I(0,1), I(0.0,0), I(0.83,0), I(0.23,1)\} = 0.17$$

and,

$$\mu_{\overline{R_P}}X(ul1) = \sup_{y\in\mathbb{U}} \{I(\mu_{R_P}(ul1,y), \mu_X(y)\}$$
$$= \sup\{T(0,1), T(0,0), T(0.83,0), T(0.23,1)\} = 0.23$$

Similarly for the decision concept $X = no$:

$$\mu_{\underline{R_P}}X(ul1) =$$
$$\inf\{I(0,0), I(0,1), I(0.83,1), I(0.23,0)\} = 0.77$$

$$\mu_{\overline{R_P}}X(ul1) =$$
$$\sup\{T(0,0), T(0,1), T(0.83,1), T(0.23,0)\} = 0.83$$

Note that for each of the unlabelled test objects, the object is allowed to belong to the class under consideration to degree 1.0 as the 'true' class is unknown. It can be seen that the upper and lower approximation membership values for test object $ul1$ for the class label $X = yes$ are equal to 0.17, and 0.23 respectively. When $X = yes$ the corresponding values are 0.77 and 0.83. Note that the FRSL algorithm in the first instance will only label objects with membership $\mu_{\underline{R_P}}$ X = 1.0 and that the example employed here is to show how these membership values are obtained. If we are to assume that ul1 and ul2 are remaining objects after all others have been labelled then, the algorithm will therefore label $ul1$ naïvely. This is done using the upper and lower approximation memberships and given that: (0.77 + 0.83)/2 = 0.80 for $X = no$ and (0.17 + 0.23)/2 = 0.20 for $X = yes$. Data object $ul1$ will be therefore labelled as belonging to the class $X = no$.

Similarly, the procedure is then repeated for object $ul2$ which results in the following upper and lower approximation values for $X = no$:

$$\mu_{\underline{R_P}}X(ul2) =$$
$$\inf\{I(0.2,1), I(0.4,0), I(0,0), I(0,1)\} = 0.6$$

$$\mu_{\overline{R_P}}X(ul2) =$$
$$\sup\{T(0.2,1), T(0.4,0), T(0,0), T(0,1)\} = 0.2$$

And, $X = yes$:

$$\mu_{\underline{R_P}}X(ul2) =$$
$$\inf\{I(0.2,0), I(0.4,1), I(0,1), I(0,0)\} = 0.8$$

$$\mu_{\overline{R_P}}X(ul2) =$$
$$\sup\{T(0.2,0), T(0.4,1), T(0,1), T(0,0)\} = 0.4$$

IV. Experimental Evaluation

There is no clear consensus or commonly agreed benchmark datasets for the comparison of semi-supervised learning techniques. The most common way of testing new techniques involves taking the labelled datasets available in [19] and removing labels from a percentage of the data objects. The problem with such an approach is that well-distributed absent labels are rarely the case in the real-world. Indeed, the removal of labels in such a manner may not demonstrate sufficiently the true utility of most semi-supervised approaches.

In light of the above statement, two different approaches have been adopted for the experimental evaluation: (i) Two artificial datasets are examined and compared with some existing methods (ii) a real-world labelling problem for mammographic risk assessment is presented along with some prototype labelled examples.

1) Experimental Setup: For the artificial data, two datasets have been generated which reflect some common realistic problems, and demonstrate how the FRSL method copes with such problems. The data objects contained in the datasets have 2 conditional attributes and belong to two separate classes. The labels of only 5% of the objects are known for the problem shown in Fig. 2 (and represented by ■ for class + and ● for class ○) - thus 2.5% for one class and 2.5% for the other, giving a total of 410 labelled and unlabelled objects. For problem 2 in Fig.6, 10% of the labels are known (again represented by ■ and ●), thus giving a total of 420 labelled and unlabelled objects for this dataset. In the case of the mammographic data there are 322 objects in total, and four decision classes based on the BIRADS [20] labelling scheme to reflect risk of development of breast cancer. 10% of the data (32 data objects) has been labelled using the consensus of three expert radiologists - i.e. where all three agree completely on the classification for a given mammogram.

The FRSL method is compared with some common SSL techniques - SSFCM [5] and another self-learning technique based on FNN [21]. SSFCM was proposed as an extension to the popular FCM clustering algorithm. It uses the labelled data as seed points for the cluster prototypes which are essentially ignored when the clusters are updated. The rationale behind the approach is that all labelled examples should be trusted, which is a reasonable assumption but this can affect the objective function of FCM.

The FNN-based self-learning approach uses a fuzzy classifier to estimate class membership for unlabelled examples and learns in an iterative fashion by adding learned examples to the classifier training data at the end of each iteration and

then retraining. This approach has a number of parameters which must be tuned however: number of nearest neighbours, fuzzifier value, and threshold for class membership. For the experimental evaluation carried out in this paper, the fuzzifier value (m) was set to 2.0, the labelling threshold was varied between 0.8-0.95, and the number of nearest neighbours was varied between 1 and 20. The parameter settings which resulted in the best performance are presented here. No restrictions were imposed algorithm itself in terms of number of iterations, number of examples selected from the unlabelled data for labelling (per iteration), or number of most confidently labelled examples that are added at each iteration to the labelled data.

Although the FRSL approach does not have any subjective tunable parameters, a similarity relation must be selected. The fuzzy similarity relation defined in (9) is employed here as this has been shown to produce good results for the task of supervised learning.

A. Artificial Data

The first artificial dataset as shown in Fig. 2, represents two clusters of data, and has only two conditional features. The problem is that for the given class labels, the clusters do not characterise the classes very well and a supervised classifier will be easily misled. The labelled data objects have been chosen at random from the distribution.

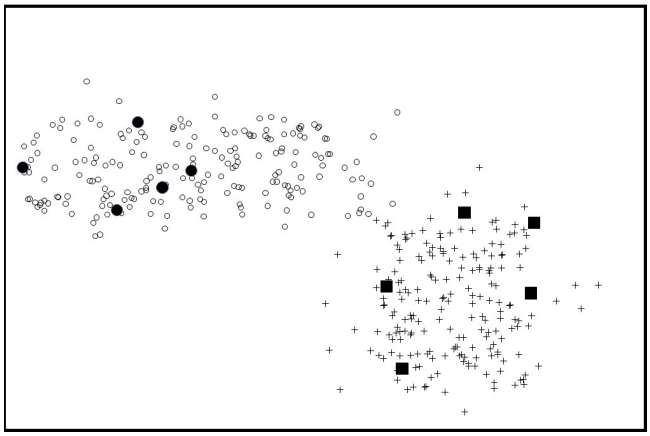

Fig. 2. Artificial Data - Problem 1

SS-FCM was applied to this problem and the results are shown in Fig.3. It can be seen that SS-FCM manages to classify 76% of the objects correctly and fails mostly around the decision boundary between the two classes. Given that the two concepts are very close at this point, and there is some overlap between classes, this performance is quite good.

The FNN wrapper method seems to produce better results that that of SS-FCM but still suffers from poor performance around the decision boundary. It manages to increase classification accuracy to 88% correct classification however.

FRSL manages to label 92% of all objects correctly. Once again the objects are at the boundary between two classes which demonstrates that the overlapping boundary presents a challenge for all methods.

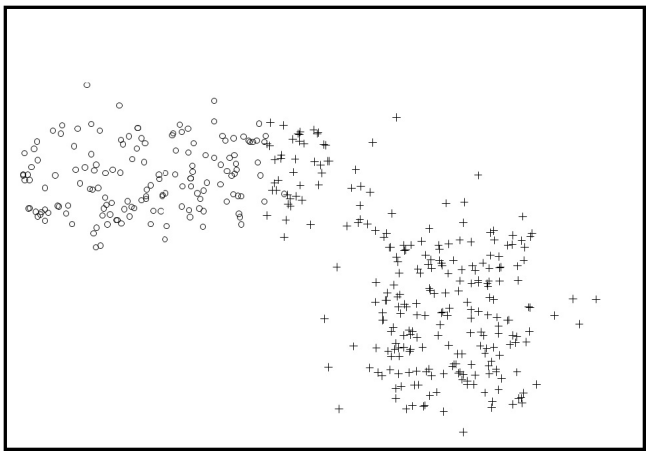

Fig. 3. Artificial Data Problem 1 - SS-FCM

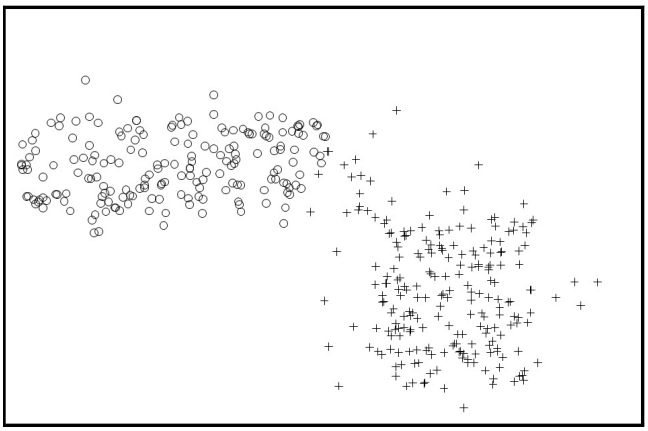

Fig. 4. Artificial Data Problem 1 - FNN Wrapper

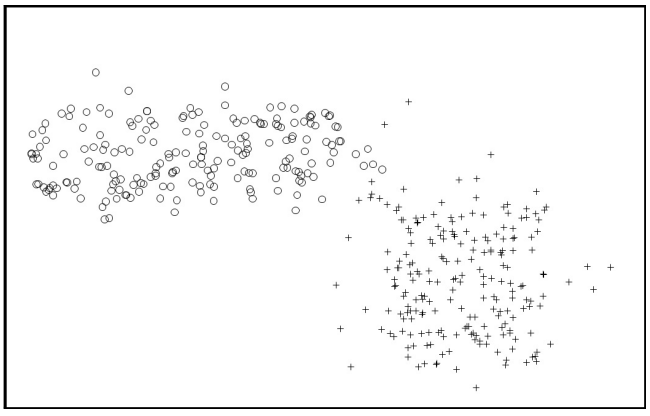

Fig. 5. Artificial Data Problem 1 - FRSL

The second artificial dataset shown in Fig.6 is more complex than that of the previous example. In this case one of the classes has been split into two regions. Once again the labelled objects have been chosen at random, although they now represent 10% of the overall data (20 objects) rather than 5% used in the previous example. This dataset has particularly badly defined decision boundaries and it is certain that a completely unsupervised method would fail in this case.

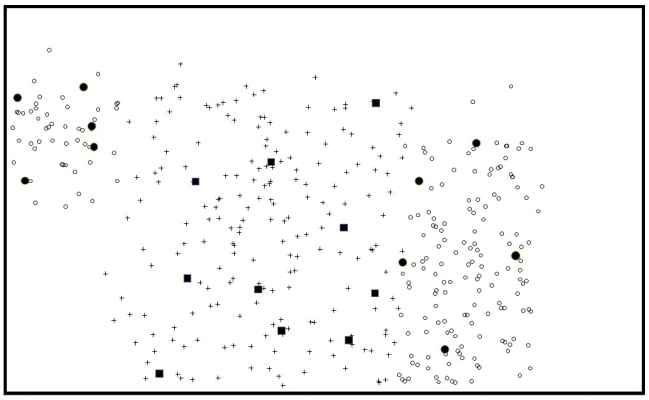

Fig. 6. Artificial Data Problem 2

The SS-FCM method failed completely to correctly label any of the unlabelled data objects that lie in the second cluster which is part of class 1 represented by "O" in Fig.7. The reason for this failure is that SS-FCM does not allow for the induction of more than one cluster for each concept. It also manages to mis-label a number of objects on the decision boundary which is to be expected to a certain degree as the boundary is extremely cluttered. The overall accuracy of the method for correctly labelled instances is 66%.

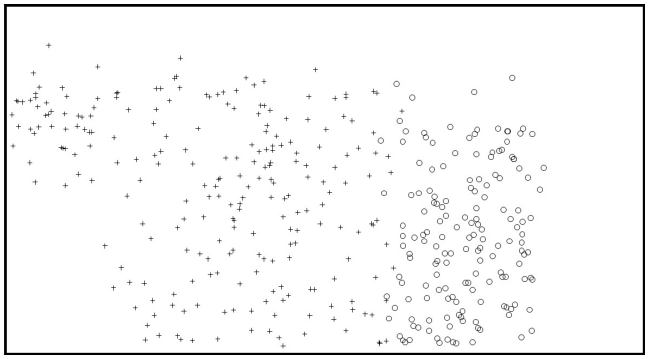

Fig. 7. Artificial Data Problem 2 - SS-FCM

In the case of the FNN wrapper method, performance is quite good and both clusters are identified. However there is a significant amount of mis-labelling of objects. Despite this, the method correctly labels 78% of all objects. Interestingly, some of the assignments appear to be quite strange around the boundaries, with some objects that are distant from the relevant labelled examples. This may be more to do with the sequence of self-learning and value for the number of neighbours than any inherent properties of FNN however.

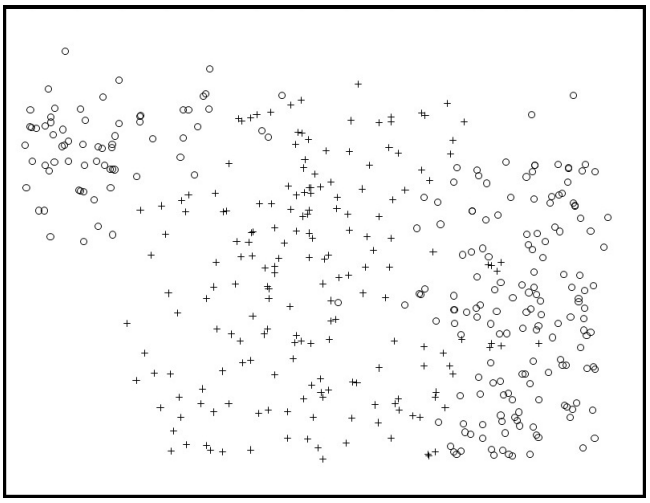

Fig. 8. Artificial Data Problem 2 - FNN

FRSL correctly labels 83% of all of the unlabelled objects for problem 2. Perhaps more importantly however, it manages to label all of those objects represented by the class "O" correctly, the only confusion that arises is with regard to incorrectly labelling objects of the other class.

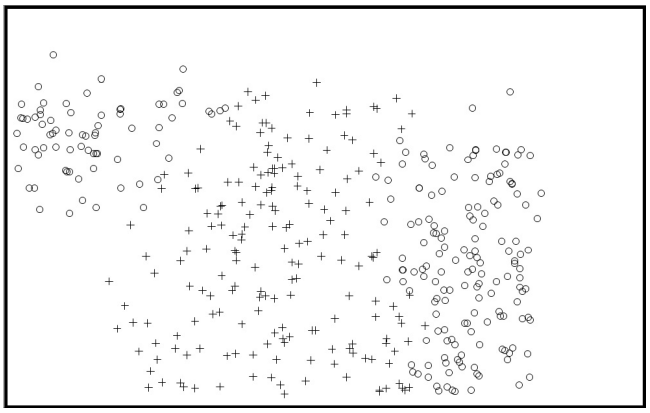

Fig. 9. Artificial Data Problem 2 - FRSL

B. Mammographic Risk Assessment Data

Although artificial data examples often provide useful performance indicators, a mammographic risk assessment problem has been included here in order to demonstrate that FRSL is also useful for such real-world tasks.

Breast cancer is a major health issue, and perhaps the most common amongst women in the EU. It is estimated that between 8% and 13% of all women will develop breast cancer at some point during their lives. Breast tissue characteristics are widely accepted as important indicators of the likelihood of the developing breast cancer [22]. The BIRADS [20] classification scheme allows the division of breast tissue density into 4 distinct classes where 1 represents tissue that is fatty and 4 represents tissue that is dense. The data that is used here has been obtained from [23] and the features have been extracted

TABLE III
CONFUSION MATRICES AND LABEL CLASSIFICATION ACCURACIES FOR THE MIAS DATASET.

FNN
(*Classification accy* = 51.50%)

Consensus opinion	*1*	*2*	*3*	*4*
1	62	15	8	2
2	40	48	15	0
3	32	22	35	6
4	6	4	6	21

FRSL
(*Classification accy* = 65.22%)

	1	*2*	*3*	*4*
1	74	13	0	0
2	15	68	17	3
3	0	36	44	15
4	0	7	6	24

using the method described in [22]. Each of the labelled objects has been labelled using the consensus of three expert radiologists (i.e. where they *all* agree on the classification).

The confusion matrices in Fig. III show the results obtained by both the FNN Wrapper method and the FRSL method. The results for SS-FCM method was not presented for this problem as it fails almost completely to identify any distinct classes. This probably due in the most part to the fact that this is not a clustering task.

The true accuracy for this dataset is 68% when all of the objects have been annotated by experts, FRSL manages 65.21% correct label assignment which is close to this figure. FNN seems to fail to label classes 1 and 2 in particular, whereas one would expect the confusion to lie between classes 2 & 3 as these are conceptually close and are the classes upon which experts disagree most. FNN however shows a large amount of confusion between classes 1 and 3, and also between 1 and 4 which of course are not neighbouring classes. FRSL demonstrates results which do seem to follow a diagonal trend with low non-neighbouring class confusions and a better correct number of label assignments.

V. CONCLUSION

This paper has presented a novel algorithm for the semi-supervised labelling of unlabelled data based on the fuzzy-rough upper and lower approximation membership. Note that no user-defined thresholds are required for the FRSL method, although a choice must be made regarding fuzzy similarity relations and connectives.

Further work in this area will include a more in-depth experimental investigation of the proposed method and the impact of the choice of fuzzy relations, connectives as well as the learning speed of FRSL and number of instances labelled at each iteration etc. Another area worthy of investigation is the combination of the use fuzzy discernibility matrices on the unlabelled data and the use of the fuzzy-rough method on the labelled data, such that the information in both could be aggregated to build classifiers. This may help to address the current assumption for the FRSL method that the labelled objects are fully representative of the class distribution which of course may not be the case. One area is particular which may yield improvements in performance is that of multi-view learning or ensemble semi-supervised classification, where a number of weakly supervised classifiers are aggregated in order to label unlabelled data.

ACKNOWLEDGMENT

Neil Mac Parthaláin would like to acknowledge the financial support for this research through *The Research Institute of Visual Computing - Wales (RIVIC)*.

REFERENCES

[1] O. Chapelle, B. Schölkopf, and A. Zien, *Semi-Supervised Learning*. MIT Press, Cambridge, MA, 2006.
[2] M. De Cock, C. Cornelis, and E.E. Kerre, Fuzzy rough sets: The forgotten step, IEEE Trans. Fuzzy Syst., vol. 15, no. 1, pp. 121-130, 2007.
[3] A. Verikas, A. Gelzinis, and K. Malmqvist, Using unlabeled data for learning classification problems. In New learning paradigms in soft computing, Lakhmi C. Jain and Janusz Kacprzyk (Eds.). *Physica-Verlag Studies In Fuzziness And Soft Computing Series*, Vol. 84, Physica-Verlag GmbH, Heidelberg, Germany, pp. 367–402, 2002.
[4] K. Nigam, and R.Ghani, Analyzing the effectiveness and applicability of co-training. *Ninth International Conference on Information and Knowledge*, Management, pp. 86-93, 2000.
[5] A.M. Bensaid, L.O. Hall, J.C. Bezdek, and L.P. Clarke, Partially supervised clustering for image segmentation, *Pattern Recognition*, vol. 29 no.2, pp. 859-871. 1996.
[6] K.P. Bennett, A. Demiriz, Semi-supervised support vector machines, *Proceedings of Neural Information and Processing System*, pp. 368-374. 1998.
[7] B. Gabrys, A. Bargiela, *General fuzzy minmax neural network for clustering and classification*, IEEE Transactions on Neural Networks, vol.11, no. 3, pp.769-783, 2000.
[8] X.J. Zhu, and A.B. Goldberg, Introduction to semi-supervised learning, *Synthesis Lectures on Artificial Intelligence and Machine Learning*, vol. 3, no.1, pp. 1-130, 2009.
[9] Z. Pawlak, Rough sets. *Int. J. Comput. Inf. Sci.* 11, pp. 341–356. 1982.
[10] D. Dubois and H. Prade. Putting rough sets and fuzzy sets together. In R. Slowinski, editor. *Intelligent Decision Support*. Kluwer Academic Publishers, Dordrecht. 1992., pp. 203–232. 1992.
[11] R. Jensen and Q. Shen. *Computational Intelligence and Feature Selection: Rough and Fuzzy Approaches*, IEEE Press and Wiley & Sons, 2008.
[12] L. Shi, X. Ma, L. Xi, Q. Duan, and J. Zhao, Rough set and ensemble learning based semi-supervised algorithm for text classification, *Expert Systems with Applications*, In Press, Corrected Proof, Available online 19 November 2010, ISSN 0957-4174, DOI: 10.1016/j.eswa.2010.11.069.
[13] Z. Xue, Y. Shang and A. Feng, Semi-supervised outlier detection based on fuzzy rough C-means clustering, *Mathematics and Computers in Simulation*, vol. 80, no. 9, pp. 1911–1921, 2010.
[14] R. Jensen and Q. Shen. New Approaches to Fuzzy-Rough Feature Selection. *IEEE Transactions on Fuzzy Systems*, vol.17, no.4, pp. 824–838, 2009.
[15] R. Mihalcea. Co-training and Self-training for Word Sense Disambiguation, *Proceedings of the Conference on Natural Language Learning* (CoNLL 2004), Boston, 2004.
[16] D. Yarowsky, Unsupervised word sense disambiguation rivaling supervised methods. *Proc. of the 33rd Annual Meeting of the Association for Computational Linguistics*, pp. 189-196, 1995.
[17] A.M. Radzikowska and E.E. Kerre, A comparative study of fuzzy rough sets, *Fuzzy Sets and Systems*, vol. 126, no. 2, pp. 137–155, 2002.

[18] A. Blum, T. Mitchell, Combining labeled and unlabeled data with co-training. *COLT: Proceedings of the Workshop on Computational Learning Theory*, Morgan Kaufmann, pp. 92–100, 1998.

[19] D.J. Newman, S. Hettich, C.L. Blake, and C.J. Merz, *UCI Repository of machine learning databases* [http://www.ics.uci.edu/ mlearn/MLRepository.html]. Irvine, CA: University of California, Department of Information and Computer Science, 1998.

[20] American College of Radiology. *Illustrated Breast Imaging Reporting and Data System BIRADS*. 3rd Edition, American College of Radiology, 1998.

[21] J.M. Keller, M.R. Gray and J.A. Givens. A fuzzy K-nearest neighbor algorithm. *IEEE Trans. Systems Man Cybernet.*, vol. 15, no. 4, pp. 580-585, 1985.

[22] A. Oliver, J. Freixenet, R. Marti, J. Pont, E. Perez, E.R.E. Denton, R. Zwiggelaar. A Novel Breast Tissue Density Classification Methodology. *IEEE Transactions on Information Technology in Biomedicine*, vol. 12, no. 1, pp. 55–65, 2008.

[23] J Suckling, J. Partner, D.R. Dance, S.M. Astley, I. Hutt, C.R.M. Boggis, I. Ricketts, E. Stamatakis, N. Cerneaz, S.L. Kok, P. Taylor, D. Betal, and J. Savage. The Mammographic Image Analysis Society digital mammogram database. *International Workshop on Digital Mammography*, pp 211–221, 1994.

[24] X. Zhu, B.R. Gibson, K. Jun, T.T. Rogers, J. Harrison, and C. Kalish. Cognitive models of test-item effects in human category learning,Proc. of the 27th International Conference on Machine Learning (ICML), 2010.

2011 IEEE International Conference on Fuzzy Systems
June 27-30, 2011, Taipei, Taiwan

An Application of Genetic Fuzzy Systems for Wireless Sensor Networks

Líliam Barroso Leal,
Raimir Holanda Filho
and Marcus Vinícius de S. Lemos
Applied Comp. Sciences Department
University of Fortaleza, Brazil
Email: liliamleal,marvinlemos@gmail.com
and raimir@unifor.br

Ricardo A. L. Rabelo,
Fabio A. S. Borges
Unified Teaching Center of Teresina
Teresina, PI, Brazil
Email: ricardor_usp@yahoo.com.br
and fabbioanderson@gmail.com

***Abstract*—Wireless sensor networks (WSNs) are composed of sensor nodes in order to detect and transmit features from the physical environment. Generally, the sensor nodes transmit information to a special node called sink. Some recent researches have led to the selection of routes in sensor networks with multiple sink nodes. The approach proposed by this paper presents the application of Genetic Fuzzy System (GFSs) for the selection of routes in WSNs, in order to make the communication between multiple sensor nodes and sink nodes. The results obtained through simulations demonstrated a sensor network with a longer lifetime, through the choice of the adequate sink used for sending packets through the network in order to find the best routes.**

***Index Terms*—Fuzzy Inference System, Genetic Algorithms, Wireless Sensor Networks, Mamdani, Sink Nodes.**

I. Introduction

In recent years we have witnessed a considerable increase in researches involving Wireless Sensor Networks (WSNs) due to their applicability to various areas like safety, health, agriculture, smart environments, industrial automation, among others [1],[2]. Some of the most common paradigms of communication in WSNs involve the communication of multiple sensor nodes placed in an observation area reporting information to a special node named sink (many-to-one). In [3] it is said that the use of a unique sink represents a bottleneck in a network, especially for applications in real-time and continuous data flow. In this sense, some researches have directed studies to the use of multiple sinks, in which communication addresses an alternative paradigm composed of multiple sensor nodes to multiple sinks (many-to-many). For instance, we can cite some papers that address the aspects of WSN with multi-sinks: Tradeoff Between Security and Communication Cost [4], Data Dissemination of Emergency Messages in Mobile Multi-sink Wireless Sensor Networks [5], Topology Control Algorithm Based on Bottleneck Node for Large-Scale WSNs [6], Data Caching Based Queries in Multi-sink Sensor Networks [7].

The approach used in this work focuses on the communication between the sensor nodes and the multiple sink nodes of a WSN. This scenario was chosen because of the growing popularization of applications that require networks with multiple sinks, for example, applications using multimedia wireless sensor networks [8] applications using acting nodes [9], as well as other applications where there might be more than one sink node. Some of these applications intended to promote the selection of routes in WSN, such as: An Energy Efficient Load-Balanced Multi-Sink Routing Protocol for Wireless Sensor Networks [10], Routing in Wireless Sensor Networks Using an Ant Colony Optimization (ACO) Router Chip [11], NSN based Multi-Sink Minimum Delay Energy Efficient Routing in Wireless Sensor Networks [12].

One approach often used to deliver data to multiple sink nodes involves the technique of load balancing [13]. In this approach the data collected by the sensors are distributed throughout the network in order to use all the paths available for routing algorithm. However, the isolated use of the technique of load balancing does not guarantee the energy efficiency of the network, because the path may serve more than one sensor node and thus can have paths with different energy levels. Thus, this technique can force a particular sensor node using a route with low energy capacity.

The methodology implemented in this work for routes selection in WSN combines fuzzy inference systems (FIS) of Mamdani [14] and Genetic Algorithms (GA) [15]. We employed a FIS of Mamdani, in that we tried to model approximate reasoning [16] in order to imitate the human ability to make reasonable decisions in an environment of imprecision, uncertainties and noise. This is because FIS are potentially able to express and process qualitative information. In this paper, fuzzy inference systems of Mamdani are used to determine the most appropriate sink node through consideration of some characteristics of the sensors network, such as energy and number of hops. The production rules in an inference model have linguistic variables both in their antecedents as in their consequents. Genetic Algorithms are employed to obtain the optimal adjustment of fuzzy inference system parameters. By applying GAs, we intend to achieve both a fuzzy database and a fuzzy rules base to maximize performance of the application of Mamdani's inference system in the selection of routes in Wireless Sensor Networks. Therefore, the obtained fuzzy system should be able to help the routing algorithm to choose the best communication path between the sensor nodes and the

978-1-4244-7316-8/11/$26.00 ©2011 IEEE

sink nodes so as to maximize the network lifetime. The design of a fuzzy inference system can be seen as an optimization problem in a high-dimensional search space where each point represents a specific fuzzy rule base and a fuzzy data base. The performance of the FIS forms a hypersurface in the search space. Implementing the optimal FIS corresponds to obtain the optimal location of this hypersurface. However this hypersurface is infinitely large, nondifferentiable, complex, noisy, multimodal and deceptive [17]. It is important to highlight that GAs are global optimization algorithms, based on natural selection mechanisms and genetics, which have shown themselves efficient in a wide variety of problems, in that they override many limitations found in the traditional search/optimization methods [18]. The systems achieved from the integration between the fuzzy inference models and genetic algorithms are called Genetic Fuzzy Systems (GFSs) [19].

II. Related Works

In [3] we have a wireless sensors network consisting of multiple sinks arranged in a cluster that use a database management system distributed in each sink of the network. This proposal requires two modifications in the routing protocol: the first is that the protocol should enable the creation and storage of the multiple routes during message propagation, and the second requires that the network offer QoS (Quality of Service), for the delivery of event notification messages. While the message is propagated through the network, the paths are created and stored in each clusterhead (CH).

The research in [20] proposes a scheme based on Fuzzy Logic to select a better path and increase survival time in MANETs (Mobile Ad hoc Networks). This proposal presents, as contributions, an adaptive path selection scheme and protocol independent. In addition, the correlation of the network characteristics and the safety criterion are made through the use of Fuzzy Logic, to improve the path selection in order to minimize safety limitations found in routing protocols.

In [21], the scenario is of a flat WSN that has only one sink and investigates problems of optimization of the data routing to the sink, based on metrics to choose the best path. In this proposal, a fuzzy inference system is used to select the best candidate node to send packets to the sink at any given time. One drawback to this protocol is the fact that it does not approach the use of multiple sinks, what makes it vulnerable to problems such as bottlenecks and greater energy waste of the nodes next to the sink.

Our work differs from the ones mentioned, since it was proposed to use a Genetic Fuzzy approach to enable choosing the best path for sending data. We propose an algorithm that works together with a routing protocol, in order to help the sensor node in the selection process of the best path among the various possible routes at a given time. This route selection process is made through the use of a Mamdani's fuzzy inference system responsible for classifying routes based on criteria, like energy and number of hops, with the aim of increasing the uptime of the network, since bad ways, such as longer paths, with little energy, should be avoided.

III. The algorithm proposed to assist the Choice of the Best Route in Multi-Sink Environments

A. General Aspects

In our proposal we consider a network in which the sensor nodes are positioned so as to reach the coverage of the whole area and the multiple sinks are arranged according to the network design. It is noteworthy that the sink nodes are devices with superior characteristics to the sensor nodes, having no energy limitations.

Each sink node is responsible for receiving notification messages of events occurring anywhere on the network. For such, each sensor node must select the most appropriate sink at a given moment, taking characteristics of the network into consideration, such as energy, number of hops, collisions and delay. We must emphasize that on this paper we considered initially only two characteristics, energy and number of hops, main metrics considered in WSNs [22].

It is important to highlight that choosing a routing protocol is necessary, since our solution will work together with it. The choice of the routing protocol is made according to the needs of the network designer, being required only that the protocol be capable of providing multiple paths (multipath). To test, we used the routing protocol Directed Diffusion [23] whose operation is detailed in section 5.

B. The Solution Proposed

We present the steps of the implemented algorithm by means of Figure 1. After the positioning stage of all nodes in the network, they are started and the sinks generate a *V*-list containing their neighbor nodes. This list is used by the sinks to send a signalling message β^n, as illustrated in Figure 1. The signalling message sent by the sinks is propagated through the network by the neighbor sensor nodes.

At receiving a signalling message a sensor node *X* will check the following fields:

- *Energy*: this field is used to store the lowest energy value found on the course so far;
- *Base_station*: indicates which sink originated the signalling message;
- *Number_of_hops*: distance traveled in hops from the sink which originated the message to the current sensor node;
- *Predecessor_node*: identifies the node from which *X* node received the message;
- *Last_sequence*: identifies the signalling message. Every time sinks need to reconstruct the routes, a new signalling message is generated and the field *Last_sequence* will be incremented, so that the nodes may distinguish the current message from the messages sent previously.

If a given node *Y* receives a signalling message whose value of the field Predecessor_node is different from some of the neighbor nodes that it uses as the current route it will disregard this message discarding it, so as to save resources of the sensor node such as: processing, storage and energy used. Figure 2 illustrates a situation of signalling message discard in which the network interconnection has already been established at

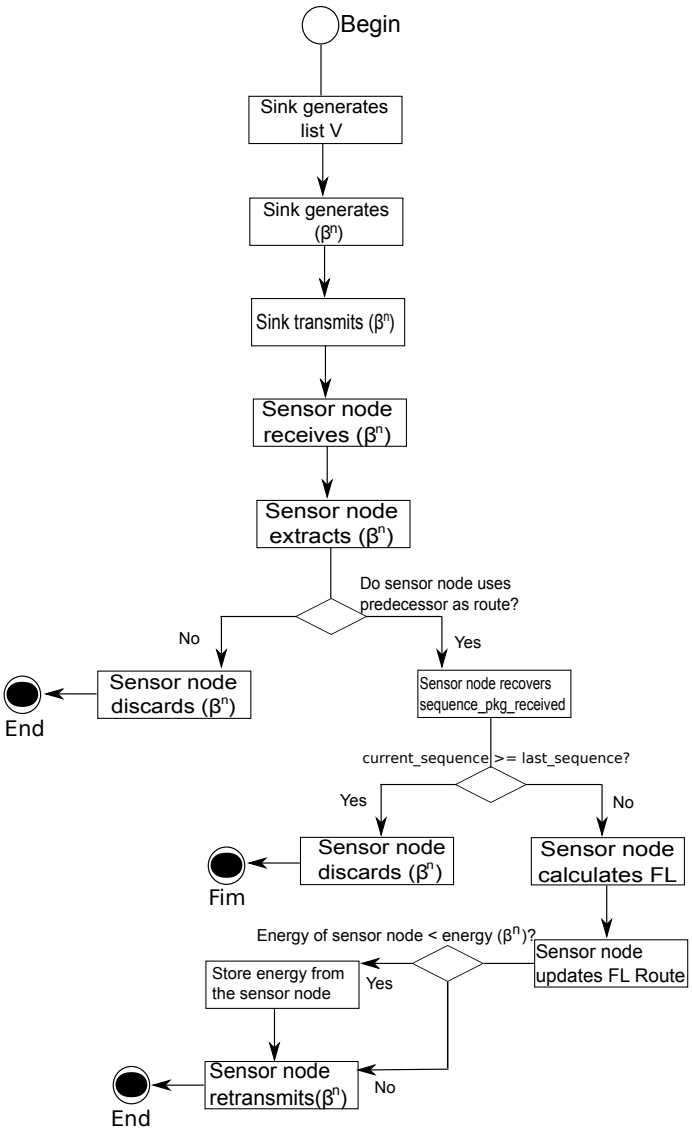

Fig. 1. Flowchart that represents the algorithm.

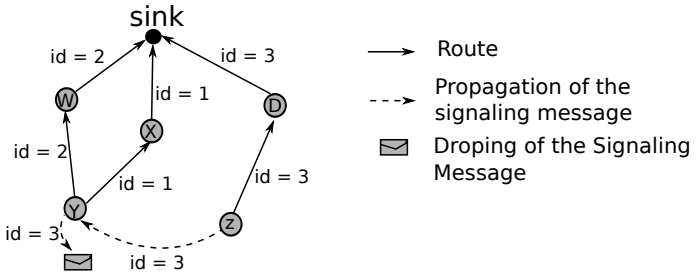

Fig. 2. Droping of the signalling message.

the boot by the routing algorithm used and the sensor nodes have multiple routes. Thus, the sensor node *Y* has two routes to reach the sink node established through the nodes *X*, id = 1 and *W*, id = 2. When the signalling message β^n is transmitted by the sink node, the neighbor nodes propagate the message through the network. Thus, when node *Z* receives the message β^n, it passes it on to all neighbor nodes it can reach, including sensor nodes that are not part of its route, as it is the case of node *Y*, when receiving the message β^n from node *Z* will discard it immediately.

In order to avoid old messages from remaining traveling through the network, some routines are established according to algorithm presented in Figure 1. A given node *X* at receiving a signalling message checks the field Last_Sequence to verify whether it refers to a new signalling message, or if it is only the propagation of a message received previously. The next step is to calculate the fuzzy level (FL) associated with each route. This parameter allows the node to select the best route at a given moment, according to the last signalling message received. For each route that a node may use, there is an FL associated with it. Routes with higher FL value are regarded as preferential. The FL value is obtained through Mamdani's fuzzy inference model, whose entries correspond to the values of energy and number of hops. Finally, node *X* tests if its energy is lower than the energy contained in the received message, if so, it updates the field energy signalling message with the value of its remaining power, if not, it goes to the next step and relays the message over the network.

In our work, we consider that each sink node will send signalling messages β^n periodically to the network, in order to update the FL of each route set up by the routing algorithm. Thus, there will be a better use of the energy of the sensor nodes, in that the routes are chosen at each transmitted signalling message. We call α window the period in which signalling messages are transmitted. The value attributed to α cannot be very small so that the network is overcharged with the constant transmission of signalling messages nor can it be a value large enough to affect the choice of routes. Details related to the α value determination will be submitted in section 7.

IV. Genetic Fuzzy System

A. Fuzzy Inference Systems

Fuzzy Inference Systems are able to handle very complex processes, based on imprecise, uncertain and qualitative information. Fuzzy Inference Systems are very suitable for modelling complex systems where it is very complicated to describe the system mathematically. Generally, the fuzzy inference systems are based on linguistic rules of type "if ... then" in which the fuzzy set theory [24] and the Fuzzy Logic [25], [26] provide the mathematical basis.

In general, fuzzy inference systems operate based on three steps: Fuzzification, inference procedures, and defuzzification. In fuzzy inference systems, generally, non fuzzy (quantitative, accurate, crisp) inputs are taken into consideration, derived from observation or measurement, which is the case of most practical applications. Fuzzification is a mapping of the domain of the entrance variable to the fuzzy domain, representing the attribution of linguistic values defined by membership

functions to the input variables of the Fuzzy Inference System. The fuzzy inference procedure is responsible for evaluating the primary terms (linguistic labels) of the input variables applying the production rules so as to obtain the value of the fuzzy output from the inference system. Once the fuzzy output set has been obtained at the step of defuzzification an interpretation of that information is made. This step is necessary because in practical applications, quantitative outputs are generally required. Defuzzification is typically used to assign a numeric value to the output fuzzy set.

B. Genetic Algorithms

Genetic Algorithms are search and/or optimization algorithms based on the mechanisms of genetics and natural selection. Their operation follows biologic inspiration, which presupposes that in a given population individuals with "good" characteristics are more likely to survive and to beget even stronger individuals (fit), while the less fit individuals tend to disappear during the evolutionary process. When using GAs, each individual of the population, called chromosome, represents a potential solution to the problem to be solved. Each piece of the chromosome is called the gene. GAs emphasize combination of the most promising candidates for the solution of the problem. This combination of the fittest individuals is obtained through the application genetic operators that manipulate the genetic composition of chromosomes in order to explore and to exploit the search space so as to find better solutions to the problem. The genetic operators mentioned are computational aproximations of phenomena seen in nature, such as genetic mutation and sexual reproduction.

Though apparently simple, in part due to their bioinspired foundation, GAs are able to solve complex problems in very elegant way. Moreover, they are not affected by suppositions about differentiability or continuity of the objective function of the problem, in that GAs do not use information from derivatives in the evolutionary process, nor do they need information about the individuals' neighborhood. This implies that GAs can be very appropriate to deal with problems with non-differential and non-continuous functions. In addition, GAs differ themselves from randomic search and/or optimization techniques, since they apply the fitness index, which is important information relevant to the search space obtained by the use of the evaluation function.

C. Genetic Fuzzy System Implementation Aspects

The implemented fuzzy inference system has two input linguistic variables, Energy and number of hops, and a output linguistic variable, the Fuzzy Level (FL). The syntax of the rules of the fuzzy system is represented by the following linguistic conditional declarations:

- Rule 1: If (Energy is A_1) and (Number of hops is B_1), Then (FL is C_1) or
- ...
- Rule n_r: If (Energy is A_p) and (Number of hops is B_q), Then (FL is C_r)

where: n_r is the number of rules; A_j, B_k, C_l are the primary terms (linguistic values) associated with the linguistic variables, Energy, number of hops and FL, respectively; *p*, *q* and *r* correspond to the number of primary terms of the linguistic variables Energy, Number of hops and FL, respectively.

Thus, we have a Mamdani's fuzzy system, consisting of N_r disjunctive inference rules. The rules are inferred in a parallel way, without considering the order in which they are implemented. The inference of each rule consists of the evaluation of the antecedent, followed by the application of the implication operator to determine the consequent fuzzy set. The defuzzification procedure obtains the FL's numeric value. The implication operator used was Mamdani's minimal operator; the aggregation of the consequents was performed by the maximum operator and the defuzzification method employed was the area center method (or centroid method) [27], [28].

The approach adopted in this paper proposes the use of GAs to determine the number of primary terms for the linguistic variables, the adjustment of the membership functions associated with each primary term, and the set of linguistic rules of Mamdani's fuzzy system, simultaneously.

The first aspect to be considered in the use of GAs for the solution of a problem is the chromosomal representation of the problem, so that the GAs can solve it appropriately [17]. In this study the chromosomes have information related to the number of primary terms and the membership functions of the input and output linguistic variables, as well as information on the rules bases of the fuzzy inference system.

The chromosome structure to store the parameters of the fuzzy inference system was divided into three parts. The first part codifies the amount of primary terms of the linguistic variables. This part of the chromosome has 9 bits, where each set of 3 bits represents the number of primary terms of a linguistic variable. The second part stores information of the fuzzy rules base. According to experience of authors in relation to the behavior of WSNs, the top number of primary terms of each linguistic variable was defined as being equal to 5, and the amount of rules is then set by a multiplication between the numbers of primary terms of the input linguistic variables (Energy and Number of hops). Thus, the maximum number of rules in the system is equals to 25. Therefore, the second part is represented by 75 bits, and each set of 3 bits represents the primary term associated with a rule of the inference system. The third part codifies the parameters of the membership functions of each linguistic variable of the system. As membership functions have continuous parameters that require a great precision, the representation of the chromosome by real numbers was adopted [29], instead of binary representation [30] used in the two first parts. The membership functions used for the linguistic variables are triangular (Figure 3).

However, instead of the chromosomes storing the values a_i, m_i and b_i for each membership function, they store the adjustment coefficients (parameters) δ_i and η_i. Each membership function i can be assembled from the following equations [31]:

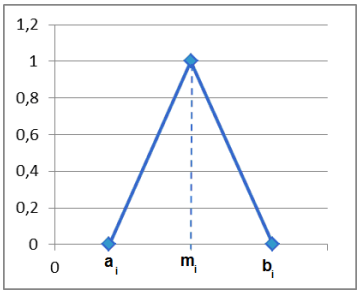

Fig. 3. Triangular membership function.

- $a_i = (a_i + \delta_i) - \eta_i$;
- $m_i = (m_i + \delta_i)$;
- $b_i = (b_i + \delta_i) + \eta_i$.

The coefficient δ_i is responsible for moving the membership function to the right or to the left, while the coefficient η_i can expand or shrink the support of the membership function [28] in relation to its universe of discourse. As each linguistic variable has 5 primary terms at most, and each membership function associated with a primary term is represented by the two parameters δ_i and η_i, 10 genes, at most, are necessary to represent the membership functions of a linguistic variable of the applied fuzzy inference system. Therefore, the third part of the chromosome has size 30. As each chromosome stores the information about the parameters of the inference fuzzy system (fuzzy database and fuzzy rule base), we have one chromosome of 114 (9 + 75 + 30) genes. The GA implemented has adopted a population of 80 individuals (chromosomes).

After the chromosome representation definition, the GA design focuses on the specification of an evaluation function. Since the goal of the fuzzy system is to help the routing algorithm choose the best way to communicate between the sensor nodes and the sink nodes, this work employed the time it takes for the first sensor node of the network to die as evaluation function. Therefore, this is a maximization problem whose objective is to tune the Mamdani's fuzzy inference system that selects the best routes to maximize the lifetime of the network.

After the attribution of the fitness index by the evaluation function, the selection process chooses a subset of individuals of the current population to compose an intermediate population in order to apply the genetic operators. The selection method adopted in this work was the tournament method. It is worth mentioning that the size of the adopted tournament was set equal to 2. In combination with the selection module an elitist strategy was used with the maintenance of the best individual from one generation to the other.

To evolve the population go through an evolution one should apply the genetic operators (crossover and mutation). Crossover is the process for sharing information through of the exchange of portions (genes) of the parent chromosomes. The crossover operator has always been considered as the primary search operator in GAs because it exploits the available information from chromosomes about the search space. As this operator combines the features of parent chromosomes to form offsprings, it is highly probable that good chromosomes may generate better ones. Therefore the crossover can be considered one of the main components for improving the behavior of the GA [32]. In this study, we used discrete crossover [33]. The mutation genetic operator [34] is necessary to introduce and maintain genetic diversity of the population through randomic changes of genes within the chromosomes, what provides a means for incorporation of new genetic characteristics within the population. Therefore, mutation ensures the possibility of reaching any point of the search space, besides to avoid to get trapped in local minima. However, mutation is applied less frequently than crossover in order to preserve the exploration-exploitation-relationship [35].

Several criteria may be applied to finalize the execution of a GA. In this work the maximum limit of generations fixed in 100 interactions was adopted as stopping criterion.

As a result of the GAs operation in the adjustments of fuzzy systems, Figures 4 and 5 show the membership functions associated with the linguistic variable energy and number of hops.

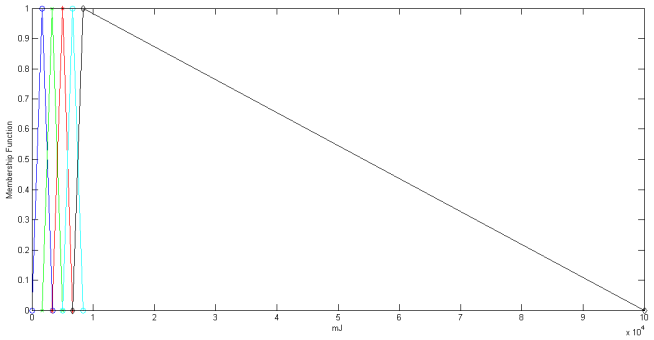

Fig. 4. Membership function of the energy variable.

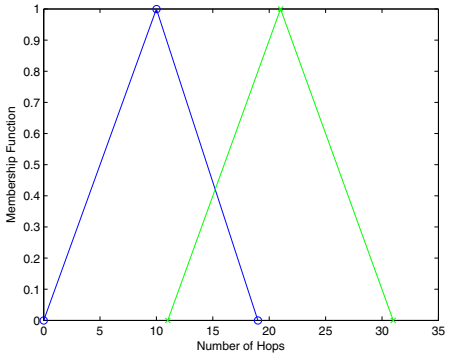

Fig. 5. Membership function of the number of the hops variable.

V. Simulation

This section presents comments about the simulations carried out to validate the routes selection algorithm using the implemented Genetic Fuzzy System.

A. Simulator

In our experiments, we use the Sinalgo simulator [36]. Sinalgo is a framework implemented in Java language, for testing and validating the networks algorithms. Contrary to other tools such as the *Network Simulator* 2 [37], which allows the simulation of networks in several layers of the protocol stack, our approach focuses the use of Sinalgo to verificate the efficiency of the algorithms to selection of routes.

B. Network Characteristics

The main characteristics of the network are:

1) Topology: the simulated network is steady and includes only two types of nodes: sink nodes and sensor nodes. The sensor nodes have similar characteristics, featuring a flat network, where each node of the network has a single identifier and steady radio range.
2) Scenarios used: in our simulations we used four scenarios with similar environment. All scenarios are usually composed of 100 sensor nodes distributed uniformly throughout the network and for the scenarios that use multiple sinks we used 4 sink nodes located at the end of the network initially, with a range area of 700 m x 700 m. We configured a sensor node located in the center of the network to transmit packets continuously at a ratio of one packet per second in the four scenarios.

Next we describe the simulated scenarios:

- Scenario 1: in this scenario we used the Directed Diffusion routing protocol in its traditional form, without the use of fuzzy inference systems and without multiple sinks.
- Scenario 2: we used the Directed Diffusion routing protocol with multiple sinks and applyed the load balancing among the existing multiple paths. It is important to emphasize that we did not use Fuzzy Inference Systems.
- Scenario 3: the application through Mamdani's fuzzy inference system influences the routes formation through the Directed Diffusion protocol, in order to choose the best route to one of the sinks. Nevertheless, the design of the fuzzy inference system is made in an empiric way, in which the adjustments of the fuzzy database and the fuzzy rule base are made manually, based on tests with various different configurations.
- Scenario 4: just as in scenario 3, the application through Mamdani's fuzzy inference system influences the formation of routes through the Directed Diffusion protocol, in order to choose the best route to one of the sinks. However, in this scenario, the parameters of the fuzzy inference system are not adjusted empirically anymore, but by using Genetic Algorithms, characterizing the approach as fuzzy-genetic.

C. The Routing Algorithm

For the communication of the nodes with the sinks, we used the Direct Diffusion routing protocol, which is designed for wireless sensor networks, where the network designer is responsible for defining the type of event that should be observed by the sensor nodes and the area of interest.

VI. Results and Discussions

The results of the proposed approach application are presented based on three metrics. The metrics are:

- First node death time: it expresses the death time of the first node in the network. Here, we intend to analyze how long sensor nodes remain living;
- Network death time: it records how long the network remains alive, that is, how long the network will be able to keep the necessary communications active.
- Sink nodes number: in this metric, we evaluate how the amount of sink nodes influences our work;

Although our solution is aimed at environments with multiple sinks, we firstly analyzed the network behavior through simulations in the same scenarios described in section V using only one sink node, as illustrated by the figures 6 and 7. We conducted these experiments with the purpose of verifying the feasibility and efficiency of the proposed solution, since an environment with a single sink did not receive satisfactory results, possibly the realization of these simulations environments with multiple sinks would be unsatisfactorily similar.

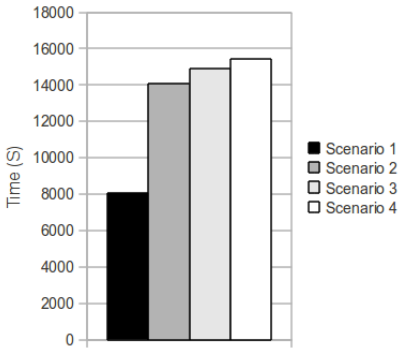

Fig. 6. Death time of the first node of the network.

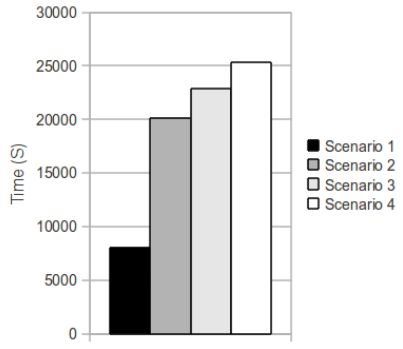

Fig. 7. Death Time the Network.

We also evaluated the behavior of the sensors in a WSN with multiple sink nodes for each scenario according to the three metrics addressed. For the first metric, first node death time

in the network, we can see from Figure 8 that in scenario 1, where we used the Directed Diffusion protocol in its traditional form, without the use of fuzzy inference systems and without multiple sinks. The results showed weakness in the lifetime of the network, where a sensor node participates actively in a route in use. In scenario 2, without using Fuzzy Inference Systems, with multiple sinks and the usage of load balancing. We obtained an improvement of approximately 11% compared to scenario 1. In scenario 3 we have a solution that uses fuzzy inference systems adjusted empirically, associated with the use of multiple sinks. In this scenario, the gain compared with scenario 1 is approximately 234%. Finally, in scenario 4 we have the representation of the proposed solution that uses a genetic fuzzy system and multiple sinks in which the gain when compared with scenario 1, approaches 373%. This gain was due to the use of multiple sinks, increasing the number of routes each node can use for the transmission of data over the network and the use of the genetic fuzzy system which makes the node avoid the bad routes (low energy, long distances).

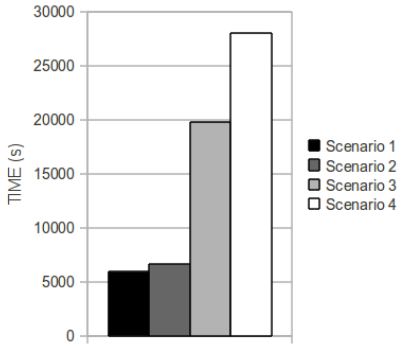

Fig. 8. Death time of the first node of the network.

We represented in Figure 9 the network death time, time when the network communication is discontinued due to the death of some sensor nodes that compose the routes of the sender. In the column representing scenario 1 (without fuzzy inference system and without multiple sinks), we have that the network death time corresponds to the network's first node death time because this network does not have multiple routes and multiple sinks. In scenario 2, due to load balancing across multiple paths to network remains active around 104% more than scenario 1. In scenario 3, the network remains active for a long period of time. Approximately 478% higher than the scenario 1, this gain was achieved by using multiple routes, associated with the use of empirical fuzzy inference in the best routes selection process at a certain moment. The great difficulty encountered in this simulation scenario was due to the empirical adjustment of the inference system that consumed much time, in that they were carried out based on trial and errors. Still, it was not possible to firmly tell whether the chosen parametres of fuzzy inference system were the best. We obtained in scenario 4, an uptime of the network higher than all simulated scenarios; about 541% higher than scenario 1, this gain was promoted through the use of genetic fuzzy system and multiple sinks.

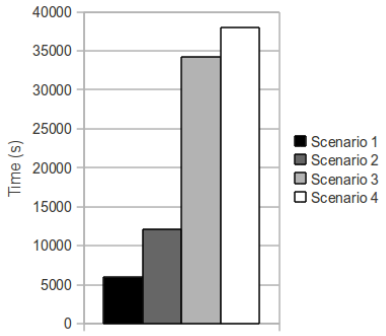

Fig. 9. Death Time the Network.

VII. α Window

As mentioned previously, in our algorithm, we consider that each sink node waits for an α time window to send signalling messages so that the sensor nodes update their fuzzy levels.

We conducted simulations with different α values and we evaluated the performance based on the network's first node death time (Figure 10). We could realize that the values close to the desired are between 800 and 900 seconds.

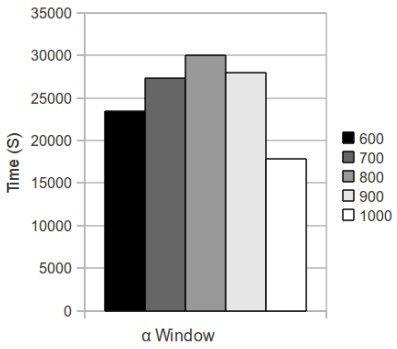

Fig. 10. Window α.

VIII. Conclusions

This paper proposes a fuzzy genetic system-based algorithm for the selection of routes in WSN with multiple sinks. Fuzzy inference systems of Mamdani are used to determine the most appropriate sink node through consideration of some characterstics of the sensors network, such as energy and number of hops. However, the optimal design of a Mamdani's fuzzy inference system is a complicated task due to some characteristics of the search space. Generally, this search space is characterized as infinitely large, nondifferentiable, complex, noisy, multimodal and deceptive. These characteristics induce the authors to apply Genetic Algorithms on tuning of Mamdani's fuzzy inference system. The main objective of the algorithm is to extend the network's lifetime which can be achieved by making the nodes avoid bad routes during the sending of packets through the network. For such, we applied

fuzzy inference systems in order to build a knowledge base which makes the process of finding the best routes possible.

Results obtained through simulations, demonstrated that our approach is feasible increasing the network's lifetime satisfactorily. In future works we intend to analyze the behavior of algorithms in more complex scenarios, as well as select new linguistic variables for the fuzzy inference.

When you opt for a fuzzy inference system to determine the selection of routes in a wireless sensor network with multiple sink nodes, you have an action/control strategy that can be monitored and interpreted, even from the linguistic viewpoint. Another advantage found in using fuzzy inference systems during the development of this work refers to the inclusion of the authors' experience in the definition of some parameters of the implemented fuzzy system. That experience could be used directly to aid the construction of the rules base and the initial definition of the primary terms (fuzzy sets) of the linguistic variables.

REFERENCES

[1] Y. chee Tseng, Y. chiun Wang, and L. wu Yeh, "ipower: An energy conservation system for intelligent buildings by wireless sensor networks," 2009.

[2] A. Mainwaring, D. Culler, J. Polastre, R. Szewczyk, and J. Anderson, "Wireless sensor networks for habitat monitoring," in *WSNA '02: Proceedings of the 1st ACM international workshop on Wireless sensor networks and applications*. New York, NY, USA: ACM, 2002, pp. 88–97.

[3] A. Boukerche and A. Martirosyan, "An energy efficient and low latency multiple events' propagation protocol for wireless sensor networks with multiple sinks," in *PE-WASUN '07: Proceedings of the 4th ACM workshop on Performance evaluation of wireless ad hoc, sensor,and ubiquitous networks*. New York, NY, USA: ACM, 2007, pp. 82–86.

[4] Y. Lu and J. Li, "Forward-secure certificate-based encryption and its generic construction," *JNW*, vol. 5, no. 5, pp. 527–534, 2010.

[5] A. Tüysüz Erman and P. Havinga, "Data dissemination of emergency messages in mobile multi-sink wireless sensor networks," in *Proceedings of the 9th IFIP Annual Mediterranean Ad Hoc Networking Workshop, Med-Hoc-Net 2010*. IEEE, June 2010, pp. 1–8. [Online]. Available: http://doc.utwente.nl/73133/

[6] Y. Fan, Q. Chen, and J. Yu, "Topology control algorithm based on bottleneck node for large-scale wsns," in *Proceedings of the 2009 International Conference on Computational Intelligence and Security - Volume 01*, ser. CIS '09. Washington, DC, USA: IEEE Computer Society, 2009, pp. 592–597. [Online]. Available: http://dx.doi.org/10.1109/CIS.2009.11

[7] J. Li, S. Ji, and J. Zhu, "Data caching based queries in multi-sink sensor networks," in *Proceedings of the 2009 Fifth International Conference on Mobile Ad-hoc and Sensor Networks*, ser. MSN '09. Washington, DC, USA: IEEE Computer Society, 2009, pp. 9–16. [Online]. Available: http://dx.doi.org/10.1109/MSN.2009.20

[8] I. F. Akyildiz, T. Melodia, and K. R. Chowdhury, "A survey on wireless multimedia sensor networks," *Comput. Netw.*, vol. 51, no. 4, pp. 921–960, 2007.

[9] P. Ciciriello, L. Mottola, and G. P. Picco, "Efficient routing from multiple sources to multiple sinks in wireless sensor networks," in *EWSN'07: Proceedings of the 4th European conference on Wireless sensor networks*. Berlin, Heidelberg: Springer-Verlag, 2007, pp. 34–50.

[10] A. Eghbali, N. Javan, A. Dareshoorzadeh, and M. Dehghan, "An Energy Efficient Load-Balanced Multi-Sink Routing Protocol for Wireless Sensor Networks," in *Telecommunications, 2009. ConTEL 2009. 10th International Conference on*, 2009, pp. 229 – 234.

[11] S. Okdem and D. Karaboga, "Routing in wireless sensor networks using an ant colony optimization (aco) router chip," *Sensors*, vol. 9, no. 2, pp. 909–921, 2009. [Online]. Available: http://www.mdpi.com/1424-8220/9/2/909/

[12] K. N. Chaaran, M. Younus, and M. Y. Javed, "NSN based Multi-Sink Minimum Delay Energy Efficient Routing in Wireless Sensor Networks ," *European Journal of Scientific Research*, vol. 41, 2010.

[13] L. Mottola and G. P. Picco, "Muster: Adaptive energy-aware multi-sink routing in wireless sensor networks," *IEEE Transactions on Mobile Computing*, vol. 99, no. PrePrints, 2010.

[14] E. H. Mamdani, "Application of Fuzzy Algorithms for Control of Simple Dynamic Plant," *Proceedings of IEE Control and Science*, vol. 121, no. 12, pp. 1585–1588, 1974.

[15] D. E. Goldberg, *Genetic Algorithms in Search, Optimization and Machine Learning*. Addison-Wesley Longman Publishing Co., Inc. Boston, MA, USA, 1989.

[16] E. H. Mamdani, "Application of Fuzzy Logic to Approximate Reasoning Using Linguistic Synthesis," *IEEE Transactions on Computers*, vol. 26, no. 12, pp. 1182–1191, 1977.

[17] Y. Shi, R. Eberhart, and Y. Chen, "Implementation of Evolutionary Fuzzy Systems," *IEEE Transactions on Fuzzy Systems*, vol. 7, no. 2, pp. 109–119, 1999.

[18] R. L. Haupt and S. E. Haupt, *Practical Genetic Algorithms*. Wiley New York, 1998.

[19] F. Herrera, "Genetic Fuzzy Systems: Taxonomy, Current Research Trends and Prospects," *Evolutionary Intelligence*, vol. 1, no. 1, pp. 27–46, 2008.

[20] M. N. Lima, H. W. da Silva, A. L. dos Santos, and G. Pujolle, "Survival multipath routing for manets," in *NOMS*, 2008, pp. 425–432.

[21] M. A. Azim and A. Jamalipour, "Optimized forwarding for wireless sensor networks by fuzzy inference system," 2007.

[22] C. F. Garca-hernndez, P. H. Ibargengoytia-gonzlez, J. Garca-hernndez, and J. A. Prez-daz, "Wireless sensor networks and applications: a survey," 2007.

[23] C. Intanagonwiwat, R. Govindan, D. Estrin, J. Heidemann, and F. Silva, "Directed diffusion for wireless sensor networking," *IEEE/ACM Trans. Netw.*, vol. 11, pp. 2–16, February 2003. [Online]. Available: http://dx.doi.org/10.1109/TNET.2002.808417

[24] L. Zadeh, "Fuzzy Sets*," *Information and control*, vol. 8, no. 3, pp. 338–353, 1965.

[25] L. A. Zadeh, "Fuzzy logic = computing with words," *IEEE Transactions on Fuzzy Systems*, vol. 4, no. 2, 1996.

[26] J. Yen, "Fuzzy Logic-a Modern Perspective," *IEEE Transactions on Knowledge and Data Engineering*, vol. 11, no. 1, pp. 153–165, 1999.

[27] T. J. Ross, *Fuzzy Logic with Engineering Applications*. Wiley, 2004.

[28] H. J. Zimmermann, *Fuzzy Set Theory – and its Applications*. Kluwer Academic Publishers, 2001.

[29] T. Srikanth and V. kamala, "A real coded genetic algorithm for optimization of cutting parameters in turning," *IJCSNS International Journal of Computer Science and Network Security*, vol. 8, no. 6, pp. 189 – 193, 2008.

[30] J. H. Holland, *Adaptation in Natural and Artificial Systems*. Ann Arbor: The University of Michigan Press, 1975.

[31] D. Park, A. Kandel, and G. Langholz, "Genetic-based New Fuzzy Reasoning Models with Application to Fuzzy Control," *IEEE Transactions on Systems, Man and Cybernetics*, vol. 24, no. 1, pp. 39–47, 1994.

[32] F. Herrera, M. Lozano, and A. M. Snchez, "A taxonomy for the crossover operator for real-coded genetic algorithms: An experimental study," *International Journal of Intelligent Systems*, vol. 18, no. 3, pp. 309–338, 2003.

[33] ——, "Hybrid crossover operators for real-coded genetic algorithms: an experimental study," *Soft Computing-A Fusion of Foundations, Methodologies and Applications*, vol. 9, no. 4, pp. 280 – 298, 2005.

[34] R. Hinterding, H. Gielewski, and T. Peachey, "The Nature of Mutation in Genetic Algorithms," in *Proceedings of the Sixth International Conference on Genetic Algorithms*. Citeseer, 1995, pp. 65–72.

[35] F. Herrera, M. Lozano, and J. Verdegay, "Tackling Real-Coded Genetic Algorithms: Operators and Tools for Behavioural Analysis," *Artificial Intelligence Review*, vol. 12, no. 4, pp. 265–319, 1998.

[36] sinalgo, "http://disco.ethz.ch/projects/sinalgo/index.html," 2010.

[37] NS2, "http://nsnam.isi.edu/nsnam/index.php/main_page," 2008.

2011 IEEE International Conference on Fuzzy Systems
June 27-30, 2011, Taipei, Taiwan

On Predicting Learning Styles in Conversational Intelligent Tutoring Systems using Fuzzy Classification Trees

Keeley Crockett, Annabel Latham, David Mclean, Zuhair Bandar, James O'Shea
The Intelligent Systems Group, School of Computing, Mathematics and Digital Technology,
The Manchester Metropolitan University, Chester Street,
Manchester, M1 5GD, UK
K.Crockett@mmu.ac.uk

Abstract— **Oscar is a conversational intelligent tutoring system (CITS) which dynamically predicts and adapts to a student's learning style throughout the tutoring conversation. Oscar aims to mimic a human tutor to improve the effectiveness of the learning experience by leading a natural language tutorial and adapting material to suit an individual's learning style. Prediction of learning style is undertaken through capturing independent variables during the conversation. The variable with the highest value determines the individuals learning style. This paper proposes a new method which uses a fuzzy classification tree to build a fuzzy predictive model using these variables which are captured through natural language dialogue Experiments have been undertaken on two of the learning style dimensions: perception (sensory-intuitive) and understanding (sequential-global). Early results show the model has substantially increased the predictive accuracy of the Oscar CITS and discovered some interesting relationships amongst these variables.**

Keywords- Fuzzy classification tree, conversational agent; intelligent tutoring systems;

I. INTRODUCTION

Intelligent Tutoring Systems (ITS) are computer-based educational systems which employ intelligent technologies to provide individualised instruction [1]. In order to personailise the students learning experience, a number of factors can be used such as user affect, such as emotion [2], personality [3] and learning style [4]. Learning styles recognise that people have instructional preferences in how they absorb and process information. One of the most established learning style models is known as the Index of Learning Styles model (ILSM). ILSM was proposed by Felder and Silverman [5] to describe the learning styles in engineering education and suggested different teaching styles to address learners' needs. Each person has their own learning strategy for learning specific subject matter in a particular context [5]. If the teacher knows the students' learning styles then delivery of a subject can be adapted.

Existing ITS capture learning styles using a formal questionnaire [6], [7] or by analysing a student's behaviour within the ITS [8], [9]. The main problem with questionnaires is that they are time consuming and onerous and people do not tend to complete them accurately. Predicting learning style using a history of student behaviour means adaptation is delayed until several modules have been completed, and also a student's learning style may change over time or for different topics. EDUCE [10] and WELSA [11] both estimate learning style dynamically for curriculum sequencing, but do not include a conversational interface or incorporate other intelligent tutoring technologies.

Most ITS do not have a natural language interface but rely instead on navigation around the tutoring material through buttons and hyperlinks. This is due to the fact that conversational interfaces are complex to develop [6..11]. However, to adequately mimic a human tutor, an ITS should support the construction of knowledge through discussion [12]. One way of providing a natural language interface is through the incorporation of a Conversational Agent (CA) [13]. A CA uses natural language dialogue to communicate with users [14] and will have the ability to reason and pursue a course of action based on its interactions with humans and other agents. Some work has been done in incorporating CAs with ITS but this has been to help the learning management system, rather than undertake a tutorial with a learner [15,16]. AutoTutor [16] is a conversational intelligent tutoring system (CITS), which helps students construct knowledge about computer literacy and physics. CIRCSIM-tutor [16] engages students in discussion to solve physiology problems. Discussions that take place in either system do not consider learning styles during tutoring. Knowledge of an individual's learning style is essential when developing a CITS which can adapt its teaching style to individual learner preferences [12].

Oscar is a CITS that dynamically predicts learning style throughout the tutoring conversation and adapt its intelligent tutoring style to suit an individual's learning style [12]. Prediction of learning style occurs during the conversational tutoring session by capturing the values independent variables. The variable with the highest value determines the individuals learning style in accordance with the Index of Learning Styles Model (ILSM) [5]. The current method has had some degrees of success but its fundamental weakness is that it does not consider the relationships between these variables in predicting the learning style.

Fuzzy models have been developed for educational learning since 1996 when Hawkes and Derry [18] proposed

978-1-4244-7316-8/11/$26.00 ©2011 IEEE

a model that captured the way in which human tutor's evaluated borderline tutoring decisions in accordance with student behavior. One of the most recent areas of research is in making learning object recommendations for a specific domain based on an individual's learning style [19..22]. In [20] a fuzzy inference system comprising of six rules is applied to a recommender system in order to assign a student a suitable learning object in the field of computer networks. Cabada et al [21] used a combined fuzzy-neuro approach to recommend learning objects. The approach learns student behavior based upon types of tutoring materials students have previously used and their learning styles. In [22] a fuzzy-neuro approach was used to infer the learning characteristics of a student in an interactive learning environment. This method was used to obtain an optimal learning path both instructor and learner through the tutoring domain. Whilst each of the above systems have shown degrees of success using small experimental groups none attempt to predict the learning style through obtaining variables captured through natural language dialogue which occurs naturally through a tutoring conversation.

This paper proposes an approach to modeling these variables using fuzzy classification trees in order to improve the predictive accuracy. The concepts of fuzzy decision trees are well established [23..27].The main features of fuzzy trees, compared with crisp trees, are the gradual transitions that exist between continuous attribute values and the inference process that allows all branches within the tree to be fired to some degree. Existing methodologies for creating fuzzy trees present different approaches on how to determine fuzzy regions at nodes within the tree [28] and the fuzzy inference strategy which is applied [23-24]. In this paper, a modified version of the Fuzzy Inference Algorithm (FIA) [24] is used to produce a fuzzy predictive model using variables extracted through natural language dialogue during the tutoring conversation.

The paper is organized as follows: Section II describes Oscar, the conversational intelligent tutoring system used within this paper. Section III describes the modified FIA and how it has been applied to the learner's data set. Section IV explains the experimental process which was undertaken on two of the learners dimensions: perception (sensory-intuitive) and understanding (sequential-global) [5]. Finally section V presents the results and discussion.

II. OSCAR: A CONVERSATIONAL INTELLIGENT TUTORING SYSTEM

The Oscar CITS is a conversational intelligent tutoring system designed to dynamically predict a student's learning style during a tutoring conversation, and to adapt the tutoring style to suit the individual learner [17]. Oscar's pedagogical aim is to provide the learner with the most appropriate learning material for their learning style leading to a more effective learning experience and a deeper understanding of the topic. Rather than being designed with the purpose of picking up learning styles (such as [5]), the Oscar CITS attempts to mimic a human tutor by leading a two-way discussion and using cues from the student dialogue and behaviour to predict and adapt to their learning style. Oscar's natural dialogue interface and classroom tutorial style are intuitive to learners, enabling them to draw on experience to feel more comfortable and confident in using the CITS. Oscar CITS is a personalised tutor which can answer questions, provide hints and assistance using natural dialogue, and which favours learning material to suit each individual's learning style. The Oscar CITS offers 24-hour personalised learning support at a fixed cost. Oscar's intelligent approach includes presenting learning material in the sequence and style most suited to the individual's learning style (curriculum sequencing [15]), analysing and giving feedback on incomplete and erroneous solutions (intelligent solution analysis [29]) and giving intelligent hints and discussing questions (problem solving support [30]). By combining all three intelligent technologies with a conversational interface, Oscar's intelligent support aims to build the confidence of the learner and improve motivation and deep understanding of the subject.

A. The Index of Learning Styles

In their Index of Learning Styles (ILS) model [5], Felder and Silverman described the learning styles in engineering education and suggested different teaching styles to address learners' needs. The ILS model defines four separate dimensions of preferred learning style, each relating to a step in the process of receiving and processing information as follows:

- *Perception* – this dimension categorises learners as *sensory* (SNS) or *intuitive* (INT) and relates to the type of information a student prefers to perceive (e.g. external, by observation (sensory) or internal, by speculation (intuitive)).
- *Input* – this dimension classes learners as *visual* or *verbal* by considering the way in which learners prefer to receive external information (e.g. by looking at diagrams (visual) or by listening to explanations (verbal)).
- *Processing* – this dimension groups learners as *active* or *reflective* according to the way perceived information is converted into knowledge (e.g. by the active discussion (active) or introspective consideration (reflective) of a topic).
- *Understanding* – this dimension categorises learners as *sequential* (SEQ) or *global* (GLO) depending on the way they progress towards understanding (e.g. by continual steps (sequential) or holistically in large jumps (global)).

Learning styles are central to the decision making within Oscar CITS. Following an initial study, a subset of the best ILS predictor questions for each learning style dimension was identified [31] and this was used to generate tutoring material for each learning style within Oscar.

For the purpose of this work, a conversational tutorial on structured query language (SQL) was developed. The target audience for the pilot study would be undergraduate computing students, for whom a Databases course including SQL is compulsory. Tutoring revision scenarios were designed based around the syllabus and the database

lecturers' experience of revision tutorials. Each revision question was mapped to the ILS model using the model's descriptions of indicative behaviour, such as a preference for theoretical questions.

B. Prediction and Adaptation

The Oscar CITS aims to mimic a human tutor by using knowledge of learning styles and cues from student behaviour to predict individual learning style. During a tutorial, information is recorded about learner behaviours and then used to predict learning style. The experiments reported in [12, 31] compared the results of the formal ILS questionnaire to student behaviour to compute an accuracy of prediction based on 17 hypotheses. Three of the 17 hypotheses are shown as an example below.

H1: a student's learning path through the tutorial is indicative of learning style.

H2: choosing to be guided through a process (or not) is indicative of learning style.

H3: The amount of discussion a student enters into with the tutor is indicative of learning style.

The variables with the best accuracy for an ILS dimension are then used to predict student learning style and adapt the tutoring style accordingly.

Oscar CITS uses an algorithm to determine the best adaptation for each tutoring question based on the student learning style strengths. The algorithm is fairly complex in that it considers all four learning style dimensions. Rather than simply adapting to the strongest student learning style, the algorithm separately considers each question and its ability to adapt for certain learning styles as well as a student's learning styles. This allows for tutorial questions where it is not possible to include adaptive learning material for all learning styles, as occur in real life. The development of the adaptive Oscar CITS is reported in [17].

Figure 1 shows two examples of logic rules used by the system to increment learning style values during tutoring. Learning styles are held in eight values within the student model, representing each pole of the four dimensions (perception (sensory-intuitive), input (visual-verbal), processing (active-reflective) and understanding (sequential-global) [17].

1. Example rule to test whether presenting information visually helps the student's information perception:

```
IF    student does not know the answer
THEN show student image/diagram;
IF    student shown image/diagram
AND   student gives correct answer
THEN increase VISUAL;
```

2. Example rule to test how comfortable the student is with words and with detail:

```
IF    answer is given in the explanation text
AND   student does not know the answer
THEN increase INTUITOR
AND   increase VISUAL;
```

Fig. 1. Example of logic rules used to adjust student learning style based on tutoring conversation

C. Conversational Agent and Dialogue Design

Oscar was developed using a type of conversational agent (CA) known as a goal-orientated conversational agent (GO-CA) [13]. GO-CA's are a specific family of conversational agents that are designed to converse with humans through the use of natural language dialogue to achieve a specific task. In this case to act as an intelligent tutor to guide the learner through the tutorial based upon their learning style. The GO-CA used in this work utilised pattern matching algorithms to capture the values of specific attributes through dialogue interaction with a user. This is achieved through the use of scripts which contain sets of rules about the domain (SQL) and a knowledge base to guide the conversation towards achieving a specific goal (Oscar adaptation rules). In the Oscar CITS, the dialogue for each tutorial was scripted using Convagent's GO-CA [19]. Overall, there were 38 contexts containing around 400 rules. The full architecture and methodology for developing Oscar CITS is described in [32]. Throughout tutoring, the CITS records and logs information about the behaviour of the student, such as timing of interactions, the number of words used, the number of times FAQs are asked and the type of tutor resource accessed. The tutoring conversation is also recorded, along with information about the student knowledge of the topic being discussed and the adaptation employed.

Figure 2 shows a screenshot of the Oscar CITS user interface showing a user interaction where the student is being asked to write an SQL query with the results limited by two values. Oscar is guiding the student through each step of writing the query. The chat window shows the student's previous utterance, which is incorrect, and Oscar's response, followed by a reminder of the question. An image relevant to the stage of the query is shown to the right, and movies pop up in a new window if appropriate. Oscar's response helps the student by hinting at the solution by recommending an approach to writing the WHERE clause, rather than simply showing the answer. By adopting the constructivist style of teaching like human tutors, Oscar endeavors to provoke a deeper understanding of a topic.

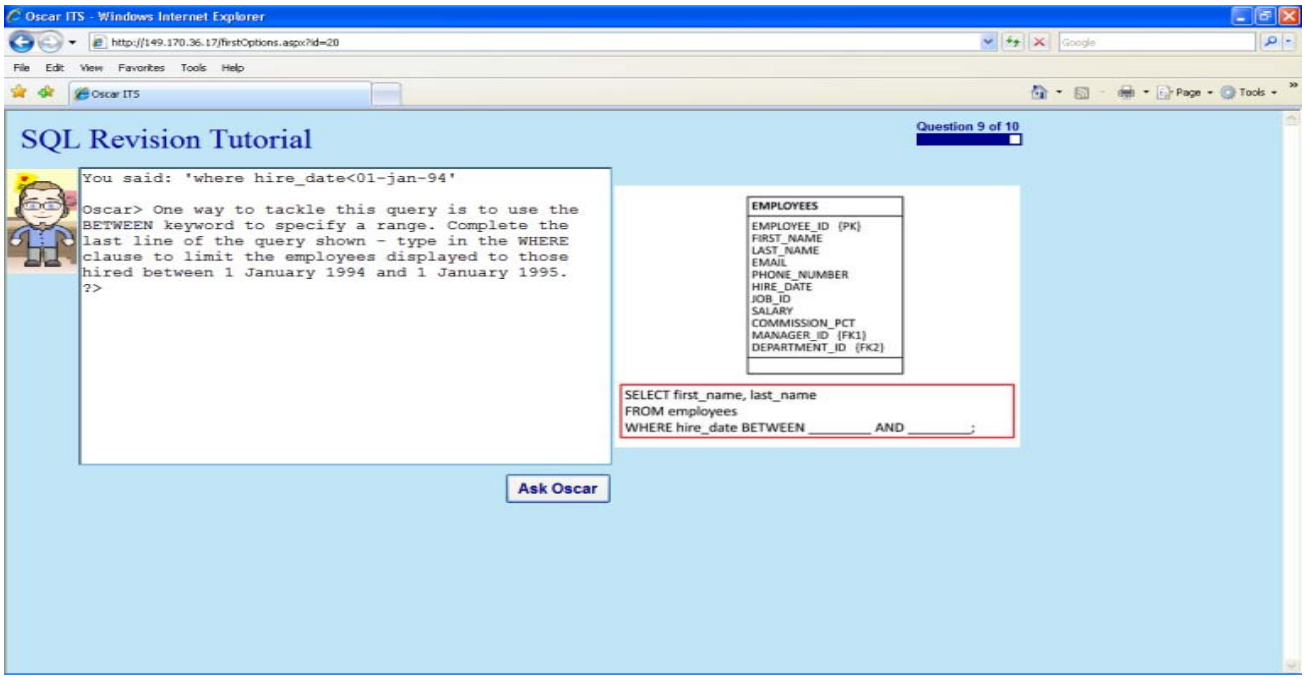

Fig. 2. Oscar CITS

D. *Example Learner Dialogue*

Table I shows part of a student's tutoring dialogue logged during experiments used for this work. In utterance 33, Oscar continues a question about data types. The student gives the wrong data type in utterance 34, and next Oscar indicates that the answer is wrong and gives the student a second chance to answer in case of spelling errors, repeating the question. In utterance 36 the student tries again, still with the wrong answer. Oscar gives feedback that the answer is wrong (utterance 37), and helps by showing an image of the most common data types to see if the student is able to pick out the required answer. In this action, Oscar is helping the student learn by reminding them of the common data types and asking them to think about the correct data type rather than simply telling them the answer. In utterance 38 the student enters the correct data type, extended to include the decimal places, and Oscar then confirms that they have the right answer and repeats the solution to reinforce the knowledge.

TABLE I. EXAMPLE TUTORING DIALOGUE SNIPPET LOGGED DURING THE EXPERIMENT.

Utterance	Dialogue
33. Oscar>	Now, in our books table suppose we want to store the price of the book where the maximum price of a book is 99.99. What would be the datatype?
34. Student>	VARCHAR2
35. Oscar>	I'm sorry, that's wrong. Check your spelling and try again - type in the datatype for book price (with a maximum of 99.99).
36. Student>	VARCHAR2 MAX 99.99
37. Oscar>	That's still wrong. Take a look at the table of common datatypes - can you now type in the datatype for book-price where the maximum price is 99.99?
38. Student>	NUMBER(2,2)
39. Oscar>	That's correct - we need a datatype of NUMBER(2,2) in order to show the decimal point in book-price, with a maximum of 99.99.

III. GENERATING FUZZY CLASSIFICATION TREES

Previous work [23,24,28] has shown that the generation of a fuzzy classifier from crisp induced trees produces a generalized and robust rule set without the need for human expert intervention during the fuzzification process. For the purpose of this paper the fuzzy classification trees will be constructed using the FIA algorithm [24] which will now be briefly described. FIA is an algorithm designed to build fuzzy classification trees from raw datasets. One of the strengths of the algorithm is that no pre-fuzzification of the data is required. FIA provides a mechanism for the direct fuzzification of both discrete and continuous attributes and the ability to use any T-norm/ T-conorm pair for determining fuzzy inference

A. *Fuzzy Inference Algorithm (FIA)*

A high level description of the stages of FIA is as follows:

1. Generate a crisp classification decision tree using pre-defined pruning criteria (in this work Quinlan's C4.5 decision tree algorithm was used [32]).
2. For each node, *i* within the tree identify whether discrete or continuous attributes and define an opposing membership function pair. Each membership function will have an associated domain (dm_i, dn_i) whose scope is determined by the attribute at that specific branch which is defined as

$$dm_i = dt_i - n_j\sigma_i \quad \text{and} \quad dn_i = dt_i + n_{j+1}\sigma_i \qquad (1)$$

Where σ_i is the standard deviation of attribute *i*,

n is a real number $n \rightarrow [0,5]$ used to extend fuzziness

across the domain of the attribute,

dt is the decision threshold and

dm and *dn* are the lower and upper bounds respectively of membership function *i*.

3. Select T-norm pair with inference strategy.

Let a set of data ***S*** consist of ***i***-attributes $\{A_1,A_2....A_i\}$ of domain D which are used to describe a single object. The process of learning from ***S*** involves a transformation function ***F*** which accepts as input ***S*** and produces a defuzzified outcome ***O***, which is a mapping

$$\boldsymbol{F(S) \rightarrow O} \tag{2}$$

Applying an inference technique onto an existing tree consisting of ***x*** branches involves the combination of ***V*** membership function values $\{\mu_1, \mu_2,...\mu_v\}$ of all root to leaf node paths. Let ***T*** be a set of all possible outcomes $\{t_1,t_2,..t_y\}$ defined from an existing crisp tree where ***y*** is the total number of outcomes. Fuzzy inference of ***S*** will involve an inference mechanism, ***IM*** which consists of an intersection function $f\wedge$, which takes in ***V*** and a t-norm ***TMin*** , which produces a set of minimum outcomes $\{TMin_1,TMin_2.....T.Min_j\}$ where *j* is the number of leaf nodes, and a union function $f\vee$, which combines output from $f\wedge$ to produce a maximum membership grade ***O***. Let $f\wedge, f\vee$ $\boldsymbol{O} \in \{0.0,1\}$ consisting of real numbers, $\Re$.

i. Applying the fuzzy intersection function, $f\wedge$

This involves combining membership grades down all paths, from root to leaves within the tree.

$$f\wedge\ (\{\mu_1, \mu_2,...\mu_v\}) \rightarrow \boldsymbol{TMin}\ \{TMin_1,TMin_2.....T.Min_j\} \tag{3}$$

ii. Apply possibilistic strength of leaf node

The possibilistic strength of a leaf node represents the possibility that an example reaching a leaf node will have the same outcome as the leaf. Let ***P*** be a set of leaf possibilities $\{p_1,p_2...p_y\}$ where ***y*** is the total number of leaf outcomes then

$$f\wedge\ (\{\mu_1, \mu_2,...\mu_v\}) \rightarrow TMin \{(TMin_1*p_1),(TMin_2*p_2).....(TMin_j*p_y)\} \tag{4}$$

Each leaf possibility p_y is applied to the corresponding membership grade at each leaf node $TMin_j$, after the intersection operation has been applied to combine grades of membership down one tree path.

iii. Applying fuzzy union function $f\vee$

The fuzzy union operator is applied in-order to combine the membership grades from all leaf nodes in order to produce a representative final grade of membership.

$$f\vee\ (\{(TMin_1*p_1),(TMin_2*p_2).....(TMin_j*p_y)\rightarrow \boldsymbol{O} \tag{5}$$

O is the fuzzy singleton used to determine the success of correct classification having taken place for ***S***.

4. Interpret and implement the tree as a set of Fuzzy IF-THEN rules. Each rule within the classifier may be defined as:

$$R\,j_1..j_n : IF\ x_1\ is\ A_{1j1}\ .....\ AND\ X_n\ is\ A_{njn}$$
$$THEN\quad y\ is\ b_{\,j1.jn},$$
$$Where\ \ j1 = 1,2,...K_1;\quad jn = 1,2,...,Kn \tag{6}$$

$R\,j_1..j_n$ is the label of each fuzzy if-then rule,
$b_{\,j1.jn}$, is the consequent real number and
K is the number of fuzzy sub-spaces.

5. Optimize membership function and inference weightings (if applicable)

A full description of the original FIA can be found in [24].

B. Defuzzification

The unique characteristics of a specific classification problem will often determine the defuzzification strategy used. The experiments in this paper have been undertaken using discrete outcome data set. In this instance the fuzzy singleton is first used to construct the consequence part of the rule after the min intersection operator has been applied. Each consequence is then combined using the max fuzzy union operator to produce a real valued outcome.

IV. GENERATING A FUZZY DECISION TREE FROM CONVERSATIONAL TUTORIALS

A. Data Set

75 undergraduate university students who had previous experience of SQL completed the formal ILS questionnaire and the Oscar CITS SQL Revision tutorial. During the tutorial their behavior and test scores were logged. Information relevant to the prediction of learning styles was captured in 41 different variables during the tutorial. The value of each variable in table II was determined by a series of logic rules (see Section II, B) being fired during the tutoring conversation. Table II shows all 41 variables within the data set that were captured. Each variable is associated with predicting at least one learning style dimension. For example, one variable, *no_interactions*, captured the number of conversational interactions the user had with Oscar during the session. The variables *Q5_choice* and *Q5steps2* captured the student's approach to writing queries (i.e. whether they try all at once or want to try one step at a time). These two variables along with *Q9_choice* and *Q9_steps2* are indicative of the SEQUENTIAL/GLOBAL and SENSORY/INTUTIVE learning dimensions. Most learning

style dimensions had an approximately even split of students, apart from the Visual/Verbal dimension where most students were Visual. This was not unexpected and in accordance with the ILS model [5] for students studying science and engineering based subjects.

TABLE II. OSCAR DATA SET DESCRIPTION

Variable name	Type	Values / Range	Mean	Standard Deviation
Rules_VIS	Numeric	1 to 11	6.733	2.767
Rules_VRB	Numeric	0 to 11	3.400	2.427
Rules3_VIS	Numeric	0 to 16	4.413	2.881
Rules3_VRB	Numeric	0 to 12	3.053	2.117
Rules_SEQ	Numeric	1 to 11	6.200	2.307
Rules_GLO	Numeric	1 to 10	4.933	1.848
Rules3_SEQ	Numeric	0 to 10	6.067	2.662
Rules3_GLO	Numeric	0 to 8	4.347	1.573
Q5_choice	Discrete	4		
Q5_steps2	Discrete	3		
Q9_choice	Discrete	4		
Q9_steps2	Discrete	3		
Q4_detail	Discrete	4		
Q_prac	Numeric	0.2 to 1	0.673	0.174
Q_thep	Numeric	0.125 to1	0.678	0.183
Keywd_eg	Numeric	0 to 3	0.04	0.346
Keywd_show	Numeric	0 to 3	0.627	0.749
Keywd_see	Numeric	0 to 1	0.013	0.115
Keywd_tell	Numeric	0 to 2	0.04	0.257
Keywd_picture	Numeric	0 to 1	0.013	0.115
Keywd_discuss	Numeric	0 to 2	0.027	0.231
Rules_ACT	Numeric	0 to 11	5.52	2.549
Rules_REF	Numeric	0 to 11	3.013	2.883
Rules3_ACT	Numeric	0 to 10	3.907	1.62
Rules3_REF	Numeric	0 to 3	3.267	0.6
Rules_SNS	Numeric	0 to 11	4.72	3.451
Rules_INT	Numeric	0 to 11	4.52	2.811
Rules3_SNS	Numeric	0 to 4	1.307	0.822
Rules3_INT	Numeric	1 to 14	4.293	2.358
MCQ_theory	Numeric	0 to 1	0.524	0.37
MCQ_pract	Numeric	0 to 1	0.532	0.373
Duration	Numeric	845 to 14527	444.68	1637.56
Mean_Duration	Discrete	2		
Time_per_int	Numeric	18 to 415	52.906	45.906
Mean_time_int	Discrete	2		
Read_time	Numeric	4.305 to 102.303	12.33	11.295
MeanRdTime	Discrete	2		
Wordcount	Numeric	67 to 352	164.022	68.67
Mean_WC	Discrete	2		
No_interactions	Numeric	24 to 84	48.84	9.895
Mean_interact	Discrete	2		
Class	Discrete	2		

B. Experimental Methodology

For each experiment set, stratified 10-fold cross validation was used. For the purpose of this work, experiments were undertaken on two of the learning style dimensions: perception (sensory-intuitive) and understanding (sequential-global). Following the FIA methodology, first crisp decision trees were created from the data set using the statistical chi-square pruning technique with significance levels of 0.1% in order to produced highly optimized crisp trees which would allow good generalization to take place. Figure 3 shows a sample crisp decision tree for the sequential-global learning dimension. Table III, provides a high level description of variables used within the tree in Figure 3.

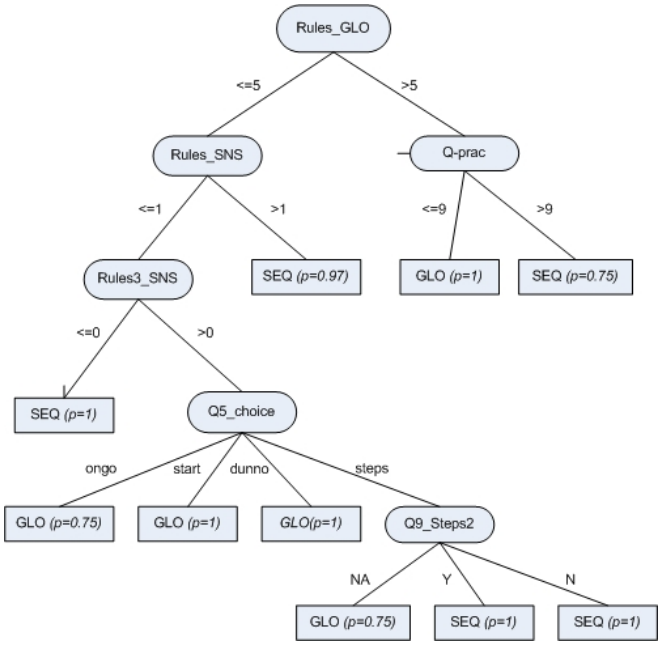

Fig. 3. Crisp tree representing sequential-global dimension

TABLE III. VARIABLE DESCRIPTION

Variable	Description
Rules_GLO	The number of user interactions which mapped to Global logic rules that fired during the tutoring conversation.
Rules_SNS	The number of user interactions which mapped to Sensory logic rules that fired during the tutoring conversation.
Rules3_SNS	The number of Sensory rules that fired during user interaction AND whether the student got the answer right directly afterwards.
Q5_choice	Records the approach taken by the student in the first attempt in answering a complex query (Q5).
Q9_Steps2	Records a change in approach taken by the student during their answer to complex query Q9.
Q_prac	Records the number of correct practical based questions during the tutorial.

Fuzzy membership functions were generated for both discrete and continuous attributes. Initial membership functions were selected to be equivalent to crisp sets with the initial fuzzy classifier system becoming an alternative representation of the decision tree. For experiments reported in this paper the amount of fuzzification either side of each tree node was increased linearly. Figure 4 shows an example

membership function generated from the training data for the attribute RulesSen.

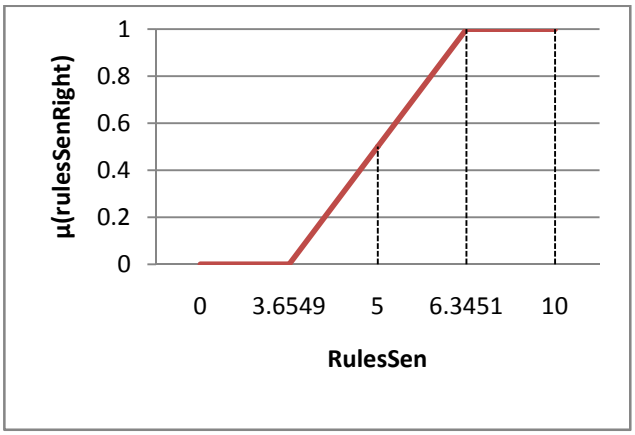

Fig. 4. μ(rulesSenRight)

Using a one-to-one mapping, each tree was then transformed into a set of Fuzzy IF-THEN rules. For example, the tree in figure 3 would be transformed into 10 rules. Zadeh's Min-Max inference technique [33] was to combine grades of memberships of all rules within the fuzzy classification trees. In each experiment, results were generated using 10-fold cross validation. The classification accuracy of the fuzzy classification tree can be defined as

$$F_1 = \frac{\sum_{i=1}^{i=n} \frac{\text{Number of Correctly Classified Records in Class } i}{\text{Total Number of Records in Class } i}}{n} \quad (7)$$

where i = Class i, and n= Number of classes.

Accuracy was measured by comparing the system predicted learning style to the ILS questionnaire result of the same participant.

V. Results and Discussion

Tables IV and V present the results of the sequential-global and sensory-intuitive dimensions respectively using three methods. In each table the average results of 10 fold cross validation are shown. For the sequential-global dimension (Table IV), columns %AVG SEQ and %AVG GLO show the %accuracy of predicting sequential learners and global learners respectively, with the overall prediction accuracy for the sequential-global learning dimension being shown in the %AVG SEQ/GLO column. Table V presents the results for the sensory-intuitive dimension in a similar way. In tables IV and V; OneVar gives the classification accuracy of using one variable predictor to classify the learning style; DT(C4.5) provides the classification accuracy of a crisp decision tree model where multiple variables are combined based upon their effect on the outcome; Fuzzy DT show the results obtained by the fuzzy classification trees generated by FIA.

TABLE IV Sequential - Global

Method	%AVG SEQ	% AVG GLO	% AVG SEQ/GLO
OneVar (Q5choice)	70	59	65
DT (C4.5)	80	70	76
Fuzzy DT	93	83	88

TABLE V Sensory-Intuitive

Method	%AVG SEN	% AVG INT	% AVG SEN/INT
OneVar(Q5choice)	70	59	65
DT (C4.5)	84	80	82
Fuzzy DT	98	73	86

The results in tables IV and V show that in the case of both learning dimensions, when only one variable is used (OneVar); the same variable (Q5choice) was identified as being the most significant in terms of prediction accuracy. An initial observation of the results shows that correlation does exist between the two learning dimensions as sequential people like to learn step by step and sensory people like to go slowly and carefully, whereas global people like to jump straight in and intuitive people are fast and careless. The results in Tables IV for OneVar show that 70% of students who choose to answer the Question 9 query in the tutorial, one step at a time are Sequential learners. Using this variable (Q5choice) the Oscar CITS would predict that students in this group are Sequential learners and be accurate 70% of the time.

The results of inducing fuzzy classification trees yielded some interesting results with regards to the models that were produced. In modeling the sequential-global dimension, the attribute Rules_GLO (representing the number of global related rules that had fired during the conversation) was seen to be the most significant detector of learning style. However, what was surprising was the number of sensory attributes (Rules_SNS and Rules3_SNS) that were also included in the model. This again supported the correlation between sequential-global and sensory-intuitive dimensions.

The results in Tables IV and V also show that combining the attributes from the dataset generates a model which can be used to improve the prediction accuracy of the learner through the conversational agent tutorial. For the sequential-global dimension, the fuzzy classification trees produced gave a 23% improvement over prediction using one variable and a 12% increase over the crisp C4.5 decision tree. For the sensory–intuitive dimension, a 21% improvement was obtained over the one variable predictor and a 4% improvement over the crisp C4.5 decision tree.

VI. CONCLUSION

This paper proposes a new method which uses fuzzy classification trees to build a fuzzy predictive model in order to predict a students learning style through a conversational intelligent tutoring system. Using a dataset of 41 independent variables captured during the tutorial, experiments were carried out on two of the learning style dimensions: perception (sensory-intuitive) and understanding (sequential-global). The results have shown that the fuzzy predictive model has substantially increased the predictive accuracy of the Oscar CITS compared with the one variable predictor currently used within the system. Further work will incorporate the fuzzy predictive model into the adaptive Oscar CITS in order to provide an improved and more personalized learning experience.

REFERENCES

[1] Brusilovsky, P., Peylo, C.: Adaptive and Intelligent Web-based Educational Systems. Int.J. Artificial Intelligence in Education 13, 2003, pp.156–169.

[2] Ammar, M.B., Neji, M., Alimi, A.M., Gouarderes, G.: The Affective Tutoring System. Expert Systems with Applications 37, 2010, pp.3013–3023.

[3] Leontidis, M., Halatsis, C.: Integrating Learning Styles and Personality Traits into an Affective Model to Support Learner's Learning. In: Spaniol, M., et al. (eds.) Advances in Web Based Learning – ICWL 2009. LNCS, vol. 5686, 2009, pp. 225–34.

[4] Papanikolaou, K.A., Grigoriadou, M., Kornilakis, H., Magoulas, G.D.: Personalizing the Interaction in a Web-based Educational Hypermedia System: the case of INSPIRE. User Modeling and User-Adapted Interaction 13, 2003, pp.213–267.

[5] Felder, R., Silverman, L.K.: Learning and Teaching Styles in Engineering Education. J. Engineering Education 78(7), 1988, pp.674–681.

[6] Wang, H.C., Li, T.Y., Chang, C.Y.: A web-based tutoring system with styles-matching strategy for spatial geometric transformation. Interacting with Computers 18, 2006, pp.331–355.

[7] Cha, H.J., Kim, Y.S., Park, S.H., Yoon, T.B., Jung, Y.M., Lee, J.H.: Learning styles diagnosis based on user interface behaviours for the customization of learning interfaces in an intelligent tutoring system. In: Ikeda, M., Ashley, K.D., Chan, T.-W. (eds.) LNCS, vol. 4053, 2006, pp. 513–524.

[8] Spallek, H.: Adaptive Hypermedia: A New Paradigm for Educational Software. Advances in Dental Research 17(1), 2003, pp.38–42.

[9] Garcia, P., Amandi, A., Schiaffino, S., Campo, M.: Evaluating Bayesian networks' precision for detecting students' learning styles. Computers & Education 49, 2007, pp.794–808.

[10] Kelly, D., Tangney, B.: Adapting to intelligence profile in an adaptive educational system. Interacting with Computers 18, 2006, pp.385–409.

[11] Popescu, E.: An Artificial Intelligence Course Used to Investigate Students' Learning Style. In: Li, F., Zhao, J., Shih, T.K., Lau, R., Li, Q., McLeod, D. (eds.) LNCS, vol. 5145, 2008, pp. 122–131.

[12] Latham, A. Crockett, K. McLean, D, Edmonds, B. "Predicting Learning Styles in a Conversational Intelligent Tutoring System", in X. Luo et al (eds.), LNCS, vol. 6483, 2010, pp. 131-140.

[13] Crockett, K. Bandar, Z. O'Shea, J. Mclean, D. Goal Orientated Conversational Agents - the rocky road to commercialization. IEEE World Congress on Computational Intelligence, July 2010, pp.1820-1827.

[14] Crockett, K, O'Shea, J, Bandar, Z. Goal Orientated Conversational Agents: Applications to Benefit Society. Springer-Verlag, KES 2011, LNCS, 2011, in press.

[15] Weber, G., Brusilovsky, P.: ELM-ART: An adaptive versatile system for Web-based instruction Int. J. Artificial Intelligence in Education vol. 12(4), 2001, pp.351–384.

[16] Graesser, A., Chipman, P., Haynes, B.C., Olney, A.: AutoTutor: An Intelligent Tutoring System With Mixed-Initiative Dialogue. IEEE Trans. Education vol. 48(4), 2005, pp.612–618.

[17] Latham, A. Crockett, K, Mclean, D, Edmonds, B. Oscar: An Intelligent Adaptive Conversational Agent Tutoring System'. Springer-Verlag, KES 2011, LNCS, 2011, in press.

[18] Hawkes, L. Derry, S. Advances in local student modeling using informal fuzzy reasoning. International Journal of Human-Computer Studies, vol. 45(6), 1996, pp. 697-722.

[19] Xu, D., Wang, H., & Su., K. (2002). Intelligent student profiling with fuzzy models. In HICSS'02, 35th Annual Hawaii international conference on system sciences, vol. 3, 2002.

[20] Garcia-Valdez, M. Alanis, A. Parra, B. Fuzzy inference for Learning Object Recommendation, IEEE International Conference on Fuzzy Systems, 2010, pp.1-6.

[21] Cabada, R.Z.; Estrada, M.L.B.; Garcia, C.A.R.; A Fuzzy-Neural Network for Classifying Learning Styles in a Web 2.0 and Mobile Learning Environment, 2009 Latin American Web Congress (la-web 2009), 2009, pp.177-182.

[22] Fazlollahtabar H.,Mahdavi, I. User/tutor optimal learning path in e-learning using comprehensive neuro-fuzzy approach, Educational Research Review, vol.4(2), 2009, pp.142-155.

[23] Crockett, K. Bandar, Z., O'Shea, J, Fowdar, J. A fuzzy numeric inference strategy for classification and regression problems. KES Journal vol. 12(4), 2008, pp.255-269.

[24] Crockett, K., Bandar, Z., O'Shea, J. Mclean, D. On Constructing a Fuzzy Inference Framework using Crisp Decision Trees. Fuzzy Sets and Systems, vol. 157(21), 2006, pp.2809-2832.

[25] Marsala, C. Bouchon-Meunier, B. Ranking Attributes to Build Fuzzy Decision Trees: a Comparative Study of Measures. 2006 IEEE International Conference on Fuzzy Systems, 2006, pp.8436-8442.

[26] Chen, Yi-lai, Wang, T, Wang, B, Li, Z, A survey of fuzzy decision tree classifier, Fuzzy Information and Engineering, Springer Berlin Heidelberg, in co-publication with Fuzzy Information and Engineering Branch of the Operations Research Society of China, vol. 1(2), 2009, pp.149-159.

[27] Piero P. Bonissone, José Manuel Cadenas, M. Carmen Garrido, R. Andrés Díaz-Valladares: A fuzzy random forest. Int. J. Approx. Reasoning vol. 51(7), 2010, pp.729-747.

[28] Crockett, K. Bandar, Z. O'Shea, J. Fuzzification of Discrete Attributes From Financial Data in Fuzzy Classification Trees, IEEE International conference on Fuzzy Systems, South Korea, 2009, pp.1320-1325.

[29] Mitrovic, A.: An Intelligent SQL Tutor on the Web. Int. J. Artificial Intelligence in Education vol. 13, 2003, pp171–195.

[30] Melis, E., Andrès, E., Büdenbender, J., Frishauf, A., Goguadse, G., Libbrecht, P., Pollet, M., Ullrich, C.: ActiveMath: A web-based learning environment. Int. J. Artificial Intelligence in Education vol. 12(4), 2001, pp.385–407.

[31] Latham, A. Crockett, K. Mclean, D, Edmonds. B. Oscar: An Intelligent Conversational Agent Tutor to Estimate Learning Styles. IEEE World Congress on Computational Intelligence, July 2010, pp.2533-2540.

[32] Quinlan, J, R. C4.5: Programs for Machine Learning. Morgan Kaufmann Publishers, 1993.

[33] Zadeh, L. Knowledge Representation In Fuzzy Logic. In An Introduction To Fuzzy Logic Applications In Intelligent systems, eds. Yager, R and Zadeh, L, Kluwer Academic Publishers, 1992.

2011 IEEE International Conference on Fuzzy Systems
June 27-30, 2011, Taipei, Taiwan

Signal Transduction Ability Measurement of Signaling Pathways in Intracellular Communication via Fuzzy Method

Chia-Chou Wu and Bor-Sen Chen
Department of Electrical Engineering, Lab. of Control and Systems Biology
National Tsing Hua University
Hsinchu, Taiwan
d9761820@oz.nthu.edu.tw; bschen@ee.nthu.edu.tw

***Abstract*—Signal transduction plays an important role in biological organisms. Here, we proposed a method to access the information of the signal transduction ability of signal transduction pathway in the cells. Due to the nonlinear signal transduction pathway model, we have to solve the Hamilton-Jacobi inequalities (HJIs) to get the measurement. Instead of directly solving HJIs, fuzzy interpolation method was employed such that we can systematically measure signal transduction ability by solving the linear matrix inequalities (LMIs). The measurement will provide an insight to the characteristics of the signal transduction networks.**

Keywords-signal transduction ability, fuzzy interpolation, T-S fuzzy model, MAP kinase cascades, linear matrix inequalities (LMIs)

I. INTRODUCTION

Metabolic processes (homeostasis) [1], the growth and differentiation of tissues (endocrine signaling) [2], the synthesis and secretion of proteins (blood clotting, immune-responses) and the composition of intracellular and extracellular fluids (photoreception, olfaction) are all closely related to signaling pathways. It is apparent that signaling pathways are indispensable for life. In general, a signaling pathway is initiated by protein-protein interaction between ligands and receptors. Conformation changes of a receptor usually occurs when a ligand binds to its specific receptor. This change ultimately induces specific cellular responses. Such converting processes from ligand binding to specific cellular response are termed as signal transductions. On molecular level, signaling pathways involve production or degradation of substances, molecular modification and activation or inhibition of chemical reaction. Thus there are many researches on the signaling pathways have focused on signaling molecules, cell-surface receptors, or the second messengers. Besides mass transferring, signaling pathways can be viewed as the information processing and transferring systems [3]. There are also many researches on the properties of signaling pathways, such as amplification [1], specificity, adaption, ultrasensitivity [4], oscillation [4], or synchronization. In this paper, we investigated the amplification of signaling pathways.

Signaling pathways need an amplification mechanism to reduce expense of signaling molecules and to respond as soon as possible. From the viewpoint of energy expedition, signal amplification can effectively reduce the initial key substances and can cause significant effects. Also, signaling pathways are responsible for the responses to the environmental variation that means the response should be as soon as possible if some deleterious stress was presented to organisms. There are many researches indicated the importance of signal amplification as well as the functional role of signal amplification. In osmo-adaptation in yeast under osmotic stress, Klipp and et al. provided an integrated mathematical model of the signaling pathway which indicated the relationship between rate constants of kinases and phosphatases and signal amplification [5]. In liver glycogenolysis and release of glucose, 10^{-10}M epinephrine in blood can generate an intracellular cAMP concentration of 10^{-6}M, an amplification of 10^{4} [6].

In electrical engineering, there are several electrical components having the property of signal amplification, such as transistors. The analysis of amplification property of those gadgets had been done. The same analysis may be performed on the amplification property of a signaling pathway [7]. However, because of nonlinearity of signaling pathways, knowledge about the systematic properties of signaling pathways is still limited and incomplete. The interpretation of experimental data of signaling pathway is still context and knowledge-dependent. In this study, the signaling pathway is studied from the dynamic system perspective for which a signal transduction ability measurement is proposed based on signal and system theory from the systematic point of view. It is according to the ratio of output to input signal energy of the studied signaling pathway. This measurement is only dependent on the system characteristics of the studied signaling pathway.

Nevertheless, the proposed measurement scheme for nonlinear signaling pathways needs to solve the corresponding nonlinear Hamilton-Jacobi inequalities (HJIs). At present, we still have no analytic or numerical solution for HJIs, except some simple cases. Recently, Takagi-Sugeno (T-S) fuzzy systems have efficiently interpolated several local linear systems via fuzzy bases to approximate a nonlinear system [8].

978-1-4244-7316-8/11/$26.00 ©2011 IEEE

Then the nonlinear signal transduction ability measurement problem can be solved via a set of linear matrix inequalities (LMIs) based on a set of fuzzy local linear signaling systems, which could be easily solved via LMI toolbox in Matlab® [9]. Based on fuzzy system theory and signal transmission method, the transduction ability of nonlinear signal transduction pathway could be investigated from these local linear signal transduction pathways. In this situation, more biological transduction insight can be investigated from linear signal system point of view. In near future, the transduction ability measurement may be as the characterization of the signal transmission systems for biotechnological, therapeutic applications and development of drug design.

The following sections include description of the generalized nonlinear signal transduction model, proposed measurement of signal transduction ability, fuzzy approximation of the nonlinear signal transduction model, and simulation example of MAP kinase and JAK/STAT signaling pathways, which are widely involved in eukaryotic signal transduction of cellular growth and differentiation and immune-responses respectively.

II. Methods And Results

A. Dynamic model of signaling pathways

Mathematical modeling for metabolic networks has been studied extensively and is useful for describing experimental data, deducing regulatory principle and understanding more complex dynamic phenomena such as oscillation. However, in modeling of signaling pathways, there are few examples have been studied since no available experimental data. According to the structure of signaling pathways which is consisted of consecutive activations and deactivations of proteins, we still can model the signaling pathways as series of chemical reactions. That means the signaling pathways can be modeled by a system of rate equations. The choice of the expressions for the rates is a matter of the elaborateness of experimental knowledge and of modeling taste. Linear and bilinear expressions or Michaelis-Menten kinetics have been used to model the signaling pathway [3]. A ubiquitous signaling pathway, mitogen-activated protein (MAP) kinase cascades, which regulate fundamental cellular functions including cell growth and death, differentiation, transformation and motility, is used here to demonstrate the proposed measurement scheme. A general scheme of a MAP kinase cascade (Fig.1) consists of general levels (three or more), where the activated kinase at

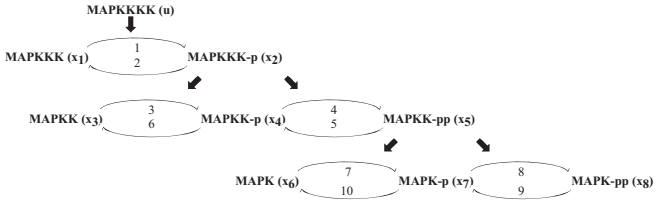

Figure 1. The general scheme of mitogen-activated protein (MAP) kinase cascade.

each level phosphorylates the kinase for the next level. The MAP kinase (MAPK) is at the terminal level of the whole cascade. It is activated by MAPK kinase (MAPKK), which is activated by MAPKK kinase (MAPKKK). Those sequential phosphorylations can be referred as activation of the signaling pathway. Dephosphorlyation of those kinases is thought to inactivate the signaling pathway. At each level, protein phosphatases can inactivate the corresponding kinase. The dynamics of a MAP kinase cascade can be represented by the following ODE system.

$$\begin{aligned}
\frac{d}{dt}MAPKKK &= -v_1 + v_2 \\
\frac{d}{dt}MAPKKKP &= v_1 - v_2 \\
\frac{d}{dt}MAPKK &= -v_3 + v_6 \\
\frac{d}{dt}MAPKKP &= v_3 - v_6 - v_4 + v_5 \\
\frac{d}{dt}MAPKKP_2 &= v_4 - v_5 \\
\frac{d}{dt}MAPK &= -v_7 + v_{10} \\
\frac{d}{dt}MAPKP &= v_7 - v_{10} - v_8 + v_9 \\
\frac{d}{dt}MAPKP_2 &= v_8 - v_9
\end{aligned} \tag{1}$$

where $v_i, i = 1,2,\ldots,10$ are reaction rates. The assumed values for the constants and rate equations are listed in Table 1.

TABLE I. Rate equations and parameters' values of the MAP kinase cascade model.

Reaction number	Rate equation	Constant
v_1	$\frac{k_1 x_1 u}{K_1 + x_1}$	$k_1 = 0.025, K_1 = 15$
v_2	$\frac{k_2 x_2}{K_2 + x_2}$	$k_2 = 0.25, K_2 = 8$
v_3	$\frac{k_3 x_2 x_3}{K_3 + x_3}$	$k_3 = 0.025, K_3 = 15$
v_4	$\frac{k_4 x_2 x_4}{K_4 + x_4}$	$k_4 = 0.025, K_4 = 15$
v_5	$\frac{k_5 x_5}{K_5 + x_5}$	$k_5 = 0.75, K_5 = 15$
v_6	$\frac{k_6 x_4}{K_6 + x_4}$	$k_6 = 0.75, K_6 = 15$
v_7	$\frac{k_7 x_5 x_6}{K_7 + x_6}$	$k_7 = 0.025, K_7 = 15$
v_8	$\frac{k_8 x_5 x_7}{K_8 + x_7}$	$k_8 = 0.025, K_8 = 15$
v_9	$\frac{k_9 x_8}{K_9 + x_8}$	$k_9 = 0.5, K_9 = 15$
v_{10}	$\frac{k_{10} x_7}{K_{10} + x_7}$	$k_{10} = 0.5, K_{10} = 15$

In general, the scheme of a signaling cascade can be represented by the following nonlinear dynamic system:

$$\begin{aligned} \dot{x} &= f(x) + g(x) \cdot u \\ y &= C \cdot x \end{aligned} \tag{2}$$

where the vector $x = \begin{bmatrix} x_1 & \cdots & x_n \end{bmatrix}^T$ denote states of protein involved in the signaling pathway. $f(x)$ denotes the interaction among these proteins. $g(x)$ denotes the coupling between m input signals $u = \begin{bmatrix} u_1 & \cdots & u_m \end{bmatrix}^T$ and the signaling pathway. y denotes the outputs of the signaling pathway. For example, if x_n is the output signal to be discussed, then $C = \begin{bmatrix} 0 & \cdots & 0 & 1 \end{bmatrix}$.

B. Signal transduction ability measurement

There are many properties of the signaling way to be investigated such as the signaling time, the signal duration or the signal amplitude. As we mentioned previously, our interest is in the signal amplification that is, the signal amplitude. We define the transduction ability from the system gain point of view as follows:

$$T_a = \sup_{u(t) \in L_2[0,t_f]} \frac{\|y(t)\|_2}{\|u(t)\|_2} \tag{3}$$

where $u(t)$ and $y(t)$ are the inputs and outputs of the signaling pathway respectively. The physical meaning of transduction ability is the maximum ratio of signal energy of output to the signal energy of all possible bounded input signals within the time interval $[0, t_f]$. The reason why we consider the maximum energy ratio of output signal to all input signals is that input signals may change under different conditions and the signal energy ratio may change depending on those input signals. However, transduction ability is based on the worst-case effect of all input signals on outputs and is dependent on the characteristics of dynamic systems. Actually, the transduction ability cannot be measured directly by trying each possible bounded input signal which is a measure of system characteristics of the signaling pathway. In general, the maximization problem for measurement of signal transduction ability of a signal transduction pathway cannot be solved directly. It can only be solved indirectly by a systematic analysis method in the following.

Let us denote an upper bound of transduction ability as follows:

$$\frac{\|y(t)\|_2^2}{\|u(t)\|_2^2} \le \rho^2, \forall u(t) \in L_2[0, t_f] \tag{4}$$

or

$$\|y(t)\|_2^2 \le \rho^2 \|u(t)\|_2^2, \forall u(t) \in L_2[0, t_f] \tag{5}$$

Therefore, we can find an upper bound them decrease the upper bound as small as possible to approach the transduction ability, i.e., to minimize the upper bound to estimate the signal transduction ability.

Theorem 1

If there exists a positive function $V(x)$ with $V(0) = 0$ satisfying the following Hamilton-Jacobi inequality (HJI):

$$\left(\frac{\partial V(x)}{\partial x}\right)^T f(x) + \frac{1}{4\rho^2}\left(\frac{\partial V(x)}{\partial x}\right)^T g(x) g(x)^T \frac{\partial V(x)}{\partial x} + x^T C^T C x \le 0 \tag{6}$$

then the signal transduction ability of the signal pathway is less than ρ.

C. Fuzzification

In general, it is still very difficult to solve the nonlinear HJI-constrained optimization problem in proposition 1. Fuzzy interpolation method is employed to overcome this situation and simplify the procedure to solve the transduction ability measurement problem.

Recently, fuzzy dynamic model has been widely employed to interpolate several local linear dynamic systems to approximate a nonlinear dynamic system to simplify nonlinear control problem [10], [11]. Takagi-Sugeno (T-S) fuzzy dynamic model [8] is described by fuzzy If-Then rules and employed here to efficiently deal with the problem of transduction ability measurement of the signaling pathway. The *i*-th rule of fuzzy model of nonlinear signal transduction pathway is proposed as the following form: [10],[11]

Rule i

If $x_1(t)$ is F_{i1}, $x_2(t)$ is F_{i2},..., $x_l(t)$ is F_{il}, then

$$\begin{aligned} \dot{x} &= A_i x(t) + B_i u(t) \\ y &= Cx(t) \end{aligned}$$

where $i = 1, 2, \ldots, L$, F_{ij} is the fuzzy set, A_i and B_i are known constant matrices, L is the number of fuzzy rules, and l is the number of premise variables. If all state variables are used as premise variables then $l = n$. The physical meaning of fuzzy rule i is that if the state variables $x_1(t), x(t), \ldots, x_l(t)$ are with fuzzy sets $F_{i1}, F_{i2}, \ldots F_{il}$, then the nonlinear signaling pathway could be represented by the linear systems. The fuzzy system is referred as follows:[10], [11], [8]

$$\begin{aligned} \dot{x} &= \frac{\sum_{i=1}^{L} \mu_i(x(t)) \left[A_i x(t) + B_i u(t)\right]}{\sum_{i=1}^{L} \mu_i(x(t))} \\ &= \sum_{i=1}^{L} m_i(x(t)) \left[A_i x(t) + B_i u(t)\right] \\ y &= Cx(t) \end{aligned} \tag{7}$$

where $\mu_i\left(x\left(t\right)\right)=\prod_{i=1}^{l}F_{ij}\left(x_j\left(t\right)\right)$, and $m_i\left(x\left(t\right)\right)=\dfrac{\mu_i\left(x\left(t\right)\right)}{\sum_{i=1}^{L}\mu_i\left(x\left(t\right)\right)}$. $F_{ij}\left(x_j\left(t\right)\right)$ is the grade of membership of $x_j\left(t\right)$ in F_{ij} and $m_i\left(x\left(t\right)\right), i=1,2,\ldots,L$ are called the fuzzy bases. The denominator $\sum_{i=1}^{L}\mu_i\left(x\left(t\right)\right)$ is only for normalization so that the total fuzzy sum of fuzzy bases $\sum_{i=1}^{L}m_i\left(x\left(t\right)\right)=1$. The physical meaning of the fuzzy system is local linear signaling pathways are interpolated through nonlinear bases $m_i\left(x\left(t\right)\right)$ to approximate the nonlinear signaling pathway. Actually, except fuzzy bases, other interpolation bases could be also employed to interpolate linear signaling pathways to approximate a nonlinear signaling pathway.

By fuzzy approximation, the nonlinear signaling pathway can be represented by the following fuzzy interpolated signaling pathway:

$$\begin{aligned}\dot{x}&=f\left(x\right)+g\left(x\right)u\\&=\sum_{i=1}^{L}m_i\left(x\left(t\right)\right)\left[A_ix\left(t\right)+B_iu\left(t\right)\right]\\&\quad+\Delta f\left(x\right)+\Delta g\left(x\right)u\left(t\right)\end{aligned}\tag{8}$$

where $\Delta f\left(x\right)=f\left(x\right)-\sum_{i=1}^{L}m_i\left(x\left(t\right)\right)A_ix\left(t\right)$ and $\Delta g\left(x\right)=g\left(x\right)-\sum_{i=1}^{L}m_i\left(x\left(t\right)\right)B_i$ denote fuzzy approximation errors. There are many methods to find A_i and B_i for the fuzzy model identification. We would use fuzzy toolbox in Matlab® to find A_i and B_i easily. After finding A_i and B_i, we could easily find bounds of fuzzy approximation error as follows:

$$\left\|\Delta f\left(x\right)\right\|_2^2\le a\left\|x\left(t\right)\right\|_2^2\tag{9}$$

$$\left\|\Delta g\left(x\right)\right\|_2^2\le b\tag{10}$$

for some positive constants a and b. Then based on fuzzy approximation, we get the following transduction ability measurement for the nonlinear signaling pathway.

Theorem 2:

For the nonlinear signaling pathway, there exists a positive definite symmetric matrix P by solving the following Riccati-like inequalities.

$$\begin{aligned}&A_i^TP+PA_i+\frac{2}{\rho^2}PB_iB_i^TP+\frac{2}{\rho^2}PP\\&\qquad+\frac{\rho^2a}{2}I+\frac{2b}{\rho^2}PP+C^TC\le 0,\\&i=1,2,\cdots,L\end{aligned}\tag{11}$$

In order to solve the above Riccati-like inequalities by the conventional LMI method, we let the positive definite symmetric matrix $W=P^{-1}$. Then above Riccati-like inequalities can be equivalent to

$$\begin{aligned}&A_iW+WA_i^T+\frac{2}{\rho^2}\left[B_iB_i^T+I+bI\right]\\&\qquad+WC^TCW+\frac{\rho^2a}{2}WW\le 0,\\&i=1,2,\ldots,L\end{aligned}\tag{12}$$

By the Schur complements, the Riccati-like inequalities is equivalent to the following LMIs:

$$\begin{aligned}&\begin{bmatrix}A_iW+WA_i^T+\frac{2}{\rho^2}\left(B_iB_i^T+I+bI\right) & WC^T & W\\ CW & -I & 0\\ W & 0 & -\frac{2}{\rho^2a}I\end{bmatrix}\le 0,\\&i=1,2,\ldots,L\end{aligned}\tag{13}$$

Then the signal transduction ability of nonlinear signaling pathway is less than ρ, i.e., is an upper bound of the signal transduction ability.

By fuzzy approximation, the HJI is approximated by a set of algebraic inequalities. Therefore, the signal transduction ability of the nonlinear signaling pathway could be obtained by solving the following constrained optimization.

$$T_a=\min_{\substack{\text{subject to } W>0\\ \rho>0 \text{ and } (12)}}\rho\tag{14}$$

which could be solved by decreasing until no positive definite symmetric matrix exists.

Remark 1. The Riccati-like inequalities are an approximation of HJI at local linear systems. Similarly, the constrained optimization problem for signal transduction ability measurement of nonlinear signaling pathway is also a conventional method based on fuzzy interpolation method to replace the very difficult constrained optimization subject to HJI by the constrained optimization subject to LMIs. In general, the constrained optimization problem for signal transduction ability measurement is called "eigenvalue problem", which can be efficiently solved by Matlab® LMI toolbox.

Remark 2. If ρ is smaller, then the last term in (11) should be larger so that the eigenvalues of A_i would be in the far left hand complex plane (i.e. with more negative real part) and then the total sums would be negative. If ρ is larger, then the eigenvalues of A_i would be near the imaginary axis (i.e. with smaller negative real part). In general, the signaling pathways always amplify the input signals (i.e. $T_a > 1$). In this situation, the eigenvalues of A_i would be near the imaginary axis, in order to amplify the extracellular signals to activate the corresponding genes in the cell.

III. Experimental Simulations

A. Simulation 1

Here we took into account that enzymes catalyze all steps and therefore consider Michaelis-Menten kinetics for the individual step. In these expressions, the concentrations of the donor and acceptor of the transferred phosphate group, ATP and ADP, are not explicitly expressed but are included in the rate constants. The dynamic of the nonlinear model and the fuzzy model of MAPK kinase cascade were shown in Fig.2 and Fig.3 respectively. The performance of MAPK kinase cascade, i.e., the ability to amplify the signal and to notably enhance the concentration of double-phosphorylated MAPK and the speed of activation, depends on the dynamic system of the signaling pathway and their rate constants. The simulation procedure started from fuzzy interpolation for the nonlinear model and the parameters of the fuzzy model, A_i and B_i , can be identified. Then, the approximation errors, a and b , can be determined. Next, according to *Theorem 2*, the augmented LMIs can be solved via LMI toolbox in Matlab®. Finally, signal transduction ability can be obtained by decreasing the prescribed ρ until no positive definite symmetric matrix solutions for the augmented LMIs exist.

First, using method of least-squares estimator, the parameters, A_i and B_i , of the fuzzy model can be identified. Since there are 8 substances or state variables in the ODE model, and by choosing 2 fuzzy sets for each variable, we have totally 256 fuzzy rules for the fuzzy model. By comparing the fuzzy model with the original ODE model, the approximation errors, $a = 2.35 \times 10^{-16}$ and $b = 1.86 \times 10^{-7}$ were determined. In the end, by solving the eigenvalue problem with LMI toolbox in Matlab®, the signal transduction ability of the fuzzy signaling pathway is $T_a = 6.39 \times 10^6$ and the corresponding positive definite symmetric matrix is

$$W = \begin{bmatrix} 0.9988 & -0.9988 & -0.0156 & 0.0083 & 0.0073 & + & - & - \\ & 0.9988 & 0.0156 & -0.0083 & -0.0073 & - & + & + \\ & & 0.1165 & -0.0613 & -0.0552 & - & + & + \\ & & & 0.0987 & -0.0374 & + & - & - \\ & & & & 0.0926 & - & + & + \\ & & & & & + & - & - \\ & & & & & & + & - \\ & & & & & & & + \end{bmatrix}$$

where $+$ and $-$ mean the very small positive and negative numbers (~10^{-12}), respectively. (The elements in the lower triangular matrix were not shown for symmetry).

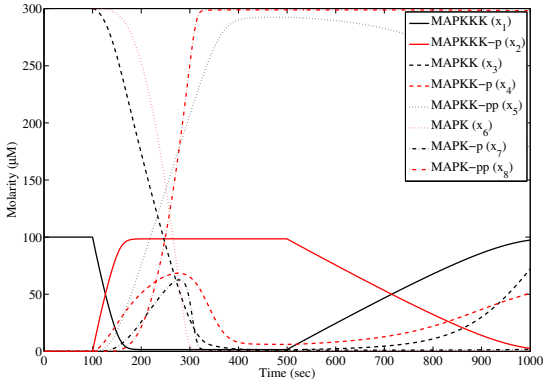

Figure 2. The nonlinear model of mitogen-activated protein (MAP) kinase cascade.

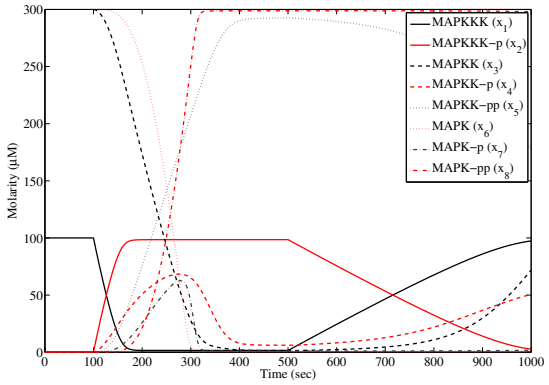

Figure 3. The fuzzy model of mitogen-activated protein (MAP) kinase cascade.

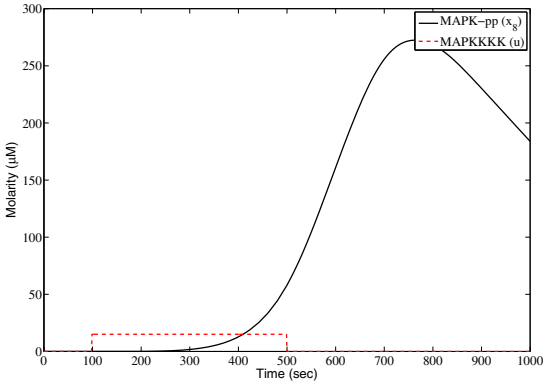

Figure 4. The input (red) and output (blue) of mitogen-activated protein (MAP) kinase cascade.

IV. DISCUSSION

In this work, the proposed measurement provided a new way to access the ability of signal transduction in intracellular communication from a systematic view. The signal transduction ability is not easy to be quantified or determined by a single biological experiment on measuring the concentration of the input and output signals. Hence, a way to quantify the ability which is independent to the measurement of the concentration of the input and output signals is demanded. According to the concept of a system gain, our proposed method can determine the ability of signal transduction and is only dependent on the structure of the signaling pathway and the components involved in. Our result said that the signal transduction ability of MAP kinase cascade is about 10^6. That matched the description from the textbook [12] which says each level of a signaling pathway can cause about 10^2 times concentration amplification since the cascade is consisted of three-level cascade. It implied the usefulness of our proposed method. However, for a more precise estimation of the signal transduction ability, it needs to be confirmed by biological experiments. Also with the improvement of the knowledge on the structure of the signaling pathway, this method can give a better estimation on the ability of signal transduction.

Moreover, in this study, the nonlinear ODE equations are adopted to describe the signaling pathway, which also have been widely used in quantitative description to metabolism. However, we have to notice the difference between these two modules in the biology. First, signaling pathways serve for information processing and transfer of information, while metabolism provides mainly mass transfer. Second, the metabolic network is determined by the present set of enzymes catalyzing the reactions. Third, the different amounts of components have an effect on the concentration ration of catalysts and substrates.[3] The models for signaling pathway can always be improved according to the improvement on the experimental techniques and the knowledge about signaling pathways. Nevertheless, based on our purposed measurement, the signal transduction ability can always be accessed no matter which model is used to describe the whole signaling pathways.

In reality, the modules operated in a living system always have inherent noise due to random events. The amount of noise is a property of the system itself, and it may or may not cause significant deviation from the deterministic model. Some stochastic models [13] have been developed due to the consideration of the nature of the signaling pathways, that is, signaling pathways execute their functions under external disturbances and internal noises. One way to improve the estimation is to modify our proposed measurement with noise term $v(t)$, i.e.,

$$T_a = \sup_{u(t)\in L_2[0,t_f]} \frac{\|y(t)\|_2}{\|u(t)\|_2 + \|v(t)\|_2} \qquad (15)$$

Then, the signal transduction ability can also be investigated under such noisy environments, which is more real. Hence we can also investigate the robustness of signaling pathways with this proposed measurement [14]. The more robust the signaling pathway is the smaller variation the signal transduction ability is.

This methodology characterize the output-to-input energy ratio of the signal transduction systems and can apply on the biological modular device, such as amplifiers, logic elements, and actuators, or biochemical circuit designs to estimate signal transduction ability. Through the measurement, the signaling pathways can be analyzed and the importance of each component in the pathway can also be estimated. In the end, through the analysis of the signal transduction ability, each step in the signaling pathway can be analyzed and calculated its signal transduction ability which may be determined by the properties of reactants (for example: kinases or phosphatases) and the state of the interested cell. According to the conception of the BioBrick, we can also build the library of the building bricks of signaling pathways, and then the signaling pathway with desired signal transduction ability can be designed.

V. ACKNOWLEDGMENT

This work was supported by the National Science Council under the contract NSC 78-2221-E-007-113-MY3.

VI. REFERENCES

[1] S. Hohmann, "Osmotic stress signaling and osmoadaptation in Yeasts," *Microbiology and Molecular Biology Reviews,* vol. 66, pp. 300-+, Jun 2002.

[2] J. Herrington and C. Carter-Su, "Signaling pathways activated by the growth hormone receptor," *Trends in Endocrinology and Metabolism,* vol. 12, pp. 252-257, Aug 2001.

[3] E. Klipp, *Systems biology in practice : concepts, implementation and application.* : Wiley-VCH, Weinheim., 2005.

[4] B. N. Kholodenko, "Negative feedback and ultrasensitivity can bring about oscillations in the mitogen-activated protein kinase cascades," *European Journal of Biochemistry,* vol. 267, pp. 1583-1588, Mar 2000.

[5] E. Klipp*, et al.*, "Integrative model of the response of yeast to osmotic shock," *Nature Biotechnology,* vol. 23, pp. 975-982, Aug 2005.

[6] A. B. Harvey Lodish, S Lawrence Zipursky, Paul Matsudaira, David Baltimore, and James Darnell., *Molecular Cell Biology, 4th edition*: New York: W. H. Freeman, 2000.

[7] P. B. Detwiler*, et al.*, "Engineering aspects of enzymatic signal transduction: Photoreceptors in the retina," *Biophysical Journal,* vol. 79, pp. 2801-2817, Dec 2000.

[8] T. Takagi and M. Sugeno, "Fuzzy Identification of Systems and Its Applications to Modeling and Control," *Ieee Transactions on Systems Man and Cybernetics,* vol. 15, pp. 116-132, 1985.

[9] G. Balas, Chiang, R., Packard, A. and Safonov, M., *Robust Control Toolbox User's Guide*, 2008.

[10] B. S. Chen*, et al.*, "Robustness design of nonlinear dynamic systems via fuzzy linear control," *Ieee Transactions on Fuzzy Systems,* vol. 7, pp. 571-585, Oct 1999.

[11] B. S. Chen*, et al.*, "Mixed H-2/H-infinity fuzzy output feedback control design for nonlinear dynamic systems: An LMI approach," *Ieee Transactions on Fuzzy Systems,* vol. 8, pp. 249-265, Jun 2000.

[12] A. B. Harvey Lodish, Paul Matsudaira, Chris A. Kaiser, Monty Krieger, Matthew P. Scott, Lawrence Zipursky, and James Darnell., *Molecular Cell Biology*, 5 ed., 2003.

[13] A. Hoffmann*, et al.*, "The IkappaB-NF-kappaB signaling module: temporal control and selective gene activation," *Science,* vol. 298, pp. 1241-5, Nov 8 2002.

[14] B. S. Chen*, et al.*, "A new measure of the robustness of biochemical networks," *Bioinformatics,* vol. 21, pp. 2698-705, Jun 1 2005.

2011 IEEE International Conference on Fuzzy Systems
June 27-30, 2011, Taipei, Taiwan

Long-term Business Cycle Forecasting Using Intuitionistic Fuzzy Least-squares Support Vector Regression

Kuo-Ping Lin
Department of Information Management
Lunghwa University of Science and Technology, Taoyuan, Taiwan
kplin@mail.lhu.edu.tw

Kuo-Chen Hung
Department of Logistics Management
National Defense University
Taipei, Taiwan
Kuochen.hung@msa.hinet.net

Ming-Chang Wu
Department of Information Management
Lunghwa University of Science and Technology, Taoyuan, Taiwan
andonebypapa@hotmail.com

***Abstract*—Long-term business cycle forecasting is a very important issue in economic evaluation. This study presents a novel intuitionistic fuzzy least-squares support vector regression (IFLS-SVR) model for accurately forecasting long-term index of business cycle. Traditional support vector regression (SVR) and least-squares support vector regressions (LS-SVR) have been successfully applied in forecasting problems especially complex/nonlinear system. In this paper, the prediction model adopts two least-squares support vector regressions with intuitionistic fuzzy sets to approach fuzzy upper and lower bounds respectively, and then approach the crisp predict values. Genetic algorithms (GAs) are also employed in order to select two parameters of IFLS-SVR models. In this study, IFLS-SVR, LS-SVR and SVR are employed for the Taiwan business index forecasting. Empirical results indicate that the IFLS-SVR has better performance in terms of forecasting accuracy. Therefore, the IFLS-SVR model can efficiently provide credible long-term prediction for the Taiwan business index forecasting**

Keywords- long-term business cycle forecasting; intuitionistic fuzzy support vector regression; support vector regression; least-squares support vector regressions

I. INTRODUCTION

Accuracy forecasting long-term business cycle is an important issue in economic research. Business cycle is often determined by a panel of macroeconomic experts from analyzing movements in the set of components making up the Commerce Department's coincident variables of economic activity. Index of business cycle can be easily observes that has nonregular business cycle in past serial time, and index of business cycle belongs nonlinear data set especially in Taiwan. For accuracy measuring/forecasting, stochastic/statistics method is usually employed to analysis business cycle. Many researches have devoted to study of business cycle ([17], [18], [4], [32], [33], [27], and [20]). However, it is difficult to predict the business cycle with time serial, and many researches forecast short-term index of business cycle for reducing complexity. The difficulty derives from assumptions made by the probability distributions and a lack of adequate business cycle models for long-term prediction. Moreover, in real world information usually belongs vague, uncertain, imprecise and incomplete. In Taiwan the index of business cycle is composed of nine exogenous variables. This may make the index of business cycle exist some uncertain factors. Hence, to overcome the problem intuitionistic fuzzy sets (IFSs) and generalization of fuzzy interval data is employed to represent Taiwan business cycle which uses five lights/intervals to represent different economic actives. In order to handle the uncertain situation and insufficient vague information, a concept IFSs developed by [1] is introduced in this paper. The fundamental characteristics of IFSs are that the values of its membership function and non-membership vague values rather than exact numbers. Therefore, it could be used to simulate any activities and process requiring human expertise and knowledge, which are inevitably imprecise values.

In this paper, we discuss multivariate fuzzy nonlinear regression by support vector regression (SVR). SVR [30] has been extended so as to solve forecasting problems and has provided many exciting results especially nonlinear regression and time series problems with the introduction of Vapnik's ε-insensitive loss function. Unlike most of the traditional technology SVR implement neural network models, and SVR adopts the structural risk minimization principle which seeks to minimize an upper bound of the generalization error rather than minimize the training error. In recent years, SVR schemes have been extended to cope with forecasting problems, and have provided many promising results in customer demand [19], finance ([29], [16], and [14]) intermittent demand [13], tourism demand [25], air quality ([22] and [21]), wind speed [24], plant control systems [31], rainfall [12], prices for the electricity market [8] and flood control [35]. Furthermore, for representing fuzzy data the support vector fuzzy regression machines have been proposed by[11]. This method modified the principle of SVR which changes convex optimization problems to multivariate fuzzy linear regression models. And the support vector interval regression networks (SVIRNs) are proposed by [15] which can efficiently handle interval output data. Yao and Yu [34] develop a fuzzy regression based on asymmetric support vector machines which extend the support vector fuzzy regression machines. Chuang [7] extended SVIRNs develops

978-1-4244-7316-8/11/$26.00 ©2011 IEEE

interval support vector interval regression networks (ISVIRNs) which can handle interval input/output data. Hao and Chiang [9] develops a fuzzy regression analysis by support vector learning. In this paper we proposed a novel IFLS-SVR to forecast index of business cycle. Our proposed method find upper and lower bound by LS-SVR respectively, and use intuitionistic fuzzy sets technology to approach training data. Our proposed method can get benefit LS-SVR. In addition to our method adopts genetic algorithms (GAs) to search optimal parameters of LS-SVR. This make our method can obtain better performance.

II. Related works

A. IFSs Theroy

Fuzzy sets theory, proposed by Zadeh [36], has shown successful applications in various fields. In this theory, the membership of an element to a fuzzy set is a single value between zero and one. But in reality, it may not always be certain that the degree of non-membership of an element to a fuzzy set is just equal to 1 minus the degree of membership, i.e. there may be some hesitation degree. Thus, as a generalization of fuzzy sets, the concept of IFSs was introduced by [1]. Bustince and Burillo [6] showed that this notion coincides with the notion of vague sets (VSs).

The IFSs is as an extension of fuzzy sets. An IFSs A in a fixed set E is an objective with the expression

$$A=\left\{\left\langle x,\mu_A(x),\nu_A(x)\right\rangle\middle|x\in E\right\}, \tag{1}$$

where the functions $\mu_A: E\to[0,1]$ and $\nu_A: E\to[0,1]$ denote the degree of membership and the degree of non-membership of the element $x\in E$, respectively. For every $x\in E$,

$$0\le\mu_A(x)+\nu_A(x)\le 1 \tag{2}$$

when $\mu_A(x)+\nu_A(x)=1$, for every $x\in E$, then the IFSs will degenerate to a fuzzy set. Hence, we can consider a fuzzy set with its membership function $u_A(x)$, having the IFSs expression as

$$A=\left\{\left\langle x,\mu_A(x),1-\mu_A(x)\right\rangle\middle|x\in E\right\} \tag{3}$$

under the condition of $v_A(x)=1-u_A(x)$, for every $x\in E$.

For each IFSs A in E, "hesitation degree" has consideration. We call the hesitation degree of an element $x\in E$ in A by the following expression:

$$\pi_A(x)=1-\mu_A(x)-\nu_A(x), \tag{4}$$

We can consider $\pi_A(x)$ as a hesitancy degree of x to A. From (4) it is evident that

$$0\le\pi_A(x)\le 1 \text{ for all } x\in E. \tag{5}$$

Therefore, to describe an intuitionistic fuzzy set completely; we need at least two functions from the triplet ([2][3]): (1) membership function; (2) non-membership function; (3) hesitation degree.

B. Least-squares Support Vector Regressions with Genetic Algorithm

A successful method for regression problem is the least squares support vector regression ([26] and [28]), which attempts to minimize the sum square errors (SSEs) of training data set while simultaneously minimizing the margin error. The LS-SVR approach is to approximate an unknown function by a training data set $\{(x_i, y_i), i=1, \ldots, N\}$. The regression function can be formulated as follows:

$$y=f(x)=w^T\varphi(x_i)+b \tag{6}$$

where $\varphi(x_i)$ denotes the feature of the inputs, and w and b indicate coefficients. LS-SVR introduces a least squares version to SVR by formulating the regression problem as

$$\begin{aligned}&Min\ J_1(w,b,e)=\frac{1}{2}\|w\|^2+\frac{1}{2}C\sum_{i=1}^{N}e_i^2\\&subjective\ to\\&y_i=w^T\varphi(x_i)+b+e_i,\ i=1,2,\cdots,N\end{aligned} \tag{7}$$

Introduce the Lagrangian as

$$L_1(w,b,e,\alpha)=J_1(w,b,e)+\sum_{i=1}^{N}\alpha_i(y_i-w^T\varphi(x_i)-b-e_i). \tag{8}$$

where α is the Lagrangian multiplier vector. The conditions for optimality are

$$\begin{aligned}&\frac{\partial L_1}{\partial w}=0\Rightarrow w=\sum_{i=1}^{N}\alpha_i\varphi(x_i),\\&\frac{\partial L_1}{\partial b}=0\Rightarrow\sum_{i=1}^{N}\alpha_i=0,\\&\frac{\partial L_1}{\partial e_i}=0\Rightarrow e_i=\frac{1}{C}\alpha_i,\ i=1,\ldots,N,\\&\frac{\partial L_1}{\partial \alpha_i}=0\Rightarrow y_i=w^T\varphi(x_i)+b+e_i,\ i=1,\ldots,N.\end{aligned} \tag{9}$$

Herein, $k(x_i, x_j)$ denotes a Kernel function whose value equals the inner product of two vectors, x_i and x_j, in the feature space $\varphi(x_i)$ and $\varphi(x_j)$, meaning that $k(x_i, x_j)=\varphi^T(x_i)\ \varphi(x_j)$. Any function that satisfies Mercer's condition [23] can act as the Kernel function. This work uses the Gaussian function. Hence, we can denote the $K=(k_{ij})_{N\times N}$, $k_{ij}=k(x_i, x_j)$, and $V=\mathrm{diag}\{1/C,1/C,\ldots,1/C\}$, LS-SVR can be described as

$$\begin{bmatrix}A & 1\\ 1^T & 0\end{bmatrix}\begin{bmatrix}\alpha\\ b\end{bmatrix}=\begin{bmatrix}y\\ 0\end{bmatrix}, \tag{10}$$

where $A=K+V$. Hence, the regression model (see (6)) is found by solving (10). The resulting LS-SVR becomes then

$$f(x)=\sum_{i=1}^{N}\alpha_i k(x,x_i)+b. \tag{11}$$

Note that in the case of Gaussian kernels, one has only two additional tuning parameters (C, σ), which is less than for standard SVR.

The experiment uses genetic algorithms (GA) [10] to search optimal parameter of LS-SVR. In this study, binary encoding is specified in GA search. The size of the population is set fifty. The roulette wheel selection principle is used to select chromosomes for reproduction. In the crossover operation,

chromosomes are paired randomly. The single-point-crossover principle is employed in the GA search. In this study, the probabilities of crossover and mutation are set to 0.5 and 0.1, respectively. By the GA search the optimal parameters C andσ can be obtained. To minimize forecasting error of the LS-SVR model, the negative values of *MAPE* were treated as the objective values of the GA; thus, each iteration generates a smaller MAPE value. The parameter search procedure is conducted until the stop criterion is reached. The two parameters resulting in the smallest validation error are then used to develop a appropriate LS-SVR model. Finalized forecasting vales are obtained by LS-SVR. Finally, after comparison with the testing data, the testing errors are obtained.

III. INTUITIONISTIC FUZZY LEAST-SQUARES SUPPORT VECTOR REGRESSIONS

The IFLS-SVR approach has mainly different with LS-SVR/SVR which constructs the intuitionistic fuzzy sets to represent uncertain degree of data. IFSs D_i in a fixed set E is an objective with the expression

$$D_i = \left\{ \left\langle X_i = (x_i, y_i), \mu_D(y_i), \nu_D(y_i) \right\rangle \middle| X \in E \right\}, i \in 1, ..., N. \quad (12)$$

In this paper, intuitionistic fuzzy generator or fuzzy complement is created from Yager generating function [5]. The fuzzy complement functional is defined as:

$$N(\mu(y_i)) = g^{-1}(g(1) - g(\mu(y_i))) \quad (13)$$

where $g(.)$ is an increasing function and g:[0,1]→[0,1].

Yager class can be generated by using the following function in the above (13)

$$g(y_i) = y_i^{\alpha} \quad (14)$$

So, Yager's intuitionistic fuzzy complement is written as:

$$N(y_i) = (1 - y_i^{\alpha})^{1/\alpha}, \alpha > 0 \text{ where} N(1)=0, N(0)=1. \quad (15)$$

Non-membership values are calculated from Yager's intuitionistic fuzzy complement $N(y_i)$. Thus, with the help of Yager's intuitionistic fuzzy complement, IFSs becomes:

$$D_i = \left\{ \left\langle X_i = (x_i, y_i), \mu_D(y_i), (1 - \mu_D(y_i)^{\alpha})^{1/\alpha} \right\rangle \middle| X \in E \right\}. \quad (16)$$

and the hesitation degree is :

$$\pi_D(Y_i) = 1 - \mu_D(y_i) - (1 - \mu_D(y_i)^{\alpha})^{1/\alpha} \quad (17)$$

In IFLS-SVR, based on the expert's viewpoints the membership function can be determined, and then the hesitation degree can be obtained by (16). Following we can use definition of triangular fuzzy numbers (TFNs) to approach the intuitionistic fuzzy lower (IY_{Li}) and upper bounds (IY_{Ui}) with α=0.5 which can be formulated as following:

$$IY_{Li} = Y_{Li} + (Y_{Ci} - Y_{Li}) \times (\mu_D(y_i) + \pi_D(y_i)) \quad (18)$$

$$IY_{Ui} = Y_{Ui} - (Y_{Ui} - Y_{Ci}) \times (\mu_D(y_i) + \pi_D(y_i)) \quad (19)$$

where Y_{Li} is lower bound of TFNs, Y_{Ci} is the mode of TFNs, and Y_{Ui} is upper bound of TFNs. Fig. 1 shows that the data point construct intuitionistic fuzzy lower and upper bounds.

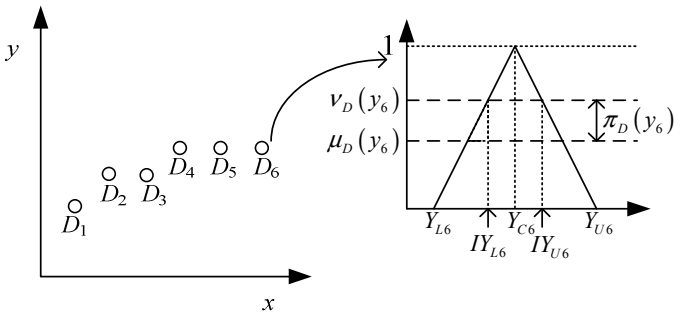

Figure 1. Illustration of construction of the intuitionistic fuzzy sets.

Then, in the IFLS-SVR model the intuitionistic fuzzy lower and upper regression lines must be constructed by the LS-SVR method with the lower bound of $\{(x_i, IY_{Li}), i=1, 2, \ldots, N\}$ and the upper bound of $\{(x_i, IY_{Ui}), i=1, 2, \ldots, N\}$, respectively, which can be written as follows:

$$Y_L(x_i) = w_{Li}^* + b_L = \sum_{i=1}^{N} \alpha_{Li} k(x, x_i) + b_L. \quad (20)$$

where the Lagrange multipliers, α_{Li} and an optimal weight vector w_{Li}^* of the lower bound regression hyperplane can be estimated by (6):

$$Y_U(x_i) = w_{Ui}^* + b_U = \sum_{i=1}^{N} \alpha_{Ui} k(x, x_i) + b_U. \quad (21)$$

where the Lagrange multipliers, α_{Ui} , and an optimal weight vector w_{Ui}^* of the upper bound regression hyperplane can be estimated by (7). Then the fuzzy prediction model uses (20) and (21) to estimate the estimated central vale $Y_C(x_i)$ by a simple calculation as follows:

$$Y_C(x_i) = \sum_{i=1}^{N} ((\alpha_{Li} + \alpha_{Ui}) K(x, x_i) + b_L + b_U)/2. \quad (22)$$

Furthermore, the IFLS-SVR model uses GA algorithms to select the two parameters of LS-SVR. Fig. 2 shows the flowchart of the proposed IFLS-SVR model.

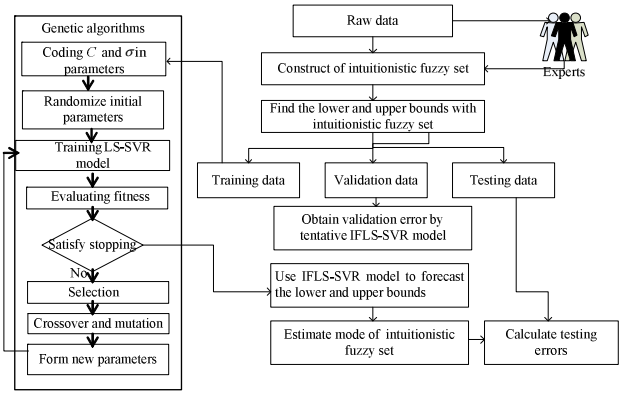

Figure 2. A flowchart of the IFLS-SVR

IV. NUMERICAL EXAMPLES AND EXPERIMENTAL RESULTS

To represent the vague characteristics of business cycles index in Taiwan, the Council of Economic Planning and Development uses five business lights to indicate the various degrees of business cycles. Table I shows the lights, intervals, and meanings of economic activities of the different degrees of business cycles from the Council of Economic Planning and Development. These intervals can be regarded as TFNs. Fig. 3 shows the monthly Taiwanese business index from October 1990 to November 2010. The monthly data were divided into three sets: the training set (October 1990 to December 2008), the validation set (January 2009 to December 2009), and the testing set (from January 2010 to November 2010). Moreover, Fig. 3 also shows IFSs of business cycles index in October 2008. The training data were used to design the forecasting model, and the testing data were employed to measure the forecasting performance of the different forecasting models. In addition, the root mean square error (*RMSE*) and mean absolute percentage error (*MAPE*) were used to measure the forecasting accuracy of the two models. (23) to (24) illustrate the expression of RMSE, MAPE respectively.

$$RMSE = \left\{ \frac{1}{M} \sum_{t=1}^{M} \left(Y_{Ct} - Y_C(x_t) \right)^2 \right\}^{0.5} \tag{23}$$

$$MAPE(\%) = \frac{100}{M} \sum_{t=1}^{M} \left| \frac{Y_{Ct} - Y_C(x_t)}{Y_{Ct}} \right| \tag{24}$$

where M is the number of forecasting periods; Y_{Ct} is the actual value, and $Y_C(x_t)$ is the forecasting value at period t.

TABLE I. THE INDEX OF BUSINESS CYCLES IN TAIWAN

Lights	Intervals of business cycle	Meanings of business activities
Red	[38, 45]	Excellent
Yellow-Red	[32, 37]	Good
Green	[23, 31]	Medium
Yellow-Blue	[17, 22]	Retrieving
Blue	[9 , 16]	Not good

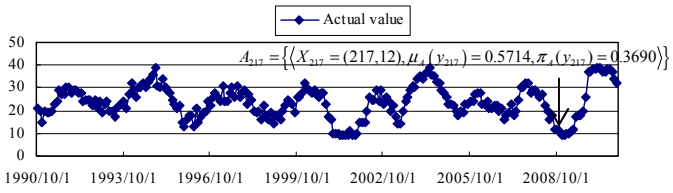

Figure 3. Illustration of actual values from October 1990 to November 2010

Table II illustrates the actual values and experimental results of the IFLS-SVR model from January 2010 to November 2010. In addition, Table II shows the optimal parameters of the proposed IFLS-SVR model. Fig. 4 makes a point-to-point comparison of actual values and predicted values of IFLS-SVR. Fig. 4 shows that the IFLS-SVR model can efficiently capture the trend of data. From observing the Fig. 4 we can find that the LS-SVR and SVR have lower forecasting values from January 2010 to November 2010. This may be because that LS-SVR and SVR have over fitting phenomenon in the forecasting index of business cycles. The forecasting values are similarity the validation set by using LS-SVR and SVR technologies. The Table III shows and ranks the performances of three models. Again, the IFLS-SVR outperforms others models in terms of forecasting accuracy.

Finally, the Wilcoxon signed rank test was implemented to test the forecasting result. The test results, presented in Table IV, show significant differences among the IFLS-SVR, the LS-SVR and SVR models, indicating the forecasting result of IFLS-SVR is better than those of the traditional LS-SVR and SVR approaches based on *MAPE* and *RMSE*.

TABLE II. COMPARISON OF THE FORECASTING RESULTS AND PARAMETERS

Date	Actual value	IFLS-SVR (C/σ= 100.74/ 0.01)	LS-SVR (C/σ= 317.39/ 0.19)	SVR ($C/\varepsilon/\sigma$= 35.84/0.22/0.88)
2010/1/1	38	41.7312	19.1038	8.4093
2010/2/1	38	41.1553	18.9448	8.7809
2010/3/1	39	39.4172	18.7833	9.2896
2010/4/1	39	36.9449	18.6193	10.651
2010/5/1	37	34.2029	18.4530	12.9979
2010/6/1	37	31.5830	18.2843	15.211
2010/7/1	38	29.3428	18.1133	16.2752
2010/8/1	38	27.5961	17.9400	16.4975
2010/9/1	37	26.3409	17.7645	16.1791
2010/10/1	34	25.5041	17.5868	14.6248
2010/11/1	32	24.9845	17.4070	10.8380

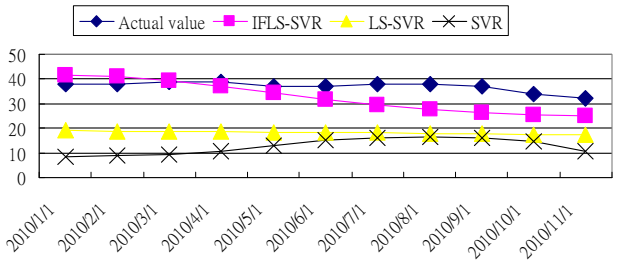

Figure 4. Illustration of actual values and forecasting values of three models

TABLE III. FORECASTING PERFORMANCES OF THREE MODELS

	IFLS-SVR	LS-SVR	SVR
MAPE(%)	15.6856	50.515	65.5035
RMSE	6.6308	18.8022	24.6016
Rank	(1)	(2)	(3)

TABLE IV. WILCOXON SIGNED RANK TEST FOR THE FORECASTING RESULTS

	LS-SVR	SVR
IFLS-SVR	-2.93(0.003) *	-2.93 (0.003) *
SVR	-2.93 (0.003) *	

Cell: standardize value(p value).
*significant different at α= 0.05.

V. CONCLUSIONS

Due to the recent global economic recession, analysis of business cycles is increasingly crucial. This study develops a novel IFLS-SVR model to exploit the unique strength of the intuitionistic fuzzy set theory and the LS-SVR technique, in order to predict long-term business cycles in Taiwan.

Simulation results indicate that the IFLS-SVR model offers a promising alternative in business cycles in uncertain circumstances. The superior performance of the IFLS-SVR model can be ascribed to two causes. First, the LS-SVR can efficiently capture trends of nonlinear data. Second, the IFLS-SVR model can provide creditable predictions for long-term Taiwanese business cycle predictions. For future work, forecasting other types of uncertain time series data by the IFLS-SVR model is a challenging issue for study. Future studies can also consider using data preprocessing techniques to improve the forecasting accuracy of the IFLS-SVR model.

ACKNOWLEDGMENTS

The authors would like to thank the National Science Council of the Republic of China for financially supporting this research under Contract No. NSC 99-2410-H-262-005.

REFERENCES

[1] K. T. Atanassov, "Intuitionistic fuzzy sets," *Fuzzy Sets and Systems*, vol. 20, pp. 87–96, 1986.

[2] K. T. Atanassov, "More on intuitionistic fuzzy sets," *Fuzzy Sets and Systems*, vol. 33, pp. 37–46, 1989.

[3] K. T. Atanassov, *Intuitionistic Fuzzy Sets: Theory and Applications*, Physica-Verlag, Heidelberg, 1999.

[4] A. Banerji and L. Hiris, "A framework for measuring international business cycles," *International Journal of Forecasting*, vol. 17, pp. 333–348, 2001.

[5] P. Burillo and H. Bustince, "Entropy on intuitionistic fuzzy set and on interval-valued fuzzy set," *Fuzzy Sets and Systems*, vol. 78, pp. 305–316, 1996.

[6] P. Burillo and H. Bustince, "Entropy on intuitionistic fuzzy sets and on interval-valued fuzzy sets," *Fuzzy Sets and Systems*, vol. 78, pp. 305–316, 1996.

[7] C.-C. Chuang, " Extended support vector interval regression networks for interval input-output data," *Information Sciences*, vol. 178, pp. 871–891, 2008.

[8] C. Gaoa, E. Bompard, R. Napoli, and H. Cheng, "Price forecast in the competitive electricity market by support vector machine," *Physica A*, vol. 382, pp. 98–113, 2007.

[9] P.-Y. Hao and J.-H. Chiang, "Fuzzy regression analysis by support vector learning approach," *IEEE Transactions on Fuzzy Systems*, vol. 16, pp. 428–441, 2008.

[10] J. H. Holland, *Adaptation in Natural and Artificial System*, University of Michigan Press, Ann Arbor, 1975.

[11] D. H. Hong and C. Hwang, "Support vector fuzzy regression machines," *Fuzzy Sets and Systems*, vol. 138, pp. 271–281, 2003.

[12] W. C. Hong and P. F. Pai, "Potential assessment of the support vector regression technique in rainfall forecasting," *Water Resources Management*, vol. 21, pp. 495–513, 2007.

[13] Z. S. Hua and B. Zhang, " A hybrid support vector machines and logistic regression approach for forecasting intermittent demand of spare parts," *Applied Mathematics and Computation*, vol. 181, pp. 1035–1048, 2006.

[14] W. Huang, Y. Nakamori, and S. Y. Wang, "Forecasting stock market movement direction with support vector machine," *Computer and Operations Research*, vol. 32, pp. 2513–2522, 2005.

[15] J.-T. Jeng, C.-C. Chuang, and S.-F. Su, "Support vector interval regression networks for interval regression analysis," *Fuzzy Set and Systems*, vol. 138, pp. 283–300, 2003.

[16] K. J. Kim, "Financial time series forecasting using support vector machines," *Neurocomputing*, vol. 55, pp. 307–319, 2003.

[17] A. P. Layton, "Dating and predicting phase changes in the U.S. business cycle," *International Journal of Forecasting*, vol. 12, pp. 417–428, 1996.

[18] A. P. Layton, "A further test of the influence of leading indicators on the probability of US business cycle phase shifts," *International Journal of Forecasting*, vol. 14, pp. 63–70, 1998.

[19] A. A. Levis and L. G. Papageorgiou, "Customer demand forecasting via support vector regression analysis," *Chemical Engineering Research and Design*, vol. 83, pp. 1009–1018, 2005.

[20] K.-P. Lin and P.-F. Pai, "A Fuzzy Support Vector Regression Model for Business Cycle Predictions," *Expert Systems with Applications*, vol. 37, pp. 5430–5435, 2010.

[21] K.-P. Lin, P.-F. Pai, and S.-L. Yang, "Forecasting concentrations of air pollutants by support vector regression models with data preprocessing procedures and immune algorithms," *Applied Mathematics and Computation*, vol. 217, pp. 5318–5327, 2011.

[22] W. Z. Lu and W. J. Wang, "Potential assessment of the "support vector machine" method in forecasting ambient air pollutant trends," *Chemosphere*, vol. 59, pp. 693–701, 2005.

[23] J. Mercer, "Function of positive and negative type and their connection with the theory of integral equations," *Philosophical Transactions of the Royal Society*, vol. A209, pp. 415–446, 1909.

[24] M. A. Mohandes, T. O. Halawani, S. Rehman, and A. A. Hussain, "Support vector machines for wind speed prediction," *Renewable Energy*, vol. 29, pp. 939–947, 2004.

[25] P. F. Pai and W. C. Hong, "An improved neural network model in forecasting tourist arrivals," *Annals of Tourism Research*, vol. 32, pp. 1138–1141, 2005.

[26] X. Peng and Y. Wang, "A normal least squares support vector machine (NLS-SVM) and its learning algorithm," *Neurocomputing*, vol. 72, pp. 3734–3741, 2009.

[27] K. L. Seip and R. McNown, "The timing and accuracy of leading and lagging business cycle indicators: A new approach," *International Journal of Forecasting*, vol. 23, pp. 277–287, 2007.

[28] J. A. K. Suykens, T. Van Gestel, J. De Brabanter, B. De Moor, and J. Vandewalle, *Least Squares Support Vector Machines*, World Scientific, Singapore, 2002.

[29] F. E. H. Tay and L. Cao, "Modified support vector machines in financial time series forecasting," *Neurcomputing*, vol. 48, pp. 847–861, 2002.

[30] V. Vapnik, S. Golowich, and A. Smola, "Support vector machine for function approximation, regression estimation, and signal processing," *Advances in Neural Information Processing Systems*, vol. 9, pp. 281–287, 1996.

[31] X. C. Xi, A. N. Poo, and S. K.Chou, "Support vector regression model predictive control on a HVAC plant," *Control Engineering Practice*, vol. 15, pp. 897–908, 2007.

[32] B. Wu and N.-F. Tseng, "A new approach to fuzzy regression models with application to business cycle analysis," *Fuzzy Set and Systems*, vol. 130, pp. 33–42, 2002.

[33] J.-M. Yang and T.-W. Kim, "A search for leading sectors over the business cycle: The case of Korea," *Japan and the World Economy*, vol. 17, pp. 480–495, 2005.

[34] C. C. Yao and P. T. Yu, "Fuzzy regression based on asymmetric support vector machines," *Applied Mathematics and Computation*, vol. 182, pp. 175–193, 2006.

[35] P. S. Yu, S. T. Chen, and I. F. Chang, "Support vector regression for real-time flood stage forecasting," *Journal of Hydrology*, vol. 328, pp. 704–716, 2006.

[36] L. A. Zadeh, "Fuzzy sets," *Information and Control*, vol. 8, pp. 338–353, 1965.

2011 IEEE International Conference on Fuzzy Systems
June 27-30, 2011, Taipei, Taiwan

Fuzzy Clustering Approach for Star-Structured Multi-Type Relational Data

Jian-Ping Mei and Lihui Chen
Division of Information Engineering, School of EEE
Nanyang Technological University
50 Nanyang Avenue, Singapore
Email: meij0002@e.ntu.edu.sg, elhchen@ntu.edu.sg

***Abstract*—Recently, mining interrelated data among multiple types of objects attracts a lot of attention due to its importance in many real-world applications. Despite of extensive study on fuzzy clustering of vector space data and homogeneous relational data, very limited exploration has been made on fuzzy clustering of relational data involving several object types. In this paper, we propose FC-SMR, a fuzzy approach for clustering star-structured multi-type relational data, where the central type is related to multiple attribute types. In FC-SMR, objects of the central type are clustered based on the rankings of objects of different attribute types. We formulate the clustering problem as a constrained maximization problem and give an efficient algorithm for finding local solutions of the defined objective function. Experimental studies conducted on real-world document data show the effectiveness of the new approach.**

***Index Terms*—Fuzzy clustering; co-clustering; multi-type; heterogeneous relational data; document categorization**

I. Introduction

Compared with hard clustering, fuzzy clustering which allows overlaps among clusters is generally agreed to be able to provide a more accurate and natural description of the underlying structure of real-world data. The same as k-means, most existing studies on fuzzy clustering such as fuzzy c-means (FCM) [1] deal with vector space data, of which each object is represented as a vector in some feature space, e.g. a document is represented as a vector where each feature or dimension of the vector is a distinctive word. Other than the vector-feature represented data, the pairwise relational data also has been studied for a long time [2], [3], [4]. Most typically, the relationships are similarities or dissimilarities between each pair of objects from a given data set, e.g. similarity between two documents. These document-document relation is referred as homogeneous as it exist between objects of the same type, i.e., document. Although the vector space data and homogeneous relational data are two basic data representation models based on which extensive studies have been carried out, new challenges come out when the technique of clustering is applied to the data mining domain for handling various real-world data sets, which is more natural to be represented as multi-type relational data, where inter-relations exist among objects of several types.

In some recent studies [5], [6], fuzzy co-clustering approaches have been proposed for document categorization which simultaneously cluster documents and words. Different from the two basic data representations, in co-clustering, *document* and *word* are treated as two object types, and the *document-word* co-occurrence data is a bi-type heterogeneous relational data. While traditional clustering generates clusters of one type of objects, co-clustering simultaneously clusters objects of each of the two types. It has been shown in the literature that co-clustering approaches are always more effective and informative than those traditional one-side clustering approaches [7].

However, co-clustering is not applicable on data involving more than two object types. For document data sets, other than *document* and *word*, which form the *document-word* relation, document may also be related to other object types. For example, in hierarchical taxonomy mining, each document belongs to a category, which forms a *document-category* relation. The relations among objects of different types may form different structures. A star-structure is a special case where the central type is related to several attribute types as illustrated in Fig. 1. For document clustering, *document* is the central type and other object types, such as *word* and *category* are attribute types, and the *document-word* relation corresponds to a bi-type star-structure, while the *document-word* together with the *document-category* relations form a tri-type star-structure. It is possible to transform multi-type relational data to one of the basic data representation forms with respect to the object type that is interested, and then use an existing approach to get the clusters of the objects of this type. For example, a vector representation for the central-type objects may be obtained by concatenating all attribute-type objects as its features. However, this leads to a very sparse data in a high dimensional space which is a very difficult problem for most clustering approaches to solve.

To fully make use of those central-attributes relations, multi-type relational clustering approaches have been proposed in [8], [9], [10], [11], [12], [13], [14]. Most of these approaches are formulated as high-level co-clustering approaches, where [9], [11], [15], [12] formulate clustering as matrix factorization problems, [14], [13] are model-based approaches solved by the EM algorithm, [8] solves the problem with semi-definite programming and [10] is an iterative spectral clustering which needs eigenvalue decomposition at each iteration. In this paper, we develop a fuzzy clustering approach for star-structured multi-type relational data mining (FC-SMR). The proposed approach is a natural extension of the fuzzy co-clustering

978-1-4244-7316-8/11/$26.00 ©2011 IEEE

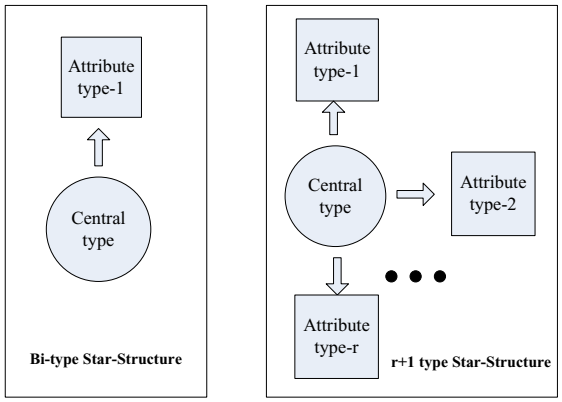

Fig. 1. Multi-type relational data with a star-structure

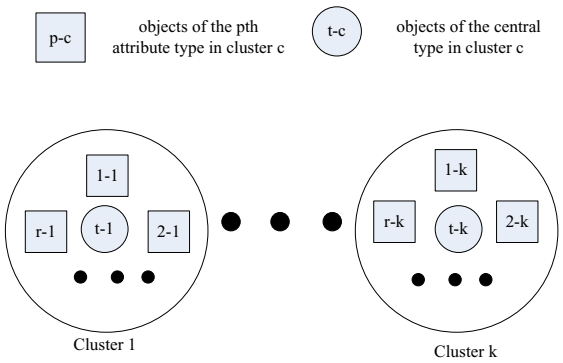

Fig. 2. The clustering problem for multi-type star-structured relational data.

approach (FCoDok) in [5]. In FCoDok, a co-cluster is a document cluster associated with a word cluster, while in FC-SMR, each document cluster is associated with r clusters with each of them corresponding to an attribute type. This multi-type relational clustering problem has some similarity to the multi-view clustering [16] and collaborative clustering [17] in the sense that all these three problems make use of more than one data descriptions or views, i.e. relational matrices between the central type and different attribute types, views by different feature sets or data source distributed in multiple places. However, in [16] and [17], clustering is performed locally on each data view during which the partition information on other views are collaborated to some degree, while in the problem of this study, only a global partition of the documents is produced as an optimal solution for taking care of all relations. Moreover, the clusters of objects of each of the attribute types are also obtained.

The rest of the paper is arranged as follows: we first review some related work in Section 2. The detailed formulation of the proposed approach is then presented in Section 3. Experimental results on benchmark document data sets are reported and discussed in Section 4. Finally, we make the conclusion of this paper in Section 5.

II. Fuzzy co-clustering for documents

Several fuzzy co-clustering approaches have been proposed in the literature, and here we only review the most related one referred as FCoDok proposed in [5]. This approach is an improved version of [18] for document categorization. Given the document-word co-occurrence matrix $r_{ij} \in \mathbf{R}_{n\times m}$ of n documents and m words, the objective of FCoDok is to maximize the following criterion:

$$J_{FCoDok} = \sum_{c=1}^{k}\sum_{i=1}^{n}\sum_{j=1}^{m} u_{ic} r_{ij} v_{jc} - T_u \sum_{c=1}^{k}\sum_{i=1}^{n} u_{ic}^2 - T_v \sum_{c=1}^{k}\sum_{j=1}^{m} v_{jc}^2 \quad (1)$$

subject to

$$\forall c, i, j, \quad u_{ic} \geq 0, v_{jc} \geq 0 \quad (2)$$

$$\forall i, \sum_{c=1}^{k} u_{ic} = 1; \quad \forall c, \sum_{j=1}^{m} v_{jc} = 1 \quad (3)$$

where k is the number of clusters, u_{ic} is the membership of document i with respect to cluster c, and v_{jc} is the membership of word j with respect to cluster c. From (3), it can be observed that u_{ic} is the standard fuzzy membership as for each document, the sum of its u values in all clusters is 1; differently, for each word j, the sum of its v values in all clusters is not required to be 1, instead, the sum of v values over all words in each cluster is 1. To differentiate these two kinds of measures, from now on, we refer u the membership while v the ranking. The first term of (1) called degree of aggregation measures the quality of the clustering and the second and third terms of (1) are quadratic regularization of u and v, respectively. This quadratic regularization has also been used as an alternative way to generate the fuzziness of memberships in fuzzy c-means [19].

The updating equations of u_{ic} and v_{jc} are derived by the method of Lagrange Multiplier, which is shown as below [5]:

$$u_{ic} = \frac{1}{2T_u} g_{ic} + \frac{1}{k}\left(1 - \frac{1}{2T_u}\sum_{f=1}^{k} g_{if}\right) \quad (4)$$

$$v_{jc} = \frac{1}{2T_v} h_{jc} + \frac{1}{m}\left(1 - \frac{1}{2T_v}\sum_{p=1}^{m} h_{pc}\right) \quad (5)$$

where $g_{ic} = \sum_{j=1}^{m} v_{jc} r_{ij}$ and $h_{jc} = \sum_{i=1}^{n} u_{ic} r_{ij}$. Since the above updating formulas do not guarantee nonnegativity of u_{ic} and v_{jc}, during each iteration, negative values of u_{ic} and v_{jc} are set to 0, and re-normalization is performed accordingly to satisfy the summation constraints in (3). Solutions that guarantee nonnegativity are also derived in [5] with the KKT (Karush-Kuhn-Tucker) conditions.

III. Fuzzy Clustering for Star-Structured Multi-Type Relational Data (FC-SMR)

The FCoDok handles the *document-word* co-occurrence data, which can be regarded as bi-type star-structured relational

data, where *word* is the only attribute type. Now, we present the proposed approach FC-SMR for star-structured relational data with $r > 1$ attribute types.

A. Problem Formulation

Given a document data involving $r > 1$ attribute types, we have r matrices $\{\mathbf{R}_p\}_{p=1}^r$, where $r_{ij}^p \in \mathbf{R}_p$ is the relationship between the ith object of the central type, i.e., document x_i, and the jth object of the pth attribute type denoted as y_j^p. We assume that each relation matrix is weighted by β_p. As illustrated in Fig. 2, the problem is to produce k document clusters based on r relation matrices $\{\mathbf{R}_p\}_{p=1}^r$, and each document cluster is associated with a cluster of objects of each of the attribute types. We use u_{ic} to represent the fuzzy membership of x_i in cluster c, and v_{jc}^p the ranking of y_j^p in cluster c. The proposed approach is to maximize the following objective:

$$J_{FC-SMR} = \sum_{p=1}^{r}\sum_{c=1}^{k}\sum_{i=1}^{n}\sum_{j=1}^{m_p}\beta_p u_{ic} r_{ij}^p v_{jc}^p \tag{6}$$

$$-\frac{\rho}{2}\sum_{c=1}^{k}\sum_{i=1}^{n}(u_{ic})^2 - \frac{\eta_p}{2}\sum_{p=1}^{r}\sum_{c=1}^{k}\sum_{j=1}^{m_P}(v_{jc}^p)^2 \tag{7}$$

subject to

$$\forall i, c, \quad u_{ic} \geq 0; \quad \forall p, j, c, \quad v_{jc}^p \geq 0; \tag{8}$$

$$\forall i, \sum_{c=1}^{k} u_{ic} = 1, \quad \forall p, j, \quad \sum_{j=1}^{m_p} v_{jc}^p = 1. \tag{9}$$

where n and m_p are the number of documents and the number of objects of the pth attribute type, respectively. The document clusters obtained as the solution of the above problem may not be the optimal with respect to the relation between *document* and each individual attribute type, but it is an overall optimum considering the relations between *document* and all attribute types. We use the classic method of Lagrange multiplier to derive the local solutions of the constrained optimization problem formulated above. The Lagrangian is formed as

$$L = J_{FC-SMR} + \sum_{i=1}^{n}\gamma_i(\sum_{c=1}^{k}u_{ic} - 1) + \sum_{p=1}^{r}\sum_{c=1}^{k}\lambda_c^p\sum_{j=1}^{m_p}(v_{jc}^p - 1)$$
$$+\sum_{c=1}^{k}\sum_{i=1}^{n}\alpha_{ic}u_{ic} + \sum_{p=1}^{r}\sum_{c=1}^{k}\sum_{j=1}^{m_p}\theta_{jc}^p v_{jc}^p \tag{10}$$

where all γ_i and λ_c^p, α_{ic}, θ_{jc}^p are Lagrange multipliers. According to the KKT (Karush-Kuhn-Tucker) conditions, after some algebraic manipulations, u_{ic} can be derived as

$$u_{ic} = \begin{cases} \frac{1}{\rho}g_{ic} + \frac{1}{|\mathcal{K}_i^+|}(1 - \frac{1}{\rho}\sum_{f\in\mathcal{K}_i^+} g_{if}), & \text{for } \ c \in \mathcal{K}_i^+ \\ 0, \quad otherwise \end{cases} \tag{11}$$

with

$$g_{ic} = \sum_{p=1}^{r}\sum_{j=1}^{m_p}\beta_p v_{jc}^p r_{ij}^p \tag{12}$$

where

$$\mathcal{K}_i^+ = \{f : u_{if} > 0\}$$

is the set that consists of cluster ids of which the memberships of x_i is positive, and

$$v_{jc}^p = \begin{cases} \frac{1}{\eta_p}h_{jc}^p + \frac{1}{|\mathcal{N}_c^+|}(1 - \frac{1}{\eta_p}\sum_{l\in\mathcal{N}^+} h_{lc}^p), & \text{for } \ j \in \mathcal{N}_c^+ \\ 0, \quad otherwise \end{cases} \tag{13}$$

with

$$h_{jc}^p = \beta_p \sum_{i=1}^{n} r_{ij}^p u_{ic} \tag{14}$$

where

$$\mathcal{N}_c^+ = \{l : v_{lc}^p > 0\}$$

is the set of object ids of which the rankings in cluster c is positive. The derivation is similar as in FCoDok and we can use Procedure-K and Procedure-N in [4] to decide $\mathcal{K}_i^+$ and $\mathcal{N}_c^+$.

The first term of (11) decides the membership distribution of each x_i in k clusters while the second term is a normalization to ensure the summation constraint to be satisfied. From (12), it can be observed that given the rankings of attribute objects in each cluster, the membership of x_i in a cluster c is larger than in cluster f if more objects of r attribute types related to x_i have large ranking values in cluster c than in cluster f. Similarly, the first term in (13) decides the distribution of rankings among objects of the pth attribute type in cluster c, and the second term is there to ensure the satisfaction of the summation constraints on the ranking values. From (14), we may know that the rankings of objects of the same attribute type are only decided by the memberships of the documents. Given the memberships of documents in a cluster c, the ranking of attribute object y_i^p in this cluster is larger than that of another attribute object y_j^p if more documents related to y_i^p have larger memberships in this cluster.

B. Algorithm

For implementation, we can update $u_{ic} \in \mathbf{U}_{n\times k}$ and $v_{jc}^p \in \mathbf{V}_p(m_p \times k)$ in matrix form as below and use the same simplified way as in [5] to deal with negative memberships and rankings.

Calculate $\mathbf{U}$:

$$\mathbf{U} = \frac{1}{\rho}\mathbf{G} + \frac{1}{k}(\ -\frac{1}{\rho}\ \mathbf{G}) \tag{15}$$

$$\mathbf{G} = \sum_{p=1}^{r}\beta_p\mathbf{R}_p\mathbf{V}_p \tag{16}$$

For each row i of $\mathbf{U}$, find

$$\mathcal{K}_i^+ = \{f : u_{if} > 0\} \tag{17}$$

modify

$$u_{ic} = \begin{cases} 0, & \text{for} \quad c \notin \mathcal{K}_i^+ \\ \frac{u_{ic}}{\sum_{f\in\mathcal{K}_i^+} u_{if}}, & \text{for} \quad c \in \mathcal{K}_i^+ \end{cases} \tag{18}$$

for each p, calculate $\mathbf{V}_p$:

$$\mathbf{V}_p = \frac{1}{\eta_p}\mathbf{H}_p + \frac{1}{m_p}(\quad -\frac{1}{\eta_p}\quad \mathbf{H}_p) \tag{19}$$

$$\mathbf{H}_p = \beta_p \mathbf{R}_p^T \mathbf{U} \tag{20}$$

For each column c of $\mathbf{V}_p$, find

$$\mathcal{N}_c^+ = \{l : v_{lc}^{\mu} > 0\} \tag{21}$$

modify

$$v_{jc}^p = \begin{cases} 0, & \text{for} \quad j \notin \mathcal{N}_c^+ \\ \dfrac{v_{jc}^p}{\sum_{l \in \mathcal{N}_c^+} v_{lc}^p}, & \text{for} \quad j \in \mathcal{N}_c^+ \end{cases} \tag{22}$$

where is a matrix with a proper size, of which every entry is 1. The detailed algorithm is given as below:

Algorithm 1 FC-SMR

Input: $n \times m_p$ Relation matrix $\{\mathbf{R}_p\}_{p=\{1,2,\ldots,r\}}$, the number of clusters k, parameter ρ, $\{\eta_p\}_{p=\{1,2,\ldots,r\}}$, and positive weights $\{\beta_p\}_{p=\{1,2,\ldots,r\}}$.

Output: Fuzzy memberships of the central objects $\mathbf{U}$ and rankings of the attribute objects $\mathbf{V}_p$ for each $p = \{1, 2, \ldots, r\}$.

Method:

1: Initialize $\mathbf{U}^{(0)}$ with nonnegative values.
2: **repeat**
3: **for** each $p = \{1, 2, \ldots, r\}$ **do**
4: Update $\mathbf{V}_p^{(l)}$ as (19) with $\mathbf{H}_p^{(l)}$ calculated from (20).
5: Modify $\mathbf{V}_p^{(l)}$ according to (21) and (22).
6: **end for**.
7: Update $\mathbf{U}^{(l+1)}$ as (15) with $\mathbf{G}^{(l+1)}$ calculated from (16).
8: Modify $\mathbf{U}^{(l+1)}$ according to (17) and (18).
9: **until** convergence

IV. Experimental Results

This section presents experimental studies of the proposed FC-SMR approach for document clustering. We use the benchmark data set 20newsgroups [20].

A. Data

The original data of 20newsgroups downloaded at http://people.csail.mit.edu/jrennie/20Newsgroups/ contains 18828 non-duplicated documents, which are categorized into 20 topics. Following [8] and [10], we generate three subsets consisting of different subtopics as listed in Table I. For example, data set TM1 consists of clusters C_1 and C_2, where C_1 is the *rec.sport* cluster which contains two subtopics or categories on *baseball* and *hockey*, and C_2 is the *talk.politics* cluster that has three subtopics on *guns*, *mideast* and *misc*. Each of the three data sets is formed by randomly selecting 100 documents from each of the chosen subtopics. For each data set, we obtain two relation matrices *document-word* and *document-category* which are denoted as $\mathbf{R}_1$ and $\mathbf{R}_2$, respectively. The *rainbow* toolkit [21] is used to get the *document-word* occurrence data. Stop-words have been removed and 2000 words with the largest information gain are kept. Non-text documents are skipped by *rainbow*. After preprocessing, documents consisting of less than two words are removed and finally we have 497, 598 and 794 documents for TM1, TM2 and TM3, respectively. The *tf-idf* weighting [22] is used for weighting the words in each document. Each subtopic is a category and $\mathbf{R}_2$ is a binary matrix with an entry is 1 if the document is from that subtopic otherwise is 0.

TABLE I
Structure of Newsgroup Datasets

TM1	C_1: {rec.sport.baseball, rec.sport.hockey} C_2: {talk.politics.guns, talk.politics.mideast, talk.politics.misc}
TM2	C_1: {comp.graphics, comp.os.ms-windows.misc} C_2: {rec.autos, rec.motorcycles} C_3: {sci.crypt, sci.electronics}
TM3	C_1: {comp.sys.ibm.pc.hardware, comp.sys.mac.hardware} C_3: {rec.autos, rec.motorcycles} C_3: {sci.med, sci.space} C_4: {talk.politics.guns, talk.politics.mideast}

B. Setting Up

We tested the proposed approach FC-SMR on the TM1, TM2 and TM3 three data sets. For comparison, we also implemented four existing approaches: Hyperspherical Fuzzy c-Means (HFCM) [23], fuzzy co-clustering (FCoDok) [5], Non-negative matrix factorization approach referred as (NMF-H) [12] and spectral relational clustering (SRC) [10]. HFCM is a modified fuzzy c-means clustering with cosine distance for documents; NMF-H and SRC are two existing multi-type relational clustering approaches. The results of HFCM and FCoDok are obtained based on $\mathbf{R}_1$, the *document-word* bi-type relational data. Three multi-type relational clustering approaches, FC-SMR, NMF-H and SRC are based on $\mathbf{R}_1$ and $\mathbf{R}_2$, i.e. the *word-document-category* tri-type relational data.

In our experiment, the number of clusters k is set to be equal to the real number of classes for each data set. We set $T_u = 0.001, T_v = 1$ for FCoDok and $\rho = 0.01, \eta_1 = \eta_2 = 1$ for FC-SMR. The fuzzifier $m = 1.02$ is used for HFCM. We let $\beta_1 + \beta_2 = 1$ in FC-SMR. For all fuzzy approaches, truncated clusters are obtained by assigning each object to the cluster with the largest membership.

C. FC-SMR vs. HFCM and FCoDok

We first compare the performance of the proposed FC-SMR with existing fuzzy approaches HFCM and FCodok. Table II to Table IV give the best clustering results that HFCM, FCoDok and FC-SMR can achieve among 30 trials with random initializations on the three data sets, respectively.

It can be seen from these contingency tables that with the additional *document-category* relation, FC-SMR is able to achieve 100% accuracy on all the three data sets. The results of FCoDok and HFCM on TM1 and TM2 are close, but FCoDok performs better than HFCM on TM3. Although FCoDok and HFCM make use of the same *document-word* matrix, HFCM treats each document as a vector and use the cosine similarity to measure the closeness of two documents, while FCoDok

treats document and word as two different object types and documents are clustered based the ranking of words. There is no explicit similarity measure defined in FCoDok and FC-SMR.

Fig. 3 plots $\mathbf{u}_1 = \{u_{1,1}, u_{2,1} \ldots, u_{500,1}\}$, the membership values of documents in C_1 of TM1 produced by HFCM and FC-SMR, respectively. According to the summation constraints, the memberships in the other cluster follow $\mathbf{u}_2 = 1 - \mathbf{u}_1$. For TM1, the ground truth partition is that the first 198 documents are in C_1: *rec.sport* and the rest are in C_2: *talk.politics*. It can be seen from Fig. 3a that in HFCM, for the 21th document, $u_{21,1} < u_{21,2}$, although this document should be in C_1. At the same time, six documents (labeled by circles) which should be in C_2 are assigned larger memberships in C_1. These results indicate that the representation of these documents in terms of word frequency is not sufficient enough for correctly assigning those documents into the right clusters. The *document-category* relation help to clarify the uncertainty or correct the misleading information in the *document-word* relation. This can be seen from Fig. 3b that, when the *document-category* relation are further incorporated, those previously mis-clustered documents are now assigned reasonable memberships in two clusters which are consistent with the ground truth. Although it can be told from the document-category matrix that which documents are in the same subtopic, this matrix alone delivers no information on the hierarchy structure of the subtopics, i.e. which subtopics should be combined into a high-level cluster. Therefore, clustering only based on the *document-category* relation does not produce any meaningful result as it merely combines those subgroups into the specified number of clusters in a random way.

D. Comparison of NMI Values

Now we compare FC-SMR with four other approaches in terms of *Normalized Mutual Information* (NMI) [24]. The higher the NMI value, the more closer of the algorithm generated results to the ground truth. The NMI value equals to 1 only when the partition produced by an algorithm is identical to the ground truth of the partition. Each approach is run 30 trials on each data set. Random initializations are used for HFCM, and other approaches are initialized with document fuzzy memberships produced by HFCM. Table V shows the mean and standard deviation (numbers in brackets) of NMI values over 30 trials. For FC-SMR, we give results with different values of β_1 and β_2.

It can be seen that FC-SMR achieves significant better results than other approaches on all three data sets. Generally, three multi-type relational clustering approaches making use of both $\mathbf{R}_1$ and $\mathbf{R}_2$ perform better than HFCM and FCoDok where $\mathbf{R}_2$ is not used. FCoDok and HFCM give close results on TM2 but HFCM outperforms FCoDok on TM1, while FCoDok performs better than HFCM on TM3. Among three multi-type relational approaches, FC-SMR is the best and NMF-H is better than SRC. Like FC-SMR, NMF-H also produces the ideal result on TM1, but its performances on the other two data sets are not as good as those of FC-SMR.

TABLE V
COMPARISON OF NMI VALUES

	TM1	TM2	TM3
HFCM	0.8862 (0.0149)	0.7183 (0.0076)	0.7862 (0.0395)
FCoDok	0.8506 (0.0138)	0.7127 (0.0024)	0.8129 (0.0408)
NMF-H	1.0000 (0.0000)	0.8008 (0.1757)	0.8925 (0.1032)
SRC	0.9595 (0.1541)	0.7207 (0.1679)	0.8053 (0.1331)
FC-SMR ($\beta_2 = 1 - \beta_1$)			
($\beta_1 = 0.1$)	1.0000 (0.0000)	1.0000 (0.0000)	0.9866 (0.0525)
($\beta_1 = [0.2, 0.8]$)	1.0000 (0.0000)	1.0000 (0.0000)	0.9917 (0.0455)
($\beta_1 = 0.9$)	1.0000 (0.0000)	1.0000 (0.0000)	1.0000 (0.0000)

It also shows that the results of FC-SMR on three data sets do not change much with respect to β_1 in [0.1, 0.9].

E. Ranking of Words and Categories

Together with the documents clusters, we also obtain the word rankings and category rankings. The ranking values of each category in each cluster is shown in the three matrices given in (23) to (25) for TM1, TM2 and TM3, respectively, where each row indicates a category and each column indicates a cluster or a topic. Top 10 words of each cluster are also listed in Table VI. As attribute types, *category* and *word* can be used for description or characterization of the document cluster. We can see that those key categories and key words which have large ranking values provide meaningful information to tell what topic each document cluster possibly related to. If we take C_1 of TM1 for example, from its associated key categories named *basedball* and *hockey*, and key words, such as *game*, *hockey*, *team*, *players*, *baseball*, we may guess that documents of this cluster are about sports, possibly on hockey and baseball. Such kind of information can be used as a short summary of the cluster which provides a quick sense of the whole document cluster without looking through each of the long documents.

$$\begin{array}{c} \\ \textit{baseball} \\ \textit{hockey} \\ \textit{guns} \\ \textit{mideast} \\ \textit{misc} \end{array} \begin{array}{c} \begin{array}{cc} \textit{rec.sport} & \textit{talk.politics} \end{array} \\ \begin{pmatrix} 0.4327 & 0 \\ 0.5673 & 0 \\ 0 & 0.3067 \\ 0 & 0.3506 \\ 0 & 0.3428 \end{pmatrix} \end{array} \tag{23}$$

$$\begin{array}{c} \\ \textit{graphics} \\ \textit{os.ms-windows.misc} \\ \textit{autos} \\ \textit{motorcycles} \\ \textit{crypt} \\ \textit{electronics} \end{array} \begin{array}{c} \begin{array}{ccc} \textit{comp} & \textit{rec} & \textit{sci} \end{array} \\ \begin{pmatrix} 0.4716 & 0 & 0 \\ 0.5284 & 0 & 0 \\ 0 & 0.4579 & 0 \\ 0 & 0.5421 & 0 \\ 0 & 0 & 0.7018 \\ 0 & 0 & 0.2982 \end{pmatrix} \end{array} \tag{24}$$

TABLE II
CONTINGENCY TABLE OF CLUSTERING RESULTS ON TM1

	HFCM		FCoDok		FC-SMR	
	Clust 1	Clust 2	Clust 1	Clust 2	Clust 1	Clust 2
Class 1	197	1	196	2	198	0
Class 2	6	293	4	295	0	299

TABLE III
CONTINGENCY TABLE OF CLUSTERING RESULTS ON TM2

	HFCM			FCoDok			FC-SMR		
	Clust 1	Clust 2	Clust 3	Clust 1	Clust 2	Clust 3	Clust 1	Clust 2	Clust 3
Class 1	193	3	3	194	4	1	199	0	0
Class 2	2	188	10	2	190	8	0	200	0
Class 3	20	9	170	21	11	167	0	0	199

TABLE IV
CONTINGENCY TABLE OF CLUSTERING RESULTS ON TM3

	HFCM				FCoDok				FC-SMR			
	Clust 1	Clust 2	Clust 3	Clust 4	Clust 1	Clust 2	Clust 3	Clust 4	Clust 1	Clust 2	Clust 3	Clust 4
Class 1	189	4	5	1	194	1	4	0	199	0	0	0
Class 2	3	188	5	3	4	190	4	1	0	199	0	0
Class 3	4	9	180	6	6	6	182	5	0	0	199	0
Class 4	0	6	2	189	1	6	4	186	0	0	0	197

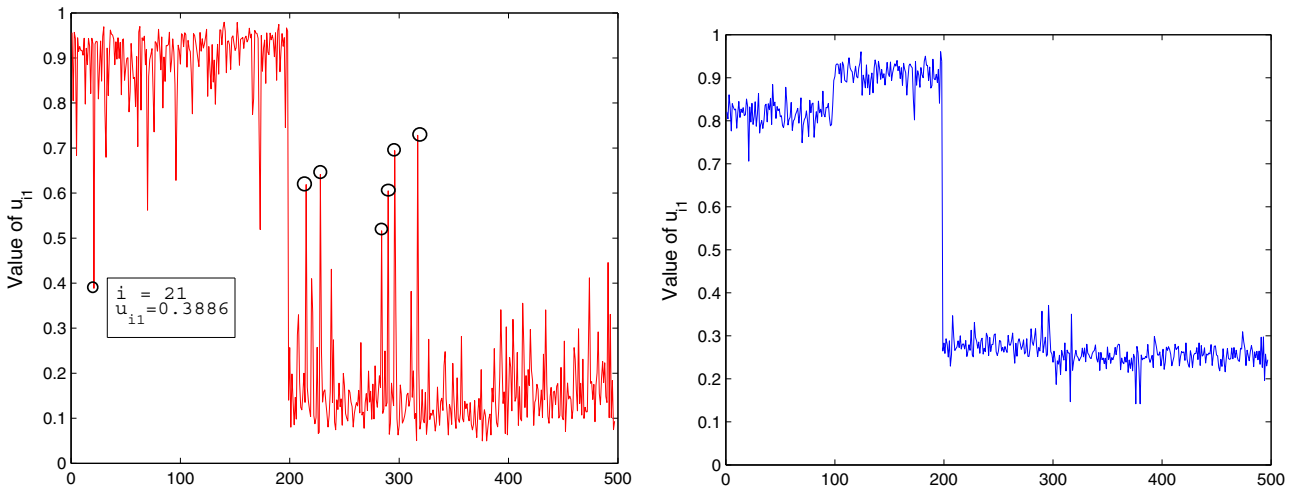

(a) HFCM (b) FC-SMR

Fig. 3. Fuzzy memberships of documents with respect to C_1 of TM1 by HFCM and FC-SMR. The (horizontal) x-axis denotes the document id ($i = 1, \ldots, 500$) and the (vertical) y-axis shows the value of the membership u_{i1}. In (a), small circles label objects that are clustered incorrectly.

TABLE VI
TOP 10 WORDS IN EACH CLUSTER OF THREE DATA SETS GENERATED BY FC-SMR

TM1		TM2			TM3			
C_1: *rec.sport*	C_2: *talk.politics*	C_1: *comp*	C_2: *rec*	C_3: *sci*	C_1: *comp.sys*	C_2: *rec*	C_3: *sci*	C_4: *talk.politics*
game	jews	windows	car	key	mac	bike	space	israel
hockey	israel	file	bike	clipper	drive	car	nasa	israeli
team	people	graphics	dod	chip	card	dod	moon	jews
games	government	files	bmw	keys	scsi	bikes	launch	arab
players	gun	tiff	dog	nsa	apple	list	pat	arabs
ca	state	version	cars	encryption	disk	ride	shuttle	turkish
baseball	children	ftp	insurance	netcom	mb	honda	henry	jewish
season	cramer	site	bikes	phone	software	bmw	orbit	mr
win	fbi	program	audi	des	drives	oil	alaska	armenians
espn	cosmo	dos	motorcycle	government	driver	miles	mission	muslim

$$
\begin{array}{l}
\\
\textit{ibm.pc.hardware} \\
\textit{mac.hardware} \\
\textit{autos} \\
\textit{motorcycles} \\
\textit{med} \\
\textit{space} \\
\textit{guns} \\
\textit{mideast}
\end{array}
\begin{array}{c}
\begin{array}{cccc}
\textit{comp.sys} & \textit{rec} & \textit{sci} & \textit{talk.politics}
\end{array} \\
\left(\begin{array}{cccc}
0.5265 & 0 & 0 & 0 \\
0.4735 & 0 & 0 & 0 \\
0 & 0.3749 & 0 & 0 \\
0 & 0.6251 & 0 & 0 \\
0 & 0 & 0.4056 & 0 \\
0 & 0 & 0.5944 & 0 \\
0 & 0 & 0 & 0.3530 \\
0 & 0 & 0 & 0.6470
\end{array}\right)
\end{array}
\tag{25}
$$

V. Conclusion

In this paper, we work on a fuzzy clustering approach for star-structured multi-type relational data analysis, where relations exist between the central type and r attribute types. The main idea of the new approach is to estimate the fuzzy memberships of the central-type objects based on the rankings of all related attribute-type objects, and the memberships of central-type objects are in turn used for updating the rankings of all attribute-type objects. Our experimental study on benchmark document data sets demonstrates the benefit of using information from multiple relation matrices for clustering as well as the feasibility and effectiveness of the proposed approach.

References

[1] J. C. Bezdek, *Pattern Recognition with Fuzzy Objective Function Algorithms*. New York: Plenum, 1981.

[2] R. J. Hathaway, J. W. Devenport, and J. C. Bezdek, "Relational duals of the c-means clustering algorithms," *Pattern Recogn.*, vol. 22, pp. 205–212, 1988.

[3] R. Krishnapuram, A. Joshi, O. Nasraoui, and L. Yi, "Low-complexity fuzzy relational clustering algorithms for web mining," *IEEE Trans. Fuzzy Syst.*, vol. 9, pp. 595–607, 2001.

[4] J.-P. Mei and L. Chen, "Fuzzy clustering with weighted medoids for relational data," *Pattern Recognition*, vol. 43, pp. 1964–1974, 2010.

[5] K. Kummamuru, A. Dhawale, and R. Krishnapuram, "Fuzzy co-clustering of documents and keywords," in *12th IEEE Int. Conf. Fuzzy Systems*, 2003.

[6] W.-C. Tjhi and L. Chen, "Dual fuzzy-possibilistic coclustering for categorization of documents," *IEEE Trans. Fuzzy Syst.*, vol. 17, pp. 532–543, 2009.

[7] I. S. Dhillon, S. Mallela, and D. S. Modha, "Information-theoretic co-clustering," in *Proc. KDD '03*, 2003, pp. 89–98.

[8] B. Gao, T.-Y. Liu, X. Zheng, Q.-S. Cheng, and W.-Y. Ma, "Consistent bipartite graph co-partitioning for star-structured high-order heterogeneous data co-clustering," in *Proc. KDD'05*.

[9] B. Long, X. Wu, Z. Zhang, and P. S. Yu, "Unsupervised learning on k-partite graphs," in *KDD'06*.

[10] B. Long, Z. Zhang, X. Wu, and P. S. Yu, "Spectral clustering for multi-type relational data," in *Proc. 23th Int. Conf. Machine Learning*, 2006, pp. 585–592.

[11] A. P. Singh and G. J. Gordon, "Relational learning via collective matrix factorization," in *Proc. KDD'08*.

[12] Y. Chen, L. Wang, and M. Dong, "Non-negative matrix factorization for semisupervised heterogeneous data coclustering," *IEEE Trans. Knowl. Data Eng.*, vol. 22, no. 10, pp. 1459–1474, 2010.

[13] B. Long, Z. Zhang, and P. S. Yu, "A probabilistic framework for relational clustering," in *KDD'07*.

[14] Y. Sun, Y. Yu, and J. Han, "Ranking-based clustering of heterogeneous information networks with star network schema," in *Proc. KDD'09*.

[15] F. Wangy, T. Li, and C. Zhang, "Semi-supervised clustering via matrix factorization," in *SIAM International Conference on Data Mining, SDM'08*, 2008.

[16] G. Cleuziou, M. Exbrayat, L. Martin, and J.-H. Sublemontier, "Cofkm: a centralized method for multiple-view clustering," in *Proc. 9th IEEE Int. Conf. Data Mining*, 2009.

[17] W. Pedrycz, "Collaborative fuzzy clustering," *Pattern Recogn. Lett.*, no. 14, pp. 1675–1686, 2002.

[18] C.-H. Oh, K. Honda, and H. Ichihashi, "Fuzzy clustering for categorical multivariate data," in *Proc. Joint 9th IFSA World Cong. and 20th NAFIPS Int. Conf.*, Vancouver, 2001, pp. 2154–2159.

[19] S. Miyamoto and K. Umayahara, "Fuzzy clustering by quadratic regularization," in *IEEE Int. Conf. Fuzzy Systems*, 1998.

[20] K. Lang, "NewsWeeder: learning to filter netnews," in *Proc. 12th Int. Conf. Machine Learning*, 1995, pp. 331–339.

[21] A. K. McCallum, "Bow: A toolkit for statistical language modeling, text retrieval, classification and clustering," 1996. [Online]. Available: http://www.cs.cmu.edu/ mccallum/bow/

[22] G. Salton and C. Buckley, "Term-weighting approaches in automatic text retrieval," *Information Processing and Management*, vol. 24, no. 5, pp. 513–523, 1988.

[23] M. E. S. Mendes and L. Sacks, "Evaluating fuzzy clustering for relevance-based information access," in *12th IEEE Int. Conf. Fuzzy Systems*, 2003, pp. 648–653.

[24] A. Strehl and J. Ghosh, "Cluster ensembles—a knowledge reuse framework for combining multiple partitions," *Journal on Machine Learning Research*, vol. 3, pp. 583–617, 2002.

2011 IEEE International Conference on Fuzzy Systems
June 27-30, 2011, Taipei, Taiwan

Predicting Septic Shock Outcomes in a Database with Missing Data using Fuzzy Modeling

Influence of Pre-processing Techniques on Real-World Data-based Classification

Rúben D.M.A. Pereira,
André S. Fialho, Federico Cismondi
MIT-Portugal Program, Bio-Engineering Systems
MIT / HMS / IST
Cambridge, MA, USA / Lisbon, Portugal

Rui J. Almeida, Uzay Kaymak
Erasmus School of Economics, Econometric Institute
Erasmus University Rotterdam
Rotterdam, The Netherlands

Susana M. Vieira, João M.C. Sousa
Dept. of Mechanical Engineering, CIS/IDMEC-LAETA
Instituto Superior Técnico (IST)
Lisbon, Portugal

Shane R. Reti, Michael D. Howell
Beth Israel Deaconess Medical Center
Harvard Medical School (HMS)
Boston, MA, USA

Stan N. Finkelstein
Engineering Systems Division and Harvard-MIT Division of Health Sciences & Technology
Massachusetts Institute of Technology (MIT)
Cambridge, MA, USA

Abstract – **Real-world databases often contain missing data and existing correction algorithms deliver varying performance. Also, most modeling techniques are not suitable to deal with them automatically. In this study we examine different approaches to predicting septic shock in the presence of missing data. Some pre-processing techniques for managing missing data include disregarding data, or replacing it with information that by design introduces bias. In this study, we show that predictive performance improves by employing a minimum pre-processing technique, the Zero-Order-Hold (ZOH) method, by applying a Fuzzy C-Means clustering technique based on the partial distance calculation strategy (FCM-PDS) and by computing the final classification regarding the samples from each patient. Performance improvements continue to occur where up to approximately 60% of the data is missing, though for higher percentage the classification performance still is statistically improved. We further validate this approach by making comparisons with previous studies.**

Missing Data; Septic Shock; Fuzzy C-Means; Partial Distance Strategy; Zero-Order-Hold

I. INTRODUCTION

Severe sepsis remains both an important clinical challenge and an economic burden in intensive care. This is especially so for septic shock, which is characterized by the persistence of a hypotensive state, despite adequate fluid resuscitation [1]. The mortality rate among septic shock patients is very high (about 50%), as are the comparative costs of treatment. Cost-of-illness studies in the US focusing on direct costs per sepsis patient support the premise of, and attention to, increasing global health care costs [2]. Prevention and quality are therefore embraced as cost efficient contributors to a solution, and it so the ability to predict and prevent expensive septic shock hospitalizations.

A review of the literature highlights previous studies in this area that have applied knowledge-based soft computing techniques to various scenarios associated with septic shock [3, 4, 5, 6]. In [5], however, feature selection is applied in order to reduce data dimensionality by removing inputs that do not improve the prediction performance of the model.

The aim of this study is explore the influence of pre-processing and new modeling techniques for the prediction of septic shock. By using two sets of 12 and 28 selected features from the pre-processed MEDAN database [6] described in [4] and [5], respectively, results were compared to these studies.

Real-world databases often contain many missing values and artifacts, either due to lack of sampling or post-acquisition processing techniques (e.g. re-sampling). Most learning rule-based algorithms deal poorly with this. However, different pre-processing techniques can be applied to minimize this issue. In some cases, if the amount of missing data is small, it is possible to delete all incomplete data. In other cases, it can be more useful to attempt to find suitable replacement values.

This work is supported by the Portuguese Government under the programs: Project PTDC/SEM-ENR/100063/2008, Fundação para a Ciência e Tecnologia (FCT), and by the MIT-Portugal Program and FCT grants SFRH/BD/51028/2010, SFRH/43043/2008 and SFRH/43081/2008.

There are two types of missing data: missing not at random (MNAR) and missing at random (MAR) [7]. The second group can be further divided into missing completely at random (MCAR) and general MAR. MCAR values can be interpreted as a random reduction of the dataset, because their probability does not depend on the observed data or the unobserved data [8, 9]. Thus, they provide no further information for assigning incomplete features vectors to clusters. Alternatively, MAR values are not randomly distributed across all observations, but are randomly distributed within one or more subsamples instead. This is the scenario for the database used in this study.

Having discussed the unsatisfactoriness of disregarding missing data, replacing missing values creates problems of bias with the introduction of new data [10]. An alternative then to these two methods is to extend the data analysis method so that the method can deal directly with incomplete data. In this work we use a modified fuzzy c-means (FCM) clustering method that allows the identification of Takagi-Sugeno fuzzy models from incomplete data by means of product-space clustering [11]. This method uses the extension of the Fuzzy C-Means algorithm with the Partial Distance Strategy (FCM-PDS), discussed in [12, 13], and does not require any kind of imputation or iterative guess-estimation of the missing values. The algorithm possesses all the standard convergence properties of FCM. Additionally, both the global convergence theory and the local alternating optimization convergence theory are applicable [13]. Previous works [11] showed that the performance of these models is comparable to the one obtained when using a complete data set [11] making it a suitable tool for the present study.

The modeling technique used will be briefly discussed in Section II. In Section III the methodology is described followed by results and discussion in Section IV. Section V concludes the paper.

II. MODELING

Takagi-Sugeno (TS) fuzzy models can be used as universal approximators in non-linear studies as this.

A. Takagi-Sugeno Fuzzy Modeling

A TS fuzzy model [14] is a fuzzy rule-based model where the rule consequents are crisp functions of the model input:

$$R^k : \text{If } \mathbf{x} \text{ is } A^k \text{ then } y^k = f^k(\mathbf{x}),\ k = 1,\ 2,\ ...,\ K, \qquad (1)$$

where R^k denotes the k-th rule, K is the number of rules, $\mathbf{x}$ is the antecedent variable, y is the one dimensional consequent variable and A^k are the (multidimensional) antecedent fuzzy sets of the k-th rule. Each rule k has a different function f^k yielding a different value y^k for the output. The most simple consequent function f^k in (1) is the linear affine form:

$$R^k: \text{If } \mathbf{x} \text{ is } A^k \text{ then } y^k = \left(\mathbf{a}^k\right)^T \mathbf{x} + b^k \qquad (2)$$

where $\mathbf{a}^k$ is a vector of parameter and b^k is a scalar offset. This model is called an affine TS model.

B. Fuzzy Modeling with Missing Values

Several techniques can be used in fuzzy identification. One possibility is to use identification by product-space clustering [15]. This principle involves approximating a nonlinear problem by decomposing it into several sub-problems. In general, the identification of fuzzy models is solved in two steps: structure identification and parameter estimation. Structure identification can be obtained by fuzzy clustering. Parameter identification consists of determining the parameters for the antecedent functions and the parameters of the rule consequents.

With missing values, product-space clustering can also be used as long as the distance metric is modified in order to deal with those values. It is possible to calculate partial distances using all non-missing feature values, and scaling afterwards this quantity by the reciprocal of the proportion of components used [16]. An example of the D^2_{ik} calculation of the Euclidean distance is [13]:

$$\begin{aligned} D_{ik}^2 &= \|z_k - v_i\|_2^2 \\ &= \left\|(?\,2\,?\,?\,5)^T - (6\,7\,8\,9\,10)\right\|_2^2 \\ &= \frac{5}{5-3}\left((2-7)^2 - (5-10)^2\right) \end{aligned} \qquad (3)$$

The general formula for the partial distance calculation of D^2_{ik} is given by:

$$D_{ik}^2 = \frac{n}{I_k}\sum_{j=1}^{n}\left(x_{kj} - v_{ij}\right)^2 I_{kj} \qquad (4)$$

where

$$I_{kj} = \begin{cases} 0, if\ x_{kj} \in X_M \\ 1, if\ x_{kj} \in X_P \end{cases}, for\ 1 \le j \le n \text{ and } 1 \le k \le N \qquad (5)$$

and $I_k = \sum_{j=1}^{n} I_{kj}$

X_M and X_P are the subsets of X containing the missing and the present values from the total datum, respectively. This is the partial distance strategy (PDS) mentioned before and the operational basis of modified FCM the algorithm used in this study. The FCM-PDS is the regular FCM algorithm where the calculation of the distance D^2_{ik} is substituted by (4) and also the cluster prototype centers, v_{ij}, are calculated according to:

$$v_{ij} = \sum_{k=1}^{N}(\mu_{ik})^m I_{kj} x_{kj} \Big/ \sum_{k=1}^{N}(\mu_{ik})^m I_{kj} \qquad (6)$$

where μ_{ik} is the membership degree of x_k to the cluster center v_i.

The antecedent membership functions can be obtained by projecting the multidimensional fuzzy sets defined point wise in the rows of the partition matrix of the model onto the individual antecedent variables of the rules. However, by computing the membership degrees directly in the space of the antecedent variables, each cluster represents one fuzzy rule, as in (2). The multidimensional membership functions A^k are given analytically by computing the distance from the projection of the cluster center v_i onto X, and then computing the membership degree, $\beta_i(\mathbf{x})$, in an inverse proportion to the distance, with the form:

$$\beta_i(\mathbf{x}) = \left[\sum_{j=1}^{c} \left(D_{ik}^2 \left(\mathbf{x}, v_i^x \right) / D_{jk}^2 \left(\mathbf{x}, v_j^x \right) \right)^{\frac{2}{m-1}} \right]^{-1} \quad (7)$$

The consequent parameters for each rule are estimated by the least-squares method. The set of optimal parameters with respect to the model output is estimated by minimizing the global prediction error, taking into account the aggregation of the rules [11].

III. METHODOLOGY

A. MEDAN Database Pre-processing

The pre-processed MEDAN database [6] originates from 71 German intensive care units (ICUs) using several data quality techniques [3] (e.g. data re-sampling, errors filtration, standardization of measuring units). However, to use the database for our objectives, several pre-processing methodologies are required such as identification and removal of outliers and management of missing data.

In [4], data from a suitable normal distribution (noise) was inserted randomly so that the algorithms could not learn from the added noise data. In particular, the aim was to prevent situations where data with missing value replacements might be alternatively classified [17]. Contrastingly, a linear regression strategy followed by the Zero-Order-Hold (ZOH) method was used in [5]. The ZOH method can be applied causally by holding in time a sample value until a new one is acquired. This was done for each feature along the time. In the case where no value is present in the initial time stamp of a patient, the dataset will contain missing values until one value is acquired for that feature. This method constitutes a suitable pre-processing technique for medical data records as we are dealing with time-dependent signals series, many of them with low changing frequencies [5]. Schematically, the dataset preprocessing will happen as follows:

(Without ZOH pre-processing)

$$original\ dataset = \begin{bmatrix} ? & ? & ? & 13 & 17 & 21 & ? & 29 \\ 2 & ? & 10 & ? & ? & 22 & ? & ? \\ 3 & 7 & ? & ? & 19 & ? & ? & ? \\ 4 & 8 & 12 & 16 & ? & ? & 28 & ? \end{bmatrix} \quad (8)$$

(With ZOH pre-processing)

$$ZOH\ dataset = \begin{bmatrix} ? & ? & ? & 13 & 17 & 21 & ? & 29 \\ 2 & ? & 10 & 13 & 17 & 22 & ? & 29 \\ 3 & 7 & 10 & 13 & 19 & 22 & ? & 29 \\ 4 & 8 & 12 & 16 & 19 & 22 & 28 & 29 \end{bmatrix} \quad (9)$$

Approximately 24h spaced samples were used for comparison with [4]. Though in [4] the daily mean values (after input of missing data) were used, comparison with this work still is valid. Two studies were performed here: Predicting septic shock by applying the FCM-PDS method without any pre-processing of the dataset (FCM-PDS); and predicting septic shock by applying the FCM-PDS method with the ZOH pre-processing method (ZOH-FCM-PDS). Thus, for the first study the datasets contain all the missing data from the original MEDAN database. For the second, the datasets will only contain missing data until at least one value is acquired in every feature, in the original database.

From these studies we can compare the use of the FCM-PDS algorithm with the results obtained in [4] and evaluate the differences in performance when using a suitable pre-processing technique.

B. Experimental Setup

This study makes use of a publicly available database [6], containing data from a total of 382 patients with septic shock associated with abdominal causes. For each patient, the database holds personal records, physiological parameters, diagnoses/therapies, medication, and respective outcomes (survived or deceased).

As in previous works we focused exclusively on the physiological parameters (a total of 103 features). However, only 139 patients were found to meet initial inclusion criteria and not all of them have entries for the 103 features [3, 4]. From the total features available then, two different datasets of 12 features [4] and 28 features [5] were selected to perform the studies, resulting in a total of 121 patients and 81 patients in each set, respectively.

The models were iteratively built (100 times for statistical purposes) for the two sets of features and the performance of the models was evaluated in terms of accuracy (correct classification rate), sensitivity (true positive classification rate) and specificity (true negative classification rate), and area under the ROC (Receiver Operating Characteristic) curve (AUC):

$$Accuracy = \frac{TP + TN}{TP + FP + TN + FN} \quad (10)$$

$$Sensitivity = \frac{TP}{TP + FN} \quad (11)$$

$$Specificity = \frac{TN}{TN + FP} \tag{12}$$

Where *TP* is the number of true positive classifications obtained, *FP* is the number of false positive classifications, *TN* is the number of true negative classifications and *FN* is the number of false negative classifications. The ROC curve is obtained by plotting the true positive classifications rate (TPR, or sensitivity) against the false positive classifications rate (FPR, or 1-specificity) obtained for a binary classifier system as its discrimination threshold is varied. The area under that curve is calculated as:

$$AUC = \int_0^1 ROC = \int_0^1 TPR.dFPR \tag{13}$$

The train and test sets in each set of features were obtained by randomly dividing the available data (50% train and 50% test). These subsets were maintained the same throughout the simulation.

The results were then compared with [4], where a neural-network-based modeling approach is used to classify abdominal septic shock patients using the same subset of 12 features that was used in this work.

C. Computing Classification

When performing the first tests with the FCM-PDS algorithm the accuracy obtained was very similar to that obtained in [4] (in contrast, sensitivity and specificity were balanced). This is not unexpected as neither of the pre-processing techniques adds any additional information to the missing dataset. Therefore, after testing the model created with the test set, the results were aggregated so that the predicted classification for each patient results from the mean of all its predicted classifications for each time samples. Schematically, consider the dataset configuration used:

$$\begin{bmatrix} id & time & feature1 & \dots & featureN & Classification \\ id_{p1} & t_{p1,1} & x_{1,p1,1} & \dots & x_{N,p1,1} & class_{p1} \\ \dots & \dots & \dots & \dots & \dots & \dots \\ id_{p1} & t_{p1,T1} & x_{1,p1,T1} & \dots & x_{N,p1,T1} & class_{p1} \\ id_{p2} & t_{p2,1} & x_{1,p2,1} & \dots & x_{N,p2,1} & class_{p2} \\ \dots & \dots & \dots & \dots & \dots & \dots \\ id_{p2} & t_{p2,T2} & x_{1,p2,T2} & \dots & x_{N,p2,T2} & class_{p2} \\ \dots & \dots & \dots & \dots & \dots & \dots \\ id_{pk} & t_{pk,1} & x_{1,pk,1} & \dots & x_{N,pk,1} & class_{pk} \\ \dots & \dots & \dots & \dots & \dots & \dots \\ id_{pk} & t_{pk,Tk} & x_{1,pk,Tk} & \dots & x_{N,pk,Tk} & class_{pk} \end{bmatrix} \tag{14}$$

Where id_{pk} is the identifier of patient *pk*, x_N is the value of feature *N*, *Tk* is the number of time stamps for patient *pk*, and $class_{pk}$ is the observed classification. The clustering method treats each time sample individually. Consequently, we can compute the predicted classification of each patient using the predicted classification for each of its time stamps:

$$\hat{class}_{pk,final} = \frac{1}{Tk}\sum_{i=1}^{Tk} \hat{class}_{pk}(t_{pk,i}) \tag{15}$$

This procedure maintains some of the time series information by not treating each time sample as an individual sample. This method was used in both approaches (with and without pre-processing) presented in this work.

IV. Results and Discussion

The 12 feature and 28 feature datasets created without pre-processing contained approximately 54% and 67% missing data, respectively. In contrast, same datasets obtained using the ZOH method only contained 2% and 4% missing data, respectively (the remaining missing values are placed in the initial positions of each feature (9)).

In Fig.1 one can observe the performance test of the ZOH-FCM-PDS method for the 12 feature dataset. The threshold value selected for comparison was one for which accuracy is near the maximum, and sensitivity and specificity are relatively balanced. In this case we selected 0.35.

Table I presents the percentage of correct classifications achieved by each of the approaches. Although the ZOH-FCM-PDS approach performs better than the other methods for the 12 feature dataset, the differences between this method and the FCM-PDS method become faded for the 28 feature dataset. In Table II, sensitivity and specificity are presented for the 12 features dataset studies and, again, the best results for these criteria are achieved by the ZOH-FCM-PDS method. This method performs well overall as the missing data percentage decreases. In Table III, where the results for sensitivity and specificity for the studies using the 28 feature dataset are presented, the clearest differences between the two approaches are the standard deviations. The mean values are very similar which means that the FCM-PDS approach is not as robust as it is when preceded by the pre-processing. This is also observed in Table I and is due to the fact that we are not dealing with MCAR values, and therefore the configuration of the dataset influences the results drastically. This effect is best observed when dealing with the 28 feature dataset (67% missing values downgraded to 4%) where, by replacing the great majority of the missing values using the ZOH method, the model becomes more robust maintaining its prediction power. This means that the information contained in each time sample is related to the previous ones, as expected by physicians, otherwise the ZOH-FCM-PDS method would perform worse overall. Additionally, this reinforces the observations that for percentages of missing data up to approximately 70% the FCM-PDS model can perform well though the mean error increases as one approaches upper limits [11].

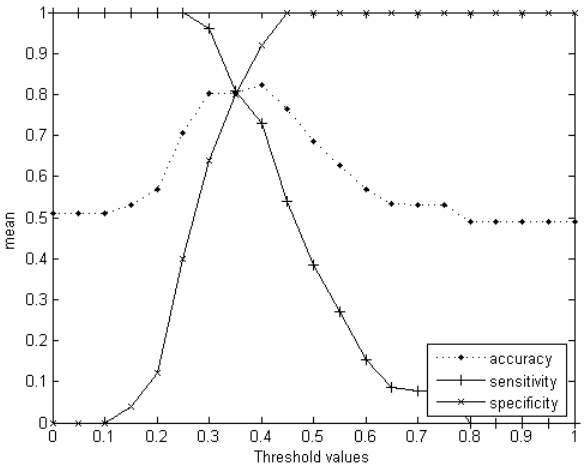

Figure 1. Performance of the ZOH-FCM-PDS method using the 12 feature dataset. The threshold value chosen for presenting the results here was 0.35.

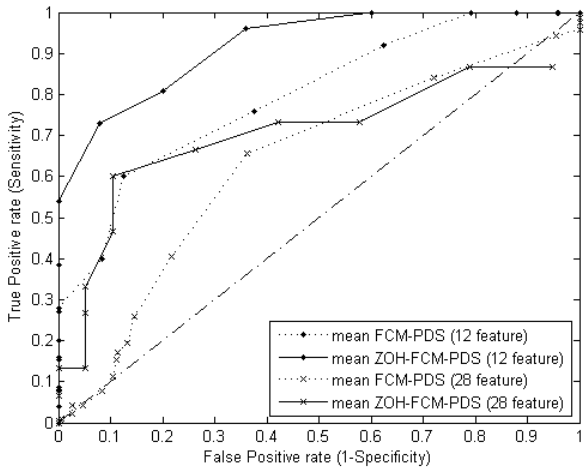

Figure 2. ROC curves obtained for the 12 and 28 feature datasets studies.

TABLE I. ACCURACY (PERCENTAGE OF CORRECT CLASSIFICATIONS)

	12 feature		28 feature	
	Mean	***Std***	***Mean***	***Std***
NN [4]	69.00	4.37	-	-
ZOH-FCM-PDS	80.39	0.00	70.59	0.00
FCM-PDS	69.39	0.00	64.76	7.73

TABLE II. SENSITIVITY AND SPECIFICITY USING 12 FEATURES

	12 feature			
	Sensitivity		Specificity	
	Mean	***Std***	***Mean***	***Std***
NN [4]	15.01	-	92.26	-
ZOH-FCM-PDS	80.77	0.00	80.00	0.00
FCM-PDS	76.00	0.00	62.50	0.00

TABLE III. SENSITIVITY AND SPECIFICITY USING 28 FEATURES

	28 feature			
	Sensitivity		Specificity	
	Mean	***Std***	***Mean***	***Std***
ZOH-FCM-PDS	66.67	0.00	73.68	0.00
FCM-PDS	65.67	12.98	63.75	24.03

The method used in [4] performs similarly in terms of accuracy to FCM-PDS method. However, for sensitivity and specificity the approach used in this study clearly performs better.

In Table IV the AUC values obtained for the two datasets of features when using the two approaches discussed are presented. Again, the use of the ZOH pre-processing method constitutes a significant difference for the 12 feature dataset, resulting in better AUC values. The variability of the results due to the high percentage of missing data is noticeable for the 28 feature dataset. Fig.2 permits graphical comparison of the ROC curves obtained for all the studies. Both methods perform similarly for the 28 feature dataset.

The technique used in this study to compute the predicted classification of each patient clearly improves the classification when compared to results in [4]. Although the accuracy of both is similar, the differences can be seen in Table II as the balance between sensitivity and specificity. As mentioned before, both [4] and the FCM-PDS approach do not use pre-processing techniques that could bias the information contained in the dataset.

TABLE IV. AUC

	12 feature		28 feature	
	Mean	***Std***	***Mean***	***Std***
ZOH-FCM-PDS	89.85	0.00	64.91	0.00
FCM-PDS	78.58	0.00	63.14	11.73

In [4], a potential improvement to the classification performance was to use only the three last 24h time samples from each patient. However, this work demonstrates a viable alternative method, and notes that other techniques could also be used in order to favor the positive or negative classifications, for example, as in the "balanced accuracy". Computing the classification of each patient after using the FCM-PDS method in datasets containing limited time windows (e.g. last three days) could constitute a better improvement to the septic shock prediction study.

In reference [17] missing values are replaced by centers of gravity associated with fuzzy rules. This procedure unjustly improves the statistical properties of the original data by replacing the missing values in the best possible manner for the system [3, 4]. However, such a replacement strategy, like performing a linear regression in the existing values [5], offers some advantages that warrant further examination and comparison in the development of more robust models (e.g. applications in data-based knowledge extraction).

V. CONCLUSIONS

Real-world databases usually contain missing values. Using the MEDAN database we studied the application of a modified fuzzy c-means (FCM) clustering method that allows the identification of Takagi-Sugeno fuzzy models from incomplete data, without using complex pre-processing methods. This paper demonstrates a real-time modeling strategy for medical data that is reliable, with high fidelity and non-complex interpretability. Applying the models developed in this study with time limited physiological datasets and suitable pre-processing techniques demonstrates the opportunities to improve classification performance and risk prediction in clinical settings.

REFERENCES

[1] American College of Chest Physicians/Society of Critical Care Medicine Consensus Conference, "Definitions for sepsis and organ failures guidelines for the use of innovative therapies in sepsis," Critical Care Medicine, vol. 20, pp. 864–874, 1992.

[2] H. Burchardi and H. Schneider, "Economic aspects of severe sepsis: a review of intensive care unit costs, cost of illness and cost effectiveness of therapy," Pharmacoeconomics, vol. 22, no. 12, pp. 793–813, 2004.

[3] J. Paetz, B. Arlt, K. Erz, K. Holzer, R. Brause and E. Hanisch, "Data quality aspects of a database for abdominal septic shock patients," Computer Methods and Programs in Biomedicine, vol. 75, pp. 23–30, 2004.

[4] J. Paetz, "Knowledge-based approach to septic shock patient data using a neural network with trapezoidal activation functions," Artificial Intelligence in Medicine, vol. 28, pp. 207–230, 2003.

[5] A. S. Fialho and F. Cismondi, et al., "Predicting outcomes of septic shock patients using feature selection based on soft computing techniques," Communications in Computer and Information Science, Part II, vol. 81, pp. 65–74, 2010.

[6] E. Hanisch, R. Brause, B. Arlt, J. Paetz, K. Holzer, "The MEDAN Database," 2003 (http://www.medan.de).

[7] H. Timm, C. Döring, and R. Kruse, "Differentiated treatment of missing values in fuzzy clustering," in Proceedings of the 10th International Fuzzy Systems Association World Congress, Lecture Notes in Artificial Intelligence, T. Bilgic, B. D. Baets, and O. Kaynak, Eds. Istanbul, Turkey: Springer-Verlag, vol. 2715, June 2003, pp. 354–361.

[8] R. J. A. Little and D. B. Rubin, Statistical Analysis with Missing Data, 2nd ed. New York: Wiley and Sons, 2002.

[9] J. L. Schafer, Analysis of Incomplete Multivariate Data. London: Chapman & Hall, 1997.

[10] A. Farhangfar, L. Kurgan and J. Dy, "Impact of imputation of missing values on classification error for discrete data," Pattern Recognition, vol. 41, no. 12, pp. 3692–3705, 2008.

[11] R. J. Almeida, U. Kaymak and J. M. C. Sousa, "A new approach to dealing with missing values in data-driven fuzzy modeling," IEEE International Conference on Fuzzy Systems, pp. 1–7, July 2010.

[12] H. Timm and R. Kruse, "Fuzzy cluster analysis with missing values," Conference of the North American Fuzzy Information Processing Society, pp. 242–246, Aug 1998.

[13] R. J. Hathaway and J. C. Bezdek, "Fuzzy c-means clustering of incomplete data," IEEE Transactions on Systems, Man and Cybernetics, Part B, vol. 31, no. 5, pp. 735–744, October 2001.

[14] T. Takagi and M. Sugeno, "Fuzzy identification of systems and its aplication to modeling and control," IEEE Transactions on Systems, Man and Cybernetics, vol. 15, no. 1, pp. 116–132, 1985.

[15] R. Babuska and H. B. Verbruggen, "Constructing fuzzy models by product space clustering," in Fuzzy Model Identification: Selected Approaches, H. Hellendoorn and D. Driankov, Eds. London, UK: Springer-Verlag, 1997, pp. 53–90.

[16] J. Dixon, "Pattern recognition with partly missing data," IEEE Transactions on Systems, Man and Cybernetics, vol. 9, no. 1, pp. 617–621, 1979.

[17] M. R. Berthold, "Fuzzy-models and potential outliers," in Proceedings of the 18th International Conference of the North America Fuzzy Information Processing Society, R. N. Dave, T. A. Sudkamp, Eds. New York, USA, Los Alamitos: IEEE Press, 1999, pp. 532–535.

2011 IEEE International Conference on Fuzzy Systems
June 27-30, 2011, Taipei, Taiwan

A Normalized Soft Window-Based Similarity Measure To Extend The Rand Index

Romain Quéré
Lab. Mathématiques, Image et Applications
Université de La Rochelle
PRES Limousin-Poitou-Charentes
France
Email: romain.quere@univ-lr.fr

Carl Frélicot
Lab. Mathématiques, Image et Applications
Université de La Rochelle
PRES Limousin-Poitou-Charentes
France
Email: carl.frelicot@univ-lr.fr

***Abstract*—This article addresses the problem of the construction of concordance measures between two crisp, fuzzy and possibilistic partitions from their coincidence matrices. Two existing approaches are reviewed and their advantages and drawbacks are exhibited so that a new Rand index taking profits of both is proposed. Numerous experimental results show that it outperforms other extensions of the Rand index.**

***Index Terms*—Soft partitions, similarity measure, Rand index**

I. Introduction

A partition of a dataset $X = \{\mathbf{x}_1, ..., \mathbf{x}_n\}$ of n objects is a set of c non-empty subsets of X. These subsets, called *clusters* thereafter, generally regroup objects along common properties they share. Partitions can be represented by a $(c \times n)$ partition matrix U, whose general term u_{ik} represents the membership degree of each $\mathbf{x}_k$ $(k = 1, n)$ to the ith cluster $(i = 1, c)$. Each column of U is then the membership vector $\mathbf{u}_k$ of the object $\mathbf{x}_k$. For the sake of clearness and simplicity, a partition will be identified with its corresponding partition matrix in the following. Depending on whether or not clusters are mutually exclusive and on whether or not objects of X totally belong to each cluster, partitions can be of different nature. We distinguish the three main categories [1], called the sets of *possibilistic*, *fuzzy* and *crisp* partitions, respectively defined as :

- $\mathcal{M}_{pcn} = \{U \in \mathbb{R}^{c\,n} : u_{ik} \in [0, 1]\}$,
- $\mathcal{M}_{fcn} = \{U \in \mathcal{M}_{pcn} : \sum_{i=1}^{c} u_{ik} = 1\}$,
- $\mathcal{M}_{hcn} = \{U \in \mathcal{M}_{fcn} : u_{ik} \in \{0, 1\}\}$.

Moreover, we will refer to the set $\mathcal{M}_{pcn} - \mathcal{M}_{hcn}$ as the set of *soft partitions*, according to the definition in [2].

In many fields, figuring out how close are two partitions of the same dataset X is a problem of great interest. Generally speaking, it can indeed be useful to confront how different experts class different objects. In clustering, and more precisely in cluster validity, it also enables to evaluate and compare the quality of different algorithms, or the same algorithm with different parameters. This important problem has been tackled since decades by attempting to define concordance measures assessing the degree of agreement between partitions, so that a large number of measures exist in the literature. One can distinguish two kinds of measures, depending on the use made of them, see [3] : an *external index* will be used when one wants to assess the quality of a partition compared to a reference one, while a *relative index* will be used to only evaluate how close two partitions are. Since the frontier between these two categories is thin, we will more generally refer to both of them as *comparison indices* in this paper.

Early comparison indices have been dedicated to crisp partitions, and a new interest has recently emerged for this topic thanks to the definition of the new class of soft partitions mentioned above. Many fuzzy or soft concordance measures have been recently proposed, and one can distinguish between them those relying on direct approaches from those extending historical crisp ones. Among the formers, one can cite measures based on the comparison of the whole set of α-cuts of the two partitions [4], or on a measure of uncertainty of both partitions [5]. The latters, such as the fuzzy transfert distance [6], extend existing crisp indices in the sense they reduce to crisp ones while comparing two crisp partitions. This category of soft indices also regroup a class of propositions called *coincidence-based indices*, extending well known indices such as the Rand, Jaccard and Fowlkes-Mallow ones [7]. Such soft indices solve most of the intrinsic problems of the comparison of partitions, and specifically :

- the *correspondance* or *cluster matching* problem, as discussed in [2],
- the problem of comparing partitions with different number of clusters.

Indeed, by comparing how objects are paired, i.e. belong or not belong to the same cluster in both partitions, no preliminary cluster matching is required, and the number of clusters has computationally no importance with these indices. The comparison is based on the construction, for each partition to be compared, of a coincidence matrix crossing the partition with itself. Many propositions have been made to compute and compare such matrices. Most of them are based on fuzzy set-theoretic tools, extending thus directly the set-theoretic approach used for the crisp indices, *e.g.* in [8], [9] and [10]. Another approach is possible, as proposed in [11]. It consists in using a similarity measure between the two coincidence matrices based on a distance between the membership vectors of the partitions. Because each of these constructions presents drawbacks and advantages, we propose in this paper a new

978-1-4244-7316-8/11/$26.00 ©2011 IEEE

soft Rand index taking profits of both approaches.
This paper is organized as follows. A review of existing soft Rand indices is presented in section II and their strengths and weaknesses are confronted. In section III, the new Rand index is proposed. Its main characteristics are investigated in section IV through an intensive comparative experimental study. A conclusion is given in section V.

II. Some existing coincidence-based soft Rand Indices

Let $U \in \mathcal{M}_{hcn}$ be a crisp partition of a dataset X. The *coincidence matrix* Ψ_U of U is a symmetric $(n \times n)$ matrix whose general term

$$\psi_{U,kl} = \sum_{i=1}^{c} u_{ik} \wedge u_{il} = \begin{cases} 1 & \text{if } \mathbf{u}_k = \mathbf{u}_l \\ 0 & \text{else} \end{cases} \tag{1}$$

describes the degree to which the objects $\mathbf{x}_k$ and $\mathbf{x}_l$ of X belong to the same cluster in U. Given a second partition V of the same dataset and its coincidence matrix Ψ_V, the crisp Rand Index measuring the concordance between U and V is defined as follows:

$$RI(U,V) = \frac{n_{11} + n_{00}}{n_{11} + n_{10} + n_{01} + n_{00}}. \tag{2}$$

As defined, the Rand index takes values in $[0,1]$ and equals 1 when $U \equiv V$. The number of pairs of objects $(\mathbf{x}_k, \mathbf{x}_l)$ belonging to the same cluster (respectively to different clusters) in both U and V is given by n_{11} (respectively n_{00}), so that the numerator in (1) represents the agreement of U and V. On the other side, disagreement between both partitions is represented by the numbers of pairs belonging to the same cluster in U (respectively V) and in different clusters in V (respectively U), namely n_{10} and n_{01}. Let us assume $\alpha, \beta \in \{0,1\}$, the different numbers of pairs $n_{\alpha\,\beta}$ are given:

$$n_{\alpha\,\beta} = \sum_{k=2}^{n} \sum_{l=1}^{k-1} \big((1-\alpha) + (2\,\alpha - 1)\ \psi_{U,kl}\big) \wedge \big((1-\beta) + (2\,\beta - 1)\ \psi_{V,kl}\big). \tag{3}$$

This index, as many other crisp indices constructed on the same principle, *e.g.* in [7], can be equally computed from the contingency matrix crossing the two partitions to be compared, see [12]. This equivalence, that do not generally holds in the soft case, has led to two different classes of soft extensions, namely the *contingency-based*, see the recent work by Anderson et al [2], and the *coincidence-based* ones we are interested in. We recall hereafter two recent extensions of the Rand index belonging to this latter class to which we will compare our proposition.

A. The fuzzy set-theoretic approach

Since the crisp Rand index as defined by (2) is built on a logical and set-theoretic approach, some authors have proposed to extend it by use of fuzzy set-theoretic tools. Namely, the t-norm and the sum (or Σ-count) operators are used to extend the classical concepts of intersection (or conjunction) and cardinality, respectively. Briefly, a t-norm is a commutative, associative and monotonic function $\top : [0,1]^2 \to [0,1]$ having 1 for neutral element. The most common t-norms are given in table I and an interest reader can refer to [13] for a complete review.

TABLE I
Basic triangular norms and some parametrized families of t-norms.

Standard	$\top_M(a,b) = \min(a,b)$
Product	$\top_P(a,b) = a\,b$
Łukasiewicz	$\top_L(a,b) = \max(a+b-1, 0)$
Frank $\lambda \in \mathbb{R}_+^\star \backslash \{1\}$	$\top_{F_\lambda}(a,b) = \ln_\lambda\left(1 + \frac{(\lambda^a - 1)\,(\lambda^b - 1)}{\lambda - 1}\right)$
Hamacher $\lambda \in \mathbb{R}_+$	$\top_{H_\lambda}(a,b) = \frac{a\,b}{\lambda + (1-\lambda)\,(a+b-a\,b)}$

Extending (1) to the soft domain results in defining the elements of the soft coincidence matrix $\Psi_U^\top$ of a soft partition matrix U by [3]:

$$\psi_{U,kl}^\top = \sum_{i=1}^{c} \top(u_{ik}, u_{il}). \tag{4}$$

However, it has been recently shown that such a direct extension leads to counterintuitive values for the diagonal elements $\psi_{U,kk}^\top$ of the soft matrix, see [9], [10]. Indeed, these elements, which represent the degree to which each object $\mathbf{x}_k$ belongs to the same cluster as itself, is generally not 1, and can moreover be much less than 1 because of the $\top$ aggregation operator. The authors thus recommend to normalize the matrix $\Psi_U^\top$ to bring its diagonal terms to ones. A generic solution can be found in [10], leading to a soft normalized coincidence matrix $\Phi_U^\top$ whose general term is defined by:

$$\phi_{U,kl}^\top = \frac{\psi_{U,kl}^\top}{\top\left(K_\top\left(\psi_{U,kk}^\top\right), K_\top\left(\phi_{U,ll}^\top\right)\right)} \tag{5}$$

where $K_\top : [0,1] \to [0,1]$ is a t-norm dependant function such that $\top\big(K_\top(a), K_\top(a)\big) = a$. Given another soft normalized coincidence matrix $\Phi_V^\top$ computed from another soft partition V, the numbers $n_{\alpha\beta}$ (3) are extended to the soft domain by:

$$n_{\alpha\,\beta}^\top = \sum_{k=2}^{n} \sum_{l=1}^{k-1} \top\big((1-\alpha) + (2\,\alpha - 1)\ \phi_{U,kl}^\top, (1-\beta) + (2\,\beta - 1)\ \phi_{V,kl}^\top\big). \tag{6}$$

The derived *Normalized Soft Rand Index* ($NSRI$) is then computed directly from (2), and it is easy to show it reduces to its crisp counterpart when U and V are crisp.

B. The distance-based measure of equivalence approach

In [11], Hüllermeier and Rifqi propose another extension of the Rand index lying on a distance-based measure of equivalence between the membership vectors $\mathbf{u}_k$ of a soft partition U, so that the terms of the coincidence matrix Ψ_U^{HR} of U are defined as:

$$\psi_{U,kl}^{HR} = 1 - \frac{||\mathbf{u}_k - \mathbf{u}_l||}{\sqrt{2}}. \tag{7}$$

Given another soft partition V, the *Soft Equivalence Rand Index* ($SERI$) is then given by:

$$SERI(U,V) = \frac{1}{q}\sum_{k=2}^{n}\sum_{l=1}^{k-1} 1 - |\psi_{U,kl}^{HR} - \psi_{V,kl}^{HR}| \qquad (8)$$

where $q = \frac{n(n-1)}{2}$ is the number of different pairs of objects in X. It is shown that $SERI$ reduces as well to the crisp Rand index when comparing two crisp partitions. Furthermore it presents the great advantage to take its maximum value of 1 when $U \equiv V$ whatever the space in which U and V are defined ; which is not the case for the previously presented $NSRI$. This lead to an interesting discussion about how the two coincidence matrices are aggregated to build the index, depending on the approach. Indeed, keep in mind the terms of the coincidence matrices describe the degree to which two elements belong to the same cluster in a given partition, and remember the Rand index is meant to assess how much the two partitions are in agreement. Then, while $\psi_{U,kl}$ is close to $\psi_{V,kl}$, one can intuitively conclude in an agreement between U and V concerning the $(\mathbf{x}_k, \mathbf{x}_l)$ pair of objects. As a direct consequence, the given pair should then have a high contribution to the value of the Rand index. However, this is not the case with the $NSRI$ presented in section II-A. As an example, let $a = 0.3$ and $b = 0.29$ be the degrees to which two objects $\mathbf{x}_k$ and $\mathbf{x}_l$ are paired in two partitions. With the standard t-norm $\top_M$, and according to (6) and (2), the contribution of a and b to the agreement $n_{11} + n_{00} = \min(0.3, 0.29) + \min(1-0.3, 1-0.29) = 0.99$, which is a value one can expect. Nevertheless, their overall impact on the Rand index is drastically pulled down by their contribution to the disagreement $n_{10} + n_{01} = \min(0.3, 1-0.29) + \min(1-0.3, 0.29) = 0.59$. At the opposite, the contribution of a and b to the $SERI$, given by $s^{HR}(a,b) = 1 - |a-b| = 0.99$ in (8), is total and avoid the previously exposed drawback.
It is interesting to point out that this s^{HR} function, called *degree of concordance* by its authors, is actually a *similarity measure* since it satisfies the following axioms:

$$s(a,b) = s(b,a) \qquad \text{(symmetry)} \qquad (9)$$
$$s(a,a) \geq s(a,b),\ \forall\ b \qquad \text{(maximality)} \qquad (10)$$
$$s(a,a) = 1 \qquad \text{(unity)} \qquad (11)$$

This remark lies at the heart of this paper. On one hand, by preserving the set-theoretic sense of the original Rand index, $NSRI$ presents the strong advantage to lie on a strong and admitted theory, and its well behaviour has been shown in [10]. However, as exhibited above, it also presents a serious drawback because of the way the terms of the coincidence matrices are aggregated. On the other hand, the $SERI$, by redefining the original Rand index formula by means of a similarity measure, correct this. In the next section, we propose a new Rand index which takes profit of both approach, based on a new family of similarity measures.

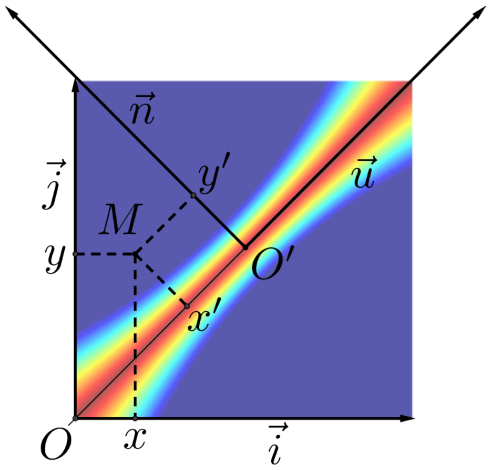

Fig. 1. Isosurface of s_p^w computed with w_T, $t = 0.1$, $r = 0.3$ and $o = \frac{1}{2}$ and geometrical explanation of its construction

III. The Normalized Soft Window-based similarity Rand Index

Let $O' = {}^t(o,o)$ be a point lying on the diagonal line $\Delta : x = y$ of the unit square and let $\vec{u}$ and $\vec{n}$ be two unit orthogonal vectors as shown in Fig. 1. Each point $M = {}^t(x,y) \in [0,1]^2$, whose coordinates express in $(O, \vec{i}, \vec{j})$, can be transformed into $M' = {}^t(x', y')$, with respect to $(O', \vec{u}, \vec{n})$. Given a zero-mean symmetric window function w taking values in $[0,1]$ such that $w(0) = 1$ and a symmetric profile function p taking values in $[0,1]$ satisfying $p(x) > 0,\ \forall x$, the function $s_p^w \colon [0,1]^2 \to [0,1]$ defined by

$$s_p^w(x,y) = w\left(\frac{y'}{p(x')}\right) \qquad (12)$$

is a measure of similarity between x and y w.r.t. axioms (9), (10) and (11). The proof being trivial, it is left to the reader. In (12), w controls the way x and y are considered similar with regard to their difference. Formally, it is a weighting function acting on the distance between M and Δ such that the farther M is from Δ, the smaller $s_p^w(x,y)$ is. Thus, choosing a window function w dropping quickly from 1 leads to a drastic similarity function s_p^w, *i.e* only close x and y values will be considered similar. Many symmetric window functions exist, some usual ones are reported in Table II. Fig. 2(b) presents the cuts of three s_p^w obtained with the three window functions w_U, w_T and w_G and whose isosurfaces are presented in Fig. 2(a). This example demonstrates how the behaviour of the similarity function s_p^w can be drastically modified according to w.

TABLE II
Usual window functions

Uniform	$w_U(x) = 1_{(x\leq 1)}$
Triangular	$w_T(x) = (1-\lvert x\rvert)1_{(x\leq 1)}$
Gaussian	$w_G(x) = \exp(-x^2)1_{(x\leq 1)}$
Epanechnikov	$w_E(x) = (1-x^2)1_{(x\leq 1)}$

In the same manner, the profile function p influences the similarity between x and y with respect to the distance between

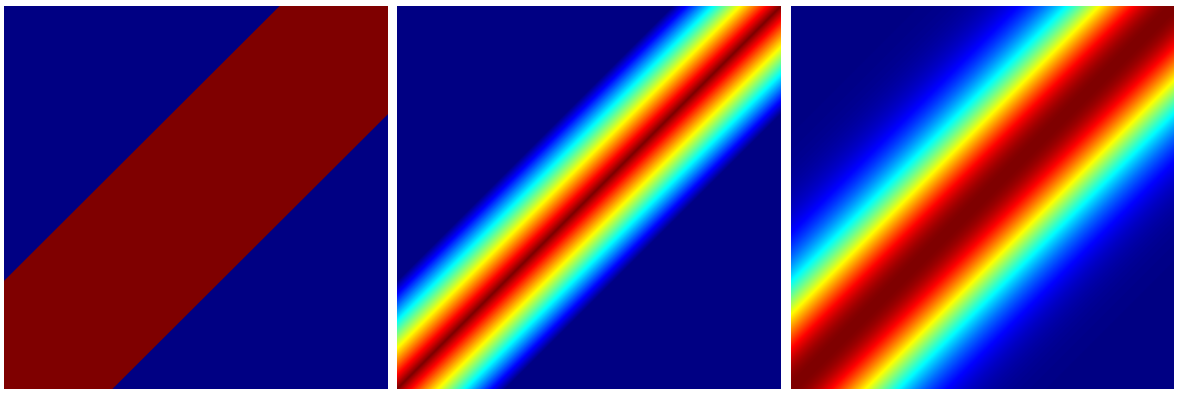

(a) $w = w_U, w_T$ and w_G (from left to right) , $t = 0.2, r = 0, o$ is undefined

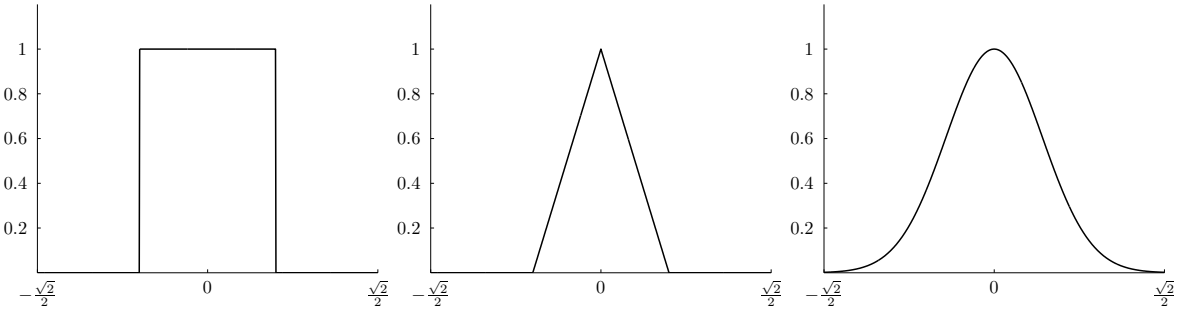

(b) Cut views of s_p^w plotted above along $x + y = 1$

Fig. 2. Isosurfaces and cut views of some s_p^w

M and O'. This allows to favour or not some specific ranges of values, according to the chosen *origin* parameter o. We propose to use the following p function:

$$p(x') = t + r\,x'^2 \tag{13}$$

where $t \in]0, \sqrt{2}]$ and $r \in \mathbb{R}_+$ are user defined parameters, called respectively the *thickness* and *curvature* parameters.

It is easy to show that with this particular profile function, O' has no influence whenever $r = 0$, so that no value for o is required.

As an example, Fig. 1 presents the isosurface of s_p^w with the following settings: $w = w_T$, a thickness $t = 0.1$, a curvature $r = 0.3$ and an origin $o = \frac{1}{2}$. One can observe that, for all M, the closer x and y are to $\frac{1}{2}$, the more selective $s_p^w(x, y)$ is, as expected. Fig. 3 also show examples of s_p^w functions using most of w functions of Table II with particular values for t, r and o, so that each row exhibits the role of each parameter. For instance, Fig. 3(a) shows the influence of t on the selectivity of s_p^w, according to its value (a small one, a middle one and the maximum one).

From this construction, we propose to define a new index measuring the concordance between two soft partitions U and V, called the *Normalized Soft Window-based similarity Rand Index* ($NSWRI$), by:

$$NSWRI(U, V) = \frac{1}{q} \sum_{k=2}^{n} \sum_{l=1}^{k-1} s_p^w(\phi_{U,kl}^{\top}, \phi_{V,kl}^{\top}) \tag{14}$$

where $\phi_{U,kl}^{\top}$ and $\phi_{V,kl}^{\top}$ are the terms of the normalized coincidence matrices Φ_U and Φ_V constructed according to (5).

Whatever the parameters used for the similarity function s_p^w, it is easy to show that this index reduces to the original crisp Rand index while comparing two crisp partitions. Moreover, like the $SERI$, it reaches its maximum value of 1 when $U \equiv V$, whatever their nature.

The set of parameters an user has to choose in order to compute $NSWRI(U, V)$ is $\{\top, w, t, r, o\}$. Since the range of values of each parameter is wide, we will only show some examples in the the following experimental results.

IV. Experimental results

A. Numerical experiments on fuzzy partitions.

In this section, we propose to investigate the specificities and possibilities of this new index by mean of a simple set of synthetic partitions composed of one crisp partition $U_1 = \begin{pmatrix} 0 & 0 & 1 & 1 \\ 0 & 1 & 0 & 0 \\ 1 & 0 & 0 & 0 \end{pmatrix} \in \mathcal{M}_{h34}$ and eight fuzzy partitions in $\mathcal{M}_{f34}$:

$$U_2 = \begin{pmatrix} 0.05 & 0.10 & 0.85 & 0.95 \\ 0.00 & 0.90 & 0.15 & 0.00 \\ 0.95 & 0.00 & 0.00 & 0.05 \end{pmatrix}, U_3 = \begin{pmatrix} 0.10 & 0.10 & 0.80 & 0.90 \\ 0.00 & 0.80 & 0.20 & 0.00 \\ 0.90 & 0.10 & 0.00 & 0.10 \end{pmatrix},$$

$$U_4 = \begin{pmatrix} 0.20 & 0.20 & 0.70 & 0.80 \\ 0.00 & 0.70 & 0.20 & 0.10 \\ 0.80 & 0.10 & 0.10 & 0.10 \end{pmatrix}, U_5 = \begin{pmatrix} 0.20 & 0.30 & 0.60 & 0.70 \\ 0.10 & 0.60 & 0.30 & 0.10 \\ 0.70 & 0.10 & 0.10 & 0.20 \end{pmatrix},$$

$$U_6 = \begin{pmatrix} 0.30 & 0.30 & 0.50 & 0.60 \\ 0.10 & 0.50 & 0.30 & 0.20 \\ 0.60 & 0.20 & 0.20 & 0.20 \end{pmatrix}, U_7 = \begin{pmatrix} 0.30 & 0.35 & 0.40 & 0.50 \\ 0.20 & 0.40 & 0.35 & 0.25 \\ 0.50 & 0.25 & 0.25 & 0.25 \end{pmatrix},$$

$$U_8 = \begin{pmatrix} 0.35 & 0.35 & 0.35 & 0.35 \\ 0.30 & 0.35 & 0.35 & 0.30 \\ 0.35 & 0.30 & 0.30 & 0.35 \end{pmatrix}, U_9 = \begin{pmatrix} 0.40 & 0.45 & 0.30 & 0.35 \\ 0.30 & 0.35 & 0.45 & 0.25 \\ 0.30 & 0.20 & 0.25 & 0.40 \end{pmatrix}.$$

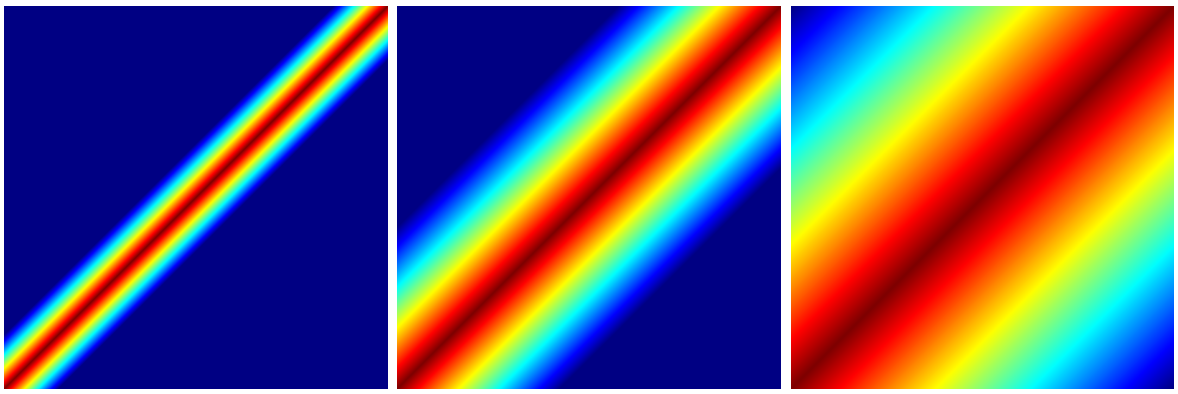

(a) $w_T, t = 0.1, 0.3$ and $\frac{\sqrt{2}}{2}$ (from left to right) , $r = 0, o$ is undefined

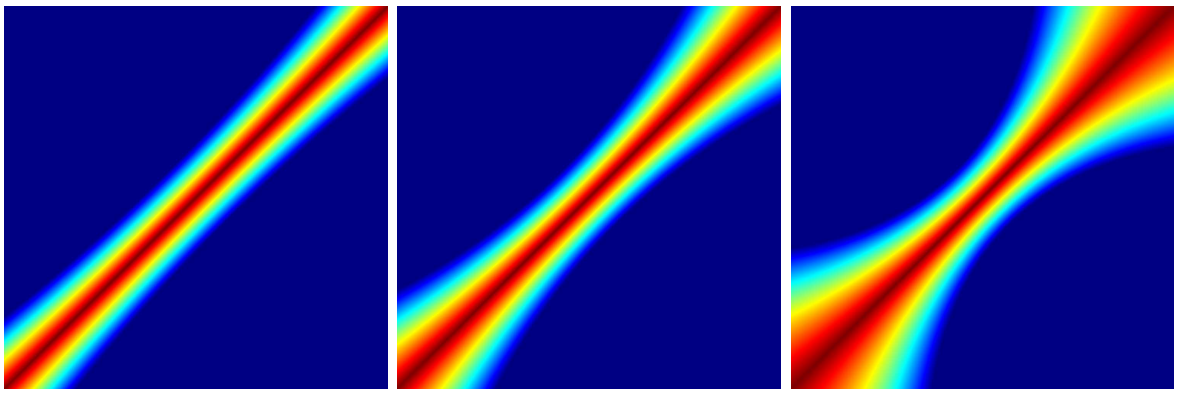

(b) $w_T, t = 0.1, r = 0.1, 0.3$ and 0.8 (from left to right) , $o = 0.5$

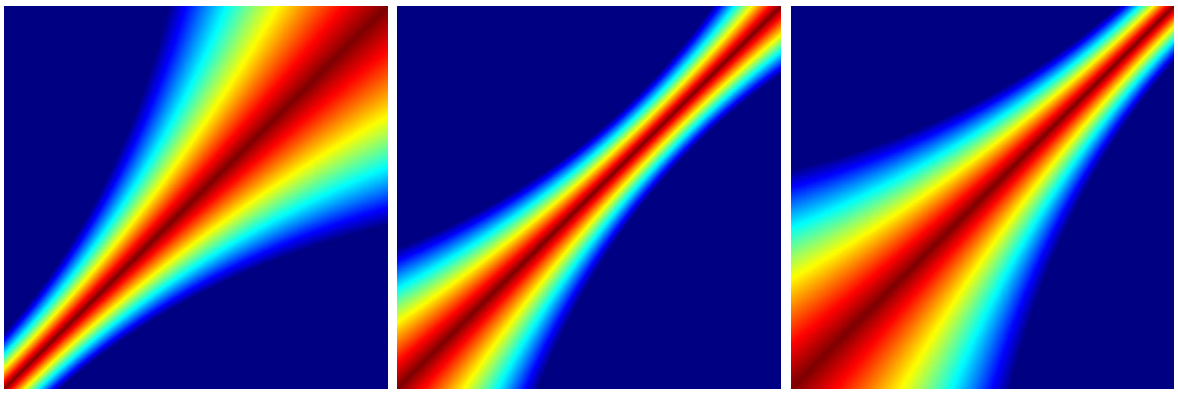

(c) $w_T, t = 0.1, r = 0.3, o = 0, 0.7,$ and 1 (from left to right)

Fig. 3. Isosurfaces of some s_p^w

These partitions are chosen such that:

- $U_2, ..., U_7$ reduce to U_1 if hardened according to the maximal membership degree, while U_8 may not because of ties and U_9 does not
- $U_{\alpha+1}$ is fuzzier than U_α, $\forall \alpha \in \{1, ..., 7\}$ according to the *Partition Entropy* [1] (see table III), which indicates the amount of fuzziness in a given partition:

$$PE(U) = -\frac{1}{n} \sum_{i=1}^{c} \sum_{k=1}^{n} u_{ik} \log(u_{ik}) \qquad (15)$$

One can intuitively state that, according to their proximity with U_1, these partitions can thus be sorted decreasingly as $\{U_2, U_3, U_4, U_5, U_6, U_7, U_9, U_8\}$. Note that U_9 is considered closer to U_1 than U_8. Altought this may seems counterintuitive, it can be explained simply. Indeed, U_1 is fully determinist whereas U_8 presents, at the extreme opposite, complete uncer-

TABLE III
FUZZINESS OF PARTITIONS U_α, $\forall \alpha \in \{1, ..., 8\}$

	U_1	U_2	U_3	U_4	U_5	U_6	U_7	U_8
$PE(U)$	0	0.29	0.45	0.69	0.85	0.98	1.06	1.10

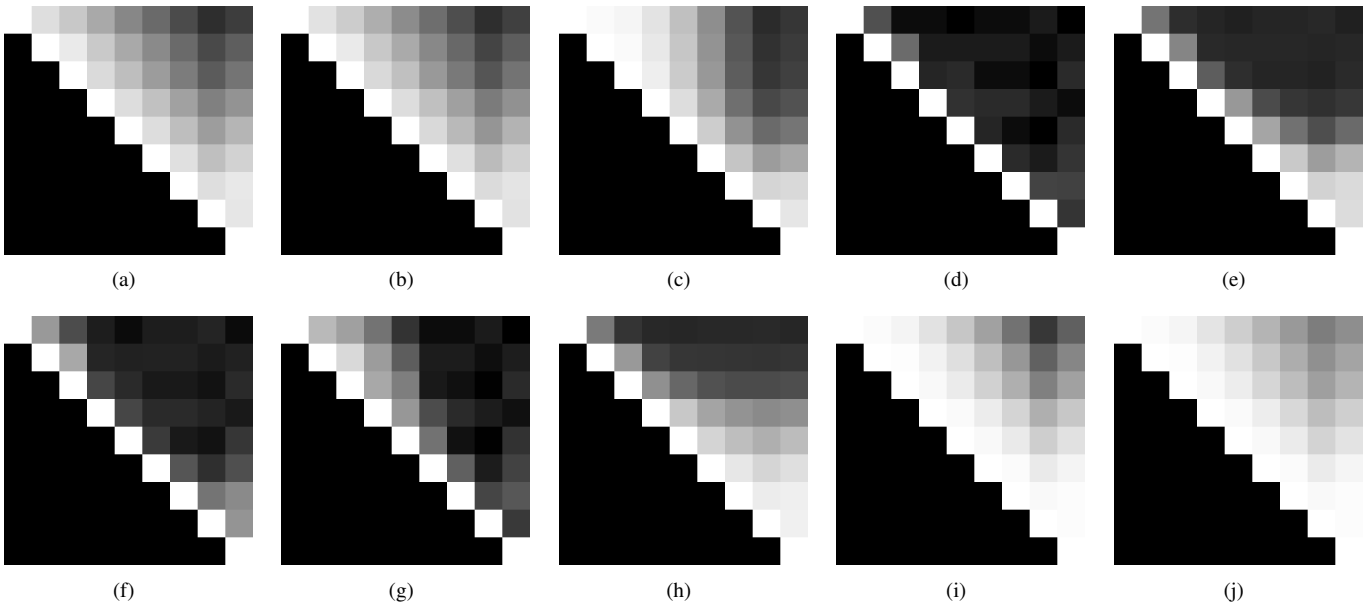

Fig. 4. Dissimilarity matrices crossing the nine partitions U_α with $SERI$ (a) and $NSWRI$ with different parameters (b)–(j) described in table IV

tainty. Thanks to a possible permutation of clusters, U_9 then shares more information in common with U_1 than U_8 does, as confirmed by the partition entropy $PE(U_9) = 1.07$.

So as to validate our proposal regarding to the intuitive proximities discussed above, nine dissimilarity matrices crossing all the pairs of partitions (U_i, U_j) with $NSWRI$ are computed for different values of each of the five parameters $\{\top, w, t, r, o\}$. These nine dissimilarity matrices are presented in Fig. 4 with an additional matrix computed with $SERI$ for comparison, presented in Fig. $4(a)$. The parameters used to compute the nine dissimilarity matrices (b)–(j) are reported in table IV. For each of them, partitions are ordered in rows and columns according to their index. The brighter a cell of a matrix is, the higher is the value of the index.

As one can directly see, the statemment made earlier about the relative proximities between the nine partitions mostly holds, according to the first row of each dissimilarity matrix, especially for (b), (c), (e), (h), (i) and (j) where $NSWRI$ is not to much drastic. While the statement does not hold, *i.e.* with (d), (f) and (g), it is interesting to note that $NSWRI$ almost provides a strong separation between the partitions, so that a threshold could be easily tuned to decide whether two partitions are similar or not. Moreover, other statements can be made while comparing some couples or triples of dissimilarity matrices:

- (a) and (b) clearly show that $NSWRI$ can be tuned to behave in the same way $SERI$ does.
- (b) and (c) demonstrate the influence of the t-norm. Indeed, by choosing a drastic t-norm such as $\top_{H_{100}}$, our proposal favour the less fuzzy partitions.
- the influence of the thickness parameter t is crucial as it enables to tune how drastic the index is, as shown by (b) and (d).
- (e), (f) and (g) show the influence of the chosen origin parameter o while the curvature r is not null: choosing o near 0 leads $NSWRI$ to favour extremely fuzzy partitions, while choosing o near 1 will lead $NSWRI$ to the opposite behaviour.
- (e) and (h) demonstrate the influence of the degree of curvature chosen for r on the previously described behaviour, *i.e.* a high value of r reinforce it.
- (b), (i) and (j) testify of the influence the window function w has on the selectivity and the range of response our proposal have. For instance, partitions U_α and $U_{\alpha+1}$ are considered closer by $NSWRI$ using w_E than using w_T.

All these remarks show that our $NSWRI$ is a really versatile tool for comparing partitions, that can be tuned to behave in many different ways.

TABLE IV
PARAMETERS USED TO COMPUTE $NSWRI$ IN THE EXPERIMENTATIONS DECRIBED BY FIG. 4

Dissimilarity matrix	$\top$	w	t	r	o
(b)	$\top_M$	w_T	$\frac{\sqrt{2}}{2}$	0	$\times$
(c)	$\top_{H_{100}}$	w_T	$\frac{\sqrt{2}}{2}$	0	$\times$
(d)	$\top_M$	w_T	0.1	0	$\times$
(e)	$\top_M$	w_T	0.1	0.3	0
(f)	$\top_M$	w_T	0.1	0.3	0.5
(g)	$\top_M$	w_T	0.1	0.3	1
(h)	$\top_M$	w_T	0.1	0.8	0
(i)	$\top_M$	w_E	$\frac{\sqrt{2}}{2}$	0	$\times$
(j)	$\top_M$	w_G	$\frac{\sqrt{2}}{2}$	0	$\times$

B. Numerical experiments on possibilistic partitions.

Consider the set composed of the crisp partition U_1 of the previous section and eight possibilistic $U^p_{\{2\ldots9\}}$ partitions defined from the previous fuzzy partitions $U_{\{2\ldots9\}} \in \mathcal{M}_{p34}$ such as $U^p_\alpha = \frac{U_\alpha}{2}$. As previously, the nine partitions are crossed

using $SERI$ and $NSWRI$ to compute two dissimilarity matrices presented in Fig. 5. The parameters used for the computation of $NSWRI$ are the same as those used for Fig. 4(b), see table IV.

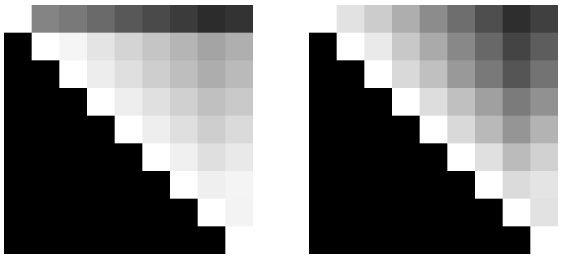

Fig. 5. Dissimilarity matrices crossing nine possibilistic partitions U_α^p, obtained with $SERI$ (left) and $NSWRI$ (right) with $\{\top_M, w_T, t = \frac{\sqrt{2}}{2}, r = 0\}$

One can observe that the $SERI$ makes a strong distinction between the crisp and the possibilistic partitions. At the opposite, results given here by $NSWRI$ strictly present no differences with the ones obtained with the previous set of fuzzy partitions U_α, as described in Fig. 4(b). This behaviour is the consequence of the normalization applied to the coincidence matrix of each partition. Moreover, this property holds for any set of parameters $\{\top, w, t, r, o\}$ while $\top \in \{\top_M, \top_P\}$ and barely holds with little differences with other t-norms, so that results obtained in previous section holds for possibilistic partitions. An interesting discussion is that no existing statement has already been made about the way possibilistic partitions must be compared to crisp or fuzzy ones, so that both $SERI$ and $NSWRI$ behaviour can be defended and used, depending on the application.

C. Comparing two fuzzy partitions provided by FCM.

We consider four well known datasets from the UCI Machine Learning Repository [14] presenting various characteristics in terms of: number n of samples, number p of features, true number $c^\star$ of classes/clusters and degree of overlap between clusters, as summarized in table V. For each dataset, the *Fuzzy C-Means algorithm* (FCM) [15] is run to produce a reference fuzzy partition R and a collection of 14 fuzzy c-partitions Q_c, $c \in 2, ..., 14$. Each partition Q_c is compared to R with different indices, namely $NSRI$, $SERI$ and our proposal $NSWRI$ with different parameters, provided the index requires some parametrization. For each index I, the computed value of $I(R, Q_c)$ is stored for each value of c. Fig. 6 presents some examples ofresulting curves. Each column is for a dataset, the first, second, third and fourth rows are respectively the results obtained by computing $NSWRI$ with $\{\top_P, w_T, 0.1, 0.1, 0\}$, $\{\top_P, w_T, 0.1, 0.8, 0\}$, $\{\top_P, w_T, 0.1, 0.1, 1\}$ and $\{\top_P, w_T, 0.1, 0.8, 1\}$. $NSRI$ is computed with $\top_P$ as well.

As expected, each index expresses its maximum value when c reaches the real number of classes $c^\star$, and they share the tendency to drop from this maximum toward an asymptotic value, different in each case and for each index and depending on the overlap of the dataset. $NSWRI$ does not always reach a value as large as the other two indices, but it presents a better dynamic and is thus more discriminant. One can observe that this behaviour is influenced by the choice of the origin parameter o. Indeed, the separation is emphasized in the whole set of examples when $o = 1$, backing the statements made in previous experiments, see section IV-A. Nevertheless, it seems that choosing a large value for r weakens the discriminant power of $NSWRI$, according to the results presented in each second and fourth row of Fig. 6.

TABLE V
REAL DATASETS AND THEIR CHARACTERISTICS.

dataset	n	p	$c^\star$	clusters property
Ionosphere	351	34	2	very strong overlap
Pima	768	9	2	strong overlap
Iris	150	4	3	slight overlap
Thyroid	215	5	3	slight overlap

V. CONCLUSION

In this article, we propose a new extension of the Rand index, meant to take benefits of two existing ones that belong to the class of conincidence-based comparison indices. These approaches lie respectively on fuzzy set-theoretic and similarity principles. It is shown that the former, although it is based on a direct extension of the crisp Rand index to the soft domain, presents some drawbacks because of the way the coincidence matrices are aggregated. These drawbacks are avoided by the latter, thanks to the use of a similarity measure. A new parametrized similarity measure is proposed to correct the drawbacks. It allows us to define a new versatile Rand index. Thanks to its flexibility, this index outperforms the existing ones as shown by numerous experimental results on both synthetic and real data. Moreover, by allowing to compare possibilistic partitions in a new way, the proposed concordance measure could become a privilegied tool for many practitioners.

ACKNOWLEDGMENT

This work is partially supported by the French Ministry of Research through a PhD grant.

REFERENCES

[1] J. Bezdek, *Pattern Recognition with fuzzy objective function algorithm*. Plenum Press, 1981.

[2] D. Anderson, J. Bezdek, M. Popescu, and J. Keller, "Comparing fuzzy, probabilistic, and possibilistic partitions," *IEEE Transactions on Fuzzy Systems*, vol. 18, no. 5, pp. 906–918, 2010.

[3] C. Borgelt, "Prototype-based classification and clustering," 2005, habilitation Thesis, Fakultat fur Informatik der Otto von Guericke, Universitat Magdeburg.

[4] S. Bodjanova, "Comparison of fuzzy partitions based on their α-cuts," *Fuzzy Sets and Systems*, vol. 105, no. 1, pp. 99–112, 1999.

[5] A. G. Di Nuovo and V. Catania, "On external measures for validation of fuzzy partitions," in *Lecture Notes in Computer Science 4529*, 2007, pp. 491–501.

[6] I. Charon, L. Denoeud, A. Guenoche, and O. Hudry, "Maximum transfer distance between partitions," *Journal of Classification*, vol. 23, no. 1, pp. 103–121, June 2006.

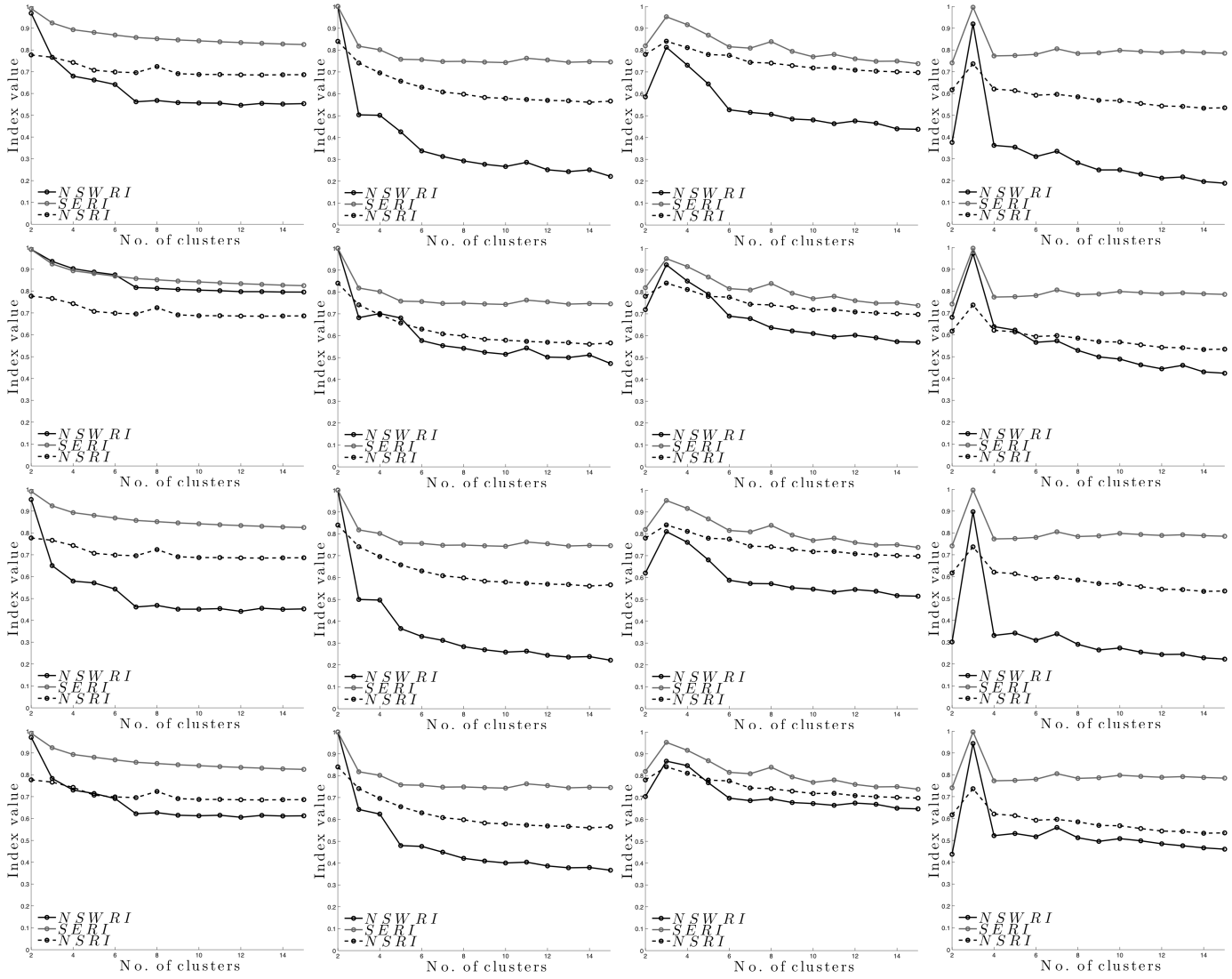

(a) Ionosphere dataset (b) Pima dataset (c) Iris dataset (d) Thyroid dataset

Fig. 6. $SERI(R, Q_c)$, $NSRI(R, Q_c)$, $NFRI(R, Q_c)$ and $NSWRI(R, Q_c)$ for four datasets, with $\{\top_P, w_T, 0.1, 0.1, 0\}$, $\{\top_P, w_T, 0.1, 0.8, 0\}$, $\{\top_P, w_T, 0.1, 0.1, 1\}$ and $\{\top_P, w_T, 0.1, 0.8, 1\}$

[7] A. Albatineh, M. Niewiadomska-Bugaj, and D. Mihalko, "On similarity indices and correction for chance agreement," *Journal of Classification*, vol. 23, pp. 301–313, 2006.

[8] C. Borgelt, "Resampling for fuzzy clustering," *International Journal of Uncertainty, Fuzziness and Knowledge-Based Systems*, vol. 15, no. 5, pp. 595–614, 2007.

[9] R. Brouwer, "Extending the rand, adjusted rand and jaccard indices to fuzzy partitions," *Journal of Intelligent Information Systems*, vol. 32, no. 3, pp. 213–235, 2009.

[10] R. Quéré, H. L. Capitaine, N. Fraisseix, and C. Frélicot, "On normalizing fuzzy coincidence matrices to compare fuzzy and/or possibilistic partitions with the rand index," in *10th. IEEE Int.ernational Conference on Data Mining*, 2010, pp. 977–982.

[11] E. Hüllermeier and M. Rifqi, "A fuzzy variant of the rand index for comparing clustering structures," in *13th International Fuzzy Systems Association World Congress*, 2009, pp. 1294–1298.

[12] M. Kendall and A. Stuart, *The Advanced Theory of Statistics*. Griffin, 1981, vol. 2.

[13] E. Klement, R. Mesiar, and E. Pap, *Triangular Norms*, T. in Logic, Ed. Kluwer Academic, 2000.

[14] A. Asuncion and D. Newman, "UCI machine learning repository," 2007. [Online]. Available: http://www.ics.uci.edu/∼mlearn/MLRepository.html

[15] J. Bezdek, J. Keller, R. Krishnapuram, and N. Pal, *Fuzzy Models and Algorithms for Pattern Recognition and Image Processing*. Kluwer Academic, 1999.

2011 IEEE International Conference on Fuzzy Systems
June 27-30, 2011, Taipei, Taiwan

Fuzzy Clustering With Learnable Cluster Dependent Kernels

Ouiem Bchir
CECS department
Multimedia Research Laboratory
University of Louisville
Louisville, KY, 14208
Email: ouiem.bchir@gmail.com

Hichem Frigui
CECS department
Multimedia Research Laboratory
University of Louisville
Louisville, KY, 14208
Email: h.frigui@louisville.edu

***Abstract*—We propose a new relational clustering approach, called Fuzzy clustering with Learnable Cluster dependent Kernels (FLeCK), that learns multiple kernels while seeking compact clusters. A Gaussian kernel is learned with respect to each cluster. It reflects the relative density, size, and position of the cluster with respect to the other clusters. These kernels are learned by optimizing both the intra-cluster and the inter-cluster similarities. Moreover, FLeCK is formulated to work on relational data. This makes it applicable to data where objects cannot be represented by vectors or when clusters of similar objects cannot be represented efficiently by a single prototype. The experiments show that FLeCK outperforms several other algorithms. In particular, we show that when data include clusters with various inter and intra cluster distances, learning cluster dependent kernel is crucial in obtaining a good partition.**

***Index Terms*—Fuzzy clustering, kernel learning, Gaussian kernel.**

I. Introduction

Clustering consists of partitioning a data set into subsets, so that data in each subset share some common aspects. In other words, according to a defined distance measure, objects in the same cluster should be as similar as possible and objects in different clusters should be as dissimilar as possible. Clustering has been used in many applications related to understanding and exploring the structure of the data. In particular, fuzzy clustering techniques have been shown to be suitable to describe real situations with overlapping boundaries [1].

Typically, the set of objects to be clustered could be described in two ways: object based representation, and relational based representation. While for object data representation, each object is represented by a feature vector, for the relational representation only information of how two objects are related is available. Relational data representation is more general in the sense that it can be applied when only the degree of (dis)similarity between objects is available or when groups of similar objects cannot be represented efficiently by a single prototype.

Despite the large number of existing clustering methods, clustering remains a challenging task when the structure of the data does not correspond to easily separable categories, and when clusters vary in size, density and shape. Kernel based approaches [2], [3], [4] allow to adapt a specific similarity measure in order to make the problem easier. Gaussian kernel is the most common similarity function. Although good results were obtained using this kernel, it relies on the selection of a scale parameter. This selection is commonly done manually. Moreover, as it is a global parameter over the entire data, it may not be appropriate when the distributions of the different clusters in the feature space exhibit large variations. Thus, in the absence of apriori knowledge, the choice of a scaling parameter that can adapt to different clusters and discriminate between them is difficult. In such situations, the geometry of the data should be explored to learn local similarity measures by finding intrinsic properties, such as local dimensionality, and local parametrization.

In this work, we introduce a new fuzzy relational clustering technique. The proposed algorithm, called Fuzzy clustering with Learnable Cluster dependent Kernels (FLeCK), learns the underlying cluster dependent dissimilarity measure while finding compact clusters. The learned measure is a local dissimilarity based on the Gaussian kernel function defined with respect to each cluster. In particular, we propose to learn a scaling parameter σ_i with respect to each cluster i. This scaling parameter is designed to distinguish and separate the objects of cluster i from the rest of the data. We achieve this by considering one cluster at a time, and learning a scaling parameter that maximizes the intra-cluster similarity and minimizes the inter-cluster similarity.

The organization of the rest of this paper is as follows. In section 2, we highlight related clustering algorithms. In section 3, we present our algorithm. In section 4, we describe the experiments conducted to validate the proposed algorithm. Finally, section 5 contains the conclusions and potential future work.

II. Related works

In most applications categories are rarely well separated and boundaries are overlapping. Describing these real world situations by crisp sets does not allow the user to quantitatively distinguish between objects which are strongly associated with a particular category from those that have only a marginal association with multiple ones, particularly, along the overlap-

978-1-4244-7316-8/11/$26.00 ©2011 IEEE

ping boundaries. Fuzzy clustering methods are good at dealing with these situations [5]. In fact, data elements can belong to more than one cluster with fuzzy membership degrees. These memberships indicate the strength of the association between that data element and a particular cluster. One of the most widely used fuzzy clustering algorithms is the Fuzzy C-Means (FCM) Algorithm [6] and its relational dual, Relational Fuzzy C-means algorithm (RFCM) [7].

Although FCM based approaches are quite efficient, they are not suitable for all types of data, and cannot handle clusters of different sizes and densities effectively [8]. Another major drawback of FCM based approaches is that they cannot separate clusters that are non-linearly separable in the input space. Two recent approaches have emerged for tackling such a problem. They allow mapping of the data into a new space in such a way that computing a linear partitioning in this feature space results in a nonlinear partitioning in the input space [2], [3], [4], [9]. These are mainly approaches based on kernel and spectral clustering.

Kernel methods allow the incorporation of a priori knowledge. This knowledge is implicit and is integrated in the learning process through the use of a kernel function. However, despite the existence of a large number of kernel clustering algorithm (e.g., kernel K-means [2], [10], kernel FCM [11], [12], [13], kernel SOM [3], [14] and kernel Neural Gas [4]), the choice of a good kernel function and the adaptation of its parameters to the data remains a challenging task. For instance, in the Kernelized Non-Euclidean Relational Fuzzy c-Means Algorithm (kNERF) [15], a relational Gaussian kernel is used with one global scaling parameter for all the data. The selection of the scaling parameter is discussed but there has been no attempt to devise methods to automatically select it. Moreover, a global scaling parameter may not be appropriate when clusters are of widely differing shapes, sizes, and densities.

Spectral clustering algorithm methods solve a similar problem as kernel methods, but use a different approach. Its theory arises from the graph cut concept [9]. As for kNERF, spectral clustering use the Gaussian similarity function in order to model the local neighborhood relationships between data points. Thus, it has the same challenging task of determining and adapting the scaling parameter to the data set.

The Gaussian similarity function, used in kernel and spectral clustering, is defined as

$$\mathbf{S}_{jk} = exp\left(-\frac{dist\left(\mathbf{x}_j, \mathbf{x}_k\right)}{\sigma^2}\right) \tag{1}$$

where $dist$ measures the dissimilarity between patterns and σ controls the rate of decay of S. The scaling parameter σ is commonly set manually.

Ng et al. [16] suggested selecting σ that provides the least distorted clusters by running the algorithm for different values of σ. However, the range of values to be tested still has to be set manually. Moreover, a global σ for mapping all the data may not provide a good clustering when the input data includes clusters with different local statistics.

In [17], the authors proposed to calculate a local scaling parameter σ_j for each data point $\mathbf{x}_j$ and defined the similarity between a pair of points as

$$\mathbf{S}_{jk} = exp\left(-\frac{dist\left(\mathbf{x}_j, \mathbf{x}_k\right)}{\sigma_j \sigma_k}\right) \tag{2}$$

The selection of the local scale σ_j is defined in [17] as the distance between point $\mathbf{x}_j$ and its P^{th} neighbor. Nevertheless, this approach is still dependent on the selection of the neighborhood parameter P which is fixed empirically for each data set. Moreover, if $\mathbf{x}_j$ is a noise point, adapting σ_j to this point will distort this fact.

To the best of our knowledge, no automatic way to select the optimal scaling parameter and adapt it to each cluster has been proposed even though the performance of Gaussian kernel based approaches is highly dependent on this parameter. In this paper, we propose a clustering algorithm, called Fuzzy clustering with Learnable Cluster dependent Kernels (FLeCK), that learns the underlying cluster dependent scaling parameters while finding compact clusters.

III. Fuzzy clustering with learnable cluster dependent kernels

Considering the Gaussian similarity function as defined in (1), the optimal choice of the scaling parameter is the one that allows to segregate and distinguish between the clusters. Thus, this scaling parameter has to ensure a high intra-cluster similarity and low inter-cluster similarity. A very large value of σ would minimize the intra-cluster similarity. However, this choice would also minimize the inter-cluster similarity and merge all the objects into a single cluster. One possible approach to avoid this trivial solution is to seek scaling parameters that minimize the intra-cluster similarities and maximize the intra-cluster similarities simultaneously.

Let $\{\mathbf{x}_1, \cdots, \mathbf{x}_N\}$ be a set of N data points and let $\mathbf{R} = [\mathbf{r_{jk}}]$ be a relational matrix where r_{jk} represent the degrees to which pairs of objects are similar. The FLeCK algorithm minimizes the intra-cluster similarity

$$\begin{aligned} J^{intra} &= \sum_{i=1}^{C}\sum_{j=1}^{N}\sum_{k=1}^{N}\beta_{jk}^{i}\left(1 - exp\left(-\frac{\mathbf{r}_{jk}}{\sigma_i}\right)\right) \\ &- \sum_{i=1}^{C}\frac{K}{\sigma_i} \end{aligned} \tag{3}$$

and maximizes the inter-cluster similarity

$$J^{inter} = \sum_{i=1}^{C}\sum_{j=1}^{N}\sum_{k=1}^{N}\alpha_{jk}^{i} exp\left(-\frac{\mathbf{r}_{jk}}{\sigma_i}\right) - \sum_{i=1}^{C}\frac{K}{\sigma_i} \tag{4}$$

In (3) and (4), C is the number of clusters. The constant K provides a way of specifying the relative importance of the regularization term compared to the sum of intra-cluster and inter-cluster distances. When K is zero, minimizing (3) with respect to σ_i gives the trivial solution of a very large σ_i that merges all points into a single cluster. Instead of treating K as a constant, we propose to determine the optimal K

by simultaneously minimizing the intra-cluster similarity and maximizing the inter-cluster similarity.

The term β^i_{jk} in (3) is the likelihood that two points $\mathbf{x}_j$ and $\mathbf{x}_k$ belong to the same cluster i and is defined as

$$\beta^i_{jk} = u^m_{ij} u^m_{ik} \tag{5}$$

where u_{ij} is the fuzzy membership of $\mathbf{x}_j$ in cluster i and satisfies the constraints

$$0 \leq u_{ij} \leq 1 \;\; and \;\; \sum_{i=1}^{C} u_{ij} = 1, \; for \; j \in \{1, \ldots N\}. \tag{6}$$

Similarly, the term α^i_{jk} in (4) refers to the likelihood that two points $\mathbf{x}_j$ and $\mathbf{x}_k$ do not belong to the same cluster i. It can also be defined using the fuzzy memberships of the two points using

$$\alpha^i_{jk} = u^m_{ij}\left(1 - u^m_{ik}\right) + u^m_{ik}\left(1 - u^m_{ij}\right). \tag{7}$$

In (5) and (7), $m \in (1, \infty)$ is a constant that determines the level of cluster fuzziness. A larger m results in fuzzier clusters. Typically, m is set to 2 [18].

The first term in (3) seeks clusters that have compact local relational distances

$$\mathbf{D}^i_{jk} = 1 - exp\left(-\frac{\mathbf{r}_{jk}}{\sigma_i}\right) \tag{8}$$

with respect to each cluster i. The scaling parameter, σ_i, controls the rate of decay of $\mathbf{D}^i_{jk}$. We should note here that our approach learns a cluster dependent σ_i in order to deal with the large variations between the distributions and the geometric characteristics of each cluster. The second term in (3) and (4) is a regularization term to avoid the trivial solution where all σ_i are infinitely large.

The proposed FLeCK algorithm attempts to optimize (3) and (4) by learning the C clusters, the scaling parameter, σ_i, of each cluster, and the membership values, u_{ij}, of each sample $\mathbf{x}_j$ in each cluster i.

In order to optimize (3) and (4) with respect to σ_i, we assume that σ_i's are independent from each others and reduce the optimization problem to C independent problems. That is, we convert the set of objective functions in (3) and (4) to the following C simpler set of functions

$$J^{intra}_i = \sum_{j=1}^{N}\sum_{k=1}^{N} \beta^i_{jk}\left(1 - exp\left(-\frac{\mathbf{r}_{jk}}{\sigma_i}\right)\right) - \frac{K}{\sigma_i}, \tag{9}$$

and

$$J^{inter}_i = \sum_{j=1}^{N}\sum_{k=1}^{N} \alpha^i_{jk} exp\left(-\frac{\mathbf{r}_{jk}}{\sigma_i}\right) - \frac{K}{\sigma_i} \tag{10}$$

for $i = 1, \ldots, C$. To obtain an update equation for the scaling parameters, we first set the derivative of J^{intra}_i with respect to σ_i to zero and solve for K. Then, we substitute the expression of K back in (10). Assuming that the values of σ_i do not change significantly from one iteration $(t-1)$ to the next one (t) and setting the derivative of J^{inter}_i to zero, we obtain

$$\sigma^{(t)}_i = \frac{Q^i_1}{Q^i_2} \tag{11}$$

where

$$Q^i_1 = \sum_{j=1}^{N}\sum_{k=1}^{N} \beta^i_{jk}\mathbf{r}^2_{jk} exp\left(-\frac{\mathbf{r}_{jk}}{\sigma^{(t-1)}_i}\right) \tag{12}$$

and

$$\begin{aligned} Q^i_2 &= \sum_{j=1}^{N}\sum_{k=1}^{N} \alpha^i_{jk}\mathbf{r}_{jk} exp\left(-\frac{\mathbf{r}_{jk}}{\sigma^{(t-1)}_i}\right) \\ &+ \sum_{j=1}^{N}\sum_{k=1}^{N} \beta^i_{jk}\mathbf{r}_{jk} exp\left(-\frac{\mathbf{r}_{jk}}{\sigma^{(t-1)}_i}\right) \end{aligned} \tag{13}$$

The expression of the scaling parameter defined by equation (11) depends on both the inter-cluster and the intra-cluster distances.

Optimization of (3) and (4) with respect to u_{ij} is not trivial and does not lead to a closed form expression. To keep the computation simple, we optimize only (3) with respect to u_{ij}. We achieve this by using the relational dual of the fuzzy C-means algorithm formulated by Hathaway et al. [7]. As it has been proved in [7], the Euclidean distance, $d^2_{ik} = \|\mathbf{x}_k - \mathbf{c}_i\|^2$, from feature $\mathbf{x}_k$ to the i^{th} cluster, $\mathbf{c}_i$, can be written in terms of the relational matrix $\mathbf{D}^i$ as

$$d^2_{ik} = \left(\mathbf{D}^i\mathbf{v}_i\right)_k - \frac{\mathbf{v}^t_i\mathbf{D}^i\mathbf{v}_i}{2}. \tag{14}$$

In (14), $\mathbf{v}_i$ is the membership vector of all N samples in cluster i defined by

$$\mathbf{v}_i = \frac{(u^m_{i1}, \ldots, u^m_{iN})^t}{\sum_{j=1}^{N} u^m_{ij}}. \tag{15}$$

Using Lagrange multiplier technique, it can be shown that optimization of (3) with respect to u_{ij}, subject to (6), yields the following membership update equation

$$u_{ij} = \frac{1}{\sum_{t=1}^{C}\left(d^2_{ij}/d^2_{tj}\right)^{\frac{1}{m-1}}}. \tag{16}$$

The resulting FLeCK algorithm is summarized below.

Algorithm 1 The FLeCK algorithm

Fix number of clusters C and m $\in [1\infty)$;
Initialize the fuzzy partition matrix $\mathbf{U}$;
Initialize the scaling parameter σ_i to 1;
REPEAT
  Compute the dissimilarity D^i for all clusters using (8) ;
  Compute the membership vectors $\mathbf{v}_i$ using (15);
  Compute the distances using (14);
  Update the fuzzy membership using (16);
  Update the scaling parameter σ_i using (11);
UNTIL (fuzzy membership do not change)

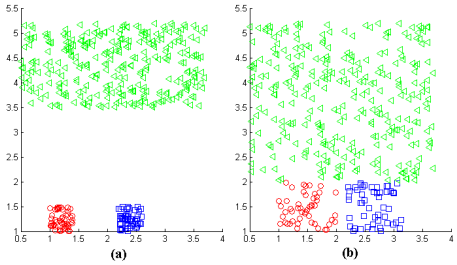

Fig. 1. 2D datasets. Each cluster is shown by a different color.

IV. Experimental Results

The performance of the proposed algorithm is illustrated and compared to kNERF [15] and Self tuning spectral [17]. We also illustrate the advantage of learning cluster dependent σ_i's compared to one global σ.

A. Synthetic data sets

To illustrate the ability of FLeCK to learn appropriate local scaling parameters and cluster the data simultaneously, we use it to categorize synthetic data sets. We use 2 data sets that include categories of different sizes and densities. We should mention here that for the purpose of visualizing the results, we use feature based and 2-dimensional data. Relational dissimilarity matrices are obtained by computing the Euclidean distance between these feature vectors. Results on real and high-dimensional data sets will be reported in the next section. Figure 1 displays the 2 synthetic data sets where each cluster is displayed with a different color.

For kNERF, and Self tuning spectral, we repeat the clustering with different parameters and report the best results. In particular, for Self tuning spectral, we tune the neighborhood parameter from 1 to 20 by an increment of 1. For kNERF, we tune the scaling parameter between 0.001 and 10 with a step of 0.01.

Figure 2 displays the clustering results of the three algorithms on data set 1. As shown in figure 2 (b), self tuning spectral was able to categorize it correctly after tuning the scaling parameter. Although, similar to spectral clustering kNERF is based on a non linear mapping of the input data, it was not able to categorize this data correctly (Fig. 2 (a)). This is due mainly to the fact that one global scaling parameter is not sufficient when the input data includes clusters with different local statistics. FLeCK and self tuning spectral provide local exponential mapping of the data and were able to partition this data correctly. The main difference between these approaches, as explained in section III, is that FLeCK learns the local scaling parameters and performs clustering simultaneously, while the self tuning spectral tunes the neighborhood within a user specified range to find local scaling parameters.

The scaling parameters learned by FLeCK reflect the relative position of each cluster with respect to the other clusters. For this data, cluster 1 and cluster 2 are close to each other, and cluster 3 is quite distant from both of them. Consequently, FLeCK learns a large scaling parameter $(\sigma_3 = 106.64)$ for

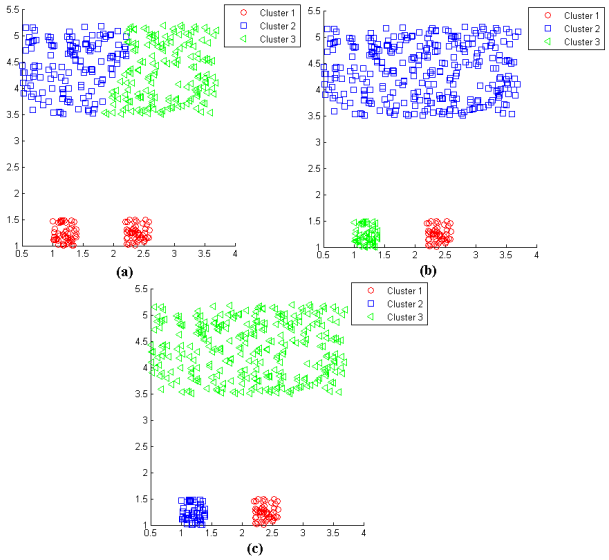

Fig. 2. Results of clustering the data in fig. 1 (a) using (a) kNERF, (b) Spectral, and (c) FLeCK

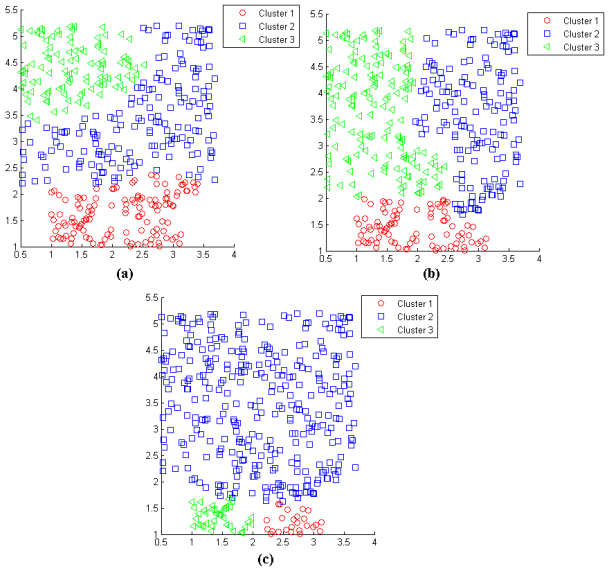

Fig. 3. Results of clustering the data in fig. 1 (b) using (a) kNERF, (b) Spectral, and (c) FLeCK

cluster 3. This large σ_3 allows points that are spatially dispersed to be grouped into one cluster without including points from the other clusters. On the other hand, FLeCK learns smaller σ_i's for the two small and dense clusters $(\sigma_1 = 24.94 \; and \; \sigma_2 = 30.17)$. These small σ_1 and σ_2 prevent points that are not spatially very close from being assigned to these clusters.

The second data set, shown in figure 1 (b), contains two clusters that have the same shape, density, and size, and a third cluster that is larger. The clustering results of the three algorithms on this data are shown in figure 3. As it can be seen, only FLeCK was able to partition this data correctly. This was possible due to the learned scaling parameters for each cluster.

TABLE I
NUMBER OF SAMPLES FORM EACH CATEGORY

Category	0	1	2	3	4	5	6	7	8	9
No. of samples	128	131	107	122	108	119	114	117	109	111

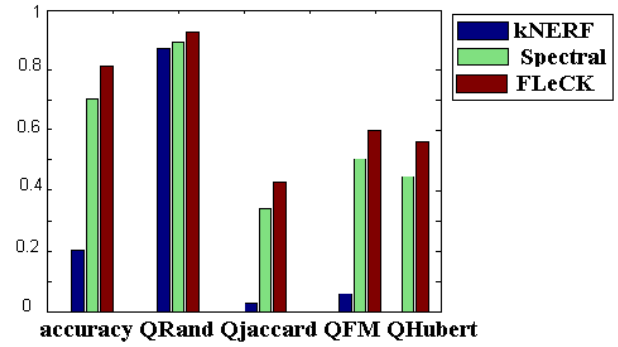

Fig. 4. Performance measures obtained on Handwritten Digits Data set using kNERF, Spectral and FLeCK clustering approaches.

For instance, cluster 2 has the smallest scaling parameter ($\sigma_2 = 0.0007$). This reflects the fact that points within this cluster are dispersed and some of them are closer to cluster 1 and cluster 3 than other points within this cluster. This small σ_2 ensures that cluster 2 does not include points from the other clusters. FLeCK learns a relatively bigger scaling parameters for cluster 1 and cluster 3 ($\sigma_1 = 12.21$ *and* $\sigma_3 = 11.3$). In fact, these two scaling parameters can be relatively larger (to maximize the intra-cluster similarity) without including points from the other cluster.

Besides giving a better clustering results than kNERF and self tuning spectral, FLeCK has two more main advantages over these two algorithms. First, it does not require the specification of the scaling parameter or the neighborhood parameter. Instead, it learns a cluster dependent scaling parameter in a completely unsupervised manner. Second, the learned scaling parameters provide a better description of the data and can be explored in subsequent learning steps.

B. Real data set

To illustrate the ability of FLeCK to learn local kernels and to cluster relational data derived from real and high dimensional data, we use it to categorize the Handwritten Digits database. We use a subset of 1166 handwritten digits from the Pen-Based Recognition of Handwritten Digits collection [19] available at the UCI Machine Learning data set. The handwritten samples were collected using a pressure sensitive tablet that sends the x and y coordinates of the pen at fixed time intervals. The raw data is processed so that each digit is represented by 8 (x,y) coordinates resulting in a 16-D feature vector. Table I displays the number of samples form each category.

We compare our clustering results to those obtained using the kNERF [15], and self tuning spectral clustering [17]. To quantify the performance of the different clustering algorithms and compare them, we assume that the ground truth is known,

TABLE II
KNERF CLUSTERING RESULTS ON THE HANDWRITTEN DIGIT DATA

		True class									
		'0'	'1'	'2'	'3'	'4'	'5'	'6'	'7'	'8'	'9'
Clusters	1	0	0	0	0	0	0	0	0	0	0
	2	0	0	0	1	0	0	0	0	0	0
	3	0	0	0	103	0	3	0	0	0	2
	4 - 13	0	0	0	0	0	0	0	0	0	0
	14	0	0	0	0	0	0	0	0	0	1
	15	0	0	0	0	0	0	0	0	0	0
	16	128	131	107	18	108	116	114	117	109	108

TABLE III
SELF TUNING SPECTRAL CLUSTERING RESULTS ON THE HANDWRITTEN DIGIT DATA

		True class									
		'0'	'1'	'2'	'3'	'4'	'5'	'6'	'7'	'8'	'9'
Clusters	1	0	7	0	4	0	0	0	7	0	3
	2	0	1	0	0	0	0	0	44	0	0
	3	0	0	0	0	37	0	0	0	0	7
	4	0	0	0	0	65	0	0	0	0	0
	5	14	0	0	0	0	0	0	0	0	0
	6	0	19	0	0	0	0	0	0	0	0
	7	0	0	0	0	0	0	108	0	0	0
	8	50	0	0	0	0	0	0	0	0	0
	9	1	1	0	1	6	59	6	14	0	27
	10	0	5	58	0	0	0	0	0	0	0
	11	0	0	0	0	0	0		41	0	0
	12	0	15	0	0	0	0	0	0	0	0
	13	63	0	0	1	0	57	0	0	109	70
	14	0	51	49	0	0	0	0	1	0	0
	15	0	0	0	115	0	3	0	0	0	4
	16	0	32	0	1	0	0	0	10	0	0

and we evaluate the performance of the algorithms by using the accuracy, Rand statistics, *QRand*, Jaccard coefficient, *Qjaccard*, Folkes-Mallows index, *QFM*, and Hubert index, *QHubert*, [20]. All these measures provide larger values when the two partitions are more similar.

For all algorithms, we use the Euclidean distance and we fix the number of clusters to 16. For the fuzzy algorithms, we fix the fuzzifier m to 1.1. For Self tuning spectral, we tune the

TABLE IV
FLECK CLUSTERING RESULTS ON THE HANDWRITTEN DIGIT DATA

		True class									
		'0'	'1'	'2'	'3'	'4'	'5'	'6'	'7'	'8'	'9'
Clusters	1	0	0	0	0	0	0	0	0	41	0
	2	0	55	59	0	0	0	0	1	1	0
	3	45	0	0	0	0	0	0	0	1	0
	4	9	0	0	0	0	0	0	0	0	0
	5	45	0	0	0	0	0	0	0	0	0
	6	0	0	0	0	0	0	0	0	59	1
	7	0	0	0	0	0	0	105	1	0	0
	8	0	0	0	1	0	2	0	0	0	76
	9	0	1	0	116	0	34	0	12	0	14
	10	0	19	0	0	5	26	8	0	1	1
	11	0	0	0	0	68	0	0	0	0	3
	12	0	54	0	5	0	0	0	18	0	8
	13	0	0	0	0	0	57	0	0	5	0
	14	0	2	8	0	0	0	0	85	0	0
	15	29	0	0	0	0	0	1	0	1	0
	16	0	0	0	0	35	0	0	0	0	8

TABLE V
THE SCALING PARAMETERS LEARNED BY FLECK, NO. OF SAMPLES PER CLUSTER, AND THE INTRA AND INTER CLUSTER DISTANCES

Clusters	No. of samples	σ_i
1	41	16.4
2	156	49.2
3	46	20.3
4	9	3.4
5	45	23.6
6	60	18.5
7	106	29.3
8	79	27.4
9	177	50.7
10	60	17.3
11	71	17.4
12	85	27.8
13	62	31.7
14	95	25.6
15	31	11.2
16	43	10.11

neighborhood parameter from 1 to 20 by an increment of 1. For kNERF, we tune the scaling parameter between 0.01 and 100 with a step of 0.1. Since we should not use the ground truth to select the optimal parameter, for each algorithm, we select the parameter that gives the minimum intra-cluster similarity.

Figure 4 compares the performance of the three considered algorithms. As it can be seen, FLeCK outperforms the other methods with respect to all five measures. Although, kNERF and self tuning spectral use a similar Gaussian kernel, they were not able to cluster this data properly. This is due to their sensitivity to the choice of the scaling parameter.

As it can be seen from table II, kNERF has succeeded to segregate only the digit "3" (cluster 3). In fact, almost all the other elements of the data set are gathered in a big cluster (cluster 16) and the remaining clusters are empty. This is due to the fact that one global σ for mapping all the data can not provide the correct partition when the input data includes clusters with different local statistics.

The self tuning spectral did relatively better than kNERF because it uses a local scaling parameter that is defined as the distance between $\mathbf{x}_j$ and its P^{th} neighbor. However, as it can be seen from table III, it still creates one big cluster that contains 300 elements from categories '0', '6', '8' and '9'. Moreover, although category '1' was split in five clusters (cluster 1, 6, 12, 14, and 16), it was not well segregated in clusters 1 and 14. This may be due to the fact that adapting σ to each sample can distort the structure of the data.

FLeCK on the other hand, was able to partition the data better than kNERF and Self tuning spectral. Referring to the FLeCK clustering results shown in table IV, some digits have been categorized using more than one cluster (clusters 0, 4, 5 and 8). This is due to the different writing styles. For instance, digit '4' has been categorized using two clusters (cluster 11 and 16). Figure 5 displays the top 10 representatives of these two clusters (corresponding to the highest memberships). We can notice that each cluster contains one style of writing the digit '4'. On the other hand, FLeCK categorized other digits using one cluster (clusters 1, 2, 3, 6, 7, and 9). These are categories

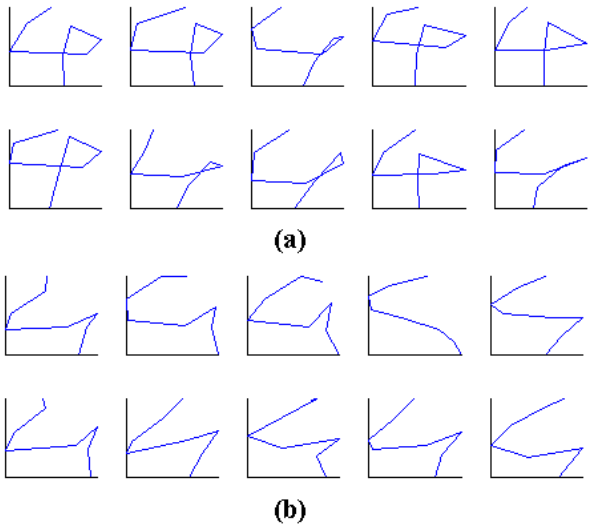

Fig. 5. The top 10 representatives of (a) cluster 11 and (b) cluster 16.

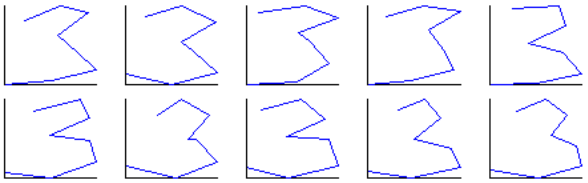

Fig. 6. The top 10 representatives of cluster 9.

with more consistent writing style. Figure 6 displays the top 10 representatives of one such cluster representing digit 3.

FLeCK learned a scaling parameter for each cluster. These parameters are reported in table V. For instance, cluster 4 is the smallest cluster and contains only 9 digits. These digits form the densest region in the feature space (small sum of intra cluster similarity) and are relatively close to other digits categories (small sum of inter cluster distances). Consequently, FLeCK learns a small scaling parameter ($\sigma_4 = 3.4$) for this cluster. This Small σ prevent digits that are spatially close but not within the dense region, from being assigned to this clusters.

On the other hand, FLeCK leaned a relatively larger scaling parameter for cluster 9 ($\sigma_9 = 50.65$) representing the digit 3. This is due to the fact that this cluster includes a large number of samples with large intra-cluster distances (without being split into small clusters).

V. CONCLUSIONS

We have proposed an approach that performs relational fuzzy clustering and local kernel learning. The learned kernel is based on a Gaussian function with a cluster dependent scaling parameter. The proposed approach minimizes both the inter-cluster dissimilarity and the intra-cluster dissimilarity to learn a scaling parameter with respect to each cluster. This allows FLeCK to adapt the distance to the characteristics of each cluster. FLeCK is formulated to work on pairwise relational

data. This makes it applicable when data is available only in relational form and when similar objects cannot be represented efficiently by a single prototype.

Using synthetic and real data sets, we have shown that our approach outperforms kNERF and self tuning spectral. In particular, we have shown that when data include clusters with various inter and intra cluster distances, learning cluster dependent scaling parameters is crucial in obtaining a good partition.

Currently, FLeCK uses fuzzy memberships that are constrained to sum to one. This type of membership does not discriminate between typical points that are close to multiple clusters and noise points. Consequently, FLeCK is not robust to noise and outliers. One way to overcome this limitation is to replace the fuzzy memberships with possibilistic memberships [21]. We are currently investigating this alternative.

ACKNOWLEDGMENTS

This work was supported in part by U.S. Army Research Office Grants Number W911NF-08-0255 and by a grant from the Kentucky Science and Engineering Foundation as per Grant Agreement No. KSEF-2079-RDE-013 with the Kentucky Science and Technology Corporation.

REFERENCES

[1] F. Klawonn, “Fuzzy Clustering: Insights and a New Approach”, *Mathware & Soft Computing 11*, Vol 11, No 3, 2004.

[2] M. Girolami, “Mercer kernel based clustering in feature space”, *IEEE Transactions on Neural Networks*, Vol. 13, No. 3, 2002.

[3] R. Inokuchi and S. Miyamoto, “LVQ clustering and SOM using a kernel function”, *IEEE Conf. on Fuzzy Systems*, 2004.

[4] A. K. Qinand and P. N. Suganthan, “Kernel neural gas algorithms with application to cluster analysis”, *ICPR*, 2004.

[5] Raju G., Binu Thomas, Sonam Tobgay, Th. Shanta Kumar, “Fuzzy Clustering Methods in Data Mining: A Comparative Case Analysis,” *icacte*, pp.489-493, 2008

[6] J.C Bezdek, “Pattern Recognition with fuzzy objective function algorithm”, *Plenum Press*, New york, 1981.

[7] R. J Hathaway, J.W. davenport, and J,C Bezdek, “Relational duals of the c-means algorithms”, *Pattern Recognition*, vol. 22, p.205 , 1989.

[8] Pang-Ning Tan, Michael Steinbach, Vipin Kumar,” Introduction to data mining”, *Addison Wesley,* 2006.

[9] Luxburg, “U. A tutorial on spectral clustering”, *Statistics and Computing* , 2007.

[10] B. Scholkopf, A.J. Smola, and K. R. Muller, “Nonlinear component analysis as a kernel eigenvalue problem”, *Neural Computation*, vol 10, p. 1299-1319,1998.

[11] T. Graepel and K. Obermayer, “Fuzzy topographic kernel clustering”, *5th GI Workshop Fuzzy Neuro Systems*, 1998.

[12] Z. D. Wu, W. X. Xie, and J. P. Yu, “Fuzzy c-means clustering algorithm based on kernel method”, *CIMA*, 2003.

[13] D.-Q. Zhang and S.-C. Chen, “Fuzzy clustering using kernel method”, *ICCA*, 2002.

[14] D. Macdonald and C. Fyfe, “The kernel self-organising map”, *KBIESAT*, 2000.

[15] R.J.Hathaway, J.M. Huband, and J.C.Bezdek, ”A Kernelized Non-Euclidean Relational Fuzzy c- Means Algorithm”, *FUZZ-IEEE*, 2005.

[16] P. Perona and W. T. Freeman, “A Factorization Approach to Grouping”, *5th European Conference on Computer Vision*, 1998.

[17] L. Zelnik-Manor, P. Perona, “Self-Tuning spectral clustering”, *NIPS*, 2004.

[18] Enrique Frias-Martinez, Sherry Y. Chen, and Xiaohui Liu. “Survey of Data Mining Approaches to User Modeling for Adaptive Hypermedia”, *IEEE Transactions on systems, man and cybernetics,* Vol. 36, No. 6, 2006.

[19] F. Alimoglu, E. Alpaydin, "Methods of Combining Multiple Classifiers Based on Different Representations for Pen-based Handwriting Recognition," *TAINN*, 1996, Istanbul.

[20] C. Borgelt and R. kruse, “Finding the number of fuzzy clusters by resampling”, *IEEE Conf. on Fuzzy Systems*, 2006.

[21] Krishnapuram, R. and Keller, J., "A Possibilistic Approach to Clustering", *IEEE Transactions on Fuzzy Systems*, Vol. 1, No. 3, pp. 222-233, 1993.

2011 IEEE International Conference on Fuzzy Systems
June 27-30, 2011, Taipei, Taiwan

The Interval Autoregressive Time Series Model

Xun Wang
Department of Applied Mathematics
Beijing University of Technology
Beijing, China 100124
Email: wangxun@emails.bjut.edu.cn

Shoumei Li
Department of Applied Mathematics
Beijing University of Technology
Beijing, China 100124
Email: lisma@bjut.edu.cn

***Abstract*—This paper mainly suggests a new type of interval time series: interval autoregressive (IAR) model. Firstly we state why we should introduce the interval time series models. Then we give necessary definitions about random intervals and interval time series. Thirdly, we introduce some methods of efficiency evaluation for forecasting of interval time series. And then we discuss parameter estimation and forecasting in IAR model, in which the methods of parameter estimation are based on the evaluation forecasting for interval data. Furthermore, we give the simulation results and apply it to real data from Shanghai Stock Index, which is to illustrate our modeling methodology. This model makes it possible for decision makers to forecast the best and worst possible situations based on interval-valued observations.**

Keywords: Interval time series; IAR model; parameter estimation; forecasting of stock price

I. Introduction

It is well-known that traditional time series models play an important role in many application areas. For instance, Box-Jenkins provided autoregressive integrated moving average (ARIMA) time series model in [4], which has been applied in engineering, economics, foreign current exchange, data analysis of stock markets, etc. In those traditional times series models, authors assumed that that the future values of a time series have a determined function relationship with current, past values and white noises. However, there are a great deal of economic problems that can not be explained and handled by these models since the actions of individuals in investment are affected not only by the random factors in financial market but also by the mental factors of investors. Therefore, interval-valued time series emerges quite naturally in some situations, which indicates uncertainty and variability.

Song and Chissom [11]-[13] believed in that fuzzy numbers would be better to describ the mental factors. So they introduced the concepts of fuzzy time series, and they assumed that the model parameters were fuzzy numbers. Tseng *et. al.* [15] built a fuzzy ARIMA model and gave the methods of parameter estimation and forecasting, and applied it to the foreign current exchange market.

The sample data usually are one-dimensional or multidimensional numbers in traditional time series analysis. However, in practice, the sample data sometimes are intervals in economics. For example, when the economists are surveyed to predict the economic increasing rate, they tend to give the answers like "5% to 7%", "5.2% to 6.7%" and so on . So we get the interval-valued sample data. Therefore, it is necessary to build the models of interval time series. The interval time series models show up the information in the form of a series of interval-valued data and make predictions based on the interval-valued data. Furthermore, such models also provide the upper boundary and lower boundary of possible selections for decision-makers or investors.

Hsu and Wu did a preliminary study on interval time series, and gave three evaluation criteria of forecasting efficiency for interval time series in [7], [8], that is, mean square error of interval (MSEI), mean relative interval error (MRIE), mean ratio of symmetric difference. Based on their works, we develop a new interval time series model in this paper ,which is called interval autoregressive (IAR) model .

This paper is organized as follows. Some definitions of random interval and interval time series are given in Section 2, especially interval autoregressive model is formulated and proposed. In Section 3, the methods of efficiency evaluation of forecasting for interval time series are presented. Methods of parameter estimation in IAR model are given in Section 4. In Section 5 and Section 6, simulation result and real data analysis are given respectively, which illustrate our modeling methodology.

II. Random Intervals and Interval Time Series

Random interval, as well as its operations, is the foundation in terms of analyzing the interval time series. Therefore, before the discussions of interval time series, we give some definitions of random interval and its operations.

Assume that $(\Omega, \mathcal{A}, P)$ is a probability space, $\mathbb{R}$ is the set of all real numbers.

Definition 2.1 The interval $X = [a, b]$ is called a random interval, if a, b: $\Omega \to \mathbb{R}$ are real-valued random variables with $a(\omega) \leq b(\omega)$ for all $\omega \in \Omega$. Then $c = (a + b)/2$ is called the center of the random interval X, $r = (b - a)/2$ is called the radius of the random interval X, and X is also denoted as $X = (c; r)$.

Let $X = [a, b] = (c; r)$ be a random interval, the interval length of X is $2r = b - a$, and denoted as $\|X\| = 2r$.

Remark 2.2 Actually the above concept of a random interval is the special case of that of a set-valued random variable (or a random set, or a multifunction in literature). Readers may refer to [2], [3], [6], [10], [16]. It was defined in a general way as follows.

978-1-4244-7316-8/11/$26.00 ©2011 IEEE

Let $\mathfrak{X}$ be a separable Banach space with its dual space $\mathfrak{X}^*$. A set-valued mapping X from Ω to the family of all nonempty closed subsets of $\mathfrak{X}$ is called a set-valued random variable if, for each open subset O of $\mathfrak{X}$,

$$X^{-1}(O) = \{\omega \in \Omega : X(\omega) \cap O \neq \emptyset\} \in \mathcal{A}.$$

If X takes compact convex subsets of $\mathfrak{X}$, then that X is a set-valued random variable is equivalent to that, for any $x^* \in \mathfrak{X}^*$, its support function

$$s(x^*, X(\omega)) = \sup\{\langle x^*, x\rangle : x \in X(\omega)\}$$

is a real-valued random variable.

So it is obvious that, if we limit $\mathfrak{X} = \mathbb{R}$, X takes compact convex set values in $\mathbb{R}$, then the concept of a random interval above is consistent with that of a set-valued random variable.

Definition 2.3 Let $X_1 = [a_1, b_1] = (c_1; r_1)$, $X_2 = [a_2, b_2] = (c_2; r_2)$ be two random intervals. The interval addition, scalar multiplication and interval subtraction are defined as

(i) interval addition:

$$X_1 \oplus X_2 = (c_1; r_1) \oplus (c_2; r_2) = (c_1 + c_2; r_1 + r_2);$$

(ii) scalar multiplication:

$$k \cdot X_1 = kX_1 = k(c_1; r_1) = (kc_1; |k|r_1), \forall k \in \mathbb{R};$$

(iii) interval subtraction:

$$X_1 \ominus X_2 = X_1 \oplus (-X_2) = (c_1 - c_2; r_1 + r_2).$$

Remark 2.4 (1) Note that above definitions of interval addition, scalar multiplication are the special case of the definitions of addition and scalar multiplication of set-valued random variables in a separable Banach space.

(2) Let $\mathbf{K}_{kc}(\mathbb{R})$ be the set of all finite intervals of $\mathbb{R}$. We define interval addition and scalar multiplication on $\mathbf{K}_{kc}(\mathbb{R})$ as above definition. But we have to notice that $(\mathbf{K}_{kc}(\mathbb{R}), \oplus, \cdot)$ is not a linear space! This is because for any $[a, b]$ with $a < b$, $[a, b] \oplus (-[a, b]) \neq \{0\}$. Thus, above interval interval subtraction operator is not inverse operator of interval addition.

In the set theory, set difference $A \setminus B$ is defined by $A \setminus B = \{x : x \in A \text{ and } x \notin B\}$. While we use this definition of the set difference on the family of closed intervals, the difference of two closed intervals is a half-closed interval. Since we want it to be a closed set, we have to revise the definition of interval difference as follows.

Definition 2.5 Let $X_1 = [a_1, b_1] = (c_1; r_1)$, $X_2 = [a_2, b_2] = (c_2; r_2)$ be two random intervals, then the interval difference $X_1 - X_2$ is defined by

$$X_1 - X_2 = \mathrm{cl}(X_1 \bigcap X_2^c),$$

where $\mathrm{cl}(A)$ means the closure of the set A.

If $a_1 \leq a_2 \leq b_1 \leq b_2$, then $X_1 - X_2 = [a_1, b_1] - [a_2, b_2] = [a_1, a_2]$ by the above definition.

Definition 2.6 Let $X_1 = [a_1; b_1] = (c_1; r_1)$, $X_2 = [a_2; b_2] = (c_2; r_2)$ be two random intervals, then the symmetric difference is defined by $X_1 \triangle X_2 = (X_1 - X_2) \bigcup (X_2 - X_1)$.

If $a_1 \leq a_2 \leq b_1 \leq b_2$, then by the above definition, $X_1 \triangle X_2 = (X_1 - X_2) \bigcup (X_2 - X_1) = [a_1, a_2] \bigcup [b_1, b_2]$.

Definition 2.7 Let $X = (c; r)$, c and r are two real-valued random variables, then $X = (c; r)$ is called a generalized random interval.

Obviously, if r is positive, $X = (c; r)$ is a random interval defined in Definition 2.1. Similarly, we may define the addition and scalar multiplication for generalized random interval as we do in definition 2.3.

Definition 2.8 The expectation of the random interval $X = [a, b] = (c; r)$ is defined by

$$E[X] = [E(a), E(b)],$$

where $E(a), E(b)$ are the expectations of real-valued random variables a and b respectively.

Obviously, we have $E[X] = (E(c); E(r))$. If $X_i = [a_i, b_i]$, $i = 1, 2$, then $E[X_1 \oplus X_2] = E[X_1] \oplus E[X_2]$, $E[kX_1] = kE[X_1]$, for any $k \in \mathbb{R}$.

Remark 2.9 (1) The expectation of a random interval above is consistent with Aumann integral of a compact convex set-valued random variable in $\mathbb{R}$ (cf. [3], [10]). Hence, we may obtain the same properties of the expectations of random intervals as that of Aumann integrals.

(2) In [2] and [10], authors defined the concepts of the distribution of a set-valued random variable, independence of a sequence of set-valued random variables. Here we used them to the random interval case and we omit them. By the Chapter 3 in [10], we know that, if two random intervals $X_1 = [a_1, b_1] = (c_1; r_1)$ and $X_2 = [a_2, b_2] = (c_2; r_2)$ are independent, so are a_1 and a_2, b_1 and b_2, c_1 and c_2, r_1 and r_2 respectively.

Assume that a simple random sample $X_i = [a_i, b_i]$, $i = 1, 2, \cdots, n$, is taken from a random interval $X = [a, b]$, i.e. $X_1, X_2, \cdots, X_n$ are independent and identically distributed with X. Let

$$\overline{X} = \frac{1}{n}[X_1 \oplus X_2 \oplus \cdots \oplus X_n]$$

denote the random sample average. By using the strong law of large numbers of set-valued random variables (cf. [2] and [10]), we may estimate the expectation $E[X]$ of random interval X by using the random sample average

$$\overline{X} = \Big[\frac{1}{n}\sum_{i=1}^{n} a_i, \frac{1}{n}\sum_{i=1}^{n} b_i\Big].$$

It is obvious that $\overline{X}$ is an unbiased estimator of $E[X]$.

Now we introduce the definition of interval autoregressive model (IAR).

Definition 2.10 An interval time series is a sequence of random intervals, $X_t = [a_t, b_t] = (c_t; r_t), \ \ t = 1, 2, 3, \cdots$, denoted by $\{X_t\} = \{X_t = [a_t, b_t] = (c_t; r_t) : \ t = 1, 2, 3, \cdots\}$.

Assume that $\widetilde{\varepsilon}_t = (c_{\varepsilon_t}; r_{\varepsilon_t}),\ \ t = 1, 2, \cdots$ is a generalized random interval (r_{ε_t} may be negative), c_{ε_t} and r_{ε_t} are independent white noise processes $WN(0, \sigma_c^2)$ and $WN(0, \sigma_r^2)$ respectively, then the p-order equation

$$X_t = a_1 X_{t-1} + a_2 X_{t-2} + \cdots + a_p X_{t-p} + \widetilde{\varepsilon}_t, t \in \mathbb{Z}$$

is called a p-order interval autoregressive model, denoted as IAR(p), where $a_1, a_2, \cdots a_p$ ($a_p \neq 0$) are called autoregressive coefficients of the IAR(p) model.

III. Efficiency Evaluation of Forecasting with Interval Time Series

A. The Mean Square Error of Interval Time Series

Let $X_t = [a_t, b_t] = (c_t; r_t)$, $t = 1, 2, \cdots$, be an interval time series, and $\hat{X}_t = [\hat{a}_t, \hat{b}_t] = (\hat{c}_t; \hat{r}_t)$, $t = 1, 2, \cdots$, be the forecast interval with respect to $X_t = [a_t, b_t] = (c_t; r_t)$. In the analysis and forecasting of interval time series, we may meet four forecasting situations:

(1) If $\hat{a}_t \leq a_t \leq b_t \leq \hat{b}_t$, then the forecast interval is too wide, and denoted by FIW;

(2) If $a_t \leq \hat{a}_t \leq \hat{b}_t \leq b_t$, then the forecast interval is too narrow, and denoted by FIN;

(3) If $a_t \leq \hat{a}_t \leq b_t \leq \hat{b}_t$, then the forecast interval inclines to the right, and denoted by FIR;

(4) If $\hat{a}_t \leq a_t \leq \hat{b}_t \leq b_t$, then the forecast interval inclines to the left, and denoted by FIL.

In the classical time series models, we use the distance between actual value and forecast value to describe the efficiency of prediction. In the interval time series models, what we are concerned about are not only the forecasting of interval length, but also the location disparity between the predicted interval and the actual interval. Therefore, it is necessary to define new criteria for analyzing of interval time series forecasting.

Assume that $X_t = (c_t; r_t)$, $t = 1, 2, \cdots$, is an interval time series, $\hat{X}_t = (\hat{c}_t; \hat{r}_t)$, $t = 1, 2, \cdots$, is the forecasting interval series of X_t, mean square error of interval is given in the following.

Definition 3.1 The mean squared error of interval position (MSEP) is given by

$$MSEP = \frac{1}{s}\sum_{t=1}^{s}(c_{n+t} - \hat{c}_{n+t})^2,$$

and the mean squared error of interval length (MSEL) is defined as

$$MSEL = \frac{1}{s}\sum_{t=1}^{s}(r_{n+t} - \hat{r}_{n+t})^2,$$

where n denotes the current time, and s is the number of the preceding intervals.

Definition 3.2 The error between the forecast interval $\{\hat{X}_t = (\hat{c}_t; \hat{r}_t)\}$ and the actual interval $\{X_t = (c_t; r_t)\}$ consists of two parts: the position error and the length error. The mean square error of interval time series (MESI) is given by

$$\begin{aligned} MSEI &= MSEP + MSEL \\ &= \frac{1}{s}\sum_{t=1}^{s}(c_{n+t} - \hat{c}_{n+t})^2 + \frac{1}{s}\sum_{t=1}^{s}(r_{n+t} - \hat{r}_{n+t})^2, \end{aligned}$$

where n denotes the current time, and s is the number of the preceding intervals.

In practice, different people may have different standards in terms of the prediction of interval time series due to different situation of problems. One important case, we take into account, is that mean squared error of interval with respect to position and mean squared error of interval with respect to length should pose different influence to the total error. Thus we define a generalized mean squared error of interval time series as follows.

Definition 3.3 The generalized mean squared error of interval (GMSEI) between the forecast interval $\{\hat{X}_t = (\hat{c}_t; \hat{r}_t)\}$ and the actual interval $X_t = (c_t; r_t)$ of a time series is

$$\begin{aligned} GMSEI &= f(MSEP) + g(MSEL) \\ &= f\Big(\frac{1}{s}\sum_{t=1}^{s}(c_{n+t} - \hat{c}_{n+t})^2\Big) \\ &\quad + g\Big(\frac{1}{s}\sum_{t=1}^{s}(r_{n+t} - \hat{r}_{n+t})^2\Big), \end{aligned}$$

where f and g are strictly increasing functions with $f(0) = 0$, $g(0) = 0$, n is the current time and s is the number of the preceding intervals.

For instance, if we let $f(x) = e^x - 1, g(x) = x, \forall x \geq 0$, that is

$$GMSEI = \exp(MSEP) - 1 + MSEL.$$

Under this evaluation criteria of forecasting error, we believe that the $MSEP$ is more significant than $MSEI$ in terms of contribution to the total error.

B. Other Evaluation Criteria

Symmetric difference between the actual interval and the forecast interval shows their non-intersecting parts. The smaller the length of their symmetric difference is, the more the forecast interval covers the actual interval. By virtue of this character of symmetric difference, we offer another method of the efficiency evaluation for the interval time series forecasting, i.e. mean ratio of symmetric difference.

Definition 3.4 Let $\{X_t = (c_t; r_t), t = 1, 2, \cdots, s\}$, be an interval time series, and $\{\hat{X}_t = (\hat{c}_t; \hat{r}_t), t = 1, 2, \cdots, s\}$, be the forecast interval time series. Then the mean ratio of symmetric difference, denoted by MRSD, is defined as

$$MRSD = \frac{1}{s}\sum_{t=1}^{s}\frac{\|X_{n+t} \triangle \hat{X}_{n+t}\|}{\|X_{n+t}\|}.$$

Definition 3.5 [The efficiency of MRSD] Let $\{X_t = (c_t; r_t)\}$ be an interval time series, and the forecast interval

time series $\{\hat{X}_{1t} = (\hat{c}_{1t}; \hat{r}_{1t})\}$ and $\{\hat{X}_{2t} = (\hat{c}_{2t}; \hat{r}_{2t})\}$ are obtained by two different forecast methods. If the MRSD of $\{\hat{X}_{1t}\}$ (denoted as $MRSD_1$) is smaller than that of $\{\hat{X}_{2t}\}$ (denoted as $MRSD_2$), i.e. $MRSD_1 < MRSD_2$, we say the forecast interval $\{\hat{X}_{1t}\}$ is more efficient than the forecast interval $\{\hat{X}_{2t}\}$.

Hsu and Wu [7] also referred to another evaluation criterion, called mean relative interval error (MRIE). Roughly speaking, we believe that a forecast result is better if the center of this forecast interval is closer to the center of the actual interval, and the intersection of their intervals is larger. The definition of mean relative interval error is as follows.

Definition 3.6 Let $\varepsilon_t = \frac{|c_t - \hat{c}_t|}{r_t + \hat{r}_t}$ be the relative error between the forecast interval $\hat{X}_t$ and the actual interval X_t, the mean relative interval error (MRIE) is given by

$$MRIE = \frac{1}{s} \sum_{t=1}^{s} \frac{|c_t - \hat{c}_t|}{r_t + \hat{r}_t}.$$

In practical use, we may be confronted with the case that the importance of FIR errors and FIL errors are different. With respect to how to treat this case, we shall discuss it in future works since the page limitation of this paper.

IV. Parameter Estimation in IAR Model

In this section, we will estimate the order p, autoregressive coefficients $a_1, a_2, \cdots, a_p$ and the variances of white noises σ_c^2, σ_r^2 in IAR(p) model

$$X_t = a_1 X_{t-1} + a_2 X_{t-2} + \cdots + a_p X_{t-p} + \tilde{\varepsilon}_t, \quad t = 1, 2, \cdots$$

through the observation data $x_1, x_2, \cdots, x_N$.

A. Methods of coefficient estimation

Firstly, we assume that the order p is known. Now we will choose an evaluation criterion of prediction efficiency. Without loss of generality, we take mean square error of interval (MSEI) as an example here, if other evaluation criteria are taken, a similar conclusion can be derived.

The basic idea of parameter estimation here is similar to the least squares estimation in the classic statistics.

Now we use the linear combination of $x_{j-1}, x_{j-2}, \cdots, x_{j-p}$ with coefficients $a_1, a_2, \cdots, a_p$, i.e. $a_1 x_{j-1} + a_2 x_{j-2} + \cdots + a_p x_{j-p}$, to predict x_j, the reasonable estimators of $a_1, a_2, \cdots, a_p$ should minimize the square error

$$\begin{aligned} & S(a_1, a_2, \cdots, a_p) \\ = & \sum_{j=p+1}^{N} [c_j - (a_1 c_{j-1} + a_2 c_{j-2} + \cdots + a_p c_{j-p})]^2 \\ & + \sum_{j=p+1}^{N} [r_j - (|a_1| r_{j-1} + |a_2| r_{j-2} + \cdots + |a_p| r_{j-p})]^2. \end{aligned}$$

Thus, we take the values $\hat{a}_1, \hat{a}_2, \cdots, \hat{a}_p$ which minimize the $S(a_1, a_2, \cdots, a_p)$ as the estimators of autoregressive coefficients. And the estimators of the variances of the white noises, $c_{\varepsilon_t}, c_{\varepsilon_t}$ are

$$\widehat{\sigma_c^2} = \frac{1}{N-p} \sum_{j=p+1}^{N} [c_j - (\hat{a}_1 c_{j-1} + \hat{a}_2 c_{j-2} + \cdots + \hat{a}_p c_{j-p})]^2,$$

$$\widehat{\sigma_r^2} = \frac{1}{N-p} \sum_{j=p+1}^{N} [r_j - (|\hat{a}_1| r_{j-1} + |\hat{a}_2| r_{j-2} + \cdots + |\hat{a}_p| r_{j-p})]^2.$$

B. Order Selection

Parameter estimation in IAR model described above is based on that the order p is known. But order p is usually unknown when we cope with some practical problems. Therefore, order p should be estimated.

In terms of order selection problem in traditional single-valued time series models, one of the most applicable criteria is Akaike information criterion (AIC), which was given by Akaike in 1973 [1]. Here we use an interval version of AIC to select an order p. We assume order $p \leq P_0$, where $P_0 \in \mathbb{N}$. The AIC statistics, defined as

$$\begin{aligned} AIC(k) &= \ln \frac{S(\hat{a}_1, \hat{a}_2, \cdots, \hat{a}_p)}{N-k} + \frac{4k}{N} \\ &= \ln \left(\widehat{\sigma_c^2} + \widehat{\sigma_r^2} \right) + \frac{4k}{N}, \end{aligned}$$

where $k = 0, 1, \cdots, P_0$. We select the value of p as the order in our model which minimizes $AIC(k)$.

C. Diagnostic Checking

Typically, the goodness of fit of a statistical model to a set of data is judged by comparing the observed values with the corresponding predicted values obtained from the fitted model. If the fitted model is appropriate, the residuals should behave in a manner that is consistent with the model.

By the interval observation data $x_1, x_2, \cdots, x_N$, if now we have the estimation $\hat{p}$ and $(\hat{a}_1, \hat{a}_2 \cdots, \hat{a}_p)$ of the order p and the autoregressive coefficient $a_1, a_2, \cdots, a_p$ of IAR model

$$X_t = a_1 X_{t-1} + a_2 X_{t-2} + \cdots + a_p X_{t-p} + \tilde{\varepsilon}_t, \quad t = 1, 2, \cdots,$$

the residuals are defined as follows

$$\hat{\varepsilon}_{ct} = c_t - \sum_{j=1}^{p} \hat{a}_j c_{t-j}, \quad t = \hat{p}+1, \hat{p}+2, \cdots, N,$$

$$\hat{\varepsilon}_{rt} = r_t - \sum_{j=1}^{p} \hat{a}_j r_{t-j}, \quad t = \hat{p}+1, \hat{p}+2, \cdots, N.$$

If we can check that $\{\hat{\varepsilon}_{ct}\}$ and $\{\hat{\varepsilon}_{rt}\}$ are white noise processes, i.e. $\{\hat{\varepsilon}_{ct}\} \sim WN(0, \widehat{\sigma_c^2})$, $\{\hat{\varepsilon}_{rt}\} \sim WN(0, \widehat{\sigma_r^2})$, then the assertion that the above model is the true process in terms of generating $x_1, x_2, \cdots, x_N$ is acceptable.

V. SIMULATIONS

In this section, we conduct simulation experiments to illustrate the methodology of parameter estimation in IAR model. We indicate the mean square error of interval ($MSEI$) as the evaluation criterion in this section.

Our simulated data is generated from the IAR model

$$X_t = a_1 X_{t-1} + a_2 X_{t-2} + \tilde{\varepsilon}_t, \quad t = 3, 4, \cdots, n$$

(the order is p=2), where $\tilde{\varepsilon}_t = (c_{\varepsilon_t}; r_{\varepsilon_t}),\ t = 3, 4, \cdots, n$ is a generalized random interval, $c_{\varepsilon_t}, r_{\varepsilon_t}$ are independent normal white noise processes $WN(0, \sigma_c^2)$, $WN(0, \sigma_r^2)$, and let $a_1 = 0.85, a_2 = 0.152, \sigma_c = \sigma_r = 0.1$. Fix $X_1 = (10; 1), X_2 = (10.1; 0.9)$, then we can compute

$$\begin{aligned} X_t &= a_1 X_{t-1} + a_2 X_{t-2} + \tilde{\varepsilon}_t \\ &= 0.85 X_{t-1} + 0.152 X_{t-2} + \tilde{\varepsilon}_t, \quad t = 3, 4, \cdots, n, \end{aligned}$$

where $\tilde{\varepsilon}_t = (c_{\varepsilon_t}; r_{\varepsilon_t})$ is the generalized random intervals and $c_{\varepsilon_t}, r_{\varepsilon_t}$ are generated by normal random variables $N(0, \sigma_c^2) = N(0, 0.1^2)$, $N(0, \sigma_r^2) = N(0, 0.1^2)$ respectively.

Take the sample size n to be 50, Fig.1. shows a simulated orbit generated by the above IAR model.

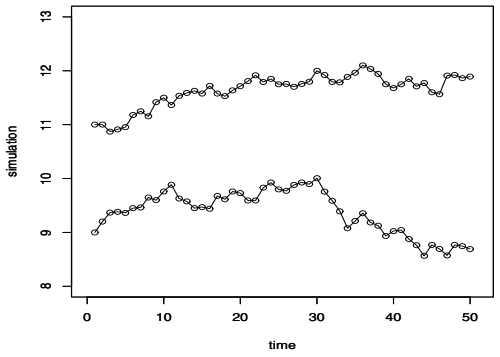

Fig.1.

We use the method introduced in Section 4.1 to estimate the autoregressive coefficient.

Now we simulate $\{X_t\}$ 500 times. Then we obtain 500 different estimators $\hat{a}_1, \hat{a}_2$ of autoregressive coefficients a_1, a_2. The mean values of this 500 different estimators are 0.847818 and 0.1541758 (the actual values are 0.85 and 0.152). Also, we get 500 estimators $\hat{\sigma}_c, \hat{\sigma}_r$ of standard deviation of white noise σ_c, σ_r, their mean value are 0.0989, 0.0989 (the actual values are 0.1, 0.1).

Again, we simulate $\{X_t\}$ 1000 times. Then we get 1000 different estimators $\hat{a}_1, \hat{a}_2$ of autoregressive coefficients a_1, a_2. The mean values of this 1000 different estimators are 0.8494906 and 0.1524187 (the actual values are 0.85 and 0.152). Also, we get 1000 estimators $\hat{\sigma}_c, \hat{\sigma}_r$ of standard deviation of white noise σ_c, σ_r, their mean value is 0.0991782, 0.0991782 (the actual values are 0.1, 0.1).

Such results show that the method of parameter estimation in Section 4.1 is fairly good.

VI. EMPIRICAL STUDY

In this section, we use an example to illustrate the parameter estimation and forecasting technique in IAR model.

While using the traditional time series models to forecast the stock price, we usually take the closing prices as the analyzing data. Then the information of fluctuations of stock price during each day is not able to be utilized. And the forecast value is also single-valued, so the information provided to the decision makers is also lack of flexibility. In the following, we will take the highest and the lowest daily price as the upper and lower boundary of the interval respectively, and the forecast will also be the interval-valued.

Here we collect data of the highest and lowest daily price of the Shanghai Stock Index from April 1 to June 17 in the year of 2009 (53 trading days in all). See Fig.2.

To select the order, $p = 2$, using the method described in Section 4.1, we obtain the estimated values of autoregressive coefficients, which are $\hat{a}_1 = 1.033, \hat{a}_2 = -0.03$.

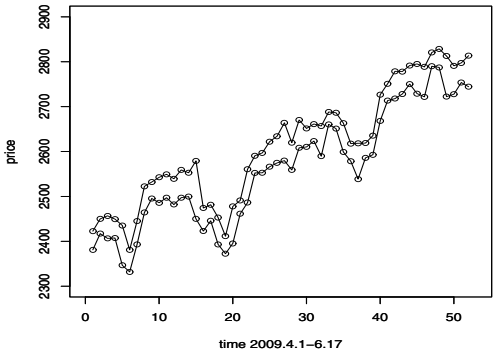

Fig.2.

Then check the residuals

$$\hat{\varepsilon}_{ct} = c_t - \sum_{j=1}^{2} \hat{a}_j c_{t-j}, \quad t = 3, 4, \cdots, 52,$$

$$\hat{\varepsilon}_{rt} = r_t - \sum_{j=1}^{2} \hat{a}_j r_{t-j}, \quad t = 3, 4, \cdots, 52,$$

by the method introduced in Section 4.3, $\{\hat{\varepsilon}_{ct}\}$ and $\{\hat{\varepsilon}_{rt}\}$ are white noise processes.

Now we can forecast the stock prices. We use the linear combination of the stock prices of the preceding two trade days X_{t-1}, X_{t-2} with coefficients which are the autoregressive coefficients $\hat{a}_1, \hat{a}_2$:

$$\begin{aligned} \widetilde{X_t} &= \hat{a}_1 X_{t-1} + \hat{a}_2 X_{t-2} \\ &= 1.033 X_{t-1} - 0.03 X_{t-2}, \quad t = 53, 54, \cdots \end{aligned}$$

as the forecast interval series.

We compare the forecast interval with the actual interval of the latter ten trading days.

The forecast intervals of latter ten trading days are
[2752.169,2822.535], [2821.281,2865.241],
[2856.997,2896.092], [2893.885,2933.112],

[2849.159,2950.418], [2890.083,2931.713],
[2918.681,2956.444], [2919.119,2946.144],
[2927.386,2987.030], [2963.269,3006.872].

The actual intervals of the latter ten trading days are
[2810.85,2855.42], [2847.36,2886.50],
[2884.13,2923.24], [2841.90,2941.06],
[2880.29,2923.47], [2909.09,2946.90],
[2910.35,2937.61], [2918.39,2976.92],
[2953.36,2997.27], [2947.69,3009.71].

The mean square error of interval (MSEI) of this ten-day forecasting is 729.2548. As is shown in Fig.3., the red lines depict the forecast interval series while the black lines describe the actual interval series.

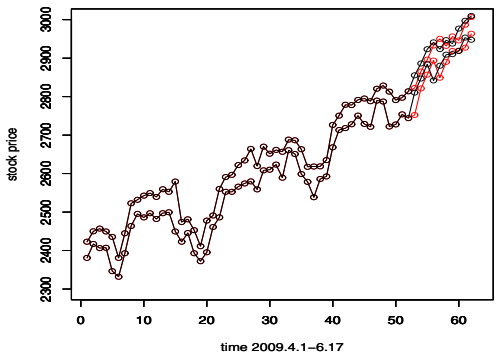

Fig.3.

VII. Conclusions

In this paper, based on the concepts of interval time series and efficiency evaluation of forecasting for interval time series, we suggest a new type of interval time series (IAR model), and present the methods of parameter estimation and forecasting in this model. Furthermore, we apply it to forecast the Shanghai Stock Index.

Both the examples regarding simulated data and real data show that the methods of parameter estimation are pretty good, which is based on the efficiency evaluation of forecasting for interval-valued data. The evaluation criterion we chosen is $MSEI$, and the parameter estimation based on other evaluation criteria can also be derived.

One advantage of the IAR model is that it is possible for decision makers to know the best and worst possible situations, and it requires fewer amount of observations than traditional time series models.

Acknowledgment

This research is partially supported by PHR(IHLB), NSFC(No.10771010) and NSFB(No.1112001).

References

[1] H. Akaike, “Information theory and an extension of the maximum likelihood principle”, in The Proceeding of the 2nd International Symposium on Information Theory, B.N. Petrov and F. Csaki(eds), Akademia Kiado, Budapest, 1973.

[2] Z. Artstein and R.A. Vitale, “A strong law of large numbers for random compact sets”, Ann. Probab., vol:3, pp. 879-882, 1975.

[3] R. Aumann, “Integrals of set valued functions”, J. Math. Anal. Appl., vol: 12, pp. 1-12, 1965.

[4] G.P. Box and G.M. Jenkins, Time Series Analysis: Forecasting and Control, Holden-day Inc., San Francisco, CA, 1976.

[5] P.J. Brockwell and R.A. Davis, Introduction to time series and forecasting, Springer, 2002.

[6] F. Hiai and H. Umegaki, “Integrals, conditional expectations and martingales of multivalued functions”, J. Multivar. Anal., vol:7, pp. 149-182, 1977.

[7] H.L. Hsu and B. Wu, “Evaluating forecasting performance for interval data”, Computers and Mathematics with Applications, vol: 56, pp, 2155-2163, 2008.

[8] H.L. Hsu and B. Wu, “On the forecasting accuracy of fuzzy time series”, to appear, 2010.

[9] T.L. Lai and H. Xing, Statistical Model and Methods for Financial Markets, Springer, 2007.

[10] S. Li, Y. Ogura and V. Kreinovich, Limit Theorems and Applications of Set-Valuded and Fuzzy Set-Valued Random Variables, Kluwer Academic Publishers, Dordrecht, 2002.

[11] Q. Song and B.S. Chissom, “Forecasting enrollments with fuzzy time series - part 1”, Fuzzy Set and Systems, vol:54, pp. 1-9, 1993.

[12] Q. Song and B.S. Chissom, “Fuzzy time series and its models”, Fuzzy Set and Systems, vol:54, pp. 269-277, 1993.

[13] Q. Song and B.S. Chissom, “Forecasting enrollments with fuzzy time series - part 2”, Fuzzy Set and Systems, vol:62, pp. 1-8, 1994.

[14] R.S. Tsay, Analysis of Financial Time Series, Wiley, New York, 2005.

[15] F. Tseng, G. Tzeng, H. Wu and B. Yuan, “Fuzzy ARIMA model for forecasting the foreign exchange market”, Fuzzy Sets and Systems, vol:118, pp. 9-19, 2001.

[16] W. Zhang, S. Li, Z. Wang and Y. Gao, Set-Valued Stochastic Processes, Science Publisher (in Chinese), 2007.

2011 IEEE International Conference on Fuzzy Systems
June 27-30, 2011, Taipei, Taiwan

Feature Evaluation Based Fuzzy C-Mean Classification

Mostafa A. Salama
Department of Computer Science
British University in Egypt
Cairo, Egypt
E-mail: mostafa.salama@gmail.com

Aboul Ella Hassanien and Aly A. Fahmy
Faculty of Computers and Information
Computer Engineering
Cairo University
E-mail: aboitcairo, aly.fahmy@gmail.com

***Abstract*—Fuzzy C-Means Clustering, FCM, is an iterative algorithm whose aim is to find the center or centroid of data clusters that minimize an assigned dissimilarity function. The degree of being in a certain cluster can be defined in terms of the distance to the cluster-centroid. The domain knowledge is used to formulate an appropriate measure. However the Euclidean distance is considered as a general measure for such value. The calculation of the Euclidean distance doesn't take into consideration the degree of relevance of each feature to the classification model. In this paper, scoring methods like ChiMerge and Mutual information are used in the FCM model to improve the calculation of the Euclidean distance. Experimental results demonstrate the better performances of the improved FCM on UCI benchmark data sets rather than the ordinary FCM, where the ordinary FCM uses in classification either all features or the most important features while the improved FCM uses all the features but the Euclidean Distance will be calculated according to the relevance degree of each feature.**

***Index Terms*—Fuzzy C-Means; Feature selection; ChiMerge.**

I. Introduction

Fuzzy C-Mean (FCM) is a model of data clustering which allows one piece of data to belong to two or more clusters. It is based on minimization of an objective or dissimilarity function [1], [2]. With Fuzzy C-Means, the centroid of a cluster is computed as being the mean of all points, weighted by their degree of belonging to the cluster. The degree of being in a certain cluster is related to the inverse of the distance to the cluster. For high dimensional data, a popular measure is used for calculating the distance which is the Minkowski metric [3], Euclidean distance is a special case of such equation. The calculation of the Euclidean distance ignore the degree of relevance of each feature to the classification problem and treats all the features equally. On the other hand, high number of features may contain irrelevant or redundant features to the classification [4]. To handle this curse of dimensionality problem, feature reductions methods are used. The number of features are reduced to the minimum value either by selecting the best features or extracting a lower number of feature from the higher ones. Consequently, applying the classifier on the resulted and reduced features should show a better performance. Classifiers could use the ChiMerge and the Mutual Information (MI) methods as feature selection methods in the pre-processing step of the Classification system design procedure [5]. Chi-square testing χ^2 is a well-known discrete data hypothesis testing method from statistics, for continuous data sets, the ChiMerge method can automatically select a proper χ^2 values and determining the intervals of numeric attributes [6]. On the other hand MI indicates the strong informative relationships among the attributes. In this paper, the ChiMerge or MI methods are applied to evaluate the worth of each attribute by computing the value of the chi-squared statistic with respect to the class. The resulted value is scaled to the range or interval between 0 and 1 and will be defined as ranks. Previously, the result from the feature selection methods are either 0 or 1 and used in the classifier, but here we put into account all features but with different ranks. Then these ranks are used in the calculation of the Euclidean distance used in the Fuzzy C-Mean model. The new factor is that the features with less chi-square χ^2 or MI values will have a less influence on the classification procedure rather than being removed completely and rather than using the total set of feature. According to the results this modification generates a better classification performance. Also the results in the case of using ChiMerge and MI methods are compared and it shows that ChiMerge has a better results.

The rest of this paper is organized as follows. Section II discusses the related work. Section III explains the Fuzzy C-Mean clustering model. Section IV explain the calculation of the distance to the cluster center. Section V shows the feature evaluation method used in details which are the ChiMerge and Mutual information methods. section VI shows how the chi-Square values will be used in the Fuzzy C-Mean classification. Results and comparisons with other classifiers are illustrated in section VII. Conclusion and future work is discussed in section VIII.

II. Related Work

Most of the improvements in the Fuzzy C-Mean models are applied on the selection the most relevant or informative features. The benefits of feature selection [7] includes a lot of aspects like facilitating data visualization and data understanding, reducing the measurement and storage requirements, providing faster and more cost-effective classifiers, and defying the curse of dimensionality to

978-1-4244-7316-8/11/$26.00 ©2011 IEEE

improve prediction performance. A paper like in [8] has an addition is that the fuzzy feature clustering and feature selection are based on the interdependence among features using chi-square methods. Other feature selection methods like in [9] has improved the MI formula for feature ranking which is used for feature selection in the pattern classification task. The problem of the current work in this area is that it stresses on the improvement of the feature selection methods, while ignores the use of the feature ranks of the selected features in the classification models. A similar study has been applied in [10] that propose an approach to feature-weight learning which is based on the gradient-desent technique. This method suffers from the high complexity due to the feature-weight learning which depends on the convergence of iterations in the traditional convergence technique. Also this method has a pre-assumption that the distribution of data is uniform which is not the case in real life data-sets.

III. Fuzzy C-Mean clustering

The discreteness of each cluster makes the C-Means analytically and algorithmically intractable. Partitioning the data set in a fuzzy manner avoid this problem. The FCM clustering treats each cluster as a fuzzy set and each feature vector is assigned to multiple clusters with some degree of certainty measured by the membership function [11]. The FCM optimizes the following objective function

$$J^m = \sum_{j:1..K} \sum_{i:1..N} \mu_{ji}^m * d_{ij} \tag{1}$$

Where: K is the number of clusters,
N is the number of objects,
m is the fuzziness controller which reduce the influence of small membership values, m is greater than 1,
d_{ij} represents the Euclidean distance between the object i of value x_i and the centroid of cluster j of value c_j which is represented by the following equation:

$$d_{ij} = \|x_i - c_j\| \tag{2}$$

and μ_{ji} denotes the membership of object i in cluster j; the values of μ_{ji} are initialized randomly such that the following condition is valid:

$$\sum_{j:1..K} \mu_{ji}^m = 1, i = 1, .., N \tag{3}$$

and c_j is the centroid of cluster j which it is calculated as follows:

$$c_j = \frac{\sum_{i:1..N} \mu_{ji}^m * x_i}{\sum_{i:1..N} \mu_{ji}^m} \tag{4}$$

After calculating the objective function J^m by equation (1), the value of μ_{ji} is updated by the following equation

$$\mu_{ji}^m = \frac{1}{\sum_{j:1..K} \frac{d_{ij}}{d_{ik}}} \tag{5}$$

The calculation of the J^m is repeated iteratively until the difference between the current J^m and the previous one is smaller than a certain threshold value ε such that:

$$J_{current}^m - J_{last}^m < \varepsilon \tag{6}$$

The correctness of equation (6) indicates the conversion of the objective function.

IV. Distance calculation to clusters center

A popular measure used for calculating the distance between any object and the cluster center, is the Minkowski metric. This measure is required for high dimensional data and it is calculated as follows:

$$d_p(x_i, x_j) = (\sum_{k=1..D} \mid x_{ik} - x_{jk} \mid^p)^{\frac{1}{p}} \tag{7}$$

Where x_i and x_j are two objects in the input data set. D is the dimensionality of the input data set, i.e. number of attributes. p is a parameter that represents the type of Minkowski measure. The Euclidean distance [12] is a special case of this measure, where in this case, p = 1, while Manhattan metric is the case where p = 2. However, there are no general theoretical guidelines for selecting a measure for any given application.

V. Feature Evaluation Methods

The selected feature evaluation techniques used in this paper are ChiMerge and Mutual Information approaches, which are considered as the most reliable methods for feature selection purpose with no significant difference between them [13].

A. ChiMerge feature evaluation

One of the most popular feature selection methods is the chi-Square χ^2 method, which measures the lack of independence between each attribute A and the target class c. ChiMerge or Chi2-Square is a χ^2-based discretization method [14]. It uses the χ^2 statistic to discretize numeric attributes repeatedly until some inconsistencies are found in the data that achieves feature selection via discretization. The χ^2 value is calculated for each continuous attribute as follows: Initially, each distinct value of a numeric attribute A is considered to be one interval. The values,intervals, of attribute A are sorted and the χ^2 is applied for every pair of adjacent intervals as follows:

$$\chi^2 = \sum_{i:1..2} \sum_{j:1..k} \frac{(A_{ij} - E_{ij})^2}{E_{ij}} \tag{8}$$

Where:
A_{ij} is the number of values in the ith interval and jth class,
R_{ij} is the number of values in the jth class = $\sum_{j:1..k} A_{ij}$,
C_{ij} is the number of values in the ith interval = $\sum_{i:1..2} A_{ij}$,
N is the total number of values = $\sum_{i:1..2} R_{ij}$,
and E_{ij} is the expected frequency of A_{ij} = $\frac{R_{ij} * C_{ij}}{N}$

Adjacent intervals with the least χ^2 values are merged together, because low χ^2 values for a pair indicates similar

class distributions. This merging process proceeds recursively until all χ^2 values of all pairs exceeds a parameter $signlevel$ (initially 0.5). Then repeat the previous steps with a decreasing $signlevel$ until an inconsistency rate is exceeded, where two patterns are the same but classified into different categories.

B. Mutual Information feature evaluation

The mutual information MI (also called cross entropy or information gain) is a widely used information theoretic measure for the stochastic dependency of discrete random variables. The mutual information $I(A;C)$ between values of feature A and the set of classes C can be considered as a measure of the amount of knowledge on C provided by A (or conversely on the amount of knowledge on A provided by C). In other words $I(A;C)$ measures the interdependence between A and C where it can be computed as follows:

$$I(A;C) = H(C) - H(C|A) \tag{9}$$

The entropy $H(C)$ measures the degree of uncertainty entailed by the set of classes C , and can be computed as

$$H(C) = -\sum_{c \in C} p(c) \log p(c) \tag{10}$$

where $p(c)$ is the probability density function (PDF) of c. The conditional entropy $H(C|X)$ measures the degree of uncertainty entailed by the set of classes C given the set of feature values X , and can be computed as

$$H(C|A) = \sum_{c \in C} \int_{a \in A} p(a,c) \log \frac{p(a|c)p(c)}{p(a)} dx \tag{11}$$

The integration in the expression above signifies that the feature space is continuous.

VI. Classification using the improved Fuzzy C-Mean model

By iteratively updating the cluster centers and the membership grades for each data point, FCM iteratively moves the cluster centers to the right location within a data set. But increasing the number of features may lead to ambiguity in training so that it would not even converge. The usual solution for this problem is to eliminant the features using the feature reduction methods, like applying feature selection of the most important and relevant features. After feature selection is applied, the data will be ready for training and testing by the classifier selected. The problem of this procedure is that not all features, even the selected features, are as important as each other to the classifier. On the other hand, in the calculations of the distance each object to the centroid in the Fuzzy C-Mean classifier model, all the attributes are used in the calculation in the same way.

In order to solve this problem, this paper uses a ranking procedure like the chi2-square method to give a percentage of importance to each feature. The results from the chiMerge method, χ^2 values, are processed such that these values range from 0 to 1 and the sum of all values are 1. Then uses the percentage that corresponds to each feature in the calculation of the Euclidean distance. Such that this percentage will be multiplied by the difference between the values of each object and the centroid corresponding to this attribute. So equation (7) will be adjusted to be as follows:

$$d_p(x_i, c_j) = (\sum_{k=1..D} r_k * \mid x_{ik} - c_{jk} \mid^p)^{\frac{1}{p}} \tag{12}$$

Where r_k represents the rank of attribute k, x_i represents the object i and c_j represents the centroid of class j.

The calculation of the rank values r_k will be as follows:

First, the values that are resulted from the feature selection methods are saved, in our paper these values are the χ^2 values. Then, the degree of importance of each feature is calculated according to the sorting of χ^2 values in an increasing order. The formula of the degree of importance will be in the form:

$$d_k = \frac{D - o_k}{\sum_{k=1..D} o_k} \tag{13}$$

Where o_k represents the order of the attribute from the chi-square method, for example, if o_k=1, this means that the attribute k is the best attribute, while if o_k= D, it means that attribute k is the worst attribute.

Then the χ^2 value of each feature k multiplied by d_k is divided by the sum of χ^2 values of all feature, and the result is assigned to the rank value r_k. So, r_k will be calculated as shown in the following formula (14):

$$r_k = \frac{\chi_k^2 * d_k}{\sum_{k=1..D} \chi_k^2} \tag{14}$$

In the case when the data set produces all χ^2 values have zero value, so formula (14) should be replaced by following formula (13). As shown in figure (1), the input from the training data set is evaluated by the chiMerge method then the χ^2 values are adjusted as in formula (14), and this input is introduced to Fuzzy C-Mean model for training. The evaluation from the chi2-square method will be used in the calculation of the distance to the centroid. When the termination condition is reached; either by convergence or elapsed number of iterations, the calculated centroids and the adjusted χ^2 values will be used in the testing of the classifier.

This improvement could be applied using the Mutual information method, such that the information gain resulted in equation (9) or the MI value for each attribute will be used in formula (14) as follows:

$$r_k = \frac{MI_k * d_k}{\sum_{k=1..D} \chi_k^2} \tag{15}$$

where MI_k value represents the mutual information between feature k and the set of target classes. The complete steps of the enhanced FCM model is shown in figure (1), in the steps of the model, scaling of the input data is important as it showed a better results in case of the scaled data than unscaled one.

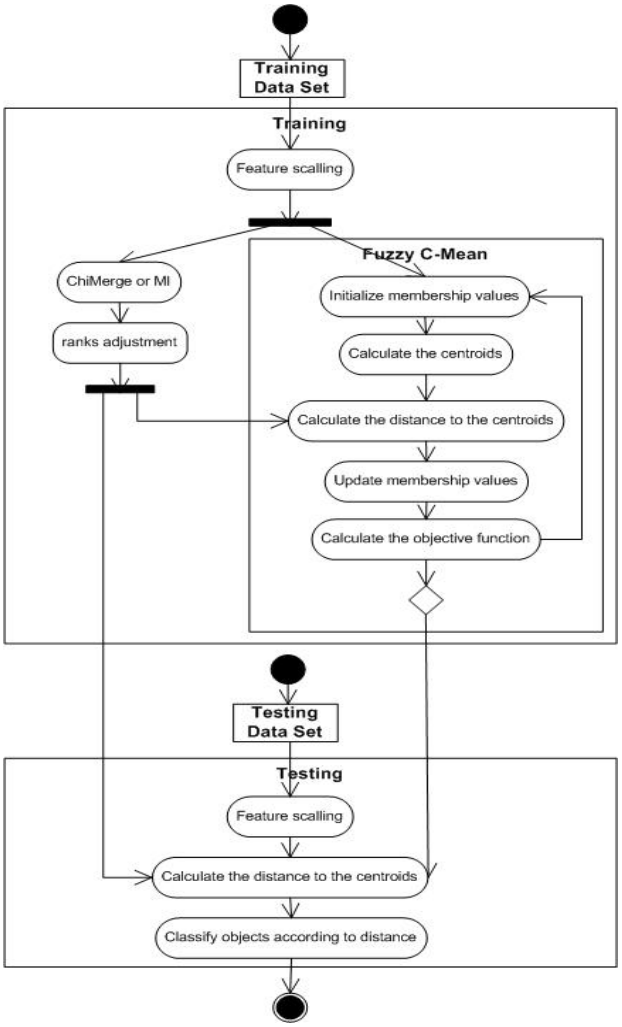

Fig. 1. Improved Fuzzy C-Mean model

VII. Experimental results and discussions

The proposed improvement is applied on two data sets and compared to the case when all features are used. Also it is compared to the case when only the important features are used in classification, in order to perform this, the test is applied on the first important feature only, then the first two important features, and so on until all feature are used in classification test. On the other hand the FCM with the proposed improvement is compared to other classifiers.

A. Data sets used in classification

This proposed enhancement is applied on two different data sets to ensure its capability and competency among other classifiers. These data sets are obtained from UCI machine learning repository [15]. Which are the pima-indians-diabetes data set of 536 objects and 8 features, and the Yeast data set of 600 objects and 8 features. 90% of the input data used for training while the rest of 10% is used for testing.

B. Classifiers used in the comparison analysis

The model is tested against other different classification techniques like Bayesian network, Support Vector Machine, Multilayered Neural Network and Decision table.

C. Classification results

1) Performance Measure: The classification effectiveness of the improved model is calculated in terms of $precision$ and $recall$ [16] which are defined as follows:

$$precision = \frac{a}{a+b}, a+b>0 \tag{16}$$

$$recall = \frac{a}{a+c}, a+c>0 \tag{17}$$

Where a counts the assigned and correct cases, b counts the assigned and incorrect cases, c counts the not assigned but incorrect cases and d counts the not assigned and correct cases. To evaluate the performance across categories, $F-measure$ is averaged. There are two kinds of averaged values, namely, micro average and macro average. The micro value is the average of the two values, $precision$ and $recall$, of all classes, while the macro average is the average of all micro values, this average represents the $F-measure$. Table (I) shows the Macro averaged $F-measure$ of the improved model when applying the ranking values in the improvement shown in equation (10). The results in the case of pima-indians-diabets and yeast data sets are compared to the FCM model without the improvement.

TABLE I
The $F-Measure$ results comparison

Data Set Used	IndianDiabets	Yeast
$F-Measure$ of FCM	0.796	0.601
$F-Measure$ of Improved FCM Ranking:ChiMerge	0.833	0.642
$F-Measure$ of Improved FCM Ranking:MI	0.833	0.627

2) Applying feature selection before classification: The following table (II) shows the results when perform the classification using the Fuzzy C-Mean after feature selection. The first row shows the result when only the first feature is used in classification, then the second row shows the results when the first two features are selected, and so on until all the features are used. The last row shows the results appear from the improved FCM model shown in table (I).

3) Comparison to the other classifiers: Table (III) shows the results of other classifiers in comparison to the enhanced FCM model where it appears to have best results.

D. Results analysis

Pima-indians-diabetes is continuous multi-variate features data set. So Fuzzy C-Mean model shows a better results

TABLE II
FCM CLASSIFICATION RESULTS OF THE PIMA-INDIANS-DIABETES (PID) DATA SET AND THE YEAST DATA SET

features used	$F-Measure$ of PID	$F-Measure$ of yeast
1 feature selected	0.740	0.500
2 features selected	0.777	0.600
3 features selected	0.777	0.600
4 features selected	0.777	0.533
5 features selected	0.796	0.533
6 features selected	0.796	0.533
7 features selected	0.796	0.516
8 features selected	0.777	0.566
Ranking features Improved FCM	0.833	0.642

TABLE III
COMPARISON BETWEEN DIFFERENT CLASSIFICATION MODELS ACCORDING TO ERROR PERCENTAGES AND RUNNING TIME IN SECONDS AND THE IMPROVED FCM MODEL (I-FCM)

Classifier	pima-indians-diabetes Classification $F-Measure$
I-FCM	0.814
Multilayer Perceptron	0.776
IB1	0692
BFTree	0.759
Decision Table	0.763
Naïve Bayes	0.746
Bayes Network	0.761
LibSVM	0.527

of 0.777 than other classifiers. As Decision trees and Decision tables tend to perform better when dealing with discrete/categorical features, while Bayes belief models like Bayesian Network (BN) and Naïve Bayesian Network due to the "independence assumption". Moreover, if feature selection is applied before the Fuzzy C-Mean classifier, the maximum classification performance appeared is 0.796 for five selected features. When applying the improvement on the Fuzzy C-Mean model, the classification results is raised more to 0.833. Also the enhancement in the classification performance from the Fuzzy C-Mean to the improved Fuzzy C-Mean model appears to be raised from 0.60 to 0.642 when being applied on the Yeast data set. Chi-Merge ranks leads to a better classification performance than that of Mutual information method due to the better discretization algorithm embedded in the Chi-Merge method. This proves that not all of the selected features have the same importance as each other. In the case of pima-indians-diabetes and yeast data sets, the chi-square method produces different values for each attributes and only few attributes have zero values, formula (14) will be applied without changes. In cases where all features are ordered with different importance but all have the zero rank values, r_k values could be replaced by d_k values.

VIII. CONCLUSIONS

This paper introduces a new application of the feature selection method in the classification model. It uses the ranks of each feature resulted from feature evaluation methods like ChiMerge and Mutual Information in the calculations of the Euclidian distance as a main parameter in the Fuzzy C-Mean model. This introduced modification in the Fuzzy C-Mean model enhanced the performance of the Fuzzy C-Mean model. The modified FCM has been applied on real life data sets including pima-indians-diabetes and yeast data sets, and it provides the best classification accuracy. The reason of these results is that even the selected features from the feature reduction methods have no equal relevance or contribution to the classifier, so if the degree of relevance in each classifier is taken into consideration, a better results can appear.

REFERENCES

[1] Tina Gewenigera, Dietlind Zlkeb, Barabara Hammerc and Thomas Villmann, "Median fuzzy c-means for clustering dissimilarity data", Neurocomputing, vol. 73, issue. 7-9, pp. 1109-1116, Mar. 2010.

[2] Abdelwadood Moh'd, "Chi Square Feature Extraction Based Svms Arabic Language Text Categorization System", Journal of Computer Science, ISSN 1549-3636, vol. 3, pp. 430-435, 2007.

[3] Tai-hoon Kim, "Procedure of Partitioning Data Into Number of Data Sets or Data Group", Communications in Computer and Information Science, vol. 78, pp. 104-115, 2010.

[4] A.G.K. Janecek, W.N. Gansterer, M. Demel and G.F. Ecker, "On the relationship between feature selection and classification accuracy", JMLR Workshop and Conference Proceedings, vol. 4, pp. 90-105, 2008.

[5] Thabtah F., Eljinini M., Zamzeer M. and Hadi W., "Naïve Bayesian based on Chi Square to Categorize Arabic Data", In proceedings of The 11th International Business Information Management Association Conference (IBIMA) Conference on Innovation and Knowledge Management in Twin Track Economies, Cairo, Egypt, pp. 930-935, Jan. 4-6, 2009.

[6] Surendra Kumar, C.S.P. Rao, "Application of ant colony, genetic algorithm and data mining-based techniques for scheduling", Robotics and Computer-Integrated Manufacturing, vol. 25, issue 6, pp. 901-908, Dec. 2009.

[7] Mostafa A. Salama, Aboul Ella Hassanien and Aly A. Fahmy, "Uni-Class Pattern-based Classification Model", In proceeding of the 10th IEEE International Conference on Intelligent Systems Design and Applications, Cairo, Egypt, Dec. 2010.

[8] Elham Chitsaz, Mohammd Taheri, Seraj D. Katebi, Mansour Zolghadri Jahromi, "An Improved Fuzzy Feature Clustering and Selection based on Chi-Squared-Test", In proceedings of the International MultiConference of Engineers and Computer Scientists 2009, Hong Kong, vol. 1, Mar. 18-20, 2009.

[9] Jin-Jie Huang, Yun-Ze Cai, Xiao-Ming Xu, "A parameterless feature ranking algorithm based on MI", Neurocomputing, vol. 71, pp. 1656-1668, 2008.

[10] Xizhao Wang, Yadong Wang and Lijuan Wang, "Improving fuzzy c-means clustering based on feature-weight learning", Pattern Recognition Letters, vol. 25, issue. 10, pp. 11231132, jul. 2004. Neural networks, vol. 23, issue 1, pp. 89-107, Jan. 2010.

[11] K-L Du, "Clustering: A neural network approach", Neural networks, vol. 23, issue 1, pp. 89-107, Jan. 2010.

[12] Jing Lia and Bao-Liang Lu, "An adaptive image Euclidean distance", Pattern Recognition, vol. 42, issue 3, pp. 349-357, Mar. 2009.

[13] J. R. Mndez, B. Corzo, D. Glez-Pea, F. Fdez-Riverola and F. Daz, "Analyzing the Performance of Spam Filtering Methods When Dimensionality of Input Vector Changes", In proceedings of the 5th international conference on Machine Learning and Data Mining in Pattern Recognition, vol. 4571, pp. 364-378, 2007.

[14] Huan Liu, Rudy Setiono, ”Chi2: Feature Selection and Discretization of Numeric Attributes”, In proceedings of the Seventh International Conference on Tools with Artificial Intelligence, Virginia, USA, pp.388, Nov. 8, 1995.
[15] UCI Machine Learning Repository, http://archive.ics.uci.edu/ml/datasets.html.
[16] Yiming Yang, ”An evaluation of statistical approaches to text categorization”, Inform Retrieval, vol. 1, pp. 69-90, 1999.

2011 IEEE International Conference on Fuzzy Systems
June 27-30, 2011, Taipei, Taiwan

A Clustering Method for Geometric Data based on Approximation using Conformal Geometric Algebra

Minh Tuan Pham
Nagoya University
minhtuan@cmplx.cse.nagoya-u.ac.jp

Kanta Tachibana
Kogakuin University
kanta@cc.kogakuin.ac.jp

Tomohiro Yoshikawa
Nagoya University
yoshikawa@cse.nagoya-u.ac.jp

Takeshi Furuhashi
Nagoya University
furuhashi@cse.nagoya-u.ac.jp

***Abstract*—Clustering is one of the most useful methods for understanding similarity among data. However, most conventional clustering methods do not pay sufficient attention to the geometric properties of data. Geometric algebra (GA) is a generalization of complex numbers and quaternions able to describe spatial objects and the relations between them. This paper uses conformal GA (CGA), which is a part of GA, to transform a vector in a real vector space into a vector in a CGA space and presents a proposed new clustering method using conformal vectors. In particular, this paper shows that the proposed method was able to extract the geometric clusters which could not be detected by conventional methods.**

***Index Terms*—conformal geometric algebra, hyper-sphere, inner product, distance, clustering.**

I. Introduction

Because nowadays enormous amounts of data are available in various fields, data mining, which analyzes data to reveal interesting information, becomes increasingly necessary. Clustering is an important technique in data mining. Methods of clustering [1] iteratively minimize an objective function based on a distance measure to label each individual data point. To take the geometric structure of data into consideration, [2] adopted a distance measure based on straight lines, and [3] adopted a distance measure based on spherical shells. The straight line measure and the spherical shell measure are applicable to datasets which have clusters generated respectively by translational motion and by rotational motion in m-dimensional space. But so far, a distance measure which detects a mixture of clusters generated by either translational or rotational motions has not been proposed. Furthermore, the spherical shell measure cannot detect a cluster around a spherical shell with dimension less than m. For example, it cannot express a data distribution around a circle in three-dimensional space because it optimizes an objective function based on distance from a three-dimensional spherical shell. This paper proposes a clustering method which can detect clusters with either translational or rotational relations. The proposed method can also detect clusters around spheres and planes of any dimension less than m because they are well expressed as elements of conformal geometric algebra.

In this study, we use geometric algebra (GA), which can describe spatial vectors and the higher-order subspace relations between them [4],[5],[6]. There are already many successful examples of its use in image processing, signal processing, color image processing, and multi-dimensional time-series signal processing with complex numbers or quaternions, which are low-dimensional GAs [7],[8],[9],[10],[11],[12],[13]. In addition, GA-valued neural network learning methods for learning input–output relationships [14] and the feature extraction based on GA [15] are well studied. This paper uses the vectors in conformal GA (CGA) [16] space, which is a part of GA to propose a new approach of approximation and a new clustering method for geometric data. A vector in CGA is called a conformal vector, and it can express both m-dimensional spheres and planes (infinite radius spheres). A conformal bivector, called a 2-blade in CGA, expresses the intersection of two m-dimensional elements, and thus it is able to express an $m-1$-dimensional sphere or plane. Likewise, a k-blade in CGA expresses an $m-k$-dimensional element. A conformal vector can also express a point as a sphere with zero radius.

In this paper, data vectors in the original space are first translated into conformal vectors expressing the data points. Then, the conformal vectors expressing the cluster centers are optimized using a distance measure on the cluster center conformal vectors and the data points. This optimization problem is solvable as an eigen-value decomposition using the Lagrange multiplier formulation. Each eigen-value is proportional to the sum of distances from an m-dimensional element expressed by the corresponding eigen conformal vectors to each of the data points. The sum of k eigen-values can be considered to be the sum of the distances from the intersection of k elements to the data points. The k eigen conformal vectors corresponding to the smallest k eigen-values can detect a cluster which is distributed over an $m-k$-dimensional spherical or planar surface.

A characteristic of the proposed method is that it is able to detect a cluster distributed over a sphere, plane, or intersection of some combination of the three, for example, a straight line or arc. Section II describes our proposal to approximate geometric data as conformal vectors and shows an algorithm of the proposed clustering method. Section III demonstrates the effectiveness of the proposed method through two experiments. One experiment estimates the probability density distribution of geometric data, and the other is a clustering experiment. The results of the first experiment demonstrate that the proposed method can approximate 2 express geometric data precisely.

978-1-4244-7316-8/11/$26.00 ©2011 IEEE

The results of the second experiment demonstrate that the kernel alignment [17] between the true labels and the labels detected by clustering using the proposed method is better than those from using conventional methods.

II. Proposed Method

A. Conformal Geometric Algebra and Estimation of Hyperspheres (-planes) from Geometric Data Sets

CGA is a special part of GA, which is also called Clifford algebras. GA defines the signature of $p+q$ orthonormal basis vectors $\mathcal{O} = \{\mathbf{e}_1, \ldots, \mathbf{e}_p, \mathbf{e}_{p+1}, \ldots, \mathbf{e}_{p+q}\}$, $\{\mathbf{e}_i\}$, such that $\mathbf{e}_i^2 = +1, \forall i \in \{1, \ldots, p\}$ and $\mathbf{e}_i^2 = -1, \forall i \in \{p+1, \ldots, p+q\}$. This paper denotes the geometric algebra determined from $\mathcal{O}$ by $\mathcal{G}_{p,q}$. For example, the geometric algebra determined from the m-dimensional real vector space $\mathbf{R}^m$ is denoted by $\mathcal{G}_{n,0}$.

A CGA space is extended from the real vector space $\mathbf{R}^m$ by adding 2 orthonormal basis vectors. Thus, a CGA space is determined by $m+2$ basis vectors $\{\mathbf{e}_1, \ldots, \mathbf{e}_m, \mathbf{e}_+, \mathbf{e}_-\}$, where $\mathbf{e}_+$ and $\mathbf{e}_-$ are defined so that

$$\begin{aligned} \mathbf{e}_+^2 = \mathbf{e}_+ \cdot \mathbf{e}_+ &= 1, \\ \mathbf{e}_-^2 = \mathbf{e}_- \cdot \mathbf{e}_- &= -1, \\ \mathbf{e}_+ \cdot \mathbf{e}_- = \mathbf{e}_+ \cdot \mathbf{e}_i = \mathbf{e}_- \cdot \mathbf{e}_i &= 0, \forall i \in \{1, \ldots, m\}. \end{aligned} \quad (1)$$

Therefore, a CGA space can be expressed by $\mathcal{G}_{m+1,1}$. This paper then defines the converted basis vectors $\mathbf{e}_0$ and $\mathbf{e}_\infty$ as

$$\mathbf{e}_0 = \frac{1}{2}(\mathbf{e}_- - \mathbf{e}_+), \mathbf{e}_\infty = (\mathbf{e}_- + \mathbf{e}_+). \quad (2)$$

From Eq. (1) and Eq. (2), we get

$$\begin{aligned} \mathbf{e}_0 \cdot \mathbf{e}_0 = \mathbf{e}_\infty \cdot \mathbf{e}_\infty &= 0, \\ \mathbf{e}_0 \cdot \mathbf{e}_\infty = \mathbf{e}_\infty \cdot \mathbf{e}_0 &= -1, \\ \mathbf{e}_0 \cdot \mathbf{e}_i = \mathbf{e}_\infty \cdot \mathbf{e}_i &= 0, \forall i \in \{1, \ldots, m\}. \end{aligned} \quad (3)$$

We also make use of a transform based upon that proposed by Hestenes[16]. The real vector $\mathbf{x} = \sum_i^m x_i \mathbf{e}_i \in \mathbf{R}^m$ is extended to a point $P \in \mathcal{G}_{m+1,1}$ according to the equation

$$P = \mathbf{x} + \frac{1}{2}\|\mathbf{x}\|^2 \mathbf{e}_\infty + \mathbf{e}_0. \quad (4)$$

Note that the inner product of P with itself, $P \cdot P$, is 0. Then, a sphere is represented as a conformal vector

$$\begin{aligned} S &= P - \frac{1}{2} r^2 \mathbf{e}_\infty \\ &= \mathbf{x} + \frac{1}{2}\{\|\mathbf{x}\|^2 - r^2\}\mathbf{e}_\infty + \mathbf{e}_0, \end{aligned} \quad (5)$$

where the sphere has center $\mathbf{x}$ and radius r in real space $\mathbf{R}^m$. The inner product $S \cdot Q$ is 0 for any point Q on the surface of the sphere. From Eqs. 4 and 5, we can see that a point is naturally expressed as a sphere with radius $r = 0$ in CGA space $\mathcal{G}_{m+1,1}$.

CGA also expresses a plane as a conformal vector:

$$L = \mathbf{n} + d\mathbf{e}_\infty, \quad (6)$$

where $\mathbf{n}$ is the normal vector, and d is a scalar coefficient of the plane $\mathbf{n} \cdot \mathbf{x} + d = 0$ in real space $\mathbf{R}^m$. The inner product $L \cdot Q$ is 0 for any point Q in the plane.

A conformal vector S in $\mathcal{G}_{n+1,1}$ is generally written in the following form:

$$S = \mathbf{s} + s_\infty \mathbf{e}_\infty + s_0 \mathbf{e}_0. \quad (7)$$

$\mathbf{s} = \sum_i^m s_i \mathbf{e}_i$ is a vector in the real vector space $\mathbf{R}^m$. s_∞ and s_0 are the scalar coefficients of the basis vectors $\mathbf{e}_\infty$ and $\mathbf{e}_0$.

In this paper, we use that the inner product between a point P and a conformal vector S in CGA space is proportional to the distance between them. From Eqs. (3), (4), and (7), the inner product of P and S is

$$\begin{aligned} d(P,S) &\propto P \cdot S \\ &= \left(\mathbf{x} + \frac{1}{2}\|\mathbf{x}\|^2 \mathbf{e}_\infty + \mathbf{e}_0\right) \cdot (\mathbf{s} + s_\infty \mathbf{e}_\infty + s_0 \mathbf{e}_0) \\ &= \mathbf{x} \cdot \mathbf{s} - s_\infty - \frac{1}{2}\|\mathbf{x}\|^2 s_0. \end{aligned} \quad (8)$$

When $d(P,S) = 0$, we get

$$\begin{aligned} & \mathbf{x} \cdot \mathbf{s} - s_\infty - \frac{1}{2}\|\mathbf{x}\|^2 s_0 = 0 \\ \Leftrightarrow & \begin{cases} \mathbf{x} \cdot \mathbf{s} - s_\infty = 0 & (s_0 = 0), \\ \|\mathbf{x} - \frac{1}{s_0}\mathbf{s}\|^2 = \frac{\|\mathbf{s}\|^2 - 2 s_\infty s_0}{s_0^2} & (s_0 \neq 0). \end{cases} \end{aligned} \quad (9)$$

Eq. (9) shows that when $d(P,S) = 0$, the point P lies on the hyper-plane or hyper-sphere expressed in CGA space as conformal vector S. Herein, we use this characteristic to approximate geometric data having rotational or the translational relations and propose a new approach for clustering.

Given a set of vectors $\mathcal{X} = \{\mathbf{x}_k = \sum_i^m x_{k;i} \mathbf{e}_i \in \mathbf{R}^m, k = 1, \ldots, n\}$, the proposed method transforms each m-dimensional vector to a point in CGA space using Eq. (4) to yield the set $\mathcal{P} = \{P_k = \mathbf{x}_k + \frac{1}{2}\|\mathbf{x}_k\|^2 \mathbf{e}_\infty + \mathbf{e}_0, k = 1, \ldots, n\}$ in $\mathcal{G}_{m+1,1}$. Then, the proposed method approximates the set of points $\mathcal{P}$ using a vector $S = \mathbf{s} + s_\infty \mathbf{e}_\infty + s_0 \mathbf{e}_0$ in $\mathcal{G}_{m+1,1}$, which is estimated using least squares. The error function E is defined as

$$\begin{aligned} E &= \sum_{k=1}^n d^2(P_k, S) \\ &= \sum_{k=1}^n \left(\mathbf{x}_k \cdot \mathbf{s} - s_\infty - \frac{1}{2}\|\mathbf{x}_k\|^2 s_0\right)^2. \end{aligned} \quad (10)$$

Eq. 9 can be solved by modifying the equation while preserving the equality, such as by multiplying both sides by a scalar value. Therefore, $\mathbf{s}$ can be restricted to $\|\mathbf{s}\|^2 = 1$. In this case, the optimization problem becomes

$$\min \sum_{k=1}^n \left(\mathbf{x}_k \cdot \mathbf{s} - s_\infty - \frac{1}{2}\|\mathbf{x}_k\|^2 s_0\right)^2 \quad (11)$$

subject to

$$\|\mathbf{s}\|^2 = 1. \quad (12)$$

Therefore, we might be tempted to express the previous problem by means of a non-negative Lagrange multiplier λ as the minimization of

$$L = \frac{1}{n}\sum_{k=1}^{n}\left(\mathbf{x}_k \cdot \mathbf{s} - s_\infty - \frac{1}{2}\|\mathbf{x}_k\|^2 s_0\right)^2 - \lambda\left(\|\mathbf{s}\|^2 - 1\right). \quad (13)$$

The critical values of L occur when its gradient is zero. The partial derivatives are

$$\frac{\partial L}{\partial \mathbf{s}} = \frac{2}{n}\sum_{k=1}^{n}\left(\mathbf{x}_k \cdot \mathbf{s} - s_\infty - \frac{1}{2}\|\mathbf{x}_k\|^2 s_0\right)\mathbf{x}_k - 2\lambda\mathbf{s} = 0, \quad (14)$$

$$\frac{\partial L}{\partial s_\infty} = -\frac{2}{n}\sum_{k=1}^{n}\left(\mathbf{x}_k \cdot \mathbf{s} - s_\infty - \frac{1}{2}\|\mathbf{x}_k\|^2 s_0\right) = 0, \quad (15)$$

$$\frac{\partial L}{\partial s_0} = -\frac{1}{n}\sum_{k=1}^{n}\left(\mathbf{x}_k \cdot \mathbf{s} - s_\infty - \frac{1}{2}\|\mathbf{x}_k\|^2 s_0\right)\|\mathbf{x}_k\|^2 = 0. \quad (16)$$

From Eqs. (15) and (16),

$$s_\infty = \mathbf{f}_\infty \cdot \mathbf{s}, \quad (17)$$

$$\frac{1}{2}s_0 = \mathbf{f}_0 \cdot \mathbf{s}, \quad (18)$$

where

$$\mathbf{f}_\infty = \frac{-\sum_{k=1}^{n}\|\mathbf{x}_k\|^4\sum_{k=1}^{n}\mathbf{x}_k + \sum_{k=1}^{n}\|\mathbf{x}_k\|^2\sum_{k=1}^{n}\|\mathbf{x}_k\|^2\mathbf{x}_k}{\sum_{k=1}^{n}\|\mathbf{x}_k\|^2\sum_{k=1}^{n}\|\mathbf{x}_k\|^2 - \sum_{k=1}^{n}\|\mathbf{x}_k\|^4\sum_{k=1}^{n}1}, \quad (19)$$

$$\mathbf{f}_0 = \frac{\sum_{k=1}^{n}\|\mathbf{x}_k\|^2\sum_{k=1}^{n}\mathbf{x}_k - \sum_{k=1}^{n}1\sum_{k=1}^{n}\|\mathbf{x}_k\|^2\mathbf{x}_k}{\sum_{k=1}^{n}\|\mathbf{x}_k\|^2\sum_{k=1}^{n}\|\mathbf{x}_k\|^2 - \sum_{k=1}^{n}\|\mathbf{x}_k\|^4\sum_{k=1}^{n}1}. \quad (20)$$

More simply, we define the equation

$$\mathbf{f}(\mathbf{x}) = \mathbf{x} - \mathbf{f}_\infty - \|\mathbf{x}\|^2\mathbf{f}_0 \in \mathbf{R}^m. \quad (21)$$

Then, Eq. (13) can be rewritten as

$$L = \mathbf{s}^T\mathbf{A}\mathbf{s} - \lambda\left(\|\mathbf{s}\|^2 - 1\right), \quad (22)$$

where

$$\mathbf{A} = \frac{1}{n}\sum_{k=1}^{n}\mathbf{f}(\mathbf{x}_k)\,\mathbf{f}^T(\mathbf{x}_k). \quad (23)$$

Therefore, the optimization problem is solved by the eigen decomposition

$$\mathbf{A}\mathbf{s} = \lambda\mathbf{s}. \quad (24)$$

An eigen vector $\mathbf{s}$ is an eigen conformal vector defining the hyper-sphere (-plane) $S = \mathbf{s} + s_\infty\mathbf{e}_\infty + s_0\mathbf{e}_0$, and the eigen-value λ is the variance, i.e., the sum of the squared distances between P_k and S. The estimated hyper-sphere or -plane will exactly fit the data set if the eigen-value λ is 0. Because there are m eigen-values when the original data space is m-dimensional, we can find m solutions of hyper-spheres (or planes). Thus, we can also detect the $m-k$-dimensional hyper-spheres (or planes) using the k eigen conformal vectors corresponding to the smallest k eigen-values. For example, in the case of three-dimensional data, we can detect a circle which is a intersection between two spheres having the smallest eigen-values. Furthermore, by also using the sphere with the largest eigen-value, we can detect a cluster of data with an arc, i.e., part of a circle. So, the proposed method is expected to improve clustering performance.

B. Geometric Clustering Method

This paper proposes a new clustering method based on the proposed approximation for data with both the mixture of rotational and translational relationships. For each cluster $\mathcal{X}_c = \{\mathbf{x}_k = \sum_i^m x_{k;i}\mathbf{e}_i \in \mathbf{R}^m \mid y_k = c, k \in \{1,\ldots,n\}\}$, the proposed method uses Eqs. (17), (18), and (24) to estimate the m pairs of hyper-spheres (-planes) $S_{c,l} = \mathbf{s}_{c,l} + s_{\infty c,l}\mathbf{e}_\infty + s_{0c,l}\mathbf{e}_0, l \in \{1,\ldots,m\}$ and eigen-values $\lambda_{c,l}$, where the eigen-values are the variances based on the distance $d(P, S_{c,l})$ between a point $P = \mathbf{x} + \frac{1}{2}\|\mathbf{x}\|^2\mathbf{e}_\infty + \mathbf{e}_0, \mathbf{x} \in \mathcal{X}_c$ and the hyper-sphere (-plane) $S_{c,l}$. Herein, we assume that the variance based on $d(P, S_{c,l})$ follows a Gaussian distribution. Then the density function is

$$p(\mathbf{x} \mid \lambda_{c,l}) = \frac{1}{\sqrt{2\pi\lambda_{c,l}}}\exp\left(-\frac{d^2(P, S_{c,l})}{2\lambda_{c,l}}\right). \quad (25)$$

Next, we assume that the variances corresponding to the eigenvalues are mutually statistically independent. Under these assumptions, the posterior probability density function for $\mathbf{x}$ given the cluster $y = c$ can be defined as

$$p(\mathbf{x} \mid c) = \prod_l^m p(\mathbf{x} \mid \lambda_{c,l}). \quad (26)$$

Then the following shows an algorithm of the proposed method using Eq. (26).

- Step1 Choose the number of clusters, C.
- Step2 Randomly assign label $y_k \in \{1,\ldots,C\}$ for each data point k.
- Step3 Estimate the posterior probability density function $p(\mathbf{x} \mid c)$ for all clusters $\mathcal{X}_c = \{\mathbf{x}_k \mid y_k = c\}$.
- Step4 Update the data label by $y_k = \arg\max_c p(\mathbf{x} \mid c)\,P(c)$, where $P(c) = \frac{|\mathcal{X}_c|}{n}$ is the prior distribution of cluster $\mathcal{X}_c$, and $|\mathcal{X}_c|$ is the number of data in cluster $\mathcal{X}_c$.
- Step5 Repeat the two previous steps until the algorithm has converged.

III. Experiments and Discussion

A. Estimation of Probability Density Function for Geometric Data Set

This subsection focuses on estimation of the probability density function for three kinds of two-dimensional geometric data: a circle, a line, and an arc. Tables I, II, and III show

the generating parameters and the parameters of the estimated conformal vectors. α and ϵ are random variables following the uniform distribution. x and y are the coordinates of the generated data. λ, $\mathbf{s}$, s_∞, and s_0 are the parameters which are estimated by the proposed method. $r = \sqrt{\frac{\|\mathbf{s}\|^2 - 2s_\infty s_0}{s_0^2}}$ is a radius calculated from the estimated parameters.

TABLE I
GENERATING AND ESTIMATED PARAMETERS FOR THE CIRCLE.

Generating Parameters				
α	uniform distribution on $[-\pi; \pi]$			
ϵ	uniform distribution on $[-0.5, -0.5]$			
x	$5 + (3.5 + \epsilon)\sin\alpha$			
y	$5 + (3.5 + \epsilon)\cos\alpha$			
Estimated Parameters				
λ	$\mathbf{s}$	s_∞	s_0	r
0.017	-0.71, -0.70	-2.70	-0.14	3.61
6.626	0.70, -0.71	0.12	-0.02	46.69

TABLE II
GENERATING AND ESTIMATED PARAMETERS FOR THE LINE.

Generating Parameters				
α	uniform distribution on $[1.5, 8.5]$			
ϵ	uniform distribution on $[-0.5, -0.5]$			
x	α			
y	$\alpha + \epsilon$			
Estimated Parameters				
λ	$\mathbf{s}$	s_∞	s_0	r
0.038	-0.75, 0.66	-0.17	-0.01	83.40
0.283	-0.66, -0.75	-3.07	-0.14	2.98

TABLE III
GENERATING AND ESTIMATED PARAMETERS FOR THE ARC.

Generating Parameters				
α	uniform distribution on $[-\frac{\pi}{3}; \frac{\pi}{3}]$			
ϵ	uniform distribution on $[-0.5, -0.5]$			
x	$5 + (3.5 + \epsilon)\sin\alpha$			
y	$5 + (3.5 + \epsilon)\cos\alpha$			
Estimated Parameters				
λ	$\mathbf{s}$	s_∞	s_0	r
0.013	-0.78, -0.63	-3.18	-0.13	2.85
0.399	0.63, -0.78	3.37	-0.04	28.77

Table I shows that the circle data is approximated by a circle with radius $r_{circle} = 3.61$ when the smallest eigen-value equals 0.017. The approximated circle is very similar to the circle of the generating parameters. Table II shows that the line data is approximated by a circle with a large radius ($r_{line} = 83.40$) when the smallest eigen-value equals 0.038. Thus, it is easy to see that the parameters which are estimated using the proposed method shown in Table II are reasonable if one considers a line as a circle with infinite radius. Table III shows the generating and estimated parameters for the arc data. As shown, the radius $r_{arc} = 2.85$ of the estimated circle is smaller than the generating radius $\hat{r}_{arc} = 3.5$. This shows that the radius of the estimated circle with smallest eigen-value in the case of arc data is different from the case of circle or line data. Thus, the proposed method is expected to be able to express arc data using a combination of all the estimated circles.

Next, we will use Eq. (26) to estimate the probability density function for geometric data. Fig. 1 shows the data distribution and the estimation results of the probability density function using the proposed method. Figs. 1(a), (b), and (c) show the data distributions for the circle, line, and arc data generated using the parameter values listed in Tables I, II, and III, respectively. Fig. 1(d), (e), and (f) show the estimated probability densities corresponding respectively to the data shown in Figs. 1(a), (b), and (c) using the proposed method. The results shown in Fig. 1 demonstrate that the proposed method can estimate the probability density for an arc, not just circles and lines. For a general m-dimensional vector space, it is easy to understand that the proposed method can estimate exactly the probability density for the hyper-sphere, -plane, and -arc.

B. Clustering Experiment

This subsection uses 2 kinds of triangular pyramid data for an experiment of clustering. Table IV shows the coordinate of vertexes of triangular pyramids which was used in this experiment. For each triangular pyramid $i \in \{1, 2\}$, we have a set of vectors $\xi_i = \{\mathbf{p}_{ij} = (\mathbf{p}_{ij,x}, \mathbf{p}_{ij,y}, \mathbf{p}_{ij,z}) \in \mathbf{R}^3; j = 1, 2, 3, 4\}$. We generated a data set $D = \{f(\xi_i, \Sigma)\}\}$ that randomly rotated each triangular pyramid 250 times, where Σ is a random rotation matrix. For each rotated triangular pyramids, we have a feature vector $f(\xi_i) = [\mathbf{p}_{i1}\Sigma, \ldots, \mathbf{p}_{i1}\Sigma] \in \mathbf{R}^{12}$ made by arranging 4 groups of 3 coordinates of each vector in a row. This experiment compares k-means[1], hard C Spherical Shells (HCSS) [3] and proposed clustering algorithm. In this paper, we choose true cluster number $C = 2$ for all algorithms.

TABLE IV
COORDINATE OF VERTEXES OF TRIANGULAR PYRAMIDS.

	Triangular pyramid 1			Triangular pyramid 2		
	x	y	z	x	y	z
$\mathbf{p}_1$	0	1	1	1	0	0
$\mathbf{p}_2$	1	0	1	0	1	0
$\mathbf{p}_3$	1	1	0	0	0	1
$\mathbf{p}_4$	0	0	0	-1	-1	-1

Because the results depend on the randomly assigned initial labels in most clustering methods, this experiment is performed using five different random sets of initial labels for each clustering method. The following kernel alignment function is used to evaluate the performance of the clustering results:

$$A(Y_t, Y_e) = \frac{\sum_{k,l} y_{kl;t} y_{kl;e}}{\sqrt{\sum_{k,l} y_{kl;t}^2} \sqrt{\sum_{k,l} y_{kl;e}^2}} \in [0, 1], \tag{27}$$

where $Y_t = [y_{kl;t}]$ and $Y_e = [y_{kl;e}]$ are symmetric matrices with n rows and n columns corresponding respectively to the generating data labels and the estimated data labels. y_{kl} indicates whether labels are different between instance k and instance l, and is defined by

$$y_{kl} = \begin{cases} 1 & (y_k = y_l), \\ 0 & (y_k \neq y_l). \end{cases} \tag{28}$$

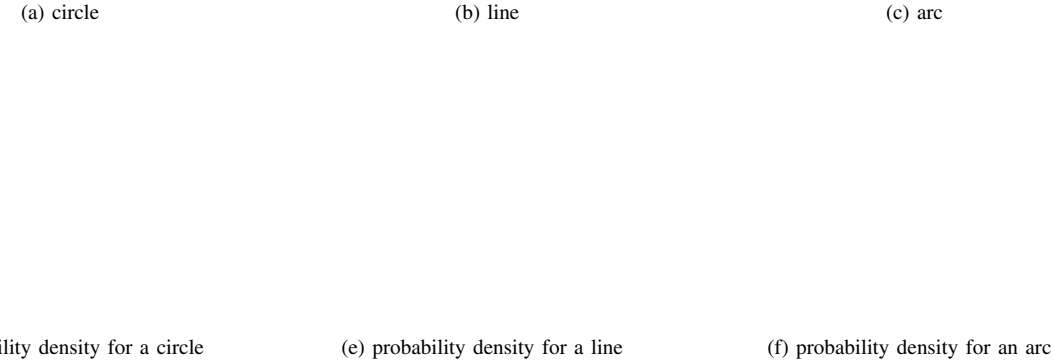

(a) circle (b) line (c) arc

(d) probability density for a circle (e) probability density for a line (f) probability density for an arc

Fig. 1. Estimated probability densities for the (a) circle, (b) line, and (c) arc.

Table V shows the average of the kernel alignment when using k-means, HCSS, and the proposed method. As shown in Table V, the kernel alignment when using the proposed method was better than when using k-means or HCSS.

TABLE V
AVERAGE ALIGNMENTS OF K-MEANS, HCSS, AND THE PROPOSED METHOD.

Method	Average alignment
k-mean	0.50053
HSSC	0.50082
CGA	1.00000

The clustering based on k-means uses the center of each cluster as representative, and so it is not able to cluster geometric data based on hyper-spheres. HCSS can cluster the data based on hyper-spheres. But in this experiment, the vectors made by rotating from two triangular pyramids have a norm $\|f(\xi_i)\|_2 = \sum_j \|\mathbf{p}_{ij}\|^2 = 6, \forall i \in \{1,2\}$. So, these vectors lie on the same hyper-sphere in 12-dimensional space. Therefore, the clustering result of HCSS was not good. Unlike k-means and HCSS, the proposed method can detect clusters around spheres of any dimension less than 12 because they are well expressed as elements of conformal geometric algebra. Together, the results of this experiment verifies that the clustering results using the proposed method are better than those using these conventional methods.

IV. CONCLUSION

This paper proposed a new approach of approximating geometric data, including that based on hyper-spheres or hyper-plane using CGA. The proposed method used a Lagrange function and eigen decomposition to find eigen conformal vectors for constructing the approximation. In m-dimensional space, the proposed method could find m solutions of hyper-spheres (-planes) and m eigen-values. The method expresses various data distributions, such as those based on hyper-spheres (-planes), circles (lines), or arcs, by using probability density functions based on the Gaussian function for the distance defined by CGA. Then, this paper proposed a new clustering method using the proposed approximation. The results of the first experiment showed that the proposed method was able to express exactly geometric data based on circles, lines, or arcs. The results of the second experiment showed that the kernel alignment based on the clustering results using the proposed method was better than those of clustering using conventional methods.

REFERENCES

[1] J. B. MacQueen, Some Methods for classification and Analysis of Multivariate Observations, Proceedings of 5th Berkeley Symposium on Mathematical Statistics and Probability, vol. 1, pp. 281–297, 1967.

[2] J. C. Bezdek, C. Coray, R. Gunderson and J. Watson, Detection and characterization of cluster substructure I. Linear structure fuzzy c-lines, SIAM Jour. of Appl. Math., vol.40, no.2, pp. 339-357, 1981.

[3] R. Krishnapuram, O. Nasraoui and H. Frigui, The fuzzy c spherical shells algorithms: a new approach, IEEE Trans. on Neural Networks, vol.3, no.5, pp. 663–671, 1992.
[4] C. Doran and A. Lasenby, Geometric algebra for physicists, Cambridge University Press, 2003.
[5] D. Hestenes, New foundations for classical mechanics, Dordrecht, 1986.
[6] L. Dorst, D. Fontijne, and S. Mann, Geometric Algebra for Computer Science: An Object-oriented Approach to Geometry (Morgan Kaufmann Series in Computer Graphics), 2007.
[7] I. Sekita, T. Kurita, and N. Otsu, Complex Autoregressive Model for Shape Recognition, IEEE Trans. on Pattern Analysis and Machine Intelligence, Vol. 14, No. 4, 1992.
[8] A. Hirose, Complex-Valued Neural Networks: Theories and Applications, Series on Innovative Intelligence, Vol. 5, 2006.
[9] N. Matsui, T. Isokawa, H. Kusamichi, F. Peper, and H. Nishimura, Quaternion neural network with geometrical operators, Journal of Intelligent and Fuzzy Systems, Volume 15, Numbers 3–4, pp. 149–164, 2004.
[10] S. Buchholz and N. Le Bihan, Optimal separation of polarized signals by quaternionic neural networks, 14th European Signal Processing Conference, EUSIPCO 2006, September 4–8, Florence, Italy, 2006.
[11] T. Nitta, An Extension of the Back-Propagation Algorithm to Complex Numbers, Neural Networks, Volume 10, Number 8, pp. 1391–1415(25), November 1997.
[12] D. Hildenbrand and E. Hitzer, Analysis of point clouds using conformal geometric algebra, 3rd International conference on computer graphics theory and applications, Funchal, Madeira, Portugal, 2008.
[13] E. Hitzer, Quaternion Fourier Transform on Quaternion Fields and Generalizations, Advances in Applied Clifford Algebras, 17(3), pp. 497–517 (2007).
[14] G. Sommer, Geometric Computing with Clifford Algebras, Springer, 2001.
[15] M. T. Pham, K. Tachibana, E. M. S. Hitzer, T. Yoshikawa, and T. Furuhashi, Classification and Clustering of Spatial Patterns with Geometric Algebra, AGACSE 2008 Leipzig, 2008.
[16] D. Hestenes and G. Sobczyk. Clifford Algebra to Geometric Calculus: A unified language for mathematics and physics, Reidel, 1984.
[17] N. Cristianini, J. Kandola, A. Elisseeff, and J. Shawe-Taylor, On kernel target alignment. Journal of Machine Learning Research, 2002.

2011 IEEE International Conference on Fuzzy Systems
June 27-30, 2011, Taipei, Taiwan

Fuzzy Bipolar Conditions of Type "or else"

Ludovic Liétard
IRISA/IUT/Univ. Rennes 1,
Rue Edouard Branly, BP 30219
22302 Lannion Cedex, France
Email: ludovic.lietard@univ-rennes1.fr

Nouredine Tamani
IRISA/ENSSAT/Univ. Rennes 1,
6, rue de Kerampont, BP 80518,
22305 Lannion Cedex, France
Email: tamani@enssat.fr

Daniel Rocacher
IRISA/ENSSAT/Univ. Rennes 1,
6, rue de Kerampont, BP 80518,
22305 Lannion Cedex, France
Email: rocacher@enssat.fr

***Abstract*—Previously studied fuzzy bipolar conditions of type "and if possible" are made of a mandatory condition c and an optional condition w. They allow expressing complex preferences of a conjunctive nature. We define in this paper, a new kind of fuzzy bipolar conditions of the form "or else" which express complex preferences of a disjunctive nature. We show that the "or else" form can be used as a negation operator of the "and if possible" form and vice versa. We also show that these both forms are compatible and, therefore, fuzzy bipolar conditions of both types can be used together in the same bipolar query.**

***Keywords*—Flexible querying, bipolar conditions, negation of bipolar conditions, fuzzy sets theory.**

I. Introduction

Flexible querying allows expressing preferences in user queries, which are addressed to regular databases and deliver a set of ranked answers from the most to the least preferred. In this context, the fuzzy sets theory [10] provide a general framework for the expression and the interpretation of queries involving preferences modelled by fuzzy predicates (or conditions). It is also possible to consider fuzzy bipolar conditions to model complex preferences [4], [5]. In this context, a bipolar condition is made of two components: a constraint and a wish. More precisely, for the expression of user preferences, we rely on fuzzy bipolar conditions in which the constraint and the wish are defined by fuzzy sets. We define then a bipolar query as a query that involves bipolar conditions.

Several interpretations have been introduced for the evaluation of queries involving fuzzy bipolar conditions of type "and if possible" (see [4], [5], [9], [11], [12]). The algebraic operators (selection, projection, join, union, intersection) have also been extended to fuzzy bipolar conditions [7], [2] of type "and if possible". It is therefore possible to express the usual query statements over relational bipolar relations, but in order to build a bipolar relational algebra, it stills to define a global operator for the negation of bipolar conditions. Several operators have been proposed in the literature but none of them fits in well with the framework of flexible querying.

We introduce in this paper a new kind of fuzzy bipolar conditions noted "or else", which expresses fuzzy bipolar conditions of a disjunctive nature. Its definition and properties allow us to define a negation operator of fuzzy bipolar conditions of the form "and if possible".

We show that each of these forms of bipolarity expresses a negation form of one another. These forms of bipolarity are also compatible in the sense that it is possible to mix in the same bipolar queries an "and if possible" fuzzy bipolar condition with an "or else" fuzzy bipolar condition.

The remainder of this paper is organized as follows. In section II, a short reminder about fuzzy bipolar conditions of type "and if possible" is introduced. In section III, we sum up different negation operators of fuzzy bipolar conditions of the form "and if possible", which have been proposed. Section IV is dedicated to our contribution; we introduce, firstly, the definition of fuzzy bipolar conditions of type "or else" and we show, secondly, that such fuzzy bipolar conditions can be used to define a negation operator for fuzzy bipolar conditions of type "and if possible". In section V, we show that these forms of fuzzy bipolar conditions are mutually compatible and can be used together in the same bipolar query. Section VI recalls our contribution and draws some lines for future works.

II. Fuzzy Bipolar Conditions

A bipolar condition is an association of a negative condition (negative pole) and positive condition (positive pole). In this paper, a bipolar condition is made of two conditions defined on the same universe: i) a constraint c, which describes the set of acceptable elements, ii) a wish w which defines the set of desired or wished elements. The negation of c is the set of rejected elements since it describes non-acceptable elements. Since it is not coherent to wish a rejected element, the following property of coherence holds: $w \subseteq c$.

In addition, condition c is mandatory since an element which does not satisfy c is rejected; $\neg c$ is then considered as the negative pole of the bipolar condition. Condition w is optional because its non-satisfaction does not automatically mean the rejection; w is then considered as the positive pole of the bipolar condition. In this paper, a bipolar condition is noted (c,w) and means, *"to satisfy c and if possible to satisfy w"* [4], [5].

If c and w are boolean conditions, the satisfaction with respect to (c,w) is an ordered pair from $\{0,1\}^2$. When querying a database with such a condition, tuples satisfying the constraint and the wish are returned in priority to the user. If such answers do not exist, tuples satisfying only the constraint are delivered.

If c and w are fuzzy conditions (defined on the universe U), the property of coherence becomes: $\forall u \in U, \mu_w(u) \leq \mu_c(u)$.

The satisfaction with respect to (c,w) is an ordered pair of degrees from the unit interval $[0,1]^2$. Each element u from U is then attached with a pair of grades $(\mu_c(u), \mu_w(u))$ that

978-1-4244-7316-8/11/$26.00 ©2011 IEEE

expresses the degrees of its satisfaction respectively to the constraint and the wish.

When querying a relation R with a fuzzy bipolar condition, each tuple t from R is then attached with a pair of grades $(\mu_c(t), \mu_w(t))$ that expresses the degrees of its satisfaction respectively to the constraint c and the wish w (and a so-called fuzzy bipolar relation is obtained). A tuple t is then denoted $(\mu_c, \mu_w)/t$. Any tuple u such that $\mu_c(u) = 0$ does not belong to the fuzzy bipolar relation.

In such a context, tuples cannot be ranked from the most preferred to the least preferred using an aggregation of μ_c and μ_w because the constraint and the wish are not commensurable. However, they can be ranked using the lexicographical order: t_1 is preferred to t_2 if and only if:

$\mu_c(t_1) > \mu_c(t_2)$ or $(\mu_c(t_1) = \mu_c(t_2) \wedge \mu_w(t_1) > \mu_w(t_2))$,
which is noted $(\mu_c(t_1), \mu_w(t_1)) > (\mu_c(t_2), \mu_w(t_2))$.
In this case, the satisfaction with respect to the constraint is firstly used to discriminate among answers (the constraint being mandatory). The satisfactions with respect to the wish being optional, they can only be used to discriminate among answers having the same evaluation with respect to the constraint. A total order is then obtained on μ_c and μ_w (with $(1,1)$ as the greatest element and $(0,0)$ as the least element).

Based on the lexicographical order, the *lmin* and *lmax* operators [6], [2] are introduced in order to define the conjunction (resp. intersection) and the disjunction (resp. union) of bipolar conditions (resp. relations). They are respectively defined as follows:

$$\begin{array}{rcl} ([0,1]\times[0,1])^2 & \rightarrow & [0,1]\times[0,1] \\ ((\mu,\eta),(\mu',\eta')) & \mapsto & lmin((\mu,\eta),(\mu',\eta')) = \\ & & \begin{cases} (\mu,\eta) & if\ \mu < \mu' \vee (\mu = \mu' \wedge \eta < \eta'), \\ (\mu',\eta') & else. \end{cases} \end{array} \quad (1)$$

$$\begin{array}{rcl} ([0,1]\times[0,1])^2 & \rightarrow & [0,1]\times[0,1] \\ ((\mu,\eta),(\mu',\eta')) & \mapsto & lmax((\mu,\eta),(\mu',\eta')) = \\ & & \begin{cases} (\mu,\eta) & if\ \mu > \mu' \vee (\mu = \mu' \wedge \eta > \eta'), \\ (\mu',\eta') & else. \end{cases} \end{array} \quad (2)$$

The *lmin* (resp. *lmax*) operator is commutative, associative, idempotent and monotonic. The pair of grades $(1,1)$ is the neutral (resp. absorbing) element of the operator *lmin* (resp. *lmax*) and the pair $(0,0)$ is the absorbing (resp. neutral) element of the operator *lmin* (resp. *lmax*).

Remark 1: Fuzzy bipolar conditions generalize fuzzy conditions since a fuzzy condition C can be rewritten (C,C) to express *"to satisfy C and if possible to satisfy C"*. As a consequence, a fuzzy relation R is a particular case of a fuzzy bipolar relation such that $\forall t \in R, \mu_R(t) = \mu_c(t) = \mu_w(t)$. Therefore, it is easy to demonstrate that the *lmin* (resp. *lmax*) generalizes the triangular norm *min* (resp. the triangular co-norm *max*).

More formally, bipolar conditions of the form "C and if possible W" can be defined with the following properties:

1) $\neg C$ corresponds to the rejection (C denotes acceptable elements),
2) W corresponds to the optimal values,
3) The acceptability condition C is more important than the optimality (the condition W),
4) The set of optimal values is included in the set of acceptable values ($W \subseteq C$).

Remark 2: The property 3 means that the non-rejection (or the acceptability) is more important than the optimality, therefore, the lexicographical order can be used to rank between elements.

III. The negation of Fuzzy Bipolar Conditions

Many works have been carried out to define a negation operator of fuzzy bipolar conditions.

To be consistent, any negation operator must verify the following properties, which have been introduced in [1]:

Let (C',W') denotes the negation of a fuzzy bipolar condition (C,W).

a) Property 1. Order reversing: The negation operator must deliver tuples in reverse order in which they are delivered by the condition (C,W):

$$\begin{array}{r} \forall t_1,t_2, (\mu_C(t_1),\mu_W(t_1)) < (\mu_C(t_2),\mu_W(t_2)) \Leftrightarrow \\ (\mu_{C'}(t_2),\mu_{W'}(t_2)) < (\mu_C(t_1),\mu_W(t_1)). \end{array} \quad (3)$$

b) Property 2. Consistency condition: The negation operator must deliver a consistency bipolar condition, which means: $\forall t, \mu_{W'}(t) \leq \mu_{C'}(t)$.

This property means that the negation of a bipolar condition of the form "and if possible" must also be a bipolar condition.

c) Property 3. Involutivity: The negation operator must be an involutive operator, it means that: $\neg(\neg(C,W)) = (C,W)$.

Several negation operators have been proposed in the literature. Some of them are summarized in what follows.

A. The Negation Operator Inspired by Twofold Fuzzy Sets

This negation operator is proposed in [3]. In this context, the negation of the wish corresponds to the constraint and the negation of the constraint defines the wish of the obtained condition. More formally, let (C,W) be a bipolar condition, its negation is: $\neg(C,W) = (\neg W, \neg C)$.

This kind of negation is not intuitive and does not satisfy the property of order reversing as it is shown in the following example 1.

Example 1: Let (C,W) be a bipolar condition and R a relational table containing tuples t_1 and t_2 such that: $(\mu_C(t_1),\mu_W(t_1)) = (0.8,0)$ and $(\mu_C(t_2),\mu_W(t_1)) = (0.6,0.6)$, we obtain $t_1 > t_2$.

The negation of (C,W) delivers the following result: $(\mu_{C'}(t_1),\mu_{W'}(t_1)) = (1,0.2)$ and $(\mu_{C'}(t_2),\mu_{W'}(t_2)) = (0.4,0.4)$, we obtain, then $t_1 > t_2$. □

B. The Negation Operator Based on the Product and the Division

This operator has been proposed in [1]. It is defined as follows: $\neg(C,W) = (C',W')$, where:

$$\mu_{C'} = 1 - \mu_C, \tag{4}$$

and

$$\mu_{W'} = \begin{cases} (1-\mu_C) * (1 - \frac{\mu_W}{\mu_C}) & if\ \mu_C \neq 0, \\ 1 & else. \end{cases} \tag{5}$$

This operator is not involutive; indeed:
$\neg(\neg(1, b \neq 0)) = \neg(0,0) = (1,1) \neq (1, b \neq 0)$.

In order to make this operator involutive, it is necessary to accept ordered pairs of grades of the form $(0, b > 0)$ and to define the negation as follows:

$$\mu_{C'} = 1 - \mu_C \tag{6}$$

$$\mu_{W'} = \begin{cases} 1 - \mu_W & if\ \mu_C = \{0,1\}, \\ (1-\mu_C) * (1 - \frac{\mu_W}{\mu_C}) & else. \end{cases} \tag{7}$$

The above properties 1, 2 and 3 hold only if the following conditions are satisfied:

- do not substitute (C,W) by $(C, C \wedge W)$ when $\mu_C = 0$,
- substitute (C,W) by $(C, W \wedge (C \vee (\neg C \Rightarrow_{RG} true)))$, where $\Rightarrow_{RG}$ is the Rescher-Gaines fuzzy implication,
- do not discard from the bipolar relation, tuples which have an ordered pair of grades of the form $(0, b \neq 0)$.

Despite the satisfaction of properties $1, 2$ and 3 under above conditions, the following drawbacks are pointed out:

- this operator does not express a natural negation form from the user point of view,
- its implementation is difficult and complex,
- the three added conditions can be seen as an infringement to properties of fuzzy bipolar conditions.

C. The Negation Operator of the Form $(\neg C, false)$

This operator is proposed in [2] and it is defined as follows:

$$\neg(C,W) = (\neg C, false) \tag{8}$$

This operator means that if tuples satisfying the constraint are discarded, then the wish becomes meaningless.

This form of negation is not involutive:
$\neg(\neg(C,W)) = \neg(\neg C, false) = (C, false) \neq (C,W)$.

D. The Negation Operator of the Form $(\neg C, \neg W)$

This operator is proposed in [7], [6]. The negation operator in this approach is defined as follows: $\neg(C,W) = (\neg C, \neg W)$.

This operator does not satisfy the consistency condition because $\neg W \nsubseteq \neg C$. The obtained operator is no more bipolar and can leads to non-consistent queries as in the following example 2.

Example 2: The negation of *"Train tickets which cost less than* 100 *\$ and if possible less than* 75 *\$"* is defined in this context as *"Train tickets which cost more than* 100 *\$ and if possible more than* 75 *\$"*.

This query is not consistent because the set of tickets which cost more than 75 \$ in not included in the set of tickets which cost more than 100 \$, but rather the opposite. □

IV. Fuzzy bipolar conditions of the form "or else"

We introduce in this section a new kind of fuzzy bipolar conditions. They are of the form "or else". We, firstly, provide a formal definition for such bipolar conditions; then, we study semantic relationships and similarities between "or else" and "and if possible" fuzzy bipolar conditions. Finally, we show that these two forms can be used in a negation context to define a global negation operator for fuzzy bipolar conditions.

A. Definition

A bipolar condition of the form "E, or else F" is made of two parts: (i) a positive pole corresponding to the condition E, which expresses perfect values and (ii) a negative pole corresponding to the condition F that expresses acceptable values (any element does not satisfy F is discarded).

We define bipolar conditions of the form "E, or else F", denoted $[E,F]$, with the following properties:

1) $\neg F$ corresponds to the rejection (F denotes acceptable elements),
2) E corresponds to the optimal values,
3) The optimality condition E is more important than the acceptability condition F,
4) The set of optimal values is included in the set of acceptable values ($E \subseteq F$): $\forall x, \mu_E(x) \leq \mu_F(x)$.

The ordered pair of grades, denoted $[\mu_E(x), \mu_F(x)]$, expresses the satisfaction of an element x to the condition "E, or else F".

Since the satisfaction with respect to the optimality E is more important than the satisfaction with respect to the acceptability F, the lexicographical order can be used to rank between elements. Indeed, if an element x satisfies completely the optimal condition E then it gets a pair of grades $[1,1]$ because $\forall x, \mu_E(x) \leq \mu_F(x)$, and by definition, the lexicographical order shows that this element is optimal. If the satisfaction to the optimal condition E of an element x_1 is better than the satisfaction to the same condition by another element x_2, then x_1 is more preferred than x_2.

Finally, if both x_1 and x_2 have the same satisfaction to the optimal condition E, for want of anything better, the condition F is used to distinguish between them.

Remark 3: It is worth noticing that a fuzzy condition C can be expressed "C or else C" within the framework of bipolar conditions of the form "or else". This generalization of fuzzy conditions expresses that perfect and acceptable values are the same.

As is the case of fuzzy conditions of the form "and if possible", the *lmin* (resp. *lmax*) operator applied on bipolar conditions of the form "or else" defines an extended triangular norm (resp. co-norm).

B. Relationships Between "or else" and "and if possible" Fuzzy Bipolar Conditions

Let "E, or else F" and "C, and if possible W" be two fuzzy bipolar conditions. The former is denoted $[E,F]$, with $\forall x, \mu_E(x) \leq \mu_F(x)$ and the latter is denoted (C,W), with $\forall x, \mu_W(x) \leq \mu_C(x)$.

TABLE I
EXAMPLE OF THE BEHAVIOR OF THE (C,W) FORMALISM.

	$\mu_C(x_i)$	$\mu_W(x_i)$
t_1	1	1
t_2	0.8	0.2
t_3	0.7	0.5
t_4	0.4	0.3

TABLE II
EXAMPLE OF THE BEHAVIOR OF THE $[W,C]$ FORMALISM.

	$\mu_W(x_i)$	$\mu_C(x_i)$
t_1	1	1
t_3	0.5	0.7
t_4	0.3	0.4
t_2	0.2	0.8

We notice strong similarities between these two formalisms, since in both cases we have:

- C and F express the acceptable values (or a non rejected values),
- $\neg C$ and $\neg F$ correspond to the discarded values,
- W and E express the perfect or optimal values,
- the set of perfect values is included in the set of acceptable values.

Moreover, these two conditions generalize fuzzy conditions in the same way: a fuzzy condition C is expressed (C,C) or $[C,C]$.

Since W (resp. C) plays the same role as E (resp. F), it is interesting to study the behavior of (C,W) and $[W,C]$. First of all, we notice that in the boolean case, both formalisms have the same meaning, as shown in the example 3.

Example 3: Let x,y and z be three elements attached respectively to the following pair of grades: $(1,1),(1,0)$ and $(0,0)$ with respect to conditions C and W.

The lexicographical order delivers the same order in both situations (C,W) and $[W,C]$: $x > y > z$. □

However, when C and W are fuzzy conditions, the two formalisms do not express the same semantic because the lexicographical order does not deliver the same order.

Tables I and II show that tuples t_1,t_2,t_3 and t_4 are not sorted according to the same order, depending on whether the formalism (C,W) or $[W,C]$ is used.

The basic difference between these two formalisms is the fact that the formalism "C, and if possible W" gives more importance to the non rejected elements (that means the satisfaction with respect to the condition of acceptance C is privileged), whereas the formalism "E, or else F" gives more importance to the optimal elements (i.e. the satisfaction with respect to the optimal condition E is privileged).

In this context, a fuzzy bipolar condition of the form (C,W) can be defined as a pair of fuzzy conditions, which define a set of optimal values (W) and a set of acceptable values (C) under the consideration that the non-rejection is more important than the optimality; and a fuzzy bipolar condition of the form $[E,F]$ is defined as a pair of fuzzy conditions, which define a set of optimal values (E) and a set of acceptable values (F) under the consideration that the optimality is more important than the non-rejection.

TABLE III
EXAMPLE OF TUPLES ATTACHED WITH THEIR ORDERED PAIRS OF GRADES W.R.T THE FUZZY BIPOLAR CONDITION $(Young, Young \wedge WellPaid)$.

#Employee	$\mu_{Young}(\#Employee)$	$\mu_{Young}(\#Employee) \wedge \mu_{WellPaid}(\#Employee)$
10	1	1
11	0.75	0.56
12	0.6	0.36
13	0.5	0.25

C. The Negation Context

In this subsection, we show that the negation of the fuzzy bipolar condition (C,W) is the fuzzy bipolar condition $[\neg C,\neg W]$ and, reciprocally, the negation of the fuzzy bipolar condition $[E,F]$ is the fuzzy bipolar condition $(\neg E,\neg F)$.

1) Negation of (C,W): We recall that a bipolar condition (C,W) is defined by the following properties:

1) $\neg C$ corresponds to the rejection (C denotes acceptable elements),
2) W corresponds to the optimal values,
3) The acceptability condition C is more important than the optimality condition W.

In addition, the set of optimal values is included in the set of acceptable values ($W \subseteq C$).

If we express these properties in the context of a negation $\neg(C,W)$, we obtain:

1) $\neg C$ corresponds to the optimal values (C contains rejected and acceptable elements),
2) W corresponds to the rejected values ($\neg W$ denotes acceptable elements),
3) The optimality condition $\neg C$ is more important than the acceptability condition $\neg W$.

In addition, since $W \subseteq C$, we have $\neg C \subseteq \neg W$.

Therefore, we obtain a fuzzy bipolar condition which fits within the definition of the "or else" fuzzy bipolar conditions and we denote it by $[\neg C,\neg W]$. That means:

$$\neg(C,W) = [\neg C,\neg W]. \quad (9)$$

It is important to notice that in (C,W), the importance is put on C and the concept attached to C stills the most important for $\neg(C,W)$. As an example, when considering *"young and if possible young and well-paid employees"*, the importance is put on the *age* (young). In its negation, the *age* stills the most important aspect to consider.

Example 4: Let $(Young, Young \wedge WellPaid)$ be a fuzzy bipolar condition of type "and if possible" which defines *young and if possible young and well-paid employees*. Let table III be a set of returned tuples from a relational table. The negation of the fuzzy bipolar condition $(Young, Young \wedge WellPaid)$ is defined as $[notYoung, not(Young \wedge WellPaid)]$, which corresponds to *employees which are not young, or else are not (young and well-paid)*. We notice that concepts used to define the fuzzy bipolar condition $(Young, Young \wedge$

TABLE IV
EXAMPLE OF TUPLES ATTACHED WITH THEIR ORDERED PAIRS OF GRADES W.R.T THE FUZZY BIPOLAR CONDITION $[notYoung, not(Young \wedge WellPaid)]$.

#Employee	$\mu_{notYoung}(\#Employee)$	$\mu_{not(Young\ and\ WellPaid)}(\#Employee)$
13	0.5	0.75
12	0.4	0.64
11	0.25	0.44

WellPaid) are the same ones used to express its negation $[notYoung, not(Young \wedge WellPaid)]$. More precisely, the concept *age* is used to define the most important fuzzy condition in both fuzzy bipolar condition $(Young, Young \wedge WellPaid)$ and $[notYoung, not(Young \wedge WellPaid)]$.

The obtained ordered pairs of degrees for the fuzzy bipolar condition $[notYoung, not(Young \wedge WellPaid)]$ are summed up in the table IV. The tuple #10 is completely discarded. □

2) Negation of $[E,F]$*:* We recall that a fuzzy bipolar condition $[E,F]$ is defined by the following properties:

- $\neg F$ corresponds to the rejection (F denotes the acceptable elements),
- E corresponds to the optimal values,
- The optimality condition E is more important than the acceptability.

In addition, the set of optimal values is included in the set of acceptable values ($E \subseteq F$).

If we express these properties in the context of a negation, we obtain:

- $\neg F$ corresponds to the optimal values,
- E corresponds to the rejected values ($\neg E$ denotes the acceptable elements),
- The acceptability condition $\neg E$ is the more important condition.

In addition, since $E \subseteq F$, we have $\neg F \subseteq \neg E$. This property states that, in the context of negation of a fuzzy bipolar condition of the form $[E,F]$, the set of optimal values is included in the set of acceptable values.

Therefore, we obtain a fuzzy bipolar condition, which fits within the definition of the "and if possible" fuzzy bipolar conditions and we denote it by $(\neg E, \neg F)$. That means:

$$\neg[E,F] = (\neg E, \neg F). \tag{10}$$

As for bipolar conditions of type "and if possible", we notice that in $[E,F]$, the importance is put on E and the concept attached to E stills the most important for $\neg[E,F]$.

This form of negation is involutive and reverses the lexicographical order (either for $\neg(E,F)$ or $\neg[E,F]$).

Proof: Reversing of the lexicographical order.

The proof is based on the following properties:

$$(x_1,y_1) > (x_2,y_2) \Rightarrow (1-x_1, 1-y_1) < (1-x_2, 1-y_2).$$

Let $[E,F]$ or (E,F) be a fuzzy bipolar condition. A tuple t_i is preferred to t_j means that:

$(\mu_E(t_i), \mu_F(t_i)) > (\mu_E(t_j), \mu_F(t_j))$,
or $[\mu_E(t_i), \mu_F(t_i)] > [\mu_E(t_j), \mu_F(t_j)]$

From the definition of the lexicographical order, we get:

(t_i is preferred to t_j) $\Leftrightarrow \mu_E(t_i) > \mu_E(t_j)$ or
$(\mu_E(t_i) = \mu_E(t_j)$ and $\mu_E(t_i) > \mu_F(t_j))$
$\Leftrightarrow (1-\mu_E(t_i) < 1-\mu_E(t_j))$ or $((1-\mu_E(t_i) = 1-\mu_E(t_j))$
and $(1-\mu_E(t_i) < 1-\mu_F(t_j)))$

$\Leftrightarrow t_j$ is preferred to t_i for $(\neg E, \neg F)$ or $[\neg E, \neg F]$, with $(\neg E, \neg F) = \neg[E,F]$ and $[\neg E, \neg F] = \neg(E,F)$. The order is then reversed for the negation. ■

Proof: Involutivity.

$\neg(\neg(C,W)) = \neg[\neg C, \neg W] = (\neg\neg C, \neg\neg W) = (C,W)$ and $\neg(\neg[E,F]) = \neg(\neg E, \neg F) = [\neg\neg E, \neg\neg F] = [E,F]$. ■

V. MUTUAL COMPATIBILITY OF "AND IF POSSIBLE" AND "OR ELSE" FUZZY BIPOLAR CONDITIONS

It is possible to express fuzzy bipolar conditions of both forms "and if possible" and "or else" together in the same bipolar query. This means that it is possible to use *lmin* and *lmax* operators to compare and to handle ordered pairs of scores of these types of fuzzy bipolar conditions. This is due to the fact that both of them are semantically equivalent in the sense that they are defined similarly. Indeed, fuzzy bipolar conditions of types "and if possible" and "or else" consist of two parts: a first part which corresponds to the most important concept (the concept attached to C for the fuzzy bipolar condition (C,W) and the concept attached to E or the fuzzy bipolar condition $[E,F]$) and a second part which corresponds to the least important concept of the bipolar condition. Therefore, in order to rank between tuples, the first choice is made on the condition which corresponds to the most important concept in the fuzzy bipolar condition, and the second choice is made on the condition which corresponds to the least important concept of the same fuzzy bipolar condition. We show in the following example a bipolar query in which both forms of fuzzy bipolar conditions are used, and its returned tuples with their attached ordered pairs of degrees.

Example 5: Let R be a relational table about *journeys* from *Paris* to *Brest* (see table V), delivered from a multimodal transport information system.

One can express a bipolar query about preferred journeys in the following terms:

"Find journeys from Paris to Brest which are ***(fast, and if possible fast and cheap)****, or journeys with* ***(an early departure and a late arrival, or else an early departure)"****.*

In the above query, the preferred journeys are those which have a short duration and cost as low as possible, or journeys in which the user takes the time to travel, which correspond to journeys having an early departure and a late arrival, otherwise journeys which have an early departure.

Based on the fuzzy predicates *fast*, *cheap*, *early* and *late*, we define from the relation R the following bipolar relations $Journey_{(Fast, Fast \wedge Cheap)}$ (see table VI), which corresponds to fast *and if possible* cheap journeys, and $Journey_{[Early \wedge Late, Early]}$ (see table VII), which corresponds journeys having an early departure and a late arrival *or else* an early departure. Tuples of these relations are ranked from the most satisfactory to the least satisfactory with regard to fuzzy bipolar conditions $(Fast, Fast \wedge Cheap)$ and $[Early \wedge Late, Early]$ respectively.

TABLE V
EXAMPLE OF EXTENSION OF THE RELATION R.

#Journey	Duration	Departure	Mode	Cost	...
10	2h	11h30 am	Plane	60	...
11	2h45	11h am	Plane	150	...
12	2h30	8h30 am	Plan	260	...
13	3h10	8h am	Train	80	...
14	3h30	10h am	Train	80	...
15	4h10	7h30 am	Train	90	...
16	5h15	7h15 am	Bus	85	...

TABLE VI
THE FUZZY BIPOLAR RELATION $Journey_{(Fast,Fast \wedge Cheap)}$.

#Journey	$\mu_{Fast}(\#Journey)$	$\mu_{Fast \wedge Cheap}(\#Journey)$
10	1	1
11	0.80	0.64
12	0.80	0.25
13	0.60	0.36
14	0.40	0.36
15	0.40	0.16
16	0.25	0.25

The ordered pair of grades of satisfaction, with regard to the combination of the fuzzy bipolar conditions $(Fast, Fast \wedge Cheap)$ and $[Early \wedge Late, Early]$, attached to each tuple is obtained by the application of the $lmax$ operator on each tuple of both fuzzy bipolar relations as follows:

- #journey = 10: $lmax((1,1),[0.25,0.6]) = (1,1)$,
- #journey = 11: $lmax((0.8,0.64),[0.25,0.5]) = (0.8,0.64)$,
- #journey = 12: $lmax((0.8,0.25),[0.3,1]) = (0.8,0.25)$,
- #journey = 13: $lmax((0.6,0.36),[0.6,1]) = [0.6,1]$,
- #journey = 14: $lmax((0.4,0.36),[0.6,0.7]) = [0.6,0.7]$,
- #journey = 15: $lmax((0.4,0.16),[0.8,1]) = [0.8,1]$,
- #journey = 16: $lmax((0.25,0.25),[1,1]) = [1,1]$,

We notice that journeys are delivered depending on the grade of satisfaction w.r.t the most important fuzzy condition: *fast* for the fuzzy bipolar condition $(Fast, Fast \wedge Cheap)$ and *early* for the fuzzy bipolar condition $[Early \wedge Late, Early]$. In the case where the two most important conditions have the same satisfaction, the distinction is made on the least important conditions.

The maximum ordered pair of degrees is attached to tuples #10 and #16, because the corresponding fuzzy bipolar condition is completely satisfied (both are fully satisfactory and not distinguishable).

In the case of tuples #11, #12, #14, #15, the returned ordered pair of grades corresponds to the ordered pair in which the satisfaction w.r.t the most important fuzzy condition in both used fuzzy bipolar conditions is the highest.

TABLE VII
THE FUZZY BIPOLAR RELATION $Journey_{[Early \wedge Late, Early]}$.

#Journey	$\mu_{Early \wedge Late}(\#Journey)$	$\mu_{Early}(\#Journey)$
16	1	1
15	0.80	1
13	0.60	1
14	0.60	0.70
12	0.30	1
10	0.25	0.60
11	0.25	0.50

In the case of tuple #13, the satisfaction is the same with regard to the most important fuzzy condition in both fuzzy bipolar conditions; therefore, the least important condition is used to determine which ordered pair of degrees to attach to the resulting tuple.

Finally, journeys are delivered in the following order: $(1,1)$/#10, $[1,1]$/#16, $[0.8,1]$/#15, $(0.8,0.64)$/#11, $(0.8,0.25)$/#12, $[0.6,1]$/#13, $[0.6,0.7]$/#14.

VI. CONCLUSION AND FUTURE WORKS

A new kind of fuzzy bipolar conditions is introduced in this paper. These conditions are of the form "or else" and allow users to express complex preferences of a disjunctive nature in their queries. We showed that this form of fuzzy bipolar conditions are compatible with fuzzy bipolar conditions of the form "and if possible" in the sense that (i) each one can be used as the negation form of the other and that (ii) it is possible to combine them in the same query and to handle them using the lexicographical order based operator *lmin* and *lmax*.

As future work, we aim at studying this form of negation within the scope of a bipolar relational language and at integrating it into the bipolar SQLf language, which is an extension of the SQLf language to fuzzy bipolar conditions.

ACKNOWLEDGMENTS

This work is funded by the Brittany region and the department of Côtes-d'Armor and is partially supported by the National Agency for Research (AOC Ref. ANR-08-CORD-009).

REFERENCES

[1] P. Bosc and O. Pivert. A propos de la négation de conditions bipolaires floues. on the negation of fuzzy bipolar conditions. In *Rencontre francophone sur la logique floue et ses applications*, pages 21–28, 2010.
[2] P. Bosc, O. Pivert, L. Liétard, and A. Mokhtari. Extending relational algebra to handle bipolarity. In *25th ACM Symposium on Applied Computing, SAC'10*, pages 1717–1721, 2010.
[3] D. Dubois and H. Prade. Twofold fuzzy sets and rough sets–some issues in knowledge representations. *Fuzzy sets and Systems*, 23(1):3–18, 1987.
[4] D. Dubois and H. Prade. Bipolarity in flexible querying. *LNAI*, 2522:174–182, 2002.
[5] D. Dubois and H. Prade. An introduction to bipolar representations of information and preference. *International Journal of Intelligent Systems*, 23:866–877, 2008.
[6] L. Liétard and D. Rocacher. On the definition of extended norms and co-norms to aggregate fuzzy bipolar conditions. In *IFSA/EUSFLAT*, pages 513–518, 2009.
[7] L. Liétard, D. Rocacher, and P. Bosc. On the extension of SQL to fuzzy bipolar conditions. In *The 28th North American Information Processing Society Annual Conference (NAFIPS'09)*, 2009.
[8] E. Trillas, C. Moraga, S. Guadarrama, S. Cubillo, and E. Castineira. Computing with antonyms. In M. Nikravesh, J. Kacprzyk, and L. Zadeh, editors, *Forging New Frontiers: Fuzzy Pioneers I*, Studies in Fuzziness and Soft Computing, pages 133–153. Springer Berlin / Heidelberg, 2007.
[9] G. D. Tré, S. Zadrozny, T. Matthé, J. Kacprzyk, and A. Bronselaer. Dealing with positive and negative query criteria in fuzzy database quering bipolar satisfaction degrees. *LNAI, FQAS*, 5822:593–604, 2009.
[10] L. Zadeh. Fuzzy sets. *Information and control*, 8(3):338–353, 1965.
[11] S. Zadrozny and J. Kacprzyk. Bipolar queries using various interpretations of logical connectives. *LNAI, IFSA*, 4529:182–190, 2007.
[12] S. Zadrozny and J. Kacprzyk. Bipolar queries: An approach and its various interpretations. In *In Proceedings of IFSA/EUSFLAT*, pages 1288–1293, 2009.

2011 IEEE International Conference on Fuzzy Systems
June 27-30, 2011, Taipei, Taiwan

Fuzzy Optimization Model Based Tolerance Approach to Timetable Rescheduling for High Speed Railway in China

Yong Qin[1], Li Wang[1], Huan Lian[2]
[1]State Key Laboratory of Rail Traffic Control and Safety
Beijing Jiaotong University
Beijing, China
qinyong2146@126.com,08114168@bjtu.edu.cn,
lianhuan369@yahoo.com.cn

Xuelei Meng[1], Xuewen Li[2], Fugui Shi[2], Limin Jia[1]
[2]School of Science
Beijing Institute of Technology
Beijing, China
mengxuelei@gmail.com, lixuewen@bit.edu.cn,
fuguishi@bit.edu.cn,jialm@vip.sina.com

***Abstract*—A fuzzy optimization model based tolerance approach is proposed to handle timetable rescheduling in high speed railway during speed restriction period. As the limited speed and headway time are not crisp figures in practice especially when some natural hazards happen or some equipment failure, tolerance approach is introduced with the fuzzy membership functions of the original objective and soft constraints to find an new optimal objective with little slack of constraints. The original objective is treated in the same manner as the soft constraints, so the model is symmetric. The proposed fuzzy rescheduling model is simulated on the busiest part of a high speed railway line in China. The entire case study shows the significance of fuzzy optimization in case of speed restriction. The results shed light on how we could choose a better limited speed and headway time, so that the number of seriously impacted trains can be reduce greatly with little cost and risk.**

Keywords- timetable rescheduling; fuzzy optimization; tolerance approach

I. INTRODUCTION

At present, China is extensively developing the infrastructure of high speed railway. The target is to cover its major economic areas with a high speed railway network, which consists of four horizontal and four vertical lines [1], in the following several years. The network scale is much larger than any existing ones in the world. Train timetable rescheduling is a focal point to improve the operation mode with the characteristics of high train speed, high train frequency and mixed train speed (HHM), which is of great theoretical and practical significance for safety and efficiency operation of China high speed railway network.

In China, train rescheduling is mostly manual developed by the operator with the suport of computer in the existing line or the high speed railway, which is depends on human experience to dominate only one line or some section in one line with fixed three hours period. In future China will establish five comprehensive operation centers of the railway network, each of which will dominate several lines that total length over thousands of kilometers [2]. The scale of rescheduling object is far larger and the relationship between lines is far more complex than the existing situation, so the inefficient manually rescheduling, which seriously affect the use of the ability of high-speed rail and bring risk to railway safety, cannot support the advanced operation command mode.

Over the years, the research on the train operation automatic adjustment has been paid great attention and many different algorithms for optimal rescheduling have been put forward. The integer programming, such as branch and bound, linear programming and other traditional optimization method [3] are usually used for the simple transportation organization mode (only high speed or medium speed train running). In China, there are usually mixed high-speed and medium-speed trains running in one line, so there are great differences on the variable size, type of constraints and target values in the actual situation of the Chinese high-speed railway, and these methods cannot be directly applied to the train rescheduling problems in China.

Since the railway network is extensively developed and transportation organization mode is more complex in recent years, many heuristic methods of artificial intelligence, like DEDS-based simulation method [4], expert system [5], tabu search [6, 7], and some computational intelligence methods [8-14], like genetic algorithm, particle swarm optimization algorithm, are used to solve the large-scale combinatorial optimization problem by many scholars.

To some extent, these mathematical model and optimization algorithm have given a feasible solution for train operation automatic adjustment problem; actually there are many uncertainties of decision variables, parameters, constraints and goals for high speed railway timetable rescheduling optimization. For example, the running time at a section and the dwell time at a station of the train, which are typical uncertain variables, are easily impacted by railway and equipment status, technological level of crew and weather condition [15, 16]. So these methods that only consider the crisp parameters cannot adapt to the actual operation environment of high-speed railway under the great influence of uncertainty, and it can not achieve the purpose of automatic rescheduling, even play the role of decision support in practical applications. Therefore, the uncertainty character of high-speed

978-1-4244-7316-8/11/$26.00 ©2011 IEEE

train operation automatic adjustment model should be considered in substance.

II. TIMETABLE RESCHEDULING PROBLEM

The aim of train rescheduling is to get a new timetable that adjustes the train movements to be consistent with the planned schedule as much as possible under some interference. The follow model focuses on minimizing the total delay as well as the number of seriously impacted trains.

A. Input Data

The numerical inputs are described as follows:

$inis_p$, $inie_p$: Initial start and end time of interval p according to original timetable.

z_p : The minimum size of interval p. If p is the possession of a station, d_p stands for the minimum dwell time of the train associated with p. Otherwise, it stands for the minimum running time of the train.

f_k : The minimum separation time of two intervals on station k, i.e. end time of an interval – start time of the subsequent interval.

hw_k : The headway of section k, i.e. start time of an interval – start time of the subsequent interval.

c_i^{delay} : The cost per time unit delay for train i.

w_i : Delay tolerance for train i.

W_i : Weight for objective i;

$$h_p = \begin{cases} 1, \ if \ \text{interval} \ p \ is \ a \ planned \ stop, \\ where \ p \in Itv \\ 0, otherwise \end{cases}$$

M : A very big integer, e.g. 100000.

TABLE I. SETS DEFINED FOR MODELING

Set Name	Description	Size	Index of set
Trn	All the trains.	T	i
Seg	All the segments.	S	k
$Stn \subseteq Seg$	All the stations.	N	--
$Sec \subseteq Seg$	All the sections.	S-N	--
Itv	All the intervals where an interval is the possession of a segment by a train with specified start and end time.	--	p
$Itv_i \subseteq Itv$	The ordered set of intervals for train i according to the original timetable.	--	--
$Itv_i^{stn} \subseteq Itv_i$	The ordered set of intervals associated with stopping at stations for trains i.	--	--
$Itv_k \subseteq Itv$	The ordered set of intervals for segment k according to the original timetable.	--	--
Trk_k	All the tracks of station k	L_k	l

Remarks: For the ease of understanding, we use p as the index for every interval-related set (i.e. Itv , Itv_i , Itv_i^{stn} and Itv_k). In each of the interval-related sets, p+1 indicates the first subsequent interval of p, and $\tilde{p}$ indicates all the subsequent intervals of p.

Some sets are defined in TABLE I for modeling. Note that the segment between two stations is called "section", while the station segment is called "station" for short.

B. Decision variables

s_p , e_p : Start time and end time of interval p.

d_p : Delay of interval p, which is defined as the difference between the departure time after adjustment and the planned departure time in the original timetable.

$$b_i = \begin{cases} 1, \ if \ train \ i \ reaches \ its \ final \ considered \ stop \\ with \ a \ delay \ larger \ than \ w_i, where \ i \in Trn \\ 0, otherwise \end{cases}$$

$$\eta_{pl} = \begin{cases} 1, \ if \ \text{interval} \ p \ uses \ track \ l, where \ p \in Itv_k, \\ l \in Trk_k \ and \ k \in Stn \\ 0, otherwise \end{cases}$$

$$\alpha_{p\tilde{p}} = \begin{cases} 1, \ if \ \text{interval} \ p \ occurs \ before \ \tilde{p} \ as \ in \ the \\ initial \ timetable, where \ p, \tilde{p} \in Itv_k, k \in Seg \\ 0, otherwise \end{cases}$$

$$\beta_{p\tilde{p}} = \begin{cases} 1, \ if \ \text{interval} \ p \ is \ changed \ to \ occur \ after \ \tilde{p}, \\ where \ p, \tilde{p} \in Itv_k, k \in Seg \\ 0, otherwise \end{cases}$$

C. Objective functions

i) To minimize the delay cost:

$$\text{Minimize} \sum_{i \in Trn} \left(c_i^{delay} \cdot \sum_{p \in Itv_i^{stn}} d_p \right) \quad (1)$$

ii) To minimize the number of trains exceeding delay tolerance:

$$\text{Minimize} \sum_{i \in Trn} b_i \quad (2)$$

$$S = W_1 \sum_{i \in Trn} \left(c_i^{delay} \cdot \sum_{p \in Itv_i^{stn}} d_p \right) + W_2 \sum_{i \in Trn} b_i \quad (3)$$

D. Constraints

i) Interval restrictions

$$e_p - s_p \geq z_p, \ p \in Itv \quad (4)$$

The real departure time cannot be earlier than the original departure time:

$$e_p \geq inie_p, \ p \in Itv \ \text{and} \ h_p = 1 \quad (5)$$

$$e_p - inie_p = d_p, \ p \in Itv \quad (6)$$

ii) Track restrictions

$$\sum_{l \in Trk_k} \eta_{pl} = 1,\ p \in Itv_k \text{ and } k \in Stn \tag{7}$$

iii) Connectivity restrictions

$$e_p = s_{p+1},\ p \in Itv_i,\ p \neq last(Itv_i) \text{ and } i \in Trn \tag{8}$$

For each station, if two intervals use the same track, at least one of α and β is forced to be 1:

$$\eta_{pl} + \eta_{\tilde{p}l} - 1 \leq \alpha_{p\tilde{p}} + \beta_{p\tilde{p}},\quad p, \tilde{p} \in Itv_k,\ p < \tilde{p},\ l \in Trk_k \text{ and } k \in Stn \tag{9}$$

One train can enter a station after the preceding train, which uses the same track, leaves it:

$$s_{\tilde{p}} - e_p \geq f_k \alpha_{p\tilde{p}} - M\left(1 - \alpha_{p\tilde{p}}\right),\quad p, \tilde{p} \in Itv_k \text{ and } k \in Stn \tag{10}$$

$$s_p - e_{\tilde{p}} \geq f_k \beta_{p\tilde{p}} - M\left(1 - \beta_{p\tilde{p}}\right),\quad p, \tilde{p} \in Itv_k \text{ and } k \in Stn \tag{11}$$

For each section, at least one of α and β is forced to be 1 because there is only one track:

$$\alpha_{p\tilde{p}} + \beta_{p\tilde{p}} = 1,\ p, \tilde{p} \in Itv_k \text{ and } k \in Sec \tag{12}$$

Headways for each section:

$$s_{\tilde{p}} - s_p \geq hw_k \alpha_{p\tilde{p}} - M\left(1 - \alpha_{p\tilde{p}}\right),\ p, \tilde{p} \in Itv_k \text{ and } k \in Sec \tag{13}$$

$$s_p - s_{\tilde{p}} \geq hw_k \beta_{p\tilde{p}} - M\left(1 - \beta_{p\tilde{p}}\right),\ p, \tilde{p} \in Itv_k \text{ and } k \in Sec \tag{14}$$

iv) Auxiliary restrictions

$$d_{last(Itv_i)} - w_i \leq Mb_i \tag{15}$$

In practice, some constraints of the model are not satisfied strictly because of the inexact operation time. Two kinds of constraints are changed as below:

i) Interval restrictions

z_p stands for the minimum running time or the minimum dwell time of the train associated with p. Both of them may be impacted by some weather and human factors. The running time of the train at a section is formed by pure running time at the section and addition time for departure and arrival at a station, which is easily impacted by railway and equipment status, technological level of crew and weather condition. Since the average running speed of the train usually changes within a certain range, especailly in speed restriction under some emergency, it is very important to find a safety and reasonable average speed that far below the limited speed to improve the optimization result greatly. Furthermore, many factors, like the train type, on and off time of passengers, preparation time for drivers and crew and station technology operation of the train may increase the uncertainty of the dwell time of the train at a station. So there should be a tolerance for z_p, and the constraint is changed as below:

$$g_1 = e_p - s_p \gtrsim z_p,\ p \in Itv \tag{16}$$

ii) Headway restrictions

The headway time for each station is decided by the number of receiving-departure track, the operation time of turnout and holding time of the track, which is also an uncertainty constraint due to the factors of equipment status and human technological level. So there should be a tolerance for f_k. The headway constraint for each station is changed as below:

$$g_2 = s_{\tilde{p}} - e_p \gtrsim f_k \alpha_{p\tilde{p}} - M\left(1 - \alpha_{p\tilde{p}}\right),\quad p, \tilde{p} \in Itv_k \text{ and } k \in Stn \tag{17}$$

$$g_3 = s_p - e_{\tilde{p}} \gtrsim f_k \beta_{p\tilde{p}} - M\left(1 - \beta_{p\tilde{p}}\right),\quad p, \tilde{p} \in Itv_k \text{ and } k \in Stn \tag{18}$$

The headway time for each section is decided by the number and length of the block between two tracking trains and the speeds of the trains, which ranges from 2.4 minutes to 3 minutes according to [17]. The headway constraint for each section is changed as below:

$$g_4 = s_{\tilde{p}} - s_p \gtrsim hw_k \alpha_{p\tilde{p}} - M\left(1 - \alpha_{p\tilde{p}}\right),\ p, \tilde{p} \in Itv_k \text{ and } k \in Sec \tag{19}$$

$$g_5 = s_p - s_{\tilde{p}} \gtrsim hw_k \beta_{p\tilde{p}} - M\left(1 - \beta_{p\tilde{p}}\right),\ p, \tilde{p} \in Itv_k \text{ and } k \in Sec \tag{20}$$

For this condition, the model above turns meaningless in the sense of mathematical viewpoints. To construct a reasonable mathematical model under the uncertain environment, the tolerance approach based timetable rescheduling model will be introduced in the next section.

III. FUZZY OPTIMIZATION MODEL BASED TIMETABLE RESCHEDULING

In the paper, we use the fuzzy optimization based tolerance approach to solve the uncertainty program, some necessary backgrounds and notions of the approach are reviewed.

A. Fuzzy optimization based tolerance approach

Tolerances are indicated in any technical process, that is the admissible limit of variation around the object value and the deviations allowed from the specified parameters.

A general model of a fuzzy linear programming problem (FLP-programming) is presented by the following system.

$$\text{Minimize } \tilde{C}_1 x_1 \oplus \tilde{C}_2 x_2 \oplus \cdots \oplus \tilde{C}_n x_n \tag{21}$$

$$\text{Subject to } \tilde{A}_{i,1} x_1 \oplus \tilde{A}_{i,2} x_2 \oplus \cdots \oplus \tilde{A}_{i,n} x_n \gtrsim \tilde{B}_i,\quad i = 1, \cdots m \tag{22}$$

$\tilde{A}_{i,j}, \tilde{B}_i, \tilde{C}_j$ ($i = 1, \cdots, m$; $j = 1, \cdots, n$) are fuzzy set in R. The symbol $\oplus$ represents the extended addition. Each real number a can be modeled as a fuzzy number.

$$\tilde{A} = \{(x, f_A(x)); x \in R\}$$
$$with \quad f_A(x) = \begin{cases} 1 & x = a \\ 0 & x \neq a \end{cases} \tag{23}$$

Here we only discuss the special case where the objective function is crisp and some constraints have the soft form and the rest constrains are crisp.

$$\text{Minimize } z(x) = c_1 x_1 + c_2 x_2 + \cdots + c_n x_n \tag{24}$$

Subject to

$$g_i(x) = a_{i,1}x_1 + a_{i,2}x_2 + \cdots + a_{i,n}x_n \gtrsim \tilde{B}_i, \quad i = 1, \cdots, m_1 \tag{25}$$

$$a_{i,1}x_1 + a_{i,2}x_2 + \cdots + a_{i,n}x_n \geq b_i, \quad i = m_1 + 1, \cdots, m \tag{26}$$

$$x_1, \cdots, x_n \geq 0$$

The m_1 soft constraints (25) may be described more precisely by the fuzzy set with the support $[b_i - d_i, b_i]$, and d_i is the tolerance according to b_i. Moreover the membership function $g_i(x)$ can be specified as the follow function.

$$\mu(g_i) = \begin{cases} 0, & g_i \leq b_i - d_i \\ \dfrac{g_i - (b_i - d_i)}{d_i}, & b_i - d_i < g_i \leq b_i, \\ i = 1, \cdots, m_1 & \\ 1, & b_i \leq g_i \end{cases} \tag{27}$$

Directly assigns a measure of the satisfaction of the i-th constraint to the solution $X = (x_1, x_2, \cdots x_n)$.

For the objective function $z(x)$, there is a fuzzy set $\tilde{Z} = \{(z, \mu_Z(z)) \mid z \in R\}$ Let

$$X_L = \{x \in R \mid a_{i1}x_1 + a_{i2}x_2 + \cdots a_{in}x_n \geq b_i - d_i, \forall i = 1, 2, \cdots, m_1 \quad and \quad a_{i1}x_1 + a_{i2}x_2 + \cdots a_{in}x_n \geq b_i, \forall i = m_1 + 1, \cdots m\} \tag{28}$$

$$X_U = \{x \in R \mid a_{i1}x_1 + a_{i2}x_2 + \cdots a_{in}x_n \geq b_i, \forall i = 1, 2, \cdots, m\} \tag{29}$$

$$\overline{z} = \underset{x \in X_U}{Min}\, z(x) \tag{30}$$

and

$$\underline{z} = \underset{x \in X_L}{Min}\, z(x) \tag{31}$$

So the membership function $\mu_Z(z)$ of $\tilde{Z}$ is given by

$$\mu_z(z) = \begin{cases} 0, & \overline{z} \leq z \\ 1 - \dfrac{z - \underline{z}}{\overline{z} - \underline{z}}, & \underline{z} < z \leq \overline{z} \\ 1, & z \leq \underline{z} \end{cases} \tag{32}$$

In order to determine a compromise solution, it is usually assumed in the literature that the total satisfaction of a decision maker may be described by

$$\lambda(x) = \min(\mu_Z(x), \mu_1(x), \cdots \mu_{m_1}(x)) \tag{33}$$

We treat the objective in the same manner as the soft constraints, so this is a symmetric model.

The optimization system is clearly equivalent to

$$\text{Maximize } \lambda \tag{34}$$

$$\text{Subject to } \mu_Z(x) \geq \lambda \tag{35}$$

$$\mu_i(x) \geq \lambda, \quad i = 1, \cdots m_1 \tag{36}$$

$$x \in X, \ \lambda \in [0,1]$$

Using linear membership functions or piecewise linear, concave membership function, the system can easily be solved by well-known algorithms.

B. Fuzzy optimization model based tolerance approach to timetable rescheduling

In the rescheduling model mentioned above, three additional inputs are involved to describe the tolerances of minimum running time or dwell time, headway time for section and station respectively. An additional decision variable λ is involved to describe the fuzzy number for the objective and constraints. All the additional parameters are list as below:

c_{z_p} : Tolerance of z_p

c_{f_k} : Tolerance of f_k

c_{hw_k} : Tolerance of hw_k

λ : Decision variable for the fuzzy number

s^0 : The objective value of the original model according to z_p, f_k, hw_k.

s^* : The objective value of the original model according to $z_p - c_{z_p}$, $f_k - c_{f_k}$, $hw_k - c_{hw_k}$.

So fuzzy membership function of objective is given by

$$\mu_0 = \begin{cases} 1, & S < s^* \\ 1 - \dfrac{S - s^*}{s^0 - s^*}, & s^* \leq S \leq s^0 \\ 0, & S > s^0 \end{cases} \tag{37}$$

Fig. 1 shows the objective fuzzy membership function.

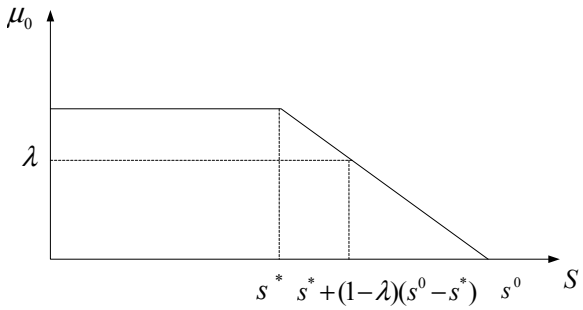

Figure 1. The objective fuzzy membership functione

Fuzzy membership function of run time constraint is given by

$$\mu_1=\begin{cases}1, & g_1>z_p\\ 1-\dfrac{z_p-g_1}{c_{z_p}}, & z_p-c_{z_p}\le g_1\le z_p\\ 0, & g_1<z_p-c_{z_p}\end{cases} \tag{38}$$

Fig. 2 shows the fuzzy membership function of run time constraint.

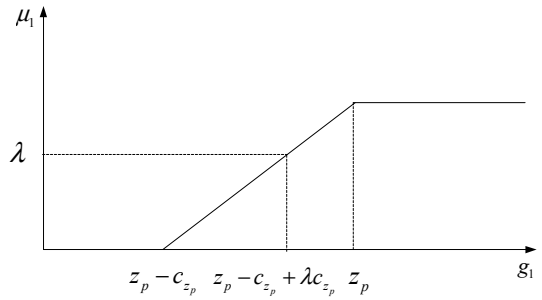

Figure 2. The run time constraint fuzzy membership function

Fuzzy membership functions of headway time constraints and their graphics are similar to figure 2.

$$\mu_2=\begin{cases}1, & g_2>f_k\\ 1-\dfrac{f_k-g_2}{c_{f_k}}, & f_k-c_{f_k}\le g_2\le f_k\\ 0, & g_2<f_k-c_{f_k}\end{cases} \tag{39}$$

$$\mu_3=\begin{cases}1, & g_3>f_k\\ 1-\dfrac{f_k-g_3}{c_{f_k}}, & f_k-c_{f_k}\le g_3\le f_k\\ 0, & g_3<f_k-c_{f_k}\end{cases} \tag{40}$$

$$\mu_4=\begin{cases}1, & g_4>hw_k\\ 1-\dfrac{hw_k-g_4}{c_{hw_k}}, & hw_k-c_{hw_k}\le g_4\le hw_k\\ 0, & g_4<hw_k-c_{hw_k}\end{cases} \tag{41}$$

$$\mu_5=\begin{cases}1, & g_5>hw_k\\ 1-\dfrac{hw_k-g_5}{c_{hw_k}}, & hw_k-c_{hw_k}\le g_5\le hw_k\\ 0, & g_5<hw_k-c_{hw_k}\end{cases} \tag{42}$$

So the model is changed as follow:

C. Objective functions

i) To maximize the fuzzy number:

Maximize λ (43)

D. Constraints

i) Objective restrictions

$$W_1\sum_{i\in Trn}\left(c_i^{delay}\cdot\sum_{p\in Itv_i^{stn}}d_p\right)+W_2\sum_{i\in Trn}b_i \le s^*+(1-\lambda)(s^0-s^*) \tag{44}$$

ii) Interval restrictions

$$e_p-s_p\ge z_p+(\lambda-1)c_{z_p},\ p\in Itv \tag{45}$$

The real departure time cannot be earlier than the original departure time:

$$e_p\ge inie_p,\ p\in Itv \text{ and } h_p=1 \tag{46}$$

$$e_p-inie_p=d_p,\ p\in Itv \tag{47}$$

iii) Track restrictions

$$\sum_{l\in Trk_k}\eta_{pl}=1,\ p\in Itv_k \text{ and } k\in Stn \tag{48}$$

iv) Connectivity restrictions

$$e_p=s_{p+1},\ p\in Itv_i,\ p\ne last(Itv_i) \text{ and } i\in Trn \tag{49}$$

For each station, if two intervals use the same track, at least one of α and β is forced to be 1:

$$\eta_{pl}+\eta_{\tilde{p}l}-1\le\alpha_{p\tilde{p}}+\beta_{p\tilde{p}},\quad p,\tilde{p}\in Itv_k,\ p<\tilde{p},\ l\in Trk_k \text{ and } k\in Stn \tag{50}$$

One train can enter a station after the preceding train, which uses the same track, leaves it:

$$s_{\tilde{p}}-e_p\ge(f_k+(\lambda-1)c_{f_k})\alpha_{p\tilde{p}}-M\left(1-\alpha_{p\tilde{p}}\right),\quad p,\tilde{p}\in Itv_k \text{ and } k\in Stn \tag{51}$$

$$s_p-e_{\tilde{p}}\ge(f_k+(\lambda-1)c_{f_k})\beta_{p\tilde{p}}-M\left(1-\beta_{p\tilde{p}}\right),\quad p,\tilde{p}\in Itv_k \text{ and } k\in Stn \tag{52}$$

For each section, at least one of α and β is forced to be 1 because there is only one track:

$$\alpha_{p\tilde{p}} + \beta_{p\tilde{p}} = 1,\ p, \tilde{p} \in Itv_k \text{ and } k \in Sec \quad (53)$$

Headways for each section:

$$s_{\tilde{p}} - s_p \geq (hw_k + (\lambda - 1)c_{hw_k})\alpha_{p\tilde{p}} - M\left(1 - \alpha_{p\tilde{p}}\right),$$
$$p, \tilde{p} \in Itv_k \text{ and } k \in Sec \quad (54)$$

$$s_p - s_{\tilde{p}} \geq (hw_k + (\lambda - 1)c_{hw_k})\beta_{p\tilde{p}} - M\left(1 - \beta_{p\tilde{p}}\right),$$
$$p, \tilde{p} \in Itv_k \text{ and } k \in Sec \quad (55)$$

v) Auxiliary restrictions

$$d_{last(Itv_i)} - w_i \leq Mb_i \quad (56)$$

Since M is a very integer, the headway time constraints can be changed as below:

$$s_{\tilde{p}} - e_p \geq f_k + (\lambda - 1)c_{f_k} - M\left(1 - \alpha_{p\tilde{p}}\right) \quad (57)$$

$$s_p - e_{\tilde{p}} \geq f_k + (\lambda - 1)c_{f_k} - M\left(1 - \beta_{p\tilde{p}}\right) \quad (58)$$

$$s_{\tilde{p}} - s_p \geq hw_k + (\lambda - 1)c_{hw_k} - M\left(1 - \alpha_{p\tilde{p}}\right) \quad (59)$$

$$s_p - s_{\tilde{p}} \geq hw_k + (\lambda - 1)c_{hw_k} - M\left(1 - \beta_{p\tilde{p}}\right) \quad (60)$$

IV. CASE STUDY

This model is simulated on the busiest part of Jing-Hu high speed line, between Nanjing (Ning for short) and Shanghai (Hu for short). In the rest of this paper, "Hu-Ning Part" is used to represent this part of the Jing-Hu high speed line. Since Jing-Hu high speed line is double-track, we only consider the direction from Ning to Hu without loss of generality. All the models are solved by IBM ILOG CPLEX 12.2.

There are seven stations on the Hu-Ning Part, thereby 6 sections, whose lengths are 65110m, 61050m, 56400m, 26810m, 31350m and 43570m. Its daily service starts at 6:30am and ends at 11:30pm. As currently planned, there are 52 trains (14 high speed trains and 38 medium speed trains) from Jing-Hu line and 8 medium speed trains from Riverside line that go from Ning to Hu by the Hu-Ning part. The trains from Jing-Hu line are called self-line trains, while those from Riverside line are called cross-line trains. As in reality, self-line trains have higher priority than cross-line trains. As for self-line trains, the high speed trains have higher priority than the quasi-high speed trains. We did two studies as follows.

A. speed restriction in all section

When some natural hazards happened, like heavy storm and strong wind, railway will be greatly affected in a large area. In the simulation, we assume there is a speed restriction in all sections and the average limited speed ranges from 170km/h to 150km/h; the headway is set from 3 minutes to 2.5 minutes and the minimum separation time on track possession in each station is set to 1min.

First we use the original model to solve the problem, and get the follow results. When we set the speed as 150km/h and headway time as 3 minutes, the solution value is 2580587; there are 54 trains late for 30 minutes and 6 trains late for one hour; and the total delay time is 3052.95 minutes. When the speed is 170km/h and headway time is 2.5 minutes, the Solution value is 1481413; there are 55 trains late for 30 minutes and no train late for one hour; and the total delay time is 2248.45 minutes. Although the latter result is very exciting, it is a significant risk to take the speed of 170km/h, as the highest speed must brings the high operation cost and may arouse some new delays. Then we using the above results as the inputs of the fuzzy model the paper described before and get the follow results. The fuzzy member λ is 0.689117, which means the average speed is 156km/h and headway time is 2.8445 minutes; there are 60 trains late for 30 minutes, no train late for one hour; and the total delay time is 2799.4 minutes. We can see that the fuzzy optimization result improved greatly with little slack of constraints that means little risk and operation cost. Fig. 3 is the rescheduling timetable by fuzzy model. The gray lines mean the initial timetable and blue lines mean the rescheduling timetable.

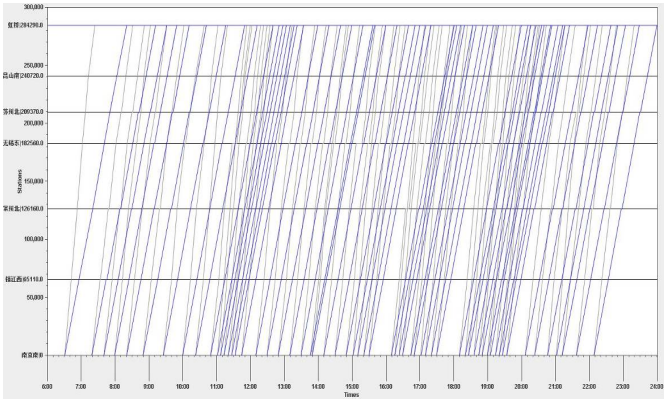

Figure 3. Rescheduling timetable with limited speed in all sections

B. speed restriction in one section

Sometimes equipment failure, like train signal failure, happens in some but not all the sections. In the simulation, we assume there is a speed restriction in first section and the limited speed ranges from 60km/h to 50km/h; the headway is also set from 3 minutes to 2.5 minutes; and the minimum separation time on track possession in each station is 1min.

First we use the original model to solve the problem and get the follow result. When the speed is 50km/h and headway time is 3 minutes, the solution value is 4040593; there are 52 trains late for 30 minutes and 8 trains late for one hour, and the total delay time is 3109.95 minutes. When the speed is 60km/h and headway time is 2.5 minutes, the solution value is 2518709; there are 56 trains late for 30 minutes and no train late for one hour, and the total delay time is 2328.45 minutes. Then we get the follow result using the fuzzy model the paper described before. The fuzzy member λ is 0.70606, which means the average speed is 53km/h and headway time is 2.85303 minutes; there are 60 trains late for 30 minutes, no train late for one hour, the total delay time is 2766.4 minutes. We can see that the optimization result also improved greatly with little slack of constraints. Fig. 4 is the rescheduling timetable with speed restriction in the first section.

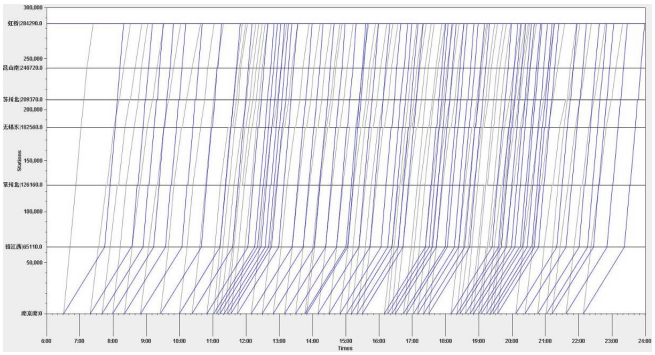

Figure 4. Rescheduling timetable with speed restriction in first section

These simulations are realized on the computer with Intel Core 2 Duo CPU E7500 and 2G Memory. Calculation time for the original model is about 4 seconds and it is less than 20 seconds for the fuzzy model.

V. CONCLUSION AND FUTURE WORK

This paper presents a fuzzy optimization model based tolerance approach for train rescheduling in speed restriction, which deal with the train running time at sections, train dwell time at stations, the headway time at sections and station as the fuzzy parameters. The simulation on Jing-Hu high speed line reveals that the fuzzy optimization result improved greatly with little slack of constraints, which means we can get a new timetable with fewer total delay time as well as the number of seriously impacted trains in safety and lower limited speed and enough headway time .

There remain many interesting areas to explore around membership functions of fuzzy parameters, which may be piecewise linear or more complex form in practice. In addition, there are also some stochastic factors in the timetable rescheduling problem. The more accurate the membership function is, the better result the uncertain optimization model gets. Our ultimate goal is to develop a real-time rescheduling system to significantly improve operation management and scheduling efficiency in the future.

ACKNOWLEDGMENT

This work has been supported by National Natural Science Project (Grant: 61074151), China National Technique Supporting Plan Project (Grant: 2008BAG11B01, 2009BAG12A10) and Chinese State Key Laboratory of Rail Traffic Control and Safety Independent Project (Grant: RCS2008ZZ003, RCS2009ZT002).

REFERENCES

[1] Medium-Long Term Railway Network Plan (2008 Revision), China Railway Ministry, August 2008.

[2] S. Zhang, The Beijing-Shanghai high-speed railway system optimization research, China Railway Publishing House, 2009.

[3] A.D'Arianoa, D. Pacciarellib and M. Pranzoc, A branch and bound algorithm for scheduling trains in a railway network, European Journal of Operational Research, vol.183, pp.643-657, 2007.

[4] M.J. Dorfman and J. Medanic, Scheduling trains on a railway network using a discrete event model of railway traffic, Transportation Research Part B, vol.38, pp.81-98, 2004.

[5] T.W. Qiang and H.Y. Hau, Knowledge-based system for railway scheduling, Data & Knowledge Engineering, vol.27, pp. 289-312, 1998.

[6] S.Q. Dong, J.Y. Wang, H.F. Yan, Tabu search for train operation adjustment on double-track line, China Railway Science, vol.26, pp.114-l19, 2005.

[7] C.Z. Yi, Tabu search algorithm on location for railway baggage and parcel base and distribution Sites, Control and Decision, vol.21, pp.1316-1320, 2006.

[8] W.S. Lin and J.W. Sheu, Adaptive critic design of automatic train regulation of MRT system, IEEE ICIT. China, pp.1-7, 2008.

[9] P. Ren, N. Li, L.Q. Gao, Bi-criteria passenger trains scheduling optimal planning based on integrated particle swarm optimization. Journal of System Simulation, vol.19, pp.1449-1452, 2007.

[10] X.S. Zhou and M. Zhong, Bi-criteria train scheduling for high-speed passenger railroad planning applications, European Journal of Operational Research, vol.16, pp.752—771, 2005.

[11] L.M. Jia, Fuzzy control and decision-making with its application in railway automation, doctoral thesis of China Academy of Railway Science, 1991.

[12] K. Huang, Study on the application of rough Set-Based knowledge acquisition and decision in train traffic control. doctoral thesis of China Academy of Railway Science, 2004.

[13] L. Kroon, Stochastic improvement of cyclic railway timetables, Transportation Research Part B, vol.42, pp.553–570, 2008.

[14] Y. Lee, C.Y. Chen, A heuristic for the train pathing and timetabling problem, Transportation Research Part B, vol.43, pp.837–851,2009.

[15] W.X. Zha, G. Xiong. Study on the dynamic performance of the train running time in the section. Systems Engineering, vol.19, pp.47-51, 2001.

[16] X.C. Zhang, A.Z. Hu, Analysis of β-function distribution for deviation of train running time in section. Journal of The China Railway Society, vol.18, pp.1-6, 1996.

[17] X.M. Shi, Research on train headway time of high speed railway in China. Chinese Railways, vol.5, pp.32-35, 2005.

2011 IEEE International Conference on Fuzzy Systems
June 27-30, 2011, Taipei, Taiwan

Online Neuro-Fuzzy CANFIS Hidden-Node Teaching

Eiji Mizutani
Department of Industrial Management
National Taiwan University of Science and Technology
Taipei, Taiwan
Email: eiji@mail.ntust.edu.tw

Jing-Yun Carey Fan
Coach Team/Mobile Division
Zoran Corporation
Hsinchu, Taiwan
Email: goldfish@gmail.com

***Abstract*—On-line first-order backpropagation (BP) has been widely employed for optimizing a multi-layer neural network and a fuzzy neural network. When BP is applied to a TSK fuzzy system, the interpretability of fuzzy rules may be lost. We describe a simple and effective remedy for the loss by casting the posed optimization problem into a general Bolza-type optimal-control mold so as to include stage costs on top of the terminal cost; this is what we called the (on-line) hidden-node teaching. Our on-line learning scheme turns out to be useful not only in optimizing a large model, a so-called CANFIS neuro-fuzzy modular network, but also in enhancing its generalization capacity. The fundamental concept is that each (local) expert network is supervised individually by hidden-node teaching for minimizing a stage cost while all local-expert modules are encouraged to cooperate in reducing the terminal cost simultaneously. Furthermore, we show how to construct a CANFIS modular network in order to alleviate the so-called curse of dimensionality that frequently hampers the design of fuzzy systems. In simulation, our concepts have been demonstrated in the letter recognition benchmark problem as well as in small regression and XOR-classification tasks.**

Keywords–CANFIS modular networks; hidden-node teaching.

I. Introduction

Consider a typical single-output fuzzy model with a given set of M fuzzy "if-then" rules; its final output y may be produced as

$$y = \sum_{p=1}^{M} w_p h_p, \tag{1}$$

where h_p, each of *then*-part outputs, is weighted by w_p, the firing strength of rule p, which is determined by *if*-part of fuzzy membership functions (MFs). When each h_p is expressed as a *linear* system, as shown next, the preceding fuzzy model is a well-known TSK (Takagi-Sugeno-Kang) fuzzy system:

$$h_p = \theta_{0,p} + \sum_{i=1}^{S} x_i \theta_{i,p}, \tag{2}$$

where S is the dimension of the input vector $\mathbf{x}$, and $\theta_{i,p}$ (with bias $\theta_{0,p}$) are the linear parameters. Since TSK was developed in 1980s [22], [21], it has enjoyed great popularity in diverse contexts, probably due to its simple linear then-part structure.

Our motivating example is a simple data fitting (regression) task described for Fig.1 on p.118 in [22], a task described for the original Takagi-Sugeno fuzzy system. In our interpretation, linear then-parts are given as h_p in the form of Equation (2), where $p = 1, 2$, for the following two fuzzy rules: (Rule 1) if input x is "small," then use linear h_1, and (Rule 2) if input x is "large," then use linear h_2. Those two fuzzy rules cooperate in producing final responses; this is what we call *complementary learning*. When we attack the posed regression task in conjunction with the "standard" on-line first-order backpropagation (BP), a problem often arises that h_p, the *then*-part of Rule p, may deviate from the data distribution beyond our expectation (hence, the loss of interpretability); Figure 1 shows such a situation. In the original Takagi-Sugeno fuzzy system [22], given *if*-part MF setups, RLSE (recursive least-squares estimation), implemented by the well-known Sherman-Morrison inverse formula, is applied in "batch" mode to optimizing *then*-part *linear* parameters. (The same method is used in ANFIS hybrid-learning.) Such a batch-mode RLSE-based approach may yield more interpretable then-part results than on-line first-order BP, but its batch-mode use of the Sherman-Morrison formula is not recommendable (see [8], [7]). More important, direct RLSE is not applicable to "nonlinear" then-part that can overcome the so-called curse of dimensionality when S, the dimension of inputs, is large. Later in Sec.III-B, we demonstrate our approach to the letter recognition benchmark problem ($S = 16$).

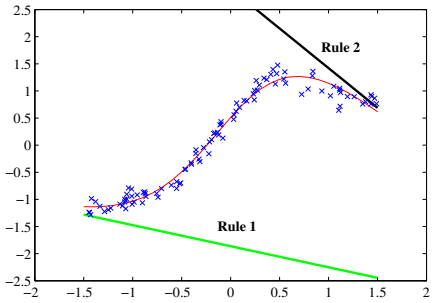

Fig. 1. An after-learning result obtained by "standard" on-line first-order BP on a TSK fuzzy system with two rules in a regression task that involves 100 data (marked by "×"), adapted from p.118 in [22]. The *then*-part linear rule's output deviates significantly from the data distribution in an unexpected manner.

In what follows, we describe a Bolza-type optimal-control formulation that can resolve the preceding problem indicated in Figure 1. We then discuss how to mitigate the curse of dimensionality, which becomes a serious obstacle in the design of fuzzy systems when the number of inputs increases. Throughout this paper, we highlight CANFIS (Co-Active Neuro-Fuzzy Inference System) [5], for its systematic design methodology offers a useful and consistent framework for describing representative adaptive-network models; such as

an aforementioned TSK, MLP (multilayer perceptron), RBFN (radial basis function network), and modular networks. In all numerical tests that follow, the bell-shaped Gaussian MF is used for the if-part of each fuzzy rule, and its center and width parameters are fine-tuned during the learning phase.

II. On-line CANFIS hidden-node learning

The first-order backpropagation (BP) is a simplified form of the Kelley-Bryson optimal-control gradient procedure (see [6] and references therein); it is originally contrived to attack a general Bolza-type optimal-control problem. We explain how such a general problem formulation inspires an elaborate neuro-fuzzy learning algorithm.

A. The Bolza-type optimal-control formulation

We describe an N-stage (discrete-time) optimal-control problem of Bolza in the framework of N-layer MLP-learning, where stage s (i.e., layer s) has P_s states (or nodes), and stage 1 corresponds to the first (nominal) input layer. The objective function J below includes an intermediate *stage cost* L^s at the hidden layer s as well as the *terminal cost* E at layer N (last stage):

$$J(\boldsymbol{\theta}) = \sum_{s=2}^{N-1} L^s(\mathbf{y}^s, \boldsymbol{\theta}^s) + E(\mathbf{y}^N), \quad (\text{with } \mathbf{y}^1 \text{ given}) \tag{3}$$

where $E(.)$, the terminal cost at stage N, depends only on terminal *state* vector $\mathbf{y}^N$ of length P_N (per datum), and $L^s(.,.)$, the cost at stage s, depends on both the P_s-dimensional *state* vector $\mathbf{y}^s$ of "after-node" outputs and the n_s-dimensional *control* vector $\boldsymbol{\theta}^s$ of weight parameters (including thresholds); hence, the length $n_s \equiv (1+P_s)P_{s+1}$ in MLP-learning. Equation (3) may consist of squared residuals on each (training) datum d (for $d=1,...,D$) at each stage s, where each residual vector $\mathbf{r}_d^s$ (of length P_s) is evaluated as the difference between the node-output vector $\mathbf{y}_d^s$ and the target vector $\mathbf{t}_d^s$. In fact, it is often the case that the terminal cost is defined as the squared-error measure below:

$$\begin{aligned} E(\mathbf{y}^N) &= \frac{1}{2}\sum_{d=1}^{D}\sum_{k=1}^{P_N}(y_{k,d}^N - t_{k,d}^N)^2 \\ &= \frac{1}{2}\sum_{d=1}^{D}\|\mathbf{y}_d^N - \mathbf{t}_d^N\|_2^2 = \frac{1}{2}\sum_{d=1}^{D}\mathbf{r}_d^{N\top}\mathbf{r}_d^N. \end{aligned} \tag{4}$$

Likewise, the stage cost $L^s(.,.)$ $(1<s<N)$ can be defined as

$$\begin{aligned} L^s(\mathbf{y}^s, \boldsymbol{\theta}^s) &= \frac{1}{2}\sum_{d=1}^{D}\sum_{k=1}^{P_s}(y_{k,d}^s - t_{k,d}^s)^2 + \frac{1}{2}\sum_{j=1}^{n_s}\left(\theta_j^s\right)^2 \\ &= \frac{1}{2}\sum_{d=1}^{D}\mathbf{r}_d^{s\top}\mathbf{r}_d^s + \frac{1}{2}\boldsymbol{\theta}^{s\top}\boldsymbol{\theta}^s, \end{aligned} \tag{5}$$

where the last quantity is a so-called weight-decay term for penalizing large weights in modulus, and $\mathbf{r}_d^s$ is the P_s-length vector of hidden residuals on datum d evaluated at intermediate layer s $(1 < s < N)$. The introduction of such a stage

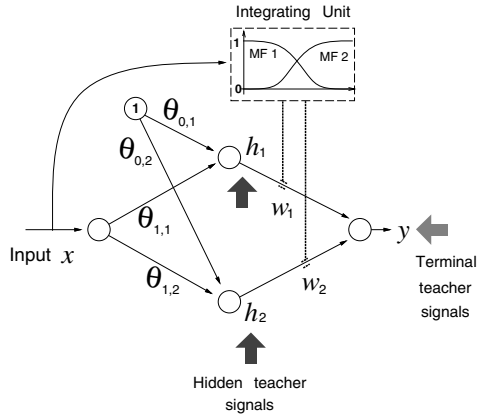

Fig. 2. A 1-2-1 MLP representation of CANFIS with two linear rules, in which two terminal weights, w_1 and w_2, are the firing strengths of corresponding two rules, Rule 1 and Rule 2, respectively, obtainable from the fuzzy membership functions. The posed network is equivalent to a TSK fuzzy system (see p.377 [5]). For hidden-node teaching, teacher signals are presented to the hidden layer as well as to the terminal output layer. In this model, each of two local-expert is a linear perceptron; expanding each of them to an MLP leads to a CANFIS modular network (see Figure 4).

cost $L^s(.,.)$ at intermediate stages (i.e., at *hidden layers*; $1<s<N$) is what we call *hidden-node teaching* [6], [9], [13]. For MLP-type node dynamics at layer s, $\mathbf{y}^s \equiv \mathbf{f}(\mathbf{x}^s, \boldsymbol{\theta}^s)$, we define two types of *node sensitivities*: (1) after-node sensitivity: $\boldsymbol{\xi}^s \equiv \frac{\partial J}{\partial \mathbf{y}^s}$ and (2) before-node sensitivity: $\boldsymbol{\delta}^s \equiv \frac{\partial J}{\partial \mathbf{x}^s}$; the former is used (as state sensitivity) in optimal control, whereas the latter is well-known for a generalized delta rule in the neural-network literature (e.g., see [6], [13]). Then, the Kelley-Bryson optimal-control gradient formula (on datum d with subscript d suppressed) is given by

$$\underbrace{\boldsymbol{\xi}^s}_{P_s\times 1} = \boldsymbol{\Theta}_{\text{void}}^{s^T}\boldsymbol{\delta}^{s+1} + (\mathbf{y}^s - \mathbf{t}^s), \tag{6}$$

where $\boldsymbol{\Theta}_{\text{void}}^s$ denotes a $P_{s+1}\times P_s$ matrix of parameters at stage s excluding "threshold" parameters (if any at stage s). By the above formula, the node sensitivities are propagated backwards in a layer-by-layer (i.e., stagewise) fashion.

B. CANFIS with linear rules

As shown in Equation (2), the *then*-part of TSK fuzzy rules is identical to a "linear" *perceptron*. Given M fuzzy rules, TSK combines (at most) M perceptrons in a fuzzy fashion on each datum. This can be organized into our familiar MLP-type architecture. In this perspective, a single-output TSK can be expressed as an S-M-1 MLP with M "linear" *hidden* nodes (hence, $P_1 = S$; $P_2 = M$; $P_3 = 1$). Each hidden-node output is given by h_p, as defined in Equation (2), where the parameters $\theta_{i,p}$ are the weights between the input layer and hidden layer (with bias $\theta_{0,p}$). The weights (with no bias) between the terminal and hidden layers correspond to firing strengths w_p, which are *data-dependent* values.

Example: A single-input single-output TSK with two rules.

A TSK with two fuzzy rules ($M=2$) can be constructed as a CANFIS neuro-fuzzy network with two perceptrons since

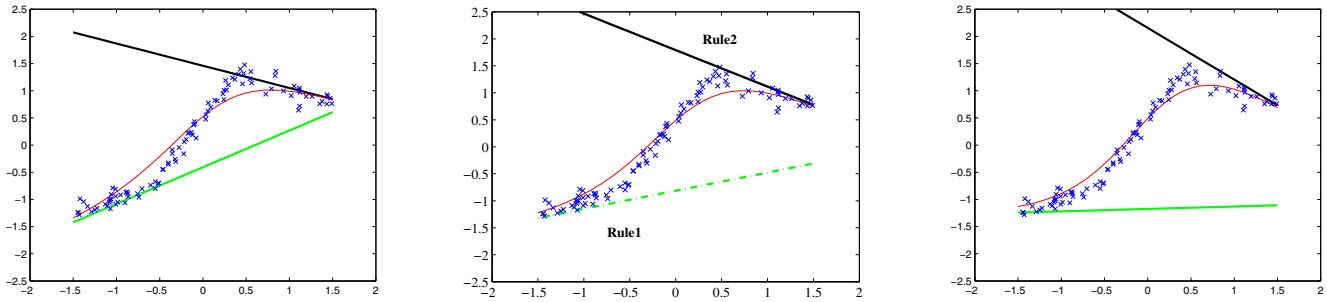

(a) $\tau = 0.7$ (b) $\tau = 0.8$ (c) $\tau = 0.9$

Fig. 3. Data fitting results obtained by on-line hidden-node teaching with three choices of τ (for designating the local-expert region) in Equation (8): (a) $\tau = 0.7$; (b) $\tau = 0.8$; and (c) $\tau = 0.9$. The results indicate that $\tau \approx 0.7$ would be a good choice in the posed problem. Compared with Figure 1, where no hidden-node teaching is applied, it is clear that hidden-node teaching is effective in maintaining rules' *then*-part interpretability to meaningful limits. In each case, all the parameters in both *if*-part and *then*-part are updated on-line until the same error level is achieved.

it can be put in a three-layer ($N = 3$) 1-2-1 MLP mold having single-input and single-output nodes ($P_1 = P_3 = 1$) with two *linear* hidden-node functions ($P_2 = 2$), as illustrated in Figure 2: Here, two terminal weights, denoted by w_1 and w_2, are the *firing strengths* calculated at the integrating unit of fuzzy MFs in response to each input x, and two hidden-node "linear" outputs h_i correspond to *then*-part of fuzzy rules; that is, Equation (2) reduces to

$$h_i = \theta_{0,i} + x\theta_{1,i} \quad \text{for } i = 1, 2. \tag{7}$$

The final output y is generated by $y = w_1 h_1 + w_2 h_2$, as shown in Equation (1) with $M = 2$. □

The above transformation of a fuzzy system to such an MLP-type network as in Figure 2 is a key ingredient in design for CANFIS (see p.371 [5] for more details).

C. TSK hidden-node teaching effects in a motivating example

On-line first-order BP-based algorithms may be attractive in attacking a large-scale problem. However, when on-line BP is applied to optimizing both *if*-part and *then*-part of fuzzy rules, after-learning knowledge extraction may not always be possible. Here, for the initial setup of fuzzy rules, the *then*-part *linear* parameters are randomly initialized in a small range, as usually done for MLP-learning. In order to attain a higher input-output mapping precision, on-line BP may adapt the parameters of initial fuzzy rules significantly, ending up with meaningless fuzzy rules. This is a dilemma between mapping precision and interpretability (see pp.382–387 [5]). Back to our motivating example, Figure 1 illustrates such a dilemma; this phenomenon is partly due to a fact that the standard supervised learning uses a terminal cost alone, as in Equation (4), and thus only encourages the final combined output to be close to the desired output; this is the nature of *complementary* learning. In the spirit of fuzzy systems, however, the *then*-part linear output of each rule should match up to the desired output when its firing strength is large enough; this is the original claim made for a TSK (see p.118 in [22]).

Hidden-node teaching can handle this situation with a CANFIS network depicted in Figure 2. The posed two-rule CANFIS has two terminal weights: $\mathbf{\Theta}_{\text{void}} \equiv [w_1, w_2]$. Now, suppose that a "terminal" teacher signal, denoted by t^3, is presented to the terminal node at layer 3 and another "hidden" teacher signal, t_i^2, to hidden-node i at layer 2; then, the scalar version of the on-line hidden-node teaching BP-formula (6) is given by

$$\xi_i^2 = w_i(y_1^3 - t^3) + (y_i^2 - t_i^2) = w_i(y - t^3) + (h_i - t_i^2),$$

where $\xi^3 = \delta^3 = (y - t^3)$; y_k^s is the kth node output at layer s; and the last equality holds owing to Equations (1) and (2). In our numerical experiments that follow, we introduce scalar τ as a threshold for designating local-expert regions, and the same desired outputs t are presented at both terminal and hidden layers in our model, yielding the following BP-formula (with superscripts omitted for simplicity):

$$\xi_i = \begin{cases} w_i(y - t) + (h_i - t), & \text{if } w_i \geq \tau \\ w_i(y - t), & \text{otherwise.} \end{cases} \tag{8}$$

Since the hidden-node functions are also *linear*, as shown in Equation (7), we have $\delta_i = \xi_i$ at hidden node i. We thus obtain the gradient vector below for then-part parameters $\boldsymbol{\theta}$ in response to input x:

$$\frac{\partial J}{\partial \boldsymbol{\theta}} = \left[\frac{\partial J}{\partial \theta_{0,1}}, \frac{\partial J}{\partial \theta_{1,1}}, \frac{\partial J}{\partial \theta_{0,2}}, \frac{\partial J}{\partial \theta_{1,2}}\right]^T = [\delta_1, x\delta_1, \delta_2, x\delta_2]^T,$$

for which the weight-decay term is omitted from Equation (5). Once a (scalar) gradient element $g = \frac{\partial J}{\partial \theta}$ is evaluated for any parameter θ, it is used to update θ on-line by

$$\begin{cases} \Delta\theta = -\eta g + \beta \Delta\theta_{\text{old}}, \\ \theta_{\text{new}} = \theta_{\text{old}} + \Delta\theta, \\ \Delta\theta_{\text{old}} \leftarrow \Delta\theta, \end{cases} \tag{9}$$

where η is a learning rate and β a momentum term.

Figure 3 shows our numerical demonstration with three different choices of τ for the hidden-node teaching BP-formula (8). The larger the value τ is, the smaller each local-expert region is. When $\tau = 1$ in Equation (8), essentially no hidden-node teaching applies. This preliminary investigation

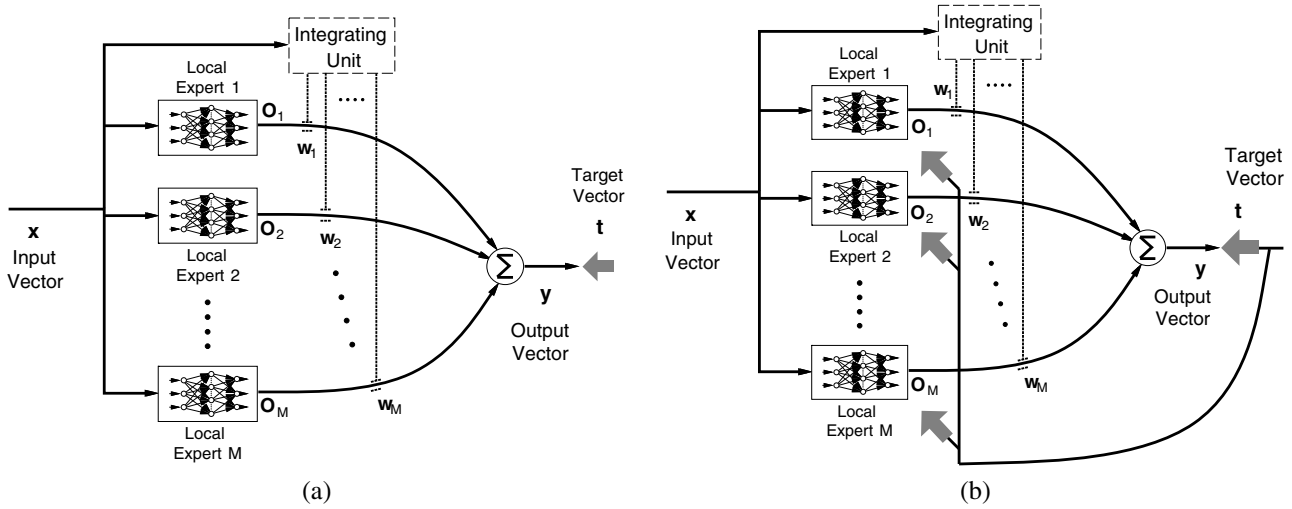

Fig. 4. An architectural comparison between CANFIS modular networks (a) without and (b) with hidden-node teaching [see Eq.(11)]. Here, *then*-part local-expert MLPs are encouraged to cooperate with each other within overlapped regions, where their corresponding *if*-part fuzzy MFs are overlapped in the input space.

suggests $\tau \approx 0.7$. Compared with Figure 1, the then-part outputs are kept within the data-distribution limits. In this way, hidden-node teaching can maintain fuzzy rules' interpretability.

D. CANFIS modular networks

Next, we advance to "non-linear" then-part of fuzzy rules that can circumvent many problems arising in "linear" then-part fuzzy rules. In Equation (7), each then-part h_i is a simple "linear" perceptron (with only two weights in a single-input case). If each h_i is expanded to include any number of "hidden" layers (with nonlinear hidden-node functions), then each amounts to an MLP (see p.377 [5] for such a transformation); the resulting model is a CANFIS with "neural" rules; or, a CANFIS modular network with local-expert MLPs. Figure 4 describes a typical CANFIS modular network, in which the final combined output is given by

$$\mathbf{y} = \sum_{i=1}^{M} w_i \mathbf{o}_i, \tag{10}$$

where w_i is the firing strength of Rule i, and $\mathbf{o}_i$ the output of *then*-part local-expert MLP i. To emphasize the usefulness of the posed model, we later show how to approach the UCI letter recognition benchmark (26-class pattern classification) problem that involves with 16 input features.

As described earlier for Figure 1, in standard supervised learning with terminal residuals in Equation (4) alone, the output of each then-part expert-MLP may differ substantially from the desired output even in its own local-expert region (e.g., see Fig.13.15 on p.391 [5]) due to the nature of *complementary learning*. That is, when a modular network (that consists of M local-expert MLPs) is optimized simultaneously, only the final outcome $\mathbf{y}$ is made close to the terminal desired output $\mathbf{t}$; here, each local-expert output $\mathbf{o}_i$ may not reproduce the terminal desired output $\mathbf{t}$ accurately even when the input $\mathbf{x}$ comes right into its own territory. In the spirit of fuzzy systems, it may be adequate to encourage each expert to generate the terminal desired outputs when the input $\mathbf{x}$ falls into its own local-expert area. For this reason, hidden-node teaching may apply to a CANFIS modular network, as shown in Figure 4(b).

By hidden-node teaching, we may designate a "principal" local-expert MLP based on the magnitude of firing strengths w_i. From the concept behind Equation (8), we say that on each datum, local-expert MLP i is a principal expert if its firing strength w_i is greater than or equal to a threshold τ. By hidden-node teaching, the principal local-expert MLP is encouraged to reproduce the same target $\mathbf{t}$ as presented at the terminal layer. To this end, Equation (8) is modified as

$$\boldsymbol{\xi}_i = \begin{cases} w_i(\mathbf{y}-\mathbf{t}) + (\mathbf{o}_i - \mathbf{t}), & \text{if } w_i \geq \tau \\ w_i(\mathbf{y}-\mathbf{t}), & \text{otherwise} \end{cases}, \tag{11}$$

where term $(\mathbf{o}_i - \mathbf{t})$ is a "hidden" residual vector for each expert-MLP i evaluated at its final output layer [see Fig.4(b)].

We summarize a general computing procedure below for CANFIS modular-network learning with hidden-node teaching using the same symbols used in Figure 4:

Algorithm for CANFIS with M local-expert MLPs in Fig.4:

(1) Do forward pass in the integrating unit of fuzzy (Gaussian) MFs to calculate M rules' firing strengths w_i (typically by the product rule).
(2) Do forward pass in each local-expert MLP i to evaluate MLP's output vector $\mathbf{o}_i$, the output of *then*-part of Rule i, (when $w_i > 0$) for $i = 1, ..., M$.
(3) Evaluate the final CANFIS output $\mathbf{y} = \sum_{i=1}^{M} w_i \mathbf{o}_i$, and then compute the terminal residual vector $\mathbf{r} = \mathbf{y} - \mathbf{t}$.
(4) For each local-expert MLP i ($i = 1, ..., M$), repeat the following backward-pass procedure:
   (a) Propagate back the terminal after-node sensitivity vector, residual vector $\mathbf{r}$, to local-expert MLP i.
   (b) If Rule i is fired strongly enough [i.e., $w_i \geq \tau$ in Eq.(11); see also Eq.(8)], then compute the hidden

residual vector and add it to the back-propagated after-node sensitivity signals.

(c) Continue the backward pass for the remaining stages to update the weights.

(5) Do backward pass on the integrating unit of fuzzy MFs. □

General parameter-updating formulas for use in Steps (4) and (5) can be found on p.379 [5]. In Step (5), MF-parameters may be updated on-line (on each datum); alternatively, the gradient information of MF-parameters may be accumulated over all the training data for the "batch-mode" fine-tunings (see [4], [10]), while the other parameters of local-expert MLPs are updated on-line.

Furthermore, a so-called *truncation filter* function (see p.380 [5]) may be introduced; for instance, in attacking classification problems with binary target values, the kth residual at node k is set equal to zero for any final output y_k beyond the target value t_k, *ON* $(+1)$ or *off* (-1); this implies the following residual evaluation:

$$r_k = \begin{cases} 0 & \text{if } t_k = \textit{ON} \text{ and } y_k \geq \textit{ON} \\ 0 & \text{if } t_k = \textit{off} \text{ and } y_k \leq \textit{off} \\ y_k - t_k & \text{otherwise.} \end{cases} \quad (12)$$

Here, the kth element of final outputs $\mathbf{y}$ [see Equation (10) and Figure 4(b)] is given by

$$y_k = \sum_{i=1}^{M} w_i o_{i,k},$$

when M expert-MLPs are employed. The posed scheme is related to a threshold least-mean-square procedure (e.g., see [20]). If "hidden" target signals at the output layer of each expert-MLP are the same as the "terminal" target ones for hidden-node teaching [see Fig.4(b)], then those associated hidden residuals may also be subject to Equation (12), for which y_k is replaced with $o_{i,k}$, the kth output of expert-MLP i.

III. Numerical Experiments

We explain more about the learning capacity of CANFIS models, showing numerical evidence obtained in the well-known XOR (two-class pattern classification) problem and the UCI letter recognition benchmark problem.

A. The XOR problem by CANFIS with two linear rules

In the literature, the XOR problem is usually solved by a 2-2-1 MLP; yet, when the so-called weight-sharing is applied to hidden weights, it can be solved by a 1-2-1 MLP with $x_1 + x_2$ as input. The solution weights of the 1-2-1 MLP can be always expanded as those of a corresponding 2-2-1 MLP (see [14] for details). Similarly, for attacking the XOR problem, a conventional fuzzy system usually needs four rules: two MFs on each input x_i $(i = 1, 2)$. In this section, we demonstrate a 1-2-1 MLP-structured CANFIS in Figure 2 for solving the XOR problem. By the weight-sharing concept, the original four XOR-data reduce to three data, as shown in the right-most column in Table I. In "standard" MLP-learning, the hidden-node activation function should be nonlinear. For instance, an MLP with any number of "linear" hidden nodes is unable to solve the XOR problem because a linear transformation of another linear transformation is just *linear*. One may wonder why a CANFIS with two *linear* hidden nodes has a "nonlinear" mapping capacity. This is simply because the terminal weights w_i are firing strengths, whose values are data-dependent (see Figure 2).

TABLE I

FOUR DATA OF THE XOR, TWO-BIT PARITY, PROBLEM: (COLUMN 1) TARGET VALUE, t; (COLUMNS 2 AND 3) TWO-BIT INPUTS, x_1 AND x_2; AND (COLUMN 4) $x_1 + x_2$ FOR THE WEIGHT-SHARING CASE.

Target	Two inputs		Sum of inputs
t	x_1	x_2	$x_1 + x_2$
-1	$+1$	$+1$	$+2$
$+1$	-1	$+1$	0
$+1$	$+1$	-1	0
-1	-1	-1	-2

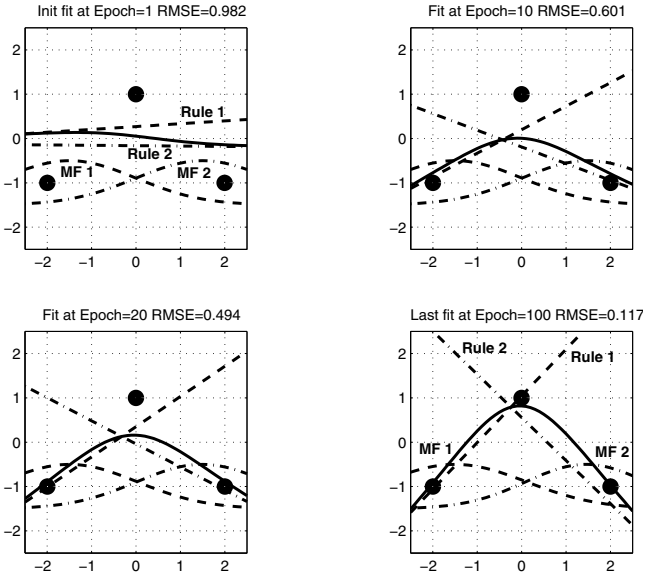

Fig. 5. A learning progress of a CANFIS with two linear rules, a 1-2-1 MLP-structured CANFIS in Figure 2, for solving the XOR problem: Displayed are the terminal CANFIS output (solid line) as well as two *if*-part MF outputs & two *then*-part linear outputs at epochs 1 (upper left), 10 (upper right), 20 (lower left), and 100 (lower right). The three dots denote the three data points, resulting from our weight-sharing; see the right-most column in Table I. The CANFIS is trained by on-line hidden-node teaching with $\tau = 0.95$ in Equation (8).

Figure 5 shows four snapshots of the CANFIS output during on-line learning. As the number of epochs increases, the output approaches the three data points. In this way, it can be readily confirmed that the CANFIS with only two *linear* rules solves the XOR problem perfectly. The 1-2-1 MLP-structured CANFIS (in Figure 2) even with (two) *linear* hidden nodes has a great nonlinear mapping capacity, which is derived from the *data-dependent* terminal weights, firing strengths of two linear rules. By contrast, in the standard MLP-learning, terminal weights are *common* to all data points (hence, an MLP with "linear" hidden nodes would never solve XOR). This is a fundamental distinction between a MLP-structured CANFIS

and a standard MLP.

In the XOR or higher-dimensional parity problems, a standard MLP (with sigmoidal-shaped hidden-node functions) tends to fail due to hidden-node saturations. Originally, our hidden-node teaching scheme has been designed to alleviate such malicious hidden-node saturation problems for MLP-learning [9], although saturations may be necessary to some extent for parity solutions (see [14] for proofs). In seven-bit parity, for instance, a 7-4-1 MLP (with only four tanh hidden nodes) can develop *insensitivity* to initial weights owing to hidden-node teaching; that is, it can always solve the 7-bit parity problem (128 data) * "perfectly."

The above *weight-sharing* concept is applicable to any number of (input) bits of parity; in 21-bit parity, for instance, the weight-sharing concept leads to a 1-11-1-MLP-structured CANFIS with 11 linear rules; this is because 21-bit parity can be readily solved by a standard 1-11-1 MLP, which yields a solution weight vector for a 21-11-1 MLP (see [14]). By contraries, the standard TSK fuzzy system needs to use at least 2^{21} rules since at least two fuzzy MFs, the minimum number of MFs, must be set up on each input feature. This is the so-called "curse of dimensionality" problem, which commonly arises in the design of many other fuzzy systems also. Unfortunately, the weight-sharing concept may not apply in general (see the letter recognition problem). In such a case, CANFIS modular networks may be useful in bypassing the curse of dimensionality through the subset selection of input features (see other applications in [4], [10]).

B. The UCI letter recognition benchmark problem

Next, we attack a larger and more realistic letter recognition (26-class pattern classification) benchmark problem available at the UCI machine learning repository [1]. The problem contains 16,000 patterns for training and 4,000 for test; each pattern consists of 16 extracted attributes (inputs) and 26 capital letters, English alphabet: A to Z (of 20 different fonts); hence, 26 classes in total. As a preprocessing, the training data set is normalized to *zero mean* and *unit variance* for each attribute. Accordingly, the test data set is preprocessed using the average of the training data set; here, we did not use any information of the average of test data. A straightforward application of TSK-type fuzzy system may end up with 2^{16} *then*-part linear functions (i.e., linear local-expert perceptrons in Figure 2) when two MFs, the minimum number of MFs, are designed on each input feature. This is the aforementioned "curse of dimensionality" problem, which often occurs in many fuzzy systems. To circumvent this dimensionality obstacle, we apply fuzzy partitioning only to a subset of inputs (see [4], [10]) and use local-expert MLPs as nonlinear *then*-part of fuzzy rules.

In the UCI-letter recognition problem, the 12th input (x_{12}) alone may be partitioned in a fuzzy fashion; e.g., with two "intuitively-obvious" linguistic labels on it: *small* and *large*.

*The Matlab code for 7-bit parity attacked by a 7-4-1 MLP is available at www.ieor.berkeley.edu/People/Faculty/dreyfus-pubs/hidteach.m for reference.

TABLE II
THE ERROR-RATE RESULTS IN THE UCI-LETTER RECOGNITION, AVERAGED OVER TEN TRIALS, OBTAINED AT (PRE-SET LIMIT) EPOCH 500 BY CANFIS HAVING TWO 16-70-50-26 (LOCAL EXPERT) MLPS, (IN COLUMNS 2 AND 3) WITH HIDDEN-NODE TEACHING ($\tau = 0.7$) AND (IN COLUMNS 4 AND 5) WITHOUT IT, IN CONJUNCTION WITH THE TRUNCATED FILTER FUNCTION FOR BOTH HIDDEN AND TERMINAL RESIDUALS. THE LAST ROW SHOWS THE ERROR RATE OBTAINED BY A SIMPLE COMMITTEE METHOD THAT EMPLOYED TEN TRAINED CANFIS MODELS.

	With hid-teach		No hid-teach	
	Train	Test	Train	Test
Average error (%)	0.19	3.43	0.35	3.42
Committee error (%)	0.13	2.35	0.25	2.43

This is because the distribution of x_{12} appeared to spread relatively widely, but our "improvisatory" choice of a single input feature x_{12} is purely for our testing purpose of CANFIS modeling to the letter recognition problem. In our experiment, we employ a CANFIS modular network with two local experts ($M = 2$), each of which is a two-hidden-layer 16-70-50-26 MLP (with 6,066 weights), the same-size MLP architecture used in [19], [12] with tanh hidden-activation and *linear*-output nodes. The posed CANFIS is optimized by *on-line* first-order BP (with or without hidden-node teaching) using momentum term 0.8 [$\beta = 0.8$ in Eq.(9)] and learning rates: $\eta_{h1} = 1 \times 10^{-4}$ for the hidden weights at Stage 1, $\eta_{h2} = 8 \times 10^{-5}$ for those at Stage 2, $\eta_o = 5 \times 10^{-5}$ for terminal weights. The integrating unit consists of two Gaussian MFs having the initial center positions -1.5 and 1.5 with the same width 1.0 initially. Those MFs are updated in batch-mode with a very small learning rate 1×10^{-8} merely for the fine-tuning purpose, whereas the two local-expert MLPs are trained in on-line mode with the above learning rates.

Table II shows the results obtained (at the pre-set limit epoch 500) by a CANFIS modular network with two local-expert 16-70-50-26 MLPs with or without hidden-node teaching. The last row shows the results obtained by the simple committee method (for model-averaging; see Ch.8 in [2]) using ten weight-value sets obtained at final (i.e., pre-set limit) epoch; each of those resulted from the ensemble over ten optimized CANFIS models. In general, hidden-node teaching may serve as a constraint, slowing down the learning process and resulting in a lower mapping precision. In this application, however, the hidden-node teaching results allude to an improvement in speed and accuracy with respect to training error rates; this may be due to increased "hidden" residuals (in addition to terminal residuals).

IV. CONCLUDING REMARKS AND FUTURE DIRECTIONS

The CANFIS design methodology may be regarded most simply as a way of converting an original TSK model into an MLP-type structure, but it can be readily extended to a more sophisticated CANFIS modular network (see p.377 [5]). This perspective makes CANFIS conceptually differ greatly from other network-based fuzzy models including a fuzzy neural network (e.g., see [3]). A key concept behind CANFIS modular-network learning is that, by selecting an appropriate

subset of input features, we can circumvent the so-called curse of dimensionality that frequently arises in any fuzzy systems. Since each local-expert MLP has a great learning capacity, any choice of small input subsets to the integrating unit may not deteriorate the overall learning performance. In the preceding application examples, we have designed CANFIS models by choosing only one feature for fuzzy partitioning, but our numerical test shows encouraging results (see also [4], [10] for other applications).

Yet another advantage of our CANFIS design is that all the parameters of any-size CANFIS modular network can be readily optimized by what we have developed, the (on-line) hidden-node teaching backpropagation algorithm, which exploits its multi-stage structure. Our hidden-node teaching method, which was originally developed to avoid hidden-node saturations in MLP-learning [9], may be significant for neuro-fuzzy learning for several different reasons: (1) for attacking a large-scale problem due to its easy on-line implementation; (2) for maintaining rules' interpretability in the spirit of a fuzzy system; (3) for improving generalization capacity; (4) for escaping from plateaus in learning. Merit (1) is obvious, and (2) was explained for Figure 3. For (3), in our experiments; the same target signals were presented at the hidden layer [i.e., the final output layer of each expert-MLP; see Figure 4(b)] as well as at the terminal layer of a CANFIS network. In consequence, the output variance of local experts could be reduced. Furthermore, the variance of linear weights may be decreased as well, compared with some other (neural) fuzzy systems that employ RLSE to determine the linear weights, as mentioned in Section I, because such a least squares estimator tends to yield quite large linear weights in magnitude; this is an important issue common to *separable nonlinear least squares* learning algorithms (e.g., see [17]). In any event, smaller variance in either output or weight or in both would furnish a better performance in response to previously unseen (test) data. Lastly, item (4) is new (our future work): The problem is that if hidden-node outputs get very similar to each other on all (training) data during learning, then a matrix of hidden-node outputs becomes *rank-deficient*, giving rise to plateaus in learning (e.g., see in [16] our Hessian-matrix analysis for indefiniteness in MLP-learning and references therein). Since the Hessian matrix of J in Equation (3) can be evaluated efficiently by our recently-developed second-order stagewise backpropagation [13], [15], [18], it would be of our great interest to investigate plateaus in CANFIS neuro-fuzzy modular-network learning.

ACKNOWLEDGMENT

Eiji Mizutani would like to thank Stuart Dreyfus (UC Berkeley) for a countless number of useful discussions on discrete-time optimal-control methods that led to the development of hidden-node teaching.

REFERENCES

[1] A. Asuncion and D.J. Newman. UCI Machine Learning Repository: *http://www.ics.uci.edu/∼mlearn/MLRepository.html*, University of California, Irvine, School of Information and Computer Sciences, 2007.

[2] T. Hastie, R. Tibshirani, and J. Friedman. *The Elements of Statistical Learning*. Springer-Verlag, 2001 (Corrected printing 2002).

[3] S. Horikawa, T. Furuhashi and Y. Uchikawa. On Fuzzy Modeling Using Fuzzy Neural Networks with the Back-Propagation Algorithm. *IEEE Trans. on Neural Networks*, Vol.3, No.5, pp. 801–806, 1992.

[4] E. Mizutani, J.-S. R. Jang, K. Nishio, H. Takagi, and D. M. Auslander. Coactive neural networks with adjustable fuzzy membership functions and their applications. In *Proc. of the International Conference on Fuzzy Logic and Neural Networks*, pp. 581–582, Iizuka, Japan, August 1994.

[5] Eiji Mizutani. Chapter 13: Coactive Neuro-Fuzzy Modeling: Toward Generalized ANFIS. In *Neuro-Fuzzy and Soft Computing: a computational approach to learning and machine intelligence* (J.-S. R. Jang, C.-T. Sun and E. Mizutani), pages 369–400. Prentice Hall, 1997.

[6] E. Mizutani, S. Dreyfus, and K. Nishio. On derivation of MLP backpropagation from the Kelley-Bryson optimal-control gradient formula and its application. In *Proc. of the IEEE International Conference on Neural Networks (vol.2)*, pages 167–172, Como, Italy, July 2000.

[7] E. Mizutani and J. W. Demmel. On separable nonlinear least squares algorithms for neuro-fuzzy modular network learning. In *Proceedings of the International Joint Conference on Neural Networks*, pages 2399–2404, Honolulu USA, May 2002.

[8] E. Mizutani and K. Nishio. Fuzzy Mixtures of Complementary Local Experts: Towards Neuro-Fuzzy Modular Networks. In *Proceedings of the IEEE International Conference on Fuzzy Systems (FUZZ-IEEE)*, 2, 1192–1197, Honolulu USA, May 2002.

[9] E. Mizutani and S. E. Dreyfus. MLP's hidden-node saturations and insensitivity to initial weights in two classification benchmark problems: parity and two-spirals. In *Proceedings of the International Joint Conference on Neural Networks*, pages 2831–2836, Honolulu USA, May 2002.

[10] E. Mizutani and K. Nishio. Multi-Illuminant Color Reproduction for Electronic Cameras Via CANFIS Neuro-Fuzzy Modular Network Device Characterization. *IEEE Transactions on Neural Networks*, Vol. 13, No. 4, pages 1009—1022, July 2002.

[11] E. Mizutani and J. Demmel. On structure-exploiting trust-region regularized nonlinear least squares algorithms for neural-network learning. *Neural Networks*, 16(5-6): 745-753, 2003.

[12] E. Mizutani and J. W. Demmel. Iterative scaled trust-region learning in Krylov subspaces via Pearlmutter's implicit sparse Hessian-vector multiply. In S. Thrun, L. Saul, and B. Schölkopf, editors, *Advances in Neural Information Processing Systems 16 (NIPS 2003)*, volume 16, pages 209–216. MIT Press, 2004.

[13] E. Mizutani and S. E. Dreyfus. On derivation of stagewise second-order backpropagation by invariant imbedding for multi-stage neural-network learning. In *Proceedings of the IEEE-INNS International Joint Conf. on Neural Networks*, pages 4762–4769, Vancouver, Canada, July 2006.

[14] E. Mizutani and J.-Y. C. Fan. On exploiting symmetry for multilayer perceptron learning. In *International Joint Conference on neural networks*, pp. 2857-2862, Aug 2007.

[15] E. Mizutani and S. E. Dreyfus. Second-order stagewise backpropagation for Hessian-matrix analyses and investigation of negative curvature. *Neural Networks*, 2008 Special Issue: Advances in Neural Networks Research: IJCNN 2007, pages 193–203, Vol.21, 2008.

[16] E. Mizutani and S. E. Dreyfus. An analysis on negative curvature induced by singularity in multi-layer neural-network learning. In *Advances in Neural Information Processing Systems*, Vol. 23, MIT Press, NIPS 2010.

[17] E. Mizutani and J. W. Demmel. Trust-region variable projection algorithms for separable nonlinear least squares learning. To appear in *Proceedings of the IEEE-INNS International Joint Conference on Neural Networks*, San Jose, California, USA, August 2011.

[18] Eiji Mizutani. On exploiting sparsity in CANFIS neuro-fuzzy modular network learning by second-order stagewise backpropagation. To appear in *Proceedings of the eighth International Conference on Fuzzy Systems and Knowledge Discovery*, Shanghai, China, July 2011.

[19] H. Schwenk and Y. Bengio. Boosting Neural Networks. Neural Computation. 12: page1869-1887.2000

[20] E. D. Sontag and H. J. Sussmann. Backpropagation separates when perceptrons do. In *Proceedings of the International Joint Conf. on Neural Networks (IJCNN'89)*, pages 639–642, vol.1, Washington, DC, USA, June, 1989.

[21] M.Sugeno and G.Kang. Structure Identification of Fuzzy Model. *Fuzzy Sets and Systems*, pp.329–346, Vol.28, 1986.

[22] T. Takagi and M. Sugeno. Fuzzy identification of systems and its application to modeling and control. *IEEE Trans. on Systems Man and Cybernetics*, Vol.15, pp. 116-132, 1985.

2011 IEEE International Conference on Fuzzy Systems
June 27-30, 2011, Taipei, Taiwan

Fuzzy Fusion Fairness Relations for the Evaluation of User Preference

Mario Köppen
NDRC
Kyushu Institute of Technology
Iizuka, Fukuoka 820-8502, Japan
Email: mkoeppen@ieee.org

Jun Okamoto
Service Integration Laboratories
NTT Corporation
Tokyo 180-8585, Japan
Email: okamoto.jun@lab.ntt.co.jp

Aoi Honda
Computer Science and Systems Engineering
Kyushu Institute of Technology
Iizuka, Fukuoka 820-8502, Japan
Email: aoi@ces.kyutech.ac.jp

***Abstract*—In this paper, formal representations for user preferences will be provided, which also take fairness in the achievement of probably conflicting goals into account. The analysis of the Bottleneck Flow Control (BFC) algorithm for congestion avoidance in traffic networks will serve as a base to specify extensions of relations among preference sets. In particular, these relations are the lexicographic minimum, the maxmin fairness, and the newly introduced ordered-ordered weighted averaging operator. All of them are shown to become, in a relational sense, maximized by the BFC algorithm. Their further expansion by introducing fuzzy fusion operators in their formal definitions than establishes a comprehensive sets of relations. The application of these relations to the Multiple Relation Analysis (MRA) of subjective video quality evaluation data is demonstrated and gives the conclusion that also fairness criterions are present in such evaluations, at least as a secondary preference criterion.**

***Keywords*-fairness; maxmin fairness; ordered weighted averaging operator; preference modelling; fuzzy information fusion**

I. Introduction

Preference modelling, and the related preference prediction have become research fields of increasing importance. This tendency has been established by the wide-spread use of the internet, social networks, and vendor systems, all of them comprising systems that receive a strong impact from the user's attitude. So far, the focus of user preference modelling was on either binary systems ("yes-no", "like-neutral") or numerical evaluations given by the user (ratings, stars). However, recent research is already focussing on the limitations of such a point a view. For example, CP-nets were introduced as graphical representations of conditional preferences [1]. Also older works that were not considered for a long time newly came under focus, as for example the Landau theorems on scoring sequences (i.e. necessary and sufficient conditions for scoring systems in a network context) [2]. In this work, we also want to promote the point of view to represent preferences by means of (set-theoretic) relations, in order to allow for a rich analysis of various aspects of user decisions. In particular, the goal is to extend the analysis to additionally represent (possibly hidden) trade-offs that are inherent in user preferences, by a formalization of the concept of user fairness. As a means for such an analysis, a field was choosen were much progress in the modelling of fairness was achieved for a long time, i.e. the introduction of maxmin fairness in the field of data communication [3]. By a rigorous analysis of one of the fundamental algorithms in this field, the so-called Bottleneck Flow Control (BFC) algorithm [4] for congestion avoidance in traffic networks, we could find opportunities for the generalization of relations that are established by this algorithm. The generalization of these relations can be successfully achieved by employing concepts from fuzzy fusion. At the end of our exposition, we will have a suite of formal relations at hand that is capable to issue a Multiple Relation Analysis (MRA) for general data analysis, also taking the attitude of users towards unachievable goals into account. The MRA will be demonstrated on a subjective video quality evaluation dataset.

This paper is organized as follows: the following Section II will recall the BFC algorithm, and discuss the relevant aspects of the state that is achieved at the end of this algorithm. These characteristics of the algorithm will guide to the specification of a suite of formal relations for MRA in Section III, and the application of this suite to the video quality dataset will be given in Section IV. The paper ends with a short conclusion section.

II. Fairness Relations

In this section, we will focus on the formal representations of fairness. In general, fairness, as a daily life concept, can be understood in many ways and fashions. Problems with global optimization easily lead to a motivation to also take fairness into account [5][6]. We can find various attempts to represent fairness in the past, but mostly there was no notable progress. For example, in processor scheduling tasks, often related to hard combinatorial optimization problems, the concept of n-fairness was introduced, with the notion meaning that in a processor regime, each processor should ensure that the processor before can perform at least n tasks [7]. Also in common means like credit granting, fairness can be used as an indicator for a relevant assessment. Here, the criterion could be that two customers that have the same evaluation criterions should receive the grant with the same likelihood.

However, all such specifications do not guide to a formal representation of fairness in such a way that it can be effectively used for the finding of suitable "fair" states. Here, the best progress so far was achieved in the field of data communications. Starting with the proposal of the Bottleneck

978-1-4244-7316-8/11/$26.00 ©2011 IEEE

Flow Control (BFC) algorithm, an effective way of a fair resource assessment was introduced, probably for the first time [4].

A. The Bottleneck Flow Control Algorithm

We assume a traffic network congestion avoidance problem. A network for carrying traffic is given as an un-directed graph G with nodes N and links L. Also, a *maximum capacity* is assigned to each link. Then, there are a number of users that want to send traffic units through this network. Thus, also a set of n triples (Π_i, s_i, r_i) of sender-receiver pairs and paths connecting them is given, where s_i represents the sending node, r_i the receiver node for user u_i. Paths Π_i are given as a sequence of joined links starting from s_i and ending at r_i. We also consider the union of all links l_i used by all paths, each link with a multiplicity w_i according to the number of paths using the link l_i. Then the Bottleneck Flow Control algorithm assigns traffic amounts t_i to all users u_i in the following way:

Bottleneck Flow Control

---

1) Set the *remaining paths* to the set of all paths. Set the traffics t_i for users u_i along their corr. paths Π_i to 0.
2) While the *remaining paths* set is not empty, perform the following steps:
3) For all links l_i used by the *remaining paths*, get the number w_i of paths that pass through this link.
4) Find the links with minimum value of $m_i = c_i/w_i$.
5) Add m_i to the traffics for all users through the links with minimal m_i.
6) Remove the paths of all users of links, for which m_i is minimal, from the *remaining paths*.
7) Set new capacities of network links $c_i \rightarrow c_i - m_i * w_i$.

An example for the BFC algorithm is given in Fig. 1. It shows a network with 7 nodes and links between these nodes as indicated in the figure. It is assumed that the link connecting nodes 3 and 4 has a maximum capacity of 200 units, and the link connecting nodes 4 and 7 has a maximum capacity of 100 units. All other links will have some higher maximum capacity. Three users wants to send traffic through this network: user 1 sends traffic t_1 via the nodes 1, 3, 4 and 7; user 2 sends traffic t_2 via the nodes 2, 4 and 7; and user 3 sends traffic t_3 via 5, 3, 4 and 6. It means that some users have to share links for their traffic: users 1 and 3 share the link between nodes 3 and 4, and users 1 and 2 share the link between nodes 4 and 7. The BFC algorithm now will assign specific values for the traffic amounts t_1, t_2 and t_3, starting with amount 0, and increasing equally for a subgroup of users. At the beginning (Level 0) the amount will increase for all users. In some later stage, for example at Level 20, the traffic amount assignment of 20 (units) to all users is still feasible. However, at Level 50, the link between nodes 4 and 7 has to transport a total traffic of 100: 50 from user 1, and 50 from user 2. This gives a so-called *bottleneck*. Any attempt to further increase the traffic for either user 1 or user 2 will result in exceeding the maximum capacity of this link. Thus, the BFC algorithm stops to further

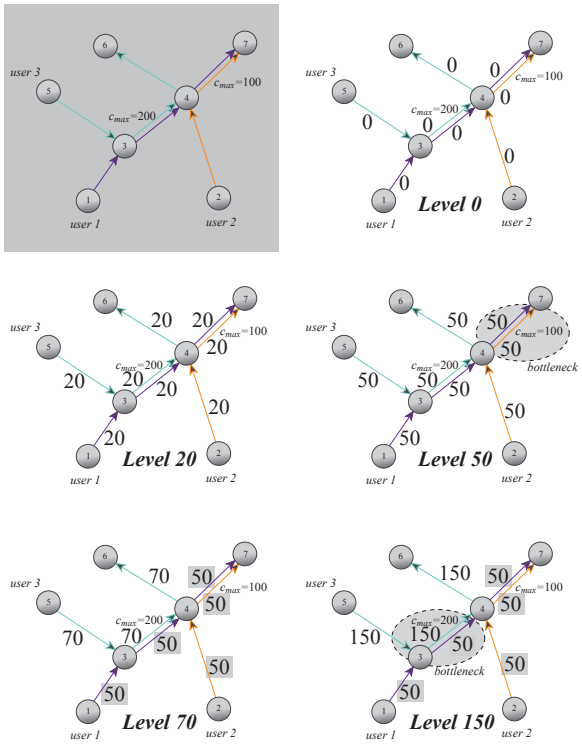

Fig. 1. Example for the Bottleneck Flow Control Algorithm: the algorithm starts traffic assignments for users along given paths at level 0, and gradually increases this level until bottlenecks are appearing. Then, the algorithm stops the further increase for the affected users, but continues for the other users. Thus, it is attained to assign the same traffic to subsets of users as long as possible. This algorithm also utilizes the specific network in the best way.

increase the traffic amount for users 1 and 2, and fixes the assignment $t_1 = 50$ and $t_2 = 50$.

However, user 3 is not affected by this bottleneck, since her traffic is not using the link between nodes 4 and 7. So, the BFC algorithm continues. Later on, for example at Level 70, the traffic assignment $t_3 = 70$ (while keeping $t_1 = t_2 = 50$) is still feasible. This level increase will continue until Level 150. Now, the total traffic for the link between nodes 3 and 4 becomes 200: user 1 was fixed before at the level $t_1 = 50$, and $t_3 = 150$ for user 3.

Any further increase of traffic is not possible, and the BFC algorithm stops. Thus, the final traffic assignment is $t_1 = 50, t_2 = 50, t_3 = 150$. In the implementation of this algorithm, of course, there are no increasing level sets, as the values of bottlenecks can be directly inferred from the network configuration and the values of maximum capacities.

It has to be noted that the BFC algorithm also specifies the feasible space of traffic assignments. We can write the result of the algorithm by a set of linear equalities (bottleneck equations):

$$\begin{aligned}\lambda_{11}t_1 + \cdots + \lambda_{1n}t_n &= b_1\\ \lambda_{21}t_1 + \cdots + \lambda_{2n}t_n &= b_2\\ &\cdots\\ \lambda_{k1}t_1 + \cdots + \lambda_{kn}t_n &= b_k\end{aligned} \quad (1)$$

where all $\lambda_{ij} \in \{0, 1\}$, t_i is the traffic amount allocated to the sender-receiver pair (s_i, r_i) and k is the number of bottlenecks found by the BFC algorithm, in the same order by which they are found by the algorithm. It can also be seen that the t_i can be numbered (arranged) in such a way that the set of equations fulfills the following properties:

- In row 1, all t_i with $\lambda_{1i} = 1$ are equal.
- In each row $r > 1$ there exists a "border" index i_r such that for all $i < i_r$ and $\lambda_{ri} = 1$ in at least one row $r_1 < r$ also $\lambda_{r_1,i} = 1$, and for $i \geq i_r$, all t_i are equal, larger than any t_j with $j \leq i_r$, and there is an index $r_2 \leq r$ such that $\lambda_{r_1,i} = 0$ for all $r_1 < r_2$ and $\lambda_{r_1,i} = 1$ for all $r_2 \leq r_1 < r$. This means that the traffics comprising a particular bottleneck equation (their λ-values are 1) can be divided into two groups: the first group contains only traffic amounts already assigned by foregoing bottleneck equations. Thus, in the progress of the algorithm, while reaching another maximum capacity (bottleneck), the remaining traffic amount at that bottleneck will be equally shared among another new group of sender-receiver pairs. These traffics then comprise the second group. Note that the first group might be empty.
- If $i > j$ then for the largest k_i and k_j from $\{1, \ldots, n\}$ with $\lambda_{i,k_i} = 1$ and $\lambda_{j,k_j} = 1$ resp. it holds that $t_{k_i} \geq t_{k_j}$. This means the last elements in the equations are sorted in non-decreasing order, according to the flow of the BFC algorithm.

For clarity (we will need this structure of the bottleneck equations later on) here the bottleneck equations for the example given above:

$$\begin{aligned}t_1|_{=50} + t_2|_{=50} &= 100\\ t_1|_{=50} + t_3|_{=150} &= 200\end{aligned}$$

thus, for the second row the index i_2 is 2: all traffics appearing in the equation (i.e. their λ factor is 1 and not 0) with lower index appear in at least one foregoing bottleneck equation (here, t_1 appears in the first equation and was fixed to 50), and the remaining capacity of $200 - 50 = 150$ at the second bottleneck will be equally shared for the third traffic. Since there is only one sender-receiver pair, its value will become 150.

Writing the bottleneck equations in such an index-ordered way has the additional advantage that, after replacing each equal sign in the Eqns. (1) with a lower-or-equal sign specifies the feasible space of all possible traffic assignments.

After this analysis of the BFC algorithm, the question is about the characterization of the final state achieved by the algorithm. The BFC algorithm is effective in the sense that for any given network structure, and given sender-receiver pairs, it will uniquely assign traffic amounts to all sender-receiver pairs, and thus select one and only one element of the feasible space. How is this element be qualified against all other elements of the feasible space?

In the following, we will recall two already known notations of that final state, and provide another (up to our best knowledge) new characteristic. Then, we will discuss the extension of these characteristics into the fuzzy fusion domain.

B. Characterization of the BFC result

There are several ways to characterize the final state of the BFC algorithm. Here, we will focus on three ways. In a less formal way, the BFC algorithm can be seen as a prototype to achieve fairness in the assignment of traffic amounts among the various users (i.e. sender-receiver pairs) in such a network model. The algorithm assigns the same traffic to all user as long as possible. Then, when this increase is no longer possible, as the assignment is reaching a bottleneck, it is no longer possible to give a larger same amount to all users. But, in contrary to other "equalizing" approaches to fairness, the BFC algorithm does not stop here. It acknowledges the fact that a number of users is *not* affected by this bottleneck, and continues to raise their traffic amounts equally — until the next bottleneck is reached.

From this argument, we can see the first characteristic of the BFC algorithm.

(1) **Lexmin relation**. The lexmin relation is defined as a relation between two points from R^n. Given two vectors x and y from R^n, we consider the coordinates of both vectors sorted in increasing order. It is said that $x >_{lexmin} y$ if and only if the first coordinate of x, in that sorting, which is different from y, is larger than the corresponding coordinate of y, in that sorting. For simplicity, if the smallest coordinate of x is larger than the smallest coordinate of y or if both are equal but the second-smallest coordinate of x is larger than the second-smallest coordinate of y etc. - than x is lexmin-related to y.

We also want to recall here that for any relation $>_R$, formally seen as a subset of $A \times A$, where A is an arbitrary but fixed set, we can define a *maximum set* and a *best set*: the maximum set contains all elements x from A such that there is no different $y \neq x$ in A with $y >_R x$. The best set, on the other hand, contains all elements x of A such that for each different $y \neq x$ $x >_R y$ holds.

In this sense, the best set of the feasible space of a network traffic assignment problem under the lexmin relation contains exactly one element, and this is the one found by the BFC algorithm. This can be seen from the index-ordered bottleneck equations: the minimum traffic is given in the first of the equations, and it cannot be increased. Then, for states with the same minimum traffic, the second-smallest traffic will appear in the second equation. Also this one cannot be increased without exceeding the second bottleneck. The argument can be continued for the third-smallest traffic, fourth-smallest traffic etc.

(2) **Maxmin fair dominance relation**. It has already been established [3][8] that the BFC algorithm is selecting the best set element of another relation, the so-called *maxmin fairness dominance*.

Definition 1. *An element x of the feasible space is* maxmin fair dominating *an element y of same space, if for each component y_i of y, which is larger than the corresponding component x_i of x there is another component x_j of x which is (already) smaller than or equal to x_i and such that y_j is smaller than x_j.*

This can be directly seen from the index-ordered bottleneck equations. If one traffic is increased, there will be a bottleneck equation r where this traffic appears for the first time (and there belonging to the second group, i.e. with index $i \geq i_r$, using former convention). To maintain the bottleneck equation, another traffic has to be decreased in order to compensate for the increase (note that the compensation can be larger than the increase). But each other traffic in this equation will be the same (before increase) or smaller (if belonging to the first group with indizes $i < i_r$). So, any increase of a traffic amount can only happen if some other traffic amount, which is already the same or smaller, is decreased. This is exactly the definition of the maxmin fair dominance relation. Note that maxmin fair dominance relation and lexmin relation are different relations.

In the next subsection, we will introduce a generalization of the maxmin fair dominance relation, based on using fuzzy fusion operators. Here, we will already note that *maxmin fairness* (referring to the quality of the best element of this relation) has already found a number of alternatives in the data network domain (where it was first introduced). The most popular one is the so-called *proportional fairness*. It can be defined as follows:

Definition 2. *A point x of feasible space (a subset of R_n^+) is considered proportional fair dominating another feasible point y, if and only if*

$$\sum_{i=1,\ldots,n} \frac{y_i - x_i}{x_i} \leq 0 \tag{2}$$

holds.

The reason to introduce proportional fairness were a number of problems with maxmin fairness, including the negligence of user utility, and the overvaluation of the least element, for example as it was noted by Kelly[9]: "*The maxmin fairness criterion gives an absolute priority to the smaller flows, in the sense that if $x_{s^*} < x_s$ then no increase in x_s, no matter how large, can compensate for any decrease in x_{s^*}, no matter how small.*"

We can find the further extension of proportional fairness to the so-called weighted alpha fairness dominance relation:

Definition 3. *A point x of feasible space (a subset of R_n^+) is considered weighted alpha fair dominating another feasible point y, if and only if for a given fixed set of weights w_i*

$$\sum_{i=1,\ldots,n} w_i \frac{y_i - x_i}{x_i^\alpha} \leq 0 \tag{3}$$

holds.

It can be shown that for $\alpha \to \infty$ alpha-fairness nearly everywhere converges to maxmin fairness, but equals proportional fairness for $\alpha = 1$.

(3) **Exponential OOWA**. While the former two definitions show how to use a relation between points in the feasible space, and to characterize the BFC algorithm as the one that finds the best element for each relation, the question comes up if there is also a scalar function that is directly maximized by the BFC algorithm. As a new result, we will show that there is such a function. We define a special case of the ordered weighted averaging (OWA) operator. As a reminder, the OWA of a point x of R_n, given a weight vector $w \in R_n$, is defined as $\sum w_i x_{(i)}$. In this expression, $x_{(i)}$ indicates the i-th largest element of all coordinates of x. We specialize the OWA by also requiring the weights to be sorted in the opposite order.

Definition 4. *Given a point x from R_n and a set of weights $w \in R_n$, the Ordered-Ordered Weighted Averaging (OOWA) of x by w is defined as*

$$OOWA_w(x) = \sum_{i=1}^{n} w_{(n-i+1)} x_{(i)} \tag{4}$$

Thus, in the OOWA, the largest value is multiplied with the smallest weight, the second-largest value with the second-smallest weight etc. As a special case of the OOWA, we also introduce the exponential OOWA. The additional requirement here is

$$w_{(i)} > \sum_{k=1}^{i-1} w_{(k)} \tag{5}$$

so that the weights itself are exponentially increasing. A possible choice is $w_i = 2^i$ for any n. Then it holds:

Theorem 1. *The BFC algorithm is maximizing any exponential OOWA.*

For an outline of the proof, see the Appendix.

Back to the example from the former subsection, and using the weights $(1, 2, 4)$ to compute

$$OOWA_{exp}(t_1, t_2, t_3) = t_{(1)} + 2t_{(2)} + 4t_{(3)} \tag{6}$$

we can see that any feasible modification of the t_i will reduce this expression for the state $(50, 50, 150)$ assigned by the BFC algorithm. This state has the exponential OOWA value $1 \cdot 150 + 2 \cdot 50 + 4 \cdot 50 = 450$. If for example t_2 is increased, this has to be compensated by a decrease of t_1. The increase can be at most 50 due to the first bottleneck at 100, and t_2 will always become the second largest traffic, and the exponential OOWA is changing to

$$f^* = 1 \cdot 150 + 2 \cdot (50 + \delta) + 4 \cdot (50 - \delta_1) \tag{7}$$

where $\delta_1 \geq \delta$. This expression is clearly smaller than 450, as it reduces the former value by at least 2δ. If t_1 is increased, than

t_2 and t_3 have to be decreased, and the argument is basically the same. An increase of t_3 forces a decrease of t_1. Since the increased t_3 will still be the largest value, and thus weighted by 1, the smaller t_1 now will be weighted by 2 or 4 (which depends on a possible modification of t_2). So, also here the net change in the exponential OOWA expression will be negative.

The exponential condition is also necessary. It suffices to consider a network structure, where one traffic shares links with k other users, all of same maximum capacity and exactly one other user per link to share, and the remaining $n-k$ links will have only one sending user, all with a lower maximum capacity. Then, an increase of all the k sharing users will require the one sharing user to compensate all k traffics. This, its weight must be at least as large as the sum of the weights of all other k increased traffics.

As a last comment, we may note that the exponential condition is a result of link sharing. With regard to fairness, single user sharing links with many other users at once can be considered the worst case, as assigning any traffic to such a user affects the traffic of many other users, in fact enforces their reduction.

III. Suite of Relations

In order to apply the concepts that were presented in the foregoing section, we will have to study the unrevealed relations independently from the BFC algorithm and the underlying network traffic assignment problem. In fact, there are a number of formal ways to expand these definitions, and they will be discussed in the following.

A. Maxmin fairness and fuzzy fusion

The definition of maxmin fair dominance is rather complex. However, its implementation can be much simplified [5]: in general it would need to check the fairness condition for all pairs of components, but for simplification, we define index sets as follows (see Fig. 2). Given two vectors x and y we want to test if x maxmin fair dominates y. Then, we compute

- $A = \{i \,|\, x_i > y_i\}$
- $B = \{i \,|\, x_i = y_i\}$
- $C = \{i \,|\, x_i < y_i\}$
- $min_A = \min_{i \in A} x_i$, or ∞ if A is empty
- $min_C = \min_{i \in C} x_i$, or ∞ if C is empty

The definition of maxmin fairness requires to check the following for every increasing component x_i: is there any $j \neq i$ such that $x_j \leq x_i$ and $y_j < x_j$? It means that $i \in C$ and $j \in A$. We omit the case that either A or C is empty at the moment. Then, for such an index j to exist, it is necessary that for every $i \in C$ there is at least one element j of A with $x_j \leq x_i$, in particular it is necessary that there is a $j \leq min_C$ and thus $min_A \leq min_C$. We can see that this is a sufficient condition as well: for any i from C, already one j with $x_j = min_A$ fulfills the check: the j-th component (min_A) is smaller than or equal to any x_i with $i \in C$, and $x_j > y_j$ since $j \in A$. If we also take formally $z < \infty$ for any real z, we can evaluate maxmin fair dominance as follows: *Given two vectors x and y, then x will maxmin fair dominate y if and only if $min_A \leq min_C$.*

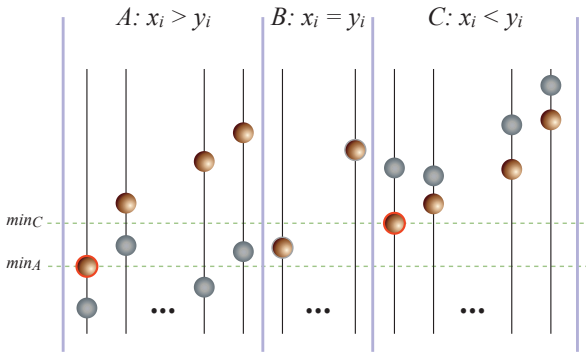

Fig. 2. Maxmin fairness relation can be more easily defined, if we consider the sets of components of x larger (set A) and smaller (set C) than corresponding components of y. Vector x will maxmin fair dominate y if and only if the smallest larger component of x is smaller than or equal to the smallest smaller component of x [5]. In the figure, corresponding components of x and y are placed on the same line, with height indicating their magnitude, and the lines are re-arranged to show first x-components larger than the corr. y-component, then equal components, and third smaller components (each of the three sections are additionally arranged by increasing size of the corr. x-component).

Note that equal components do not have any influence on maxmin fair dominance, and that the definition includes Pareto dominance. If C is empty, but A not, then each component of x is larger than or equal to the corresponding component of y, and at least one is larger.

From this way of testing the maxmin fair dominance relation, we can see that the relation actually refers to a fusion of all smaller and all larger components of a vector, compared to another vector. The fusion used here is the minimum operation. In this regard, we consider an extension of the maxmin fair dominance by formally generalizing on the fusion aspect. Thus, instead of comparing $\min A$ and $\min C$ we use other means to fuse the information of the sets A and C into single values. In present study, we will use other t-norms (incl. Dubois Prade t-norm, and algebraic t-norm), and OWA operators with different weights.

B. OOWA

Also the exponential OOWA that was shown to be maximized by the BFC algorithm offers some straightforward extensions, esp. by requiring a different law of weights increase. Here, we will consider also a linear OOWA, where weight i is choosen to be i.

Such operations will reflect sharing aspects. In the network problem, the exponential increase of weights was necessary in order to ensure that even the situation where one sender shares links with ALL other users is covered. In the simple scenario of no link sharing at all, a linear OOWA would be sufficient to ensure maximization by BFC algorithm. Thus, comparing linear and exponential OOWA in a situation, where the interpretation of "link sharing" is not obvious, it can still refer to a relevant problem of the studied feasible space -

technically, these expressions can be computed without any reference to a networking problem at all.

C. Data processing suite of relations

With the modifications mentioned in the former subsections, we propose a suite of relations that can be used together for a Multiple Relation Analysis.

- Fuzzy fusion fairness relations fff_{op}, where op indicates the used fuzzy fusion operator. To decide for two points x and y whether $x >_R y$ or not, we first compute the set A of all components of x that are larger than the corr. component of y, and the set C of all components of x that are smaller than the corr. component of y. Then, if A is not-empty, op is applied to A, giving a value f_A, and if C is not-empty, op is applied to the set C, giving a value f_C. If either of these sets is empty, the corr. f-value is set to ∞. Then, $x >_R y$ if and only if $f_A \leq f_C$. More specifically, we will consider Dubois-Prade T-norm for fusion (which is for two reals a and b from $(0, 1)$ and a parameter α defined as $ab/\max[a, b, \alpha]$, and for more than two arguments by associativity of the expression for two arguments), the "simple" algebraic t-norm as product of components, and several OWA operators, with larger weights for smaller values, or nearly equal weights, thus focussing on averaging. Also, plain average of the sets A and C will be considered.
- Other fairness relations, as introduced in subsection II-B(2): proportional fair dominance, and alpha fair dominance with various values of α.
- Exponential OOWA, as introduced in section II-B(3), the variant linear OOWA as discussed in the foregoing subsection, and in this context also the lexmin relation.
- Other general relations that are not primarily related to the concept of fairness: more than half of the components of x is larger than the corresponding components of y; the largest component of x is larger than the largest component of y; and the average of the components of x is larger than the average of the components of y in order to x be in relation to y.
- We also consider Pareto dominance relation with regard to maximization and minimization. For maximization, x is larger than (or: in relation to) y iff all components of x are larger or equal to the corresponding components of y, and at least one component is larger (minimization Pareto dominance is defined accordingly).

D. Mathematical properties

For space reasons, we will not provide a thorough analysis of the mathematical properties of the introduced relations. Here we only mention that the introduced fuzzy fusion fairness relations are all not complete (i.e. it is possible that for some x and y neither $x >_R y$ nor $y >_R x$ holds) and not (always) transitive. For example, for the maxmin fair dominance relation, consider the tripel of vectors $x = (70, 50), y = (40, 40), z = (30, 60)$. Here x maxmin fair dominates y, and y maxmin fair dominates z but x does not maxmin fair dominate z. Nevertheless, the relations will not produce conflicts, as from $x >_R y$ and $y >_R z$ always $z >_R x$ can be excluded. On the other hand, the lexmin relation as well as the OOWA are complete and transitive.

IV. Experimental Validation: Subjective Evaluation of Video Quality

A. Used data and recent findings

For the application of the relations, we are considering a dataset of subjective evaluations of video data quality. The dataset contains two kinds of information for 1139 sample videos: five objective measures of video quality, in particular values numerically representing overall noise, degradation caused by block distortion, degradation associated with blurring, local spatial degradation, and freeze degradation, and an average ranking of a number of users for each of these 5-tuples of data. The dataset is part of a larger experiment performed at NTT Corp.[1]

The data have already been analyzed in a recent publication[10]. There, the goal was to use a newly-proposed fuzzy integral, the inclusion-exclusion integral, to derive the user ranking from the quality measures by direct computation. The approach was shown to improve the recommended rule by the Telecommunication Standardization Sector of International Telecommunication Union (ITU-T), and an approach based on the Choquet integral as well. It was also confirmed that the 5-th quality measure shows a logarithmic utility for the user, while the other four correspond directly to the user utility.

B. Data Pre-Processing

Here, we are interested in specifying the user attitude towards increase or decrease of the quality measures in total. While it can be expected that video material with lower degradation measures will be more likely higher ranked, the question that can be handled by the introduced fairness relations is also about the acceptance of trade-offs by the user. So, the question for the analysis is if an increase in quality according to one criterion is less favored, if the cost for this increase is the decrease of another criterion, which is already lower in quality.

For this processing, we have to represent the quality values by their utility. Also we have to consider that the introduced relations are focussing on increasing magnitudes of components. Thus, the following pre-processing of the data was performed:

1) Data sets containing unsafe measurements (about 20) were removed.
2) All 5-th measurements x_{i5} were replaced by the decimal logarithm $\log_{10} x_{i5}$.
3) All datasets were normalized by their average and standard deviation (μ_j is the average of the j-measurement, and σ_j the corresponding standard deviation):
$$x_{ij} \leftarrow \frac{x_{ij} - \mu_j}{2\sigma_j} \tag{8}$$
4) Datasets with strong outliers were removed (about 200), as we are more focussing on the average behaviour.

[1]The dataset itself is not publicly available.

5) The single data were rescaled to the $(0, 1)$ range, such that larger values represent better quality:

$$x_{ij} \leftarrow 1 - \frac{x_{ij} + 1}{2} \tag{9}$$

After preprocessing, the frequency correlation for each proposed relation was computed. Thus, we are considering the normalized measurements for each possible pair (x, y) of datasets in two ways:

- Precision: in case that x is in relation to y, we are counting how often then also $s_x > s_y$ holds, i.e. how often the users also ranked the video higher.
- Recall: in case that $s_x > s_y$, we count how often this is indication for the relation $x >_R y$ to hold as well.

In the processing, equal pairs of values were ignored. It was also noted how often the relation was actually occurring. The total number of pairs used in the comparison for each relation was 938961.

C. Results and Discussion

The result for all used relations can be seen in Table I.

We describe the main properties of the result by the following items, see also Fig. 3.

- Most of the relations achieve precision and recall measures between 0.1 and 0.8. The largest precision value is achieved by the Pareto dominance (maximizing), but it is accompanied by a low recall value. This indicates that an improvement in ALL measures usually also results in a higher rating of the videos, but that it is not required from the user perspective. The low measures for the Pareto dominance minimizing strengthen this conclusion: a higher rating of a video with all lower quality measures is highly unlikely. Note the small number of occurrences of the Pareto dominance relation as well.
- We find the fuzzy fusion fairness relations located in the lower right part of the precision-recall plot, in an area with the maxmin fair dominance relation (as a special case of fuzzy fusion fairness) in its center. This indicates that these relations are focussing on related aspects of user preferences. Remember that these relations are focussing on the modality of accepting a decrease in some quality measures for the benefit of increasing other measures. In a fair state, the decrease should not happen to quality measures that are already lower. The rather low recall values indicates that the user is not considering this a primary criterion, and is more focussing on general improvements. Nevertheless, the recall values can become rather large, esp. when the algebraic t-norm is used for fuzzy fusion. This is a relevant issue, as most t-norms have the tendency to depend (in their numerical range) strongly from the number of arguments, and this effect is most extreme for the product. It can also be seen from the tendency of the Dubois-Prade t-norm to provide larger recall values with increasing α parameter. It is known that this parameter smoothly transits the operation result from the minimum ($\alpha \to 0$) to the product of its arguments for $\alpha \to 1$.
- We can find OOWA and lexmin rather close together, and with comparable large precision and recall values. Especially, there is the same result for exponential and linear OOWA. Recalling the discussion of the introduction of these operators, and their motivation from the maximizing property of the BFC algorithm, this is an indication that there is no strong "sharing" between the quality measures. It means that the increase of a quality measure can be gracefully done without the need to decrease other quality measures. On the other hand, lexmin can also be seen as an OOWA with weights converging to infinity, and the results are rather similar, just a little bit smaller.
- Averaging relations in general do perform less well, compared to other relations. Especially for the fuzzy fusion fairness with nearly equal OWA weights it gives the lowest precision and recall values (except Pareto minimum). Also the largest component alone is not much indicative for the user rating.
- The default suite of relations, esp. the number of larger components relation, confirms the findings from the other relations: the number of larger quality measures can be seen as the primary criterion for the user rating, and the corr. trade-off as secondary criterion. But it seems in this trade-off the user is not much considering the choice of which of the other measures is actually decreased.

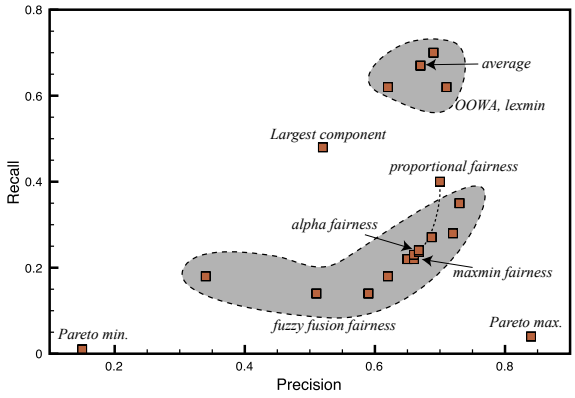

Fig. 3. Precision vs. Recall for the used relations.

V. Conclusions

We have provided formal representations for user preferences, also taking fairness among the achievement of probably conflicting goals into account. Their further expansion by introducing fuzzy fusion operators in their formal definitions than established a comprehensive set of relations. The application of these relations for a Multiple Relation Analysis (MRA) for the analysis of subjective video quality evaluation data is demonstrated and gives the conclusion that also fairness criterions are present in such evaluations, at least as a secondary preference criterion. Further work will have to focus on the

TABLE I
PRECISION AND RECALL FOR VARIOUS RELATION-BASED EVALUATIONS.

Relation	Parameter	Number of related pairs	Total ratio	Precision	Recall
maxMinFairness = fff_{min}	-	159024	0.110257	0.651015	0.223613
fff_{owa}	$w = (0.8, 0.2, 0, 0, 0)$	130073	0.0863007	0.622981	0.175027
fff_{owa}	$w = (0.6, 0.3, 0.1, 0, 0)$	123956	0.0675385	0.511601	0.136976
fff_{owa}	$w = (0.3, 0.2, 0.2, 0.2, 0.1)$	242104	0.0875755	0.339647	0.177613
$\text{fff}_{dubois-prade}$	$\alpha = 0.2$	159010	0.110258	0.651078	0.223616
$\text{fff}_{dubois-prade}$	$\alpha = 0.5$	156492	0.109369	0.656219	0.221812
$\text{fff}_{dubois-prade}$	$\alpha = 0.8$	183208	0.140454	0.719843	0.284857
$\text{fff}_{algebraic}$	-	222989	0.174354	0.734171	0.35361
$\text{fff}_{average}$	-	111732	0.0702915	0.590708	0.142559
proportional fairness	-	265724	0.197693	0.698567	0.400943
alpha fairness	alpha=3	186517	0.136353	0.686425	0.276539
alpha fairness	alpha=7	164952	0.117707	0.670025	0.238722
alpha fairness	alpha=10	161627	0.114446	0.664864	0.232109
exp. OOWA	-	468996	0.325803	0.652278	0.660764
lin. OOWA	-	468996	0.325803	0.652278	0.660764
lexmin	-	468996	0.308115	0.616867	0.624892
Pareto dominance (maximizing)	-	20341	0.0182233	0.841207	0.036959
Pareto dominance (minimizing)	-	20341	0.00316414	0.14606	0.00641722
number of larger components	-	401481	0.304671	0.712547	0.617906
largest component	-	426865	0.237688	0.522835	0.482058
average	-	468996	0.332448	0.665583	0.674242

more elaborate analysis of mathematical properties of these relations, and their employment in other domains, especially preference prediction.

ACKNOWLEDGMENT

This work was partly supported by the Japan Society for the Promotion of Science, Grant-in-Aid for Scientific Research (S) (No. 18100001).

REFERENCES

[1] C. Boutilier, R. I. Brafman, C. Domshlak, H. H. Hoos, and D. Poole, "Preference-based constrained optimization with cp-nets," *Computational Intelligence*, vol. 20, no. 2, pp. 137–157, 2004. [Online]. Available: http://dx.doi.org/10.1111/j.0824-7935.2004.00234.x

[2] H. Landau, "On dominance relations and the structure of animal societies: III the condition for a score structure," *Bulletin of Mathematical Biology*, vol. 15, pp. 143–148, 1953, 10.1007/BF02476378. [Online]. Available: http://dx.doi.org/10.1007/BF02476378

[3] D. Bertsekas and R. Gallager, *Data Networks*. Englewood Cliffs, N: Prentice Hall, 1992.

[4] J. Jaffe, "Bottleneck flow control," *IEEE Trans. Commun.*, vol. COM-29, July 1981.

[5] M. Koeppen, K. Yoshida, and M. Tsuru, "Fuzzification of maxmin fairness relation based on subvector dominance degree," in *Proc. 2nd International Conference on Intelligent Networking and Collaborative Systems (INCoS 2010), Thessaloniki, Greece*, November 2010.

[6] M. Koeppen, R. Verschae, K. Yoshida, and M. Tsuru, "Heuristic maxmin fairness for the wireless channel allocation problem," in *Proc. Fifth International Conference on Broadband and Wireless Computing, Communication and Applications (BWCCA 2010), Nov. 2010, Fukuoka, Japan*, 2010.

[7] S. Haldar and D. K. Subramanian, "Fairness in processor scheduling in time sharing systems," *SIGOPS Oper. Syst. Rev.*, vol. 25, no. 1, pp. 4–18, 1991.

[8] M. Koeppen, K. Yoshida, M. Tsuru, and Y. Oie, "Evolutionary routing-path selection in congested communication networks," in *Proceedings of the 2009 IEEE International Conference on Systems, Man, and Cybernetics, San Antonio, TX, USA - October 2009*, 2009, pp. 2224–2229.

[9] F. Kelly, "Charging and rate control for elastic traffic," *Eur. Trans. Telecomm.*, vol. 8, pp. 33–37, Jan./Feb. 1997.

[10] A. Honda and J. Okamoto, "Inclusion-exclusion integral and its application to subjective video quality estimation," in *Information Processing and Management of Uncertainty in Knowledge-Based Systems. Theory and Methods - 13th International Conference, IPMU 2010, Dortmund, Germany, June 28 - July 2, 2010. Proceedings, Part I*, E. Hüllermeier, R. Kruse, and F. Hoffmann, Eds., 2010, pp. 480–489.

APPENDIX

Outline of the proof for Theorem 1

The following lemma indicates a minimizing property of the OOWA against all OWA using the same set of weights:

Lemma 1. *Given a set of n weights w in non-decreasing order, and any permutation $w*$ of these weights. Then for any $x \in R^n$*

$$OOWA_w(x) \leq OWA_{w*}(x) \tag{10}$$

Proof: We will use bracketed subscripts to refer to the different orderings. By $x_{(i)}$ we indicate the i-th largest element of x, by $w_{(i*)}$ the i-th element in the permutation $w*$ of the weights. We also define $h_i = x_{(n-i+1)} - x_{(n-i+2)}$ for $i > 1$ and $h_1 = x_{(n)}$. Then, $x_{(i)} = \sum_{k=1}^{n-i+1} h_k$ and it follows:

$$
\begin{aligned}
OWA_{w*}(x) &= \sum_{i=1}^{n}\left[w_{(i*)}\sum_{k=1}^{n-i+1}h_k\right] \\
= \sum_{i=1}^{n}\left[h_i\sum_{k=1}^{n-i+1}w_{(k*)}\right] &\geq \sum_{i=1}^{n}\left[h_i\sum_{k=1}^{n-i+1}w_k\right] \\
= \sum_{i=1}^{n}\left[w_i\sum_{k=1}^{n-i+1}h_k\right] &= OOWA_w(x)
\end{aligned}
$$

since the weights are sorted in non-decreasing order and thus, the sum of the first k weights will be always smaller or equal to the sum of the first k permuted weights. ■

We indicate the assignment T^* of traffics achieved by the BFC algorithm with a star t_i^*. Now we have to consider any other feasible assignment T of t_i traffic values to users. By T^+ we indicate the set of traffics that become larger in T and by T^- the set of values that become smaller (if needed, arrange the traffic indices such that for equal t^* values, T^+ traffics appear before T^- traffics). We consider a bipartite directed graph with nodes set (T^+, T^-) constructed as follows: each node represents a traffic that was modified when changing from T^* to T and keeps two values: the change δ and the weight of the traffic in the original order O. A directed link goes from a node t_1 in the "right" set of the T^--nodes to a node t_2 in the "left" set of the T^+-nodes if t_1 appears in the same bottleneck equation(s), where t_2 appears for the first time. Thus, we use a link to indicate that a reduced traffic can *compensate* for an increase in traffic in the same bottleneck equation.

Now we generate the following sum S: for each link, we multiply the weight of the incident node (i.e. for an increased traffic) and the δ-value of the outgoing node (i.e. of a decreased traffic) and sum up all products for all links. Then, from the condition for the weight increase of the exponential OOWA we can see that

$$\sum_{i,t_i\in T^-}\delta_i w_i > S \tag{11}$$

since each node on the right side is at most connected to $(k-1)$ nodes to the left, where k is the index of its weight, and all links will have a different weight factor in S with smaller weight index. On the other hand

$$S \geq \sum_{i,t_i\in T^+}\delta_i w_i \tag{12}$$

since S contains, for each increasing node, the compensating terms in the same bottleneck equation (the δ-values of decreasing traffics, to which it is connected) with the same weight as the increase appears in the modified $oowa^*$ expression. Thus, by this modification, the original OOWA expression becomes smaller. By Lemma 1, after re-arranging the weights into the correct order, the value will not increase. Thus, the total OOWA expression becomes smaller.

For assisting these arguments, figure 4 gives an example. Assuming a setup with the following bottleneck equations as a result T^* of the BFC algorithm:

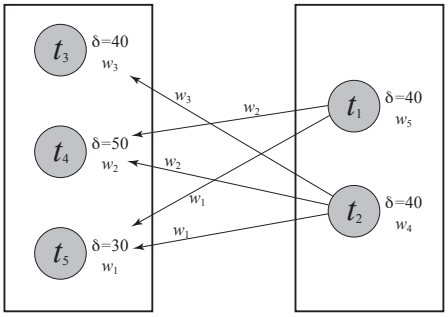

Fig. 4. Example for the bi-graph used in the proof.

$$
\begin{aligned}
t_1|_{=50} + t_2|_{=50} &= 100 \\
t_2|_{=50} + t_3|_{=60} &= 110 \\
t_1|_{=50} + t_2|_{=50} + t_4|_{=70} + t_5|_{=70} &= 240
\end{aligned}
$$

Then, we assume a change to another feasible state T as follows: $t_1 = 10, t_2 = 10, t_3 = 100, t_4 = 120, t_5 = 100$.

The set T^+ contains the elements t_3, t_4 and t_5, and the set T^- the two elements t_1 and t_2. The directed links are as shown in the figure, for example, node t_2 is connected to node t_5, since t_5 appears the first time in the 3rd bottleneck equation, and t_2 as element of T^- appears also in the same bottleneck equation.

Now there are five links and the value of S is computed as follows:

$$40 \cdot w_1 + 40 \cdot w_1 + 40 \cdot w_2 + 40 \cdot w_2 + 40 \cdot w_3 \tag{13}$$

and from $w_4 > w_1 + w_2 + w_3$ and $w_5 > w_1 + w_2 + w_3 + w_4 > w_1 + w_2$ it can be seen that the weighted sum for the right nodes exceeds S: $40 \cdot w_4 + 40 \cdot w_5 > S$.

For the left nodes, we can see that S contains all terms needed to compensate the weighted sum of all T^+ changes as well:

- For t_3, which increases the $oowa^*$ value by $40w_3$, S contains the (necessary) compensation of the increase in the second bottleneck equation from node t_2 ($40w_3$).
- For t_4, which increases the $oowa^*$ value by $50w_2$, S contains a compensation from decreasing t_1 by 40 and t_2 by 40, both weighted by w_2 in S.
- For t_5 with increase $30w_1$, the connecting links from t_1 and t_2 provide a compensation for the increase by a decrease of 40 and are weighted with w_1 in S.

So it can be seen that the sum of all changes for T^+ nodes (smaller or equal to S) increases the original OOWA by a smaller amount than the sum of all changes for T^- nodes (larger than S).

2011 IEEE International Conference on Fuzzy Systems
June 27-30, 2011, Taipei, Taiwan

Multiple Criteria Group Decision Making with Triangular Interval Type-2 Fuzzy Sets

Kuo-Ping Chiao
Department of Industrial Management and Enterprise Information, Aletheia University
Tamsui, Taipei, Taiwan
chiao@mail.au.edu.tw

***Abstract*—In this paper, the triangular interval type-2 fuzzy set extension of the Analytic Hierarchy Process is introduced. The priority vectors are elicited from the pairwise comparison matrix with triangular interval type-2 fuzzy sets which represent the linguistic relative importance judged by experts. First, the triangular interval type-2 fuzzy set logarithmic regression function is defined with respect to the pairwise comparison matrix of the criteria. Then, the sets of linear systems corresponding to the end points of the upper and lower membership functions are formulated by minimizing the logarithmic regression function. The non-normalized weights are solved. It is shown in this paper that the sets of linear systems are all dependent. Accordingly, the final normalized weights can be obtained. A quadratic programming model for finding the optimum normalized weights is constructed in the sense of minimizing the fuzziness of the interval type-2 fuzzy weights. Analogously, if the pairwise comparisons are for the alternatives, then the final normalized triangular interval type-2 fuzzy rates are also obtained. The aggregation process of the triangular interval type-2 fuzzy sets is proposed to obtain the overall rate of each alternative. The interval type-2 fuzzy set ranking method is proposed and used to find the final preference of the alternatives. A numerical example about selecting the best professor candidate is examined.**

Keywords: Analytic Hierarchy Process, Interval Type-2 Fuzzy Sets, Multiple Criteria Decision Making, Pairwise Comparison Matrix

I. Introduction

Analytic hierarchy process (AHP) is developed by Saaty[1] to find the priority of a set of alternatives under the given relative importance opinions to the pairs of criteria. In real life, some judgments might not be given as an exact relative scale. The linguistic scales are used instead. The fuzzy version of the extensions of Saaty's priority theory was proposed by de Graan[2] and Loostma[3]. Based on their fuzzy extension, van Laarhoven and Pedrycz[4] formally presented a method to find the fuzzy priority vector from a fuzzy pairwise comparison matrix(FPCM) with the triangular fuzzy numbers(TFN) as the matrix elements. By proposing a normalization modification of the fuzzy priority vector from Loostma's LSMR algorithm, Boender, Graan and Lootsma[5] pointed out that the normalized solution violates the first-order conditions, i.e. the applied normalization destroys optimality. Another approach to find the priority vector was based on the row and column geometric means(RCGM) which was studied by Uppuluri[6], Aczel[7] and Koczkodaj[8]. Buckley[9] was the first one to develop the fuzzy geometric mean method to find the fuzzy priority vector(weights). Actually, Buckley developed the interval geometric mean method for obtaining the interval priority vector for interval comparison matrix. His algorithm can be applied to any general fuzzy numbers and not just for TFN. However, the numerical evaluation process is tedious. The original Saaty's AHP model is of crisp opinions, which is too restrictive for experts to judge. Almost all the studies dealing with the extension to fuzzy criteria are using type-1 fuzzy sets. The uncertainty of the relative importance among criteria can be further given by words which are modelled by interval type-2 fuzzy sets(IT2FSs)([10]).

In this paper, the triangular IT2FS extension of the classical AHP is introduced and the IT2FS priority vector(weighting vector) are elicited from the pairwise comparison matrix with triangular IT2FS elements which represent the linguistic relative importance judged by experts. First, the triangular IT2FS logarithmic regression function is defined with respect to the triangular IT2FS pairwise comparison matrix of the criteria. Secondly, five sets of linear systems corresponding to the end points of the upper and lower membership functions are formulated by minimizing the logarithmic regression function. Finally, the non-normalized triangular IT2FS weight of the criteria are solved. It is shown in this paper that the sets of linear systems are all dependent. Accordingly, the final normalized weights can be obtained. A linear programming model for finding the optimum normalized weights is constructed in the sense of minimizing the fuzziness of the interval type-2 fuzzy weights. The final normalized weights can be obtained. Analogously, if the pairwise comparison are given for the alternatives, then the final normalized triangular IT2FS rates are also obtained by the same mathematical analysis. The aggregation process of the triangular IT2FS is also proposed to obtain the overall rate of each alternative. After obtaining the triangular IT2FS overall rates of the alternatives, the IT2FS ranking method is introduced and used to find the preference of the alternatives.

The rest of this paper is organized as follows: Section 2 presents definitions of the triangular IT2FS and some arithmetic and transcendental operations. Section 3 formulates the mathematical model by proposing the triangular IT2FS logarithmic regression function. The non-normalized solutions are obtained. Section 4 proposes the normalized solutions by applying the dependent conditions of the linear systems. It is shown that the sets of linear systems are all dependent. Accordingly, the final normalized weights can be obtained. A quadratic programming model for finding the optimum

978-1-4244-7316-8/11/$26.00 ©2011 IEEE

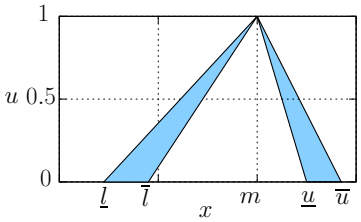

Figure 1. Footprint of uncertainty(FOU) of the triangular interval type-2 fuzzy number.

normalized weights is constructed in the sense of minimizing the fuzziness of the interval type-2 fuzzy weights. Section 5 proposes the aggregation process of the triangular IT2FS weights of the criteria and the rates of the decision alternatives. Section 6 proposes the IT2FS ranking method. Section 7 is a numerical example about the decision of selecting the best candidate of a college professor in Operations Research.

II. Triangular Interval Type-2 Fuzzy Sets

A. Some Definitions of Expressions

We need to define some terms and approximation operations for the model.

The triangular interval type-2 fuzzy number is defined as in the following.

Let $\tilde{\tilde{a}} = \left(\left[\underline{l}, \overline{l}\right], m, [\underline{u}, \overline{u}]\right)$ be a triangular interval type-2 fuzzy number. The upper and lower membership functions of $\tilde{\tilde{a}}$ is

$$\mathrm{UMF}_{\tilde{\tilde{a}}}(x) = \begin{cases} \dfrac{x-\underline{l}}{m-\underline{l}}, & \underline{l} \le x \le m \\ \dfrac{x-\overline{u}}{m-\overline{u}}, & m \le x \le \overline{u} \end{cases},$$

$$\mathrm{LMF}_{\tilde{\tilde{a}}}(x) = \begin{cases} \dfrac{x-\overline{l}}{m-\overline{l}}, & \overline{l} \le x \le m \\ \dfrac{x-\underline{u}}{m-\underline{u}}, & m \le x \le \underline{u} \end{cases}.$$

The footprint of uncertainty(FOU) of the membership function is depicted on Fig. 1.

Some approximation operations are defined as follows.

Definition 1. The inverse of a triangular interval type-2 fuzzy number is defined as

$$\frac{1}{\tilde{\tilde{a}}} = \left(\left[\frac{1}{\overline{u}}, \frac{1}{\underline{u}}\right], \frac{1}{m}, \left[\frac{1}{\overline{l}}, \frac{1}{\underline{l}}\right]\right).$$

Definition 2. The logarithm of a triangular interval type-2 fuzzy number is defined as

$$\ln \tilde{\tilde{a}} = \left(\left[\ln \underline{l}, \ln \overline{l}\right], \ln m, [\ln \underline{u}, \ln \overline{u}]\right).$$

Definition 3. The exponential of a triangular interval type-2 fuzzy number is defined as

$$\exp \tilde{\tilde{a}} = \left(\left[\exp \underline{l}, \exp \overline{l}\right], \exp m, [\exp \underline{u}, \exp \overline{u}]\right).$$

Definition 4. The power to the positive integer n of a triangular interval type-2 fuzzy number is defined as

$$\tilde{\tilde{a}}^n = \left(\left[\underline{l}^n, \overline{l}^n\right], m^n, [\underline{u}^n, \overline{u}^n]\right).$$

Definition 5. The negative of a triangular interval type-2 fuzzy number is defined as

$$-\tilde{\tilde{a}} = \left(\left[-\overline{u}, -\underline{u}\right], -m, \left[-\overline{l}, -\underline{l}\right]\right).$$

Based on the definitions above, we can define the binary operations as follows.

Definition 6. Let $\tilde{\tilde{a}} = \left(\left[\underline{a}^l, \overline{a}^l\right], a^m, [\underline{a}^u, \overline{a}^u]\right)$ and $\tilde{\tilde{b}} = \left(\left[\underline{b}^l, \overline{b}^l\right], b^m, \left[\underline{b}^u, \overline{b}^u\right]\right)$ be two triangular interval type-2 fuzzy numbers. The sum of $\tilde{\tilde{a}}$ and $\tilde{\tilde{b}}$ is

$$\tilde{\tilde{a}} + \tilde{\tilde{b}} = \left(\left[\underline{a}^l + \underline{b}^l, \overline{a}^l + \overline{b}^l\right], a^m + b^m, \left[\underline{a}^u + \underline{b}^u, \overline{a}^u + \overline{b}^u\right]\right).$$

Definition 7. Let $\tilde{\tilde{a}} = \left(\left[\underline{a}^l, \overline{a}^l\right], a^m, [\underline{a}^u, \overline{a}^u]\right)$ and $\tilde{\tilde{b}} = \left(\left[\underline{b}^l, \overline{b}^l\right], b^m, \left[\underline{b}^u, \overline{b}^u\right]\right)$ be two triangular interval type-2 fuzzy numbers. The difference of $\tilde{\tilde{a}}$ and $\tilde{\tilde{b}}$ is defined thru the negation as $\tilde{\tilde{a}} - \tilde{\tilde{b}} = \tilde{\tilde{a}} + \left(-\tilde{\tilde{b}}\right)$.

Definition 8. Let $\tilde{\tilde{a}} = \left(\left[\underline{a}^l, \overline{a}^l\right], a^m, [\underline{a}^u, \overline{a}^u]\right)$ and $\tilde{\tilde{b}} = \left(\left[\underline{b}^l, \overline{b}^l\right], b^m, \left[\underline{b}^u, \overline{b}^u\right]\right)$ be two triangular interval type-2 fuzzy numbers. The product of $\tilde{\tilde{a}}$ and $\tilde{\tilde{b}}$ is

$$\begin{aligned} \tilde{\tilde{a}} \cdot \tilde{\tilde{b}} = \Bigg(\Bigg[& \min\left\{\underline{a}^l \cdot \underline{b}^l, \underline{a}^l \cdot \overline{b}^l, \overline{a}^l \cdot \underline{b}^l, \overline{a}^l \cdot \overline{b}^l\right\}, \\ & \max\left\{\underline{a}^l \cdot \underline{b}^l, \underline{a}^l \cdot \overline{b}^l, \overline{a}^l \cdot \underline{b}^l, \overline{a}^l \cdot \overline{b}^l\right\}\Bigg], \\ & a^m \cdot b^m, \Big[\min\left\{\underline{a}^u \cdot \underline{b}^u, \underline{a}^u \cdot \overline{b}^u, \overline{a}^u \cdot \underline{b}^u, \overline{a}^u \cdot \overline{b}^u\right\}, \\ & \max\left\{\underline{a}^u \cdot \underline{b}^u, \underline{a}^u \cdot \overline{b}^u, \overline{a}^u \cdot \underline{b}^u, \overline{a}^u \cdot \overline{b}^u\right\}\Big]\Bigg). \end{aligned}$$

Definition 9. Let $\tilde{\tilde{a}} = \left(\left[\underline{a}^l, \overline{a}^l\right], a^m, [\underline{a}^u, \overline{a}^u]\right)$ and $\tilde{\tilde{b}} = \left(\left[\underline{b}^l, \overline{b}^l\right], b^m, \left[\underline{b}^u, \overline{b}^u\right]\right)$ be two triangular interval type-2 fuzzy numbers, where $\underline{b}^l > 0$ or $\overline{b}^u < 0$. The quotient $\tilde{\tilde{a}}$ and $\tilde{\tilde{b}}$ is defined thru the inverse and multiplication as $\tilde{\tilde{a}}/\tilde{\tilde{b}} = \tilde{\tilde{a}} \cdot \left(1/\tilde{\tilde{b}}\right)$.

All the definitions above are well-defined, because if the type-2 fuzzy numbers are reduced to the type-1 fuzzy numbers or even further to the crisp numbers, then the operations would result in the ordinary traditional definitions of the operations of real numbers.

III. Mathematical Model of Logarithmic Regression Function

The interval type-2 fuzzy pairwise comparison matrix (IT2FPCM) is like

$$\begin{pmatrix} 1 & \tilde{\tilde{\mathbf{r}}}_{12} & \cdots & \tilde{\tilde{\mathbf{r}}}_{1n} \\ \tilde{\tilde{\mathbf{r}}}_{21} & 1 & \cdots & \tilde{\tilde{\mathbf{r}}}_{2n} \\ \vdots & \vdots & \ddots & \vdots \\ \tilde{\tilde{\mathbf{r}}}_{n1} & \tilde{\tilde{\mathbf{r}}}_{n2} & \cdots & 1 \end{pmatrix}$$

where $\tilde{\tilde{\mathbf{r}}}_{ij} = \left[\tilde{\tilde{r}}_{ij1}, \tilde{\tilde{r}}_{ij2}, \cdots, \tilde{\tilde{r}}_{ij\delta_{ij}}\right]^T$ and δ_{ij} is the number of judgments given by experts for the preference of the criterion i to the criterion j. The triangular interval type-2 fuzzy number $\tilde{\tilde{r}}_{ijk}$ is the relative comparison judgment of the criterion i to the criterion j given by the k^{th} expert. Note that $\delta_{ij} = \delta_{ji}$ and some δ_{ij} could be 0 but not all $\delta_{ij} = 0$ for $i = 1, 2, \cdots, n; i \neq j$. In other words, it is not reasonable that no any judgments of criterion i to other criteria are given.

Let $\tilde{\tilde{w}}_i$ be the absolute weight for the criterion i. Based on the assumption that $\tilde{\tilde{r}}_{ijk} \approx \tilde{\tilde{w}}_i / \tilde{\tilde{w}}_j$, and to obtain the optimal solutions for $\tilde{\tilde{w}}_i$, it is required that

$$\text{Min} J = \sum_{i=1}^{n} \sum_{\substack{j=1 \\ j\neq i}}^{n} \sum_{k=1}^{\delta_{ij}} \left(\ln \tilde{\tilde{r}}_{ijk} - \ln \frac{\tilde{\tilde{w}}_i}{\tilde{\tilde{w}}_j} \right)^2. \quad (1)$$

Let $\tilde{\tilde{r}}_{ijk} = \left(\left[\underline{r}^l_{ijk}, \overline{r}^l_{ijk} \right], r^m, \left[\underline{r}^u_{ijk}, \overline{r}^u_{ijk} \right] \right)$ and $\tilde{\tilde{w}}_i = \left(\left[\underline{w}^l_i, \overline{w}^l_i \right], w^m_i, [\underline{w}^u_i, \overline{w}^u_i] \right)$. Using the definitions, the logarithmic regression equation (2) can be expressed as

$$\begin{aligned} \text{Min } J &= \sum_{i=1}^{n} \sum_{\substack{j=1 \\ j\neq i}}^{n} \sum_{k=1}^{\delta_{ij}} \left(\ln \tilde{\tilde{r}}_{ijk} - \ln \frac{\tilde{\tilde{w}}_i}{\tilde{\tilde{w}}_j} \right)^2 \\ &= \sum_{i=1}^{n} \sum_{\substack{j=1 \\ j\neq i}}^{n} \sum_{k=1}^{\delta_{ij}} \left(\ln \tilde{\tilde{r}}_{ijk} - \ln \tilde{\tilde{w}}_i + \ln \tilde{\tilde{w}}_j \right)^2. \quad (2) \end{aligned}$$

Extending the type-1 fuzzy models from [4], [5], [11] and using the definitions 2, 5, 9, the approximation of (2) can be expressed as

$$\begin{aligned} &\text{Min } J = \\ &\sum_{i=1}^{n} \sum_{\substack{j=1 \\ j\neq i}}^{n} \sum_{k=1}^{\delta_{ij}} \left(\ln \underline{r}^l_{ijk} - \ln \underline{w}^l_i + \ln \overline{w}^l_j \right)^2 \quad (3) \\ &+ \sum_{i=1}^{n} \sum_{\substack{j=1 \\ j\neq i}}^{n} \sum_{k=1}^{\delta_{ij}} \left(\ln \overline{r}^l_{ijk} - \ln \overline{w}^l_i + \ln \underline{w}^l_j \right)^2 \quad (4) \\ &+ \sum_{i=1}^{n} \sum_{\substack{j=1 \\ j\neq i}}^{n} \sum_{k=1}^{\delta_{ij}} \left(\ln r^m_{ijk} - \ln w^m_i + \ln w^m_j \right)^2 \\ &+ \sum_{i=1}^{n} \sum_{\substack{j=1 \\ j\neq i}}^{n} \sum_{k=1}^{\delta_{ij}} \left(\ln \underline{r}^u_{ijk} - \ln \underline{w}^u_i + \ln \overline{w}^l_j \right)^2 \quad (5) \\ &+ \sum_{i=1}^{n} \sum_{\substack{j=1 \\ j\neq i}}^{n} \sum_{k=1}^{\delta_{ij}} \left(\ln \overline{r}^u_{ijk} - \ln \overline{w}^u_i + \ln \underline{w}^l_j \right)^2. \quad (6) \end{aligned}$$

To get the minimum of J, it is required that

$$\frac{\partial J}{\partial \underline{w}^l_i} = \frac{-2}{\underline{w}^l_i} \sum_{\substack{j=1 \\ j\neq i}}^{n} \sum_{k=1}^{\delta_{ij}} \left(\ln \underline{r}^l_{ijk} - \ln \underline{w}^l_i + \ln \overline{w}^l_j \right) = 0, \quad (7)$$

$$\frac{\partial J}{\partial \overline{w}^l_i} = \frac{-2}{\overline{w}^l_i} \sum_{\substack{j=1 \\ j\neq i}}^{n} \sum_{k=1}^{\delta_{ij}} \left(\ln \overline{r}^l_{ijk} - \ln \overline{w}^l_i + \ln \underline{w}^l_j \right) = 0, \quad (8)$$

$$\frac{\partial J}{\partial w^m_i} = \frac{-2}{w^m_i} \sum_{\substack{j=1 \\ j\neq i}}^{n} \sum_{k=1}^{\delta_{ij}} \left(\ln r^m_{ijk} - \ln w^m_i + \ln w^m_j \right) = 0, \quad (9)$$

$$\frac{\partial J}{\partial \underline{w}^u_i} = \frac{-2}{\underline{w}^u_i} \sum_{\substack{j=1 \\ j\neq i}}^{n} \sum_{k=1}^{\delta_{ij}} \left(\ln \underline{r}^u_{ijk} - \ln \underline{w}^u_i + \ln \overline{w}^l_j \right) = 0, \quad (10)$$

$$\frac{\partial J}{\partial \overline{w}^u_i} = \frac{-2}{\overline{w}^u_i} \sum_{\substack{j=1 \\ j\neq i}}^{n} \sum_{k=1}^{\delta_{ij}} \left(\ln \overline{r}^u_{ijk} - \ln \overline{w}^u_i + \ln \underline{w}^l_j \right) = 0, \quad (11)$$

for $i = 1, 2, \cdots n$. The equations (7)~(11) can be divided into three uncoupled linear systems,

$$\begin{aligned} \begin{bmatrix} D & E \\ E & D \end{bmatrix} \begin{bmatrix} \underline{\mathbf{l}} \\ \overline{\mathbf{u}} \end{bmatrix} &= \begin{bmatrix} \underline{\mathbf{b}}^l \\ \overline{\mathbf{b}}^u \end{bmatrix}, \quad (12) \\ [D+E]\,\overline{\mathbf{m}} &= \mathbf{b}^m, \quad (13) \\ \begin{bmatrix} D & E \\ E & D \end{bmatrix} \begin{bmatrix} \overline{\mathbf{l}} \\ \underline{\mathbf{u}} \end{bmatrix} &= \begin{bmatrix} \overline{\mathbf{b}}^l \\ \underline{\mathbf{b}}^u \end{bmatrix}., \quad (14) \end{aligned}$$

where $D = diag(\sum_{j=2}^{n} \delta_{1j}, \sum_{\substack{j=1 \\ j\neq 2}}^{n} \delta_{2j}, \cdots, \sum_{j=1}^{n-1} \delta_{nj})$, and $E = [e_{ij}]$ with $e_{ij} = \begin{cases} 0, & i = j \\ -\delta_{ij}, & i \neq j \end{cases}$, and the unknowns are $\mathbf{t} = [\ln w^t_i]$, $t = l$ or u, the knowns are $\mathbf{b}^t = [b^t_i]$, $b^t_i = \sum_{\substack{j=1 \\ j\neq i}}^{n} \sum_{k=1}^{\delta_{ij}} \ln \underline{r}^l_{ijk}$, $t = l$ or u or m. Both $\mathbf{t}$ and $\mathbf{b}$ can be appended the underline or overline. Furthermore, let $A = \begin{bmatrix} D & E \\ E & D \end{bmatrix}$, $A^m = D + E$, the linear systems (12)~(14) can be expressed as

$$\begin{aligned} A\mathbf{w}_1 &= \mathbf{b}_1, \quad (15) \\ A^m \mathbf{w}^m &= \mathbf{b}^m, \quad (16) \\ A\mathbf{w}_2 &= \mathbf{b}_2. \quad (17) \end{aligned}$$

The linear systems (15)~(17) which are uncoupled can be solved independently. If each $\delta_{ij} \neq 0$, then it can be easily shown that A and A^m are not of full rank. Each of the linear system (15)~(17) has infinite many solutions. The solutions exist for systems (15)~(17).

A. Theorems

Since the judgment matrix is reciprocal, we have $\tilde{\tilde{r}}_{jik} = 1/\tilde{\tilde{r}}_{ijk}$ and $\ln \tilde{\tilde{r}}_{jik} = -\ln \tilde{\tilde{r}}_{ijk}$. It follows that

$$\begin{aligned}&\ln\left(\left(\left[\underline{r}^l_{jik}, \overline{r}^l_{jik}\right], r^m_{jik}, \left[\underline{r}^u_{jik}, \overline{r}^u_{jik}\right]\right)\right)\\ &= -\ln\left(\left[\underline{r}^l_{ijk}, \overline{r}^l_{ijk}\right], r^m, \left[\underline{r}^u_{ijk}, \overline{r}^u_{ijk}\right]\right).\end{aligned}$$

The rank of A and the rank of the augmented matrices $\left[\begin{array}{cc} A & \mathbf{b}_1 \end{array}\right]$ and $\left[\begin{array}{cc} A & \mathbf{b}_2 \end{array}\right]$ are the same and the dimension of the null space of A is 1. Also, the rank of A^m and the augmented matrix $\left[\begin{array}{cc} A^m & \mathbf{b}^m \end{array}\right]$ are the same and the dimension of the null space of A^m is equal to 1. Therefore, all the three linear systems (15)~(17) have infinite many solutions.

It is suffice to assume that each of δ_{ij}, $i = 1, 2, \cdots, n; i \neq j$ is not equal to 0 on the following theorems and corollaries. Let $\mathbf{1} = [1, 1, \cdots, 1]^t$ in the sequel.

Theorem 1. *The nullity of the coefficient matrix A of the linear system (15) is 1 and the null space of A is span $\{\mathbf{1}\}$.*

Proof: The proof can be easily followed by the row reduced echelon form of A. ■

Theorem 2. *The rank of A is the same as the augmented matrix $\left[\begin{array}{cc} A & \mathbf{b}_1 \end{array}\right]$ of the linear system (15).*

Proof: The proof can be easily followed by the row reduced echelon form of the augmented matrix $\left[\begin{array}{cc} A & \mathbf{b}_1 \end{array}\right]$. ■

Theorem 3. *The rank of A is the same as the augmented matrix $\left[\begin{array}{cc} A & \mathbf{b}_2 \end{array}\right]$ of the linear system (17).*

Proof: The proof is the same as in Theorem 2. ■

Corollary 1. *The linear system (15) has infinite solutions with two degrees of freedom.*

Proof: The solution space has two degrees of freedom, because the nullity of the coefficient matrix is 1. ■

Corollary 2. *The linear system (17) has infinite solutions with two degrees of freedom.*

Proof: The proof is the same as in 1. ■

Let A^+ be the Moore-Penrose pseudo-inverse of A[12, p.432], then the particular solutions of (15) and (17) are

$$\mathbf{w}^p_1 = A^+\mathbf{b}_1, \tag{18}$$
$$\mathbf{w}^p_2 = A^+\mathbf{b}_2. \tag{19}$$

The general solution can be expressed as

$$\mathbf{w}_1 = A^+\mathbf{b}_1 + p_1\mathbf{1},\ p_1 \in \mathbb{R}. \tag{20}$$
$$\mathbf{w}_2 = A^+\mathbf{b}_2 + p_2\mathbf{1},\ p_2 \in \mathbb{R}. \tag{21}$$

Theorem 4. *The nullity of the coefficient matrix A^m of the linear system (16) is 1 and the null space of A^m is span $\{\mathbf{1}\}$.*

Proof: The proof can be easily followed by the row reduced echelon form of A^m. The nullity of A^m is 1, and the null space is span $\{\mathbf{1}\}$. ■

Theorem 5. *The rank of A^m is the same as the augmented matrix $\left[\begin{array}{cc} A^m & \mathbf{b}^m \end{array}\right]$ of the linear system (16).*

Proof: The proof can be easily followed by the row reduced echelon form of the augmented matrix $\left[\begin{array}{cc} A^m & \mathbf{b}^m \end{array}\right]$. The rank of the augmented matrix $\left[\begin{array}{cc} A^m & \mathbf{b}^m \end{array}\right]$ is $(n-1)$ which is equal to the rank of A^m. ■

Corollary 3. *The linear system (16) has infinite solutions with one degrees of freedom.*

Proof: The solution space has one degrees of freedom, because the nullity of the coefficient is 1. ■

Let A^{m+} be the Moore-Penrose pseudo-inverse of A^m[12, p.432], then the particular solution $\mathbf{w}^{m,p}$ is $A^{m+}\mathbf{b}^m$. The general solution can be expressed as

$$\mathbf{w}^m = A^{m+}\mathbf{b}^m + p_m\mathbf{1},\ p_m \in \mathbb{R}. \tag{22}$$

IV. Normalization

The weight $\tilde{\tilde{w}}_i = \left(\left[\underline{l}_i, \overline{l}_i\right], m_i, \left[\underline{u}_i, \overline{u}_i\right]\right)$ is a triangular interval type-2 fuzzy weights for the criteria. It should be well-defined and satisfied the inequalities

$$\underline{l}_i \leq \overline{l}_i \leq m_i \leq \underline{u}_i \leq \overline{u}_i. \tag{23}$$

From Corollaries 1 and 3, the final solution of the weight of a certain criterion has three degrees of freedom. The suitable or the optimal parameters can be selected such that the final solution of the weight is a well-defined triangular interval type-2 fuzzy number.

From (20) and (22), we have

$$\ln \tilde{\tilde{w}}_i = \left(\left[\underline{l}_i + p_1, \overline{l}_i + p_2\right], m_i + p_m, \left[\underline{u}_i + p_2, \overline{u}_i + p_1\right]\right),$$

where s, t, v are three arbitrary parameters. The parameter v can be independently determined by normalizing modal vector in the sense of unit vector sum. Namely, $\sum_{i=1}^n \exp(m_i + p_m) = 1$,then we have

$$p_m = -\ln\left(\sum_{i=1}^n \exp m_i\right). \tag{24}$$

The other two parameters s, t can be determined by minimizing the spans of the supports of the FOU. A quadratic programming(QP) model can be constructed to find the optimal

solution for p_1 and p_2.

$$\begin{aligned}
&\min J \\
&= \sum_{i=1}^{n} \Big(\big((\bar{l}_i + p_2) - (\underline{l}_i + p_1) \big)^2 \\
&+ \big((m_i + p_m) - (\bar{l}_i + p_2) \big)^2 \\
&+ \big((\underline{u}_i + p_2) - (m_i + p_m) \big)^2 \\
&+ \big((\overline{u}_i + p_1) - (\underline{u}_i + p_2) \big)^2 \Big) \\
&\underline{l}_i + p_1 \le \bar{l}_i + p_2,\ i = 1, 2, \cdots, n \\
&\underline{u}_i + p_2 \le \overline{u}_i + p_1,\ i = 1, 2, \cdots, n \\
&\bar{l}_i + p_2 \le m_i + p_m,\ i = 1, 2, \cdots, n \\
&m_i + p_m \le \underline{u}_i + p_2,\ i = 1, 2, \cdots, n \\
&p_1, p_2 \text{ unbounded.}
\end{aligned}$$

Let

$$\begin{aligned}
J' = J - \sum_{i=1}^{n} \big(& \underline{l}_i^2 + 2\bar{l}_i^2 + 2\underline{u}_i^2 + \bar{u}_i^2 \\
& + 2m_i^2 + 2p_m^2 - 2p_m \bar{l}_i \\
& - 2\bar{l}_i \underline{l}_i - 2m_i \underline{u}_i - 2p_m \underline{u}_i \\
& - 2\bar{u}_i \underline{u}_i + 4p_m m_i - 2m_i \bar{l}_i \big)
\end{aligned}$$

and introduce the following matrices and vectors,

$$\mathbf{x} = \begin{bmatrix} p_1 \\ p_2 \end{bmatrix},\ Q = \begin{bmatrix} 4n & -4n \\ -4n & 8n \end{bmatrix},$$
$$\mathbf{c} = \begin{bmatrix} \sum_{i=1}^{n} \left(-2\bar{l}_i + 2\underline{l}_i + 2\bar{u}_i - 2\underline{u}_i \right) \\ \sum_{i=1}^{n} \left(4\bar{l}_i - 2\underline{l}_i - 2\bar{u}_i + 4\underline{u}_i - 4m_i - 4v \right) \end{bmatrix},$$

the objective function of the QP model can be expressed as

$$\text{Min } J' = \frac{1}{2}\mathbf{x}^t Q \mathbf{x} + \mathbf{x}^t \mathbf{c}.$$

Since Q is a positive definite matrix, the minimizer exists and is unique. Suppose the optimal solution exists at $p_1 = p_1^\star$ and $p_2 = p_2^\star$, the optimal normalized ith IT2 triangular fuzzy weight can be expressed as

$$\begin{aligned}
\tilde{\tilde{w}}_i = & \Big(\left[\exp(p_1^\star) \cdot \exp \underline{l}_i, \exp(p_2^\star) \cdot \exp \bar{l}_i \right], \\
& \frac{\exp m_i}{\sum_{j=1}^{n} \exp m_j}, \\
& \left[\exp(p_2^\star) \cdot \exp \underline{u}_i, \exp(p_1^\star) \cdot \exp \overline{u}_i \right] \Big).
\end{aligned}$$

V. Aggregation

Let $\tilde{\tilde{r}}_i = \left(\left[\underline{r}_i^l, \overline{r}_i^l \right], r_i^m, \left[\underline{r}_i^u, \overline{r}_i^u \right] \right)$ be the rate for a certain alternative corresponding to the i^{th} criterion whose weight is $\tilde{\tilde{w}}_i = \left(\left[\underline{w}_i^l, \overline{w}_i^l \right], w_i^m, \left[\underline{w}_i^u, \overline{w}_i^u \right] \right)$. We propose two approaches to find the IT2 fuzzy weighted average(FWA) for IT2 TFNs. One is using the linear programming models to find the uncertainty supports of the lower membership function (LMF) and upper membership function(UMF). The other is a direct extension from the interval weighted average to the IT2 FWA of the IT2 TFNs.

A. Aggregation by Linear Programming

Model-I(lower bound of UMF)

$$\begin{aligned}
\text{Min } \underline{r}_{\text{ave}}^l &= \sum_{i=1}^{n} \underline{r}_i^l \cdot w_i, \\
\frac{\underline{w}_i^l}{\sum_{j=1}^{n} \overline{w}_j^u} &\le w_i \le \frac{\overline{w}_i^u}{\sum_{j=1}^{n} \underline{w}_i^l},\ i = 1, 2, \cdots n, \\
\sum_{i=1}^{n} w_i &= 1.
\end{aligned}$$

Model-II(lower bound of LMF)

$$\begin{aligned}
\text{Min } \overline{r}_{\text{ave}}^l &= \sum_{i=1}^{n} \overline{r}_i^l \cdot w_i, \\
\frac{\overline{w}_i^l}{\sum_{j=1}^{n} \underline{w}_j^u} &\le w_i \le \frac{\underline{w}_i^u}{\sum_{j=1}^{n} \overline{w}_j^l},\ i = 1, 2, \cdots n, \\
\sum_{i=1}^{n} w_i &= 1.
\end{aligned}$$

Model-III(upper bound of LMF)

$$\begin{aligned}
\text{Max } \underline{r}_{\text{ave}}^u &= \sum_{i=1}^{n} \underline{r}_i^u \cdot w_i, \\
\frac{\overline{w}_i^l}{\sum_{j=1}^{n} \underline{w}_j^u} &\le w_i \le \frac{\underline{w}_i^u}{\sum_{j=1}^{n} \overline{w}_j^l},\ i = 1, 2, \cdots n, \\
\sum_{i=1}^{n} w_i &= 1.
\end{aligned}$$

Model-IV(upper bound of UMF)

$$\begin{aligned}
\text{Max } \overline{r}_{\text{ave}}^u &= \sum_{i=1}^{n} \overline{r}_i^u \cdot w_i, \\
\frac{\underline{w}_i^l}{\sum_{j=1}^{n} \overline{w}_j^u} &\le w_i \le \frac{\overline{w}_i^u}{\sum_{j=1}^{n} \underline{w}_i^l},\ i = 1, 2, \cdots n, \\
\sum_{i=1}^{n} w_i &= 1.
\end{aligned}$$

Let $\underline{r}_{\text{ave}}^{l\star}, \overline{r}_{\text{ave}}^{l\star}, \underline{r}_{\text{ave}}^{u\star}, \overline{r}_{\text{ave}}^{u\star}$ be the optimal solutions of the above four linear programming models, respectively, and let the modal weighted average be $r_{\text{ave}}^m = \frac{\sum_{i=1}^{n} r_i^m \cdot w_i^m}{\sum_{j=1}^{n} w_i^m}$, then interval type-2 fuzzy weighted average is

$$\tilde{\tilde{r}}_{\text{ave}} = \left(\left[\underline{r}_{\text{ave}}^{l\star}, \overline{r}_{\text{ave}}^{l\star} \right], r_{\text{ave}}^m, \left[\underline{r}_{\text{ave}}^{u\star}, \overline{r}_{\text{ave}}^{u\star} \right] \right).$$

B. Aggregation from Extension of Type-1 FWA

By extending the type-1 fuzzy weighted average, [13] introduced a set of formulas which can be used to find the supports of the LMF and UMF of the IT2 FWA as follows,

$$\underline{r}_{ave}^{l} = \frac{\sum_{i=1}^{\underline{k}^{l}} \underline{r}_{i}^{l} \cdot \overline{w}_{i}^{u} + \sum_{i=\underline{k}^{l}+1}^{n} \underline{r}_{i}^{l} \cdot \underline{w}_{i}^{l}}{\sum_{i=1}^{\underline{k}^{l}} \overline{w}_{i}^{u} + \sum_{i=\underline{k}^{l}+1}^{n} \underline{w}_{i}^{l}}, \quad (25)$$

$$\overline{r}_{ave}^{l} = \frac{\sum_{i=1}^{\overline{k}^{l}} \overline{r}_{i}^{l} \cdot \underline{w}_{i}^{u} + \sum_{i=\overline{k}^{l}+1}^{n} \overline{r}_{i}^{l} \cdot \overline{w}_{i}^{l}}{\sum_{i=1}^{\overline{k}^{l}} \underline{w}_{i}^{u} + \sum_{i=\overline{k}^{l}+1}^{n} \overline{w}_{i}^{l}}, \quad (26)$$

$$\underline{r}_{ave}^{u} = \frac{\sum_{i=1}^{\underline{k}^{u}} \underline{r}_{i}^{u} \cdot \underline{w}_{i}^{l} + \sum_{i=\underline{k}^{u}+1}^{n} \underline{r}_{i}^{u} \cdot \underline{w}_{i}^{u}}{\sum_{i=1}^{\underline{k}^{u}} \underline{w}_{i}^{l} + \sum_{i=\underline{k}^{u}+1}^{n} \underline{w}_{i}^{u}}, \quad (27)$$

$$\overline{r}_{ave}^{u} = \frac{\sum_{i=1}^{\overline{k}^{u}} \overline{r}_{i}^{u} \cdot \underline{w}_{i}^{l} + \sum_{i=\overline{k}^{u}+1}^{n} \overline{r}_{i}^{u} \cdot \overline{w}_{i}^{u}}{\sum_{i=1}^{\overline{k}^{u}} \underline{w}_{i}^{l} + \sum_{i=\overline{k}^{u}+1}^{n} \overline{w}_{i}^{u}}, \quad (28)$$

where $\underline{k}^{l}$, $\overline{k}^{l}$, $\underline{k}^{u}$, $\overline{k}^{u}$ are the indexes satisfying the following inequalities respectively,

$$\begin{aligned} \underline{r}_{\underline{k}^{l}}^{l} &\leq \underline{r}_{ave}^{l} \leq \underline{r}_{\underline{k}^{l}+1}^{l}, \\ \overline{r}_{\overline{k}^{l}}^{l} &\leq \overline{r}_{ave}^{l} \leq \overline{r}_{\overline{k}^{l}+1}^{l}, \\ \underline{r}_{\underline{k}^{u}}^{u} &\leq \underline{r}_{ave}^{u} \leq \underline{r}_{\underline{k}^{u}+1}^{u}, \\ \overline{r}_{\overline{k}^{u}}^{u} &\leq \overline{r}_{ave}^{u} \leq \overline{r}_{\overline{k}^{u}+1}^{u}. \end{aligned}$$

These indexes are commonly referred to as the thresholds for the supports of the LMFs and UMFs of the IT2 fuzzy weights and have been proved to be unique[14], [13]. Some algorithms [15], [14], [16] were developed to determine these thresholds. We adopt the algorithm from [16]. The algorithm for finding $\underline{r}_{ave}^{l}$ is as follows:

Stage1: Sort $\underline{r}_{i}^{l}$, for $i = 1, 2, \cdots, n$ in non-decreasing order and rearrange $\left[\underline{w}_{i}^{l}, \overline{w}_{i}^{u}\right]$ with respect to the reordered $\underline{r}_{i}^{l}$.

Stage2: Construct the function of index

$$\tau(i) = \frac{\sum_{j=1}^{i} \left(\underline{r}_{j}^{l} - \underline{r}_{i}^{l}\right) \cdot \overline{w}_{i}^{u} + \sum_{j=i+1}^{n} \left(\underline{r}_{j}^{l} - \underline{r}_{i}^{l}\right) \cdot \underline{w}_{i}^{l}}{\sum_{j=1}^{i} \overline{w}_{j}^{u} + \sum_{j=i+1}^{n} \underline{w}_{j}^{l}}.$$

Stage3: The threshold $\underline{k}^{l}$ exists at the index where $\tau\left(\underline{k}^{l}\right) > 0$ and $\tau\left(\underline{k}^{l}+1\right) \leq 0$.([16] proved that such index exists and is unique.)

Stage4: Substitute the threshold $\underline{k}^{l}$ into (25) to get $\underline{r}_{ave}^{l}$.

The algorithms for determining the thresholds for other supports can be constructed similarly by defining the corresponding specific index functions.

VI. Ranking of IT2FSs

The final stage of the decision making process is to rank the overall ratings of the alternatives. It is not trivial to rank a set of IT2FSs. Most of the ranking algorithms are for type-1 FSs. So far there are two mature ranking algorithms proposed in literature. [17] adopted a statistical viewpoint and interpret each type-2 fuzzy number as an ensemble of ordinary fuzzy numbers. By ranking the 32 IT2FSs which represents words for computation, [18] pointed out that Mitchell's method is highly impractical and prohibitive. Wu and Mendel proposed an extension of the type-1 FSs centroid method to obtain the centroids of a set of IT2FSs, which are used for ranking these IT2FSs. The centroid of an IT2FS is approximated by discretizing the primary domain. Let x_i be the ith sample point of the primary variable x in ascending order with index i, then the IT2FS centroid can be obtained from the following formulas

$$\begin{aligned} c_{l}(j) &= \frac{\sum_{i=1}^{j} x_i \overline{\mu}(x_i) + \sum_{i=j+1}^{n} x_i \underline{\mu}(x_i)}{\sum_{i=1}^{j} \overline{\mu}(x_i) + \sum_{i=j+1}^{n} \underline{\mu}(x_i)}, \\ c_{u}(j) &= \frac{\sum_{i=1}^{j} x_i \underline{\mu}(x_i) + \sum_{i=j+1}^{n} x_i \overline{\mu}(x_i)}{\sum_{i=1}^{j} \underline{\mu}(x_i) + \sum_{i=j+1}^{n} \overline{\mu}(x_i)}, \end{aligned}$$

for a specific switching indexes is $c = [c_l, c_u]$ where indexes k_l and k_u are the switching index such that

VII. Numerical Example

The fuzzy logarithmic least squares for fuzzy pairwise comparison matrix was proposed by [4] and modified by [5]. We investigate the same numerical example in both papers in which the type-1 fuzzy judgments are all extending to the IT2 triangular fuzzy numbers.

One of the three candidates (A, B and C) seeking for a post of professor in Operations Research is to be determined by a committee of three members. The following four criteria are identified by the committee for selecting the best candidates.

C1: Mathematical creativity,
C2: Implementation creativity,
C3: Administrative capability,
C4: Human maturity.

Fig. 2 shows the hierarchy structure of the decision making problem.

The committee members need to give the pairwise comparison judgments. All the linguistic judgments from committee members are transformed to the corresponding IT2 triangular fuzzy numbers. The set of IT2 triangular fuzzy scales that is the type-2 fuzzy extension of Saaty's scale ([19]) defined as

$$\begin{aligned} \tilde{\tilde{1}} &= ([1,1], 1, [3/2, 2]), \\ \tilde{\tilde{2}} &= ([1, 3/2], 2, [5/2, 3]), \\ \tilde{\tilde{3}} &= ([2, 5/2], 3, [7/2, 4]). \end{aligned}$$

Additionally, the reciprocals are defined by Definition 1.

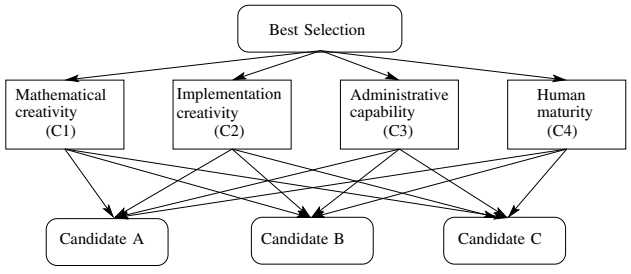

Figure 2. Hierarchy structure for the best candidate decision problem

Table I
THE PAIRWISE COMPARISON JUDGMENTS OF THE FOUR CRITERIA

$C_1 - C_2$	$C_1 - C_3$	$C_1 - C_4$	$C_2 - C_3$	$C_2 - C_4$	$C_3 - C_4$
$\left\{\tilde{\tilde{1}}, \tilde{\tilde{\frac{1}{2}}}, \tilde{\tilde{2}}\right\}$	$\left\{\tilde{\tilde{1}}\right\}$	$\left\{\tilde{\tilde{\frac{1}{3}}}, \tilde{\tilde{\frac{1}{3}}}, \tilde{\tilde{\frac{1}{2}}}\right\}$	$\left\{\tilde{\tilde{3}}, \tilde{\tilde{3}}\right\}$	$\left\{\tilde{\tilde{1}}, \tilde{\tilde{1}}, \tilde{\tilde{2}}\right\}$	$\left\{\tilde{\tilde{\frac{1}{2}}}\right\}$

Table II
PAIRWISE COMPARISONS OF THE THREE CANDIDATES WITH RESPECT TO THE FOUR CRITERIA

	A-B	A-C	B-C
C1	$\left\{\tilde{\tilde{1}}, \tilde{\tilde{1}}\right\}$	$\left\{\tilde{\tilde{1}}, \tilde{\tilde{\frac{1}{2}}}\right\}$	$\left\{\tilde{\tilde{\frac{1}{2}}}\right\}$
C2	$\left\{\tilde{\tilde{3}}\right\}$	$\left\{\tilde{\tilde{2}}\right\}$	
C3	$\left\{\tilde{\tilde{5}}, \tilde{\tilde{3}}, \tilde{\tilde{2}}\right\}$	$\left\{\tilde{\tilde{3}}\right\}$	$\left\{\tilde{\tilde{1}}\right\}$
C4		$\left\{\tilde{\tilde{2}}, \tilde{\tilde{\frac{1}{2}}}\right\}$	$\left\{\tilde{\tilde{2}}\right\}$

Table I shows the pairwise comparison judgments of the four criteria. Note that, not each of the committee members is required to give judgment for pairs of criteria. For example, only one member gives the judgment $\tilde{\tilde{\frac{1}{2}}}$ for the pair (C_3, C_4).

Table II contains the pairwise comparison judgments of the three candidates with respect to the four criteria.

Using the IT2 FLLSM and the optimal normalization process developed in this paper, the IT2 TFN weights for the four criteria are obtained and is shown in Table III and Fig. 3.

Table IV shows the IT2 fuzzy rates for three candidates with respective to the four criteria.

We apply two approaches from Section V-A and Section V-B to finding the overall aggregated IT2 fuzzy rates of the three candidates as in Tables V and VI.

Fig. 4 and Fig. 5 show the overall aggregated IT2 fuzzy rates for the three candidates. It is clear that candidate A is the best candidate.

Table III
THE IT2 FUZZY WEIGHTS FOR FOUR CRITERIA NORMALIZED BY MINIMIZING THE QUADRATIC SUM OF FOUR SPANS.

C1	$([0.1718, 0.1836], 0.1945, [0.2283, 0.2680])$
C2	$([0.2609, 0.2904], 0.3192, [0.3617, 0.3977])$
C3	$([0.1149, 0.1246], 0.1398, [0.1490, 0.1649])$
C4	$([0.2531, 0.2982], 0.3466, [0.3708, 0.3946])$

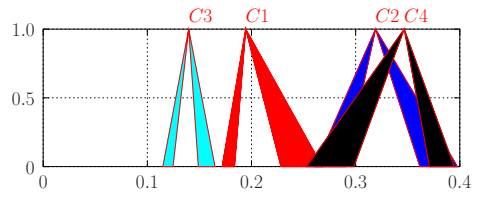

Figure 3. The IT2 fuzzy weights for four criteria normalized by minimizing the quadratic sum of four spans.

Table IV
THE IT2 FUZZY RATES FOR THREE CANDIDATES WITH RESPECTIVE TO THE FOUR CRITERIA

	candidate A
C1	$([0.2891, 0.2891], 0.2891, [0.3448, 0.3694])$
C2	$([0.3782, 0.4664], 0.5455, [0.6186, 0.6872])$
C3	$([0.4620, 0.5375], 0.5789, [0.6326, 0.6991])$
C4	$([0.2184, 0.2321], 0.2500, [0.2752, 0.3150])$
	candidate B
C1	$([0.1801, 0.2171], 0.2651, [0.2730, 0.2818])$
C2	$([0.1718, 0.1767], 0.1818, [0.1865, 0.1891])$
C3	$([0.1975, 0.2040], 0.2167, [0.2572, 0.2988])$
C4	$([0.3783, 0.4494], 0.5000, [0.5328, 0.5456])$
	candidate C
C1	$([0.2679, 0.3652], 0.4458, [0.4840, 0.5136])$
C2	$([0.2291, 0.2474], 0.2727, [0.3109, 0.3782])$
C3	$([0.1616, 0.1760], 0.2045, [0.2094, 0.2136])$
C4	$([0.1819, 0.2131], 0.2500, [0.2996, 0.3783])$

Table V
THE IT2 FUZZY RATES FOR THE OVERALL GLOBAL FUZZY RATES USING APPROACH IN SECTION V-A

	Linear programming model(V-A)
A	$([0.2894, 0.3398], 0.3979, [0.4833, 0.5682])$
B	$([0.2185, 0.2611], 0.3132, [0.3560, 0.3947])$
C	$([0.1998, 0.2411], 0.2890, [0.3406, 0.4081])$

Table VII provides the comparative results from [4] and [5], in which the triangular fuzzy sets represented by (l, m, r) are used. It shows that candidate A is also the best candidate. Note that the middle points of the results, 0.40 for candidate A, 0.31 for candidate B and 0.29 for candidate C, are exactly the same (despite of the decimal digits) as our approach in Tables V and VI, namely 0.3979 for candidate A, 0.3131 for candidate B and 0.2890 for candidate C.

VIII. CONCLUSION

In this article, we have introduced an overall process for implementing interval type-2 fuzzy sets on group decision

Table VI
THE IT2 FUZZY RATES FOR THE OVERALL GLOBAL FUZZY RATES USING APPROACH IN SECTION V-B.

	Fuzzy Weighted Average(V-B)
A	$([0.3037, 0.3495], 0.3979, [0.4668, 0.5385])$
B	$([0.2260, 0.2679], 0.3132, [0.3445, 0.3687])$
C	$([0.2058, 0.2457], 0.2890, [0.3359, 0.3976])$

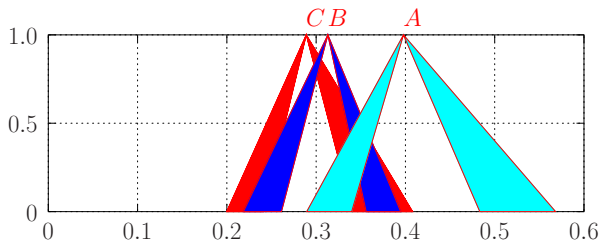

Figure 4. The global fuzzy rates of three candidates using linear programming model

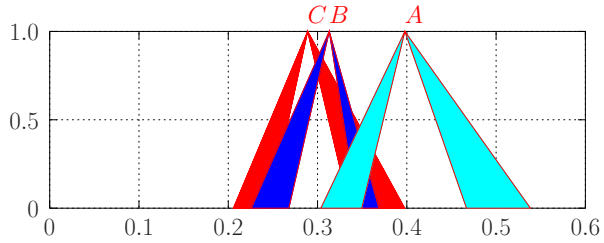

Figure 5. The global fuzzy rates of three candidates using IT2 fuzzy weighted average

Table VII
RESULTS OBTAINED IN [4] AND [5]

	Laarhoven and Pedrycz[4]	Boender,Graan and Lootsma[5]
A	(0.23, 0.40, 0.71)	(0.30, 0.40, 0.54)
B	(0.17, 0.31, 0.58)	(0.22, 0.31, 0.42)
C	(0.19, 0.29, 0.51)	(0.23, 0.29, 0.36)

making problems with uncertain judgments. Since most decision making problems exist in real world. The judgments are always made by human beings. Not all the experts are familiar with the mathematical properties of the decision making process. If the type of judgments given by experts can be allowed to as flexible as possible, then the collected decision data would be much more valuable. Type-2 fuzzy sets are the better mathematical quantities than type-1 fuzzy sets and even better than the crisp scales. Using type-2 fuzzy sets on decision making problems can lead to more realistic and accurate results. This paper proposes a very important approach on decision making problem with type-2 fuzzy sets specifically on the very popular decision tool, Analytic Hierarchy Process.

We extend the logarithmic least squares method proposed by [4] and formulate a quadratic model for the optimal solutions of the interval type-2 fuzzy priority weights. We also give a detail discussion about the simultaneous linear equations of the logarithmic decision variables. After obtaining these interval type-2 fuzzy weights, we construct a linear programming model to get the overall rate of interval type-2 fuzzy rates. Finally, the individual overall type-2 fuzzy rates are sorted using the centroids of the type-2 fuzzy sets.

The proposed model is for triangular type interval type-2 fuzzy sets. For different purposes, other kinds lower and upper membership functions can be used. For example, one can use triangular membership function for lower membership function and trapezoidal membership function for upper membership function or both trapezoidal membership functions for lower and upper membership function. In addition to the logarithmic least square method, other algorithms (for example, [9]) can be used to obtain the optimal type-2 fuzzy priority weights and rates. We need further studies on these topics.

REFERENCES

[1] T. L. Saaty, *The Analytical Hierarchy Process*. New York, 1980.
[2] J. de Graan, "Extensions to the multiple criteria analysis method of t.l. saaty," National Institute for Water Supply, Tech. Rep., 1980.
[3] F. Loostma, "Performance evaluation of non-linear optimization methods via multi-criteria decision analysis and via linear model analysis," in *Nonlinear Optimization*, London.
[4] P. Van Laarhoven and W. Pedrycz, "A fuzzy extension of saaty's priority theory," *Fuzzy sets and Systems*, vol. 11, pp. 199–227, 1983.
[5] C. G. E. Boender, J. G. de Graan, and F. A. Lootsma, "Multi-criteria decision analysis with fuzzy pairwise comparisons," *Fuzzy Sets and Systems*, vol. 29, pp. 133–143, 1989.
[6] V. Uppuluri, "Logarithmic least-squares approach to saaty's decision problems," in *Mathematics and Statistics Research Department Progress Report*, R. W. D. W. W.E. Lever, D.E. Shepherd, Ed. Oak Ridge, TN: Oak Ridge National Laboratory, 1978, pp. 19–21.
[7] J. Aczel and T. Saaty, "Procedures for synthesizing ratio judgments," *J. Math. Psychology*, vol. 27, pp. 93–102, 1983.
[8] W. Koczkodaj and M. Orlowski, "Computing a consistent approximaiton to a generalized pairwise comparison matrix," *Computers and Mathematics with Applications*, vol. 37, pp. 79–85, 1999.
[9] J. Buckley, "Fuzzy hierarchical analysis," *Fuzzy Sets and Systems*, vol. 17, pp. 233–247, 1985.
[10] J. Mendel, R. John, and F. Liu, "Interval type-2 fuzzy logic systems made simple," *IEEE Transactions on Fuzzy Systems*, vol. 14, no. 6, pp. 808–821, 2006.
[11] M. Kwiesielewicz, "A note on the fuzzy extension of saaty's priority theory," *Fuzzy sets and systems*, vol. 95, no. 2, pp. 161–172, 1998.
[12] P. Lancaster and M. Tismenetsky, *The theory of matrices: with applications*. Academic Pr, 1985.
[13] D. Wu and J. Mendel, "Aggregation using the linguistic weighted average and interval type-2 fuzzy sets," *IEEE Transactions on Fuzzy Systems*, vol. 15, no. 6, pp. 1145–1161, 2007.
[14] D. Lee and D. Park, "An efficient algorithm for fuzzy weighted average," *Fuzzy Sets and Systems*, vol. 87, pp. 39–45, 1997.
[15] W. Dong and F. Wong, "Fuzzy weighted average and implementation of the extension principle," *Fuzzy Sets and Systems*, vol. 21, pp. 183–199, 1987.
[16] K. Chiao, "Direct fuzzy weighted average algorithm for fuzzy multiple attributes decision making," *Tamsui Oxford Journal of Mathematical Sciences*, vol. 16, no. 2, pp. 311–327, 2000.
[17] H. Mitchell, "Ranking type-2 fuzzy numbers," *Fuzzy Systems, IEEE Transactions on*, vol. 14, no. 2, pp. 287–294, 2006.
[18] D. Wu and J. M. Mendel, "A comparative study of ranking methods, similarity measures and uncertainty measures for interval type-2 fuzzy sets," *Information Sciences*, vol. 179, no. 8, pp. 1169 – 1192, 2009.
[19] T. L. Saaty, *Multicriteria Decision Making: The Analytic Hierarchy Process*. Pittsburgh: RWS Publications, 1990.

2011 IEEE International Conference on Fuzzy Systems
June 27-30, 2011, Taipei, Taiwan

Noise Control in Document Classification Based On Fuzzy Formal Concept Analysis

Sheng-Tun Li
Institute of Information Management
National Cheng Kung University
Tainan, Taiwan
stli@mail.ncku.edu.tw

Fu-Ching Tsai
Institute of Information Management
National Cheng Kung University
Tainan, Taiwan
r7895104@mail.ncku.edu.tw

***Abstract*—Document classification is critical due to explosive increasing of text in modern world. However, most of existing document classification algorithms are easily affected by noise data. Therefore, in document classification tasks, the ability of noise control is as important as the ability to classify exactly. In this paper, we propose a novel classification framework based on fuzzy formal concept analysis to moderate the impact from noise. In addition, the well-organized concepts also provide inherent relations, which support knowledge codification and distribution effectively. Experimental results using Reuters 21578 dataset demonstrates significant noise control benefit and superior classification accuracy.**

Keywords-text classification; fuzzy formal concept analysis; noise control; information retrieval

I. INTRODUCTION

The explosive increasing of text in modern world contributes the increasing need to provide automatic document classification and categorization. The well-organized categories of document are efficient in browser, retrieval and dissemination. Most existing document classification algorithms operate in a high dimensional vocabulary space while computing document similarities and relevance. However, the document classification procedure are easily affected by term-based inner product, cosine coefficient operations and noise data, such as synonym, antonym or words with multiple meanings [1]. Thus, the ability of handling noise is one of the important indicators for a text analysis algorithm and the reason why it can produces more useful results than others [2]. Moreover, for effectively controlling noise without eliminating relevant information, the parameter setting is another delicate topic. For example, when excessive parameter is applied for filtering irrelevant data, it is possible to remove some significant messages as well. Thus, the tradeoff parameter settings may vary regarding to different sources of data and needs to be careful examined especially in practical implementations.

One way to solve the noise problem in document classification is to decrease the impact from terms in document vectors. Since a vector is composed of a document and key terms, we consider that the technique, which can transforms the inherent relations between document and terms to a more abstract form, may appropriate for noise control. The more general elements are capable of resisting specific noise-sensitive variations. Formal concept analysis (FCA) formulates concepts in terms of documents and their properties, terms, and provides a way of combining and organizing individual concepts of a given context into a hierarchical ordered conceptual structure [3]. In the last few years, several researches have shown the capacity of FCA in information retrieval and management. In FCA lattice, the document collection can be organized into a reasonable consensus with good efficiency in retrieval performance, its structural comprehension is valuable to extract implication rules and classify documents in a suitable category [4], [5]. The path, location and hierarchical relations of concepts in FCA are successful to provide significant relations of keywords and documents [6]. While the weight of each term in a document is not simply belongs or does not belongs, we further utilize fuzzy formal concept analysis (FFCA) to take uncertain information into consideration.

The objective of this research is to develop a document classification scheme which can tolerate noise data. The structure of the paper is organized as follows. Section 2 reviews underlying technologies on formal concept analysis and Section 3 describes the specifics of the research methodology and system development process. Section 4 illustrates the results and discusses performance evaluation. Finally, Section 5 draws conclusions on the paper and provides insights on future work.

II. FUZZY FORMAL CONCEPT ANALYSIS

A. Formal Concept Analysis

Formal concept analysis (FCA) is a mathematical approach proposed by Wille[7] used for structuring, analyzing and visualizing data, based on a notion of duality called Galois connection[8]. Data consisting of a set of entities and their features are structured into formal abstractions called formal concepts, which together form a concept lattice ordered by a partial order relation. Concept lattices are constructed by identifying the objects and their corresponding attributes for a specific domain, called conceptual structures, and then displaying the relationships between them.

In FCA, a context is represented as a triple *(O, A, R)* where *O* is a set of objects, *A* is a set of elements and *R* is a binary relation between *O* and *A*. If for an object o and an attribute a, *oRa* holds, when we say that "object *o* has attribute *a*", or "attribute *a* applies to object *o*". Table 1 shows an context of an animal environment, where each row is an object representing

978-1-4244-7316-8/11/$26.00 ©2011 IEEE

an animal, each column is an attribute, and each X represents the existence of the relationship.

TABLE I. THE CONTEXT OF A ANIMAL ENVIRONMENT

	Hunt	Fly	Bird	Mammal
Lion	×			
Warbler		×	×	
Eagle	×	×	×	
Rabbit				×
Ostrich			×	

Two sets can be derived from a given formal context (*O, A, R*), one from the perspective of objects and another form the viewpoint of attributes. The former is a subset of objects $I \subseteq O$ such that I' is defined by the attributes that apply to all objects belonging to I and the later is a subset of attributes $J \subseteq A$ such that J' is defined by the objects that have all attributes belonging to J. Correspondingly,

$$I' = \{a \subseteq A | oRa \ \forall o \in I\},$$

$$J' = \{o \subseteq O | oRa \ \forall a \in J\},$$

thus the pair *(I, J)*, where $I \subseteq O$ and $J \subseteq A$, is a formal concept of the context (*O, A, R*) if *I'=J* and *J'=I*. The formal concept (*I, J*) is a pair where I consist of those objects that have all attributes from the set J, and equally, J consists of those attributes that apply to all objects from the set I. additionally, the set of objects is known as the extent of the concept and the set of attributes as the intent.

B. *Fuzzy Formal Concept Analysis*

Fuzzy formal concept analysis (FFCA) was introduced by Tho et al.[9] by incorporating fuzzy logic into FCA in order to represent vague information. Traditional FCA uses a binary approach indicating the presence or absence of the relation between an object and an attribute and cannot take uncertain information into consideration, while FFCA extends the relation into a value in the interval of real numbers between 0 and 1 called membership value. In this way, the relation is not simply belongs or does not belong anymore, but can take a set of values indicating a degree of belonging. This membership value of an attribute towards an object is proportional to its significance and can be used to calculate a similarity value between two formal concepts. These notions are represented in the following definitions.

Definition 1 (Fuzzy formal context) A fuzzy formal context is a triple (G, M, F=φ(G×M)). Where G is a set of objects, M is a set of attributes, and F is a fuzzy relation between G and M. Each relation $(g, m) \in F$ has a membership value $\mu(g, m)$ in [0, 1].

Definition 2 (Fuzzy formal concept). A fuzzy formal concept of a fuzzy formal concept of a fuzzy context (G, M, F) is a pair $(\varphi(Y), Z)$ for $Y \subseteq G$ and $Z \subseteq M$, where each object $g \in \varphi(Y)$ has a membership value $\mu_Y(g) = \min_{m \in Z} \mu(g, m)$ with $\mu(g, m)$ being the membership value of $(g, m) \in F$.

Definition 3 (Fuzzy formal concept cardinality). The fuzziness of a fuzzy formal concept is represented by membership values of objects of the concept, hence the cardinality of a fuzzy formal concept $(\varphi(Y), Z)$ is defined as $|\varphi(Y)|$, where $|\varphi(Y)|$ is the cardinality of the fuzzy set $\varphi(Y)$.

Definition 4 (Fuzzy formal concept similarity). The similarity of a fuzzy formal concept $(\varphi(Y_1), Z_1)$ and its subconcept $(\varphi(Y_1), Z_1)$ is defined as (1)

$$E\big((\varphi(Y_1), Z_1), (\varphi(Y_1), Z_1)\big) = E\big(\varphi(Y_1), \varphi(Y_2)\big) = \frac{|\varphi(Y_1) \cap \varphi(Y_2)|}{|\varphi(Y_1) \cup \varphi(Y_2)|} \quad (1)$$

where $\cap$ and $\cup$ are the intersection and union operations of fuzzy sets $\varphi(Y_1)$ and $\varphi(Y_2)$, respectively.

III. TEXT CLASSIFICATION WITH FFCA

This research uses FFCA to generalize documents to concepts in order to decrease the impact from noise term features. The documents are preprocessed by natural language processing to identify significant terms. Subsequently, FFCA is employed to provide the more generalized perspective, concept, by the way of analyzing inherent relationships between documents and its term features. Every formal concept on lattice diagram is used to recommend the precise category for new documents. An overview of the proposed FFCA document classification system is shown in Fig. 1. Five main phases, namely natural language processing, lattice construction, attribute-concept transformation, document-concept mapping and collaborative recommendation, are discussed in the following subsections.

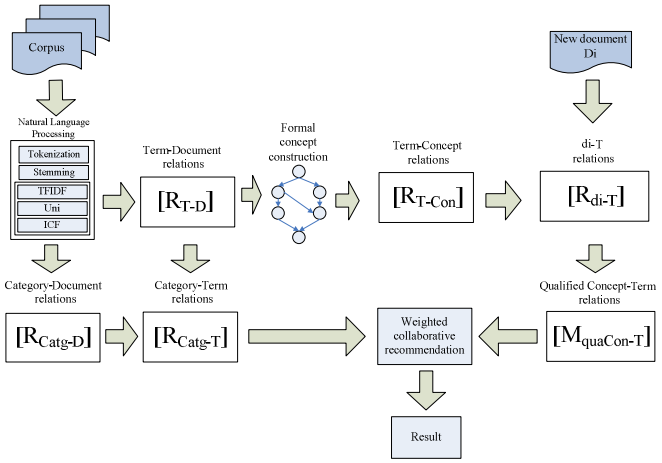

Figure 1. The FFCA classification framework

A. *Natural Language Processing*

Documents containing data in natural language format are useful sources of information, but due to the several variations in human language, it is problematical for automated systems to understand its meaning accurately. Natural language using computers, but has faced numerous problems and limitations since in order to really understand its connotation, extensive

knowledge about the outside world is required. The general process starts by separating textual input into tokens, followed by stemming to map related words to the same root and reduce the amount of tokens, stop-word elimination, part-of-speech tagging and finally syntax analysis.

In order to retrieve significant features from the corpus, information retrieval technique is applied to estimate the importance of retrieved tokens. Three indexes, term frequency and inverse document frequency (TF-IDF), Uni and ICF provide effective criteria to identify important keywords, which are TF-IDF> 26, Uni<0.2 and ICF>log2. Terms, which meet these three criteria, are treated as significant features of a specific document[10].

B. Lattice Construction

The source of lattice is composed of the relationships between key terms and documents. For more precisely demonstrate the degree of significance of the key terms, the traditional binary relations are improved to fuzzy numbers. The TF-IDF values that previously calculated for terms are used as membership degrees to build up fuzzy formal context. A α-cut acting as a membership degree threshold is set to eliminate relations that have low membership and in this way, reduce a accordingly the complexity of the analysis process. All membership values below the α-cut are considered equivalent to zero. Fig. 2(b) shows the fuzzy formal context in Fig. 2(a) with α=0.5, where the null values signify the absence of the topic or its exclusion due to low significance. In each row, d, represents a document, and each column, t, represents a key term.

	t1	t2	t3
d1	0.8	0.12	0.61
d2	0.9	0.85	0.13
d3	0.1	0.14	0.87

(a)

	t1	t2	t3
d1	0.8	-	0.61
d2	0.9	0.85	-
d3	-	-	0.87

(b)

Figure 2. The formal context with α-cut=0.5

The lattice organizes the documents and key terms via partial order which reveals the inherent hierarchical relationships of knowledge. The formal concepts which produced by FFCA further provide more general perspective than documents to represent the content of corpus. Therefore, this research focuses on operating concepts instead of documents in classification problems. The relationships between concepts and key terms are transformed from lattice structure with matrix shows in Fig. 3.

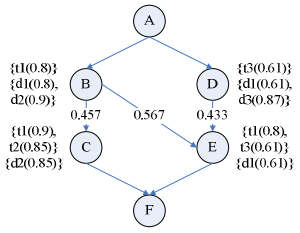

	t1	t2	t3
B	0.8	-	-
C	0.9	0.85	-
D	-	-	0.61
E	0.8	-	0.61

Figure 3. The transformation from lattice structure to concept-term relations

C. Term-category Transformation

The objective of this research is to provide concepts, a more general perspective than document, to facilitate noise control in document classification issue. However, the category information is mainly tagged on documents. Neither terms nor concepts can be the basis to decide the category of a new document. Therefore, the term-category transformation is necessary for a concept-based classification approach. The transformation mechanism is based on fuzzy compositions[11]. The standard composition of two fuzzy relations $P(X, Y)$ and $Q(Y, Z)$ is represented by $P(X, Y) \circ Q(Y, Z)$ which generate $R(X, Z)$ on $X \times Z$. The $R(X, Z)$ is calculated by (2).

$$R(x,z) = [P \circ Q](x,z) = \max_{y \in Y} \min [P(x,y), Q(y,z)] \quad (2)$$

where all $x \in X$ and all $z \in Z$. Therefore, the relations between terms and categories, M_{T-Catg}, can be derived by compositing term-document relations, and document-category relations, as shown in (3).

$$R_{T-Catg} = R_{T-D} \circ R_{D-Catg} \quad (3)$$

where R_{T-D} is term-document relations and M_{D-Catg} are document-category relations. The values in M_{T-D} are the previously calculated TF-IDF value. In traditional approaches, each row represents a document vector which is used for similarity calculation of documents. In M_{D-Catg}, the binary data, 1 or 0, is used to represent document and category relations. The value 1 indicates the document belongs to the category. Otherwise, the value will be 0.

D. Concept-category Transformation

Since the a more abstract perception, concepts, are proposed to replace documents in text classification task, the category information for each concept is essential to conclude the appropriate category for a new incoming document. As mentioned above, the category information from documents has been transformed to terms in M_{T-Catg}, the next challenge is how to reveal the concept-category relations, $M_{Con-Catg}$. Similarly, the standard composition of concept-key term and key terms-category relations can be composited by $M_{Con-T} \circ M_{T-Catg}$. Thus, the category information, which previously based on documents, has been successively transformed to concepts.

E. Unclassified document mapping

The main objective of FFCA classification approach is to classify new documents based on well-organized concepts in the lattice space. As $M_{Con-Catg}$ has provided concept-category relations, it is capable of mapping unclassified documents to a set of relevant concepts and assigning the most appropriate category by collaborative recommending of its significant neighbor concepts. In order to search relevant concepts for a new document, we represent the new document as fuzzy formal concepts with TF-IDF values. Further, the fuzzy similarity operation, (1), is applied to calculate the similarity measure between new document and fuzzy formal concepts. The parameter δ is designed to determine the similarity criterion that the qualified fuzzy formal concepts should include in classification procedure. A more detailed pseudo code is presented in Fig. 4.

Procedure $Build_MSC(d_i, \delta, R_{Con-T})$
d_i : new document
δ : most similar concept threshold, $0 < \delta < 1$
R_{Con-T} : concept-term relations
MSC : the most similar concept set

$MSC = \varnothing$
FOR each $concept_i$ exists in R_{Con-T}
  IF $fuzzysimilarity(d_i, concept_i) > \delta$
    $MSC \leftarrow concept_i$
  END IF
END FOR

return MSC

Figure 4. Algorithm to find relevant concepts of new document

F. Classification

After retrieving the qualified concepts which highly correlated with a new document, the classification procedure are based on weighted collaborative recommendation of retrieved concepts as (4).

$$\text{weighted_sum}(C_i) = \sum_{k=1}^{j} fuzzysimilarity(d, concept_k) \times membership(concept_k, C_i) \quad (4)$$

where $fuzzysimilarity(d, concept_k)$ is the fuzzy similarity between document, d, and $concept_k$. As $membership(concept_k, C_i)$ is the part of $M_{Con-Catg}$ which provide the category information of qualified concepts. A more detailed pseudo code is presented in Fig. 5.

Procedure $Categorize(d_i, MSC)$
d_i : new document
MSC : the most similar concept set
C : assigned category

FOR each C_i
  FOR each $concept_j \in MSC$
    $weighteds_sum(C_i) = fuzzysimilarity(d_i, concept_j) \times membership(concept_j, C_i)$
  END FOR
END FOR
$C = \arg\max_{c_i} weighteds_sum(C_i)$
return C

Figure 5. Algorithm to categorize new document

IV. Experiments and Analysis

We conduct several experiments to evaluate the effectiveness of proposed FFCA classification. In the first experiment, we demonstrate the performance in terms of f-measure, the weighted harmonic mean of recall and precision, based on ten-fold cross-validation. In the second experiment, we investigate the impact of different parameter settings on classification performance. Further, the information which contributed from various lattice construction perspectives are analyzed with regards to their structure to affect the classification results. In the following section, we first describe the experimental dataset and then analyze the evaluation results.

A. Data Collection

In this research, we choose a public corpus, Reuters 21578, to evaluate the performance of classification. Reuters 21578 is the main benchmark for text classification evaluation. Each article is well tagged with several properties. The tag, TOPIC, indicates what categories each article belongs to. Articles with multiple classes are allowed in Reuters 21578, which means there are multiple values in TOPIC tag. However, our research is mainly focus on the single classification problem. Thus, articles belongs to multiple classes are ignored in this experiment. In order to avoid the effects of small sample, the classes which have less than one hundred articles are not included in this experiment as well. The qualified five classes containing 5550 articles are implemented using ten-fold cross-validation experiment. The statistics of experimental data are demonstrated in table 2.

TABLE II. THE STATISTICS OF EXPERIMENTAL DATASET

Category	Testing data	Training data	Total
acq	151	1359	1510
crude	26	234	260
earn	355	3195	3550
ship	10	90	100
trade	13	117	130

B. Evaluation of accuracy

Since the FFCA classification approach is affected by two parameters, α and δ, we investigate their effect and correlation by conducting different parameter settings. α represents the tfidf threshold of terms in new documents based on the training data. Only terms with tfidf value higher than α are included in

lattice construction. Higher α denotes less keywords are qualified as the features of new document and vice versa. δ depicts the similarity criterion between new document and concepts. Since k concepts which are similar enough to new document are chosen as neighbors to predict the category, δ provides the information to manipulate the number of concepts participating in classification. The range of δ is between 0 and 1. When δ=0, all concepts are involving in classification procedure. On the contrary, only the concept which is exact the same with new document is involving the classification procedure when δ=1. The results of different combinations of α and δ are shown in Fig 6.

Fig. 6 depicts that the highest classification f-measure is when α=0.1 and δ=0.1. α=0.1 demonstrates that the terms of new document should be kept as factors to provide information in classification. The same situation, δ=0.1, also shown in deciding δ, the results also support that when more the concepts involving in classification the accuracy is higher.

	α								
δ	0.1	0.2	0.3	0.4	0.5	0.6	0.7	0.8	0.9
0.1	**96.03%**	95.86%	95.80%	95.58%	94.53%	93.80%	88.39%	88.46%	87.14%
0.2	93.56%	93.49%	95.42%	95.34%	92.47%	89.32%	86.87%	86.65%	85.39%
0.3	90.43%	91.17%	91.57%	90.18%	81.85%	85.36%	85.29%	85.39%	84.38%
0.4	85.82%	87.14%	83.33%	81.78%	65.79%	72.10%	85.00%	85.13%	84.29%
0.5	74.74%	84.10%	75.29%	71.45%	63.13%	67.68%	85.07%	84.95%	84.17%
0.6	66.60%	73.55%	63.79%	62.57%	62.65%	67.49%	85.07%	84.95%	84.17%
0.7	63.95%	68.85%	58.96%	61.53%	62.65%	67.49%	85.07%	84.95%	84.17%
0.8	63.77%	67.36%	58.70%	61.52%	62.65%	67.49%	85.07%	84.95%	84.17%
0.9	63.77%	67.36%	58.70%	61.52%	62.65%	67.49%	85.07%	84.95%	84.17%
1	63.77%	67.36%	58.70%	61.52%	62.65%	67.49%	85.07%	84.95%	84.17%

Figure 6. Prediction accuracy for different parameter combinations

C. *Implications for KNN-based approaches*

For KNN-based approaches, how to decide the most appropriate *K* neighbors remains a great challenge. Information may lose when choosing small *K*, but choosing big *K* may also produce poor results due to too many noise data. In practical KNN applications, *K* is always suggested to be neither too big nor too small, but lack of an efficient way to determine the most appropriate number. In this research, the parameters, α and δ, are used to determine the number of terms and concepts for classification, which is comparable to *K* in KNN approaches. Therefore, we further investigate the results from different levels of parameters and analyze the impacts of different parameter setting strategies.

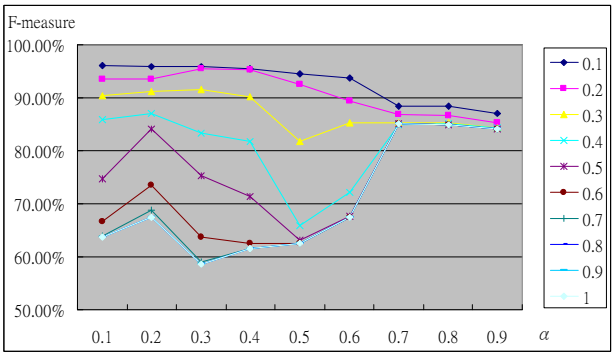

Figure 7. F-measure curves under different level of α

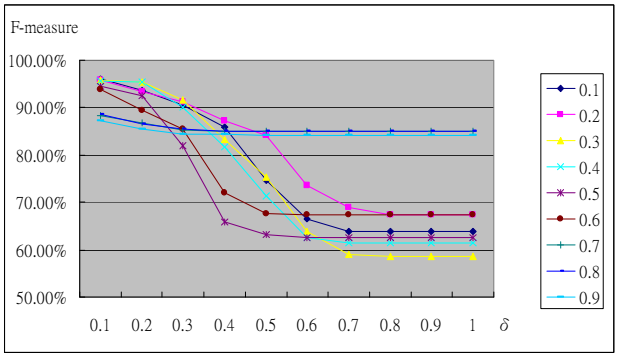

Figure 8. F-measure curves under different level of δ

Fig. 7 demonstrates the curves of δ under different levels of α. For all δ F-measure curves, their rank from high to low under different level of α are the same sequence as its value from 0.1 to 1. This fact indicates that under different thresholds of TF-IDF, more concepts are capable of providing information for document classification. As for the perspective of each single δ curve, we observe that drop and up patterns obviously appears except when δ=0.1. Since α represents TF-IDF which controls the amount of key terms involving in classification task, the drop F-measure tendency between α equals 0.2 and 0.5 reflects that the valuable key terms are eliminated by rising α and contribute decline in performance. However, tendencies reverse when α>0.5 indicate that the rising α further eliminate moderate terms and strictly keep significant ones facilitate the performance of F-measure. The F-measure for all levels of δ are stable when α is larger than 0.7. It is worth noting that, the drop and up pattern is not obvious when δ is 0.1 and 0.2. The

reason is that when δ is low indicates most of the concepts are engaging in classification task, thus, the impact of reducing key terms is negligible in F-measure.

As for Fig. 8, the tendencies of different α are divided into two different typical patterns. The first pattern, when α is between 0.1 and 0.6, demonstrate that the F-measure is declined when δ is rising. This pattern reveals that the decreasing concept caused by rising δ not only neglect relevant information but also impede the F-measure significantly. However, the disproportional relations between α and δ are limited when δ<0.7. While only important concepts are kept for document classification, δ>0.7 , the impact from key term selection also becomes not significant. The second pattern appeals when α>0.6 which are stable confronting the variation of δ. The second pattern reveals that the number of concept involving in document classification is slightly affected F-measure when only high TF-IDF value key terms are selected. It is worth noting that there is no drop and up tendency appears in Fig. 8. As mentioned above, the drop and up tendency is caused by eliminating noise data, however, each tendencies of α in Fig. 8 are monotonically decreasing, which means every concept is capable of providing valuable information and none of them should be eliminated in the process of document classification. In traditional k-means methodology, how to decide *K* is very critical and may vary from different parameter settings. Thus, finding appropriate *K* remains a great challenge. In this experiment, the monotonically descending reveals that all concepts are suitable for providing valuable information. The highest F-measure of all α are consistently located when α=0.1. This fact indicates that the transformation from terms to concepts can successively retrieve the abstractness of terms and avoid the noise terms, which is inevitable in feature selection phase.

V. CONCLUSION

Nowadays, with the fast increasing of text, document classification is important to knowledge management and distribution. However, noise data is inevitable in practical document classification tasks. How to eliminate the impact from noise data is as important as achieving high classification accuracy. For this purpose, we develop a novel classification approach to generalize document to concept and successively reduce the impact from noise. Furthermore, according to accuracy assessment results, FFCA method demonstrates the impressive ability by achieving 96.17% in Reuters 21578 dataset. By further investigate the result tendencies of different parameter settings, FFCA method also provide benefits in determining parameter settings. Future research directions may include exploring more experimental data for evaluation and retrieving IF-THEN rules from lattice to support decision-making issues.

REFERENCES

[1] O.-W. Kwon and J.-H. Lee, "Text categorization based on k-nearest neighbor approach for Web site classification," in *Information Processing and Management*. vol. 39 Elsevier Science, 2003, pp. 25-44.

[2] P. JÃÃrgensen, "Incorporating context in text analysis by interactive activation with competition artificial neural networks," in *Information Processing and Management*. vol. 41: Elsevier Science, 2005, pp. 1081-1099.

[3] R. K. Rajapakse and M. Denham, "Text Retrieval with More Realistic Concept Matching and Reinforcement Learning," in *Information Porcessing and Management*. vol. 42, 2006, pp. 1260-1275.

[4] M. Kim and P. Compton, "Evolutionary document management and retrieval for specialized domains on the web," *International Journal of Human-Computer Studies,* vol. 60, pp. 201-241, 2004.

[5] L. E. Zárate, S. Mariano Dias, and M. A. Junho Song, "FCANN: A new approach for extraction and representation of knowledge from ANN trained via Formal Concept Analysis," in *Neurocomputing*. vol. 71: Elsevier Science, 2008, pp. 2670-2684.

[6] T.-C. Hsieh and T.-I. Wang, "A mining-based approach on discovering courses pattern for constructing suitable learning path," *Expert Systems with Applications,* vol. 37, pp. 4156-4167, 2010.

[7] R. Wille, "Formal Concept Analysis as Mathematical Theory of Concepts and Concept Hierarchies," *Lecture Notes in Computer Science,* vol. 3626, pp. 1-33, 2005.

[8] U. Priss, "Formal concept analysis in information science," *Annual Review of Information Science and Technology,* vol. 40, pp. 521-543, 2006.

[9] Q. T. Tho, "A fuzzy FCA approach for citation-based document retrieval," in *Proceedings of the 2004 IEEE conference on cybernetics and intelligent systems*, Singapore, 2004, pp. 578-583.

[10] T. Y. Wang and H. M. Chiang, "Fuzzy support vector machine for multi-class text categorization," *Information Processing and Management,* vol. 43, pp. 914-929, 2007.

[11] G. J. Klir and B. Yuan, *Fuzzy sets and fuzzy logic: theory and applications*. NJ: Prentice Hall, 1995.

2011 IEEE International Conference on Fuzzy Systems
June 27-30, 2011, Taipei, Taiwan

Deriving the Input-Output Mathematical Relationship for a Class of Interval Type-2 Mamdani Fuzzy Controllers

Haibo Zhou
State Key Lab of High Performance Complex Manufacturing
Central South University
Changsha, China
csuhaibo@hotmail.com

Hao Ying
Department of Electrical and Computer Engineering
Wayne State University
Detroit, USA
hao.ying@wayne.edu

Abstract—**Most fuzzy controllers, type-1 (T1) or type-2 (T2), have been used and treated as black boxes in that their explicit mathematical input-output mappings (i.e., analytical structures) are unknown. Revealing and analyzing the analytical structure is important as it will lay a solid foundation for better understanding, more insightful analysis, and more effective design of fuzzy control systems. We previously developed a general technique to derive the analytical structures of the type-1 fuzzy controllers that employed Zadeh AND operator. We now extend our study to a class of typical interval type-2 fuzzy controller that adopt Zadeh AND operator and the popular Karnik-Mendel iterative center-of-sets type reducer. A novel analytical structure deriving technique is developed. And the resulting input-output mathematical relationship for the controller is received.**

Keywords- Type-2 fuzzy control; analytical structure; input-output mathematical relationship

I. INTRODUCTION

In the past several years, research results on type-2 (T2) fuzzy control have started to emerge in the literature [1-5]. Many results claim that T2 fuzzy control outperforms its counterpart type-1 (T1) fuzzy control (e.g., traditional fuzzy control). Logically, many questions arise. Why is this the case? Do the T2 fuzzy controllers work well because their input-output structures are more peculiar than T1 fuzzy controllers and other conventional nonlinear controllers? What are their structures then? All these questions are of considerable importance. And moreover, once the mathematical relationship information becomes available, analyzing and designing T2 fuzzy control systems can be studied in the framework of the well-developed conventional (nonlinear) control theory as the fuzzy control problems will be transformed to nonlinear control problems.

Actually, deriving the input-output mathematical relationship is no easy in most cases. The reality is that many fuzzy controllers are constructed via the "knowledge engineering approach" as opposed to the mathematical approaches exclusively adopted in conventional control. All the fuzzy controllers have been treated and used as black-box controllers in the sense that their analytical structures are unknown. And for conventional control, this is never an issue because the analytical structure of the conventional control, linear or nonlinear, is always readily available for analysis and design. For T1 fuzzy controller, we previously did a lot of research on its analytical structure [6, 7]. Our research methods and results on the analytical structure of T1 fuzzy controllers create great help for better analysis and design of fuzzy controller, which have been widely used in literature [8]. Few of the present literatures about T2 fuzzy control, however, are concerned with mathematical input-output relationship of a T2 fuzzy controller [9, 10].

In the present paper, the input-output relationship of a class of interval T2 Mamdani fuzzy controller is derived. Their configurations are typical - any types of input fuzzy sets and output fuzzy sets, arbitrary fuzzy rules, Zadeh AND operator, the Karnik-Mendel center-of-sets type reducer, and the centroid defuzzifier.

II. CONFIGURATION OF A CLASS OF INTERVAL T2 MAMDANI FUZZY CONTROLLERS

The T2 fuzzy controllers in this study have two input variables, $x_1(n)$ and $x_2(n)$, and one output variable, $\triangle u(n)$, which is the change of controller output, where n represents the sampling instance. For simplicity, x_1, x_2 and $\triangle u$ will be used instead of $x_1(n)$, $x_2(n)$ and $\triangle u(n)$. We suppose that x_1 is defined on $[L_1, R_1]$ that is divided into $N_1 - 1$ subintervals: $[S_1, S_2]$,..., $[S_i, S_{i+1}]$,..., $[S_{N_1-1}, S_{N_1}]$, $1 \le i \le N_1$. There are N_1 interval T2 fuzzy sets, $A_1, \cdots, A_i, \cdots, A_{N_1}$. A_i is defined over $[S_{i-1}, S_{i+1}]$ and its membership value is zero everywhere else. The upper and lower primary membership functions of A_i are designated as $\overline{\mu}_{A_i}(x_1)$ and $\underline{\mu}_{A_i}(x_1)$, respectively. We assume that: (1) $\overline{\mu}_{A_i}(x_1) \ge \underline{\mu}_{A_i}(x_1)$, and (2) $\overline{\mu}_{A_i}(x_1)$ (and $\underline{\mu}_{A_i}(x_1)$) increases from 0, reaches its maximum (can be a range of the same maximum), and then decreases to 0. Most of the widely-used fuzzy sets in the literature (e.g., the trapezoidal ones) meet the assumptions. To illustrate the assumptions, Fig. 1 provides some example T2 fuzzy sets. Likewise, we suppose that x_2 is

This work was supported in part by National Natural Science Foundation of China under Grant 51005253.

defined in $[L_2, R_2]$ that is divided into $N_2 - 1$ subintervals, namely $[M_1, M_2]$,..., $[M_j, M_{j+1}]$,..., $[M_{N_2-1}, M_{N_2}]$, over which N_2 interval T2 fuzzy sets meeting the same assumptions above are defined. Each of them is denoted B_j $(1 \le j \le N_2)$ whose upper and lower primary membership functions are $\overline{\mu}_{B_j}(x_2)$ and $\underline{\mu}_{B_j}(x_2)$, respectively.

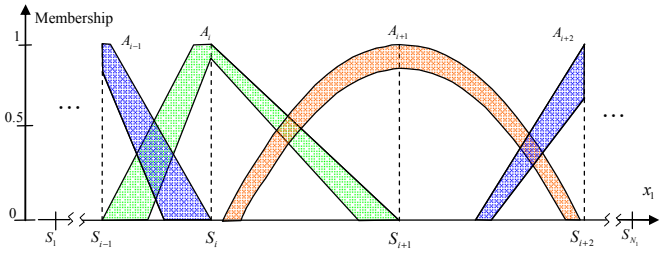

Fig. 1. Example interval T2 fuzzy sets for input variable x_1.

We use a total of $N_1 \times N_2$ Mamdani fuzzy rules to cover all the possible combinations of the input fuzzy sets. At any sampling instance, only two adjacent A_i and two adjacent B_j will be involved in the fuzzification of x_1 and x_2, respectively, due to the manner that the fuzzy sets are defined. Without losing generality, we assume that A_i, A_{i+1}, B_j, B_{j+1} are the ones that are involved. Accordingly, the following four fuzzy rules are executed:

IF x_1 is A_i AND x_2 is B_j THEN Δu is $G_{h(i,j)}$. (Rule 1)

IF x_1 is A_i AND x_2 is B_{j+1} THEN Δu is $G_{h(i,j+1)}$. (Rule 2)

IF x_1 is A_{i+1} AND x_2 is B_j THEN Δu is $G_{h(i+1,j)}$. (Rule 3)

IF x_1 is A_{i+1} AND x_2 is B_{j+1} THEN Δu is $G_{h(i+1,j+1)}$ (Rule 4)

where Zadeh fuzzy AND operator (i.e., min()) is used and $G_{h(i,j)}$, $G_{h(i,j+1)}$, $G_{h(i+1,j)}$ and $G_{h(i+1,j+1)}$ are interval T2 fuzzy sets for Δu, which can be any continuous T2 fuzzy sets, interval type or not. These output fuzzy sets are indexed by integer subscripts whose values are computed using function $h(\cdot)$ so that the input and output fuzzy sets are mathematically linked. Because $h(\cdot)$, chosen by the controller designer, can be any function, the fuzzy rules subsequently can be arbitrary in terms of input and output relation.

The firing interval for the input fuzzy sets in Rule k ($k = 1,2,3,4$), denoted $[\underline{f}_k(x_1,x_2), \overline{f}_k(x_1,x_2)]$, is first calculated [2]:

$$\begin{aligned} f_1(x_1,x_2) &= [\underline{f}_1(x_1,x_2), \overline{f}_1(x_1,x_2)] \\ &= [\min(\underline{\mu}_{A_i}(x_1), \underline{\mu}_{B_j}(x_2)), \min(\overline{\mu}_{A_i}(x_1), \overline{\mu}_{B_j}(x_2))] \end{aligned} \quad (1)$$

$$\begin{aligned} f_2(x_1,x_2) &= [\underline{f}_2(x_1,x_2), \overline{f}_2(x_1,x_2)] \\ &= [\min(\underline{\mu}_{A_i}(x_1), \underline{\mu}_{B_{j+1}}(x_2)), \min(\overline{\mu}_{A_i}(x_1), \overline{\mu}_{B_{j+1}}(x_2))] \end{aligned} \quad (2)$$

$$\begin{aligned} f_3(x_1,x_2) &= [\underline{f}_3(x_1,x_2), \overline{f}_3(x_1,x_2)] \\ &= [\min(\underline{\mu}_{A_{i+1}}(x_1), \underline{\mu}_{B_j}(x_2)), \min(\overline{\mu}_{A_{i+1}}(x_1), \overline{\mu}_{B_j}(x_2))] \end{aligned} \quad (3)$$

$$\begin{aligned} f_4(x_1,x_2) &= [\underline{f}_4(x_1,x_2), \overline{f}_4(x_1,x_2)] \\ &= [\min(\underline{\mu}_{A_{i+1}}(x_1), \underline{\mu}_{B_{j+1}}(x_2)), \min(\overline{\mu}_{A_{i+1}}(x_1), \overline{\mu}_{B_{j+1}}(x_2))] \end{aligned} \quad (4)$$

In this paper, the Karnik-Mendel center-of-sets type reducer is used to reduce the T2 output sets to $\Delta U = [\Delta u_L, \Delta u_R]$, a T1 fuzzy set, which is then defuzzified to produce a crisp number Δu. In the Karnik-Mendel type reducer, the centroid for Rule k's output fuzzy set, denoted $[\alpha_k, \gamma_k]$, is computed first, on-line or off-line [1]. The rather complex calculation procedure is described in [1]. Because we will only need the outcome of the reducer prior to the structure derivation and do not care how it is produced, the procedure is omitted here for better presentation. γ_k's and α_k's are then respectively arranged in the ascending orders and the results are represented by: $\gamma_1^* \le \gamma_2^* \le \gamma_3^* \le \gamma_4^*$ and $\alpha_1^* \le \alpha_2^* \le \alpha_3^* \le \alpha_4^*$. We then arrange $\overline{f}_k(x_1,x_2)$ and $\underline{f}_k(x_1,x_2)$ to correspond to $\gamma_1^* \le \gamma_2^* \le \gamma_3^* \le \gamma_4^*$ and $\alpha_1^* \le \alpha_2^* \le \alpha_3^* \le \alpha_4^*$, respectively, resulting in $\overline{f}_1^*(x_1,x_2) \le \overline{f}_2^*(x_1,x_2) \le \overline{f}_3^*(x_1,x_2) \le \overline{f}_4^*(x_1,x_2)$ and $\underline{f}_1^*(x_1,x_2) \le \underline{f}_2^*(x_1,x_2) \le \underline{f}_3^*(x_1,x_2) \le \underline{f}_4^*(x_1,x_2)$. The left-most point Δu_L and right-most point of the interval ΔU_R can then be represented as [2]:

$$\Delta u_L = \frac{\sum_{i=1}^{P_L} \overline{f}_i^*(x_1,x_2)\alpha_i + \sum_{j=P_L+1}^{4} \underline{f}_j^*(x_1,x_2)\alpha_j}{\sum_{i=1}^{P_L} \overline{f}_i^*(x_1,x_2) + \sum_{j=P_L+1}^{4} \underline{f}_j^*(x_1,x_2)} \quad (5)$$

$$\Delta u_R = \frac{\sum_{i=1}^{P_R} \underline{f}_i^*(x_1,x_2)\gamma_i + \sum_{j=P_R+1}^{4} \overline{f}_j^*(x_1,x_2)\gamma_j}{\sum_{i=1}^{P_R} \underline{f}_i^*(x_1,x_2) + \sum_{j=P_R+1}^{4} \overline{f}_j^*(x_1,x_2)} \quad (6)$$

where integers P_L ($1 \le P_L \le 3$) and P_R ($1 \le P_R \le 3$) are switching points that depend on the input and output fuzzy sets and the values of x_1 and x_2, and hence vary with n. Their calculation procedure is fully described in [2]. Since ΔU_R is an interval set, the centroid defuzzifier is used to produce the crisp output Δu [4]:

$$\Delta u = \frac{1}{2}(\Delta u_L + \Delta u_R) \quad (7)$$

III. New Technique for Deriving Analytical Structure of the Fuzzy Controllers

Without loss of generality, suppose arbitrarily that A_i, A_{i+1}, B_j, and B_{j+1} are as shown in Fig. 2 with the mathematical

definitions given in Table 1 (outside the intervals in the right column of Table 1, the membership values are 0).

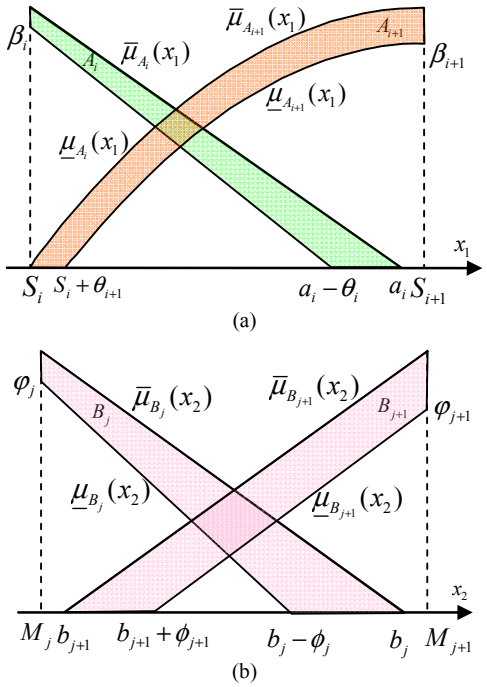

Fig. 2. Example interval T2 fuzzy sets used for (a) x_1, and (b) x_2 at sampling time n.

TABLE I. MATHEMATICAL DEFINITIONS FOR THE PARTS OF THE PRIMARY MEMBERSHIP FUNCTIONS OF A_i, A_{i+1}, B_j, AND B_{j+1}.

Mathematical definition	Interval
$\bar{\mu}_{A_i}(x_1)=\frac{-1}{a_i-S_i}x_1+\frac{S_i}{a_i-S_i}+1$	$x_1\in[S_i,a_i]$
$\underline{\mu}_{A_i}(x_1)=\frac{-\beta_i}{a_i-\theta_i-S_i}x_1+\frac{S_i\beta_i}{a_i-\theta_i-S_i}+\beta_i$	$x_1\in[S_i,a_i-\theta_i]$
$\bar{\mu}_{A_{i+1}}(x_1)=-\left(\frac{x_1-S_{i+1}}{S_i-S_{i+1}}\right)^2+1$	$x_1\in[S_i,S_{i+1}]$
$\underline{\mu}_{A_{i+1}}(x_1)=-\beta_{i+1}\left(\frac{x_1-S_{i+1}}{S_i+\theta_{i+1}-S_{i+1}}\right)^2+\beta_{i+1}$	$x_1\in[S_i+\theta_{i+1},S_{i+1}]$
$\bar{\mu}_{B_j}(x_2)=\frac{-1}{b_j-M_j}x_2+\frac{M_j}{b_j-M_j}+1$	$x_2\in[M_j,b_j]$
$\underline{\mu}_{B_j}(x_2)=\frac{-\varphi_j}{b_j-\phi_j-M_j}x_2+\frac{M_j\varphi_j}{b_j-\phi_j-M_j}+\varphi_j$	$x_2\in[M_j,b_j-\phi_j]$
$\bar{\mu}_{B_{j+1}}(x_2)=\frac{1}{M_{j+1}-b_{j+1}}x_2-\frac{M_{j+1}}{M_{j+1}-b_{j+1}}+1$	$x_2\in[b_{j+1},M_{j+1}]$
$\underline{\mu}_{B_{j+1}}(x_2)=\frac{\varphi_{j+1}}{M_{j+1}-b_{j+1}-\phi_{j+1}}x_2-\frac{M_{j+1}\varphi_{j+1}}{M_{j+1}-b_{j+1}-\phi_{j+1}}+\varphi_{j+1}$	$x_2\in[b_{j+1}+\phi_{j+1},M_{j+1}]$

To derive the explicit Δu expressions from (7), one must first determine the resulting membership value for each of the four rules involving the min() operation in (1)-(4) as a mathematical expression, as opposed to a numerical value. The only way to achieve this goal is to divide the area $[S_i,S_{i+1}]\times[M_j,M_{j+1}]$ into a number of regions, each of which is called IC (input combination) so that in each region, the inequality relationship between x_1 and x_2 is exclusive [6]. Without loss of generality, we assumed that $\varphi_{j+1}\le\beta_{i+1}\le\varphi_j\le\beta_i$ in Table 1. Fig. 3 and 4 then show the input space division results for (1)-(4), where $\underline{\mu}_{A_i}^{-1}(\varphi_j)$, $\underline{\mu}_{A_i}^{-1}(\varphi_{j+1})$, $\underline{\mu}_{B_j}^{-1}(\beta_{i+1})$ and $\underline{\mu}_{A_{i+1}}^{-1}(\varphi_{j+1})$ are the inverse functions of the linear parts of the these four lower membership functions. For instance, Fig. 3(a) shows the divisions for $\underline{f}_1(x_1,x_2)=\min(\underline{\mu}_{A_i}(x_1),\underline{\mu}_{B_j}(x_2))$ from Rule 1. There are three regions and they are labeled as $\underline{f}_1$-IC1, $\underline{f}_1$-IC2 and $\underline{f}_1$-IC3. In $\underline{f}_1$-IC3, $\underline{\mu}_{A_i}(x_1)\le\underline{\mu}_{B_j}(x_2)$, thus $\underline{f}_1(x_1,x_2)=\underline{\mu}_{A_i}(x_1)$. For $\underline{f}_1$-IC1, because either $\underline{\mu}_{A_i}(x_1)=0$ or $\underline{\mu}_{B_j}(x_2)=0$, the result of min() is always 0. Accordingly, there should be eight different divisions for whole input space to determine the firing intervals in (1)-(4): division for $\underline{f}_1$ in (1), for $\bar{f}_1$ in (1), for $\underline{f}_2$ in (2), for $\bar{f}_2$ in (2), for $\underline{f}_3$ in (3), for $\bar{f}_3$ in (3), for $\underline{f}_4$ in (4), for $\bar{f}_4$ in (4). For space limitation, just two of them list in Fig. 3. And take Fig. 3(b) as another example. Boundary A, on which $\underline{\mu}_{A_{i+1}}(x_1)=\underline{\mu}_{B_j}(x_2)$, is obtained by solving the following equation:

$$\varphi_j-\frac{\varphi_j}{b_j-\phi_j-M_j}x_2+\frac{M_j\varphi_j}{b_j-\phi_j-M_j}=\beta_{i+1}-\beta_{i+1}\left(\frac{x_1-S_{i+1}}{S_i+\theta_{i+1}-S_{i+1}}\right)^2 \quad (8)$$

Yielding

$$x_2=\frac{\beta_{i+1}(b_j-\phi_j-M_j)}{\varphi_j(S_i+\theta_{i+1}-S_{i+1})^2}(x_1-S_{i+1})^2+\frac{(\varphi_j-\beta_{i+1})(b_j-\phi_j-M_j)}{\varphi_j}+M_j \quad (9)$$

Once the boundary is determined, just compute the values of $\underline{\mu}_{A_{i+1}}(x_1)$ and $\underline{\mu}_{B_j}(x_2)$ using any pair of x_1 and x_2 in either IC. The function producing the smaller value should be the result of min( ) for that IC.

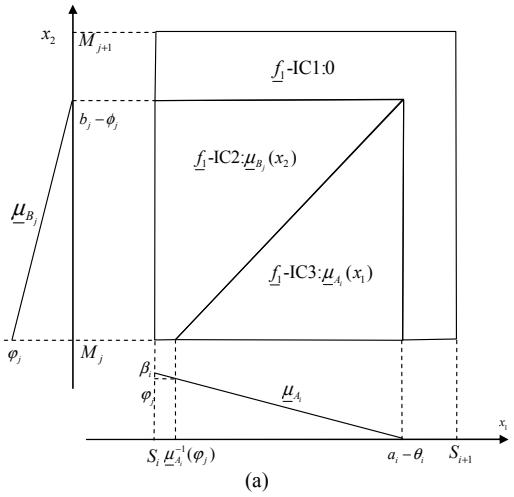

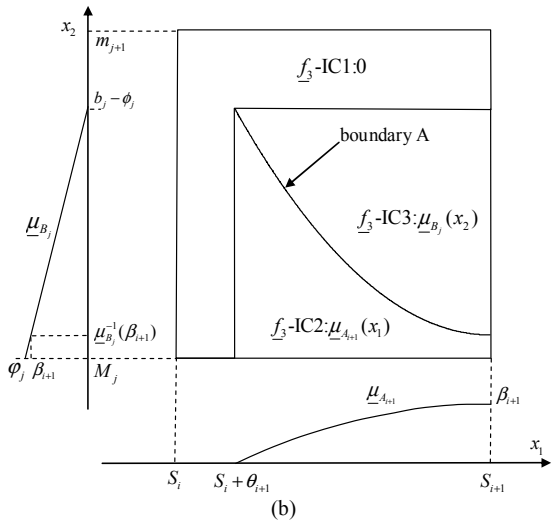

(b)

Fig. 3. Part of eight divisions of the input space to determine the firing intervals in (1)-(4): (a) for $\underline{f}_1$ in (1), (b) for $\underline{f}_3$ in (3).

These divisions are for each individual fuzzy rule only. Because all the rules are involved in calculating controller output $\triangle u$, all the four rules must be simultaneously considered to derive the controller structure. This simultaneous consideration is achieved if we superimpose the eight individual input space divisions shown in Fig. 3 to form an overall input space division (Fig. 4). It turns out that there are a total of 78 regions, labeled from IC1 to IC78.

Now, for each region in Fig. 4, we can decide $f_k(x_1, x_2)$ (i.e., $[\underline{f}_k(x_1, x_2), \overline{f}_k(x_1, x_2)]$). For example, for IC40 (i.e., the region labeled 40 in Fig. 4), $\underline{f}_1(x_1, x_2) = \underline{\mu}_{B_j}(x_2)$, $\underline{f}_2(x_1, x_2) = \underline{\mu}_{A_i}(x_1)$, $\underline{f}_3(x_1, x_2) = \underline{\mu}_{B_j}(x_2)$, $\underline{f}_4(x_1, x_2) = \underline{\mu}_{B_{j+1}}(x_2)$, $\overline{f}_1(x_1, x_2) = \overline{\mu}_{B_j}(x_2)$, $\overline{f}_2(x_1, x_2) = \overline{\mu}_{A_i}(x_1)$, $\overline{f}_3(x_1, x_2) = \overline{\mu}_{B_j}(x_2)$ and $\overline{f}_4(x_1, x_2) = \overline{\mu}_{B_{j+1}}(x_2)$. This process is carried out for all the 78 ICs. We do not list all the results here for space limitation. We emphasize that the result can be different if the input fuzzy sets are different.

For better notations, assume $\gamma_k^* = \gamma_k$ and $\alpha_k^* = \alpha_k$, and accordingly, $\overline{f}_k^*(x_1, x_2) = \overline{f}_k(x_1, x_2)$ and $\underline{f}_k^*(x_1, x_2) = \underline{f}_k(x_1, x_2)$. Putting the eight membership functions resulted from the min() operations in the four rules and the resulting centroids for an IC into the type reducer represented by (5) and (6), we will obtain $\triangle u_R$ and $\triangle u_L$. Putting them into the defuzzifier (7) and making some algebraic simplifications, we will attain the analytical structure of the fuzzy controller for that particular IC if P_L and P_R in (5) and (6) are known.

According to the Karnik-Mendel type reducer, the exact values of P_L and P_R can always be computed as long as all the parameters of the input fuzzy sets, controller inputs, and the centroids of all the output fuzzy sets are numerically available. Hence, in principle for any specific fuzzy controller, the structure can always be derived. Nevertheless, our interest is on general controller configuration where these parameter values are not specified. As a result, P_L and P_R are unknown, making the analytical structure derivation significantly more complicated. Given that P_L=1~3 and P_R=1~3, there are a total of 3×3 =9 possible outcomes, each of which is called a case, that (5) and (6) can produce for an IC. When P_L=1 and P_R=1, we define the case number as 1, the corresponding analytical structure of the T2 fuzzy controller with the general configuration is (10), the other eight cases can also be easily computed by Karnik-Mendel type reducer, which are omitted here.

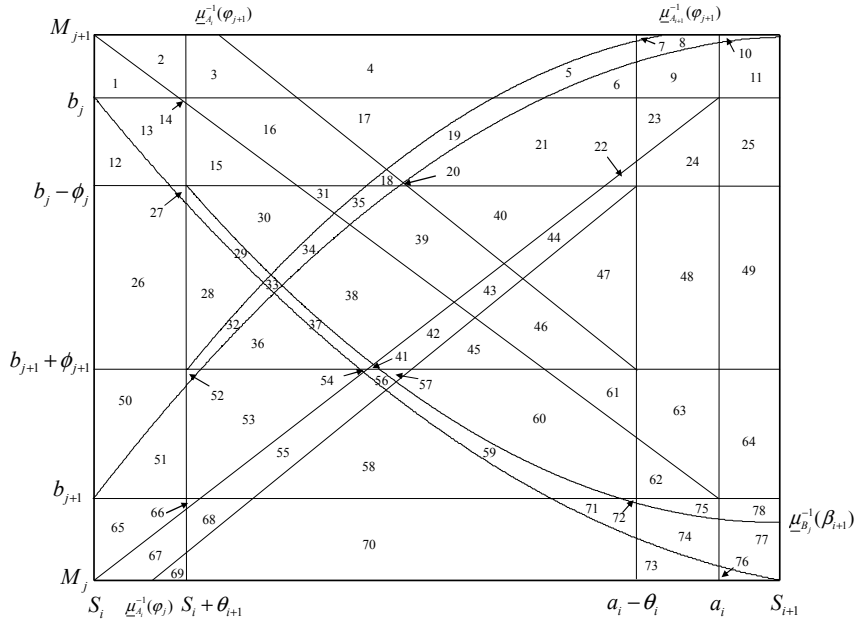

Fig. 4. Superimposing the ICs in Figs. 3(a)-3(h) to create an overall input space division (each region is labeled by an IC number)

$$\Delta u = \frac{1}{2}\left(\begin{array}{l} \dfrac{\overline{f}_1^*(\cdot)\alpha_1 + \underline{f}_2^*(\cdot)\alpha_2 + \underline{f}_3^*(\cdot)\alpha_3 + \underline{f}_4^*(\cdot)\alpha_4}{\overline{f}_1^*(\cdot) + \underline{f}_2^*(\cdot) + \underline{f}_3^*(\cdot) + \underline{f}_4^*(\cdot)} \\ + \dfrac{\underline{f}_1^*(\cdot)\gamma_1 + \underline{f}_2^*(\cdot)\gamma_2 + \overline{f}_3^*(\cdot)\gamma_3 + \overline{f}_4^*(\cdot)\gamma_4}{\underline{f}_1^*(\cdot) + \underline{f}_2^*(\cdot) + \overline{f}_3^*(\cdot) + \overline{f}_4^*(\cdot)} \end{array} \right) \tag{10}$$

Continuing the IC40 example above, with different inputs, one can derive nine different analytical structures from the nine cases. We provide case No. 1 below: Eq. (11). As another instance, the analytical controller structure for another case number (P_L=1 and P_R=2) for IC28 is Eq.(12). For the 78 ICs shown in Fig. 4, there exist a total of 9×78 = 702 analytical structure expressions. We have derived all of them and found that their mathematical structures to be all similar to either (11) or (12).

The new structure-deriving method presented above is not restricted to the T2 fuzzy controllers with two input variables. Its principle is applicable to the fuzzy controllers involving more than two input variables. Nevertheless, the derivation task will be more challenging. The biggest difficulty is to divide the n-dimension input space ($n \geq 3$) into a number of n-dimensional ICs. Take n=3 as example - one must properly divide the 3D input space into many 3D ICs so that Zadeh AND operation can be carried out for each of the fuzzy rules (at least 2^3 = 8 rules). This step is the same, in spirit, as what is shown in Fig. 3 except each IC is no longer two-dimensional, but 3D. Also, for all the 2^3 = 8 rules, there will be $2\times2^3=16$ individual divisions that will be superimposed to generate overall 3D ICs, as suppose to $2\times2^2=8$ individual divisions in Fig. 3. The number of switching points will be more - P_L=1~7 and P_R=1~7, resulting in a total of 7×7 =49 different cases.

IV. CONCLUSION

A novel general analytical structure-deriving technique for a class of interval T2 Mamdani fuzzy controllers that employ Zadeh fuzzy AND operator is developed. The mathematical input-output mapping of this class of T2 fuzzy controllers is derived then. From the results we concluded that the universe of inputs can be divided into several regions, the mathematical input-output structure is not the same in different region. It depends on controller and controller inputs. The mathematical input-output relationships are complicated nonlinear function of inputs.

REFERENCES

[1] N. N. Karnik and J. M. Mendel, "Centroid of a type-2 fuzzy set," Information Sciences, vol. 132, pp. 195-220, 2001.

[2] Q. L. Liang and J. M. Mendel, "Interval type-2 fuzzy logic systems: Theory and design," IEEE Transactions on Fuzzy Systems, vol. 8, pp. 535-550, 2000.

[3] J. M. Mendel, Uncertain Rule-Based Fuzzy Logic Systems: Introduction and New Directions. Upper Saddle River, NJ: Prentice-Hall, 2001.

[4] J. M. Mendel, "Advances in type-2 fuzzy sets and systems," Information Sciences, vol. 177, pp. 84-110, 2007.

[5] H. Zhou, H. Ying, and J. a. Duan, "Adaptive Type-2 Fuzzy Control for Uncertain Nonlinear System," Journal of Central South University of Technology, vol. (in press), 2011.

[6] H. Ying, "Deriving analytical input-output relationship for fuzzy controllers using arbitrary input fuzzy sets and Zadeh fuzzy AND operator," IEEE Transactions on Fuzzy Systems, vol. 14, pp. 654-662, 2006.

[7] H. Ying, "A general technique for deriving analytical structure of fuzzy controllers using arbitrary trapezoidal input fuzzy sets and Zadeh AND operator," Automatica, vol. 39, pp. 1171-1184, 2003.

[8] C. L. Chen, S. N. Wang, C. T. Hsieh, and F. Y. Chang, "Theoretical analysis of a fuzzy-logic controller with unequally spaced triangular membership functions," Fuzzy Sets and Systems, vol. 101, pp. 87-108, 1999.

[9] N. Maowen and T. Woei Wan, "Derivation of the analytical structure of symmetrical IT2 fuzzy PD and PI controllers," in 2010 IEEE International Conference on Fuzzy Systems, Barcelona, 2010, pp. 1-8.

[10] X. Y. Du and H. Ying, "Derivation and Analysis of the Analytical Structures of the Interval Type-2 Fuzzy-PI and PD Controllers," IEEE Transactions on Fuzzy Systems, vol. 18, pp. 802-814, Aug 2010.

$$\Delta u = \frac{\left(\frac{-\gamma_2}{a_i - S_i}\right)x_1 + \left(\frac{-\gamma_3}{b_j - M_j} - \frac{\gamma_4}{b_{j+1} - M_{j+1}} + \frac{\gamma_1\varphi_j}{M_j + \phi_j - b_j}\right)x_2 + \gamma_2 + \gamma_3 + \gamma_4 + \gamma_1\varphi_j - \frac{\gamma_1 M_j\varphi_j}{M_j + \phi_j - b_j} + \frac{\gamma_2 S_i}{a_i - S_i} + \frac{\gamma_3 M_j}{b_j - M_j} + \gamma_4\frac{M_{j+1}}{b_{j+1} - M_{j+1}}}{\left(\frac{-2}{a_i - S_i}\right)x_1 + \left(\frac{-2}{b_j - M_j} - \frac{2}{b_{j+1} - M_{j+1}} + \frac{2\varphi_j}{M_j + \phi_j - b_j}\right)x_2 + 6 + 2\varphi_j + \frac{2S_i}{a_i - S_i} + \frac{2M_j}{b_j - M_j} + \frac{2M_{j+1}}{b_{j+1} - M_{j+1}} - \frac{2M_j\varphi_j}{M_j + \phi_j - b_j}}$$
$$+ \frac{\left(\frac{-\alpha_2\beta_i}{a_i - S_i - \theta_i}\right)x_1 + \left(\frac{-\alpha_1}{b_j - M_j} + \frac{\alpha_4\varphi_{j+1}}{M_{j+1} - b_{j+1} - \phi_{j+1}} + \frac{\alpha_3\varphi_j}{M_j + \phi_j - b_j}\right)x_2 + \alpha_1 + \frac{\alpha_1 M_j}{b_j - M_j} + \alpha_2\beta_i + \frac{\alpha_2 S_i\beta_i}{a_i - S_i - \theta_i} + \alpha_3\varphi_j - \frac{\alpha_3\varphi_j M_j}{M_j + \phi_j - b_j} + \alpha_4\varphi_{j+1} - \frac{\alpha_4\varphi_{j+1}M_{j+1}}{M_{j+1} - b_{j+1} - \phi_{j+1}}}{\left(\frac{-2\beta_i}{a_i - S_i - \theta_i}\right)x_1 + \left(\frac{-2}{b_j - M_j} + \frac{2\varphi_{j+1}}{M_{j+1} - b_{j+1} - \phi_{j+1}} + \frac{2\varphi_j}{M_j + \phi_j - b_j}\right)x_2 + 2\beta_i + \frac{2S_i\beta_i}{a_i - S_i - \theta_i} + 2 + \frac{2M_j}{b_j - M_j} + 2\varphi_j - \frac{2\varphi_j M_j}{M_j + \phi_j - b_j} + 2\varphi_{j+1} - \frac{2\varphi_{j+1}M_{j+1}}{M_{j+1} - b_{j+1} - \phi_{j+1}}} \tag{11}$$

$$\Delta u = \frac{\frac{(\alpha_3 + \alpha_4)\beta_{i+1}}{(S_i - S_{i+1} + \theta_{i+1})^2}x_1^2 + \frac{-2(\alpha_3 + \alpha_4)\beta_{i+1}S_{i+1}}{(S_i - S_{i+1} + \theta_{i+1})^2}x_1 + \left(\frac{\alpha_2\varphi_{j+1}}{M_{j+1} - b_{j+1} - \phi_{j+1}} - \frac{\alpha_1}{b_j - M_j}\right)x_2 + (\alpha_3 + \alpha_4)\beta_{i+1} + (\alpha_3 + \alpha_4)\beta_{i+1}\frac{S_{i+1}^2}{(S_i - S_{i+1} + \theta_{i+1})^2} + \alpha_1 + \frac{\alpha_1 M_j}{b_j - M_j} + \alpha_2\varphi_{j+1} - \frac{\alpha_2\varphi_{j+1}M_{j+1}}{M_{j+1} - b_{j+1} - \phi_{j+1}}}{\frac{4\beta_{i+1}}{(S_i - S_{i+1} + \theta_{i+1})^2}x_1^2 + \frac{-8\beta_{i+1}S_{i+1}}{(S_i - S_{i+1} + \theta_{i+1})^2}x_1 + \left(\frac{2\varphi_{j+1}}{M_{j+1} - b_{j+1} - \phi_{j+1}} - \frac{2}{b_j - M_j}\right)x_2 + 4\beta_{i+1} + \frac{4\beta_{i+1}S_{i+1}^2}{(S_i - S_{i+1} + \theta_{i+1})^2} + 2 + \frac{2M_j}{b_j - M_j} + 2\varphi_{j+1} - \frac{2\varphi_{j+1}M_{j+1}}{M_{j+1} - b_{j+1} - \phi_{j+1}}}$$
$$+ \frac{\frac{-(\gamma_3 + \gamma_4)}{(S_i - S_{i+1})^2}x_1^2 + \frac{2(\gamma_3 + \gamma_4)S_{i+1}}{(S_i - S_{i+1})^2}x_1 + \left(\frac{\gamma_1\varphi_j}{M_j + \phi_j - b_j} + \frac{\gamma_2\varphi_{j+1}}{M_{j+1} - b_{j+1} - \phi_{j+1}}\right)x_2 + \gamma_3 + \gamma_4 - \frac{(\gamma_3 + \gamma_4)S_{i+1}^2}{(S_i - S_{i+1})^2} + \gamma_1\varphi_j + \frac{\gamma_1\varphi_j M_j}{M_j + \phi_j - b_j} + \gamma_2\varphi_{j+1} - \frac{\gamma_2\varphi_{j+1}M_{j+1}}{M_{j+1} - b_{j+1} - \phi_{j+1}}}{\frac{-4}{(S_i - S_{i+1})^2}x_1^2 + \frac{8S_{i+1}}{(S_i - S_{i+1})^2}x_1 + \left(\frac{2\varphi_j}{M_j + \phi_j - b_j} + \frac{2\varphi_{j+1}}{M_{j+1} - b_{j+1} - \phi_{j+1}}\right)x_2 + 4 - \frac{4S_{i+1}^2}{(S_i - S_{i+1})^2} + 2\varphi_j + \frac{2\varphi_j M_j}{M_j + \phi_j - b_j} + 2\varphi_{j+1} - \frac{2\varphi_{j+1}M_{j+1}}{M_{j+1} - b_{j+1} - \phi_{j+1}}} \tag{12}$$

2011 IEEE International Conference on Fuzzy Systems
June 27-30, 2011, Taipei, Taiwan

Design of Interval Type-2 Fuzzy Logic Controllers for Flocking Algorithm

Seung-Mok Lee
Department of Civil and Environmental Engineering, Robotics Program
KAIST
Daejeon, Korea
E-mail: seungmok@kaist.ac.kr

Jong-Hwan Kim
Department of Electrical Engineering and Computer Science, Robotics Program
KAIST
Daejeon, Korea
E-mail: johkim@rit.kaist.ac.kr

Hyun Myung
Department of Civil and Environmental Engineering, Robotics Program
KAIST
Daejeon, Korea
E-mail: hmyung@kaist.ac.kr

***Abstract*—This paper presents a novel interval type-2 fuzzy logic control architecture for flocking system when the system has noisy sensor measurements. The traditional type-1 fuzzy logic controller (FLC) using precise type-1 fuzzy sets cannot fully model and handle the uncertainties of sensor data. However, type-2 FLC using type-2 fuzzy sets with a footprint of uncertainty (FOU) produces better performances under noisy environments. In this paper, therefore, we present a reactive control architecture for flocking algorithm that is based on interval type-2 FLC to implement the flocking behaviors consisting separation, obstacle avoidance, and velocity matching behaviors. The type-2 based control system could cope with the uncertainties of noisy sensor measurements and resulted in good performances that outperformed the type-1 FLC.**

Keywords-Type-2 fuzzy logic controller (FLC), flocking algorithm, reactive control, multi-agent systems

I. INTRODUCTION

In 1970s, the concept of type-2 fuzzy logic system (FLS) was first introduced by Zadeh [1]. Compared to traditional type-1 fuzzy sets which have membership functions that are precise, the type-2 fuzzy sets are described by membership functions that are themselves fuzzy. Thus, type-2 FLS can be successfully used to model and handle data uncertainties in many applications. However, the type-2 FLS has some difficulties in 1) characterization of type-2 fuzzy sets; 2) performing operations; 3) inferencing, and 4) obtaining a defuzzified value which is type-0 set from the output of a type-2 inference engine which is type-2 fuzzy set [2]. After the publication of Karnik and Mendel [3] which introduces some new concepts to overcome the difficulties stated above, a lot of papers up to recently have been published about type-2 FLS [4]- [6].

Fuzzy logic controllers (FLCs) have been successfully implemented for reactive control of robots. However, most of the researches in robot control fields are based on the traditional type-1 FLC [7]-[10]. Recently, several researchers have applied type-2 FLC to mobile control. For instance, Hagras [4] applied type-2 FLS to mobile robot control in real-time for changing and dynamic environments, and the type-2 FLC resulted in good control responses compared with the type-1 FLCs. Martinez *et al*. [5] have investigated the usage of tuning technique to tune the parameters of type-2 FLC for mobile robots by using genetic algorithms.

There have been many studies for flocking behavior of multi-agent systems. For the simulation of flocking birds, Reynolds [11] introduced three heuristic rules that lead to the creation of the first computer animation model of flock. The three rules are for cohesion, separation, and alignment. In Reynolds' model, there is no leader in the flock and each bird has a local control strategy. After that, several researches on flocking motion applied the heuristic rules used in Reynolds' model to their algorithms. Olfati-Saber [12] designed artificial potentials based on graph theory to form a lattice-shape formation of robots and Bennet and McInnes [13] proposed bifurcating potential field by considering pattern formation and reconfigurability in flocking system. Moshtagh and Jadbabaie [14] proposed a method that considered velocity alignment in a group of kinematic nonholonomic robots. By analyzing the velocity vectors on a circle or sphere, they proposed a distributed control law that results in an agreement of velocity vectors and flocking. Recently, fuzzy logic based approaches to flocking algorithm are developed. Gu and Hu [15] proposed a fuzzy logic solution to the separation control problem by applying Takagi-Sugeno (TS) rules and Gaussian membership functions. Yu *et al*. [16] designed an attractive/repulsive potential function based on fuzzy logic.

To date there have been many studies on type-1 FLC for multi-robot and flocking control [15], [16], whereas few studies on control of flocking robots with considering uncertainty in environments are found in the literatures. There is one paper written by Gu and Hu [15] which discusses robustness of flocking algorithm with bounded random noise, but it has limitations in handling the noise because they used type-1 fuzzy sets.

In this paper, we use the interval type-2 fuzzy logic to design controllers for flocking algorithm. The controllers enable robots to behave toward flocking by Reynolds' model. The robots used in this paper are modeled by second order dynamical system which is fully actuated. The simulation results of type-2 FLCs are presented and their results are compared with the results of type-1 FLCs to verify the robustness of type-2 FLCs with noisy sensor measurements.

978-1-4244-7316-8/11/$26.00 ©2011 IEEE

The rest of the paper is organized as follows. Section II presents a flock model for robots with second order dynamical system. Section III proposes interval type-2 FLCs for flocking algorithm. The simulation results of the proposed type-2 FLCs are provided and discussed in Section IV. Finally, conclusions are presented in Section V.

II. FLOCK MODEL

A. Robot Dynamics

Let us consider a group of n robots (or particles) modeled by second order dynamical system with the following equation of motion:

$$\begin{aligned} \dot{q}_i(t) &= p_i(t) \\ \dot{p}_i(t) &= u_i(t) \end{aligned} \tag{1}$$

where $q_i(t)$, $p_i(t) \in \mathbb{R}^m$ are the position and velocity vectors of robot i, respectively, and $u_i(t) \in \mathbb{R}^m$ is a control vector which will be introduced later. It is assumed that all robots can communicate with each other and are fully actuated. The states of all n robots can be joined into vectors $q=[q_1,\ldots,q_n]^T \in \mathbb{R}^{mn}$, $p=[p_1,\ldots,p_n]^T \in \mathbb{R}^{mn}$, and $u=[u_1,\ldots,u_n]^T \in \mathbb{R}^{mn}$.

Let $q_d(t)$ and $p_d(t)$ be the desired position and velocity states for the group center. To track the desired position and velocity, a state feedback control law is applied to all robots in a group as follows:

$$u_i^{track} = -c_1(q_i - q_d) - c_2(p_i - p_d) \tag{2}$$

where c_1 and c_2 are the feedback gains, which can be represented by n-dimensional diagonal matrices. Then, the collective dynamics of a group of robots with the control input $u^{track} = [u_1^{track},\ldots,u_n^{track}]^T \in \mathbb{R}^{mn}$ can be represented in the following form:

$$\begin{aligned} \dot{q}(t) &= p(t) \\ \dot{p}(t) &= u^{track}(t). \end{aligned} \tag{3}$$

By using the control input $u^{track}(t)$, all robots belonging to the same group move to follow the desired trajectory.

The center of the group can be represented by the average of all states as follows:

$$q_c = \frac{1}{N}\sum_{i=1}^{N} q_i(t), \quad p_c = \frac{1}{N}\sum_{i=1}^{N} p_i(t). \tag{4}$$

From (1)-(4), the control input of the group center has the following form:

$$u_c^{track} = -c_1(q_c - q_d) - c_2(p_c - p_d). \tag{5}$$

Then, the dynamics of the center of the group can be represented by:

$$\begin{aligned} \dot{q}_c(t) &= p_c(t) \\ \dot{p}_c(t) &= u_c^{track}(t). \end{aligned} \tag{6}$$

B. Definition of Flocking Model

The flocking model was proposed by Reynolds [11] in 1986 for computer simulation of flocking behavior like flocking birds. The flocking model consists of the following three heuristic rules:

1) Cohesion behavior: attempt to stay close to nearby flockmates

2) Separation behavior: avoid collisions with nearby flockmates

3) Velocity matching behavior: attempt to match velocity with nearby flockmates

In this paper, not only the three rules of Reynolds but also obstacle avoidance behavior is designed through three interval type-2 FLCs in order to achieve the flocking behavior in environments with obstacles. Here we use interval type-2 fuzzy sets to design the FLCs, and then the robustness of the internal type-2 FLCs is tested with noisy sensor measurements. The three FLCs are designed to achieve cohesion-separation, velocity matching, and obstacle avoidance behaviors respectively.

III. TYPE-2 FUZZY LOGIC CONTROLLERS (FLCS) FOR FLOCKING ALGORITHM

In developing type-2 FLC for flocking algorithm, fuzzy sets are represented by Gaussian interval type-2 fuzzy sets. In Gaussian type-2 fuzzy sets, uncertainties are associated with the value of mean or standard deviation. In this paper the fuzzy sets with uncertain mean value is considered because uniform random noise is used to test the robustness of the type-2 FLCs.

For the simulation of flocking behaviors, three FLCs corresponding to each of the flocking behaviors are designed as shown in Fig. 1. Each FLC receives a crisp input value and then produces control output u_i^{sep}, u_i^{vel}, and u_i^{obs}. To determine the movement of each robot in the next step, the sum of the control outputs including u_i^{track} in (2) is used as u_i in (1). Thus, the total control function u_i is

$$u_i = u_i^{sep} + u_i^{vel} + u_i^{obs} + u_i^{track}. \tag{7}$$

In the rest of this section, three FLCs for each behavior in flocking algorithm based on interval type-2 fuzzy sets will be described to verify the robustness of the interval type-2 FLCs in the presence of uncertainty.

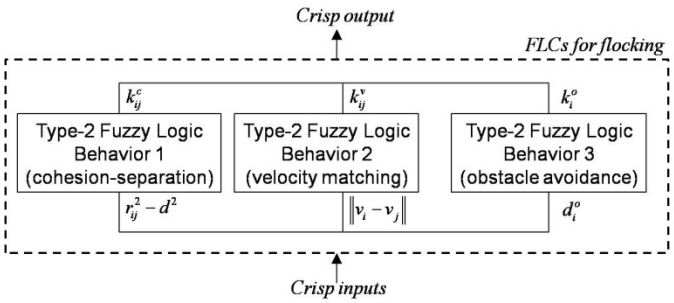

Fig. 1. Type-2 FLCs for flocking

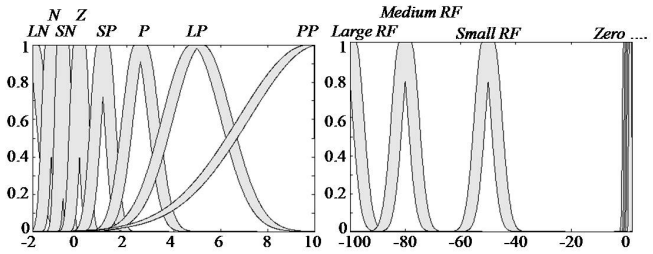

Fig. 2. Input (left) and output (right) membership functions for cohesion-separation behavior

A. Type-2 FLC for Cohesion-Separation Behavior

The FLC for cohesion-separation behavior make the robots in a group gather together around the group center while keeping robots with constant distance from others to avoid collisions with nearby robots. In order to achieve the cohesion-separation behavior, the type-1 FLC developed by Gu and Hu [15] is reformulated into an interval type-2 FLC, and it is used for cohesion-separation control. In developing the type-2 FLC for cohesion-separation control, eight type-2 Gaussian fuzzy sets which have a footprint of uncertainty (FOU) to model and handle the uncertainties of sensor data are designed as shown in Fig. 2. In the figure, the area of FOU is shaded in gray. Also eight fuzzy rules are designed as follows in a similar manner to [15]:

IF	$r_{ij}^2 - d^2$	is	*LN*	**THEN**	k_{ij}^s	is	*Large RF*
IF	$r_{ij}^2 - d^2$	is	*N*	**THEN**	k_{ij}^s	is	*Medium RF*
IF	$r_{ij}^2 - d^2$	is	*SN*	**THEN**	k_{ij}^s	is	*Small RF*
IF	$r_{ij}^2 - d^2$	is	*Z*	**THEN**	k_{ij}^s	is	*Zero*
IF	$r_{ij}^2 - d^2$	is	*SP*	**THEN**	k_{ij}^s	is	*Small AF*
IF	$r_{ij}^2 - d^2$	is	*P*	**THEN**	k_{ij}^s	is	*Medium AF*
IF	$r_{ij}^2 - d^2$	is	*LP*	**THEN**	k_{ij}^s	is	*Large AF*
IF	$r_{ij}^2 - d^2$	is	*PP*	**THEN**	k_{ij}^s	is	*Very Large AF*

where r_{ij} is the distance between robot i and robot j and d is desired distance between two robots. The control function of the robot i which include all effects from all robots in the group is

$$u_i^{sep}(t) = -\sum_i^n k_{ij}^s \left(q_i - q_j\right) \tag{8}$$

where $k_i^s=[k_{i1},\ldots,k_{in}]^T \in \mathbb{R}^n$ is the fuzzy output vector. The control function acts as a potential function on the robots, i.e. if the fuzzy input $r_{ij}^2 - d^2$ becomes negative value, then repulsive force (RF) acts on the robots; on the contrary, if the value becomes positive, then attractive force (AF) acts on the robots. In this manner, robots in a group can congregate without collisions with each other.

To measure the degree in which robots take the cohesion-separation behavior, we introduce the following *potential energy function*:

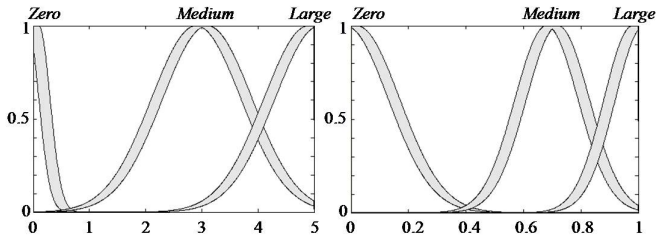

Fig. 3. Input (left) and output (right) membership functions for velocity matching behavior

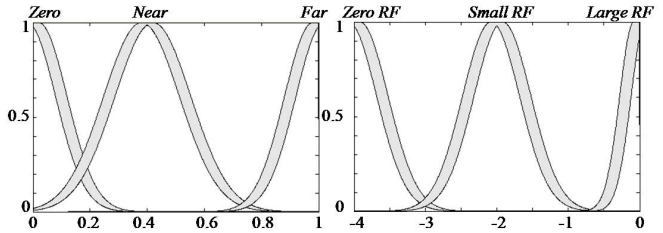

Fig. 4. Input (left) and output (right) membership functions for obstacle avoidance behavior

$$E(q) = \sum_i^n \sum_{j=i}^n \psi\left(\left\|q_i - q_j\right\| - d\right) \tag{9}$$

where $\psi(x)=x^2$. With this potential energy function, if the value becomes smaller, the flocking of robots is more stable.

B. Type-2 FLC for Velocity Matching Behavior

The FLC for velocity matching behavior is designed to align the velocity of each robot considering the others. The FLC receives only one crisp input value $\|v_i - v_j\|$ to determine fuzzy output value k_i^v. For the FLC, we represented the input and output fuzzy membership functions as *Zero*, *Medium*, and *Large* with FOU as shown in Fig. 3, and three simple fuzzy rules are designed as follows:

IF	$\left\|v_i - v_j\right\|$	is	*Zero*	**THEN**	k_{ij}^v	is	*Zero*
IF	$\left\|v_i - v_j\right\|$	is	*Medium*	**THEN**	k_{ij}^v	is	*Medium*
IF	$\left\|v_i - v_j\right\|$	is	*Large*	**THEN**	k_{ij}^v	is	*Large.*

The control function of robot i for velocity matching behavior is

$$u_i^{vel}(t) = -\sum_i^n k_{ij}^v \left(v_i - v_j\right) \tag{10}$$

where $k_i^v=[k_{i1},\ldots,k_{in}]^T \in \mathbb{R}^n$ is the fuzzy output vector. With this control function, a robot tends to align its velocity with other robots which have large velocity difference with it.

To measure the degree of velocity alignment, we use the following *deviation energy function*:

$$V(p) = \sum_i^n \sum_{j=i}^n \psi\left(\left\|p_i - p_j\right\|\right). \tag{11}$$

If the velocity $p_i(t)$ reaches an average velocity of all the robots, their headings and speed will be the same. Thus, the deviation energy function $V(p)$ becomes zero.

C. Type-2 FLC for Obstacle Avoidance Behavior

The obstacle avoidance behavior is needed for safe navigation in environments with obstacles. To design the type-2 FLC, we assume that there is one static obstacle and each robot has a range sensor which can detect the range from a robot to the obstacle when the obstacle is located within the r_{max} maximum detectable range of the sensor. Under this assumption, the range sensor value is represented by three interval type-2 fuzzy sets; *Zero*, *Near*, and *Far*; and the output fuzzy sets *Zero RF*, *Small RF*, and *Large RF* as shown in Fig. 4. The three simple fuzzy rules are designed as follows:

IF d_i is *Zero* **THEN** k_i^o is *Zero RF*
IF d_i is *Near* **THEN** k_i^o is *Small RF*
IF d_i is *Far* **THEN** k_i^o is *Large RF*.

The control function of robot i for obstacle avoidance behavior is as follows:

$$u_i^{obs}(t) = -\sum_i^n k_i^o \left(q_i - q^{obs}\right) \tag{12}$$

where k_i^o is the fuzzy output and q^{obs} is the position of obstacle. If the distance between the robot and the obstacle becomes smaller, then the robot feels large repulsive force from the obstacle. Thus, the type-2 FLC results in obstacle avoidance behavior.

IV. Simulation Results and Discussions

In this section, we present several simulation results of interval type-2 FLCs for flocking and compare their results with those of type-1 FLCs. In the simulations, a group of 10 robots in 2-D (i.e. m=2) is used, and all of them are networked with each other, i.e. the locations and velocity vectors of all robots are available to any robots belonging to the group for cohesion-separation and velocity matching behaviors.

For simulations, the robots are initially located randomly within a square of [-2.5m, 2.5m] and [-2.5m, 2.5m] in X and Y directions, respectively. The velocities are initially set randomly in the interval of [-1m/s, 1m/s]. The following parameters remain fixed throughout all simulations: d=0.3m for the cohesion-separation behavior, r_{max}=1m for the obstacle avoidance (range sensor), c_1=1 and c_2=1 for tracking a given reference trajectory. The reference trajectory which should be followed by the center of the flock is given by a straight line represented by

$$q^d = \begin{bmatrix} 0.5t & 0 \end{bmatrix}^T. \tag{13}$$

A. Tracking reference trajectory without obstacles

In the first test, the type-1 and type-2 FLCs for flocking are tested without obstacle avoidance behavior. To test the robustness of the FLCs, uniform random noise which produces data points that have the standard uniform distributions is applied to the measurements of range and velocity.

Figs. 5-6 show robot trajectories controlled by type-1 and type-2 FLCs respectively. As shown in the figures, the robots are initially located at random, and congregate around a center of the flock. As time goes on, the flocking becomes stable, and

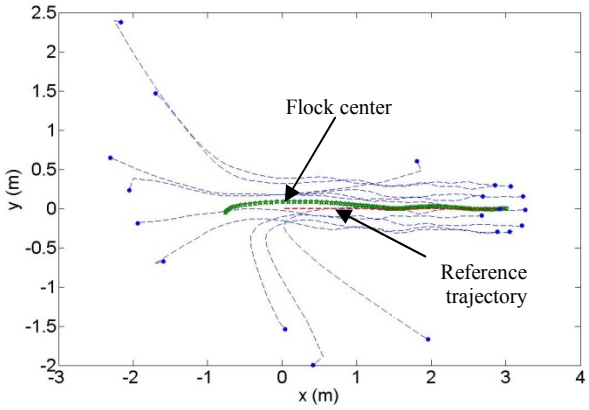

Fig. 5. Trajectories of robots by type-1 FLCs

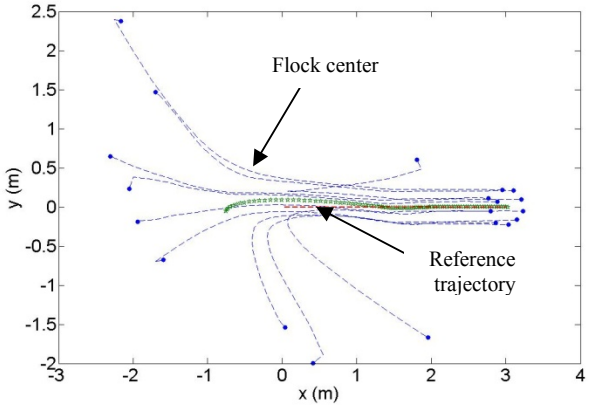

Fig. 6. Trajectories of robots by type-2 FLCs

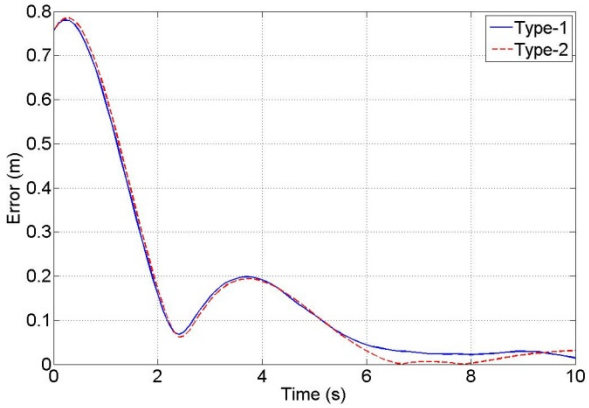

Fig. 7. Tracking error of the flock center

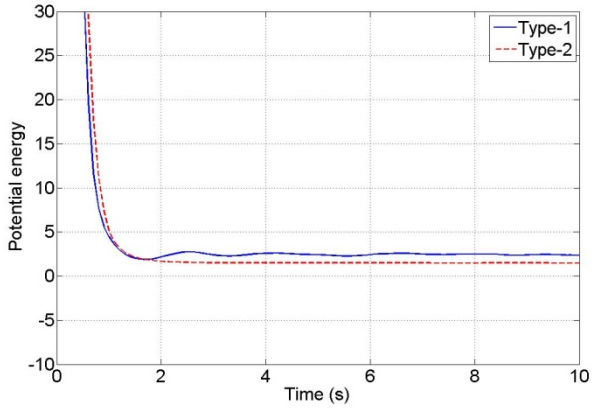

Fig. 8. Potential energy of flocking robots

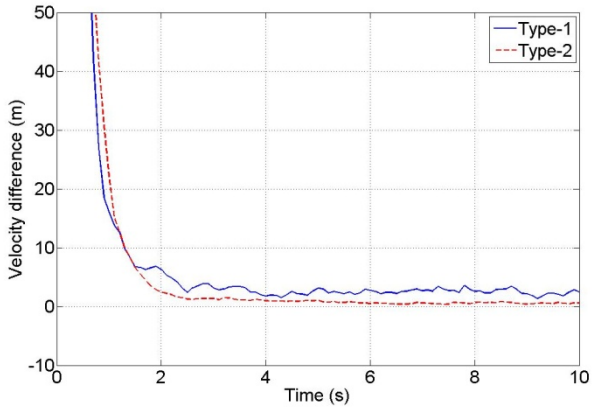

Fig. 9. Degree of velocity difference between robots

its center tracks the reference trajectory q_i^d. As shown in Fig. 5, the type-1 FLC-based cohesion-separation and velocity matching behaviors produce wobbling paths in tracking the reference path. In contrast to the type-1 FLCs, the type-2 FLCs produce smooth paths during flocking even though noisy sensor measurements are used as shown in Fig. 6. Fig. 7 shows the errors between the reference path and the center of flock trajectory. Fig. 8 shows that the potential function of type-2 have lower energy level compared with that of type-1. Also, considering the degree of velocity difference of type-1 and type-2, we can find that the type-2 shows not only lower degree but also smoother than type-1 as shown in Fig. 9. As can be seen in the results, the type-2 FLCs show robust performances under noisy environments compared to the type-1 FLCs.

B. Tracking reference trajectory with static obstacle

In the second test, the FLCs for the total flocking behaviors including obstacle behavior are tested, where the range sensors for detecting obstacles are noisy. For obstacle avoidance behavior, we assume that there is a static obstacle modeled by single point (i.e. no volume) located at q^{obs} = (3m, 0.3m). Figs. 10-11 show obstacle avoidance behaviors of type-1 and type-2 during flocking. As seen in the figures, the type-2 FLCs perform obstacle avoidance more smoothly than the type-1 FLCs, when robots detect an obstacle. Fig. 12 shows that the tracking error of the type-2 show slightly better performance than type-1. With respect to the potential energy, the type-2 show lower level of potential energy than the type-1 as shown in Fig. 13. Also, considering the degree of velocity difference, we can find that the value of the degree of robots controlled by

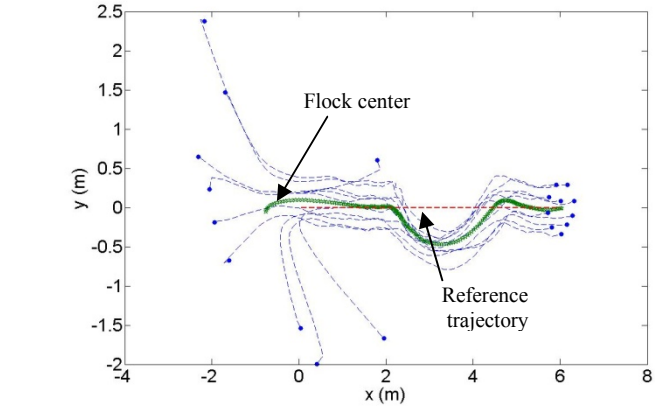

Fig. 10. Trajectories of robots by type-1 FLCs

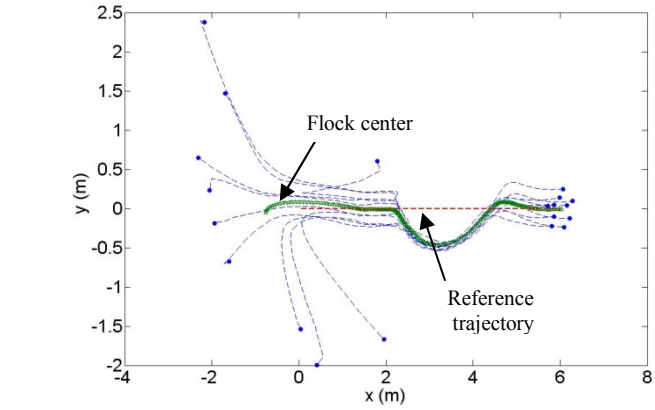

Fig. 11. Trajectories of robots by type-2 FLCs

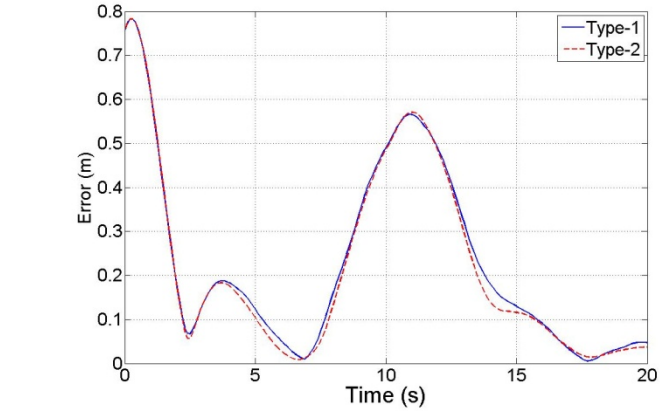

Fig. 12. Tracking error of flock center

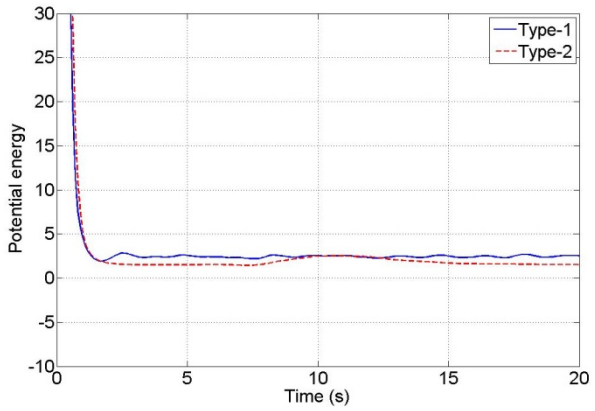

Fig. 13. Potential energy of flocking robots

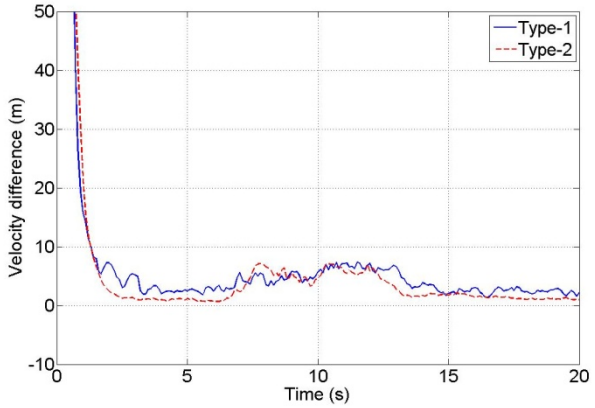

Fig. 14. Degree of velocity difference between robots

the type-2 FLCs shows better performance than the type-1 FLCs as shown in Fig. 14.

V. CONCLUSIONS

In this paper, we presented interval type-2 FLCs for flocking behaviors of robots which are modeled by the second order dynamical system, and its simulation results are compared to the type-1 FLCs with noisy sensor measurements. For flocking simulation, we proposed a structure composed of the three FCLs corresponding to flocking behaviors which consist of three components: cohesion-separation, velocity matching, and obstacle avoidance behaviors. From several simulations, we conclude that the interval type-2 FLCs are robust under uncertainties and that they resulted in better control responses than type-1 FLCs. As the use of interval type-2 FLC enables to model and handle the uncertainties effectively, the suggested FLC could provide robust performance on systems with uncertainties.

ACKNOWLEDGMENT

This research was supported by the MKE (The Ministry of Knowledge Economy), Korea, under the National Robotics Research Center for Robot Intelligence Technology support program supervised by the NIPA (National IT Industry Promotion Agency) (NIPA-2010-N02100128). It was also supported by Basic Science Research Program through the National Research Foundation of Korea (NRF) funded by the Ministry of Education, Science and Technology (grant number 2010-0006465).

REFERENCES

[1] L. A. Zadeh, "The concept of a linguistic variable and its application to approximate reasoning-1," *Inf. Sci.*, vol. 8, pp. 199-249, 1975.

[2] J. Mendel, *Uncertain Rule-Based Fuzzy Logic Systems: Introduction and New Directions*. Upper Saddle River, NJ: Prentice-Hall, 2001.

[3] N. N. Karnik and J. M. Mendel, "An introduction to type-2 fuzzy logic systems," Universtiy of Sourthern Califonia, Tech. Rep., June 1998.

[4] H. A. Hagras, "A hierarchical type-2 fuzzy logic control architecture for autonomous mobile robots," *IEEE Trans. Fuzzy Syst.*, vol. 12, no. 4, pp. 524-539, 2004.

[5] R. Martinez, O. Castillo, and L. T. Aguilar, "Optimization of interval type-2 fuzzy logic controllers for a perturbed autonomous wheeled mobile robot using genetic algorithms," *Inf. Sci.*, vol. 179, issue 13, pp. 2158-2174, 2009.

[6] C. Wagner and H. Hagras, "Toward general type-2 fuzzy logic systems based on zSlices," *IEEE Trans. Fuzzy Syst*, vol. 18. No. 4, pp. 637-660, Aug. 2010.

[7] A. Saffiotti, "The uses of fuzzy logic in autonomous robot navigation," *J. Soft Comput.*, vol. 1, no. 4, pp. 180-197, 1997.

[8] A. Bonarini, "Anytime learning and adaptation of hierarchical fuzzy logic behaviors," *Adapt. Behavior J.,* vol. 5, no. 3-4, pp. 281-351, 1997.

[9] H. Hagras, V. Callaghan, and M. Colley, "Outdoor mobile robot learning and adaptation," *IEEE Robot. Automat. Mag.*, vol. 8, no. 3, pp. 53-69, Sep. 2001.

[10] H. Hagras, M. Colley, and V. Callaghan, "Learning and adaptation of an intelligent mobile robot navigator operating n unstructured environments based on a novel online fuzzy-genetic system," *J. Fuzzy Sets Syst.*, vol. 141, no. 1, pp. 107-160, Jan. 2004.

[11] C. W. Reynolds, "Flocks, herds, and schools: A distributed behavioural model," *Comput. Graph.*, vol. 21, no. 4, pp. 25-34, 1987.

[12] R. Olfati-Saber, "Flocking for multi-agent dynamic systems: Algorithms and theory," *IEEE Trans. Autom. Control*, vol. 51, no. 3, pp. 401-420, Mar. 2006.

[13] D. J. Bennet and C. R. McInnes, "Distributed control of multi-robot systems using bifurcating potential fields," *Robot. Auton. Syst.*, vol. 58, pp.256-264, 2009.

[14] N. Moshtagh and A. Jadbabaie, "Distributed geodesic control laws for flocking of nonoholonomic agents," *IEEE Trans. Autom. Control*, vol. 52, no. 4, pp. 681-686, April 2007.

[15] D. Gu and H. Hu, "Using fuzzy logic to design separation function in flocking algorithms," *IEEE Trans. Fuzzy Syst.*, vol. 16, no. 4, pp. 826-838, Aug. 2008.

[16] H. Yu, J. Jian, and Y. Shen, "Flocking control of a group of agents using a fuzzy-logic-based attractive/repulsive function," *Int. J. Communications Network and System Sciences*, vol. 6, no. 3, pp. 567-577, 2010.

2011 IEEE International Conference on Fuzzy Systems
June 27-30, 2011, Taipei, Taiwan

Is It Rational To Partition A Data Set Using Kernel-Clustering?

Kaushik Sarkar
Department of Electronics & Communication Engineering
Narula Institute of Technology (JIS Group)
81, Nilgunj Road, Agarpara, Kolkata-700109, India
(Email: kaushik.srkr@gmail.com)

Nikhil R. Pal
Electronics and Communication Sciences Unit
Indian Statistical Institute
203, B.T. Road,Calcutta-700108
(Email: nikhil@isical.ac.in)

***Abstract*—Many interesting papers have been written in the recent past on kernel clustering and many attractive results have also been demonstrated. Here we question the rationality behind such clustering approaches. Using simple data sets we argue and demonstrate that it is not a good idea to find clusters in the kernel space when the objective is to look for clusters in the original data because in the kernel space the data may have a different geometry from that in the original feature space. In particular we demonstrate the following : (1) improper choice of the number of clusters may lead to very counterintuitive clusters (e.g., instead of merging nearby clusters, it may merge clusters that are far from each other) and (2) improper choice of kernel parameters has a significant effect on the extracted clusters and it can even impose arbitrary cluster structures that are undoubtedly absent in the original data. However, we definitely do not imply that kernel clustering can never produce desirable results. In fact, kernel clustering could be useful provided we can choose right kernel parameters. But the process being unsupervised, we do not have a solution to this issue yet. In this study, for illustration, we use one variant of the kernel Fuzzy C-Means (KFCM) clustering algorithm in conjunction with Polynomial kernels.**

Keywords: Fuzzy C-means, FCM, Kernel fuzzy C-means, feature space, Kernel space.

I. Introduction

A cluster seeking algorithm partitions a given data set $X = \{\mathbf{x_1}, \mathbf{x_2}, ..., \mathbf{x_n}\}$, $\mathbf{x}_i \in R^p$ into c number of clusters so that members of the same cluster are similar to one another and members of different cluster are dissimilar. Clustering has many applications covering almost all areas of science and technology [1], [2] and hence there are many algorithms [1], [3], [4], [5], [6] and the research efforts are still going on to develop more effective algorithms. Some algorithms use probabilistic concepts, while others use fuzzy and/or possibilistic modeling [3], [4], [7].

Crisp clustering methods assume that each data point belongs to one and only one cluster, which may not be true in some real life applications such as land-cover classification. In such cases, fuzzy clustering is considered a better alternative for extracting sub-structures in the data. In a fuzzy cluster, a data point may partially belong to more than one cluster and the membership degrees/grades lie in [0,1]. The most popular fuzzy clustering algorithm is the Fuzzy C-Means (FCM) [3] which works fine when the data set has hyperspherical clusters. However, if a pair of clusters is not linearly separable (eg., two nested spherical-shells), such algorithms usually fail. To identify such clusters there have been many extentions/variants of the FCM algorithm [8], [9], [10], [11]. In the recent past there have been many attempts to kernelize clustering algorithms. These algorithms are demonstrated to be useful in clustering data such as a disk surrounded by a shell, which are otherwise difficult to cluster [5], [12], [13], [14], [15], [16], [17]. These algorithms project the data implicitly into a high dimensional space with a hope that the "clusters" in the original space (we shall call it feature space) will be well separated in the kernel space. These algorithms then find the clusters in the kernel space.

There are different types of kernelized version of FCM. We shall consider a version which assumes that the cluster centers/prototypes are in the Kernel space [18], [19], [20], [21]. This family of algorithms requires an inverse mapping of prototypes from the kernel space to feature space. This type of algorithms will be called as KFCM-K (Kernel FCM with prototypes in the kernel space).

The objective of any clustering algorithm is to find the clusters (i.e., natural groups) in the *original* data space. Does a kernel clustering algorithm do so? Sometimes 2-Dimensional data sets are used to demonstrate the success of a kernel clustering algorithm. Usually some "suitable" kernel parameter values are chosen and results are demonstrated. Do we know if the algorithm will work for a wide range of choices of parameters? We shall see that even for some simple data sets, the answer to the previous question is "No". When the data sets are in 2-D we can visualize easily the performance. But when the data are in high dimension visual assessment is difficult. For such cases, usually the cluster centroids or the partition are used in conjunction with a labeled data set (the data set is for a classification problem) to assess the resubstitution or classification error. This approach makes an assumption that number of natural clusters is equal to the number of classes. But this may not necessarily be true as clustering and classification are philosophically two different problems. For example, a two class problem may have four distinct clusters and we may not know it (A high dimensional generalization of the Ex-OR problem). If the resubstitution or classification error is low, we should be happy, but if not, we cannot make any inference because the number of clusters may be equal

978-1-4244-7316-8/11/$26.00 ©2011 IEEE

to the number of classes but the clustering could be poor or the number of clusters could be more than the number of classes and that may lead to poor classification performance. So assuming number of classes equal to the number of clusters and then checking the resubstitution error or classification error is not a good way of justifying kernel clustering.

Here we investigate whether clustering in the kernel space is justified or not. Our investigation suggests that Kernel clustering can lead to strange (counterintuitive) results if the choice of number of clusters and/or the choice of kernel parameters are not appropriate. We discuss and demonstrate this issue using some simple data sets.

II. Kernelized Version FCM

A data set may have clusters in it, but it may be difficult for an algorithm like FCM to extract those clusters. One reasons for this may be that a pair of clusters is not linearly separable. In such a case, the original data can be mapped to a higher dimensional space (kernel space) with a hope that clusters will be easily identifiable [19], [20], [21]. For this a non linear mapping function f is used such that $\phi : R^d \longrightarrow H$, where H is the kernel space. Typically kernel-clustering algorithms use the kernel trick that takes the advantage of the fact that the dot products in the kernel space can be represented by a Mercer kernel K where $K(\mathbf{x},\mathbf{y}) = \phi(\mathbf{x})^T\phi(\mathbf{y})$, where, $\mathbf{x},\mathbf{y} \in R^p$. Thus the distance/similarity in the kernel space can be replaced by the Mercer kernel. Some of the popular kernel functions are:

1) RBF kernel : $e^{-||\mathbf{x}-\mathbf{y}||^2/\sigma^2}, \sigma^2 > 0$
2) Polynomial kernel : $(\mathbf{x^T}.\mathbf{y}+a)^b, a \geq 0, b \in N$
3) Hyper-tangent : $tanh(\mathbf{x^T}.\mathbf{y}+a), a \geq 0$

In this study, we shall consider only one Kernel based FCM algorithm, KFCM-K and use only the Polynomial kernel (PK). We shall not consider the other versions, such as KFCM-F [18], [5], [22], where cluster centers are considered in the feature space itself.

A. KFCM-K [13], [14], [15], [16], [18]

Here the prototypes are located in the kernel space, so the pre-images of prototypes in the feature space have to be computed by taking the inverse mapping from kernel space to feature space. KFCM-K algorithm minimizes the following objective function at (1).

$$Q = \sum_{i=1}^{c}\sum_{k=1}^{n} u_{ik}^m ||\phi(\mathbf{x_k}) - \mathbf{v_i}||^2 \tag{1}$$

subject to the constraints

1) $u_{ik} \in [0,1] \forall i,k$
2) $0 < \sum_{k=1}^{n} u_{ik} < n \ \forall i$
3) $\sum_{i=1}^{c} u_{ik} = 1 \ \forall k$

In (1) $\mathbf{v}_i$ is i^{th} prototype in the kernel space. Using the Lagrange Multiplier technique, optimization of Q with respect to $\mathbf{v}_i$, results in

$$\mathbf{v_i} = \frac{\sum_{k=1}^{n} u_{ik}^m \phi(\mathbf{x_k})}{\sum_{k=1}^{n} u_{ik}^m} \tag{2}$$

Similarly, the expression for the membership values are derived as

$$u_{ik} = \frac{1}{\sum_{j=1}^{c} (\frac{||\phi(\mathbf{x_k}) - \mathbf{v_i}||}{||\phi(\mathbf{x_k}) - \mathbf{v_j}||})^{\frac{2}{m-1}}}; i = 1, \cdots, c; k = 1, \cdots, n \tag{3}$$

where

$$\begin{aligned} ||\phi(\mathbf{x_k}) - \mathbf{v_i}||^2 &= (\phi(\mathbf{x_k}) - \mathbf{v_i})^T(\phi(\mathbf{x_k}) - \mathbf{v_i}) \\ &= \phi(\mathbf{x_k})^T\phi(\mathbf{x_k}) - 2\phi(\mathbf{x_k})^T\mathbf{v_i} + \mathbf{v_i}^T\mathbf{v_i}. \end{aligned} \tag{4}$$

Using the expression for the prototypes (2) into the expression (4) , one gets

$$\begin{aligned} ||\phi(\mathbf{x_k}) - \mathbf{v_i}||^2 \quad = \quad & K(\mathbf{x_k},\mathbf{x_k}) - 2\frac{\sum_{j=1}^{n} u_{ij}^m K(\mathbf{x_k},\mathbf{x_j})}{\sum_{j=1}^{n} u_{ij}^m} \\ & + \frac{\sum_{j=1}^{n}\sum_{l=1}^{n} u_{ij}^m u_{il}^m K(\mathbf{x_k},\mathbf{x_l})}{(\sum_{j=1}^{n} u_{ij}^m)^2} \end{aligned} \tag{5}$$

Following, [18], [14], the expression for the prototypes in the feature space $V = \{\tilde{\mathbf{v}}_i; i = 1, 2, ..., c\}$ with Polynomial kernel is given in (6).

$$\tilde{\mathbf{v}}_i = \frac{\sum_{k=1}^{n} u_{ik}^m (\mathbf{x_k^T}\tilde{\mathbf{v}}_i + a)^{b-1}\mathbf{x_k}}{(\tilde{\mathbf{v}}_i{}^T\tilde{\mathbf{v}}_i + a)^{b-1}\sum_{j=1}^{n} u_{ij}^m} \tag{6}$$

Algorithm KFCM-K

1) Fix $c, t_{max}, m > 1$ and $\epsilon > 0$, the tolerance level for termination.
2) Initialize membership matrix U.
3) Repeat
   Update $U = [u_{ik}]$ according to equation (3) via (5).

   until $\sum_{i=1}^{c}\sum_{k=1}^{n} |u_{ik}^{(t+1)} - u_{ik}^{(t)}| < \epsilon$ is satisfied. (7)
4) Return U.
5) Initialize prototypes V
6) Repeat
   Update $\tilde{\mathbf{v}}_i$s according to equation (6) for Polynomial kernel

   until $\sum_{i=1}^{c}\sum_{k=1}^{p} |\tilde{v}_{k,i}^{(t+1)} - \tilde{v}_{k,i}^{(t)}| < \epsilon$ is satisfied. (8)
7) Return V.

Note that, there are many other equivalent termination criteria that can be used in place of (7) and (8).

III. Experimental studies

We use three synthetic data sets, all in R^2:Ring, Five-Cluster, and Uniform-Disc.

- **Ring** : The Ring Data set is depicted in Fig.1a, where the inner disk contains 100 points and the outer ring contains 200 points.

- **Five-Cluster** : Fig.1b shows the Five-Cluster data set where the inner disk, like Ring contains 100 data points forming a cluster. Surrounding this cluster, there are four smaller clusters, each with 50 points.
- **Uniformdisk** : Fig.1c depicts the Uniform data set with 441 points that are uniformly distributed. This data set does not have any cluster in it.

For each data set, X, every feature x is normalized by $\frac{(x-\mu)}{\sigma}$, where μ and σ are the mean and standard deviation of x as estimated from the given data set. This protocol is followed in [18].

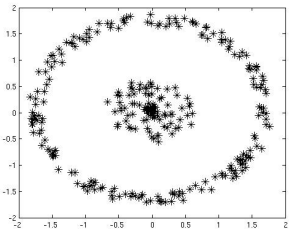

(a) Ring dataset

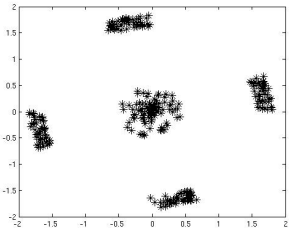

(b) FiveCluster dataset

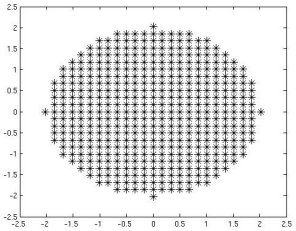

(c) Uniform dataset

Fig. 1: The three Synthetic datasets used in this study

A. Kernel Clustering with Polynomial Kernel

We study the behavior of FCM, and KFCM-K with Polynomial kernel on the three data sets Ring, Five-Cluster, and Uniform. We use $m = 1.2, \epsilon = 10^{-8}, t_{max} = 100$. For the Polynomial Kernel,we have experimented with different choices for $a \in \{1, 2, 3, 4, 5, 7, 10, 15\}$ and $b \in \{2, 4, 6, 8, 10, 12, 14, 16\}$, a total of 64 combinations. The initial prototypes are taken randomly from the input data set.

First we consider the Ring data, Fig.1a. Clearly there is a disk-shaped cluster at the center. Many authors share the view that the shell around the disk is also a cluster. We also share the same view here. For this data set with c=2, FCM, as expected, divides the data set as shown in Fig.2a. For some choices of a and b, the KFCM-K behaves similar to FCM, but for none of the 64 choices of parameters, KFCM-K could extract the shell as a separate cluster. Sometimes, part of the shell is extracted as a cluster and the remaining data points as another cluster. One such partition is exhibited in Fig. 2b. We also noticed that when a is high and b is low, then for this data set KFCM-K behaves like FCM. Fig 2c shows one such partition with a=15 and b=2. For this data set we find that the choice of a and b has a significant influence on the clustering output. Moreover, in this case, KFCM-K failed to produce the desired partition. Hence we do not make any further analysis on this data set.

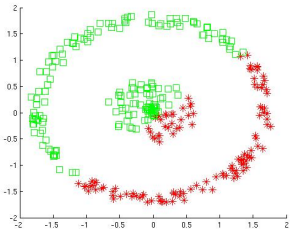

(a) FCM

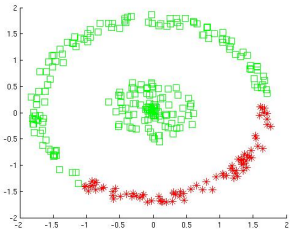

(b) KFCM-K (a=1,b=2)

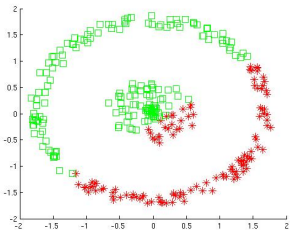

(c) KFCM-K (a=15,b=2)

Fig. 2: Clustering of Ring data with FCM and KFCM-K for c=2

Next we focus our attention on the Five-Cluster data set (Fig.1b), which has five distinct clusters. As expected, FCM finds all the five clusters correctly when c=5 (Fig.3g), so does KFCM-K with a=1, b=2 (Fig.3h). Fig.3, also compares the results with c=2,3, and 4. For example, when c= 4 (with a=1,b=2), the FCM result is quite intuitive (Fig.3e), while KFCM-K merges two clusters, which are on the *opposite sides* of the central disk, into one clusters (Fig. 3f). Thus KFCM-K

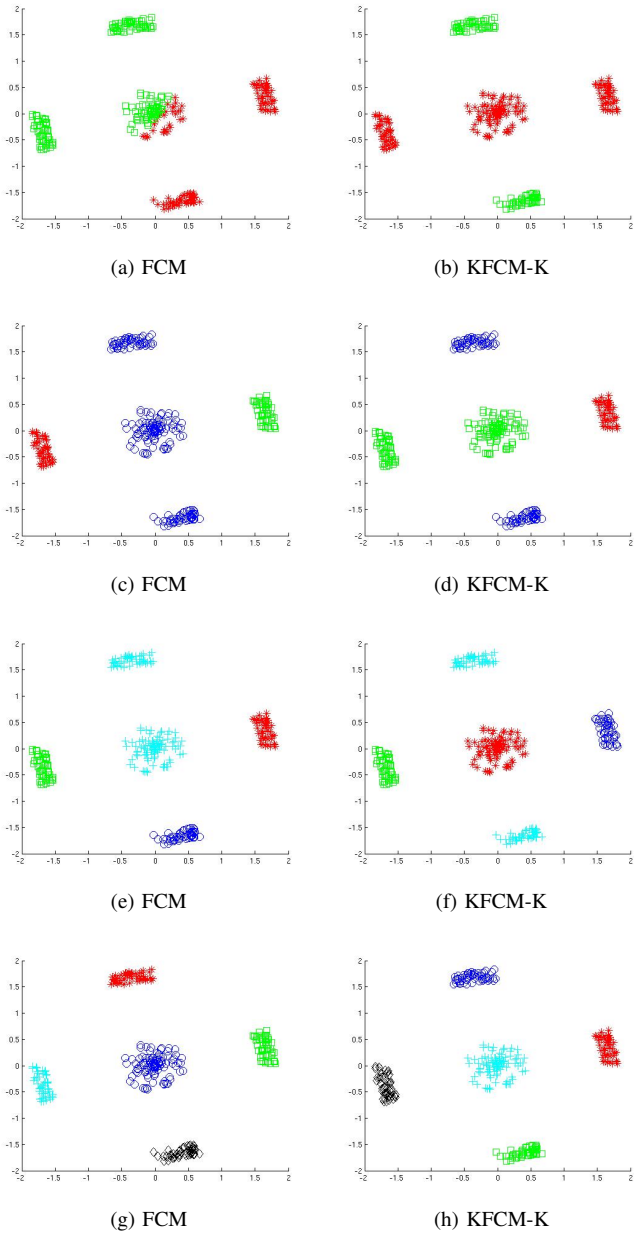

(a) FCM (b) KFCM-K

(c) FCM (d) KFCM-K

(e) FCM (f) KFCM-K

(g) FCM (h) KFCM-K

Fig. 3:
(a) FCM Clusters with c=2; (b)KFCM-K Clusters with c=2;
(c) FCM Clusters with c=3; (d)KFCM-K Clusters with c=3;
(e) FCM Clusters with c=4; (f)KFCM-K Clusters with c=4;
(g) FCM Clusters with c=5; (h)KFCM-K Clusters with c=5;

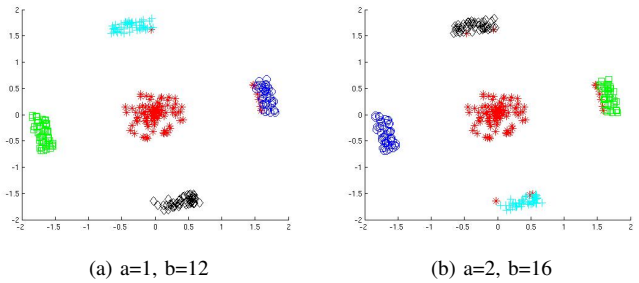

(a) a=1, b=12 (b) a=2, b=16

Fig. 4: Few bad clusters on the Five-Cluster dataset using KFCM-K

TABLE I: Value of Correlations for different kernel parameters [a,b-Kernel parameters, Q-Quality, PC-Pearson Correlation, KC=Kendall Correlation, SP-Spearman Correlation]

DATA	a,b	Q	a,b	Q	a,b	Q
FiveCluster	1,2	Good	5,2	Good	10,2	Good
	1,4	Good	5,4	Good	10,4	Good
	1,6	Good	5,6	Good	10,6	Good
	1,8	Good	5,8	Good	10,8	Good
	1,10	Good	5,10	Good	10,10	Good
	1,12	Bad	5,12	Good	10,12	Good
Uniform Disk	1,2	Good	5,2	Good	10,2	Good
	1,4	Medium	5,4	Good	10,4	Good
	1,6	Bad	5,6	Good	10,6	Good
	1,8	Bad	5,8	Medium	10,8	Good
	1,10	Bad	5,10	Bad	10,10	Good
	1,12	Bad	5,12	Bad	10,12	Medium

merges two small clusters when they are quite far from each other. Note that, we have run the clustering algorithms with different initializations, and we got similar results in several runs. However, for c=2 and c=3, FCM produces intuitively acceptable results (Fig.3a and Fig. 3c), while KFCM-K does not (Fig.3b and Fig. 3d) as it merges two clusters which are not nearby. In this case, since the data are in 2-D we can assess the results visually. But for high dimensional data, we may not know the desired number of clusters and hence we may end up with very undesirable results (merging of two distant clusters) and we would not even know that. This is one facet of the problems associated with kernel clustering.

The other problems is associated with the choice of kernel parameters. To demonstrate this issue, we consider c=5, the best choice for number of clusters for this data set. Then we ran KFCM-K for all 64 combinations of a and b as mentioned above. Table I, summarizes the results. Table I reveals that when a=1, and b is high (12 or higher), KFCM-K fails to extract the correct partition. Fig.4 (a) reveals that with a=1 and b=12, a few points of the cyan (plus) and blue (circle) clusters get merged with the central disk. Similarly, with a=2 and b=14 or higher, the partition starts departing from the desirable one (Fig.4 (b)). Thus we find that the choice of kernel parameters is crucial to the success of the algorithm even for very simple data sets. Since, for high dimensional data we would not know the sub-structures present in the original data, we shall not know whether KFCM-K has found a good solution or not. One can make the same arguments with FCM, but the differences are : (a) with improper choices of c, the number of clusters, FCM splits or merges clusters in such a manner that they agree with our intuition and FCM does not impose strange geometric structures on the data and (b) FCM does not have these two extra parameters, which may change the geometry of the data.

Now we consider the data set, Uniform (Fig.1c). Clearly Uniform does not have any sub-structure or cluster. Hence any clustering algorithm, with c=2, should partition the data into approximately two halves, where the approximate line partitioning the data may have one of many possible orientations. Fig. 5a shows that FCM does the same. Similarly, KFCM-K also does the same with a=1, b=2 (Fig.5b); as b increases, one of the clusters starts becoming bigger (Fig.5c). With a=1,

b=12 or above, KFCM-K extracts a *nice shell* (Fig. 5d) as one of the clusters. This behavior is also repeated with other choices of a. In fact, when a is increased, KFCM-K starts extracting a shell for further high values of b. This is a very serious limitation of the KFCM-K algorithm. As an illustration in Fig. 6 we show the membership values of different points to the cluster they belong to. Figure 6 corresponds to Fig. 5d. In Fig. 6, for each point we find the maximum membership value and depending on its cluster label we plot it either in green (square) or in red (circle). Figure 6 shows that for most of the points in the central big cluster the membership values to the cluster are very high, while for most points belonging to the imposed outer-shell cluster, the membership values are above 0.6. There are some points in the bigger cluster with memberships varying from values slightly higher than 0.5 to further high values suggesting a kind of gradual transition from one cluster to the other. In this data set, there is no reason to assume such a strange cluster structure.

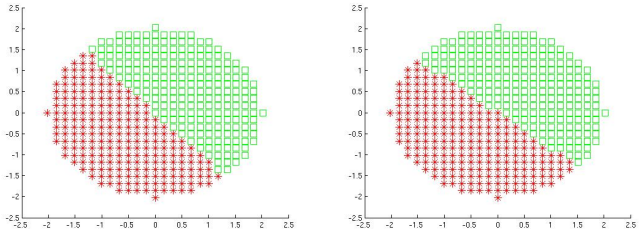

(a) FCM (b) KFCM-K (a=1, b=2)

(c) KFCM-K (a=1, b=6) (d) KFCM-K (a=1, b=12)

Fig. 5: Results on the Uniform dataset by FCM and KFCM-K for different parameters

Table I summarizes the visual assessment of quality of the partitions generated by kernel clustering for some illustrative sets of a and b. In Table I, Medium indicates minor departure from ideal partition while Bad indicates significant departure from the ideal partition.

So what do we learn from these experiments?

- Knowledge of the number of clusters present in the data is essential for the success of KFCM-K; otherwise, some cluster may include data points which are far from each other. In particular when c is less than the actual number clusters, KFCM-K may merge two subclusters which are far from each other in the actual data (feature) space ignoring nearby clusters. Thus producing counterintuitive clusters.

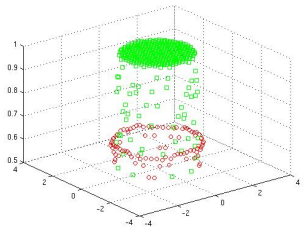

Fig. 6: Pictorial representation of the maximum membership values to the clusters.

- When a data set does not have any cluster structure, depending on the choice of kernel-parameters, it can impose very artificial substructures (e.g., the KFCM-K extracts a shell from the uniform data). To summarize, KFCM-K may impose arbitrary structures on the data.
- Even when the number of clusters is known, appropriate choice of the kernel parameters is essential to get the desirable results.

These problems are quite serious because for any real life application, data are usually in a high dimensional space. But why do all these happen? We think, this happens because we are trying to extract clusters in a space which may alter the geometry of the original data. This does not mean that for some data set KFCM-K type clustering cannot help. For example, if we have two touching clusters and in the projected space the two clusters become separated, then it would be easy to find the clusters in the kernel space. There could be other interesting cases where kernelized version could be useful. For example, using RBF kernel with an appropriate choice of the kernel width, it is possible to extract the shell and the central disk as two different clusters [18], but we need to use the right kernel with the right choice of parameters.

IV. Discussion and Conclusion

The performance of the kernel clustering algorithm, KFCM-K raises a very fundamental question : Should we really cluster a given data set in the kernel space? Although in the kernel space the data points might be more sparsely distributed, we cannot say that the clusters that we find in the kernel space will represent the same groups as those in the original feature space. We have illustrated this using a few synthetic data sets. In some of the studies involving kernel clustering the results are justified by matching the clusters with the classes [18]. In other words, one starts with a data set on k classes where every point has an associated class label indicating the class that the data point comes from. Such a data set is then clustered into c=k clusters ignoring the class labels. Finally, one assesses how good the partition matches with class structure. If there is a good match we should be happy. But we need to remember that cluster structure in a data set may be quite different from the structure imposed by class labels. The situation is actually more complicated because most kernel needs specification of some parameters. We have demonstrated that the choice of the kernel parameters has a

significant impact on the performance of clustering algorithm. When the problem is of classification, we can use different ways, such as cross-validation, to choose a desirable value for the kernel parameters. But for cluster seeking problems, it is difficult to choose the optimal parameters because the problem is unsupervised.

We have demonstrated / justified that Kernel clustering may lead to very unexpected results. When the goal of clustering a data set is to find the clusters / substructures in the original data (feature) space, unless one is careful, kernelization may impose undesirable structures on the data and hence the clusters obtained in the kernel space may not exhibit the structure of the original data. But, this does not mean that kernel clustering cannot be useful at all. If one wants to cluster in the kernel space, then proper choice of the parameters of the kernel function has to be used. We do not have a mechanism to choose the desirable parameters and currently we are investigating this issue. We hope to report our findings on this in near future.

REFERENCES

[1] M.R. Anderberg, Cluster Analysis for Application, Academic Press, New York,1973.

[2] E. Backer, A.K. Jain, A clustering performance measure based on fuzzy set decomposition, IEEE Trans. Pattern Anal. Mach Intell. 3 (1) (1981) 6674.

[3] J. C. Bezdek, Patteren Recognition With Fuzzy Objective Function Algorithms. New York: Plenum, 1981.

[4] Nikhil R. Pal, Kuhu Pal, James M. Keller and James C. Bezdek, A Possibilistic Fuzzy c-Means Clustering Algorithm, IEEE Transactions on Fuzzy Systems, Vol. 13, N0. 4, August 2005.

[5] D.Q. Zhang, S.C. Chen, Clustering incomplete data using Kernel-based Fuzzy C-Means algorithm, Neural Processing Letters 18 (3) (2003) 155162.

[6] I.S. Dhillon, Y. Guan, B. Kulis, A unified view of kernel k-means, spectral clustering and graph partitioning, Technical Report TR-04-25, UTCS, 2005.

[7] S. Theodoridis , K. Koutroumbas, Pattern Recognition, Academic Press, 2003.

[8] J. C. Bezdek, R. J. Hathaway and N. R. Pal, Norm-induced shell-prototypes (NISP) clustering, *Neural, Parallel and Scientific Computations* , Vol. 3, pp 431-450, 1995.

[9] E. E. Gustafson and W. Kessel, Fuzzy Clustering with a Fuzzy Covariance Matrix, Proc. 1978 IEEE CDC, IEEE Press, 1979. Piscataway, NJ, 761-766.

[10] Dav, R. N. and Bhaswan, K. (1992). Adaptive fuzzy c-shells clustering and detection of ellipses, IEEE Trans. on Neural Networks, 3(5), 643-662.

[11] Krisnapuram, R., Frigui, H. and Nasroui, O. (1995). Fuzzy and possibilistic shell clustering algorithms and their application

[12] Z. D. Wu, W. X. Xie, J. P.Yu, Fuzzy c-means clustering algorithm based on kernel method, in: Proc. Of the Internat. Conf. on Computational Intelligence and Multimedia Applications, 2003, pp. 49-54.

[13] D. Zhang, S. Chen, Fuzzy clustering using kernel method, in: Proc. of the Internat. Conf. on Control and Automation, 2002, pp. 123127.

[14] S. Zhou, J. Gan, Mercer kernel fuzzy c-means algorithm and prototypes of clusters, in: Proc. of Conf. on Internat. Data Engineering and Automated Learning, Vol. 3177, 2004, pp. 613618.

[15] L. Zeyu, T. Shiwei, X. Jing, J. Jun,Modied FCMclustering based on kernel mapping, in: Proc. of the Internat. Society for Optical Engineering, Vol. 4554, 2001, pp. 241245.

[16] J. H. Chiang, P. Y. Hao, A new kernel-based fuzzy clustering approach: support vector clustering with cell growing, IEEE Transactions on Fuzzy Systems 11 (4) (2003) 518-527.

[17] D. W. Kim, K. Y. Lee, D. Lee, K. H. Lee, Evolution of the performance of clustering algorithms kernel-induced feature space, Pattern Recognition 38 (4) (2005) 607-611.

[18] Daniel Graves, Witold Pedrycz, Kernel-based fuzzy clustering and fuzzy clustering: A comperative experimental study, Fuzzy Sets and Systems, 161 (2010) 522-543.

[19] R. Herbrich, Learning Kernel Classiers, MIT Press, Cambridge, MA, 2002.

[20] K.R. Muller, S. Mika, G. Ratsch, K. Tsuda, B. Scholkopf, An introduction to kernel-based learning algorithms, IEEE Transactions on Neural Networks 12 (2) (2001) 181201.

[21] B. Scholkopf, A. Smola, K.R. Muller, Nonlinear component analysis as a kernel eigenvalue problem, Neural Computation 10 (1998) 12991319.

[22] H. Shen, J. Yang, S. Wang, X. Liu, Attribute weighted Mercer kernel based fuzzy clustering algorithm for general non-spherical datasets, Soft Computing 10 (11) (2006) 10611073.

[23] I.S. Dhillon, Y. Guan and B. Kulis, Kernel k-means: spectral clustering and normalized cuts, KDD 04: Proceedings of the Tenth ACM SIGKDD International Conference on Knowledge Discovery and Data Mining, ACM Press, New York, NY, USA (2004), pp. 551556.

[24] M. Filippone, F. Camastra, F. Masulli, and S. Rovetta. A survey of kernel and spectral methods for clustering. Pattern Recognition, 41(1):176-190, January 2008.

[25] F.R. Bach, M.I. Jordan, Learning spectral clustering, Technical Report UCB/CSD-03-1249, EECS Department, University of California, Berkeley, 2003.

[26] F.R. Bach, M.I. Jordan, Learning Spectral Clustering, With Application To Speech Separation, The Journal of Machine Learning Research, 7, p.1963-2001, 12/1/2006

[27] N. Cristianini, J.S. Taylor, A. Elisseeff and J.S. Kandola, On kernel-target alignment, NIPS (2001), pp. 367373.

[28] I. Fischer, I. Poland, New methods for spectral clustering, Technical Report IDSIA-12-04, IDSIA, 2004.

[29] M. Meila, J. Shi, Learning segmentation by random walks, in: NIPS, 2000, pp. 873879.

[30] B. Kulis, S. Basu, I.S. Dhillon and R. Mooney, Semi-supervised graph clustering: a kernel approach, ICML 05: Proceedings of the 22nd International Conference on Machine Learning, ACM Press, New York, NY, USA (2005), pp. 457464.

[31] N. Lanckriet, N. Cristianini, P. Bartlett, L. El-Ghoui, and M.I Jordan. Learning the kernel matrix using semi-definite programming. In International Conference on Machine Learning (ICML 2002), 2002.

[32] X. Yin, S. Chen, E. Hu, D. Zhang. Semi-supervised clustering with metric learning: An adaptive kernel method. Pattern Recognition, Volume 43, Issue 4, April 2010, Pages 1320-1333

[33] M. Filippone. Dealing with non-metric dissimilarities in fuzzy central clustering algorithms. International Journal of Approximate Reasoning, 50(2):363-384, February 2009.

[34] John W. Sammon Jr, A nonlinear Mapping for Data Structure Analysis, IEEE Transactions on Computers, Vol. C-18, No. 5, pp 401-409, May 1969.

2011 IEEE International Conference on Fuzzy Systems
June 27-30, 2011, Taipei, Taiwan

Fuzzy Quantum Computation Based Thermal Unit Commitment Strategy with Solar-battery System Injection

Shantanu Chakraborty, Tomonobu Senjyu, Atsushi Yona
Dept. of Electrical and Electronics Engineering
University of the Ryukyus, Japan
Email: b985542@tec.u-ryukyu.ac.jp

Toshihisa Funabashi
Meidensha Corporation, Tokyo, Japan
Email: funabashi-t@mb.meidensha.co.jp

***Abstract*—This article presents a strategy to solve thermal unit commitment (UC) integrated with an equivalent solar-battery system using Fuzzy based Quantum inspired Evolutionary Algorithm (FQEA). As a renewable power source, solar power is injected stochastically with the model. To handle the uncertainty and intermittency involved while integrating solar power and load forecasting, the trivial crisp problem formulations are modified by fuzzification. An evolutionary algorithm based on the concept and principle of quantum computation is applied to solve the UC problem. The conventional Quantum Evolutionary Algorithm (QEA) is advanced by using several operators such as binary differential operator, mutation and crossover along with trivial rotation operator with a re-defined rotational angle look-up table. The QEA is further modified by introducing multi-population based scheme. The fitness function is formulated by combining the objective function, penalty function and the aggregated fuzzy membership function. The proposed FQEA is applied to UC problem in different scaled power systems up to 100 units. Provided simulation results will show the effectiveness of FQEA.**

Keywords*—Unit Commitment, Fuzzy Logic, Quantum Computation, Evolutionary Method.

I. Introduction

The generation planning problem is an important problem in planning and operation of power system which required to be solved very carefully in order to accomplish maximum benefit. UC requires determining the on/off schedules of thermal units over a particular schedule horizon as well as resolves the hourly thermal output power (known as economic load dispatch; ELD) as well as satisfying a large set of system and operational constraints while keeping the production cost as minimum as possible. UC is introduced as one of the most complex combinatorial optimization problems in power system economics. A bibliographical survey on UC discloses that a good amount of numerical and meta-heuristic optimization techniques such as priority list [1], Lagrangian relaxation (LR)[2,3], genetic algorithm (GA)[4,5], evolutionary programming (EP)[6], particle swarm optimization (PSO)[7,8], simulated annealing (SA)[9,10], dynamic programming (DP)[11], constraint logic programming (CLP)[13] have been successfully applied to achieve efficient and near optimal solutions for UC problem. The concept of applying quantum mechanics in the field of computer science is a new prototype in the research of evolutionary programming. Some key principles of quantum mechanics such as uncertainty, superposition, interference are the main working force in quantum inspired evolutionary programming [14,15]. QEA is also successfully applied on thermal UC problem [16]. Moreover, one variant of QEA coupled with binary particle swarm optimization was skillfully deployed on UC problem [17], showing its versatility in power system economical optimization field. Thermal unit generation requires extensive use of fossil fuels which have negative effect on environment. Renewable energy sources come as a remedy of such scenarios and rightfully receive significant importance in recent researches and studies. Solar power is widely investigated such renewable source. However its integration with UC is imprecise due to the prediction error in forecasted load demand, solar radiation and spinning reserve requirement. Hence the crisp methods fell short especially when imprecise solar power system is coupled. Such uncertainties in imprecise parameters have been considered in mainly two ways: fuzzy systems approach [12] and stochastic/probabilistic approach.

This paper proposes a fuzzy logic based thermal UC strategy integrated with solar-battery by facilitating a modified quantum inspired evolutionary algorithm. Battery is modeled with solar system to supply power in case of peak load shaving and also to smooth out the load leveling. The solutions are initialized by a sophisticated weighted priority list method which helps to determine feasible as well as diverse solutions. The solutions are then 're-observed' and converted into quantum individuals. The QEA process, comprised with multi-population scheme is applied on the quantum individuals. The load demand, solar radiation, spinning reserve and total production cost is re-formulated by defining fuzzy membership degrees considering their uncertain nature. To evaluate the individual's fitness and contribution, a fitness function is defined which includes the aggregated fuzzy membership function and penalty function for constraints violations. The individuals are updated using several operators to facilitate the exploration and

978-1-4244-7316-8/11/$26.00 ©2011 IEEE

exploitation syndrome.

The organization of the paper is briefed as follows: Section II details about the quantum computation. The problem formulation including the objective function and constraints is elucidated in Section III. Section IV shows the fuzzy formulation of the imprecise constraints. The details algorithms with associated technical aspects are briefed in Section V. Numerical simulations and results analysis are detailed in Section VI. Finally concluding remarks are described in Section VII.

II. Quantum Computation

The combination of quantum mechanical computers and quantum algorithms is the key concept of quantum computation. Many efforts on quantum computers, such as Grover's database search algorithm, and Shor's quantum factoring algorithm, have been progressed actively due to its superiority to classical computers in various fields. To begin with, a novel Q-bit chromosome representation is adopted based on the concept and principles of quantum computing such as Q-bits and linear superposition. The smallest unit of information stored in two-state quantum computer is called a quantum bit (Q-bit), which may be in the "1" stage, or in the "0" state, or in any superposition of the two. The state can be represented as

$$| \Phi\rangle = \alpha \mid 0\rangle + \beta \mid 1\rangle \tag{1}$$

where α and β are complex numbers that specify the probability amplitude of the corresponding states. $|\alpha|^2$ and $|\beta|^2$ give the probabilities that Q-bit will be located in "0" state and "1" state, respectively. Normalization of the state to the unity guarantees

$$|\alpha|^2 + |\beta|^2 = 1 \tag{2}$$

A Q-bit individual as a string of λ Q-bits is defined as

$$\left[\begin{array}{c|c|c|c} \alpha_1 & \alpha_2 & \dots & \alpha_\lambda \\ \beta_1 & \beta_2 & \dots & \beta_\lambda \end{array}\right] \tag{3}$$

where the normalization condition holds for each of the λ Q-bits as per Eq. (2). Q-bit representation has advantages such as to present a linear superposition of states and able to represent 2^λ states in probabilistic manner. For example, the following 2 Q-bit

$$\left[\begin{array}{c|c} 1/\sqrt{2} & 1/2 \\ 1/\sqrt{2} & \sqrt{3}/2 \end{array}\right] \tag{4}$$

can represent 4-states, each of which with a specific probability ($|00\rangle$ is $1/8$, $|01\rangle$ is $3/8$, $|10\rangle$ is $1/8$ and $|11\rangle$ is $3/8$. The high-level (three levels) outline of quantum evolutionary algorithm (QEA) is shown in Figure 1. The following subsections will brief the components of QEA.

A. Quantum individuals

The lowest level of QEA corresponds to Q-individuals. As shown in Eq. (3), it contains a number of Q-bits. $Q_i(t)$ denotes the Q-individual i at tth generation. Each Q-individual has to be viewed as a distribution of bit strings of length λ. The fitness

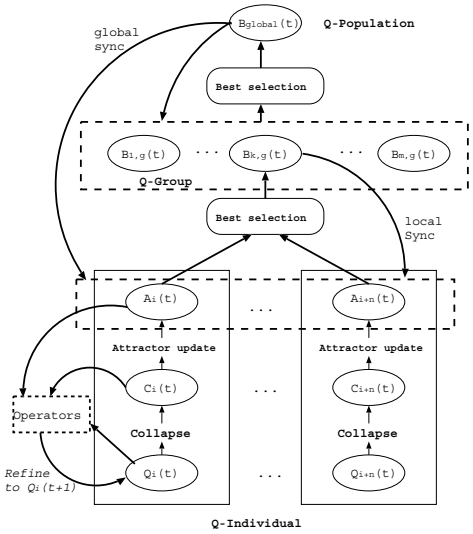

Fig. 1. High level outline diagram of QEA.

of Q-individual is re-evaluated at every generation according to a realization of distribution even if the individual is unchanged. Which is why, each $Q_i(t)$ is measured to form a binary corresponds namely $C_i(t)$ by the process called $collapse$ or $observe$. Q_i is the genotype while C_i is the phenotype in the context of classical EA. The individual Q_i is further attached to a binary string A_i which acts as an $attractor$ for Q_i. In every generation, C_i and A_i are compared in terms of both fitness and bit values. Operators, such as quantum gate, bit flipping, etc. trigger to a corresponding Q-bit when A_i is better than C_i and their bit values differ. Thus the distribution of Q_i is slightly moved toward a given solution A_i. On the other hand, $attractor$ is updated if C_i is better than A_i.

B. Quantum groups

The population is divided into m Q-groups each containing n Q-individuals having the ability to synchronize their attractors. Therefore, the best attractor of group k, $B_{k,g}$ is stored at every generation and is periodically distributed to the group attractors.

C. Quantum population

The set of all $n \times m$ Q-individuals forms the *quantum population*. As for Q-groups, the individuals of a Q-population can synchronize their attractors. Therefore, the best attractor (in terms of fitness) among all Q-groups, noted B_{global}, is stored every generation and is periodically distributed to the group attractors.

III. Formulation of UC Problem

A. Objective function

The objective function of thermal unit commitment problem is to minimize the total production cost (TC) while satisfying several constraints.

$$Min\ TC = \sum_{i=1}^{N}\sum_{t=1}^{T}[F(P_{i,t} + SC_i(1 - I_{i,t-1})]I_{i,t} \quad (5)$$

where $F(P_{i,t}) = a + b.P_{i,t} + c.P_{i,t}^2$, is the quadratic fuel cost function of $P_{i,t}$ which is the thermal power output of unit i at hour t, $I_{i,t}$ is the status of i-th unit at hour t, N and T are the number of production units and time horizon, respectively. a, b and c are the fuel coefficients and SC_i is the startup cost for unit i which is defined as follows

$$SC_i = \begin{cases} hcost_i & :T_i^{off} \le X_i^{off} \le H_i^{off} \\ ccost_i & :X_i^{off} > H_i^{off} \end{cases}$$
$$H_i^{off} = T_i^{off} + cshour_i. \quad (6)$$

where $T_i^{on/off}$ is the minimum up/down time for unit i, while $X_i^{on/off}$ is the duration for which unit i is being on/off. $hcost$ and $ccost$ are the hot and cold start cost for unit i, respectively. $cshour$ is the cold start hour of unit i.

B. Constraints

The following constraints are considered in this study which needs to be satisfied while optimizing the total production cost.

1) System power balance: The total power output from the thermal generators and solar-battery source should satisfy the load demand for that hour. Thus the system power balance equation for hour t can be expressed as

$$\sum_{i=1}^{N} P_{i,t} + P_{s,t} = D_t. \quad (7)$$

where $P_{s,t}$ is the solar power output at hour t and D_t is the forecasted load demand. The power output from solar energy system is expressed as the following equation

$$P_{pv}(S(t)) - p_{b,t} - P_{s,t} = 0 \quad (8)$$

where $S(t)$ is the solar radiation at hour t (in W/m^2), P_{pv} is the conversion function regarding solar radiation to energy and $p_{b,t}$ is the output of the battery at hour t. P_{pv} is defined as

$$P_{pv}(S(t)) = \begin{cases} P_{sn}\frac{S(t)^2}{S_{std}R_c} & 0 < S(t) < R_c \\ P_{sn}\frac{S(t)^2}{S_{std}} & S(t) > R_c \end{cases} \quad (9)$$

where S_{std} is the solar radiation for standard environment and set as 1,000 W/m^2 and R_c is the cut in radiation point set as 150 W/m^2. Since the solar energy system is incorporated with battery, trivial battery constraints such as charge/discharge limit, initial and ending state of charge, penetration limit are considered in this study.

2) Generation limit: The power output of each generating unit must be limited within a specified range.

$$P_i^{min} \le P_{i,t} \le P_i^{max}. \quad (10)$$

where $P_i^{min/max}$ is the minimum/maximum power output limit for unit i.

3) Ramp constraint: For each unit in each hour output is limited by the following ramp constraint:

$$P_{i,t}^{min} \le P_{i,t} \le P_{i,t}^{max}. \quad (11)$$

where $P_{i,t}^{min} = max(P_{i,t-1} - DR_i, P_i^{min})$ and $P_{i,t}^{max} = min(P_{i,t-1} + UR_i, P_i^{max})$. UR_i and DR_i are the up and down ramp limit for unit i, respectively.

4) System spinning reserve requirements: In order to ensure reliability, the system spinning reserve requirement must be satisfied. The spinning reserve requirement is expressed by following equation

$$\sum_{i=1}^{N} I_{i,t}P_{i,t}^{max} \ge D_t + SR_t. \quad (12)$$

where SR_t is the required spinning reserve for hour t.

5) Unit minimum up/down time: Due to operational limitations, once a unit is committed/decommitted it should be kept stable for a minimum period of time before a transition. This scenario can be expressed as

$$\left.\begin{array}{rcl} T_i^{\text{on}} & \le & X_{i,t}^{\text{on}} \\ T_i^{\text{off}} & \le & X_{i,t}^{\text{off}} \end{array}\right\}. \quad (13)$$

6) Emission constraint: Burning fuel emit contaminated gases which should be limited by the following equation

$$\sum_{i=1}^{N}\sum_{t=1}^{T} H_i(P_{i,t}) \le E_{limit}. \quad (14)$$

where $H_i(P_{i,t})$ is a quadratic function associated with several emission types and E_{limit} is the emission limit.

IV. Fuzzy Formulation

In thermal UC, the constraints related to the imprecise hourly load demand the system load balance, spinning reserve requirement invite uncertainty. Therefore, they can be treated as fuzzy constraints instead of crisps constraints. Moreover, the solar power generation, which is directly related to the solar radiation, is also a contender of fuzzy representation. The following subsections describe the fuzzy constraints with associated membership functions.

A. Fuzzy load demand

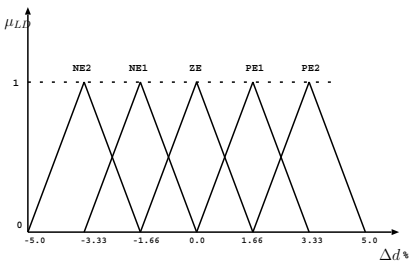

Fig. 2. Load demand error membership function.

The forecasted load demand is imprecise and can vary with the actual load demand. Therefore, the crisp notation is changed into the fuzzified load demand. The predicted load

demand usually deviates (Δd) from the actual one by $\pm 2\%$ to $\pm 5\%$. The membership function for fuzzy load percentage (Δd vs. μ_{LD}) error is shown in Figure 2. The load deviation error is equally distributed in $\pm 5\%$. Five linguistic values (NE2, NE1, ZE, PE1, PE2) are defined for negative, zero and positive errors. The load demand error thus can be represented as the following fuzzy equality relation

$$D_{f,t} \cong \sum_{i=1}^{N} P_{i,t}. \tag{15}$$

where $D_{f,t}$ is the calculated forecasted load demand for tth hour.

B. Fuzzy spinning reserve

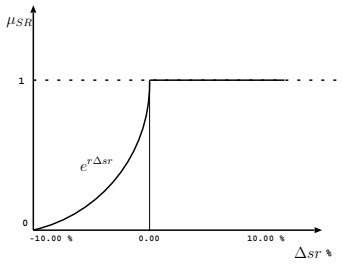

Fig. 3. Spinning reserve error membership function.

To ensure the secure operation during the outage, spinning reserve is required. Since the load demand is modeled by fuzzy logic, spinning reserve requirement can also be represented as non-crispy notations. In this proposed method, the spinning reserve membership function μ_{SR}, shown in Figure 3, can be defined as following equations

$$\mu_{SR} = \begin{cases} 1 & if\ Eq.(17)\ holds \\ e^{r.\Delta sr} & Otherwise \end{cases} \tag{16}$$

$$\sum_{i=1}^{N} I_{i,t}.P_{i,t}^{max} \geq SR_t + D_{f,t}. \tag{17}$$

where r is the weighting factor and Δsr is the error percentage of spinning reserve.

C. Fuzzy cost function

The total production cost can also be taken under fuzzy wings by imposing the lower membership function value to a higher production cost schedule. The membership function is a reverse one of that of spinning reserve which can be define as follow

$$\mu_{TC} = \begin{cases} 1 & if\ \Delta tc < 0 \\ e^{-w.\Delta tc} & Otherwise \end{cases} \tag{18}$$

$$\Delta tc = \frac{TC - \sigma TC_{max}}{\sigma TC_{max}} \tag{19}$$

where w is the weighting factor, σ is the cost tolerance factor and TC_{max} is a predefined value elucidates the maximum production cost.

D. Fuzzy solar power

Solar radiation error needs to be fuzzified in order to deal with such uncertainty. The membership function μ_{LR}, for solar radiation is equated as follows

$$\mu_{LR} = \begin{cases} \frac{1}{1+2.33(\Delta v/v^{+})^2}, & if\ \Delta V \geq 0 \\ \frac{1}{1+2.33(\Delta v/v^{-})^2}, & if\ \Delta V < 0 \end{cases} \tag{20}$$

where $v^{\pm}$ is the average error percentage of the error deviation, ranging from ± 0.40 to ± 0.13 depending on the margin of error.

V. FQEA Details

This section details about the key components of FQEA method. The following subsections are presented for this purpose.

A. Solution structure

The control variables of the UC method are the units' on/off status for the entire horizon. Therefore, the data structure for each individual contains the binary status, the corresponding power output, etc. Moreover, the Q-bit representation is also needs to be incorporated. Figure 4 shows the data structure of the entire population (of size P). The usage of flag vector will

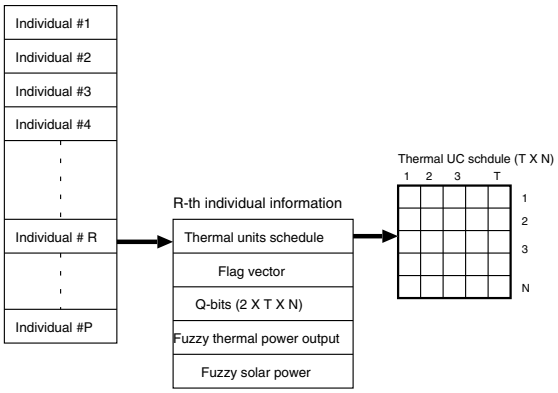

Fig. 4. High level data structure for FQEA population.

be used to boost up ELD performance.

B. Generating initial solution

In trivial QEA algorithm for mixed integer problem, the Q-bits are initialized as $[\sqrt{(0.5)}, \sqrt{(0.5)}]^T$ in order to make units' status equally probable of ON/OFF. But such initialization may produce highly infeasible individuals which eventually lead to slower convergence. In FQEA method, the initialization process is done by providing priority list depending on the load demand. The process is shown in Figure. 5. The units are prioritized using a sophisticated weighted priority list method. Then based on the load demand and spinning reserve requirements, the units are turned ON. The corresponding Q-individual is also set by reflecting the binary bit by weighting associated Q-bit depending on the units' status. Assuming that, on the peak load time, all units will be committed. To satisfy minimum up/down constraints, some

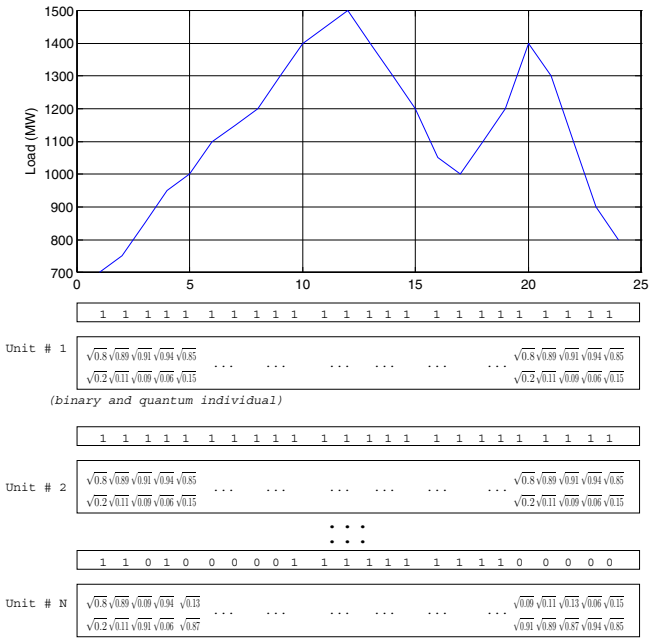

Fig. 5. Generating initial solution process.

excess units are needed to be ON. A logarithmic probability distribution function is used stochastically set such units status.

C. Fitness function

The quality of a particular individual is presented by the fitness function. In the proposed FQEA method, the fitness function is comprised with the objective function (Eq. 5), penalty function for constraints violation and aggregated fuzzy membership function to integrate the involved uncertainties. The aggregated fuzzy membership function for an individual j is defined as

$$\mu_{A_j} = min(\mu_{LD*}, \mu_{SR*}, \mu_{TC}, \mu_{LR*}) \quad (21)$$

where

$$\mu_{LD*} = min(\mu_{LD^1}, \mu_{LD^2}, \ldots, \mu_{LD^T}) \quad (22)$$
$$\mu_{SR*} = min(\mu_{SR^1}, \mu_{SR^2}, \ldots, \mu_{SR^T}) \quad (23)$$
$$\mu_{LR*} = min(\mu_{LR^1}, \mu_{LR^2}, \ldots, \mu_{LR^T}) \quad (24)$$

The penalty function needs to be defined to measure up the violation index of an individual. For the inequality constraints, a generic violation function is defined as per following equation

$$V = \sum_{k=1}^{ic} C_k |min(ULD, LLD)| \quad (25)$$

where ic is the number of inequality constraints, C_k are a constant associated with related constraints. ULD and LLD are the upper limit and lower limit constraints violations for inequality constraints respectively. The penalty function is therefore written as

$$PF = K.|D_t - \sum_{i=1}^{N} P_{i,t} - P_{w,t}| + V \quad (26)$$

TABLE I
LOOK UP TABLE FOR DETERMINING THE ROTATION ANGLE FOR QUANTUM ROTATION OPERATION.

X_j	B_j	$f(r) \geq f(global)$	$\Delta\theta_j$	$s(\alpha_j,\beta_j)$ $\alpha_j\beta_j > 0$	$\alpha_j\beta_j < 0$	$\alpha_j = 0$	$\beta_j = 0$
0	0	False	0	0	0	0	0
0	0	True	0	0	0	0	0
0	1	False	0	0	0	0	0
0	1	True	θ	-1	+1	±1	0
1	0	False	θ	-1	+1	±1	0
1	0	True	θ	+1	-1	0	±1
1	1	False	θ	+1	-1	0	±1
1	1	True	θ	+1	-1	0	±1

where K is a scaling factor. So, the evaluation function is finally defined as

$$E = \frac{10^{round(log_{10}^{F_{max}})}}{F + PF} \times \mu_{A_j}. \quad (27)$$

where F_{max} is a priori value of maximum fuel cost which is determined by several trials and errors.

D. Quantum operators

The proposed method applies several quantum operators based on the associated assigned probabilities assigned. The operators work on either single Q-bit individual or multiple Q-bit individuals.

1) Rotation gate: The rotation gate, $U(\theta)$ is employed on a singe Q-bit individual as a variation operator. $(\alpha_{i,j}, \beta_{i,j})$ of the jth Q-bit of ith individual is updated for $(t+1)$-th iteration as follows

$$\begin{bmatrix} \alpha_{i,j}(t+1) \\ \beta_{i,j}(t+1) \end{bmatrix} = U(\theta_{i,j}) \begin{bmatrix} \alpha_{i,j}(t) \\ \beta_{i,j}(t) \end{bmatrix} \quad (28)$$
$$= \begin{bmatrix} \cos(\theta_{i,j}) & -\sin(\theta_{i,j}) \\ \sin(\theta_{i,j}) & \cos(\theta_{i,j}) \end{bmatrix} . \begin{bmatrix} \alpha_{i,j}(t) \\ \beta_{i,j}(t) \end{bmatrix}.$$

where $\theta_{i,j}$ is rotation angle, $\theta_{i,j} = s(\alpha_{i,j}, \beta_{i,j})\Delta\theta_{i,j}$, where $s(\alpha_{i,j}, \beta_{i,j})$ is the sign of θ_i that determines the direction, $\Delta\theta_{i.j}$ is the magnitude of rotation angle whose lookup table is shown in Table 1. The angle θ is determined based on several trial and error considering their sensitivity towards the FQEA (explained in Section VI). In the table, B_j and X_j represents the jth quantum bit of best solution B and binary corresponding bit of Q-bit individual, X.

2) Mutation: The mutation operator on Q-individual works as follows

$$\left[\begin{array}{c|c|c|c|c} \alpha_1 & \alpha_2 & \ldots & \alpha_r & \ldots \\ \beta_1 & \beta_2 & \ldots & \beta_r & \ldots \end{array}\right] \Rightarrow \left[\begin{array}{c|c|c|c|c} \alpha_1 & \alpha_2 & \ldots & \beta_r & \ldots \\ \beta_1 & \beta_2 & \ldots & \alpha_r & \ldots \end{array}\right] \quad (29)$$

This operator is used with a probability of 0.1.

3) Crossover: The crossover operator is operated on two randomly chosen Q-individuals. The operator is analogous to genetic algorithms crossover operator. This method applies two-point crossover where the offspring will get two slices of the better fitted individual. The probability of crossover is 0.5.

4) Differential operator: A new differential operator is used in the FQEA method to provide diversified Q-bits. The trivial mutation operator does not assure a better offspring. To overcome such deficiency, the FQEA uses the information of the best Q-individual in Q-groups. Therefore, the new Q-individual, $Q_{new}(t+1)$ is defined as

$$Q_{new}(t+1) = Q_{r1}(t) + (B_{global}(t) - Q_{r2}(t)) \quad (30)$$

where Q_{r1} and Q_{r2} are two randomly chosen Q-individuals where $r1 \neq r2$, $r1 < r2$ and since the Q-individuals are in ascending order according to their fitness, $f(Q_{r1}(t)) < f(Q_{r2}(t))$. Now, the arithmetical operators on the above equation should be transformed to work with Q-individuals or the corresponding *collapsed* binary solutions. Therefore, the above equation is revisited such as follows

$$\begin{aligned} Q_{new}(t+1) \quad = \quad & Q_{r1}(t)\&\&(B_{global}(t)||Q_{r2}(t))|| \\ & (B_{global}(t)\&\&Q_{r2}(t)) \end{aligned} \quad (31)$$

The probability of this operator is set to 0.7.

E. Algorithm steps

The procedure of FQEA is stepped below.

1. Set $t = 0$ as a generation counter.

2. Initialize Q-individual as described in previous section. Divide the individuals into m groups of size n (as shown in Figure 1). Now for each group k the following steps are conducted.

a. Generate binary corresponding string $C_i(t)$ of ith Q-individual $Q_i(t)$ by *collapsing*. When a Q-bit $[\alpha\beta]^T$ is *collapsed*, its corresponding binary character c is determined by

$$c = \begin{cases} 1, & random[0,1] \ < t \ |\beta|^2 \\ 0, & otherwise \end{cases} \quad (32)$$

Thus $C_i(t)$ contains the binary strings of length of $N \times T$ (Figure 4).

b. Check for the constraint violation and repair the individual if necessary.

c. Evaluate the performance of $C_i(t)$. Determine the fuzzy membership functions for each of the imprecise constraints as stated in Section IV. The fuzzy solar-battery power output is determined by Eq. (8) and (9) using the forecasted solar radiation and considering the forecasting error. A forward dynamic programming approach is undertaken to figure out the optimal battery power output. Then calculate the ELD output for the thermal units using system lambda operation.

d. When $t = 0$, set the local attractor $A_i(t)$ to $C_i(t)$. Otherwise, compare $C_i(t)$ to $A_i(t)$ as described in Section II-A.

e. Select the best individual from the attractors list and save it as $B_{k,g}(t)$.

3. Select the best individual from m Q-groups and save it as $B_{global}(t)$.

4. Apply the operators briefed in Section V.D on Q-individual(s) based on the fuzzy probability scheme stated in Section V.E. Note that, the look up table in Table 1 is used here by replacing X to $C_i(t)$ and B to $A_i(t)$.

5. Synchronize $B_{global}(t)$ with attractors and Q-group best values using rotation gate operator.

7. Set $t = t + 1$. If t reaches to maximum, stop the process and B_{global} contains the best result. Return to Step 2(a) otherwise.

VI. Simulation

The proposed FQEA is applied on a thermal power system of 10 units with an equivalent solar power rating of 185 MW and battery-storage of 200 MW. PHP 5.0 is used to write the core program where the graphs are drawn by Matlab. The generators parameters and load data were reported on reference [4]. In order to check the scalability of FQEA, the 10 units' system is enhanced with corresponding load demand and solar power rating up to 100 units. For practical power system, FQEA is also tested on a 38-unit Taiwan power system. However solar power was not integrated in Tai-power case. Two analyses of parameters' sensitivity of FQEA are presented. First, the rotational angle θ is scrutinized. Since θ varies with the nature of applied problem domain, it should be chosen carefully. Which is why, several trials are conducted for 10-units system and the results are shown in Figure 6. The figure points out the frequency of hitting the optimal solution range ($563942-$564210) for various values of θ. θ is varied from 0.005 to 0.05 with step size of 0.0025. It can be seen that, θ is sensitive of FQEA. Among the best performed θ-values 0.03 is chosen. The second analysis is performed on the population size and maximum iteration. Table III shows the sensitivity of Q-population size ($G = m \times n$) and maximum iteration (MX_T) on 10 units system. FQEA is trialed 100 times for each of the system configurations. The solution quality of FQEA when performed under pair (G, MX_T):$(40, 150)$ is better than the other configuration. Moreover, the reported standard deviation for this pair is also not significant. The Q-population is then divided into 8-groups where each group contains 5 Q-individuals.

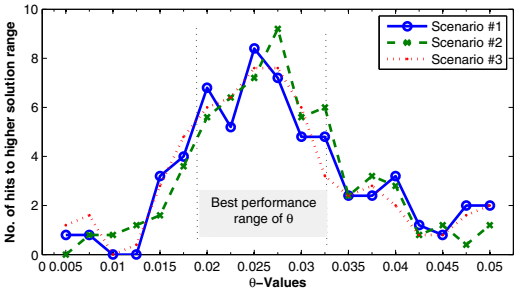

Fig. 6. Sensitivity of θ on the performance of FQEA.

Table III shows the best result achieved by FQEA by considering different combinations of the system configuration e.g. with/without solar battery system. The minimum, maximum and average cost are also reported on the table. Figure 7 shows the thermal power output with solar/battery

TABLE II
PARAMETER ANALYSIS FOR 10-UNITS SYSTEM.

	$G = 20$			$G = 30$			$G = 40$			$G = 50$		
	MX_T			MX_T			MX_T			MX_T		
	50	75	150	60	100	150	100	150	200	100	150	200
Min.	536884	535428	532048	532173	528471	528890	529461	**525478**	527025	5291048	531584	530247
Mean	539871	539875	538481	538728	531484	531614	532238	**530734**	532746	534197	537044	536310
Max.	544069	545036	543094	542403	531484	535293	536109	**535807**	537048	538991	541879	540094
Std. dev.	8.791	7.665	9.064	5.602	4.685	5.172	6.074	**5.358**	5.914	7.725	9.815	8.223

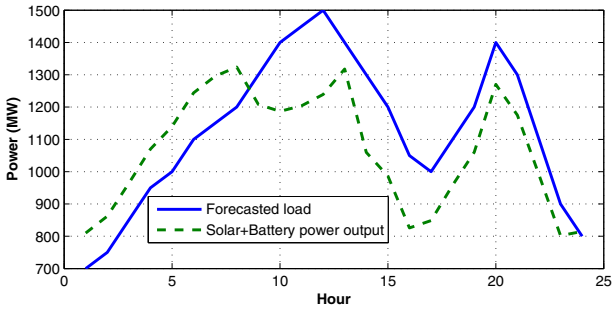

Fig. 7. Forecasted load with solar-battery power generation (10-units system).

TABLE III
RESULTS FOR FQEA CONSIDERING WITH/WITHOUT SOLAR POWER.

	Standalone			With solar/battery		
Cost($)	Min.	Mean.	Max.	Min.	Mean.	Max.
10-unit	563942	566170	568047	525478	530434	535807
20-unit	1123304	1126304	1129701	1101649	1105709	1110840
40-unit	2242627	2247841	2252417	2229985	2234728	2239029
60-unit	3361816	3365743	3369030	3321054	3325563	3329274
80-unit	4480635	4484097	4488663	4415658	4419240	4423738
100-unit	5597190	5601657	5604725	5552570	5556319	5559406

system and corresponding forecasted load. Table IV shows the cost comparison with established method. Note that, all of these comparing methods did not consider the solar power integration. Therefore, the comparison is limited only to the standalone thermal system. From the table, it is evident that, for high scaled power system (from 40 units to more), FQEA is capable to provide best results among comparing methods even no renewable energy sources are integrated. The fuzzy membership degrees (μ_{LD}, μ_{SR} and μ_{LR}) for different scaled power systems are reported on Table V. FQEA is able to manage the membership degrees to a higher value. The convergences of FQEA on 10-units' system for two randomly chosen runs are figured in Figure 8. The aggregated fuzzy membership function (μ_A) is also pointed in the figure from the starting point of the convergence graph to the settling cost. The μ_A also converged to 0.94 when the method reaches the optimal point.

Next simulation is conducted by applying FQEA to a 38-units' Taiwan power system[12]. Due to the unavailability of proper data on solar radiation, the simulation is run for the standalone system. The comparisons with other methods as well as the achieved result are tabled in Table VI. Like the 10 units' system, FQEA also able to produce the higher quality solutions among the established methods considering both production cost and average execution time (AET). The

TABLE IV
BEST SOLUTION COMPARISON WITH OTHER ESTABLISHED METHOD.

Method	10-unit	20-unit	40-unit
ELR[2]	563977	1123297	2244237
GA[4]	565825	1126243	2251911
EP[6]	564551	1125494	2249093
HPSO[7]	563942	-	-
SA[9]	565828	1126254	2250063
UCC-GA[5]	563977	1125516	2249715
IQEA-UC[16]	**563938**	**1123297**	2242980
QBPSO[17]	563977	1123297	2242957
FQEA	563942	1123304	**2242627**
Method	60-unit	80-unit	100-unit
ELR[2]	3363491	4485633	5605678
GA[4]	3376625	4504933	5627437
EP[6]	3371611	4498479	5623825
HPSO[7]	-	-	-
SA[9]	-	4498076	5617876
UCC-GA[5]	3375065	4505614	5626514
IQEA-UC[16]	3362010	4482826	5602387
QBPSO[17]	3361980	4482085	5602486
FQEA	**3361816**	**4480635**	**5597190**

two scenarios are considered here; one with ramp rate and one without ramp rate. The cost of the system becomes higher when the ramp rate is considered because this constraint restricts the power output of some units to certain capacities during rising and lowering loads. The FQEA outperforms most of the methods such as DP since it cannot reach all states of UC especially for a large power system which explains the high execution time. LR often suffers to obtain feasible solution and minimize the duality gap. As for SA, execution time is the highest among the competitors due to infeasible solution generations. CLP[13] provides good result as this approach applied problem UC specific logic while designing the algorithm. FA [12] is better performer in terms of execution time as it undertakes the similar approach as FQEA. However FQEA provides better result than FA [12]. Figure 9 shows the curves of crisp and fuzzy load demands of the optimal solution (Taiwan power system of 38 generating units) with membership degrees of fuzzy load and satisfied spinning reserve for 24 hours. The crisp load has been modified with fuzzy load by considering fuzziness of load demand. Depending on load statistics, in some hours (e.g. 9-12, 14-23) the fuzzy load is lower and the other hours it is higher than the forecasted crisp load. However the total fuzzy load is greater than total crisp load since the mean positive percentage load error is greater than the mean absolute negative percentage error. It is noticeable that, the spinning reserve membership degree is always 1 which indicates the reserve amount seems to be crisp although the fuzzy approach is taken.

TABLE V
FUZZY MEMBERSHIP DEGREES FOR DIFFERENT NUMBER UNITS' SYSTEM.

Unit	μ^*_{LD}	μ^*_{SR}	μ^*_{LR}
10	0.9538	0.9410	0.9742
20	0.9206	0.9177	0.9365
40	0.9152	0.9034	0.9241
60	0.9241	0.9071	0.8924
80	0.8962	0.8875	0.9004
100	0.8634	0.8742	0.8593

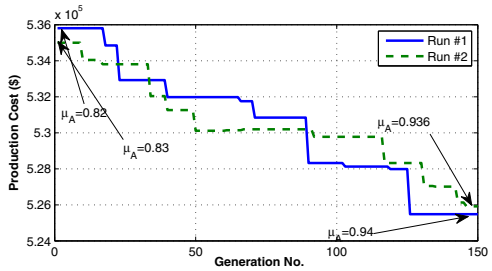

Fig. 8. Convergence of the proposed method for 10-units system.

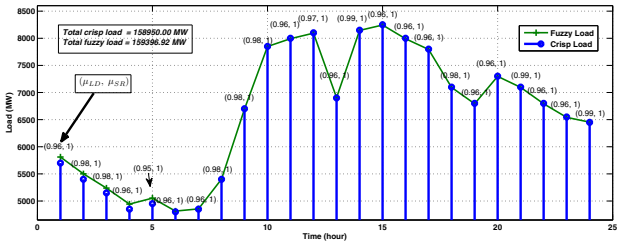

Fig. 9. Crisp and fuzzy load with associated load and reserve membership value for 38-unit power system.

TABLE VI
PERFORMANCE COMPARISON OF FQEA FOR TAIWAN POWER SYSTEM WITH OTHER METHODS.

Cost (MNT$)	FQEA	DP [13]	LR [13]	SA [13]	CLP [13]	FA [12]
W. Ramp	208.71	215.5	214.5	215.6	213.8	213.9
W/out Ramp	201.35	201.5	209.0	207.8	208.1	207.9
AET	11.95	199	29	2589	17	5

VII. CONCLUSION

This paper presents a fuzzy logic based unit commitment strategy facilitating the quantum inspired evolutionary algorithm. This model comprises thermal generators, coupled with solar/battery system to provide the attention toward the global warming effects. In order to incorporate the uncertainties regarding load demand, solar radiation, spinning reserve, the formulations are modified using fuzzy logic. Trivial QEA approach is modified by applying several operators such as differential operator, crossover, and mutation to diversify the solutions. The solutions are reformed by Q-bit representation and further re-arranged into several Q-groups. Such features provide greater search space to enhance exploration as well as exploitation. The performance of the algorithm is tested in two different power systems. For the first case of 10-units system and higher, FQEA is able to produce best solutions for 40-units and above. In case of 10 and 20-units system, the cost difference is also marginal with global best. FQEA is also effective is practical power system for Taiwan 38-units since it provides the best results among comparing methods. Thus, the reported simulation results confirmed the superiority and effectiveness of FQEA. For future studies, the author will try to explore the potential of FQEA in other power system optimization problems such as ELD, optimal power flow, voltage control, optimum capacitor placement, feeder balancing etc. considering their complexity as combinatorial optimization problems involving uncertainties.

REFERENCES

[1] T. Senjyu, K. Shimabukuro, K. Uezato, and T. Funabashi: "A fast technique for unit commitment problem by extended priority list", *IEEE Trans. Power Syst.*, vol. 18, no. 2, pp. 882-888, May 2003.

[2] W. Ongsakul and N. Petcharaks, "Unit commitment by enhanced adaptive lagrangian relaxation," *IEEE Trans. Power Syst.*, Vol 19, no. 1, pp. 620-628, Feb, 2004.

[3] W.L. Peterson, S.R. Brammer," A capacity based Lagrangian relaxation unit commitment with ramp rate constraints", *IEEE Trans. Power Syst.*, vol. 10, no. 2, pp. 1077-1088, May 1995.

[4] S. A. Kazarlis, A. G. Bakirtzis, and V. Petridis, "A genetic algorithm solution to the unit commitment problem," *IEEE Trans. Power Syst.*, Vol 11, no. 1, pp. 83-92, Feb. 1996.

[5] T. Senjyu, H. Yamashiro, K. Uezato, and T. Funabashi, "A unit commitment problem by using genetic algorithm based on unit characteristic classification," *Proc. 2002 IEEE Power Eng. Soc. Winter Meeting*, Vol 1, pp. 58-63.

[6] K. A. Juste, H. Kita, E. Tanaka, and J. Hasegawa, "An evolutionary programming solution to the unit commitment problem," *IEEE Trans. Power Syst.*, Vol 14, no. 1, pp. 1452-1459, Nov. 1999.

[7] T. O. Ting, M. V. C. Rao, and C. K. Loo, "A Novel approach for unit commitment problem via an effective hybrid particle swarm optimization," *IEEE Trans. Power Syst.*, Vol 21, no. 1, pp. 411-418, Feb. 2006.

[8] S. Chakraborty, T. Senjyu, A. Y. Saber, A. Yona, and T. Funabashi, "Optimal thermal unit commitment integrated with renewable energy sources using advanced particle swarm optimization," *IEEJ- Trans. on Electrical and Electronics Eng.*, Vol 4, no. 5, Sept. 2009.

[9] D. N. Simopoulos, S. D. Kavatza, and C. D. Vournas, "Unit commitment by an enhanced simulated annealing algorithm," *IEEE Trans. Power Syst.*, Vol 21, no. 1, pp. 68-76, Feb. 2006.

[10] F. Zhuang, F.D. Galiana,"Unit commitment by simulated annealing", *IEEE Trans. Power Syst.* vol. 5, no. 1, pp. 311-318. Feb. 1990.

[11] Z. Ouyang, S.M. Shahidehpour,"An intelligent dynamic programming for unit commitment application", *IEEE Trans. Power Syst.*, vol. 6, no. 3, pp 1203-1209, August 1991.

[12] M.M. El-Saadawi, M.A. Tantawi, E. Tawfik,"A fuzzy optimization based approach to large scale thermal unit commitment", *Electr. Power Syst. Res.* vol. 72 pp. 245-252, 2004.

[13] K.Y. Huang, H.T. Yang, C.L. Huang,"A new thermal unit commitment approach using constraint logic programming", *IEEE Trans. Power Syst.* vol. 13 no. 3 pp. 936-945, Aug. 1998.

[14] K. H. Han, J. H. Kim, "Quantum-inspired evolutionary algorithm for a class of combinatorial optimization," *IEEE Trans. Evol. Compute.*, Vol 6, no. 6, pp. 580-593, Feb. 2006.

[15] K. H. Han, J. H. Kim, "Quantum-inspired evolutionary algorithms with a new termination condition, H_ε gate, and two-phase scheme," *IEEE Trans. Evol. Compute.*, Vol 8, no. 2, pp. 156-169, Feb. 2006.

[16] C. Y. Chung, H. Yu, and K. P. Wong, "An advanced quantum-inspired evolutionary algorithm for unit commitment", *IEEE Trans. Power Syst.*, paper accepted for publication. DOP: Aug. 2010

[17] Y Jeong, J, Park, S Jang, and K. Y. Lee, "A new quantum-inspired binary PSO: Application to unit commitment problems for power systems", *IEEE Trans. Power Syst.*, vol. 25, no. 3, pp. 1486-1495, Aug. 2010.

2011 IEEE International Conference on Fuzzy Systems
June 27-30, 2011, Taipei, Taiwan

Control of Doubly-Fed Induction Generator System Using PFNN

Faa-Jeng Lin[#△] Kuang-Hsiung Tan[*] Zong-Han Lu[#◎] Yung-Ruei Chang[§]

[#]Dept. of Electrical Engineering
National Central University
Chungli, Taiwan
[△]linfj@ee.ncu.edu.tw
[◎]scott31025@hotmail.com

[*]Dept. of Electrical and Electronic Engineering
National Defense University
Taoyuan, Taiwan
s913115@gmail.com.tw

[§]Engineering Technology and Facility Operation Division
Institute of Nuclear Energy Research
Taoyuan, Taiwan
raymond@iner.gov.tw

***Abstract*—An intelligent controlled doubly-fed induction generator (DFIG) system using probabilistic fuzzy neural network (PFNN) is proposed in this study. This system can be applied as a stand-alone power supply system or as the emergency power system when the electricity grid fails for all sub-synchronous, synchronous and super-synchronous conditions. The rotor side converter is controlled using the field-oriented control to produce three-phase stator voltages with constant magnitude and frequency at different rotor speeds. Moreover, the stator side converter, which is also controlled using field-oriented control, is primarily implemented to maintain the magnitude of the DC-link voltage. Furthermore, an intelligent PFNN controller is proposed for both the rotor and stator side converters to improve the transient and steady-state responses of the DFIG system for different operating conditions. The network structure, on-line learning algorithm and convergence analyses of the PFNN are introduced in detail. Finally, the feasibility of the proposed control scheme is verified using some experimental results.**

Keywords-doubly-fed induction generator; field-oriented control; probabilistic fuzzy neural network

NOMENCLATURE

v_{abs} , v_{bcs} , v_{cas}	3-Phase stator line voltage.
i_{as} , i_{bs} , i_{cs}	3-Phase stator current.
i_{al} , i_{bl} , i_{cl}	3-Phase load current.
i_{ar} , i_{br} , i_{cr}	3-Phase rotor current.
i_a , i_b , i_c	3-Phase current of stator side converter.
L_a , L_b , L_c	3-Phase inductor at stator side converter.
v_{an} , v_{bn} , v_{cn}	3-Phase stator phase voltage.
C	DC-link capacitance.
V	Magnitude of stator phase voltage.
V_n	Magnitude of phase *A* stator voltage.
V_n^*	Command magnitude of phase *A* stator voltage.
V_{dc}	DC-link voltage.
V_{dc}^*	Command of DC-link voltage.
d,q	*d-q* Axis.
v_{ds} , v_{qs}	2-Axis stator voltage.
R_s	Stator resistance.
λ_{ds} , λ_{qs}	2-Axis stator flux linkage.
i_{ds} , i_{qs}	2-Axis stator current.
i_{dr} , i_{qr}	2-Axis rotor current.
L_s	Stator inductance.
L_m	Magnetizing inductance.
P	Pole numbers.
θ_e , ω_e	Electric angle and angular speed of stator phase voltage.
θ_r , ω_r	Rotor angle and angular speed.
θ_{sl} , ω_{sl}	Slip angle and angular speed.
θ_m , ω_m	Mechanical angle and angular speed.
P_s	Real power of stator side converter.
Q_s	Reactive power of stator side converter.
v_d , v_q	2-Axis voltage of stator side converter.
i_d , i_d^*	*d*-Axis current and command current of stator side converter.
i_q , i_q^*	*q*-Axis current and command current of stator side converter.

I. INTRODUCTION

Recently, the concept of incorporating fuzzy logic into a neural network (NN) has been grown into a popular research topic. In contrast to the pure NN or fuzzy system, the fuzzy neural network (FNN) possesses both advantages including the capability of fuzzy reasoning in handling uncertain information and the capability of artificial neural networks in learning from processes. Moreover, FNNs do not require mathematical models and have the ability to approximate nonlinear and uncertainties systems. Therefore, there were many researches which are using FNNs to represent complex plants and construct advanced controllers based on the back-propagation (BP) algorithm. Furthermore, probabilistic neural network (PNN) is a feedforward neural network, and its structure is neural network implementation of Parzen nonparametric

This work was supported in part by the National Science Council (NSC) of Taiwan, R.O.C. under Grant NSC 98-3114-E-008-001-CC2.

probability density function (PDF) estimation and Bayes classification rule [1]. The PNN can handle the uncertainties in industry applications effectively, and have been widely used in pattern classification, nonlinear mapping, and fault detection and classification. Due to the above advantages of FNN and PNN, the PFNN, which combines the characteristics of FNN (degree of truth) and PNN (probability of truth) [2], has been proposed in some applications, such as modeling and control problems [3] and stochastic modeling.

The DFIG systems have been widely used on large variable-speed fixed-frequency wind power generation systems, hydro power systems and turbine engine power generation systems. In contrast to the squirrel-cage induction generator (SCIG) system and the synchronous generator system, the power capacity of the rotor side and stator side converters of the DFIG system required only 30% of the rated power [4]. This means that the desired variable-speed range is $\pm$ 30% around the rated turbine speed. Thus, compared to the SCIG system where the converters have to handle the total power, the costs and losses in the power electronics converters can be much reduced.

There are two types of applications of a DFIG system, grid-connected type and stand-alone type. Several field-oriented control schemes for the DFIG have been proposed for the applications of both types [3], and the control strategies of the stator side and rotor side converters for the grid-connected type and stand-alone type are quite different.

The grid-connected DFIG system is quit mature and is widely used today and a lot of control schemes have been reported. However, only little attention has been paid toward the development of the control schemes of the stand-alone type DFIG system. On the other hand, satisfied transient performance can't be achieved using the traditional PID control for the DFIG system due to time-varying and nonlinear control characteristics of the DFIG system. Therefore, this study addresses the issue to develop an intelligent control scheme for the DFIG system for stand-alone application.

II. FIELD-ORIENTED CONTROL DFIG SYSTEM

A direct drive DFIG system using both the rotor side and stator side converters is shown in Fig. 1 and is consists of a doubly-fed induction machine with slip rings, and a back-to-back PWM converter between the rotor slip rings and the transformer. The stator is directly connected to the 3-phase load.

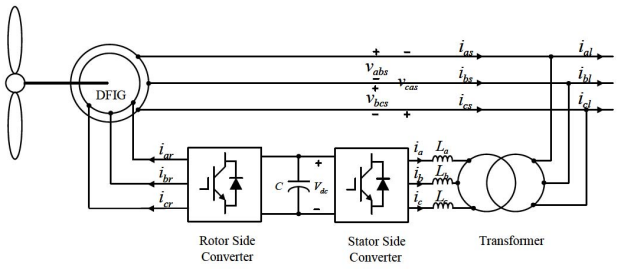

Figure 1. System block of DFIG.

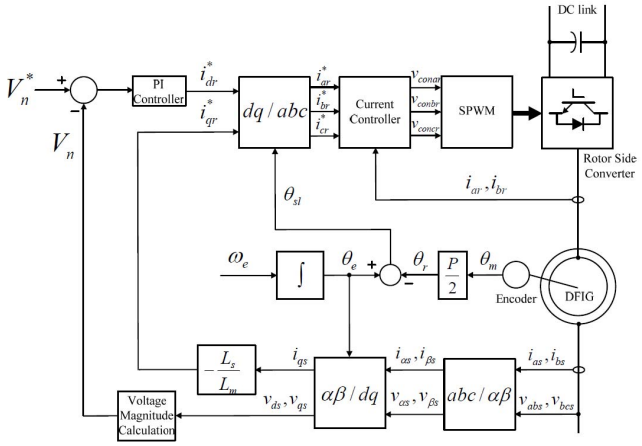

Figure 2. Control block of rotor side converter.

The control block diagram of the rotor side converter, which comprises a DFIG, a 3-phase current controlled voltage source inverter (VSI) using sinusoidal pulse-width-modulation (SPWM) and field-oriented control mechanism, is shown in Fig. 2 [5-6]. There are two control loops: one is for the regulation of the magnitude of the stator voltage; and the other one is for the field-oriented control using the command angular speed for the stator output voltage. The machine model of a DFIG can be described in the synchronous rotating reference frame as:

$$v_{ds} = R_s i_{ds} + \frac{d\lambda_{ds}}{dt} - \omega_e \lambda_{qs} \tag{1}$$

$$v_{qs} = R_s i_{qs} + \frac{d\lambda_{qs}}{dt} + \omega_e \lambda_{ds} \tag{2}$$

$$\lambda_{ds} = L_s i_{ds} + L_m i_{dr} \tag{3}$$

$$\lambda_{qs} = L_s i_{qs} + L_m i_{qr} \tag{4}$$

For the purpose of field-orientation in the synchronous rotating reference frame of the stator flux, the spatial vector of the stator flux is aligned with the *d*-axis in steady-state. That is

$$\lambda_{qs} = 0 \tag{5}$$

Substitute (5) into (4), then

$$i_{qr} = -\frac{L_s}{L_m} i_{qs} \tag{6}$$

It is possible to keep the spatial vector of the stator flux aligned to the reference frame *d*-axis despite of the load and rotor speed conditions if (6) is imposed. Moreover, the voltage control loop is used to control the magnitude of the stator voltage defined as follows:

$$V_n = \sqrt{(v_{ds})^2 + (v_{qs})^2} \tag{7}$$

Substituting (5) into (1), (2) and (3), the following equations are yielded

$$v_{ds} = R_s i_{ds} + \frac{d\lambda_{ds}}{dt} \tag{8}$$

$$v_{qs} = R_s i_{qs} + \omega_e \lambda_{ds} \tag{9}$$

$$\lambda_{ds} = L_s i_{ds} + L_m i_{dr} \tag{10}$$

Moreover, substitute (10) into (8) and (9), then

$$v_{ds} = R_s i_{ds} + L_s \frac{di_{ds}}{dt} + L_m \frac{di_{dr}}{dt} \tag{11}$$

$$v_{qs} = R_s i_{qs} + \omega_e L_s i_{ds} + \omega_e L_m i_{dr} \tag{12}$$

It can be seen from (11) and (12) that the spatial components of the stator voltage v_{ds} and v_{qs} are dependent on i_{dr} , i_{ds} and i_{qs} . However, i_{ds} and i_{qs} are load dependent perturbations. Therefore, only i_{dr} can be adopted as an independent control variable as shown in Fig. 2. Furthermore, for the sub-synchronous condition, the slip angular speed ω_{sl} is positive and the slip angular angle θ_{sl} is increasing, the direction of the power flow is from the DC-link to the rotor. On the other hand, for the super-synchronous conditions, the slip angular speed ω_{sl} is negative and the slip angular angle θ_{sl} is decreasing, the direction of the power flow is from the rotor to the DC-link.

The block diagram of the field-oriented control stator side converter with the stator voltage orientation is shown in Fig. 3. The 3-phase current controlled VSI using SPWM is also adopted in the current loop. Moreover, a voltage loop is designed for the regulation of the DC-link voltage. The active and reactive powers of the stator side converter can be described as [4,7]

$$P_s = \frac{3}{2}(v_d i_d + v_q i_q) \tag{13}$$

$$Q_s = \frac{3}{2}(v_d i_q - v_q i_d) \tag{14}$$

The *d*-axis voltage component v_d is fixed with the orientation of the stator voltage and the *q*-axis v_q voltage component is zero. Therefore, (13) and (14) can be simplified as follows:

$$P_s = \frac{3}{2} v_d i_d \tag{15}$$

$$Q_s = \frac{3}{2} v_d i_q \tag{16}$$

From (15) and (16), if i_q is set to zero, then the reactive power Q_s is zero. Thus, unit power factor of the stator side converter can be achieved. Moreover, if i_d is positive, the direction of the power flow is from the DC-link to the stator side. On the other hand, if i_d is negative, the direction of the power flow is from the stator side to the DC-link.

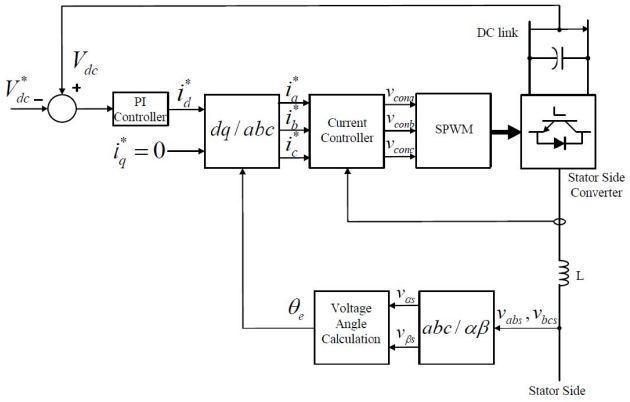

Figure 3. Control block of stator side converter.

III. PFNN CONTROLLER

In this section, the PFNN controller is proposed to replace the PI controllers shown in Figs. 2 and 3 for both the rotor side and stator side converters in order to improve the transient and steady-state responses of the DFIG system. In the proposed PFNN, not only the tracking error but also its derivative is considered as the inputs to achieve precise tracking performance in both the transient and steady-state phases to deal with instant uncertainties including system parameters variations and external disturbances. Moreover, in order to make the output of the PFNN sensitive to the history data, self-connection of the output neuron is also added. Therefore, the proposed PFNN can improve the convergence error and reduce the learning time effectively.

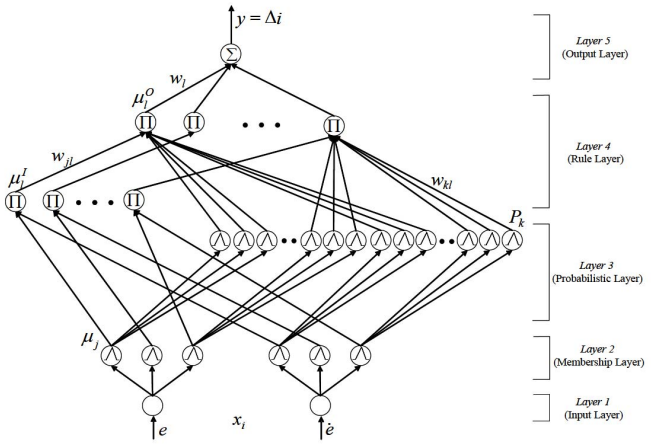

Figure 4. Network structure of PFNN.

A. Probabilistic Fuzzy Neural Network

The architecture of the PFNN including the input layer (layer 1), the membership layer (layer 2), the probabilistic layer (layer 3), the rule layer (layer 4) and the output layer (layer 5) with two inputs and one output is shown in Fig. 4. Moreover, the signal propagation and the basic function of each layer are introduced in the following:

1) Input layer(layer1): In the input layer, the node input and the node output are represented as:

$$x_i(N) = e_i(N), \quad i = 1, 2 \tag{17}$$

where x_i represents the ith input to the input layer; N represents the Nth iteration. In this study, the inputs of the PFNN are $e_1(N) = e$ and $e_2(N) = \dot{e}$, which are the tracking error and its derivative, respectively.

2) Membership layer(layer2): In the membership layer, the receptive field function is usually a Gaussian function in FNN. In order to reduce the computational requirements, a triangular function $f_m(x_i)$ is selected as the receptive field function. The equations of the triangular function $f_m(x_i)$ are in the following:

$$\mu_j(x_i) = f_m(x_i) = \begin{cases} 0 & if \quad x_i \ge m_j + \sigma_j,\ x_i \le m_j - \sigma_j \\ \dfrac{x_i - m_j + \sigma_j}{\sigma_j} & if \quad m_j - \sigma_j < x_i \le m_j \\ \dfrac{-x_i + m_j + \sigma_j}{\sigma_j} & if \quad m_j < x_i \le m_j + \sigma_j \end{cases} \tag{18}$$

$$i = 1, 2. \qquad j = 1, 2, \ldots, 6$$

where $\mu_j(x_i)$ is the output of the jth node of the ith input variable; m_j is the center of the triangle; σ_j is the center's width of the triangle.

3) Probabilistic layer(layer3): In the probabilistic layer, the receptive field function is usually a Gaussian function. For the same reason in membership layer, another triangular function $f_p(\mu_j)$ is selected as the receptive field function and its equations are as follows:

$$P_k(\mu_j) = f_p(\mu_j) = \begin{cases} 0 & if \quad \mu_j \ge m_k + \sigma_k,\ \mu_j \le m_k - \sigma_k \\ \dfrac{\mu_j - m_k + \sigma_k}{\sigma_k} & if \quad m_k - \sigma_k < \mu_j \le m_k \\ \dfrac{-\mu_j + m_k + \sigma_k}{\sigma_k} & if \quad m_k < \mu_j \le m_k + \sigma_k \end{cases} \tag{19}$$

$$k = 1, 2, \ldots, 18$$

where $P_k(\mu_j)$ is the output of the kth node of the jth input variable; m_k is the center of the triangle; σ_k is the center's width of the triangle.

4) Rule layer(layer4): In the rule layer, each node corresponds to a rule in the knowledge base. In the Mamdani inference, the node itself performs the t-norm operation (product operation) to obtain the inference set according to the rules as shown in (20). The probabilistic information is processed using the Bayes' theorem [1,3] in consideration of the group of fuzzy grade being independent variables as shown in (21). Therefore, the node input and the node output are represented as:

$$\mu_l^I = \prod_j w_{jl} \mu_j \tag{20}$$

$$P_l^I = \prod_k w_{kl} P_k \tag{21}$$

$$\mu_l^O = \mu_l^I P_l^I \qquad l = 1, 2, \ldots, 9. \tag{22}$$

where μ_l^I and P_l^I are the input of rule layer; w_{jl} is the connective weight between the membership layer and the rule layer which is set to be 1; w_{kl} is the connective weight between the probabilistic layer and the rule layer which is also set to be 1; μ_l^O is the output of the rule layer.

5) Output layer(layer5): In the output layer, the node input and the node output are represented as:

$$\Delta i = y(N) = \sum_{l=1}^{9} w_l \mu_l^O \tag{23}$$

where $\Delta i = y(N)$ is the output of the PFNN; w_l is the connective weight between the rule layer and the output layer.

B. On-Line Learning Algorithm Using Delta Adaptation Law

The central part of the learning algorithm for the PFNN

concerns how to recursively obtain a gradient vector in which each element in the learning algorithm is defined as the derivative of an energy function with respect to a parameter of the network. This is done by means of the chain rule, and the method is generally referred to as the BP learning rule. To describe the on-line learning algorithm of the PFNN using supervised gradient decent method, first the energy function E is defined as:

$$E = \frac{1}{2}(\omega_r^* - \omega_r)^2 = \frac{1}{2}e^2 \tag{24}$$

Then the learning algorithm is described as follows:

1) Layer5: The error term to be propagated is given by:

$$\delta_o = -\frac{\partial E}{\partial y(N)} = -\frac{\partial E}{\partial \omega_r}\frac{\partial \omega_r}{\partial y(N)} \tag{25}$$

and the weights are updated by the amount:

$$\Delta w_l = -\eta_1 \frac{\partial E}{\partial w_l} = -\eta_1 \frac{\partial E}{\partial y(N)}\frac{\partial y(N)}{\partial w_l} = \eta_1 \delta_o \mu_l^O \tag{26}$$

where the factor η_1 is the learning rate. The connective weight w_l is updated according to the following equation:

$$w_l(N+1) = w_l(N) + \Delta w_l \tag{27}$$

2) Layer4: In this layer, the error terms to be propagated are given by:

$$\delta_l = -\frac{\partial E}{\partial \mu_l^O} = -\frac{\partial E}{\partial y(N)}\frac{\partial y(N)}{\partial \mu_l^O} = \delta_o w_l \tag{28}$$

3) Layer2: The error terms to be propagated are given by:

$$\delta_j = -\frac{\partial E}{\partial \mu_j} = -\frac{\partial E}{\partial y(N)}\frac{\partial y(N)}{\partial \mu_l^O}\frac{\partial \mu_l^O}{\partial \mu_l^I}\frac{\partial \mu_l^I}{\partial \mu_j} = \sum_l \delta_l P_l^I \tag{29}$$

By using of the chain rule, the update laws of center and center's width of the triangle are

$$\Delta m_j = -\eta_2 \frac{\partial E}{\partial m_j} = -\eta_2 \frac{\partial E}{\partial y(N)}\frac{\partial y(N)}{\partial \mu_l^o}\frac{\partial \mu_l^o}{\partial \mu_l^I}\frac{\partial \mu_l^I}{\partial \mu_j}\frac{\partial \mu_j}{\partial m_j}$$
$$= \begin{cases} -\eta_2 \delta_j \dfrac{1}{\sigma_j} & if \quad m_j - \sigma_j < x_i \le m_j \\ \eta_2 \delta_j \dfrac{1}{\sigma_j} & if \quad m_j < x_i \le m_j + \sigma_j \end{cases} \tag{30}$$

$$\Delta \sigma_j = -\eta_3 \frac{\partial E}{\partial \sigma_j} = -\eta_3 \frac{\partial E}{\partial y(N)}\frac{\partial y(N)}{\partial \mu_l^o}\frac{\partial \mu_l^o}{\partial \mu_l^I}\frac{\partial \mu_l^I}{\partial \mu_j}\frac{\partial \mu_j}{\partial \sigma_j}$$
$$= \begin{cases} \eta_3 \delta_j \dfrac{m_j - x_i}{(\sigma_j)^2} & if \quad m_j - \sigma_j < x_i \le m_j \\ \eta_3 \delta_j \dfrac{x_i - m_j}{(\sigma_j)^2} & if \quad m_j < x_i \le m_j + \sigma_j \end{cases} \tag{31}$$

where the factors η_2 and η_3 are the learning rates. The center of the triangle m_j and center's width of the triangle σ_j are updated according to the following equation:

$$m_j(N+1) = m_j(N) + \Delta m_j \tag{32}$$

$$\sigma_j(N+1) = \sigma_j(N) + \Delta \sigma_j \tag{33}$$

In order to reduce the computation load, in layer 3, the center of the triangle m_k and the center's width of the triangle σ_k are constants where m_k is set to be 0.4 for $k = 1, 4, 7, 10, 13, 16$, 0.5 for $k = 2, 5, 8, 11, 14, 17$, and 0.6 for $k = 3, 6, 9, 12, 15, 18$; σ_k is set to be 1. Furthermore, the exact calculation of the Jacobian of the system, $\partial \omega_r / \partial y(N)$, is difficult to be determined due to the unknown dynamics of the control system. To overcome this problem, a delta adaptation law is adopted as follows [8]:

$$\delta_o \cong e(N) + \dot{e}(N) \tag{34}$$

Moreover, the on-line learning algorithm for the PFNN controller of the stator side converter is the same as PFNN controller of the rotor side converter only $V_n(N)$ is replaced by $V_{dc}(N)$ in related derivations.

IV. Design and Experimentation

A. Design

The computer controlled DFIG system is shown in Fig. 5. The block diagram of the personal computer (PC)-based control computer for the PFNN controlled DFIG system is shown in Fig. 5(a), where the inductor in the stator side converter is 3*m*H and the DC-link capacitor is 2820 μ F. The field-oriented control algorithms, synchronization algorithm and the PFNN controllers are realized in a PC. Three-phase current commands are sent to both the rotor side converter and stator side converter using digital/analog (D/A) converters. The current-controlled VSI SPWM converters are implemented using an intelligent power modules (PM30CSJ060) manufactured by Mitsubishi Co. with a switching frequency of 10kHz. Matlab & Simulink Real-Time Control package is adopted for the implementation of the proposed algorithms and

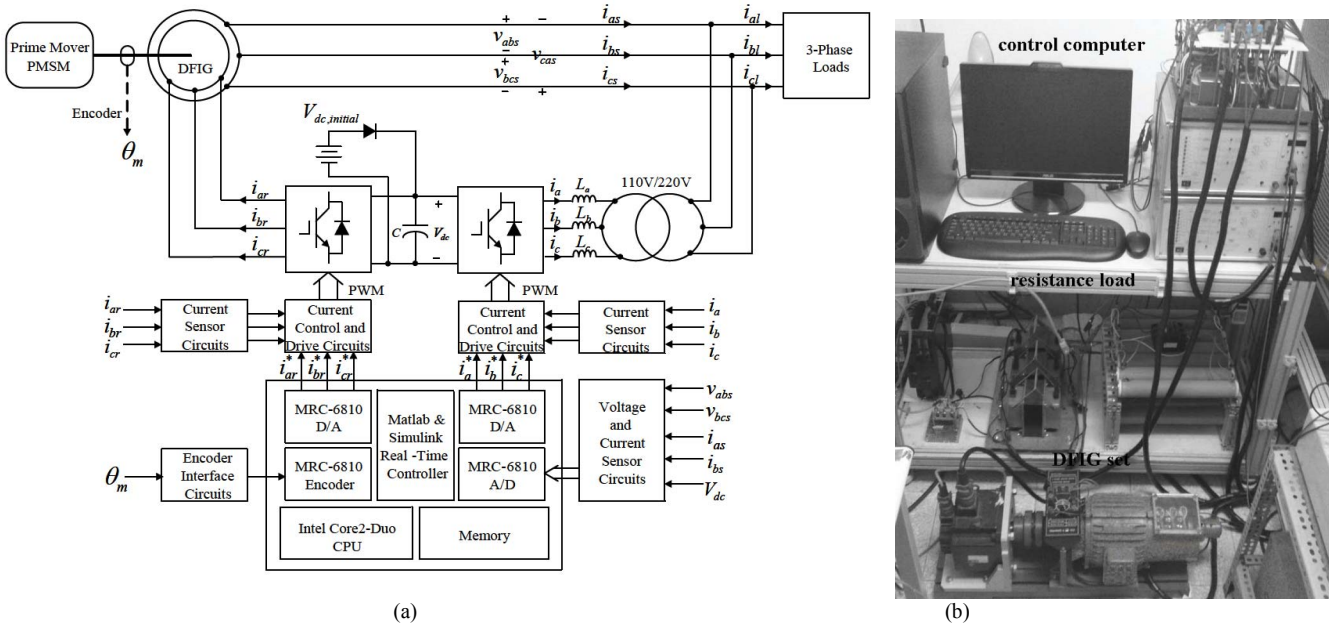

(a) (b)

Figure 5. Computer controlled DFIG system. (a) Computer control system. (b) Photo of DFIG set, resistance load and control computer.

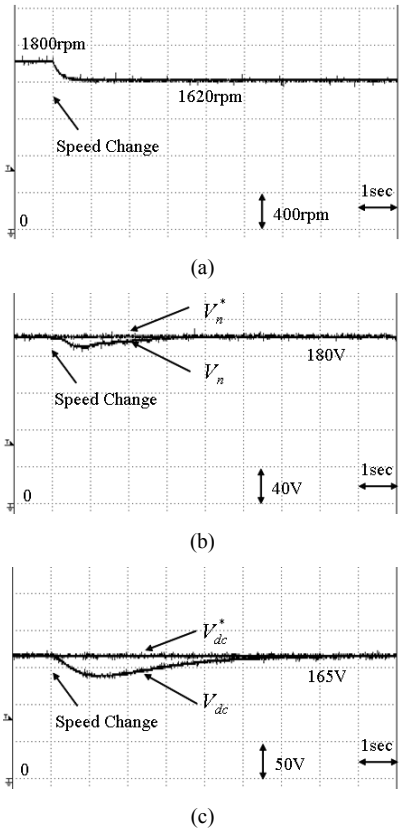

Figure 6. Experimental results of PI controlled DFIG system from 1800rpm to 1620rpm. (a) Speed response. (b) Magnitude response of phase *A* voltage. (c) Magnitude response of DC-link voltage.

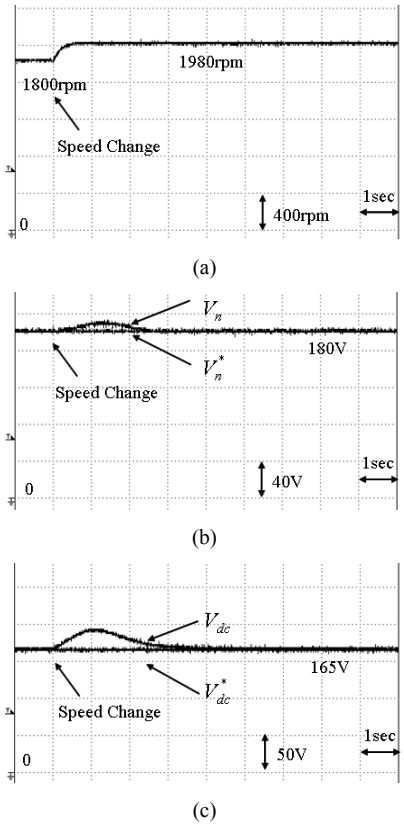

Figure 7. Experimental results of PI controlled DFIG system from 1800rpm to 1980rpm. (a) Speed response. (b) Magnitude response of phase *A* voltage. (c) Magnitude response of DC-link voltage.

the fix-step solver in the Real-Time Control package is set to be 0.5ms. In the program, first, the v_{abs}, v_{bcs}, V_{dc}, i_{as}, i_{bs} signals are obtained via A/D converters and the θ_m signal is obtained via encoder interface. Then, both the rotor side and stator side converters are controlled using either PI controller or PFNN controller to generated i_{ar}^*, i_{br}^*, i_{cr}^* and i_a^*, i_b^*, i_c^*,

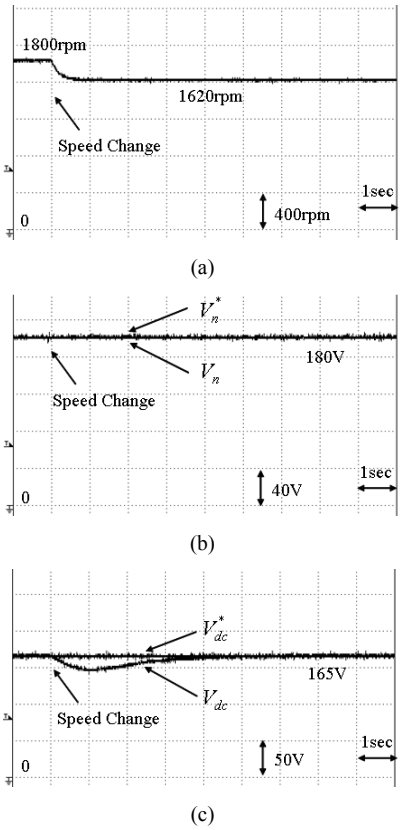

Figure 8. Experimental results of PFNN controlled DFIG system from 1800rpm to 1620rpm. (a) Speed response. (b) Magnitude response of phase *A* voltage. (c) Magnitude response of DC-link voltage.

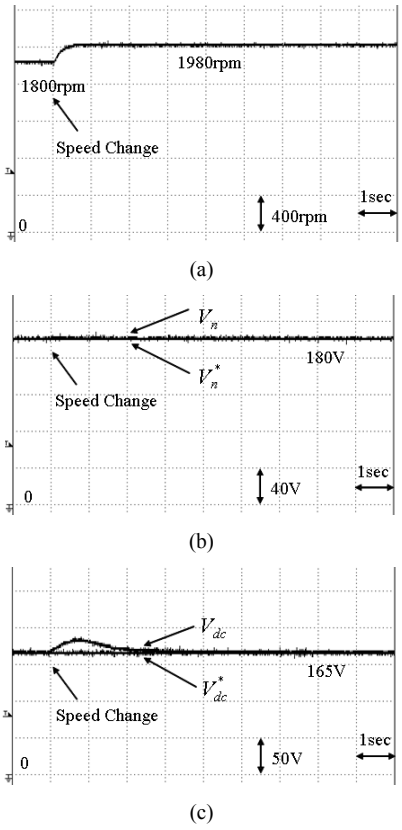

Figure 9. Experimental results of PFNN controlled DFIG system from 1800rpm to 1980rpm. (a) Speed response. (b) Magnitude response of phase *A* voltage. (c) Magnitude response of DC-link voltage.

respectively. The generated current commands are sent to the analog current controllers through D/A converters to generate the pulse-width-modulation (PWM) signals for both the converters. The initial DC-link voltage $V_{dc,initial}$ is also necessary for the stand-alone applications of the DFIG system as shown in Fig. 5(a) to provide the initial rotor excitation. Furthermore, the photo of DFIG set, resistance load and control computer is shown in Fig. 5(b). In addition, in the DFIG set, the prime mover is a field-oriented controlled permanent magnet synchronous motor (PMSM).

B. Experimentation

The adopted DFIG is a three-phase Y-connected four-pole 1Hp 220V/3.5A 1700rpm type. The parameters of the DFIG at the nominal condition are:

$$R_s = 2.85\Omega,\ R_r = 2.34\Omega,\ L_s = 0.1967H,\ L_r = 0.1970H \quad (35)$$

Moreover, the prime mover is a three-phase Y-connected four-pole 3.5kW 120V/26.4A 2000rpm type PMSM. Furthermore, sub-synchronous control 1620rpm (s=0.1), synchronous control 1800rpm (s=0) and super-synchronous control 1980rpm (s=-0.1) three operating conditions all with 484W 3-phase load are test.

To emulate the variation of the wind speed, some experimental results using both the PI and PFNN control are provided to further test the transient control performance of both the PI and PFNN controlled DFIG system. The variation of the rotor speed, the responses of the magnitude of phase *A* stator voltage V_n and DC-link voltage V_{dc} from 1800rpm to 1620rpm using the PI controller are shown in Figs. 6(a), 6(b) and 6(c). Moreover, the variation of the rotor speed, the responses of the magnitude of phase *A* stator voltage V_n and DC-link voltage V_{dc} from 1800rpm to 1980rpm using the PI controller are shown in Figs. 7(a), 7(b) and 7(c). Furthermore, the variation of the rotor speed, the responses of the magnitude of phase *A* stator voltage V_n and DC-link voltage V_{dc} from 1800rpm to 1620rpm using the PFNN controller are shown in Figs. 8(a), 8(b) and 8(c). In addition, the variation of the rotor speed, the responses of the magnitude of phase *A* stator voltage V_n and DC-link voltage V_{dc} from 1800rpm to 1980rpm using the PFNN controller are shown in Figs. 9(a), 9(b) and 9(c). From the experimental results, compared to the PI controlled DFIG system, excellent magnitudes tracking responses of the phase voltage can be obtained for the PFNN controlled DFIG system. However, the improvement of the responses of the DC-link voltage is limited due to the requirement of the stable phase voltage for the construction of the stable DC-link voltage.

V. CONCLUSION

This study has successfully demonstrated the applications of a PFNN controller on both the rotor side and stator side converters for the voltage magnitudes tacking control of an intelligent controlled DFIG system. First, the dynamic model of a field-oriented control DFIG system via the rotor side converter was introduced. Then, the control methodology of the stator side converter and the synchronization method to the stator were both introduced. Moreover, the network structure, online learning algorithm and convergence analyses of the PFNN were introduced in detail. The PFNN was proposed to control both the magnitudes of phase *A* stator voltage in the rotor side converter and DC-link voltage in the stator side converter at sub-synchronous, synchronous and super-synchronous conditions for stand-alone applications. Furthermore, the effectiveness of the proposed control scheme has been confirmed via experimentation. Form the experimental results, the control performance of the proposed PFNN controlled DFIG system is robust with regard to different operating conditions.

REFERENCES

[1] E. Parzen, "On estimation of a probability density function and mode," Ann. Math. Statist., vol. 33, no. 3, pp. 1065-1076, September 1962.

[2] A. H. Meghdadi and M.-R. Akbarzadeh-T, "Probabilistic fuzzy logic and probabilistic fuzzy systems," IEEE International Conf. Fuzzy Syst., Melbourne, Australia, 2001, pp. 1127-1130.

[3] Z. Liu and H. X. Li, "A probabilistic fuzzy logic system for modeling and control," IEEE Trans. Fuzzy Syst., vol. 13, no. 6, pp. 848-859, December 2005.

[4] R. Pena, J. C. Clare, and G. M. Asher, "Doubly fed induction generator using back-to-back PWM converters and its application to variable-speed wind-energy generation," IEE Proc.-Electr. Power Appl., vol.143, no. 3, pp. 231-241, May 1996.

[5] D. Forchetti, G. Garcia, and M. I. Valla, "Vector control strategy for a doubly-fed stand-alone induction generator," IEEE Annual Conf. Industrial Electronics Society, pp. 991-995, November 2002.

[6] G. Iwanski and W. Koczara, "DFIG-based power generation system with UPS function for variable-speed applications," IEEE Trans. Ind. Electron., vol. 55, no. 8, pp. 3047-3054, August 2008.

[7] J. Yao, H. Li, and Z. Chen, "An improved control strategy of limiting the DC-link voltage fluctuation for a doubly fed induction wind generator," IEEE Trans. Power Electron., vol. 23, no. 3, pp. 1205-1213, May 2008.

[8] F. J. Lin, R. J. Wai, and C. C. Lee, "Fuzzy neural network position controller for ultrasonic motor drive using push-pull DC-DC converter," IEE Proc.- Control Theory Appl., vol. 146, no. 1, pp. 99-107, January 1999

2011 IEEE International Conference on Fuzzy Systems
June 27-30, 2011, Taipei, Taiwan

Web User Identification with Fuzzy Fingerprints

Nuno Homem
TULisbon – Instituto Superior Técnico
INESC-ID
R. Alves Redol 9, 1000-029 Lisboa
nuno.homem@hotmail.com

Joao Paulo Carvalho
TULisbon – Instituto Superior Técnico
INESC-ID
R. Alves Redol 9, 1000-029 Lisboa
Portugal
joao.carvalho@inesc-id.pt

***Abstract*— Fingerprint identification is a well-known technique in forensic sciences. The basic idea of identifying a subject based on a set of features left by the subject actions or behavior can be applied to other domains. Identifying a web user based on a user fingerprint is one such application. This paper considers the problem of extracting fingerprints from web usage logs and matching them with those obtained from a set of known users. It presents an innovative fuzzy fingerprint algorithm based on vector valued fuzzy sets. Used sites are used as base features to create the fingerprint. The assumption is that sites accessed by each user remain approximately stable and are distinctive. The paper presents the proposed algorithm and shows some experimental results that validate the approach. The use of fast and compact algorithms is critical due to the possible huge number of users, and allows this method to be used on near real time.**

Keywords-component; fuzzy fingerprints, vector valued fuzzy sets, similarity, frequent elements, approximate algorithms, data streams

I. INTRODUCTION

In this paper, one considers the problem of extracting a fingerprint from web usage logs and then using that fingerprint to identify the user behind a distinct web session.

Identifying users based in their previously known usage is a known procedure in several areas such as telecommunications and financial fraud detection. For security and judicial purposes, identifying a user based on a specific usage behavior is also relevant. These detection methods are based on the fact that although a suspect or fraudster may present different identification credentials or simply no identification at all, its behavior and its relationships remain the same. Every individual keeps some relationships and habits, either personal or businesswise, stable for some time. Even if some of those relationships and habits change along time (the individual starts working in a different company, a distinct business, marries another person, etc.), some will remain stable (same family, some job, same interests). This provides the basis for the fingerprint as relationships and habits are translated into usage events. By using the destination number as a proxy for the individual behind a specific communication event, we can gather information out of a person's calls to its relationship network. The sites the user accesses in the web are also a clue to the user habits and interests and therefore can be used to identify him in a pool of suspected web sessions.

Within the scope of this paper, one will consider a web session as the sequence of web log records that belong to a single user, either known or unknown. For anonymous web access, one will consider that some method is available to group these records into a single session. Although out of the scope of this paper, user identity could be linked to a single fixed IP address or a single provider login.

Each web log record represents a user visit to a single web site, regardless of the used protocol. The set of known users for whom a fingerprint is available will constitute the suspects for unknown user sessions identification.

Fingerprint identification is a well-known technique in forensic sciences and widely documented. In computer sciences a fingerprint is a procedure that maps an arbitrarily large data item (such as a computer file, or author set of texts) to a much compact information block, its fingerprint, that uniquely identifies the original data for all practical purposes, just as human fingerprints uniquely identify people for practical purposes.

In computer sciences, fingerprints are typically used to avoid the comparison and transmission of bulky data. For example, a web browser or proxy server can efficiently check if a remote file has been modified simply by fetching its fingerprint and comparing it with the fingerprint of the previously fetched copy. Fingerprints are a fast and compact way to identify items.

To serve the user identification purposes, a fingerprint must be able to capture the identity of that user. In other words, the probability of a collision, i.e., two users yielding the same fingerprint, must be small. The fingerprint has also to be robust; a user should be identified even if he changes some aspects of the web use. The idea of identifying users based on a fingerprint is a very appealing one, because identification can theoretically be made on near real time.

To be useful, the fingerprint should comply with some basic criteria:

- Include a minimal set of features that describe the user (the suspect) in a compact format.
- Allow for update operations whenever new information (new logs) on the user is available.
- Allow for a fast comparison process once a new session owner needs to be identified.

978-1-4244-7316-8/11/$26.00 ©2011 IEEE

- Scalability, i.e., performance should not degrade significantly when the number of sessions and suspects in the pool increases.
- Flexibility, i.e., should allow new suspects to be included in the process, whenever information is available.

This paper proposes a new method for identifying web users given a set of possible suspects. By using the web site access frequencies as a proxy for the individual behind a specific session, one can gather information on the user and identify other unidentified sessions.

The first step in the proposed method is to gather the top-*k* site access frequencies in all known logs of each known user. An approximated algorithm is used for this purpose since classical exact top-k algorithms are inefficient and require the full list of distinct elements to be kept. The Filtered Space-Saving algorithm [1], [7] is used for this purpose since it provides a fast and compact answer to the top-*k* problem although it only gives an approximate solution. This paper defends that the algorithm approximation is not an issue, as a degree of change or randomness has to be expected and incorporated into the detection method.

Once the top-k site access frequencies are available, the fingerprint is constructed by applying a fuzzifying function to each frequency. This paper proposes the innovative method of fuzzifying the set of features based on their order on the top-*k* list instead of their frequency value.

The last part in the process is to perform the same calculations for the session being identified and then to compare this fuzzy fingerprint with all the available users fuzzy fingerprints. The most similar fingerprint is chosen and the session is assigned to the fingerprint author.

II. Relation with previous work

A. Signatures and fingerprints

Boltan and Hand [1] and Phua and al. [12] survey multiple methods for fraud detection using statistical and data-mining techniques but no mention is made of research aiming to identify individual fraudsters based on their behavior. A more common, although distinct, approach is the use of usage signatures but to detect behavior changes as in [3], [4] and [5]. Signatures are used to monitor the individual activity and detect changes in that activity, or to compare against known fraud signatures to detect similarity of patterns, not the individuals behind the fraud. In [3] and [5] signatures are created extracting relevant features out of the individual usage, such as number of local, national and international calls, etc., based on pre-defined types of traffic classifications and summarized. In [5] a list of the top-k countries and destinations called, and a count of calls that do not go to any of the top-k is used but with the purpose of detecting changes in the usage.

A recent work by Cormode et al. [1] presents the concept of signature algorithms applied to iterations between individuals and provides some signature schemes to network traffic and telecommunication calls. A generic approach and a theoretical framework for signatures communication graphs analysis are provided. The "signatures" concept has some common points to the proposed user fingerprint. However, one prefers to use the "fingerprint" designation, as the algorithm aims at extracting information about the user that he has not provided knowingly, while a "signature" usually refers to information that was created specifically to identify someone or something. In [1] the feature extraction is exact; the use of approximated algorithms is suggested and several distinct distances are proposed.

B. Fuzzy Signatures

The fuzzy fingerprint concept is a generalization of the Vector Valued Fuzzy Sets (VVFS) concept introduced by Kóczy [8]. The qualitative meaning of an object is represented by the quantities of the VVFS.

The vector valued fuzzy sets concept has also been used in [9] to introduce the fuzzy signature concept. Fuzzy signatures can model sparse and hierarchically correlated data with the help of hierarchically structured VVFS and a set of not-necessarily homogenous and hierarchically organized aggregation functions.

III. The Filtered Space-Saving Algorithm

To allow the use of user identification techniques in near real time and for a large number of potential suspects and sessions, a key issue is to be able to extract the relevant features using an efficient algorithm with reduced memory usage. In this case, features are the most frequent visited sites in the user usage. The choice was to use an approximate top-*k* algorithm capable of generating good quality estimates using a reduced memory footprint. The Filtered Space-Saving algorithm [7] was chosen. Filtered Space-Saving, originally presented in [6], is an evolution from Space-Saving algorithm presented by Metwally and al. [10].

The Filtered Space-Saving (FSS) algorithm uses a bitmap counter with h cells, each containing two values, α_i and c_i, standing for the error and the number of monitored elements in cell i. The hash function needs to be able to transform the input values (site) into an uniformly distributed integer range. The hashed value *hash(x)* is then used to increment the corresponding counter. Initially all values of α_i and c_i are set to 0.

The second storage element is a list of monitored elements A with size m. The list is initially empty. Each element contains three parts; the value itself v_j, the estimate count f_j and the associated error e_j.

The minimum required value to be included in the monitored list is always the minimum of the estimate counts, $\mu = min\ \{f_j\}$. While the list has free elements, the minimum is set to 0.

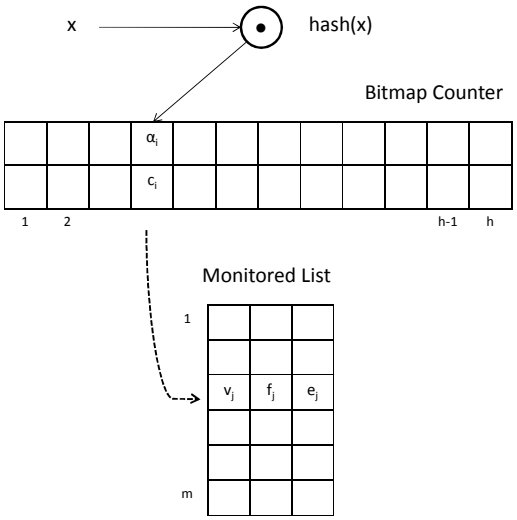

Figure 1 – FSS Algorithm Diagram.

The algorithm is quite simple. When a new element is received, its hash is calculated and the bitmap counter is checked. If there are already monitored elements with that same hash *($c_i > 0$)* the list is searched to see if this particular element is already there. If the element is in the list then the estimate count f_j is incremented. If the element is not in the list then it is checked to see if it should be added.

A new element will be inserted into the list if $\alpha_i + 1 \geq \mu$. If the element is not monitored then α_i is incremented. In fact this α_i stands for the number of elements with hash value i that have not been counted in the monitored list; it is the maximum number of times an element that is not in the list and that has this hash value could have been observed.

```
Algorithm: FSS(h cells, m counters, S stream)

begin
for each element, x, with value w, in S {
    set min to min {fj}
    let i be the hash(x) mod h
    if ci is not 0 {
        if x is monitored {
            let j be the index of x in the list
            increment fj
            continue for next x
        }
    } // this will only be executed if x is not monitored

    if  αi + 1 >= min {
        if list size equals m {
            let m be the index with lower fj
            and for same fj with higher ej
            let k be the hash(x) mod h
            decrement ck
            set αk = fi
            remove vm
        }
        include x in the list in index j
        set vj to x
        set ej to αi and fj to αi+1
        increment counter ci
    } else {
        increment αi
    }
}// end for
end
```

Figure 2 – The FSS Algorithm

IV. The Fuzzy Fingerprint Algorithm

The main concept behind this algorithm is that users have a stable enough behavior that allows a set of features to be extracted, fuzzified and then compared. The most frequent visited sites of a single user present the required stability.

User web traffic can then be analyzed as a set of site accesses generated by a stable distribution that depends only on the user. Only site visit counts are in fact relevant and used as variables.

The set of sites to consider in the fingerprint should be large enough to allow a comprehensive sample of the user behavior along time. The FSS algorithm requires two parameters, the size of the monitored list *m* and the size of the bitmap counter *h*. In all the tests the parameters were set proportional to the number of visited sites used in the fingerprint: $m = 3k$, $h = 9k$.

A. Fuzzy Fingerprint Creation

The full set of known texts are processed through the modified FSS algorithm to compute the approximated top-*k* list and frequencies for each user. Consider T_j is the set of logs by the user *j*. The result consists of a list of *k* tuplets $\{v_i, n_i\}$ where v_i is the *i*-th most frequent visited site and n_i the corresponding count estimate.

To create the actual fingerprint, the top-*k* list has to be fuzzified. The choice of the fuzzifying function is critical and the chosen approach is to assign a membership value to each site in the set based only on the order in the list. In fact, experiments have shown that the order of the frequency seems more relevant than its actual value. The more frequent sites will have a higher membership value.

Several alternative membership attribution functions for each element *i* of the top-*k* list are tested in this paper. The simplest one is:

$$\mu_{flat}(i) = \frac{k-i}{k}. \tag{1}$$

Function μ_{par}, inspired in the Pareto rule, where 80% of the membership value is assigned to first 20% elements in the ranking:

$$\mu_{par}(i) = \begin{cases} 1-(1-b)\dfrac{i}{k} & \text{if } i < a \\ a\left(1-\dfrac{i-a}{k-a}\right) & \text{if } i \geq a \end{cases} \tag{2}$$

The third function is μ_{erfc}, based on the complementary error function:

$$\mu_{erfc}(i) = 1 - erf\left(\frac{2i}{k}\right), \tag{3}$$

where *erf()* is the Gauss error function. Figure 3 presents the used functions.

The fingerprint based on the top-*k* list (size-*k* fingerprint, Φ), consists on a size-*k* fuzzy vector where each position *i*

contains a element v_i and a value μ_i representing the fuzzified value of v_i's rank (the membership of the rank).

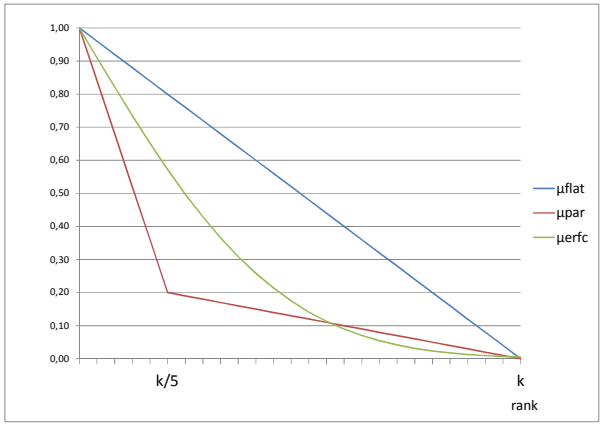

Figure 3 – Fuzzyfying functions

An user j will be represented by its fingerprint $\Phi_j = \Phi(T_j)$. Formally, fingerprint $\Phi_j = \{(v_{ji}, \mu_{ji}) | i = 1..k_j\}$ has length k_j, let $S_j = \{v_{ji} | i = 1..k_j\}$ be the set of v's in Φ_j.The set of all user fingerprints will constitute the fingerprint library.

B. *Fuzzy Fingerprint Detection*

In order to find the user of an unknown session L, one starts by computing the size-k fingerprint of L, Φ_L. Then one compares the fingerprint of L with the fingerprints Φ_j of all users present in the fingerprint library. The unknown user is identified as user j if he has the most similar fingerprint to Φ_L. Fingerprint comparision, $sim(\Phi_L, \Phi_j)$, is calculated using (4):

$$sim(\Phi_L, \Phi_j) = \sum_{v \in S_L \cup S_j} \frac{\min\left(\mu_v(\Phi_L), \mu_v(\Phi_j)\right)}{k}, \qquad (4)$$

where $\mu_v(\Phi_x)$ is the membership value associated with the rank of element v in fingerprint x. This function is based on the minimum or Gödel t-norm, but other t-norms could be used.

V. Experimental Results

A. *Experimental data set*

Experiments were performed using a data set consisting of 10 days of web logs collected from a large company (including a weekend, with much less records). The data is annonymized but every user in the web access record is identified by a unique tag. Records detailing access to .jpg, .bmp, .gif objects were filtered and are not present in the data set. Filtering the images from the web logs reduces the number records to circa 10%. Note that this company has implemented a web access policy that limits access to some sites

To create the suspect library the logs from the 8 initial days were used, constituting the training set. The sessions to be used as the test set were created with the remaining 2 days of web logs. A total of 21 669 597 records were included in the training set, and 6 621 078 records in the test set. Although both the training and test sets were created using a much reduced sample period, this may in fact be similar to real life situations where data is usually much less than ideal.

A total of 1630 users were considered for these tests, each with a minimum 750 records in the training set and 250 records in the test set. Note that this is a small number of access records; many of the users generate more than a thousand records per day (excluding images).

The site name and port part of the url were used as base features. Site name and port were prefered to the IP address because, first, many sites use multiple servers and IP addresses for load balancing, second, many sites share the same IP address as they are hosted in a single server, third, because with the emergence of cloud hosting services IP addresses are easily changed and the site name is what effectivly distinguishes one site from another. The use of the site name requires also requires some care as some services may use the name to convey some information for user or load distribution, in this case some cleaning is required to transform the site name and port to the generical format of *server.domain:port* or *server.domain*.

Although the sample period is not long it is interesting to see the site access distribution per user. Figure 4 presents the percentage of accesses for each of the most visited sites of each user. On average 90% of the users accesses are made to just 55 sites. Figure 4 also presents distribution of consecutive site accesses, and the mixture of the two distributions. Consecutive site accesses are relevant because one user may visit one site and then visit another. This path may be distinct from other users paths and helps distinguising the users.

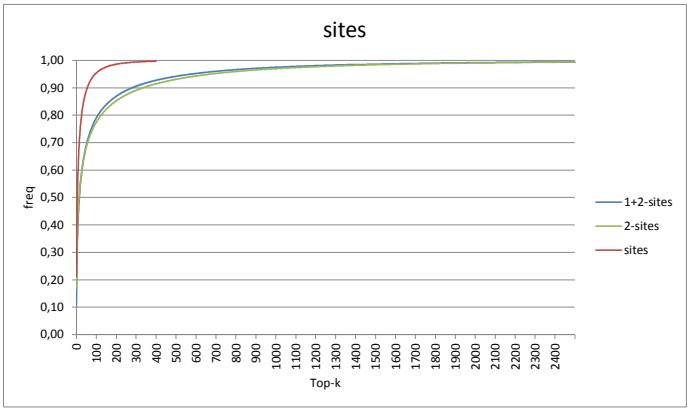

Figure 4 – Web site accesses distribution

B. *Test methodology*

The distinct fuzzifying functions were tested on each of the available users and sessions. Each test returns a ranked list of the suspects. A test is considered to be positive if the real user is returned in the first position of the ranked list. Accuracy measures the ratio of positive tests for each of the function. For each of the tested algorithms tests were performed for multiple values of k.

To evaluate the accuracy of the proposed algorithms against crisp signature algorithms one will present experimental results

obtained using equivalent methods proposed in [2]. In [2] a variety of distance functions were presented to compare signatures. They are generalized from known measures, and take into account both set overlap as well as weighted occurrence. In [2] signatures are k sized tuples with element v_i and a value w_i representing the frequency of the element. Each signature $\Omega_i = \{(v_{ij}, w_{ij}) | j = 1..k_i\}$ has length k_i, let $S_i = \{v_{ij} | j = 1..k_i\}$ be the set of v's in Ω_i. The distances considered were adapted from [2]:

$$D_{jac}(\Omega_1, \Omega_2) = 1 - \frac{S_1 \cap S_2}{S_1 \cup S_2} \quad (5)$$

$$D_{dice}(\Omega_1, \Omega_2) = 1 - \frac{\sum_{v \in S_1 \cap S_2} \min(w_1, w_2)}{\sum_{v \in S_1 \cup S_2} \max(w_1, w_2)} \quad (6)$$

$$D_{hel}(\Omega_1, \Omega_2) = 1 - \frac{\sum_{v \in S_1 \cap S_2} \sqrt{w_1 \cdot w_2}}{\sum_{v \in S_1 \cup S_2} \max(w_1, w_2)} \quad (7)$$

It is easy to verify that all these distance functions yield values in [0, 1]. D_{jac} is based on Jaccard coefficient, where the node weights are not taken into account; it is minimized when S1 = S2, and it equals 1 when their overlap is empty. D_{dice} is an scaled version of the distance based on Dice criterion, which factors in node weights; it gives an added premium if the individual weights in S_1 and S_2 are similar. D_{hel} is based on Hellinger distance .

To better characterize the classifier response ROC curves are presented for every algorithm. ROC curves are a standard measure in statistics [10]. ROC curves map the ratio of false positives against the ratio of true positives, with the false positives in the x-axis and true positives in the y-axis. ROC curves were constructed by first running every test sample against the suspect library and obtaining a ranked list. Let T be the number of tests and U the number of suspects. The total number of elements in the answer lists is TU. The total number of positive tests is T (there is always one correct user for each unknown session) and the number of incorrect tests is $T(U-1)$. The ROC curve starts at the origin (0, 0). For each rank, in ascending order, the number of positive tests p with that rank are used to draw a vertical line upwards by p/T. For the same rank a horizontal line is draw to the right by $(T-p)/(T(U-1))$.

Also a standard measure in statistics, the Area Under the ROC Curve (AUC) [10] can also be computed. AUC is an indicator of the overall accuracy of the classifier, if the AUC is 0.5, the classifier is no better than random selection; higher values indicate better precision. An AUC of 1 indicates a perfect classifier.

C. *Single site fuzzy fingerprints*

The first set of experiments use single site name and port fingerprints. Figure 5 presents the accuracy of fuzzy fingerprints using the three fuzzifying functions described and the results obtained using the three crisp distance functions. The difference between fuzzy and crisp algorithms is very significant. The fuzzy fingerprints deal better with the very sparse nature of the web accesses and significant differences of use in the training and test periods. Differences between the three proposed fuzzifying functions are not very relevant, the Pareto based function achieves the best results, followed closely by the complementary gaussian error function. These functions weight more the most frequent elements.

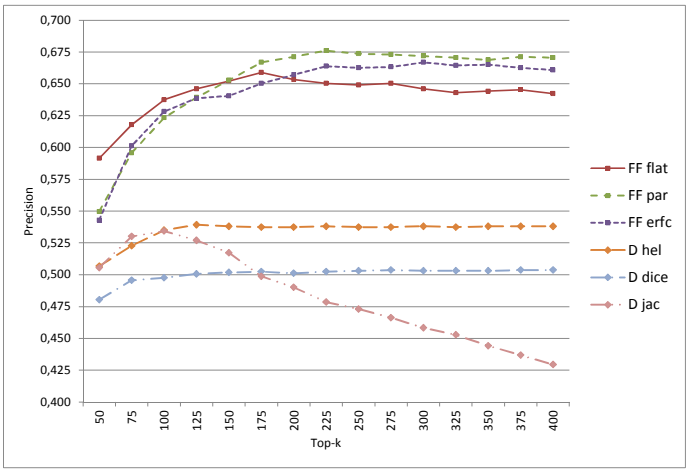

Figure 5 – Algorithms accuracy for single web site access

Figure 6 presents the ROC curve for each of the tested algorithms. To better show the differences Figure 7 presents the zoom of the most relevant area of the ROC.

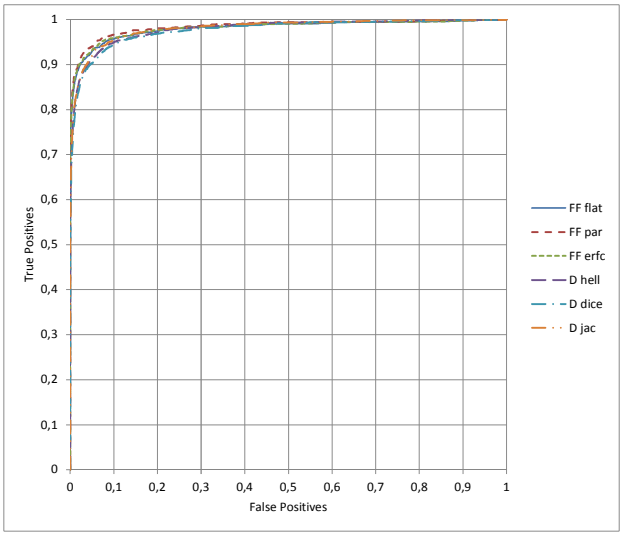

Figure 6 – Algorithms ROC for single web site access

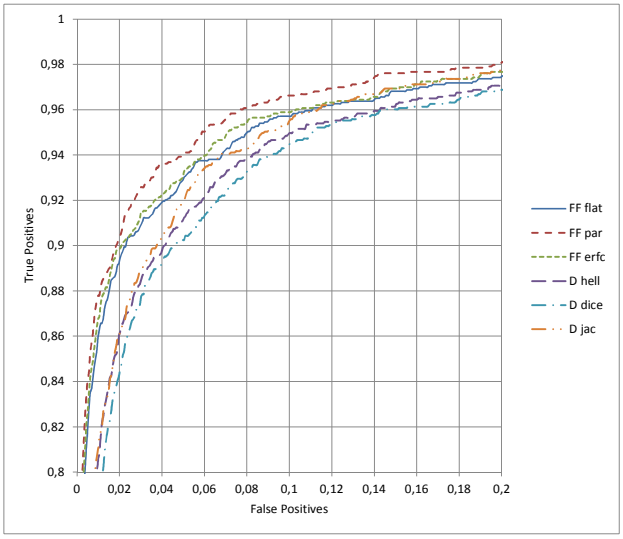

Figure 7 – Detailed ROC for single web site access

D. *Consecutive sites fuzzy fingerprints*

The second set of experiments uses pairs of consecutive site name and port fingerprints. Figure 8 presents accuracy for each of the algorithms. Both crisp and fuzzy algorithms present better results, both can use the extra information contained in the order of the accesses. But this performance increase is only achieved at the expense of much higher number of top-*k* elements. Fuzzy algorithms perform much better than crisp algorithms but is interesting to see that the worst performing algorithm in the single site tests, the Jaccard based distance performes much better with consecutive sites. Fuzzy fingerprints using the Pareto based function achieves the best results, followed closely by the complementary gaussian error function.

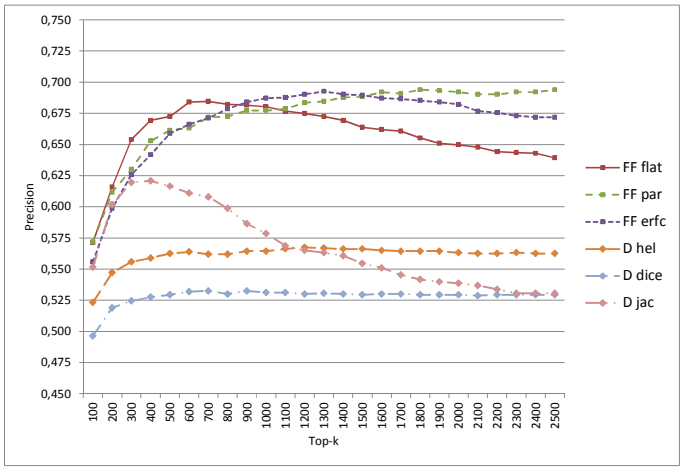

Figure 8 – Algorithms accuracy for consecutive web site accesses

Figure 9 presents the ROC curves. To better show the differences Figure 10 presents the zoom of the most relevant area of the ROC.

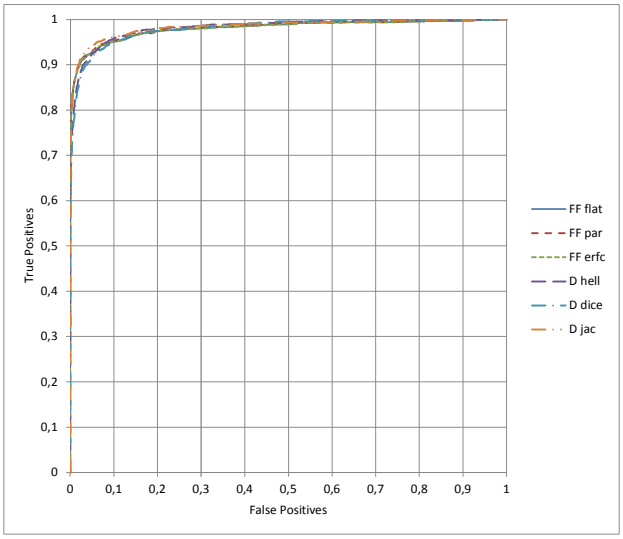

Figure 9 – Algorithms ROC for consecutive web site accesses

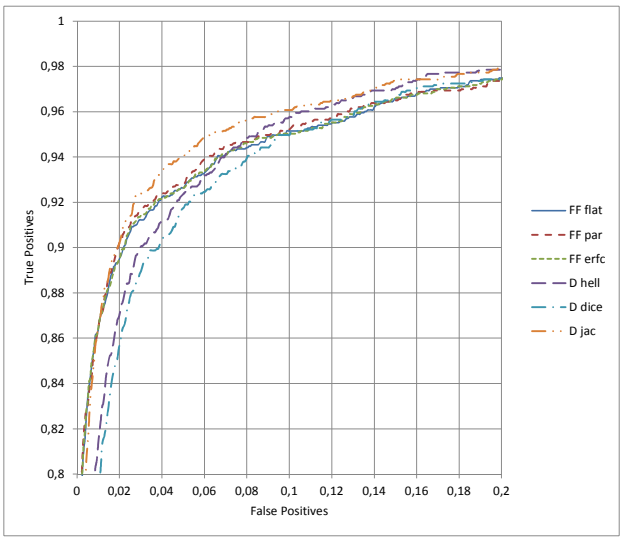

Figure 10 – Detailed ROC for consecutive web site accesses

Interestingly the ROC shows that the Jaccard based distance behaves quite well overall. Although the accuracy of the top choice is not the best of all algorithms, it generates less false positives when the list is enlarged.

E. *Mixture fuzzy fingerprints*

The final set of experiments use both the single site and pairs of consecutive site name and port fingerprints. Both elements are mixed in a single top-k list. Figure 11 presents the accuracy for each of the algorithms.

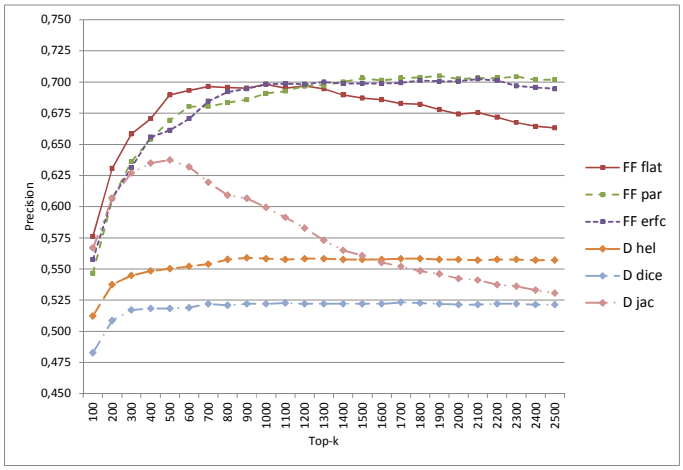

Figure 11 – Algorithms accuracy for mixture fingerprints

Figure 12 and Figure 13 present the corresponting ROC curves.

There is a slight increase in performance of all fuzzy algorithms and for the Jaccard based distance, a slight reduction for the Dice and Hellinger based distances. The most relevant benefict for the use of the mixture is that performance remains stable for a wider range of k. For Pareto and complementary gaussian error based functions the performance remains stable between k values of 1000 to 2500.

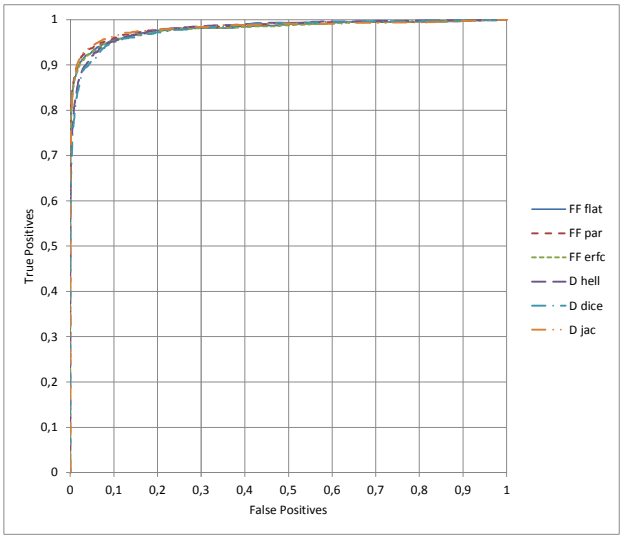

Figure 12 – Algorithms ROC for mixture fingerprints

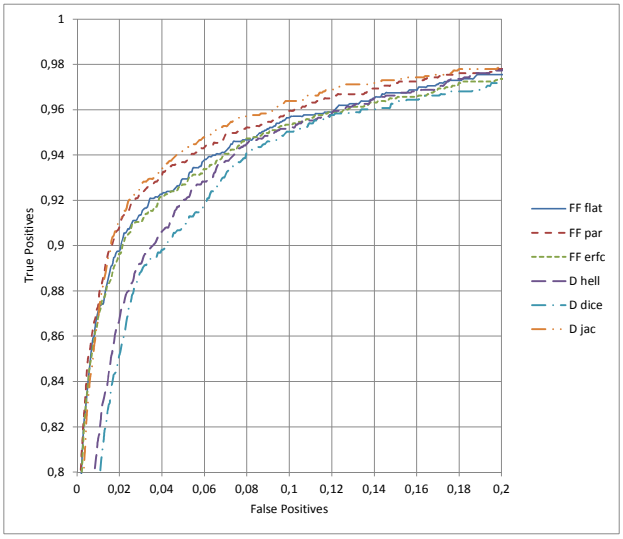

Figure 13 – Detailed ROC for mixture fingerprints

Table I presents the peak performance values for all of the experiments and algorithms. It includes the Area Under the ROC Curve (AUC) [10]. AUC is an indicator of the overall accuracy of the classifier, if the AUC is 0.5, the classifier is no better than random selection; higher values indicate better precision. An AUC of 1 indicates a perfect classifier.

TABLE I. RESULTS FOR EXPERIMENTS WITH WEB SITE ACCESSES

		Fuzzy Fingerprints			**Crisp Distances**		
		flat	***par***	***erfc***	***hell***	***dice***	***jac***
Tests		1630	1630	1630	1630	1630	1630
Users		1630	1630	1630	1630	1630	1630
Single Site	***Peak k***	175	225	300	125	275	100
	Peak Accuracy	0,6589	0,6761	0,6669	0,5393	0,5037	0,5344
	AUC	0,9811	0,9848	0,9819	0,9792	0,9765	0,9810
2 Sites	***Peak k***	700	1800	1300	1200	700	400
	Peak Accuracy	0,6847	0,6939	0,6926	0,5675	0,5325	0,6209
	AUC	0,9802	0,9809	0,9802	0,9822	0,9800	0,9840
1+2 Sites	***Peak k***	1000	1900	2100	900	1700	500
	Peak Accuracy	0,6982	0,7049	0,7025	0,5589	0,5233	0,6374
	AUC	0,9807	0,9829	0,9798	0,9809	0,9786	0,9826

VI. Conclusions and Future Work

This work shows how fuzzy methods may be used to identify the users behind an unidentified web session. The use of simple fuzzy techniques based on approximate algorithms leads to very interesting results.

The fact that the results remain stable for a wide range of values of *k* and for several fuzzification functions shows that the proposed method is robust.

The large number of suspects it supports and the ability to include new suspects or update existing user fuzzy fingerprints is critical to the use of the method in long-term detection processes. New fuzzy fingerprints can be created and added to the suspect's library at any time, and new session logs from known users can be added to the fuzzy fingerprint. Update to one fuzzy fingerprint does not influence all the others.

In this work the method is applied to identifying a author within a list of possible suspects but it can also be applied to the single author problem or to the one or none author within a list by considering the distance (or the inverse comparison) between fuzzy fingerprints as a distinguishing feature. One can then apply a binary classifier, such as a Bayes classifier to determine if the author is a probable one. There is however a significant risk in reducing the complexity of a very high level dimension problem to a single dimension. A candidate should only be tested in this way if all other candidates have been eliminated (i.e., it should only be applied to the top of a list of suspects).

The use of order information, by using consecutive events as base features, enriches the fingerprints, even with such as sparse data as web site names. One can expect that this approach could lead to even better improvements in domains where event order is more relevant.

The proposed method should not be seen as a specific method; it can be used in other domains to identify individual behavior based on events. The proposed method will identify individuals as long as they present a stable event distribution. Future work should also test the inclusion of additional features available in the web logs.

References

[1] R. Bolton and D. Hand, Statistical Fraud Detection: A Review, Statistical Science, Vol. 17, No. 3, 235–255, 2002

[2] G. Cormode, F. Korn, S. Muthukrishnan, Yihua Wu, On signatures for communication graphs, IEEE 24th International Conference on Data Engineering (ICDE), 2008.

[3] C. Cortes and D. Pregibon, Signature-Based Methods for Data Streams. Data Mining and Knowledge Discovery 5: 167-182, 2001

[4] T. Fawcett, and F. Provost, Activity monitoring: Noticing Interesting Changes in Behavior. Proc. of SIGKDD99, 53-62, 1999

[5] P. Ferreira, R. Alves, O. Belo and L. Cortesão, Establishing Fraud Detection Patterns Based on Signatures, Proceedings of the 6th Industrial Conference on Data Mining, ICDM2006, Lecture Notes in Computer Science, Springer, 2006

[6] N. Homem and J. Carvalho, Estimating Top-k Destinations in Data Streams, Computational Intelligence for Knowledge-Based Systems Design, Springer Berlin / Heidelberg, pages 290-299, 2010.

[7] N. Homem and J. Carvalho, Finding top-k elements in data streams, Information Sciences, 180(24), pp. 4958-4974, Dec. 2010, Elsevier.

[8] L. Kóczy, Vector valued fuzzy sets, BUSEFAL- BULL STUD EXCH FUZZIN APPL, pages 41–57, 1980.

[9] L. Kóczy, T. Vámos, G. Biró, Fuzzy signatures, in: EUROFUSE-SIC99, 1999.

[10] S. Mason and N. Graham, Areas beneath the relative operating characteristics (ROC) and relative operating levels (ROL) curves: Statistical significance and interpretation. Q. J. R. Meteorol. Soc, 30:291–303, 1982.

[11] A. Metwally, D. Agrawal and A. Abbadi, Efficient Computation of Frequent and Top- k Elements in Data Streams, Technical Report 2005-23, University of California, Santa Barbara, September 2005.

[12] C. Phua, V. Lee, K. Smith and R. Gayler, Comprehensive Survey of Data Mining-based Fraud Detection Research, Artificial Intelligence Review, 2005.

2011 IEEE International Conference on Fuzzy Systems
June 27-30, 2011, Taipei, Taiwan

Fuzzy Multiattribute Evaluation of Airport Performance

Chung-Hsing Yeh and Yu-Liang Kuo
Faculty of Information Technology
Monash University
Clayton, Victoria 3800, Australia
E-mail: ChungHsing.Yeh@infotech.monash.edu.au

Yu-Hern Chang
Department of Transportation and Communications Management
National Cheng Kung University, Tainan, Taiwan
E-mail: yhchang@mail.ncku.edu.tw

Abstract— **This paper presents a fuzzy multiattribute decision making (MADM) approach to evaluating airport performance in terms of the airport operator, the passenger, and the airline dimensions. Assessments for quantitative measures are represented by crisp values, and assessments for qualitative measures and attribute weights are represented by triangular fuzzy numbers, obtained via surveys using linguistic terms. An effective algorithm is developed by using the α-cut concept for incorporating the decision-maker's confidence level about respondents' fuzzy assessments on performance ratings and attribute weights. Based on the concept of the degree of optimality, the algorithm obtains a quantitative performance index for each airport evaluated, relative to other comparable airports with respect to each of three evaluation dimensions individually and all three evaluation dimensions as a whole. The performance index obtained would help individual airports understand the comparative level of their performance on measures relating to operational management, airport facilities, and passenger service quality. An empirical study of performance evaluation of 11 Asia-Pacific major international airports is conducted to illustrate how the approach works.**

Keywords-Fuzzy multiattribute decision making; Airport performance evaluation; TOPSIS

I. INTRODUCTION

The operation efficiency and service quality of international airports are critical in the modern-day context where businesses are international and people are more mobile. To help an airport identify functional areas for improvement, it is advisable to evaluate its performance relative to other comparable airports with respect to a number of manageable attributes (evaluation criteria). As the evaluation is based on a comparative process, the evaluation result can be used as a service benchmarking and management tool for airports. The most comprehensive study of comparing service performance of international airports is probably the International Air Transport Association (IATA) Global Airport Monitor. Despite a wide coverage of performance indicators for airport services, no attempt was made by IATA to develop an integrated airport performance index.

Quite a few studies on airport performance evaluation have been reported in the literature with focus on specific functional areas of airport operations, such as productivity [1]–[4], capacity and delays [5], efficiency [6]–[8], airline services [9], competitiveness [10], [11], financial performance [12], service quality [13]–[15]. Although there is no universal and exact definition for airport performance, the overall performance of airports can be measured from the viewpoints of passengers, airlines, and the airport operator [16]. The most widely used airport performance evaluation methods are perhaps the data envelopment analysis (DEA) and total factor productivity (TFP) [3], [6]–[8], [17], [18]. Although these methods are well suited for measuring the efficiency of airport operations based on resource input measures and performance output measures, they do not intend to address the effectiveness issue with respect to the overall performance of airports from the viewpoints of the airport operator, passengers, and airlines as a whole.

The evaluation of the overall performance of airports is a complex decision-making process, as it usually involves (a) multiple conflicting criteria with non-commensurable units and (b) both crisp and fuzzy data derived from precise measures of quantitative criteria and imprecise judgments of qualitative criteria resulting from human subjectivity. Multiattribute decision making (MADM) has proven to be an effective approach for ranking a finite number of alternatives characterized by multiple conflicting criteria [19]. The most widely used theory in solving MADM problems is multiattribute utility theory [20] or multiattribute value theory (MAVT) [21], with which a cardinal preference or ranking of the decision alternatives is generated. Fuzzy set theory has proven to be a powerful modeling tool for coping with the subjectiveness and imprecision of human judgments [22], [23]. In the applications of MAVT-based MADM for evaluation and selection problems involving subjective judgments of the decision maker, fuzzy MADM has demonstrated its applicability in ranking decision alternatives such as transportation systems (e.g. [10], [24]–[28]).

In this paper, we formulate the evaluation of airport performance as a fuzzy MADM problem that requires cardinal ranking. To obtain a quantitative airport performance index, we develop an algorithm based on the concept of the degree of optimality. In subsequent sections, we first discuss the performance measures suitable for evaluating the airport performance from the perspectives of the airport operator, passengers, and airlines. We then present the fuzzy MADM

978-1-4244-7316-8/11/$26.00 ©2011 IEEE

approach to the performance evaluation problem. Finally we conduct an empirical study to measure and compare the overall performance of 11 major Asia-Pacific international airports.

II. AIRPORT PERFORMANCE MEASURES

The use of performance measures (attributes) in airport evaluation problem is crucially important because of its specific economic characteristics. In the business competitive environment optimal performance can be equated with profitability. However, the conditions under which airports operate are far from competitive. Regulatory, geographical, economic, social and political constraints all hinder direct competition between airports [29]. Various performance attributes or measures can be used to evaluate the airport performance from the perspectives of different stakeholders of the airport operation, depending on the objectives of the evaluation problem. In the case of airport performance evaluation, the airport operator (service provider) would focus more on measures concerned with the operational efficiency of the airport. Passengers are more interested in measures relating to service quality and safety. Airlines are more concerned about the facilities provided by the airport. As such, to reflect the operating characteristics of international airports, the criteria for performance evaluation should be constructed from the perspectives of the airport operator, passengers, and airlines. Fig. 1 shows the hierarchical structure of the airport evaluation problem to be addressed in the paper. The three evaluation dimensions and their associated performance measures are discussed below.

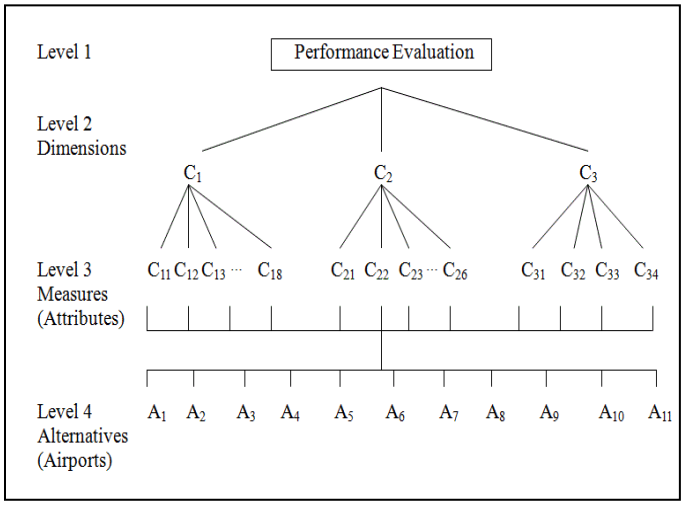

Figure 1. Hierarchy structure for airport performance evaluation.

The airport operator dimension (C_1) is mainly concerned with airport operational management and the facilities provided for the airport users. The airport operator is assessed quantitatively based on the airport operational data, including revenue (C_{11}) (total operating revenue), annual growth rate (C_{12}) (annual growth rate of total passenger volume), airport terminal size (C_{13}) (total terminal surface area of airport), navigation Aids (C_{14}) (category of the navigation aid system), ground access facilities (C_{15}) (types of ground transportation to/from city), distance to CBD (C_{16}) (distance from the airport to the central business district), car park (C_{17}) (number of parking car bays), noise pollution (C_{18}) (number of aircraft movement per day).

The passenger dimension (C_2) relates to the services provided by the airport and the quality level as perceived by the passengers. These service measures include comfort (C_{21}) (congestion level and cleanliness in the terminal building), processing time (C_{22}) (total time required during check-in, immigration inspection and customs), convenience (C_{23}) (availability and accessibility of airport facilities within the terminal building), courtesy of staff (C_{24}) (helpfulness and friendliness of airport staff), information visibility (C_{25}) (information display for flights, airport facilities, and signposting), security (C_{26}) (safety measures and security facilities). These service attributes are to be measured based on passengers' perception, which are to be assessed subjectively by a survey process using a set of linguistic terms characterized by fuzzy numbers.

The airline dimension (C_3) is mainly concerned with the facilities provided by airports such as gates, operating hours, aircraft movement and runways. Its performance measures include aircraft movement (C_{31}) (total number of aircraft movement), gates (C_{32}) (number of gates), operating hours (C_{33}) (total daily operating hours of the airport), runway (C_{34}) (number of runways).

The performance measures discussed above involve both quantitative and qualitative assessments, for which numerical data and fuzzy numbers are to be used respectively. These measures are independent of each other, thus suitable for use in an MAVT-based MADM model.

III. THE FUZZY MULTIATTRIBUTE DECISION MAKING APPROACH

A. The Evaluation Problem

In this paper, we formulate the airport performance evaluation as a fuzzy MADM problem that requires cardinal ranking. The problem involves a set of m airports (alternatives) A_i ($i = 1, 2, ..., m$), which are to be evaluated based on n evaluation dimensions C_j ($j = 1, 2, ...,n$), each of which is represented by a set of p_j performance measures (attributes) C_{jk} ($k = 1, 2, ..., p_j$). Assessments are to be given to determine (a) the weight vectors $W = (w_1, w_2, \ldots, w_j, ..., w_n)$ and $W_j = (w_{j1}, w_{j2}, ..., w_{jk}, ..., w_{jp_j})$ ($j = 1, 2, ..., n; k = 1, 2, ..., p_j$), and (b) the decision matrices $Y_{C_j} = \{y_{ki}, k = 1, 2, ..., p_j; i = 1, 2, ..., m\}$ ($j = 1, 2, ..., n$) and $X = \{x_{ij}, i = 1, 2, ..., m; j = 1, 2, ..., n\}$.

The weight vectors W and W_j represent the relative importance of n evaluation dimensions C_j ($j = 1, 2, ..., n$) and p_j performance measures C_{jk} ($k = 1, 2, ...,p_j$) for the problem and their corresponding dimension respectively. The weight vectors are to be assessed subjectively by airport experts via surveys, using the set of linguistic terms defined in Table I. Linguistic terms have been found intuitively easy to use in

expressing the subjectiveness and imprecision of the decision maker's assessments [23], [30]–[32]. To facilitate the making of qualitative assessments by respondents, a set of linguistic terms is used. Each linguistic term is characterized by a triangular fuzzy number for representing its approximate value range between 1 and 9, denoted as (a_1, a_2, a_3), where $1 \le a_1 \le a_2 \le a_3 \le 9$. a_2 is the most possible value of the term, and a_1 and a_3 are the lower and upper bounds respectively used to reflect the fuzziness of the term. As such, w_j in W and w_{jk} in W_j are the fuzzy weights of evaluation dimensions C_j (j = 1, 2, ..., m) and performance measures C_{jk} (k = 1, 2, ..., p_j), respectively.

TABLE I. LINGUISTIC TERMS USED FOR DETERMINING THE WEIGHT VECTOR

Linguistic Term	Not Important (NI)	Somewhat Important (SI)	Important (I)	Very Important (VI)	Extremely Important (EI)
Membership Function	(1,1,3)	(1,3,5)	(3,5,7)	(5,7,9)	(7,9,9)

In practical applications, the triangular form of the membership function is used most often for representing fuzzy numbers that characterize linguistic information [33], [34]. The popular use of triangular fuzzy numbers is mainly attributed to their simplicity in both concept and computation. Theoretically, the merits of using triangular fuzzy numbers in fuzzy modeling have been well justified [35]. With the simplest form of the membership function, triangular fuzzy numbers constitute an immediate solution to the optimization problems in fuzzy modeling.

The decision matrices Y_{C_j} represent the performance ratings (y_{ki}) of airport A_i with respect to each performance measure C_{jk} (k = 1, 2, ..., p_j) of the corresponding evaluation dimension C_j. These performance ratings are given based on quantitative and qualitative assessments. While the quantitative assessments are straightforward based on the data available, the qualitative assessments require subjective judgments of airport experts to reflect the degree to which each airport satisfies each qualitative safety measure. The set of linguistic terms defend in Table II is used by airport experts to assess the qualitative performance ratings via surveys.

TABLE II. LINGUISTIC TERMS USED FOR DETERMINING PERFORMANCE RATINGS

Linguistic Term	Very Poor (VP)	Poor (P)	Fair (F)	Good (G)	Very Good (VG)
Membership Function	(1,1,3)	(1,3,5)	(3,5,7)	(5,7,9)	(7,9,9)

The decision matrix $X = \{x_{ij}, i = 1, 2, ..., m; j = 1, 2, ..., n\}$ represents the performance ratings of airport A_i with respect to evaluation dimension C_j. While Y_{C_j} (j = 1, 2, ..., n) are given based on the assessments made on the airports, the decision matrix X is constructed by aggregating the weighted assessments from lower-level performance measures of each evaluation dimension C_j. Given the fuzzy weight vectors (W and W_j) and fuzzy decision matrices (X and Y_{C_j}), the objective of the problem is to rank all the airports by giving each of them an overall airport performance index with respect to all evaluation dimensions.

B. The Solution Procedure

The algorithm begins with the generation of the decision matrix X by multiplying the weight vector W_j by the decision matrix Y_{C_j}, as

$$\left(x_{1j}, x_{2j}, ..., x_{mj}\right) = W_j Y'_{C_j} \Big/ \sum_{k=1}^{p_j} w_{jk}, \; j = 1, 2, ..., n. \quad (1)$$

where Y'_{C_j} (i = 1, 2, ..., m) are the normalized decision matrices by

$$y'_{ki} = y_{ki} \Big/ \sqrt{\sum_{i=1}^{n} (y_{ki})^2}, \; i = 1, 2, ..., m; \; k = 1, 2, ..., p_j. \quad (2)$$

The normalization process is required to allow a comparable scale for all performance measures, assessed by different measurement units.

In (1), (x_{1j}, x_{2j}, …, x_{mj}) is a fuzzy decision vector in X, which is obtained from a normalized value function that multiplies the weight vector W_j for its lower-level sub-criteria C_{jk} by the corresponding normalized decision matrix Y'_{Cj}. With the use of triangular fuzzy numbers, the arithmetic operations on fuzzy numbers are based on interval arithmetic [36].

The algorithm then generates a fuzzy performance matrix by multiplying the weight vector W by the decision matrix X, as given in (3).

$$Z = \begin{bmatrix} w_1 x_{11} & w_2 x_{12} & \cdots & w_n x_{1n} \\ w_1 x_{21} & w_2 x_{22} & \cdots & w_n x_{2n} \\ \cdots & \cdots & \cdots & \cdots \\ w_1 x_{m1} & w_2 x_{m2} & \cdots & w_n x_{mn} \end{bmatrix} \quad (3)$$

By using the concept of α-cut on the fuzzy numbers in the performance matrix, an interval performance matrix is derived as given in (4), where $0 \le \alpha \le 1$. For a given α, z_{ijl}^{α} and z_{ijr}^{α} (i = 1, 2, ..., m; j = 1, 2, ..., n) are the average of the lower bounds and upper bounds of the crisp intervals respectively, resulted from all α-cuts using the alpha values equal to or greater than the specified value of α.

$$Z_{\alpha} = \begin{bmatrix} \left[z_{11l}^{\alpha}, z_{11r}^{\alpha}\right] & \left[z_{12l}^{\alpha}, z_{12r}^{\alpha}\right] & \cdots & \left[z_{1nl}^{\alpha}, z_{1nr}^{\alpha}\right] \\ \left[z_{21l}^{\alpha}, z_{21r}^{\alpha}\right] & \left[z_{22l}^{\alpha}, z_{22r}^{\alpha}\right] & \cdots & \left[z_{2nl}^{\alpha}, z_{2nr}^{\alpha}\right] \\ \cdots & \cdots & \cdots & \cdots \\ \left[z_{m1l}^{\alpha}, z_{m1r}^{\alpha}\right] & \left[z_{m2l}^{\alpha}, z_{m2r}^{\alpha}\right] & \cdots & \left[z_{mnl}^{\alpha}, z_{mnr}^{\alpha}\right] \end{bmatrix} \quad (4)$$

The value of α represents the decision maker's degree of confidence in the fuzzy assessments, given by the respondents with respect to attribute weights and performance ratings of airports. A larger α value indicates that the decision maker is

more confident in choosing a crisp value interval to represent the corresponding fuzzy number, as the interval is smaller and has a higher possibility. This implies that a confident decision maker would not consider less possible values embedded in a fuzzy number.

To reflect the decision maker's relative preference between z_{ijl}^{α} and z_{ijr}^{α} in (4), a preference index λ in the range of 0 and 1 is incorporated in the algorithm. As a result, a crisp performance matrix is obtained as

$$Z_{\alpha}^{\lambda'} = \begin{bmatrix} z_{11\alpha}^{\lambda'} & z_{12\alpha}^{\lambda'} & \cdots & z_{1m\alpha}^{\lambda'} \\ z_{21\alpha}^{\lambda'} & z_{22\alpha}^{\lambda'} & \cdots & z_{2m\alpha}^{\lambda'} \\ \cdots & \cdots & \cdots & \cdots \\ z_{n1\alpha}^{\lambda'} & z_{n2\alpha}^{\lambda'} & \cdots & z_{nm\alpha}^{\lambda'} \end{bmatrix} \quad (5)$$

where $z_{ij\alpha}^{\lambda'} = \lambda z_{ijr}^{\alpha} + (1-\lambda) z_{ijl}^{\alpha}$, $0 \le \lambda \le 1$, *i = 1, 2, ..., m; j = 1, 2, ..., n*. The use of λ allows the algorithm to reflect the decision maker's attitude towards risk, which may be optimistic, pessimistic or somewhere in between. In actual decision settings, λ = 1, λ = 0.5, or λ = 0 can be used to indicate that the decision maker has an optimistic, moderate, or pessimistic view respectively on fuzzy assessment results. An optimistic decision maker is apt to prefer higher values of the crisp value interval derived from fuzzy assessments, while a pessimistic decision maker tends to favor lower values.

To solve the multiattribute evaluation problem characterized by the perform matrix in (5), an effective method is applied. The method is based on the concept of the degree of optimality rooted in an alternative where multiple attributes (criteria) characterize the notion of the best [37]. In the context of MADM, the concept suggests that the most preferred alternative should not only have the shortest distance from the positive ideal solution (or the best alternative), but also have the longest distance from the negative ideal solution (or the worst alternative). The positive (or negative) ideal solution consists of the best (or worst) attribute values attainable from all the alternatives if each attribute takes monotonically increasing or decreasing values [19]. This concept has been implemented by a widely used MADM method called the technique for order preference by similarity to ideal solution (TOPSIS) [19] and has been applied under different decision contexts [38]–[44]. This is mainly due to (a) its applicability in solving various practical decision problems, (b) its simplicity and comprehensibility, (c) its computational efficiency, and (d) its ability to measure the relative performance of the alternatives in a simple mathematical form.

Based on the concept presented above, the positive ideal solution $A_{\alpha}^{\lambda+}$ and the negative ideal solution $A_{\alpha}^{\lambda-}$ can be determined from (5) by selecting the maximum value and the minimum value respectively across all alternatives (airports) with respect to each service attribute, as given in (6) and (7).

$$\begin{aligned} A_{\alpha}^{\lambda+} &= \left(z_{1\alpha}^{\lambda+}, z_{2\alpha}^{\lambda+}, \ldots, z_{n\alpha}^{\lambda+}\right) \\ A_{\alpha}^{\lambda-} &= \left(z_{1\alpha}^{\lambda-}, z_{2\alpha}^{\lambda-}, \ldots, z_{n\alpha}^{\lambda-}\right) \end{aligned} \quad (6)$$

where

$$\begin{aligned} z_{j\alpha}^{\lambda+} &= \max\left(z_{1j\alpha}^{\lambda}, z_{2j\alpha}^{\lambda}, \ldots, z_{mj\alpha}^{\lambda}\right) \\ z_{j\alpha}^{\lambda-} &= \min\left(z_{1j\alpha}^{\lambda}, z_{2j\alpha}^{\lambda}, \ldots, z_{mj\alpha}^{\lambda}\right) \end{aligned}, \; j = 1, 2, \ldots, n \quad (7)$$

$A_{\alpha}^{\lambda+}$ and $A_{\alpha}^{\lambda-}$ represent the performance vectors of the best possible airport and the worst possible airport on *n* service attributes respectively.

Like the performance vectors in (6), the weighted overall performance of airport A_i on service attributes C_j (*j=1, 2,..., n*) can be expressed as a performance vector of *n* elements. Thus, we can apply the vector matching technique to measure how close a particular airport is to the best possible airport and to the worst possible airport, given respectively as

$$S_{i\alpha}^{\lambda+} = \frac{A_{i\alpha}^{\lambda} A_{\alpha}^{\lambda+}}{\max\left(A_{i\alpha}^{\lambda} A_{i\alpha}^{\lambda}, A_{\alpha}^{\lambda+} A_{\alpha}^{\lambda+}\right)} \quad (8)$$

$$S_{i\alpha}^{\lambda-} = \frac{A_{i\alpha}^{\lambda} A_{\alpha}^{\lambda-}}{\max\left(A_{i\alpha}^{\lambda} A_{i\alpha}^{\lambda}, A_{\alpha}^{\lambda-} A_{\alpha}^{\lambda-}\right)}, \; i=1, 2, \ldots, m \quad (9)$$

$A_{i\alpha}^{\lambda}$ is the i^{th} row of the performance matrix in (5), representing the corresponding performance vector of airport A_i with respect to service attribute C_j. $S_{i\alpha}^{\lambda+}$ and $S_{i\alpha}^{\lambda-}$ represent the degree of similarity between airport A_i and the positive ideal solution and the negative ideal solution respectively.

For a given decision maker's degree of confidence level (α) in fuzzy assessments and a given index of optimism (λ), an overall performance index for each airport can be determined by

$$P_{\alpha i}^{\lambda} = \frac{S_{i\alpha}^{\lambda+}}{S_{i\alpha}^{\lambda+} + S_{i\alpha}^{\lambda-}}, \; i=1, 2, \ldots, m. \quad (10)$$

The rationale behind (10) is that that a preferred alternative should have a higher degree of similarity to the positive ideal solution and a lower degree of similarity to the negative ideal solution [19]. The larger the performance index, the better the overall service performance of the airport, relative to other airports. As such, the performance index generated is a relative concept, and indicates the relative ranking of the airports evaluated in terms of service attributes.

IV. Empirical Study of 11 Asia-Pacific International Airports

To illustrate how the fuzzy MADM approach works, we conducted an empirical study on 11 major international airports in the Asia-Pacific region. Air travel demand in the Asia-Pacific region had an average annual growth rate of 10.1% during the past decade, the highest in the world. A high rate of economic growth in Asia has spurred the rapid expansion of commercial aviation industries serving the Asia-Pacific region. With 16 of the world's 25 busiest air routes, Asia's major airports are already near capacity. Asia's explosive economic growth has been accompanied by rapid expansion and the transformation of the region's aviation industry. Air transportation is expected to play a larger role in this region more than anywhere else in the world. First, the high

population and income growth rates in many Asian countries are expected to produce an astounding increase in the demand for air transportation services. The region already accounts for more than 50 per cent of the world's population. Second, vast distances separate many Asia-Pacific countries. About 60 per cent of the air routes in the region are between cities that are at least 2,000 kilometers apart, and a number of countries in the region are islands or archipelagos with few alternatives to air passenger travel [45].

The purpose of this study is to evaluate the performance of Asia-Pacific's 11 major international airports on measures relating to operational management, passenger service quality, and airport facilities. The 11 major airports selected process more than half of the region's international traffic. These airports are (A_1) Incheon International Airport - Incheon (ICN), (A_2) Chek Lap Kok International Airport - Hong Kong (HKG), (A_3) Suvarnabhumi International Airport - Bangkok (BKK), (A_4) Narita International Airport - Tokyo (NRT), (A_5) Changi International Airport - Singapore (SIN), (A_6) Kingsford Smith International Airport - Sydney (SYD), (A_7) Kansai International Airport - Osaka (KIX), (A_8) Capital International Airport - Beijing (PEK), (A_9) Taoyuan International Airport - Taipei (TPE), (A_{10}) Tullamarine International Airport - Melbourne (MEL) and (A_{11}) Pudong International Airport - Shanghai (PVG). The performance of these 11 airports is to be evaluated based on the three dimensions and their associated performance measures as shown in Fig. 1.

In this study, we use equal weights for the three evaluation dimensions, i.e. W = (1, 1, 1). The weights of performance measures within each dimension are assessed by airport experts using the linguistic terms defined in Table I. Table III shows the assessment result.

TABLE III. WEIGHT VECTOR FOR EVALUATION DIMENSIONS

Weight Vector	Fuzzy Weights for Performance Measures
W	(1, 1, 1)
W_1 (Airport operator)	(VI, EI, VI, I, I, I, VI, I)
W_2 (Passenger)	(VI, VI, VI, EI, I, VI)
W_3 (Airline)	(I, VI, VI, I)

The assessment results of the performance measures for the airport operator and the airline dimensions are obtained from the available data for 2008 as crisp data, as given in Tables IV and V respectively. The assessment for qualitative performance measures of the passenger dimension is made by surveys of 15 international tour guides using the linguistic terms defined in Table II. Table VI shows the assessment result.

With the data in Tables III - VI, the decision matrix for the three evaluation dimensions can be calculated by (1). The fuzzy performance matrix in (3) can then be obtained by multiplying this decision matrix by the weight vector W of equal weights. By applying the algorithm given as in (4)-(10) with $\alpha = 0$ and $\lambda = 0.5$, we can obtain an airport performance index for each airport with respect to each evaluation dimension individually and all the three dimensions as a whole. Table VII shows the result and the corresponding ranking order.

TABLE IV. ASSESSMENT DATA FOR THE AIRPORT OPERATOR DIMENSION

Air-port	Revenue 000,000 ' (C_{11})	Annual Growth Rate % (C_{12})	Airport Terminal Size '000 m^2 (C_{13})	Navig-ation Aids (C_{14})	Ground Access (C_{15})	Distance to CBD km (C_{16})	Car Park (C_{17})	Noise Pollution (C_{18})
A_1	973	-4	600	2	3	52	11,303	578
A_2	1,120	1.7	710	3	2	40	4,010	811
A_3	206	-6.3	283	3	2	25	5,000	208
A_4	1,830	-5.6	789	2	2	65	9,144	530
A_5	921	2.7	1,043	2	2	20	5,420	614
A_6	773	3	387	2	2	8	11,500	819
A_7	959	-2.5	330	2	3	50	6,133	366
A_8	561	4.4	1,382	2	2	26	7,000	1,177
A_9	346	-4	487	2	1	40	6,441	367
A_{10}	370	7.9	127	3	1	24	6,700	530
A_{11}	482	-2.4	824	1	3	30	3,000	728

TABLE V. ASSESSMENT DATA FOR THE AIRLINE DIMENSION

Airport	Aircraft Movements (C_{31})	Gates (C_{32})	Operating Hours (C_{33})	Runway (C_{34})
A_1	211,102	90	24	3
A_2	296,000	106	24	2
A_3	267,480	51	24	2
A_4	193,321	87	17	3
A_5	231,900	102	24	2
A_6	298,964	65	17	3
A_7	133,502	52	24	2
A_8	429,646	120	24	3
A_9	134,072	55	24	2
A_{10}	193,500	62	24	2
A_{11}	265,735	98	24	3

TABLE VI. ASSESSMENT DATA FOR THE PASSENGER DIMENSION

Airport	Comfort (C_{21})	Processing Time (C_{22})	Conve-nience (C_{23})	Courtesy of Staff (C_{24})	Information Visibility (C_{25})	Security (C_{26})
A_1	G	G	F	F	F	G
A_2	G	G	G	G	G	G
A_3	F	F	F	F	F	F
A_4	G	F	F	G	G	G
A_5	VG	G	G	G	G	G
A_6	F	F	F	F	F	F
A_7	G	G	F	G	F	G
A_8	F	F	F	F	F	F
A_9	F	G	F	F	F	F
A_{10}	F	F	F	F	F	G

A_{11}	F	F	F	F	F	F

TABLE VII. AIRPORT PERFORMANCE INDEX AND RANKING OF 11 AIRPORTS

Airport	Overall		C_1		C_2		C_3	
	Index	*Ranking*	*Index*	*Ranking*	*Index*	*Ranking*	*Index*	*Ranking*
A_1 (Incheon)	1.414	7	0.369	8	0.512	4	0.533	4
A_2 (Hong Kong)	1.595	4	0.470	5	0.557	2	0.568	3
A_3 (Bangkok)	1.392	8	0.445	6	0.481	7	0.465	8
A_4 (Tokyo)	1.446	6	0.431	7	0.525	3	0.490	7
A_5 (Singapore)	1.681	2	0.587	2	0.570	1	0.524	5
A_6 (Sydney)	1.527	5	0.566	3	0.439	11	0.522	6
A_7 (Osaka)	1.235	10	0.354	9	0.506	5	0.374	11
A_8 (Beijing)	1.695	1	0.552	4	0.463	10	0.680	1
A_9 (Taipei)	1.122	11	0.257	11	0.485	6	0.379	10
A_{10} (Melbourne)	1.671	3	0.763	1	0.480	8	0.428	9
A_{11} (Shanghai)	1.367	9	0.329	10	0.465	9	0.572	2

The settings used for α and λ reflect that the decision maker has no particular preference for the fuzzy assessment results made by the respondents. $\alpha = 0$ implies that the mean value of a fuzzy number; that is, the average of value intervals of all α-cuts on the fuzzy number is used. $\lambda = 0.5$ indicates that the decision maker has a moderate attitude towards the respondents' assessments; that is, the decision maker weights all the values derived from fuzzy assessments equally.

In terms of the overall performance, the Beijing, Singapore, and Melbourne airports perform best, while the Taipei, Osaka and Shanghai airports have the worst performance. On the airport operator dimension, the Melbourne airport ranks first with a good performance in all measures, while the Taipei airport ranks last, mainly because of its poor performance in the areas of revenue, annual growth rate, and ground access. The Melbourne airport performs exceptionally well on this dimension as compared with its performance on other dimensions, mainly due to its highest annual growth rate among all the airports. On the passenger dimension, the Singapore, Hong Kong, and Tokyo airports perform exceptionally well based on passengers' perception of airport service quality, while the Sydney, Beijing and Shanghai airports provide relatively poor passenger service quality. On the airline dimension, the Beijing, Shanghai and Hong Kong airports have the best performance, while the Osaka and Taipei airports perform worst.

To examine whether the confidence level (the α value) and the risk attitude (the λ value) may affect the evaluation result presented in Table VII, a sensitivity analysis process was carried out by changing the values of α and λ. Table VIII shows three representative evaluation results under three typical settings of λ regardless of the settings of α. Fig. 2 shows some representative evaluation results under various settings of α and λ. As shown in Table VIII and Fig. 2, when the risk attitude is pessimistic or moderate ($\lambda = 0$ or $\lambda = 0.5$), the ranking result is not consistent. This implies that the decision maker's attitude towards the handling of the uncertainty associated with the fuzzy assessments in this case study does have significant influence on the evaluation result in terms of relative ranking. This is mainly due to the fact that these airports have relatively similar performances on the passenger service quality dimension than the other two dimensions. No airport appears to have a dominating performance in all three evaluation dimensions.

TABLE VIII. OVERALL AIRPORT PERFORMANCE INDEX AND RANKING UNDER VARIOUS RISK ATTITUDES

Airport	$\lambda = 0$		$\lambda = 0.5$		$\lambda = 1$	
	Index	*Ranking*	*Index*	*Ranking*	*Index*	*Ranking*
A_1 (Incheon)	1.439	7	1.414	7	1.395	8
A_2 (Hong Kong)	1.679	3	1.595	4	1.558	4
A_3 (Bangkok)	1.119	10	1.392	8	1.478	6
A_4 (Tokyo)	1.496	5	1.446	6	1.419	7
A_5 (Singapore)	1.777	1	1.681	2	1.636	3
A_6 (Sydney)	1.485	6	1.527	5	1.527	5
A_7 (Osaka)	1.235	9	1.235	10	1.223	10
A_8 (Beijing)	1.703	2	1.695	1	1.677	1
A_9 (Taipei)	1.104	11	1.122	11	1.119	11
A_{10} (Melbourne)	1.656	4	1.671	3	1.667	2
A_{11} (Shanghai)	1.345	8	1.367	9	1.363	9

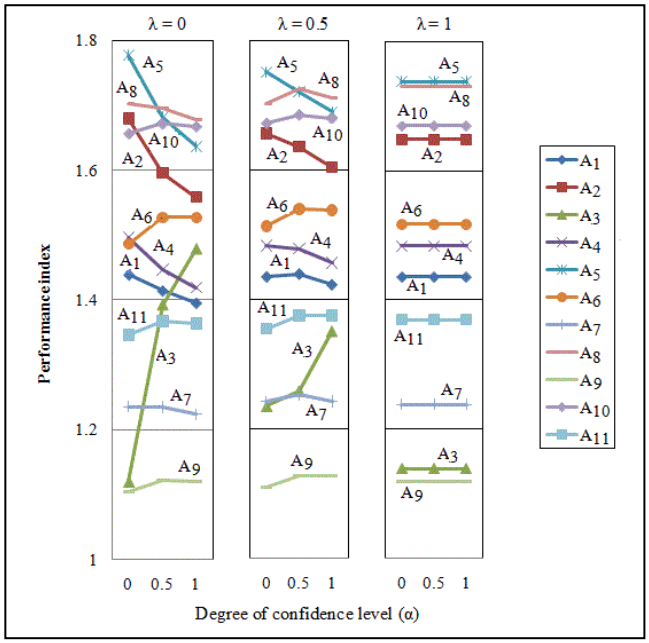

Figure 2. Overall airport performance index and ranking under various decision settings.

The performance index obtained would help airports understand the comparative level of their performance on

measures relating to operational management, airport facilities, and passenger service quality. With its relative concept, the index serves as a performance benchmarking and management tool for airports, as it can identify functional areas for performance improvement.

V. CONCLUSION

Airport performance evaluation requires considering multiple evaluation criteria structured in multi-level hierarchies. The evaluation often involves both quantitative and qualitative assessment data. In this paper, we have formulated airport performance evaluation as a fuzzy MADM problem that requires cardinal ranking of all airports. As an effective alternative to airport performance evaluation, the fuzzy MADM approach developed can effectively handle both quantitative and qualitative performance measures with a multilevel hierarchy. The empirical study of 11 Asia-Pacific international airports has demonstrated the effectiveness of the approach. The evaluation result would provide an airport with indicative information about its relative strengths and weaknesses in terms of performance measures associated with the airport operator, the passenger, and the airline. With its simplicity in concept and computation, the approach has general application in solving multiattribute evaluation problems involving both crisp assessments of quantitative attributes and fuzzy assessments of qualitative attributes.

ACKNOWLEDGMENT

This research was supported the National Science Council of Taiwan (Grant NSC100-2811-H-006-002) and the National Cheng Kung University (Grant HUA 98-21T-06-078). We are grateful to Taiwan's airport management and travel experts involved for providing assistance in problem formulation and data collection.

REFERENCES

[1] D. Gillen, and W.G. Waters II, "Introduction airport performance measurement and airport pricing," Transportation Research Part E, vol. 33, pp. 245–247, 1997.

[2] P.G. Hooper, and D.A. Hensher, "Measuring total factor productivity of airports - an index number approach," Transportation Research Part E, vol. 33, pp. 249–259, 1997.

[3] D. Gillen, and A. Lall, "Developing measures of airport productivity and performance: an application of data envelopment analysis," Transportation Research Part E, vol. 33 pp. 261–273, 1997.

[4] T.H. Oum, C. Yu, and X. Fu, "A comparative analysis of productivity performance of the world's major airports: summary report of the ATRS global airport benchmarking research report – 2002," Journal of Air Transport Management, vol. 9, no. 5, pp. 285–297, 2003.

[5] L. Brunetta, L., Righi, and G. Andreatta, "An operations research model for the evaluation of an airport terminal: SLAM.," Journal of Air Transportation Management, vol. 5, pp. 161–175, 1999.

[6] J. Sarkis, "An analysis of the operational efficiency of major airports in the United States," Journal of Operations Management, vol. 18, pp. 335–351, 2000.

[7] E. Pels, P. Nijkamp, P. Rietveld, "Inefficiencies and scale economies of European airport operations," Transportation Research Part E, vol. 39, pp. 341–361, 2003,

[8] M.-M., Yu, "Assessment of airport performance using the SBM-NDEA model," Omega, vol. 38, pp. 440–452, 2010.

[9] N. Adler, and J. Berechman, "Measuring airport quality from the airlines' viewpoint: an application of data envelopment analysis," Transport Policy, vol. 8, pp. 171–181, 2001.

[10] Y. Park, "Application of a fuzzy linguistic approach to analyse Asian airports' competitiveness," Transportation Planning and Technology, vol. 20, pp. 291–309, 1997.

[11] Y. Park, "An analysis for the competitive strength of Asian major airports," Journal of Air Transport Management, vol. 9, pp. 353–360, 2003.

[12] B. Vasigh, and R.G. Hamzaee, "A comparative analysis of economic performance of US commercial airports," Journal of Air Transport Management, vol. 4, pp. 209–216, 1998.

[13] C.-H. Yeh, and Y.-L. Kuo, "Evaluating passenger services of Asia-Pacific international airports," Transportation Research Part E, vol. 39, pp. 35–48, 2003

[14] E. Fernandes, and R.R. Pacheco, R.R., "A quality approach to airport management," Quality and Quantity, vol. 44, pp. 551–564, 2010.

[15] C.-C. Chou, "Evaluating the quality of airport service using the fuzzy multi-criteria decision-making method: a case study of Taiwanese airports," Expert Systems, vol. 28, pp. 1–15, 2011.

[16] A.C. Lemer, "Measuring performance of airport passenger terminals," Transportation Research Part A, vol. 26, pp. 37–45, 1992.

[17] I. Humphreys, and G. Francis, "Traditional airport performance indicators: a critical perspective," Transportation Research Record, vol. 1703, pp. 24–30, 2000.

[18] A.Y. Chi-Lok, and A. Zhang, "Effects of competition and policy changes on Chinese airport productivity: an empirical investigation," Journal of Air Transport Management, vol. 15, pp. 166–74, 2009.

[19] C.L. Hwang, and K. Yoon, Multiple Attribute Decision Making: Methods and Application. Berlin: Springer-Verlag, 1981.

[20] R. Keeney, and H. Raiffa, Decisions with Multiple Objectives, Preferences and Value Tradeoffs. New York: Cambridge University Press, 1993.

[21] J.S. Dyer, and R.K. Sarin, "Measurable multi-attribute value functions," Operations Research, vol. 27, pp. 810–822, 1979.

[22] R.E. Bellman, and L.A. Zadeh, "Decisionmaking in a fuzzy environment," Management Science, vol. 17, pp. 141–164, 1970.

[23] H.-J. Zimmermann, Fuzzy Set Theory and Its Applications, third edition. Boston: Kluwer Academic Publishers, 1996.

[24] P.N. Smith, "Fuzzy evaluation of potential suburban railway station locations," Journal of Advanced Transportation, vol. 27, pp. 153−179, 1993.

[25] C.-H. Yeh, H. Deng, and H. Pan, "Multi-criteria analysis for dredger dispatching under uncertainty," Journal of the Operational Research Society, vol. 50, pp. 35–43, 1999.

[26] C.-H. Yeh, H. Deng, and Y.-H. Chang, "Fuzzy multicriteria analysis for performance evaluation of bus companies," European Journal of Operational Research, vol. 126, no. 3, pp. 459–473, 2000.

[27] Y.-H. Chang, and C.-H. Yeh, "A survey analysis of service quality for domestic airlines," European Journal of Operational Research, vol. 139, pp. 166−177, 2002.

[28] Y.-H. Chang, and C.-H. Yeh, "A new airline safety index," Transportation Research Part B: Methodological, vol. 38, pp. 369–383, 2004.

[29] R. Doganis, and A. Graham, Airport Management - The Role of Performance Indicators. Transport Studies Group Research Report No. 13. London: Polytechnic of Central London, 1987.

[30] L.A. Zadeh, "The concept of a linguistic variable and its application to approximate reasoning: I; II," Information Science, vol. 8, pp. 199–249; 301–357, 1975.

[31] C.-H. Yeh, R.J. Willis, H. Deng, and H. Pan, "Task oriented weighting in multi-criteria analysis," European Journal of Operational Research, vol. 119, pp. 130–146, 1999.

[32] F. Herrera, and E. Herrera-Viedma, "Linguistic decision analysis: steps for solving decision problems under linguistic information," Fuzzy Sets and Systems, vol. 115, pp. 67–82, 2000.

[33] C.-H. Yeh, and H. Deng, "A practical approach to fuzzy utilities comparison in fuzzy multi-criteria analysis," International Journal of Approximate Reasoning, vol. 35, pp. 179–194, 2004.

[34] H.-K. Chiou, G.-H. Tzeng, and D.-C. Cheng, "Evaluating sustainable fishing development strategies using fuzzy MCDM approach," Omega, vol. 33, pp. 223 – 234, 2005.

[35] W. Pedrycz, "Why triangular membership functions?" Fuzzy Sets and Systems, vol. 64, pp. 21–30, 1994.

[36] A. Kaufmann, and M.M. Gupta, Introduction to Fuzzy Arithmetic, Theory and Applications. Boston: International Thomson Computer Press, 1991.

[37] M. Zeleny, Multiple Criteria Decision Making. New York: McGraw-Hill, 1982.

[38] H. Deng, C.-H. Yeh, and R.J. Willis, "Inter-company comparison using modified TOPSIS with objective weights," Computers & Operations Research, vol. 27, pp. 963–973, 2000.

[39] Y.-H. Chang, and C.-H. Yeh, "Evaluating airline competitiveness using multiattribute decision making," Omega, vol. 29, pp. 405–415, 2001

[40] S.J. Chen, and C.L. Hwang, Fuzzy Multiple Attribute Decision Making: Methods and Applications. New York: Springer-Verlag, 1991.

[41] G.S. Liang, "Fuzzy MCDM based on ideal and anti-ideal concepts", European Journal of Operational Research, vol. 112, pp. 682–691, 1999.

[42] M.-S. Kuo, G.-H. Tzeng, and W.-C. Huang, "Group decision-making based on concepts of ideal and anti-ideal points in a fuzzy environment," Mathematical and Computer Modelling, vol. 45, pp. 324–339, 2007.

[43] H.-Y. Wu, G.-H. Tzeng, and Y.-H. Chen, "A fuzzy MCDM approach for evaluating banking performance based on Balanced Scorecard," Expert Systems with Applications, vol. 36, pp. 10135–10147, 2009.

[44] C.-H. Yeh and Y.-H. Chang, "Modeling subjective evaluation for fuzzy group multicriteria decision making," European Journal of Operational Research, vol. 194, pp. 464 – 473, 2009.

[45] L.A. Croix, and D.J. Wolff, The Asia-Pacific Airline Industry: Economic Boom and Political Conflict. Hawaii: East-West Centre, 1995.

2011 IEEE International Conference on Fuzzy Systems
June 27-30, 2011, Taipei, Taiwan

An Intelligent Decision Support Tool Based on Belief Rule-Based Inference Methodology

Alberto Calzada, Jun Liu and Hui Wang
School of Computing and Mathematics
Faculty of Computing and Engineering
University of Ulster, Northern Ireland, UK
albertocalsa@gmail.com; {j.liu, h.wang}@ulster.ac.uk

Luis Martinez
School of Computing
University of Jaén
Jaén, Spain
luis.martinez@ujaen.es

Anil Kashyap
School of the Built Environment
University of Ulster
Northern Ireland, UK
a.kashyap@ulster.ac.uk

***Abstract* — Taking into account the need of handling hybrid information with uncertainty in human decision making, a new belief rule-base inference methodology (RIMER) has been recently proposed. RIMER approach and its relevant extensions have proved to be highly positive solving decision problems. However, for an end user it is difficult to implement the methods and algorithms from the raw equations in order to solve a specific problem. This paper presents a decision support tool based on the RIMER approach that facilitates its implementation and use to end-users. The overall structure and main functionalities of the tool are outlined, followed by an example to illustrate the use of this tool for applications.**

Keywords — knowledge-based system, belief rule base, decision making, uncertainty, decision support system.

I. INTRODUCTION

Nowadays, large amount and heterogeneous information provided by different sources is common for decision making problems, this fact implies a high complexity that is rather difficult of managing for human beings without any support. Consequently, more and more computer based decision-making support has been accepted and developed, to provide a stress-free view of the situation, joining the individuals intellectual resources with the capabilities of computers for improving the quality of decisions [1].

The use of rules is one of the most common ways in many tools for knowledge representation and inference in decision problems. Knowledge-based systems, usually constructed from human knowledge by means of if-then rules, have been one of the most visible and fastest growing branches of artificial intelligence [2]. In the design and implementation of knowledge-based systems for supporting human decision making, it is necessary and inevitable to use a scheme for representing and processing imprecise, incomplete and uncertain information in conjunction with precise data. Because of the need of handling hybrid information with uncertainty in human decision making, the belief Rule-base Inference Methodology using the Evidential Reasoning approach – RIMER was introduced in [3]. This methodology uses a belief structure for modelling hybrid rule-bases and an evidential reasoning (ER) approach [4] for making inference in the belief rule-based system by combining decision science [5], rule-based systems, and Dempster-Shafer (D-S) theory of evidence [6-7]. Therefore in RIMER a rule-base is designed with belief degrees embedded in the entire consequent terms of a rule, called belief rule-base (BRB), to capture nonlinear causal relationships as well as uncertainty. RIMER approach has been further investigated and extended in [8], denoted as RIMER$^+$, where an extended rule base is designed with belief degrees embedded in the entire consequent terms as well as in the entire antecedent terms of each rule. In addition, a simple but efficient method for automatically generating such extended belief rule-base from numerical data is proposed involving low time cost iterative learning procedure and simple rule generation mechanisms [8]. RIMER results and its relevant extensions have proved to be highly positive solving decision problems applied to different areas, such as, among others, safety and risk analysis, oil pipe leak detection and some other application in engineering systems [9-13].

This paper presents a decision support software tool which aims to facilitate the implementation and use of RIMER and RIMER$^+$ to solve complex decision making problems. This tool presents a friendly end-user interface that allows the implementation of RIMER and RIMER$^+$ in a transparent, informative and integrated way. Concretely, it offers the following functionalities: 1) A data base to store the input-output data; 2) a friendly user interface for problem structuring, information collection, and data presentation in both graphical and text formats; 3) The necessary modules for the rule-base which would be automatically generated based on the input-output sample data or assigned by domain experts and can be then represented in the interface; 4) management of heterogeneous input information in an integrated way; 5) inference algorithms to be applied once the rule-base is generated and the inputs are obtained; 6) a module to save and load solutions of a problem in both textual and graphical formats. Each functionality will be further detailed in the following sections.

This paper is organized as follows: RIMER and RIMER$^+$ are briefly overviewed in Section II. The architecture of the decision support tool and its functionalities are presented in Section III. Section IV introduces an illustrative example. This paper is concluded in Section V.

978-1-4244-7316-8/11/$26.00 ©2011 IEEE

II. OUTLINING RIMER APPROACH

RIMER [3] presents a new belief rule representation scheme to extend traditional IF–THEN rules using a belief structure. The belief rule base (BRB) introduced in RIMER approach is designed with belief degrees embedded in the consequent terms. It has been then extended into a new belief rule base with belief degrees embedded in the entire consequent terms as well as in the entire antecedent terms of each rule [8].

Suppose a BRB is given by $\boldsymbol{R}=\{R_1, R_2,\ldots, R_L\}$ with the k^{th} rule represented as follows [3]:

R_k: IF $\boldsymbol{U}$ is $\boldsymbol{A^k}$ THEN D with belief degrees $\boldsymbol{\beta^k}$, with a rule weight θ_k and attribute weights $\delta_1, \delta_2,\ldots, \delta_T$ (1)

where $\boldsymbol{U}$ represents the antecedent attribute vector ($U_1,\ldots, U_T$), $\boldsymbol{A^k}$ the packet antecedents $\{A_1^k,\ldots, A_T^k\}$, and A_i^k (i=1,…, T) the referential value of the antecedent attribute U_i in the k^{th} rule; T the total number of antecedent attributes used in the rule base; $\boldsymbol{D}$ the consequent vector ($D_1,\ldots, D_N$), and $\boldsymbol{\beta^k}$ the vector of the belief degrees ($\beta_{1k},\ldots, \beta_{Nk}$) for $k\in\{1,\ldots, L\}$, and β_{sk} ($s\in\{1,\ldots, N\}$ the belief degree to which D_i is believed to be the consequent if in the k^{th} packet rule the input satisfies the packet antecedents $\boldsymbol{A^k}$. θ_k is the relative weight of the k^{th} rule and $\delta_1,\ldots, \delta_T$ are the relative weights of the T antecedent attributes. L is the number of all the packet rules in the rule-base. $\sum_{s=1}^{N}\beta_{sk}\le 1$. If $\sum_{s=1}^{N}\beta_{sk}=1$, the k^{th} packet rule is said to be complete; otherwise, it is incomplete.

Take for example the belief rule in safety analysis [10-11]:

R_k: IF the **failure rate** is *frequent* and the **consequence severity** is *critical* and the **failure consequence probability** is *unlikely,* THEN the **safety estimate** is {(*good,* 0), (*average,* 0), (*fair,* 0.7), (*poor,* 0.3)}, (2)

where the consequent is a belief distribution representation for safety consequent, stating that it is 70% sure that safety level is fair and 30% sure is poor. This kind of rule reflects another kind of uncertainty caused because an expert is unable to establish a strong correlation between premise and conclusion.

In [8], to facilitate the more general application cases and more flexible and simpler rule-base generation scheme, this belief rule is extended with belief degrees embedded in the entire possible antecedent terms of each rule as well, for example, belief rule (2) can be extended as follows:

R_k: IF the **failure rate** is {(*very low,* 0), (*low,* 0), (*reasonably low,* 0), (*average,* 0), (*reasonably frequent,* 0), (*frequent,* 0), (*highly frequent,* 1) AND the **consequence severity** is {(*negligible,* 0), (*marginal ,* 0), (*moderate ,* 0.3), (*critical,* 0.7), (*catastrophic,* 0)} AND the **failure consequence probability** is {(*highly unlikely,* 0.1), (*unlikely ,* 0.7), (*reasonably unlikely,* 0.2), (*likely ,* 0), (*reasonably likely,* 0), (*highly likely,* 0), (*definite,* 0)} THEN the **safety estimate** is {(*Good*, 0), (*Average*, 0.1), (*Fair*, 0.6), (*Poor*, 0.3)} (3)

This kind of extended belief rule is able to not only capture vagueness (with linguistic terms), uncertainty (with beliefs), incompleteness (partially known beliefs in antecedents and/or consequents) and nonlinear relationships (IF-THEN rules) between these three parameters and the safety level but also provide the flexible way to incorporate the hybrid input information as well as more efficient rule generation scheme.

Generally, rule (1) can be extended in the following form:

R_k^*: IF $\boldsymbol{U}$ is ($\boldsymbol{A}$, $\boldsymbol{\alpha^k}$) THEN $\boldsymbol{D}$ with belief degrees $\boldsymbol{\beta^k}$, with a rule weight θ_k and attribute weights $\delta_1, \delta_2,\ldots, \delta_T$ (4)

where ($\boldsymbol{A}$, $\boldsymbol{\alpha^k}$) is the packet antecedents $\{\{(A_{ij}, \alpha_{ij}^k), j=1,\ldots, J_i\}; i=1,\ldots, T\}$ (as illustrated in (3)) representing antecedent with belief structure; here A_{ij} ($j\in\{1,\ldots, J_i\}$) is the jth referential value of the i^{th} antecedent attribute U_i (i=1, …, T), α_{ij}^k the likelihood to which U_i is evaluated to be the referential value A_{ij} in the kth rule with $\alpha_{ij}^k\ge 0$ and $\sum_j^{J_i}\alpha_{ij}^k\le 1$ (i=1,… T), k=1,…, L^*, L^* is the total number of all the packet rules in the rule-base. A rule base with rules in the form of (4) is called an extended belief rule base (EBRB) compared with (1). Note that all the rules in an EBRB share the same antecedent terms and consequent terms, but have different belief distributions for each antecedent attribute and the consequent. The use of the superscript k in (4) reflects this feature.

Once given an input, the activation weight w_k which measures the degree to which the k^{th} rule is weighted and activated, will be calculated using various ways depending on the nature of an antecedent attribute as detailed in [3, 8]. Having determined the activation weight of each rule in the rule base, the ER approach can be directly applied to combine the rules and generate final conclusions. The final conclusion generated by aggregating all activated rules by the current input vector $\boldsymbol{x}=\{x_i, i=1,\ldots, T\}$ can be represented as follows:

$$f(\boldsymbol{x})=\{(D_s, \beta_s), s=1,\ldots, N\}. \quad (5)$$

The final result is still estimated a belief distribution, which gives a panoramic view about estimate for a given input [3, 8]. The inference methodology based on (1) is referred to RIMER, and the one based on (4) as RIMER$^+$. The following introduced software tool includes both methodologies, for the convenience, we use only RIMER as a representative.

III. DECISION SUPPORT SYSTEM BASED ON RIMER

This section introduces a decision support software tool that implements the RIMER method.

A. Architecture

This system has been developed under the object-oriented programming paradigm. So abstract concepts can be defined and grouped into packages. The general structure of the packages follows the classic MVC architecture [14]. Each main package – Model, View and Controller – communicate with the rest through interface classes, i.e. with non-implemented methods. The main feature of this design pattern is that permits the encapsulation of each part of the system with a minimal decoupling with the rest. The MVC architecture allows us to build the system iteratively, from the first basic window with the basic features, until the final result, which is improved due to the versioning system until all the functionalities required are achieved.

B. *Features of RIMER support system*

This section introduces the main features of the system. Firstly it presents the features related to the *problem definition* and secondly related to the *solving process.*

1) Problem definition

The system provides the flexibility to define the hierarchical decision structure which is composed of several attributes. Attributes (also referred to as parameters) are variables that represent decision sub-problems. They are organized hierarchically so the attributes in higher levels of the hierarchy depend on lower-level attributes. The system presents a clear-cut interface to define the hierarchical structure and its attributes. The interface has been designed in a way that each attribute in the structure can be directly modified. Therefore, all the elements of the problem definition can be managed directly in an integrated way, just by clicking on them. These elements are subsequently described.

The system interface is based on two main windows that show the details of every parameter and keep them visible in the window to facilitate their management. Hence, an accessible and fast way to navigate between both windows is provided. Figure 1 (a) illustrates the layout of attributes management and Figure 1 (b) shows a general hierarchical structure window (also taken as the main window).

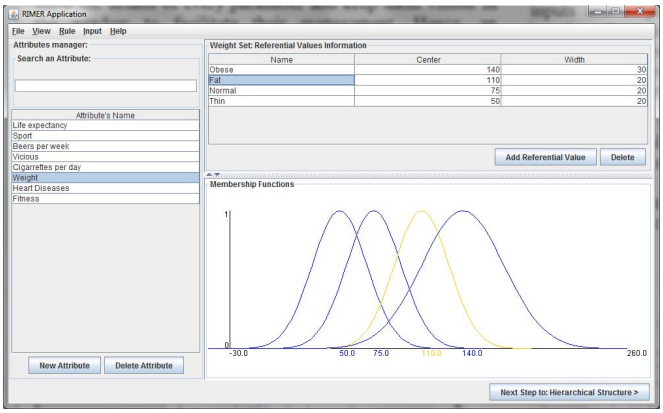

Figure 1 (a) Attribute window

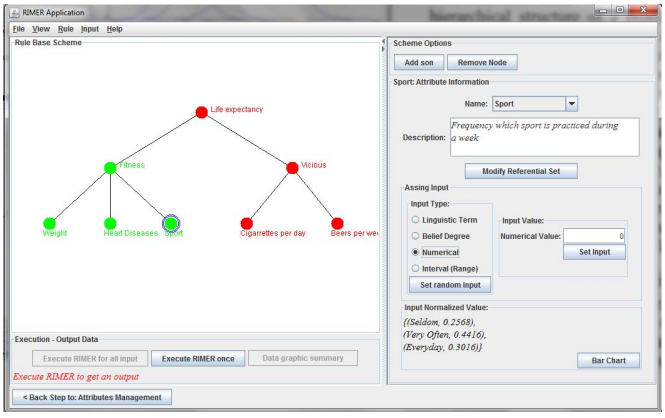

Figure 1 (b) Hierarchical structure window as main window

a) Attributes management

The attributes management window manages every aspect regarding the attributes and their referential values (a set of meaningful and distinctive evaluation standards for describing an attribute, which is commonly described by subjective linguistic terms). The definition of each attribute is essential to obtain proper results when executing RIMER, since both inputs and outputs are transformed into belief distribution based on the referential values of each attribute (see Section II). The attributes management window is divided into three parts – attributes manager (on the left), referential values manager (top-centre) and functions graph (bottom-centre).

It is possible to choose among different types of functions for the referential values when creating a new attribute in the attributes manager. Figure 2 shows examples about different functions can be graphically represented in the system– from top-left to bottom: Triangular, Trapezoidal and Gaussian fuzzy membership functions, qualitative linguistic terms and utility functions.

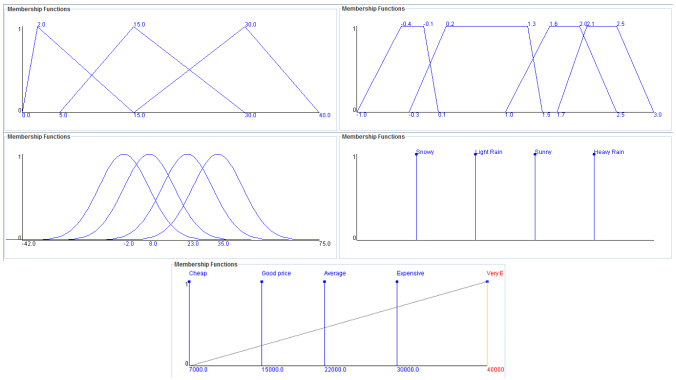

Figure 2. Possible representations in the functions graph

b) Generate hierarchal structure of the problem

From the main window, it is possible to generate a hierarchical structure of a problem by adding and removing nodes. In this case, each node of the hierarchy is associated with one of the attributes defined previously in the attributes window. By selecting a node included in the hierarchy, users will be able to modify its properties. Note that the leaf nodes have different properties from the non-leaf nodes: for a leaf node, it is possible to assign an input and for the non-leaf nodes, users can create and manage rules which form a sub-rule base in the hierarchical structure. Therefore, the content of the panel on the right side of the main window will change depending on the type of the current selected node. In Figure 1, this panel corresponds to a leaf node, since the selected node – surrounded by blue circles – is a leaf node.

c) Belief rule-bases generation and representation

Once the attributes are defined and organized into a hierarchical structure, the next step is to generate the belief rule base to model the causal relationship among the attributes. Rule based can be generated automatically from a data set, or can be manually defined and adjusted by an expert. Rules can be manually assigned in a sub rule-base by selecting one of the non-leaf nodes in the hierarchical structure. The right-side panel will shows the information related to the management of the sub rule-base correspondent to this non-leaf node. Figure 3 illustrates the appearance of the main window when a non-leaf

node (i.e. sub rule-base) is selected. Rules can be assigned automatically by selecting the option "Load Rules File" in the "Rule" menu, in the menu bar.

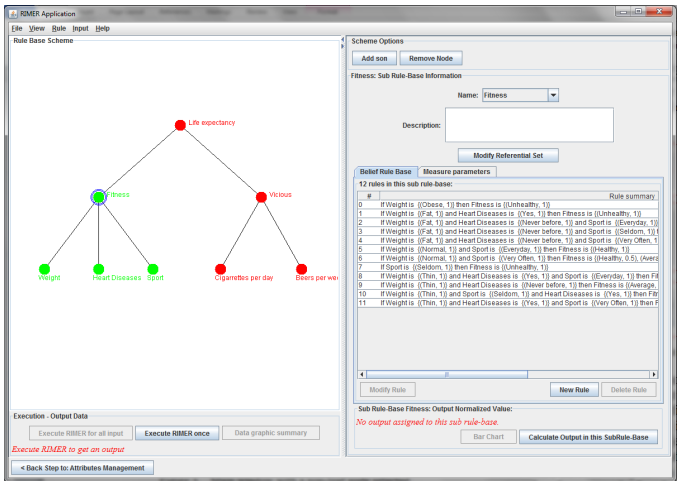

Figure 3. Main window with a non-leaf node selected

There are several options to modify the type of rules in the hierarchical structure are included. For the comparison purposes in the RIMER algorithm, the system can adopt three different types of rules:

- RIMER original rules: Rules with belief degree distributions in the antecedents of each rule. This is RIMER algorithm originally developed and executed in [3].
- RIMER^{+} extended rules: Rules with belief degree distributions not only in the antecedents of the rules, but also in each consequent. This is the extended RIMER algorithm in [8]. In the system, the rules can be automatically generated from the input-output sample data based on the simple but efficient generation proposed in [8].
- Wang-Mendel rules: Rules which do not include belief degree distributions, but linguistic terms in both antecedents and consequents. The Wang-Mendel algorithm [15] is executed when these rules are selected in the system.

In order to obtain an improved analysis of the results, the system includes data to measure the inconsistence [16] of each sub-rule base. This is an important parameter to explain the results returned by the algorithm, since it indicates the quality of the data set the system is working with.

Repeated rules are not necessary when executing the decision algorithm. Options to remove similar rules – based on a threshold – are therefore included in the system.

d) Facilate different types of inputs

Inputs can be assigned manual or automatically. To assign an input manually, click one of the leaf nodes in the hierarchical structure and select one of the options that appear in the right-side panel. Therefore, the system will ask for the required information to generate the input. Figure 4 illustrates the different types of the input format which the system could offer:

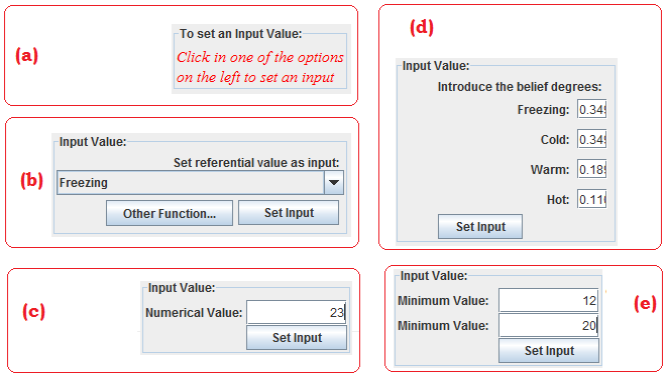

Figure 4. Different inputs that can be assigned

Fig. 4 (a) shows the initial panel, when there is no option selected; Fig. 4 (b) sets a referential value (linguistic terms) or another function that can be defined by the user as an input; Fig. 4 (c) indicates a numerical input; Fig. 4 (d) sets a belief degree distribution and Fig. 4 (e) creates an interval (range) input. Once the button "Set Input" is pressed, the input will be transformed automatically into a belief degree distribution and assigned to the current leaf node.

However, to assign inputs automatically from a properly defined input CSV file the option *Load Input File*, in the *Input* menu, included in the menu bar must be selected. In a CSV file, it is possible to specify any type of input (i.e. numerical, range, etc.). The system will automatically recognize each one of these types when loading a CSV file. Once the inputs are loaded, the system will be ready to execute the algorithm for all of them (in multi-execution mode).

Sometimes it is necessary to test a problem with random data. Thus, the system includes options to define a single random input or directly assign random values to every leaf node in the hierarchical structure.

2) Solving process

Once all the elements required for a problem definition are assigned, it is then ready to generate results by executing the RIMER approach algorithm embedded into the tool.

Depending on how the inputs have been assigned, the system could be running in different execution modes:

- If the inputs have been assigned manually, the system will be ready for single execution (with the inputs currently assigned in every leaf node). To carry out a single execution, it is just necessary to press the button so-called *Execute RIMER once* in the main window. The system will report the results of the execution through a label at the bottom part of the window. Errors during the execution process will be also specified in this label, if applicable. Users can obtain graphical representations of every input and output regarding the last single execution. The *Bar Chart* button is included in the right-side panel in the main window. It is also possible to obtain an entire graphical summary of the execution selecting the *Data Graphic Summary* included in the main window. Figure 5 shows the window where users can observe different graphical data.

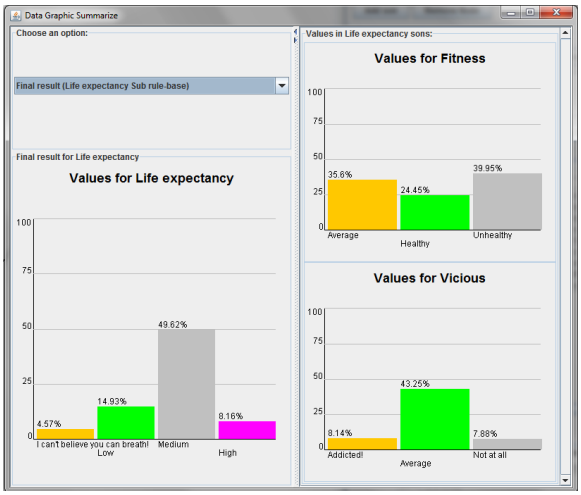

Figure 5. Data graphic summary window

- If the inputs have been loaded from a CSV file, the system will be ready for a multi-execution (one execution for each input loaded in the CSV file). For a multi-execution, the button titled "Execute RIMER for all Input" in the main window should be enabled. After this multi-execution, a log window with the results will automatically appear.

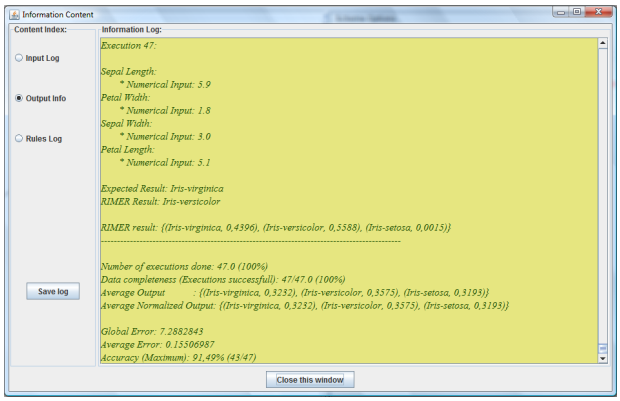

Figure 6. Statistics of the multi-execution mode for the Iris data set

Figure 6 illustrates the information log retrieved after a multi-execution process. As it can be observed, specific details are shown in this figure for the last execution (Execution 47th):

- List of original inputs used in this execution, before its transformation into belief degree distributions
- Expected result
- Result of the RIMER approach
- Result of the RIMER approach, in belief degree distribution

As aforementioned, in the multi-execution mode, general statistics about all the execution performed will be generated and showed in a log window. The statistics calculated by the system (See Figure 5) are summarized as follows:

- *Executions done*: This percentage tells us how many executions were done above the total that was supposed to be done (In case that users stop the execution, if not, this percentage always will be 100%).
- *Executions successfully done*: This percentage data acts as an indicator to show us the completeness of our rule bases. If an execution is not successfully done it is because the input data does not activate any rule. Therefore, if no rule is activated, means that a rule is not defined for this input. Thus, there is a lack of completeness in the rule-base.
- *Global and average error*: This data will show us the total and average error in RIMER predictions or classifications.
- *Accuracy*: This percentage statistic displays in how many cases RIMER predict the correct classification.
- *Average Output*: This statistic in a belief degree shape shows us which referential values of our output are more likely to be predicted. The data in the Average Normalized Output eliminates the uncertain degree and shows the average output with its values normalized.
- *T parameter*: In case that the root attribute in the hierarchical scheme has Utility functions defined within it, the system will calculate a special figure based on the distance between the output calculated and the expected one, assessing the T statistic for T=0.25, T=0.5 and T=1.

Another important feature in the system is to provide methods to load and save in external files all the information related with the application, which includes loading and saving the rules and inputs included in the current belief rule-bases and the information logs that keep information about it.

IV. Case Study

A numerical example is provided in this section to demonstrate the implementation and potential applications of the proposed system. The main focus is given on the illustration of the functionality of the developed system.

A. Problem Description

For this illustrative simulation, Iris data set for classification was chosen. Its characteristics are: 1) 150 instances (50 in each of three classes); 2) 4 attributes - Sepal length in cm, Sepal width in cm, Petal length in cm and Petal width in cm - and three possible output values - Iris Setosa, Iris Virginica and Iris Versicolor; 3) Does not contain missing values. In this example, a K-fold cross validation method by be applied, with K=5. In each test, 120 samples will be used for training and the rest 30 samples will be used for testing.

B. Implementation

Firstly, the attributes should be defined in the attributes window. In this simulation, each attribute has been assigned three linguistic terms as referential values (high, medium and low) which are defined with utility functions, so those three terms correspond the value of the maximum, average and minimum value for this attribute in the data set respectively). Figure 7 shows the attributes manager window with the definition of the five attributes for this problem (four for the input attributes and one output attribute, so called Iris).

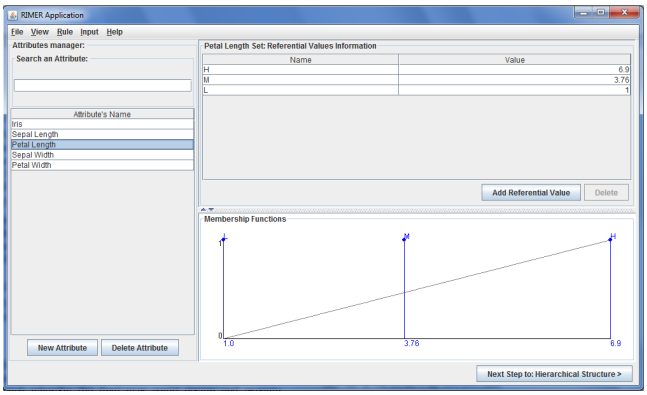

Figure 7. Attributes manager window with the Iris problem attributes

After defining all the attributes, it is needed to design the hierarchical structure for the problem. In the main window, the structure is built just by adding four son nodes to the root node, which will be the output attribute Iris.

Afterwards, the data set was downloaded and adapted into 10 CSV files, five for training and another five for testing each of the training files to apply the K-fold cross validation method. After loading one of the training files, the right-panel of the main window is updated and the rules table is filled with the rules loaded. Figure 8 shows the main window after defining the problem structure and loading one of the training files. The last element remaining to complete the definition of the problem is the input one. It is possible to assign manually inputs to the leaf nodes in the hierarchical structure. However, in this simulation one of the test CSV files that has been created before will be loaded.

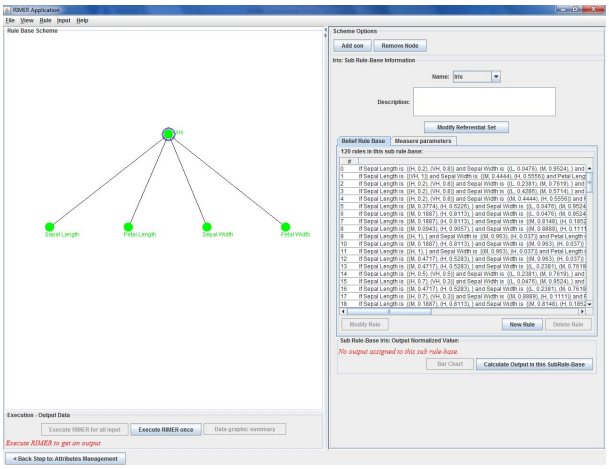

Figure 8. Main window with Iris problem structure defined

Finally, the algorithm is executed in multi-execution mode and after that the results log appears in the window, showing the results of the test executed (See Figure 6). The results for this test are 0.966 accuracy, with an average error of 0.141. For the 5 tests carried out in this simulation, the accuracy is 0.96, and the average error of 0.136.

V. CONCLUSIONS

This paper presented a decision support tool which facilitates the implementation of the recently presented RIMER approach whereby the final user could design and execute problems to obtain the decision result. The architecture and features of the system are outlined and illustrated. The system is expected to be applied for different application and we are working on further improvement about the overall presentation and functionality of the system.

ACKNOWLEDGMENT

This paper has been partially supported by the UU strategy fund, and the research projects TIN2009-08286, P08-TIC-3548 and Feder Fonds.

REFERENCES

[1] E. Turban, and J.E. Aronson, *Decision Support Systems and Intelligent Systems*, Fifth Edition, Prentice Hall, 1997.

[2] R. Sun (1995), "Robust reasoning: Integrating rule-based and similarity-based reasoning," *Artif. Intell.,* vol. 75, no. 2, pp. 241–295.

[3] J. B. Yang, J. Liu, J. Wang, H. S. Sii, and H. W. Wang, "A generic rule-base inference methodology using the evidential reasoning approach—RIMER," *IEEE Transactions on Systems, Man, and Cybernetics-Part A*: *System and Humans*, vol. 36, no. 2, pp. 266–285, Mar. 2006.

[4] J. B. Yang and D. L. Xu, "On the evidential reasoning algorithm for multiple attribute decision analysis under uncertainty," *IEEE Trans. Syst. Man Cybern., A, Syst. Humans*, vol. 32, no. 3, pp. 289–304, May 2002.

[5] J. S. Dyker, P. C. Fishburn, R. E. Steuer, J. Wallenius, and S. Zionts, "Multiple criteria decision making, multiattribute utility theory: The next ten years," *Manag. Sci.*, vol. 38, no. 5, pp. 645–654, May 1992.

[6] G. Shafer (1976), *A Mathematical Theory of Evidence*. Princeton, NJ: Princeton Univ. Press.

[7] A. P. Dempster, "A generalization of Bayesian inference," *J. R. Stat. Soc., Ser. B*, vol. 30, no. 2, pp. 205–247, 1968.

[8] J. Liu, L. Martínez, A. Calzada, and Hui Wang, "An extended belief rule based inference methodology and its rule-base generation by learning from examples", submitted to *IEEE Transactions on Knowledge and Data Engineering*.

[9] J.B. Yang, J. Liu, D.L. Xu, J. Wang, H.W. Wang, "Optimization models for training belief-rule-based systems", *IEEE Transactions on Systems, Man, and Cybernetics-Part A*, 37(4)(2007) pp. 569-585.

[10] J. Liu, J.B. Yang, D. Ruan, L. Martinez, and J. Wang. Self-tuning of fuzzy belief rule bases for engineering system safety analysis, Annals of Operations Research, 163(1): 143-168, 2008.

[11] J. Liu, J.B. Yang, J. Wang, H.S. Sii and Y.M. Wang. "Fuzzy rule-based evidential reasoning approach for safety analysis", *International Journal of General Systems*, 33(2-3): 183-204, 2004.

[12] D. L. Xu, J. Liu, J. B. Yang, G. P. Liu, J. Wang, I. Jenkinson and J. Ren (2007), "Inference and learning methodology of belief-rule-based expert system for pipeline leak detection", *Expert Systems with Applications*, Volume 32, Issue 1, pages 103-113, ISSN 0957-4174.

[13] Z.J. Zhou, C.H. Hu, J.B. Yang, D.L. Xu, and D.H. Zhou, "Online updating belief-rule-based system for pipeline leak detection under expert intervention". *Expert Systems with Applications*, 36(3): 7700-7709, 2008.

[14] Reenskaug T. *Models - views – controllers*, Technical report, *Xerox PARC*, Dec. 1979.

[15] L. X. Wang, J.M. Mendel, "Generating fuzzy rules by learning from examples", *IEEE Transactions on Systems, Man, and Cybernetics*, 22:6 (1992) 1414-1427.

[16] J. Liu, L. Martínez, D. Ruan, R.M. Rodriquez, and A. Calzada (2010), "Optimization algorithm for learning consistent belief rule-base from examples", *Journal of Global Optimization*, in press: 10.1007/s10898-010-9605-x (22-09-2010).

2011 IEEE International Conference on Fuzzy Systems
June 27-30, 2011, Taipei, Taiwan

Production Planning with Uncertain Demands

Romain Guillaume
Université de Toulouse-IRIT
5, Allées A. Machado
31058 Toulouse Cedex 1,France
Email: Guillaum@irit.fr

Przemysław Kobylański
Institute of Mathematics
and Computer Science
Wrocław University of Technology
Wybrzeże Wyspiańskiego 27
50-370 Wrocław, Poland
Email: Przemyslaw.Kobylanski@pwr.wroc.pl

Paweł Zieliński
Institute of Mathematics
and Computer Science
Wrocław University of Technology
Wybrzeże Wyspiańskiego 27
50-370 Wrocław, Poland
Email: Pawel.Zielinski@pwr.wroc.pl

***Abstract*—The paper deals with a single-item production planning problem with uncertain demands modeled by fuzzy intervals whose membership functions are possibility distributions for the values of the uncertain demands. Optimization criteria, in the setting of possibility theory, that lead to choose robust production plans under fuzzy demands are given. Algorithms for determining optimal robust production plans with respect to the proposed criteria are provided and some computational experiments are presented.**

***Index Terms*—Production Planning, Uncertain Demand, Fuzzy Optimization, Possibility Theory.**

I. Introduction

Nowadays, companies do not compete as independent entities but as a part of collaborative supply chains. The uncertainty on demands creates a risk in the supply chain as backordering, obsolete inventory due to the bullwhip effect [1]. To reduce this risk two different approaches exist: the collaboration between the customer and the supplier or the integration of the uncertainty into a planning process. In this paper, we cope with the approaches. Within these supply chains, collaborative processes are usually characterized by a set of point-to-point (customer/supplier) relationships with partial information sharing [2], [3]. More precisely, a procurement plan are built and propagated through the supply chain, moreover in stronger relationship between the customer and the supplier, the supplier can share her/him delivering capacity constraints to the customer. Another way to reduce a risk of the supply chain is to integrate the uncertainty in a planning process. Industries used the *Material requirements planning method* (MRP) [4] to plan a production. The use of *possibility theory* [5] to model the uncertainty in a production planning is due to the difficulties to access to available historical data allowing to compute a probability distribution. Different models (based on possibility theory) have been used to represent imperfections on demands to compute the gross requirements (in MRP context): [6] takes into account the imprecision on quantities with trapezoidal fuzzy intervals; [7] integrates the uncertainty on the order and the imprecision on quantities by a union of fuzzy intervals; and [8] adds to the previous model the imprecision on the date by a trapezoidal fuzzy interval. The gross requirements, in case of integration of imperfection, become fuzzy gross requirements (or a set of fuzzy gross requirements [8]) where the required quantities by period are fuzzy quantities. In the context of collaborative supply chain the customer sends a procurement plan to the supplier but this procurement plan can not be fuzzy, also the problem is to compute from the fuzzy gross requirement a procurement plan. In this communication, we are interested in computing a robust procurement plan (with and without delivering capacity of the supplier sharing). The delivering capacity are composed of two bounds: the lower one being the minimal accepted quantity that is sent to the customer and the upper bound which is due to a production capacity of the supplier. Moreover the customer accepts to have backordering but it is more penalized that inventory. This problem is equivalent to the *problem of production planning* with backordering, more precisely to a certain version of the *lot sizing problem* (see, e.g., [9], [10]), where: the procured quantities are production quantities, a *production plan*; delivering constraints are production constraints, *capacity limits on production plans*; and the gross requirements are *demands*. Thus, the problem consists in finding a production plan that fullfils capacity limits and minimizes the total cost of storage and backordering subject to the conditions of satisfying each demand. It is efficiently solvable when the demands are precisely known (see, e.g., [11], [12], [13]). However, the demands are seldom precisely known in advance and the uncertainty must be taken into account.

In this paper, we wish to investigate the above problem with uncertain demands modeled by fuzzy intervals. The membership function of a fuzzy interval is a *possibility distribution* describing, for each value of the demand, the extent to which it is a possible value. In other words, it means that the value of this demand belongs to a λ-cut of the fuzzy interval with the degree of necessity (confidence) $1-\lambda$. To evaluate a production plan, we assign to it, a *degree of necessity* that its cost does not exceed a given threshold and a degree of necessity that costs of the plan fall within a given fuzzy goal. In order to find "robust solutions" under fuzzy demands, we apply two criteria. The first one consists in choosing a production plan which maximizes the degree of necessity (certainty) that its cost does not exceed a given threshold. This criterion is similar in spirit to *threshold model* (see, e.g., [14]) in *stochastic optimization* in which we seek a solution maximizing the probability that its random value does not exceed a given threshold. The second criterion is weaker than the first one and consists in choosing

978-1-4244-7316-8/11/$26.00 ©2011 IEEE

a plan with the maximum degree of necessity that costs of the plan fall within a given fuzzy goal. A similar criterion has been proposed in [15] for discrete optimization problems with fuzzy costs. We provide some methods for finding a robust production plan with respect to the proposed criteria under fuzzy-valued demands which heavy rely on methods for finding a robust production plan, called *optimal robust production plan*, in the problem of production planning under interval-valued demands with the *min-max* criterion. Namely, it turns out that the considered fuzzy problems can be reduced to examining a family of the interval problems with the min-max criterion.

II. The Deterministic Problem

We are given T periods. For period t, $t = 1, \ldots, T$, let d_t be the demand in period t, $d_t \geq 0$, x_t the production amount in period t, $x_t \geq 0$, l_t, u_t the production capacity limits on x_t. Let $\mathbb{X} \subseteq \mathbb{R}^T_{\geq 0}$ be the set of feasible production amounts. Two cases are distinguished, the case *with no capacity limits* $\mathbb{X} = \{(x_1, \ldots, x_T) \ : \ x_t \geq 0, t = 1, \ldots, T\}$ and the one *with capacity limits* $\mathbb{X} = \{(x_1, \ldots, x_T) \ : \ l_t \leq x_t \leq u_t, t = 1, \ldots, T\}$. Set $\mathbf{D}_t = \sum_{i=1}^{t} d_i$ and $\mathbf{X}_t = \sum_{i=1}^{t} x_i$, $\mathbf{D}_t$ and $\mathbf{X}_t$ stand for the cumulative demand up to period t and the production level up to period t, respectively. Obviously, $\mathbf{X}_{t-1} \leq \mathbf{X}_t$ and $\mathbf{D}_{t-1} \leq \mathbf{D}_t$, $t = 2, \ldots, T$.

We make the assumption: the costs of carrying one unit of inventory from period t to period $t+1$ for every $t = 1, \ldots, T$ are equal, we denote it by c_I and the costs of backordering one unit from period $t+1$ to period t for every $t = 1, \ldots, T$ are equal, we denote it by c_B. Furthermore, we assume that $c_I < c_B$. The nonnegative real function $L(u, v)$ represents either the cost of storing inventory from period t to period $t+1$ or the cost of backordering quantity from period $t+1$ to period t, namely $L(\mathbf{X}_t, \mathbf{D}_t) = c_I(\mathbf{X}_t - \mathbf{D}_t)$ if $\mathbf{X}_t \geq \mathbf{D}_t$; $c_B(\mathbf{D}_t - \mathbf{X}_t)$ otherwise. The Function has the form $L(\mathbf{X}_t, \mathbf{D}_t) = \max\{c_I(\mathbf{X}_t - \mathbf{D}_t), c_B(\mathbf{D}_t - \mathbf{X}_t)\}$.

The production planning problem consists in finding a feasible production plan $\boldsymbol{x} = (x_1, \ldots, x_T)$, $\boldsymbol{x} \in \mathbb{X}$, that minimizes the total cost of storage and backordering subject to the conditions of satisfying each demand, namely

$$\min_{\boldsymbol{x} \in \mathbb{X}} F(\boldsymbol{x}) = \min_{\boldsymbol{x} \in \mathbb{X}} \sum_{t=1}^{T} L(\mathbf{X}_t, \mathbf{D}_t). \tag{1}$$

Without loss of generality, we can assume that an initial inventory I_0 and an initial backorder B_0 are equal to zero. Otherwise, one can append period 0 and assign $x_0 = I_0$ and $d_0 = 0$ with zero inventory cost if $I_0 > 0$ or assign $x_0 = 0$ and $d_0 = B_0$ with zero backorder cost if $B_0 > 0$.

In the case with no capacity limits problem (1) has a trivial optimal solution equal to $\boldsymbol{d}$. In the case with capacity limits, (1) can be formulated as the minimum cost flow problem (see, e.g., [16]):

$$\begin{array}{lll} \min & \sum_{t=1}^{T}(c_I I_t + c_B B_t) & \\ \text{s.t.} & B_t - I_t = \sum_{j=1}^{t}(d_j - x_j), & t = 1, \ldots, T, \\ & l_t \leq x_t \leq u_t, & t = 1, \ldots, T, \\ & B_t, I_t \geq 0, & t = 1, \ldots, T. \end{array} \tag{2}$$

Problem (2) can efficiently solved, for instance, by an algorithm presented in [13] that takes into account a special structure of the underling network.

III. Robust Problem

Assume that demands d_t, $t = 1, \ldots, T$, in problem (1), are only known to belong to intervals $D_t = [d_t^-, d_t^+]$, $d_t^- \geq 0$. This means that we neither know the exact demands, nor can we set them precisely. We assume that the demands are unrelated to one another and there is no probability distribution in D_t, $t = 1, \ldots, T$. A vector $S = (d_1, \ldots, d_T)$, $d_t \in D_t$, that represents an assignment of demands d_t to periods t, $t = 1, \ldots, T$, is called a *scenario*. Thus every scenario expresses a realization of the demands. We denote by Γ the set of all the scenarios, i.e. $\Gamma = [d_1^-, d_1^+] \times \cdots \times [d_T^-, d_T^+]$. Among the scenarios of Γ *extreme scenarios* can be distinguished, that is the ones, which belong to $\{d_1^-, d_1^+\} \times \cdots \times \{d_T^-, d_T^+\}$, the set of extreme scenarios is denoted by Γ_{ext}. We denote by S^+ (resp. S^-) the extreme scenario in which all the demands are set to their upper (resp. lower) bounds. The demand and the cumulative demand in period t under scenario S are denoted by $d_t(S) \in D_t$ and $\mathbf{D}_t(S)$, respectively, $\mathbf{D}_t(S) = \sum_{i=1}^{t} d_i(S)$. Clearly, for every $S \in \Gamma$ it holds $\mathbf{D}_{t-1}(S) \leq \mathbf{D}_t(S)$, $t = 2, \ldots, T$, and $\mathbf{D}_t(S) \in [\mathbf{D}_t(S^-), \mathbf{D}_t(S^+)]$. The function $L(\mathbf{X}_t, \mathbf{D}_t(S)) = \max\{c_I(\mathbf{X}_t - \mathbf{D}_t(S)), c_B(\mathbf{D}_t(S) - \mathbf{X}_t)\}$, represents either the cost of storing inventory from period t to period $t+1$ or the cost of backordering quantity from period $t+1$ to period t under scenario S. Now $F(\boldsymbol{x}, S)$ denotes the total cost of a production plan $\boldsymbol{x} \in \mathbb{X}$ under scenario S, i.e. $F(\boldsymbol{x}, S) = \sum_{t=1}^{T} L(\mathbf{X}_t, \mathbf{D}_t(S))$.

In order to choose a robust production plan, one of robust criteria, called the *min-max* can be adopted. In the *min-max* version of problem (1), we seek a feasible production plan with the minimum the worst total cost over all scenarios, that is

$$\begin{aligned} \text{ROB}: \ \boldsymbol{x}^r &= \arg \min_{\boldsymbol{x} \in \mathbb{X}} A(\boldsymbol{x}) = \min_{\boldsymbol{x} \in \mathbb{X}} \max_{S \in \Gamma} F(\boldsymbol{x}, S) \\ &= \min_{\boldsymbol{x} \in \mathbb{X}} \max_{S \in \Gamma} \sum_{t=1}^{T} L(\mathbf{X}_t, \mathbf{D}_t(S)). \end{aligned}$$

In other words, we wish to find among all production plans the one that minimizes the maximum production plan cost over all scenarios, that minimizes $A(\boldsymbol{x})$, $A(\boldsymbol{x})$ is the *maximal cost of production plan* $\boldsymbol{x}$. An optimal solution $\boldsymbol{x}^r$ to the problem ROB is called *optimal robust production plan*. Let $\boldsymbol{x} \in \mathbb{X}$ be a given production plan. A scenario $S^w \in \Gamma$ that maximizes cost $F(\boldsymbol{x}, S)$ in problem ROB for $\boldsymbol{x}$ is called *the worst case scenario*.

Let us first study the problem of computing a worst case scenario for a given production plan $\boldsymbol{x}^* \in \mathbb{X}$, that is:

$$A(\boldsymbol{x}^*) = F(\boldsymbol{x}^*, S^w) = \max_{S \in \Gamma} F(\boldsymbol{x}^*, S). \tag{3}$$

Since $F(\boldsymbol{x}^*, S)$ is a continuous function on a bounded closed set Γ, it attains maximum for some $S \in \Gamma$. Furthermore, determining S can be restricted to the vertices of Γ, that is to the set of extreme scenarios Γ_{ext}, since $F(\boldsymbol{x}^*, S)$ is convex on Γ for any fixed production plan $\boldsymbol{x}^* \in \mathbb{X}$. The problem (3)

can be formulated as a mixed integer programming problem (MIP):

$$\begin{array}{lll} \max & \sum_{t=1}^{T}(c_I I_t + c_B B_t) & \\ \text{s.t.} & B_t - I_t = \sum_{j=1}^{t}(s_j - x_j^*), & t = 1,\ldots,T, \\ & s_t \in [d_t^-, d_t^+], & t = 1,\ldots,T, \\ & B_t, I_t \geq 0, & t = 1,\ldots,T, \\ & I_t \leq (1-\delta_t)\sum_{j=1}^{t}(x_j^* - d_j^-), & t = 1,\ldots,T, \\ & B_t \leq \delta_t \sum_{j=1}^{t}(d_j^+ - x_j^*), & t = 1,\ldots,T, \\ & \delta_t \in \{0,1\}, & t = 1,\ldots,T. \end{array} \quad (4)$$

Let s_t^w, B_t^w, I_t^w and δ_t, $t = 1,\ldots,T$, be an optimal solution to problem (4). Then $S^w = (s_1^w,\ldots,s_T^w)$ is a worst case scenario for $\boldsymbol{x}^*$ (a pessimistic realization of uncertain demands) and I_t^w is storing inventory amount from period t to period $t+1$ and B_t^w is backordering amount from period $t+1$ to period t under the worst case scenario S^w. The last two constraints model (4) and the binary variables δ_t ensure that storing inventory from period t to period $t+1$ and backordering from period $t+1$ to period t is not performed simultaneously (either $I_t > 0$ or $B_t > 0$). If $\delta_t = 1$ then backordering is performed $B_t > 0$; otherwise storing inventory is performed $I_t > 0$.

In order to assert *necessity* that the cost of a given plan $\boldsymbol{x}^* \in \mathbb{X}$ does not exceed a given threshold g under interval demands, i.e. evaluating whether $F(\boldsymbol{x}^*, S) \leq g$ for every scenario $S \in \Gamma$, we only need to determine worst case scenario S^w by solving (4) and evaluate $F(\boldsymbol{x}^*, S^w) \leq g$. Moreover, by means of worst case scenario S^w, for a given solution $\boldsymbol{x}^* \in \mathbb{X}$, one can determine the upper bound on its possible values of costs, namely $F(\boldsymbol{x}^*, S) \leq F(\boldsymbol{x}^*, S^w)$ for every scenario $S \in \Gamma$.

Let us consider the problem ROB with no capacity limits, i.e. the problem with the set $\mathbb{X} = \{(x_1,\ldots,x_T) : x_t \geq 0, t = 1,\ldots,T\}$. Note that function $F(\boldsymbol{x}, S)$ is continuous on $\mathbb{X}$ and Γ, Γ is a closed bounded set, and so $A(\boldsymbol{x})$ is well defined continuous function on $\mathbb{X}$ (see, e.g., [17, Theorem 1.4]). One can show that an optimal robust production plan $\hat{\boldsymbol{x}} = (\hat{x}_1,\ldots,\hat{x}_T)$, i.e. $\hat{\boldsymbol{x}} = \arg\ \min_{\boldsymbol{x}\in\mathbb{X}} A(\boldsymbol{x})$, can be computed by the following formulae:

$$\begin{array}{ll} \hat{\mathbf{X}}_1 := \frac{c_B \mathbf{D}_1(S^+) + c_I \mathbf{D}_1(S^-)}{c_B + c_I}, & \hat{x}_1 := \hat{\mathbf{X}}_1 \\ \hat{\mathbf{X}}_t := \frac{c_B \mathbf{D}_t(S^+) + c_I \mathbf{D}_t(S^-)}{c_B + c_I}, & \hat{x}_t := \hat{\mathbf{X}}_t - \hat{\mathbf{X}}_{t-1}, \quad t \geq 2. \end{array} \quad (5)$$

An algorithm for determining optimal robust production plan $\hat{\boldsymbol{x}}$ according to (5) can be implemented in $O(n)$ time. Note that if an initial backorder B_0 or an initial inventory I_0 are not equal to zero then one can modify the interval demand D_1 as follows: $D_1 := [d_1^- + B_0, d_1^+ + B_0]$ if $B_0 > 0$ or $D_1 := [d_1^- - I_0, d_1^+ - I_0]$ if $0 < I_0 \leq d_1^-$, and apply formulae (5) to determine an optimal robust production plan for problem ROB with the modified demand. If $I_0 > d_1^-$ then one appends period 0, as it has been described in Section II, and applies an algorithm (Algorithm 1 - presented later in this section) for the case with capacity limits, $l_t = 0$, $u_t = M$, $t = 1,\ldots,T$, where M is a large number.

Let us turn to the problem ROB with capacity limits, i.e. the problem with the set $\mathbb{X} = \{(x_1,\ldots,x_T) : l_t \leq x_t \leq u_t, t = 1,\ldots,T\}$. Notice Γ is a bounded closed set. Function $F(\boldsymbol{x}, S)$ is continuous on $\mathbb{X}$ and Γ and hence $A(\boldsymbol{x})$ is continuous function on $\mathbb{X}$ (see, e.g., [17, Theorem 1.4]). From this and the fact $\mathbb{X}$ is a bounded closed set it follows that $A(\boldsymbol{x})$ attains its minimum on $\mathbb{X}$.

We now construct an iterative algorithm for solving problem ROB based on on iterative relaxation scheme for min-max problems proposed in [18]. Similar methods were developed for min-max regret linear programming problems with an interval objective function [19], [20]. Let us consider the problem (RX-ROB) being a relaxation of problem ROB that consists in replacing a given scenario set Γ with a discrete scenario set $\Gamma_{\text{dis}} = \{S^1,\ldots,S^K\}$:

$$\begin{array}{lll} \text{RX-ROB:} & a^* = \min a & \\ & \text{s.t.} \quad a \geq F(\boldsymbol{x}, S^k) & \forall S^k \in \Gamma_{\text{dis}}, \\ & \boldsymbol{x} \in \mathbb{X}, & \end{array} \quad (6)$$

where $S^k = (s_t^k)_{t=1}^T$. The constraint $a \geq F(\boldsymbol{x}, S^k)$, called *scenario cut*, is associated with exactly one scenario $S^k \in \Gamma_{\text{dis}}$. Obviously, the maximal cost a^* of an optimal solution $\boldsymbol{x}^*$ of problem RX-ROB over discrete scenario set Γ_{dis} is a lower bound on the maximal cost of an optimal robust production plan $\boldsymbol{x}^r$ for problem ROB, i.e. $a^* \leq A(\boldsymbol{x}^r)$. Note that the scenario cut, $a \geq F(\boldsymbol{x}, S^k)$, associated with S^k is not a linear constraint. One can linearize the cut by replacing it in RX-ROB with the following $T+1$ constraints and $2T$ new decision variables:

$$\begin{array}{ll} a \geq \sum_{t=1}^{T}(c_I I_t^{S^k} + c_B B_t^{S^k}), & \\ B_t^{S^k} - I_t^{S^k} = \sum_{j=1}^{t}(s_j^k - x_j), & t = 1,\ldots,T, \\ B_t^{S^k}, I_t^{S^k} \geq 0, & t = 1,\ldots,T. \end{array}$$

Our algorithm (Algorithm 1) starts with zero lower bound on the maximal cost of an optimal robust production plan $\boldsymbol{x}^r$, $LB = 0$, a candidate $\boldsymbol{x}^* \in \mathbb{X}$ for an optimal solution for ROB and empty discrete scenario set, $\Gamma_{\text{dis}} = \emptyset$. At each iteration, a worst case scenario S^w for $\boldsymbol{x}^*$ is computed by applying the method (4) - this is the most time consuming part. Clearly, $A(\boldsymbol{x}^*) = F(\boldsymbol{x}^*, S^w)$ is an upper bound on $A(\boldsymbol{x}^r)$, $A(\boldsymbol{x}^r) \leq A(\boldsymbol{x}^*)$. If a termination criterion is fulfilled (usually $A(\boldsymbol{x}^*) \leq LB + \epsilon$, $\epsilon > 0$ is a given tolerance) then algorithm stops with production plan $\boldsymbol{x}^*$, which is an approximation of an optimal robust production plan. Otherwise the worst case scenario $S^w = (s_t^w)_{t=1}^T$ is added to Γ_{dis}, the corresponding to S^w scenario cut is appended to problem RX-ROB. Next the updated linear programming problem RX-ROB is solved to obtain a better candidate $\boldsymbol{x}^*$ for an optimal solution for ROB and new lower bound $LB = a^*$. Since set Γ_{dis} is updated during the course of the algorithm, the computed values lower bounds are nondecreasing sequence of their values. Then new iteration is started.

In order to choose a good initial production plan $\boldsymbol{x}^* \in \mathbb{X}$ in Algorithm 1, we suggest to solve the classical production planning problem (1) with capacity limits (the model (2)) under the midpoint demand scenario S^m, i.e. $d_t(S^m) = (d_t^- + d_t^+)/2$, $t = 1,\ldots,T$ and take an optimal production plan under the midpoint scenario as an initial production plan.

Algorithm 1: Finding an optimal robust production plan.

Input: Interval demands $D_t = [d_t^-, d_t^+]$, $t = 1, \dots T$, costs c_I, c_B, initial production plan $\boldsymbol{x}^* \in \mathbb{X}$, a convergence tolerance parameter $\epsilon > 0$.

Output: A production plan $\hat{\boldsymbol{x}}^r$, an approximation of an optimal robust production plan, and its worst case scenario S^w.

Step 0. $k := 0$, $LB := 0$, $\Gamma_{\text{dis}} := \emptyset$.

Step 1. $\boldsymbol{x}^k := \boldsymbol{x}^*$.

Step 2. Compute a worst case scenario S^w for $\boldsymbol{x}^k$ by applying the method (4).

Step 3. If $F(\boldsymbol{x}^k, S^w) \leq LB + \epsilon$ then output $\boldsymbol{x}^k, S^w$ and STOP.

Step 4. $k := k + 1$.

Step 5. $S^k := S^w$, $\Gamma_{\text{dis}} := \Gamma_{\text{dis}} \cup \{S^k\}$ and append scenario cut $a \geq F(\boldsymbol{x}, S^k)$ to problem RX-ROB.

Step 6. Compute an optimal solution $(\boldsymbol{x}^*, a^*)$ for RX-ROB, $LB := a^*$, and go to Step 1.

Theorem 1: Algorithm 1 terminates in a finite number of steps for any given $\epsilon > 0$.

Proof: The proof is almost the same as those given in [21, Theorem 2.5] and [18, Theorem 3]. ■

Note that if an initial inventory I_0 or an initial backorder B_0 are not equal to zero then one appends period 0, as it has been described in Section II, and applies Algorithm 1 for $T + 1$ periods.

In order to check the efficiency of Algorithm 1, we performed some computational tests. For every $T = 100, 200, \dots, 1000$, ten instances of the problem ROB with capacity limits were generated. In every instance, $c_I = 1$, $c_B = 10$, the demands and the production capacities were randomly generated intervals $[X, Y]$, where X is an integer-valued random variable uniformly distributed in $\{0, 1, \dots, 99\}$ and Y is an integer-valued random variable uniformly distributed in $\{100, 101, \dots, 199\}$. To solve the generated instances, we used IBM ILOG CPLEX 12.2 library and a computer equipped with Intel Core 2 Duo 2.5 GHz. In Table I, minimal, average and maximal computation times in seconds, required to find optimal robust production plans, are presented. All computations finished in a few iterations and about 98% of the total running time was spent on computing worst case scenarios by MIP model (4). As we can see from the obtained results, Algorithm 1 allows us to solve quite large problems having up to 1000 periods in reasonable time.

TABLE I
MINIMAL, AVERAGE AND MAXIMAL COMPUTATION TIMES IN SECONDS

T	**100**	**200**	**300**	**400**	**500**
MIN	0.22	0.44	1.23	3.91	5.73
AVG	0.42	2.29	7.88	13.28	41.96
MAX	0.90	4.76	25.04	37.38	96.62
T	**600**	**700**	**800**	**900**	**1000**
MIN	9.22	43.22	7.70	35.13	33.94
AVG	104.07	203.86	155.97	335.56	581.95
MAX	396.30	358.20	398.78	580.79	1152.54

IV. FUZZY PROBLEM

In this section, we apply a more elaborate approach to model uncertain demands. Namely, the uncertain demands, in problem (1), are modeled by fuzzy intervals $\widetilde{D}_t$, $t = 1, \dots, T$. A *fuzzy interval* $\widetilde{A}$ is a fuzzy set in $\mathbb{R}$ whose membership function $\mu_{\widetilde{A}}$ is normal, quasi concave and upper semicontinuous. Usually, it is assumed that the support of a fuzzy interval is bounded. The main property of a fuzzy interval is the fact that all its λ-cuts, that is the sets $\widetilde{A}^{[\lambda]} = \{x : \mu_{\widetilde{A}}(x) \geq \lambda\}$, $\lambda \in (0, 1]$, are closed intervals. We will assume that $\widetilde{A}^{[0]}$ is the smallest closed set containing the support of $\widetilde{A}$. So, every fuzzy interval $\widetilde{A}$ can be represented as a family of closed intervals $\widetilde{A}^{[\lambda]} = [a^{-[\lambda]}, a^{+[\lambda]}]$, parametrized by the value of $\lambda \in [0, 1]$. In many applications, the class of *trapezoidal fuzzy intervals* is used. A trapezoidal fuzzy interval, denoted by a quadruple $(a^-, a^+, \alpha, \beta)$, can be represented as a family of intervals $[a^- - \alpha(1-\lambda), a^+ + \beta(1-\lambda)]$ for $\lambda \in [0, 1]$. Notice that this representation contains classical intervals ($\alpha = \beta = 0$) and real numbers (additionally $a^- = a^+$) as special cases.

Here, a membership function of $\widetilde{D}_t$ is regarded as a *possibility distribution* for the values of the unknown demand d_t (see book [5], that is entirely devoted to possibility theory). The *possibility degree* of the assignment $d_t = s$ is $\Pi(d_t = s) = \pi_{d_t}(s) = \mu_{\widetilde{D}_t}(s)$. Let $S = (s_t)_{t=1}^T$ be a scenario that represents a state of the world where $d_t = s_t$, for $t = 1, \dots, T$. It is assumed that the demands are unrelated one to each other. Hence, the possibility distributions associated with the demands induce the following possibility distribution over all scenarios in $S \in \mathbb{R}^T$ (see [22]):

$$\begin{aligned} \pi(S) &= \Pi((d_1 = s_1) \wedge \dots \wedge (d_T = s_T)) \\ &= \min_{t=1,\dots,T} \Pi(d_t = s_t) = \min_{t=1,\dots,T} \mu_{\widetilde{D}_t}(s_t). \end{aligned} \quad (7)$$

The value of $\pi(S)$ stands for the possibility of the event that scenario $S \in \mathbb{R}^T$ will occur. We have thus extended scenario set Γ given by the intervals (see Section III) to the fuzzy case and now $\widetilde{\Gamma}$ is a fuzzy set of scenarios with membership function $\mu_{\widetilde{\Gamma}}(S) = \pi(S)$, $S \in \mathbb{R}^T$. We see at once that the λ-cuts of $\widetilde{\Gamma}$ for every $\lambda \in (0, 1]$ fulfill the following equality:

$$\widetilde{\Gamma}^{[\lambda]} = \{S : \pi(S) \geq \lambda\} = [d_1^{-[\lambda]}, d_1^{+[\lambda]}] \times \dots \times [d_T^{-[\lambda]}, d_T^{+[\lambda]}],$$

which is from (7) and the definition of λ-cut. We also define $\widetilde{\Gamma}^{[0]} = [d_1^{-[0]}, d_1^{+[0]}] \times \dots \times [d_T^{-[0]}, d_T^{+[0]}]$. Notice that $\widetilde{\Gamma}^{\lambda}$, $\lambda \in [0, 1]$, is the classical scenario set containing all scenarios whose possibility of occurrence is not less than λ.

In order to choose a reasonable production plan under fuzziness, we first show how to evaluate a given production plan $\boldsymbol{x} \in \mathbb{X}$. Notice that a cost of a production plan is unknown quantity, denoted by $f_{\boldsymbol{x}}$, since demands are unknown and modeled by fuzzy intervals in the setting of possibility theory. Thus, the unknown cost $f_{\boldsymbol{x}}$ falls within fuzzy interval $\widetilde{F}_{\boldsymbol{x}}$, called *fuzzy cost*, whose membership function $\mu_{\widetilde{F}_{\boldsymbol{x}}}$ is a possibility distribution for the values of fuzzy variable $f_{\boldsymbol{x}}$, $\pi_{\widetilde{F}_{\boldsymbol{x}}} = \mu_{\widetilde{F}_{\boldsymbol{x}}}$,

defined as follows:

$$\mu_{\widetilde{F}_{\boldsymbol{x}}}(v) = \Pi(f_{\boldsymbol{x}} = v) = \sup_{\{S:\, F(\boldsymbol{x},S)=v\}} \pi(S), \quad v \in \mathbb{R}. \tag{8}$$

Making use of (8), we can define the *degree of necessity* that a cost of a given plan $\boldsymbol{x} \in \mathbb{X}$ does not exceed a given threshold g:

$$\begin{aligned} \mathrm{N}(f_{\boldsymbol{x}} \leq g) &= 1 - \Pi(f_{\boldsymbol{x}} > g) = 1 - \sup_{v>g} \pi_{\widetilde{F}_{\boldsymbol{x}}}(v) \\ &= 1 - \sup_{\{S:\, F(\boldsymbol{x},S)>g\}} \pi(S). \end{aligned} \tag{9}$$

It is easily seen that $\mathrm{N}(f_{\boldsymbol{x}} \leq g) = 1 - \lambda$ means that for all scenarios S such that $\pi(S) > \lambda$, costs of plan $\boldsymbol{x}$ under these scenarios do not exceed g.

We now propose two criteria of choosing a robust solution in the fuzzy-valued problem (1). We have a threshold g, and we would like to find a production plan which maximizes the degree of certainty (necessity) that its cost does not exceed threshold g. Thus, we would like to solve the following problem:

$$\max_{\boldsymbol{x}\in\mathbb{X}} \mathrm{N}(f_{\boldsymbol{x}} \leq g). \tag{10}$$

There are no doubts that an optimal production plan computed according to (10) is a robust one, since with the highest degree of certainty costs of the plan over scenarios will not exceed threshold g. Problem (10) is equivalent to the following mathematical programming problem:

$$\begin{array}{ll} \min & \lambda \\ \text{s.t.} & f_{\boldsymbol{x}}^{+[\lambda]} \leq g, \\ & \lambda \in [0,1], \\ & \boldsymbol{x} \in \mathbb{X}. \end{array} \tag{11}$$

If λ^* is the optimal objective and $\boldsymbol{x}^*$ is an optimal solution for problem (11) then $\mathrm{N}(f_{\boldsymbol{x}^*} \leq g) = 1 - \lambda^*$ and $\boldsymbol{x}^*$ is an optimal production plan for (10). If (11) is infeasible then $\mathrm{N}(f_{\boldsymbol{x}} \leq g) = 0$ for all $\boldsymbol{x} \in \mathbb{X}$.

We now present a more general criterion of choosing a robust production plan than (10). Namely, suppose that a decision maker knows her/his preferences about a cost of a production plan $f_{\boldsymbol{x}}$ and expresses it by a *fuzzy goal* $\widetilde{G}$, which is a fuzzy interval with a bounded support and a nonincreasing upper semicontinuous membership function $\mu_{\widetilde{G}} : \mathbb{R}_{\geq 0} \to [0,1]$, such that $\mu_{\widetilde{G}}(v) = 1$ for $v \in [0,g]$. The value of $\mu_{\widetilde{G}}(f_{\boldsymbol{x}})$ is the extent to which cost $f_{\boldsymbol{x}}$ satisfies the decision maker. Now the requirement "$f_{\boldsymbol{x}} \leq g$" is replaced softer one, i.e. "$f_{\boldsymbol{x}} \in \widetilde{G}$". So, using (8), the necessity that event "$f_{\boldsymbol{x}} \in \widetilde{G}$" holds can be expressed as follows:

$$\begin{aligned} \mathrm{N}(f_{\boldsymbol{x}} \in \widetilde{G}) &= 1 - \Pi(f_{\boldsymbol{x}} \notin \widetilde{G}) \\ &= 1 - \sup_{v\in\mathbb{R}} \min\{\pi_{f_{\boldsymbol{x}}}(v), 1 - \mu_{\widetilde{G}}(v)\} \\ &= 1 - \sup_{S} \min\{\pi(S), 1 - \mu_{\widetilde{G}}(F(\boldsymbol{x},S))\}. \end{aligned} \tag{12}$$

Thus, if $\mathrm{N}(f_{\boldsymbol{x}} \in \widetilde{G}) = 1 - \lambda$ means that for all scenarios S such that $\pi(S) > \lambda$, the degree that costs of plan $\boldsymbol{x}$ fall within fuzzy goal $\widetilde{G}$, is not less than $1 - \lambda$. Note that $\mathrm{N}(f_{\boldsymbol{x}} \in \widetilde{G})$ is more general and weaker than $\mathrm{N}(f_{\boldsymbol{x}} \leq g)$. If $\mu_{\widetilde{G}}(v) = 0$ for $v \in (g, \infty)$ then they are the same. Moreover, $\mathrm{N}(f_{\boldsymbol{x}} \leq g) \leq \mathrm{N}(f_{\boldsymbol{x}} \in \widetilde{G})$.

Let us give the second criterion of choosing a robust plan. We have a fuzzy goal $\widetilde{G}$, and we wish to find a production plan which maximizes the necessity degree that costs of the plan fall within fuzzy goal $\widetilde{G}$. Thus we need to solve the following optimization problem,

$$\max_{\boldsymbol{x}\in\mathbb{X}} \mathrm{N}(f_{\boldsymbol{x}} \in \widetilde{G}). \tag{13}$$

We check at once that problem (13) is equivalent to the following mathematical programming problem:

$$\begin{array}{ll} \min & \lambda \\ \text{s.t.} & f_{\boldsymbol{x}}^{+[\lambda]} \leq g^{+[1-\lambda]}, \\ & \lambda \in [0,1], \\ & \boldsymbol{x} \in \mathbb{X}. \end{array} \tag{14}$$

If $(\boldsymbol{x}^*, \lambda^*)$ is an optimal solution for problem (14), then $\mathrm{N}(f_{\boldsymbol{x}^*} \in \widetilde{G}) = 1 - \lambda^*$. If (14) is infeasible then $\mathrm{N}(f_{\boldsymbol{x}} \in \widetilde{G}) = 0$ for all $\boldsymbol{x} \in \mathbb{X}$.

An algorithm for solving problem (14) (resp. (11)) is based on the standard binary search technique in $[0,1]$ (the interval of possible values of λ) which follows from the fact that $f_{\boldsymbol{x}}^{+[\lambda]}$ and $g^{+[1-\lambda]}$ (resp. g) are nonincreasing and nondecreasing functions of λ, respectively. We call the algorithm the *binary search based algorithm*. To find an optimal (x^*, λ^*), $x^* \in \mathbb{X}$, $\lambda^* \in [0,1]$, with a given error tolerance $\xi > 0$, we seek at each iteration, for a fixed λ, a plan $\boldsymbol{x} \in \mathbb{X}$ satisfying $f_{\boldsymbol{x}}^{+[\lambda]} \leq g^{+[1-\lambda]}$ (resp. $f_{\boldsymbol{x}}^{+[\lambda]} \leq g$), which boils down to seeking an optimal robust production plan $\boldsymbol{x}^r$ and its worst case scenario under scenario set $\widetilde{\Gamma}^{[\lambda]}$, i.e. to solving problem ROB (see Section III). Note that $f_{\boldsymbol{x}}^{+[\lambda]} = A(\boldsymbol{x})$ and also that $f_{\boldsymbol{x}}^{+[\lambda]} \leq g^{+[1-\lambda]}$ (resp. $f_{\boldsymbol{x}}^{+[\lambda]} \leq g$) holds for some $\boldsymbol{x} \in \mathbb{X}$ if and only if it holds for an optimal robust production plan under $\widetilde{\Gamma}^{[\lambda]}$. Thus, at each iteration, we use either formulae (5) for the case without capacity limits or Algorithm 1 for the case with capacity limits. If the length of determined interval of possible values of λ is less than ξ, then an optimal robust production plan $\boldsymbol{x}^r$ for a fixed λ, $(\boldsymbol{x}^r, \lambda)$, is an approximation of an optimal solution for problem (14) (resp. (11)) with precision ξ. The running time of the above algorithm is $O(I(T)\log \xi^{-1})$ time, where $\xi > 0$ is a given error tolerance and $I(|T|)$ is time required for finding an optimal robust production plan and its worst case scenario under interval scenario set $\widetilde{\Gamma}^{[\lambda]}$ (the running time of either (5) or Algorithm 1).

In order to evaluate the efficiency of the binary search based algorithm, we show some results of computational experiments. For every $T = 100, 200, \ldots, 1000$, ten instances of the problem (13) with capacity limits were generated. In every instance, $c_I = 1$, $c_B = 10$, the production capacities were randomly generated intervals $[X, Y]$, where X is an integer-valued random variable uniformly distributed in $\{0, 1, \ldots, 99\}$ and Y is an integer-valued random variable uniformly distributed in $\{100, 101, \ldots, 199\}$, the demands are triangular fuzzy intervals with the supports equal to $[0, 199]$ and the modal values equal to Z, where Z is an integer-valued random

TABLE II
AVERAGE COMPUTATION TIMES IN SECONDS.

T	0.00	0.25	0.50	0.75	1.00
100	0.75	0.76	0.74	0.73	0.70
200	3.47	3.47	3.40	3.38	3.37
300	14.03	13.96	13.95	13.93	13.93
400	25.64	25.60	25.64	25.60	25.61
500	34.70	34.68	34.64	34.66	34.56
600	86.74	86.73	86.90	86.78	86.87
700	141.40	141.41	141.05	141.08	141.31
800	210.70	210.81	210.68	210.79	207.91
900	338.86	338.49	338.65	338.86	338.36
1000	668.77	672.50	672.18	672.61	671.49

variable uniformly distributed in $\{0, 1, \ldots, 199\}$, the fuzzy goal $\widetilde{G}$ was modeled as a trapezoidal fuzzy interval $(0, g, 0, \beta)$, where g was chosen as the maximal cost of an optimal robust production plan for the problem ROB without capacity limits (an ideal supplier) and under the interval demands being the supports of the generated triangular fuzzy demands. The values of β were equal to $0.00 \cdot g, 0.25 \cdot g, 0.50 \cdot g, 0.75 \cdot g$ and $1.00 \cdot g$ and the error tolerance $\xi = 0.01$. We used IBM ILOG CPLEX 12.2 library and a computer equipped with Intel Core 2 Duo 2.5 GHz to solve the generated instances. In Table II average computation times in seconds are presented. As we can see from the obtained results, the binary search based algorithm, which calls Algorithm 1 at each iteration, can solve efficiently the problem (13) with capacity limits having up to 1000 periods.

V. CONCLUSION

In this paper, we have investigated a certain version of production planning problem with uncertain demands modeled by fuzzy intervals, whose membership functions are possibility distributions for the values of the unknown demands. We have introduced, in this setting, the degree of necessity that the cost of a plan does not exceed a given threshold and the degree of necessity that costs of a plan fall within a given fuzzy goal, which allows us to evaluate a given production plan. For finding robust production plans under fuzzy demands, we have proposed two criteria: the first one consists in choosing a production plan which maximizes the degree of necessity that its cost does not exceed a given threshold, the second criterion is softer than the first one and consists in choosing a plan with the maximum degree of necessity that costs of the plan fall within a given fuzzy goal. We have constructed the algorithms for determining optimal robust production plans with respect to the criteria and confirmed their efficiency experimentally. The criteria are a generalization, to the fuzzy case, of the known from literature the min-max criterion. Consequently, we have shown in the paper that there exists a link between interval uncertainty with the min-max criterion and possibilistic uncertainty with the necessity based criteria. Therefore, we have discussed first the interval-valued case and then we have extended the methods introduced for the interval-valued problem to the fuzzy-valued one.

ACKNOWLEDGMENT

The second author of the paper was partially supported by Polish Committee for Scientific Research, grant N N206 492938.

REFERENCES

[1] H. L. Lee, V. Padmanabhan, and S. Whang, "Information Distortion in a Supply Chain: The Bullwhip Effect," *Management Science*, vol. 43, pp. 546–558, 1997.
[2] F. Galasso and C. Thierry, "Design of cooperative processes in a customer-supplier relationship: An approach based on simulation and decision theory," *Engineering Applications of Artificial Intelligence*, vol. 22, pp. 865–881, 2009.
[3] S. Agrawal, R. N. Senguptaa, and K. Shanker, "Impact of information sharing and lead time on bullwhip effect and on-hand inventory," *European Journal of Operational Research*, vol. 192, pp. 576–593, 2009.
[4] J. Orlicky, *Material Requirements Planning*. McGraw-Hill, 1975.
[5] D. Dubois and H. Prade, *Possibility theory: an approach to computerized processing of uncertainty*. New York: Plenum Press, 1988.
[6] H. Fargier and C. Thierry, "The Use of Possibilistic Decision theory in manufacturing planning and control: Recent results in fuzzy master production scheduling," in *Advances in Scheduling and Sequencing under fuzziness*, R. Slowiński and M. Hapke, Eds. Spingler-Verlag, 2000, pp. 45–59.
[7] B. Grabot, L. Geneste, G. Reynoso-Castillo, and S. Vérot, "Integration of uncertain and imprecise orders in the MRP method," *Journal of Intelligent Manufacturing*, vol. 16, pp. 215–234, 2005.
[8] R. Guillaume, C. Thierry, and B. Grabot, "Modelling of ill-known requirements and integration in production planning," *Production Planning and Control*, 2010 (to appear).
[9] H. M. Wagner and T. M. Whitin, "Dynamic Version of the Economic Lot Size Model," *Management Science*, vol. 5, pp. 89–96, 1958.
[10] M. Florian, K. J. Lenstra, and A. H. G. Rinnooy Kan, "Deterministic Production Planning: Algorithms and Complexity," *Management Science*, vol. 26, pp. 669–679, 1980.
[11] A. Drexl and A. Kimms, "Lot sizing and scheduling – Survey and extensions," *European Journal of Operational Research*, vol. 99, pp. 221–235, 1997.
[12] B. Karimi, S. M. T. Fatemi Ghomi, and J. M. Wilson, "The capacitated lot sizing problem: a review of models and algorithms," *Omega*, vol. 31, pp. 365–378, 2003.
[13] R. K. Ahuja and D. S. Hochbaum, "Solving Linear Cost Dynamic Lot Sizing Problems in O(n log n) Time," *Operations Research*, vol. 56, pp. 255–261, 2008.
[14] E. Nikolova, J. A. Kelner, M. Brand, and M. Mitzenmacher, "Stochastic shortest paths via quasi-convex maximization," in *ESA*, 2006, pp. 552–563.
[15] A. Kasperski and M. Kulej, "Choosing robust solutions in discrete optimization problems with fuzzy costs," *Fuzzy Sets and Systems*, vol. 160, pp. 667–682, 2009.
[16] R. K. Ahuja, T. L. Magnanti, and J. B. Orlin, *Network Flows: theory, algorithms, and applications*. Englewood Cliffs, New Jersey: Prentice Hall, 1993.
[17] R. Meyer, "The Validity of a Family of Optimization Methods," *SIAM Journal on Control and Optimization*, vol. 8, pp. 41–54, 1970.
[18] K. Shimizu and E. Aiyoshi, "Necessary Conditions for Min-Max Problems and Algorithms by a Relaxation Procedure," *IEEE Transactions on Automatic Control*, vol. 25, pp. 62–66, 1980.
[19] M. Inuiguchi and M. Sakawa, "Minimax regret solution to linear programming problems with an interval objective function," *European Journal of Operational Research*, vol. 86, pp. 526–536, 1995.
[20] H. E. Mausser and M. Laguna, "A heuristic to minimax absolute regret for linear programs with interval objective function coefficients," *European Journal of Operational Research*, vol. 117, pp. 157–174, 1999.
[21] A. M. Geoffrion, "Generalized Benders Decomposition," *Journal of Optimization Theory and Applications*, vol. 10, pp. 237–260, 1972.
[22] D. Dubois, H. Fargier, and V. Galvagnon, "On latest starting times and floats in activity networks with ill-known durations," *European Journal of Operational Research*, vol. 147, pp. 266–280, 2003.

2011 IEEE International Conference on Fuzzy Systems
June 27-30, 2011, Taipei, Taiwan

Min-Max and Two-Stage Possibilistic Combinatorial Optimization Problems

Adam Kasperski
Institute of Industrial Engineering and Management
Wrocław University of Technology
Wybrzeże Wyspiańskiego 27
50-370 Wrocław, Poland
Email: Adam.Kasperski@pwr.wroc.pl

Paweł Zieliński
Institute of Mathematics and Computer Science
Wrocław University of Technology
Wybrzeże Wyspiańskiego 27
50-370 Wrocław, Poland
Email: Pawel.Zielinski@pwr.wroc.pl

***Abstract*—This paper deals with a class of combinatorial optimization problems with uncertain costs. The uncertainty is modeled by specifying a scenario set containing a finite number of possible realizations of the costs called scenarios. Additionally, a possibility distribution on the scenario set can be defined. Two robust models, namely the min-max and two-stage, for hedging against uncertainty of the costs in the possibilistic setting are considered. A general framework for solving the problems is proposed. For the linear sum objective a mixed integer programing formulation is shown. For the bottleneck objective, an algorithm is constructed which runs in polynomial time if the deterministic problem, i.e. the one with a single scenario, is polynomially solvable.**

***Index Terms*—Min-Max, Uncertain Cost, Fuzzy Optimization, Possibility Theory.**

I. Introduction

A *combinatorial optimization problem* discussed in this paper consists of a finite set of elements E and a set Φ of subsets of E, called the set of *feasible solutions*. In the deterministic case, each element in E has a precise cost and we wish to find a feasible solution whose total cost is minimal (the *linear sum* objective) or whose the largest element cost is minimal (the *bottleneck* objective). This formulation encompasses a large variety of problems. It contains, for example, the important class of *network problems*, where E is a set of the edges of a given graph G and Φ consists of some objects in G such as trees, paths or matchings (see, e.g., [1]).

The usual assumption in combinatorial optimization is that the element costs are precisely known. However, in real life this requirement is seldom satisfied and, in many optimization models, a possible uncertainty of costs must be taken into account. In general, this uncertainty can be modeled by specifying a *scenario set* which contains all possible cost realizations, called *scenarios*. This scenario set can be defined in several ways. In the *discrete scenario representation*, which is considered in this paper, we simply list all the possible scenarios. In the *interval scenario representation*, we specify for each cost a closed interval containing all its values. This means that we neither know the exact costs, nor can we set them precisely. The scenario set is then the Cartesian product of all the uncertainty intervals (see, e.g., [2]). For this representation, it is assumed that the costs are unrelated, that is the value of a cost does not depend on the values of the remaining costs. The interval scenario representation can be generalized by assuming that the scenario set is any convex set (see, e.g., [3]), which allows us to model the relationships between the costs. We can also use a combination of discrete and interval uncertainty representations (see, e.g., [4]).

A criterion of choosing a solution depends on additional information provided with the scenario set. If a probability distribution on the scenario set is specified, then the *stochastic optimization* can be used [5], where the typical goal is to optimize the expected cost of a solution built. If there is no probability distribution on the scenario set, then the *robust optimization can be* applied [2], [6]. In order to choose a solution in this setting, the *min-max* criterion can be used. Under this criterion, we seek a solution which minimizes the largest cost over all scenarios. We can consider a *single-stage model* in which a complete solution must be determined before a cost scenario is observed (see, e.g., [2]) or a *two-stage model*, where only a partial solution must be computed when the costs are precisely known and completed when a cost scenario is observed (see, e.g., [7], [8]). Finally, if a possibility distribution on the scenario set is given, then the *fuzzy optimization* is appropriate [9], [10], [11]. In the fuzzy optimization, the goal is to choose a solution optimizing a criterion based on the *possibility* or *necessity* measures.

In this paper, we consider the discrete scenario uncertainty representation. So, we assume that the scenario set contains a finite number of distinct scenarios (element cost realizations). A decision maker can additionally specify a possibility distribution on the scenario set which describes more or less plausible scenarios. Namely, she/he can assign a number from the interval [0,1] to each scenario, which is the possibility of the event that this scenario will occur. Such a more elaborate description of scenario sets is often required in practical applications, where decision makers may know likely scenarios, but the probability distributions are unknown or there is lack of statistical data validating the choice of the probability distributions. In this paper, we propose the solution concepts which generalize the single and two stage models with the min-max criterion. We thus extend the robust approach to the fuzzy one by using *possibility theory* [12] which offers

978-1-4244-7316-8/11/$26.00 ©2011 IEEE

a framework of decision making under uncertainty and allows us to extend the robust models in a natural way.

II. Combinatorial Optimization Problem with Deterministic Costs

Let $E = \{e_1, \ldots, e_n\}$ be a finite ground set and let $\Phi \subseteq 2^E$ be a set of subsets of E called the set of the *feasible solutions*. A nonnegative cost c_e is given for each element $e \in E$. In a combinatorial optimization problem $\mathcal{P}$ with the linear sum objective, we seek a solution $X \in \Phi$ whose total cost, $f(X) = \sum_{e \in X} c_e$, is minimal. In a combinatorial optimization problem $\mathcal{BP}$ with the bottleneck objective, we wish to find a solution $X \in \Phi$ whose largest element cost, $f(X) = \max_{e \in X} c_e$, is minimal. The formulations $\mathcal{P}$ and $\mathcal{BP}$ encompass a large variety of classical combinatorial optimization problems such as the shortest path, the minimum spanning tree, the minimum cost matching, the 0-1 knapsack *etc.* (see, e.g. [13], [1], [14]). The problem $\mathcal{P}$ is often formulated as the following mathematical programming problem:

$$\begin{array}{ll} \min & \sum_{i=1}^{n} c_i x_i \\ & (x_1, \ldots, x_n) \in \Phi' \\ & x_i \in \{0,1\} \qquad\qquad i = 1, \ldots, n, \end{array} \tag{1}$$

where x_i is a binary variable equal to 1 if and only if element e_i belongs to the solution computed. Thus Φ' is the set of all characteristic vectors of Φ and the condition $(x_1, \ldots, x_n) \in \Phi'$ is specified in the form of constraints involving variables $x_1, \ldots, x_n$. It is worth pointing out that many important combinatorial problems are NP-hard (see e.g., [1]). The framework proposed in this paper can also be applied to the NP-hard problems if one can represent them in the form of (1).

III. Basic Notions of Possibility Theory

Possibility theory [12] is an approach for dealing with incomplete information and is based on two dual measures: *possibility* and *necessity*, which express plausibility and certainty of events. Both measures are built from a *possibility distribution*. Let Z be a real valued quantity whose value is not precisely known. We specify for Z a *possibility distribution* π_{Z}, which describes the set of more or less plausible, mutually exclusive values of Z. The value of $\pi_{\mathrm{Z}}(z) = \Pi(\mathrm{Z} = z)$ is a possibility of the event that Z will take the value of z. In particular, $\pi_{\mathrm{Z}}(z) = 0$ means that $\mathrm{Z} = z$ is impossible and $\pi_{\mathrm{Z}}(z) > 0$ means that $\mathrm{Z} = z$ is plausible. The possibility distribution encodes a family of probability functions and a degree of possibility can be viewed as an upper bound on a degree of probability [15]. A detailed interpretation of the possibility distribution and some methods of obtaining it from a knowledge possessed about Z are described in [12].

Let $\tilde{A}$ be a fuzzy set in $\mathbb{R}$ with membership function $\mu_{\tilde{A}}$. Then $\mathrm{Z} \in \tilde{A}$ is a *fuzzy event* and we can determine the possibility that this event will occur in the following way:

$$\Pi(\mathrm{Z} \in \tilde{A}) = \sup_{z \in \mathbb{R}} \min\{\pi_{\mathrm{Z}}(z), \mu_{\tilde{A}}(z)\}. \tag{2}$$

Thus $\Pi(\mathrm{Z} \in \tilde{A})$ evaluates the extent to which "$\mathrm{Z} \in \tilde{A}$" is possibly true. We can also determine the necessity of the event $\mathrm{Z} \in \tilde{A}$ in the following way:

$$\mathrm{N}(\mathrm{Z} \in \tilde{A}) = 1 - \Pi(\mathrm{Z} \in \tilde{A}'), \tag{3}$$

where $\tilde{A}'$ is the complement of $\tilde{A}$ with the membership function $1 - \mu_{\tilde{A}}(z)$. Hence, $\mathrm{N}(\mathrm{Z} \in \tilde{A})$ evaluates the extent to which "$\mathrm{Z} \in \tilde{A}$" is certainly true. If A is a crisp subset of $\mathbb{R}$, then it is easy to verify that $\Pi(\mathrm{Z} \in A) = \sup_{z \in A} \pi_{\mathrm{Z}}(z)$ and $\mathrm{N}(\mathrm{Z} \in A) = \inf_{z \notin A}(1 - \pi_{\mathrm{Z}}(z))$.

IV. Possibilistic Min-Max Problem

Consider a situation in which the costs of the elements $e_1, \ldots, e_n$ are uncertain. This uncertainty is modeled by specifying a scenario set Γ which is defined by explicitly listing all the possible element cost vectors. Thus $\Gamma = \{S_1, \ldots, S_K\}$ is finite and contains exactly K scenarios, where a scenario S_j, $j = 1, \ldots, K$, is a vector of the element costs $S_j = (c_{1j}, c_{2j}, \ldots, c_{nj})$. Additionally, a possibility distribution on the scenario set is specified. This possibility distribution expresses the fact that some scenarios are more plausible than others. Hence, for each scenario S_j a number $\pi(S_j) \in [0, 1]$ is given, which denotes the possibility of the event that S_j will occur. The value of $\pi(S_j)$ can also be seen as an upper bound on the probability of occurring S_j [15]. It is convenient to represent the uncertain costs in the form of Table I whose columns contain all the cost scenarios in Γ.

TABLE I
The scenario representation of the uncertain costs

	$\pi(S_1)$	$\pi(S_2)$	$\ldots$	$\pi(S_K)$
	S_1	S_2	$\ldots$	S_K
e_1	c_{11}	c_{12}	$\ldots$	c_{1K}
e_2	c_{21}	c_{22}	$\ldots$	c_{2K}
e_3	c_{31}	c_{32}	$\ldots$	c_{3K}
$\vdots$	$\vdots$	$\vdots$	$\ldots$	$\vdots$
e_n	c_{n1}	c_{n2}	$\ldots$	c_{nK}

A. Linear Sum Criterion

Let $f(X, S_j) = \sum_{e_i \in X} c_{ij}$ be the cost of solution X under scenario S_j. We will denote by $\mathrm{f(X)}$ the uncertain cost of X, i.e. a real variable whose value depends on scenario $S_j \in \Gamma$. The uncertain cost $\mathrm{f(X)}$ has the following possibility distribution $\pi_{\mathrm{f(X)}}$:

$$\pi_{\mathrm{f(X)}}(z) = \max_{\{j : f(X, S_j) = z\}} \pi(S_j) \tag{4}$$

and $\pi_{\mathrm{f(X)}}(z) = 0$ if $f(X, S_j) \neq z$ for all $j = 1, \ldots, K$. Hence, $\pi_{\mathrm{f(X)}}(z) = \Pi(\mathrm{f(X)} = z)$ is the possibility of the event that the cost of X will take value of z. To illustrate this idea, let us consider the example of the shortest path problem presented in Fig. 1.

In this problem $E = \{e_1, \ldots, e_5\}$ is the set of arcs of a given graph G and $\Phi = \{\{e_1, e_4\}, \{e_1, e_3, e_5\}, \{e_2, e_5\}\}$ contains all directed paths between s and t in G. There are six cost scenarios listed in the table and each scenario has some possibility of occurrence. The possibility distribution of

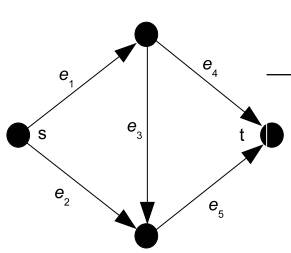

	0.6	0.8	0.8	0.5	1	0.3
	S_1	S_2	S_3	S_4	S_5	S_6
e_1	3	4	1	5	4	2
e_2	1	6	3	4	3	7
e_3	2	3	2	2	2	1
e_4	3	8	1	7	2	4
e_5	1	1	7	2	2	1

Fig. 1. An example of the shortest path problem with uncertain costs

the cost $\mathrm{f(X)}$ for the path $X = \{e_1, e_3, e_5\}$ is shown in Fig. 2. Observe that the path X has a cost of 8 under two scenarios S_2 and S_5 and, according to (4), $\pi_{\mathrm{f(X)}}(8) = \Pi(\mathrm{f(X)} = 8) = \max\{\pi(S_2), \pi(S_5)\} = 1$.

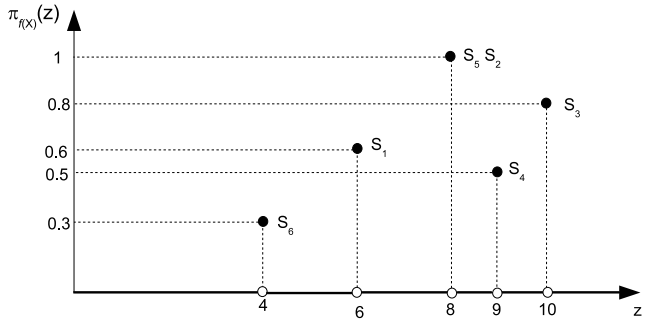

Fig. 2. The possibility distribution for $\mathrm{f}(X)$, where $X = \{e_1, e_3, e_5\}$

Now assume that a decision maker expresses her/his preferences about solution costs by means of a *fuzzy goal* $\tilde{G}$. The membership function of $\tilde{G}$ has the following form:

$$\mu_{\tilde{G}}(z) = \begin{cases} 1 & \text{if} \quad z \leq g \\ 1 - \frac{g-z}{\beta} & \text{for} \quad z \in [g, g+\beta] \\ 0 & \text{if} \quad z \geq g+\beta \end{cases} \tag{5}$$

The interpretation of $\tilde{G}$ is as follows. The solution costs less than g are totally accepted and the solution costs greater than $g + \beta$ are not at all accepted. The acceptance of the solution costs decreases linearly between g and $g + \beta$. In general, a fuzzy goal $\widetilde{G}$ can be any fuzzy set in $\mathbb{R}$ with a bounded support and the membership function $\mu_{\widetilde{G}}$ being a nonincreasing mapping from $[0, \infty)$ into $[0, 1]$ such that $\mu_{\widetilde{G}}(z) = 1$ for $z \in [0, g]$. In this paper we use the membership function (5) to simplify the presentation. We will denote by $\tilde{G}'$ the complement of $\tilde{G}$ with the membership function $1 - \mu_{\tilde{G}}(z)$.

Now, we are ready to give a criterion of choosing a robust solution in problem $\mathcal{P}$ with the uncertain costs. Having a fuzzy goal $\tilde{G}$ we would like to find a solution $X \in \Phi$, whose cost belongs to $\tilde{G}$ with the highest necessity (certainty). Thus, we would like to solve the following problem:

$$\text{POSS MIN-MAX } \mathcal{P}: \quad \max_{X \in \Phi} \mathrm{N}(\mathrm{f(X)} \in \tilde{G}). \tag{6}$$

There are no doubts that every optimal solution to (6) is robust, since the cost of such a solution falls within $\tilde{G}$ with the highest degree of certainty. Since $\mathrm{N}(\mathrm{f(X)} \in \tilde{G}) = 1 - \Pi(\mathrm{f(X)} \in \tilde{G}')$, problem (6) is equivalent to

$$\min_{X \in \Phi} \Pi(\mathrm{f(X)} \in \tilde{G}'). \tag{7}$$

By (2) and (4) we obtain

$$\begin{aligned} \Pi(\mathrm{f(X)} \in \tilde{G}') &= \sup_{z \in \mathbb{R}} \min\{\pi_{\mathrm{f(X)}}(z), \mu_{\tilde{G}'}(z)\} \\ &= \max_{j=1,\ldots,K} \min\{\pi(S_j), \mu_{\tilde{G}'}(f(X, S_j))\}, \end{aligned} \tag{8}$$

which is illustrated in Fig. 3.

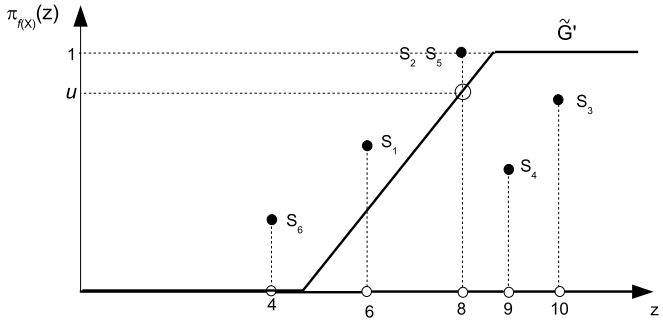

Fig. 3. $\Pi(\mathrm{f(X)} \in \tilde{G}') = u$ for the path $X = \{e_1, e_3, e_5\}$

Observe that $\mathrm{N}(\mathrm{f(X)} \in \tilde{G}) = 1$ if $\Pi(\mathrm{f(X)} \in \tilde{G}') = 0$, i.e. when the cost of X under every scenario $S_j \in \Gamma$ such that $\pi(S_j) > 0$ is totally accepted. On the other hand, $\mathrm{N}(\mathrm{f(X)} \in \tilde{G}) = 0$ if $\Pi(\mathrm{f(X)} \in \tilde{G}') = 1$, i.e. when the cost of X under some scenario S_j such that $\pi(S_j) = 1$ is not at all accepted. In the example presented in Fig. 3 an intermediate situation is shown, where $\mathrm{N}(\mathrm{f(X)} \in \tilde{G}) \in (0, 1)$. Note that the solution costs under scenarios S_3 and S_4, which are not at all accepted (i.e. belong to $\tilde{G}'$ with degree 1), occur with possibility less than 1. Using (7) and (8), we can represent POSS MIN-MAX $\mathcal{P}$ as the following mathematical programming problem:

$$\begin{array}{l} \min u \\ u \geq \min\{\pi(S_j), \mu_{\tilde{G}'}(f(X, S_j))\}, \quad 1 \leq j \leq K, \\ X \in \Phi, \\ u \geq 0 \end{array} \tag{9}$$

Let us introduce additional binary variables $\delta_j \in \{0, 1\}$, $j = 1, \ldots, K$, and a sufficiently large constant M. We then get the following equivalent formulation:

$$\begin{array}{ll} \min u & \\ u \geq \pi(S_j) - M\delta_j, & 1 \leq j \leq K, \\ u \geq \mu_{\tilde{G}'}(f(X, S_j)) - M(1 - \delta_j), & 1 \leq j \leq K, \\ X \in \Phi, & \\ \delta_j \in \{0, 1\}, & 1 \leq j \leq K, \\ u \geq 0. & \end{array} \tag{10}$$

From (5) and the equality $f(X, S_j) = \sum_{i=1}^{n} c_{ij} x_i$, we obtain:

$$\begin{array}{ll} \min u & \\ u \geq \pi(S_j) - M\delta_j, & 1 \leq j \leq K, \\ u \geq \frac{1}{\beta} \sum_{i=1}^{n} c_{ij} x_i - \frac{g}{\beta} - M(1 - \delta_j), & 1 \leq j \leq K, \\ (x_1, \ldots, x_n) \in \Phi', & \\ \delta_j \in \{0, 1\} & 1 \leq j \leq K, \\ x_i \in \{0, 1\}, & 1 \leq i \leq n, \\ u \geq 0, & \end{array} \tag{11}$$

where x_i is a binary variable equal to 1 if and only if element e_i belongs to the solution computed. For a particular problem, $(x_1, \ldots, x_n) \in \Phi'$ can be replaced with a set of linear constraints. As the result we obtain a mixed integer linear programming (MIP) model which can be solved by the available and powerful software such as CPLEX. If X^* is an optimal solution to (11) with an objective value of u^*, then $\mathrm{N}(\mathrm{f}(\mathrm{X}^*) \in \tilde{G}) = 1 - u^*$. We now illustrate the approach using two examples. In the first example the deterministic problem is polynomially solvable while in the second one it is NP-hard.

Example 1: Consider the following *shortest path problem* with imprecise costs (POSS MIN-MAX SHORTEST PATH). We are given a digraph $G = (V, A)$ with uncertain arc costs. Namely, for each arc $(k, l) \in A$ a cost $c_{(k,l)j}$ of this arc under scenario S_j, $j = 1, \ldots, K$, is specified. We distinguish two nodes s and t in G and seek a directed path X from s to t which maximizes $\mathrm{N}(\mathrm{f}(\mathrm{X}) \in \tilde{G})$. Let us introduce a binary variable $x_{(k,l)}$ for each arc $(k, l) \in A$, $x_{(k,l)}$ is equal to 1 if and only if the arc (k, l) belongs to the path computed. The set Φ' is described by the standard mass balance constraints (see e.g., [14]). Hence, we obtain the following MIP model for the problem:

$$
\begin{array}{ll}
\min u & \\
u \geq \pi(S_j) - M\delta_j, & 1 \leq j \leq K, \\
u \geq \frac{1}{\beta} \sum_{(k,l)\in A} c_{(k,l)j} x_{(k,l)} - \frac{g}{\beta} - M(1 - \delta_j), & 1 \leq j \leq K, \\
\sum_{\{l:(k,l)\in A\}} x_{(k,l)} - \sum_{\{l:(l,k)\in A\}} x_{(l,k)} = b(k), & k \in V, \\
x_{(k,l)} \in \{0, 1\}, & (k, l) \in A, \\
\delta_j \in \{0, 1\}, & 1 \leq j \leq K, \\
u \geq 0, &
\end{array}
$$

where $b(s) = 1$, $b(t) = -1$ and $b(k) = 0$ for all $k \in V \setminus \{s, t\}$.

Example 2: Consider the following *minimum cost knapsack problem* (POSS MIN-MAX MINIMUM COST KNAPSACK). We are given a set of items $E = \{e_1, \ldots, e_n\}$. Each item e_i has a precise weight w_i and imprecise cost, where c_{ij} is the cost of e_i under scenario S_j, $j = 1, \ldots, K$. We would like to find a subset X of the items of the total weight at most W which maximizes $\mathrm{N}(\mathrm{f}(\mathrm{X}) \in \tilde{G})$. Contrary to the shortest path problem discussed in the previous example, the deterministic knapsack problem with one scenario is NP-hard. Nevertheless, by introducing binary variable x_i for each item $e_i \in E$, where x_i is equal to 1 if and only if item e_i belongs to the subset computed, we can propose the following mixed integer programming model for the problem:

$$
\begin{array}{ll}
\min u & \\
u \geq \pi(S_j) - M\delta_j, & 1 \leq j \leq K, \\
u \geq \frac{1}{\beta} \sum_{i=1}^{n} c_{ij} x_i - \frac{g}{\beta} - M(1 - \delta_j), & 1 \leq j \leq K, \\
\sum_{i=1}^{n} w_i x_i \leq W, & \\
x_i \in \{0, 1\}, & 1 \leq 1 \leq n, \\
\delta_j \in \{0, 1\}, & 1 \leq j \leq K, \\
u \geq 0. &
\end{array}
$$

Examples 1 and 2 show that our approach is general and can also be applied to the problems whose deterministic versions are NP-hard. The obtained MIP model can be solved by using some standard off-the-shelf MIP solvers.

Now we show that POSS MIN-MAX $\mathcal{P}$ is a generalization of the min-max robust problem $\mathcal{P}$, i.e. the problem $\mathcal{P}$ with the min-max criterion, where no probability and possibility distributions on the scenario set are given. Suppose that $\pi(S_j) = 1$ for all scenarios $S_j \in \Gamma$, which means that a decision maker believes that all the scenarios in Γ are equally possible to occur. Let us choose a fuzzy goal $\tilde{G}$ such that $g = 0$ and β is sufficiently large, so that the inequality $\frac{1}{\beta} \sum_{i=1}^{n} c_{ij} x_i \leq 1$ always holds. We can set, for example, $\beta = \sum_{i=1}^{n} \sum_{j=1}^{K} c_{ij}$. Then the model (11) can be simplified as follows:

$$
\begin{array}{ll}
\min u & \\
u \geq \frac{1}{\beta} \sum_{i=1}^{n} c_{ij} x_i & 1 \leq j \leq K \\
(x_1, \ldots, x_n) \in \Phi' & \\
u \geq 0 &
\end{array}
\tag{12}
$$

Substituting $z = \beta u$ in (12) yields:

$$
\begin{array}{ll}
\min z & \\
z \geq \sum_{i=1}^{n} c_{ij} x_i & 1 \leq j \leq K \\
(x_1, \ldots, x_n) \in \Phi' & \\
z \geq 0 &
\end{array}
\tag{13}
$$

which is the well known min-max robust combinatorial optimization problem with scenario set Γ [2]. This implies that all the negative complexity results known for (13) hold true for POSS MIN-MAX $\mathcal{P}$. The robust min-max problems are typically NP-hard and also hard to approximate. Hence, POSS MIN-MAX $\mathcal{P}$ cannot be easier. We refer the reader to [6], [2], [16], [17] for some complexity results for the min-max versions of the classical combinatorial optimization problems.

B. Bottleneck Criterion

It turns out that the problem becomes easier to solve if we replace the linear sum criterion with the bottleneck one. Assume that the cost of solution X under scenario S_j is expressed as $f(X, S_j) = \max_{e_i \in X} c_{ij}$. The uncertain cost $\mathrm{f}(X)$ of solution X is defined exactly the same as (4) and we seek a solution X maximizing $\mathrm{N}(\mathrm{f}(\mathrm{X}) \in \tilde{G})$ (or, equivalently, minimizing $\Pi(\mathrm{f}(\mathrm{X}) \in \tilde{G}')$). From (8) we get:

$$
\Pi(\mathrm{f}(\mathrm{X}) \in \tilde{G}') = \max_{j=1,\ldots,K} \min\{\pi(S_j), \mu_{\tilde{G}'}(\max_{e_i \in X} c_{ij})\}.
$$

Function $\mu_{\tilde{G}'}$ is nondecreasing ($\mu_{\tilde{G}}$ is nonincreasing), therefore

$$
\begin{aligned}
\Pi(\mathrm{f}(\mathrm{X}) \in \tilde{G}') &= \max_{j=1,\ldots,K} \min\{\pi(S_j), \max_{e_i \in X} \mu_{\tilde{G}'}(c_{ij})\} \\
&= \max_{e_i \in X} \max_{j=1,\ldots,K} \min\{\pi(S_j), \mu_{\tilde{G}'}(c_{ij})\}
\end{aligned}
$$

Set $c_i^* = \max_{j=1,\ldots,K} \min\{\pi(S_j), \mu_{\tilde{G}'}(c_{ij})\}$, $e_i \in E$, and in consequence

$$
\min_{X \in \Phi} \Pi(\mathrm{f}(\mathrm{X}) \in \tilde{G}') = \min_{X \in \Phi} \max_{e_i \in X} c_i^*,
$$

which is a deterministic bottleneck combinatorial optimization problem. So, POSS MIN-MAX $\mathcal{BP}$ can be reduced to problem $\mathcal{BP}$ with deterministic costs c_i^*, $e_i \in E$. We have thus proved the following theorem:

Theorem 1: If problem $\mathcal{BP}$ is polynomially solvable, then problem POSS MIN-MAX $\mathcal{BP}$ is also polynomially solvable.

The above result holds true for a wide class of classical polynomially solvable bottleneck combinatorial ooptimization problems [18], [19], [20], [21].

V. Possibilistic Two-Stage Problem

Suppose that we are given first stage element costs C_i for all $e_i \in E$ and these costs are precisely known. In the second stage the costs are imprecise and all the possible cost scenarios are listed in scenario set $\Gamma = \{S_1, \ldots, S_K\}$. Additionally, a possibility distribution π is specified in Γ and its interpretation is the same as for the single-stage problem discussed in the previous section. An instance of the problem can be represented in the form of Table II.

TABLE II
The representation of costs in two stages

	stage I	stage II			
		$\pi(S_1)$	$\pi(S_2)$	$\ldots$	$\pi(S_K)$
		S_1	S_2	$\ldots$	S_K
e_1	C_1	c_{11}	c_{12}	$\ldots$	c_{1K}
e_2	C_2	c_{21}	c_{22}	$\ldots$	c_{2K}
e_3	C_3	c_{31}	c_{32}	$\ldots$	c_{3K}
$\vdots$	$\vdots$	$\vdots$	$\vdots$	$\ldots$	$\vdots$
e_n	C_n	c_{n1}	c_{n2}	$\ldots$	c_{nK}

Let $X \subseteq E$ be a part of a feasible solution determined in the first stage. The cost of X under scenario $S_j \in \Gamma$ is then

$$f(X, S_j) = \sum_{e_i \in X} C_i + \min_{\{Y_j : X \cup Y_j \in \Phi\}} \sum_{e_i \in Y_j} c_{ij}.$$

So, a decision consists of choosing a partial solution X in the first stage and augmenting it optimally to a complete feasible solution $X \cup Y_j$ after observing that scenario S_j has occurred in the second stage. The cost f(X) of a partial solution X is uncertain and its possibility distribution is defined in the same way as (4).

Consider the following example. A set of eight elements $E = \{e_1, \ldots, e_8\}$ is given and we must select exactly 5 out of them. We can select any $X \subset E$ such that $|X| \leq 5$ in the first stage and complete it, after observing which of the six scenarios in $\Gamma = \{S_1, \ldots, S_6\}$ has occurred. The representation of the costs in both stages for this problem is shown in Table III.

TABLE III
The representation of costs for the sample problem

	stage I	stage II					
		0.4	0.3	0.6	0.8	1	0.7
		S_1	S_2	S_3	S_4	S_5	S_6
e_1	5	5	1	2	1	3	2
e_2	4	5	3	2	9	3	5
e_3	2	8	1	6	1	1	9
e_4	7	4	4	7	8	3	5
e_5	4	9	1	1	8	7	7
e_6	7	6	3	1	9	8	8
e_7	5	1	1	4	6	1	5
e_8	3	1	1	1	2	1	2

Suppose that a decision maker decides to select two elements, say e_3 and e_5, in the first stage. Therefore, $X = \{e_3, e_5\}$ and the cost in the first stage is 6. The cost $f(X, S_j)$ depends now on a scenario S_j that will occur. For instance, if scenario S_1 is observed, then the subset X is completed to form a feasible solution (a five element subset of E) by choosing the elements in $Y_1 = \{e_5, e_8, e_7\}$, which gives the smallest cost $f(X, S_1)$ equal to 12. A similar reasoning can be performed for the remaining scenarios. The possibility distribution for f(X) is presented in Fig. 4.

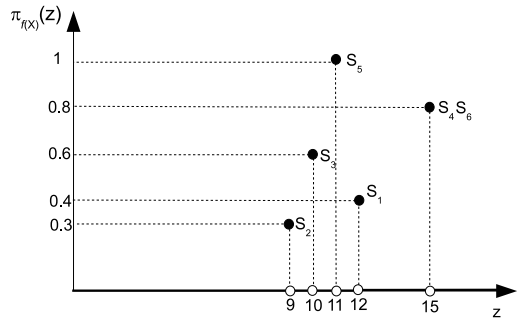

Fig. 4. The possibility distribution for f(X) where $X = \{e_3, e_5\}$

In order to choose a solution, we use exactly the same solution concept as in Section IV. Namely, a decision maker specifies a fuzzy goal $\tilde{G}$ and we seek a solution which maximizes the necessity that its costs will fall within $\tilde{G}$. Thus Poss 2-Stage is the optimization problem $\max_{X \in \Phi} \mathrm{N}(\mathrm{f(X)} \in \tilde{G})$ or equivalently $\min_{X \in \Phi} \Pi(\mathrm{f(X)} \in \tilde{G}')$. The same reasoning as in Section IV leads to a model similar to (10). Let us introduce binary variables x_i and y_{ij}, $i = 1, \ldots, n$, $j = 1, \ldots, K$. Variable x_i is equal to 1 if and only if element e_i is selected in the first stage, y_{ij} is equal to 1 if and only if element e_i is selected in the second stage if scenario S_j occurs. Then a feasible solution $X \cup Y_j$ under scenario S_j is described by variables $x_1, \ldots, x_n, y_{1j}, \ldots, y_{nj}$, which form a vector $(x_1, \ldots, x_n, y_{1j}, \ldots, y_{nj}) \in \Phi'$. The cost $f(X, S_j)$ can be then expressed as $\sum_{i=1}^{n} C_i x_i + \sum_{i=1}^{n} c_{ij} y_{ij}$. The model takes the following form:

$$\begin{array}{ll}
\min u & \\
u \geq \pi(S_j) - M\delta_j, & 1 \leq j \leq K, \\
u \geq \frac{1}{\beta}(\sum_{i=1}^{n} C_i x_i + \sum_{i=1}^{n} c_{ij} y_{ij}) - \frac{g}{\beta} - M(1 - \delta_j), & 1 \leq j \leq K, \\
(x_1, \ldots, x_n, y_{1j}, \ldots, y_{nj}) \in \Phi', & 1 \leq j \leq K, \\
\delta_j \in \{0, 1\}, & 1 \leq j \leq K, \\
u \geq 0. &
\end{array} \tag{14}$$

For a particular problem we should only replace $(x_1, \ldots, x_n, y_{1j}, \ldots, y_{nj}) \in \Phi'$ with some linear constraints involving the variables $x_1, \ldots, x_n, y_{1j}, \ldots, y_{nj}$. We now apply the above MIP approach to the following examples of combinatorial problems.

Example 3: Consider the 2-stage *minimum cost selecting items* with imprecise costs (Poss 2-Stage Minimum Cost Selecting Items). A set of items $E = \{e_1, \ldots, e_n\}$ and integer p, $1 < p < n$ are given. The set of feasible solutions consists of all the subsets of E with cardinality p. We select

some elements in the first stage, where the item costs C_i are known for each $e_i \in E$ and complete it to a feasible solution after a scenario from Γ is observed. The cost of item e_i under scenario S_j is c_{ij}. This problem can be solved by using the following MIP formulation:

$$\begin{aligned}
&\min u \\
&u \geq \pi(S_j) - M\delta_j && 1 \leq j \leq K, \\
&u \geq \frac{1}{\beta}(\sum_{i=1}^{n} C_i x_i + \sum_{i=1}^{n} c_{ij} y_{ij}) - \frac{g}{\beta} - M(1-\delta_j), && 1 \leq j \leq K, \\
&\sum_{i=1}^{n} x_i + \sum_{i=1}^{n} y_{ij} = p, && 1 \leq j \leq K, \\
&\delta_j \in \{0,1\}, && 1 \leq j \leq K, \\
&x_i \in \{0,1\}, && 1 \leq i \leq n, \\
&y_{ij} \in \{0,1\}, && 1 \leq i \leq n, \\
& && 1 \leq j \leq K, \\
&u \geq 0.
\end{aligned}$$

Example 4.: Consider the 2-stage *minimum cost matching* with imprecise costs (POSS 2-STAGE MINIMUM COST MATCHING). Let E be the set of the edges of a complete bipartite graph $G = (U \cup V, E)$, where $|U| = |V| = n$. The solution set Φ consists of all perfect matchings (assignments) in G. We can build a partial assignment in the first stage X, when the edge costs are equal to $C_{(k,l)}$ for $(k,l) \in E$ and complete it in the second stage when a cost scenario from Γ is observed. The cost of edge (k,l) under scenario S_j is equal to $c_{(k,l)j}$. This problem can be solved by using the following MIP formulation:

$$\begin{aligned}
&\min u \\
&u \geq \pi(S_j) - M\delta_j, && 1 \leq j \leq K, \\
&u \geq \frac{1}{\beta}(\sum_{(k,l)\in E} C_{(k,l)} x_{(k,l)} \\
&+ \sum_{(k,l)\in E} c_{(k,l)j} y_{(k,l)j}) - \frac{g}{\beta} - M(1-\delta_j), && 1 \leq j \leq K, \\
&\sum_{k\in U} (x_{(k,l)} + y_{(k,l)j}) = 1, && l \in V, 1 \leq j \leq K, \\
&\sum_{l\in V} (x_{(k,l)} + y_{(k,l)j}) = 1, && k \in U, 1 \leq j \leq K, \\
&x_{(k,l)} \in \{0,1\}, && (k,l) \in E, \\
&y_{(k,l)j} \in \{0,1\}, && (k,l) \in E, \\
& && 1 \leq j \leq K, \\
&\delta_j \in \{0,1\}, && 1 \leq j \leq K, \\
&u \geq 0.
\end{aligned}$$

By assuming that $\pi(S_j) = 1$ for each $S_j \in \Gamma$ and choosing a suitable fuzzy goal, we can show that POSS 2-STAGE $\mathcal{P}$ is is a generalization of the robust two-stage problem $\mathcal{P}$ known from the literature (see, e.g., [7], [8], [17]). This implies that all the negative complexity results for robust two-stage problem $\mathcal{P}$ hold true for POSS 2-STAGE $\mathcal{P}$.

VI. CONCLUSIONS

In this paper, we have proposed a general framework for dealing with possibilistic combinatorial optimization problems with uncertain costs in the single and two-stage decision models. The uncertainty has been modeled by a specified scenario set with a possibility distribution given on it. We have provided the solution concepts that lead to robust solutions in the setting of possibility theory. The concepts are consistent with popular and widely accepted robust approach to single and two stage optimization, where decision makers are interested in minimizing a solution cost in the worst case. Apart from showing the general framework, we have provided some methods based on mixed integer models for computing a solution with respect to the given solution concepts and we have illustrated them by examples.

ACKNOWLEDGMENT

The second author of the paper was partially supported by Polish Committee for Scientific Research, grant N N206 492938.

REFERENCES

[1] C. H. Papadimitriou and K. Steiglitz, *Combinatorial Optimization*. Mineola, New York: Dover Publications, INC, 1998.
[2] P. Kouvelis and G. Yu, *Robust Discrete Optimization and its applications*. Kluwer Academic Publishers, 1997.
[3] A. Ben-Tal and A. Nemirovski, "Robust solutions of uncertain linear programs," *Operations Research Letters*, vol. 25, pp. 1–13, 1999.
[4] A. Kasperski and M. Kulej, "Choosing robust solutions in discrete optimization problems with fuzzy costs," *Fuzzy Sets and Systems*, vol. 160, pp. 667–682, 2009.
[5] P. Kall and S. W. Wallace, *Stochastic Programming*. John Wiley and Sons, 1994.
[6] H. Aissi, C. Bazgan, and D. Vanderpooten, "Min-max and min-max regret versions of combinatorial optimization problems: A survey," *European Journal of Operational Research*, vol. 197, pp. 427–438, 2009.
[7] K. Dhamdhere, V. Goyal, and R. Ravi, "Pay Today for a Rainy Day: Improved Approximation Algorithms for Demand-Robust Min-Cut and Shortest Path Problems," in *STACS 2006*, ser. Lecture Notes in Computer Science, vol. 3884. Springer-Verlag, 2006, pp. 206–217.
[8] I. Katriel, C. Kenyon-Mathieu, and E. Upfal, "Commitment under uncertainty: Two-stage matching problems," *Theoretical Computer Science*, vol. 408, pp. 213–223, 2008.
[9] M. Inuiguchi and M. Sakawa, "Robust optimization under softness in a fuzzy linear programming problem," *International Journal of Approximate Reasonning*, vol. 18, pp. 21–34, 1998.
[10] M. Inuiguchi and J. Ramik, "Possibilistic linear programming: a brief review of fuzzy mathematical programming and a comparison with stochastic programming in portfolio selection problem," *Fuzzy Sets and Systems*, vol. 111, pp. 3–28, 2000.
[11] A. Kasperski and P. Zieliński, "Computing Min-Max regret Solutions in Possibilistic Combinatorial Optimization Problems," in *Fuzzy Optimization. Recent Advances and Applications*, ser. STUDFUZZ, W. A. Lodwick and J. Kacprzyk, Eds. Springer-Verlag, 2010, vol. 254, pp. 287–312.
[12] D. Dubois and H. Prade, *Possibility theory: an approach to computerized processing of uncertainty*. New York: Plenum Press, 1988.
[13] B. Korte and J. Vygen, *Combinatorial Optimization. Theory and Algorithms*. Springer-Verlag, 2006.
[14] R. K. Ahuja, T. L. Magnanti, and J. B. Orlin, *Network Flows: theory, algorithms, and applications*. Englewood Cliffs, New Jersey: Prentice Hall, 1993.
[15] D. Dubois and H. Prade, "When upper probabilities are possibility measures," *Fuzzy Sets and Systems*, vol. 49, pp. 65–74, 1992.
[16] A. Kasperski and P. Zieliński, "On the approximability of minmax (regret) network optimization problems," *Information Processing Letters*, vol. 109, pp. 262–266, 2009.
[17] ——, "On the approximability of robust spanning tree problems," *Theoretical Computer Science*, vol. 412, pp. 365–374, 2011.
[18] A. P. Punnen, "A linear time algorithm for the maximum capacity path problem," *European Journal of Operational Research*, vol. 53, pp. 402–404, 1991.
[19] H. N. Gabow and R. E. Tarjan, "Algorithms for two bottleneck optimization problems," *Journal of Algorithms*, vol. 9, pp. 411–417, 1988.
[20] P. M. Camerini, "The minimax spanning tree problem and some extensions," *Information Processing Letters*, vol. 7, pp. 10–14, 1978.
[21] A. P. Punnen, "A fast algorithm for a class of bottleneck problems," *Computing*, vol. 56, pp. 397–401, 1996.

2011 IEEE International Conference on Fuzzy Systems
June 27-30, 2011, Taipei, Taiwan

A Fuzzy Concept for Climate Management in Preventive Conservation

An Approach to Define and Manage Climate Setpoints using Fuzzy Decision Making

Christian Arnold, Steven Lambeck
University of Applied Sciences Fulda, Department of Electrical Engineering and Information Technology
Fulda, Germany
{christian.arnold, steven.lambeck}@et.hs-fulda.de

Christoph Ament
Technical University of Ilmenau
Institute for Automation and Systems Engineering
Ilmenau, Germany
christoph.ament@tu-ilmenau.de

***Abstract* — Especially for air conditioning tasks with applications in the area of preventive conservation, requirements can only be described by using vague and incomplete information. In this field of application a fuzzy formulation, which considers stationary, dynamical and economy demands of climate values, turned out to be appropriate. The presented paper describes an unifying approach of formulating fuzzy setpoints as well as using fuzzy decision making, in order to develop a automated climate management system for the best possible preventive conservation.**

Keywords - setpoint optimization; fuzzy decision making; process management system; preventive conservation

I. INTRODUCTION

Climate describes the state of physical values of an ambiance, mostly of the air. The automation task is to control these values in an effective way, so that they are stabilized in defined climate goals. Climate values are classified into a thermal and non-thermal group. The values concerning the non-thermal group are mainly those, which describe a local concentration of substances, for example the concentration of carbon dioxide. These values mostly represent measures of pollution. They originate from indoor sources and the goal is to reduce their concentration to an accepted limit. Usually the only way to fulfill this demand is to change air volumes with the environment using a ventilation system. [1]

As opposed to this, thermal values (we take the focus on temperature ϑ and relative humidity φ) should not be reduced to a limiting threshold, they have to reach a specified setpoint with an allowed deviation. The aim of keeping these values in a specified range is established by demands of people, caused by aspects of comfort and health.

It is an important fact that climate goals are usually formulated not crisp, but fuzzy. Looking into standards (for this ISO 7730, [2]) only vague parameters define specifications like the predicted mean vote (PMV-Index) and the predicted percentage of dissatisfied (PPD-Index). Hence, in the area of air conditioning and climate management there are only rough values of setpoints (or ranges of setpoints) available. That is why climatic requirements are often described linguistically and are provided with lack of knowledge [3]. These characteristics leads to the application of Zadeh's fuzzy theory [4], using fuzzy numbers and intervals [5] to formulate setpoints and evaluate controlled variables [6], [7] by creating a membership function (like in figure 1).

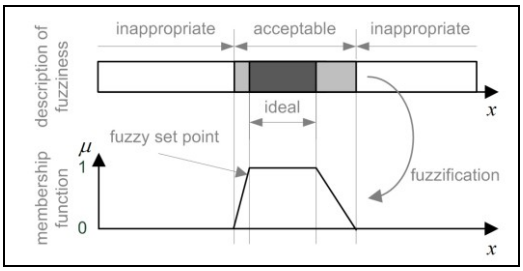

Figure 1. Fuzzification of a vaguely known setpoint

Conventional applications of air conditioning already use intervals of setpoints in order to realize energy-efficient operations and to reduce operation costs. Furthermore, state of the art concepts use theory of fuzzy decision making in order to generate setpoints and to find compromises between comfort and economical demands. These concepts to integrate requirements concerning the preventive conservation of cultural heritage, where the velocity of changes in the controlled values has to be minimized, will be enhanced in the presented paper. In this paper two concepts to calculate fuzzy setpoints are proposed: the first one will be used for an offline calculation (section V-*A*) and the second one will be used to make an online adaption of setpoints (section V-*B*).

II. CLIMATE DEMANDS IN PREVENTIVE CONSERVATION

Methods in saving cultural heritage objects may be classified into restoration and conservation. Restoration methods are treatments of the object, with a manipulation of the material substance (maybe by exchanging or repairing). In contrast, conservation methods are characterized by operations, which do not interact directly with the material. Fundamentally, the use of conservation methods is preferred for saving the original state of the object. Especially methods of preventive conservation are coming up, where (among other things) the

environment of objects should be designed in a way that material ageing and damaging get slowed and delayed. The topic of analyzing the present climate, determining reasonable setpoints for the different climate values and optimization of climate control, is in focus of many research groups, as appeared to reports and proceedings like [8].

A. Stationary demands

Except for a few applications, the significant thermal climate value is the relative humidity φ and not the temperature ϑ. This can be explained by looking at chemical and biological damaging processes: they slow down, if the temperature is low. In defining a reasonable range for the relative humidity, such a simplified rule cannot be defined. Figure 2 shows different goals for relative humidity of different materials. It is obvious to use fuzzy theory to formulate setpoints of relative humidity as fuzzy number or fuzzy interval, to utilize the range of setpoints in management systems and to define compromises in applications with different demands.

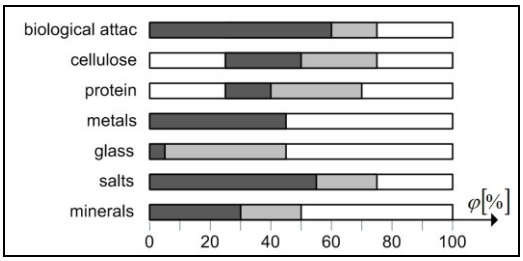

Figure 2. Stationary demands of relative humidity (modified from [9])

B. Dynamical demands

Furthermore, materials react on climate changes in their environment. In the stationary case, there is an equilibrium of environment and object climate (or the object state). If temperature in the environment changes, a heat flow at the material surface will start to reach another point of equilibrium, since the object's material serves as a heat storage. The same effect can be noticed on changes in humidity: the relation between the humidity in the air and the material states (like water content or inner stress) causes moisture flows. Based on the saturated vapor pressure of material and air, the relative humidity and not the absolute humidity should be focused. [10]

Hence, if there is a heat or moisture flow into or out of the material, the inner structure of the material has to transport energy or mass. This transport process fatigues the material, and if it is too fast, the inner structure will be damaged. But some materials are acclimatized during the transport process over the course of the years. They accustom their inner structure to historic climate cycles. [10]

C. Guidelines and standards

Some standards [11], [12] and guidelines [13] are published concerning the avoidance of such damaging processes. Also there are some quality climate classes published in [14]. Material-specific demands, the calculation of individual historical climates and the acceptable climate fluctuations in a time span can be found there. But it is not yet defined,

- how these fuzzy demands can be realized by an air conditioning system,
- how the setpoints can be calculated, if the historical climate (for all objects in a room!) is unknown,
- how to define a compromise between stationary and dynamical demands as well as to economical aspects and
- how to manage basic automation and planning setpoint trajectories in the case of an error.

III. Decision Making in Fuzzy Environment

The task of decision making is to find the best solution for a value (or multiple values) inside a decision space. So we talk about an optimization problem. For the frequent case of several objectives, we even have a multi criteria optimization problem. Searching the best solution will be more difficult, if objectives are only inexactly, imprecisely or vaguely known.

A. Basic concept of fuzzy decision making

The theory of fuzzy decision making aims primarily at finding the best solution x^* from a set of alternatives x. Objectives are formulated as fuzzy sets. Objectives are classified in a set of n goals $\mu_{Gi}(x)$ (objectives to aim requirements, with $i=1,\ldots n$) and a set of m constraints $\mu_{Cj}(x)$ (objectives to avoid damages, with $j=1,\ldots,m$). The question arises, how to aggregate all single objectives to an overall objective function for the elements of the decision space. Initially Bellman and Zadeh [15] suggest to create the intersection of all objectives and to determine the maximum of the resulting function as the best solution. Hence, we can aggregate all the goals to a new fuzzy set and all the constraints to a new fuzzy set. All goals and constraints may be combined to the set of decisions by creating the intersection [16]:

$$\mu_D(x)=\left(\bigcap_{i=1}^{n}\mu_{Gi}(x)\right)\cap\left(\bigcap_{j=1}^{m}\mu_{Cj}(x)\right) \tag{1}$$

The optimal decision x* can be determined (shown in figure 1):

$$\mu_D(x^*)=\max\{\mu_D(x)\} \tag{2}$$

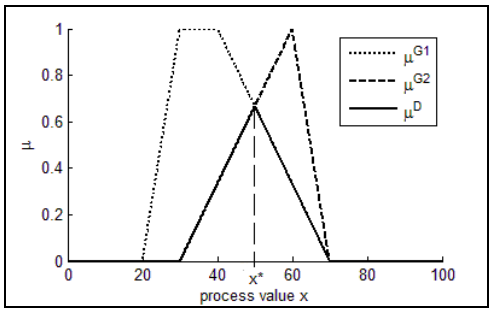

Figure 3. Fuzzy decision making of two fuzzy goals

Theoretical constraints can also be formulated as goals. For instance, if an objective is nominated to avoid a bad state, it will be possible to formulate this in a way that it will be good to reach the opposite. Hence, after reformulating the constraints it is sufficient to focus the goals [17]. Further information about fuzzy decision making can be found in [16], [18], [19] and [20]. Applying this theory in climate management, there are two major issues to be discussed: how to weight the goals and how to handle extremely contrasting demands.

B. Weighting objectives

In the concept described in section *A*, the importance of all goals in the intersection is equivalent. In some applications this is not correct, because single objectives have to be weighted. Bellman and Zadeh [16] suggest at first to weight single goals by using multiplicative factors. Instead of the aggregation using the intersection, the sum of all sets is advised:

$$\mu_D(x) = \sum_{i=i}^{n} a_i \cdot \mu_{Gi}(x) \tag{3}$$

To stay in the fuzzy world, it is necessary that the maximum of the decision set is not higher than one. For equation (3) this may be reached, if the sum of all weighting factors a_i is equal to one. As an alternative concept, exponents between zero and infinity may be used to weight single objectives. If the exponent is near infinity, the set will be equal to the kernel-function of the initial set (all elements round down to zero, except the elements with the degree of one), which means that the objective is very high weighted. In the opposite case, if the exponent is near zero, the set will be equal to the support (all elements will be round to one, except the elements with the degree of zero), which means that the objective is not very important. So, the intersection may be used for aggregation:

$$\mu_D(x) = \bigcap_{i=1}^{n} \mu_{Gi}(x)^{a_i} \tag{4}$$

This concept is also known in the area of fuzzy modifiers, where these powering operations are used as methods to describe the fuzziness in a linguistic term and to consider linguistic hedges in modeling of knowledge based systems [21], [22]. That is pretty much the same as weighting of objectives. A drawback of this concept is that the weighting process is not very obviously, because there are different ranges for dilatation (between zero and one) and concentration (between one and infinity). As an extension of this concept, we suggest to introduce an additional value λ_i by using the following mark:

$$\mu_{Gi}^{\langle\lambda_i\rangle}(x) = \mu_{Gi}(x)^{a_i} \tag{5}$$

The parameter is scaled from –1 to 1 and defined as:

$$a_i = \begin{cases} \dfrac{1}{1-\lambda_i} & for \quad 0 \le \lambda_i < 1 \\ 1+\lambda_i & for \quad -1 < \lambda_i < 0 \end{cases} \tag{6}$$

Figure 4 shows the effect of the modification using equation (6). If the weighting value λ_i moves toward –1, the shape will be deformed equal to the support-function and if the λ tends to 1, the shape will be deformed to the kernel-function.

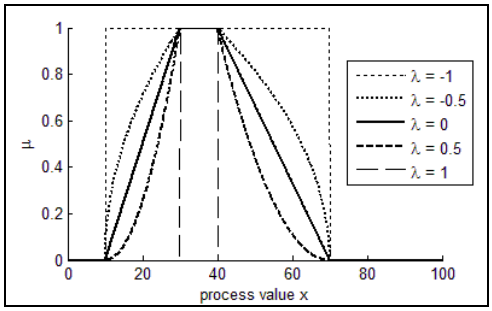

Figure 4. Effect of the weighting parameter λ_i to the membership function

C. Extremely contrasting demands

In some applications it can happen that a creation of an intersection is impossible. There will be no element in the set of alternatives where all membership functions are different to zero at once and finally an empty decision is resulting. This case occurs, if the demands are in an extreme contrast. In fuzzy decision making also values outside the appropriate area must be evaluated and it has to come to a decision about the reaction in such cases. It is necessary to distinguish those states, because a value far away from the kernel should not get the same bad rating as a value more close to it. This is why we should talk about an "inappropriate" and not about a "forbidden" area. The task before was to find the solution which satisfies all objectives equally; now the task is to find the solution where all objectives are unfulfilled in the same way.

To handle such scenarios, membership functions with degrees always higher than zero should be used. That can be done if suitable parametric membership functions (like the difference between two sigmoidal functions) are used or existing membership functions are manipulated. Remember: goals and constraints have finally been defined by human, where complicated functions may not be obviously parameterizable.

We prefer to keep the clearness of trapezoidal linear functions, because it is simple to define areas like “inappropriate” (outside the support), “appropriate” (inside the support) and “ideal” (inside the kernel), as shown in figure 1. In the classical trapezoidal function

$$\mu(x) = f_{Trap}(a,b,c,d) \tag{7}$$

the shape is defined by four parameters: a linear function increase from zero at *a* till one at *b*; another linear function

decrease from one at *c* till zero at *d*; between *b* and *c* all degrees are equal to one; all other degrees are zero. After defining this, we mitigate the crossing between the acceptable and the inappropriate zone to solve special cases as described in section *A* and we extend the conventional function by an additional parameter ε:

$$\mu(x) = f_{Trap\,\varepsilon}(a,b,c,d,\varepsilon) \tag{8}$$

The shape is defined as:

$$\mu(x) = \begin{cases} \varepsilon \cdot e^{\left(\frac{x-a}{\varepsilon\cdot(b-a)}-1\right)} & for \quad x \le a+\varepsilon\cdot(b-a) \\ \frac{x-a}{c-a} & for \quad a+\varepsilon\cdot(b-a) < x < b \\ 1 & for \quad b \le x \le c \\ \frac{d-x}{d-c} & for \quad c < x < d-\varepsilon\cdot(d-c) \\ \varepsilon \cdot e^{\left(\frac{d-x}{\varepsilon\cdot(d-c)}-1\right)} & for \quad x \ge d-\varepsilon\cdot(d-c) \end{cases} \tag{9}$$

The effect of choosing ε is shown in figure 5. We justify our approach as follows: if we look at a fuzzy objective it is possible that an ideal area (with equivalent ratings inside) could be defined by an expert; but the boundaries could not be defined clearly.

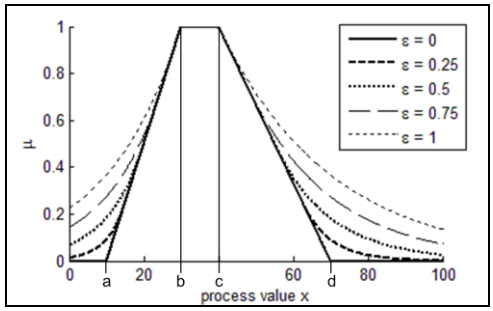

Figure 5. Effect of breaking the hard constraint

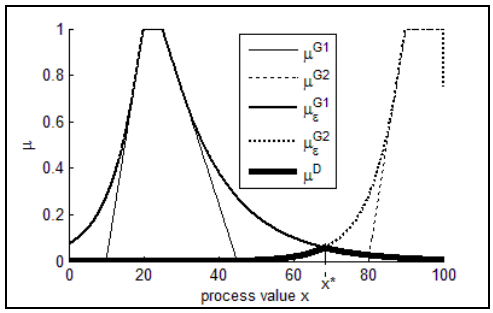

Figure 6. Decision making with controversy goals

Using this concept, it will always be possible to find a solution, also for controversial demands. An example is shown in figure 6: Two fuzzy sets defined according to equation (9) are intersected according to equation (1). The optimal process value *x** is obtained from equation (2).

D. *Manage the trajectory of setpoints*

The requirements of a controlled variable can usually be characterized by different criteria. First of all, stationary goals μ_{GS} should be reached to work in desired operating points. Generally, the necessary operations to reach the stationary goals should be done very efficient with low costs, thus aspects of economy μ_E are added. Finally, dynamical demands μ_{GD} have to be considered; these goals are dependent on past values of the controlled variable (as an example figure 7 shows a decision making process):

$$\mu_{GD}(x, x(k-1)) = f_{Trap\,\varepsilon}(x(k-1)+[a,b,c,d],\varepsilon) \tag{10}$$

All goals may be aggregated to the decision set:

$$\mu_D(x) = \mu_{GS}(x) \cap \mu_E(x) \cap \mu_{GD}(x, x(k-1)) \tag{11}$$

Hence, the question arises, how to weight the interacting of goals. It is obvious that all requirements are coupled: a higher performance may be reached by a high weighted stationary goal on the one hand and by a low weighted dynamical goal on the other. Surely, both cases will involve increasing costs. Based on the normalization, one goal may be inflexible and the other two goals may be mutually weighted .

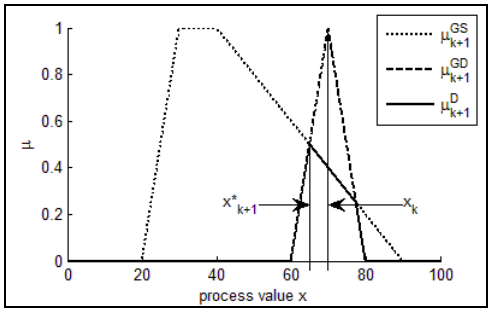

Figure 7. Decision making of stationary and dynamical demands

IV. THE AIR CONDITIONING PROCESS

Every climate value (thermal or non-thermal) can be described by a mass or energy balance. By summarizing all flows into the room, we get an universal balance equation for the indoor value σ^R, where the exchange of air with the outdoor climate is named as σ^E, buffering and storage effects are described by σ^S, transmission effects by σ^T, disturbance and non-manipulable inner loads by σ^Z and at last the manipulable inner sources named as σ^Y are added:

$$\dot{\sigma}^R(t) = \dot{\sigma}^\Sigma(t) = \dot{\sigma}^E(t) + \dot{\sigma}^S(t) + \dot{\sigma}^T(t) + \dot{\sigma}^Z(t) + \dot{\sigma}^Y(t) \tag{12}$$

A. Calculation of temperature and humidity

Taking the focus on temperature values, it is necessary to integrate the heat flows with a capacity (product of density ρ, specific capacity of air c and the room volume V_R of); using equation (12) and setting the universal value σ to the heat quantity Q:

$$\vartheta^R(t) = \frac{1}{\rho \cdot c \cdot V_R} \cdot \int \dot{Q}^{\Sigma}(t) \cdot dt \tag{13}$$

Model structures and control concepts of the temperature are well known and can be found in the corresponding literature [1], [23]. Taking the focus on the humidity, it is necessary to integrate the flows of (absolute!) humidity with a capacity (as the volume) of the room; using equation (12) and setting the universal value σ to the moisture content f:

$$f^R(t) = \frac{1}{V_R} \cdot \int \dot{f}^{\Sigma}(t) \cdot dt \tag{14}$$

As already mentioned above, the most important physical value of air conditioning is not the absolute humidity but rather the relative humidity, which is a temperature-dependent function and may be calculated by equation (15), where R^S is the specific gas constant and p^S is the saturated vapor pressure, which can be calculated by using appropriate functions (look at [24]). A structure of the process is shown in figure 8.

$$\varphi^R(t) = \frac{f^R(t) \cdot R^S \cdot \vartheta^R(t)}{p^S} \tag{15}$$

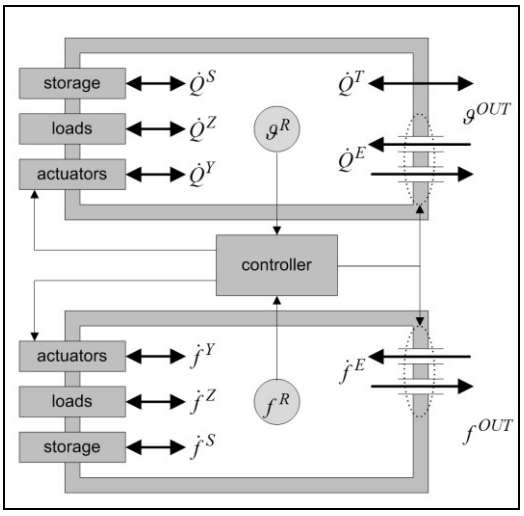

Figure 8. Control schema and influences on the indoor climate

B. Manipulating and controlling the process

It is obvious that the task of control thermal values is coupled to temperature and humidity, especially the temperature dependence of relative humidity and the influence of the ventilation rate. Additional to the manipulation of the ventilation rate, heating and cooling may be used to control the temperature. Humidifier and dehumidifier may be used to control the moisture balance. There are special requirements in the area of preventive conservation, because installations of air conditioning systems needs often a huge installation space and are also very expensive. Furthermore, it is also not allowed to damage the substance of historical buildings by additional installations. Finally, there are only a few options left to manipulate the process. Tasks of air conditioning may be divided into tasks of different time scales:

- short-term: measure process states, control of the variables in order to meet the given setpoints, aggregation of process information, time span: minutes till hours (daily fluctuations)
- medium-term: online optimization of setpoints, planning trajectories, time span: days (weather fluctuations)
- long-term: seasonal optimization, time span: weeks till month (seasonal fluctuation)

Short-term tasks are usually handled in concepts of basic automation, where standard controllers are used or manual operations (on/off switching of actuators, manual aerating) are provided to the process. Medium-term and long-term tasks can be aggregated to tasks of the process management system (PMS), which calculates the setpoints for the different control variables online (so far as online process information is available). Figure 9 shows the division of tasks and decision making in different levels of the automation structure.

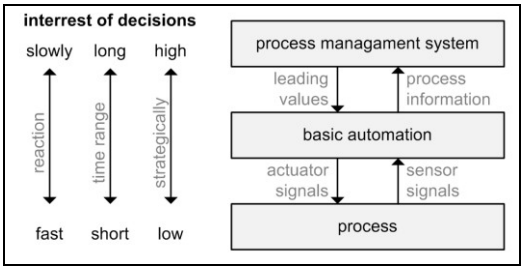

Figure 9. Levels of process automation

V. Application: Calculation of Climate Setpoints

This section describes a concept to find the optimal setpoints for the climate in applications of preventive conservation. Initially, applications where elements of basic automation are already present are considered. But this will also be a task, if the process is controlled by manual operations and the process staff is trying to reach the setpoints in that way. In this case, the PMS works as a decision support system.

A. Offline planning of fuzzy trajectories

The first approach for using fuzzy decision making is the design of a planning system. In interaction with the user, a local climate profile and stationary demands of people and cultural heritage have to be defined (maybe by using an additional configuration system). In this case there is no information about the process state, hence the system is only a

stationary offline system, dynamical aspects cannot be taken into account. Taking a priori information of the local climate in the course of the year into account, only the seasonal component is estimable, as effects of weathers and daily fluctuations are unknown.

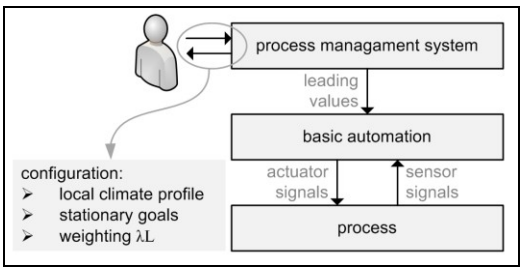

Figure 10. Structure of the planning tool

The outdoor climate of temperature and humidity can be approximated using a sine function [24]; hence, an appraisal of the economical demand to control a specific value is calculable. As an example, we plan the fuzzy setpoints of relative humidity in a room, where the indoor climate is controlled by components of the basic automation. Ignoring short-term effects, the demand of humidifying and dehumidifying may be calculated by looking at the required power in order to compensate the losses of absolute humidity by the mean of the natural air exchange $\dot{V}^E$:

$$\dot{f}^Y(t) \approx -\frac{1}{V} \cdot \left[f^{OUT}(t) - f^R(t) \right] \cdot \bar{\dot{V}}^E \tag{16}$$

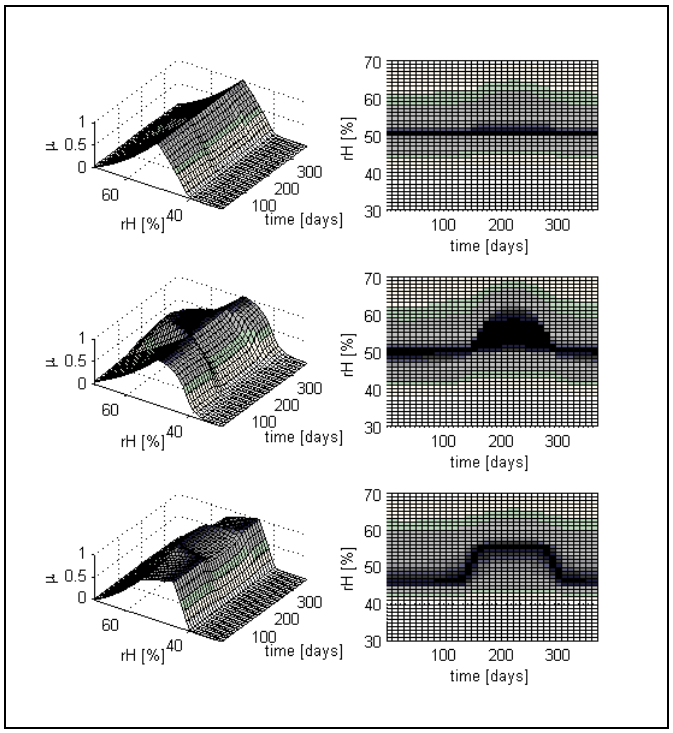

Figure 11. Fuzzy setpoints for relative humidity in the course of the year at different configurations. Left: stationary goal $f_{Trapε}$ (40, 50, 50, 70, 0.1) and λ_L =0. Middle: stationary goal $f_{Trapε}$ (40, 50, 50, 70, 0.1) and λ_L =-0.5. Right: stationary goal $f_{Trapε}$ (40, 45, 55, 70, 0.1) and λ_L =0.

Using equation (15), the economical demand may be calculated for various setpoints of relative humidity at every time step:

$$\dot{\vec{f}}^Y(t) \approx -\frac{1}{V} \cdot \left[\frac{\varphi^{OUT}(t)}{\vartheta^{OUT}(t)} - \frac{\vec{\varphi}^R(t)}{\vartheta^R(t)} \right] \cdot \frac{p^S}{R^S} \cdot \bar{\dot{V}}^E \tag{17}$$

We use the following relation to create a fuzzy membership function of the cost objective applying the result of (17):

$$\mu_{EL}\left(\varphi^R, t\right) = 1 - \frac{\left| \dot{\vec{f}}^Y(t) \right|}{\max \left| \dot{\vec{f}}^Y(t) \right|} \tag{18}$$

To reduce the complexity of configuration, we define λ_L as a weighting parameter, hence we can calculate the trajectory of fuzzy setpoints over the year. Figure 11 shows some examples for different configurations:

$$\mu_{\varphi L}\left(\varphi^R, t\right) = \mu_{GS}^{\langle \lambda_L \rangle}\left(\varphi^R\right) \cap \mu_{EL}^{\langle -\lambda_L \rangle}\left(\varphi^R, t\right) \tag{19}$$

B. *Online process management system*

Another approach for using the presented concept is an online PMS. In interaction with the user stationary and dynamical demands of people and cultural heritage have to be defined (may be using an additional configuration system again); but now there is no need of defining an outdoor climate profile (because of online measurements).

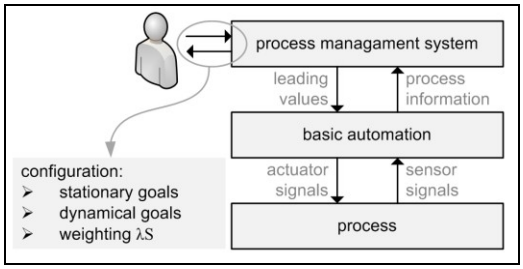

Figure 12. Structure of the process management system

Economical demands are calculated using online information of indoor and outdoor climate. We use equations like (17) and (18), but not over the course of the year (only for the present time). Furthermore, it is possible to calculate the membership function for dynamical goals, also using process information about the actual states. To reduce the configuration complexity, we do not weight the stationary demand (see above) and introduce a parameter λ_S as a weighting parameter between economical and dynamical demands, which may be justified obliviously.

$$\mu_{\varphi S}(x,t) = \mu_{GS}(x) \cap \mu_{GD}^{\langle \lambda_S \rangle}\left(x, x(k-1)\right) \cap \mu_{ES}^{\langle -\lambda_S \rangle}(x,k) \tag{20}$$

VI. Case-Study: Simulations of a the PMS

Based on simulations, in which a PMS has to generate optimal setpoints for an underlying control circuit of relative humidity, we will show the effectiveness of the proposed concept. This circuit in the basic automation level is using a feedback controller (PID) combined with a disturbance feed forward control (DFF). The structure is shown in figure 13.

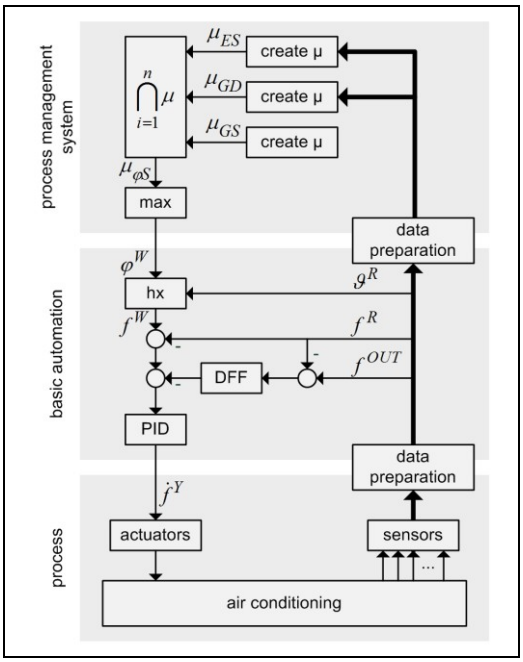

Figure 13. Structure of the controller in the case study

The PMS works dependent on the process values in medium-term range, a discrete filter (moving average of 24 hourly samples) is used to blind out short-term effects, which must be handled by basic automation. The setpoint of relative humidity gets an update every hour. Equation (20) is used for calculating the decision set. Thus the design parameter is λ_S. For the simulation we use a simulation environment of a building model in MATLAB/Simulink, which depends on first order balance equations of energy as well as additional components like storage effects for heat and moisture of the room. For details regarding to building physics and simulation look at the respective literature [25], [26] and [1].

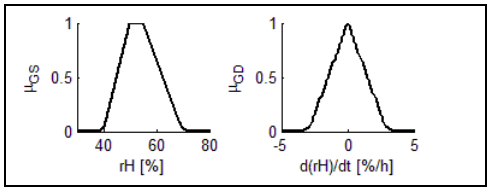

Figure 14. Stationary and dynamical goals in the case study

The goals are fuzzy values, the stationary demand is defined as appropriate in the area from 30% to 55% and in the vicinity of 35% and 50% the value is ideal. Regarding dynamical aspects, no changes would be the best solution; changes about ±3% per hour are accepted. To create a fuzzy membership function, we use equation (9) with a value ε of 0.1 for all membership functions. A scenario of outdoor climate and initial conditions is defined and simulated at different configurations of λ_S (figure 15). It is obvious that the design parameter λ_S has a significant influence on the dynamic behavior of the controlled variable. In a more detailed analysis of the simulation results, the membership of all simulation data to the stationary and the dynamical goal is determined just as the power (needed for humidification) is cumulated. The normalized and scaled values are plotted in figure 16.

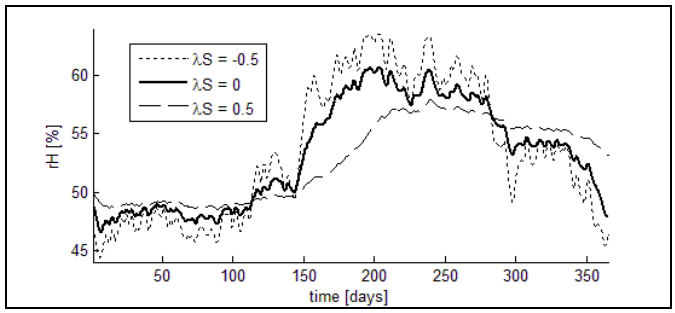

Figure 15. Simulation results: behaviour of the controlled relative humidity at various weightings.

As expected, choosing a higher λ_S (higher weighting of the prevention of high gradients) leads to lower economical effects. Considerable is the correlation of the effect of choosing λ_S to stationary and dynamical demands, which is caused at the coevally opposed weighting of economical aspects.

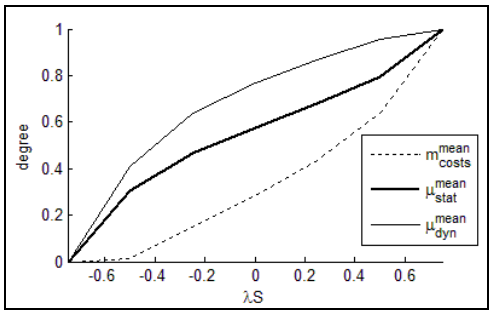

Figure 16. Simulation results (normalized and scaled): sum of power demands and means of bad ratings

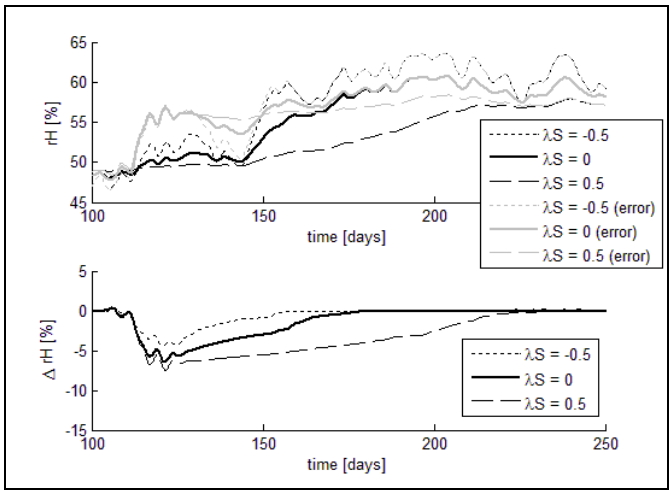

Figure 17. Dynamical behaviour of the controlled variable after an error (between the 105th and the 130th day): simulation results (above) and difference to normal behaviour (below)

Analyzing the second effect of using the PMS, an error in the technical equipment is simulated. The task of the PMS is now to guarantee the return of the process back to the optimal sequence of setpoints (depicted in figure 17). After reactivation of the equipment, the parameter λ_S defines the velocity to reach the behavior in the normal operation; the activation is also bumpless. Hence, the PMS also resumes the task of planning trajectories.

VII. Conclusion and outLook

The theory of fuzzy decision making can be used to make decisions in applications where the demands of the controlled process are only inexact, imprecise or vague known. We presented established weighting methods and suggested a simple principle for using the powering operator obviously. Furthermore, we discussed the problems of decision making in the case of controversial demands and suggested a principle to transform hard constraints in trapezoidal membership functions.

Applications of air conditioning, especially in the area of preventive conservation are complex tasks, where the demands to avoid climate damages are only roughly known. There are some goals defined in norms, but no method how to find a compromise between the different demands, for instance how to weight stationary and dynamical demands. The presented approach and the simulations of a process management system were presented in this paper. Especially for the use in preventive conservation such a system may be used to find compromises between stationary and dynamical goals as well as to economical aspects.

In following work, we will use the concept of the process management system to generate future fuzzy setpoints and to optimize future manipulating operations in cooperation with the theory of multistage fuzzy control [26], maybe for planning an optimal ventilation sequence. Furthermore, we will expand the theory for MIMO processes, especially to combine the generation of setpoints for relative humidity and temperature.

Acknowledgment

The support for these studies was provided within the framework of the projects "BestBiMa", sponsored by the German Federal Ministry of Education and Research, and "OptiFDM", sponsored by the Hessian Ministry for Sciences and Arts.

References

[1] L. Keller, "Leitfaden für Lüftungs- und Klimaanlagen," Oldenbourg Industrieverlag, 2008, 2. edition.

[2] International Organization for Standardization (ISO), "Ergonomics of the thermal environment - Analytical determination and interpretation of thermal comfort using calculation of the PMV and PPD indices and local thermal comfort criteria," Norm ISO 7730, 2005.

[3] C. Arnold, "Rating the state of distributed indoor climate considering the fuzziness in set- and actual-values," conference proceedings, automation 2010, VDI/VDE-Society Measurement and Automation, Baden-Baden, Germany, 2010.

[4] L. A. Zadeh, "Fuzzy sets," Information and Control 8, pp. 338–353, 1965.

[5] G. Bojadziev, and M. Bojadziev," Fuzzy sets, fuzzy logic, applications, " Advances in fuzzy systems, World Scientific Publishing, Singapore, 1998.

[6] C. Arnold, B. Cuno, and C. Ament, "Modifing fuzzy goals to consider the fuzziness of actual values," 3rd International Conference on Computer and Automation Engineering, Chongqing, China, 2011.

[7] C. Arnold, B. Cuno, and C. Ament, "An approach for the control error calculation under fuzziness," conference proceedings, international scientific colloquium, Ilmenau, Germany, 2010.

[8] T. Padfield, K. Borchersen, "Museum Microclimates,", Contributions on the Copenhagen conference, Copenhagen, Denmark, 2007.

[9] D. Erhardt, M. F. Mecklenburg, "Relative humidity re-examined," Preprints to the Ottawa Congress, International Institute for Conservation of Historic an Artistic Works, London, 1994.

[10] M. F. Mecklenburg, "Determining the Acceptable Ranges of Relative Humidity and Temperature in Museums and Galleries," Smithsonian Museum Conservation Institute, Report, Suitland, USA, 2007.

[11] International Organization for Standardization (ISO), "Information and documentation - Document storage requirements for archive and library materials," Norm ISO 11799, 2003.

[12] European Committee for Standardization (CEN), "Conservation of Cultural Property - Specifications for temperature and relative humidity to limit climate-induced mechanical damage in organic hygroscopic materials," European Norm EN 15757, 2010.

[13] International Association for Science and Technology of Building Maintenance and the Preservation of Monuments (WTA), "Climate and climate stability in historic buildings," Guideline 6-12, 2010.

[14] S. Michalski, " The Ideal Climate, Risk Management, the ASHRAE Chapter, Proofed Fluctuations,and Toward a Full Risk Analysis Model," Contribution to the Experts' Roundtable on Sustainable Climate Management Strategies, Tenerife, Spain, 2007.

[15] R. E. Bellmann, L. A. Zadeh, "Decision-Making in a fuzzy environment," Nasa contractor report, Washington D. C., USA, 1970.

[16] H. Bandemer, S. Gottwald, "Einführung in die Fuzzy-Methoden," Akademie Verlag, Berlin, Germany, 1993, 4. edition.

[17] T. Bernard, "Ein Beitrag zur gewichteten multikriteriellen Optimierung von Heizungsund Lüftungsregelkreisen auf Grundlage des Fuzzy Decision Making," PhD-Thesis, University Karlsruhe, Faculty for mechanical engineering, 2000.

[18] H. J. Zimmermann " Fuzzy set theory - and its applications," Kluwer Academic Publishers, Boston, 2001, 4. edition.

[19] J. M. C. Sousa and U. Kaymak, "Fuzzy Decision Making in Modeling and Control," World Scientific Publishing Company, Singapore, 2002.

[20] H. J. Rommelfanger "Fuzzy Decision Support–Systeme - Entscheiden bei Unschärfe,", Springer, Berlin, 1994, 2. edition.

[21] M. De Cock, and E. E. Kerre "Fuzzy modifiers based on fuzzy relations," Information Sciences, Vol. 160, pp. 173–199, 2004.

[22] H. Shi, R. Ward, "Expanding the Definitions of Linguistic Hedges," Joint 9th IFSA world congress and 20th NAFIPS international conference, pp. 2591-2595, 2001.

[23] Arbeitskreis der Professoren für Regelungstechnik in der Versorgungstechnik, "Regelungs- und Steuerungstechnik in der Versorgungstechnik," VDE Verlag, Berlin, Germany, 2010, 6. edition.

[24] P. Häupl, "Bauphysik : Klima, Wärme, Feuchte, Schall," Ernst & Sohn Verlag, Berlin, Germany, 2008.

[25] American Society of Heating, Refrigerating and Air-Conditioning Engineers (ASHRAE), "Handbook - HVAC Systems and Equipment," 2008.

[26] J. Kacprzyk, "Multistage fuzzy control," John Wiley & Sons, Chichester, England, 1997.

2011 IEEE International Conference on Fuzzy Systems
June 27-30, 2011, Taipei, Taiwan

Fuzzy Controller Design Using Group-Crossover Particle Swarm Optimization for Truck Reversing Control

Chia-Feng Juang, Yu-Cheng Chang, Chia-Hung Hsu
Department of Electrical Engineering
National Chung-Hsing University
Taichung, Taiwan, R.O.C
e-mail:cfjuang@dragon.nchu.edu.tw

I-Fang Chung
Institute of Biomedical Informatics
National Yang-Ming University
Taipei, Taiwan, R.O.C

***Abstract*—This paper proposes a fuzzy controller design using group-crossover particle swarm optimization (GCPSO) algorithm. The GCPSO uses a group-based framework for defining particle neighborhood topology and incorporating crossover operation into particle swarm optimization. The GCPSO dynamically forms different groups for selecting parents in crossover operations, particle updates and replacements. The objective of GCPSO is to improve fuzzy control accuracy. Comparisons with different population-based optimizations on truck reversing control problem demonstrate the performance of GCPSO algorithm.**

Keywords- fuzzy controller, particle swarm optimization, genetic algorithms.

I. INTRODUCTION

Fuzzy controllers (FCs) have been successfully applied to many optimum control problems, like robots and power systems. Evolutionary fuzzy control (EFC) concerns automatic design of FC using evolutionary computation techniques. Two popular EFC approaches are genetic algorithms (GAs) [1,2] and particle swarm optimization (PSO) [3]. The PSO algorithm studies collective behavior in decentralized systems [4]. Its development was based on mimicking the social behavior of animals or insects models in an effort to find the optima in the problem space. Original PSO models are initialized with a population of random solutions. Each individual in PSO is assigned with a randomized velocity according to its own and its companions' flying experiences, and the individuals, called particles, are the flown through hyperspace.

Many modified PSO have been proposed and successfully applied to different optimization problems [5-12], such as a hybrid of GA and PSO (HGAPSO) [5], self-organizing hierarchical PSO with time-varying acceleration coefficients (HPSO-TVAC) [6], PSO with controller random exploration velocity (PSO-CREV) [7], a species-based PSO (SPSO) [8], and a hierarchical cluster-based multi-species particle swarm optimization (HCMSPSO) [12]. In HGAPOS and several latter studies [9-11], the idea of crossover in GA is incorporated into PSO. In SPSO and HCMSPO, a swarm population is divided into species subpopulations, and the dominating particle in each species is used as a best neighborhood for particles within the same species. This paper proposes a new framework for incorporating crossover operation and species formation into PSO.

This paper proposes a group-crossover PSO, called as GCPSO. According to the adaptively formed groups in a swarm, a new group-based crossover operation (GCRO) is proposed. Unlike the SPSO and HCMSPSO, the formation of the group is used not only for particle velocity update but also for particle crossover in the EGPSO. The EGPSO uses the name "group" because individuals in different species do not perform crossovers in nature. This paper applies the GCPSO algorithm to design a fuzzy controller for a truck reversing control problem. In the simulation, this paper demonstrates the performance of GCPSO via comparisons with various advanced GA and PSO algorithms.

This paper is organized as follows: Section II introduces the FC designed by the GCPSO. Section III introduces the GCPSO. Section IV conducts the truck reversing control problem. Finally, Section V presents conclusion.

II. FUZZY CONTROLLER(FC)

This paper designs a fuzzy controller (FC) using the GCPSO. The i th rule, denoted as R_i, in the FC is represented in the formula :

$$\begin{aligned} R_i:\ &\text{If } x_1(k) \text{ is } A_{i1} \text{ And ... And } x_n(k) \text{ is } A_{in} \\ &\text{Then } u(k) \text{ is } a_i \end{aligned} \tag{1}$$

where k is time step, $x_1(k)$, …, $x_n(k)$ are the input variables, $A_{i1},\ldots,A_{in}$ are fuzzy sets, and a_i is a crisp value. The fuzzy set A_{ij} uses a Gaussian membership function

$$M_{ij}(x_j) = \exp\{-(\frac{x_j - m_{ij}}{\sigma_{ij}})^2\}, \tag{2}$$

This work was supported by the National Science Council, Taiwan, under Grants NSC-99-2221-E-005-064-MY2 and NSC 99-2221-E-010 -013.

where m_{ij} and σ_{ij} represent the center and width of the fuzzy set A_{ij}, respectively. The fuzzy AND operation in the inference engine implemented by the algebraic product in the fuzzy theory. Therefore, given an input data set $\vec{x}(k) = (x_1(k), \ldots, x_n(k))$, the firing strength $\phi_i(\vec{x}(k))$ is calculated by

$$\phi_i(\vec{x}(k)) = \prod_{j=1}^{n} M_{ij}(x_j(k)). \quad (3)$$

If there are r rules in the fuzzy controller, then the output of the controller computed by the weighted average defuzzification method and is shown

$$u(k) = \frac{\sum_{i=1}^{r} \phi_i(\vec{x}(k)) a_i}{\sum_{i=1}^{r} \phi_i(\vec{x}(k))}. \quad (4)$$

The designed of an FC training data consists of the determination of fuzzy rules and the optimization of all free parameters in each fuzzy rule. For the FC in (1) that consists of n inputs variables and r rules. Therefore, all of ties free parameters can be described by the following vector

$$\vec{s} = m_{11}, \sigma_{11}, \cdots, m_{1n}, \sigma_{1n}, a_1, \cdots, m_{r1}, \sigma_{r1}, \cdots, m_{rn}, \sigma_{rn}, a_r] \in \Re^{r(2n+1)} \quad (5)$$

In GCPSO-designed FC, the number of rules r is assigned in advance. The number of fuzzy sets in each input variable is simply equal to the number of rules. The solution vector in (5) functions as a particle. The GCPSO-designed FC optimizes all of the free parameters in an FC with the number of rules being fixed.

III. GROUP-CROSSOVER PARTICLE SWARM OPTIMIZATION (GCPSO)

In basic PSO, the initial P_s (which is the swarm size) particles forming the swarm are randomly generated. However, there are too many search points before locating the global optimum. To improve the search ability, this paper applies the idea of swarm speciation proposed in species-based PSO (SPSO) [8] for particle velocity update. Unlike the SPSO, the formation of groups is used not only for particle velocity update but also for particle crossover in GCPSO. Figure 1 shows the block diagram of the group formation, particle update, particle generation, and replacement operations in the GCPSO. Details of these operations are introduced as follows.

A. Group formation

Initially, the particles are sorted from best performance to worst performance. The first particle is the best-performing one in the sorted swarm. This particle forms the first group and functions as first group leader (denoted as $\vec{p}_1^{\,L}$). For the leader $\vec{p}_z^{\,L}$ of group z, positions of the particles ranked after $\vec{p}_z^{\,L}$ are checked one by one against $\vec{p}_z^{\,L}$ until a particle whose

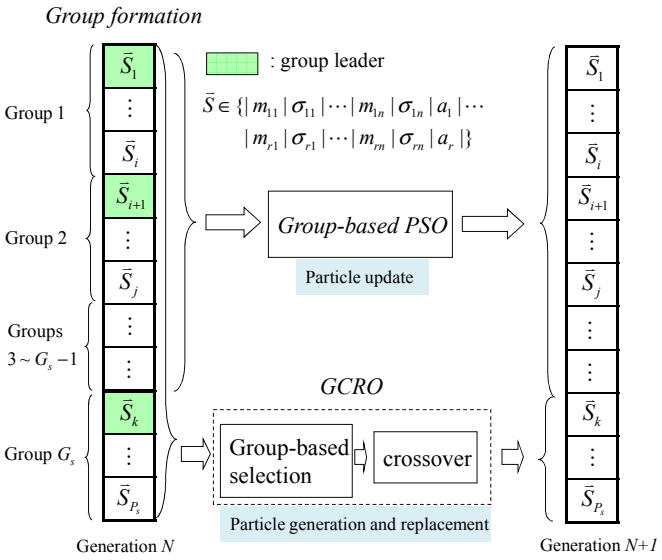

Fig. 1. The Block diagram of the GCPSO.

similarity degree with respect to $\vec{p}_z^{\,L}$ is larger than a predefined threshold ρ_{th}. The similarity degree, ρ, between a particle $\vec{s}_i$ and a group leader $\vec{p}_z^{\,L}$ is given by

$$\rho(\vec{p}_z^{\,L}, \vec{s}_i) = \sqrt{\frac{\| \vec{p}_z^{\,L} - \vec{s}_i \|_2^2}{D}}, \quad (6)$$

where D is the length of a particle vector. The ρ value can be regarded as the root-mean-squared error between twovectors. The particles with $\rho(\vec{p}_z^{\,i}, \vec{s}_i)$ being smaller than the threshold ρ_{th} are categorized into group z. The first particle with $\rho(\vec{p}_z^{\,i}, \vec{s}_i)$ being larger than the threshold ρ_{th} functions as a new leader $\vec{p}_{z+1}^{\,L}$ and forms a new group $z+1$. This paper sets the threshold ρ_{th} to be 1.5.

B. Particle Update

Suppose that there are G_S groups in the GCPSO, where G_S changes with learning iterations. The GCPSO updates particles in groups $1, \ldots, (G_S - 1)$. In the GCPSO, grouping is used for neighborhood topology definition in a swarm. That is, the neighbors of a particle are defined as the particles within the same group. Therefore, the neighborhood best position is the leader $\vec{p}_z^{\,L}$ for particles within group z. The velocity $\vec{v}_i$ of each particle i in group z is updated using its individual best position, $\vec{p}_i$, and the neighborhood best position, $\vec{p}_z^{\,L}$. The following equation with a constriction coefficient is used for velocity updating [4]:

$$v_i^j(t+1) = \chi(v_i^j(t) + c_1\varphi_1^j \cdot (p_i^j(t) - s_i^j(t)) + c_2\varphi_2^j \cdot (p_z^{Lj}(t) - s_i^j(t))), \quad j = 1,...,D \tag{7}$$

where χ is a constriction factor controls the magnitude of $\vec{v}_i^j$, c_1 and c_2 are positive acceleration coefficients, and φ_i^j is uniform random number [0, 1]. The particles in different groups are attracted by the different group leaders, which causes different groups to locate different optima. This method helps to reduce the chance of getting stuck in a local solution. Each particle changes its position according to the following velocity-dependent formula:

$$\vec{s}_i(t+1) = \vec{s}_i(t) + \vec{v}_i(t+1). \tag{8}$$

C. *Particle Generation and Replacement*

The GCPSO generates new particles by using a new group-based crossover operation (GCRO), which is inspired by the crossover operation in the GAs. The GCRO-generated particles are used to replace the worst-performing group in each iteration. In the GCRO, parents for crossover are selected from different groups except for the worst-performing group in order to avoid inbreeding. Therefore, this operation is applied only when the number of groups G_S is larger than two. To select parents for the GCRO, the group-based tournament selection scheme is used. To select one parent, $G_S/2$ groups are first randomly and uniformly selected regardless of group performance. For these $G_S/2$ groups, the one with the best performance is selected. A particle within the selected group is then randomly and uniformly selected regardless of particle performance. This selected particle is designated as one parent $\vec{s}_{p1}$. The other parent $\vec{s}_{p2}$ is selected by the same way. Two new particles, $\vec{s}_{n1}$ and $\vec{s}_{n2}$, are created by performing crossover on the two selected parents. Two crossover sites are randomly selected and are denoted by t_1 and t_2. The GCRO creates each element in the two new particle vectors using the following operations:

$$s_{n1}^j = \begin{cases} \gamma_1 s_{p1}^j + (1-\gamma_1)s_{p2}^j, & j = 1,\dots,t_1 \\ \gamma_2 s_{p1}^j + (1-\gamma_2)s_{p2}^j, & j = t_1+1,\dots,t_2 \\ \gamma_3 s_{p1}^j + (1-\gamma_3)s_{p2}^j, & j = t_2+1,\dots,D \end{cases} \tag{9}$$

and

$$s_{n2}^j = \begin{cases} (1-\gamma_1) s_{p1}^j + \gamma_1 s_{p2}^j, & j = 1,\dots,t_1 \\ (1-\gamma_2) s_{p1}^j + \gamma_2 s_{p2}^j, & j = t_1+1,\dots,t_2 \\ (1-\gamma_3) s_{p1}^j + \gamma_3 s_{p2}^j, & j = t_2+1,\dots,D \end{cases} \tag{10}$$

where γ_i is a uniform random number in [0,1]. Each crossover operation creates two new particles. For worst-group replacement, the number of crossover operations is equal to $\lceil N_w/2 \rceil$, where N_w denotes the number of particles in the worst-performing group.

Table 1. The SAE of GCPSO and Different Population-based Algorithms in for The Truck Reversing Control Problem.

Methods	EGA [1]	C-PSO [4]	HGAPSO [5]	HPSO-TVAC [6]	PSO-CREV [7]	GCPSO
Average	0.525	0.5438	0.141	0.3252	1.29	0.1204
STD	0.564	1.0643	0.176	0.257	0.67	0.1531

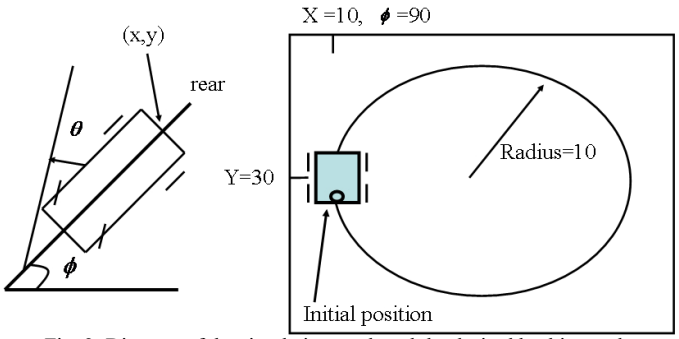

Fig. 2. Diagram of the simulation truck and the desired backing path.

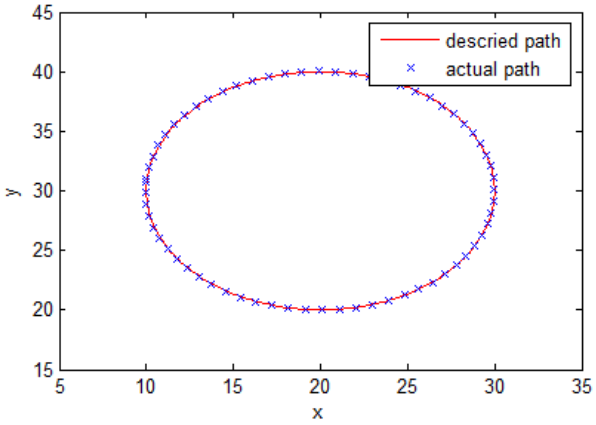

Fig. 3. The control results using GCPSO, where the desired and actual paths are denoted by solid line and "×", respectively.

For each new particle $\vec{s}_n$, its initial velocity $\vec{v}_n$ should be assigned accordingly, which is introduced as follows. The similarity degree between $\vec{s}_n$ and each of the left $G_S - 1$ group-leaders $\vec{p}_z^L$ are computed, and the leader with the minimum degree is found. That is, find

$$\hat{z} = \arg \min_{1 \le z \le G_S - 1} \rho(\vec{p}_z^L, \vec{s}_n) \tag{11}$$

The particle $\vec{s}_n$ is categorized into group $\hat{z}$. The initial velocity vector is assigned by the following formula:

$$v_n^j = \gamma_4^j \cdot (p_{\hat{z}}^{Lj} - s_n^j) + \gamma_5^j \cdot (s_{p1}^j - s_n^j) + \gamma_6^j \cdot (s_{p2}^j - s_n^j), \quad j = 1,...,D \tag{12}$$

This initial velocity is assigned according to the positions of the two parents and the group leader to which the new particle $\bar{s}_n$ belongs.

IV. SIMULATION

This paper simulates a truck reversing control problem. The FC is designed using GCPSO. Figure 2 shows the simulated truck. The truck position is precisely determined by the three state variables ϕ, x, and y, where ϕ is the angle of the truck with the horizon as shown in Fig. 2. The control signal to the truck is steering angle θ, where $\theta \in [-20°, 20°]$. Only reversing is considered. The truck moves backward by a fixed unit distance every stage. The model of the truck reversing system is [13]

$$x(k+1) = x(k) + \cos[\phi(k) + \theta(k)] + \sin[\theta(k)]\sin[\phi(k)] \quad (13)$$

$$y(k+1) = y(k) + \sin[\phi(k) + \theta(k)] - \sin[\theta(k)]\cos[\phi(k)] \quad (14)$$

$$\phi(k+1) = \phi(k) - \sin^{-1}[\frac{2\sin(\theta(k))}{b}] \quad (15)$$

where b is the length of the truck and b =4 in this simulation. Equations (13) to (15) generate the next state when the present state and control are given. The task here is to design a fuzzy controller to reverse the truck following the desired circular path

$$(x-20)^2 + (y-30)^2 = 10^2 \quad (16)$$

with an initial state of $(x, y, \phi) = (10, 30, 90^\circ)$. Figure 3 shows the initial state and the desired driving path. There are a total of 65 control steps, and control error is defined as

$$SAE = \sum_{k=1}^{65} |e(k)|, e(k) = (((x(k)-20)^2 + (y(k)-30)^2)^{1/2} - 10)^2 \quad (17)$$

FC inputs are $x(k)$, $y(k)$, and $\phi(k)$, and the input output is θ. The number of fuzzy rules is set to be four. In the GCPSO-designed FC, the particle size is set to be 40. This paper sets the parameters in (7) as follows: $\chi = 0.9$, $C1 = C2 = 1$, and the $\rho_{th} = 1.5$. The number of iterations is 1000. For statistical analysis, learning is performed for 50 runs. Table 1 shows the average SAE and standard deviation (STD) over 50 runs.

For the sake of comparisons, this paper compares the GCPSO performance with different advanced GA and PSO, including: an elite GA (EGA)[1], constriction PSO (C-PSO) [4], a hybrid of GA and PSO (HGAPSO) [5], self-organizing hierarchical PSO with time-varying acceleration coefficients (HPSO-TVAC) [6], and PSO with controller random exploration velocity (PSO-CREV) [7]. The number of rules in these methods is also set to be four *a priori*. Table 1 shows the learning average SAE and STDs of these population-based optimization algorithms used for comparison. The result shows that the GCPSO achieves the smallest control error.

V. CONCLUSION

This paper proposes a new optimization algorithm, GCPSO, for truck reversing control problem. The GCPSO generates a new swarm by using not only group-based particle update but also group-based crossover operation. The group-based crossover operation (GCRO) is incorporated into PSO for performance improvement. Effectiveness and efficiency of the GCPSO have been demonstrated through comparisons with different population-based optimization algorithms in the FC design problem. In the future, the GCPSO-designed FC will be applied to other control problems to verify its performance.

REFERENCES

[1] C.F. Juang, "A TSK-type recurrent fuzzy network for dynamic systems processing by neural network and genetic algorithms," IEEE Trans. Fuzzy Systems, vol.10, no. 2, pp. 155-170, April 2002.

[2] C. F. Juang, "Combination of on-line clustering and Q-value based GA for reinforcement fuzzy system design," *IEEE Trans. Fuzzy Systems*, Vol. 13, No. 3, pp. 289-302, June 2005.

[3] C. F. Juang and C. H. Hsu, "Temperature control by chip-implemented adaptive recurrent fuzzy controller designed by evolutionary algorithm," *IEEE Trans. Circuits and Systems- I: Regular Papers*, Vol. 52, No. 11, pp. 2376-2384, Nov. 2005.

[4] M. Clerc and J. Kennedy, "The particle swarm - explosion, stability, and convergence in a multidimentional complex space," *IEEE Trans. Evolutionary Computation*, vol. 6, no. 1, pp. 58-73, Feb. 2002.

[5] C. F. Juang, "A hybrid of genetic algorithm and particle swarm optimization for recurrent network design," *IEEE Trans. Syst., Man, and Cyber., Part B: Cybernetics*, vol. 34, no. 2, pp. 997-1006, April 2004.

[6] A. Ratnaweera, S. K. Halgamuge, and H. C. Watson, "Self-organizing hierarchical particle swarm optimizer with time-varying acceleration coefficients," *IEEE Trans. Evolutionary Computation*, vol. 8, no. 3, pp. 240-255, June 2004.

[7] X. Chen and Y. Li, "A modified PSO structure resulting in high exploration ability with convergence guaranteed," *IEEE Trans. Syst., Man, and Cyber., Part B: Cybernetics*, vol. 37, no. 5, pp. 1271-1289, Oct. 2007.

[8] D. Parrott and X. Li, "Locating and tracking multiple dynamic optima by a particle swarm model using speciation," *IEEE Trans. Evolutionary Computation*, vol.10, no.4, pp.440-458, Aug. 2006.

[9] Y. P. Chen, W. C. Peng, and M. C. Jian, "Particle swarm optimization with recombination and dynamic linkage discovery," *IEEE Trans. Syst., Man, and Cyber., Part B- Cyber.*, vol. 37, no. 6, pp. 1460-1470, Dec. 2007.

[10] F. Grimaccia, M. Mussetta, and R.E. Zich, "Genetical swarm optimization: self-adaptive hybrid evolutionary algorithm for electromagnetics," *IEEE Trans. Antennas and Propagation*, vol. 55, no. 3, Part 1, pp. 781-785, March 2007.

[11] S. Jeong; S. Hasegawa, K. Shimoyama, and S. Obayashi, "Development and investigation of efficient GA/PSO-hybrid algorithm applicable to real-world design optimization," *IEEE Trans. Computational Intelligence Mag.*, vol. 4, no.3, pp. 36-44, Aug. 2009.

[12] C. F. Juang, C. M. Hsiao, and C. H. Hsu, "Hierarchical cluster-based multi-species particle swarm optimization for fuzzy system optimization," *IEEE Trans. Fuzzy Systems*, vol. 18, no. 1, pp. 14-26, Feb. 2010..

[13] L. X. Wang, Adaptive Fuzzy Systems and Control. Englewood Cliffs, NJ: Prentice-Hall, 1994.

2011 IEEE International Conference on Fuzzy Systems
June 27-30, 2011, Taipei, Taiwan

Evolving Ensemble of Fuzzy Models

Eng Yeow Cheu†, Chai Quek* and See Siong Ng†
*Centre for Computational Intelligence
Nanyang Technological University, Singapore
Email: ashcquek@ntu.edu.sg
†Institute for Infocomm Research
A*STAR (Agency for Science, Technology and Research), Singapore
Email: engyeow_cheu@pmail.ntu.edu.sg, skng@i2r.a-star.edu.sg

***Abstract*—This paper presents an online learning-based neuro-fuzzy system called evolving Fuzzy Ensemble (eFE). The hierarchical computational structure of eFE is progressively adapted to autonomously support fuzzy data associations in accordance with neurophysiological studies. Activity-dependent synapse with global decay learning rule is incorporated to simulate the retention and active forgetting mechanisms that are involved in memory persistence. Such features incorporated in eFE model make it suitable to address the nonstationary characteristics of real-world problems. This work demonstrates the use of simple mechanisms to accomplish complex form of associative learning, an idea that has been suggested by psychologists for many years but has only recently been verified at the cellular level. The proposed eFE model is evaluated and compared with other modelling techniques in two benchmark time series experiments. The experimental results demonstrate the capabilities, and illustrate the viability of the proposed modelling technique.**

***Index Terms*—Fuzzy system, neuro-fuzzy system, ensemble, associative learning, online learning.**

I. Introduction

Soft computing has been a significant and influential computing paradigm in drawing complementary methodologies to exploit the tolerance for uncertainty, so as to achieve cost-effective intelligent solutions [1]. A typical approach is the integration of neural network and fuzzy system to create a hybrid structure called *neuro-fuzzy system* (NFS) [2]. The application of NFS has been demonstrated in a number of fields, including time-varying signal detection [3], adaptive nonlinear control [4], forecasting [5], knowledge extraction [6], decision support [7], fault detection [8], and robotics [9]. This neural-fuzzy synthesis provides flexible information processing capability, in a human comprehensible neural construct, for handling real life complex and uncertain situations [2].

A. Incremental Adaptation

Existing NFSs (see, e.g., [10], [5], [11], [12], for instance) generally employ all the training data samples multiple times either during network structure identification or network parameter adaptation. These systems generally require the representative data samples of the problem domain to be collected in advance. Hence, such batch learning models are not suitable for modelling of complex time-varying processes in dynamically changing environments. In addition, the ever increasing flow of data makes batch learning models unfeasible because these models generally make use of time consuming complex optimization with the objective of deriving a globally optimized solution that is representative of the training data. In order to use these models in online applications, it is only possible for the price of re-training the whole model structure and parameters with iterative and time-consuming procedures [13], [14].

In fact, a situation is likely to be encountered where it is not easy to collect a complete set of training samples to build a classification or forecasting system. For instance, it is almost impossible to construct a human face database without taking into consideration all the various factors that can affect an image quality. Thus, it is usually the case that an imperfect system is constructed to work well with some limited conditions, and only to revise it when more information is acquired. Therefore, in many practical situations, the presentation of training samples becomes sequential and adaptation to the system and forecasting by the system have to be alternatively carried out. In other practical applications (e.g. stock price forecasting), a static forecasting system is rendered ineffective by the changing property of the data source. Thus, a system is required to be incrementally adaptable to new information.

Progressive adaptation refers to the incremental modification of the network structure and parameters. The objective of progressive adaptation is to bring the network to produce a model close to a desired process through a gradual and progressive change of the network computational capability. In this paper, the progressive adaptation of a NFS is concerned with online learning of a data stream. The training exemplars from the data stream are assumed to arrive one at a time, and that the online learning algorithm adapts the structure and network parameters of the model based on the current training exemplar in an incremental manner. Online learning algorithms encompass the following four distinguishing features from *sequential learning algorithms* [15]: *1)* All the training observations are sequentially (one-by-one) presented to the learning system; *2)* At any time, only one training observation is seen and learned; *3)* A training observation is discarded as soon as the learning procedure for that particular observation is completed; *4)* The learning system has no prior knowledge as to how many total training observations will be presented. In addition, the following additional features are specifically considered for online learning algorithms: *1)* There is no knowledge of the lower and upper bound of the training

978-1-4244-7316-8/11/$26.00 ©2011 IEEE

observations; *2)* The system should account for time-varying data characteristics (i.e. knowledge about data should change).

B. Focus and Structure of Paper

This paper focuses on the structure and learning aspects of a NFS [2] called *evolving Fuzzy Ensemble* (eFE). The proposed eFE network is organised into a modular and hierarchical network of neurons. Starting with zero neuron, eFE adopts a single-pass progressive learning approach that is inspired from the neurobiological learning theories of synaptic plasticity. This paper is organised as follows. Section II presents the architecture of the eFE network. Section III provides an overview of the proposed progressive biologically inspired learning algorithm for eFE network. In Sect. IV, two experiments are conducted to demonstrate the modelling and tracking capabilities of the proposed eFE model. Section V summarises and concludes this paper.

II. Network Architecture

The proposed eFE is a feed-forward network comprising of five layers of neurons. Other than layer I and V, the neurons in the other layers of eFE network are organised into a modular and hierarchical structure with H levels. Figure 1 shows the hierarchical structure of eFE network with two input variable nodes, one output variable node, and H hierarchical levels of nodes in layer II, III, and IV. The symbols used in this paper denotes the following:

I	number of input features;
M	number of output features;
K_h	number of rule nodes at hth hierarchical level;
IV_i	input linguistic node for input feature x_i ($1 \leq i \leq I$);
OV_m	output linguistic node for output feature y_m ($1 \leq m \leq M$);
$J_{h,i}$	number of linguistic term node/membership functions (MFs) for input feature x_i at hth hierarchical level;
$L_{h,m}$	number of MFs for output feature y_m at hth hierarchical level;
$IL_{h,i,j}$	jth MF for input feature x_i at hth hierarchical level ($1 \leq j \leq J_{h,i}$);
$OL_{h,m,\ell}$	ℓth MF for output feature y_m at hth hierarchical level ($1 \leq \ell \leq L_{h,m}$);
$R_{h,k}$	kth rule node at hth hierarchical level ($1 \leq k \leq K_h$);
$C_{h,m,\ell,k}$	fuzzy rule connection between $R_{h,k}$ and $OL_{h,m,\ell}$.

The hierarchical organisation of eFE network corresponds to the structure of the neocortex [16]. A hierarchical level of eFE corresponds to a cortical layer. The differences in the sensory function among the cortical layers are simulated using different hierarchical levels of linguistic term/label nodes with different receptive fields (supports of fuzzy MFs). A layer of nodes in eFE network corresponds to a vertical cortical column. Every layer of neurons in the proposed eFE network is a functional module of a *fuzzy inference system* (FIS). Each layer of the eFE network performs specific fuzzy operations to realize an extended-Mamdani fuzzy reasoning model that handles *mutual inclusivity* [17]. A fuzzy rule at the hth hierarchical level of eFE network is encoded as follows:

IF x_1 is $IL_{h,1,j}$ $\ldots \wedge \ldots$ x_i is $IL_{h,i,j}$ $\ldots \wedge \ldots$ x_I is $IL_{h,I,j}$ THEN y_1 is $OL_{h,1}$, …, y_m is $OL_{h,m}$, …, y_M is $OL_{h,M}$

where $OL_{h,m}$ represents a fuzzy partition that is shaped by the output MFs ($OL_{h,m,1}, \ldots, OL_{h,m,L_{h,m}}$) of different degrees [18].

The input and output signals at any time t are respectively represented as crisp vectors $\mathbf{x}(t) = [x_1, \ldots, x_I]^T$ and $\mathbf{y}(t) = [y_1, \ldots, y_M]^T$. Every node in the first layer of the network takes in a single element from the input vector $\mathbf{x}(t)$. Every output node computes a single output element of the output vector $\mathbf{y}(t)$ with respect to the input stimulus vector $\mathbf{x}(t)$. The forward reasoning with signal propagation through each layer of the network as shown in Fig. 1 is described as follows.

A. Layer I: Input Linguistic Nodes

A node IV_i simply receives signal from the input stimulus x_i, and propagates it to the next layer nodes for processing. The output o_i^I of IV_i is defined in (1).

$$o_i^I = x_i \ . \tag{1}$$

B. Layer II: Input Linguistic Term Nodes

A neuron $IL_{h,i,j}$ denotes the jth fuzzy MF of the ith input feature at the hth hierarchical level and constitutes an antecedent of a fuzzy rule. Every node $IL_{h,i,j}$ defines a triangular fuzzy MF and its output $o_{h,i,j}^{II}$ is computed using *singleton fuzzification* operation in (2).

$$\begin{aligned} o_{h,i,j}^{II} &= \mu_{h,i,j}^{II}(o_i^I; a_{h,i,j}^{II}, b_{h,i,j}^{II}, c_{h,i,j}^{II}) \\ &= \max\left(\min\left(\frac{o_i^I - a_{h,i,j}^{II}}{b_{h,i,j}^{II} - a_{h,i,j}^{II}}, \frac{c_{h,i,j}^{II} - o_i^I}{c_{h,i,j}^{II} - b_{h,i,j}^{II}}\right), 0\right) \ , \end{aligned} \tag{2}$$

where parameters $a_{h,i,j}^{II}$ and $c_{h,i,j}^{II}$ are the minimum and maximum support, and $b_{h,i,j}^{II}$ is the kernel of the MF for $IL_{h,i,j}$ respectively. In addition, the following conditions are satisfied for the input fuzzy MFs.

$$o_{h,i,1}^{II} = \begin{cases} 1, & o_i^I \leq b_{h,i,1}^{II}; \\ \mu_{h,i,1}^{II} \text{ defined in (2)}, & \text{otherwise.} \end{cases} \tag{3}$$

$$o_{h,i,J_{h,i}}^{II} = \begin{cases} 1, & o_i^I \geq b_{h,i,J_{h,i}}^{II}; \\ \mu_{h,i,J_{h,i}}^{II} \text{ defined in (2)}, & \text{otherwise.} \end{cases} \tag{4}$$

$$\sum_{j=1}^{J_{h,i}} \mu_{h,i,j}^{II} = 1 \ ; \ b_{h,i,j}^{II} < b_{h,i,j+1}^{II} \ . \tag{5}$$

Equation (3) and (4) respectively defines the first and the last MF in $x_i \subset \mathbb{R}$, and (5) specifies the overlap level of 0.5 between any two successive MFs. The eFE network consists of H sets (each set belonging to a level of eFE) of input linguistic labels, with each of them characterized by a scale parameter $\sigma_{h,i}^{II}$ defined in (6),

$$\sigma_{h,i}^{II} = b_{h,i,j}^{II} - a_{h,i,j}^{II} = c_{h,i,j}^{II} - b_{h,i,j}^{II} \ , \tag{6}$$

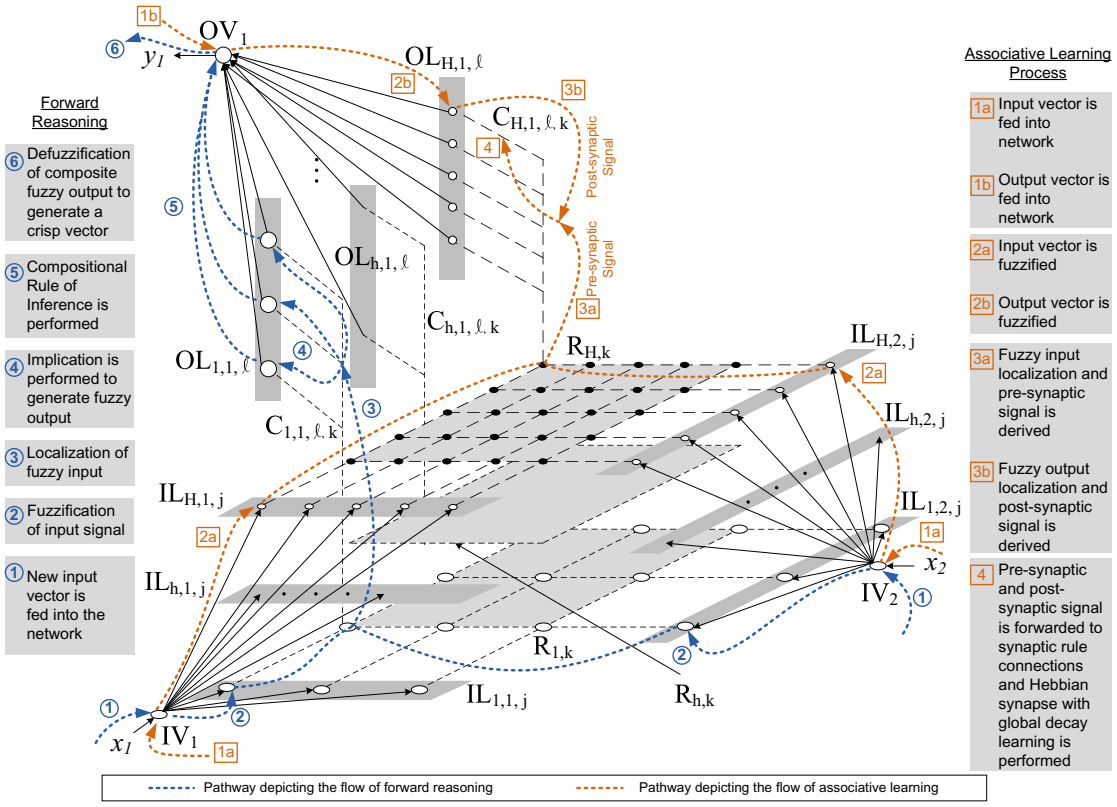

Fig. 1. Structure of eFE network.

and $\sigma^{II}_{h,i} > \sigma^{II}_{h+1,i}$. Each higher hierarchical level composes of MFs with smaller uniform entropies than the ones at the lower hierarchical level [19].

C. Layer III: Rule Nodes

A neuron $R_{h,k}$ represents the kth fuzzy rule node at the hth hierarchical level with output $o^{III}_{h,k}$ computed using a conjunctive fuzzy set operation (minimum t-norm operation) [20] defined in (7).

$$o^{III}_{h,k} = \min_{(h,i,j)\in A^{II}_{h,k}} o^{II}_{h,i,j} \ , \tag{7}$$

where $A^{II}_{h,k}$ is the set of input linguistic term nodes in layer II (antecedent) that are connected to $R_{h,k}$.

D. Layer IV: Output Linguistic Term Nodes

A neuron $OL_{h,m,\ell}$ represents the ℓth output linguistic term node of the mth output linguistic node at the hth hierarchical level. Each node implements the *Compositional Rule of Inference* (CRI) [21] scheme. The output $o^{IV}_{h,m,\ell}$ of $OL_{h,m,\ell}$ is defined in (8).

$$o^{IV}_{h,m,\ell} = \max_{k\in R^{III}_{h,m,\ell}} \left(\min(o^{III}_{h,k}, C^{f}_{h,m,\ell,k})\right) \ , \tag{8}$$

where $R^{III}_{h,m,\ell}$ is the set of rule nodes in layer III that are connected to $OL_{h,m,\ell}$, and $C^{f}_{h,m,\ell,k}$ (refer to (13)) is the certainty factor (normalized weight) of the rule node connection $C_{h,m,\ell,k}$ between $R_{h,k}$ and $OL_{h,m,\ell}$.

The eFE network consists of H sets of output linguistic labels. These labels also satisfy the same conditions ((3), (4), (5)) that are specified for the input linguistic labels. Each output linguistic label is characterized by a scale parameter $\sigma^{IV}_{h,m}$ defined in (9),

$$\sigma^{IV}_{h,m} = b^{IV}_{h,m,\ell} - a^{IV}_{h,m,\ell} = c^{IV}_{h,m,\ell} - b^{IV}_{h,m,\ell} \ , \tag{9}$$

and $\sigma^{IV}_{h,m} > \sigma^{IV}_{h+1,m}$. At each hierarchical level, the overlap of 0.5 between any two successive output MFs implies no reconstruction error in the linguistic-numerical transformation [19].

E. Layer V: Output Linguistic Nodes

The neuron or defuzzification node OV_m defuzzifies the fuzzy composite output generated in layer IV into a crisp value. The output o^{V}_{m} of OV_m is computed using the *height defuzzification* method [20] defined in (10).

$$o^{V}_{m} = y_m = \frac{\sum_{h=1}^{H}\sum_{\ell=1}^{L_{h,m}} o^{IV}_{h,m,\ell} b^{IV}_{h,m,\ell}}{\sum_{h=1}^{H}\sum_{\ell=1}^{L_{h,m}} o^{IV}_{h,m,\ell}} \ , \tag{10}$$

where $b^{IV}_{h,m,\ell}$ represents the kernel of the MF that is employed to describe $OL_{h,m,\ell}$.

III. Progressive Learning Algorithm

Figure 2 depicts the overview of the progressive learning procedure. The learning algorithm consists of three modules; namely: *network expansion*, *associative learning*, and *network*

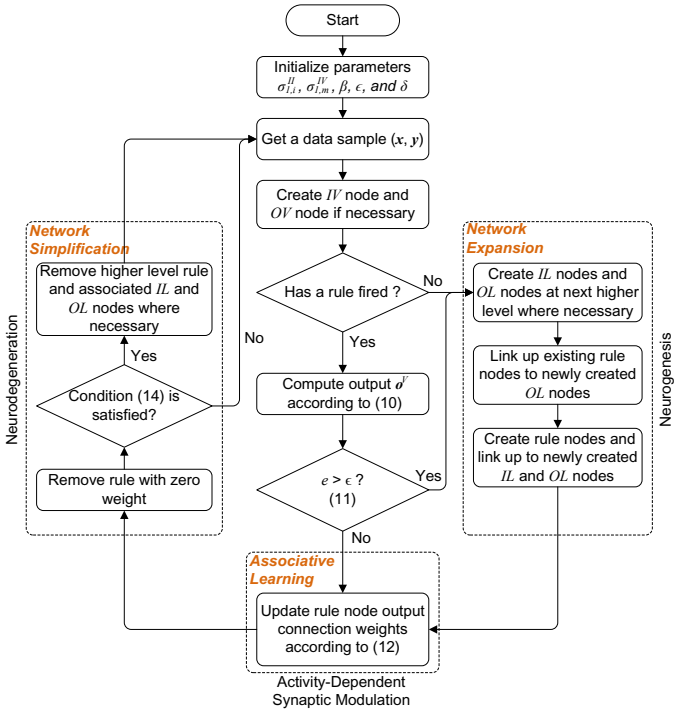

Fig. 2. Progressive learning procedure.

simplification. The learning procedure for each of the module is outlined as follows.

A. Network Expansion Module

The biological network structure plasticity is partially due to *neurogenesis* [22], [23], [24]. The function of neurogenesis was hypothesized to avoid prediction error due to *catastrophic interference* [24] by extending the encoding of new pattern with new neuron. In addition, microscopic examination of a coronal section through the neocortex shows that the neuronal cell bodies are arranged in different layers [25]. Birth dating studies showed that cortical neurons generated earlier reside in deeper layers while later-born neurons migrates past existing layers to form superficial layers [25].

First, to account and model the neurogenesis process and development in neocortex, new higher level rule node and its associated linguistic label nodes (IL and OL nodes) are added to the proposed eFE network whenever the network has a forecast error $e(t)$ exceeding a maximum acceptable error threshold ϵ defined in (11).

$$e(t) = \|\mathbf{o}^V(t) - \mathbf{y}^d(t)\|/M > \epsilon \ , \tag{11}$$

where $\mathbf{o}^V(t)$ is the output vector produced by eFE, and $\mathbf{y}^d(t)$ represents the desirable response the network should produce at time t.

The incremental insertion of new level neurons corresponds to the sequence of neurogenesis process in neocortex, in which neurons that are generated earlier reside in the deeper cortical layers (lower levels of eFE network). In addition, new neurons are added to avoid catastrophic interference and reduce prediction error according to the function of neurogenesis [24].

Second, new input and output linguistic label nodes are added with smaller fuzzy membership "width" (smaller support) at each higher level. Every new higher level linguistic label node is created with receptive field half the size of the immediate lower level linguistic label node. This creates linguistic label nodes in a hierarchical organisation with different receptive fields to simulate the laminar differences in the sensory function among the different cortical layers [16].

As a result, linguistic label nodes with smaller scales (receptive fields) will be present in those regions where the most subtle details are located. Nodes are adaptively allocated with adequate scale in the different regions of the input and output data space to form a sparse approximation of the data. The differences in the sensory function encoded by the different level of linguistic label nodes also allow the proposed network to describe the input and output feature across different scales. The lower level neurons could encode knowledge on more general information, and the higher level neurons to describe knowledge in finer detail.

Third, neurons created earlier (having wider receptive fields in lower levels) will be activated more frequently than higher level neurons. Consistent with physiological findings, in which older neurons are relatively more stable than newer neurons [26], this mechanism allows the lower and older neurons less likelihood from being removed (cf. Sect. III-C). In addition, this mechanism is also consistent with memory retention behaviour in human. Human normally remember more general than specific fact/knowledge.

Fourth, individually adding node as required limit the network complexity by preventing network to memorize training patterns and generalize poorly (large variance case). The network is also adapted according to changing pattern statistics to prevent the network being too simple that it can not even be able to represent training patterns well (large bias case) [27].

B. Associative Learning Module

Numerous evidences have suggested that rehearsal is required to support the consolidation of memories [28], [29], [30]. At the molecular level, the formation and consolidation of *long-term memory* are thought to be ultimately expressed in the form of structural changes at the synapses [31]. At the same time, other studies suggested that the decay of memory traces is the result of an active forgetting mechanism which opposes the strengthening mechanism involved in memory persistence [32], [33]. The progressive learning algorithm (cf. the associative learning process depicted in Fig. 1) captures these two key features; namely: retention and forgetting of memory traces, as follows.

- *Retention Mechanism*: First, to model the involvement of retention mechanism in long-term memory formation, the dynamics of the Hebbian learning rule [34] is incorporated to mediate the synapses between rule nodes and output linguistic term nodes. Synapse is strengthened by the retention term in (12) during correlated activation (firing) between rule node (pre-synaptic neuron) and output linguistic term node (post-synaptic neuron).

- *Forgetting Mechanism*: Second, the forgetting mechanism is interpreted as having a destabilizing effect on the existing stored memories. To account for such a process, a global synaptic decay term is included in (12) to weaken the synaptic strength.

The overall changes in the synaptic strength (Step 4 of the associative learning process depicted in Fig. 1) is simulated in (12),

$$\begin{aligned}\Delta C^{w}_{h,m,\ell,k}(t) &= C^{w}_{h,m,\ell,k}(t) - C^{w}_{h,m,\ell,k}(t-1) \\ &= \underbrace{\min(o^{III}_{h,k}(t), \mu^{IV}_{h,m,\ell}(y^{d}_{m}(t)))}_{\text{retention term}} - \underbrace{\beta \cdot C^{w}_{h,m,\ell,k}(t-1)}_{\text{forgetting term}},\end{aligned} \tag{12}$$

where $C^{w}_{h,m,\ell,k}$ denotes the synapse strength of rule node connection $C_{h,m,\ell,k}$, $\mu^{IV}_{h,m,\ell}(y^{d}_{m}(t))$ represents the membership grade of $OL_{h,m,\ell}$ for output variable node OV_m (Step 2b of associative learning process in Fig. 1), $y^{d}_{m}(t)$ denotes the mth element of the desired output vector $\mathbf{y}^{d}(t)$ at time instance t, and β represents the forgetting rate.

To prevent saturation and loss of input selectivity, the weights of the connections between rule nodes and output linguistic term nodes are normalized according to (13).

$$C^{f}_{h,m,\ell,k}(t) = \frac{C^{w}_{h,m,\ell,k}(t)}{\sum_{\ell=1}^{L_{h,m}} C^{w}_{h,m,\ell,k}(t)} \ , \tag{13}$$

where $C^{f}_{h,m,\ell,k}$ is the normalized weight of rule node connection $C_{h,m,\ell,k}$. $C^{f}_{h,m,\ell,k}$ is the degree (certainty factor) of the output MF $OL_{h,m,\ell}$ associated with $R_{h,k}$. Different certainty factors to the output MFs are used to shape an alternative output fuzzy answer space [18].

The computational model demonstrates the effect of active forgetting and retention memory processes. Only in the presence of sufficient and repeated synaptic reinforcements, either triggered by multiple repetitive training events or reactivation/recollection of such events, can memories be maintained and strengthened. This is consistent with evidence, in which the more frequently an event is recalled, the better and longer it will be remembered [28].

C. Network Simplification Module

Even though higher level rules and associated linguistic label nodes are adaptively added, the consolidated rules will be updated according to changing pattern statistics. Some rule nodes that represent the different localized regions of the data space may at a later stage of adaptation make to produce similar forecast as those rules activated at a lower level.

At each presentation of a data sample, the highest level activated rule $R^{f}_{H_f,k}$ is removed if the following condition (14) is satisfied.

$$\|\mathbf{o}^{R}_{H_f,k} - \mathbf{o}^{R}_{H_f-1,a}\|/M < \delta \ ; \ \exists a \in R^{f}_{H_f-1}, H_f \neq 1 \ , \tag{14}$$

where δ represents the output forecast similarity threshold, H_f represents the highest level of the rules that are activated, $R^{f}_{H_f-1}$ represents the set of lower immediate level rules that are activated, and $\mathbf{o}^{R}_{H_f,k}$ represents the inferred crisp output vector of $R^{f}_{H_f,k}$ using CRI scheme defined in (15) with $h = H_f$.

$$\begin{aligned}\mathbf{o}^{R}_{h,k} &= [o^{R}_{h,k,1}, \ldots, o^{R}_{h,k,m}, \ldots, o^{R}_{h,k,M}]^{T} \ ; \\ o^{R}_{h,k,m} &= \frac{\sum_{\ell=1}^{L_{h,m}} \min(o^{III}_{h,k}, C^{f}_{h,m,\ell,k}) \cdot b^{IV}_{h,m,\ell}}{\sum_{\ell=1}^{L_{h,m}} \min(o^{III}_{h,k}, C^{f}_{h,m,\ell,k})}.\end{aligned} \tag{15}$$

Such higher level rule with smaller receptive field can safely be removed as it describes the localized fuzzy region that is also enclosed by a lower immediate level rule.

In addition, if a rule node $R_{h,k}$ has all its rule node connection weights $C^{w}_{h,m,\ell,k}$ ($1 \leq \ell \leq L_{h,m}$; $1 \leq m \leq M$) reduced to zero then $R_{h,k}$ is removed from the rule base. This is because the rule node is not frequently activated to make it relevant for the present data events. Thus, the network structure is simplified in this process. This step corresponds to structure plasticity related to the removal of neurons and synapses that contributes to the loss of memory (see, e.g., [35], for instance).

IV. Experiments: Simulations

In this section, two experiments are conducted to demonstrate the quality features of the proposed eFE model.

A. Online System Identification of a Nonlinear System

The objective of this experiment is to evaluate the proposed eFE network in one-pass identification of a nonlinear system defined by (16).

$$y_d(t+1) = \frac{y_d(t)}{1 + y^{2}_{d}(t)} + u^{3}(t) \ , \tag{16}$$

where $u(t) \in$ [-1.0, 1.0] is given by $\sin(2\pi t/100)$, and $y_d(t) \in$ [-1.5, 1.5] and $y_d(0) = 0$. The proposed eFE model is benchmarked with existing works; namely, MRAN [36], RANEKF [37], SONFIN [38], SAFIS [14], Simpl_eTS [39], eTS [13], DENFIS [40], FALCON-ART [41], and EFuNN [42] under the same experimental set-up in [14].

Table I lists the consolidated generalization result achieved by the various modelling techniques. The result shows that neural network and TSK modelling techniques deliver better generalization accuracies than the proposed eFE model. The following are the reasons to explain this result.

- TSK-based fuzzy models [43], [44] are used for *precise fuzzy modelling* (PFM) in place of *linguistic fuzzy modelling* (LFM) [45]. The proposed eFE model is based on Mamdani fuzzy model used for LFM.
- The benchmark modelling techniques (MRAN, RANEKF, SONFIN, SAFIS, Simpl_eTS, eTS, DENFIS, FALCON-ART, and EFuNN[1]) utilize a clustering-based prototyping to partition the data space. In contrast, eFE makes use of the more restrictive grid based type of data space partitioning [46]. Clustering-based prototyping poses less

[1]The second layer nodes in EFuNN are fully connected to a rule node in the third layer via a set of connection weights. These connection weights represent the coordinates of the center of the hypersphere in the fuzzy input space for a rule node.

constraint as this methodology provides direct modelling of data distribution in the data space. Hence, clustering-based partitioning of data space usually requires lesser number of prototypes (rule nodes). However, systems based on clustering-based prototyping usually have opaque computing structure. For example, the input fuzzy sets derived by SAFIS have large overlaps that obstruct the understandings of the underlying data structure (refer to [14]).

- The other benchmark systems employ complex operations and perform fine tuning of network parameters. The proposed eFE model does not require such time consuming complex operations. For example, RANEKF and MRAN networks are evolving radial basis neural networks based on the principle of the Resource Allocation Network (RAN) [47]. RANEKF extends the RAN by employing the Extended Kalman Filter (EKF) algorithm in place of the Least Mean Squares (LMS) algorithm. MRAN extends RAN (and RANEKF) by combining the growth criterion of the RAN with a pruning strategy based on the relative contribution of each hidden unit to the overall network output. SAFIS computes the statistical contribution of every rule to the system output and the parameters are tuned with EKF algorithm. eTS has to recursively update its TSK model structure based on the potential of the input data. This is defined based on its distances to all other data points that have been received. As for the DENFIS online model, a weighted recursive Least-Square Estimator (LSE) is used. In SONFIN, the consequent parameters of its TSK rules are tuned either by LMS or Recursive Least Squares (RLS) algorithms and the precondition parameters are tuned by back-propagation algorithm. FALCON-ART tunes the parameters of the MFs using the back-propagation algorithm. Unconstraint accuracy-oriented parameter optimization is also one of the other reasons that will produce significant overlapping of the fuzzy MFs. This obstructs the understandings of the underlying data structure.
- The training and testing data are generated from the same difference equation (16). An accuracy-oriented modelling technique with enough training cycles to tune its network structure and parameters would definitely perform better in this case. On the other hand, the eFE learning algorithm does not try to reduce the error to zero. Under soft computing paradigm, the proposed eFE aims to contain the error between the computed output and desirable values within an acceptable threshold. Hence, the learning error is not asymptotically reduced to zero. It is seldom the case in reality that the unseen events replicate exactly the same as past events. Hence, optimization done at the present time instance has no guarantee in providing an optimal solution that will also generalize well for future unseen events. For one obvious reason, current optimization may produce a solution that over fits to the current set of training data. Section IV-B illustrates this point by evaluating EFuNN, DENFIS and eFE to track a time-varying nonlinear system.

TABLE I
FORECAST RESULTS ON ONLINE NONLINEAR SYSTEM IDENTIFICATION

Reasoning Model	Type	# Rules	Testing RMSE
MRAN[a]	NN	10*	0.0129
RANEKF[a]	NN	11*	0.0184
SONFIN[a]	TSK	10	0.0130
SAFIS[a]	TSK	8	0.0116
Simpl_eTS[a] (r=0.075, Ω=10^6)	TSK	18	0.0122
eTS[a] (r=1.0, Ω=10^6)	TSK	19	0.0082
DENFIS	TSK	8	0.0482
FALCON-ART	M	289	0.1379
EFuNN	M	18	0.0578
eFE	E-M	21	0.0751

[a] = Result adapted from [14]; NN = Neural Network; TSK = Takagi-Sugeno-Kang-based fuzzy model; M = Mamdani-based fuzzy model; E-M = Extended Mamdani-based fuzzy model that handles mutual inclusivity [17]; * = Number of hidden nodes; RMSE = Root Mean Squared Error.

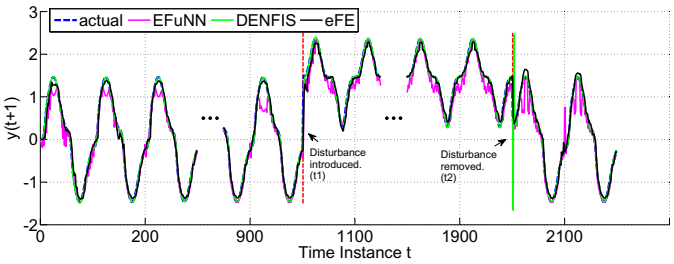

Fig. 3. Forecast of time-varying nonlinear system.

B. Online System Identification of a Time-Varying Nonlinear System

The previous nonlinear dynamic system (16) is modified as shown in (17).

$$y_d(t+1) = \frac{y_d(t)}{1+y_d^2(t)} + u^3(t) + f(t) \ , \qquad (17)$$

where $f(t)$ simulates the disturbance to be introduced, and is defined in (18),

$$f(t) = \begin{cases} 0, & 0 \le t \le 1000 \text{ and } t \ge 2001; \\ 1, & 1001 \le t \le 2000. \end{cases} \qquad (18)$$

Similar to [48], the eFE model is employed to progressively identify the characteristics of the modified nonlinear dynamic system.

Figure 3 shows the tracking capability of eFE, EFuNN, and DENFIS. The eFE model is able to track the underlying system characteristics right from the initial stage. The proposed eFE model is also able to track new system characteristics when the disturbance $f(t)$ is introduced at time t1 ($t = 1001$) and when it is removed at time t2 ($t = 2001$). EFuNN has large tracking error towards the end of the simulation. DENFIS exhibits large tracking error at time t2.

Figure 4(a) illustrates the corresponding changes to the structure of the three models. For eFE, rule nodes are progres-

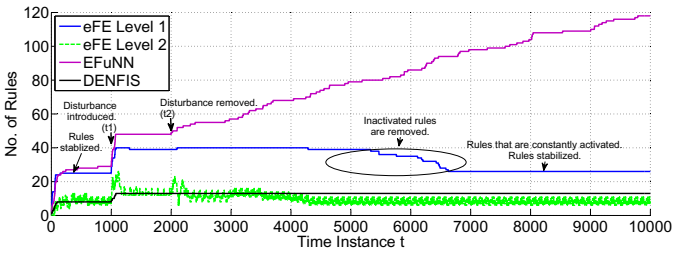

(a) Number of rule nodes.

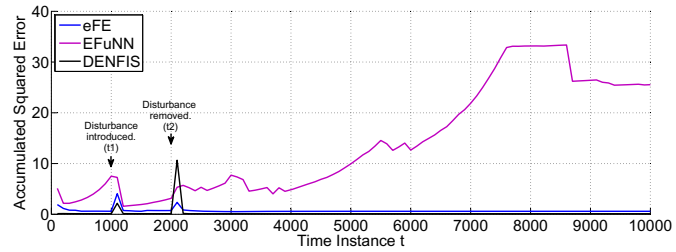

(b) Online learning error.

Fig. 4. Online learning of the time-varying nonlinear system.

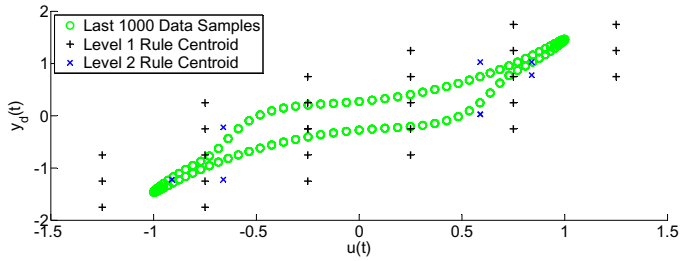

Fig. 5. Rules identified by eFE at the end of simulation ($t = 10000$).

sively added and removed. After the disturbance is removed at t2, the fuzzy rules that describe the disturbance are subsequently removed. This is because these rules are not activated frequently enough to make it relevant for the present data events. For EFuNN, rule nodes are progressively added even when disturbance has been removed at t2. The structure of DENFIS is fixed after the introduction of disturbance at time t1.

Figure 4(b) illustrates the accumulated squared error computed over 100 adjacent time steps. Spikes in the eFE learning error are observed at three instances; namely, during the initial stage at time $t = 0$, when the disturbance is introduced at time t1, and when the disturbance is removed at t2. The increase in learning error at these three instances corresponds to the time when there are changes in the underlying properties of the nonlinear system model. When the disturbance $f(t)$ is removed at t2 only a smaller increase in eFE learning error has been observed. In contrast, EFuNN performs unacceptably. The online learning error of EFuNN generally becomes larger at each time instance. On the other hand, DENFIS has overly learnt and fitted the data. This is because the online learning error accumulated by DENFIS just after the disturbance was removed, is higher than the amount of error accumulated when the disturbance was introduced. The information learnt by DENFIS before the disturbance was introduced is lost even though the number of rules has not reduced. This experiment illustrates that DENFIS accuracy-oriented optimization on the given information causes the network to quickly skew towards current information and forget the information learnt in the past.

Figure 5 plots the distribution of the last 1000 input data samples, and the centroids of the rules identified by eFE. The figure shows more rules are identified near the lower left and upper right region of the input data space. These regions correspond to the input data samples that are more closely located. The lower level eFE rules coarsely describe these regions and higher level rules are added to describe these regions in finer detail.

V. Conclusion

This paper presents an online learning-based hierarchical NFS called, eFE (evolving Fuzzy Ensemble). A progressive learning algorithm is proposed to incrementally modify the hierarchical structure of eFE in accordance with neurophysiological studies. With continuous exposure to external stimuli, the eFE network adapts its structure by allocating nodes and creating links to autonomously support fuzzy data associations. Activity-dependent synapse with global decay learning rule is incorporated such that fuzzy rules that are relevant to the observed training data are reinforced while rules that are inconsistent are weakened. This technique simulates the two opposite mechanisms that are involved in memory persistence [32], [33], [28]. At the same time, the eFE network structure is simplified by removing similar and irrelevant fuzzy knowledge. This is accomplished by removing rules that have similar forecast output, and irrelevant rules that are no longer reinforced by the external stimuli. This technique corresponds to structure plasticity related to the removal of neurons and synapses that contributes to the loss of memory (see, e.g., [35], for instance).

The learning algorithm employed by eFE possesses the distinguishing features of online learning algorithms as outlined in Sect. I. The experimental results are concluded as follows.

- The experimental result showed that the proposed eFE model is able to adequately model the underlying data characteristics of a nonlinear system compared to other benchmarked modelling techniques.
- The tracking capability of eFE model was demonstrated by learning the underlying data characteristics of a time-varying system. Without prior knowledge of the data distribution, the eFE multi-resolution hierarchy structure allows both good generalization and fine detail to be captured. Unlike other benchmark modelling techniques, the experiment also showed the capability of the proposed eFE in removing irrelevant fuzzy knowledge. The experiment also demonstrated that optimization can cause a model to quickly skew towards current information and forget the information learnt in the past.

In conclusion, most batch learning methodologies are computationally intensive with the objective of deriving a global

solution by optimizing certain criterion (e.g. parameter adaptation to minimize prediction error under supervised learning). The extension of offline learning paradigms to online learning mode questions the need for such intensive computation given that only limited information is available at a given time. After all, such form of *limited-knowledge optimization* in time-varying environment would likely not produce a globally optimized solution which directly contradicts the initial idea for optimization in a global sense. Instead, this paper presents a simple fuzzy associative learning algorithm that does not rely on computationally intensive accuracy-oriented optimization to incrementally adapt an ensemble of fuzzy models.

REFERENCES

[1] L. A. Zadeh, "Fuzzy logic, Neural networks, and Soft Computing," *Communications of the ACM*, vol. 37, no. 3, pp. 77–84, 1994.

[2] C. T. Lin and C. S. G. Lee, *Neural Fuzzy Systems: A Neuro-Fuzzy Synergism to Intelligent Systems*. Englewood Cliffs, NJ: Prentice Hall, 1996.

[3] M. E. Yüksel and E. Beşdok, "A Simple Neuro-Fuzzy Impulse Detector for Efficient Blur Reduction of Impulse Noise Removal Operators for Digital Images," *IEEE Transactions on Fuzzy Systems*, vol. 12, no. 6, pp. 854–865, 2004.

[4] C. W. Ting and C. Quek, "A Novel Blood Glucose Regulation Using TSK^0-FCMAC: A Fuzzy CMAC based on the Zero-Ordered TSK Fuzzy Inference Scheme," *IEEE Transactions on Neural Networks*, vol. 20, no. 5, pp. 856–871, 2009.

[5] K. K. Ang and C. Quek, "RSPOP: Rough Set-Based Pseudo Outer-Product Fuzzy Rule Identification Algorithm," *Neural Computation*, vol. 17, no. 1, pp. 205–243, 2005.

[6] G. Castellano, A. Fanelli, and C. Mencar, "A Neuro-Fuzzy Network to generate Human-Understandable Knowledge from Data," *Cognitive Systems Research*, vol. 3, no. 2, pp. 125–144, 2002.

[7] E. Y. Cheu, S. K. Ng, and C. Quek, "Enhancing Decision Support System with Neural Fuzzy Model and Simple Model Visualizations," in *Handbook on Decision Making, ISRL 4*, L. C. Jain and C. P. Lim, Eds. Springer-Verlag Berlin Heidelberg, 2009, ch. 4, pp. 85–116.

[8] W. Wang, F. Ismail, and F. Golnaraghi, "A Neuro-Fuzzy Approach to Gear System Monitoring," *IEEE Transactions on Fuzzy Systems*, vol. 12, no. 5, pp. 710–723, 2004.

[9] K. Kiguchi, T. Tanaka, and T. Fukuda, "Neuro-Fuzzy Control of a Robotic Exoskeleton with EMG Signals," *IEEE Transactions on Fuzzy Systems*, vol. 12, no. 4, pp. 481–490, 2004.

[10] J. Kim and N. Kasabov, "HyFIS: Adaptive Neuro-Fuzzy Inference Systems and their Application to Nonlinear Dynamical Systems," *Neural Networks*, vol. 12, no. 9, pp. 1301–1319, 1999.

[11] J. Sim, W. L. Tung, and C. Quek, "FCMAC-Yager: A Novel Yager-Inference-Scheme-Based Fuzzy CMAC," *IEEE Transactions on Neural Networks*, vol. 17, no. 6, pp. 1394–1410, Nov. 2006.

[12] W. Yu, F. O. Rodriguez, and M. A. Moreno-Armendariz, "Hierarchical Fuzzy CMAC for Nonlinear Systems Modeling," *IEEE Transactions on Fuzzy Systems*, vol. 16, no. 5, pp. 1302–1314, 2008.

[13] P. Angelov and D. P. Filev, "An Approach to Online Identification of Takagi-Sugeno Fuzzy Models," *IEEE Transactions on Systems, Man, and Cybernetics, Part B: Cybernetics*, vol. 34, no. 1, pp. 484–498, 2004.

[14] H.-J. Rong, N. Sundararajan, G.-B. Huang, and P. Saratchandran, "Sequential Adaptive Fuzzy Inference System (SAFIS) for Nonlinear System Identification and Prediction," *Fuzzy Sets and Systems*, vol. 157, no. 9, pp. 1260–1275, May 2006.

[15] G. B. Huang, P. Saratchandran, and N. Sundararajan, "A Generalized Growing and Pruning RBF (GGAP-RBF) Neural Network for Function Approximation," *IEEE Transactions on Neural Networks*, vol. 16, no. 1, pp. 57–67, jan. 2005.

[16] J. A. Hirsch and L. M. Martinez, "Laminar Processing in the Visual Cortical Column," *Current Opinion in Neurobiology*, vol. 16, no. 4, pp. 377–384, Aug. 2006.

[17] J. Tan and C. Quek, "ACPOP: Ambiguity Correction-based Pseudo-Outer-Product Fuzzy Rule Identification Algorithm," in *IEEE International Conference on Fuzzy Systems*, Aug. 2009, pp. 74–79.

[18] W. Siler and J. J. Buckley, *Fuzzy Expert Systems and Fuzzy Reasoning*. Hoboken, NJ: Wiley, 2005.

[19] W. Pedrycz, "Why Triangular Membership Functions?" *Fuzzy Sets and Systems*, vol. 64, no. 1, pp. 21–30, 1994.

[20] J. M. Mendel, *Uncertain Rule-Based Fuzzy Logic Systems: Introduction and New Directions*. Upper Saddle River, NJ: Prentice Hall, 2001.

[21] L. A. Zadeh, "Fuzzy Sets," *Information and Control*, vol. 8, no. 3, pp. 338–353, 1965.

[22] R. A. Chambers, M. N. Potenza, R. E. Hoffman, and W. Miranker, "Simulated Apoptosis/Neurogenesis Regulates Learning and Memory Capabilities of Adaptive Neural Networks," *Neuropsychopharmacology*, vol. 29, pp. 747–758, 2004, anglais.

[23] S. Becker, "A Computational Principle for Hippocampal Learning and Neurogenesis," *Hippocampus*, vol. 15, no. 6, pp. 722–738, 2005.

[24] L. Wiskott, M. J. Rasch, and G. Kempermann, "A Functional Hypothesis for Adult Hippocampal Neurogenesis: Avoidance of Catastrophic Interference in the Dentate Gyrus," *Hippocampus*, vol. 16, no. 3, pp. 329–343, 2006, automatic medline import.

[25] J. G. Parnavelas, "The Origin of Cortical Neurons," *Brazilian Journal of Medical and Biological Research*, vol. 35, pp. 1423–1429, 2002.

[26] C. Schmidt-Hieber, P. Jonas, and J. Bischofberger, "Enhanced Synaptic Plasticity in Newly Generated Granule Cells of the Adult Hippocampus," *Nature*, vol. 429, no. 6988, pp. 184–187, May 2004.

[27] R. O. Duda, P. E. Hart, and D. G. Stork, *Pattern Classification*, 2nd ed. Wiley Interscience, 2000.

[28] J. Jonides, R. L. Lewis, D. E. Nee, C. A. Lustig, M. G. Berman, and K. S. Moore, "The Mind and Brain of Short-Term Memory," *Annual Review of Psychology*, vol. 59, pp. 193–224, 2008.

[29] J. L. C. Lee, "Reconsolidation: Maintaining Memory Relevance," *Trends in Neurosciences*, vol. 32, no. 8, pp. 413–420, 2009.

[30] B. A. Kuhl, A. T. Shah, S. DuBrow, and A. D. Wagner, "Resistance to Forgetting Associated with Hippocampus-Mediated Reactivation During New Learning," *Nature Neuroscience*, vol. 13, no. 4, pp. 501–506, Apr. 2010.

[31] E. R. Kandel, "The Molecular Biology of Memory Storage: A Dialogue Between Genes and Synapses," *Science*, vol. 294, no. 5544, pp. 1030–1038, 2001.

[32] M. C. Anderson, K. N. Ochsner, B. Kuhl, J. Cooper, E. Robertson, S. W. Gabrieli, G. H. Glover, and J. D. E. Gabrieli, "Neural Systems Underlying the Suppression of Unwanted Memories," *Science*, vol. 303, no. 5655, pp. 232–235, Jan. 2004.

[33] M. Johansson, A. Aslan, K.-H. Bauml, A. Gabel, and A. Mecklinger, "When Remembering Causes Forgetting: Electrophysiological Correlates of Retrieval-Induced Forgetting," *Cerebral Cortex*, vol. 17, no. 6, pp. 1335–1341, Jun. 2007.

[34] D. O. Hebb, *The Organization of Behavior: A Neuropsychological Theory*. New York: John Wiley & Sons Inc., 1949.

[35] J. H. Morrison and P. R. Hof, "Life and Death of Neurons in the Aging Brain," *Science*, vol. 278, no. 5337, pp. 412–419, Oct. 1997.

[36] Y. Lu, N. Sundararajan, and P. Saratchandran, "A Sequential Learning Scheme for Function Approximation using Minimal Radial Basis Function Neural Networks," *Neural Computation*, vol. 9, no. 2, pp. 461–478, 1997.

[37] V. Kadirkamanathan and M. Niranjan, "A Function Estimation Approach to Sequential Learning with Neural Networks," *Neural Computation*, vol. 5, no. 6, pp. 954–975, 1993.

[38] C. F. Juang and C. T. Lin, "An On-line Self-Constructing Neural Fuzzy Inference Network and its Applications," *IEEE Transactions on Fuzzy Systems*, vol. 6, no. 1, pp. 12–32, 1998.

[39] P. Angelov and D. P. Filev, "Simpl_eTS: A Simplified Method for Learning Evolving Takagi-Sugeno Fuzzy Models," in *IEEE International Conference on Fuzzy Systems*, Ford Motor Co., Glendale Ave 24500, Detroit, United States, 2005, pp. 1068–1073.

[40] N. Kasabov and Q. Song, "DENFIS: Dynamic Evolving Neural-Fuzzy Inference System and its Application for Time-Series Prediction," *IEEE Transactions on Fuzzy Systems*, vol. 10, no. 2, pp. 144–154, April 2002.

[41] C. J. Lin and C. T. Lin, "An ART-based Fuzzy Adaptive Learning Control Network," *IEEE Transactions on Fuzzy Systems*, vol. 5, no. 4, pp. 477–496, 1997.

[42] N. Kasabov, "Evolving Fuzzy Neural Networks for Supervised/Unsupervised Online Knowledge-Based Learning," *IEEE Transactions on Systems, Man, and Cybernetics, Part B: Cybernetics*, vol. 31, no. 6, pp. 902–918, 2001.

[43] T. Takagi and M. Sugeno, "Fuzzy Identification of Systems and Its Applications to Modeling and Control," *IEEE Transactions on Systems, Man, and Cybernetics*, vol. 15, no. 1, pp. 116–132, February 1985.

[44] M. Sugeno and G. T. Kang, "Fuzzy Modelling and Control of Multilayer Incinerator," *Fuzzy Sets and Systems*, vol. 18, no. 3, pp. 329–345, 1986.

[45] J. Casillas, O. Cordón, F. Herrera, and L. Magdalena, "Interpretability Improvements to Find the Balance Interpretability-Accuracy in Fuzzy Modeling: An Overview," in *Interpretability Issues in Fuzzy Modeling, Studies in Fuzziness and Soft Computing*, J. Casillas, O. Cordón, F. Herrera, and L. Magdalena, Eds. Springer-Verlag New York, Inc., 2003, pp. 3–22.

[46] C. T. Sun, "Rule-base Structure Identification in An Adaptive-Network-Based Fuzzy Inference System," *IEEE Transactions on Fuzzy Systems*, vol. 2, no. 1, pp. 64–73, 1994.

[47] J. Platt, "A Resource Allocating Network for Function Interpolation," *Neural Computation*, vol. 3, no. 2, pp. 213–225, 1991.

[48] C. F. Juang and Y. W. Tsao, "A Self-Evolving Interval Type-2 Fuzzy Neural Network With Online Structure and Parameter Learning," *IEEE Transactions on Fuzzy Systems*, vol. 16, no. 6, pp. 1411–1424, 2008.

2011 IEEE International Conference on Fuzzy Systems
June 27-30, 2011, Taipei, Taiwan

Long Term Bank Failure Prediction using Fuzzy Refinement-based Transductive Transfer Learning

Vahid Behbood, Jie Lu and Guangquan Zhang
Decision Systems & E-Service Intelligence Research Laboratory
Centre for Quantum Computing and Intelligent System
School of Software, Faculty of Engineering and Information Technology
University of Technology Sydney
POBOX123, Broadway, NSW 2007, Australia
vahid.behbood, jie.lu & guangquan.zhang@{uts.edu.au}

***Abstract*- machine learning algorithms, which have been considered as robust methods in different computational fields, assume that the training and test data are drawn from the same distribution. This assumption may be violated in many real world applications like bank failure prediction because training and test data may come from different time periods or domains. An efficient novel algorithm known as Fuzzy Refinement (FR) is proposed in this paper to solve this problem and improve the performance. The algorithm utilizes the fuzzy system and similarity concept to modify the instances' labels in target domain which was initially predicted by shift-unaware Fuzzy Neural Network (FNN) proposed by [1]. The experiments are performed using bank failure financial data of United States to evaluate the algorithm performance. The results address a significant improvement in the predictive accuracy of FNN due to applying the proposed algorithm.**

Keywords-Transfer Learning; Fuzzy Neural Network; Fuzzy Sets; Long Term Prediction; Bank Failure Prediction

1. INTRODUCTION

Although machine learning technologies have gained remarkable attention among researches in different computational fields including classification, clustering and prediction, most of them work very well under a common assumption that the training data and test data has the same future space and same distribution. So once the distribution or feature space changes, the models need to be rebuild and retrained from the scratch using new collected training data. In many real world applications, particularly finance business, recollecting new training data and retraining the model is very expensive or practically impossible. For example, more and more labeled financial data become out of date and may not follow the same distribution as time goes by and thus past labeled data cannot be used to reliably predict financial situation of an organization. It would be so useful if the necessary of the recollecting labeled data can be reduced and the data from different time periods or domains can be utilized to assist the current learning task such as failure prediction. In this situation a new field of study has been emerged recently which is called *Transfer Learning*.

Transfer learning, which is different from the traditional machine learning and semi-supervised algorithms [2-4], considers that the domains and tasks of training and testing data can be different [5]. The study of transfer learning has been inspired by this fact that human beings can utilize the knowledge, which learned previously, to solve upcoming similar but not identical problems much faster and even better. The study of Transfer learning has begun since 1995 in different names: learning to learn, life-long learning, meta learning, multi-task learning [6]. According to the definition of Transfer learning which will be explained in the next Section, this techniques can be categorized into different settings.

However there are many researches in this field, most of them have used statistical models and there are a few studies have used soft computing techniques. In this paper a novel Transductive Transfer learning algorithm is proposed for fuzzy neural network using fuzzy sets concept which has been proved to be a successful soft computing techniques in machine learning. Likewise most of existence methods aim to refine decision boundary and models while the proposed algorithm has developed a method namely bridge refinement [7] to modify the prediction labels in target domain and focus on currently given test data. This ability makes the algorithm more practical and independent from the prediction method.

The rest of paper is organized as follow. In Section 2, some preliminaries concepts including the definition of Transductive Transfer learning and related works are given. Section 3 proposes the Fuzzy Refinement (FR) algorithm and Section 4 describes the experimental illustration and results comparing Fuzzy Neural Network (FNN) with FNN-FR (FNN using Fuzzy Refinement). Section 5 concludes this paper and discusses future researches.

2. PRELIMINARIES AND RELATED WORKS

In this section the definition of transfer learning and particularly Transductive Transfer learning is introduced and then the related works are presented. Also the FNN, which is proposed by [1], is briefly explained at the end.

A. Definition 1 (Domain)

A domain consists of two components: 1) feature space X and 2) marginal probability distribution $P(X)\ where\ X = \{x_1, \dots, x_n\}$, Domain is denoted by $D = \{X, P(X)\}$.

B. *Definition 2 (Task)*

A task consists of two components: 1) a label space $Y = \{y_1, \dots, y_m\}$ and an objective predictive function $f(.)$ which is not observed and to be learned by pairs$\{x_i, y_i\}$, Task is denoted by $T = \{Y, f(.)\}$.

C. *Definition 3 (Transfer learning)*

Given a source domain D_s and learning task T_s, a target domain D_t and learning task T_t, transfer learning aims to help improve the learning of the target predictive function $f_t(.) in\ D_t$ using the knowledge in $D_s\ and\ T_s, where\ D_s \neq D_t\ or\ T_s \neq T_t$.

D. *Definition 4 (Transdutive Transfer learning)*

A category of transfer learning in which $T_s = T_t$ and $D_s \neq D_t$ which implies that either $X_t \neq X_s\ or\ P_t(x) \neq P_s(x)$, in this situation no labeled data is available in the target domain while a lot of labeled data in the source domain are available.

E. *Related works*

Transductive Transfer learning was first proposed by [8]. It mentioned that the source and target tasks are the same, although the domains are different due to their distribution. Almost all studies in Transductive Transfer learning can be categorized into two groups[6]:

1) *Transferring the knowledge of instances:* this approach is motivated by the importance of samples and it tries to find an optimum weight for each instance to learn a precise model for target domain. There are some papers in this category which can be found in a recently published book [9] by Quionero-Candela et al.

2) *Transferring the knowledge of feature representation:* this approach focuses on feature space and attempts to extract and/or convert some relevant features which reduce the difference between the domains. Blitzer et al [10-12] proposed SCL algorithm to define a pivot features on the target domain from both domains and then uses unlabeled instances from target do create the classification model. Dai et al. [13] proposed a co-clustering based algorithm to propagate the label information across domains. In [7] Xing et al. introduced a novel algorithm known as bridge refinement to modify the predicted labels of instances from target domain. This study, which is the base idea of this paper, utilizes mixture distribution of the training and test data as a bridge to transfer feature distribution from source domain to target one. Xue et al. [14] presented a cross-domain text classification known as TPLSA to integrate target instances and source instances into a unified probabilistic model.

F. *Fuzzy Neural Network*

Assume that $X = [x_1, x_2, \dots, x_n]$ and $Y = [y_1, y_2, \dots, y_m]$ represent the vector of inputs and outputs respectively to and from the network. In addition, assume the vector $D = [d_1, d_2, \dots, d_m]$ represents the desired (actual) outputs required during the learning phase.

The proposed network has five layers of nodes: (1) Input layer consisting of input nodes $It_i, i \in \{1,2, \dots, n\}$, which have a single input x_i. (2) Input cluster layer including cluster nodes $ITerm_{ij}, i \in \{1,2, \dots, n\}\ \&\ j \in \{1, \dots, k_i\}$ which represent linguistic terms for each input. For instance, $ITerm_{23}$ represents the third linguistic term of input x_2. (3) Rule layer consisting of rule nodes $R_h, h \in \{1,2, \dots, l; l = \sum_{i=1}^{n} k_i \times \sum_{i=1}^{m} k_i\}$,which are representative of each rule and connect only one labels of each input ($x_i\ ; i \in \{1,2, \dots, n\}$) to one labels of each output ($y_i; i \in \{1,2, \dots, m\}$) . (4) Output cluster layer including cluster nodes $OTerm_{ij}, i \in \{1,2, \dots, m\}\ \&\ j \in \{1, \dots, k_i\}$ which represent linguistic terms for each output. For instance, $OTerm_{35}$ represents the fifth linguistic term of output y_3. (5) Output layer consisting of output nodes $Ot_i, i \in \{1,2, \dots, m\}$, which have single output y_i. Figure 1 shows the structure of the proposed FNN.

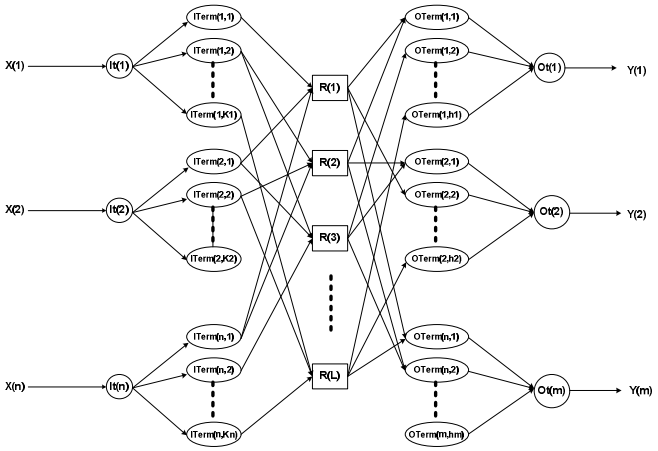

Fig1. FNN structure

The rule generation algorithm is developed by formulating an algorithm which is based on the structure of our proposed FNN. In this algorithm, ISP_h is the terms for all input linguistic terms (layer 2 nodes) that contribute to antecedent of rule node R_h and OSP_h refers to all output linguistic terms (layer 4 nodes) that form the consequent of rule node R_h:

$$ISP_h = \{ITerm_{1P_1}, ITerm_{2P_2}, \dots, ITerm_{nP_n}\} \quad and$$
$$OSP_h = \{OTerm_{1Q_1}, OTerm_{2Q_2}, \dots, OTerm_{mQ_m}\}$$

if and only if

$$R_h: \ \boldsymbol{If}\ x_1 is\ ITerm_{1P_1}\ and\ x_2\ is\ ITerm_{2P_2} and \dots and\ x_n\ is\ ITerm_{nP_n} \boldsymbol{then}\ y_1\ is\ OTerm_{1Q_1} and\ y_2\ is\ OTerm_{2Q_2}\ and \dots and\ y_m\ is\ OTerm_{mQ_m}) \quad (1)$$

The rule generation algorithm has three main steps as follows: Algorithm 1:

Step 1: Firing input and desired vectors

The input vector $X(T) = [x_1(T), \dots, x_n(T)]$ and the desired vector $D(T) = [d_1(T), \dots, d_m(T)]$ are feed to the network through layer 1 and layer 5 respectively at T-th

epoch. According input and output linguistic terms (fuzzy sets) membership function, the membership value of inputs and outputs in each term is evaluated and then the linguistic terms of each input and output with maximum membership value is selected:

$$MITerm(T) = \{ITerm_{1b_1}, ITerm_{2b_2}, \dots, ITerm_{nb_n} \mid \mu_{ITerm_{ib_i}}(x_i(T)) = Max\left\{\mu_{ITerm_{ij}}\ (x_i(T)), j \in \{1, \dots, k_i\}\right\}\} \quad (2)$$

$$MOTerm(T) = \{OTerm_{1b_1}, OTerm_{2b_2}, \dots, OTerm_{mb_m} \mid \mu_{OTerm_{ib_i}}(d_i(T)) = Max\left\{\mu_{OTerm_{ij}}\ (d_i(T)), j \in \{1, \dots, k_i\}\right\}\} \quad (3)$$

Step 2: Indicating nominated rule

In this step, the rule which has to be nominated for updating is selected in each epoch. The rule which satisfies (4) in epoch T-th is qualified for an update:

$$ISP_h = MITerm(T)\ and\ OSP_h = MOTerm(T)$$
$$h \in \{1,2, \dots, l\},\ \ l = \sum_{i=1}^{n} k_i \times \sum_{i=1}^{m} k_i \} \quad (4)$$

Step 3: Rule updating

To update the rule weight in epoch T-th, equation (5) is applied:

$$W_h(T) = W_h(T-1) + \left(M_{ISP_h}(T) \times M_{OSP_h}(T)\right),$$
$$W_h(0) = 0, h \in \{1,2, \dots, l\} \quad (5)$$

where $M_{ISP_h}(T) = \mu_{ITerm_{1b_1}} \times \mu_{ITerm_{2b_2}} \times \dots \times \mu_{ITerm_{nb_n}}$ and $M_{OSP_h}(T) = \mu_{OTerm_{1b_1}} \times \mu_{OTerm_{2b_2}} \times \dots \times \mu_{OTerm_{mb_m}}$.

To prune the weak rules at the end of the rule generation phase, a predefined threshold parameter $Thresh$ is considered and then each rule satisfying (6) will be pruned at the end of the training step.

$$l \times \left(\frac{W_h}{\sum_{k=1}^{l} w_k}\right) < Thresh \quad (6)$$

Through using this algorithm we can obtain an initial consistent and compact fuzzy rule base which needs to be modified and updated to gain more accurate results. In the next section, a learning algorithm is proposed to optimize the rule base.

The adaptive inference-based learning algorithm aims to update the fuzzy rule base, which is obtained by rule generation algorithm, to improve the prediction accuracy. This algorithm tries to adapt the parametric t-norm of inference system to reduce the significance of rules causing errors and consequently augment accuracy.

Assume that $X(T) = [x_1(T), \dots, x_n(T)]$ and $D(T) = [d_1(T), \dots, d_m(T)]$ are input and desired output vectors in T-th epoch of training respectively and there is a fuzzy rule base that includes l rules and each rule, R_i ($i^{th}\ rule$) has the form as shown in (7).

$$R_i: If\ x_1\ is\ ITerm_{1j_1} \dots and\ x_n\ is\ ITerm_{nj_n}$$
$$Then\ \ y_1\ is\ OTerm_{1h_1} \dots and\ y_m\ is\ OTerm_{mh_m} \quad (7)$$

The proposed **adaptive inference-based learning algorithm** has seven steps as follows:

Algorithm 2:

Step 1: Fuzzyfying

Input nodes act as singleton fuzzifier that fuzzyfy the crisp-valued inputs. So, the activation function of each node in layer 1 is defined as:

$$Z_i^{(1)}(T) = f^{(1)}(x_i(T)) = \mu_{\tilde{X}_i}(\tilde{x}_i(T)) = \begin{cases} 1, & if\ \tilde{x}_i(T) = x_i(T) \\ 0, & Otherwise \end{cases} \quad i \in \{1,2, \dots, n\} \quad (8)$$

where $\tilde{x}_i(T)$ is the fuzzyfied equivalent of crisp input $x_i(T)$ and $Z_i^{(1)}(T)$ is the output of node $It_i, i \in \{1,2, \dots, n\}$ at T-th epoch.

Step 2: Antecedent matching

To perform antecedent matching of fuzzyfied inputs against linguistic terms, input cluster nodes compute the similarity measure which is the input membership value in each term. The activation function of each node in layer 2 is defined as:

$$Z_{ij}^{(2)}(T) = f^{(2)}\left(Z_i^{(1)}(T)\right) = \mu_{ITerm_{ij}}(x_i(T)) = \begin{cases} 0, & if \quad x_i(T) \le l_{ij} \\ \frac{x_i - l_{ij}}{u_{ij} - l_{ij}}, & if \quad l_{ij} \le x_i \le u_{ij} \\ 1, & if \quad u_{ij} \le x_i \le v_{ij} \\ \frac{r_{ij} - x_i}{r_{ij} - u_{ij}} & if \quad v_{ij} \le x_i \le r_{ij} \end{cases}$$
$$i \in \{1,2, \dots, n\} \quad j \in \{1,2, \dots, k_i\} \quad (9)$$

where $Z_{ij}^{(2)}(T)$ is the output of node $ITerm_{ij}$ at T-th epoch.

Step 3: Rule fulfillment

To calculate the strength of activation of an antecedent for all rules with input vector $X(T)$, rule nodes compute the degree of rule fulfillment as their outputs. The higher the degree of fulfillment, the greater is the compatibility of the input to the antecedent of the rule. Hence, the activation function of each node, R_h ; $h \in \{1,2, \dots, l\}$, in layer 3 is defined as:

$$Z_{R_h}^{(3)}(T) = f^{(3)}\left(Z_{(ij)_h}^{(2)}(T), i \in \{1,2, \dots, n\}\right) =$$

$$T\left(Z_{(ij)_h}^{(2)}(T),\ i \in \{1,2,\dots,n\}\right) \quad (10)$$

where $Z_{(ij)_h}^{(2)}(T)$ is the output of the j-th term of the i-th input that is connected to the rule R_h and T is the conjunction operator. In order to adapt the inference system, this operator is considered as parameterized t-norm. Some researchers [15, 16] have shown that a tuning parameter can significantly improve the accuracy of linguistic fuzzy systems. Therefore, Dubios t-norm shown in (13) is used as conjunction operator in this step because it provides better accuracy than other parametric t-norms [15].

$$T_{Dubios}(x,y,\alpha) = \frac{x \times y}{\max(x,y,\alpha)} \quad (11)$$

Dubios t-norm operates as the minimum and an algebraic product with $\alpha = 0\ and\ \alpha = 1$ repectively. The activation function is represented as:

$$Z_{R_h}^{(3)}(T) = f^{(3)}\left(Z_{(ij)_h}^{(2)}(T), i \in \{1,2,\dots,n\}\right) = T_{Dubios}\left(Z_{(ij)_h}^{(2)}(T), i \in \{1,2,\dots,n\}, \alpha_h(T)\right) = \left(\prod_{i=1}^{n} Z_{(ij)_h}^{(2)}(T)\right)/Max\{Z_{(ij)_h}^{(2)}(T), i \in \{1,2,\dots,n\}\}, \alpha_h(T)\Big) \quad (12)$$

where $Z_{R_h}^{(3)}(T)$ is the output of node R_h at T-th epoch. In addition,$\alpha(0) = (\alpha_1(0), \alpha_2(0), \dots, \alpha_l(0))$ is initialized as 0 at the beginning of the learning algorithm, and then, during the feedback learning phase, each α_h may be increased separately.

Step 4: Consequent derivation

In this step, an aggregator operator is used to derive the consequent of fuzzy rules. Max operator which is considered as s-norm uses rule weights and rule outputs to compute the inferred output according to each rule in the rule base. Therefore, the activation function for each node in layer 4 becomes:

$$Z_{ij}^{(4)}(T) = f_{ij}^{(4)}\left(Z_{R_h}^{(3)}(T), h \in \{1,\dots,l\}, W_h\right) = Max\left(\prod_{h=1}^{l} W_h \times Z_{R_h}^{(3)}(T)\right) \quad (13)$$

where $Z_{R_h}^{(3)}(T)$ is the output of the h-th rule node in layer 3 that is connected to $OTerm_{ij}$ as its consequent.

Step 5: Deffuzyfying

To deffuzify the derived fuzzy outputs, the weighted center of averaging (COA) technique [17] is used. So, the activation function in layer 5 is as follows:

$$y_i(T) = Z_i^{(5)}(t) = f_i^{(5)}\left(z_{ij}^{(4)}(T), j = (1,2,\dots,h_j)\right) = \frac{\sum_{j=1}^{h_j}(Z_{ij}^{(4)}(T) \times \tilde{m}_{ij})}{\sum_{j=1}^{h_j} Z_{ij}^{(4)}(T)} \quad (14)$$

where $\tilde{m}_{ij} = \frac{u_{ij}+v_{ij}}{2}$ and $y_i(T)$ is the output of i-th node Ot_i in layer 5.

Step 6: Error evaluation

During the feed forward phase, the input vector $X(T)$ is presented to the network and the output vector $Y(T)$ results in T-th epoch. At the beginning of the feed backward pass, $Y(T)$ is compared against the desired output vector D(T) and the error is used to modify the vector $\alpha(T)$ in T-th epoch. Regarding the framework of imbalanced data-sets, the geometric mean presented in (2) should be used to calculate the error for all outputs. The following equation denotes the error in the t-th epoch.

$$Error(T) = \left(1 - G(T)\right) = \left(1 - \sqrt{\frac{TP(T)}{TP(T) \times FN(T)} \times \frac{TN(T)}{FP(T) \times TN(T)}}\right) \quad (15)$$

where $G(T)$ is the accuracy of model till T-th epoch of training.

Step 7: Modifying t-norm

All links in the proposed network do not have a particular weight which affects the error in the feed backward phase. The first issue to be taken into consideration in order to achieve better accuracy is the significance of antecedents that make inaccuracy should be reduced. Dobius t-norm performs like minimum t-norm if the following equation (15) becomes satisfied and Dobius t-norm approaches to product t-norm, which reduces the significance of the antecedent causing inaccuracy, by increasing $\alpha_h(T)$. Hence, better prediction can be achieved by increasing $\alpha_h(T)$ of ruleR_h which participates in producing $Error(T)$.

$$Z_{(ij)_h}^{(2)}(T) \geq \alpha_h(T) \quad (16)$$

To modify the parameter $\alpha_h(T)$ in each iteration (17) is used.

$$\alpha_h(T+1) = \alpha_h(T) - \sigma \times (Error(T) \times W_h) \quad (17)$$

where σ is a positive experimental consistent less than 1.

3. FUZZY REFINEMENT ALGORITHM

The bridge refinement algorithm[7] is motivated by PageRank algorithm [18] and it assumes that the conditional probability of a specified label C given an instance$d$, does not vary among different distributions: $P_{D_s}(C|d) = P_{D_{sUt}}(C|d) = P_{D_t}(C|d)$ although the marginal probability of instance d, $P(d)$, varies. The reason is based on the fact that if an identical instance appears in the target and source domain, the predicted label should be the same. In further, the more similar instances are in the target domain, the more the probability is they have the same label. This situation forms a mutual reinforcement relationship between instances in target domain

and source domain and can be used to correct the predicted labels. Not only is this assumption considered in our research but also a complementary idea of that is applied. We assume that more different instances in the target domain, the less the probability is they have the same label.

Given $\widetilde{F^s} = \{\widetilde{f^s}_1, \dots, \widetilde{f^s}_m\}$ and $\widetilde{F^t} = \{\widetilde{f^t}_1, \dots, \widetilde{f^t}_m\}$ are the fuzzy feature sets for source and target domain respectively. The number of these features is the same for both target and source domains but the membership function of these fuzzy sets are different. This assumption implies a Transductive Transfer learning problem in which the feature space is the same but the distribution is different. Given $X^s = \{x_1^s, \dots, x_{n_s}^s\}$ and $X^t = \{x_1^t, \dots, x_{n_t}^t\}$ are the instances of source and target domain respectively. Given $\tilde{Y} = \{\tilde{y}_1, \dots, \tilde{y}_l\}$ is the predictive fuzzy label set which is the same for both domains. Given $G(.)$ is a predictive model, which is fuzzy neural network (FNN) proposed by [1], such that $G(x_i) = \{\mu_{\tilde{y}_1}(x_i), \dots, \mu_{\tilde{y}_l}(x_i)\}$ is the vector of membership value of x_i that belongs to each label. The parameter k is the number of the most and least similar instances which is applied to refine the predicted labels and α is used to specify the degree of refinement in each iteration. The steps of Fuzzy Refinement (FR) algorithm are described as follow.

[Fuzzy Refinement algorithm]

Input: F^s , F^t , X^s, X^t, $\tilde{Y}$, $G(.)$, k and $\propto$.

Output: Label matrix for instances of target domain, MR.

[Begin]

Step 1: At the first step the singleton fuzzifier is used as follow to fuzzyfy the crisp-valued of instances from both domains.

$$\mu_{\tilde{X}_i}(\tilde{x}_i(T)) = \begin{cases} 1, & if\ \tilde{x}_i(T) = x_i \\ 0, & Otherwise \end{cases} \quad i \in \{1,2,\dots,n\} \qquad (18)$$

where $\tilde{x}_i$ is the fuzzyfied equivalent of crisp input x_i , $i \in \{1,2,\dots,n\}$.

Step 2: In this step the similarity matrix is calculated by following equation:

$$M_{n_s \times n_t} = \{m_{(i,j)} | m_{(i,j)} = 1 - \sqrt{\sum_{k=1}^{m}((\mu_{\widetilde{f_k^s}}(x_i^s) - \mu_{\widetilde{f_k^t}}(x_i^t))^2}\} \qquad (19)$$

Step 3: In this step the pseudo label matrix for target domain instances and label matrix for source domain instances are calculated by FNN as follow.

$$G_{n_s \times l}^s = \{g_{(i,j)}^s | g_{(i,j)}^s = FNN(x_i^s) = \mu_{\widetilde{y_j}}(x_i^s)\} \qquad (20)$$

$$G_{n_t \times l}^t = \{g_{(i,j)}^t | g_{(i,j)}^t = FNN(x_i^t) = \mu_{\widetilde{y_j}}(x_i^t)\} \qquad (21)$$

Step 4: In this step for each target instance, k most similar and k least similar instances from source domain are found. N^i and V^i includes the k most similar and k least similar instances from source domain to target instance i.

$for\ i = 1\ to\ n_t$

$$N_{1\times k}^i = \{n_1^i, \dots, n_k^i\} = \{n_j^i = x_p^s | m(p,i) = Max\{M(.,i)\}, j = 1, \dots, k\} \qquad (22)$$

$$V_{1\times k}^i = \{v_1^i, \dots, v_k^i\} = \{v_j^i = x_p^s | m(p,i) = Min\{M(.,i)\}, j = 1, \dots, k\} \qquad (23)$$

$Next\ i$

Step 5: The pseudo label for each instance from target domain is refined in this step according to the following equation. $\widetilde{MR}_{n_t \times l}$ is the fuzzy label matrix for instances of target domain.

$For\ i = 1\ to\ n_t$

  $For\ j = 1\ to\ l$

    Do

$$MR_{(i,j)}(t) = (1-\propto) g_{(i,j)}^t + \propto \left(\frac{(\sum_{p=1}^{k} \mu_{\widetilde{y_j}}(n_p^i) - \sum_{p=1}^{k} \mu_{\widetilde{y_j}}(v_p^i))}{k}\right)(MR_{(i,j)}(t-1)) \qquad (24)$$

    Until MR converges

  Next j

Next i

[End]

As can be seen from the equation (24) the refinement is based on the fact that the label of most similar and least similar instances to the target instance is used to modify the pseudo label of target instance which was initialized by FNN. As result of this algorithm a fuzzy label matrix for all instances of target domain is achieved. Each row of this matrix indicates the membership value of one instance to all label classes. To find the final label for each instance namely x_i^t , the following equation can be used.

$$\text{MR} = \arg max_j \{\widetilde{MR}_{i,j} | j = 1, \dots, l\} \qquad (25)$$

It should be mentioned that the above algorithm is implemented by Matlab which has the ability of matrix language programming.

4. EXPERIMENTS

In this section we would like to validate the proposed algorithm using real world financial data considering different scenarios. The task in this experiment is bank failure prediction and the prediction label has two classes: Failed; Survived. We perform the experiments to examine the algorithm whether it can transfer knowledge from different time periods.

A. Data Sets

The data set and financial variables are extracted from Call Report Data, which is downloaded from the website of Federal Reserve Bank of Chicago (http://www.chicagofed.org) and the status of each bank is identified according Federal Financial Institutions Examination Council (http://www.ffiec.gov/nicpubweb/nicweb/NicHome.aspx). The dataset, which is showed in Table 1, includes the observation period of the Survived banks of 21 years from Jun 1980 to Dec 2000 and based on the history of each bank in FFIEC.

There are 548 Failed banks and 2555 Survived ones which are presented by [19, 20] . Although, Tung et al. [19] used nine financial features, according to their statistical significance and correlation, it is observed that the model with three features has less created rules, less computational load and more prediction accuracy. Each feature is ranked based on the importance of a feature as a result of a future selection process and three features with the highest grade are selected [20]. The definition of all features and their expected impacts on bank failure are described in Table 2. The proposed approach is run by nine inputs and three inputs separately and the results are then compared.

TABLE 1
DATA SETS

Year	Total Number banks	Number of Survived banks	Number of Failed banks
1990	2156	1843(85.48%)	313 (14.52%)
1995	2539	2192(86.34%)	347(13.66%)
1998	2943	2585(87.84%)	358(12.16%)
2000	3103	2555(82.34%)	548(17.66%)

Number of available records in second data set for each scenario

TABLE 2
VARIABLES

Financial Variable
1) *CAPADE: average total equity capital /average total assets
2) OLAQLY: average (accumulated)loan loss allowance/average total loans and leases, gross
3) PROBLO: Loans 90+days late/average total loans & leases, gross
4) *PLAQLY: Loan loss provision /average total loans and leases, gross
5) NIEOIN: noninterest expense/operating income
6) NINMAR: (total interest income – interest expense)/average total asset
7) *ROE: (net income after tax +applicable income taxes)/average total equity capital
8) LIQUID: (average cash + average federal funds sold)/ (average total deposit + average fed funds purchased + average banks' liability on acceptance + average other liabilities)
9) GROWLA: (total loans & leases (t) – total loans & leases (t-1))/ total loans & leases (t-1)

Definition of variables (three selected variables are marked with *).

B. Research design and preprocessing

The domain instances (training data) are selected from data until year 1990 and the target instances (test data) are selected from records of year 1995, 1998 and 2000, 5, 8 and 10 years after 1990 (see Table 1). We compare the results of FNN using proposed algorithm denoted as FNN-FR with FNN to find out the improvement gained due to fuzzy refinement. Likewise the evaluation is performed using two categories of feature sets: nine variables; three variables. In conclusion the experiments have been performed based on 12 scenarios.

To reduce the influence of imbalance data-sets problem, the SMOTE technique is applied to train data sets. The number of Failed banks increases to the number of Survived ones to achieve balanced data set which improves the accuracy of prediction without losing important information.

In each scenario, the training data set splits into two pools: (1) Failed banks denoted with output 1; (2) Survived banks denoted with output 0. There are five cross-validation groups which include instances of both pools randomly to form the training set. The training set of the five groups are mutually exclusive. The FNN and FNN-FR are trained using training data sets and then evaluated by the testing data sets. The accuracy of the each experiment, which is the mean value of cross-validation groups' accuracy, is calculated using following equation.

$$GM = \sqrt{\frac{TP}{TP+FN} \times \frac{TN}{FP+TN}} \tag{9}$$

where $\frac{TP}{TP+FN}$ is called *sensitivity* and $\frac{TN}{FP+TN}$ is called *specificity,* measure the effectiveness of the prediction algorithm in any class. The proposed metric (9) is a geometric mean of *sensitivity* and *specificity,* because both of them are expected to be high simultaneously

C. Experiment results analysis

In this section the results which are gained from the experiment is reported. To ensure that the Fuzzy Refinement (FR) algorithm for Transfer learning makes significant improvement, the performance of FNN applying FR (FNN-FR) is compared with FNN which generates unrefined results.

As a result of this comparison, the Figure 2 represents the difference of FNN and FNN-FR performance using three financial features. In all data sets the FNN-FR outperforms the FNN. The relative increase is achieved by 10%, 14% and 15% on 1995, 1998 and 2000 data sets. Surprisingly it shows that the influence of proposed algorithm become more significant once the period of prediction become farther and so the difference between target domain and source domain become greater. Figure 3 shows the results of FNN and FNN-FR using nine financial features. The relative growth is 10%, 20% and 25% on 1995, 1998 and 2000 data sets. This growth in accuracy, which is gained due to applying proposed algorithm, is more than previous experiments. The reason may be that the proposed algorithm works better on larger feature space and more number of features. The summary of all 12 scenarios results are shown in the Table 3.

To clarify this improvement clearly the t-test is applied on the level of confidence of 0.05 on 12 scenarios. As it is showed in Table 4, the null hypothesis of the equality of average accuracy is rejected for FNN-FR. So it can be concluded that the proposed algorithm can significantly improve the predictive accuracy of FNN for long term prediction.

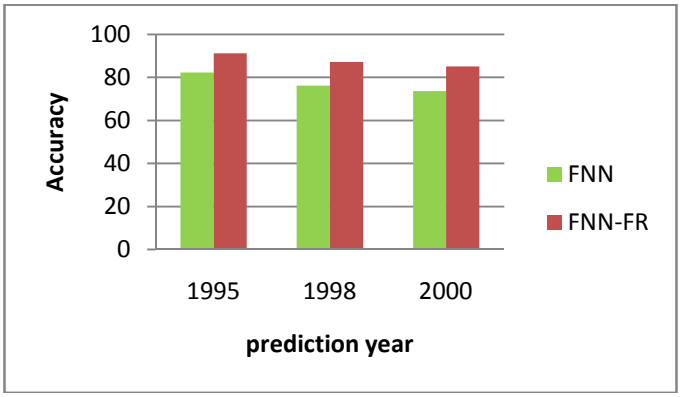

Fig. 2 Comparison FNN and FNN-FR accuracy using three variables

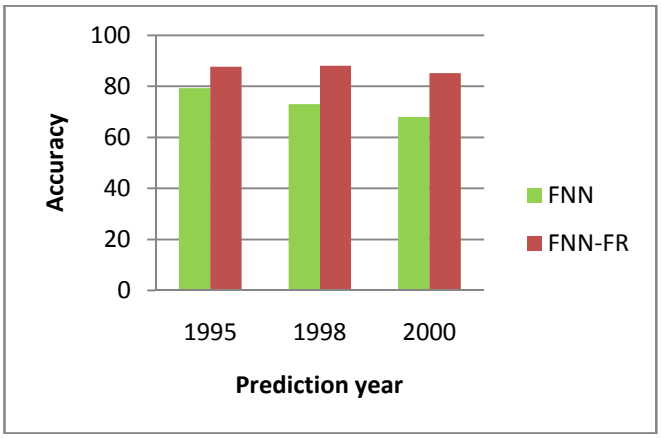

Fig. 3 Comparison FNN and FNN-FR accuracy using nine features.

TABLE 3
RESULTS

		12 Scenarios		
Method	N.O feature	1995	1998	2000
FNN	3	82.36	76.15	73.29
	9	79.25	72.98	68.03
FNN-FR	3	91.15	87.22	85.07
	9	87.66	88.10	85.17

The accuracy of FNN and FNN-FR

TABLE 4
T-TEST RESULT

Algorithm	Mean Value	Hypothesis	t	DF	P-Value
FNN	75.4167	FNN vs. FNN-FR	-8.323	5	0.00
FNN_FR	87.3950				

The t-test result for comparison of FNN and FNN-FR

D. Parameter sensitivity

The proposed algorithm has two parameters, *k and* ∝, which need to be set in performing experiments. In this section we investigate the influence of these parameters on the performance of the Fuzzy refinement algorithm. To do this the performance of the algorithm is examined using different value of these parameters on 6 scenarios. The accuracy of the algorithm for different value of *k* is shown in the Figure 4. It shows that the performance is not greatly sensitive to *k* as long as *k* is large enough. According to this figure the value of 80 is the best value for *k* which is chosen in this research. Figure 5 shows the accuracy by applying different values of ∝. It shows that 0.66 is the best value for ∝ which is selected in this paper.

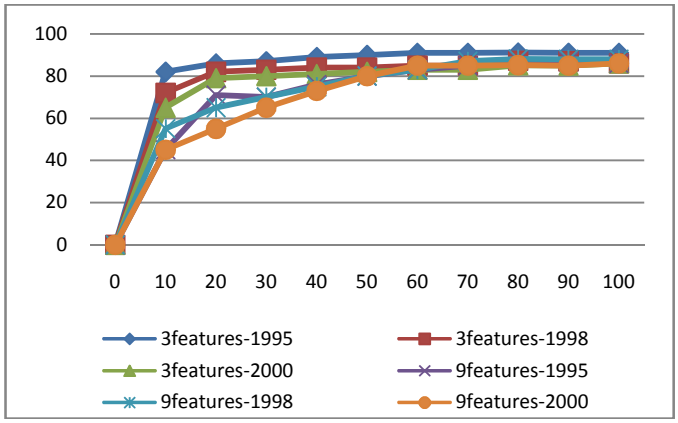

Figure 4. The accuracy of FNN-RF using different value of K

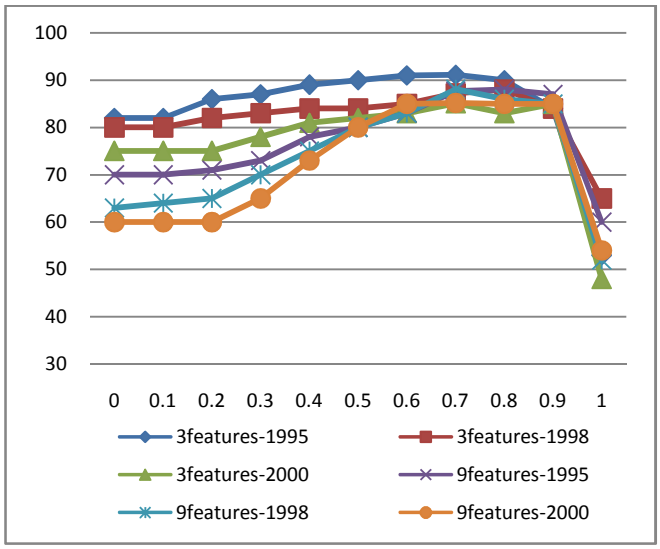

Figure 5. The accuracy of FNN-RF using different value of α

5. CONCLUSION AND FUTURE STUDY

In this paper Fuzzy Refinement algorithm is proposed to solve the Transductive Transfer Learning problem. The algorithm concentrates on the modification the instances' labels in target domain and uses the fuzzy concepts to improve the predictive accuracy. The FNN which is proposed by [1] is considered as prediction model to determine the initial labels for target instances. According to the empirical results, the proposed algorithm brings about remarkable improvement in performance. It demonstrates a

significant increase in predictive accuracy when the algorithm is applied particularly for farther time period ahead prediction

The approach which is mentioned in [7] to apply two refinement steps can be applied in the algorithm as future research. Also developing an algorithm based the proposed algorithm which can extract the relevant features to reduce the difference between domains is desirable for future work. Finally evaluating the proposed algorithm in the situation that there are some labeled data in target domain can be an interesting study for future as well.

RERERENCES

[1] V. Behbood, J. Lu, and G. Zhang, "Adaptive Inference-based learning and rule generation algorithms in fuzzy neural network for failure prediction," in *2010 IEEE International Conference on Intelligent Systems and Knowledge Engineering (ISKE 2010)* China, 2010, pp. 33-38.

[2] K. Nigam, A. K. McCallum, S. Thrun, and T. Mitchell, "Text Classification from Labeled and Unlabeled Documents using EM," *Mach. Learn.,* vol. 39, pp. 103-134, 2000.

[3] A. Blum and T. Mitchell, "Combining labeled and unlabeled data with co-training," in *Proceedings of the eleventh annual conference on Computational learning theory* Madison, Wisconsin, United States: ACM, 1998.

[4] T. Joachims, "Transductive Inference for Text Classification using Support Vector Machines," in *Proceedings of the Sixteenth International Conference on Machine Learning*: Morgan Kaufmann Publishers Inc., 1999.

[5] F. Gabriel Pui Cheong, J. X. Yu, L. Hongjun, and P. S. Yu, "Text classification without negative examples revisit," *Knowledge and Data Engineering, IEEE Transactions on,* vol. 18, pp. 6-20, 2006.

[6] P. Sinno Jialin and Y. Qiang, "A Survey on Transfer Learning," *Knowledge and Data Engineering, IEEE Transactions on,* vol. 22, pp. 1345-1359, 2010.

[7] D. Xing, W. Dai, G.-R. Xue, and Y. Yu, "Bridged Refinement for Transfer Learning," in *Knowledge Discovery in Databases: PKDD 2007*. vol. 4702: Springer Berlin / Heidelberg, 2007, pp. 324-335.

[8] A. Arnold, R. Nallapati, and W. W. Cohen, "A Comparative Study of Methods for Transductive Transfer Learning," in *Data Mining Workshops, 2007. ICDM Workshops 2007. Seventh IEEE International Conference on*, 2007, pp. 77-82.

[9] J. Quionero-Candela, M. Sugiyama, A. Schwaighofer, and N. Lawrence, *Dataset Shift in Machine Learning*: The MIT Press, 2009.

[10] J. Blitzer, R. McDonald, and F. Pereira, "Domain adaptation with structural correspondence learning," in *Proceedings of the 2006 Conference on Empirical Methods in Natural Language Processing* Sydney, Australia: Association for Computational Linguistics, 2006.

[11] J. Blitzer, M. Dredze, and F. Pereira, "Biographies, Bollywood, Boom-boxes and Blenders: Domain Adaptation for Sentiment Classification," in *Proceedings of the 45th Annual Meeting of the Association of Computational Linguistics*, 2007, pp. 440-447.

[12] J. Blitzer, K. Crammer, A. Kulesza, F. Pereira, and J. Wortman, "Learning Bounds for Domain Adaptation," in *Advances in Neural Information Processing Systems*, 2007.

[13] W. Dai, G.-R. Xue, Q. Yang, and Y. Yu, "Co-clustering based classification for out-of-domain documents," in *Proceedings of the 13th ACM SIGKDD international conference on Knowledge discovery and data mining* San Jose, California, USA: ACM, 2007.

[14] G.-R. Xue, W. Dai, Q. Yang, and Y. Yu, "Topic-bridged PLSA for cross-domain text classification," in *Proceedings of the 31st annual international ACM SIGIR conference on Research and development in information retrieval* Singapore, Singapore: ACM, 2008.

[15] J. Alcalá-Fdez, F. Herrera, F. Márquez, and A. Peregrín, "Increasing fuzzy rules cooperation based on evolutionary adaptive inference systems," *International Journal of Intelligent Systems,* vol. 22, pp. 1035-1064, 2007.

[16] F. A. Marquez, A. Peregrin, and F. Herrera, "Cooperative Evolutionary Learning of Linguistic Fuzzy Rules and Parametric Aggregation Connectors for Mamdani Fuzzy Systems," *Fuzzy Systems, IEEE Transactions on,* vol. 15, pp. 1162-1178, 2007.

[17] C.-T. Lin and C. S. G. Lee, *Neural fuzzy systems: a neuro-fuzzy synergism to intelligent systems*: Prentice-Hall, Inc., 1996.

[18] L. Page, S. Brin, R. Motwani, and T. Winograd, "The PageRank Citation Ranking: Bringing Order to the Web," in *7th International World Wide Web Conference* Australia, 1998, pp. 161-172.

[19] W. L. Tung, C. Quek, and P. Cheng, "GenSo-EWS: a novel neural-fuzzy based early warning system for predicting bank failures," *Neural Networks,* vol. 17, pp. 567-587, 2004.

[20] G. S. Ng, C. Quek, and H. Jiang, "FCMAC-EWS: A bank failure early warning system based on a novel localized pattern learning and semantically associative fuzzy neural network," *Expert Systems with Applications,* vol. 34, pp. 989-1003, 2008.

2011 IEEE International Conference on Fuzzy Systems
June 27-30, 2011, Taipei, Taiwan

Developing a Fuzzy Search Engine Based on Fuzzy Ontology and Semantic Search

Lien-Fu Lai Chao-Chin Wu Pei-Ying Lin
Dept. of Computer Science and Information Engineering
National Changhua University of Education
Changhua, R.O.C.
{lflai,ccwu}@cc.ncue.edu.tw, ester6236@gmail.com

Liang-Tsung Huang
Department of Biotechnology
Mingdao University
Changhua, R.O.C.
larry@mdu.edu.tw

***Abstract*—Most of existing search engines retrieve web pages by means of finding exact keywords. Traditional keyword-based search engines suffer several problems. First, synonyms and terms similar to keywords are not taken into consideration to search web pages. Users may need to input several similar keywords individually to complete a search. Second, traditional search engines treat all keywords as the same importance and cannot differentiate the importance of one keyword from that of another. Third, traditional search engines lack an applicable classification mechanism to reduce the search space and improve the search results. In this paper, we develop a fuzzy search engine, called Fuzzy-Go. First, a fuzzy ontology is constructed by using fuzzy logic to capture the similarities of terms in the ontology, which offering appropriate semantic distances between terms to accomplish the semantic search of keywords. The Fuzzy-Go search engine can thus automatically retrieve web pages that contain synonyms or terms similar to keywords. Second, users can input multiple keywords with different degrees of importance based on their needs. The totally satisfactory degree of keywords can be aggregated based on their degrees of importance and degrees of satisfaction. Third, the domain classification of web pages offers users to select the appropriate domain for searching web pages, which excludes web pages in the inappropriate domains to reduce the search space and to improve the search results.**

Keywords- Fuzzy Search Engine; Fuzzy Ontology; Semantic Search

I. INTRODUCTION

As the massive data on the internet is increasing rapidly, internet search engines have become the essential ways to find information. Most of existing search engines, such as Google, Yahoo, MSN, ASK, Baidu, and Bing, retrieve web pages by means of finding exact keywords. These keyword-based search engines collect and analyze web pages through web crawlers. While users input keywords to search web pages, web pages that contain exact keywords are retrieved and ranked. For example, the Google search engine sorts the search results by their Page-rank scores, Relevance scores and Local scores. However, traditional keyword-based search engines suffer several problems:

- Synonyms and terms similar to keywords are not taken into consideration to search web pages. Users may need to input several similar keywords individually to complete a search. The restriction of exact keywords makes it inconvenient for users to search web pages. Many valuable web pages would be omitted if users did not search for several similar keywords individually.
- While users input several keywords to search web pages, different keywords may have different degrees of importance in their opinions. Traditional search engines treat all keywords as the same importance and cannot differentiate the importance of one keyword from that of another.
- The problem of information overload makes it difficult for users to find really useful information from a large amount of search results. Traditional search engines lack an applicable classification mechanism to reduce the search space and improve the search results.

To alleviate the mentioned problems, we have applied the fuzzy logic theory and the semantic search techniques to develop a fuzzy search engine, called Fuzzy-Go. First, a fuzzy ontology is constructed by using fuzzy logic [15] to capture the similarities of terms in the ontology, which offering appropriate semantic distances between terms to accomplish the semantic search of keywords. The Fuzzy-Go search engine can thus automatically search web pages that contain synonyms or terms similar to keywords. Second, users can input multiple keywords with different degrees of importance based on their needs. The totally satisfactory degree of keywords can be aggregated based on their degrees of importance and degrees of satisfaction. Third, the domain classification of web pages offer users to select the appropriate domain for searching web pages, which excludes web pages in the inappropriate domains to reduce the search space and to improve the search results.

An overview of the Fuzzy-Go search engine is shown in Figure 1. The Web Crawler is developed to gather and classify web pages. Web pages are classified and stored based on their domains. The characteristic information of web pages is recorded in the Web Document. The Ontology Manager constructs and maintains a Fuzzy Ontology. A data mining approach is applied on the Web Document to calculate the fuzzy similarity between terms in the Fuzzy Ontology. The User Interface provides users to select an appropriate domain and to input multiple keywords with different degrees of

978-1-4244-7316-8/11/$26.00 ©2011 IEEE

importance based on their needs. The Fuzzy Search Mechanism would exclude web pages in the inappropriate domains to reduce the search space and to improve the search results. The keywords are expanded by the Fuzzy Ontology to find out synonyms and terms similar to keywords. The search results are ordering based on several fuzzy factors including the satisfaction degrees of keywords, the importance degrees of keywords, the relevance of domains, the page ranks [3], the page in-links [2], titles, and last modified dates.

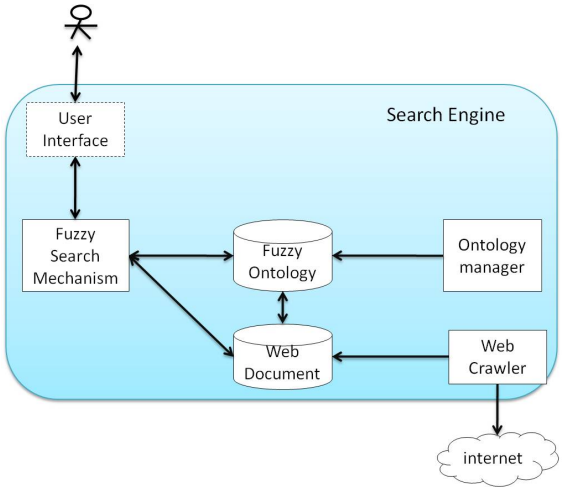

Figure 1. An overview of the Fuzzy-Go search engine

II. CONSTRUCTING THE FUZZY ONTOLOGY

Domain dependency is an important character of knowledge: the meaning of a term may be different in different domains. We construct a two-layered fuzzy ontology to organize terms that are elicited from WordNet [6]. WordNet is a large lexical database of English, built by Princeton University. Nouns, verbs, adjectives and adverbs are grouped into sets of cognitive synonyms, each expressing a distinct concept. In the two-layered fuzzy ontology, the first layer forms a domain hierarchy (see Figure 2). We adopt the Suggested Upper Merged Ontology (SUMO) [5] to classify domains. SUMO is owned by the IEEE and defines a group of domain ontologies which have been mapped to the WordNet domains. In our approach, the domain hierarchy is treated as gen-spec relationships. The upper level in the domain hierarchy

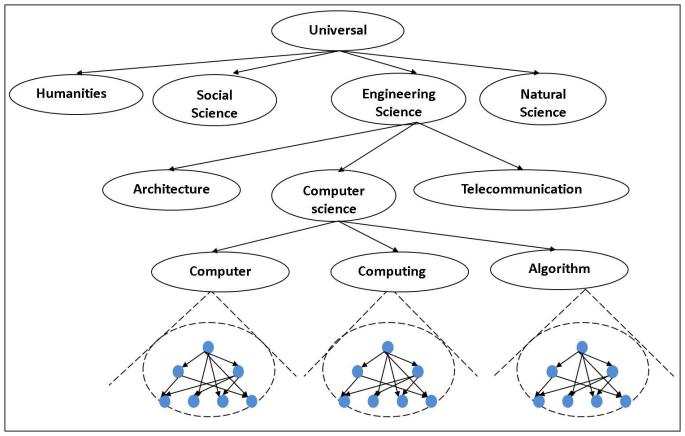

Figure 2. The domain hierarchy in the two-layered fuzzy ontology

maintains terms in a more general domain, while the lower level maintains terms in a more specific domain. Each domain contains a term lattice in the second layer (see Figure 3). A sub-domain can inherit the term lattice from its super-domain, add new terms specific to the sub-domain itself, and override (i.e., redefine) fuzzy similarity between terms in the super-domain.

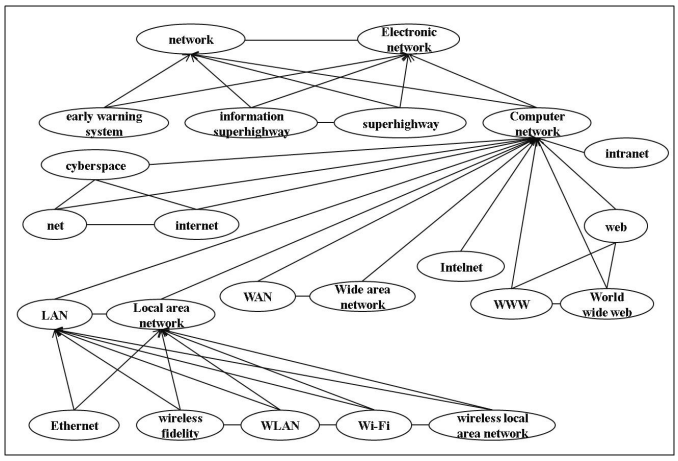

Figure 3. The term lattice in a domain

Church et al. [9] had extended the word association in psycholinguistics to provide the basis for a statistical description of the semantic relationship between words through the co-occurrence of words. To determine the similarity degree between terms, we use the data mining method to find out the degree of co-occurrence for two terms in web pages. The measure of mutual information [9] is adopted to calculate the degree of a children node conforming to a parent node in the term lattice. For any two terms x and y, the mutual information $I(x,y)$ is defined as

$$I(x,y) \equiv \log_2 \frac{P(x,y)}{P(x)P(y)} \quad (1)$$

Where $P(x)$ and $P(y)$ is the probabilities of observing x and y independently in web pages, and $P(x,y)$ is the probabilities of observing x and y together in web pages. The higher the semantic relationship between x and y, the larger the co-occurrence degree (i.e. $P(x,y)$ is larger), and consequently the larger the mutual Information $I(x,y)$.

To normalize the mutual information into a similarity degree in interval $[0,1]$, we adopt the maximizing set [16] to assign the fuzzy similarity degree between terms. For all mutual Information $x \in X$, let f be a real-valued function in X. The maximizing set $\tilde{M} = \{(x, \mu_{\tilde{M}}(x))\}, x \in X$ assigns the degrees of membership $\mu_{\tilde{M}}(x)$ for all $x \in X$ with

$$\mu_{\tilde{M}}(x) = \frac{f(x) - \inf(f)}{\sup(f) - \inf(f)} \quad (2)$$

Where $inf(x)$ is the minimum of f and $sup(x)$ is the maximum of f.

The Ontology Manager is responsible to apply the data mining approach to give the similarity degrees between terms in all term lattices based on the Web Document. Figure 4 shows a term lattice with the similarity degrees. Note that the similarity degree between two synonyms defined by WordNet is assigned 1.0 directly.

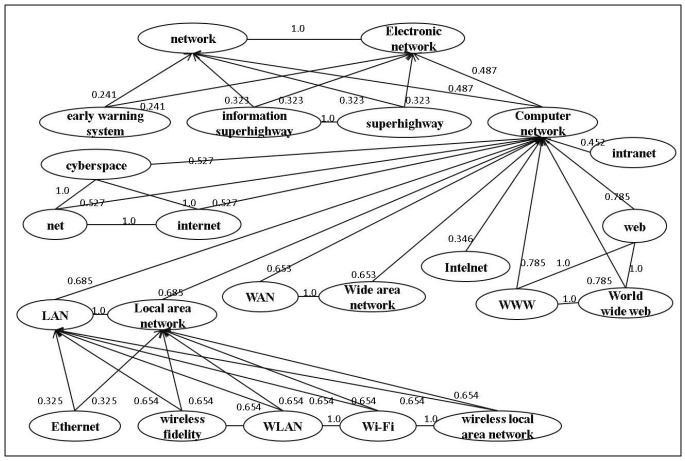

Figure 4. A term lattice with similarity degrees

III. THE WEB CRAWLER

We develop a crawler agent to automatically extract web pages and inventory them by finding out keywords and characteristic values. While the Web Crawler retrieves web pages, some important information of web pages is analyzed and stored, including titles, keywords, the page ranks of web pages, the last modified dates etc. Figure 5 shows the work flow of the Web Crawler.

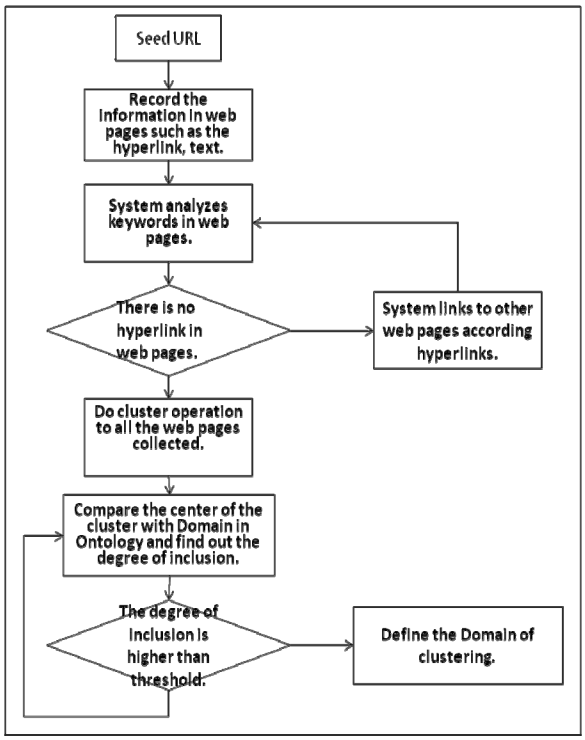

Figure 5. The work flow of the Web Crawler

The Web Crawler is also responsible to classify retrieved web pages by determining their domains. Since the amount of retrieved web pages is huge, we adopt the notions of Fuzzy C-Mean (FCM) [7] to cluster web pages based on their keywords. In our approach, each web page is translated into a vector of keywords. Each vector doesn't belong to only one cluster but belongs to several clusters with different degrees. By comparing to the terms within domains in the Fuzzy Ontology, the keywords in the center of a cluster are useful to determine what domain the cluster belongs to.

Keywords in web pages are regarded as the characteristic values and each web page is translated into a vector of keywords in the web page. Assume that all web pages in the Web Document are gathered into k clusters. The Euler distance between two web pages x_i and x_j would be

$$dist(x_i, x_j) = \left(\sum_{d=1}^{k} \left| x_{id} - x_{jd} \right|^2 \right)^{\frac{1}{2}} \quad (3)$$

The center of a cluster will be changed after iteration. In each iteration, we calculate the total deviation for changing the center of the cluster. In the case of k clusters, the total deviation E can be obtained by $E = \sum_{i=1}^{k} \sum_{x \in S_i} \left\| x - C_i \right\|^2$, where C_i is the center of each cluster S_i and x is the web page in cluster S_i. If the total deviation for the m+1's iteration is smaller than the m's, the center of the cluster would be changed into m+1's iteration -- otherwise the center would remain unchanged (see Figure 6).

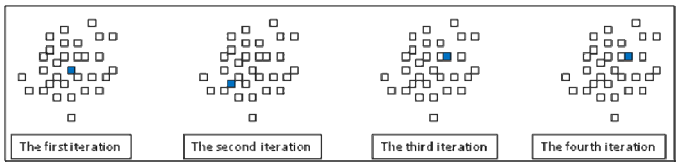

Figure 6. Changing of the FCM center of the clustering

Since the centers of clusters will be changed again and again, we use an objective function J to check if the result of clustering is stable.

$$J = \sum_{i=1}^{k} J_i = \sum_{i=1}^{k} \sum_{j=1}^{n} w_{ji}^m \left\| x_j - C_i \right\|^2 \quad (4)$$

Where w_{ji} is the degree of the web page x_j belongs to the cluster S_i with $w_{ji} = \frac{1}{\sum_{s=1}^{k} \left(\frac{\left\| X_j - C_i \right\|}{\left\| X_j - C_s \right\|} \right)^{\frac{2}{m-1}}}$, $\sum_{i=1}^{k} w_{ji} = 1$, w_{ji}^m forms a weighting matrix, and C_i is the center of each cluster S_i with $C_i = \frac{\sum_{j=1}^{n} w_{ji}^m x_j}{\sum_{j=1}^{n} w_{ji}^m}$. If the value of the objective function J is stable, the result of clustering is stable.

Finally, the characteristic values set of the center of the cluster is captured to compare with terms of domains. We applied N-Gram [4] to find out the degree of match between a cluster and a domain. Assume that C_K is the keywords set extracted from a cluster K and C_D is the keywords set of a domain D. The degree of match between a cluster K and a domain D is

$$Sim(C_K, C_D) = \frac{|C_K \cap C_D|}{|C_K|}, \{C_K\} \neq \phi \qquad (5)$$

A web page may belong to several domains. While the degree of match between a cluster and a domain is above the threshold, we assign all web pages in the cluster into the domain. The domain classification mechanism can reduce the search space and improve the search results.

IV. THE FUZZY SEARCH MECHANISM

The User Interface of the fuzzy search engine provides users to select an appropriate domain and to input multiple keywords with different degrees of importance based on their needs (see Figure 7). On the one hand, web pages in the inappropriate domains can be excluded to reduce the search space and to improve the search results, since all web pages are already classified by domains. On the other hand, a better search result can be obtained by differentiating between keywords according to the degrees of importance. We use linguistic degrees of importance [13] (i.e. don't care, unimportant, rather unimportant, moderately important, rather important, very important, and most important) to make it easier for users to grade relative importance. Each linguistic degree of importance can be mapped to a triangular fuzzy number as shown in Figure 8.

Figure 7. The user interface of the fuzzy search engine

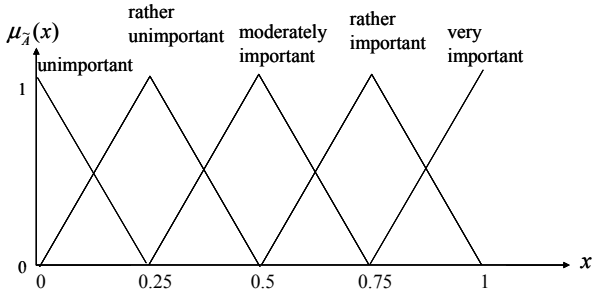

Figure 8. Membership functions for degrees of importance

It is inconvenient for users to be restricted to input precise keywords. Users may need to input several similar keywords individually to complete a search. To alleviate the problem, we use the term expansion to find out synonyms and terms similar to keywords based on the semantics inherited from the selected domain. While the user selects an appropriate domain and inputs keywords to search web pages, the Fuzzy Search Mechanism would expand keywords to synonyms and terms similar to keywords based on the term lattice of the selected domain. For the example in Figure 9, when the keyword is 'Computer Network' and the α-cut is set to 0.475, we would acquire 12 terms whose similarity degrees to 'Computer Network' are greater than 0.475.

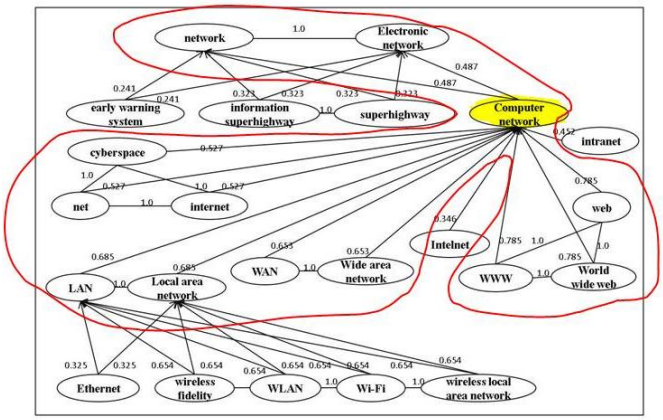

Figure 9. The term expansion of keywords in the term lattice

The fuzzy similarity between two non-adjacent terms T_A and T_B can be calculated by the multiplication principle for a path from T_A to T_B. That is, we can obtain the fuzzy similarity between T_A and T_B via another term T_C in the term lattice of the domain D.

$$Sim(T_A, T_B) = \underset{\forall\, Tc \in D}{Max}\{Sim(T_A, T_C) \times Sim(T_C, T_B)\} \qquad (6)$$

Therefore, the terms similar to a keyword with degree $\geqq$ α-cut could be found through the term lattice of the selected domain. All synonyms and terms similar to keywords are taken into account while we calculate the degree of satisfaction between the keyword and a web page. In our approach, the keyword density is used to determine the degrees of satisfaction between keywords and web pages. The keyword density is the percentage of times a keyword appears on a web page compared to the total number of words on the web page. Many SEO (Search Engine Optimization) experts consider the optimum keyword density to be 1 to 3 percent [1]. Others claim that the optimum keyword density would be 3%, 4% even as high as 2%~8%. We add the density of the keyword and all similar terms together, and adopt the largest range (i.e. 2 to 8 percent), S functions and Z functions [16] to establish the membership function of the optimum keyword density (see Figure 10). If the keyword density falls within 2% to 8%, the degree of satisfaction between the keyword and the web page would be set to 1. In the case of 0% to 2%, the S function is applied to set the degree value; whereas in the case of 8% to 12%, the Z function is applied to set the degree value.

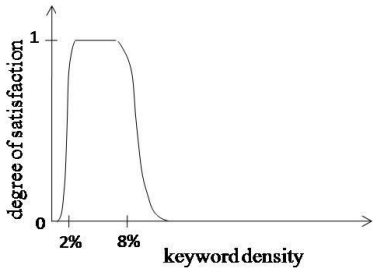

Figure 10. The membership function of the optimum keyword density

Since users may input multiple keywords with different degrees of importance to search web pages, the totally satisfactory degree of multiple keywords should be aggregated based on their degrees of importance and degrees of satisfaction. The fuzzy weighted average (FWA) [8,11] is applied to calculate the totally satisfactory degree of multiple keywords using triangular fuzzy numbers. In our approach, the degree of satisfaction between a keyword and a web page is the indicator (x_i), and the degrees of importance are weights (w_i) that act upon indicators. Therefore, the fuzzy weighted average y can be defined as

$$y = f(x_i,...,x_n,w_1,...,w_n) = \frac{\sum_{i=1}^{n} w_i x_i}{\sum_{i=1}^{n} w_i} \qquad (7)$$

Where there is n keywords, the degree of satisfaction x_i, $1 \le i \le n$ is a crisp value, and the degree of importance w_i, $1 \le i \le n$ is represented by a triangular fuzzy number. We adopt the approximate expressions on $\oplus$ and $\otimes$ operators for the computation of L-R fuzzy numbers, which is suggested by Dubois and Prade [10]. For example, a user may input two keywords to search web pages: 'expert systems' with moderately important and 'soft computing' with very important. In the term lattice, the term 'expert systems' links to a similar term 'knowledge-based systems' with the similarity degree 0.786, and 'soft computing' links to 'fuzzy logic' with 0.623. Assume that the keyword densities of 'expert systems', 'knowledge-based systems', 'soft computing' and 'fuzzy logic' for the web page *P* are 1.5%, 1.2%, 0% and 2.1% respectively. The expanded keyword density of 'expert systems' would be $1.5\%+1.2\%\times 0.786=2.4432\%$, and the degree of satisfaction between 'expert systems' and *P* would be 1. The expanded keyword density of 'soft computing' would be $0\%+2.1\%\times 0.623=1.3083\%$, and the degree of satisfaction between 'soft computing' and *P* would be $S(1.3083)=1-2\left(\frac{2-1.3083}{2-0}\right)^2 \cong 0.76$. FWA is applied to calculate *P*'s totally satisfactory degree of keywords as

$$y = \frac{(0.25,0.5,0.75)\otimes 1.0 \oplus (0.75,1,1)\otimes 0.76}{(0.25,\ 0.5,\ 0.75)\oplus(0.75,\ 1,\ 1)} = \frac{(0.82,1.26,1.51)}{(1,\ 1.5,\ 1.75)}$$

$$\cong \frac{1.1517}{1.3536} = 0.8508$$

Applying the mathematical operations on fuzzy numbers [10,16], we get two fuzzy numbers (0.82, 1.26, 1.51) and (1, 1.5, 1.75). The center of gravity is adopted to defuzzify a fuzzy number [14], which is achieved by mathematical integral. Therefore, *P*'s totally satisfactory degree of keywords is 0.8508 .

The search results are ordering based on several fuzzy factors including the totally satisfactory degrees of keywords, the page ranks, the page in-links, titles, and last modified dates. Through the mutual compensation of all fuzzy factors, an ordering of search results which is considered in every respect can be generated. The fuzzy weighted average [8,11] is utilized to aggregate all fuzzy factors based on their degrees of importance and degrees of satisfaction. The users can manually select appropriate fuzzy factors with different importance degrees to meet their specific requirements (see Figure 11) -- otherwise the importance degrees of fuzzy factors would be default values. Figure 12 shows the ordering of search results which the grade is generated by aggregating all fuzzy factors.

Figure 11. The selection of fuzzy factors with different importance degrees

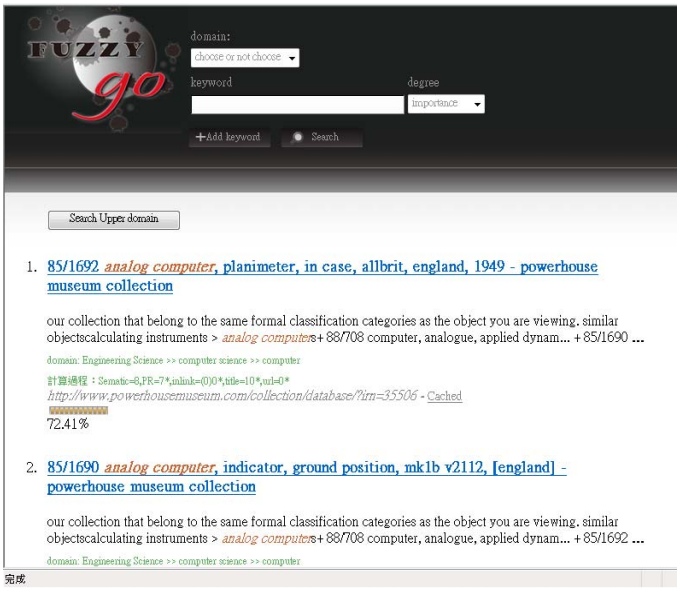

Figure 12. The ordering of search results

However, the original setting is not optimal, and it needs continuous learning and adaptation to fit users' expectations gradually. We have applied the genetic algorithm to propose a self-adaptation approach to Fuzzy-Go search engine [12]. For each search, the fuzzy search engine records the difference between the ordering of search results and user's real behavior on clicking web pages. This feedback is gathered and analyzed to adjust the fuzzy similarities between terms in the fuzzy ontology, the domain classification of web pages, and the default importance degrees of fuzzy factors. The ordering of search results can thus be improved gradually by continuous learning and adaptation.

V. CONCLUSION

In this paper, we develop a fuzzy search engine, called Fuzzy-Go. First, the Ontology Manager constructs and maintains a Fuzzy Ontology. A data mining approach is applied on the Web Document to calculate the fuzzy similarity between terms in the Fuzzy Ontology. The Fuzzy Ontology is constructed by using fuzzy logic to capture the similarities of terms in the ontology, which offering appropriate semantic distances between terms to accomplish the semantic search of keywords. The Fuzzy-Go search engine can thus automatically retrieve web pages that contain synonyms or terms similar to keywords. Second, the Web Crawler is developed to gather and classify web pages. Web pages are classified and stored based on their domains. To deal with the huge amount of retrieved web pages, we propose a data mining approach to cluster web pages based on their keywords. Third, the User Interface provides users to select an appropriate domain and to input multiple keywords with different degrees of importance based on their needs. The totally satisfactory degree of keywords can be aggregated based on their degrees of importance and degrees of satisfaction. Finally, the Fuzzy Search Mechanism would exclude web pages in the inappropriate domains to reduce the search space and to improve the search results. The keywords are expanded by the Fuzzy Ontology to find out synonyms and terms similar to keywords. The search results are ordering based on several fuzzy factors including the totally satisfactory degrees of keywords, the page ranks, the page in-links, titles, and last modified dates. The advantages of the proposed approach are as follows.

- Using fuzzy logic to capture the similarities of terms in the ontology, which offers appropriate semantic distances between terms to accomplish the semantic search of keywords. The domain classification of web pages offers users the selection of the appropriate domain to search web pages, which excludes web pages in the inappropriate domains to reduce the search space and to improve the search results.
- Users can input multiple keywords with different degrees of importance based on their needs, and all fuzzy factors are aggregated based on their degrees of importance and degrees of satisfaction. Through the mutual compensation of all fuzzy factors, the ordering of search results which is considered in every respect can be generated.

ACKNOWLEDGMENT

This research is partially sponsored by National Science Council (Taiwan, R.O.C.) under the grant NSC 98-2221-E-018-008-MY2.

REFERENCES

[1] Keyword Density, http://en.wikipedia.org/wiki/Keyword_density

[2] Page Inlink Analysis, http://ericmiraglia.com/inlink/

[3] Page Rank Check, http://www.prchecker.info/check_page_rank.php

[4] The Stochastic Language Models (N-Gram) Specification, http://www.w3.Org/tr/ngram-spec/

[5] The Suggested Upper Merged Ontology (SUMO), http://www.ontologyportal.org/

[6] WordNet, http://wordnet.princeton.edu/

[7] J. C. Bezdek, Pattern Recognition with Fuzzy Objective Function Algorithms. New York: Plenum, 1981.

[8] P.T. Chang, K.C. Hung, K.P. Lin, and C.H. Chang, a Comparison of Discrete Algorithms for Fuzzy Weighted Average, IEEE Transactions on Fuzzy Systems, pp.:663-675, Oct. 2006.

[9] K.W. Church and P. Hanks Word Association Norms, Mutual Information and Lexicography, Computational Linguistics 16(1):22-29, Mar. 1990.

[10] D. Dubois and H. Prade. *Fuzzy sets and systems: theory and applications*. New York, London, 1980.

[11] L.F. Lai, C.C. Wu, M.Y. Shih, L.T. Huang, and W. Chiou. Parallel Processing for Fuzzy Queries in Human Resources Websites. *Journal of Internet Technology*, 7(11):943-953, Dec. 2010.

[12] Y.C. Lin, L.F. Lai, C.C. Wu, and L.T. Huang. A Self-Adaptation Approach to Fuzzy-Go Search Engine. *The 2010 International Computer Symposium (ICS 2010)*, pp. 1020-1025, Dec. 2010.

[13] E.W.T. Ngai and F.K.T. Wat. Fuzzy Decision Support System for Risk Analysis in E-Commerce Development. Decision Support Systems. pp.:235-255, Aug. 2005.

[14] T.Y. Tseng and C.M. Klein. A New Algorithm for Fuzzy Multicriteria Decision Making. *International Journal of Approximate Reasoning*, 6:45-66, 1992.

[15] L.A. Zadeh. Fuzzy Sets. Information and Control, pp.338-353, 1965.

[16] H.J. Zimmermann. Fuzzy set theory and its applications. 2nd revised edition, Kluwer Academic Publishers, 1991.

2011 IEEE International Conference on Fuzzy Systems
June 27-30, 2011, Taipei, Taiwan

Multi-Agent Automatic Negotiation and Argumentation for Courses Scheduling

Jong Yih Kuo
Department of Computer Science and Information Engineering
National Taipei University of Technology
Taipei, Taiwan
jykuo@ntut.edu.tw

Hsuan-Kuei Cheng
Department of Computer Science and Information Engineering
National Taipei University of Technology
Taipei, Taiwan
iamkaspar@gmail.com

Yong-Yi FanJiang
Department of Computer Science and Information Engineering
Fu Jen Catholic University
Taipei, Taiwan
yyfanj@csie.fju.edu.tw

Shang-Pin Ma
Department of Computer Science and Engineering
National Taiwan Ocean University
Keelung, Taiwan
albert@mail.ntou.edu.tw

***Abstract*—this paper proposes an argumentation and negotiation mechanism for multi-agent systems. Through argumentations and negotiations, agents obtain more information on the topics of common interests or on those they have odds with. At the inception of the negotiation, agents can hardly understand completely the goals and beliefs other agents have toward related issues. Through argumentations and negotiations, the beliefs evolve, and agents will have better understanding about each other's target needs and preferences. During negotiations, agents can select the proposal that better suits other agents, further improving the chances for the agents to reach a consensus. Lastly, this paper illustrates our proposed methods through a simple course-scheduling negotiating system.**

Keywords-agent; Negotiation; argumentation

I. INTRODUCTION

In a multi-agent system, agents, in order to complete tasks with others through various forms of interaction, negotiation is the most commonly used method. Negotiation is a form of interaction in which a group of agents, with conflicting interests and a desire to cooperate try to come to a mutually acceptable agreement on the division of scarce resources. Resources are scarce in the sense that not all demands can be simultaneously satisfied [7][8]. For the information in the surroundings, agents can hardly obtain complete information about them. Therefore, agents often have to make decisions based on incomplete information, or to use a different way trying to obtain more information on the subject in order to make the decision making more precise. In traditional negotiations, an agent can only refute or submit another proposal when it doesn't agree with it. Recently, it has been proposed that argumentation mechanisms can be used to facilitate negotiation among computational agents. These mechanisms attempt to overcome some of the limitations of bargaining-based frameworks by allowing agents to exchange additional information or to argue about their beliefs and other internal characteristics during the negotiation process. This process of argumentation allows an agent to justify its negotiation stance and/or influence that of another agent [10][14][15]. Adding in the argumentation mechanism allows agents to understand the reasons and considerations behind these rejections of other's. In the end of the Negotiation and Argumentation System [1][13], agents can understand the reason behind other agents' decisions in favor of or against the proposal.

In a general course scheduling problem, a set of courses need to be arranged into a certain number of time slot under a set of constraints. This often makes the problem very hard to solve in real world circumstances [5]. It consists of efficiently arranging a set of courses into class periods. Scheduling consists of assigning offered courses to available time periods so that the teachers' satisfaction factor is maximized while preserving the unbreakable academic rules such as two distinct courses cannot be scheduled during the same period of time.

It is practically impossible to exhaustively consider and evaluate all possible schedules. The number of such schedules is exponential in the number of courses and time periods. Many papers proposed different approaches to solve this tough problem, such as genetic algorithm, case-based reasoning and fuzzy reasoning [4][6][9]. The present work applied negotiation and argumentation approaches for the courses scheduling problem. Each teacher is regarded as an agent called *course negotiation agent*. Through the negotiation and argumentation process of multi-agent, a suitable course timetable is scheduled. The paper is organized as follows. In the next section, we provide a conceptual framework of the negotiation and argumentation mechanism. Section 3 presents the processes of the negotiation and argumentation. Section 4 shows the results of the experiment. Section 5 is the conclusions of this work.

II. THE FRAMEWORK OF NEGOTIATION AND ARGUMENTATION

The work was supported by the National Science Council of Taiwan, Republic of China under research contract NSC 99-2220-E-027-009.

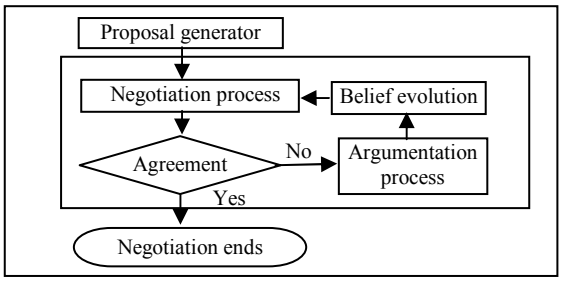

Figure 1 the System Pocess

The System Process is shown in Figure 1. The System obtains the User Belief from each agent, then generates numbers of different proposals through the Proposal Generator according to agents' various preferences and enters the Negotiation Process phase. During the negotiation process, each agent will select the acceptable proposal from all the proposals. The agents then submit this proposal and make efforts to reach a consensus with other agents. If there is a consensus among all the agents on a specific proposal, this proposal becomes the final agreement proposal and the Negotiation ends. If the attempt to reach a consensus has been unsuccessful, the System goes to Argumentation process where agents create arguments according to their own beliefs, and proceed with Argumentation with other agents. After the Argumentation phase comes the Belief Evolution, where beliefs are updated and intensified according to the outcome of Argumentation. The system then goes back to the start and proceeds with the next negotiation, re-evaluating proposals until a general consensus is reached.

A. Negotiation Mechanism

TABLE 1 DEFINITION OF NEGOTIATION SYMBOL

Symbol	Definition
bp_i	The most suitable proposal for $agent_i$.
bp_i'	The most personally effective proposal for $agent_i$.
P	Negotiation proposal.
NS (Negotiation set)	The set of available proposals.
T_i	The proposed proposal by agent.
$Utility_i$	The utility of the agent for the proposal.
$Risk_i$	The risk of the agent.

The so called Negotiation is a series of interactions performed by a group of conflicting agents when they need to work together, finding a way they all agree to allocate limited resources within an environment. The complete definition of Negotiation Symbol is shown in Table 1. During the process of Negotiation, agents select a proposal for the agent negotiation from existing proposals through a specific evaluating method. The purpose of Negotiation is to reach a consensus, and different negotiating proposal may have different value for the objects within the negotiation. The entire agent proposal can be defined by the equation (1).

$$P = \{(issue.name, issue.value) \mid issue, issue \in NO\} \quad (1)$$

The NO represents the entire Negotiation object; where issue is an issue within the Negotiation object. Agents select the best proposal by evaluating the best utility as a whole from those that have the highest utility. The expression for evaluating the utility of a proposal is presented in expression (2).

$$Utility_k(P) = \frac{\sum_{i=1}^{N}\sum_{j=1}^{M} f_j(issue_i)}{max(LevelPriority_k \mid K \in M) * N} \quad (2)$$

The system obtains the agent's preference on $issue_i$ based on $f_j(issue_i)$. $issue_i$ represents the *ith* issues of the agent; where fj represents the level of *jth* preference time of the $issue_i$. In the equation (2), *k, N, M*, and *LevelPriority* are used to represent the agent number, the number of issues agent *k* has, the number of time level of the agent *k's* preference and assign weighting values according to its Level respectively. *max* and *Σ* are used to present the maximum value within a group and its summation. Evaluating with equation (2), the agent can then evaluate which proposal has the highest utility for itself.

The raising of a proposal is based on an agent's individual preference. The utility degree the agent evaluates on in this proposal is the preference this proposal has for this agent. We can divide the level of preference into different levels according to how strong it is, and average them evenly as a general utility of the proposal.

$$bpi = \{P \mid P \in bpi' \text{ and } Utility(P) = max\{ Utility(P') \mid P' \in bpi'\}\} \quad (3)$$

Equation (3) evaluates the proposal that is most suitable for agent *i*. Agents decide whether to join bp_i based on the utility of each proposal. The proposal of bp_i will be submitted as a negotiating proposal during the negotiation and then be joined into T_i, which records every proposal agent submitted. The Negotiation Set is a set of all the available proposals. If the set is not empty, it means there is at least one proposal on which there exists a general consensus among all the agents.

To select which agent to concede during the negotiation, it is often decided by figuring out which agent has the lowest risk value. The risk value is evaluated by how much utility an agent will lose during the concession, as shown in equation (4). The equation calculates the maximum cost of giving in to other agent's proposal and the utility of its own proposal in order to obtain how much the agent will lose. This is the risk value for concession.

$$Risk_k = \frac{(Utility_k(SP_k) - min(Utilit\ y_k(SP_j) \mid K \in N)}{Utility_k(SP_k)} \quad (4)$$

The *priority* is the calculation of *priority* value according to the teacher's teaching years and its job title; *N* is the number of selected proposals submitted by other agents. SP_k*(Selected Proposal)* is the negotiation proposal submitted by the *k*th agent during this round of negotiation. If there are many agents that share the same lowest risk value, the selection of which agent to concede will take turns in fair. In that case, the agent that has conceded for the least times in history will be selected.

B. Argumentation Mechanism

In order to pass on additional information between agents, the Negotiation system relies on the argumentation system to generate arguments and to evaluate them. [1][2][3][11][12].

For the architecture in this paper, the purpose behind the agents submitting argument contents is to persuade others in the negotiation. The content of the submitted argument by the agent is a series of reasoning principles intended to praise the benefits of its own argument. The argumentation content A is represented by formula (5).

$$A = (H, h) \quad (5)$$

The purpose of the argumentation system is to provide agents with the ability to evaluate and generate arguments. Our research extended the argumentation system in [3] to generate suitable arguments using reasoning principles according to agents' beliefs, and to provide conflicts between beliefs in order for the agents' beliefs to evolve after argumentation. It also assigns priorities to beliefs that help the agents to compare them more easily.

A represents the argument content. H is the knowledge set that the reasoning is based on. h is the reasoning-formed conclusion. The knowledge includes the reasoning principle knowledge base available for the agents; the argumentation content is the set of used reasoning principles. When the arguments submitted by different agents in the system clash with each other, use *Undercut* to resolve the conflict, as shown in equation (6) and (7). Assume *(H1, h1)*, *(H2, h2)* to be two arguments.

(H1, h1) undercuts *(H2, h2):*

(1) If $h1 \equiv h2$ or If $\exists h \in H2$ *such that* $h \equiv h1$, *Using Rule of* Inference. (6)

(2) Undercut $= \{(A_i, A_j) \mid A_i, A_j \in Arguments\}$ (7)

For example, A_i and A_j represents two arguments respectively, where A_i *undercuts* A_j as in equation (7). A_i is *(H1, h1)*, and A_j is *(H2, h2)*. The two arguments, based on (6):

$h1 \wedge h2 \Rightarrow False$, *If* $h \in H2$, $h \wedge h1 \Rightarrow False$, *(H1, h1)* can then refute *(H2, h2)*.

For example, in equation (7), A_i and A_j represents proposal by agent i and j, respectively. The A_i submitted by agent i is P. By using the *Modus ponens:* $\{P, PQ\} \vdash Q\}$ in (6), agent j can submit A_i as Q, and A_i *undercuts* A_j.

This ordering is considered the priority of *Knowledge_Preference*. The definition of argumentation symbol is shown in Table 2.

TABLE 2 DEFINITION OF ARGUMENTATION SYMBOL

<A(∑), Undercut, Knowledge_Preference>	
∑	The knowledge base.
A(∑)	Output the suitable arguments for the agent according to the given ∑.
Undercut	Describes the conflicts between arguments.
Knowledge_Preference	Divide the available knowledge into several prioritized levels.

During the process of argumentation, agents can submit, query, and accept proposal by other agents. Agent submits a new proposal P by *assert(p)*; query other agents' proposal by *question(p)*, and accept other's proposal using *accept(p)*.

In the agent argumentation process, each argumentation is preceded with two agents, submitting proposal in turns. For those conflicting items, both agents are required to explain the reason of their own once. The proposal of both agents and other's that passes the argumentation wins. For the agent that loses, its belief needs to be updated and intensified.

III. NEGOTIATION AND ARGUMENTATION PROCESS

Negotiation process uses the conceding policy shown in Figure 2. If the negotiation fails, the system will enter argumentation process shown in Figure 3. Upon the completion of the argumentation, the beliefs are updated and the next round of negotiation begins.

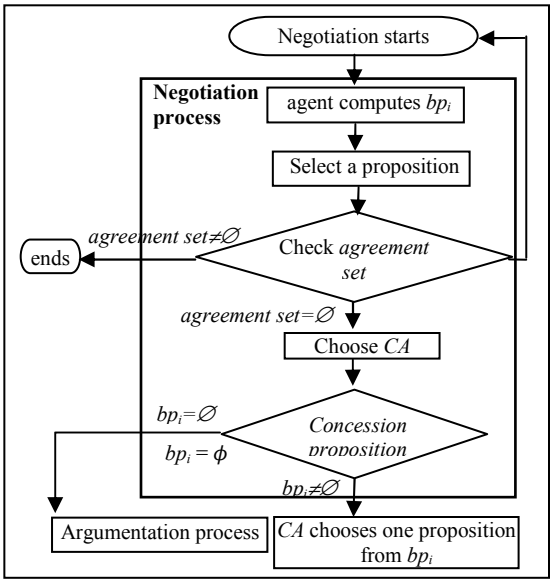

Figure 2 Negotiation process

A. Negotiation Process

This research proposes the negotiation process as follows:

- The agent calculates the utility value of the proposal. Select the proposal that best meets the agent requirement standards based on the utility value to form bp_i.
- Each agent chooses a proposal from bp_i to submit. The submitted proposal is then removed from bp_i and added to T_i.
- Evaluate whether the Negotiation Set is empty; if it is not empty, then at least one consensus has been reached, and the negotiation ends.
- Calculate the risk value of each agent. The agent with the least risk value will concede in the next turn. If numerous agents share the same minimum risk value,

the system chooses the agent who has conceded for the least times in the past to concede.

- The conceding agent then checks if bp_i is empty. If it is, which means that the agent does not have any other proposals that meet the requirements during this negotiation, it enters the argumentation process.
- On the other hand, if bp_i is not empty, choose a proposal from it. The chosen one should be the proposal that hasn't been submitted before, and goes back to step 1 to continue the negotiation.

B. Argumentation Process

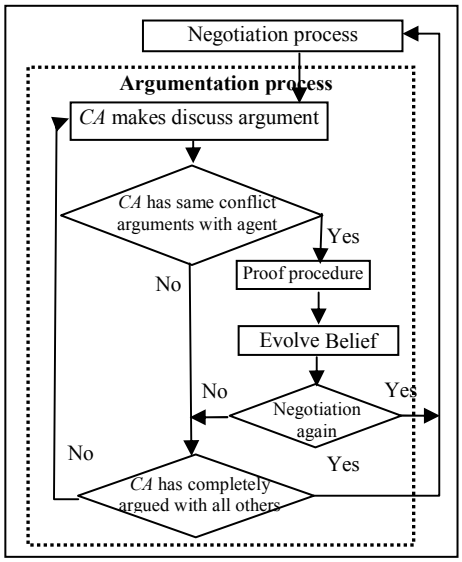

Figure 3 Argumentation process

The proposed argumentation process is specified as follows: (1) The conceding agent picks $agent_i$ who has the minimum risk value during negotiations, and compare the value for any conflicting issues. (2) The two agents search for any conflicting issue between them. If there is a conflicting issue, proceed with argumentation on this conflicting issue; if there is not, the conceding agent checks whether it has completed argumentations with all the other agents. (3) If the arguments conflict each other, use the argumentation reasoning. (4) The agents that fail the argumentation must evolve their beliefs. (5) After evolving, the failed agents re-check whether the negotiation can be carried on again. (6) Checking whether the conceding agents have completed argumentations with all the others. If they all have, the process goes back to the negotiation process and proceeds with the next negotiation; otherwise, it goes back to negotiation process step 1 and continues with argumentations.

C. Belief Evolvement

During the argumentation process, the agents pass on the argument to each other. The failed agents in the argumentation process get persuaded, and their beliefs must be evolved. The process includes: (1) Acquire the conflicting relations between beliefs through argumentation system. (2) Evolve the agent's belief according to the conflicting relations and the obtained results. (3) Remove the conflicting relation from the agent's belief. (4) Adjust and evolve the agent's belief.

IV. CASE STUDY

This paper uses a simple course-scheduling system to illustrate our negotiation and argumentation architecture written by Java and Jade (Java Agent Development Framework). A teacher represents the equivalence of a negotiation agent in this system, and each teacher obtains a suitable school timetable scheduling through negotiations.

A central coordinator obtains the preference time of each teacher agent, and with the help of the general school timetable generator, it submits a general school timetable proposal. For each teacher agent involved in the negotiation, according to this general timetable, each of them forms their own set of proposals. Based on the timetable set, the teacher agent submits proposal to the central coordinator, who then checks if any consensus can be reached within all the submitted proposals submitted by fellow agents. If there is no consensus, the conceding generator will decide which agent to concede. The conceding agent will carry on with the next round of negotiation later on, until a consensus has been reached.

A. Agent Belief

In this paper, agent's preference, and their thoughts on the available proposals affect how agents choose the negotiating proposal. We classify agent's preference into their beliefs. The agent can provide others with how it thinks about each proposal, making others' proposals more suitable to itself. The teacher agents' beliefs can be set by themselves; the beliefs are represented in XML, which includes the following elements: (1) Course: The courses name. (2) Degree: Agent's preference over the course timetable scheduling. Smaller value means higher preference; Degree = 1 represents the favorite time schedule. (3) Time_Preference: The preferred time schedule of the teacher. Each Time_Preference includes the ArgumentDep of the related arguments. (4) ArgumentDep: The arguments related to teachers' preferred time schedule, associated with the arguments in argumentation. (5) Argumentation: The argument that the agent (teacher) holds, which is classified into "Arguments" and "Counter-Arguments". (6) Arguments: The argument of the agent (teacher) its own. (7) Counter-Argument: Refute the argument of other agents.

TABLE 3 CANDIDATES PROPOSALS

Course Name \ Proposal Number	1	2	3	4	5
Web 2.0	Monday, afternoon	Tuesday, afternoon	Thursday, morning	Monday, afternoon	Monday, afternoon
Network Fundamental	Tuesday, afternoon	Friday, morning	Friday, afternoon	Thursday, morning	Friday, morning
Algorithm	Monday, morning	Monday, morning	Monday, morning	Monday, morning	Monday, morning
Linear Algebra	Wednesday, morning	Thursday, morning	Friday, morning	Friday, afternoon	Tuesday, afternoon
Java	Thursday, afternoon	Thursday, afternoon	Thursday, afternoon	Tuesday, morning	Thursday, afternoon
AI	Tuesday, morning	Wednesday, morning	Monday, afternoon	Wednesday, morning	Friday, afternoon

The agent belief includes its preffered time and the school timetable. The time format includes the day of the week and whether it's in the morning or afternoon. The purpose of negotiation is to arrange the course timetable for each teacher agent, therefore the issue contained in the proposal of the agent is the course schedule. The complete proposal candidates are listed in Table 3, where five course schedules are designated with the day of the week, and the time during the day.

The argumentation system allows the agents to generate suitable arguments. With specific information, agents can predict the arguments, conflicting knowledge relations, and knowledge usage level. The course schedule is the focus of argumentation among teacher agents in this experiment, which begins after negotiation fails to reach consensuses. If two teachers have same preference over certain schedules, they must provide with the reasons behind their choices. This paper designs the possible reasons behind teacher's preference over the schedule and assigns priority according to these reasons' characteristics. This priority is the *Knowledge_Prederence*. The process of assigning priorities can be discussed in public, or be decided by an unbiased third-party. Next we design possible preference reasons and their *Knowledge_Preference*. The reasons why having lower *Knowledge_Preference* value is better are: (1) Having regular executive meetings: ExecutiveCouncil (Agent, Time), Knowledge_Preference: 1. (2) Agent having courses from other department: HasCourse(Agent, Time), Knowledge_Preference: 2. (3) Single family: SingleFamily (Agent), Knowledge_Preference: 3. (4) Picking up kids from and to school: SendChildToSchool(Agent, Status), Knowledge_Preference: 4. (5) Preference over a schedule: Prefer(AgentName, (day, time)). (day, time) is the time the agent wishes others to concede, Knowledge_Preference: 5. (6) How intense the agent wishes the schedule to be: DaysOfCourse(Agent, Density), Knowledge_Preference: 6.

B. Negotiation and Argumentation Process

During the negotiation process, agent needs first to select the target proposal and then proceed with the argumentation in order to evolve its beliefs. Finally, it obtains the negotiation-argumentation result. Using the utility equation below, we can calculate the utility value that each agent can obtain for all the proposals in this round. They are listed in Table 12. We assume that the agent will set the proposal with the highest utility value as the most suitable proposal (bp_i), as Table 13 illustrates.

In round 1, teacher A chooses proposal 2, teacher B chooses proposal 1, 2, and teacher C chooses proposal 1. Obviously, in the first round, there are no proposals that can satisfy all the agents. Risk values of agents in round 1 are A: 0.17, B: 0 and C: 0.17. B has the lowest risk of all, so B has to concede in the first round. B submits another proposal for the next round, and other agents propose the same proposal on the next round. There is still no consensus in this round. Risk values of agents on round 2 are A: 0.17, B: 0 and C: 0.17. B has the lowest risk of all, and B has to concede in the second round. B's bp_i is empty, which means there is no proposal, so the negotiation process enters the argumentation process. B in the argumentation continues to concede. B argues with A. Based on the teacher's beliefs, both of them prefer Monday morning. B cast out reasons why it loves this particular time.

- B asserts SendChildToSchool(B, AfterClass).
- A asserts ¬SendChildToSchool(B, AfterClass)).
- B Supposes P=SendChildToSchool(B,AfterClass). P asserted by A, P=¬SendChildToSchool(B, AfterClass). Teacher B according to Modus ponens {{¬P, P∨Q} ⊢ Q}, inference Q=SingleFamily (B), then asserts SingleFamily (B).
- A accepts SingleFamily (B).

TABLE 4 THE EFFECTIVENESS OF AN AGENT TO RE-CALCULATE THE VALUE OBTAINED

Teacher \ Proposal Number	1	2	3	4	5
A	1	1	0.67	0.83	0.83
B	1	1	0.83	0.83	0.83
C	1	0.83	0.83	0.83	0.67

Finally, agent A won the argumentation. B evolves its beliefs, and makes a concession on the Monday morning time and removes it from its belief. Next, B selectes from the preference of session degree two which is the closest to Monday. After teacher B updated its beliefs, the perceptions of the environment are changed, and the assessment of the proposal on the curriculum will be different. All agents re-calculate *Utility* value and the bp_i for the curriculum proposal in Table 4, and check whether to continue with the negotiations.

Return to the negotiation process. During round 3, teacher A chooses proposal 1, teacher B chooses proposal 1 and teacher C chooses proposal 1. The negotiation focuses on a proposal to find an agreement, and the agent concludes the negotiations. Proposal is a schedule that can be used as a school curriculum and is acceptable to all the teachers. All agents make their own proposals for the most desired curriculum at the beginning of the negotiation. After a few concessions, if it is still unable to reach consensus on the proposal, the negotiations breaks down. So that agents can use the argument mutual understanding of each other's needs and then update the agent's beliefs. The proposals will close other agent's demands in next round of consultations.

We compared method [15] with this study. In research [15], if the proposal set is empty, the agent withdraws from negotiation. Because conventional trading negotiation will not change agent's beliefs, an agent will not interact with other agents of change in spite of understanding the environment. In our method, agents interact with other agents. This allows a better understanding of the needs of others, further changing the perceptions of the environment and updates their beliefs. For example, after the teacher argumentation, B is persuaded by A, and B will change its beliefs. The curriculum for the proposal in Table 1 candidate proposals will have a different assessment.

TABLE 5 THE FINAL PROPOSALS

Approach / Teacher	Negotiation	Negotiation and Argumentation
A	1	1
B	1	1
C	0.83	1

Table 5 shows the argumentation and negotiation of the final proposal with their values for comparison. In the traditional negotiation method, if there is no more proposal that can be chosen, the negotiation process would be withdrew. In this experiment, the final outcome of the negotiations is proposal 2. However, C is not very satisfied with proposal 2. A evolves its beliefs through argumentation; the proposal 2 may be accepted. Proposal 1, which satisfies all the agents, is the best result of the negotiation. After adding the argumentation method in negotiation, agents can interact with other agents and obtain more information and evolve their beliefs and then cause the perceptions of the environment to change. The agent who withdraws from the negotiation can re-evaluate the proposal, and goes back to the negotiation process once again to put forward a new proposal. Conceding agents can put forward new proposals more in line with all the agents.

V. CONCLUSION

Many research papers have addressed to the problem of agents' decision making accuracy being affected by the incomplete environment information in multi-agent systems. Through negotiation and argumentation, this paper makes agents understand others in the environment better, further achieving the evolvement of their beliefs.

REFERENCES

[1] Leila Amgoud, and S. Vesic, "On the Role of Preferences in Argumentation Frameworks," 22nd IEEE International Conference on Tools with Artificial Intelligence, vol. 1, pp. 219-222, 2010.

[2] Leila Amgoud, Claudette Cayrol. "A reasoning model based on the production of acceptable arguments," Annals of Mathematics and Artificial Intelligence, vol. 34 (1-3), pp.197-215, 2002.

[3] Leila Amgoud, Florence Dupin de Saint-Cyr, "A new semantics for ACL based on commitments and penalties," International Journal of Intelligent Systems, vol. 23 (3), pp. 286-312, 2008.

[4] Hishammuddin Asmuni, Edmund K. Burke, Jonathan M. Garibaldi, Barry McCollum, "A novel fuzzy approach to evaluate the quality of examination timetabling," Lecture Notes in Computer Science, vol. 3867, pp.327-346, 2007.

[5] Edmund K. Burkea, Barry McCollumb, Amnon Meiselsc, Sanja Petrovica and Rong Qu, "A graph-based hyper-heuristic for educational timetabling problems," European Journal of Operational Research, vol. 176 (1), pp. 177-192, 2007.

[6] Edmund K. Burke, Sanja Petrovic, Rong Qu, "Case-based heuristic selection for timetabling problems," Journal of Scheduling, vol. 9 (2), pp. 115-132, 2006.

[7] Yann Chevaleyre, Ulle Endriss, Nicolas Maudet, "Simple negotiation schemes for agents with simple preferences: sufficiency, necessity and maximality," Autonomous Agents and Multi-Agent Systems, vol. 20, pp. 234-259, 2010.

[8] Y. Dimopoulos, P. Moraitis, L. Amgoud, "Characterizing the Outcomes of Argumentation-Based Integrative Negotiation," IEEE/WIC/ACM International Conference on Web Intelligence and Intelligent Agent Technology, vol. 2, pp. 456 - 460, 2008.

[9] Ying-Shen Juanga, Shui-Shun Lin, Hsing-Pei Kao, "An adaptive scheduling system with genetic algorithms for arranging employee training programs," Expert Systems with Applications, vol. 33 (3), pp. 642-651, 2007.

[10] Fernando Lopes, Michael Wooldridge, A. Q. Novais, "Negotiation among autonomous computational agents: principles, analysis and challenges," Artificial Intelligence Review, vol. 29, pp. 1-44, 2008.

[11] Sanjay Modgil, "Reasoning about preferences in argumentation frameworks," Artificial Intelligence, Vol. 173 (9-10), pp. 901-934, 2009.

[12] Henry Prakken, "Models of persuasion dialogue", Argumentation in Artificial Intelligence, pp. 281-300, 2009.

[13] Iyad Rahwan, Liz Sonenberg, Peter McBurney, "Bargaining and argument-based negotiation," Lecture Notes in Computer Science, vol. 3366, pp.176-191, 2005.

[14] Iyad Rahwan and Leila Amgoud, "An argumentation-based approach for practical reasoning," Argumentation in Multi-Agent Systems Lecture Notes in Computer Science, vol. 4766/2007, pp. 74-90, 2007.

[15] M. Wooldridge, S. Bussmann, and M. Klosterberg, "Production sequencing as negotiation," Proceedings of the 1st International Conference on the Practical Application of Intelligent Agents and Multi-Agent Technology, pp. 709-726, 1996.

2011 IEEE International Conference on Fuzzy Systems
June 27-30, 2011, Taipei, Taiwan

Investment Decision Making by Using Fuzzy Candlestick Pattern and Genetic Algorithm

Chiung-Hon Leon Lee, Yi-Ching Liaw, and Lindroos Hsu
Department of Computer Science and Information Engineering
Nanhua University
Dalin, Chia-Yi, 620, Taiwan
chlee@mail.nhu.edu.tw, ycliaw@mail.nhu.edu.tw, somewhereibeing@gmail.com

***Abstract*—This paper proposed an approach to extract fuzzy candlestick patterns from financial time series and select a set of patterns for investment decision making. The candlestick chart in stock market is a widely used technical analysis model. The investor observes the candlestick chart and makes investment decisions by identifying patterns in the chart. We use fuzzy linguistic variables to model candlestick chart and extract patterns from the chart. A Genetic algorithm based approach is used to select a set of extracted pattern as the background knowledge in the system for investment decision making. The advantage of the proposed approach is the investment knowledge is comprehensible, editable, and visible. The user can set different range of historical financial time series to extract and select different set of patterns. The experimental results shows that the investment decisions based on selected fuzzy patterns have better investment performance than using original non-fuzzy patterns.**

Keywords-component; fuzzy candlestick pattern; time series; genetic algorithm

I. INTRODUCTION

How to modeling and implementing domain knowledge is an important part when design and implement an intelligent decision supporting system. For example, if an intelligent investment expert system has rich background knowledge from human expert, the system can give more precise suggestions to the user [1].

There are a lot of fundamental and technical analysis concepts and techniques have been established in financial investment domain such as Relative Strength Index (RSI), Moving Average Convergence Divergence (MACD), and Fast and Slow Stochastic (KD-line), etc. These technical analysis tools are the basis when design some investment decision supporting systems [2].

However, the set of data used to calculate RSI, MACD, and KD indicators is the closing price in a time point. There is rich information which exists in the financial time series database, but most of the traditional approaches only scratch the surface of the wealth of knowledge buried in the data. Many financial time series prediction approaches only use daily closing price as raw data to construct the forecasting model.

Figure 1 shows three general ways to represent the stock trading price during a time period. Figure 1(a) indicates a single closing price. Figure 1(b) represents the bar line which contains richer information than 1(a). The data required to produce a standard bar chart consists of the open, high, low, and close prices for the time period under study. A bar chart consists of vertical lines representing the high to low range in prices for that trading time period. The high price refers to the highest price that the issue traded during that trading time period. Likewise, the low price refers to the lowest price traded that trading time period. Figure 1(c) illustrates the candlestick line which is similar to the bar line but using a box to makes up the difference between the open and close price.

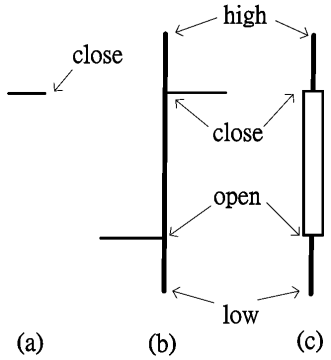

Figure 1. Different represention of financial data.

The candlestick chart in stock market is a widely used empirical model for investment decision making [3]. The investor observes the candlestick chart and makes investment decisions by identifying patterns in the chart. Figure 2 shows two examples of the daily candlestick chart in a stock market. Daily opening, closing, highest, and lowest prices are recorded in the candlestick lines for days d1, d2, d3, and d4. On d1, the stock opens in a higher price, but close at a lower price. On the next day d2, the opening price is lower than previous closing price, but closes at the highest price and is much higher than the lowest price. This situation might be interpreted by an experienced investor as the candlestick line on the day d1 reflecting a downtrend of the stock price, because there are many investors want to sell their stock and make the closing price much lower than the opening price. However, the downtrend might reverse itself on the day d2, because there are investors to buy the stock in the trading period that makes

978-1-4244-7316-8/11/$26.00 ©2011 IEEE

the price close at the highest price and much higher than the lowest price. In other word, the candlestick lines at d1 and d2 might represent a bouncing back. At d3, the closing price is higher than the opening price, and at d4, the opening price is much higher than the previous closing price, but closes at lowest price. The lines at d3 and d4 might be interpreted by the investor that the trend is returned, because the uptrend is broken at d4. It is obvious that the interpretation between the lines at d1, d2 and d3, d4 is very different, but the closing prices of d1, d2 and d3, d4 are the same.

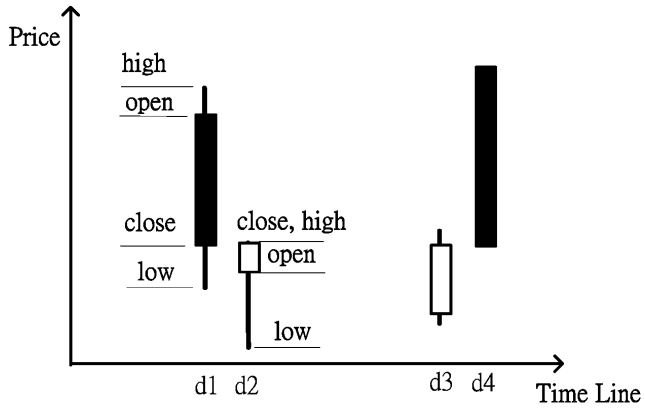

Figure 2. A candlestick chart.

Candlestick patterns which exist in the candlestick chart are empirical models of investment decision. The experienced investors can make their investment decision based on the observation of some specific candlestick patterns such as Bullish Engulfing, Hanging Man, Hammer, etc which are defined by the pioneer investors. However, to a human investor, to identify an effective pattern from a lot of imprecise and vague candlestick patterns needs years of investment experience and expertise. In addition, to retrieve the candlestick patterns from a large amount of financial trading data is time consuming.

In this paper, we propose a fuzzy candlestick pattern based financial decision supporting system to acquire the stock trading data in the Taiwan stock market (TAIEX) [4] from the Internet, provide an interface for the users to edit their own fuzzy candlestick patterns which are represented by fuzzy linguistic variables, extract fuzzy candlestick patterns from financial time series, and use a Genetic Algorithm (GA) based approach to select a set of extracted pattern as the background knowledge in the system for investment decision making. The advantage of the proposed approach is the investment knowledge is comprehensible, editable, and visible. The user can use different range of historical financial time series as basis for candlestick patterns construction.

This paper is organized as follows. In Section 2, the fuzzy-based candlestick pattern representation method is introduced. Section 3 describes the Genetic algorithm (GA) based fuzzy candlestick pattern extraction approach and the experimental results. Finally, Section 4 concludes this paper.

II. MODELING CANDLESTICK CHART

By the trading experience, the investor tries to identify the candlestick patterns to help themselves to make the investment decisions such as to buy, sell, or hold the stock. There are many existing defined candlestick patterns which are widely used by the investors. Figure 3(a) shows a hierarchy to represent the relationships among the candlestick pattern, candlestick line, and the prices. A visual candlestick pattern which called Bearish Engulfing is demonstrated in Figure 3(b).

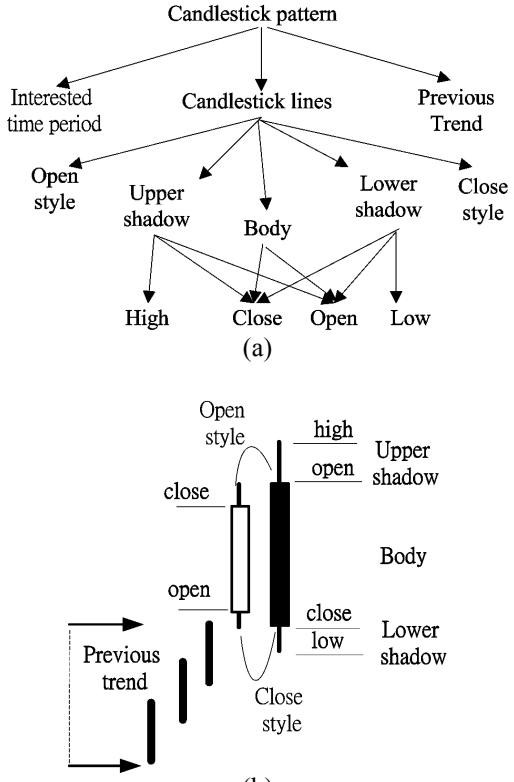

Figure 3. An example of the candlestick pattern.

The advantage of candlestick chart to investors is that the candlestick chart is visual, and a reversal or continuation candlestick pattern can be easily identified by an experienced investor. However, identifying the candlestick pattern from a large amount of trading data is time consuming, and there are no crisp and standard definitions to the candlestick patterns. The imprecise and vague definitions of the candlestick patterns make the automated searching, mining, and processing the candlestick patterns with computer software difficult. In this paper, we adapted the approach proposed in [5] to solve this problem.

A. Modeling Candlestic Patterns

A candlestick chart is composed by a series of continual candlestick lines. The lines consist of the open, high, low, and close prices in a time period under study. The time period can be of any duration, such as five minute, fifty minute, one hour, one day, one week, or one month. The first trading price in the interested trading time period is called open price; the last

trading price is called close price; the highest price is called high price, and the lowest price is called low price. These four prices compose a candlestick line. A candlestick pattern is composed by several serial candlestick lines.

The box that makes up the difference between the open and close is called the real body of a candlestick line. The height of the body is the range between a trading day's open price and the day's close price. When the body is black, it means that the closing price was lower than the opening price. When the closing price is higher than the opening, the body is white.

Four fuzzy linguistic variables EQUAL, SHORT, MIDDLE, and LONG are defined to indicate the fuzzy sets of the shadows and body length. Figure 4 shows the fuzzy membership function $\mu(x)$ of the linguistic variables.

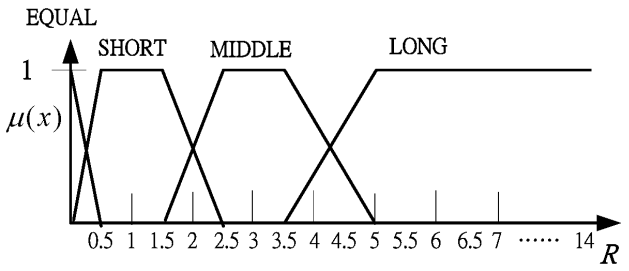

Figure 4. The membership functions of the length of the body and shadows.

The time period used in this paper is one day and the range of body and shadow length are set to 0 to 14 percent of the fluctuation of stock price, because the varying percentage of the stock prices are limited to 14 percent in TAIEX. Although we limit the fluctuation of body and shadow length in 14 percent in this paper, it is up to the system designer to change the range of the lengths to fit the needs of other applications.

In Figure 4, the unit of X axis is the percentage of price change in a stock and it indicates the lengths of body or shadows. The crisp input value of the membership function can be calculated by the following equations.

$$L_{upper} = [high - \max(open, close)]/open$$
$$L_{lower} = [\min(open, close) - low]/open$$
$$L_{body} = [\max(open, close) - \min(open, close)]/open \quad (1)$$

The character "*L*" of the equation indicates the length of the upper shadow, lower shadow, and body. The terms of open, close, high, and low are the prices in an interested time period. The function of **max** is used to calculate the greater value between the open price and the close price while and the function **min** is for the smaller value between them.

A right linear membership function is used to model the EQUAL fuzzy set and is defined by the following formula. The parameters (a, b) are equal to (0, 0.5) in this paper.

$$right_linear(x:a,b) = \begin{cases} 1 & x < a \\ (b-x)/(b-a) & a \le x \le b \\ 0 & x > b \end{cases} \quad (2)$$

The LONG fuzzy set is defined by the following left linear membership function. The parameters (a, b) are equal to (3.5, 5).

$$left_linear(x:a,b) = \begin{cases} 0 & x < a \\ (x-a)/(b-a) & a \le x \le b \\ 1 & x > b \end{cases} \quad (3)$$

The membership function of SHORT and MIDDLE is a trapezoid function and the following formula is used.

$$trapezoid(x:a,b,c,d) = \begin{cases} 0 & x < a \\ (x-a)/(b-a) & a \le x < b \\ 1 & b \le x < c \\ (d-x)/(d-c) & c \le x < d \\ 0 & x \ge d \end{cases} \quad (4)$$

Four parameters (a, b, c, d) of this function to describe the linguistic variables SHORT and MIDDLE are (0, 0.5, 1.5, 2.5) and (1, 2.5, 3.5, 5).

The body color is also an import feature of a candlestick line and can be simply defined by three terms BLACK, WHITE, and CROSS. The situation where open price equals close price has specific meaning in the candlestick pattern, so a "CROSS" term is defined to describe this situation. In this case, the height of the body is 0, and the shape is represented with a horizontal bar. The definition of body color is defined as follows.

If open - close > 0 then the body color is BLACK.

If open - close < 0 then the body color is WHITE. (5)

If open - close = 0 then the body color is CROSS.

Figure 5 shows the membership function of the linguistic variables of the open style and close style. The candlestick line in the bottom of Figure 5 is the candlestick line of previous trading time. The unit of X axis is the trading prices of previous day and the unit of Y axis is the possibility values of the membership function.

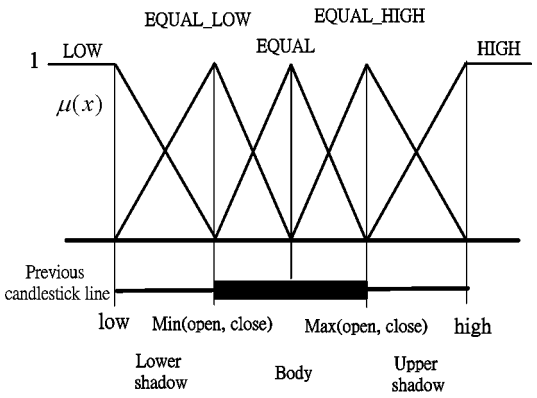

Figure 5. The membership function of the open and close style.

Five linguistic variables are defined to represent the open style relationships: OPEN LOW, OPEN EQUAL_LOW, OPEN EQUAL, OPEN EQUAL_HIGH, and OPEN HIGH, and five linguistic variables are defined to represent the close style relationships: CLOSE LOW, CLOSE EQUAL_LOW, CLOSE EQUAL, CLOSE EQUAL_HIGH, and CLOSE HIGH.

The function used to represent OPEN LOW and CLOSE LOW is the right linear function in (2), and (3) is also used to represent the fuzzy sets of OPEN HIGH and CLOSE HIGH. The other fuzzy sets are described by the triangle function in (6).

$$triangle(x:a,b,c)=\begin{cases}0 & x<a\\ (x-a)/(b-a) & a\le x\le b\\ (c-x)/(c-b) & b<x\le c\\ 0 & x>c\end{cases} \quad (6)$$

The parameters for the linguistic variables of open and close style are determined by the prices of previous candlestick line. For example, if the open price in a interested time period is equal to the price of min(*open,close*), then the open style is OPEN EQUAL_LOW and if the close price is equal to the price max(*open,close*), then the close style is CLOSE EQUAL_HIGH.

B. Modeling the Investment Knowledge

The description of a fuzzy candlestick pattern stored in the system consists of two parts: the pattern description part and the pattern information part. The description part is composed by the name of the candlestick pattern, a previous trend of the pattern, candle lines which composed the pattern, and the time period information. The information part records the candlestick pattern related information such as the pattern identification rules and the meaning of the pattern, etc. The information part is optional and is defined by the investors if the investor is interested in the pattern. If a candlestick pattern is described with the description information, it becomes more comprehensible to the other investors.

Table 1 shows a fuzzy candlestick pattern example which demonstrates a possible way to represent the Bearish Engulfing candlestick pattern and other candlestick patterns can be defined in the same way. The previous trend defined here is a crisp rule such as "down 15% in recent 10 days" to represent a downtrend or "up 15% in recent 10 days" to represent an uptrend. It should be noted that, for implementation convenience, we define the candlestick line which appear at the day *t* line 0, and the line appear in previous trading day *t-1* line 1.

Assume that the pattern appears at day *t*, the close price of day *t* is denoted *close(t)*, the highest close price in recent *k* days is denoted *highest(k)*, and the lowest close price in recent *k* days is denoted *lowest(k)*. The rules to determine the downtrend and uptrend can be defined as follows.

If $\frac{highest(k)-close(t)}{close(t)} > p$ then the stock price is in a downtrend.

If $\frac{close(t)-lowest(k)}{close(t)} > q$ then the stock price is in an uptrend,

where *p* and *q* are the thresholds to determine the trend of stock price is in uptrend or downtrend, and the unit of *p* and *q* is percentage of the fluctuation of stock prices.

Table 1
An example of the fuzzy candlestick pattern.

Pattern description part	**Pattern information part**
Pattern name: Bearish Engulfing	***Confirmation suggest:*** Suggest
Previous trend: Uptrend	***Confirmation information:*** The open price after the pattern should not be higher than the open price of candle line 0.
Candle lines: ***Candle line 0:*** ***Open style:*** OPEN HIGH ***Close style:*** CLOSE LOW ***Upper shadow:*** null ***Body:*** ABOVE MIDDLE ***Body color:*** BLACK ***Lower shadow:*** null ***Candle line 1:*** ***Open style:*** ABOVE OPEN EQUAL_LOW ***Close style:*** CLOSE HIGH ***Upper shadow:*** null ***Body:*** ABOVE SHORT ***Body color:*** WHITE ***Lower shadow:*** null	***Recognition rule:*** 1. A definite downtrend must be underway. 2. The second day's body must completely engulf the prior day's body. 3. The first day's color should reflect the trend: black for a downtrend and white …
Interested time period: DAY	***Pattern explanation:*** The first day of the Engulfing pattern has a small body and the second day has a long real body. Because the second day's move. ….

C. Pattern recognition

Since the patterns have been defined by the investor, the defined patterns can be easily transferred into fuzzy rules. For example, the Bearish Engulfing pattern can be transferred as following fuzzy rule.

IF trend = UP_TREND
AND line0.open_style = OPEN HIGH
AND line0.close_style = CLOSE LOW
AND line0.body = ABOVE MIDDLE
AND line0.body_color = BLACK
AND line1.open_style = ABOVE OPEN EQUAL_LOW
AND line1.close_style = CLOSE HIGH
AND line1.body = ABOVE SHORT
AND line1.body_color = WHITE
THEN the pattern = BEARISH ENGULFING.

A pattern recognition rule consists of the crisp part and the fuzzy part. The crisp part includes the previous trend of the pattern and the body color. The others of the rule are the fuzzy part such as the body and shadow length and the open and close style. From observation, well arranged identification rule will reduce the pattern recognition processing time.

Comparing with the processing time of the fuzzy part, the crisp part takes less processing time. For example, the body

Identify applicable sponsor/s here. *(sponsors)*

color includes three possibilities: BLACK, WHITE, and CROSS. For judging the value of the body color, the pattern recognition module only needs to compare the value of open price and close price. The pattern identifying time can be reduced if the judgment of the crisp part is placed before the process of the fuzzy part.

The concept of Hamming distance [6] is used to measure the similarity among fuzzy candlestick patterns. Assume that A and B represent two different fuzzy candlestick patterns which described by n linguistic variables, the similarity is defined as:

$$S(A,B)=\frac{1}{n}\sum_{i=1}^{n}\left|\mu_A(x_i)-\mu_B(x_i)\right|,\qquad 0<S(A,B)\le 1. \tag{7}$$

The user can set a threshold T to determine a pattern is recognized or not. If $S(A,B)\ge T$ then the pattern is identified.

III. Investment Knowledge Extracting

When using the candlestick chart, the investment decision is based on a set of candlestick patterns rather than only use a single pattern. In other word, how to select a set of patterns becomes an important problem.

Using fuzzy candlestick pattern to make investment decisions has several steps.

1. Transfer a range of financial time series into candlestick chart for pattern extraction.
2. Extracting original fuzzy candlestick patterns by using predefined heuristic rules.
3. Selecting patterns from extracted patterns by GA.
4. Using the selected patterns as the investment knowledge for decision making.

Step 1 fellows the method introduced in section 2 to transfer financial time series into candlestick chart. Three heuristic rules are defined for pattern extraction in step 2.

1. Bullish pattern recognition rule: if the previous trend is downtrend and the up_index of following N days up $P\%$ then the pattern is a bullish pattern.
2. Bearish pattern recognition rule: if the previous trend is uptrend and the down_index of following N days down $P\%$ then the pattern is a bearish pattern.
3. Other patterns: don't care.

The up and down indexes are used to indicate the maximum and minimum variation of the stock price after a specific pattern has happened. The calculation of up and down indexes is similar to previous trend of the candlestick pattern. Assume that the pattern appears on day t, the close price of day t is denoted *close(t)*, the highest close price in recent k days is denoted as *highest(k)*, and the lowest close price in recent k days is denoted as *lowest(k)*. The up and down index are defined in (8).

$$up_index=\frac{highest(k)-close(t)}{close(t)}\times 100$$
$$down_index=\frac{close(t)-lowest(k)}{close(t)}\times 100 \tag{8}$$

The *total_up_down* index is used to indicate the possibility investment result when using a specified pattern in an assigned time period, and the *mean_fluctuation* index is used to reflect the mean fluctuation of the stock prices when the pattern appears. To a reversal pattern, these two parameters should as large as possible. The total up times and total down times are also calculated. If the up index is higher than the down index, the total up times are increased by 1, and if the up index is lower than the down index, the total down times are increased by 1. The total up and down index and mean fluctuation are calculated as follows.

$$total_up_down=\sum(up_index-down_index)$$
$$mean_fluctuation=\frac{1}{T}\sum_{i=1}^{T}(up_index+down_index) \tag{9}$$
$$T=total_up_times+total_down_times$$

Figure 6 shows a reversal pattern called "Hanging Man" testing results. The selected stock number is 2409 (AUO), and the validation range is 1000 trading days before 2004-12-10. The maximum and minimum close prices from trading day t to t - 5 are selected to calculate the up and down index. In the selected range of trading days, the pattern appeared 10 times. In other words, the frequency of this pattern is 0.01. The *total_up_down* index is equal to about 20 percent, and *mean_fluctuation* index is equal to about 11 percent.

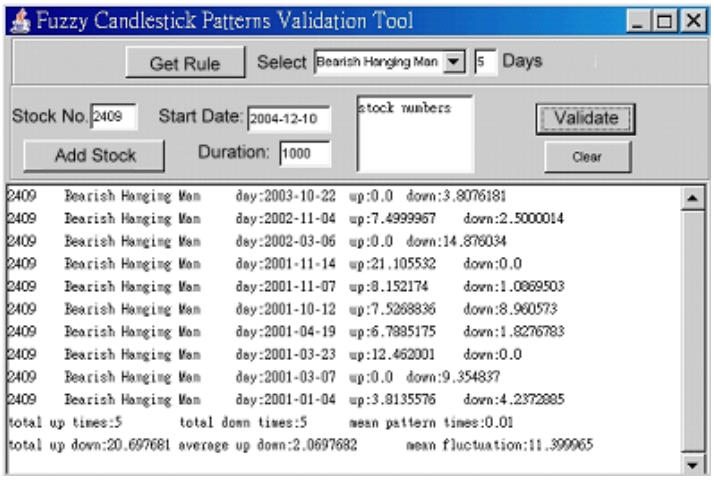

Figure 6. A pattern validation results.

In step 3, we use the extracted patterns as gene to consist a chromosome for GA. The relationship of pattern rules and chromosomes is shown in Figure 7.

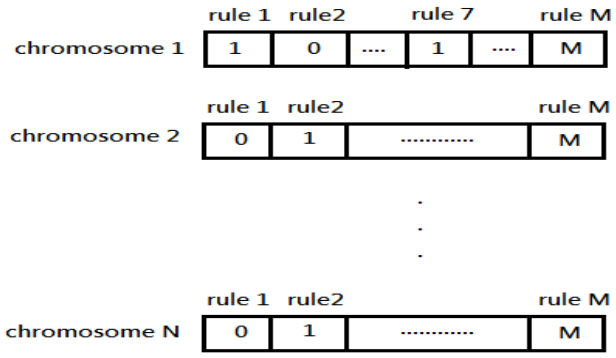

Figure 7: The chromosome used in GA.

If the pattern extracted in step 2 is 576 the *M* will be 576. In chromosome, bit 1 indicate the rule is used for investment decision making, bit 0 indicate this rule do not be used. In the beginning of GA, we set bits in chromosome randomly.

The fitness function is define as:

$$f(x_n) = \frac{x+m}{\sum_{i=1\sim N}(x_i+m)} \qquad (10)$$

Where x is the earned or lost point when using patterns indicated in chromosome and m is the stop value if earned point reached this value. We use Taiwan Stock Exchange Capitalization Weighted Stock Index (TAIEX) from 2001 to 2005 for patterns selection. The experimental results by running GA are shown in Figure 8.

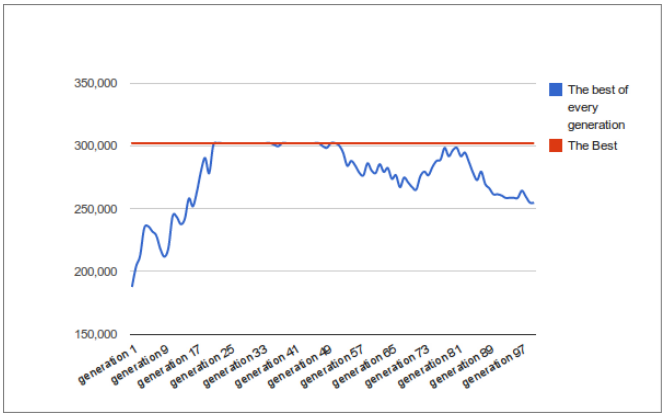

Figure 8: A comparison of different GA generation.

Finally we compared the performance by using different pattern sets. First results use extracted fuzzy candlestick pattern as background knowledge, second use user defined patterns, and third use GA to get better pattern set. The experimental results in Table 2 show fuzzy candlestick patterns with GA have best performance.

Table 2: a comparison among using different pattern set.

	Time series for pattern extraction	Evaluation Time series	Results
Extracted patterns	2001~2005	2006~2009	5027
Predefined patterns	No	2006~2009	6114
Selected patterns	2001~2005	2006~2009	8452

IV. CONCLUSION

In this paper, we proposed a knowledge based method to represent the financial time series. The variance of the stock price is represented in fuzzy candlestick patterns which make the imprecise and vague investment knowledge comprehensible, computable, visual, and editable. We also propose a GA based approach for patterns selection. The system can give investment suggestion to the investor by using these patterns as background knowledge.

The fuzzy candlestick patterns carry rich information and also can be used to increase the efficiency of the data mining, machine learning, and pattern recognition models. Pattern construction and recognition approach is introduced and implemented in a system prototype to illustrate the usage of the fuzzy candlestick patterns. Moreover, investors can save and share their investment experience. By reusing and modifying the stored candlestick pattern information, the investor can also increase the efficiency of their investing strategies. We believe that the fuzzy candlestick pattern representation method can still be used in other areas in which the time series has some properties like the stock price.

ACKNOWLEDGEMENT

This research was partially supported by the National Science Council in Taiwan through Grant NSC-99-2221-E-343-006.

REFERENCES

[1] J. C. P. Shieh, *Contemporary Investments—Analysis And Management*, Taipei, Taiwan, Best-Wise,pp. 317-431, 1998.

[2] R.S.T. Lee, "iJADE stock advisor: an intelligent agent based stock prediction system using hybrid RBF recurrent network," IEEE Trans. on Systems, Man and Cybernetics, Part A, vol. 34, no. 3, pp. 421-428, 2004.

[3] G.L. Morris, Candlestick Charting Explained: Timeless Techniques for Trading Stocks and Futures, 2nd ed., McGraw-Hill Trade, 1995.

[4] http://www.twse.com.tw/en/products/indices/tsec/tsec_index.php

[5] C.H.L Lee, A. Liu, and Wen-Sung Chen, "Pattern Discovery of Fuzzy Time Series for Financial Prediction," IEEE Trans. on Knowledge and Data Engineering, vol. 18, no. 5, pp. 613-625, 2006.

[6] Klir, G.J. & Yuan, B. (1995). Fuzzy sets and fuzzy logic theory and application. Upper Saddle River, NJ: Prentice Hall.

2011 IEEE International Conference on Fuzzy Systems
June 27-30, 2011, Taipei, Taiwan

Fuzzy Logic as a Basic for Use Case Point Estimation

Jonathan Lee
Department of Computer Science and Information Engineering
National Central University
Jhongli, Taiwan
Email: yjlee@selab.csie.ncu.edu.tw

Wen-Tin Lee
Department of Software Engineering
National Kaohsiung Normal University
Kaohsiung, Taiwan
Email: wtlee@nknu.edu.tw

Jong-Yih Kuo
Department of Computer Science and Information Engineering
National Taipei University of Technology
Taipei, Taiwan
Email: jykuo@ntut.edu.tw

***Abstract*—Project estimation based on function point or use case point (UCP) methods provide only fixed complexity grades which can not deal with the uncertain and imprecise conditions. This study, therefore, provides a fuzzy size estimation procedure for goal-driven use case model based on UCP using fuzzy theory. We propose a metric to calculate the unadjusted use case points of goal-driven use cases based on the relations between each use cases and goals with the fuzzy membership functions and the fuzzy rules. Furthermore, the technical and environmental factors are considered to calculate the use case points which can be used to estimate the implementation time and effort of the system under development. The proposed approach is illustrated by a benchmark problem domain of a meeting scheduler systems.**

***Index Terms*—function point analysis, use case point, goal-driven use cases, fuzzy theory.**

I. Introduction

Software estimation is an important and difficult activity in project planning and management process. Several estimation models have been proposed to estimate the software size [3], [5], [14] based on function point (FP) [1]. In object oriented development process, use case analysis is a crucial activity to develop software system. Therefore, the use case points method, a software sizing and estimation method based on use case counts called use case points (UCP) [6], [12], [13] is provided to estimate functional size of software in early stage of a project. The use case point method can be divided into five parts: Weighting actors by indicating the three actor types, simple, average and complex to generate unadjusted actor weights (UAW); Weighting use cases by indicating the three use case types based on transactions or classes to generate unadjusted use case weights (UUCW); Weighting technical complexity factors (TCF) to indicate the expectations of the users for the delivered software; Weighting environment factor (EF) to indicate the experience level of people on project; Finally, calculate use case points (UCP) by the formula UCP = (UAW + UUCW) $\times$ TCF $\times$ EF.

Nevertheless, FP and UCP methods provides only fixed complexity grades which can not deal with the uncertain and imprecise conditions. Therefore, some studies have been proposed to estimate the software size using fuzzy set theory. Xia et al [15] provide a neuro-fuzzy FP calibration model that integrate fuzzy logic, statistical regression and neuro network techniques to improve the accuracy of software effort estimation. Braz and Vergilio [2] present two metrics, use case size points (USP) which considers the internal structure of the use case and fuzzy use case size point (FUSP) which uses fuzzy set theory for gradual change of complexity. Rodrigo et al [11] propose a task fuzzy estimator based on the UCP techniques with three inputs: complexity to modify the modules, experience of developers and the size of the alteration. The inference result is the effort in days for software development.

However, those studies do not consider the relationships between use cases and goals that would affect the complexity and implementation effort of each use cases. In this work, we propose a fuzzy software sizing and estimation method that considers the relationships between use cases and goals based on our previous work on goal-driven use case (GDUC) [7]–[10], in which use cases are derived based on the analysis of goals interactions. The meeting scheduler problem [4], a widely used benchmark problem domain in requirements engineering community, is adopted throughout this work as an example to illustrate the proposed approach.

The paper is organized as follows. Section 2 describes the concept of goal-driven use cases. Section 3 introduces the proposed method. Section 4 shows the results of the application of the introduced method. Section 5 concludes the paper.

II. Goal-Driven Use Cases (GDUC)

A brief summary of our goal-driven use case model [8] to construct a use case model with goals is outlined below for the readers' reference. To identify goals from domain descriptions and system requirements, we propose a faceted classification scheme so that each goal can be classified with three facets: *competence*, *view*, and *content*. The *competence* describes whether a requirement is satisfied completely or only to a degree. A *rigid* type of goal describes a minimum requirement that a target system must satisfy utterly. A *soft* goal describes properties or concerns that stakeholder care about for a target system, and can be satisfied to a degree. The *view* facet concerns whether a goal is *actor-specific* or *system-specific*. Actor-specific goals are actor's objectives in using a system; system-specific goals are requirements on services that the system provides. A goal can be further distinguished based

978-1-4244-7316-8/11/$26.00 ©2011 IEEE

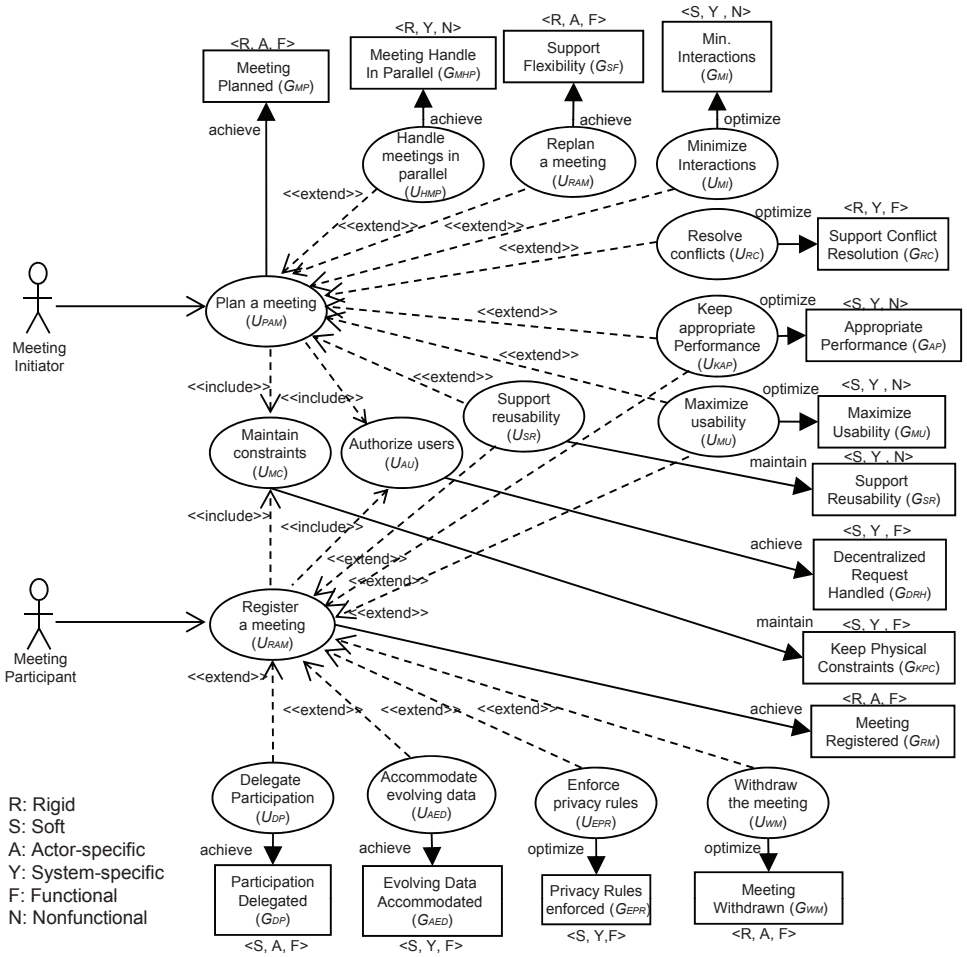

Fig. 1. Use Case Model for Meeting Scheduler System

on its *content* and can be either related to a system's *functional* aspects or associated with the system's *nonfunctional* aspect.

A goal can be achieved, optimized or maintained by its associated use case. The use cases of the meeting scheduler system are established for actors *meeting initiator* and *meeting participant* (see Figure 1). For the actor *meeting initiator*, the use case *plan a meeting* covers the scenario for an initiator to achieve an original goal *MeetingPlanned*, which is a goal of rigid, actor-specific, and functional. Meanwhile, in the case of the actor *meeting participant*, the use case *register a meeting* covers the case for a participant to achieve an original goal *MeetingRegistered*, which is a goal that is rigid, actor-specific, and functional.

To achieve a system-specific goal, an extension use case may be created. Referring to our example, the original use case *plan a meeting* describes the process to create a meeting from the view of the actor *initiator*. The extension use cases *Handle meetings in parallel* and *Resolve conflicts* extends it to take all initiators into account, that is, to achieve the system-specific goals *MeetingHandleInParallel* and *SupportConflictResolution*. The extension use cases *Accommodate evolving data* and *Enforce privacy rules* extends the original use case *Register a meeting* to achieve the soft, system-specific and functional goals *EvolvingDataAccommondated* and *PrivacyRulesEnforced*, respectively.

To achieve a nonfunctional goal, an extension use case serves as a constraint to qualify its original use case. In our example, several constraints (may be rigid or soft) on a meeting are considered as extension use cases to extend or constrain the behavior of the original use case *Plan a meeting* which is a direct course to create a meeting, including *Minimize Interactions, Keep Appropriate Performance, Support Reusability and Maximize Usability*. To enhance reusability, the use case models are further elaborated by extracting the common fragments among various use cases into an included use case by using "include" relationships. For example, the use cases *Maintain constraints* and *Authorize users*, are included by the use case *Plan a meeting* and use case *Register a meeting*.

A. Evaluate Relation from Use Case to Goal

To analyze the satisfaction values from use cases to goals, we examine the relationships among goals and use cases in a pairwise manner, which results in the satisfaction values in Use Case to Goal *U2G* matrix (see *U2G* Matrix in Figure 2).

	U_{PAM}	U_{RAM}	U_{RC}	U_{MI}	U_{HMP}	U_{AU}	U_{MC}	U_{KAP}	U_{RM}	U_{DP}	U_{AED}	U_{WM}	U_{EPR}	U_{SR}	U_{MU}
G_{MP}	5	3	1	1	1	1	1	0	0	0	0	0	0	0	0
G_{SF}	3	5	2	-1	0	0	0	0	0	0	0	0	0	0	0
G_{RC}	2	2	5	-2	0	0	0	0	0	0	0	0	0	0	0
G_{MI}	2	-1	-2	5	0	0	0	0	0	0	0	0	0	0	0
G_{MHP}	2	0	0	0	5	0	0	0	0	0	0	0	0	0	0
G_{DRH}	0	0	0	0	0	5	0	0	0	0	0	0	0	0	0
G_{KPC}	0	0	0	0	0	0	5	0	0	0	0	0	0	0	0
G_{AP}	1	0	0	0	0	0	0	5	1	0	0	0	0	-2	-1
G_{RM}	0	0	0	0	0	1	1	0	5	1	1	1	1	0	0
G_{DP}	0	0	0	0	0	0	0	0	2	5	1	0	0	0	0
G_{AED}	0	0	0	0	0	0	0	0	2	1	5	0	0	0	0
G_{WM}	0	0	0	0	0	0	0	0	2	0	0	5	0	0	0
G_{EPR}	0	0	0	0	0	0	0	0	2	0	0	0	5	0	0
G_{SR}	1	0	0	0	0	2	2	-2	1	0	0	0	0	5	-1
G_{MU}	1	0	0	0	0	0	0	-1	1	0	0	0	0	-1	5

Fig. 2. Satisfaction Values of Use Case to Goal (U2G) Matrix

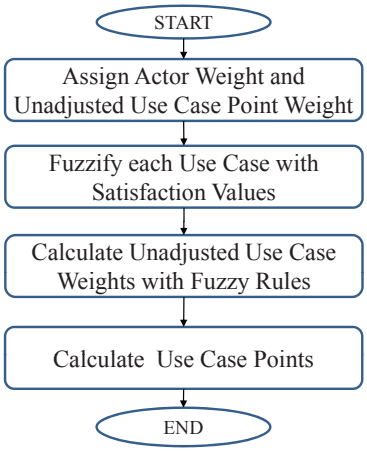

Fig. 3. Fuzzy Size Estimation Method

The gauge of satisfaction values is from 5 to -5. 5/-5 means that the goal is fully satisfied/fully denied after the use case is performed. 1/-1 means that the goal is partially satisfied/partially denied after the use case is performed. 0 means that the goal is not affected after the use cases is performed. Others represent the degrees between scores listed above. Detail explanation of the rating of satisfaction degree can be found in Table I.

TABLE I
RATINGS DEFINITION OF SATISFACTION VALUES

Score	Explanation
5	The goal is fully satisfied after the use case is performed
4	Represent the degrees between scores 5 and 3
3	The goal is largely satisfied after the use case is performed
2	Represent the degrees between scores 3 and 1
1	The goal is partially satisfied after the use case is performed
0	The goal is not affected after the use cases is performed
-1	The goal is partially denied after the use case is performed
-2	Represent the degrees between scores -1 and -3
-3	The goal is largely denied after the use case is performed
-4	Represent the degrees between scores -3 and -5
-5	The goal is fully denied after the use case is performed

For example, the effect of performing use case U_{PAM} is evaluated with respect to all goals in the system. G_{MP} is rated as 5 since performing U_{PAM} can fully satisfy the goal. G_{SF} is rated as 3 to indicate that performing U_{PAM} can largely satisfy the goal. The effect of performing use case U_{RC} with respect to goal G_{MI} is rated as -2 to show that performing U_{RC} can partially to largely deny the goal.

III. FUZZY SIZE ESTIMATION METHOD

In order to estimate the size and analyze the complexity of the goal-driven use case model, there are four steps involved in our fuzzy size estimation method (see Figure 3 for an overview). The method extends UCP method by considering the relations between use cases and goals with fuzzy theory. The details are explained below:

A. Assign Actor Weight and Unadjusted Use Case Point Weight

The unadjusted actor weights (UAW) and unadjusted use case weights (UUCW) are assigned base on UCP method with table II, III and IV [13]. Table II indicates the three actor types in UCP method. Table III and IV indicate the three use case types which are used to weight use cases based on transaction or class, respectively. The unadjusted use case weights (UUCW) is calculated by summing the weights of each use case.

TABLE II
ACTOR WEIGHTING FACTORS [13]

Actor Type	Description	Factor
Simple	Program interface	1
Average	Interactive, or protocol-driven, interface	2
Complex	Graphical interface	3

TABLE III
TRANSACTION-BASED WEIGHTING FACTORS [13]

Use Case Type	Description	Factor
Simple	3 or fewer transactions	5
Average	4 to 7 transactions	10
Complex	More than 7 transactions	15

TABLE IV
ANALYSIS CLASS-BASED WEIGHTING FACTORS [13]

Use Case Type	Description	Factor
Simple	Fewer than 5 analysis classes	5
Average	5 to 10 analysis classes	10
Complex	More than 10 analysis classes	15

B. Fuzzify each use case with satisfaction values

Since each use case satisfies each goals in different degree, *rValue*, represents the relevance from a use case to the goals of the system, can be calculated using equation 1 according to the satisfaction values in *U2G* matrix (see figure I).

U_iG_j, the satisfaction values in column i of *U2G* matrix, represents the relationships between use case U_i and the goals of the system. Equation 1 generates *rValue* of use case U_i by finding the maximum value of U_iG_j except the satisfaction value of use case U_i to its goal G_i and adding the average of the rest satisfaction values of U_iG_j where $U_iG_j \neq 0$. That is, except goal G_i of use case U_i, the satisfaction value of most complex goal of use case U_i should achieve is regarded and the average of the sum of the rest satisfaction values which are not zero is added to indicate the degree that the use case should satisfy the goals. The result generated in equation 1 denotes the relevance between use case U_i and the goals of the system.

$$rValue_i = max(|U_iG_j|) + avg(\sum |U_iG_j| - max(|U_iG_j|)) \quad \text{where } n = \#\text{ of goals}, i = 1...n, j = 1...n, i \neq j, U_iG_j \neq 0 \tag{1}$$

To allow a gradual change from one complexity category to another, we define the fuzzy input membership function *F(x)* that classify *rValue* which is between $0 \sim 10$ into five linguistic terms. (see figure 4).

$$F(x) = \begin{cases} \frac{2.5 - x}{2.5} & 0 \le x < 2.5 \quad \text{Simple} \\ \frac{x}{2.5} & 0 \le x < 2.5 \quad \text{Average} \\ \frac{5 - x}{2.5} & 2.5 \le x < 5 \quad \text{Average} \\ \frac{x - 2.5}{2.5} & 2.5 \le x < 5 \quad \text{Complex} \\ \frac{7.5 - x}{2.5} & 5 \le x < 7.5 \quad \text{Complex} \\ \frac{x - 5}{2.5} & 5 \le x < 7.5 \quad \text{Very Complex} \\ \frac{10 - x}{2.5} & 7.5 \le x < 10 \quad \text{Very Complex} \\ \frac{x - 7.5}{2.5} & 7.5 \le x < 10 \quad \text{Most Complex} \end{cases}$$

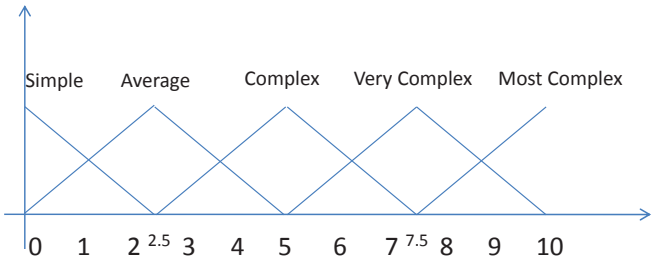

Fig. 4. The Membership Function *F(x) of* rValue

C. Calculate Unadjusted Use Case Weights with Fuzzy Rules

Table V defines the fuzzy rules with the use case types and the membership function *F(x)*. For each use case, we use min-max fuzzy inference method to match the rules with its use case types and the result of *F(rValue)*. The center of gravity defuzzification is made through the application of the rules matched with the output membership function. (see figure 5). After this, the fuzzy unadjusted use case weight (FUUCW) of each use case can be calculated.

TABLE V
FUZZY RULES

use case type / F(x)	**Simple**	**Average**	**Complex**	**Very Complex**	**Most Complex**
Simple	Simplest	Very Simple	Simple	Average	Complex
Average	Very Simple	Simple	Average	Complex	Very Complex
Complex	Simple	Average	Complex	Very Complex	Most Complex

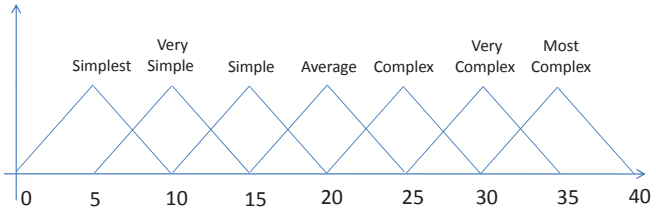

Fig. 5. The Membership Function of Fuzzy Rules

D. Calculate Use Case Points

We adopt the technical complexity factors (TCF) and environment factors (EF) [13] to take the characteristics of the system-to-be into count to generate use case points. Table VI shows the technical complexity factors which indicate the characteristics of the delivered software. The TFactor is calculated by adding all the numbers resulting from multiplying the value of each technical factors (T1-T13) by its weight.
TFactor = $\sum_i$ (*Ti* $\times$ Weight) , where i = 1,...,13
The following formula is then applied to get the TCF value:
TCF = 0.6 + (0.01 $\times$ TFactor)

TABLE VI
WEIGHTING TECHNICAL COMPLEXITY FACTORS (TCF) [13]

Factor number	Factor Description	Weight
T1	Distributed system	2
T2	Response or throughput	1
T3	End-user efficient	1
T4	Complex internal processing	1
T5	Code must be reusable	1
T6	Easy to install	0.5
T7	Easy to use	0.5
T8	Portable	2
T9	Easy to change	1
T10	Concurrent	1
T11	Includes special security feature	1
T12	Access for third parties	1
T13	Special user training facilities required	1

Table VII [13] shows the 8 environment factors which indicate the experience level of people on project. The EFactor is calculated by adding all the numbers resulting from multiplying the value of each environment factors (F1-F8) by its weight.
EFactor = $\sum_i$ (F*i* $\times$ Weight) , where i = 1,...,8

The following formula is then applied to get the EF value: EF = 1.4 + (-0.03 × EFactor).

TABLE VII
WEIGHTING ENVIRONMENT FACTOR (EF) [13]

Factor number	Factor Description	Weight
F1	Familiar with RUP	1.5
F2	Application experience	0.5
F3	OO experience	1
F4	Lead analyst capability	0.5
F5	Motivation	1
F6	Stable requirements	2
F7	Part-time workers	-1
F8	Difficult programming language	-1

The value of unadjusted use case points (UUCP) is calculated by adding unadjusted actor weights (UAW) and unadjusted use case weights (UUCW) in UCP method. In this study, we use fuzzy unadjusted use case weights (FUUCW) to replace UUCW (see equation 2).

$$UUCP = UAW + FUUCW \tag{2}$$

The use case points of the system-to-be is generated by considering the technical complexity factors and environment factors using equation 3.

$$\text{Use Case Points} = UUCP \times TCF \times EF \tag{3}$$

IV. CASE STUDY

The meeting scheduler system is used to explain how our fuzzy size estimation method be applied. The detail steps are illustrated below.

A. Step 1: Assign Actor Weight and Unadjusted Use Case Point Weight

TABLE VIII
ACTOR WEIGHTS OF MEETING SCHEDULER SYSTEM

Actor	Actor Type	UAW
Meeting Initiator	complex	3
Meeting Participant	complex	3

Table VIII represents the unadjusted actor weights (UAW) of meeting scheduler system. The total UAW is calculated as: Total UAW = 2 complex = 2 × 3 = 6

Table IX represents the unadjusted use case weights (UUCW) of meeting scheduler system. The total UUCW is calculated as:
Total UUCW = 6 simple + 6 average + 3 complex = 6 × 5 + 6 × 10 + 3 × 15 = 30 + 60 + 45 = 135

B. Step 2: Fuzzify each Use Case with satisfaction value

Taking U_{PAM} as an example, we use the satisfaction values in the first column of table 2 to calculate *rValue* of U_{PAM} below.
$rValue = max(|U_{PAM}G_j|) + avg(\sum |U_{PAM}G_j| - max(|U_{PAM}G_j|))$ where n = # of goals, j= 1...n
$= 3 + 1.5 = 4.5$

The fuzzy input membership function then takes 4.5 as input to classify the relevance of U_{PAM} to the goals of meeting scheduler system into 0.2 average and 0.8 complex (see figure 6)

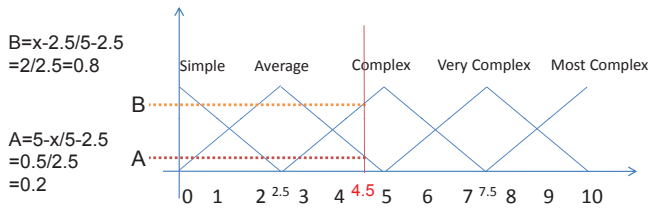

Fig. 6. U_{PAM} Example of Fuzzy Input Membership Function

C. Step 3: Calculate Unadjusted Use Case Weights with Fuzzy Rules

The fuzzy unadjusted use case weight (FUUCW) can be calculated by using center of gravity defuzzification with the output membership function of fuzzy rules. Since the complexity of U_{PAM} is complex and the results of the input membership function of *rValue* are 0.2 average and 0.8 complex, the rules matched is 0.2 complex and 0.8 very complex. We use the output membership function of fuzzy rules and center of gravity defuzzification to calculate the FUUCW which is 23.79 (see figure 7).

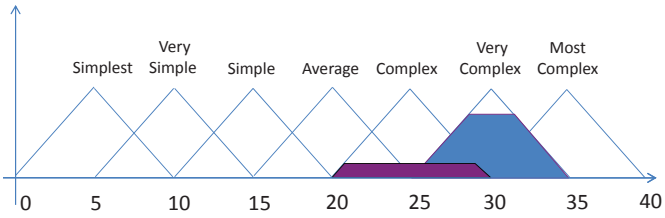

Fig. 7. U_{PAM} Example of Fuzzy Output Membership Function

Table IX represents the unadjusted use case points of meeting scheduler system.

TABLE IX
UNADJUSTED USE CASE POINTS OF MEETING SCHEDULER SYSTEM

Use Case	Use Case Type	UUCW	*rValue*	FUUCW
U_{PAM}	complex	15	4.5	23.79
U_{RAM}	simple	5	4.5	13.79
U_{RC}	complex	15	3.5	22.10
U_{MI}	average	10	3.0	16.21
U_{HMP}	simple	5	1.0	7.10
U_{AU}	average	10	3.0	16.21
U_{MC}	average	10	3.0	16.21
U_{KAP}	simple	10	3.0	16.21
U_{RM}	complex	15	3.5	22.10
U_{DP}	average	10	2.0	13.79
U_{AED}	average	10	2.0	13.79
U_{WM}	simple	5	1.0	7.10
U_{EPR}	simple	5	1.0	7.10
U_{SR}	simple	5	3.0	11.21
U_{MU}	simple	5	2.0	8.79
Total		135	40.0	215.50

D. Step 4: Calculate Use Case Points

To calculate the use case points of meeting scheduler system, we should consider TCF and EF of the system-to-be to adjust the overall complexity. Table X represents the technical complexity weights of meeting scheduler system. The TFactor is calculated as:
TFactor = 0+3+3+3+3+0.5+2.5+0+3+3+1+0+3 = 25
The TCF value is calculated as:
TCF = 0.6 + (0.01 $\times$ TFactor) = 0.6 + (0.01 $\times$ 25) = 0.85

TABLE X
TECHNICAL COMPLEXITY FACTORS OF MEETING SCHEDULER SYSTEM

Factor number	Weight	Assigned Value	Extended Value	Reason
T1	2	0	0	Not at first release
T2	1	3	3	Time response is one of the important criteria
T3	1	3	3	Needs to be efficient
T4	1	3	3	Needs to resolve conflicts
T5	1	3	3	Some code should be reused
T6	0.5	1	0.5	End users can use it through browser
T7	0.5	5	2.5	Needs to be easy for non-technical people
T8	2	0	0	Not at this time
T9	1	3	3	Yes
T10	1	3	3	Handle meeting in parallel
T11	1	1	1	Simple security
T12	1	0	0	No
T13	1	3	3	Require some training

Table XI represents the environment complexity weights of meeting scheduler system. The EFactor is calculated as:
EFactor = 3+1.5+3+2.5+5+6+0+(-1) = 20
The EF value is calculated as:
EF = 1.4 + (-0.03 $\times$ EFactor) = 1.4 + (-0.03 $\times$ 20) = 0.8

TABLE XI
ENVIRONMENT FACTORS OF MEETING SCHEDULER SYSTEM

Factor number	Weight	Assigned Value	Extended Value	Reason
F1	1.5	2	3	Some of team familiar
F2	0.5	3	1.5	Some of team familiar
F3	1	3	3	Some of team familiar
F4	0.5	5	2.5	Team is really good
F5	1	5	5	Team is really eager
F6	2	3	6	Changes may occur
F7	-1	0	0	No part-timers
F8	-1	1	-1	We are looking at Java

Calculated by the equation 3, the total use case points of meeting scheduler system = (6+215.5) $\times$ 0.85 $\times$ 0.8 = 150.62

V. CONCLUSION

This article proposes a fuzzy size estimation method of goal-driven use cases using fuzzy theory by extending the use case point analysis method with the relations between use cases and goals. We evaluate and analyze the relations from use cases to goals to generate the relevance value which can be used as inputs of the fuzzy input membership function. The fuzzy unadjusted use case weight (FUUCW) can be calculated using center of gravity defuzzification with the matched fuzzy rules and output membership function. FUUCW not only considers the internal functionality of a use case but also its relations with other use cases and goals, which indicates the complexity of each use case. The total use case points shows the overall system size by considering the technical complexity factors and environment factors of the system under consideration.

Our future research plan will focus on applying our fuzzy size estimation method in more case studies and collecting historical data in the historical database for regression analysis.

REFERENCES

[1] A. Albrecht. Measuring Application Development Productivity. In *IBM Application Development Symp.*, pages 83–92, October 1979.

[2] M. R. Braz and S. R. Vergilio. Software effort estimation based on use cases. In *Proceedings of the 30th Annual International Computer Software and Applications Conference*, pages 221–228, 2006.

[3] COSMIC. *COSMIC-FFP measurement manual - The COSMIC implementation guide for ISO/IEC 19761:2003, version 2.2.* Common Software Measurement International Consortium (COSMIC), 2003.

[4] M. S. Feather, S. Fickas, A. Finkelstein, and A. van Lamsweerde. Requirements and specifications exemplars. *Automated Software Engineering*, 4(4):419–438, October 1997.

[5] IFPUG. *Function point counting practices manual, Release 4.2*. International Function Point Users Group (IFPUG), Princeton Junction, USA, 2004.

[6] G. Karner. Resource Estimation for Objectory Projects. *Objectory Systems*, 1993.

[7] J. Lee and K.-H. Hsu. Modeling software architectures with goals in virtual university environment. *Information and Software Technology*, 44(6):361–380, April 2002.

[8] J. Lee and N.-L. Xue. Analyzing user requirements by use cases: A goal-driven approach. *IEEE Software*, 16(4):92–101, July/August 1999.

[9] J. Lee, N.-L. Xue, and J.-Y. Kuo. Structuring requirements specifications with goals. *Information and Software Technology*, 43(2):121–135, February 2001.

[10] W.-T. Lee, W.-Y. Deng, J. Lee, and S.-J. Lee. Change impact analysis with a goal-driven traceability-based approach. *International Journal of Intelligent Systems*, 25(8):878–908, August 2010.

[11] R. P. Pantoni, E. A. Mossin, and D. Brandao. Task effort fuzzy estimator for software development. *INFOCOMP Journal of Computer Science*, 7(2):84–89, 2008.

[12] K. Ribu. Estimating object-oriented software projects with use cases. Master's thesis, November 2001.

[13] G. Schneider and J. P. Winters. *Applying Use Cases: A Practical Guide (2nd Edition)*. Addison-Wesley, 2001.

[14] UKSMA. *Mk II Function Point Analysis, Counting Practices Manual, version 1.31*. United Kingdom Software Metrics Association (UKSMA), 1998.

[15] W. Xia, L. F. Capretz, D. Ho, and F. Ahmed. A new calibration for function point complexity weights. *Information and Software Technology*, 50:670–683, June 2008.

2011 IEEE International Conference on Fuzzy Systems
June 27-30, 2011, Taipei, Taiwan

Fuzzy Lymphedema Assessment based on Clinical and Functional Criteria

Patricia Vicentini
Health Informatics Department (DIS)
Universidade Federal de São Paulo (UNIFESP)
São Paulo, SP, Brazil, 04023-062
Email: patricia.vicentini@unifesp.br

M. del Carmen J. Perez
Vascular Surgery Division (DCV)
Universidade Federal de São Paulo (UNIFESP)
São Paulo, SP, Brazil, 04023–062
Email: patricia.vicentini@unifesp.br

Ernesto Araujo
Hospital Municipal Dr. José de Carvalho Florence (HMJCF)
São José dos Campos, SP, Brazil, 12243–000

Health Informatics Department (DIS)
Universidade Federal de São Paulo (UNIFESP)
São Paulo, SP, Brazil, 04023–062

Assoc. Paulista para o Desenvolvimento da Medicina (SPDM)
São Paulo, SP, Brazil, 04024–002

Email: ernesto.araujo@unifesp.br, ernesto.araujo.br@gmail.com

***Abstract*—A fuzzy lymphedema clinical and functional assessment for classifying the risk of developing and its severity is proposed in this paper. Different from the previous approach where reversibility, skin infection, and skin changes were the input variables, this new fuzzy lymphedema clinical assessment takes into account the elements that compose the Brazilian Society of Lymphology (SBL). Such a SBL-based metric not only takes into account pre-clinical cases with risk of worsening and infective-degenerative local complications but also points out functional data of limb edema with the involvement of articular joints. The proposed approach includes both clinical (Pitting, Skin Changes, Stemmer Signal and Reversibility) and functional criteria (Joint Involvement). The fuzzy lymphedema assessment based on clinical and functional criteria allows establishing therapeutic global rehabilitative programs, degree of assistance necessity of patients, and reduction of the daily living activities.**

***Index Terms*—Lymphedema, Classification, Decision Support System, Fuzzy Logic, Artificial Intelligence, Computational Intelligence**

I. Introduction

Lymphedema is a condition of localized fluid retention and tissue swelling caused by compromised lymphatic systems. Often found in the extremities of the body, lymphedema is a sort of protein-rich edema that does not cause pain to the patient. Nevertheless, it is a syndrome with high prevalence in the worldwide population. In later stages, lymphedema can be a social disease that disqualify patients in their daily functional and labor activities [1].

If, for one side, lymphedema definition and characteristics are well established, on the other side, its classification is a question that remains open. The importance of classifying lymphedema concerns recognizing such a syndrome when presenting higher chance of evolving to health complications. Further, an adequate classification allows assigning appropriate treatment and, thus, reducing the morbidity risk [2].

Most of the cases of lymphedema are diagnosed by clinical findings such as reversibility, pitting, stemmer signal, among others. Lymphedema can also be classified according to its cause as primary (congenital, precocious or late presentation) or secondary (mainly associated to inflammatory processes, cancer, neoplasy, and trauma).

The etiological classification mechanisms of lymphedema present adhesion among experts in daily practice. Classifying them, however, according to their etiological aspects can be restrained. Existing etiological–based classifications not always takes into account the severity of their clinical or functional impairment [3], [4], [5].

The severity classification mechanisms of lymphedema, on the other hand, often take into account the clinical and functional characteristics. They are recommended because play a relevant role in the elaboration of criteria for measuring the risk and the development level of lymphedema. These classifications, however, present the inconvenient of not always being accessible to all experts. They or use expensive methods such as imaging tests either are too complex in its applicability due to subjective variables that depend on the observer's viewpoint. The later aspect concerns vague, imprecise, and uncertain qualification [6].

An alternative to represent the inherent subjectivity concerning the human decision to quantify the severity of lymphedema is to use fuzzy set theory and fuzzy logic. They present great appeal in the real world, being of special interest to biosciences as confirmed by the considerable increase of medical studies related to the fuzzy logic in last decades. The literature has shown that the application of fuzzy sets has a great capacity for application to biomedical problems, due to the type of uncertainty involved in medical, biological, and epidemiological procedures. Fuzzy sets associate degrees of membership values in a subset instead a rigid yes or no decision. It also uses the partiality concept by a computationally effective way while fuzzy logic allows inference in approximate reasoning [7], [8].

The proposed approach uses the Mamdani method for representing the heuristic knowledge of experts to build the

978-1-4244-7316-8/11/$26.00 ©2011 IEEE

TABLE I
LYMPHEDEMA CLINICAL AND FUNCTIONAL SEVERITY ASSESSMENT ACCORDING TO THE BRAZILIAN SOCIETY OF LYMPHOLOGY (SBL).

Stage	Clinics
0	No edema in a risk patient
1	Edema which reduces spontaneously with anti–gravitation position, Pitting ++, Stemmer +, Involvement of at least two joints
2	Edema which do not reduce spontaneously but only with treatment, Pitting +, Stemmer +, Involvement of at least two joints
3	Edema which do not reduce spontaneously but partially only after treatment, Pitting +, Stemmer +, Involvement of at least three joints
4	Edema which do not reduce spontaneously but partially only after treatment, Pitting +, Stemmer +, Involvement of at least three joints, with skin changes

rule base of a Fuzzy Decision Support System (FDSS) to assess the clinical and functional severity of lymphedema. The proposed fuzzy system is based on the expertise obtained in the design of a previous lymphedema fuzzy system which is based on the classification adopted by World Health Organization (WHO) [9], [10]. This paper extends previous approach to the Lymphedema classification mechanism adopted by the Brazilian Society of Lymphology since it includes both clinical and functional criteria.

II. LYMPHEDEMA FUZZY DECISION SUPPORT SYSTEM

Current classification mechanisms for measuring the risk and the development level of lymphedema are accomplished by using classic (Aristotelian) set theory. According to it, the patient belongs to a set (class), or not, as exemplified in Table I. Therein are exposed the variables and criteria of classification for lymphedema clinical and functional severity assessment according to the Brazilian Society of Lymphology (SBL – Sociedade Brasileira de Linfedema). Nevertheless, it does not seem appropriate to attribute a Boolean classification for lymphedema severity since pitting, stemmer signal, reversibility (edema reduction) variables and terms as "partially" are inherently subjective, arbitrary, and dependent on the observer's viewpoint and expertise. Further, a patient can simultaneously belong to grade 1 because it has a good reversibility, but presents 3 involvement joints that characterize grade 3 or 4.

Building a decision support system as a grading system for clinical and functional lymphedema assessment by using fuzzy logic can be an interactive and flexible alternative that represents the approximate reasoning or experts in supporting and improving the process of decision making.

Note that all the figures herein are normalized in the range from 0 to 1.

A. Input Linguistic Variable

The proposed FDSS for fuzzy lymphedema assessment based on clinical and functional criteria is based on the lymphedema evaluation method as recommended by the Brazilian Society of Lymphology as presented in Table I.

Clinical signals evaluated by experts in the diagnosis of the severity of lymphedema forms the input variables of the proposed model. These are: Pitting (P), Skin Changes (C), Stemmer Signal (S), Reversibility (R), and Articular Joint, forming the Fuzzy (Skin)–Changes–Stemmer–Pitting–Reversibility–Articular–Joint Lymphedema Assessment.

1) Pitting (P):

Pitting refers to the consistency of the symptom of swelling in lymphedema. The consistency is evaluated by the palpation (touching) of the area presenting fluid retention and/or Godet signal, which consists of compression of the swollen area with the thumb. After removal of the thumb, it must be noticed the pitting. In hypertrophic, lipid, or spongy tissues, the depression caused by digital pressure disappears immediately (+++), which can characterize a soft or elastic type of swelling, for example, being defined as depressible edema. When the digital signal in the skin disappears in less than 1 minute, i.e., quickly (++); it is characterized a soft, malleable type of swelling being defined as partially depressing. Finally, but not less important, when the depression slowly disappears (+), or disappear in the range of 5 minutes or persists (0), the edema is defined as being non–depressing, also classified as hard or non-elastic type [11]. Additionally, it is important to emphasize that the soft swelling concerns better prognosis by charactering the liquid present in this type of edema as being easier treated and by associating this sort of signal as presenting a tissue of less fibrosis [5]. The pitting variable and the partition of the universe of discourse in depicted in Fig. 1. The linguistic terms are Immediately, Quickly, and Slowly, characterizing the speed in which the swelling due to the pitting is reduced.

2) Skin Changes (C):

Skin changes are factors associated to progression or regression concerning developmental stages of lymphedema. Examples are surgical or burns scars, signs of venous stasis, fissures, bumps, dermatofibrosclerosis, dermatitis, and skin ulcers and warty lesions that can be considered as gateways

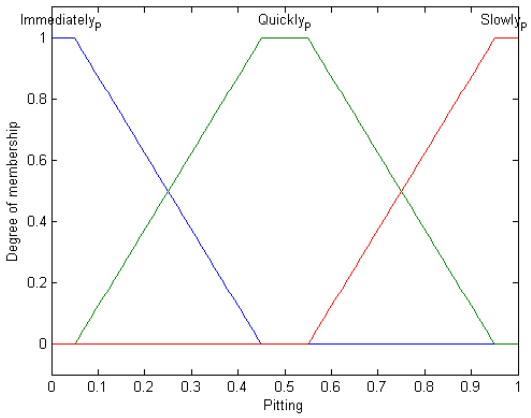

Fig. 1. Input Linguistic Variable: Pitting.

to infections. Some lesions are present and definitive while others (such as ulcers) may be transitory, making their classification still more difficult [2]. The classification of the Brazilian Society of Lymphology uses this variable to indicate greater severity, using only in the Grade 4. Clinically, it is a variable largely used for the assessment and grading the severity of lymphedema. Nevertheless, because it is a signal frequently discussed and presenting no consensus, it is difficult to determine a standard when taking into account all the current lymphedema classifications. Consequently, it brings forward a dangerous situation. The same classification term of skin changes employed by an expert can represent a complete different classification and meaning for another expert, resulting to erroneous problems in analysis, diagnosis, and treatment according to each reviewer. Further, this variable of classifications sometimes is used to quantify while others is employed to qualify the skin modifications. Due to that, this variable is also inherently subjective, arbitrary, and depends on the observer's viewpoint and expertise being able to be represented by employing fuzzy sets. The skin change variable and the partition of the universe of discourse in presented in Fig. 2 such that the linguistic terms comprise three classes of occurrence: Low, Moderate, and Intense.

3) Stemmer Signal (S):

This signal consists on skin thickening of the second toe and is obtained by the examiner when trying to do a grip of the skin from this region. In patients with lymphedema, it can be seen that there is an infiltration of the tissues, restricting an adequate grip of the skin [11]. Totally subjective and expert dependent, the universe of discourse and the fuzzy sets are shown in Fig. 3. Due to the nature of stemmer signal it is assigned only two linguistic fuzzy sets whose linguistic terms are None and Total.

4) Reversibility (R):

Reversibility is the input variable that refers to the property of edema be reverted to its previous state. Such a capacity can occur spontaneously and natural, spontaneously when elevated, or after being subjected to treatment. Some classifications only admit the possibility of edema, regardless being reversible, or not, while others stratify it based on the speed rating that lymphedema can reverse [3], [6], [10], [12], [13]. The classification recommended by the Brazilian Society of Lymphology uses the last two modes of reversibility. Moreover, the SBL classification is the only one that takes into account the treatment as a factor that boosts the reversibility speed [10] as presented in Table I. From the perspective of the variable reversibility, this classification comprises edemas that can reverse spontaneously but when in anti–gravitation position – i.e., the member put in elevate position –, featuring as Grade 1; edemas in which the swelling does not reduce spontaneously but reduces with treatment, being classified as Grade 2; and edemas in which the swelling does not reduce spontaneously but reduces partially with treatment, encompassing the Grades 3 and 4. It is worth pointing out that this classification does not contemplate the possibility of an edema does not revert. The reversibility variable and the partition of the universe of discourse in illustrated in Fig. 4 and the fuzzy sets are assigned in order to encompass the SBL requirements:

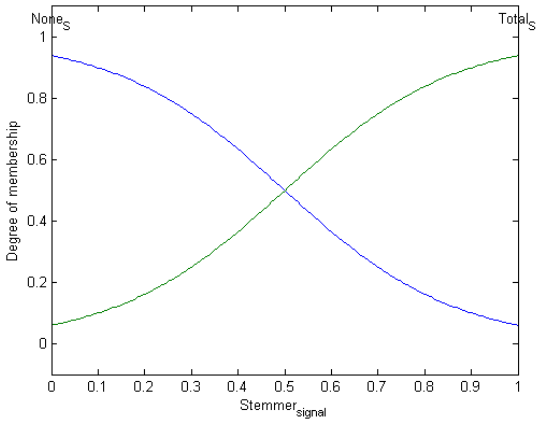

Fig. 3. Input Linguistic Variable: Stemmer Signal.

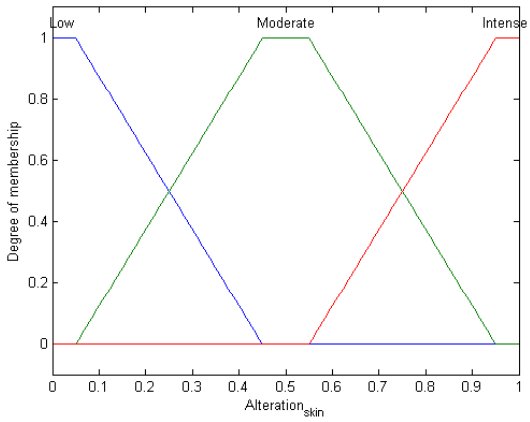

Fig. 2. Input Linguistic Variable: Skin Changes.

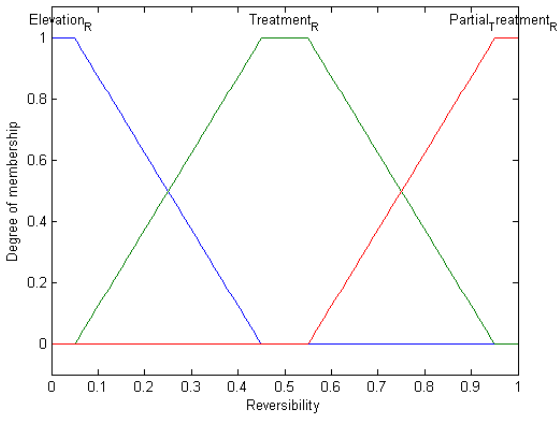

Fig. 4. Input Linguistic Variable: Reversibility.

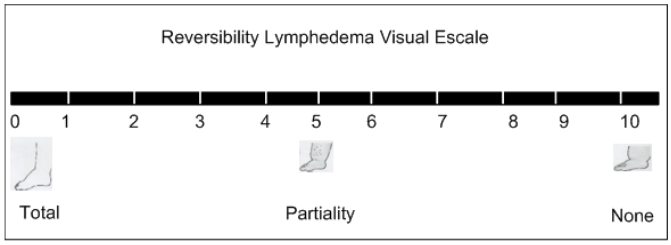

Fig. 5. Reversibility Lymphedema Visual Scale.

Elevation, Treatment, and Partial Treatment. Observe that it is considered that in all conditions the reversibility takes place. Additionally, the proposed fuzzy assessment innovate in presenting a qualitative reversibility assessment where the healthcare professional ask the patient to mark on a scale from 0 to 10 how the signal representing edema reverts (Fig. 5) according to previous approach suggested in [14]. Inspired on pain intensity scales, the proposed lymphedema reversibility scale (LRS) can deal with both singleton and fuzzy measurement following the same mechanism and understanding as presented for the fuzzy pain intensity scale in [15].

5) Articular Joint Involvement (AJI):

Articular joint involvement is a functional criterion used for evaluating the severity of Lymphedema. The articular joint involvement analysis points out functional data of limb edema when interested in dealing with big articular joint problems. According to this criterion it can evaluate only one big joint of the limb, two or the all three big articular joints. This aspect allows establishing the therapeutic global rehabilitative program, the degree of necessity of assistance of the patient, and the reduction of the daily living activities. Likewise stemmer signal, due to the nature of articular joint involvement analysis it is assigned only two linguistic fuzzy sets whose linguistic terms are Low and Total (Fig. 6).

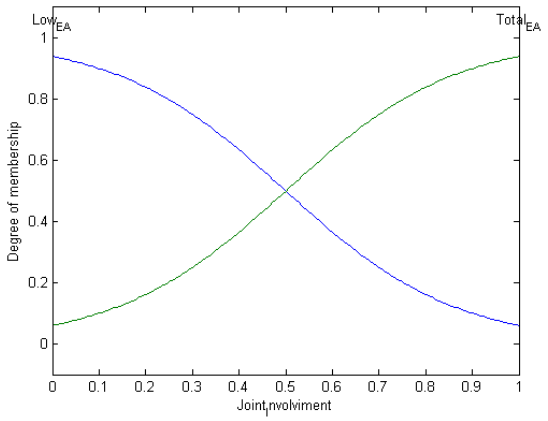

Fig. 6. Input Linguistic Variable: Articular Joint.

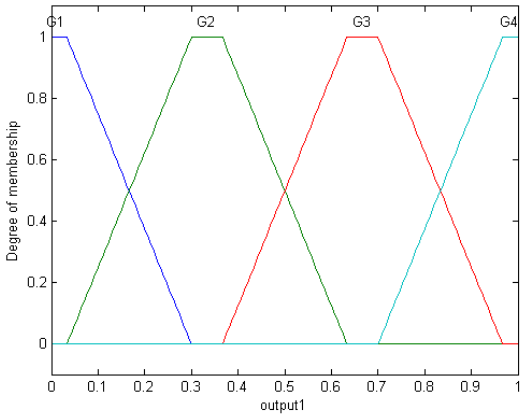

Fig. 7. Output Linguistic Variable: Lymphedema Severity.

B. Output Linguistic Variable

The outcome assessment of clinical and functional lymphedema is the severity linguistic variable. The linguistic terms that characterize the output variable are: $G1$, $G2$, $G3$ and $G4$, where $G(\cdot)$ means the grade of lymphedema severity in a discourse universe which ranges from 0 to 10 (Fig. 7). The classification of the Brazilian Society of Lymphology also uses the possibility of lymphedema presenting grade 0 that means the risk of developing lymphedema. When using the Fuzzy Lymphedema System the risk of developing lymphedema is imbedded since it can also compute the null value according to the inputs furnished to it. Further, the proposed system is able to grade the risk of developing lymphedema when the syndrome is in its initial stages.

C. Fuzzy Rules

The Mamdani fuzzy system presents its structure as a nonlinear mapping based on IF-THEN rules. Based on a review of the literature and internationally, worldwide valid classifications, the set of 3–3–3–2–2 linguistic terms that part the input universes of discourse, respectively, pitting, skin changes, stemmer signal, reversibility, and articular joint, yield a set of 89 valid fuzzy regions in a five-dimensional input space. Despite a complete 3–3–3–2–2 rule base contains 108 rules, there are rules not valid at all due to human health conditions as stated by the standard of clinical and functional criteria recommended by the Brazilian Society of Lymphology. Further, although rules could be merged in some circumstances, here they are formally separated to help enhancing transparency, mainly because there would be healthcare professionals not able to handle mathematical, logical languages.

The Fuzzy Lymphedema assessment based on clinical and functional criteria recommended by the Brazilian Society of Lymphology is, thus, represented as IF-THEN *fuzzy rules* in

the form:

$$
\begin{aligned}
\mathrm{R}_1 : \text{IF } &\langle \textit{Pitting} \text{ reduces Immediately} \rangle \text{ AND } \ldots \\
&\langle \textit{Stemmer} \text{ is None} \rangle \text{ AND } \ldots \\
&\langle \textit{Skin Changes} \text{ is Low} \rangle \text{ AND } \ldots \\
&\langle \textit{Reversibility} \text{ is Elevation} \rangle \text{ AND} \\
&\langle \textit{Articular Joint} \text{ is Low} \rangle \ldots \\
\text{THEN } &\langle \textit{Lymphedema Severity} \text{ is G1} \rangle \ , \\
\mathrm{R}_2 : \text{IF } &\langle \textit{Pitting} \text{ reduces Quickly} \rangle \text{ AND } \ldots \\
&\langle \textit{Stemmer} \text{ is None} \rangle \text{ AND } \ldots \\
&\langle \textit{Skin Changes} \text{ is Low} \rangle \text{ AND } \ldots \\
&\langle \textit{Reversibility} \text{ is Elevation} \rangle \text{ AND} \\
&\langle \textit{Articular Joint} \text{ is Low} \rangle \ldots \\
\text{THEN } &\langle \textit{Lymphedema Severity} \text{ is G1} \rangle \ , \\
&\ldots \\
\mathrm{R}_{88} : \text{IF } &\langle \textit{Pitting} \text{ reduces Quickly} \rangle \text{ AND } \ldots \\
&\langle \textit{Stemmer} \text{ is None} \rangle \text{ AND } \ldots \\
&\langle \textit{Skin Changes} \text{ is Intense} \rangle \text{ AND } \ldots \\
&\langle \textit{Reversibility} \text{ is Partial} \rangle \text{ AND} \\
&\langle \textit{Articular Joint} \text{ is Total} \rangle \ldots \\
\text{THEN } &\langle \textit{Lymphedema Severity} \text{ is G4} \rangle \ , \\
\mathrm{R}_{89} : \text{IF } &\langle \textit{Pitting} \text{ reduces Slowly} \rangle \text{ AND } \ldots \\
&\langle \textit{Stemmer} \text{ is None} \rangle \text{ AND } \ldots \\
&\langle \textit{Skin Changes} \text{ is Intense} \rangle \text{ AND } \ldots \\
&\langle \textit{Reversibility} \text{ is Partial} \rangle \text{ AND} \\
&\langle \textit{Articular Joint} \text{ is Total} \rangle \ldots \\
\text{THEN } &\langle \textit{Lymphedema Severity} \text{ is G4} \rangle \ ,
\end{aligned}
\tag{1}
$$

such that linguistic terms part the respective universes of discourse, X_k and Y and the input vector of the premise is given by $x = [x_1, x_2, x_3]^T$, while the output is associated to y.

III. Results and Discussion

At the XX International Congress of Lymphology, in a special session concerning consensus on lymphedema staging, the Brazilian Society of Lymphology proposed a classification mechanism for lymphedema [10]. This classification is, here, chosen to design a Fuzzy Decision Support System to classify the lymphedema clinical and functional severity as a comparative metric. This choice is carried out because such a SBS-based lymphedema assessment is the classification that best represents the intermediate states of the clinical and functional signals assessed by healthcare professionals.

The proposed fuzzy classification, however, advantages upon the inspired classification method by the fact that depressibility (pitting) can be graded as immediately, quickly and slowly reduced, instead of, depressing or not. Contrary to the inspired model that does not achieve the real demand in diagnosing patients porting the two concomitant intermediate possibilities, the fuzzy lymphedema assessment satisfy this demand when employing fuzzy set theory. This aspect makes fuzzy set theory effectively applied; it allows the quantitative mapping of membership degree of evaluated clinical signs and the overlapping of classes. The SBL classification allows yet that the functionality assessment be evaluated when associated to the linguistic variable articular joint involvement.

In order to demonstrate the effectiveness of the proposed fuzzy decision support system for classifying the lymphedema severity, data from literature and experts are employed. Results obtained by the comparison between the proposed method of lymphedema classification and the SBL approach is shown in Table II. Seven patients presenting diverse severity levels of lymphedema are distributed therein.

In daily practice, experts hardly face patient with lymphedema presenting the same clinical conditions. Subtle or large differences are present and the severity assessment mechanism must be able to capture these variations. For instance, when using the traditional method for classifying lymphedema, the patient can present reversibility only after treatment, thus characterizing it as grade 3 or 4, but not more than two articular joints are involved, which characterizes a grade 1. Pitting, skin changes, stemmer sign are healthcare

TABLE II
Results comparison between the Brazilian Society of Lymphology classification and the proposed model.

Pitting		Skin Changes		Stemmer Signal		Reversibility		Joint Involvement		SBL Classification	PASRIJ Classification	Severity Value
0.1	Immediately	0.1	Low	0.1	None	0.1	Limb Elevat	0.1	Low	Grade 1	Grade 1	0.15
0.1	Immediately	0.2	Low	0.3	None	0.1	Limb Elevat	0.3	Low	Grade 1	Grade 1 & 2	0.39
0.1	Immediately	0.2	Low	0.3	None	0.5	Treatment	0.3	Low	Grade 2	Grade 2	0.43
0.5	Quickly	0.9	Intense	0,6	Total	0.5	Treatment	0.5	Total	Grade 3	Grade 2 & 3	0.51
0.7	Slowly	0.6	Low	0.7	Total	0.6	Treatment	0.4	Low	Grade 3	Grade 3	0,63
0.8	Slowly	0.7	Intense	0.7	Total	0.6	Treatment	0.7	Total	Grade 3	Grade 3 & 4	0,74
0.8	Slowly	0.6	Intense	0.8	Total	0.8	Partial Treatm	0.8	Total	Grade 4	Grade 4	0,87

professional dependent. Such an inherent subjectivity in the process of staging the severity of lymphedema demonstrates vagueness and uncertainty which hampers the standardization of a classification that can be easy, simple, and widely applied. The seven patients presented in Table II feature subtle differences among the input parameters of evaluation. Observe that when the objective is to analyze classes, the results obtained with the fuzzy lymphedema system are quite similar to the method of classification used by the SBL. They barely differ except when the patient presents clinical characteristics simultaneously belonging to two classes when using the proposed fuzzy assessment. The fuzzy system allows this possibility because the classes accept the relevance of severity in different degrees being an advantage, more than a problem, mainly because the final result of evaluation can cope not only with qualitative but quantitative results.

Due to that, the proposed fuzzy lymphedema clinical and functional severity assessment not only is compatible to SBL-inspired model but carries two other important features. First, not only a class of severity is presented but there is a value, score associate to the classification allowing the value be used for objective comparative analysis and for being employed as the factor for determining the medication. Second, both qualitative and quantitative values are able to be determined by using computers or any of now–a–day available electronic devices.

It is noteworthy that this paper is a result of activities in research and development at the Hospital Municipal Dr. José de Carvalho Florense (HMJCF) and Universidade Federal de São Paulo (UNIFESP), and approved by two Committees for Research Ethics.

IV. Conclusion

The use of Fuzzy Logic becomes an alternative to stage the clinical and functional severity of lymphedema. Diagnosing and grading the diverse levels of severity of lymphedema requires dealing with diverse subjective parameters and variables that depends on the observer's viewpoint and expertise. The proposed approach turns out to be an effective tool of classification method that may cooperate with the standardization of therapeutic management of lymphedema and its classification, which is essential for the systematization of health care and decreasing morbidity in patients with high developed lymphedema.

The clinical parameters comprise pitting, skin changes, stemmer signal and reversibility whereas the functional criterion is the articular joint Involvement. The fuzzy lymphedema assessment based on clinical and functional criteria allows establishing therapeutic global rehabilitative programs, degree of assistance necessity of patients, and reduction of the daily living activities.

References

[1] M. Földi, E. Földi, and al., *Földis Textbook of Lymphology for Physicans and Lymphedema Therapists*. San Francisco: Elsevier Urban and Fisher, 2006, 2nd Ed.

[2] M. C. J. Perez, "Classificao dos linfedemas," in *Linfologia: Diagnstico, Clnica e Tratamento*, H. J. G. Neto and C. E. Q. Belczak, Eds. São Caetano do Sul, SP: Yendis Editora, 2009, pp. 77–84.

[3] *The Diagnosis and Treatment of Peripheal Lymphedema*, Internacional Society of Lymphology, 2009.

[4] A. K. Cordeiro and F. F. Baracat, "Etiologia e patogenia," in *Linfologia*, A. K. Cordeiro and F. F. Baracat, Eds. São Paulo, SP: Fundo Editorial BYK-Procienx, 1983, pp. 81–85.

[5] M. F. C. Andrade, "Linfedema: Epidemiologia, classificao e fisiopatologia," in *Doenas Vasculares Perifricas*, F. H. A. Maffei, S. Lastoria, W. B. Yoshida, H. Rollo, and et al., Eds. Rio de Janeiro, RJ: Fundo Editorial BYK-Procienx, 2002, pp. 1641–1646, 3rd Ed.

[6] B. B. Lee and J. Bergan, "New clinical and laboratory staging systems to improve management of chronic lymphedema," *Lymphology*, vol. 38, pp. 122–129, 2005.

[7] K. P. Adlassnig, "Fuzzy set theory in medicine," *International Institute for Apllied Systems Analysis*, pp. 2–17, 1984.

[8] S. M. Shamin, A. S. Enam, and U. Qidway, "Fuzzy logic in neurosurgery: predicting poor outcomes after lumbar disk surgery in 501 consecutive patients," *Surgical Neurology*, vol. 72, pp. 565–572, 2009.

[9] P. Vicentini and E. Araujo, "Lymphema severity classification by using fuzzy logic," in *Brazilian Congress of Health Informatics*. SBIS, 2010, in Portuguese.

[10] F. Boccardo, C. Campisi, A. Failla, S. Michelini, and G. Moneta, *Staging of Lymphedema: Comparing different proposals*, European Society of Lymphology, 2010, cited 2010 May 10. [Online]. Available: http://www.g-el.org/gestion_articles/show_articles.php?art_id=12

[11] J. C. Ferrandez, S. Theys, and J. Y. Bouchet, *Reeducao vascular nos edemas dos membros inferiores*. São Paulo: Manole, 2001.

[12] J. R. C. Smith, M. Földi, T. J. Ryan, and et al., "Lymphedema: Summary of the international congress of lymphology working group discussions and recommendations," *Lymphology*, vol. 18, pp. 175–55, 1985.

[13] S. Nietto, "Classificacion de linfedema," in *Congresso Latinoamericano para el tratamiento Del linfedema*, Buenos Aires, 2003.

[14] P. Vicentini and E. Araujo, "Lynphedema reversibility scale (LRS)," *Lymphology*, 2010, submitted.

[15] E. Araujo and S. A. Miyahira, "Unidimensional fuzzy pain scale," in *International Conference on Fuzzy Systems*. IEEE, 2009, pp. 185–190.

2011 IEEE International Conference on Fuzzy Systems
June 27-30, 2011, Taipei, Taiwan

Decision Making Based on Reinforcement Learning and Emotion Learning for Social Behavior

Atsushi Matsuda*, Hideaki Misawa* and Keiichi Horio*
*Graduate School of Life Science and Systems Engineering
Kyushu Institute of Technology,
2-4 Hibikino, Wakamatsu, Kitakyushu 808-0196 Japan
Email:{matsuda-atsushi, misawa-hideaki}@edu.brain.kyutech.ac.jp, horio@brain.kyutech.ac.jp

***Abstract*—In this paper, we propose a decision making method based on reinforcement learning and emotion learning (DRE) for inducing social behaviors of robots. Emotion of animals has an important role in their social interactions. We attempt to incorporate emotion into decision making of robots. To make a social decision making, the DRE combines a decision based on intrinsic fear emotion with a strategic decision obtained by reinforcement learning. Agents with the DRE learn state values by reinforcement learning and learn emotion values by fear emotion learning. In simulation experiments, the effectiveness of the DRE is verified concerning the emergence of social behaviors and the adaptability to an environmental change through an unmoving target search problem.**

***Keywords*—decision making; reinforcement learning; emotion; fear emotion learning; social behavior**

I. Introduction

Robot technologies have been under rapid development during recent years. Robots are expected as a new labor force in the coming aging society with fewer children and are expected to work with humans in our daily life. Nursing-care and medical robots have been developed and some of them have already worked instead of humans [1]. In this situation, robots are required to coexist and cooperate with humans.

Emotion of animals determines whether or not their feelings are pleasure from their own experience and situation at the time. This ability is very important for animals to decide their actions such as approaching or avoidance action. Furthermore, emotion has an important role in social interaction between animals which have the sociality like humans. The influence of emotion on decision making has been investigated in neuro-physiological and neuropsychological studies [2], [3]. Emotion is now attracting attention as the ability to enhance robots' sociality [4], [5]. Currently, most of robotics studies regarding emotion employ emotion for expressing the internal states of robots when the robots interact with humans (e.g., [6]). To realize robots with sociality, we consider that emotion should be incorporated into decision making of robots.

In this paper, we propose a Decision making method based on Reinforcement learning and Emotion learning (DRE) for inducing social behaviors and for realizing robots with sociality. The DRE combines a decision based on intrinsic fear emotion with a strategic decision obtained by reinforcement learning. Reinforcement learning has been successfully used as an action learning method in the field of robotics to make decision and take actions based on the experience of robots [7]. Fear emotions are involved with avoidance behaviors of animals. In simulation experiments, the effectiveness of the DRE is investigated through an unmoving target search problem. We confirm the emergence of social behaviors and the adaptability of agents with DRE to an environmental change.

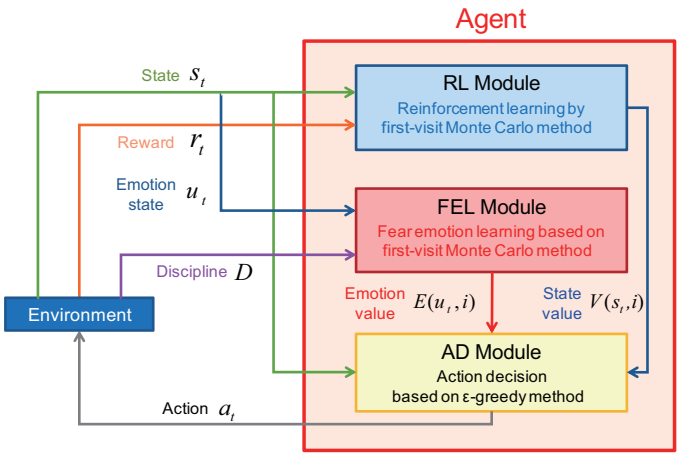

Fig. 1. Agent with DRE. The DRE comprises three modules: reinforcement learning (RL) module, fear emotion learning (FEL) module and action decision (AD) module.

II. DRE

In this research, an unmoving target search problem is considered. The task of agents is to reach one of the targets first within a limit of time steps. In addition to this task, the agents are disciplined when some conditions are met. However, they do not know this condition, that is, why they are disciplined. This is considered as fear emotional experience for the agents. The agents need to take in account not only achieving the task but also avoiding disciplines. In this paper, the condition of disciplines is that the agents do not perform social behaviors. Under this situation, the emergence of social behaviors is investigated. Social behaviors defined in this research are described in the next section.

The architecture of an agent with DRE is shown in Fig. 1. The DRE consists of three modules: reinforcement learning (RL) module, fear emotion learning (FEL) module and action decision (AD) module. Agents with DRE learn state values by

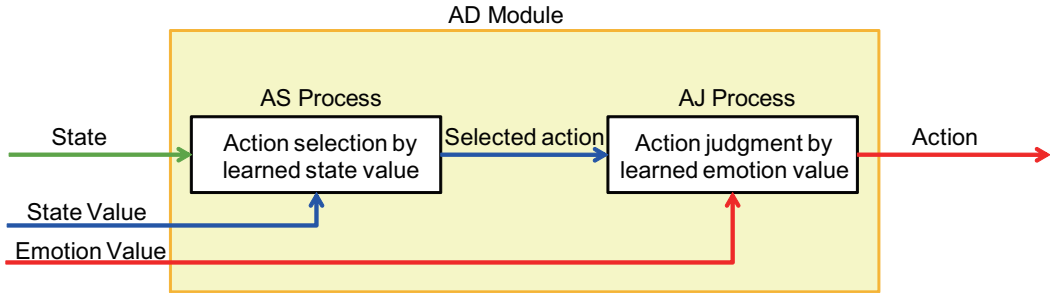

Fig. 2. Action decision (AD) module. The AD module has two processes: action-selection (AS) process and action-judgment (AJ) process.

reinforcement learning in the RL module and learn emotion values by fear emotion learning in the FEL module. In the AD module, the agents decide their actions based on both state and emotion values. These modules are described in detail below.

A. RL module

Reinforcement learning is an unsupervised learning method of machine learning. In reinforcement learning, agents can learn adequate actions to complete tasks by trial and error in interaction with an environment [7]. This learning is achieved by maximizing the cumulative rewards from the environment.

In the DRE, a basic Monte Carlo method is used for learning actions of agents to complete tasks. Actions are selected by using state values. In the RL module, the first-visit MC method is employed, that is, a state value in the position of an agent is updated only once even if the agent visits the position twice.

If an agent can reach the targets at time step t' in the i-th episode, a return R (a positive constant) is given to the agent and state values $V(s_t, i)(t = 1, 2, \ldots, t')$ are updated by

$$V(s_t, i+1) = V(s_t, i) + \alpha \cdot (r_t - V(s_t, i)), \qquad (1)$$

where t, s_t and α are time step, state and learning rate, respectively.

The discount return r_t for the state s_t is given by

$$r_t = \gamma^{t'-t} \cdot R, \qquad (2)$$

where γ is a discount rate. On the other hand, if the agents cannot reach the targets in the i-th episode, all the state values decay with a decay rate η as follows.

$$V(s, i+1) = \eta \cdot V(s, i) \quad \forall\ s. \qquad (3)$$

B. FEL module

Emotion of animals induces their feelings and affects their action selection. Recent researches in brain science show that the amygdala of cerebral limbic system processes fear emotions and plays an important role for the survival of animals [8]. Fear emotions are involved with avoidance behaviors of animals such as avoiding natural enemies and areas where they previously suffered fear experience. The concept of fear emotion is used as emotion in this paper.

The agents decide their actions based not only on the strategic judgment obtained by reinforcement learning but also on their intrinsic fear emotion. Namely, the agents select their behaviors using both state and emotion values. An emotion value is defined for an emotion state u_t. Th emotion state u_t represents the situation inducing disciplines (e.g., the combination of the agents' positions). In the FEL module, the first-visit MC method is also employed. If the agents are disciplined at time step t^* in the i-th episode, the emotion values $E(u_t, i)$ $(t = 1, 2, \ldots, t^*)$ are updated by the following equation.

$$E(u_t, i+1) = \zeta^{t^*-t} \cdot \{E(u_t, i) + \alpha' \cdot (D - E(u_t, i))\}, \qquad (4)$$

where ζ, α' and D are a discount rate, learning rate and discipline value (a negative constant) given at time step t^*, respectively. To enhance the latest emotion experience, the emotion values of the emotion states that are not updated in this episode decay with a decay rate β as follows.

$$E(u, i+1) = \beta \cdot E(u, i) \quad \text{for} \quad u \notin U_i, \qquad (5)$$

where U_i is a set of the emotion states experienced in the ith episode. If the agents are not disciplined in ith episode, the emotion values $E(u, i)$ are updated by

$$E(u, i+1) = E(u, i) \quad \forall\ u. \qquad (6)$$

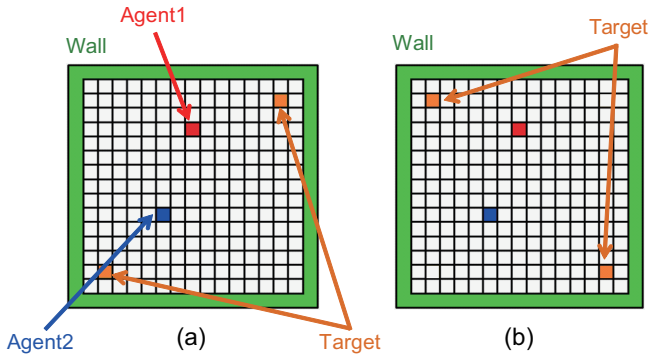

Fig. 3. Discrete grid field (15×15 cells). Each cell corresponds to a state in the DRE. (a) Target positions in the first experiment. (b) Target position after 1000th episode in the second experiment.

C. AD module

Fig. 2 shows the action decision process of the agents. The AD module has two processes: action-selection (AS) process

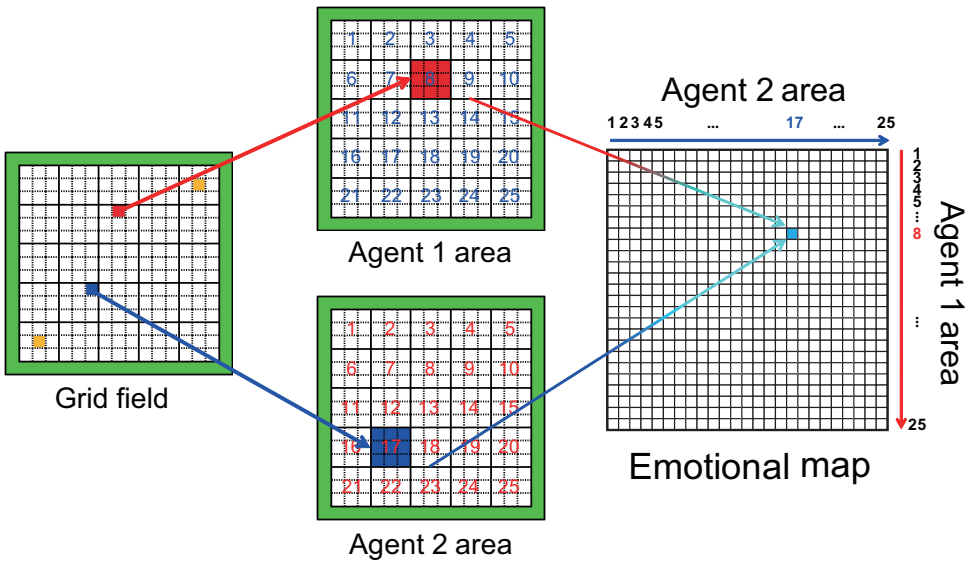

Fig. 4. Agent areas and emotion states. The grid field is separated into 25 (5×5) areas. An emotion state in the DRE corresponds to a combination of one agent area and the other agent area.

and action-judgment (AJ) process. The ε-greedy strategy is employed in the both processes. In the AS process, an action is randomly selected at probability ε_s (random selection) and is selected based on the state values at probability $1-\varepsilon_s$ (greedy selection). In the greedy selection, the agent selects an action to move to a state with the highest state value around them. In the AJ process, the action selected in the AS process is decided as the next action at probability ε_e (state-value judgment) and the next action is decided based on the emotion values at probability $1-\varepsilon_e$ (emotion-value judgment). In the emotion-value judgment, the agents select an action that the agents can approach a state with the highest emotion value around them. In other words, an action is randomly selected at probability $\varepsilon_s \cdot \varepsilon_e$, greedily at probability $(1-\varepsilon_s)\cdot\varepsilon_e$ and emotionally at probability $1-\varepsilon_e$.

III. Simulation Experiments

We conducted simulation experiments to verify the effectiveness of the DRE concerning the emergence of social behaviors and the adaptability to an environmental change.

Experimental setting

Two agents and two unmoving targets in a discrete grid field (15×15 cells) were used as shown in Fig. 3(a). The agents can observe and reach the targets if the targets are in the cells next to the agents. The task of the agents is to reach one of the targets first within a limit of time steps T_L. If the agent completes this task, a return R is given to the agent. A state s used in the RL module corresponds to a cell.

In this paper, "cooperative behaviors" that the agents reach the different targets, were defined as social behaviors. The agents were disciplined if they did not achieve the cooperative behaviors within the time limit T_L. Furthermore, if the agents collided with each other at an episode, they were disciplined and the episode was terminated. To achieve the cooperative behaviors, the agents need to take in account not only achieving the task but also avoiding disciplines.

An emotion state u used in the FEL module was defined as a combination of one agent area and the other agent area. An agent area was comprised of 3×3 cells. Thus, the grid field was separated into 25 (5×5) areas as shown in Fig. 4. Each agent can sense the area where the other agent is. Emotion map was comprised of 625 (25×25) emotion states that were all possible combinations of the agent areas (Fig. 4). The reason of using not the cells but the areas is that animals may avoid not a point but a rough area around the point if they previously suffered fear experience at the point.

The agents can move in the field by selecting one of actions: up, down, right and left. In the greedy selection of the AS process, the agents select an action that the agents can move to a cell with the highest state value around them. In the emotion-value judgment of the AJ process, the agents select an action that the agents can approach an area with the highest emotion value around them.

In the following experiments, agents with DRE were compared with agents with RL and agents with cooperative behavior learning (CL). In the rest of this section, we represent agent with DRE, agent with RL and agent with CL as DRE agent, RL agent and CL agent, respectively.

The RL agents have the RL and AD modules. State values of the RL agents were learned by the first-visit MC method. Only the parameter ε_s was used in the AD module of the RL agents. The RL agent was identical to the DRE agent with $\varepsilon_e = 1$. If the agents collided with each other at an episode, the episode was terminated. The effectiveness of the emotion-value judgment was investigated by the comparison between the DRE agents and RL agents.

The CL agents have the RL and AD modules. State values

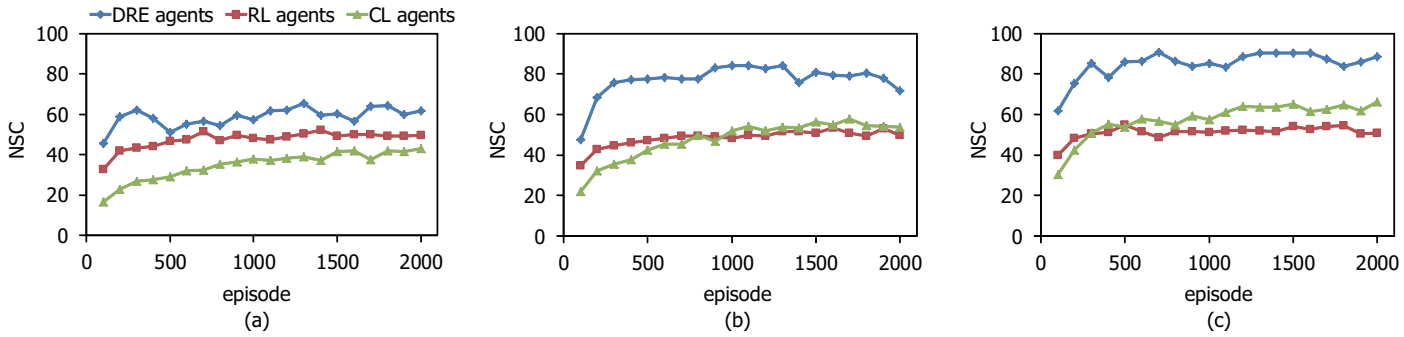

Fig. 5. Number of successful cooperative behaviors (NSC) in the first experiment. The limits of time steps T_L were (a) 30, (b) 40, and (c) 50 steps, respectively.

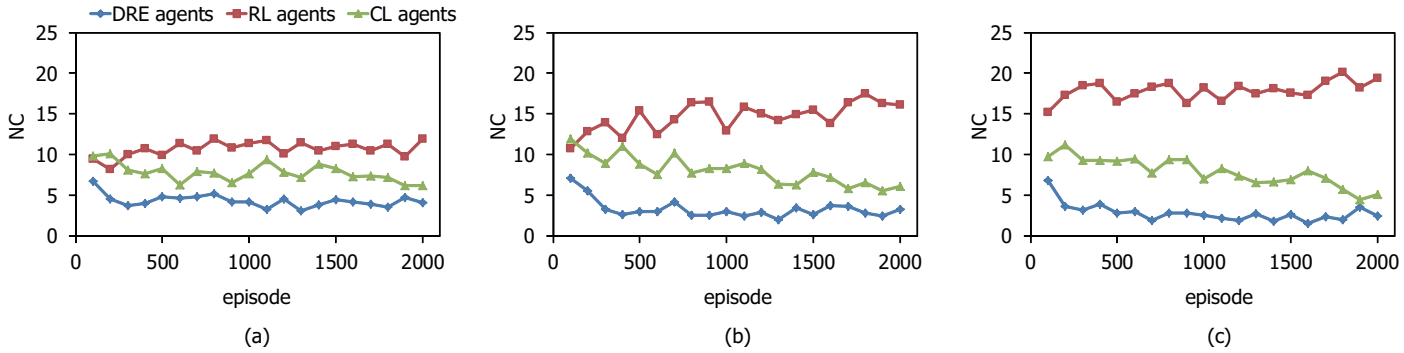

Fig. 6. Number of collisions (NC) in the first experiment. The limits of time steps T_L were (a) 30, (b) 40, and (c) 50 steps, respectively.

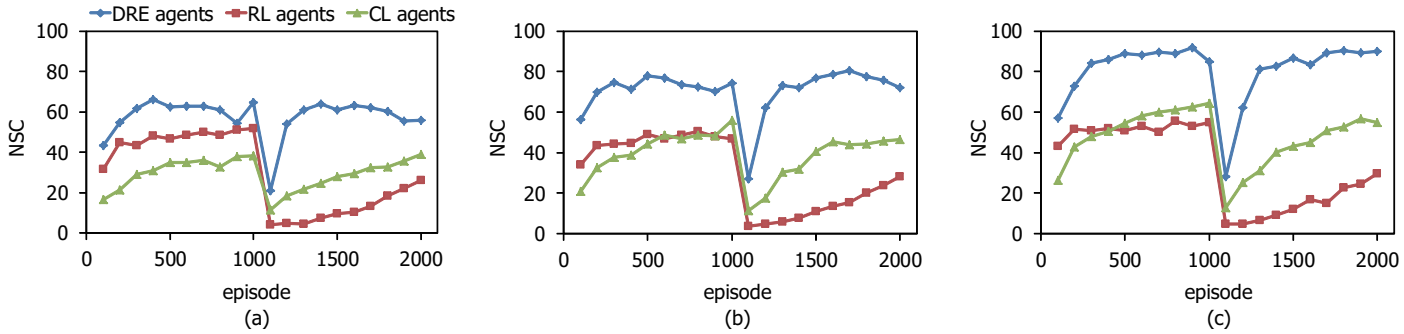

Fig. 7. The number of successful cooperative behaviors (NSC) in the second experiment. The positions of targets were changed after the 1000th episode. The limits of time steps T_L were (a) 30, (b) 40, and (c) 50 steps, respectively.

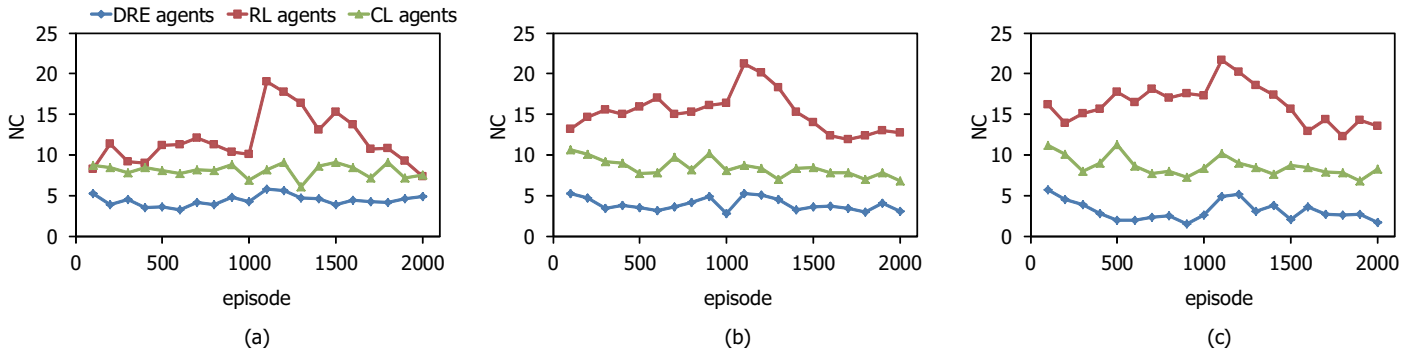

Fig. 8. The number of collisions (NC) in the second experiment. The positions of targets were changed after the 1000th episode. The limits of time steps T_L were (a) 30, (b) 40, and (c) 50 steps, respectively.

of the CL agents were learned by the first-visit MC method. Unlike the DRE and RL agents, a state of the CL agents was defined as a combination of one agent's cell and the other agent's cell. A positive return R was given to the CL agents if they achieved the cooperative behaviors and a negative return D if they did not. Therefore, the task of the CL agents is to achieve the cooperative behaviors. Only the parameter ε_s was used in the AD module of the CL agents. If the agents collided with each other at an episode, the negative return D was given to the CL agents and the episode was terminated. The effectiveness of the separation of RL and FEL was investigated by the comparison between the DRE agents and CL agents.

In the experiments, the parameters were set as follows; $\varepsilon_s = 0.1, \varepsilon_e = 0.1, R = 10, \alpha = 0.1, \gamma = 0.95, \eta = 0.99, D = -10, \alpha' = 0.9, \beta = 0.9$ and $\zeta = 0.5$. At the beginning of each episode, the positions of the agents were randomly assigned. The state and emotion values were set to zero at the beginning of the first episode. Two thousand episodes were defined as one trial. During trial, the number of successful cooperative behaviors (NSC) and the number of collisions (NC) were counted every 100 steps.

Experiment 1: Emergence of cooperative behavior

The first experiment was conducted to confirm the emergence of cooperative behaviors by using the emotion values. Figs. 5(a), (b) and (c) show the NSCs when T_L was 30, 40 and 50, respectively. The results presented in Fig. 5 are the average values of the NSC over ten trials. The NSC of the DRE agents increased with episodes and was more than those of the RL and CL agents. The NSC of the DRE and CL agents increased as T_L increased. The NSC of the RL agents converged around fifty. The RL agents approached the nearest target from their initial positions and the cooperative behaviors occurred by chance since the RL agents were not intended for the cooperative behavior. The NSC of the CL agent increased with episodes but was less than that of the DRE agents. This was because the number of the states of the CL agents was 50,625 (225×225) and was more than that of the DRE agents. The number of episodes may be insufficient to learn the whole of the state values of the CL agents although the CL agents were intended for the cooperative behavior. The DRE agents were not directly intended for the cooperative behavior. However, the first priority was given to the emotional judgment in the AJ process and this resulted in the emergence of the cooperative behavior.

Figs. 6(a), (b) and (c) show the NCs when T_L was 30, 40 and 50, respectively. The results presented in Fig. 6 are the average values of the NC over ten trials. The NC of the DRE agents was less than that of the RL agents. This was because the DRE agents were disciplined and the RL agents were not when the agents collided with each other. The NC of the CL agents was more than that of the DRE agents due to the enormous number of states although the CL agents were also disciplined when the collision occurred.

We confirmed that the cooperative behaviors (social behaviors) emerged in the DRE agents through this experiment.

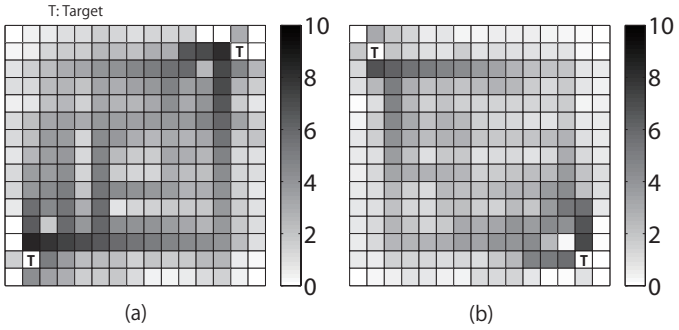

Fig. 9. State values of one of the DRE agents in a run of the second experiment with $T_L = 40$. (a) After 1000th episode. (b) After 2000th episode.

Experiment 2: Adaptation to environmental change

The second experiment was conducted to examine the adaptability of the DRE agents to an environmental change. As an environmental change, the positions of target were changed from those shown in Fig. 3(a) to those shown in Fig. 3(b) after the 1000th episode.

Figs. 7(a), (b) and (c) show the NSCs in the second experiment when T_L was 30, 40 and 50, respectively. Figs. 8(a), (b) and (c) show the NCs in the second experiment when T_L was 30, 40 and 50, respectively. The results presented in Fig. 7 an Fig. 8 are the average values over ten trials. The NSCs of all the agents remarkably decreased just after the environmental change. The NSC of the DRE agents rapidly rose with episodes even after the environmental change. Figs. 9(a) and (b) show the state values of one of the DRE agents after the 1000th episode and the 2000th episode in a run of the second experiment with $T_L = 40$, respectively. As can be seen from Fig. 9, the state values were high around the targets. Figs. 10(a) and (b) show the emotion values of the DRE agents after the 1000th episode and the 2000th episode in a run of the second experiment with $T_L = 40$, respectively. Each panel shows the emotion values on the agent 2 areas (5×5) where the number and star symbol indicate the agent 1 area. Each panel corresponds to one row in the emotion map shown in Fig. 4. From the panel 16 in Figs. 10(a) and (b), it is seen that the DRE agents were frequently disciplined due to the collisions when the both agents were in area 16 before and after the environmental change. On the other hand, from the panel 20 in in Figs. 10(a) and (b), it is considered that the DRE agents were disciplined due to the unsuccessful cooperative behaviors. The emotion values were less dependent on the positions of targets than the state values. Therefore, the DRE agents could utilize some of the emotional values learned before the environmental change. The NSC of the RL agents slowly increased with episodes after the environmental change since the state values have a high dependency on the positions of the targets. Thus, the RL agents needed to learn the state values again. The NSC of the CL agents gradually rose with episodes after the environmental change but was less than that of the DRE agents due to the enormous number of states.

The NC of the RL agents rapidly increased just after the

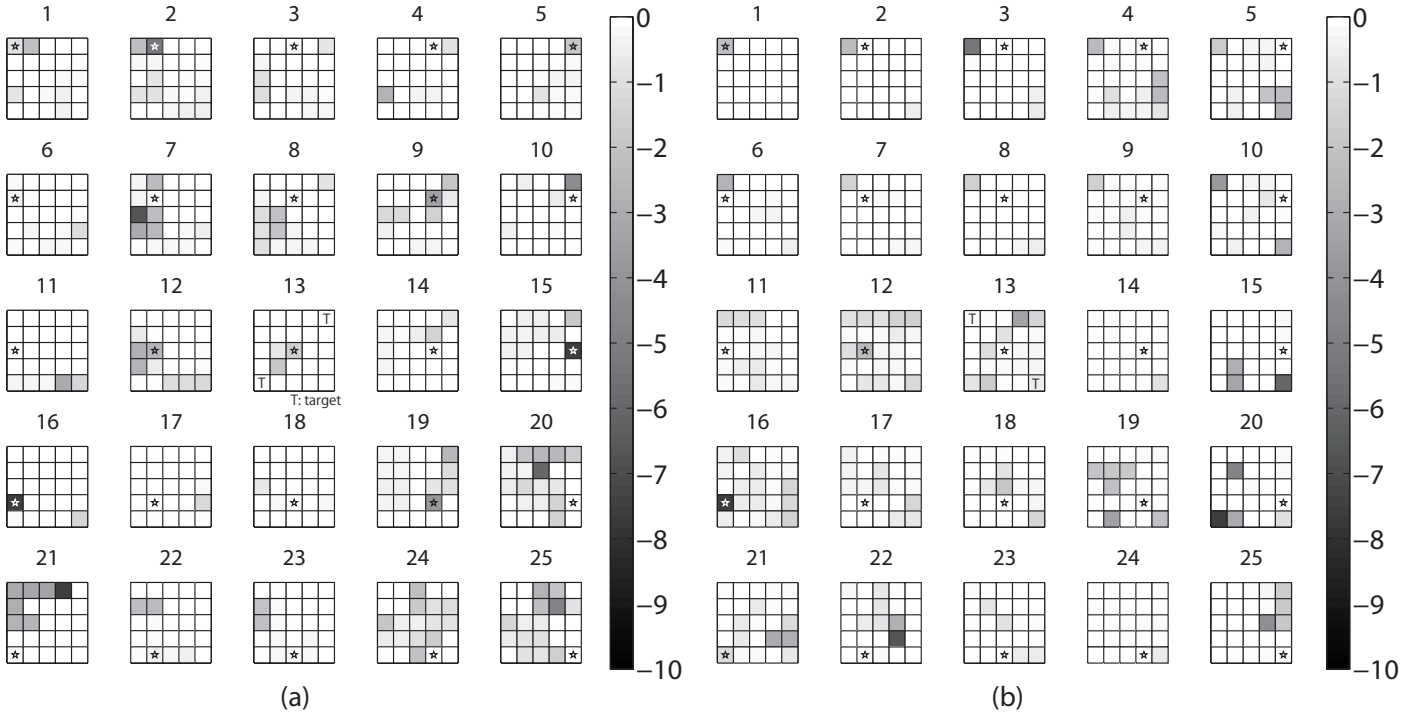

Fig. 10. Emotion values of the DRE agents in a run of the second experiment $T_L = 40$. (a) After 1000th episode. (b) After 2000th episode. Each panel shows the emotion values on the agent 2 areas (5×5) where the number and star symbol indicate the agent 1 area. The areas where the targets exit are shown as T in the panel 13.

environmental change. The state values of the RL agents were in the transition from those for the previous environment to those for the current environment at that time. This led to the increase of the NC. The NCs of the DRE and CL agents slightly increased after the environmental change.

The results of the NSC and NC suggest that the DRE agents have a high adaptability to the environmental change.

IV. Conclusion

In this paper, we proposed the DRE for inducing social behaviors of agents. In the DRE, the agents decide their actions based not only on the strategic judgment obtained by reinforcement learning but also on their intrinsic fear emotion. In the simulation experiments, we confirmed that the agents with the DRE took actions for realizing the social behaviors and adapted to the environmental change. In a future work, we will investigate the effects of the parameters ε_s and ε_e in the AD module on the emergence of social behaviors.

References

[1] Y. Bar-Cohen and D. Hanson, *The Coming Robot Revolution : Expectations and Fears About Emerging Intelligent, Human like Machines*, New York:Springer-Verlag, 2009.

[2] G. Coricelli, R. Dolan and A. Sirigu, "Brain, emotion and decision making: the paradigmatic example of regret," *Trends in cognitive sciences*, Vol. 11, No. 6, pp. 258–265, 2007.

[3] N. Naqvi, B. Shiv and A. Bechara, "The Role of Emotion in Decision Making," *Current directions in psychological science*, Vol. 15, No. 5, pp. 260–264, 2006.

[4] S. Gadanhon and J.Hallam, "Robot learning Driven by Emotions," *Adaptive Behavior*, Vol. 9, No. 1, pp. 42–64, 2002.

[5] M. Arbib and J. Fellous, "Emotions: from brain to robot," *Trends in cognitive sciences*, Vol. 8, No. 12, pp. 554–561, 2004.

[6] S. Sonoh, K. Horio, S. Aou and T.Yamakawa, "An Emotional Expression Model Inspired by the Amygdala," *International Journal of Innovative Computing, Information and Control*, Vol. 5, No. 5, pp. 1147–1160, 2009.

[7] R. S. Sutton and A. G. Barto, *Reinforcement Learning: An Introduction*, Cambridge, MA:MIT Press, 1998.

[8] M. Davis, "The role of the amygdala in fear and anxiety," *Annual Reviews of Neuroscience*, Vol. 15, pp. 353–375, 1992.

2011 IEEE International Conference on Fuzzy Systems
June 27-30, 2011, Taipei, Taiwan

Analysis of Relationship between Characteristics of Driver's Eye Movements and Visual Scene in Driving Events

Tetsuya MIYOSHI
Faculty of Business and Informatics
Toyohashi Sozo University
Toyohashi, Japan
miyoshi@sozo.ac.jp

Hidetoshi Nakayasu
Faculty of Intelligence and Informatics
Konan University
Kobe, JAPAN
nakayasu@konan-u.ac.jp

Abstract— **It has been reported in many papers that the number of eye movements increases and the mean fixation durations on individual objects decreases when the road situation becomes more complex. In this paper eye-movement analysis has been used for understanding the mechanism of visual search of drivers. For the aim, two experiments in which the subjects drove the driving simulators have been conducted. We analyzed the relationship between the eye movement of drivers and the characteristics of their front scenes while driving in driving conditions. In the first experiment it was confirmed that the frequency of saccade became higher and fixation time became shorter in case of the turn event condition among three driving events, where the pixel difference extracted as the visual information from the driver's front scene became larger. In the second experiment the same relationship between the characteristics of eye movements and the driver's front scenes were confirmed by considering the three driving events, running straight, turning corners at a crossing and prediction task of hazard in the urban course. The pixel difference of the driver's front scene influenced the eye movements while driving. These results of experiments about driver's cognitive processing while driving suggested that eye movements depends on the amount of information contained in the front scene defined by the pixel difference.**

Keywords—**Visual perception of driver, eye movement, useful field of vision, visual attention, safety engineering**

I. INTRODUCTION

Driving is such a complex task that the drivers must control steering, accurate level, display of going direction by signals every moment based on the configuration around own car, simultaneously. The driving environment has become more complex as the cars increases on the road and also amount of structures as the traffic signs, the eye-catching shop front and advertising billboards are constructed along the road. Then, the drivers visual environment has become more complex [1][2]. In such the complex and restless driving environment, lack of visual attention to the situation of their own car and the other cars causes traffic accidents or crashes. Therefore, the driver must concentrate on the driving task. Keeping the visual attention for the driving environments high level required the resource of the cognitive perception and recognition for the visual information processing. For example, the driving performance suffered during cell phone and remote passenger conversations as compared with in-car passenger conversations [3]. Since the conversation by the cell phone makes the driver's driving performance decrease and thereby causes the traffic accident, the use of cell phone while driving is prohibited by the law in Japan. A high complex environment on the road is congested with the cars or pedestrians, demands the more cognitive resources for the visual processing in order to keep the car safe.

The eye movements are generated so as to gather the visual information about the driving environment. Informative regions of a scene are fixated for significantly longer than less informative regions [4]. In general, the frequency of saccade and mean fixation durations provide a good measure of the visual attention. Increasing the complexity of the visual scene (by adding vehicles, road furniture, or irrelevant signing), increases the frequency of eye movements and decreases the mean fixation durations on individual objects while driving[5][6][7][8][9]. However, when the driving situations become more dangerous, the presence of a hazard in the scene causes a focusing of attention such that the fixation duration increase, saccade lengths decrease, the spread of search reduces[10]. The policy of visual information processing while driving is different according to the driving situation in order to avoid the traffic accident or risk[11].

A driver must process much visual information while driving a car. For the driving task they gather the meaning visual information of environment by the eye movement. Since the fixation duration and the frequency of saccade which characterize the eye movement depend on the visual scene of driving situation, the eye movement is function of visual scene. Although a lot of factors to effect the eye movement as experience of driving[12], driving situation, the visual scene cause the eye movement in this paper, therefore, it is assumed that the drivers eye movements was a function of visual stimuli of the driver.

In this paper we investigate the characteristics of the eye movements of driver while driving with regard to the driving events and analyze the relationship between the characteristics of eye movements and the peripheral vision. For the aim of present research the eye movements of drivers are measured

978-1-4244-7316-8/11/$26.00 ©2011 IEEE

(1) A view of driving simulator

(2) A front image of cabin of driving simulator

Figure 1. Driving simulator((DA-DOO: HONDA Motor Co. Ltd.))

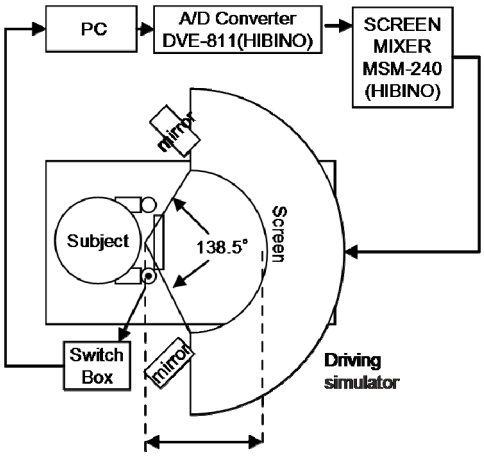

Figure 2. Diagram of DS and devices

Figure 3. Driver wearing eye tracking system in driving simulator

using the driving simulator and the driver's front view on their peripheral vision are recorded. The mean fixation duration and the frequency of saccade of eye movements were summarized as the characteristics in the period of driving events and the difference of the driver's front view were calculated as the index of complexity of the driving task. We attempt to identify the underlying reasons for change of the policy of eye movements according to the driving configuration, such as going straight, turning corner etc., while driving.

This paper is organized as follows: Section 2 describes the experimental methods and equipments, and the configuration of the two experiments. Section 3 describes the results of two experiments about the eye movements and the front view of drivers, and shows the relationship between the eye movement and the front view of drivers. Lastly the final conclusions are presented in Section 4.

II. Experimental Method

A. *Expeimental Equipments*

(1)Driving simulator

The automobile driving simulator (DA-D1102: HONDA Motor Co. Ltd.) was used to simulate a driving work. Fig. 1 shows the driving simulator used in this study. This simulator is usually used for driver trainees or novices to learn safe driving techniques. The simulator is implemented on an advanced 6-axis motion base (sway-motion device) that can simulate closely automobile dynamics in real traffic situations, and visual scenes of driving a road from a viewpoint of the driver is presented on a front screen and three mirror-CRTs. The driver's front view is illustrated in Fig.1 (b). A distance from the front screen to the driver's seat is 1511mm. The front screen is wide and curved so as to surround the driver, and then the driver's visual field is covered by the front screen as shown in Fig.1 (b). The configurations of the driver in the simulator are illustrated in Fig. 2. Using the driving simulator, the driver can drive several kind of driving courses with varying in some kinds of automobile conditions, such as weather and car and human actions (e.g., dashing out in front of a driver's automobile). In this driving simulator two driving modes are selected, the automatic transmission changing mode and the manual transmission changing mode. The automatic mode was used since the driver must concentrate the visual stimuli while driving in the experiments.

(2) Eye movement tracker

During simulated driving, eye movements of the driver and driving road scene were recorded by a head-mounted eye tracking system (EyeLink II: SR Research Ltd., see also Fig. 3). Two eye cameras track right and left eyes respectively. A scene camera on a head band records visual scene that the participant views. In a scene camera either a color or high resolution black and white scene camera is used to generate 30

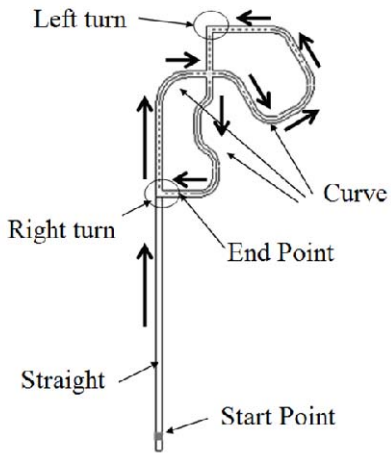

(1) course used in the first experiments

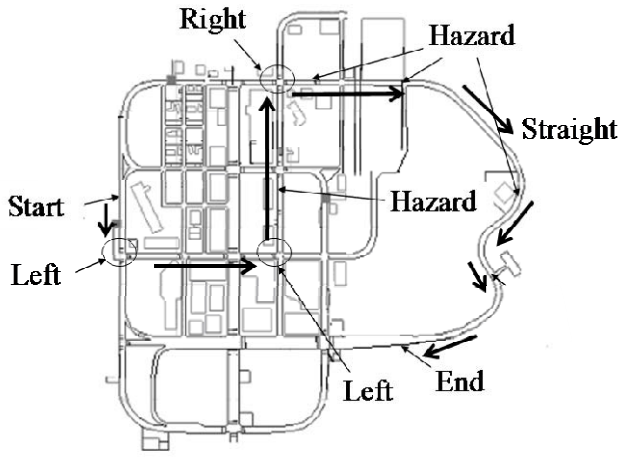

(2) course used in the second experiments

Figure 4 Driving course of driving simulator in first experience.

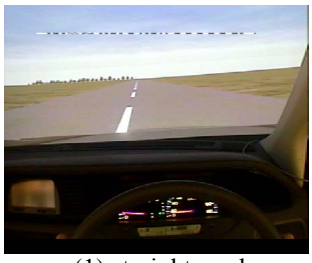

(1) straight road

(2) curve

(3) crossing

Figure 5 Example screenshot of driving simulator in first experiment.

frames (60 fields) of a scene image per second. The scene image is also streamed to the overlay box, by which participants' gaze position (indicated by a fulfilled circle) is superimposed with the visual scene. The host PC converts gaze position data, obtained by the eye cameras, into position data on the visual scene image captured by the head mounted scene camera. The host PC also analyzes eye movement events in real-time.

B. Participants

Participants were five males, who were 22 aged students of the university. All the participants have regular class automobile licenses in Japan with normal or corrected-to-normal vision. All the participants were given enough explanation for the present experiments and gave informed consents to the experiments before participation. The participants were instructed through a practical lesson and verbal instruction as the driving lessons in the driving simulator.

C. Driving Scene in two experiments

In this paper two experiments with different driving configurations using the driving simulator were conducted in order to investigate the visual information strategy of drivers while driving. The driving configurations of two experiments are changed in the view point of the simplicity of driving scenery and driving velocity so as that the visual task required while driving would be the different level in two experiments.

In the first experiment the driving configuration is set to the situation of driving in a suburb of the city, where there is only road in a wide field without any buildings and traffic facilities, such as shops, traffic equipments and so on. The condition of weather is set to a clear and fine day. The abstract of driving course is shown in Fig. 4(1), in which there are the straight road, curve, and the crossing. The front views in these driving conditions are simple or monotonous sceneries as shown in Fig. 5. In the rural roads situation there are few stationary objects and no moving objects. e.g., no cars and no pedestrians appear on the driving course. In this configuration the drivers see the only road and a distant view as the front scene while driving. Therefore, it is seemed that the cognitive work load of a driver was set relatively lower level in the first experiment since all the driver has to do are only to concentrate the road situation for driving safety.

In the second experiment the driving configuration was set to the situation of driving in the city (urban) on a sunshine day. The visual scenes of drivers on urban roads were more complex or complicated than on the rural ones. The abstract of driving course of the second experiment is shown in Fig.

(1)Merging to the main road

(2) Car sudden-out(Hazard)

(3) Door of truck opens

(4) Turning at the crossing

Figure 6 Example screenshot of the front visual scene during second experiment.

i th frame

i+1 frame

(1) two front scenes in *i* th and *i*+1 th frame

(2) residual of pixel of front scenes

Figure 7. Residual picture of driver's front scene while driving

4(2) and the front views in these driving conditions are shown in Fig. 6. In this configuration, the pedestrians, the buildings and shop front located along the road and the traffic equipments such as the traffic signs and signal. The moves of other cars and the pedestrians keep step based on the driving scenario in the driving scenes. This driving simulator contains a risk awareness program that is designed to take participants through a route containing several hazards such as children crossing the road and unexpected door open of a parking car. The driving course used in the second experiment contains two hazards, unexpected door open of a parking trailer and sudden crossing of a car as shown in Fig. 4(2). The front view scenes of the second experiment are shown in Fig. 7. The driving environments of the second experiment fall into three categories, normal (driving on a straight road), turn event (turning at crossing and joining to the main road), and hazard event (door open and car sudden-out).

Mentioned above, it was seemed that the cognitive visual resources were required more in the second experiment than in the first experiment since the driver's visual tasks while driving were loaded more in the second experiment. For keeping safety drivers not only have to pay attention the other cars and pedestrians movement consciously, but also have to predict the likely driving events as the pedestrians rush out into the road and the front car suddenly stop every time. In the second experiment the objects and the driving events to be particularly concerned are set as a driving scenario.

D. Procedure

Participants drove the predetermined courses on the DA-D1102 driving simulator wearing the eye tracking camera (see Fig. 3). After calibration of the eye tracking system they were seated at the simulator and asked to adjust the seat. The participants were instructed to drive the predetermined course as they would do normally and follow the traffic regulations.

In the first experiment the participants drove the course in a suburb of the city at the predetermined speeds, 30 km/h or 60 km/h. Since it was difficult to turn the corner in the crossing at the predetermined speed, they were instructed to reduce the car speed so as to turn the corner well in the crossing. Although the driving speed was not kept at predetermined speed, the driver had to be encouraged to speed up the car to the predetermined speed 30 km/h or 60 km/h in the driving course. Therefore, it was seemed that the driver's cognitive mental workload while driving at 60 km/h is larger than at 30 km/h.

The iteration number of trials was three in each speed condition for each participant. In a trial at the predetermined speed a driver drove the course three times. After calibration of the eye tracker the participants drove the predetermined course three times at 30km/h speed condition, and then did it three times at 60km/h speed condition. The next trial was performed after the intervals of several minutes as a rest and last trial was done with same procedure. While the driving experiments using the driving simulator eye movements of the participants were measured and the front view of them were recorded in digital video. The characteristics of eye movement such as the saccade and fixation were extracted from the recorded eye movement data after the all trials were completed.

In the second experiment the participants were asked to drive the simulator on the predetermined course with the current of the other car. The iteration number of trials was three. In a trial they drove once around the course as shown in Fig. 4(b). The task to keep the predetermined speed was not imposed to them since it is difficult to keep the fixed velocity due to a lot of

TABLE I. SAMPLES OF TIME SEQUENT OF EVENT PERIOD (SUBJECT A)

(1) Time sequence of an event period in an experiment 1.

(sec)

Event	period		Event	period	
	30km/h	*60km/h*		*30km/h*	*60km/h*
Straight	45.69	24.12	Straight	11.74	6.90
Curve	11.98	5.67	Curve	10.85	5.61
Straight	3.91	2.54	Straight	4.30	2.53
Curve	5.44	2.80	Curve	6.27	2.70
Straight	3.48	2.40	Straight	4.37	2.34
Curve	18.09	10.27	Curve	21.19	10.31
Straight	4.12	2.71	Straight	4.94	3.01
Curve	5.80	2.30	Curve	5.91	2.50
Straight	9.08	4.90	Straight	8.91	5.51
Turn(Left)	2.94	6.59	Turn(Left)	4.44	3.95
Straight	9.51	4.22	Straight	9.32	4.06
Curve	24.83	15.38	Curve	25.85	14.85
Straight	3.67	2.81	Straight	3.40	2.54
Turn(Right)	3.74	3.87	Total	273.77	157.39

(2) Time sequence of an event period in an experiment 2.

(sec)

Event		Event	
Straight	15.42	Straight	5.85
Turn(Right)	6.00	Hazard	6.00
Straight	12.85	Straight	6.71
Turn(Right)	6.00	Hazard	6.00
Straight	13.59	Turn(Right)	6.00
Turn(Left)	6.00	Straight	14.63
		Total	105.05

events. In the second experiment the driving. The participants were same with ones of the first experiment, but the second experiments were carried out on the different day with the first experiment because of the fatigue of participants.

E. Extract of charactoristics of eye movement and front view while driving

In these experiments eye movements of drivers were measured while driving in two road conditions. For considering the relationship between the eye movements and the peripheral vision, the characteristics of eye movements and peripheral vision should be extracted from the eye movement data and driver's frontal scene during the experiments. Generally speaking, the frequency of saccade and mean fixation durations provide a good measure of the visual attention. The frequency of saccade and mean fixation duration were extracted as an eye movement property in each period according to the driving events.

The difference of gray levels between two pictures represents the edge of objects. In Fig.7 shows the two consecutive frame images and the picture representing the gray level difference of them. The increase of the gray level difference means that the number of objects in the visual scene increases and the complexity of the visual scene for the driver becomes higher level. This index for the complexity of the front scene of a driver was defined using the difference of the front picture, and the relationship between this index and driver's eye movements are discussed through the results of experiments. The visual information of the front scene was quantified based on the pixel change of them. The i -th quantity of the pixel change of the picture is defined by the difference of pixel-value between i -th frame image and (i+1)-the frame image included in the front view. In the total quantity of the difference of each frame included in a period of driving event is calculated by summation of the difference value in each frame. This total gray level difference of frame image was defined as the characteristics of the front scene in the period according to the driving task.

In the first experiment three categories of driving events, running straightly on the course, running curve along course and turning the corner at the crossing, were considered as the task seemed to be required the different cognitive level. The characteristics of the eye movements and the front scene of drivers were calculated in case of the periods according to the three categories about driving tasks in two speed condition, 30 km/h and 60 km/h. In the second experiment, the periods of three driving categories, operation of running straightly, operation of turning the corner in the crossing and hazard prediction event, were determined in the driving course. The driving task periods of the turning operation and hazard prediction were set to 6 sec, 3sec before the event and 3sec after the event. The start time and end time of period was determined so as to center the driving event on the middle of the period.

III. EXPERIMENTAL RESULS

A. Time period of driving evets

The frequency of saccades and mean fixation duration were recorded as the characteristics of eye movements of drivers while driving. For the aim to investigate the eye movement while driving in relation to the front scene, the driving scenes were categorized into three driving events. Thus, the segments of the driving were determined so that these measures were summarized in three kinds of driving events according to the three road situations. The examples of time sequent of the events and the period time are shown in TABLE I. The time sequence of driving events was different between the subjects because of the difference of the car speed of each subject, and also the driving event periods were different with ones of other subjects.

In the first experiment the whole course was divided into three categories and the start and end times of the period corresponding to the three driving events were identified in each trial by analyzing the recorded front scene video. An example of the event period was one in the first trial driving of subject A which was shown in TABLE I (a). The total time for driving the course in 30km/h and 60km/h was 273.77sec and 157.39sec, respectively. 7 straight road events, 10 curvature events and 3 turning events were contained in the one driving trial. The driving trials were repeated three times. The average

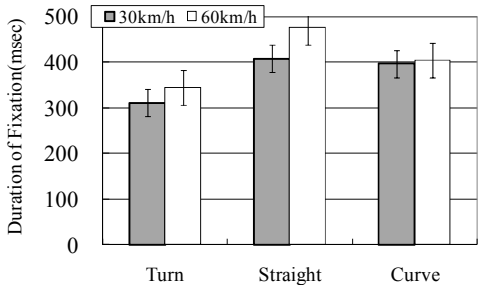

Figure 8. Mean fixation duration in first experiment.

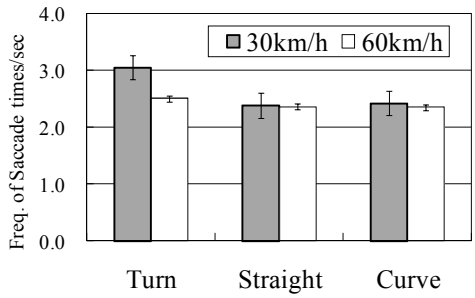

Figure 9. Frequency of saccade in first experiment.

of the frequency of saccades and mean fixation duration during the same events were summarized in each subject.

In the second experiment the driving event periods were also identified by analyzing the scene video, running straight, turning at a crossing, and prediction of hazard. The period time of the turning operation and prediction of hazard was fixed as 6sec. The example of the driving task period in the second experiment is shown in TABLE I (b).

B. Results of first experiment

(1) Eye movement while driving events

The eye movements of five subjects were recorded while driving in the suburb course in the first experiment. The characteristics of eye movements in three driving events, straight event, curve event and turn event, were summarized as the results of eye movements. The mean fixation duration and the frequency of the saccade in each driving event are illustrated in Fig.8 and Fig.9, respectively. The mean fixation duration in left or right turning at a crossing was shortest among the three events, and the one in driving on the straight road was longest in both 30km/h and 60 km/h conditions. While, the frequency of saccade in left or right turning at a crossing is highest and one while driving at a straight road is lowest. The same tendency of eye movements while the driving events was similar to the result of the subjects.

The results of one way ANOVA with respect to the traffic event conditions are shown in TABLE II (1) and (2). For the mean fixation duration, the significant main effects of the driving events were detected in four subjects expect "subject E" in 60km/h speed condition. For the frequency of saccade, the significant main effects of the traffic events were detected in four subjects expect "subject E" in both speed conditions.

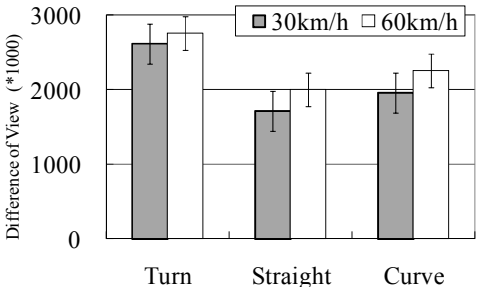

Figure 10. Difference of front view of drivers in first experiment.

TABLE II. RESULTS OF ANOVA FOR EYE MOVEMENT WITH RESPECT TO TRAFFIC EVENTS.

(1) Results of ANOVA for the duration of fixation.

subject	30km/h		60km/h	
	$F(2,78)$ value	p value	$F(2,78)$ value	p value
A	4.84	0.01*	3.99	0.022*
B	1.83	0.16	4.54	0.013*
C	2.69	0.074	4.05	0.002*
D	1.95	0.14	4.95	0.009*
E	0.22	0.79	0.17	0.83

note : * means that the significant effect is detected

(2) Results of ANOVA for the frequency of saccade.

subject	30km/h		60km/h	
	$F(2,78)$ value	p value	$F(2,78)$ value	p value
A	21.5	<0.0001*	3.99	0.018*
B	5.53	0.0056*	4.54	<0.001*
C	6.9	0.0017*	4.05	0.0069*
D	5.65	0.005*	4.95	0.0057*
E	1.33	0.26	0.17	0.28

note : * means that the significant effect is detected

(2) Pixel difference of front scene as index of complexity

In this paper the complexity of the visual scene were defined by the ever-changing front view of driver as shown in Fig. 7. The increase of the gray level difference means that the number of objects in the visual scene increases and the complexity of the visual scene for the driver became higher level. The gray level difference of the front scene of subjects during the experiment were calculated and summarized in each traffic event as shown in Fig. 10. The average of the gray level difference of the front scene during the period of each traffic event is illustrated. The gray level difference in turning at the crossing is larger than one in the other events, driving on the straight road or curvature. The same tendency of front scene while the driving events as each other is confirmed in each result of the subjects.

(3) Comparison between characteristics of eye movement and the complexity of front view

For considering the relationship between eye movement and the front scene, the correlation coefficients between the

TABLE III. CORRELATION BETWEEN CARACTORISTICS OF EYE MOVEMENTS AND DIFFERENCE OF PICTU IN FIRST EXPERIMENT.

Subject	trial	30km/h		60km/h	
		Fixation duration.	Frequency Sac.	Fixation duration.	Frequency Sac.
Sub-A	1	-0.376	0.762	-0.359	0.579
	2	-0.445	0.689	-0.224	0.403
	3	-0.506	0.39	-0.240	0.18
Sub-B	1	-0.230	0.291	-0.205	0.359
	2	-0.205	0.224	-0.461	0.633
	3	-0.323	0.427	-0.385	0.515
Sub-C	1	-0.137	0.057	-0.273	0.389
	2	-0.438	0.655	-0.096	0.216
	3	-0.260	0.292	-0.128	0.087
Sub-D	1	-0.397	0.548	-0.491	0.682
	2	-0.202	0.346	-0.462	0.669
	3	-0.227	0.402	-0.076	0.155
Sub-E	1	-0.174	0.066	-0.523	0.512
	2	-0.009	0.235	-0.471	0.607
	3	-0.303	0.141	-0.130	0.041

difference of pictures and gazing time, times of saccade were calculated as shown in TABLE III. Even though there exits the variance the positive correlation between the frequency of saccade and the difference of front scene and the negative correlation between the mean fixation duration and the difference were detected for all subjects. These results suggest that the change of peripheral vision influences the visual information processing while driving and consequently causes the quick and instantaneous eye movements, and also, this busy eye movements were required to compensate the lack of visual information to keep the vehicle safe.

C. Results of second experiment

(1) Eye movement while driving events

In the second experiment the eye movements of five subjects were recorded while driving in the city course, in which several events were prepared containing the two hazard events provided by the risk awareness program of the driving simulator. The analyzing periods were defined with three categories, normal (driving on a straight road), turn event (turning at a crossing and merging to the main road), and prediction event of hazard (door open and car sudden-out). The characteristics of eye movements in three driving events were summarized as the results of eye movements. The mean fixation duration and the frequency of the saccade while each driving event are illustrated in Fig.11 and Fig.12, respectively. The ANOVA of frequency of saccadic eye movement and fixation time while the driving with respect to the driving events were conducted ant significant effect were confirmed as shown in TABLE VI.

(2) Pixel difference of front scene as index of complexity

The gray level difference of the front view of subjects during the experiment were calculated and summarized in each traffic event as shown in Fig. 13. The average of the gray level difference of the front view during the period of each traffic event is illustrated. The mean fixation duration became longer in order to “Straight”, “Turn”, and “Hazard”. The frequency of

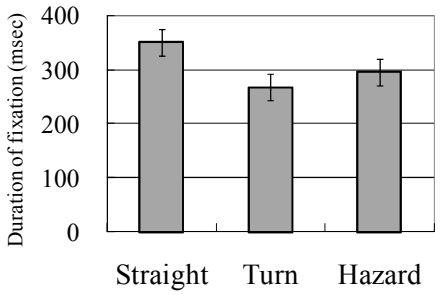

Figure 11. Mean fixation duration in second experiment.

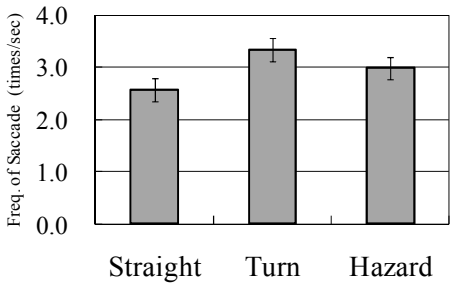

Figure 12. Frequency of saccade in second experiment.

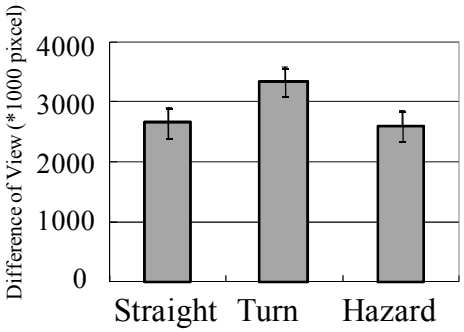

Figure 13. Difference of front view of drivers in second experiment.

saccade and the difference of the view became larger in the reverse order. The gray level difference in the turn event is larger than one in the other events.

(3) Comparison between characteristics of eye movement and the complexity of front view

It was confirmed that the relationship between the eye movements and background view also existed in case of the drive of the city course except the hazard situation. In the hazard situation the relationship between them were different with one in the normal driving situation since the eye movement was caused by the different mechanism. The correlation coefficient between the two kinds of characteristics of eye movements and the front scenes were shown in TABLE V. I a lot of driving trials the correlation between them were confirmed

D. Discussion

In general, the frequency of saccade becomes higher and the duration of fixation became longer in the more complicated

situation so as to get more information from environment. However, the saccadic movements are required frequently so as to get the information around own car for avoiding the accidents, therefore, the fixation duration of drivers became shorter [5][6][8]. Considering these results about characteristics of eye movements while driving in the first experiment, the results of the first experiments suggested that the complexity of the front views in the three traffic events were different, and the traffic events effected the eye movement of drivers. In other words, the results of the first experimented that the driving operation on the straight or curve road was an easier task for the driver than the one on the turning operation at the crossing since the frequency of saccade became smaller and the duration of fixation became longer.

In the second experiment, the differences of the properties of eye movements among the driving events were not detected significantly by the ANOVA as shown in TABLE IV. The correlation between the characteristics of eye movements and the front scene was confirmed as shown in TABLE V. It was reported as "focusing of attention" that the mean fixation duration became longer than the normal situation in the hazard situation [3]. Thus, since the hazard situation required the more visual resources to keep safe or occupied the visual attention, the relationship between eye movements and the front scene was not detected in the hazard situation.

TABLE IV. RESULTS OF ANOVA FOR EYE MOVEMENT TO DRIVING EVENTS.

subject	Duration of Fixation		Frequency of Saccade	
	F(2,78) value	p value	F(2,78) value	p value
A	2.93	0.060	5.62	0.008*
B	2.41	0.100	2.28	0.110
C	4.56	0.093	6.65	0.004*
D	2.55	0.38	4.49	0.013*
E	0.97	0.0001*	2.01	0.140

note : * means that the significant effect is detected

TABLE V. CORRELATION BETWEEN CHARACTERISTICS OF EYE MOVEMENTS AND DIFFERENCE OF PICTU IN SECOND FIRST EXPERIMENT.

Subject	trial	Fixation duration	Frequency Saccade
Sub-A	1	-0.544	0.549
	2	-0.623	0.731
	3	-0.579	0.57
Sub-B	1	-0.370	0.229
	2	-0.508	0.61
	3	-0.238	0.119
Sub-C	1	0.306	-0.255
	2	-0.605	0.674
	3	-0.458	0.537
Sub-D	1	-0.568	0.554
	2	-0.503	0.571
	3	-0.617	0.692
Sub-E	1	-0.466	0.524
	2	-0.842	0.887
	3	-0.585	0.705

IV. CONCLUSION AND FUTUREWORK

In this paper, the two driving experiments were conducted on the course in rural area and urban area, in which the driving events, such as running straightly or turning at the crossing, were contained. The different amount of cognitive resources of drivers was required according to the driving events to keep the car safe in these experiments. After driving experiments, the characteristics of eye movements and the driver's front scene corresponding to the driving events were extracted from the eye movement data and the recorded video. The present study illustrated the relationship between the characteristics of eye movements and the front scene. The larger became the frequency of eye movements, the larger became the extracted characteristics of the scene video in two experiments. These results suggested that when the index defined by the difference of pixel in the front scene became larger, the eye movement might be generated more frequently.

In this paper the characteristics of the front scene were simply defined by the difference of pixel contained in it. It is the future work to consider the index of their attention in relation to the eye movements.

REFERENCES

[1] B. Wallace, "Driver distraction by advertising: genuine risk or urban myth?," Municipal Eng. vol.156, pp. 185–190, 2003.

[2] D. Crundall, E.V. Loon and G. Underwood, "Attraction and distraction of attention with roadside advertisements," Accident Analysis & Prevention, vol. 38, Issue 4, pp.671-677, 2006.

[3] S. G. Charlton, "Driving while conversing: Cell phones that distract and passengers who react," Accident Analysis & Prevention, vol. 41, Issue 1, January 2009, pp.160-173, (http://www.sciencedirect.com/ science/ article/B6V5S-4TWSRPC-2/2/7628c7da43d7483686f95216df 65db3f)

[4] J.R.Antes, "The time course of picture viewing," Journal of Experimental Psychology, vol. 103, no.1, pp.62-70, 1974.

[5] T. Miura, "Visual search in intersections — An underlying mechanism," IATSS RESEARCH, vol. 16, no.1, pp.42-49,1992.

[6] P. Chapman and G. Underwood, "Visual search of driving situations: Danger and experience," Perception, vol. 27, pp. 951-964, 1998.

[7] P. Miltenburg and M. Kuiken, "The effects of driving experience on visual search strategies : Results of a laboratory experiment" , Haren, the Netherlands : Traffic research centre, University of Groningen , 1990.

[8] D.Crundall, B.Andrews, E.van Loon and, P.Chapman, "Commentary training improves responsiveness to hazards in a driving simulator," Accid Anal Prev.vol. 42, no.6, pp.2117-24, 2010.

[9] D. Crundall, G. Underwood and P. Chapman, "Attending to the peripheral world while driving," Appl. Cognit. Psychol., pp.459-475, 2002.

[10] D. Crundall, G. Underwood and P. Chapman,"Eye movements during intentional car following," Perception, vol.33, no.8, pp.975-986, 2004.

[11] P. Chapman, D. Crundall, N. Phelps and G. Underwood : Police drivers ' visual search in hazardous situations, Behavioral Research in Road Safety:12th seminar, 57-67, 2002.

[12] P.Konstantopoulos, P.Chapman and D.Crundall, "Driver's visual attention as a function of driving experience and visibility. Using a driving simulator to explore drivers' eye movements in day, night and rain driving," Accid Anal Prev. vol.42, no.3, pp.827-834, 2010

2011 IEEE International Conference on Fuzzy Systems
June 27-30, 2011, Taipei, Taiwan

Directional Control of an Omnidirectional Walker for Walking Support with Forearm Pressures

Yinlai Jiang
School of Systems Engineering
Kochi University of Technology
Kochi, Japan
jiang.yinlai@kochi-tech.ac.jp

Shuoyu Wang
School of Systems Engineering
Kochi University of Technology
Kochi, Japan
wang.shuoyu@kochi-tech.ac.jp

Kenji Ishida
Department of Physical Medicine and Rehabilitation
Kochi University
Kochi, Japan
ishidake@kochi-u.ac.jp

Takeshi Ando, Masakatsu G. Fujie
Department of Modern Mechanical Engineering
Waseda University
Tokyo, Japan
ando@aoni.waseda.jp, mgfujie@waseda.jp

***Abstract*— Walking is a fundamental human ability necessary for everyday life. We have developed an omnidirectional walker (ODW) for walking support to those who have walking disabilities. It is necessary for the ODW to know which direction the user is intending to go during walking support. A novel interface is proposed for the ODW to recognize directional intention according to the user's forearm pressures which are measured by force sensors embedded in the armrest. The relationship between forearm pressures and directional intention was extracted as fuzzy rules and an algorithm is proposed for directional intention identification based on distance type fuzzy reasoning method. In this paper, we conduct walking support experiments with the proposed method. The results show that the algorithm is applicable to directional control in walking support.**

Keywords- walking support; omnidirectional walker; directional intention identification; distance type fuzzy reasoning method

I. INTRODUCTION

There are many people with walking disabilities due to either age or accidents. Therefore, the development of walking machines that can efficiently conduct walking rehabilitation and walking support is highly desirable. In previous studies, the authors along with colleagues have developed an omnidirectional walker (ODW) [1][2]. This walker allows omnidirectional movement. In walking rehabilitation, training programs are stored in the walker so that rehabilitation can be carried out without the presence of physical therapists. Its effectiveness in walking rehabilitation was verified by clinical tests [3][4].

In walking support, it is necessary for the ODW to know the direction the user intends to go based on user manipulation. Actual directional intent must, however, be identified from physical manipulation because a user's directional intent and physical manipulation are not always mutually consistent. In this paper, a novel interface is proposed to recognize a user's directional intention according to the forearm pressures exerted to the ODW by the user with wrists and elbows. The forearm pressures are measured by 4 sensors embedded in the ODW's armrest [5][6]. The relationship between forearm pressure and directional intention was extracted as fuzzy rules and an algorithm was proposed for directional intention identification based on distance type fuzzy reasoning method (DTFRM) [7][8]. The effectiveness of the algorithm was verified by experiment results. However, in the previous experiments the ODW was fixed on the ground. The intentioned directions were identified only when the ODW was stationary. If the ODW moves while the subject pushes it, forearm pressures should differ due to body sway and change of the supporting foot. This is not convenient in real walking support. Therefore, in this paper, we examine the effectiveness of the proposed method in walking support experiments when the ODW moves. The results show that users can control the ODW with the proposed method by adjusting direction as they walk.

II. STRUCTURE AND MODEL OF THE OMNIDIRECTIONAL WALKER

The structure of the ODW is shown in Fig. 1. The most important feature of the walker is the use of omniwheels. An arrangement of four omniwheels at the bottom of the walker body enables the walker to move in any direction while maintaining its orientation.

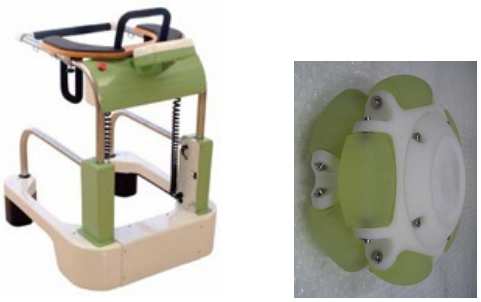

Figure 1. ODW and one of its omni wheels.

TABLE I. PHYSICAL PARAMETERS OF THE WALKER

Parameter	Value	Unit
Height	900–1200	mm
Arm	600	mm
Mass	58	kg
Maximum load	77	kg
Maximum speed	0.25	m/s

The physical parameters of the ODW are listed in Table 1. Two telescopic poles are designed to support both the upper part of the walker and the load from the user. The walker height is adjustable from 900 to 1200 mm to accommodate the different heights of the users. The mass of the walker is 77 kg and the maximum speed is set to 0.25 m/s to ensure user safety. The coordinate settings and structural model are shown in Fig. 2.

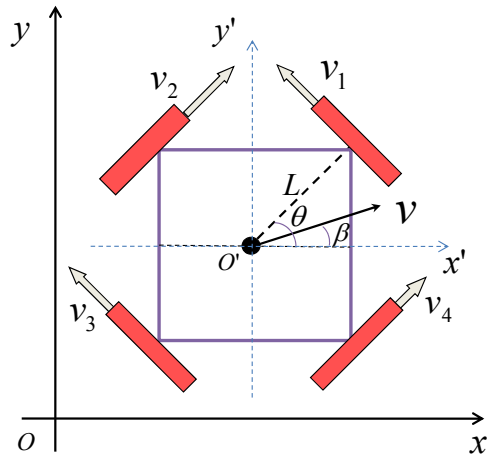

Figure 2. Structural model of the omnidirectional walker.

$\sum(x, y, O)$: Absolute coordinate system.

$\sum(x', y', O')$: Translation coordinate system of $\sum(x, y, O)$.

v: Speed of the ODW.

v_i: Speed of an omniwheels (i=1,2,3,4).

L: Distance from the center of the walker to each omniwheel.

β: Angle between the x'-axis and the direction of v.

θ: Angle between the x'-axis and the position of the first omniwheel.

Using the coordinate system shown in Fig. 2, the kinematic equations of the ODW are

$$\begin{cases} v_1 = -v_x \sin\theta + v_y \sin(\frac{\pi}{2} - \theta) + L\dot{\theta} \\ v_2 = v_x \cos\theta + v_y \cos(\frac{\pi}{2} - \theta) - L\dot{\theta} \\ v_3 = -v_x \sin\theta + v_y \sin(\frac{\pi}{2} - \theta) - L\dot{\theta} \\ v_4 = v_x \cos\theta + v_y \cos(\frac{\pi}{2} - \theta) + L\dot{\theta} \end{cases} \quad (1)$$

where $v_x = v\cos\beta$ and $v_y = v\sin\beta$ are the x and y components of the walker's velocity, respectively.

III. DIRECTIONAL CONTROL BY FOREARM PRESSURES USING DISTANCE TYPE FUZZY REASONING METHOD[7][8]

Force sensors to measure the user's forearm pressure are embedded in the ODW armrest as shown in Fig.3, to identify directional intention based on the pressure information from the sensors. This novel interface can also be applied to other apparatuses such as wheelchairs. It has the following three advantages: 1) Safety during walking is ensured because the users need not intentionally manipulate devices to input directional instructions. 2) Cost is lower without using any biological measurement system compared with other direct interfaces that determine the human intentions through EEG or EMG [9].

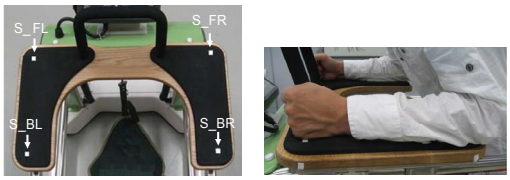

Figure 3. Equipment of load sensors.

The relationship between directional intention and forearm pressures was investigated in a measurement experiment. Eight healthy male volunteers aged 20-25 yr participated in the experiment. Subjects were instructed to push the ODW with their forearms as if they wanted to go in the following 8 directions: 1) 0° - Right (R), 2) 45° - Forward right (FR), 3) 90° - Forward (F), 4) 135° - Forward left (FL), 5) 180° - Left (L), 6) 225° - Backward left(BL), 7) 270° - Backward (B), and (8) 315° - Backward right (BR). There is great relevance between forearm pressures and directional intention, which can be referenced to identify directional intention from forearm pressure. Means and standard deviations (SD) of sensor output for the 8 subjects on each intended direction are listed in Table 1 (The unit is 0.025kgf, abridged for convenience below).

TABLE II. SENSORS' OUTPUT STATISTICS

	w_fr		w_fl		w_br		w_bl	
	mean	***SD***	***mean***	***SD***	***mean***	***SD***	***Mean***	***SD***
R	216.5	58.1	17.1	15.3	454.1	165.5	81.9	45.7
FR	290.3	66.1	23.9	18.2	121.7	110.6	34.8	20.4
F	255.7	57.8	249.5	55.0	51.1	44.5	69.4	44.4
FL	17.6	13.9	321.3	93.65	41.5	41.2	128.3	83.2
L	4.7	4.65	199.9	55.4	81.0	49.9	465.1	117.0
BL	3.4	3.2	74.1	30.7	82.6	32.9	607.9	174.8
B	3.0	2.7	16.9	9.7	454.9	117.7	440.5	83.8
BR	66.9	30.8	3.2	2.7	575.4	179.4	109.8	36.9

w_fr, w_fl, w_br, and w_bl are outputs of sensors S_FR, S_FL, S_BR and S_BL.

Directional intention can be reasoned from forearm pressures using the fuzzy rules about relevance between forearm pressures and directional intentions extracted in Section 3. Based on these results, the following fuzzy rules were extracted as fuzzy rules, used as knowledge in fuzzy reasoning.

$$Rule^i : if \quad w_fr = A^i_{fr} \quad w_fl = A^i_{fl}, \quad w_br = A^i_{br}, \quad w_bl = A^i_{bl} \quad \Rightarrow \quad y = \beta^i \quad i = 1,2,\cdots,8$$

where i is numbers 1) - 8) in Table 1 and β^i ith directional intention. A is a triangle-type fuzzy set defined by the data in Table 1, with its vertices being (mean – SD, 0), (mean, 1) and (mean + SD, 0). The fuzzy sets in the fact to be input are fuzzy singletons whose membership functions are 1 at the points of average outputs of the four sensors. Reasoning result, the intended direction, is also a fuzzy singleton.

$$Fact: \; w_fr = a_fr, w_fl = a_fl, w_br = a_br, w_bl = a_bl$$

$$Result: \; y = \beta$$

The DTFRM is used to reason directional intention from forearm pressure. An angle can be specified by innumerable degrees. However, the conclusion of DTFRM is affected by the specific degrees due to its asymptotic characteristic. If, for example, the distances between input fact and $Rule^1$, $Rule^8$ are much smaller than those between facts and the other rules, the reasoning conclusion, or intended direction, should be between R and BR due to the asymptotic characteristic. When calculating the conclusion, if R is specified as 0° and BR is specified -45°, then conclusion $\beta \in (0,-45)$, between R and BR. However, if R is specified as 0° and BR is specified 315°, then conclusion $\beta \in (0,315)$, not between R and BR, because direction R and BR are adjacent to each other while 0° and 315° are far distant. Therefore, when calculating the reasoning result, the degrees for specifying directions are determined as follows. The consequent degree of the fuzzy rule whose antecedent has the smallest distance among all the rules is determined as $\alpha \in [0,360)$. The degrees for specifying the other directions are determined as $\gamma \in (\alpha - 180, \alpha + 180]$. If, for example, when $Rule^7$ has the smallest distance, $\beta^1 \sim \beta^8$ are determined as 360°, 45°, 90°, 135°, 180°, 225°, 270°, 315°. When $Rule^1$ has the smallest distance, $\beta^1 \sim \beta^8$ are determined as, 0°, 45°, 90°, 135°, 180°, -135°, -90°, -45°.

IV. Direction Control Experiment

A path tracking experiment was carried out to verify the directional intention identification method. In the experiment, a healthy male volunteers aged 31 yr was instructed to push the ODW using his forearms to follow a 1.5m×1.5m square on the ground. Since the subject placed his arm against the armrest to partially support body weight throughout the experiments, even when not intending to go any direction. Therefore, the pressures for direction identification should be stable and significantly larger than the baseline due to body support. In the experiment, the directional intention was calculated when one second of data meet the two following conditions: 1) During this second, outputs of at least one sensor were all larger than 100. 2) During this second, SDs of outputs of all the sensors were less than 20. The first condition ensures that increases in pressures are significant. The second condition ensures that the pressures are stable.

The experiment results were shown in Fig.4, Fig.5 and Fig.6. Fig.4 shows the path tracking results of 6 attempts. Fig.5 shows the sensor's outputs during the 6th attempt. Fig 6 shows the reasoning results of the 6th attempt. In the experiment, the subject adjusted the direction of the walker as he walked. He revised the direction from time to time on the way until reaching the goal. It is indicated by the results that the proposed algorithm is applicable in walking support.

There might be three main reasons for the errors in the path tracking experiment: 1) Human beings cannot control their forearm pressure accurately. 2) The fuzzy rules are based on statistical experiment results. Individual differences are not considered. 3) During path tracking, error happens due to the center of gravity shift and the load changes caused by the user [10-12].

V. Conclusions

This study examined the effectiveness of the proposed directional intention identification method. The path tracking experiment indicated the applicability of the method in walking support.

In addition to the straight movements in the experiment, rotation movements, clockwise and anticlockwise rotation, are also very important during walking. Rotation movements are not considered in the current study because rotational intentions cannot be denoted by angles, which are different from the straight directional intentions. Rotational intentions can also be expressed by the forearm pressures. For example, we can define that pushing S_FR and S_BL means to rotate clockwise and S_FL and S_BR means to rotate anticlockwise. Future work will deal with this problem by adding knowledge of rotational intentions to the knowledge base.

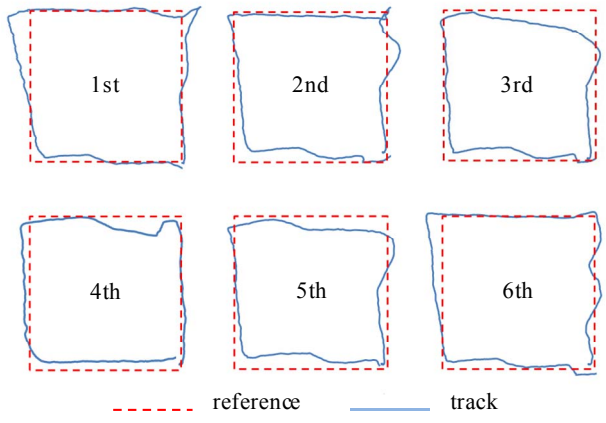

Figure 4. Path tracking results

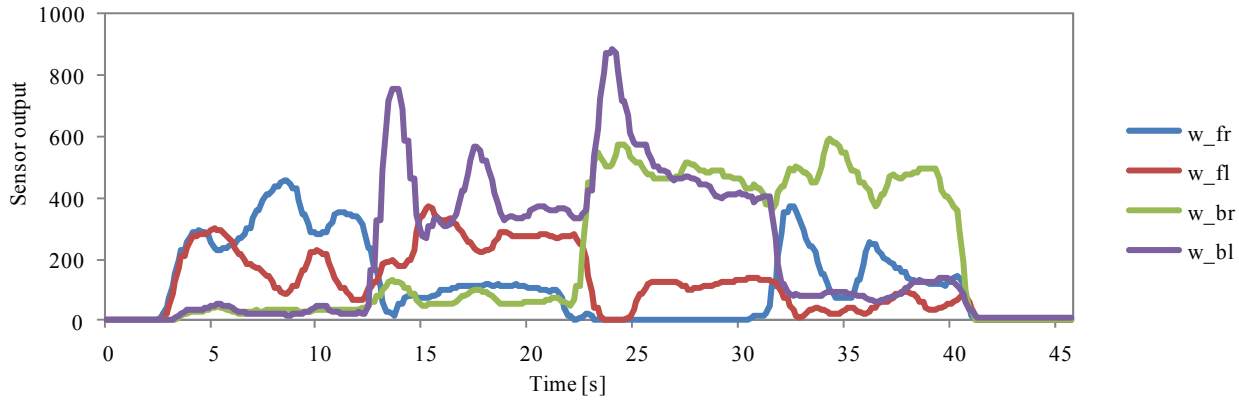

Figure 5. Sensors' outputs of the 6th attempt

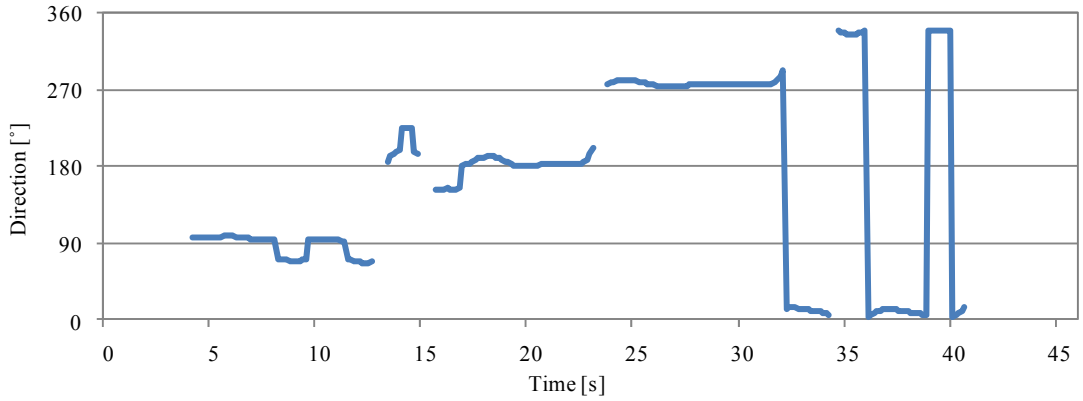

Figure 6. Reasoning results of the 6th attempt. The blank period is caused by the data that do not meet the 2 conditions. Although the reasoning results vibrate shaply from 34s to 42s, their directions are similiar.

ACKNOWLEDGMENT

This work is supported by Grants-in-Aid for Scientific Research Nos. 20240058 and 21300212 from the Japan Society for the Promotion of Science.

REFERENCES

[1] S.Y. Wang, K. Kawata, K. Ishida, H. Yamamoto and T. Kimura, "Omni-directional mobile walker for rehabilitation of walking", The 17th Society of Life Support Technology, pp. 48, 2001 [in Japanese].

[2] S.Y. Wang, K. Kawata, Y. Inoue, K. Ishida and T. Kimura, "Omni-directional mobile walker for rehabilitation of walking which can prevent tipping over", Japan Society of Mechanical Engineers Symposium on Welfare Engineering, vol. 39, pp. 145-146, 2003.

[3] S.Y. Wang, H. Inoue, K. Kawata, Y. Inoue, M. Nagano, S. Ino, K. Ishida and T. Kimura, "Developing the omni-directional mobile walker and verifying its effect of increase in the muscle power", JSME Symposium on Welfare Engineering 2007, pp. 176-177, 2007 [in Japanese].

[4] K. Ishida, S.Y. Wang, T. Nagano and T. Kishi, "Development of an all-way mobile walker", J. Physical Medicine, vol. 19, no. 4, pp. 246-250, 2008 [in Japanese].

[5] Y. L. Jiang, S.Y Wang, K. Ishida, T. Ando and M. G. Fujie, "Directional intention identification based on the force interaction between an omnidirectional walker and a human", ICIC Express Letters, Part B: Applications, vol.1, no.2, pp.195-200, 2010.

[6] Y. L. Jiang, S. Y. Wang, K Ishida, T. Ando and M. G. Fujie, "Directional intention identification for running control of an omni-directional walker", Journal of Advanced Computational Intelligence and Intelligent Informatics, vol.14, no.7, pp.784-792, 2010.

[7] S.Y. Wang, T. Tsuchiya, and M. Mizumoto, "Distance-Type Fuzzy Reasoning Method", Journal of Biomedical Fuzzy Systems Association, vol. 1, no. 1, pp. 61-78, 1999[in Japanese].

[8] S.Y. Wang, T. Tsuchiya, and M. Mizumoto, "A learning algorithm for distance-type fuzzy reasoning method", Journal of Biomedical Fuzzy Systems Association, vol. 6, no. 1, pp. 61-68, 2000.

[9] J.N. Mak and J.R.Wolpaw, "Clinical applications of brain–computer interfaces: current state and future prospects," IEEE Reviews in Biomedical Engineering, vol.2, pp. 187-199, 2009.

[10] R.P. Tan, S.Y. Wang, Y.L Jiang, K. Ishida, M. G. Fujie, and M. Nagano, "Adaptive control method for path tracking control of an omni-directional walker considering center of gravity shift and load change, International Journal of Innovative Computing, Information and Control, vol.7, no.9, 2011 (in press).

[11] R.P. Tan, S.Y. Wang, Y.L Jiang, K. Ishida and M. G. Fujie, "Adaptive control algorithm with parameter optimization using neural networks for an omni-directional walker", ICIC Express Letters, Part B: Applications, vol.1, no.2, pp.201-208, 2010.

[12] R.P. Tan, S.Y. Wang, Y.L Jiang, K. Ishida, M. G. Fujie, and M. Nagano, "Motion control of an omni-directional walker using adaptive control method", ICIC Express Letters, vol.4, no.6(A), pp.2195-2199, 2010.

2011 IEEE International Conference on Fuzzy Systems
June 27-30, 2011, Taipei, Taiwan

Construction of Collision Avoidance Behavior Model Induced by Visual Motion

Norifumi Watanabe
Brain Science Institute
Tamagawa University
6-1-1 Tamagawa-gakuen, Machida-shi
Tokyo, Japan
Email: norifumi@lab.tamagawa.ac.jp

Hiroaki Mikado
Graduate School of Engineering
Tamagawa University
6-1-1 Tamagawa-gakuen, Machida-shi
Tokyo, Japan
Email: mkdhi6ec@engs.tamagawa.ac.jp

Takashi Omori
Brain Science Institute
Tamagawa University
6-1-1 Tamagawa-gakuen, Machida-shi
Tokyo, Japan
Email: omori@lab.tamagawa.ac.jp

***Abstract*—We decide and execute our action from many types of environmental information in our daily lives even if we are not conscious of being guided. The human action induced from the oncoming person's movement is the collision avoidance of passing each other. In collision avoidance, we chiefly judge the avoidance direction from visual information. Especially, it is important to get the information from oncoming person's body part and avoidance timing in each other. Then, we make an experiment to judge the avoidance direction by watching the masking movie of oncoming person's body part. By evaluating this judgment time, it was clarified oncoming person's body part is leg in collision avoidance. Next, it especially paid attention to oncoming person's leg, and the relation between the walking cycle and leg position in avoidance judgment is evaluated. From this result, the avoidance judgment is possible because the traveling direction can be controlled by the leg when the leg is lifting and landing. It was clarified that oncoming person's walking cycle is important in the action decision during collision avoidance. So we propose the action decision model based at the walking cycle.**

***Index Terms*—action decision model, collision avoidance, visual motion, walking cycle**

I. Introduction

As for us, a safe walking is possible in the crowded situation. We plan not to collide with the other person, and the purpose of this is to execute it the decision of the action. However, it is difficult in the situation very crowded at the event site and the disaster, etc. to walk safely [1]. Attention is distributed in the inducement by the emergency light and the arrow when trying to head for a target place in such a place and the situation, and consideration is not turned by the inducement presentation thing. Then, it is important to make a unconscious inducement system thought that the congestion situation doesn't influence us easily, and our safety is kept direction where it should walk by controlling person's flow.

We examine the use of the galvanic vestibular stimulation (GVS) as a device of such an unconscious inducement. GVS behave on the vestibular apparatus, and change the perception of the direction of gravitational force. The movement related in the direction of center of gravity undertakes the influence of unconsciousness by this action. For example, it is reported that the direction of walking changes right and left into giving the illusion that posture has collapsed to the pedestrian by giving GVS , and the unconscious correction of the posture [2-3]. Up to now, the possibility that the effect of the inducement is achieved in a consecutive periodic motion has been pointed out from the walking [4] and minion [5-6] inducement by GVS.

On the other hand, we are generating the walking rhythm by using CPG(Central Pattern Generator) [7-8] that exists in the spinal cord while walking. Therefore, a smooth, steady walking is achieved in the place where it walks the plain, the stairs, the crowd, and for the first time. It is thought that the rhythm of CPG is related to the timing generation in various processes included in walking of perception and the action decisions and the motion executions etc. It is necessary to stimulate drawing out the effect of the inducement on the pedestrian by GVS to its maximum in the appropriate timing based on the walking cycle. Then, we construct a model of pedestrian's action decision process based on a walking cycle to optimize the intervention effect to walking with the device such as GVS. Concretely, the scene of passing each other of the one to one is taken up as a daily walking. We presume the influence specifying oncoming person's body necessary for the action decision at the time of passing each other. And, the influence of the self-movement when passing each other on generation is discussed.

II. Action Decision Process of Passing Each Other

In this study, we targets an action of passing each other to which the others observation, the self-decision making and motion generation for the action decision by walking. In addition, to make the model simple, the pedestrian goes straight, and the situation in which the direction is that oncoming person may evade the collision with the pedestrian. In this case, the pedestrian observes others, judges the direction of evasion from information in other's body site, decides own evasive action based on it, and is executing his movement (Fig. 1).

As for the judgment of others' evasion directions, the body site that seems to be important. So we evaluated to the judgment by using movie of passing each other by masiking others' body sites. From the result of the using others' body sites, we consider the influence of own evasive action. Finally, we measure the body site thought to receive the influence by using the motion capture system and evaluate whether the motion generation based on the self action decision gives the

978-1-4244-7316-8/11/$26.00 ©2011 IEEE

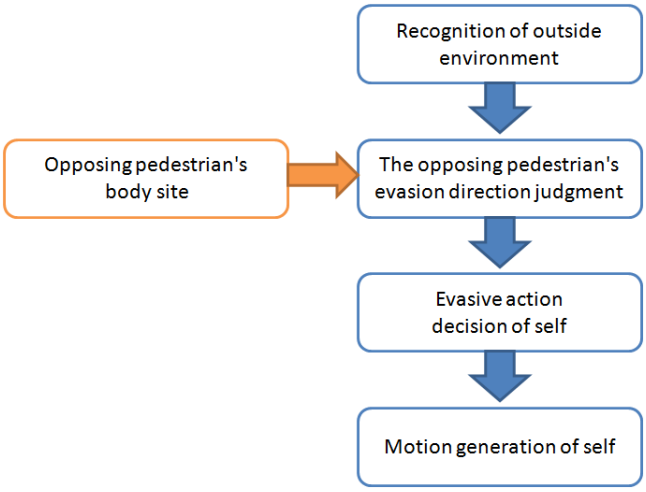

Fig. 1. Pedestrian's Action Decision Process

Fig. 2. Masking Movie of Passing Each Other Used by Experiment

effect to own body site.

A. Gazing Body Part in Passing Each Other

When passing each other with the person, we judge own direction of evasion from body features of those who oppose it by obtaining from the sight. Then, we measure the time that hangs to the judgment when the movie that does oncoming person's body site in masking is presented, and presume the body site necessary for the judgment.

1) Method: Subjects see the movie that those who oppose it projected onto the projector pass each other leaving the screen by about three meters in standing position, and judges oncoming person's direction of evasion. And subjects were stepping to image walking, and push the button in oncoming person's direction of evasion momentarily at the time of understood oncoming person's direction of evasion. However, the correction in the direction of evasion is no object.

The movie used by the experiment masked the specific body site all of about 300 frames, and integrated it again (Fig. 2). Oncoming person's body was classified into three (head, body, and foot), and the either was masked because the pedestrian had gazed at oncoming person's foot and breast by using eye track camera. Information obtained from the body site is limited by using the masked movie, and an important body site is specified from delay of the judgment by the limitation for the estimation of the direction of evasion.

2) Results: Figure 3 is a result of having totaled the number of judgments of body sites where the evasion judgment is delayed (N=3). The result that the judgment time became long when it had the foot in masking was shown. Then, it is thought that we do the evasion judgment by using information on our feet when passing each other. However, the delay has been generated by not only one's feet but also the masking of the head and the upper-body. It is thought that the head and the upper-body are seen and judged when the judgment is difficult only by oncoming person's feet. Thus, we examined the possibility that the body site where the evasion judgment was done according to the walking phase (position of the foot when walking) is different (Fig. 4).

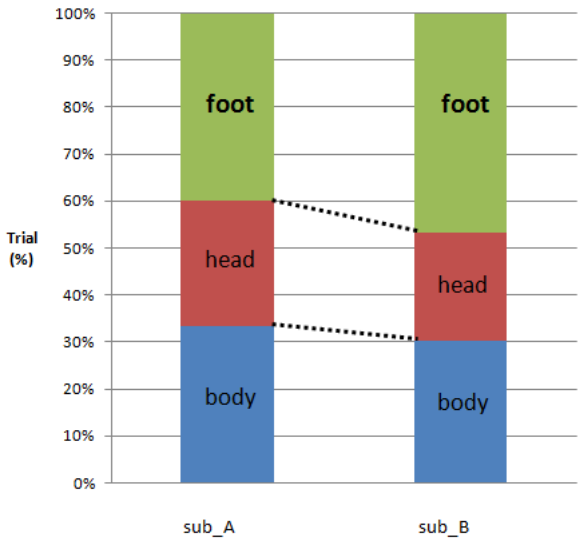

Fig. 3. Body Site Where the Delay of Judgment by Masking

B. Walking Phase in Evasion Judgment

We make a hypothesis with different body site at which it gazed when the evasion judgment is done according to oncoming person's walking phase at the time of passing each other. Next, how the walking phases of the body site and those who opposed it by the gaze influenced was examined.

1) Method: The subjects stand leaving the screen by 3 meters, step to image walking. They push the button in the direction momentarily at the time of understood oncoming person's direction of evasion. However, the correction in the direction of evasion is no object.

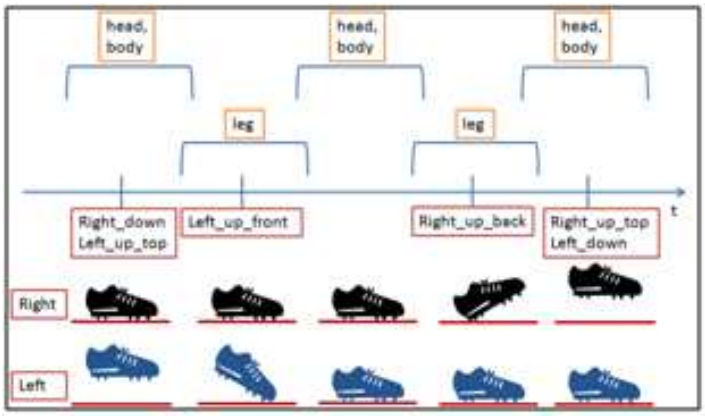

Fig. 4. Conceptual Chart of Walking Cycle and Evasion Judgment Body Part

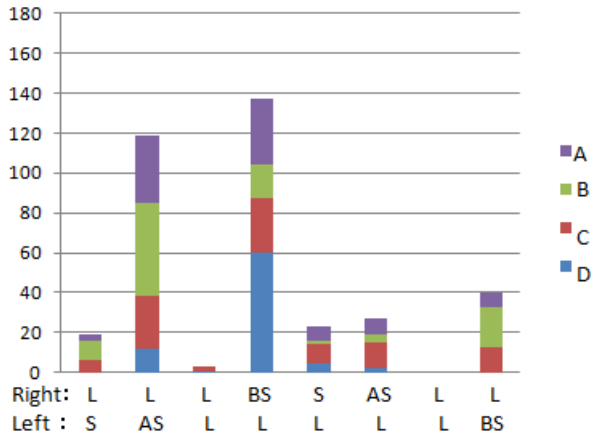

Fig. 5. Evasion judgment distribution when left leg is stepped forward. L: Landing, BS: Before Swing, S: Swing, AS: After swing.

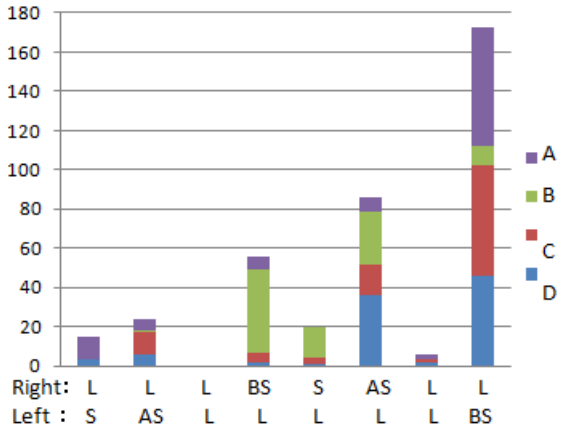

Fig. 6. Evasion judgment distribution when right leg is stepped forward. L: Landing, BS: Before Swing, S: Swing, AS: After swing.

The movie used took the situation of passing each other of the one to one from the other subject side. Four of those who opposed it directed the right and left foot stepped forward, and walked ten times of left evasion ten times of right evasion. In addition, to evaluate the walking phase, the movie of the side foot position was recorded synchronizing with movie of passing each other.

2) Results: Four subjects saw 378 animations a day in the experiment, the evasion judgment was done, and it experimented on it for five days. Average judgment timing of each movie was calculated from the experiment, and the walking phase when judged that was analyzed. The walking phase classified a foot right and left respectively in four states "Landed phase", "Before swing phase", "Swing phase", and "After swing phase".

Figures 5 and 6 are graphs where the number of judgments of walking phases of a momentary each foot that the evasion judgment was done was shown dividing into four oncoming pedestrians. In the graph, the phase is shown, "L: Landing, BS: Before Swing, S: Swing, AS: After swing". Figure 5 is distribution of the phase in the judgment trice when stepping forward from the left leg. The judgment result has concentrated for the period of AS for the period of BS in the right leg in the left leg. Figure 5 is distribution of the phase in the judgment trice when stepping forward from the right leg. The judgment result is Figure 5, the oncoming phase, and has a lot of judgments in the period of BS in the left leg in AS in the right leg. As a result, it is suggested that a lot of evasion judgments be done in "Before swing phase" and "After swing phase" in the walking phase in operation of passing each other.

C. Walking Phase in Generating Evasion Motion

As for pedestrian's action decision process, it has been understood that there is a judgment process of depending on oncoming person's walking phase in addition to the process of others observation and decision of self-action and execution of self-movements. Not only these factors however but also in own motion generation, it is possible to a distance of self and oncoming pedestrian and the influence of own walking phase. Then, the moved distance of subject's body (especially, feet) at the time of passing each other is measured by using the motion capture system, the physical exertion for passing each other is begun, and timing is examined.

1) Method: The distance between oncoming pedestrian and subject is about 5.2 meters, and they start at time when the oncoming pedestrian put down his hand both simultaneous. At this time, both oncoming pedestrian and subject go straight. The subject evades to the right and left directed beforehand, and the oncoming pedestrian goes straight and passes each other. The evasion distance was directed to avoid it when seeming to collide with subject with oncoming pedestrian.

The subject threaded 13 point in total marker of head 3 points, shoulder 2 points, waist 2 points, knee 2 points, and ankle 4 points, and oncoming pedestrian threaded 8 points of waist 2 points, knee 2 points, and ankle 4 points in total. The subjects walked ten times respectively in right evasion and left evasion. The motion capture device used the one of made of Motion Analysis, 12 cameras, and the sampling rate 250Hz.

2) Results: A right and left rate vector greatly changes into straight advancement so that the subject may evade right and left so as not to collide with the oncoming pedestrian. We analyzed the moment when a right and left speed of the ankle had greatly changed into the right and left as 0.16m/second or more as for the threshold as motion generation timing. Figures 7 and 8 show the frequency of the walking phase when the motion of each subject being tested is generated. In the graph, the phase is shown, "L: Landing, BS: Before Swing, S: Swing, AS: After swing". Figure 7 is a momentary walking phase with which subjects generated the evasion motion left, and the motion generation is often done in the section where the left leg has landed. Figure 8 shows a momentary walking phase in which the evasion motion to the right side is generated, and subjects generate the motion with both of right legs when landing and the left leg have landed. As a result, the timing at the motion generation is suggested that the foot in the direction of evasion landed. However, when the left leg had landed, the motion was generated about right evasion. Here, the motion generation tends to do generally by own working foot. The tendency to generate the motion when the foot in the direction of evasion had landed was suggested from experimental result at left evasion. On the other hand, the motion that moved at half cycle is generated in the direction of evasion by the left leg at right evasion. As a result, we assume whether subject's working foot influences.

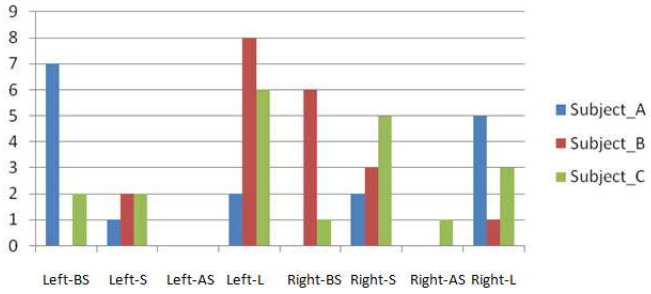

Fig. 7. Walking Phase at Motion Generation When the Left Side is Evaded

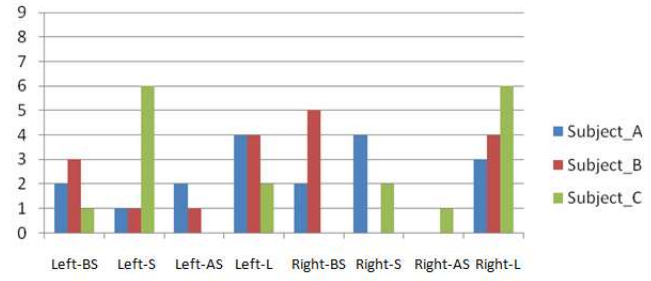

Fig. 8. Walking Phase at Motion Generation When the Right Side is Evaded

III. Discussion

A. The pedestrian's action decision based on walking cycle

From these experiments, it was shown that we have been influenced when passing each other at the action decision and the motion generation according to an oncoming pedestrian and own walking cycle.

Oncoming person's body site is observed and the direction of evasion is judged the start when the pedestrian passes each other (Fig. 9-1). Concretely, the direction of evasion is judged from information on oncoming person's feet in "Before swing phase" and "After swing phase" by which those who oppose it can control the direction of the foot. In L and S that the control of the foot is difficult, it is thought that the direction of the upper-body and the face is seen, and the direction for which the oncoming person's heads is judged.

The pedestrian action decision after the direction of evasion is judged undertakes the influence of oncoming person's walking phase (Fig. 9-2). Because the pedestrian has decided it the action according to the body site (especially, walking cycle) at which it gazed by the evasion judgment, the influence is undertaken from oncoming person's walking phase though it only has to do the evasion judgment according to arbitrary timing.

This timing at the motion generation depends on own walking phase though the exercise is generated after the decision of the self action. That is, the motion is generated when the foot in the direction of evasion can be controlled, and a lot of the timing occurs to after swing phase (Fig. 9-3).

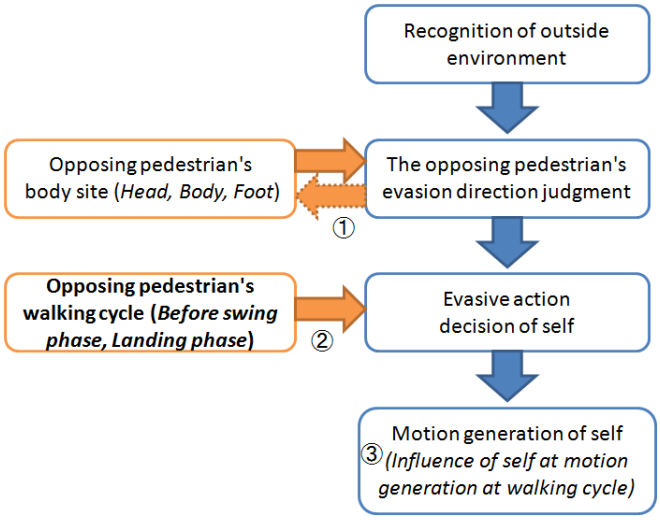

Fig. 9. Pedestrian's Action Decision Process Model in Passing Each Other

B. Possibility of Inducement of Pedestrian Based on Action Decision Model

In this study, we have experimented the understanding of the action decision process at the time of person's passing each other based on the hypothesis that an effective inducement by aiming at human action inducement under unconsciousness,

and putting out the inductive stimulus according to the walking cycle according to appropriate timing.

It is thought that we observe others' body sites and presume others' directions of evasion. However, there is a possibility of correcting the evasion judgment that the self decided when inducing it here with the sight device etc. so that the self may do the evasion judgment. Therefore, it is improper as the timing of the inducement presentation.

On the other hand, self decides the action according to others' walking cycle (3.2). Because the action decision timing has synchronized with the others' behavior, there is a possibility that it is caused to the inducement by inducing the pedestrian before the action decision. It is expected that the action decision of unconsciousness is performed by the inducement as for this method because there is no correction feedback by own intention. In addition, the action decision causes a high effect of the inducement because it influences the motion generation that the self controls. It is thought that it is the most effective before own evasive action is decided to induce it under such consideration.

IV. Conclusion

In this study, it experimented passing each other of the one to one for the clarification of the decision process of the walking action that aimed at the action inducement of unconscious. As a result, it was suggested that an oncoming pedestrian and own walking cycle influence at an action decision of the self and own motion generation. However, it is necessary to increase the number of subjects so that the possibility that the motion generation is influenced by the working foot may remain.

In addition, it wants to examine the inducement device including GVS, and to examine the inducement experiment.

Acknowledgment

This research is supported by Core Research for Evolutional Science and Technology (CREST), Japan Science and Technology agency (JST). Professor Taro Maeda and associate professor Hideyuki Ando gave us a lot of important advices. We thank their efforts.

References

[1] N. Fridman, Gal A. Kaminka, "Towards a Cognitive Model of Crowd Behavior Based on Social Comparison Theory", AAAI 2007, pp. 731-737, 2007.

[2] T. Murofushi, S. Iwasaki, H. Ozeki, M. Ushio, Y. Chihara, "Tone burst-galvanic ratio of vestibular evoked myogenic potential amplitudes: A new parameter of vestibular evoked myogenic potential?," Clinical Neurophysiology vol. 118, pp. 1685-1690, 2007.

[3] R. C. Fitzpatrick and B. L. Day, "Probing the human vestibular system with galvanic stimulation," J Appl Physiol vol. 96, pp. 2301-2316, 2004.

[4] M. Sugimoto, J. Watanabe, H. Ando, T. Maeda, "Inducement of walking direction using vestibular stimulation-The Study of Parasitic Humanoid (XVII)-," Virtual Reality Society of Japan. 8, pp. 339-342, Sep. 2003. (In Japanese)

[5] I. Toshima, N. Watanabe, T. Omori: Possibility of guidance of arm movement in circle-writing experiment, Proc. of the 2009 IEEE International Conference on System, Man, and Cybernetics, pp. 448-453, 2009

[6] N. Watanabe, T. Omori: Trigger Model for Guiding Arm Movement in Circle Drawing, Proc. IEEE INNS/FUZZ'10(WCCI'10), pp.18-23, 2010.

[7] S. Grillner, P. Zangger, On the initiation of swing phase oflocomotion in chronic spinal cat, Brain Res, 146 (1979) , 169-277.

[8] G. S. Stent et al., Neuronal Generation of the Leech Swimming Movement, Science, 200 (1978), 1348-1357.

2011 IEEE International Conference on Fuzzy Systems
June 27-30, 2011, Taipei, Taiwan

Instruction Knowledge Acquisition for Reinforcement Learning Scheme by PSO Algorithm

Toru Sawa
Osaka Electro-Communication University
Neyagawa, Osaka, Japan
m10709@oecu.jp

Toshihiko Watanabe
Osaka Electro-Communication University
Neyagawa, Osaka, Japan
t-wata@isc.osakac.ac.jp

***Abstract*— In order to realize intelligent agents such as autonomous mobile robots, Reinforcement Learning is one of the necessary techniques in control systems. It is desirable in terms of knowledge or skill acquisition of agents that reinforcement learning is based only upon rewards instead of teaching signals. However, there exist many problems to apply reinforcement learning to real-world tasks. The most severe problem is a huge number of iterations in the learning phase. In order to deal with the problem, the instruction approach for reinforcement learning agents based on sub-rewards and forgetting mechanisms were proposed and shown to be effective. However, the relationship between the instruction and the learning performance of reinforcement learning has not been adequately clarified. In this study, in order to clarify the instruction performance in the reinforcement learning, we propose an instruction knowledge acquisition method for the reinforcement learning scheme by the particle swarm optimization (PSO) algorithm. Through numerical experiments of the mountain car task and the Acrobat task, we show the validness of the proposed approach in terms of learning speed and accuracy.**

Keywords: Reinforcement Learning, Q-Learning, Fuzzy Q-Learning, Instruction, PSO, Machine Learning

I. INTRODUCTION

The Reinforcement Learning[1-4] will be one of the necessary techniques to realize intelligent agents such as autonomous mobile robots. The reinforcement learning is a desirable idea that can acquire the skill and knowledge without using the teaching signal based upon only the rewards from environments. However, the huge iterations of the trial for accomplishment of the reinforcement learning become a problem in actual applications in which the appropriate learning of the compound task or complicated task is needed. This huge trial frequency is one of the issues of the reinforcement learning. In order to deal with the complicated task problem, several effective approaches are studied. For relaxation of task complexity, several types of hierarchical reinforcement learning have been proposed to apply to actual applications[5,6]. The hierarchical reinforcement learning has been widely recognized as an effective scheme for complicated tasks. However, the approach is based on the assumption that the compound task is decomposed hierarchically into subtasks as internal models of the agent in advance. The assumption is sometimes not suitable for learning of agents in an unknown environment, i.e. basic concepts of the reinforcement learning. When we consider realizing the automatic task decomposition function by means of the reinforcement learning, improvement of learning performance such as iterations and precision of acquisition is indispensable for the reinforcement learning technique as well as a concrete segmentation technique of the learning results. The authors proposed an instruction based reinforcement learning applying sub-rewards and forgetting mechanisms[7,8] in order to improve the learning performance of reinforcement learning agents. In the study, we aimed at constructing a new learning scheme that can utilize the instruction, i.e. not strictly teaching, in the reward based reinforcement learning scheme and showed effectiveness in terms of the necessary learning speed in the reinforcement learning process through numerical experiments of not so complicated tasks. However, the relationship between the instruction and the learning performance of the reinforcement learning has not been adequately clarified. In this study, in order to clarify the instruction performance further in the reinforcement learning, we propose an instruction knowledge acquisition method for reinforcement learning scheme by the particle swarm optimization (PSO) algorithm[9]. The efficacy is shown by the numerical experiment of the mountain car task and the Acrobot task.

The paper is organized as follows. In section 2, we discuss the issue of instructions for task acquisition. In section 3, we introduce a learning method based on the instruction. An instruction knowledge acquisition algorithm is proposed in section.4. Then the results of numerical experiments are shown in section 5. Finally, conclusions are drawn in section 6.

II. INSTRUCTIONS FOR TASK ACQUISITION

The skillful task performed by human experts is indispensable even in the modern society. Even in a highly automated factory, skillful experts usually take part in important tasks. Moreover, tasks in traditional artistic crafts such as ceramic art or woodwork are also highly skillful. On the other hand, techniques in sports can also be said to be skillful for not only the athlete but also general people in our daily life. Since it is obvious that the sports are good for health, learning the techniques(task acquisition) in the sports is necessary process to all the people. Even injured people under treatment, struggle to restore their movement functions through rehabilitation physical trainings which are difficult tasks for themselves as though skillful techniques of the sports.

978-1-4244-7316-8/11/$26.00 ©2011 IEEE

There exist many skillful tasks to acquire in many areas.

Though the skillful task is highly complicated at a glance through an observation, many tasks consist of the combination of simple sub-tasks. As seen from the potential ability of human recognition, the simple task is clearly performed from the selected inputs among huge information, such as vision, sound, and measured data. The comprised simple task is not difficult itself to be developed into an automated machine owing to the modern technology progress. However the task decomposition without knowledge is not easy to develop. In the soft computing area, the automatic task decomposition by the computer system has been studied. Modular neural network[10,11] is proposed to realize the modularization of learning results. This is equivalent to the task decomposition represented as "gating network." Modular fuzzy model[12] is also proposed to deal with the problem. The task decomposition without knowledge is more difficult without explicit teaching.

This problem corresponds substantially to the reinforcement learning concept. The model for the reinforcement learning is usually constructed as a memory type, neural network, fuzzy model, locally weighted regression, CMAC and so on. However, non structured model acquired is essentially a mimic system that is not robust for changes of environment, condition, and so on. Moreover, the segmentation of native acquired model is an important problem to realize the task decomposition. Recently, study of the task decomposition is advanced by learning by the intrinsic motivation[13,14]. The methods are based on internal rewards to formulate behavioral rules abstracted from the results of the reinforcement learning expressed as action rules. In the abstraction process, the segmentation of learning is an indispensable and essential technique. Although they are promising techniques in terms of task decomposition or task acquisition of complicated tasks of the agent, the substantial difficulty of the intrinsic reward concept is still remained in actual applications.

On the other hand, in terms of realization of applicable task decomposition or task acquisition, the authors proposed an "Instruction based reinforcement learning"[7,8] applying environmental sub-rewards and forgetting mechanism in the agent and showed promising results through not so complicated tasks. We consider that there exist some situations that the environmental sub-reward is more suitable than the intrinsic concept in the task acquisition. "Instruction" plays an important role in acquiring the task of human works. For example, when we teach someone the skill we already have, we often give only an instruction as a knack or a point that is necessary to perform the skill, instead of teaching every detail including trivial matters in the task procedure. Our motivation of "Instruction based reinforcement learning" is to realize such instructions in the reinforcement learning scheme. The basic concept is to give "instruction" that is not strict and fragmental compared with the teaching data used in the teaching based learning such as the multi-layered perceptron,

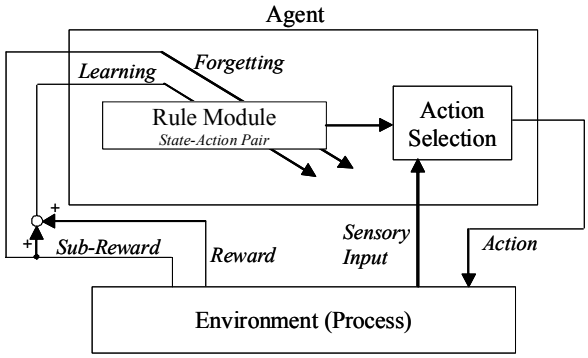

Figure 1. Conceptual Diagram of Instruction Based RL Architecture

to the reinforcement learning agent. The instruction concept can be realized as sub-rewards in addition to the main reward as well as forgetting mechanism to improve the learning performance in the reinforcement learning process.

However, there exist a lot of tasks difficult to give the instructions even by the skillful human experts. Moreover, the instruction concept is essentially subjective and is not clear its optimality or validness in terms of the reinforcement learning. Our primary motivation in this study is to investigate the relationship between instructions and learning performance of the reinforcement learning. Since the instruction can be considered as additive information to accelerate the learning process of the task, valid instruction is necessary to the task acquisition. Furthermore the instruction acquisition might lead to significant tools to analyze the skillful task and to hand down the skillful task to the next generation by interacting human and agent(robot) models. In this study, in order to clarify the instruction performance further in the reinforcement learning, we propose an instruction knowledge acquisition method for the reinforcement learning scheme

III. LEARNING METHOD BASED ON INSTRUCTION

In order to commission sub-rewards mechanism appropriately, the issue of consistence maintenance between sub-rewards and the main reward should be dealt with. Then we proposed a learning algorithm based on sub-rewards with forgetting mechanism and eligibility trace[7, 8]. The sub-rewards are defined corresponding to necessary state-action pairs. Moreover, when the agent obtains the sub-reward, forgetting mechanism is applied at the same time. Fig.1 shows the conceptual diagram of proposed learning architecture.

A. Q-learning algorithm

In Q-learning reinforcement learning algorithm, an optimal policy is formulated by maximizing rewards received over time. Q-function is defined as values for each pair of state and action:

$$Q(x_t, a_t) = Q(x_t, a_t) + \alpha\left(r_{t+1} + \gamma \max_{\eta} Q(x_{t+1}, \eta) - Q(x_t, a_t) \right) \quad (1)$$

where x_t is the state vector of t-th input, a_t is the t-th action,

r_{t+1} is a reward, γ is a discount rate, and α is a learning rate. The reward based on the sub-reward is defined as:

$$r_{t+1} = hr_{t+1} + R_{t+1} \tag{2}$$

where hr_{t+1} denotes a sub-reward, and R_{t+1} is a main reward. At learning, neither a sub-reward nor a main reward distinguishes the kind. Therefore, the possibility of inconsistency of the expectation reward in the reinforcement learning is not negligible. Then, forgetting is executed also at giving the instruction to maintain consistency of the expectation reward. Forgetting mechanism is defined as:

$$Q(x,b) = \Gamma \cdot Q(x,b), \qquad b \neq a_t, 0 \leq \Gamma \leq 1 \tag{3}$$

where Γ is a forgetting parameter and a_t is the current action.

B. Fuzzy Q-learning algorithm

In Fuzzy Q-Learning[15], Q-function is approximated by the fuzzy model. The fuzzy model is defined by FCS (Fuzzy Classifier System) form[16] as:

$$if\ x_t\ is\ A_j\ then\ a_t\ is\ c_j^k\ with\ q_j^k \tag{4}$$

where c^k_j is a k-th concrete action, A_j denotes the fuzzy set defined in the input states, and q^k_j is the Q-value of the j-th rule. The output Q-value is calculated as:

$$Q(x_t, c^k) = \frac{\sum_{s=1}^{m} h_s \cdot q_s^k}{\sum_{s=1}^{m} h_s} \tag{5}$$

where h_s denotes the membership degree of the rule and m is the number of the fuzzy rules. From (1), the TD error that should be corrected is defined as:

$$\Delta Q(x_t, a_t) = \left(r_{t+1} + \gamma \max_{\eta} Q(x_{t+1}, \eta) - Q(x_t, a_t) \right) \tag{6}$$

The correction of the q-value in the rule is defined as follows by the request of the gradient of (5) and (6).

$$\Delta q_j^k = \Delta Q(x_t, a_t) \cdot \frac{\partial Q(x_t, a_t)}{\partial q_j^k} = \Delta Q(x_t, a_t) \cdot \frac{h_j}{\sum_{s=1}^{m} h_s} \tag{7}$$

where a_t is the action c^k in this equation. The maximum Q value at the right of (6) is obtained from (5).

Moreover, when the sub-reward and forgetting are applied to the fuzzy Q-learning, (2) and (4) are applied based on the next equation that modifies the Q value.

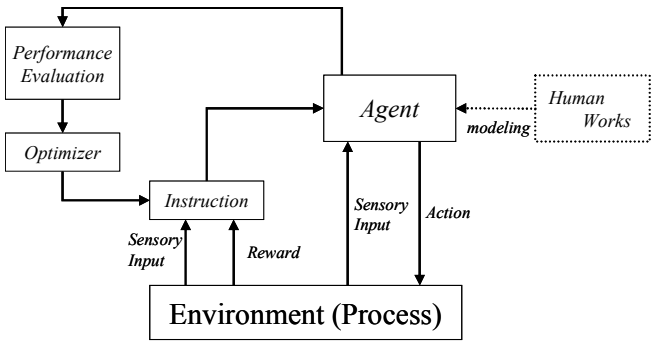

Figure 2. Conceptual Diagram of Instruction Knowledge Acquisition

$$\begin{aligned} q_j^b &= \Gamma \cdot q_j^b \\ \Gamma &= 1 - (1-\beta)\left(1 - \mu(d,b)\right) \cdot h_j, \ \ 0 \leq \beta \leq 1 \end{aligned} \tag{8}$$

where μ is a membership function that shows the degree of agreement of selected action d and the other actions b, and β is a forgetting parameter. The degree of forgetting becomes high when we set a small value as the parameter.

The eligibility trace can also be successfully applied at the same time of the instruction[8].

IV. Instruction Knowledge Acquisition by PSO Algotrithm

Our objective in this study is to acquire effective instructions through reinforcement learning simulations. Fig.2 shows the conceptual diagram of instruction knowledge acquisition. Let us assume that the human works such as actions or movement are modeled as the agent or the robot. By evaluating the learning performance using episode lengths, appropriate instructions are decided through optimization procedures. Empirically, there could exist many alternatives of good instructions. In order to deal with such nature, we adopt PSO algorithm to acquire the instructions.

A. Particle swarm optimization algorithm

Particle swarm optimization[9] is a population-based iterative search procedure, which simulates the social behavior such as flocks of birds or schools of fish. N individuals, referred to as particles, constitute a swarm. Each particle is a candidate solution to the D dimensional problem. The position of the *i-th* particle at *t-th* iteration is represented by:

$$X_i^{(t)} = \left(x_{i1}, x_{i2}, \cdots, x_{iD} \right) \tag{9}$$

During the search process, the particle successively adjusts its position toward the global optimum according to two factors. The best position encountered by itself (pbest) is denoted as:

$$P_i = \left(p_{i1}, p_{i2}, \cdots, p_{iD} \right) \tag{10}$$

The best position encountered by the whole swarm (gbest) is denoted as:

$$P_g = \left(p_{g1}, p_{g2}, \cdots, p_{gD}\right) \tag{11}$$

Its velocity at t iteration is represented by:

$$V_i^{(t)} = \left(v_{i1}, v_{i2}, \cdots, v_{iD}\right) \tag{12}$$

The position at the next iteration is calculated according to the following equations:

$$V_i^{(t)} = \lambda\left(\begin{array}{l} w * V_i^{(t-1)} + c_1 * rand(\,) * \left(P_i - X_i^{(t-1)}\right) \\ \qquad + c_2 * rand(\,) * \left(P_g - X_i^{(t-1)}\right) \end{array}\right) \tag{13}$$

$$X_i^{(t)} = X_i^{(t-1)} + V_i^{(t)} \tag{14}$$

where c_1 and c_2 are two positive constants, called cognitive learning rate and social learning rate respectively; *rand*() is a random function in the range [0;1] ; w is inertia factor; and , λ is a constriction factor. In addition, the velocities of the particles are confined within $[V\text{min}, V\text{max}]^D$. If an element of velocities exceeds the threshold Vmin or Vmax; it is set equal to the corresponding threshold. From equation (13) and (14), it can be seen that the velocity determines search direction and step-size simultaneously for the particle according to the social learning and the cognitive learning.

The point of the instruction for the reinforcement learning is defined as a particle (position X) for PSO algorithm in this study. The particles(instruction points) search towards the point in which the trial episode lengths of learning are minimized.

V. NUMERICAL EXPERIMENTS

In order to evaluate the performance of the proposed approach, the numerical experiments are conducted for the mountain car task and the Acrobot task. The search of the instruction points is performed by using PSO algorithm.

Each parameter of PSO is as follows. c_1 and c_2 are 2.0, respectively. The number of particles in the swarm is 10. Constriction factor λ is set as 0.1. Inertia factor w is set as 1.0. Let us assume that the positions of particles are also confined within the rage $[X\text{min}, X\text{max}]^D$. In this study, Xmax is set as 100, and Xmin is set as -100. The state variables including the action for the instruction are normalized to $[X\text{min}, X\text{max}]^D$ according to the task. In the mountain car task, the dimension of the state is three(position, speed, and acceleration operation of the car agent). In acrobat task, the dimension of the state is five (angle and angular velocity of the first link, angle and angular velocity of the second link, and torque operation of the Acrobot).

Initial positions of particles are decided at random within the range of Xmin and Xmax. The number of generations of PSO is set as 100 in this study.

A. Mountain Car Task(Crisp)

Fig.3 shows the settings of the mountain car task. The purpose of this task is to climb a right-hand mountain. The power of the car agent is restrained as lower value than the gravity. Therefore, the acquisition of the action knowledge that shuttles several times, enlivens, and reaches a goal becomes indispensable. The state of the agent (car) is two continuous values of speed v_t and position p_t. The action can be selected from {-1, 0, 1}. The action is each full throttle retreat (-1), zero throttle (0), and full throttle advancement (+1). When the car finishes climbing the mountain, the reward is given. Agent's initial state was assumed to be p_0=-0.5 and v_0=0. The state is quantized by the crisp partition. The number of partitions is 15, the learning rate α is 0.10, and the discount rate γ is 0.95. The simulations are conducted 100 times. The averaging value is used to evaluate. The agent tries the mountaineering 5 times by one simulation. When the following condition is satisfied, the instruction is given to the agent. When the state and the action of the agent falls into the range of the instruction point(particle) as shown in Fig.4, the instruction is applied to the agent. In the figure, position p and

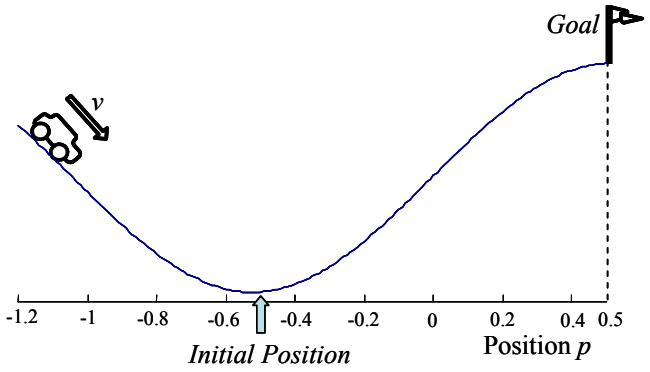

Figure 3. Mountain Car Task

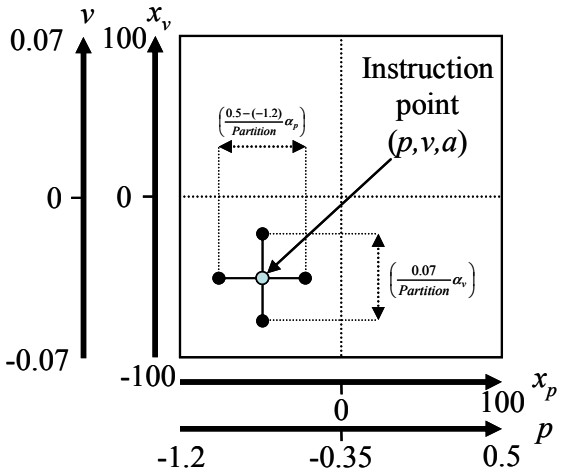

Figure 4. Normalization of Mountain Car Task

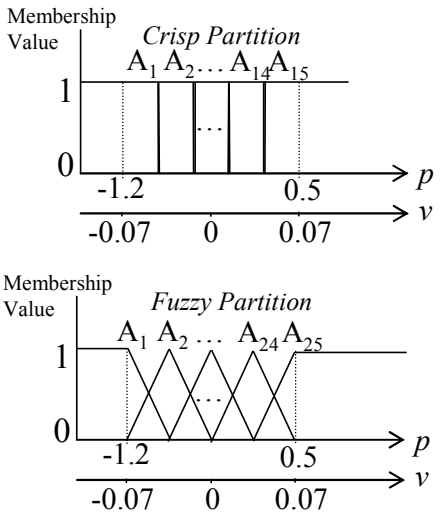

Figure 5. Membership Function

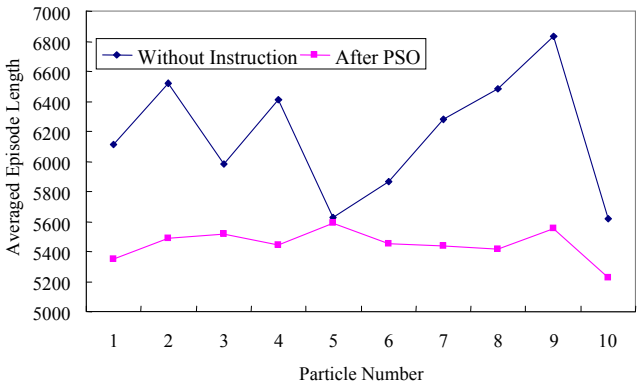

Figure 6. Results of Crisp Mountain Car Task

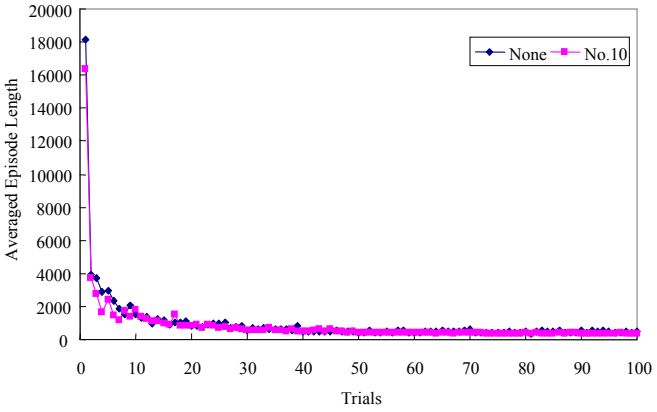

Figure 7. Results of Crisp Mountain Car Task*(No.10)*

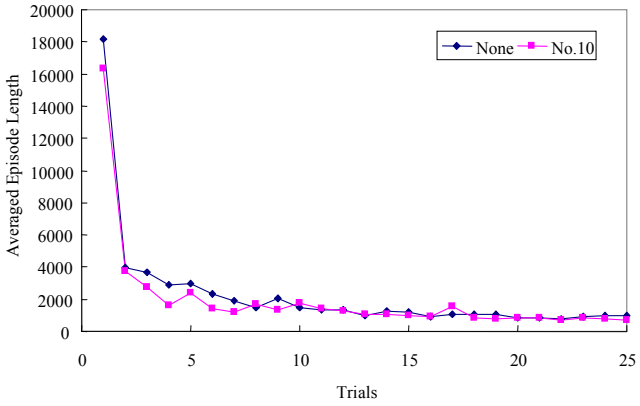

Figure 8. Results of Crisp Mountain Car Task*(No.10)*

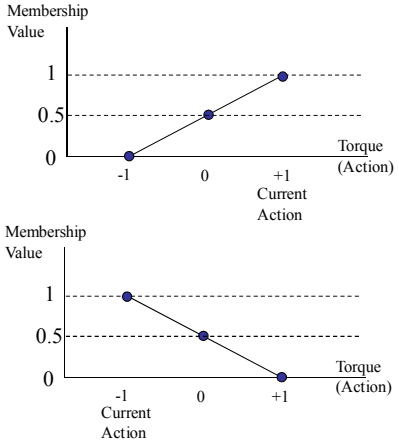

Figure 9. Membership Function for Forgetting

speed v of the instruction are normalized from position x_p and x_v of the particle in PSO. Moreover, the action a is defined as +1(full throttle advancement) when x_a is positive, and action a is defined as -1(full throttle retreat) when x_a is negative. α_v and α_p are predefined parameters to decide the range of the instruction, and $0<\{\alpha_v, \alpha_p\}<= 1.0$. The range of the instruction becomes wider if they are set near 1.0. α_v and α_p are set as 0.1, in this study.

The membership function for the state quantization for the agent is shown in Fig.5. The averaged episode lengths of the initial states of the particles and the averaged episode lengths after the 100 generations in PSO are shown in Fig.6. About 700 or more of the averaged episode length is decreased by the proposed method. As for the #9, we can see the averaged episode length becomes 5551 from initial value of 6831, i.e. decrease over 1200 episodes. Fig.7 shows the initial 100 trial process of the #10, i.e. the best instruction, after the optimization as well as the results without the instructions. Fig.8 also shows the initial 25 trial process. It is confirmed that the episode lengths are decreased by the proposed algorithm.

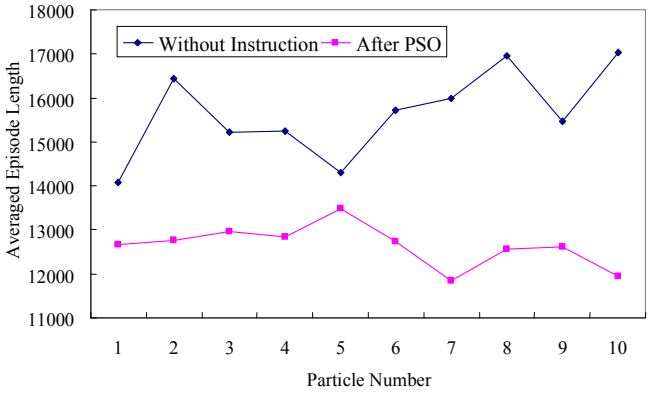

Figure 10. Results of Fuzzy Mountain Car Task

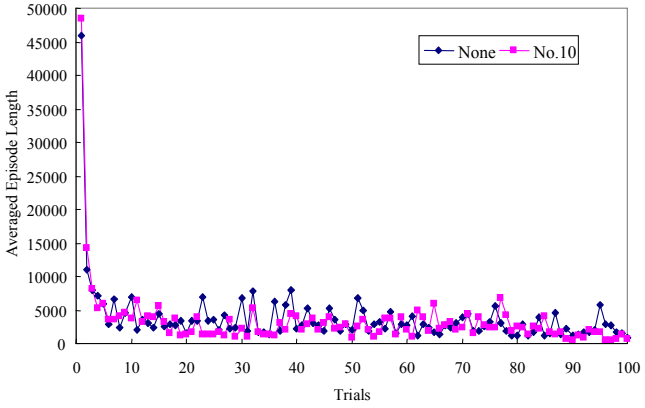

Figure 11. Results of Fuzzy Mountain Car Task*(No.10)*

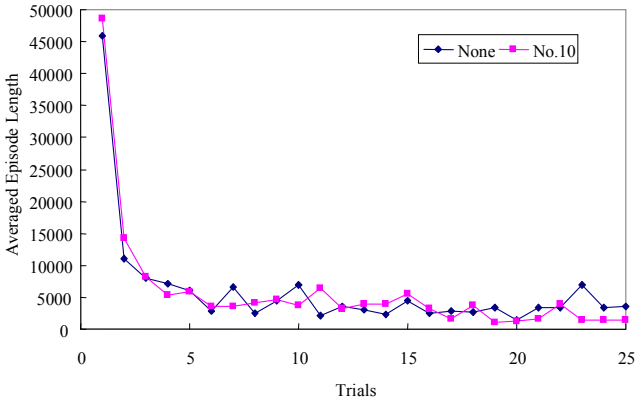

Figure 12. Result of Fuzzy Mountain Car Task*(No.10)*

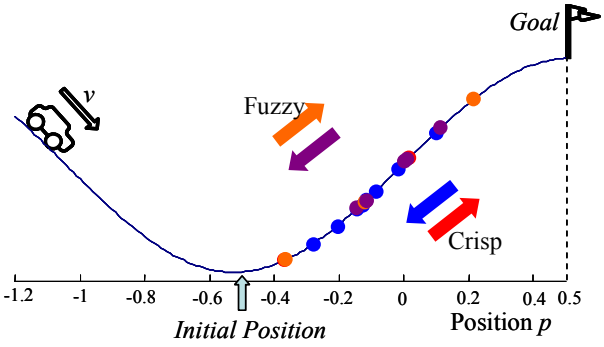

Figure 13. Crisp and Fuzzy Instruction Points

B. *Mountain Car Task(Fuzzy)*

Fuzzy Q-Learning agent is evaluated applying the instruction acquisition. The state is partitioned according to the membership functions of 25 fuzzy sets as shown in Fig.5. The degree of agreement in (8) that employs forgetting is assumed to be formulated as the membership functions shown in Fig.9. The averaged episode lengths of the initial states of the particles and the averaged episode lengths after the 100 generations in PSO are shown in Fig.10. About 3000 or more of the averaged episode length is decreased by the proposed method. As for the #10, we can see the averaged episode length becomes 11931 from initial value of 17036, i.e. decrease over 5000 episodes. Fig.11 shows the initial 100 trial process of the #10 after the optimization along with the results without the instructions. Fig.12 also shows the initial 25 trial process. It is confirmed that the total episode lengths are decreased by the proposed algorithm (from 367906 to 324872).

Examples of typical instruction points are shown in Fig.13. The action of a full throttle advances is decided around the initial position and the goal as the instruction. The full throttle retreat is decided in the other parts. These results are similar to the results by the Crisp partitioned agents.

C. *Acrobot task (Crisp)*

Acrobot is a mimic system of the "horizontal bar" of human gymnastics. The objective of the task is to swing the tip of the robot up to the predefined height as shown in Fig.14. A unique characteristic of the task is that the robot adjusts only the second joint torque being affected by its dynamics to achieve the goal. The dynamical equations of the Acrobot are as follows:

$$
\begin{aligned}
&d_{11}\ddot{\theta}_1 + d_{12}\ddot{\theta}_2 + h_1 + \phi_1 = 0 \\
&d_{21}\ddot{\theta}_1 + d_{22}\ddot{\theta}_2 + h_2 + \phi_2 = T \\
&d_{11} = m_1 r_1^2 + m_2 l_1^2 + m_2 r_2^2 + 2m_2 l_1 r_2 \cos\theta_2 + I_1 + I_2 \\
&d_{12} = m_2 r_2^2 + m_2 l_1 r_2 \cos\theta_2 + I_2 \\
&d_{21} = m_2 r_2^2 + m_2 l_1 r_2 \cos\theta_2 + I_2 \\
&d_{22} = m_2 r_2^2 + I_2 \\
&h_1 = -m_2 l_1 r_2 \left(2\dot{\theta}_1 + \dot{\theta}_2\right)\dot{\theta}_2 \sin\theta_2 \\
&h_2 = m_2 l_1 r_2 \dot{\theta}_1^2 \sin\theta_2 \\
&\phi_1 = \left(m_1 r_1 + m_2 l_1\right) g \sin\theta_1 + m_2 r_2 g \sin\left(\theta_1 + \theta_2\right) \\
&\phi_2 = m_2 r_2 g \sin\left(\theta_1 + \theta_2\right)
\end{aligned}
$$

where θ_1, θ_2 are the angles of joint1 and joint2, $\dot{\theta}_1$, $\dot{\theta}_2$ are the angular velocities of joint1 and joint2, and $\ddot{\theta}_1$, $\ddot{\theta}_2$ are the angular accelerations of joint1 and join2, respectively. T is the torque applied to the joint2. m_i is mass, l_i is length, r_i is length to center of mass, and I_i is moment of inertia of link$i$, respectively. Actual setting of constant parameters is as m_i =1, l_i =1, r_i =1, I_i=1 (i=1,2), and g=9.8 in this study. The angular velocities are bounded by $\dot{\theta}_1 \in [-4\pi, 4\pi]$ and $\dot{\theta}_2 \in [-9\pi, 9\pi]$. The target height H is set as 0.5. The equations of motion are numerically solved by means of Runge-Kutta method in 0.05sec interval. The sampling period is 0.2 sec. The agent chooses the torque T from {-1,0,1} as action at every sampling

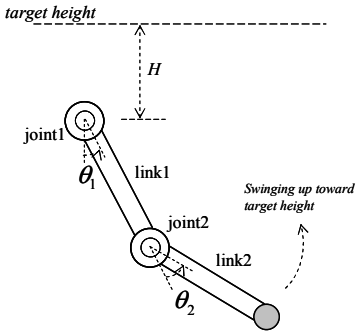

Figure 14. Acrobot Task

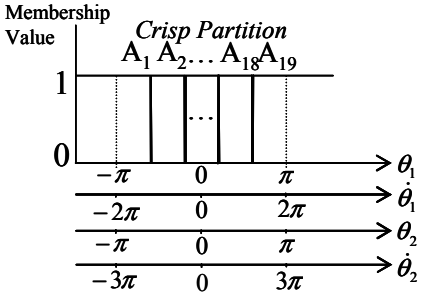

Figure 15. Membership Function

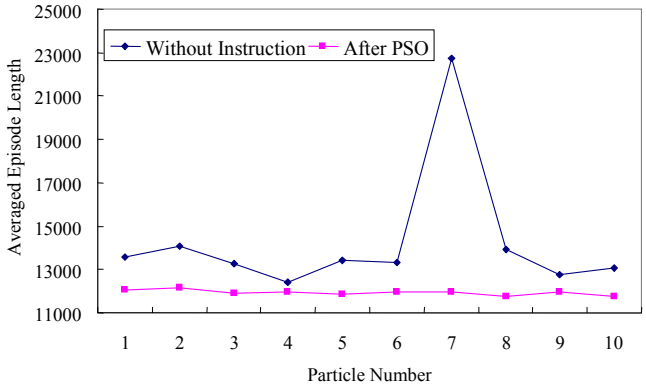

Figure 16. Results of Crisp Acrobot Task

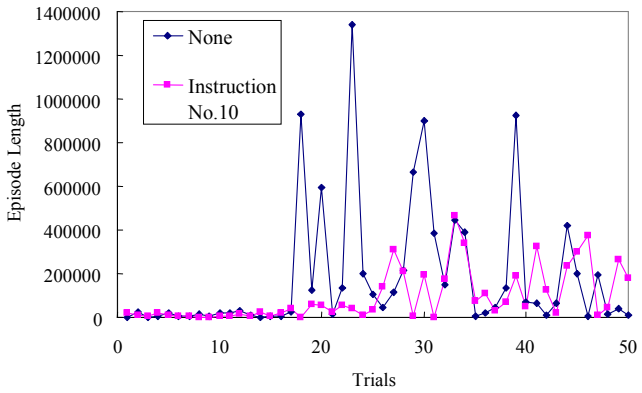

Figure 17. Results of Crisp Acrobot Task*(No.10)*

TABLE I. ACROBOT INSTRUCTION POINTS

Particle number	Acrobot Instruction Points				
	θ_1	$\dot{\theta}_1$	θ_2	$\dot{\theta}_2$	*act*
1	0.49	3.44	-0.53	1.79	1
2	0.83	3.85	-0.60	2.83	1
3	0.64	6.81	0.27	-3.25	1
4	1.04	0.64	-1.11	4.83	-1
5	0.57	3.55	-0.42	2.73	1
6	0.70	3.77	-0.31	2.81	1
7	1.44	7.04	-1.41	0.93	1
8	-0.21	2.34	-0.29	0.89	-1
9	-0.70	-6.56	2.52	-18.1	1
10	0.19	2.59	-1.37	-2.98	1

time(step). The number of partitions is 19 as shown in Fig.15, the learning rate α is 0.20, and the discount rate γ is 0.95. The agent tries the mountaineering 5 times in one simulation and the simulation is conducted 100 times. The averaged episode length is used to evaluate the learning performance.

When the following condition is satisfied, the instruction is given to the agent. The condition of the angle is defined in the same way of the mountain car task experiments as follows:

$$\frac{|\theta\max|\cdot x_\theta}{|X\max|}-\frac{|\theta\max|}{Partition\ size}\le\theta\le\frac{|\theta\max|\cdot x_\theta}{|X\max|}+\frac{|\theta\max|}{Partition\ size} \quad (15)$$

where θ denotes the state value of the angle, x_θ is the normalized particle state corresponding to the angle value, and $|X\ \max|$ is the maximum range value of the particle state. $|\theta\ \max|$ is the maximum range value of the angle. *Partition size* is a parameter of granularity of PSO search. The other conditions of states such as angular velocities are defined in the same manner.

The averaged episode lengths of the initial states of the particles and the averaged episode length after the 100 generations in PSO are shown in Fig.16. About 2000 or more of the averaged episode length is decreased by the proposed method. As for the #7, we can see the averaged episode length becomes 11951 from initial value of 22724, i.e. decrease over 10000 episodes. Fig.17 shows the initial 50 trial process of the #10 after the optimization along with the results without the instructions. It is confirmed that the total episode lengths are decreased drastically by the proposed algorithm (from 9169856 to 4721048 episodes). The acquired instructions by PSO algorithm are shown in TABLE.I. Fig.18 schematically depicts the examples of the acquired instruction points of Acrobot by the proposed algorithm. Although the Acrobot task is high dimensional and complicated task that the appropriate instruction is not clear intuitively, the proposed algorithm performs successfully the acquisition of the instruction in the reinforcement learning. Moreover, the episode length, i.e. the learning performance, can be drastically decreased by giving

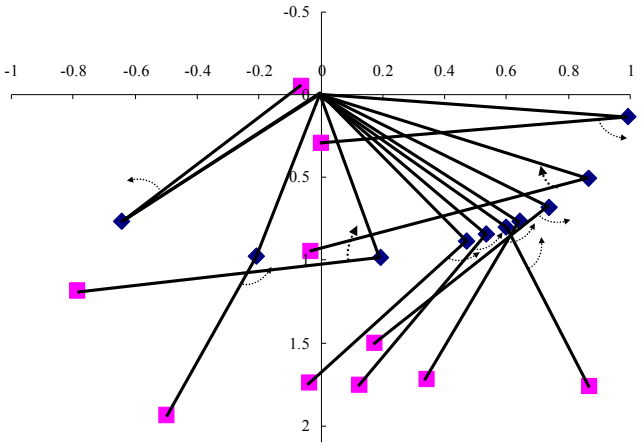

Figure 18. Acquired Instructions of Crisp Acrobot Task

even only one instruction point acquired by the proposed algorithm. It can be considered that this is because the necessary knack existing in the task is successfully acquired by the proposed algorithm.

VI. CONCLUSION

In this study, in order to clarify the instruction performance in the reinforcement learning, we proposed an instruction knowledge acquisition method for the reinforcement learning scheme by the particle swarm optimization (PSO) algorithm. Through numerical experiments of the mountain car task and the acrobat task, we showed the validness of the proposed approach in terms of learning speed and accuracy. Moreover, the effective instruction point for the reinforcement learning process was successfully acquired even in the Acrobot task that was the complicated task. In this study, the number of the instruction was assumed as 1 for simplicity. Our future plan includes acquisition of appropriate combination of some instructions for high dimensional and complicated tasks.

REFERENCES

[1] R. S. Sutton and A. G. Barto, "Reinforcement Learning", MIT Press, 1998.

[2] C. J. H. Watkins and P.Dayan, "Technical Note: Q-Leaning", Machine Learning, Vol.8, pp.58-68, 1992.

[3] K. Miyazaki, H. Kimura, and S. Kobayashi, "Theory and Application of Reinforcement Learning Based on Profit Sharing, " J. of JSAI, Vol.14, No.5, pp. 800-807, 1999.

[4] K. Miyazaki, S. Arai, and S. Kobayashi, "A Theory of Profit Sharing in Multi-agent Reinforcement Learning," J. of JSAI, Vol. 14, No.6, pp.1156-1164, 1999.

[5] Y. Takahashi and M. Asada, "Behavior Acquisition by Multi-Layered Reinforcement Learning, " Proc. of the 1999 IEEE Int. Conf. on Syst., Man, and Cybern., pp.716-721, 1999.

[6] J. Morimoto and K. Doya, "Acquisition of Stand-up Behavior by a Real Robot using Hierarchical Reinforcement Learning," Proc. of International Conference on Machine Learning, pp. 623-630, 2000.

[7] T. Watanabe and T. Sawa, "Instruction for Reinforcement Learning Agent Based on Sub-Rewards and Forgetting", Proc. of the IEEE World Congress on Computational Intelligence, FUZZ-IEEE 2010, pp.1984-1990, 2010.

[8] T. Sawa and T. Watanabe, "A Study on Evaluation of Eligibility Trace in Instruction Method for Fuzzy Q-learning Agent," Proc. of Joint 5th International Conference on Soft Computing and Intelligent Systems and 11th International Symposium on Advanced Intelligent Systems, pp.310-315, 2010.

[9] Yu Liu, Zheng Qin, and Zhewen Shi, "Hybrid Particle Swarm Optimizer with Line Search", Proceedings of the 2004 IEEE International Conference on Systems, Man & Cybernetics, pp. 3751-3755

[10] R. A. Jacobs, M. I. Jordan, and A. G. Barto, "Task Decomposition through Competition in a Modular Connectionist Architecture: The What and Where Vision Tasks," Neural Computation, Vol.3, pp.79-87, 1991.

[11] G. Auda and M. Kamel, "Modular Neural Networks: A Survey," International Journal of Neural Systems, Vol.9, No.2, pp.129-151, 1999.

[12] T. Watanabe and Y. Takahashi, "Hierarchical Reinforcement Learning Using A Modular Fuzzy Model for Multi-Agent Problem," Proc. of the 2007 IEEE International Conference on Systems, Man, and Cybernetics, pp.1681-1686, 2007.

[13] A. Stout, G. D. Konidaris, and A. G. Barto: "Intrinsically motivated reinforcement learning: A promising framework for developmental robot learning," Proc. of the AAAI spring symposium workshop on developmental robotics, 2005.

[14] Y. Tanaka and M. Ishikawa: "Reinforcement Learning with Internal Rewards Based on Error in a Grid-based Map," IEICE Technical Report, NC2008-151, pp.285-290, 2009.

[15] P. Y. Glorennec, "Reinforcement Learning: Overview," Proc. of ESIT, pp. 17- 35, 2000.

[16] D. Gu and H. Hu, "Fuzzy Multi-Agent Cooperative Q-Learning," Proc. of the 2005 IEEE International Conference on Information Acquisition, pp.193-197, 2005.

2011 IEEE International Conference on Fuzzy Systems
June 27-30, 2011, Taipei, Taiwan

Daily Reservoir Inflow Forecasting Using Fuzzy Inference Systems

Ivette Raymunda Luna Huamaní and Rosangela Ballini
Institute of Economics
UNICAMP
Campinas, Brasil
{ivette, ballini}@eco.unicamp.br

Ieda Geriberto Hidalgo
Faculty of Technology
UNICAMP
Limeira, Brasil
iedahidalgo@ft.unicamp.br

Paulo Sérgio Franco Barbosa and Alberto Luiz Francato
Faculty of Civil Engineering
UNICAMP
Campinas, Brasil
{franco, francato}@fec.unicamp.br

***Abstract*— This paper presents the application of a methodology for daily reservoir inflow forecasting in Brazilian hydroelectric plants. The methodology is based on Fuzzy Inference Systems (FIS) and the technique used for adjusting of the model parameters is an offline version of the Expectation Maximization (EM) algorithm. In order to automate the application of the methodology and facilitate the analysis of the results, a tool that allows managing streamflow forecasting studies and visualizing their information in graphical form was developed. A case study was applied to the data from three Brazilian hydroelectric plants whose operation is under the coordination of the Electric System National Operator. They are located in the Grande basin, a part of the Parana basin with two main rivers: the Grande and the Pardo. The benefits of the model are analyzed using statistics calculations, such as: root mean square error, mean absolute percentage error, mean absolute error and mass curve coefficient. Besides that, graphics that compare the registered and predicted streamflow are presented. The results show an adequate performance of the model, leading to a promising alternative for daily streamflow forecasting.**

Keywords: Inflow forecasting; Fuzzy systems; Hydroelectric plants; Reservoir management; Computacional tool.

I. INTRODUCTION

One of the great economic and environmental challenges facing humanity nowadays is the production of electricity. In Brazil, the power generation is assigned to the task of planning and scheduling of hydroelectric plants. The objective of this task is to ensure an economic and reliable operation policy for the system.

Forecasting of streamflows is an important step for planning and scheduling of hydroelectric power system. However, this step is still one of the most difficult issues in hydrological science because it is characterized as a problem dynamic, uncertain and nonlinear. The purpose of forecasting is to support decision-making, help operate reservoirs, assess resource capabilities and determine pricing for the out-of-province sale of energy.

Several researches have been devoted to the formulation and development of models that aims to improve the quality of hydrological prediction. In general, the models are assigned to one of three broad categories: *deterministic*, *conceptual* or *parametric*.

Deterministic models describe the rainfall-runoff process using physical laws of mass and energy transfer. Conceptual models provide simplified representations of key hydrological process using a perceived system. Parametric models use mathematical transfer functions to relate meteorological variables to runoff [1].

Deterministic and conceptual models require a large amount of high-quality data associated with hydrological, meteorological and natural geographical characteristics as well as human activities. Parametric models do not presuppose a detailed understanding of the basin's physical characteristics, nor does it require extensive data preprocessing [2]. Therefore, neural network and fuzzy systems are particularly powerful in situation where it is difficult to determine the physical process or when it is not possible to obtain a physical interpretation of the mathematical model representation [3]. Their potential for inflow forecasting is demonstrated in [4], [5] and [6].

In [7], an offline Fuzzy Inference System (FIS) was used for predicting annual inflows that are disaggregated in the respective monthly samples used for long-term hydropower scheduling. The use of these tools for the daily or hourly forecasting may be an interesting alternative that complements time series analysis for inflow modeling, usually performed in hydroinformatics via physical and conceptual models [8].

Given the importance of streamflow forecasting for power generation systems, this paper presents a Takagi-Sugeno (TS) FIS for daily inflow forecasting. The learning algorithm is based on the offline version of the Expectation Maximization (EM) algorithm. The objective is to improve the quality of this information, contributing to the choice of an operational policy that meets the consumer market in an economic and safe way.

The context of this paper is organized as follow. Initially, Section II presents the model general structure and the optimization algorithm. Then, in Section III a case study is shown. This section is divided in four items. The first describes the study area and the data collection; in the second item the methodology and the modeling are explained; the third shows the tool used in this work and the fourth item presents the

978-1-4244-7316-8/11/$26.00 ©2011 IEEE

results and discussions. After that, in Section IV the conclusions are presented.

II. MODEL DESCRIPTION

Model detailed is already used in different applications involving time series forecasting. It was originally proposed as a model initialization of the adaptive fuzzy system model proposed in [8]. In order to increase the clarity of this paper a general description of the model structure is presented next.

A. General Structure

The model structure adopted, as its name indicates, is mainly based on the first order TS-FIS [9].

Let denote the input vector at instant time k as $x^k = [x_1^k \quad x_2^k \quad ... \quad x_p^k]$. The output model for the correspondent input x^k is denoted by y^k. The input space represented $x^k \in R^p$ is partitioned into M sub-regions, each represented by a fuzzy rule (Fig. 1).

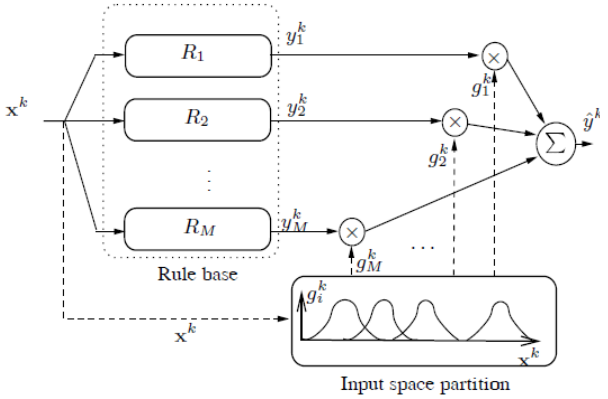

Figure 1. General model structure.

The antecedents of each If-Then fuzzy rule (R_i) are represented by their respective centers $c_i \in R^p$ and covariance matrices $V_i|_{p\times p}$. The consequents are represented by local linear models, with outputs y_i^k, $i = 1,..,M$ defined by:

$$y_i^k = \phi^k \times \theta_i^T \tag{1}$$

where $\phi^k = [1 \quad x_1^k \quad x_2^k \quad ... \quad x_p^k]$ is the extended input vector where the first component is increased for considering a constant term in the local linear model; $\theta_i = [\theta_{i0} \quad \theta_{i1} \quad ... \quad \theta_{ip}]$ is the coefficient vector of the local linear model related to the i^{th} rule.

Each input pattern has a membership degree associated with each region of the input space partition. This is calculated through membership functions $g_i(x^k) \in [0,1]$ that vary according to centers and covariance matrices related to the fuzzy partition, and are computed by:

$$g_i(x^k) = g_i^k = \frac{\alpha_i P[i \mid x^k]}{\sum_{q=1}^{M} \alpha_q P[q \mid x^k]} \tag{2}$$

where α_i are positive coefficients satisfying $\sum_{i=1}^{M} \alpha_i = 1$ and $P[i \mid x^k]$ is defined according to:

$$P[i \mid x^k] = \frac{1}{(2\pi)^{p/2} \det(V_i)^{1/2}} \exp(-(x^k - c_i) V_i^{-1} (x^k - c_i)^t) \tag{3}$$

where $\det(\cdot)$ is the determinant function. The final model output $\hat{y}^k$ is calculated by a non-linear weighted average of the local outputs and its respective membership degrees. Thus, the predicted value of the output variable for future time instant k is given by:

$$\hat{y}^k = \sum_{i=1}^{M} g_i^k y_i^k \tag{4}$$

B. Optimization Algorithm

The EM algorithm has been used for the optimization of several computational intelligence based methods, such as the works presented in [8], [10] and [11]. Therefore, this work suggests the use of the offline EM algorithm for the optimization of the FIS parameters.

First, the FIS structure is initialized. In order to define the number of rules M to codify in the model structure, the unsupervised Subtractive Algorithm (SC) is used over the input-output training data set [12]. Initial values for spreads codified in the covariance matrix are the same used by the SC algorithm. Therefore, the FIS structure is initialized as follows:

- $c_i^0 = \psi_i^0|_{1...p}$ where $\psi_i^0|_{1...p}$ is composed of the first p components of the i^{th} center found by the SC algorithm;
- $\sigma_i^0 = 1.0$;
- $\theta_i^0 = \left|\psi_i^0\right|_{p+1} 0...0\Big|_{1\times p+1}$, where $\psi_i^0|_{p+1}$ is the $(p+1)^{th}$ component of the i^{th} center found by the SC algorithm;
- $V_i^0 = r_a^2 I$, where I is a $p \times p$ identity matrix and r_a is the spread parameter used by the SC algorithm;
- $\alpha_i^0 = 1/M$.

After this initialization, model parameters are readjusted on the basis of the offline EM algorithm, (see [13] for the complete formulation), with the objective of maximizing the log-likelihood $\Im$ of the observed values of y^k at each M step of the learning process. This objective function is defined by:

$$\Im(D,\Omega)=\sum_{k=1}^{N}\ln\left(\sum_{i=1}^{M}g_i\left(x^k,C\right)\times P\left(y^k\middle|x^k,\theta_i\right)\right) \quad (5)$$

where N is the number of input-output patterns used for model optimization, $D=\{x^k,y^k\mid k=1,\ ..,\ N\}$, Ω contains all model parameters and C contains just the antecedents parameters (centers and covariance matrices). As noticed, for maximizing $\Im$, it is necessary to know the data distribution. Due to the lack of knowledge of the real distribution of precipitation and inflow data, the model is adjusted assuming a normal distribution of the observed records.

III. CASE STUDY

A. Study Area and Data Collection

The case study considers a part of the Paraná basin, located in the south of Brazil. It considers three power plants located in the Grande basin, a part of the Parana basin with two main rivers, the Grande and Pardo rivers. Caconde (CAC) reservoir plant and Euclides da Cunha (EDC) run off hydro plant are part of a cascade at the Pardo river, whereas the Água Vermelha (AVE) reservoir hydro plant is located in the Grande river cascade. All these power plants are under the management of AES-Brasil company.

Data available correspond to a continuous period of three years from 1st January 2005 to 31st December 2007. Accumulated daily rainfall data for the catchment area associated with each plant were supplied by SOMAR company while average daily inflow data were supplied by AES. Table I summarizes some statistics observed during the indicated period for the overall time series where *Max* = Maximum, *Min* = Minimum and *S Dev* = Standard Deviation.

From this table, we can notice that Agua Vermelha inflows present the highest mean and variability, whereas Canconde has the lowest ones. On the other hand, Agua Vermelha presents an average rainfall lower than the ones registered in the other two hydro plants, but both – Caconde and Euclides da Cunha – present similar rainfall statistics in terms of mean and standard deviation, specially in terms or magnitude level if compared to Agua Vermelha.

TABLE I SOME STATISTICS FOR ALL THE TIME SERIES USED IN THE CASE STUDY.

Alias	Inflows				Runoff			
	Max	*Min*	*Mean*	*S. Dev*	*Max*	*Min*	*Mean*	*S. Dev*
CAC	339	14	59	53	711	0	4.07	9.23
EDC	714	21	95	90	686	0	4.13	9.45
AVE	8641	537	2316	2066	2573	0	3.65	8.38

B. Methodology and Modeling

Input patterns consider both, past and future precipitation information and past inflow data. Therefore, a general input pattern is defined as:

$$x^k=[x_1^{\,k}\quad x_2^{\,k}\quad ...\quad x_p^{\,k}]=[r_1^{\,k}\quad ...\quad r_a^{\,k}\quad s_1^{\,k}\quad ...\quad s_b^{\,k}] \quad (6)$$

where $a\in Z^+$ indicates the number of components of the input vector containing past and future rainfall information represented by r and $b\in Z^+$ represents the number of input vector terms containing past inflow records (s), with $p=a+b$. It means that if we are forecasting the streamflow for time instant k, rainfall terms composing the input patterns will consider the last a-1 accumulated D days rainfall lags, the expected accumulated D days rainfall for instant k, as well as the last b inflows recorded up to k-1 as input variables. For the next h steps ahead, forecasted inflows and rainfall will be necessary.

With the purpose of improving the explanatory power of rainfall time series for each hydro plant, the FIS model uses as rainfall variable the accumulated precipitation of the last D days, where D is selected by maximizing the correlation coefficients between observed runoff and accumulated precipitation during those D days. Optimal D values for all the three inflow time series as well as correlation coefficient achieved are presented in Table II.

TABLE II OPTIMAL D VALUES, CORRELATION COEFFICIENTS AND LAGS CONSIDERED FOR BUILDING INPUT PATTERNS CONSIDERING RAINFALL AND RUNOFF INFORMATION.

Alias	D	Correlation	a	b
CAC	5	0.73	5	3
EDC	5	0.71	5	3
AVE	11	0.75	4	3

Table II also shows the number of lags a and b considered as input variables for modeling each model. These numbers of lags to were selected by maximizing the model performance for a multi-step ahead daily inflow forecasting task, with time horizon varying from one to twelve days ahead. As observed, in the case of runoff (b), the first three lags of each streamflow time series were considered as input variables. In the case of accumulated precipitation, lags considered varied from 5 to 11 days.

After input-output patterns are built, data set is normalized to the unit interval and then split up in two subsets, a training data set and a testing data set. The training data set was composed by the first two years of historical data whereas the testing data set was composed by the last one. Initial spreads for the SC algorithm ($r_a^{\,2}$) was equal to 1.25.

Performance assessment and model validation was performed considering the root mean square error (RMSE (m^3/s)), mean absolute percentage error (MAPE (%)), mean absolute error (MAE (m^3/s)) and mass curve coefficient (E), which is frequently used in hydrology for the validation of hydrological models [14] and is defined by the following equation:

$$E = \frac{\sum_{k=1}^{N}(y^k - \bar{y})^2 - \sum_{k=1}^{N}(y^k - \hat{y}^k)^2}{\sum_{k=1}^{N}(y^k - \bar{y})^2} \quad (7)$$

where $\bar{y}$ is the observed mean inflow. The first sum in the numerator denotes the total square error (SE) achieved assuming as forecast inflow the historical mean for all *k*. The second sum denotes the SE achieved by the evaluated model (FIS). Therefore, the closer E is to the unity, the better the model is, since the respective SE will be lower than the SE given by the mean. In this case the use of a more complex model would be justified by the improvement of the accuracy in the forecasting process.

C. *Tool Developed*

A tool to automate the application of the proposed methodology was developed. The software project and the computational implementation of this tool use the object-oriented paradigm and the C++ programming language. For searching information in the database the Structured Query Language (SQL) is used.

Fig. 2 presents the main interface of the system. It allows managing streamflow forecasting studies. Besides that, it facilitates the analysis of the results because these can be visualized in graphical form.

The interface presented in Fig. 2 is divided in frames. In the first frame on the left, the studies of streamflow forecasting are shown using a hierarchical structure for visualization. In the next frame, on the middle, the hydroelectric plants and the measurements stations are listed. Different icons distinguish them. The last frame on the right presents five sheets of which three have highlighted. The first one make possible to choose the period for which the study will be realized. So, this tool is able to predict the future streamflows or trying to reproduce the past streamflows. The second sheet shows one chart of recorded and predicted inflows and one chart of the precipitations for the period. The third sheet presents the results in spreadsheets.

This tool allows eight actions with the studies: create, duplicate, rename, delete, save, import data, edit data and run the study. Besides, it is possible export the results of a study for electronic spreadsheets, like Excel.

D. *Results and Discussions*

Performance metrics are summarized in Table III, for a given forecasting horizon *h* varying from *1,..12*. Since the FIS provides a different forecasted trajectory for each time instant, columns 2 to 13 present average errors of the last 353 trajectories predicted from one to twelve steps ahead.

As expected, observing any of the metrics, because of the prediction error of previous steps are fed into the input pattern for the next step ahead, the model performance becomes degraded as the forecast horizon aparts from the actual time instant. However, given that the minimum value of the mass curve coefficient goes from almost 77% to 99%, we can consider that the model presents an adequate performance due to its capability of explaining the hydrological process in at least 77%.

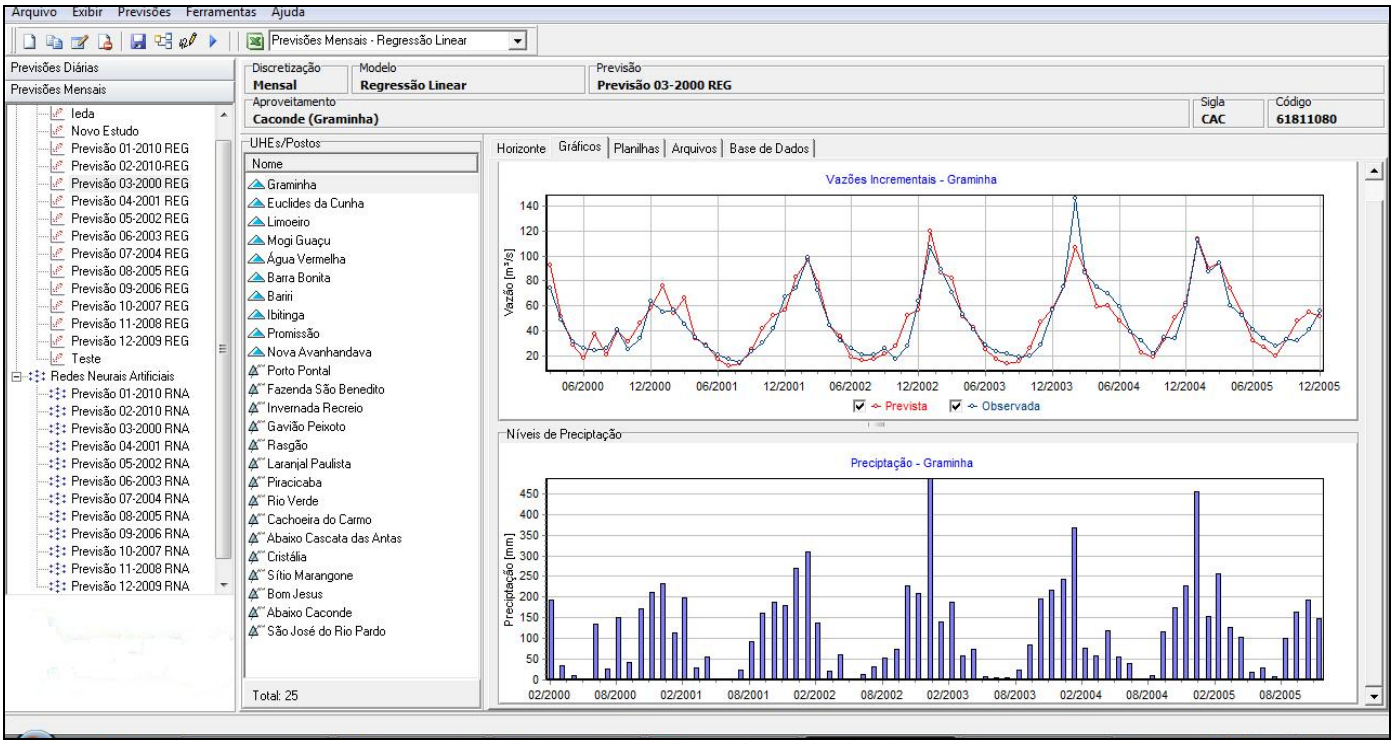

Figure 2. Main interface of the tool developed for forecasting streamflows.

TABLE III PERFORMANCE METRICS.

Alias	Horizon (h)											
	1	**2**	**3**	**4**	**5**	**6**	**7**	**8**	**9**	**10**	**11**	**12**
MAPE (%)												
CAC	8.96	11.32	12.91	14.43	15.78	16.91	17.85	18.66	19.36	20.01	20.67	21.29
EDC	6.98	8.91	10.33	11.40	12.27	12.98	13.56	14.01	14.41	14.75	15.05	15.33
AVE	1.62	2.46	3.35	4.20	5.05	5.84	6.61	7.35	8.06	8.74	9.39	10.00
RMSE (m^3/s)												
CAC	0.74	0.88	0.97	1.04	1.10	1.15	1.20	1.24	1.27	1.30	1.33	1.35
EDC	1.25	1.55	1.71	1.82	1.90	1.99	2.06	2.13	2.17	2.21	2.25	2.29
AVE	6.16	8.00	10.25	12.20	14.32	16.21	18.07	19.78	21.44	23.01	24.53	25.95
MAE (m^3/s)												
CAC	6.04	7.56	8.53	9.37	10.05	10.64	11.11	11.53	11.89	12.23	12.57	12.89
EDC	9.76	11.75	13.29	14.33	15.17	15.86	16.46	16.87	17.24	17.53	17.80	18.07
AVE	44.23	63.97	84.66	103.55	122.54	140.94	158.92	176.22	192.85	208.56	223.22	236.83
E												
CAC	0.94	0.92	0.90	0.88	0.86	0.85	0.83	0.82	0.80	0.79	0.78	0.77
EDC	0.94	0.91	0.88	0.87	0.85	0.84	0.82	0.81	0.80	0.79	0.78	0.77
AVE	0.99	0.99	0.99	0.99	0.98	0.98	0.97	0.97	0.96	0.96	0.95	0.94

Fig. 3 depicts the evolution of MAPE and E from one up to twelve days ahead of forecasted inflow records. Since Caconde and Euclides da Cunha inflows belong to a different magnitude level if compared to Agua Vermelha, their results will be compared and analyzed simultaneously.

The worse performance in terms of MAPE was achieved for Caconde hydroplant. Nevertheless, given that this metric is a relative index, it is necessary to consider at least one other absolute performance metric. So, analyzing RMSE and MAE values, results achieved for Caconde outperformed the ones obtained for Euclides da Cunha. Though, considering the mass curve coefficient, the fuzzy system achieved a similar performance for both inflow time series, as also depicted in Fig. 3.

Forecasted trajectories for one step ahead and for one up to twelve steps ahead are depicted in Fig. 4 and 5, for Caconde and Euclides da Cunha, respectively. We can observe that, the difficulty for predicting inflows increase during humid periods, since the different trajectories obtained at the beginning of the year tend to apart from the observed one with the increase of the lead time and specially before the peak flows. In general, performance metrics point to an adequate and similar model performance in both cases, which is expected due to the nature of Euclides da Cunha hydroelectric (a run off plant).

On the other hand, considering results obtained for Agua Vermelha, the FIS presented the lowest MAPE but the highest MAE, which is expected due to the inflows levels. In terms of explanatory power, the FIS presented a mass curve coefficient varying from 94% to 99%. Forecasted results are illustrated in Fig. 6. Again, we can notice the effect of the lead time and uncertainties over the forecasted inflow trajectories.

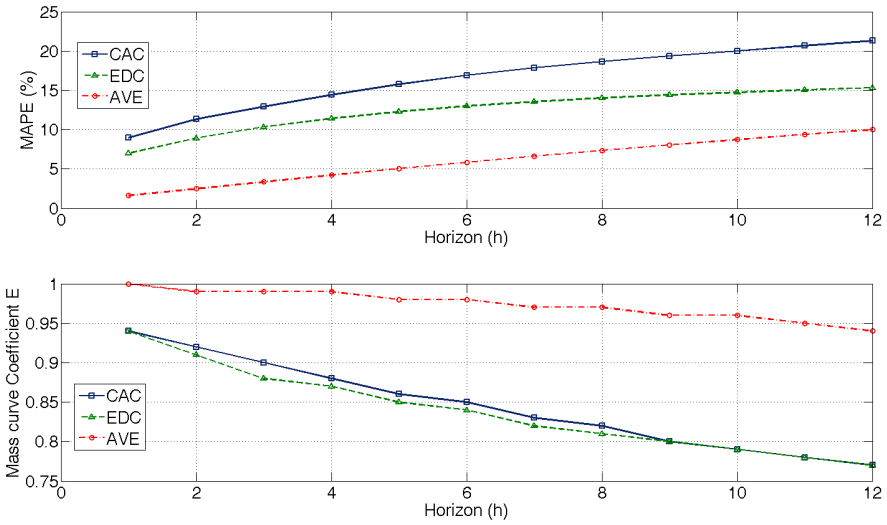

Figure 3. Mean absolute percentage error and mass curve coefficient evolution.

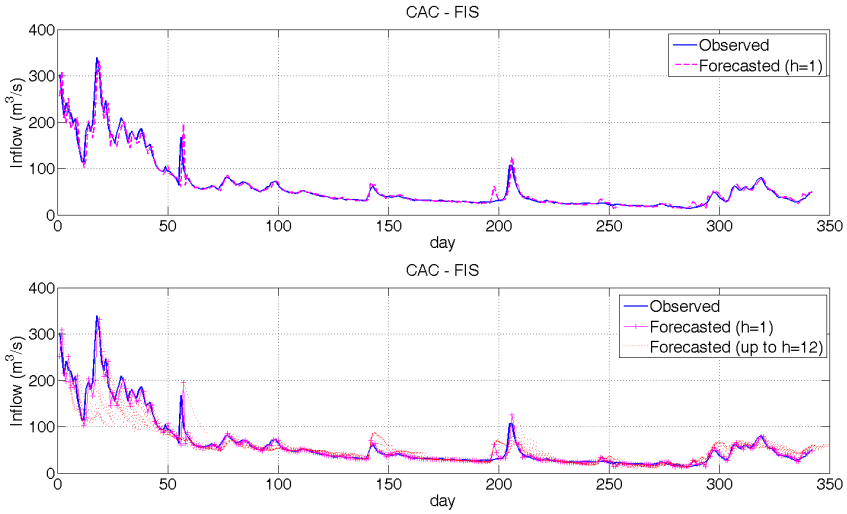

Figure 4. One step ahead and one up to twelve steps ahead daily inflow forecasting for Caconde hydroplant.

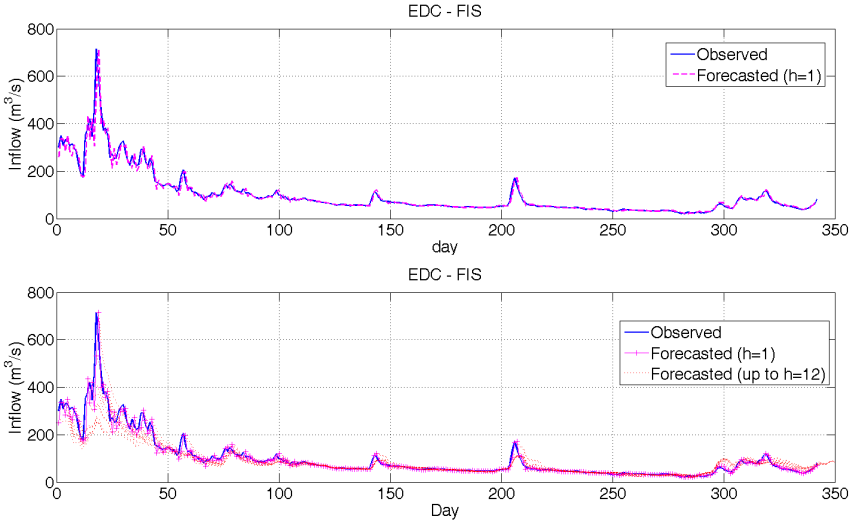

Figure 5. One step ahead and one up to twelve steps ahead daily inflow forecasting for Euclides da Cunha hydroplant.

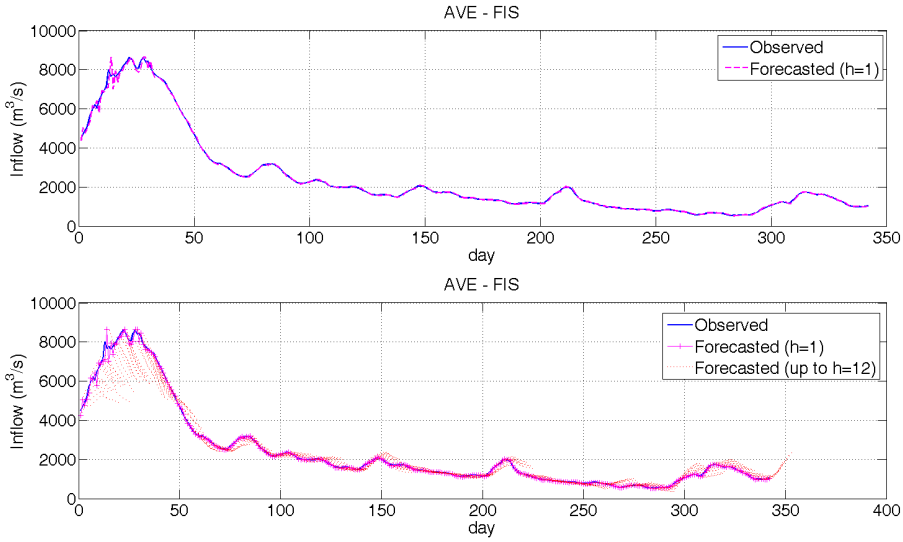

Figure 6. One step ahead and one up to twelve steps ahead daily inflow forecasting for Agua Vermelha hydroplant.

IV. CONCLUSIONS

This work presented an application of Fuzzy Inference Systems (FIS) for multi-step ahead daily inflow time series forecasting. The technique used for adjusting of the model parameters is an offline version of the Expectation Maximization (EM) algorithm.

The case study considered three Brazilian hydroelectric plants: Caconde (CAC), Euclides da Cunha (EDC) and Água Vermelha (AVE) that are located in the Parana basin. Theirs operation is under the coordination of Electric System National Operator and under management of AES-Brasil company.

A tool was developed in order to automate the application of the methodology and facilitate the analysis of the results. This tool allows managing streamflow forecasting studies and visualizing their information in graphical form.

Although the results shows very promising, it is evident the need research about alternative for improving multi-step ahead forecasting results. Future works involve the use of a different learning algorithm for the fuzzy inference system in order to avoid the normality hypothesis over the time series distribution, as well as the use of adaptive reorganizable fuzzy model in order to deal with the higher variability presented during humid periods. Comparison with other proposals is also considered.

REFERENCES

[1] C. Dawson and R. Wilby, "Hydrological modelling using artificial neural networks," Progress in Physical Geography, vol. 25, no. 1, pp. 80–108, 2001.

[2] Jun Zhang, Chun-tian Cheng, Sheng-li Liao, Xin-yu Wu, and Jian-jian Shen "Daily reservoir inflow forecasting combining QPF into ANNs model". Hydrol. Earth Syst. Sci. Discuss., 6, 121-150, 2009.

[3] R. Price, "Lecture on knowing the context between hydroinformatics and flood modelling," UNESCO-IHE Institute for Water Edutation, Tech. Rep., November 2008.

[4] C. M. Zealand, D. H. Burn, and S. P. Simonovic, "Short term streamflow forecasting using artificial neural networks," Journal of Hydrology, no. 214, pp. 32–48, 1999.

[5] P. Nayak, K. Sudheer, D. Rangan, and K. Ramasastri, "A neuro-fuzzy computing technique for modeling hydrological time series," Journal of Hydrology, vol. 291, pp. 52–66, 2004.

[6] G. J. Bowden, H. R. Maier, and G. C. Dandy, "Input determination for neural network models in water resources applications. Part 2. Case Study: forecasting salinity in a river," Journal of Hydrology, no. 301, pp. 93–107, 2005.

[7] M. Zambelli, I. Luna, and S. Soares, "Long-Term hydropower scheduling based on deterministic nonlinear optimization and annual inflow forecasting models." Procs. of the PowerTech Conference, pp. 1–8, 2009.

[8] I. Luna, S. Soares, J.E.G. Lopes, and R. Ballini. Verifying the use of evolving fuzzy systems for multi-step ahead daily inflow forecasting. 15th International Conference on Intelligent System Applications to Power Systems – ISAP '09, pages 1–6, November 2009.

[9] T. Takagi and M. Sugeno, "Fuzzy identification of systems and its applications to modeling and control," IEEE Transactions on Systems, Man and Cybernetics, no. 1, pp. 116–132, January/February 1985.

[10] R. Jacobs, M. Jordan, S. Nowlan, and G. Hinton, "Adaptive mixture of local experts." Neural Computation, vol. 3, no. 1, pp. 79–87, 1991.

[11] Lázaro, M., Santamariaa, I. e Pantaleón, C. (2003). A new EM-based training algorithm for RBF networks, Neural Networks 16(1): 69–77.

[12] S. Chiu, "A cluster estimation method with extension to fuzzy model identification," in Proceedings of The IEEE International Conference on Fuzzy Systems, vol. 2, June 1994, pp. 1240–1245.

[13] Ivette Luna, Leandro Maciel, Rodrigo Lanna F. da Silveira, and Rosangela Ballini. Estimating the Brazilian central bank's reaction function by fuzzy inference system. In Eyke Hüllermeier, Rudolf Kruse, and Frank Hoffmann, editors, IPMU (2), volume 81 of Communications in Computer and Information Science, pages 324--333. Springer, 2010.

[14] A. Aitken, "Assessing systematic errors in rainfall-runoff models," Journal *of Hydrology*, vol. 20, pp. 121–136, 1973.

2011 IEEE International Conference on Fuzzy Systems
June 27-30, 2011, Taipei, Taiwan

A Study on Hybrid Model of HMMs and GMMs for Mirror Neuron System Modeling using EEG Signals

Seung-Min Park
School of Electrical Electronics Engineering
Chung-Ang University
Seoul, KOREA
Smpark85@gmail.com

Junheong Park
School of Electrical Electronics Engineering
Chung-Ang University
Seoul, KOREA
fullsamo@wm.cau.ac.kr

Kwang-Eun Ko
School of Electrical Electronics Engineering
Chung-Ang University
Seoul, KOREA
kke@wm.cau.ac.kr

Kwee-Bo Sim
School of Electrical Electronics Engineering
Chung-Ang University
Seoul, KOREA
kbsim@cau.ac.kr

***Abstract*—For our present life anytime, anywhere access to the network can communicate with the ubiquitous computing. it is essential to human life. We should be able to agree that communication will be enabled. For our present life, anytime, anywhere access to the network can communicate with the ubiquitous computing. Such as the ubiquitous era approached, interaction between the user and the computer has become an important issue. In this paper we use EEG signals to extract the user's intention recognition data, which the Mirror Neuron System Based on HMMs and GMMs to model the convergence of the hybrid model is proposed. This is based on a kind of biological signals using EEG signals to the user's intention recognition techniques have been studied. In addition, EEG signals is generated based on the model, using the user intention recognition method have been studied. The proposed model will be applied in the field of neuro robotics.**

Keywords-Mirror Neuron System, HMMs(Hidden Markov Models), GMMs(Gaussian Mixture Models), EEG, Intention recognition

I. INTRODUCTION

The last century, AI(Artificial Intelligent) field (problem solving, pattern recognition, decision-making) was a tremendous progress. The idea for the robot AI robot 'thinks' you want to empower people to start in the desires. AI robot, such as differences of level perceptual, emotional, and cognitive, was insufficient points. Therefore, we implemented a much more seamless system for human robot interaction is required. Meanwhile, today's information and communication technology breakthrough by the user computing system through anywhere, anytime access to information needed to build an infrastructure that can have been going. Accordingly, the ubiquitous and user-centered environment built on active service, the core technologies necessary to provide the domestic and foreign research institutes and universities have been actively focusing on. In ubiquitous computing environment, the circumstances of the computer and the user intent is consistent with the self-awareness must be able to provide the best service. To implement this, a critical underlying technology is the user's intention recognition technology. Recognition technology is intended to process the information collected from various centers, fusion is applied to the reasoning and learning. Thus, to infer the intent of people, recognized as the technology to existing information and emotional situation for the individual to perform the recognition, there are many case studies[1][2].

According to the latest neuroscience research into the human brain called mirror neurons, the nerve was the existence of the doctrine[3][4]. Mirror neurons are brain cells in the premotor cortex. First identified in macaque monkeys in the early 1990s, the neurons also known as "monkey-see, monkey-do cells" fire both when a monkey performs an action itself and when it observes another living creature perform that same action[5]. Though it has been impossible to directly study the analogue of these neurons in people (since human subjects cannot be implanted with electrodes), several indirect brain-imaging measures, including EEG, have confirmed the presence of a mirror neuron system in humans[6]. The human mirror neuron system is now thought to be involved not only in the execution and observation of movement, but also in higher cognitive process, language, for instance, or being able to imitate and learn from other's actions, or decode their intentions and empathize with their pain[7][8].

There have been many studies Mirror neurons in the department of brain neuroscience, and psychology. But so far the engineering models of mirror neurons are the basic steps.

In this paper, the user intent recognition, a method for effectively is proposed for engineering modeling of mirror neurons. Original intent of the user to recognize the techniques used in the HMMs and GMMs are created by combining a hybrid model. This is based on a kind of biological signals using EEG signals to the user's intention recognition techniques have been studied. In addition, EEG signals is generated based

978-1-4244-7316-8/11/$26.00 ©2011 IEEE

on the model, using the user intention recognition method have been studied. The proposed model will be applied in the field of neuro robotics. This paper is organized as follows.

In chapter 2, mirror neurons, and background information on user intent recognition is described, Section 3 describes the proposed hybrid model, and Section 4 describes the conclusions and future research.

II. THEORY FOR SYSTEM

A. *Mirror neuron system in humans*

Action observation studies in the mid 1990s using both TMS(Transcranial Magnetic Stimulation) and PET(Positron Emission Tomography) provided some evidence for the existence of the human MNS(Mirror Neuron System)[6][9]. Especially imitation was closely associated with MNS when researchers began to report the relation between mirror neurons and imitation in humans using MRI(Magnetic Resonance Imaging) and fMRI(Functional Magnetic Resonance Imaging). These reports provided the foundation for examining whether human areas relating to imitation of hand actions had mirror properties. Based on the research that mirror neurons discharge more during the execution than the observation of an action, and that an individual simultaneously observes and performs an action during imitation, it was predicted that human mirror neuron areas would show higher activity during execution than during observation of an action, and highest activity during imitation. This in sum reflects the activity attributable to action observation and execution[10][11].

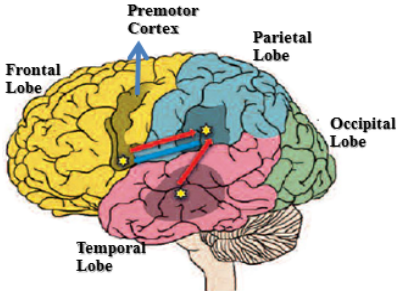

Figure 1. The distribution of mirror neurons

The human MNS is especially important for imitative behavior early in life. And imitation is a pervasive type of learning in humans, and the understanding of its primary neural mechanisms is noticeably important. It is associated with the user's intention recognition. Because, according to other people's words and actions that recognize the person's intent is for the most basic instincts. Therefore, when describing the behavior of actors, by analyzing the signals, as opposed to the user's intent is to identify.

B. *Intention recognition using EEG data extraction*

In the previous study, when each of the letters imagine the ideation center and Broca's area was measured from the EEG signals. This is based on the person you imagine what a particular word on when the change in EEG was found[12]. Using this data, data to recognize the user's intention were analyzed by ERSP(Event-Related Spectral Perturbation) and ITC(Inter-Trial Coherence) methods. We were building a database to recognize user's intention based on these data.

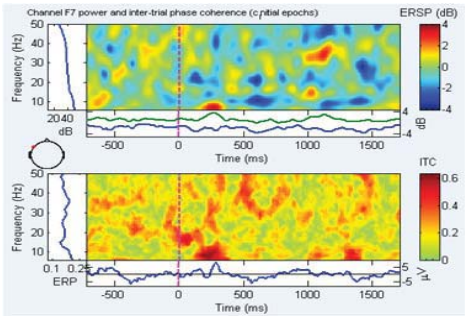

Figure 2. When we imagine letter C, spectrum of ERSP and ITC

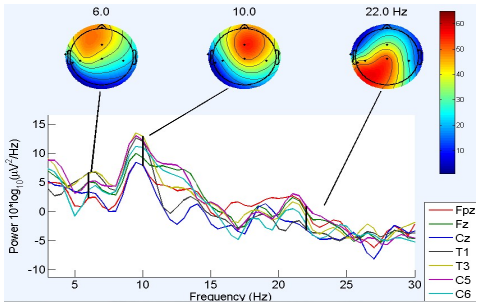

Figure 3. Analysis with EEGLAB, when we listen to dance music and the frequency by the average power spectrum EEG data

C. *Hidden Markov Models*

HMMs (Hidden Markov Models) has been widely used in pattern classification, speech recognition and gesture recognition. In addition, the user with the user's intent is to produce a secreted sequence data to determine whether the top because you can see a problem in the field of intention recognition can be effectively applied[13][14].

HMMs Hidden States that we do not know the status of the probabilistic transition process Observable symbol that raises the probability of realistically modeling the transition process is a double stochastic process.

HMMs as the symbols $\lambda = (\pi, A, B)$ is expressed as the number of hidden state variables, N, Observable symbol that when the number of M, has the following components[15].

1) $Q = \{q_1, q_2, \cdots\cdots, q_n\}$: set of hidden states
2) $V = \{v_1, v_2, \cdots\cdots, v_m\}$: set of observable symbol
3) $O = \{o_1, o_2, \cdots\cdots o_{t-1}, o_t\}$: sequence consists of observable symbol
4) π_i : initial probability vector of hidden state
5) A_{ij} : state transition matrix
6) B_{ij} : confusion matrix

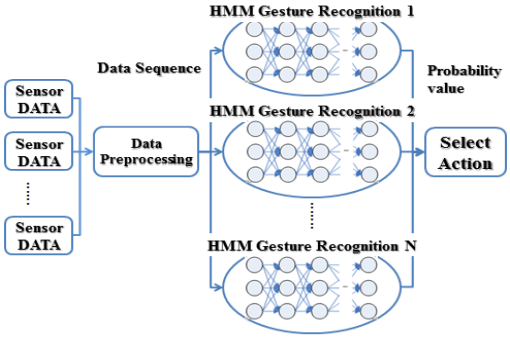

Figure 4. HMM models for recognizing the different behaviors

HMMs Hidden States that we do not know the status of the probabilistic transition process Observable symbol that raises the probability of realistically modeling the transition process is a double stochastic process.

HMMs as the symbols $\lambda = (\pi, A, B)$ is expressed as the number of hidden state variables, N, Observable symbol that when the number of M, has the following components[15].

7) $Q = \{q_1, q_2, \cdots\cdots\cdots, q_n\}$: set of hidden states
8) $V = \{v_1, v_2, \cdots\cdots\cdots, v_m\}$: set of observable symbol
9) $O = \{o_1, o_2, \cdots\cdots o_{t-1}, o_t\}$: sequence consists of observable symbol
10) π_i : initial probability vector of hidden state
11) A_{ij} : state transition matrix
12) B_{ij} : confusion matrix

After the fact, the model defined by HMMs in order to use the following three problems (Evaluation, Decoding, Learning) must solve. Therefore, the three kinds of solutions to the problem, several algorithms have been widely used. When estimating the probability of the problem, Forward / Backward algorithm can be solved using, and determine the issue of optimal order is one of the Viterbi algorithm of dynamic programming techniques are used. Finally, estimate the parameters of the EM algorithm called the Baum-Welch algorithm is employed and can be solved[15]. For more information on HMM and then you can see in the paper[16].

D. Gaussian Mixture Models

Gaussian probability distribution, albeit the most widely used distribution data, based on the average of the group together as a form of a unimodal only one possible representation is limited. Therefore, the general form of probability model capable of expressing need, this time to consider it the most easily combined with the multiple Gaussian model is being created. This is called GMMs (Gaussian Mixture Models). M simple probability density function (or component [component]) is defined as a linear combination of the entire probability density function is expressed as the following equation.

$$p(x \mid \Phi) = \sum_{j=1}^{M} p(x \mid w_j, \Phi) P(w_j) \tag{1}$$

Where w_i is a component, $P(w_i)$ is the prior probability or mixed parameters. And $p(X \mid w_i, \Phi)$ is the vector of the parameters Φ, when told, is the probability density of the ingredients. $X = \{x_k\}$ log-likelihood of the sample were as follows.

$$\begin{aligned} L(\Phi \mid x) &= \sum_k \log p(x_k \mid \Phi) \\ &= \sum_k \log \sum_j p(x_k \mid w_j, \Phi) P(w_j) \end{aligned} \tag{2}$$

Equation (2) does not have an immediate solution. Therefore, these problems can be solved using EM(Expectation Maximization)algorithm[17]. EM algorithm is performed in two stages, as follows: posterior probabilities was calculated using Bayes' theorem.

$$p(w_j \mid x_k, \Phi) = \frac{p(x_k \mid w_j, \Phi) P(w_j)}{\sum_l p(x_k \mid w_l, \Phi) P(w_l)} \equiv h_{kj} \tag{3}$$

Where the d-dimensional gaussian density components if you choose to be, $p(x \mid w_j, \Phi) \sim N_d(\mu_j, \sum j)$ is as follows.

$$p(x \mid w_j, \Phi) = \frac{1}{(2\pi)^{d/2} \left| \sum j^{1/2} \right|} \exp[-\frac{1}{2}(x - \mu_j)^T \sum j^{-1} (x - \mu_j)] \tag{4}$$

So , the equation (3) can be expressed equation(4). As a result, equation (5) is represented by Gaussian probability.

$$h_{kj} = \frac{g_j \left| \sum j \right|^{-1/2} \exp[-\frac{1}{2}(x_k - \mu_j)^T \sum j^{-1} (x_k - \mu_j)]}{\sum_l g_l \left| \sum^{l} \right|^{-1/2} \exp[-\frac{1}{2}(x_k - \mu_l)^T \sum j^{-1} (x_k - \mu_l)]} \tag{5}$$

However, $g_l \equiv P(w_j)$

III. Hybrid Model of HMMs and GMMs

Hybrid model based on the class variable mixture GMMs and HMMs based on the components are configured. Hybrid models take advantage of the positive aspects of each model used in the combination. Each of the types of models included in the training data, it is possible to collect specific information. For example, GMMs are more likely to capture the structural information. While HMMs in the sequence, the transition is to extract information. The choice of a single model, it can interfere with the performance of the classification. Before making a decision of the classification, the hybrid model has output to improve the stability of method and performance. We think this situation, combined results from two models that use a hybrid model of the sum rule is proposed. Sum rule for the probabilities of each model in estimating the error is known to be robust. Given a set of weights $\{w_i; i = 1 \cdots L\}$ for L number of classifiers, and k classes, a given brain activity data, x is assigned to a model of M_n.

$$\sum_{i=1}^{L} w_i P(M_n \mid x_i) > \sum_{i=1}^{L} w_i P(M_l \mid x_i) \qquad l = 1, \cdots, k \; ; l \neq n \quad (6)$$

A small training set to minimize the error rate classifier decides the value weighted. Figure 5. Illustrates the proposed model.

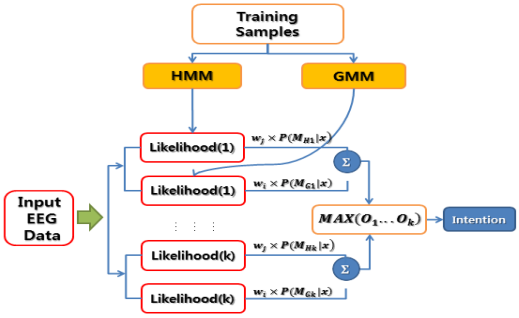

Figure 5. Hybrid model of HMMs and GMMs

HMMs and GMMs in Figure 5, M is the result of the hybrid model we ultimately need to find the error rate of recognition model, removing the maximum value of the optimized sequence.

IV. Conclusions

In this paper, HMMs and GMMs as shown in Figure 5, the convergence of the proposed hybrid model. Hybrid models take advantage of the positive aspects of each model used in the combination. Each of the types of models included in the training data, it is possible to collect specific information. The choice of a single model, it can interfere with the performance of the classification. Before, both models making a decision on the classification of a performance and how to improve the stability of the output. Conventional HMMs to recognize only the user's intentions in the posterior probability classifier to minimize the error rate of Gaussian Neural Network based on GMMs were added. Error rate as shall be determined appropriately weighted values and operations are expected to increase the speed and accuracy. Next simulation compares the performance of the proposed algorithm will be tested.

Acknowledgment

This work was supported by the National Research Foundation of KOREA[NRF] grant funded by the KOREA government[MEST] [No.2010-0029226].

References

[1] K.E KO, K.B Sim, "Development of Context Awareness and Service Reasoning Technique for Handicapped People", Journal of Korean Institute of Intelligent Systems, Vol.19, No.1, pp.34-39.

[2] C. Zhu, Q Cheng, and W. Sheng, "Human Intention Recognition in Smart Assitsted Living Systems Using A Hierarchical Hidden Markov Model", 4th IEEE Conference on Automation Science and Engineering Key Bridge Marriott, Washington DC, USA August 23-26, 2008, pp.253-258.

[3] G. Rizzolatti "The Mirror Neuron System and its function in humans" Anatomy and embryology, vol.210, Dec. 2005, pp.419-21.

[4] M. Fabbri-Destro and G. Rizzolatti, "Mirror neurons and mirror systems in monkeys and humans.," *Physiology (Bethesda, Md.)*, vol. 23, Jun. 2008, pp. 171-9.

[5] a Murata, L. Fadiga, L. Fogassi, V. Gallese, V. Raos, and G. Rizzolatti, "Object representation in the ventral premotor cortex (area F5) of the monkey.," *Journal of neurophysiology*, vol. 78, Oct. 1997, pp. 2226-30.

[6] V. Gallese, L. Fadiga, L. Fogassi, and G. Rizzolatti, "Action recognition in the premotor cortex.," *Brain : a journal of neurology*, vol. 119 (Pt 2), Apr. 1996, pp. 593-609.

[7] M. a Umiltà, E. Kohler, V. Gallese, L. Fogassi, L. Fadiga, C. Keysers, and G. Rizzolatti, "I know what you are doing. a neurophysiological study.," *Neuron*, vol. 31, Jul. 2001, pp. 155-65.

[8] L. Cattaneo, M. Fabbri-Destro, S. Boria, C. Pieraccini, A. Monti, G. Cossu, and G. Rizzolatti, "Impairment of actions chains in autism and its possible role in intention understanding.," *Proceedings of the National Academy of Sciences of the United States of America*, vol. 104, Nov. 2007, pp. 17825-30.

[9] L. Fadiga, L. Fogassi, G. Pavesi, and G. Rizzolatti, "Motor facilitation during action observation: a magnetic stimulation study.," *Journal of neurophysiology*, vol. 73, Jun. 1995, pp. 2608-11.

[10] M. Iacoboni, "Cortical Mechanisms of Human Imitation," *Science*, vol. 286, Dec. 1999, pp. 2526-2528.

[11] L. Koski, A. Wohlschläger, H. Bekkering, P. Woods, M.-charlotte Dubeau, J.C. Mazziotta, and M. Iacoboni, "Modulation of Motor and Premotor Activity during Imitation of Target-directed Actions," *Cerebral Cortex*, 2002, pp. 847-855.

[12] H G Yeom., I H Jang, K B Sim, "Brain-Computer Interface based on Changes of EEG on Broca's Area", Journal of Korean Institute of Intelligent Systems, Vol.19, No.1, pp.122-127, 2009

[13] K S Kim, D M Kim, T B Yoon, and J H Lee, " Intention-Awareness Method using Behavior Model Based User Intention" Proceedings of KFIS Autumn Conference , Vol.12, No.2, pp.3-6, 2007

[14] J E Lee, and J H Lee, "User Intention-Awareness System for Goal-oriented context-awareness service", Proceedings of KFIS Autumn Conference, Vol.16, No.2, pp.239-242, 2006

[15] J H Kim, E B Kong, S H Cho, "HMM Based Anomaly Intrusion Detection System", Proceedings of KIISE Spring Conference, Vol.30, No.1, pp.449-450

[16] Lawrence R. Rabiner, " A Tutorial on Hidden Markov Models and Selected Applications in Speech Recognition", Proceedings of the IEEE, Vol.77, No.2, Feb, 1989

[17] Roy I Streit, Tod E. Luginbuhl, "Maximum Likelihood training of Probabilitic Neural Networks", IEEE Trans on Neural Networks, Vol.5, No.5,pp.764-782,1994

2011 IEEE International Conference on Fuzzy Systems
June 27-30, 2011, Taipei, Taiwan

Optimal Input Selection for Neural Fuzzy Modelling With Application to Charpy Energy Prediction

Yong Y. Yang, Mahdi Mahfouf, Qian Zhang
Department of Automatic Control and Systems Engineering
IMMPETUS, The University of Sheffield
Mappin Street, Sheffield S1 3JD, United Kingdom
y.y.yang@sheffield.ac.uk

Abstract— **Input variables selection plays a critical role in data-driven modelling, especially for complex systems with high dimensionality between the input/output space. In this paper, a new artificial neural network based forward input selection scheme is proposed. The objective of the proposed scheme is to select the smallest number of important variables as model inputs, which will then be used for neural-fuzzy data modelling. The proposed input selection scheme is applied to a case study of Charpy impact energy prediction, with data extracted from an industrial database. Model performance has been compared with previous results where a much larger input set was used. Simulation results show that the number of inputs for the Charpy data model can be significantly reduced with little performance degradation. Also, the performance of the proposed scheme outperforms both the standard correlation analysis and fuzzy clustering based input selection schemes**

Keywords: Model input selection; fuzzy clustering; neural network; neural fuzzy system; Charpy impact energy.

I. INTRODUCTION

Data-driven modelling is becoming more popular due to the rapid growth in computing power, the wide availability of data/information, and the readily available software packages where different data modelling strategies can be readily implemented and tested. Modelling tools and algorithms have also evolved into more complex structures capable of dealing with highly non-linear and multi-dimensional input/output data. However, in many real-world modelling scenarios, the available data often contain hundreds or even thousands variables, and the influences of many variables on associated outputs are not well understood. For such complex modelling tasks, a heavy-handed input selection method is essential, so that the dimension of the final model input space can be reduced to a manageable size. Due to the increasing demand for modelling large scale data, as is almost always the case in data mining [1], research in model input selection methodologies is becoming a hot topic area. Artificial neural network (NN) is a very popular model framework, due to the existence of well-established error back-propagation training algorithms and its capability of being a universal approximator for complex nonlinear mapping [2]. As the computational intensity and the number of training samples required increase exponentially with the input space dimension, applications of NN model in very high dimensional problems quickly become prohibitive. Several methods have already been investigated for input selection in the past, aimed at assisting NN modelling for a large number of potential inputs. A concise review can be found in [3], with the focus being on input selection methods using mutual information criterion and genetic algorithms. Fuzzy logic systems are another popular modelling paradigm, and a variety of related input selection schemes have been developed [4-5]. It is even more important to use a small input set in fuzzy modelling than NN, as one of the key advantage of transparency related to a fuzzy logic system will be lost even when the number of inputs is moderate. Feature transformation [1, 6], including principal component analysis and independent component analysis, is often very effective in order to reduce the nominal number of inputs, but one needs to be reminded of the fact that the individual features thus formatted involve a combination of the original variables, and the physical interpretation of such features may not be easy. Input selection via feature transformation is not considered further in this paper.

In this paper, an NN-based forward input selection scheme is proposed. The input selection scheme belongs to the category of model based direct search [5], and it starts by selecting only one input from all the potential inputs such that the corresponding model trained on the selected input produces the best model performance when compared to all other NN models with a different single input. The first input identified is thus ranked as the most important input variable, and will always be included in the subsequent enlarged input set. As an exhaustive search of input combinations leads to an exponential growth with the number of potential inputs in computation, hence it is infeasible for a search particularly involved with a large number of variables. The forward input selection scheme provides a pragmatic yet an effective solution to find the smallest number of important variables, and upon which a compact data model can be developed. The remainder of the paper is organized as follows. Section 2 introduces the aim, objective and motivation for input selection in neural-fuzzy data modelling, and describes two commonly used input selection methods based on correlation analysis and fuzzy importance ranking. In Section 3, an NN-based forward input

Financial support from the UK-EPSRC is acknowledged under Grant EP/F023464/1.

978-1-4244-7316-8/11/$26.00 ©2011 IEEE

selection scheme is developed, together with the key techniques for the implementation of the forward input selection scheme. Section 4 is devoted to the application of the proposed input selection scheme to a case study problem of Charpy impact energy data modelling, with the data extracted from an industrial database. The preliminary results of the developed model are compared to models derived from other input configuration schemes, including correlation coefficient analysis, fuzzy importance ranking, and to some previously developed models using the full input data. Finally, Section 5 concludes the paper with suggestions for future research.

II. Some Common Input Selection Methods

Input variable selection is a vital step in complex system modelling where the input–output relationship is often not well understood. An unnecessarily large number of inputs can be detrimental for effective data modelling, not only that the high dimensional space will cause difficulties due to 'the curse of dimensionality', but also the irrelevant inputs tend to confuse the true input-output relationships. Moreover, it is well-known that the number of data examples needed to tune a model grows exponentially with the dimension of the input space, and the resource required for collecting an increasing large data set with good quality is very expensive. As pointed out in [7], the objective of input variable selection is three-fold: improving the model prediction performance, providing faster and more cost-effective predictors, and providing a better understanding of the underlying process that generated the data in the first place.

Most of human experience is limited to low-dimensional spaces, partly due to the fact that we live in a low 3D space. A large degree of unease will be felt if humans are confronted with a high dimensional space, even if it is slightly larger than 3D. Our visualization ability and degree of imagination will easily run out of limit when facing a higher dimensional space, and many properties of these high dimensional spaces often appear to be counter-intuitive. Smits et al [8], for example, summarised some of these counter-intuitive properties: (i) samples sizes with the same data density increase exponentially with dimensionality; (ii) an increasingly large radius is needed to enclose a given fraction of data points even when the data are uniformly distributed; (iii) most data points are closer to an edge than to another internal data point, which indicates extrapolation is the norm rather than the exception in higher dimensional space; and (iv) almost every point is an outlier in its own projection on the line defined by the prediction point and the origin. In the following, two common input selection methods based on correlation analysis and fuzzy clustering ranking are briefly introduced, and later they will be compared with the NN-based forward input selection scheme to be developed in Section III.

A. Input Selection Based on Correlation Analysis

The correlation coefficient analysis can prove sufficient enough to help identify the input/output dependency if the process under investigation is linear [3]. Even if the system relating the original data is nonlinear, correlation analysis is often worthwhile as it can help to reach a better understanding of the data to be modelled. The Pearson's correlation coefficient can be calculated via the following equation:

$$\rho_{ij} = \frac{\sum_{k=1}^{N}(x_i(k)-\bar{x}_i)(x_j(k)-\bar{x}_j)}{\sqrt{\sum_{k=1}^{N}(x_i(k)-\bar{x}_i)^2 \sum_{k=1}^{N}(x_j(k)-\bar{x}_j)^2}} \quad (1)$$

where $\rho_{ij} \in [-1, 1]$ is the correlation coefficient between variable x_i and x_j, $x_i(k)$ is the value of the kth sample, N is the total number of samples, and $\bar{x}_i$ is the corresponding sample mean. When one of the variables is an output, ρ_{ij} represents the linear dependency between the output and the given input, otherwise it indicates the co-linearity between the two involved inputs.

A compact form to summarize all the correlation coefficients is a correlation matrix, which is particularly useful when a large amount of variables are involved. A correlation matrix $\boldsymbol{R}$ is defined as follows:

$$\boldsymbol{R} = [\rho_{ij}]_{n\times n} = \begin{pmatrix} \rho_{11} & \cdots & \rho_{1n} \\ \vdots & \ddots & \vdots \\ \rho_{n1} & \cdots & \rho_{nn} \end{pmatrix} \quad (2)$$

Where ρ_{ij} is the correlation coefficient defined in (1), n is the total number of data variables. $\boldsymbol{R}$ is a symmetric matrix with $\rho_{ij} = \rho_{ji}$, and all the diagonal elements $\rho_{ii} = 1$.

The full correlation matrix provides one with the mutual linear dependency among each pair of variables. A large $|\rho_{ij}|$ value represents a strong linear correlation, hence a large dependency between the two variable i and j. As such, the application of correlation analysis for model input selection can be of double fold. First, the dominant correlation coefficients among the potential input variables are identified and they can then be used to detect the redundant input variables, which can and need to be eliminated to reduce the potential input space dimension. Second, the large correlation coefficients among the input variables and the outputs can be used to identify those variables to be selected as the important model inputs, while these variables corresponding to insignificant correlation coefficients are removed from the model input consideration. It should be noted here that the correlation coefficients defined in (1-2) only indicate the linear dependency between the involved variables, while no causal relationship can be inferred. Table I lists the input-output correlation coefficients obtained from the Charpy impact energy data, ordered in columns by the magnitude. The full correlation matrix also reveals that there is no severe redundancy among the 16 original input variables, with the most dominant correlation coefficients being $\rho_{12,13} = 0.59$, $\rho_{8,9} = 0.53$, $\rho_{7,8} = 0.48$, and $\rho_{14,16} = 0.46$. The association of the variable x_i, $i = 1, 2, \ldots, 16$ and its physical name is given in Table IV.

TABLE I. The Input-Output Correlation Coefficients

x_i	ρ	x_i	ρ	x_i	ρ	x_i	ρ
x_{15}	0.38	x_{10}	-0.19	x_{12}	0.12	x_{11}	*0.02*
x_4	-0.28	x_6	0.18	x_1	-0.12	x_5	*0.02*
x_{14}	0.24	x_2	-0.15	x_3	0.08	x_7	*0.01*
x_{13}	0.20	x_{16}	0.13	x_9	0.08	x_8	*0.00*

B. Input Selection via Fuzzy Clustering

There exist many different methods of using fuzzy logic for input selection [4], including fuzzy c-means clustering, optimal Mahalanobis distances, 'fuzzy curves' method, etc. In this paper, the input selection method presented in [9] has been adapted for identifying the important input variables. An initial fuzzy model was first generated through the competitive clustering method using all possible m variables as the initial inputs. The initial fuzzy model has p fuzzy rules, which best divide the full model data into p clusters centred at $c_i \in R^m$ (i = 1, 2, …, p). The fuzzy model structure used for input selection is shown in Fig. 1, where ϕ_i is the membership function set (consists of p members) related to the ith input variable, and Rz_i is the range of z_i which represents the output change attributed to the ith input x_i taking values from across the corresponding centre locations in $\{ c_{ki} , k = 1, 2, \ldots, p\}$.

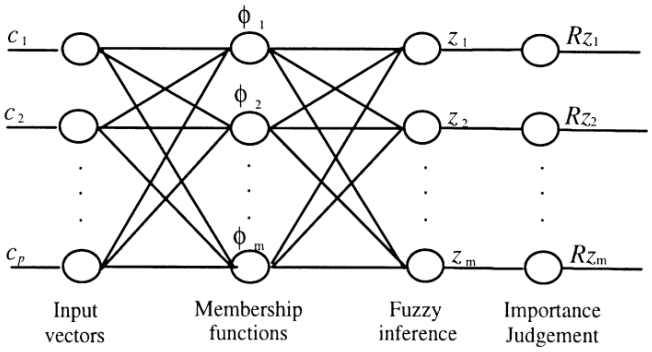

Figure 1. Fuzzy model structure for input variable selection [9]

The basic idea of ranking the importance of each input variable from the above initial model is based on calculating the contribution of individual input variations to the model output. The larger the output change caused by a specific input variable variations quantifying by its central locations of in the p clusters, the more important this input variable is. The fuzzy model shown in Fig. 1 provides an effective mechanism to test the importance of individual input variables. If all antecedent clauses except the one associated with a particular input x_i under scrutinizing are kept constant, the resulting fuzzy model output variations can be captured in the specific output route Rz_i while all the other output routes Rz_j, $j \neq i$, will be constant. Hence, with the inputs including the full variations specified by the cluster centers $\{c_k , k = 1, 2, \ldots, p\}$, output variations for each input variable can be extracted from the corresponding output nodes Rz_1, Rz_2,… Rz_m in Fig. 1. An importance factor designed to provide criteria for input variable selection is based on the magnitude of output variations attributed to individual inputs, defined as follows:

$$F_i = Rz_i / \max(Rz_1, Rz_2, \ldots, Rz_m) \quad (3)$$

Where $F_i \in (0, 1]$ is the importance factor for the ith variable x_i, and Rz_j, j = 1, 2, …, m are the output variation range associated with the corresponding input x_j variations. The x_i associated with F_i = 1 is the most important input variable.

Two important design parameters, the cluster radius r_c and the membership width σ_c, are responsible for controlling the initial fuzzy partition of the full input data space, and hence determine the initial fuzzy rule structure. These parameters need to be tuned carefully, as they directly influence the quality of input variable ranking. For the Charpy impact energy data after being normalized into a high dimensional hyper-cube, these two design parameters are selected as r_c = 0.7 and σ_c = 0.2. The initial fuzzy model obtained contains 36 fuzzy rules, and the importance factor for all the original input variables are listed in Table II, ordered in columns according the value of the associated importance factor F_i.

TABLE II. THE INPUT IMPORTANCE FACTOR

x_i	F_i	x_i	F_i	x_i	F_i	x_i	F_i
x_9	1.00	x_8	0.59	x_2	0.40	x_{10}	*0.26*
x_5	0.85	x_{15}	0.58	x_{16}	0.31	x_{14}	*0.13*
x_4	0.84	x_{12}	0.56	x_{11}	0.30	x_3	*0.13*
x_{13}	0.60	x_1	0.53	x_7	0.26	x_6	*0.10*

III. NN-BASED FORWARD INPUT SELETCION

A. NN-Based Forward Input Seletcion

An artificial neural network model based forward selection procedure is proposed here to assist identifying the most important input variables for data-driven modelling. A 3-layer feed-forward neural network is adopted as the base model, and its output can be expressed as follows [10]:

$$\hat{y}(k) = \sum_{j=1}^{M} w_j \varphi_j (\sum_{i=1}^{n} w_{ij} x_i(k) + w_{j0}) + w_0 \quad (3)$$

where $\hat{y}(k)$ is the NN output prediction for the kth sample, w_j and w_{ji} are the relevant NN weighting coefficients at the output layer and hidden layer, respectively, w_0 and w_{j0} are the bias of the output layer and hidden layer, respectively, ϕ_j is the nonlinear activate function of the jth hidden neuron, n is the dimension of the NN input space, and M is the total number of hidden neurons.

A forward input selection procedure is proposed with the above NN model as a performance evaluator. The input selection is implemented through an iterative process, starting from selecting a single input for the NN modelling. All the potential inputs are sampled as the single input candidate, and the neural network model with the minimum root mean squared error (RMSE) is identified as NN*. The inputs corresponding to the ones used in NN* are ranked as the most important inputs identified so far. In the next iteration of input selection, the inputs of the NN is increased by one from the identified input set, with the newly increased input selected from all remaining potential input candidates. The above forward input selection procedure is repeated until either a sufficient number of inputs identified or no performance improvement achieved by adding more inputs. The NN training procedure used here is adapted from the one used in [11], with critical training parameters fixed via trial-and-error tuning. The number of hidden neurons is determined by the dimension of the input using heuristic rules, as optimisation here will be too computationally cost. The iterative forward input selection algorithm is summarized as follows:

Step i: Initialisation. Set $\boldsymbol{x}^* = \{\}$ and n_{max} - the maximum number of inputs allowed. Put all the variables into the potential input candidate set $\boldsymbol{X} = [x_1, x_2, \ldots, x_N]$, where N is the maximum number of potential input variables.

Step ii: Start a new iteration of input selection. For each of the potential input candidate $x_j \in \boldsymbol{X}$ perform neural network modelling with extended input $\boldsymbol{x}^j = [\boldsymbol{x}^*, x_j]$ and $H = \min(5, 2*\dim(\boldsymbol{x}^j))$. Compute the corresponding NN model performance $J(\boldsymbol{x}^j)$, j = {1, 2, …, $dim(\boldsymbol{X})$}. In this step, all the NN models has the same number of inputs $n = \dim(\boldsymbol{x}^*) + 1$, and there is a total number of $N - \dim(\boldsymbol{x}^*)$ neural network models trained.

Step iii: Identify the optimal inputs obtained so far. Determine the optimal inputs in the current iteration $\boldsymbol{x}^* = \boldsymbol{x}^{j*}$, where j^* is determined by using the criterion $j^* = \text{argmin}_j J(x^j)$. Update the potential input set $\boldsymbol{X}$ by eliminating the associated x_{j*} ($\boldsymbol{X} = \boldsymbol{X} \setminus x_{j*}$). Notice here that the dimension of the potential input candidate set is reduced by one in each iteration.

Step iv: Termination check. If the best NN performance in the current round $J(x^*)$ does not improve over the previous one, or if $dim(\boldsymbol{x}^*) >= n_{max}$, or if $\boldsymbol{X}$ is empty, then go to Step v, otherwise return to Step ii for the next iteration of optimal input selection.

Step v: Final input ranking. The elements in $\boldsymbol{x}^*$ are the most important input variables identified by the NN forward selection procedure. The importance ranking is the order of inclusion of the elements in $\boldsymbol{x}^*$.

Table III summarises the input variable ranking results for the Charpy impact energy data using the NN-based forward input selection procedure. Due to its powerful input-output mapping capability, a NN-based framework can deal with nonlinear behaviour in the data set effectively. However, the computations involved in this NN-based forward input ranking are rather heavy, especially when a large high dimensional data set is involved. For the Charpy data input ranking task with a moderate 16 potential inputs, a total number of 120 neural networks need to be trained via some kind of error back-propagation algorithm. The procedure may meet some difficulties for ranking very high dimensional input space, as not only the number of neural networks need to be trained will be much larger, but also the training for each individual NN with a large number of inputs will be computing and resource intensive.

TABLE III. INPUT RANKING USING THE NN FORWARD SELECTION

Rank	$\boldsymbol{x_i}$	***Rank***	$\boldsymbol{x_i}$	***Rank***	$\boldsymbol{x_i}$	***Rank***	$\boldsymbol{x_i}$
1	x_{15}	5	x_6	9	x_8	13	x_5
2	x_2	6	x_7	10	x_{11}	14	x_{12}
3	x_4	7	x_1	11	x_{10}	15	x_{14}
4	x_{16}	8	x_3	12	x_{13}	16	x_9

B. Neural Fuzzy Modelling with Reduced Input Variables

Neural networks and adaptive fuzzy systems are two widely used data modelling paradigms, due to the existing of well-established training algorithms and their ability as universal approximator [11, 12]. Both models can approximate any continuous non-linear function with arbitrary accuracy, provided that enough hidden neurons or fuzzy rules have been used. After the optimal model inputs with significantly reduced dimension has been identified, a final data model can be developed using an appropriate neural fuzzy modelling framework. In this paper, a feed-forward neural network is chosen for the final stage of data modelling. The number of hidden neurons H, which is the most critical NN structure parameter, is optimised through an interactive search method. Fig. 2 shows the iterative NN training strategy incorporating structure optimisation, implemented using the built-in training utilities provided by the MATLAB Neural Network toolbox [13]. The search range for the hidden neurons [H_{min} ~H_{max}] for the NN structure optimisation should be tuned according to the complexity of the data, as well as the dimension of the input space. The Levenberg-Marquardt training algorithm [14-15] is adopted to carry out the error back-propagation, and an earlier training stopping option is also added within the NN training routine in order to prevent the NN model from being over-fitting.

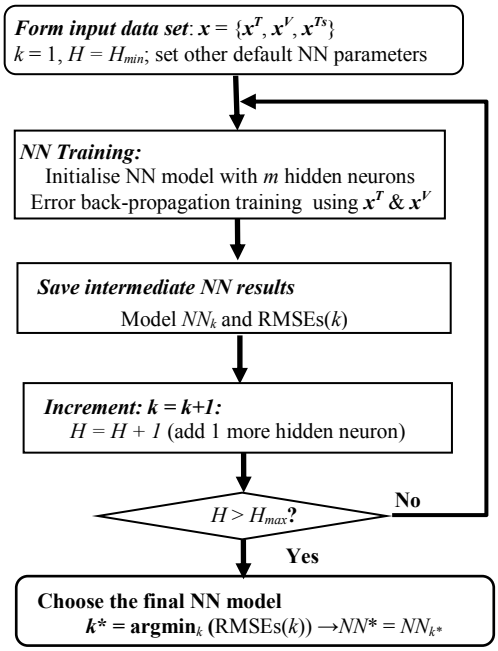

Figure 2. An iterative NN training scheme with structure optimisation

IV. CASE STUDY - CHARPY IMPACT DATA MODELLING

A. Overview of the Charpy Imapct Energy Data

The Charpy impact energy data, together with its relevant input variables, were extracted from an industrial database pertaining to TATA Steel Europe. The data set consists of 1661 records, each with measurements of the steel chemical compositions, heat treatment specifications, and Charpy impact

test conditions. Some important statistics of the Charpy data are summarised in Table IV.

TABLE IV. CHARPY IMPACT DATA STATISTICS

x_i	*variable name*	*min - max*	*mean*	*σ (std.)*
x_1	Test Depth (mm)	5.5 - 146.0	20.8	14.5
x_2	Specimen Size (mm)	11 - 381	172.5	80.8
x_3	Test Site (coded)	2 - 6	3.80	1.12
x_4	C (% wt)	0.13 - 0.52	0.394	0.058
x_5	Si (% wt)	0.11 - 0.38	0.255	0.032
x_6	Mn (% wt)	0.41 - 1.75	0.841	0.217
x_7	S (% wt)	0.001 - 0.052	0.019	0.009
x_8	Cr (% wt)	0.11 - 3.25	1.075	0.245
x_9	Mo (% wt)	0.02 - 0.98	0.239	0.086
x_{10}	Ni (% wt)	0.03 - 4.21	0.368	0.519
x_{11}	Al (% wt)	0.003 - 0.047	0.027	0.005
x_{12}	V (% wt)	0.001 - 0.260	0.009	0.029
x_{13}	Hardening Temp.	810 - 980	865.1	17.1
x_{14}	Cool Medium	1 - 3	2.8	0.482
x_{15}	Temper Temp. (C)	450 - 730	651.6	49.2
x_{16}	Testing Temp. (C).	-59 - 23	-8.0	26.0
y (output)	Impact Energy (J)	6.1 - 241.3	89.70	6.13

It is known that the above Charpy impact energy data are difficult to model, due to the existence of a large scatter in the measurements, the poor repeatability of the Charpy impact test and the highly sparse sample distribution. Several previous studies have been conducted on the modelling of this data set, where the focus is on model performance improvement by using advanced modelling strategies [16-19]. The work presented in this paper represents a first attempt aimed at further model input optimisation.

B. NN Modelling Results for Reduced Inputs

The reduced input sets containing 9 variables are selected from the original 16 input variables according to the different input selection methods discussed` earlier, and are used as the final inputs for the Charpy impact energy data modelling. The reduced input Charpy data are then divided into three data subsets, for training ($\boldsymbol{x}^T$), validation ($\boldsymbol{x}^V$) and testing ($\boldsymbol{x}^{Ts}$). The data ratio of $\boldsymbol{x}^T$:$\boldsymbol{x}^V$:$\boldsymbol{x}^{Ts}$ is set to 60:25:15, identical to most of the previous modelling work so that the performances are directly comparable. The maximum number of iterations (epochs) for the inner NN training is set to 200, and the training algorithm is fixed to the Levenberg-Marquardt algorithm. The search range for the hidden neurons is set to H_{min} = 5 and H_{max} = 20. Some typical results obtained via the iterative NN modelling scheme as shown in Fig. 2 are presented below.

According to the NN-based forward input selection scheme (see Table III), the reduced model input set $\boldsymbol{x}_N$* is as follows:

$$\boldsymbol{x}_N^* = [x_{15}, x_2, x_4, x_{16}, x_6, x_7, x_1, x_3, x_8]^T \quad (4)$$

The optimal NN model trained from $\boldsymbol{x}_N$* has m* = 12 hidden neurons, and the model performance achieved is RMSE(T, V, Ts) = (15.52, 18.36, 19.83). Fig. 3 shows the NN model predictions of the Charpy impact energy against the measurements for the validation and testing data set. Prediction accuracy is better for the training data set, which is not shown due to the constraints in space.

Similar modelling practices have also been carried out for the reduced model inputs selected using the correlation coefficient criterion and the fuzzy input importance ranking criterion. The corresponding constituents for the reduced model input sets, according to Tables I-II, are given as follows:

$$\boldsymbol{x}_F^* = [x_9, x_5, x_4, x_{13}, x_8, x_{15}, x_{12}, x_1, x_2]^T$$
$$\boldsymbol{x}_C^* = [x_{15}, x_4, x_{14}, x_{13}, x_{10}, x_6, x_2, x_{16}, x_{12}]^T \quad (5)$$

Where $\boldsymbol{x}_F^*$ is the reduced input set selected using the fuzzy input importance ranking, and $\boldsymbol{x}_C^*$ is the reduced inputs obtained by the input-output correlation. The optimised NN model trained using $\boldsymbol{x}_F^*$ produces a RMSE(T, V, Ts) = (18.84, 23.47, 27.49), with H* = 15 hidden neurons. Similarly, the NN model generated based on $\boldsymbol{x}_C^*$ has a RMSE(T, V Ts) = (15.57, 20.99, 20.53), with H* = 16. The NN predictions for the testing data set from these two models are shown in Fig. 4, and Table V summarises the RMSE performance comparisons, including performances from some previously developed models [17-19].

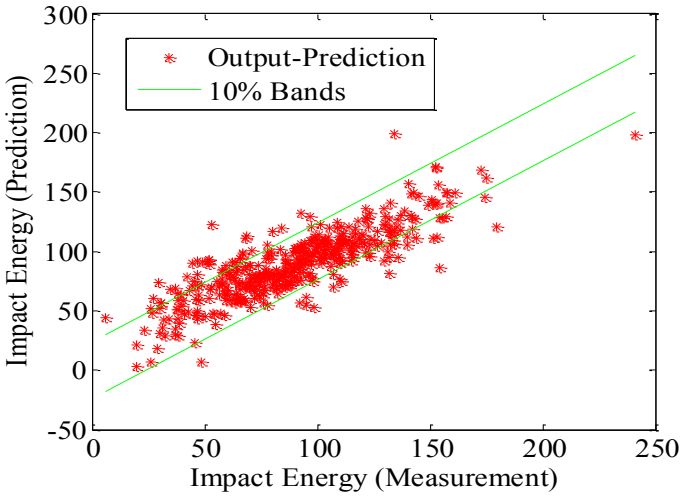

(a) For the validation data set $\boldsymbol{x}^V$

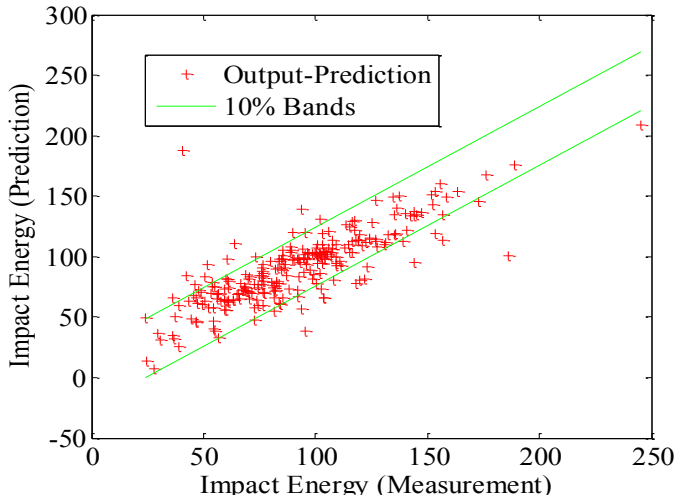

(b) For the testing data set $\boldsymbol{x}^{Ts}$

Figure 3. NN (using $\boldsymbol{x}_N$*) predictions for Charpy impact energy

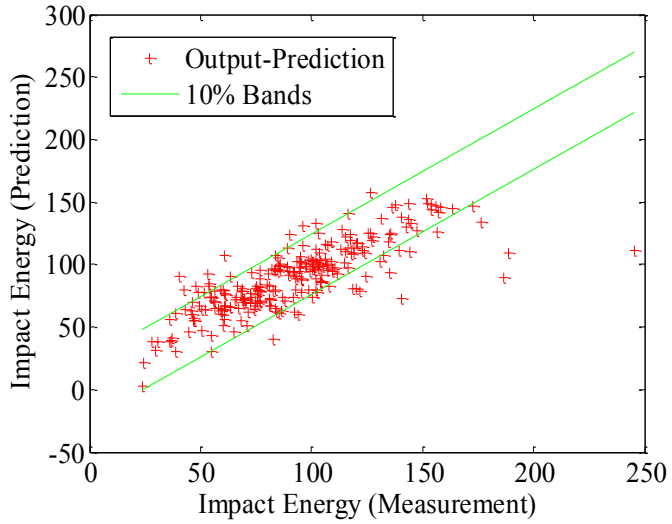

(a) NN model using correlation based inputs x_C^*

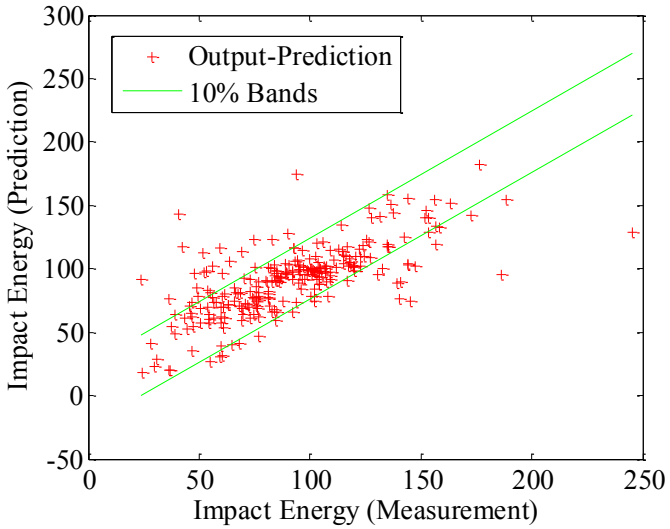

(b) NN model based on fuzzy ranking inputs x_F^*

Figure 4. NN predictions of the Charpy impact energy (testing data)

TABLE V. RMSE PERFORMANCE COMPARISONS

Modelling Methods	**Number of Inputs**	**Train Error**	**Validation Error**	**Test Error**
Neural-Fuzzy [17]	16	16.7	-	20.40
GrC – NF [18]	16	14.66	21.24	20.42
GA – NN [19]	16	14.32	17.94	18.96
NN – Corr. Inputs	9	15.57	20.99	20.53
NN – Fuzzy Inputs	9	18.84	23.47	27.49
NN – NN Inputs	9	15.52	18.36	19.83

C. Brief Discussions

The NN based forward input selection scheme performs best among the three input selection methods considered in this paper. Considering the large uncertainty involved in the Charpy impact energy measurements, the RMSE error performance of below 20 achieved by the proposed modelling scheme is good. The reduced input set identified by the correlation analysis leads to a better NN model than that of using fuzzy ranking input selection. This may indicate that a more careful tuning is needed when complicated methodology such as the fuzzy input ranking is to be used.

The model performance using a reduced 9-input obtained via NN-based forward input selection scheme is in par with the previous developed models where the full 16 input variables were used. The NN-based forward input selection scheme outperforms the Neural-Fuzzy model being reported in [7]. It also produces better RMSE performances for the validation and testing data sets, as compared to the Granular Computing Neural Fuzzy (GrC-NF) model [18], but a slightly worse RMSE value for the training data set. The performances for the validation and testing data are deemed to be more important than that of the training data, due to the possible model over-fitting phenomenon. The GA-NN model, with the structure and the parameters optimised using a GA-based algorithm, did produce an overall better RMSE performance than the current reduced input model, but the difference is not significant. It may be argued that the significant reduction of input dimension (from 16 to 9), may be worth the slight increase in RMSE.

V. CONCLUSIONS

In this paper, an NN-based forward input selection scheme is proposed to deal with the optimal input selection problem. The principle for selecting the most importance input variables relies on a direct search among the potential candidates for model performance optimisation. Input selection plays an important role in data-driven modelling in general, especially for complex systems with a large number of potential inputs. After the reduced input set is identified, it can be used in an appropriate modelling scheme for the final data model development. In this paper, a feed-forward NN model framework is employed to deliver the final data model. The integrated model-input selection and model optimisation are implemented using the MATLAB Neural Network toolbox, with the training guided by an error back-propagation algorithm. The number of hidden neurons, a critical parameter determining the NN structure, is also optimised in the final NN modelling stage. The model prediction performance, in terms of RMSE, is then compared to two other input selection methods, one based on correlation analysis, and the other based on fuzzy input ranking. Preliminary results obtained in the case study for Chary impact energy prediction show that the NN-based forward input selection method produces the best overall model performance among the three input selection methods compared.

The model performance obtained from the NN-based forward input selection is also compared with the performances of some previous developed Charpy impact energy prediction models, including the neural-fuzzy model, the granular computing neural fuzzy model, and the NN model with structure optimised via a genetic algorithm. Even though all the previous models used the full 16 model inputs, the NN model developed in this paper with a reduced 9 inputs managed to outperform two out of three previous models, while a slight RMSE performance deterioration is recorded in the third case of full input NN model with genetic algorithm based structure

optimisation. However, the benefit of a much compact model, resulting from a smaller input space, should generally outweigh the small RMSE-based performance loss. In training data requirement, for example, 512 training samples will be needed to train for the reduced input model proposed in this paper assuming a training data density of 2 samples per input, while a huge number of 655336 training data samples will be required to provide the same training data density across the high input space of 16 dimensions. This is an overwhelming 128 fold increase in training data requirement from a 9-input model to a 16 input model. This shows one of the 'counter intuitive' properties of a high dimensional space: the effect of reducing the number of inputs is also exponential, albeit in the reverse direction.

One disadvantage of using the proposed NN-based forward input selection is that the computational resources required are still high, and may be prohibitive for very large scale data with a high dimension. Hence, designing novel fast input raking algorithms based on the forward input selection principle will be beneficial. Also, due to the intensive calculations involved in error back-propagation algorithm, developing a fast NN training algorithm will be worth the effort. We will investigate new methodologies relating to these fields in future research.

ACKNOWLEDGMENT

Financial support from the UK-EPSRC is acknowledged under Grant EP/F023464/1. The authors wish to thank Tata Steel Europe for providing the Charpy impact energy data used in this research as well as expert knowledge for the data pre-processing and modelling.

REFERENCES

[1] I. H. Witten, and E. Frank, Data Mining - Practical Machine Learning Tools and Techniques, 2nd Ed., Morgan Kaufmann Publishers, San Francisco, 2005.

[2] K. Hornik, "Approximation capabilities of multilayer feedforward networks", Neural Networks, vol. 4, no. 2, pp. 251-257. 1991.

[3] M. P. C. Couto, "Review of input determination techniques for neural network models based on mutual information and genetic algorithms", Neural Comput & Application, vol. 18, pp. 891–901, 2009.

[4] Y. Hou, J. M. Zurada, W. Karwowski, W. S. Marras, and K. Davis, "Identification of key variables using fuzzy average with fuzzy cluster distribution", IEEE Transactions On Fuzzy Systems, vol. 15, no. 4, pp. 673-685, 2007.

[5] R. Sindelár, and R. Babuska, "Input selection for nonlinear regression models", IEEE Transactions On Fuzzy Systems, vol. 12, no. 5, pp. 688-696, 2004.

[6] S. Theodoridis, and K. Koutroumbas, Pattern Recognition, 4th Ed., Elsevier Inc., 2009.

[7] I. Guyon, and A. Elisseeff, "An introduction to variable and feature selection". Journal of Machine Learning Research, vol. 3, pp. 1157-1182, 2003.

[8] G. Smits, A. Kordon, K. Vladislavleva, E. Jordaan, and M. Kotanche, "Variable selection in industrial datasets using pareto genetic programming". International Congress on Modelling and Simulation MODSIM 05, December 2005, Melbourne University, Vic.

[9] D. A. Linkens, and M. Y. Chen, "Input selection and partition validation for fuzzy modelling using neural network", Fuzzy Sets and Systems, vol. 107, pp. 299-308, 1999.

[10] M. Mahfouf, and Y. Y. Yang, "A GA-optimised ensemble neural network model for charpy impact energy predictions", IFAC MMM2010, The 13th Symposium on Automation in Mining, Mineral and Metal Industry, 2-4 August 2010, Cape Town, South Africa.

[11] K. Hornik, "Approximation capabilities of multilayer feedforward networks", Neural Networks; vol. 4, no. 2, pp. 251-257, 1991.

[12] B. Kosko, "Fuzzy systems as universal approximators", IEEE Transactions on Computers, vol. 43, no. 11, pp. 1329-1333, 1994.

[13] The MathWorks Inc., Neural Network Toolbox 7 User's Guide, http://www.mathworks.com/help/pdf_doc/nnet/nnet.pdf , 2010.

[14] C. M. Bishop, Neural Networks for Pattern Recognition, Clarendon Press, Oxford. pp. 290-292, 1995.

[15] C. M. Bishop, Pattern Recognition and Machine Learning, Springer. London, 2006.

[16] J. Tenner, Optimisation of the Heat Treatment of Steel using Neural Networks, PhD Thesis, The University of Sheffield, 1999.

[17] M. Y. Chen, and D. A. Linkens, "A systematic neural-fuzzy modelling framework with application to material properties of alloy steels". IEEE Transactions on System, Man and Cybernetics – Part B: Cybernetics, vol. 31, no. 5. pp. 781-790. 2001.

[18] G. Panoutsos, and M. Mahfouf, "Granular computing and evolutionary fuzzy modelling for mechanical properties of alloy steels", Proceeding of 16th IFAC World Congress, Prague, Czech Republic, 4-8 July, 2005.

[19] M. Mahfouf, Y. Y. Yang, and Q. Zhang, "Modelling Charpy impact energy of heat-treated-steel using efficient neural-networks and genetic-algorithms", IFAC MMM2009 Workshop on Automation in Mining, Mineral and Metal Industry, 14-16 October 2009; Viña del Mar, Chile.

2011 IEEE International Conference on Fuzzy Systems
June 27-30, 2011, Taipei, Taiwan

Stereo Vision-Based Self-Localization System for RoboCup

Jen-Shiun Chiang
Department of Electrical Engineering
Tamkang University
New Taipei city, Taiwan
chiang@ee.tku.edu.tw

Chih-Hsien Hsia
Department of Electrical Engineering, National Taiwan University of Science and Technology
Taipei city, Taiwan
chhsia@ee.tku.edu.tw

Hung-Wei Hsu
Department of Electrical Engineering
Tamkang University
New Taipei city, Taiwan
hung.weiwei.hsu@gmail.com

Chun-I Li
Department of Electrical Engineering
Tamkang University
New Taipei city, Taiwan
698450417@s98.tku.edu.tw

***Abstract*—This work proposes a new Stereo Vision-Based Self-Localization System (SVBSLS) for the RoboCup soccer humanoid league rules for the 2010 competition. The humanoid robot integrates the information from the pan/tilt motors and stereo vision to accomplish the self-localization and measure the distance of the robot and the soccer ball. The proposed approach uses the trigonometric function to find the coarse distances from the robot to the landmark and the robot to the soccer ball, and then it further adopts the artificial neural network technique to increase the precision of the distance. The statistics approach is also used to calculate the relationship between the humanoid robot and the position of the landmark for self-localization. The experimental results indicate that the localization system of SVBSLS in this research work has 100% average accuracy ratio for localization. The average error of distance from the humanoid soccer robot to the soccer ball is only 0.64 cm.**

Keywords- Back propagation neural network; humanoid robot; Robo Cup 2010; self-localization, stereo vision

I. INTRODUCTION

The research of robots is one of the most important issues in recent years. In the numerous robot researches, the development of autonomous robots is attracted mostly. Accompanying the advancement of robotics and artificial intelligence, the autonomous robots cannot only handle simple and monotonous problems, but also have independent thoughts to deal with the complex states in the unpredictable and dynamic environments. All these functions rely on a powerful vision system, and therefore the vision system is one of the most critical techniques for the autonomous robot system. In the RoboCup soccer humanoid league competition, the vision system is used to collect various environment information as the terminal data to finish the functions of object recognition, coordinate building, robot localization, robot tactic, barrier avoiding, etc. A good self-localization system for a humanoid soccer robot cannot only make the robot acquire the information quickly and accurately in the whole field, but also make an appropriate decision correspondingly. For easy manipulation we can preset all the locations in the field as a Cartesian coordinate system, and the robot will self-localize itself by the coordinate system. In recent years, the competition fields of RoboCup [1] and FIRA Cup [2] become more and more conformed to human environments. Fig. 1 shows the RoboCup soccer fields for humanoid kid-size of 2009 and 2010, respectively. The sizes of the landmark pole and landmark goal in the field become smaller [3-4]. In other words, the reference checkmarks for self-localization become less and less, and how to use less landmarks and increase the degree of accuracy become important issues [5-6].

Zhong et al. [7] proposed three types of techniques for robot localization. The first approach is based on the stereo vision. This approach can obtain a lot of information such that the distance measurement between the camera and the target is accurate enough [8] to increase the accuracy of localization. The second one is based on the omni-directional vision. Although this method obtains better features, the omni-directional device causes geometry distortions to the perceived scene [9]. The third one uses the monocular vision technique. However, it must have robust features within a specific region [10]. SLAM [11] is an algorithm for localization and mapping simulation and is appreciated by many researchers. Although this algorithm has better efficiency, it needs complex image processing procedures and is difficult to be applied to the embedded system for real time humanoid soccer robot applications. For the implementation of the humanoid soccer robot, real time is the main issue, and we need a less complicated but high efficient localization method. Therefore for the humanoid soccer robot competition purpose, we propose a visual self-localization approach, stereo vision-based self-localization system (SVBSLS), which uses two CCD cameras and a set of pan/tilt motors on the robot head to find the various features and analyze the environmental information of the RoboCup 2010 soccer field [4].

The rest of this paper is organized as follows. Section II presents the related background such as the general color based object recognition methods, intrinsic parameters of the CCD, and distance measurement. Section III describes the proposed approach, SVBSLS. The experimental results of SVBSLS applied to the humanoid soccer robot are described in Section IV. Section V compares and analyzes the self-localization for humanoid robot by SVBSLS and other approaches. Finally, Section VI gives a brief conclusion.

978-1-4244-7316-8/11/$26.00 ©2011 IEEE

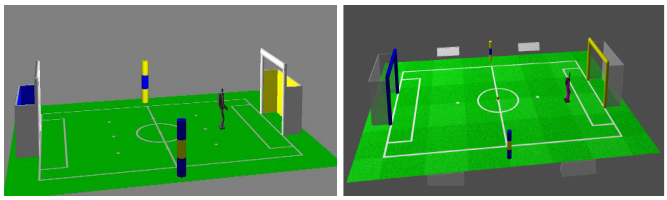

(a) (b)

Figure 1. The configuration of RoboCup soccer fields for humanoid kid-size: (a) for 2009, (b) for 2010.

II. BACKGROUND

A. Intrinsic Parameters of the CCD Camera

The vision-based distance measurement needs the intrinsic parameters, such as focal distance and horizontal viewpoints, of the CCD camera. Generally the camera makers rarely provide such parameters. Even if they provide such parameters, the mechanical mechanism, processing circuits, and lens distortion may cause deviations of the parameters. Actually we can find the intrinsic parameters of the CCD cameras regardless of the CCD branes.

The relationship of the distance between the CCD camera and the object and some parameters are shown in Fig. 2. In Fig. 2, OP is the optical origin; $2\theta_H$ is the horizontal viewpoints, and D_{OP} is the distance between OP and the edge of the CCD lens.

In order to find the distance between the CCD center and the object, θ_H and D_{OP} must be found first. We can capture the width of an object, $D_{H1}(max)$, with a pre-defined position, D_A, and the width of the same object, $D_{H2}(max)$, with a pre-defined position, D_B. The two captured frames can be combined to form Fig. 3. By the trigonometric functions we can derive θ_H in (1):

$$\theta_H = \cot^{-1}\left(2\times\frac{D_{K2}-D_{K1}}{D_{H2}(max)-D_{H1}(max)}\right) \tag{1}$$

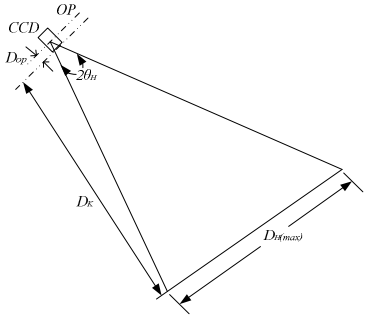

Figure 2. The internal parameters diagram of a CCD camera.

By the theorem of similar triangles, D_{OP} can be found as shown in (2) and (3).

$$\frac{D_{OP}+D_{K1}}{D_{OP}+D_{K2}}=\frac{D_{H1}(max)}{D_{H2}(max)} \tag{2}$$

$$D_{op}=\frac{D_{K2}D_{H1}(max)-D_{K1}D_{H2}(max)}{D_{H2}(max)-D_{H1}(max)} \tag{3}$$

The above approach can be applied to find the intrinsic parameters for any kind of CCD cameras. Once D_{OP} is found, the distance between the camera and the object can be measured by IBDMS (image-based distance measuring system) [12-13].

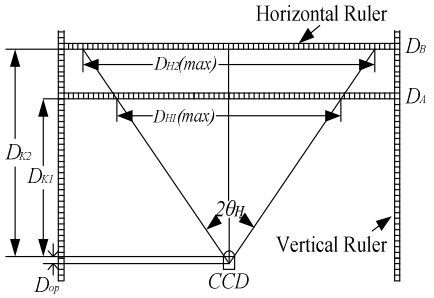

Figure 3. The intrinsic parameters measuring system[12-13].

B. Image-Based Distance Measuring System (IBDMS) [12-13]

The IBDMS (image-based distance measuring system) uses two fixed lasers to project the laser beams to the object to measure the distance between the CCD camera and the object. Fig. 4 is the diagram of the location relationship of the CCD camera and the object. The unit of D_{SH} is cm that is the actual length of the distance between the two lasers. F_H is the pixel numbers that the laser beams project to the object in a picture frame. If the maximum horizontal pixels that a CCD camera can catch in a picture frame is $F_H(max)$, the maximum width (in cm as unit) that a CCD camera can reach can be calculated as (4):

$$D_H(max)=\frac{F_H(max)}{F_H}\times D_{SH} \tag{4}$$

According to Fig. 4, the distance D_K (with unit of cm) between the CCD camera and object can be calculated with the intrinsic CCD parameters as mentioned in the previous subsection as (5):

$$D_K=\frac{1}{2}\times D_H(\max)\times D_{SH}\times\cot(\frac{\theta_H}{2})-D_{op} \tag{5}$$

In the RoboCup 2010 rule, the landmark pole is a cylinder with diameter equal to 10cm. when the IBDMS is applied to measure the distance between the CCD camera and the landmark pole, the two lasers of the original IBDMS can be removed, and we call this approach without lasers as modified IBDMS.

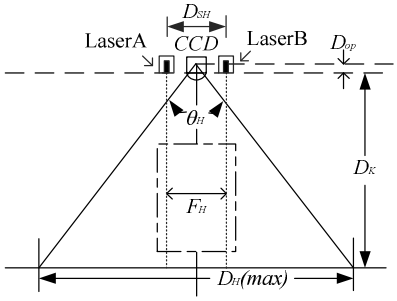

Figure 4. The location relationship of the CCD camera and the object.

III. THE PROPOSED METHOD

This research work uses the parallax of a stereo (binocular) vision system to establish the stereo vision-based self-localization system (SVBSLS) for a humanoid soccer robot used in the Robo-Cup 2010 kid-size humanoid robot soccer competition. Basically there are two main issues in this research: *1)* how to utilize the landmarks, such as the landmark poles and landmark goals, of the competition field to find the coordinate of the humanoid robot in a 2-D coordinate system, *2)* how to measure the accurate distance of the humanoid robot and the soccer ball. Here we have to overcome the difficulties caused by the CCD camera intrinsic parameters such as focal distance and visual angle. The humanoid soccer robot can be adjusted by the tactics dynamically, such as localizing before competition, measuring the distance of the robot and the soccer ball during competition, or localizing during competition.

For the localization algorithm, it needs several procedures: establishment of the coordinate system, object searching, object identification, the distance measurement between the robot and object, refinement of the measured distance, and the adjustment of the location of the robot and the landmarks. In the distance measurement, we use the modified IBDMS approach and the parallax of the stereo vision system. For precision and convenience considerations, the soccer field is treated in a 2-D coordinate system. In the object detection, the two cameras of the stereo vision system catch images in RGB 24-bit colorful formats, respectively. The RGB images are then converted to the HSV colorful formats, and here we only utilize *H* and *S* data and further convert them to the binarization format with proper threshold values. The binarization data are processed to reduce noises to increase the correctness and integrity for object recognition. According to the processed binarization data we can distinguish the object as landmark pole, landmark goal, or soccer ball. If the object is a landmark pole or landmark goal, it will try to localize the robot itself and output the coordinate values to the system. If the object is a soccer ball (we call this as a distance mode), it will try to measure the distance between the robot and soccer ball and output the distance value to the system.

A. Establishment of the Coordinate System

If the coordinate of a geometric map is available, it will be convenient to retain a lot of information in the whole field. For easy manipulation of the self-localization of a robot, the coordinate system of the field must be established in advance. In this research work, before processing the localization we must establish two appropriate coordinate systems. One is called "absolute coordinate system" on the field, and the other is called "relative coordinate system" in the picture frame. It needs four steps to establish the absolute coordinate system: *1)* to estimate the sizes of the soccer field and the robot; *2)* to find the interested position in the soccer field; *3)* to divide the field into several blocks with the same size and assign the interested position block; *4)* according to the proportion of the robot in the field to adjust the value in each block. Through these coordinate systems, the location of the robot, landmark pole, and landmark goal can be located explicitly.

B. Object Searching

Since the objects (landmark poles and landmark goals) are the fixed features in the 2010 RoboCup soccer field, we treat the objects as the reference for localization. In the initialization of the orientation, the robot keeps searching one of the objects until finding it. After finding the object, the two cameras of the system will take the interested feature by converting the image from RGB to HSV space, respectively, as shown in Fig. 5. In order to remove the influence of brightness of light, it takes the *H*- and *S*- spaces only. Finally, each camera will mark five feature points, upper left (X_1,Y_1), upper right (X_2,Y_2), lower left (X_3,Y_3), lower right (X_4,Y_4), and center (X_C,Y_C), for the object in the picture frame, as shown in Fig. 6. According to the five feature points in each picture frame, we can calculate the horizontal lengths (in pixels) FH_{Lx}, FH_{Rx} and vertical lengths FH_{UPx}, FH_{DOWNx} (where x is either 1 or 2; 1 represents the left camera, and 2 represents the right camera) for each of the two cameras. The parallax (in pixels) of the two cameras can be calculated as follows:

$$\Delta N = |FH_{L1} - FH_{L2}| = |FH_{R1} - FH_{R2}| \quad (6)$$

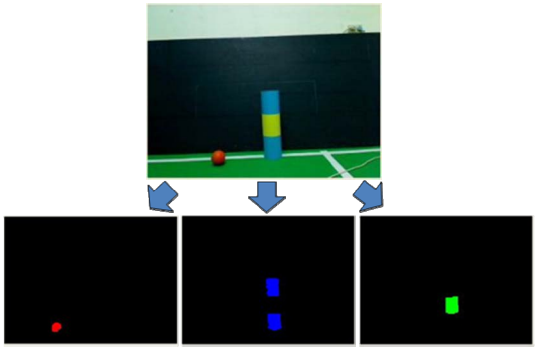

Figure 5. Color model transformation.

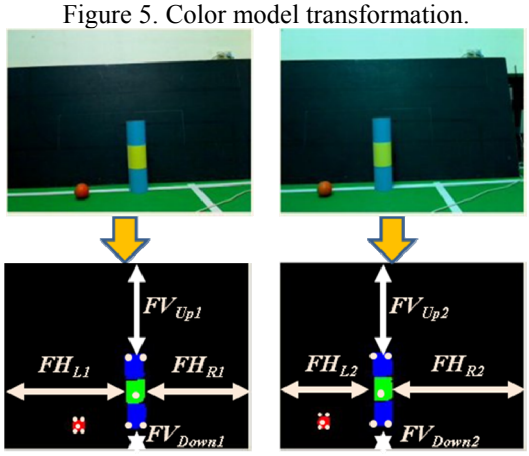

Figure 6. The upper left, upper right, lower left, lower right, and center of the object in the two cameras.

C. Object Recognition Method

According to the color segmentation method, it can fast and easily extract the orange soccer ball in the field, but it is not enough to recognize the landmark goals and landmark poles. The colors of the landmark goals and landmark poles are yellow and blue, and by color segmentation the extraction of the landmark goals and landmark poles may not be correct as shown in Fig. 7. Therefore we have to use more features and

information to extract them. Since the competition field is not complicated, a simple recognition method can be used to reduce the computation complexity. The landmark pole is a cylinder with three colors. Let us look at one of the landmark pole with the upper and bottom layers in blue, and the center layer in yellow; this one is defined as the BYB-landmark pole, and the diagram is shown in Fig.8. The color combinations of the other one are in contrast of the previous one, and the landmark pole is defined as the YBY-landmark pole. The labels of the BYB-landmark pole can be calculated by (7). The YBY landmark pole is in the same manner as the BYB-landmark pole.

$$O_{BYB}(x,y) = L_B^u(x,y) + L_B^v(x,y) + L_Y^w(x,y) \quad (7)$$
$$if \ \left|L_B^u(x_c) - L_B^v(x_c)\right| < \beta_B \cap L_B^u(y_{\max}) < L_Y^v(y_c) < L_B^w(y_{\min})$$

where L_B^u is the pixel of the u-th blue component in a picture frame, y_{min} and y_{max} the minimum value and the maximum value for the object u at y direction in the picture frame respectively, x_c and y_c the center point of the object at the horizontal and vertical direction respectively. The vertical bias value β is set as 45 empirically. The landmark pole is composed of two same color objects in the vertical line, and the center is in different color. If it can find an object with this feature, the system treats this object as the landmark pole and outputs the frame coordinate data. Equation (8) is used to define the label of the soccer ball.

$$O(x,y) = L_O^u(x,y), if \ \alpha_1 \le \frac{L_O^u(x_{\max}) - L_O^u(x_{\min})}{L_O^u(y_{\max}) - L_O^u(y_{\min})} \le \alpha_2 \cap A_u \text{ is the maximum} \quad (8)$$

where L_O^u is the pixel of the u-th orange component in a picture frame. Since the soccer ball is very small in the picture frame, in order to avoid the noise the soccer ball is treated as the maximum orange object and with a shape ratio of height to width approximately equal to 1. Empirically α_1 and α_2 are set to 0.8 and 1.2, respectively. The landmark goal recognition is defined in (9).

$$G_B(x,y) = L_B^u(x,y),$$
$$if \ L_B^u(x,y) \notin O_{BYB}(x,y) \cap L_B^u(x,y) \notin O_{YBY}(x,y) \cap A_B^u > \gamma_B \quad (9)$$

where L_B^u is the pixel of the u-th blue component in a picture frame. Since the blue landmark goal is composed of the blue object and it is not a part of the YBY-landmark pole or BYB-landmark pole. The size of the landmark goal in the field is larger than other objects, and empirically the parameter γ is set as 50. The yellow landmark goal is in the same manner as the blue landmark goal.

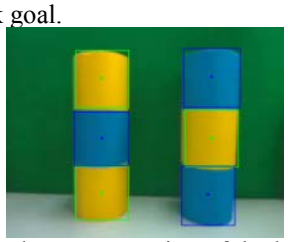

Figure 7. False segmentation of the landmark pole.

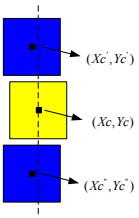

Figure 8. The diagram of the landmark pole.

To get robust FH_L, FH_R, FH_{UP}, and FH_{DOWN}, the object shape must be completely displayed in the picture frame, as shown in Fig. 9(b). Figs. 9(a) and 9(c) show the incomplete objects with partial object displayed in the picture frame. If it finds an incomplete object in the picture frame or the object could be occluded by other robots, the system will command the robot to activate some proper movements to find a complete object. In order to insure the completeness of the object, the pixel values between the edge of the object and the edge of the frame should be greater than some appropriate values.

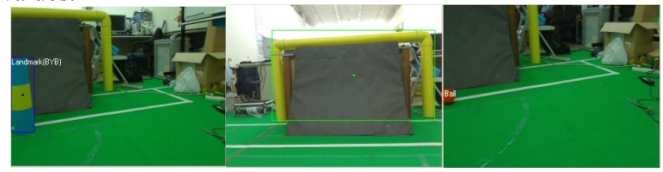

(a)

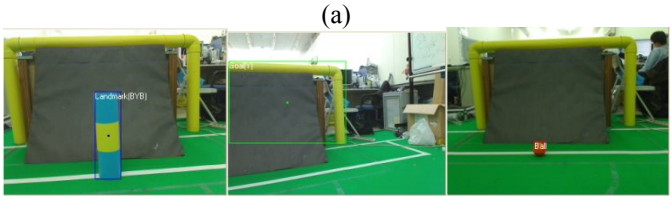

(b)

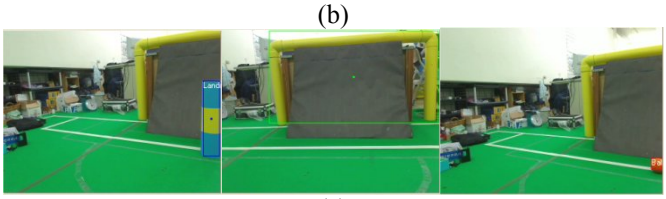

(c)

Figure 9. Object searching: (a) incomplete object, (b) complete object, (c) incomplete object.

D. Distance Measurement between the Robot and Object

The distance measurement between the robot and the object is based on the parallax of the stereo vision. The modified IBDMS as mentioned in the previous section is applied to measure the distance between the CCD camera and object (the landmark pole, landmark goal, or soccer ball) for the RoboCup 2010 rule. Fig. 10 shows the relationship of the camera and the object. In Fig. 10, Δh is the length of the distance between the two cameras and D_H is the parallax in unit of cm. D_H can be converted by the parallax ΔN (in pixels) and Δh as follows:

$$D_H = \frac{\Delta h \times F_H(max)}{\Delta N} \quad (10)$$

where $F_H(max)$ is the maximum horizontal pixels that a camera can reach in a picture frame. FH_{L1}, FH_{R1}, and FH_{L2}, FH_{R2} are the lengths in pixels for horizontal lengths of the landmark pole in the image frame. By the modified IBDMS

approach, the distance D_K (photo-distance) between the CCD camera and the landmark can be found as follows:

$$D_K = \frac{1}{2} \times D_H \times \cot\theta_H - D_{OP} \quad (11)$$

Due to the non-ideality of the CCD lens and the light illumination the measurement of D_K may not be accurate enough. It can be fine-tuned by the artificial neural network technique. The neural network technique is described in the following subsection.

E. Stereo Vision-based Self-localization System (SVBSLS)

Based on the above concepts, the self-localization system, stereo vision-based self-localization system (SVBSLS), is proposed for the humanoid soccer robot for RoboCup 2010 competition. The proposed SVBSLS consists of six steps, and the operation flow of this self-localization mechanism is shown in Fig. 11. The six steps are:

Step 1: Establish the coordinate system.
Step 2: Search objects.
Step 3: Recognize objects.
Step 4: Measure the distance between the robot and objects.
Step 5: Fine-tune the measured distance.
Step 6: Find the coordinate of the robot in the competition field.

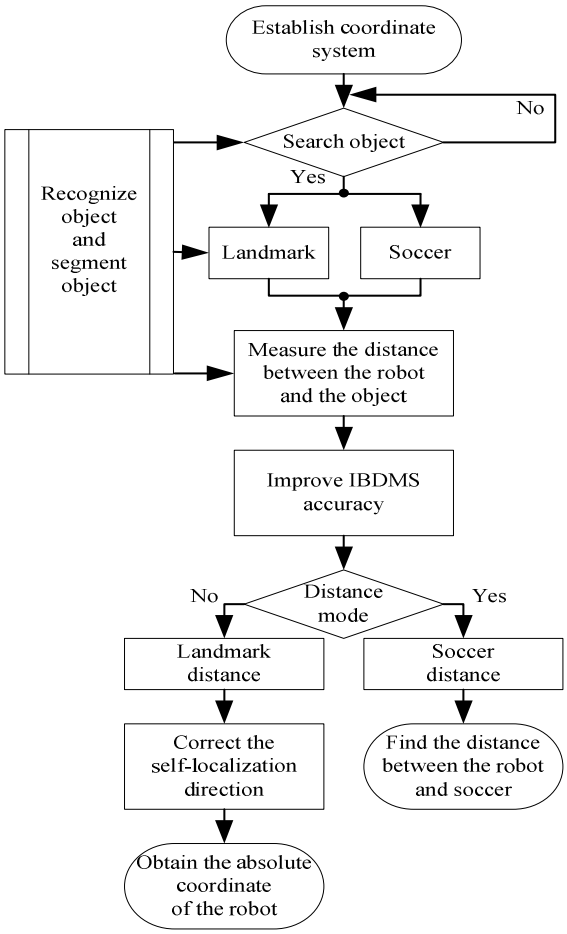

Figure 11. The SVBSLS flowchart for the humanoid robot.

IV. THE EXPERIMENT RESULTS

A. The Experimental Environment and the Robot Vision Module

The experiments are based on the feature of the competition field for 2010 RoboCup soccer humanoid league. The field contains two landmark goals and two landmark poles, and it has unique color combinations for the interesting features as shown in Fig. 12. Because the width of the robot shoulder is 26cm, we set the unit length of the coordinate to be 30cm in length and the competition field can be divided into 29×17 blocks as shown in Fig. 13.

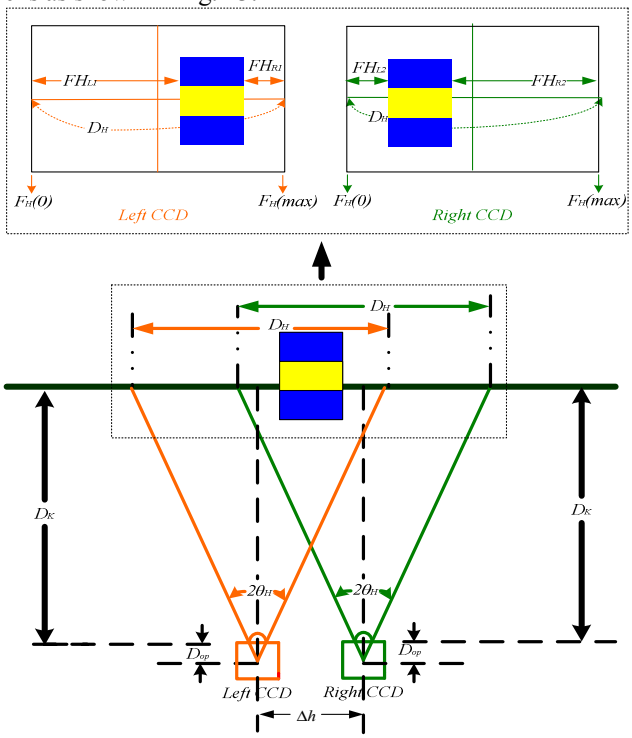

Figure 10. Three-dimension distance measurement.

Figure 12. Configuration of the RoboCup soccer field for humanoid kid-size in 2010.

The experimental robot vision module is consisted of two CCD cameras with distance of 10cm and a set of pan/tilt motors. The CCD camera is the Logitech QuickCam® Professor [14] for Notebooks, and the motor is ROBOTIS Dynamixel AX-12 [15]. The input of the robot vision module is RGB 24-bit and the resolution is 960×720 pixels, and the frame rate is 4 fps (frame per second). For simulation, the computer CPU is Intel Core 2 Duo CPU 2.1GHz, and the development tool is Borland C++ Builder 6.0. The output is the

absolute coordinate of the humanoid robot in the competition field.

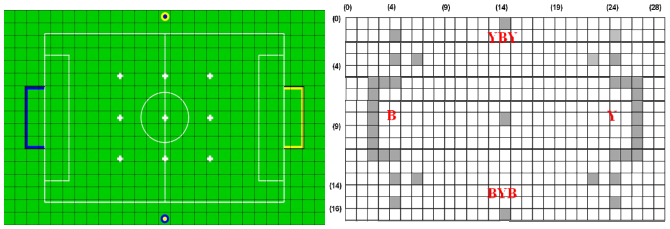

(a) (b)

Figure 13. The RoboCup soccer field: (a) the original field with 29×17 blocks, (b) the coordinate of the soccer field (2010).

B. The Parallax ΔN of Stereo Vision Analyses

We measured the parallax ΔN in a given distance with different pan/tilt motor angles, and the results are shown in Table 1. According to Table 1, as the same distance the parallax ΔN is the same with different pan/tilt motor angles. Therefore, our SVBSLS does not need to calibrate the non-linear distortion caused by the visual angle of the lens, and it can measure the distance of the object as soon as the camera sees the complete object in the picture frame.

Table 1. The parallax ΔN of the landmark pole in a given distance with different pan/tilt motor angles. (a) The parallax ΔN of the landmark pole in a given distance with different pan motor angles. (b) The parallax ΔN of the landmark pole in a given distance with different tilt motor angles.

D_k \ angle	-20	-15	-10	-5	0	5	10	15	20
50	148	148	148	148	148	148	148	148	148
100	76	76	76	76	76	76	76	76	76
150	52	52	52	52	52	52	52	52	52
210	36	36	36	36	36	36	36	36	36
270	28	28	28	28	28	28	28	28	28

(a)

D_k \ angle	-20	-15	-10	-5	0	5	10	15	20
60	128	128	128	128	128	128	128	128	128
90	84	84	84	84	84	84	84	84	84
120	64	64	64	64	64	64	64	64	64
150	52	52	52	52	52	52	52	52	52
180	40	40	40	40	40	40	40	40	40
210	36	36	36	36	36	36	36	36	36
240	32	32	32	32	32	32	32	32	32
270	28	28	28	28	28	28	28	28	28
300	24	24	24	24	24	24	24	24	24

(b)

C. Precision Simulation of the Distance Measurement

For the BPN network approach, we need data for the two neurons in the input layer (ΔN and the rough distance D_K) to measure the distance to the landmark and the input layer (ΔN and rough distance D_K) to measure the distance to the soccer ball. The total training samples are 247. The hidden layer is one. Because the absolute coordinate system of the soccer field is fixed, we can train the on-line data beforehand. The simulation result indicates that the most suitable number of neurons is six. The learning rate is 0.1, and the output layer is one. After finishing the on-line training, the relationships between the information of the frame and the distance can be found, and then it can operate the off-line process for the invariable parameters (relationships) to improve the precision of the distance. The precision can reach 0.028cm for the landmark distance measurement and 0.005cm for the soccer ball distance measurement, and the simulation results are shown in Fig. 14.

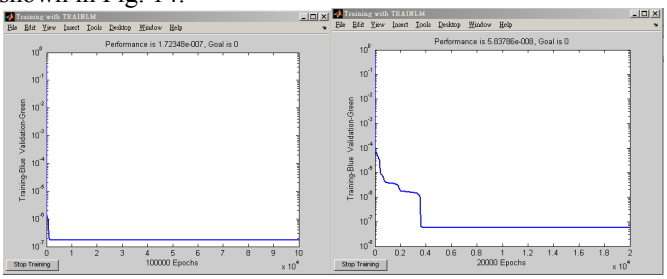

(a) (b)

Figure 14. The errors between the simulated and real distances are: (a) 0.028cm in the landmark distance measurement and (b) 0.005cm in the soccer ball distance measurement.

I. COMPARISONS AND ANALYSES

A. The Analyses for the Actual Measuring Distance

This work uses modified IBDMS and NNIBDMS techniques to measure the distance between the robot and landmark and the distance between the robot and soccer ball from 10cm to 300cm. Fig. 15 shows the errors between the measuring distance and actual distance, and the results are listed in Table 2. In the distances from 10cm to 300cm, the average and maximum errors for the modified IBDMS are 48.96cm, 51.03cm, and 162.16cm, 170.52cm, respectively. On the other hand, those of the NNIBDMS are 1.38cm, 0.64cm, and 2.49cm, 4.55cm, respectively. The proposed NNIBDMS approach improves the distance accuracy significantly.

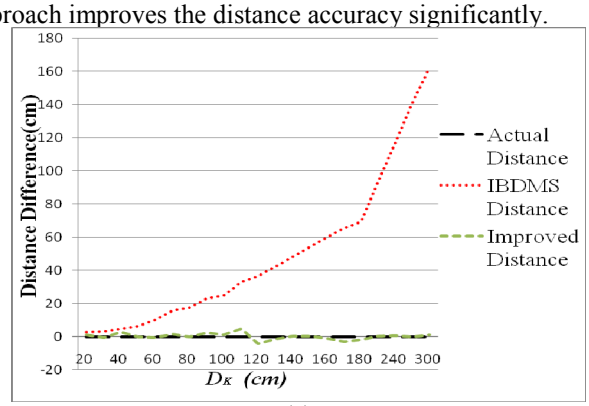

(a)

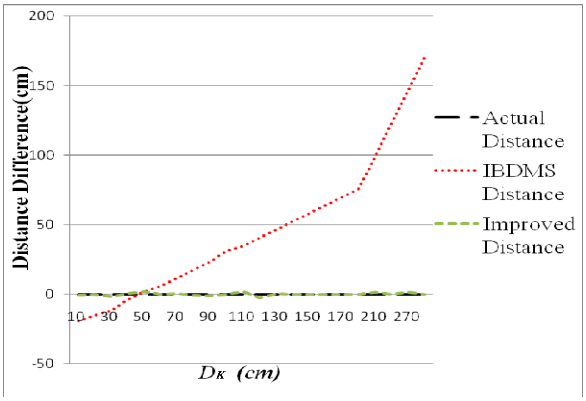

(b)

Figure 15. The distance differences of the actual distance and the modified IBDMS and NNIBDMS approaches, (a) Landmark distance, (b) Soccer ball distance.

Table 2. Comparisons of the maximum and average errors for different methods.

Landmark distance		
Methods	**Average error**	**Maximum error**
Modified IBDMS	48.96 cm	162.16 cm
NNIBDMS	1.38 cm	4.55 cm
Soccer ball distance		
Methods	**Average error**	**Maximum error**
Modified IBDMS	51.03 cm	170.52 cm
NNIBDMS	0.64 cm	2.49 cm

B. The Results of the Self-localization in the Competition Field

The distances measured between the robot and landmarks as mentioned in the previous subsection are applied to the SVBSLS to localize the robot itself. The localization results of using the distances measured by the modified IBDMS and NNIBDMS are compared. The experiments include the localization by using the distance from the robot to the landmark pole and the distance from the robot to the landmark goal. There are 247 coordinate positions in Fig. 16. The yellow and blue star signs stand for the correct localization by using the NNIBDMS approach for distance measurement. The purple star signs stand for the correct localization by using the modified IBDMS or NNIBDMS approaches for distance measurement. The red star signs stand for the correct localization with both landmark pole and landmark goal by using the NNIBDMS approach for distance measurement. Table 3 shows the comparisons for the robot localization by using SVBSLS with modified IBDMS and NNIBDMS approaches for distance measurement. The correct rate for the SVBSLS approach with the NNIBDMS approach is 100%; on the other hand that of the localization by the modified IBDMS is only 13.77%. The main reason of the lower correct rate is due to the worse accurate measuring distance results.

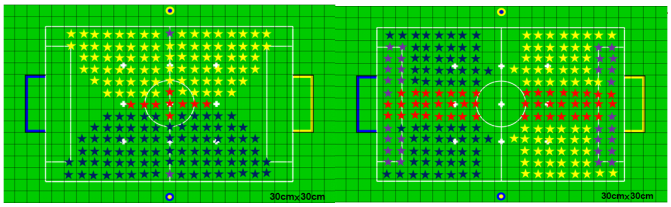

(a) (b)

Figure 16. The correct localization by using SVBSLS with modified IBDMS and NNIBDMS approaches, (a) Landmark pole, (b) Landmark goal.

Table 3. Comparisons of the correct rates for SVBSLS with different distance measurement methods.

Total experimental points = 247(blocks)			
Situation	**Correct**	**Incorrect**	**Accuracy rate**
IBDMS	34	213	13.77%
SVBSLS	247	0	100%

C. The Comparisons of Monocular Vision and Binocular Vision

In this subsection we compare the localization results of SVBSLS approach with those of the monocular vision approach, AVBSLS [16], under the same experimental environment. The errors of the distance measurement by the NNIBDMS approach with monocular vision (AVBSLS) and binocular vision (SVBSLS) are shown in Fig. 17. The results are summarized in Table 4. The average and maximum errors of the distance measurement by AVBSLS are 2.68cm and 12.86cm, respectively. On the other hand, those by SVBSLS are 1.38cm and 4.55cm, respectively. The proposed SVBSLS approach increases the distance measurement accuracy significantly.

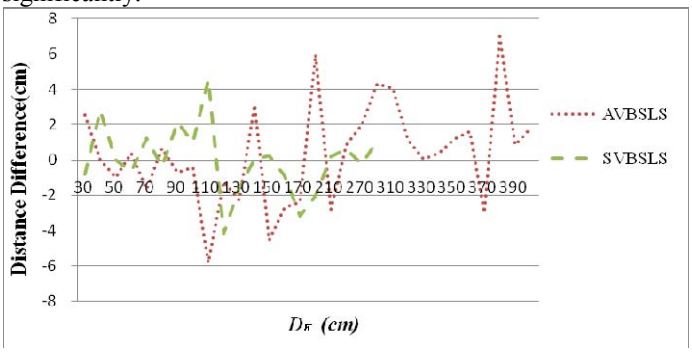

Figure 17. The distance errors by using AVBSLS and SVBSLS.

The correctness of the localization by using AVBSLS and SVBSLS is shown in Fig. 18 with 247 coordinate positions. The red star signs stand for the correct localization results. Table 5 shows the correct rates of the localization by using AVBSLS and SVBSLS approaches. The correct localization rate of the AVBSLS is 93.5%, but it must have robust features within a specific region. On the other hand, the SVBSLS approach can have a 100% correct rate without any restriction.

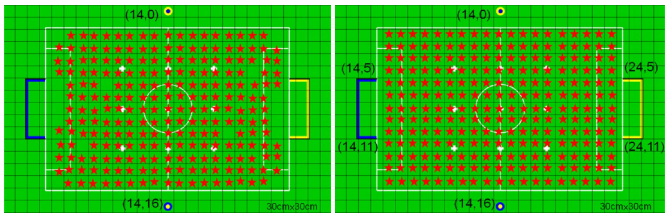

(a) (b)

Figure 18. The localization results of AVBSLS and SVBSLS, (a) AVBSLS, (b) SVBSLS.

Table 4. The average and maximum errors of the distance measurement by AVBSLS and SVBSLS.

Landmark		
Methods	**Average error**	**Maximum error**
AVBSLS	2.68 cm	12.86 cm
SVBSLS	1.38 cm	4.55 cm

Table 5. The comparisons of the correct localization rate with AVBSLS and SVBSLS.

Total experimental points = 247(blocks)			
Situation	**Correct**	**Incorrect**	**Accuracy rate**
AVBSLS	231	16	95.5%
SVBSLS	247	0	100%

CONCLUSIONS

Self-localization is one of the most important issues for the humanoid soccer robot. This research work proposes a very efficient vision approach, stereo vision-based self-localization system (SVBSLS), to localize the soccer robot itself during the soccer competition for the 2010 RoboCup rule. In order to emulate the human being, the mechanism of the SVBSLS consists of only two CCD cameras and a set of pan/tilt motors on the head of the humanoid soccer robot. We use the landmarks of the soccer field as the reference points to correctly self-localize the humanoid robot. In the SVBSLS approach, we have to measure the distance between the robot and the landmark. The modified IBDMS approach is used to measure the intrinsic parameters of the CCD camera and further to calculate the distance between the robot itself and the landmark or soccer ball. The BPN technique is used to refine the calculated distance to a more accurate one (NNIBDMS). By the SVBSLS approach with the NNIBDMS technique, the accuracy rate of the self-localization of the humanoid soccer robot can reach 100%, the average error of distance from the humanoid soccer robot to the soccer ball is only to 0.64cm. Since the resolution of the CCD camera is 960×720 pixels, the frame rate is only 4 fps. Although it is enough for the robot soccer competition, the computation efficiency can be improved by using the technique of hardware acceleration. The bottleneck (such as the color transform) can be overcome by hardware approach, and the image processing can be improved such that the robot can operate more smoothly.

ACKNOWLEDGEMENT

This work was supported by the National Science Council of Taiwan, R.O.C. under grant number: NSC 98-2218-E-032-003.

REFERENCES

[1] H. Kitano, M. Asada, Y. Kuniyoshi, I. Noda, and E. Osawa. "Robocup: The robot world cup initiative," IJCAI-95 Workshop on Entertainment and AI/ALife, pp. 19-24, 1995.

[2] FIRA RoboWorld Congress, 2010, Available: http://www.fira.net.

[3] RoboCup Soccer Humanoid League Rules and Setup for the 2009 competition, 2009 Available: http://www.robocup2009.org/

[4] RoboCup Soccer Humanoid League Rules and Setup for the 2010 competition, 2010 Available: http://www.robocup2010.org/

[5] I. Shimshoni, "On mobile robot localization from landmark bearings," IEEE Transactions on Robotics and Automation, vol. 18, no. 6, pp. 971-976, December 2002.

[6] M. Betke and L. Gurvits, "Mobile robot localization using landmarks," IEEE Transactions on Robotics and Automation, vol. 13, no. 2, pp. 251-263, April 1997.

[7] Z.-G. Zhong, J.-Q. Yi, D.-B. Zhao, Y.-P. Hong, and X.-Z. Li, "Motion vision for mobile robot localization," IEEE International Conference on Control, Automation, Robotics and Vision, vol. 1, pp. 261-266, December 2004.

[8] D.-J. Kriegman, E. Triendl, and T.-O. Binford, "Stereo vision and navigation in buildings for mobile robots," IEEE Transactions on Robotics and Automation, vol. 5, no. 6, pp. 792-802, Dec. 1989.

[9] S.-K. Choi, J. Yuh, and G.-Y. Takashiqe, "Development of the omni-directional intelligent navigator," IEEE Robotics & Automation Magazine, vol. 2, no. 1, pp. 44-53, Mar. 1995.

[10] P.-R. Liu, M.-Q. Meng, and P.-X. Liu, "Moving object segmentation and detection for monocular robot based on active contour model," Electronics Letters, vol. 41, no. 24, Nov. 2005.

[11] J. Kim, K.-J. Yoon, J.-S. Kim, and I. Kweon, "Visual SLAM by single-camera catadioptric stereo," SICE-ICASE International Joint Conference, pp. 2005-2009, Oct. 2006.

[12] S. Karin and P. Ioannis, "A novel method for automatic face segmentation, facial feature extraction and tracking," Signal Processing: Image Communication, vol. 12, no. 3, pp. 263-281, Jun. 1998.

[13] N. Herodotou, K. N. Plataniotis, and A. N. Venetsanopoulos, "Automatic location and tracking of the facial region in color video sequences," Signal Processing: Image Communication, vol. 14, pp. 359-388, 1999.

[12] C.-C. Chen, M.-C. Lu, C.-T. Chuang, and C.-P. Tsai, "Vision-based distance and area measurement system," IEEE Sensors Journal, vol. 6, no. 2, pp. 495-503, Apr. 2006.

[13] C.-C. Hsu, M.-C. Lu, W.-Y Wang, and Y.-Y. Lu, "Distance measurement based on pixel variation of CCD images," ISA Transactions, vol. 48, issue 4, pp. 389-395, Oct. 2009.

[14] Logitech, 2007, Logitech QuickCam® Pro for Notebooks, Available : http://www.logitech.com/

[15] Robotis, 2006, ROBOTIS Dynamixel AX-12, Available : http://www.robotis.com/zbxe/software_en.

[16] S.-H. Chang, W.-H. Chang, C.-H. Hsia, F. Ye, and J.-S. Chiang, "Efficient neural network approach of self-localization for humanoid robot," Joint Conference on Pervasive Computing, pp. 149-154, Dec. 2009.

2011 IEEE International Conference on Fuzzy Systems
June 27-30, 2011, Taipei, Taiwan

Training Multilayer Perceptron By Using Optimal Input Normalization

Xun Cai
School of Computer Science & Technology
Shandong University
Jinan, Shandong, P.R.China
caixunzh@sdu.edu.cn

Kanishka Tyagi
Department of Electrical Engineering
The University of Texas at Arlington
Arlington, TX, US
kanishka.tyagi@mavs.uta.edu

Michael T.Manry
Department of Electrical Engineering,
The University of Texas at Arlington
Arlington, TX, US
manry@uta.edu

***Abstract*— In this paper, we propose a novel second order paradigm called *optimal input normalization* (OIN) to solve the problems of slow convergence and high complexity of MLP. By optimizing the non-orthogonal transformation matrix of input units in an equivalent network, OIN absorbs separate optimal learning factor for each synaptic weight as well as the threshold of hidden unit, leading to an improvement in the performance for MLP training. Moreover, by using a whitening transformation of negative Jacobian matrix of hidden weights, a modified version of OIN called *optimal input normalization with hidden weights optimization* (OIN-HWO) is also proposed. The Hessian matrices in both OIN and OIN-HWO are computed by using *Gauss- Newton* method. All the linear equations are solved via *orthogonal least square* (OLS). Regression simulations are performed on several real-life datasets and the results show that the proposed OIN has not only much better convergence rate and generalization ability than *output weights optimization-back propagation* (OWO-BP), *optimal input gains* (OIG) and even *Levenberg-Marquardt* (LM) method, but also takes less computational time than OWO-BP. Although OIN-HWO takes a little expensive computational burden than OIN, its convergence rate is faster than OIN and often close to or rivals LM. It is therefore suggested that OIN-based algorithms are potentially very good choices for practical applications.**

Keywords- multilayer perceptron (MLP), orthogonal least square (OLS), Gauss-Newton, output weights optimization back propagation (OWO-BP), optimal learning factor (OLF), hidden weights optimization (HWO), Schmidt procedure

I. INTRODUCTION

The *multilayer perceptron* (MLP) has several favorable properties, such as universal approximation[1] and the ability to mimic Bayes discriminant [2] which make it a popular tool for many regression and classification applications including finance and weather predication [3,4], automatic controller [5], image and documents retrieval [6,7] and data mining [8].

A. Notation and Primary of MLP

Given a dataset with N_v training patterns $\{(\mathbf{x}_p, \mathbf{t}_p)\}$, where p=1 to N_v denotes the index of pattern, the typical topology of a fully-connected feed-forward MLP which consists of three layers, namely, input layer, hidden layer and output layer is shown in Figure 1. The numbers of units in input layer, hidden layer and output layer are denoted as N, N_h and M, respectively. All these three layers are connected to each other by synaptic weights.

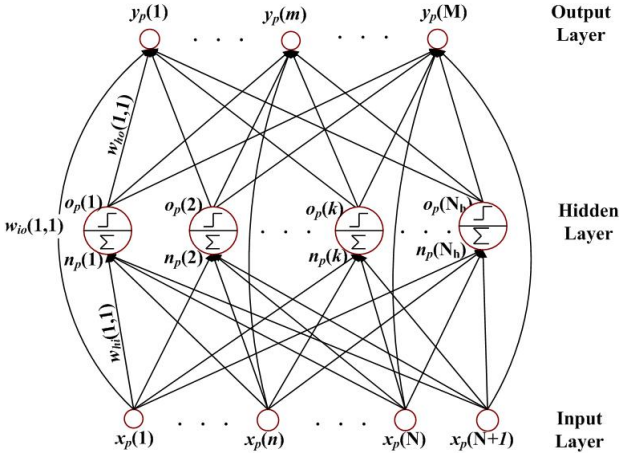

Figure 1. The architecture of a fully connected feedforward MLP

In Figure 1, $\mathbf{x}_p=[x_p(1), x_p(2),\ldots x_p(N+1)]^T$ denotes the input unit vector of p^{th} pattern which consists of N+1 input units, where $x_p(N+1)$ is an augmented input unit for conveniently handling the threshold of each hidden unit by setting $x_p(N+1)=1$ and $\mathbf{t}_p=[t_p(1), t_p(2),\ldots t_p(M)]^T$ denotes the corresponding desired output vector of p^{th} pattern which consists of M desired output units.

If i=1 to (N+1), m=1 to M and k =1 to N_h., then $\mathbf{W}_{ih}=\{w_{ih}(i,k)\}$ denotes all the hidden weights linking from input units to hidden units with N by N_h dimension. $\mathbf{W}_{ho}=\{w_{ho}(k,m)\}$ represents all the output weights linking from hidden units to output units with N_h by M dimension. For full-connected feed-forward MLP, there are another kind of weights directly link from input units to output units which called bypass weights $\mathbf{W}_{io}$. All the bypass weights.$\{w_{io}(i,m)\}$,are denoted as $\mathbf{W}_{io}$ with N by M dimension.Then, the net function of hidden units is denoted as $\mathbf{n}_p=[n_p(1),n_p(2),\cdots,n_p(N_h)]^T$. For k^{th} hidden unit, $n_p(k)$,is denoted as

This paper is sponsored by National Natural Science Foundation of China (No. 60970047) and Innovation foundation of Shandong University (No. 2010TS001).

$$n_p(k) = \sum_{i=1}^{N+1} w_{ih}(i,k)x_p(i) = (\boldsymbol{W}_{ih})^T \boldsymbol{x}_p \quad (1)$$

Thus, if the corresponding output vector of hidden units which called activation function is denoted as $\mathbf{O}_p=[O_p(1),O_p(2),\cdots,O_p(N_h)]^T$, then the output value of k^{th} hidden unit, $O_p(k)$ is given by

$$O_p(k) = f\left(n_p(k)\right) \quad (2)$$

where, $f(\cdot)$ denotes the nonlinear hidden layer activation function, which generally is taken as sigmoid function

$$f\left(n_p(k)\right) = \frac{1}{1+e^{-n_p(k)}} \quad (3)$$

Finally, the output vector of MLP $\mathbf{y}_p=[y_p(1), y_p(2),\cdots \boldsymbol{y}_p(M)]^T$ is summarized as,

$$\mathbf{y}_p = (\mathbf{W}_{io})^T \mathbf{x}_p + (\mathbf{W}_{ho})^T \mathbf{O}_p \quad (4)$$

For batch mode training of MLP, the typical error function $\mathbf{E}$ is *mean squared error* (MSE) which is defined as

$$\mathbf{E} = \frac{1}{N_v}\sum_{p=1}^{N_v}\sum_{m=1}^{M}\left[t_p(m) - y_p(m)\right]^2 \quad (5)$$

where $t_p(m)$ denotes the desired value and actual value of m^{th} output unit, respectively. If $\mathbf{W}$ denotes all the synaptic weight matrix, then the output vector, $\mathbf{y}_p$ is the function of $\mathbf{W}$ then the general main purpose of training MLP is to optimize the weight matrix, $\mathbf{W}$, by minimizing the MSE function , $\mathbf{E}$, based on some optimal training rules. In such case, $\mathbf{E}$ can also be represented as $\mathbf{E}(\mathbf{W})$.

B. Gradient Descent Algorithm

One of the earliest training algorithms for optimizing weights is gradient descent back propagation algorithm [10]. In such case, the hidden weight matrix, $\mathbf{W}_{ih}$, is updated as

$$\mathbf{W}_{ih} \leftarrow \mathbf{W}_{ih} + z \cdot \mathbf{G}_{ih} \quad (6)$$

where $\mathbf{G}_{ih}=\{g_{ih}(n, k)\}$ is a (N+1) by N_h negative Jacobian matrix of hidden weights which is given by

$$\mathbf{G}_{ih} = \frac{1}{N_v}\sum_{p=1}^{N_v}\mathbf{x}_p\left(\boldsymbol{\delta}_p\right)^T \quad (7)$$

where $\boldsymbol{\delta}_p = [\delta_p(1), \delta_p(2) \ldots, \delta_p(N_h)]^{\mathrm{T}}$. $\delta_p(k)$ is the delta function corresponding to for k^{th} hidden unit and is formulated as

$$\delta_p(k) = f'\left(n_p(k)\right) \cdot \sum_{m=1}^{M}\delta_o(m) \cdot w_{ho}(k,m) \quad (8)$$

where $[\delta_o(1), \delta_o(2), \cdots, \delta_o(M)]^T$ is denoted as $\boldsymbol{\delta}_o$ which represent the delta function for output units and is normally given by

$$\boldsymbol{\delta}_o = 2(\mathbf{t}_p - \mathbf{y}_p) \quad (9)$$

Let $\mathbf{W}_o=[\mathbf{W}_{io}: \mathbf{W}_{ho}]$ denote the combined output weight matrix with (N+1+N_h) by M dimension, then the equation for updating $\mathbf{W}_o$ is given by

$$\mathbf{W}_o \leftarrow \mathbf{W}_o + z_1\mathbf{G}_o \quad (10)$$

where z_1 is the learning factor and $\mathbf{G}_o$ is the gradient matrix of error function with respect to $\mathbf{W}_{\mathrm{o}}$.

If $\mathbf{X}_p = [\mathbf{x}_p: \mathbf{O}_p]$ with (N+N_h+1) by 1 dimension, then $\mathbf{G}_o$ is formulated as

$$\mathbf{G}_o = \frac{1}{N_v}\sum_{p=1}^{N_v}\mathbf{X}_p(\boldsymbol{\delta}_o)^T \quad (11)$$

From (6) and (10), we can easily find that the learning factors, z and z_1 have the directly effects on the convergence rate of MLP.

To choose appropriate z and z_1, many researchers have suggested that learning factor should be optimized separately for different synaptic weights [11]~[14]. However, for many MLP training algorithms, the definitions of learning factor z and z_1 were either assigned to be the fixed values or tuned empirically. Although these methods can show fast convergence rates for some specific applications, they are suffered from lots of efforts to find out the proper learning factors. Also, these methods have some error oscillations during training.

C. Output Weights Optimization Back Propagation (OWO-BP)

The OWO-BP algorithm is a fully optimal learning method which convergences fast without any error oscillation [15]. The OWO-BP algorithm includes two stages: the *output weights optimization* (OWO) and *back propagation* (BP).

In OWO stage, since the output units have linear activation functions, the OWO procedure is equal to solve a set of linear equations. In this case, the output weight vector $\mathbf{W}_{\mathrm{o}}$ is given as follows

$$\mathbf{W}_o = \mathbf{R}_o\mathbf{C}_o^T \quad (12)$$

Here, $\mathbf{R}_o$ is the autocorrelation matrix of $\mathbf{X}_p$ with (N+N_h+1) by (N+N_h+1) dimension and $\mathbf{C}_o$ is the correlation matrix of between output vector $\mathbf{y}_{\mathrm{p}}$ and $\mathbf{X}_p$ with dimension of M by (N+N_h+1). The calculations of $\mathbf{R}_o$ and $\mathbf{C}_o$ are given respectively as

$$\begin{cases} \mathbf{C}_o = \frac{1}{N_v}\sum_{p=1}^{N_v}\mathbf{y}_p\mathbf{X}_p^T \\ \mathbf{R}_o = \frac{1}{N_v}\sum_{p=1}^{N_v}\mathbf{X}_p\mathbf{X}_p^T \end{cases} \tag{13}$$

In this case, (12) can be directly solved by using orthogonal least square (OLS) which is achieved by Schmidt procedure[15].

In BP phase, the learning factor z is optimized which introduces the concept of *optimal learning factor* (OLF) z and the optimization of z for all the hidden weight is given by Newton's method as

$$z = -\frac{\frac{\partial \mathbf{E}}{\partial z}}{\frac{\partial^2 \mathbf{E}}{\partial z^2}} \tag{14}$$

where $\frac{\partial \mathbf{E}}{\partial z}$ and $\frac{\partial^2 \mathbf{E}}{\partial z^2}$ are the first order and the second order derivative of error function, with respect to the learning factor, z, which are computed , respectively as,

$$\begin{cases} \frac{\partial \mathbf{E}}{\partial z} = \frac{-2}{N_v}\sum_{p=1}^{N_v}\sum_{i=1}^{M}\left(t_p(i) - y_p(i)\right)\cdot\frac{dy(i)}{dz} \\ \frac{\partial^2 \mathbf{E}}{\partial z^2} = \frac{2}{N_v}\sum_{p=1}^{N_v}\sum_{i=1}^{M}\left[\frac{dy(i)}{dz}\right]^2 \end{cases} \tag{15}$$

where $\frac{dy(i)}{dz}$ is derived by following equation

$$\frac{dy(i)}{dz} = \sum_{k=1}^{N_h} w_{oh}(i,k) f'\left(n(k)\right)\sum_{n=1}^{N+1} g(k,n)\, x_p(n) \tag{16}$$

As the training of output weights is equivalent to solving linear equations and the learning factor z is optimized by using second order Newton's method, OWO-BP performs much better than gradient descent based BP with much less computations than LM. However, as OWO-BP only computes single OLF for all hidden weights, it cannot guarantee it is the global optimal factor for the entire error surface. Hence, OWO-BP doesn't exhibit faster convergence rate than LM.

D. The Plain Levenberg-Marquardt Algorithm

The plain *Levenberg-Marquardt* (LM) algorithm [17]~[20] is a sub-optimal learning factor method which updates all synaptic weights by following formulation

$$\mathbf{W} \leftarrow \mathbf{W} - (\mathbf{H} + \lambda \cdot \mathbf{I})^{-1}\nabla \boldsymbol{f}(\mathbf{W}) \tag{17}$$

where $\mathbf{H}$ is Hessian matrix of error function with respect to $\mathbf{W}$ with (N+N_h+1) by (N+N_h+1) dimension, λ is a controlling factor for tuning the direction of method towards first order or second order method, $\nabla \boldsymbol{f}(\mathbf{W})$is gradient matrix of a quadratic function of $\mathbf{W}$ and $\mathbf{I}$ is identity matrix. As LM algorithm optimizes all the synaptic weights by using the second order Newton's method, this algorithm converges significantly better than many other MLP training algorithms. However, due to the huge computations for calculate Hessian matrix H and its inversion matrix, which costs O(N^3), as well as lots of efforts to choose proper value of λ, LM suffers from huge computations leading to impractical application.

E. Optimal Input Gains algorithm

Compared with LM and OWO-BP, *optimal input gains* (OIG) algorithm is a fully optimal learning algorithm which embeds optimal learning factors into so-called optimal input gains [21]. OIG introduces a novel way to update hidden weights by optimizing an input unit transformation matrix in an equivalent MLP network. This transformation matrix is shown as

$$\mathbf{A} = \begin{bmatrix} a(1) & 0 & \cdots & 0 & 0 \\ 0 & a(2) & \cdots & 0 & 0 \\ \vdots & \vdots & \ddots & \vdots & \vdots \\ 0 & 0 & \cdots & a(N) & 0 \\ 0 & 0 & \cdots & 0 & a(N+1) \end{bmatrix} \tag{18}$$

where [a(1), a(2),⋯, a(N+1)] is called input gain vector and is denoted as **a**. Hence, the input transformation equation is given by

$$\bar{\boldsymbol{x}}_{\boldsymbol{p}} = \mathbf{A}\mathbf{x}_{\mathbf{p}} \tag{19}$$

By optimizing input gain vector **a**, the hidden weight can be updated as,

$$\mathbf{W}_{ih} \leftarrow \mathbf{W}_{ih} + \mathbf{a} \cdot \mathbf{G}_{ih} \tag{20}$$

Compared (20) with (6), it can be easily seen that the input gain vector , **a,** in fact takes the role of learning factor for training hidden weight matrix $\mathbf{W}_{ih}$.

Due to absorbing optimal learning factors into optimal input gains instead of obtaining optimal learning factor z directly, OIG converges much faster than OWO-BP with much less computation burden than LM.

In this paper, we proposed a more generalized optimal transformation matrix of input units. By optimizing this transformation matrix, a new algorithm which called *optimal input normalization* (OIN) improves the convergent rate and generalization than OIG.

The rest of paper is organized as follows: in the section II, we present the motivation for OIN and its mathematic derivation as well as the improved version of OIN which called OIN-HWO. In section III, the algorithm procedure of OIN as well as OIN-HWO is represented. In section IV, the simulation results on several benchmarks are analyzed. In section V, the conclusions and some suggestions on future enhancements are present. Acknowledgements and references are given in section VI and section VII, respectively.

II. OPTIMAL INPUT NORMALIZATION (OIN)

A. Motivation for OIN

The motivation for OIN comes from the well-known fact that if the input units are normalized to zero-mean, then the training error will be improved by non-orthogonal transformation of input units [22]. Thus, the non-orthogonal transformation matrix **A** is expressed as

$$\mathbf{A}=\begin{bmatrix}1 & 0 & \cdots & 0 & -m(1)\\ 0 & 1 & \cdots & 0 & -m(2)\\ \vdots & \vdots & \ddots & \vdots & \vdots\\ 0 & 0 & \cdots & 1 & -m(N)\\ 0 & 0 & \cdots & 0 & 1\end{bmatrix} \tag{21}$$

where $[m(1),(2)\cdots m(N)]$ is the mean vector of the input units. Hence, the n^{th} transformed input unit $\bar{x}_p(n)$ is given by

$$\bar{x}_p(n)=x_p(n)+m(n) \tag{22}$$

where n=1 $\cdots N$. This leads to the following lemma for the transformation of input unit to an equivalent network which is defined as [20].

Lemma: *Consider a nonlinear network with input unit vector* $\mathbf{x}_p\in R^{N+1}$*, with the restriction* $\mathbf{x}_p(N+1)=1$ *and output vector* $y\in R^M$ *and a second network in which the input unit vector* $\bar{\mathbf{x}}_p=\mathbf{A}\cdot\mathbf{x}_p$ *has corresponding output vector* $\bar{\mathbf{y}}_p\in R^M$ *then two networks are strongly equivalent if* $\forall\,\mathbf{x}_p\in R^{N+1}$, $\bar{\mathbf{y}}_p=\mathbf{y}_p$.

Based on the above theory, the negative Jacobian matrix of equivalent transformed network, $\bar{\mathbf{G}}_{ih}$ is given by derived from the original network, $\mathbf{G}_{ih}$, where

$$\bar{\mathbf{G}}_{ih}=\frac{1}{N_v}\sum_{p=1}^{N_v}\bar{\mathbf{x}}_p\left(\boldsymbol{\delta}_p\right)^T=\frac{1}{N_v}\sum_{p=1}^{N_v}(\mathbf{A}\mathbf{x}_p)\left(\boldsymbol{\delta}_p\right)^T=\mathbf{A}\mathbf{G}_{ih} \tag{23}$$

If we map the transformed input units back to the original network, then the relation between the negative Jacobian matrix of mapped MLP network, which is denoted as $\bar{\bar{\mathbf{G}}}_{ih}$, and $\mathbf{G}_{ih}$ is described as

$$\bar{\bar{\mathbf{G}}}_{ih}=(\mathbf{A}^T\mathbf{A})\mathbf{G}_{ih}=\bar{\mathbf{A}}\mathbf{G}_{ih} \tag{24}$$

where $\bar{\mathbf{A}}=\mathbf{A}^{\mathbf{T}}\mathbf{A}$ is a new transformed matrix with (N+1) by (N+1) dimension.

From (24), we can infer that only if **A** is non-orthogonal matrix, then $\bar{\mathbf{A}}$ could be useful for transformation from $\mathbf{G}_{ih}$ to $\bar{\bar{\mathbf{G}}}_{ih}$. In this case, the mapped back MLP will not be equal to the original MLP. Hence, by optimizing the non-orthogonal A, the training error of the mapped back MLP could be decreased more rapidly than that of the original one. This motivates us to propose the current OIN model.

Compared to OIG, the transformation matrix **A** of our proposed paradigm OIN has a more generalized form as

$$\mathbf{A}=\begin{bmatrix}a(1) & 0 & \ldots & 0 & b(1)\\ 0 & a(2) & \ldots & 0 & b(2)\\ \vdots & \vdots & \ddots & \vdots & \vdots\\ 0 & 0 & \cdots & a(N) & b(N)\\ 0 & 0 & \cdots & 0 & a(N+1)\end{bmatrix} \tag{25}$$

Here, [a(1), a(2), ..., a(N+1)] and [b(1), b(2), ..., b(N)] are called input gain vector which denoted as **a** and input bias vector which denoted as **b**, respectively. In these case, the $\bar{\mathbf{A}}$ is derived into the following symmetrical formation

$$\begin{aligned}\bar{\mathbf{A}}&=\mathbf{A}^{\mathbf{T}}\mathbf{A}\\ &=\begin{bmatrix}a(1)a(1) & 0 & \ldots & 0 & a(1)b(1)\\ 0 & a(2)a(2) & \ldots & 0 & a(2)b(2)\\ \vdots & \vdots & \ddots & \vdots & \vdots\\ 0 & 0 & \cdots & a(N)a(N) & a(N)b(N)\\ b(1)a(1) & b(2)a(2) & \cdots & b(N)a(N) & \sum_{n=1}^{N}a(n)b(n)\end{bmatrix}\\ &=\begin{bmatrix}\bar{a}(1) & 0 & \ldots & 0 & \bar{b}(1)\\ 0 & \bar{a}(2) & \ldots & 0 & \bar{b}(2)\\ \vdots & \vdots & \ddots & \vdots & \vdots\\ 0 & 0 & \cdots & \bar{a}(N) & \bar{b}(N)\\ \bar{b}(1) & \bar{b}(2) & \cdots & \bar{b}(N) & \bar{a}(N+1)\end{bmatrix}\end{aligned} \tag{26}$$

By substituting $\mathbf{G}_{ih}$ with $\bar{\bar{\mathbf{G}}}_{ih}$ in (6), the hidden weights of the mapped back MLP , $\bar{\bar{w}}_{ih}(n,k)$ and $\bar{\bar{w}}_{ih}(N+1,k)$,where n=1 to N ,k=1 to N_h, are updated ,respectively, as

$$\begin{cases}\bar{\bar{w}}_{ih}(n,k)\leftarrow\bar{\bar{w}}_{ih}(n,k)+z\cdot[\bar{a}(n)g_{ih}(n,k)\\ \qquad+\bar{b}(n).g_{ih}(N+1,k)]\\ \bar{\bar{w}}_{ih}(N+1,k)\leftarrow\bar{\bar{w}}_{ih}(N+1,k)+\\ z\cdot[\bar{a}(N+1)g_{ih}(N+1,k)+\sum_{j=1}^{N}\bar{b}(j).g_{hi}(j,k)]\end{cases} \tag{27}$$

If $z\cdot\bar{a}(n)$ and $z\cdot\bar{b}(n)$ are denoted as $\bar{\bar{a}}(n)$ and $\bar{\bar{b}}(n)$ respectively, then by comparing (27) with (6), it can be easily inferred that $\bar{\bar{a}}(n)$ and $\bar{\bar{b}}(n)$ absorb the learning factor z for each hidden weight of hidden unit as well as the threshold of hidden units. This results into the *optimal input normalization* (OIN) algorithm which gives more concern for thresholds of hidden units more than OIG.

B. Derivation of OIN

If $[\bar{\bar{a}}(1),\bar{\bar{a}}(2),\cdots\bar{\bar{a}}(N+1)\ ]^{\mathrm{T}}$ is denoted as **a** and $[\bar{\bar{b}}(1),\bar{\bar{b}}(2),\cdots\bar{\bar{b}}(N+1)]^{\mathrm{T}}$ is denoted as **b** , then [**a:b**] is denoted as **ab** which is a vector with (2N+1) by 1 dimension. Here, we use Gauss-Newton's method to optimize **ab**, which is formulated as

$$\mathbf{ab}=\mathbf{H}_{ab}^{-1}\mathbf{G}_{ab} \tag{28}$$

where $\mathbf{H}_{ab}=\begin{bmatrix}\mathbf{h}_{aa} & \mathbf{h}_{ab}\\ \mathbf{h}_{ba} & \mathbf{h}_{bb}\end{bmatrix}$ denotes the Hessian matrix with dimension of (2*N*+1) by (2*N*+1) and $\mathbf{G}_{ab}=[\mathbf{G}_a:\ \mathbf{G}_b]$ denotes the negative Jacobian matrix with dimension of (2*N*+1) by 1, where $\mathbf{G}_a$ and $\mathbf{G}_b$ are expressed , respectively, as

$$\begin{cases}\mathbf{G}_a=\dfrac{\partial \mathbf{E}}{\partial \mathbf{a}}=\dfrac{-2}{N_v}\cdot[\dfrac{\partial \mathbf{y}_p}{\partial \mathbf{a}}]^T\left[\mathbf{t}_p-\mathbf{y}_p\right]\\ \mathbf{G}_b=\dfrac{\partial \mathbf{E}}{\partial \mathbf{b}}=\dfrac{-2}{N_v}\cdot[\dfrac{\partial \mathbf{y}_p}{\partial \mathbf{b}}]^T\left[\mathbf{t}_p-\mathbf{y}_p\right]\end{cases} \tag{29}$$

From *m*=1to $(N+1)$, *u*=1 to *N* , then the each element of $\mathbf{h}_{ab}$, $\mathbf{h}_{ba}$ $\mathbf{h}_{aa}$ and $\mathbf{h}_{bb}$ are denoted as $h_{\mathrm{ab}}(m,u)$, $h_{\mathrm{ba}}(u,m)$, $h_{\mathrm{aa}}(m,m)$ and $h_{bb}(u,u)$, respectively and are calculated as,

$$\begin{cases}h_{ab}(m,u)=h_{ba}(u,m)=\dfrac{\partial^2\mathbf{E}}{\partial\bar{\bar{a}}(m)\partial\bar{\bar{b}}(u)}\approx 2\cdot\dfrac{1}{N_v}\sum\limits_{p=1}^{N_v}\sum\limits_{i=1}^{M}\dfrac{\partial y_p(i)}{\partial\bar{\bar{a}}(m)}\cdot\dfrac{\partial y_p(i)}{\partial\bar{\bar{b}}(u)}\\ h_{aa}(m,m)=\dfrac{\partial^2\mathbf{E}}{\partial\bar{\bar{a}}(m)^2}\approx 2\cdot\dfrac{1}{N_v}\sum\limits_{p=1}^{N_v}\sum\limits_{i=1}^{M}\dfrac{\partial y_p(i)}{\partial\bar{\bar{a}}(m)}\cdot\dfrac{\partial y_p(i)}{\partial\bar{\bar{a}}(m)}\\ h_{bb}(u,u)=\dfrac{\partial^2\mathbf{E}}{\partial\bar{\bar{b}}(u)^2}\approx 2\cdot\dfrac{1}{N_v}\sum\limits_{p=1}^{N_v}\sum\limits_{i=1}^{M}\dfrac{\partial y_p(i)}{\partial\bar{\bar{b}}(u)}\cdot\dfrac{\partial y_p(i)}{\partial\bar{\bar{b}}(u)}\end{cases} \tag{30}$$

.The net function , $n_p(k)$ in (1) is rewritten as

$$n_p(k)=\sum_{n=1}^{N}\bar{\bar{w}}_{hi}(n,k)\cdot x_p(n)+\bar{\bar{w}}_{hi}(N+1,k) \tag{31}$$

By substituting (31) and (27) into (4) and differentiating the first order of $\mathbf{y}_{\mathrm{p}}$ with respect of **a** and **b**, we obtain $\dfrac{\partial y_p(i)}{\partial\bar{\bar{a}}(m)}$ and $\dfrac{\partial y_p(i)}{\partial\bar{\bar{b}}(u)}$ by following equations

$$\begin{cases}\dfrac{\partial y_p(i)}{\partial\bar{\bar{a}}(m)}=\sum\limits_{k=1}^{N_h}w_{ho}(k,i)\cdot O_p'(k)\cdot\left[g_{ih}(m,k)\cdot x_p(m)\right]\\ \dfrac{\partial y_p(i)}{\partial\bar{\bar{b}}(u)}=\sum\limits_{k=1}^{N_h}w_{ho}(k,i)\cdot O_p'(k)\cdot\begin{bmatrix}g_{ih}(N+1,k)\cdot x_p(u)\\ +g_{ih}(u,k)\end{bmatrix}\end{cases} \tag{32}$$

where $O_p'(k)=f'\left(n(k)\right)$.

As $\mathbf{W_{ho}}$ can be obtained by using OWO from (12) shows, $\mathbf{H}_{ab}$ and $\mathbf{G}_{ab}$ in (28) can be calculated by (29)(30)and (32).

Finally, to obtain optimal **ab** in (28), here we use the *orthogonal least square* (OLS) method which is performed by using Schmidt procedure [15].

C. OIN-HWO

The concept behind HWO method [16] is that it uses separate error function for training each hidden weight. In such case, the error function of j^{th} hidden unit, $E_\delta(j)$,where *j* is from 1 to N_h, .in HWO is expressed as

$$E_\delta(j)=\sum_{p=1}^{N_v}\left[\delta_p(j)-\sum_{n=1}^{N+1}g_{hwo}(j,n)x_p(n)\right]^2 \tag{33}$$

$\mathbf{G}_{hwo}$ is derived from Newton's method as

$$\mathbf{G}_{hwo}\mathbf{R}=\mathbf{G}_{ih} \tag{34}$$

where **R** is the input auto-correlation matrix of input unit vector $\mathbf{x}_{\mathbf{p}}$. By this whitening transformation of $\mathbf{G}_{\mathrm{ih}}$, the input dependence can be eliminated, which makes the $\mathbf{H}_{\mathrm{ab}}$ is non-singular and the optimization **ab** is available. The set of linear equations in (34) is solved by using OLS. Thus, by substituting $\mathbf{G}_{ih}$ into $\mathbf{G}_{hwo}$, we can get a modified version of OIN called OIN-HWO**.**

III. PROCEDURE

The procedure of OIN in batch mode training is shown as follows:

Step1: Initialize input weight matrix $\mathbf{W}_{\mathrm{ih}}$ by using normal distribution function and net control.

Step2: Use OWO by (12) to get the optimal output weight matrix, $\mathbf{W}_o$, initially at first iteration.

Step 3: If the iteration does not end, then use (7) and (8) to get the negative Jacobian matrix $\mathbf{G}_{ih}$ for OIN or use (7), (8) and (34) to get $\mathbf{G}_{hwo}$ for OIN-HWO; else go to Step 10.

Step 4: Solve (28) ~ (32) to obtain optimal input normalization vector, **ab**, by using Schmidt procedure.

Step 5: Update the hidden weights of mapped back MLP by (27), $\bar{\bar{\mathbf{W}}}_{ih}$, for OIN based on $\mathbf{G}_{ih}$ or $\mathbf{G}_{hwo}$.

Step 7: Use these new hidden weights to get new output values of hidden units, $\mathbf{O}_p$, by (2).

Step 8: Calculate new optimal output weight matrix $\mathbf{W}_o$ in (12).

Step 9: Combine new $\bar{\bar{\mathbf{W}}}_{ih}$ and $\mathbf{W}_o$ to get actual output vector $\mathbf{y}_p$ in (4) and use (5) to get new training MSE, **E**.

Step 10: Return to Step 3 and repeat the above steps until get to the end of iterations.

IV. EXPERIMENTAL RESULTS

We perform our simulations for two versions of OIN on several datasets and show the performance by comparing the results with OWO-BP and LM. All the simulations run on Intel Core2 Duo P8700. The number of training iterations for each simulation is fixed to 100, namely, N_{it}=100. For better comparison, all the synaptic weights are initialized using the same method which is given by section III Step (1)~(2). Thus, the training iteration will start after OWO and the first training error will start at the same point.

A. Description of Datasets

The datasets which we use are called "Twod", "Single2", "Mattrn" and "Concrete", respectively. All these datasets used for simulation are publicly available and the input units

of all these datasets have been normalized to be zero-mean and unit variance..

The first three are from the Image Processing and Neural Networks Lab repository [23] and the last one is from UCI Machine Learning Repository [24,25]. Among these datasets, "Twod" is used to invert the surface scattering parameters from an inhomogeneous layer above a homogeneous half space, where both interfaces are randomly rough. "Mattrn" is used for inversion of random two-by-two matrices; "Single2" is used for inversion of surface permittivity, the normalized surface rms roughness, and the surface correlation length found in back scattering models from randomly rough dielectric surfaces. "Concrete" dataset is used to approximate the nonlinear function of age and ingredients of concrete compressive strength.

All of the numbers of patterns, input units, output units and hidden units of these datasets are denoted as N_v, N, M, and N_h , respectively, as listed in TABLE I. In order to learn how each algorithm deals with the co-linearity of each dataset, all the co-linearity of datasets are also listed in Table I.

TABLE I. THE STRUCTURE OF MLP AND CO-LINEARITY FOR EACH DATASET

Datasets	N_v	N	M	N_h	Co linearity
Twod	1768	8	7	10	high
Single2	10000	16	3	8	high
Mattrn	2000	4	4	12	high
Concrete	1030	8	1	15	low

Under the above training conditions, the training MSEs of OIN, OIN-HWO, OIG, OWO-BP and LM are plotted version the time spent after 100 iterations are shown in Figure 2, respectively.

B. Training Error Versus Computational Time

From Figure 2(a)~(d), we can see that OIN shows faster converging rates than OWO-BP and OIG , even rivals LM in (c) as well as OIG does. The total training time spent by OIN is a little longer than OIG but shorter than OWO-BP.

Also, it can be easily seen that OIN-HWO always shows better converge rate than OIN even close to or rivals LM as (a)~(c) shown. OIN-HWO takes a little longer training time then OIN, OIG and OWO-BP. However, compared with LM, the training time spent by OIN-HWO is much less.

C. K-fold Cross Validation

Furthermore, we use k-fold cross validation procedure to evaluate the generalization abilities of OIN and OIN-HWO with comparison with OIG, OWO-BP and, LM. Here, k=10. The procedure of k-fold cross validation is described as follows.

We split each dataset randomly into 10 non-overlapping parts of equal size and combine 9 parts of 10 for training leaving the remaining one part for testing. This procedure is repeated until we have exhausted all 10 combinations. Then, by training all these combinational datasets and then testing on the remaining dataset, we obtain the training MSE and validation MSE of each algorithm on each dataset. The results are listed in Table II.

From Table II, we can see that both training error and validation error of OIN are smaller than OIG and OWO-BP, even smaller than LM on "Single 2" dataset. OIN-HWO shows much better training and validation errors than OIN, even rivals LM on these four datasets. That means our proposed paradigm OIN and OIN-HWO can be seemed as a potential robust approach for practical applications.

V. CONCLUSION

In this paper, we present a novel MLP training algorithm called optimal input normalization (OIN) and its improved version OIN-HWO. Several simulations on real-life datasets and the k-fold cross validation show that the proposed OIN and OIN-HWO greatly improve the converging rates and generalization abilities of OIG, OWO-BP and even LM, respectively. Moreover, as they spend much less computational time than LM, OIN and OIN-HWO are potentially good choice for real life applications.

Future work will give more detailed analysis the effects of co-linearity of different dataset on OIN performance and develop the novel OIN algorithm combined with other network such as RBF, SVM etc..

VI. ACKNOWLEDGMENTS

Our sincere thanks are given to the Image Processing and Neural Network Lab in the Department of Electrical Engineering at the University of Texas at Arlington.

TABLE II. K-FOLD CROSS VALIDATION

Datasets	T&V	OIG	OIN	OIN-HWO	LM	OWO-BP
Twod	T	0.240	0.224	0.165	0.200	0.248
	V	0.249	0.235	0.179	0.212	0.259
Single2	T	0.452	0.168	0.104	0.582	1.445
	V	0.588	0.432	0.130	0.780	1.479
Mattrn	T	0.021	0.017	0.004	0.014	0.039
	V	0.021	0.016	0.009	0.013	0.037
Concrete	T	41.93	38.268	13.813	19.600	50.228
	V	49.39	48.564	20.444	30.239	59.399

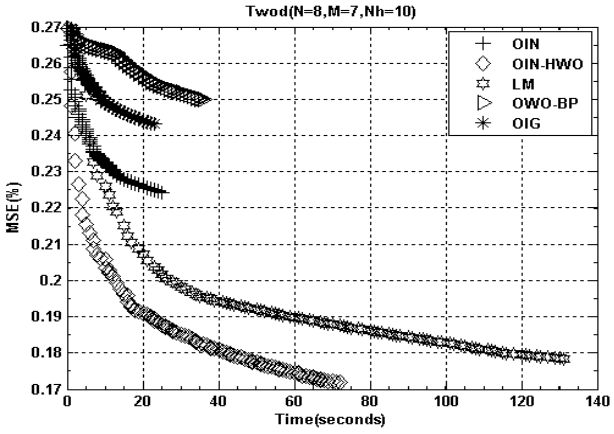

(a)"Twod"

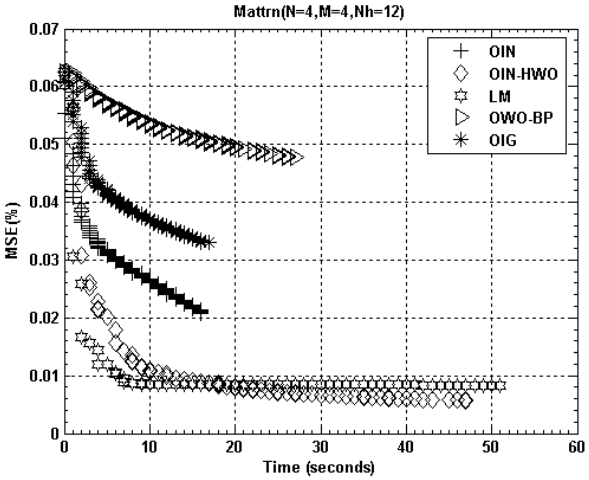

(b)"Mattrn"

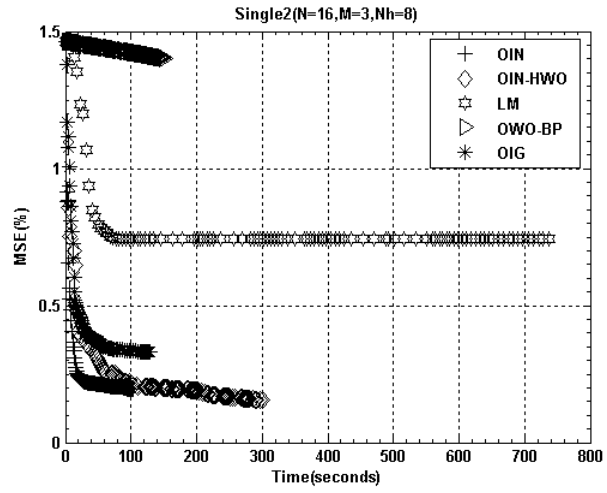

(c)"Single2"

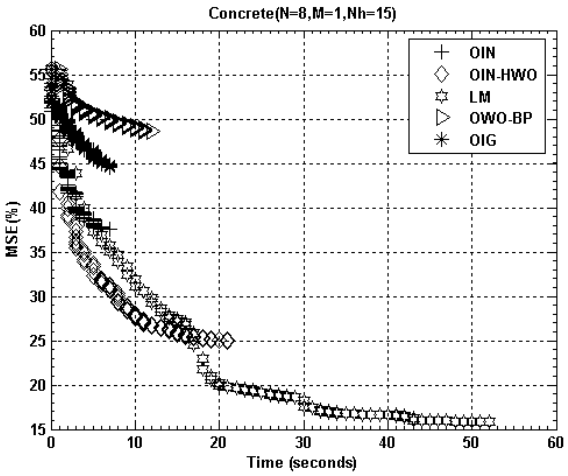

(d)"Concrete"

Figure 2. The training error versus time spent on various datasets

VII. REFERENCES

[1] G. Cybenko, "Approximations by superpositions of a sigmoidal function," Mathematics of Control, Signals, and Systems (MCSS), vol. 2, pp. 303-314, 1989.

[2] Dennis W. Ruck et al., "The mulitlayer perceptron as an approximation to a bayes optimal discriminant function," IEEE Transactions on Neural Networks, vol. 1, No. 4, pp.256-298, 1990.

[3] Meesomsarn, K., Chaisricharoen, R., Chipipop, B. and Yooyativong, T. "Forecasting the effect of stock repurchase via an artificial neural network," ICROS-SICE International Joint Conference 2009, pp.2573 - 2578, Aug , 2009.

[4] Jao-Hong Cheng, Huei-Ping Chen and Yi-Min Lin, "A hybrid forecast marketing timing model based on probabilistic neural network rough set and C4," Expert Systems with Applications, vol. 37, n.4, pp. 1814 – 1820, 2010.

[5] Rong-Jong, Wai and Zhi-Wei, Yang, " Design of fuzzy-neural-network tracking control with only position feedback for robot manipulator including actuator dynamics," .IEEE International Conference on Systems, Man and Cybernetics. (Taipei, China, Oct12-15, 2008), pp. 2349 – 2354, Oct., 2008,

[6] Marinai, S., Gori, M., Soda, G., "Artificial neural networks for document analysis and recognition," IEEE Transactions on Pattern Analysis and Machine Intelligence, vol. 27, n.1, pp. 23-35, 2005.

[7] Jyothi, B.V., Eswaran, K., "Comparative study of neural networks for image retrieval," International Conference on Intelligent Systems, Modelling and Simulation (Liverpool, UK, Jan 27-29, 2010), pp. 199 – 203, Jan . 2010.

[8] .K.-L, Du. "Clustering: A neural network approach," Neural Networks, vol. 23, n. 1, pp. 89-107, 2010,.

[9] Melacci, S.; Maggini, M.and Sarti, L., "Semi-supervised clustering using similarity neural networks," International Joint Conference on Neural Networks, (Atlanta, GA, June 14-19, 2009), pp.2065 – 2072, June 2009.

[10] Rumelhart, D.E., Hinton, G.E.and Williams, R.J., "Learning internal representations by error propagation," Parallel distributed processing: explorations in the microstructure of cognition, Mit Press Computational Models Of Cognition And Perception Series, Cambridge, MA, USA, vol. 1: foundations.1, pp. 318 – 362, 1986.

[11] Robert, A. Jacobs, "Increased rates of convergence through learning rate adaptation," Neural Networks. vol.1, n.4, pp.295-307, 1988.

[12] Sang-Hoon Oh and Soo-Young Lee., "Optimal learning rates for each pattern and Neuron in gradient descent training of multilayer

perceptrons,"International Joint Conference on Neural Networks (Washington, DC , USA 10 Jul 1999),pp. 1635 – 1638, Jul 1999.

[13] Y. LeCunn, L.Bottou, G.B.Orr, K.R.Muller, "Efficient BackProp," Lecture Notes In Computer Science, vol. 1524, Springer-Verlag, London, pp. 9-50, 1998.

[14] Hestenes M., R., and Steifel, E., "Methods of conjugate gradients for solving linear systems." Journal of Research of the National Bureau of Standards. vol. 49, n.6, pp. 409-436, 1952.

[15] F. J. Maldonado, M. T. Manry and Tae-Hoon Kim,. "Finding optimal neural network basis function subsets using the Schmidt procedure" In Proceedings of the International Joint Conference on Neural Networks,(Portland, Oregon,2003),1, pp.444 – 449, July , 2003.

[16] H-H Chen, M.T. Manry, and H. Chandrasekaran, "A neural network training algorithm utilizing multiple sets of linear equations", Neurocomputing, vol. 25, pp. 1-3, 55-72, 1999,.

[17] Fun., M,H., and Hagan., M,T., " Levenberg-marquardt training for modular networks," Proc. Of IEEE International Conference on Neural Networks'96, Washington DC,pp.468-473, 1996.

[18] Hagan., M, T., and Mehna., M,B., "Training feedforward networks with the marquardt algorihm," IEEE Trans. Of Neural Networks, vol.5, pp. 989-993, Nov.1994.

[19] Levenberg, K.,. " A method for the solution of certain problems in least squares," Quart. Appl. Math.,vol. 2, pp. 164.168, 1944,.

[20] Marquardt, D.," An algorithm for least-squares estimation of nonlinear parameters," SIAM J. Appl. Math., vol. 11, 431-441, 1963.

[21] Sanjeev S. Malalur, Manry, M. T., " Feed-forward network training using optimal input gains," Proceedings of International Joint Conference on Neural Network.(Atlanta, Georgia, USA, June 14-19, 2009),pp. 1958-1960, June 14-19, 2009

[22] Y. LeCun, "Efficient Learning and Second-Order Methods," A Tutorial at NIPS 93, Denver 1993.

[23] http://www-ee.uta.edu/eewb/ip/training_data_files.htm

[24] http://archive.ics.uci.edu/ml/

[25] Cheng Yeh., " Modeling of strength of high performance concrete using artificial neural networks," Cement and Concrete Research,vol. 28,n.12, pp.1797-1808,1998,

2011 IEEE International Conference on Fuzzy Systems
June 27-30, 2011, Taipei, Taiwan

Automatic Scene Recognition for Low-Resource Devices using Evolving Classifiers

Javier Andreu, Rashmi Dutta Baruah, Plamen Angelov
School of Computing and Communications
Infolab21, Lancaster University
Lancaster, LA1 4WA, United Kingdom
{j.andreu,r.duttabaruah,p.angelov}@lancaster.ac.uk

Abstract– **In this paper an original approach is proposed which makes possible autonomous scenes recognition performed on-line by an evolving self-learning classifier. Existing approaches for scene recognition are off-line and used in intelligent albums for picture categorization/selection. The emergence of powerful mobile platforms with camera on board and sensor-based autonomous (robotic) systems is pushing forward the requirement for efficient self-learning and adaptive/evolving algorithms. Fast real-time and online algorithms for categorisation of the real world environment based on live video stream are essential for understanding and situation awareness as well as for localization and context awareness. In scene analysis the critical problem is feature extraction mechanism for a quick description of the scene. In this paper we apply a well known technique called spatial envelop or GIST. Visual scenes can be quite different but very often they can be grouped in similar types/categories. For example, pictures from different cities across the Globe, e.g. Tokyo, Vancouver, New York, Moscow, Dusseldorf, etc. bear the similar pattern of an urban scene – high rise buildings, despite the differences in the architectural style. Same applies for the beaches of Miami, Maldives, Varna, Costa del Sol, etc. One assumption based on which such automatic video classifiers can be build is to pre-train them using a large number of such images from different groups. Variety of possible scenes suggests the limitations of such an approach. Therefore, we use in this paper the recently propose evolving fuzzy rule-based classifier, simpl_eClass, which is self-learning and thus updates its rules and categories descriptions with each new image. In addition, it is fully recursive, computationally efficient and yet linguistically transparent.**

Key words - **scene recognition, evolving fuzzy rule based classifier, GIST, image processing**

I. INTRODUCTION

The rapid evolution of MEMS (Micro-Electro-Mechanical Systems) has brought to our lives hundreds of sensors which can fit in the palm of our hand and also be embedded in personal devices such as PCs, PDAs, tablets and mobile devices. One of the sources of information (a kind of a sensor) which is integrated within such devices is the video camera. Thanks to these built-in cameras it is possible to obtain video input from nearly all portable devices nowadays.

There is a body of research which is focused on the event detection such as landmarks [1]-[2] and on scene recognition such as [3]-[4]. In the field of scene recognition, there are works that developed intelligent photo albums such as [5] or photo retrieval and classification systems as [6]. However, only in [1] the algorithm that has been used is recursive, on-line, adaptive and can be embedded on a chip. Most of the other published approaches are off-line, computationally expensive and not suitable for embedded applications.

A very important by-product of having computationally lean algorithms is the energy efficiency. In terms of energy consumption one can differentiate between two types of digital capturing images; i) one is CCD (charge coupled devices), and the other one is ii) CMOS (complementary metal oxide semiconductor). Both of them convert images into electric charges. In terms of functioning, the former determines a charge for every pixel which is transferred into another chip as an analogue signal; the latter defines a voltage charge for each pixel conversion and performs digitalization by itself. Although, both offer an excellent imaging performance, CMOS is widely used because it is more energy efficient compare to CCD [7]. It also offers more functionality such as discretization and signal digitalization integrated on the chip than CCD. However, the picture quality of CMOS is not as good as the ones that can be obtained from a CCD camera.

Consequently, in order to maximize the performance and energy consumption of these devices, quick and cheap algorithms in terms of resources will have an important role.

For this purpose, we have developed and studied new algorithms based on recursive and computationally efficient evolving classifiers [8]-[9]. We used GIST descriptor [10]-[11] to compute the features from images. The idea of this descriptor is quite simple; it aims to develop a low dimensional representation of the scene but without partitioning. Basically, GIST feature instances are defined by perceptual dimension such as roughness, openness, naturalness, expansion. All these characteristics represent the spatial structure of a scene. They are easily computed using spectral and superficial localized information. In addition, the use of GIST in scene recognition has been widely experimented [12]-[13].

The evolving fuzzy rule-based classifiers that we will apply in this study [8]-[9] represent a new paradigm of online self-learning which combines the classifier design and classification (prediction) and can also be used as unsupervised tool for clustering (the labeling of clusters can be left for the user). Similar techniques of evolving classifiers have been recently reported in human activity recognition [14] and intelligent robotics applications [15].

The remainder of the paper is organized as follows; in section II related works are presented; in section III feature

978-1-4244-7316-8/11/$26.00 ©2011 IEEE

extraction method is given; in section IV image processing methods are described, in section V the evolving classifier is portrayed, a summary of the entire approach is given in section VI; section VII analyses experimental results and finally section VIII concludes the paper.

II. Related Work

Nowadays, the topic of natural scene classification has been widely studied. Fundamentally, most of the publications focus on modeling the scene using statistical information which is fed later to classification. They differ in the selected method to compute the features. For example [16] which is one of the first works in the field, proposed a feature framework which differentiate between indoor and outdoor scenes. It uses low level features such as; texture, color, and frequency information. Some standards, such as MPEG-7 offer a detailed description of these features. Other, more complex studies, try to relate graphical model with object recognition [17]. Further approaches also try to split the scene semantics concepts [18]. For this purpose, grids of sub-regions of the image are created and later semantics concepts (depicted in semantic nets) are related to these regions. One outstanding contribution to this field was the work [10] which used GIST [11] to build efficient classifiers. However, their work is in off-line mode.

Many other studies used GIST-based scene descriptors. For example [19] used GIST combined with clustering methods to recognize landmarks in the scene. In [20] the recognition of facial expression is enhanced by using context information of the scene using GIST descriptors. In [21] a context-based recognition approach was presented for mobile robots capturing the GIST-based description of the scene.

Evolving classifiers has also been used for recognizing landmarks [22] and for autonomous self-location of mobile robots [9]. In this paper we propose an innovative approach to automatic scene analysis using on-line and evolving self-learning fuzzy rule-based (FRB) classifier that is *potential free*. This results in an algorithm which is computationally and energy efficient and very precise.

III. Gist Descritpion of a Scene

Usually, it is said that humans are able to recognize a scene from a single glance. This is because our brain captures a spatial representation of the scene, recognizing some meaningful objects or salient information of the scene. However, our rational capacities cannot process all information of a complex scene in just a single glance. What our brain does is to just construct a representative picture of perceptual and conceptual low-level (color, contours); intermediate (shapes, texture regions) and high-level information (semantic knowledge). Based on behavioral studies, Friedman [12] observed that regardless of the visual complexity of the scene, humans are able to recognize either categories or special layout of the scene.

More recently, based on Friedman's fundamental studies, a team at MIT studied the application of the GIST to images [10],[22]-[23] to analyze characteristics and properties of images, in order to create a structured summary of a real-world scene. It is stated that descriptive factors exist that can be instrumental for the diagnostic structure of the scene. Torralba et al. came up with the example that urban zones are structured vertically while the forests are textured [11].

Unlike the other approaches, which partition the scene in bins, the standard GIST-based approach considers the scene as a whole, but analyses it spectrally. Consequently, there is no need to detect individual landmarks and objects in the scene. Instead, a scene can be represented by a vector of spectral values. These values are spatial envelope properties such as expansion, openness, roughness.

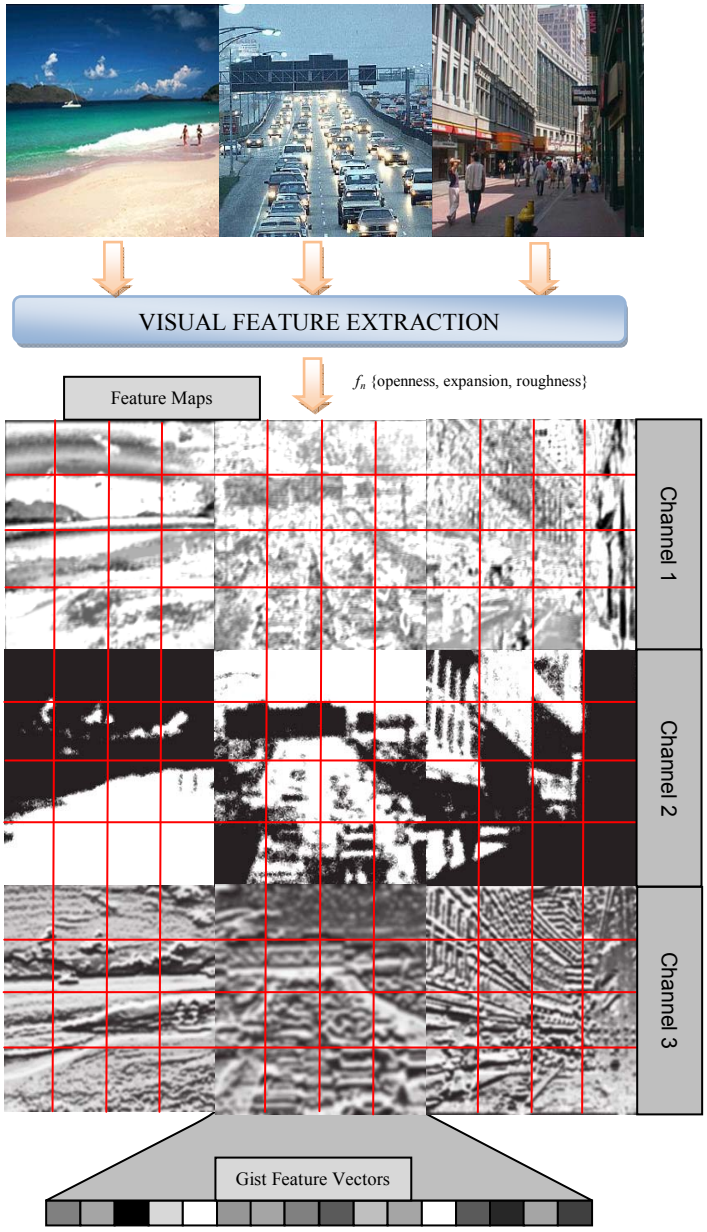

Fig 1. Feature vector of spatial envelop properties

Each property is equivalent to a dimension of the spatial envelope space. These features are meaningful enough to describe the spatial structures of the scene. To estimate these properties spectral and coarsely localized information is used.

To have a rough idea of how GIST-based analysis works let's consider the fundament of the approach.

Most widely used image-based representation for the analysis of the spectral dynamic properties is provided by the discrete Fourier Transform (FT). FT filters represent the spatial domain of the input figure in a frequency domain of sine and cosine components. The discrete form of the FT is a sampled version of it. In other words, it is a set of most representative samples of frequencies. FT-based image representations have shown to have a very good performance in scene recognition problems.

In the fundament of GIST approach are Gabor filters which bear some similarity to Fourier filters. However, the former ones are defined by harmonic functions modulated by Gaussian distributions. As a result of adjustment into Gaussians, these types of filters are limited by frequency bands. With a judicious selection of frequencies (e.g. by successive factors of 2, by octaves), a succession of Gabor filters can be assimilated to a wavelet transform. It results in a very good method of image compression and discretization.

In Figure 1 several Gabor filters with selected channels are computed on a grid of the image (4x4) and indexed into an array. This array is called GIST of the scene. This array represents the spatial layout of the scenes, i.e two images with similar array values (layout) are often similar scenes and vice versa.

IV. Online Preprocessing of Features.

For online recognition of scenes, a fast computation of features is necessary. This can be achieved by means of a fast/recursive computation of parameters. On this sense, in the literature we may find several research works which already have considered this issue. For example, [25] proposes an efficient and recursive computation of Gabor filters to cope with the multi-resolution/orientation of images (which can be a computational intense process). Other works like [26] defined a fast computation of Gabor functions using a bi-orthogonal condition to compute the dual frames. A very precise solution to increase speed on computation of Gabor features is to compute the Gaussian envelope recursively. This way, [27] proposes a recursive way to compute the Gaussian kernel of the Gabor filter general formula [28].

In most of the cases, number of Gist features from the resultant Gabor filters applied, is usually big. In our case, the resultant 4x4 grid partition leads to a feature map of 544 gist features (from 34 Gabor features per region). Consequently, a dimensionality reduction algorithm should be also considered. Although, the recursive computation of these methods is not as extended as the ones of Gabor filters, there has been some progress in this line.

Most widely, used approaches to attain this dimensional reduction are by means of methods such as Principal Component Analysis (PCA) or Fast Independent Component Analysis (FastICA). The latter is already formulated as a computationally efficient method; the former by definition is not. However, there are some works that have recently achieved to formulate the computation of PCA values online [29].

Based on the trend of some works in biology and biotechnology, PCA/ICA projections are reinforced with a Linear Discriminant Analysis (LDA) to increase the description power of features regarding to the class.

1) Recursive Principal Component Analysis (PCA)

It is one of the most commonly used approaches for feature extraction/reduction. Principal Component Analysis (PCA) addresses the issue of correlation of raw input data by orthogonalisation. PCA mainly aims to transform the raw data that are, usually, correlated into a smaller set of uncorrelated variables. Summarizing, we may say that the transformation of new variables are performed by linear combinations of the original (measured) variables. In this connection, the overall number of variables that are required to be measured is not being reduced; what is reduced is the number of inputs to the classifier (manipulated variables by the classifier) by preserving the majority of the information in terms of data variance which is useful for correct classification.

It is mainly based on producing new variables maximising the variance of the data. PCA is very helpful in revealing the hidden dynamics that is often 'hidden' in a raw signal. This method is completely unsupervised (that makes easy to compute it online) and does not take into account any category or label. Its main target is to find efficient orthogonal projections explaining the variance of the data most. In the standard (offline) version of PCA, projections are evaluated by the value of their associated eigen-values. The number of desired orthogonal directions must be defined previously. This is because each projection has to be orthogonal to its previous, independently of the first computed one that will be update according to the coming data.

As it has been discussed before, in this work we aim to perform in an online/real time basis. In order to get a recursive/fast implementation of PCA we can follow the steps suggested by [29].

PCA projections are represented by the eigen-values, *v*. They can be calculated as follows:

$$v_k = \frac{1}{k}\sum_{i=1}^{k} u_i \cdot u_i^T \cdot \frac{v_{i-1}}{\|v_{i-1}\|} \tag{1}$$

Note u denotes an orthogonal projection and k is the current time instant/sample.

This expression is based on the definition of *v* as $\gamma \cdot x = C \cdot x$ and $v = \gamma \cdot x$ where γ is the magnitude of the eigen-value, $\|v\|$, and C the covariance matrix.

Expression (1) can be expressed recursively by weighting its current and last estimates by $\frac{k-1}{k}$ and $\frac{1}{k}$ respectively; then we get:

$$v_k = \frac{k-1}{k} \cdot v_{k-1} + \frac{1}{k} \cdot u_k \cdot u_k^T \cdot \frac{v_{k-1}}{v_{k-1}} \tag{2}$$

As a result, it is possible to estimate recursively orthonormalized values to guarantee maximum independence of directions. Thus, parting from the first order eigenvector a new one is estimated by subtracting its orthogonal projection. The formula which describes this projection u_j is as follows:

$$u_k = u_{k-1} - u_{k-1}^T \cdot \frac{v_{k-1}}{\|v_{k-1}\|} \cdot \frac{v_k}{\|v_k\|} \quad (3)$$

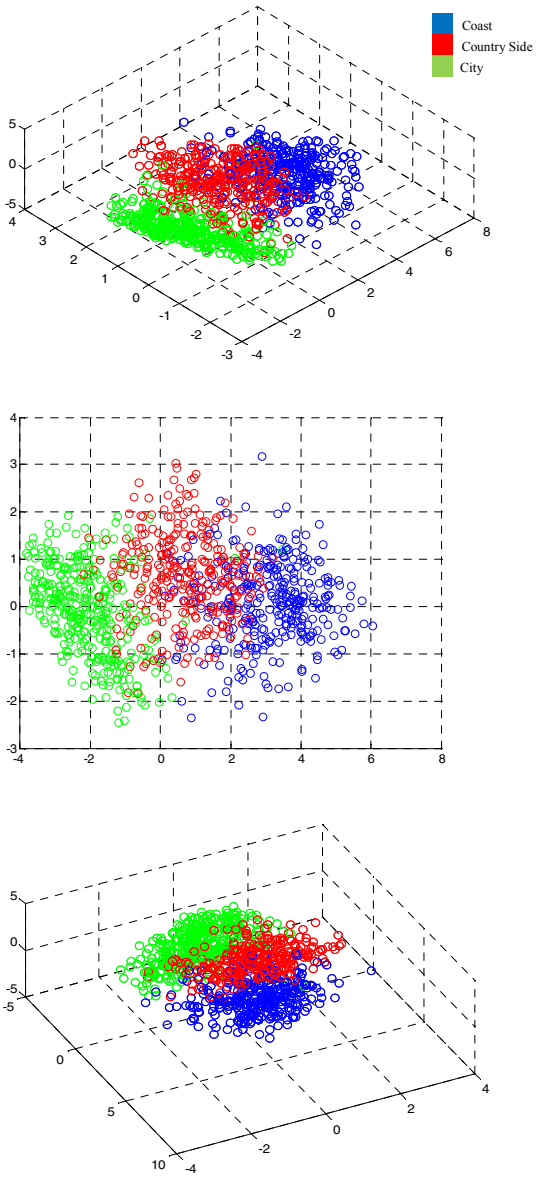

Fig 2. rPCA-LDA applied to data with three categories.

2) Recursive Linear Discriminant Analysis (LDA)

Methods explained above are very useful for reducing correlation and number of inputs to the classifier. However, they do not take into account what category of scene data belongs to. They just get the best representation of data based on its initial values (inputs) without considering the output. We want to classify and recognize categories. Hence, bearing in mind that scenes are categorized, LDA can be applied, it is considered to use LDA to improve the description power of features, this time regarding to the class label (outputs in terms of the classifier).

While PCA/ICA finds the best projections of data in a way that maximises their separability, LDA helps finding these directions which will be best to distinguish between different classes (scenes categories). A combination of both, PCA and LDA has proven to be an effective pre-processing technique in spectroscopy. LDA method is based on the sample variance (σ^2) and sample variance per class (σ_c^2). They are used to form scatter matrices (S_b and S_w). S_w denotes the within-class scatter matrix. Likewise, S_b represents a singular matrix denoted as between-classes scatter matrix. The separation between those matrices is defined as a measure of the signal-to-noise ratio for class labelling. Eigenvectors of $S_{w^{-1}}$ and S_b are consider the best coordinates to discriminate classes better. Thus, new projections of data enhance a separation between categories. In [29] a recursive method is presented to compute both LDA and PCA (fig. 2).

V. Evolving Fuzzy Rule-based Classifiers

In this paper we use evolving fuzzy-rule based (FRB) classifiers of the eClass family [8], namely *eClass1* [8] and a simplified version called *simpl_eClass1* [30]. The evolving classifiers are characterized by self-learning of both structure and parameters and use evolving Takagi-Sugeno FRB models [31]. The structure of both the classifiers is based on first-order multi-input multi-output (MIMO) type FRB model of the following form.

$$Rule^i : IF\left(x_1 \; is \sim x_1^{i*}\right) AND ... \left(x_n \; is \sim x_n^{i*}\right) THEN\left(\mathbf{y}^i = \mathbf{x}_e \boldsymbol{\theta}^i\right) \quad (4)$$

where $\mathbf{y}^i = [y_1^i \;\; y_2^i \;\; \ldots \;\; y_m^i]$ is the m-dimensional output of i^{th} rule, $\mathbf{x}_e = [1 \;\; x_1 \;\; \ldots \;\; x_n]$ is the extended input vector, $\boldsymbol{\theta}^i$ is the matrix of local sub-system parameters given as:

$$\theta^i = \begin{bmatrix} a_{01}^i & a_{02}^i & \cdots & a_{0m}^i \\ a_{11}^i & a_{12}^i & \cdots & a_{1m}^i \\ \vdots & \vdots & \cdots & \vdots \\ a_{n1}^i & a_{n1}^i & \cdots & a_{nm}^i \end{bmatrix}$$

The rules of the classifiers are formed around focal points (cluster centres), where a focal point is a representative of all the data samples within a cluster. The consequent parameters of the rules are estimated using weighted recursive least squares (wRLS) approach [31]. *Simpl_eClass1* differs from *eClass1* mainly due to the learning mechanism which is potential/density free [30]. In order to determine whether an incoming sample is a new focal point, *eClass1* requires calculation of a *potential/density* value [8],[31] for the incoming sample and update of potentials/densities of all the existing focal points. Thus, the computational complexity of *eClass1* (similarly to *eTS*) is *O(N),* where *N* is the number of

existing focal points (respectively fuzzy rules). On the other hand, the determination of focal points in *simpl_eClass1* requires only mean value calculation, and it can be calculated recursively as each sample arrives (same as in *simpl_eTS+* [32]). Thus, in *simpl_eClass1* the computational complexity is reduced from *O(N)* to *O(1)* – by a factor of *N*. A detailed description of *simpl_eClass1* is presented in [30].

In both the classifiers, before the rule learning phase, the actual label of a given sample is converted into numeric form in order to enable the consequent part of a rule to be represented in the form of (4). For example, for a two class problem, *class 1* can be represented as *y = [1 0]*, and *class 2* as *y = [0 1]*. Similarly, for a three class problem, *class 1* is *y = [1 0 0], class 2* is *y = [0 1 0]*, and *class 3* is *y = [0 0 1]*. As can be observed from the representation, the dimension (*m*) of *y* is same as the number of classes. For the classification task, the classifiers estimate the overall output (***est_Y***) by weighted sum of outputs of all the rules using (5)-(6). The index corresponding to the highest value element of ***est_Y*** is assigned as the class label for the sample as given in (7) – so called winner takes all principle which is usually used in classification. For example, suppose for a given sample the value of ***est_Y*** is determined to be *est_Y= [0.45 0.23 0.78]* in a three class problem, then the sample is assigned class label *3*.

$$\mathbf{est_Y} = \sum_{i=1}^{N} \lambda^i \mathbf{y}^i; \ \lambda^i = \frac{\tau^i}{\sum_{j=1}^{N} \tau^j} \tag{5}$$

$$\tau^i = \prod_{j=1}^{n} \mu_j^i(x_j), \quad i = [1, N], \quad \mu_j^i = e^{-\frac{\left\|\mathbf{x} - \mathbf{x}^{i*}\right\|^2}{2(r_j^i)^2}} \tag{6}$$

where **estY** is the overall estimated output, τ^i is the firing strength of the i^{th} rule, $(r_j^i), i = [1, N], \ j = [1, n]$ is the spread of the membership function.

$$Class = Class^{i*}, \quad i* = \arg\max_{i=1}^{m}(\mathbf{est_Y}) \tag{7}$$

VI. Proposed Evolving Online Method.

The procedures explained above might be concatenated in a single process instance by instance. It does mean that just from a standalone data source for example a frame from a camera. The proposed method must be able to recognize pre-defined categories and also any other that has not appeared before, as a result of the evolving nature of the algorithm.

In figure 3, the entire process is represented. A single data sample or frame for a video camera is obtained and formatted to a representative numeric model. The transformation model used in this work is based on a RGB color map, however other geometrical representations such as HSL or HSV could be considered. This image representation is handed to another module where the resultant color map is partitioned and over those partitions GIST is applied. Applying *32* different feature maps and partitioning the data on *4x4* regions per map, a total of *512* features are obtained per image. For a learning model this number of features implies a very high number of dimensions in most cases. A data compression technique is highly recommended, hence GIST features are handed to another module where PCA (for compression) in addition to LDA (enhance feature categorization) is used. A reduced data set of *22* features is obtained after this process, and then an evolving fuzzy rule base model is build up from the scratch. In first iteration, first sample will be considered as a rule and next samples update the FRB model adding, removing or updating new rules. New rules may be associated to one of existing categories and improve interpretation of that category. On other hand, by means of a small supervision or a simple rules monitoring, a new rule can be considered as a start point of a new category.

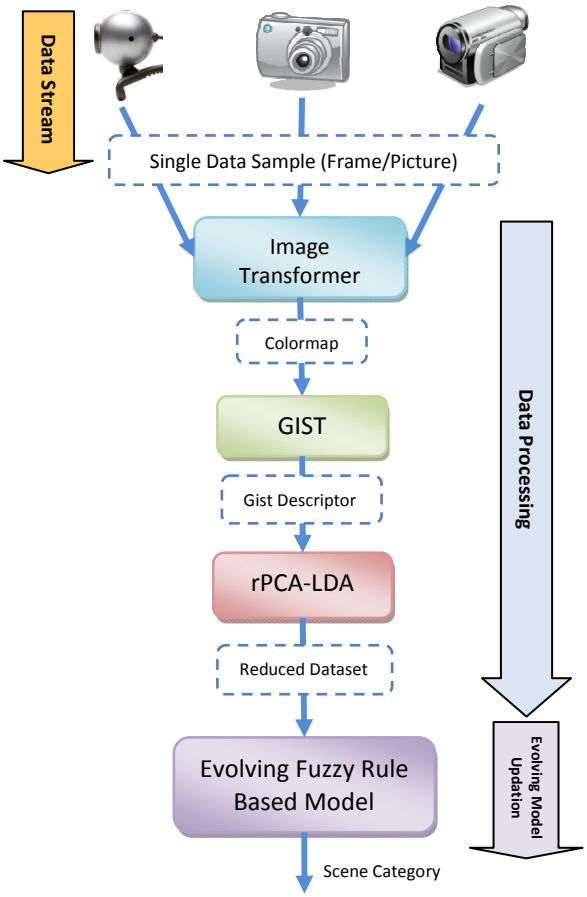

Fig. 3. Processing order of different modules (approaches) to work in a fully online (sample by sample) basis.

VII. Experimental Results and Evaluation

In this section the proposed classification scheme for scene recognition (*eClass_Scenes*) which includes recursive PCA-LDA as well as two versions of evolving classifier: a FRB (eClass) and a potential free version (simpl_eClass). These approaches are compared with several well known classifiers. These classifiers are organized in two groups: i) static, off-line classifiers, and ii) on-line and evolving classifiers. The first ones, generally, provide higher classification rate, but impose heavy requirements on the memory and computational resources. Some of them can process the data incrementally but they keep most of the data in the memory and process all

of them at once. On the other hand, the latter, process the data sample by sample (on-line) always and may be able to adapt their structure (evolve) as a reaction to the variance in the data pattern. A less complex model is obtained from their adaptation and evolution. It is principally due to the on-line processing mode they operate. Significantly less computational resources are required. For this reason, they use to have a better performance in terms of memory consumption and CPU usage which compensate a slight lower accuracy.

The selected data set [33] to test the previous mentioned methods contains *8* outdoor scene categories: street, open country, inside city, forest, coast, mountain, tall buildings and highways. In total, they are *2600* colour images of *256x256* pixels. A confusion matrix of experiments is presented in Figure 4. In this experiment features were reduced to *22* out of *512* initial inputs using rPCA-LDA. Classifications rates vary between *79%* and *81%*. Although, in some cases categories were independently recognized with more than *90%* of accuracy, for instance Inside City, Open Country, Mountain and Forest. By contrast, one category was recognized with less than a *90%*. This is the case of highways. This category could wrongly be identified as coast. It is understandable that mirages of sunny highways could resemble sea water channels.

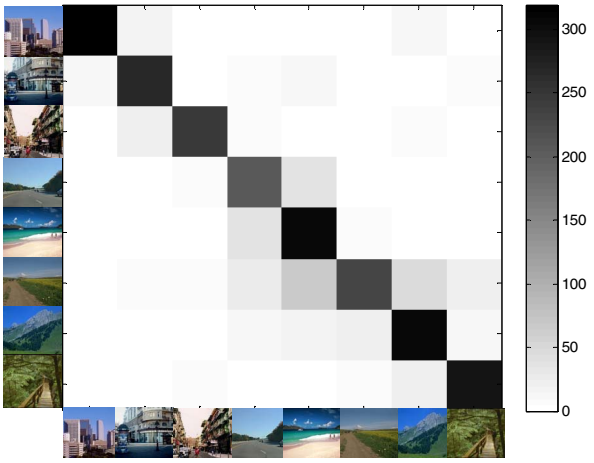

Figure 4. Confusion matrix for classification of scenes.

TABLE II. EVALUATION TIMES FOR THE WHOLE APPROACH

Method	Mean Time (seconds)
RGB Format + GIST	310.73 ms
rPCA-LDA	0.104 ms
Evolving Fuzzy Classifier	0.6/0.2 ms

TABLE I. EVALUATION PARAMETERS USING RPCA-LDA

Method	Evaluation Parameters		
	Accuracy Rate	*Time, ms*	*Number of Rules-SV-K*
Evolving			
eClass1	79.1578%	0.648	31
Simple_eClass1	80.580357%	0.240	29
Non-Evolving			
NaiveBayes	79.6646%	10	-
Nearest Neighbour	74.3187 %	0.31	8
SVM Classifier	80.2935%	2	140

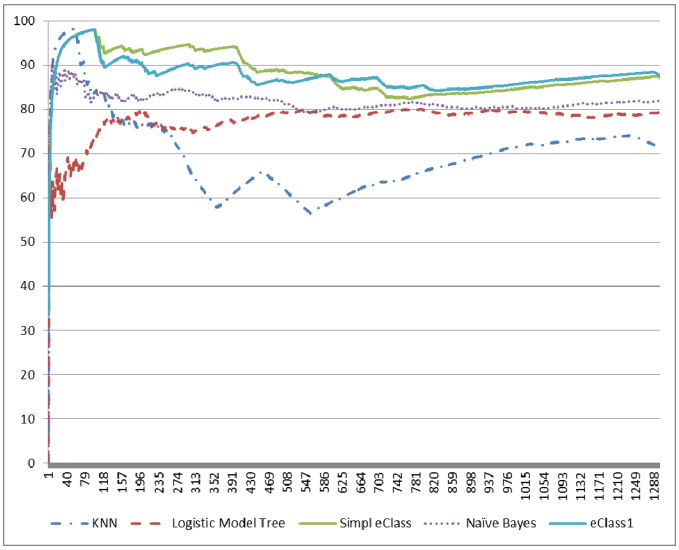

Fig 5. Evolution of rate accuracy sample by sample.

VIII. CONCLUSION

The foundation of a new approach for a fast automatic categorization of visual scenes is presented in the paper. It combines GIST feature selection and PCA-LDA methods with a self-learning evolving fuzzy rule-based classifier with very light computational load (*simpl_eClass*). *Simpl_eClass* can work in real-time, on-line and is linguistically transparent. The proposed approach is compared thoroughly with possible alternative methods including off-line and incremental approaches and the results demonstrate that it outperforms them computationally, in terms of complexity and transparency (Table I). The approach has a latency of approximately *0.3* seconds in total (including spatial descriptors, pre-processing, model updating and estimation) which makes it perfectly usable in real-time application. Moreover, this is calculated based on a Matlab application, an application using C or on-chip VHDL will further reduce this latency. It is important to stress that the computational time of model update is significantly smaller than that of the other approaches. Figure 5 clearly demonstrates that eClass1 and simpl_eClass outperform other methods in terms of accuracy.
To conclude we may say that scene classification can be important for scene analysis and a better understanding of the differences in scenes etc. The results are promising as Evolving Fuzzy Classifiers can compete with renowned SVM approach despite incrementally trained where SVM sees all

the samples at once in a batch setting; furthermore, the number of structural components (rules) is significantly lower than in case of SVM (support vectors).

IX. REFERENCES

[1] Zhou X. and Angelov P., "Real-time joint Landmark Recognition and Classifier Generation by an Evolving Fuzzy System" in *Proceedings of IEEE International Conference on Fuzzy Systems,* 2006 pp.1205-1212.

[2] Bandera A. and Marfil R., "Incremental Hybrid Approach for Unsupervised Classification: Applications to Visual Landmarks Recognition" in *Lecture Notes in Computer Science*, 2010, vol. 6111, pp.137-146.

[3] Li J. and Qian Y., "Automatic scene recognition for digital camera by semantic features" in *Proceedings of International Conference on Wavelet Analysis and Pattern Recognition*, 2008, vol.1, pp.327-332.

[4] Matsushita N., Hihara D., Ushiro T., Yoshimura S., Rekimoto J., Yamamoto Y., "ID CAM: a smart camera for scene capturing and ID recognition" in *Proceedings of The Second IEEE and ACM International Symposium on Mixed and Augmented Reality,* 2003, pp. 227-236.

[5] Chai Y., Xia T., Zhu J. and Li, "Intelligent Digital Photo Management System Using Ontology and SWRL" in *Proceedings of International Conference on Computational Intelligence and Security*, 2010, pp.18-22.

[6] La Cascia M., Morana M. and Sorce S., "Mobile Interface for Content-Based Image Management," in *Proceedings of Complex, Intelligent and Software Intensive Systems*, 2010, pp. 718-723.

[7] Rizkalla M.E. and Gundrum H.C., "Design of analog CMOS integrated circuits input stage for the operation at zero temperature coefficient using PSPICE" in *Proceedings of the 35th Midwest Symposium on Circuits and Systems,* 1992, vol.1, pp.16-19.

[8] Angelov P. and Zhou X., "Evolving Fuzzy-Rule-based Classifiers from Data Streams in *Proceedings of IEEE Trans. on Fuzzy Systems,* 2008, vol. 16(6) *Evolving Fuzzy Systems,* pp.1462-1475.

[9] Zhou X. and Angelov P., "An Approach to Autonomous Self-localization of a Mobile Robot in Completely Unknown Environment using Evolving Fuzzy Rule-based Classifier" in *Proceedings of IEEE Intern. Conf. on Comp. Intel. App. for Defense & Security*, 2007, pp.131-138.

[10] Oliva A. and Torralba A., "Modeling the shape of the scene: a holistic representation of the spatial envelope" in *International Journal in Computer Vision*, 2001, vol. 42, pp. 145-175.

[11] Oliva, A. and Torralba, A.. Building the Gist of a Scene: The Role of Global Image Features in Recognition *in Progress in Brain Research: Visual perception*, 2006, vol. 155, pp. 23-36.

[12] A. Friedman, "Framing pictures: The role of knowledge in automatized encoding and memory for gist", in *J. Exp. Psychol. Gen.*, 1979 vol. 108 pp. 316-355.

[13] Murillo A.C., Kosecka J., "Experiments in place recognition using gist panoramas" *in Proceedings of IEEE 12th International Conference on Computer Vision Workshops (ICCV Workshops), 2009,* pp. 2196-2203.

[14] Andreu J. and Angelov P., "Real-time human activity recognition from wireless sensors using evolving fuzzy systems" in *Proceedings of IEEE International Conference on Fuzzy Systems*, 2010, pp. 1-8.

[15] Sadeghi-Tehran P., Andreu J., Angelov P. and Zhou X.,"Intelligent Leader-Follower Behaviour for Unmanned Ground-based Vehicles" *Journal of Automation, Mobile Robotics and Intelligent Systems (JAMRIS)*,, vol. 5 (1), pp.1-11, 2011

[16] Szummer M. and Picard R. "Indoor-outdoor image classification" *In Proceedings of International Workshop on Content-based Access of Image and Video Databases,* 1998, pp. 42-55.

[17] Murphy K., Torralba A. and Freeman, W.: Using the forest to see the trees: exploiting context for visual object detection and localization. *In Communications of the ACM*. 2004 vol. 16 (3).

[18] Ankenbrandt C.A, Buckles B.P and Petry F.E, "Scene recognition using genetic algorithms with semantic nets" *in Pattern Recognition Letters*, 1990, Vol.11 (4), pp. 285-293.

[19] Li X., Wu C., Zach C., Lazebnik S. and Frahm J. "Modeling and Recognition of Landmark Image Collections Using Iconic Scene Graphs" in *Proceedings of the 10th European Conference on Computer Vision,* 2008, pp. 427-440.

[20] Ruthger R., De Gelder B., "Recognition of facial expression is influenced by emotional scene gist" *in Cognitive, Affective and Beahavioural Neuroscience*, 2008, vol 8 (3), pp. 264-272.

[21] Siagian C., Itti L., "Gist: A Mobile Robotics Application of Context-Based Vision in Outdoor Environment" in *IEEE Computer Society Conference on Computer Vision and Pattern Recognition*, 2005, pp. 285-293.

[22] Zhou X. and Angelov P., "Real-Time joint Landmark Recognition and Classifier Generation by an Evolving Fuzzy System" in *IEEE World Congress on Computational Intelligence*, 2006, pp.6314-6321.

[23] Lazebnik S., Schmid C. and Ponce J., "Beyond Bags of Features: Spatial Pyramid Matching for Recognizing Natural Scene Categories" *in IEEE Computer Society Conference on Computer Vision and Pattern Recognition,* 2006, pp. 2169-2178.

[24] Oliva A., and Schyns P.G., "Diagnostic colors mediate scene recognition" *in Cognitive Psychology*, 2006, vol. 41, pp. 176–210.

[25] Kameswara R.N., Mehrotra R., Ranganathan N., "Efficient computation of gabor filter based multiresolution responses" in *Pattern Recognition* vol 27(7), pp. 925-938

[26] Youhong L., Morris J.M., "Fast Computation of Gabor Functions" in *IEEE Signal Processing Letters*, 1996, vol 3(3), pp. 75-78.

[27] Young I.T, Van Vliet L.J. and Van Ginkel M., "Recursive Gabor Filtering" in *IEEE Transactions on Signal Processing,* vol. 50(11), pp. 2798-2805.

[28] Gabor D., "Theory of communications," *in Proc. Inst. Elect. Eng.,* 1946, vol. 93, pp. 429-459.

[29] Dagher I.; "Incremental PCA-LDA algorithm" in *Computational Intelligence for Measurement Systems and Applications (CIMSA), 2010* pp. 97-101

[30] Dutta-Baruah R., Angelov P. and Andreu J., "Simpl_eClass: Simplified Potencial-free Evolving Fuzzy Rule-Based Classifiers" in *IEEE International Conference on Systems, Man, and Cybernetics,* Oct. 9-12, 2011. Submitted.

[31] Angelov P. and Filev D., "An approach to online identification of Takagi-Sugeno fuzzy models" in *IEEE Transactions on Systems Man and Cybernetics Part B-Cybernetics,* 2004, vol. 34, pp. 484-498.

[32] Angelov P., "Fuzzily connected multi-model systems evolving autonomously from data streams" *IEEE Transactions on Systems Man and Cybernetics.* In Press.

[33] Spatial Envelope [online]. Available: http://people.csail.mit.edu/

2011 IEEE International Conference on Fuzzy Systems
June 27-30, 2011, Taipei, Taiwan

Real Time Recognition of Human Activities from Wearable Sensors by Evolving Classifiers

Javier Andreu, Rashmi Dutta Baruah, Plamen Angelov
School of Computing and Communications
Infolab21, Lancaster University
Lancaster, LA1 4WA, United Kingdom
{j.andreu,r.duttabaruah,p.angelov}@lancaster.ac.uk

***Abstract*—A new approach to real-time human activity recognition (HAR) using evolving self-learning fuzzy rule-based classifier (eClass) will be described in this paper. A recursive version of the principle component analysis (PCA) and linear discriminant analysis (LDA) pre-processing methods is coupled with the eClass leading to a new approach for HAR which does not require computation and time consuming pre-training and data from many subjects. The proposed new method for evolving HAR (eHAR) takes into account the specifics of each user and possible evolution in time of her/his habits. Data streams from several wearable devices which make possible to develop a pervasive intelligence enabling them to personalize/tune to the specific user were used for the experimental part of the paper.**

Keywords- human activity recognition, fuzzy rule-based classifiers, evolving systems, wearable sensors, accelerometers.

I. INTRODUCTION

Nowadays due to the increase of the average age of the population in the world as well as due to the dramatic increase of the capacities and availability (including lower costs, power consumption, size) of versatile computing and communication platforms there is a rising interest in areas of research such as Ambient Intelligence (AmI), Ubiquitous and Pervasive Computing, autonomous machine learning etc. Traditional machine learning and intelligent systems can only partially address all of the challenges because of the requirements such as personalization, adaptation, human-intelligible (often linguistic) interface and transparency (reluctance to use 'black-box' solutions even if they perform well. Inside this AmI there is an important interest in the Human Activity Analysis. It may serve as a basis for a better understanding of human habits and relations.

Trying to address all of these challenges, an emerging trend in computational intelligence which borrows heavily from adaptive systems, systems identification, fuzzy rule-based models, machine learning and pattern recognition have recently been prominent – the development of evolving systems [1]. They are characterized by the ability to self-learn and self-adapt their structure as well as to tune their parameters. They are also, usually, human-intelligible (transparent). Evolving systems, and classifiers, in particular [2] can evolve their structure to reflect the habits and behavior of a specific human user. In this way, they can be personalized. This is very useful because, for example, same type of activities (such as *walking*) is usually performed by younger individuals in a quite different manner as compared to more mature individuals. Users with different complexions perform activities with a different intension or energy.

Evolving systems is a new paradigm which requires a different type of real-time, on-line learning which combines structure learning with the parameter learning. In this study we will take the evolving fuzzy rule-based (FRB) type classifier (eClass) as a starting point and will develop a more advanced pre-processing mechanism specifically suitable for the activity –recognition task that we have.

HAR is also an area of intensive research recently [3] [4]. Very often it relies on cameras and video signals [4], however these methods often have problems related to person occlusion in the camera range, selecting a good viewpoint to track the person, privacy connotations, etc. More recently, wearable sensors have offered a very promising and attractive opportunity to collect information directly from the human body. This approach has the advantage of monitoring the human/subject continuously and without invading his privacy.

HAR problem was already addressed in several works in real-time mode using wearable sensors. For example, in [5] an activity recognition system which retrieves information from several wearable sensors is used. In [6] an *iPhone* is used to recognize simple activities such as *running, walking, bicycling*. In these works the training is carried out collecting expert knowledge from many subjects and creating a general model or creating a personal model from training provided from a particular user. However, a cross-personal model which is just trained from one subject and evolves itself with the next one, without expert knowledge or large training sets of different users would be more attractive.

A previous work [8] has involved evolving classifier in the HAR field for the first time, but it was limited to using binary data from light power switches. However, evolving system has not been involved yet in a HAR context using a complex signal domain such as acceleration from wearable sensors.

This paper is organized as follows; section II provides a description of various sensors used; in section III the pre-processing and feature selection approach, that is particularly suitable for this problem, is presented; in section IV the eHAR system is described along with the mechanism of its self-learning and adaptation, and in section V the proposed approach is being evaluated and compared with the possible alternatives. Finally, section VI concludes and outlines the future perspectives.

978-1-4244-7316-8/11/$26.00 ©2011 IEEE

II. WEARABLE SENSORS

The miniaturization of electronic circuits has made possible increasing the number of devices that one can pervasively wear or even carry in a pocket or as a part of another device. One of the most prominent pervasive micro sensors which can be applied close to the body or as a wearable item is the accelerometer. A large number of manufactured products bring on board accelerometers such as smart phones, high-tech shirts, sports watches, hearings and so on. Hence, in this research we will consider accelerometers as preferred devices of study across in the wearable context.

There are analogue and digital accelerometers; the former produce a voltage that is proportional to the acceleration while the latter outputs pulse with modulated (PWM) signal. Accelerometers can be classified based on the number of axes they consider. For easy recognition tasks, two axes are often enough. However, the higher the number of axes the more sources of information we get for the motion of the object. Although, accelerometer data seems to be highly correlated, the influence of centripetal and gravitational forces leads to randomisation of the correlation either negatively or positively according to the movement. A well planned pre-processing procedure (see next section) can further significantly minimise the correlation effect. Another characteristic to bear in mind is the maximum swing of the accelerometer. It can be computed using the tilt which is the inverse of the tangent of the quotient of two vectors. In order to measure the tilt, only a swing of $\pm 1.5g$ can be enough; in order to conduct very basic recognition of activities such as walking, running or stopping a swing of $\pm 2g$ may be required; however, in order to measure more complex activities such as sudden switches between different types of motion (sudden stop - abrupt movement, etc.) the accelerometer have to handle a swing of $\pm 5g$ or more. Sensitivity is also very important, but it directly depends on the quality of the device itself or the inter-mediation of other devices; for example, when an accelerometer is embedded in a smart phone, its accuracy could be reduced by conflicts with other in-built devices or can be influenced by the position of the sensor inside the phone. Finally, the bandwidth is, perhaps, the most critical aspect of the experiment, because it can restrict or facilitate the level of cognition of a movement. In order to take into account the vibration as well as the acceleration changes or tilt during the movement the bandwidth should be set up accordingly (for example, at least *150 Hz*).

Accelerometers use a *3D* Cartesian coordinate system to represent the direction of the vector of acceleration. When a device is moving along an axis, the acceleration is positive is moving towards positive coordinates, on the contrary, the acceleration is negative.

A. Placement of the Sensors on the Body

Devices that a user can carry such as phones, MP3 players, etc. can have different placement on the body. The location on the human body of the sensors which are part of these devices is very important in respect to facilitating the recognition of specific activities. For example, in case we aim to recognise if someone is *standing up*, it is best to attach the sensor to the leg of the subject; however, in case we aim to recognise if an individual is "*writing on the white board*", a combination of sensors placed on body's arms and legs would be required. Hence, the position of the sensor on the body is of a crucial importance in order to collect informative signal for activity recognition using wearable sensors. The need to add multiple sensing points increases with the complexity of the activity.

A lot of research has been carried out recently aiming to clarify the number of sensors and locations where sensors can be applied aiming to maximise the recognition rate. For example, statistical analysis has been used in [7] to discover the most significant placements of sensors as well as a heuristic method have been defined to cope with this problem. However, in real life applications activity recognition should be made as pervasively as possible avoiding affecting individual's behaviours and habits. For example, it is expected not to force an individual to wear a sensitive object every time in the same place and same position in order to keep certain level of freedom of movement for the user. Moreover, this individual cannot have the same motion habits/patterns as the other. Consequently, the data that are collected from the sensor will not be the same for each individual. Therefore, personalisation is an important issue in human activity recognition and self-adaptive/evolving models [8] can address this problem by self-learning classifiers aiming to recognise human activity of a specific individual adapting to the personal specifics and self-developing their mechanism of classification. In evolving classifiers learning can take place on-line and the classifier structure evolves adapting to an individual's specifics

B. Hardware Instrumentation

In order to get data samples and test the algorithms, we have used several portable devices which can be considered as wearable. Some of these sensors have processing capacities on-board and others are data transducers. In particular, we considered:

1) SunSPOT: It is a hardware/software platform developed by Oracle/Sun Microsystems in 2007 [9]. It has characteristics of a wireless sensor, i.e data can be relayed to a base station via sockets and also forwarded to all sensors. The radio range is 10 meters (USA version allows up to 100m). SunSPOT sensors have embedded a *3*-axial accelerometer that can be set to measure accelerations over a scale of $\pm 6g$. The device is programmable in Java ME through an embedded virtual machine (Squawk VM), Figure 1.

Fig 1. SunSPOT (on a palm and attached to the arm; size 63x38x25mm)

2) Nokia N97: It is a Smart Phone which can be used as a data collection platform. The reason we consider *Nokia N97* is to study a commonly used device as a sensor platform. Usually mobile/cell phones are carried in different locations: a pocket, a bag, on a mobile belt bag, etc. They are completely personal which allows training procedures to be adapted to the specific phone owner (personalised). Consequently, the data collected from these devices is highly representative. *Nokia N97* has a fully programmable Symbian Environment on board and a *3*-axial accelerometer with a scale of ±*8g*, Figure 2.

Fig 2. Nokia 97 Smartphone. Size 117 x 55 x 16 mm.

3) Porcupine: This device is a small wearable sensing module which was developed initially at Lancaster University, UK. A further, improved version of *Porcupine* was developed at the Embedded Sensing Systems group, Techincal University, Darmstadt, Germany. *Porcupine* is based on a *Zigbee* board [10]. The latest version of the *Porcupine* has up to 4GB of memory, 6 tilt switches, 2 light sensors, a temperature sensor, real time clock and a low power 3-axis 3-D accelerometer. The sampling frequency of the accelerometer can be tuned in the range between *0.5Hz* to *1.6kHz* for *X* and *Y* axes, and a range of *0.5Hz* to *550Hz* for the *Z* axis, Figure 3.

Fig 3. Porcupine Sensor v2.5 with modular sensor and plastic cases (Image Source: Embedded Sensing System Group, TU Darmstadt, Germany).

III. PRE-PROCESSING AND FEATURE SELECTION

A. *Pre-processing*

As a result of the chaotic nature of acceleration data, it is extremely complex to recognise human activities based on the raw data. The main characteristic of a human activity is often hidden in the raw data. In addition, due to the non-stationary nature of the motion and other characteristics of human activity an adaptive approach (including in respect to feature selection) requires online update of classifier structure as well as of its parameters. This means the classifier structure (including its inputs – features) to be updated in parallel with the recognition task which means to evolve.

Pre-processing is an important stage of any machine learning and pattern recognition algorithm which provides a valuable level of interpretability from raw data in respect to the input data. This stage is usually done off line on the basis of a large number of training data from a number of subjects. This approach has obvious disadvantages in respect of the representativeness of the training data, the large amount of time and memory needed to process the data. It includes several tasks, such as; i) outliers and missing data detection, ii) data cleaning and filtering, iii) data normalisation or standardisation, iv) feature extraction and feature selection. Pre-processing is often done off-line. It is important to mention that pre-processing can increase the recognition rate by up to 40%. In this study we propose and test several pre-processing methods which are particularly suitable for adaptive and evolving classifiers.

B. *Feature Selection*

Feature selection aims to reduce the computation level and enhance recognition characteristics based on the analysis of the importance of each feature (usually in terms of statistical characteristics) [7]. Although real-time algorithms work in a sample-per-sample basis, for recognizing human activity from motion sensor it is recommendable to use short time windows as instances [11]. For example, if the sampling frequency is *50Hz* a data instance represents *20ms* which is a very short period to get a representative motion pattern.

The features for the classifier that is supposed to recognise the human activity are usually different statistical characteristics of the signal. For example, [5] suggest using the following features:

- *Mean value of the signal;* this represents the local posture of the body;
- *Standard deviation:* It corresponds to the amount of motion presented in the signal. This is very valuable information to differentiate activities with a very different pattern such as *walking* and *running*, for example;
- *Energy of the signal:* It represents the stress. The energy of the signal indicates the dynamics of the motion.
- *Correlation:* It helps differentiate simple from complex movements. For example, both *walking* and *running* have similar acceleration pattern in all dimensions whereas *climbing stairs* have a very different pattern in two dimensions.

All these features are computed for a window with size of 268 samples with an overlap of 128 samples, Figure 4.

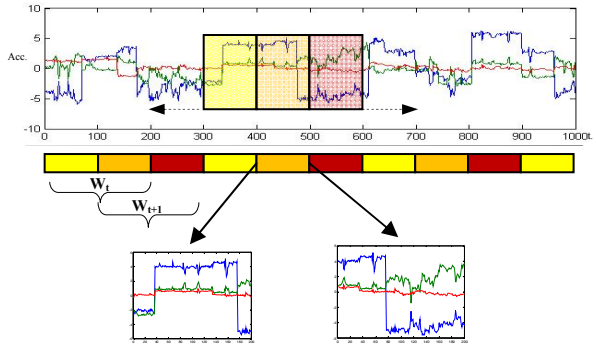

Fig.4 Sampling Windows

C. Feature Extraction.

Due to the same physical principles, different accelerometer axes exhibit some correlation regardless of which human activity is being monitored. For example, significant values of the correlation has been found between axes *(R^2=0.4)* in human motion.

1) Principal Component Analysis (PCA): One of the most widely used approaches for feature extraction which successfully addresses the issue of correlation of raw input data by orthogonalisation is the Principal Component Analysis (PCA). PCA aims to transform the raw data that are, usually, correlated into a smaller set of uncorrelated variables. In this transformation the new variables are linear combinations of the original (measured) variables and in this sense, the overall number of variables that are required to be measured is not being reduced; what is reduced is the number of inputs to the classifier (manipulated variables by the classifier) by preserving the majority of the information in terms of data variance which is useful for correct classification.

PCA has been applied widely in various areas, including spectroscopy, computing vision, intelligent sensors. It is based on producing new variables maximising the variance of the data. PCA is very helpful in revealing the hidden dynamics that is often '*hidden*' in a raw signal. It relies on so called singular value decomposition (SVD) by which the most efficient direction in terms of classifying the data is being determined. This efficient representation is achieved by projection in a least-squares (LS) sense. To get these projections a covariance matrix, C is computed and thereafter a new matrix, V of eigen-values and eigen-vectors, which diagonalise the previously computed matrix, are worked out. Once the matrix V has been computed, eigenvectors, denoted as matrix w are sorted in decreasing order regarding their respective eigen-values. Data is standardized and projected onto the matrix, w.

2) Linear Discriminant Analysis (LDA): PCA is very useful in reducing the correlation and reducing the number of inputs to the classifier (thus the computational complexity). However, PCA does not take into account what activity corresponds to certain motion pattern, i.e. it takes only input data into account and not the class labels (outputs in terms of the classifier).

If data is arranged based on the classes (activity types), that we expect to have, so called Linear Discriminant Analysis (LDA) approach can be applied. While PCA get projections of input data in a way that maximises their separability, LDA helps finding these directions which will be best to distinguish between different classes (activities). A combination of both, PCA and LDA has proven to be an effective pre-processing technique in spectroscopy. Sample variance (σ^2) and sample variance per class (σ_c^2) are used to form scatter matrices (S_b and S_w). S_w denotes the **within**-class scatter matrix.

Likewise, S_b represents a singular matrix denoted as **between**-classes scatter matrix. The separation between those matrices is defined as a measure of the signal-to-noise ratio for class labelling.

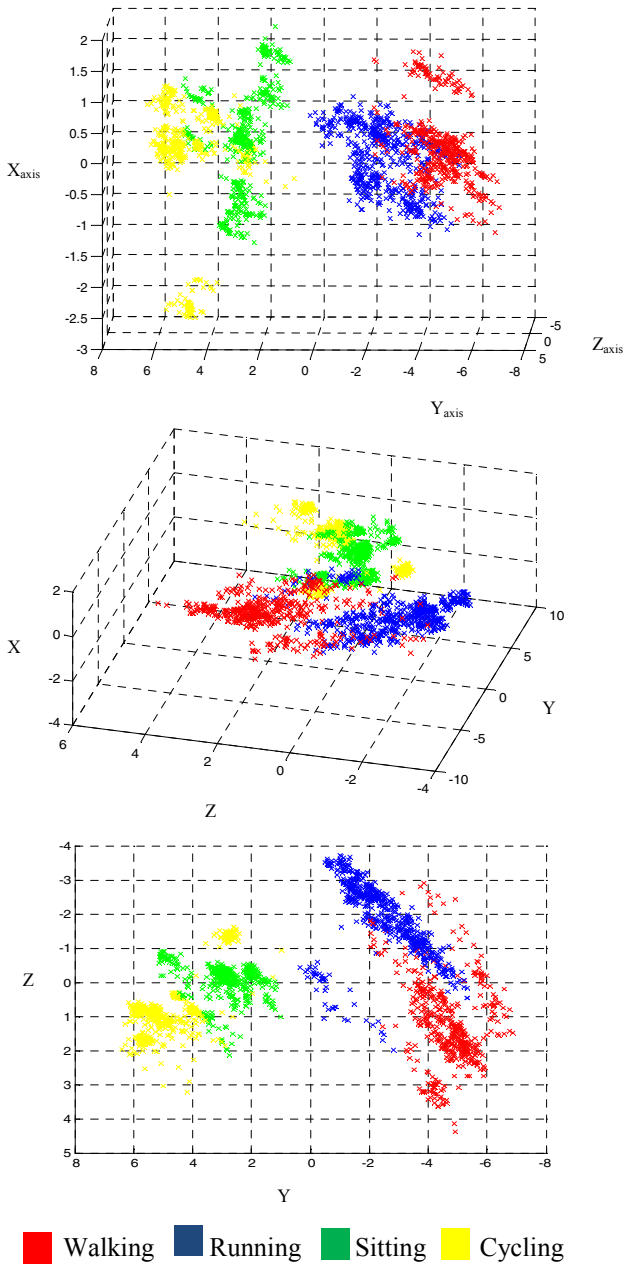

Fig. 5 Features grouped by labels after rLDA-PCA applied

Hence, a criterion function J is computed on the basis of these two matrices, in the following form:

$$J(w) = \frac{w^T S_b w}{w^T S_w w} \quad (1)$$

Values of w which maximizes J are taken as desirable projections of data regarding not just their features (inputs to the classifier) but the class label (output) such as activity type.

3) On-line, recursive PCA, rPCA: All the procedures described above regarding pre-processing techniques such as PCA and LDA are calculated off-line and require, therefore, all the training data to be available beforehand, high memory/storage and high computational power capacities. They have been applied in face recognition problems [12], but are not suitable for real-time, on-line applications in their original form. In this study we need a recursive implementation of the combination of PCA-LDA [12]. This approach is applicable on-line and in real-time. PCA and LDA are compatible techniques because whereas PCA tries to find better projections of data according features, LDA finds what projections discriminate classes better.

PCA projections represented by the eigen-values, v can be calculated expressed as suggested by [11] as follows:

$$v_k = \frac{1}{k}\sum_{i=1}^{k} u_i \cdot u_i^T \cdot \frac{v_{i-1}}{\|v_{i-1}\|} \tag{2}$$

where u denotes an orthogonal projection and k is the current time instant/sample.

This expression is based on the definition of v as $\lambda \cdot x = C \cdot x$ and $v = \lambda \cdot x$ where λ is the magnitude of the eigen-value, $\|v\|$ and C the covariance matrix.

This expression, (2) can be expressed recursively by weighting its current and last estimates by $\frac{k-1}{k}$ and $\frac{1}{k}$ respectively; then we get:

$$v_k = \frac{k-1}{k} \cdot v_{k-1} + \frac{1}{k} \cdot u_k \cdot u_k^T \cdot \frac{v_{k-1}}{v_{k-1}} \tag{3}$$

The algorithm estimates ortho-normalized vectors to ensure maximum independence of the directions. Thus, from the first order eigenvector a new one is computed by subtracting its orthogonal projection. The formula which describes this projection u_j is as follows:

$$u_k = u_{k-1} - u_{k-1}^T \cdot \frac{v_{k-1}}{\|v_{k-1}\|} \cdot \frac{v_k}{\|v_k\|} \tag{4}$$

4) On-line recursive LDA, rLDA: In order to get the desired projections in terms of LDA we have to calculate the between-, and within- classes scatter, S_b and S_w recursively:

$$S'_{wk} = S'_{wk-1} + \left(Y_k - \left(\sigma_c^2 - \sigma^2\right)\right) \cdot \left(Y_k - \left(\sigma_c^2 - \sigma^2\right)\right)^T \tag{5}$$

$$S_{wk}^{-1} = \frac{S'^{-1}_{w(k-1)} + \left(Y_k - \left(\sigma_c^2 - \sigma^2\right)\right) \cdot \left(Y_k - \left(\sigma_c^2 - \sigma^2\right)\right)^T S'^{-1}_{w(k-1)}}{1 + \left(Y_k - \left(\sigma_c^2 - \sigma^2\right)\right)^T \cdot S'^{-1}_{w(k-1)} \left(Y_k - \left(\sigma_c^2 - \sigma^2\right)\right)} \tag{6}$$

$$S_{wk} = A_{k-1} \cdot S'_{wk} \cdot A_{k-1}^T \tag{7}$$

$$S_{wk}^{-1} = A_{k-1} \cdot S'^{-1}_{wk} \cdot A_{k-1}^T \tag{8}$$

$$S_b = A_{k-1} \cdot \left(\sum_{i=1}^{c} n_i \cdot \left(\sigma_c^2 - \sigma^2\right) \cdot \left(\sigma_c^2 - \sigma^2\right)^T \right) \cdot A_{k-1}^T \tag{9}$$

where $Y_k = x_k - \mu$ is the variance; A_k is the matrix of desired orthogonal projections (eigenvectors) S_w^{-1} and S_b.

An explanatory diagram of the combination of both methods in a same time step, *k* is shown in Fig. 6. At the end of the algorithm desired eigenvectors which guarantee best projections and features that enhance the separation between classes of activities are provided. Consequently, the raw data, *x* are being mapped onto the feature space, *f* (see Fig. 5).

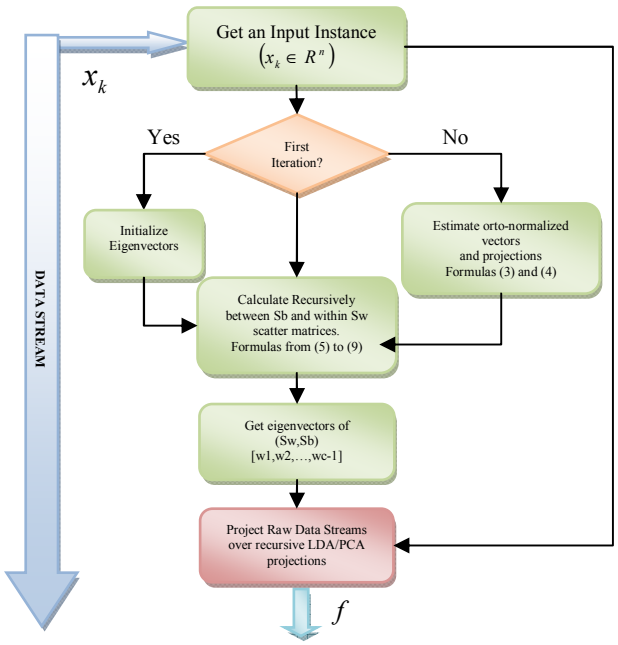

Fig. 6 rLDA-PCA scheme

IV. Evolving Classifier

A classifier is a mapping from the feature space to the class label space. In this study we will develop and apply a self-learning evolving fuzzy rule-based (FRB) classifier, eClass [2]. The structure of the FRB classifiers consists of a set of fuzzy logic (IF-THEN) rules, the fuzzy sets that define the linguistic terms such as '*Low*', '*Medium*', '*High*' etc., aggregation operators such as '*AND*', '*OR*', '*NOT*' and number of inputs/features, *n*. In our study we consider an evolving FRB classifier, *eClass* which is characterised by having an evolving (not fixed) structure of the following form [1]:

$$R^i: \; IF\left(f_1 \; is \; \sim f_1^{i*}\right) \; AND \; ...\left(f_n \; is \; \sim f_n^{i*}\right) \; THEN \; \left(L^i\right) \tag{10}$$

where $f = [f_1, f_2, ..., f_n]^T$ is the vector of features – for our study we consider *n=16*; R^i denotes the i^{th} fuzzy rule; *i=[1, N];N* is the number of fuzzy rules; $\left(f_j \; is \; \sim f_j^{i*}\right)$ denotes the j^{th} fuzzy set of the i^{th} fuzzy rule; *j=[1,n]* ; f^{i*} is the focal point of the i^{th} rule antecedent (note that this is a prototype - a real, existing data sample not the mean). L^i is the label of the class of the i^{th} prototype (focal point).

This set of fuzzy rules (note, that due to its evolving nature their number, N is not fixed) defines with its antecedent/premise (IF) part a *16-D* feature space, $f \in R^{16}$ and with its consequent part it determines in a fuzzy way (with a degree of fulfilment) the class label (activity), L_i, $i=[1, K]$.

The inference in *eClass* is produced by 'winner takes all' rule [1]:

$$L = L^{i^*}; i^* = \arg\max_{i=1}^{N}\left(\tau^i\right) \tag{11}$$

where τ^i denotes the firing level of (degree of confidence in) the i^{th} fuzzy rule, which is determined as a product of the membership values, u_j^i of the j^{th} feature, $j=[1,n]$ to the fuzzy set $(f_j \, is \sim f_j^{i^*})$:

$$\tau^i = \prod_{j=1}^{n} \mu_j^i(f_j); \; i = [1, N] \tag{12}$$

The membership functions that describe the degree of association with a specific prototype are usually of Gaussian form (characterized by good generalization capabilities and coverage of the whole feature space):

$$\mu_j^i = e^{-\frac{1}{2}\left(\frac{d_j^i}{r_j^i}\right)^2}; \quad i = [1, N]; \quad j = [1, n] \tag{13}$$

Where d_j^i is the distance between a sample and the prototype (focal point) of the i^{th} fuzzy rule; r_j^i is the spread of the membership function, which also represents the radius of the zone of influence of the fuzzy rule.

A. Learning eClass

Normally, classifiers use evolutionary algorithms or gradient-based based schemes to be trained-offline. Some examples of this are NN combined with back propagation. Evolving intelligent systems such as eClass are designed to be fully on-line in estimating and training. This is achieved by means of an evolving (self-developing) FRB structure. This FRB structure is created from data-stream inputs $z = \left[f^T, L\right]^T$. Focal points are generated to describe the nature and dynamics of the signal.

This process of self-calibration resembles adaptive control and estimation. Two phases are formed during the process:

i) class estimation (classification);
ii) Update or evolution of the model.

In the first phase the class label is unknown, consequently it is estimated. During the second phase this same class label is used as a supervisory information to update the model structure (so named process of ***structure evolution***), as well as its internal parameters.

There are a couple of differences between *eClass* and conventional classifiers:

i) Starting from scratch, the fuzzy rule-base structure self-develops itself. On the other hand, the structure of a conventional classifier is determined off-line (and then fixed).
ii) Also the on-line learning process considers this flexible rule-base structure.

The overall fuzzy rule base structure has a K number of sub-rule based with the same number of consequents. However, the number of rules must be not less than the number of classes ($N \geq K$). That's to say, every data from a non-previously seen label, automatically becomes a prototype. Model updating procedures (replacement and removal of rules) makes this situation temporal. Later, this prototype is usually replaced by more descriptive prototypes. In this sense, *eClass* learns from the scratch and a fixed class number does not need to be set.

The partitioning model is generated by a density model which defines the potential or density of each point in the feature space. For this reason, a Cauchy function of the sum of distance between a particular data sample and all other data samples of its same class label *(L)*, in the feature space [2];

$$D_k^i(z_k) = \frac{1}{2 - \left[1/\sqrt{\sum_{j-1}^{n+1}(z_k^i)^2}\right]\sum_{j-1}^{n+1} z_k^i b_{k-1}^i} \tag{14}$$

$$k = 2,3,... \qquad D_1(z_1) = 1$$

where $b_k^i = b_{k-1}^i + \sqrt{\frac{\left(z_k^i\right)}{\sum_{j=1}^{n+1}(z_k^j)^2}}, b_1^i = \sqrt{\frac{(z_1^i)^2}{\sum_{j=1}^{n+1}(z_1^j)^2}}$

$i = [1, n+1]$ and $z = [f^T, L]^T$ is the input/output vector.

The use of a density model comes from the following principle: "every point with the highest density is chosen to be the focal point (prototype) for the antecedent of a fuzzy rule'. By means of this procedure, it is possible to define rules with high descriptive power.

The data density model needs to be updated each time a new data sample is added; logically, density values of the existing prototypes have to be updated. This procedure is also done in a recursive way:

$$D_K^L(z_l^{i^*}) = \frac{(N_k^l - 1)D_{k-1}^l(z_l^{i^*})}{N_k^l - 1 + \left[(N_k^l - 2)\left(\frac{1}{D_{k-1}^l(z_l^{i^*})} - 1\right) + d(z_l^{i^*}, z_k)\right]} \tag{15}$$

The updating of the model procedure is a follows: The density of the new data sample is calculated recursively using formula (14) and after this calculation, updating of the density/potential of each existing prototype is computed recursively using (15). After both densities have been computed/updated, conditions are inspected. If the density of the new data sample is higher than any other previously existing prototypes of the same class *L;* then it is a good candidate to become a prototype of a new rule. It means that this point has enough descriptive power.

$$D_k^L(z_k) > D_k^L\left(z_L^{i^*}\right), \; \forall i^* \in N^L \tag{16}$$

In the previous case, a new fuzzy rule around the new added

prototype is formed. This condition leads to a gradual increase of the sub-rule-base. This is one of the fundaments why this computational process is named "evolving".

$$z^{(N^L+1)*} \leftarrow z_k \quad (17)$$

One the new generated prototype has been created; its new density is set to 1. Its density value is updated, according to the influence of this prototype on each new collected data sample (15):

$$D_k^L\left(z^{(N^L+1)*}\right) \leftarrow 1 \quad (18)$$

It is possible that after adding a rule from a new prototype to the model, this rule would be ambiguous or existing prototypes already describe this behaviour/characteristic. Hence, each time a fuzzy rule is added it is also verified whether any of the existing prototypes of the current sub-rule base are already described by this rule to a degree higher than e^{-1}:

$$\exists i, i = [1, N^L]; \quad \mu_i^j(z^{N^L+1}) > e^{-1} \quad \forall j, j = [1, n] \quad (19)$$

If any of the existing prototypes satisfy condition (19), all rules that correspond to them are removed from the sub-rule-base (indeed, they are replaced for the new formed rule).

The spread of membership functions of the sub-rule-base of the respective class are also recursively updated on the basis of the data distribution:

$$r_k^i = \rho r_{k-1}^i + (1-\rho)\sigma_{k-1}^i; \; i = [1, N^L] \quad (20)$$

Note ρ as learning parameter; it sets how fast the spread of the membership functions will concur to the local scatter of that prototype; the normal used value is 0.5.

V. Experimental Results and Evaluation

In this section the proposed classification scheme for human activity recognition (*eClass_HAR*) which includes recursive PCA and LDA as well as the evolving FRB Classifier, *eClass* is compared with several well known classifiers. These classifiers are grouped in two groups: i) static, off-line classifiers, and ii) on-line and evolving classifiers. The former, generally, provide higher classification rate, but impose heavy requirements on the memory and computational resources. They keep most of the data in the memory and process all of them at once. On the other hand, the latter, process the data sample by sample (on-line) and may be able to adapt their structure (evolve) as a reaction to the variance in the data pattern. As a result of this adaptation and evolution they result in less complex models and due to the on-line processing manner they require significantly less computational resources. For this reason, they use to have a better performance in terms of CPU and memory usage which compensate the somewhat lower accuracy.

All the results of the comparison are tabulated in Table I. As it can be seen, the proposed *eClass_HAR* classifier is very competitive. It has very low memory requirements and CPU usage. Classification rate is also higher than that of any other on-line classifier and very competitive with the off-line classifiers.

TABLE I Comparison Table

Off-line Classifiers	Memory, KB	Max. CPU, %	Class. rate
Hoeffding Adaptive Tree	2.3	10%	81%
Incremental Naïve Bayes	4.868	14%	76.53%
Nearest Neigbour (Euclidean Distance)	3.64	47%	72%
Kstar (Entropic Distance Measure)	4.624	50%	83.55%
Locally-Weighted Learning + Naïve Bayes	1.853	48%	75.16%
On-line Classifiers			
OzaBagASHT (Adaptative Tree)	0.105	18%	70.53%
OzaBagADWIN (Adaptative Windowing + Adaptative Tree)	0.992	13%	70.61%
SingleClassifierDrift (Drift Detection+ Adaptative Tree)	0.012	8%	49.99%
SingleClassifierDrift (Drift Detection + Incremental Naïve Bayes)	0.01	6%	63.41%
AdaHoeffdingOptionTree (Adaptative Tree + Incremental Naïve Bayes)	0.01	8%	70.45%
eClass_HAR (proposed)	**0.02**	**5%**	**71.4%**

Figure 7 shows an evolution graph of the classification rate produced by eClass_HAR. The top plot shows that recognition rate may drop during the first subject of test (the classifier can start with a pre-training on a different set of subjects or 'from scratch'). Following the first subject, the classifier self-tunes its parameters as well as its self-learns its structure (evolves) and, as a result, raises its classification rate. After an increase to values around 70-80% there is some saturation (and even reverse). This is due to the known phenomena in signal and data processing that 'more data not always brings more useful information'.

The bottom plot illustrates the effect of self-learning by temporal re-training. Because of the low computational requirements of the algorithm, it is also possible to update the classifier online by providing in real-time ground truth (activity labels). Several such update periods (with duration of 1 to 2 min) were used in real-time. It is obvious that they helped eClass_HAR to increase the classification rate to 83-84% which surpasses all off-line classifiers. It is due to the fact that the classifier adapts its structure (fuzzy rules) to match better the nature and dynamic of the data stream.

In Table II, a confusion matrix is presented which includes all activities that has been considered. It can be seen that the general activities such as *walking, running*, *lying down* or even sporty ones (such as *bicycling*) are classified with higher rates. On the other hand, there are also two intermediate activities that are composed of several sub-activities. These are *vacuuming* and *stretching*. The classification rates for these activities are fluctuating because they involve several general activities. In order to overtake this issue, larger windows or

feedback from objects via integrated sensors would help to increase the classification rates. This will be studied and reported in a further publication.

TABLE II. CONFUSION MATRIX

	Walking	Running	Bicycling	Standing	Lay down	Vacuuming	Stretching	Sitting
Walking	**89.42**	0	9.12	1.46	0	0	0	0
Running	18.11	**76.38**	3.15	2.36	0	0	0	0
Bicycling	4.67	0	**89.25**	5.61	0	0	0.47	0
Standing	0	0	0	**99.14**	0.43	0	0.43	0
Lay down	0	0	0	9.02	**90.98**	0	0	0
Vacuuming	7.25	0	19.85	10.31	2.29	**58.78**	1.53	0
Stretching	4.17	0	23.33	27.50	0.00	37.50	**7.50**	0
Sitting	0	0	0	1.33	23.11	0	4.44	**71.11**

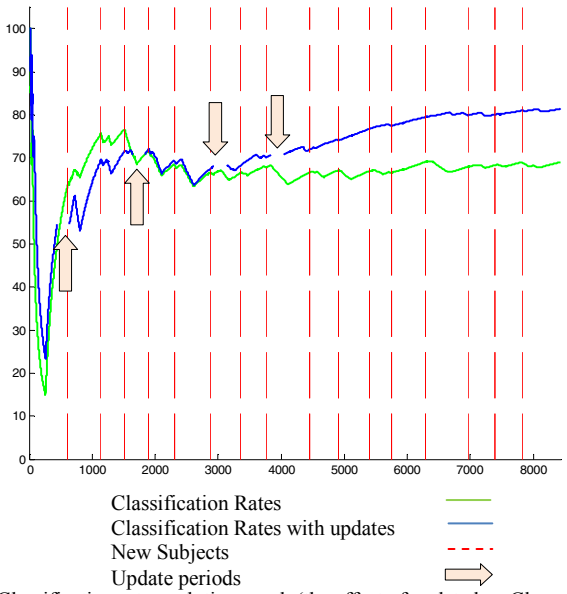

Fig 7. Classification rate evolution graph (the effect of update by eClass_HAR is clearly seen to improve the classification rate despite switching to new subjects).

VI. CONCLUSION

This work presents the ground of a new paradigm of processing HAR data - eHAR. Evaluation and experimentation has shown that results are very promising. This new evolving paradigm applied to the HAR systems provides self-adaptation and self-learning capabilities. In this sense, the classifier is able to evolve its FRB structure to reflect the evolution of the habits and behaviour of a specific human user or a change to a new user (see Figure 7). In this way, eHAR enabled intelligent devices can be personalized. For example, same type of activities (such as *walking*) is usually performed in a different manners by different people depending on age, habits etc. Users with different complexions perform activities with a different intension or energy. The performance of eHAR is very competitive in comparison with existing off-line and incremental approaches (see Table I). Off-line approaches, however, require a huge amount of training data, time and computational resources and less relevant for new users (see also Figure 7). Incremental approaches are outperformed by eHAR, but more importantly, they do not keep an evolving structure as the proposed approach does. The proposed approach is also linguistic (IF-THEN rules can be easily extracted that are human-intelligible.

REFERENCES

[1] P. Angelov, *Evolving Rule-based Models: A Tool for Design of Flexible Adaptive Systems*, Heidelberg: Springer, ISBN 3-7908-1457-1, 2002

[2] P. Angelov, X. Zhou, "Evolving Fuzzy-Rule-based Classifiers from Data Streams" in *IEEE Trans. on Fuzzy Systems*, vol. 16, no. 6, 2008, pp. 1462-1475,

[3] N. Robertson and I. Reid, "A general method for human activity recognition in video" in *Comput. Vis. Image Underst.*, Vol. 104, 2006, pp. 232-248.

[4] W. Chen, H. Aghajan , "Real-Time human pose estimation: a case study in algorithm design for smart camera networks" in *Proceedings of the IEEE*, vol. 96, no. 10, 2006, pp.1715-1732.

[5] E.M Tapia, S.S. Intille, W. Haskell, K. Larson, J. Wright, A. King, , R. Friedman , "Real-Time recognition of physical activities and their Intensities using wireless accelerometers and a heart rate monitor" in *11th IEEE Intern. Symposium on Wearable Computing*, 2007, pp.37-40.

[6] S. Saponas, J. Lester, J. Froehlich, J. Fogarty and J. Landay "iLearn on the iPhone: Real-Time Human Activity Classification on Commodity Mobile Phones". Univ. of Washington, Tech. Report, UW-CSE-08-04-02, 2008.

[7] U. Maurer, A. Smailagic, D.P. Siewiorek and M. Deisher, "Activity recognition and monitoring using multiple sensors on different body positions" in *Intern. Workshop on Body Sensor Networks*, 2006, pp.104-116.

[8] J. Andreu, and P. Angelov, "Real-time human activity recognition from wireless sensors using evolving fuzzy systems" in *IEEE World Congress on Computational Intelligence*, 2010, pp. 18-23.

[9] SunSPOT World [Online]. Available: http://sunspotworld.com/

[10] K. Van Laerhoven, G. Hans-Werner and Y.G. Malliaris, "Long-term activity monitoring with a wearable sensor node." in *Intern. Workshop on Wearable and Implantable Body Sensor Networks*, 2006, pp. 171-174.

[11] N. Ravi, N. Dandekar, P. Mysore, and M.L. Littman, "Activity recognition from accelerometer data" in *IAAI'05*, vol. 3, 2005, pp. 1541-1546.

[12] I. Dagher, "Incremental PCA-LDA algorithm" in *IEEE Intern. Conf. on Computational Intelligence for Measurement Systems and Applications*, 2010, pp. 97-101.

2011 IEEE International Conference on Fuzzy Systems
June 27-30, 2011, Taipei, Taiwan

Fuzzy Granular Evolving Modeling for Time Series Prediction

Daniel Leite and Fernando Gomide
School of Electrical and Computer Engineering
University of Campinas
Campinas SP, Brazil
Email: {danfl7,gomide}@dca.fee.unicamp.br

Rosangela Ballini
Institute of Economics
University of Campinas
Campinas SP, Brazil
Email: ballini@eco.unicamp.br

Pyramo Costa
Graduate Program in Electrical Engineering
Pontifical Catholic University of Minas Gerais
Belo Horizonte MG, Brazil
Email: pyramo@pucminas.br

***Abstract*—Modeling large volumes of flowing data from complex systems motivates rethinking several aspects of the machine learning theory. Data stream mining is concerned with extracting structured knowledge from spatio-temporally correlated data. A profusion of systems and algorithms devoted to this end has been constructed under the conceptual framework of granular computing. This paper outlines a fuzzy set based granular evolving modeling - FBeM - approach for learning from imprecise data. Granulation arises because modeling uncertain data dispenses attention to details. The evolving aspect is fundamental to account endless flows of nonstationary data and structural adaptation of models. Experiments with classic Box-Jenkins and Mackey-Glass benchmarks as well as with actual Global40 bond data suggest that the FBeM approach outperforms alternative approaches.**

***Index Terms*—Data Stream, Evolving System, Granular Computing, Online Learning, Time Series.**

I. Introduction

Continuous data stream processing has become a task of primary importance mainly due to the emergence of industrial sensor networks and small scale computing devices that produce massive amounts of data from their environments. In online settings, large unbounded datasets stream in high frequency and bring uncertainty in their instances. Data streams demand fast single-scan-through-the-data algorithms to identifying and storing essential information. Rethinking many existing data mining and machine learning techniques is necessary to consider structural adaptation of information systems based on sequences of never-seen-before instances.

Recent research on evolving granular systems [1]-[7] lays emphasis on granulated views of detailed data and computing with granules coarser than the data in order to simplify complex real-world problems and provide low cost solutions. As stated by Zadeh [8] and Yao [9], granular computing exploits the tolerance for imprecision, uncertainty and partial truth to achieve tractability, robustness and better rapport with reality. The flexibility of handling dynamics within granular framework enables us to describe granules in different application domains without deep knowledge about the underlying problem. Narrow time and space constraints of online environment as well as understandability requirements inspire granulated views of the data and computing at coarser granularities.

Fuzzy set based evolving modeling FBeM approach belongs to the framework of granular computing because it uses fuzzy-type information granules to construct granular maps that associate input granular datum to output granular datum. Fuzzy granules warrant the generality of the structure of the data and give algorithms with simple math and rules describing their meaning. Building fuzzy sets from uncertain data is the FBeM strategy for lodging noise and disturbances. Basically, FBeM systems look to streaming data under different resolutions and decide when to shift back or forth between simpler or more detailed granularities. Structured representation of data streams by means of a set of fuzzy rules that carry the very essence of the information mirrored in the data is a wealthy contribution.

FBeM benefits from fuzzy granular objects to summarize information-in-motion and assist decision making. Models in FBeM are created on the fly and evolved as requested by the data stream. Supported data sources include sensors, web traffic, audio and video, financial data, climate data, etc. The FBeM learning algorithm creates and fosters granules recursively, steered by the information flow. Eventually, the quotient granular structure may be optimized, refined or coarsed, agreeing with inter-granule relationships.

Structurally, FBeM models combine functional and linguistic fuzzy systems to provide singular and granular approximations of nonstationary functions. Functional fuzzy systems are generally more precise whereas linguistic fuzzy systems are more interpretable. Accuracy and interpretability require tradeoffs and one usually prevails over the other. By combining functional and linguistic systems into a single modeling framework, $\cup$-closure for short, FBeM takes advantage of both systems simultaneously. At the practical level, experts usually prefer that online systems give approximated results as well as tolerance bounds on the approximations.

This paper addresses time series prediction. Examples on predicting the Box-Jenkins, Mackey-Glass and Global40 time series emphasize the complementarity of the functional and linguistic parts of FBeM and illustrate the usefulness of the approach. The FBeM predictor makes no specific assumption about the properties of the data sources in experiments, but rather lets the data stream guide learning freely.

The remainder of this paper is organized as follows. Section II addresses the granular fuzzy modeling approach, the FBeM structure and its characteristics. The associated data-stream-driven recursive learning algorithm is detailed in Section III. Section IV presents results of time series predictions with

978-1-4244-7316-8/11/$26.00 ©2011 IEEE

FBeM playing the role of an evolving predictor. Section V concludes the paper and suggests issues for further investigation.

II. Fuzzy Set Based Evolving Modeling

FBeM is an evolving modeling approach that produces higher level information granules based on more detailed streaming data and recursive learning algorithm. A $\cup$-closure granular structure ensues from more specific local models. Incremental learning procedures cast the FBeM structure to track new concepts, cope with uncertainty, and provide singular and granular approximations of nonlinear functions. FBeM addresses the problem of unbounded databases and the scalability issue. It deals with computationally hard problems outer approximating the solution.

An FBeM model conveys a set of If-Then fuzzy rules extracted from the data. The set of rules means a granular representation of a complex system. Learning in FBeM starts from scratch, i.e., no granules and rules need to be preconceived nor the amount of evolved granules ceiled. Granules and rules are created and adapted on the fly, dynamically, steered by the behavior of the process function over time. Whenever data instances arrive, a decision mechanism is trigged and either granules and rules are inserted into the FBeM structure or parameters of existing granules are adapted.

FBeM rules manage information granules. For each granule there exists a corresponding rule. They are gradually evolved over time. Experts may wish to provide a verbal description about the process using their intuition and experience. Evolving fuzzy modeling, Fig. 1, supports both, learning from data streams and learning from experience.

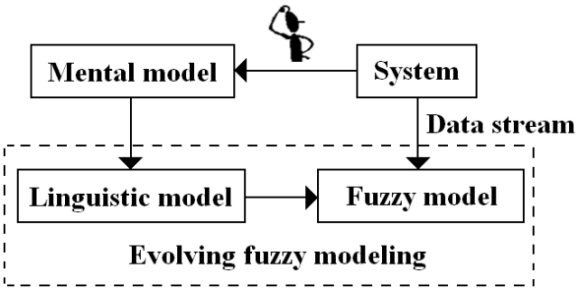

Fig. 1. Evolving fuzzy modeling

In FBeM models, rules R^i governing information granules γ^i are of the type

$$\begin{aligned}\text{IF } &(x_1 \text{ is } A_1^i) \text{ AND...AND } (x_j \text{ is } A_j^i) \text{ AND...AND } (x_n \text{ is } A_n^i)\\ \text{THEN } &(y_1 \text{ is } B_1^i) \quad \text{AND} \quad \bar{y}_1 = p_1^i(x_j \forall j) \quad \text{AND}\\ &\ldots\\ &(y_k \text{ is } B_k^i) \quad \text{AND} \quad \bar{y}_k = p_k^i(x_j \forall j) \quad \text{AND}\\ &\ldots\\ &\underbrace{(y_m \text{ is } B_m^i)}_{\text{linguistic}} \quad \text{AND} \quad \underbrace{\bar{y}_m = p_m^i(x_j \forall j)}_{\text{functional}} \quad ,\end{aligned}$$

where x_j and y_k are variables of the data stream $(x, y)^{[h]}$, $h = 1, ...$; A_j^i and B_k^i are membership functions built in light of the data being available; p_k^i are approximation polynomials. The collection of rules R^i, $i = 1, ..., c$, forms the rule base. Rules born and grow on-demand whenever the structure of the data calls for improvements in the current model. It is worth noting that an FBeM rule combines both, linguistic and functional consequents. The linguistic part of the consequent outer approximates functions and provides interpretability of the results. The functional part of the consequent offers singular approximation of functions and precision. Using this structure, FBeM takes advantage of both, linguistic and functional systems, within a single modeling framework.

A. Rule Antecedent

Granulation of data into fuzzy objects A_j, $j = 1, ..., n$, can be based on grid, tree or scatter partitioning. Grid partition divides attributes in finer parts $\{A_j^1, ..., A_j^c\} \prec A_j$ of equivalent size (top-down approach). Low-level granules represent more specific concepts; $\prec$ is a fine relation. A fixed fuzzy grid is easily interpretable but suffers with concept change, learning in unknown domain, and coexistence of different granularities in the data stream. Tree partition results from cuts of larger granules. Trees are more flexible than grids since sub-trees A_j^i, refinements of A_j, can be sliced independently. Trees may experience the problem of excessive partitioning due to large amount of features and concept drift. Scatter fuzzy partitioning uses subsets A_j^i which can be extended to fuzzy hyperboxes in a product space by means of alpha level sets. The scattering process clusters the data into information granules when appropriate. Granules are positioned at arbitrary locations into the product space. An aspect to be taken into account with scattering-type granulation refers to searching for a suitable amount of partitions, their positions and sizes. Figure 2 illustrates the different types of data granulation.

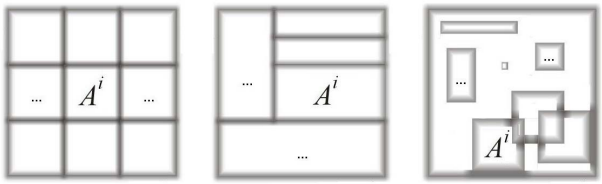

Fig. 2. Grid, tree and scattering granulation

In this work, the FBeM system is equipped with scattering-type granulation mechanism. Accommodating data into conveniently placed and sized granules leaves substantial flexibility for incremental recursive adaptation and freedom in choosing the internal representation of the granules. Online environment claims for opportune creation and rearrangement of fuzzy structural objects from time to time. Essentially, FBeM seizes Gaussian membership functions as formal granular objects to wrap uncertainty in the data of streams. Gaussians are quite easily converted to hyperboxes by means of alpha level sets.

A Gaussian fuzzy subset $A_j^i = \mathcal{G}(\mu_j^i, \sigma_j^i)$ is characterized by a modal value μ_j^i and spread σ_j^i. Features that make the Gaussian representation suitable include: (*i*) easiness of acquiring the necessary parameters. The modal and spread values are captured straightforwardly from a data stream; (*ii*) infinite support does not ignore data. Because data ranges are

unknown before learning, the support of Gaussians extends across the whole domain; (*iii*) smoothness and continuously differentiable surface. On representing uncertainty, Kreinovich [10] under certain assumptions has shown that Gaussian functions are the most adequate choice for representing imprecise measurements.

B. Rule Consequent

Consequent of FBeM rules joins functional and linguistic fuzzy information to approximate actual system outputs and provide tolerance bounds on the approximation. The functional part of the consequent p_k^i comprises singular local functions whereas the linguistic part depicts corresponding information granules B_k^i occurring along the domain of output variables k.

Here we assume affine local functions of the type

$$p_k^i = a_{0k}^i + \sum_{j=1}^{n} a_{jk}^i x_j \tag{1}$$

for all instances measured from the process function f and that activate the fuzzy hyperbox delineated by the granule γ^i. In general, each p_k^i can be of different type and is not required to be linear. For instance, higher order polynomials could be used to approximate f. However, the number of coefficients to be identified increases substantially, especially when the number or variables n is large. FBeM approximands p_k^i estimate f within the domain of granule γ^i. The recursive least mean square (RLMS) algorithm is used to determine the corresponding coefficients a_{jk}^i.

Gaussian representation allows all granules to overlap. Therefore, each rule in FBeM contributes to the system output. FBeM singular output is determined as a weighted mean value over all rules,

$$p_k = \frac{\sum_{i=1}^{c} min(A_1^i, ..., A_n^i) p_k^i}{\sum_{i=1}^{c} min(A_1^i, ..., A_n^i)}. \tag{2}$$

This assure smooth transition between overlapped functions.

Similarly to the approach for embodying antecedent of rules A_j^i, consequents of rules B_k^i benefit from scattering-based granulation and fuzzy hyperboxes to cluster output data streams skillfully. We assume Gaussian fuzzy subsets $B_k^i = \mathcal{G}(\mu_k^i, \sigma_k^i)$ to assemble granular objects in the output space by the same motivations previously described for A_j^i.

Granular output such as B_k^i may enrich decision making and sometimes provides more useful information than the specific numerical output p_k. Whilst being very specific using p_k we risky being incorrect, being unspecific from B_k^i we turn ourselves assure with a certain confidence of being correct. Sacrificing accuracy pays the price of the guarantee of correctness. Information granules tend to reflect the essence of the structure of the underlying data stream and emphasize the interpretability of the result.

III. Recursive Online Learning

FBeM learns online from a stream of instances $(x, y)^{[h]}$, $h = 1, ...$, where $y^{[h]}$ is known given $x^{[h]}$ or will be known at some latter step. Each pair (x, y) is an observation of the target function f. When f changes with the time we say that the function is nonstationary. Modeling nonstationary functions requires tracking time-varying functions $f^{[h]}$. Data streams require choosing a modeling framework and designing recursive algorithm to decide when and how to proceed structural and parametric adaptation of models.

The learning procedure to evolve fuzzy granular systems FBeM can be summarized as follows:

Begin
 Do
  1: Input a new instance $(x, y)^{[h]}$, $h = 1, ...$
  2: Accommodate possible new information
   2.1: Create a new information granule and a rule
   2.2: Adapt existing granules and rules
  3: Discard instance $(x, y)^{[h]}$
  4: Optimize the quotient granular structure
End

Steps 1 and 3 of the learning procedure emphasize the essence of data stream driven algorithms, i.e., instances are read and discarded one at a time. Historical data are dispensable and evolution stands continuously. Granular systems evolve whenever new information appears in the data, step 2. When a new instance does not fit current knowledge, the procedure is to create a new information granule and a rule governing the granule, step 2.1. Conversely, if a new instance fits current knowledge, the procedure adapts existing granules and rules, step 2.2. Eventually, the quotient structure may be optimized, coarsed or refined, according with inter-granules relationships, step 4. Next sections detail the procedure.

A. Creating Rules

In FBeM no rule does necessarily exist before learning starts. Rules are born and evolve when data are input. A new granule γ^{c+1} is created adding a rule R^{c+1} to the current collection of rules $R = \{R^1, ..., R^i, ..., R^c\}$. Whenever the current collection of rules is not sufficiently activated by an instance $x^{[h]}$ so to support a confident output, a new granule is created. FBeM assumes that the instance $x^{[h]}$ brings new information about the process.

Formally, let $\rho \in [0, 1]$ be a threshold value that determines whether to create or adapt rules. If

$$min(A_1^i, ..., A_n^i) \leq \rho \quad \forall i, \tag{3}$$

then the FBeM structure is extended. Note that if ρ is set to 0, then the FBeM system is structurally stable and unable to capture eventual concept shift. Conversely, if ρ equals 1, the FBeM system creates a rule for each new instance, which is not practical. Life-long adaptability is reached through maintaining a condition between the extremes, see Fig. 3.

The role of ρ is crucial in determining the granularity of FBeM models. Choices of ρ impact model accuracy and model transparency, e.g, shifting back and forth between values of ρ

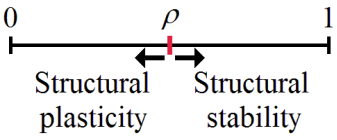

Fig. 3. Plasticity-stability tradeoff and the role ρ in FBeM systems

results in different granulated views of the same process in different levels of detail.

A new granule γ^{c+1} is initially represented by membership functions, A_j^{c+1} and B_k^{c+1}, with parameters

$$\begin{aligned} \mu_j^{c+1} &= x_j^{[h]}, \\ \mu_k^{c+1} &= y_k^{[h]} \text{ and} \\ \sigma_j^{c+1} = \sigma_k^{c+1} &= 1/2\pi, \end{aligned} \tag{4}$$

i.e., the Stigler approach for standard Gaussian functions [11]. The coefficients of local-valued polynomials p_k^{c+1} are set to

$$\begin{aligned} a_{0k}^{c+1} &= y_k^{[h]} \\ a_{jk}^{c+1} &= 0, \ j \neq 0. \end{aligned} \tag{5}$$

With that initial parameterization, preference is given to the design of granules balanced along all dimensions rather than granules with unbalanced geometry. Therefore, FBeM follows the principle of the balanced information granularity [12] and tends to give more specific rules in the sense of Yager [13].

B. Adapting Rules

Rule adaptation consists in (*i*) expand or contract objects A_j^i and B_k^i to accommodate new data; (*ii*) move granules γ^i toward denser regions of data over the input and output domains; and simultaneously (*iii*) adjust coefficients of local approximation functions p_k^i.

A rule R^i is adapted always it is sufficiently activated by a data instance $x^{[h]}$ according to

$$min(A_1^i, ..., A_n^i) > \rho. \tag{6}$$

Geometrically, the instance rests into a region highly influenced by the granule γ^i. To include $x^{[h]}$, FBeM updates the modal value and the spread of membership functions A_j^i recursively as follows:

$$\mu_j^i(\text{new}) = \frac{(\varpi - 1)\mu_j^i(\text{old}) + x_j}{\varpi^i} \tag{7}$$

$$\sigma_j^i(\text{new}) = \frac{(\varpi^i - 1)}{\varpi^i}\sigma_j^i(\text{old}) + \frac{1}{(\varpi^i - 1)}(x_j - \mu_j^i(\text{new}))^2 \tag{8}$$

where ϖ^i stands for the number of times that the granule γ^i has been activated by the data stream. Notice that values are recursively computed and they do not need data accumulation. Also, only the most active rule for $x^{[h]}$ is chosen for adaptation.

Adaptation of fuzzy sets of rules consequents B_k^i uses output data $y_k^{[h]}$. Polynomial coefficients a_{jk}^i are updated based on the standard RLMS algorithm and takes advantage of the new instance that has activated γ^i. Storage of a number of recent instances may be useful to guide alternative coefficient identification algorithms, e.g., data chunks oriented algorithms. However, it comes with some additional cost concerning memory and processing time.

C. Setting the Granularity

The granularity threshold ρ takes values in the unit interval according to prediction errors. Levels of activation of rules for a given input $x^{[h]}$ are compared to the value of $\rho^{[h]}$ to define either structural or parametric changes of FBeM systems. Values of ρ influence the granularity and understandability of local models. In the most general case, FBeM starts learning with an empty rule base and ignorance about the task and the properties of the data. Therefore, it is fair to initialize ρ in an intermediate condition to permit structural stability and plasticity equally. We use $\rho^{[0]} = 0.5$ as default initial value.

Let E be the maximum square error between predictions $p_k(x^{[h]})$ and actual values $y_k^{[h]}$, then

$$e_k = (y_k^{[h]} - p_k(x^{[h]}))^2, \ k = 1, ..., m, \tag{9}$$

and

$$E = max(e_1, ..., e_k, ..., e_m). \tag{10}$$

Assume E_D is the desired prediction error, and let ρ learn values for itself from

$$\rho(\text{new}) = \rho(\text{old}) + \alpha(E_D - E), \tag{11}$$

where α is a learning rate. Decision makers have authority over the value of E_D and may wish it to be zero. Clearly, very small values of E_D conduct ρ to 0 and lead data overfitting. Practice suggests trade-offs to attain acceptable approximation error and useful granular abstractions and compactness of the original dataset into interpretable rules. Recursive adaptation of the granularity of FBeM systems alleviates guesses on how fast and how often the structure of the data changes.

D. Coarsening the Quotient Structure

As the data arrive and granules are identified, relationships between pairs of granules may be strong enough to justify forming a larger and more abstract granule that inherits the essence and nature of the lower level smaller granules. Quantitative analysis of inter-granule relations requires a suitable metric to measure the distance between uncertain objects.

With Gaussian membership functions as internal representatives of granules, the expected distance between uncertain instances belonging to two different granules, say γ^{i_1} and γ^{i_2}, may be given by:

$$\begin{aligned} D(\gamma^{i_1}, \gamma^{i_2}) = \frac{1}{n}\sum_{j=1}^{n} ||\mu_j^{i_1} - \mu_j^{i_2}||^2 + \sigma_j^{i_1} + \\ + \sigma_j^{i_2} - 2\sqrt{\sigma_j^{i_1}\sigma_j^{i_2}}. \end{aligned} \tag{12}$$

This distance has demonstrated to be of fast calculation and more accurate than e.g. distance between means in L^p spaces [14]. The relation considers uncertain data and the specificity of the information, which is in turn inversely proportional to the spread. FBeM combines granules using the lowest entry of $D(.)$ for any pair of granules of the current collection and a decision criterion, which may be either based on a threshold value Δ, or expert judgment in respect of the convenience of the combination.

A new granule γ^i, coarsening of γ^{i_1} and γ^{i_2}, is constituted by Gaussian membership functions with modal value

$$\mu_j^i = \frac{\frac{\sigma_j^{i_1}}{\sigma_j^{i_2}}\mu_j^{i_1} + \frac{\sigma_j^{i_2}}{\sigma_j^{i_1}}\mu_j^{i_2}}{\frac{\sigma_j^{i_1}}{\sigma_j^{i_2}} + \frac{\sigma_j^{i_2}}{\sigma_j^{i_1}}},\ j = 1, ..., n, \tag{13}$$

and spread

$$\sigma_j^i = \sigma_j^{i_1} + \sigma_j^{i_2},\ j = 1, ..., n. \tag{14}$$

These are heuristic relations that basically take into account the proportion of uncertainty of each granule being combined to determinate the location and size of the new granule. The same coarsening relations hold for output variables k. The coefficients of the new local polynomial are

$$a_{jk}^i = \frac{1}{2}(a_{jk}^{i_1} + a_{jk}^{i_2}),\ j = 0, ..., n. \tag{15}$$

Naturally, combining granules reduces the number of rules in FBeM systems and redundancy.

E. Removing Granules

A granule should be removed from the FBeM structure if it seems to be inconsistent with the current concept. Common removing strategies either (*i*) retire stale granules by age, (*ii*) exclude the weakest granules based on error values or (*iii*) delete the most inactive granules. In FBeM, we opt by the strategy of deleting inactive granules. Stale granules may still be useful in the current environment while weak granules are attempted to be invigorated through adapting parameters of singular and granular functions.

FBeM granules are deleted when they become inactive during a number of processing steps, h_r. If the application requires memorization of rare events, or if cyclical drifts are expected, then it may be the case to let all granules live forever. Removing inactive granules periodically helps to keep the rule base updated.

IV. Time Series Prediction

Observing past outcomes of a system to estimate its future behavior: time series prediction is based on the idea that the series carry the potential information needed to predict their future values. Analyzing data produced by actual phenomena can give good insights into the phenomena itself and knowledge about the rules underlying the data.

Chaotic time series are commonly found in natural phenomena [15]-[16]. Models of chaotic time series are useful both to test some hypothesis or theory about the generating phenomena to predict future values of the series, and to decide on mechanisms to control future values. In this avenue, researchers have relied on methods based mainly on looking at trends, moving averages, and graphical patterns to perform predictions. Most of these are linear approaches, e.g. the Box-Jenkins method, linear regression, Kalman filtering, and suffer of some shortcomings [17]. More recently, predicting approaches into the realm of soft computing, e.g. wavelet networks, fuzzy and neuro-fuzzy predictors, have emerged. These approaches have advantages over the traditional statistical ones [18] because generally they are nonlinear in nature thus approximating complex dynamics more easily.

Although classical neural networks and fuzzy systems can approximate any nonlinear continuous function, they usually demand high quality training data and time-consuming off-line learning. Learning system models from data streams in online mode is a challenging task for most of the classical statistical and emergent computing techniques. Therefore, there exists substantial room for further developments of predictors able to perform online learning using data streams.

A. Problem Statement

Forward prediction of a time series can be stated as follows. Given a finite sequence of observations of a discrete time series, namely, $x^{[h]}$, $x^{[h-1]}$, ..., $x^{[h-M]}$, find the continuation $x^{[h+1]}$, $x^{[h+2]}$, ... This involves setting a scalar M and encountering a function f such that a future value, e.g. $x^{[h+1]}$, can be predicted by

$$\hat{x}^{[h+1]} = f(x^{[h]}, x^{[h-1]}, ..., x^{[h-M]}). \tag{16}$$

This is equivalent to modeling the time series as

$$x^{[h+1]} = f(x^{[h]}, x^{[h-1]}, ..., x^{[h-M]}) + \zeta^{[h+1]} \tag{17}$$

with $\zeta^{[h+1]}$ being a white noise process. If the statistics of the time series are non-Gaussian or the time series is the result of some nonlinear operation, the function f is nonlinear. When the characteristics of the time series change with time we say f is nonstationary. Nonlinear nonstationary functions require that online adaptive models identify time varying relations $f^{[h]}$ to perform prediction.

B. Box-Jenkins Gas Furnace

The Box and Jenkins gas furnace benchmark data [19] consist of 9-second-sampling measurements recorded from a combustion process of an oxygen-methane gas mixture. The proportion of gases was randomly changed during the process. The original dataset consists of 296 time indexed instances of the gas flow rate into the furnace $x^{[h]}$ and the concentration of carbon dioxide $y^{[h]}$ emitted.

The task of the FBeM system is to identify the level of carbon dioxide at instant h, $y^{[h]}$, using the preview observation

$y^{[h-1]}$ and the gas rate four steps before $x^{[h-4]}$. This premise prevails in literature works due to positive correlation between these state variables. FBeM scans the data only once to build the system structure and adjust parameters. This is to emulate a data stream. The rule base is initially empty.

Starting parameters to be set include $\alpha = .05$, $E_D = .04$, $\Delta = .08$ and $h_r = 300$. These are values that have particularly worked well for a range of problems. In this experiment we prioritized the compactness and performance of the model.

Training and testing are performed concomitantly from $h = 5$ to 296. First, the estimation $y^{[h]}$ for a given instance $(x^{[h-4]}, y^{[h-1]})$ is provided by the system (testing). Then, parametric and structural adaptation is carried out when necessary (training). Training is necessary whenever an instance carries new information significantly mismatching the current knowledge. Sample-per-sample testing-before-training approach portrays the true online data stream context.

Performance evaluation is made based on the root mean square error:

$$RMSE = \sqrt{\frac{1}{H}\sum_{h=1}^{H}(y^{[h]} - p^{[h]})^2} \tag{18}$$

and the non-dimensional error index:

$$NDEI = \frac{RMSE}{std(y^{[h]} \forall h)}, \tag{19}$$

which ponders the $RMSE$ by the inverse of the standard deviation of the underlying data.

Table I summarizes the results. It emphasizes the FBeM performance against alternative models in identifying levels of carbon dioxide smoked out of the furnace. The results of Table I show that FBeM is the most accurate model according to the $RMSE$ and $NDEI$ indices. FBeM reaches the best performance using an average of 2.61 ± 0.55 rules during learning with a maximum of 3 rules, as shown in Fig. 4. The algorithm does not take advantage from large amount of local processing units as evidenced in the figure, but from a combination of ingredients concerning with structural assumptions, peculiarities of the learning algorithm, and fuzzy granular framework to achieve the performance.

TABLE I
GAS FURNACE - PREDICTION PERFORMANCE

Model	Ref.	Rules	$RMSE$	$NDEI$
ARMA	[19]	–	0.8426	3.8687
TS	[20]	2	0.2608	1.1973
ANFIS	[21]	25	0.0854	0.3923
HyFIS*	[22]	15	0.0648	0.2975
eTS*	[23]	5	0.0490	0.3057
Simp-eTS*	[23]	3	0.0484	0.3004
FBeM*	This paper	3	0.0421	0.1932

* Online model

Figure 4 illustrates FBeM one-step singular and granular predictions for the gas furnace problem. The granular prediction $\mu \pm \sigma$ associated to the more meaningful singular prediction p is an important information which may help decision making giving an idea about a range of values around the prediction.

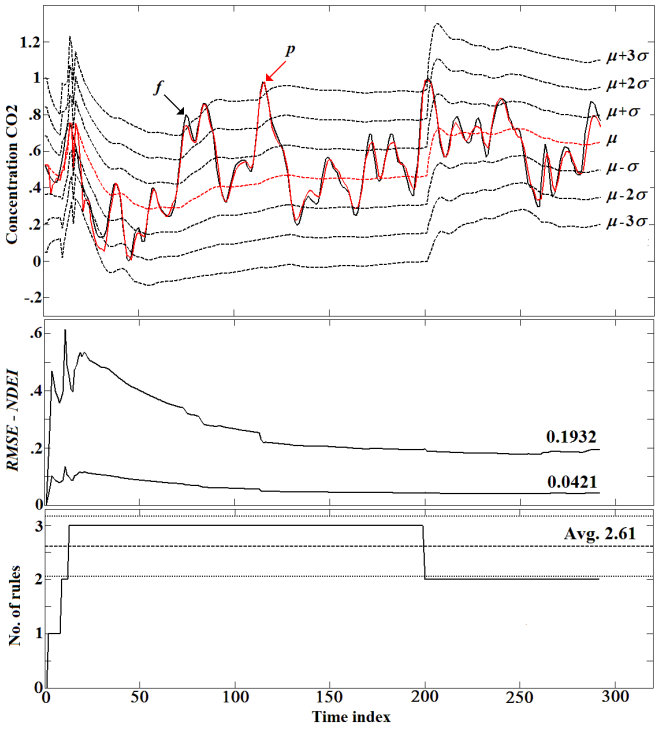

Fig. 4. FBeM singular and granular one-step prediction, and evolution of the error indices and number of rules for the Box and Jenkins gas furnace data

Rules of particular interest can be displayed at any time. For example, a rule at $h = 296$ is:

R^i: IF $x^{[h-4]}$ is $\mathcal{G}(.4192, .1269)$ AND $y^{[h-1]}$ is $\mathcal{G}(.6523, .1516)$ THEN $y^{[h]}$ is $\mathcal{G}(.6503, .1497)$ AND $p^i = .2514 - .0656x^{[h-4]} + .8128y^{[h-1]}$.

C. Mackey-Glass

The Mackey-Glass equation described by:

$$\frac{dx}{dt} = \frac{Ax^{[t-\tau]}}{1 + (x^{[t-\tau]})^C} - Bx^{[t]}, \; A, B, C > 0, \tag{20}$$

is a time delay differential equation that behaves chaotically or periodically depending on the values of its parameters and on the time delay τ. The equation may represent a model of feedback control systems.

The task of FBeM is constructing a function:

$$x^{[t+\xi]} = p(x^{[t]}, x^{[t-\Delta]}, ..., x^{[t-D\Delta]}). \tag{21}$$

Similar to many studies on this series we admit $\xi = 85$, $\Delta = 6$, $D = 3$; and $A = 0.2$, $B = 0.1$, $C = 10$, $\tau = 17$ for the parameters of the Mackey-Glass equation to generate a state

vector. Data are presented sequentially to the FBeM system one at a time. The system starts learning from scratch, with no rules nor pre-training.

To evaluate the effect of different parameterizations, we conduct two experiments. Firstly, FBeM^1 prioritizes a compact structure and adopts $\alpha = .05$, $E_D = .06$, $\Delta = .2$ and $h_r = 2000$. Second, FBeM^2 focuses high accuracy at the price of a larger structure and employs $\alpha = .1$, $E_D = .01$, $\Delta = .1$ and $h_r = 8000$. We resort to the sample-per-sample testing-before-training approach from $h = 105$ to $h = 11898$. Table II shows the performance of the FBeM models and that of other online models for the Mackey-Glass prediction problem.

Table II shows that FBeM^1 is supported by a relatively compact structure, 3.23 ± 0.56 rules with a maximum of 5 rules, similar to eTS, IBeM and xTS, to give competitive results in terms of the $RMSE$ and $NDEI$ indices. Figure 5 details the results of this experiment. The figure illustrates the singular prediction p of the Mackey-Glass series provided by FBeM^1, and the evolution of the number of rules and error indices during the learning steps. Granular prediction is omitted for clarity. Lastly, FBeM^2 makes use of 27.87 ± 4.11 rules with a maximum of 33 rules to sponsor the smallest prediction error and overcome the performance of the remaining approaches.

In case equation f represents the production of white blood cells to defend the human body against pathogen, as in Glass and Mackey [29], FBeM granular prediction may represent, for example, the range of normal activity of hematopoietic stem cells. The effectiveness of the approach in predicting chaotic time series without prior knowledge about the data is clearly verified in this experiment.

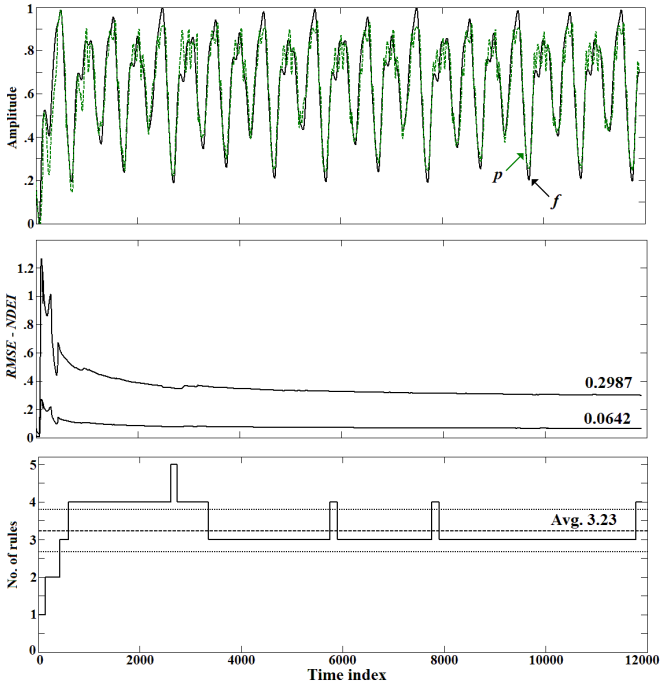

Fig. 5. FBeM singular one-step prediction and evolution of the number of rules and error indices for the Mackey-Glass time series

TABLE II
MACKEY-GLASS - PREDICTION PERFORMANCE

Model	Ref.	Rules	$RMSE$	$NDEI$
EFuNN*	[24]	193	0.0822	0.4010
RAN	[25]	113	0.0802	0.3730
eTS*	[26]	9	0.0799	0.3720
IBeM*	[7]	5	0.0769	0.3577
xTS*	[26]	10	0.0711	0.3310
FBeM^1*	This paper	5	0.0642	0.2987
DENFIS*	[27]	58	0.0593	0.2760
Neural Gas	[28]	1000	0.0133	0.0620
IBeM*	[7]	98	0.0126	0.0586
FBeM^2*	This paper	33	0.0122	0.0568

* Online model

D. Brazilian Global40

Currently, the most negotiated Brazilian sovereign bonds are the Global 2040, which were issued in 2000, with 40 years maturity. Price movements define the bond rentability: higher prices imply lower rentability. Thus, if investors believe that the bond price will increase and the rentability decrease, they should buy the bond before this expected movement. On the other hand, if the investors believe the bond price will decrease and the rentability increase, they should behave contrariwise. Predicting bond price movements is a crux issue from the point of view of the investors on their portfolio decisions.

Variable selection may enhance the prediction ability of FBeM as well as provide useful insights about the data source. Time series carry a limited number of indispensable variables, while the remainders tend to confuse the underlying predictor. The input variables of FBeM may be M consecutive measurements of the time series or we may perform selection of $n < M$ variables, which are not necessarily sequential. In this experiment, variables were chosen based on a partial autocorrelation function of the Global40 bond price, similar to [30]. Coincidently, autocorrelation analysis has suggested $x^{[h-1]}$ and $x^{[h]}$ for one step ahead, $x^{[h+1]}$, prediction.

To evaluate the relative performance of the FBeM predictor, we consider daily bond prices from August 11, 2000 to January 16, 2007, testing-before-training in a sample-per-sample basis, and the following parameters: $\alpha = .03$, $E_D = .01$, $\Delta = .1$ and $h_r = 500$. Table III shows the results on one-step-ahead prediction of the bond price. The result using FBeM makes use of 2.25 ± 1.05 rules, with a high of 4 rules during steps $h = 863$ to $h = 1149$ as portrayed in Fig. 6. The FBeM approach achieved error indices equivalent to the ePL approach employing a structure almost as compact as ePL. However, FBeM offers additional information concerning with

TABLE III
GLOBAL 2040 - PREDICTION PERFORMANCE

Model	Ref.	Rules	RMSE	NDEI
eTS*	[23]	7	0.1362	0.5069
xTS*	[26]	12	0.1355	0.5043
AR	[19]	–	0.0136	0.0506
ePL*	[30]	2	0.0123	0.0458
FBeM*	This paper	4	0.0121	0.0452

* Online model

tolerance bounds around the numerical prediction, as highlights the zoom-in of Fig. 6. Granular output in this case may be read as optimistic and pessimistic bias of the rentability of the Global40 bond.

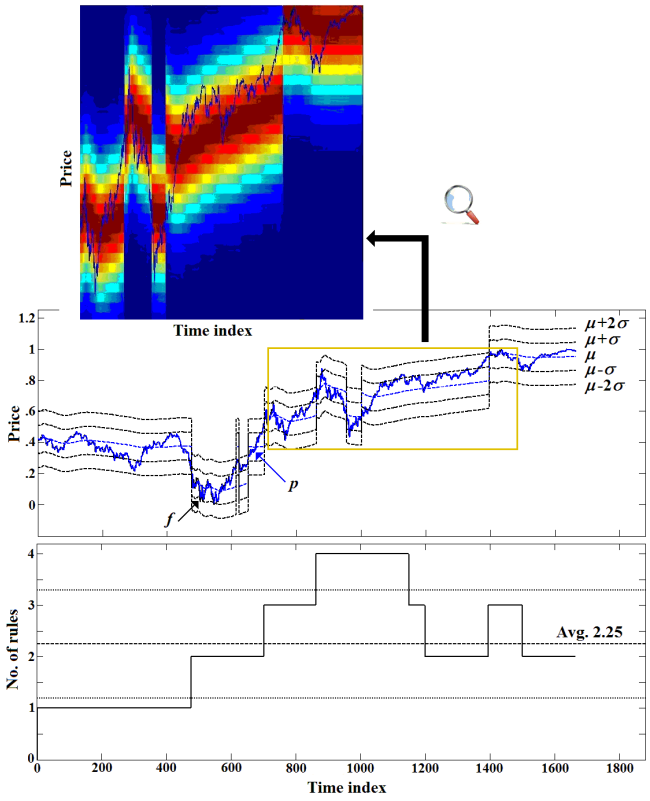

Fig. 6. FBeM singular and granular one-step prediction and evolution of the number of rules for the Global40 bond price

V. Conclusion

This work has suggested fuzzy set based evolving modeling as a framework to learn from online data streams. The FBeM algorithm recursively granulates data instances to output singular and linguistic granular approximations of nonstationary functions. The system combines good accuracy of functional fuzzy models with the advantage of better semantic interpretation of linguistic models. The usefulness of the FBeM approach in prediction was verified using the classic benchmarks Box-Jenkins and Mackey-Glass and actual data of the Global40 time series. Comparisons with alternative approaches have shown the effectiveness of the FBeM modeling approach. Further work shall discuss different forms of manifestation of information granules in data streams and the role FBeM to capture the essence of the information in the data.

Acknowledgment

The first author acknowledges CAPES, Brazilian Ministry of Education, for his fellowship. The second author thanks CNPq, the Brazilian National Research Council, for grant 304596/2009-4. The last author is grateful to the Energy Company of Minas Gerais - CEMIG, Brazil, for grant P&D178.

References

[1] W. Pedrycz, "Evolvable fuzzy systems: some insights and challenges," Evolving Systems, Vol. 1, Issue 2, pp: 73-82, 2010.
[2] A. Bargiela, W. Pedrycz, "Granulation of temporal data: a global view on time series," NAFIPS'03, pp: 191-196, 2003.
[3] P. Angelov, D. Filev, "An approach to online identification of Takagi-Sugeno fuzzy models," IEEE Transactions on Systems, Man, and Cybernetics - Part B, Vol. 34, Issue 1, pp: 484-498, 2004.
[4] D. Leite, F. Gomide, "Evolving linguistic fuzzy models from data streams," To appear in: E. Trillas, P. Bonissone, L. Magdalena, J. Kacprycz (Eds.), Studies in Fuzziness and Soft Computing: A Homage to Abe Mamdani, Springer-Verlag, 15p., 2011.
[5] D. Leite, P. Costa, F. Gomide, "Evolving granular neural network for semi-supervised data stream classification," International Joint Conference on Neural Networks, pp: 1-8, 2010.
[6] D. Leite, P. Costa, F. Gomide, "Interval-based evolving modeling," IEEE Symposium Series on Comp. Intelligence-ESDIS'09, pp: 1-8, 2009.
[7] D. Leite, P. Costa, F. Gomide, "Granular approach for evolving system modeling," In: E. Hullermeier, R. Kruse, F. Hoffmann (Eds.), Lecture Notes in AI, Vol. 6178, pp: 340-349, Springer, 2010.
[8] L. A. Zadeh, "Towards a theory of fuzzy information granulation and its centrality in human reasoning and fuzzy logic," Fuzzy Sets and Systems, Vol. 19, pp: 111-127, 1997.
[9] Y. Y. Yao, "Perspectives of granular computing," IEEE International Conference on Granular Computing, pp: 85-90, 2005.
[10] V. Kreinovich, C. Quintana, L. Reznik, "Gaussian membership functions are most adequate in representing uncertainty in measurements," NAFIPS'92, pp: 618-624, 1992.
[11] S. M. Stiegler, "A modest proposal: a new standard for the normal," The American Statistician, Vol. 36, Issue 2, JSTOR, 1982.
[12] A. Bargiela, W. Pedrycz, Granular Computing: An Introduction, Kluwer Academic Publishers - Boston, Dordrecht, London, 452p., 2003.
[13] R. R. Yager, "Measures of specificity over continuous spaces under similarity relations," Fuzzy Sets and Sys., Vol.159, pp: 2193-2210, 2008.
[14] L. Xiao, E. Hung, "An efficient distance calculation method for uncertain objects," IEEE Symposium on Computational Intelligence and Data Mining, pp: 10-17, 2007.
[15] C. Gao, J. Qian, "Evidence of chaotic behavior in noise from industrial process," IEEE Trans. on Signal Processing, Vol.55-6, pp:2877-84, 2007.
[16] H. Kantz, T. Schreiber, Nonlinear Time Series Analysis, Cambridge Univ. Press, 390p., 2004.
[17] S. Haykin, Adaptive Filter Theory, 4^{th} ed., Prentice-Hall, 936p., 2001.
[18] G. S. Maddala, Introduction to Econometrics, 3^{th} edition, Wiley, 664p., 2001.
[19] G. Box, G. Jenkins, Time Series Analysis: Forecasting and Control, Holden-Day San Francisco, US, 2^{nd} edition, 1976.
[20] M. Sugeno, T. Yasukawa, "A fuzzy-logic-based approach to qualitative modelling," IEEE Trans. on Fuzzy Systems, Vol.1, Iss.1, pp: 7-31, 1993.
[21] J. Jang, "ANFIS: adaptive-network-based fuzzy inference systems," IEEE Transactions on SMC, Vol. 23, Issue 3, pp: 665-685, 1993.
[22] J. Kim, N. Kasabov, "HyFIS: adaptive neuro-fuzzy inference systems and their application to nonlinear dynamical systems," Neural Networks, Vol. 12, Issue 9, pp: 1301-1319, 1999.
[23] P. Angelov, D. Filev, "Simpl-eTS: a simplified method for learning evolving Takagi-Sugeno fuzzy models," IEEE International Conference on Fuzzy Systems, pp: 1068-1073, 2005.
[24] N. Kasabov, "Evolving Fuzzy Neural Networks - Algorithms, Applications and Biological Motivation," In: T. Yamakawa, G. Matsumoto (Eds.), Methodologies for the Conception, Design and Application of Soft Computing, World Scientific, pp: 271-274, 1998.
[25] J. Platt, "A resource-allocating network for function interpolation," Neural Computation, Vol. 3, pp: 213-225, 1991.
[26] P. Angelov, X. Zhou, "Evolving fuzzy systems from data streams in real-time," Int. Symp. on Evolving Fuzzy Systems, pp: 29-35, 2006.
[27] N. Kasabov, Q. Song, "DENFIS: Dynamic evolving neural-fuzzy inference system and its application for time-series prediction," IEEE Transactions on Fuzzy Systems, Vol. 10, Issue 2, pp: 144-154, 2002.
[28] B. Fritzke, "A growing neural gas network learns topologies," Advances in Neural Information Processing Systems, Vol. 7, pp: 625-632, 1995.
[29] M. Mackey, L. Glass, "Oscillation and chaos in physiological control systems," Science, Vol. 197, Issue 4300, pp: 287-289, 1977.
[30] R. Ballini, A. Mendonca, F. Gomide, "Evolving fuzzy modeling of sovereign bonds," The Journal of Financial Decision Making - special issue: The Fuzzy Logic in the Financial Uncertainty, Vol.5, Iss.2, 2009.

2011 IEEE International Conference on Fuzzy Systems
June 27-30, 2011, Taipei, Taiwan

Combustion Engine Modelling using an Evolving Local Model Network

Christoph Hametner* and Stefan Jakubek†
Christian Doppler Laboratory for Model Based Calibration Methodologies
Vienna University of Technology
1040 Vienna, Austria
*christoph.hametner@tuwien.ac.at
†stefan.jakubek@tuwien.ac.at

***Abstract*—In this paper a new evolving parameter estimation algorithm for a local model network under special consideration of combustion engine modelling is presented. For practical applications computational speed, incorporation of prior knowledge and the interpretability of the local models is of great interest. Accordingly, a robust and efficient online training algorithm with a particular focus on computational requirements involved in dynamic system identification of complex nonlinear processes is presented. The incremental construction of the model tree allows to gradually increase the model complexity while a proper initialisation of new model parameters is easily possible. The proposed evolving local model network is validated using real measurement data from a state-of-the-art 4-cylinder EURO5 diesel engine.**

***Index Terms*—System identification, local model network, online learning, engine modelling**

I. Introduction

Evolving model structures are becoming a more and more essential factor in the automotive industry. Recent publications have addressed automatic adaptation techniques and evolving schemes for data-based modelling, e. g. [1], [2], [3], [4]. Such models are trained *online* and it is necessary to adjust, refine, extend, and evolve the already trained model when new data are available, [1]. The model is evolved sample by sample and its complexity is gradually increased due to the fact that it is not practicable to completely rebuild the model using all measurement data. Accordingly, new rules are created and an update of the model parameters during the operation of the system is required.

In the context of data-driven modelling, fuzzy systems are an established approach for nonlinear system identification. These so-called *grey-box* models allow to reduce the model complexity, if physical (or other) insight into the nature of the object is available, [5]. In automotive industry, *local model networks* (LMN) are a widely used concept, e. g. [6], [7]. Local model networks offer a versatile structure for the identification of nonlinear static and dynamic systems and provide not only accurate but also *interpretable* models and therefore allow a better understanding of the true system than pure black-box models, e. g. [8], [9], [10].

Especially in engine modelling, evolving model structures are of great interest in order to provide an online model of the engine during testbed runs, see e. g. [11]. Internal combustion (IC) engines are typically calibrated on testbeds which involves the determination of a number of functional relationships between measured input and output data. In this context, the *design of experiments* (DoE) for testbed runs is closely related to the model adaptation. Generally, *optimal* experiment design is targeted to retrieve the information which is required to properly parameterise a model with as little effort as possible, [12]. Typically, the experiment design is performed offline and prior to the testbed run based on prior knowledge about the process under consideration. The availability of an evolving model allows to optimise the experiment design online (model based) during the testbed run. Accordingly, *model based DoE* employs an intermediate model in combination with a statistical criterion to design optimal experiments, e. g. [13]. Model based DoE can also be used to take into account local process limits in terms of engine protection and combustion stability (i. e. the driveable area of the engine) which are not known in advance. In such cases a model which has been trained online allows to predict and avoid the violation of certain operational limits.

The main contribution of the present paper is a new evolving optimisation algorithm for a local model network that can build the model incrementally whenever new data are available. Important requirements for the practical applicability in engine modelling are low computational effort, proper initialisation, and robustness of the optimisation algorithm. The proposed online training algorithm is based on the local model network presented in [14]. Here, the global process description is obtained by recursively bisecting the input space. The bisection is carried out in such a way that the nonlinear process can reasonably accurately be described by the local models in the resulting subdomains. The use of an incremental tree has proven to be an effective model building strategy in both offline and online modelling, e. g. [15], [16], [17]. An important advantage of these hierarchically constructed models is their robustness and training speed.

The proposed algorithm is not restricted to axis orthogonal splits and offers a higher flexibility compared to e. g. [15], [6]. Especially in online system identification, where the operating range of a process (e. g. driveable area of the engine) is generally not known a priori, arbitrary (axis oblique) splits are required for an optimal partitioning of the input space. Thereby, the incremental construction of the model tree allows

978-1-4244-7316-8/11/$26.00 ©2011 IEEE

to gradually increase the model complexity while a proper initialisation of new model parameters is easily possible. A difficult part in online learning of incremental trees is the decision when to grow the tree, see [16]. In this paper a splitting rule based on statistical measures is proposed.

The remainder of this paper is structured as follows: In section II the architecture of the local model network is shortly reviewed. In section III the online training algorithm is presented. In section IV a practical application of *dynamic* online system identification using real measurement data from a state-of-the-art diesel engine is presented.

II. Local Model Network Architecture

Local model networks interpolate between different local models, each valid in a certain region of a input space. Each local model - indicated by subscript i - consists of two parts: The *validity function* $\Phi_i(\tilde{\boldsymbol{x}}(k))$ and its *model parameter vector* $\boldsymbol{\theta}_i$. Thereby, Φ_i defines the region of validity of the i-th local model.

The *local* estimate for the output is obtained by

$$\hat{y}_i(k) = \boldsymbol{x}^T(k)\boldsymbol{\theta}_i, \tag{1}$$

where $\boldsymbol{x}^T(k)$ denotes the regressor vector. In dynamic system identification, the regressor vector $\boldsymbol{x}(k)$ comprises past system inputs and outputs. For static models, the regressor vector contains arbitrary functions (e. g. polynomials) of the input signals.

All local estimations $\hat{y}_i(k)$ are used to form the global model output $\hat{y}(k)$ by weighted aggregation

$$\hat{y}(k) = \sum_{i=1}^{M} \Phi_i(k)\hat{y}_i(k), \tag{2}$$

where

$$\Phi_i(k) = \Phi_i(\tilde{\boldsymbol{x}}(k)) \tag{3}$$

and M denotes the number of local linear models. Thereby, the elements in $\tilde{\boldsymbol{x}}(k)$ span the so-called partition space and are chosen on the basis of prior knowledge about the process and the expected structure of its nonlinearities. Especially in dynamic identification, the dimension of the partition space and furthermore the complexity of the optimisation problem can thus be reduced dramatically when prior knowledge about the nonlinear behaviour of the process is available, see also [6].

The computation of the validity functions Φ_i is based on a logistic discriminant tree. Exemplarily, a hierarchical model tree with three local models is depicted in Fig. 1. Each node corresponds to a split of the partition space into two parts and the free ends of the branches represent the actual local models with their parameter vector $\boldsymbol{\theta}_i$ and their validity functions Φ_i. The overall nonlinear model thus comprises M local models and $M-1$ nodes which determine their regions of validity.

Generally, for the representation of the discriminant function in the d-th node a logistic sigmoid activation function is chosen, c. f. [18]:

$$\varphi_d(\tilde{\boldsymbol{x}}(k)) = \frac{1}{1+\exp(-a_d(\tilde{\boldsymbol{x}}(k)))} \tag{4}$$

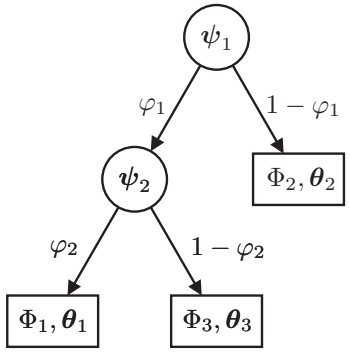

Fig. 1. Logistic discriminant tree

with

$$a_d(\tilde{\boldsymbol{x}}(k)) = \begin{bmatrix}1 & \tilde{\boldsymbol{x}}^T(k)\end{bmatrix}\begin{bmatrix}\psi_{d0}\\ \tilde{\boldsymbol{\psi}}_d\end{bmatrix}. \tag{5}$$

Here, $\tilde{\boldsymbol{\psi}}_d^T = \begin{bmatrix}\psi_{d1} \dots & \psi_{dp}\end{bmatrix}$ denotes the weight vector and ψ_{d0} is called bias term. The discriminant functions φ_d are used to calculate the validity functions Φ_i, c. f. [19].

The validity functions for the layout in Fig. 1 are obtained by

$$\Phi_1 = \varphi_1\varphi_2, \tag{6}$$

$$\Phi_2 = 1-\varphi_1, \tag{7}$$

$$\Phi_3 = \varphi_1(1-\varphi_2). \tag{8}$$

A main advantage of this hierarchical discriminant tree is that a partition of unity throughout the partition space is guaranteed and no normalisation side effects like reactivations can occur.

III. Evolving Local Model Network

An incremental model construction allows to gradually increase the complexity of the local model network: When the number of local models M is increased by one, the *worst* local model (indexed by l) of the logistic discriminant tree in Fig. 1 is replaced by a new node and two adjoining local models are appended, see Fig. 2. On the one hand this strategy allows a proper initialisation of the new model parameters while on the other hand the computational demand is low.

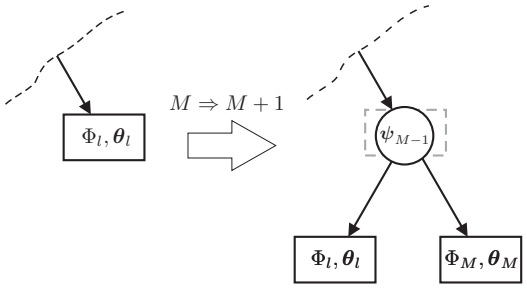

Fig. 2. Incremental tree construction

In order to reduce the computational demand, only the weight vector of the new node $\boldsymbol{\psi}_{M-1}$ is optimised while

all other weight vectors are retained. A disadvantage of this strategy is that the computation of the weight vector $\boldsymbol{\psi}_{M-1}$ and the consequent parameters substantially depends on previous splits. Due to the fact that each split is optimised subject to previous splits, a *global* optimum can generally not be guaranteed. However, a global (simultaneous) optimisation of *all* weight vectors and local model parameters of the LMN results in a much higher computational effort which is not desired and inapplicable for online engine modelling.

A flowchart of the *online* training algorithm is depicted in Fig. 3. The online identification task comprises four subtasks:

- *Build initial model:* The construction of the initial model is based on an *initial data block* using the batch training algorithm, c. f. [14].
- *Split optimisation and parameter update (see section III-A):* Optimisation *and* update of the actual node (discriminant function). Update of the consequent parameters of each local model (LM) using the new data sample.
- *Model extension (see section III-B):* Statistical assessment of the actual LMN in order to decide whether to extend the model tree.
- *Initialisation of new LMs (see section III-C):* Determine a proper initialisation of new parameters.

A. Split Optimisation and Parameter Update

In the online training, the *actual* number of data - indicated by N - is increased by one in each loop. The online adaptation of the local model network can be divided into two subtasks:

1) *Partitioning process:* Find an optimal weight vector $\boldsymbol{\psi}_{M-1}^T = \begin{bmatrix} \psi_{M-1,0} & \tilde{\boldsymbol{\psi}}_{M-1}^T \end{bmatrix}$ for the new node.
2) *Local model parameter estimation:* Update of the consequent parameters of *all* local models.

In this section, the optimisation of the actual (most recent) split and the parameter update of all local model parameters is presented.

1) Partitioning Process: Due to the incremental model construction, only the weight vector of the actual node $\boldsymbol{\psi}_{M-1}$ is optimised while all other weight vectors are retained. The optimisation of the weight vector is based on the cost function

$$\begin{aligned} J &= \frac{1}{2}\sum_{k=1}^{N} \Phi_l(k)\left[y(k)-\hat{y}_l(k)\right]^2 + \\ &\quad +\Phi_M(k)\left[y(k)-\hat{y}_M(k)\right]^2 \\ &= \frac{1}{2}\sum_{k=1}^{N} e_l^2(k) + e_M^2(k), \end{aligned} \tag{9}$$

where

$$e_l(k) = \sqrt{\Phi_l(k)}\left[y(k)-\hat{y}_l(k)\right] \tag{10}$$

and

$$e_M(k) = \sqrt{\Phi_M(k)}\left[y(k)-\hat{y}_M(k)\right] \tag{11}$$

are the *weighted* local prediction errors of the adjoining models l and M, respectively.

Obviously, the weight vector $\boldsymbol{\psi}_{M-1}$ and the two adjoining models with their local model parameters $\boldsymbol{\theta}_l$, $\boldsymbol{\theta}_M$ have to be optimised simultaneously, see also Fig. 1.

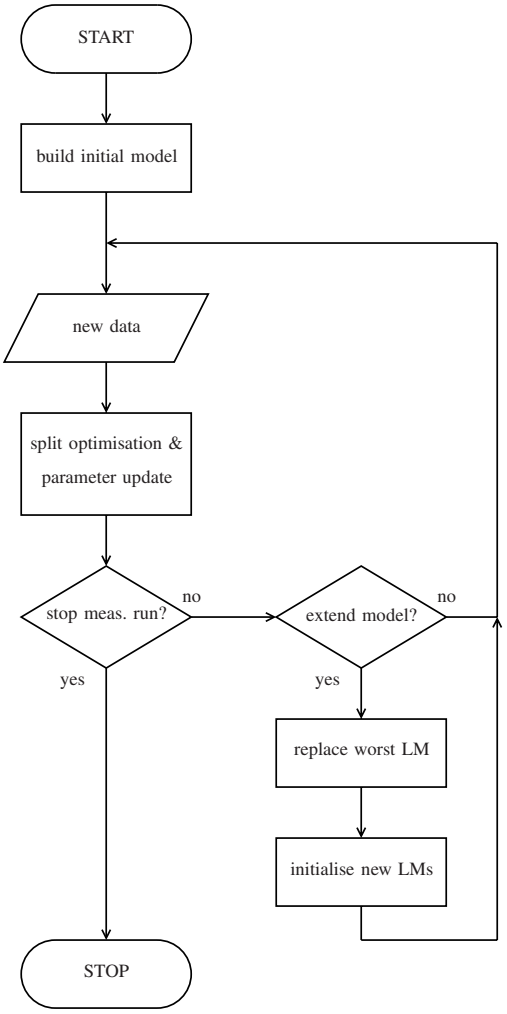

Fig. 3. Flowchart diagram for the online training

With $\Phi_l = \Phi_l(\boldsymbol{\psi}_{M-1})$ and $\Phi_M = \Phi_M(\boldsymbol{\psi}_{M-1})$ a direct solution for the optimisation problem with respect to $\boldsymbol{\theta}_l$, $\boldsymbol{\theta}_M$ and $\boldsymbol{\psi}_{M-1}$ is not possible because the computation of the consequent parameters $\boldsymbol{\theta}_l$ and $\boldsymbol{\theta}_M$ depends on the weight vector $\boldsymbol{\psi}_{M-1}$ and vice versa. Consequently, a *nonlinear least squares* method is applied for the minimisation of (9). A recursive formulation of the nonlinear least squares algorithm, in order to reduce the computational demand, can be found in e. g. [20].

Another important issue in fuzzy modelling is the interpretability of the local models, [21], [10]. Only consequent parameters obtained by local estimation (weighted least squares) allow the interpretation of the consequent parameters as a local linearisation of the nonlinear system, [9]. The particular choice of (9) aims at a *locally* weighted least squares optimisation of the consequent parameters so that local interpretability is conserved.

2) Parameter Update: While the update of the consequent parameters $\boldsymbol{\theta}_l$ and $\boldsymbol{\theta}_M$ is based on a nonlinear least squares algorithm, the online training of the local model network also

requires the update of all other local model parameters when a new observation is available. Due to the fact that the validity functions, i. e. the weight vectors $\boldsymbol{\psi}_j, j = 1, \ldots, M-2$, of these models are not modified during the split optimisation, these parameters can be updated using the conventional weighted least squares method. A recursive formulation of the weighted least squares algorithm is easily possible which helps to reduce the computational demand, see e. g. [22].

B. Model Extension

In online learning the number of local models strictly depends on the currently available data. Too many local models can result in overfitting or even loss of identifiability while a simplistic model yields an inaccurate description of the process. In this section a statistically motivated splitting rule is proposed in order to automatically detect when an extension of the model structure is reasonable.

The splitting rule is based on the assumption that the residual distribution of each local linear model follows a χ^2 distribution for Gaussian white noise and a proper choice of the model structure, i. e. the number of local models.

Using the χ^2 distribution the confidence interval for the variance of the model error of the i-th local model $\sigma_{e_i}^2$ is obtained as

$$\frac{DOF_i}{\chi^2_{1-\alpha/2,DOF_i}} s_i^2 \leq \sigma_{e_i}^2 \leq \frac{DOF_i}{\chi^2_{\alpha/2,DOF_i}} s_i^2, \qquad (12)$$

with the error probability α and the remaining statistical degrees of freedom DOF_i. In (12) s_i^2 is the estimated variance of the model error based on the currently available data and $\sigma_{e_i}^2$ the *unknown* true variance.

In the online training the estimated variance and the degrees of freedom change over time as the number of data increases, i. e. in each iteration step new data (a new observation) are available. The χ^2 distribution is used to determine if a local model of the updated LMN performs significantly worse using the additional data sample. The hypothesis that the current local model structure properly describes the process in its region of validity is accepted with an error probability α, if the estimated variance does not exceed the corresponding confidence interval. Otherwise the hypothesis is rejected and the corresponding local model is replaced by two new local models.

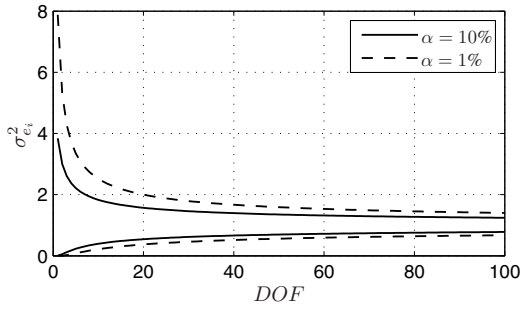

Fig. 4. Upper and lower bounds of the χ^2 distribution

In Fig. 4 the upper and lower bounds of the χ^2 distribution are depicted for $\alpha = 1\%$ and $\alpha = 10\%$, respectively. In the χ^2 distribution the probability α is a good means to control regularisation. Accordingly, a small error probability results in a small number of local models while the robustness of the parameter estimation process is increased. An increased error probability will in turn yield a more accurate description of the process with a higher number of local models while the robustness is decreased (overfitting).

C. Initialisation of new Local Models

The robustness of the training algorithm is closely related to the initialisation of new parameters when the model complexity is increased. Thus the initialisation of new local models, i. e. the consequent parameters $\boldsymbol{\theta}_l$ and $\boldsymbol{\theta}_M$ as well as the weight vector of the most recent split $\boldsymbol{\psi}_{M-1}$, must not depend on a random variables.

The incremental model construction allows a proper initialisation of these parameters: The weight vector $\boldsymbol{\psi}_{M-1}$ of new node is chosen based on the weighted mean and the weighted covariance matrix of the observations with respect to the worst local model. The initialisation of the local model parameters $\boldsymbol{\theta}_l$ and $\boldsymbol{\theta}_M$ is then based on the conventional weighted least squares algorithm.

IV. Example

In order to demonstrate the capabilities of the proposed evolving model tree construction scheme the online training of a complex *dynamic* nonlinear local model network using real measurement data from a state-of-the-art 4-cylinder EURO5 diesel engine is presented.

The inputs into the system are *engine speed* N [rpm] and *main injection mass* Q [mg/stroke]. Exemplarily, the *turbine speed* N_{Turbo} [rpm] is considered as the system output $y(k)$. Accordingly, the input-output dynamics are described by the nonlinear difference equation

$$N_{Turbo}(k) = f\left(\boldsymbol{x}(k)\right)$$

where the dynamic regressor vector in (1) is made up according to

$$\boldsymbol{x}(k) = \begin{bmatrix} 1 \\ Q(k-1) \\ \vdots \\ Q(k-m) \\ N(k-1) \\ \vdots \\ N(k-m) \\ N_{Turbo}(k-1) \\ \vdots \\ N_{Turbo}(k-m) \end{bmatrix}.$$

The dynamic system order for the local models is chosen as $m = 3$.

The dynamic input and output data are depicted in Fig. 5. All in all 5000 data samples are available for the training of the local model network. Here, amplitude modulated pseudo random binary (APRB) signals are used for the input signals in order to ensure proper excitation of the system, see e. g. [6],

[23]. The bandwidth of the input signals is defined by their minimum and maximum hold times which are chosen in consideration of the expected system dynamics.

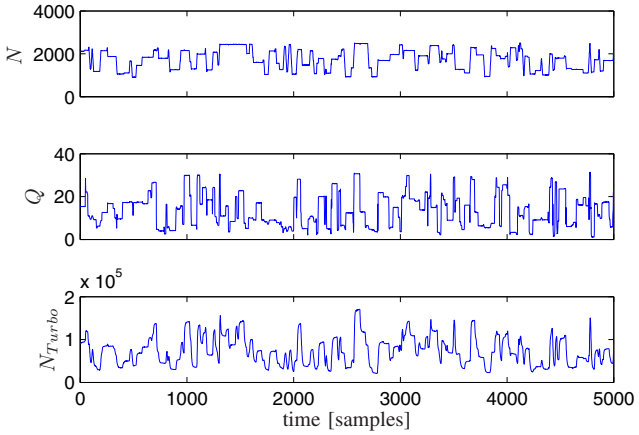

Fig. 5. Measured input and output data

The *initial* local model network with two local models is constructed using the first 1000 samples, see Fig. 6. The partition space is spanned by $N(k-1)$ and $Q(k-1)$ which are the main influence parameters on the highly nonlinear behaviour of the engine. In Fig. 6 a contour plot of the membership functions indicates the region of validity of the two local models. The trajectory of the initial data record is depicted in grey.

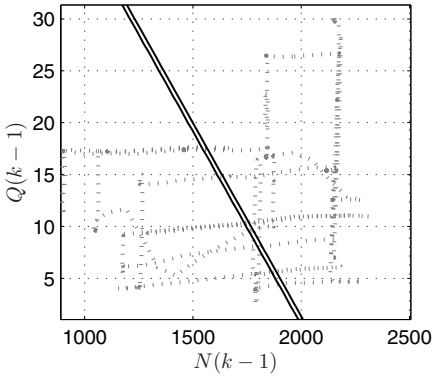

Fig. 6. Initial engine model with 1000 samples

In Fig. 7 the evolvement of the first two local models during the online training procedure is illustrated, c. f. Fig. 6. The validity functions (black) are continuously adapted to the growing data base using the online optimisation algorithm from section III-A. The lower plot in Fig. 7 illustrates how the estimated variances $\sigma^2_{e_i}$ of the two local models evolve as the number of data and the operating range of the LMN increase. Obviously, the estimated variance of the second local model exceeds the upper bound of the χ^2 distribution at some stage. According to section III-B, the second local model is then replaced by two new models in the next iteration step. Their validity functions are indicated by the dashed black contour lines.

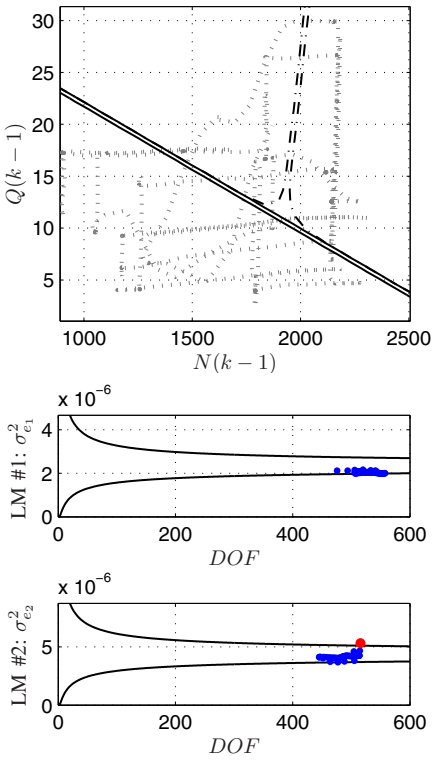

Fig. 7. Online training: Validity functions and χ^2 criterion

The sample-wise online training of the evolving local model tree using the χ^2 splitting rule from section III-B with $\alpha = 1\%$ results in a local model network with seven local models. The final model with the shape and extent of each validity function (black) as well as the training data record (grey) are shown in Fig. 8.

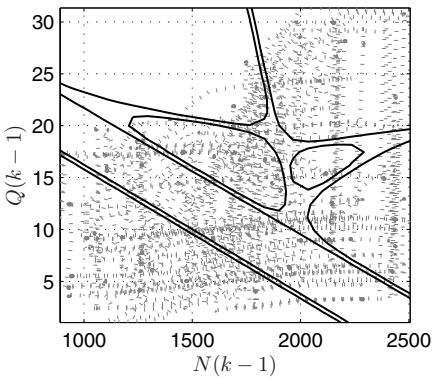

Fig. 8. Final model with 5000 samples and 7 local models

The performance of the local model network obtained from online training is highlighted using a dynamic generalisation data record. In Fig. 9 a section of the measured output and the simulated model output are compared. It is clearly visible that

the LMN accurately describes the nonlinear behaviour of the engine throughout the operating range of the engine.

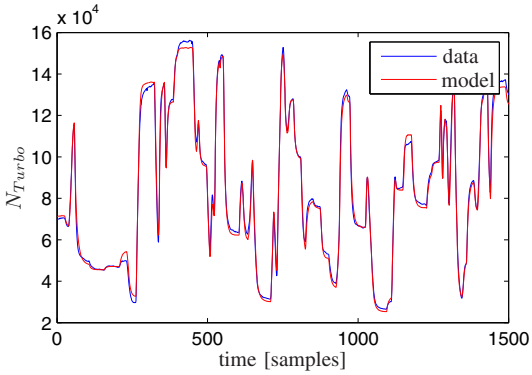

Fig. 9. Simulated model output using generalisation data

In table I the performance of the models obtained from the evolving online training and the classic batch algorithm is indicated by means of the R^2 statistics

$$R^2 = 1 - \frac{\sum_{k=1}^{N} (y(k) - \hat{y}(k))^2}{\sum_{k=1}^{N} (y(k) - \bar{y})^2}, \qquad (13)$$

where $\bar{y}$ is the mean value of all $y(k)$.

TABLE I
COMPARISON OF ONLINE AND OFFLINE TRAINING

	online training	offline training
R^2	0.99277	0.99353

V. CONCLUSION AND OUTLOOK

In this paper an evolving local model network concept especially suited for engine modelling is presented. Especially in dynamic system identification the computational speed is an important requirement for online training. The incremental model construction allows a proper initialisation of the model parameters in order to increase the robustness while the computational demand is low. A new evolving optimisation algorithm for the online training of the local model network is proposed where the particular choice of the cost function for the split optimisation aims at obtaining locally interpretable models.

A statistically motivated splitting rule is proposed in order to automatically detect when an extension of the model structure is reasonable.

The practical applicability of the evolving local model network is validated by means of real dynamic measurement data from a state-of-the-art 4-cylinder diesel engine.

ACKNOWLEDGEMENTS

This work was supported by the Christian Doppler Research Association and AVL List GmbH, Graz.

REFERENCES

[1] E. Lughofer, "FLEXFIS: A Robust Incremental Learning Approach for Evolving Takagi-Sugeno Fuzzy Models," *Fuzzy Systems, IEEE Transactions on*, vol. 16, no. 6, pp. 1393 –1410, dec. 2008.

[2] P. Angelov and D. Filev, "An approach to online identification of takagi-sugeno fuzzy models," *Systems, Man, and Cybernetics, Part B: Cybernetics, IEEE Transactions on*, vol. 34, no. 1, pp. 484 – 498, feb. 2004.

[3] N. Kasabov and Q. Song, "Denfis: dynamic evolving neural-fuzzy inference system and its application for time-series prediction," *Fuzzy Systems, IEEE Transactions on*, vol. 10, no. 2, pp. 144 –154, apr 2002.

[4] P. Angelov and X. Zhou, "Evolving fuzzy systems from data streams in real-time," in *Evolving Fuzzy Systems, 2006 International Symposium on*, sept. 2006, pp. 29 –35.

[5] L. Ljung, "Perspectives on system identification," *Proceedings of the 17th IFAC World Congress*, 2008.

[6] O. Nelles, *Nonlinear System Identification*, 1st ed. Springer Verlag, 2002.

[7] M. Hafner, M. Schler, O. Nelles, and R. Isermann, "Fast neural networks for diesel engine control design," *Control Engineering Practice*, vol. 8, no. 11, pp. 1211 – 1221, 2000.

[8] R. Murray-Smith and T. A. Johansen, *Multiple Model Approaches to Modelling and Control*. Taylor & Francis, 1997.

[9] J. Abonyi and R. Babuska, "Local and global identification and interpretation of parameters in takagi-sugeno fuzzy models," in *Fuzzy Systems, 2000. FUZZ IEEE 2000. The Ninth IEEE International Conference on*, vol. 2, 2000, pp. 835 –840 vol.2.

[10] T. A. Johansen, R. Shorten, and R. Murray-Smith, "On the Interpretation and Identification of Dynamic Takagi-Sugeno Fuzzy Models," *IEEE Transactions on Fuzzy Systems*, vol. 8, no. 3, pp. 297–313, 2000.

[11] P. Angelov, V. Giglio, C. Guardiola, E. Lughofer, and J. M. Lujan, "An approach to model-based fault detection in industrial measurement systems with application to engine test benches," *Measurement Science and Technology*, vol. 17, no. 7, p. 1809, 2006. [Online]. Available: http://stacks.iop.org/0957-0233/17/i=7/a=020

[12] L. Pronzato, "Optimal experimental design and some related control problems," *Automatica*, vol. 44, no. 2, pp. 303–325, 2008.

[13] G. Franceschini and S. Macchietto, "Model-based design of experiments for parameter precision: State of the art," *Chemical Engineering Science*, vol. 63, no. 19, pp. 4846–4872, 2008.

[14] C. Hametner and S. Jakubek, "Neuro-fuzzy modelling using a logistic discriminant tree," *American Control Conference, 2007. ACC '07*, pp. 864–869, July 2007.

[15] L. Breiman, J. Friedman, R. Olshen, and C. Stone, *Classification and Regression Trees*. Monterey, CA: Wadsworth and Brooks, 1984.

[16] D. Potts and C. Sammut, "Online nonlinear system identification using linear model trees," in *Proceedings of the 16th IFAC World Congress*, 2005.

[17] O. Nelles, "Local linear model trees for on-line identification of time-variant nonlinear dynamic systems," in *Artificial Neural Networks ICANN 96*, ser. Lecture Notes in Computer Science, C. von der Malsburg, W. von Seelen, J. Vorbrggen, and B. Sendhoff, Eds. Springer Berlin / Heidelberg, 1996, vol. 1112, pp. 115–120.

[18] C. M. Bishop, *Neural networks for pattern recognition*. USA: Oxford University Press, 1995.

[19] P. Pucar and M. Millnert, "Smooth hinging hyperplanes - an alternative to neural networks," in *Proceedings of the 3rd ECC*, 1995.

[20] L. Ngia, J. Sjoberg, and M. Viberg, "Adaptive neural nets filter using a recursive levenberg-marquardt search direction," in *Signals, Systems Computers, 1998. Conference Record of the Thirty-Second Asilomar Conference on*, vol. 1, Nov. 1998, pp. 697 –701 vol.1.

[21] R. Babuska, *Fuzzy Modeling for Control*. Norwell, MA, USA: Kluwer Academic Publishers, 1998.

[22] N. R. Draper and H. Smith, *Applied Regression Analysis*, 3rd ed., ser. Wiley Series in Probability and Statistics. John Wiley & Sons, 1998.

[23] R. Isermann, *Identifikation dynamischer Systeme 2*, 2nd ed. Springer Verlag, 1992.

2011 IEEE International Conference on Fuzzy Systems
June 27-30, 2011, Taipei, Taiwan

Rough Set Approach to User Modeling

Binghui Helen Wu
FS Consulting
Wichita, Kansas
Swhelen21@hotmail.com

***Abstract*—The intelligence of an interactive system is exhibited through the evolution of its intelligent behaviors, namely, its effectiveness in performing tasks and its adaptiveness to both variations of task conditions and different users. Having a good user modeling component in any intelligent interactive system becomes crucial to the performance of that system. We have developed a computational approach to building intelligent tutoring systems (ITS) in conjunction with our framework for ITS [1]. This computational approach employs two exploratory AI techniques—a hybrid knowledge representation model as an implementation mechanism of ITS and a rough set [2] approximation approach to user modeling. In this article, we focus on discussing the rough set approach to user modeling of the system in detail.**

Keywords-rough sets; user modeling; computational approach to knowledge representations; intelligent tutoring systems

I. INTRODUCTION

Research in building intelligent computer assisted learning environments (more often known as intelligent tutoring systems, ITS) has been ongoing for more than 20-25 years. Existing ITS research, including well-known tutoring systems such as Clancey's GUIDON and its revision [3], Anderson's ACT Tutors [4], Johnson's PROUST [5], and many others, have shown that the key feature of tutoring systems is their ability to diagnose students' misconceptions in learning during a tutoring process and, based upon those diagnoses, to provide students with remedial learning. However, many psychological questions underlying learning, teaching and understanding have not received convincing answers. In addition, enormous difficulties in creating a precise machine representation of the students' learning stages and in identifying students' possible misconceptions lend to a diversification of ITS research. Many urged the importance of evaluation of such systems, for example, the special issue on evaluation in IJ. of Artificial intelligence in Education (1993) 4(2/3).

In spite of difficulties in existing ITS research, we believe that tutoring by computers is an attractive alternative to human tutors in providing assistance, both to instructors who are responsible for students' learning and to individual students who are supposed to learn the subject to be taught, especially when human tutors are not available or not willing to spend more time. In fact, one study has shown [6], tutoring by a human instructor–a one-on-one help session to improve an individual student's learning—is more effective than that in a classroom instruction setting.

Aiming at building an effective tutoring system, which is as adaptable to different students and instructors as possible, we have proposed a framework (ATA, i.e., Artificial Teaching Assistant) for ITS [1] based on the constructivist theory of knowledge, learning, and understanding. Constructivism is a model of how learning takes place. It has drawn considerable attention among science education researchers and ITS researchers who aim at building computer based learning environment [7] [8] [9]. In the constructivist view, learning is an active process of constructing a conceptual framework. Although sharing the basic view of learning, different interpretations of this view result in different approaches to science education. Our understanding of constructivist theory is based on Cobern's interpretation [10], in which our ATA framework for ITS reflects.

This ATA framework consists of three models—presentation, question, and test models—attempting to capture the two most important aspects of a tutoring process. One of the two aspects is how the presented knowledge is organized, so that it can be presented automatically and effectively. The other is how questions and tests are to be given to ensure that students have developed a meaningful interpretation of the presented knowledge and can apply it to solve related problems. To exemplify our ATA framework for ITS, we have been implementing a prototyped tutoring system with number systems, a topic in Foundations of Computer Science [11], as its domain. A systematic approach has been developed for the implementation. In this paper, we first give an overview of our computational approach to building ITS, in which a hybrid knowledge representation model (SG, i.e., Graph-Sets) provides both an automated presentation process of domain knowledge and automated interpretation of student learning and/or understanding of the presented knowledge. Then, we present a novel approach to user modeling—rough set approximation—that we have used in the user modeling component of the implementation of our tutoring system.

II. OVERVIEW OF OUR COMPUTATIONAL APPROACH TO ITS

Our hybrid representation model (GS model), which mixes two levels of knowledge representation schemes, subject network—a fully connected, directed, and acyclic graph with a semantic interpretation and "knowledge base"—a two tuple, a universal discourse and a class of relations imposed on the universal set. There are two types of knowledge possessed by the paradigm of our tutoring system: the knowledge of the subject materials to be represented and the knowledge of how to make an effective presentation dynamically based on various student responses during tutoring so that the quality of tutoring can be ensured. Based on these, we use a variation of semantic networks (named subject network), as the coarse grain of representation of domain knowledge; and we use "knowledge base" (coined by Pawlak, see the chapter in [2]), as the fine grain representation of the domain knowledge.

978-1-4244-7316-8/11/$26.00 ©2011 IEEE

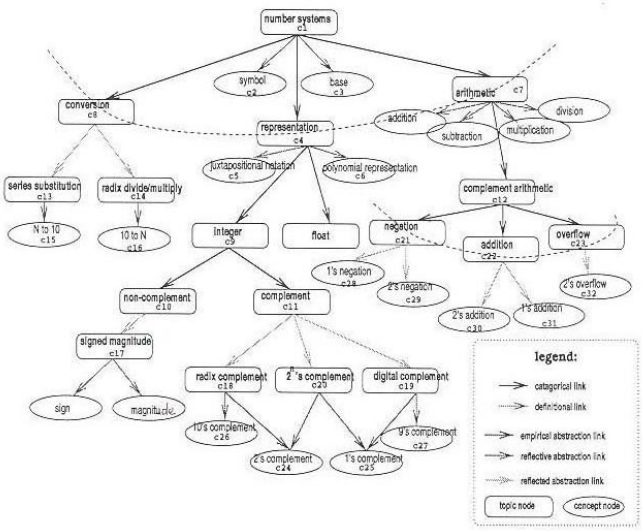

Figure 1: An Example to illustrate the ATA representation model of our framework for ITS (see Appendix for a clear version)

A. Knowledge Representation Scheme I: Subject Network

In semantic networks, knowledge is represented in terms of nodes, which can represent objects, and are connected by links that represent the interrelations among nodes. This graphical form of knowledge representation is most appealing and has long been used in AI systems including ITS [12] [13]. In the context of our tutoring system where abstract knowledge has been chosen as the domain of tutoring materials, naturally, we have adopted this knowledge representation scheme. However, there are two important features that have distinguished our way of using this scheme.

First, as shown in Figure 1, there are two different kinds of nodes: topic and concept, in which knowledge of the subject material has been stored. There are also two kinds of links to capture two kinds of relations among nodes: inclusion and dependency. An inclusion link describes the relation between two nodes in which the destination node always elaborates its source node (i.e., is a subtopic of the topic represented in the source node). On the other hand, a dependency link describes a dependency relation between two nodes with two possibilities. If a topic node depends on a concept node, the concept is used to define the topic node; and, if a dependency link exists between two topic nodes, the source node would be the prerequisite topic of the destination node. For example (see Figure 1), the topic, *number systems*, can be defined using concepts, *symbol* and *base* (dependency) and can be elaborated with subtopics, *representation*, *arithmetic*, and conversion of numbers with different bases (inclusion). Further, in our number systems example, in order to introduce the subtopic *conversion* (between numbers with different bases), we need to have introduced how a number is represented (*representation*). Therefore, the relation between number representation and number conversion is a dependency relation. Also, note that both topic and concept nodes are used to store knowledge in a subject network; they are both literally concepts. The difference between the two, besides their names, is that the concept in a concept node in a subject network is atomic in the sense that it doesn't need to be further elaborated. Therefore, concept nodes are minimal elements of subject graphs.

Second, in addition to the nodes and links described above, special kinds of nodes depicted in the dashed notations and named supplementary nodes, are utilized in the subject graph to represent supplementary material as options for students who desire to know more and learn further about the subject. A supplementary node may be either a topic or concept node. Continuing with our example, since the subtopic conversion mainly provides a better understanding of numbers, it may not be necessary to teach this subtopic if we present the topic, number systems, in connection with digital computers. Thus, we define the subtopic as a supplementary material to students' learning of number systems.

Overall, the knowledge representation scheme described above provides not only a way of establishing a network of subject material, but also an automatic presentation procedure: that is, an automatic scheme for traversing nodes by following links which may be optionally set by a user (an instructor). Now the problem left to be investigated is how can we ensure that a student is learning while following through a presentation? We believe that the behaviorist instructional teaching [14] can be effective. Specifically, we use Gagne's nine-significant-event model—recursively utilizing the nine events while instructing: gaining learner's attention, informing learner of objectives, stimulating the recall of prerequisites, presenting stimuli, providing guidance, eliciting performance, providing feedback, assessing performance, and enhancing retention and transfer. Overall, we ask questions while presenting materials and give exercise problems as homework so that we can assess students' performance in their learning. Then, the question is how can we implement this kind of tutoring so that our system can do it effectively?

B. Knowledge Representation Scheme II: Knowledge Base

Pawlak has proposed a formal definition of knowledge in terms of Knowledge Base and its basic property [2]. Directly motivated by his understanding and formalization of "knowledge" and "concepts," we employ his set notations, known as Knowledge Base, as a fine grain representation of the presented knowledge in tutoring systems.

In our representation, concepts in a subject network of a tutoring system used to evaluate students' learning are encoded in questions and problems, which are accessed through interactions between students and the system during tutoring. That is, those of concepts are used for questioning and testing students, and evaluating students' answers. For instance, in our number systems example, there are about 35 concepts, including 11 supplementary concepts used for testing and evaluating students' learning of the subject material; and there are about 50 questions and problems that have been stored in the associated database of the tutoring system, which may be

assigned to students as exercises, where each problem embeds several concepts among the fifty. In general, let

$$C=\{c_1, c_2, \cdots, c_n\} \quad (1)$$

be the set of n concepts that are presented in a subject network. Further, let there be m problems in the problem set

$$P=\{p_1, p_2, \cdots, p_m\} \quad (2)$$

that have included these n concepts in the subject network. One way of representing such knowledge is to use n by m matrix as the following.

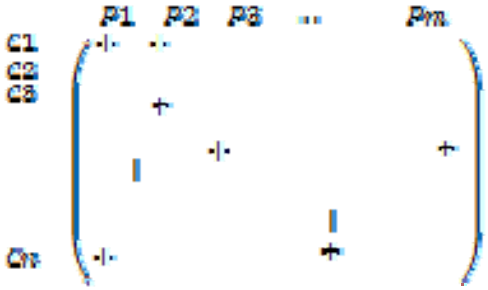

In this matrix, a cell is checked means that the concept identified by the row of that cell is embedded in the problem identified by the column of that cell. Further, a student's answer to the problem can be checked against these concepts. We then keep track of students' answers to problems, which should be a reflection of their understanding of those concepts.

Although we have found a method to represent subject material (the use of GS-model) and student learning stages (eliciting performance of student's learning of each concept) mechanically and to test and evaluate students' learning through their answering questions and solving problems, there are many possible kinds of uncertainties inherent in this paradigm of tutoring.

III. User Modeling to Cope with Uncertainties

We have identified two kinds of uncertainties, namely, vagueness and incomplete information. Vagueness may exist in the methods of evaluating students' answers and in the answers that students give to problems. First, as to the methods of evaluating students' answers, it is likely that relations between concepts may not be simple, but instead, hierarchical. For example, in the subject domain of our tutoring system, complement is an important number representation in digital computers, which provides uniform computation for arithmetic operations of both positive and negative numbers. There are two variations of this representation, radix and digit complements. Complement, radix complement, and digit complement are considered to be different concepts in our representation model. Obviously, they are closely related. That is, one's understanding of radix complement may imply his understanding of complement and partial understanding of digit complement. Generally depending on how an instructor would view these related concepts, the subject material in a tutoring system could be rearranged with significant differences, so can problems to test students' mastery level to those concepts.

Second, as to the students' answer, again according to the behaviorist model of understanding students' learning, if a students' answer to a problem is incorrect, generally, we infer that the student has not yet mastered the concept(s) that the problem tries to test. However, the information on the cause of students' wrong answers is somewhat incomplete (perhaps, it would be impossible to obtain it fully), and may result from students' psychological factors, their mental states during a tutoring session. Simply presenting the tutoring material again to students may not be an effective remedial learning. Instead, testing students with more problems and approximating their answers could be a better solution. This means that more flexible ways of evaluating students' answers may be desirable or even necessary.

Motivated by seeking how to build an accurate user model, we have explored the rough set formalism and adopted it in the user-modeling component of our tutoring system to compensate for these uncertainties.

A. The Rough Set Approximation

Pawlak has succinctly described [15]:

"In the rough set theory each vague concept is replaced by a pair of precise concepts called its lower and upper approximations; the lower approximation of a concept consists of all objects which surely belong to the concept, whereas the upper approximation of the concept consists of all objects which possibly belong to the concept." (p. 73 in [2])

Corresponding to his description of vague concept, we have here the vagueness of evaluating students' learning and the vagueness of understanding of the relations between concepts depending upon instructors' preference.

Formally, let U be a set of universe of discourse (called universe); let **R** be a set of equivalence relations imposed on the universe U.

The Knowledge Base K is defined as K = (U, **R**); and the concept X in K is defined as a subset of U, i.e., $X \subseteq U$.

Further, the upper approximation of the concept X in K under a given equivalence relation **R** is defined as

$$\overline{X_R} = \{\, x : [x]_R \cap X \neq 0 \,\} \quad (3)$$

and the lower approximation of the concept X is defined as

$$\underline{X_R} = \{ x : [x]_R \subseteq X \} \quad (4)$$

Here $[x]_R$ represents the equivalence class of x under the given relation R. If $\overline{X}_R = \underline{X}_R$, then the concept X is considered to be precise; otherwise, we say the concept is vague. For a vague concept, these two approximations under the given relation in the Knowledge Base K can be calculated and obtained.

For example, as we have previously written, let (1) be the set of n concepts that are presented in a subject network. An interrelationship among concepts can be expressed as an equivalence relation (a partition). Then, there are many

possible partitions to form equivalence classes on the set C. Further, because there are m problems in the problem set (2) that have included these n concepts in the subject network, there should be various combinations for an instructor to assign a student problems according to the instructor's preference (expressed in his way of partitioning concepts in the subject network) and using this partition, problems are assigned. Further, an evaluation of the students' answers involving each concept can be obtained. Among the possible answers that a student may give, an evaluation based on the rough set approximation may be performed.

In our tutoring system, specifically, in one of the subject networks of the tutoring system, we can presumably represent all concepts that we would like students to learn with the possibility of varying granularity level of each node; and we also can select sufficient problems to embed these concepts, and for students to solve. Formally, let Pi be a subset of the problem set P, that is,

$$P = \cup P_i,\ i \in 1,2,\cdots,m \tag{5}$$

in the subject network. Let C_i be a subset of the concept set C, that is,

$$C = \cup C_i,\ i \in 1,2,\cdots,n \tag{6}$$

in the subject network. We can impose relations between P and C functionally as

$$f_{P_i} : P_i \to C \text{ where } i \in 1,2,\cdots,l \tag{7}$$

and each of these l functions is subjective; and

$$f_{C_i} : C_i \to P \text{ where } i \in 1,2,\cdots,k\ ; \tag{8}$$

and it (f_{C_i}) indicates that, given a group of concepts, a corresponding set of problems can be selected to test students' learning of this group of concepts. PC (Note that $P_i \in 2^P$ and $C_i \in 2^C$.) Providing the mechanism based on the rough set theory, our system allows instructors to group concepts (C_i) and to select problems (P_i) differently so that the evaluation of students' answers to problems can vary according to instructors' preferences. Our objective here is to find good selection algorithms such that the vagueness in ensuring and evaluating students' learning in the tutoring processes will be minimized.

B. Comparison with Other Approximation Approaches

Katz et al.[16] have proposed using fuzzy probabilistic variables to measure performance conditions when students are learning with their tutoring system. More recently, Kavcic [19] has conjectured with fuzzy and probabilistic user modeling. In fact, probability theory [17] and fuzzy set theory [18] are popularly used in approximate reasoning. However, the advantage of the rough set approximation over these two in our case is that the numerical value of imprecision is calculated according to a pre-defined formula which is based on the fundamental concepts used to express imprecision of knowledge. For example, Pawlak has proposed one numerical calculation of the rough set imprecision, namely,

$$a_R = \frac{card\ \underline{R}}{card\ \overline{R}} \tag{9}$$

where card denotes the cardinality of sets ($\overline{R}$ or $\underline{R}$). To illustrate this point, we use a simple example as follows. Let there be 10 concepts that have been chosen to be presented to students. One instructor may partition these 10 concepts as

$$[c_1]_R = \{c_1, c_2, c_3\ \}, \tag{10}$$

$$[c_4]_R = \{\ c_4, c_5\ \}, \tag{11}$$

$$[c_6]_R = \{\ c_6\ \}, \tag{12}$$

$$[c_7]_R = \{\ c_7, c_8\ \}, \tag{13}$$

$$[c_9]_R = \{\ c_9, c_{10}\ \}, \tag{14}$$

That means that concepts in the same equivalent class are substitutable. Suppose one student has mastered the following concepts:

$$\{c_1, c_2, c_4, c_6, c_7, c_9, c_{10}\ \}; \tag{15}$$

Then the upper approximation of his performance under the given relation is

$$\{c_1, c_2, c_3, c_4, c_5, c_6, c_7, c_8, c_9, c_{10}\ \}; \tag{16}$$

while the lower approximation of his performance is

$$\{c_6, c_9, c_{10}\ \} \tag{17}$$

Consequently, the accuracy using Pawlak's calculation would be $2/5$. On the other hand, the fuzzy probability variables in [16] are obtained by expert estimations without a predefined membership function. As a result, the inconsistency of human performance would bias the approximation processes inevitably.

IV. CONCLUSION AND FURTHER INDICATION

We have developed the rough set approach to user modeling under our ATA framework for ITS and our hybrid knowledge representation model (GS model) and implemented it in the user modeling component of our tutoring system. Theoretically, our development approaches are based on the constructivist understanding of scientific knowledge [9] [10] and the constructivist view of learning mathematical knowledge [8]. After we have formulated our hybrid representation model (GS model), the rough set approximation

fits well in the implementation of our tutoring system. As we have briefly described, under the ATA framework, GS model provides an automated presentation mechanism (both initial and remedial presentations). Thus, the rough set approach can be used on top of the model to make the tutoring process more adaptable.

Our intention has been using exploratory AI approaches to build a tutoring system with observable intelligent behavior in its performance. Other important factors confronted in our implementation have been interface design issues. These issues may contribute to user modeling, and could be crucial to the performance of our system as well. As we have tried to show in this article, our automation mechanism is based on the high consensus approach—i.e., providing questions with multiple choices, and exercises that have solutions with well-defined steps— in evaluating students' learning. Wasilewska has recently formulated Knowledge Systems [20] based on Pawlak's Knowledge base in the context of data mining. It can also be applied to the user modeling component of our ITS. We strongly believe that with these exploratory AI approaches—i.e., the hybrid representation model and the rough set approximation—our tutoring system has had a lot to offer to ITS developers and will have a significant potential in the development of ITS.

ACKNOWLEDGMENT

Thanks to the Electrical Engineering and Computer Science Department of Lehigh University for the financial support of this work. Thanks also to T. Boult and G. Blank, associate professors of EECS Department of Lehigh University for their support, especially for providing criticism on this work.

APPENDIX

Figure 1 in large size

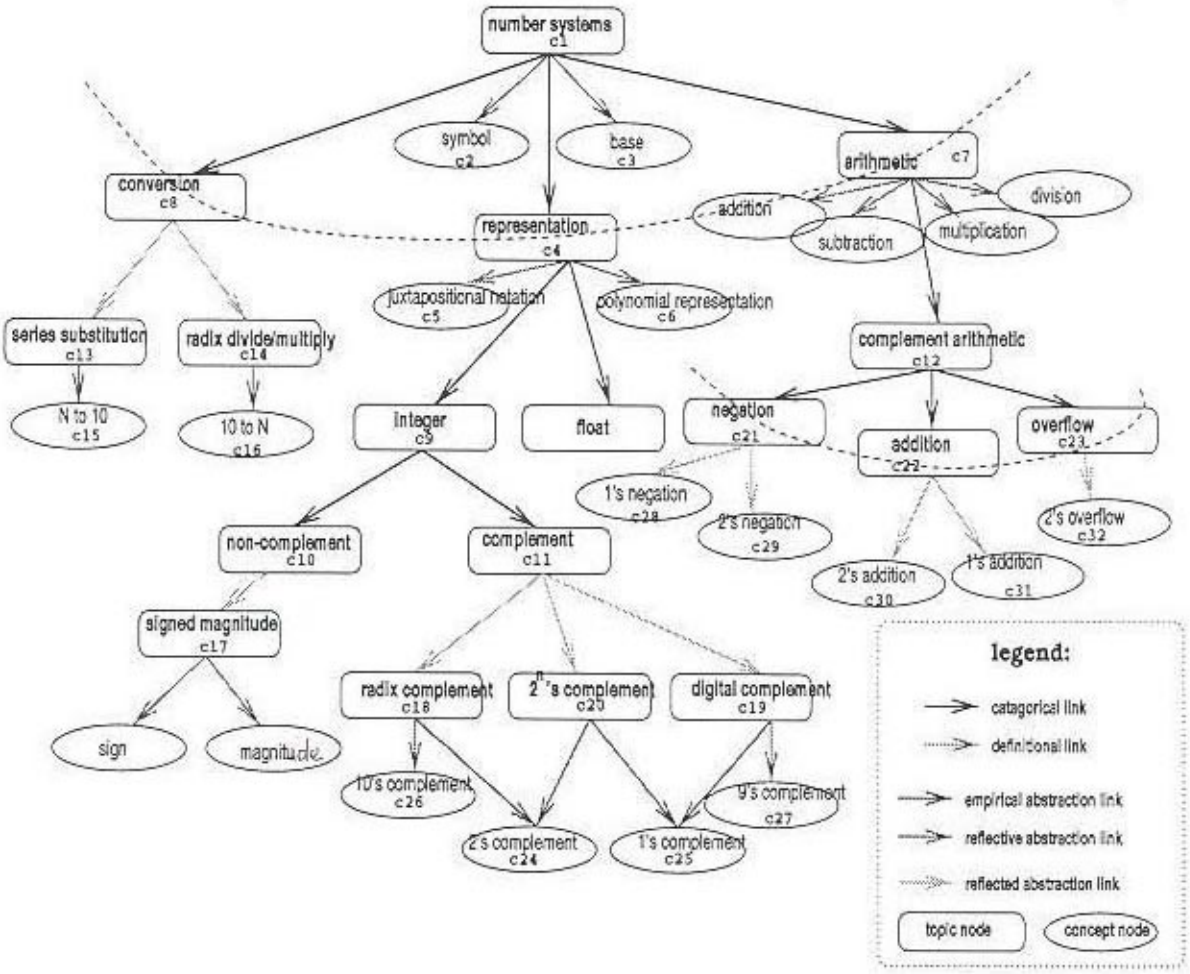

REFERENCES

[1] Binghui Helen Wu. A framework for intelligent tutoring systems. In The 7th World Conference on Artificial Intelligent in Education (AI-ED 95), page 599. AACE and GMU, Aug. 1995.

[2] Zdzislaw Pawlak. Rough Sets: Theoretical Aspects of Reasoning about Data. Kluwer Academic, The Netherlands, 1991.

[3] William J. Clancey. Guidon-manage revisited: A socio-technical systems approach. JI. of Artificial Intelligence in Education, vol.4, no. 1 p5-34, 1993.

[4] John R. Anderson. Cognitive tutors: Lessons learned. In The 4th International Conference on User Modeling, page 71. MITRE Corp., Aug. 1994.

[5] W. Lewis Johnson. Understanding and debugging novice programs. Artificial Intelligence, vol. 42, p51-97, 1990.

[6] John R. Anderson and Brian J. Reiser. The lisp tutor. BYTE, vol. 4, p159-175, 1985.

[7] Warren Sack, Elliot Soloway, and Peri Weingrad. Re: Writing Cartesian student models. JI. of Artificial Intelligence in Education, vol. 3, no. 4, p381-399, 1992..

[8] Paul Cobb, Erna Yackel, and Terry Wood. A constructivist alternative to the representational view of mind in mathematics education. Journal for Research in Mathematics Education, vol. 4, no.1,p2-33, 1992.

[9] John P. Smith, Andrea A. diSessa, and Jeremy Roschelle. Misconceptions reconceived: A constructivist analysis of knowledge in transition. The Journal of the Learning Sciences, vol. 3, no. 2, p115-164, 1993/94.

[10] J. William W. Cobern. Constructivism. Journal of Educational and Psychological Consultation, vol. 4, no.1, p105-112, 1993.

[11] Alfred V. Aho; Jeffrey D. Ullman. Foundations of Computer Science. Computer Science Press, an Imprint of W. H. Freeman and Company, New York, 1992.

[12] Renee Elio and Peternela B. Scharf. Modeling novice-to-expert shifts in problem solving strategy and knowledge organization. Cognitive Science, vol. 14, no.4,p 579-639, 1990..

[13] Denise Whitson Gurer. A Bi-level Physics Student Diagnostic Utilizing Cognitive Models for an Intelligent Tutoring System. PhD thesis, Lehigh University, Aug. 1993.

[14] Robert M. Gagne, Leslie J. Briggs, and Walter W. Wager. Principles of Instructional Design. Harcourt Brace Jovanovich College Publishers, Orlando, Fl, 1992.

[15] Zdzislaw Pawlak. Rough sets present state and further prospects. In The Third International Workshop on Rough Set and Soft Computing (RSSC '94), pages 72-76. AAAI, EPRI, IAMCS, ISF, IEEE, and SJSU, Nov. 1994

[16] Sandra Katz, Alan Lesgold, Fary Eggan, and Maria Gordin. Modelling the student in sherlock ii. JI. of Artificial Intelligence in Education, vol. 3, no.4,p 495-518, 1992..

[17] P. Cheeseman. In defense of probability. In Proceedings IJCAI-85, 1985.

[18] L.A. Zadeh. A theory of approximate reasoning. In Machine Intelligence. Halstead Press, New York, 1979

[19] Alenka Kavcic. Fuzzy User Modeling for Adaptation in Educational Hypermedia. IEEE Transactions on Systems, Man, and Cybernetics—Part C: Applications and Reviews, vol. 34, no. 4, November 2004

[20] Anita Wasiewska. Descriptive Granularity. 2010 IEEE International Conference on Granular Computing, San Jose, California, 14-16 August 2011

2011 IEEE International Conference on Fuzzy Systems
June 27-30, 2011, Taipei, Taiwan

A Rough-based Robust Support Vector Regression Network for Function Approximation

Chih-Ching Hsiao
Department of Electrical Engineering
Kao Yuan University
Kaohsiung City, Taiwan, R.O.C
t20051@cc.kyu.edu.tw

Shun-Feng Su, *Fellow*, *IEEE*
Department of Electrical Engineering
National Taiwan University of Science and Technology
Taipei City, Taiwan, R.O.C
sfsu@mail.ntust.edu.tw

Chen-Chia Chuang
Department of Electrical Engineering,
National Ilan University
I-Lan County, Taiwan, ROC
ccchuang@niu.edu.tw

***Abstract*—Support vector regression (SVR) employs the support vector machine (SVM) to tackle problems of function approximation and regression estimation. SVR has been shown to have good robust properties against noise. Besides, in SVR, outliers may also possibly be taken as support vectors. Such an inclusion of outliers in support vectors may lead to seriously overfitting phenomena. The rough set theory is successes to deal with imprecise, incomplete or uncertain for information system. In this paper, a novel regression approach, termed as the Rough Margin Support Vector Regression (RMSVR) network, is proposed to enhance the robust capability of SVR. The basic idea of the approach is to adopt the concept of rough sets to construct the model obtained by SVR and fine tune it with a robust learning algorithm. Simulation results of the proposed approach have shown the effectiveness of the approximated function in discriminating against outliers.**

Keywords-support vector regression(SVR); outlier; rough sets; robust learning

I. INTRODUCTION

The support vector machine (SVM) is a universal approach for solving the problems of multidimensional function estimation. Those approaches are all based on the Vapnik–Chervonenkis (VC) theory [1-2]. When SVM is employed to tackle the problems of function approximation and regression estimation, the approaches are often referred to as the support vector regression (SVR) [3]. The SVR type of function approximation is very effective, especially for the case of having a high-dimensional input space. Another important advantage for using SVR in function approximation is that the number of free parameters in the function approximation scheme is equal to the number of support vectors. Such a number can be obtained by defining the width of a tolerance band. Thus, the selection of the number of free parameters can be directly related to the approximation accuracy and does not have to depend on the dimensionality of the input space or other factors as that in the cases of multilayer feedforward neural networks.

Outliers may occur due to various reasons, such as erroneous measurements or noisy phenomenon appearing in the tail portion of some noise distribution functions. When the obtained observations contain noise or outliers, the learning process being unaware of those situations may try to fit those unwanted data and this behavior may lead to a corrupted approximation function. This phenomenon is often called overfitting [4-5]. In [6], SVR has been shown to have better robust properties for various signal-to-noise ratios. In [7], SVR has also been shown to have excellent performance for both the ε -insensitive function and Huber's robust function matching the correct type of noise in an application of time series prediction. Besides, a general cost function for SVR has also been proposed in considering error distributions [8]. In [9], the SVM with weighted least square (LS-SVM) is proposed to overcome the effects of outliers. However, when the parameters in those approaches are not properly chosen, the final results may be affected by its parameters. This property has also been mentioned in [9]. The selection of parameters in SVR is not straightforward. In [10], a robust SVR (RSVR) network is proposed to enhance the robust capability of SVR. The basic idea of the approach is to adopt the concept of traditional robust statistics to fine tune the model obtained by SVR.

In the last two decades, rough sets and fuzzy sets turned out to be two contemporary progresses in analyzing inexact, imprecise, uncertain, or vague knowledge. The former captures the distinct aspect of indiscernibility in knowledge, while the latter describes the inherent feature of vagueness in linguistics and decision-making. The rough set theory proposed by Pawlak [11-12] is a mathematical theory dealing with uncertainty in data. Rough sets rely on the notion of lower and upper approximations of a set and are applied to rough fuzzy control [13], modeling, system identification[14] , discovery of discussion rules from experimental data [15] and clustering [16-17]. Recently, combining both rough and SVM [18-24], Lingras [19] proposed a rough set approach to SVM classification removes the necessity of exact classification and is especially useful when dealing with noisy data. By utilizing the boundary region in rough sets shorten the training time and reduced storage requirements compared to the conventional techniques. In [20] proposed a so-call RST–SVM, the redundant attributes in multi-attribute information table can be reduced by RST approach, is utilized as a preprocessor to improve business failure prediction capability by SVM. Asharaf [18] incorporates rough set theoretic flavor in support vector clustering paradigm to achieve soft clustering. The user-defined parameters allow to control the extent of softness by controlling the width of boundary region and number of outliers. Chen [21] proposed fuzzy transitive kernels based fuzzy rough sets, and then reformulated hard margin support vector machines into fuzzy rough set based SVMs (FRSVMs)

978-1-4244-7316-8/11/$26.00 ©2011 IEEE

with new constraints in which the memberships are taken into account. It has certain capacity to deal with noise. In [22], a called rough support vector regression (RSVR), is proposed to improve the modeling of rough patterns. rough insensitive loss function by applying separate SVR for patterns of lower and upper values. The main advantage of rough-SVR was that it almost never over-predicted the upper values. Based on *v*-SVM(SVR) [25], Zhang [23] gave a rough margin based support vector machine for classification to escape from the overfitting problem due to outliers. In [24] focus on the rough margin based *v*-SVR which constructs the rough margin with double tolerance bands. In this paper, a novel regression approach, termed as the Rough Margin Support Vector Regression (RMSVR) network, is proposed to enhance the robust capability of SVR. The basic idea of the approach is to adopt the concept of rough sets to construct the model obtained by SVR and fine tune it with a robust learning algorithm. Simulation results of the proposed approach have shown the effectiveness of the approximated function in discriminating against outliers.

The reminder of this paper is outlined as follows. Section II describes the concept of rough sets and the fundamental ideas for SVR. In Section III, the RMSVR network is proposed and its learning process is introduced. Section IV gives experimental results. Concluding remarks are given in Section V.

II. SUPPORT VECTOR REGRESSION AND ROUGH SETS

A. Support vector regression

A function approximation problem can be formulated as to obtain a function from a set of observations $\{(\vec{x}_1, y_1),(\vec{x}_2, y_2),...,(\vec{x}_N, y_N)\}$ with $\vec{x}_i \in R^m$ and $y_i \in R$, where N is the number of training data, $\vec{x}_i$ is the i-th input vector, and y_i is the desired output for the input $\vec{x}_i$. Based on the SVM theory, SVR is to approximate the given observations in an m-dimensional space by a linear function in another feature space F. The function in SVR is of the form

$$f(\vec{x}, \vec{w}) = \langle \vec{w}, \Phi(\vec{x}) \rangle + b \tag{1}$$

where $\langle \cdot, \cdot \rangle$ is an inner product defined on F, $\Phi(\cdot)$ is a nonlinear mapping function from R^m to F, $\vec{w} \in F$ is a weight vector to be identified in the function, and b is a threshold. Usually, the considered cost function [26] is

$$R_{SV}[f] = R_{emp}[f] + C \cdot \|\vec{w}\|^2 \tag{2}$$

where $R_{emp}[f] = \frac{1}{N}\sum_{i=1}^{N} L(y_i - f(\vec{x}_i, \vec{w})) = \frac{1}{N}\sum_{i=1}^{N} L(e_i)$ [27], $L(y - f(\vec{x}, \vec{w}))$ is the loss function measuring the error between y and the estimated output $f(\vec{x}, \vec{w})$ for a given input , and $C > 0$ is a regular constant. In traditional SVR, the ε-insensitive function is used as the loss function in (2).

It was shown in [2] that the solution of the above problem can be expressed in terms of support vectors $\vec{w} = \sum_{i=1}^{N} \theta_i \Phi(\vec{x}_i)$, and the function f is then written as.

$$f(\vec{x}, \vec{w}) = \sum_{i=1}^{N} \theta_i \langle \Phi(\vec{x}_i), \Phi(\vec{x}) \rangle + b \tag{3}$$

In (3), the inner product $\langle \Phi(\vec{x}_i), \Phi(\vec{x}) \rangle$ in the feature space is usually considered as a kernel function [28]. The kernel function determines the smoothness properties of solutions and should reflect a prior knowledge on data. The choice of the kernel function is usually left for users. The coefficients θ_i s in (3) can be solved by quadratic programming methods with suitable transformation of the above problem into constraint optimization problems In (3), the constant b is unknown. Various forms can be found in the literature [6].

According to the SVM theory, SVR has the advantage of self-determining its structure. Hence, there are no initialization problems for SVR. For training data sets with certain noise distributions, SVR also has shown excellent performance under the ε-insensitive function or Huber's robust function [3,5,7]. However, the robust effects against training data sets with outliers are not obvious in SVR.

B. Rough sets

The theory of rough sets [11-12] has recently emerged as another major mathematical tool for managing uncertainty that arises from granularity in the domain of discourse—that is, from the indiscernibility between objects in a set. The intention is to approximate a rough (imprecise) concept in the domain of discourse by a pair of exact concepts, called the lower and upper approximations. These exact concepts are determined by an indiscernibility relation in the domain, which, in turn, may be induced by a given set of attributes ascribed to the objects of the domain. The lower approximation is the set of objects definitely belonging to the vague concept, whereas the upper approximation is the set of objects possibly belonging to the same. A rough set X is characterized by its lower and upper approximations $\underline{B}X$ and $\overline{B}X$, respectively, with the following properties.

1) An object $\vec{x}_k$ can be part of at most one lower approximation.
2) If $\vec{x}_k \in \underline{B}X$ of cluster X, then simultaneously $\vec{x}_k \in \overline{B}X$.
3) If $\vec{x}_k$ is not a part of any lower approximation, then it belongs to two or more upper approximations.

III. ROUGH MARGIN SUPPORT VECTOR REGRESSION ALGORITHM

A novel approach, termed as Rough Margin Support Vector Regression (RMSVR) Algorithm, is proposed. Support vector regression (SVR) [3] which is constructed by minimizing Vapnik's ε-insensitive loss function residuals between the outputs of SVR and the target values and the

model complexity. Instead of selecting an appropriate ε, Schölkopf et al [25] proposed a *v*-support vector regression (*v*-SVR), which introduces a new parameter *v* which can control the number of support vectors and training errors without defining ε a prior. They proved that *v* is an upper bound on the fraction of margin errors and lower bound of the fraction of support vectors.

In [24] focus on the rough margin based *v*-SVR, which constructs the rough margin with double ε instead of single ε for *v*-SVR such as Fig.1. Following the rough theory, ε_l and ε_u is the lower margins and the upper margins, respectively. The regions between those two margins are equivalent to the boundary regions; the region inside the lower margins is equivalent to the positive region; and the regions outside the upper margins are equivalent to the negative regions. When the datum lies in the positive region, it is regarded as non-support vector. The datum lying in the boundary and negative regions are all support vectors. The farther the datum deviates from the target function, the more important it is, so it emphasizes the residuals introduced by the data lying in the negative regions. Although the experimental results on benchmark datasets have been conformed the effectiveness of this idea, but if the outliers exist that will result in overfitting phenomena. In our approach, the datum lying in the boundary regions are considered as support vectors, i.e. ε_l and ε_u is the lower bound and upper bound of the fraction of support vectors, respectively. The datum lying in negative regions are viewed as outliers.

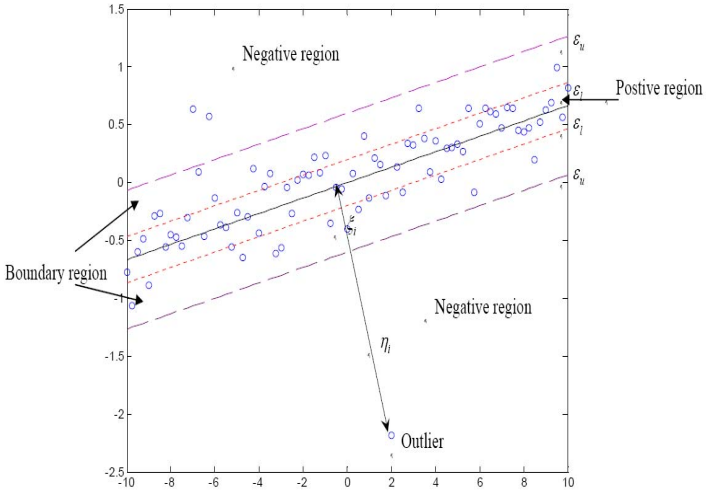

Fig.1 Rough margin SVR

Similar to the classical *v*-SVR and rough *v*-SVR, the primal problem can be described as:

$$\min_{\vec{w},\varepsilon_l,\varepsilon_u,\xi_i,\xi_i^*,\eta_i,\eta_i^*} \frac{1}{2}\|\vec{w}\|^2 + C\left(v\left(\varepsilon_l+\delta^b\varepsilon_u\right)+\frac{1}{l}\sum_{i=1}^{l}\left(\xi_i+\xi_i^*\right)+\frac{\delta^n}{l}\sum_{i=1}^{l}\left(\eta_i+\eta_i^*\right)\right) \quad (4)$$

subject to

$$\begin{aligned}
&\left(\vec{w}\cdot\Phi\left(\vec{x}_i\right)+b\right)-y_i \le \varepsilon_l+\xi_i+\eta_i,\\
&y_i-\left(\vec{w}\cdot\Phi\left(\vec{x}_i\right)+b\right) \le \varepsilon_l+\xi_i^*+\eta_i^*,\\
&0\le\xi_i\le\varepsilon_u-\varepsilon_l,\ \ 0\le\xi_i^*\le\varepsilon_u-\varepsilon_l,\\
&\eta_i\ge 0,\ \ \eta_i^*\ge 0,\ \ \varepsilon_l\ge 0,\ \ \varepsilon_u\ge 0,
\end{aligned}$$

The Lagrange function is defined as

$$\begin{aligned}
L=&\frac{1}{2}\|\vec{w}\|^2+C\left(v\left(\varepsilon_l+\delta^b\varepsilon_u\right)+\frac{1}{l}\sum_{i=1}^{l}\left(\xi_i+\xi_i^*\right)+\frac{\delta^n}{l}\sum_{i=1}^{l}\left(\eta_i+\eta_i^*\right)\right)\\
&-\sum_{i=1}^{l}\alpha_i\left(\varepsilon_l+\xi_i+\eta_i+y_i-\left(\vec{w}\cdot\Phi\left(\vec{x}_i\right)+b\right)\right)\\
&-\sum_{i=1}^{l}\alpha_i^*\left(\varepsilon_l+\xi_i^*+\eta_i^*-y_i+\left(\vec{w}\cdot\Phi\left(\vec{x}_i\right)+b\right)\right)\\
&-\sum_{i=1}^{l}\beta_i\left(\varepsilon_u-\varepsilon_l-\xi_i\right)-\sum_{i=1}^{l}\beta_i^*\left(\varepsilon_u-\varepsilon_l-\xi_i^*\right)\\
&-\sum_{i=1}^{l}\gamma_i\xi_i-\sum_{i=1}^{l}\gamma_i^*\xi_i^*-\sum_{i=1}^{l}\sigma_i\eta_i-\sum_{i=1}^{l}\sigma_i^*\eta_i^*-\lambda_l\varepsilon_l-\lambda_u\varepsilon_u
\end{aligned} \quad (5)$$

where $\alpha_i\ge 0,\alpha_i^*\ge 0,\beta_i\ge 0,\beta_i^*\ge 0,\gamma_i\ge 0,\gamma_i^*\ge 0,\sigma_i\ge 0,\sigma_i^*\ge 0$, $\lambda_l\ge 0$, $\lambda_u\ge 0$ are Lagrangian multipliers. According to KKT conditions and then the dual problem can be written as

$$\min_{\alpha_i,\alpha_i^*}\ \frac{1}{2}\sum_{i,j=1}^{l}\left(\alpha_i-\alpha_i^*\right)\left(\alpha_j-\alpha_j^*\right)K(\vec{x}_i,\vec{x}_j)-\sum_{i=1}^{l}\left(\alpha_i-\alpha_i^*\right)y_i \quad (6)$$

subject to

$$\begin{aligned}
&\sum_{i=1}^{l}\left(\alpha_i-\alpha_i^*\right)=0\\
&\alpha_i,\alpha_i^*\in\left[0,\delta_n\frac{C}{l}\right]\\
&\sum_{i=1}^{l}\left(\alpha_i+\alpha_i^*\right)\le\left(1+\delta_b\right)Cv
\end{aligned}$$

The regression estimate then takes the form,

$$f(x)=\sum_{i=1}^{l}\theta_i K(\vec{x}_i,\vec{x}_j)+b, \quad (7)$$

where $\theta_i=\alpha_i-\alpha_i^*$ and $K(\vec{x}_i,\vec{x}_j)$ is a kernel function.

We let $v\ge 0,\delta^b\ge 0,\delta^n\ge 0$. If $\delta^b=0,\delta^n=1$, RMSVR is equivalent to the classical *v*-SVR. In other word, let $\delta^b=1,\delta^n\ge 1$, RMSVR becomes the rough *v*-SVR. In this function approximation approach, we select $\delta^b>1$ to emphasize those support vectors lying in the boundary regions, and select $\delta^n<1$ give the penalty to the datum lying in negative regions. Hence, *b* can be computed as:

$$\begin{aligned}
b=\frac{1}{2}\Bigg\{&\min_{i\notin NG}\left(y_i-\sum_{i=1}^{N}\left(\alpha_j-\alpha_j^*\right)K(\vec{x}_i,\vec{x}_j)\right)\\
&+\max_{i\notin NG}\left(y_i-\sum_{i=1}^{N}\left(\alpha_j-\alpha_j^*\right)K(\vec{x}_i,\vec{x}_j)\right)\Bigg\}
\end{aligned} \quad (8)$$

where NG expressed the datum lying in negative regions.

The initial phase is to determine the network structure and the corresponding initial network weights through the RMSVR approach. In this paper, the kernel function is chosen as Gaussian function and defined as

$$K(\vec{x},\vec{x}_i)=\exp\left[-\left\|\vec{x}-\vec{x}_i\right\|^2/2\tau^2\right] \quad (9)$$

where is τ a constant. After applying the RMSVR approach, an initial network is obtained which has been with a level of accuracy against outliers. Furthermore, to improve the accuracy, it should to adjust those weights by the robust learning approach. A robust learning algorithm called ARBP [5] is proposed, in this algorithm, it is simply embedding an annealing process into the learning process, and a deterministic annealing process is used to replace the scale estimator. Based on this idea, the robust cost function of ARBP is defined as:

$$E_{ARBP}=\sum_{i=1}^{l}\chi\left(e_k,\kappa(\tau)\right), \quad (10)$$

where $\chi(\cdot)$ is the loss function. $e_k=y_k-\hat{y}_k$ .The annealing schedule, $\kappa(\tau)$ is usually selected to decrease toward zero as the epoch number increases to infinite; that is $\lim_{\tau\to\infty}\kappa(\tau)=0$.

In the learning algorithm, $\vec{\theta}$ can be updated as

$$\vec{\theta}(t+1)=\vec{\theta}(t)+\Delta\vec{\theta}(t) \quad (11)$$

with

$$\Delta\vec{\theta}(t)=\varsigma\frac{\partial E_{ARBP}(t)}{\partial\vec{\theta}}, \quad (12)$$

where ς is the learning constant.

The proposed Algorithm is described in the following:

[Step 1] Initialize the RMSVR structure with the given kernel functions, the loss function, and the constant C,v,δ^b,δ^n .

[Step 2] For each training pattern, compute the estimated result by Equ.(7) and its error.

[Step 3] Update the weight vector incrementally by (11) and (12).

[Step 4] Compute the robust cost function defined by (10).

[Step 5] If the termination conditions are not satisfied, then go to Step 2; otherwise, terminate the learning process.

IV. Simulation Example

A sinc function is considered and defined as

$$y=\frac{\sin(x)}{x},\ -10\le x\le 10 .$$

80 input-output data are used. In this example, outliers are added artificially by moving some points away from designated locations. The parameters selected as $\tau=3, C=0.5$. Based on the above procedure, the approximated results of RMSVR are presented in Fig. 1 and RMSVR with robust learning are shown as Fig.2. It can be found that the proposed RMSVR can reduce the overfitting phenomena.

V. Conclusion

Rough set theory turned out to be particularly adequate for the analysis of various types of data with inexact, uncertain or vague knowledge. In this paper, a novel regression approach, termed as the Rough Margin Support Vector Regression (RMSVR) network, is proposed to enhance the robust capability of SVR. The basic idea of the approach is to adopt the concept of rough sets to construct the model obtained by SVR and fine tune it with a robust learning algorithm. Simulation results of the proposed approach have shown the effectiveness of the approximated function in discriminating against outliers.

Acknowledgment

This work was supported in part by National Science Council of Taiwan under Grant NSC 98-2221-E-244 -004 -.

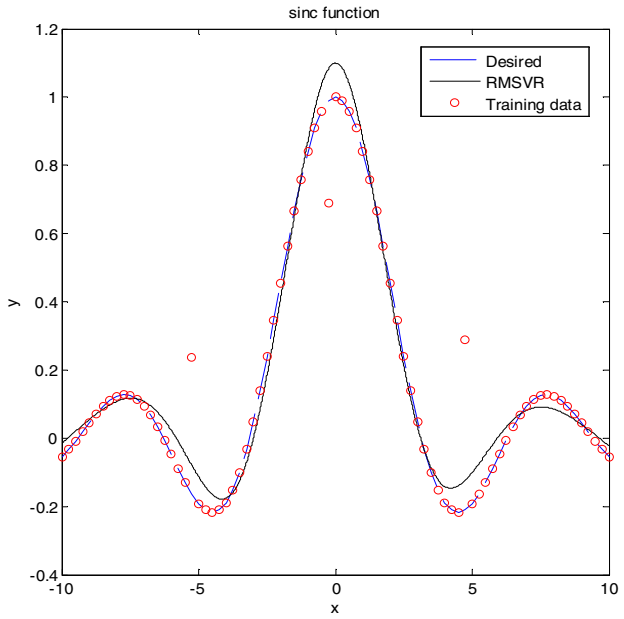

Fig.1 The approximated results

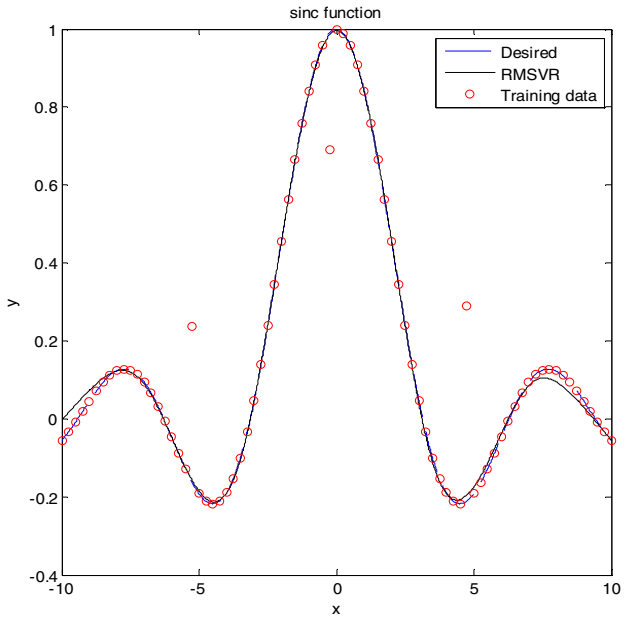

Fig.2 The approximated results with robust learning

.

REFERENCES

[1] C. Cortes and V. Vapnik, "Support vector networks," *Machine Learning*, vol. 20, pp. 273–297, 1995.

[2] V. Vapnik, *The Nature of Statistical Learning Theory*. New York: Springer-Verlag, 1995.

[3] V. Vapnik, S. Golowich, and A. J. Smola, "Support vector method for function approximation, regression estimation, and signal processing," in *Neural Information Processing Systems*. Cambridge, MA: MIT Press, 1997, vol. 9 .

[4] D. S. Chen and R. C. Jain, "A robust back-propagation learning algorithm for function approximation," *IEEE Trans. Neural Networks*, vol. 5, pp. 467–479, May 1994.

[5] C.-C. Chuang, S.-F. Su, and C.-C. Hsiao, "The annealing robust backpropagation (ARBP) learning algorithm," *IEEE Trans. Neural Networks*, vol. 11, pp. 1067–1077, Sept. 2000.

[6] A. J. Smola and B. Schölkopf, "A tutorial on support vector regression," Royal Holloway College, London, U.K., Neuro COLT Tech. Rep. TR-1998-030, 1998.

[7] S. Mukherjee, E. Osuna, and F. Girosi, "Nonlinear prediction of chaotic time series using a support vector machine," in *Proc. NNSP*, 1997, pp. 24–26.

[8] A. J. Smola, "Regression estimation with support vector learning machines," Master's thesis, Technical Univ. Munchen, Munich, Germany, 1998.

[9] J. A. K. Suykens, J. De Brabanter, L. Lukas, and J. Vandewalle, "Weighted least squares support vector machines: Robustness and sparse approximation," Neurocomput., 2001.

[10] C. C. Chuang, S. F. Su, J. T. Jeng and C. C. Hsiao, "Robust support vector regression networks for function approximation with outliers," *IEEE Trans. Neural Networks*, vol. 13, no. 6, pp. 1322-1330, 2002.

[11] Pawlak. Z, "Why rough set?," *Proceedings of IEEE international conference on Fuzzy systems,* New Orleans, Louisiana. USA, 1996, pp. 738-743.

[12] Pawlak. Z, "Rough sets," *Int. J. Coinput. Inf. Sci.,* 1982, vol.11,pp. 341-356.

[13] T. Y. Lin, "Rough Logic Formalism For Fuzzy Controllers-A Hard and Soft Computing Approach," *Jouranl of Approximate Reasoning*,pp.395-414,1996.

[14] C. C. Hsiao, "A Rough-Set-Based for fuzzy modeling with outlier," *2008 International Conference on Instrumentation, Control and Information Technology(SICE 2008)*, pp.364-368, August, 2008.

[15] X. Wang, Eric C.C. Tsang, S. Zhao, D. Chen and Daniel S. Yeung, "Learning fuzzy rules from fuzzy samples based on rough set technique", *Information Sciences* , vol.177, pp.4493–4514, 2007.

[16] Sushmita Mitra, Haider Banka, and Witold Pedrycz, "Rough–Fuzzy Collaborative Clustering", *IEEE Trans. Syst., Man, Cybern-Part B,* vol. 36, no. 4, pp.795-805, 2006.

[17] Pradipta Maji, Sankar K. Pal, "Rough Set Based Generalized Fuzzy *C*-Means Algorithm and Quantitative Indices", *IEEE Trans. Syst., Man, Cybern-Part B,* vol. 37, no. 6, pp.1529-1540, 2007.

[18] S. Asharaf, S.K. Shevade,M. and Narasimha Murty, "Rough support vector clustering", *Pattern Recognition*, vol.38 , pp.1779 – 1783, 2005.

[19] P. Lingras, C.J. Butz, "Rough set based 1-v-1 and 1-v-r approaches to supportvector machine multi-classification," *Information Sciences*, vol.177, pp. 3782–3798, 2007.

[20] C.C. Yeh , D.J. Chi and M.F. Hsu, "A hybrid approach of DEA, rough set and support vector machines for business failure prediction," *Expert Systems with Applications*, vol. 37, pp.1535–1541, 2010.

[21] D. Chen, Q. He and X. Wang, "FRSVMs: Fuzzy rough set based support vector machines," *Fuzzy Sets and Systems* , vol.161, pp.596–607, 2010.

[22] P. Lingras, C.J. Butz, "Rough support vector regression," *European Journal of Operational Research*, 2009.

[23] Zhang, J., & Wang, Y., "A rough margin based support vector machine," *Information Sciences*, vol.178, pp.2204–2214, 2008.

[24] Y. Zhao and J. Sun, "Rough *v*-support vector regression," *Expert Systems with Applications*, vol.36, pp.9793–9798, 2009.

[25] Schölkopf, B., Smola, A., Williamson, R., and Bartlett, P., "New support vector algorithms," *Neural Computation*, vol.12, pp.1207–1245, 2000.

[26] A. J. Smola and B. Schölkopf, "From regularization operators to support vector kernels," in *Neural Information Processing Systems*. Cambridge, MA: MIT Press, 1997, vol. 9.

[27] V. Vapnik, *Estimation of Dependences Based on Empirical Data*. New York: Springer-Verlag, 1982.

[28] M. A. Aizerman, E. M. Braverman, and L. I. Rozonoér, "Theoretical foundations of the potential function method in pattern recognition learning," *Automat. Remote Contr.*, pp. 821–837, 1964.

2011 IEEE International Conference on Fuzzy Systems
June 27-30, 2011, Taipei, Taiwan

An Immune Symbiotic Evolution Learning for Compensatory Neural Fuzzy Networks and Its Applications

Cheng-Hung Chen, *Member*, *IEEE*
Department of Electrical Engineering
National Formosa University
Yunlin County 632, Taiwan, R.O.C.
E-mail: chchen.ee@nfu.edu.tw

Cheng-Jian Lin, *Member*, *IEEE*
Department of Computer Science and Information Engineering
National Chin-Yi University of Technology
Taichung County 411, Taiwan, R.O.C.
E-mail: cjlin@ncut.edu.tw

Chin-Teng Lin, *Fellow*, *IEEE*
Department of Electrical Engineering
National Chiao-Tung University
Hsinchu 300, Taiwan, R.O.C.
E-mail: ctlin@mail.nctu.edu.tw

***Abstract*—This study presents an efficient immune symbiotic evolution learning algorithm for the compensatory neural fuzzy network (CNFN). The proposed immune symbiotic evolution learning method (ISEL) includes three major components - initial population, subgroup symbiotic evolution and immune system algorithm. The advantage of the proposed ISEL method are that the subgroup symbiotic evolution method uses the subgroup-based population to evaluate the fuzzy rules locally and the adopted immune system algorithm can accelerate the search and increase global search capacity. Finally, the simulation results have shown that the proposed CNFN-ISEL can outperform other methods.**

Keywords- Compensatory fuzzy operator; neural fuzzy network; symbiotic evolution; immune system algorithm ; control problems.

I. INTRODUCTION

Many researchers have developed GAs to implement fuzzy systems and neural fuzzy networks in order to automate the determination of parameters and structures [1]-[3]. Unfortunately, the number of fuzzy rules (i.e., the length of each chromosome in the GA) increased exponentially as the number of inputs increased. However, such GAs encounter some important issues: 1) the input space is partitioned into a grid; 2) the number of fuzzy rules is determined by trial and error or by a expert system; 3) a fuzzy system was encoded into a chromosome; and 4) the rate of convergence of the evolution process is low.

This study presents an efficient immune symbiotic evolution learning algorithm (ISEL) for the compensatory neural fuzzy network. The proposed compensatory neural fuzzy network (CNFN) is based on our previous research [4]. The immune symbiotic evolution learning method (ISEL) includes three major components - initial population, subgroup symbiotic evolution and immune system algorithm. First, the self-clustering algorithm that determines proper input space partitioning and finds the mean and variance of the membership function and the number of rules, is applied to the initial population. Second, the subgroup symbiotic evolution method in which each sub-antibody represents a single fuzzy rule differs from traditional GAs. A fuzzy system with *R*-rules is constructed by selecting and combining *R* sub-antibodies from a given population, and allowing the evolution of the rule itself. Third, the immune system algorithm uses the clonal selection principle to cancel antibodies between others of high similar degree, and these antibodies, after the process, will be of higher quality, accelerating the search and increasing the global search capacity.

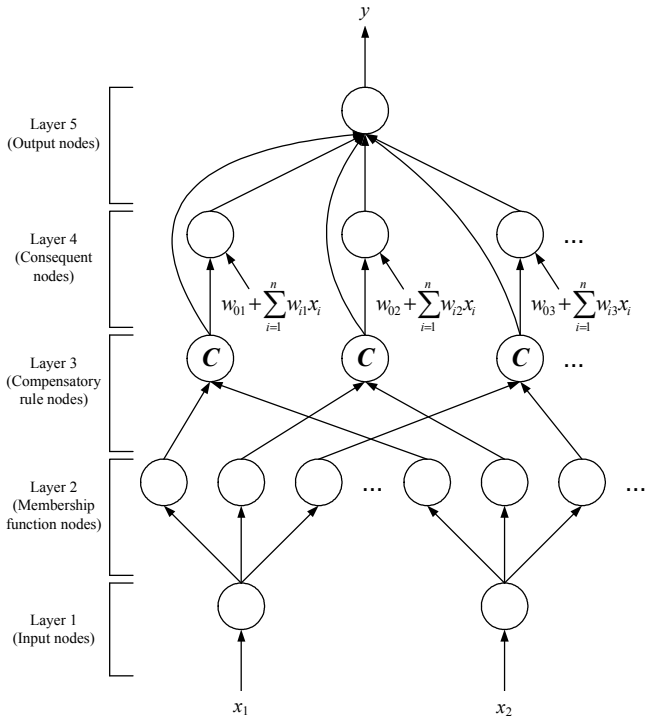

Figure 1. Structure of the proposed CNFN.

II. STRUCTURE OF COMPENSATORY NEURAL FUZZY NETWORK

The section describes the compensatory neural fuzzy network (CNFN) [4]. Compensatory operators are used to optimize fuzzy logic reasoning and to select optimal fuzzy operators. Therefore, an effective neural fuzzy network should be able not only to adaptively adjust fuzzy membership functions but also to dynamically optimize adaptive fuzzy operators. Figure 1 shows the structure of the CNFN.

The CNFN realizes a fuzzy model in the following form.

$$\text{Rule}-j: \quad \text{IF}\left[x_1 \text{ is } A_{1j} \text{ and } x_2 \text{ is } A_{2j} \ldots \text{and } x_i \text{ is } A_{ij} \ldots \text{and } x_N \text{ is } A_{Nj}\right]^{1-\gamma_j+\frac{\gamma_j}{N}} \quad (1)$$
$$\text{THEN } y' \text{ is } w_{0j}+w_{1j}x_1+w_{2j}x_2+\ldots+w_{ij}x_i+\ldots w_{Nj}x_N$$

where x_i is the input variable; y' is the output variable; A_{ij} is the linguistic term of the precondition part; $\gamma_j \in [0,1]$ is the

compensatory degree, and w_{0j} and w_{ij} are the corresponding parameters of consequent part.

III. An Immune Symbiotic Evolution Learning for the CNFN

This section describes an immune symbiotic evolution learning method (ISEL) for constructing the CNFN. The ISEL method comprises of three major components - initial population, subgroup symbiotic evolution and immune system algorithm. First, the initial population uses the self-clustering algorithm that determines proper input space partitioning and finds the mean and variance of the Gaussian membership function and the number of rules. Second, in traditional symbiotic evolution, all rules generally evolve together; however, in the subgroup symbiotic evolution method, each rule evolves separately. Third, the immune system algorithm uses the clonal selection principle to accelerate the search and increase global search capacity. Figure 2 presents the immune symbiotic evolution learning of the CNFN.

A. Initial Population

This subsection introduces the production of initial population, covering the coding and initialization steps. The coding step involves the membership functions and the fuzzy rules of a fuzzy system that represent sub-antibodies and are suitable for subgroup symbiotic evolution. The initialization step assigns the population values before the evolution process begins.

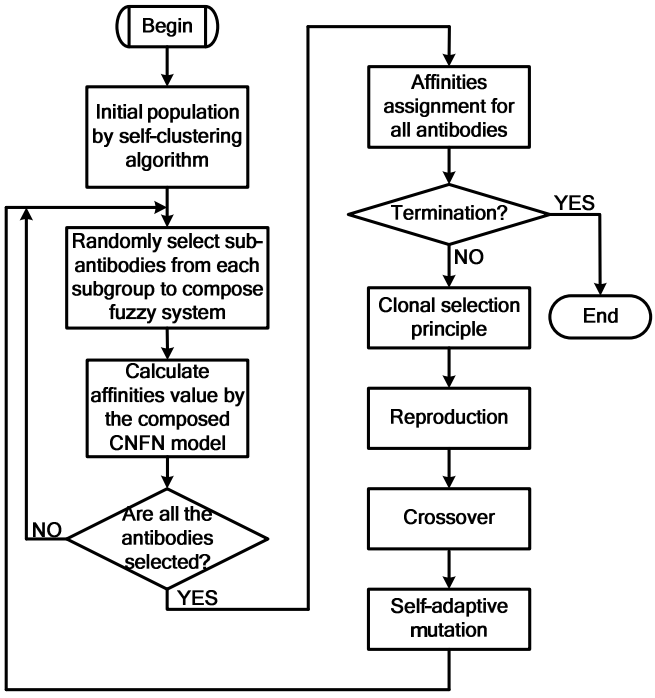

Figure 2. Flowchart of the proposed ISEL method.

1) Coding Step

The first step in ISEL method is the coding of a fuzzy rule into a sub-antibody. Figure 3 shows an example of a fuzzy rule coded into a sub-antibody where *i* and *j* are the *i*th dimension and the *j*th rule. Figure 3 describes a fuzzy rule given by Eq. (1), where m_{ij} and σ_{ij} are the mean and variance of a Gaussian membership function, respectively; c_j and d_j are compensatory parameters, and w_{ij} is the corresponding parameter of the consequent part associated with the *j*th rule node.

Sub-antibody

m_{1j}	σ_{1j}	m_{2j}	σ_{2j}	.....	m_{ij}	σ_{ij}	.....	c_j	d_j	w_{0j}	w_{1j}	w_{2j}	.....	w_{ij}	.....

Figure 3. Coding a fuzzy rule into a sub-antibody in subgroup symbiotic evolution.

2) Initialization Step

Before the ISEL method is designed, the individuals that will constitute an initial population must be created. In this study, the initial population was created according to the range of the mean and variance of the membership function, which were computed by the self-clustering algorithm (SCA) method [5]. The following formulations show the generation of the initial population.

Mean: $Sub\text{-}antibody[index] = m_{ij} + random[0,1] \times \sigma_{ij}$
where $index=1,3,\ldots,2\times N\text{-}1$

Variance: $Sub\text{-}antibody[index] = 4 \times random[0,1] \times \sigma_{ij}$
where $index=2,4,\ldots,2\times N$

Other parameters: $Sub\text{-}antibody[index] = random[-1,1]$
where $index>2\times N$

where *index* is the site of a sub-antibody; m_{ij} and σ_{ij} are the mean and variance, respectively of the Gaussian membership function of the *j*th rule of the *i*th input variable. The size of the population depends on the complexity of the problem. Many experiments showed that the population size of 20 is most effective. Besides the population size, other parameters must be set. This is the number of fuzzy systems to be formed and evaluated in each generation. The crossover rate, and the mutation rate and these parameters also depend on the complexity of the problem.

B. Subgroup Symbiotic Evolution

This subsection presents a novel method of subgroup symbiotic evolution. As described above, in the subgroup symbiotic evolution, the affinity value of a rule (a sub-antibody) is computed as the sum of the affinity values of all the feasible combinations of that rule with all other randomly selected rules, and then dividing this sum by the total number of combinations. Figure 4 shows the structure of the sub-antibody in the subgroup symbiotic evolution. The stepwise assignment of the affinity value is as follows.

Step 0: Divide the rules into subgroups of size *ps*.

Step 1: Randomly select *R* fuzzy rules (sub-antibody) from each of the above subgroups, and compose the fuzzy system using these *R* rules.

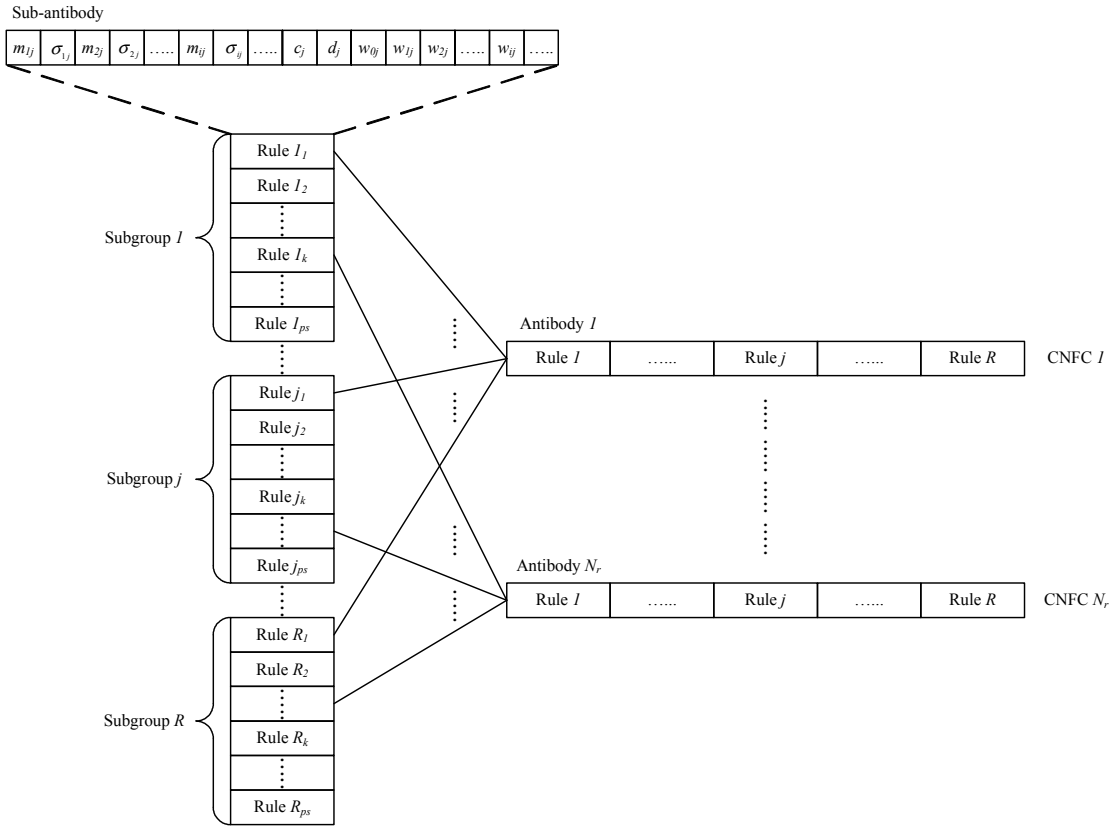

Figure 4. Structure of sub-antibody in subgroup symbiotic evolution.

Step 2: Calculate affinities of the antibodies using the CNFN thus composed. In this study, the affinity value is given by the follow formula;

$$Affinity\ value = \frac{1}{1+\sqrt{\frac{1}{N_t}\sum_{k=1}^{N_t}\left(y_k - y_k^d\right)^2}} \qquad (2)$$

where y_k represents the *kth* model output; y_k^d represents the desired output, and N_t represents the number of input data.

Step 3: Divide the affinity value by R and accumulate the divided affinity value to the affinity record of the R selected rules with their recorded affinity values initially set to zero.

Step 4: Repeat the above steps until each rule (sub-antibody) in each subgroup has been selected a sufficient number of times, and record the number of fuzzy systems to which each sub-antibody has contributed.

Step 5: Divide the accumulated affinity of each sub-antibody by the number of times it has been selected.

Step 6: Sort these sub-antibodies in each subgroup in order of decreasing affinity.

C. Immune System Algorithm

This subsection introduces the implementation of the immune system algorithm that is based on the clonal selection principle, the reproduction step, the crossover step and the self-adaptive mutation step.

1) Clonal Selection Principle

The antibodies of this immune system that eliminate the antigen should exhibit at least a minimal threshold of diversity. Accordingly, the diversity operator is applied to these antibodies such that those between others of high similar degree are canceled, guaranteeing and improvement in quality. This process is called clonal selection principle. Therefore, if the affinity between two antibodies exceeds the suppression threshold Th_{aff}, then these two antibodies are called similar. Now, the subgroup is assumed to be composed of *ps* sub-antibodies with L genes, as shown in Fig. 5.

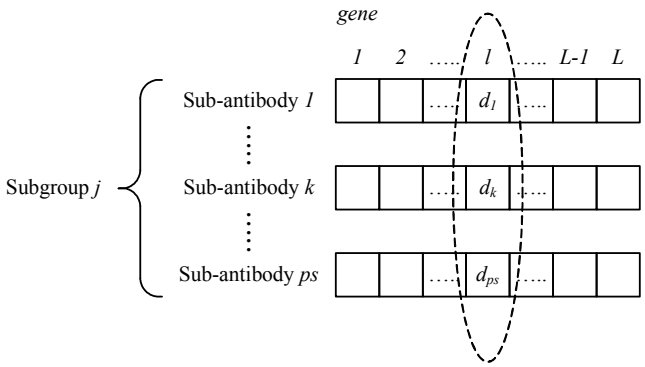

Figure 5. Composition of subgroup with these sub-antibodies.

Information theory yields the entropy value $EV_l(ps)$ of the lth gene in this jth subgroup:

$$EV_l(ps) = \sum_{k=1}^{ps} -P_{kl} \log P_{kl} \quad (3)$$

where P_{kl} is the probability of the kth allele from the lth gene, and $P_{kl} = 1/\left(1 + \left\| d_k - d_{k'} \right\|\right)$ is defined, where d_k and $d_{k'}$ are the genes of the kth and the k'th sub-antibody, respectively. The diversity of the genes is calculated using Eq. (3). If all alleles of the lth gene are of the same form, then the entropy value $EV_l(ps)$ will be zero.

The average entropy value *EV(ps)* of diversity is also given as follows;

$$EV(ps) = \frac{\sum_{l=1}^{L} EV_l(ps)}{L} \quad (4)$$

where L is the size of the gene in a sub-antibody. Equation (4) yields the diversity of the sub-antibody pool in terms of the entropy. Two affinity expression are considered in the proposed approach. The first explains the relationships between the antibody and the antigen, and is given by Eq. (2). The second describes the degree of association between sub-antibodies. The following equation computes the affinity between sub-antibodies;

$$Affinity_Ab_{kk'} = \frac{1}{1 + EV(2)} \quad (5)$$

where $Affinity_Ab_{kk'}$ is the affinity between two sub-antibodies k and k', and *EV(2)* is the entropy of only the sub-antibodies k and k'. This affinity is constrained from zero to one. When *EV(2)* is zero, the genes of the kth sub-antibody and the k'th sub-antibody are the same. Therefore, the clonal selection principle is that if the $Affinity_Ab_{kk'}$ exceeds Th_{aff}, then the sub-antibody should be canceled. Reproduction, crossover and mutation steps follow, according to the flowchart presented in Fig. 6.

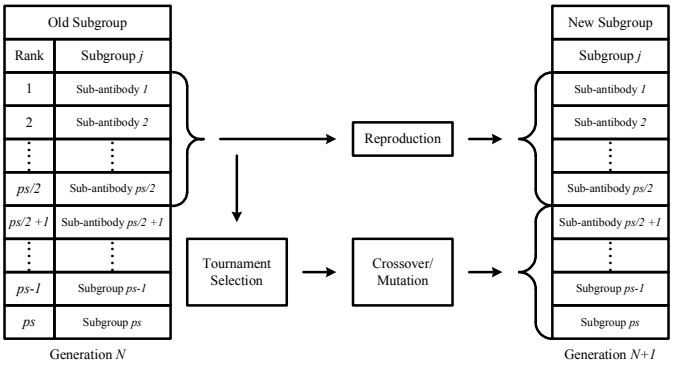

Figure 6. Flowchart of reproduction, crossover and mutation steps.

2) Reproduction Step

Reproduction is a process in which sub-antibody strings are copied according to their affinity values. This process is an artificial version of natural selection. This study uses the roulette-wheel selection method [6] - a simulated roulette is spun - in this reproduction step. The best performing sub-antibodies in the top half of the subgroup evolves to the next generation. The other half is generated to perform crossover on sub-antibodies in the top half of the parent generation.

3) Crossover Step

Reproduction directs the search toward the best existing sub-antibodies but does not create any new sub-antibodies. In nature, an offspring has two parents and inherits genes from both. The main operator working on the parents is the crossover operator, the operation of which occurred for a selected pair with a crossover rate that was set to 0.5 in this study. Therefore, the new sub-antibodies are principally generated by crossover. In this process, the first step is to select two sub-antibodies for crossover. Two sub-antibodies for crossover are selected by tournament selection [6] on the top half of the best-performing sub-antibodies. Tournament selection shown in Fig.7 randomly selects three sub-antibodies in each subgroup, and the sub-antibody with the best affinity is adopted as the designated sub-antibody. The other designated sub-antibody is selected in the same way. Two new sub-antibodies are generated by performing crossover on the selected designated sub-antibodies.

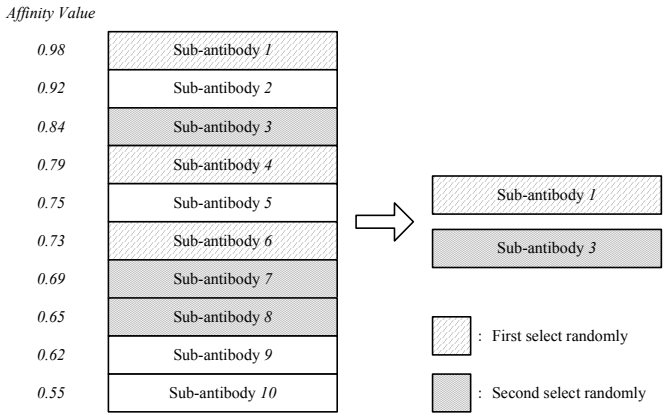

Figure 7. Tournament selection.

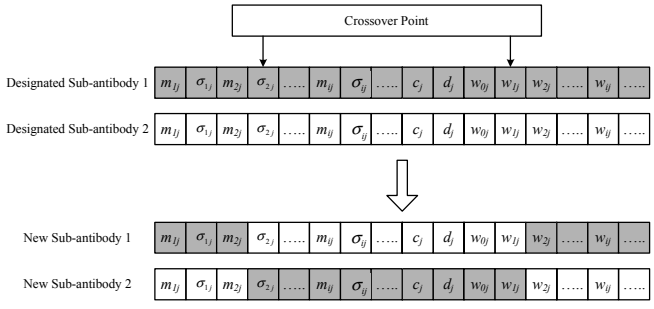

Figure 8. Two-point crossover.

In the second step, the two designated sub-antibodies are crossed and separated using a two-point crossover, as shown in Fig. 8, in which new sub-antibodies are created by exchanging the gene between the selected sites of the two designated sub-antibodies. In the crossover step, we also keep the same number of sub-antibodies in the other half of the population for each subgroup. After this operation, the new sub-antibodies replace the designated sub-antibodies with poor performances.

4) Self-Adaptive Mutation Step

After reproduction and the crossover step yielded new strings, no new information is introduced to the subgroup at the site of a sub-antibody. As a source of new sites, mutation

should be used sparingly because it is a random search operator. In the following simulations, a mutation rate was set to 0.3. Mutation is an operator that randomly alters the allele of a gene. The self-adaptive mutation adopted in the immune system algorithm yields high diversity. The sub-antibody suffers from a mutation to avoid falling in a local optimal solution and to ensure the searching capacity of approximate global optimal solution. The self-adaptive mutation with real-valued representation can be used to produce mutants by adding a number randomly selected from some interval to a given antibody. Figure 9 shows the self-adaptive mutation of a sub-antibody. The mutation value is generated according to Eq. (6). Following self-adaptive mutation, a new sub-antibody can be introduced into the population.

$$SAb[index] = \begin{cases} SAb[index] + (\max(SAb[:]) - SAb[index]) \times \lambda, \text{if } \alpha > 0.5 \\ SAb[index] + (\min(SAb[:]) - SAb[index]) \times \lambda, \text{if } \alpha \le 0.5 \end{cases} \quad (6)$$

where $\lambda = \beta \times (t/T)^{\beta}$, $\alpha, \beta \in [0,1]$ are random values; *index* represents the gene in a sub-antibody (*SAb*); t is the tth generation, and T is the maximum number of generations.

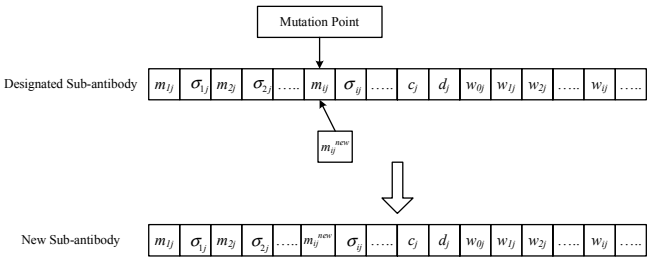

Figure 9. Self-adaptive mutation.

TABLE I. INITIAL PARAMETERS BEFORE TRAINING.

Parameter	Value
Size of Subgroup (*ps*)	20
Crossover Rate	0.5
Mutation Rate	0.3
Threshold of Affinity (Th_{aff})	0.95
Coding Type	Real Number

IV. ILLUSTRATIVE EXAMPLES

This study evaluated the performance of the proposed compensatory neural fuzzy network using immune symbiotic evolution learning algorithm (CNFN-ISEL) for nonlinear control systems. This section presents several examples and compares the performance with that of other neural fuzzy networks using symbiotic evolution (NFN-SE) [7], [8]. In the nonlinear control system problems, CNFN-ISEL is adopted to design controllers in four simulations - multi-input single-output plant control, multi-input multi-output plant control [9] and backing up the truck [10]. Table I presents the initial parameters before training used in the four computer simulations.

Example 1: Multi-input Single Output (MISO) Control

The controlled plant is the same as that used elsewhere [9], and is described by

$$y_p(k+1) = f[y_p, y(k-1)] + u(k) \quad (23)$$

where $f[y_p, y(k-1)] = \dfrac{y_p(k)y_p(k-1)[y_p(k)+2.5]}{1+y_p^2(k)+y_p^2(k-1)}$.

In designing the CNFN, the desired output y_r is specified by the following 250 pieces of data;

$$y_r(k+1) = 0.6y_r(k) + 0.2y_r(k-1) + r(k) \quad (24)$$

where $r(k) = 0.5\sin(2\pi k/45) + 0.2\sin(2\pi k/15) + 0.2\sin(2\pi k/90)$.

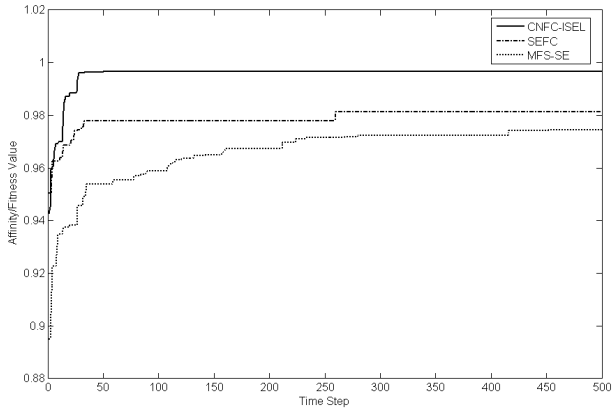

Figure 10. Learning curves of best performance of the CNFN-ISEL, SEFC and MFS-SE in Example 1.

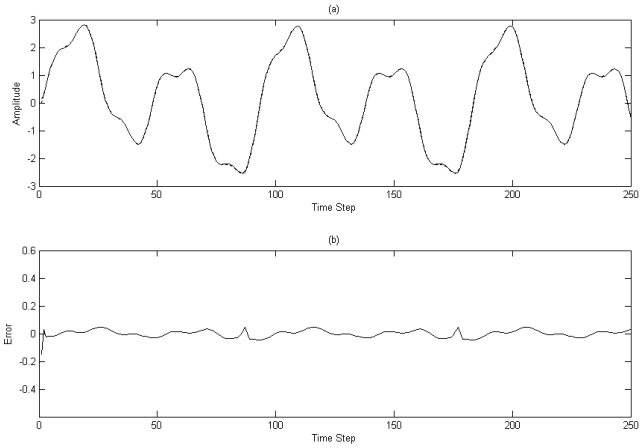

Figure 11. (a) Desired (solid line) and model (dotted line) output generated by CNFN designed with ISEL in Example 1. (b) Errors of proposed CNFN-ISEL.

The inputs to the CNFN are $y_p(k)$, $y_p(k+1)$, $y_r(k)$ and $y_r(k+1)$ and the output is $u(k)$. For the self-clustering algorithm (SCA), we chose the parameter D_{thr}=0.85 and then four rules are generated by SCA in CNFN; hence, R=4, and the number of total parameters is 60. Accordingly, the number of genes is also 15 in each subgroup. Figure 10 plots the learning curves of the best performance of the CNFN-ISEL for the affinity/fitness value, the symbiotic evolution of the fuzzy controller (SEFC) [7] and the Mamdani-type fuzzy system using the symbiotic evolution algorithm (MFS-SE) [8], after the learning process of 500 generations. Figure 11 (a) plots the control results of the desired output and the model output after a learning process of 500 generations. Figure11 (b) shows the errors of the proposed method. Table II presents the best and averaged affinity/fitness

values after 500 generations of training. The comparison indicates that the best and averaged affinity/fitness values of CNFN-ISEL are better than those obtained using other methods.

TABLE II. PERFORMANCE COMPARISONS WITH CNFN-ISEL, SEFC AND MFS-SE IN EXAMPLE 1.

Method	CNFN-ISEL	SEFC [7]	MFS-SE [8]
Affinity/Fitness Value (Ave)	0.9916	0.9793	0.9655
Affinity/Fitness Value (Best)	0.9961	0.9802	0.9745

Example 2: Multi-input Multi-output (MIMO) Control

In this example, the MIMO plants [9] to be controlled are described by the equations

$$\begin{bmatrix} y_{p1}(k+1) \\ y_{p2}(k+1) \end{bmatrix} = \begin{bmatrix} 0.5\dfrac{y_{p1}(k)}{1+y_{p2}^2(k)} \\ 0.5\dfrac{y_{p1}(k)y_{p2}(k)}{1+y_{p2}^2(k)} \end{bmatrix} + \begin{bmatrix} u_1(k) \\ u_2(k) \end{bmatrix}. \quad (25)$$

The controlled outputs should follow the desired output yr1 and yr2 as specified by the following 250 pieces of data;

$$\begin{bmatrix} y_{r1}(k) \\ y_{r2}(k) \end{bmatrix} = \begin{bmatrix} \sin(k\pi/45) \\ \cos(k\pi/45) \end{bmatrix}. \quad (26)$$

The inputs of the CNFN are $y_{p1}(k)$, $y_{p2}(k)$, $y_{r1}(k)$ and $y_{r2}(k)$, and the outputs are $u_1(k)$ and $u_2(k)$. For the self-clustering algorithm (SCA), we chose the parameter D_{thr}=1 and then six rules generated by SCA in CNFN, R=6. Therefore, the total number of parameters is 120 and the number of genes is 20 in each subgroup.

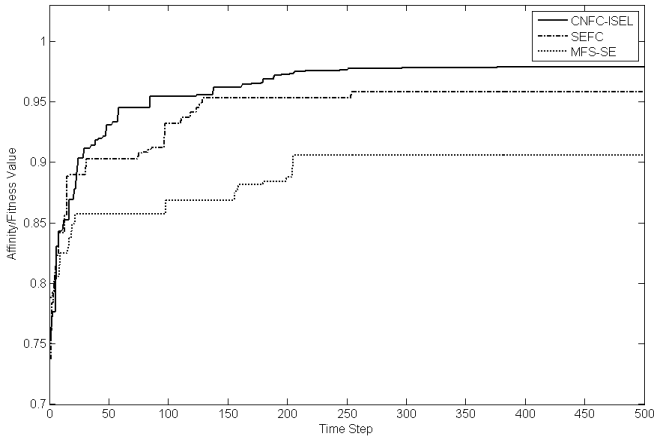

Figure 12. Learning curves of best performance of the CNFN-ISEL, SEFC and MFS-SE in Example 2.

Figure 12 plots the learning curves of the best performance of the CNFN-ISEL model for the affinity/fitness value, the symbiotic evolution of the fuzzy controller (SEFC) [7] and the Mamdani-type fuzzy system using symbiotic evolution algorithm (MFS-SE) [8], after the learning process of 500 generations. To demonstrate the control result, Figures 13(a) and (b) plot the control results of the desired output and the model output after the learning process of 500 generations. Figures 13 (c) and (d) show the errors of the proposed method. Table III presents the best and averaged affinity/fitness values after 500 generations of training. The comparison indicates that the best and averaged affinity/fitness values of CNFN-ISEL are better than those of other methods.

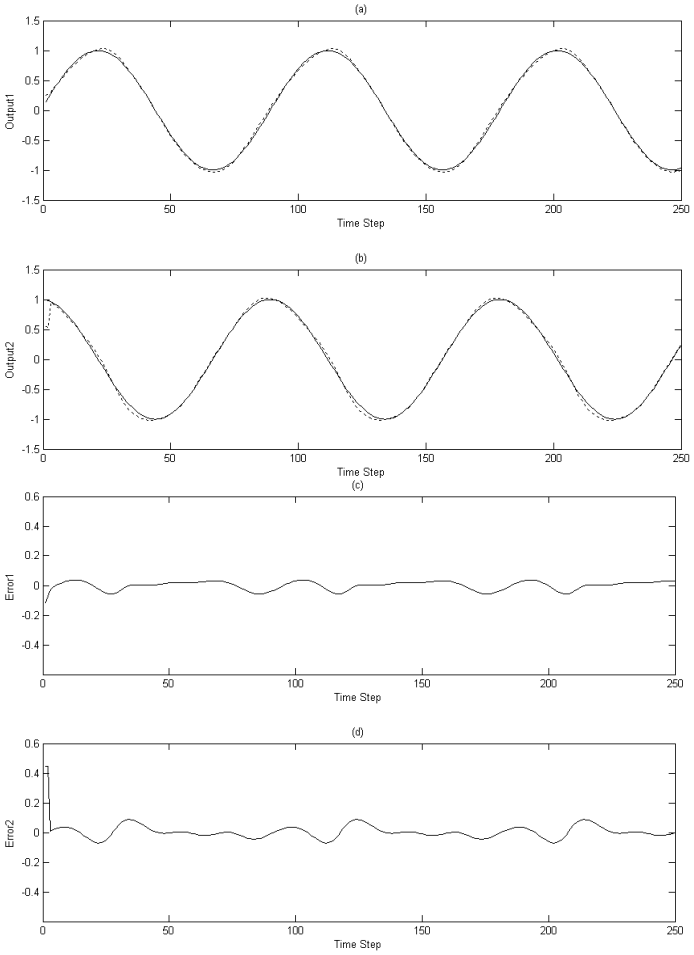

Figure 13. Desired (solid line) and model (dotted line) output generated by CNFN designed with ISEL in Example 1. (a) Output 1. (b) Output 2. Errors of proposed CNFN-ISEL for (c) output 1 and (d) output 2.

TABLE III. COMPARISON OF PERFORMANCE OF CNFN-ISEL, SEFC AND MFS-SE IN EXAMPLE 2.

Method	CNFN-ISEL	SEFC [7]	MFS-SE [8]
Affinity/Fitness Value (Ave)	0.9721	0.9553	0.8503
Affinity/Fitness Value (Best)	0.9786	0.9581	0.8560

Example 3: Control of Backing Up the Truck

Backing a truck into a loading dock is difficult. It is a nonlinear control problem for which no traditional control method exists [10]. Figure 14 shows the simulated truck and loading zone. The truck position is exactly determined by three state variables ϕ, x and y, where ϕ is the angle between the truck and the horizontal, and the coordinate pair (x, y) specifies

the position of the center of the rear of the truck in the plane. The steering angle θ of the truck is the controlled variable. Positive values of θ represent clockwise rotations of the steering wheel and negative values represent counterclockwise rotations. The truck is placed at some initial position and is backed up while being steered by the controller. The objective of this control problem is to use backward only motions of the truck to make the truck arrive in the desired loading dock (x_{desired}, y_{desired}) at a right angle (ϕ_{desired}=90°). The truck moves backward as the steering wheel moves through a fixed distance (*df*) in each step. The loading region is limited to the plane [0,100] × [0,100].

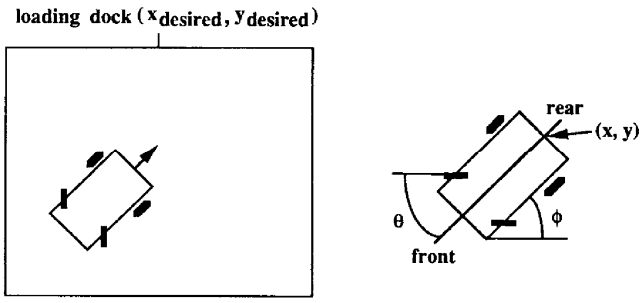

Figure 14. Diagram of simulated truck and loading zone.

The input and output variables of the CNFN must be specified. The controller has two inputs, truck angle ϕ and cross position *x*. When the clearance between the truck and the loading dock is assumed to be sufficient, the *y* coordinate is not considered as an input variable. The output of the controller is the steering angle θ. The ranges of the variables *x*, ϕ and θ are as follows.

$$0 \le x \le 100 \tag{27}$$

$$-90° \le \phi \le 270° \tag{28}$$

$$-30° \le \theta \le 30° \tag{29}$$

The equations of backward motion of the truck are,

$$\begin{aligned} x(k+1) &= x(k) + d_f \cos\theta(k) + \cos\phi(k) \\ y(k+1) &= y(k) + d_f \cos\theta(k) + \sin\phi(k) \\ \phi(k+1) &= \tan^{-1}\left[\frac{l\sin\phi(k) + d_f \cos\phi(k)\sin\theta(k)}{l\cos\phi(k) - d_f \sin\phi(k)\sin\theta(k)}\right] \end{aligned} \tag{30}$$

where *l* is the length of the truck. Equation (30) yields the next state from the present state.

Learning involves several attempts, each starting from an initial state and terminating when the desired state is reached; the CNFN is thus trained. For the self-clustering algorithm (SCA), we chose the parameter D_{thr}=0.45. After SCA learning, 13 fuzzy logic rules are generated and the parameters of the membership functions are determined. Hence, the total number of parameters is 117 and the number of genes is 9 in each subgroup. The training process continues for 500 generations. The affinity of the CNFN is approximately 0.95587 and the learning curve of CNFN is compared with those obtained using various existing models [7], [8], as shown in Fig. 15. Figures 16(a)-(b) plot the trajectories of the moving truck controlled by the CNFN, starting at initial positions (*x*, *y*, ϕ) = (a) (10 ,20 ,150°) and (b) (70, 20, -30°), after the training process has been terminated. The considered performance indices include the best affinity/fitness and the average affinity/fitness value. Table IV compares the results. According to these results, the proposed CNFN-ISEL outperforms various existing models.

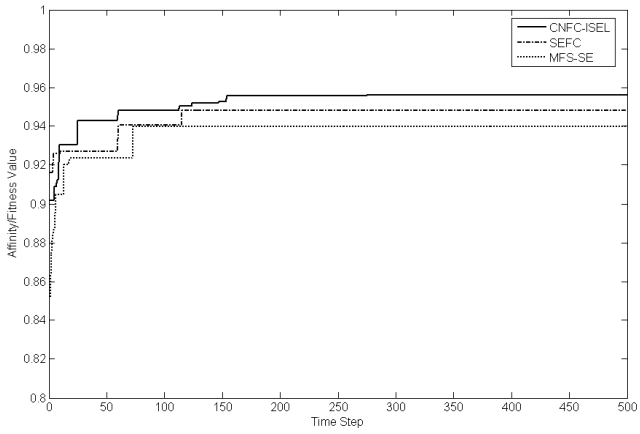

Figure 15. Learning curves of best performance of the CNFN-ISEL, SEFC and MFS-SE in Example 3.

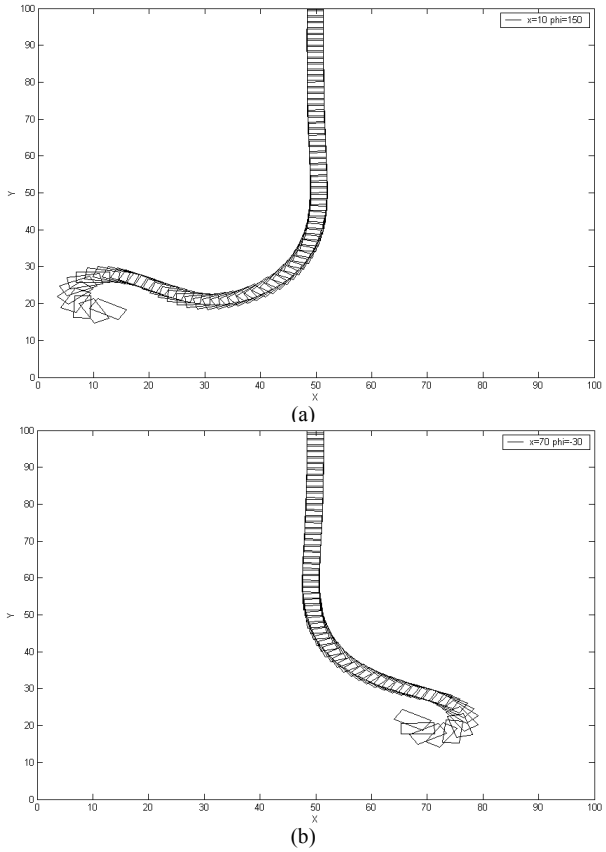

(a)

(b)

Figure 16. Trajectories of truck, starting at four initial positions under the control of the CNFN-ISEL after learning using training trajectories.

TABLE IV. COMPARISONS OF PERFORMANCE OF CNFN-ISEL, SEFC AND MFS-SE IN EXAMPLE 3.

Method	CNFN-ISEL	SEFC [7]	MFS-SE [8]
Affinity/Fitness Value (Ave)	0.9511	0.9451	0.9332
Affinity/Fitness Value (Best)	0.9558	0.9516	0.9398

V. CONCLUSION

This study proposes an efficient immune symbiotic evolution learning algorithm for the compensatory neural fuzzy network. The immune symbiotic evolution learning method (ISEL) includes three major components - initial population, subgroup symbiotic evolution and immune system algorithm. However, the self-clustering algorithm, an evolution of the rule itself, the clonal selection principle of antibodies, and self-adaptive mutation are achieved by ISEL method. Moreover, the proposed CNFN-ISEL obtains better simulation results than alternative models in some circumstances, for example achieving faster learning and higher design accuracy in many nonlinear control problems.

ACKNOWLEDGMENT

This research was sponsored by the National Science Council, Taiwan, R.O.C., under Grant NSC 99-2218-E-150-047.

REFERENCES

[1] Y. Shi, R. Eberhart and Y. Chen, "Implementation of evolutionary fuzzy systems," IEEE Trans. Fuzzy Syst., vol. 7, pp. 109-119, Apr. 1999.

[2] T. L. Seng, M. B. Khalid, and R. Yusof, "Tuning of a neuro-fuzzy controller by genetic algorithm," IEEE Trans. Syst., Man, Cybern. B, vol. 29, pp. 226-236, Apr. 1999.

[3] H. K. Lam, F. H. F. Leung, and P. K. S. Tam, "Design and stability analysis of fuzzy model based nonlinear controller for nonlinear systems using genetic algorithm," IEEE Trans. Syst., Man, Cybern. B, vol. 33, pp. 250-257, Apr. 2003.

[4] C. J. Lin and C. H. Chen, "Identification and prediction using recurrent compensatory neuro-fuzzy systems," Fuzzy Sets and Systems, vol. 150, no. 2, pp.307-330, Mar. 2005.

[5] C. J. Lin, C. H. Chen and C. Y. Lee, "A self-adaptive quantum radial basis function network for classification applications," Proc. IEEE International Joint Conference Neural Networks, vol. 4, pp. 25-29, 2004.

[6] O. Cordon, F. Herrera, F. Hoffmann, and L. Magdalena, "Advances in Fuzzy Systems-Applications and Theory," Genetic fuzzy systems evolutionary tuning and learning of fuzzy knowledge bases., vol. 19, NJ: World Scientific Publishing, 2001.

[7] C. F. Juang, J. Y. Lin and C. T. Lin, "Genetic reinforcement learning through symbiotic evolution for fuzzy controller design," IEEE Trans. Syst., Man, Cybern. B, vol. 30, no. 2, Apr. 2000.

[8] M. Jamei, M. Mahfouf and D. A. Linkens, "Elicitation and fine-tuning of fuzzy control rules using symbiotic evolution," Fuzzy Sets and Systems, vol. 147, no. 1, pp. 57-74, Oct. 2004.

[9] K. S. Narendra and K. Parthasarathy, "Identification and control of dynamical systems using neural networks," *IEEE Trans. Neural Networks*, vol. 1, no. 1, pp. 4-27, Mar. 1990.

[10] D. Nguyen and B. Widrow, "The truck backer-upper: An example of self-learning in neural network," *IEEE Conf. Syst. Mag.*, vol. 10, no. 3, 1990, pp. 18-23.

2011 IEEE International Conference on Fuzzy Systems
June 27-30, 2011, Taipei, Taiwan

Identification of Time-Delay Chaotic System with Outliers: Fuzzy Neural Networks Using Hybrid Learning Algorithm

Chia-Nan Ko
Department of Automation Engineering
Nan Kai University of Technology
Nantou, Taiwan, R.O.C.
t105@nkut.edu.tw

Guan-Yu Liu
Department of Electronic Engineering
Nan Kai University of Technology
Nantou, Taiwan, R.O.C.
guanyu@nkut.edu.tw

Yu-Yi Fu
Department of Automation Engineering
Nan Kai University of Technology
Nantou, Taiwan, R.O.C.
t098@nkut.edu.tw

Cheng-Ming Lee
Department of Computer and Communication Engineering
Nan Kai University of Technology
Nantou, Taiwan, R.O.C.
t104@nkut.edu.tw

***Abstract*—A hybrid learning algorithm is proposed to train fuzzy neural networks (FNNs) for identifying a time-delay chaotic system with outliers. In the proposed algorithm, integrating support vector regression (SVR) and annealing robust time-varying learning algorithm (ARTVLA) to optimize FNNs. In the evolutionary procedure, first, SVR is adopted to determine the number of hidden layer nodes and the initial structure of the FNNs. After initialization, ARTVLA with nonlinear time-varying learning rate is then applied to train FNNs. In ARTVLA, the determination of the learning rate would be an important work for the trade-off between stability and speed of convergence. A computationally efficient optimization method, particle swarm optimization (PSO) method, is adopted to simultaneously find optimal learning rates. Due to the advantages of SVR and ARTVLA (SVR-ARTVLA), the proposed FNNs (SVR-ARTVLA-FNNs) have good performance for identifying a time-delay chaotic system: Mackey Glass system with outliers. Simulation results are illustrated the effectiveness and feasibility of the proposed SVR-ARTVLA-FNNs.**

Keywords-fuzzy neural networks; support vector regression; time-delay chaotic system; annealing robust time-varying learning algorithm; particle swarm optimization

I. INTRODUCTION

A chaotic system is a nonlinear deterministic system that has some special features of sensitive dependence on initial conditions and unstable bounded trajectories in the phase space. Control and synchronization of chaotic systems have been investigated in various fields during recent years [1-3]. Due to their characteristics sensitivity to initial conditions, chaotic systems are not easy to identify. Recently, some researchers have endeavored to improve the identification of chaotic time series [4-6].

In the field of artificial intelligence, a fuzzy system using the human-like reasoning and expert knowledge can model complex nonlinear process characterized with ill-defined and uncertain factors. However, a fuzzy system lacks the learning capacity, it is difficult to fine tune fuzzy rules and membership functions from the training data. Neural networks have learning, adaption, and nonlinear mapping capacities, but the mapping rules in the networks is hard to understand. Therefore, FNNs combine the benefits of fuzzy logic and neural network, which is a popular research topic in system identification and control [7-9]. However, the number of fuzzy rule in the simplified fuzzy inference system and the initial parameters of FNNs are difficult to determine.

Recently, SVR [10] incorporated with FNNs has become a popular research topic. In this article, in order to overcome the above problems of training FNNs, first, an SVR method with Gaussian kernel function is adopted to determine the initial structure of the FNNs for identifying nonlinear systems [11, 12]. After initialization, an annealing robust concept in [12, 13] with ARTVLA is then applied to train the FNNs (ARTVLA-FNNs), in which PSO method is adopted to find optimal learning rates during learning procedure. A time-delay chaotic system will be given to illustrate the feasibility and efficiency of the proposed SVR-based ARTVLA-FNNs (SVR-ARTVLA-FNNs) for system identification of the Mackey Glass system.

II. ARCHITECTURE OF FUZZY NEURAL NETWORKS

A. Identification of Chaotic Time series

Let $\{\boldsymbol{x}\}$ be a chaotic system with time delay generated by an m-dimensional nonlinear dynamical system. According to Takens's delay embedding theorem [14], an embedding of

chaotic attractors can be obtained by constructing delay vectors

$$x(t+\tau) = f(x(t), x(t-\tau), x(t-2\tau), \cdots, x(t-(m-1)\tau)), \quad (1)$$

where $[x(t-\tau), x(t-2\tau), \cdots, x(t-(m-1)\tau)]$ is a proper vector, τ is the time-delay parameter, and m is the embedding parameter. If m is large enough, there exists a smooth function $f(\cdot)$ [15].

In this paper, the FNN will be applied to identify nonlinear systems due to the advantages of the self-learning ability of neural networks and the adaptive ability of fuzzy logic. The current output can be expressed as

$$\hat{x}_k(t+1) = \sum_{i=1}^{r} w_{ik} \exp\left(-\frac{(\boldsymbol{x} - b_i)^2}{2a_i^2} \right) \quad \text{for } k = 1, 2, \ldots, p, \quad (2)$$

where $\boldsymbol{x} = [x(t), x(t-1), \cdots, x(t-n)]$ is the input vector to FNNs, w_{ik} is the synaptic weight of the ith fuzzy rule for the kth FNN output, a_i and b_i are the widths and the centers of the ith membership function for all input data $\boldsymbol{x}$, respectively.

B. Fuzzy Neural Networks Model

The proposed architecture of FNNs is depicted in Fig. 1. It is a four-layered network structure that consists of input, membership function, inference rule, and output layers. In the FWNNs, a wavelet function is adopted as the membership function. Generally, the fuzzy rule of FNNs is expressed as

$$R_i: \text{IF } x_1 \text{ is } A_{i1} \text{ and } \ldots \text{ and } x_n \text{ is } A_{in},$$
$$\text{THEN } \hat{y}_{i1} = w_{i1} B_i \text{ and } \ldots \text{ and } \hat{y}_{ik} = w_{ik} B_i, \quad (3)$$

where R_i is the ith fuzzy rule, $1 \le i \le r$, x_j is the jth input, $1 \le j \le n$, y_{ik} is the kth output contributed by the ith fuzzy rule, $1 \le k \le p$, A_{ij} is the membership function for the ith fuzzy rule of the jth input characterized by a wavelet function, w_{ik} is the synaptic weight of the ith inference rule for kth system output, and B_i is the constant consequent of the ith fuzzy rule. The semantic meaning and operation function of the nodes in each layer are described as follows：

***Layer* 1** (input layer): In this layer, the number of nodes is equal to the number of input variables. These nodes are used to transmit the input linguistic values to the next layer directly.

***Layer* 2** (membership function layer): In this layer, each node corresponds to one input linguistic term in Layer 1. In other words, the membership value specifying the degree to which an input value belongs to a fuzzy set is calculated in this layer. To describe the linguistic terms, Gaussian function representing fuzzy membership functions is adopted as

$$\mu_{ij}(x_j) = \exp\left(-\frac{(x_j - b_{ij})^2}{2a_{ij}^2} \right), \quad (4)$$

where a_{ij} and b_{ij} for $i = 1, 2, \ldots, r$, $j = 1, 2, \ldots, n$ are the dilation and the translation of the ith wavelet membership function for the jth input variable x_j, respectively.

***Layer* 3** (inference rule layer): Each node represents one fuzzy rule in this layer. The AND (min) operation is applied to calculate the output of each node. That is, product inference method is used to determine the firing strength of each node. Each inference rule can be expressed as

$$B_i = \prod_{j=1}^{n} \mu_{ij}(x_j) \quad \text{for } i = 1, 2, \ldots, r, \quad (5)$$

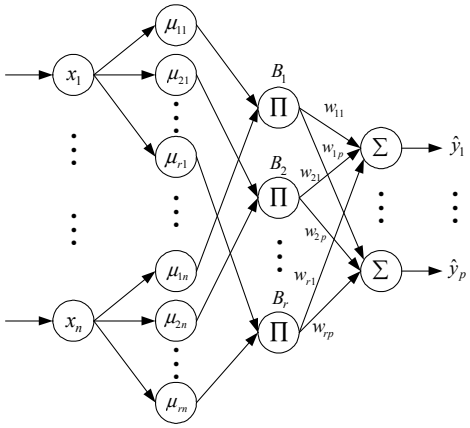

Figure 1. The architecture of fuzzy neural networks (FNNs).

***Layer* 4** (output layer): In this layer, each node represents an individual output of the FNN by using a simple weighted sum. The mathematic function of the kth output is shown as

$$\hat{y}_k = \sum_{i=1}^{r} w_{ik} B_i = \sum_{i=1}^{r} w_{ik} \prod_{j=1}^{n} \exp\left(-\frac{(x_j - b_{ij})^2}{2a_{ij}^2} \right), \quad (6)$$

where $\hat{y}_k$ for $k = 1, 2, \ldots, p$ is the kth FNN output.

It is very difficult, if not impossible, to solve the above problem directly. In usual cases, the initial values of r, w_{ik}, b_{ij}, and a_{ij} are chosen first. Then a training algorithm is applied to FNNs to search for the optimal combination of these values in an iterative manner. However, as mentioned above, there is no way to choose these initial values systematically. Therefore, in the following section, an SVR approach will be proposed to serve for this purpose.

III. SVR-ARTVLA-FNNS BASED ON PSO

A. SVR-Based Initial Structure of FNNs

When approximating an unknown function, SVR method can be adopted to build the initial structure of FNNs [10]. Meanwhile, assume that a set of basis functions, $g_l(\mathbf{x})$, $l = 1, 2, \cdots, L$, is given. Then the problem of function

approximation is transformed into finding the parameters of the following basis linear expansion

$$f(\mathbf{x},\boldsymbol{\theta}) = \sum_{l=1}^{L} \theta_l g_l(\mathbf{x}) + bias\,, \tag{7}$$

where $\boldsymbol{\theta} = (\theta_1, \theta_2, \cdots, \theta_L)$ is a parameter vector to be identified and *bias* is a constant to be determined.

From SVR method, one can find that the solution is to find $f(\mathbf{x},\boldsymbol{\theta})$ in (7) that minimizes

$$R(\boldsymbol{\theta}) = \frac{1}{N}\sum_{j=1}^{N} L_\varepsilon(y_1^{(j)} - f(\mathbf{x}^{(j)}, \boldsymbol{\theta}))\,, \tag{8}$$

subject to the constraint

$$\|\boldsymbol{\theta}\|^2 < C\,, \tag{9}$$

where $L_\varepsilon(\cdot)$ is the ε-insensitive loss function defined as

$$L_\varepsilon(e) = \begin{cases} 0 & \text{for } |e| \le \varepsilon \\ |e| - \varepsilon & \text{otherwise} \end{cases} \tag{10}$$

for some nonnegative number ε.

Vapnik [10] has applied the kernel function $K(\mathbf{x}_r, \mathbf{x}_s)$ to replace the inner product of basis functions $g_l(\mathbf{x}_r)$ and the Lagrange multiplier method has been adopted to minimize (8). Then the dual optimization problem can be expressed as follows:

$$\begin{aligned} \text{Min } Q(\alpha, \alpha^*) = \varepsilon\sum_{r=1}^{N}(\alpha_r + \alpha_r^*) - \sum_{r=1}^{N} y_r(\alpha_r - \alpha_r^*) \\ + \frac{1}{2}\sum_{r,s=1}^{N}(\alpha_r^* - \alpha_r)(\alpha_s^* - \alpha_s)K(\mathbf{x}_r, \mathbf{x}_s), \end{aligned} \tag{11}$$

subject to the constraint

$$\sum_{r=1}^{N}\alpha_r^* = \sum_{r=1}^{N}\alpha_r\,,\ 0 < \alpha_r^*, \alpha_r < C \tag{12}$$

and the solution is in the form of the following linear expansion of kernel functions

$$f(\mathbf{x}, \alpha, \alpha^*) = \sum_{l=1}^{L}(\alpha_l^* - \alpha_l)K(\mathbf{x}, \mathbf{x}_l) + bias\,. \tag{13}$$

Note that some of $(\alpha_l^* - \alpha_l)$'s are not zeros and the corresponding vectors $\mathbf{x}_l$'s are called *support vectors* (SVs).

The Gaussian function is used as the kernel function, then (13) can be rewritten as

$$f(\mathbf{x},\lambda) = \sum_{l=1}^{\#SV}\lambda_l \exp\left(-\frac{\|\mathbf{x} - \mathbf{x}_l\|^2}{2\sigma_l^2}\right) + bias\,, \tag{14}$$

where $\#SV$ is the number of SVs, $\lambda_l = (\alpha_l^* - \alpha_l) \neq 0$, and $\mathbf{x}_l$ denotes SVs. Comparing (14) with (2), *#SV*, *l*, λ_l, $\mathbf{x}_l$, and σ_l in (14) can be regarded as the *r*, *i*, w_{ik}, b_i, and a_i in (2), respectively.

B. ARTVLA-Based FNNs

With an initial structure, a learning algorithm must be established to train FNNs. In the training procedure of the proposed FNNs, the annealing concept in the cost function of robust back-propagation learning algorithm was adopted to overcome the existing problems in robust back-propagation learning algorithm, such as slow convergence rate and getting into local minimum. A cost function for the ARTVLA is defined here as

$$J_k(h) = \frac{1}{N}\sum_{j=1}^{N}\rho\left[e_k^{(j)}(h); \beta(h)\right] \text{ for } k = 1, 2, \cdots, p\,, \tag{15}$$

where

$$\begin{aligned} e_k^{(j)}(h) &= y_k^{(j)} - \hat{f}_k(\mathbf{x}^{(j)}) \\ &= y_k^{(j)} - \sum_{i=1}^{L} w_{ik}\exp\left(-\frac{\|\mathbf{x}^{(j)} - b_i\|^2}{2a_i^2}\right), \end{aligned} \tag{16}$$

h is the epoch number, $e_k^{(j)}(h)$ is the error between the *k*th desired output and the *k*th output of FNNs at epoch *h* for the *k*th input-output training data in a nonlinear system, $\beta(h)$ is a deterministic annealing schedule acting like the cut-off point, and $\rho(\cdot)$ is a logistic loss function defined as

$$\rho[e_k^{(j)}; \beta] = \frac{\beta}{2}\ln\left[1 + \frac{(e_k^{(j)})^2}{\beta}\right] \text{ for } k = 1, 2, \cdots, p\,. \tag{17}$$

Based on the gradient-descent kind of learning algorithms, the synaptic weights w_{ik}, the centers b_i, and the widths a_i of Gaussian functions are updated as

$$\Delta w_{ik} = -\eta_{w_k}\frac{\partial J_k}{\partial w_{ik}} = -\frac{\eta_{w_k}}{N}\sum_{j=1}^{N}\varphi_k(e_k^{(j)}; \beta)\frac{\partial e_k^{(j)}}{\partial w_{ik}}\,, \tag{18}$$

$$\Delta b_i = -\eta_b\frac{\partial J_k}{\partial b_i} = -\frac{\eta_b}{N}\sum_{j=k}^{p}\sum_{j=1}^{N}\varphi_k(e_k^{(j)}; \beta)\frac{\partial e_k^{(j)}}{\partial b_i}\,, \tag{19}$$

$$\Delta a_i = -\eta_a\frac{\partial J_k}{\partial a_i} = -\frac{\eta_a}{N}\sum_{k=1}^{p}\sum_{j=1}^{N}\varphi_k(e_k^{(j)}; \beta)\frac{\partial e_k^{(j)}}{\partial a_i}\,, \tag{20}$$

$$\varphi_k(e_k^{(j)}; \beta) = \frac{\partial\rho(e_k^{(j)}; \beta)}{\partial e_k^{(j)}} = \frac{e_k^{(j)}}{1 + (e_k^{(j)})^2 / \beta(h)}\,, \tag{21}$$

where η_{w_k}, η_b, and η_a are the learning rates for the synaptic weight w_{ik}, $k = 1, 2, \cdots, p$, the center b_i, and the width a_i, respectively; $\varphi(\cdot)$ is usually called the influence function. In the ARTVLA, the annealing schedule $\beta(h)$ has the properties:

(A) β_{initial}, $\beta(h)$ for the first epoch, has large values;

(B) $\beta(h) \to 0^+$ for $h \to \infty$;

(C) $\beta(h) = \kappa / h$ for any h epoch, where κ is a constant.

When the learning rates are constant in (18) to (10), the work for selecting an appropriate learning rate is tedious; moreover, there exists a tendency to get stuck in a near-optimal solution or to converge slowly. To overcome the stagnation in searching a globally optimal solution, an ARTVLA is proposed to approach the optimal solution closely in this paper. In the learning procedure, considering the search space, a large learning rate is selected at the beginning. Once the algorithm is found to converge more and more towards the optimum, the evolution process is gradually converted to a finer and finer tuning by a smaller learning rate in later epochs. Then, in the ARTVLA, a nonlinear time-varying evolution concept is adopted over iterations, in which the learning rates η_w, η_b, and η_a with a high value $\eta_{\max}$ and nonlinearly decreases to $\eta_{\min}$ at the maximal number of epochs, respectively. This means that the mathematical expressions are given as shown as

$$\eta_w = \eta_{\min} + \left(1 - \frac{h}{epoch_{\max}}\right)^{pw} (\eta_{\max} - \eta_{\min}), \tag{22}$$

$$\eta_b = \eta_{\min} + \left(1 - \frac{h}{epoch_{\max}}\right)^{pb} (\eta_{\max} - \eta_{\min}), \tag{23}$$

$$\eta_a = \eta_{\min} + \left(1 - \frac{h}{epoch_{\max}}\right)^{pa} (\eta_{\max} - \eta_{\min}), \tag{24}$$

where $epoch_{\max}$ is the maximal number of epochs and h is the current number of epochs. In the updated procedure, appropriate functions for the learning rate η_w, η_b, and η_a can promote the performance of FNNs. However, simultaneously determining the optimal combination of *pw*, *pb*, and *pa* is a time-consuming work. An efficient evolutionary algorithm, PSO, will be adopted to determine the optimal solution (*pw*, *pb*, *pa*).

C. Particle Swarm Optimization

PSO is a population-based stochastic searching technique developed by Kennedy and Eberhart [16]. It is similar to the continuous genetic algorithms, in which it begins with a random population matrix and searches for the optimum by updating generations. However, the PSO has no evolution operations such as crossover and mutation. The potential of this technique makes it be a powerful optimization tool which has been successfully applied to many fields. Nowadays PSO has been developed to be real competitors with other well-established techniques for population-based evolutionary computation [17-19].

In this paper, the PSO method is adopted to find the optimal combination (*pw*, *pb*, *pa*) of learning rates in (22) to (24) for system identification. When applying the PSO method, possible solutions must be encoded into particle positions and a fitness function must be chosen. In the system identification, the goal is to minimize the error between the desired outputs and the trained outputs. Therefore, the root mean squares error (*RMSE*) should be used to define a fitness function. This means that the fitness function will be defined as

$$RMSE = \sqrt{\frac{1}{N}\sum_{j=1}^{N}\left(y^{(j)} - \hat{y}^{(j)}\right)^2}, \tag{25}$$

where $y^{(j)}$ is the desired output, $\hat{y}^{(j)}$ is the trained output for *N* sampling data.

IV. Simulation Results

In the identification scheme of a chaotic system, training input-output data are obtained by feeding a time series $[x(t), x(t-\tau), x(t-2\tau), \cdots, x(t-(m-1)\tau)]$ to the system and to predict its corresponding output $x(t+\tau)$ Then subject to the same input data, the objective of identification is to construct an SVR-ARTVLA-FNNs model based on PSO method, which produces an output $\hat{x}(t+\tau)$ to approximate $x(t+\tau)$ as closely as possible.

In this section, a time-delay chaotic system with outliers is used to verify the feasibility of the proposed SVR-ARTVLA-FNNs. When applying the proposed algorithm, the population size, the maximal iteration number, and the maximal epoch number are chosen to be 30, 200, and 500, respectively. As for the parameters in PSO, the best ranges were presented [19]. The variables *pw* *pb* and *pa* in learning rate functions (22) through (24) are all chosen as real numbers in the range $[0.1, 5]$. In PSO, the particles are updated by linearly time-varying evolutionary algorithm in [19]. Meanwhile, the values of $\eta_{\max}$ and $\eta_{\min}$ are set as 1.0 and 0.01, respectively. To evaluate the performance of the proposed FNNs, *RMSE* of the training data is adopted as

$$RMSE = \sqrt{\frac{1}{N}\sum_{j=1}^{N}\left(x_j(t) - \hat{x}_j(t)\right)^2}, \tag{26}$$

where $x_j(t)$ is the desired output of the chaotic time series, $\hat{x}_j(t)$ is the trained output of the proposed FNNs.

***Example*:** A typical chaotic system, Mackey Glass time-delay series, is considered as an example described as follows [6]:

$$x = \frac{px(t-\tau)}{1 + x^r(t-\tau)} - qx(t), \tag{27}$$

where $p = 0.2$, $q = 0.1$, $r = 10$, τ is the time-delay parameter. If $\tau \geq 17$, the time series show the chaotic phenomenon. To compare with [6, 20], the time series are chosen as

$$x(t+6) = f(x(t), x(t-6), x(t-12), x(t-18\tau)), \qquad (28)$$

where $x(t)$, $x(t-6)$, $x(t-12)$, and $x(t-18)$ are the inputs of the proposed FNNs; $x(t+6)$ is the output of the FNNs.

In the simulation, 1000 time-delay series are generated from (27) with initial value $x(0) = 1.2$. The former 500 data are selected as the training data for identifying the Mackey Glass system shown in Fig. 2. Assume that the membership function is Gaussian function and initial structures are obtained by an ε-SVR approach, in which the parameters are set as $C = 10$, $\varepsilon = 0.3775$ in (9) and (10).

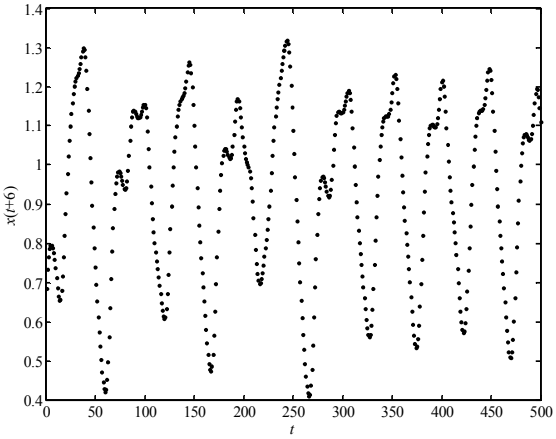

Figure 2. Training data without outliers for identifying time-delayMackey Glass system.

Problem 1:

The training data with no outliers are fed into the FNNs. The initial values of w_{ik}, b_i, and a_i in (2) can be determined by ε-SVR approach. Meanwhile, the number of fuzzy rules is obtained as 23.

Based on the above initial structure of FNNs, ARTVLA with nonlinear learning rates to train the SVR-FNNs, in which the optimal learning rates are determined by PSO method. Then, the optimal sets (pw, pb, pa) in (22) to (24) are obtained as (4.241218, 2.050131, 3.700988). Meanwhile, the final value of *RMSE* with ARTVLA-FNNs is found to be 0.005886. With the optimal learning rates, the errors of training data after 500 epochs are illustrated in Fig. 3.

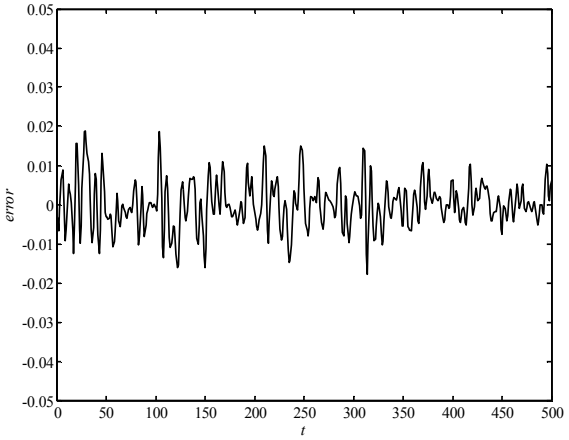

Figure 3. The plots of $error = x(t) - \hat{x}(t)$ for 500 training data without outliers after 500 training epoch.

Problem 2:

The training data with 10 artificial outliers shown in Fig. 4 are fed into the FNNs. The initial values of w_{ik}, b_i, and a_i in (2) can be determined by ε-SVR method. Meanwhile, the number of fuzzy rules is obtained as 25.

Based on the above initial structure of FNNs, ARTVLA with nonlinear learning rates to train the SVR-FNNs, in which the optimal learning rates are determined by PSO method. Then, the optimal sets (pw, pb, pa) in (22) to (24) are obtained as (2.306907, 0.979595, 2.961404). Meanwhile, the final value of *RMSE* with ARTVLA-FNNs is found to be 0.007477. With the optimal learning rates, the errors of training data after 500 epochs are illustrated in Fig. 5.

From the above results, the feasibility of the ARTVLA-FNNs has been confirmed. The final *RMSEs* of the proposed FNNs and other FNNs of [6] are shown in Tables I. From the results, show that the proposed ARTVLA-FNNs can overcome the outliers and get a good performance for training data. Moreover, the comparison of *RMSE* with other NNs for Mackey-Glass time series without outliers after 500 training epochs is shown in Table II, in which the superiority of the proposed ARTVLA-FNNs can be verified.

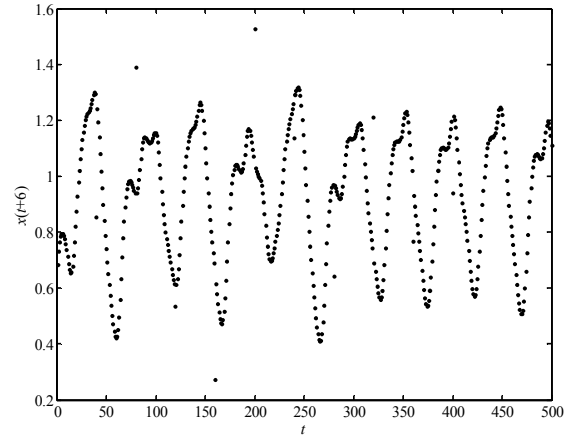

Figure 4. Training data with 10 artificial outliers for identifying time-delay Mackey Glass system.

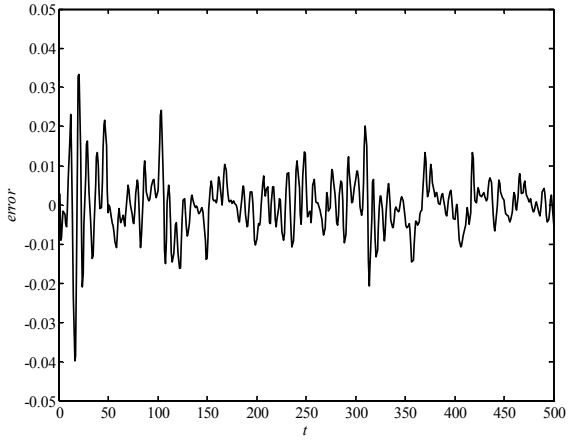

Figure 5. The plots of $error = x(t) - \hat{x}(t)$ for 500 training data with 10 artificial outliers after 500 training epoch.

TABLE I. COMPARISON OF *RMSE* USING VARIOUS METHODS FOR MACKEY-GLASS TIME-SERIES WITH ARTIFICIAL OUTLIERS.

ARTVLA-FNNs	ARFNNs [6]	ANFIS	RBFNs
0.0075	0.0091	0.0201	0.0204

TABLE II. COMPARISON OF *RMSE* USING VARIOUS METHODS FOR MACKEY-GLASS TIME-SERIES WITHOUT OUTLIERS.

Method	Training data	*RMSE*
ANFIS	500	0.0837
Gu and Wang [20]	500	0.1095
ARFNNs [6]	500	0.0073
ARTVLA-FNNs	500	0.0059

V. CONCLUSIONS

This paper presents the integrating SVR and ARTVLA to train FNNs for identification of a time-delay chaotic system. With the initial structure of the FNNs using SVR method, the nonlinear time-varying learning rates are simultaneously determined by PSO method to perform the ARTVLA. Then the optimal FNNs are obtained to identify the Mackey-Glass chaotic system. From the simulation results, one can conclude that the proposed SVR-ARTVLA-FNNs using PSO method have good performance for identification of the time-delay series system. Meanwhile, the superiority of the proposed ARTVLA-FNNs with nonlinear learning rates over the other NNs for identification has been verified. The proposed SVR-ARTVLA-FNNs can be further extended to identify more complex chaotic systems.

ACKNOWLEDGMENT

This work was supported in part by the National Science Council, Taiwan, R.O.C., under grants NSC 99-2221-E-252-017.

REFERENCES

[1] J. H. Kim, C. W. Park, E. Kim, and M. Park, "Fuzzy adaptive synchronization of uncertain chaotic systems," Physics Letters A, vol. 334, pp. 295–305, 2005.

[2] X. Wu, Z. H. Guan, Z. Wu, and T. Li, "Chaos synchronization between Chen system and Genesio system," Physics Letters A, vol. 364, pp. 484–487, 2007

[3] J. H. Park, "Adaptive control for modified projective synchronization of a four-dimensional chaotic system with uncertain parameters," Journal of Computational and Applied Mathematics, vol. 213, pp. 288–293, 2008.

[4] H. Gu and H. W. Wang, "Fuzzy prediction of chaotic time series based on singular value decomposition," Applied Mathematics and Computation, vol. 185, pp. 1171–1185, 2007.

[5] S. T. Pan and C. C. Lai, "Identification of chaotic systems by neural network with hybrid learning algorithm," Chaos, Solitons and Fractals, vol. 37, no. 1, pp. 233–244, 2008.

[6] Y. Y. Fu, C. J. Wu, J. T, Jeng, and C. N. Ko, "ARFNNs with SVR for prediction of chaotic time series with outliers," Expert Systems with Applications, vol. 37, pp. 4441–4451, 2010.

[7] C. F. Juang and C.T. Lin, "A recurrent self-organizing neural fuzzy inference network," IEEE Transactions on Neural Networks, vol. 10, no. 4, pp. 828–845, 1999.

[8] S. Abbasbandy and M. Otadi, "Numerical solution of fuzzy polynomials by fuzzy neural network," Applied Mathematics and Computation, vol. 181, no. 2, pp. 1084–1089, 2006.

[9] A. Azadeh, S. F. Ghaderi, M. Anvari, M. Saberi, and H. Izadbakhsh, "An integrated artificial neural network and fuzzy clustering algorithm for performance assessment of decision making units," Applied Mathematics and Computation, vol. 187, no. 2, pp. 584–599, 2007.

[10] V. N. Vapnik, The Nature of Statistical Learning Theory. New York: Springer-Verlag, 1995.

[11] S. Gao, H. W. Dai, Y. Y. Zhu, and Z. Tang, "Annealing chaotic pattern search learning method for multi-layer neural networks," International Journal of Computer Science and Network Security, vol. 7, no. 6, pp. 137–145, 2007.

[12] C. C. Chuang, S. F. Su, and C. C. Hsiao, "The annealing robust backpropagation (BP) learning algorithm," IEEE Transactions on Neural Networks, vol. 11, no. 5, pp. 1067–1077, 2000.

[13] C. C. Chuang, J. T. Jeng, and P. T. Lin, "Annealing robust radial basis function networks for function approximation with outliers," Neurocomputing, vol. 56, pp. 123–139, 2004.

[14] F. Takens, Detecting strange attractors in turbulence. Dynamical systems and turbulence. Berlin: Springer. pp. 336–381, 1981.

[15] L. Cao, A. Mees, and K. Judd, "Dynamics from multivariate time series," Physica D, vol. 121, 75–88, 1998.

[16] J. Kennedy and R. Eberhart, "Particle swarm optimization," In Proceeding of the IEEE International Conference on Neural Networks, Washington, DC, USA, vol. 4, pp. 1942–1948, 1995.

[17] D. W. Boeringer and D. H. Werner, "Particle swarm optimization versus genetic algorithms for phased array synthesis," IEEE Transactions on Antennas and Propagation, vol. 52, no. 3, pp. 771–779, 2004.

[18] E. Elbeltagi, T. Hegazy, and D. Grierson, "Comparison among five evolutionary-based optimization algorithms," Advanced Engineering Informatics, vol. 19, no. 1, pp. 43–53, 2005.

[19] A. Ratnaweera, S. K. Halgamuge, and C. Watson, "Self-organizing hierarchical particle swarm optimizer with time-varying acceleration coefficients," IEEE Transactions on Evolutionary Computation, vol. 8, no. 3, pp. 240–255, 2004.

[20] H. Gu and H. Wang, "Fuzzy prediction of chaotic time series based on singular value decomposition," Applied Mathematics and Computation, vol. 185, 1171–1185, 2007.

2011 IEEE International Conference on Fuzzy Systems
June 27-30, 2011, Taipei, Taiwan

A New Framework of Fuzzy Clustering Algorithm

Horng-Lin Shieh
Department of Electrical Engineering
St. John's University
Taipei, Taiwan
shieh@mail.sju.edu.tw

Abstract—**In this paper, a novel data clustering algorithm based on the *subtractive clustering* (SC) algorithm and a new validity index are proposed. The SC algorithm is a simple method for data clustering; however, it has two problems which must be overcome. The first problem is such that the cluster centers found by SC are taken from data with the highest potential values, but that this data may not be the real cluster centers. The second problem is such that the cluster number generated by the SC algorithm is influenced by a predefined parameter. The proposed algorithm is based on distance relations between data and centers and is designed to ascertain the real centers generated by the SC algorithm. In addition, a novel robust cluster index is proposed to identify the real cluster number generated by SC algorithm.**

Keywords- validity index, subtractive clustering (SC) algorithm, clustering algorithm

1. INTRODUCTION

In classical set theory, the membership of datum to a set is assigned using a value of 0 or 1. Let $\mu_A(x)$ denote the membership value of x belonging to cluster A (or set A). If one datum x belongs to cluster A, the membership value $\mu_A(x)$ is 1, otherwise, its value is 0; this clustering method is called hard partition. However, in practical applications, there are ambiguities found in the data set such that some data may or may not be partitioned into one cluster. In this situation, the membership value $\mu_A(x)$ of x is assigned to a range of [0,1]; this method is called *soft partition*. The fuzzy clustering algorithm based on fuzzy set theory is the most well known soft partition method. In the context of a fuzzy set, a value close to 1 for $\mu_A(x)$ denotes a high degree of membership, while a value close to 0 denotes a low degree of membership. Numerous successful applications of fuzzy clustering have been proposed, such as handwritten digit recognition [1], function approximation [2][3][4], and image processing [5].

There have been numerous fuzzy clustering methods proposed in the literature [6]-[11]. The fuzzy c-means algorithm (FCM) [7][8] has become the most popular fuzzy clustering approach for both theoretical and practical applications in recent decades. However, the FCM algorithm has two disadvantages: (1) the number of clusters has to be known in advance but, in many applications, this knowledge is often not available; (2) when the data training contains outliers, the resultant centers are always influenced by outliers. To overcome the first disadvantage, the results of the analyses pertaining to different numbers of clusters have to be compared to each other using a validity function in order to ascertain an optimal cluster number. As regards the second disadvantage, when the training data contains noise/outliers, the results obtained by FCM are always affected by noise/outliers.

2. A New Clustering Algorithm

The *mountain method* (MM) proposed by Yager and Filev in 1994 [12] is an effective and simple method for identifying the cluster center of the sampling data. The mountain method divides data space into several intervals to construct grids and then evaluates its energies by substituting the distance from the grid to the data points into the objective exponential function in order to determine the approximated cluster centers at the grid with the maximum energy.

Let $X=\{x_1,x_2,\ldots,x_n\}$ be a set of n vectors in a d-dimensional feature space, that is, $x_i \in \Re^d$ is a vector, and x_{kj} denotes the j-th coordinate of the k-th data point, where $k = 1,2,\ldots, n$ and $j = 1,2,\ldots, d$.

The MM for data clustering is divided into three steps:

Step1: first, the mountain function involves constructing a grid on the data space where the intersections of the grid lines are considered to be candidates for the cluster centers.

Step2: the second step entails constructing a mountain function representing a data energy measurement. The value of the mountain function at grid node N_i is calculated by:

$$M(N_i) = \sum_{k=1}^{n} \exp(-\alpha \cdot d(x_k, N_i)), \qquad (1)$$

where α is an application-specific positive constant and $d(x_k,N_i)$ is the distance between the data point x_k and the grid node N_i. The value of the mountain function can be seen to represent the potential ability of any of the grid nodes to be a cluster center. The higher mountain function value of the data is selected as the cluster center.

Step 3: the third step involves an iterative selection of the next cluster centers and a sequential deconstruction of the mountain function value. In each iterative process, the grid node that has the largest energy is selected as the cluster center and the energies of the remaining grid nodes must be eliminated in order to identify the next one. Let N_k^* , $k=1,2,\ldots,c_{max}$, denote the grid node that

978-1-4244-7316-8/11/$26.00 ©2011 IEEE

has the maximal value of the mountain function at the k-th iteration. The maximal value of the mountain function M_k^* is denoted as:

$$M_k^* = \max_i M_k(N_i) \quad (2)$$

The new modified value of the mountain function is defined as follows:

$$M_{k+1}(N_i) = M_k(N_i) - M_k^* \times e^{-\beta d(N_i - N_k^*)} \quad (3)$$

Where β is a predefined positive constant. The MM continually produces new cluster centers and reduces the value of the mountain function until the level of the current maximum M_k^* compared with the original maximum M_1^* becomes too low.

Although the mountain method is a simple method for data clustering and has robust properties against outliers and noise, it has a notable problem that must be overcome. That is, because the mountain function calculates its energies on the grid nodes, the grid nodes and computational loads increase exponentially as the dimensions increase. In 1994, Chiu [13] modified the mountain method to construct a potential function for calculating the clustering center of the sampling data. The proposed method is also called the subtractive clustering (SC) algorithm. In the SC algorithm, the data points are likened to energy sources. The potential generated by each feature point has a peak value at the location of the data point which decreases rapidly at any point away from the data point [14]. The potential of each data point x_i is defined as:

$$P(x_i) = \sum_{k=1}^{n} \exp(-\alpha \cdot d(x_i, x_k)), \quad (4)$$

where $\alpha = \frac{4}{r_a}$, and r_a is a positive constant that is effectively the radius defining a neighborhood. In Equation (4), the total potential of any data point x_i is defined as the sum of the potentials contributed by each data point at x_k. It is reasonable to assume that the peaks of the total potential function correspond to cluster prototypes and that the valleys correspond to the decision boundaries between the clusters [14].

After the potential of each data point is obtained, the data point with the highest potential is selected as the first cluster center. Assume x_1^* is the first cluster center and its potential value is p_1^*. Then, the potential of each data point can be revised by:

$$P(x_i) = P(x_i) - p_1^* e^{-\beta d(x_i, x_1^*)}, \quad (5)$$

where $\beta = \frac{4}{r_b}$, and r_b is a positive constant which is effectively the radius defining a neighborhood that will have measurable reductions in potential. In [13], a good choice for r_b is 1.5 r_a. To find the next cluster center, x_2^*, the new revised potential is maximized and the effects of this cluster center are again removed. The process is repeated until a given threshold for the potential is obtained so that:

$$\frac{p_j^*}{p_1^*} < \delta. \quad (6)$$

In the above equation, δ is a given threshold. The choice of δ is an important factor affecting the clustering results; if δ is too large, then too few data points will be accepted as cluster centers and if δ is too small, then too many cluster centers will be generated [13].

There are two problems that must be overcome: (1) the SC algorithm assumes that the clustering center is x_i^* obtained by the i^{th} iteration. However, the x_i^* may be a rough cluster center which does not represent the actual cluster center; (2) there is no index to indicate what the optimal number of clusters for a data set is. For overcoming the first problem, this paper proposes a new algorithm based on distance measurements to identify the actual cluster centers. For overcoming second problem, this paper proposes a new validity index for the SC algorithm to indicate the goodness of the partitions in various cluster numbers. The proposed validity index combines the compactness in each cluster, the separation between clusters, and the correct ratio of data being properly partitioned into clusters to whole data set.

Let x_i^*, $i = 1,2,\ldots,c_{max}$ are the cluster centers obtained by the SC algorithm, the distance relation between the centers x_i^* and data x_j is defined by the following equation:

$$D_{ij} = \exp(-\alpha \| x_j - x_i^* \|^2), i = 1, 2, \ldots, c_{\max}, j = 1, 2, \ldots, n, \quad (7)$$

where $\|x_j - x_i^*\|$ represents the Euclidean distance between x_j and x_i^* and where α is a constant defined in Equation (4). The value of D_{ij} indicates the distance relationship between x_j and x_i^*. In other words, for a cluster center x_i^*, any data x_j that has high value of D_{ij} indicates that this data x_j is close to the cluster i. Set N_ϵ denotes the number of data which has $D_{ij} \geq \epsilon$, where $\epsilon \geq 0$ is a constant. In this paper, ϵ is set to 0.5. The new center of cluster i is defined by the following equation:

$$v_i = \frac{\sum_{k=1}^{N_\varepsilon} x_k^i}{N_\varepsilon}, \quad (8)$$

where x_k^i are the data which have $D_{ik} \geq \epsilon$. In Equation (8), v_i is the mean of data close to cluster i. In each iterative epoch of the SC algorithm, when a new rough cluster center x_i^* is found, Equation (8) is adopted to evaluate the real cluster center; the potential of the data point can be revised by:

$$P(x_k^i) = P(x_k^i) - p_i^* e^{-\beta d(x_k^i, v_i)}. \quad (9)$$

The differences between the proposed method and the original SC algorithm are such that: (1) the cluster centers obtained by the proposed method provide a more accurate real cluster center than the cluster centers obtained by the SC algorithm; and (2), in each iterative epoch of the proposed method, the revised potential of Equation (9) uses relative data, x_k^i, that is close to the cluster center *i*, while the revised potential of the SC algorithm in Equation (5) uses all sampling data. That is to say that the proposed method requires less computation of data than SC algorithm.

3. A ROBUST VALIDITY INDEX

A *validity index* is a function which assigns to the output of the clustering algorithm a value to measure the qualities of the partitions provided by the output. The cluster number of SC algorithm is determined in Equation (6) but it is not used for evaluating the fitness of partitions obtained through fuzzy clustering. The validity index for finding an optimal *c,* denoted c^*, which can completely describe the data structure, has become the most studied topic in cluster validity. Several popular validity indexes are reviewed in [15][16].

The partition coefficient (PC) index proposed by Bezdek [17] in 1974 was the first index for the FCM algorithm. et $X=\{x_1,x_2,\ldots x_n\} \subset \Re^d$ be a data set in a *d*-dimensional feature space and μ_{ik} be the membership value of data x_i belonging to cluster *k*. The PC index is defined as:

$$\mathrm{PC}(c) = \frac{1}{n}\sum_{k=1}^{c}\sum_{i=1}^{n}(\mu_{ik})^2 , \quad (10)$$

$$\text{and} \quad \sum_{k=1}^{c}\mu_{ik} = 1, \quad \frac{1}{c} \le PC(c) \le 1 .$$

As regards a clustering algorithm for the partitioning of a data set, the optimal cluster number occurs when the PC (*c*) is at maximal value. The core idea of the PC index is such that the optimal cluster number occurs when the data are most unambiguously partitioned into clusters. The disadvantage of the PC index is that it only considers the fuzzy membership degree μ_{ik} for each cluster without considering the structure of the clusters.

The other index proposed by Bezdek is the partition entropy (PE) index [17][18]. The PE index is defined as:

$$PE(c) = -\frac{1}{n}\sum_{k=1}^{c}\sum_{i=1}^{n}\mu_{ik}\log_a(\mu_{ik}) , \quad (11)$$

where *a* is the base of the logarithm and the range of the PE(c) is $[0, \log_a(c)]$. For finding an optimal c^*, we solve min $_{2\le c\le c_{\min}}$ PE(c) to produce the best clustering performance for a data set. The disadvantage of the PE index is analogous to the PC index, i.e., the PE index will take the minimum value on every hard partition. These two indexes only evaluate the fuzziness and do not consider the data structure of the clusters.

The Xie and Beni (XB) index [19], combined compactness and separation properties, is defined as follows:

$$XB(c) = \frac{\sum_{k=1}^{c}\sum_{i=1}^{n}\mu_{ik}^2 \,\| x_i - v_k \|^2}{n \times min_{i\ne j}(\| v_i - v_j \|)} . \quad (12)$$

Where v_i and v_j represent the centers of cluster *i* and *j*, respectively, while $\|v_i - v_j\|$ represents the Euclidean distance between v_i and v_j. In Equation (12), the numerator indicates the compactness of the fuzzy partition while the denominator indicates the strength of the separation between clusters [20]. A small value in the numerator of the XB index represents a high level of compactness, while a high value in the denominator denotes good separation between clusters. Hence, the lowest $\mathrm{XB}(c), 2 \le c \le c_{\max}$ indicates the optimal cluster number for a data set *X*. However, the separation measurement of the XB index adopts the minimal distance between cluster centers; when cluster number *c* is close to the candidate of the data set, the XB index decreases to the lowest value.

The Fukuyama and Sugeno (FS) index [21] is another index which combines the properties of compactness and separation measurements. The FS index is defined as follows:

$$\mathrm{FS(c)} = \sum_{i=1}^{n}\sum_{k=1}^{c}(\mu_{ik})^m \| x_i - v_k \|^2 - \sum_{k=1}^{c}\left\{\left[\sum_{i=1}^{n}(\mu_{ik})^2\right]\cdot\| v_k - \bar{v}\|\right\}, \quad (13)$$

where $1 < m < \infty$, and $\bar{v} = \frac{1}{c}\sum_{i=1}^{c} v_i$ represents the mean of the cluster centroids. In Equation (13), the first term represents the geometrical compactness of the clusters and the second term indicates the separation between the clusters. When *m* is 2, the first term of the FS index equals the numerator of the XB index. The second term of the FS index is used for the separation measurements. The optimal cluster number is obtained by solving $\min_{2\le c\le n-1} FC(\mathrm{c})$.

The I-index was proposed by Maulik and Bandyopadhyay [22] in 2002. The I-index is defined as:

$$I(c) = \left(\frac{1}{c}\times\frac{E_1}{E_c}\times D_c\right)^2 . \quad (14)$$

Where

$$E_c = \sum_{i=1}^{n}\sum_{j=1}^{c}\mu_{ij}\| x_i - v_j \| , \quad (15)$$

and

$$D_c = \max_{i,j=1}^{c}\| v_i - v_j \| . \quad (16)$$

To find the optimal c^*, the authors tried to solve the max $_{2\le c\le c_{\max}}$ I(c) in order to obtain the best clustering performance for the data set.

In real applications, data domains are often affected by noises and outliers. The resultant partitions obtained by clustering algorithms are consistently affected by those variables and, surprisingly, there has been little discussion in

the literature about the influence of noises and outliers on validity indexes. In this paper, a novel robust validity index is proposed to indicate the adequacy of partitions in a data set with regard to noise and outliers.

Let $X=\{x_1,x_2,\ldots,x_n\} \subset \Re^d$ be a data set in a d-dimensional feature space and $W=\{w_{ik} \mid 0 \le w_{ik} \le 1\}$, $1 \le i \le n, 1 \le k \le c$ be a matrix, where w_{ik} is the membership degree of x_i belonging to cluster k, and $v=\{v_1, v_2, \ldots, v_c\}$ is a set of the cluster centers, where $v_k \in \Re^d$. The w_{ik} is defined by:

$$w_{ik} = \exp(-\frac{\| x_i - v_k \|^2}{\rho^2}), \quad (17)$$

where $\|x_i - v_k\|$ represents the Euclidean distance between x_i and v_k, and ρ is the width of the Gaussian function. In the proposed method, $\rho = \sqrt{\alpha}$, where α is defined by Equation (4). Let F represent a fuzzy set of data x_i belonging to cluster k. Hence, F can be characterized by Equation (17). An α- cut of a fuzzy set F is a crisp set F_α that contains all the elements in X which have membership values in F greater than or equal to α, that is:

$$F_\alpha = \{x_i \in X | w_{ik} \ge \alpha\} \quad (18)$$

This paper assumes that $\alpha = 0.5$ and that Γ represents the number of data satisfying $w_{ik} \ge \alpha$, that is:

$$\Gamma = |F_{0.5}|, \quad (19)$$

where $|\ |$ is the number of elements in a set. When a data x_i closes to cluster k, then w_{ik} is greater than or equal to 0.5 and x_i can be partitioned into cluster k. Hence, this paper defines a parameter τ named *partitioned index* to indicate the ratio of data that has been properly partitioned to all data. Thus, τ is defined as:

$$\tau = \frac{\Gamma}{|X|}. \quad (20)$$

For indicating the fitness of the number of partitions in a data set with noises and outliers, this paper combines compactness, separation, and τ properties to propose a new validity index, CSα, as follows:

$$CS\alpha(c) = (\frac{1}{\tau \times D_{\min}}) \times com. \quad (21)$$

Where,

$$D_{\min} = \min_{i \ne j} (\| v_i - v_j \|), \quad (22)$$

$$com = (\frac{1}{n^2} \sum_{k=1}^{c} \sum_{i=1}^{n} \mu_{ik}^2 \| x_i - v_k \|^2 \times \sum_{k=1}^{c} \sum_{i=1}^{n} \mu_{ik} \| x_i - v_k \|), \quad (23)$$

and,

$$\sum_{k=1}^{c} \mu_{ik} = 1. \quad (24)$$

To find the optimal number of clusters, this paper solves the $\min_{2 \le c \le c_{max}} CS\alpha$. The CSα is subject to three factors: $\frac{1}{\tau}$, $\frac{1}{D_{\min}}$, and *com*.

4. Experimental Results

In this section, two data sets are used to show that the validity index proposed in this paper outperforms other indexes proposed in the literature. For all experiments undertaken in this paper, it is reasonable to regard the square root of n as the upper limit of the optimal number of clusters [23], that is $c_{max} = \sqrt{n}$, where n is the candidate of data set.

Example 1: this example is used to test the performance of various indexes for a data set without noise. Fig. 1(a) shows a data set made up of four clusters and the stars denote the cluster centers obtained by the proposed method. Each cluster has fifty data points, hence, the $c_{max} = \sqrt{200} = 14$. Figs. 1(b)-(f) show the results obtained by PE, XB, FS, I-index and CSα, respectively. The results show that the XB, FS, I-index and CSα indexes can correctly indicate the cluster number of this data set, but the PE index indicate that the optimal numbers of clusters is two. This result shows that the XB, FS, I-index and CSα indexes performe equally as well, but that PE did not have good performance.

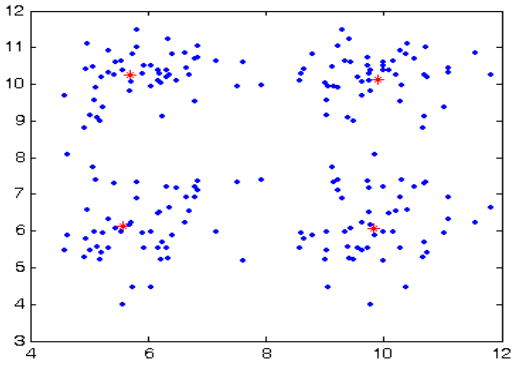

(a)

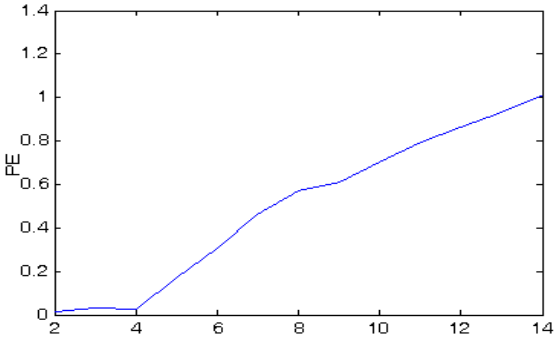

(b)

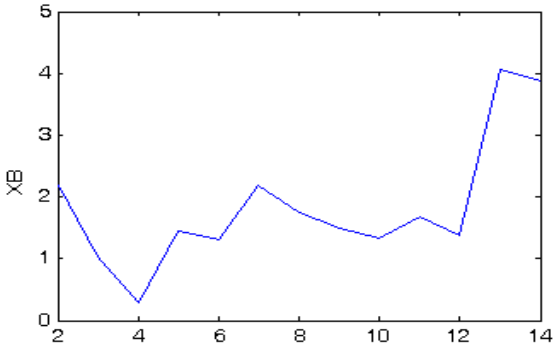

(c)

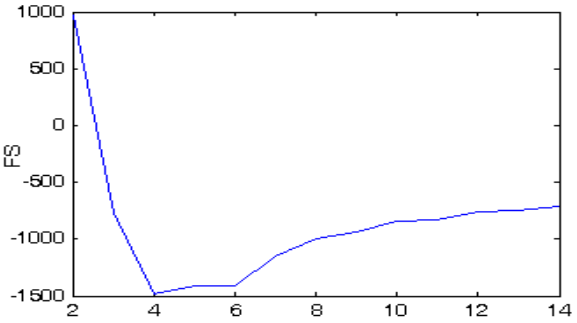

(d)

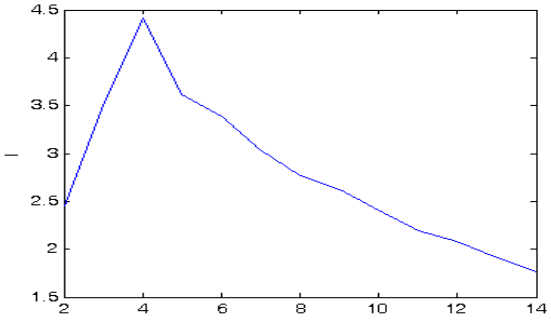

(e)

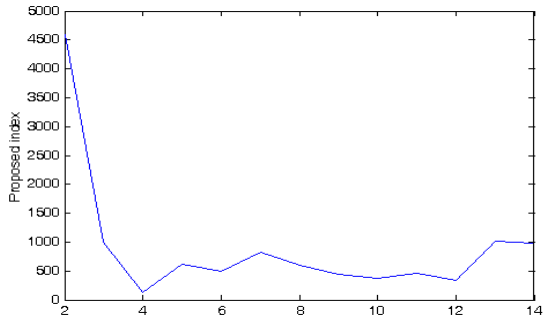

(f)

Fig.1: A data set contains four clusters.

Example 2: In this experiment, 100 noises are added to the data set used in Example 1 to test the proposed clustering and validity index. Fig. 2(a) shows the data set containing three clusters and noises and stars denote the cluster centers obtained by the proposed clustering algorithm. The performances of various indexes for this data set are shown in Figs. 2(b)-(f). The results show that only the proposed index can correctly indicate the optimal number of clusters. The PE, XB, FS, and I-index obtain the optimal number of clusters at two clusters.

5. Conclusions

In this paper, a novel data clustering algorithm based on the SC algorithm and a new validity index are proposed. The proposed clustering algorithm adopts the distance relations between data points and cluster centers obtained by using the SC algorithm to evaluate real cluster centers. In addition, a new validity index composed of compactness, separation, and a partitioned index is proposed to measure the fitness of various cluster numbers. Two examples show that the proposed clustering algorithm can obtain correctly the cluster centers, and the proposed index can indicate correctly the cluster numbers of data set with noises.

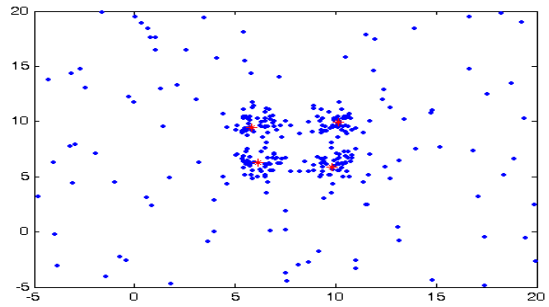

(a)

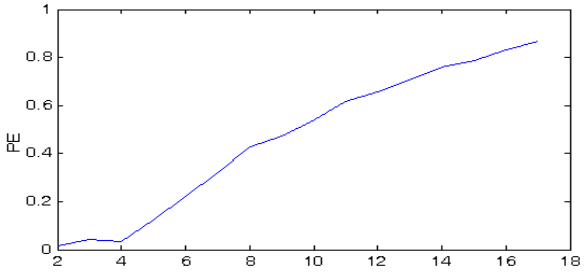

(b)

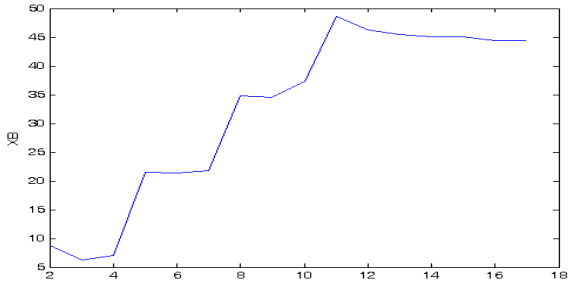

(c)

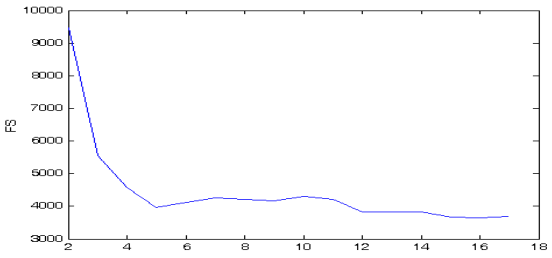

(d)

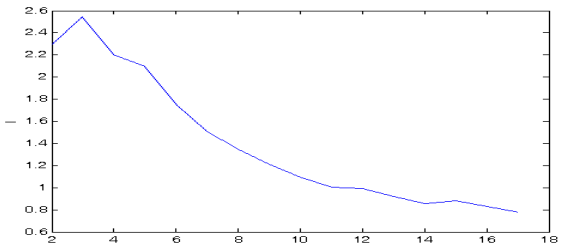

(e)

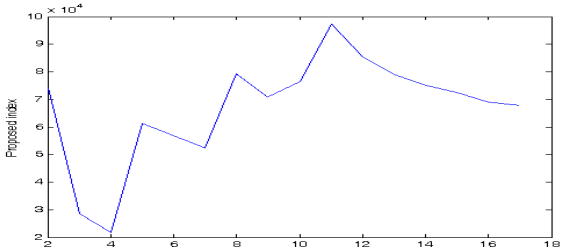

(f)

Fig. 2: A data set containing 4 clusters with 100 noises

References

[1] S. Chatzis, and T. Varvarigou, "Factor Analysis Latent Subspace Modeling and Robust Fuzzy Clustering Using t-Distributions," IEEE Trans. on Fuzzy Systems, vol. 17, no. 3, pp.505-517, 2009.

[2] H.-L. Shieh, Y.-K. Yang, P.-L. Chang, J.-T. Jeng, "Robust Neural-Fuzzy Method for Function Approximation," Expert Systems with Applications, 36, pp.6903-6913, 2009,

[3] H-L Shieh, Y. K. Yang and C.-N. Lee, "A Robust Approach of Fuzzy Clustering on Data Sets with Noise and Outliers", Cybernetics and Systems: An International Journal, Vol.37, No.7, pp.755-778, 2006

[4] H.-L Shieh, Y.-K. Yang, P.-L. Chang, J.-T. Jeng, "Robust Neural-Fuzzy Method for Function Approximation," Expert Systems with Application*s*, 36, pp.6903-6913, 2009.

[5] U. Maulik, and I. Saha, "Automatic Fuzzy Clustering Using Modified Differential Evolution for Image Classification," IEEE Trans. on Geoscience and Remote sensing, vol. 48, no. 9, pp. 3502-3510, 2010.

[6] M. S. Yang and K.-L. Wu, "A Similarity-Based Robust Clustering Method," IEEE Trans. On Pattern Analysis and machine Intelligence, Vol. 25, No. 4, pp. 434-448, April, 2004.

[7] R. J. Hathaway, J. C. Bezdek, and Y. Hu, "Generalized Fuzzy c-Means Clustering Strategies Using L_p Norm Distances," IEEE Trans. on Fuzzy Set, vol. 8, no. 5, pp.576~582, 2000.

[8] J.C. Bezdek, "A convergence theorem for the fuzzy ISODATA clustering algorithms," IEEE Trans. on Pattern Analysis and Machine Intelligence, pp.1-8, 1980.

[9] G. Zouridakis, B. H. Jansen and N. N. Boutros, "A Fuzzy Clustering Approach to EP Estimation," IEEE Tran. On Biomedical Engineering, Vol. 44, no. 8, pp.673-680, 1977.

[10] C. Borgelt, "Accelerating fuzzy clustering," Information Sciences, 179, pp.3985-3997, 2009.

[11] S.-M. Chen, Y.-C. Chang, "Multi-variable fuzzy forecasting based on fuzzy clustering," Information Sciences 180, pp.4772-4783, 2010.

[12] R. R. Yager and D. P. Filev, "Approximate Clustering Via the Mountain Method," IEEE Trans. on Systems, Man and Cybernetics, vol. 24, no. 8, pp.1279-1284, 1994.

[13] S. Chiu, "Fuzzy model identification based on cluster estimation," Journal of Intelligent & Fuzzy Systems, 2, pp.267-278, 1994.

[14] R. N. Dave and R. Krishnapuram, "Robust Clustering Methods: A Unified View," IEEE Trans. on Fuzzy System, vol. 5, no. 2, pp.270-293, 1997.

[15] K. L. Wu, M. S. Yang, "A cluster validity index for fuzzy clustering," Pattern Recognition Letters, 26, pp.1275–1291, 2005.

[16] H.-L. Shieh, C.-C. Kuo, "A Novel Validity Index for the Subtractive Clustering Algorithm," to be appeared in International Journal of Pattern Recognition and Artificial Intelligence.

[17] J. C. Bezdek, "Numerical Taxonomy with Fuzzy Sets," Journal of Mathematical Biology, 1, pp.57-71, 1974.

[18] J. C. Bezdek, "Cluster validity with fuzzy sets, "Cybernetics and Systems, 3, pp.58-73, 1973.

[19] X. L. Xie and G. Beni, "A Validity Measure for Fuzzy Clustering," IEEE Trans. on Pattern Analysis and Machine Intelligence, vol.13 pp. 841–847, 1991.

[20] W. Wang and Y. Zhanga, "On fuzzy cluster validity indices," Fuzzy Sets and Systems, 158, pp.2095-2117, 2007.

[21] Y. Fukuyama and M. Sugeno, "new method of choosing the number of clusters for the fuzzy c-means method." In Proc. 5th Fuzzy Systems Symposium, pp. 247-250, 1989, Japanese.

[22] U. Maulik, and S. Bandyopadhyay, "Performance evaluation of some clustering algorithms and validity indices," IEEE Trans. on Pattern Analysis Machine Intelligence, vol. 24, no. 12, pp. 1650-1654, 2002.

[23] J.C. Bezdek and N.R, Pal, "Some new indexes of cluster validity," IEEE Trans. Systems, Man Cybernetics. Part B: Cybernetics, 28(3), pp.301-15, 1998.

2011 IEEE International Conference on Fuzzy Systems
June 27-30, 2011, Taipei, Taiwan

Modeling of Fuzzy Integral Based Nonlinear Multi-regressions Systems with QPSO-GS

You-Min Jau
Graduate School of Engineering Science and Technology
National Yunlin University of Science & Technology
Yunlin, Taiwan, R.O.C
g9510809@yuntech.edu.tw

Jin-Tsong Jeng* and Kuo-Lan Su
*Department of Computer Science & Information Engineering
National Formosa University
Huwei, Taiwan, R.O.C
tsong@nfu.edu.tw

***Abstract*—A nonlinear multi-regression based on fuzzy integral (NAFI) model that include outliers under inherent interaction among feature attributes is considered in this paper. The modeling of the proposed model is also performed via a modified algorithm base on particle swarm optimization with quantum-behavior (MQPSO) and the high breakdown value estimator, least trimmed squares (LTS). That is, we successfully integrate mechanisms of the genetic algorithm and the simulated annealing into the QPSO algorithm to estimate parameters of the NAFI model; meanwhile, the LTS estimator is also introduced to filter out outliers. From simulation results, the proposed MQPSO algorithm with LTS estimator (named QPSO-GS) readily corrects the deviation caused by outliers and swiftly achieves convergences on estimating the parameters of the proposed NAFI model with outliers.**

Keywords- Fuzzy integral; nonlinear multi-regression based on fuzzy integral; particle swarm optimization with quantum-behavior; least trimmed squares.

I. INTRODUCTION

In the modern world, to accomplish an optimal decision in aeronautics, economics, industry, science, manufacturing, traffic control, and many other military and civilian applications extremely depend on useful and crucial information which is drawn from messages or data via transformation, classification and/or other procedure. Therefore, multi-sensor systems providing these messages or data are becoming increasingly important in meeting the goal of optimal decision-making. Besides, a feasible model to elaborate on information fusion and a soft computing technique to perform the heavy computations are also critical.

Within the consideration to a feasible model, traditionally, the most common forms are the weighted average model and the linear regression model. These models are all linear and must assume that there is no interaction among feature attributes (i.e. inputs). However, in many real-world systems, the inherent interaction among feature attributes must be considered circumspectly and these kinds of systems are essentially non-additive systems. Hence, a nonlinear multi-regression based on fuzzy integral (NAFI) model with respect to non-additive set function is a powerful consideration to cope with these kinds of systems. In general, Choquet integral is the most frequent form of the fuzzy integral and there are a few literatures have been proposed [1-4]. Liu et al. [1] proposed a NAFI model derived from one of the following three kinds of fuzzy supports, that is, the bespoke fuzzy support, the sample relative fuzzy support and the response correlative fuzzy support. This model deals with the interaction among feature attributes based on the correlation in statistics. Wang et al. proposed the original [2] and weighted [3-4] NAFI model to deal with the information with numerical and categorical feature attributes, respectively. In fact, the weighted NAFI model is the generalized form of the original one. In these two models, the interaction among the feature attributes toward the objective attributes (i.e. outputs) is described as non-additive set functions and is practically deferent from the co-relationship in the statistics. The problem that exactly finds out these parameters is an essential optimization problem and the basic idea is making the residuals as small as possible. Residuals here are defined as the difference between what is actually observed and what is estimated. To minimize residuals, the well-known tool, Least Square (LS) method is introduced and always makes a remarkable estimation in the circumstance that all attributes are uncontaminated with outliers. Unfortunately, these feature and objective attributes are usually subject to outliers in the real world applications. That is, outliers may occur due to various reasons, such as erroneous measurements or the data with a heavy-tailed distribution functions. Whenever the outliers exist, they make a serious deviation of what is estimated all the time. Within outlier detection literatures [5-7], the least trimmed squares (LTS) estimator which possesses not only high breakdown value but also several advantages over the other methods is the most popular form to eliminate effects caused by outliers. In this study, therefore, we focus our efforts on the LTS estimator to eliminate the inference from outliers.

Subsequent to confirming the feasible model and previous analysis, to efficiently and swiftly estimate parameters satisfying appointed criteria from observations, a timesaving soft computing technique is necessary for the information fusion system with contaminated attributes. In literatures, there are many outstanding soft computing techniques qualify for this work; they are neural network [8], genetic algorithm (GA) [9], hybrid learning [10], etc. Particle swarm optimization with quantum-behavior (QPSO) which is an improved type on the traditional particle swarm optimization (PSO) would be one of the powerful choices [11-12]. The QPSO algorithm behaves

978-1-4244-7316-8/11/$26.00 ©2011 IEEE

high performance in single mode systems, because of the property of swift convergence. However, particles usually fall into local extreme state in multimode optimization systems and then take on the premature phenomenon. In order to overcome these defects, we proposed a QPSO algorithm with elitist crossover mechanism of the GA (named MQPSO) in our previous work [13] and performed a superior performance. In this paper, we improve the MQPSO algorithm to manipulate systems with outliers which make serious deviations. That is, the mechanism of the LTS estimator is introduced to eliminate deviation caused by outliers and enhance robustness of the MQPSO, and it is named QPSO-GS. The significant improvement is that the QPSO-GS algorithm combines the concepts of the GA and the simulated annealing (SA) within the QPSO algorithm to achieve global search and overcome prematurity in optimal process, respectively; meanwhile, the LTS estimator is also performed to eliminate the inference from outliers. In order to verify the proposed QPSO-GS algorithm, a numerical example is also performed in this study. From the results of experiment, the proposed QPSO-GS algorithm is able to make a reasonable estimation on parameters of the NAFI model and then, quite precise objective attributes are also acquired.

The rest of paper is organized as follows: in Section II, the NAFI model is proposed. Section III, the least trimmed square estimator and the QPSO algorithm are briefly described. Next, we propose the QPSO-GS algorithm in detail. Section V, the numerical simulation results are demonstrated and then the paper is concluded in Section VI.

II. CHARACTERIZATION OF THE NAFI MODEL

In traditional linear aggregations, the most frequent model to describe the relation between feature attributes X and objective attribute Y is the Lebesgue-like integral [14]. However, in many real-world systems, the inherent interaction among feature attributes must be considered circumspectly. Hence, to reasonably describe the inherent interaction among feature attributes, Wang and Klir [15-16] proposed a regular non-additive set function μ defined on the power set of feature attributes and named fuzzy measure (FM). The formal definition of the FM can be express as

$$\mu(\varnothing)=0,\ \mu(X)=1,\ \varnothing\in P(X), \tag{1}$$

$$A\in P(X),\ B\in P(X), \text{ and } A\subset B\Rightarrow \mu(A)\le\mu(B). \tag{2}$$

Besides, a fuzzy integral is also introduced to aggregate the feature attributes. That is, whenever we deal with information fusion systems where information possesses inherent interaction, the fuzzy integral with respect to the FM is the most reasonable tools. In practical applications, there are many kinds of fuzzy integrals such as Choquet integral [17], Sugeno integral [18] and Wang integral [19], and so on. Considering simplicity and accuracy, the Choquet integral is the most frequent form and then, the Choquet integral with respect to the FM is defined as follows

$$\int f d\mu=\int_0^{\infty}\mu(F_\alpha)d\alpha, \tag{3}$$

where f is non-negative measureable function with n-dimensions on X, and $F_\alpha=\{x\mid f(x)\ge\alpha, x\in X\}$, $\alpha\in[0,\infty)$, is called the α-cut set of function f. Since X is a finite set, in this work, and the value of measureable function f can be sorted as

$$\min_{1\le i\le n} f(x_i)=f(x_1^*)\le\cdots\le f(x_n^*)=\max_{1\le i\le n} f(x_i), \tag{4}$$

where $\{x_1^*,x_2^*,\cdots,x_n^*\}$ is a permutation of $\{x_1,x_2,\cdots,x_n\}$. Then, the discrete type of Choquet integral with respect to the FM defined above can be express as

$$\int f d\mu=\sum_{i=1}^{n}\left(f(x_i^*)-f(x_{i-1}^*)\right)\cdot\mu(\{x_i^*,\cdots,x_n^*\}). \tag{5}$$

In addition, to deal with observations with categorical attributes, i.e., these feature attributes have only finitely many states, and numerical attributes, simultaneously, the NAFI model which indicates the relation between hybrid attributes and objective attributes can be expressed by the following formula [4]

$$y=c+q\cdot\int(\omega\cdot f)d\mu+er, \tag{6}$$

where c and q are constants, $\int f d\mu$ is the Choquet integral of function f with respect to the FM μ, vector $\omega=(\omega_1,\omega_2,\cdots,\omega_n)$ is an n-dimensional weighting vector which is used for coping with categorical attributes, i.e. vector ω is used for balancing the units among various attributes and satisfies the following constrain

$$0<\omega_i\le 1 \text{ and } \max_{1\le i\le n}\omega_i=1,\ i=1,2,\cdots,n. \tag{7}$$

In the NAFI model, totally, there are 2^n+n unknown parameters and increase exponentially with the dimension of feature attributes. In order to complete the NAFI model, these parameters have to be determined in advance. That is so called the learning state or the training state of the NAFI model. In this state, associating (6) with available observations constitute an over-determined system with Choquet integral. Thus, the analytic solution of the model parameters cannot be exact figured out. Furthermore, constants c and q are essential of difference from the other parameters which are governed by the Choquet integral. Therefore, the dual optimization procedures must be performed, simultaneously; meanwhile, the performance index of optimization J (called fitness function) is also introduced and expressed as

$$J=\text{Min}\left\{\sum_{j=1}^{k}\left(y_j-c-q\cdot\int(\omega\cdot f_j)d\mu\right)^2\right\}, \tag{8}$$

where k is the length of available observations for the training state. Because the kernel of the performance index of optimization is the LS estimator, it usually suffers from outliers in real world systems. Fortunately, there are many high breakdown value regression estimators have been proposed to

eliminate the effect of outliers [6-7]. For the reason of simplicity and efficiency, the least median of squares (LMS) and the LTS are the most popular regression estimators in scientific applications. Furthermore, the LTS estimator possesses not only the same breakdown value as LMS, but also several merits: for instance, its objective function is smoother; its statistical efficiency is better, and so on. Therefore, we focus the treatment of outliers on LTS method and then the fitness function J is revised as the form

$$J = \text{Min}\left\{\sum_{j=1}^{h}\left(y_j^* - c - q\cdot\int(\omega\cdot f_j^*)d\mu\right)^2\right\}, \qquad (9)$$

where y_j^* and f_j^* are a permutation of observations under the best model parameters and h is a trimmed parameter of the LTS estimator. The block diagram of the proposed structure for the training state and information fusion systems are shown in Fig. 1. Where the block named QPSO-GS receives the differences of objective attributes between observations and estimations when the terminative criterion is not satisfied yet, and then the parameters of the NAFI model are updated base on these differences; meanwhile, in the LTS block used for filtering out these atypical observations, the trimmed parameter h is also revised by the global optimal parameters so far.

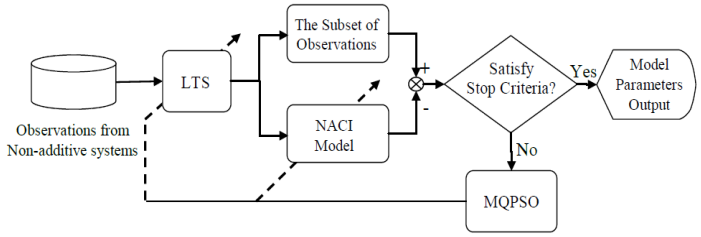

Figure 1. Block diagram of the proposed structure for the parameters estimation of the NACI model via MQPSO and LTS.

III. THE LTS ESTIMATOR AND THE QPSO ALGORITHM

In robust regression analysis [6], the LTS estimator is formulated as

$$\text{Min}\left\{\sum_{i=1}^{h} r^2(d_i)\right\},\ r^2(d_1)\le\cdots\le r^2(d_h)\le\cdots\le r^2(d_k), \quad (10)$$

where d_i is the i_{th} observation, $r^2(d_i)$ is the i_{th} squared residual, k is the length of observations and h is the number of data points which are not trimmed from the data set. The maximum tolerance of the LTS estimators to outliers (named Maximum Breakdown Point) for any equi-variant regression estimator satisfies

$$\text{Breakdown Point} \le \frac{1}{k}\left(\left((k-\zeta)/2\right)+1\right), \qquad (11)$$

where ζ is the dimension of variables. Intuitively, 50% is the upper bound that can be expected and it is actually attained for $h=(k+\zeta+1)/2$. In theorem, the solution of (10) always exists. Of course, one can achieve the optimal solution by performing $C(k,h)$ ordinary least square problems for all subsets of $\{1,2,\cdots,k\}$ with h elements and selecting the best one among all candidates. Obviously, it is laborious and impractical for real world systems with large observations. In order to cope with a great deal of observations, the FAST-LTS method was been proposed [7]. The major distinguishing features are the initial h-subset, the C-step and the nested extensions. By and large, the initial h-subset is a preselecting mechanism to confirm that a clean h-subset $\{d_1,d_2,\cdots,d_h\}$ drawn from all observations can be attained and the C-step is a recursive procedure and used for increasing accuracy of the estimated model parameters. For a small to moderate data size k, these two procedures work well and do not take much time. When observations are large enough, the procedure named nested extension is introduced to avoid the heavy computation.

After drawing observations without contaminations, a proper soft computing technique is essential and can help us to efficiently estimate parameters of the NAFI model. The QPSO algorithm is one of these soft computing techniques, and possesses a significant ability of global and local search. In the QPSO algorithm, particles move in a quantum multi-dimensional space, the state of particles is usually depicted by normalized wave function $\Psi(\rho,t)$, i.e., the probability amplitude of position where particles are presence; and the wave function satisfies the constrain

$$\int_{\text{whole space}}\left|\Psi(\rho,t)\right|^2 d\rho = 1, \qquad (12)$$

where ρ is the n-dimensional coordinates. That is, a single particle with mass m is subjected to the influence of a potential field $V(\rho,t)$ in the quantum space and the wave function is governed by the Schrödinger equation:

$$i\hbar\frac{\partial}{\partial t}\Psi(\rho,t) = -\frac{\hbar^2}{2m}\nabla^2\Psi(\rho,t) + V(\rho,t)\Psi(\rho,t), \quad (13)$$

where $\hbar$ is the Planck constant and ∇^2 is the Laplacian operator. In the environment with potential field, the particles are then attracted to the center of potential field through the optimization process, and such attraction leads to the global optimum. Base on the assumption that the attractive potential field is time-independent (called stationary state); the solution of the time-independent Schrödinger equation has the form [20]

$$\Psi(\rho,t) = \varphi(\rho)\cdot\exp(-i\omega t), \qquad (14)$$

where ω has the dimensions of an angular frequency. In theorem, any type of potential well can describe this system which is bounded and attracted by a potential field, but the simplest one is the Delta Potential Well and the potential field is given by

$$V(\rho) = -\gamma\delta(\rho), \qquad (15)$$

where γ is a positive number proportional to the "depth" of the potential well. For the sake of simplicity, the solution of time-independent Schrödinger equation for this system in one dimensional space is considered and expressed as

$$Q(z) = |\varphi(z)|^2 = \frac{1}{L} e^{-\frac{2|z|}{L}},\ L = \frac{\hbar^2}{m\gamma}, \tag{16}$$

where $Q(z)$ is the probability density function for measuring a particle's state and L is the characteristic length of Delta Potential Well which specifies the search scope of a particle. In order to obtained the precise position of particles, Monte Carlo Method is used for simulating the procedure that the quantum state collapses to the classic state, and the particle's position can be expressed as

$$\varphi_i = pf^{cnt}(i) \pm L/2 \cdot \ln\left(1/u\right),\ i = 1,2,\cdots,NP, \tag{17}$$

where NP is the number of particles in a population, u is random number uniformly distribute on $[0,1]$ and pf^{cnt} is the center of potential field which is proposed by Clerc and Kennedy [21] and defined as

$$pf^{cnt}(i) = \frac{\left(c_1 \cdot p_i^{loc} + c_2 \cdot p^{gol}\right)}{\left(c_1 + c_2\right)},\ i = 1,2,\cdots,NP, \tag{18}$$

where c_1 , c_2 are constriction coefficients and p_i^{loc} , p^{gol} are the best position of the i_{th} particle and the global best position found so far. In order to improve performance of the QPSO algorithm, Sun et al [12] employ a Mean Best Position (*mbest*) to evaluate parameter *L*. However, to extend the global search of the QPSO algorithm, the *mbest* is modified and then these two parameters can be expressed as the following form

$$mbest = \left[\sum_{i=1}^{NP} \frac{\phi_{i,1}}{NP}, \sum_{i=1}^{NP} \frac{\phi_{i,2}}{NP}, \cdots, \sum_{i=1}^{NP} \frac{\phi_{i,n}}{NP}\right], \tag{19}$$

$$L = 2 \cdot \beta \left| mbest - \varphi_i \right|, \tag{20}$$

where β is a creative coefficient which is used to adjust the convergent speed of individual particle and the performance of the QPSO algorithm.

IV. THE QPSO-GS ALGORITHM

Within empirical applications, however, the QPSO algorithm usually represents stagnating phenomenon for searching the global optimal solution in multi-mode problems and systems; meanwhile, it is also strongly influenced by the creative coefficient β . In order to improve these defects, a nonlinearly updating mechanism of the creative coefficient β and instantaneously monitoring the convergence of optimization procedure are introduced. The nonlinearly revising mechanism which is similar to the SA is expressed as the form

$$\beta = \beta_{ini} - \Delta\beta \cdot (1 + \exp(-(\Delta fit)))^{-1}, \tag{21}$$

where $\Delta\beta$ is step length of β , Δfit is the changing rate of optimal estimation so far and β_{ini} is the initial value of β .

The other improvement of the proposed QPSO-GS algorithm is the mechanism to overcome prematurity. Inspired by these mechanisms of mutation and elite crossover in the GA, an index of conquering stagnation (named *ECM* which is an abbreviation of elite crossover and mutation) is used for monitoring the status of optimization procedure. That is, during the optimization procedure, the QPSO-GS algorithm preserves each different p^{gol} ; meanwhile, the index of conquering stagnation, *ECM* is set to zero whenever p^{gol} is updated. Of course, the *ECM* increases by one whenever p^{gol} is unchanged. Before finishing current iteration, the QPSO-GS algorithm makes a judgment whether *ECM* exceeds the specific criteria. If it is true, the QPSO-GS algorithm lets the new population be these collected p^{gol} instead of original population (all/or these worse particles) and sets the *ECM* to zero, instantaneously.

Because the kernel of estimating fitness is the LS estimator, the MQPSO algorithm presents superior performances for estimating parameters for observations without outliers in our previous work. However, the MQPSO algorithm always makes a serious deviation in the contaminated circumstance. Hence, the LTS estimator is introduced to sieve out the observations without contamination and the proposed QPSO-GS algorithm is detailed below:

Step 1: Perform the LTS estimator to sieve out these *h* observations without contamination.

Step 2: Randomly initialize the population of particles with dimension $2^n - 2 + n$ and then, evaluate their fitness values by (9).

Step 3: Sort particles according to their fitness values and then initialize p_i^{loc} , p^{gol} .

Step 4: Calculate pf^{cnt} , *mbest* and *L* by (18), (19) and (20), respectively.

Step 5: Select (22) or (23) with randomly probability to update φ_i .

$$\varphi_{i+1} = pf^{cnt}(i) + \beta \cdot \left\| mbest - \varphi_i \right\| \cdot \ln(1/u), \tag{22}$$

$$\varphi_{i+1} = pf^{cnt}(i) - \beta \cdot \left\| mbest - \varphi_i \right\| \cdot \ln(1/u). \tag{23}$$

Step 6: Evaluate the fitness values of all particles by (9).

Step 7: According to evaluation in Step 6, update p_i^{loc} .

Step 8: Check over whether the maximum iteration is reached or the terminative criterion is satisfied? If yes, go to Step 11, else perform next Step.

Step 9: Check over whether p^{gol} is updated? If p^{gol} is updated, sets *ECM* to 0 and perform the LTS

procedure, then go to Step 4. If p^{gol} is unchanged, increase ECM by 1 and perform next Step.

Step 10: Check over whether the maximum ECM is reached? If yes, let these collected p^{gol} instead of φ_{i+1} and go to Step 4, else keep φ_{i+1} and go to Step 4.

Step 11: Check over whether p^{gol} should be updated and then output results.

V. Numerical Simulation and Results

To demonstrate and verify the effectiveness and feasibility of the proposed systems are shown in Figure 1, an artificial observation profile which simulates 4 continuous sampling data with outliers is made to estimate the model parameters by associating the proposed QPSO-GS algorithm based on the NAFI model. All simulations are implemented in the Matlab environment and conducted on Intel Core 2 Duo CPU P8400, 4GB Ram capacity PC.

Example 1: The original model parameters are set as: c=4, q=1.5, μ = { 0.22, 0.3, 0.45, 0.28, 0.42, 0.49, 0.6, 0.25, 0.45, 0.52, 0.62, 0.74, 0.82, 0.88,1 } , w = { 0.3, 0.26, 1, 0.48 } . Then, we randomly create 400 4-dimensional feature attributes with 10% random contamination (marked with shadows) to produce training data as shown in Table I, where y_{true} and y_{cont} are the original and contaminated objective attributes, respectively. After performing the proposed QPSO-GS algorithm for many times, the average results of estimating model parameters are shown in Tables II, where y_{esti} is the estimated objective attributes, p_{esti} and p_{true} are the contaminated and original model parameters, respectively. In addition, we also show plots of the training data and estimated results in Figures 2~3. In this Example, the terminative criteria of program are maximum iterations which reach 1500 times or the mean square error which is less than 10^{-4}. From Table II and Figures 2~3, these estimated results almost the same as original objective attributes and these estimated model parameters are really precise. That is, the QPSO-GS algorithm is able to efficiently filter out outliers from observations. That is, the proposed QPSO-GS readily corrects the deviation caused by outliers and swiftly achieves convergences on estimating the parameters of the proposed NAFI model with outliers.

VI. Conclusions

In this paper, the NAFI model association with the QPSO-GS algorithm is considered and developed to deal with a non-additive system with outliers. Whenever atypical observations are presence, the estimation method of parameters based on the LS estimator is no longer feasible. Therefore, there is an excellently alternative ways to replace the LS estimator with the LTS estimator. That is, we successfully integrate mechanisms of the GA and the SA into the QPSO algorithm to estimate parameters of the NAFI model with outliers; meanwhile, the LTS estimator is also introduced to filter out outliers. From the simulation results, the proposed QPSO-GS algorithm can precisely estimate parameters of the NAFI model for observations contaminated with outliers; meanwhile, it still maintains high coincidence between the estimated and original objective attributes.

Acknowledgments

This work was supported by the National Science Council of Taiwan, R. O. C. under Grand NSC 99-2221-E150-079 and National Formosa University EN99B-B1005.

TABLE I. Tanning data with and without contaminations used for verifying the proposed NACI model and LTS-MQPSO algorithm

	x_1	x_2	x_3	x_4	y_{true}	y_{cont}
01	0.70	0.73	0.65	0.32	4.4605	4.4605
02	0.01	0.33	0.30	0.46	4.2969	4.2969
03	0.56	0.50	0.28	0.27	4.2657	2.6707
04	0.94	0.39	0.47	0.65	4.4739	4.4739
05	0.09	0.73	0.78	0.83	4.6472	4.6472
06	0.59	0.10	0.13	0.47	4.2169	4.2169
07	0.32	0.56	0.99	0.49	4.6259	4.6259
08	0.35	0.78	0.29	0.81	4.4204	5.7115
09	0.62	0.49	0.78	0.68	4.6095	4.6095
10	0.28	0.64	0.49	0.83	4.5308	4.5308
⋮	⋮	⋮	⋮	⋮	⋮	⋮
391	0.05	0.80	0.93	0.16	4.5037	4.5037
392	0.85	0.77	0.51	0.77	4.5539	4.5539
393	0.26	0.99	0.72	0.96	4.6884	3.5601
394	0.46	0.51	0.35	0.53	4.3749	4.3749
395	0.86	0.08	0.27	0.46	4.3057	4.3057
396	0.52	0.74	0.90	0.93	4.7545	4.7545
397	0.22	0.50	0.79	0.22	4.4464	4.4464
398	0.43	0.97	0.51	0.59	4.4858	4.4858
399	0.86	0.03	0.63	0.82	4.5693	4.5693
400	0.03	0.37	0.14	0.47	4.2093	4.2093

TABLE II. The average results of model parameters estimated by the proposed LTS-MQPSO algorithm

	p_{esti}	p_{true}	Data	y_{esti}	y_{cont}	y_{true}
μ_1	0.2243	0.22	d(1)	4.4605	4.4605	4.4605
μ_2	0.2988	0.30	d(2)	4.2969	4.2969	4.2969
$\mu_{1,2}$	0.4532	0.45	d(3)	4.2657	2.6707	4.2657
μ_3	0.2795	0.28	d(4)	4.4740	4.4739	4.4739
$\mu_{1,3}$	0.4216	0.42	d(2)	4.6472	4.6472	4.6472
$\mu_{2,3}$	0.4890	0.49	d(6)	4.2167	4.2169	4.2169
$\mu_{1,2,3}$	0.6010	0.60	d(7)	4.6259	4.6259	4.6259
μ_4	0.2495	0.25	d(8)	4.4204	5.7115	4.4204
$\mu_{1,4}$	0.4528	0.45	d(9)	4.6096	4.6095	4.6095
$\mu_{2,4}$	0.5186	0.52	d(10)	4.5308	4.5308	4.5308
$\mu_{3,4}$	0.6213	0.62	⋮	⋮	⋮	⋮
$\mu_{1,2,4}$	0.7385	0.74	d(391)	4.5036	4.5037	4.5037
$\mu_{1,3,4}$	0.8195	0.82	d(392)	4.5541	4.5539	4.5539
$\mu_{2,3,4}$	0.8787	0.88	d(393)	4.6885	4.6884	3.5601
$\mu_{1,2,3,4}$	1.0000	1.00	d(394)	4.3750	4.3749	4.3749
ω_1	0.2963	0.30	d(395)	4.3055	4.3057	4.3057
ω_2	0.2598	0.26	d(396)	4.7545	4.7545	4.7545
ω_3	1.0000	1.00	d(397)	4.4464	4.4464	4.4464
ω_4	0.4803	0.48	d(398)	4.4858	4.4858	4.4858
c	3.99999	4.00	d(399)	4.5692	4.5693	4.5693
q	1.50236	1.50	d(400)	4.2093	4.2093	4.2093

REFERENCES

[1] H. C. Liu, Y. C. Tu, C. C. Chen, and W. S. Weng, "The Choquet integral with respect to λ measure based on γ support," Proc. of the 7th International Conference on Machine Learning and Cybernetics, Kunming, 2008.

[2] Z. Wang, K. S. Leung, M. L. Wong, J. Fang, and K. Xu, "Nonlinear nonnegative multi-regressions based on Choquet integrals," International Journal of Approximate Reasoning, vol. 25, pp. 71-87, 2000.

[3] K. Xu, Z. Wang, K. S. Leung, and M. L. Wong, "Discover dependency pattern among attributes by using a new type of nonlinear multi-regression," International Journal of Intelligent Systems, vol. 16, pp. 949-962, 2001.

[4] K. S. Leung, M. L. Wong, W. Lam, Z. Wang, and K. Xu, "Learning nonlinear multi-regression networks based on evolutionary computation," IEEE Transactions on Systems, Man, and Cybernetics, vol. 32, pp. 630-643, 2002.

[5] C. C. Chuang, S. F. Su, J. T. Jeng, and C. C. Hsiao "Robust Support Vector Regression Networks for Function Approximation with Outliers," IEEE Trans. on Neural Networks, Vol. 13, No. 6, pp1322-1330, 2002.

[6] P. J. Rousseeuw, and M. A. Leroy, "Robust Regression and Outlier Detection," Wiley, New York, 1987.

[7] P. J. Rousseeuw, and K. V. Driessen, "Computing LTS regression for large data sets," Data Mining and Knowledge Discovery, vol. 12, pp. 29-45, 2006.

[8] C. C. Chuang and J. T. Jeng, "CPBUM Neural Networks for Modeling with Outliers and Noise," Applied Soft Computing, Vol. 7, No. 3, pp. 957-967, 2007.

[9] J. T. Tsai, T. K. Liu, and J. H. Chou, "Hybrid Taguchi-Genetic Algorithm for Global Numerical Optimization," IEEE Transactions On Evolutionary Computation, vol. 8, no. 4, pp. 365-377, August 2004.

[10] Y. Y. Fu, C. J. Wu, C. N. Ko and J. T. Jeng, "Radial Basis Function Networks with Hybrid Learning for System Identification with Outliers," Applied Soft Computing, Vol. 11, Issue 3, PP 3083-3092, 2011.

[11] J. Sun, B. Feng and W.B. Xu, "Particle swarm optimization with particles having quantum behavior," Proc. of CEC 2004 Congress on Evolutionary Computation, Portland, USA, 2004.

[12] J. Sun, B. Feng, and W.B. Xu, "A global search strategy of quantum-behaved particle swarm optimization," Proc. of 2004 IEEE Conference on Cybernetics and Intelligent Systems, Singapore, 2004.

[13] Y. M. Jau, C. J. Wu, and J. T. Jeng, "A fast parameters estimation for nonlinear multi-regressions based on Choquet integral with quantum-behaved particle swarm optimization," Artificial Life and Robotics, vol. 15, pp. 199-202, 2010.

[14] P. R. Halmos, "Measure Theory," Van Nostrand, New York, 1967.

[15] Z. Wang, and G. J. Klir, "Fuzzy Measure Theory," Plenum Press, New York, 1992.

[16] Z. Wang, and G. J. Klir, "Generalized Measure Theory," Springer, New York, 2008.

[17] G. Choquet, "Theory of Capacities," Annales de l'Institut Fourier, vol. 5, pp. 131–295, 1953.

[18] M. Sugeno, "Ph. D. Thesis: Theory of Fuzzy Integrals and Applications," Tokyo Institute of Technology, Tokyo, 1974.

[19] Z. Wang, K. S. Leung, M. L. Wong, and J. Fang, "A new type of nonlinear integrals and the computational algorithm," Fuzzy Sets and Systems, vol. 112, pp. 223-231, 2000.

[20] C. T. Claude, and B. Diu, F. Laloë, "Quantum Mechantics, vol. 1," Wiley-Interscience, 2006.

[21] M. Clerc, and J. Kennedy, "The particle swarm: explosion, stability, and convergence in a multidimensional complex space," IEEE Transactions on Evolutionary Computation, vol. 6, pp. 68-73, 2002..

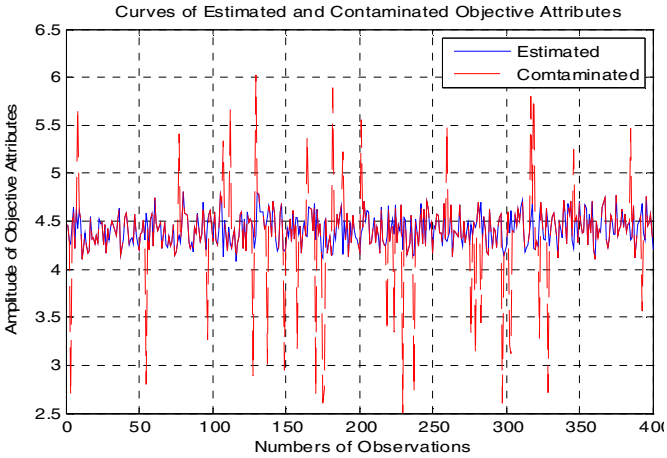

Figure 2. Shown the results for the contaminated objective attributes and the estimated objective attributes.

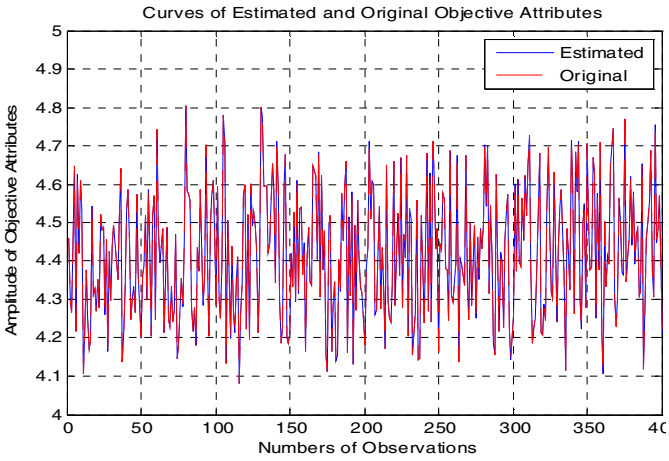

Figure 3. Shown the results for the original objective attributes and the estimated objective attributes.

2011 IEEE International Conference on Fuzzy Systems
June 27-30, 2011, Taipei, Taiwan

A Formula for Fuzzy Linear Regression Analysis

Chi-Tsuen Yeh
Department of Applied Mathematics, National University of Tainan
33, Sec. 2, Shu-Lin St., 70005, Tainan, Taiwan
Email: ctyeh@mail.nutn.edu.tw

***Abstract*—The purpose of this paper is to deal with the problem of least-squares multiple regression with fuzzy data. The constant regression coefficient is assumed to be symmetric triangular, and other coefficients are real (crisp). By applying symmetric triangular approximations of fuzzy numbers, a new method for computing the regression coefficients is proposed. The new method is efficient and easy to determine the coefficients.**

***Index Terms*—fuzzy linear regression, symmetric triangular approximation, least-squares estimates.**

I. Introduction

An arbitrary fuzzy number $\tilde{A}$ can be represented by an ordered pair of left continuous functions $[A^l(\alpha), A^u(\alpha)]$, $0 \leq \alpha \leq 1$, which both satisfy the following conditions:

1) A^l is increasing on [0,1],
2) A^u is decreasing on [0,1],
3) $A^l(1) \leq A^u(1)$.

Let $\mathbb{R}$ and $F(\mathbb{R})$ denote the sets of all real numbers and fuzzy numbers, respectively. In this paper, we always place a $\sim$ over a letter to denote a fuzzy number, for example $\tilde{X}_i$, $\tilde{A} \in F(\mathbb{R})$ and $a, \tau, \sigma \in \mathbb{R}$. Let $\tilde{A}$ and $\tilde{B} \in F(\mathbb{R})$. The Euclidean distance between $\tilde{A}$ and $\tilde{B}$ is defined as

$$\mathrm{d}(\tilde{A}, \tilde{B}) = \Big[\int_0^1 (|A^l(\alpha) - B^l(\alpha)|^2 + |A^u(\alpha) - B^u(\alpha)|^2) \mathrm{d}\alpha \Big]^{\frac{1}{2}}.$$

Given fuzzy vectors $\vec{\tilde{Y}} = (\tilde{Y}_1, \ldots, \tilde{Y}_n)$ and $\vec{\tilde{X}}_i = (\tilde{X}_{i1}, \ldots, \tilde{X}_{in}) \in F(\mathbb{R})^n$, $1 \leq i \leq m$, the problem of fuzzy linear regression analysis is to find the regression coefficients $\tilde{A}_i \in F(\mathbb{R})$, $0 \leq i \leq m$, which minimize the observation error

$$\begin{aligned} &\mathrm{d}^2(\vec{\tilde{Y}}, \tilde{A}_0 \vec{1} + \tilde{A}_1 \vec{\tilde{X}}_1 + \cdots + \tilde{A}_m \vec{\tilde{X}}_m) := \\ &\sum_{j=1}^{k} \mathrm{d}^2(\tilde{Y}_j, \tilde{A}_0 + \tilde{A}_1 \tilde{X}_{1j} + \cdots + \tilde{A}_m \tilde{X}_{mj}), \end{aligned} \tag{1}$$

where $\vec{1} := (1, \ldots, 1)$.

In 1982, Tanaka et al. [21] first examined fuzzy regression analysis with real independent (or explanatory) and fuzzy dependent (or response) variables, in which the regression coefficients are assumed to be symmetric triangular fuzzy numbers. Afterwards, many scholars studied this type fuzzy regression analysis by generalizing the coefficients to more general fuzzy numbers [2], [6], [8], [9], [10], [14], [16], [18], [19], [22]. In 1992, Sakawa and Yano [20] considered fuzzy linear regression models with fuzzy data, that means the independent variables and dependent variable are all fuzzy numbers. Subject to the regression coefficients are all real, the least-squares estimation was further studied by Diamond [4], and the existence was proved by Kratschmer [17]. In 1992, Bardosy et al. [11] presented normal equations systems depended on signs of regression coefficients to estimate the regression coefficients. And, in 2002 Kao and Chyu [12] proposed a two-stage method. Most of the recent approaches have to consider optimization cones, then determine the regression coefficients by comparing observation errors of these possible estimators. It will take a lot of time to find the best one. An iterative algorithm (numerical method) was proposed by Bargiela et al. [1]. In 2009, Yeh [27] showed that the multiple regression problem can be replaced with a 0-1 programming problem. Furthermore, he proposed a formula for computing the regression coefficients in one-variable models (see the following Theorem 5). For more general case that the constant coefficient is fuzzy, Diamond and Korner [5] generalized their previous results via Hukuhara difference. Wunsche and Nather [23] turned to study on the restriction that the data are of normal distributions. Chen and Hsueh [3] used the least-squares method to determine regression coefficients in multiple-variable models. There are also many other contributions to this type [2], [8], [9], [13], [15], [18].

This paper is organized as follows. In Section 2, we introduce the mean of fuzzy numbers. In Section 3, we present an formula for solving the regression model whose regression coefficients are all real. The present formula is simple and clear. In Section 4, we completely solve the regression problem whose constant coefficient is assumed to be symmetric triangular. In Section 5, we work on the example designed by Sakawa and Yano. It is shown that our estimator is better than the previous.

II. The mean of fuzzy numbers

Let $\tilde{Z}_i$, $1 \leq i \leq n$ be fuzzy numbers. We define the *mean* of $\tilde{Z}_i$ as follows

$$E(\tilde{Z}) = \frac{1}{n} \sum_{i=1}^{n} \tilde{Z}_i. \tag{2}$$

Theorem 1. *Let $\tilde{Z}_i$, $1 \leq i \leq n$ be fuzzy numbers. Then,*

$$\sum_{i=1}^{n} \mathrm{d}^2(\tilde{Z}_i, \tilde{A}) = \sum_{i=1}^{n} \mathrm{d}^2(\tilde{Z}_i, E(\tilde{Z})) + n\mathrm{d}^2(E(\tilde{Z}), \tilde{A}),$$

for each $\tilde{A} \in F(\mathbb{R})$.

Let $\tilde{A} = [A^l(\alpha), A^u(\alpha)]$ and $\tilde{B} = [B^l(\alpha), B^u(\alpha)] \in F(\mathbb{R})$. The *vector difference* between $\tilde{A}$ and $\tilde{B}$ is described as follows

$$\tilde{A} \ominus \tilde{B} := [A^l(\alpha) - B^l(\alpha), A^u(\alpha) - B^u(\alpha)].$$

978-1-4244-7316-8/11/$26.00 ©2011 IEEE

The vector difference between $\tilde{A}$ and $\tilde{B}$ may not belong to $F(\mathbb{R})$. For example,

$$[\alpha, 2-\alpha] \ominus [2\alpha, 2] = [-\alpha, -\alpha] \notin F(\mathbb{R}).$$

Notice that, we can still compute the distance $\mathrm{d}(\tilde{A}, \tilde{B})$, defined in Section 1, even if $\tilde{A} = [A^l(\alpha), A^u(\alpha)]$ and $\tilde{B} = [B^l(\alpha), B^u(\alpha)] \notin F(\mathbb{R})$.

Theorem 2. *Let $\vec{\tilde{Y}} = (\tilde{Y}_1, \ldots, \tilde{Y}_n)$ and $\vec{\tilde{X}} = (\tilde{X}_1, \ldots, \tilde{X}_n) \in F(\mathbb{R})^n$ be fuzzy vectors. Then,*

$$\mathrm{d}^2(\vec{\tilde{Y}}, \tilde{A}\vec{1} + b\vec{\tilde{X}}) = \sum_{i=1}^{n} \mathrm{d}^2(\tilde{Y}_i \ominus E(\tilde{Y}), b\tilde{X}_i \ominus bE(\tilde{X})) + n\mathrm{d}^2(E(\tilde{Y}) \ominus bE(\tilde{X}), \tilde{A}),$$

for each $\tilde{A} \in F(\mathbb{R})$ and each $b \in \mathbb{R}$.

III. A FORMULA FOR COMPUTING REAL REGRESSION COEFFICIENTS

In this section, we are going to study fuzzy regression analysis with real regression coefficients, that is to find $a, b \in \mathbb{R}$ minimizing the observation error

$$\mathrm{d}^2(\vec{\tilde{Y}}, a\vec{1} + b\vec{\tilde{X}}),$$

where $\vec{\tilde{Y}} = (\tilde{Y}_1, \ldots, \tilde{Y}_n)$ and $\vec{\tilde{X}} = (\tilde{X}_1, \ldots, \tilde{X}_n)$ are given data.

Let $\tilde{A} \in F(\mathbb{R})$ and Ω be a closed convex subset of $F(\mathbb{R})$. Then, an element $P_\Omega(\tilde{A}) \in \Omega$ is called the *best approximation* of $\tilde{A}$ in Ω if

$$\mathrm{d}(\tilde{A}, P_\Omega(\tilde{A})) \le \mathrm{d}(\tilde{A}, \tilde{X}), \quad \forall \tilde{X} \in \Omega.$$

If we set $\Omega = \mathbb{R}$ (i.e. each $\tilde{A} \in \Omega$ is real), then

$$P_{\mathbb{R}}(\tilde{A}) := \int_0^1 A^c(\alpha)\, d\alpha.$$

Proposition 3. *Let $\tilde{A}, \tilde{B} \in F(\mathbb{R})$ and $a, b \in \mathbb{R}$. Then,*

$$P_{\mathbb{R}}(a\tilde{A} + b\tilde{B}) = aP_{\mathbb{R}}(\tilde{A}) + bP_{\mathbb{R}}(\tilde{B}),$$
$$P_{\mathbb{R}}(a\tilde{A} \ominus b\tilde{B}) = aP_{\mathbb{R}}(\tilde{A}) - bP_{\mathbb{R}}(\tilde{B}),$$

and

$$\mathrm{d}^2(\tilde{A}, a) = \mathrm{d}^2(\tilde{A}, P_{\mathbb{R}}(\tilde{A})) + |P_{\mathbb{R}}(\tilde{A}) - a|^2.$$

From Theorem 2 we find

$$\mathrm{d}^2(\vec{\tilde{Y}}, a\vec{1} + b\vec{\tilde{X}}) = \sum_{i=1}^{n} \mathrm{d}^2(\tilde{Y}_i \ominus E(\tilde{Y}), b\tilde{X}_i \ominus bE(\tilde{X})) + n\mathrm{d}^2(E(\tilde{Y}) \ominus bE(\tilde{X}), a).$$

Consequently, by Proposition 3 we have

$$\begin{aligned} &\mathrm{d}^2(E(\tilde{Y}) \ominus bE(\tilde{X}), a) \\ &\ge \mathrm{d}^2(E(\tilde{Y}) \ominus bE(\tilde{X}), P_{\mathbb{R}}(E(\tilde{Y})) - bP_{\mathbb{R}}(E(\tilde{X}))). \end{aligned}$$

Hence, to minimize $\mathrm{d}^2(\vec{\tilde{Y}}, a\vec{1} + b\vec{\tilde{X}})$ we must choose that

$$a = P_{\mathbb{R}}(E(\tilde{Y})) - bP_{\mathbb{R}}(E(\tilde{X})),$$

and then we have

$$\begin{aligned} &\mathrm{d}^2(\vec{\tilde{Y}}, a\vec{1} + b\vec{\tilde{X}}) \\ =&\mathrm{d}^2(\vec{\tilde{Y}}, [P_{\mathbb{R}}(E(\tilde{Y})) - bP_{\mathbb{R}}(E(\tilde{X}))]\vec{1} + b\vec{\tilde{X}}) \\ =&\sum_{i=1}^{n} \mathrm{d}^2(\tilde{Y}_i \ominus P_{\mathbb{R}}(E(\tilde{Y})), b\tilde{X}_i \ominus bP_{\mathbb{R}}(E(\tilde{X}))). \end{aligned}$$

Recall that every closed interval can be represented by its center and radius (half width). For instance, the center of $[A^l(\alpha), A^u(\alpha)]$ is

$$A^c(\alpha) := \frac{A^l(\alpha) + A^u(\alpha)}{2}, \tag{3}$$

and the radius of $[A^l(\alpha), A^u(\alpha)]$ is

$$A^r(\alpha) := \frac{A^u(\alpha) - A^l(\alpha)}{2}. \tag{4}$$

That means we can use the symbol

$$[A^c(\alpha), A^r(\alpha)]_{CR}$$

to rewrite the fuzzy number $\tilde{A} = [A^l(\alpha), A^u(\alpha)]$, which is called the CR-*representation* of $\tilde{A}$, see [24].

Proposition 4 (Proposition 1, [27])**.** *Let*

$$\tilde{A} = [A^c(\alpha), A^r(\alpha)]_{CR} \quad \textit{and} \quad \tilde{B} = [B^c(\alpha), B^r(\alpha)]_{CR}$$

be fuzzy numbers with CR*-representations, and $a \in \mathbb{R}$. Then the addition and scalar multiplication of fuzzy numbers can be described as follows:*

$$\tilde{A} + \tilde{B} = [A^c(\alpha) + B^c(\alpha), A^r(\alpha) + B^r(\alpha)]_{CR}$$

and

$$a\tilde{A} = [aA^c(\alpha), |a|A^r(\alpha)]_{CR},$$

respectively. Moreover,

$$(\sum_i a_i\tilde{X}_i)^c(\alpha) = \sum_i a_i\tilde{X}_i^c(\alpha)$$

and

$$(\sum_i a_i\tilde{X}_i)^r(\alpha) = \sum_i |a_i|\tilde{X}_i^r(\alpha),$$

for all $\tilde{X}_i \in F(\mathbb{R})$ and $a_i \in \mathbb{R}$.

For each fuzzy vector $\vec{\tilde{Z}} = (\tilde{Z}_1, \ldots, \tilde{Z}_n)$, where

$$\tilde{Z}_j = [Z_j^c(\alpha), Z_j^r(\alpha)]_{CR}, \quad 1 \le j \le n,$$

are represented with CR-representations, define two real functional vectors as follows:

$$\vec{Z}^c := (Z_1^c(\alpha), \ldots, Z_n^c(\alpha))$$

and

$$\vec{Z}^r := (Z_1^r(\alpha), \ldots, Z_n^r(\alpha)).$$

Recall that, for any two real vector functions $\vec{f} = (f_1, \ldots, f_n)$ and $\vec{g} = (g_1, \ldots, g_n)$ the *inner product* of $\vec{f}$ and $\vec{g}$ is

$$\langle \vec{f}, \vec{g} \rangle := \sum_{i=1}^{n} \int_0^1 f_i(x) g_i(x)\ dx. \tag{5}$$

Now, let $\vec{\tilde{X}} = (\tilde{X}_1, \ldots, \tilde{X}_n)$ and $\vec{\tilde{Y}} = (\tilde{Y}_1, \ldots, \tilde{Y}_n) \in F(\mathbb{R})^n$. Define

$$\begin{aligned}
S^c_{xx} &:= \langle \vec{X}^c - P_{\mathbb{R}}(E(\tilde{X}))\vec{1}, \vec{X}^c - P_{\mathbb{R}}(E(\tilde{X}))\vec{1} \rangle,\\
S^c_{xy} &:= \langle \vec{X}^c - P_{\mathbb{R}}(E(\tilde{X}))\vec{1}, \vec{Y}^c - P_{\mathbb{R}}(E(\tilde{Y}))\vec{1} \rangle,\\
S^r_{xx} &:= \langle \vec{X}^r, \vec{X}^r \rangle,\\
S^r_{xy} &:= \langle \vec{X}^r, \vec{Y}^r \rangle.
\end{aligned}$$

It is easy to verify $S^c_{xx} \geq 0$, $S^r_{xx} \geq 0$, and $S^r_{xy} \geq 0$.

Theorem 5 (Theorem 6, [27]). *Let $\vec{\tilde{Y}}$ and $\vec{\tilde{X}} \in F(\mathbb{R})^n$, and let $(-1)^s$ denote the sign of S^c_{xy}. If $S^c_{xx} + S^r_{xx} \neq 0$, then the regression coefficients can be computed by the following formula*

$$b = (-1)^s (|S^c_{xy}| + S^r_{xy})(S^c_{xx} + S^r_{xx})^{-1}, \tag{6}$$

$$a = P_{\mathbb{R}}(E(\tilde{Y})) - bP_{\mathbb{R}}(E(\tilde{X})). \tag{7}$$

IV. A theorem for more general regression model

Let Δ denote the set of all symmetric triangular fuzzy numbers. In this section, we are going to study fuzzy regression model whose constant regression coefficient is symmetric triangular, that is to find $\tilde{A} \in \Delta$ and $b \in \mathbb{R}$ minimizing the observation error

$$\mathrm{d}^2(\vec{\tilde{Y}}, \tilde{A}\vec{1} + b\vec{\tilde{X}}).$$

For each $\tilde{A} \in F(\mathbb{R})$, an element $P_\Delta(\tilde{A}) \in \Delta$ is called the *symmetric triangular approximation* of $\tilde{A}$ if

$$\mathrm{d}(\tilde{A}, P_\Delta(\tilde{A})) \leq \mathrm{d}(\tilde{A}, \tilde{X}), \quad \forall \tilde{X} \in \Delta.$$

In [28], the author proved that:

Proposition 6. *Let $\tilde{A} \in F(\mathbb{R})$. Then, its the symmetric triangular approximation $P_\Delta(\tilde{A}) = [\tau, \sigma]_{CR}$ can be computed by the following formula*

$$\tau = \tau(\tilde{A}) := \int_0^1 A^c(\alpha)\ d\alpha, \tag{8}$$

$$\sigma = \sigma(\tilde{A}) := 3\int_0^1 A^r(\alpha)(1-\alpha)\ d\alpha. \tag{9}$$

It is easy to verify that

$$\tau(a\tilde{A}) = a\tau(\tilde{A})$$

$$\sigma(a\tilde{A}) = |a|\sigma(\tilde{A})$$

for all $\tilde{A} \in F(\mathbb{R})$ and $a \in \mathbb{R}$. For more general approximations of fuzzy numbers, we refer to [7], [25], [26], [29], [30].

Proposition 7. *Let $\tilde{A}, \tilde{B} \in F(\mathbb{R})$ and $a, b \in \mathbb{R}$. Then,*

$$P_\Delta(a\tilde{A} + b\tilde{B}) = aP_\Delta(\tilde{A}) + bP_\Delta(\tilde{B}),$$

$$P_\Delta(a\tilde{A} \ominus b\tilde{B}) = aP_\Delta(\tilde{A}) \ominus bP_\Delta(\tilde{B}). \tag{10}$$

Furthermore,

$$\mathrm{d}^2(\tilde{A}, \tilde{X}) = \mathrm{d}^2(\tilde{A}, P_\Delta(\tilde{A})) + \mathrm{d}^2(P_\Delta(\tilde{A}), \tilde{X}), \forall \tilde{X} \in \Delta. \tag{11}$$

Let $\tilde{A} \in \Delta$. From Theorem 2 we find

$$\begin{aligned}
&\mathrm{d}^2(\vec{\tilde{Y}}, \tilde{A}\vec{1} + b\vec{\tilde{X}}) =\\
&\sum_{i=1}^{n} \mathrm{d}^2(\tilde{Y}_i \ominus E(\tilde{Y}), b\tilde{X}_i \ominus bE(\tilde{X})) + n\mathrm{d}^2(E(\tilde{Y}) \ominus bE(\tilde{X}), \tilde{A}).
\end{aligned}$$

Consequently, by Proposition 7 we have

$$\begin{aligned}
&\mathrm{d}^2(E(\tilde{Y}) \ominus bE(\tilde{X}), \tilde{A}) \qquad \text{(by Eq.(10))}\\
&\geq \mathrm{d}^2(E(\tilde{Y}) \ominus bE(\tilde{X}), P_\Delta(E(\tilde{Y}) \ominus bE(\tilde{X}))) \qquad \text{(by Eq.(11))}\\
&= \mathrm{d}^2(E(\tilde{Y}) \ominus bE(\tilde{X}), P_\Delta(E(\tilde{Y})) \ominus bP_\Delta(E(\tilde{X}))).
\end{aligned}$$

Hence, if $P_\Delta(E(\tilde{Y})) \ominus bP_\Delta(E(\tilde{X})) \in \Delta$, we only choose

$$\tilde{A} = P_\Delta(E(\tilde{Y})) \ominus bP_\Delta(E(\tilde{X}))$$

and then we have

$$\begin{aligned}
&\mathrm{d}^2(\vec{\tilde{Y}}, \tilde{A}\vec{1} + b\vec{\tilde{X}})\\
=&\sum_{i=1}^{n} \mathrm{d}^2(\tilde{Y}_i \ominus P_\Delta(E(\tilde{Y})), b\tilde{X}_i \ominus bP_\Delta(E(\tilde{X}))).
\end{aligned} \tag{12}$$

Thus, the rest is to find $b \in \mathbb{R}$ which minimizes the above value (i.e. Eq.(12)). But in general case, it may happen

$$P_\Delta(E(\tilde{Y})) \ominus bP_\Delta(E(\tilde{X})) \notin \Delta.$$

Note that, Proposition 7 implies

$$\begin{aligned}
P_\Delta(E(\tilde{Y})) \ominus bP_\Delta(E(\tilde{X})) = \Big[&\tau(E(\tilde{Y})) - b\tau(E(\tilde{X})),\\
&(\sigma(E(\tilde{Y})) - |b|\sigma(E(\tilde{X})))(1-\alpha)\Big]_{CR}
\end{aligned} \tag{13}$$

Hence, we obtain $P_\Delta(E(\tilde{Y})) \ominus bP_\Delta(E(\tilde{X})) \notin \Delta$ if and only if

$$\sigma(E(\tilde{Y})) < |b|\sigma(E(\tilde{X})).$$

Let $\vec{\tilde{X}} = (\tilde{X}_1, \ldots, \tilde{X}_n)$ and $\vec{\tilde{Y}} = (\tilde{Y}_1, \ldots, \tilde{Y}_n)$. Define

$$\begin{aligned}
T^c_{xx} &:= \langle \vec{X}^c - \tau(E(\tilde{X}))\vec{1}, \vec{X}^c - \tau(E(\tilde{X}))\vec{1} \rangle,\\
T^c_{xy} &:= \langle \vec{X}^c - \tau(E(\tilde{X}))\vec{1}, \vec{Y}^c - \tau(E(\tilde{Y}))\vec{1} \rangle,\\
T^r_{xx} &:= \langle \vec{X}^r - \sigma(E(\tilde{X}))(1-\alpha)\vec{1}, \vec{X}^r - \sigma(E(\tilde{X}))(1-\alpha)\vec{1} \rangle,\\
T^r_{xy} &:= \langle \vec{X}^r - \sigma(E(\tilde{X}))(1-\alpha)\vec{1}, \vec{Y}^r - \sigma(E(\tilde{Y}))(1-\alpha)\vec{1} \rangle.
\end{aligned}$$

Note that, by Eq.(5), (8), and (9) it is easy to verify that

$$\begin{aligned}
\langle \vec{X}^c, \tau(E(\tilde{X}))\vec{1} \rangle &= n\tau(E(\tilde{X}))^2,\\
\langle \vec{X}^c, \tau(E(\tilde{Y}))\vec{1} \rangle &= \langle \vec{Y}^c, \tau(E(\tilde{X}))\vec{1} \rangle = n\tau(E(\tilde{X}))\tau(E(\tilde{Y})),\\
\langle \vec{X}^r, \sigma(E(\tilde{X}))(1-\alpha)\vec{1} \rangle &= \frac{n}{3}\sigma(E(\tilde{X}))^2,\\
\langle \vec{X}^r, \sigma(E(\tilde{Y}))(1-\alpha)\vec{1} \rangle &= \langle \vec{Y}^r, \sigma(E(\tilde{X}))(1-\alpha)\vec{1} \rangle\\
&= \frac{n}{3}\sigma(E(\tilde{X}))\sigma(E(\tilde{Y})).
\end{aligned}$$

Hence, we have

$$T^c_{xx} := \langle \vec{X}^c, \vec{X}^c \rangle - n\tau(E(\tilde{X}))^2, \tag{14}$$

$$T^c_{xy} := \langle \vec{X}^c, \vec{Y}^c \rangle - n\tau(E(\tilde{X}))\tau(E(\tilde{Y})), \tag{15}$$

$$T^r_{xx} := \langle \vec{X}^r, \vec{X}^r \rangle - \frac{n}{3}\sigma(E(\tilde{X}))^2, \tag{16}$$

$$T^r_{xy} := \langle \vec{X}^r, \vec{Y}^r \rangle - \frac{n}{3}\sigma(E(\tilde{X}))\sigma(E(\tilde{Y})). \tag{17}$$

Theorem 8. *Input $\vec{\tilde{Y}}$ and $\vec{\tilde{X}} \in F(\mathbb{R})^n$. Suppose that*

$$T^c_{xx} + T^r_{xx} \neq 0.$$

Let $(-1)^t$ denote the sign of T^c_{xy} and

$$\delta^+ := \frac{|T^c_{xy}| + T^r_{xy}}{T^c_{xx} + T^r_{xx}} \tag{18}$$

and

$$\delta^- := \frac{-|T^c_{xy}| + T^r_{xy}}{T^c_{xx} + T^r_{xx}}. \tag{19}$$

Then the regression coefficients can be computed in the following cases:

1) *If $\delta^+ \geq 0$ and $\sigma(E(\tilde{Y})) \geq \delta^+\sigma(E(\tilde{X}))$, then*

$$b = (-1)^t\delta^+, \tag{20}$$

$$\tilde{A} = P_\Delta(E(\tilde{Y})) \ominus bP_\Delta(E(\tilde{X})). \tag{21}$$

2) *If $\delta^+ \geq 0$ and*

$$\delta^+\sigma(E(\tilde{X})) > \sigma(E(\tilde{Y})) \geq \delta^-\sigma(E(\tilde{X})),$$

then set

$$b^{(1)} = (-1)^t\delta^-, \tag{22}$$

$$\tilde{A}^{(1)} = P_\Delta(E(\tilde{Y})) \ominus b^{(1)}P_\Delta(E(\tilde{X})), \tag{23}$$

and applying Theorem 5, by Eqs.(6) and (7) compute real regression coefficients, say $a^{(2)}$ and $b^{(2)}$. Finally, compare the two observation errors

$$\mathrm{d}^2(\vec{\tilde{Y}}, \tilde{A}^{(1)}\vec{1} + b^{(1)}\vec{\tilde{X}}) \quad \textit{and} \quad \mathrm{d}^2(\vec{\tilde{Y}}, a^{(2)}\vec{1} + b^{(2)}\vec{\tilde{X}})$$

and output the best estimators.

3) *If $\delta^+ < 0$ or $\sigma(E(\tilde{Y})) < \delta^-\sigma(E(\tilde{X}))$, then compute real regression coefficients by Theorem 5.*

V. An illustrative example

Example 1 ([1], [2], [8], [13], [18], [20])**.** In order to cross-reference to the previous contributions let's consider the following example designed by Sakawa and Yano [20]:

	$\vec{Y}_i$	$\vec{X}_i$
1.	$[3.5 + 0.5\alpha, 4.5 - 0.5\alpha]$	$[1.5 + 0.5\alpha, 2.5 - 0.5\alpha]$
2.	$[5 + 0.5\alpha, 6 - 0.5\alpha]$	$[3 + 0.5\alpha, 4 - 0.5\alpha]$
3.	$[6.5 + \alpha, 8.5 - \alpha]$	$[4.5 + \alpha, 6.5 - \alpha]$
4.	$[6 + 0.5\alpha, 7 - 0.5\alpha]$	$[6.5 + 0.5\alpha, 7.5 - 0.5\alpha]$
5.	$[8 + 0.5\alpha, 9 - 0.5\alpha]$	$[8 + 0.5\alpha, 9 - 0.5\alpha]$
6.	$[7 + \alpha, 9 - \alpha]$	$[9.5 + \alpha, 11.5 - \alpha]$
7.	$[10 + 0.5\alpha, 11 - 0.5\alpha]$	$[10.5 + 0.5\alpha, 11.5 - 0.5\alpha]$
8.	$[9 + 0.5\alpha, 10 - 0.5\alpha]$	$[12 + 0.5\alpha, 13 - 0.5\alpha]$

By applying Eqs.(3) and (4), represent all fuzzy numbers with CR-representations, as follows:

	$\vec{Y}_i$	$\vec{X}_i$
1.	$[4.0, 0.5(1-\alpha)]_{CR}$	$[2.0, 0.5(1-\alpha)]_{CR}$
2.	$[5.5, 0.5(1-\alpha)]_{CR}$	$[3.5, 0.5(1-\alpha)]_{CR}$
3.	$[7.5, 1.0(1-\alpha)]_{CR}$	$[5.5, 1.0(1-\alpha)]_{CR}$
4.	$[6.5, 0.5(1-\alpha)]_{CR}$	$[7.0, 0.5(1-\alpha)]_{CR}$
5.	$[8.5, 0.5(1-\alpha)]_{CR}$	$[8.5, 0.5(1-\alpha)]_{CR}$
6.	$[8.0, 1.0(1-\alpha)]_{CR}$	$[10.5, 1.0(1-\alpha)]_{CR}$
7.	$[10.5, 0.5(1-\alpha)]_{CR}$	$[11.0, 0.5(1-\alpha)]_{CR}$
8.	$[9.5, 0.5(1-\alpha)]_{CR}$	$[12.5, 0.5(1-\alpha)]_{CR}$

By Eq.(2) we obtain the mean of $\tilde{Y}_i$ is

$$E(\tilde{Y}) = [6.875 + 0.625\alpha, 8.125 - 0.625\alpha].$$

Consequently, by applying Eqs.(3) and (4) the CR-representation of $E(\tilde{Y})$ is

$$E(\tilde{Y}) = [7.5, 0.625(1-\alpha)]_{CR}.$$

In the same way, we obtain

$$\begin{aligned} E(\tilde{X}) &= [6.9375 + 0.625\alpha, 8.1875 - 0.625\alpha] \\ &= [7.5625, 0.625(1-\alpha)]_{CR}. \end{aligned}$$

Now, by Eqs.(8) and (9) we obtain

$$\begin{aligned} &\tau(E(\tilde{X})) = 7.5625, \\ &\sigma(E(\tilde{X})) = 0.625, \\ &\tau(E(\tilde{Y})) = 7.5, \\ &\sigma(E(\tilde{Y})) = 0.625. \end{aligned}$$

Hence, by Eq.(5) and (14)-(17) we obtain

$$\begin{aligned} &T^c_{xx} := 97.71875, \\ &T^c_{xy} := 50.75, \\ &T^r_{xx} := 0.125, \\ &T^r_{xy} := 0.125. \end{aligned}$$

T^c_{xy} is positive, so $(-1)^t = 1$. Consequently, by Eqs.(18) and (19) we obtain

$$\delta^+ = 0.520$$

and

$$\delta^- = -0.517.$$

Since $\delta^+ \geq 0$ and $\sigma(E(\tilde{Y})) \geq \delta^+\sigma(E(\tilde{X}))$, by Eqs.(20) and (21) (Theorem 8, Case 1) we obtain

$$b = (-1)^t\delta^+ = 0.520$$

and

$$\begin{aligned} \tilde{A} &= P_\Delta(E(\tilde{Y})) \ominus bP_\Delta(E(\tilde{X})) \qquad \text{(by Eq.(14))} \\ &= [\tau(E(\tilde{Y})) - b\tau(E(\tilde{X})), \\ &\qquad (\sigma(E(\tilde{Y})) - |b|\sigma(E(\tilde{X})))(1-\alpha)]_{CR} \\ &= [3.5675, 0.3(1-\alpha)]_{CR} \\ &= [3.2675 + 0.3\alpha, 3.8675 - 0.3\alpha] \end{aligned}$$

Table 1. Comparison of the observation errors for previous estimators

			$d^2(\tilde{Y}_i, \tilde{A} + b \odot \tilde{X}_i)$		
	$\vec{X}_i$	$\vec{Y}_i$	D.	C.-H.	Thm. 8
1.	$(1.5, 2, 2.5)$	$(3.5, 4, 4.5)$	0.7344	0.7466	0.7417
2.	$(3, 3.5, 4)$	$(5, 5.5, 6)$	0.0282	0.0273	0.0275
3.	$(4.5, 5.5, 6.5)$	$(6.5, 7.5, 8.5)$	2.3177	2.3265	2.3200
4.	$(6.5, 7, 7.5)$	$(6, 6.5, 7)$	1.0106	0.9965	1.0049
5.	$(8, 8.5, 9)$	$(8, 8.5, 9)$	0.5195	0.5359	0.5267
6.	$(9.5, 10.5, 11.5)$	$(7, 8, 9)$	2.1578	2.1086	2.1352
7.	$(10.5, 11, 11.5)$	$(10, 10.5, 11)$	2.9113	2.9743	2.9403
8.	$(12, 12.5, 13)$	$(9, 9.5, 10)$	0.6648	0.6285	0.6476
Observation errors			10.3443	10.3442	10.3439

Using the data set in Example 1, Diamond [4] obtained the following regression coefficients

$$\tilde{A} = [3.263 + 0.3\alpha, 3.863 - 0.3\alpha],$$
$$b = 0.521.$$

And, Chen and Hsueh [3] obtained

$$\tilde{A} = [3.272 + 0.3\alpha, 3.872 - 0.3\alpha],$$
$$b = 0.521.$$

Table 1 shows that the observation errors corresponding to the above three estimators, where the observation errors are computed by Eq.(1). It is easy to see that our estimators are the best, as follows

$$\tilde{A} = [3.2675 + 0.3\alpha, 3.8675 - 0.3\alpha],$$
$$b = 0.520.$$

VI. Conclusion

In the paper, we apply the CR-representations of fuzzy numbers and symmetric triangular approximations to solve the regression model whose constant coefficient is assumed to be symmetric triangular and other coefficients to be real. The proposed formulae are simple and clear. In the future, one may consider applying more general approximations (such as triangular approximations [30], trapezoidal approximations [7], [26], and symmetric trapezoidal approximations [28]) to solve the following regression model

$$d^2(\vec{\tilde{Y}}, \tilde{A}\vec{1} + b\vec{\tilde{X}}),$$

where $b \in \mathbb{R}$ and $\tilde{A}$ is triangular (trapezoidal or symmetric trapezoidal).

Acknowledgment

This work is supported by National Science Council of Taiwan (99-2115-M-024-002). The author also gratefully acknowledges the helpful comments and suggestions of the reviewers, which have improved the presentation.

References

[1] A. Bargiela, W. Pedrycz, T. Nakashima, "Multiple regression with fuzzy data," Fuzzy Sets and Systems, vol.158, pp.2169-2188, 2007.
[2] L.-H. Chen and C.-C. Hsueh, "A mathematical programming method for formulating a fuzzy regression model based on distance criterion," IEEE Transactions on Systems, Man, and Cybernetics-Part B: Cybernetics, vol.37, no.3, pp.705-712, 2007.
[3] L.-H. Chen and C.-C. Hsueh, "Fuzzy Regression Models Using the Least-Squares Method Based on the Concept of Distance," IEEE Transactions on Fuzzy Systems, vol.17, no.6, pp.1259-1272, 2009.
[4] P. Diamond, "Fuzzy least squares," Information Science, vol.46, pp.141-157, 1988.
[5] P. Diamond and R. Korner, "Extended fuzzy linear models and least squares estimates," Computers and Mathematics with Applications, vol.33, no.9, pp.15-32, 1997.
[6] P. D'Urso and A. Santoro, "Goodness of fit and variable selection in the fuzzy multiple linear regression," Fuzzy Sets and Systems," vol.157, pp.2627-2647, 2006.
[7] P. Grzegorzewski and E. Mrowka, "Trapezoidal approximations of fuzzy numbers preserving the expected interval - algorithms and properties," Fuzzy Sets and Systems, vol.159, pp.1354-1364, 2008.
[8] M. Hojati, C.R. Bector and K. Smimou, "A simple method for computation of fuzzy linear regression," European Journal of Operational Research," vol.166, pp.172-184, 2005.
[9] D.H. Hong and C. Hwang, "Extended fuzzy regression models using regularization method," Information Science, vol.164, pp.31-46, 2004.
[10] D.H. Hong and C. Hwang, "Interval regression analysis using quadratic loss support vector machine," IEEE Transactions on Fuzzy Systems, vol.13, no.2, pp.229-237, 2005.
[11] J. Kacprzyk and M. Fedrizzi, Eds., "Fuzzy least squares regression: theory and application," in Fuzzy Regression Analysis, Omnitech Press Warsaw and Physica-Verlag, Heidelberg, 1992, pp.181-193.
[12] C. Kao and C.L. Chyu, "A fuzzy linear regression model with better explanatory power," Fuzzy Sets and Systems, vol.126, pp.401-409, 2002.
[13] C. Kao and C.L. Chyu, "Least-squares estimates in fuzzy regression analysis," European Journal of Operational Research, vol.148, pp.426-435, 2003.
[14] B. Kim and R.R. Bishu, "Evaluation of fuzzy linear regression models by comparing membership functions," Fuzzy Sets and Systems, vol.100, pp.343-352, 1998.
[15] H.K. Kim, J.H. Yoon, Y. Li, "Asymptotic properties of least squares estimation with fuzzy observations," Information Science, vol.178, pp.439-451, 2008.
[16] R. Korner and W. Nather, "Linear regression with random fuzzy variables: extended classical estimates, best linear estimates, least squares estimates," Information Science, vol.109, pp.95-118, 1998.
[17] V. Kratshmer, "Least-squares estimation in linear regression models with vague concepts," Fuzzy Sets and Systems, vol.157, pp.2579-2592, 2006.
[18] M.H. Mashinchi, M.A. Orgun, M. Mashinchi and W. Pedrycz, "A tabu-harmony search based approach to fuzzy linear regression," IEEE Transactions on Fuzzy Systems, accepted.
[19] M. Modarres, E. Nasrabadi and M.M. Nasrabadi, "Fuzzy linear regression models with least square errors," Applied Mathematics and Computation, vol.163, pp.977-989, 2005.

[20] M. Sakawa and H. Yano, "Multiobjective fuzzy linear regression analysis for fuzzy input-output data," Fuzzy Sets and Systems, vol.47, pp.173-181, 1992.
[21] H. Tanaka, S. Uejima, K. Asai, "Linear regression analysis with fuzzy model," IEEE Transactions on Systems Man Cybernetics, vol.12, No.6, pp.903-907, 1982.
[22] N. Wang, W.X. Zhang, C.L. Mei, "Fuzzy nonparametric regression based on local linear smoothing technique," Information Science, vol.177, pp.3882-3900, 2007.
[23] A. Wunsche and W. Nather, "Least-squares fuzzy regression with fuzzy random variables," Fuzzy Sets and Systems, vol.130, pp.43-50, 2002.
[24] C.-T. Yeh, "Reduction of fuzzy linear systems of dual equations," International Journal of Fuzzy Systems, Vol.9, No.3, pp.173-178, 2007.
[25] C.-T. Yeh, "On improving trapezoidal and triangular approximations of fuzzy numbers," International Journal of Approximate Reasoning, vol.48, no.1, pp.297-313, 2008.
[26] C.-T. Yeh, "Weighted trapezoidal and triangular approximations of fuzzy numbers," Fuzzy Sets and Systems, vol.160, pp.3059-3079, 2009.
[27] C.-T. Yeh, "Reduction to least-squares estimates in multiple fuzzy regression analysis," IEEE Transactions on Fuzzy Systems, vol.17, no.4, pp.935-948, 2009.
[28] C.-T. Yeh, "Approximations by interval, triangular and trapezoidal fuzzy numbers," Proceeding of 2009 International Fuzzy Systems Association World Congress, pp.143-148, 2009.
[29] C.-T. Yeh, "Weighted semi-trapezoidal of fuzzy numbers," Fuzzy Sets and Systems, vol.165, pp.61-80, 2011.
[30] W. Zeng and H. Li, "Weighted triangular approximation of fuzzy numbers," International Journal of Approximate Reasoning, vol.46, no.1, pp.137-150, 2007.

2011 IEEE International Conference on Fuzzy Systems
June 27-30, 2011, Taipei, Taiwan

A Real-Time Analysis of Granular Information: Some Initial Thoughts on a Convex Hull-based Fuzzy Regression Approach

Azizul Azhar Ramli[1,3], Witold Pedrycz[2], Junzo Watada[1], and Nureize Arbaiy[1,3]

[1]Graduate School of Information, Production and Systems, Waseda University, 2-7, Hibikino, Wakamatsu, Kitakyushu, 808-0135 Japan

[2]Department of Electrical and Computer Engineering, University of Alberta, Edmonton, Alberta, Canada T6G 2V4 and Systems Research Institute, Polish Academy of Sciences, Warsaw, Poland

[3]Faculty of Computer Science and Information Technology, Universiti Tun Hussein Onn Malaysia, Parit Raja, 86400 Batu Pahat, Johor Darul Takzim, Malaysia

{azizulazhar@moegi.waseda.jp, pedrycz@ece.ualberta.ca, junzow@osb.att.ne.jp, nureize@uthm.edu.my}

Abstract— **Regression models are well known and widely used as one of the important categories of models in system modeling. In this paper, we extend the concept of fuzzy regression in order to handle real-time implementation of data analysis of information granules. An ultimate objective of this study is to develop a hybrid of a genetically-guided clustering algorithm called genetic algorithm-Fuzzy C-Means (GA-FCM) and a convex hull-based fuzzy regression approach being regarded as a potential solution to the formation of information granules. It is anticipated that the setting of Granular Computing will help us reduce the computing time, especially in case of real-time data analysis, as well as an overall computational complexity. We propose an efficient real-time granular fuzzy regression analysis based on the convex hull approach in which a Beneath-Beyond algorithm is employed to design a convex hull. In the proposed design setting, we emphasize a pivotal role of the convex hull approach, which becomes crucial in alleviating limitations of linear programming manifesting in system modeling.**

Keywords-convex hull, fuzzy regression, Fuzzy C-Means, genetic algorithm, granular computing

I. INTRODUCTION

Nowadays, we witness a significant growth of interest in Granular Computing（GrC) being regarded as a promising vehicle supporting the design, analysis and processing of information granules [1]. With regard of all processing faculties, information granules are collections of entities (elements), usually originating at the numeric level, that are arranged together due to their similarity, functional adjacency and indistinguishability or alike [1]. Given the similarity function to measure the closeness between the samples these data are clustered into certain granules, categories or classes [2]. The process of forming information granules is referred as information granulation.

GrC has begun to play important roles in bioinformatics, pattern recognition, security, high-performance computing and so on in terms of efficiency, effectiveness, robustness as well as a structural representation of uncertainty [3]. Therefore, the needs for sophisticated intelligent data analysis (IDA) tools are highly justifiable when dealing with this type of information.

Ramli *et al.* proposed a real-time fuzzy regression model incorporating a convex hull method, specifically a Beneath-Beyond algorithm [3]. They have deployed a convex hull approach useful in the realization of data analysis in a dynamic data environment. The developed method exhibits good performance as far as computing time and an overall computation complexity are concerned. Fuzzy C-Means (FCM) clustering algorithm, introduced by Dunn in 1973 and generalized by Bezdek in 1981, becomes one of the commonly used techniques of GrC when it comes to the formation of information granules [4] [5]. There has been a great deal of improvements and extensions of this clustering technique. One can refer here to the genetically-guided clustering algorithm called genetic algorithm-FCM (GA-FCM) and proposed by Hall *et al.* It has been shown that the GA-FCM algorithm can successfully alleviate the difficulties of choosing a suitable initialization of the FCM method [6].

Associated with these two highlighted models (that is fuzzy regression and fuzzy clustering), the main objective of this study is to propose an enhancement of the fuzzy regression analysis for the purpose of analysis of information granules. From the IDA perspective, this research intends to augment the model given originally proposed by Bezdek by including the Ramli *et al.*'s approach. It will be shown that such a hybrid combination is capable of supporting real-time granular based fuzzy regression analysis.

In general, the proposed approach helps perform real-time fuzzy regression analysis in presence of information granules. The proposed approach comprises three main phases. First, we use the GA-FCM clustering to granulate the entire data set into a limited number of chunks–information granules. The second phase consists of constructing convex hull polygons for the already formed information granules. Finally, in the last phase, the selected vertices of the constructed convex hull, which covers all information granules, are used to build a fuzzy regressions model. To illustrate the efficiency and effectiveness of the proposed method, a numeric example is presented.

This study is structured as follows. Section 2 serves as a concise and focused review of the fuzzy regression model, convex hull approach, principles of GrC as well as GA-FCM. Section 3 discusses some essentials of fuzzy linear regression

978-1-4244-7316-8/11/$26.00 ©2011 IEEE

augmented by the convex hull approach. Section 4 discusses a processing flow of the proposed approach; a real-time granular-based fuzzy regression models. Section 5 is devoted to a numerical experiment. Finally, Section 6 presents some concluding remarks.

II. SOME RELETED PRILIMINARIES

A. Review of Fuzzy Regression Model

In statistical regression, deviations between observed and estimated values are assumed to be due to the random errors. Regression analysis is one of commonly encountered approaches in describing relationships among the analyzed data. The regression models explain dependencies between independent and dependent variables. The variables, which are used to explain the other variable(s) are called explanatory ones [7].

Although conventional regression has been applied to various applications, problems may arise when we encounter vague relationships between input and output variables in which cases there assumptions made for regression models are not valid any longer. This situation becomes a major reason of a lack of relevance of regression models.

Recall that a standard numeric linear regression model comes in the following form

$$y = a_0 + a_1 x_1 + ... + a_K x_K . \tag{1}$$

As an interesting and useful extension, Tanaka *et al.* [7] introduced an enhancement of the regression model by accommodating fuzzy sets thus giving rise to the term of fuzzy regression or possibilistic regression. The models of this category reflect the fuzzy set based nature of relationships between the dependent and independent variables. The upper and lower regression boundaries in the fuzzy regression are used to quantify the fuzzy distribution of the output values.

As an alternative to the fuzzy specification, an inexact relationship among those dependent and independent variables can be represented via fuzzy linear regression expressed in the following form

$$\widetilde{Y} = \widetilde{A}_0 X_0 + \widetilde{A}_1 X_1 + ... + \widetilde{A}_K X_K = \widetilde{\mathbf{A}}\mathbf{X}^t , \tag{2}$$

where $\mathbf{X} = [X_0, X_1, ..., X_K]$ is a vector of independent variables; $\widetilde{\mathbf{A}} = [\widetilde{A}_0, \widetilde{A}_1, ...\widetilde{A}_K]$ is a vector of fuzzy coefficients represented in the form of symmetric triangular fuzzy numbers and denoted by $\widetilde{A}_j = (\alpha_j, c_j)$. Their membership function is described in the form:

$$u_{\widetilde{A}_j}(a_j) = \begin{cases} 1 - \dfrac{|\alpha_j - a_j|}{c_j}, & : c_j \neq 0, \alpha_j - c_j \le a_j \le \alpha_j + c_j \\ 1, & : c_j = 0, \alpha_j = a_j \\ 0, & : otherwise \end{cases} \tag{3}$$

$$(j = 0, \ldots, K)$$

In addition, from the computational perspective, the estimation of the membership functions of the fuzzy parameters of the regression is concerned with a certain problem of linear programming (LP) [8] [9].

Given the notation used above, (2) can be rewritten as

$$\widetilde{Y}_i = (\alpha_0, c_0) + (\alpha_1, c_1) X_1 + (\alpha_2, c_2) X_2 + ... + (\alpha_K, c_K) X_K \tag{4}$$

where α_j and c_j are the central (modal) value and the spread of triangular fuzzy number, respectively.

Related to the above model (4), we assume that the numeric input and output data are available, while the relation between the input and output data is defined by some fuzzy function in which the distribution of the parameter is governed by the membership functions [10].

By making use of the extension principle, the membership function of the fuzzy number $\widetilde{Y}_i$ comes in the following form

$$u(Y_i) = \begin{cases} 1 - \dfrac{|\, Y_i - \boldsymbol{\alpha}\mathbf{X}_i^t \,|}{\mathbf{c}\,|\,\mathbf{X}_i^t\,|}, & : \mathbf{c}\,|\,\mathbf{X}_i^t\,| \neq 0, \boldsymbol{\alpha}\mathbf{X}_i^t - \mathbf{c}\,|\,\mathbf{X}_i^t\,| \le Y_i \le \boldsymbol{\alpha}\mathbf{X}_i^t + \mathbf{c}\,|\,\mathbf{X}_i^t\,| \\ 1, & : \mathbf{c}\,|\,\mathbf{X}_i^t\,| = 0, \; Y_i = \boldsymbol{\alpha}\mathbf{X}_i^t \\ 0, & : otherwise \end{cases} \tag{5}$$

where $\mathbf{c} = [c_0, c_1, ..., c_K], \boldsymbol{\alpha} = [\alpha_0, \alpha_1, ..., \alpha_K]$ and $\mathbf{c}\,|\,\mathbf{X}_i^t\,| = \sum_{j=0}^{K} c_j \,|\, x_{ij} \,|$, $x_{i0} = 1 : (\forall i = 1, ..., n)$.

Moreover, when we consider an optimization of some objective function, its minimization reduces the total spread of the fuzzy number, $\widetilde{Y}_i$. More specifically we have

$$\underset{\boldsymbol{\alpha},\mathbf{c}}{\text{MIN}} \sum_{i=1}^{n} \mathbf{c}\,|\,\mathbf{X}_i^t\,| = \underset{\boldsymbol{\alpha},\mathbf{c}}{\text{MIN}} \sum_{i=1}^{n} \sum_{j=0}^{K} c_j \,|\, x_{ij} \,| \tag{6}$$

along with the constraints which require that each observation Y_i comes with at least h degree of membership to $\widetilde{Y}_i$, that is $u(Y_i) \ge h \; (i = 1, ..., n),$. This requirement can be expressed in an equivalent form

$$1 - \frac{|\, Y_i - \boldsymbol{\alpha}\mathbf{X}_i^t \,|}{\mathbf{c}\,|\,\mathbf{X}_i^t\,|} \ge h, \qquad \forall i = 1, ..., n \tag{7}$$

The above formulation of the problem leads to the following problem of LP

$$\underset{\boldsymbol{\alpha},\mathbf{c}}{\text{MIN}} \sum_{i=1}^{n} \sum_{j=0}^{K} c_j \,|\, x_{ij} \,| \tag{8}$$

$$\text{subject to } \sum_{j=0}^{K}\alpha_j x_{ij} + (1-h)\sum_{j=0}^{K} c_j \mid x_{ij} \mid \geq Y_i,$$
$$\sum_{j=0}^{K}\alpha_j x_{ij} - (1-h)\sum_{j=0}^{K} c_j \mid x_{ij} \mid \leq Y_i, \qquad (9)$$
$$c_j \geq 0, \quad \alpha_j \in \Re, \quad x_{i0} = 1 \quad (0 \leq h < 1; \quad \forall i = 1,...,n).$$

Additionally, the fuzzy regression model is constructed in such a way so that it "covers" all data points under consideration, cf. [11].

We use the notation $(\tilde{y}_i, \mathbf{x}_i), \tilde{y}_i = (y_i, d_i)$, to denote the fuzzy output data and $\mathbf{x}_i = [x_{i0}, x_{i1}, x_{i2}, ..., x_{iK}]$ $(i = 1,...,n)$ to describe the numeric input data. The notation of $(\boldsymbol{\alpha}, \mathbf{c})$ is used to describe fuzzy coefficients. The development of the fuzzy regression model results in the following LP problem:

$$\underset{\boldsymbol{\alpha},\mathbf{c}}{\text{MIN}} \sum_{i=1}^{n} \mathbf{c} \mid \mathbf{x}_i^t \mid \qquad (10)$$

$$\text{subject to } y_i + L^{-1}(h)d_i \leq \boldsymbol{\alpha}\mathbf{x}_i^t + L^{-1}(h)\mathbf{c} \mid \mathbf{x}_i^t \mid$$
$$y_i - L^{-1}(h)d_i \geq \boldsymbol{\alpha}\mathbf{x}_i^t - L^{-1}(h)\mathbf{c} \mid \mathbf{x}_i^t \mid \qquad (11)$$
$$\mathbf{c} \geq 0 \quad (i = 1,...,n),$$

where $L(u)$ refers to the shape of the membership function of the parameters of the fuzzy regression model while h is a possibility degree expressing to which extent a given datum is "covered" by the model. Based on the above explanation, fuzzy regression becomes the possibilistic model that can be used in the context of possibility theory [12]. Furthermore, it is possible in this formulation of the fuzzy regression model to treat non-fuzzy data with zero width setting the value of, d to 0 as described in the above formulas.

B. Convex Hull Approach

Let us recall that the convex hull of a set S of points while $hull(S)$ is defined to be a minimum convex set containing S. A point $P \in S$ is an extreme point of S if $P \notin hull(S - P)$. In general, if S is finite, then $hull(S)$ are a convex polygon and the extreme points of S are the corners of this polygon. The edges of this polygon are referred to as the edges of the $hull(S)$. Figure 2 illustrates the convex hull realization.

The concept closely related here is the affine hull of a set S in Euclidean space $\Re^K$. It is the smallest affine set containing S, or equivalently, the intersection of all affine sets containing S. Here, an affine set is defined as the translation of a vector subspace. The affine hull $aff(S)$ of S is the set of all affine combinations of elements of S, namely,

$$aff(S) = \{\sum_{j=1}^{K}\alpha_j x_j \mid x_j \in S, \alpha_j \in \Re, \alpha_j \geq 0, \sum_{j=1}^{K}\alpha_j = 1\}. \qquad (12)$$

The Beneath-Beyond algorithm is developed to incrementally build up the convex hull by keeping track of the current convex hull P_i and using an incidence graph [13]. In a nutshell, the Beneath-Beyond algorithm comprises the following steps:

Step_1 : Select and sort points along one direction, say x_1. Let $s = \{p_0, p_1, ..., p_{n-1}\}$ be input points after sorting. Process the points in increasing order.

Step_2 : Take the first n points, which define a facet (*dimensional faces*) as the initial hull.

Step_3 : Let P_i be the point to be added to the hull at the i th stage. Let $p_i = conv(p_0, p_1, ..., p_{i-1})$ be the convex hull polytope built so far. This step includes two kinds of hull updates;

(a) A pyramidal update is done when $p_i \notin aff(p_0, p_1, ..., p_{i-1})$ - when P_i is not on the hyperplane defined by the current hull. A pyramidal update consists of adding a new node representing P_i to the incidence graph and connecting this node to all existing hull vertices by new edges.

(b) A non-pyramidal update is done when the above condition is not met, *i.e.* P_i is in the affine subspace defined by the current convex hull. In this case, faces that are visible from P_i are removed and new facets are created.

C. Review of Granular Computing with Genetic Clustering

As said earlier, GrC is a general computing paradigm that effectively deals with processing information granules. The underlying formalism relies on a way in which information granules are represented; here we may consider set theory, fuzzy sets, rough sets, to name a few of the available alternatives [1] [14].

In this context, FCM arises as a way of formation of information granules represented by fuzzy sets [5]. In essence, the FCM algorithm is developed based on the minimization of the following objective function

$$J_m(U,V) = \sum_{i=1}^{c}\sum_{k=1}^{n}(U_{ik})^m D_{ik}^2(\mathbf{v}_i, \mathbf{x}_k) \qquad 1 \leq i \leq c; 1 \leq k \leq n \qquad (13)$$

where $U \in M_{fcn}$ is a fuzzy partition matrix, $V = (\mathbf{v}_1, \mathbf{v}_2, ..., \mathbf{v}_c)$ is a collection of cluster centers *(prototypes).* $\mathbf{v}_i \in \Re^K$ $\forall i$ and $D_{ik}(\mathbf{v}_i, \mathbf{x}_k)$ is a distance between x_k and the i^{th} prototype while m is a certain parameter known as a fuzzification coefficient, $m > 1$.

The FCM optimizes (13) by iteratively updating the prototypes and the partition matrix. More specifically, we choose some values of c, m and ε (termination condition – a small positive constant), then generate a random a fuzzy partition matrix U^0 and set an iteration index $t = 0$. An iterative process is organized as follows. Given the

membership value $\mu_{ik}^{(t)}$, the cluster centers $\mathbf{v}_i^{(t)}(i=1,\ldots,c)$ are calculated by

$$\mathbf{v}_i^{(t)} = \frac{\sum_{k=1}^{n}(\mu_{ik}^{(t)})^m \mathbf{x}_k}{\sum_{k=1}^{n}(\mu_{ik}^{(t)})^m} \quad for \quad 1 \le k \le n.. \tag{14}$$

Given the new cluster centers $\mathbf{v}_i^{(t)}$, we update the membership values of the partition matrix $\mu_{ik}^{(t)}$

$$\mu_{ik}^{t+1} = \left[\sum_{j=1}^{c} \left(\frac{\left\| \mathbf{x}_k - \mathbf{v}_i^{(t)} \right\|}{\left\| \mathbf{x}_k - \mathbf{v}_j^{(t)} \right\|} \right)^{\frac{2}{m-1}} \right]^{-1} \quad 1 \le j \le c. \tag{15}$$

This process terminates when $\left| U^{(t+1)} - U^{(t)} \right| \le \varepsilon$, or a predefined number of iterations have been reached [15].

We focus here on the practice of genetically-guided clustering algorithm, which proposed by Hall *et al.* in 1999 [6]. Based on Hall *et al.*, in any generation, element i of the population, V_i, a $c \times s$ matrix of cluster centers or prototypes. The initial population of size P is built by some random assignment of real numbers to each of the features of the c cluster centers. The initial values are constrained to be in the range of the attribute to which they are assigned (determined empirically from the experimental data sets) but are otherwise random [6].

In addition, as the cluster centers are to be used by the GA, it becomes necessary to reformulate the objective function for optimization purposes. Expression (13) can be given in terms of distances from the prototypes (as done in the FCM algorithm). As long as $D_{jk}(\mathbf{v}_j, \mathbf{x}_k) > 0 \forall j,k$, $1 \le j \le c; 1 \le k \le n$ we can use the following formula

$$U_{ik} = 1 / \sum_{j=1}^{c} \left(\frac{D_{ik}(\mathbf{v}_i, \mathbf{x}_k)}{D_{jk}(\mathbf{v}_j, \mathbf{x}_k)} \right)^{\frac{2}{m-1}} \quad for \quad 1 \le i \le c; 1 \le k \le n \tag{16}$$

in the calculations of the fuzzy partition matrix. Therefore the reformulated version of the FCM objective function comes in the form

$$R_m(V) = \sum_{k=1}^{n} \left(\sum_{i=1}^{c} D_{ik}^{\frac{1}{1-m}} \right)^{1-m} \quad for \quad 1 \le i \le c; 1 \le k \le n \tag{17}$$

Next we optimize R_m by running a genetically-guided algorithm (GGA). As usual, the important features of the GA-based clustering algorithm relate with the choice of the selection, crossover as well as mutation operators of the genetic optimization; for details one may refer to [6].

Moreover, the complete process of the GGA algorithm is outlined as follows [6].

GGA_1 : Choose m, c and D_{ik}.

GGA_2 : Randomly initialize P sets of c cluster centers. Constrain the initial values within the space defined by the data to be clustered.

GGA_3 : Calculate R_m by using (17) for each population member and apply modified objective function $R_m'(V) = R_m(V) + b \times R_m(V)$, where $b \in [0, c]$ is the number of empty clusters.

GGA_4 : Convert population members to binary equivalents (*using the Gray code*).

GGA_5 : For $i = 1$ to number of generations, Do

i. Used k-fold tournament selection (default $k = 2$) to select $P/2$ parent pairs for reproduction.

ii. Complete a two-point crossover and bitwise mutation for each feature of the parent pairs.

iii. Calculate R_m by using (17) for each population member and apply modified objective function $R_m'(V) = R_m(V) + b \times R_m(V)$, where $b \in [0, c]$ is the number of empty clusters.

iv. Create a new generation of size P which is selected from the two best members of the previous generation and the best children that are generated by using crossover and mutation.

GGA_6 : Provide the cluster centers to the terminal population with the smallest R_m' value and report R_m'

III. Fuzzy Linear Regression Models with Convex Hull Approach

Ordinarily, the weaknesses of the implementation of the multi-dimensional fuzzy linear regression can be addressed by incorporating the convex hull approach [12]. In the introduced modification, the construction of vertices of the convex hull becomes realized in real-time by using related points (convex points) of the graph. Furthermore, the real-time implementation of the method has to deal with a large number of samples (data). Therefore, each particular analyzed sample stands for a convex point and is possibly selected as a convex hull vertex. Some edges connecting the vertices need to be re-constructed as well.

Recall that the main purpose of fuzzy linear regression is to form the upper and lower bounds of the linear regression model. Both the upper line Y^U and lower line Y^L for fuzzy linear regression are expressed in the form:

$$Y^U = \{A_0 + A_1 x_1 + \ldots + A_K x_K\}^U : \{\mathbf{A}\mathbf{x}_i^t\}^U = \boldsymbol{\alpha}\mathbf{x}_i^t + \mathbf{c}\left|\mathbf{x}_i^t\right| \tag{18}$$

$$Y^L = \{A_0 + A_1 x_1 + \ldots + A_K x_K\}^L : \{\mathbf{A}\mathbf{x}_i^t\}^L = \boldsymbol{\alpha}\mathbf{x}_i^t - \mathbf{c}\left|\mathbf{x}_i^t\right| \tag{19}$$

By using (18) and (19), we convert the problem to a general fuzzy regression that is similar to the one shown below:

(i) Evaluation (objective) function

$$\min_{\boldsymbol{\alpha},\mathbf{c}} \sum_{i=1}^{n}\sum_{j=2}^{K} c_j \left|P_{ij}\right|. \tag{20}$$

(ii) Constraints

$$P_{i1} \in Y_i \Leftrightarrow \begin{cases} P_{i1} \le \alpha_0 + c_0 + \sum_{j=2}^{K} \alpha_j P_{ij} + \sum_{j=2}^{K} c_j \left|P_{ij}\right| \\ P_{i1} \ge \alpha_0 - c_0 + \sum_{j=2}^{K} \alpha_j P_{ij} - \sum_{j=2}^{K} c_j \left|P_{ij}\right| \\ (i = 1,\ldots,n) \end{cases} \tag{21}$$

The above expression can be further rewritten as follows:

$$\begin{aligned} Y^U &= \{Y_i^U \,|\, i = 1,\ldots,n\} \\ Y^L &= \{Y_i^L \,|\, i = 1,\ldots,n\}. \end{aligned} \tag{22}$$

We also arrive at the following simple relationships for P_{i1}

$$P_{i1} \le Y_i^U, \quad P_{i1} \ge Y_i^L \qquad (i = 1,\ldots,n). \tag{23}$$

It is well known that any discrete topology is a topology which is formed by a collection of subsets of a topological space X and the discrete metric ρ on X is defined as

$$\rho(x,y) = \begin{cases} 1 & if\ x \ne y \\ 0 & if\ x = y \end{cases} \tag{24}$$

for any $x, y \in X$. In this case, (X,ρ) is called a discrete metric space or a space of isolated points. According to the definition of discrete topology, expression (23) is rewritten as follows:

$$\begin{aligned} S(Y^U) &= \sum_{j=1}^{K} \{Y_j P_{ij}\}^U \ge 0 \\ S(Y^L) &= \sum_{j=1}^{K} \{Y_j P_{ij}\}^L \le 0 \end{aligned} \tag{25}$$

where we assume that $P_{i1} = 1$.

This formula corresponds to the definition of the support hyperplane. Under the consideration of the range of

$$S \bigcap P \ne \phi \ \text{ and } \ P \subset S^+ \text{ or } P \subset S^-, \tag{26}$$

the following relation is valid:

$$\bigcap S(Y^U) = \bigcap S(Y^L). \tag{27}$$

This is explained by the fact that regression formula Y^U and Y^L are formed by vertices of a convex hull. Therefore, it is apparent that the constructed convex hull polygon or more specifically, its vertices clearly define the as discussed constraints of fuzzy mathematical programming, which were becomes more reliable as well as significant for the subsequent processes.

Recall that the convex hull of a set S of points while $hull(S)$ is defined to be a minimum convex set containing S. A point $P \in S$ is an extreme point of S if $P \notin hull(S - P)$. Hence P denotes the set of points (input samples) and P_C is the set of vertices of the convex hull where $P_C \in P$. Therefore, the convex hull has to satisfy the following relationship:

$$conv(P) = conv(P_C) \tag{28}$$

Let us introduce the following set

$$P_C = \left\{x_{Cl} \in \Re^K \,\middle|\, l = 1,\ldots,m\right\} \subseteq P \tag{29}$$

where m is the number of vertices of the convex hull. Plugging this relationship into (21), we arrive at the following constraints:

$$P_{i1} \in Y_i \Leftrightarrow \begin{cases} P_{i1} \le \alpha_0 + c_0 + \sum_{j=2}^{K} \alpha_j P_{ij} + \sum_{j=2}^{K} c_j \left|P_{ij}\right| \\ P_{i1} \ge \alpha_0 - c_0 + \sum_{j=2}^{K} \alpha_j P_{ij} - \sum_{j=2}^{K} c_j \left|P_{ij}\right| \\ (i = 1,\ldots,m). \end{cases} \tag{30}$$

By using (30), the constraints of the LP of the fuzzy linear regression can be written down in the following manner:

$$y_i \in Y_i \Leftrightarrow \begin{cases} y_i \le \boldsymbol{\alpha}\mathbf{x}_i^t + \mathbf{c}\left|\mathbf{x}_i^t\right| \\ y_i \ge \boldsymbol{\alpha}\mathbf{x}_i^t - \mathbf{c}\left|\mathbf{x}_i^t\right| \\ (i = 1,\ldots,m). \end{cases} \tag{31}$$

Moreover, in order to form a suitable regression model based on the constructed convex hull, the connected vertex points are used as the constraints in the LP formulation of the fuzzy linear regression. Considering this process, the use of

the limited number of selected vertices contributes to the minimized computing complexity associated with the model [1].

IV. A Real-Time Granular Based Fuzzy Regression Models with a Convex Hull Implementation

In what follows, we present a hybrid combination of a fuzzy linear regression analysis based on convex hull algorithm, in particular the Beneath-Beyond algorithm to facilitate a real-time fuzzy regression analysis of granular data implementation. The detailed flow of processing is shown in Figure 1.

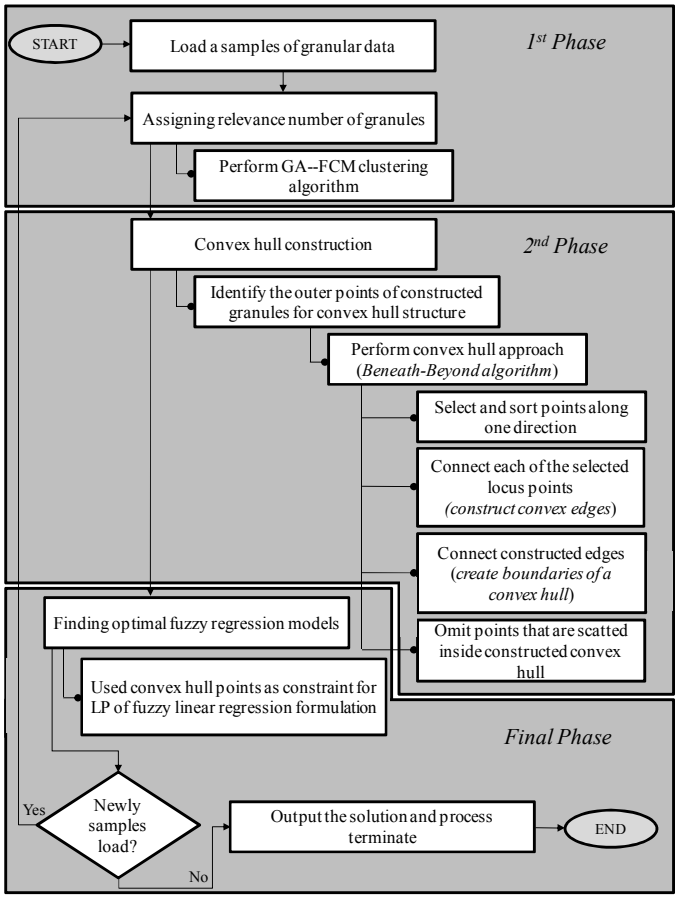

Figure 1. A general flow of processing of the proposed approach.

During the first phase we perform an assigning of appropriate number of granules augmented by GA-FCM clustering algorithm. Then, at the next phase, a construction of convex hull polygon is realized by selecting the outer points among the assigned granules. Therefore, the connection between these selected points (vertices) were became a boundary of the entire analyzed data samples as well as obtained information granules. As a result, with this constructed convex hull, we create the optimal regression lines as realized in the final phase, see Figure 1. In addition, we complete some iterations of the overall procedure considering that more data become available. Say, new samples are provided within a certain time interval, *e.g.*, they could be arriving every 5 or 10 seconds.

In light of the comments made above, it becomes apparent that the quality of granular based fuzzy regression model can be improved by the hybrid combination of fuzzy regression approach with the convex hull approach. The efficiency refers to the computing time as well as the overall computational complexity.

We do not have to consider the complete feature vectors for building regression models; just we utilize the selected vertices which are used for the construction of the convex hull. Therefore, this situation will lead to the decrease of computation load. On the other hand, related to the computational complexity factor for the subsequent iteration, it will only consider the newly added samples of data together with the selected vertices of the previous convex hull. For that reason, this computing scenario will reduce the computational complexity because of the lower number of the feature vectors used for the subsequent processing of regression models [3].

V. A Numerical Example

We present a simple numerical example, which shows the efficiency of the proposed approach in the implementation of real-time granular based fuzzy regression. Below, shows an illustration of real-time data analysis which involve dynamic record/database, see Figure 2. For instant, each of iteration might be having a same amount of newly arrived data. As early mentioned, the size of data were increase along with time spending. We can see here, the volume of data becomes enlarge as regard to the time increased.

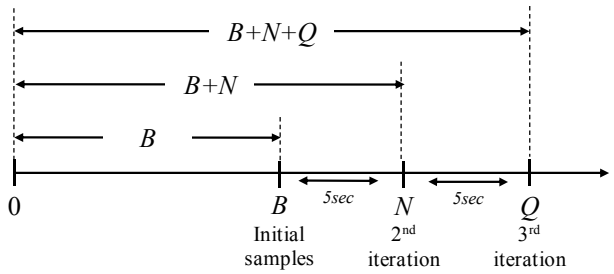

Figure 2. An Illustration of an increasing record/database along with time consumption.

Based on the above figure, we assume that an initial group of samples (*for 1st iteration*) consists of 100 data of the well-known *Iris* data set [11]. Next, considering a distribution of these data, we construct a convex hull polygon, which becomes the boundary of the overall analyzed samples. Among 100 obtained loci points (*clustered feature vectors*), only 11 points were selected as convex hull vertices, see Figure 3. In addition, these selected vertices are located as the outside points of the constructed clusters. By solving the associated LP problem that considered these selected vertices as a part of the constraint portion standing in the problem, we obtained the optimal regression coefficients, see Table I. In addition, we selected $h = 0.05$ to express goodness of fit or compatibility of data and the regression model.

TABLE I. The Center and Width Values of Initial Group of Data Samples

Variables	Center, m_i	Width, c_i
Intercept	2.071	0.163
$C1$	0.612	0.096
$C2$	0.639	0.075
$C3$	-0.412	0.000

Figure 2 shows the obtained feature vectors.

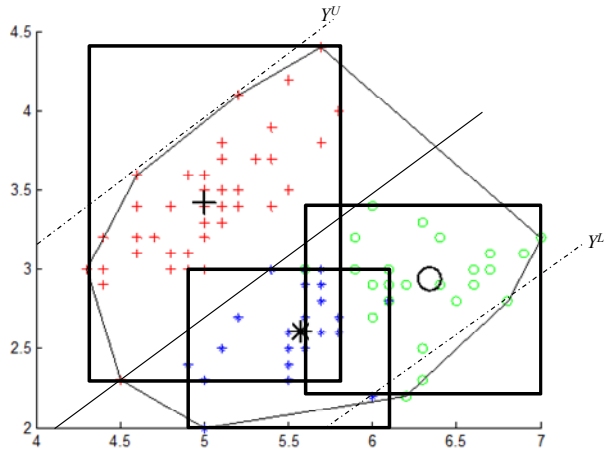

Figure 3. An Ilustration of obtained clustered feature vectors for the initial group of data samples.

To deal with a real-time scenario, we added a group of samples taken from the same data set, which consists of 50 patterns. In this case, we assume that a same as previous parameter setting has been set up and an iteration process has been completed. For this 2nd iteration, only 9 points were considered as convex hull vertices.

Finally, Table II includes the parameters as well as the values of the fuzzy regression which have been obtained and Figure 4 shows the of clustered feature vectors.

TABLE II. CENTER AND WIDTH VALUES OF INITIAL GROUP TOGETHER WITH NEWLY ADDED DATA SAMPLES

Variables	Center, m_i	Width, c_i
Intercept	1.856	0.173
$C1$	0.651	0.102
$C2$	0.709	0.095
$C3$	-0.556	0.000

Let us highlight some essential features related to the time analysis. In general, an increasing number of potential vertices present in the subsequent iterations may not directly influence the required time analysis because some of vertices, which have been previously selected, might be reused in the consecutive iteration. Therefore, this situation might reduce required computing time. Furthermore, due to the decrease in the number of considered vertices, this effect will influence (*reduce*) the computational complexity.

On the other hands, as a supporting evidence for evaluating the performance as well as efficiency of this proposed approach, we use the same set of data samples/parameters and each of experiment was run five times for some other regression approaches; LP approach and fuzzy least-squares regression (FLSR) [16]. Each run presents samples of data sequentially in different order depending on their own procedure. Table III shows the performance of the proposed approach and the remaining regression models in time consumption point of view.

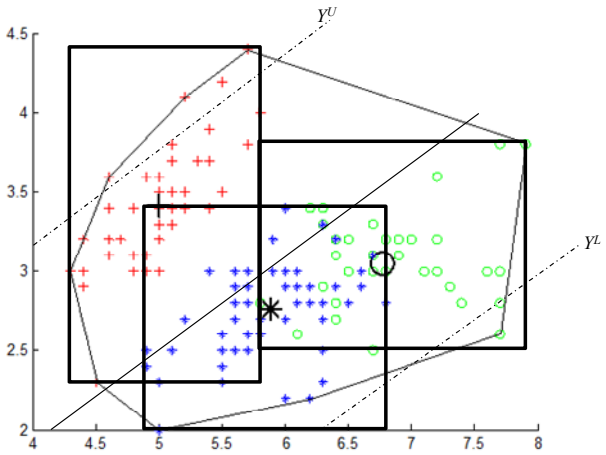

Figure 4. Ilustration of obtained clustered feature vectors for initial group together with newly added data samples.

TABLE III. PERFORMANCE ANALYSIS-TIME CONSUMPTION FACTOR: DETAILS

Model	Iteration	Points Total (*Considered Vertices*)	Time Used (*seconds*)
LP approach	1st iteration	100 (*100*)	0.58
	2nd iteration	150 (*150*)	1.22
FLSR approach	1st iteration	100 (*100*)	0.47
	2nd iteration	150 (*150*)	1.04
Proposed approach	1st iteration	100 (*11*)	0.33
	2nd iteration	150 (*9*)	0.39

Based on above table, we can summarized that, our proposed approach was utilized the minimal time consumption. In addition, noted that, those, LP and FLSR regression approach was not appropriate for dealing with dynamic data analysis. Therefore, these results illustrate the potential of our proposed approach to solve real-time fuzzy regression problem especially for granular computing fields that demand incremental adaptability.

VI. CONCLUDING REMARKS

In this study, we have developed an enhancement of the IDA tool of fuzzy regression in case of information granules. The method first constructs a limited number of information granules and afterwards those granules are processed by running the convex hull-based fuzzy regression. In this way, we have successfully developed a new idea of real-time granular based fuzzy regression models as a modeling alternative to deal with real-world regression problems.

It is shown that information granules are formed as a result of running the genetic version of the FCM called GA-FCM. The second phase of the overall method is completed depending upon the outer plots of the clusters. The sequential flow of processing was carried out to deal with dynamically increasing data set.

Based on the experimental developments, one could note that this approach becomes a suitable design alternative especially when solving real-time fuzzy regression problems with information granules. It works efficiently for real-time data analysis given the reduced processing time as well as the associated computational complexity.

This proposed approach can be applied to real-time fuzzy regression problems in large-scale systems presented in real-world scenarios. In addition, each of selected approach (*GA-FCM and convex hull-based fuzzy regression*) has their own features to be faced with dynamically changes of samples volume within a certain time interval. Therefore, as a result, this extended enhancement or hybrid combination will provide an efficient platform for regression purposes which require only plenty of time as well as reduce computational complexity with lower computing overhead. Although in this paper we dealt with small data sets (*and this was done for illustrative purposes*), it is worth noting that method scales up quite easily.

In further studies, we plan to expand the proposed approach by incorporating some other technologies of soft computing and swarm intelligence.

ACKNOWLEDGMENT

The first author was supported by Ministry of Higher Education Malaysia (MOHE) under *Skim Latihan Akademik IPTA* (*SLAI-UTHM*) scholarship program at Graduate School of Information, Production and Systems (IPS), Waseda University, Fukuoka, Japan.

REFERENCES

[1] A. Bargiela and W. Pedrycz, "Granular computing: An introduction," *Kluwer Academic Publishers*, 2003.

[2] D. Shifei, X. Li, Z. Hong and Z. Liwen"Research and progress of cluster algorithms based on granular computing," *International Journal of Digital Content Technology and its Applications*, Volume 4, Number 5, 2010, pp. 96-104.

[3] A. A. Ramli, J. Watada and W. Pedrycz, "Real-time fuzzy regression analysis: A convex hull approach," *European Journal of Operational Research*, Volume 210, Issue 3, 1 May 2011, pp. 606-617.

[4] A. Bargiela and W. Pedrycz, "Toward a theory of granular computing for humancentered information processing," *IEEE Transactions on Fuzzy Systems*, Volume 16, Issue 16, 2008, pp. 320-330.

[5] B. Chen, P. C. Tai, R. Harrison and Y. Pan, "FIK model: Novel efficient granular computing model for protein sequence motifs and structure information discovery," *Sixth IEEE International Symposium on BioInformatics and BioEngineering (BIBE 2006)*, 16-18 October 2006, Arlington, Virginia, USA, pp. 20-26.

[6] L. O. Hall, I. B. Ozyurt and J. C. Bezdek, "Clustering with a genetically optimized approach," *IEEE Transactions on Evolutionary Computation*, Volume 3, Issue 2, 1999, pp. 103-112.

[7] J. Watada and W. Pedrycz, "A possibilistic regression approach to acquisition of linguistic rules," in: W. Pedrycz, A. Skowron and V. Kreinovich (eds.), *Handbook on Granular Commutation*, John Wiley and Sons Ltd, Chapter 32, 2008, pp. 719-740.

[8] J. Watada, Y. Toyoura and S. G. Hwang, "Convex hull approach to fuzzy regression analysis and its application to oral age model," *International Fuzzy System Association World Congress and 20th North American Fuzzy Information Processing Society International Conference 2001*, Joint 9th, Canada, 2001, pp. 867-871.

[9] H. Tanaka, S. Uejima and K. Asai, "Linear regression analysis with fuzzy model," *IEEE Transactions Systems, Man and Cybernetics*, Volume 12, No. 6, 1982, pp. 903-907.

[10] H-F. Wang and R-C. Tsaur, "Insight of a possibilistic regression model," *Fuzzy Sets and Systems*, Volume 112, Issues 3, 2000, pp. 355-369.

[11] A. Frank and A. Asuncion, *UCI Machine Learning Repository* [*http://archive.ics.uci.edu/ml*]. Irvine, CA: University of California, School of Information and Computer Science, 2010.

[12] A. A. Ramli, J. Watada and W. Pedrycz. "Real-time fuzzy switching regression analysis: a convex hull approach," *11th International Conference on Information Integration and Web-based Applications and Services (iiWAS2009)*. Kuala Lumpur, Malaysia, 14-16 December 2009, pp. 284-291.

[13] B. Barber B., D. P. Dobki, H. Hupdanpaa "The quickhull algorithm for convex hull," A*CM Transaction on Mathematical Software*, Vol. 22, No. 4, 1996, pp. 469-483.

[14] B. Apolloni, D. Iannizzi, D. Malchiodi and W. Pedrycz, "Granular regression," *Neural Nets. 16th Italian Workshop on Neural Nets, WIRN 2005 and International Workshop on Natural and Artificial Immune Systems, (NAIS 2005)*, Vietri sul Mare, Italy, 2005, Lecture Notes in Computer Science, Volume 3931, 2006, pp. 147-156.

[15] S. Nascimento, B. Mirkin and F. Moura-Pires, "A fuzzy clustering model of data and fuzzy c-means," *IEEE Conference on Fuzzy Systems (FUZZ-IEEE2000)*, San Antonio, Texes, USA, 2000, pp. 302-307.

[16] C. Kao and C. Chyu, "Least-squares estimates in fuzzy regression analysis," *European Journal of Operational Research*, Vol. 148, Issue 2, 2003, pp. 426-435.

2011 IEEE International Conference on Fuzzy Systems
June 27-30, 2011, Taipei, Taiwan

An Interval-Based Approach to Fuzzy Regression for Fuzzy Input-Output Data

Jalal Chachi
and S. Mahmoud Taheri
Department of Mathematical Sciences
Isfahan University of Technology
Isfahan 84156–83111, Iran
Email: j.chachi@math.iut.ac.ir
Email: taheri@cc.iut.ac.ir

H. Rezaei Pazhand
Maharab Geotechnical
Water Resources and Dam Consulting Engineers
Mashhad 91861–33664, Iran
Email: hrpazhand@yahoo.com,
info@Tmaharab.com

***Abstract*—A novel approach is introduced to construct a fuzzy regression model when the data available of independent and dependent variables are fuzzy numbers. The approach, consisting on the least-squares method, uses the $\alpha-$level sets of fuzzy observations to estimate the crisp parameters of the model. A competitive study shows the performance and efficiency of the proposed approach with respect to some well-known methods.**

***Keywords*— capability index; fuzzy regression; hydrology; interval arithmetic; least squares method**

I. Introduction

Identification and analysis of the functional relationship between a dependent and some independent variables have made great interest in statistical analysis. Based on such functional relationship, which is called regression model, one can describe and predict the values of the dependent variable using the observations of independent variables.

However, when the data are reported as imprecise quantities we need to develop some soft methods to construct and analyze regression models. Fuzzy set theory provides appropriate tools for modeling regression when imprecise data have been observed. Over the last decades, different approaches to regression modeling have been widely proposed in the statistical literature, focussing on the situation of fuzzy environment. We refer the reader to [3], [4], [8], [12], [13], [15] for some recent works as well as some reviews of the main approaches to regression analysis in fuzzy environment.

In the present work, we investigate the situation in which the data available of independent and dependent variables are fuzzy numbers. We introduce a novel approach to model such a fuzzy data set. In the proposed approach, we apply a squared distance on the space of real intervals. Then, consisting on minimizing the total least-squares of errors, a linear regression model is expressed in terms of interval arithmetic between the α-level sets of fuzzy input-output data at each level of $\alpha \in [0,1]$. The errors are considered based on the differences between the interval-valued data obtained from the α-level sets of the observations and the estimations of the dependent variable. Finally, by aggregating the coefficients obtained from the interval regression model, we estimate the coefficients of the fuzzy regression model. The proposed method is investigated by two numerical competitive examples, which indicate the performance of the proposed model with respect to some well-known models.

The rest of this paper is organized as follows. In the next section, some preliminaries of fuzzy arithmetic that will be used in the sequel are recalled. Section III presents a novel approach to fuzzy regression for fuzzy input output data. In this section, the method of estimation of the parameters of the model is explained. In Section IV, two numerical examples are given to clarify the proposed approach. Finally, in Section V some concluding remarks are made.

II. Preliminaries from fuzzy arithmetic

A fuzzy set $\tilde{A}$ on the universal set $\mathbb{X}$ is defined by its membership function $\tilde{A}(x) : \mathbb{X} \to [0,1]$. Through this paper we will consider that $\mathbb{X} = \mathbb{R}$ (the real line). The α-level set of a fuzzy set $\tilde{A}$ is defined as $A_\alpha = \{x \in \mathbb{R} : \tilde{A}(x) \geq \alpha\}$, $\alpha \in (0,1]$, and $A_0 = \text{closure}\{x \in \mathbb{R} : \tilde{A}(x) > 0\}$. A fuzzy set $\tilde{A}$ of $\mathbb{R}$ is called a fuzzy number if any α-level set of $\tilde{A}$ is a non-empty compact interval, for any $\alpha \in [0,1]$. Such intervals are represented by $A_\alpha = [A_\alpha^l, A_\alpha^u]$.

A specific type of fuzzy number, which is rich and flexible enough to cover most of the applications, is the so-called LR-fuzzy number, denoted by $\tilde{N} = (n, l, r)_{LR}$ with central value $n \in \mathbb{R}$, left and right spread values $l, r \in \mathbb{R}$, decreasing left and right shape functions $L, R : \mathbb{R}^+ \to [0,1]$, with $L(0) = R(0) = 1$. Such LR-fuzzy numbers have the following membership function [16]

$$\tilde{N}(x) = \begin{cases} L(\frac{n-x}{l}) & \text{if} \quad x \leq n, \\ R(\frac{x-n}{r}) & \text{if} \quad x > n. \end{cases}$$

It is easy to see that each α-level set of the LR-fuzzy number $\tilde{N}$ is a closed interval as follows

$$N_\alpha = [n - L^{-1}(\alpha)l, n + R^{-1}(\alpha)r], \quad \alpha \in [0,1].$$

978-1-4244-7316-8/11/$26.00 ©2011 IEEE

In the special case, where $L(x) = R(x) = max\{0, 1 - |x|\}$, $\tilde{N}$ is called a triangular fuzzy number and is denoted by $\tilde{N} = (n, l, r)_T$.

Algebraic operations on LR-fuzzy numbers are defined based on the interval arithmetic. For our proposes, we recall some definitions and results on this topic [16].

Proposition 2.1: Let $\tilde{M} = (m, l_m, r_m)_{LR}$ and $\tilde{N} = (n, l_n, r_n)_{LR}$ be two LR-fuzzy numbers, and λ be a real number. Then

$$\begin{aligned} \lambda \otimes \tilde{M} &= \begin{cases} (\lambda m, \lambda l_m, \lambda r_m)_{LR} & \text{if} \quad \lambda > 0, \\ \mathcal{I}_{\{0\}} & \text{if} \quad \lambda = 0, \\ (\lambda m, |\lambda| r_m, |\lambda| l_m)_{RL} & \text{if} \quad \lambda < 0, \end{cases} \\ \tilde{M} \oplus \tilde{N} &= (m + n, l_m + l_n, r_m + r_n)_{LR}. \end{aligned}$$

where $\mathcal{I}_A$ represents the indicator function of a crisp set A.

Definition 2.1: Let $I = [i_1, i_2]$ and $J = [j_1, j_2]$ be two intervals, and λ be a real number. Then scaler multiplication and addition of two intervals are defined as follows

$$\begin{aligned} \lambda \otimes I &= \begin{cases} [\lambda i_1, \lambda i_2] & \lambda > 0, \\ \mathcal{I}_{\{0\}} & \lambda = 0, \\ [\lambda i_2, \lambda i_1] & \lambda < 0, \end{cases} \\ I \oplus J &= [i_1 + j_1, i_2 + j_2]. \end{aligned}$$

Definition 2.2: The distance between two intervals $I = [i_1, i_2]$ and $J = [j_1, j_2]$ is defined as

$$\mathcal{D}(I, J) = (i_1 - j_1)^2 + (i_2 - j_2)^2.$$

The reader is refereed to [10] for more on interval arithmetic.

III. Fuzzy regression model

In this section, we investigate the following fuzzy linear regression model

$$\tilde{y}_i = \beta_0 \oplus \beta_1 \otimes \tilde{x}_i, \qquad i = 1, \ldots, n, \tag{1}$$

in which the data $(\tilde{y}_i, \tilde{x}_i)$, $i = 1, \ldots, n$, are fuzzy observations on n statistical units, and the coefficients β_0 and β_1 are crisp values.

In order to estimate the regression coefficients β_0 and β_1, we first transform the fuzzy observations $(\tilde{y}, \tilde{x})$ into a set of interval-valued data obtained from the $\alpha-$level sets of the observations, i.e. $x_\alpha = [x_\alpha^l, x_\alpha^u]$ and $y_\alpha = [y_\alpha^l, y_\alpha^u]$, for any $\alpha \in [0, 1]$. Then, we use the distance $\mathcal{D}$ in Definition 2.2 to minimize the following objective function

$$\begin{aligned} \mathcal{D}(b_0, b_1) &= \sum_{i=1}^{n} \mathcal{D}(y_{i\alpha}, b_0 \oplus b_1 \otimes x_{i\alpha}) \\ &= \sum_{i=1}^{n} \mathcal{D}([y_{i\alpha}^l, y_{i\alpha}^u], b_0 \oplus b_1 \otimes [x_{i\alpha}^l, x_{i\alpha}^u]). \end{aligned}$$

By such a minimization problem we can determine the best values for b_0 and b_1 in the following interval regression model

$$[y_{i\alpha}^l, y_{i\alpha}^u] = b_0 \oplus b_1 \otimes [x_{i\alpha}^l, x_{i\alpha}^u], \qquad i = 1, \ldots, n,$$

which models y_α on x_α at each α-level set, $\alpha \in [0, 1]$.

Note that, the objective function $\mathcal{D}(b_0, b_1)$ represents the sum of squared errors between the observed and estimated values of the $\alpha-$level sets of dependent variable. Now, concerning the sign of b_1, we have the two following expressions for the objective function

$$\begin{aligned} \mathcal{D}^+(b_0, b_1) &= \sum_{i=1}^{n} [(y_{i\alpha}^l - b_0 - b_1 x_{i\alpha}^l)^2 \\ &\qquad + (y_{i\alpha}^u - b_0 - b_1 x_{i\alpha}^u)^2] \quad b_1 \geq 0. \\ \mathcal{D}^-(b_0, b_1) &= \sum_{i=1}^{n} [(y_{i\alpha}^l - b_0 - b_1 x_{i\alpha}^u)^2 \\ &\qquad + (y_{i\alpha}^u - b_0 - b_1 x_{i\alpha}^l)^2] \quad b_1 < 0. \end{aligned}$$

In this step, we can follow the procedure in two ways:
1) We may, first, pre-determine the sign of b_1, for example, by fitting a classical regression model to the centers of the fuzzy observations, and then follow one of the above expressions with respect to the sign of the slope of the classical linear regression model.
2) We can also employ both expressions and estimate the related coefficients. In such a case, we consider the amounts b_0 or b_1 for which the related objective function is smaller than the other one. To do this, we have to solve the following equations

$$\tfrac{\partial}{\partial b_0}\mathcal{D}^+(b_0, b_1) = 0, \quad \tfrac{\partial}{\partial b_1}\mathcal{D}^+(b_0, b_1) = 0, \qquad \text{for } b_1 \geq 0,$$

and

$$\tfrac{\partial}{\partial b_0}\mathcal{D}^-(b_0, b_1) = 0, \quad \tfrac{\partial}{\partial b_1}\mathcal{D}^-(b_0, b_1) = 0, \qquad \text{for } b_1 < 0.$$

For the positive case, we obtain

$$\begin{aligned} b_0^+(\alpha) &= \bar{Y}(\alpha) - b_1^+(\alpha)\bar{X}(\alpha), \\ b_1^+(\alpha) &= \frac{\sum_{i=1}^n [x_{i\alpha}^l y_{i\alpha}^l + x_{i\alpha}^u y_{i\alpha}^u] - 2n\bar{X}(\alpha)\bar{Y}(\alpha)}{\sum_{i=1}^n [(x_{i\alpha}^l)^2 + (x_{i\alpha}^u)^2] - 2n\bar{X}^2(\alpha)}, \end{aligned}$$

where, $\bar{Y}(\alpha) = \frac{1}{n}\sum_{i=1}^n \frac{y_{i\alpha}^l + y_{i\alpha}^u}{2}$ and $\bar{X}(\alpha) = \frac{1}{n}\sum_{i=1}^n \frac{x_{i\alpha}^l + x_{i\alpha}^u}{2}$. For the negative case, we obtain

$$\begin{aligned} b_0^-(\alpha) &= \bar{Y}(\alpha) - b_1^-(\alpha)\bar{X}(\alpha), \\ b_1^-(\alpha) &= \frac{\sum_{i=1}^n [x_{i\alpha}^l y_{i\alpha}^u + x_{i\alpha}^u y_{i\alpha}^l] - 2n\bar{X}(\alpha)\bar{Y}(\alpha)}{\sum_{i=1}^n [(x_{i\alpha}^l)^2 + (x_{i\alpha}^u)^2] - 2n\bar{X}^2(\alpha)}. \end{aligned}$$

Finally, by integration, we aggregate the functions $b_0^+(\alpha)$ ($b_0^-(\alpha)$) and $b_1^+(\alpha)$ ($b_1^-(\alpha)$) to estimate the regression coefficients β_0 and β_1, as follows

$$\widehat{\beta}_0 = \int_0^1 b_0^+(\alpha)d\alpha \qquad (\text{or } \widehat{\beta}_0 = \int_0^1 b_0^-(\alpha)d\alpha),$$
$$\widehat{\beta}_1 = \int_0^1 b_1^+(\alpha)d\alpha \qquad (\text{or } \widehat{\beta}_1 = \int_0^1 b_1^-(\alpha)d\alpha).$$

Therefore, the estimate of the dependent variable, denoted by $\widehat{\tilde{y}}$, can be obtained by the following fuzzy linear regression model

$$\widehat{\tilde{y}}_i = \widehat{\beta}_0 \oplus \widehat{\beta}_1 \otimes \tilde{x}_i, \qquad i = 1, \ldots, n.$$

Goodness of fit criteria: To evaluate the goodness of fit of the fuzzy regression models we employ a well-known criteria due to Kim and Bishu [7] (see also [2], [6]).

TABLE I
FUZZY DATA IN EXAMPLE 4.1

i	$\tilde{x}_i = (x_i, l_i)_T$	$\tilde{y}_i = (y_i, s_i)_T$
1	$(2.0, 0.5)_T$	$(4.0, 0.5)_T$
2	$(3.5, 0.5)_T$	$(5.5, 0.5)_T$
3	$(5.5, 1.0)_T$	$(7.5, 1.0)_T$
4	$(7.0, 0.5)_T$	$(6.5, 0.5)_T$
5	$(8.5, 0.5)_T$	$(8.5, 0.5)_T$
6	$(10.5, 1.0)_T$	$(8.0, 1.0)_T$
7	$(11.0, 0.5)_T$	$(10.5, 0.5)_T$
8	$(12.5, 0.5)_T$	$(9.5, 0.5)_T$

Definition 3.1 ([7]): The capability index ($\mathcal{CI}$) of the fuzzy regression model (1) is defined by

$$\mathcal{CI} = \frac{1}{n}\sum_{i=1}^{n} \mathcal{CI}(i),$$

where

$$\mathcal{CI}(i) = \frac{\int |\tilde{y}_i(x) - \widehat{\tilde{y}}_i(x)|\, dx}{\int \tilde{y}_i(x)\, dx}.$$

The capacity index $\mathcal{CI}$ represents the average of errors in estimation and, therefore, smaller values of $\mathcal{CI}$ indicates that the fuzzy linear regression model fits better to the data.

Remark 3.1: It should be noted that Bargiela et al. [1] considered a more or less similar approach to regression modelling with fuzzy data. They used the distance $\mathcal{D}$ for the $\alpha-$level sets of fuzzy observations and then aggregated such distances to obtain the distance between fuzzy estimate and fuzzy observed values of the dependent variable. But, in our proposed approach, we first used the distances between the $\alpha-$level sets of fuzzy observations and fuzzy estimations of $\tilde{y}$ to provide an interval-valued regression model. Then, we integrated the coefficients of the interval-valued regression model to provide the coefficients of the fuzzy regression model.

Remark 3.2: While, most common methods in fuzzy regression modeling require all the observations to have the same type of membership functions for the fuzzy observations, in the proposed approach there is no limitation in the types of the membership functions of the fuzzy observations. The proposed model, therefore, is applicable when the observations have different types of membership functions.

Remark 3.3: Note that, when fuzzy observations reduce to crisp values, the proposed method reduces to the conventional least-squares regression method.

IV. COMPETITIVE STUDY

In this section, we provide two numerical examples to explain how the proposed method is applicable to derive the regression model for fuzzy observations. We also compare the proposed model with some other models.

Example 4.1: In this example, we compare the proposed method in this paper with some other models, using the triangular fuzzy input-output data set given by Sakawa and Yano [14] (Table I).

By applying the introduced procedure in Section III, we obtain the following functions for each $\alpha \in [0, 1]$

$$\widehat{b}_0^+(\alpha) = \frac{-7\alpha^2 + 14\alpha + 11164}{112\alpha^2 - 224\alpha + 3239},$$
$$\widehat{b}_1^+(\alpha) = \frac{112\alpha^2 - 224\alpha + 1736}{112\alpha^2 - 224\alpha + 3239}.$$

Therefore, the estimated coefficients are derived as $\widehat{\beta}_0 = 3.53$ and $\widehat{\beta}_1 = 0.525$. So, the fuzzy linear regression model is as follows

$$\widehat{\tilde{y}} = 3.53 \oplus 0.525 \otimes \tilde{x}.$$

To compare the proposed method with some other methods in fuzzy regression modeling, the index $\mathcal{CI}$ is employed to evaluate the goodness of fit of the models. Different models and their $\mathcal{CI}$ indices are given in Table II. The results indicate that the proposed method outperforms all the models.

Example 4.2: One of the classical problem in hydrology studies is the measurement of suspended load ($\frac{\text{Ton}}{Day}$) and discharge ($\frac{m^3}{s}$) in watersheds [9]. Based on a study in a part of Darband, situated in the province of Khorasan (North west of Iran) between the cities Bojnord and Esferayen, some water characteristics were measured using standard procedures. The daily discharge and suspended load of the watershed are measured for 51 days. But, due to some limitations in experimental environments, the observed data were reported as fuzzy numbers shown in Table IV. Since, in practical studies, it is important to estimate the amount of suspended load in term of discharge, we wish to model the relationship between suspended load as the dependent variable and discharge as independent variable.

According to the proposed method, the estimated coefficients are obtained as $\widehat{\beta}_0 = 5.0845$ and $\widehat{\beta}_1 = 0.3040$, and the fuzzy linear regression model is, therefore

$$\widehat{\tilde{y}} = 5.0845 \oplus 0.3040 \otimes \tilde{x}.$$

For a competitive study we employ some well-known methods to model such a fuzzy data set, as well. Different models and their goodness of fit indices are given in Table III. The results show that the proposed method provides a better performance equal to that of Bargiela et al. and better performance with respect to three other models.

V. CONCLUSIONS

A fuzzy regression model was investigated for fuzzy input-output data set. By utilizing the method of least-squares as a fitting criterion and applying it to each interval-valued data obtained from $\alpha-$level sets of imprecise observations, a regression model is provided at each level of α. The estimates of the parameters were obtained as functions of α. Then, by integrating the coefficients of the provided regression models, the coefficients of the fuzzy regression model were derived.

The proposed model is applicable when the observations have different types of membership functions. When all fuzzy observations reduce to crisp values, the proposed method

TABLE II
FUZZY REGRESSION MODELS AND THEIR CAPABILITY INDICES IN EXAMPLE 4.1

Proposed by	Model	$\mathcal{CI}$
Bargiela et al. [1]	$\widehat{\tilde{y}}_i = (3.446 + 0.536x_i, 0.536l_i)_T$	1.3428
Kao and Chyu [6]	$\widehat{\tilde{y}}_i = (3.554 + 0.522x_i, 0.951 + 0.522l_i, 0.949 + 0.522l_i)_T$	1.9951
Nasrabadi and Nasrabadi [11]	$\widehat{\tilde{y}}_i = (3.5767 + 0.5467x_i, l_i)_T$	1.4879
The proposed model	$\widehat{\tilde{y}}_i = (3.53 + 0.525x_i, 0.525l_i)_T$	1.3285

† For the values of $\tilde{E}_i$ see [2]

TABLE III
FUZZY REGRESSION MODELS AND THEIR CAPABILITY INDICES IN EXAMPLE 4.2

Proposed by	Model	$\mathcal{CI}$
Bargiela et al. [1]	$\widehat{\tilde{y}}_i = (5.0674 + 0.3072x_i, 0.3072l_i)_T$	1.0107
Kao and Chyu [6]	$\widehat{\tilde{y}}_i = (5.6371 + 0.1993x_i, 3.1887 + 0.1993l_i)_T$	2.1217
Nasrabadi and Nasrabadi [11]	$\widehat{\tilde{y}}_i = (5.4464 + 0.1465x_i, 2.0058 + 1.2718l_i)_T$	1.6158
The proposed model	$\widehat{\tilde{y}}_i = (5.0845 + 0.3040x_i, 0.3040l_i)_T$	1.0106

† For the values of $\tilde{E}_i$ see [2]

TABLE IV
FUZZY DATA IN EXAMPLE 4.2

i	$\tilde{x}_i = (x_i, l_i)_T$	$\tilde{y}_i = (y_i, s_i)_T$	i	$\tilde{x}_i = (x_i, l_i)_T$	$\tilde{y}_i = (y_i, s_i)_T$	i	$\tilde{x}_i = (x_i, l_i)_T$	$\tilde{y}_i = (y_i, s_i)_T$
1	$(2.98, 0.30)_T$	$(4.90, 0.30)_T$	18	$(2.01, 0.20)_T$	$(5.36, 0.76)_T$	35	$(2.68, 0.30)_T$	$(5.30, 0.69)_T$
2	$(5.56, 0.60)_T$	$(7.23, 4.01)_T$	19	$(2.53, 0.25)_T$	$(8.47, 3.86)_T$	36	$(8.53, 1.00)_T$	$(7.99, 4.99)_T$
3	$(3.59, 0.40)_T$	$(5.53, 1.62)_T$	20	$(10.2, 2.50)_T$	$(7.96, 5.30)_T$	37	$(4.16, 0.60)_T$	$(6.72, 3.50)_T$
4	$(1.91, 0.20)_T$	$(4.63, 0.41)_T$	21	$(10.2, 2.50)_T$	$(5.73, 3.07)_T$	38	$(2.73, 0.30)_T$	$(7.84, 3.64)_T$
5	$(6.67, 0.70)_T$	$(8.03, 5.03)_T$	22	$(10.2, 2.50)_T$	$(5.37, 2.71)_T$	39	$(9.00, 1.25)_T$	$(9.62, 6.81)_T$
6	$(10.25, 2.50)_T$	$(7.41, 4.75)_T$	23	$(10.53, 2.50)_T$	$(7.96, 5.30)_T$	40	$(2.43, 0.25)_T$	$(5.81, 1.20)_T$
7	$(11.12, 2.70)_T$	$(7.90, 5.37)_T$	24	$(10.53, 2.50)_T$	$(5.14, 2.48)_T$	41	$(4.97, 0.65)_T$	$(6.80, 3.58)_T$
8	$(4.76, 0.50)_T$	$(6.57, 3.35)_T$	25	$(4.28, 0.60)_T$	$(7.15, 3.65)_T$	42	$(4.46, 0.60)_T$	$(6.26, 2.35)_T$
9	$(1.36, 0.20)_T$	$(6.31, 1.02)_T$	26	$(5.03, 0.60)_T$	$(8.10, 4.88)_T$	43	$(9.68, 1.25)_T$	$(7.79, 4.98)_T$
10	$(2.36, 0.30)_T$	$(4.98, 0.37)_T$	27	$(7.20, 0.80)_T$	$(8.04, 5.04)_T$	44	$(3.05, 0.40)_T$	$(4.83, 0.22)_T$
11	$(3.11, 0.40)_T$	$(6.34, 2.43)_T$	28	$(7.20, 0.80)_T$	$(7.56, 4.56)_T$	45	$(2.32, 0.30)_T$	$(5.37, 0.77)_T$
12	$(1.54, 0.20)_T$	$(6.26, 0.96)_T$	29	$(7.20, 0.80)_T$	$(8.29, 5.29)_T$	46	$(6.53, 0.75)_T$	$(7.83, 4.61)_T$
13	$(1.98, 0.25)_T$	$(5.14, 0.54)_T$	30	$(8.75, 1.00)_T$	$(8.96, 6.14)_T$	47	$(2.45, 0.35)_T$	$(6.90, 2.30)_T$
14	$(3.97, 0.45)_T$	$(5.51, 1.83)_T$	31	$(6.72, 0.75)_T$	$(5.50, 2.40)_T$	48	$(1.58, 0.20)_T$	$(7.66, 2.36)_T$
15	$(5.20, 0.60)_T$	$(7.86, 4.64)_T$	32	$(2.04, 0.20)_T$	$(4.69, 0.20)_T$	49	$(2.25, 0.25)_T$	$(4.90, 0.30)_T$
16	$(6.94, 0.75)_T$	$(7.24, 4.24)_T$	33	$(2.92, 0.30)_T$	$(5.95, 2.03)_T$	50	$(4.24, 0.55)_T$	$(6.91, 2.99)_T$
17	$(4.16, 0.50)_T$	$(5.98, 2.48)_T$	34	$(3.16, 0.40)_T$	$(6.68, 2.77)_T$	51	$(9.97, 1.75)_T$	$(7.88, 5.22)_T$

becomes the conventional least-squares method in crisp environment, while some of the existing methods still generate fuzzy regression coefficients in such a case.

Although the discussion of this paper is confined to simple regression with one explanatory variable, the approach studied in this paper, could be extended to more general situation including several independent variables.

ACKNOWLEDGMENT

The first and second authors would like to thank the Research Council at Isfahan University of Technology. They also thanks the Fuzzy Systems and Applications Center of Excellence, Shahid Bahonar University of Kerman, Kerman, Iran, for partially supporting of this work. The authors thanks the anonymous reviewers for their useful comments.

REFERENCES

[1] A. Bargiela, W. Pedrycz and T. Nakashima, "Multiple regression with fuzzy data", Fuzzy Sets Syst., vol. 158, pp. 2169-2188, 2007.

[2] S.P. Chen and J.F. Dang, "A variable spread fuzzy linear regression model with higher explanatory power and forecasting accuracy", Inform. Sci., vol. 178, pp. 3973-3988, 2008.

[3] R. Coppi, P. D' Urso, P. Giordani and A. Santoro, "Least squares estimation of a linear regression model with LR-fuzzy response", Comp. Stat. Data Anal., vol. 51, pp. 267-286, 2006.

[4] H. Hassanpour, H.R. Maleki and M.A. Yaghoobi, "Fuzzy linear regression model with crisp coefficients: A programming approach", Iranian J. Fuzzy Syst., vol. 7, pp. 19-39, 2010.

[5] C. Kao and C.L. Chyu, "A fuzzy linear regression model with better explanatory power", Fuzzy Sets Syst., vol. 126, pp. 401-409, 2002.

[6] C. Kao and C.L. Chyu, "Least-squares estimates in fuzzy regression analysis", European J. Oper. Res., vol. 148, pp. 426-435, 2003.

[7] B. Kim and R.R. Bishu, “Evaluation of fuzzy linear regression models by comparison membership function”, Fuzzy Sets Syst., vol. 100, pp. 343-352, 1998.
[8] M.H. Mashinchi, M.A. Orgun, M.Mashinchi and W. Pedrycz, “Tabu harmony search based approach to fuzzy linear regression”, IEEE Tran. Fuzzy Syst., 2011. DOI:10.1109 TFUZZ.2011.2106791.
[9] L.W. Mays, “Water Resources Engineering”, 2nd ed., John wiley and sons, Arizona State Univ., 2011.
[10] R.E. Moore, R.B. Kearfott and M.J. Cloud, Introduction to Interval Analysis, Society for Industrial and Applied Mathematics, Philadelphia, PA, 2009.
[11] M.M. Nasrabadi, and E. Nasrabadi, “A mathematical-programming approach to fuzzy linear regression analysis”, Appl. Math. Comput., vol. 155, pp. 873-881, 2004.
[12] W. Näther, “Regression with fuzzy random data”, Comput. Statist. Data Anal., vol. 51, pp. 235-252, 2006.
[13] S. Pourahmad, S.M.T. Ayatollahi and S.M. Taheri, “Fuzzy logistic regression: A new possibilistic model and its application in clinical vague status”, Iranian J. Fuzzy Syst., vol. 8, pp. 1-17, 2011.
[14] M. Sakawa and H. Yano, “Multiobjective fuzzy linear regression analysis for fuzzy input-output data”, Fuzzy Sets Syst., vol. 157, pp. 173-181, 1992.
[15] S.M. Taheri and M. Kelkinnama, “Fuzzy Least Absolutes Regression”, Proc. 4th Inter. IEEE Conf. Intell. Syst., vol. 11, pp. 55-58, 2008.
[16] H.J. Zimmermann, Fuzzy Set Theory and Its Applications, 4th ed., Kluwer Nihoff, Boston, 2001.

2011 IEEE International Conference on Fuzzy Systems
June 27-30, 2011, Taipei, Taiwan

Study of Dependency between the Input Noise and the Parameter in Fuzzy Linear Regression Model

Hongwei Ge, Shitong Wang and Wei Song
School of Internet of Things, Jiangnan University
Wuxi, Jiangshu , People's Republic of China
ghw8601@163.com

***Abstract*—When noise exists in data, it is a very meaningful topic to reveal the dependency between the parameter h (i.e. the threshold value used to measure degree of fit) in Fuzzy linear regression (FLR) model and the input noise. In this paper, the FLR model is first extended to its regularized version, i.e. regularized fuzzy linear regression (RFLR) model, so as to enhance its generalization capability; then RFLR model is explained as the corresponding equivalent *maximum a posteriori* MAP problem; finally, the approximately inverse proportional dependency relationships that the parameter h with Laplacian noisy input and Uniform noisy input should follow are derived, respectively. Our experimental results also confirm this theoretical claim. We believe that this conclusion provides an important reference for us to determine h in FLR model with noisy input.**

Keywords—Fuzzy linear regression model; MAP; Optimal parameter choice

I. INTRODUCTION

Fuzzy linear regression model plays a pivotal role in fuzzy modeling. However, how to choose the parameter h for FLR model with noisy input still keeps an open problem. A bad choice for threshold h will heavily deteriorate the performances of these models. In recent years, how to choose the loss function and the corresponding parameters for support vector regression (SVR) machine with noisy input has been studied well. J.B.Gao and S.R.Gunn pointed out that SVR problem could be transformed into the equivalent MAP problem [1]. Based on this idea, J.T.Kwok derived the linear dependency between ε and the input noise in ε-SVR [2], Shitong Wang et al. investigated the theoretically optimal parameter choices for Huber-SVR and r-SVR [3], and Hongwei Ge et al. investigated the optimal parameter choices for FLR model with Gaussian noisy input [4,5]. Although Gaussian noise is typically adopted in most robustness analyses, there are still other types of noise such as Laplacian distribution noise and uniform noise in real datasets. So, in this paper, particular attention is paid on the dependency relationships between free threshold h and the standard deviations of Laplacian and uniform noisy input. We first extend the traditional FLR model to its regularized version, i.e. regularized fuzzy linear regression (RFLR) model, so as to enhance its generalization capability; and then explain this regularized model by using MAP framework [1-3]; and finally, with the help of this MAP framework, study the dependency between h and the standard deviation of input noise.

The rest of this paper is organized as follows. In section 2, we will introduce the FLR model and the corresponding RFLR model and show the equivalent relationship between RFLR model and MAP. The analysis of the inverse linear dependency between h and the standard deviation of Laplacian noisy input and Uniform noisy input are theoretically derived in section 3, respectively, while section 4 gives the experimental results and last section concludes this paper.

II. FUZZY LINER REGRESSION MODEL AND MAP

A. Fuzzy liner regression model

The FLR model can be summarized as follows. Consider the function:

$$Y = f(\mathbf{x}, \mathbf{A}) = A_0 + A_1 x_1 + A_2 x_2 + \cdots + A_n x_n, \qquad (1)$$

where $\mathbf{x} = (1, x_1, x_2, \cdots, x_n)^T$ is a vector of non-fuzzy inputs, and $\mathrm{A} = (A_0, A_1, \cdots, A_n)^T$ is a vector of fuzzy model parameters. Parameters $A_i (0 \le i \le n)$ are symmetric triangular fuzzy coefficients, and they can be described by $\{\xi_i, \eta_i\}$, where ξ_i is the center and η_i is the spread of A_i.

In vector notation, the fuzzy parameters $\mathbf{A}$ can be written as $\mathrm{A} = (\boldsymbol{\xi}, \boldsymbol{\eta})$ where $\boldsymbol{\xi} = (\xi_0, \xi_1, \xi_2, \cdots, \xi_n)^T$ and $\boldsymbol{\eta} = (\eta_0, \eta_1, \eta_2, \cdots, \eta_n)^T$. Following the principle of extension, the fuzzy membership function for the output can be obtained by

$$\mu_Y(y) = \begin{cases} 1 - \dfrac{\left| y - \boldsymbol{\xi}^T \mathbf{x} \right|}{\boldsymbol{\eta}^T |\mathbf{x}|}, & \mathbf{x} \neq 0, \\ 1, & \mathbf{x} = 0, y = 0, \\ 0, & \mathbf{x} = 0, y \neq 0, \end{cases} \qquad (2)$$

where $|\mathbf{x}| = (1, |x_1|, |x_2|, \cdots, |x_n|)^T$, The center of Y is $\boldsymbol{\xi}^T \mathbf{x}$, and the spread of Y is $\boldsymbol{\eta}^T |\mathbf{x}|$ with $\boldsymbol{\eta}^T |\mathbf{x}| \ge 0$.

Assume we have a dataset with n-dimensional non-fuzzy input $\mathbf{x}$ and one-dimensional non-fuzzy output variable y:

$$D = \{(\mathbf{x}_1, y_1), (\mathbf{x}_2, y_2), \cdots, (\mathbf{x}_N, y_N)\}, \quad \mathbf{x}_i \in R^{n+1}, y_i \in R, i = 1,2,\cdots,N. \qquad (3)$$

We can establish the following FLR model $Y_i^* = \mathbf{A}^{*T} \mathbf{x}_i$, where $\mathbf{x}_i = (1, x_{i1}, x_{i2}, \cdots, x_{in})^T$, $\mathbf{A} = (A_0, A_1, A_2, \cdots, A_n)^T$, $\mathbf{A}^* = (A_0^*, A_1^*, A_2^*, \cdots, A_n^*)^T$, $i = 1,2,\cdots,N$, and $Y_i^*, \mathbf{A}^*$ denote the

This work is supported by National Natural Science Foundation of China (Grant No.60975027), New century Outstanding Young Scholar Grant of Ministry of Education of China.

978-1-4244-7316-8/11/$26.00 ©2011 IEEE

estimates of Y_i, $\mathbf{A}$ respectively. The objective is to minimize the fuzziness of the fuzzy linear model and the following linear programming problem can be formulated [4,5]:

$$\min \Phi(\boldsymbol{\eta},\xi,\Delta) = \sum_i \boldsymbol{\eta}^T |\mathbf{x}_i| + C\sum_i (\Delta_i^- + \Delta_i^+), \tag{4}$$

$$s.t. \begin{cases} \dfrac{y_i - \xi^T \mathbf{x}_i}{\boldsymbol{\eta}^T |\mathbf{x}_i|} \le (1-h) + \Delta_i^-, \\ \dfrac{\xi^T \mathbf{x}_i - y_i}{\boldsymbol{\eta}^T |\mathbf{x}_i|} \le (1-h) + \Delta_i^+, \\ \Delta_i^-, \Delta_i^+ \ge 0, \\ i = 1,2,\cdots,N, \end{cases}$$

where C is a predefined constant, Δ_i^- and Δ_i^+ denote the latent variables of the upper/lower bounds of output respectively, h $(h \in [0,1))$ is the threshold of fitness.

In order to enhance the generalization capability of FLR model and to be easy to analyze, just like SVR techniques in [3, 7, 8], a regularized term $\frac{1}{2}\xi^T\xi$ can be introduced into Eq. (4), i.e.

$$\min \Phi(\boldsymbol{\eta},\xi,\Delta) = \sum_i \boldsymbol{\eta}^T |\mathbf{x}_i| + \frac{1}{2}\xi^T\xi + C\sum_i (\Delta_i^- + \Delta_i^+) \cdot \tag{5}$$

Equation (5) formulates the RFLR model. In the rest of this paper, how to choose the parameter h for RFLR model with Laplacian noisy input and Uniform noisy input will be studied. Obviously, the conclusion will also be very helpful for the practical applications of FLR model.

B. The regression model and MAP

In this subsection, in terms of the evidence theory [1,2], we will demonstrate the RFLR model is equivalent to *maximum a posteriori* MAP estimation, based on maximum likelihood estimation.

Now, the focus is on obtaining a weight vector $\tilde{\xi}$ in the generalized linear regression model such as

$$y_i = \tilde{\xi}^T \mathbf{x}_i + n_i, i = 1,2,\cdots,N \ , \tag{6}$$

for all the data in the dataset (3), where all the data $\mathbf{x}_i$ follow distribution $p(\cdot)$ and all n_i are i.i.d noise following some distribution $\phi(\cdot)$. Thus, the corresponding density function on y can be denoted as $p(y|\mathbf{x}) = \phi(y - \tilde{\xi}^T\mathbf{x})$. The degree of such an approximation can be measured by a loss function $L(\xi^T\mathbf{x}, \boldsymbol{\eta}^T\mathbf{x}, y)$, i.e.

$$L(\xi^T\mathbf{x}, \boldsymbol{\eta}^T\mathbf{x}, y) = \begin{cases} 0, & \dfrac{|\xi^T\mathbf{x} - y|}{\boldsymbol{\eta}^T|\mathbf{x}|} \le 1-h, \\ \dfrac{|\xi^T\mathbf{x} - y|}{\boldsymbol{\eta}^T|\mathbf{x}|} - 1 + h, & otherwise, \end{cases} \tag{7}$$

Assume the loss function $L(\xi^T\mathbf{x}, \boldsymbol{\eta}^T\mathbf{x}, y)$ leads to the following Gaussian probability density function on y:

$$p(y_i|\mathbf{x}_i, \xi, \boldsymbol{\eta}, \beta, h) = \frac{1}{C(\beta,h)} \exp[-\beta L(\xi^T\mathbf{x}_i, \boldsymbol{\eta}^T\mathbf{x}_i, y_i)] \tag{8}$$

where $C(\beta,h) = \iint_D \exp[-\beta L(\xi^T\mathbf{x}, \boldsymbol{\eta}^T\mathbf{x}, y)] d\mathbf{x}dy$, and β is a parameter.

Just as the mathematical analysis in [1,2] does, we adopt the Gaussian prior on $\boldsymbol{\eta}$ and ξ, i.e.

$$p(\boldsymbol{\eta}|\alpha, \mathbf{x}_i) = \frac{1}{M(\alpha)} \exp(-\alpha\boldsymbol{\eta}^T|\mathbf{x}_i|), \tag{9}$$

where $M(\alpha) = \int \exp(-\alpha\boldsymbol{\eta}^T|\mathbf{x}_i|) d\boldsymbol{\eta}$,

$$p(\xi|\gamma) = \frac{1}{F(\gamma)} \exp\left(-\frac{\gamma}{2}\xi^T\xi\right), \tag{10}$$

where $F(\gamma) = \int \exp\left(-\frac{\gamma}{2}\xi^T\xi\right) d\xi$,

and by applying the Bayes rule:

$$p(\boldsymbol{\eta},\xi|D,\beta,h) \propto p(D|\boldsymbol{\eta},\xi,\beta,h) p(\xi|\gamma) \prod_{i=1}^N p(\boldsymbol{\eta}|\alpha,\mathbf{x}_i) p(\mathbf{x}_i), \tag{11}$$

we have

$$\ln p(\boldsymbol{\eta},\xi|D,\beta,h) = -\alpha \sum_{i=1}^N \boldsymbol{\eta}^T|\mathbf{x}_i| - \frac{\gamma}{2}\xi^T\xi - \beta \sum_{i=1}^N L(\boldsymbol{\eta}^T\mathbf{x}_i, \xi^T\mathbf{x}_i, y_i) - N\ln C(\beta,h) + const \cdot \tag{12}$$

With setting $\gamma = \alpha$ and $C = \beta/\alpha$, optimizing (5) can be interpreted as finding for the MAP estimate of $\boldsymbol{\eta},\xi$ at given values of β, h. That is to say, the RFLR model in (5) is equivalent to *maximum a posteriori* MAP estimation.

In order to make the analysis easier, $\frac{1}{N}\sum_{i=1}^N L(\boldsymbol{\eta}^T\mathbf{x}_i, \xi^T\mathbf{x}_i, y_i)$ in (12) is replaced by its expectation:

$$\begin{aligned} E(L(\boldsymbol{\eta}^T\mathbf{x}, \xi^T\mathbf{x}, y)) &= \iint_D L(\boldsymbol{\eta}^T\mathbf{x}, \xi^T\mathbf{x}, y) p(y|\mathbf{x}) p(\mathbf{x}) d\mathbf{x}dy \\ &= \int_D \left[\int_{-\infty}^{\xi^T\mathbf{x} - (1-h)\boldsymbol{\eta}^T|\mathbf{x}|} \left(\frac{\xi^T\mathbf{x} - y}{\boldsymbol{\eta}^T|\mathbf{x}|} - 1 + h \right) p(y|\mathbf{x}) dy \right. \\ &\quad \left. + \int_{\xi^T\mathbf{x} + (1-h)\boldsymbol{\eta}^T|\mathbf{x}|}^{+\infty} \left(\frac{y - \xi^T\mathbf{x}}{\boldsymbol{\eta}^T|\mathbf{x}|} - 1 + h \right) p(y|\mathbf{x}) dy \right] p(\mathbf{x}) d\mathbf{x}, \end{aligned} \tag{13}$$

and $\frac{1}{N}\sum_{i=1}^N \boldsymbol{\eta}^T|\mathbf{x}_i|$ in (12) can also be approximated by

$$E(\boldsymbol{\eta}^T|\mathbf{x}|) = \int_D \boldsymbol{\eta}^T|\mathbf{x}| \, p(\mathbf{x}) d\mathbf{x} \tag{14}$$

Thus, Eq.(12) becomes

$$\ln p(\boldsymbol{\eta},\xi|D,\beta,h) = -\alpha N * E(\boldsymbol{\eta}^T|\mathbf{x}|) - \frac{\gamma}{2}\xi^T\xi - \beta N * E(L(\boldsymbol{\eta}^T\mathbf{x}, \xi^T\mathbf{x}, y)) - N\ln C(\beta,h) + const \, . \tag{15}$$

In order to maximize (15), its derivatives with respect to $\boldsymbol{\eta},\xi,\beta,h$ must be zero.Thus, we can obtain

$$E(L(\hat{\boldsymbol{\eta}}^T\mathbf{x}, \hat{\xi}^T\mathbf{x}, y)) = -\frac{\partial C(\beta,h)/\partial\beta}{C(\beta,h)}, \tag{16}$$

$$\int_D \left[\int_{-\infty}^{\hat{\xi}^T\mathbf{x}-(1-h)\hat{\boldsymbol{\eta}}^T|\mathbf{x}|} p(y\mid\mathbf{x})dy + \int_{\hat{\xi}^T\mathbf{x}+(1-h)\hat{\boldsymbol{\eta}}^T|\mathbf{x}|}^{+\infty} p(y\mid\mathbf{x})dy \right] p(\mathbf{x})d\mathbf{x} = \frac{-\partial C(\beta,h)/\partial h}{\beta C(\beta,h)}. \quad (17)$$

When $\boldsymbol{\eta}=\hat{\boldsymbol{\eta}},\boldsymbol{\xi}=\hat{\boldsymbol{\xi}}$, maximizing (15) actually becomes the following optimization problem:

$$\arg\min_{\alpha,\beta,h} \alpha E(\hat{\boldsymbol{\eta}}^T\mid\mathbf{x}\mid) + \beta E(L(\hat{\boldsymbol{\eta}}^T\mathbf{x},\hat{\boldsymbol{\xi}}^T\mathbf{x},y)) + \ln C(\beta,h). \quad (18)$$

Please note $C(\beta,h)$ in (18). According to its corresponding MAP, we have

$$C(\beta,h) = 2\left(\int_0^{1-h}\exp(0)dt + \int_{1-h}^{+\infty}\exp(-\beta(t-1+h))dt\right) = \frac{2(1+(1-h)\beta)}{\beta}. \quad (19)$$

By substituting (19) into (16) and (17), we obtain

$$E(L(\hat{\boldsymbol{\eta}}^T\mathbf{x},\hat{\boldsymbol{\xi}}^T\mathbf{x},y)) = \frac{1}{\beta(1+(1-h)\beta)}, \quad (20)$$

$$\int_D \left[\int_{-\infty}^{\hat{\xi}^T\mathbf{x}-(1-h)\hat{\boldsymbol{\eta}}^T|\mathbf{x}|} p(y\mid\mathbf{x})dy + \int_{\hat{\xi}^T\mathbf{x}+(1-h)\hat{\boldsymbol{\eta}}^T|\mathbf{x}|}^{+\infty} p(y\mid\mathbf{x})dy \right] p(\mathbf{x})d\mathbf{x} = \frac{1}{1+(1-h)\beta}. \quad (21)$$

III. The Dependency Between h and the Input Noise

A. Laplacian Noise

For the Laplacian noise model,

$$p(y\mid\mathbf{x}) = \frac{1}{2\mu}\exp\left[-\frac{\left|y-\tilde{\boldsymbol{\xi}}^T\mathbf{x}\right|}{\mu}\right], \quad (22)$$

Here, we only consider the simpler case when $\mathbf{x}$ is one-dimensional, with uniform density over the range $[-L,L]$ (i.e. $X\sim U([-L,L])$). When $\mathbf{x}$ is multi-dimensional, we can also arrive at the similar conclusion, if we select suitable integral region for each dimension.

Let $\varepsilon=1-h$, $E=\int_D \hat{\eta}|x|p(x)dx$. After tedious computation, it can be shown that (21) reduce to

$$\begin{aligned}\frac{1}{1+\varepsilon\beta} &= \int_D\left[\int_{-\infty}^{\tilde{\xi}x-\varepsilon\hat{\eta}|x|}\frac{1}{2\mu}\exp\left(-\frac{|y-\tilde{\xi}x|}{\mu}\right)dy + \int_{\tilde{\xi}x+\varepsilon\hat{\eta}|x|}^{+\infty}\frac{1}{2\mu}\exp\left(-\frac{|y-\tilde{\xi}x|}{\mu}\right)dy\right]p(x)dx\\ &= 2\int_{-L}^{0}\left(\int_{\hat{\xi}x+\varepsilon\hat{\eta}x}^{+\infty}\frac{1}{2\mu}\exp\left(-\frac{y-\tilde{\xi}x}{\mu}\right)dy\right)\frac{1}{2L}dx\\ &\quad + 2\int_{0}^{L}\left(\int_{\tilde{\xi}x}^{+\infty}\frac{1}{2\mu}\exp\left(-\frac{y-\tilde{\xi}x}{\mu}\right)dy\right)\frac{1}{2L}dx\\ &\quad + 2\int_{-L}^{0}\left(\int_{\tilde{\xi}x}^{\hat{\xi}x-\varepsilon\hat{\eta}x}\frac{1}{2\mu}\exp\left(-\frac{y-\tilde{\xi}x}{\mu}\right)dy\right)\frac{1}{2L}dx\end{aligned}$$

$$\begin{aligned}&= 1+\frac{\mu}{2L(\tilde{\xi}-\hat{\xi}-\varepsilon\hat{\eta})}\left(1-\exp\left(\frac{-(\tilde{\xi}-\hat{\xi}-\varepsilon\hat{\eta})L}{\mu}\right)\right)\\ &\quad + \frac{\mu}{2L(\tilde{\xi}-\hat{\xi}+\varepsilon\hat{\eta})}\left(\exp\left(\frac{-(\tilde{\xi}-\hat{\xi}+\varepsilon\hat{\eta})L}{\mu}\right)-1\right).\end{aligned} \quad (23)$$

Similarly, from (13), (20) and (21), we obtain

$$\begin{aligned}\frac{1}{\beta} &= \frac{(\tilde{\xi}-\hat{\xi})L}{2E} + \frac{\mu^2}{LE}\cdot\frac{(\tilde{\xi}-\hat{\xi})^3-3(\tilde{\xi}-\hat{\xi})\varepsilon^2\hat{\eta}^2}{\left((\tilde{\xi}-\hat{\xi})^2-\varepsilon^2\hat{\eta}^2\right)^2}\\ &\quad + \frac{\mu}{2E}\exp\left(-\frac{(\tilde{\xi}-\hat{\xi})L}{\mu}\right)\\ &\quad \left(\frac{(\tilde{\xi}-\hat{\xi}-\varepsilon\hat{\eta})\varepsilon\hat{\eta}L-(\tilde{\xi}-\hat{\xi})\mu+2\mu\varepsilon\hat{\eta}}{(\tilde{\xi}-\hat{\xi}-\varepsilon\hat{\eta})^2L}\exp\left(\frac{\varepsilon\hat{\eta}L}{\mu}\right)\right.\\ &\quad \left.-\frac{(\tilde{\xi}-\hat{\xi}+\varepsilon\hat{\eta})\varepsilon\hat{\eta}L+(\tilde{\xi}-\hat{\xi})\mu+2\mu\varepsilon\hat{\eta}}{(\tilde{\xi}-\hat{\xi}+\varepsilon\hat{\eta})^2L}\exp\left(-\frac{\varepsilon\hat{\eta}L}{\mu}\right)\right).\end{aligned} \quad (24)$$

By using (20), (23) and (24), we have

$$\begin{aligned}E(L(\hat{\eta}x,\hat{\xi}x,y)) &= \frac{(\tilde{\xi}-\hat{\xi})L-2\varepsilon E}{2E}\\ &\quad + \frac{\mu}{LE}\cdot\frac{(\tilde{\xi}-\hat{\xi})^3\mu-(\tilde{\xi}-\hat{\xi})^2\varepsilon^2\hat{\eta}E-3(\tilde{\xi}-\hat{\xi})\varepsilon^2\hat{\eta}^2\mu+\varepsilon^4\hat{\eta}^3E}{\left((\tilde{\xi}-\hat{\xi})^2-\varepsilon^2\hat{\eta}^2\right)^2}\\ &\quad + \frac{\mu}{2E}\exp\left(-\frac{(\tilde{\xi}-\hat{\xi})L}{\mu}\right)\\ &\quad \left(\frac{(\tilde{\xi}-\hat{\xi}-\varepsilon\hat{\eta})\varepsilon\hat{\eta}L-(\tilde{\xi}-\hat{\xi})\mu+2\mu\varepsilon\hat{\eta}+(\tilde{\xi}-\hat{\xi})\varepsilon E-\varepsilon^2\hat{\eta}E}{(\tilde{\xi}-\hat{\xi}-\varepsilon\hat{\eta})^2L}\exp\left(\frac{\varepsilon\hat{\eta}L}{\mu}\right)\right.\\ &\quad \left._-\frac{(\tilde{\xi}-\hat{\xi}+\varepsilon\hat{\eta})\varepsilon\hat{\eta}L+(\tilde{\xi}-\hat{\xi})\mu+2\mu\varepsilon\hat{\eta}+(\tilde{\xi}-\hat{\xi})\varepsilon E+\varepsilon^2\hat{\eta}E}{(\tilde{\xi}-\hat{\xi}+\varepsilon\hat{\eta})^2L}\exp\left(-\frac{\varepsilon\hat{\eta}L}{\mu}\right)\right).\end{aligned} \quad (25)$$

We have defined $E=\int_D\hat{\eta}|x|p(x)dx$, $C=\beta/\alpha$, so we obtain

$$\alpha E(\hat{\eta}|x|) = \beta E C^{-1} \quad (26)$$

and

$$\varepsilon\hat{\eta}L = 2\varepsilon E \quad (27)$$

Define $y-\tilde{\xi}x\approx\hat{\xi}x-\tilde{\xi}x=\delta(x)$. It can be shown that

$$E_X\left(\delta^2(x)\right)\approx E_X\left((y-\tilde{\xi}x)^2\right)=2\mu^2. \quad (28)$$

With $X\sim U([-L,L])$, we also obtain $\mathrm{var}(X)=L^2/3$. Consequently

$$E_X\left(\delta^2(x)\right)\approx\mathrm{var}\left((\tilde{\xi}-\hat{\xi})X\right)\approx(\tilde{\xi}-\hat{\xi})^2L^2/3, \quad (29)$$

and hence

$$\mu=(\tilde{\xi}-\hat{\xi})L/\sqrt{6}. \quad (30)$$

After substituting(19), (23), (24), (25), (26), (27) and (30) into (18), minimizing (18) becomes minimizing

$$\begin{aligned}g(\frac{\varepsilon}{\mu}) &= \left(\frac{\sqrt{6}}{2E}+f_1(\frac{\varepsilon}{\mu})+\frac{\exp\left(-\sqrt{6}\right)}{4E}f_2(\frac{\varepsilon}{\mu})\right)^{-1}\\ &\quad \left(\frac{\sqrt{6}-2\frac{\varepsilon E}{\mu}}{2E}+\frac{3\sqrt{6}-\left(6+6\sqrt{6}\right)\frac{\varepsilon^2E^2}{\mu^2}+4\frac{\varepsilon^4E^4}{\mu^4}}{18E-24\frac{\varepsilon^2E^3}{\mu^2}+8\frac{\varepsilon^4E^5}{\mu^4}}\right.\\ &\quad \left.+\frac{\exp\left(-\sqrt{6}\right)}{4E}f_3(\frac{\varepsilon}{\mu})+\frac{E}{\mu C}\right)\end{aligned}$$

$$-\ln\left(1+\frac{\frac{\varepsilon E}{\mu}}{3-2\frac{\varepsilon^2E^3}{\mu^2}}+\frac{\exp(-\sqrt{6})}{2}\left(\frac{\exp\left(-2\frac{\varepsilon E}{\mu}\right)}{\sqrt{6}+2\frac{\varepsilon E}{\mu}}-\frac{\exp\left(2\frac{\varepsilon E}{\mu}\right)}{\sqrt{6}-2\frac{\varepsilon E}{\mu}}\right)\right)$$

$$+\ln\left(\frac{\sqrt{6}}{2E}+f_1(\frac{\varepsilon}{\mu})+\frac{\exp\left(-\sqrt{6}\right)}{4E}f_2(\frac{\varepsilon}{\mu})\right)+const, \quad (31)$$

where

$$f_1(\frac{\varepsilon}{\sigma})=\frac{3\sqrt{6}-6\sqrt{6}\frac{\varepsilon^2E^2}{\mu^2}}{18E-24\frac{\varepsilon^2E^3}{\mu^2}+8\frac{\varepsilon^4E^5}{\mu^4}},$$

$$f_2(\frac{\varepsilon}{\sigma})=\frac{-\sqrt{6}+\left(4+2\sqrt{6}\right)\frac{\varepsilon E}{\mu}-4\frac{\varepsilon^2E^2}{\mu^2}}{3-2\sqrt{6}\frac{\varepsilon E}{\mu}+2\frac{\varepsilon^2E^2}{\mu^2}}\exp\left(2\frac{\varepsilon E}{\mu}\right)$$

$$-\frac{\sqrt{6}+\left(4+2\sqrt{6}\right)\frac{\varepsilon E}{\mu}+4\frac{\varepsilon^2E^2}{\mu^2}}{3+2\sqrt{6}\frac{\varepsilon E}{\mu}+2\frac{\varepsilon^2E^2}{\mu^2}}\exp\left(-2\frac{\varepsilon E}{\mu}\right)$$

$$f_3(\frac{\varepsilon}{\sigma})=\frac{-\sqrt{6}+\left(4+3\sqrt{6}\right)\frac{\varepsilon E}{\mu}-6\frac{\varepsilon^2E^2}{\mu^2}}{3-2\sqrt{6}\frac{\varepsilon E}{\mu}+2\frac{\varepsilon^2E^2}{\mu^2}}\exp\left(2\frac{\varepsilon E}{\mu}\right)$$

$$-\frac{\sqrt{6}+\left(4+3\sqrt{6}\right)\frac{\varepsilon E}{\mu}+6\frac{\varepsilon^2E^2}{\mu^2}}{3+2\sqrt{6}\frac{\varepsilon E}{\mu}+2\frac{\varepsilon^2E^2}{\mu^2}}\exp\left(-2\frac{\varepsilon E}{\mu}\right)$$

Obviously, when $(\frac{\varepsilon}{\mu})$ takes some fixed value, $g(\frac{\varepsilon}{\mu})$ will achieve its minimum, which indicates that there is a linear dependency between ε and μ. Thus, there is an inverse linear dependency between the parameter h and the standard variance σ of the Laplacian input noise because of $\varepsilon=1-h$ and $\sigma=\sqrt{2}\mu$.

B. Uniform Noise

Next, we consider the uniform noise model

$$\phi(n)=\frac{1}{2\mu},\quad n\in[-\mu,\mu] \quad (32)$$

Again, we only consider the simpler case when $\mathbf{x}$ is one-dimensional, with uniform density over the range $[-L,L]$. Let $\varepsilon=1-h$, $E=\int_D\hat{\eta}|x|p(x)dx$. Eq. (21) becomes

$$\frac{1}{1+\varepsilon\beta}=\int_D\left[\int_{-\infty}^{\hat{\xi}x-\varepsilon\hat{\eta}|x|}\frac{1}{2\mu}dy+\int_{\hat{\xi}x+\varepsilon\hat{\eta}|x|}^{+\infty}\frac{1}{2\mu}dy\right]p(x)dx$$

$$=2\int_0^L\left(\int_{\hat{\xi}x+\varepsilon\hat{\eta}x}^{\tilde{\xi}x+\mu}\frac{1}{2\mu}dy\right)\frac{1}{2L}dx$$

$$+2\int_0^{\frac{\mu}{\tilde{\xi}-\hat{\xi}+\varepsilon\hat{\eta}}}\left(\int_{\tilde{\xi}x-\mu}^{\hat{\xi}x-\varepsilon\hat{\eta}x}\frac{1}{2\mu}dy\right)\frac{1}{2L}dx$$

$$=\frac{(\tilde{\xi}-\hat{\xi})^2L^2-\varepsilon^2\hat{\eta}^2L^2+2\mu(\tilde{\xi}-\hat{\xi}+\varepsilon\hat{\eta})L+\mu^2}{4\mu(\tilde{\xi}-\hat{\xi}+\varepsilon\hat{\eta})L}. \quad (33)$$

Using (13), (20), (21)and(33), after a little tedious computation, it can be shown that

$$\frac{1}{\beta}=\frac{(\tilde{\xi}-\hat{\xi}+\varepsilon\hat{\eta})(\tilde{\xi}-\hat{\xi}-\varepsilon\hat{\eta})^2L^3+3((\tilde{\xi}-\hat{\xi})^2-\varepsilon^2\hat{\eta}^2)L^2(\mu+\varepsilon E)}{12\mu(\tilde{\xi}-\hat{\xi}+\varepsilon\hat{\eta})LE}$$

$$+\frac{3\mu(\tilde{\xi}-\hat{\xi}+\varepsilon\hat{\eta})L(\mu+2\varepsilon E)+3\mu^2\varepsilon E+\mu^3}{12\mu(\tilde{\xi}-\hat{\xi}+\varepsilon\hat{\eta})LE}, \quad (34)$$

$$E(L(\hat{\eta}x,\hat{\xi}x,y))=$$

$$\frac{(\tilde{\xi}-\hat{\xi}+\varepsilon\hat{\eta})(\tilde{\xi}-\hat{\xi}-\varepsilon\hat{\eta})^2L^3+3\mu(\tilde{\xi}-\hat{\xi}+\varepsilon\hat{\eta})(\tilde{\xi}-\hat{\xi}-\varepsilon\hat{\eta})L^2}{12\mu(\tilde{\xi}-\hat{\xi}+\varepsilon\hat{\eta})LE}$$

$$+\frac{3\mu^2(\tilde{\xi}-\hat{\xi}+\varepsilon\hat{\eta})L+\mu^3}{12\mu(\tilde{\xi}-\hat{\xi}+\varepsilon\hat{\eta})LE}. \quad (35)$$

As in Section 3.A, consider $\delta(x)=(\hat{\xi}-\tilde{\xi})x$ and assume that

$$E_X\left(\delta^2(x)\right)\approx E_X\left((y-\tilde{\xi}x)^2\right)=\mu^2/3 \quad (36)$$

Using (29) again, we obtain

$$\mu=(\tilde{\xi}-\hat{\xi})L \quad (37)$$

Analogous to Section 3.A, by plugging in (19), (33), (34), (35), (26), (27) and (37), it can be shown that the problem reduces to minimizing

$$g(\frac{\varepsilon}{\mu})=\left(\frac{3E+6\frac{\varepsilon E^2}{\mu}}{2+4\frac{\varepsilon E}{\mu}-\frac{\varepsilon^2E^2}{\mu^2}-\frac{\varepsilon^3E^3}{\mu^3}}\right)\left(\frac{2+\frac{\varepsilon E}{\mu}-4\frac{\varepsilon^2E^2}{\mu^2}+2\frac{\varepsilon^3E^3}{\mu^3}}{3E+6\frac{\varepsilon E^2}{\mu}}+\frac{E}{\mu C}\right)$$

$$-\ln\left(\frac{1+\frac{\varepsilon E}{\mu}-\frac{\varepsilon^2E^2}{\mu^2}}{1+2\frac{\varepsilon E}{\mu}}\right)+\ln\left(\frac{2+4\frac{\varepsilon E}{\mu}-\frac{\varepsilon^2E^2}{\mu^2}-\frac{\varepsilon^3E^3}{\mu^3}}{3E+6\frac{\varepsilon E^2}{\mu}}\right)+const. \quad (38)$$

Again, we can see from (38) that there is a linear dependency between ε and μ. Obviously, because the standard variance σ of the uniform input noise equals to $\mu/\sqrt{3}$ and $\varepsilon=1-h$, there is an the inverse linear dependency relationship between the parameter h and σ.

C. Dependency Between h and the Input Noise

From Section 3.A and 3.B, we come to the conclusion that there are approximately inverse proportional dependency relationships between the parameter h and the standard variance σ of Laplacian input noise and uniform input noise. At the same time, in [4,5], we have derived the analogical conclusion with Gaussian noisy input. Following the same spirit in [2], we can draw the more generic conclusion that the dependency between h and input noise is approximately inverse proportion.

It should be mentioned here that although we investigate the dependency relationship between the parameter h in RFLR model and the input noise, the conclusion is very helpful for the practical applications of both FLR and RFLR model, for FLR model is just a special case of RFLR model.

IV. EXPERIMENTAL STUDIES

In this experiment, we apply RFLR model to a real dataset taken from [6] (see Table1). In [6], fuzzy linear regression was used successfully to analyze the dependence relationship of the atmospheric concentration of carbon monoxide (CO) on a set of meteorological variables, including relative humidity (RH) (%), rain (R) (mm) and wind speed (WS) (m/s).

By using the same method from [6], we also take CO as the output data, RH, R and WS as the input data. Let h=0.5. Now the corresponding regression values $(\xi_i,\eta_i), i=1,2,\cdots,21$ can be obtained, where ξ_i denotes the center and η_i denotes the spread. Next, in order to investigate the dependency relationship between h and the noisy input, let $y_i' = y_i + k\cdot n$, $i=1,2,\cdots,21$, where k is a noise-signal ratio and n represents the Laplacian noise. Then the corresponding sampling dataset $(x_i, y_i'), i=1,2,\cdots,21$ can be generated. Similarly, its corresponding regression values $(\xi_i',\eta_i'), i=1,2,\cdots,21$ can be obtained by using the same RFLR model. In order to make the experimental results fair, σ is taken from [0.1,2.0] with the step length 0.1, and the Laplacian noise distribution is used to generate 20 groups of the corresponding sampling datasets for each given σ. For each given σ, h is taken as the average result of all 20 h values which can minimize $\sum_{i=1}^{21}\sqrt{(\xi_i-\xi_i')^2+(\eta_i-\eta_i')^2}$ respectively for each group of the sampling datasets.

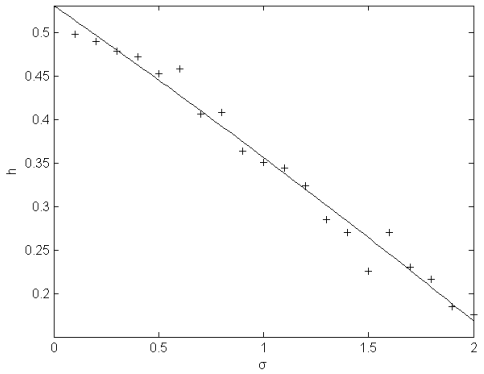

Fig. 1. With Laplacian noisy input，the relationship between h and σ when $k=0.05$

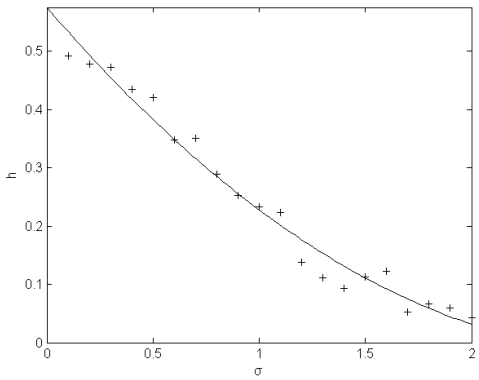

Fig. 2. With Laplacian noisy input，the relationship between h and σ when $k=0.1$

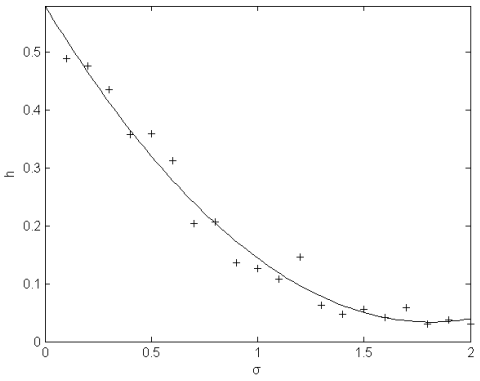

Fig. 3. With Laplacian noisy input，the relationship between h and σ when $k=0.2$

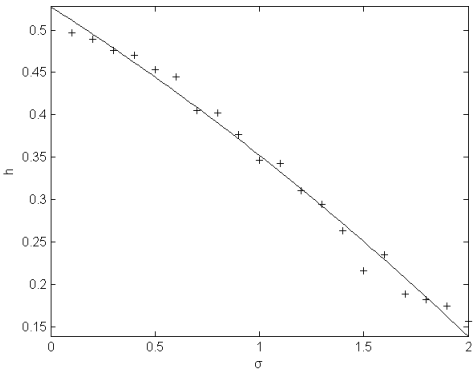

Fig. 4. With uniform noisy input，the relationship between h and σ when $k=0.05$

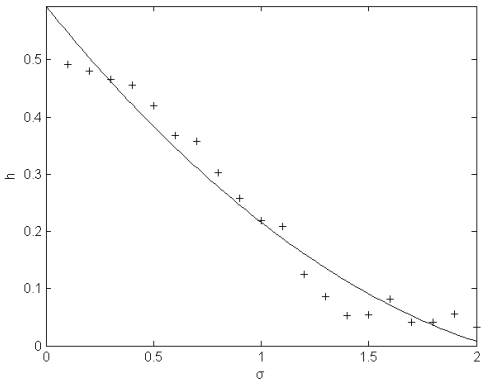

Fig. 5. With uniform noisy input，the relationship between h and σ when $k=0.1$

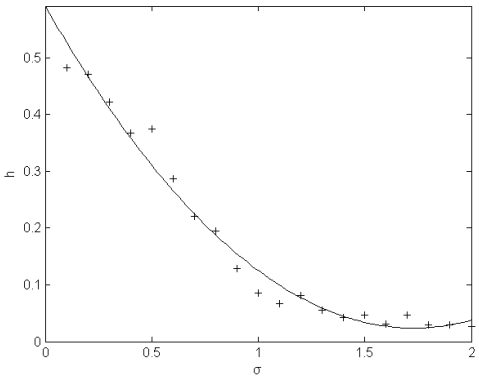

Fig. 6. With uniform noisy input，the relationship between h and σ when $k=0.2$

Fig.1, 2 and 3 depict the dependency relationships between h and σ for all 20 σ values with different k (see + in the figures), where the curves are used to roughly indicate the change tendencies between h and σ, respectively. With the same experimental method as above and the Uniform noise distribution, Figures 4-6 show the experimental results, which again validate our theoretical conclusion.

It can be easily seen from Fig.1-6 that when noise is small, i.e. k and σ is comparatively small, there is an obvious inverse linear dependency relationship between h and σ. However, when k and/or σ are comparatively large, i.e. the datasets are seriously distorted, the inverse linear relationship between h and σ does not exist anymore. In other words, RFLR model may become ineffective for seriously distorted datasets. Of course, although we have arranged many experiments and all these experimental results validate the above obtained conclusion on RFLR model, we just show several experimental results here so as to save the paper's space.

V. Conclusions and Future Work

In this paper, based on the Bayesian frame, the approximately inversely linear dependency relationships between the parameter h and the standard variance σ of Laplacian input noise and uniform input noise are derived. And the experimental results also validate our theoretical conclusion. In fact, the optimal choices of the parameter h are actually dependent on the variance of the input noise. Because Gaussian noise, Laplacian noise and uniform noise are all typical noise, and with the theoretical and experimental results from [4, 5], we can arrive at the more generic conclusion that there is an approximately inverse proportional dependency between h and input noise. The theoretical result here is very useful for the optimal choices of the parameter h. Of course, in order to apply the inversely linear dependency result in practical applications, one has to first arrive at an estimate of the noise level σ. One way to obtain this is by using Bayesian methods [7]. In the future, we will investigate better methods to solve the problem.

References

[1] J.B.Gao, S.R.Gunn and C.J. Ham's, "A probabilistic framework for SVM regression and Error Bar Estimation," Machine Learning, vol., 46, pp.71-89, 2002

[2] J. T. Kwok and Ivor W. Tsang, "Linear dependency between ε and the input noise in ε-support vector regression," IEEE Transaction on Neural Networks, vol.14, no.3, pp.544-553, 2003

[3] Wang shitong, "Theoretically optimal parameter choices for support vector regression machines with noisy input," Int. J. Soft Computing, vol.9, no.10, pp.732-741, 2005

[4] Hongwei Ge and Shitong Wang, "Dependency between degree of fit and input noise in fuzzy linear regression using non-symmetric fuzzy triangular coefficients," Fuzzy Sets and Systems, vol.158, no.19, pp.2189-2202, 2007

[5] Hongwei Ge , Fu-lai Chung and Shitong Wang, "Theoretical Choice of the Optimal Threshold for Possibilistic Linear Model with Noisy Input," IEEE Transactions on Fuzzy Systems, vol.16, no.4, pp.1027-1037, 2008

[6] Renato Coppi and Pierpaolo D'Urso, "Least squares estimation of a linear regression model with LR fuzzy response," Computational Statistics & Data Analysis, vol.51, pp.267-286, 2006

[7] M.H.Law and J.T.Kwok, "Bayesian support vector regression," in Proc English Int.Workshop Artif.Intell.Statist.,2001, pp.239-244

[8] D. H. Hong and C. Hwang, "Support vector fuzzy regression machines," *Fuzzy Sets and Syst.*, vol.138, pp.271-281, 2003

[9] Mehran Hojati and C.R.Bector, "A simple method for computation of fuzzy linear regression," European Journal of Operational Research, vol.166, pp.172-184, 2005

TABLE I
INPUT-OUTPUT DATA IN [8]

Number	Relative Humidity (RH)(%)	Rain R(mm)	Wind Speed WS(m/s)	Concentrations of carbon monoxide (CO)(mg/m^3)
1	82.27	0.90	2.87	1.15
2	88.70	0.90	1.12	2.98
3	82.51	0.02	0.85	3.92
4	79.46	0.00	0.45	4.65
5	68.85	0.00	0.91	3.98
6	79.39	0.02	1.07	3.35
7	88.87	1.30	0.69	3.13
8	88.92	0.09	0.40	4.15
9	83.52	0.00	0.83	3.96
10	87.51	0.05	2.09	4.07
11	86.04	0.04	0.90	3.30
12	91.77	0.93	1.22	4.02
13	83.62	0.02	3.00	2.06
14	73.10	0.02	1.75	1.37
15	80.38	0.09	0.73	3.35
16	87.98	0.24	1.87	1.45
17	90.13	0.02	2.39	2.74
18	64.95	0.00	1.25	2.44
19	80.16	0.01	1.02	2.79
20	86.14	0.44	0.70	3.31
21	89.12	0.01	1.17	4.02

2011 IEEE International Conference on Fuzzy Systems
June 27-30, 2011, Taipei, Taiwan

Direct Adaptive Fuzzy Control for Nonaffine Nonlinear Systems with Unknown Control Direction

Salim Labiod
LAMEL, Faculty of Science and Technology,
University of Jijel,
18000, Jijel, Algeria.
e-mail: labiod_salim@yahoo.fr

Thierry Marie Guerra
LAMIH, UMR CNRS 8530, Université de Valenciennes
et du Hainaut-Cambrésis, Le Mont Houy,
59313, Valenciennes Cedex 9, France.
e-mail: thierry.guerra@univ-valenciennes.fr

***Abstract*—This paper deals with direct adaptive fuzzy control for a class of uncertain nonaffine nonlinear systems with unknown control direction. Within this scheme, a fuzzy system is used to generate directly the control input signal without dynamic system estimation. The adjustable parameters in the used fuzzy system are updated using a gradient descent adaptation algorithm that incorporates a Nussbaum-type function to deal with the unknown control direction. The stability of the closed-loop system is performed using a Lyapunov approach. Simulation results are provided to verify the effectiveness of the proposed design.**

Keywords- fuzzy control, adaptive control, nonaffine nonlinear systems, Nussbaum function.

I. INTRODUCTION

In the past years, based on the universal approximation property of fuzzy systems, adaptive fuzzy control of uncertain nonlinear systems has been intensively conducted and some developments have been achieved in the literature [1, 2]. The stability study in such adaptive methods is performed by using the Lyapunov design approach. Most of the proposed adaptive fuzzy control methods can be roughly classified into two types: the direct adaptive fuzzy control approach where fuzzy systems are used to approximate unknown ideal controllers [1-4], and the indirect adaptive fuzzy control approach where fuzzy systems are used to identify the plant dynamics [1-3, 5]. In [1-5], adaptive fuzzy control design for the affine-in-control nonlinear systems is presented. Adaptive fuzzy control design for nonaffine systems is discussed in [6-9].

In the direct schemes [1-4, 6, 8, 9], the parameter adaptation laws used are designed based on a Lyapunov approach, where an error signal between the desired output and the actual output is used to update the adjustable parameters. However, since in the direct adaptive control approach, the purpose is to approximate an unknown ideal controller by using a fuzzy controller, so it is more convenient to try to adjust the free parameters of the fuzzy controller by using directly the error between the ideal controller and the fuzzy controller [4, 7]. In [7], a direct adaptive fuzzy controller was designed for a class of nonaffine systems where the gradient descent method was used to design the parameter adaptation law in order to minimize the error between an ideal controller and the fuzzy controller.

However, in [7], the control direction is assumed known a priori, i.e., the sign of the control gain (the control gain is the partial derivative over control variable for nonaffine systems) is assumed known for the designer. Without this assumption, the adaptive control design becomes much more difficult, because in this case, one cannot decide the direction along which the control operates and/or the direction of the search of controller parameters. In the adaptive control literature, the unknown control direction problem is mainly solved by using the Nussbaum-type function [10, 11], and it has been successfully applied for robust control design [12, 13] adaptive control design for nonlinear systems [14-17], and adaptive fuzzy control for nonaffine systems [18, 19]. In the literature, other approaches solved the unknown control direction problem by using: the correction vector method for first order nonlinear systems [20]; a switching scheme based on a monitoring function [21]; a hysteresis-type function for indirect adaptive fuzzy control [22, 23]; or by estimating unknown parameters involved in the control gain [24].

In this work we present a direct adaptive fuzzy control scheme for a class of uncertain nonaffine nonlinear systems with unknown control direction. In the design; instead of using fuzzy systems to approximate the unknown nonlinearities in the system, a fuzzy system is used to approximate an unknown desired controller that can achieve control objectives, and a Nussbaum function is introduced in the parameter adaptation law to solve the problem of unknown control direction. The parameter adaptation law is designed to minimize the error between the ideal controller and the fuzzy controller by using the gradient descent method. Using the Lyapunov approach, it is proved that the proposed adaptive fuzzy controller can guarantee the boundedness of all the signals of the closed-loop system and the asymptotic convergence of the tracking error. In fact, this paper presents an extension of our previous work [7] to the case of unknown control direction.

The remainder of the paper is organized as follows. The problem formulation and preliminaries are given in section II. The proposed direct adaptive control scheme is presented in section III with its adaptive law and stability analysis. In section IV, the proposed adaptive control algorithm is used to control a simple nonaffine nonlinear system.

978-1-4244-7316-8/11/$26.00 ©2011 IEEE

II. PROBLEM FORMULATION AND PRELIMINARIES

A. Problem Formulation

Consider the class of single-input single-output (SISO) nonlinear systems modeled by

$$\begin{cases} \dot{x}_i = x_{i+1}, i = 1,\ldots,n-1 \\ \dot{x}_n = f(\boldsymbol{x},u) \\ y = x_1 \end{cases} \tag{1}$$

or, equivalently

$$y^{(n)} = f(\boldsymbol{x},u) \tag{2}$$

where $\boldsymbol{x} = [x_1,\ldots,x_n]^T \in \mathbb{R}^n$, is the state vector of the system which is assumed available for measurement, $u \in \mathbb{R}$ is the scalar control input, $y \in \mathbb{R}$ is the scalar system output, and $f(\boldsymbol{x},u)$ is an unknown smooth nonlinear function.

In respect of the dynamic system (1), the following assumption will be made:

Assumption 1: The function $g(\boldsymbol{x},u) = \dfrac{\partial f(\boldsymbol{x},u)}{\partial u}$ is nonzero and bounded. Moreover, its sign, i.e. control direction, is unknown.

The objective is to design an adaptive fuzzy controller for system (1) such that the system output $y(t)$ follows a desired trajectory $y_d(t)$ while all signals in the closed-loop system remain bounded.

Regarding the development of the control law, the following assumption should also be made:

Assumption 2: The desired trajectory $y_d(t)$ and its first n derivatives are smooth and bounded.

Now, let us define the tracking error as

$$e = y_d - y \tag{3}$$

and let s be a sliding surface defined as

$$s = \left(\frac{d}{dt} + \lambda\right)^{n-1} e, \quad \lambda > 0 \tag{4}$$

From (4), $s(t) = 0$ represents a linear differential equation whose solution implies that the tracking error $e(t)$ converges to zero with a time constant $(n-1)/\lambda$ [22]. Thus, the control objective becomes the design of a controller to keep $s(t)$ at zero.

The time derivative of s is given by

$$\dot{s} = \upsilon_0 - f(\boldsymbol{x},u) \tag{5}$$

where

$$\upsilon_0 = y_d^{(n)} + \beta_{n-1} e^{(n-1)} + \cdots + \beta_1 \dot{e} \tag{6}$$

with $\beta_j = \dfrac{(n-1)!}{(n-j)!(j-1)!}\lambda^{n-j}$, $j = 1,\ldots,n-1$.

By adding and subtracting $k_1 s + k_2 \tanh(s/\varepsilon)$ to the right-hand side of (6), one obtains

$$\dot{s} = -k_1 s - k_2 \tanh(s/\varepsilon) - \left(f(\boldsymbol{x},u) - \upsilon\right) \tag{7}$$

where k_1 and k_2 are positive design parameters, and $\upsilon = \upsilon_0 + k_1 s + k_2 \tanh(s/\varepsilon)$.

From Assumption 1 and the fact that the signal υ, does not explicitly depend upon the control input u, the partial derivative of $f(\boldsymbol{x},u) - \upsilon$ with respect to the input u satisfies

$$\frac{\partial\left(f(\boldsymbol{x},u) - \upsilon\right)}{\partial u} = \frac{\partial f(\boldsymbol{x},u)}{\partial u} \neq 0 \tag{8}$$

Based on the implicit function theorem [5, 13], we know that the nonlinear algebraic equation $f(\boldsymbol{x},u) - \upsilon = 0$ is locally solvable for the input u for each $\boldsymbol{x}$ and υ. Therefore, there exists some ideal controller $u^*(\boldsymbol{x},\upsilon)$ satisfying the following equality for all $\boldsymbol{x}$ and υ

$$f\left(\boldsymbol{x},u^*(\boldsymbol{x},\upsilon)\right) - \upsilon = 0 \tag{9}$$

If the control input u is chosen as the ideal control law u^*, i.e., $u = u^*(\boldsymbol{x},\upsilon)$, the closed-loop error dynamic (7) becomes

$$\dot{s} = -k_1 s - k_2 \tanh(s/\varepsilon) \tag{10}$$

From which one can conclude that $s(t) \to 0$ as $t \to \infty$ and, therefore, $e(t)$ and all its time derivatives up to $n-1$ converge to zero [25].

However, the implicit function theory only guarantees the existence of the ideal controller u^* for system (1), and does not prescribe a technique for constructing it even if the dynamics of the system are well-known. In the next section, a fuzzy system will be used to construct adaptively this unknown ideal implicit controller and Nussbaum technique will be used to cope with the unknown control direction.

B. Fuzzy Systems

We use in this work the zero-order Takagi-Sugeno fuzzy system that performs a mapping from an input vector $\boldsymbol{z} = [z_1,\ldots,z_m]^T \in \Omega_z \subset \mathbb{R}^m$ to a scalar output variable $y_f \in \mathbb{R}$, where $\Omega_z = \Omega_{z_1} \times \cdots \times \Omega_{z_m}$ and $\Omega_{z_i} \subset \mathbb{R}$. If we define M_i fuzzy sets F_i^j, $j = 1,\ldots,M_i$, for each input z_i, then the fuzzy

system will be characterized by a set of if-then rules of the form [1, 2]

$$\begin{aligned} \mathrm{R}^{k}: &\text{ If } z_1 \text{ is } G_1^k \text{ and} \ldots \text{and } z_m \text{ is } G_m^k \\ &\text{Then } y_f \text{ is } y_f^k \quad (k=1,\ldots,N) \end{aligned} \tag{11}$$

where $G_i^k \in \left\{F_i^1,\ldots,F_i^{M_i}\right\}$, $i=1,\ldots,n$, y_f^k is the crisp output of the k-th rule, and N is the total number of rules.

By using the singleton fuzzifier and the product inference engine, the final output of the fuzzy system is given by [1, 2]

$$y_f(z)=\frac{\sum_{k=1}^{N}\mu_k(z)\,y_f^k}{\sum_{k=1}^{N}\mu_k(z)} \tag{12}$$

where

$\mu_k(z)=\prod_{i=1}^{m}\mu_{G_i^k}(z_i)$, with $\mu_{G_i^k}\in\left\{\mu_{F_i^1},\ldots,\mu_{F_i^{M_i}}\right\}$,

with $\mu_{F_i^j}(x_i)$ is the membership function of the fuzzy set F_i^j.

By introducing the concept of fuzzy basis functions [1], the output given by (10) can be rewritten in the following compact form

$$y_f(z)=\boldsymbol{w}^T(z)\theta \tag{13}$$

where $\theta=\left[y_f^1,\ldots,y_f^N\right]^T$ is a vector grouping all consequent parameters, and $\boldsymbol{w}(z)=\left[w_1(z),\ldots,w_N(z)\right]^T$ is a set of fuzzy basis functions defined as

$$w_k(z)=\frac{\mu_k(z)}{\sum_{j=1}^{N}\mu_j(z)},\ k=1,\ \ldots,N. \tag{14}$$

The fuzzy system (11) is assumed to be well-defined so that $\sum_{j=1}^{N}\mu_j(z)\neq 0$ for all $z\in\Omega_z$.

It has been proved in [1] that fuzzy systems in the form of (12) with Gaussian membership functions can approximate continuous functions over a compact set to an arbitrary degree of accuracy provided that enough number of rules are considered.

C. Nussbaum Functions

In order to deal with the unknown control direction (sign of $g(\boldsymbol{x},u)$), the Nussbaum gain technique is used in this paper. The Nussbaum function technique was originally proposed in [10] and has been effectively used in controller design in solving the difficulty of unknown control directions [11-17]. A function $N(\tau)$ is called a Nussbaum-type function if it has the following properties [10]

$$\limsup_{\nu\to+\infty}\left(\frac{1}{\nu}\int_0^{\nu}N(\tau)\,d\tau\right)=+\infty \tag{15}$$

$$\liminf_{\nu\to+\infty}\left(\frac{1}{\nu}\int_0^{\nu}N(\tau)\,d\tau\right)=-\infty \tag{16}$$

For example, the continuous functions $e^{\tau^2}\cos(\tau)$ and $\tau^2\cos(\tau)$ are Nussbaum-type functions. In this paper, the even Nussbaum function $\tau^2\cos\left(\frac{\pi}{2}\tau\right)$ is used.

The following Lemma regarding the property of Nussbaum functions is used in the controller design and theorem proof of next section.

Lemma 1: Le $V(\cdot)$ and $\tau(\cdot)$ be smooth functions defined on $\left[0,t_f\right)$ with $V(t)\geq 0$, $\forall t\in\left[0,t_f\right)$, $N(\cdot)$ be an even smooth Nussbaum-type function. If the following inequality holds: $V(t)\leq c_0+\int_0^t\left(g(\zeta)N(\tau(\zeta))+c_1\right)\dot{\tau}(\zeta)\,d\zeta$ for $\forall t\in\left[0,t_f\right)$, where $g(\cdot)$ is a piecewise continuous time function which takes values in the unknown closed interval $I=\left[\underline{g},\overline{g}\right]$ with $0\notin I$, c_1 any positive number and c_0 is a constant, then $V(t)$, $\tau(t)$ and $\int_0^t\left(g(\zeta)N(\tau(\zeta))+c_1\right)\dot{\tau}(\zeta)\,d\zeta$ are bounded on $\left[0,t_f\right)$.

Proof: For the proof, please refer to [12].

III. Adaptive Fuzzy Controller Design

In the previous section, based on the implicit function theory, it has been shown that there exists an ideal control law $u^*(\boldsymbol{x},\upsilon)$ that can achieve control objectives. Since the implicit function theory only ensures the existence of this ideal controller and does not provide a way or a procedure for building it. In this section, we propose to use a fuzzy system to adaptively build this unknown ideal implicit controller.

To develop the control law, we assume that the ideal controller $u^*(\boldsymbol{x},\upsilon)$ can be approximated by a fuzzy system in the form of (11) as follows

$$u^*(z)=\boldsymbol{w}^T(z)\theta^* \tag{17}$$

where z is the input vector of the fuzzy system, $\boldsymbol{w}(z)$ is a fuzzy basis function vector fixed by the designer, and θ^* is a unknown bounded time-varying parameter vector with bounded time derivative.

Since the ideal parameter vector θ^* is unknown, let us use its estimate θ instead to form the adaptive control

$$u(z)=\boldsymbol{w}^T(z)\theta \tag{18}$$

To design an adaptation law for the free parameters θ, if the control direction (sign of $g(\boldsymbol{x},u)$) is known, one can consider the minimization problem of the cost function [7]

$$J(\theta)=\frac{1}{2}\left(u^*-u\right)^2=\frac{1}{2}\left(u^*-\boldsymbol{w}^T(z)\theta\right)^2$$

By using the gradient descent method, the following parameters update law can be obtained [7]

$$\dot{\theta}=\gamma\,\mathrm{sgn}\left(g(\boldsymbol{x},u)\right)\boldsymbol{w}(z)\left(\dot{s}+k_1 s+k_2\tanh(s/\varepsilon)\right)$$

with $\gamma>0$. However, since the control direction (sign of $g(\boldsymbol{x},u)$) is unknown, we have to use a Nussbaum-type function instead for designing the parameter adaptation law as the following

$$\dot{\theta}=\gamma N(\tau)\boldsymbol{w}(z)\left(\dot{s}+k_1 s+k_2\tanh(s/\varepsilon)\right) \tag{19}$$

$$\dot{\tau}=\eta\left(\dot{s}+k_1 s+k_2\tanh(s/\varepsilon)\right)^2 \tag{20}$$

$$N(\tau)=\tau^2\cos\left(\frac{\pi}{2}\tau\right) \tag{21}$$

where γ and η are strictly positive constants.

Theorem 1: For nonlinear system (1), under Assumptions 1 and 2 and Lemma 1, the control law (18) with adaptation laws (19)–(21) guarantee the boundedness of all the signals in the closed-loop system and the asymptotic convergence of the tracking error.

Proof: By invoking the mean value theorem, there exists a constant $\bar{\lambda}$ with $0<\bar{\lambda}<1$, such that the nonlinear function $f(\boldsymbol{x},u)$ can be expressed around u^* as follows

$$f(\boldsymbol{x},u)=f\left(\boldsymbol{x},u^*\right)+g(\boldsymbol{x},\bar{u})\left(u-u^*\right) \tag{22}$$

where $\bar{u}=\bar{\lambda}u+\left(1-\bar{\lambda}\right)u^*$.

By substituting (22) into (7), we get

$$\dot{s}=-k_1 s-k_2\tanh(s/\varepsilon)+g(\boldsymbol{x},\bar{u})\left(u^*-u\right) \tag{23}$$

With (17) and (18), one can rewrite (23) as

$$\dot{s}=-k_1 s-k_2\tanh(s/\varepsilon)+g(\boldsymbol{x},\bar{u})\boldsymbol{w}^T(z)\tilde{\theta} \tag{24}$$

where $\tilde{\theta}=\theta^*-\theta$ is the parameter error vector.

Now, consider the following positive definite function

$$V=\frac{1}{2}s^2+\frac{1}{2\gamma}\tilde{\theta}^T\tilde{\theta} \tag{25}$$

The time derivative of V is

$$\dot{V}=s\dot{s}-\frac{1}{\gamma}\tilde{\theta}^T\dot{\theta}+\frac{1}{\gamma}\tilde{\theta}^T\dot{\theta}^* \tag{26}$$

Substituting (19) and (24) into (26), and using the equality $\boldsymbol{w}^T(z)\tilde{\theta}=\tilde{\theta}^T\boldsymbol{w}(z)$, it follows that

$$\begin{aligned}\dot{V}=&-k_1 s^2-k_2 s\tanh(s/\varepsilon)+sg(\boldsymbol{x},\bar{u})\boldsymbol{w}^T(z)\tilde{\theta}+\frac{1}{\gamma}\tilde{\theta}^T\dot{\theta}^*\\&-g(\boldsymbol{x},\bar{u})N(\tau)\boldsymbol{w}^T(z)\tilde{\theta}\left(\dot{s}+k_1 s+k_2\tanh(s/\varepsilon)\right)\end{aligned} \tag{27}$$

From (24) one can obtain

$$\dot{s}+k_1 s+k_2\tanh(s/\varepsilon)=g(\boldsymbol{x},\bar{u})\boldsymbol{w}^T(z)\tilde{\theta} \tag{28}$$

Thus, (26) can be rewritten as

$$\begin{aligned}\dot{V}=&-k_1 s^2-k_2 s\tanh\left(\frac{s}{\varepsilon}\right)-\frac{N(\tau)}{g(\boldsymbol{x},\bar{u})}\left(\dot{s}+k_1 s+k_2\tanh\left(\frac{s}{\varepsilon}\right)\right)^2\\&+sg(\boldsymbol{x},\bar{u})\boldsymbol{w}^T(z)\tilde{\theta}+\frac{1}{\gamma}\tilde{\theta}^T\dot{\theta}^*\end{aligned} \tag{29}$$

Using (20) and the inequality

$$\begin{aligned}sg(\boldsymbol{x},\bar{u})\boldsymbol{w}^T(z)\tilde{\theta}&\le\frac{1}{4\eta}s^2+\eta\left(g(\boldsymbol{x},\bar{u})\boldsymbol{w}^T(z)\tilde{\theta}\right)^2\\&\le\frac{1}{4\eta}s^2+\eta\left(\dot{s}+k_1 s+k_2\tanh(s/\varepsilon)\right)^2\end{aligned} \tag{30}$$

Equation (29) can be bounded as

$$\dot{V}\le-\left(k_1-\frac{1}{4\eta}\right)s^2-k_2 s\tanh\left(\frac{s}{\varepsilon}\right)+\dot{\tau}-\frac{N(\tau)}{g(\boldsymbol{x},\bar{u})}\dot{\tau}+\frac{1}{\gamma}\tilde{\theta}^T\dot{\theta}^* \tag{31}$$

Now, we suppose that the following inequality holds

$$\begin{aligned}\left\|\tilde{\theta}^T\dot{\theta}^*\right\|&\le\kappa_1 s^2+\kappa_2\left(g(\boldsymbol{x},\bar{u})\boldsymbol{w}^T(z)\tilde{\theta}\right)^2+\delta^2\\&\le\kappa_1 s^2+\kappa_2\left(\dot{s}+k_1 s+k_2\tanh(s/\varepsilon)\right)^2+\delta^2\\&\le\kappa_1 s^2+\frac{\kappa_2}{\eta}\dot{\tau}+\delta^2\end{aligned} \tag{32}$$

where κ_1 and κ_2 are positive constants, and δ is a bounded square integrable function.

With (32), (33) can be upper bounded by

$$\begin{aligned}\dot{V}\le&-\left(k_1-\frac{1}{4\eta}-\frac{\kappa_1}{\gamma}\right)s^2-k_2 s\tanh\left(\frac{s}{\varepsilon}\right)\\&+\left(h(\boldsymbol{x})N(\tau)+c_1\right)\dot{\tau}+\frac{1}{\gamma}\delta^2\end{aligned} \tag{33}$$

with $c_1=1+\frac{\kappa_2}{\gamma\eta}$ and $h(\boldsymbol{x},\bar{u})=-1/\left(\eta g(\boldsymbol{x},\bar{u})\right)$.

Assuming that $k_1 > 1 \Big/ \left(\frac{1}{4\eta} + \frac{\kappa_1}{\gamma} \right)$, then by integrating (33) over $[0,t]$, one can obtain the following inequality

$$V(t) \le c_0 + \int_0^t \left(h(\zeta) N(\tau(\zeta)) + c_1 \right) \tau(\zeta) d\zeta \qquad (34)$$

where $c_0 = V(0) + \frac{1}{\gamma} \int_0^\infty \delta^2(t) dt$.

According to Assumption 1, we can consider $h(\cdot)$ as a time-varying parameter which takes values in the interval $I_h = \left[-(\eta \underline{g})^{-1}, -(\eta \overline{g})^{-1} \right]$ with $0 \notin I_h$. Thus, Using Lemma 1, we can conclude from (33) the boundedness of the signals $V(t)$, $N(t)$ and $\int_0^t \left(h(\zeta) N(\zeta) + c_1 \right) \dot{\tau}(\zeta) d\zeta$ for $t \in [0, t_f)$. According to [13], since no finite-time escape phenomenon may happen, then $t_f = \infty$. Therefore, $s(t)$, $\tilde{\theta}(t)$, $\boldsymbol{x}(t)$, and $u(t)$ are bounded. As an intermediate result, $s(t)$ is square integrable and $\dot{s}(t)$ is bounded. Moreover, by invoking Barbalat's lemma, we can conclude the asymptotic convergence of $s(t)$, which further implies the asymptotic convergence of the tracking error $e(t)$ and its first $(n-1)$ derivatives.

Remark 1: In this paper, since the signal $\dot{s}(t)$ in the adaptive laws (19) and (20) is not available for measurement, the following approximation is used $\dot{s}(t) \approx \left(s(t) - s(t - \Delta t) \right) \Big/ \Delta t$ where Δt is a small positive constant. Notice that because of the integral structure of adaptive laws (19) and (20), the noise effect will be considerably reduced.

IV. Simulation Results

To demonstrate the effectiveness of the above proposed adaptive controller, the following second-order nonlinear nonaffine system is used for simulation [7]

$$\begin{cases} \dot{x}_1 = x_2 \\ \dot{x}_2 = x_1^2 + 0.15u + 0.1\left(1 + x_2^2\right)u + \sin(0.1u) \end{cases} \qquad (35)$$

The control objective is to force the system output $y(t) = x_1(t)$ to track the desired trajectory $y_d(t) = \sin(t) + \cos(0.5t)$.

Within this simulation, the unknown ideal controller is approximated by a fuzzy system in the form of (15). The input variables of the fuzzy system are chosen as $\boldsymbol{z} = [x_1, x_2]^T$. For each variable z_i, $i = 1, 2$, five Gaussian membership functions are used with centers -1, -0.5, 0, 0.5 and 1, and a variance equal to 4.

In this simulation, the system initial conditions are $\boldsymbol{x}(0) = [0.1, 0]^T$, the adjustable parameters θ are initialized with zero values, and the design parameters are $\lambda = 1$, $k_1 = 0.5$, $k_2 = 0.5$, $\gamma = 0.1$, $\eta = 0.01$ and $\varepsilon_0 = 0.01$.

Simulation results for the case of an unknown control direction (where $\mathrm{sgn}\left(g(\boldsymbol{x}, u)\right) = 1$) are shown through Figs. 1 to 4. We can see that actual trajectories converge to the desired ones and that the control input signal is bounded.

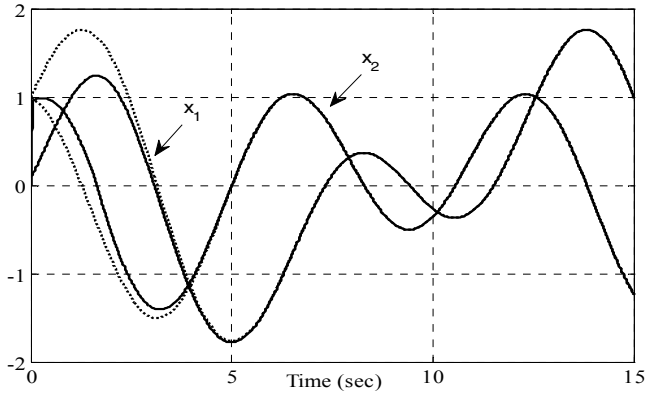

Fig. 1. Actual system trajectories (solid lines) and desired trajectories (dotted lines)

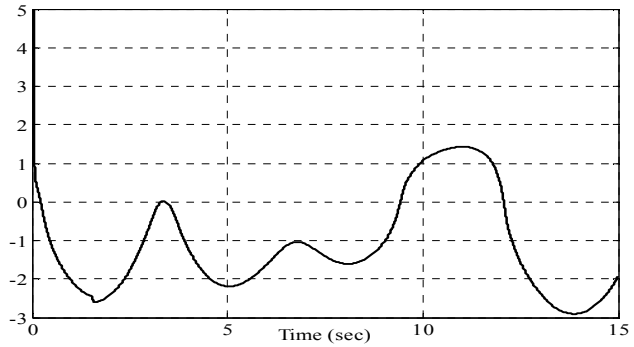

Fig. 2. Control input signal

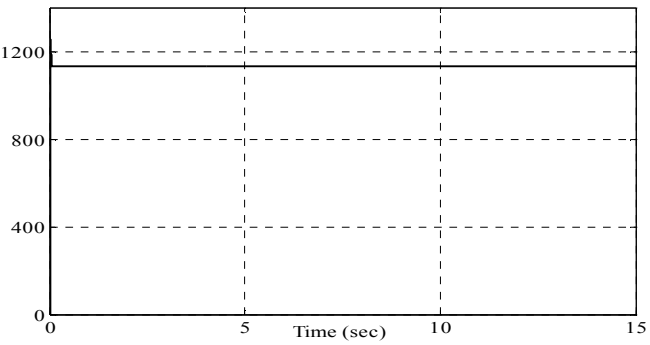

Fig. 3. Nussbaum function $N(\tau)$

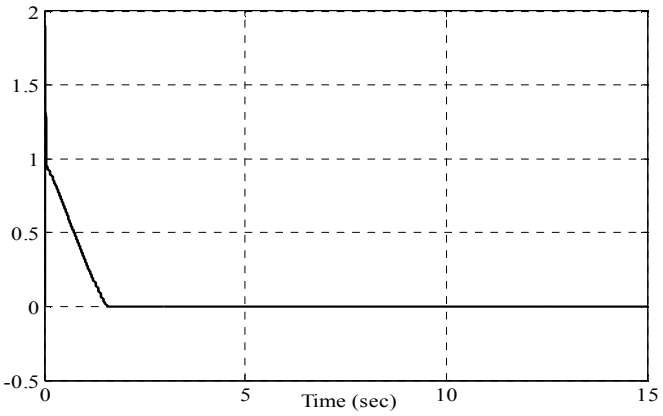

Fig. 4. Sliding surface $s(t)$

V. CONCLUSION

This paper proposed a stable direct adaptive fuzzy control scheme for a class of uncertain SISO nonaffine nonlinear systems with unknown control direction. The scheme consists of an adaptive fuzzy controller with its adaptive law. Within this scheme, a fuzzy system is used to construct adaptively an unknown ideal implicit controller, and its adjustable parameters are updated, by using the gradient descent method, in order to minimize the error between the unknown controller and the fuzzy controller. The parameters adaptation law incorporates a Nussbaum function in order to cope with the unknown control direction problem. Using the Lyapunov synthesis method, all signals in the closed-loop control system have been theoretically shown to be bounded and the tracking error has been shown to be asymptotically stable. Simulation results have verified the effectiveness of the proposed adaptive control approach.

REFERENCES

[1] L.X. Wang, *Adaptive Fuzzy Systems and Control: Design and Stability Analysis*, Prentice-Hall, Englewood Clifs, NJ, 1994.

[2] J.T. Spooner and K.M. Passino, "Stable adaptive control using fuzzy systems and neural networks," *IEEE Trans. Fuzzy Systems*, vol. 4, pp. 339-359, 1996.

[3] J. T. Spooner, M. Maggiore, R. Ordonez, and K. M. Passino, *Stable adaptive control and estimation for nonlinear systems*. John Wiley & Sons, 2002.

[4] S. Labiod and T.M. Guerra, "Direct adaptive fuzzy control for a class of MIMO nonlinear systems," *International Journal of Systems Science*, vol. 38, no. 8, pp. 665-675, 2007.

[5] S. Labiod, M.S. Boucherit, and T.M. Guerra, "Adaptive fuzzy control of a class of MIMO nonlinear systems," *Fuzzy Sets and Systems*, vol. 151, no. 1, pp. 59-77, 2005.

[6] N. Essounbouli and A. Hamzaoui, "Direct and indirect robust adaptive fuzzy controllers for a class of nonlinear systems," *International Journal of Control, Automation, and Systems*, vol. 4, no. 2, pp. 146-154, 2006.

[7] S. Labiod and T. M. Guerra, "Adaptive fuzzy control of a class of SISO nonaffine nonlinear systems," *Fuzzy Sets and Systems*, vol. 158, no. 10, pp. 1098-1126, 2007.

[8] C. P. Bechlioulis and G. A. Rovithakis, "Robust adaptive fuzzy control of nonaffine systems guaranteeing transient and steady state error bounds," 17th Mediterranean Conference on Control and Automation, pp. 862-867, 2009, Greece.

[9] X. Li, D. Wang, Z. Peng, G. Sun, "Adaptive fuzzy control for a class of non-affine systems," In Proc. International Conference on Intelligent Control and Information Processing (ICICIP), 2010.

[10] R. D. Nussbaum, "Some Remarks on the Conjecture in parameter Adaptive Control," *Systems Control Letter*, vol. 3, pp. 243-246, 1983.

[11] Ioannou and J. Sun, *Robust adaptive control*. Prentice Hall, Englewood Cliffs, NJ, 1996.

[12] L. Liu and J. Huang, "Global robust stabilization of cascade-connected systems with dynamic uncertainties without knowing the control direction," *IEEE Trans. Automat. Contr.*, vol. 51, pp. 1693-1699, 2006.

[13] L. Liu and J. Huang, "Global robust output regulation of lower triangular systems with unknown control direction," *Automatica*, vol. 44, pp. 1278–1284, 2008.

[14] X. Ye and J. Jiang, "Adaptive nonlinear design without a priori knowledge of control directions," *IEEE Trans. Automatic Control*, vol. 43, pp. 1617–1621, 1998.

[15] S. S. Ge, F. Hong, and T. H. Lee, "Adaptive neural control of nonlinear time-delay systems with unknown virtual control coefficients," *IEEE Trans. Syst., Man, Cybern. B*, vol. 34, no. 1, pp. 499-516, 2004.

[16] T.P. Zhang, and S.S. Ge, "Adaptive neural control of MIMO nonlinear state time-varying delay systems with unknown dead-zones and gain signs," *Automatica*, vol. 43, pp. 1021-1033, 2007.

[17] X. Li, D. Wang, Y. Yao, W. Lan, Z. Peng, G. Sun, Adaptive Fuzzy Control for a Class of Nonlinear Time-delay Systems with Unknown Control Direction, *In Proc. 29th Chinese Control Conference*, 2010, pp. 2593-2597.

[18] B. Ren, S.S. Ge, and T.H. Lee, "Adaptive NN control for a class of non-affine nonlinear systems with unknown control gain," *In Proc. 3rd IFAC Workshop on Advanced Fuzzy and Neural Control*, 2007, France.

[19] Y. J. Liu and Z. F. Wang, "Adaptive fuzzy controller design of nonlinear systems with unknown gain sign," *Nonlinear Dynamics*, vol. 58, pp. 687–695, 2009.

[20] B. Brogliato and R. Lozano, "Adaptive control of first-order nonlinear systems with reduced knowledge of the plant parameters," *IEEE Trans. on Automatic Control*, vol. 39, pp. 1764-1768, 1994.

[21] W. H. Dong, X. X. Sun and Y. Lin, "Variable Structure Model Reference Adaptive Control with Unknown High Frequency Gain Sign," *Acta Automatica Sinica*, vol. 33, no. 4, pp. 404-408, 2007.

[22] J. H. Park, S. H. Kim, and C. J. Moon, "Adaptive fuzzy controller for the nonlinear system with unknown sign of the input gain," *International Journal of Control, Automation, and Systems*, vol. 4, no.2, 178-186, 2006.

[23] S. Labiod and T. M. Guerra, "Indirect adaptive fuzzy control for a class of nonaffine nonlinear systems with unknown control directions," *International Journal of Control, Automation, and Systems*, vol. 8, no. 4, 903-907, 2010.

[24] J. Kaloust and Z. Qu, "Robust Control Design for Nonlinear Uncertain Systems with an Unknown Time-Varying Control Direction," *IEEE Trans. Automat. Contr.*, vol. 42, no. 3, 393-399, 1997.

[25] J.E. Slotine and W. Li, *Applied nonlinear control*. Prentice Hall, Englewood Cliffs, NJ, 1991.

2011 IEEE International Conference on Fuzzy Systems
June 27-30, 2011, Taipei, Taiwan

An Observer Based Adaptive Iterative Learning Control for Robotic Systems

Ying-Chung Wang
Department of Electronic Engineering
Huafan University
Taipei County, Taiwan
ycwang@cc.hfu.edu.tw

Chiang-Ju Chien
Department of Electronic Engineering
Huafan University
Taipei County, Taiwan
cjc@huafan.hfu.edu.tw

***Abstract*—In this paper, an observer based adaptive iterative learning control is proposed for robotic systems. Due to the joint velocities are assumed to be not measurable, a state observer is introduced to design the iterative learning controller. We first derive an observation error model based on an tracking error observer. Then we apply an averaging filter to design the ILC algorithm. A fuzzy neural learning component using a filtered fuzzy neural network is presented to solve the problem of unknown nonlinearities. A robust learning component using sliding-mode like design is used to overcome the uncertainties, including fuzzy neural approximation error and the error induced by using state estimation errors. We show that all the adjustable parameters as well as internal signals remain bounded for all iterations. Finally, the norm of output tracking error will asymptotically converge to a tunable residual set as iteration goes to infinity.**

***Index Terms*—adaptive iterative learning control; observer; robotic systems; filtered fuzzy neural network; averaging filter approach**

I. Introduction

Due to the repeatability of operation for robotic systems, it is suitable to perform the control task by using the technique of iterative learning control (ILC). The ILC is a non-model based learning approach which is very effective in dealing with repetitive control tasks. Based on the contraction mapping theory and a certain priori knowledge, the ILC algorithms for robotic systems were initially developed in [1]. In general, the most popular designs of the ILC algorithms for robotic system can be roughly classified into D-type ILC [1], [2] and P-type ILC [3], [4]. In D-type ILC, the acceleration error of joint variable is used to construct the learning controller. In order to guarantee the convergence of the learning systems, it is necessary to assume that the nonlinearity of the plant is Lipschitz in states. Although the condition is mild, the acceleration measurement is unfortunately not realizable in practice and becomes the major disadvantage of D-type ILC. On the other hand, P-type ILC uses only the velocity error for the design of updated learning function. Although the requirement of acceleration measurement is removed, more strict conditions on the plant are needed for technical analysis. Recently, adaptive iterative learning control (AILC) have been widely studied [5], [6] for robotic systems. In order to relax the restrict Lipschitz condition on the plant's nonlinearity, the Lyapunov-like approach is applied to analyze the stability and convergence instead of contraction mapping theory. However, both PID-type ILCs and AILCs require at least the joint velocities to develop the ILC algorithms. If only the measurement of joint positions is available, an observer is one of the possible choice to design the ILC.

Actually, observer based ILCs were developed in [7], [8] for a class of nonlinear systems. Same as the case of the most ILC works, the plant nonlinearities must be known or satisfy Lipschitz continuous condition in [7], [8]. In this paper, to solve the relative degree problem caused by the condition that joint velocities are not measurable, an s-domain transfer function technique is adopted to derive an output error model based on a tracking error observer. An averaging filter is then proposed for the controller design. Under the derived error model, a filtered FNN using state estimation vector as the network input is used to design a fuzzy neural learning component for approximation of the unknown nonlinearities. A robust learning component is also constructed to compensate for the uncertainties from approximation error and state estimation error. Based on a Lyapunov like analysis, we show that all the adjustable parameters and internal signals remain bounded during the learning process. Furthermore, the norm of output tracking error will asymptotically converge to a tunable residual set if iteration number is large enough.

In the subsequent discussions, the following notations will be used.

(1) $|\cdot|$ denotes the absolute value of a scalar or the Euclidean or any other consistent norm of a vector or matrix.
(2) $\|(\cdot)_t\|_\infty = \sup_{\tau \le t} |(\cdot)(\tau)|$ denotes the truncated L_∞ norm of the argument function or vector [10].
(3) $\|P(s)\|_\infty$ denotes the H_∞ norm of the transfer function $P(s)$.
(4) $G(s)[u]$ denotes the filtered version of u with any proper or strictly proper transfer function $G(s)$.

II. Problem Formulation

In this paper, we consider an uncertain robotic system with n rigid bodies which can perform a given task repeatedly over a finite time interval $[0, T]$ as follows:

$$D(q^j(t))\ddot{q}^j(t) + B(q^j(t), \dot{q}^j(t))\dot{q}^j(t) + F(q^j(t), \dot{q}^j(t)) = u^j(t) \quad (1)$$

where $j \in Z_+$ denotes the index of iteration number and $t \in [0,T]$ denotes the time index[1]. The signals $q^j, \dot{q}^j, \ddot{q}^j \in R^n$ are respectively the generalized joint position, joint velocity and joint acceleration vectors. $D(q^j) \in R^{n\times n}$ is the inertia matrix, $B(q^j,\dot{q}^j) \in R^{n\times n}$ is the centripetal plus Coriolis force vector, $F(q^j,\dot{q}^j) \in R^n$ is the gravitational plus frictional forces and $u^j \in R^n$ is the joint torque vector. It is noted the inertia matrix $D(q^j)$ is assumed to be positive definite and bounded for all $t \in [0,T]$ and iteration $j \geq 1$ as

$$0 < m_1 I \leq D(q^j) \leq m_2 I$$

where $m_1, m_2 > 0$ and I is an $n \times n$ identity matrix. Since the inverse of inertia matrix exists for all joint variables, the dynamic formulation of the robotic system can be written as follows,

$$\ddot{q}^j = -D^{-1}(q^j)\left[B(q^j,\dot{q}^j)\dot{q}^j + F(q^j,\dot{q}^j)\right] + D^{-1}(q^j)u^j \quad (2)$$

Let $f(q^j,\dot{q}^j) = D^{-1}(q^j)[B(q^j,\dot{q}^j)\dot{q}^j + F(q^j,\dot{q}^j)] \in R^n$ and $b(q^j) = D^{-1}(q^j) \in R^{n\times n}$ and choose the output variable as $y^j = q^j \in R^n$, state variable as $X^j = [x_1^{j\top}, x_2^{j\top}]^\top = [y^{j\top}, \dot{y}^{j\top}]^\top = [q^{j\top}, \dot{q}^{j\top}]^\top \in R^{2n}$, then we have

$$\begin{aligned} \dot{x}_1^j &= x_2^j \\ \dot{x}_2^j &= -f(X^j) + b(X^j)u^j \\ y^j &= x_1^j \end{aligned} \quad (3)$$

or equivalently in the following state-space form :

$$\begin{aligned} \dot{X}^j &= AX^j + B\left[-f(X^j) + b(X^j)u^j\right] \\ y^j &= C^\top X^j \end{aligned} \quad (4)$$

where

$$A = \begin{bmatrix} 0 & I \\ 0 & 0 \end{bmatrix},\ B = \begin{bmatrix} 0 \\ I \end{bmatrix},\ C = \begin{bmatrix} I \\ 0 \end{bmatrix},$$

Here $0 < b(X^j) \leq m_1^{-1} I$. In this paper, we assume that only joint position y^j is measurable for controller design. Let the desired state trajectory be defined as $X_d = [y_d^\top, \dot{y}_d^\top]^\top$. Now, given a specified desired output trajectory y_d, $t \in [0,T]$ and a possible initial resetting error $y_d(0) \neq y^j(0)$ for all $j \geq 1$, the control objective for the robotic systems doing a repeatable task is to force the system output y^j to follow y_d as close as possible.

III. Derivations of Error Model and Controller

A. Derive the Error Model

Define the output error as $e^j = y_d - y^j$ and the state tracking error vector as $E^j = X_d - X^j = \left[e^{j\top}, \dot{e}^{j\top}\right]^\top \in R^{2n}$, then we can derive $\ddot{e}^j$ as follows,

$$\begin{aligned} \ddot{e}^j &= \ddot{y}_d + f(X^j) - b(X^j)u^j \\ &= -K_c^\top E^j + f(X^j) + \ddot{y}_d + K_c^\top E^j - b(X^j)u^j \end{aligned} \quad (5)$$

[1]the time index t will be omitted unless otherwise specified.

where $K_c = [k_2^c I, k_1^c I]^\top \in R^{2n\times n}$ is the feedback gain matrix such that the characteristic polynominal of $A_c = A - BK_c^\top$ is Hurwitz. Therefore, the tracking error dynamics will satisfy

$$\begin{aligned} \dot{E}^j &= A_c E^j + B\Big(f(X^j) + \ddot{y}_d + K_c^\top E^j - b(X^j)u^j\Big) \\ &= A_c E^j + B\Big(f(X^j) + \ddot{y}_d + K_c^\top X_d - K_c^\top X^j \\ &\quad - u^j + (1 - b(X^j))u^j\Big) \\ &= A_c E^j + B\Big(h(X^j) + \alpha - u^j + (1 - b(X^j))u^j\Big) \\ e^j &= C^\top E^j \end{aligned} \quad (6)$$

where $h(X^j) \equiv f(X^j) - K_c^\top X^j$, $\alpha \equiv \ddot{y}_d + K_c^\top X_d$. Note that the state tracking error vector E^j in the tracking error dynamics (6) is not assumed to be available for measurement. Hence, it is necessary to construct a state estimation vector $\widehat{X}^j = [\widehat{x}^{j\top}, \dot{\widehat{x}}^{j\top}]^\top \in R^{2n} \times [0,T]$ for estimation of the state vector. In order to construct a state estimation vector, we define a state tracking error estimation vector $\widehat{E}^j$ as

$$\widehat{E}^j = X_d - \widehat{X}^j = [\widehat{e}^{j\top}, \dot{\widehat{e}}^{j\top}]^\top \in R^{2n} \times [0,T]$$

The tracking error observer is designed as

$$\begin{aligned} \dot{\widehat{E}}^j &= A_c \widehat{E}^j + K_o(e^j - \widehat{e}^j) \\ \widehat{e}^j &= C^\top \widehat{E}^j \end{aligned} \quad (7)$$

where $K_o = [k_1^o I, k_2^o I]^\top \in R^{2n\times n}$ is the observer gain vector such that the characteristic polynomial of $A_o = A_c - K_o C^\top$ is Hurwitz. If we further define the observation error vector as $\widetilde{E}^j = E^j - \widehat{E}^j$, the observation error dynamics can be derived by using (6) and (7) as follows

$$\begin{aligned} \dot{\widetilde{E}}^j &= A_o \widetilde{E}^j + B\Big(h(X^j) + \alpha - u^j + (1 - b(X^j))u^j\Big) \\ \widetilde{e}^j &= C^\top \widetilde{E}^j \end{aligned} \quad (8)$$

Based on the universal approximation theorem, we know that the nonlinear function $h(X^j)$ can be approximated by an FNN [9] $O^{(4)}(X^j, W^j) = W^{j\top} O^{(3)}(X^j)$. Here $O^{(3)}(X^j) \in \mathcal{R}^M$ is the basis function vector with M being the number of rule nodes and W is the weight matrix of the output layer. According to the universal approximation theorem, there will exist an optimal weight matrix W^* such that $h(X^j) = O^{(4)}(X^j, W^*) + \epsilon^j = W^{*\top} O^{(3)}(X^j) + \epsilon^j$, where ϵ^j is the approximation error satisfying $|\epsilon^j| \leq \epsilon^*$ in a certain compact set. This implies that (8) can be rewritten as

$$\begin{aligned} \dot{\widetilde{E}}^j &= A_o \widetilde{E}^j + +B\Big(W^{*\top} O^{(3)}(X^j) + \epsilon^j + \alpha - u^j \\ &\quad + (1 - b(X^j))u^j\Big) \\ &= A_o \widetilde{E}^j + +B\Big(W^{*\top} O^{(3)}(\widehat{X}^j) - u^j + \delta^j \\ &\quad + (1 - b(X^j))u^j\Big) \\ \widetilde{e}^j &= C^\top \widetilde{E}^j \end{aligned} \quad (9)$$

where $\delta^j = W^{*\top}\Big(O^{(3)}(X^j) - O^{(3)}(\widehat{X}^j)\Big) + \epsilon^j + \alpha$ is the lumped uncertainty term which includes the difference between

FNN network with input using state and estimated state, the network approximation error and the desired state trajectory. It is easily proven that the lumped uncertainty term satisfying $|\delta^j| \leq \delta^*$. However, it is noted that the value of the unknown constant δ^* might be large.

To see how to design the iterative learning controller u^j to achieve the control objective, we now adopt the mixed use of a time signal and a Laplace transfer function to obtain the explicit expression of $\widetilde{e}^j$ in (9) in time domain with a filtered version as follows,

$$\widetilde{e}^j = H(s)\Big[W^{*\top}O^{(3)}(\widehat{X}^j) - u^j + \delta^j + (1 - b(X^j))u^j\Big] \quad (10)$$

where $H(s) = C^\top(sI - A_o)^{-1}B = \frac{1}{s^2+(k_1^c+k_1^o)s+(k_1^ck_1^o+k_2^ck_2^o)}$. The observer gain vector $K_o = [k_1^oI, k_2^oI]^\top$ is chosen such that $H(s) = \frac{1}{\ell(s)L(s)}$ with $\ell(s) = s + \lambda$ and $L(s)$ being any Hurwitze polynomial of order 1. Then (10) can be rewritten as

$$\begin{aligned}\widetilde{e}^j &= H(s)L(s)\Big[W^{*\top}\frac{1}{L(s)}\big[O^{(3)}(\widehat{X}^j)\big] - \frac{1}{L(s)}\big[u^j\big] \\ &\quad + \frac{1}{L(s)}\big[(1 - b(X^j))u^j + \delta^j\big]\Big] \\ &= \frac{1}{\ell(s)}\Big[W^{*\top}\xi^j - \frac{1}{L(s)}\big[u^j\big] + \delta_L^j\Big] \end{aligned} \quad (11)$$

where $\xi^j = \frac{1}{L(s)}[O^{(3)}(\widehat{X}^j)]$ and $\delta_L^j = \frac{1}{L(s)}[(1 - b(X^j))u^j + \delta^j]$.

B. Construct Some Useful Signals

According to the filtered version of output tracking error model (11), we define an augmented signal with filtered version as

$$y_a^j = \frac{1}{\ell(s)}\left[v^j - \frac{1}{L(s)}\Big[u^j\Big]\right],\ y_a^j(0) = 0 \quad (12)$$

where v^j is an auxiliary input to be designed later. Then, design an auxiliary error signal as

$$e_a^j = \widetilde{e}^j - y_a^j \quad (13)$$

The initial condition $e_a^j(0)$ will satisfy $|e_a^j(0)| = |\widetilde{e}^j(0) - y_a^j(0)| = |\widetilde{e}^j(0)| \equiv \varepsilon^j$. Substituting (11) and (12) into (13), we can find that

$$e_a^j = \widetilde{e}^j - y_a^j = \frac{1}{\ell(s)}\Big[W^{*\top}\xi^j - v^j + \delta_L^j\Big] \quad (14)$$

It is noted that we apply the Laplace operation to derive the tracking error model (14) for technical analysis later as that used in the traditional model reference adaptive control [10]. The equivalent time-domain state space representation of (14) is

$$\dot{e}_a^j = -\lambda e_a^j + W^{*\top}\xi^j - v^j + \delta_L^j \quad (15)$$

In order to overcome the uncertainty from initial output tracking error, a new signal e_ϕ^j is introduced as follows,

$$e_\phi^j = e_a^j - \phi^j\mathbf{sat}\left(\frac{e_a^j}{\phi^j}\right),\ \phi^j = \varepsilon^j e^{-\lambda t} \quad (16)$$

where $\mathbf{sat}(\frac{e_a^j}{\phi^j}) = [\mathbf{sat}(\frac{e_{a,1}^j}{\phi^j}), \cdots, (\frac{e_{a,n}^j}{\phi^j})]^\top \in R^n$ and

$$\mathbf{sat}\left(\frac{e_{a,i}^j}{\phi^j}\right) = \begin{cases} 1 & \text{if } e_{a,i}^j > \phi^j \\ \frac{e_{a,i}^j}{\phi^j} & \text{if } |e_{a,i}^j| \leq \phi^j,\ i = 1, \cdots, n \\ -1 & \text{if } e_{a,i}^j < -\phi^j \end{cases}$$

and ϕ^j is the width of boundary layer. Note that ϕ^j is designed to decrease along time axis with the initial condition chosen as $\phi^j(0) = \varepsilon^j$ for jth iteration and $0 < \varepsilon^j e^{-\lambda T} \leq \phi^j \leq \varepsilon^j, \forall t \in [0, T], j \geq 1$. According to (16), it is easy to show that $e_\phi^j(0) = 0, \forall j \geq 1$. Now let us differentiate $\frac{1}{2}e_\phi^{j\top}e_\phi^j$ as follows,

$$\begin{aligned}\frac{1}{2}\frac{d}{dt}e_\phi^{j\top}e_\phi^j &= e_\phi^{j\top}\dot{e}_\phi^j \\ &= e_\phi^{j\top}\Big(\dot{e}_a^j - \mathbf{sgn}\Big(e_\phi^j\Big)\dot{\phi}^j\Big) \\ &= e_\phi^{j\top}\Big\{-\lambda e_a^j - \mathbf{sgn}\Big(e_\phi^j\Big)\dot{\phi}^j\Big\} \\ &\quad + e_\phi^{j\top}\Big\{W^{*\top}\xi^j - v^j + \delta_L^j\Big\} \\ &= -\lambda e_\phi^{j\top}e_\phi^j + e_\phi^{j\top}\Big\{W^{*\top}\xi^j - v^j + \delta_L^j\Big\} \end{aligned} \quad (17)$$

where $\mathbf{sgn}(e_\phi^j) = [\mathbf{sgn}(e_{\phi,1}^j), \cdots, \mathbf{sgn}(e_{\phi,n}^j)]^\top$ is the typical signum function vector. In the following, we will show that the uncertainty term δ_L^j in (11) can be bounded in a linearly parameterized form if the following normalization signal m^j [11] is utilized

$$m^j = \frac{\delta_2}{s + \delta_1}\Big[1 + \big|u^j\big|\Big],\quad m^j(0) > \frac{\delta_2}{\delta_1} \quad (18)$$

where $\delta_1, \delta_2 > 0$ and $\delta_1 < \delta^*$. Here δ^* is the least positive constant such that $\frac{1}{L(s-\delta^*)}$ is a stable system. In practical, δ_1 can be chosen as small as possible. Note that $1 - b(X^j)$, α and δ^j are bounded and $\frac{1}{L(s)}$ is a strictly proper stable transfer function. This implies that

$$\Big|\delta_L^j\Big| \leq \theta_1^* m^j + \theta_2^* = [\theta_1^*, \theta_2^*]\begin{bmatrix} m^j \\ 1 \end{bmatrix} \equiv \theta^{*\top}Y^j \quad (19)$$

for some positive constants θ_1^*, θ_2^*.

C. Design the Iterative Learning Controller Using Filtered FNN

Based on the derived error model and the useful signals, we design u^j and v^j as follows

$$u^j = \frac{L(s)}{F^{n-1}(\tau s)}[v^j] \quad (20)$$

$$v^j = W^{j\top}\xi^j + \mathbf{sat}\left(\frac{e_a^j}{\phi^j}\right)\theta^{j\top}Y^j + e_\phi^jY^{j\top}Y^j \quad (21)$$

where W^j is the weight matrix of the network and θ^j is control parameter vector which are used to compensate for the unknown W^* and θ^* respectively. Furthermore, $F(\tau s) = (\tau s + 1)^2$ with $\tau > 0$ being a small constant. In the literature, $\frac{1}{F(\tau s)}$ is referred to as an *averaging filter*, which is obviously a low-pass filter whose bandwidth can be arbitrarily enlarged

as τ approaches 0. If we define the parameter error as $\widetilde{W} = W^j - W^*$ and $\widetilde{\theta}^j = \theta^j - \theta^*$ and substitute (21) into (17), we have the following error dynamics for technical analysis later,

$$\begin{aligned}
&\frac{1}{2}\frac{d}{dt}e_\phi^{j\top}e_\phi^j \\
&= -\lambda(e_\phi^j)^2 + e_\phi^j\Big\{-\widetilde{W}^{j\top}\xi^j - \mathbf{sat}\left(\frac{e_a^j}{\phi^j}\right)\theta^{j\top}Y^j \\
&\quad - e_\phi^j Y^{j\top}Y^j + \delta_L^j\Big\} \\
&\leq -\lambda(e_\phi^j)^2 - e_\phi^j\widetilde{W}^{j\top}\xi^j - \Big|e_\phi^j\Big|\widetilde{\theta}^{j\top}Y^j - (e_\phi^j)^2 Y^{j\top}Y^j
\end{aligned} \tag{22}$$

A set of stable adaptive laws is necessary to tune the control parameters. The adaptive laws combining time domain and iteration domain adaptation without knowledge of known bounds on optimal parameters or deadzone mechanism are proposed as follows,

$$(1-\gamma_1)\dot{W}^j = -\gamma_1 W^j + \gamma_1 W^{j-1} + \beta_1 e_\phi^j \xi^j \tag{23}$$

$$(1-\gamma_2)\dot{\theta}^j = -\gamma_2\theta^j + \gamma_2\theta^{j-1} + \beta_2|e_\phi^j|Y^j \tag{24}$$

with $W^j(0) = W^{j-1}(T), \theta^j(0) = \theta^{j-1}(T)$ for $j \geq 1$, and $0 < \gamma_1, \gamma_2 < 1$, $\beta_1, \beta_2 > 0$. In these adaptive laws, γ_1, γ_2 and β_1, β_2 are defined as the weighting gains and adaptation gains, respectively. The setting of initial network parameter vector W^0 and θ^0 are specified in [12].

IV. Analysis of Stability and Convergence

To prove the stability and convergence of the proposed learning system, we first give the following two facts.

• **Fact 1** : Choose a Lyapunov-like positive function as

$$V_a^j = \frac{1}{2}e_\phi^{j\top}e_\phi^j + \frac{(1-\gamma_1)}{2\beta_1}tr\Big\{\widetilde{W}^{j\top}\widetilde{W}^j\Big\} + \frac{(1-\gamma_2)}{2\beta_2}\widetilde{\theta}^{j\top}\widetilde{\theta}^j$$

and compute its derivative with respective to time t, we have the following result by using similar technique in [12] as

$$\dot{V}_a^j \leq -kV_a^j + \bar{k}^{j-1} \tag{25}$$

where $k = \min\{2\bar{\lambda}, \frac{\gamma_1}{1-\gamma_1}, \frac{\gamma_2}{1-\gamma_2}\}$, and $\bar{k}^{j-1} = \frac{\gamma_1}{2\beta_1}tr\Big\{\widetilde{W}^{j-1\top}\widetilde{W}^{j-1}\Big\} + \frac{\gamma_2}{2\beta_2}\widetilde{\theta}^{j-1\top}\widetilde{\theta}^{j-1}$. It is noted that $\bar{W}^0 = W^0 - W^* = W^{ini} - W^* \equiv \bar{W}^0$ and $\widetilde{\theta}^0 = \theta^0 - \theta^* = \theta^{ini} - \theta^* \equiv \bar{\theta}^0$ are bounded for all $t \in [0, T]$ so that if $j = 1$, (25) can be rewritten as

$$\begin{aligned}
\dot{V}_a^1 &\leq -kV_a^1 + \bar{k}^0 \\
&= -kV_a^1 + \frac{\gamma_1}{2\beta_1}tr\Big\{\bar{W}^{0\top}\bar{W}^0\Big\} + \frac{\gamma_2}{2\beta_2}\bar{\theta}^{0\top}\bar{\theta}^0
\end{aligned} \tag{26}$$

Note that the initial value $V_a^1(0)$ is bounded since $e_\phi^1(0) = 0$, $\widetilde{W}^1(0) = W^1(0) - W^* = W^0(T) - W^* = \bar{W}^0$, and $\widetilde{\theta}^1(0) = \theta^1(0) - \theta^* = \theta^0(T) - \theta^* = \bar{\theta}^0$. Together with the result of (26), it readily implies $V_a^1, e_\phi^1, \widetilde{W}^1, \widetilde{\theta}^1, W^1, \theta^1 \in L_{\infty e}[0, T]$. Since the basis function vector $O^{(3)^j}$ is bounded for all $j \geq 1$, we conclude that e_a^1 (by (16)) and $\dot{W}^1$ (by 23) $\in L_{\infty e}[0, T]$.

• **Fact 2** : Define a positive function $V^j(T)$ as

$$\begin{aligned}
V^j(T) &= \int_0^T \left[\frac{\gamma_1}{2\beta_1}\widetilde{W}^{j\top}\widetilde{W}^j + \frac{\gamma_2}{2\beta_2}\widetilde{\theta}^{j\top}\widetilde{\theta}^j\right]dt \\
&\quad + \frac{(1-\gamma_1)}{2\beta_1}tr\Big\{\widetilde{W}^j(T)^\top\widetilde{W}^j(T)\Big\} \\
&\quad + \frac{(1-\gamma_2)}{2\beta_2}\widetilde{\theta}^j(T)^\top\widetilde{\theta}^j(T)
\end{aligned} \tag{27}$$

Using the technique of integration by parts, we can show that

$$\begin{aligned}
&V^j(T) - V^{j-1}(T) \\
&\leq \int_0^T \left(e_\phi^{j\top}\widetilde{W}^{j\top}\xi^j + |e_\phi^j|\widetilde{\theta}^{j\top}Y^j\right)dt
\end{aligned} \tag{28}$$

Integrating both side of (22) from 0 to T gives

$$\begin{aligned}
&\int_0^T \left(e_\phi^{j\top}\widetilde{W}^{j\top}\xi^j + |e_\phi^j|\widetilde{\theta}^{j\top}Y^j\right)dt \\
&\leq -\int_0^T \left(\lambda e_\phi^{j\top}e_\phi^j + e_\phi^{j\top}e_\phi^j Y^{j\top}Y^j\right)dt \\
&\quad - \frac{1}{2}e_\phi^{j\top}(T)e_\phi^j(T)
\end{aligned} \tag{29}$$

where we use the property of $\frac{1}{2}e_\phi^{j\top}(0)e_\phi^j(0) = 0$. Substituting (29) into (28), it yields

$$\begin{aligned}
&V^j(T) - V^{j-1}(T) \\
&\leq -\frac{1}{2}e_\phi^{j\top}(T)e_\phi^j(T) - \int_0^T \left(\lambda e_\phi^{j\top}e_\phi^j + e_\phi^{j\top}e_\phi^j Y^{j\top}Y^j\right)dt
\end{aligned} \tag{30}$$

Since $V^1(T)$ is bounded by **Fact 1** and $V^j(T)$ is positive and monotonically decreasing, we conclude by the result of (30) that $V^j(T)$ is bounded for all $j \geq 1$ and will converge as j approaches infinity to some limit value V_T which is independent of j. Furthermore, (30) also implies

$$\int_0^T e_\phi^{j\top}e_\phi^j Y^{j\top}Y^j dt \leq V^{j-1}(T) - V^j(T) \leq V^1(T) \tag{31}$$

$$\int_0^T \lambda e_\phi^{j\top}e_\phi^j dt \leq V^{j-1}(T) - V^j(T) \leq V^1(T) \tag{32}$$

$$\frac{1}{2}e_\phi^{j\top}(T)e_\phi^j(T) \leq V^{j-1}(T) - V^j(T) \leq V^1(T) \tag{33}$$

It follows that $\widetilde{W}^j(T)$, $\widetilde{\theta}^j(T)$ and $e_\phi^{j\top}(T)e_\phi^j(T)$ are bounded for all $j \geq 1$. Furthermore, $\lim_{j\to\infty}\int_0^T e_\phi^{j\top}e_\phi^j dt = 0$, and $\lim_{j\to\infty} e_\phi^{j\top}(T)e_\phi^j(T) = 0$.

Lemma 1 : Consider the robotic system (1) performing a repetitive control task. If we apply the output based fuzzy neural adaptive iterative learning controller (12), (13), (16), (18), (20), and (21) with adaptation laws (23) and (24), then we ensure that all the internal signals are bounded, i.e., e_ϕ^j, e_a^j, $\widetilde{e}^j$, y_a^j, $\widehat{e}^j$, e^j, $\widetilde{E}^j$, $\widehat{E}^j$, E^j, W^j, θ^j, u^j, $\dot{W}^j$, $\dot{\theta}^j \in L_{\infty e}[0, T]$.

Proof : Integrating (25) from 0 to t, we have

$$\begin{aligned}
V_a^j &\leq V_a^j(0) + \int_0^t \bar{k}^{j-1}(z)dz \\
&\leq V_a^j(0) + \int_0^T \bar{k}^{j-1}(t)dt
\end{aligned} \tag{34}$$

Then we can conclude that $V_a^j, e_\phi^j, W^j, \theta^j, e_a^j, \dot{W}^j \in L_{\infty e}[0,T]$ by using Fact 2.

However, the boundedness of $V_a^j, e_\phi^j, \widetilde{W}^j, \widetilde{\theta}^j, e_a^j, \dot{W}^j$ can not guarantee the boundedness of Y^j (or equivalently m^j) and input u^j. In order to show the boundedness of Y^j for all $t \in [0,T]$, we first note that the boundedness of $\int_0^T \gamma \widetilde{e}_\phi^{j\top} \widetilde{e}_\phi^j Y^{1\top} Y^1 dt$ are then established from (31). Furthermore, since $\int_0^t e_\phi^{j\top} e_\phi^j Y^{j\top} Y^j dz \leq \int_0^T e_\phi^{j\top} e_\phi^j Y^{j\top} Y^j dt$, it implies that $\int_0^t e_\phi^{j\top} e_\phi^j Y^{j\top} Y^j dz \in L_{\infty e}[0,T]$. But the boundedness of e_ϕ^j and $\int_0^t e_\phi^{j\top} e_\phi^j Y^{j\top} Y^j dz$ only ensure that Y^j is bounded everywhere except on a set of measure zero. Now we adopt some techniques given in chapter 2 of [10]. Consider u^j in (20),

$$\begin{aligned} u^j &= \frac{L(s)}{F^{n-1}(\tau s)}[v^j] \\ &= \frac{L(s)}{F^{n-1}(\tau s)}\left[W^{j\top}\xi^j + \mathbf{sat}\left(\frac{e_a^j}{\phi^j}\right)\theta^{j\top} Y^j\right] \\ &\quad + \frac{sL(s)}{F^{n-1}(\tau s)}\left[\int_0^t e_\phi^j Y^{j\top} Y^j dz\right] \end{aligned} \tag{35}$$

Since W^j, ξ^j, θ^j and $\int_0^t e_\phi^j Y^{j\top} Y^j dz$ are bounded for $t \in [0,T]$, and $\frac{L(s)}{F^{n-1}(\tau s)}$, $\frac{sL(s)}{F^{n-1}(\tau s)}$ are strictly proper stable transfer functions, (35) implies that u^j will satisfy

$$|u^j| \leq k_1 \|(Y^j)_t\|_\infty + k_1 \leq k_2 |(m^j)_t|_\infty + k_2 \tag{36}$$

for some $k_1, k_2 > 0$ by lemma 2.6 (output is bounded by truncated L_∞ norm of input for a stable linear system) in [10]. Now we construct an extended dynamic equation by using (**??**), (8) and (18) as follows :

$$\begin{aligned} &\begin{bmatrix} \dot{E}^j \\ \dot{m}^j \end{bmatrix} \\ &= \begin{bmatrix} A_c & 0 \\ 0 & -\delta_1 \end{bmatrix}\begin{bmatrix} E^j \\ m^j \end{bmatrix} \\ &\quad + \begin{bmatrix} B \\ 0 \end{bmatrix}\Big(-b(X^j)u^j + W^{*\top} O^{(3)}(\widehat{X}^j) + \delta^j \Big) \\ &\quad + \begin{bmatrix} 0 \\ \delta_2\left(1 + |u^j|\right) \end{bmatrix} \end{aligned} \tag{37}$$

Let X_a^j be the state vector of the extended dynamic equation (37). Taking norms on (37) will yield

$$\|\dot{X}_a^j\| \leq k_3 \|X_a^j\| + k_3 |u^j| + k_3 \leq k_4 \|(X_a^j)_t\|_\infty + k_4 \tag{38}$$

for some $k_3, k_4 > 0$. This implies that X_a^j is regular [10] so that X_a^j and hence, E^j, m^j can grow at most exponentially fast and no finite time escape during a finite time interval $[0,T]$. This condition guarantees a certain degree of smoothness of signal m^j. Therefore, we show that Y^j is a certain degree of smooth signal. Together with the result of $\int_0^t e_\phi^j Y^{j\top} Y^j dz \in L_{\infty e}[0,T]$, we can conclude that $Y^j \in L_{\infty e}[0,T]$. Due to $W^j, \xi^j, \theta^j, Y^j, e_\phi^j \in L_{\infty e}[0,T]$, this also implies that $v^j \in L_{\infty e}[0,T]$ (by (21)). Because $e_\phi^j, W^j, \theta^j, \xi^j, Y^j \in L_{\infty e}[0,T]$, we conclude that $\dot{W}^j(t)$ (by 23)), $\dot{\theta}^j(t)$ (by 24) $\in L_{\infty e}[0,T]$. Since $v^j \in L_{\infty e}[0,T]$ and $\frac{L(s)}{F^{n-1}(s)}$ is a proper stable transfer function, this implies that $u^j \in L_{\infty e}[0,T]$ (by (20)). Since $v^j, u^j \in L_{\infty e}[0,T]$, $\frac{1}{L(s)}$ and $\frac{1}{\ell(s)}$ are strictly proper stable transfer functions, this implies that $y_a^j \in L_{\infty e}[0,T]$ (by (12)). As noted above, $e_a^j, y_a^j \in L_{\infty e}[0,T]$, we have $\widetilde{e}^j \in L_{\infty e}[0,T]$ (by (13)). Moreover, because A_c is a Hurwitz matrix and $\widetilde{e}^j \in L_{\infty e}[0,T]$, this implies that $\widehat{e}^j, \widehat{E}^j \in L_{\infty e}[0,T]$ (by (7)). Finally, since A_c and A_o are Hurwitz matrices and $-b(X^j)u^j + W^{*\top} O^{(3)}(\widehat{X}^j) + \delta^j \in L_{\infty e}[0,T]$, we have $\widetilde{e}^j, \widetilde{E}^j \in L_{\infty e}[0,T]$ (by (8)) and $e^j, E^j \in L_{\infty e}[0,T]$ (by (6)). This completes the proof. Q.E.D.

Based on **Fact 1, Fact 2** and **Lemma 1**, we now get the main result of this learning system.

Theorem 1 : Consider the system set-up in Lemma 1. The proposed adaptive iterative learning controller guarantees the tracking performance and system stability as follows :

(T1) $\lim_{j\to\infty} e_\phi^j(t)^\top e_\phi^j(t) = 0$, for all $t \in [0,T]$.

(T2) $\lim_{j\to\infty} |e_a^j(t)| \leq e^{-\lambda t}\varepsilon^\infty$, for all $t \in [0,T]$.

(T3) $\lim_{j\to\infty} |e^j(t)| \leq e^{-\lambda t}\varepsilon^\infty + \tau k_6$, for all $t \in [0,T]$.

(T4) Let δ be the positive constant such that $\Delta(D-\delta)$ is still a Hurwitz polynomial, then $\lim_{j\to\infty} |\widehat{e}^j(t)| = |\widehat{e}^\infty(t)| \leq m_2\left(\varepsilon^\infty \frac{e^{-\lambda t} - e^{-\delta t}}{\delta - \lambda} + \tau k_6 \frac{1 - e^{-\delta t}}{\delta}\right)$, for all $t \in [0,T]$.

(T5) $\lim_{j\to\infty} |e^j(t)| = |e^\infty(t)| \leq e^{-\lambda t}\varepsilon^\infty + \tau k_6 + m_2\left(\varepsilon^\infty \frac{e^{-\lambda t} - e^{-\delta t}}{\delta - \lambda} + \tau k_6 \frac{1 - e^{-\delta t}}{\delta}\right)$, for all $t \in [0,T]$.

Proof : Based on Fact 1, Fact 2 and Lemma 1, then we can conclude the result of (T1) and (T2). For (T3), Substituting (20) into (12), we can find that e_a^j actually satisfies

$$\begin{aligned} e_a^j &= \widetilde{e}^j - y_a^j \\ &= \widetilde{e}^j - \frac{1}{\ell(s)}\left(1 - \frac{1}{F^{n-1}(\tau s)}\right)\left[v^j\right] \\ &\triangleq \widetilde{e}^j - R^j \end{aligned} \tag{39}$$

Since v^j is bounded and the H_∞ norm of $\|\frac{1}{s}(1 - \frac{1}{F^{n-1}(\tau s)})\|_\infty = 2(n-1)\tau$ and $\|\frac{s}{\ell(s)}\|_\infty = k_5$ for some $k_5 > 0$, we can conclude that

$$|R^j| \leq \left\|\frac{1}{s}\Big(1 - \frac{1}{F^{n-1}(\tau s)}\Big)\right\|_\infty \left\|\frac{s}{\ell(s)}\right\|_\infty \|(v^j)_t\|_\infty \leq \tau k_6$$

for some $k_6 > 0$. Taking norms on (39), we find that

$$|\widetilde{e}^j| \leq |e_a^j| + |R^j| \leq |e_a^j| + \tau k_6$$

As iteration goes to infinity,

$$\lim_{j\to\infty} |\widetilde{e}^j| \leq e^{-\lambda t}\varepsilon^\infty + \tau k_6 \leq \phi^\infty + \tau k_6$$

Finally, we apply a similar technique in [13], (T4) and (T5) are achieved.

V. Simulation Example

In this example, we apply the observer based adaptive iterative learning controller to robotic system [14]

$$\begin{bmatrix} D_{11} & D_{12} \\ D_{21} & D_{22} \end{bmatrix}\begin{bmatrix} \ddot{q}_1^j \\ \ddot{q}_2^j \end{bmatrix} + \begin{bmatrix} -h\dot{q}_2^j & -h(\dot{q}_1^j + \dot{q}_2^j) \\ h\dot{q}_1^j & 0 \end{bmatrix}\begin{bmatrix} \dot{q}_1^j \\ \dot{q}_2^j \end{bmatrix} = \begin{bmatrix} u_1^j \\ u_2^j \end{bmatrix}$$

where $D_{11} = m_1 l_{c1}^2 + m_2(l_1^2 + l_{c2}^2 + 2l_1 l_{c2}\cos(q_2^j)) + I_1 + I_2$, $D_{12} = D_{21} = m_2 l_1 l_{c2}\cos(q_2^j) + m_2 l_{c2}^2 + I_2$, $H_{22} = m_2 l_{c2}^2 + I_2$, $h = m_2 l_1 l_{c2}\sin(q_2^j)$. Here m_i, I_i, l_i and l_{c_i} represent mass, inertia, length of link i, and the distance from the previous joint to the center of mass of link i, respectively. In this simulation, $m_1 = 10$kg, $m_2 = 5$kg, $l_1 = 1$m, $l_2 = 0.5$m, $l_{c1} = 0.5$m, $l_{c2} = 0.25$m, $I_1 = 0.83$kg-m^2 and $I_2 = 0.3$kg-m^2. The control objective is to let $q^j = [q_1^j, q_2^j]^\top$ track the desired trajectory $q_d = [q_{d1}, q_{d2}]^\top = [\sin(t), \cos(t)]^\top$ as close as possible over a finite time interval $[0, 15]$ when only the angular position q^j is measurable. In this simulation, we set $\lambda = 10$, $\gamma_1 = \gamma_2 = 0.5$ and $\beta_1 = \beta_2 = 10$. In this simulation, we assume that the initial output for the first five iterations : $q^j(0) = [0.05, 0.3]^\top, [0.25, 0.8]^\top, [0.14, 0.6]^\top, [0.09, 0.4]^\top, [-0.1, 0.5]^\top$. Finally, we show the learning performance even there exist initial output error in Fig. 1. It is clear that the effectiveness of the proposed controller can be obtained by the simulation results.

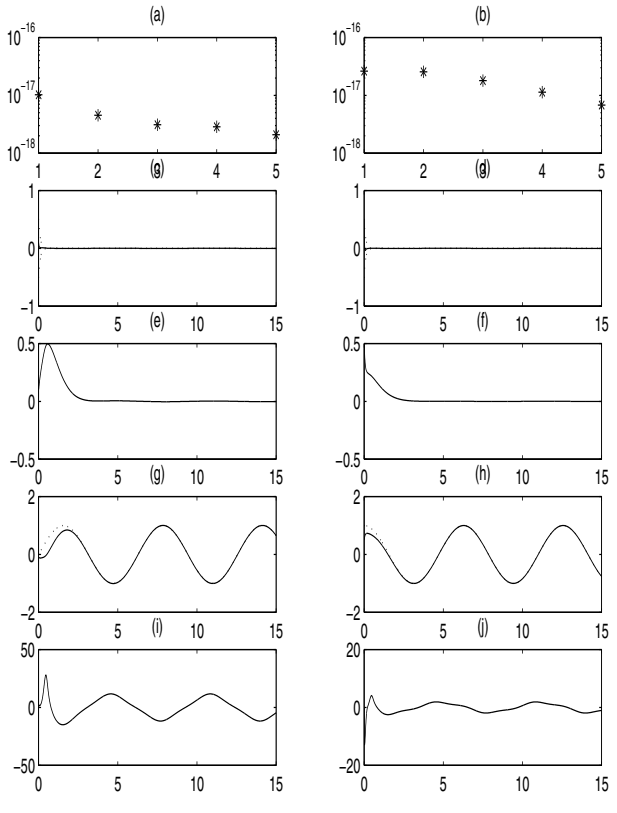

Fig. 1. (a) $\sup_{t\in[0,15]} |e_{\phi_1}^j(t)|$ versus iteration j; (b) $\sup_{t\in[0,15]} |e_{\phi_2}^j(t)|$ versus iteration j; (c) $e_{a_1}^5(t)$ (solid line) and $\pm\phi^5(t)$ (dotted lines) versus time t; (d) $e_{a_2}^5(t)$ (solid line) and $\pm\phi^5(t)$ (dotted lines) versus time t; (e) $e_1^5(t)$ (solid line) versus time t; (f) $e_2^5(t)$ (solid line) versus time t; (g) $q_1^5(t)$ (solid line) and $q_{d_1}(t)$ (dotted line) versus time t; (h) $q_2^5(t)$ (solid line) and $q_{d_2}((t)$ (dotted line) versus time t; (i) $u_1^5(t)$ versus time t; (j) $u_2^5(t)$ versus time t.

VI. Conclusion

An observer based AILC for repeated tracking control of uncertain robotic systems is proposed in this paper. Only joint positions are assumed to be measurable so that a tracking error observer is designed to estimate the unknown joint variables. An error observation dynamic based on the tracking error observer is derived for the design of the AILC. Using a technique of averaging filter, a fuzzy neural learning component based on a filtered FNN is used to approximate the unknown nonlinear function and a robust learning component is designed to compensate for the other uncertainties. Based on a Lyapunov like analysis, we show that all adjustable parameters and the internal signals inside the closed-loop system remain bounded and the output tracking error asymptotically converge to a tunable residual set as iteration goes to infinity.

VII. Acknowledgement

This work is supported by National Science Council, R.O.C., under Grant NSC 99-2221-E-211-011-MY2

References

[1] S. Arimoto, S. Kawamura and F. Miyazaki, "Bettering operation of robotics by learning," *J. of robotic. Syst.*, vol. 1, no. 2, pp. 123-140, 1984.

[2] T.J. Jang, C.H. Choi and H.S. Ahn, "Iterative learning control in feedback systems," *Automatica*, vol. 31, no. 2, pp. 243-248, 1995.

[3] B.H. Park, T.Y. Kuc and J.S. Lee, "Adaptive learning of uncertain robotic systems," *International Journal of Control*, vol. 65, no. 5, pp. 725-744, 1996.

[4] C.J. Chien and J.S. Liu, "A P-type iterative learning controller for robust output tracking of nonlinear time-varying systems," *International Journal of Control*, vol. 64, no. 2, pp. 319-334, 1996.

[5] J.Y. Choi and J.S. Lee, "Adaptive iterative learning control of uncertain robotic systems," *IEE Proc. D, Control Theory Application*, vol. 147, no. 2, pp. 217-223, 2000.

[6] A. Tayebi, "Adaptive iterative learning control for robot manipulators," *Automatica*, vol. 40, pp. 1195-1203, 2004.

[7] A. Tayebi and J-X Xu, "Observer-based iterative learning control for a class of time-varying nonlinear systems," *IEEE Trans. Circuits and Systems-I*, vol. 50, no. 3, pp. 452-455, 2003.

[8] J-X Xu and J Xu, "Observer based learning control for a class of nonlinear systems with time-varying parametric uncertainties," *IEEE Trans. Automat. Contr.*, vol. 49, no. 2, pp. 275-281, 2004.

[9] Y.-C. Wang, C.-J. Chien, and D.-T. Lee, "A hybrid adaptive scheme of fuzzy-neural iterative learning controller for nonlinear dynamic systems," *International Journal of Fuzzy Systems*, Vol. 7, No. 4, pp. 147-157, 2005.

[10] Annaswamy, A. M., and Narendra, K.S., *Stable Adaptive Systems*, Prentice-Hall, 1988.

[11] P.A. Ioannou and K.S. Tsakalis, "A robust direct adaptive control," *IEEE Trans. Automat. Contr.*, vol. 31, pp. 1033–1043, 1986.

[12] C. J. Chien, "A combeined adaptive law for fuzzy iterative learning control of nonlinear systems with varying control tasks," *IEEE Trans. Fuzzy Syst.*, vol. 16, no. 1, pp. 40–51, 2008.

[13] Y.-C. Wang and C.-J. Chien, "Observer Based Adaptive Fuzzy Neural Iterative Learning Control for Nonaffine Nonlinear Systems," *2009 CACS International Automatic Control Conference.*.

[14] J. J. Slotine and W. Li, *Applied Nonlinear Control*, Englewood Cliffs, NJ: Prentice-Hall, 1991.

2011 IEEE International Conference on Fuzzy Systems
June 27-30, 2011, Taipei, Taiwan

Synchronization of Uncertain Fractional Order Chaotic Systems via Adaptive Interval Type-2 Fuzzy Sliding Mode Control

Tsung-Chih Lin
Feng-Chia University
Department of Electronic Engineering
Taichung, Taiwan, R.O.C.
tclin@fcu.edu.tw

Tun-Yuan Lee
Feng-Chia University
Department of Electronic Engineering
Taichung, Taiwan, R.O.C.
m9901315@fcu.edu.tw

Valentina Emilia Balas
University of Arad
Department of Automation and Applied Engineering
Informatics
Arad, Romania
balas@drbalas.ro

***Abstract*—In this paper, a novel adaptive interval type-2 fuzzy sliding mode control (AITFSMC) is proposed to handle high level uncertainties facing the fuzzy logic controller (FLC) in dynamic fractional order chaotic systems such as uncertainties in inputs to the FLC, uncertainties in control outputs, linguistic uncertainties and uncertainties associated with the noisy training data. Based on the learning algorithm combining Lyapunov approach and sliding mode control, free parameters of the AITSMC can be tuned on line by output feedback control law and adaptive law to synchronize two different uncertain fractional order chaotic systems. Meanwhile, the chattering phenomena in the control efforts can be reduced. During the design procedure, not only the stability and robustness can be guaranteed but also the external disturbance on the synchronization error can be attenuated. The numerical simulation is performed to illustrate the effectiveness of the proposed control strategy.**

Keywords- Adaptive fuzzy, sliding mode control, fractional order, chaotic synchronization, Lyapuinov synthesis

I. INTRODUCTION

In recent years, dynamics described by fractional differential equations are becoming more and more popular as the underlying facts about the differentiation and integration is significantly different from the integer counterparts and beyond this, many real life systems are described better by fractional order differential equations. For instance, electrochemical processes and flexible structures are modeled by fractional order models [1]-[4], the behavior of some biological systems is explored using fractional calculus [5] and dielectric polarization, electromagnetic waves and viscoelastic systems are involved with fractional order operators. It is observed that the description of some systems is more accurate when the fractional derivative is used [6]-[7]. Nowadays, many fractional-order differential systems behave chaotically, such as the fractional-order Chua's system [8-9], the fractional-order Duffing system [10-11], the fractional-order Lu system [12], the fractional-order Chen's system [13-14], the fractional-order cellular neural network [15-16], and the fractional-order neural network [17].

Recently, synchronization of chaotic system is attractive in many applications such as power converters, biological systems, chemical reactions, information processing and secure communication. Over the past few years, fractional operators have been applied with satisfactory results in modeling and control of complex systems and synchronization of chaos has been investigated in many papers [18-20,40-42]. The algorithms based on active sliding mode controller employed to synchronize two different chaotic systems are proposed in [21]-[23]. However, there exists a chattering phenomenon implementing a sliding mode control (SMC), and this may excite high-frequency dynamics [24]-[26]. In order to eliminate chattering, Palm [27] noted the similarity between fuzzy controller and sliding mode controller with a boundary layer, and provided a fuzzy sliding mode design approach.

Although, type-1 fuzzy logic controllers (FLCs) have been successfully applied in many different applications, for dynamic unstructured environments and many real world applications, there is a need to cope with large amount of uncertainties such as uncertainties in inputs to the FLC, uncertainties in control outputs, linguistic uncertainties and uncertainties associated with the noisy training data. Type-2 FLCs have potential to overcome the limitations of type-1 FLCs and provide improved performance for many applications [32]-[36]. In this paper, a novel adaptive interval type-2 fuzzy sliding mode controller is developed to synchronize two different uncertain fractional order chaotic systems with high level uncertainties.

This paper is organized as follows: In section II, an introduction to fractional derivative and its relation to the approximation solution will be addressed. A brief of the interval type-2 fuzzy neural network (FNN) is presented in section III. Section IV generally proposes the employment of

978-1-4244-7316-8/11/$26.00 ©2011 IEEE

the AITFSMC for synchronizing the fractional order chaotic system in presence of uncertainty and its stability analysis. In Section V, application of the proposed method on fractional order expression of Duffing–Holmes chaotic system is investigated. Finally, the simulation results and conclusion will be presented in Section VI.

II. BASIC DEFINITION AND PRELIMINARIES FOR FRACTIONAL ORDER SYSTEMS

Fractional calculus is a mathematical topic more than 300 years. It is a generalization of integration and differentiation to non-integer order fundamental operator, denoted by ${}_aD_t^q$, where a and t are the limits of the operator. This operator is a notation for taking both the fractional integral and functional derivative in a single expression defined as

$$ {}_aD_t^q = \begin{cases} \dfrac{d^q}{dt^q}, & q > 0 \\ 1 & q = 0 \\ \displaystyle\int_a^t (d\tau)^{-q}, & q < 0 \end{cases} \tag{1} $$

There are some basic definitions of the general fractional integration and differentiation. The commonly used definitions are Grunwald-Letnikov and Riemann-Liouville. The Grunwald-Letnikov definition is expressed as

$$ {}_aD_t^q f(t) = \lim_{h\to 0} \sum_{j=0}^{\left[\frac{t-a}{h}\right]} (-1)^j \binom{q}{j} f(t-jh) \tag{2} $$

where $[\cdot]$ is the integer part. The simplest and easiest definition is Riemann-Liouville definition given as

$$ {}_aD_t^q f(t) = \frac{1}{\Gamma(n-q)} \frac{d^n}{dt^n} \int_0^t \frac{f(\tau)}{(t-\tau)^{q-n+1}} d\tau \tag{3} $$

where n is the first integer which is not less q, i.e., $n-1 < q < n$, and Γ is the Gamma function.

The numerical simulation of a fractional differential equation is not simple as that of an ordinary differential equation. In this paper, the algorithm which is an improved version of Adams–Bashforth–Moulton algorithm [28-30] to find an approximation for fractional order systems based on predictor-correctors [30-31] is given. Consider the following differential equation

$$ \begin{aligned} &{}_0D_t^q y(t) = r(y(t), t), \quad 0 \le t \le T \\ &\text{and } y^{(k)}(0) = y_0^{(k)}, k = 0, 1, 2, \cdots, m-1 \end{aligned} \tag{4} $$

where

$$ {}_0D_t^q y(t) = \begin{cases} \dfrac{1}{\Gamma(m-q)} \displaystyle\int_0^t \frac{f^{(m)}(\tau)}{(t-\tau)^{q-m+1}} d\tau, & m-1 < q < m \\ \dfrac{d^m}{dt^m} y(t) & q = m \end{cases} \tag{5} $$

and m is the first integer larger the q. The solution of the equation (4) is equivalent to Volterra integral equation [32] described as

$$ y(t) = \sum_{k=0}^{[q]-1} y_0^{(k)} \frac{t^k}{k!} + \frac{1}{\Gamma(q)} \int_0^t (t-\lambda)^{q-1} r(y(\lambda), \lambda) d\lambda \tag{6} $$

Let $h = T/N$, $t_n = nh$, $n = 0, 1, 2, \cdots N$. Then (6) can be discretized as follows.

$$ \begin{aligned} y_h(t_{n+1}) = &\sum_{k=0}^{[q]-1} y_0^{(k)} \frac{t_{n+1}^k}{k!} + \frac{h^q}{\Gamma(q+2)} r(y_h^p(t_{n+1}), t_{n+1}) \\ &+ \frac{h^q}{\Gamma(q+2)} \sum_{j=0}^{n} a_{j,n+1} r(y_h(t_j), t_j) \end{aligned} \tag{7} $$

where predicted value $y_h^p(t_{n+1})$ is determined by

$$ y_h^p(t_{n+1}) = \sum_{k=0}^{[q]-1} y_0^{(k)} \frac{t_{n+1}^k}{k!} + \frac{h^q}{\Gamma(q)} \sum_{j=0}^{n} b_{j,n+1} r(y_h(t_j), t_j) \tag{8} $$

and

$$ a_{j,n+1} = \begin{cases} n^{q+1} - (n-q)(n+1)^q, & j = 0 \\ (n-j+2)^{q+1} + (n-j)^{q+1} - 2(n-j+1)^{q+1} & 1 \le j \le n \\ 1 & j = n+1 \end{cases} \tag{9} $$

$$ b_{j,n+1} = \frac{h^q}{q} ((n+1-j)^q - (n-j)^q) \tag{10} $$

The approximation error is given as

$$ \max_{j=0,1,2,\cdots N} \left| y(t_j) - y_h(t_j) \right| = \mathrm{O}(h^p) \tag{11} $$

where $p = \min(2, 1+q)$. Therefore, the numerical solution of a fraction order system can be obtained by applying the above mentioned algorithm.

III. BRIEF DESCRIPTION OF INTERVAL TYPE-2 FNN [32]-[36]

In this section, we will describe the interval type-2 fuzzy set and the inference of type-2 fuzzy logic system which leads to interval type-2 fuzzy neural network (T2FNN). Due to the complexity of the type reduction, the general type-2 FLS becomes computationally intensive. In order to make things simpler and easier to compute meet and join operations, the secondary MFs of an interval type-2 FLS are all unity which leads finally to simplify type reduction. The 2-D interval type-2 Gaussian membership function (MF) with uncertain mean $m \in [m_1, m_2]$ and a fixed deviation σ is shown in Fig. 1.

$$ \mu_{\tilde{A}}(x) = \exp\left[-\frac{1}{2} \left(\frac{x-m}{\sigma} \right)^2 \right], \quad m \in [m_1, m_2] \tag{12} $$

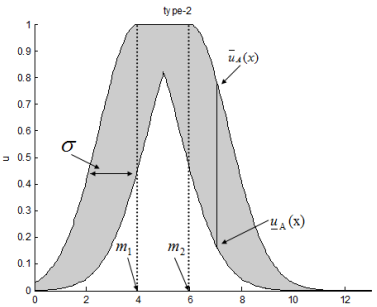

Figure 1. Interval type-2 fuzzy set with uncertain mean

It is obvious that the type-2 fuzzy set is in a region bounded by an upper MF and a lower MF denoted as $\overline{\mu}_{\tilde{A}}(x)$ and $\underline{\mu}_{\tilde{A}}(x)$, respectively, and is called a foot of uncertainty (FOU). In the meantime, the firing strength F^i for the ith rule can be an interval type-1 set [9] expressed as

$$F^i = \begin{bmatrix} \underline{f}^i \\ \overline{f}^i \end{bmatrix} \tag{13}$$

Where

$$\underline{f}^i = \underline{\mu}_{\tilde{F}_1^i}(x_1) * \cdots * \underline{\mu}_{\tilde{F}_n^i}(x_n) = \Pi_{j=1}^n \underline{\mu}_{\tilde{F}_j^i}(x_j) \tag{14}$$

$$\overline{f}^i = \overline{\mu}_{\tilde{F}_1^i}(x_1) * \cdots * \overline{\mu}_{\tilde{F}_n^i}(x_n) = \Pi_{j=1}^n \overline{\mu}_{\tilde{F}_j^i}(x_j) \tag{15}$$

Based on the center of sets type reduction, the defuzzified crisp output from an interval type-2 FLS is the average of y_l and y_r, i.e.,

$$y(\underline{x}) = \frac{y_l + y_r}{2} = \frac{1}{2}(\underline{\xi}_r^T \underline{\Theta}_r + \underline{\xi}_l^T \underline{\Theta}_l) = \frac{1}{2}\begin{bmatrix} \underline{\xi}_r^T & \underline{\xi}_l^T \end{bmatrix}\begin{bmatrix} \underline{\Theta}_r \\ \underline{\Theta}_l \end{bmatrix} = \underline{\xi}^T \underline{\Theta} \tag{16}$$

where $(1/2)[\underline{\xi}_r^T \ \underline{\xi}_l^T] = \underline{\xi}^T$ and $[\underline{\Theta}_r^T \ \underline{\Theta}_l^T] = \underline{\Theta}^T$.

where y_l and y_r are the left most and right most points of the interval type-1 set which can be obtained as

$$y_l = \frac{\sum_i^M f_l^i w_l^i}{\sum_i^M f_l^i} = \frac{\sum_{i=1}^L \overline{f}^i w_l^i + \sum_{i=L+1}^M \underline{f}^i w_l^i}{\sum_{i=1}^L \overline{f}^i + \sum_{i=L+1}^M \underline{f}^i} = \sum_{i=1}^L \underline{q}_l^i y_l^i + \sum_{i=L+1}^M \overline{q}_l^i y_l^i = [\underline{Q}_l \ \overline{Q}^l]\begin{bmatrix} \underline{y}_l \\ \overline{y}^l \end{bmatrix} = \underline{\xi}_l^T \underline{\Theta}_l \tag{17}$$

where $\underline{q}_l^i = \underline{f}^i / D_l$, $\overline{q}_l^i = \overline{f}^i / D_l$ and $D_l = (\sum_{i=1}^L \underline{f}^i + \sum_{i=L+1}^M \overline{f}^i)$. In the meantime, we have $\underline{Q}_l = [\underline{q}_l^1, \underline{q}_l^2, \cdots, \underline{q}_l^R]$, $\overline{Q}^l = [\overline{q}_l^1, \overline{q}_l^2, \cdots, \overline{q}_l^R]$, $\underline{\xi}_l^T = [\underline{Q}_l \ \overline{Q}^l]$ and $\underline{\Theta}_l^T = [\underline{y}_l \ \overline{y}^l]$.

and

$$y_r = \frac{\sum_i^M f_r^i w_r^i}{\sum_i^M f_r^i} = \frac{\sum_{i=1}^R \underline{f}^i w_r^i + \sum_{i=R+1}^M \overline{f}^i w_r^i}{\sum_{i=1}^R \underline{f}^i + \sum_{i=R+1}^M \overline{f}^i} = \sum_{i=1}^R \underline{q}_r^i y_r^i + \sum_{i=R+1}^M \overline{q}_r^i y_r^i = [\underline{Q}_r \ \overline{Q}^r]\begin{bmatrix} \underline{y}_r \\ \overline{y}^r \end{bmatrix} = \underline{\xi}_r^T \underline{\Theta}_r \tag{18}$$

where $\underline{q}_r^i = \underline{f}^i / D_r$, $\overline{q}_r^i = \overline{f}^i / D_r$ and $D_r = (\sum_{i=1}^R \underline{f}^i + \sum_{i=R+1}^M \overline{f}^i)$. In the meantime, we have $\underline{Q}_r = [\underline{q}_r^1, \underline{q}_r^2, \cdots, \underline{q}_r^R]$, $\overline{Q}^r = [\overline{q}_r^1, \overline{q}_r^2, \cdots, \overline{q}_r^R]$, $\underline{\xi}_r^T = [\underline{Q}_r \ \overline{Q}^r]$ and $\underline{\Theta}_r^T = [\underline{y}_r \ \overline{y}^r]$, and M is the total number of rules in the rule base of the RIT2FNN. The weighting factors w_l^i and w_r^j of the consequent part represent the centroid interval set of the consequent type-2 fuzzy set of the $i$the rule. In the meantime, R and L can be determined by using the iterative Karnik-Mendel procedure [32]-[36].

An interval T2FNN system which is an implementation of interval type-2 fuzzy logic system, and some of their parameters and components are presented by fuzzy logic terms, is shown in Fig. 2 [34]. The interval T2FNN is a four layers structure [34]. Layer I and layer II represent input nodes and type-2 fuzzification nodes, respectively, which form the antecedent part of this T2FNN. A classical 2-layer NN with fuzzy rule nodes and output nodes is used to construct layer III and layer IV, respectively, which compose the consequent part of this T2FNN. d_i , $i = 1 \sim z$ are reference signals.

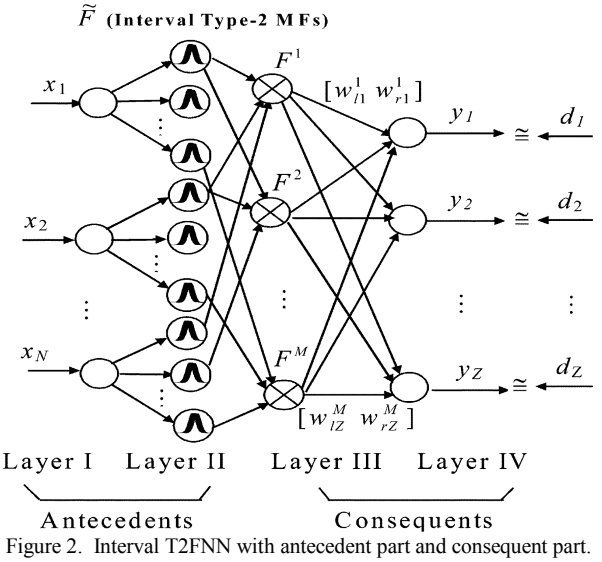

Figure 2. Interval T2FNN with antecedent part and consequent part.

IV. ADAPTIVE INTERVAL TYPE-2 FUZZY SLIDING MODEL SYNCHRONIZATION OF FRACTIONAL ORDER CHAOTIC SYSTEMS

Let's consider two chaotic systems with fractional order derivative, driven system and response system, as follows:

Driven system:

$$D^{(q)} x_1 = x_2$$
$$D^{(q)} x_2 = f(x,t) \tag{19}$$

Response system:

$$D^{(q)} y_1 = y_2$$
$$D^{(q)} y_2 = g(y,t) + u(t) + d(t) \tag{20}$$

where x_1, x_2, y_1 and y_2 are the state variables, $f(x,t)$ and $g(y,t)$ are unknown but bounded nonlinear functions which express system dynamics, $d(t)$ is the external bounded disturbance and $u(t)$ is the control input of the response system. The control objective to synchronize both driven and response systems by designing a nonlinear controller which obtains signals from driven system to tune behavior of the response system.

The synchronization error vector is defined as

$$e = [e_1, e_2] \tag{21}$$

where $e_i = y_i - x_i$. Then, in the space of the synchronization error, sliding surface is given by

$$S(t) = k_1 e_1 + k_2 e_2 \tag{22}$$

where k_1, k_2 are arbitrary constants which are chosen such that dynamic of the sliding surface vanished quickly. The process can be classified into two phases, approaching phase with $S(t) \neq 0$ and sliding phase with $S(t) = 0$. In order to guarantee the trajectory of the synchronization error vector *e* will move from approaching phase to sliding phase, a sufficient condition to is to design the control effort such that sliding condition

$$S(t)\dot{S}(t) \leq -\eta |S(t)|, \quad \eta > 0 \tag{23}$$

is satisfied. We have $S(t) = 0$ and $\dot{S}(t) = 0$ in the sliding phase, if $f(x,t)$ and $g(x,t)$ are known and free of external disturbance, $d(t) = 0$, the corresponding equivalent control effort u_{eq} to force the system dynamics to stay on the sliding surface can be derived from $\dot{S}(t) = 0$.

$$\dot{S}(t) = D^{(1-q)}(D^{(q)}(S(t))) = 0 \rightarrow D^{(q)}(S(t)) = 0 \tag{24}$$

Substituting (22) into (24), we have

$$\begin{aligned} D^{(q)}(S(t)) &= D^{(q)}(k_1 e_1 + k_2 e_2) = k_1 D^{(q)} e_1 + k_2 D^{(q)} e_2 \\ &= k_1 D^{(q)}(y_1 - x_1) + k_2 D^{(q)}(y_2 - x_2) \\ &= k_1 (y_2 - x_2) + k_2 [g(y,t) - f(x,t) + u_{eq}(t)] \\ &= k_1 e_2 + k_2 [g(y,t) - f(x,t) + u_{eq}(t)] = 0 \end{aligned}$$

Then the equivalent control effort can be obtained as

$$u_{eq}(t) = -\frac{k_1}{k_2} e_2 + f(x,t) - g(y,t) \tag{25}$$

During the approaching phase, in order to satisfy the sliding condition (23), a switching control action $u_{sw} = \eta_{sw} \operatorname{sgn}(S(t))$ must be included in the complete sliding control which can be expressed as

$$\begin{aligned} u(t) &= u_{eq}(t) - \eta_{sw} \operatorname{sgn}(S(t)) \\ &= -\frac{k_1}{k_2} e_2 + f(x,t) - g(y,t) - \eta_{sw} \operatorname{sgn}(S(t)) \end{aligned} \tag{26}$$

where η_{sw} i is a positive constant such the approaching condition can be guaranteed for,

$$\eta_{sw} > \left| D^{1-q} d(t) \right| + \left| D^{1-q} \omega \right| \tag{27}$$

where ω is the minimum approximation error, $|d(t)|$ and $|\omega|$ are assumed to be bounded.

However, $f(x,t)$ and $g(x,t)$ are unknown and external disturbance, $d(t) \neq 0$, the ideal control effort (23) cannot be implemented. We replace $f(x,t)$ and $g(x,t)$ by the interval type-2 fuzzy logic system $f(x|\underline{\theta}_f)$ and $g(y|\underline{\theta}_g)$, respectively, in specified form as (16), i.e.,

$$\begin{aligned} f(x|\underline{\theta}_f) &= \frac{1}{2}\left(\underline{\theta}_{fr}^T \underline{\xi}_r(x) + \underline{\theta}_{fl}^T \underline{\xi}_l(x)\right) = \underline{\theta}_f^T \underline{\xi}(x), \\ g(x|\underline{\theta}_g) &= \frac{1}{2}\left(\underline{\theta}_{gr}^T \underline{\xi}_r(y) + \underline{\theta}_{gl}^T \underline{\xi}_l(y)\right) = \underline{\theta}_g^T \underline{\xi}(y) \end{aligned} \tag{28}$$

where $\underline{\theta}_f^T = [\underline{\theta}_{fr}\ \underline{\theta}_{fl}]^T$ and $\underline{\theta}_g^T = [\underline{\theta}_{gr}\ \underline{\theta}_{gl}]^T$. Here the parameters $\underline{\xi}_r(x)$, $\underline{\xi}_l(x)$, $\underline{\xi}_r(y)$ and $\underline{\xi}_l(y)$ depend on the fuzzy membership functions and are supposed to be fixed, while $\underline{\theta}_{fr}^T$, $\underline{\theta}_{fl}^T$, $\underline{\theta}_{gr}^T$ and $\underline{\theta}_{gl}^T$ are adjusted by adaptive laws based on Lyapunov stability criterion. Therefore, the resulting control effort can be obtained as

$$u(t) = -\frac{k_1}{k_2} e_2 + f(x|\underline{\theta}_f) - g(y|\underline{\theta}_g) - \eta_{sw} \operatorname{sgn}(S(t)) \tag{29}$$

Following the proceeding consideration, the following theorem can be obtained.

Theorem: Consider the two fractional order chaotic systems, driven system (16) and response system (17), the control effort of the response system is given in (26) and the fuzzy-based adaptive laws are chosen as

$$D^{(q)} \underline{\theta}_{fr} = -\frac{1}{2} r_1 S(t) \underline{\xi}_r(x) \tag{30}$$

$$D^{(q)} \underline{\theta}_{fl} = -\frac{1}{2} r_2 S(t) \underline{\xi}_l(x) \tag{31}$$

$$D^{(q)} \underline{\theta}_{gr} = \frac{1}{2} r_3 S(t) \underline{\xi}_r(y) \tag{32}$$

$$D^{(q)} \underline{\theta}_{gl} = \frac{1}{2} r_4 S(t) \underline{\xi}_l(y) \tag{33}$$

Then, the overall adaptive scheme guarantees the global stability of the resulting closed-loop system in the sense that all signals involved are uniformly bounded and the synchronization error will converge to zero asymptotically.

Proof: The optimal parameter estimations $\underline{\theta}_f^*$ and $\underline{\theta}_g^*$ are defined as

$$\underline{\theta}_f^* = \arg\min_{\underline{\theta}_f \in \Omega_f} \left[\sup_{x \in \Omega_x} |f(x|\underline{\theta}_f) - f(x,t)| \right] \tag{34}$$

$$\underline{\theta}_g^* = \arg\min_{\underline{\theta}_g \in \Omega g} \left[\sup_{y \in \Omega_y} |g(y|\underline{\theta}_g) - g(y,t)| \right] \tag{35}$$

where Ω_f, Ω_g, Ω_y and Ω_x are constraint sets of suitable bounds on $\underline{\theta}_f$, $\underline{\theta}_g$, y and x respectively and they are defined as $\Omega_f = \{\underline{\theta}_f \,|\, |\underline{\theta}_f| \leq M_f\}$, $\Omega_g = \{\underline{\theta}_g \,|\, |\underline{\theta}_g| \leq M_g\}$, $\Omega_y = \{y \,|\, |y| \leq M_y\}$ and $\Omega_x = \{x \,|\, |x| \leq M_x\}$, where M_f, M_g, M_y and M_x are positive constants. Then, we have

$$\begin{aligned} D^{(q)}(S(t)) &= D^{(q)}(k_1 e_1 + k_2 e_2) = k_1 D^{(q)} e_1 + k_2 D^{(q)} e_2 \\ &= k_1 e_2 + k_2 [g(y,t) - f(x,t) + u(t) + d(t)] \\ &= k_1 e_2 + k_2 \{[g(y,t) - f(x,t)] + [-\frac{k_1}{k_2} e_2 + f(x|\underline{\theta}_f) \\ &\quad - g(y|\underline{\theta}_g) - \eta_{sw} \operatorname{sgn}(S(t))] + d(t)\} \\ &= k_2 \{\frac{1}{2}[(\underline{\theta}_{gr}^* - \underline{\theta}_{gr})^T \underline{\xi}_r(y) + (\underline{\theta}_{gl}^* - \underline{\theta}_{gl})^T \underline{\xi}_l(y) - (\underline{\theta}_{fr}^* - \underline{\theta}_{fr})^T \underline{\xi}_r(x) \\ &\quad - (\underline{\theta}_{fl}^* - \underline{\theta}_{fl})^T] \underline{\xi}_l(x)\} - k_2 [\eta_{sw}(\operatorname{sgn}(S(t)) - d(t) - \omega] \end{aligned}$$

$$= k_2 \frac{1}{2}[\tilde{\underline{\theta}}_{gr}^T \xi_r(y) + \tilde{\underline{\theta}}_{gl}^T \xi_l(y) - \tilde{\underline{\theta}}_{fr}^T \xi_r(x) - \tilde{\underline{\theta}}_{fr}^T \xi_r(x)] - k_2[\eta_{sw}\,\mathrm{sgn}(S(t)) - d(t) - \omega] \quad (36)$$

where $\tilde{\underline{\theta}}_{fr} = \underline{\theta}_{fr}^* - \underline{\theta}_{fr}$, $\tilde{\underline{\theta}}_{fl} = \underline{\theta}_{fl}^* - \underline{\theta}_{fl}$, $\tilde{\underline{\theta}}_{gr} = \underline{\theta}_{gr}^* - \underline{\theta}_{gr}$, $\tilde{\underline{\theta}}_{gl} = \underline{\theta}_{gl}^* - \underline{\theta}_{gl}$ and the minimum approximation error is

$$\omega = [g(y,t) - g(y|\underline{\theta}^*{}_g)] - [f(x,t) - f(x|\underline{\theta}^*{}_f)] \quad (37)$$

Now consider the Lyapunov function candidate

$$V = \frac{1}{2}S^2(t) + \frac{k_2}{2r_1}\tilde{\underline{\theta}}_{fr}^T\tilde{\underline{\theta}}_{fr} + \frac{k_2}{2r_2}\tilde{\underline{\theta}}_{fl}^T\tilde{\underline{\theta}}_{fl} + \frac{k_2}{2r_3}\tilde{\underline{\theta}}_{gr}^T\tilde{\underline{\theta}}_{gr} + \frac{k_2}{2r_4}\tilde{\underline{\theta}}_{gl}^T\tilde{\underline{\theta}}_{gl} \quad (38)$$

where r_1, r_2, r_3 and r_4 are positive constants. Taking the derivative of the (38) with respect to time, we get

$$\begin{aligned} V^{(q)} &= S(t)S^{(q)}(t) + \frac{k_2}{r_1}(D^{(q)}\tilde{\underline{\theta}}_{fr}^T)(\tilde{\underline{\theta}}_{fr}) + \frac{k_2}{r_2}(D^{(q)}\tilde{\underline{\theta}}_{fl}^T)(\tilde{\underline{\theta}}_{fl}) \\ &\quad + \frac{k_2}{r_3}(D^{(q)}\tilde{\underline{\theta}}_{gr}^T)(\tilde{\underline{\theta}}_{gr}) + \frac{k_2}{r_4}(D^{(q)}\tilde{\underline{\theta}}_{gl}^T)(\tilde{\underline{\theta}}_{gl}) \\ &= S(t)k_2\frac{1}{2}[\tilde{\underline{\theta}}_{gr}^T\xi_r(y) + \tilde{\underline{\theta}}_{gl}^T\xi_l(y) - \tilde{\underline{\theta}}_{fr}^T\xi_r(x) - \tilde{\underline{\theta}}_{fr}^T\xi_r(x)] \\ &\quad - k_2[\eta_{sw}\,\mathrm{sgn}(S(t)) - d(t) - \omega] + \frac{k_2}{r_1}(D^{(q)}\tilde{\underline{\theta}}_{fr}^T)(\tilde{\underline{\theta}}_{fr}) \\ &\quad + \frac{k_2}{r_2}(D^{(q)}\tilde{\underline{\theta}}_{fl}^T)(\tilde{\underline{\theta}}_{fl}) + \frac{k_2}{r_3}(D^{(q)}\tilde{\underline{\theta}}_{gr}^T)(\tilde{\underline{\theta}}_{gr}) + \frac{k_2}{r_4}(D^{(q)}\tilde{\underline{\theta}}_{gl}^T)(\tilde{\underline{\theta}}_{gl}) \\ &= k_2\tilde{\underline{\theta}}_{gr}^T[\frac{1}{2}S(t)\xi_r(y) + \frac{1}{r_3}(D^{(q)}\tilde{\underline{\theta}}_{gr})] + k_2(\tilde{\underline{\theta}}_{gl}^T)[\frac{1}{2}S(t)\xi_l(y) \\ &\quad + \frac{1}{r_4}(D^{(q)}\tilde{\underline{\theta}}_{gl})] - k_2\tilde{\underline{\theta}}_{fr}^T[\frac{1}{2}S(t)\xi_r(x) - \frac{1}{r_1}(D^{(q)}\tilde{\underline{\theta}}_{fr})] \\ &\quad - k_2(\tilde{\underline{\theta}}_{fl}^T)[\frac{1}{2}S(t)\xi_l(x) - \frac{1}{r_2}(D^{(q)}\tilde{\underline{\theta}}_{fl})] \\ &\quad - k_2\eta_{sw}|S(t)| + k_2S(t)d(t) + k_2S(t)\omega \end{aligned} \quad (39)$$

Substituting (30)-(33) into (39) and using (27), we have

$$\begin{aligned} V^{(q)} &\le -k_2\{\eta_{sw}|S(t)| - |S(t)||d(t)| - |S(t)||\omega|\} \\ &= -k_2|S(t)|\{\eta_{sw} - |d(t)| - |\omega|\} < 0 \end{aligned} \quad (40)$$

The existence of adaptive fuzzy sliding mode dynamics is confirmed by (40) and the closed-loop system is globally asymptotically stable. The proof is completed.

V. Simulation Example

In this section, we will apply our adaptive interval type-2 fuzzy sliding model controller to synchronize two different uncertain fractional order Duffing-Holmes chaotic systems, the drive system and the response system.

Example: Let us consider two different uncertain fractional order Duffing-Holmes chaotic systems, the drive system and the response system, as follows [37]:

Drive system:

$$\begin{cases} D^{(q)}x_1 = 2.2x_2 \\ D^{(q)}x_2 = -0.40x_1^3 - 0.40x_1 - 0.10x_2 + 22\cos(1.29t) \end{cases} \quad (41)$$

Response system

$$\begin{cases} D^{(q)}y_1 = 2.2y_2 \\ D^{(q)}y_2 = -0.55y_1^3 - 0.30y_1 - 0.20y_2 + 18\cos(1.29t) + u(t) + d(t) \end{cases} \quad (42)$$

The external disturbance is $d(t) = 0.5\sin(t)$. The initial conditions of drive and response systems are chosen as: $\begin{bmatrix} x_1(0) \\ x_2(0) \end{bmatrix} = \begin{bmatrix} 0 \\ 0 \end{bmatrix}$ and $\begin{bmatrix} y_1(0) \\ y_2(0) \end{bmatrix} = \begin{bmatrix} -1 \\ -2 \end{bmatrix}$, respectively. All design constants are selected as, k_1=0.2, k_2=1, r_1=60, r_2=2, r_3=60, $r4$=4, $\eta_{sw} = 1$ and step size h=0.002. The values of $q = 0.98$ is considered.

For free of control input, the 3-D phase portrait of the drive and response systems is given in Figure. 3. It is obvious that both systems are not synchronized without control effort added in response system.

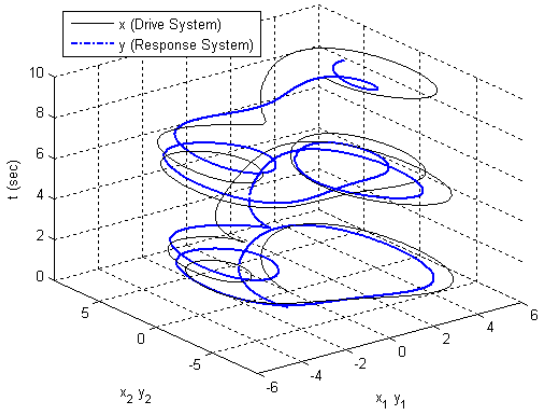

Figure 3. 3-D Phase portrait of chaotic drive and response systems.

From the adaptive laws (30)-(33), the control effort of the response system is given by

$$u(t) = -\frac{k_1}{k_2}e_2 + f(x|\underline{\theta}_f) - g(y|\underline{\theta}_g) - \eta_{sw}\,\mathrm{sgn}(S(t)) \quad (43)$$

The simulation results of both adaptive type-1 FNN SMC and adaptive interval type-2 FNN SMC are listed as follows: Figure 4 and Figure 5 show the trajectories of the states x_1, y_1 and x_2, y_2, respectively. Control effort trajectory is given in Figure 6 and 3-D phase portrait, synchronization performance, of the drive and response systems is shown in Figure 7. Sliding surface trajectory, *S*(t), is given in Figure 8. Figure 9 shows the graph of $V^{(q)}(t)$ which is always negative defined and consequently is stable.

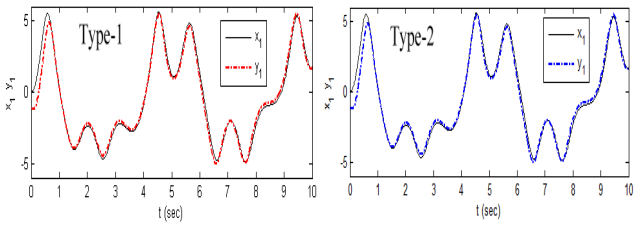

Figure 4. The trajectories of the states x_1 and y_1 .

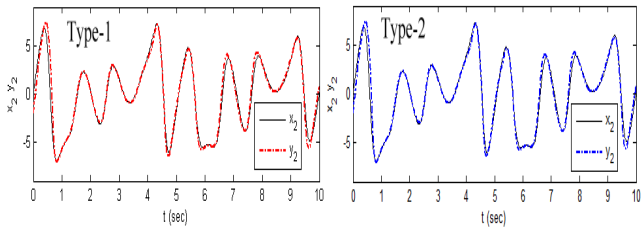

Figure 5. The trajectories of the states x_2 and y_2.

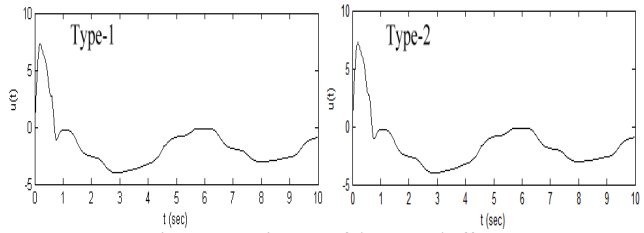

Figure 6. Trajectory of the control effort.

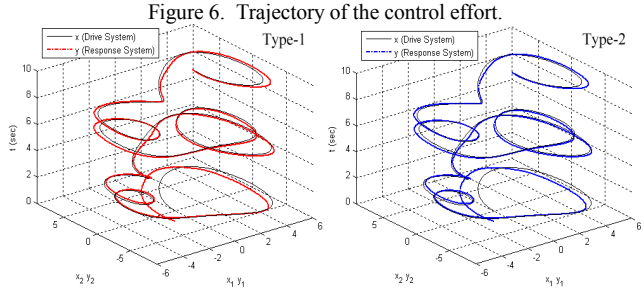

Figure 7. 3-D Phase portrait, synchronization performance, of the drive and response systems.

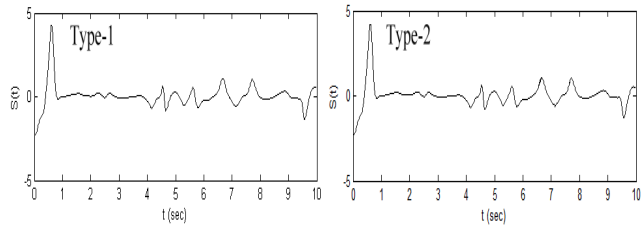

Figure 8. Sliding surface trajectory , S(t).

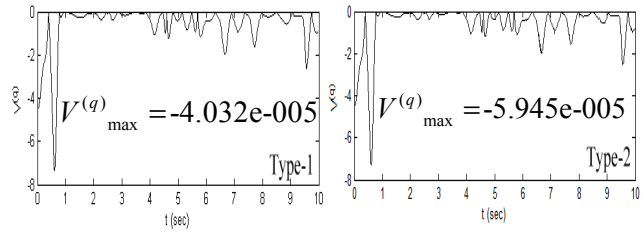

Figure 9. The graph of $V^{(q)}(t)$.

In order to show that the interval type-2 FLS can handle the measurement uncertainties, training data are corrupted by white Gaussian noise with signal-to-noise ratio (SNR) 20 dB. The trajectories of the states x_1, y_1 and x_2, y_2, respectively, are given in Figure 10 and Figure 11. Figure 12 show the control effort trajectory and 3-D phase portrait, synchronization performance, of the drive and response systems is shown in Figure 13. Sliding surface trajectory, S(t), is given in Figure 14. Figure 15 shows the graph of $V^{(q)}(t)$ which is always negative defined and consequently is stable.

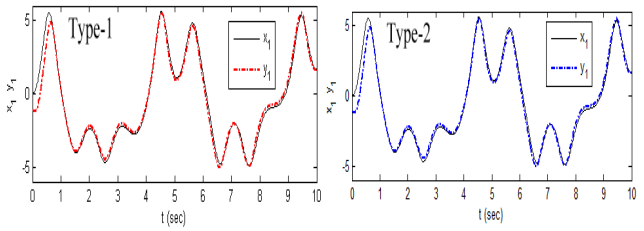

Figure 10. The trajectories of the states x_1 and y_1.

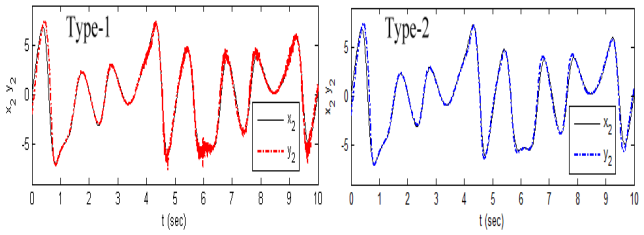

Figure 11. The trajectories of the states x_2 and y_2.

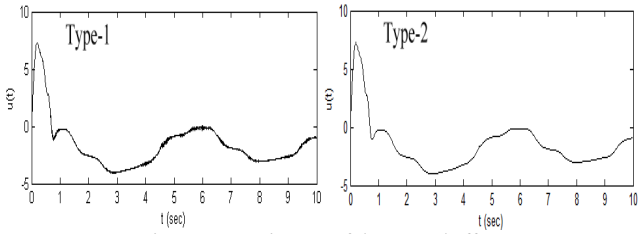

Figure 12. Trajectory of the control effort.

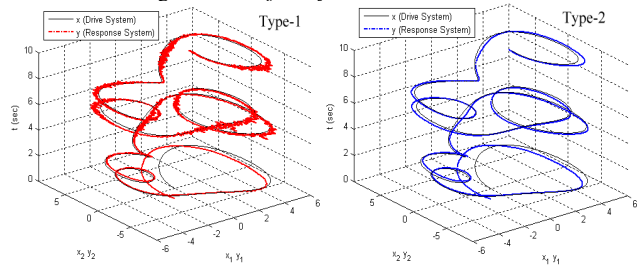

Figure 13. 3-D Phase portrait, synchronization performance, of the drive and response systems.

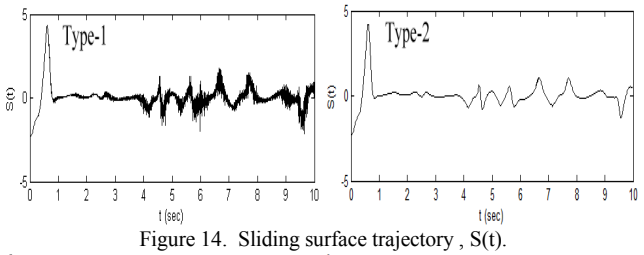

Figure 14. Sliding surface trajectory , S(t).

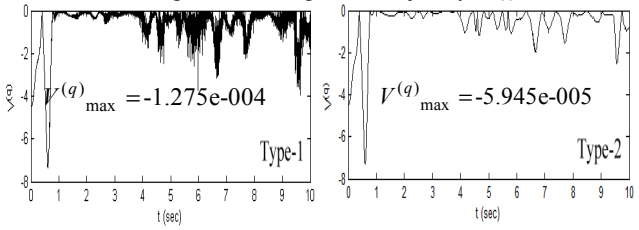

Figure 15. The graph of $V^{(q)}(t)$.

The synchronization performance, mean square errors of $\text{MESE1} = \sum_{k=0}^{5000} (y_1(k) - x_1(k))^2$ and $\text{MSE2} = \sum_{k=0}^{5000} (y_2(k) - x_2(k))^2$, for different values of q are shown in Figure 16 and Figure 17,

respectively. We can see that a fast synchronization of drive and response systems can be achieved and q is reduced the chaos is seen reduced, i.e., the synchronization error is reduced, accordingly. MSE1 and MSE2 of different q for type-1 and interval type-2 FNN controllers are given in Table I and Table II. MSU of different q for type-1 and interval type-2 FNN controllers are shown in Table III, where $\mathrm{MSU} = \sum_{k=0}^{5000} u(k)^2$.

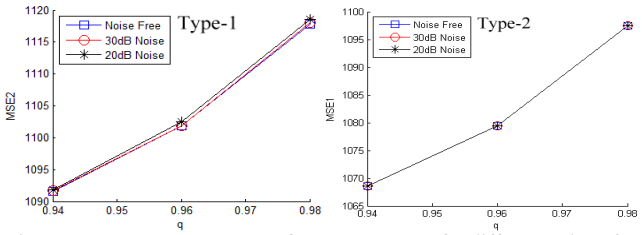

Figure 16. Mean square errors of $\mathrm{MSE1} = y_1 - x_1$ for different value of q.

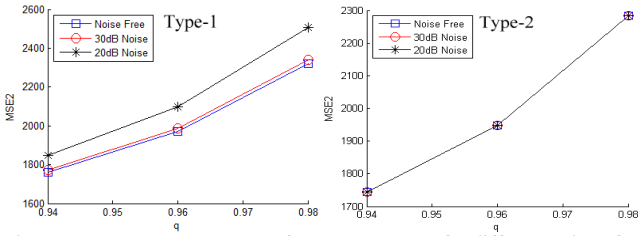

Figure 17. Mean square errors of $\mathrm{MSE2} = y_2 - x_2$ for different value of q.

Table I. MSE1 of the type-1 and the interval type-2 FNN controllers

MSE1	***q=0.98***		***q=0.96***		***q=0.94***	
	Type-1	***Type-2***	***Type-1***	***Type-2***	***Type-1***	***Type-2***
Noise Free	1117.8	1097.5	1101.8	1079.4	1091.6	1068.5
30dB Noise	1118.0	1097.5	1101.9	1079.4	1091.7	1068.5
20dB Noise	1118.6	1097.5	1102.5	1079.4	1091.8	1068.5

Table II. MSE2 of the type-1 and the interval type-2 FNN controllers

MSE2	***q=0.98***		***q=0.96***		***q=0.94***	
	Type-1	***Type-2***	***Type-1***	***Type-2***	***Type-1***	***Type-2***
Noise Free	2318.9	2283.5	1970.4	1947.8	1760.9	1743.5
30dB Noise	2341.5	2283.5	1987.8	1947.8	1772.0	1743.5
20dB Noise	2508.3	2283.5	2098.5	1947.8	1848.9	1743.5

Table III. MSU of the type-1 and the interval type-2 FNN controllers

MSU	***q=0.98***		***q=0.96***		***q=0.94***	
	Type-1	***Type-2***	***Type-1***	***Type-2***	***Type-1***	***Type-2***
Noise Free	34601	34452	38415	38298	40143	40004
30dB Noise	34606	34452	38427	38298	40145	40004
20dB Noise	34609	34452	38430	38298	40147	40004

VI. CONCLUSIONS

In this paper adaptive interval type-2 FNN SMC is proposed to deal with chaos synchronization between two different uncertain fractional order chaotic systems with linguistic uncertainties and internal noise. During the process of design, the free parameters of the adaptive fuzzy controller can be tuned on line by output feedback control law and adaptive law by using Lyapunov synthesis approach, and the chattering phenomena in the control efforts can be reduced. The simulation example, chaos synchronization of two different fractional order Duffing-Holmes chaotic systems, is given to demonstrate that interval type-2 FLC can overcome the limitations of type-1 FLC in high uncertain environments. The significance of the adaptive fuzzy sliding model control in the simulations for different values of q is manifest. Simulation results show that a fast synchronization of drive and response systems can be achieved and q is reduced the chaos is seen reduced, i.e., the synchronization error is reduced, accordingly.

REFERENCES

[1] I. Podlubny, "Fractional differential equations," Academic Press, San Diego 1999.

[2] S.G. Samko, A.A. Kilbas and O.I. Marichev, "Fractional integrals and derivatives: theory and applications," Gordon and Breach, Yverdon 1993.

[3] A.A. Kilbas, H.M. Srivastava and J.J. Trujillo, "Theory and applications of fractional differential equations," Elsevier, Amsterdam, 2006.

[4] BM Vinagre, V Feliu, "Modeling and control of dynamic systems using fractional calculus: Application to electrochemical processes and flexible structures," Proceedings of 41st IEEE conference on decision and control, Las Vegas, 2002.

[5] R.-L. Magin, "Fractional calculus in bioengineering," Begell House, Inc., 2006.

[6] B. Ross, "Fractional calculus and its applications, Lecture notes in mathematics," proceedings of the international conference, New Haven, Springer, Berlin 1974.

[7] R. Hilfer, "Applications of fractional calculus in physics," World Scientific, New Jersey, 2001.

[8] T.T. Hartley, C.F. Lorenzo and H.K. Qammer, "Chaos on a fractional Chua's system," IEEE Trans Circ Syst Theory Appl,vol. 8, pp. 485–490, 1995.

[9] Ivo Petras, "A note on the fractional-order Chua's system," Chaos, Solitons & Fractals, 33 vol.1, pp. 140-147, 2006.

[10] P. Arena, R. Caponetto, L. Fortuna and D. Porto, "Proceedings of ECCTD," Technical University of Budapest, Budapest, pp. 1259, 1997.

[11] X. Gao and J. Yu, "Chaos in the fractional order periodically forced complex Duffing's oscillators," Chaos, Solitons & Fractals, pp.1125–1133, 2005.

[12] W.H. deng and C.P. Li, "Chaos synchronization of the fractional Lu system," Physica A, pp. 61–72, 2005.

[13] C.P. Li and G.J. Peng, “Chaos in Chen’s system with a fractional order,” Chaos, Solitons & Fractals, pp. 443–450, 2004.
[14] J.G. Lu and G. Chen, “A note on the fractional-order Chen system,” Chaos, Solitons & Fractals, pp. 685–688, 2006.
[15] P. Arena and R. Caponetto, “Bifurcation and chaos in noninteger order cellular neural networks,” Int J Bifurcat Chaos , vol. 7, pp. 1527–1539, 1998.
[16] I. Petras, “A note on the fractional-order cellular neural networks,” Proceedings of the IEEE world congress on computational intelligence, international joint conference on neural networks, Vancouver, Canada, pp. 16–21, 2006.
[17] Z. Shangbo, L.i. Hua and Z. Zhengzhou, “Chaos control and synchronization in a fractional neuron network system,” Chaos, Solitons & Fractals vol. 4, pp. 973-984, 2008.
[18] D. Matigon, “Computational engineering in systems and application multiconference,” IMACS, IEEE-SMC, France, vol. 12, pp. 963, 1996.
[19] A. Kiani-B, K. Fallahi, N. Pariz and H. Leung, “A chaotic secure communication scheme using fractional chaotic systems based on an extended fractional Kalman filter,” Commun Nonlinear Sci Numer Simulat vol. 14, 2009, pp. 863–879.
[20] Grigorenko and E. Grigorenko, “Chaotic dynamics of the fractional Lorenz system,” Phys Rev Lett vol. 3, 2003.
[21] W.H. Deng and C.P. Li, “Chaos synchronization of the fractional Lü system,” Physica A vol. 353, pp. 61–72, 2005.
[22] G. Chen and T. Ueta, “Yet another chaotic attractor,” Int. J. Bifurcat Chaos vol. 9, pp. 1465–1466, 1999.
[23] C.P. Li and G. Chen, “A note on hopf bifurcation in chen's system,” Int. J. Bifurcat Chaos vol. 6, pp. 1609-1615, 2003.
[24] W.H. Deng and C.P. Li, “Synchronization of Chaotic Fractional Chen System,” J. Phys. Soc. Vol. 74, pp. 1645, Jpn. 2005.
[25] V.I. Utkin, “Variable structure systems with sliding mode,” IEEE Trans Autom Control vol. 22, pp. 212–222, 1977.
[26] J. J. E. Slotine, “Sliding controller design for non-linear systems,” International Journal of Control, vol.2, pp. 465-492, 1984.
[27] R. Palm, “Sliding mode fuzzy control,” Proceedings of IEEE Conference on Fuzzy Systems, San Diego, pp. 517-526, 1992.
[28] K. Diethelm, N.J. Ford and A.D. Freed, “Detailed error analysis for a fractional Adams method,” Numer. Algorithms vol. 36, 2004, pp. 31–52.
[29] C. Li and G. Peng, “Chaos in Chen's system with a fractional order,” Chaos Solitons Fractals vol. 22, pp. 443–450, 2004.
[30] K. Diethelm, N.J. Ford and A.D. Freed, “A predictor-corrector approach for the numerical solution of fractional differential equations,” Nonlinear Dyn., Vol.29, 2002, pp. 3–22.
[31] K. Diethelm, “An algorithm for the numerical solution of differential equations of fractional order,” Elec. Trans. Numer. Anal. Vol. 5 , pp. 1–6.
[32] Mendel, J. M. and John R. I. B., “Type-2 fuzzy sets made simple”, IEEE Trans. Fuzzy Systems 10, pp.117-127, 2000.
[33] Karnik, N. N., Mendel, J. M. and Liang Q, “Type-2 fuzzy logic systems”, IEEE Trans. Fuzzy Systems 7, pp. 643-658, 1999.
[34] C. H. Wang, C. S. C. S. Cheng, T. T. Lee, “Dynamical Optimal Training for Interval Type-2 Fuzzy Neural Network (T2FNN),” IEEE Trans. Systems, Man and Cybernetics, Part B, 34, Vol. 3, pp.1462-1477, 2004.
[35] Tsung-ChihLin, Han-LeihLiu, Ming-Jen Kuo, “Direct adaptive interval type-2 fuzzy control of multivariable nonlinear systems,” Engineering Applications of Artificial Intelligence, 22, pp.420–430, 2009.
[36] Tsung-Chih Lin, Ming-Jen Kuo, and Chao-Hsing Hsu, “Robust Adaptive Tracking Control of Multivariable Nonlinear Systems Based on Interval Type-2 Fuzzy approach,” International Journal of Innovative Computing, Information and Control, 6, Vol. A, pp. 941-961, 2010.
[37] S.H. Hosseinnia, R. Ghaderi, A. Ranjbar N., M. Mahmoudian, S. Momani, “Sliding mode synchronization of an uncertain fractional order chaotic system,” Computers and Mathematics with Applications, pp. 1637-1643, 2010.

2011 IEEE International Conference on Fuzzy Systems
June 27-30, 2011, Taipei, Taiwan

Fractional Order Chaotic System Tracking Design Based on Adaptive Hybrid Intelligent Control

Tsung-Chih Lin[1*]
[1]Department of Electronic Engineering Feng-Chia University Taichung
Taiwan
R.O.C.
tclin@fcu.edu.tw

Chia-Hao Kuo[2]
[2]Ph.D Program in Electrical and Communications Engineering Feng-Chia University Taichung
Taiwan
R.O.C.
peterqo022@hotmail.com

Valentina Emilia Balas[3]
[3]Department of Automation and Applied Informatics
University of Arad
Arad
Romania
balas@drbalas.ro

***Abstract*—In this paper, an adaptive hybrid fuzzy neural network (FNN) controller is proposed to achieve prescribed tracking performance of fractional order chaotic systems. Based on the trade-off between plant knowledge and control knowledge, a weighting factor can be adjusted by combining the indirect adaptive FNN control effort and the direct FNN adaptive control effort. Nonlinear fractional order chaotic response system is fully illustrated to track the trajectory generated from fractional order chaotic drive system. The numerical results show that tracking error and control effort can be made smaller and the proposed hybrid intelligent control scheme is more flexible during the design process.**

Keywords- Fractional order chaotic systems; fuzzy neural network (FNN), adaptive hybrid control.

I. INTRODUCTION

In recent years, fractional calculus deals with derivatives and integrations of arbitrary order [30]-[32] and numerous applications of fractional order systems in many areas of science and engineering have been proposed such as control theory, electromagnetic waves, viscoelastic systems, diffusion signal processing and bio-engineering [33]-[36]. It is observed that the description of some systems is more accurate when the fractional derivative is used. Nowadays, many fractional-order differential systems behave chaotically, such as the fractional-order Chua's system [37], [38], the fractional-order Duffing system [39], [40], the fractional-order Lu system [41], the fractional-order Chen's system [42], [43], the fractional-order cellular neural network [15]-[16], the fractional-order neural network [17].

Owing to its potential applications in secure communication and control processing [18], study of chaos tracking, synchronization, in fractional order dynamical systems and related phenomena is receiving growing attention [19], [20]. The tracking problem of fractional order chaotic systems is first investigated by Deng and Li [21] who carried out tracking in case of the two fractional Lü systems. Afterwards, they studied chaos tracking of the Chen system with a fractional order in a different manner [22]-[24].

Furthermore, the advent of fuzzy set techniques provides us with a powerful tool to solve demanding real word problem with uncertain and unpredictable environments. Based on the universal approximation theorem, [1]-[5] (fuzzy logic controllers are general enough to perform any nonlinear control actions) there is rapidly growing interest in systematic design methodologies for a class of nonlinear systems using fuzzy adaptive control schemes. By equipping with a training algorithm an adaptive fuzzy controller is synthesized from a collection of fuzzy IF-THEN rules and the parameters of the membership functions characterizing the linguistic terms in the IF-THEN rules changed according to some adaptive law for the purpose of controlling a plant to track a reference trajectory.

Like the conventional adaptive control, the adaptive FNN control is classified into direct and indirect FNN adaptive control categories [27]-[29]. A direct adaptive FNN controller uses fuzzy logic systems as controller in which linguistic fuzzy control rules can be directly incorporated into the controller. On the other hand, an indirect adaptive FNN controller uses fuzzy descriptions to model the plant in which fuzzy IF-THEN rules describing the plant can be directly incorporated into the indirect FNN controller. Moreover, a hybrid adaptive FNN controller can be constructed using a weighting factor to sum together the control efforts from indirect adaptive FNN controller and direct adaptive FNN controller [44],[45].

In this paper, by combining the approximate mathematical model, linguistic model description and linguistic control rules into a single adaptive FNN controller, an adaptive hybrid fuzzy neural network (FNN) controller is proposed to achieve prescribed tracking performance of fractional order chaotic systems. A new adaptive H^{∞} fuzzy control algorithm

978-1-4244-7316-8/11/$26.00 ©2011 IEEE

incorporated Lyapunov stability criterion is proposed so that not only the stability of adaptive fuzzy control system is guaranteed but also the influence of the approximation error and external disturbance on the tracking error can be attenuated to an arbitrarily prescribed level.

This paper is organized as follows: In section II, an introduction to fractional derivative and its relation to the approximation solution will be addressed. A brief description of the fuzzy neural networks is presented in section III. Section IV generally proposes adaptive hybrid FNN control of uncertain fractional order systems in presence of uncertainty and its stability analysis. In Section V, application of the proposed method on fractional order expression chaotic system is investigated. Finally, the simulation results and conclusion will be presented in Section VI.

II. BASIC DEFINITION AND PRELIMINARIES FOR FRACTIONAL ORDER SYSTEMS

The fractional calculus has been known more than 300 years, since the development of regular calculus. It is a generalization of integration and differentiation to non-integer order fundamental operator, denoted by ${}_aD_t^q$, where a and t are the limits of the operator. This operator is a notation for taking both the fractional integral and functional derivative in a single expression defined as

$$ {}_aD_t^q = \begin{cases} \dfrac{d^q}{dt^q}, & q > 0 \\ 1 & q = 0 \\ \int_a^t (d\tau)^{-q}, & q < 0 \end{cases} \tag{1} $$

There are some basic definitions for the general fractional and the commonly used definitions are Grunwald-Letnikov and Riemann-Liouville. The Grunwald-Letnikov definition is expressed as

$$ {}_aD_t^q f(t) = \lim_{h\to 0} \sum_{j=0}^{\left[\frac{t-a}{h}\right]} (-1)^j \binom{q}{j} f(t-jh) \tag{2} $$

where $[\cdot]$ is the integer part. The simplest and easiest definition is Riemann-Liouville definition given as

$$ {}_aD_t^q f(t) = \frac{1}{\Gamma(n-q)} \frac{d^n}{dt^n} \int_0^t \frac{f(\tau)}{(t-\tau)^{q-n+1}} d\tau \tag{3} $$

where n is the first integer which is not less q, i.e., $n-1 < q < n$, and Γ is the Gamma function.

The numerical simulation of a fractional differential equation is not simple as that of an ordinary differential equation. In this paper, the algorithm which is an improved version of Adams–Bashforth–Moulton algorithm [12]-[13] to find an approximation for fractional order systems based on predictor-correctors [12], [14] is given. Consider the following differential equation

$$ {}_0D_t^q y(t) = r(y(t),t), \quad 0 \le t \le T \quad \text{and } y^{(k)}(0) = y_0^{(k)}, k = 0,1,2,\cdots,m-1 \tag{4} $$

where

$$ {}_0D_t^q y(t) = \begin{cases} \dfrac{1}{\Gamma(m-q)} \int_0^t \dfrac{f^{(m)}(\tau)}{(t-\tau)^{q-m+1}} d\tau, & m-1 < q < m \\ \dfrac{d^m}{dt^m} y(t) & q = m \end{cases} \tag{5} $$

and is the first integer larger the q. The solution of the equation (4) is equivalent to Volterra integral equation [34] described as

$$ y(t) = \sum_{k=0}^{[q]-1} y_0^{(k)} \frac{t^k}{k!} + \frac{1}{\Gamma(q)} \int_0^t (t-\lambda)^{q-1} r(y(\lambda),\lambda) d\lambda \tag{6} $$

Let $h = T/N$, $t_n = nh$, $n = 0,1,2,\cdots N$. Then (6) can be discretized as follows.

$$ y_h(t_{n+1}) = \sum_{k=0}^{[q]-1} y_0^{(k)} \frac{t_{n+1}^k}{k!} + \frac{h^q}{\Gamma(q+2)} r(y_h^p(t_{n+1}),t_{n+1}) + \frac{h^q}{\Gamma(q+2)} \sum_{j=0}^{n} a_{j,n+1} r(y_h(t_j),t_j) \tag{7} $$

where predict value $y_h^p(t_{n+1})$ is determined by

$$ y_h^p(t_{n+1}) = \sum_{k=0}^{[q]-1} y_0^{(k)} \frac{t_{n+1}^k}{k!} + \frac{h^q}{\Gamma(q)} \sum_{j=0}^{n} b_{j,n+1} r(y_h(t_j),t_j) \tag{8} $$

and

$$ a_{j,n+1} = \begin{cases} n^{q+1} - (n-q)(n+1)^q, & j = 0 \\ (n-j+2)^{q+1} + (n-j)^{q+1} - 2(n-j+1)^{q+1} & 1 \le j \le n \\ 1 & j = n+1 \end{cases} \tag{9} $$

$$ b_{j,n+1} = \frac{h^q}{q} ((n+1-j)^q - (n-j)^q) \tag{10} $$

The approximation error is given as

$$ \max_{j=0,1,2,\cdots N} \left| y(t_j) - y_h(t_j) \right| = \mathrm{O}(h^p) \tag{11} $$

where $p = \min(2, 1+q)$. Therefore, the numerical solution of a fraction order system can be obtained by applying the above mentioned algorithm.

III. A BRIEF DESCRIPTION OF THE FUZZY NEURAL NETWORKS [6]-[9], [25]

Fuzzy logic systems are knowledge-based or rule-based systems which consist of so called fuzzy IF-THEN rules. The basic configuration the T-S FNN system includes a fuzzy rule base, which comprises of a collection of fuzzy IF-THEN rules in the following form:

$$ R^{(l)}: \text{ IF } x_1 \text{ is } F_1^l, \text{ and } \cdots, \text{ and } x_n \text{ is } F_n^l, \text{THEN } y_l = q_0^l + q_1^l x_1 + \cdots + q_n^l x_n = \underline{\theta}_l^T [1\ \underline{x}^T]^T \tag{12} $$

where F_i^l are fuzzy sets and $\underline{\theta}_l^T = [q_0^l, q_1^l, \cdots, q_n^l]$ is a vector of the adjustable weight factors of the consequence part of the fuzzy rule. Also y_l is a fuzzy inference engine to combine the fuzzy IF-THEN rules in the fuzzy rule base into a mapping from an input linguistic vector $\underline{x}^T = [x_1, x_2, \cdots, x_n] \in R^n$ to an output variable $y \in R$. Let M be the number of the fuzzy IF-THEN rules. The output of the fuzzy logic systems with central average defuzzifier, product inference and singleton fuzzifier can be expressed as

$$ y(\underline{x}) = \frac{\sum_{l=1}^{M} \phi^l \cdot y_l}{\sum_{l=1}^{M} \phi^l} = \frac{\sum_{l=1}^{M} \phi^l \cdot \underline{\theta}_l^T [1\ \underline{x}^T]}{\sum_{l=1}^{M} \phi^l} \tag{13} $$

where $\mu_{F_i^l(x_i)}$ is the membership function value of the fuzzy variable x_i and $\phi^l = \prod_{i=1}^{n} \mu_{F_i^l(x_i)}$ is the true value of the l^{th} implication. Equation (13) can be rewritten as

$$y(\underline{x}) = \underline{\theta}^T \underline{\psi}(\underline{x}) \quad (14)$$

where $\underline{\theta}^T = \left[\underline{\theta}_1^T \ \underline{\theta}_2^T \ \cdots \ \underline{\theta}_M^T\right]$ is an adjustable parameter vector and $\underline{\psi}^T(\underline{x}) = [\psi^1(\underline{x}), \psi^2(\underline{x}), \cdots, \psi^M(\underline{x})]$ is a fuzzy basis function vector defined as

$$\psi^l(\underline{x}) = \frac{\phi^l[1 \ \underline{x}^T]}{\sum_{l=1}^{M} \phi^l} \quad (15)$$

When the inputs are fed into the T-S FNN, the true value υ^l of the lth implication is computed. Applying the common defuzzification strategy, the output of the neural networks expressed as (13) is pumped out. The overall configuration of the T-S FNN is shown in Fig.1 [27]-[29].

Based on the universal approximation theorem [26], the above fuzzy logic system is capable of uniformly approximating any well-defined nonlinear function over a compact set U_c to any degree of accuracy. Also it is straightforward to show that a multi-output system can always be approximated by a group of single-output approximation systems.

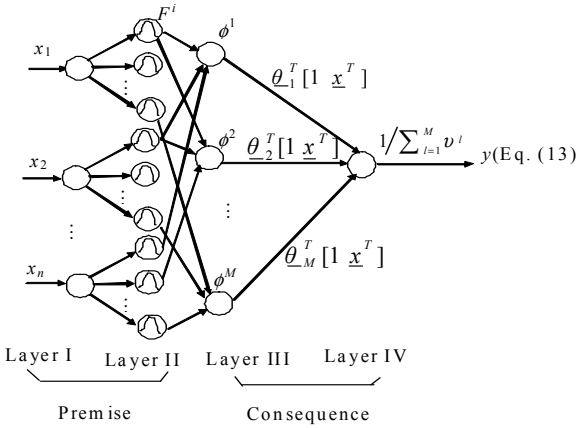

Figure1 The configuration of the T-S fuzzy-neural networks.

IV. Adaptive Hybrid Fuzzy H^∞ Tracking Control of Uncertain Fractional Order Chaotic Systems

In this section, we study adaptive H^∞ tracking control of uncertain fractional order chaotic systems, i.e., to force output trajectory of the response system to track output trajectory of the drive system.

Consider a fractional order chaotic dynamic system

$$\begin{aligned} x^{(nq)} &= f(\underline{x},t) + g(\underline{x},t)u + d(t) \\ y &= x_1 \end{aligned} \quad (16)$$

where $\underline{x} = [x_1, x_2, \cdots, x_n]^T = [x, x^{(q)}, x^{(2q)}, \cdots, x^{((n-1)q)}]^T$ is the state vector, $f(\underline{x},t)$ and $g(\underline{x},t)$ are unknown but bounded nonlinear functions which express system dynamics, $d(t)$ is the external bounded disturbance and $u(t)$ is the control input. The control objective is to force the system output y to follow a bounded reference signal y_d which is the output trajectory of a drive system, under the constraint that all signals involved must be bounded. To begin with, the reference signal vector $\underline{y}_d$ and the tracking error vector $\underline{e}$ will be defined as

$$\underline{y}_d = \left[y_d, y_d^{(q)}, \cdots, y_d^{((n-1)q)}\right]^T \in R^n,$$
$$\underline{e} = \underline{y}_d - \underline{x} = [e, e^{(q)}, e^{(2q)}, \cdots, e^{((n-1)q)}]^T \in R^n, e^{(iq)} = y_d^{(iq)} - x^{(iq)} = y_d^{(iq)} - y^{(iq)}$$

Let $\underline{k} = \left[k_1, k_2, \cdots, k_n\right]^T \in R^n$ to be chosen such that $p(s) = s^{(nq)} + k_n s^{(n-1)q} + \cdots + k_1$ is a Hurwitz polynomial. If the functions $f(\underline{x},t)$ and $g(\underline{x},t)$ are known and the system is free of external disturbance d, then control law of the certainty equivalent controller is obtained as [38]

$$\bar{u} = \frac{1}{g(\underline{x},t)}\left(-f(\underline{x},t) + y_d^{(nq)} + \underline{k}^T \underline{e}\right) \quad (17)$$

Substituting (17) into (16), we have [30]

$$e^{(nq)} + k_n e^{(n-1)q} + \cdots + k_1 e = 0$$

which is the main objective of control, $\lim_{t\to\infty} e(t) = 0$.

However, $f(\underline{x},t)$ and $g(\underline{x},t)$ are unknown and external disturbance, $d(t) \neq 0$, the ideal control effort (17) cannot be implemented. We replace $f(\underline{x},t)$ and $g(\underline{x},t)$ by the fuzzy logic system $f(\underline{x}|\underline{\theta}_f)$ and $g(\underline{y}|\underline{\theta}_g)$ in specified form as (14), i.e.,

$$f(\underline{x}|\underline{\theta}_f) = \xi^T(\underline{x})\underline{\theta}_f, \quad g(\underline{x}|\underline{\theta}_g) = \xi^T(\underline{x})\underline{\theta}_g \quad (18)$$

Here the fuzzy basis function $\xi(\underline{x})$ depends on the fuzzy membership functions and is supposed to be fixed, while $\underline{\theta}_f$ and $\underline{\theta}_g$ are adjusted by adaptive laws based on Lyapunov stability criterion.

However, depending on plant knowledge and control knowledge, a hybrid adaptive FNN controller can be constructed by incorporating both fuzzy description and fuzzy control rules using a weighting factor α to combine the indirect adaptive FNN controller and the direct adaptive FNN controller. Based on the trade-off between plant knowledge and control knowledge, the weighting factor $\alpha \in [1, 1]$ can be adjusted. Therefore, the total control effort can be expressed as

$$u = \alpha u_i + (1-\alpha)u_d \quad (19)$$

where the direct adaptive FNN controller u_d and the indirect adaptive FNN controller u_i are given as follows:

$$u_d = u_D(\underline{x}|\underline{\theta}) - \frac{u_a}{g(\underline{x}|\underline{\theta})} \quad (20)$$

$$u_i = \frac{1}{g(x|\theta_g)}[-f(x|\theta_f) + y_d^{(nq)} + \underline{k}^T \underline{e} + u_a] \quad (21)$$

where the robust compensator u_a is employed to attenuate the external disturbance and the fuzzy approximation errors and $u_D(\underline{x}|\underline{\theta})$ is obtained by fuzzy logic system specified as

$$u_D(\underline{x}|\underline{\theta}_D) = \xi^T(\underline{x})\underline{\theta}_D \quad (22)$$

By substituting (19) into (16), the error dynamic equation can be obtained in state space representation as

$$\begin{aligned} \underline{e}^{(q)} = A\underline{e} + B\{&\alpha\left(\left[f(\underline{x}|\theta_f) - f(\underline{x},t)\right] + \left[g(\underline{x}|\theta_g) - g(\underline{x},t)\right]u_i\right) \\ &-(1-\alpha)\left(g(\underline{x},t)\left[u_D(\underline{x}|\theta) - \bar{u}\right]\right) + u_a - d(t)\} \end{aligned} \quad (23)$$

where $A=\begin{bmatrix} 0 & 1 & 0 & 0 & \cdots & 0 & 0 \\ 0 & 0 & 1 & 0 & \cdots & 0 & 0 \\ \vdots & \vdots & \vdots & \vdots & \ddots & \vdots & \vdots \\ 0 & 0 & 0 & 0 & \cdots & 0 & 1 \\ -k_1 & -k_2 & -k_3 & -k_4 & \cdots & -k_{(n-1)} & -k_n \end{bmatrix}$ and $B=\begin{bmatrix} 0 \\ 0 \\ \vdots \\ 0 \\ 1 \end{bmatrix}$

The optimal parameter estimations $\underline{\theta}_f^*$, $\underline{\theta}_g^*$ and $\underline{\theta}_D^*$ are defined as

$$\underline{\theta}_f^* = \arg\min_{\underline{\theta}_f \in \Omega_f}[\sup_{x \in \Omega_x} | f(\underline{x}|\underline{\theta}_f) - f(\underline{x},t) |] \quad (24)$$

$$\underline{\theta}_g^* = \arg\min_{\underline{\theta}_g \in \Omega g}[\sup_{x \in \Omega_x} | g(\underline{x}|\underline{\theta}_g) - g(\underline{x},t) |] \quad (25)$$

and

$$\underline{\theta}_D^* = \arg\min_{\underline{\theta}_D \in \Omega_D}[\sup_{x \in \Omega_x} | u_D(\underline{x}|\underline{\theta}_g) - \overline{u} |] \quad (26)$$

where Ω_f, Ω_g, Ω_D and $\Omega_{\underline{x}}$ are constraint sets of suitable bounds on $\underline{\theta}_f$, $\underline{\theta}_g$, $\underline{\theta}_D$ and $\underline{x}$ respectively and they are defined as $\Omega_f = \{\underline{\theta}_f \,|\, |\underline{\theta}_f| \le M_f\}$, $\Omega_g = \{\underline{\theta}_g \,|\, |\underline{\theta}_g| \le M_g\}$, $\Omega_D = \{\underline{\theta}_D \,|\, |\underline{\theta}_D| \le M_D\}$ and $\Omega_x = \{x \,|\, |x| \le M_x\}$, where M_f, M_g, M_D and M_x are positive constants.

By using (24)-(26), error dynamic equation (23) can be rewritten as

$$\begin{aligned} \underline{e}^{(q)} = \mathrm{A}\underline{e} + \mathrm{B}\{ & \alpha\left(\left[f(\underline{x}|\theta_f) - f(\underline{x}|\theta_f^*)\right] + \left[g(\underline{x}|\theta_g) - g(\underline{x}|\theta_g^*)\right]u_i\right) \\ & -(1-\alpha)\, g(\underline{x},t)\left[u(\underline{x}|\theta) - u(\underline{x}|\theta^*)\right] + u_a + \omega\} \end{aligned} \quad (27)$$

where the minimum approximation errors is defined as

$$\begin{aligned} \omega = & \alpha\left(f(\underline{x}|\theta_f^*) - f(\underline{x},t) + \left[g(\underline{x}|\theta_g^*) - g(\underline{x},t)\right]u_i\right) \\ & -(1-\alpha)\, g(\underline{x},t)\left[u_D(\underline{x}|\theta^*) - \overline{u}\right] - d(t) \end{aligned} \quad (28)$$

If $\tilde{\underline{\theta}}_f = \underline{\theta}_f - \underline{\theta}_f^*$, $\tilde{\underline{\theta}}_g = \underline{\theta}_g - \underline{\theta}_g^*$ and, $\tilde{\underline{\theta}}_D = \underline{\theta}_D - \underline{\theta}_D^*$, we have

$$\underline{e}^{(q)} = A\underline{e} + B[\underline{\xi}(\underline{x})^T \tilde{\underline{\theta}}_f + \underline{\xi}(\underline{x})^T \tilde{\underline{\theta}}_g u_i + \underline{\xi}(\underline{x})^T \tilde{\underline{\theta}}_D + u_a + \omega] \quad (29)$$

Following the proceeding consideration, the following theorem can be obtained.

Theorem: Consider the fractional order SISO nonlinear chaotic system (16) with control input (19), if the robust compensator u_a and the fuzzy-based adaptive laws are chosen as

$$u_a = -\frac{1}{r} B^T P \underline{e} \quad (30)$$

$$\underline{\theta}_f^{(q)} = -r_1 \underline{\xi}(\underline{x}) B^T P \underline{e} \quad (31)$$

$$\underline{\theta}_g^{(q)} = -r_2 \underline{\xi}(\underline{x}) B^T P \underline{e} u_i \quad (32)$$

$$\underline{\theta}_D^{(q)} = r_3 \underline{\xi}(\underline{x}) g(x,t) B^T P \underline{e} \quad (33)$$

where $r > 0, r_i > 0, i = 1 \sim 3$, and $P = P^T > 0$ is the solution of the following Ricatti-like equation

$$PA + A^T P + Q - PB\left(\frac{2}{r} - \frac{1}{\rho^2}\right) B^T P = 0 \quad (34)$$

where $Q = Q^T > 0$ is a prescribed weighting matrix. Therefore, the H^∞ tracking performance can be achieved for a prescribed attenuation level ρ and all the variables of the closed-loop system are bounded.

Proof: In order to analyze the closed-loop stability, the Lyapunov function candidate is chosen as

$$V = \frac{1}{2}\underline{e}^T P \underline{e} + \frac{\alpha}{2r_1}\tilde{\underline{\theta}}_f^T \tilde{\underline{\theta}}_f + \frac{\alpha}{2r_2}\tilde{\underline{\theta}}_g^T \tilde{\underline{\theta}}_g + \frac{(1-\alpha)}{2r_3}\tilde{\underline{\theta}}_D^T \tilde{\underline{\theta}}_D \quad (35)$$

Taking the derivative of the (35) with respect to time, we get

$$\begin{aligned} V^{(q)}(t) = & \frac{1}{2}(\underline{e}^{(q)}(t))^T P \underline{e}(t) + \frac{1}{2}\underline{e}^T(t) P \underline{e}^{(q)}(t) \\ & + \frac{\alpha}{r_1}(\tilde{\underline{\theta}}_f^T)(\tilde{\underline{\theta}}_f^{(q)}) + \frac{\alpha}{r_2}(\tilde{\underline{\theta}}_g^T)(\tilde{\underline{\theta}}_g^{(q)}) + \frac{1-\alpha}{r_3}(\tilde{\underline{\theta}}_D^T)(\tilde{\underline{\theta}}_D^{(q)}) \end{aligned} \quad (36)$$

$$\begin{aligned} V^{(q)} = & \frac{1}{2}\underline{e}^T \mathrm{A}^T P \underline{e} + \left[\alpha\left(\underline{\xi}^T \tilde{\underline{\theta}}_f + \underline{\xi}^T \tilde{\underline{\theta}}_g u_i\right) - (1-\alpha)\, g(x,t)\underline{\xi}^T \tilde{\underline{\theta}}_D + \omega\right]^T \mathrm{B}^T P \underline{e} \\ & + \frac{1}{2}\underline{e}^T P \mathrm{A}\underline{e} + \underline{e}^T P \mathrm{B}\left[\alpha\left(\underline{\xi}^T \tilde{\underline{\theta}}_f + \underline{\xi}^T \tilde{\underline{\theta}}_g u_i\right) - (1-\alpha)\, g(x,t)\underline{\xi}^T \tilde{\underline{\theta}}_D + u_a + \omega\right] \\ & + \frac{\alpha}{r_1}\tilde{\underline{\theta}}_f^T \tilde{\underline{\theta}}_f^{(q)} + \frac{\alpha}{r_2}\tilde{\underline{\theta}}_g^T \tilde{\underline{\theta}}_g^{(q)} + \frac{(1-\alpha)}{r_3}\tilde{\underline{\theta}}_D^T \tilde{\underline{\theta}}_D^{(q)} \\ & = \frac{1}{2}\underline{e}^T (PA + A^T P - \frac{2}{r} PBB^T P)\underline{e} + (\alpha \underline{e}^T PB\underline{\xi}^T(\underline{x}) + \frac{\alpha}{\gamma_1}\tilde{\underline{\theta}}_f^{(q)T})\tilde{\underline{\theta}}_f \\ & + (\alpha \underline{e}^T PB\underline{\xi}^T(\underline{x})u_i + \frac{\alpha}{\gamma_2}\tilde{\underline{\theta}}_g^{(q)T})\tilde{\underline{\theta}}_g - \left((1-\alpha)\,\underline{e}^T PBg(\underline{x},t)\underline{\xi}(\underline{x})^T - \frac{(1-\alpha)}{\gamma_3}\tilde{\underline{\theta}}_D^{(q)T}\right)\tilde{\underline{\theta}}_D \\ & + \frac{1}{2}(\omega^T B^T P\underline{e} + \underline{e}^T PB\omega) \end{aligned} \quad (37)$$

From the robust compensator u_a and the fuzzy-based adaptive laws are given (30)-(33), after simple manipulation, we have

$$\begin{aligned} V^{(q)}(t) = & -\frac{1}{2}\underline{e}^T Q\underline{e} - \frac{1}{2\rho^2}\underline{e}^T PBB^T \underline{e} + \underline{e}^T PB\omega \\ = & -\frac{1}{2}\underline{e}^T Q\underline{e} - \frac{1}{2}(\frac{1}{\rho}B^T P\underline{e} - \rho\omega)^T(\frac{1}{\rho}B^T P\underline{e} - \rho\omega) + \frac{1}{2}\rho^2\omega^T\omega \\ \le & -\frac{1}{2}\underline{e}^T Q\underline{e} + \frac{1}{2}\rho^2\omega^T\omega \end{aligned} \quad (38)$$

Integrating (38) from $t = 0$ to $t = T$, we have

$$V(T) - V(0) \le -\frac{1}{2}\int_0^T (\underline{e}^T Q\underline{e} + \frac{1}{2}\rho^2\omega^T\omega)\, dt \quad (39)$$

Since $V(T) \ge 0$, (39) can be rewritten as follows:

$$\int_0^T \underline{e}^T Q\underline{e}\ dt \le \underline{e}^T(0)P\underline{e}(0) + \underline{\theta}^T(0)\underline{\theta}(0) + \rho^2\int_0^T \omega^T\omega\ dt \quad (40)$$

Therefore, the H^∞ tracking performance can be achieved. The proof is completed.

V. SIMULATION EXAMPLE

In this section, we will apply our adaptive hybrid H^∞ FNN controller to force the fractional order chaotic response system to track the trajectory of the fractional order chaotic drive system.

Example: The fractional order chaotic drive and response systems are given as follows:

Drive System:

$$\begin{cases} D^{(q)}y_1 = y_2 \\ D^{(q)}y_2 = 1.2y_1 - y_2 - y_1^2 + 0.5\cos(t) \end{cases}$$

Response System:

$$\begin{cases} D^{(q)}x_1 = x_2 \\ D^{(q)}x_2 = x_1 - 1.8x_2 - x_1^2 + 0.9\cos(t) + u(t) + d(t) \end{cases}$$

where external disturbance $d(t) = 0.1\sin(t)$. The main objective is to control the trajectories of the response system to track the reference trajectories obtained from the drive system. The initial conditions of drive and response systems are chosen as $\begin{bmatrix} y_1(0) \\ y_2(0) \end{bmatrix} = \begin{bmatrix} 0 \\ 0 \end{bmatrix}$ and $\begin{bmatrix} x_1(0) \\ x_2(0) \end{bmatrix} = \begin{bmatrix} 1 \\ -1 \end{bmatrix}$, respectively. values of $q = 0.95$ are considered. All design constants are specified as k_1=k_2=1, $r_1 = 200$, $r_2 = 40$, $r_3 = 100$, $r_4 = 10$, $r = 0.005$, $\rho = 0.05$ and step size h=0.01.

Case 1. q=0.95, α=0.7 : For $q = 0.95$ and free of control input, the phase portrait of the drive and response systems is given in Fig. 2.

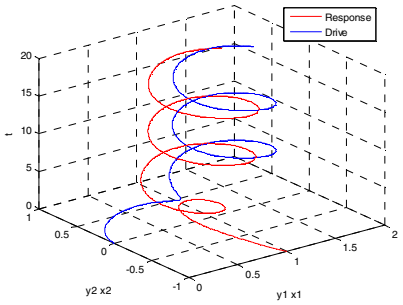

Figure 2. Phase portrait of chaotic drive and response systems.

The membership functions for x_i $i = 1, 2$ are shown in Fig. 3 and are selected as follows:

$$\mu_{F_1^i}(x_i) = \exp\left[-0.5\left(\frac{x_i - 2}{0.8}\right)^2\right],\ \mu_{F_2^i}(x_i) = \exp\left[-0.5\left(\frac{x_i - 1.5}{0.8}\right)^2\right],$$

$$\mu_{F_3^i}(x_i) = \exp\left[-0.5\left(\frac{x_i - 1}{0.8}\right)^2\right],\ \mu_{F_4^i}(x_i) = \exp\left[-0.5\left(\frac{x_i - 0.5}{0.8}\right)^2\right],$$

$$\mu_{F_5^i}(x_i) = \exp\left[-0.5\left(\frac{x_i}{0.8}\right)^2\right],\ \mu_{F_6^i}(x_i) = \exp\left[-0.5\left(\frac{x_i + 0.5}{0.8}\right)^2\right],$$

$$\mu_{F_7^i}(x_i) = \exp\left[-0.5\left(\frac{x_i + 1}{0.8}\right)^2\right]$$

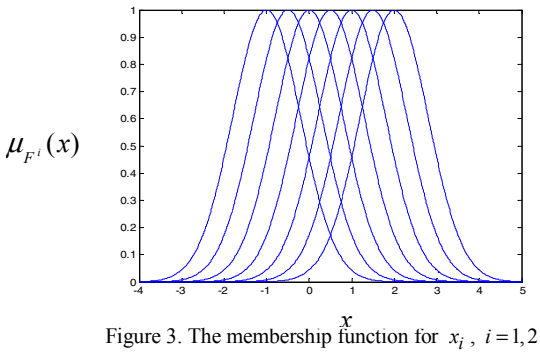

Figure 3. The membership function for x_i, $i = 1, 2$.

From the adaptive laws (33)-(36) and the robust compensator (32), the control effort of the response system can be obtained as

$$u = \alpha u_i + (1 - \alpha)u_d \tag{41}$$

Fig. 4 and 5 show the trajectories of the states x_1, y_1 and x_2, y_2, respectively. Control effort trajectory is given in Fig 6 and phase portrait, tracking performance, of the drive and response systems is shown in Fig. 7. Fig. 8 shows the graph of $V^{(q)}(t)$ which is always negative defined and consequently is stable.

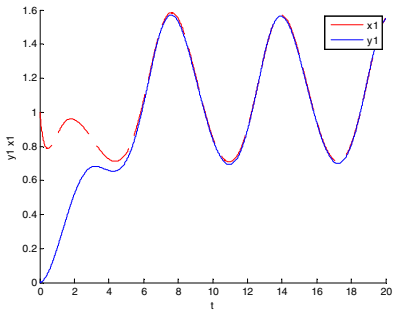

Figure 4. The trajectories of the states x_1 and y_1.

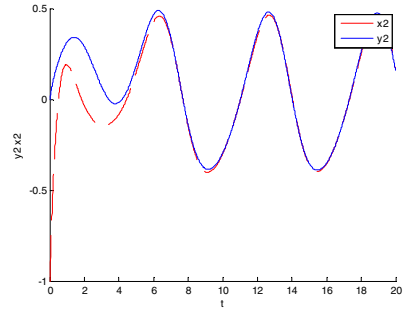

Figure 5. The trajectories of the states x_2 and y_2.

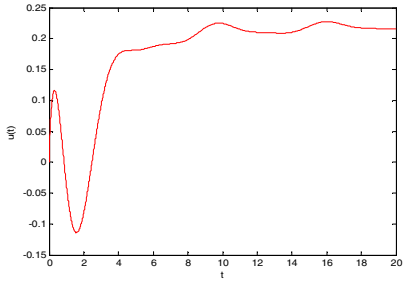

Figure 6. Trajectory of the control effort.

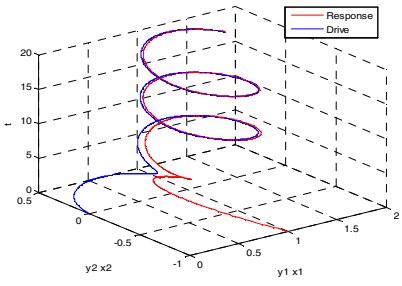

Figure 7. Phase portrait, tracking performance, of the drive and response systems.

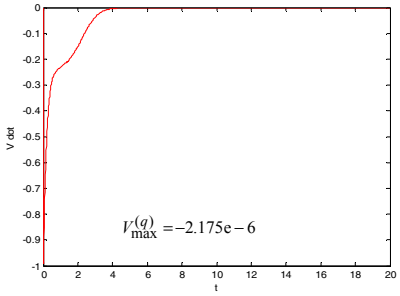

Figure 8. The graph of $V^{(q)}(t)$.

In order to show the robustness of the proposed adaptive fuzzy H^{∞} control, the control effort is activated at 5 second. The phase portrait, tracking performance, of the drive and response systems is given in Fig. 9. Fig. 10 and 11 show the trajectories of the states x_1, y_1 and x_2, y_2, respectively. We can see that a fast synchronization of drive and response is achieved as the control effort is activated. Control effort trajectory is given in Fig 12.

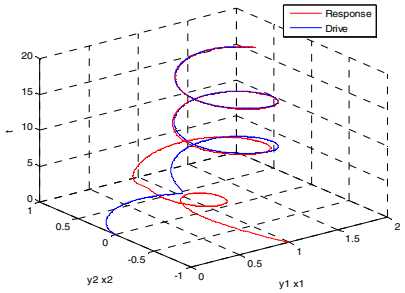

Figure 9. Phase portrait, tracking performance, of the drive and response systems.

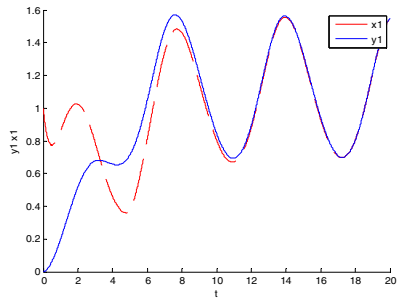

Figure 10. The trajectories of the states x_1 and y_1.

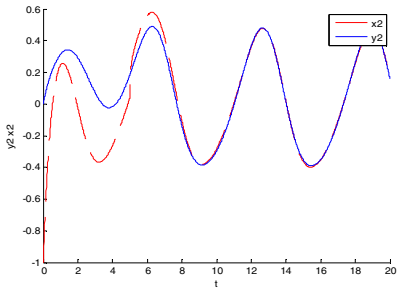

Figure 11. The trajectories of the states x_2 and y_2.

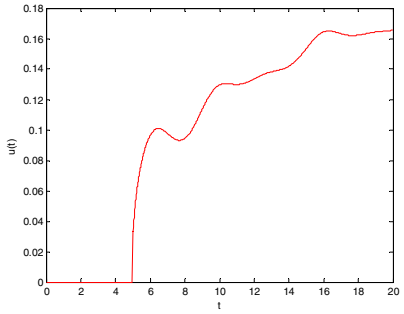

Figure 12. Trajectory of the control effort.

VI. Conclusions

A novel adaptive hybrid FNN controller is proposed to achieve prescribed tracking performance of fractional order chaotic systems in this paper. It is a flexible design methodology by the trade-off between plant knowledge and control knowledge using a weighting factor α adopted to sum together the control effort from indirect adaptive FNN controller and direct adaptive FNN controller. Based on the Lyapunov synthesis approach, free parameters of the adaptive fuzzy controller can be tuned on line by output feedback control law and adaptive laws. The simulation example, the output trajectory of the fractional order chaotic response system to tracking the trajectory of the fractional order chaotic drive system, is given to demonstrate the effectiveness of the proposed methodology. The significance of the adaptive fuzzy H^{∞} control in the simulations for different values of q is manifest. Simulation results show that a fast synchronization of the drive and response systems can be achieved and q is reduced the chaos is seen reduced, i.e., the synchronization error is reduced, accordingly.

References

[1] L. **X.** Wang, Stable adaptive fuzzy control of nonlinear systems, *IEEE Trans. Fuzzy Syst.,* vol. 1, pp. 146-155, 1993.

[2] L. X. Wang, and J. M. Mendel, Fuzzy basis function, universal approximation, and orthogonal least square learning, *IEEE Trans. Neural Networks,* vol. 3, no. 5, pp. 807-814, 1992.

[3] L. X. Wang, *Adaptive **Fuzzy** Systems and Control: Design and Stability Analysis*. Englewood Cliffs, NJ: Prentice-Hall, 1994.

[4] **J.** J. Buckley, 'Theory of fuzzy controller: An introduction," *Fuzzy Sets Syst.,* vol. 51, 1992, pp. 249-258.

[5] G. C. Hwang and *S.* C. Lin, "A stability approach to fuzzy control design for nonlinear systems," *Fuzzy Sets Syst.,* vol. 48, 1992pp. 279-287.

[6] T. Takagi and M. Sugeno, "Fuzzy Identification of Systems and Its Applications to Modeling and control," *IEEE Trans. Syst., Man, Cybern*., vol. 15, Jan./Feb., 1985, pp. 116-132.

[7] M. Sugeno, "On Stability of Fuzzy Systems Expressed by Fuzzy Rules with Singleton Consequents," *IEEE Trans. Fuzzy Syst.*, vol. 7, Apr. 1999, pp.201-224.

[8] F. Cuesta, F. Gordillo, J. Aracil, and A. Ollero, "Stability Analysis of Nonlinear Multivariable Takagi-Sugeno Fuzzy Control Systems," *IEEE Trans. Fuzzy Syst.*, vol. 7, Oct., 1999, pp.508-519.

[9] Marcelo C. M. Teixeira and S. H. Zak, "Stabilizing Controller Design for Uncertain Nonlinear Systems Using Fuzzy Models," *IEEE Trans. Fuzzy Syst.*, vol. 7, Apr.1999, pp.133-142.

[10] K. Diethelm, N.J. Ford and A.D. Freed, Detailed error analysis for a fractional Adams method, *Numer. Algorithms* **36** 2004, pp. 31–52.

[11] C. Li and G. Peng, Chaos in Chen's system with a fractional order, *Chaos Solitons Fractals* **22** (2004), pp. 443–450.

[12] K. Diethelm, N.J. Ford and A.D. Freed, A predictor-corrector approach for the numerical solution of fractional differential equations, *Nonlinear Dyn.* **29** (2002), pp. 3–22.
[13] K. Diethelm, An algorithm for the numerical solution of differential equations of fractional order, *Elec. Trans. Numer. Anal.* **5** 1997, pp. 1–6.
[14] K. Diethelm and N.J. Ford, Analysis of fractional differential equations, *J. Math. Anal. Appl.* **265** (2002), pp. 229–248.
[15] P. Arena and R. Caponetto, Bifurcation and chaos in noninteger order cellular neural networks, *Int J Bifurcat Chaos* **8** (7) 1998, pp. 1527–1539.
[16] Petras I. A note on the fractional-order cellular neural networks. In: Proceedings of the IEEE world congress on computational intelligence, international joint conference on neural networks, Vancouver, Canada; 2006. p. 16–21.
[17] Zhou Shangbo, L.i. Hua and Zhu Zhengzhou, Chaos control and synchronization in a fractional neuron network system, *Chaos, Solitons & Fractals* 2006.
[18] D. Matigon, Computational engineering in systems and application multiconference, IMACS, IEEE-SMC, vol. 2, France; 1996. p. 963.
[19] A. Kiani-B, K. Fallahi, N. Pariz and H. Leung, A chaotic secure communication scheme using fractional chaotic systems based on an extended fractional Kalman filter, *Commun Nonlinear Sci Numer Simulat* **14** 2009, pp. 863–879.
[20] Grigorenko and E. Grigorenko, Chaotic dynamics of the fractional Lorenz system, *Phys Rev Lett* **91** (3) 2003, p. 034101.
[21] W.H. Deng and C.P. Li, Chaos synchronization of the fractional Lü system, *Physica A* **353** 2005, pp. 61–72.
[22] G. Chen and T. Ueta, *Int. J. Bifurc. Chaos* **9** 1999, p. 1465.
[23] C.P. Li and G. Chen, A note on hopf bifurcation in chen's system, 2003 International Journal of Bifurcation and Chaos in Applied Sciences and Engineering, 13 (6), pp. 1609-1615.
[24] W.H. Deng and C.P. Li, Synchronization of Chaotic Fractional Chen System, *J. Phys. Soc. Jpn.* **74** 2005, p. 1645.
[25] O. Begovich, E. N. Sanchez, and M. Maldonado, "T-S Scheme for Trajectory Tracking of an Underactuated Robot," in Proc. *Fuzzy_IEEE.* 2000*,* San Antonio, Texas, USA May, 2000, pp.798-803.
[26] J. L. Castro, "Fuzzy logical controllers are universal approximators," *IEEE Trans. Syst., Man, Cybern*., vol. 25, Apr. 1995 , pp. 629-635.
[27] Chi-Hsu Wang, Tsung-Chih Lin, , Tsu-Tan Lee and Han-Leih Liu, "Adaptive Hybrid Intelligent Control for Unknown Nonlinear Dynamical Systems", IEEE Transaction on Systems, Man, and Cybernetics Part B , vol. 32, no. 5, October, 2002, pp. 583-597.
[28] Chi-Hsu Wang, Han-Leih Liu and Tsung-Chih Lin, "Direct Adaptive Fuzzy-Neural Control with Observer and Supervisory Control for Unknown Nonlinear Systems", IEEE Transaction on Fuzzy Systems, Vol. 10, no. 1, 2002, pp. 39-49.
[29] Tsung-Chih Lin Chi-Hsu Wang and Han-Leih Liu, "Observer-based Indirect Adaptive Fuzzy-Neural Tracking Control for Nonlinear SISO Systems Using VSS and H^{∞} " Fuzzy Sets and Systems 143, 2004, pp.211-232.
[30] I. Podlubny, Fractional differential equations, Academic Press, San Diego 1999.
[31] S.G. Samko, A.A. Kilbas and O.I. Marichev, Fractional integrals and derivatives: theory and applications, Gordon and Breach, Yverdon 1993.
[32] A.A. Kilbas, H.M. Srivastava and J.J. Trujillo, Theory and applications of fractional differential equations, Elsevier, Amsterdam 2006.
[33] Vinagre BM, Feliu V. Modeling and control of dynamic systems using fractional calculus: Application to electrochemical processes and flexible structures. In: Proceedings of 41st IEEE conference on decision and control, Las Vegas; 2002.
[34] R.-L. Magin, Fractional calculus in bioengineering, Begell House, Inc. 2006.
[35] B. Ross, Fractional calculus and its applications, *Lecture notes in mathematics. proceedings of the international conference*, *New Haven*, Springer, Berlin 1974 June.
[36] R. Hilfer, Applications of fractional calculus in physics, World Scientific, New Jersey 2001.
[37] T.T. Hartley, C.F. Lorenzo and H.K. Qammer, Chaos on a fractional Chua's system, *IEEE Trans Circ Syst Theory Appl* **42** (8) 1995, pp. 485–490.
[38] Ivo Petras, A note on the fractional-order Chua's system, *Chaos, Solitons & Fractals* 2006.
[39] P. Arena, R. Caponetto, L. Fortuna and D. Porto, *Proceedings of ECCTD*, Technical University of Budapest, Budapest 1997 p. 1259, September.
[40] X. Gao and J. Yu, Chaos in the fractional order periodically forced complex Duffing's oscillators, *Chaos, Solitons & Fractals* **26** 2005, pp. 1125–1133.
[41] W.H. deng and C.P. Li, Chaos synchronization of the fractional Lu system, *Physica A* **353** 2005, pp. 61–72.
[42] C.P. Li and G.J. Peng, Chaos in Chen's system with a fractional order, *Chaos, Solitons & Fractals* **20** 2004, pp. 443–450.
[43] J.G. Lu and G. Chen, A note on the fractional-order Chen system, *Chaos, Solitons & Fractals* **27** 2006, pp. 685–688.
[44] Tsung-Chih Lin, Chia-Hao Kuo, Adaptive Fuzzy H^{∞} Synchronization of Uncertain Fractional Order Chaotic Systems, 2011 3rd International Conference on Computer and Automation Engineering, V1, pp.86-90.
[45] Tsung-Chih Lin, Tun-Yuan Lee, H^{∞} Tracking Design of SISO Uncertain Nonlinear Fractional Order Time-Delay Systems: Adaptive Fuzzy Approach, 2011 3rd International Conference on Computer and Automation Engineering, V1, pp. 74-79.

2011 IEEE International Conference on Fuzzy Systems
June 27-30, 2011, Taipei, Taiwan

Towards the Learning from Low Quality Data in a Fuzzy Random Forest ensemble

Jose M. Cadenas M. Carmen Garrido Raquel Martinez
Dpt. Engineering Information and Communications
Faculty of Informatic, University of Murcia
Campus of Espinardo, Murcia, Spain
Email: jcadenas, carmengarrido, raquel.m.e@um.es

Piero P. Bonissone
GE Global Research
One Research Circle
Niskayuna, NY 12309, USA
Email: bonissone@ge.com

***Abstract*—Imperfect information inevitably appears in real situations for a variety of reasons. Although efforts have been made to incorporate imperfect data into classification techniques, there are still many limitations as to the type of data, uncertainty and imprecision that can be handled. In this paper, we will present a Fuzzy Random Forest ensemble for classification and show its ability to handle imperfect data into the learning and the classification phases. Then, we will describe the types of imperfect data it supports. We will devise an augmented ensemble that can operate with others type of imperfect data: crisp, missing, probabilistic uncertainty and imprecise (fuzzy and crisp) values. Additionally, we will perform experiments with datasets used in other papers to show the advantage of being able to express the true nature of imperfect information.**

***Index Terms*—Fuzzy Random Forest; Imperfect Data**

I. Introduction

Classification has always been a challenging problem [1], [2]. Many techniques and algorithms have been developed to address this issue. There is a wide range of classification techniques based on different theoretical proposals [3]–[6]. Unfortunately, most of the conventional techniques did not consider the sources of uncertainty. As a result, incomplete and imprecise data have usually been discarded or ignored in the classifier's learning and in its subsequent classification process. However, this data is inevitable when dealing with real-world applications.

Imperfect information inevitably appears in realistic domains and situations. Instrument errors or corruption from noise during experiments may give rise to information with incomplete data when measuring a specific attribute. In other cases, the extraction of exact information may be excessively costly or unfeasible. Moreover, it might be useful to complement the available data with additional information from an expert, which is usually elicited by imperfect data (interval data, fuzzy concepts, etc). In most real-world problems, data have a certain degree of imprecision. Sometimes, this imprecision is small enough for it to be safely ignored. On other occasions, the imprecision of the data can be modeled by a probability distribution. However, there is a third kind of problem, where the imprecision is significant, and a probability distribution is not the most natural way to model it. This is the case of certain practical problems where the data are inherently fuzzy [7]–[10]. For these cases, it is necessary to incorporate the handling of information with attributes which may present missing and imprecise values in the classifier's learning and classification phases.

In general, we can say that there are many restrictions to the type of imperfection allowed in the input examples or in the data. For this reason, we propose to extend the treatment of imperfect information with a classification technique based on multiple classifier systems. This technique is a Fuzzy Random Forest (FRF) ensemble. Beside its ability to handle imperfect information, FRF also proved to be effective when dealing with regular data, e.g., without imperfect information [11].

FRF uses a fuzzy decision tree as base classifier. Therefore, FRF leverages the robustness of fuzzy decision trees and tree ensembles, the power of randomness to increase the diversity of the trees in the forest, and the flexibility of fuzzy logic to manage imperfect data. In Section II we review the major elements that constitute the FRF ensemble. In Section III, we describe the types of imperfect data supported by the FRF ensemble and we devise an augmented ensemble that can operate with others type of imperfect data. In Section IV, we perform experiments with imperfect datasets used in other papers to show the advantage of being able to express the true nature of imperfect information. Finally, we present our conclusions in Section V.

II. An ensemble based on Fuzzy Decision Trees

FRF was originally presented in [11]. In this section we describe the basic elements that compose a FRF ensemble and the types of data that are supported by this ensemble in both learning and classification phases.

A. Fuzzy Random Forest Learning

FRF learning phase uses Algorithm 1 to generate the FRF ensemble whose trees are fuzzy decision trees. Each tree in the FRF ensemble is a fuzzy tree. Algorithm 2 shows the fuzzy decision tree learning algorithm.

Although the user chooses the size of the FRF, computational studies have shown that good accuracy is obtained on sizes between [100,150] trees, [11]. Algorithm 2 has been designed so that the trees can be constructed without considering all the attributes to split the nodes. Algorithm 2 is an algorithm to construct trees based on ID3, where the numeric attributes have been discretized by a fuzzy partition. The domain of each numeric attribute is represented by trapezoidal fuzzy sets,

978-1-4244-7316-8/11/$26.00 ©2011 IEEE

Algorithm 1 - FRF ensemble Learning

FRFlearning(*in:E, Fuzzy Partition; out:Fuzzy Random Forest*)
begin

1. Take a random sample of $|E|$ examples with replacement from the dataset E.
2. Apply Algorithm 2 to the subset of examples obtained in the previous step to construct a fuzzy tree, using the fuzzy partition.
3. Repeat steps 1 and 2 until T fuzzy trees are built to constitute the FRF ensemble.

end

Algorithm 2 - Fuzzy Decision Tree Learning

FuzzyDecisionTree(*in: E, Fuzzy Partition; out: Fuzzy Tree*)
begin

1. Start with the examples in E with values $\chi_{Fuzzy_Tree,root}(e) = 1$.
2. Let M be the set of attributes where all numeric attributes are partitioned according to the Fuzzy Partition.
3. Choose an attribute to do the split at the node N.

3.1. Make a random selection of attributes from the set of attributes M.

3.2. Compute the information gain for each selected attribute using the values $\chi_{Fuzzy_Tree,N}(e)$ of each e in node N.

3.3. Choose the attribute such that information gain is maximal.

4. Divide N in children nodes according to possible outputs of the attribute selected in the previous step and remove it from the set M. Let E_n be the dataset of each child node.
5. Repeat steps 3, 4 with each (E_n,M) until the stopping criteria is satisfied.

end

$A_1, \ldots, A_f$ so each internal node of the tree, whose division is based on a numerical attribute, generates a child node for each fuzzy set of the partition. Moreover, Algorithm 2 uses a function, denoted by $\chi_{t,N}(e)$, that indicates the degree with which the example e satisfies the conditions that lead to node N of tree t. Each example e is composed of attributes which can take crisp, missing or fuzzy values belonging to the fuzzy partition of the corresponding attribute. Each of these examples (according of the attribute value) has the following treatment:

- Each example e used in the training of the tree t has been assigned an initial value 1 ($\chi_{t,root}(e) = 1$).
- According to the membership degree of the example e to different fuzzy sets of partition of a split based on a numerical attribute:
  - If the value of e for that attribute is crisp, the example e may belong to one or two children nodes ($\mu_{fuzzy_set_partition}(e) > 0$). In this case $\chi_{t,childnode}(e) = \chi_{t,node}(e) \times \mu_{fuzzy_set_partition}(e)$.
  - If the value of e for that attribute is a fuzzy value, it must match one of the sets of the fuzzy partition of the attribute (e will descend to the child node associated with that set). In this case, $\chi_{t,childnode}(e) = \chi_{t,node}(e)$.
  - When the example e has a missing value on the attribute used as split in a node, the example e descends to each child node with value $\chi_{t,childnode}(e) = \chi_{t,node}(e) \times \frac{1}{number_outputs_{split}}$.

The construction process of this fuzzy tree is a modification of fuzzy ID3 algorithm [12] to allow treatment of the attributes with crisp, fuzzy and missing values [11].

B. Fuzzy Random Forest Classification

In this section we describe how the classification is carried out using the FRF ensemble. We present two alternative strategies to obtain the decision of the FRF ensemble for a target example.

When the example e runs through each tree t, we obtain the matrix L_FRF of size $(T \times MAX_{N_t})$ with $MAX_{N_t} = max\{N_1, N_2, \ldots, N_T\}$ and N_i the number of reached leaves in tree i. Each element of the matrix is a vector of size I containing the support for every class provided by every activated leaf n on each tree t. Therefore, the matrix L_FRF contains all the information generated by the FRF ensemble when it is used to classify an example e and from which it makes its decision or class with certain methods of combination[1]. In the Appendix, we present concrete instances of these methods of combination used in the experiments.

The fuzzy classifier module operates on fuzzy trees of the FRF ensemble using one of these two possible strategies:

Strategy 1: Combining the information from the different leaves reached in each tree to obtain the decision of each individual tree and then applying the same or another combination method to generate the global decision of the FRF ensemble. In order to combine the information of the leaves reached in each tree, the $Faggre1_1$ function is used and the $Faggre1_2$ function is used to combine the outputs obtained with $Faggre1_1$ (functions that define the combination method), and so, we obtain vector D_FRF (vector with size I that indicates the confidence assigned by the FRF ensemble to each class i).

Strategy 2: Combining the information from all reached leaves from all trees to generate the global decision of the FRF ensemble. We use function $Faggre2$ (function that define the combination method) to combine the information generated by all the leaves obtaining vector D_FRF (vector with size I that indicates the confidence assigned by the FRF ensemble to each class i).

From vector D_FRF, obtained with Strategy 1 or 2, FRF ensemble assigns class c to example e such that

$$c = \arg \max_{i,\ i=1,\ldots,I} \{D_FRF_i\}$$

[1]In [11] a set of combination methods are defined.

As we can see, the output of FRF ensemble (regardless of the strategy) is obtained from vector D_FRF, which contains the membership degree of the target example to each class. Finally, the FRF ensemble assigns the class c with maximum value to example e.

III. Extending FRF ensemble

FRF ensemble is a versatile technique, which is able to adapt itself to new elements. Having introduced the FRF ensemble, we now describe an extension of this technique to allow the incorporation of new imprecise data. This extension involves changes in the learning and classification phases of the technique. In this section, we will describe the new types of imprecise data that we will incorporate and the new elements and changes needed to carry out the FRF ensemble's extension.

A. New types of imprecise data

In Section II-A we described the types of data supported by the FRF ensemble, in both the learning and classification phases, as originally proposed in [11]. Now, we want to extend the information processing in the FRF ensemble to incorporate data containing attributes measured by fuzzy values (which may be different from the fuzzy values which constitute the fuzzy partition of the attribute), and attributes with interval values. Furthermore, we want to allow the class attribute to be set-valued. Figure 1 illustrates the proposed extension.

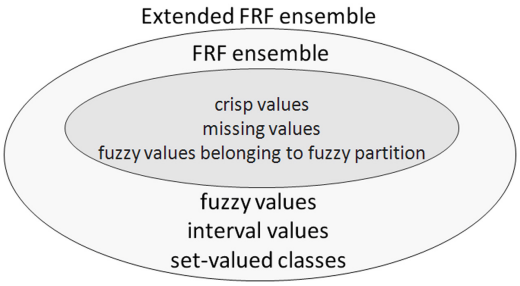

Fig. 1. Extending information processing in FRF

To incorporate these new types of data, we need to modify the following elements of FRF ensemble:

- Define an extended function to measure the membership degree of these new types of data in the fuzzy partitions of the numerical attributes used by the ensemble.
- The definition of this function requires a modification of the *information gain* function in both learning and classification phases of FRF ensemble.
- To incorporate set-valued classes, we need to modify and to define the learning and classification phases.

Let's further analyze these new elements and their required modifications.

B. Fuzzy and Interval values

To incorporate attribute values measured by a fuzzy value (fuzzy set) different from the sets of the partition of the attribute, or attributes measured by interval values, we must extend the function that measures the membership degree of these types of values to the different fuzzy sets forming the partition of the numeric attributes. In [13] we can find a review of similarity measures. We define the measure $\mu_{simil}(\cdot)$ which captures change in the value $\chi_{t,node}(e)$ of the example e when it descends in the fuzzy tree. e has attributes whose values are expressed by intervals or fuzzy values that do not match any of the fuzzy values of the partition used by the fuzzy tree and therefore by the ensemble. This function μ_{simil} will be used in both learning and classification phases of extended FRF ensemble.

In these cases, we use a membership function ($\mu_{simil}(\cdot)$) that, given the attribute "$Attr$" to be used to split a node, measures the similarity between the values of the fuzzy partition of the attribute and fuzzy values or intervals of the example in that attribute. When the example e must descend to different child nodes, the function $\chi(\cdot)$ is calculated as $\chi_{t,childnode^i}(e) = \chi_{t,node} \times \mu^i_{simil}(e)$.

Function $\mu^i_{simil}(e)$ is defined as:

$$\mu^i_{simil}(e) = \frac{\int_{\mathbb{R}}(\min\{\mu_e(x), \mu_{A_i}(x)\})dx}{\sum_{i=1}^{f}\int_{\mathbb{R}}(\min\{\mu_e(x), \mu_{A_i}(x)\})dx}, \quad i = 1, \ldots, f$$

where:

- $\mu_e(x)$ is the membership function that represents the fuzzy or interval value in the example e
- $\mu_{A_i(x)}$ is the membership function that represents the i-th fuzzy value of the partition of the attribute $Attr$
- f is the cardinality of the partition of the attribute $Attr$

C. Set-valued classes

We assume that if an example is labeled with a set-valued we are not stating that it belongs to all categories at time (which is not an imprecise assert). We are expressing that we are not sure about the class of the example, [14].

As described in Section II, the examples in the dataset are weighted examples (initially with weight 1). When we incorporate in FRF ensemble examples whose class can be expressed by a set of values, it is necessary to modify the way we treat this weight in the learning phase of FRF ensemble. Thus, step 3.2 of Algorithm 2 should calculate the information gain considering the example as belonging to *each* potential class. For this, the example in step 1 of the algorithm, must be replicated for each class of its class attribute, using an associated weight of $1/(n\ values\ classes\ of\ example)$. Therefore, the initial weight of the replicated examples will be $1/(n\ values\ classes\ of\ example)$.

When the ensemble is learned, we need to extend the classification phase in which the function $\mu_{simil}(e)$ is used.

As an example descends through various branches of the tree (using function $\mu_{simil}(e)$), different leaf nodes are activated. Each of these activated leaf nodes assigns a weight to each possible classes. According to the combination method used, we obtain from the FRF ensemble a weight for each class. The resulting weight vector of classes is denoted by D_FRF.

At this point, when we perform a test of the FRF ensemble results to classify a dataset we can follow the decision process:

If class(e)==class$_{FRF}$(e) and size(class(e)==1) then successes++
else
If class(e)$\cap$ class$_{FRF}$(e)$\neq \emptyset$ then success_or_error++
else errors++

As result of this test, we obtain the interval $[min_error, max_error]$ where min_error is calculated considering only errors indicated in the variable $errors$ from the previous process and max_error is calculated considering as errors $errors + success_or_error$.

D. Changes of learning and classification algorithms

Learning and classification phases should now be modified to allow the FRF ensemble to learn, infer, and classify from an example expressed with the types of values presented in Section III-A. This subsection shows these modification.

Algorithm 2 is modified in steps 1 and 3.2. The new step 1 is "Start with the examples in E with values $\chi_{Fuzzy_Tree,root}(e) = 1/(n\ values\ classes\ of\ example)$" and the new step 3.2 is "Compute the information gain for each selected attribute using the values $\chi_{Fuzzy_Tree,N}(e)$ of each e in node N taking into account the function $\mu_{simil(e)}$ for the cases required."

FRF Classification with Strategy 1 is modified. The decisions of trees are modified because obtaining of matrix L_FRF takes into account the function μ_{simil} for the cases required. On the other hand, the decision of FRF ensemble is modified due to FRF ensemble assigns the set of classes c to example e such that $c = \arg \max_{i,\ i=1,\ldots,I} \{D_FRF_i\}$.

Finally, FRF Classification with Strategy 2 is modified. The decisions of tree are modified because obtaining of matrix L_FRF takes into account the function $\mu_{simil(e)}$ for the cases required. Again, FRF ensemble assigns the set of classes c to example e such that $c = \arg \max_{i,\ i=1,\ldots,I} \{D_FRF_i\}$.

IV. Experiments and Results

In this section we describe several experiments. These experiments are designed to measure the behavior of FRF ensemble using datasets and results proposed in [14], [15]. We define the experimental settings quite similar to those proposed in [14], [15] to compare with their results.

A. Datasets and parameters for FRF ensemble

To obtain these results we have used real-world datasets about medical diagnosis and high performance athletics [14], [15], whose characteristics are shown in Table I.

TABLE I
Datasets

Dataset	Abbr	$\|E\|$	$\|M\|$	I
Long-4	Long-4	25	4	2
100ml-4-I	ml-4-I	52	4	2
100ml-4-P	ml-4-P	52	4	2
Dyslexia	Dyslexic	65	12	4

The table shows the number of examples ($|E|$), the number of attributes ($|M|$) and the number of classes (I) for each dataset. "Abbr" indicates the abbreviation of the dataset used in the experiments.

All FRF ensembles use a forest size of 100 trees. The number of attributes chosen at random at a given node is $\log_2(|\cdot| + 1)$, where $|\cdot|$ is the number of available attributes at that node, and each tree of the FRF ensemble is constructed to the maximum size (node pure or set of available attributes is empty) and without pruning.

In experiments described in [14], [15], fuzzy partitions used are uniform. We will use both uniform and non-uniform fuzzy partitions. These last ones are obtained by the NIP1.5 tool available in "http://heurimind.inf.um.es/".

B. Experimentation with low quality data

These experiments were conducted to test the accuracy of FRF ensemble applied to real-world datasets with imperfect values and compare the results with the ones obtained by the GFS classifier proposed in [14].

In these experiments we used the available datasets in "http://sci2s.ugr.es/keel/" and the available results in [14], [15]. These are datasets from two different real-world problems. The first one is related to the composition of teams in high performance athletics and the second one is a medical diagnosis problem.

1) High performance athletics: The score of an athletics team is the sum of the individual scores of the athletes in the different events. It is the coach's responsibility to balance the capabilities of the different athletes in order to maximize the score of a team according to the regulations. The variables that define each problem are as follows:

- There are four indicators for the long jump that are used to predict whether an athlete will pass a given threshold: the ratio between the weight and the height, the maximum speed in the 40 meters race, and the tests of central (abdominal) muscles and lower extremities;
- There are also four indicators for the 100 meters race: the ratio between weight and height, the reaction time, the starting or 20 m speed, and the maximum or 40 m speed.

A more detailed description of this problem may be found in [14]. The datasets used in this experiment are the following:

- Dataset "Long-4": Dataset used to predict whether an athlete will improve certain threshold in the long jump, given the indicators mentioned before. The set has 25 examples (25 athletes), 4 attributes, 2 classes, and no missing values. All attributes, including the output attribute, are interval-valued.
- Dataset "100ml-4-I": Used for predicting whether a mark in the 100 meters sprint race is being achieved. Actual measurements are taken by three observers, and are combined into the smallest interval that contains them. The set has 52 examples, 4 attributes, 2 classes, and no missing values. All attributes, including the output attribute, are interval-valued.
- Dataset "100ml-4-P": Same dataset as "100ml-4-I" but the measurements have been replaced by the subjective grade

TABLE II
RESULTS FOR DATASETS ML-4-I, ML-4-P AND LONG-4 WITH UNIFORM (FIVE LABELS/ATTRIBUTE) AND NON-UNIFORM FUZZY PARTITIONS.

		Dataset					
		ml-4-I		ml-4-P		Long-4	
	Technique	Train	Test	Train	Test	Train	Test
Uniform fuzzy partition	FFR_{SM1}	[0.229,0.421]	[0.250,0.443]	[0.075,0.269]	[0.120,0.333]	[0.156,0.436]	[0.217,0.483]
	FRF_{SM2}	[0.226,0.419]	[0.233,0.427]	**[0.081,0.274]**	**[0.100,0.297]**	**[0.151,0.427]**	**[0.217,0.483]**
	FRF_{MWL1}	[0.209,0.402]	[0.233,0.427]	[0.092,0.287]	[0.120,0.317]	[0.196,0.467]	[0.217,0.483]
	FRF_{MWL2}	[0.207,0.399]	[0.250,0.443]	[0.094,0.286]	[0.120,0.317]	[0.187,0.462]	[0.217,0.483]
	FRF_{MWLT1}	**[0.207,0.399]**	**[0.233,0.427]**	[0.094,0.286]	[0.120,0.317]	[0.196,0.475]	[0.217,0.483]
	FRF_{MWLT2}	[0.199,0.391]	[0.250,0.443]	[0.094,0.286]	[0.120,0.317]	[0.191,0.471]	[0,217,0.483]
Non-uniform Fuzzy partition	FFR_{SM1}	[0.139,0.331]	[0.150,0.343]	[0.098,0.291]	[0.133,0.310]	[0.120,0.404]	[0.200,0.467]
	FRF_{SM2}	[0.141,0.333]	[0.150,0.343]	[0.096,0.288]	[0.093,0.290]	[0.115,0.391]	[0.200,0.467]
	FRF_{MWL1}	[0.077,0.269]	[0.093,0.287]	[0.075,0.269]	[0.073,0.270]	[0.116,0.396]	[0.100,0.417]
	FRF_{MWL2}	**[0.060,0.252]**	**[0.093,0.287]**	[0.077,0.269]	[0.073,0.270]	[0.102,0.382]	[0.100,0.367]
	FRF_{MWLT1}	[0.077,0.269]	[0.093,0.287]	**[0.075,0.267]**	**[0.073,0.270]**	[0.107,0.387]	[0.150,0.417]
	FRF_{MWLT2}	[0.062,0.254]	[0.093,0.287]	[0.077,0.269]	[0.073,0.270]	**[0.094,0.373]**	**[0.067,0.333]**
	Crisp [14]	0.259	0.384	0.288	0.419	0.327	0.544
	GGFS [14]	[0.089,0.346]	[0.189,0.476]	[0.076,0.320]	[0.170,0.406]	[0.000,0.279]	[0.349,0.616]

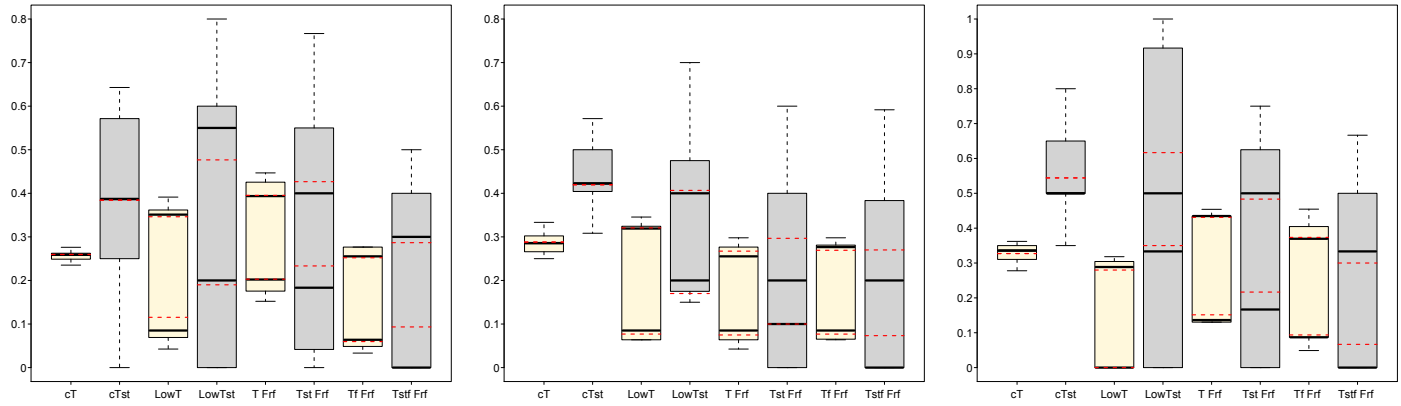

Fig. 2. Boxplots ml-4-I, ml-4-P and Long-4 with five labels/attribute. cT and cTst are the results for train and test respectively of the crisp algorithm proposed in [14]. LowT and LowTst are the results for train and test of the extended algorithm proposed in [14]. T-Frf, Tst-Frf, Tf-Frf adn Tstf-Frf are the results for train and test of FRF with uniform and non-uniform fuzzy partitions (results marked in bold).

the trainer has assigned to each indicator (i.e. "reaction time is low" instead of "reaction time is 0.1 sec").

As in [14], we have used a 10 fold cross-validation design for all datasets. Table II shows the results obtained in [14] and the ones obtained by the FRF ensemble with the six combination methods proposed in Appendix. Except for the crisp algorithm proposed in [14], in this table, the interval $[mean_min_error, mean_max_error]$ obtained for each dataset according to the decision process described in Section III-C, is shown.

In these experiments we used different types of fuzzy partitions of the attributes. We used uniform fuzzy partitions with size of five labels/attribute, as commented in [14]. In addition, we used non-uniform fuzzy partitions. These last ones are obtained by the NIP1.5 tool and they have (3,0,3,3), (0,2,3,6) and (3,3,2,0) labels/attribute for "100ml-4-I", "100ml-4-P" and "100ml-4-P", respectively. To obtain these fuzzy partitions for each dataset, attributes with interval values have been changed by its average value.

In Figure 2 is shown the boxplots with the best results of FRF ensemble. Observe that the boxplots of the imprecise experiments are not standard. We have used the extended boxplot proposed in [14]. They propose to use a box showing the 75% percentile of the maximum and the 25% percentile of the minimum error (thus the box displays at least the 50% of data). In addition, they represent the interval-valued median of the maximum and minimum result. For this reason, they draw two marks inside the box.

In Figure 2, we show the results of FRF with uniform and non-uniform fuzzy partitions marked in bold and the results of Crisp [14] and GGFS [14].

The results obtained by the extended GPS proposed in [14] and FRF ensemble, are very promising because we are representing the information in a more natural and appropriate way, and in this problem, we are allowing the collection of knowledge of the coach by ranges of values and linguistic terms. The results of FRF ensemble are very competitive.

TABLE III
COMPARATIVE RESULTS OF FRF WITH UNIFORM AND NON-UNIFORM FUZZY PARTITIONS FOR DATASETS DYSLEXIC-12, DYSLEXIC-12-01 AND DYSLEXIC-12-12.

		Dataset					
		Dyslexic-12		Dyslexic-12-01		Dyslexic-12-12	
	Technique	Train	Test	Train	Test	Train	Test
Uniform fuzzy partition	FRF_{SM1} (four labels)	[0.000,0.235]	[0.011,0.441]	[0.000,0.288]	[0.000,0.443]	[0.000,0.265]	[0.000,0.434]
	FRF_{SM2} (four labels)	[0.000,0.231]	[0.014,0.447]	**[0.000,0.205]**	**[0.000,0.412]**	**[0.000,0.247]**	**[0.000,0.415]**
	FRF_{MWL1} (four labels)	[0.002,0.258]	[0.004,0.436]	[0.000,0.308]	[0.000,0.436]	[0.000,0.290]	[0.000,0.435]
	FRF_{MWL2} (four labels)	[0.001,0.259]	[0.006,0.443]	[0.000,0.312]	[0.000,0.445]	[0.000,0.292]	[0.000,0.436]
	FRF_{MWLT1} (four labels)	**[0.002,0.260]**	**[0.005,0.435]**	[0.000,0.279]	[0.000,0.425]	[0.000,0.286]	[0.000,0.432]
	FRF_{MWLT2} (four labels)	[0.001,0.256]	[0.006,0.441]	[0.000,0.286]	[0.000,0.430]	[0.000,0.285]	[0.000,0.432]
Uniform fuzzy partition	FRF_{SM1} (five labels)	[0.000,0.250]	[0.004,0.465]	[0.000,0.307]	[0.000,0.459]	[0.000,0.275]	[0.000,0.443]
	FRF_{SM2} (five labels)	[0.000,0.251]	[0.001,0.515]	**[0.000,0.205]**	**[0.000,0.421]**	[0.000,0.264]	[0.000,0.473]
	FRF_{MWL1} (five labels)	[0.003,0.284]	[0.008,0.448]	[0.000,0.339]	[0.000,0.448]	[0.000,0.308]	[0.000,0.451]
	FRF_{MWL2} (five labels)	[0.001,0.278]	[0.004,0.443]	[0.000,0.335]	[0.000,0.449]	[0.000,0.305]	[0.000,0.447]
	FRF_{MWLT1} (five labels)	[0.002,0.280]	[0.007,0.442]	[0.000,0.309]	[0.000,0.431]	**[0.000,0.307]**	**[0.000,0.435]**
	FRF_{MWLT2} (five labels)	**[0.001,0.277]**	**[0.004,0.440]**	[0.000,0.309]	[0.000,0.435]	[0.000,0.303]	[0.000,0.445]
Non-uniform Fuzzy partition	FRF_{SM1}	[0.000,0.320]	[0.002,0.511]	[0.000,0.282]	[0.000,0.413]	[0.000,0.405]	[0.000,0.477]
	FRF_{SM2}	[0.000,0.327]	[0.001,0.515]	[0.000,0.253]	[0.000,0.389]	[0.000,0.402]	[0.000,0.469]
	FRF_{MWL1}	[0.000,0.261]	[0.003,0.419]	[0.000,0.264]	[0.000,0.400]	[0.000,0.335]	[0.000,0.422]
	FRF_{MWL2}	[0.000,0.270]	[0.003,0.423]	[0.000,0.276]	[0.000,0.407]	**[0.000,0.343]**	**[0.000,0.414]**
	FRF_{MWLT1}	[0.000,0.264]	[0.004,0.419]	**[0.000,0.243]**	**[0.000,0.386]**	[0.000,0.331]	[0.000,0.422]
	FRF_{MWLT2}	**[0.000,0.267]**	**[0.003,0.417]**	[0.000,0.259]	[0.000,0.394]	[0.000,0.343]	[0.000,0.418]
	Crisp CF^0 (four labels) [15]	0.444	[0.572,0.694]	0.336	[0.452,0.533]	0.390	[0.511,0.664]
	GGFS (four labels) [14]	–	[0.421,0.558]	–	[0.219,0.759]	–	[0.199,0.757]
	GGFS CF^0 (four labels) [15]	[0.003,0.237]	[0.405,0.548]	[0.005,0.193]	[0.330,0.440]	[0.003,0.243]	[0.325,0.509]
	Crisp CF^0 (five labels) [15]	0.556	[0.614,0.731]	0.460	[0.508,0.605]	0.485	[0.539,0.692]
	GGFS (five labels) [14]	–	[0.490,0.609]	–	[0.323,0.797]	–	[0.211,0.700]
	GGFS CF^0 (five labels) [15]	[0.038,0.233]	[0.480,0.621]	[0.000,0.187]	[0.394,0.522]	[0.000,0.239]	[0.393,0.591]

2) Diagnosis of dyslexic: Dyslexia is a learning disability in people with normal intellectual coefficient, and without further physical or psychological problems explaining such disability. A more detailed description of this problem can found in [14], [15].

In these experiments, we have used three different datasets. Their names are "Dyslexic-12', "Dyslexic-12-01" and "Dyslexic-12-12". Each dataset has 65 examples, 4 classes and 12 attributes. The output variable for each of these datasets is a subset of the labels that follow: • No dyslexic; • Control and revision; • Dyslexic; and • Inattention, hyperactivity or other problems.

Both input and the output exhibit imprecision and missing values. These three datasets differ only in their outputs:

- "Dyslexic-12" comprises the four mentioned classes.
- "Dyslexic-12-01" does not make use of the class "control and revision", whose members are included in class "no dyslexic".
- "Dyslexic-12-12" does not make use of the class "control and revision", whose members are included in class "dyslexic".

All experiments are repeated 100 times for bootstrap resamples with replacement of the training set. The test set comprises the "out of the bag" elements. As mentioned above, the boxplots of the imprecise experiments are not standard. We have used the extended boxplot proposed in [14].

In these experiments we used different types of fuzzy partitions of the attributes. We used uniform fuzzy partitions with size of four and five labels/attribute, as commented in [14], [15]. In addition, we used non-uniform fuzzy partitions. These last ones are obtained by the NIP1.5 tool and they have (0,0,2,0,0,7,4,0,0,0,3,3), (0,2,2,2,3,3,4,0,0,2,0,2) and (0,0,3,2,2,3,0,0,2,2,2,2) labels/attribute for "Dyslexic-12", "Dyslexic-12-01" and "Dyslexic-12-12P", respectively. To obtain these fuzzy partitions for each dataset, attributes with interval values have been changed by its average value.

In Table III, we show the results obtained when we run FRF ensemble with these type of partitions for datasets "Dyslexic-12", "Dyslexic-12-01" and"Dyslexic-12-12'. Also, in Table III, we compare the results obtained by FRF ensemble with the best ones obtained in [15]. Again, in this table, the interval $[mean_min_error, mean_max_error]$ obtained for each dataset according to the decision process described in Section III-C, is shown. The statistical significance of the differences is displayed in Figure 3. In Figure 3, we show the results with FRF with uniform and non-uniform fuzzy partitions marked in bold and the results of Crisp CF^0 [15], GGFS [14] and GGFS CF^0 [15] with four labels.

As we can see, FRF with non-uniform fuzzy partitions obtains better results in test that FRF with uniform fuzzy partitions. FRF ensemble is a significant improvement over the crisp GFS. As also discussed in [15] is preferable to use an algorithm which is capable of learning with low quality data than removing the imperfect information and using a

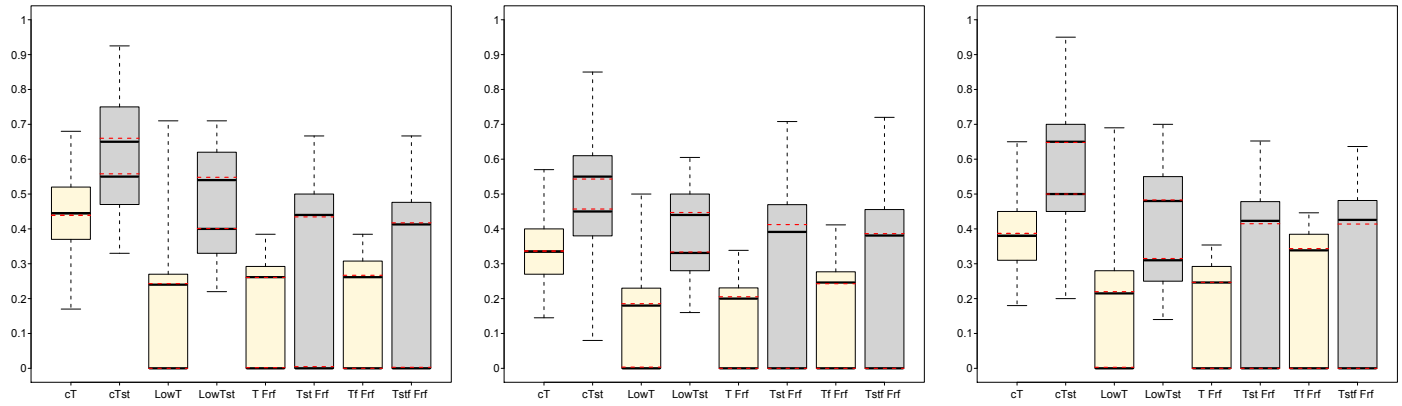

Fig. 3. Boxplots Dyslexic-12, Dyslexic-12-01 and Dyslexic-12-12 with four labels/attributes. cT and cTst are the results for train and test, respectively, of crisp algorithm CF_0 proposed in [15]. LowT and LowTst are the results of the extended algorithm CF_0 proposed in [15]. T-Frf, Tst-Frf, Tf-Frf and Tstf-Frf are the results for train and test of FRF with uniform and non-uniform fuzzy partitions (results marked in bold).

conventional algorithm.

The results of the dataset "Dyslexic-12-01" are better than "Dyselxic-12" and "Dyslexic-12-12". Moreover, if the class "control and revision" is not used, the individuals in this class tend to be assigned to the group "no dyslexic" rather than to the group "dyslexic".

V. Conclusions

We have presented FRF ensemble, which is an ensemble based on fuzzy decision trees. The FRF ensemble can manage imperfect data directly and has a good classification performance with relatively small ensembles sizes. The FRF ensemble has been extended to include the treatment of new types of imperfect data in both input and output attributes. This technique is very versatile due to the ease with which we can extend it to new situations.

We have presented experimental results obtained by applying the FRF ensemble to various datasets. FRF ensemble has been applied to real-problems datasets, such as the composition of teams in high performance athletics and a medical diagnosis problem. The results obtained by FRF ensemble are promising, concluding, as in [14], [15], that by using ranges of values and linguistic terms instead of crisp, imputed numbers, we better capture the nature of the underlying information.

Our conclusion, as many papers in the literature are indicating, is that it is necessary to design and/or adapt classification techniques so they can manipulate real data that can be imperfect in some cases. The transformation of these imperfect values to (imputed) crisp values may cause undesirable effects with respect to accuracy of the technique.

Acknowledgment

Supported by the project TIN2008-06872-C04-03 of the MICINN of Spain and European Fund for Regional Development. Thanks also to the Funding Program for Research Groups of Excellence with code 04552/GERM/06 granted by the "Fundación Séneca", Murcia, Spain. R. Martínez is supported by the scholarship program FPI from the "Fundación Séneca" of Spain. Thanks to Luciano Sánchez and Ana Palacios for their help in creating extended boxplot.

Appendix

In this appendix, we use the notation above defined in Section II-B. For each strategy for fuzzy classifier module in the FRF ensemble that is described in Section II we can define several functions $Faggre1_1$, $Faggre1_2$ and $Faggre2$. The overall set of functions is described in [11]. In this appendix, the utilized methods in this paper are described in detail:

Non-trainable methods - In these combination methods, a transformation is applied to the matrix L_FRF so that each leaf reached assigns a simple vote to the majority class.

For $t = 1, \ldots, T$

For $n = 1, \ldots, N$

For $i = 1, \ldots, I$

$$L_FRF_{mod_{t,n,i}} = \begin{cases} 1 & if\ i = \arg \max_{j,\ j=1,\ldots,I} \{L_FRF_{t,n,j}\} \\ 0 & otherwise \end{cases}$$

Within this group we define the following methods. We get two versions depending on the strategy used:

- *Simple Majority vote:*

Strategy 1→ method SM1

The function $Faggre1_1$ is defined as:

$Faggre1_1(t, i, L_FRF) =$

$$= \begin{cases} 1 & if\ i = \arg \max_{j,\ j=1,\ldots,I} \left\{ \sum_{n=1}^{N_t} L_FRF_{mod_{t,n,j}} \right\} \\ 0 & otherwise \end{cases}$$

In this method, each tree t assigns a simple vote to the most voted class among the N_t reached leaves by example e in the tree. We will denote by T_FRF to the out matrix of $Faggre1_1$.

The function $Faggre1_2$ is defined as:

$Faggre1_2(i, T_FRF) = \sum_{t=1}^{T} T_FRF_{t,i}$

Strategy 2 → method SM2

For Strategy 2 it is necessary to define the function $Faggre2$ combining information from all leaves reached in the ensemble by example e. Thus, the function $Faggre2$ is defined as:
$Faggre2(i, L_FRF) = \sum_{t=1}^{T} \sum_{n=1}^{N_t} L_FRF_{modt,n,i}$

Trainable explicitly dependent methods-

• *Majority vote Weighted by Leaf:*

In this combination method, a transformation is applied to the matrix L_FRF so that each leaf reached assigns a weighted vote to the majority class. The vote is weighted by the degree of satisfaction with which example e reaches the leaf.

For $t = 1, \ldots, T$
For $n = 1, \ldots, N$
For $i = 1, \ldots, I$

$L_FRF_{mod_{t,n,i}} =$

$$= \begin{cases} \chi_{t,n}(e) & if\ i = \arg \max_{j,\ j=1,\ldots,I} \{L_FRF_{t,n,j}\} \\ 0 & otherwise \end{cases}$$

Again, we have two versions according to the strategy used.

Strategy 1 → method MWL1

The functions $Faggre1_1$ and $Faggre1_2$ are defined as:
$Faggre1_1(t, i, L_FRF) =$

$$= \begin{cases} 1 & if\ i = \arg \max_{j,\ j=1,\ldots,I} \left\{ \sum_{n=1}^{N_t} L_FRF_{mod_{t,n,j}} \right\} \\ 0 & otherwise \end{cases}$$

$Faggre1_2(i, T_FRF) = \sum_{t=1}^{T} T_FRF_{t,i}$

Strategy 2 → method MWL2

The function $Faggre2$ is defined as:
$Faggre2(i, L_FRF) = \sum_{t=1}^{T} \sum_{n=1}^{N_t} L_FRF_{t,n,i}$

• *Majority vote Weighted by Leaf and by Tree:*

Again, in this combination method, a transformation is applied to the matrix L_FRF so that each leaf reached assigns a weighted vote to the majority class. The vote is weighted by the degree of satisfaction with which example e reaches the leaf.

For $t = 1, \ldots, T$
For $n = 1, \ldots, N$
For $i = 1, \ldots, I$

$L_FRF_{mod_{t,n,i}} =$

$$= \begin{cases} \chi_{t,n}(e) & if\ i = \arg \max_{j,\ j=1,\ldots,I} \{L_FRF_{t,n,j}\} \\ 0 & otherwise \end{cases}$$

In addition, in this method a weight for each tree obtained is introduced by testing each individual tree with the OOB dataset. Let $\overline{p} = (p_1, p_2, \ldots, p_T)$ be the vector with the weights assigned to each tree. Each p_t is obtained as $\frac{N_success_OOB_t}{size_OOB_t}$ where $N_success_OOB_t$ is the number of examples classified correctly from the OOB dataset used for testing the t-th tree and $size_OOB_t$ is the total number of examples in this dataset.

Strategy 1 → method MWLT1

The function $Faggre1_1$ is defined as:

$Faggre1_1(t, i, L_FRF) =$

$$= \begin{cases} 1 & if\ i = \arg \max_{j,\ j=1,\ldots,I} \left\{ \sum_{n=1}^{N_t} L_FRF_{mod_{t,n,j}} \right\} \\ 0 & otherwise \end{cases}$$

Vector $\overline{p}$ is used in the definition of function $Faggre1_2$:
$Faggr1_2(i, T_FRF) = \sum_{t=1}^{T} p_t \cdot T_FRF_{t,i}$

Strategy 2 → method MWLT2

The vector of weights $\overline{p}$ is applied to Strategy 2.
$Faggre2(i, L_FRF) = \sum_{t=1}^{T} p_t \sum_{n=1}^{N_t} L_FRF_{t,n,i}$

REFERENCES

[1] H. Ahn, H. Moon, J. Fazzari, N. Lim, J. Chen and R. Kodell, "Classification by ensembles from random partitions of high dimensional data," Computational Statistics and Data Analysis, vol. 51, pp. 6166–6179, 2007.

[2] A. Fernández, M. J. del Jesus and F. Herrera, "Hierarchical fuzzy rule based classification systems with genetic rule selection for imbalanced data-sets," Int. J. Approx. Reasoning, vol. 50, no. 3, pp. 561–577, 2009.

[3] R. O. Duda, P. E. Hart and D. G. Stork, Pattern classification. John Wiley and Sons, Chichester, 2001.

[4] D. J. C. Mackay, Information theory, inference and learning algorithms. Cambridge University Press, Cambridge, 2003.

[5] J. R. Quinlan, C4.5: Programs for machine learning. Morgan Kaufmann Publishers, California, 1993.

[6] I. H. Witten and E. Frank E, Data mining. Morgan Kaufmann Publishers, San Francisco, 2000.

[7] P. P. Bonissone, "Approximate reasoning systems: handling uncertainty and imprecision in information systems," in Uncertainty Management in Information Systems: From Needs to Solutions, A. Motro and Ph. Smets, Eds. Kluwer Academic Publishers, 1997, pp. 369–395.

[8] J. Casillas and L. Sánchez, "Knowledge extraction from data fuzzy for estimating consumer behavior models," IEEE conference on Fuzzy Systems, pp. 164–170, 2006.

[9] M. C. Garrido, J. M. Cadenas and P. P. Bonissone, "A classification and regression technique to handle heterogeneous and imperfect information," Soft Computing, vol. 14, no. 11, pp. 1165–1185, 2010.

[10] A. Otero, J. Otero, L. Sánchez and J. R. Villar, "Longest path estimation from inherently fuzzy data acquired with GPS using genetic algorithms," Int. Symposium on Evolving Fuzzy Systems, pp. 300–305, 2006.

[11] P. P. Bonissone, J. M. Cadenas, M. C. Garrido and R. A. Díaz-Valladares, "A fuzzy random forest," Int. J. Approx. Reasoning, vol. 51, no. 7, pp. 729–747, 2010.

[12] M. Umano, H. Okamoto, I. Hatono, H. Tamura, F. Kawachi, S. Umedzu and J. Kinoshita, "Fuzzy decision trees by fuzzy ID3 algorithm and its application to diagnosis systems," IEEE Conference on Fuzzy Systems, vol. 3, pp. 2113–2118, 1994.

[13] B. Sridevi and R. Nadarajan, "Fuzzy similarity measure for generalized fuzzy numbers," Int. J. Open Problems Compt. Math. vol. 2, no. 2, pp. 240–253, 2009.

[14] A. M. Palacios, L. Sánchez and I. Couso I, "Extending a simple genetic coopertative-competitive learning fuzzy classifier to low quality datasets," Evolutionary Intelligence, vol. 2, pp. 73–84, 2009.

[15] A. M. Palacios, L. Sánchez and I. Couso I, "Diagnosis of dyslexia with low quality data with genetic fuzzy systems," Int. J. Approx. Reasoning, vol. 51, pp. 993–1009, 2010.

2011 IEEE International Conference on Fuzzy Systems
June 27-30, 2011, Taipei, Taiwan

Non-monotone Averaging Aggregation

Gleb Beliakov, Shui Yu
School of Information Technology
Deakin University
VIC 3125, Australia
Email: {gleb, syu}@deakin.edu.au

Daniel Paternain
Departamento de Automática y Computación
Universidad Pública de Navarra
31006 Pamplona, Spain.
Email: daniel.paternain@unavarra.es

***Abstract*—We advance the theory of aggregation operators and introduce non-monotone aggregation methods based on minimization of a penalty for inputs disagreements. The application in mind is processing data sets which may contain noisy values. Our aim is to filter out noise while at the same time preserve signs of unusual values. We review various methods of robust estimators of location, and then introduce a new estimator based on penalty minimisation.**

***Index Terms*—Aggregation operator, penalty function, estimators of location, outliers.**

I. Introduction

The need to aggregate several inputs into a single representative output frequently arises in fuzzy systems. Aggregation of membership values is typically performed in fuzzy rule-based systems by using triangular norms and conorms (t-norms and t-conorms). Averaging aggregation functions, including weighted arithmetic means, ordered weighted averaging (OWA) functions and fuzzy integrals (Choquet and Sugeno integrals in particular) are also frequently used in multicriteria decision making, image analysis and machine learning, see [1]–[3].

By their definition, aggregation functions are monotone in all variables. The role of averaging functions is to provide a representative value of the inputs. Some of the existing averaging functions, however, are not monotone. A particular example is the mode, illustrated in Section II. One can argue that the mode does provide a representative value, as it returns the most frequently observed input. But when the inputs are not repeated, the mode is not defined uniquely: any input is the mode in that case. In this article we investigate other non-monotone averaging functions which play the same role as the mode, but can be used when all inputs are different. This is important when the number of inputs is small, but they can take many values, and specifically any real value from $[0, 1]$, as it happens in fuzzy logic.

Our motivation is the following. Suppose we have a flow of noisy inputs, such as computer network traffic, or digital images. We want to combine the inputs into representative values, for example to reduce the size of the data in image reduction. On the other hand, we want to preserve some interesting aspects of the data, such as narrow spikes in pixel intensity or network traffic. When we aggregate the data using standard averaging functions, these interesting features may be lost. For example a small detail in an image will disappear in the background. However, we wish to reduce the noise in the data at the same time.

We think of a datum as noise when its value is distinct from some group of similar values of the neighboring data. In the image processing context, too large or too small a value of an individual pixel compared to the neighboring pixels is considered noise. But if two or more neighboring pixels take similar values distinct form the background, they possibly represent a fine detail of an object. Such values should be preserved when averaging across the neighboring pixels. A similar reasoning applies to a flow of network packets in network traffic analysis. A narrow spike in the intensity may be an early indication of a cyberattack.

Our objective is to study averaging operators which have the capability to filter out noise, yet preserve interesting but not dominant features of the inputs.

The structure of the paper is as follows. In Section II we provide preliminary definitions. In Section III we review various definitions of existing non-monotone means. In Section IV we introduce a new type of mode-like aggregation. Conclusions are presented in Section V.

II. Preliminaries

A. Aggregation functions

The research effort concerning aggregation functions, their behavior and properties, has been disseminated throughout various fields including decision making, knowledge based systems, artificial intelligence and image processing. Recent books providing a comprehensive overview include [1]–[3].

Definition 1: A function $f : [a, b]^n \to [a, b]$ is called an aggregation function if it is monotone non-decreasing in each variable and satisfies $f(\mathbf{a}) = a$, $f(\mathbf{b}) = b$, with $\mathbf{a} = (a, a, \ldots, a), \mathbf{b} = (b, b, \ldots, b)$.

Definition 2: An aggregation function f is called *averaging* if it is bounded by the minimum and maximum of its arguments

$$\begin{aligned} \min(\mathbf{x}) := \min(x_1, \ldots, x_n) &\leq f(x_1, \ldots, x_n) \\ \leq \max(x_1, \ldots, x_n) &:= \max(\mathbf{x}). \end{aligned}$$

It is immediate that averaging aggregation functions are idempotent (i.e., $\forall t \in [a, b] : f(t, t, \ldots, t) = t$) and (because of monotonicity) vice versa. Then clearly the boundary conditions $f(\mathbf{a}) = a$, $f(\mathbf{b}) = b$ are satisfied.

978-1-4244-7316-8/11/$26.00 ©2011 IEEE

A function is called *internal* if its output coincides with one of the inputs. A function f is called *shift-invariant*, if $f(\mathbf{x}+\mathbf{a}) = f(\mathbf{x}) + a$, where $\mathbf{a} = (a, a, \ldots, a)$. A function f is *homogeneous* (of degree one) if $f(\lambda \mathbf{x}) = \lambda f(\mathbf{x})$.

Well known examples of averaging functions are the arithmetic mean and the median. It is known that the arithmetic means and the median are solutions to simple optimization problems, in which a measure of disagreement between the inputs is minimized (see [2], [4]–[6]). The reasoning is as follows. Let $\mathbf{x}$ be the inputs and y the output. If all the inputs coincide $x = x_1 = \ldots = x_n$, then the output is $y = x$, and we have a unanimous vote. If some input $x_i \neq y$, then we impose a "penalty" for this disagreement. The larger the disagreement, and the more inputs disagree with the output, the larger (in general) is the penalty. We look for an aggregated value which minimizes the penalty.

Let us define a suitable measure of disagreement, or dissimilarity.

Definition 3: Let $P : [a, b]^{n+1} \to \Re$ be a penalty function with the properties

i) $P(\mathbf{x}, y) \geq 0$ for all $\mathbf{x}, y$;
ii) $P(\mathbf{x}, y) = 0$ if all $x_i = \mathbf{y}$;
iii) $P(\mathbf{x}, y)$ is quasiconvex in y for any $\mathbf{x}$.

The penalty based function is

$$f(\mathbf{x}) = \arg\min_y P(\mathbf{x}, y),$$

if y is the unique minimizer. If the set of minimizers is the interval $[a, b]$ then $y = \frac{a+b}{2}$.

Remark 1: $f(y)$ is quasiconvex if $f(ay_1 + (1-a)y_2) \leq \max\{f(y_1), f(y_2)\}$ for all $a \in [0, 1]$ and all y_1, y_2 within its domain.

In [4] it was shown that any averaging aggregation function can be represented as a penalty based function. Further, the classical means, such as the arithmetic mean and the median are represented via the following penalty functions. The arithmetic mean is the solution to

$$minimize_y \sum_{i=1}^{n} (x_i - y)^2$$

whereas the median is a solution to

$$minimize_y \sum_{i=1}^{n} |x_i - y|.$$

Not all penalty-based functions are monotone. Let $P(\mathbf{x}, y) = \sum_{i=1}^{n} p(x_i, y)$, with $p(t, s) = 1, t \neq s$ and $p(t, t) = 0$. Then the minimizer of P is the mode. Note that the mode is not monotone non-decreasing, for example

$$Mode(5, 5, 5, 3, 3, 2, 2) = 5 > 3 = Mode(5, 5, 5, 3, 3, 3, 3).$$

Hence mode is not an aggregation function.

III. Non-monotone averaging functions

As we mentioned, the mode has a disadvantage in that it is not well defined when the inputs are distinct. The usual practice to discretize the inputs by assigning frequency values to intervals of equal distance is too sensitive to the choice of the intervals. Here we look at other alternatives which provide a mode-type average.

Our motivation is the following. We think of y as a representative value of the inputs x_i if at least some of the inputs are grouped together around y, i.e. form a compact cluster around y. Other inputs could be far from y, in which case we do not take them into account to avoid any bias toward them. Consider the following inputs $\mathbf{x} = (1, 2, 3, 6, 6.1)$. It appears that the two largest values form a cluster, whereas the first three inputs are dispersed. Hence we may want to choose y near 6 as a representative of the inputs. If x_5 were 6, then the mode would have given us $y = 6$.

The median is one aggregation function robust with respect to outliers in the data. In our example the median is 3, and it does not represent a cluster around 6. Let us now recall other robust estimators of location, which appeared in statistical literature, see e.g., [7].

Definition 4: The *shorth* of a sample is the arithmetic mean of the shortest contiguous subsample with the half of the observations.

To calculate the shorth, we sort the inputs in ascending order and then find the smallest of the differences $x_{(h)} - x_{(1)}, x_{(h+1)} - x_{(2)}, \ldots, x_{(n)} - x_{(n-h+1)}$, with $h = [\frac{n}{2}] + 1$. Let the smallest difference be $x_{(h+j-1)} - x_{(j)}$. Here and in the rest of this paper $x_{(i)}$ denotes the i-th smallest input. Then the inputs falling into the interval $[x_{(h+j-1)}, x_{(j)}]$ are averaged.

A related quantity is the least median of squares estimator [7], [8], defined by

$$LMS(\mathbf{x}) = \arg\min_y Med(x_i - y)^2.$$

Here we also take the shortest contiguous half of the sample, but instead of taking the mean, we take the midpoint of the shortest half. If several shortest halves exist, one could take the average of their midpoints. LMS is based on minimizing a special penalty function, cf. Definition 3, which is not quasiconvex in y (and hence several optima may exist).

Another interesting example is the least trimmed squares estimator, see [7], [8],

$$LTS(\mathbf{x}) = \arg\min_y \sum_{i=1}^{h} r_{(i)}^2.$$

with the residuals $r_i = x_i - y$ and $r_{(i)}$ denoting the i-th smallest (by absolute value) residual. Here, in difference to the LMS estimator, the mean of each contiguous half of $\mathbf{x}$ is computed,

$$\bar{x}^{(i)} = \frac{1}{h} \sum_{j=i}^{i+h-1} x_{(j)},$$

and then the corresponding sum of squares is computed

$$SQ^{(i)} = \sum_{j=i}^{i+h-1} (x_{(j)} - \bar{x}^{(j)})^2.$$

The LTS solution is the mean $LTS(\mathbf{x}) = \bar{x}^{(i)}$ which corresponds to the smallest $SQ^{(i)}$. However, it may be different from the shorth.

The least Winsorized squares estimator is

$$LWS(\mathbf{x}) = \arg\min_y \sum_{i=1}^{h} r_{(i)}^2 + (n-h) r_{(h)}^2.$$

Explicitly, the LWS is the midpoint of the contiguous half which leads to the lowest value of the objective function above.

The averaging functions in this section are symmetric, homogeneous and shift-invariant, but not necessarily monotone or continuous in x_i. Take, for instance, the shorth. We have $Shorth(0, 0.6, 1) = 0.8 > Shorth(0.4, 0.6, 1) = 0.5$.

We note that the functions considered in this section are robust to outliers, the components of $\mathbf{x}$ with aberrantly large or small values. The median is also robust to outliers. The resulting value y remains the same even if half of the components of $\mathbf{x}$ are replaced with arbitrary (possibly infinite) values. However, none of the mentioned functions provides the output close to the desired value 6 in our example.

IV. Non-monotone averages minimizing a penalty

Let us return to Definition 3 and consider other types of penalties.

We are interested in identifying clusters of similar values in the inputs, and taking as the output representative values of such clusters. An input vector may have more than one cluster, and in this case we choose the most compact and large cluster, in some way balancing these two contradictory selection criteria. This can be achieved, in principle, by a clustering algorithm, such as k-means. However, the input vector can also contain only one cluster, which makes clustering methods struggle.

We define an averaging function as follows

$$f(\mathbf{x}) = \arg\min_y P(\mathbf{x}, y) = \arg\min_y \sum_{i=1}^{n} w_i p(|r_{(i)}|), \qquad (1)$$

where p is a penalty term for disagreement with the output. We observe that as in the LTS estimator, the residuals $r_i = x_i - y$ are ordered according to their magnitude. As opposed to LTS, all residuals are taken into account. The function p is chosen as

$$p(t) = \begin{cases} t & \text{if } t \le C, \\ Cs & \text{otherwise.} \end{cases}$$

C is a threshold which reflects scale, and s is a parameter which reflects the relative weighting of the inputs far from the output y.

The reasoning is as follows. On one hand we want y to represent compact clusters of the inputs, and not be affected by inputs far away from y, which can be seen as noise. On the other hand, we want to account for the number of inputs far from y: the smaller is such number, i.e., the larger is the cluster around y, the smaller is the penalty. Finally, we want to have a robust estimate of scale, i.e., C should be related to the inputs values rather than fixed a priori.

For a fixed y, we define C as a multiple of the smallest residual which is not zero. If all the inputs are different, and y coincides with one of the inputs, we take $C = M \times |r_{(2)}|$, and we fix M at 3. Then p will account for all the residuals within C units from y. The inputs outside this range will also contribute to the total penalty P, but only in terms of their number, not their distances from y. This way C is determined automatically.

By construction, the penalty P is aimed to: a) penalize non-compact clusters (through the choice of p and C), b) penalize small clusters (controlled by s), c) penalize y away from the centers of clusters. Among two clusters of inputs of the same size C, P will be smaller for the cluster which contains more data. Among two clusters of the same number of inputs, P will be smaller for the more compact cluster with smaller C. The parameter s controls the relative weighting of two criteria: the size and compactness of clusters. The larger s, the more emphasis is on the size of the cluster. The value s is the only user-defined parameter in our approach.

The weights w_i are associated with the individual inputs, not their distances from y. That is, they can be seen as weights of relative importance of the inputs, and can be omitted if all the inputs have the same importance.

Let us now examine some properties of the function f. First, f is shift-invariant, and symmetric when all the weights are equal. Second, f is also homogeneous. This can be seen from the fact that $p(\lambda x) = \lambda p(x)$, and that the residuals r_i are shift-invariant and homogeneous. The function f is also idempotent, but it is not monotone. The latter can be seen by aggregating the values in the following example: $\mathbf{x}_1 = (0, 1, 2, 3, 3)$ and $\mathbf{x}_2 = (2, 2, 2, 3, 3)$, which results in $f(\mathbf{x}_1) = 3 > 2 = f(\mathbf{x}_2)$.

Minimization of (1) has to be performed numerically, and it requires a global optimization method. For univariate minimization as in (1) we suggest Pijavski-Shubert method [9], see also [10]–[12], which is deterministic and numerically efficient. A significant simplification comes when the function f can be internal. Then the values of $P(\mathbf{x}, y)$ are calculated for all the inputs, and the input with the smallest value of P is returned. The computational complexity in this case is $O(n^2)$, n is the length of the input vector, because a selection algorithm to determine C runs in $O(n)$ time. This is the same complexity as that of a clustering method, when all x_i are tested as cluster centers (we remind that k-means clustering also leads to a global optimization problem, whose objective has complexity $O(n)$, same as in the proposed method).

For the example input vector we considered earlier $\mathbf{x} = (1, 2, 3, 6, 6.1)$, our approach gives $f(\mathbf{x}) = 6$ or 6.1, as desired. In contrast, $med(\mathbf{x}) = 3$, $Shorth(\mathbf{x}) = LMS(\mathbf{x}) = LTS(\mathbf{x}) = 2$, and mode can be any of the inputs.

Let us now look at the following illustrative example. Consider calculation of the moving average, which is often

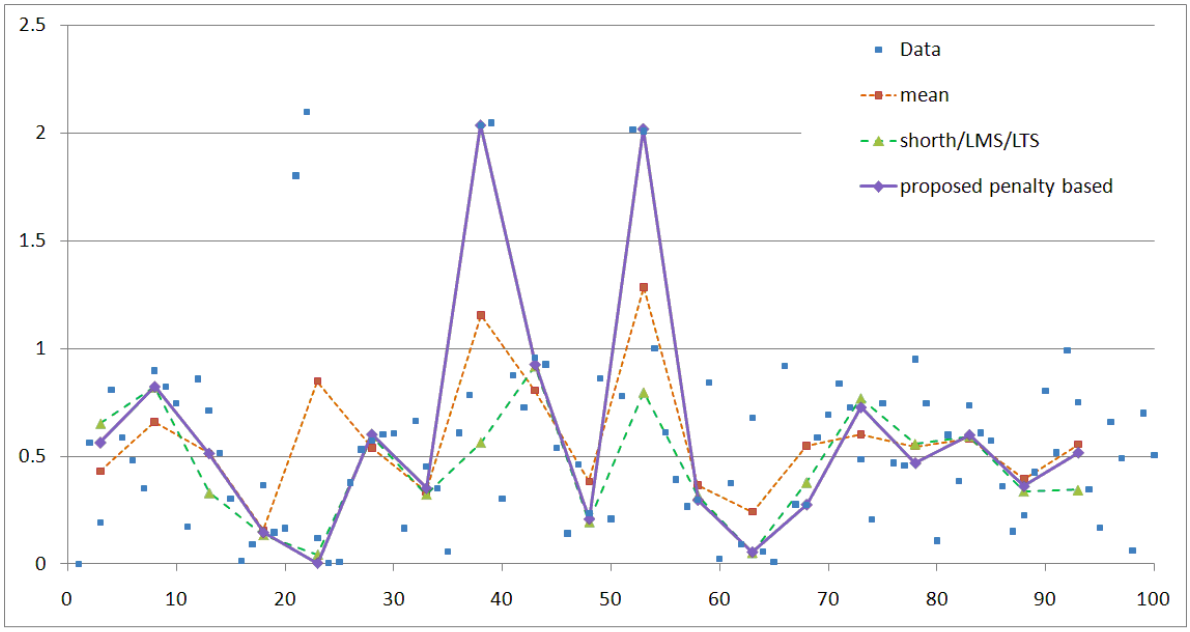

Fig. 1. Illustration of various averages in the moving average example with $m = 5$. The shorth, LMS and LTS estimators give almost the same values in this example and are represented with the dashed line. The arithmetic mean is illustrated with the dotted line. The proposed penalty based average is the solid line. It is the only method which picks two events of interest near 2, and discards abnormal data at positions 21 and 22, because they do not form a compact cluster. Hence these values are considered noise. At other places this method gives the averages similar to shorth/LMS/LTS methods.

used to reduce the size of a time series. We calculate an average of each m consecutive values in the data set, and reduce the length of the data set by the same factor m. Here we randomly generated 100 points with the uniform distribution $U(0, 1)$, and we replaced the data at positions 21,22,38,39, 52 and 53 with (unequal) random values near 2. These spikes in data represent events of interest (e.g., in anomaly detection). The data and various means we considered, along with the simple moving average (for $m = 5$), are illustrated in Figure 1.

We observe that the existing methods filter out the events of interest at the above mentioned positions. The arithmetic mean is affected by the outliers, and results in the values not representative of the corresponding subsamples. The proposed method gives averages close to those of shorth/LMS/LTS methods, but pinpoints the outliers, if they form clusters.

V. Conclusions

We discussed aggregation operators which are not monotone with respect to the inputs. Our motivation was to calculate the outputs representative of inputs that form clusters. Several robust location estimators have been recalled. We introduced a penalty-based averaging function, which favors the values representative of compact clusters.

Compared with the median, and several existing robust estimators of location, the proposed method delivers the outputs similar to those of the mode function, which are representatives of compact clusters of the input values. Unlike the mode, it works when all the inputs are distinct. In the subsequent research we aim at applying such averaging to image processing and analysis of network traffic.

References

[1] G. Beliakov, A. Pradera, and T. Calvo, *Aggregation Functions: A Guide for Practitioners*. Heidelberg, Berlin, New York: Springer, 2007.
[2] Y. Torra and V. Narukawa, *Modeling Decisions. Information Fusion and Aggregation Operators*. Springer, 2007.
[3] M. Grabisch, J.-L. Marichal, R. Mesiar, and E. Pap, *Aggregation Functions*. Cambridge: Cambridge University Press, 2009.
[4] T. Calvo and G. Beliakov, "Aggregation functions based on penalties," *Fuzzy Sets and Systems*, vol. 161, pp. 1420–1436, 2010.
[5] T. Calvo, R. Mesiar, and R. Yager, "Quantitative weights and aggregation," *IEEE Trans. on Fuzzy Systems*, vol. 12, pp. 62–69, 2004.
[6] R. Yager and A. Rybalov, "Understanding the median as a fusion operator," *Int. J. General Syst.*, vol. 26, pp. 239–263, 1997.
[7] P. Rousseeuw and A. Leroy, *Robust Regression and Outlier Detection*. New York: Wiley, 2003.
[8] P. Rousseeuw, "Least median of squares regression," *Journal of the American Statistical Association*, vol. 79, pp. 871–880, 1984.
[9] S. Pijavski, "An algorithm for finding the absolute extremum of a function," *USSR Comput. Math. and Math. Phys.*, vol. 2, pp. 57–67, 1972.
[10] G. Beliakov, "Extended cutting angle method of global optimization," *Pacific J. of Optimization*, vol. 4, pp. 153–176, 2008.
[11] G. Beliakov and J. Ugon, "Implementation of novel methods of global and non-smooth optimization: GANSO programming library," *Optimization*, vol. 56, pp. 543–546, 2007.
[12] G. Beliakov, "The cutting angle method - a tool for constrained global optimization," *Optimization Methods and Software*, vol. 19, pp. 137–151, 2004.

2011 IEEE International Conference on Fuzzy Systems
June 27-30, 2011, Taipei, Taiwan

Linguistic Local Change Comparison Of Time Series

Rita Castillo-Ortega and Nicolás Marín
University of Granada
Granada, Spain
Email: {rita,nicm}@decsai.ugr.es

Daniel Sánchez
European Centre for Soft Computing
Mieres, Asturias, Spain
Email: daniel.sanchezf@softcomputing.es

***Abstract*—In this paper a methodology is proposed for providing a linguistic summary of the comparison of time series. This series are obtained as a result of queries which the user defines over a data cube with time dimension. Our objective is that the final summary describe the similarity between series by using local changes. Definitions of the degree and sign of local changes are proposed. The understandability of the linguistic summary is achieved by means of linguistically quantified sentences. So are the coverage and brevity by using a hierarchical partition of time dimension inherited from the data warehouse. Our linguistic summaries are well suited to be included in an interface layer of a data warehouse system, improving the quality of human-machine interaction and the understandability of the results.**

***Index Terms*—Linguistic Summarization, Time series, OLAP, Business Intelligence, Multidimensional Data Model, Fuzzy Logic.**

I. Introduction

Summarization is widely accepted as a data mining task, since summaries of data are extracted non-trivially, they are very useful since they contribute to a better understanding, and they provide a novel, previously unseen view of data.

In the setting of data mining, summaries are expected to be an understandable description of knowledge present in the data. The simpler form of such knowledge are plain facts, as in the case of using statistics (i.e., the average value of a certain variable in a database, etc.). However, much complex summaries may be obtained using more sophisticated knowledge representation languages with richer semantics. Due to its good understandability to the user, one very interesting possibility is to obtain linguistic summaries of data, i.e., summaries expressed in (usually a subset of) natural language.

One of the areas where linguistic summaries can be very useful is that of Business Intelligence solutions, intended to help managers in order to obtain a better understanding of its commercial procedure and operations and, this way, supporting decision-making. Data warehousing systems use to incorporate an interface layer responsible of providing such information (see for example the case of scorecards [1]). One of the tools that undoubtedly can help in building this kind of interfaces is to use natural language as a vehicle to describe data, as a human assistant in charge of this task would do [2].

Part of the research was supported by the Andalusian Government (Junta de Andalucía, Consejería de Innovación, Ciencia y Empresa) under project P07-TIC-03175 *Representación y Manipulación de Objetos Imperfectos en Problemas de Integración de Datos: Una Aplicación a los Almacenes de Objetos de Aprendizaje*. Part of the research was supported by the Spanish Government (Science and Innovation Department) under project TIN2009-08296.

Many queries to data warehousing systems involve the evolution of data along time. Data cubes usually have a time dimension because time plays a crucial role in any commercial activity. Hence, many OLAP queries in data cubes with time dimension produce as result time series data. In particular, many queries are intended to provide a comparison between datasets, like for example the total amount of sales in different shops of a supermarket chain or, involving time, about the evolution of those sales in the same shops. As a consequence, there is a necessity for tools able to provide understandable, accurate, and relevant information about the similarities and differences between time series.

In this work we propose a methodology for providing a linguistic summary of the comparison of time series obtained as a result to a user's query. The summary comes in the form of a collection of *accurate* linguistic quantified sentences describing the similarity between local changes in the whole time domain considered. On the basis of a hierarchical partition of the time dimension, available through the datacube structures, we not only achieve a complete *coverage* of the time domain, but we also avoid obtaining two sentences for the same time period and, in this sense, our summary is also *brief*. The *relevance* of the information is assumed since it is the user who asks for the comparison of the series by means of a specific query , and since we choose the most representative among all the possible sentences for a given time period, also on the basis of the user's preferences. Finally, as we indicated before, *understandability* is taken into account in that the information is provided in the form of a linguistic description in natural language.

As related work, many approaches to data summarization with the use of Soft Computing concepts can be found in the literature. Among these proposals, linguistic summarization is of special interest because of the above mentioned need for sentences close to natural language to describe data. An important seminal part of this research can be found in Ronald R. Yager's works, where he first proposes the use of quantified sentences in the sense of L. Zadeh [3] and later introduces his own way of quantification with OWA (Ordered Weighted Averaging) operators in [4], [5]. Also following Zadeh's footsteps, we can find J. Kacprzyk et al. ([6], [7], [8], [9]) introducing new quality measures and using the protoform concept in order to reach different summary profiles. The same author

The query language employed is not relevant for the purpose of our work.

978-1-4244-7316-8/11/$26.00 ©2011 IEEE

has provided methods for linguistic comparison of time series [10], though of a different kind and with different objectives than we intend here. Raschia et al. have created a model named SaintEtiQ [11], working with hierarchies composed by summaries with different abstraction levels. From a different point of view, Bosc and Dubois propose the use of association rules to obtain knowledge from data and even for case based prediction [12]. Our work here is based on an approach to the linguistic summarization of a single time series on the basis of a hierarchical partition of time dimension [13]. The basis for a better understanding of this work can be found in [14], [15] and a detailed study is available at [16].

The document is organized as follows: Section II is devoted to present the source our data come from, introducing OLAP queries on fuzzy data cubes as a mean to obtain the time series to compare. The use of fuzzy data cubes with time dimension provides us with a hierarchical organization of the time domain that plays a determining role in our approach. Section III introduces our proposal to compare two query results in the form of two time series that share the same time line. In this section, we first analyze the characteristics of the series where the comparison focus on and then we set the linguistic framework used to build the summaries. Two greedy algorithms to compute the linguistic summaries are also presented in this section. Section IV contains a descriptive example of the use of the proposed approach and, finally, section V concludes the paper.

II. Describing time series coming from OLAP cubes

Time plays a main role in data warehouses that store *historical* information regarding the daily operation of the organization. This way, decision-makers can analyze the evolution of several aspects of the business along the time. One of the most extended models for building data warehouses is the use of datacubes (also known as OLAP cubes).

We can briefly describe a data cube as a n-dimensional set of cells. Each dimension consists of a set of members that can be arranged along a hierarchy or many hierarchies. Thanks to the hierarchical organization of dimensions, granularity in the data cube can vary according to the selected level chosen in each dimension. OLAP operations permit the user to take advantage of this fact and query the data cube in order to get the desired data in each moment. According to the previous paragraph, among the dimensions of a data cube, we usually find the time dimension.

OLAP cubes have been extended in order to add the capability of dealing with fuzzy data. In our approach, we use as basis the model proposed in [17], [18]. One of the main characteristics of this model is that the hierarchical organization of dimensions can be made by means of linguistic partitions. The use of this model provides a suitable framework for the linguistic description of time series.

Figure 1 describes a (generic) data cube with a time dimension. Each cell contains the value of the variable *V* according to the context defined by the members of each dimension. As we can see, using conventional OLAP operations, we can query the data cube focusing on a given member of each of the non-time dimensions: the result of this query is a time series of data.

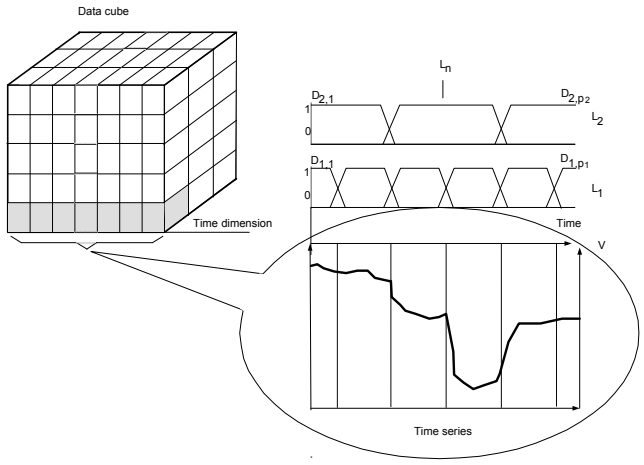

Fig. 1. Time series from OLAP cubes

Suppose that the time dimension is described in its finest grained level of granularity by members $T = \{t_1, ..., t_m\}$. Then, the above mentioned query result will have the following form: $\{< t_1, v_1 >, ..., < t_m, v_m >\}$, where every v_i is a value of the basic domain of the variable V. We will use $TS(t_i)$ to refer to v_i when necessary.

In order to linguistically describe the time information in our approach, the time dimension is hierarchically organized in n levels, namely, L=$L_1, ..., L_n$. Each level L_i has a partition $\{D_{i,1}, ..., D_{i,p_i}\}$ of the basic time domain associated. There is no restriction concerning the form of the membership function of a label apart from that it must be normalized. In our approach, we will use trapezoidal functions. When necessary, labels $D_{i,j}$ in time dimension can be the union of a set of trapezoidal functions.

In this work, a set of labels $\{X_1, ..., X_r\}$ is a partition on X iff:

1) $\forall x \in X, \exists X_i, i \in \{1..r\} | \mu_{X_i}(x) > 0$.
2) $\forall i, j \in \{1..r\}, i \neq j, core(X_i) \cap core(X_j) = \emptyset$.

Additionally, considering the hierarchy of the time dimension, we add the following constraints:

1) $\forall i, j \in \{1..n\}, i < j, p_i > p_j$ (i.e, as we move upward in the hierarchy, the number of labels of the partition decreases).
2) $\forall i \in \{2..n\}, \forall j \in \{1..p_i\}, \forall k \in \{1..p_{i-1}\} | (D_{i,j} \subseteq D_{i-1,k}) \rightarrow (D_{i,j} = D_{i-1,k})$ (i.e., labels cannot generalize another label of an upper level).

As an example, consider a data warehouse with data related to medical centers in a given country. A data cube of this data warehouse can be built with information regarding the patient inflow according to the dimensions *medical center*, *service*, and *time*. If we focus (slice and dice) on a given medical center C and aggregate (roll up) across the service dimension, we obtain the time series "Total patient inflow in center C

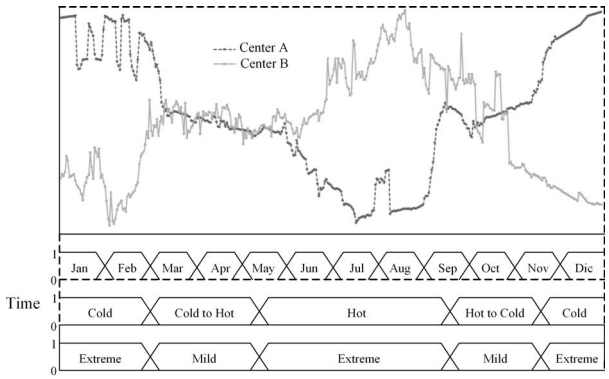

Fig. 2. Patient inflow data series

along the time". In this example, the time dimension is fuzzy hierarchically organized using a meteorological criteria.

Figure 2 contains two time series that shows the patient inflow along a given year to two medical centers. As we can see, the time dimension is hierarchically organized thanks to three fuzzy partitions of the time domain, namely: one based on approximate months (in order to avoid a strong dependence of the obtained summaries with respect to the crisp boundaries of conventional months) and two others based on a meteorological criteria with two levels of granularity. Fuzziness is specially useful in these two last partitions because transitions between periods are clearly fuzzy.

In previous works, we have focused on the linguistic summarization of a single time series [13]. In this work, we extend our approach to the case of the linguistic comparison of the trends of two time series like the ones depicted in Figure 2.

III. Local change based comparison of time series

Once we have described the framework where the time series are defined, the next step is to introduce the new approach to linguistically compare the information related to two time series. There are several ways to compare series. Among them, special attention has been paid to value-based comparison and trend-based comparison. In a previous work [13] we introduced an approach to value-based comparison of two time series. With respect to trend-based comparison, Kacprzyk et al.'s work is of interest [10]. This approach compares the trends trough the analysis of significant segments in the series with respect to duration, dynamics (slope), and variability.

In this work, our interest is centered on the comparison of trends but with a different perspective: we study the dynamics of change through the local variations in the points of the series and we take advantage of the hierarchical partition of the time domain when building the summaries. Our summaries are comprised of several linguistically quantified sentences.

A. Comparing the dynamics of change

The current subsection is devoted to describe the process we follow in order to compare de dynamics of change. The bases will be set by means of the introduction of some important definitions.

We use consecutive points in order to analyze the dynamics of change in the series. To do that, we measure the local change for every time point with respect to the next one in each individual series. This local change can be formalized with the next definitions.

Definition 1 (Local change): Let $TS = \{< t_1, v_1 >, ..., < t_m, v_m >\}$ be a time series and t_i with $i \in [1, m-1]$ be a given time point. The local change $\Delta_{TS}(t_i)$ of t_i in TS is defined as follows: $\Delta_{TS}(t_i) =$

$$= \arctan\left(\frac{TS(t_{i+1}) - TS(t_i)}{t_{i+1} - t_i}\right) = \arctan\left(\frac{v_{i+1} - v_i}{t_{i+1} - t_i}\right)$$

Hence, we are defining local change as the slope of the line joining two consecutive points in the time series. We assume that this slope comes in the form of a value in $[-\pi/2, \pi/2]$.

In Figure 3 the reader can graphically see the intuitive semantics behind our definitions concerning the local change at a given point t_i.

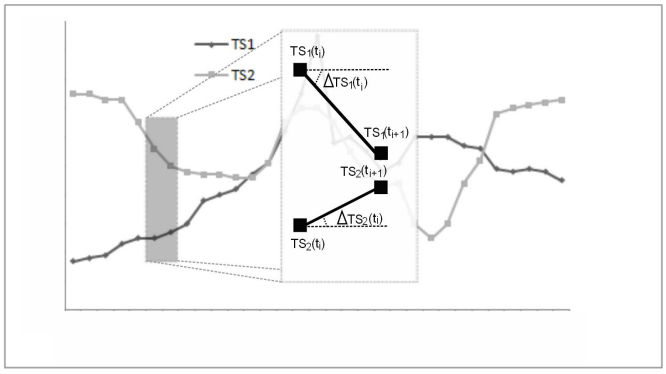

Fig. 3. Local change

Our approach tries to linguistically compare the local change of two time series. To do that, we need a linguistic framework in order to express this comparison by means of natural language. The following definitions are devoted to this aim.

Definition 2 (Same sign function): Let TS_1 and TS_2 be two time series defined on $t_1..t_m$. The same sign function SS_{TS_1,TS_2} is defined, for every $t_i \in \{t_i, ..., t_m - 1\}$ as follows:

$$SS_{TS_1,TS_2}(t_i) = \begin{cases} 1, & \text{if } (\Delta_{TS_1}(t_i) * \Delta_{TS_2}(t_i) \geq 0) \\ 0, & \text{otherwise} \end{cases}$$

Similarly, we can define the different sign function.

Definition 3 (Different sign function): Let TS_1 and TS_2 be two time series defined on $t_1..t_m$. The different sign function DS_{TS_1,TS_2} is defined, for every $t_i \in \{t_i, ..., t_m - 1\}$ as follows:

$$DS_{TS_1,TS_2}(t_i) = \begin{cases} 0, & \text{if } (\Delta_{TS_1}(t_i) * \Delta_{TS_2}(t_i) \geq 0) \\ 1, & \text{otherwise} \end{cases}$$

It is obvious that $SS_{TS_1,TS_2}(t_i) = 1 - DS_{TS_1,TS_2}(t_i)$. If we only focus on the magnitude of the change, we can define two additional functions.

Definition 4 (Degree of similar variation): Let TS_1 and TS_2 be two time series defined on $t_1..t_m$ and t_i with $i \in [1, m-1]$ be a given time point. The degree of similar variation $SV_{TS_1,TS_2}(t_i)$ in point t_i between series TS_1 and TS_2 is defined as follows:

$$SV_{TS_1,TS_2}(t_i) = 1 - \frac{||\Delta_{TS_1}(t_i)| - |\Delta_{TS_2}(t_i)||}{\pi/2}$$

By means of the computation of the degree of similar variation we obtain the similarity observed between the two angles responsible of the local change at a given t_i in both series, without taking into account the sign.

Similarly, we can define the degree of different variation:

Definition 5 (Degree of different variation): Let TS_1 and TS_2 be two time series defined on $t_1..t_m$ and t_i with $i \in [1, m-1]$ be a given time point. The degree of different variation $DV_{TS_1,TS_2}(t_i)$ in point t_i between series TS_1 and TS_2 is defined as follows:

$$DV_{TS_1,TS_2}(t_i) = \frac{||\Delta_{TS_1}(t_i)| - |\Delta_{TS_2}(t_i)||}{\pi/2}$$

Again, it is obvious that $SV_{TS_1,TS_2}(t_i) = 1 - DV_{TS_1,TS_2}(t_i)$.

B. Linguistically quantified sentences

Fuzzy quantification extends classical quantification by considering (fuzzy) linguistic quantifiers, a generalization of the ordinary quantifiers $\exists$ and $\forall$ of first order logic [19]. A large number of applications can be found in the literature in areas like quantifier-guided aggregation, linguistic summarization, computing with words, and quantification in fuzzy description logics, among many others.

The most usual quantified sentences considered in the literature are of the form "Q of X are A" or "Q of D are A", where Q is a linguistic quantifier, X is a (finite) crisp set, and A, D are fuzzy subsets of X. These sentences are called type I and type II sentences, respectively. Linguistic quantifiers are normal, convex fuzzy subsets of integers $\mathbb{Z}$ (absolute quantifiers) or $[0, 1]$ (relative quantifiers). Particularly, in this paper, linguistic quantifiers are represented by trapezoidal functions.

There are many different approaches for evaluating quantified sentences; we shall use the method called GD introduced in [20] as follows: the evaluation of "Q of D are A" by means of GD is

$$GD_Q(A/D) = \sum_{\alpha_i \in \triangle(A/D)} (\alpha_i - \alpha_{i+1}) Q\left(\frac{|(A \cap D)_{\alpha_i}|}{|D_{\alpha_i}|}\right) \quad (1)$$

where $(A \cap D)(x) = \text{Min}(A(x), D(x))$, $\triangle(A/D) = \Lambda(A \cap D) \cup \Lambda(D)$, $\Lambda(D)$ being the level set of D, and $\triangle(A/D) = \{\alpha_1, ..., \alpha_p\}$ with $\alpha_i > \alpha_{i+1}$ for every $i \in \{1, ..., p\}$, we consider $\alpha_1 = 1$ and $\alpha_{p+1} = 0$ (although α_{p+1} is not in the level set we consider it in the formula). The set D is assumed to be normalized. If not, D is normalized and the same normalization factor is applied to $A \cap D$ (D and $A \cap D$ will be divided by the greater value in D) .

The GD method has been used due to its efficiency and non-strict character. The method also fulfills some interesting properties related to relative quantifiers (defined in [20]). Another point is that it is easy to implement. Anyway, let us remark that the strategies presented in this paper are not dependent on the evaluation method.

As we have mentioned, we consider that the user is interested in linguistic comparisons that take the form of a collection of quantified sentences. In this sense, our approach will deliver a collection of sentences of the form "Q of $D^S_{i,j}$ are A^S" where:

- Q is a linguistic quantifier.
- $D_{i,j}$ is a label member of a certain level i of the hierarchy associated to the time dimension and

$$D^S_{i,j}(< t, v >) = D_{i,j}(t). \quad (2)$$

- A is a label or the union of a subset of labels of the partition of the variable V under study. In this case V represents the local change, and

$$A^S(< t, v >) = A(v). \quad (3)$$

With this kind of sentences, the approach will be able to produce results like "Most (Q) days of the cold season ($D^S_{i,j}$), both series exhibit a local change with the same sign and similar variation (A^S)".

With respect to the quantifier Q, the user must provide a collection of quantifiers defining the kind of fuzzy quantities and percentages she/he is interested in. This can be defined by choosing among a collection of predefined quantifiers. In this work, we consider that the user provides a *totally ordered* subset $\{Q_1, ..., Q_{qmax}\}$ of a coherent family of quantifiers $\mathcal{Q}$ [21] to be used in the summarization process.

Definition 6 (Coherent family of quantifiers): Let $\mathcal{Q}$=$\{Q_1$, ..., $Q_l\}$ be a linguistic quantifier set, we shall say it is coherent if it verifies that:

- The membership functions of elements in $\mathcal{Q}$ are non-decreasing functions.
- A partial order relation $\succeq$ is defined in $\mathcal{Q}$. It has as its maximal element $Q_1 = \exists$ and as its minimal one $Q_l = \forall$. Furthermore $\forall Q_i, Q_j \in \mathcal{Q}$, $Q_i \subseteq Q_j \Rightarrow Q_j \succeq Q_i$.
- The membership function of the quantifier $\exists$ is given by $Q_1(x) = 1$ if $x \neq 0$ and $Q_1(0) = 0$, whereas the membership functions of $\forall$ will be $Q_l(x) = 0$ if $x \neq 1$ and $Q_l(1) = 1$.

To play the role of D, we can take any of the labels $D_{i,j}$ defined in the hierarchy associated to the time domain in our fuzzy OLAP cube.

Finally, we can consider the definition of A according to the previous definitions:

As the data set X is assume to be finite, D is considered to be finite, and hence the number of relevant α-cuts is also finite.

- Points where local change has the same sign (whatever the variation). In this case:

$$A(t_i) = SS_{TS_1,TS_2}(t_i)$$

- Points where local change has different sign (whatever the variation). In this case:

$$A(t_i) = DS_{TS_1,TS_2}(t_i)$$

- Points where local change has similar variation (whatever the sign). In this case:

$$A(t_i) = SV_{TS_1,TS_2}(t_i)$$

- Points where local change has different variation (whatever the sign). In this case:

$$A(t_i) = DV_{TS_1,TS_2}(t_i)$$

C. Obtention of the summaries

According the above defined linguistic framework, our approach will deliver a summary composed by a collection of sentences of the form "Q of D^S are A^S" with the above described semantics. To obtain this collection, apart from the linguistic framework analyzed in the previous subsection, the user will provide a threshold τ for the minimum accomplishment degree she/he wishes for the quantified sentences comprising the summaries. It is also necessary that the user specify wether she/he is interested in summarizing the local changes according to the sign or the variation.

Once we have defined all the parameters we need, it is time to launch a process able to compute the desired summary. Algorithm 1 explores all the possible A labels of C before exploring solutions with a less strict quantifier, beginning with the *strictest* quantifier provided by the user.

In order to look for *brevity*, we start from the time periods at the top level of the hierarchy. Each level has its own quantifier bound ($Qbound_i$) that indicates the least strict quantifier to be considered. The set $ToSummarize$ is the collection of time periods for which a quantified sentence is missing. The set $Summarized$ is the collection of time periods for which a quantified sentence is found. If it is possible to obtain an accomplishment degree greater than or equal to τ for a certain period using a quantifier Q and an A label of C, the procedure obtains a summary for that period.

If all A labels are tried without success, the algorithm repeats the process again, but with a less strict quantifier, until $Qbound_i$ is reached. When a summary is found in a certain time period we say that the period is $covered$.

If there is no result for a given period $D_{i,j}$, we try to obtain such sentences with the *corresponding children* $ch(D_{i,j})$ in the next level of the time domain (line 21).

For every $D_{i,j}$, $ch(D_{i,j})$ is defined as follows:

- $ch(D_{1,j}) = \emptyset$ for all j.
- Otherwise, $ch(D_{i,j}) = \{D_{i-1,k}, k \in \{1..p_{i-1}\} | D_{i-1,k} \cap D_{i,j} \neq \emptyset$ and $\neg\exists D \in ToSummarize \cup Summarized$, $(D_{i-1,k} \cap D_{i,j}) \subseteq D\}$.

Algorithm 1 to obtain linguistic summaries.

Input

Two time series TS_1 and TS_2
A hierarchical fuzzy partition of the time dimension D
A totally ordered subset $\{Q_1..Q_{qmax}\}$ of a coherent family of quantifiers Q.
A threshold τ as minimum accomplishment for quantified sentences.
For each L_i, maximum number of quantifiers to use ($Qbound_i$).
Two collections of alternatives for A, $C \subseteq \{SS_{TS_1,TS_2}, DS_{TS_1,TS_2}\}$ or $C \subseteq \{SV_{TS_1,TS_2}, DV_{TS_1,TS_2}\}$.

Output

A Summary of the comparison of time series TS_1 and TS_2

Algorithm

1: $ToSummarize \leftarrow L_n$;
2: $Summary \leftarrow \emptyset$; $Summarized \leftarrow \emptyset$;
3: **while** $ToSummarize \neq \emptyset$ **do**
4: Take $D_{i,j} \in ToSummarize$
5: $ToSummarize \leftarrow ToSummarize \backslash \{D_{i,j}\}$;
6: $p \leftarrow qmax$; $covered \leftarrow false$;
7: **while** $p \geq Qbound_i$ and $not\ covered$ **do**
8: Let $A \leftarrow argmax_{B \in C_k} GD_{Q_p}(B^S / D^S_{i,j})$;
9: **if** $GD_{Q_p}(B^S / D^S_{i,j}) \geq \tau$ **then**
10: $Summary \leftarrow Summary \cup \{Q_p$ of $D^S_{i,j}$ are $A^S\}$;
11: $Summarized \leftarrow Summarized \cup (D_{i,j})$;
12: $covered \leftarrow true$;
13: **end if**
14: $p \leftarrow p - 1$;
15: **end while**
16: **if** $not\ covered$ and $i > 1$ **then**
17: $ToSummarize \leftarrow ToSummarize \cup ch(D_{i,j})$;
18: **end if**
19: **end while**

With regards to the computational complexity of the algorithms, as can be seen, it exponentially depends on $|A|$ (the number of labels defined in A) and linearly depends on $\sum_i p_i$ (the number of labels in the time partitions) and $qmax$ (the number of quantifiers). In any case, $|E|$ is usually low and it is not necessary to explore its entire powerset due to the user-defined bounds.

IV. Experimentation

This section is devoted to show the performance of the proposed approach. With that purpose we use two series representing the gasoline price in New York and Texas during the same period of time.

As it was mentioned before, once the user has the corresponding time series data, he/she is in charge of defining the linguistic background and setting the parameters following his/her specific needs. The different partitions on the variable and time domains will define the type of sentences he/she will be able to obtain at the end of the summarization process. Moreover, he/she has to set the parameters values to inform the algorithm of his/her exploration preferences (sign/variation, threshold and boundaries).

The series used in this example represent the weekly all grades all formulation retail gasoline prices (in cents per gallon) in New York and Texas during the decade 2000-2010. In this example we do not have all the measures on year 2000 but only those corresponding to the second half of the year. The same thing occurs when dealing with 2010 where we only have

values for the first quarter of the year. In total, we count on 513 measures representing the 513 weeks. Series are depicted in Figure 4.

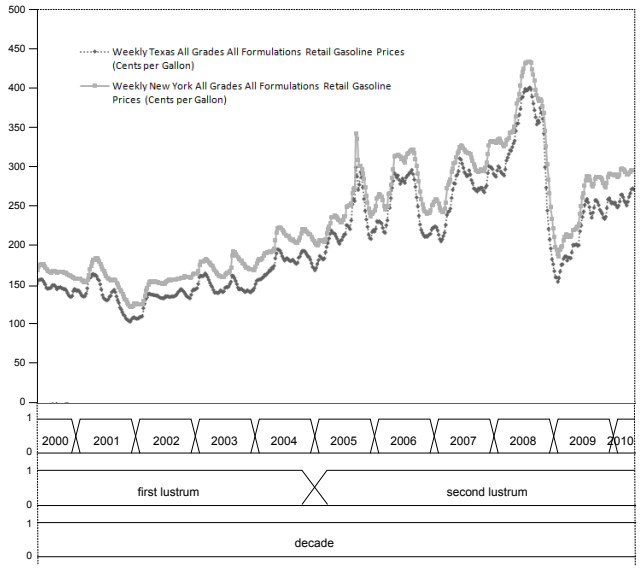

Fig. 4. Weekly all grades all formulation retail gasoline prices (in cents per gallon)

As we can see in Figure 4, the time dimension is hierarchically organized in three levels. The more general level represents the whole decade, while the second is made up of partitions representing two approximate periods of five years (lustrums). Finally, the finest grained level partition represents approximate years. In this context, fuzziness is used in order to avoid sharp transitions between time periods. The hierarchical partition of the time domain is defined in Table I.

Level	Label	Definition
1	Second half of year 2000	(0, 0, 28, 32)
	Year 2001	(28, 34, 80, 84)
	Year 2002	(80, 84, 132, 136)
	Year 2003	(132, 136, 184, 188)
	Year 2004	(184, 188, 236, 240)
	Year 2005	(236, 240, 288, 292)
	Year 2006	(288, 292, 341, 345)
	Year 2007	(341, 345, 393, 397)
	Year 2008	(393, 397, 445, 449)
	Year 2009	(445, 449, 497, 501)
	First quarter of year 2010	(497, 501, 513, 513)
2	First lustrum	(0, 0, 230, 249)
	Second lustrum	(230, 249, 513, 513)
3	Whole decade	(0, 0, 513, 513)

TABLE I
PARTITION OF THE TIME DIMENSION

The example has been carried out using the set of linguistic quantifiers shown at Table II. The threshold value has been set as $\tau = 0.7$. Regarding $Qbound_i$, this parameter has value 1 in levels 3 and 2, and value 2 in level 1 ($Qbound_3 = Qbound_2 = 1$ and $Qbound_1 = 2$). This is due to the fact that the user wants to use stricter quantifiers in levels holding bigger periods of time, and less strict quantifiers in the finest grained partition in order to obtain representative summaries.

Quantifier	Definition
Most	(0, 0.7, 0.9, 1)
At least 70%	(0, 0.6, 0.8, 1)
At least 60%	(0, 0.5, 0.7, 1)
At least 50%	(0, 0.4, 0.6, 1)

TABLE II
QUANTIFIERS

In the first case, we are going to consider that the user is interested or she/he considers useful only those labels representing the local changes in terms of sign as C. As a result, we obtain this set of quantified sentences.
- Most days of second lustrum, both series exhibit a local change with the same sign (0.716765).
- At least 70% of the days of a half of year 2000, both series exhibit a local change with the same sign (0.770035).
- Most days of year 2001, both series exhibit a local change with the same sign (0.714104).
- At least 70% of the days of year 2003, both series exhibit a local change with the same sign (0.821261).
- Most days of year 2004, both series exhibit a local change with the same sign (0.812402).

In the second case, the user focusses the attention on those labels representing the local changes in terms of variation as C. The obtained set of quantified sentences is:
- At least 70% of the days of a half of year 2000, both series exhibit a local change with similar variation (0.727618).
- At least 70% of the days of year 2002, both series exhibit a local change with similar variation (0.707482).
- At least 70% of the days of year 2003, both series exhibit a local change with similar variation (0.763968).
- At least 70% of the days of year 2004, both series exhibit a local change with similar variation (0.784934).
- Most days of year 2005, both series exhibit a local change with similar variation (0.761454).
- Most days of year 2006, both series exhibit a local change with similar variation (0.736421).
- At least 70% of the days of year 2007, both series exhibit a local change with similar variation (0.75718).
- Most days of year 2008, both series exhibit a local change with similar variation (0.736357).
- At least 70% of the days of year 2009, both series exhibit a local change with similar variation (0.754698).
- It has not been possible to find any kind of information referring to the rest of time periods.

The reader can see that the algorithm has obtained a short summary using sign local changes while the summary is a little bit longer using variation local changes. In the first execution the algorithm has come up with a suitable sentence describing the whole second lustrum. In the second execution

the accuracy of the sentence produce for the same period of time using variation is not enough and smaller periods have to be analyzed. We can conclude that the series are more similar according to local changes in sign that according to local changes related to variation.

We have to keep in mind that the presented method analyzes local trends by doing the calculation with pairs of consecutive time points. It could be possible that the obtained results surprised the user if he/she was expecting a summary comprising a global trend description. In some occasions the local trends can coincide with the global one, but this is not necessarily true.

V. Conclusion and future work

Linguistic summarization of data is a very interesting data mining task providing highly understandable knowledge. In this work we have proposed a methodology for providing linguistic summaries to answer a usual kind of queries in data warehouses, i.e., the comparison of time series. These queries are frequent as data cubes use to have a time dimension.

The comparison is focused on the analysis of the degree and sign of the local change observed in every time point. The summary is a collection of *accurate* linguistic quantified sentences describing the similarity between local changes in the whole time domain considered. A hierarchical partition of the time dimension permits us not only to achieve a complete *coverage* of the time domain, but also to obtain *brief* summaries. The *relevance* of the information is assumed since it is the user who asks for the comparison of the series by means of a specific query, and since we choose the most representative among all the possible sentences for a given time period, also on the basis of the user's preferences. Our linguistic summaries are well suited to be included in an interface layer of a data warehouse system, improving the quality of human-machine interaction and the understandability of the results.

We are currently extending the approach so that the user can interleave both the analysis in term of sign and in term of variation at the same time. This way, different levels of granularity can be managed by the algorithm in its look for a *brief* and *accurate* summary of the comparison of the dynamic of local changes in the series.

References

[1] R. S. Kaplan and D. P. Norton, *The Balanced Scorecard: Translating Strategy into Action*. Harvard Business Press, 1 ed., September 1996.

[2] F. Bobillo, M. Delgado, J. Gómez-Romero, and E. López, "A semantic fuzzy expert system for a fuzzy balanced scorecard," *Expert Syst. Appl.*, vol. 36, no. 1, pp. 423–433, 2009.

[3] R. R. Yager, "A new approach to the summarization of data," *Information Sciences*, no. 28, pp. 69–86, 1982.

[4] R. R. Yager, "Toward a language for specifying summarizing statistics," *IEEE Transactions on Systems, Man, and Cybernetics, Part B*, vol. 33, no. 2, pp. 177–187, 2003.

[5] R. R. Yager, "A human directed approach for data summarization," in *IEEE International Conference on Fuzzy Systems*, pp. 707–712, 2006.

[6] J. Kacprzyk, "Fuzzy logic for linguistic summarization of databases," in *IEEE International Fuzzy Systems Conference*, pp. 813–818, 1999.

[7] J. Kacprzyk and R. R. Yager, "Linguistic summaries of data using fuzzy logic," in *International Journal of General Systems*, vol. 30, pp. 133–154, 2001.

[8] J. Kacprzyk, R. R. Yager, and S. Zadrozny, "A fuzzy logic based approach to linguistic summaries in databases," *International Journal of Applied Mathematical Computer Science*, vol. 10, pp. 813–834, 2000.

[9] J. Kacprzyk and S. Zadrozny, "Linguistic database summaries and their protoforms: towards natural language based knowledge discovery tools," *Inf. Sci. Inf. Comput. Sci.*, vol. 173, no. 4, pp. 281–304, 2005.

[10] J. Kacprzyk and A. Wilbik, "Using fuzzy linguistic summaries for the comparison of time series: an application to the analysis of investment fund quotations," in *IFSA-EUSFLAT 2009* (U. K. J. P. Carvalho, D. Dubois and J. M. C. Sousa, eds.), pp. 1321–1326, 2009.

[11] G. Raschia and N. Mouaddib, "Saintetiq: a fuzzy set-based approach to database summarization," *Fuzzy Sets Syst.*, vol. 129, no. 2, pp. 137–162, 2002.

[12] P. Bosc, D. Dubois, O. Pivert, H. Prade, and M. D. Calmes, "Fuzzy summarization of data using fuzzy cardinalities," in *Int. Conf. Inf. Process. Manag. Uncertainty Knowl. Based Syst.*, pp. 1553–1559, 2002.

[13] R. Castillo-Ortega, N. Marín, and D. Sánchez, "Time series comparison using linguistic fuzzy techniques," in *International Conference on Information Processing and Management of Uncertainty in Knowledge-Based Systems. IPMU 2010*, pp. 330–339, 2010.

[14] R. Castillo-Ortega, N. Marín, and D. Sánchez, "Fuzzy quantification-based linguistic summaries in data cubes with hierarchical fuzzy partition of time dimension," in *IDEAL'09* (H. Yin and E. Corchado, eds.), vol. 5788 of *LNCS*, pp. 578–585, Springer, Heidelberg, 2009.

[15] R. Castillo-Ortega, N. Marín, and D. Sánchez, "Linguistic summary-based query answering on data cubes with time dimension," in *FQAS'09* (T. Andreasen, R. R. Yager, H. Bulskov, H. Christiansen, and H. L. Larsen, eds.), vol. 5822 of *LNAI*, pp. 560–571, Springer, Heidelberg, 2009.

[16] R. Castillo-Ortega, N. Marín, and D. Sánchez, "A fuzzy approach to the lingusitic summarization of time series," *Journal of Multiple-Valued Logic and Soft Computing, Special Issue Soft Computing Techniques in Data Mining*, vol. 17, no. 2,3, pp. 157–182, 2011.

[17] N. Marín, C. Molina, J.-M. Serrano, and M. A. V. Miranda, "A complexity guided algorithm for association rule extraction on fuzzy datacubes," *IEEE T. Fuzzy Systems*, vol. 16, no. 3, pp. 693–714, 2008.

[18] C. Molina, L. R. Ariza, D. Sánchez, and M. A. V. Miranda, "A new fuzzy multidimensional model," *IEEE T. Fuzzy Systems*, vol. 14, no. 6, pp. 897–912, 2006.

[19] L. A. Zadeh, "A computational approach to fuzzy quantifiers in natural languages," *Computing and Mathematics with Applications*, vol. 9, no. 1, pp. 149–184, 1983.

[20] M. Delgado, D. Sánchez, and M. Vila, "Fuzzy cardinality based evaluation of quantified sentences," *International Journal of Approximate Reasoning*, vol. 23, pp. 23–66, 2000.

[21] M. A. Vila, J. C. Cubero, J. M. Medina, and O. Pons, "The generalized selection: an alternative way for the quotient operations in fuzzy relational databases," in *Fuzzy Logic and Soft Computing* (B. Bouchon-Meunier, R. Yager, and L. Zadeh, eds.), World Scientific Press, 1995.

2011 IEEE International Conference on Fuzzy Systems
June 27-30, 2011, Taipei, Taiwan

Ant Colony Optimization with Dual Pheromone Tables for Clustering

Chun-Wei Tsai
Department of Applied Geoinformatics
Chia Nan University of Pharmacy & Science
Tainan, Taiwan, R.O.C.
Email: cwtsai0807@gmail.com

Kai-Cheng Hu and Ming-Chao Chiang
Department of Computer Science and Engineering
National Sun Yat-sen University
Kaohsiung, Taiwan, R.O.C.
Email: spring69953@hotmail.com and mcchiang@cse.nsysu.edu.tw

Chu-Sing Yang
Department of Electrical Engineering
National Cheng Kung University
Tainan, Taiwan, R.O.C.
Email: csyang@ee.ncku.edu.tw

***Abstract*—This paper presents a novel pheromone update strategy for improving the clustering results of ant colony optimization (ACO). The proposed algorithm is motivated by the observation that most of the ACOs only keep track of the *promising* foraging information, which has the potential to lead to better solutions than all the other search directions in the pheromone table. This eventually makes the search converge to particular search directions in later iterations because the pheromone values on good routing paths will be reinforced. As such, the breadth of search (diversity) will be reduced, thus limiting the clustering results of ACO. The proposed algorithm adds a second pheromone table to ACO for recording the *unpromising* foraging information that is worse than all the other search directions and using a novel construction method to explore the new search directions. In other words, by leveraging the strengths of diversification and intensification, the proposed algorithm can find better solutions than traditional ACO. To evaluate the performance of the proposed algorithm, we use it to solve the data clustering problem. Our experimental results indicate that the proposed algorithm can significantly improve the quality of ant colony optimization.**

keyword: ant colony optimization; pheromone table, and clustering.

I. Introduction

Partitional clustering is a traditional clustering approach [1], [2], [3] that partitions n patterns in d-dimensional space into k groups according to some predefined criteria. The ultimate goal of clustering is to find a partitioning that minimizes the distance between all patterns and their centroids while at the same time maximizing the distance between clusters. In practice, the most popular metric used to measure the clustering results is the sum of squared errors (SSE) defined as

$$\text{SSE} = \sum_{i=1}^{k} \sum_{j=1}^{n_i} \|x_{ij} - c_i\|^2, \tag{1}$$

where k denotes the number of clusters; n_i the number of patterns in the ith cluster; x_{ij} the jth pattern in the ith cluster; $c_i = (1/n_i) \sum_{j=1}^{n_i} x_{ij}$ the mean (centroid) of the ith cluster; and $n = \sum_{i=1}^{k} n_i$ the number of patterns. On the other hand, metrics other than SSE such as f-measure or entropy can be used when the same clustering algorithm is applied to solve other clustering problems.

Clustering technologies are important because many applications such as search engine [4], [5], [6], document analysis [7], [8], bio-information [9], [10], financial analysis [11], and human face recognition [12], [13] rely on the clustering technologies. More recently, how to find an approximate solution to a clustering problem, which is NP-hard [14], in a reasonable time has become a very important research topic partially because the dataset size has become larger and larger and partially because finding the optimum solution to a clustering problem takes an extraordinary amount of time.

Since 1950's, many methods have been proposed to solve the clustering problem. Some of them are deterministic, some stochastic, and some statistic. The k-means [15], [16] algorithm is undoubtedly one of the most well known clustering algorithms because it is very easy to implement and it will converge to a local optimum very quickly. However, the clustering results of k-means are not satisfied for many applications because the k-means algorithm has several drawbacks. Of them are: the final result is very sensitive to the initial solutions; it is incapable of separating clusters that are non-linearly separable; and it may fall into local minima at early iterations. In addition to k-means, metaheuristics provide another way for clustering the data to mitigate the problems of k-means. Over the past, many metaheuristics have been employed to solve the clustering problem such as genetic algorithm (GA) [17], [18], tabu search (TS) [19], particle swarm optimization (PSO) [20], [21], and ant colony optimization (ACO) [22], [23]. Of them, ACO is among one of the most efficient metaheuristic algorithms because it uses social behavior to search for the clustering solution.

Although ACO can provide better results than other metaheuristic algorithm algorithms, it is still facing the local minima problem on its convergence process because by reinforcing the pheromone values on some routing paths that provide better solutions, the breadth of the search directions is limited. However, solutions on worse routing paths may provide partial solutions of the optimum soltuion or better search directions

978-1-4244-7316-8/11/$26.00 ©2011 IEEE

even though the chance is very small. For this reason, ACO-based algorithms may lose partial optimum solutions at the future search process by only reinforecing the promising paths. As such, how to improve the end results has recently become a promising research topic. In this paper, we present a novel ACO-based algorithm based on ant colony system (ACS), called ant colony optimization with dual pheromone tables (ACODPT), that adds a second pheromone table to it for keeping track of a different kind of information for improving the end results. A new recombination method for solution construction is also presented to explore the new search directions that may find better solution of clustering. To evaluate the performance of the proposed algorithm, we compare it to three state-of-the-art clustering algorithms: standard k-means [16], ant colony system [24], and genetic k-means algorithm [17].

The remainder of the paper is organized as follows. Section II gives a brief introduction to the genetic algorithm and approaches taken to enhance its performance. Section III describes in detail the proposed algorithm. Also given in Section III is a simple example to demonstrate how the proposed algorithm works. Performance evaluation of the proposed algorithm is presented in Section IV. Conclusion is drawn in Section V.

II. Related Work

Generally speaking, the clustering algorithms [25] that are inspired by the behavior of ants can be divided into two categories: ant-based clustering algorithm (ACA) [26], [27], [28], [29] and ant colony optimization (ACO) [30], [24], [31], [32]. In this section, we will give a brief introduction to these clustering algorithms.

A. Ant-based clustering algorithms

The ant-based clustering algorithm is inspired by the behavior of ant colonies in clustering their corpses and sorting their larvae [33]. The initial study was done by Deneubourg et al. [26] in which they proposed a model to make the ants move randomly and used the behavior of ants in "picking up" and "dropping" patterns to cluster the patterns. In [27], Lumer and Faieta extended the study in [26] to improve the quality of the clustering results. Generally, the clustering algorithms in this class are called the ant-based clustering algorithm (or ACA for short). Fig. 1 shows the basic concept and the major operators used by ACA [27].

```
1 Initialize()
2 while the termination criterion is not met
3     randomly select an ant to move
4     s = DropItem()
5     s = PickupItem()
6 end
7 OutputResult()
```

Fig. 1. Outline of the ACA.

As shown in Fig. 1, the very first step ACA takes is to initialize all the parameters, randomly scatter data items on the toroidal grid, and randomly place ants on the toroidal grid. The *DropItem* operator checks to see if ant j carries a pattern and is placed at a free grid position. It decides probabilistically whether to drop the pattern at the current position by Eqs. (2) and (4). The *PickupItem* operator checks to see if ant j does not carry any pattern and has arrived at a grid position occupied by a data pattern. It decides probabilistically whether to pick up this pattern by Eqs. (3) and (4).

$$p_{\text{drop}}(i) = \begin{cases} 2f(i) & \text{if} f(i) < k^-, \\ 1 & \text{otherwise}, \end{cases} \tag{2}$$

$$p_{\text{pick}}(i) = \frac{k^+}{k^+ + f(i)}, \tag{3}$$

$$f(i) = \max\left\{0, \frac{1}{\sigma^2}\sum_{j\in L}\left(1 - \frac{d(i,j)}{\alpha}\right)\right\}. \tag{4}$$

where k^+ and k^- are constants, $f(i)$ is a neighborhood function, $d(i,j)$ is the similarity measurement between patterns i and j, α is a data-dependent scaling parameter, and σ^2 is the size of the local neighborhood L.

In [33], Yang and Kamel presented a parallel model by using the multi-ant colonies model that contains independent ant colonies and a queen ant. The proposed three information exchange methods between the queen ant and ant colonies. They are: keeping predecessor, circular exchange, and lowest outliers. The experimental results show that the multi-ant colonies algorithm [33] outperforms single-ant-based algorithm and k-means in terms of several different criteria. In [34], Boryczka presented an extended version of ACA, by modifying the density function $f(i)$ to solve the problem in which the stable value of neighborhood scaling parameter may sometimes cause inappropriate behavior. Another modification is the new α-adaptation scheme that uses simulated annealing to determine its value. In summary, the advantages of ACA are in that it can automatically determine the number of clusters and the clustering results outperforms the statistical methods [25].

B. ACO-based algorithms for clustering

Ant Colony Optimization (ACO) [30], [24], [31], [32] is an efficient method proposed in the early 1990s for attacking the combinatorial optimization problems. It is inspired by the foraging behavior of real ant colonies. Fig. 2 shows the basic concept and the major operators used by ACO to find good solutions.

```
1 Initialize()
2 while the termination criterion is not met
3     s = SolutionConstruction()
4     τ = PheromoneUpdate()
5     LocalSearch(s) // optional
6 end
7 OutputResult()
```

Fig. 2. Outline of the ACO.

As shown in Fig. 2, the very first step ACO takes is to initialize all the parameters such as the best-so-far solution, the iteration-best solution, and the pheromone values τ. After that, the main procedure on lines 2 through 6 will be repeated until the stop condition is met. In general, the main procedure is composed of two required operators *SolutionConstruction*() and *PheromoneUpdate*() and one optional operator *LocalSearch*().

The *SolutionConstruction*() operator on line 3 that calculates the probability p_{ij}^k for choosing the next sub-solution is defined as follows:

$$p_{ij}^k = \begin{cases} \frac{[\tau_{ij}]^\alpha [\eta_{ij}]^\beta}{\sum_{j \in \mathcal{N}_i^k} [\tau_{ij}]^\alpha [\eta_{ij}]^\beta} & \text{if } j \in \mathcal{N}_i^k, \\ 0 & \text{otherwise,} \end{cases} \tag{5}$$

where $\mathcal{N}_i^k$ denotes the set of feasible (or candidate) sub-solutions that can be the next sub-solution of i; τ_{ij} the pheromone value between the sub-solutions i and j; η_{ij} a heuristic value, which is also referred to as the *heuristic information*, used to denote the quality of sub-solution s_{ij}^k that will affect each ant's determination to move to j when at i; and α and β the weight of exploration and exploitation.

The *PheromoneUpdate*() operator on line 4 that is employed in updating the pheromone value τ_{ij} on each edge e_{ij} is defined as follows:

$$\tau_{ij} = (1-\rho)\tau_{ij} + \rho \sum_{k=1}^{m} \triangle \tau_{ij}^k, \tag{6}$$

$$\triangle \tau_{ij}^k = \frac{1}{L^k} \tag{7}$$

where m denotes the number of ants; L^k either the length of the tour created by ant k, the length of the iteration-best solution, or the length of the best-so-far solution. Normally, local search, such as problem-specific permutation method, is used as an option for improving the quality of the solution of ACO if ACO cannot find an applicable solution.

Recently, several studies [35], [36], [37], [38], [39], [40], [41], [42] have used ACO to solve the clustering problem because it can provide better result than the other traditional clustering algorithms such as k-means. Šilc et al. [35] used the generalized Lloyd algorithm to create a partition, which is then used as the initial solution for ACO to solve the mesh-partitioning problem. Kuo et al. [36], [37] presented another combination to solve the clustering problem that integrates ACO and k-means, called ant k-means algorithm (AK). This algorithm adds four operators to ACO, that is, *divide*, *agglomerate_obj*, *agglomerate*, and *remove*. Initially, all the patterns are grouped into a root cluster. The divide operator plays the role of dividing the root cluster into several new clusters by the predefined criteria. The agglomerate_obj operator is then used to agglomerate the patterns into the suitable clusters while the agglomerate operator is used to merge clusters that are simliar to each other. The remove operator is employed to remove patterns that are dissimilar in the cluster to which they belong. The simulation results show that AK [37] outperforms self organizing maps with k-means and self organizing maps with genetic algorithm. Tsai et al. [38] presented another modified version of ACO to solve the clustering problem by adding several efficient strategies, called ant colony optimization with different favor (ACODF). One of the efficient strategies is that ACODF does not require ant to visit all the patterns (nodes) to be clustered. Another efficient strategy is that ACODF splits patterns the pheromone value between them is less than a predefined threshold into different groups. Li et al. [39] parallelized the ACO for the codebook generation problem (CGP) by using MPI. The simulation results show that the parallel strategy can improve the quality of ACO for CGP by about 0.1 up to 0.2 dB of peak signal-to-noise ratio (PSNR). Han and Shi [40] presented an efficient ant-based algorithm for fuzzy clustering the image segmentation problem. First, k centers are selected based on the image histogram. Then, the gradients of the k centers are used to determine the neighboring features to reduce the computation time.

Ramos et al. [41] combined hyperboxes and ACO to solve the clustering problem, called hyperbox clustering with ACO (HACO). More precisely, the hyperboxes are placed in the search space to reduce the number of patterns that ACO needs to compute. The hyperboxes are then grouped by using the nearest-neighbor (NN) method. The computation time of HACO can then be reduced so that it is faster than ACO. Korürek and Nizam [42] used ACODF [38] to cluster unknown patterns to train the arrhythmia detection system. The nearest neighborhood classifier is used to test the system. The results show that ACO can be used to improve the analysis results of the medical signals such as electrocardiography (ECG).

III. The Proposed Algorithm

In this section, we present an efficient ACO-based algorithm based on two pheromone tables, called ant colony optimization with dual pheromone tables (ACODPT). We will begin with a brief introduction to the proposed algorithm and an example of ACODPT before we move on to the details of the proposed algorithm.

A. The concept

In general, most of the ACO-based algorithms use pheromone to record and propagate the *positive information* between ants in the population. Consequently, when one or more ants find a good path (search direction or solution), the other ants in the population will follow this path by a positive feedback to the pheromone table. That is, the ACO-based algorithms only keep the positive information to the pheromone table. As such, the breadth of the search directions will be reduced as the number of iterations increases. In this paper, we add a second pheromone table to lay down the negative information. As shown in Fig. 3, the proposed algorithm, ACODPT, has two different kinds of pheromone tables: the positive pheromone table and the negative pheromone table. After the transition and mean update operator, the pheromone values of some paths in the positive pheromone table will be strengthened when ants routing on these paths find better results than the other ants. At the same time, the pheromone

values of some paths in the negative pheromone table will be increased when ants routing on these paths find worse results than the other ants.

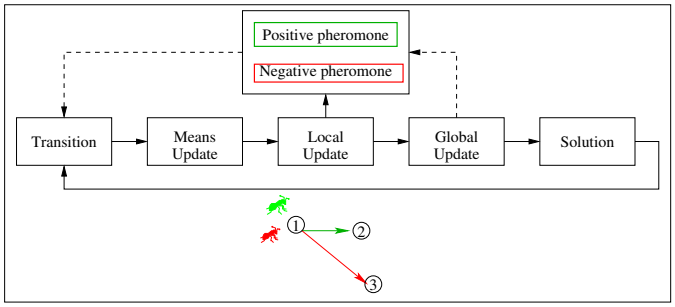

Fig. 3. An illustration of the proposed algorithm.

For example, as depicted at the bottom of Fig. 3, the green ant finds a better route path (starting with node 1 to node 2) than the red ant (node 1 to node 3). The green ant then updates the positive pheromone table to keep its route path whereas the red ant updates the negative pheromone table to keep its route path. Simply speaking, the underlying idea is to prevent the ant from routing the some paths they have already traveled that are worse than paths (solutions) created by the other ants. From this perspective, it is used to avoid only searching the similar directions that can find better result.

B. The ant colony optimization with dual pheromone tables

In order to integrate two pheromone tables into the proposed algorithm, the way the probability is calculated has to be modified, which in turn changes the solution construction operators, as given below.

$$s = \begin{cases} \arg\max_{u \in \mathcal{N}_r^k} \{[\tau_{ru}] \cdot [\eta_{ru}]^\beta\} & \text{if } q \le q_0, \\ v & \text{if } q_0 < q \le q_1, \\ w & \text{otherwise,} \end{cases} \quad (8)$$

$$q_{rz}^k = \begin{cases} \frac{[\tau_{rz}] \cdot [\eta_{rz}]^\beta}{\sum_{u \in J(r)} [\tau_{ru}] \cdot [\eta_{ru}]^\beta} & \text{if } z \in \mathcal{N}_r^k \setminus B_r^k, \\ 0 & \text{otherwise,} \end{cases} \quad (9)$$

$$B_r^k = B_r^k \cup \{\overline{rz}\} \quad \forall z \in \mathcal{N}_r^k \text{ and } \tau_{rz}^b < q_b, \quad (10)$$

where q is a random value to determine which strategy will be used to construct the next sub-solution, q_0 and q_1 are used to predefine the intervals of the three strategies used in ACODPT. Similar to ACS, as defined in Eq. (8), the first two selection strategies are: select the best next sub-solution (when $q \le q_0$) and select the next solution with the probability calculated by Eq. (5) (when $q_0 < q \le q_1$).

When $q > q_1$, the proposed algorithm will, of course, use Eqs. (9) and (10) to determine the next sub-solution. As defined in Eq. (10), B_r^k represents the path that will not be selected, $q_b \in (0, 1)$ is a random value, and $\tau^b \in (0, 1)$ represents the second kind of pheromone on the path. In other words, the path will be included to the set B_r^k if the pheromone value τ^b is less than q_b. As a consequence, the paths (solutions) that are worse than the other existing paths found by ants will not be selected when the ACODPT uses q_{rz}^k to determine the next sub-solutions.

```
1  Initialization
2  while the termination criterion is not met
3     for each ant k
4        1. assign all patterns to the clusters to which they belong by
5           Eqs. (8), (9) and (10).
6        2. update centroids
7        3. local update each path rs ant k moved
8     end
9     global update each path rs by Eqs. (11) and (12)
10 end
11 Output the best result
```

Fig. 4. Outline of ACODPT

Fig. 4 gives an outline of the proposed algorithm. ACODPT will first initialize the positive pheromone table and the negative pheromone table by setting all the paths to the initial value, followed by setting the parameters, such as α, β, ρ, and SSE to their initial values. Next, ACODPT will enter the main loop, which will be performed until the stop criterion is met. At the solution construction step (lines 3–7), each ant in the population will take care of assigning the input patterns to the clusters by using the equations Eqs. (8), (10) and (9).

In this paper, the proposed algorithm uses the group ID of all patterns to represent the clustering result. As shown in Fig. 5, suppose that we have four input patterns to be partitioned into three groups (clusters). The solution of each ant k of the proposed algorithm can be denoted by $s^k = \{s_1^k, s_2^k, s_3^k, s_4^k\}$, with s_i^k indicating to which cluster pattern i belongs, determined by Eqs. (8), (10) and (9) (see also lines 4 and 5).

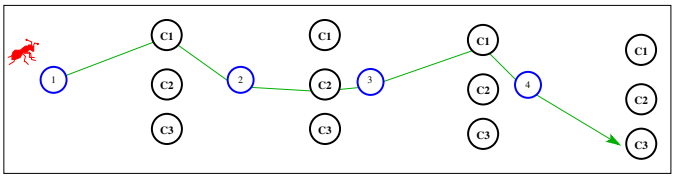

Fig. 5. Example illustrating how ACODPT assigns a pattern to the cluster to which it belongs.

This procedure will be repeated for all the input patterns. The centroids of the solution created by the ant k will then be updated when that ant completed the tour. In addition to local update the pheromone values in the positive pheromone table, ACODPT will also global update the pheromone values in the positive pheromone table defined as

$$\tau_{rs} = (1 - \rho)\tau_{rs} + \rho\Delta\tau_{rs}^{\text{bs}}, \quad \forall \overline{rs} \in T^{\text{bs}}, \quad (11)$$

where T^{bs} denotes the best-so-far tour and τ^{bs} the pheromone value that will be increased by the global update of this path, and the pheromone values in the negative pheromone table defined as

$$\tau_{rs}^b = \gamma\tau_{rs}^b, \quad \forall \overline{rs} \in T^{\text{iw}}, \quad (12)$$

where T^{iw} denotes the iteration-worst tour. Moreover, γ is set to 0.999 as far as this paper is concerned. When the termination criterion is met, ACODPT will output the best-so-far solution as the final solution.

IV. Simulation Results

In this section, the performance of the proposed algorithm is evaluated by comparing it with several state-of-the-art clustering algorithms. But before that, we will first give the parameter settings and datasets used.

A. Parameter settings and datasets

To evaluate the performance of ACODPT, we compare it with three state-of-the-art clustering algorithms: standard k-means [16], genetic k-means algorithm [17], and ant colony system [24]. The empirical analysis is conducted on an Intel i7 CPU 920 with 2.67 GHz CPU and 4GB of memory running on Fedora 12 with Linux 2.6.31.5-127. Also, the programs are written in C and compiled by gcc version 4.4.2 20091027 (Red Hat 4.4.2-7). Moreover, for GKA, the population size is fixed at 25, so is the population size of ACS (i.e., the number of ants). Same as the GKA, the crossover operator is replaced by a 2-iteration k-means operator, the mutation probability is 0.01, and the number of generations is 1,000. For the ACS and ACODPT, α is set to 0.1, β to 11.0, ρ to 0.1, and τ to 0.01. q_0 and q_1 are set to 1 and 75, respectively. To avoid premature convergence, the proposed method is started at iteration 2. For comparison, the datasets used in this paper to evaluate the performance of these clustering algorithms are iris, wine, yeast, and abalone, all from [43].

B. Results

Table I compares the performance of ACODPT with the following clustering algorithms: k-means, GKA, and ACS. It shows that GKA provides a better result than k-means while ACS providing a better result than GKA for the benchmarks yeast and abalone. In contrast, our observation shows that the proposed algorithm, ACODPT, provides a better result than ACS because these two benchmarks (yeast and abalone) are more difficult than the others (iris and wine). For this reason, the proposed algorithm can further improve the quality of ACS by about 1.43% and 29.24% for the benchmarks ecoli, yeast, and abalone. Moreover, although the clustering results of ACODPT of benchmarks wine, ecoli, and yeast are worse than GKA, we believe that it is because the ACS and the proposed algorithm do not use the local search to fine tune the clustering results but GKA does.

TABLE I
Simulation results

Data set	$x \times y \times z$	k-means	GKA
iris	$3 \times 4 \times 150$	85.34	78.94
wine	$3 \times 13 \times 178$	2,370,690.00	2,370,689.69
glass	$9 \times 6 \times 214$	394.58	340.82
ecoli	$8 \times 7 \times 336$	2,284.85	1,815.70
yeast	$10 \times 8 \times 1484$	49.06	45.83
abalone	$29 \times 8 \times 4177$	1,144.10	572.99
Data set	$x \times y \times z$	**ACS**	**ACODPT**
iris	$3 \times 4 \times 150$	78.94	78.94
wine	$3 \times 13 \times 178$	2,370,690.00	2,370,690.00
glass	$9 \times 6 \times 214$	336.06	336.06
ecoli	$8 \times 7 \times 336$	2,579.26	1,995.67
yeast	$10 \times 8 \times 1484$	47.44	46.30
abalone	$29 \times 8 \times 4177$	484.93	482.57

x, y, z denote, respectively, the number of clusters, attributes, and patterns.

V. Conclusion

In this paper, we proposed an efficient method, called ACODPT, to improve the quality of ACS-based clustering algorithms. The major concept is to add a negative pheromone table to record the route paths which may lead the ants to create worse solutions. It is inspired by how to prevent the ants from falling into the local minima region again and again. For this reason, the solution construction operator is modified to take into account the way the strategies are selected. In addition to a simple example given to show the design concept, we also describe in detail the proposed algorithm. Our simulation results showed that the proposed algorithm outperforms all the other clustering algorithms compared in this paper in terms of the quality of the end result, especially for large scale datasets. Our future goal is to reduce the computation time of the proposed algorithm while at the same time improving the quality of the end result such as local search methods..

Acknowledgment

This work was supported in part by the National Science Council, Taiwan, R.O.C., under Contract Nos. NSC100-2218-E-041-001-MY2 and NSC99-2221-E-110-052.

References

[1] A. K. Jain and R. C. Dubes, *Algorithms for clustering data*. Englewood Cliffs, NJ: Prentice Hall, 1988.

[2] A. K. Jain, M. N. Murty, and P. J. Flynn, "Data clustering: A review," *ACM Computing Surveys*, vol. 31, no. 3, 1999.

[3] R. Xu and D. W. II, "Survey of clustering algorithms," *IEEE Transaction on neural netowrks*, vol. 16, no. 3, pp. 645–678, 2005.

[4] F. Giannotti, M. Nanni, D. Pedreschi, and F. Samaritani, "Webcat: Automatic categorization of web search results," *Proceedings of SEBD'2003*, pp. 507–518, 2003.

[5] P. Ferragina and A. Gulli, "A personalized search engine based on web-snippet hierarchical clustering," *International World Wide Web Conference (WWW2005)*, pp. 801–810, 2005.

[6] H. J. Zeng, Q. C. He, Z. Chen, W. Y. Ma, and J. Ma, "Learning to cluster web search results," *Proceedings of the 27th annual international ACM SIGIR conference on Research and development in information retrieval (SIGIR'04)*, pp. 210–217, 2004.

[7] W. Xu, X. Liu, and Y. Gong, "Document clustering based on non-negative matrix factorization," in *Proceedings of the 26th Annual International ACM SIGIR Conference on Research and Development in Information Retrieval*, pp. 267–273, 2003.

[8] A. Leuski, "Evaluating document clustering for interactive information retrieval," in *Proceedings of the Tenth International Conference on Information and Knowledge Management*, pp. 33–40, 2001.

[9] M. P. S. Brown, W. N. Grundy, D. Lin, N. Cristianini, C. W. Sugnet, T. S. Furey, M. Ares, and D. Haussler, "Knowledge-based analysis of microarry gene expression data by using support vector machines," *Proceedings of the National Academy of Sciences of the United States of America*, vol. 97, no. 1, pp. 262–267, 2000.

[10] G. Getz, H. Gal, I. Kela, D. A. Notterman, and E. Domany, "Coupled two-way clustering analysis of breast cancer and colon cancer gene expression data," *Bioinformatics*, vol. 19, pp. 12079–12084, 2003.

[11] H. Lawrence, "Face recognition: A literature survey," *Review of Financial Studies*, vol. 4, no. 3, pp. 389–415, 1991.

[12] R. W. Zhao, Chellappa, P. J. Philips, and A. Rosenfeld, "Face recognition: A literature survey," *ACM Computing Surveys (CSUR)*, vol. 35, no. 4, pp. 399–458, 2003.

[13] T. Fromherz, P. Stucki, and M. Bichsel, "A survey of face recognition," *MML Technical Report*, 1997.

[14] P. Brucker, "On the complexity of clustering problems," *Lecture Notes in Economics and Mathematical Systems*, vol. 157, pp. 45–54, 1978.

[15] A. L. Jain, "Data clustering: 50 years beyond K-means," *Pattern Recognition Letters*, vol. 31, no. 8, pp. 651–666, 2010.

[16] J. B. McQueen, "Some methods of classification and analysis of multivariate observations," in *Proceedings of the 5th Berkeley Symposium on Mathematical Statistics and Probability*, pp. 281–297, 1967.

[17] K. Krishna and M. N. Murty, "Genetic k-means algorithm," *IEEE Transactions on System, Man and Cybernetics—Part B:Cybernetics*, vol. 29, no. 3, pp. 433–439, 1999.

[18] S. Bandyopadhyay and U. Maulik, "An evolutionary technique based on k-means algorithm for optimal clustering in R^N," *Information Sciences*, vol. 146, no. 1-4, pp. 221–237, 2002.

[19] M. K. Ng and J. C. Wong, "Clustering categorical data sets using tabu search techniques," *Pattern Recognition*, vol. 35, no. 12, pp. 2783–2790, 2002.

[20] D. van der Merwe and A. P. Engelbrecht, "Data clustering using particle swarm optimization," in *Proceedings of the 2003 Congress on Evolutionary Computation*, pp. 215–220, 2003.

[21] X. Cui, T. E. Potok, and P. Palathingal, "Document clustering using particle swarm optimization," in *Proceedings of the IEEE Swarm Intelligence Symposium*, pp. 185–191, 2005.

[22] R. J. Kuo, L. M. Ho, and C. M. Hu, "Integration of self-organizing feature map and k-means algorithm for market segmentation," *International Journal of Computers and Operations Research*, vol. 29, no. 11, pp. 1475–1493, 2002.

[23] A. Ghosh, A. Halder, M. Kothari, and S. Ghosh, "Aggregation pheromone density based data clustering," *Information Sciences*, vol. 178, no. 13, pp. 2816–2831, 2008.

[24] M. Dorigo and L. M. Gambardella, "Ant colony system: A cooperative learning approach to the traveling salesman problem," *IEEE Transactions on Evolutionary Computation*, vol. 1, no. 1, pp. 53–66, 1997.

[25] J. Handl and B. Meyer, "Ant-based and swarm-based clustering," *Swarm Intelligence*, vol. 1, no. 2, pp. 95–113, 2007.

[26] J.-L. Deneubourg, S. Goss, N. Franks, A. Sendova-Franks, C. Detrain, and L. Chretien, "The Dynamics of Collective Sorting: Robot-Like Ant and Ant-Like Robot," in *Proceedings of the First Conference on Simulation of Adaptive Behavior: From Animals to Animats* (J. Meyer and S. Wilson, eds.), (Cambridge, MA), pp. 356–365, MIT Press, 1991.

[27] E. D. Lumer and B. Faieta, "Diversity and adaptation in populations of clustering ants," in *Proceedings of the third international conference on Simulation of adaptive behavior : from animals to animats 3: from animals to animats 3*, pp. 501–508, MIT Press, 1994.

[28] J. Handl and B. Meyer, "Improved ant-based clustering and sorting," in *Proceeding of 7th International Conference Parallel Problem Solving from Nature - PPSN VII*, pp. 913–923, 2002.

[29] J. Handl, J. Knowles, and M. Dorigo, "Ant-based clustering: a comparative study of its relative performance with respect to k-means, average link and 1d-som," in *Proceedings of the Third International Conference on Hybrid Intelligent Systems, IOS Press*, 2003.

[30] M. Dorigo, V. Maniezzo, and A. Colorni, "The ant system: Optimization by a colony of cooperating agents," *IEEE Transactions on Systems, Man, and Cybernetics—Part B*, vol. 26, no. 1, pp. 29–41, 1996.

[31] C. Blum, "Ant colony optimization: Introduction and recent trends," *Physics of Life Reviews*, vol. 2, no. 4, pp. 353–373, 2005.

[32] M. Dorigo and T. Stützle, *Ant Colony Optimization*. The MIT Press, 2004.

[33] Y. Yang and M. S. Kamel, "An aggregated clustering approach using multi-ant colonies algorithms," *Pattern Recognition*, vol. 39, no. 7, pp. 1278–1289, 2006.

[34] U. Boryczka, "Finding groups in data: Cluster analysis with ants," *Applied Soft Computing*, vol. 9, no. 1, pp. 61–70, 2009.

[35] J. Šilc, P. Korošec, and B. Robič, "Combining vector quantization and ant-colony algorithm for mesh-partitioning," in *Proceedings of 5th International Conference Parallel Processing and Applied Mathematics (PPAM)*, pp. 113–118, 2003.

[36] R. J. Kuo, C. L. Cha, S. H. Chou, C. W. Shih, and C. Y. Chiu, "Integration of ant algorithm and case based reasoning for knowledge management," in *Proceedings of International Conference on IJIE*, 2003.

[37] R. J. Kuo, H. S. Wang, T.-L. Hu, and S. H. Chou, "Application of ant k-means on clustering analysis," *Computers & Matematics with Applications*, vol. 50, pp. 1709–1724, 2005.

[38] C.-F. Tsai, C.-W. Tsai, H.-C. Wu, and T. Yang, "Acodf: a novel data clustering approach for data mining in large databases," *Journal of Systems and Software*, vol. 73, pp. 133–145, 2004.

[39] X. Li, X. Yu, and X. Luo, "Parallel implementation of ant colony optimization for vector quantization codebook design," in *Proceedings of theInternational Conference on Natural Computation*, vol. 4, pp. 787–791, 2007.

[40] Y. Han and P. Shi, "An improved ant colony algorithm for fuzzy clustering in image segmentation," *Neurocomputing*, vol. 70, no. 4-6, pp. 665–671, 2007.

[41] G. N. Ramos, Y. Hatakeyama, F. Dong, and K. Hirota, "Hyperbox clustering with ant colony optimization (haco) method and its application to medical risk profile recognition," *Applied Soft Computing*, vol. 9, no. 2, pp. 632–640, 2009.

[42] M. Korürek and A. Nizam, "Clustering mit-bih arrhythmias with ant colony optimization using time domain and pca compressed wavelet coefficients," *Digital Signal Processing*, vol. 20, no. 4, pp. 1050–1060, 2010.

[43] UCI Datasets. URL: http://archive.ics.uci.edu/ml/datasets/Iris.

2011 IEEE International Conference on Fuzzy Systems
June 27-30, 2011, Taipei, Taiwan

Job Shop Scheduling Based on ACO with a Hybrid Solution Construction Strategy

Shih-Pang Tseng
Department of Computer Science and Engineering
National Sun Yat-sen University
Kaohsiung, Taiwan, R.O.C.
Email: tsp@mail.tajen.edu.tw

Chun-Wei Tsai
Department of Applied Geoinformatics
Chia Nan University of Pharmacy & Science
Tainan, Taiwan, R.O.C.
Email: cwtsai0807@gmail.com

Jui-Le Chen
Department of Electrical Engineering
National Cheng Kung University
Tainan, Taiwan, R.O.C.
Email: reler@mail.tajen.edu.tw

Ming-Chao Chiang
Department of Computer Science and Engineering
National Sun Yat-sen University
Kaohsiung, Taiwan, R.O.C.
Email: mcchiang@cse.nsysu.edu.tw

Chu-Sing Yang
Department of Electrical Engineering
National Cheng Kung University
Tainan, Taiwan, R.O.C.
Email: csyang@ee.ncku.edu.tw

***Abstract*—This paper presents a novel ant colony optimization (ACO) based on an efficient solution construction strategy (transition operator) for improving the quality of the end results of job shop scheduling problem (JSSP). Inspired by the observation that the quality of the end results of ACO is largely affected by their operators—especially the transition operator, a novel solution construction strategy is presented in this paper. The proposed algorithm uses two different strategies to compute the probability of solution construction to improve the end results. Our experimental results show that the proposed algorithm outperforms all state-of-the-art job shop scheduling algorithms evaluated in this paper and can significantly improve the quality of ant colony optimization for JSSP.**

Keyword: ant colony optimization; job shop scheduling problem; transition operator.

I. Introduction

As one of the most well known combinatorial optimization problems, the job shop scheduling problem (JSSP) [1], [2], [3], [4], [5] is to assign a finite set of jobs, each of which consists of a sequence of operations, to a finite set of machines in such a way that the maximum completion time or makespan is minimized while assuming that each operation of a job is assigned to a different machine in the order given and is processed to completion without being preempted. Formally, the JSSP is usually defined as follows: Given a set of m machines and a set of n jobs—each of which consists of a sequence of operations $\langle O_{1j}, O_{2j}, \ldots, O_{mj} \rangle$, with O_{ij} to be processed on a given machine μ_{ij} for p_{ij} time where $\mu_{ij} \neq \mu_{i+1,j}$ for $i = 1, 2, \ldots, m-1$—the problem is to find an assignment of the n jobs to the m machines that minimizes the maximum completion time or makespan. In symbols,

$$C_{\max} = \min \max_{1 \leq j \leq n} C_j$$

where C_j denotes the completion time of the jth job.

Recently, the JSSP has become an important research topic for several reasons. The first is that it has become extremely important to minimize the computation time, or maximize the throughput, in this era because it is important to conserve the energy so as to protect the environments or reduce the cost. For example, the cost can be reduced by fabricating the same products with less energy. The second is that an efficient solution to the JSSP can be used to solve many other problems. As such, several variants of JSSP have been introduced in recent years to solve the nurse scheduling problem, the flexible job shop scheduling problem, the fuzzy job shop scheduling problem, and the flow shop scheduling problem. However, even after all these efforts, the NP-hard job shop scheduling problem [6] is still very hard to be solved to optimality even if the size of benchmark is small. For this reason, it has always been a popular research topic of combinatorial optimization problems because a better solution can be used to enhance the work efficiency or reduce the energy cost of a factory.

One of the most well known examples to explain the difficulty of JSSP was introduced by Fisher and Thompson [1] in 1960s, which is a 10×10 instance (i.e., $n = 10$ and $m = 10$), and its optimal solution was not found until 20 years after this problem was introduced. The good news is that the optimum solution has been found by Carlier and Pinson [7]. They used a branch and bound algorithm to solve the JSSP in 1989. However, although the exhaustive search algorithm can find the optimum solution of this benchmark (i.e., the 10×10 instance), it is still very hard to find the optimum solution when the size of benchmark becomes 20×20 [8]. For this reason, since 1990's, approximation algorithms (some of which are called metaheuristics) such as priority dispatch, shifting bottleneck procedure [9], tabu search (TS) [10], [11], simulated annealing (SA) [12], genetic algorithm (GA) [13], [14], and ant colony

978-1-4244-7316-8/11/$26.00 ©2011 IEEE

optimization (ACO) [15], [16], [17], [18], [19] have been used to solve the JSSP in a reasonable time. In addition to using the original version of the above metaheuristic algorithms, many studies have tried to integrate these algorithms to find a better result. A good example is the TSSA by Zhang et al. [8], which combines TS with SA.

Among these researches, ACO is apparently one of the most promising metaheuristic algorithms to solve the JSSP because its search abilities are very efficient for the combinatorial optimization problems. More important, ACO is not sensitive to the initial solutions. In this paper, we present an efficient algorithm, called hybrid selection strategy for ant colony optimization (HSSACO), to solve the JSSP that provides a better result than traditional metaheuristics can. The new transition operator of the proposed algorithm is designed to modify the solution construction strategy which integrates more than one objective compared to the traditional ACO for JSSP, which considers only one objective at a time (e.g., earliest starting time; or EST for short) so as to improve the quality of the end results. To evaluate the performance of the proposed algorithm, we compare it with four ACO-based algorithms for several well known benchmarks for the JSSP. Experimental results show that the proposed algorithm, HSSACO, outperforms all state-of-the-art algorithms for the JSSP compared in this paper.

The remainder of the paper is organized as follows. Section II gives a brief introduction to the genetic algorithm and approaches taken to enhance its performance. Section III provides a detailed description of the proposed algorithm. Also given in Section III is a simple example to demonstrate how the proposed algorithm works. Performance evaluation of the proposed algorithm is presented in Section IV. Analysis of the proposed algorithm is given in Section IV. Conclusion is drawn in Section V.

II. Related Work

Proposed by Dorigo et al. in the 90s, the ant colony optimization (ACO) [20], [21], [22] is a promising metaheuristic algorithm inspired by the foraging behavior of real ants. The focus of the early version of ACO has been on solving the combinatorial optimization problems such as the traveling salesman problem and the quadratic assignment problem. Basically, ACO is made up of two required operators *SolutionConstruction*() and *PheromoneUpdate*() as well as one optional operator *LocalSearch*().

The *SolutionConstruction*() operator plays the role of calculating the probability of choosing the next sub-solution of i, which is defined as follows:

$$p_{ij}^k = \begin{cases} \frac{[\tau_{ij}]^\alpha [\eta_{ij}]^\beta}{\sum_{j \in \mathcal{N}_i^k} [\tau_{ij}]^\alpha [\eta_{ij}]^\beta} & \text{if } j \in \mathcal{N}_i^k, \\ 0 & \text{otherwise,} \end{cases} \quad (1)$$

where $\mathcal{N}_i^k$ denotes the set of feasible (or candidate) sub-solutions that can be the next sub-solution of i; τ_{ij} the pheromone value between the sub-solutions i and j; and η_{ij} the quality of the sub-solution j that will affect each ant's determination to move to j when at i. The parameters α and β are used to adjust the weight of exploration and exploitation. The *PheromoneUpdate*() operator is employed in updating the pheromone value τ_{ij} on each edge e_{ij}, which is defined as follows:

$$\tau_{ij} = (1-\rho)\tau_{ij} + \rho \sum_{k=1}^{m} \triangle \tau_{ij}^k, \quad (2)$$

where m denotes the number of ants; $\triangle \tau_{ij}^k = 1/L^k$; L^k the quality of solution created by ant k. Moreover, $\rho \in (0, 1]$ denotes the evaporation rate of pheromone values on the pheromone table. The optional operator *LocalSearch*() is employed in improving the quality of the solution of ACO. A good example is problem-specific permutation method.

Recently, several studies [15], [16], [18], [19] have attempted to use ACO to solve the JSSP because of its potential to find solutions that are closer to the optimum solution than all traditional heuristic algorithms. In 1994, Colorni et al. [15] used the early version of ACO, ant system (AS), to solve the JSSP in which the way the solution is represented is similar to that of the traveling salesman problem, which consists of $n+1$ nodes and $n(n-1)/2+n$ edges. Their simulation results showed that AS can find approximate solution to the JSSP that is about 7% to 10% away from the optimum solution of the benchmark they tested. In 1999, Zwaan and Marques [16] first analyzed the performance of the parameter settings of AS and then used the information so obtained to fine-tune the parameter values of AS. More precisely, the interaction between α and β was first tested, followed by the values of ρ and the numbers of ants. Then, Zwaan and Marques suggested that the number of ants of AS be close to $n \times m$ where n and m are the number of jobs and the number of machines, respectively.

More recently, Heinonen and Pettersson [18] combined ACO with efficient local search method to improve the results of ACO in solving the JSSP. The local search method first identifies the critical path in the schedule constructed by ACO. The critical path can be decomposed into a number of blocks each of which is a maximal sequence of adjacent operations that require to be processed by the same machine. Then, the local search method is used to swap operations to improve the makespan of the schedule. Their simulation results showed that ACO with efficient local search method can find a near-optimum solution to the MT10 problem the relative error of which is about 3.9%. In [19], Huang and Liao presented a hybrid algorithm, called ACO combined with fast TS (ACOFT), that uses ant colony optimization to find the global search directions and tabu search to fine-tune the soltuion. Their simulation results showed that ACOFT can find a near-optimum soltuion the relative error of which is 1.798% on average. In addition to using ACO to solve the JSSP, some studies [23], [24] also apply ACO to solve the variants of JSSP. Examples are the felxible job shop scheduling problem and the fuzzy job shop scheduling problem.

III. The Proposed Algorithm

In this section, we will begin with the concept, followed b is a detailed description of the proposed algorithm.

A. The concept

Generally speaking, most ACO-based algorithms for JSSP use only one kind of strategy to optimze the makespan such as earliest starting time (EST), most remaining operations (MRO), shortest processing time (SPT), and most work remaining (MWR). More precisely, $\eta(o_{ij})$ can be computed as EST, MRO, or the others. However, even though all the heuristic methods are aimed to minimize the makespan, the strategies they use are very different. For example, the EST is aimed to perform the jobs at the earliest possible starting time whereas the SPT is aimed to perform the shortest jobs first.

In this paper, we integrate two different heuristics into the solution construction method of the ACO-based algorithms for solving JSSP. As shown in Eq. (3), the probability, p_{ij}^k, of the proposed algorithm is made up of two different search strategies. One is the earliest starting time (as shown in Eq. (5)) while the other is the most remaining operations (as shown in Eq. (6)).

$$p_{ij}^k = \frac{[\tau_{ij}]^\alpha [\eta_{\text{em}}(o_{ij})]^\beta}{\sum_{o_{ij} \in \mathcal{N}_i} [\tau_{ij}]^\alpha [\eta_{\text{em}}(o_{ij})]^\beta}, \tag{3}$$

$$\eta_{\text{em}}(o_{ij}) = \eta_{\text{est}}^{w_1}(o_{ij}) \times \eta_{\text{mro}}^{w_2}(o_{ij}), \tag{4}$$

$$\eta_{\text{est}}(o_{ij}) = \frac{\frac{1}{s_{ij}+1}}{\sum_{o_{ij} \in \mathcal{N}_i} \frac{1}{s_{ij}+1}}, \tag{5}$$

$$\eta_{\text{mro}}(o_{ij}) = \frac{r_{ij}+1}{\sum_{o_{ij} \in \mathcal{N}_i} r_{ij}+1}, \tag{6}$$

where s_{ij} denotes the possible starting time of o_{ij}; r_{ij} the number of remaining operations of o_{ij}; $\mathcal{N}_i$ the remaining operations that satisfy the processing order restriction but have not started yet; w_1 and w_2 (where $w_1, w_2 \in [0, 1]$ and $w_1 + w_2 = 1$) the weights of the two makespan optimization strategies. As shown in Eq. (4), more than one makespan optimization strategy is considered at a time to avoid the ACO-based algorithms from falling into local minima at early iterations. Moreover, $\eta_{\text{em}}(o_{ij})$ is the weighted geometric mean of these two strategies $\eta_{\text{est}}^{w_1}(o_{ij})$ and $\eta_{\text{mro}}^{w_2}(o_{ij})$. The proposed algorithm not only considers searching the possibility of earliest possible starting time of the job, it also takes into account performing the job thatwhich has a larger number of operations that are not started yet. For instance, suppose $w_1 = w_2 = 0.5$. Then, $\eta_{\text{em}} = \eta_{\text{est}}^{0.5} \times \eta_{\text{mro}}^{0.5} = \sqrt{\eta_{\text{est}}} \times \sqrt{\eta_{\text{mro}}}$. Moreover, to avoid converging to a single direction, we also normalize the values of these two makespan optimize strategies, as shown in Eqs. (5) and (6).

B. The hybrid selection strategy for ant colony optimization

In the previous section, we present a new solution construction strategy (also called the transition operator) for the ACO-based algorithm. As Eqs. (3)–(6) show, the hybrid selection strategy for ant colony optimization is as follows.

1) Input the dataset and its parameters.
2) Initialization:
   a) Set the values of all paths τ_{ij} in the pheromone table to τ_{init}.
   b) Initialize the parameters of ACO.
   c) Put all the ants on the start node.
3) Solution Construction:
   For each ant,
   a) Compute the probability distribution by using Eq. (3).
   b) Construct the solution by using the probability distribution p_{ij}^k.
   c) Update the local pheromone by using Eq. (2).
4) Update the pheromone of the best solution.
5) Perform local search to improve the solution.
6) If the stop condition is not met, go to 2.
7) Otherwise, output the best so far solution as the final solution.

Because our aim is to apply the proposed algorithm to all the ACO-based algorithms, the description of the proposed algorithm herein is for the general design of ACOs. First, the proposed algorithm will read the dataset and its parameters. Next, set all the paths in the pheromone table (an $m \times n$ array) to the initial value τ_{init}. Then, initialize all the other parameters of ACO such as α, β, ρ, w_1, and w_2. In the solution construction stage, HSSACO will first use Eq. (3) to compute the probability distribution of ant k. Then, ant k will use the probability distribution p_{ij}^k to determine which will be the next sub-solution. For the JSSP, it means the next operation. After the next sub-solution is determined, the proposed algorithm will then perform the local pheromone update if required by the ACO we use. In addition to the local pheromone update, the global pheromone update will then be performed. In this paper, the proposed algorithm also performs local search to improve and fine-tune the final results. The above operators will be repeatedly performed until convergence or the stop condition is met.

IV. Simulation Results

To simplify the discussion of the simulation results, the following conventions are employed in this paper.

$$\Delta = \frac{\Delta_{\text{HSS}+\psi} - \Delta_\psi}{\Delta_\psi} \times 100\%, \tag{7}$$

where Δ denotes the enhancement of $\Delta_{\text{HSS}+\psi}$ compared with Δ_ψ in percentage of makespan. That is, ψ denotes either earliest starting time (EST) or most remaining operations (MRO) used by the ant system (AS) [15], elitist ant system (EAS) [25], [20], rank ant system (RAS) [26], and ant colony system (ACS) [21].

A. Parameter settings and datasets

The empirical analysis was conducted on an SUN X4150 machine with 2.5 GHz Xeon CPU and 4GB of memory running CentOS 5.4 with Linux 2.6.18. Moreover, all the programs are written in C++ and compiled using g++ (GNU C++ compiler).

TABLE II
IMPACT OF w_1 AND w_2.

	0.1/0.9	0.2/0.8	0.3/0.7	0.4/0.6	0.5/0.5	0.6/0.4	0.7/0.3	0.8/0.2	0.9/0.1
AS	-2.48	-2.62	-2.59	-2.52	-2.56	-2.45	-1.98	-1.59	-1.15
EAS	-2.21	-2.29	-2.40	-2.39	-2.45	-2.48	-2.29	-2.06	-1.41
RAS	-2.02	-2.08	-2.19	-2.24	-2.23	-2.27	-2.15	-1.94	-1.36
ACS	-4.84	-4.89	-4.88	-4.89	-4.93	-4.96	-5.02	-5.03	-4.74

TABLE III
SIMULATION RESULTS OF ACO WITHOUT LOCAL SEARCH

Dataset		BKS	AS		HSS+AS			EAS		HSS+EAS		
			EST	MRO	ESTMRO	δ_{est}	δ_{mro}	EST	MRO	ESTMRO	δ_{est}	δ_{mro}
la01	10× 5	666	725	737	706	-2.64	-4.14	716	722	701	-1.99	-2.89
la05	10× 5	593	595	593	593	-0.27	0.00	593	593	593	-0.06	0.00
la10	15× 5	958	981	958	958	-2.32	0.00	969	958	958	-1.12	0.00
la15	20× 5	1,207	1,394	1,378	1,364	-2.11	-1.02	1,366	1,377	1,365	-0.08	-0.87
la20	10×10	902	1,070	1,028	1,014	-5.27	-1.43	1,056	1,020	995	-5.81	-2.51
la25	15×10	977	1,228	1,182	1,165	-5.13	-1.49	1,209	1,179	1,155	-4.50	-2.06
la30	20×10	1,355	1,668	1,591	1,570	-5.88	-1.32	1,645	1,584	1,554	-5.52	-1.94
la31	30×10	1,784	2,082	1,951	1,935	-7.04	-0.81	2,026	1,943	1,906	-5.93	-1.91
la32	30×10	1,850	2,203	2,088	2,070	-6.05	-0.90	2,157	2,071	2,039	-5.47	-1.54
la33	30×10	1,719	2,008	1,950	1,916	-4.57	-1.74	1,987	1,927	1,884	-5.15	-2.22
la34	30×10	1,721	2,078	1,977	1,945	-6.37	-1.63	2,034	1,958	1,924	-5.42	-1.73
la35	30×10	1,888	2,243	2,226	2,164	-3.53	-2.79	2,181	2,222	2,142	-1.79	-3.60
la36	15×15	1,268	1,624	1,506	1,497	-7.82	-0.60	1,592	1,490	1,464	-8.03	-1.73
la37	15×15	1,397	1,735	1,744	1,695	-2.35	-2.83	1,705	1,720	1,680	-1.46	-2.33
la38	15×15	1,196	1,538	1,522	1,499	-2.58	-1.56	1,513	1,507	1,479	-2.24	-1.85
la39	15×15	1,233	1,577	1,537	1,505	-4.60	-2.11	1,554	1,513	1,478	-4.91	-2.33
la40	15×15	1,222	1,561	1,498	1,474	-5.63	-1.66	1,520	1,479	1,450	-4.60	-1.95
Average						-4.36	-1.53				-3.77	-1.85

Dataset		BKS	RAS		HSS+RAS			ACS		HSS+ACS		
			EST	MRO	ESTMRO	δ_{est}	δ_{mro}	ESTMRO	MRO	HSS	δ_{est}	δ_{mro}
la01	10× 5	666	706	723	700	-0.89	-3.19	802	765	740	-7.78	-3.39
la05	10× 5	593	593	593	593	-0.01	0.00	603	593	593	-1.72	0.00
la10	15× 5	958	971	958	958	-1.30	0.00	999	958	958	-4.13	0.00
la15	20× 5	1,207	1,372	1,373	1,356	-1.19	-1.25	1,389	1,432	1,374	-1.02	-3.99
la20	10×10	902	1,046	1,004	996	-4.77	-0.75	1,182	1,105	1,068	-9.58	-3.34
la25	15×10	977	1,199	1,177	1,148	-4.26	-2.47	1,262	1,168	1,151	-8.83	-1.51
la30	20×10	1,355	1,623	1,583	1,553	-4.33	-1.88	1,674	1,615	1,537	-8.19	-4.87
la31	30×10	1,784	2,020	1,935	1,910	-5.48	-1.30	2,004	1,923	1,835	-8.43	-4.60
la32	30×10	1,850	2,144	2,066	2,032	-5.21	-1.61	2,210	2,081	1,973	-10.71	-5.16
la33	30×10	1,719	1,978	1,924	1,882	-4.88	-2.17	1,974	1,876	1,810	-8.28	-3.52
la34	30×10	1,721	2,038	1,953	1,916	-5.97	-1.91	2,056	2,000	1,886	-8.26	-5.68
la35	30×10	1,888	2,185	2,217	2,143	-1.90	-3.31	2,179	2,223	2,128	-2.34	-4.26
la36	15×15	1,268	1,578	1,484	1,457	-7.67	-1.81	1,628	1,489	1,461	-10.24	-1.84
la37	15×15	1,397	1,706	1,716	1,678	-1.66	-2.21	1,632	1,732	1,645	0.81	-4.98
la38	15×15	1,196	1,503	1,509	1,473	-2.02	-2.42	1,533	1,533	1,444	-5.79	-5.77
la39	15×15	1,233	1,555	1,513	1,481	-4.73	-2.11	1,485	1,493	1,430	-3.71	-4.21
la40	15×15	1,222	1,519	1,481	1,445	-4.85	-2.40	1,483	1,492	1,428	-3.71	-4.28
Average						-3.60	-1.81				-6.00	-3.61

TABLE I
PARAMETER SETTINGS OF THE ACO ALGORITHMS.

Algorithm	α	β	ρ	τ
AS	1	10	0.1	$1/C$
ACS	—	10	0.1	1.0
EAS	1	10	0.1	a_n/C
AS-rank	1	10	0.1	$0.5w(w-1)/C$

Moreover, all the simulations are carried out for 30 runs, and all the ACO-based algorithms tested in this paper use 25 ants and 100 iterations. The parameter κ of EAS is set to 25. C denotes the makespan produced randomly; a_n the number of ants. The number of elitist ants w of AS-rank is set to 6. For the other settings, some of them are repeated below in Table I for easy reference.

The datasets used in this paper are the la series from la01 up to la40. These datasets contain from 10 up to 30 jobs and from 5 up to 15 machines. Moreover, these datasets are available for download from OR-Library at http://people.brunel.ac.uk/~mastjjb/jeb/info.html.

TABLE IV
SIMULATION RESULTS OF ACOS WITH LOCAL SEARCH

Dataset		BKS	AS		HSS+AS			EAS		HSS+EAS		
			EST	MRO	ESTMRO	δ_{est}	δ_{mro}	EST	MRO	ESTMRO	δ_{est}	δ_{mro}
la01	10× 5	666	666	681	677	1.60	-0.63	670	676	671	0.15	-0.68
la05	10× 5	593	593	593	593	0.00	0.00	593	593	593	0.00	0.00
la10	15× 5	958	958	958	958	0.00	0.00	958	958	958	0.00	0.00
la15	20× 5	1,207	1,323	1,279	1,274	-3.67	-0.34	1,297	1,274	1,268	-2.22	-0.42
la20	10×10	902	97 5	944	946	-2.95	0.25	970	939	939	-3.19	-0.04
la25	15×10	977	1,134	1,092	1,084	-4.39	-0.67	1,108	1,079	1,079	-2.66	0.01
la30	20×10	1,355	1,551	1,460	1,462	-5.72	0.14	1,507	1,463	1,454	-3.53	-0.63
la31	30×10	1,784	1,919	1,811	1,807	-5.82	-0.20	1,887	1,803	1,795	-4.85	-0.45
la32	30×10	1,850	2,062	1,914	1,920	-6.90	0.30	1,995	1,904	1,901	-4.71	-0.16
la33	30×10	1,719	1,927	1,784	1,784	-7.44	-0.04	1,857	1,766	1,767	-4.84	0.04
la34	30×10	1,721	1,946	1,835	1,829	-6.00	-0.30	1,901	1,819	1,812	-4.68	-0.41
la35	30×10	1,888	2,039	2,037	2,010	-1.41	-1.34	2,045	2,034	1,997	-2.35	-1.83
la36	15×15	1,268	1,536	1,409	1,413	-7.99	0.32	1,475	1,398	1,387	-5.99	-0.75
la37	15×15	1,397	1,632	1,627	1,612	-1.22	-0.94	1,600	1,602	1,590	-0.61	-0.70
la38	15×15	1,196	1,404	1,403	1,404	-0.02	0.06	1,407	1,392	1,386	-1.47	-0.42
la39	15×15	1,233	1,398	1,392	1,401	0.22	0.62	1,445	1,387	1,380	-4.46	-0.49
la40	15×15	1,222	1,394	1,395	1,382	-0.86	-0.95	1,419	1,376	1,358	-4.28	-1.30
Average						-3.09	-0.22				-2.92	-0.48

Dataset		BKS	RAS		HSS+RAS			ACS		HSS+ACS		
			EST	MRO	ESTMRO	δ_{est}	δ_{mro}	EST	MRO	ESTMRO	δ_{est}	δ_{mro}
la01	10× 5	666	668	673	671	0.41	-0.38	719	693	689	-4.16	-0.58
la05	10× 5	593	593	593	593	0.00	0.00	593	593	593	-0.02	0.00
la10	15× 5	958	958	958	958	0.00	0.00	958	958	958	0.00	0.00
la15	20× 5	1,207	1,294	1,275	1,267	-2.12	-0.60	1,328	1,321	1,314	-1.04	-0.53
la20	10×10	902	960	937	937	-2.34	0.09	1,098	992	998	-9.12	0.66
la25	15×10	977	1,102	1,083	1,075	-2.46	-0.71	1,168	1,095	1,098	-5.98	0.28
la30	20×10	1,355	1,504	1,454	1,452	-3.50	-0.14	1,578	1,470	1,453	-7.90	-1.16
la31	30×10	1,784	1,881	1,802	1,800	-4.30	-0.10	1,925	1,787	1,784	-7.32	-0.18
la32	30×10	1,850	1,984	1,899	1,897	-4.36	-0.09	2,125	1,919	1,866	-12.18	-2.77
la33	30×10	1,719	1,844	1,764	1,762	-4.42	-0.11	1,917	1,745	1,728	-9.84	-0.92
la34	30×10	1,721	1,900	1,821	1,814	-4.53	-0.39	1,987	1,823	1,795	-9.67	-1.51
la35	30×10	1,888	2,030	2,029	1,996	-1.64	-1.63	2,073	2,001	1,971	-4.93	-1.52
la36	15×15	1,268	1,470	1,394	1,382	-5.99	-0.89	1,564	1,420	1,409	-9.90	-0.76
la37	15×15	1,397	1,592	1,598	1,586	-0.39	-0.73	1,582	1,615	1,604	1.39	-0.64
la38	15×15	1,196	1,394	1,387	1,383	-0.78	-0.32	1,454	1,399	1,396	-3.95	-0.18
la39	15×15	1,233	1,438	1,381	1,377	-4.22	-0.25	1,431	1,378	1,356	-5.23	-1.56
la40	15×15	1,222	1,403	1,375	1,356	-3.35	-1.43	1,409	1,392	1,377	-2.27	-1.12
Average						-2.59	-0.45				-5.42	-0.73

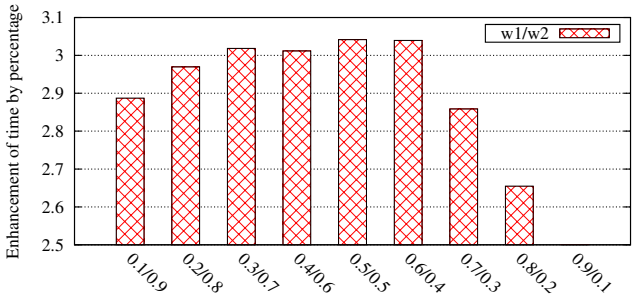

Fig. 1. Impact of w_1 and w_2 on average.

B. Results and Analysis

Table II shows the impact of w_1 and w_2 on the performance of different ACO-based algorithms. Moreover, Table II also shows the results of setting $w_1 = 1.0$ and $w_2 = 0.0$ for the 40 la series datasets from la10 up to la40 on average. As shown in Fig. 1, the settings of $w_1 = w_2 = 0.5$ and $w_1 = 0.6, w_2 = 0.4$ provide better results than the other settings. For this reason, we set $w_1 = w_2 = 0.5$ for all the simulations to be given later in this paper. Tables III and IV show the results of applying the proposed algorithm to four ACO-based algorithms—AS, EAS, RAS, and ACS. For each of these algorithms, two heuristic methods, EST and MRO, are used to compute η. In other words, δ_{est} and δ_{mro} denote, respectively, the enhancement of the proposed algorithm compared with the ACO-based algorithms with EST and MRO. Also, BKS denotes the best known solution of each benchmark.

Table III shows the results of ACO and ACO with the proposed algorithm but no local search. For all the benchmarks tested, the results show that the proposed algorithm can improve the makespan by from 1.53% up to 6.00% on average, by 0.00% in the worst case, and by 10.71% in the best case. Some of the results show that the improvement of HSS is 0.00%. That is because like AS and HSS+AS with MRO for la05 and la10, HSS and MRO get the BKS. In addition, Table III shows that the proposed algorithm can find the better results compared with the original ACO for all the benchmarks tested. Table IV gives the results with local search

proposed by Nowicki and Smutnicki [27]. The results show that the ACO-based algorithms can find solutions closer to the optimum value. However, even in this case, the proposed algorithm can still improve the makespan by from 0.22% up to 5.42% on average, by -1.60% in the worst case, and by 12.18% in the best case. This shows that the proposed algorithm can effectively improve the makespan.

According to our observation, the proposed algorithm, HSSACO, can improve the final results of ACO-based algorithms, especially for the large scale datasets. This characteristic is shown in using the AS to solve la01 with the EST method. The proposed algorithm cannot improve the final results of the original version of AS for some of the benchmarks. It is because the results are very close to the optimum solution. However, the good news is that the proposed algorithm can improve the final results as the size of the dataset increases such as AS for la33. The proposed algorithm can improve the results by about 7.44% compared with AS using the EST method. Moreover, the proposed algorithm can also improve the results of EAS, RAS, and ACS. In summary, even though some of the final results of these simulations are not very close to the BKS, these comparisons have shown that the proposed algorithm has the potential to improve the quality of the end results of the ACO-based algorithms, especially when the solutions are not close to the optimum solution.

V. Conclusion

This paper presents a novel technique for improving the quality of ACO-based algorithms, called hybrid selection strategy for ant colony optimization (HSSACO). The proposed algorithm uses two different heuristic stragegies to compute the probability for the solution construction operator so as to maintain the diversity of the solutions. To evaluate the performance of the proposed algorithm, we apply it to four state-of-the-art ACO-based algorithms—AS, EAS, RAS, and ACS. Moreover, we also use it to solve 10 JSSP datasets, the size of which are from 10 up to 20 jobs and from 5 up to 20 machines. The simulation results show that the proposed algorithm can effectively improve the results of ACO and its variants from 1.23% up to 4.05% on average. Our future focus will be on speeding up the proposed algorithm.

Acknowledgment

This work was supported in part by the National Science Council, Taiwan, R.O.C., under Contract Nos. NSC100-2218-E-041-001-MY2 and NSC99-2220-E-006-008.

References

[1] H. Fisher and G. L. Thompson, "Probabilistic learning combinations of local job-shop scheduling rules," in *Industrial Scheduling* (J. F. Muth and G. L. Thompson, eds.), pp. 225–251, Prentice-Hall, 1963.

[2] R. L. Graham, E. L. Lawler, J. K. Lenstra, and A. H. G. R. Kan, "Optimization and approximation in deterministic sequencing and scheduling: a survey," *Annals of Discrete Mathematics*, vol. 4, pp. 287–326, 1979.

[3] F. A. Rodammer and J. K. Preston White, "A recent survey of production scheduling," *IEEE Transactions on Systems, Man and Cybernetics*, vol. 18, no. 6, pp. 841–851, 1988.

[4] A. S. Jain and S. Meeran, "A state-of-the-art review of job-shop scheduling techniques," *European Journal of Operations Research*, no. 113, pp. 390–434, 1999.

[5] M. L. Pinedo, *Scheduling: Theory, Algorithms, and Systems*. Springer Publishing Company, Incorporated, 3rd ed., 2008.

[6] M. R. Garey, D. S. Johnson, and R. Sethi, "The complexity of flowshop and jobshop scheduling," *Mathematics of Operations Research*, vol. 1, pp. 117–29, 1976.

[7] J. Carlier and E. Pinson, "An algorithm for solving the job-shop problem," *Management Science*, vol. 35, pp. 164–176, 1989.

[8] C. Y. Zhang, P. Li, Y. Rao, and Z. Guan, "A very fast ts/sa algorithm for the job shop scheduling problem," *Computers & Operations Research*, vol. 35, pp. 282–294, 2008.

[9] J. Adams, E. Balas, and D. Zawack, "The shifting bottleneck procedure for job shop scheduling," *Management Science*, vol. 34, pp. 391–401, 1988.

[10] É. D. Taillard, "Parallel taboo search techniques for the job shop scheduling problem," *ORSA Journal on Computing*, vol. 6, no. 2, pp. 108–117, 1994.

[11] M. Dell'Amico and M. Trubian, "Applying tabu search to the job-shop scheduling problem," *Annals of Operations Research*, vol. 41, pp. 231–252, 1993.

[12] P. J. M. van Laarhoven, E. H. L. Aarts, and J. K. Lenstra, "Job shop scheduling by simulated annealing," *Operations Research*, vol. 40, pp. 113–125, 1992.

[13] T. Yamada and R. Nakano, "Conventional genetic algorithm for job shop problems," in *Proceedings of the 4th International Conference on Genetic Algorithms*, pp. 474–479, 1997.

[14] F. D. Croce, R. Tadei, and G. Volta, "A genetic algorithm for the job shop problem," *Computers & Operations Research*, vol. 22, no. 1, pp. 15–24, 1995.

[15] A. Colorni, M. Dorigo, V. Maniezzo, and M. Trubian, "Ant System for Job-shop Scheduling," *JORBEL - Belgian Journal of Operations Research, Statistics and Computer Science*, vol. 34, no. 1, pp. 39–53, 1994.

[16] S. van der Zwaan and C. Marques, "Ant Colony Optimisation for Job Shop Scheduling," in *Proceedings of the 3rd Workshop on Genetic Algorithms and Artificial Life*, 1999.

[17] J. Zhang, X.-M. Hu, X. Tan, J. hui Zhong, and Q. Huang, "Implementation of an ant colony optimization technique for job scheduling problem," *Transactions of the Institute of Measurement and Control*, vol. 28, no. 1, pp. 93–108, 2006.

[18] J. Heinonen and F. Pettersson, "Hybrid ant colony optimization and visibility studies applied to a job-shop scheduling problem," *Applied Mathematics and Computation*, vol. 187, no. 2, pp. 989–998, 2007.

[19] K.-L. Huang and C.-J. Liao, "Ant colony optimization combined with taboo search for the job shop scheduling problem," *Computers & Operations REsearch*, vol. 35, no. 4, pp. 1030–1046, 2008.

[20] M. Dorigo, V. Maniezzo, and A. Colorni, "The ant system: Optimization by a colony of cooperating agents," *IEEE Transactions on Systems, Man, and Cybernetics—Part B*, vol. 26, no. 1, pp. 29–41, 1996.

[21] M. Dorigo and L. M. Gambardella, "Ant colony system: A cooperative learning approach to the traveling salesman problem," *IEEE Transactions on Evolutionary Computation*, vol. 1, no. 1, pp. 53–66, 1997.

[22] M. Dorigo and T. Stützle, *Ant Colony Optimization*. The MIT Press, 2004.

[23] N. Liouane, I. Saad, S. Hammadi, and P. Brone, "Ant systems & local search optimization for flexible job shop scheduling production," *International Journal of Computers, Communications & Control*, vol. 2, no. 2, pp. 174–184, 2007.

[24] J. Šilc, P. Korošec, and B. Robič, "Combining vector quantization and ant-colony algorithm for mesh-partitioning," in *Proceedings of 5th International Conference Parallel Processing and Applied Mathematics (PPAM)*, pp. 113–118, 2003.

[25] M. Dorigo, *Optimization, Learning and Natural Algorithms (in Italian)*. PhD thesis, Dipartimento di Elettronica, Politecnico di Milano, Milan, Italy, 1992.

[26] B. Bullnheimer, R. F. Hartl, and C. Straus, "A new rank based version of the ant system - a computational study," *Central European Journal for Operations Research and Economics*, vol. 7, pp. 25–38, 1997.

[27] E. Nowicki and C. Smutnicki, "A fast taboo search algorithm for the job shop problem," *MANAGEMENT SCIENCE*, vol. 42, no. 6, pp. 797–813, 1996.

2011 IEEE International Conference on Fuzzy Systems
June 27-30, 2011, Taipei, Taiwan

The Sensing System for the Autonomous Mobile Robot Emmy III

Cláudio Rodrigo Torres
Faculdade de Exatas e Tecnologia
Universidade Metodista de São Paulo
São Bernardo do Campo, Brazil
c.r.t@uol.com.br

Jair Minoro Abe
Paulista University - UNIP
São Paulo, Brazil

Germano Lambert-Torres
Artificial Intelligence Application Group - GAIA
Federal University of Itajubá
Itajubá, Brazil

João Inácio da Silva Filho
Universidade Santa Cecilia - UNISANTA
Santos, Brazil

***Abstract* — This paper shows the results of the sensing system which was designed for the autonomous mobile robot Emmy III. The proposed Sensing System has as its mean part the Paraconsistent Neural Network. This artificial neural network is based on the Paraconsistent Evidential Logics – Eτ. The objective of the Sensing System is to inform the other robot components about the obstacle position. The reached results have been satisfactory.**

***Keywords* - Paraconsistent Neural Network; Paraconsistent Logics; Automous Mobile Robot; Sensing System.**

I. INTRODUCTION

This article describes the Emmy III robot architecture emphasizing the sensing system of the robot [1]. The Emmy III robot is designed to achieve a set point in an environment which is divided into coordinates [2]. The Emmy III robot may be considered as a system divided into three other subsystems: the Planning Subsystem, the Sensing Subsystem and the Mechanical Subsystem.

The Planning Subsystem is responsible for generating the sequence of movements the robot must perform to achieve a set point. The Sensing Subsystem has the objective of informing the Planning Subsystem about the position of obstacles; and the Mechanical Subsystem is the robot itself, it means, the mobile mechanical platform which carries all devices away from the other subsystems. This platform must also perform the sequence of movements which are borne by the Planning Subsystem.

The Planning Subsystem and the Sensing Subsystem have already been implemented, but the Mechanical Subsystem has not been implemented yet.

The Sensing Subsystem uses the Paraconsistent Artificial Neural Network [3] and [4]. This artificial neural network is based on the Paraconsistent Evidential Logics – Eτ.

It is described some concepts about the Paraconsistent Evidential Logics – Eτ in the next section.

II. PARACONSISTENT EVIDENTIAL LOGICS

The Paraconsistent Evidential Logics – Eτ [5] is a type of paraconsistent logic in which there may be a Favorable Evidence Degree - μ and a Contrary Evidence Degree - λ in each analyzed sentence.

The Favorable Evidence Degree (μ) is a value between 0 and 1 that represents the favorable evidence in which the sentence is true.

The Contrary Evidence Degree (λ) is a value between 0 and 1 that represents the contrary evidence in which the sentence is true.

Through the Favorable and Contrary Degrees it is possible to represent the four extreme logic states, as shown in the figure 1.

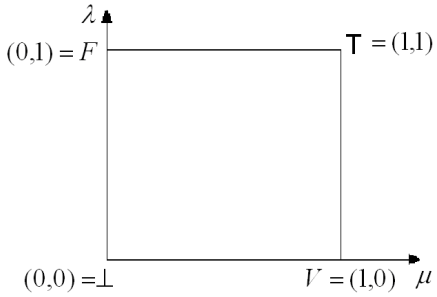

Figure 1. Extreme logic states

The four extreme logic states are:

- True (V)
- False (F)
- Paracomplete (⊥)
- Inconsistent (T)

In [6] it is proposed the Paranalyzer Algorithm. By this algorithm it is also possible to represent the non-extreme logic state. The figure 2 shows this.

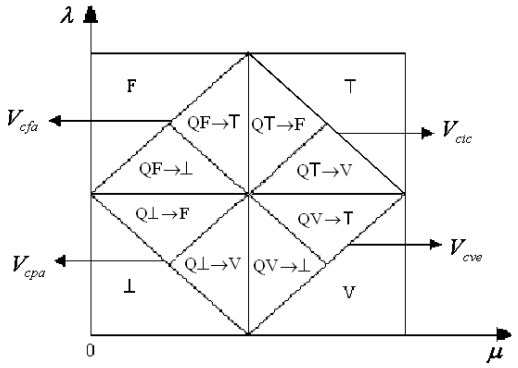

Figure 2. Non extreme logic states

The eight non-extreme logic states are:

- Quasi-true tending to Inconsistent - QV→T
- Quasi-true tending to Paracomplete - QV→⊥
- Quasi-false tending to Inconsistent - QF→T
- Quasi-false tending to Paracomplete - QF→⊥
- Quasi-inconsistent tending to True - QT→V
- Quasi-inconsistent tending to False - QT→F
- Quasi-paracomplete tending to True - Q⊥→V
- Quasi-paracomplete tending to False - Q⊥→F

The Uncertainty Degree: $G_{un}(\mu, \lambda) = \mu + \lambda - 1$ and the Certainty Degree: $G_c(\mu, \lambda) = \mu - \lambda$ $(0 \leq \mu, \lambda \leq 1)$

Some additional control values are:

- V_{cic} = maximum value of uncertainty control
- V_{cve} = maximum value of certainty control
- V_{cpa} = minimum value of uncertainty control
- V_{cfa} = minimum value of certainty control

In the next section we describe the proposed sensing system.

III. SENSING SYSTEM

The sensing system is a set of electronic components and softwares responsible for analyzing the environment around the robot and detecting the obstacle positions. After that, it must inform the other components of the robot the position of the obstacles.

The sensing system may get information from any type of sensor. It is shown in this paper a sensing system able to deal with information from just one ultrasonic sensor. But, if there is more than one sensor in the robot, it is possible to build a sensing system similar to the one shown here for each sensor.

In [7] it is presented a method of robot perception and world's modeling that uses a probabilistic tessellated representation of spatial information called the Occupancy Grid. It is proposed here a similar method, but instead of using probabilistic representation, it is used the Paraconsistent Evidential Logic Eτ.

The proposed sensing system aims to generate a Favorable Evidence Degree in each environment position. The Favorable Evidence Degree is related to the sentence: there is obstacle in the analyzed position.

The sensing system is divided into two parts. The first part is responsible for receiving the data from the sensors and sending information to the second part of the system. And the second part is the Paraconsistent Artificial Neural Network itself. The figure 3 shows this idea.

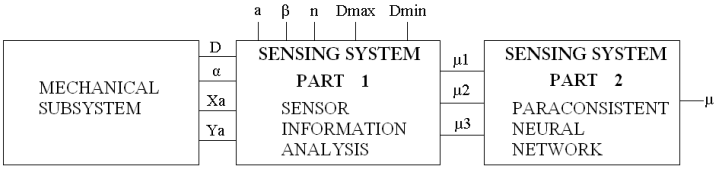

Figure 3. Representation of the sensing system

The proposed sensing system is prepared to receive data from ultrasonic sensors. The robot sensors are on the Mechanical Subsystem. So, this subsystem must treat the data generated by the sensors and send information to the first part of the Sensing Subsystem. The data the Mechanical Subsystem must send to the first part of the Sensing Subsystem are: D, α, Xa and Ya.

a) The distance between the sensor and the obstacle (D).

b) The angle between the horizontal axis of the environment and the direction to the front of the sensor (α). The figure 4 shows the angle α.

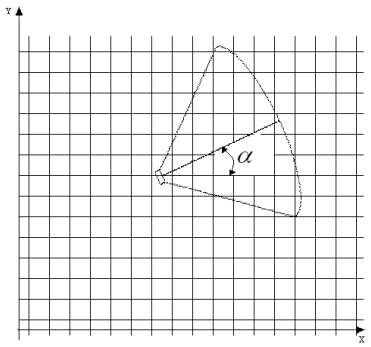

Figure 4. Angle α

c) The coordinate where the robot is (Xa, Ya).

In the first part of the Sensing Subsystem there are also some configuration parameters. They are:

a) The distance between the environment coordinates (a). The figure 5 shows this.

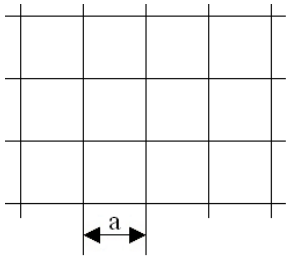

Figure 5. Distance between coordinates

a) The angle of the ultrasonic sensor conical field of view (β). The figure 6 shows this.

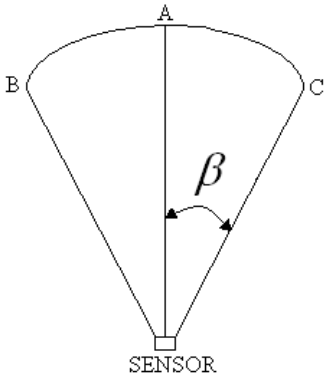

Figure 6. Ultrasonic sensor conical field of view (β)

a) The number of positions on the arch BC, shown in the figure 6, considered by the system (n).

b) The maximum distance measured by the sensor which the system considers (Dmax).

c) The minimum distance measured by the sensor which the system considers (Dmin).

The first part of the Sensing System generates three Favorable Evidence Degree, μ_1, μ_2 and μ_3.

The Favorable Evidence Degree μ_1 is related to the distance between the sensor and the obstacle. The nearer the obstacle is to the sensor the bigger μ_1 value is.

The Favorable Evidence Degree μ_2 is related to the coordinate position on the arch AC shown in the figure 6. As the analyzed coordinate is near to the point A as bigger is μ_2 value. And as the analyzed coordinate is near to the points A and C, as smaller is the μ_2 value. The inspiration of this idea comes from [8] which says that the probability of the obstacle be near to the point A is high. And this probability decreases as we analyze the region near to the points B and C.

Eventually, the Favorable Evidence Degree μ_3 is the previous value of the coordinate Favorable Evidence Degree.

IV. PARACONSISTENT ARTIFICIAL NEURAL NETWORK

The Sensing Subsystem neural network of the robot is composed of two types of cells: Analytic Paraconsistent Artificial Neural Cell – CNAPa and Passage Paraconsistent Artificial Neural Cell - CNAPpa. In the follow it is described the cells.

A. Analytic Paraconsistent Artificial Neural Cell - CNAPa

This cell has two in-puts (μ_{RA} and μ_{RB}) and two out-puts (S1 and S2). Also there are two configuration parameter in-puts (Ftct and Ftc). The figure 7 shows the graphic representation of this cell.

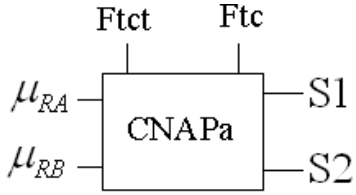

Figure 7. Graphic representation of the Analytic Paraconsistent Artificial Neural Cell

The in-put evidence degrees are:

μ_{RA}, such as: $0 \leq \mu_{RA} \leq 1$

μ_{RB}, such as: $0 \leq \mu_{RB} \leq 1$

There are also two control values:

Contradiction Tolerance Factor – Ft_{ct}, such as: $0 \leq Ft_{ct} \leq 1$

Certainty Tolerance Factor – Ft_c, such as: $0 \leq Ft_c \leq 1$

The Analytic Paraconsistent Artificial Neural Cell – CNAPa has two out-puts. The out-put 1 (S1) is the Resultant Evidence Degree - μ_E.

μ_E, such as: $0 \leq \mu_E \leq 1$

The out-put 2 (S2) is the Resultant Evidence Interval – φ_E.

φ_E, such as: $0 \leq \varphi_E \leq 1$

The Analytic Paraconsistent Artificial Neural Cell calculates the maximum value of certainty - V_{cve}, the minimum value of certainty control - V_{cfa}, the maximum value of uncertainty control - V_{cic} and the minimum value of uncertainty control - V_{cpa} by this way:

$$V_{cve} = \frac{1 + Ft_c}{2} \quad (1)$$

$$V_{cfa} = \frac{1 - Ft_c}{2} \quad (2)$$

$$V_{cic} = \frac{1 + Ft_{ct}}{2} \quad (3)$$

$$V_{cpa} = \frac{1 - Ft_{ct}}{2} \quad (4)$$

The Resultant Evidence Degree – μ_E, is determined in this way:

$$\mu_E = \frac{G_c + 1}{2} \quad (5)$$

As $G_c = \mu - \lambda$:

$$\mu_E = \frac{\mu - \lambda + 1}{2} \quad (6)$$

It is called as Certainty Interval (φ) the Certainty Degree interval that can be modified without changing the Uncertainty Degree value. This value is determined in this way.

$$\varphi = 1 - |G_{ct}| \quad (7)$$

B. Passage Paraconsistent Artificial Neural Cell - CNAPpa

The Passage Paraconsistent Artificial Neural Cell – CNAPpa has one in-put (μ), one out-put (S1) and one parameter control in-put (Ftc). The figure 8 shows the graphic representation of CNAPpa.

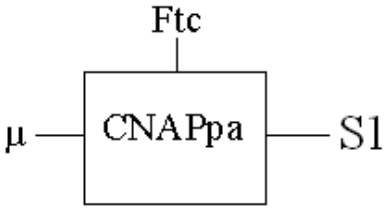

Figure 8. Graphic representation of the Passage Paraconsistent Artificial Neural Cell

The in-put is the Favorable Evidence Degree (μ).

μ, such as: $0 \leq \mu \leq 1$

The value of the out-put S1 is the same as the in-put μ. But, the out-put value may be limited through the parameter control in-put Ftc.

The Passage Paraconsistent Artificial Neural Cell calculates the maximum value of certainty - V_{cve} and the minimum value of certainty control - V_{cfa} by the equations (1) and (2).

It also determines the Resultant Evidence Degree - μ_E by the equation (6). For this, λ is considered as the following.

$$\lambda = 1 - \mu \quad (8)$$

The out-put S1 assumes the same value as in the in-put μ when the follow situation is true:

$$[(V_{cve} \leq \mu_E) \text{ or } (\mu_E \leq V_{cfa})]$$

Otherwise, S1 is 0,5.

C. Paraconsistent Artificial Neural Architecture

It is possible to see in the figure 9 the chosen Paraconsistent Neural Network Architecture for the Sensing Subsystem.

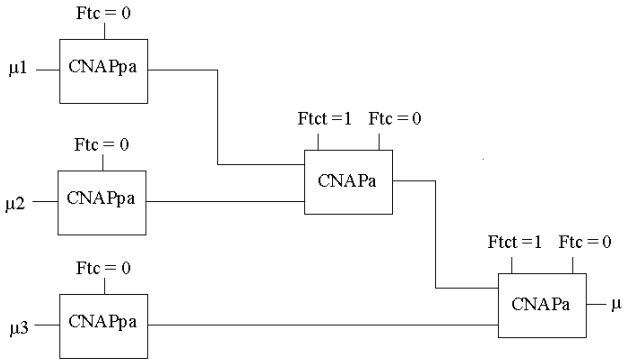

Figure 9. The chosen Paraconsistent Neural Network Architecture for the Sensing System

V. REACHED RESULTS

The Sensing System has been tested by simulating its in-puts and analyzing the database generated. The database stores the Favorable Evidence Degree in each environment position analyzed. It is shown here the result of three tests. The information from one ultrasonic sensor was considered as the Sensing System in-puts.

A. First test

The configuration parameters of this test were the following. The distance between the environment coordinates (a): 10. The angle of the ultrasonic sensor conical field of view (β): 30. The number of positions on the arch of the sensor conical field of view considered by the system (n): 10. The maximum distance measured by the sensor which the system considers (Dmax): 800. The minimum distance measured by the sensor which the system considers (Dmin): 8.

The Mechanical Subsystem treats the data from the sensors and generates the Sensing Subsystem in-puts. It was needed to simulate the Sensing Subsystem in-puts because the Mechanical Subsystem has not been implemented yet.

Thus, the simulated Sensing Subsystem data were the ones described in the follow. The distance between the sensor and the obstacle (D): 200. The angle between the horizontal axis of the environment and the direction to the front of the sensor (α): 30. The coordinate where the robot is (Xa, Ya): (0, 0).

It was simulated the first measuring of the sensor, then, μ_3 initially was 0.

It is shown in the figure 10 the representation of the coordinates in which the Sensing System considered to have obstacles in. Summarizing, the figure 10 is a graphical representation of the database generated by the Sensing Subsystem.

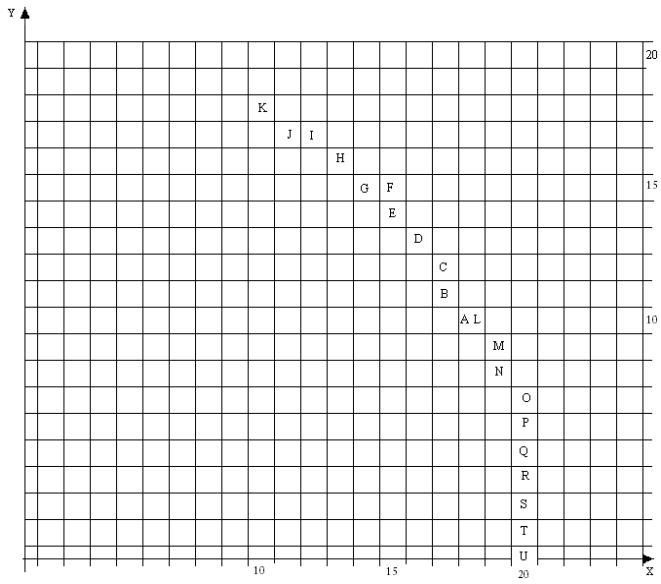

Figure 10. The graphical representation of the database generated by the first test of the Sensing Subsystem.

The analyzed coordinates and their Favorable Evidence Degree are shown in the table 1.

TABLE I. RESULTS OF THE FIRST TEST

Coordinate	μ
A (18,10)	0.438
B (17,11)	0.413
C (17,12)	0.388
D (16,13)	0.363
E (15,14)	0.338
F (15,15)	0.313
G (14,15)	0.288
H (13,16)	0.263
I (12,17)	0.238
J (11,17)	0.213
K (10,18)	0.188
L (18,10)	0.413
M (19,9)	0.388
N (19,8)	0.363
O (20,7)	0.338
P (20,6)	0.313
Q (20,5)	0.288
R (20,4)	0.263
S (20,3)	0.238
T (20,2)	0.213
U (20,0)	0.188

B. Second test

The configuration parameters of this test were the same as the ones from the first test.

The simulated Sensing Subsystem data were the ones described in the follow. The distance between the sensor and the obstacle (D): 400. The angle between the horizontal axis of the environment and the direction to the front of the sensor (α): 45. The coordinate where the robot is (Xa, Ya): (0, 0).

It was simulated the first measuring of the sensor, then, μ_3 was initially 0.

It is shown in the figure 11 the graphical representation of the database generated by the Sensing Subsystem.

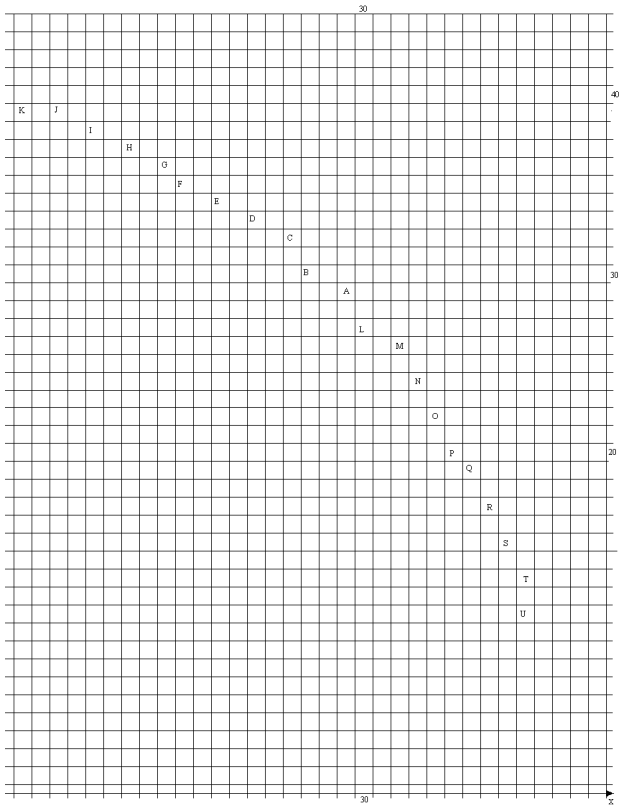

Figure 11. The graphical representation of the database generated by the second test of the Sensing Subsystem

The analyzed coordinates and their Favorable Evidence Degree are shown in the table 2.

TABLE II. RESULTS OF THE SECOND TEST

Coordinate	μ
A (29,29)	0.375
B (27,30)	0.35
C (26,32)	0.325
D (24,33)	0.3
E (22,34)	0.275
F (20,35)	0.25
G (19,36)	0.225
H (17,37)	0.2
I (15,38)	0.175
J (13,39)	0.15
K (11,39)	0.125
L (30,27)	0.35
M (32,26)	0.325
N (33,24)	0.3
O (34,22)	0.275
P (35,20)	0.25
Q (36,19)	0.225
R (37,17)	0.2
S (38,15)	0.175
T (39,13)	0.15
U (39,11)	0.125

C. Third Test

The configuration parameters and the Sensing Subsystem data were the same ones of the second test, then; the analyzed coordinates were the same as the second test. The third test has been done just after the second, therefore, their Favorable Evidence Degree were different from the second test because μ_3 was the Favorable Evidence Degree generated by the second test.

The analyzed coordinates and their Favorable Evidence Degree are shown in the table 3.

TABLE III. RESULTS OF THE THIRD TEST

Coordinate	μ
A (29,29)	0.565
B (27,30)	0.525
C (26,32)	0.49
D (24,33)	0.45
E (22,34)	0.415
F (20,35)	0.375
G (19,36)	0.34
H (17,37)	0.3
I (15,38)	0.265
J (13,39)	0.225
K (11,39)	0.19
L (30,27)	0.525
M (32,26)	0.49
N (33,24)	0.45
O (34,22)	0.415
P (35,20)	0.375
Q (36,19)	0.34
R (37,17)	0.3
S (38,15)	0.265
T (39,13)	0.225
U (39,11)	0.19

If it is considered the sequence of positions from K to U as an arch in the three tests, it is perceived that the Favorable Evidence Degree (μ) decreases as the coordinate is farther distant from the center of the arch. It means that the system is working as desired.

VI. CONCLUSIONS

This paper presents a proposal for the autonomous mobile robot Emmy III. This robot is composed of three modules: Sensing Subsystem, Planning Subsystem and Mechanical Subsystem. The Mechanical Subsystem has not been implemented yet. It is emphasized here the Sensing Subsystem.

The aim of the Sensing Subsystem is to inform the Planning Subsystem about the positions in which obstacles may happen. It considers the environment divided into coordinates.

The Sensing Subsystem is based on the Paraconsistent Artificial Neural Network. The Sensing Subsystem neural network is composed of two types of cells: Analytic Paraconsistent Artificial Neural Cell – CNAPa and Passage Paraconsistent Artificial Neural Cell - CNAPpa.

The out-put of the Sensing Subsystem is the Favorable Evidence Degree related to the statement: there is an obstacle in the position. In fact, the Sensing Subsystem generates a database with the Favorable Evidence Degree for each analyzed coordinate.

Some tests have been made with the Sensing Subsystem. The reached results are satisfactory.

The next step is the implementation of the Mechanical Subsystem and the connection of the three subsystems.

REFERENCES

[1] C. R. Torres, J. M. Abe, G. Lambert-Torres, J. I. da Silva Filho, H. G. Martins . A sensing system for an autonomous mobile robot based on the paraconsistent artificial neural network. *Lecture Notes in Computer Science*. Berlin/Heidelberg: Springer-Verlag, 2010, v. 6278, p. 154-163.

[2] C. R. Torres, "Sistema inteligente baseado na lógica paraconsistente anotada Eτ para controle e navegação de robôs móveis autônomos em um ambiente não estruturado", in Portuguese, Ph. D. Thesis, Federal University of Itajubá, Itajubá, MG, Brazil, 2010.

[3] J. I. da Silva Filho, J. M. Abe, G. Lambert-Torres "Inteligência artificial com redes de análises paraconsistentes: teoria e aplicação", in Portuguese. Rio de Janeiro: LTC, 2008.

[4] J. I. da Silva Filho, G. Lambert-Torres, J. M. Abe, Uncertainty treatment using paraconsistent logic. 1. ed. Amsterdam: IOS Press, 2010. v. 1. 311 p.

[5] J. M. Abe, "Fundamentos da lógica anotada" (Foundations of Annotated Logics), in Portuguese, Ph. D. Thesis, University of São Paulo, São Paulo, 1992.

[6] J. I. da Silva Filho, "Métodos de Aplicações da Lógica Paraconsistente Anotada de Anotação com Dois Valores LPA2v com Construção de Algoritmo e Implementação de Circuitos Eletrônicos", in Portuguese, Ph. D. Thesis, University of São Paulo, São Paulo, 1999.

[7] A. Elfes, Using occupancy grids for mobile robot perception and navigation, Comp. Mag., vol. 22, No. 6, pp. 46-57, June 1989.

[8] J. Boreinstein & Y. Koren, The vector field histogram: fast obstacle avoidance for mobile robots. IEEE Journal of Robotics and Automation. v. 7, p. 278-288, jun. de 1991.

2011 IEEE International Conference on Fuzzy Systems
June 27-30, 2011, Taipei, Taiwan

On a benchmark related assessment of the performance of mutual (investment) funds

Anna Wilbik
Systems Research Institute
Polish Academy of Sciences
Warsaw, Poland
and
Electrical and Computer Engineering
University of Missouri
Columbia, MO, USA
Email: wilbik@ibspan.waw.pl

Janusz Kacprzyk, Fellow of IEEE
Systems Research Institute
Polish Academy of Sciences
Warsaw, Poland
and
Department of Electrical
and Computer Engineering
Cracow University of Technology
Cracow, Poland
Email: kacprzyk@ibspan.waw.pl

***Abstract*—We deal with the problem of how to evaluate the performance of an investment (mutual) fund, over a past period. We assume a widely assumed attitude that an investment fund is said to have performed well if its unit price have been rising faster than its benchmark during a period of growth, and has been falling slower than its benchmark during the period of decline. We develop a novel, flexible and human consistent comparison method that operates on the comparison of trends (segments) extracted from the times series representing the behavior of the fund and its benchmark. The result of comparison becomes a new data set that is linguistically summarized using the method proposed in our previous works.**

***Index Terms*—Linguistic summaries, computing with with words, fuzzy logic, mutual (investment) fund comparison.**

I. Introduction

This paper is a continuation of our previous works (cf. Kacprzyk, Wilbik, Zadrożny [1], [2], [3] or Kacprzyk, Wilbik [4]) which deal with the problem of how to effectively and efficiently support a human decision maker in making decisions concerning investments in some financial instruments, notably in investment (mutual) funds. Decision makers are here basically interested in future gains/losses. We follow the decision support paradigm (as in Fig. 1), that is, assume primarily the user autonomy and a need to support, not replace, him/her. We are not concerned with the forecasting of future daily prices.

We deal with investment decisions that are made on a continuous basis over some period of time. Though the revenues resulting from those decisions are certainly very important, an omnipresent uncertainty calls for a different basis on which those decisions are to be based which is more robust under changing conditions. That is, we are less interested in exact values of quotations of the investment fund considered but more on the stability of their behavior, in relation to its benchmark. This stability is basically meant as the growth and/or decline, and variability.

Basically, in our work we advocate a view that the most promising paradigm is that of decision support, that is, that the system should provide the decision maker with results of some additional analyses of data that may give more insight into the situation. Then, the decision maker can make decision by himself/herself.

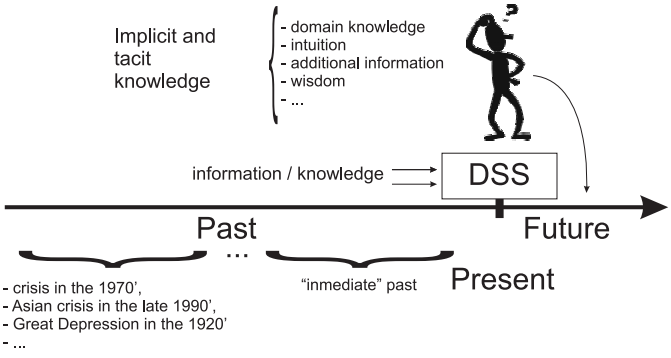

Fig. 1. Decision support paradigm

We deal with analysis of past performance of mutual funds. In our previous papers we have worked in two directions. One topic is the analysis of past performance for which we have proposed and used linguistic summaries of time series. In our works [3], [5], [4] segments (trends) derived from consecutive values have been used. We have used the following (classical) protoforms of linguistic summaries employed: "among all y's Q are P" exemplified by "among all segments (of time series), most are slowly increasing" and "among all Ry's Q are P" exemplified by "among all short segments (of time series), most are slowly increasing". Later we (cf. Kacprzyk and Wilbik [6]) have introduced new, so-called temporal protoforms: "E_T among all y's Q are P" exemplified by "recently among all segments (of time series), most are slowly increasing" and "E_T among all Ry's Q are P" exemplified by "initially, among all short segments (of time series), most are slowly increasing", that explicitly take into account importance of the time of occurrence. We have proposed several quality criteria to evaluate the linguistic summaries derived.

978-1-4244-7316-8/11/$26.00 ©2011 IEEE

The second area of our analysis is the comparison of past performance of the fund and past performance of its benchmark. A mutual fund benchmark can provide information on whether the mutual fund is performing up to the expectations. Every type of mutual funds should have a benchmark that can be used for the comparison purposes.

This is obvious and mentioned in every analysis, guideline, advice, etc. For instance [7]: "Evaluate the funds performance. Every fund is benchmarked against an index .... Investors should compare fund performance over varying time frames vis-a-vis both the benchmark index and peers. Carefully evaluate the funds performance across market cycles particularly the downturns" or even stronger "the best way to evaluate the performance of any mutual fund is to compare it to an appropriate benchmark" [8]. Moreover, they say: "Measure your results. How do your funds stack up against the rest? One of the best ways to know is to compare the funds results with those of its benchmarks. The idea behind benchmarks is to see how your mutual fund compares with an index, one that most closely resembles the holdings of your fund. ... Another way to measure your fund results is to see how a funds returns compare with one of the major market indexes" [9], or "Often cited in news reports, market indexes can be especially helpful to mutual fund investors by offering market 'standards' to help them evaluate the risk and the return history of their own investments. ... While indexes are good methods of gauging how a mutual fund performs in relation to the overall market, they shouldn't be the deciding factor in determining if a fund may meet your needs and objectives. ... The benchmark listed in your fund's prospectus will give you a good idea of what to expect from your mutual fund. However, remember that standardized tests are just that standardized" [10]". We could cite here much more similar articles and opinions.

However investors should be careful while choosing the benchmark, as "recent study from the University of Southern California shows that 42% of actively managed domestic stock funds list benchmarks in their prospectuses that do not match their investment style. No wonder investors have a hard time deciding on a relevant benchmark! Fund management is well aware that its results are being compared to benchmark indexes. In many cases, managers can most easily beat their benchmark by simply changing the index to which their fund is compared" [11]. However in this paper we will not deal with the problem if benchmark is proper for the analyzed fund or not.

In our previous works [12], [13] we had evaluated only the similarity between two time series. The degree of similarity of two time series was meant here as the degree to which, for instance, "most" of the long, overlapping segments are similar (for instance, such that "almost all" of their features are similar). Later [14], [15] we evaluated the similarity on linguistic summaries describing each time series. In such case the degree of similarity of two time series was meant as the degree to which, e.g., "most" of the valid summaries of the fund have the truth values similar to a majority of similar summaries of the benchmark.

Here we go one step further and assess if the fund is better then the benchmark. This is often done by calculating only the benchmark returns, i.e. a fund's returns compared to its benchmark. However we may compare those two time series over some defined time span, and check how the fund is performing. We take a widely assumed general principle that an investment fund is said to have performed well if its unit price have been rising faster than its benchmark during a period of growth, and has been falling slower than its benchmark during the period of decline. In other words, the funds is said to outperform its benchmark when these two conditions have been met.

II. Time series segmentation

The first step in many application and also here in the proposed method is segmentation. We have assumed that segments are linear. There are many methods for a piecewise linear segmentation of time series, e.g., on-line (sliding window) methods, top-down or bottom-up strategies or employing hybrid or genetic strategies [16], [17]. Generally, the algorithm has a minor impact on the obtained segments (cf. [18]) and what really matters is the assumed granulation, expressed in the form of maximal accepted (vertical) distance from the point to the segment, ε.

For the purposes of this work we use an on-line algorithm (also called sliding window). In general the algorithms work by checking if it is possible to add the new point to the currently constructed segment, and if so, then the segment is extended. However, if not, for instance because of the exceeding of the threshold value of the accepted error, ε, then the currently constructed segment is terminated and this new point creates a new segment. In the algorithm used here the segment links two points: the first and the last covered by the segment, as proposed by Sklansky and Gonzalez [19].

Each segment is described by three features:

- dynamics of change,
- duration, and
- variability.

By *dynamics of change* we understand the speed of change of the consecutive values of time series. It may be described by the slope of a line representing the trend (segment). Thus, to quantify dynamics of change we may use the interval of possible angles $\eta \in \langle -90; 90 \rangle$.

However it might be impractical, and not human consistent, to use such a scale directly while describing dynamics of change of the trends. We may use a fuzzy granulation in order to meet the users' needs and task specificity. The user may construct a scale of linguistic terms corresponding to various inclinations of a trend line as, e.g.:

- quickly decreasing,
- decreasing,
- slowly decreasing,
- constant,
- slowly increasing,
- increasing,
- quickly increasing

Figure 2 illustrates possible lines corresponding to the particular linguistic terms.

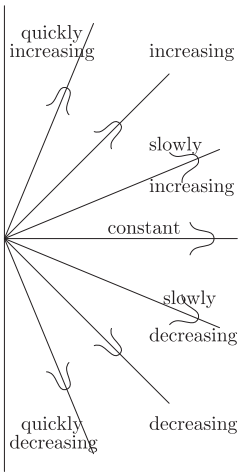

Fig. 2. A visual representation of angle granules defining the dynamics of change

In fact, each term represents a fuzzy granule of directions. In Batyrshin et al. [20], [21] there are presented many methods of constructing such a fuzzy granulation. The user may define a membership functions of particular linguistic terms depending on his or her needs.

We map a single value α characterizing dynamics of change of a trend identified by the algorithm chosen into a fuzzy set (linguistic label) best matching a given angle. We can use, for instance, some measure of a distance or similarity, cf. the book by Cross and Sudkamp [22]. Then we say that a given trend is, e.g., "decreasing to a degree 0.8", if $\mu_{decreasing}(\alpha) = 0.8$, where $\mu_{decreasing}$ is the membership function of a fuzzy set representing "decreasing" that is the best match for angle α.

Duration describes the length of a single trend, meant as a linguistic variable whose linguistic value (label) may be exemplified by a "long trend" defined as a fuzzy set.

The definitions of linguistic terms describing the duration depend clearly on the perspective or purpose assumed by the user.

Variability refers to how "spread out" ("vertically", in the sense of values taken on) a group of data is. We compute it as a weighted average of values taken by some measures used in statistics:

- the range (maximum – minimum),
- the interquartile range (IQR),
- the variance,
- the standard deviation,
- the mean absolute deviation (MAD).

Similarly as in the case of dynamics of change, we find for a given value of variability obtained as above a best matching fuzzy set (linguistic label) using, e.g., some measure of a distance or similarity, cf. the book by Cross and Sudkamp [22]. Again, the measure of variability is treated as a linguistic variable and expressed using linguistic terms (labels) modeled by fuzzy sets defined by the user.

III. Linguistic summaries of trends

A linguistic summary of data (database) is a (usually short) sentence (or a few sentences) that captures the very essence of the data; the date is assumed here numeric, its amount is large and not comprehensible for human users. We use here Yager's [23] basic approach, and a linguistic summary includes:

- a summarizer P,
- a quantity in agreement Q, i.e. a linguistic quantifier,
- truth (validity) $\mathcal{T}$ of the summary and
- optionally, a qualifier R.

An extended, implementable approach was shown in Kacprzyk and Yager [24], and Kacprzyk, Yager and Zadrożny [25].

Thus, the core of a linguistic summary is a linguistically quantified proposition in the sense of Zadeh [26] which may be written, respectively, as

$$Qy's \text{ are } P \tag{1}$$

$$QRy's \text{ are } P \tag{2}$$

which may be exemplified, respectively by: "*Most* of employees earn *low* salary", $\mathcal{T}$=0.7, or "*Most* of *young* employees earn *low* salary", $\mathcal{T}$=0.82.

For clarity and convenience we employ Zadeh's protoforms for dealing with linguistic summaries – cf. Kacprzyk and Zadrożny [27]. A *protoform* is a more or less abstract prototype (template) of a linguistically quantified proposition. The two basic types of protoforms of linguistic summaries of trends are:

- a simple (short) form:

  $$\text{Among all segments, } Q \text{ are } P \tag{3}$$

  e.g., "Among all segments, *almost all* are *slowly increasing*".
- an extended form:

  $$\text{Among all } R \text{ segments, } Q \text{ are } P \tag{4}$$

  e.g., "Among all *very short* segments, *most* are *increasing*".

The basic quality criterion is the truth value (degree) [23]. Using Zadeh's calculus of linguistically quantified propositions [26] it is calculated as:

$$\mathcal{T}(\text{Among all } y\text{'s, } Q \text{ are } P) = \mu_Q\left(\frac{1}{n}\sum_{i=1}^{n}\mu_P(y_i)\right) \tag{5}$$

$$\begin{aligned}\mathcal{T}(\text{Among all } Ry\text{'s, } Q \text{ are } P) &= \\ = \quad \mu_Q&\left(\frac{\sum_{i=1}^{n}\mu_R(y_i)\wedge\mu_P(y_i)}{\sum_{i=1}^{n}\mu_R(y_i)}\right)\end{aligned} \tag{6}$$

where n is the number of extracted segments, Q is a fuzzy set representing the linguistic quantifier in the sense of Zadeh [26], i.e. regular, nondecreasing and monotone and $\wedge$ is the minimum (or a t-norm, cf. Kacprzyk, Wilbik and Zadrożny [28]).

There are also some other quality criteria introduced for the evaluation of linguistic summaries, like degrees of focus,

specificity, covering or appropriateness and measure of informativeness and others. Those quality criteria were discussed in our works (cf. Kacprzyk and Wilbik [29], [30], [31], [32]).

IV. Comparison of the mutual fund and its benchmark

There are several possibilities how to assess if the fund is better than its benchmark. A very simple approach is to compare just the absolute return rate of the fund and benchmark after a certain period. Then we can just compare those two values to assess if the fund is better than benchmark. This is known as a *benchmark return*.

The second option is to compare the return rates of the fund and its benchmark over a certain period. First, we obtain two time series of daily return rates of an investment and its benchmark. Then we subtract the values of the time series of the benchmark from that of the time series of the fund. Next we can analyze the results, e.g., if most of the values of the new time series is above 0 or a certain value, then the fund is better than the benchmark, if most values are close to 0 then the fund is comparable with the benchmark, otherwise it is worse. Such an approach is somewhat similar to the method proposed by Castillo-Ortega, Marín and Sánchez [33].

However that approach can be inappropriate in our context of mutual funds since, usually, the difference between the fund and its benchmark may be very fluctuating. This may be caused because the daily values are compared, not the segments (or trends), and usually there is a small temporal shift between the values of the benchmark and the fund. We will show this later in the section on numerical example.

Therefore we propose to make the assessment on the basis of some trends (or linear segments), in order to avoid those rapid changes in values. We want to globally asses the interplay between the benchmark and the investment fund quotations. This is much more then the analysis of quotations and its related benchmark values but also the analysis of dynamics and behavior. Fund quotations are not directly comparable in financial terms with the values of the benchmark (the WIG index in our case), but they are related.

We assess whether the fund is better than its benchmark using the following widely accepted principle: it is said that a mutual (investment) fund is better than its benchmark when it rises faster than the benchmark and falls slower than the benchmark.

The time series is represented by its segments (trends). Each segment is described by the following four values:
- starting time, called here a partition point,
- duration of the segment (expressed in time units),
- dynamics of change (expressed as the slope of the segment),
- variability occurring in the segment, describing the variability of differences between the trend (segment line) and the particular time series values over the duration of this trend.

Let us assume that we wish to assess which of the two time series A and B is better. As a result of the segmentation procedure time series A is divided into k segments, represented by a_j, $j = 1, \ldots, k$ and time series B is divided into l segments, represented by b_j, $j = 1, \ldots, l$.

A simple approach would be that the segments have the same partition points. This may be attained at the expense of using an artificial fixed point segmentation. In our case we follow a different way and assume that segmentations of the investment fund and benchmark time series are taken as they are, and there may be different partition points between the segments. This clearly complicates the analysis.

Next we create the set of partition points of the two time series considered, i.e. this set contains the time points when at least one segment has started. There are at most $k + l$ such partition points. Those times are sorted, so that the earlier ones come first.

Now between any consecutive partition points (e.g. p_i and p_{i+1}) there is only one segment (or a part of it) of each time series. We may denote those segments as a_{p_i} and b_{p_i}, i.e., a_{p_i} is the segment representing time series A that take place between p_i and p_{i+1}, as in Figure 3.

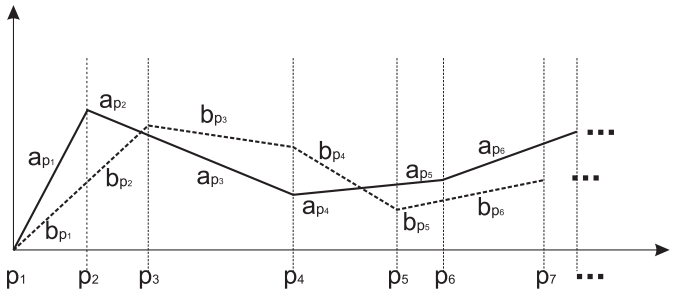

Fig. 3. Partition points for two time series

For the assessment purposes the values of the dynamic and duration are only used. First, we assess if the fund is better than its benchmark between two consecutive partition points, i.e., we compare the segments between those partition points. We subtract the value of the dynamics of change of the segment representing the benchmark's time series, from the value of the dynamics of change of the segment representing the benchmark's time series. This difference is treated as a linguistic variable and expressed using linguistic terms (labels) modeled by fuzzy sets defined by the user. Three linguistic labels should be sufficient, notably "better", "indifferent" and "worse". We could aggregate those partial scores, via a quantifier driven aggregation. However, the definition mentioned above distinguish 2 situations, an increase and a decrease of the values of the benchmark. Therefore it would be interesting to present this relationship in the form of a linguistic summary.

V. Numerical example

In this numerical example we analyze the mutual fund quotations from the last two years, i.e., from January 5, 2009 until January 3, 2011, presented in Fig. 4. The investment fund considered is an equity fund that invests at least 66% assets in shares listed at the Warsaw Stock Exchange. It may also invest at the Zagreb Stock Exchange or Moscow Interbank

Currency Exchange. The fund aims at achieving a long term capital growth (the minimal saving time is recommended to be 5 years) and promises a high profit, however at a high risk, in particular in short term.

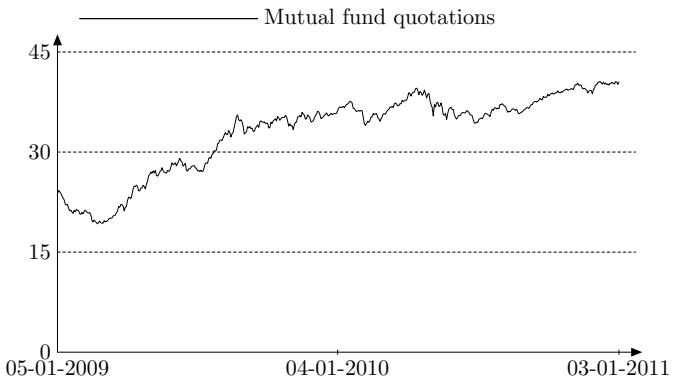

Fig. 4. Daily quotations of the investigated fund

In the analyzed time span, the benchmark of this fund was the WIG index, a total return index, which includes dividends and pre-emptive rights. More information about this index can be found at `www.gpw.pl`. The performance of the WIG index is presented in Fig. 5.

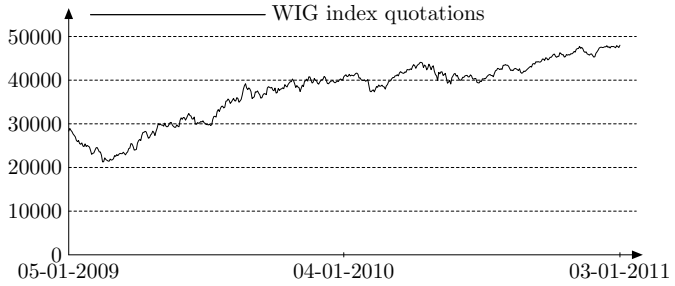

Fig. 5. Daily quotations of the WIG index

Just for information, the return rates for the fund and the WIG index over the given period are equal, respectively, to 1.60% and 1.82%. The benchmark return rate is -0.22%, so it is very small.

We could scale the both time series, i.e. interpreting the scaled values as the value of our investment of the same sum of money at a specific time point. Then we could easily subtract those values. As a result we would obtain the time series as in Fig. 6 and obtain the linguistic summaries "most values are practically the same" meaning that the difference in profit of the two instruments, meant as given above, is irrelevant in most days.

We may notice very big oscillations, and this time series looks similar to a white noise.

Let us now analyze the results of the method proposed. Using a piecewise linear segmentation method with a moderate value of the maximum accepted error we have found 28 segments for the fund quotations time series and 40 segments for the WIG quotations time series. We computed also the degree of similarity of the fund and WIG time series using

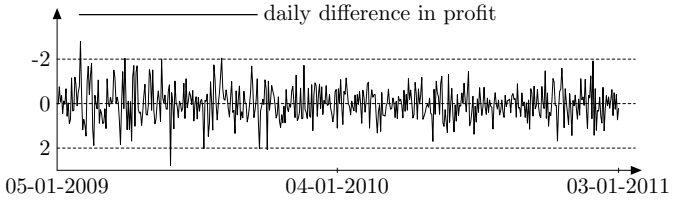

Fig. 6. Daily difference in profit of two investment instruments

a method propsed in our previous paper [12], and it is equal 0.7830, so both time series are quite similar.

Some of the linguistic summaries describing the dynamics of change of two time series and the difference of angles (slopes of the segments) are the following:

- In most cases if the dynamics of change of the investment fund was decreasing, the dynamics of change of WIG index was also decreasing, $\mathcal{T}$ = 1.0000
- In most cases if the dynamics of change of the WIG index was constant, the dynamics of change of investment fund was also constant, $\mathcal{T}$ = 1.0000
- In most cases if the dynamics of change of the investment fund was increasing, the dynamics of change of WIG index was also increasing, $\mathcal{T}$ = 0.9140
- In most cases if the dynamics of change of the WIG index was increasing, dynamics of change of the fund was worse, $\mathcal{T}$ = 1.0000
- In most cases if the dynamics of change of the WIG index was constant, dynamics of change of the fund was indifferent, $\mathcal{T}$ = 0.9107
- In most cases if the dynamics of change of the WIG index was decreasing, dynamics of change of the fund was better, $\mathcal{T}$ = 0.7727

The first 3 summaries describe relationships betweens segments describing the fund and WIG time series. The next 3 summaries compare the fund and WIG stating that, generally, the fund outperforms its benchmark, when it falls, but underperforms the benchmark when it rises. This basically means that the fund is not performing as we have wished it to do. This may be a very important clue for the funds managers. Also this may be a valuable conclusion in the context of bad situation on the economic and financial market that we have observed for a few last years.

This intuitive, human consistent assessment is a "raw estimate" and in investments practices much more sophisticated criteria are used. This is however beyond the scope of this paper.

VI. Concluding remarks

We dealt with the problem of how to evaluate the performance of an investment (mutual) fund, over a past period. We took as a point of departure a widely assumed attitude that an investment fund was said to have performed well if its unit price had been rising faster than its benchmark during a period of growth, and had been falling slower than its benchmark during the period of decline. We developed a

novel, flexible and human consistent comparison method that operated on the comparison of trends (segments) extracted from the times series representing the behavior of the fund and its benchmark. The result of comparison became a new data set that was linguistically summarized using the method proposed in our previous works. The new method proposed was tested on an open investment fund listed on Polish and international financial market whose benchmark was the most important, general index of the Warsaw Stock Exchange. The results obtained provided a valuable insight into the very essence of the behavior of the fund's quotations in relation to its benchmark, and could be useful while making investment decisions.

REFERENCES

[1] J. Kacprzyk, A. Wilbik, and S. Zadrożny, "Linguistic summarization of trends: a fuzzy logic based approach," in *Proceedings of the 11th International Conference Information Processing and Management of Uncertainty in Knowledge-based Systems*, 2006, pp. 2166–2172.

[2] ——, "On some types of linguistic summaries of time series," in *Proceedings of the 3rd International IEEE Conference "Intelligent Systems"*. IEEE Press, 2006, pp. 373–378.

[3] ——, "Linguistic summarization of time series using a fuzzy quantifier driven aggregation," *Fuzzy Sets and Systems*, vol. 159, no. 12, pp. 1485–1499, 2008.

[4] J. Kacprzyk and A. Wilbik, "An extended, specificity based approach to linguistic summarization of time series," in *Proceedings of the 12th International Conference Information Processing and Management of Uncertainty in Knowledge-based Systems*, 2008, pp. 551–559.

[5] J. Kacprzyk, A. Wilbik, and S. Zadrożny, "An approach to the linguistic summarization of time series using a fuzzy quantifier driven aggregation," *International Journal of Intelligent Systems*, vol. 25, no. 5, pp. 411 – 439, 2010.

[6] J. Kacprzyk and A. Wilbik, "Temporal linguistic summaries of time series using fuzzy logic," in *Information Processing and Management of Uncertainty in Knowledge-Based Systems*, ser. Communications in Computer and Information Science, E. Hüllermeier, R. Kruse, and F. Hoffmann, Eds., vol. 80. Springer, 2010, pp. 436–445.

[7] "www.personalfn.com/detail.asp?date=5/18/2007&story=2, A 10-step guide to evaluating mutual funds."

[8] "http://www.fundalarm.com/decid2sl.htm, Deciding to sell a mutual fund."

[9] "http://americanfundsretirement.retire.americanfunds.com/tools/learning/reading-fund-quotes.htm, Reading mutual fund quotes and benchmarks."

[10] "http://budgeting-investing.ameriprise.com/financial-planning-articles/mutual-fund-investing/market-benchmark.asp, Choosing the right benchmarks for your mutual fund."

[11] A. B. Kish, "http://www.fool.com/investing/mutual-funds/2007/06/28/are-your-funds-really-performing.aspx, Are your funds really performing?"

[12] J. Kacprzyk and A. Wilbik, "Using fuzzy linguistic summaries for the comparison of time series: an application to the analysis of investment fund quotations," in *Proceedings of IFSA/EUSFLAT 2009*, 2009, pp. 1321 – 1326.

[13] ——, "Linguistic summaries for the comparison of time series: an application to the analysis of investment fund quotations," in *Information Systems Architecture and Technology*, Z. Wilmowska, L. Borzemski, A. Grzech, and J. Świątek, Eds. Wrocaw University of Technology, 2009, pp. 139 – 148.

[14] ——, "A comprehensive comparison of time series described by linguistic summaries and its application to the analysis of performance of a mutual fund and its benchmark," in *Proceedings of WCCI2010*. IEEE Press, 2010, pp. 25–32.

[15] ——, "Comparison of time series via classic and temporal protoforms of linguistic summaries: an application to mutual funds and their benchmarks," in *Combining Soft Computing and Statistical Methods in Data Analysis*, C. Borgelt, G. Gonzalez-Rodriguez, W. Trutschnig, M. A. Lubiano, M. A. Gil, P. Grzegorzewski, and O. Hryniewicz, Eds. Springer-Verlag, Berlin and Heidelberg, 2010, pp. 369–377.

[16] E. Keogh, S. Chu, D. Hart, and M. Pazzani, "An online algorithm for segmenting time series," in *Proceedings of the 2001 IEEE International Conference on Data Mining*, 2001.

[17] ——, "Segmenting time series: A survey and novel approach," in *Data Mining in Time Series Databases*, M. Last, A. Kandel, and H. Bunke, Eds. World Scientific Publishing, 2004.

[18] A. Wilbik, "Linguistic summaries of time series using fuzzy sets and their application for performance analysis of investment funds," Ph.D. dissertation, Systems Research Institute, Polish Academy of Sciences, 2010.

[19] J. Sklansky and V. Gonzalez, "Fast polygonal approximation of digitized curves," *Pattern Recognition*, vol. 12, no. 5, pp. 327–331, 1980.

[20] I. Batyrshin, "On granular derivatives and the solution of a granular initial value problem," *International Journal Applied Mathematics and Computer Science*, vol. 12, no. 3, pp. 403–410, 2002.

[21] I. Batyrshin and L. Sheremetov, "Perception based functions in qualitative forecasting," in *Perception-based Data Mining and Decision Making in Economics and Finance*, I. Batyrshin, J. Kacprzyk, L. Sheremetov, and L. A. Zadeh, Eds. Springer-Verlag, Berlin and Heidelberg, 2006.

[22] V. Cross and T. Sudkamp, *Similarity and Compatibility in Fuzzy Set Theory: Assessment and Applications*. Heidelberg and New York: Springer-Verlag, 2002.

[23] R. R. Yager, "A new approach to the summarization of data," *Information Sciences*, vol. 28, pp. 69–86, 1982.

[24] J. Kacprzyk and R. R. Yager, "Linguistic summaries of data using fuzzy logic," *International Journal of General Systems*, vol. 30, pp. 33–154, 2001.

[25] J. Kacprzyk, R. R. Yager, and S. Zadrożny, "A fuzzy logic based approach to linguistic summaries of databases," *International Journal of Applied Mathematics and Computer Science*, vol. 10, pp. 813–834, 2000.

[26] L. A. Zadeh, "Toward a theory of fuzzy information granulation and its centrality in human reasoning and fuzzy logic," *Fuzzy Sets and Systems*, vol. 9, no. 2, pp. 111–127, 1983.

[27] J. Kacprzyk and S. Zadrożny, "Linguistic database summaries and their protoforms: toward natural language based knowledge discovery tools," *Information Sciences*, vol. 173, pp. 281–304, 2005.

[28] J. Kacprzyk, A. Wilbik, and S. Zadrożny, "Linguistic summarization of time series under different granulation of describing features," in *Rough Sets and Intelligent Systems Paradigms - RSEISP 2007*, M. Kryszkiewicz, J. F. Peters, H. Rybinski, and A. Skowron, Eds. Springer-Verlag, Berlin and Heidelberg, 2007, pp. 230–240.

[29] J. Kacprzyk and A. Wilbik, "Linguistic summaries of time series: On some additional data independent quality criteria," in *Foundations of Reasoning under Uncertainty*, B. Bouchon-Meunier, L. Magdalena, M. Ojeda-Aciego, J.-L. Verdegay, and R. R. Yager, Eds. Springer Berlin / Heidelberg, 2010, pp. 143–166.

[30] ——, "Linguistic summaries of time series using a degree of appropriateness as a measure of interestingness," in *Proceedings of 2009 Ninth International Conference on Intelligent Systems Design and Applications*. IEEE Press, 2009, pp. 385–390.

[31] ——, "Towards an efficient generation of linguistic summaries of time series using a degree of focus," in *Proceedings of the 28th North American Fuzzy Information Processing Society Annual Conference – NAFIPS 2009*, 2009.

[32] ——, "A new insight into the linguistic summarization of time series via a degree of support: Elimination of infrequent patterns," in *Soft Methods for Handling Variability and Imprecision*, D. Dubois, M. A. Lubiano, H. Prade, M. A. Gil, P. Grzegorzewski, and O. Hryniewicz, Eds. Springer-Verlag, Berlin and Heidelberg, 2008, pp. 393–400.

[33] R. Castillo-Ortega, N. Marín, and D. Sánchez, "Time series comparison using linguistic fuzzy techniques," in *Computational Intelligence for Knowledge-Based Systems Design*, ser. Lecture Notes in Computer Science, E. Hüllermeier, R. Kruse, and F. Hoffmann, Eds., vol. 6178. Springer, 2010, pp. 330–339.

2011 IEEE International Conference on Fuzzy Systems
June 27-30, 2011, Taipei, Taiwan

Discerning Suicide Notes Causality Using Fuzzy Cognitive Maps

Ethan White
Applied Computational Intelligence Laboratory
University of Cincinnati
Cincinnati, Ohio USA
whitee4@mail.uc.edu

Lawrence J. Mazlack
Applied Computational Intelligence Laboratory
University of Cincinnati
Cincinnati, Ohio USA
mazlack@uc.edu

***Abstract*—An important question is how to determine if a person is exhibiting suicidal tendencies in behavior, speech, or writing. This paper demonstrates a method of analyzing written material to determine whether or not a person is suicidal. The method involves an analysis of word frequencies that are used in a fuzzy cognitive map. The fuzzy cognitive map determines if there are suicidal tendencies. The method could have substantial potential in suicide prevention as well as in other forms of sociological behavior studies that also might exhibit their own identifying patterns.**

Keywords-fuzzy cognitive maps; causality; suicide; language; natural language processing

I. INTRODUCTION

Computationally recognizing causality is a very difficult task. However, discovered causality can be one of the most useful predictive tools. One utilitarian outcome that causality can provide is the prediction of human behavioral patterns, either in a broad domain such as nations or religious groups, or in groups of individuals. One group of individuals that can be analyzed is the people who commit suicide. Describing the causalities involved is difficult to do quantitatively, so it must be represented qualitatively. The purpose of this work is to use fuzzy cognitive maps to discover and isolate root causal relationships based on words in suicide notes.

The long term goal of this work is to discover causal patterns in written material. The focus is on patterns in the frequency of words as opposed to grammatical structure. The objective of this work, which will be the first step toward the long term goal, is to analyze a specific human behavioral pattern, i.e. suicide, in the form of suicide notes in a way as to contrast it with non-suicide notes. The central hypothesis is that suicidal behavioral patterns can be extracted from word frequencies in written material, and that these patterns can be represented using fuzzy cognitive maps.

To test the central hypothesis and accomplish the objective of this research, three specific aims are pursued:

A. Discover and extract patterns in written material in order to produce an initial fuzzy cognitive map to describe causality.

The first step toward this aim is the analysis of suicide notes according to the working hypothesis that using discovered word frequency patterns can discover causal patterns. This will be done for both the original written material and a set of the same data with spelling corrections.

The reason for making the distinction between spelling errors and corrected errors is that misspellings in suicide notes could have patterns that are exclusive to such writings as opposed to other written material. If, on the other hand, it turns out that misspellings are not significantly tied in with either suicide or non-suicide notes then notes that have had their spelling corrected will not be considered in the analysis, then only the original notes will be used in developing the fuzzy cognitive map.

The second step is an analysis of non-suicide notes based on the same working hypothesis. Again this has to be done for both the original and corrected versions of the data. Once this analysis has been done, the frequency patterns of the data will be used to produce an initial fuzzy cognitive map for analysis in the second aim.

B. Perform rigorous testing on the fuzzy cognitive map on the original data and make adjustments where necessary.

Once the first aim has been accomplished and the patterns discovered are converted to a fuzzy cognitive map, then testing must be performed in order to ensure that the map will be able to tell the difference between the suicide notes and the non-suicide notes that were originally tested.

Again, as in the first aim, this must be broken up into testing the original data and the data with spelling corrections. These must be further divided up into testing groups of notes and testing individual notes. This will show how sensitive the fuzzy cognitive map is to the amount of data available. Once the map has been altered to a point where the results are acceptably reliable then aim three will be performed.

978-1-4244-7316-8/11/$26.00 ©2011 IEEE

C. *Perform rigorous testing on the fuzzy cognitive map based on different material.*

Once the cognitive map is able to distinguish between the two original data sets used to build it, the map must be able to find the patterns in different written sources to ensure that it can work on a variety of writing. This is also broken up into two steps as in the first two aims.

The first step is using the misspelled words as written, and the second step is using the corrected words. As with the second aim, this must be tested for both individual notes and for groups of notes to determine if the amount of data affects the outcome. If satisfactory results have not been attained, then the new data must be factored into the fuzzy cognitive map until the results are reliably accurate. Then aim three must be performed again using a different source of data.

II. BACKGROUND

A. *Suicide research*

Much of the research on suicide has been in two major areas: clinical studies and analysis of suicide notes. Clinical studies usually involve two types of studies. The first type of study is statistical analysis. This usually involves analyzing suicides based on age and gender as well as other demographics such as social and educational status [5]. This method has been traditionally a primary means of analysis in researching suicide [6]. For example, some studies have shown that nearly one-third of all suicides are found in the elderly over 60 years of age [1]. By using this technique, it is possible to discover what kinds of people are more likely to commit suicide and when. This allows researchers and suicide prevention organizations to identify particular trends in the demographics where they can focus their work in discovering ways to prevent such suicides.

The second type of clinical study involves psychological analysis of individual patients that are displaying suicidal thoughts and actions. This allows for discovering reasons for committing suicide on an emotional and psychological level. This method is done by studying people with suicidal thoughts in order to correlate emotional, mental, or physical state with suicide. An example would be to study the emotional state of people who are losing eyesight, who especially have a fear of losing sight, and how it correlates with suicidal thoughts [7]. If the thought processes of people who are undergoing blindness can be thoroughly understood, than it would be possible to anticipate and treat psychopathological symptoms before they lead to suicide [7].

The analysis of suicide notes has been primarily a study into the content of the notes in an attempt to discover the state of the persons thinking and thereby understand what circumstances and emotional states were driving the individual to commit suicide. These circumstances can be divided up into situations, relationships, emotional state, cognitive state, and demographic variables [3]. These different aspects are then analyzed to determine causes and motivations for suicide similar to the clinical studies approach.

B. *Causality*

Causality is a description of what causes a particular event or group of events in order to happen [10]. Causality is more than a statistical correlation as it contains both a direction, i.e. one event causes another event and not the other way around. Causality also has a particular order in a string of events that, if changed, would alter the result of the events [10]. If causality can be extracted from outside information, it would help intelligent systems in modeling its environment for decision making [11]. Also, causal relationships are more stable in describing the world than probabilistic models [12]. However, constructing causal relationships is difficult as often it is difficult to determine whether a particular event is necessary for the causal relationship or is merely coincidental [13]. Two methods used for modeling causality are text information extraction and graphs.

One of the challenging aspects of analyzing language is that language is highly complicated and often ambiguous; consequently making computer understanding difficult [14]. Extracting causal knowledge from text is of interest because the internet can provide a huge amount of text that is machine-readable. These documents have a great deal of information in them that can be used to establish causal models, e.g. analyzing newspaper articles in order to determine causal economic trends [15]. Another use in computationally extracting causal patterns from text documents is to answer questions by analyzing lexical and semantic constructions within the sentences [16].

Graph structures can be used for both modeling outside events, such as Mideast relations [9], as well as to describe causal relations in textual data [17]. The reason why these networks are powerful is that the graphs are made up of simple elements but create complex models that can be used to describe complex relationships [18]. One type of graph structure that can capture causality is a fuzzy cognitive map.

C. *Fuzzy Cognitive Maps*

Fuzzy cognitive maps are a fairly recent development in the attempt to capture causality in a way that can be useful for studying the real world. These maps are directed weighted graphs that describe relationships between events. The nodes and edges together capture domain information allowing the fuzzy cognitive map to depict uncertain causal reasoning [8]. The individual nodes represent particular events and the directed weighted edges represent what kind of an influence each node has on the other nodes that it connects to. If node one has a positive influence on node two, then if the event of node one increases, the event of node two will also increase; if they are connected with a negative edge, then if node one increases, node two will decrease [9]. Each node in the graph is a fuzzy set that goes from 0% to 100% [9]. Also, each edge can be a set of concepts such as “a little” up to “a lot” or a range of numbers such as 0% to 100% as with the nodes [9] [2].

III. CREATING THE INITIAL FUZZY COGNITIVE MAP

A. *Extracting patterns in general categories from written material*

The first step in accomplishing the first aim, and, developing the initial fuzzy cognitive map was to analyze the written data of both suicide notes and non-suicide notes. The group of suicide notes that were studied consisted of notes written by those that successfully committed suicide. The non-suicide notes consist of three sets that are approximately the same size as the number of words used in the group of suicide notes.

The data sets are taken from informal sources, i.e., each source represents a natural human form of communication as opposed to magazine articles, professional journals, and other such written works. The first set is a collection of various product reviews extracted from Amazon.com. This sample set was taken from a number of different products over a range of different ratings that ranged from the highest rating of five stars to the lowest rating of one star. The second set is a collection of notes from a private blog at archbishopcranmer.blogspot.com. This is different from the Amazon.com data because it represents an individual instead of a group of people. The final set comes from a political website called www.biggovernment.com. This set contains more specific topics than are covered by random product reviews on Amazon.com and random notes from an individual.

All of the words were grouped into investigator defined abstract general categories and sorted in order from most frequently used to least frequently used words. Each grouping was defined by how dense they are by percentage compared to the entire dataset, i.e., how frequently each group is used in a given set of data. The categories used are references to self, others, financial terms, medical terms, religious terms, negative and positive words, and misspelled words. The densities of these categories are shown in Fig. 1.

In addition to these categories, past tense and present tense words were also included along with their corresponding negative and positive references as shown in Fig. 2.

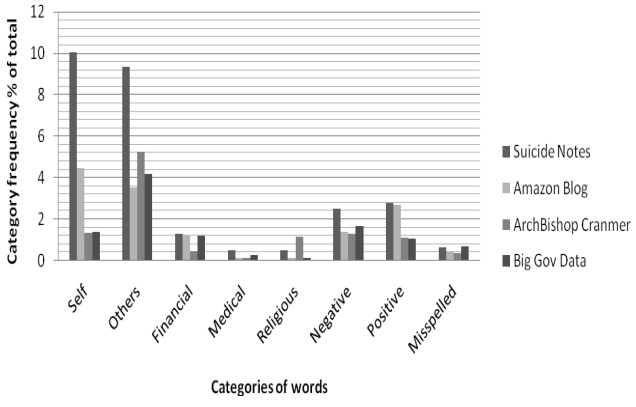

Figure 1. Word densities by percentage part 1

The results show that the greatest differentiation between the suicide notes and the non-suicide notes is found in the references to self and others as shown in Fig. 1, and, present tense as shown in Fig. 2. Also, according to the data, there is not a significant amount of misspellings and even the small amount that there is, does not show significant variation between suicide and non-suicide notes. However, these are chiefly dominated by the set of suicide notes. This means that there would be no nodes in the fuzzy cognitive map that would push the final result toward a non-suicidal classification as if it was analyzing a non-suicidal case. Therefore, the patterns have to be extracted on a word by word basis.

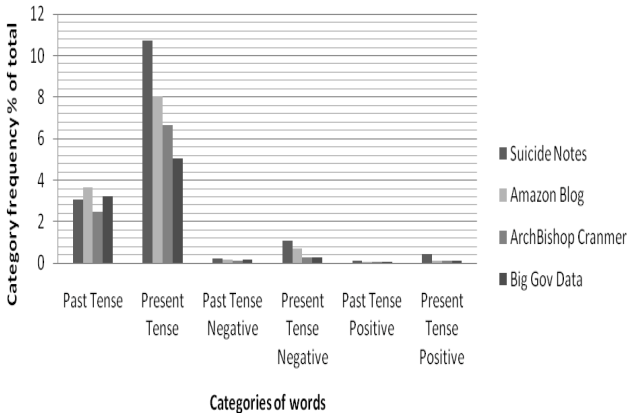

Figure 2. Word densities by percentage part 2

B. *Extracting patterns from specific words in written material*

The three best places to gather words that can provide varying reliable patterns are the groups for self references, references to others, and present tense. These groups contain the most references than any other kind and, therefore, the words in these categories are most likely to be found in a random set of notes to be analyzed and classified as suicidal or non-suicidal. The densities for these words, however, are not based on how many of each word is used in the entire dataset but rather on how many of each word is used in the group it occupies.

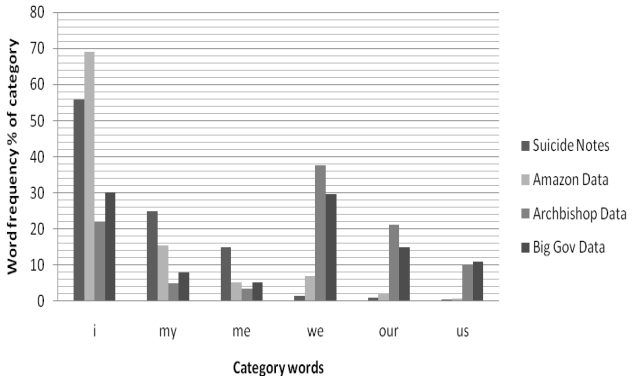

Figure 3. Word densities in self references by percentage

Upon further analysis of the three groups, there were a number of words that proved to have either distinct suicidal influences or distinct non-suicidal influences. All words that had small percentages over all four datasets or did not vary significantly between suicide and non-suicide were removed from consideration. Fig. 3 shows the final results for references to self.

On average each word has a specific affiliation to either the suicide notes or non-suicide notes. However, the Amazon.com data shows definite anomalies in the words "I," "we," "our," and "us" as compared with the other two non-suicide collection of notes. However, the apparent pattern is that suicide notes have more singular self references, i.e. "I," "my," and "me," while non-suicide notes seem to have more group self references, i.e. "we," "our," and "us." Fig. 4 shows the results for references to others.

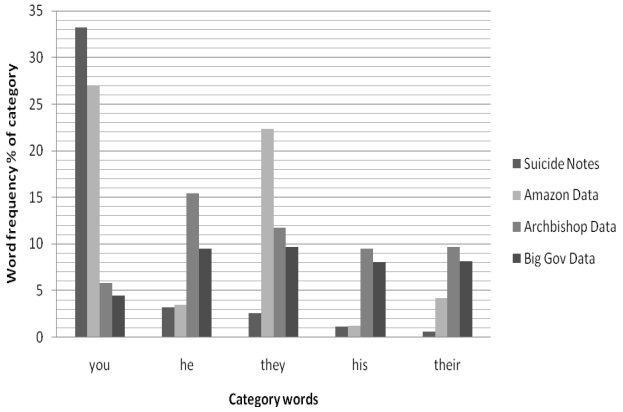

Figure 4. Word densities in others references by percentage

As before, there was a definite pattern with suicide notes having a large amount of references to the word "you" and the non-suicide notes having larger references to "he," "they," "his," and "their." Again, the Amazon.com data shows anomalies being similar to the suicide data in the word "you" but showing a great deal more influence in the word "they." The final results for present tense words are shown in Fig. 5.

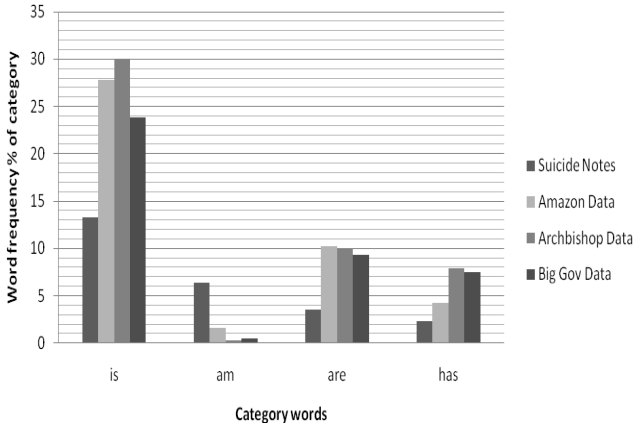

Figure 5. Word densities in present tense by percentage

In this group, the Amazon.com data acts similarly to the other non-suicide data except that the percentage for the word "has" is a little low, although not entirely problematic.

C. Developing the Initial Fuzzy Cognitive map

The fuzzy cognitive maps consist of a series of connected nodes that will represent the words being used from Fig. 3-5. These words will in some way connect to a suicidal node that will determine the classification of the dataset. The simplest graph that can be constructed, is for the suicidal node to be central with all word nodes connected to only that one node as shown in Fig. 6.

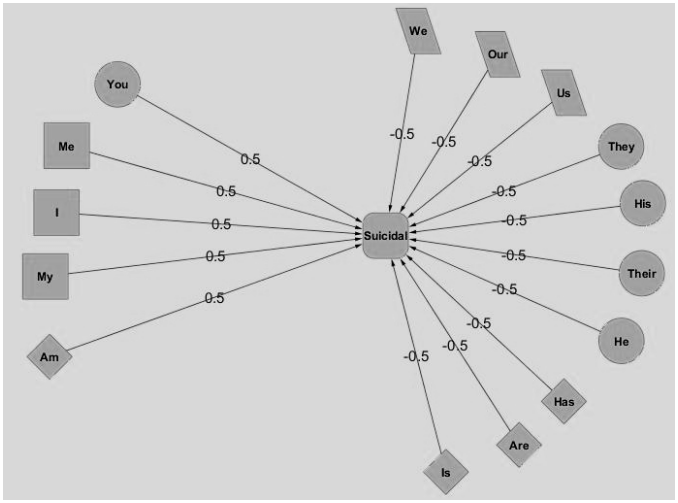

Figure 6. Initial fuzzy cognitive map

Each of the edges has a weight between -1.00 and 1.00 that is attached to it to determine how much influence and what kind of influence a particular node has on the suicidal node. The nodes on the left of Fig. 6 are all the nodes that are associated with suicide notes and thus have a positive influence, while all the nodes on the right represent non-suicide notes and are therefore negative in their influence.

All of the initial weights start at 0.5 or -0.5. This was making the simplifying assumption that all nodes have equal influence on the classification; this simplifying assumption is most likely not correct. However, by starting at this assumption, it can be determined whether or not the general structure of the map is good or bad.

Each of the nodes starts at a particular value between 0.00 and 1.00 and then the graph is allowed to iterate in a computer program until the program either reaches a breaking point or until the graph reaches equilibrium. If the graph has reached equilibrium, then the final value of the suicide node is examined. If the value is over 0.80, i.e. over 80%, then the graph has determined the dataset to be suicidal. If the value is under 30%, then the dataset would be non-suicidal, and if the value is between 30% and 80%, then the classification is uncertain.

The starting values of the nodes were determined by normalizing the data in the particular group, e.g. in Fig. 5, all four datasets would be normalized according to the

archbishop result for the word "is." This means that about 30% is the new 100% which all other values are compared to within that group. Fig. 3 and 4 would have their own number for normalization. The starting number for the suicidal node is 0.00 because it is assumed that there is no initial influence from this node.

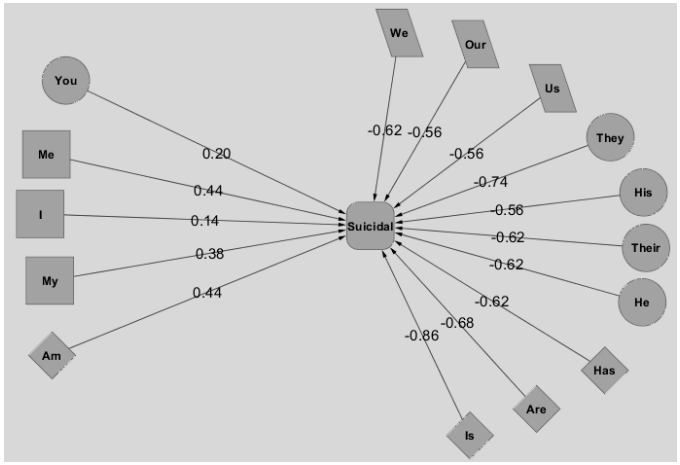

Figure 7. Final fuzzy cognitive map for testing

The final results for the fuzzy cognitive maps for each dataset were not entirely successful. The Amazon.com data was particularly unsuccessful because of its anomalies that made it similar to the suicide notes. Therefore, in order to determine if this map structure can distinguish between the datasets correctly, a set of weights must be found that can find the dividing line. By using machine learning techniques (supervised learning), it was discovered that there is a set of weights which allows the fuzzy cognitive map to correctly classify each dataset. The graph with its final weights is shown in Fig. 7.

IV. TESTING THE FUZZY COGNITIVE MAP

Once a fuzzy cognitive map had been developed that could accurately classify the four datasets, this design was tested against other collections of notes to see if the map could properly classify a random set of data.

A. General Category Testing

Three more datasets were used for testing. These consist of two sets of suicide notes and one non-suicide with each one only a fraction the size of the original four datasets. The first data set was a collection of suicide notes that contains some notes from the original suicide note collection as well as new ones. This was obtained from the website www.well.com/~art/suicidenotes.html and is labeled as suicide notes 2 in the analysis. The second set is a collection of suicide notes from famous actors, poets, and musicians labeled as suicide notes 3 in the analysis that was obtained from the website www.corsinet.com/braincandy/dying3.html. The final dataset is a collection of non-suicide notes from the private blog gregmankiw.blogspot.com. Before going straight into the word analysis, the results for the general categories were compared with the original datasets. This was for the purpose of making sure that all of the datasets are following a predictable pattern. Fig. 8 and 9 show the results for each of the general categories.

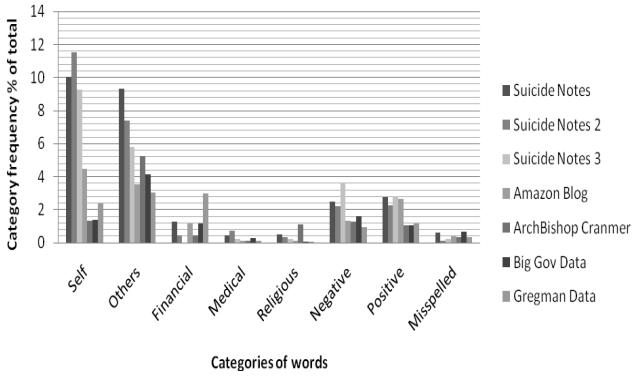

Figure 8. Results of all seven datasets in general categories part 1

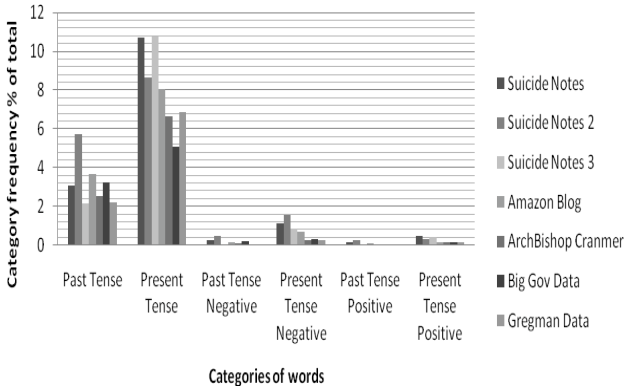

Figure 9. Results of all seven datasets in general categories part 2

As can be seen from Fig. 8 and 9, the three new datasets follow similar patterns in both the suicide and non-suicide cases. Since there were no significant differences, then the specific word analysis could begin.

B. Specific Word Analysis

The final results for the word analysis are shown in Fig. 10, 11, and 12. As can be seen from the graphs, the three new datasets follow the same pattern for their respective classification with the exception of suicide notes 3 which produces some anomalies in the form of very large values in Fig. 12 for the words "is" and "are" which are very close to non-suicide patterns.

Each of the new cases was normalized into the starting values for the nodes of Fig. 7. Each time, the fuzzy cognitive map accurately identified each dataset as either suicidal or non-suicidal. These findings suggest that this fuzzy cognitive map design is somewhat robust in that it was able to handle a random relatively small collection of suicide notes, i.e. suicide notes 3, and correctly identify them as such

even with the non-suicidal like behavior that were found in Fig. 12.

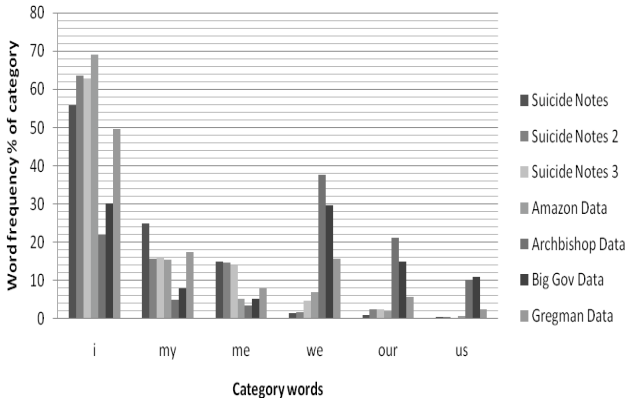

Figure 10. Word densities in self references by percentage

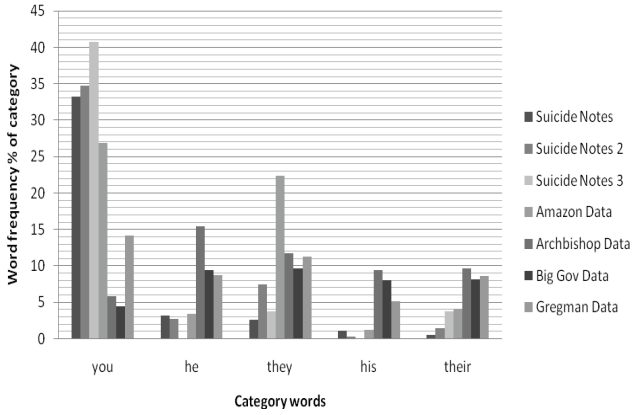

Figure 11. Word densities in others references by percentage

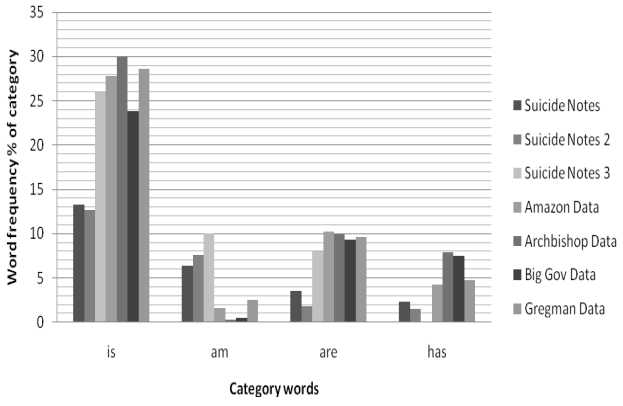

Figure 12. Word densities in present tense by percentage

V. Further Testing

One of the further tests done was an analysis based on gender distinction. A set of male and female notes were taken from the first set of suicide notes and separated to see if gender was a factor in word frequency patterns. In addition, a separate set of male and female suicide notes were taken from [3]. None of these four sets of notes showed any significant difference in word frequency patterns and were correctly identified by the fuzzy cognitive map in Fig. 7. Two non-suicide note collections were then added. The first was from a personal blog colinhughes.blogspot.com that was correctly identified. The second collection was a set of personal letters from the 1820's that were written by patients to Dr. James Carmichael. These were part of a collection from the University of Virginia found at carmichael.lib.virginia.edu. The fuzzy cognitive map was unable to distinguish these notes from the suicide notes. By performing a principle component analysis (PCA), Fig. 13, on the values of the values of the nodes in the map, it is easy to see why the Carmichael notes do not separate.

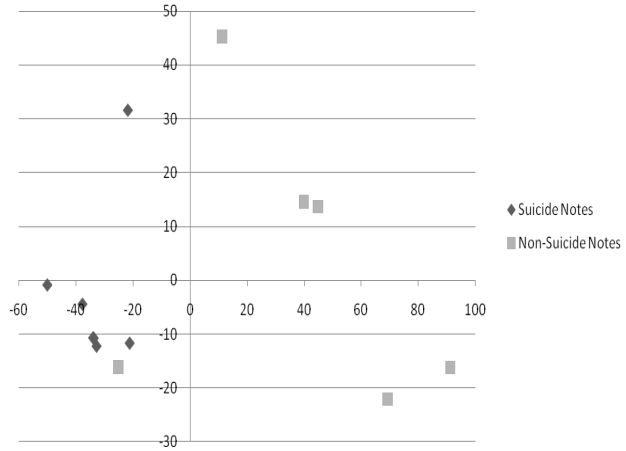

Figure 13. PCA of 13 notes

As can be seen in Fig. 13, the suicide and non-suicide notes are clearly separate from one another with the exception of the Carmichael notes which are found in with the cluster of suicide notes on the bottom left of Fig. 13. One possible explanation for why these particular notes are similar to suicide notes is that suicide notes generally take the form of a personal letter that is directed from one individual to another. This could cause particular word patterns to form that would be similar to other personalized letters. This could be especially true for the words found in the self references and references to others categories.

The problem was solved by adding more words from a new general category. Five more words were chosen from the past tense general category. The five words are "tried," "got," "told," "wanted," and "were." By adding these words, there were enough distinct word patterns that were able to separate the Carmichael notes from the cluster of suicide notes. All that was left to be done was to find a new set of weights that would be able to separate the suicide from the non-suicide notes. After redistributing the weights, the new fuzzy cognitive map, Fig. 14, was able to successfully identify the Carmichael notes as non-suicidal.

Finally, two more sets of personal letters were added to datasets for a total of 15. The first set was a collection of

letters from Alexander Bell to his wife. These were most similar to the Carmichael data. The last dataset was a collection of personal letters from a soldier during the Spanish American War. Both sets came from the digital collection at the Library of Congress. The final results are shown in the PCA of the data, Fig. 15.

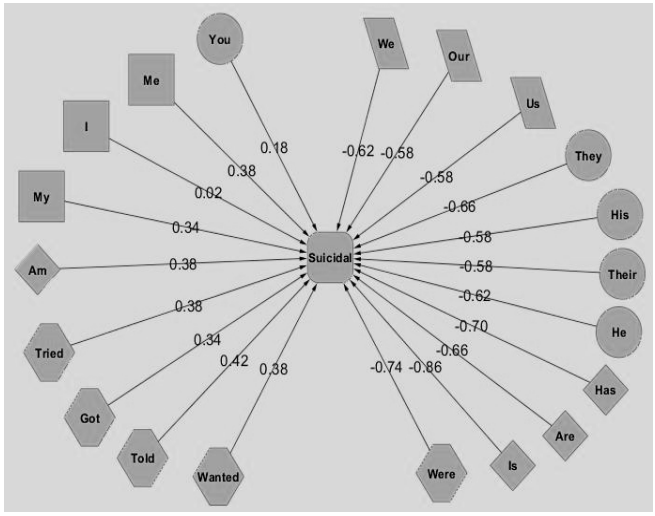

Figure 14. New fuzzy cognitive map

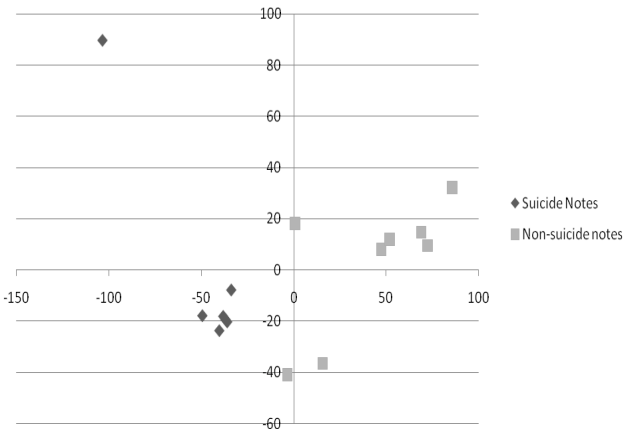

Figure 15. Final results for all 15 datasets

With the addition of the five past tense words, the Carmichael notes have shifted away from the suicide cluster and are almost at the y-axis at y ≈ -40. Immediately to the right is the collection of Alexander Bell's letters. Finally, the Spanish American War letters are found in the cluster on the right hand side of the graph near x ≈ 75.

VI. Conclusion

The results appear to provide strong evidence that it is possible to differentiate between suicidal behavioral patterns and non-suicidal patterns. Further testing must be done in order to ensure that this method can be used in all given situations. Testing needs to be done on age based collections. There is the possibility that notes from adolescents, for example, are different from adults. Another such testing would be an analysis of suicidal ideation or intent to commit suicide [1] which may or may not result in an attempted suicide. Also, further tests can be done from other collections of suicide notes and non-suicide notes that may result in further adjustments to the fuzzy cognitive map.

This work is creative and original because it employed the use of fuzzy cognitive maps based on word frequencies in order to define human behavioral patterns. It is expected that the results of this research can further the understanding of causality discovery in text and the prediction of human behavior. The broad application and positive impact of this work is a further development in the techniques for capturing causal relationships. Identification of causal relationships may allow the ability to predict the consequences of actions from military activities, governmental restructuring or societal rebuilding [2] [4]. In the context of this work, fuzzy cognitive mapping was used to analyze writing and potentially it may be used to predict suicidal acts and allow possible intervention that could save lives.

References

[1] S. Barnow and M. Linden, "Suicidality and tiredness of life among very old persons: Results from the Berlin Aging Study (BASE)," *Archives of Suicide Research*, 1997, pp. 171-182.

[2] B. Kosko, "Fuzzy Cognitive Maps," *Academic Press, Inc.*, vol. 24, 1986, pp. 65-75.

[3] A. A. Leenaars, Suicide Notes Predictive Clues and Patterns, Windsor Ontario, Canada: Human Sciences Press, Inc., 1988.

[4] L. Mazlack, "Approximate Representations In The Medical Domain," *Proceedings of the 2010 IEEE/WIC/ACM International Conference on Web Intelligence*, Toronto, August 31 – September 3, 2010.

[5] A. S. Richardson, H. A. Bergen, G. Martin, L. Roeger and S. Allison, "Perceived Academic Performance as an Indicator of Risk of Attempted Suicide in Young Adolescents," *Archives of Suicide Research*, 9, 2005, 163-176.

[6] B. L. Paulson and R. D. Everall, "The Teen Suicide Research Project," *The Alberta Journal of Educational Research*, 47, 2001, 91-94.

[7] D. Leo, P. A. Hickey, G. Meneghel and C. H. Cantor, "Blindness, Fear of Sight Loss, and Suicide," *Psychosomatics*, 40, 1999, 339-344.

[8] M. Hagiwara, "Extended Fuzzy Cognitive Maps," *IEEE International Conference on Fuzzy Systems*, San Diego, CA, March 8-12, 1992, 795-801.

[9] B. Kosko, 1993, Fuzzy Thinking: The New Science of Fuzzy Logic, Hyperion, New York.

[10] G. D. Weber, "Discovering Causal Relations by Experimentation: Causal Trees," *Proceedings of MAICS*, 1997, 91-98.

[11] J. Pearl and T. S. Verma, "A Theory of Inferred Causation," *Second International Conference on the Principles of Knowledge Representation and Reasoning*, 1991, 441-452.

[12] S. Stromsten, "First-Order Causal Knowledge," 2003.

[13] D. Buchsbaum, A. Gopnik, T. L. Griffiths and P. Shafto, "Children's Imitation of Causal Action Sequences is Influenced by Statistical and Pedagogical Evidence," *Cognition*, In Press, Corrected Proof, 2011.

[14] K. Chan and W. Lam, "Extracting Causation Knowledge from Natural Language Texts," *International Journal of Intelligent Systems*, 20, 2005, 327-358.

[15] H. Sakaj, S. Sekine and S. Masuyama, "Extracting Causal Knowledge Using Clue Phrases and Syntactic Patterns," *Proceedings of the 7th International Conference on Practical Aspects of Knowledge Management*, Springer-verlag, Berlin, 2008, 111-122.

[16] R. Girju, "Automatic Detection of Causal Relations for Question Answering," *Proceedings of the ACL 2003 workshop on Multilingual Summarization and Question Answering*, 2003, 76-83.

[17] C. S. G. Khoo, S. Chan and Y. Niu, "Extracting Causal Knowledge from a Medical Database Using Graphical Patterns," *Proceedings of the 38th Annual Meeting on Association for Computational Linguistics*, Hong Kong, Association for Computational Linguistics, Stroudsburg, PA, USA, 2000, 336-343.

[18] W. Buntine, "A Guide to the Literature on Learning Probabilistic Networks from Data," *IEEE Transactions on Knowledge and Data Engineering*, 8, 1996, 195-210

2011 IEEE International Conference on Fuzzy Systems
June 27-30, 2011, Taipei, Taiwan

Constant Penalty Functions to Simplify Optimization of the Choquet Integral under Constraints

Tanja Magoč
Center for Bioinformatics and Computational Biology
University of Maryland
College Park, MD
Email: t.magoc@gmail.com

***Abstract*—The Choquet integral have been used in many decision making problems as the optimization function that needs to be maximized or minimized. The complexity of these optimization problems is often increased by numerous constraints that are imposed to the solution. Several methods have been developed for optimization under constraints, one of them being penalty functions method. This method transforms a constrained optimization problem in an equivalent unconstrained optimization problem by adding penalties to the solutions that do not satisfy one of more constraints. Penalty functions method is an iterative process, which adjusts penalty functions in each iteration, often yielding a large number of iterations until a satisfying solution is found. To speed the process of the Choquet integral optimization under constraints, we propose to use constant penalty functions. This approach requires only one iteration, and is therefore much faster than the generic penalty function method. In this paper, we derive the constant penalty function that guarantees that the optimal solution found in the first iteration satisfies all constraints.**

Keywords-the Choquet integral; optimization; constant penalty function; decision making

I. Introduction

The Choquet integral has often been used as an optimization function in decision making such as finance [1], geographic information systems [2], evaluation of mental workload [3], and environmental structure evaluation [4]. Many real-life and scientific problems can be formulated in terms of decision making. Some decisions are relatively straightforward. However, other problems may require more strategizing such as in the case of decision under uncertainty and multi-criteria decision making. Multi-criteria decision making seeks an optimal solution among a set of alternatives that are characterized by several attributes, i.e., criteria. For example, if an individual wants to buy a car, this individual would most probably consider the price, miles per gallon, safety rating, color, and other characteristics of cars. The first difficulty faced with different criteria used to make decisions is the domain of values that each criterion could take. Some criteria take qualitative values while others take quantitative values that might be discrete or continuous. The color could be expressed using qualitative values (.e.g., {red, blue, black}); the safety rating could be expressed using discrete integers representing the number of stars rating a car's safety (e.g., {1,2,3,4,5}); and the price could be expressed in terms of a continuous variable taking values within an interval (e.g., [11000,50000]).

Furthermore, a decision maker usually has preferences within each criterion in terms of the values he/she would rather choose compared to other possible values of the criterion. For example, a car buyer would like to buy the car that is the cheapest, has the highest safety rating, travels the most miles per gallon of gas, and is of the decision buyer's favorite color. However, only in miracle situations, an available alternative (e.g., a car) is characterized by the best value for each criterion. In general, the alternative that reaches the maximum value of one attribute does not reach the maximum value of another attribute (e.g., the cheapest car usually does not have five stars safety rating). Thus, a decision maker has to accept some tradeoff between criteria, and maximize the total payoff of choosing a particular alternative. The total payoff could be calculated in various ways. Maximax, maximin, weighted sum, and the Choquet integral are most commonly used methods to combine values of each criterion into a global value. While maximax, maximin, and weighted sum are attractive approaches in decision making situation where criteria are mutually independent, the Choquet integral is well suited for situations where there are dependences between criteria used in decision making. Different approaches have been employed to optimize the Choquet integral including genetic algorithm [5], branch and bound method [6], and particle swarm optimization technique [7].

In many situations, certain constraints are imposed to the possible solution, which results in a more complex optimization problem. Numerous methods have been developed to deal with constraints while optimizing a function including simplex method ([8],[9]), Lagrange multiplier approach ([10],[11]), branch and prune method [12], and penalty functions technique [13]. The method of penalty functions relies on adding the penalty (i.e., decreasing the value of a maximizing function, or increasing the value of a minimizing function) at the points or intervals that do not satisfy constraints. Typically, the penalty function is defined as a polynomial (often the first degree polynomial) function of the inputs representing the values of the criteria considered in the decision making. The coefficients of the penalty function are adjusted in each iteration of the optimization process. However, in some situations, this functions could be replaced by a constant function, which simplifies optimization process while guaranteeing that the points not satisfying the constraint will not be selected as an

978-1-4244-7316-8/11/$26.00 ©2011 IEEE

optimal solution.

In this paper, we first present the basics of the Choquet integral and its use in multi-criteria decision making (section 2). In the section 3, we present a few common constraints to an optimizing function such as the Choquet integral. The common method of penalty functions to deal with constraints is presented in the section 4. Finally, in the section 5, we describe how a constant function could be used as a penalty function in optimizing the Choquet integral. We conclude the paper with future work in extending the proposed method to other optimizing functions.

II. The Choquet Integral as the Optimization Function in Multi-Criteria Decision Making

A multi-criteria decision making (MCDM) problem seeks the optimal choice among a (usually finite) set of alternatives. It can formally be defined as a triple $(X, I, (\succeq_i)_{i\in I})$ where

- $X \subset X_1 \times \cdots \times X_n$ is the set of alternatives with each set X_i representing a set of values of the criterion i.
- I is the (finite) set of criteria (or attributes).
- $\forall i \in I$, $\succeq_i$ is a preference relation (a weak order) over X_i.

The next task is to "combine" the partial preference relations $\succeq_i$ of an alternative into a global value for the alternative such that the final order of the alternatives is in the agreement with the decision maker's partial preferences. The natural way to construct a global preference is by using a utility function for each criterion to reflect partial preferences of a decision-maker, and then combine these monodimensional utilities into a global utility function using an aggregation operator. The utility functions

$$u_i : X_i \to \mathbb{R} \tag{1}$$

such that

$$\forall x_i, y_i \in X_i, u_i(x_i) \geq u_i(y_i) \text{ if and only if } x_i \succeq_i y_i \tag{2}$$

map the values of all attributes onto a common scale (often the interval [0,1]). The existence of monodimensional utility functions is guaranteed under relatively loose hypotheses by the work presented in [14].

Numerous aggregation operators could be used to combine monodimensional utilities into a single number that represents the value of an alternative. Two simple approaches that correspond to optimistic and pessimistic behavior of the decision maker are maximax and maximin strategies, respectively, assuming that the goal of a decision-maker is to maximize the utility. The maximax method compares the utilities of all criteria of an alternative and chooses the highest utility value, $\max_i u_i(x_i)$, to represent the global utility of the alternative $\mathbf{x} = (x_1, ..., x_n)$. This approach reflects an optimistic behavior of the decision-maker since he/she is concerned only with the attribute that has the highest utility for the given alternative. The maximax method tries to maximize the best criterion:

$$\max_{\mathbf{x}\in X}(\max_{i\in\{1,...,n\}} u_i(x_i)). \tag{3}$$

On the contrary, the maximin method reflects a pessimistic behavior of the decision-maker as the decision-maker is concerned only with the criterion that could result in the worst value. This method compares the utilities of all attributes of an alternative and chooses the lowest utility value, $\min_i u_i(x_i)$, to represent the global utility of the alternative $\mathbf{x}$. The decision-maker tries to maximize the value of the worst case scenario:

$$\max_{\mathbf{x}\in X}(\min_{i\in\{1,...,n\}} u_i(x_i)). \tag{4}$$

To allow for a position between these extremes when making a decision, a simple combination of maximax and maximin approaches is achieved by a weighted aggregation operator, named Hurwicz criterion [15],

$$\max_{\mathbf{x}\in X}(\alpha \max_i u_i(x_i) + (1-\alpha)\min_i u_i(x_i)), \tag{5}$$

where $\alpha \in [0, 1]$ is the weight given by the decision maker. This approach simplifies to the optimistic case if $\alpha = 1$ and to the pessimistic case if $\alpha = 0$.

These simple approaches are very tempting to use for quick decisions. However, they focus only on one or two criteria and ignore the impact of other characteristics of alternatives. This approach often does not suit a given situation in which a decision has to be made. Thus, we usually need to consider more complex aggregation operators that take into consideration all attributes. The simplest and most natural of them is a weighted sum approach, in which the decision-maker is asked to provide weights, w_i, that reflect the importance of each criterion. Thus, the global utility of the alternative $\mathbf{x} = (x_1, ..., x_n) \in X$ is given by

$$u(\mathbf{x}) = \sum_{i=1}^{n} w_i u_i(x_i). \tag{6}$$

The best alternative is the one that maximizes this value. Even though this approach is attractive due to its low complexity, it can be shown that using an additive aggregation operator, such as weighted sum, is equivalent to assuming that all the attributes are independent [16]. In practice, this is usually not realistic and therefore, we need to turn to non-additive approaches, that is to aggregation operators that are not linear combinations of partial preferences.

Before approaching non-additive methods, we give the definition of a non-additive measure, a tool for building non-additive aggregation operators such as the Choquet integral. For practical purposes, we restrict ourselves to measures defined on a finite set I.

Definition 1. [Non-additive (fuzzy) measure]: *Let I be the set of attributes and $\mathcal{P}(I)$ the power set of I. A set function $\mu : \mathcal{P}(I) \to [0, 1]$ is called a non-additive measure (or a fuzzy measure) if it satisfies the following three axioms:*

(1) $\mu(\emptyset) = 0$ *: the empty set contains no information.*
(2) $\mu(I) = 1$ *: the maximal set contains all the information.*
(3) $\mu(B) \leq \mu(C)$ *if B, $C \subset \mathcal{P}(I)$ and $B \subset C$: a new criterion added cannot make the importance of a coalition (a set of criteria) diminish.*

A non-additive integral, such as the Choquet integral [17], is a type of a general averaging operator that can model the behavior of a decision maker. The decision-maker provides a set of values of importance, this set being the values of the non-additive measure on which the non-additive integral is computed from. Formally, the Choquet integral in finite case is defined as follows:

Definition 2. [Choquet integral]: *Let μ be a fuzzy measure on $(I, \mathcal{P}(I))$ and an application $f : I \to \mathbb{R}^+$. The Choquet integral of f w.r.t. μ is defined by:*

$$(C)\int_I f d\mu = \sum_{i=1}^{n}(f(\sigma(i)) - f(\sigma(i-1)))\mu(A_{(i)}), \qquad (7)$$

where σ is a permutation of the indices in order to have $f(\sigma(1)) \leq \cdots \leq f(\sigma(n))$, $A_{(i)}$ is $A_{(i)} = \{\sigma(i), \ldots, \sigma(n)\}$, and $f(\sigma(0)) = 0$, by convention.

It can be shown that many aggregation operators can be represented by Choquet integrals with respect to some fuzzy measure. Although the Choquet integral is well suited for quantitative measurements, it has a major drawback. The decision maker needs to input a value of importance of each subset of attributes, that is total of 2^n values, which is intractable due to its exponential complexity. However, we can overcome intractability by using 2-additive measure to limit the complexity to a $O(n^2)$ (as shown in [18]) and still get accurate results.

Before giving the definition of a 2-additive measure, we need to define notion of interaction indices of orders 1 and 2. The importance of a criterion (or the interaction index of degree 1) is best described as the value this attribute brings to each coalition it does not belong to. It is given by the Shapley value [19]:

Definition 3. [Shapley value]: *Let μ be a non-additive measure over I. The Shapley value of index i is defined by:*

$$v(i) = \sum_{B \subset I \setminus \{i\}} \gamma_I(B)[\mu(B \cup \{i\}) - \mu(B)] \qquad (8)$$

with

$$\gamma_I(B) = \frac{(|I| - |B| - 1)! \cdot |B|!}{|I|!} \qquad (9)$$

and $|B|$ denoting the cardinal of B.

While the Shapley value gives the importance of a single attribute to the entire set of attributes, the interaction index of degree 2 represents the interaction between two attributes, and is defined by ([20],[21]):

Definition 4. [Interaction index of degree 2]: *Let μ be a non-additive measure over I. The interaction index between i and j is defined by:*

$$I(i,j) = \sum_{B \subset I \setminus \{i,j\}} (\xi_I(B) \cdot (\mu(B \cup \{i,j\}) - \mu(B \cup \{i\}) - \mu(B \cup \{j\}) + \mu(B))$$

with

$$\xi_I(B) = \frac{(|I| - |B| - 2)! \cdot |B|!}{(|I| - 1)!}. \qquad (10)$$

The interaction indices belong to the interval $[-1, +1]$ and

- $I(i,j) > 0$ if the attributes i and j are complementary;
- $I(i,j) < 0$ if the attributes i and j are redundant;
- $I(i,j) = 0$ if the attributes i and j are independent.

Even though we can define interaction indices of any order, defining the importance of attributes and the interaction indices between two attributes is generally enough in multi-criteria decision making problems. Thus, 2-additive measures constitute a feasible and accurate tool in this setting. The formal definition of a 2-additive measure follows [20]:

Definition 5. [2-additive measure]: *A non-additive measure μ is called 2-additive if all its interaction indices of order equal to or larger than 3 are null and at least one interaction index of degree two is not null.*

It has been shown [22] that the Shapley values and the interaction indices of order two offer us an elegant way to represent a Choquet integral. Therefore, in a decision-making problem, we can ask the decision maker to give the Shapley values, I_i, and the interaction indices, I_{ij}, and then use the Choquet integral with respect to a 2-additive measure, μ, to obtain the aggregation operator:

$$\begin{aligned}(C)\int f d\mu = &\sum_{I_{ij}>0} (f(i) \wedge f(j))I_{ij} \\ &+ \sum_{I_{ij}<0} (f(i) \vee f(j))|I_{ij}| \\ &+ \sum_{i=1}^{n} f(i)(I_i - \frac{1}{2}\sum_{j \neq i} |I_{ij}|).\end{aligned}$$

This form of the Choquet integral is a practical approach to many multi-criteria decision making situations ([1],[2],[3],[4]).

III. Examples of Constraints

Numerous constraints could be imposed on the input variables (i.e., variables representing the values of criteria in multi-criteria decision making). A typical constraint in many optimization problems is that (some) variables could not take negative values, $x_i \geq 0$. As we have seen in the previous section, the values of variables in a multi-criteria decision making are often mapped to the interval [0,1]; thus the non-negativity constraint is imposed to all variables. Moreover, in this particular situation, the maximum value of each variable is

1, thus another constraint should be imposed to each variable, $x_i \leq 1$.

However, not every constraint should be imposed to all variables. For example, when buying a car, we might want to buy a car only if it is relatively safe, so we might decide to consider only cars with a safety rating of at least three stars. Using utility functions, the rating of 3 stars would map to the value of 0.5. Thus, the constraint that we need to consider is $x_{\text{safety}} \geq 0.5$.

All of the above examples of constraints are hard constraints, so they must always be satisfied. On the other hand, there might be soft constraints, which we would like to be satisfied, but it is not necessary that they are satisfied. For example, we might not want to buy a car that costs more than $20,000, thus yielding the constraint $x_{\text{price}} \leq 20,000$. However, if there is a great deal available for a car that is a bit more expensive, we might be willing to somewhat sacrifice this soft constraint and buy a car that doesn't satisfy this constraint.

Finally, a constraint does not have to be imposed to only a single variable. It could be imposed to a combination of variables, such as a sum of two or more variables. Let us consider the problem of selecting an optimal financial investment portfolio where the variables represent the portion of money invested in each financial investment assets. A multi-criteria decision making problem is designed to determine the best distribution of money among n assets so that the largest amount of money will be earned in a year [2]. Certain amount of money needs to be invested in each of n assets in order to reduce risk of losing all money ([23],[24]) (we assume here that the n assets were previously selected from thousands of investment assets that exist in the world, so that n is a realistic number for the size of an investment portfolio). Thus, all the variables should be positive (rather than just non-negative), $x_i > 0$, and strictly smaller than 1, $x_i < 1$, since not all money could be invested in the same asset. Moreover, not more than all money could be invested in the portfolio (we are making simplifying assumptions that an investor can not borrow money from one institution to invest it in another asset), thus the sum of all money should be no more than 1 (i.e., 100% of money), $\sum_{i=1}^{n} x_i \leq 1$. This is a typical example of a hard constraint when the value of one variable depends on the values of other variables.

Soft constraints could also be imposed to the variables that depend on each other. For example, we might require that at least 50% of all money is invested in the financial assets, $\sum_{i=1}^{n} x_i \geq 0.5$. However, in some situations (e.g., in economic recessions, gain of investing money could be very low compared to the risk of investing money), we might accept to invest smaller amount of money if no good investment option is available.

Even though the presented examples are all represented by linear inequalities, a more complex constrains could be imposed to the solution of an optimization problem.

IV. Penalty Functions

Several methods have been developed to deal with constraints imposed to the solution of an optimization problem. The method of penalty functions ([11],[13]) transforms a constrained optimization problem into an unconstrained optimization problem, which is accomplished by adding penalties in a minimization problem (or subtracting penalties in a maximization problem) to the solutions that do not satisfy one or more constraints. A penalty function is assigned to each constraint and is adjusted through iterative process of the algorithm. Each penalty function is designed so that its value is equal to 0 if the constraint is satisfied, and greater than 0 if the constraint is not satisfied. Let $c_i(\mathbf{x})$ be the i^{th} constraint. Then the penalty function is defined as:

$$p_i(\mathbf{x}) = 0 \text{ if } c_i(\mathbf{x}) \text{ is satisfied.}$$
$$p_i(\mathbf{x}) > 0 \text{ if } c_i(\mathbf{x}) \text{ is not satisfied.} \quad (11)$$

Let us consider a constrained optimization problem:

maximize $f(\mathbf{x})$

subject to the following constraints:

$$g_i(\mathbf{x}) \geq 0, i = 1, \ldots, m;$$
$$h_j(\mathbf{x}) = 0, j = 1, \ldots, s.$$

This problem is transformed into maximizing the function $f'(\mathbf{x}) = f(\mathbf{x}) - \sum_{i=1}^{m} r_i(\mathbf{x}) - \sum_{j=1}^{s} q_j(\mathbf{x})$, where r_i and q_j are penalty functions. The goal of penalty functions is to decrease the values of the objective function at the elements of the search space that do not satisfy all the constraints. However, finding the maximum of the function $f'(\mathbf{x})$ does not guarantee that the solution is found since the maximum of this function still might not satisfy all the constraints. In order to find a solution that maximizes the objective function and satisfies all the constraints, the penalty functions are changed and the objective function is evaluated again. The process is iterated until an optimal solution that satisfies all the constraints is reached.

The method could be simply described by the following algorithm:

```
PenaltyFunctions
{
   for each constraint
   {
      initialize penalty function
   }
   while (solution not found)
   {
      evaluate objective function
      for each constraint
      {
       add penalties to objective function
      }
      increase penalty functions
   }
}
```

Note that each minimization problem, $min\ f(\mathbf{x})$, could be transformed in the maximization problem $max\ (-f(\mathbf{x}))$. Thus, in this paper, without loss of generality, we assume that we have a maximization problem.

V. A Constant Penalty Function to Optimize the Choquet Integral with Respect to a 2-additive Measure

Even though the penalty functions method could be very effective in solving constrained optimization problems, it suffers a few drawbacks, one of them being the complexity of selecting a good starting penalty function. It is not clear how to initialize a penalty function. The most common approach used to define a penalty function is to square the subrange of the objective function that does not satisfy the constraint. The next question is how to adjust the penalty functions after each iteration of the optimization process. Usually, the adjusted penalty function is simply a multiply of the original penalty function. However, this method might lead towards numerous iterations until the optimal solution is found, which yields another drawback, namely how to define the end of the iterative optimization process.

While the general form of the penalty function method is designed so that it could be applied in any constrained optimization problem regardless of the type of the optimization function, it sometimes takes a large amount of time to obtain the optimal solution. Instead, the penalty function could be defined by a much simpler form such as a constant function. This form is well suited for optimization functions that are bounded on the entire interval that input variables could take. Note that it is enough that the optimization function be bounded from above in an maximization problem, and from below in a minimization problem. One such an optimization function is the Choquet integral with respect to a 2-additive measure constructed by the utility method, which maps the values of all criteria to the interval [0,1] (as described in the section 2).

In this situation, the penalty applied should be a value that is greater or equal to any value that the Choquet integral with respect to a 2-additive measure could possibly take. The reason for this penalty is that if the constraint is not satisfied at a particular point in the search space, we do not want to consider this point as a possible solution to the problem since the problem becomes impractical if a (hard) constraint is not satisfied. Thus applying the penalty whose value is larger than the maximum value the Choquet integral could theoretically take will ensure that the value of the objective function is a negative value and therefore will certainly not be selected as a maximum value.

To determine the value of the penalty, let us consider the formula of the Choquet integral with respect to a 2-additive measure:

$$(C)\int f d\mu = \sum_{I_{ij}>0} (f(i) \wedge f(j)) I_{ij} + \sum_{I_{ij}<0} (f(i) \vee f(j)) |I_{ij}| + \sum_{i=1}^{n} f(i)(I_i - \frac{1}{2}\sum_{j\neq i} |I_{ij}|).$$

If we consider the first two sums, we conclude that each interaction index of order 2 is covered by at most one of the sums (the interaction indices of 0 are not covered at all). Each element of each summation is a minimum or a maximum of two utility values multiplied by the absolute value of the corresponding interaction index of order 2. Each utility value and the absolute value of each interaction index belong to the interval [0,1]. Using interval computation arithmetics (see e.g., [25]), we conclude that each element of any of the first two summation is at most equal to one. The maximum number of elements in two summations is the number of interaction indices of order 2, which is $\frac{n\cdot(n-1)}{2}$, where n is the number of criteria considered. Further, the third summation is the multiplication of a Shapley value and a utility value decreased by a certain amount. Thus, to find its maximum value, we can disregard the subtracted part, and only find the maximum value of the utility value multiplied by a Shapley value. As both of these values fall into the interval [0,1], the maximum value of each element of the third summation is one, and thus, the value of the summation can not exceed n. The maximum value that the Choquet integral can theoretically take is therefore the sum of the maximum value the first two sums could take, $\frac{n\cdot(n-1)}{2}$, and the maximum value the third sum could take, n:

$$\frac{n\cdot(n-1)}{2} + n = \frac{n^2+n}{2} < \frac{n^2+n^2}{2} = n^2. \quad (12)$$

Thus, the penalty that should be applied for a violation of each hard constraint should be equal to at least n^2 to ensure that even if just one constraint is not satisfied at a particular point, the penalty will decrease the value of the optimization function at this point below zero, and therefore this point will surely not yield the maximum value of the optimization function.

However, when considering soft constraints, we would like that they are satisfied, but would accept a solution that yield an optimal value even if the soft constraint is not satisfied. In this situation, we could consider a lower penalty function for soft constraints than for hard constraints. Moreover, since we would allow an optimal solution to not satisfy soft constraints, we do not want to decrease the value of the optimization function below zero if only one soft constraint is not satisfied. In some situations, we might allow for multiple soft constraints to be unsatisfied. If we allow i soft constraints to be unsatisfied, the constant penalty function should be defined as

$$\frac{n^2}{i-1}. \quad (13)$$

The proposed penalty function will assure that if i soft constraints are unsatisfied, the optimization function still might

yield a positive value; however, if the $(i+1)^{\text{th}}$ soft constraint is not satisfied, the optimization function will yield a non-positive value.

Furthermore, if not all soft constraints have the same importance, we might define penalty functions differently for each soft constraints. For example, if not satisfying a soft constraint $C1$ is less important than not satisfying a soft constraint $C2$, then the penalty function for the constraint $C1$ should be smaller than the penalty function for the constraint $C2$.

Finally, in some situations, we might prefer a solution that barely missed to satisfy a soft constraint over a solution that is far from satisfying a soft constraint. In these situations, we apply a penalty function to the objective function. However, the constant penalty function is increased by the distance from satisfying the constraint. The distance is usually calculated as the Euclidean distance between the proposed solution and the constraints.

VI. Conclusion

Numerous situation is life require decision making of some sort. Some situations are so simple that we do not even realize that we are making a decision. However, many situations require more strategies to be employed when making a decision. Different approaches have been taken to select an optimal alternative among available options, one of them being the Choquet integral with respect to a 2-additive measure, which is especially well suited for situations where criteria considered in making decision are mutually dependent.

Optimization of the Choquet integral is not a trivial process itself. The complexity of this process is increased even more by imposing constraints to possible solutions. The constraints could range from simple linear equalities or inequalities applied to one variable at a time to non-linear equalities or inequalities that combine multiple variables. Moreover, constraints could be hard (i.e., constraints that must be satisfied) or soft (i.e., constraints that we would like to be satisfied, but would accept that some of them not be satisfied if that yields a much better optimal solution than if these constraints were satisfied).

Numerous approaches have been used to deal with constraints, one of them being the penalty functions method, which adds penalty to the value of the optimization function if a constraint is not satisfied by subtracting (adding in minimization problem) the value of the penalty function from the maximizing function. The penalty functions method could result in a large number of iterations due to difficulty in adjusting the penalty from one iteration to another. To simplify this method, a constant penalty function could be applied when maximizing the Choquet integral since the Choquet integral is bounded from above. In the case of hard constraints, the penalty function should take the value n^2, where n is the number of criteria used in the decision making problem to ensure that each point that does not satisfy even one hard constraint will yield a non-positive value, and therefore will not be selected as an optimal value. In the case of soft constraints, the constant penalty function should be defined in proportion to the number of soft constraints allowed, and could also be increased based on the distance from satisfying the constraint to give a better chance of being selected as the optimum to points that are closer to satisfying the constrains than the points that are further away from satisfying the constraints.

In this paper, we presented how constant penalty functions could be used in the optimization of the Choquet integral with respect to a 2-additive measure. However, a similar approach could be applied to any other function that is bounded from above in the maximization problem, or bounded below in a minimization problem.

References

[1] T. Magoc, "New algorithms for optimal portfolio selection," Ph.D. dissertation, University of TExas at El Paso, 2009.

[2] T. Magoc, A. Kassin, and R. Romero, "A line of sight algorithm using fuzzy measures," *Proceedings of the North American Fuzzy Information Processing Society Annual Meeting*, 2010.

[3] M. Grabisch, H. Prade, E. Raufaste, P. and Terrier, "Application of the Choquet integral to subjective mental workload evaluation," it Automated Systems Based on Human Skill and Knowledge, vol. 9, no. 1, 2008.

[4] Y. Nakamori and N. Iwamoto, "Analysis of environmental evaluation structure by the Choquet integral model," *International Joint Conference of the 4th IEEE International Conference on Fuzzy Systems and the 2nd International Fuzzy Engineering Symposium*, 1995.

[5] I. Saad, S. Hammadi, M. Benrejeb, and P. Borne, "Choquet integral for criteria aggregation in the flexible job-shop scheduling problems," *Mathematics and Computeres in Simulation*, vol. 76, no, 5-6, 2008.

[6] L. Galand, P. Perny, P., and O. Spanjaard, "A branch and bound algorithm for Choquet optimization in multicriteria problems," *Multiple Criteria Decision Making for Sustainable Energy and Transportation Systems*, vol. 634, no. 4, pp. 355-365, 2010.

[7] T. Xiao, N. Zhang, and D.-M. Huang, "Solution to the model of nonlinear multiregression based on generalized Choquet integral and its application in estimating forest volume," *Proceedings of the 2010 International Conference on Computer Application and System Modeling*, 2010.

[8] G. B. Dantzig, "Maximization of alinear function subject to linear inequalities," in T. C. Koopmans (ed.), *Activity Analysis of Production and Allocation*, John Wiley & Sons, New York, 1951, pp. 339-347.

[9] D. Gale, "Linear programming and the simplex method," *Notices of the AMC*, 2007, vol. 54, no. 3, pp. 364-369.

[10] G. Arfken, "Lagrange multipliers", in *Mathematical methods for physicists*, 3^{rd} ed. Orlando, Florida: Academic Press, 1985, pp. 945-950.

[11] G. Thomas and N. Sonilah, "Use of penalty function or Lagrange multipliers for constrained deconvolution," pp. 1559-1562.

[12] A. Goldsztejn, "A branch and prune algorithm for the approximation of non-linear AE-solution set," Proceedings of the 2006 ACM Symposium on Applied Computing, 2006.

[13] A. E. Smith and D. W. Coit, "Penalty functions," *handbook of evolutionary computataion*, joint publication of Exford University Press and Institute of Physics Publishing, 1995.

[14] D. Krantz, R. Luce, P. Suppes, and A. Tverski, *Foundations of measurement*. Academic Press, 1971.

[15] J.-Y. Jaffray and M. and Jeleva, "Information processing under imprecise risk with the Hurwicz criterion," *Proceedings of International Sumposium on Imprecise Probability: Theories and Applications*, Prague, Czeck Republic, 2007.

[16] F. Modave and M. Grabisch, "Preferential independence and the Choquet integral," 8^{th} *International Conference on the Foundations and Applications of Decision Under Risk and Uncertainty*, Mons, Belgium, 1997.

[17] G. Choquet, "Theory of capacities," *Annales de l'Institut Fourier*, no. 5, 1953.

[18] M. Ceberio and F. Modave, "Interval-based multicriteria decision making," in *Modern Information Processing: from Theory to Applications*, B. Bouchon-Meunier, G. Coletti, and R. R. Yager (Editors), Elsevier ed., 2006.

[19] L. S. Shapley, "A value for n-person games," in *Contributions to the Theory of Games*, H. W. Kuhn and A. W. Tucker (Editors), no. 2, pp. 307-317, Princeton University Press, 1953.

[20] D. Denneberg and M. Grabisch, "Shapley value and interaction index," *Mathematics of Interaction Index*, 1996.
[21] M. Grabisch and M. Roubens, "Application of the Choquet integral in multicriteria decision making," in *Fuzzy Measures and Integrals: Theory and Applications*, M. Garbisch, T. Murofushi, and M. Sugeno (Editors), Physica Verlag, 2000.
[22] M. Grabisch, "The interaction and Mobius representation of fuzzy measures on finite spaces, *k*-additive measures: a survey," in *Fuzzy measures and integrals: Theory and applications*, M. Grabisch, T. Murofushi, and M. Sugeno (Editors), Physica Verlag, 2000.
[23] J. Estrada, *Finance in a nutshell: A no-nonsense companion to the tools and techniques of finance*. Prentice Hall, 2005.
[24] D. Kansas, *The Wall Street Journal: Complete money & investing guide book*. Three Rivers Press, New York, 2005.
[25] L. Jaulin, M. Kieffer, O. Didrit, and E. Walter, *Applied Interval Analysis, with Examples in Parameter and State Estimation, Robust Control and Robotics*. Springer-Verlag, London, 2001.

2011 IEEE International Conference on Fuzzy Systems
June 27-30, 2011, Taipei, Taiwan

Design of a Reliable Hub-and-spoke Network Using an Interactive Fuzzy Goal Programming

Mohammad Hossein Fazel Zarandi, Soheil Davari
Department of Industrial Engineering
Amirkabir University of Technology
Tehran, Iran
zarandi@aut.ac.ir; soheildavari@ieee.org

Ali Haddad Sisakht
Department of Industrial Engineering,
Sharif University of Technology
Tehran, Iran

***Abstract*. A Hub Location Problem (HLP) deals with finding the locations of hub facilities and assignment of demand nodes to established facilities. Hubs play a central role in many networks such as telecommunication networks and their unavailability may lead to network breakdown or poor service levels. An objective in design of a hub-and-spoke network is maximization of reliability to transfer flows. This paper puts forward design of a reliable single-allocation hub-and-spoke network using an interactive fuzzy goal programming. To model and solve the problem, a fuzzy goal programming approach was developed for design of network in an interactive manner between decision maker and the model. To validate the model and the proposed solution approach, a test problem is presented and comparison of results is made using this problem.**

Keywords. Reliable hub location problem, Interactive decision making, Fuzzy goal programming, Network design, Bi-objective programming.

I. INTRODUCTION

Decisions are usually categorized as strategic, tactical and operational. A strategic or long-term decision does not take place on a regular basis and needs major capital investments. An example of a long-term decision is determination of facility location ([1]). Facility Location (FL) has been an important concern for around 100 years. Applications of FL could be found in both public and private sectors, since more and more managers realize the importance of decisions made concerning location of facilities.

Hub location problem (HLP) has been an attractive, yet tricky variant of facility location. It arises in many different contexts such as telecommunications, cross-docking, airline industry, computer networks, etc. For example, nowadays many LTL trucking companies designed their networks based on the hub-and-spoke structure. This has led to better efficiency and improved service levels. In a typical HLP, the following questions are to be answered: a) Where to locate hub facilities b) How to allocate demand nodes to hubs, so the objective of the whole network is optimized. Since these decisions are interconnected, their separation may easily lead to sub-optimal results. Therefore, these questions are to be considered in a single model.

HLPs are often categorized as single-allocation and multiple allocation types. While in a single-allocation HLP, each spoke is allocated to one and only one hub node, in the multiple-allocation case, a spoke may be allocated to more than one hub. In this paper, a single-allocation HLP will be studied. Another interesting issue to be considered in design of hub-and-spoke networks is the discount factor associated with arcs which is a value between zero and one to represent the economies of scale. Generally, a flow in a hub-and-spoke network is in accordance with one of the seven types shown in fig. 1. In each of these types, the reliabilities of hubs and arcs play a pivotal role in a successful, on-time delivery of flow. Since hubs and arcs in a network are liable to disruption, design of a reliable network is of great value to decision makers. Kim and O'Kelly [2] proposed the reliable hub location problem and presented two models. As far as we know, this subject has not been considered much to date.

Perez et al. [3] claimed that real applications of facility location can be full of linguistic vagueness that can be appropriately modeled using fuzzy variables. In a HLP, many parameters could not be determined precisely such as demands, distances or reliabilities. In addition, it is sometimes difficult to describe parameters such as reliability as random variables. In these situations, fuzzy logic has been proven to be useful. However, reviewing the literature of HLP, we came to notice that the fuzzy version of HLP has gained little attention.

The rest of this paper is organized as follows: In the preceding section, a brief literature review of HLP and its recent publications is presented. Then, the mathematical formulation of this paper will be proposed. Section 4 is devoted to a brief introduction of fuzzy goal programming. The proposed interactive fuzzy goal programming (IFGP) will be set out in section 5. Afterwards, computational experiments are given in section 6. Finally, conclusions and areas for future research will be given in section 7.

978-1-4244-7316-8/11/$26.00 ©2011 IEEE

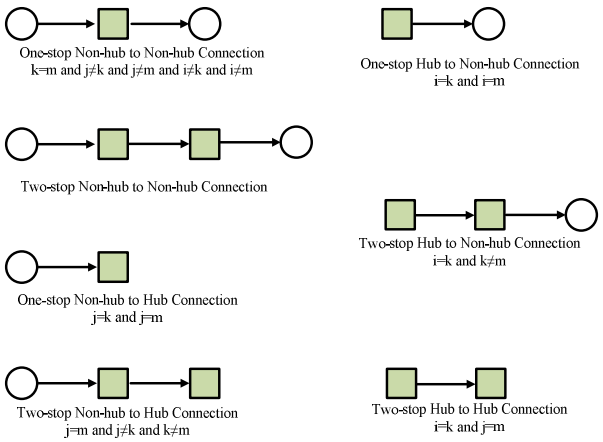

Figure 1. Different types of flows in a hub-and-spoke network

II. LITERATURE REVIEW

Hub Location Problem (HLP) has a long and wealthy background. From the beginning of the 21st century, an increase in the number of publications regarding HLP has been witnessed. The emergence of HLP dates back to late 60s when Goldman [4] defined the network hub location problem for the first time. Later, O'Kelly [5] presented the first seminal paper of HLP by proposing a mathematical formulation for a hub location problem. He studied the American airline passenger network and proposed the single allocation *p*-hub median problem which has gained the most attention so far among various hub location problems. He also proposed a well-known dataset (CAB) for hub location problems involving the passenger flows between 25 US cities. Since then, contributions to HLP have been presented in a variety of ways. It should be noted that a great deal of publications has been about the HLP models in which cost or time have been considered.

The most recent review of HLP is Alumur and Kara [6] which is an elegant and comprehensive review of network hub location problems. They classified their review into four distinct sections as *p*-hub median problem, the hub location problem with fixed costs, the *p*-hub center problem and hub covering problems. Since Alumur and Kara [6] is a comprehensive and valuable review, in this paper, only some recent publications will be presented. One may refer to [6] or other reviews and references therein to get more knowledge about the HLP literature before 2008.

Recently, some heuristics and metaheristics have been proposed to solve various HLPs. Using tabu search to solve the single-allocation hub covering HLP in incomplete networks (Calik et al. [7]), using ant colony optimization for the single-allocation *p*-hub center problem (Meyer et al. [8]). VNS for the single-allocation *p*-hub median problem (Illic et al. [9]), using Lagrangian relaxation for the single-allocation HLP (Contreras et al. [10]) are some instances, to name a few.

Using fuzzy logic in HLP has been recently considered by Chou [11]. He studied the container transshipment hub locations in southeastern Asia. He proposed a fuzzy multiple criteria decision making model to select the container transshipment hub port. Davari et al. [12] studied the single-allocation *p*-hub maximum reliability model of Kim and O'Kelly[(2] in a fuzzy sense. They considered reliability of each arc to be a fuzzy variable and presented an effective simulation-embedded simulated annealing to solve this problem.

Additionally, the Partitioning-Hub-Location-Routing Problem (PHLRP) by Catanzaro et al. [13], HLP in a competitive environment by Gelareh et al. [14] and Eiselt and Marianov [15], the time-definite *p*-hub median problem by Campbell [16], HLP assuming hub congestion by De Camargo et al. [17], considering the size of hubs as a decision variable by Correia et al. [18], stochastic *p*-hub center problem by Sim et al. [19], hierarchical HLP (Yaman [20]) are some recent extensions to the classical HLP.

Obviously, there has not been much attempt in literature to model fuzzy reliable hub location problems. Considering the publications to date, this paper contributes to the literature of HLP in two distinct aspects. First, a new method is proposed to calculate the reliability of a path in a hub-and-spoke network which seems to represent the real-world applications better. In addition, using fuzzy logic in hub location problems has not gained enough consideration so far and is addressed in this paper. Moreover, this paper will present using IFGP in solving HLP considering fuzzy aspiration levels. To the best of our knowledge, this has not been considered in the literature of HLP before.

III. MODEL FORMULATION

The model in this paper is an extension to Kim and O'Kelly [2]. Before presenting the problem formulation, let's define indices, parameters and variables.

Parameters

W_{ij} The flow between nodes *i* and *j*

R_{ij}^{km} The reliability of the flow between nodes *i* and *j* which is routed via hubs *k* and *m*

P Number of hubs to be located

Variables

X_{ij}^{km} Equals 1 if the flow between *i* and *j* is routed via hubs *k* and *m*

Z_k Equals 1 if a hub is located at hub *k*

Model:

$$Max \sum_i \sum_j \sum_k \sum_m W_{ij} R_{ij}^{km} X_{ij}^{km} \quad (1)$$

$$Max \ \omega \quad (2)$$

$$\omega \le W_{ij} R_{ij}^{km} X_{ij}^{km} + (1 - X_{ij}^{km}) M \quad \forall (i,j,k,m); i \ne j \quad (3)$$

$$\sum_k Z_{kk} = P \quad (4)$$

$$\sum_k Z_{ik} = 1 \quad \forall i \quad (5)$$

$$Z_{ik} \le Z_{kk} \quad \forall i, k (i \ne k) \quad (6)$$

$$\sum_m X_{ij}^{km} = Z_{ik} \quad \forall j > i; k \quad (7)$$

$$\sum_k X_{ij}^{km} = Z_{jm} \quad \forall j > i; m \quad (8)$$

$$Z_{ik} \in \{0,1\} \quad (9)$$

$$0 \le X_{ij}^{km} \le 1 \quad (10)$$

Equation (1) is the objective function, where the weighted reliability of the network is to be maximized. The fitness of a

solution is found by adding the weighted reliabilities of each OD pair together. Equations (2) and (3) represent the second objective presenting the center objective which maximizes the minimum reliability in the network. Constraint (4) holds that *P* hubs are to be opened. Constraint (5) states that each node must be assigned to one and only one hub. Constraint (6) states that an assignment could be made to only hub nodes. Constraints (7) and (8) force that a flow from *i* to *j* is routed via hub pair (*k*, *m*) only when hubs are established in these two nodes. Constraint (9) guarantees that the values of *Z* are binary variables. Finally, (10) represents the values that the *X* variable could take.

Kim and O'Kelly [2] presented a procedure to compute the reliability of a path based on single reliabilities of its arcs. However, it can be argued that in some cases, it is unable to represent the reliability properly.

It is known that in a hub-and-spoke network, to reach a destination, the flow must pass hubs and arcs. Therefore, the reliability of each hub is of high importance, along with the reliability of arcs. This paper adds the reliabilities of hubs to the procedure of reliability calculation by presenting a procedure to sequential multiplication of single reliabilities of hubs and arcs. Moreover, it is assumed that same as the arcs, there should be a discount factor associated with hubs which will be shown as β in the sequel. It should be noted that this value could be completely different from the arcs discount factor. Fig. 2 shows two common types of flows in a hub-and-spoke network. The reliabilities of these two types of flows could be found as:

$$(I) R_{ij}^{km} = r_{ik} * (r_{kk})^{1-\beta} * (r_{km})^{1-\alpha} * (r_{mm})^{1-\beta} * r_{mj} \quad (11)$$

$$(II) R_{ij}^{km} = r_{ik} * (r_{kk})^{1-\beta} * r_{kj} \quad (12)$$

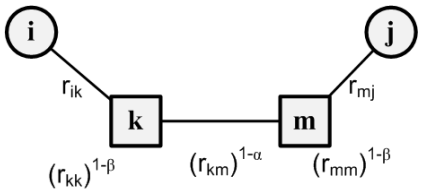

(I) Two-hub case

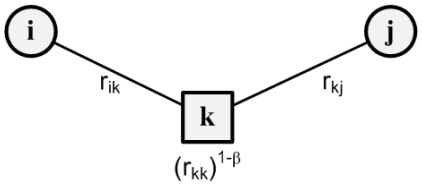

(II) One-hub case

Figure 2. The two common types of flows in hub-and-spoke networks

IV. FUZZY GOAL PROGRAMMING

Goal Programming (GP), first introduced by Charnes and Cooper [21], has been studied for many years as an efficient tool for multi-objective decision making (MODM) problems. Using a GP, decision maker(s) define aspiration levels and seeks an optimal solution where the undesirable deviations are minimized. However, determining precise aspiration levels for each objective in real world problems is a difficult task for decision makers (Yaghoobi et al. [22]).

Fuzzy Goal Programming (FGP) is a variant of the conventional GP, dealing with the imprecision came across by the DM, while expressing one's aspiration levels. The use of Fuzzy set theory (FST), proposed by Zadeh [23] to assist DMs to deal with this imprecise situation and uncertainties in GP was first proposed by Narasimhan [24] and then improved by Hannan [25].

Definition 2 (Zimmermann [26]). Assume that we are given a fuzzy goal $\widetilde{G}$ and a fuzzy constraint $\widetilde{C}$ in a space of alternatives X. Then $\widetilde{G}$ and $\widetilde{C}$ combine to form a decision $\widetilde{D}$ which is a fuzzy set resulting from intersection of $\widetilde{G}$ and $\widetilde{C}$. Bellman and Zadeh [27] proposed the min-operator to obtain a decision by intersection of the fuzzy sets of all objective functions.

DMs often need to know the crisp optimal solution, so it seems appropriate to suggest the highest degree of membership in the fuzzy set decision. Therefore, by using "maximizing solution", we have:

$$Max_{x\geq 0} Min_i\{\mu_i(x)\} = Max_{x\geq 0}\mu_{\widetilde{D}}(x) \quad (13)$$

Introducing a new variable, λ, this conventional linear programming problem can be formulated as follows:

$$Max\ \lambda \quad (14)$$

$$\mu_i(x) \geq \lambda \quad i = 1,\ldots,K \quad (15)$$

$$Ax \leq b \quad (16)$$

$$x \geq 0 \quad (17)$$

$$\lambda \in [0,1] \quad (18)$$

V. THE PROPOSED INTERACTIVE FUZZY FOAL PROGRAMMING (IFGP)

Many real-world problems are associated with a degree of uncertainty about goals and constraints. Recently, many academicians and practitioners have realized that uncertainty is an inevitable element in decision making. In addition, usually there is not enough historical data, or it is extremely difficult to gather reliable data, or even there is no underlying statistical model to build the model. Therefore, traditional probabilistic approaches are futile in many cases. In these sorts of problems, fuzzy logic has been proven to be a great tool. This paper will present how IFGP could be used to solve RHLP. Like any other MODM approach, IFGP is separated in two distinct stages. First, efficient solutions are found and then, a search is followed to find a compromise solution.

In the standard IFGP, one assumes that the DM can specify preference function with respect to the combination of the individual objective functions in advance, either as weights (utilities) or as distance functions.

Werners [28] presented a "fuzzy-and" operator which could be used in IFGP and is a strongly monotonically increasing function. It is presented as follows:

$$\mu_D(X) = Max\left\{\gamma\ Min_i\{\mu_i(x)\} + (1-\gamma)\left(\frac{1}{K}\right)\sum_i^K \mu_i(x)\right\} \quad (19)$$

where, $\mu_i(x)$ is the corresponding membership functions of *K* fuzzy objectives and constraints. DMs can interact with the

model to obtain preferred compromise solution by using γ as the coefficient of compensation defined within the interval [0, 1]. Later, Selim and Ozkarahan [29] modified the model by adding w_i as the relative weights for the membership functions of the objectives in (20):

$$\mu_D(X) = Max\left\{\gamma\ Min_i\{\mu_i(x)\} + (1-\gamma)\sum_i^K w_i\mu_i(x)\right\} \quad (20)$$

Results of using the Selim and Ozkarahan's [29] operator shows that the modified operator may provide different and even more preferable results compared to the Werners's "fuzzy and" approach. We will examine the usefulness of this operator on RHLP and analyze results.

The IFGP-based solution approach for solving RHLP is described as follows: First, individual best solutions are found using the single objective optimization and the CPLEX solver. Then, the decision maker is asked to determine if she/he is satisfied with the solution. If the results are not satisfactory, then using the payoff table (which contains the optimal values of objectives), membership functions are determined for objectives. Then, changing the values of γ gradually from 1 to 0, different solutions are obtained and presented to the decision maker. This process is followed until finding a preferred solution by the decision maker.

VI. COMPUTATIONAL EXPERIMENTS

In order to generate test problems, it was assumed that the reliability of a link is a function of its length. Therefore, the CAB dataset was modified to address the need to generate reliability values. To do so, the search was restricted to nodes 11 through 20. The set of cities is comprised of eastern, central, and western USA and include the following nodes.

- Kansas City
- Los Angeles
- Memphis
- Miami
- Minneapolis
- New Orleans
- New York
- Philadelphia
- Phoenix
- Pittsburg

Thus, it can be concluded that the dataset is sparse enough.

Then, reliability of each link was found as a function of its length. In other words, reliability value of each arc was considered to be a value between 0.5 and 0.9 based on its length. Then, the hub reliabilities (which are diagonal values in the reliability matrix) were generated uniformly between 0.9 and 1. Moreover, arc and hub discount factors were considered to be 0.95 and 0.9 respectively.

Fig. 3 shows the normalized fitness values of solutions for the test problem. Obviously, there is a tradeoff between the two objectives of the problem. Moreover, fig. 4 shows the behavior of both objectives and the aggregate function versus γ. It has been shown that although objectives change considerably by changes in γ, after a threshold (γ =0.3), the aggregated value remains almost steady.

To show the dissimilarities among the three models, fig. 5 depicts the solutions found using various values of γ. It clearly shows how the outputs differ in the locations of hubs and assignment of spokes to hubs.

Fig. 5 soundly confirms that there is an apparent discrepancy between solutions which can be attributed to changes in the value of γ. A rigorous analysis of results shows that New York is the only city which is present in all the solutions. Moreover, other cities which have been included in these solutions are Miami, Memphis, Phoenix, and Los Angeles. Since we assumed the reliabilities of arcs as a function of their length, it could be verified that the hubs are sparse in order to be able to cover the flows throughout the network.

VII. CONCLUSION AND FUTURE RESEARCH

At this point, to bring the study to a close, a conclusion is given. This paper presented a new method to compute the reliability of paths in a hub-and-spoke network. Moreover, it showed how IFGP could be used to solve RHLP. Results showed that IFGP could be a worthwhile tool to find solutions of RHLP in an interactive way with the decision maker. Another advantage of using IFGP is the fact that solutions could be found even if there is not a unanimous agreement between decision makers.

RHLP is still immature and needs more attention among academicians. An appealing future research could be considering the same problem in a stochastic environment. One may go through the performance of IFGP on other HLP variants such as incomplete hub networks or even hierarchical hub location problem. In addition, other variants of IFGP could be developed and their performance is to be assessed. Another interesting avenue for future research is building a model in which both cost and reliability are considered. Such an assumption makes the problem more realistic and in worth consideration in future Last, but not least, is the possibility of considering multiple-allocation in the HLP.

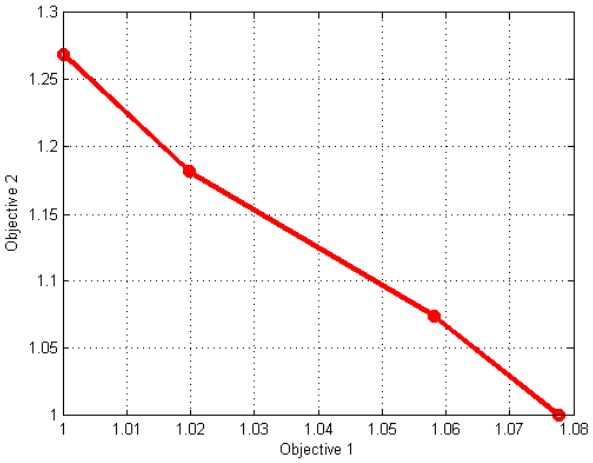

Figure 3. The normalized fitness values

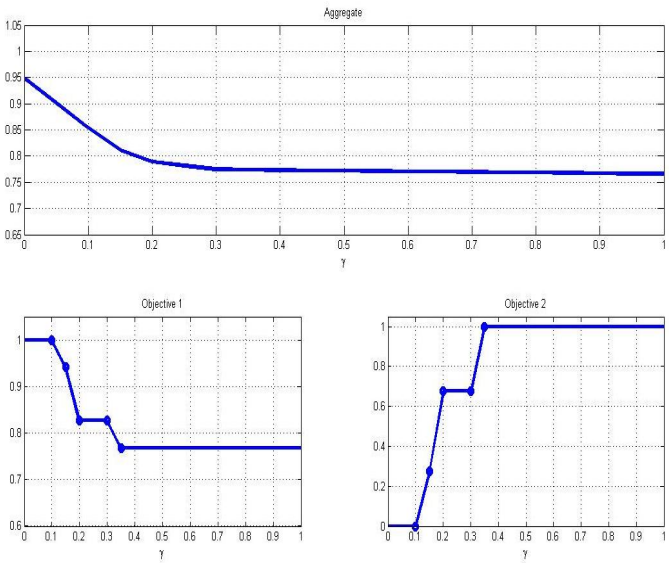

Fig 4. Results based on the values for γ

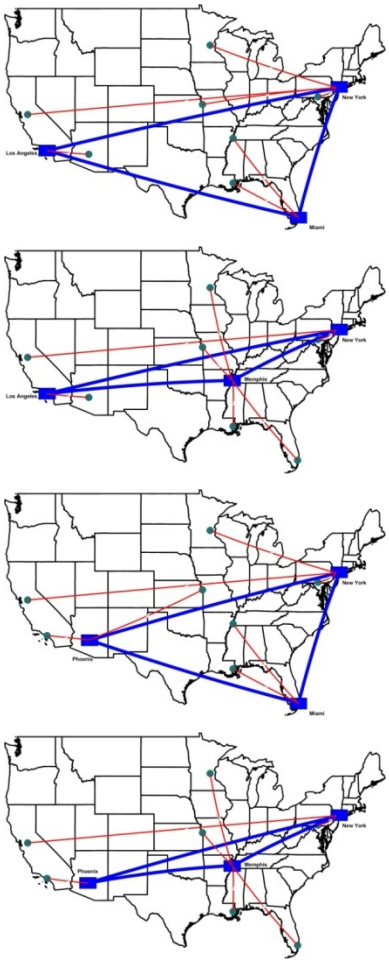

Fig 5. Comparing the solutions found

References

[1] M. H. Fazel Zarandi, A. Hemmati, and S. Davari, "The multi-depot capacitated location-routing problem with fuzzy travel times", Expert Syst. Appl., Vol. 38, 2011, pp. 10075-10084.

[2] H. Kim, and M. E. O'Kelly, "Reliable p-Hub Location Problems in Telecommunication Networks," Geogr. Analysis, vol. 41, 2009, pp. 283-306.

[3] J. A. M. Perez, J.M.M. Vega, and J.L. Verdegay, "Fuzzy location problems on networks," Fuzzy Set Syst., vol. 142, 2004, pp. 393-405.

[4] A. J. Goldman, "Optimal location for centers in a network," Transport. Sci., vol. 3, 1969, pp. 352-360.

[5] M. E. O'Kelly, "A quadratic integer program for the location of interacting hub facilities," Eur. J. Oper. Res., vol. 32, 1987, pp. 393-404.

[6] S. Alumur, and B. Y. Kara, "Network hub location problems: The state of the art," Eur. J. Oper. Res., vol. 190, 2008, pp. 1-21.

[7] H. Calik, S. A. Alumur, B. Y. Kara, and O. E. Karasan, "A tabu-search based heuristic for the hub covering problem over incomplete hub networks," Comput. Oper. Res., vol. 36, 2009, pp. 3088-3096.

[8] T. Meyer, A. T. Ernst, and M. Krishnamoortyh, "A 2-phase algorithm for solving the single allocation p-hub center problem," Comput. Oper. Res., vol. 36, 2009, pp. 3143-3151.

[9] A. Illic, D. Urosevic, J. Brimberg, and N. Mladenovic, "A general variable neighborhood search for solving the uncapacitated single allocation p-hub median problem," Eur. J. Oper. Res., vol. 206,2010, pp. 289-300.

[10] I. Contreras, J. A. Diaz, and E. Fernandez "Lagrangean relaxation for the capacitated hub location problem with single assignment," OR Spectrum, vol. 31, 2009, pp.483–505.

[11] C. C. Chou, "Application of FMCDM model to selecting the hub location in the marine transportation: A case study in southeastern Asia," Math. Comput. Model., In Press.

[12] S. Davari, M. H. Fazel Zarandi, and I. B. Turksen, "The fuzzy reliable hub location problem," Fuzzy Information Processing Society (NAFIPS), 2010 Annual Meeting of the North American, Tornoto, Canada.

[13] D. Catanzaro, E. Gourdin, M. Labbe, and F. A. Ozsoy, "A branch-and-cut algorithm for the partitioning-hub location-routing problem," Comput. Oper. Res., vol. 38, 2011, pp. 539–549.

[14] S. Gelareh, S. Nickel, and D. Pisinger "Liner shipping hub network design in a competitive environment," Transport. Res. Part E, vol. 46,2010, pp. 991–1004.

[15] H.A. Eiselt, and V. Marianov, "A conditional p-hub location problem with attraction functions." Comput. Oper. Res., vol. 36, 2009, pp. 3128-3135.

[16] J.F. Campbell, "Hub location for time definite transportation," Comput. Oper. Res., vol. 36, 2009, pp. 3107-3116.

[17] R. S. de Camargo, G. Miranda Jr, R. P. M. Ferreira, and H. P. Luna, "Multiple allocation hub-and-spoke network design under hub congestion," Comput. Oper. Res., vol. 36, 2009, pp. 3097-3106.

[18] I. Correia, S. Nickel, and F. Saldanha-da-Gama, "Single-assignment hub location problems with multiple capacity levels," Transport. Res. Part B., in press.

[19] T. Sim, T. J. Lowe, and B.W. Thomas, "The stochastic p-hub center problem with service-level constraints," Comput. Oper. Res., vol. 36, 2009, pp. 3166-3177.

[20] H. Yaman, "The hierarchical hub median problem with single assignment," Transport. Res. Part B, vol. 43, 2009, pp. 643–658.

[21] A. Charnes, and W.W. Cooper, "Management models of industrial applications of linear programming," Vol. I, Wiley, New York, 1961.

[22] M. A. Yaghoobi, and M. Tamiz, "A method for solving fuzzy goal programming problems based on MINMAX approach," Eur. J. Oper. Res., vol. 177, 2007, pp.1580–1590.

[23] L. A. Zadeh, "Fuzzy sets," Inf. Control., vol. 8, 1965, pp. 338–353.

[24] R. Narasimhan, "Goal programming in a fuzzy environment," Decis. Sci., vol. 11, 1980, pp. 325–336.

[25] E. L. Hannan, "Some further comments on fuzzy priorities," Decis. Sci., vol. 13, 1981, pp.337–339.

[26] H. J. Zimmermann, "Fuzzy set theory—and its applications," Kluwer Academic, Boston, 1996.

[27] R. E. Bellman, and L. A. Zadeh, "Decision making in a fuzzy environment," Manage. Sci., vol. 17, 1970, pp.141–164.

[28] B. Werners, "Aggregation models in mathematical programming. In: Mitra G, Greenberg HJ, Lootsma FA, Rijckaert MJ, Zimmermann H-J (eds) Mathematical models for decision support," Springer, Berlin, 1988, pp. 295–305.

[29] H. Selim, and I. Ozkarahan, "A supply chain distribution network design model: an interactive fuzzy goal programming-based solution approach," Int. J. Adv. Manuf. Technol., Vol. 36, 2008, pp. 401–418.

2011 IEEE International Conference on Fuzzy Systems
June 27-30, 2011, Taipei, Taiwan

Connection Manager : A FAHP-based System for Classifier and Decision-Making

Sheng-Tzong Cheng, Chih-Wei Hsu
Dept. of computer science and information engineering
National Cheng Kung University
Taiwan, Taiwan, R.O.C.
E-mail:stcheng@mail.ncku.edu.tw, awei@ieee.org

***Abstract*—This Connection Manager Intelligence Agent (CMIA) is an attractive feature of use the network traffic and behavior with multi-attributes to find the best network devices and connection devices meet user habits that it possible to access various multimedia contents everywhere at any time. In this agent, information process is thoroughly integrated into embedded system for connection manager of Meego or Android. We have implemented an interactive interface through this function (User interactive interface are based on Qt Creator IDE and CMIA) acquisition user behavior and to scholars of the machine. We have a successful user interaction of the agent can be decision making the choice of match the user intent.**

Keywords-attribute; decision-making; combining models; boosting; Fuzzy-AHP ; seamless network ;classifier; ranking;

I. INTRODUCTION

This is new kinds of Web apps on network connection manager of force that will be more ubiquitous and smarter than current applications and will be accessible anytime, anywhere. This will require us to development a multi-network how to switch and decision. Faced with the new wave of mobile device applications for service wide range of use, seamless network access is an important issue. Nowadays, mobile service software contains some techniques form artificial intelligence (AI) research. As for a connection manager of intelligence system (or Connection Manager of Intelligence Agent, CMIA) interaction with the owner becomes important. However, the interaction is usually limited to the predefined command or few typewriting. We propose a way for the user to define a new behavior to enhance the interaction. This human-machine interaction multi-attributes for the user to define a new degree of rating scales such [1] as received signal strength indicator (RSSI), energy consumption, traffic, throughput and other attributes of wireless devices must be based on knowledge and action mechanism of this fuzzy analytic hierarchy process (Fuzzy AHP).

This paper describes the experiences that we learned from building such devices. Based on the observation of real connected devices and their relationship with their owners, the goal that we set is to create a CMIA that may grow in its relationship with the owner. The goal of the research is to give the CMIA the following ability:

Autonomous interaction. The CMIA is to interact with the user without pre-written scripts.

Learning ability. The CMIA is to become more mature by learning skills through the training provided by the user.

Dynamic ranking. The CMIA is to adjust the three parts of attribute (RSSI, energy consumption, traffic, throughput) of behaviors dynamically through networking environment and interaction changes.

The concept of multi-attributes is the most important issue in this research. Our idea is based on the APH architecture proposed by Thomas L. Saaty in the 1990s [2] (Figure 1.), where the goal and condition input from the user environment (Figure 2.) and prepares the input attributes degree to finding Importance of rating scales for user experience. The results from the classifier module are then passed to the multi-attributes for each of classes to produce a set of use cases array comparison. After decided is switch the network connection of a use case.

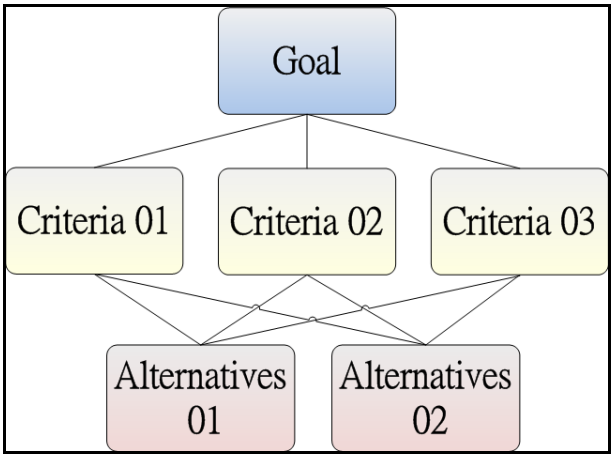

Figure 1. A sample architecture for AHP

The prototype system is described and the conclusion is given. The approach involves introduction of fuzzy theory into the Analytic Hierarchy Process developed by Saaty (1980) in

order to assess the weights of various assessed items and to sort their importance.

The rest of the paper is organized as follows. The next section explains the system concept. That is followed by the detail discussion on ranking and Fuzzy AHP.

II. SYSTEM CONCPET AND BACKGRAND

A. System Concpet

Based on the observation of Fuzzy AHP and its relationship with owner attributes, the goal was to create a use-case that enables the connection manager to find attributes automatically in its relationship with the attribute pattern-based model. The CMIA consists has five sublevel of depicted in Figure 2. : the target of sublevel, the network link type of sublevel, devices of sublevel and attribute of sublevel.

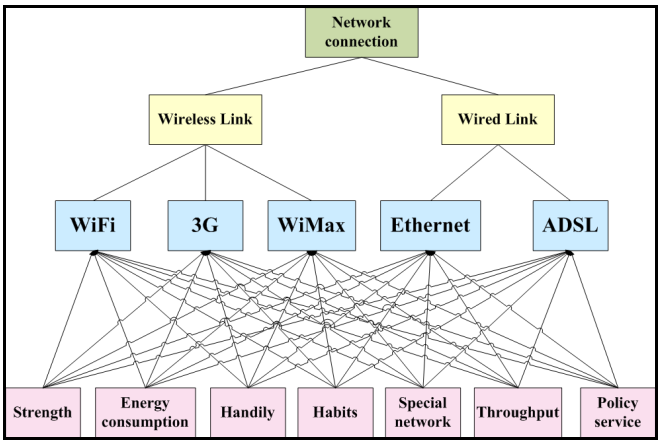

Figure 2. The five levels architecture for CMIA

However, the CMIA has combined modeling subsystem is based on the previous result for Fuzzy AHP and weighted-product model (WPM) processing which accepts the each all level weighted for WPM uses multiplication to rank alternatives with gesture of the user as the input for each kinds of levels weights in series.

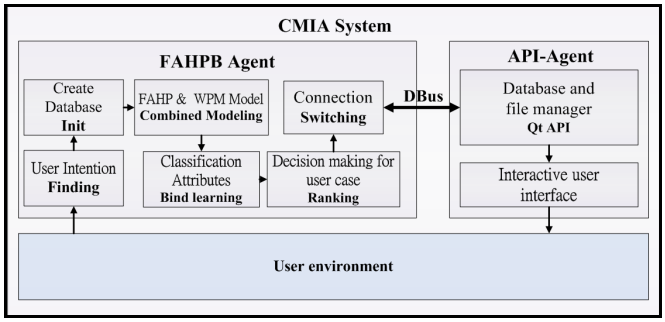

Figure 3. The System parts for CMIA

However, the implemented system contains five main modules of the elements, the input will be sent to the modeling subsystem which is the main topic reported in this paper. Within such system, learning and modeling are used for building the behavior definitions. The ranking subsystem is to carry out the behavior sequence produced by the connection switching subsystem. Such high-level behaviors are collection of basic actions that the CMIA can perform.

The attributes are processed in the combined modeling subsystem where those attributes are transformed to the user case for the CMIA to follow. The CMIA has the basic attributes (alternatives) and network devices (criteria or network classes) already defined. Thus, the main work of the combined modeling subsystem is to use such basic attributes and to construct more complicated behaviors to meet the network devices associated with the attributes. For such process, we use classification learning techniques to process the decomposition of goals to sublevels and to find the relationships associated of sublevels to the basic attributes for user case class.

The ranking subsystem is responsible for ranking the attributes (alternatives) of network class sublevel and connection link sublevel which are the collection of each levels weight in series to provide network connection recommended. The switching system (Qt API User Interface, QAUI) which shows the network device connected information of the CMIA in ConnManager list table. The interface between the switching subsystem and the QAUI is defined with ConnManager components to represent the basic connected device. This is sometimes proposed system provides the list of devices with the connMan for MeeGo network devices are currently repeat, we must establish a more updated list and delete list data. We used a state diagram approach to define the rational action relationship, which is reported in Section IV.

B. System Problems

This section describes the designing problem that system automated the processes of the dynamic parameters is difficult for convergence in CMIA. Thus, use classifier to filter a larger-scale problem given solving which can be dynamic space reduction. The storage unit is stores a network connection class, operating item, and network connection option. The processing unit performs of learning approach was self-control a dynamic parameters for classifier which in controller system can be establish an automatic network link mode. CMIA can through the user to operating some of function given a connected in network device of list table, generates a network classification link model according to the network connection class, the operating item in the network connection option which in system adopt this approach of obtained after weight calculation are ranking each all network device within user-case after classification of case of attributes in serial weights value. System have following encountered some problems:

- The characteristics of network devices are different attributes to quantify the process can not use the same method. For example, units of radiation measurement is a logarithmic expression, the user habits can simply attribute used to score.
- The environment must be immediately real-time updated parameters, the system is the application of a technology in mobile devices, the device is necessary to address the demand uncertainty and environmental

factors of space, these attributes will affect the degree of decision-making processes.

- Classification, however, parameters to be set for different connection modes will be connected by different device. Unless the user has considerable knowledge and specialty in the network and can set the connection modes by himself/herself to configuration. This network configuration is complex and difficult to install for general user. Also, they are unfamiliar connected with the network how to grasp setting manners of various network for connection modes. Which in usually because a user does not know how to set the network connection mode, an error occurs in the setting of the network connection mode so that network resources cannot be used, or a long time is required to research the setting manner, which causes trouble to the user.

III. FAHP AND CLASSIFIER

Michele Grimaldi (2011)[10] have presents a framework based on the analytic hierarchy process (AHP) methodology to select the most appropriate set of Knowledge Management (KM) tools to support the innovation and complex processes in organizations. In this study, multi-network connection mechanism is a complex of problem, which in structure will be use hierarchical architecture to solve complex problems associated with the level. The problem affected is the user of intend for interactive elements of weight-based number, we use the AHP framework to solve complex problems relationship of class and user case, there are simplify classification processes but also has affected relations between hierarchy structure.

A. FAHP and PSM Methods

We use the Fuzzy technique is used for different attributes to quantify the process include the RSSI, .When the decision maker considers the problem of ranking the m alternatives A_1,A_2,...,Am with respect to the N criteria C_1,C_2,...,C_N , it will feel great difficulty in assigning numbers, or ratios of numbers to alternatives[1] . The merit of using a fuzzy approach is to assign the relative importance of attributes using fuzzy numbers instead of crisp numbers. For numbers we use triangular fuzzy number (TFN), because they are step order for measurement data unit have dBm, mA, package rate, etc.

$$M = \{A_1, A_2, ..., A_M\} \tag{1}$$

The fuzzy weighted-product model (PWM) [3] is best alternative according to this mode is one which satisfies (2), and for the fuzzy version of this model the corresponding formula [1] is (3) :

$$R\left(\frac{A_K}{A_L}\right) = \prod_{j=1}^{N}\left(\frac{a_{Kj}}{a_{Lj}}\right)^{w_j} \tag{2}$$

where $\hat{a}_{Kj}, \hat{a}_{Lj}$, and $\hat{w}_j$ are TNF numbers. Alternative attribute A_K dominates alternative A_L if and only if the numerator (3) is greater than the denominator. We have instance in the following example:

$$R\left(\frac{A_K}{A_L}\right) = \prod_{j=1}^{N}\left(\frac{\hat{a}_{Kj}}{\hat{a}_{Lj}}\right)^{w_j} \tag{3}$$

The weighted-sum model (WSM) is a the weight of the public will use the sum of methods for decision-making [3]. A previous research discusses the notion of additive utilities in the expected-utility context when the set of consequences M can be written as the product of n other sets: $M = M1 \times M2 \times ... \times Mn$. where M is a subset of the product of n other sets: $M \subset M1 \times M2 \times ... \times Mn$. Under a finiteness restriction, an additivity axiom leads to an additive utility representation for the elements in M. The potential usefulness of the theory in connection with incomplete product sets is demonstrated with priority orderings and assignments [4]. There are M is alternatives and N criteria in a decision making problem. Then the best alternative, A^*, is the one which satisfies the following expression[3][4] :

$$P^*_{WSM} = \max_{M \geq i \geq 1} \sum_{i=1}^{N} a_{ij} W_j \tag{4}$$

There are weights in the maximization case, in each category of network devices, we find the best alternative according to (4). Currently, the performance values of the ith alternative for network devices attributes in terms of jth network device class that is a triangular fuzzy number denoted as $\hat{a}_{ij} = (a_{ijl}, a_{ijm}, a_{iju})$. Similarly, it is assumed that decision makers will use the triangular fuzzy number to express the importance of weight standards. These weights are denoted as $\hat{w}_{ij} = (w_{jl}, w_{jm}, w_{ju})$. The PSM model values of the fuzzy triangular numbers which represent the criterion weights for network device of class. It follows that best alternative is the one which satisfies the following relation [1]:

$$P^*_{WSM} = \max \sum_{j=1}^{N} \hat{a}_{ij} \hat{w}_j \text{ for } \quad i = 1,2,3,...,M . \tag{5}$$

m_l is that the lower value, m_m is that the median, m_u is located at a higher value. , show in Figure 4.

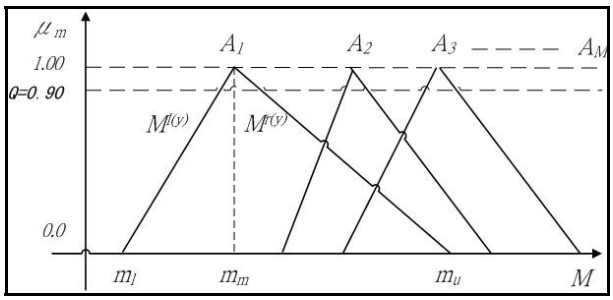

Figure 4. The fuzzy alternatives AM

So we can define each attribute fuzzy number step order for attributes scale degree mapping list, the RSSI and Energy attributes of scale degree samples such as TABLE I. In our system can be real-time update attributes values for RSSI, energy consumption, traffic, throughput. Through the reference TABLE I, we are also use a fuzzy number M on $R \in (-\infty, +be)$ is defined to be a fuzzy triangular number if its membership function $\mu_m : R \rightarrow [0, 1]$ is equal to :

$$\mu_m(x)=\begin{cases}\dfrac{1}{m-l}x-\dfrac{l}{m-l}, & x\in[l,m],\\ \dfrac{1}{m-u}x-\dfrac{l}{m-u}, & x\in[m,u],\\ 0 & otherwise,\end{cases} \tag{6}$$

A fuzzy triangular number, as denoted by (*l*,*m*,*u*).

TABLE I. ATTRIBUTES SCALE DRGREE FOR TFM TABLE LIST

Scale degree	A triangular fuzzy numbers
Weak strength	$\tilde{1}$ = (1,1,1) ≅ (1,10,20)
Degree of between	$\tilde{2}$ = (1,2,3) ≅ (21,25,30)
Low strength	$\tilde{3}$ = (2,3,4) ≅ (31,35,40)
Degree of between	$\tilde{4}$ = (3,4,5) ≅ (41,45,50)
Strength	$\tilde{5}$ = (4,5,6) ≅ (51,55,60)
Degree of between	$\tilde{6}$ = (5,6,7) ≅ (61,65,70)
Very strength	$\tilde{7}$ = (6,7,8) ≅ (71,75,80)
Degree of between	$\tilde{8}$ = (7,8,9) ≅ (81,85,90)
Higher strength	$\tilde{9}$ = (8,9,10) ≅ (91,95,100)

Finally, in this section will presents of the extent analysis method on fuzzy AHP are given and then the method classification applied to supplier selection problem. The CMIA is an AHP-Based system that goal is define and non-define for user free. The relationship between the various properties and weight (importance), we usually are based on pairwise comparison matrix properties used to calculate the average number of attributes of all weights.

Building pair-wise comparison matrix : the system have suppose classification function when the decision maker is asked to compare the nine attributes for network devices to classification these attributes to correct class.

- First: We are input a rating scale value of variables from each of attribute then use the fuzzy membership function to determine the matching variables of pair-wise comparison matrix about the ownership level degree, the process such as Figure 5.
- In this research, in synthesizing experts' opinions, the geometric mean method(GMM) proposed by Buckley (1985) [8] the average of the proposed method to integrate the views of respondents, integration formula, using the arithmetic mean method (AMM), you can calculate the ratio between the weight of property.

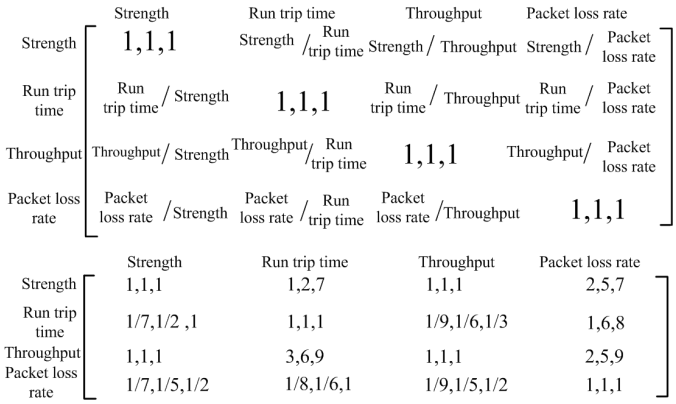

Figure 5. Using pairwis comparisons method

The fuzzy eigenvector of the above matrix is estimated. Recall that given a crisp reciprocal matrix then according with Saaty's matrix of right upper half of principal eigenvector of the matrix is expresses the importance of the attributes. We calculate the properties of the vertical for column is the average, show in Figure 6.

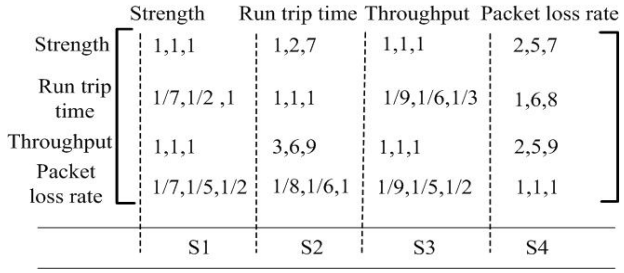

Figure 6. Vertical column for reciprocal judgment matrix of property

- And the properties of pair-wise comparison of the level of the multiplication of the sum of the field.

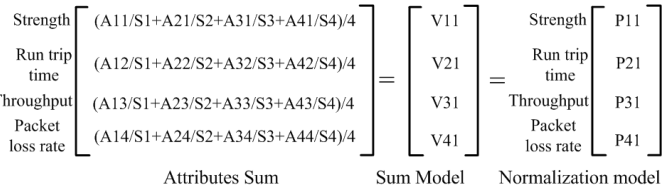

Figure 7. A pairwise comparison of the multiplication of the sum

- Above the results of the steps, only know the extent attributable to the pairing property can not be used for decision-making, with the judge to obtain measures of value, must use the fuzzy approach, a common center of gravity method (CGM), the largest collection with minimal set and so on, so before using this ambiguity to determine the value of the decision-making.
- Defuzzication :

According to the method of Teng&Tzeng(1993)[7], the DF_{ij} solution for fuzzy weight calculation process is:

$$DF_{ij}=\left[\left(R_{ij}-L_{ij}\right)+\left(M_{ij}-L_{ij}\right)\right]/3+L_{ij} \tag{7}$$

These are finished properties matching matrix, followed by the cascade (series level weight, SLW) calculation of the weight level, the process is to Class un-normalization weights and attribute sum model for the sum of the product , the fuzzy eigenvectors of the pair-wise comparisons when the four attributes are compares in the terms of each of the remaining criteria are also derived in a similar manner, along with the weights of importance of five classes, and form the vectors in the following fuzzy matrix , such as follows Figure 8. .

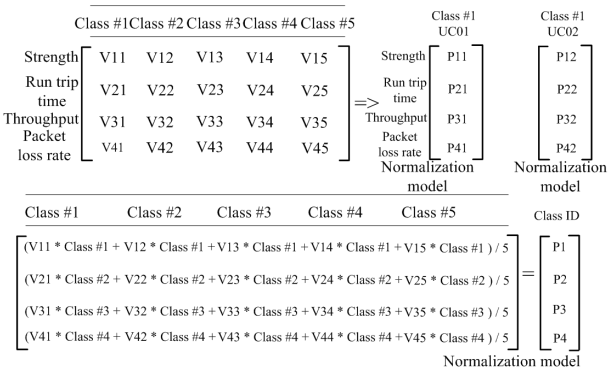

Figure 8. A pairwise comparison of the multiplication of the sum

Our approach, is based on (4) after the weights to different categories User-Case, this method is used to solve (The same device conflict., When simultaneously the occurrence of a category have more than one access point (AP), must be decision-making.

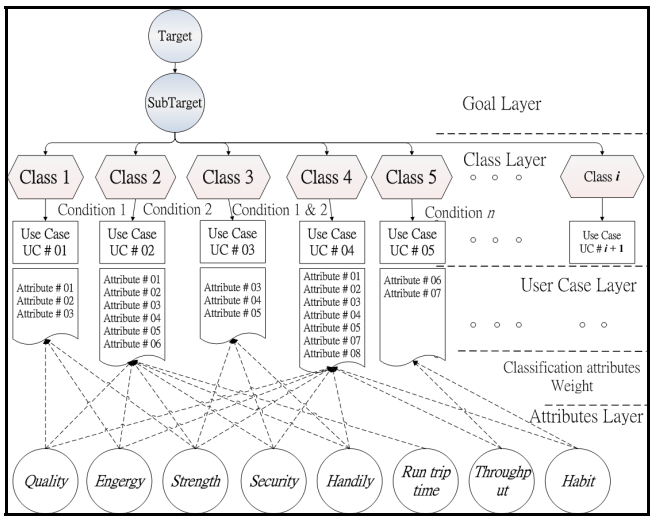

Figure 9. Fig A pairwise comparison

However, example have a decision problem with five criteria of classes (in user case, UC and include the WiFi, 3G, WiMax, Ethernet, ADSL and other classes) and four attributes in terms of first criterion by using pairwise comparisons.

We use the FAHP to building hierarchical structure for CMIA, shown in Figure 2. We are research by the FAHP [6], and modified an algorithm from fuzzy pairwise to describe our approach. The main purpose is to determine the user behavior intention as training data (TD) while satisfying constraints. The parameters, $\tilde{M}$ is a fuzzy triangular number (FTN), $1/\tilde{M}$ is a establish value of fuzzy matrix is inverted M. The FAHPTD is a training data form survey of questionnaire for 120 copies. The ConnMan is connection manager list table that record about each all devices of network device information data. Given user procession input data set:

$FAHPTD=\{(A_1,\textbf{Class}(C_1),(A_2,\textbf{Class}(C_2),\ldots,(A_N,\textbf{Class}(C_N)\}$, where A_i is a user input sample from the GD table, $\boldsymbol{Y(A_i)} \in y=\{C_1,C_2,...Class_L\}$ denotes the classes ($\boldsymbol{A_i}$) belongs to $\boldsymbol{L}$ is the number of the different classes (as like fowler formula : $Class(C_j) \in y=\{WiFi,3G,WiMax,Ethernet,ADSL,...Class_L\}$).

$\boldsymbol{N}$ is the number of training samples from to FAHPTD table for 100 questionnaires single. $\boldsymbol{i=1,2,\ldots,N}$ numbers.

procedure FAHPB (*FAHPTD,A,T*)

$FAHPTD_{Table}[i,j]$ for all $\boldsymbol{i=1,2,\ldots N}$; set for all $\boldsymbol{j=1,2,\ldots N}$;

$ConnMan_{Table}[i,j]$ for all $\boldsymbol{i=1,2,\ldots N}$; set for all $\boldsymbol{j=1,2,\ldots N}$;

//Building Comparison matrix :

$$FAHPTD_{Table}[i,j]=\frac{w_i}{w_j}=\frac{1}{FAHPTD_{Table}}>0,\forall i,j$$

//Building a fuzzy value matrix is inverted

//the value of fuzzy matrix is inverted M.

$M=[\tilde{M}_{ij}]$; $\tilde{M}_{ij}=(L_{ij},M_{ij},R_{ij})$; $\tilde{M}_{ij}=1/\tilde{M}_{ji}$,

$\forall i,j=1,2,\ldots,n$

//Groups combined

$$\tilde{m}_{ij}=(1/N)\otimes(\tilde{m}_{ij}^{\ 1}\oplus\tilde{m}_{ij}^{\ 2}\oplus\ldots\oplus\tilde{m}_{ij}^{\ N})$$

//Calculate the fuzzy weight

//Obtained by the following calculus of $\tilde{w}_i$ weight:

$$\tilde{Z}_i=(\tilde{a}_{i1}\otimes\tilde{a}_{i2}\otimes\ldots\otimes\tilde{a}_{in})^{\frac{1}{n}},\forall i=1,2,\ldots,n$$

$$\tilde{w}_i=\tilde{Z}_i\otimes(\tilde{Z}_1\oplus\tilde{Z}_2\oplus\ldots\tilde{Z}_n)^{-1}$$

//Defuzzication

DF_{ij} solution for fuzzy weight calculation process is:

$DF_{ij}=[(R_{ij}-L_{ij})+(M_{ij}-L_{ij})]/3+L_{ij}$ //Normalization

//Normalization weights for DFW_{ij} calculation process

$$DFW_{Ni}=\frac{DF_{ij}}{\sum DF_{ij}}$$

// Calculate the weight of level series, SLW

$$w_k=w_i+w_{ij}+w_{ijk}$$

//Running the Classifier core

if Rules R1 THEN UC01 update core process

if Rules R2 THEN UC02 update core process

if Rules Rn THEN UC0n update core process

//return the final hypothesis with weights for solving the //classifier

Reading $ConnMan_{Table}[i, j]$

//Update RSSI, energy consumption, traffic, throughput

Update user_parameter_weightTable[i,j]

return FAHPB process

end FAHPB

B. Classification of Approach

The Bayesian approach to classification estimates the probability that an instance Attributes (*Ai*) belongs to a class (*Cj*). Given the observed attribute values is the instance. There are L is the class labels $\{Cj\}$, $j = 1,2,\ldots,L$ numbers. When making a conditional than probabilistic classification, the class with the highest estimated posterior probability is selected. For the general problem of the user connection, each once have different conditions, there will have different the posterior probability.

The technology classified is to used for classifying different attribute and is classified in the cases of different users. According to the method of (8),(9) and [9], we can then derive the following relationship :

$$p(Y = y_i \mid X = x_i) = \frac{n_{ij}}{c_i} \tag{8}$$

$$p(Y = y_i, X = x_i) = \frac{n_{ij}}{N} = \frac{n_{ij}}{c_i} \cdot \frac{c_i}{N} = p(Y = y_i \mid X = x_i) p(X = x_i) \tag{9}$$

,which in the generating rule of probability. Conditional Probabilities of the principle with our paper is: Having constructed the GD network nodes, we will define the conditional probabilities which quantify the arcs of the GD network. We request define the second layer have two nodes are wireless link and wired link. We are reference form (8) and (9) can written (11) as follows:

$$P(WirelessLink \mid 3G) = \frac{P(3G \mid WirelessLi\ nk) P(WirelessLi\ nk)}{P(3G)} \tag{11}$$

In our system applied about the wireless link or wired link of posterior probability for connection is as flows:

Suppose there is a mixed network having 60% WiFi connection and 40% 3G link as connection switch. The wireless link 3G or WiFi in equal numbers; the wired link all Ethernet connection. An observer sees a (random) connection from a distance; all the observer can see is that this connection is 3G. What is the probability this connection is a wireless link The correct answer can be computed using Bayes' theorem.

- P(*WirelessLink*), or the probability that the wireless link is a 3G of any other information. Since the observers sees a random wireless link, meaning that all connection links have the same probability of being observed, and the percentage of connection among the wireless links is 40%, this probability equals 0.4.
- P(*WirlessLink*'), or the probability that the Wireless link connection is a WiFi regardless of any other information (*A*' is the complementary event to *A*). This is 60%, or 0.6.
- P(*3G*|*WirelessLink*), or the probability of the connection for habits given that the connection is a wireless link. As they are as likely to habits as energy consumption, this is 0.5.
- P(*3G*|W*irelessLink*'), or the probability of the wireless link to habits given that the connection is a link. This is given as 1.
- P(*3G*), or the probability of a (randomly selected) connection to 3G regardless of any other information. Since P(*3G*)=P(*3G*|*WirelessLink*)×P(*WirelessLink*)+ P(*3G*|*WirelessLink*')×P(*WirelessLink*'),this is 0.5×0.4 + 1×0.6 = 0.2+0.6=0.8.

Given all this information, the probability of the observer having spotted a 3G connection given that the observed network connection is habits can be computed by substituting these values in the formula about the entropy is by (11) posterior probability model given the features observed as show in Fig. 10.

$$P(WirelessLi\ nk \mid 3G) = \frac{P(3G \mid WirelessLi\ nk) P(WirelessLi\ nk)}{P(3G)} = \frac{0.5 \times 0.4}{0.8} = 0.25$$

We observe the values of the variables for a set of wireless link and wire link session examples. A given quantization into k of the entropy is by (11) for interval case labels, Bayesian inference for the Gaussian distribution.

The maximum likelihood framework gave point estimates for the parameters Σ. Now we develop a Bayesian treatment by introducing prior distributions over these parameters. Where Class for *i*=0,1,….,*L* and *j*=0,1,…,*L*.

$$p(Class_J \mid Attribute_i) = P(Class_J) \prod_{i=1}^{n} \prod_{j=1}^{L} P(Attribute_i \mid Class_J) \tag{12}$$

p(*Attribute*) given by a Gaussian distribution. Case profile learn method for connection manager. In this implementation, User finding to using wireless link device via the Bayesian Network probability is $P(Wireless\ link \mid \tilde{M})$ can be re-expressed as the entropy is by (12). The PTFAHP is probability for EM (Mathematical Expectation) of class, the best alternative according to this model is one which satisfies (13). For the Fuzzy AHP method of Bayesian classifier model the corresponding formula is Figure 10.

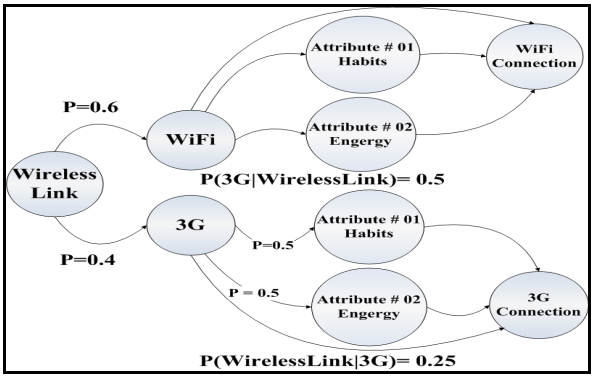

Figure 10. Connection Classifier model

$$PT_{FAHP} = \arg\max_{c \in C} P(Class) \prod_{i=1}^{n} P(\tilde{M}_i | Class) \quad (13)$$

IV. PROTOTYPE SYSTEM

The network devices connectivity of problems is currently facing in the embedded mobile device management, of multi-network connection manager problems. However, how to choose of accordance with past experience of capture user needs for system is currently an important problem, in our system will solve these technical difficulties.

A. System Architecture

We focused on the survey of questionnaire for 120 copies to build questionnaires table (*QT*a), the use of network devices for the intent of the process, after the computation of statistical methods FAHP be Training data, once again, the form through the user interface allows users to operate the network device operation process and then after FAHP understand user intent. Then, after repeated classification of learning to learn and update environment variables, classification of the property to meet the characteristics of the users of the device within the case, update the environment variables constant repeat users with FAHP operation user case *QT*a. The description to the components in is as follows, Figure 11. :

1) For Connection Manager on Intelligent System (CMIA): There are have concept of multi-attributes is the most important issue in this research. Our idea is based on the Fuzzy APH architecture by CMIA system.

a) Policy rule select: User can be selection or added this function to execution device precedence policy.

b) User input: S Selection *QT*a function will through a questionnaire to capture user intended..

c) Building relational table: Building the goal and attributes between relational values.

d) Condition rule of Pre-process: According to the user any choice the policy rules select of component, and *QT*a table input. These will be the result of user selection, back to the condition rule changes the each all weight for attributes and classes.

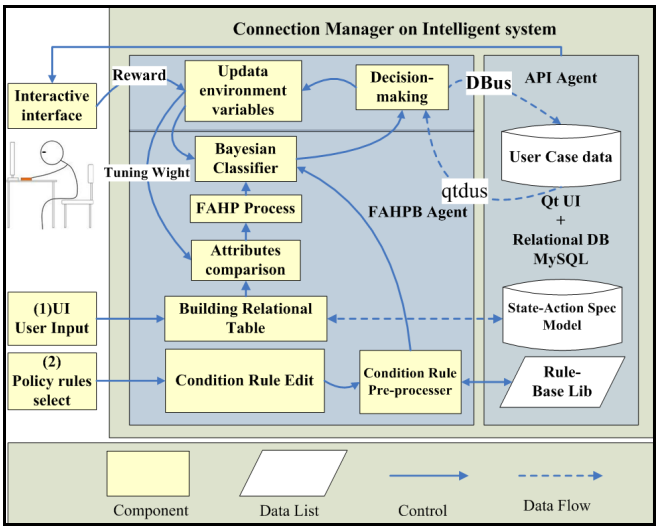

Figure 11. CMIA System Architecture

e) FAHP Process: This component is calculate the weight of Fuzzy AHP processes each attributes and level series weights.

f) Baysian of Classifier: The Bayesian network methods and trainning for classification the attributes and learning from the selection palette.

g) Decision-making: Switching for Network device

h) Updata environment variables: Update *RSSI*, energy consumption, traffic, throughput.

B. Classification about of classes

1) Classification : Accordance with the above FAHPB steps, you can calculate the properties of the network link under the main weight of each case and weight rating, as shown in TABLE II.

TABLE II. CLASSIFICATION ABOUT OF CLASSES

Classification of Class	Attributes-Normalization weights	Level weights in series	Rank
UC01 (Functional) Class #1 0.2664	Quality-0.1280	0.0351	9
	Security-0.2222	0.0582	8
	Strength-0.3169	0.0834	7
	Energy consumption-0.3328	0.0896	6
UC02 (Non-functional) Class #2 0.4520	Handily-0.3805	0.1720	1
	Habit-0.3256	0.1472	3
	Special network-0.2939	0.1318	4
UC03 (Focus factors) Class #3 0.2817	Throughput-0.3978	0.1130	5

Policy Service-0.6022	0.1696	2	

2) Interactive questionnaire : Our analysis of wired connection and wireless connection are each all through a questionnaire and statistical results, such as TABLE III.

TABLE III. QUESTIONNAIRE ABOUT WIRELESS AND LIRED LINK

Item	Wireless	Link (%)	Wired	Link (%)
Handily	Handily	Not Handily	Handily	Not Handily
	90	10	82	18
Habit	Habit	Not Habit	Habit	Not Habit
	52	46	96	4

C. Description of the Computational Results

It is ranking user case to provider a method that it is will automatically sort through Bayesian classification and find the weights in front of the properties of the three users for one case, while we get the evaluation result based on FAHP with constant weight by each all attributes weighting for actual questionnaire statistics of FAHPB process, as show in TABLE IV.

TABLE IV. THE ACTUAL QUESTIONNAIRE STATISTICS SAMPLE SET

	WiFi link		3G link		Wired link	
Item	Attributes	Weighting	Attributes	Weighting	Attributes	Weighting
1	Quality	0.038147	Quality	0.052358	Quality	0.038152
2	Security	0.043515	Security	0.059726	Security	0.043515
3	Strength	0.017694	Strength	0.024285	Strength	0.017695
4	Energy consumption	0.042312	Energy consumption	0.058074	Energy consumption	0.042312
5	Handily	0.03672	Handily	0.0504	Handily	0.03672
6	Throughput	0.056396	Throughput	0.077406	Throughput	0.056398
7	Habit	0.009643	Habit	0.013236	Habit	0.009625
8	Special	0.042312	Special	0.058074	Special	0.042329
9	Policy Service	0.009773	Policy Service	0.013414	Policy Service	0.009769
	Total weighting	0.296512	Total weighting	0.406973	Total weighting	0.296515

WiFi link: 0.043515+0.042312+0.056396 = 0.142223
3G link: 0.059726+0.058074+0.077406 = 0.195206
Wired link: 0.043515+0.042312+0.056398= 0.142225
Ranking : 3G > Wired link > WiFi

Using by FAHPB approach (Red line) is the rate which the WSM(blue line) , WPM(Green line) and FAHPB fuzzy method disagree in the indication of the best attribute. In Figure 12. the fuzzy AHP by WSM, fuzzy WPM and FAHPD respectively.

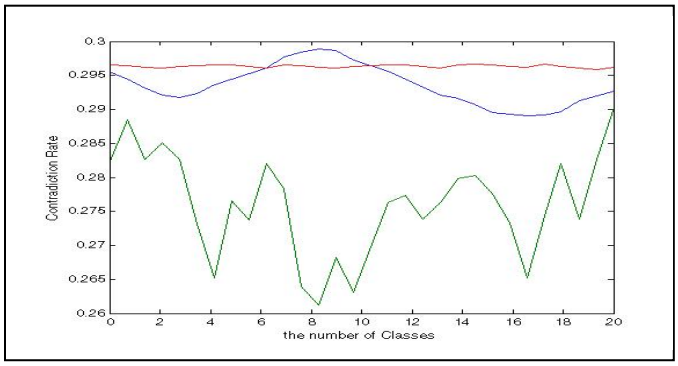

Figure 12. Contradiction rate when the number of attributes is classification

V. CONCLUSIONS

This research focuses on the connection manager of network equipment using fuzzy analytic hierarchy process in decision-making and classification classes for CMIA. The main contribution of this paper is to propose a flexible policy implementation model, including the training of classification and ranking of the optimal scheduling mechanism.

ACKNOWLEDGMENT

The authors thank the colleagues at the Institute for Information Industry (III) for providing the intelligence connection manager for Meego platform. The analysis is based on a pair-wise comparison among the user and then putted to matrix to resolve the ranking via Bayesian classifier model to selected user case.

REFERENCES

[1] E.T. and Chi-Tun,Lin, "Development and Evaluation of Five Fuzzy Multiattribute Decision-Making Methods",International Journal of Approximate Reasoning, vol. 14, Issue 4, pp. 281-310, 1996.

[2] T. L. Saaty, "How to make a decision: The Analytic Hierarchy Process," European Journal of Operation Research, Vol.48, No.1, pp.9-26, 1990.

[3] Chen,S.J., Hwang, C.L., "Fuzzy Multiple Decision Marking," Lecture Notes in Econom and Math.Systems, Springer-Verlag, New York, 1992.

[4] Fishburn, Peter C., "Additive Utilities with Incomplete Product Sets: Application to Priorities and Assignments", Oper. Res. Soc. of America, 1967.

[5] Laarhoven, P.J.M., Pedrycz, W., "A fuzzy extension of Saaty's priority theory", Fuzzy Sets and Systems, vol. 11, pp.229-241, 1983.

[6] Boender, C. G. E., de Graan, J.G., Lootsma, F.A., "Multi-criteria decision analysis with fuzzy pairwise comparisons", Fuzzy Sets and Systems, Vol. 29, pp.133-143, 1989.

[7] Teng, J Y., Tzeng, G.H., "Transportation Investment Project Selection with Fuzzy Multi-objective", Transportation Planning and Technology, vol. 17, pp.91-112, 1993.

[8] Buckley,J.J., "Ranking alternatives using fuzzy numbers", Fuzzy Sets and Systems, vol. 15, pp.21-31, 1985.

[9] M. Bishop., "Pattern Recognition and Machine Learning",Journal of Satistical software, vol. 17, Book Review 5, January 2007.

[10] Michele Grimald and Pierluigi Rippa,"An AHP-based framework for selecting knowledge management tools to sustain innovation process", Wiley,Jouarn of Knowledge and Process Management,vol. 18,pp.45-55, 2011.

2011 IEEE International Conference on Fuzzy Systems
June 27-30, 2011, Taipei, Taiwan

Approximate Confidence Interval for Generalized Taguchi Process Capability Index

Abbas Parchami and Mashaallah Mashinchi
Department of Statistics, Faculty of Mathematics and Computer Sciences, Shahid Bahonar University of Kerman, Kerman, Iran
parchami@mail.uk.ac.ir , mashinchi@mail.uk.ac.ir

M. Hadi Mashinchi
Department of Computing, Macquarie University, NSW 2112, Australia
hadi.mashinchi@mq.edu.au

Abstract— **The impreciseness happens in the quality control same as other statistical problems. In quality control where specification limits are better expressed by fuzzy sets, the generalized process capability indices $C_{\tilde{p}}$, $C_{\widetilde{pk}}$ and $C_{\widetilde{pm}}$ can be helpful and necessary for measuring the capability. We propose a generalized form of Taguchi index $C_{\widetilde{pm}}$ to assess the ability of the fuzzy process to be clustered around the target value. An approximate $100(1-\gamma)\%$ confidence interval for the generalized process capability index $C_{\widetilde{pm}}$ by using fuzzy specification limits is also presented.**

Keywords- Fuzzy quality; Taguchi process capability index; Confidence interval cmponent

I. BACKGROUND

Traditional process capability indices (PCIs) can be classified into two major kinds. The first one, such as index C_p, deals solely with the process variation in relation to a specified tolerance region. The second one, such as indices C_{pk} and C_{pm}, considers not only the process variation relative to the tolerance region but also the deviation of process mean from target value. In [3] it is pointed out that the exact sampling properties of the estimates of C_{pk} were more complex than those for C_{pm}. The process capability index C_{pm}, named Taguchi capability index, is defined as $C_{pm}=\frac{USL-LSL}{6\sqrt{E(X-T)^2}}=\frac{USL-LSL}{6\sigma_T}=\frac{USL-LSL}{6\sqrt{\sigma^2+(\mu-T)^2}}$ [1, 3, 20]. Here, T, LSL and USL are the target value, lower and upper specification limits (SLs), respectively.

In quality control, we may confront imprecise concepts. Ordinary capability indices cannot measure the capability if for example upper and lower SLs are imprecise. The impreciseness exists in SLs can be express by fuzzy terms. Recently, several PCIs developed deal with impreciseness [9, 19, 24, 25, 26, 27, 28, 32, 34, 38, 42] and they are applied in real cases [12, 13, 14, 15, 21]. We further investigate the point and interval estimators of the generalized capability index C_{pm} which has been introduced in [16, 17, 18].

In this paper, the problems of point and interval estimations of the generalized process capability index $C_{\widetilde{pm}}$ are considered which are based on the observed random sample for an in-control fuzzy process. Statistical inference based on fuzzy arithmetic is used to introduce a $100(1-\gamma)\%$ confidence interval for generalized capability index $C_{\widetilde{pm}}$, where we have two membership functions for SLs.

The organization of this paper is as follows. In Section II, some preliminaries on fuzzy arithmetic are presented and then generalized PCIs are introduced. Tow point estimators and an interval estimator is introduced in Section III for $C_{\widetilde{pm}}$. The final section is the conclusions part.

II. ARITHMETIC OPERATIONS ON FUZZY SPECIFICATION LIMITS

Let R be the set of all real numbers and $F(R)=\{\tilde{A}\mid \tilde{A}:R\to[0,1],\ \tilde{A}$ is a continuous function$\}$ be the set of all fuzzy sets on R. The α-cut of $\tilde{A}\in F(R)$ is the crisp set defined by $\tilde{A}_\alpha=\{x\mid \tilde{A}(x)\geq\alpha\}$, for any $\alpha\in[0,1]$. Although fuzzy SLs are introduced in [24], but we introduce new flexible formulas for the fuzzy SLs in Definition 2.1, inspired LR fuzzy numbers [7, 23]. The motivation of introducing fuzzy SLs in fuzzy processes is already introduced in [24].

Definition 2.1 Let $\widetilde{USL}$ and $\widetilde{LSL}$ be two fuzzy sets with membership functions

$$\widetilde{USL}(x)=\begin{cases}1 & \text{if} \quad x<q\\ U(\frac{x-q}{b}) & \text{if} \quad x\geq q\end{cases}$$

and

$$\widetilde{LSL}(x)=\begin{cases}L(\frac{p-x}{a}) & \text{if} \quad x\leq p\\ 1 & \text{if} \quad x>p\end{cases}$$

in which reference functions $L, U : [0,+\infty] \longrightarrow [0,1]$ are non-increasing functions, $U(0) = L(0) = 1$, and the upper and lower spreads a, $b > 0$. Then, $\widetilde{USL}$ and $\widetilde{LSL}$ are called upper fuzzy specification limit and lower fuzzy specification limit, and symbolically are denoted by $(q,b)_U$ and $(p,a)_L$, respectively. Also, $F_U(R)$ and $F_L(R)$ denote two sets of all upper and lower fuzzy SLs, respectively.

In Definition 2.1, the reference function L (or similarly U) can be described by any of the following functions:

(1) $L(x) = 1$ for $x \in [0,1]$ and 0 outside,

(2) $L(x) = \max\{0, 1 - |x|^r\}$,

(3) $L(x) = e^{-|x|^r}$,

(4) $L(x) = \dfrac{1}{1+|x|^r}$,

(5) $L(x) = \dfrac{1}{1+r|x|}$,

in which $r > 0$.

Remark 2.1 The fuzziness increases in $(p,a)_L$ and $(q,b)_U$, with the increase in the spreads a and b.

Definition 2.2 A process with fuzzy SLs $(q,b)_U$ and $(p,a)_L$, which we call a fuzzy process for short, is one which satisfies the normal distribution condition, that is $X_1, \ldots, X_n$ are independent, identically distributed random variables with $N(\mu, \sigma^2)$.

Definition 2.3 Let $\widetilde{USL} \in F_U(R)$ and $\widetilde{LSL} \in F_L(R)$ are the upper and the lower fuzzy SLs, such that $p \le q$. Then

$$\widetilde{USL} \oplus \widetilde{LSL} = \int_0^1 g(\alpha)(u_\alpha + l_\alpha) d\alpha$$

and

$$\widetilde{USL} \ominus \widetilde{LSL} = \int_0^1 g(\alpha)(u_\alpha - l_\alpha) d\alpha,$$

are called addition and subtraction of $\widetilde{USL}$ and $\widetilde{LSL}$, respectively, in which

$$\widetilde{USL}_\alpha = (-\infty, u_\alpha], \ \widetilde{LSL}_\alpha = [l_\alpha + \infty), \quad (1)$$

u_0, l_0 are finite real numbers and g is a real valued non-decreasing function on [0,1] with $g(0) = 0$ and $\int_0^1 g(\alpha)\, d\alpha = 1$ (for instance $g(\alpha) = (m+1)\alpha^m$ where $m = 1, 2, 3, \ldots$).

Note that in Definition 2.3, $u_\alpha + l_\alpha$ is the addition and $u_\alpha - l_\alpha$ is the subtraction of the left and the right end points of the α-cut of $\widetilde{USL}$ and $\widetilde{LSL}$. The value of $g(\alpha)$ can be understood as the weight of $u_\alpha \pm l_\alpha$, and the non-decreasing property of g means that the higher the membership of α-cut, the more important it is in determining the addition and subtraction of $\widetilde{USL}$ and $\widetilde{LSL}$. These defined operations synthetically reflect the information on every membership degree. The application of the arithmetic operations given in Definition 2.3 on fuzzy SLs allows different α-cuts to play different roles.

For observing some properties of the arithmetic operations on fuzzy SLs and numerical examples on fuzzy SLs, see [24]. Now, by extending the addition and subtract operations on fuzzy SLs, one can use $\ominus$ and $\oplus$ operations to generalize the classical PCIs, when the SLs are fuzzy rather than crisp [24].

Definition 2.4 Let in a fuzzy process $\widetilde{USL} \in F_U(R)$ and $\widetilde{LSL} \in F_L(R)$ be the engineering upper and lower fuzzy SLs, respectively, where $p \le q$. Then the extended process capability indices are defined as follows:

$$C_{\tilde{p}} = \frac{\widetilde{USL} \ominus \widetilde{LSL}}{6\sigma}, \quad (2)$$

$$C_{\widetilde{pk}} = \frac{\widetilde{USL} \ominus \widetilde{LSL} - 2\left|\mu - \dfrac{\widetilde{USL} \oplus \widetilde{LSL}}{2}\right|}{6\sigma} \quad (3)$$

and

$$C_{\widetilde{pm}} = \frac{\widetilde{USL} \ominus \widetilde{LSL}}{6\sqrt{E(X-T)^2}} = \frac{\widetilde{USL} \ominus \widetilde{LSL}}{6\sqrt{\sigma^2 + (\mu - T)^2}}, \quad (4)$$

where T is the target value. Note that $C_{\tilde{p}}$ is useful when $\mu = m$ in which $m = \dfrac{\widetilde{USL} \oplus \widetilde{LSL}}{2}$.

In the next section, we will discuss on the point and interval estimations of $C_{\widetilde{pm}}$.

III. Estimation of the Generalized Taguchi Index

A. Point estimation of $C_{\widetilde{pm}}$

The rationale behind the point estimation is quite simple. When sampling is from a population described by a Probability Density Function (PDF) or Probabiliy Mass Function (PMF) f_θ, knowledge of unknown parameter θ yields knowledge of the entire population. Hence it is natural to seek a good estimator of the unknown point θ, that is a good estimator as a function of sample. In this subsection, we

are going to obtain two point estimators for unknown parameter $C_{\widetilde{pm}}$.

The sample mean of random sample $X_1,...,X_n$ from a process is $\overline{X} = \sum_{i=1}^{n} X_i \big/ n$ and the sample variances are $S_{n-1}^2 = \frac{1}{n-1}\sum_{i=1}^{n}(X_i - \overline{X})^2$ and $S_n^2 = \frac{n-1}{n} S_{n-1}^2$. The estimators for $\sigma_T{}^2 = E(X-T)^2$ are $S_{T(n-1)}^2 = \frac{1}{n-1}\sum_{i=1}^{n}(X_i - T)^2$ and $S_{T(n)}^2 = \frac{n-1}{n} S_{T(n-1)}^2$.

Substituting the estimators of $\sigma_T{}^2$ in the formula of the Taguchi capability index will provides two point estimators for C_{pm} index. Therefore, the original estimate of C_{pm} is defined as $\hat{C}_{pm(n-1)} = \frac{USL - LSL}{6S_{T(n-1)}}$ in [3]. Another estimator is defined in [1] as

$$\hat{C}_{pm(n)} = \frac{USL - LSL}{6S_{T(n)}} = \sqrt{\frac{n}{n-1}}\hat{C}_{pm(n-1)}. \quad (5)$$

Considering the above discussion for the point estimations of C_{pm} and using Definition 2.4, one can easily define two fuzzy estimators for $C_{\widetilde{pm}}$. The below estimators (6) and (7) are computed by substituting two estimators $S_{T(n-1)}^2$ and $S_{T(n)}^2$ of $\sigma_T{}^2$ in the formula of $C_{\widetilde{pm}}$.

$$\hat{C}_{\widetilde{pm}(n-1)} = \frac{\widetilde{USL} \ominus \widetilde{LSL}}{6S_{T(n-1)}}, \quad (6)$$

$$\hat{C}_{\widetilde{pm}(n)} = \frac{\widetilde{USL} \ominus \widetilde{LSL}}{6S_{T(n)}} = \sqrt{\frac{n}{n-1}}\hat{C}_{\widetilde{pm}(n-1)}. \quad (7)$$

Like to traditional PCIs, for each of these generalized indices, a large value of estimate implies a better distribution of the quality characteristic. In sequel subsection, we only discuss the inference of the generalized index $C_{\widetilde{pm}(n)}$, since the case of $C_{\widetilde{pm}(n-1)}$ can be treated similarly.

B. Confidence interval for $C_{\widetilde{pm}}$

In this subsection, we obtain a confidence interval for the unknown parameter $C_{\widetilde{pm}}$, based the sampling distributions of the corresponding estimators.

Substituting $S_{T(n)}^2$ and $S_{T(n-1)}^2$ in $C_{\widetilde{pm}}$ will provide two fuzzy estimates for $C_{\widetilde{pm}}$, which we denote them by $\hat{C}_{\widetilde{pm}(n)}$ and $\hat{C}_{\widetilde{pm}(n-1)}$, respectively. Like other statistics $\hat{C}_{\widetilde{pm}(n)}$ is also subject to sampling variation and it is critical to compute a confidence interval. The confidence level provides a range which includes the true $C_{\widetilde{pm}}$ with high probability. The confidence interval for $C_{\widetilde{pm}}$ is based on the distribution of $S_{T(n)}^2$, where $S_{T(n)}^2$ is a uniformly minimum variance unbiased estimator of $E(X-T)^2$ [35], and $\hat{C}_{\widetilde{pm}(n)}$ is defined as a simple function of $S_{T(n)}^2$ in (7). Hence, to obtain any $100(1-\gamma)\%$ confidence interval for $C_{\widetilde{pm}}$ index, we need a statistical distribution of $S_{T(n)}^2$. This statistical distribution is presented in Chapter 29 of [10].

The approximate confidence interval for $C_{\widetilde{pm}}$ is given in Theorem 3.1.

Theorem 3.1 If $X_1,...,X_n$ is a random sample set from normal distribution with mean μ and variance σ^2, then the approximate equal-tailed $100(1-\gamma)\%$ confidence interval for $C_{\widetilde{pm}}$ is

$$\left[\hat{C}_{\widetilde{pm}(n)}\sqrt{\chi^2_{\frac{\alpha}{2},\hat{\nu}_n}\big/\hat{\nu}_n}\ ,\ \hat{C}_{\widetilde{pm}(n)}\sqrt{\chi^2_{1-\frac{\alpha}{2},\hat{\nu}_n}\big/\hat{\nu}_n}\right],$$

where $\hat{\nu}_n = n(1+\hat{\delta}_n{}^2)^2\big/(1+2\hat{\delta}_n{}^2)$, $\hat{\delta}_n = (\bar{x}-T)\big/s_n$ and $\chi^2_{\alpha,\hat{\nu}_n}$ is the 100α percentile of a central chi-square variable with $\hat{\nu}_n$ degree of freedom.

IV. Conclusions

This paper further improves the fuzzy process where it is more appropriate to define SLs by two fuzzy sets. In this paper, we presented two point estimators for $C_{\widetilde{pm}}$. But as they are not exactly equal to the true value of parameter, so $100(1-\gamma)\%$ confidence interval for the generalized process capability index $C_{\widetilde{pm}}$ is proposed and an approximate $100(1-\gamma)\%$ confidence interval for $C_{\widetilde{pm}}$ is presented. For future research one can consider the following topics: (1) Generalizing the point and interval estimations of other precise process capability indices, (2) testing hypotheses on the generalized process capability indices, (3) validating of the generalized process capability indices for real-world industrial applications.

Acknowledgment

The first and second authors are partially supported by Fuzzy Systems and its Application Center of Excellence at Shahid Bahonar University of Kerman, Kerman, Iran.

REFERENCES

[1] R. A. Boyles, "The Taguchi capability index," Journal of Quality Technology. Vol. 23, No. 1, pp. 17-26, 1991.

[2] G. Casella, R. L. Berger, Statistical Inference. Brooks/Cole Publishing, California, 1990.

[3] L. K. Chan S. W. Cheng and F. A. Spring, "A new measure of process capability: *Cpm*," Journal of Quality Technology. Vol. 20, No. 3, pp. 162-175, 1988.

[4] K. S. Chen and T. W. Chen, "Multi-process capability plot and fuzzy inference evaluation," International Journal of Production Economics. Vol. 111, No. 1, pp. 70–79, 2008.

[5] T. W. Chen, K. S. Chen and J. Y. Lin, "Fuzzy Evaluation of Process Capability for Bigger-the-Best Type Products," International Journal of Advanced Manufacturing Technology. Vol. 21, pp. 820-826, 2003.

[6] T. W. Chen, J. Y. Lin and K. S. Chen, "Selecting a supplier by fuzzy evaluation of capability indices *Cpm*," International Journal of Advanced Manufacturing Technology. Vol. 22, pp. 534-540, 2003.

[7] D. Dubois and H. Prade, Fuzzy Sets and Systems Theory and Applications. Academic Press, Inc., Toronto, 1980.

[8] Y. Gao and M. Huang, "Optimal Process Tolerance Balancing Based on Process Capabilities," International Journal of Advanced Manufacturing Technology. Vol. 21, pp. 501-507, 2003.

[9] B. M. Hsu and M. H. Shu, "Fuzzy inference to assess manufacturing process capability with imprecise data," European Journal of Operational Research. Vol. 186, No. 2, pp. 652-670, 2008.

[10] N. L. Johnson and S. Kotz, Continuous univariate distributions. John Wiley and Sons, New York, vol 2, 2nd, 1994.

[11] V. Kane, "Process capability indices," Journal of Quality Technology. Vol. 18, No. 1, pp. 41-52, 1986.

[12] C. Kahraman and I. Kaya, "Fuzzy process capability indices for quality control of irrigation water", Stochastic Environmental Research and Risk Assessment. Vol. 23, pp. 451-462, 2009.

[13] I. Kaya and C. Kahraman, "Development of fuzzy process accuracy index for decision making problems", Information Sciences. Vol. 180, pp. 861-872, 2010.

[14] I. Kaya and C. Kahraman, "Fuzzy process capability analyses: An application to teaching processes," Journal of Intelligent & Fuzzy Systems. Vol. 19, pp. 259–272, 2008.

[15] I. Kaya and C. Kahraman, "Fuzzy robust process capability indices for risk assessment of air pollution", Stochastic Environmental Research and Risk Assessment. Vol. 23, pp. 529-541, 2009.

[16] S. Kotz, and N. L. Johnson, "Process capability indices-A review, 1992-2000," Journal of Quality Technology. Vol. 34, pp. 2-19, 2002.

[17] S. Kotz and N. L. Johnson, Process capability indices. Chapman and Hall, New York, USA, 1993.

[18] S. Kotz and CR. Lovelace, Process capability indices in theory and practice. Arnoled, London, 1998.

[19] H. T. Lee, "C_{pk} index estimation using fuzzy numbers," European Journal of Operational Research. Vol. 129, pp. 683-688, 2001.

[20] M. O. Marcucci and C. C. Beazley, "Capability indices process performance measures," ASQC Quality Congress Transaction. pp. 516-523, 1988.

[21] M. Mashinchi, A. Parchami and H. R. Maleki, "Application of fuzzy capability indices in educational comparison," Proceeding of 3rd International Qualitative Research Convention. Sofitel Palm Resort, Senai, Johor Malaysia, pp. 42, 2005.

[22] D. C. Montgomery, Introduction to Statistical Quality Control. Fifth Ed., John Wiley and Sons, Inc., 2005.

[23] H. T. Nguyen and E. A. Walker, A first course in fuzzy logic. Chapman and Hall/CRC, London, 3rd edition, 2006.

[24] A. Parchami, and M. Mashinchi, "A new generation of process capability indices," Journal of Applied Statistics, Vol. 37, No. 1, pp. 77-89, 2010.

[25] A. Parchami, M. Mashinchi, A. R. Yavari and H. R. Maleki, "Process capability indices as fuzzy numbers," Austrian Journal of Statistics. Vol. 34, No. 4, pp. 391-402, 2005.

[26] A. Parchami, M. Mashinchi and H. R. Maleki, "Fuzzy confidence intervals for fuzzy process capability index," Journal of Intelligent and Fuzzy Systems. Vol. 17, No. 3, pp. 287- 295, 2006.

[27] A. Parchami and M. Mashinchi, "Fuzzy estimations for process capability indices," Information Sciences. Vol. 177, No. 6, pp. 1452-1462, 2007.

[28] A. Parchami and M. Mashinchi, "Testing the capability of fuzzy processes", Quality Technology and Quantitative Management. Vol. 6, No. 2, pp. 125–136, 2009.

[29] P. B. Patnaik, "The non-central χ^2 – and *F*-distributions and their applications," Biometrika. Vol. 36, pp. 202-232, 1949.

[30] W. L. Pearn, S. Kotz and N. L. Johnson, "Distribution and inferential properties of capability indices," Journal of Quality Technology. Vol. 24, pp. 216-231, 1992.

[31] W.L. Pearn and C.W. Wu, "A Bayesian approach for assessing process precision based on multiple samples," European Journal of Operational Research. Vol. 165, pp. 685-695, 2005.

[32] Z. Ramezani, A. Parchami and M. Mashinchi, "Fuzzy confidence regions for the Taguchi capability index," International Journal of Systems Science, 2010, DOI: 10.1080/00207720903267890.

[33] V. K. Rohatgi and A. K Ehsan saleh, An introduction to probability theory and mathematical statistics. 2nd Edn, J. wiley, 2001.

[34] B. Sadeghpour-Gildeh, "Comparison of C_p , C_{pk} and $\widetilde{C}_p$ process capability indices in the case of measurement error occurrence," IFSA World Congress. Istanbul, Turkey, pp. 563-567, 2003.

[35] P. Subbaiah and W. Taam, "Inference on the capability index: C_{pm}," Communications in Statistics: Theory and Methods. Vol. 22, No. 2, pp. 537-560, 1993.

[36] L. P. Sullivan, "Reducing variability: A new approach to quality," Quality Progress. Vol. 17, pp. 15-21, 1984.

[37] S. M. Taheri, "Trends in fuzzy statistics," Austrian Journal of Statistics. Vol. 32, No. 3, pp. 239-257, 2003.

[38] C. C. Tsai and C. C. Chen, "Making decision to evaluate process capability index Cp with fuzzy numbers," International Journal of Advanced Manufacturing Technology. Vol. 30, pp. 334-339, 2006.

[39] R. Viertl, "On the future of data analysis", Austrian Journal of Statistics. Vol. 31, pp. 241-244, 2002.

[40] X. Wang, "Reasonable properties for the ordering of fuzzy quantities (II)," Fuzzy Sets and Systems. Vol. 118, pp. 387-405, 2001.

[41] E. B. Wilson and M. M. Hilferty, "The distribution of chi square," Proceedings of National Academy of Science. Vol. 17, pp. 684-688, 1931.

[42] C. Yongting, "Fuzzy quality and analysis on fuzzy probability," Fuzzy Sets and Systems. Vol. 83, pp. 283-290, 1996.

[43] L. A. Zadeh, "Fuzzy sets," Information and Control. Vol. 8, pp. 338-359, 1965.

2011 IEEE International Conference on Fuzzy Systems
June 27-30, 2011, Taipei, Taiwan

Generalized Intuitionistic Fuzzy Soft Set and its Application in Practical Medical Diagnosis Problem

M. Agarwal, M. Hanmandlu, K. K Biswas
Indian Institute of Technology
New Delhi, India
magarwal@cse.iitd.ac.in, mhmandlu@ee.iitd.ac.in, kkb@cse.iitd.ac.in

***Abstract*—In this paper, a generalized intuitionistic fuzzy soft set (GIFSS) is introduced and its various properties are presented. The generalized intuitionistic soft fuzzy relations on GIFSS have been defined and their properties are discussed. We have also devised a new scoring function to compare two intuitionistic fuzzy numbers. An application of GIFSS, generalized intuitionistic soft fuzzy relations on GIFSS and the novel score function are demonstrated through a practical example of a multi-criteria medical diagnosis problem.**

Keywords-intuitionistic; fuzzy; soft; generalized; score function; multi criteria decision making; Sanchez diagnosis; medical diagnosis; relation

I. INTRODUCTION

The concept of intuitionistic fuzzy set characterized by a novel hesitancy function has been introduced by Atnassov [1, 2]. Molodtsov [3] has introduced the theory of soft sets characterized by parameterization tools for modelling the vagueness and uncertainties. The soft set theory finds wide range of applications in complex medical sciences, engineering, management, economics and social sciences, primarily due to its flexibility without restrictions on approximate description of the situation. Maji et al. [4-6] have extended the theory by proposing the concept of fuzzy soft sets and intuitionistic fuzzy soft sets, and their properties. Kong et al. [7-8] have demonstrated the application of soft set theory in decision making problems. Majumdar et al. [9-10] have explored the methods to find similarity measurement between the fuzzy soft sets, and proposed the notion of generalized fuzzy soft sets.

In this paper, we propose generalized intuitionistic fuzzy soft set (GIFSS). An intuitionistic degree is attached to the intuitionistic fuzzy soft set (IFSS) to indicate the degree of possibility of belongingness of the elements of the universal set in the IFSS. This adds to the second level of uncertainty in IFSS indicating the credibility of the values of IFSS. Relations and properties of GIFSS have been defined. A novel score function to compare intuitionistic fuzzy numbers (IFNs) has also been proposed. Finally Sanchez's method [11] of medical diagnosis is extended to demonstrate a practical medical application of GIFSS and novel score function.

The hesitancy parameter in Atnassov's [1] IFS is a feature of one's own perception, and hence itself ambiguous. It is insufficient to convey a unique meaning imperative for the correct medical diagnosis. For example, a patient might report the symptoms to a doctor as per his perceptions, and the real information might get distorted in its reporting. Unless this misrepresentation is factored in by a doctor, it would lead to wrong diagnosis. The extra generalization parameter that we introduce normalizes an IFSS with an expert's opinion which indicates the credibility of the information presented to him. For example, a doctor reposes more confidence in the symptoms reported by an educated adult patient than that reported by a child.

The paper is organized in seven sections. In section II, a few preliminaries and useful definitions are given. In section III, GIFSS and its properties are introduced. In section IV, a novel score function is introduced, designed specifically for the medical diagnosis applications. In the next section, relations on GIFSS are defined and its properties are discussed. In section VI, an application of GIFSS is shown in the area of medical diagnosis extending Sanchez's approach. And finally in Section VII, conclusions are presented.

II. PRELIMINARIES

Before describing GIFSS, a few definitions regarding intuitionistic fuzzy sets (IFS) and fuzzy soft sets are presented here.

Definition 2.1 [1]: Let $X = \{x_1, x_2, ..., x_n\}$ be a fixed finite non-empty set. Then a IFS $A = \{x_i, t_A(x_i), f_A(x_i) | x_i \in X\}$ where the functions $t_A: X \rightarrow [0,1]$ and $f_A: X \rightarrow [0, 1]$ denote the degree of membership and the degree of non-membership of the element $x \in X$ to A respectively, such that for every $x \in X$: $0 \leq t_A(x) + f_A(x) \leq 1$. Also $h_A(x) = 1 - (t_A(x) + f_A(x))$ is called the degree of hesitation or indeterminacy of x to A. For convenience, we call $\tilde{a} = (t_{\tilde{a}}, f_{\tilde{a}})$ as an intuitionistic fuzzy number (IFN), where $t_{\tilde{a}} \in [0, 1]$, $f_{\tilde{a}} \in [0, 1]$, and $t_{\tilde{a}} + f_{\tilde{a}} \leq 1$.

Definition 2.2 ([3]): Let U denote an initial universal set and E be a set of parameters. Let P (U) be the power set of U. Then pair (F, E) is called a soft set over U iff F is a mapping given by $F : E \rightarrow P(U)$.

Definition 2.3 ([4]): Let U denote an initial universal set and E be a set of parameters. Let I^U denote the power set of all

fuzzy subsets of U. Let A ⊂ E. A pair (F, E) is called a fuzzy soft set over U, where F is a mapping given by F : A → I^U.

Definition 2.4 ([4]) Let U denote an initial universal set and E be a set of parameters. Let IF^U denote the collection of all intuitionistic fuzzy subsets of U. Let A □ E. A pair (F, A) is called intuitionistic fuzzy soft set (IFSS) over U, where F is a mapping given by $\tilde{F} : A \rightarrow IF^U$.

Example 2.1: Let U={c_1, c_2, c_3, c_4} be the set of popular bicycles and E ={cost (e_1), colour (e_2), weight (e_3)} be the set of parameters. Let A ⊆ E denotes the list of select parameters that would determine Tom's buying decision. Let A = {e_1, e_3} ⊂ E.

Then, (C,A) = [C(e_1) = {c_1, c_3, c_4}, C(e_3)={c_2,c_3}] is the crisp soft set over U that describes the bicycles which Tom may buy.

Instead, if we have a fuzzy mapping, F: A → I^U with each criteria having a fuzzy membership for each sample of U, then an example of fuzzy soft set, (F, A), could be [F(e_1) = {c_1|0.8, c_2|0.2, c_3|0.5, c_4|0.4}, F(e_3)={ c_1|0.7, c_2|0.5, c_3|0.3, c_4|0.8}].

(F, A) is the fuzzy soft set over U that describes the cycles which Tom may buy.

If we have a mapping $\tilde{F} : A \rightarrow IF^U$ with each criteria having a intuitionistic fuzzy membership for each sample of U, then an example of IFSS, (I, A), could be [I(e_1) = {c_1|(0.8, 0.1), c_2|(0.2, 0.6), c_3|(0.5, 0.3), c_4|(0.4, 0.5)}, F(e_3)={c_1|(0.7, 0.1), c_2|(0.5, 0.2), c_3|(0.3, 0.6), c_4|(0.8, 0.0)}].

(I, A) is the IFSS over U that describes the cycles which Tom may buy.

Definition 2.5 ([1]): If A and B are two IFSs of the set E of form {x_i, t(x_i), f(x_i)> | x_i∈ X}, then

$$A \subset B \; iff \; \forall x \in E, [t_A(x) \leq t_B(x) \; and \; f_A(x) \geq f_B(x)] \quad (1)$$

$$A \supset B \; iff \; B \subset A \quad (2)$$

$$A = B \; iff \; \forall x \in E, [t_A(x) = t_B(x) \; and \; f_A(x) = f_B(x)] \quad (3)$$

$$\overline{A} = \{x, f_A(x), t_A(x) | x \in E\} \quad (4)$$

$$A \cup B = \{(x, \max(t_A(x), t_B(x)), \min(f_A(x), f_B(x)) | \; x \in E\} \quad (5)$$

$$A \cap B = \{(x, \min(t_A(x), t_B(x)), \max(f_A(x), f_B(x)) | \; x \in E\} \quad (6)$$

Definition 2.6 ([1])**:** An intuitionistic fuzzy relation (IFR) R from two IFSs X to Y is an IFS of $X \times Y$ characterized by the membership function t_R and non-membership function f_R, and denoted as R (X → Y)

Definition 2.7 ([11])**:** Let A be IFS in X. Let R (X → Y) be an IFR from X to Y. Then max-min-max composition of the IFR R (X → Y) with A would result in another IFS B of Y, denoted by B = R o A. The membership function of B is defined as

$$t_{R \circ A}(y) = \bigvee_x [t_A(x) \wedge t_R(x, y)] \quad (7)$$

Similarly, the non-membership function is defined as

$$f_{R \circ A}(y) = \bigwedge_x [f_A(x) \vee f_R(x, y)] \quad (8)$$

∀y ∈ Y (where $\bigvee = max, \bigvee = min$).

III. Generalized Intuitionistic Fuzzy Soft Set (GIFSS)

We hereby present a generalized version of IFSS with an extra parameter, indicating an expert's opinion regarding the authenticity of the IFSS values.

A. Basic Definitions

A few basic definitions of GIFSS are defined, and illustrated through examples.

Definition 3.1: Let U denote the universal set of elements and E = {e_1, e_2, ..., e_m} be the universal set of parameters. The pair (U, E) is called a soft universe. Let A ⊆ E and $\tilde{F}: A \rightarrow IF^U$ and $\tilde{\alpha}$ be an intuitionistic fuzzy subset of E, i.e., $\tilde{\alpha} \rightarrow IF = (t_{\tilde{a}}, f_{\tilde{a}})$, where $t_{\tilde{\alpha}} \in [0,1], f_{\tilde{\alpha}} \in [0,1], \; t_{\tilde{\alpha}} + f_{\tilde{\alpha}} \leq 1$, and IF^U is the collection of all intuitionistic fuzzy subsets of U. Mapping $\tilde{F}_{\tilde{\alpha}}: A \rightarrow IF^U \; X \; IF$ is defined as follows:

$$\tilde{F}_{\tilde{\alpha}}(e) = \left(\tilde{F}(e), \tilde{\alpha}(e)\right), \quad where \; \tilde{F}(e) \in IF^U, and \; \tilde{\alpha}(e) \in IF \quad (9)$$

$\tilde{F}_{\tilde{\alpha}}$ is called generalized intuitionistic fuzzy soft set (GIFSS in short) over the soft universe (U, E), where $\tilde{F}(e)$ refers to the elements of U in the IFSS, and the extra generalization parameter $\tilde{\alpha}(e)$ indicates degree of possibility of belongingness of the elements of U in $\tilde{F}(e_i)$.

Example 3.1: Let U={c_1, c_2, c_3, c_4} be the set of popular cycles and E ={cost (e_1), colour (e_2), weight (e_3)} be the set of parameters. Let A ⊆ E denote the list of select parameters that would determine Tom's buying decision. Let A = {e_1, e_3} ⊂ E.

Let $\tilde{\alpha} : E \rightarrow IF$ be defined as follows:
$\tilde{\alpha}(e_1) = (0.6, 0.3), \tilde{\alpha}(e_3) = (0.3, 0.5)$

So, if we assume the values of a member of IF^U, the function

$\tilde{F}_{\tilde{\alpha}}: A \rightarrow IF^U \; X \; IF$ is defined as follows:-

$\tilde{F}_{\tilde{\alpha}}(e_1)$ = {{c_1|(0.8, 0.1), c_2|(0.2, 0.6), c_3|(0.5, 0.3), c_4|(0.4, 0.5)}, (0.6, 0.3)}

$\tilde{F}_{\tilde{\alpha}}(e_3)$ = {{c_1|(0.7, 0.1), c_2|(0.5, 0.2), c_3|(0.3, 0.6),

$c_4|(0.8, 0.0)\}, (0.3, 0.5)\}$

Here, $\tilde{F}_{\tilde{\alpha}}$ is a GIFSS over (U, E). Here the value $\tilde{\alpha}(e)$ indicates an expert's confidence in the values of IFSS with regards to their correctness.

Definition 3.2: Let $\tilde{F}_{\tilde{\alpha}}$ and $\tilde{G}_{\tilde{\delta}}$ be two GIFSS over soft universe (U, E). Now, $\tilde{F}_{\tilde{\alpha}}$ would be called as generalized intuitionistic fuzzy soft subset of $\tilde{G}_{\tilde{\delta}}$, i.e., $\tilde{F}_{\tilde{\alpha}} \subseteq \tilde{G}_{\tilde{\delta}}$, if

i) $\tilde{\alpha}$ is an intuitionistic fuzzy subset of $\tilde{\delta}$.
ii) $\tilde{F}(e)$ is a intuitionistic fuzzy subset of $\tilde{G}(e)$, $\forall e \in E$.

Example 3.2: Let us consider the GIFSS, $\tilde{F}_{\tilde{\alpha}}$ as in Example 3.1. Let $\tilde{G}_{\tilde{\delta}}$ be another GIFSS over (U, E) defined as follows:

$\tilde{G}_{\tilde{\alpha}}(e_1) = \{\{c_1|\ (0.3, 0.5), c_2|\ (0.2, 0.7), c_3|\ (0.3, 0.5), c_4|\ (0.2, 0.6)\}, (0.5, 0.4)\}$
$\tilde{G}_{\tilde{\alpha}}(e_3) = \{\{c_1|\ (0.6, 0.3), c_2|\ (0.4, 0.4), c_3|\ (0.1, 0.8), c_4|\ (0.5, 0.3)\}, (0.1, 0.8)\}$

In the light of definition 3.2, the GIFSS, $\tilde{G}_{\tilde{\alpha}}$, is a intuitionistic fuzzy subset of $\tilde{F}_{\tilde{\alpha}}$.

Definition 3.3: Let $\tilde{F}_{\tilde{\alpha}}$ be a GIFSS over soft universe (U, E). Then the inverse of $\tilde{F}_{\tilde{\alpha}}$, $\tilde{F}^{i}_{\tilde{\alpha}} = \tilde{G}_{\tilde{\delta}}$ where

i) $\tilde{\delta}(e) = \tilde{\alpha}^{i}(e)$
ii) $\tilde{G}(e) = \tilde{F}^{i}(e)$, $\forall e \in E$.

Example 3.3: Find the inverse of the GIFSS, $\tilde{F}_{\tilde{\alpha}}(e_1)$ as in Example 3.1.

$\tilde{F}^{i}_{\tilde{\alpha}}(e_1) = \{\{c_1|\ (0.1, 0.8), c_2|\ (0.6, 0.2), c_3|\ (0.3, 0.5), c_4|\ (0.5, 0.4)\}, (0.3, 0.6)\}$

Definition 3.4: Let $\tilde{F}_{\tilde{\alpha}}$ be a GIFSS over soft universe (U, E). Then the complement of $\tilde{F}_{\tilde{\alpha}}$ is defined as

$$\tilde{F}^{c}_{\tilde{\alpha}} = \tilde{G}_{\tilde{\delta}}$$

where

i) $\tilde{\delta}(e) = \tilde{\alpha}^{c}(e)$
ii) $\tilde{G}(e) = \tilde{F}^{c}(e)$, $\forall e \in E$.

Definition 3.5: Let $\tilde{F}_{\tilde{\alpha}}$ and $\tilde{G}_{\tilde{\delta}}$ be two GIFSS over soft universe (U, E). Union of $\tilde{F}_{\tilde{\alpha}}$ and $\tilde{G}_{\tilde{\delta}}$, denoted by $\tilde{F}_{\tilde{\alpha}} \tilde{\cup} \tilde{G}_{\tilde{\delta}}$, would yield GIFSS $\tilde{H}_{\tilde{\nu}} : E \rightarrow IF^{U}\ X\ IF$, where

i) $\tilde{H}_{\tilde{\nu}}(e) = \left(\tilde{H}(e), \tilde{\nu}\ (e)\right), where\ \tilde{H}(e) \in IF^{U}, \tilde{\nu}\ (e) \in IF\ \tilde{F}(e)$
ii) $\tilde{H}(e) = \tilde{F}(e) \circ \tilde{G}(e)$
iii) $\tilde{\nu}(e) = \tilde{\alpha}(e) \circ \tilde{\delta}(e)$
iv) $\circ$ is a suitable t-conorm operator
v) $\tilde{\cup}$ is the union operator adapted for GIFSS.

Definition 3.6: Let $\tilde{F}_{\tilde{\alpha}}$ and $\tilde{G}_{\tilde{\delta}}$ be two GIFSS over soft universe (U, E). Then the intersection of $\tilde{F}_{\tilde{\alpha}}$ and $\tilde{G}_{\tilde{\delta}}$, denoted by $\tilde{F}_{\tilde{\alpha}} \tilde{\cap} \tilde{G}_{\tilde{\delta}}$, would yield GIFSS $\tilde{K}_{\tilde{\nu}} : E \rightarrow IF^{U}\ X\ IF$, where

i) $\tilde{K}_{\tilde{\nu}}(e) = \left(\tilde{K}(e), \tilde{\nu}\ (e)\right), \tilde{K}(e) \in IF^{U}, \tilde{\nu}\ (e) \in IF$
ii) $\tilde{K}(e) = \tilde{F}(e) * \tilde{G}(e)$
iii) $\tilde{\nu}(e) = \tilde{\alpha}(e) * \tilde{\delta}(e)$
iv) $*$ is a suitable t-norm operator
v) $\tilde{\cap}$ is the intersection operator adapted for GIFSS.

Example 3.4: Find the union of the two GIFSS, specified in examples 3.1 and 3.2. The t-conorm ($\circ$) operator is the standard union operator, as defined in (5).

Let $\tilde{F}_{\tilde{\alpha}}(e)\ \tilde{\cup}\ \tilde{G}_{\tilde{\delta}}(e) = \tilde{H}_{\tilde{\nu}}(e)$, $\forall e \in E$. Then,

$\tilde{H}_{\tilde{\nu}}(e_1) = \{\{c_1|\ (0.8, 0.1), c_2|\ (0.2, 0.6), c_3|\ (0.5, 0.3), c_4|\ (0.4, 0.5)\}, (0.6, 0.3)\}$
$\tilde{H}_{\tilde{\nu}}(e_3) = \{\{c_1|\ (0.7, 0.1), c_2|\ (0.5, 0.2), c_3|\ (0.3, 0.6), c_4|\ (0.8, 0.0)\}, (0.3, 0.5)\}$

Example 3.5: Find the intersection of the two GIFSS, as taken in examples 3.1 and 3.2. The t-norm ($*$) operator is the standard intersection operator, as defined in (6).

Let $\tilde{F}_{\tilde{\alpha}}(e)\ \tilde{\cap}\ \tilde{G}_{\tilde{\delta}}(e) = \tilde{K}_{\tilde{\nu}}(e)$, $\forall e \in E$. Then,

$\tilde{K}_{\tilde{\nu}}(e_1) = \{\{c_1|\ (0.3, 0.5), c_2|\ (0.2, 0.7), c_3|\ (0.3, 0.5), c_4|\ (0.2, 0.6)\}, (0.5, 0.4)\}$
$\tilde{K}_{\tilde{\nu}}(e_3) = \{\{c_1|\ (0.6, 0.3), c_2|\ (0.4, 0.4), c_3|\ (0.1, 0.8), c_4|\ (0.5, 0.3)\}, (0.1, 0.8)\}$

Definition 3.7: A GIFSS is said to be a generalized intuitionistic null fuzzy soft set, $\tilde{\Phi}_{\tilde{\theta}}: E \rightarrow IF^{U} \times IF$, if

$$\tilde{\Phi}_{\tilde{\theta}}(e) = \left(\tilde{F}(e), \tilde{\theta}\ (e)\right), where\ \tilde{F}(e) = (0.0, 1.0), and\ \tilde{\theta}\ (e) = (0.0, 1.0), \forall\ e\ \in E.$$

Definition 3.8: A GIFSS is said to be a generalized intuitionistic absolute fuzzy soft set, $\tilde{A}_{\tilde{\alpha}}: E \rightarrow IF^{U} \times IF$, if

$$\tilde{A}_{\tilde{\alpha}}(e) = \left(\tilde{F}(e), \tilde{\alpha}\ (e)\right), where\ \tilde{F}(e) = (1.0, 0.0), and\ \tilde{\alpha}\ (e) = (1.0, 0.0), \forall\ e\ \in E.$$

B. Properties of GIFSS

A few properties of GIFSS are stated in the following theorems.

Theorem 3.1: Let $\tilde{F}_{\tilde{\gamma}}$ be a GIFSS over (U, E), then the following holds:

i) $\tilde{F}_{\tilde{\gamma}}$ is a subset of $\tilde{F}_{\tilde{\gamma}} \tilde{\cup} \tilde{F}_{\tilde{\gamma}}$
ii) $\tilde{F}_{\tilde{\gamma}} \tilde{\cap} \tilde{F}_{\tilde{\gamma}}$ is a subset of $\tilde{F}_{\tilde{\gamma}}$
iii) $\tilde{F}_{\tilde{\gamma}} \tilde{\cup} \tilde{\Phi}_{\tilde{\theta}} = \tilde{F}_{\tilde{\gamma}}$
iv) $\tilde{F}_{\tilde{\gamma}} \tilde{\cap} \tilde{\Phi}_{\tilde{\theta}} = \tilde{\Phi}_{\tilde{\theta}}$
v) $\tilde{F}_{\tilde{\gamma}} \tilde{\cup} \tilde{A}_{\tilde{\alpha}} = \tilde{A}_{\tilde{\alpha}}$
vi) $\tilde{F}_{\tilde{\gamma}} \tilde{\cap} \tilde{A}_{\tilde{\alpha}} = \tilde{F}_{\tilde{\gamma}}$
vii) $\tilde{F}_{\tilde{\gamma}} \tilde{\cup} \tilde{F}_{\tilde{\gamma}}^{c} = \tilde{A}_{\tilde{\alpha}}$
viii) $\tilde{F}_{\tilde{\gamma}} \tilde{\cup} \tilde{F}_{\tilde{\gamma}}^{c} = \tilde{\Phi}_{\tilde{\theta}}$

Proof: The results follow trivially from definitions 3.1 to 3.7.

Theorem 3.2: Let $\tilde{F}_{\tilde{\gamma}}$, $\tilde{G}_{\tilde{\delta}}$ and $\tilde{H}_{\tilde{\nu}}$ be any three GIFSS over (U, E), then the commutative and associative properties hold:-

$$\text{i)}\quad \tilde{F}_{\tilde{\gamma}} \tilde{\cup} \tilde{G}_{\tilde{\delta}} = \tilde{G}_{\tilde{\delta}} \tilde{\cup} \tilde{F}_{\tilde{\gamma}} \tag{10}$$
$$\text{ii)}\quad \tilde{F}_{\tilde{\gamma}} \tilde{\cap} \tilde{G}_{\tilde{\delta}} = \tilde{G}_{\tilde{\delta}} \tilde{\cap} \tilde{F}_{\tilde{\gamma}} \tag{11}$$
$$\text{iii)}\quad \tilde{F}_{\tilde{\gamma}} \tilde{\cup} \left(\tilde{G}_{\tilde{\delta}} \tilde{\cup} \tilde{H}_{\tilde{\nu}}\right) = \left(\tilde{F}_{\tilde{\gamma}} \tilde{\cup} \tilde{G}_{\tilde{\delta}}\right) \tilde{\cup} \tilde{H}_{\tilde{\nu}} \tag{12}$$
$$\text{iv)}\quad \tilde{F}_{\tilde{\gamma}} \tilde{\cap} \left(\tilde{G}_{\tilde{\delta}} \tilde{\cap} \tilde{H}_{\tilde{\nu}}\right) = \left(\tilde{F}_{\tilde{\gamma}} \tilde{\cap} \tilde{G}_{\tilde{\delta}}\right) \tilde{\cap} \tilde{H}_{\tilde{\nu}} \tag{13}$$

Proof: The properties of commutativity and associativity of $\tilde{\cup}$ and $\tilde{\cap}$ trivially follows from the definitions.

Theorem 3.3: Let $\tilde{F}_{\tilde{\gamma}}$, $\tilde{G}_{\tilde{\delta}}$ and $\tilde{H}_{\tilde{\nu}}$ be any three GIFSS over (U, E), and the t-conorm (°) and t-norm ($*$) operators are the standard union (max) and intersection operators (min) (as defined in (5) and (6) respectively), then the distributive property holds:-

$$\text{i)}\quad \tilde{F}_{\tilde{\gamma}} \tilde{\cup} \left(\tilde{G}_{\tilde{\delta}} \tilde{\cap} \tilde{H}_{\tilde{\nu}}\right) = \left(\tilde{F}_{\tilde{\gamma}} \tilde{\cup} \tilde{G}_{\tilde{\delta}}\right) \tilde{\cap} \left(\tilde{F}_{\tilde{\gamma}} \tilde{\cup} \tilde{H}_{\tilde{\nu}}\right) \tag{14}$$
$$\text{ii)}\quad \tilde{F}_{\tilde{\gamma}} \tilde{\cap} \left(\tilde{G}_{\tilde{\delta}} \tilde{\cup} \tilde{H}_{\tilde{\nu}}\right) = \left(\tilde{F}_{\tilde{\gamma}} \tilde{\cap} \tilde{G}_{\tilde{\delta}}\right) \tilde{\cup} \left(\tilde{F}_{\tilde{\gamma}} \tilde{\cap} \tilde{H}_{\tilde{\nu}}\right) \tag{15}$$

Proof: Since the standard $\cup$ (max/union) and $\cap$ (min/intersection) operators as defined in (5) and (6) are commutative and associative, the above properties hold good, when these standard operators are used for t-conorm and t-norm.

Note: - If the t-conorm and t-norm operators are different from the standard union and intersection operators, the above rules may not hold good.

Theorem 3.4: Let $\tilde{F}_{\tilde{\gamma}}$, $\tilde{G}_{\tilde{\delta}}$ be any two GIFSS over (U, E), then the following holds:-

$$\text{i)}\quad \left(\tilde{F}_{\tilde{\gamma}} \tilde{\cup} \tilde{G}_{\tilde{\delta}}\right)^{c} = \tilde{F}_{\tilde{\gamma}}^{c} \tilde{\cap} \tilde{G}_{\tilde{\delta}}^{c} \tag{16}$$
$$\text{ii)}\quad \left(\tilde{F}_{\tilde{\gamma}} \tilde{\cap} \tilde{G}_{\tilde{\delta}}\right)^{c} = \tilde{F}_{\tilde{\gamma}}^{c} \tilde{\cup} \tilde{G}_{\tilde{\delta}}^{c} \tag{17}$$

Proof: The above results follow from definitions 3.3, 3.4 and 3.5.

Theorem 3.5: Let $\tilde{F}_{\tilde{\gamma}}$ be any GIFSS over (U, E) with $\tilde{G}_{\tilde{\delta}}$ being its generalized intuitionistic fuzzy soft subset, and the t-conorm (°) and t-norm ($*$) operators are the standard union (max) and intersection operators (min) (as defined in (5) and (6) respectively), then the following holds:-

$$\text{i)}\quad \tilde{F}_{\tilde{\gamma}} \tilde{\cup} \tilde{G}_{\tilde{\delta}} = \tilde{F}_{\tilde{\gamma}} \tag{18}$$
$$\text{ii)}\quad \tilde{F}_{\tilde{\gamma}} \tilde{\cap} \tilde{G}_{\tilde{\delta}} = \tilde{G}_{\tilde{\delta}} \tag{19}$$

Proof: The above results follow trivially from definitions 3.4 and 3.5, and (5) and (6).

IV. Novel Score Function

A novel score function is devised here to compare two intuitionistic fuzzy numbers (IFNs) by emphasizing the membership value over the non-membership value. Xu [12] has developed a ranking method based on the score function value and accuracy function value of interval-valued intuitionistic fuzzy numbers. Ye [13] has ranked the interval-valued intuitionistic fuzzy numbers based on a novel accuracy function. However, in particular applications, the proposed techniques using a score function and an accuracy function are not suitable to compare IFNs. Therefore, it is necessary to devise application specific score functions

Definition 4.1: Let $\tilde{F} = (t_f, f_f)$, $\tilde{G} = (t_g, f_g)$ be two IFNs. Then scores of $\tilde{F}$ and $\tilde{G}$ are given as $\Delta\tilde{F} = t_f^2 - f_f^2$, and $\Delta\tilde{G} = t_g^2 - f_g^2$ respectively. The accuracy degrees of $\tilde{F}$ and $\tilde{G}$ are given as $H_f = t_f^2 + f_f^2$, and $H_g = t_g^2 + f_g^2$ respectively.

- If $\Delta\tilde{F} < \Delta\tilde{G}$, $then\ \tilde{F} < \tilde{G}$;
- If $\Delta\tilde{F} = \Delta\tilde{G}$, $then$
  - If $H_f = H_g$, $then\ \tilde{F} = \tilde{G}$;
  - If $H_f < H_g$, $then\ \tilde{F} < \tilde{G}$; (20)

V. Relation on GIFSS

The notion of intuitionistic fuzzy soft relation is defined and generalized in the context of GIFSS.

Definition 5.1 : An intuitionistic fuzzy soft relation (IFSR) $\tilde{R}$ between two IFSS, $\tilde{F}$ and $\tilde{G}$ over soft universe (U, E) and (U, F) respectively, is defined as $\tilde{R}(e,f) = \tilde{F}(e) \tilde{\cap} \tilde{G}(f)$, $\forall e \in E\ and\ \forall f \in F$, where $\tilde{R}: K \rightarrow IF^{U}$ is an IFSS over (U, K), where K $\subseteq E \times F$.

Definition 5.2: A generalized intuitionistic fuzzy soft relation (GIFSR) $\tilde{R}_{\tilde{\tau}}$ between two GIFSS, $\tilde{F}_{\tilde{\alpha}}$ and $\tilde{G}_{\tilde{\delta}}$ over soft universe (U, E) and (U, F) respectively, is defined as:

$$\tilde{R}_{\tilde{\tau}}(e,f) = \tilde{F}_{\tilde{\alpha}}(e) \,\tilde{\cap}\, \tilde{G}_{\tilde{\delta}}(f),\ \forall e \in E \text{ and } \forall f \in F,$$

where, $\tilde{R}_{\tilde{\tau}}: K \to IF^U \times IF$ is a GIFSS over (U, K),

$K \subseteq E \times F$.

Definition 5.3: Let $\tilde{R}_1$ be GIFSR between two GIFSS, $\tilde{F}_{\tilde{\alpha}}$ and $\tilde{G}_{\tilde{\delta}}$ over soft universe (U, E) and (U, K) respectively. Let $\tilde{R}_2$ be GIFSR between GIFSS, $\tilde{G}_{\tilde{\delta}}$ and $\tilde{H}_{\tilde{\kappa}}$ over soft universe (U, K) and (U, L) respectively. Then composition of $\tilde{R}_1$ and $\tilde{R}_2$ is defined as:-

$$(\tilde{R}_1 \, composition \, \tilde{R}_2)(\mathrm{e},\mathrm{l}) = \tilde{R}_1(e,k) \,\tilde{\cap}\, \tilde{R}_2(k,l)$$

where, $\tilde{R}_1: E \times K \to IF^U \times IF$

$\tilde{R}_2: K \times L \to IF^U \times IF$ (21)

Definition 5.4: Let $\tilde{R}_1$ and $\tilde{R}_2$ be two GIFSRs between two GIFSS, $\tilde{F}_{\tilde{\alpha}}$ and $\tilde{G}_{\tilde{\delta}}$ over soft universe (U, A) and (U, B) respectively. Then the standard operations of union, intersection and inverse are defined as follows:

$$(\tilde{R}_1 \cup \tilde{R}_2)(\mathrm{a},\mathrm{b}) = \max\{\tilde{R}_1(a,b), \tilde{R}_2(a,b)\} \quad (22)$$

$$(\tilde{R}_1 \cap \tilde{R}_2)(\mathrm{a},\mathrm{b}) = \min\{\tilde{R}_1(a,b), \tilde{R}_2(a,b)\} \quad (23)$$

$$\tilde{R}_1^{-1}(\mathrm{a},\mathrm{b}) = \tilde{R}_1^{-1}(\mathrm{b},\mathrm{a}), \forall(\mathrm{a},\mathrm{b}) \in \mathrm{A} \times \mathrm{B} \quad (24)$$

where, $\tilde{R}_1: A \times B \to IF^U \times IF$

$\tilde{R}_2: A \times B \to IF^U \times IF$

VI. An Application of GIFSS in Medical Diagnosis

We present a practical example of an expert system to diagnose the disease of multiple patients among multiple diseases, deploying the proposed GIFSS and GIFSR and the score function. A medical expert system with intuitionistic medical knowledge as a GIFSR from S (set of symptoms) to D (set of diagnosis) as $S \times D$ is defined.

A. Case-Study 6.1

Tom, Bob, Ram and Edwin are four class-mates, and display the symptoms: fever, headache, body-pain, cough, and loss-of-appetite. The possible diseases could be Typhoid, Malaria, Flu, Jaundice or Throat infection.

Step 1: The symptoms of patients are noted in first five columns of table I. The last column is the newly proposed generalization parameter provided by a moderator indicating his trust in the fuzzy data furnished by the patients.

Step 2: Table II indicates standard medical knowledge relating symptoms with the set of diseases under consideration. The rows indicate the symptoms while the columns correspond to various diseases.

Step 3: In Table III, we obtain patients' diagnosis applying Sanchez's approach as per (7) and (8) to each row-column pair of the two matrices in order to arrive at patients' diagnosis. For ex., Tom's symptoms are composed with Typhoid symptoms as below:-

For membership function: $(0.5 \wedge 0.3) \vee (0.8 \wedge 0.4) \vee (0.8 \wedge 0.8) \vee (0.1 \wedge 0.1) \vee (0.6 \wedge 0.9) \vee (0.6 \wedge 1.0) = 0.8$

For non-membership function: $(0.4 \vee 0.7) \wedge (0.2 \vee 0.5) \wedge (0.1 \vee 0.1) \wedge (0.8 \vee 0.9) \wedge (0.2 \vee 0.1) \wedge (0.3 \vee 0.0) = 0.1$

Thus, the value obtained, (0.8, 0.1) gives the possibility of Tom, having Typhoid. Similarly other values of table III are obtained.

Step 4: The IFNs in Table III are compared, applying score function, as per (20), so as to find the maximum number that indicates the most probable diagnosis of the patients. The score values are populated in Table IV.

Result: The maximum score in a row indicates the diagnosis for each patient. Hence Tom (with score 0.63) and Ram (with score 0.63) suffer from Typhoid, Bob (with score 0.63) and Edwin (0.32) suffer from Malaria.

B. Validation of Results

A few additional steps, as given below, may also be performed so as to be more certain about the results obtained above.

Step 5: Obtain the inverse of the entries of Table II, and populate the values in Table V.

Step 6: Perform the composition of Table I and Table V, as explained in Step 3.

Step 7: Calculate the score of each number in the Table VI, and populate the values in Table VII.

Step 8: Calculate the difference between entries in Table IV and Table VII, to arrive at the net score, as given in Table

VIII. The higher the score, higher is the possibility of the patient affected with the respective disease.

Result: Again, it can be concluded that Tom and Ram suffers from Typhoid, Bob and Edwin suffer from Malaria.

C. Discussion of the Result

The new generalization parameter, indicating an expert's level of trust in the credibility of information, significantly makes the approach quite close to real-life situations. This helps in removing the individual bias from the input data and brings more credibility to the final decision arrived at.

The generalization parameter facilitates the decision making process by including the degree of possibility of correctness of the information presented. In the above example, the doctor appears to be more confident about the reporting by Tom, Ram and Bob (as seen by high values of the generalization parameter), while he is least sure about Edwin's reporting.

For standard medical knowledge, used as the basic rule engine, the generalization parameter is taken as (1, 0), indicating the absolute belief. The results obtained are also validated by performing the composition of non-symptoms of diseases with patients' symptoms so as to obtain the score that indicates non-possibility of a particular disease. The two scores are merged to arrive at the final diagnosis.

TABLE I. PATIENTS AND THEIR SYMPTOMS

Patients	Fever	Headache	Bodypain	Cough	Loss-of-Appetite	Degree of Belonging
Tom	(0.5, 0.4)	(0.8,0.2)	(0.8,0.1)	(0.1, 0.8)	(0.6, 0.2)	(0.6, 0.3)
Bob	(0.8, 0.1)	(0.9, 0.1)	(0.7, 0.2)	(0.1, 0.9)	(0.2, 0.7)	(0.4, 0.2)
Ram	(0.1, 0.8)	(0.3, 0.7)	(0.8, 0.1)	(0.6, 0.2)	(0.1, 0.8)	(0.5, 0.1)
Edwin	(0.6, 0.2)	(0.6, 0.2)	(0.5, 0.3)	(0,1)	(0.2, 0.7)	(0.2, 0.6)

TABLE II. SYMPTOMS AND RELATED DISEASES

Symptoms	Typhoid	Malaria	Flu	Jaundice	Throat-Infection
Fever	(0.3, 0.7)	(0.8,0.1)	(0.5,0.4)	(0.3, 0.5)	(0.5, 0.2)
Headache	(0.4, 0.5)	(0.6, 0.3)	(0.5, 0.2)	(0.2, 0.7)	(0.2, 0.7)
Bodypain	(0.8, 0.1)	(0.7, 0.2)	(0.2, 0.7)	(0.3, 0.5)	(0.4, 0.4)
Cough	(0.1, 0.9)	(0.3, 0.6)	(0.9, 0.1)	(0.2,0.7)	(0.8, 0.1)
Loss-of-Appetite	(0.9, 0.1)	(0.4, 0.5)	(0.1, 0.8)	(0.8,0.2)	(0.2, 0.7)
Degree of Belonging	(1,0)	(1,0)	(1,0)	(1,0)	(1,0)

TABLE III. PATIENTS AND THEIR DIAGNOSIS (TABLE I o TABLE II)

Patients	Typhoid	Malaria	Flu	Jaundice	Throat-Infection
Tom	(0.8, 0.1)	(0.7,0.2)	(0.5,0.2)	(0.6, 0.2)	(0.5, 0.3)
Bob	(0.7, 0.2)	(0.8, 0.1)	(0.5, 0.2)	(0.4, 0.2)	(0.5, 0.2)
Ram	(0.8, 0.1)	(0.7, 0.1)	(0.6, 0.1)	(0.5, 0.1)	(0.6, 0.1)
Edwin	(0.5, 0.3)	(0.6, 0.2)	(0.5, 0.2)	(0.3,0.5)	(0.5, 0.2)

TABLE IV. SCORE OF DIAGNOSIS OF PATIENTS

$Score_R$	Typhoid	Malaria	Flu	Jaundice	Throat-Infection
Tom	0.63	0.45	0.21	0.32	0.16
Bob	0.45	0.63	0.21	0.12	0.21
Ram	0.63	0.48	0.35	0.24	0.35
Edwin	0.16	0.32	0.21	- 0.16	0.21

TABLE V. NON-SYMPTOMS AND DISEASES

	Typhoid	Malaria	Flu	Jaundice	Throat-Infection
Fever	(0.7, 0.3)	(0.1,0.8)	(0.4,0.5)	(0.5, 0.3)	(0.2, 0.5)
Headache	(0.5, 0.4)	(0.3, 0.6)	(0.2, 0.5)	(0.7, 0.2)	(0.7, 0.2)
Bodypain	(0.1, 0.8)	(0.2, 0.7)	(0.7, 0.2)	(0.5, 0.3)	(0.4, 0.4)
Cough	(0.9, 0.1)	(0.6, 0.3)	(0.1, 0.9)	(0.7,0.2)	(0.1, 0.8)
Loss-of-Apetite	(0.1, 0.9)	(0.5, 0.4)	(0.8, 0.1)	(0.2,0.8)	(0.7, 0.2)
Degree of Belonging	(0,1)	(0,1)	(0,1)	(0,1)	(0,1)

TABLE VI. PATIENTS AND THEIR NON-DIAGNOSIS (TABLE I o TABLE V)

	Typhoid	Malaria	Flu	Jaundice	Throat-Infection
Tom	(0.5, 0.3)	(0.5,0.3)	(0.7,0.2)	(0.7, 0.2)	(0.7, 0.2)
Bob	(0.7, 0.3)	(0.3, 0.7)	(0.7, 0.2)	(0.7, 0.2)	(0.7, 0.2)
Ram	(0.6, 0.2)	(0.6, 0.3)	(0.7, 0.2)	(0.6, 0.2)	(0.4, 0.4)
Edwin	(0.6, 0.3)	(0.3, 0.3)	(0.5, 0.3)	(0.6,0.2)	(0.6, 0.2)

TABLE VII. SCORE OF NON-DIAGNOSIS VALUES FOR PATIENTS

$Score_R$	Typhoid	Malaria	Flu	Jaundice	Throat-Infection
Tom	0.16	0.16	0.45	0.45	0.45
Bob	0.40	- 0.40	0.45	0.45	0.45
Ram	0.32	0.27	0.45	0.32	0
Edwin	0.27	0	0.16	0.32	0.32

TABLE VIII. FINAL SCORE FOR PATIENTS

$Score_R$	Typhoid	Malaria	Flu	Jaundice	Throat-Infection
Tom	0.47	0.29	- 0.24	- 0.13	- 0.29
Bob	0.05	1.03	- 0.24	- 0.33	- 0.24
Ram	0.31	0.21	- 0.10	- 0.08	0.35
Edwin	- 0.11	0.32	0.05	- 0.48	- 0.11

VII. CONCLUSIONS

Information often gets distorted from the reality during its representation. This may happen due to lack of domain knowledge, vagueness of information, or similar reasons. In order to address the problem, we have introduced an extra generalization parameter in IFSS. This is another IFS, which is the perception of an expert, indicating the credibility of the information presented. The GIFSS is defined and its properties are studied in detail. Various relations on GIFSS are given and its properties are discussed. A novel score function is also devised specifically for medical diagnosis applications, strengthening the effect of the membership function and limiting that of the non-membership function.

Finally a new approach is developed applying the GIFSS and the novel score function with a view to evolve an expert system for the diagnosis of multiple patients. This approach takes the existing medical diagnosis methods using fuzzy sets to a higher level, being empowered with normalizing factor that indicates the quality of the input information. The approach could be the basis for development of an expert system for medical diagnosis that takes as input the symptoms of patient, and the doctor's opinion about the quality of the input furnished by the patients.

REFERENCES

[1] K. Atanassov, "Intuitionistic fuzzy sets," Fuzzy Sets and Systems, vol. 20, no. 1, pp. 87–96, August 1986.

[2] K. Atanassov, Intuitionistic Fuzzy Sets: Theory and Applications, Physica-Verlag, Heidelberg, 1999.

[3] D.Molodtsov, "Soft set theory--First results," Computers & Mathematics with Applications, vol. 37, no. 4-5, pp. 19-31, Feb – Mar 1999.

[4] P.K Maji, R. Biswas, and A. R. Roy, "Fuzzy soft-sets," Journal of Fuzzy Mathematics, vol. 9, no. 3, pp. 589-602, 2001.

[5] P.K Maji, A. R. Roy, and R. Biswas, "An application of soft sets in a decision making problem," Computers & Mathematics with Applications, vol. 44, pp. 1077-1083, 2002.

[6] P.K Maji, R. Biswas, and A. R. Roy, "Soft set theory," Computers & Mathematics with Applications, vol. 45, pp. 555-562, 2003.

[7] Z. Kong, L. Gao, L. Wang and S. Li, "The normal parameter reduction of soft sets and its algorithm," Computers & Mathematics with Applications, vol. 56, no. 12, pp. 3029-3037, Dec. 2008.

[8] Z. Kong, L. Gao and L. Wang, "Comment on 'A fuzzy soft set theoretic approach to decision making problems'," Computers & Mathematics with Applications, vol. 223, no. 2, pp. 540-542, Jan. 2009

[9] P. Majumdar, S.K. Samanta, "Similarity measure of soft sets," New Mathematics and Natural Computation, vol. 4, no. 1, pp. 1-12, 2008.

[10] P. Majumdar, S.K. Samanta, "Generalised fuzzy soft sets," Computers & Mathematics with Applications, vol. 59, no. 4, pp. 1425-1432, 2010.

[11] E. Sanchez, "Inverses of fuzzy relations, Application to possibility distributions and medical diagnosis," Fuzzy Sets and Systems, vol. 2, no. 1, pp. 75-86, 1979.

[12] Z. S. Xu, "Methods for aggregating interval-valued intuitionistic fuzzy information and their application to decision making," Control and Decision, vol. 22, no. 2, pp. 215-219, 2007.

[13] J. Ye, "Multicriteria fuzzy decision-making method based on a novel accuracy function under interval-valued intuitionistic fuzzy environment," Expert Systems with Applications, vol. 36, no. 3, pp. 6899-6902, April 2009.

2011 IEEE International Conference on Fuzzy Systems
June 27-30, 2011, Taipei, Taiwan

Indirect Adaptive Model Predictive Control Supervised by Fuzzy Logic

Jerry MAMBOUNDOU, Nicolas LANGLOIS
Automatic Control & Systems Research Group
Institut de Recherche en Systèmes Electroniques EMbarqués, IRSEEM
Saint Etienne du Rouvray, France
{jerry.mamboundou, nicolas.langlois}@esigelec.fr

***Abstract*—In order to get correct results using the model predictive control, one must find the suitable values of its tuning parameters. In many case this task is achieved by empirical methods. It's sufficient to control a physical system which internal parameters remain the same. The chosen controller parameters continue to provide satisfactory performances against small system variations. They become quickly inappropriate when strong variations occur in the process. One of the classical approaches consists to identify online the system model to update its controller based on this model. This solution doesn't ensure always best results. In this paper, we show how one can perform a suitable control to a system with variable parameters applying a fuzzy-logic-supervised predictive control. The fuzzy logic supervisor fulfills the online tuning of the predictive control parameters. Thus, we carry out a comparison between these two strategies.**

Keywords- MPC, Augmented state space model, Fuzzy Logic Supervisor, LTV system

I. INTRODUCTION

Model predictive control (MPC) is a powerful tool used to control a large range of physical systems. There are currently many industrial applications where the MPC has proved its efficiency having various difficulty complexities [1]. However, these good results depend on the best appropriate values of the MPC parameters which are the horizons of prediction, control and the weighting factor.

Many previous studies on this topic show that the MPC parameters values are chosen offline [2, 3]. Some methods use algorithms based on traditional stability criteria such as the gain and phase margins [2, 3]. Others intend to determine them by online tedious algorithms based on genetic [4] and mixed-integer linear program [5] optimizations. [6] proposes to build the adaptive MPC by achieving the online process identification to update the process model and compute the optimal control sequence after. In [7], the *Indirect Adaptive MPC (IAMPC)* approach is proposed. Nevertheless, when certain process parameters vary strongly in the time, this method is not able to respect the desired performances.

In this paper we will intend to overcome its limits thanks to the fuzzy-logic. Our approach determines the suitable values of the MPC parameters thanks to a fuzzy logic supervisor which input variables are the measurable performance criteria. From [8], we elaborate this control strategy in which predictive control is based on a state-space model and the supervisor gets a decision logic less complex. In addition, we reformulate two of the above criteria to reduce the computational load.

The paper is outlined as follows: section II presents the classical *IAMPC* while section III highlights the *IAMPC supervised by Fuzzy Logic*. In section IV, we carry out a comparative study of the obtained performances by applying both approaches on a Linear Time-Variant (LTV) system.

II. INDIRECT ADAPTIVE MODEL PREDICTIVE CONTROL

A. Discrete-time augmented state-space model

Let us consider a single-input and single-output (SISO) system represented by its discrete-time state-space model

$$\begin{aligned} x(k+1) &= A_d x(k) + B_d u(k), \\ y(k) &= C_d x(k), \end{aligned} \tag{1}$$

where k is the sampling instant assumed to be positive. [3] introduces the differences of the state vector and control variable such as

$$\begin{aligned} \Delta x(k+1) &= x(k+1) - x(k), \\ \Delta u(k+1) &= u(k+1) - u(k). \end{aligned}$$

Let us rewrite the state equation in (1) as follows

$$\begin{aligned} \Delta x(k+1) &= A_d \left(x(k) - x(k-1) \right) + B_d \left(u(k) - u(k-1) \right) \\ &= A_d \Delta x(k) + B_d \Delta u(k). \end{aligned} \tag{2}$$

Which leads to create the new state variable vector defined by

$$x_a(k) = \left[\Delta x(k) \quad y(k) \right]^T.$$

When one includes $\Delta x(k+1)$ in the second equation of (1), the measurement equation becomes

$$\begin{aligned} y(k+1)-y(k) &= C_d\left(x(k+1)-x(k)\right) = C_d\Delta x(k+1) \\ &= C_d A_d \Delta x(k) + C_d B_d \Delta u(k) \end{aligned} \tag{3}$$

The combinason of (1) and (3) leads to the following discrete-time state-space model:

$$\begin{aligned} x_a(k+1) &= Ax_a(k) + B\Delta u(k) \\ y(k) &= Cx_a(k), \end{aligned} \tag{4}$$

where

$$x_a(k+1) = \begin{bmatrix} \Delta x(k+1) \\ y(k+1) \end{bmatrix}, x_a(k) = \begin{bmatrix} \Delta x(k) \\ y(k) \end{bmatrix},$$

$$A = \begin{bmatrix} A_d & O_d^T \\ C_d A_d & 1 \end{bmatrix}, B = \begin{bmatrix} B_d \\ C_d B_d \end{bmatrix}, C = \begin{bmatrix} O_d & 1 \end{bmatrix},$$

$$O_d = \begin{bmatrix} 0 & 0 & \cdots & 0 \end{bmatrix}.$$

O_d is a row matrix of size n_A such as $(n_A \times n_A)$ are the dimensions of square matrix A_d. The set of matrices (A, B, C) forms the discrete-time augmented state-space model [3].

B. Predictive control formulation

Let be $HI, HP, HC,$ and λ the horizons of initialization, prediction, control and the weighting factor respectively. The control sequence ΔU and the sets of desired Y_{des} and predicted $\hat{Y}$ outputs are represented under a vector form as follows:

$$\Delta U^T = \begin{bmatrix} \Delta u(k) & \Delta u(k+1) & \cdots & \Delta u(k+HC-1) \end{bmatrix},$$

$$Y_{des}^T = \begin{bmatrix} y_{des}(k+1) & y_{des}(k+2) & \cdots & y_{des}(k+HP) \end{bmatrix},$$

$$\hat{Y}^T = \begin{bmatrix} \hat{y}(k+1|k) & \hat{y}(k+2|k) & \cdots & \hat{y}(k+HP|k) \end{bmatrix},$$

To obtain the control signal, we need to minimize the following cost function [3]:

$$J = (Y_{des} - \hat{Y})^T (Y_{des} - \hat{Y}) + \Delta U^T \bar{R} \Delta U, \tag{5}$$

where $\bar{R} = \lambda I$ and I is the identity matrix of dimension $(HP \times HP)$. It's possible to express the vector $\hat{Y}$ such as

$$\hat{Y} = Fx_a(k) + \Phi\Delta U, \tag{6}$$

where

$$F = \begin{bmatrix} CA \\ CA^2 \\ CA^3 \\ \vdots \\ CA^{HP} \end{bmatrix}, \Phi = \begin{bmatrix} CB & 0 & 0 & \cdots & 0 \\ CAB & CB & 0 & \cdots & 0 \\ CA^2B & CAB & CB & \cdots & 0 \\ \vdots & \vdots & \vdots & \vdots & \vdots \\ CA^{HP-1}B & CA^{HP-2}B & CA^{HP-3}B & \cdots & CA^{HP-HC}B \end{bmatrix}$$

Putting (6) in (5), we obtain a complete form of the criterion which the partial derivative with respect to ΔU gives :

$$\frac{\partial J}{\partial \Delta U} = -2\Phi^T\left(Y_{des} - Fx_a(k)\right) + 2\left(\Phi^T\Phi + \bar{R}\right)\Delta U. \tag{7}$$

We find the optimal control sequence ΔU by solving the following equation:

$$\frac{\partial J}{\partial \Delta U} = 0, \tag{8}$$

what leads to

$$\Delta U = (\Phi^T\Phi + \bar{R})^{-1}\Phi^T(Y_{des} - Fx_a(k)). \tag{9}$$

According to the receding horizon principle, the control signal applied to the process will be:

$$\begin{aligned} u(k) &= u(k-1) + \Delta U \\ u(k) &= u(k-1) + (\Phi^T\Phi + \bar{R})^{-1}\Phi^T(Y_{des} - Fx_a(k)) \end{aligned} \tag{10}$$

The state vector $x_a(k)$ constitutes the current plant information required to estimate the optimal control signal.

C. Recursive least square method

We illustrate the online model identification [9] by writing the discrete-time model of the plant such as

$$y_{\text{mod}}(k) = -\sum_{i=1}^{n_1} a_i y(k-i) + \sum_{i=1}^{n_2} b_i u(k-d-i) \tag{11}$$

where a_i and b_i are the unknown parameters. The model output $y_{\text{mod}}(k)$ can be also written under the form of a scalar product between the unknown parameter vector

$$\theta^T = \begin{bmatrix} a_1, \ldots, a_{n_1}, b_1, \ldots, b_{n_2} \end{bmatrix}$$

and the vectors of measurements called the plant model regressor vector

$$\phi(k)=\begin{bmatrix} -y(k-1) \\ \vdots \\ -y(k-n_1) \\ u(k-d-1) \\ \vdots \\ u(k-d-n_2) \end{bmatrix}.$$

What leads to

$$y_{\text{mod}}(k)=\theta^T\phi(k). \tag{12}$$

One can define now the prediction error (a priori) as

$$\varepsilon^o(k)=y(k)-\theta^T(k-1)\phi(k-1). \tag{13}$$

The minimization of the cost function

$$J_\theta=\sum_{i=1}^{k}\left(\varepsilon^o(k)\right)^2 \tag{14}$$

gives the optimal parameter vector

$$\theta(k)=P(k)\sum_{i=1}^{k}y(i)\phi(i-1) \tag{15}$$

where

$$P(k)=\left[\sum_{i=1}^{k}\phi(i-1)\phi^T(i-1)\right]^{-1}.$$

The recursive least squares (RLS) steps can be expressed by

$$\varepsilon(k+1)=\frac{y(k)-\theta^T(k)\phi(k)}{1+\phi(t)^T P(k)\phi(t)} \tag{16}$$

$$P(k+1)=P(k)-\frac{P(k)\phi(t)\phi(t)^T P(k)}{1+\phi(t)^T P(k)\phi(t)} \tag{17}$$

$$\theta(k+1)=\theta(k)+P(k+1)\phi(k)\varepsilon(k+1). \tag{18}$$

D. Parameter adaptation algorithm

The recursive formula of the adaptation gain $P(k+1)$ given by (17) is generalized by introducing two weighting sequences $\lambda_1(k)$ and $\lambda_2(k)$, as indicated below:

$$P(k+1)=\frac{1}{\lambda_1(k)}\left[P(k)-\frac{P(k)\phi(t)\phi(t)^T P(k)}{\alpha(k)+\phi(t)^T P(k)\phi(t)}\right] \tag{19}$$

where

$$0<\lambda_1(k)\le 1,\ 0<\lambda_2(k)\le 2,\ P(0)>0 \text{ and } \alpha(k)=\frac{\lambda_1(k)}{\lambda_2(k)}.$$

To improve the results of the previous identification method, [9] associates it to the constant trace technique as parameter adaptation algorithm (PAA). The principle is to move in the optimal direction of the RLS by maintaining the trace of matrix *P* approximately constant.

Imposing the ratio $\alpha(k)$, the two factors $\lambda_1(k)$ and $\lambda_2(k)$ are automatically calculated at each step to ensure

$$tr(P(k+1))=tr(P(k))=tr(P(0))=(n_1+n_2)P_0 \tag{20}$$

in which *GI* is the initial gain and $P(0)=P_0 I$ with *I* the identity matrix of dimension $((n_1+n_2)\times(n_1+n_2))$.

Fig. 1 helps us to visualize and understand well the *IAMPC* strategy wholeness. For simplicity reasons, we include the PAA in the block named RLS.

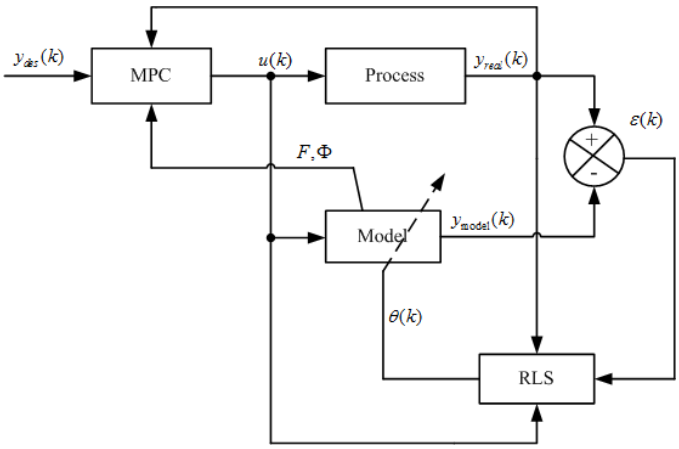

Figure 1. Equivalent structure of the IAMPC.

III. INDIRECT ADAPTIVE MODEL PREDICTIVE CONTROL SUPERVISED BY FUZZY LOGIC

Inspired by [8], it is possible to modify directly the tuning parameters of the predictive controller according to precise performance criteria. We consider four criteria estimated from controlled plant and model data. These four criteria are the inputs of the fuzzy-logic supervisor and the MPC parameters its outputs.

A. Performance criteria

We choose to evaluate the controlled plant rapidity by the controlled output convergence time (OCT). Considering the controlled output y_{cont} as a percentage γ of the desired output y_{des}, we can establish a relative error threshold (RET). It is defined such as

$$RET = \frac{y_{cont} - y_{des}}{y_{des}} = \frac{y_{des}(\gamma - 1)}{y_{des}} = \gamma - 1$$

OCT is the time interval from which the below inequality is verified:

$$\left| \left(y_{cont} - y_{des} \right) / y_{des} \right| \le RET, \tag{21}$$

Subsequently, it remains close to 0, if y_{cont} approaches y_{des}. It remains equal to -0.01, if y_{cont} is not close to y_{des}.

The controlled process stability is measured by the stability degree indicator (SDI). It is the difference between the radius of the unit circle and the modulus of the pole most remote from the unit circle center. What gives

$$SDI(k) = 1 - \max\left(|p_1|, |p_2|, \ldots, |p_{n_A}| \right), \tag{22}$$

where $p_1, p_2, \ldots, p_{n_A}$ are the eigenvalues of matrix A_d. When $0 < SDI < 1$, the system is stable. It will be in limit of stability if $SDI = 0$. It will become unstable if $SDI < 0$.

The control signal variance (VARU) allows observing the mean value of the square deviations of $u(k)$ from its average. It's expressed by

$$VARU(k) = \overline{u(k)^2} - \left[\overline{u(k)} \right]^2 \tag{23}$$

with

$$\overline{u(k)^2} = \overline{u(k-1)^2} + \frac{1}{2}\left(u(k)^2 - u(k-1)^2 \right),$$

and

$$\left[\overline{u(k)} \right]^2 = \left[\overline{u(k-1)} + \frac{1}{2}\left(u(k) - u(k-1) \right) \right]^2.$$

The trace of $\Phi^T\Phi$ provides an excellent tool to evaluate the computation conditioning of the optimal control signal [2, 8].

B. Normalization

Generally speaking, there is a difference between the real values of the mentioned performance criteria and the admissible values of the fuzzy input variables in their respective discourse universes from 0 to 1. One notices the same difference for the MPC parameters which are the fuzzy output variables. Thereby, one needs to normalize the values of these criteria and the obtained MPC horizons.

Let us add the subscript *n* to the criteria abbreviations OCT_n, SDI_n, $VARU_n$, $trace(\Phi^T\Phi)_n$ as their normalized values. Assigning them maximal and minimal values that fixe the expected performance ranges, SDI_n is evaluated by the simple operation (available for the other criteria)

$$SDI_n(k) = \left(SDI(k) - SDI_{\min} \right) / SDI_{\max}. \tag{24}$$

While the normalized supervisor outputs are designated by HP_n and HC_n respectively for *HP* and *HC*. Supposing they have maximal and minimal values that include the suitable horizons, the proposed control horizon is

$$HC(k) = round\left[HC_n(k)(HC_{\max} - HC_{\min}) + HC_{\min} \right], \tag{25}$$

where *round* is the function which rounds the real number to its nearest integer. We use the same calculus for *HP*. [8] shows how one can find the right numerical range of *HP*

$$HP_{\min} = 2\sup\left\{ n_2 + d; n_1 + 1 \right\},$$
$$HP_{\max} = HP_{\min} + 10.$$

And those of HC

$$HC_{\min} = n_1,$$
$$HC_{\max} = HP - HI.$$

C. Fuzzy logic supervisor

The purpose of the supervisor is to propose the appropriate values of *HP*, *HC* and λ depending on the plant variations. This supervisor is made of three sub-systems.

The first suggests the *HP* value based on the variance of $u(k)$ and the controlled OCT. The second gives the *HC* value according to the previous criteria. The third offers the λ value

in function of the trace of $\Phi^T\Phi$ and the controlled SDI. We illustrate this on fig. 2.

To be able to make proposals, the fuzzy logic supervisor involves the if-then rules using the Mamdani's fuzzy inference system. Thus, each linguistic input has three fuzzy sets and each linguistic output owns five fuzzy sets. All the membership functions are triangular. Tab. I, II and II present the inference tables corresponding to each supervisor sub-system.

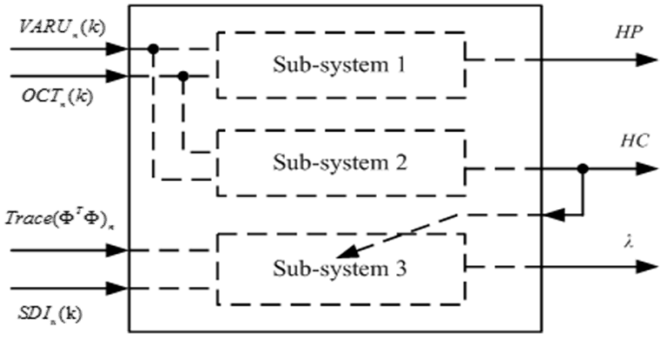

Figure 2. Sub-systems of the fuzzy logic supervisor.

TABLE I. TABLE OF RULES DEFINING HP

		$OCT_n(k)$		
		Big	***Middle***	***Small***
$VARU_n(k)$	***Small***	Very Small	Small	Middle
	Middle	Small	Middle	Big
	Big	Middle	Big	Very Big

TABLE II. TABLE OF RULES DEFINING HC

		$OCT_n(k)$		
		Big	***Middle***	***Small***
$VARU_n(k)$	***Small***	Middle	Big	Very Big
	Middle	Small	Middle	Big
	Big	Very Small	Small	Middle

TABLE III. TABLE OF RULES DEFINING λ

		$SDI_n(k)$		
		Big	***Middle***	***Small***
$\frac{\text{Trace}(\Phi^T\Phi)_n}{HC}$	***Small***	Middle	Small	Very Small
	Middle	Big	Middle	Small
	Big	Very Big	Big	Middle

D. *Control architecture*

The elaborated control architecture consists of the *IAMPC* control law enhanced by the fuzzy logic supervisor (FLS). To fulfill it this global strategy to a process, one requires to coordinate the activations of each task. The modeling error $\varepsilon(k)$ compares the real and the model outputs to guarantee good predictions. The model will track well the plant output when this error remains null. Otherwise, we take into account two adaptation cases through two positive thresholds called S_1 and S_2 $(S_1 < S_2)$.

Firstly, the condition $\varepsilon(k)$ upper than or equals to S_1 activates the RLS method enhanced by the PAA. It updates the former model parameters.

Secondly, when $\varepsilon(k)$ becomes greater than or equals to S_2, we activate the supervisor while the first adaptation still works (see fig. 3). This second updating suggests the best appropriate MPC parameters. As soon as $\varepsilon(k)$ becomes lower than or S_2, we take back the original values of *HP*, *HC* and λ.

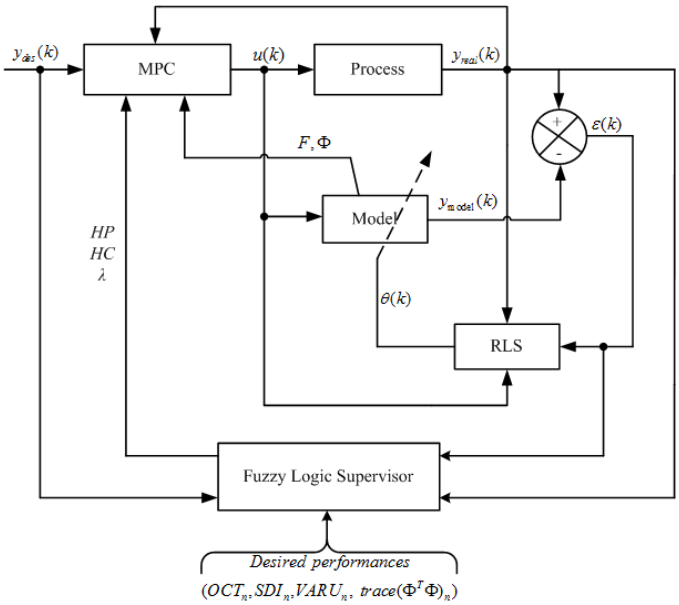

Figure 3. Equivalent structure of the IAMPC with fuzzy logic supervisor.

IV. APPLICATION AND COMPARISON

In this section we will focus on an academic application. Both detailed control strategies will be look at the overshoot or undershoot stability and rapidity. All simulations are derived via Matlab Simulink R2006b. For the computing environment set up, the solver used is "Discrete (no continuous states)" having a fixed step equals to 5 ms.

A. *System description*

The system considered is an electrical application that takes into account a flexible transmission with important variations of load inertia, which corresponds to typical applications in the machine tool area [10]. The transmission and load are modeled as a second order transfer function given in the continuous-time domain by:

$$H(s) = \frac{K}{J_n s^2 + f_n s + C} \quad with \quad \begin{cases} K = 2\ , J_n = 0.002 \\ f_n = 0.006, C = 2 \end{cases} \tag{26}$$

This SISO model is characterized by its natural pulsation and its damping factor:

$$\omega_n = \sqrt{C/J} = 31.623\ rad/s,\ \xi = f/\left(2\omega_n J\right) = 0.4743.$$

With a sampling period T_s of 5 ms, the discrete-time model coming from (26) including the digital to analogue and analogue to digital converters is given by:

$$H(q^{-1}) = \frac{0.01187q^{-1} + 0.01129q^{-2}}{1 - 1.838q^{-1} + 0.8607q^{-2}}. \qquad (27)$$

From [2], we set the original MPC parameters that produce correct results: $HI = 1$, $HC = 1$, $HP = 8$ and $\lambda = 0.42$. This set up respects the below performance criteria during the process control:

$$0 \le OCT \le 1,\ 0 \le SDI \le 1,\ 0 \le VARU \le 0.2, \left|Overshoot\right| \le S_1 \le S_2$$
$$0 \le trace(\Phi^T\Phi) \le 1.5, S_1 = 2.5\%,\ S_2 = 5\%.$$

How does the controlled plant react against the load inertia changes for a square reference signal (fig. 4)?

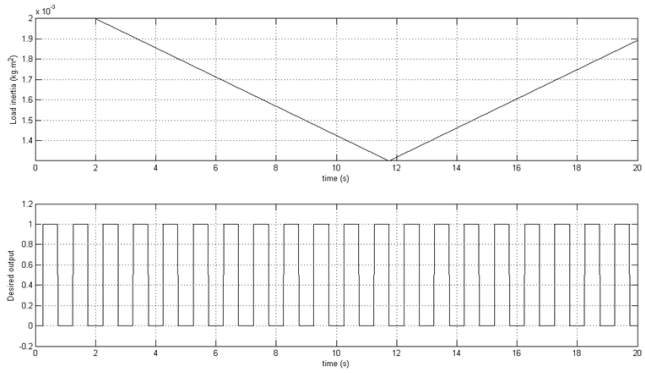

Figure 4. J profile and desired output.

B. Simulation results

1) Results with IAMPC : the plot of MPC output in fig. 5 shows us that the original controller MPC has difficulty in tracking correctly the reference signal. From 8 s to 16 s, where J reaches its lower value, the absolute overshoot is strictly greater than 5% and sometimes greater than 10% (fig. 6). In the same time, this gap increasing to $\varepsilon(k)$ activates the plant model reconfiguration (see fig. 7).

The *IAMPC* gets through to enhance the incapacities of MPC. One notices the reduction of the absolute overshoot, a smaller OCT in fig. 8 than before which prooves that the process became quicker. *IAMPC* control signal curve has decreasing and rising peaks which looks like the J profile. While MPC control signal keeps the same aspect (fig. 9).

However, an important peak of 1.21 is located around 11 s and 12 s when we use the first adaptive control law. We must solve this problem.

2) Results with fuzzy-logic-supervised IAMPC: Considering fig. 6 as the zoom of *IAMPC* output, one can observe various sudden peaks. They are limeted to 5% or 6% except between 11 s and 12 s. One visible effect of *fuzzy-logic-supervised IAMPC* is the drastic cancellation of these indisirable elements. Which leads to the smallest absolute overshoot (fig. 11). In fact, there is a modulus increase of the current control signal according to *IAMPC* control. The control signals plot shows that maximal values of control signal using FLS reach approximatively 4.3 (fig. 12).

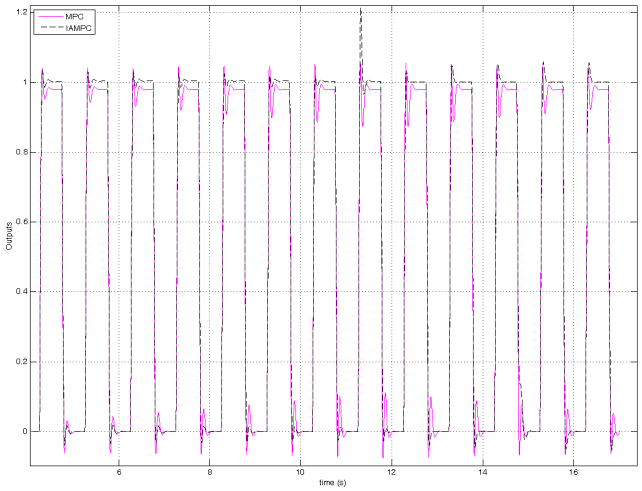

Figure 5. Output results of MPC vs IAMPC.

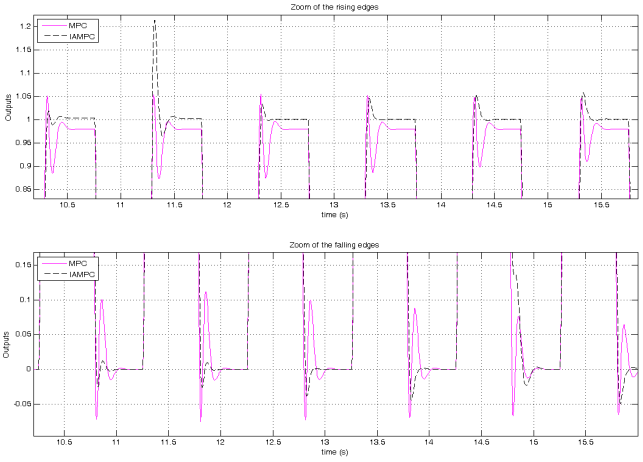

Figure 6. Output zooms of MPC vs IAMPC.

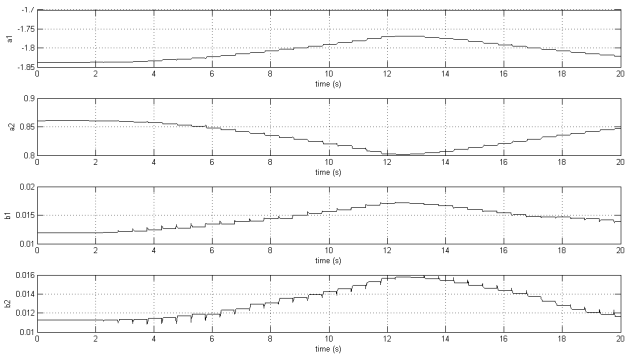

Figure 7. New estimated parameter vector.

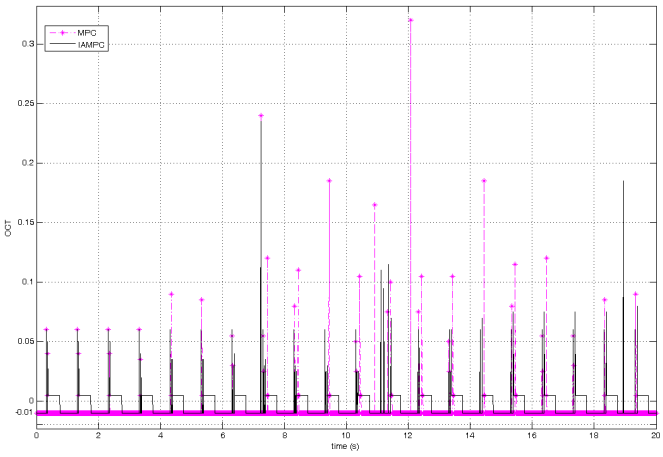

Figure 8. OCT results of MPC vs IAMPC.

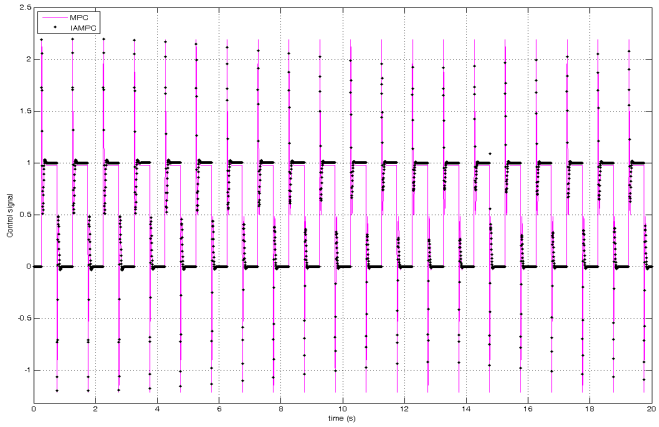

Figure 9. Control signals of MPC vs IAMPC.

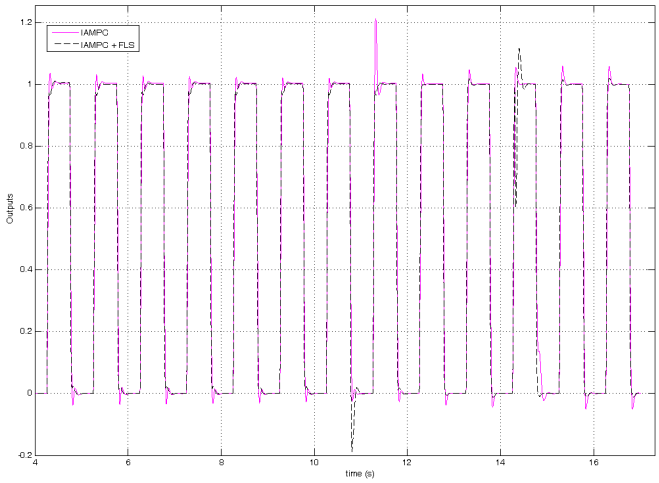

Figure 10. Output results of IAMPC vs IAMPC with FLS.

Concerning the rapidity criterion, the approach based FLS leads to a plant as quick as the process using the *IAMPC* strategy. In the above OCT plots (fig. 13), *IAMPC* proposes sometimes lower values than *IAMPC* enhanced by FLS. Otherwise, it's the opposite e.g near 7 s and from 15 s to 20 s. We perform the same analysis for SDI criterion.

During the first period i.e up to 13 s, *IAMPC* enhanced by FLS provides a better stability, while IAMPC strategy takes the advantage after (fig. 14).

This comment recalls the traditional dilemma between rapidity and stability: fluctations of one affects negatively the other.

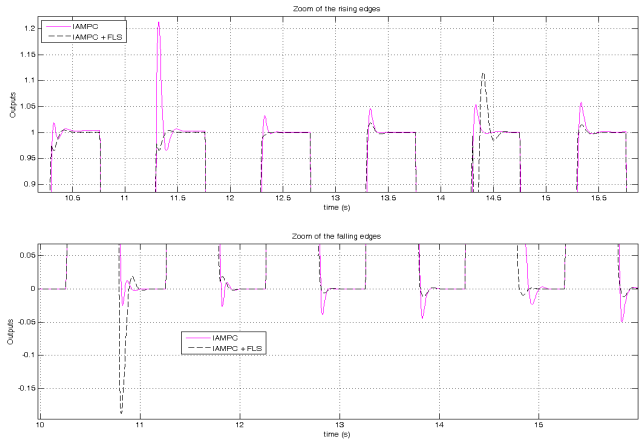

Figure 11. Output zoom of IAMPC vs IAMPC with FLS.

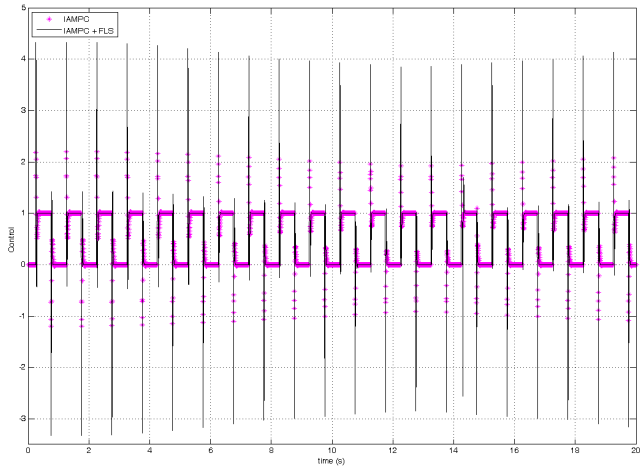

Figure 12. Control signals of IAMPC vs IAMPC with FLS.

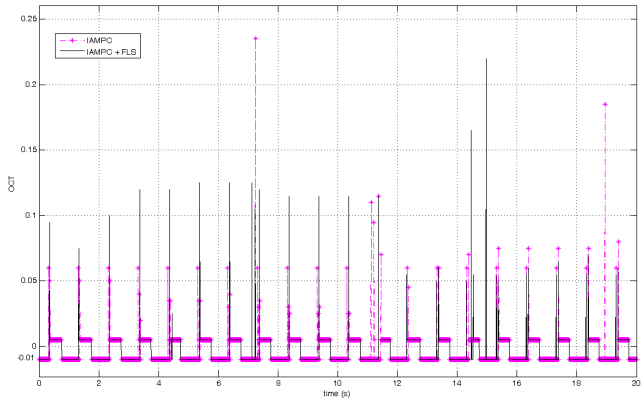

Figure 13. OCT results of IAMPC vs IAMPC with FLS.

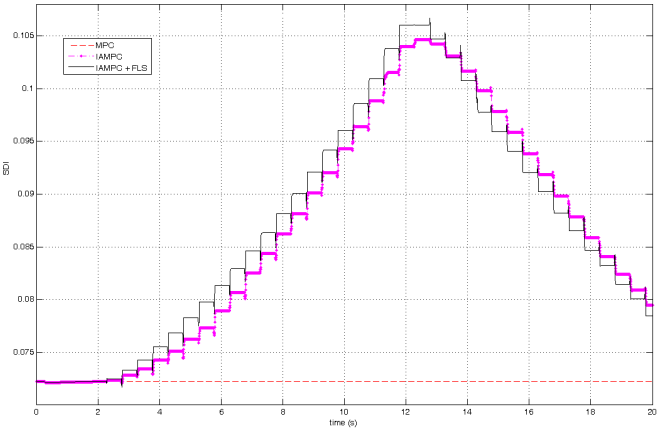

Figure 14. SDI results of IAMPC vs IAMPC with FLS.

Let us note that both reconfiguration strategies improve substantially the original stability getting an indicator closer to zero than theirs results.

All these improvements are due to the double capacity of *fuzzy-logic-supervised IAMPC* to conjugate in parallel the modifications of *HC*, *HP*, λ (see fig. 15) with the online model identification. Nevertheless, even if the irregular peak of *IAMPC* in [11 s, 12 s] disappeared, two perticular peaks (resp. -0.19 and 1.12) appear at 10.8 s and 14.4 s.

V. CONCLUSION

This paper presents an indirect adaptive MPC using fuzzy logic supervisor for which two simultaneous adaptations can be activated automatically. The first is based on the discrete-time augmented model reconfiguration thanks to RLS combining PAA. While the second provides suitable values of *HP*, *HC* and λ via a logic decision carried by the proposed supervisor.

Important abilities of IAMPC enhanced by FLS are highlighted when a Linear Time-Variant system is confronted to strong parameter variations. It gets through to repulse several limits encountered with MPC and IAMPC. The majority of performance criteria are respected. Nonetheless, two undesirable peaks appeared even if their values are lower than previously. It seems possible to eliminate these anomalies by imposing inequality constraints on the control and output signals. After that, it would be also very interesting to study how we can implement and test this enhanced control law on a real-time application.

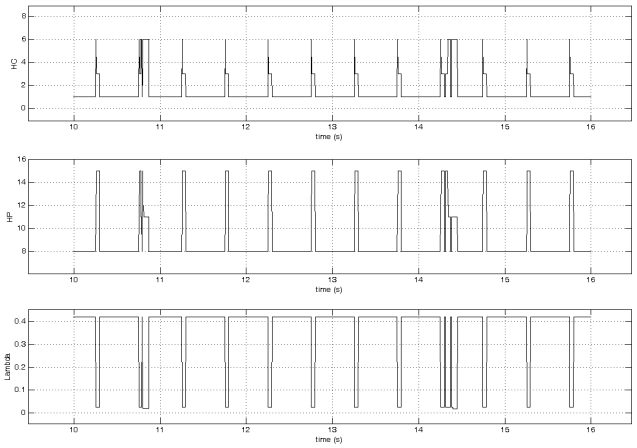

Figure 15. Variations of MPC parameters with FLS from 10 s to 16 s.

ACKNOWLEDGMENT

The authors gratefully thank "Région Haute Normandie" for financially supporting this work and its forthcoming application to diesel engine control in the frame of the ORIANNE (Outil numéRIque pour le mAquettage de foNctions de coNtrôle motEur) project labelled by the French competitiveness clusters Mov'eo and Aerospace valley.

REFERENCES

[1] S. J. Qina and T. A. Badgwell, "A survey of industrial model predictive control technology," Control Engineering Practice, vol. 11, pp. 733–764, 2003.

[2] P. Boucher and D. Dumur, La Commande Prédictive. TECHNIP, 1996.

[3] L. Wang, Model Predictive Control System Design and Implementation Using MATLAB. Springer, 2009.

[4] R. Haber, U. Schmitz, and R. Bars, "Optimal choice of horizons for predictive control by using genetic algorithms," Annual Reviews in Control, vol. 28, pp. 53–58, 2004.

[5] A. Richards and J. P. How, "Robust variable horizon model predictive control for vehicle maneuvering," Int. J. Robust Nonlinear Control, vol. 16, p. 333–351, 2006.

[6] K. Watanabet, K. Ikedat, T. Fukudas, and S. Tzafestasfl, "Adaptive generalized predictive control using a state-space approach," International Workshop on IROS, vol. 3, pp. 1609 – 1614, Nov. 3-5, 1991.

[7] L. Chisci, L. Giarri, and E. Mosca, "Indirect and implicit adaptive predictive control of the benchmark plant," Automatica, vol. 30 No 4, pp. 577–584, 1994.

[8] R. B. Abdennour, P. Borne, M. Ksouri, and F. M'sahli, Identification et commande numérique des procédés industriels. TECHINIP, 2001.

[9] I. D. Landau and G. Zito, Digital Control Systems: Design, Identification and Implementation. Springer, 2006.

[10] D. Dumur, P. Boucher, and G. Ramond, "Direct adaptive generalized predictive control. Application to motor drives with flexible modes," Annals of the CIRP, vol. 49/1/2000, pp. 271–274, August 2000.

2011 IEEE International Conference on Fuzzy Systems
June 27-30, 2011, Taipei, Taiwan

Maximum-Likelihood Principle For Possibility Distributions Viewed As Families Of Probabilities

Mathieu Serrurier,
IRIT,
University of Toulouse III,
31062 Toulouse Cedex 9, France,
E-mail: serrurie@irit.fr

Henri Prade,
IRIT,
University of Toulouse III,
31062 Toulouse Cedex 9, France,
E-mail: prade@irit.fr

Abstract— **An acknowledged interpretation of possibility distributions in quantitative possibility theory is in terms of families of probabilities that are upper and lower bounded by the associated possibility and necessity measures. This paper proposes a likelihood function for possibility distributions that agrees with the above-mentioned view of possibility theory in the continuous and in the discrete cases. Especially, we show that, given a set of data following a probability distribution, the optimal possibility distribution with respect to our likelihood function is the distribution obtained as the result of the probability-possibility transformation that obeys the maximal specificity principle. It is also shown that when the optimal distribution is not available, a direct application of this possibilistic likelihood provides more faithful results than approximating the probability distribution and then applying the probability possibility transformation. We detail the particular case of triangular and trapezoidal possibility distributions and we show that any unimodal unknown probability distribution can be faithfully upper approximated by a triangular distribution obtained by optimizing the possibilistic likelihood.**

keywords : possibility theory, probability-possibility transformation, maximum-likelihood principle.

I. Introduction

Possibility theory, based on max-decomposable set-functions, associated with possibility distributions, may have either a qualitative or a quantitative understanding, depending on the nature of the scales used for possibility degrees. Quantitative possibility theory corresponds to the case where the interval $[0, 1]$ is a ratio scale. In qualitative possibility theory, only the ordering of the possibility values makes sense. In this paper, we deal with quantitative possibility theory. Quantitative possibility measures can be viewed as upper bound of probabilities. Then, a possibility distribution represents a family of probability distributions [3]. This view was first suggested by Zadeh [10] based on the idea that what is probable must be possible. Following this intuition a probability-possibility transformation has been proposed [5]. This transformation associates a probability distribution with the maximally specific possibility distribution which is such that the possibility of any event is indeed an upper bound of the corresponding probability.

The maximum-likelihood principle is a basis for building a probability distribution from a set of data. Given a set of parameterized probability distributions and a set of data, a likelihood function is used for optimizing the choice of the parameters in order to determine the best suited distribution with respect to the data. However, this approach supposes that the shape of the distribution is apriori known or that we have a large number of data at our disposal. Moreover, due to the constraints on the probability distributions, induced by their additive nature, there are no simple distribution that allows for the faithful description of any set of data.

There exist different kinds of methods for eliciting possibility distributions from data. For instance, some approaches directly build the possibility distribution on the basis of a proximity relation defined on the universe of the data [4]. G. Mauris proposes a method for constructing a possibility distribution when only very few pieces of data are available (even only one or two) based on probability inequalities [8]. This latter method is justified in the probabilistic view of possibility theory. These methods, how different they are, have in common to build the distributions directly. In this paper, we investigate another road based on the optimization of an appropriate likelihood function. The proposed likelihood function is in agreement with the view underlying the probability-possibility transformation.

The paper is organized as follows. Section 2 provides the necessary background about possibility distributions and their interpretation in terms of families of probabilities. Section 3 presents likelihood measures for probabilities and especially a non-classical one, not based on logarithm, that can be used for approximating unbounded distributions with bounded ones. Sections 4 and 5 respectively deal with the discrete and continuous definitions of possibilistic likelihood and the specific cases of triangular or trapezoidal distributions. Finally, we provide some examples of the construction of a possibility distribution from data using the proposed possibilistic likelihood, and we discuss the usability of the approach in Section 6.

II. Background

A. Possibility distribution

Possibilty theory, introduced Zadeh [10], was initially created in order to deal with imprecision and uncertainty due

978-1-4244-7316-8/11/$26.00 ©2011 IEEE

to incomplete information. This kind of uncertainty may not be handled by probability theory, especially when a priori knowledge about the nature of the probability distribution is lacking. A possibility distribution π is a mapping from Ω to $[0,1]$ (Ω may be a discrete universe, i.e. $\Omega = \{C_1, \ldots, C_q\}$, or a continuous one, i.e. $\Omega = \mathbb{R}$). The value $\pi(x)$ is called possibility degree. For any subset of Ω, the possibility measure is defined as follows:

$$\forall A \subseteq \Omega, \Pi(A) = max\{\pi(x), x \in A\}.$$

If it exists a single value $x \in \Omega$ for which we have $\pi(x) = 1$, the distribution is normalized. We can distinguish two extreme cases of information situations:

- complete knowledge: $\exists x \in \Omega$ such as $\pi(x) = 1$ and $\forall y \in \Omega, y \neq x, \pi(y) = 0$
- total ignorance: $\forall x \in \Omega, \pi(x) = 1$.

The necessity is the dual measure of the possibility measure. We have:

$$\forall A \subseteq \Omega, N(A) = 1 - \Pi(\overline{A}).$$

Finally, α-cuts of π are subsets of Ω such that:

$$A_\alpha = \{x \in \Omega, \pi(x) \geq \alpha\}.$$

It can be checked that, if $\Omega = \mathbb{R}$ and the distribution is continuous and normalized, we have $\forall \alpha \in [0,1], \Pi(A_\alpha) = 1$ and $N(A_\alpha) = 1 - \alpha$.

B. Possibility distribution as a family of probability distributions

Possibility distributions have two types of interpretations. The first one, that is related to fuzzy set theory, is the description of gradual properties. For instance, the definition of linguistic expressions such that "long", "old" or "expensive" does not refer to a specific value, but to a set of possible values in a particular context. For instance, a possibility distribution may describe the concept "expensive" for an house in a given area. In such a case, each price will be associated with a possibility degree which quantifies how much this price is typical with respect to this particular use of the concept "expensive".

Another type of interpretation is to consider a possibility distribution as a family of probability distributions (see [1] for an overview). Thus, a possibility distribution π will represent the family of the probability distributions for which the measure of each subset of Ω will be bounded by its necessity and its possibility measures. More formally, if $\mathcal{P}$ is the set of all probability distributions defined on Ω, the family of probability distributions $\mathcal{P}_\pi$ associated with π is defined as follows:

$$\mathcal{P}_\pi = \{p \in \mathcal{P}, \forall A \in \Omega, N(A) \leq P(A) \leq \Pi(A)\}. \quad (1)$$

In this scope, the situation of total ignorance corresponds to the case where all probability distributions are possible. This type of ignorance can not be described by a single probability distribution. The case of complete knowledge corresponds to the case where only one value is possible and then where there are no randomness nor imprecision. Obviously, if π is not normalized, $\mathcal{P}_\pi$ is empty (since then $N(A) \leq \Pi(A)$ is no longer guaranteed for any A).

When $\Omega = \mathbb{R}$, this family of probability distributions can also be described in terms of confidence intervals. Given a probability distribution p, a confidence interval I_α is a subset of Ω such as $P(I_\alpha) = \alpha$. We define I^*_α, also referred as quantile, as the smallest confidence interval with probability measure equal to α. Thus, when π is continuous, an alternative to the equation (1) is:

$$\mathcal{P}_\pi = \{p \in \mathcal{P}, \forall I^*_\alpha \in \Omega, I^*_\alpha \subseteq A_{1-\alpha}\} \quad (2)$$

where $A_{1-\alpha}$ is the $(1-\alpha)$-cut of π. Thus, the possibility distribution π contains the probability distributions for which the confidence intervals associated to the α's are bounded by the $(1-\alpha)$-cuts.

C. Probability to possibility transformation

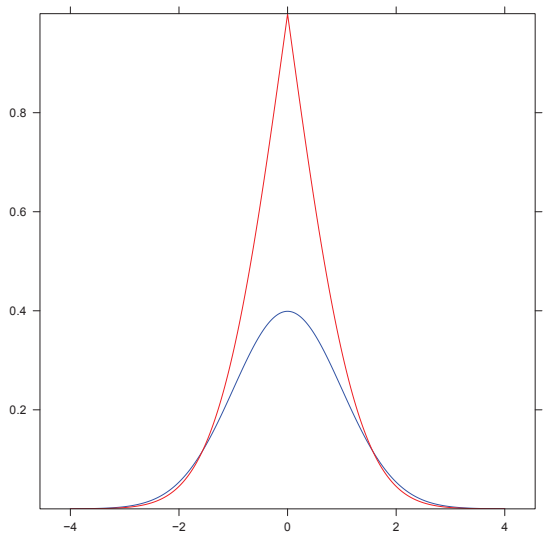

Fig. 1. probability to possibility transformation of a Gaussian distribution

According to this probabilistic interpretation, a method from transforming probability distributions into possibility distributions has been proposed in [5]. The idea behind this proposal is to consider the most informative possibility distribution, i.e. the tightest one (i.e. the smallest one in each point) that contains the probability distribution. Let us consider a probability distribution p, the possibility distribution π^* is defined in the following way:

$$\forall x \in \Omega, \pi^*(x) = max_{\alpha, x \in I_\alpha}(1-\alpha). \quad (3)$$

Then, in the spirit of equation (2), given p and its transformation π^* we have:

$$A^*_{1-\alpha} = I^*_\alpha$$

where $A^*_{1-\alpha}$ is the $(1-\alpha)$-cut of π^*. Thus, if p has a finite number of modes, π^* is the possibility distribution for which each $(1-\alpha)$-cut corresponds to the quantile of p. When p is

unimodal, the unique value x such that $\pi^*(x) = 1$ is the mode of p.

III. Probabilistic likelihood measure

Likelihood measures have been introduced in order to evaluate the adequateness of a probability distribution with respect to a set of data. Let us consider a set of data $X = \{x_1, \ldots, x_n\}$ belonging to a discrete universe $\Omega = \{C_1, \ldots, C_q\}$. We name $\alpha_1, \ldots, \alpha_q$ the frequency of the elements of X that belong respectively to $\{C_1, \ldots, C_q\}$. Given a probability distribution p on the discrete space $\Omega = \{C_1, \ldots, C_q\}$, we define $p_1, \ldots, p_q$ the probability of belonging to the unitary element of Ω, i.e. $p(x \in C_i) = p_i$. The values $p_1, \ldots, p_q$ entirely define p, and are then the parameters of p. The maximum-likelihood principle is used for estimating the parameters of a probability distribution. In the continuous case, the shape of the distribution has to be known, and the parameters are obtained through an optimization procedure with respect to the likelihood measure. In the discrete case, the parameters are $p_1, \ldots, p_q$, and obey the constraint $\sum_1^q p_i = 1$. The most used likelihood function is the logarithmic-based likelihood defined as follows (under the strict constraint $\sum_1^q p_i = 1$):

$$\mathcal{L}_{log}(p|x_1, \ldots, x_n) = -\sum_{i=1}^{n} log(p(x_i))$$

or, when considering frequency directly

$$\mathcal{L}_{log}(p|x_1, \ldots, x_n) = -\sum_{i=1}^{q} \alpha_i log(p_i).$$

It is equivalent to compute the joint probability of the elements of x with respect to p. This definition of the likelihood has a strong limitation, since it gives a very high weight to the error when probability is very low. This is especially true when Ω is continuous. Since $\mathcal{L}_{log}$ is not defined when $p(x_i) = 0$, an unbounded density cannot be approximated by a bounded one by optimization of $\mathcal{L}_{log}$. We propose another likelihood function that overcomes these limitations:

$$\mathcal{L}_{surf}(p|x_1, \ldots, x_n) = (\sum_{i=1}^{n} p(x_i)) - \frac{1}{2} * \sum_{i=1}^{q} p_i^2$$

or, when considering frequency directly

$$\mathcal{L}_{surf}(p|x_1, \ldots, x_n) = (\sum_{i=1}^{q} \alpha_i * p_i) - \frac{1}{2} * \sum_{i=1}^{p} p_i^2.$$

Roughly speaking, L_{surf} favors the probability distributions that are close to the optimal one in terms of surface. Thus, when, Ω is continuous, it allows for the approximation of unbounded densities by bounded ones.

Proposition 1: Given a set of data $X = \{x_1, \ldots, x_n\}$ belonging to a discrete universe $\Omega = \{C_1, \ldots, C_q\}$, we have

$$argmax_{p \in \mathcal{P}}(\mathcal{L}_{log}(p|x_1, \ldots, x_n)) = argmax_{p \in \mathcal{P}}(\mathcal{L}_{surf}(p|x_1, \ldots, x_n)).$$

Proof: Let $p_{log} = argmax_{p \in \mathcal{P}}(\mathcal{L}_{log}(p|x_1, \ldots, x_n))$ be the optimal probability distribution given X. This distribution is such as the probability of an event C_i is equal to the frequency of element of X in C_i, i.e. $p_{log}(x \in C_i) = p_i = \alpha_i$. We now look for the probability distribution p_{surf} that maximizes $\mathcal{L}_{surf}$. We have:

$$\forall i = 1 \ldots q, \frac{\delta \mathcal{L}_{surf}(p|x_1, \ldots, x_n)}{\delta p_i} = \alpha_i - p_i$$

thus

$$\forall i = 1 \ldots q, \frac{\delta \mathcal{L}_{surf}(p|x_1, \ldots, x_n)}{\delta p_i} = 0 \Leftrightarrow p_i = \alpha_i.$$

Since the derivative of $\mathcal{L}_{surf}(p|x_1, \ldots, x_n)$ with respect to p_i (the parameters of p) does not depend on the other parameters p_j, $j \neq i$, we obtain $p_{surf}(x \in C_i) = p_i = \alpha_i$. Thus $p_{surf} = p_{log}$ ■

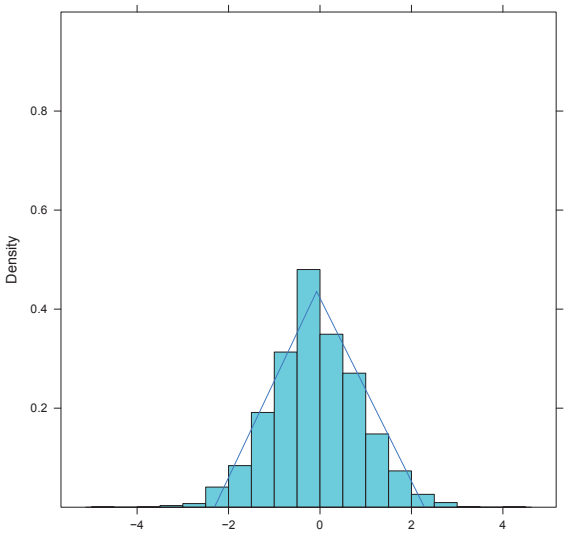

Fig. 2. Approximation of a Gaussian density with a triangular density by maximization of $\mathcal{L}_{surf}$

This proposition shows that, given X, the probability distribution that maximizes $\mathcal{L}_{log}$ is the same as the one that maximizes $\mathcal{L}_{surf}$.

$\mathcal{L}_{surf}$ can be extended to the case of $\Omega = \mathbb{R}$ in the following way:

$$\mathcal{L}_{surf}(p|x_1, \ldots, x_n) = (\sum_{i=1}^{n} p(x_i)) - \frac{1}{2} * \int_{\mathbb{R}} p(t)^2 dt.$$

Proposition 1 remains true when $\Omega = \mathbb{R}$. Figure 2 shows the triangular density that maximizes $\mathcal{L}_{surf}$ given a set of 3000 values that are generated by a Gaussian distribution with mean equal to 0 and standard derivation equal to 1. This triangular probability distribution is parametrized by m,

l and r which are respectively the mode, the left and the right spread of the probability distribution. We have used an optimization procedure in order to find the parameters that maximizes $\mathcal{L}_{surf}$. What we obtain is the triangular probability distribution that shares the maximum of surface with the histogram computed from the sample set. If we have used $\mathcal{L}_{log}$, the support of the triangle would have grow to infinity as the number of values increases.

IV. Possibilistic likelihood: discrete case

In this section we show how to use the $\mathcal{L}_{surf}$ likelihood function in order to define a likelihood function for a possibility distribution that supports the interpretation of a possibility distribution in terms of a family of probability distributions. Roughly speaking, the idea is to have a likelihood function that is maximal for the result of the probability-possibility transformation of the distribution and that favors the approximations of the distribution that share the maximum of surface with the optimal one (as for $\mathcal{L}_{surf}$ in the probabilistic case). We first consider the case of a discrete universe, i.e. $\Omega = \{C_1, \ldots, C_q\}$.

We now assume that the frequencies of examples in the different classes C_i are put in increasing order ($\alpha_1 \geq \ldots \geq \alpha_q$). In this case, the probability distribution p^* that maximizes the likelihood is such that $p(x \in C_i) = p_i = \alpha_i$. In the following, given a possibility distribution π, we note π_i the value $\pi(x \in C_i)$. It has been shown in [5] that the transformation of p^* into a possibility distribution π^* that satisfies the maximal specificity requirement, is:

$$\forall i \in \{1, \ldots, q\}, \pi_i^* = \sum_{j=i}^{q} \alpha_j. \tag{4}$$

This possibility distribution is one of the cumulated functions of p^*. It is worth noticing that it is the tightest one. What we expect from possibility likelihood is that the maximum of this function is reached for π^*. In the following, we assume that $\pi_1 \geq \ldots \geq \pi_q$ (and not necessarily $\alpha_1 \geq \ldots \geq \alpha_q$). We propose the following function:

$$\begin{aligned}\mathcal{L}_{pos}(\pi|x_1, \ldots, x_n) =& (\sum_{i=1}^{q}(1-\pi_i) * (1 - (\sum_{j=i}^{q} \alpha_i))) \\ & - \sum_{i=1}^{q} \frac{(1-\pi_i)^2}{2}\end{aligned} \tag{5}$$

which can be rewritten as this:

$$\begin{aligned}\mathcal{L}_{pos}(\pi|x_1, \ldots, x_n) =& \sum_{i=1}^{q}(-\alpha_i * \sum_{j=1}^{i}(1-\pi_j)) \\ & - \sum_{i=1}^{q} \frac{(1-\pi_i)^2}{2} \\ & + \sum_{i=1}^{q}(1-\pi_i)\end{aligned} \tag{6}$$

If we only consider one piece of data, we obtain:

$$\begin{aligned}\mathcal{L}_{pos}(\pi|x) =& \sum_{j=1}^{i|x\in C_i}(1-\pi_j)) \\ & - C * \sum_{i=1}^{q} \frac{(1-\pi_i)^2}{2} \\ & + C * \sum_{i=1}^{q}(1-\pi_i)\end{aligned} \tag{7}$$

where C is a constant (usually $\frac{1}{n}$, where n is the number of independent data considered). The rationale behind this is to evaluate the cumulated distribution in the spirit of $\mathcal{L}_{surf}$. Thus, the terms $((1-\pi_i) * (1 - (\sum_{j=i}^{q} \alpha_i))) - \frac{(1-\pi_i)^2}{2}$ correspond to the evaluation of $\mathcal{L}_{surf}$ for the set $\overline{C_i \cup \ldots \cup C_q}$. Note that, if you consider $C_i \cup \ldots \cup C_q$ instead of $\overline{C_i \cup \ldots \cup C_q}$, what is obtained is the largest cumulative distribution instead of the tightest one.

Proposition 2: Given a set of data $X = \{x_1, \ldots, x_n\}$ belonging to a discrete universe $\Omega = \{C_1, \ldots, C_q\}$, the possibility distribution π^* that maximizes the function $\mathcal{L}_{pos}$ is the transformation of the probability distribution p^*, according to equation (4), which maximizes $\mathcal{L}_{surf}$ ($\forall i \in \{1, \ldots, q\}, p_i^* = \alpha_i$).

Proof: We look for the probability distribution π^* that maximizes $\mathcal{L}_{surf}$.
We have:

$$\forall i = 1 \ldots q, \frac{\delta \mathcal{L}_{pos}(\pi|x_1, \ldots, x_n)}{\delta \pi_i} = -1 + \sum_{j=i}^{q} \alpha_i - \pi_i + 1$$

thus

$$\forall i = 1 \ldots q, \frac{\delta \mathcal{L}_{pos}(\pi|x_1, \ldots, x_n)}{\delta \pi_i} = 0 \Leftrightarrow p_i = \sum_{j=i}^{q} \alpha_i.$$

Since the derivative of $\mathcal{L}_{pos}(\pi|x_1, \ldots, x_n)$ with respect to π_i (the parameters of π) does not depend on the other operator π_j, $j \neq i$, we obtain $\pi_i^* = p_i = \sum_{j=i}^{q} \alpha_i$ which exactly corresponds to Equation (4). ■

This proposition shows that $\mathcal{L}_{pos}$ is an acceptable likelihood function for possibility distributions viewed as families of probabilities. As for $\mathcal{L}_{surf}$ the likelihood depends on the surface shared between the considered possibility distribution and the optimal one.

It is worth noticing that, when optimal distributions can only be approximated, finding the best approximation with respect to $\mathcal{L}_{pos}$ is not equivalent to find the best probability approximation with respect to $\mathcal{L}_{surf}$ and then turn it into a possibility distribution. For instance, we consider X that leads to the frequency $\alpha_1 = 0.5, \alpha_2 = 0.3, \alpha_3 = 0.2$. We know require that $p_3 = 0$ and $\pi_3 = 0$. In this context, the optimal p with respect to $\mathcal{L}_{surf}$ ($\mathcal{L}_{log}$ is not applicable here) is $p_1 = 0.6$, $p_2 = 0.4$, $p_3 = 0$. The optimal π with respect to $\mathcal{L}_{poss}$ is

$\pi_1 = 1$, $\pi_2 = 0.5$, $\pi_3 = 0$. The transformation π' of p is $\pi'_1 = 1$, $\pi'_2 = 0.4$, $\pi'_3 = 0$. We observe that π' is different than π and that π is a better approximation of the optimal possibility distribution.
This result is fundamental since it illustrates that using a probabilistic likelihood and then the probability-possibility transformation is not an effective approach for constructing a possibility distribution from data. The maximization of $\mathcal{L}_{pos}$ is more adapted in this scope.

V. Possibilistic likelihood: continuous case

We now consider the continuous case where $\Omega = \mathbb{R}$.

A. Definition

In the continuous case, the assumption of the values put in an increasing order of π is naturally replaced by the consideration of α-cuts. We adapt the equation (6) as follows:

$$\begin{aligned}\mathcal{L}_{pos}(\pi|x_1,\ldots,x_n) = &-(\sum_{i=1}^{n}\int_{A_{\pi(x_i)}}(1-\pi(t))dt)\\ &-\int_{\mathbb{R}}\frac{(1-\pi(t))^2}{2}dt\\ &+\int_{\mathbb{R}}(1-\pi(t))dt\end{aligned} \tag{8}$$

where $A_{\pi(x_i)}$ is the $\pi(x_i)$-cut of π. If we only consider one piece of data, we obtain:

$$\begin{aligned}\mathcal{L}_{pos}(\pi|x) = &-\int_{A_{\pi(x)}}(1-\pi(t))dt\\ +C*(&-\int_{\mathbb{R}}\frac{(1-\pi(t))^2}{2}dt+\int_{\mathbb{R}}(1-\pi(t))dt)\end{aligned} \tag{9}$$

where C is a constant (usually $\frac{1}{n}$, where n is the number of independent data considered). Property 2 remains true in the continuous case. The possibilistic counterpart of likelihood being defined, we will now considered the particular cases of triangular and trapezoidal distributions.

B. Triangular distribution

We define a triangular possibility distribution as the triple $\pi_{tri} = (m, l, r)$ where m is the mode of the triangle and l and r the left and the right spread respectively. Since the 0-cut is infinite for a triangular distribution, we assume that X is bounded and has a maximal size equal to the constant MAX_{size}.
We consider a piece of data $x \in X$. We note $\mu = \pi_{tri}(x)$ the possibility degree of x and $[a, b]$ the μ-cut of π_{tri}. There are two cases for the term that depends on $\pi_{tri}(x)$ in (9). We consider the case of $x \in]m-l, m+r[$. We have:

$$\begin{aligned}MemSurf(\pi_{tri}|x) &= -\int_{A_{\pi_{tri}(x)}}(1-\pi_{tri}(t))dt\\ &= -\int_a^b(1-\pi_{tri}(t))dt\\ &= -\int_a^m(1-\pi_{tri}(t))dt+\int_m^b(1-\pi_{tri}(t))dt\\ &= -\int_a^m(1-(1-\frac{m-t}{l}))dt-\int_m^b(1-(1-\frac{t-m}{r}))dt\\ &= -\int_a^m\frac{m-t}{l}dt-\int_m^b\frac{t-m}{r}dt\\ &= -(1-\mu)^2*\frac{l}{2}-(1-\mu)^2*\frac{r}{2}\\ &= -(1-\mu)^2*\frac{l+r}{2}.\end{aligned}$$

In the case of $x \notin]m-l, m+r[$, with the bounding assumption, we obtain:

$$MemSurf(\pi_{tri}|x) = -MAX_{size}+\frac{l+r}{2}.$$

Note that a more flexible approach on the bounding can be used, for instance by considering that the weight MAX_{size} depends on the distance between x and the triangle. The other part of the equation (9) is computed such as:

$$\begin{aligned}&-\int_{\mathbb{R}}\frac{(1-\pi_{tri}(t))^2}{2}dt+\int_{\mathbb{R}}(1-\pi(t))dt=\\ &\int_{m-l}^{m+r}-\frac{(1-\pi_{tri}(t))^2}{2}+(1-\pi_{tri}(t))dt\\ &+\int_{R/[m_l,m+r]}-\frac{(1-\pi_{tri}(t))^2}{2}+(1-\pi_{tri}(t))dt=\\ &-\frac{l+r}{6}-\frac{MAX_{size}}{2}.\end{aligned}$$

The terms MAX_{size} depends neither on π_{tri} and nor on x and can then be omitted. Finally, we obtain:

$$\mathcal{L}_{pos}(\pi_{tri}|x) = MemSurf(\pi_{tri}|x) - C*\frac{l+r}{6}. \tag{10}$$

C. trapezoidal distribution

We define a trapezoidal possibility distribution as the quadruple $\pi_{trap} = (a, b, c, d)$ where $[a, d]$ and $[b, c]$ are respectively the support and the core of the distribution. As in the triangular case, we assume that X is bounded and has a maximal size equal to the constant MAX_{size}. We note $\mu = \pi_{trap}(x)$ the possibility degree of x. There are three cases for the term that depends on $\pi_{tri}(x)$ in Equation (9).

- $x \in]b, c[$:
$$MemSurf(\pi_{trap}|x) = 0$$
- $x \in]a, b[$ or $x \in]c, d[$:
$$MemSurf(\pi_{trap}|x) = -(1-\mu)^2*\frac{b-a+d-c}{2}$$

- $x \notin]a, d[$:

$$MemSurf(\pi_{trap}|x) = -MAX_{size} + \frac{-b-a+d+c}{2}.$$

The other part of the equation (9) is computed such as:

$$-\int_{\mathbb{R}} \frac{(1-\pi_{trap}(t))^2}{2} dt + \int_{\mathbb{R}} (1-\pi(t))dt = -\frac{b-a+d-c}{6} - \frac{c-b}{2} - \frac{MAX_{size}}{2}.$$

As in the triangular case, the terms $-\frac{MAX_{size}}{2}$ can be omitted. Finally, we obtain:

$$\mathcal{L}_{pos}(\pi_{trap}|x) = MemSurf(\pi_{tri}|x) - C*(\frac{b-a+d-c}{6} - \frac{c-b}{2}). \quad (11)$$

Note that, having the likelihood function defined for triangular (resp. trapezoidal) distribution, we can obtain the optimal triangular (resp. trapezoidal) by finding the parameters that maximizes $\mathcal{L}_{pos}$. Since this problem cannot be solved analytically, we have to use a meta heuristic such as simulated annealing [7] or particle swarm optimization [6].

VI. Illustrations and Discussion

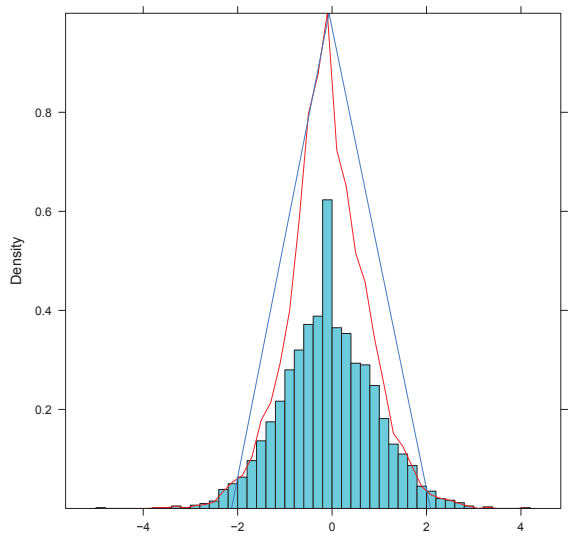

Fig. 3. Possibility transformation that maximizes $\mathcal{L}_{pos}$ with respect to a set of data that follows a Gaussian distribution

In this section, we will use possibilistic likelihood in order to build a possibility distribution from a set of data. Figure 3 represents the triangular possibility distribution obtained from a set of 3000 data that obey a Gaussian distribution with a mean equal 0 and a standard deviation equals to 1. The possibility distribution obtained from a probability-possibility transformation of the histogram is in red. It corresponds to the optimal possibility distribution with respect to data. The triangular possibility distribution that maximizes $\mathcal{L}_{pos}$ is in blue. We can first notice that the mode of the triangular distribution corresponds to the mode of the Gaussian distribution. The triangular distribution is very close to the optimal one and dominates its on the majority of the data. The support contains 96% of the data. Figure 4

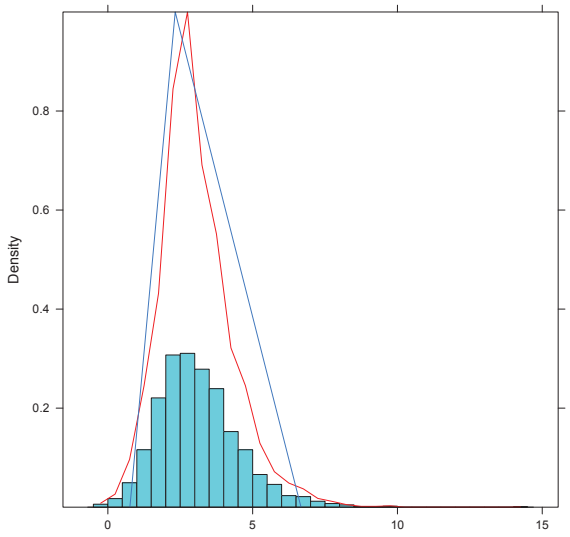

Fig. 4. Possibility transformation that maximize $\mathcal{L}_{pos}$ with respect to a set of data that follow a Student distribution

represents the triangular possibility distribution obtained from a set of 3000 data that follow a non central student distribution with 5 degrees of freedom. Although the distribution is not symmetric, we can observe similar results to the one observed with the Gaussian distribution. The support contains 96% of the data. In Figure 5, the distribution is multi modal. Here

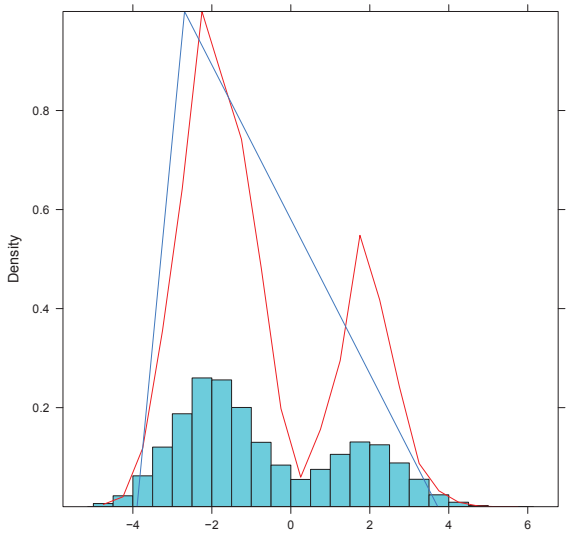

Fig. 5. Possibility transformation that maximizes $\mathcal{L}_{pos}$ with respect to a set of data that follows a multimodal distribution

we can observe that the mode of the triangular distribution is the highest mode of the probability distribution. However, it underestimates the second mode. The support still contains 96% of the data.

These results illustrates the following property, proved in [2]:

Proposition 3: The triangular symmetric possibility distribution of support $[x_1, x_2]$ and of mode $\frac{x_1+x_2}{2}$ is the least upper bound of all the possibility transforms of symmetric probability distributions of support $[x_1, x_2]$ and of mode $\frac{x_1+x_2}{2}$.

This proposition shows that triangular distributions may approximate any possibility transformation of bounded symmetric unimodal distributions. We have shown in Section 4 that approximating a possibility distribution by maximizing $\mathcal{L}_{pos}$ is more efficient that approximating the probability distribution and then turning it into a possibility distribution. It validates the use of possibilistic likelihood for building triangular distributions from data. Even Proposition 3 is not always true if the distribution is asymmetric, triangular possibilistic distribution performs well in general for any type of unimodal distribution. Thus, the use of triangular possibility distributions and of $\mathcal{L}_{pos}$ is a good alternative for bounding densities when the shape of the probability distribution is not known. Results are less good if the distribution is multimodal, but the mode of the triangular possibilistic distribution always identifies the highest mode of the probability distribution. Note that we do not present a result with a trapezoidal distribution because triangular distributions (which are a particular case of trapezoidal distributions) are always obtained.

VII. Conclusion

In this paper we have proposed a definition of possibilistic likelihood that agrees with the view of possibility distributions as families of probability distributions and with the probability-possibility transformation based on the maximum-specificity principle. This function can be used for evaluating and comparing a possibility distribution with respect to data or can be embedded into an optimization process in order to build a possibility distribution from a set of data. We have defined the possibilistic likelihood function both for discrete and for continuous universes. In the continuous case, we have shown that, in spite of its sophisticated definition, it is easy to compute for triangular and trapezoid distributions. Lastly, the good properties of triangular possibility distributions for bounding unimodal probability distributions make the building of possibility distributions by optimization of $\mathcal{L}_{pos}$ a good approach when no a priori information on the type of distribution is available. This optimization approach may be interesting in a machine learning context, for instance for Bayesian learning or for a k-nearest neighbor approach where distributions have to be computed from data. It can be also used as quality function for imprecise regression [9].

In the future, it may be interesting to define a possibilistic likelihood that allows us to obtain genuine trapezoidal distributions. Moreover, the proposed approach does not take into account the quantity of data available. Indeed, if only one value is available, the best possibility distribution is a Dirac, and there will be no difference with the case where a thousand of identical values are available. Less data should lead to less specific distributions. This should be taken into account in representations.

References

[1] D. Dubois. Possibility theory and statistical reasoning. *Computational Statistics and Data Analysis*, 51:47–69, 2006.

[2] D. Dubois, L. Foulloy, G. Mauris, and H. Prade. Probability-possibility transformations, triangular fuzzy sets, and probabilistic inequalities. *Reliable Computing*, 10:273–297, 2004.

[3] D. Dubois and H. Prade. When upper probabilities are possibility measures. *Fuzzy Sets and Systems*, 49:65–74, 1992.

[4] D. Dubois and H. Prade. On data summarization with fuzzy sets. In *Proc. of the 5th Inter. Fuzzy Systems Assoc. World Congress (IFSA'93), Seoul*, pages 465–468, 1993.

[5] D. Dubois, H. Prade, and S. Sandri. On possibility/probability transformations. In *Proceedings of Fourth IFSA Conference*, pages 103–112. Kluwer Academic Publ, 1993.

[6] J. Kennedy and R. Eberhart. Particle swarm optimization. In *Neural Networks, 1995. Proceedings., IEEE International Conference on*, pages 1942 –1948, 1995.

[7] S. Kirkpatrick, C. D. Gelatt, and M. P. Vecchi. Optimization by simulated annealing. *Science*, 220:671–680, 1983.

[8] G. Mauris. Inferring a possibility distribution from very few measurements. In *Soft Methods for Handling Variability and Imprecision*, volume 48 of *Advances in Soft Computing*, pages 92–99. Springer Berlin / Heidelberg, 2008.

[9] M. Serrurier and H. Prade. A general framework for imprecise regression. In *FUZZ-IEEE 07, London*, pages 1597–1602, 2007.

[10] L.A. Zadeh. Fuzzy sets as a basis for a theory of possibility. *Fuzzy sets and systems*, 1:3–25, 1978.

Author Index

A

Abbass, Hussein A. 2039
Abdelaziz, Hamzaoui 1388
Abe, Jair 2928
Acampora, Giovanni 123
Acampora, Giovanni 139
Acampora, Giovanni 146
Acampora, Giovanni 202
Acampora, Giovanni 223
Acampora, Giovanni 1783
Acampora, Giovanni 2018
Acampora, Giovanni 2073
Adam, Kasperski 2650
Adly, Moustafa 1918
Agarwal, Manish 2972
Aickelin, Uwe 1193
Aisbett, Janet 2185
Alimi, Adel M. 971
Almeida, Rui 2507
Althoefer, Kaspar 2232
Ament, Christoph 2656
Amin, Faijul 614
Amin, Faijul 1572
Amina, Mahdi 1033
Anderson, Derek 924
Anderson, Derek 2080
Anderson, Derek 2274
Anderson, Melissa 2274
Ando, Takeshi 2728
Andreu, Javier 2786
Angelov, Plamen 2786
Anil, Kashyap 2638
Antonelli, Michela 1286
Anugolu, Madhavi 932
Aoki, Shingo 1061
Aoki, Shingo 1701
Araki, Daisuke 1436
Araki, Daisuke 1447
Araki, Daisuke 1453
Araujo, Ernesto 1634
Araujo, Ernesto 2708
Arbaiy, Nureize 557
Arbaiy, Nureize 2851
Arcay, Bernardino 2123
Arnold, Christian 2656
Asmuss, Svetlana 1598
Asmuss, Svetlana 1610
Attarzadeh, Iman 2458
Auephanwiriyakul, Sansanee 1171
Avella, Pasquale 1783
Aymerich, F. Xavier 751

B

Baader, Franz 1735
Baccour, Leila 971
Bai, Ying 1510
Baili, Naouel 490
Balazs, Krisztian 2116
Baldinger, Jean-Louis 1466
Ballini, Rosangela 2745
Ballini, Rosangela 2794
Bandar, Zuhair 283
Bandar, Zuhair 2481
Barbosa, Paulo Sergio Franco 2745
Baruah, Rashmi Dutta 2786
Bastos, Carlos 1621
Bchir, Ouiem 2521
Beamish, Kathryn 2288
Behbood, Vahid 2676
Beliakov, Gleb 2905
Benatar, Naisan 1193
Berenji, Hamid 1689
Bernal, Miguel 1615
Besheer, Ahmad 2350
Bezdek, James 924
Bhowmik, Pavel 1902
Bisgambiglia, Paul Antoine 895
Bisgambiglia, Paul-Antoine 895
Biswas, Kanad K. 2972
Bobillo, Fernando 1727
Boixader, D. 1628
Bonissone, Piero P. 2897
Borges, Fabbio 2473
Borjalilu, Naimeh 564
Bosc, Patrick 1233
Bosworth, Ken 932
Boudy, Jerome 1466
Braga, Rosana 1111
Bustince, Humberto 1247

C

Cadenas, Jose M. 2897
Cadenas, Jose Manuel 202
Cai, Xun 248
Cai, Xun 2771
Cai, Yi 1719
Calderaro, Vito 231
Calzada, Alberto 2638
Cao, Longbing 691
Cao, Shu 2391
Carlsson, Christer 1799
Carneiro, Adriano 1111
Carrino, Stefano 86
Carvalho, Joao 2622
Castillo-Ortega, Rita 2909
Castro, Alfonso 2123
Cavalcanti, George 1621
Cecati, Carlo 231
Celi, Leo 2296
Chaabane, Mohamed 334
Chachi, Jalal 2859
Chakraborty, Aruna 1902
Chakraborty, Shantanu 656
Chakraborty, Shantanu 2606
Chamorro-Martinez, Jesus 537
Chamorro-Martinez, Jesus 759
Chan, K.Y. 572
Chan, K.Y. 2253
Chan, K.Y. 2261
Chang, Bao Rong 210
Chang, Chih-Hsiang 210
Chang, En-Chih 236
Chang, En-Chih 609
Chang, Feng-Yu 2155
Chang, Jyh-Yeong 939
Chang, Jyh-Yeong 1003
Chang, Shuo-Chieh 643
Chang, Tsung-Han 517
Chang, Wen-Jer 2213
Chang, Yu-Cheng 2664
Chang, Yu-Chuan 346
Chang, Yu-Chuan 448
Chang, Yu-Hern 2630
Chang, Yung-Ruei 2426
Chang, Yung-Ruei 2614
Chang, Yu-Yun 1491
Chau, Minh Ky 2013
Chen, Bor-Sen 2489
Chen, C.L. Philip 2193
Chen, C.L. Philip 2199
Chen, Cheng-Hung 932
Chen, Cheng-Hung 2108
Chen, Cheng-Hung 2819
Chen, Chen-Tung 1504
Chen, Chih-Chieh 643
Chen, Chih-Chuan 1587
Chen, Chin-Sheng 304
Chen, Chin-Sheng 859
Chen, Chin-Sheng 872
Chen, Chin-Sheng 1844
Chen, Chin-Yi 1497
Chen, Chung-Chieh 543
Chen, Chun-Hao 278
Chen, Chun-Sheng 1960
Chen, Hong-Ming 1127
Chen, Jui-Le 2922
Chen, Jun-Horng 160
Chen, Jyun-Yu 2104
Chen, Lihui 2500
Chen, Shinn-Horng 1774
Chen, Shyi-Ming 346
Chen, Shyi-Ming 448
Chen, Ta-Tau 304
Chen, Ta-Tau 1860
Chen, Ti-Hung 643
Chen, Wang-Kun 364
Chen, Wen-Hui 160
Chen, Xue Tao 1538
Chen, Xue Tao 2147
Chen, Yen-Tzu 2007
Chen, Yi-Chang 2426
Chen, Ying-Huang 2104
Chen, Ying-Jen 1305
Chen, Yon-Ping 195
Chen, Yung-Yue 368
Chen, Yung-Yue 1312
Chen, Zhi-Wei 1791
Cheng, Dun-Wei 210
Cheng, Hsuan-KueiI 2690
Cheng, Hui-Hua 1791
Cheng, Li Chen 2060

Cheng, Sheng-Tzong 2960
Cheng, Wen-Chang 1946
Cheng, Yangjie 110
Cheng, Yu-Hsin 1640
Chenkun, Qi 374
Cheu, Eng Yeow 2668
Chiang, Chia-Ching 1946
Chiang, Jen-Shiun 2763
Chiang, Ming-Chao 2916
Chiang, Ming-Chao 2922
Chiao, Kuo-Ping 2575
Chien, Chiang-Ju 2876
Chien, Sheng-Wei 2046
Chin, Chiun-Li 1933
Chitta, Radha 463
Chiu, Huang-Jen 2432
Chiu, Shih-Yuan 185
Chiu, Steve 932
Cho, Se-Hyoung 917
Chou, Cheng-Wei 185
Chou, Jyh-Horng 1380
Chou, Po-Huan 872
Chou, Po-Huan 1844
Chu, Hui-Shan 1927
Chu, Jianxin 1648
Chua, Teck Wee 484
Chuang, Chen-Chia 2814
Chuang, Tzung-Nan 1670
Chuang, Tzung-Nan 2013
Chuang, Yen-Ching 1491
Chung, Hsunhsun 1568
Chung, Hsunhsun 1593
Chung, I-Fang 2664
Cismondi, Federico 2096
Cismondi, Federico 2296
Cismondi, Federico 2507
Cortez, Joaquin 1615
Costa, Anderson 497
Costa, Pyramo 2794
Couso, Ines 1263
Creelman, Jim 932
Creighton, Doug 502
Crockett, Keeley 283
Crockett, Keeley 2481
Cross, Valerie 1743

D

Datta, Manoj 2440
Davari, Soheil 2955
De Maio, Carmen 2088
De Prisco, Roberto 202
De Roo, Jos 844
Delgado, Miguel 2080
Deters, Christian 2232
Detyniecki, Marcin 455
Dewantoro, Gunawan 884
Diao, Ren 1516
Dillon, T.S. 2253
Dillon, T.S. 2261
Dilmaghani, Reza Shams 2232
Dimitrios, Koulouriotis 851
Dong, Fangyan 777
Dong, Fangyan 783
Dong, Fangyan 787
Dorizzi, Bernadette 1466
Douali, Nassim 844
Ducange, Pietro 1286
Dvorak, Antonin 2383

E

El-Fiqi, Heba 2039
El-Sherif, Hisham 1918
Endo, Yasunori 804
Endo, Yasunori 810
Endo, Yasunori 816
Entani, Tomoe 1705
Erra, Ugo 733
Essounbouli, Najib 1404

F

Fahmy, Aly A. 2534
Fan, Jing-Yun 2559
Fan, Yi Hua 867
Fan, Zhun 241

Fang, Chun-Hsiung 1380
FanJiang, Yong-Yi 2690
Farivar, Faezeh 1882
Farivar, Faezeh 1999
Farzbod, Negin 1882
Farzbod, Negin 1999
Fassih, Amir 932
Fatichah, Chastine 772
Fedrizzi, Mario 1799
Feng, Gang 1299
Fenza, Giuseppe 131
Fenza, Giuseppe 2088
Fernandes, Ricardo 1111
Fernandez, Alberto 1239
Fernandez, Alberto 1247
Fialho, Andre 2096
Fialho, Andre 2296
Fialho, Andre 2507
Filho, Joao da Silva 2928
Finkelstein, Stan 2296
Finkelstein, Stan 2507
Fischetti, Enrico 131
Francato, Alberto Luiz 2745
Francisco, Chavez de la O 256
Francisco, Fernandez de Vega 256
Francisco, Herrera Trigeros 256
Frelicot, Carl 2513
Frigui, Hichem 490
Frigui, Hichem 2521
Fu, Yu-Yi 2827
Fuente, MariaJ. 1271
Fujie, Masakatsu G. 2728
Fujita, Hiroshi 622
Fukuda, Shinji 272
Fukuoka, Kenji 1061
Fuller, Robert 1799
Funabashi, Toshihisa 2420
Funabashi, Toshihisa 2440
Funabashi, Toshihisa 2606
Furno, Domenico 131
Furuhashi, Takeshi 1339
Furuhashi, Takeshi 2540

G

Gader, Paul 741
Gaeta, Matteo 102
Gaeta, Matteo 123
Galende, Marta 1271
Gallo, Mariacristina 2088
Ganji, Behnam 2335
Gao, Huijun 2358
Gao, Qing 1299
Garcia, David 1255
Garibaldi, Jonathan M. 1185
Garibaldi, Jonathan M. 1193
Garibaldi, Jonathan M. 1580
Garrido, M. Carmen 2897
Gasir, Fathi 283
Gassara, Hamdi 334
Ge, Hongwei 2864
Gedeon, Tom 1874
Ghiasi, Tayebe Sadat 1896
Gibbon, Greg 2185
Gitas, Ioannis 1279
Gomide, Fernando 2794
Gonzalez, Antonio 1255
Gonzalez-Longatt, Francisco 164
Gosain, Anjana 1656
Grimaccia, Francesco 2454
Gu, Wei 1648
Gualtieri, Jean-Sebastien 895
Guan, Cuntai 1530
Guelton, Kevin 322
Guerra, Thierry Marie 329
Guerra, Thierry Marie 2870
Guerrero, Josep M. 609
Guitao, Cao 374
Gumrah, Giray 1751
Gupta, Sitanshu 944

H

Hagras, Hani 509
Hagras, Hani 2139

Hairi-Yazdi, M.R. 1157
Hajjaji, Ahmed EL 1411
Hajjaji, Ahmed EL 334
Halder, Anisha 1902
Hamasuna, Yukihiro 804
Hamasuna, Yukihiro 810
Hametner, Christoph 1546
Hametner, Christoph 2802
Hamzaoui, Abdelaziz 1404
Han, Hugang 1320
Han, Il Song 747
Han, Ming-Feng 939
Han, Ming-Feng 1003
Han, Shilian 1201
Han, Woo Joon 747
Hanada, Masaya 783
Hanmandlu, Madasu 2972
Hao, Minshen 957
Hao, Pei-Yi 889
Hasegawa, Ryuzo 622
Hashimoto, Kiyota 1049
Hashimoto, Takuya 766
Hashimoto, Takuya 783
Hassanien, Aboul Ella 2534
Hasuike, Takashi 531
Hata, Yutaka 1013
Hata, Yutaka 1017
Hata, Yutaka 1022
Hata, Yutaka 1026
Hata, Yutaka 1430
Havens, Timothy 463
Hayashida, Tomohiro 1767
Herrera, Francisco 1239
Herrera, Francisco 1247
Heydebreck, Peter 902
Hibino, Fuminori 721
Hidalgo, Ieda Geriberto 2745
Hirokawa, Sachio 1074
Hirota, Kaoru 772
Hirota, Kaoru 777
Hirota, Kaoru 783
Hirota, Kaoru 787
Hiwada, Eriko 1459
Ho, Wen-Hsien 1774
Holanda, Raimir 2473
Holcapek, Michal 2375
Holcapek, Michal 2383
Homem, Nuno 2622
Honda, Aoi 2566
Honda, Katsuhiro 386
Honda, Katsuhiro 394
Honda, Katsuhiro 416
Honda, Katsuhiro 792
Honda, Katsuhiro 799
Honda, Katsuhiro 1079
Honda, Katsuhiro 1695
Honda, Katsuhiro 1710
Honda, Katsuhiro 1715
Hong, Tzung-Pei 218
Hong, Tzung-Pei 278
Hong, Tzung-Pei 1674
Horio, Keiichi 2714
Horng, Wen-Ren 1380
Hoshino, Yukinobu 1369
Hossain, Amjad 614
Hosseinzadeh, Mehdi 2364
Hou, Yibin 627
Howell, Michael 2296
Howell, Michael 2507
Howlader, Abdul Motin 656
Hsia, Chih-Hsien 2763
Hsia, Kuo-Hsien 984
Hsiang, Chia-Chun 2304
Hsiao, Chih-Ching 2814
Hsiao, Ming-Ying 304
Hsiao, Ming-Ying 1860
Hsieh, Chaur-Heh 996
Hsieh, Cheng-Da 1417
Hsieh, Pei-Yang 1933
Hsu, Chia-Hung 2664
Hsu, Chih-Wei 2960
Hsu, Chin-Yuan 1791
Hsu, Han-Chung 2046

Hsu, Hung-Wei 2763
Hsu, Lindroos 2696
Hsu, Sheng-Che 1923
Hsu, Sheng-Che 2104
Hsu, Shun-Chin 190
Hu, Chenglin 1910
Hu, Kai-Cheng 2916
Hu, Miaohan 2391
Huamani, Ivette Raymunda Luna 2745
Huang, Chien-Feng 210
Huang, Chi-Yo 1474
Huang, Chi-Yo 1664
Huang, Chi-Yo 2401
Huang, Hsiao-Wen 2007
Huang, Hsiao-Wen 2026
Huang, Hsien-De 2018
Huang, Hua-Wei 2007
Huang, Jih-Jeng 1497
Huang, Jun-Yi 543
Huang, Kuang Yu 1640
Huang, Liang-Tsung 2684
Huang, Xu 2342
Huang, Zhangqin 627
Hung, Kuo-Chen 590
Hung, Kuo-Chen 2495
Hung, Wei-Zhan 1504
Hung, Ying-Hsun 1479
Huo, Chih-Li 1143
Huo, Chih-Li 1554
Hwang, Chih-Lyang 706
Hwang, Chih-Lyang 1327
Hwang, Chih-Lyang 1333

I

Iakovidis, Dimitris 821
Ibrahim, Mohamed 1918
Ibrahim, Zuwarie 1084
Ichihashi, Hidetomo 386
Ichihashi, Hidetomo 394
Ichihashi, Hidetomo 416
Ichihashi, Hidetomo 792
Ichihashi, Hidetomo 799
Ichihashi, Hidetomo 1079
Ichihashi, Hidetomo 1695
Ichihashi, Hidetomo 1710
Ichihashi, Hidetomo 1715
Ichinotsubo, Takeo 1701
Imai, Hideyuki 672
Ingold, Rolf 86
Inoue, Kazushige 1701
Ishibuchi, Hisao 264
Ishibuchi, Hisao 549
Ishida, Kenji 2728
Ishikawa, Osamu 1017
Ishikawa, Utaki 1362
Istrate, Dan 1466
Izumi, Yuya 2414

J

Jaadari, Abdelhafidh 329
Jaadari, Abdelhafidh 1615
Jabri, Dalel 322
Jacob, Jerene 666
Jahromi, Abdolhamid Eshraghniaye 564
Jain, Anil 463
Jakubek, Stefan 1546
Jakubek, Stefan 2802
Jamshidi, Mo 1689
Jangjou, Mehrdad 2396
Janiszek, David 1149
Jau, You-Min 2839
Jaulent, Marie-Christine 844
Javier, Andreu 2779
Jeng, Jin-Tsong 2839
Jeng, Jyh-Fu (Don) 523
Jensen, Alex 932
Jensen, Richard 2465
Jeon, Hyoung Seok 1989
Jesus, Alcala Fernandez 256
Jheng, Sin-Sian 2213
Jia, Limin 2552

Jiang, F. 572
Jiang, Frank 2238
Jiang, Yinlai 2728
Jin, Rong 463
John, Robert I. 971
Joo, Young Hoon 1007
Joo, Young Hoon 1989
Joo, Young Hoon 1994
Ju, Zhaojie 699
Juang, Chia-Feng 1417
Juang, Chia-Feng 2664
Juang, Jih-Gau 2311
Junratanasiri, Sittichok 1171
Jyh-Horng, Chou 1774

K

Kacprzyk, Janusz 2934
Kalaivani, O.K. 649
Kanagawa, Shuya 1568
Kanchapogu, Vaisakh 153
Kandasamy, Meenaskhi 1743
Kanoh, Masayoshi 1356
Kanzawa, Yuchi 816
Kao, Hung-Yu 2018
Kao, Jhen-Shun 311
Karakasis, Evangelos 836
Karunambigai, M.G. 649
Kashani, Mohammad Mansour Riahi 2396
Katagami, Daisuke 1374
Katagiri, Hideki 531
Katagiri, Hideki 1778
Katagiri, Hideki 1830
Kato, Kosuke 879
Kato, Naoki 766
Kaur, Prabhjot 1656
Kawaguchi, Shogo 1453
Kaymak, Uzay 2507
Kchaou, Mourad 1411
Keller, James 924
Keller, James 2080
Keller, James 2274
Ketipi, Maria 836
Khaled, Omar Abou 86
Khalid, Marzuki 1084
Khalilia, Mohammed 1805
Khayyam, Hamid 2335
Kheirikhah, Mohammad Mahdi 727
Khodayari, Alireza 727
Khosravi, Abbas 502
Kim, Jong-Hwan 917
Kim, Jong-Hwan 2170
Kim, Jong-Hwan 2594
Kinjyo, Yoshihisa 2414
Kinjyo, Yoshihisa 2420
Kiseliova, Tatiana 2073
Ko, Chia-Nan 2827
Ko, Kwang-Eun 2752
Kobashi, Syoji 1022
Kobashi, Syoji 1430
Kobashi, Yusuke 1356
Kobayashi, Daisuke 1339
Kobayashi, Hiroshi 766
Koczy, Laszlo T. 2116
Kodogiannis, Vassilis 1033
Koeppen, Mario 2566
Koga, Takanori 1966
Komori, Yuki 1079
Konar, Amit 1902
Koo, Geun Bum 1989
Koshimura, Miyuki 622
Koulouriotis, Dimitrios 836
Kouzani, Abbas Z. 2335
Kovacs, Szilveszter 436
Kozek, Martin 1546
Kramer, Kathleen 950
Krueger, Lars 902
Ku, Cheung-Chieh 2213
Ku, Hsiang-Chun 1670
Kuan, Meng-Jong 1491
Kuan, Meng-Jong 2304
Kubo, Seiji 1447
Kubo, Seiji 1453

Kubota, Naoyuki 713
Kubota, Naoyuki 1362
Kubota, Naoyuki 1459
Kumar, K.D. 1836
Kumar, Parmod 932
Kung, Chung-Chun 643
Kung, Jung-Yuan 1670
Kung, Jung-Yuan 2013
Kuo, Bor-Chen 1927
Kuo, Chia-Hao 2890
Kuo, Chih-En 2104
Kuo, Feng-Yuan 676
Kuo, Hui-Ching 1791
Kuo, Jong Yih 2690
Kuo, Jong-Yih 2702
Kuo, Shu-Ching 1587
Kuo, Su-E 1791
Kuo, Yi-Ling 1055
Kuo, Yong-Lin 884
Kuo, Yu-Liang 2630
Kuramoto, Kei 1013
Kuramoto, Kei 1022
Kuramoto, Kei 1430
Kwong, C.K. 2253
Kwong, C.K. 2261

L

Labiod, Salim 2870
Lai, Daphne Teck Ching 1580
Lai, Johnny C.Y. 2219
Lai, Lien-Fu 2684
Lai, Yang-Chih 1143
Lam, H.K. 298
Lam, Hak-Keung 2232
Lam, Li Chieu 394
Lamba, I.M.S. 1656
Lambeck, Steven 2656
Lambert-Torres, Germano 2928
Langlois, Nicolas 2979
Latham, Annabel 2481
Latrach, Chedia 1411
Le, Phuc Quang 772
Leal, Liliam 2473
Lee, Chang-Shing 783
Lee, Chang-Shing 1055
Lee, Chang-Shing 1791
Lee, Chang-Shing 2018
Lee, Chao-Feng 1844
Lee, Cheng-Ming 2827
Lee, Ching-Hsiang 1380
Lee, Ching-Hung 2155
Lee, Chiung-Hon 2696
Lee, Jonathan 2702
Lee, Lian-Wang 543
Lee, Seok Jong 595
Lee, Seung-Mok 2594
Lee, Tun-Yuan 2882
Lee, Wen Jau 1084
Lee, Wen-Tin 2702
Lee, Yeong-Chyi 278
Lee, Ying Tsun 867
Lee, Yue-Shi 996
Leite, Daniel 2794
Leman, Karianto 484
Lemos, Marcus 2473
Leung, Frank H.F. 2219
Leung, Frank H.F. 2225
Leung, Ho-fung 1719
Li, Chengdong 1974
Li, Chengdong 1982
Li, Cheng-Hsuan 1927
Li, Chun-I 2763
Li, Da 627
Li, Danyun 777
Li, Hongyi 2358
Li, I-Hsum 543
Li, Junquan 1836
Li, Lei 1953
Li, Sheng-Tun 1587
Li, Sheng-Tun 2583
Li, Shoumei 2528
Li, Tzuu-Hseng S. 1852
Li, Xuewen 2552

Li, Y. 170
Li, Y.J. 170
Li, Y.J. 178
Li, You 1090
Li, You 1096
Lian, Huan 2552
Lian, Kuang-Yow 1397
Liang, Sheng-Fu 1674
Liang, Sheng-Fu 2104
Liao, Jian-Tang 2448
Liao, Shih-Hui 1003
Liao, Wei-Cheng 1294
Liao, Zuhua 2391
Liaw, Yi-Ching 2696
Lie, Donald 666
Lien, Che-hui 2066
Lien, Shao-Fan 984
Lietard, Ludovic 2033
Lietard, Ludovic 2546
Lin, Che-Nan 1860
Lin, Cheng-Jian 2819
Lin, Chin-Teng 939
Lin, Chin-Teng 1003
Lin, Chin-Teng 1927
Lin, Chin-Teng 2819
Lin, Chun-Wei 218
Lin, Chun-Yuen 2046
Lin, Faa-Jeng 872
Lin, Faa-Jeng 1844
Lin, Faa-Jeng 2614
Lin, Kuo-Ping 590
Lin, Kuo-Ping 2495
Lin, Pei-Chun 1103
Lin, Pei-Ying 2684
Lin, Tsung-Chih 2882
Lin, Tsung-Chih 2890
Lin, Tsung-Ching 218
Lin, Yang-Yin 939
Lin, Yang-Yin 1003
Lin, Yin-Fang 1670
Lin, Yu-Hsiu 859
Linciano, Roberto 2088
Linda, Ondrej 1560
Ling, S.H. 572
Ling, S.H. 2219
Ling, S.H. 2253
Ling, S.H. 2261
Ling, Sai Ho 2225
Ling, Steve 2238
Lisowski, Michael 241
Liu, Che-Hung 2026
Liu, Chien-Hung 1397
Liu, Dong C 110
Liu, Duo 2245
Liu, Guan-Yu 2827
Liu, Honghai 699
Liu, Honghai 2358
Liu, Hsiang-Chuan 356
Liu, Huaping 2319
Liu, Jun 2638
Liu, Tung-Sheng 356
Liu, Xinwang 1179
Liu, Xinwang 1201
Liu, Xinwang 2163
Liu, Zhentao 772
Liu, Zhentao 777
Lo, Ji-Chang 311
Lo, Ji-Chang 1294
Lo, Mei-Chen 1485
Lo, Yu-Kang 2432
Loia, Vincenzo 102
Loia, Vincenzo 131
Loia, Vincenzo 139
Loia, Vincenzo 202
Loia, Vincenzo 223
Loia, Vincenzo 1783
Loia, Vincenzo 2018
Loia, Vincenzo 2088
Lopez, Cristina 1810
Lozano, Sebastian 1810
Lu, Jie 2676
Lu, Zong-Han 2614
Lung, Chung-Horng 2245
Luo, Minnan 2319

M

Ma, Shang-Pin 2690
MacParthalain, Neil 1523
Maeda, Yoichiro 721
Maeda, Yoichiro 1350
Magoc, Tanja 2948
Mahfouf, Mahdi 1041
Mahfouf, Mahdi 2205
Mahfouf, Mahdi 2288
Mahfouf, Mahdi 2756
Mahmoud, Taheri Seyed 2859
Majima, Yukie 1061
Mamboundou, Jerry 2979
Manamanni, Noureddine 322
Manceur, Malik 1388
Mandal, Rajshree 1902
Manic, Milos 1560
Manna, Sukanya 1874
Manry, Michael 248
Manry, Michael 2771
Marcelloni, Francesco 1286
Marin, Nicolas 2909
Marquez, Cornelio Yanez 910
Marsala, Christophe 455
Martinez, Luis 2638
Martinez, Raquel 2897
Martinez-Bea, Sergi 401
Martinez-Jimenez, Pedro 537
Martinez-Jimenez, Pedro Manuel 759
Mashinchi, Hadi 1953
Mashinchi, M. Hadi 2968
Mashinchi, Mashaallah 2968
Matsuda, Atsushi 2714
Matsui, Takeshi 1778
Matsui, Takeshi 1830
Matsumoto, Tomoyuki 1436
Matsumoto, Tomoyuki 1447
Matsumoto, Tomoyuki 1453
Matsumoto, Yui 416
Matsushita, Takehiko 1436
Mattioli, Gabriel 2369
Mauclair, Julie 1149
Mayr, Christian 1546
Mazlack, Lawrence 1822
Mazlack, Lawrence 2940
Mclean, David 2481
Medjahed, Hamid 1466
Mei, Jian-Ping 2500
Mendel, Jerry 957
Mendel, Jerry 2177
Mendel, Jerry 2407
Meng, Tay Kai 442
Meng, Tay Kai 1219
Meng, Xuelei 2552
Miao, Chunyan 1815
Mikado, Hiroaki 2732
Miller, Simon 1185
Minyar, Sassi 683
Misawa, Hideaki 2714
Miyahira, Suzana 1634
Miyamoto, Sadaaki 381
Miyamoto, Sadaaki 422
Miyamoto, Sadaaki 804
Miyamoto, Sadaaki 810
Miyamoto, Sadaaki 816
Miyoshi, Tetsuya 2720
Miyoshi, Tsutomu 1759
Mizumoto, Masaharu 1208
Mizumoto, Masaharu 1213
Mizutani, Eiji 2559
Modryani, Geev 231
Momoi, Shinji 1759
Montseny, Eduard 751
Mori, Yusuke 1442
Morrone, Aldo 2088
Motoki, Makoto 783
Mugellini, Elena 86
Muhando, Endusa Billy 2414
Mukherjee, Asim 944
Munoz, Enrique 123
Munoz, Enrique 202
Murase, Kazuyuki 614
Murase, Kazuyuki 1572

Mussetta, Marco 2454
Myung, Hyun 2594

N

Nagamune, Kouki 1436
Nagamune, Kouki 1447
Nagamune, Kouki 1453
Nagar, Atulya K. 1902
Nagashima, Kenichi 1568
Nagashima, Kenichi 1593
Nahavandi, Saeid 502
Naidu, D. S. 932
Naidu, D. Subbaram 2108
Naito, Akio 1791
Najib, Essounbouli 1388
Nakajima, Hiroshi 1022
Nakajima, Hiroshi 1026
Nakamura, Tsuyoshi 1356
Nakamura, Yu 1055
Nakatoh, Tetsuya 1074
Nakayasu, Hidetoshi 2720
Naoki, Tsuchiya 1022
Narimani, Mohammad 298
Narimani, Mohammad 2232
Neocleous, Costas 662
Neocleous, Costas 1119
Neog, Debanga Raj 1164
Ng, Peter 178
Ng, Peter H.F. 170
Ng, See Kiong 2668
Ngo, Thanh Long 1225
Nguyen, H.T. 572
Nguyen, Hung 2225
Nie, Maowen 635
Nie, Maowen 2131
Nieto, Oscar Camacho 910
Nii, Manabu 1442
Nishikawa, Shinya 264
Niu, Wangqiang 1648
Niwa, Keiichi 1767
Noh, Sun Young 1994
Nojima, Yusuke 264
Nojima, Yusuke 549
Nollet, Frederic 1404
Nonoguchi, Ryoichi 1710
Norris, Ian 2288
Notsu, Akira 386
Notsu, Akira 394
Notsu, Akira 416
Notsu, Akira 792
Notsu, Akira 799
Notsu, Akira 1079
Notsu, Akira 1695
Notsu, Akira 1710
Notsu, Akira 1715

O

Ohnishi, Shin-ichi 672
Ohtake, Hiroshi 1305
Okamoto, Jun 2566
Ole, Ravn 241
Olfa, Arfaoui 683
Omori, Takashi 2732
Orciuoli, Francesco 102
Orgun, Mehmet 1953
O'Shea, James 2481
Oshiro, Yoshitetsu 1017
Oskooyee, Koosha Sadeghi 2396
Othman, Ahmed 1603
Ou, C.R. 115
Ou, Chung-Ming 115
Ow, Siew Hock 2458
Own, Chung-Ming 352

P

Pagava, Karaman 2073
Pai, Ping-Feng 1504
Pal, Kishore 1572
Pal, Nikhil R 2600
Palacios, Ana 1263
Pan, Juntao 329

Pan, Shing-Tai 218
Pan, Shing-Tai 1674
Panoutsos, George 2205
Panoutsos, George 2288
Papageorgiou, Elpiniki 821
Papageorgiou, Elpiniki 828
Papageorgiou, Elpiniki 844
Papaioannou, Maria 662
Papaioannou, Maria 1119
Papakostas, George 836
Papakostas, George 851
Parchami, Abbas 2968
Park, Jin Bae 1007
Park, Jin Bae 1989
Park, Jin Bae 1994
Park, Junheong 2752
Park, Seung-Min 2752
Parthalain, Neil Mac 2465
Parvathi, R. 649
Paternain, Daniel 2905
Paul, Amit 1890
Pawel, Zielinski 2644
Pawel, Zielinski 2650
Pazhand, Hojat Rezaei 2859
Pedrycz, Witold 2851
Pegalajar, Manuel 2080
Penaloza, Rafael 1735
Peng, Lim Chee 442
Peng, Lim Chee 1219
Percannella, Gennaro 139
Pereira, Cesar 1621
Pereira, Ruben 2507
Perez, Maria C.J. 2708
Perez, Raul 1255
Petraki, Eleni 2039
Pham, Minh Tuan 2540
Pham, Nam Trung 484
Piccolo, Antonio 231
Pillala, Praveena 153
Pimentel, Bruno 497
Pitarch, Jose Luis 1615
Pivert, Olivier 1233
Plamen, Angelov 2779
Polydoros, Athanasios 851
Popescu, Mihail 924
Popescu, Mihail 1805
Popescu, Mihail 2080
Potluri, Chandrasekhar 932
Prade, Henri 2987
Pratap, Alok 2414
Priya, K. 992
Przemyslaw, Kobylanski 2644
Purnama, Irwan 2432

Q

Qin, Yong 2552
Qin, Zengchang 603
Qu, Yanpeng 1523
Quang, Minh Huynh 1404
Quek, Chai 1530
Quek, Chai 2668
Quere, Romain 2513

R

Rabelo, Ricardo 1111
Rabelo, Ricardo 2473
Rafael, Alcala Fernandez 256
Rajati, Mohammad Reza 2177
Rajesh, R. 992
Ramli, Azizul Azhar 2851
Rashmi, Dutta Baruah 2779
Raskin, Victor 94
Raza, Muhammad Amjad 1164
Recasens, J. 1628
Recasens, Jordi 2369
Reformat, Marek Z. 1751
Regulski, Pawel 164
Reti, Shane 2096
Reti, Shane 2296
Reti, Shane 2507
Rey, Alberto 2123
Rey, M.Isabel 1271

Rhee, Frank Chung-Hoon 479
Rhee, Frank Chung-Hoon 1164
Rickard, John T. 2185
Rifqi, Maria 455
Rocacher, Daniel 2033
Rocacher, Daniel 2546
Romain, Guillaume 2644
Ros, Maria 2080
Rovira, Alex 751
Ruza, Vecislavs 1598

S

Saber, Ahmed Y. 656
Sadati, Nasser 2364
Sahab, Nazanin 509
Sahebjamnia, Navid 2327
Sainz, Gregorio I. 1271
Sakawa, Masatoshi 1767
Sakawa, Masatoshi 1778
Sakawa, Masatoshi 1830
Sakoda, Masayuki 1055
Sala, Antonio 329
Salama, Mostafa A. 2534
Salmeron, Jose L. 1810
Salomon, Ralf 902
Sanchana, Rama Mohana Rao 153
Sanchez, Daniel 537
Sanchez, Daniel 2909
Sanchez, Luciano 1263
Sano, Genma 1356
Santana, Fagner 584
Santiago, Regivan 584
Sanz, Jose Antonio 1247
Sarkar, Kaushik 2600
Sataya, Takahashi 1344
Satheeshkumar, J. 992
Saverio, Salerno 1783
Sawa, Toru 2737
Sawazaki, Keisuke 381
Schizas, Christos 662
Schizas, Christos 1119
Schoen, Marco P. 932
Sebastian, Anish 932
Seki, Hirosato 1208
Seki, Hirosato 1213
Senatore, Sabrina 102
Senatore, Sabrina 733
Seneviratne, L.D. 298
Senjyu, Tomonobu 656
Senjyu, Tomonobu 2420
Senjyu, Tomonobu 2440
Senjyu, Tomonobu 2606
Senthilkumaran, N. 992
Seo, Toshiaki 1305
Serrurier, Mathieu 2987
Shah, Pritam Gajkumar 2342
Shang, Changjing 1523
Shanmuga, Priya B. 992
Shao, Shih-Chun 160
Sharma, Dharmendra 2342
Sharma, Rajneesh 1422
Shen, Aidi 1648
Shen, Chun-Sheng 1127
Shen, Qiang 428
Shen, Qiang 471
Shen, Qiang 1516
Shen, Qiang 1523
Shen, Zhiqi 1815
Shi, Edwin C. 2219
Shi, Fugui 2552
Shibanuma, Nao 1017
Shieh, Horng-Lin 2833
Shih, Kai-Shiuan 1852
Shih, Wen-Chung 965
Shill, Pintu 614
Shill, Pintu 1572
Shim, Eun-A 479
Shingo, Aoki 1069
Shingo, Yamasaki 1069
Shinkai, Kimiaki 1568
Shirzi, Moteaal Asadi 1157
Shiu, S.C.K. 170
Shiu, Simon 178
Shoorehdeli, Mahdi Aliyari 1882

Shoorehdeli, Mahdi Aliyari 1896
Shoorehdeli, Mahdi Aliyari 1999
Shu, Chun-Chin 1774
Shyu, Joseph Z. 2026
Shyu, Yi-Ping 1127
Siano, Pierluigi 231
Sil, Jaya 1890
Sim, Kwee-Bo 2752
Sisakht, Ali Haddad 2955
Sjahputera, Ozy 924
Sobrevilla, Pilar 751
Song, Min Kook 1007
Song, Wei 2864
Sostak, Alexander 1610
Soto-Cota, Adolfo 1615
Soto-Hidalgo, Jose Manuel 537
Soto-Hidalgo, Jose Manuel 759
Sousa, Joao 2096
Sousa, Joao 2296
Sousa, Joao 2507
Souza, Renata 497
Spaan, Matthijs T.J. 1422
Stavrakoudis, Dimitris 1279
Stokes, Klara 409
Straccia, Umberto 1727
Stubberud, Stephen 950
Su, Chiu-Hung 1479
Su, Juhng-Perng 984
Su, Ming-Yang 2046
Su, Shun-Feng 2814
Su, Tsan-Cheng 185
Su, Tsan-Cheng 190
Su, Xiang-He 2448
Suetake, Noriaki 1966
Sui, GuangJun 364
Sun, Changping 2282
Sun, Fuchun 2319
Sun, Fu-Shing 2268
Sun, Tsung-Ying 1143
Sun, Tsung-Ying 1554
Syoji, Kobashi 1013
Syu, Jhih-Cheng 1554

T

Tachibana, Kanta 2540
Takahama, Setsuko 290
Takahama, Tetsuyuki 290
Takahashi, Yasutake 721
Takahashi, Yasutake 1350
Takahashi, Yutaka 1442
Takashima, Yuya 1013
Takayama, Isao 804
Takayauki, Nakamura 1344
Takeda, Takahiro 1430
Takeda, Yuya 1763
Takeuchi, Kazuhiro 1049
Talari, Maryam 727
Tam, Nguyen 666
Tam, Sik Chung 2199
Tamani, Nouredine 2033
Tamani, Nouredine 2546
Tamer, Abdo 2350
Tan, Kuang-Hsiung 2614
Tan, Shing Chiang 1084
Tan, Woei Wan 635
Tan, Woei Wan 1538
Tan, Woei Wan 2147
Tanaka, Kazuo 1305
Tang, DangLing 364
Tang, Yi 932
Tanii, Hideaki 1022
Tao, Zou 374
Taylor, Julia M. 94
Terami, Akihisa 422
Terzija, Vladimir 164
Theera-Umpon, Nipon 1171
Theocharis, John 1279
Thilagavathy, C. 992
Thornton, Steve 2205
Tian, Qinghe 2391
Tizhoosh, Hamid 1603
Toda, Yuichiro 713
Toda, Yuichiro 1459
Tomomoto, Ishikawa 1013

Torabi, S.Ali 2327
Torra, Vicenc 401
Torra, Vicenc 409
Torres, Claudio 2928
Toumi, Ahmed 1411
Tourassis, Vassilios 836
Toyoshima, Takayasu 1447
Tsai, Chun-Wei 2916
Tsai, Chun-Wei 2922
Tsai, Fu-Ching 2583
Tsai, Men-Shen 859
Tsai, Shun-Hung 304
Tsai, Shun-Hung 1844
Tsai, Shun-Hung 1852
Tsai, Shun-Hung 1860
Tsang, Ren 1621
Tseng, Chung-Shi 368
Tseng, Chung-Shi 1312
Tseng, Fan-Chuan 676
Tseng, Shian-Shyong 965
Tseng, Shih-Pang 2922
Tseng, Vincent S. 996
Tsuchiya, Naoki 1026
Tsuda, Ei 1593
Tsuji, Hiroshi 1055
Tsutsumi, Kazutoshi 1763
Tung, Sau Wai 1530
Tyagi, Kanishka 248
Tyagi, Kanishka 2771
Tzeng, Chun-Hung 2268
Tzeng, Gwo-Hshiung 1474
Tzeng, Gwo-Hshiung 1479
Tzeng, Gwo-Hshiung 1485
Tzeng, Gwo-Hshiung 1491
Tzeng, Gwo-Hshiung 1664
Tzeng, Gwo-Hshiung 2304
Tzeng, Gwo-Hshiung 2401

U

Uchida, Yuzu 315
Uchino, Eiji 1966
Uchinuno, Atsuko 1442
Uehara, Akie 2414
Ueno, Nao 315
Uesu, Hiroaki 1593
Uno, Takeshi 879
Uozumi, Yosuke 1436
Urasaki, Naomitsu 656
Urasaki, Nomitsu 2420
Urfer, Alex 932

V

Valentina, Emilia Balas 2882
Valentina, Emilia Balas 2890
Van, Tam Huynh 1374
Vasileios, Tourassis 851
Vento, Mario 139
Vicentini, Patricia 2708
Vieira, Susana 2096
Vieira, Susana 2296
Vieira, Susana 2507
Vila, Amparo 2080
Villar, Pedro 1239
Vitiello, Autilia 123
Vitiello, Autilia 223
Vitiello, Autilia 1783
Vitiello, Autilia 2073
Vu, Hai An 772
Vu, Hai An 787

W

Wagatsuma, Yuki 713
Wagner, Christian 1185
Wagner, Christian 2139
Wai, Rong-Jong 2426
Wan, Chih-Wei 2401
Wan, Feng 1910
Wang, Bo 1090
Wang, Bo 1096
Wang, Chi-Hsu 2193
Wang, Chi-Hsu 2199
Wang, Chun-Chieh 1138

Wang, Dali 1510
Wang, Feng-Hsu 2053
Wang, H.B. 170
Wang, Hua An 2060
Wang, Hua O. 1305
Wang, Hui 2638
Wang, Hung-Jen 1587
Wang, Jen-Sheng 2026
Wang, Jing 2193
Wang, Li 2552
Wang, Lipeng 110
Wang, Mei-Hui 1791
Wang, Shitong 2864
Wang, Shuoyu 2728
Wang, Tiechao 1681
Wang, Tiechao 1974
Wang, Tiechao 1982
Wang, Ting-shiuan 340
Wang, Weize 1179
Wang, Xiaolu 579
Wang, Xun 2528
Wang, Yan 1953
Wang, Yao-Tien 115
Wang, Ying-Chung 2876
Wang, Yong 1299
Watada, Junzo 557
Watada, Junzo 976
Watada, Junzo 1084
Watada, Junzo 1090
Watada, Junzo 1096
Watada, Junzo 1103
Watada, Junzo 2851
Watanabe, Norifumi 2732
Watanabe, Toshihiko 2737
Wei, Hsiao-Yi 1587
Wendling, Laurent 1149
Weng, Chia-Chun 590
Wescott, Daniel 2274
White, Ethan 2940
Wilbik, Anna 2934
Wolfe, Charles 2232
Wu, Berlin 1103
Wu, Binghui Helen 2808
Wu, Chao-Chin 2684
Wu, Cheng-Wei 996
Wu, Chia-Chou 2489
Wu, Dongrui 2131
Wu, Dongrui 2177
Wu, Hsiu-Ming 706
Wu, Hsiu-Ming 1333
Wu, Min 777
Wu, Ming-Chang 2495
Wu, Rong-Ching 236
Wu, Wei 1523

X

Xianxia, Zhang 374
Xiao, Chunhua 627
Xu, Weimin 1648
Xu, Zhengguang 2282

Y

Yager, Ronald R. 1751
Yager, Ronald R. 2185
Yagi, Naomi 1017
Yaguchi, Aiko 1362
Yamaguchi, Takafumi 1442
Yamamoto, Takeshi 792
Yamanoi, Takahiro 672
Yamazaki, Yoichi 777
Yamazaki, Yoichi 783
Yamazaki, Yoichi 787
Yan, Yun-Chia 2007
Yang, Chao-Tung 965
Yang, Chu-Sing 2916
Yang, Chu-Sing 2922
Yang, Hong-Jia 1127
Yang, Hong-Tzer 2448
Yang, Jianxiong 976
Yang, Jie 691
Yang, Jin 2319
Yang, Longzhi 428

Yang, Longzhi 471
Yang, Lung-Sheng 236
Yang, Shih-Hung 195
Yang, Yong Yao 2205
Yang, Yong Yao 2756
Yano, Hitoshi 1866
Yasutake, Takahashi 1344
Ye, Jiang 374
Yeh, Chung-Hsing 2630
Yeh, I-Cheng 2066
Yen, Shi-Jim 185
Yen, Shi-Jim 190
Yen, Show-Jane 996
Yi, Jianqiang 1681
Yi, Jianqiang 1974
Yi, Jianqiang 1982
Yihun, Yimesker 932
Yin, Chengjiu 1074
Yin, Li-Peng 236
Ying, Hao 2589
Yoichiro, Maeda 1344
Yona, Atsushi 656
Yona, Atsushi 2420
Yona, Atsushi 2440
Yona, Atsushi 2606
Yoneyama, Jun 315
Yoo, Bum-Soo 917
Yoshida, Daisuke 799
Yoshida, Kyohei 721
Yoshikawa, Tomohiro 1339
Yoshikawa, Tomohiro 2540
Yu, Gwo-Ruey 1941
Yu, Ker-Wei 1134
Yu, Shui 2905
Yu, Teng-to 340
Yu, Yu-Hsiang 1143
Yu, Yu-Hsiang 1554
Yuki, Kodai 1459
Yun, Sang Min 595

Z

Zaccagnino, Rocco 202
Zaheer, Sheir Afgen 2170
Zamani, Iman 2364
Zarabadipour, Hassan 1882
Zarabadipour, Hassan 1896
Zarabadipour, Hassan 1999
Zarandi, Mohammad Hossein Fazel 2955
Zare, Alina 741
Zavala, Antonio Hernandez 910
Zeng, Jian-Hong 1674
Zeng, Xiao-Jun 1299
Zhai, Daoyuan 957
Zhang, Guangquan 2676
Zhang, Guiqing 1982
Zhang, Huiliang 1815
Zhang, Kun 1350
Zhang, Qian 1041
Zhang, Qian 2205
Zhang, Qian 2288
Zhang, Qian 2756
Zhang, Tong 2199
Zhang, Weifeng 603
Zhang, Xue-Feng 622
Zhang, Yang 2391
Zhou, Haibo 2589
Zhou, Yu-Quan 1134
Zhu, Lin 691
Zich, Riccardo E. 2454
Zowghi, Mahdi 564